Potential for mineral trapping during CO_2 storage in sedimentary basins

PER AAGAARD*, HELGE HELLEVANG, BINYAM L. ALEMU, VAN T.H. PHAM AND ANJA SUNDAL

Department of Geosciences, Univ. Oslo, Norway (*correspondence: per.aagaard@geo.uio.no)

A system perturbated by CO_2 injection reacts by dissolving primary minerals and form new secondary phases, and is also accompanied by an increase in solution trapping. The importance of such mineral reactions for safe long-term storage is highly system dependent.

Based on mineralogical and sedimentological information from siliciclastic reservoirs suitable for CO_2 storage (Sleipner (Utsira fm), Snöhvit (Tubåen fm), Johansen fm, Skagerrak (Gassum- & Haldager fm), a.o.), we performed numerical simulations on geochemical reactions induced by the CO_2 injection. The Norwegian offshore clastic reservoirs considered, represent a wide range in mineralogical composition, burial history and present day P, T, and salinity conditions. The sensitivity of dissolution and secondary mineral growth were analysed with respect to temperature, pressure, salinity and initial mineral assemblage.

In low-temperature quartz rich reservoirs, such as the Utsira fm. (Northern North Sea), we see that the potential for secondary carbonate growth is both limited by slow nucleation and growth rates of the carbonates, and on the limited amount of divalent metal cations present in primary phases such as glauconite, smectite, and chlorite. At higher temperature, the rate of carbonate growth is higher with faster response to the release of divalent metal cations. Aluminum released by feldspars and micas is preferentially precipitated out in non-carbonate secondary minerals, as dawsonite ($NaAl(OH)_2CO_3$) is not likely to form as it is only thermodynamic stable relative to other NaAl-phases at low temperatures [2].

[1] Pham *et al.* (2011) IJGGC In Press. [2] Hellevang *et al.* (2011) *Oil & Gas Sci. Technol.* **66**, 119-135.

Variable radiogenic isotopic compositions in Saharan dust across the Atlantic

S. AARONS*, S. ACIEGO AND J. GLEASON

University of Michigan, Ann Arbor, MI 48109-1005, USA (*correspondence: smaarons@umich.edu)

Isotopic characterization of aerosol mineral particles (dust) of varying sizes is essential in classifying potential source areas and determining the correct source of dust deposited over oceans and icesheets. The Sahara is considered a dominant source of aerosol dust in the Northern Hemisphere. Weathering, size, and mineral sorting can have an effect on radiogenic isotope compositions [1]. In order to investigate the isotopic variability of Hf, Nd and Sr we analyzed ten airborne dust samples in 2 size fractions collected during cruise M55 that intersected a cross-Atlantic dust storm originating in the Sahara in late 2002.

Past measurements of the isotopic composition of Hf, Nd and Sr of dust has focused primarily on coarse sized particles (1-30μm), whereas far-reaching deposition is primarily of a smaller size fractions (~2μm). Studies have shown that $^{87}Sr/^{86}Sr$ varies with grain size [2], but no systematic work has been done to show if there is a fallout distance effect on the isotopic composition. Weathering and sorting of minerals has a negligible effect upon the Nd isotopic composition [3]. The Hf isotopic composition however has been hypothesized to be highly variable due to a depleted "zircon effect" in the dust over time and distance [4].

$^{87}Sr/^{86}Sr$ measurements were performed on a Finnigan MAT 262 TIMS ($^{143}Nd/^{144}Nd$ measurements pending), and measurement of $^{176}Hf/^{177}Hf$ was performed on a Nu Instruments MC-ICPMS. Hf isotopic compositions show an east to west trend toward more radiogenic compositions across the Atlantic. While no Sr isotopic sorting trend based on distance from the dust storm is evident, the fine grained samples are consistently more radiogenic than the coarse grained samples from each site. A shift of >400 ppm in the $^{87}Sr/^{86}Sr$ ratio between coarse and fine fractions is found, with an average $^{87}Sr/^{86}Sr$ ratio of 0.7159, consistent with a Saharan dust source. The silicate versus water soluble fractions show a shift in $^{87}Sr/^{86}Sr$ ratios with ~70% of the Sr in the water soluble fraction attributable to seasalt and ~30% from dust.

[1] Dasch (1969) *Geochim. Cosmochim. Acta* **33**, 1521-1552. [2] Grousset & Biscaye (2005) *Chem. Geol.* **222**, 149-167. [3] Goldstein *et al.* (1984) *Earth Planet .Sci .Lett.* **70**, 221-236. [4] Rickli *et al.* (2010) *Geochim. Cosmochim. Acta* **74**, 540-557.

https://doi.org/10.1180/S0026461X00006502 Published online by Cambridge University Press

Geochemistry and mineralogy of the arid region, Hormozgan province (southern Iran), in relation with geo-pedological factors of soil evolution

HAKIME ABBASLOU[1], FRANCISCO MARTÍN[2]*, ALI ABTAHI[1] AND MOHAMMAD JAVAD POORGOHARDI[3]

[1]Soil Science Department, College of Agriculture, Shiraz University, Iran
[2]Soil Science Department, University of Granada, Spain (correspondence: fjmartin@ugr.es)
[3]BSc. In oil and petroleum engineering

The concentrations of trace elements in soils depend mainly upon the bedrock type, from which the soil parent material is derived, and pedogenic processes acting upon it [1]. Geochemistry of trace elements, mineralogical characteristics of soil diagnostic horizons and relevant parent rocks were measured with regard to determining amount and distribution of elements concentration in soils developed from different parent materials in Hormozgan province (southern Iran) to assess distribution, evolution and influential processes of the elements behavior in soils. The studied area has an arid climate with predominant sedimentary and basic igneous parent rocks. Elements concentration in soil and parent material are higher than the proposed range of world's soil average and relevant parent material by different references; however, Se and Pb concentrations are much lower than arid world's soil average. Statistical analysis of elements with soil properties and mineralogical characteristics suggest that different elements are classified in three cluster: i) samples with the highest amount of trace element concentration coinciding with highly developed soils and phyllosilicate minerals dominant; ii) soils with high percentage of quartz and sand; and iii) with partially lower amounts of elements coinciding with gypsiferous soils containing gypsum and dolomite minerals. No significant difference between horizons A and B in relation to C horizons were found representing early stages of weathering and pedogenic processes, and indicating that trace elements composition of the soil will be inherited from the parent material. Enrichment factor results show that lithogenic origin is the dominant source of elements, especially Mn, Fe, Sb, Bi, Sr, Sn and Co, and pedogenic origin is more notable for elements like As, Pb and Cu.

[1] Mitchell (1964) Trace elements in soils. pp:320–368.

Investigation of geochemical properties of Khonj bentonite mine (East of Iran)

H. ABBASNIA[1]* AND TORSHIZIAN[2]

[1]Iranian Mining Engineering Organization, Mashhad, Iran
[2]Islamic Azad University, Mashhad Branch, Mashhad, Iran (*correspondence: Abbasnia.hosein@gmail.com)

Bentonite usually forms from weathering of volcanic ash, most often in the presence of water. However, the term bentonite, as well as a similar clay called tonstoin, has been used for clay beds of uncertain origin. Konj Bentonite mine with area about 15 km2 locate in South Korassan province in the east of Iran. Lithology exposes of the rocks is consisting of Shale and Sandstones (Jurassic), Limestone and Marl (Cretaceous), Andesite and Dacite (Oligomiocene), green sandstone, Andesite, Tuff, Argillite and Conglomerete (Eocene). Form geological viewpoint, a Bentonite horizon with 10 m and more thickness have been extended in mine area and have been formed more than 1800000 ton Bentonite. Forming of this Bentonite horizon is because of acidic submarine colcanism activities and part of silicate rocks, Montmorillonite, Tuff and volcanic ash with Eocene age. These complexs in diagenes level undergo mineralogy changes and after that have been affected by surface weathering. Bentonite horizon divides to 4 classification super quality, high, normal and low quality. Mineralogy studies by XRD analysis show that main former mineral phase of Bentonite is consist of Montmorillonite, crystobalithe, and Calcite and secondary phase is consist Quartz, Albite and Gypsum. Chemical analysis result by XRF show that Khonj Bentonite is Soda type as maximum amount of Na20 is about 3.29 % while maximum amount of K2O is less than 1.5 %. According to chemical and physical test result like acidity (ph-9-10) and absorption index (597-705), best application for this Bentonite is using in sinker and found industrials.

https://doi.org/10.1180/S0026461X00006502 Published online by Cambridge University Press

Recycled halogen signature preserved in the Tristan hotspot

L.D. ABBOTT[1]*, R. BURGESS[1], D. MURPHY[2] AND C. BALLENTINE[1]

[1]SEAES, University of Manchester, Oxford Road, Manchester, M13 9PL, UK (*correspondence:lisa.abbott@postgrad.manchester.ac.uk)
[2]School of Natural Resource Sciences, Queensland Institute of Technology, G.P.O. Box 2434, Brisbane, Qld. 4001, Australia

The halogens (Cl, Br, I) are moderately volatile elements which exhibit incompatible behaviour during melting, and are fractionated by biological processes. Although the halgoens share similar geochemical properties to the noble gases in many systems, the heavy halogens have been underutilised as tracers because of the analytical difficulties related to determining their low abundances in geological materials.

Halogen compositions have been determined in a suite of ocean island basalts, including samples from the Tristan group of islands (Tristan and Inaccessible Is.). Analyses were completed on fluid and melt inclusions in olivine separates, using an extension of the Ar-Ar technique.

The Tristan and Inaccessible Island basalts exhibit a subducted halogen signature, showing a strong overlap in Br/Cl and I/Cl with marine pore fluids (fig. 1). Intergrated Br/Cl and I/Cl values extend up to 3.4 x 10^{-3} (molar ratio) and 4.1 x 10^{-3}, with mixing trend between MORB and marine pore fluid end-members observed. Higher ratios are obsevered in the Inaccessible Island samples, suggesting that the composition of the Tristan hotspot source has changed over time.

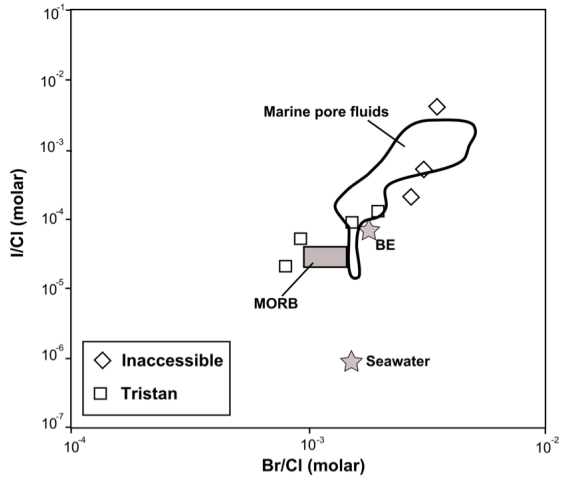

Figure 1: Observed overlap with marine pore fluids

(additional data from [1] Burgess *et al*. (2002), *EPSL* **197**, 193-203. [2] Mahn and Gieskes (2001), *Mar Geol* **174**, 323-339. [3] Martin *et al*. (1993), *GCA* **57**, 4377-4389.)

Calc-alkaline lamprophyre from Lusatia (Germany) derived from a multiply enriched mantle source

KH.M. ABDELFADIL[1], R.L. ROMER[1], TH. SEIFERT[2] AND R. LOBST[3].

[1]Deutsches GeoForschungZentrum, Potsdam, Germany (khaled@gfz-potsdam.de, romer@gfz-potsdam.de)
[2]TU Bergakademie Freiberg, Freiberg, Germany (seifert@mailserver.tu-freiberg.de)
[3]Sächsisches Landsamt für Umwelt (LfULG), Dresden, Germany (Reiner.Lobst@smul.sachsen.de)

Lusatia represents part of a 570-545 Ma old Cadomian magmatic arc that – in contrast to the adjacent areas of the Sudetes and the Erzgebirge – largely escaped metamorphism during the 350-340 Ma old Variscan orogeny. The post-Cadomian mantle beneath Lusatia was sampled by c. 400 Ma old tholeiitic gabbros and c. 230 Ma old calc-alkaline lamprophyre (spessartite), which allows to characterize the effect of the Variscan orogeny on the mantle beneath Lusatia and to compare it with the metasomatized mantle beneath the Erzgebirge and the Sudetes.

The tholeiitic gabbros originated from a mantle source that had been metasomatized during subduction beneath the Cadomian magmatic arc, which led to enrichment of LREE, Ba/Nb, and LILE relative to primitive mantle. The post-Variscan spessartites have the same trace-element pattern and Zr/Nb, Ce/Pb, and Y/Nb as the gabbros, indicating derivation from the same mantle source. The distinctly higher Rb, Ba, Pb, Sr, Th and Cs contents, higher La/Yb $^{87}Sr/^{86}Sr$, and $^{206}Pb/^{204}Pb$ ratios, and lower $^{143}Nd/^{144}Nd$ ratios in the spessartites, however, indicate a second, Variscan event of mantle enrichment. In addition, the spessartites have trace element ratios (i.e., Ba/Nb, Nb/U, Th/U, and Th/Nb) that resemble continental crust and the Sr, Nd and Pb isotope systematics demonstrate involvement of crustal material.

The trace-element signatures and Sr and Nd isotopic composition of Lusatian spessartites differ from post-Variscan calc-alkaline lamprophyres from the adjacent areas of the Sudetes and the Erzgebirge. This implies that the subduction during the Variscan orogeny resulted in geochemically and isotopically heterogenous mantle on the regional scale, possibly reflecting the contrasting nature of the subducted rocks.

https://doi.org/10.1180/S0026461X00006502 Published online by Cambridge University Press

Application of advanced nuclear magnetic resonance (NMR) spectroscopy and ultrahigh resolution mass spectrometry (MS) to studies of organic matter transformations

H. ABDULLA, P. CARICASOLE, H. CHEN, A. W. KAMGA, G. A. MCKEE, R. MESFIOUI, E. SALMON, R. L. SLEIGHTER AND P. G. HATCHER*

Department of Chemistry and Biochemistry, Old Dominion University, Norfolk, VA 23529. (habdulla@odu.edu, pcaricas@odu.edu, hxchen@odu.edu, akamga@odu.edu, gmckee@odu.edu, rmesfiou@odu.edu, esalmon@odu.edu, rsleight@odu.edu, *correspondence: phatcher@odu.edu)

The recent introduction of advanced NMR and MS methods has changed the landscape in our ability to discern the changes that natural organic matter (NOM) undergoes during processing in the environment. We can now identify molecular-scale transformations associated with both biotic reactions (biodegradation) and abiotic reactions (photodegradation, oxidation, physical separations, and thermal alteration). The strategy we have adopted for the examination of these various processes is to employ both NMR and MS together because of their complementarity in identifying molecular-level changes. Moreover, we have established ways to examine both dissolved and sedimentary OM in such a manner.

Results of our studies on biodegradation of NOM, in microcosm studies, in following terrestrial organic matter as it is exported to the oceans, have made it possible to identify suites of molecules that are recalcitrant, readily degraded, and newly produced. The MS data allow us to assign elemental formulas to these molecules, and the NMR data allow us to propose structural motifs. Our photochemical studies of DOM show that oxygenated and terrestrially-derived molecules are rapidly consumed while more aliphatic autochthonous molecules remain intact. Studies of sedimentary OM transformations have lead to the discovery of some important abiotic pathways for the reorganization of OM during diagenesis. For example, we have identified amidation reactions as important for N-sequestration in sediments. In the realm of thermal transformations, we can recognize decarboxylation as being part of a dominant process acting on kerogen.

The geochemical variation of volcanic rocks from Papandayan and Cikuray volcanoes, West Java: An existence of Gondwana continental fragment as crustal contaminant

M. ABDURRACHMAN[1,2]* M. YAMAMOTO[1] AND E. SUPARKA[2]

[1]Akita University, Akita-shi 010-8502, Japan (*correspondence: mirzam@gc.itb.ac.id)
[2]Bandung Institute of Technology, Bandung 40132, Indonesia

The Papandayan and the adjacent Cikuray Volcanoes are part of the active volcanoes in the Triangular Volcanic Complex, West Java [1]. Papandayan volcano consists of basaltic andesite (Early Stage), andesite (Middle Stage) and dacite (Late Stage); all of them belong to to medium-K series, with high $^{87}Sr/^{86}Sr$ (0.705243-0.705907) and low $^{143}Nd/^{144}Nd$ (0.512504-0.512650) ratios. In contrast to the Papandayan volcano, the Cikuray volcanic rocks exhibits a low-K series, with low $^{87}Sr/^{86}Sr$ (0.704172-0.704257) and high $^{143}Nd/^{144}Nd$ (0.512823-0.512858) ratios. Detailed petrological and geochemical studies indicate that the diversities in K_2O as well as isotopic ratios are mainly due to the influence of the Gondwana continental fragment (Fig 1a) [2] which is contaminating the Cikuray type magma to produce the Papandayan magma (Fig 1b).

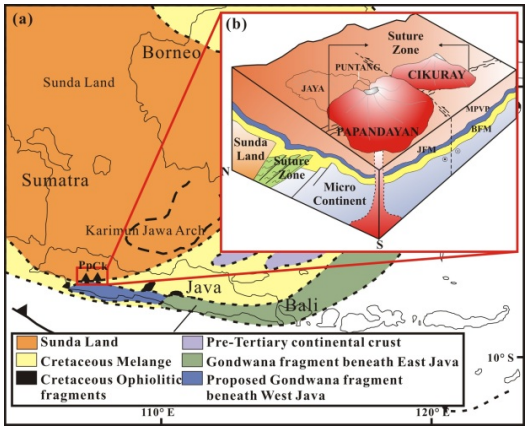

Figure 1: (a) A map showing the proposed Gondwana fragment beneath West Java [2,3,4, this study], (b) A schematic model of Papandayan-Cikuray volcanoes.

[1] Katili & Sudradjat (1984), Volcanological Survey of Indonesia, 102 pp. [2] Smyth *et al.* (2007) *Earth and Planetary Sci. Lett.* **258**, 269-282. [3] Clements & Hall (2007) *IPA31st*. [4] Sribudiyani *et al.* (2003) *IPA29th*.

https://doi.org/10.1180/S0026461X00006502 Published online by Cambridge University Press

Rutile included in the podiform chromitite from ocean floor at MAR 15°20'N FZ, Site 1271, ODP Leg 209

NATSUE ABE

IFREE, JAMSTEC, 2-15 Natsushima-cho, Yokosuka 237-0061, JAPAN, (abenatsu@jamstec.go.jp)

Several podiform chromitites includes rutile grains in abyssal peridotite are recovered from Site 1271 at Mid-Atlantic Ridge (MAR) 15°20' N fracture zone (FZ) during an ocean drilling cruise, ODP Leg 209 [1]. Only chromian spinel is preserved as the primary mantle mineral and all other primary minerals in the chromitite samples are completely altered. The primary chromian spinel has comparable Cr# (0.5) with it in the chromitite "minipod" sampled from Hess Deep [2]. The samples associated with chromitites from the drilling site consist of mainly dunite, some amphibole-bearing gabbros and troctolite, and rare in harzburgite. Therefore, the chromitites from this site are included in the rock series that composes the Moho transition zone as same in the ophiolites. It implies that a mass of melt existed, but was consumed in the uppermost mantle beneath the area. This means that the area is not magma-starved, although it is unclear when and where did interaction occurred. Some grains of the chromian spinel in the samples have thick rims of Cr-magnetite or completely replaced by magnetites. Cr content increases in the Cr-magnetite rim accompanied with Fe-enrichment. The chemical modification of the chromian spinel suggests that the chromitite from Site 1271 were metamorphosed at high temperature condition up to the upper greenschist facies because significant Al-missing from spinel cores is taken place at high temperature as a result equilibration with fluids in equilibrium with chlorite.

[1] Abe, N. (2011) Petrology of the podiform chromitite from ocean floor at MAR 15°20'N FZ, Site 1271, ODP Leg 209. *Jour. Mineral. Petrol. Sci. In Press*. [2] Arai, S. and Matsukage, K. (1996) Petrology of the gabbro-troctolite-peridotite complex from Hess Deep, equatorial Pacific. In *Proc. ODP, Sci. Results,* **147**, 135-155.

Geological, mineralogical and geochemical characteristics of Saheb Skarn (west of Iran)

NASIM ABEDI [1], MOHAMMAD YAZDI [2] AND KAMAL DANA [3]

[1](abedi42@yahoo.com)
[2](m-yazdi@sbu.ac.ir)
[3](Kamaldana@yahoo.com)

Saheb Iron Deposite is located in the northeast of Saghez in Sanandaj-Sirjan geotectonic zone, NW of Iran. Saheb Fe-skarn was developed along the contact of Saheb intrusive body with carbonatic rocks. Both endoskarn and exoskarn zone have been formed along the contact. Endoskarn is narrow while exoskarn is relatively wide and includes calc-silicates, silicates, sulphide, oxides, and carbonates minerals. Skarnification processes occurred in two separate stages (1) prograde (2) retrograde.

According to field and lab studies on Saheb intrusive body is granite to granodiorit I-type, metalumious and calk-alkalin. Calcareous host rocks have been recrystallized by this intrusive body. Also several forms of fine-grained garnet and amphibole have been formed close to skran contact while fine-grained epidote formed relatively farther from the contact. Anhydrous calc-silicates has been formed during early prograde stages at temperature range of 420-550°C. The retrograde stage began as the temperature of hydrothermal fluids decreased up to 400-420°C. During this stage, the anhydrous calc-silicate minerals were changed to a series of relatively low-temperature minerals.

Geochemical trend of major, minor and rare earth elements shows that considerable amounts of elements such as Fe, Si, Cu, K, Th, and Nb were added to the skarn system by the hydrothermal fluids derived from the pluton. In contrast, notable quantities of Ca and Mg were leached from the skarn system. It seems that garnets are the most principal host minerals for REEs, U, Y, and Th in this skarn. The main ore mineral are magnetite and hematite with up to 10 thick with Fe: 51.72%, Cu: 0.35%, Au: 0.038ppm.

https://doi.org/10.1180/S0026461X00006502 Published online by Cambridge University Press

Molecular characterisation of soil organic matter by laser-desorption ionization Fourier-transform ion cyclotron resonance mass spectrometry (LDI-FT-ICR-MS)

SAMUEL ABIVEN[1]*, JENS FUCHSER[2], MICHAEL W. I. SCHMIDT[1] AND THORSTEN DITTMAR[3]

[1]University of Zurich, Soil Science and Biogeography, Switzerland, (*correspondence: samuel.abiven@geo.uzh.ch)
[2]Bruker Daltonics, Bremen, Germany (Jens.Fuchser@bdal.de)
[3]Max Planck Research Group for Marine Geochemie, Oldenburg, Germany (tdittmar@mpi-bremen.de)

Soil organic matter (SOM) characterisation has been an analytical challenge for decades. On one hand, methods like humic substances extraction describe large pools of molecules, but these extractions target operationnally- rather than chemically-defined pools. On the other hand, specific compound analysis provides a more precise overview on the molecules present in the soil, but the sum of these molecules represents only a minor portion of the soil organic matter. Despite these shortcomings, soil organic matter characterisation is used in many concepts of soil science. For example, the soil aggregation hierarchical model describes the physical organisation of soils into fractions bound together by organic matter of different quality for each size fraction. Due to the method inadequation, most of these concepts still need to be validated.

We took advantage of a unique analytical set-up coupling laser-desorption ionization (LDI) to ultrahigh-resolution mass spectrometry via the Fourier-transform ion cyclotron resonance technique (FT-ICR-MS) to further characterise soil organic matter and to validate the soil aggregation hierarchical model. Soil aggregates (3-5 mm) were collected from two soils, a cambisol (32 % clay, 4.2 %C), and a loess-derived soil (15% clay, 1.6 %C). Aggregates were fractionated by fast wetting into <63, 63-125, 125-250 and > 250 µm fractions. These fractions were air-dried and ground to powder prior to analysis. LDI-FT-ICR-MS analyses were performed on otherwise untreated samples. Thousands of molecular formulae were identified in each samples, many of them could be associated with polyphenolic structures. The combination of LDI with ultrahigh-resolution FT-ICR-MS offers fundmentally new insights into soil organic matter, one of the largest organic matter pools on Earth.

Cadmium isotopes in Banded Iron Formations and early life in the Precambrian ocean

W. ABOUCHAMI[1,3]*, K. MEZGER[2], S.J.G. GALER[3] AND R. FREI[4]

[1]Institut für Mineralogie, Corrensstr. 24, 48149 Münster, Germany (*correspondence:wafa.abouchami@mpic.de)
[2]Institut für Geologie, Universität Bern, CH-3012 Bern, Switzerland (klaus.mezger@geo.unibe.ch)
[3]MPI f. Chemie, Postfach 3060, D-55020 Mainz, Germany (steve.galer@mpic.de)
[4]Institute of Geography and Geology, University of Copenhagen, DK-1350 Copenhagen, Denmark (robertf@geo.ku.dk)

The exact genesis of Banded Iron Formations (BIFs) is not fully understood, yet there is a consensus that they are seawater precipitates and as such provide valuable archives of Precambrian ocean chemistry, its oxygenation and perhaps clues to early life. Here we explore Cd stable isotope fractionation in BIFs to try to assess the degree of biological activity in the ancient oceans. Cadmium isotopes are particularly suited since (1) they trace differences in biological productivity between biogeochemical provinces in the modern oceans [1], (2) in contrast to Cr and Fe isotopes, Cd isotopes are not redox sensitive, and (3) they are not fractionated by Fe-Mn oxide precipitation.

Two suites of BIFs from Isua (3.8 Ga) and South Africa (2.2 Ga) were analysed using a Cd double-spike technique at MPI. Exceedingly low Cd concentrations (20-60 ng/g) are found in all BIFs, except one Isua sulfidic facies sample, independent of their provenance and age. Such concentrations are two orders of magnitude lower than found in modern Fe-Mn deposits, supporting extreme trace metal depletion in the early oceans. The Cd isotope ratios, expressed as $\varepsilon^{112/110}$Cd, are varied but systematic, ranging from essentially negative values (-3.7 to -0.3) in the 3.8 Ga-old Isua samples, except for the single sulfidic facies sample, to exclusively positive values (+0.9 to +5.5) in the 2.2 Ga-old South African samples.

The Cd isotope range of the Isua BIFs is consistent with that of modern seafloor hydrothermal systems and contrasts markedly with that of the Proterozoic. The isotope effect during the Proterozoic is similar in magnitude to that observed in the present-day oceans and seems to mark the onset of biological productivity following the Great Oxidation Event. Additional data will be crucial for constraining the timing of oxygenic photosynthesis in the early Earth.

[1] Abouchami *et al*. (2011) doi:10.1016/j.epsl.2011.02.044

https://doi.org/10.1180/S0026461X00006502 Published online by Cambridge University Press

Sorption of engineered silver nanoparticles to environmental and model surfaces

P.M. ABRAHAM AND G.E. SCHAUMANN *

University Koblenz-Landau, Institute of Environmental Sciences, Germany
(*correspondence: schaumann@uni-landau.de)

The fate of engineered nanoparticles in the environment is strongly determined not only by their tendency to form homo- or heteroaggregates but also by their interaction with environmental surfaces like plant leaves, soil particles, sediments or biofilms.

In this study we are investigating the deposition behavior of silver nanoparticles to model and environmental surfaces and to understand the role of particle-surface interaction forces for the quality and quanity of nanoparticle deposition.

Surface-nanoparticle interactions were investigated in batch experiments via equillibrium sorption isotherms to various natural and model surfaces. The model surfaces were chosen to cover a wide range of intermolecular interactions considering van-der Waals interactions as well as proton donor and acceptor interactions.

All the sorption isotherms for sorption of silver nanoparticles to different model surfaces were described best by Langmuir sorption. The Langmuir adsorption coefficient is controlled by the chemical nature of the model surfaces used.

The sorption study was accompanied by atomic force microscopy (AFM) on a qualitative and a quantitative basis for assessment of morphology and nanomechanical parameters of the covered surfaces.

In this contribution, we will discuss the physicochemical aspects of sorption and deposition of silver nanoparticles on environmental surfaces and the resulting environmental effects with special respect to quantitative aspects of sorption and interaction.

The geoengineering possibilities and impact of enhanced silicate weathering in the ocean

J. ABRAMS[1,2]*, C. VÖLKER[1], D. WOLF- GLADROW[1] AND P. KÖHLER[1]

[1]Alfred Wegener Institute for Polar and Marine Research, PO Box 12 01 61, D-27515 Bremerhaven, Germany (*correspondence: Jesse.Abrams@awi.de)
[2]Institute of Environmental Physics (IUP), University of Bremen, Otto-Hahn-Allee 1, 28359 Bremen, Germany

Geoengineering methods are being explored to counteract global warming effects on Earth's climate. The use of enhanced silicate weathering has been proposed as a method that could speed up the consumption of CO_2 by enhancing naturally occurring chemical weathering. This study investigates that method, which involves grinding, dispersing and dissolving olivine, a magnesium silicate mineral, in river catchments and over the open ocean in order to absorb excess CO_2 and oppose ocean acidification. Previous research shows that if olivine is distributed over land areas of the tropics, it has the potential to sequester as much as 1 Pg C yr^{-1} leading to a reduction of global warming by 1 K and a rise in sea surface pH by 0.1 by the year 2100 [1]. Here, different olivine distribution scenarios over the ocean are examined using the REcoM-2 biogeochemical model coupled to the MITgcm ocean general circulation model. The additional distribution of finely ground olivine over the open ocean could increase the amount of carbon sequestered. Extra input of silicate could create better growing conditions for large silicon dependant diatoms, which contribute largely to the export of organic matter. In this study, we calculate the additional contribution and consequences of olivine distribution. As one of the least expensive geoengineering methods, enhanced weathering is a promising option to help contribute to the efforts to reduce the effects of climate change. However, this can cause both intentional and unintentional changes to the climate that may have potentially important consequences on the Earth's ecosystems.

[1] Köhler, P., Hartmann, J., Wolf-Gladrow, D. (2010). *Proc. Natl. Acad. Sci. USA* **107** 20228– 20233.

https://doi.org/10.1180/S0026461X00006502 Published online by Cambridge University Press

Cenozoic intraplate volcanism in Central Europe determined by LAB topography

MICHAEL ABRATIS AND LOTHAR VIERECK-GOETTE

Institute of Geosciences, Friedrich-Schiller-Universitaet Jena, Germany

Several intraplate volcanic fields between the Eifel (Germany) and Silesia (Poland) form the northern E – W oriented zone of the Central European Cenozoic Igneous Province (CECIP). The mafic magmas show systematic regional trends in geochemistry and mineralogy that require variations of the melting processes in the upper mantle. From the Eifel to NW Bohemia the magmas exhibit increasing Si-saturation and decreasing $(La/Yb)_N$ ratios approaching the volcanic field of the Vogelsberg from both sides. The chemical variations require (1) an increasing degree of partial melting and (2) shallower equilibration depths of melt segregation indicated by increasing melt proportions from the spinel instead of garnet lherzolite mantle. A correlation of the geochemical and mineralogical data is rather obvious with the decreasing depth of the lithosphere-asthenosphere boundary (LAB) from 100 to 60 km towards the Vogelsberg. Both characteristics can thus be explained by assuming (1) a background potential for (melilite) nephelinitic melt formation along the volcanic zone due to slight buckling of the European lithosphere induced by the alpine deformation front and (2) an overprint of increasing energy supply due to increasing amounts of lithospheric uplift and rifting (or more unlikely temperature supply) towards the Vogelsberg, which marks the crossing of the northern extension of the Rhine Graben with the E-W running buckled zone.

Within the Bohemian Massif towards Silesia the chemical variations indicate an additional overprint by lithosphere penetrating NNW-running tectonic structures paralleling the Tornquist-Teisseyre-Lineament, the Elbe zone as well as the zone of earthquake swarms crossing the Cheb Basin). Approaching these structures from both sides the necessary amount of partial mantle melting decreases as well as the volumes of erupted magma, an observation similar to oceanic fracture zones. This may be explained by the cooling effect of these tectonic elements on the melting zone at the LAB or by metasomatically induced linear lithospheric mantle heterogeneities.

From the present data we propose a genetic model where the LAB topography strongly determines the composition of the Cenozoic intraplate volcanics in Central Europe.

Sources of chemical elements in fumarols of active volcanic regions (Ebeco volcano, Paramushir Island)

N.A. ABROSIMOVA* AND S.B. BORTNIKOVA

Trofimuk Institute of Petroleum Geology and Geophysics, SB of the RAS, 3, Koptuga pr., 630090 Novosibirsk, Russia (*correspondence: geonat86@mail.ru)

Volcanic fumaroles are important objects for study gas transport of chemical elements. We can directly observe chemical elements transported in gas phase in depositions of fumarole domes such as native sulfur, incrustations, and condensates.

This study presents results of geochemical analyses of native sulfur from the fumarolic fields at the volcano Ebeco, Paramushir Island. It was carried out in order to:

(1) evaluate mechanisms of trace elements transport in gas-hydrothermal discharges at the volcano;

(2) determine possible sources of elements in fumaroles.

A wide spectrum of elements was detected in the samples of native sulfur using Synchrotron XRF method, in water extracts from the samples, and in thermal solutions at the volcano by ICP-AES analysis.

Based on the obtained data, statistic analyses together with detailed comparative analyses of native sulfur composition with host andesites and metasomatites compositions the following sources of elements and mechanisms of transport ones in fumaroles can be educed:

1. Host andesites and metasomatites: Ga, Ge, Zr, Nb, Th, U, Cu, Zn which are transported by volcanic gas as aerosol particles.

2. Magmatic fluids: As, Sb, I, Se, Te, Br, Sn, Cs which are transported in a gas phase, such as pure elements, hydrides, sulphides, and halides.

3. Solutions rising throughout the volcanic edifice, interacting with wall rocks, gas phase and are enriched in geochemical barriers: V, Sr, Rb, K, Ca, Y, Fe, Cr, Mn.

https://doi.org/10.1180/S0026461X00006502 Published online by Cambridge University Press

Hydrogeological and geochemical characterisation of a mantled evaporite karst based on hydrogeochemical data

P. ACERO[1,*], F. GUTIÉRREZ[1], J.P. GALVE[1,2], M.J. GIMENO[1], L.F. AUQUÉ[1], AND P. LUCHA[1]

[1]Earth Sciences Dept., University of Zaragoza, Spain (*correspondence: patriace@unizar.es, fgutier@unizar.es, jpgalve@unizar.es, mjgimeno@unizar.es, lauque@unizar.es, plucha@unizar.es)

[2]Earth Sciences Dept., University of Modena e Reggio Emilia, Italy

The dissolution of soluble minerals present in sediments and rocks due to the action of groundwater flow may cause the subsidence of the overlying material and eventually the settlement of the ground surface with the formation of sinkholes. Very frequently the anthropogenic activities (mainly irrigation and agricultural practices) activate or accelerate the processes involved in the generation of sinkholes, favouring its development.

In this study, the hydrochemical features of the Ebro valley mantled evaporite karst in Zaragoza city area (NE Spain) are investigated in order to shed light on the functioning of the interconneted karst and alluvial aquifers and to identify the hydrogeological and hydrochemical processes and factors involved in sinkhole genesis. The surroundings of Zaragoza city are probably the area in Europe where subsidence due to evaporite karstification has a greater socio-economic impact.

With these aims, a review of the hydrochemical information contained in the public database maintained by the Ebro Waters Authority was done. Moreover, several hydrochemical field sampling campaigns were carried out and their results were interpreted with the assistance of classical ion-ion plots, statistical calculations and geochemical modelling.

The preliminary results obtained in the study suggest that the main feature controlling the hydrology and hydrochemistry in the studied area is the fluctuation of water levels and compositions seasonally caused by irrigation. Other important factors are: (1) halite and calcium sulfate dissolution, (2) differences in the chemical composition of the irrigation waters upstream and downstream Zaragoza, as clearly observed in small sinkhole lakes, and (3) local focused discharge of more saline waters from the evaporite aquifer into the overlying alluvial aquifer.

Pyroxenite xenoliths from Cenozoic alkaline basalts, Bohemian Massif

L. ACKERMAN[1]*, P. ŠPAČEK[2] AND M. SVOJTKA[1]

[1]Institute of Geology v.v.i., Academy of Sciences of the Czech Republic, Rozvojová 269, 165 00 Praha 6, Czech Republic (*correspondence: ackerman@gli.cas.cz)

[2]Institute of Geophysics v.v.i., Academy of Sciences of the Czech Republic, Boční II, 141 34, Praha 4, Czech Republic

The Cenozoic alkaline basalts from the Bohemian Massif contain abundant mantle xenoliths. They predominantly spinel lherzolites and harzburgites, but also rare wehrlites, olivine-bearing clinopyroxenites and websterites. Mantle peridotite (lherzolite-harzburgite) from Kozákov volcano (Lusatian fault, NE Bohemia) and Lutynia (SW Poland) show similar evolution – melt extraction followed by basaltic melt cryptic metasomatism [1,2]. Nevertheless, position of pyroxenites in these scenarios remains unknown.

We studied pyroxenites from Dobkovičky, Kuzov (both in Ohře/Eger graben), Kozákov and Lutynia. The studied xenoliths have different textures. While olivine/spinel-bearing clinopyroxenite from Kozákov has equigranular texture with common orthopyroxene exsolution lamellae within clinopyroxene grains, Dobkovičky clinopyroxenite show cumulate texture with large clinopyroxene grains and orthopyroxene present only on their grain boundaries. Olivine-bearing websterite from Kuzov has equigranular texture while Lutynia spinel-bearing clinopyroxenite-websterite has cumulate (clinopyroxene with orthopyroxene lamellae) texture with spinel symplectite. The pyroxenites from Kozákov, Dobkovičky and Lutynia yield a range of two-pyroxene equilibration temperatures from 820 to 900° C. In contrast, Kuzov websterite has higher equilibrium temperature of 1050° C. The #Mg numbers of clinopyroxene and orthopyroxene from Kozákov and Lutynia vary from 91.3 to 92.8 and 90.0 to 90.7, respectively and therefore fall within the same range as reported for peridotite [1,2]. Clinopyroxene from Kozákov pyroxenite show LREE enrichment suggesting its formation from basaltic melt derived in spinel-bearing peridotite stability field. Dobkovičky clinopyroxenite show lower #Mg (89.4 and 86.4, respectively). Taking into the account this low value and its texture, it is likely that represents cumulate from the host basalt.

[1] Ackerman *et al*. (2007) *Journal of Petrology* **48**, 2235-2260. [2] Matusiak-Malek *et al*. (2010) *Lithos* **117**, 49-60.

https://doi.org/10.1180/S0026461X00006502 Published online by Cambridge University Press

Hadean greenstones and the origin of the Earth's early continental crust

JOHN ADAM[1], TRACY RUSHMER[1], JONATHON O'NEIL[2] AND DON FRANCIS[3]

[1]GEMOC, Earth and Planetary Sciences, Macquarie University, 2109, Australia
[2]Department of Terrestrial Magmatism, Carnegie Institution of Washington, 5241 Broad Branch Road, N.W., Washington, DC 20015, U.S.A.
[3]Earth and Planetary Sciences Department, McGill University, 3450 University Street, Montreal, Quebec, H3A 2A7, Canada

Partial-melting experiments, at 1.0–3.0 GPa and 900–1100 ºC, were conducted on two greenstones of Early Archaean (Hadean) age from the Nuvvuagittuq Complex of northern Quebec. For comparison, similar experiments were also conducted on a modern boninite (from the North Tongan Arc) with compositional similarities to the Nuvvuagittuq greenstones. Partial-melts produced by these experiments are compositionally similar to some TTGs, including a 3.66 billion year old tonalite that encloses the Nuvvuagitttuq Complex. Because the degree of melting needed to produce the tonalitic melts is comparatively high (> 30 %), the relative concentrations of most incompatible elements in the melts are similar to those in their greenstone and bonninite parent rocks. Thus many of the incompatible element characteristics of TTGs may have been inherited from previously fractionated source rocks that already possessed similar characteristics. If this was true, early continental crust production may have been closely associated with some form of crustal re-cycling that duplicated many of the magmatic consequences of modern plate tectonics.

Evaluating new particle formation, growth, and CCN formation in global models

P.J. ADAMS*[1], D.M. WESTERVELT[1], I. RIIPINEN[1], J.R. PIERCE[2] AND W. TRIVITAYANURAK[3]

[1]Center for Atmospheric Particle Studies, Carnegie Mellon University, Pittsburgh, PA 15213, USA (*correspondence: peter.adams@cmu.edu)
[2]Department of Physics and Atmospheric Science, Dalhousie University, Halifax, NS B3H 3J5, Canada
[3]Highway Department, Transportation Ministry of Thailand, Bangkok, Thailand

Although observations of nucleation events often show rapid growth to CCN sizes, global aerosol models have typically shown modest sensitivities of CCN concentrations to uncertainties in nucleation rates. This may be because models lack good nucleation parameterizations, or they underestimate particle growth (e.g. by condensation of SOA). Alternatively, observations of strong growth events may be rare and play a minor role in the overall global CCN budget.

The ability of a global aerosol microphysics model to predict accurately the formation and growth of new particles is tested against observations for several locations: Atlanta, Hyytiälä, Pittsburgh, Saint Louis, and San Pietro Capofiume. Full-year model simulations are compared against size-distribution measurements for corresponding years. Metrics for comparison are nucleation frequency as well as daily nucleation rates, growth rates, condensation sink, sulfuric acid concentrations (where available), CCN formation rates and nuclei survival probability. The global model used is the TwO-Moment Aerosol Sectional (TOMAS) microphysics algorithm incorporated into the GEOS-CHEM global model. Separate model runs were performed using two nucleation schemes: ternary nucleation with a 10^{-5} tuning factor and activation nucleation.

In general, comparison results show that TOMAS does not understate the importance of nucleation to CCN concentrations, as most metrics show less than a 50% bias compared to ambient measurements. Averaged across all five sites, nucleation frequency is overpredicted in the model by 18% and 32% in the ternary and activation simulations, respectively. Growth rates are typically slightly overpredicted in both the ternary and activation model cases, with median growth rates of 2.9 nm h^{-1} and 3.4 nm h^{-1} compared to 2.3 nm h^{-1} in the measurements at Hyytiälä. At Hyytiälä, nuclei survival to 100 nm in the ternary case is found to be roughly 12% higher than observed, although the median survival probabilites approximately agree at 1.8%.

https://doi.org/10.1180/S0026461X00006502 Published online by Cambridge University Press

Hydrogenase enzyme assay for the quantification of microbial activity in subsurface environments

R.R. ADHIKARI* AND J. KALLMEYER

Institute of Earth and Environmental Sciences, University of Potsdam, 14476 Potsdam, Germany
(*correspondence: adhikari@geo.uni-potsdam.de)

The subsurface biosphere is the largest microbial ecosystem but very little is known about the microbially mediated processes that drive early diagenesis. Hydrogenase is an ubiquitous enzyme that catalyzes the interconversion of molecular hydrogen and/or water into protons and electrons. The protons are used for the synthesis of ATP, thereby coupling energy-generating metabolic processes to electron acceptors such as carbon dioxide or sulfate. It can therefore be used as a measure for total microbial activity as it targets a key metabolic compound rather than a specific turnover process.

Using a highly sensitive tritium assay we measured hydrogenase enzyme activity in the rather oligotrophic marine subsurface sediments of the Equatorial Pacific (EQP) and the organic-rich sedimens of Lake Van, a saline, alkaline lake in eastern Turkey.

At the EQP sites Hydrogenase activity could be detected throughout the most of the entire length of the cores down to depths of 15 to 35 meters below seafloor (mbsf). In contrary, the rather organic matter-rich Lake Van sediments exhibit measurable Hydrogenase activity only down to around 75 cm. Concomitant with the difference in organic matter content, hydrogen consumption rates are usually below 0.5 nmol H_2/g/min in EQP sediments, whereas they are around to 2 to 5 nmol H_2/g/min in Lake Van Sediments. At several EQP sites there appear to be small horizons of elevated Hydrogenase activity, indicating the location of redox fronts.

Additionally, we present enumerated microbial cell abundance in all samples in order to obtain per-cell turnover rates which allows a deeper insight into the energetics of subsurface ecosystems.

The effect of deep ocean stratification on pCO_2 and $\Delta^{14}C$

JESS F. ADKINS

MS100-23, Dept of GPS, Caltech, Pasadena, CA, 91001

Recently we have used the distribution of $\delta^{18}O$ in the deep Atlantic Ocean at the Last Glacial Maximum (LGM) to constrain the ratio of transport (psi) to vertical diffusion (kappa) in abyssal waters that flowed from around Antarctica (Lund, *et al*. 2011). This conservative tracer balance implies that psi/kappa was 8 times larger at the LGM as compared to today. As it is highly unlikely that the ocean overturning was eight times more vigorous at anytime in the past, we look to variations in kappa in the past to change this ratio. This large reduction in vertical mixing is akin to increased stratification in the LGM deep ocean.

In this work we use a 7-box ocean model to explore the consequences of deep stratification on the carbon budget of the ocean-atmosphere system. Toggweiler's 7-box model (Paleo, 1999) is modified slightly to allow explicit isolation of southern source water relative to a northern source overturning circulation. Mixing between these so called 'blue' and 'red' circulations is allowed at both the deep interface and in the Sub-Antarctic surface waters. Simulated increases in the ratio of psi/kappa lead to pCO_2 draw down, though this effect is largely due to the budget of preformed nutrients in the deep. An important sensitivity to the vertical rain ratio of organic to inorganic carbon arises in cases with deep stratification (lower kappa). Because organic matter is remineralized more in the shallow water column and carbonate in the deep, there is an important vertical stratification in the effect on pH. Preferential deposition of alkalinity in an isolated southern source water mass lowers pCO_2 in both closed and open system simulations. We will present the effects of deep stratification on both pCO_2 and the radiocarbon distribution in the past ocean.

https://doi.org/10.1180/S0026461X00006502 Published online by Cambridge University Press

Hydrothermal processes beneath the Merensky Reef and UG2 Chromitite, Bushveld Complex, RSA

E.E. ADLAKHA[1], J.J. HANLEY[1] AND C.A. HEINRICH[2]

[1]Saint Mary's University, Dept. Geology, Halifax, Canada (correspondence: erinadlakha@gmail.com)
[2]ETH Zurich, Institute of Geochemistry and Petrology, CH-8092 Zürich, Switzerland

Pegmatites in the Bushveld Complex occur as veins/pipes comprised of quartz-andesine-biotite intergrowth. Mineral thermometry indicates minimum equilibration temperatures of 610-740ºC. Mossbauer spectroscopy of biotite Fe^{3+}/Fe^{2+} ratios constrain fO_2 within 1 log unit of FMQ. The Cl isotope composition of biotite is consistent with a mantle source ($\partial^{37}Cl$ = -0.15‰ to 0.84‰). $^{40}Ar/^{39}Ar$ dating of biotite indicates pegmatite crystallization ages ranging from 2044 (±23) to 2023 (±12) Ma; therefore, late stage volatile activity persisted well beyond the accepted crystallization age of the layered rocks (2054.4±1.3 Ma[1]).

Quartz and andesine contain primary inclusions of magmatic origin, varying from early low salinity two-phase aqueous to late, nearly anhydrous NaCl-CaCl2-dominant halide melt inclusions. Silicate melt inclusions (high K-rhyodacitic) are also present, and are unambiguously coeval with the halide melt inclusions, demonstrating that the late stage felsic liquid was saturated in this salt melt. Trace element modelling shows formation of these pegmatites by low degrees of fractional crystallization (~1 vol%) of the melt composition trapped in the inclusions.

Pegmatite cores contain base metal sulfides hosting primary inclusions of Pd-bearing melonite [(Ni, Pd)Te_2]. Normative abundance patterns are most similar to those from the Platreef, showing a marked enrichment in Pd relative to Pt (Pd/Pt > 8), Cu relative to Ni (Cu/Ni > 20) and significant depletion in Ir. Analyses of melt inclusions by LA-ICP-MS indicate high concentrations of precious metals such as Pd and Au (0.2-0.6 ppm range) at the time of their entrapment.

We show direct evidence that relatively oxidizing, halide melt-saturated silicate residues were ore metal-bearing at the time of entrapment. Ore/accessory metal ratios in the melt inclusions and sulfide assemblages in the pegmatites are consistent with the bulk rock metal ratios of the pyroxenite cumulates below the Merensky Reef, suggesting that metals were scavenged from those cumulates. Quantitative modelling suggests that the residues significantly impacted metal tenor and ratios in the Upper Critical Zone magma.

[1] Scoates, J., Friedman, R., (2008), *Econ. Geol.* **103**, 456.

Electron and proton transfer equilibria of reducible moieties in humic substances

MICHAEL AESCHBACHER, RENÉ P. SCHWARZENBACH, AND MICHAEL SANDER*

Institute of Biogeochemistry and Pollutant Dynamics (IBP) Swiss Federal Institute of Technology, ETH Zurich (*correspondence: michael.sander@env.ethz.ch)

Humic substances (HS) can act as electron acceptors and electron transfer mediators and play an important role in biogochemical redox processes and in reductive pollutant transformations. Yet, key redox properties of HS remain poorly characterized. Using a novel electrochemical approach, we previously demonstrated largely reversible electron transfer to HS in reduction-O_2 reoxidation cycles and a linear correlation of electron accepting capacities with aromaticities for different HS [1]. These findings suggested quinones as major redox active moieties. The aim of this work was to characterize the electron and proton transfer equilibria of reducible moieties in HS by extending on the electrochemical methods presented in [1].

In a first step, we determined the effect of pH on the coupling of protons to electrons (molar ratios m_{H+}/n_{e-}) transferred to selected humic acids during electrochemical reduction. m_{H+}/n_{e-} gradually decreased from 1.1 to 1.0 at pH 6 to 7 to values < 0.8 at pH 10. The trend in m_{H+}/n_{e-} was consistent with increasing deprotonation of formed hydroquinones with pH, supported by the pH dependence of m_{H+}/n_{e-} during the reduction of selected model quinones. Consistent with the m_{H+}/n_{e-} ratios, potentiometric E_h-pH titration curves for HS reduced to different extents had slopes of $\Delta E_h/\Delta pH \approx -60$ mV.

In a second step, we determined the distribution in standard reduction potentials (E_h^{0}' at pH 7) of reducible moieties in HS by fitting the decrease in E_h with increasing number of electrochemically transferred electrons, n_{e-}, using a model assuming i types of redox active sites with $E_h^{0}(i)$. Attainment of redox equilibria was facilitated by addition of small amounts of radical electron transfer mediators (e.g. diquat). The E_h-n_{e-} curves showed pronounced redox buffering over a wide E_h range. The fitted $E_h^{0}(i)$ distributions were in good agreement with the standard reduction potentials of naphthoquinones and anthraquinones, suggesting that benzoquinone moieties were already present as reduced hydroquinones in the non-pretreated HS.

The proton and electron transfer equilibria of the studied HS support quinones as major reducible moieties in HS and allow, for the first time, estimating free energies of electron transfer reactions involving HS and placing HA on the redox ladder of biogeochemical redox couples and of organic and inorganic pollutants.

[1] Aeschbacher, Sander & Schwarzenbach (2010), *ES&T* **44**, 87-93.

https://doi.org/10.1180/S0026461X00006502 Published online by Cambridge University Press

Noble gas paleotemperature records: Recent developments in dating, archives, and interpretation

WERNER AESCHBACH-HERTIG, MARTIN WIESER AND THOMAS MARX

Institute of Environmental Physics, University of Heidelberg, D-69120 Heidelberg, Germany (*correspondence: aeschbach@iup.uni-heidelberg.de)

Noble gases in combination with ^{14}C dating provide the classical tools to derive paleotemperature records from groundwater. This contribution focuses on recent developments that expand the range of archives and dating methods that can be combined with the noble gas thermometer. It also addresses the interpretation of noble gas data, in particular with regard to the formation of excess air and its significance as a climate proxy.

It has been demonstrated that under certain conditions noble gas temperatures can be derived from fluid inclusions in speleothems [1]. While this method holds great potential, the difficulties imposed by disturbing gas components in stalagmites are still very challenging. On the other hand, the increasing importance of the speleothem climate archive raises the interest for applications of groundwater dating techniques such as ^{3}H-^{3}He to cave drip waters [2].

In the groundwater archive, dating remains problematic. Recent studies have tried to use all available information, including the noble gas temperatures, to constrain recharge conditions and thereby improve the dead-carbon correction in the calculation of ^{14}C ages [3]. Another promising approach to broaden the range of dating tools is the development of atom trap trace analysis for Kr and Ar radioisotopes [4]. Here too, however, big challenges remain to be solved.

It becomess increasingly evident that the excess air component in groundwater is not only a disturbance but holds paleoclimatic information. This is for example demonstrated by a recent study from the Indian monsoon region, where the neon excess correlates with stable isotopes, as both indicate changes in monsoon strength. Nevertheless, the processes of excess air formation and the corresponding models for this component are still under discussion. New field experiments to address these questions are currently conducted.

[1] Kluge *et al*. (2008) *Earth Planet. Sci. Lett*. **269**, 407-414. [2] Kluge *et al*. (2010) *Isotopes Environ. Health Studies* **46**, 299–311. [3] Blaser *et al*. (2010) *Appl. Geochem*. **25**, 437-55. [4] Welte *et al*. (2010) *N. J. Phys*. **12**, doi:10.1088/1367-2630/1012/1086/065031.

Kinetic isotopes effects in speleothems: Insight from clumped isotopes and fluid inclusions

H.P. AFFEK[1], S. ZAARUR[1], T. KLUGE[1], A. MATTHEWS[2], Y. BURSTEIN[2,3], A. AYALON[3] AND M. BAR-MATTHEWS[3]

[1]Dept. of Geology and Geophysics, Yale University, USA
[2]Inst. of Earth Sciences, Hebrew University, Jerusalem, Israel
[3]Geological Survey of Israel, Jerusalem, Israel

Carbonate clumped isotopes (Δ_{47}) is a new paleothermometer, based on ^{13}C-^{18}O abundance, providing temperature estimates that are independent of $\delta^{18}O$ of the water in which the carbonate was formed. As such it is most relevant for paleoclimate on land, where the complexity of $\delta^{18}O$ in the hydrological cycle makes temperature reconstruction difficult. A variety of biogenic carbonates adhere to one Δ_{47}-T calibration, developed by inorganic precipitation, which is assumed to reflect isotope equilibrium. Speleothems are a notable exception, with an offset to lower Δ_{47} values, yielding erroneously high temperatures. This offset, due to kinetic isotope effects in CO_2 degassing, is consistent with the offset from nominal ^{18}O equilibrium typically observed in speleothems. We hypothesize that these kinetic effects are related to speleothems forming from thin films of solution, where fast degassing leads to an isotopic offset in DIC, that is recorded in the $CaCO_3$ forming soon thereafter, due to the long time required to regain isotopic equilibrium. To gain further insight we synthesized $CaCO_3$ by surface precipitation, mimicking thin film carbonate formation. The resulting Δ_{47}-T is less steep than in biogenic carbonates, and is consistent with Δ_{47} in modern stalagmites from several caves. Such calibration may enable extraction of drip water $\delta^{18}O$, while accounting for ^{18}O kinetic offset, using a theory based assumption of a constant $\delta^{18}O$-Δ_{47} kinetic trajectory. We will explore this assumption using laboratory experiments of $\delta^{18}O$ in surface calcite precipitation, and by comparison with fluid inclusions water isotopic composition in Soreq cave.

https://doi.org/10.1180/S0026461X00006502 Published online by Cambridge University Press

Geochemical heterogeneity of the clinoform sequence by the example of neocomian sediments of the West Siberian plate

I.V. AFONIN, G.M. TATYANIN AND P.A. TISHIN

Tomsk State University, Russia, (if_w@sibmail.com)

In recent years two models of clinoform sequence forming are developing: cross-stratification and avalanche-stratification models. Potential oil content and foulness of these complexes and necessity in their fractional partition indicate the urgency about solving this problem. The conventional methods for seismic facies analysis and the biostratigraphy can't always give a necessary result. Therefore we have tried to typify different units of clinoform sequence of the achimovskaya slice (West Siberia).

Within these researches 52 argillite samples from the units AC_3-BU_{12}, AC_1-BU_{12}, AC-BU_{12}, AC_2-BU_{11}, AC-BU_{10}, AC-BU_9 were analyzed by XFA and ICP-MS. Based on the researches studied rocks were classified in two geochemical groups. The first group includes argillites of the units AC-BU_{12}, AC_2-BU_{11} which characterized by low REE accumulation (102-204 ppm) at La/Yb varied from 10 to 14, high Eu/Eu* content (0,58-0,66), and low Ce/Ce* content (0,9-1,07). These values indicate a deep-sea regime of the sedimentation. The second group consists of the units AC_3-BU_{12}, AC_1-BU_{12}, AC-BU_{10}, and AC-BU_9 with higher REE concentration (154-262 ppm), increased Ce/Ce* (1,08-1,58) and La/Yb (10,1-24,07) ratios, and decreased Eu/Eu* content (0,48-0,59). At the same time Mn/Fe, Sr/Ba variations in successions of the units AC_3-BU_{12}, AC1-BU_{12} record increasing parameters of the basin paleosalinity (Sr/Ba 0,44-0,56) and indicators of chemogeinc accumulation of sediments (Mn/Fe 0,007-0,01) on the upper levels. It shows trasgressive regime of sedimentation. For the units AC-BU_{10}, AC-BU_9 an inverse relationship was established where the Sr/Ba (0,3-0,44) and Mn/Fe (0,0076-0,011) values are decreasing up in the succession (Sr/Ba=0,33-0,35 и Mn/Fe=0,77-0,92), thus indicating their regression regime.

Thereby accomplished researches allow defining polygenetic sedimentation regime of the clinoform sequence of achimovskaya slice. It is established a consistent change of the northwest transregression (AC-BU_{12}, AC_2-BU_{11}), deep-sea sedimentation (AC-BU_{12}, AC_2-BU_{11}) and following southeast sea basin regression (AC-BU_{10}, AC-BU_9). These facies reconstructions can be used at the correlation of the units in succession.

The study was funded by the Russian Ministry of Education and Science.

Experimental compressibility of molten hedenbergite at high pressure

C.B. AGEE[1], R.G. BARNETT[1], C.M. WALLER[2], P.D. ASIMOW[2], X. GUO[3] AND R.A. LANGE[3]

[1]Inst. of Meteoritics, Univ. New Mexico, Abuquerque, NM
[2]Geological and Planetary Sciences, Caltech, Pasadena, CA
[3]Geological Sciences, Univ. Michigan, Ann Arbor, MI

The compressibility and density of molten hedenbergite ($CaFeSi_2O_6$) has been determined through a multi-lab collaborative effort to establish a new database for a range of silicate melt compositions. The database will contribute to development of an empirically based predictive model of silicate liquid density and compressibility over a wide range of P-T-X conditions where melting could occur in the Earth. Experimental methods include (i) double-bob Archimedean method for melt density and thermal expansion at 1 bar, (ii) frequency-sweep ultrasonic sound speed measurements on liquids for adiabatic melt compressibility at 1 bar, (iii) sink/float technique for melt density to 11 GPa, and (iv) preheated shock wave measurements of P-V-E equation of state to 150 GPa. The combined data from ultrasonics and shock waves yield an isentropic bulk modulus (K_s=19.81 GPa) and its pressure derivative (K'=5.19). Static compression sink/float measurements carried out in piston-cylinder and multi-anvil devices using olivine and garnet buoyancy markers are in good agreement with these elastic constants. We also determined the fusion curve for hedenbergite well beyond the pressures of earlier work [1] and observed a significant decrease in slope with pressure consistent with a temperature maximum of ~1900 °C at 10-12 GPa. This change in sign of the liquidus Clapeyron slope is also supported by our data that predict a density crossover between hedenbergite crystals and melt at approximately 10.5 GPa.

[1] Lindsley (1967) *Carnegie Yearbook*, **65**, 293.

https://doi.org/10.1180/S0026461X00006502 Published online by Cambridge University Press

Crystallization kinetics: A probe of magmatic and eruptive processes in volcanic systems

C. AGOSTINI[1]*, M.R. CARROLL[1] AND P. LANDI[2]

[1]University of Camerino, Geology Division, via Gentile III da Varano, Camerino, (MC) Italy (*correspondence: claudia.agostini@unicam.it; michael.carroll@unicam.it)
[2]INGV Pisa Division, via della Faggiola 32, Pisa, (PI) Italy

The main objective of this experimental study is to constrain and quantitatively model the complex solidification process that transforms a magma in a solid material. During this research there will be studied nucleation and growth of crystalline phases induced by both decrease in temperature and by decrease in $P(H_2O)$ at constant temperature.

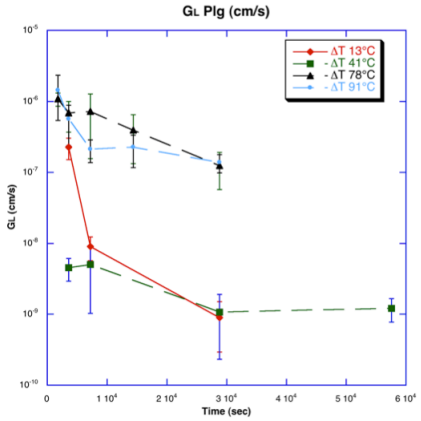

Figure 1: Figure showing Plg growth rate (GL) vs duration of decompression experiments for different ΔT, for Stromboli case.

Discussion of Results

This research concerns two different volcanic systems, Pantelleria and Stromboli, to better understand how crystallization kinetics can affect different magma compositions (in this case peralkaline rhyolites and basalts).

The study of crystallization kinetics through phases growth rates [1] (Couch *et al.*), together with the calculation of nucleation density and nucleation rates [2] (Hammer *et al.*) represent a step toward the estimation of the time scales of magmatic processes in volcanic systems and the interpretation of shallow magmatic processes such as time and velocity of magma ascent.

[1] Couch *et al.* (2003) *Am.Min.***88**, 1471-1485. [2] Hammer *et al.* (1999) *Bull Volcanol* **60**, 355-380.

Subduction-related or subdution-modified source? The case of Central-Eastern Anatolia volcanism

SAMUELE AGOSTINI[1], M. YILMAZ SAVAŞÇIN[2] AND PIERO MANETTI[3]

[1]Istituto di Geoscienze e Georisorse-CNR, Pisa – Italy (s.agostini@igg.cnr.it)
[2]Tunceli Universitesi, Tunceli – Turkey (yilmaz.savascin@deu.edu.tr)
[3]Dipartimento di Scienze della Terra, Università di Firenze, Firenze – Italy (piero.manetti@unifi.it)

Neogene volcanic rocks are widespread in Central Anatolia, between Konya and Kayseri, and Eastern Anatolia, in the region enclosed among Adana, Sivas and Diyarbakır. They occur as large ignimbrite sheets, lava plateaus, monogenetic cones as well as big stratovolcanoes. Some of these rocks are calc-alkaline, from basalts to rhyolites, while others are basanites, tephrites, alkali basalts and trachy-basalts, characterized by alkaline, mostly sodic, affinity.

No clear time and/or space separation between calc-alkaline and alkaline rocks, and no sharp chemical and/or isotopic boundary may be traced. Rather there is a gentle transition, with many samples characterized by intermediate features. As an example, alkaline rocks have Mg# varying from 72 to 45, $^{87}Sr/^{86}Sr$ from 0.7034 to 0.7055 and Ba/Nb from 5.0 to 11, whereas the same parameters span in the ranges of 71-45, 0.7039-0.7056 and 11-163, respectively, in the calc-alkaline basaltic samples. Thus, all the observed data point out for the involvement of two different mantle sources in the genesis of this magmatism, and most samples seem to be derived from interactions of these different sources.

Furthermore, the distribution of calc-alkaline rocks is not strictly linked with respect to subduction dynamics. Large volumes of very young (<2 Ma) calc-alkaline rocks are found in Kapadokyan region, in Central Anatolia, even if current subduction is very slow, or stopped at all. More to the east, some calc-alkaline rocks, are found both predating and postdating the 15 Ma Arabia-Eurasia collision, either in the upper turkish plate or the Arabian foreland.

The Miocene to Pliocene calc-alkaline rocks of Central and Central-Eastern Anatolia are sourced in a subduction-modified mantle wedge. Anyway, the occurrence of calc-alkaline magmas intimately connected with intraplate-type magmas, the presence of transitional samples, the lacking of strict connections with the subduction dynamics and geometry in the calc-alkaline rocks indicate that the metasomatizing event of the mantle wedge is in this case decoupled from the event responsible for the partial melting.

https://doi.org/10.1180/S0026461X00006502 Published online by Cambridge University Press

A review of the analytical accuracy of Cl isotope measurements in rocks by various techniques: A way to explain inconsistency between results

PIERRE AGRINIER[1]*, MAX COLEMAN[2] AND MAGALI BONIFACIE[1]

[1]Institut de Physique du Globe de Paris (IPGP), France (*correspondence: bonifaci@ipgp.fr)
[2]Jet Propulsion Laboratory, Pasadena, CA, USA

There are large inconsistencies between various Cl isotope values found for silicate rocks. Notably, mantle $\delta^{37}Cl$ is +4.7‰ [1] to near ~ 0‰ [2] and ≤ -1.6‰ [3,4], implying very different conclusions about the Earth's Cl budget and geodynamics. Each value was obtained with different analytical methods (TIMS, dual-inlet IRMS, continuous flow IRMS, SIMS). Although all use the same reference for waters (SMOC), silicate measurements require Cl extraction from the rock and only one study checked the validity of the whole analytical procedure [5]. In the absence of international rock reference materials, we analysed at IPGP two rocks 15 and 7 times in different sample sizes as well as GSJ materials provided for possible inter-lab calibrations [5]. Although less sensitive than the continuous flow technique used at University of New Mexico (UNM), the IPGP dual-inlet IRMS method is more precise and gives 100 ± 8% overall Cl yields and ± 0.12‰ $\delta^{37}Cl$ reproducibility for Cl extracted from 39 to 9042 ppm Cl rocks [5] (ie., the range of mantle-derived samples analysed [3]). Large analytical Cl isotope fractionations result from non-quantitative Cl yields (Fig. 1 in [5]). There is now a global agreement that some TIMS data in [1] are unreliable [5,6]. It is hard to evaluate discrepancies between IPGP and UNM data, as there are only few details reported for UNM method validation. The only yields reported are too high: 124 ± 17% for >1000ppm Cl samples [7]. More importantly, a new lab using an independent extraction method [8] recently reproduced the IPGP values on 3 rock samples (JB1, JB2 & Allende) – while UNM produced a 2‰ more positive value for Allende. Thus, the observed discrepancies possibly might arise from analytical artifacts in the UNM method and therefore the mantle is depleted in ^{37}Cl.

[1] Magenheim *et al*. (1994) *EPSL* **131**, 427. [2] Sharp *et al*. (2007) *Nature* **446**, 1062-1065. [3] Bonifacie *et al*. (2008) *Science* **319**, 1518-1520. [4] Layne *et al*. (2009) *Geology* **37**, 427-430. [5] Bonifacie *et al*. (2007) *Chemical Geology* **242**, 187-201. [6] Rosenbaum *et al*. (2000) *Analyt. Chem*. **72,** 2261 – 2264. [7] Barnes and Sharp (2006) *Chem. Geol*. **228**, 246-265. [8] Nakamura *et al.* (2011) *LPSC abstracts* 2513.

Neoproterozoic to Mesozoic history of Sanandaj-Sirjan Zone, West Iran

VAHID AHADNEJAD

Geology Department, Payame Noor University, Tehran 19395-4697, I. R. Iran. (v.ahadnejad@gmail.com)

Neoproterozoic tectonics is documented by U-Pb inherited zircons of Sanandaj-Sirjan Zone (SSZ) granitoids, West Iran. The 0.989 Ga inherited zircon of Malayer Syenogranite [1], Northern SSZ, is in accordance with combination of the supercontinent Rodinia at ca. 1.0 Ga. The collision between East and West Gondwana between 0.6 and 0.5 Ga is also could be pursuit by other granitoids of the SSZ which are implied a ca. 0.55 Ga. for Bubaktan biotite granite and Sheikh Chupan granodiorite [2] and ca. 0.59 Ga for Nagadeh monzogranite [3]. The magmatism at Late Neoproterozoic-Early Cambrian in SSZ [2, 3, 4] which is consistent with Pan-African orogenic event, implies that this zone was a part of Gondwana at that time.

Subsequent extension regime in Paleozoic caused rifting of Iranian microplates including SSZ away from Gondwana. Closure of Paleotethys due to its northward subduction and the synchronous opening of the Neotethys in the Late Triassic move Iranian microplates northeastward and accrete them to the Laurasia. Closure of Neotethyan oceanic crust re-amalgamated Iranian blocks at the late Mezosoic. The immense Paleozoic-Mezosoic plutonism in SSZ is the result of this opening and closure of Pale- and Neotethys.

[1] Ahadnejad, V., Valizadeh, M.V., Deevsalar, R. Rezaei-Kahkhaei, M. (2011). *Neues Jahrbuch Fur Geologie Und Palaontologie-Abhandlungen*. DOI: 10.1127/0077-7749/2011/0149. [2] Hassanzadeh, J., Stockli, D.F., Horton, B.K., Axen, G.J., Stockli, L.D., Grove, M., Schmitt, A.K., Walker, J.D., (2008). *Tectonophysics* **451**, 71–96. [3] Mazhari, S.A., Amini, S., Ghalamghash, J., Bea, F. (2009a). *Arabian Journal Geosciences*. DOI: 10.1007/s12517-009-0077-6. [4] Jamshidi-badr, M. (2010). Petrology and petrogenesis of Takab intrusive body and its sorrounding metamorphics. PhD thesis, Trabiat Moallem University of Tehran.

https://doi.org/10.1180/S0026461X00006502 Published online by Cambridge University Press

Polyphase deformation in Golpaygan metamorphic complex, Sanandaj-Sirjan Zone, Iran

G.A. AHMADI

Padidab Consultig Engineers, Northern Ordibehesht St., P.O.Box 81358-53164, Isfahan, Iran (ahmadi.gh1354@gmail.com)

Geological Setting

The Golpaygan metamorphic complex in north of Golpayegan city is a part of Sanandaj-Sirjan zone [1]. This zone is the metamorphic belt of the Zagros Orogen in the western Iran that formed by Neo-Tethys initiation and closure events between Arabian plate and Iranian microcontinent [2, 3]. This complex lithologically consists of phyllite, mica schist, garnet mica schist, marble, quartzite, amphibolite, metavolcanics and gneiss [4].

Deformations and related structures

Three stages of deformations can be recognized in this area. First deformation (D1) was associated with a regional metamorphism from lower greenschist to amphibolite facies that has developed during NE subduction of Neo-Tethys oceanic crust under Iranian microcontinent in late Jurassic. First foliation (S1) has developed during this deformation that has folded intensely by late deformations and doesn't show distinct direction. Second deformation (D2) is the most important deformation in the area and it can be recognized by isoclinals and recumbent folds with NW- SE axes, axial plane foliation (S2) and shear zones. It is considered as a progressive deformation with ductile shortening and thrusting from NE to SW. The deformation has formed during collision between Arabian plate and Iranian microcontinent in late Cretaceous to Palaeocene age [5]. Third deformation (D3) consists of en echelon gentle folds and strike - slip faults that have developed during continuous deformation with ductile- brittle condition. This deformation has developed during regional dextral transpression after collision.

[1] Stocklin (1968) *A.A.P.G.Bull*. **52**, 1229-1258.
[2] Berberian & King (1981) *Can. J. Earth Sci*.**18**, 210-265.
[3] Alavi (1994) *Tectonophysics* **229**, 211-238.
[4] Thiele *et al*. (1968) *G.S.I*. sheet number E7.
[5] Mohajjel *et al*. (2003) *J. Asian Earth Sci*. **21**,397-412.

Survey of Aeolian airborne dust over Iran from the point of view geochemistry and mineralogy (case study: Western Iran and North of Persian Gulf and Sea of Mokran)

H. AHMADY BIRGANI[1]*, S. FEIZNIA[2] AND N. CHAREHSAZ[1]

[1]Faculty of Natural Resources, University of Tehran, Iran (*correspondence: hesamahmady@ut.ac.ir)
[2]Faculty of Natural Resources, University of Tehran, Iran (sfeiznia@ut.ac.ir)

Introduction and Methods

This research aims to show the characteristics and particle-related pollution of dust storms reaching Iran and North of Persian Gulf and Sea of Mokran. Satellite images have shown that these Aeolian dust storms originate in Arabian countries in Middle East and North of Africa continent. We have conducted numbers of analysis to reveal the MMD, SEM, XRD and ICP-MS to detection of the most important source areas with regard to radioactive, heavy and toxic trace elements [1,2].

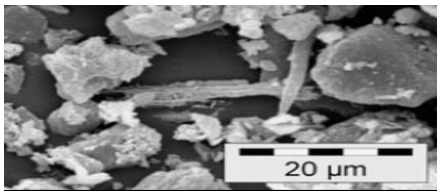

Figure 1: a sample of SEM image of Aeolian dust reaching Iran

Elements / Countries	o	c	Si	Al	Ca	Mg	k	Na	Radioactive & Toxic Traces
Iraq	47	23	13	5	2	3	3	2	2
Saudi Arabia	45	21	16	3	4	5	2	3	1
Syria	46	22	15	4	2	3	3	3.3	0.7
Kuwait	48	16	20	2	3.5	3	3	3	1.5
Occupied Palestine	52	23	16	1	2	1.6	2	1	0.4
Egypt	49	17	19	2	4	3	3	2.7	0.3

Table 1: elements compositions from the countries nearby Iran

Result has revealed that the most dangerous source areas of dust storms reaching Iran are located in Iraq country and war implications by turns have the worst effect on Iraqi environment. Soon after dust storm, Iran country be affected by Toxic, Radioactive Elements and new Microorganism (Bacteria, fungus, viruses) and make all kinds of Human disease and soil pollution and lead to decreasing of forest and plant communities.

[1] De Deckker (2008), G^3, 9, 12. [2] Lue *et al* (2010), *Atmospheric Environment,* **44**, 3477-3484.

https://doi.org/10.1180/S0026461X00006502 Published online by Cambridge University Press

Investigation of platinum group minerals (PGM) from Falcondo Ni-laterite deposit (Dominican Republic) using hydro-separation concentrates

T. AIGLSPERGER[1]*, J. A. PROENZA[1], F. ZACCARINI[2], G. GARUTI[2], F. LONGO[3]

[1]University of Barcelona, Dept. Crystal. Mineral. Ore Deposits, Barcelona, Spain (*thomas.aiglsperger@ub.edu)
[2]University of Leoben, Dept. Appl. Geol. Sci. Geophysics, Leoben, Austria
[3]Falcondo Xstrata Nickel, Santo Domingo, Dominican Republic

Two samples, one saprolite and one limonite, with total platinum group elements (PGE) contents of 62 and 212 (ppb) respectively, were processed by the innovative hydro-separation (HS) technique, with the aim to determine the presence of PGM and to understand their origin.

The studied samples were collected in the Falcondo Ni-laterite deposit, developed over the Cordillera Central serpentinized peridotite, located in the central part of Dominican Republic.

Two different types (I and II) of PGM were recognized. Type I PGM form grains less than 10 μm, occurring enclosed in fresh chromite (laurite and an unnamed [$(Rh,Ir_3)S_4$]) or included in altered awaruite (Os-Ru-Ni-Fe compound). PGM of type II consist of free grains, bigger than 10 μm. They comprise laurite and compounds of Pt-Ir-Fe-Ni, Ru-Os-Ir-Rh and Ru-Os-Ir-Fe-O characterized by porosity, irregular shape and complex chemical zoning. Type II PGM have been found only in the saprolite sample.

Composition and shape of both types I and II laurite and the an unnamed [$(Rh,Ir_3)S_4$] suggest a magmatic origin. Other type II PGM may represent the alteration product of pre-existing PGM formed at high temperature. The process that altered the magmatic PGM probably started with the serpentinization and continued during weathering and lateritization.

Our results, although preliminary, indicate that the HS technique can be successfully applied to concentrate PGM also from relatively PGE poor samples, thus providing useful information regarding their distribution and genesis.

Interpreting CO_2 measurements in volcanic gas plumes: The need for integration with geophysical data

ALESSANDRO AIUPPA[1,2]

[1]Dipartimento DiSTeM, Università di Palermo, Italy, (aiuppa@unipa.it)
[2]Istituto Nazionale di Geofisica e Vulcanologia, Sezione di Palermo, Italy

Measuring CO_2 concentrations and fluxes in volcanic gas plumes has long remained a challenge for volcanologists. Because CO_2 is the second most abundant gas species in volcanic emissions, and among the first to exsolve and separate from ascending magmas in the crust, the paucity of CO_2 plume data has prevented us from obtaining more in-depth information on magmatic degassing processes. The recent advent of new techniques, and more particularly of the MultiGAS (Multi-component Gas Analyser System), has given new impulse to CO_2 plume measurements, however, and has allowed the acquisition of unprecedented long and robust CO2 flux datasets. Observations made over the last 6 years at Etna and Stromboli (in Italy) have, in particular, demonstrated an unexpectedly large time variability of composition (e.g., CO_2/SO_2 plume ratios) and CO_2 fluxes, which interpretation still remains open and somewhat controversial. Here, I show that integrated analysis with geophysical data (volcanic tremor, deformation data) is key to interpret the dynamic processes operating in volcano's plumbing systems, which produce the observed large variations in plume composition and flux. At Etna, in particular, I demonstrate that the cyclic variations in plume CO_2/SO_2 ratios, systematically observed in 2007-2009, were paralleled by variations in tremor amplitude and location, and by inflation-deflation cycles captured by the GPS network [1]. These combined (multidisciplinary) observations have offered a more robust understanding of processes operating at depth inside Etna, which I here review. Since permanent networks for semi-continuous gas plume observations are becoming more and more in use at volcano observatory worldwide, integrated geochemical-geophysical observations will likely represent a key target of volcanic gas studies in the years to come.

[1] Aiuppa *et al*. (2010) *Geochem. Geophys. Geosyst.* **11**, doi:10.1029/2010GC003168

https://doi.org/10.1180/S0026461X00006502 Published online by Cambridge University Press

A possible model of accelerated dehydration by fluid migration in deformed amphibolite associated with Oeyama Ophiolite

RIICHI AKAI

Graduate school of Systems and Information Engineering, University of Tsukuba, Tsukuba, Ibaraki,305-8573, Japan (r1.akai@gmail.com)

In subduction zones, miscible fluids commonly would act as metasomatism agent [1]. A petrographic metasomatic model [2] for deformed amphibolite along 50m in the melange of Oeyama Ophiolite member shows continuous compositional change for parent's amphibole grains. For this model, fluid interaction was investigated in order to explain to the crystallization of secondary minerals and alterations of amphibole. The block (mono-mineralic amphibolite together with zoisite vein) that is prospected as the protolith [2] was newly found at the edge of outcrops. This field and petrographic study for vein which are assumed to have precipitated in the surroundings of porphyroclastic parent's minerals would contribute to show the whole process of metasomatism as a case of the evolution of crustal fluid.

In the petrography, some clino-zoisite and zoisite at the initial deformation stage in the vein may be the products of replacement amphibole as those size and shape are similar with fractured amphibole grain and those distributions are mostly connected. The most oligoclase precipitated at later stage doesn't have chemical heterogeneity, and some oligoclase are associated with hydro-fracturing amphibole and zoisite. Some textures seem to show the dissolving of the parent minerals.

Considering these crystallization by some fluid migration during the deformation process, the compositional evolution of the fluid must be required. The huge infiltration of Al (at early stage) and Na (at later stage) during deformation must have been changed by some coupled dissolution and precipitation process together with the reaction of amphibole along the vein.

If dissolution and replacement are key processes, and associated with this major crystallization of anhydrous-minerals during this metasomatism, the chemical system of initial amphibolite would be dehydrated.

This model for fluid interaction is concordant with the last metasomatic model based on spatial compositional trend of amphibole[2].

[1] Manning, C. E., (2004), *EPSL*, **223**, 1-16 [2] Akai, R (2010) *Goldschmidt conference*.

Geocehmical and genetic features of polymetallic Pb-Zn-Cu-Au-Ag deposits of Gümüşhane, Turkey

M. AKÇAY[1] AND R. YAŞAR[2]

[1]Dept. of Geology, Karadeniz Technical University, 61080 Trabzon. (akcay@ktu.edu.tr)

[2]Dept. of Geology, Karadeniz Technical University, 61080 Trabzon

The deposits occur as veins and lenses within dolomitic limestones nearer mainly to its upper contact with the overlying flysh. The main ore zone is 400 m long along E-W direction, 100 to 150 m wide along N-S direction and has a thichness of 1 to 17 m. The recent exploration activities and feasibility studies indicate an estimated reserve of 1,815,000 tons at 1.81 g/ton Au, 77.11 g /ton Ag, 0.6 %Cu, 5% Zn and 3% Pb. The ore zones are mainly in the form of massive shoots with sporadic pockets of sphalerite and galena, and to alesser extent, as Cu enriched lenses with chalcopyrite, Bi and Te-enriched sulphosalts, and luzonite as well as rare altaite. These minerals are also enriched in Au and Ag.

The deposition of ore occurs within voids in monolithic carbonate breccias, which is, in turn, probably related to rifting. The preferential occurence of the ore in brecciated zones, the presence of ore lenses nearer the upper contact of the Berdiga Limestone with the Upper Cretaceous flysch and along the lower contact of the flysch, as well as the weak mineralisation within units underlying the limestone point towards an epigenetic origin, despite the widespread mode of occurrence in the form of massive lenses. The presence of similar deposits in the vicinity may indicate a joint origin connected with the Eocene magmatic activity, widespread in the region, denoting that the overlying flysch unit may have behaved as a cover unit. Fluid inclusion research suggests epithermal conditions with low salinities (<8,5wt%NaCl eq.) and low to moderate temperatures (130-370 ºC; X=240 ºC). The sulphur contents of sphalerite, galena, pyrite and chalcopyrite were determined to be magmatic in origin, with near $\delta^{34}S$ values ranging from -2‰ to +3‰. Mineral pairs found to be in isotopic equilibrium support epithermal conditions. The Eocene magmatics in the close vicinity of the mineralised areas are likley to be responsible for the formation of such epithermal systems.

https://doi.org/10.1180/S0026461X00006502 Published online by Cambridge University Press

Growth-zoned chromian spinel in rodingite: Evidence for Cr mobility in hydrothermal solution

N. AKIZAWA[1]*, S. ARAI[1], A. TAMURA[2] AND J. UESUGI[1]

[1]Department of Earth Sciences, Kanazawa Univ., Ishikawa 920-1192, Japan

[2]Frontier Science Organization, Kanazawa Univ., Ishikawa 920-1192, Japan

We found growth-zoned chromian spinel in a rodingite within the layered gabbro section of the northern Oman ophiolite (Wadi Fizh). The chromian spinel coexists with Ca-rich plagioclase (An; 97-100), diopside (Mg#; 0.87-0.97), uvarovite, titanite, gismondite and chlorite (Cr_2O_3; up to 2.3 wt%). It shows a high Cr# (= Cr/(Cr+Al) atomic ratio), around 0.8, and is different from mantle spinels (in chromitites and peridotites) in the Oman ophiolite (Cr#<0.75). The procursory gabbro is rather wvolved in chemistry, and free from chromian spinel. The rodingite spinel increases Fe3+ from the core to the rim (up to >YFe=0.3). The spinel characteristically shows euhedral and skeltal shapes (Fig. 1). The spinel and uvarovite mostly occur as independent grains, which means the former does not serve as the source of Cr for the latter. The spinel and uvarovite, which enclose euhedral grains of plagioclase, chlorite and pumpellyite, show concentric and oscillatory chemical zoning (Fig. 1).

The petrological characteristics strongly indicate that the spinel and uvarovite in the Wadi Fizh rodingite were independently precipitated from hydrothermal solutions involved in rodingitization of gabbros at low pressure condition (near Moho). This suggest that the Cr was mobile in the aqueous solution at low pressure condition (<0.3 GPa). Chromium was possibly supplied from the underlying mantle via high-temperature solution, which was possibly involved in precipitation of diopsidites (Python *et al*., 2007).

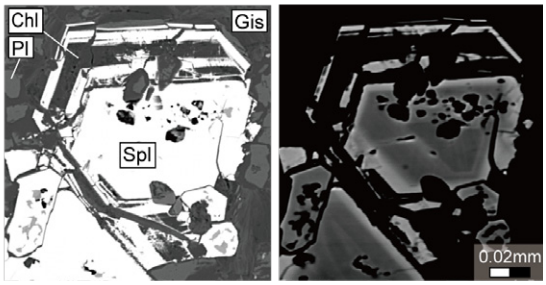

Figure 1: Composite images of spinels. Abbrreviations: spl=spinel, pl=plagioclase, chl=chlorite, gis=gismondite.

[1] Python *et al*. (2007) EPSL **255**, 289-305.

Biogenic Mn oxide formation at pH 5.5 and 7 by new Mn-oxidizing bacteria from a former U mining site

D. M. AKOB*, A. BEYER, F. SCHÄFFNER, M. HÄNDEL, D. MERTEN, G. BÜCHEL, K.U. TOTSCHE AND K. KÜSEL

Friedrich Schiller University Jena, 07743 Jena, Germany (*correspondence: denise.akob@uni-jena.de)

Uranium mining near Ronneburg, Germany resulted in widespread environmental contamination with acid mine drainage (AMD) and high concentrations of heavy metals and radionuclides. Natural attenuation of heavy metals is occurring at this site in Mn oxide rich soils and sediments ranging in pH from 5 to 7. While microorganisms readily oxidize Mn(II) and precipitate Mn oxides at pH ~7 under oxic conditions, few studies describe Mn(II)-oxidizing bacteria (MOB) at pH ~5 and/or in the presence of heavy metals. In this study we (1) isolated MOB from the contaminated Ronneburg area at pH 5.5 and 7 and (2) evaluated the biological formation of Mn oxides. We isolated nine MOB strains at pH 7 (members of the *Proteobacteria*, *Actinobacteria*, *Bacteroidetes*, and *Firmicutes* phyla) and a single isolate at pH 5.5 (Oxalobacteraceae isolate AB_14, within the *β-Proteobacteria*). While LA-ICP-MS showed that all isolates accumulated Mn and Fe in their biomass, the Oxalobacteraceae isolate AB_14 had higher intensities of Mn and Fe peaks. Preliminary FTIR analysis indicated that all isolates formed precipitates, which showed absorption bands that were characteristic for birnessite. This, the first known report of any organism capable of Mn oxidation at low pH, demonstrated that MOB can be involved in the natural attenuation of both moderately acidic and neutral pH soils and sediments via the formation of biogenic Mn oxides. Future work will fully evaluate the minerals formed in this process as well as their interactions with contaminating heavy metals and radionuclides.

https://doi.org/10.1180/S0026461X00006502 Published online by Cambridge University Press

Geothermal energy development in Turkey

A. AKPINAR[1]*, E. AKARYALI[2] AND M.I. KÖMÜRCÜ[3]

[1]Dept Civil Engn, Gümüşhane Univ, TR-29100, Gümüşhane, Turkey (*correspondence: aakpinar@ktu.edu.tr)
[2]Dept Geol Engn, Gümüşhane Univ, TR-29100, Gümüşhane, Turkey (eakaryali@gmail.com)
[3]Dept Civil Engn, Karadeniz Tech. Univ, TR-61080, Trabzon, Turkey (mkomurcu@ktu.edu.tr)

Geothermal energy is a clean and environmentally friendly energy source, as well as it is renewable and sustainable. It can be used in buildings, agriculture, industry, greenhouse heating etc. This energy source is independent of meteorological events such as wind and sun and more economic and reliable than some of the other energy sources.

In this study, historical development of geothermal energy in Turkey and balance of between geothermal potential and consumption are investigated. With this objective, the studies which have been started by General Directorate of Mineral Research & Exploration (MTA) in 1960's are examined. At the result of these studies, it was determined that, 170 numbers geothermal areas which have low and middle heat were discovered by MTA until 2000. The performed studies have shown that probable geothermal energy potential in Turkey is 31500 MWt for direct use and 4500 MWe for electric production [1]. However, the present use of geothermal energy is a very small fraction of the identified geothermal potential. Only 7% of the geothermal source potential of Turkey was used so far [2]. When Turkey uses the entire total geothermal potential, it can meet 14% of the total energy needs (head and electricity) [3]. This implies a very thought-provoking figure for Turkey which depends greatly on foreign thermal resources. For sustainable development in Turkey, it is very important to increase this percentage to upper values.

[1] Kömürcü, A., and Akpınar, A., 2009, Importance of geothermal energy and its environmental effects in Turkey, *Renewable Energy,* **34**, 1611-1615. [2] Geothermal Association of Turkey (GAT), Geothermal Energy in Turkey, http://www.jeotermaldernegi.org.tr/ (in Turkish). [3] Akpınar, A., Kömürcü, M.I., Önsoy, H., Kaygusuz, K., 2008, Status of geothermal energy amongst Turkey's energy sources, *Renewable and Sustainable Energy Reviews,* **12**, 1148-1161.

Assessing organic carbon distribution in the Koiliaris critical zone catchment (Greece) by using geostatistical techniques

E. AKSOY[1]*, P. PANAGOS[1], N. NIKOLAIDIS[2] AND L. MONTANARELLA[1]

[1]Joint Research Center of the European Commission Institute for Environment and Sustainability, Via E.Fermi, 2749, 21027 Ispra, VA, Italy (*correspondence: ece.aksoy@jrc.ec.europa.eu, panos.panagos@jrc.ec.europa.eu luca.montanarella@jrc.ec.europa.eu)
[3]Department of Environmental Engineering, Technical University of Crete, 73100 Chania, Greece (nikolaos.nikolaidis@enveng.tuc.gr)

Organic carbon amount of the soil is one of the most important geochemical parameters for defining soil characterization. It affects directly to the soil functions (biomass production, C sequestration, biodiversity, etc.) and problems about it may finalize as soil threats. Because of these reasons accuracy of the distribution assessment is an important topic.

This study implemented in Koiliaris Catchment Critical Zone, in Greece with an aim of accurate and detailed assessment of organic carbon distribution. Slope and aspect from DEM; CORINE landcover classification; geological formations and WRB soil classification information were used as covariates in this study. All layers were in the raster format with 100m resolution and the sample points has measured organic carbon values from Crete University field work. Regression – Kriging geostatistical technique was used to be able to find the distribution of the organic carbon through the catchment. As a conclusion, significant correlation between the covariates and the organic carbon dependent variable was found and organic carbon distribution map of Koiliaris CZ was produced in the digital soil mapping perspective.

https://doi.org/10.1180/S0026461X00006502 Published online by Cambridge University Press

Sampling technology of deep groundwater with Diffusive Gradient in Thin Film (DGT)

L. ALAKANGAS[1]*, M. ÅSTRÖM[2] AND B. KALINOWSKI[3]

[1]Swedish Nuclear Fuel and Waste Management Co, Box 929, SE-57229 Oskarshamn, Sweden (linda.alakangas@skb.se)
[2]Geochemistry Research Group, Linnaeus Univ., SE-39182 Kalmar, Sweden
[3]Swedish Nuclear Fuel and Waste Management Co, Box 250, SE-10124 Stockholm, Sweden

The Äspö Hard Rock Laboratory (HRL), SE Sweden, is a unique underground facility where the Swedish concept for storage of nuclear fuel waste is tested at natural repository conditions [1]. It also offers an environment for researchers interested in conducting experiments as well as testing equipment in situ at the deep subsurface.

In order to obtain as little disturbance of the sample as possible during sampling, a special designed container where the conditions in the bedrock is mimicked has been developed to be able to collect deep groundwater maintaining the pressure and the reduced state in cored boreholes. This is crucial for pH which is one of the main parameters in reaction modelling, but also for volatile species and redox sensitive elements.

In addition, the container makes it possible to sample trace elements by the new in-situ technique called Diffusive Gradients in Thin films (DGT) [2]. In the deep groundwaters at the Swedish canditate sites most trace elements such as lanthanides and actinides generally occur at concentrations below the detection limit using standard sampling methods. The DGT technique makes it possible to determine dissolved labile trace elements in-situ by trapping species in binding agents for a longer period of time, accumulating the trace elements. The container in which the DGT samplers are established is constructed in stainless steel and can maintain a high pressure of 50 bar. The PEEK material inside prevents the water to have contact with the metal. During the sampling period a constant agiation and flow through the container will be regulated.

The outcome will contribute to a better understanding the trace metal dynamics in deep groundwaters. Measurements of sensitive parameters at in situ conditions will increase the quality of the hydrogeochemical models that will be used in the safety assessment for the final respository.

[1] SKB (2009) Annual Report 2009. SKB TR-10-10 [2] Garmo *et al* (2006) *Environ Sci. Technol.* **40**: 4754-4760

Distribution of potentially toxic elements around Dolly Au-Cu Mine, Central Iran

FATEMEH ALAVI TABAEE[1], DR SOROUSH MODABBERI[2] AND DR HOOSHANG ASADI HAROONI[3]

[1]School of Geology, University of Tehran, Enghelab St. Tehran, Iran, (n.alavi63@yahoo.com)
[2]School of Geology, University of Tehran,,Enghelab St. Tehran, Iran, (modabberi@ut.ac.ir)
[3]School of Mining Engineering, Technical University of Isfahan, (hooshang_asadi@yahoo.com)

"Dolly Deposit" is the first porphyry Au-Cu deposit recognized in the Urmia-Dokhtar volcanic arc of Iran with an extent of about 9 km^2 in 40 km northwest of Delijan city in Central Iran.

Mineralization in the Dolly region is associated with a set of altered porphyry Quartzdiorite stocks and dikes intruded within a fault zone of 1-2km width at the center of a stratovolcano consisting of andesite lava and pyroclastics. Intrusive and locally volcanic rocks have been altered to potassic, fillic, argilic, propylitic and silica alteration assemblages by hydrothermal solutions. It is estimated that approximately 10 percent of Dolly deposit has an oxide and 90 percent sulfide ore mineralogy.

Copper ores are composed of chalcopyrite, bornite, chalcosite and malachite.

In order to study trace element distribution around the Dolly deposit from en environmental point of view, soil and rock samples have been taken from the areas affected by mineralization.

Concentration of As, Sb and Bi show higher values than the mean standard values, i.e. 7.2-328 ppm for As, 1.7-160 ppm for Sb, and 0.5-13.9 ppm for Bi.

Calculation of enrichment factor and also geoaccumulation index indicate that the area is naturally contaminated with these elements, for some parts it is considered to be highly contaminated requiring remediation. Noting that the deposit is supposed to be extracted in the coming years it is suggested that geochemical environmental considerations should be considered in order to delineate or restrict the contamination. On the other hand, the data obtained is a valuable piece of information from forensic geochemical views against or for possible future claims.

https://doi.org/10.1180/S0026461X00006502 Published online by Cambridge University Press

The great volatile delivery to Earth

F. ALBAREDE[1]*, C. BALLHAUS[2], C.-T. A. LEE[3], Q-Z. YIN[4] AND J. BLICHERT-TOFT[1]

[1]Ecole Normale Supérieure de Lyon, France (*correspondence: albarede@ens-lyon.fr)
[2]Steinmann Institut, Universität Bonn, Germany
[3]Dept. of Earth Sciences, Rice University, Houston, Texas
[4]University of California, Davis, California

The $^{206}Pb/^{204}Pb$ and $^{207}Pb/^{204}Pb$ ratios of the BSE indicate that Pb has been *depleted* with respect to U at some time T_1 after the beginning of the Solar System and raises the question of where the missing unradiogenic Pb resides. The Earth's gravity field is too strong for heavy Pb vapor to escape thermally. Pb has been either lost to space upon hit-and-run impacts or buried into the core, with the effect that the U/Pb ratio of the BSE has increased over time. The present Pb composition of the BSE requires that the U/Pb fractionation *increased* at T_1 >140 Ma after the formation of the Solar System. This age postdates the oldest lunar rocks [1] and also any Pb burial into the core during the lunar Giant Lunar Impact [2]. We suggest that both the proto-Earth and the Moon were extremely depleted in volatile elements, whether siderophile or not, because accretion ended while temperature was still high.

Chondritic impactors ('late veneer') dislodged from their orbits in the outer Solar System account for the strongly siderophile inventory of the BSE [3] and also explain well the late delivery of Pb and other volatiles, notably water [4]. The issue of how the impactors' U and Pb became fractionated from each other nevertheless still is outstanding. High-velocity impacts of asteroids on the Earth lead to total melting and partial vaporization of the impactors [5]. The vapor produced by impacts eventually rains back onto the Earth upon cooling, whereas molten metal separates from silicates either as diapirs or as metal rain [6]. The siderophile content of the BSE hence is accounted for by the vaporized fraction of the veneer, while the bulk of the impactor's non-siderophile volatiles adds up to the volatile content of the Earth. Using Ballhaus *et al*.'s (this meeting) metal/silicate partition coefficients, we find that 8% volatilization of a late veneer equivalent of up to 5% of the Earth's mass with metal/liquid segregation at 1600 K reproduces well the trace element concentrations in BSE. We find that 70% of Pb and Cd, 80% of Sn, 50% of W, and 7% of Cr in BSE come from the impactors. A late veneer with a rather unremarkable mean water content of ~1% adequately accounts for the terrestrial water inventory.

[1] Norman M.D *et al*. (2003) *Met. Planet. Sci*. **38**(4), 645–661 (2003) [2] Wood B.J., Halliday A. (2010) *Nature* **465**, 767-771 (2010) [3] Chou C.-L. (1978) *Proc. Lunar Planet. Sci. Conf*. **9**, 219-230 [4] Albarède F. (2009) *Nature* **461**, 1227-1233. [5] O'Keefe J.D. and Ahrens T.J. (1977) *Proc. Lunar Sci. Conf*. **8**, 3357-3374 [6] Rubie D.C. *et al*. (2003) *Earth Planet. Sci. Letters* **205**, 239-255.

Behavior of mercury in thermal sources of Kamchatka

YURY V. ALEKHIN, SERGEY A. LAPITSKY AND RENATA V. MUKHAMADIYAROVA*

Lomonosov Moscow State University, 119991 Moscow, Russian Federation (*correspondence: rinutiya@mail.ru)

For the first time for a deep-seated source of thermal waters (Kamchatka, operational holes of the Mutnovsky Geoelectric power station) are analysed compositions co-existing steam-and-gas and liquid phases and for temperatures 180 – 200 °C, the molal distribution coefficient of mercury in system a steam-liquid is defined. Results have shown, that in samples of deep-seated fluids (the borehole bottom on depth 1600) dominates the elementary mercury enriching steam-and-gas phase with the big distribution coefficient (8,17) in favour of vapour phase. Analogous results are gained on a considerable quantity of samples of other thermal sources at simultaneous selection of a liquid phase and a condensate of steam-and-gas. Results on mercury compared with distribution coefficients of other microelements.

By data in paper [2, 3] the highest content of mercury in a gas phase is fixed on an exit of Apapelsky sources 75000 ng/m^3 this result is in the contradiction with the size of a Henry's coefficient defined in paper [4] and with our data. For check and the coordination of results of these works direct measurements of mercury contents in steam-and-gas phase by the instrumentality of field atomic absorber UCM-1MC (ECON, Moscow) was realized and the thermal waters of Apapelsky sources and condensates was collected. High values of contents of mercury in condensates are in the obvious contradiction with concentration of mercury in a water phase of thermal sources and can be explained only considerable enrichment of condensates of water steam by mercury of a gas phase, i.e. its carrying over in the aerosol form.

By our results and by results described in work [1] for system of a caldera of Uzon high concentration of mercury (up to 11 ppb in Cloride Lake) not only in a steam-and-gas phase, but also in sodium chloride waters are characteristic.

[1] Naboko (1974) Coll. a volcanism, hydrothermal process and mineralisation, pp. 162-195 (in Russ.). [2] Ozerova *et al*. (1988) Coll. Modern hydrotherms and mineralization, 49, pp. 34-49 (in Russ.). [3] Smirnov, Kuznetsov, Ozerova (1972) *Geol. of Ore Deposits*, **4** (in Russ.). [4] Sorokhin, Pokrovsky, Dadze (1988) Physicochemical conditions of mercury-antimony mineralization formation, 144 p. (in Russ.).

The research has realized by supporting of RFFI (№ 11-05-93107-CNRS-a).

Experimental research of metal mercury solubility in water

YURY V. ALEKHIN, NAIL R. ZAGRTDENOV* AND RENATA V. MUKHAMADIYAROVA

Lomonosov Moscow State University, 119991 Moscow, Russian Federation
(*correspondence: nailzag@yandex.ru)

The experimental works [3, 4] was devoted to solubility of elementary mercury in water in the range of temperatures 120-500 ^{0}C. The great number of papers [1, 2, 5] for an interval 20-120 ^{0}C is in the obvious contradiction with the reliable high-temperature data. Unusual nonlinearity of dependence lg m – 1/T for simple reaction Hg^0_{liquid} - Hg^0_{aq} forces to assume change of the dominating form in a solution in the field of low temperatures.

We had been suggested the version about complete dominance of form Hg^0_{aq} (dissolved) at high temperatures when solubility of elementary mercury is high also prevalence of the oxidized forms of mercury at the low. Position of mercury in a standard electrochemical voltage range of metals isn't an obstacle for occurrence of analytically significant concentration of the oxidized forms against the lowest solubility Hg^0_{aq} at small volatility of steams Hg^0_{liquid} in the field of low temperatures. The made experiments on solubility of mercury in an interval 20-80 ^{0}C in various oxidation-reduction conditions have confirmed our version. The good concordance of our data on solubility of mercury in reductive conditions with data [4] which extrapolated on 20-80 ^{0}C is obtained. For 20 ^{0}C linear extrapolation from area of high temperatures for Hg^0_{aq} gives quantity of solubility 1,99 ppb. We experimentally receive value 1,95 ppb. This value on two order more low, than usual total solubility in oxidizing conditions. Results of research allow to offer the simple version of temperature dependence of Hg^0 solubility and Henry's coefficients for equilibrium with liquid mercury in absence of the oxidized forms.

[1] Glew, Hames (1971) *Canad. J. Chem*, **49**, pp. 3114-3118. [2] Sanemasa (1975) *Bul. of the Chem. Soc. of Japan*, **48**, pp. 1795-1798. [3] Sorokhin, Alekhin, Dadze (1978) Essay of physicochemical petrology, 8, pp. 133-149 (in Russ.). [4] Sorokhin, Pokrovsky, Dadze (1988) Physicochemical conditions of mercury-antimony mineralization formation, 144 p. (in Russ.). [5] Okouchi, Sasaki (1983) Rept. Coll. Eng. Hosei Univ., 22, pp. 57-106.

The research has realized by supporting of RFFI (№ 11-05-93107-CNRS-a).

Effect of temperature and mineralogical composition on the reactivity of shale: A comparison study of potential caprock from two potential CO_2 storage sites

B.L. ALEMU*, P. AAGAARD AND H. HELLEVANG

Department of Geosciences, University of Oslo, P.O.Box 1047 Blindern, N-0312 Olso, Norway
(*correspondence: b.l.alemu@geo.uio.no)

Two caprock shales, one from a proposed CO_2 storage site in Longyearbyen, Svalbard, and the other from a potential CO_2 storage site off-shore Norway, close to the Troll field, were used in this study. The shale from Svalbard was cored from the De Geerdalen formation close to the town of Lonyearbyen from a depth of around ~ 800m. On the other hand the shale from Troll field was cored from Upper Jurassic Draupne Formation from a depth ~ 1000m below see floor. Both samples have different mineralogical composition which is partly influenced by their respective diagentic history. The two samples were reacted in batch reactors under different temperature and constant pressure conditions. Crushed samples from both samples were reacted with a mixture of CO_2 and brine at a temperature of 250 °C, 100 °C and a constant total pressure of 110 bars. The experiment from 250 °C lasted 35 days each while the experiment from 100 °C lasted 70 days. In addition, control reactions using brine solution without CO_2 were run for high temperature experiments to discern effect of temperature-driven reactions from CO_2-enhanced reactions.

The results indicate different reactivity for both samples. The release rate of cations was affected both due to mineralogy and experimental condition. For example, K appeared to be maximum in samples reacted with brine only whereas Ca, Fe and SiO_2 were higher in samples reacted with mixture of brine and CO_2. More Ca was released from the De Geerdalen shale as it had more carbonate. On the other hand the solution from the Draupne shale released more Mg, K, Fe and SiO_2. Dissolution of carbonates was significant on the reacted solids from both samples as evidenced by the decrease in total inorganic carbon content. Compared to high temperature reactions, lower temperature reactions dissolved more carbonates. In addition, dissolution of carbonate was much more pronounced in the Draupne shale. XRD analysis of the samples also revealed some alterations of minerals in both samples.

https://doi.org/10.1180/S0026461X00006502 Published online by Cambridge University Press

Origin of N isotopic anomalies in meteoritic and cometary organic matter

JÉRÔME ALÉON

CSNSM, CNRS/IN2P3/U. Paris Sud. Bat. 104, 91405 Orsay Campus, France. (Jerome.Aleon@csnsm.in2p3.fr)

Organic molecules in meteorites and comets display a large range of nitrogen isotopic variations of unclear origin. It is widely assumed that ^{15}N excesses trace an interstellar-like chemistry in a cold dense medium, mostly by analogy with deuterium chemistry [e.g. 1]. However, chemical models face difficulties in achieving the level of ^{15}N enrichment relative to the ambient interstellar/protosolar gas observed in meteorites and the relationship between ^{15}N and D excesses remains osbcure [2,3]. Here I present isotopic fractionation calculations coupled with mixing calculations aiming at reproducing the observed distribution of ^{15}N and D excesses in acid insoluble organic matter from carbonaceous and ordinary chondrites, in subgrains nicknamed hotspots and nanoglobules, as well as in interplanetary dust particles, samples from comet Wild 2 returned by the Stardust mission and in HCN from comet Hale-Bopp. I show that the N-H isotopic compositions in these samples can be explained by a mixture of three components : (1) a late isotopic exchange with a ^{15}N-D-rich gas produced by ion-molecule reactions, possibly in the solar protoplanetary disk (PPD), (2) a D-poor, ^{15}N-rich component best preserved in the Isheyevo chondrite of abundance anti-correlated with meteoritic age, indicating a late origin in the solar PPD and (3) a minor D-rich ^{15}N-poor component of likely presolar origin, best preserved in ordinary chondrites. The anti-correlation between ^{15}N excesses and meteoritic age extends to bulk isotopic composition and differentiated objects suggesting a general trend of increasing $^{15}N/^{14}N$ ratio in organic molecules as the solar PPD ages and clears.

[1] Busemann *et al*. (2006) *Science* **312**, 727-.730 [2] Rodgers and Charnley (2008) *Mon. Not. R. Astron. Soc.* **385**, L48-L52. [3] Briani *et al*. (2009) *P. Natl. Acad. Sci.* **106**, 10522-10527.

Spectroscopic characterization of U(IV)-biomass complexes

DANIEL S. ALESSI[1], JUAN S. LEZAMA-PACHECO[2], JOANNE E. STUBBS[3], MARCUS JANOUSCH[4], PER PERSSON[5], JOHN R. BARGAR[2] AND RIZLAN BERNIER-LATMANI[1]

[1]Ecole Polytechnique Fédérale de Lausanne, EPFL, Switzerland, (daniel.alessi@epfl.ch)
[2]Stanford Synchrotron Radiation Lightsource, Menlo Park, CA 94025, USA
[3]Consortium for Advanced Radiation Sources, University of Chicago, Chicago, IL 60637, USA
[4]Swiss Light Source, Paul Scherrer Institute, Switzerland
[5]Department of Chemistry, Umeå University, Sweden

Uranium contamination in the subsurface is an enduring problem throughout Europe and North America. Current strategies for the remediation of uranium aim at transforming the soluble and mobile oxidized form of uranium, U(VI), to the reduced and relatively immobile form, U(IV). Until recently, reduction of U(VI) to U(IV) was assumed to produce solely the sparingly soluble mineral uraninite, $UO_{2(s)}$. However, recent research reveals that other species of U(IV), referred to here as 'monomeric U(IV),' can form as the product of microbial U(VI) reduction. Because monomeric U(IV) lacks the crystalline structure of uraninite, it is likely to be more labile and susceptible to reoxidation. For this reason, geochemical models that assume $UO_{2(s)}$ as the sole product of U(VI) reduction may not capture the true system behavior.

Here we use infrared spectroscopy (IR), uranium L_{III}-edge X-ray absorption spectroscopy (XAS), and phosphorus K-edge XAS analyses to determine the binding environment of monomeric U(IV) associated with *Shewanella oneidensis* MR-1 bacterial cells. Several systems were tested as a function of pH, including: cells without uranium, cells with adsorbed U(VI), cells that produced monomeric U(IV) and cells that produced uraninite as a product of U(VI) reduction. Uranium XAS analyses confirmed the reduction of U(VI) to U(IV) in U(IV)-containing systems, and the presence of either monomeric U(IV) or $UO_{2(s)}$ was confirmed by extended X-ray absorption fine structure (EXAFS). IR analyses revealed a strong coordination of U(IV) with phosphate groups in the monomeric U(IV) systems -coordination not seen in the other systems. The P EXAFS results provide further evidence of U(IV)-phosphate coordination in monomeric U(IV) when compared to an abiotic U(IV)-phosphate reference. The results of this study provide valuable insights into the binding environment of the monomeric U(IV) species associated with microbial biomass and reaffirm the conjecture that phosphate coordination is critical in the formation of the species.

https://doi.org/10.1180/S0026461X00006502 Published online by Cambridge University Press

Insights into biogenic secondary organic aerosols produced from five structurally different precursors

M.R. ALFARRA[1,2]*, N. GOOD[2], J.F. HAMILTON[3], K.P. WYCHE[4], P. MONKS[4], A. LEWIS[3] AND G.B. MCFIGGANS[2]

[1]National Centre for Atmospheric Science (NCAS), The University of Manchester, Manchester, M13 9PL, UK (*rami.alfarra@manchester.ac.uk)
[2]The University of Manchester, Manchester, M13 9PL, UK,
[3]University of York, York, YO10 5DD, UK
[4] University of Leicester, Leicester, LE1 7RH, UK

A series of novel experiments were carried out at the Manchester Aerosol Chamber in order to investigate the chemistry and microphysics of the formation and transformation of biogenic secondary aerosols. A selection of compounds covering a wide range of reactivity including monoterpenes, sesquiterpenes and oxygenated VOCs has been studied in detail. The chemical composition of the formed SOA was measured on-line using an Aerodyne Time-of-Flight Aerosol Mass Spectrometer (cToF-AMS). A hygroscopicity tandem differential mobility analyser (HTDMA) and a cloud condensation nuclei (CCN) counter were used to probe the hygroscopic properties and of the aerosols in the sub- and super-saturated regimes, respectively. A proton transfer mass spectrometer was used to study the evolution of the gas phase oxidation products.

We presents an overview and synthesis of results covering the chemical composition, hygroscopicity and cloud condensation nuclei (CCN) properties of secondary organic aerosols formed from five structurally different biogenic VOCs (β-caryophyllene, limonene, myrcene, linalool, α-pinene). The effect of the use of organic [1] and inorganic seed on the limonene SOA will be presented. Results showed that the formed SOA have a wide range of chemical properties, and that the effect of photochemical ageing on their properties was not uniform across all five precursors. A link of these results to the corresponding findings of the hygroscopic properties of the SOA particles and their CCN behaviour will be presented and discussed.

[1] Hamilton, J.F., Alfarra, M.R., Wyche, K.P., Ward, M.W., Lewis, A.C., McFiggans, G.B., Good, N., Monks, P.S., Carr, T., White, I.R. and Purvis, R.P. (2010) *Atmos. Chem. Phys. Discuss.*, **10**(10), 25117-25151.

Release rate of pollutants, nutrients and protons from pristine Eyjafjallajökull ash

H.A. ALFREDSSON[1], S.R. GISLASON[1], S.L.S. STIPP[2] AND K.W. BURTON[3]

[1]Institute of Earth Sciences, University of Iceland, Reykjavík, Iceland (haa4@hi.is)
[2]Nano-Science Centre, Department of Chemistry, University of Copenhagen, Denmark
[3]Department of Earth Sciences, University of Oxford, South Parks Road, Oxford, UK

On 14 April 2010, when magma from the Eyjafjallajökull volcano intruded glacier-meltwater, an explosive phreato-magmatic eruption sent unusually fine-grained ash into the jet stream and flood waters all the way to the ocean. Later, when meltwater did not have access to the magma, the eruption produced a larger grained magmatic ash. We were able to sample dry ash, from both these eruption phases. Both ashes were coated with salts during the eruption, and the surface area of the phreato-magmatic ash was an order of magnitude larger than the one of the magmatic ash [1]. Single pass plug flow experiments were carried out at 22 °C using DI-water and North Atlantic seawater. The outlet was connected directly to an ion chromatograph to determine release rate of anions with time without exposure to the atmosphere. The rest of the dissolved elements were measured by various ICP methods.

Magmatic ash released protons, resulting in initial pH drop in the DI-water to 3.2, and initial proton release of $10^{-6.5}$ moles/m^2/s. The surface of phreato-magmatic ash, however consumed protons, a minimum of -$10^{-7.8}$ moles/m^2/s, resulting in an initial pH of 10.3. Initial release rates, normalized to the BET-surface area, were 2-4 orders of magnitude faster than bulk dissolution rate of volcanic glasses and olivine. The rates dropped by orders of magnitude over a few hours. Surface area normalized rates from the magmatic ash was in general faster than the phreato-magmatic rates, and it is only the magmatic ash that releases Fe and Al at elevated rates, $10^{-6.6}$ and $10^{-6.4}$ moles/m^2/s, respectively. These experiments show fundamental difference in the potential environmental impact of volcanic ash of the same bulk composition, but produced by different eruption mechanism. Acid producing gases and salts dissolve in meltwaters and are transported to the ocean via flood waters. Furthermore, phreato-magmatic ash will not fertilize surface waters with water soluble iron, like the magmatic ash.

[1] Gislason S.R. *et al.* (2011), *PNAS, in press*.

https://doi.org/10.1180/S0026461X00006502 Published online by Cambridge University Press

Magmatic variety through tectonic modulation of the 27 ka Oruanui eruption, Taupo, New Zealand

A.S.R. ALLAN[1]*, C.J.N. WILSON[1], M.-A. MILLET[1] AND R.J. WYSOCZANSKI[2]

[1]SGEES, Victoria of Wellington, PO Box 600, Wellington 6140, New Zealand (*aidan.allan@vuw.ac.nz)
[2]NIWA, Private Bag 14901, Wellington, New Zealand.

Deposits of the earliest three phases (of 10) in the 530 km^3 magma, 27 ka Oruanui eruption reflect shifting vent positions and accompanying variations in compositional diversity [1, 2]. New data reveal close connections between changing vent positions and magma chemistries, involving a tectonic modulation of the eruption dynamics, thus.

1) Start of phase 1 of the eruption. Through all of the phase 1 deposits, pumice clasts from a crystal richer, biotite-bearing rhyolite magma are found that encountered the main (biotite-free) Oruanui magma in the conduit. Biotite-bearing pumices occur at 2-4% abundance, increasing to 16-17% in the uppermost phase 1 deposits. Thermobarometric constraints in combination with glass chemistry and *in situ* trace element fingerprinting of amphibole and plagioclase source this magma to an adjacent system which erupted at ~28 ka from vents ~15 km northeast of the Oruanui phase 1 vent area. This adjacent system operated entirely independent of the Oruanui magmatic system for >20 kyr prior to the 27 ka eruption and no connection was previously inferred. Lateral transport of the biotite magma is indicated, implying that a rifting event accompanied/controlled the start of the Oruanui eruption.

2) Shutdown of the phase 1 vent. After <0.1% of the Oruanui magma volume had been discharged, activity ceased for several weeks to months, despite the underlying presence of ~530 km^3 of gas-saturated rhyolite magma.

3) Renewal of explosive activity (phase 2) from the same vent site, with a renewed influx of biotite-bearing rhyolite from the adjacent independent magma system, indicating that another rifting event and dike emplacement occurred.

4) Rifting-related unzipping of new vents aligned down the E side of modern Lake Taupo in phase 3, coincident with the first appearances of high-silica (roof cupola) rhyolite and low-silica rhyolite dredged from the magma chamber roots, a spike in the abundance of juvenile mafic material and a marked increase in the tempo of the eruption.

[1] C.J.N. Wilson (2001) *J. Volcanol. Geotherm. Res.* **112**, 133-174. [2] C.J.N. Wilson *et al.* (2006) *J. Petrol.* **47**, 35-69.

Nd isotopes vs magnetic susceptibility as a double proxy for paleoclimate and paleoweathering: The Kerguelen Case

C.J. ALLEGRE[1], L. MEYNADIER[1] AND D.V. KENT[2]

[1]IPGP (Sorbonne Paris Cité, Université Paris Diderot, UMR7154 CNRS), 1 rue Jussieu, 75238 Paris Cedex 05, France (allegre@ipgp.fr, meynadier@ipgp.fr)
[2]Rutgers University, Department of Earth and Planetary Sciences, 610 Taylor Road, Piscataway, NJ 008854-8066 U.S.A. (dvk@rci.rutgers.edu)

In a seminal paper, Kent (1982) has shown that the magnetic susceptibility (MS) measured in a sediment core near the Kerguelen Island, fluctuated coherently with $\partial^{18}0$. Those variations translate the climatic change between glacial and interglacial periods. Since MS variations also fluctuate with $CaCO_3$ content (high carbonate correlates with low MS), Kent interpreted the MS variations as a dilution effect induced by $CaCO_3$. However, when we corrected MS from carbonate dilution, the fluctuations persisted and still correlated with $\partial^{18}0$. Thus, if indeed the carbonate dilution plays a role, it is not the ultimate reason for the climatic variation of MS.

We also measured both the Nd isotopic composition (ε_{Nd}) of ancient seawater and of the detrital fraction of the sediment, which is related to the local erosion. Interestingly, in this region, ε_{Nd} of ancient seawater varies with climate in coherence with MS and $\partial^{18}0$, whereas very small variations are seen on the detrital ε_{Nd}. This difference will be discussed in detail.

We will show that oceanic currents were much more active during Interglacials than Glacials and that in the region mechanical erosion and chemical erosions were also more active during Interglacials.

https://doi.org/10.1180/S0026461X00006502 Published online by Cambridge University Press

Continental growth periods deduced from river sand U-Pb-dated zircons with O and Lu-Hf isotope analyses

C.M. ALLEN[1]*, I.H. CAMPBELL[2] AND T. IIIZUKA[3]

[1]RSES, ANU, Canberra Australia 0200 (*correspondence: charlotte.allen@anu.edu.au)
[2]RSES, ANU, Canberra Australia 0200 (ian.campbell@anu.edu.au)
[3]Earth and Planetary Sciences, University of Tokyo 113-003 Japan (iizuka@eps.s.u-tokyo.ac.jp)

To evaluate continental crustal growth through time we have compiled an isotope data base for ~1400 zircons from Australian sand dunes and the world's major rivers. The data base comprises zircons that show no age zoning as shown by drilling 25 microns into zircons mounted on tape by LA-Q-ICP-MS. These selected dated zircons are mounted in epoxy and polished, cathodoluminescence imaged, analysed for oxygen isotopes using SHRIMP and analysed for Lu-Hf isotopes using LA-MC-ICP-MS. The premise behind this work is that zircon Hf model ages date the formation of continental crust. Primitive continental crust melts to form granitoid magmas from which the zircons crystallize and we can calculate this "incubation time". The Hf model ages have two major sources of uncertainty: 1. the growth curve for $^{176}Hf/^{177}Hf$ for the depleted mantle, 2. the $^{176}Lu/^{177}Hf$ used in the model age calculation. Using only those zircons with $\delta^{18}O$ of that of the mantle (5.3±1‰) reduces the uncertainty in the $^{176}Lu/^{177}Hf$ used in the calculation principally by excluding those grains that have a mixed supracrustal component indicated by $\delta^{18}O > 6.3‰$. We define juvenile zircons as those grains with incubation times <250 Ma and they are rare leading us to important model refinements and re-evaluation of when major additions to the continental crust occurred. Our data indicate that the major crustal growth periods were 3.4-2.9 Ga, 2.2-1.8 Ga, and 1.0-0.6 Ga.

Volatile solubility in phonolites from Erebus volcano: Towards a multi-component degassing model

M. ALLETTI*, A. BURGISSER, B. SCAILLET AND C. OPPENHEIMER

ISTO/CNRS, 45000, Orléans, France (*correspondence: marina.alletti@cnrs-orleans.fr, burgisse@cnrs-orleans.fr, bruno.scaillet@cnrs-orleans.fr, co200@cam.ac.uk)

The interpretation of the chemistry of volcanic gas emissions demands a firm understanding of the deep processes that control partition of volatile species between melt and gas. Volatile solubility in silicate melts is greatly affected, among other factors, by the composition of magma. Erebus volcano (Antarctica) hosts one of the few persistent active lava lakes on Earth, and the only one of anorthoclase-phonolite composition. Despite its remoteness, the lake is closely studied and its gas emissions measured during the austral summer field season using infrared spectroscopic methods. Melt inclusions (MI) in anorthoclase and pyroxene crystals have H_2O concentrations similar to or lower than those of halogens (i.e. Cl and F), indicating extensive degassing. The first studies [1] attempting to link MI data to gas composition used degassing models that neglected the multi-component fluid phase, and which did not account for experimentally-determined solubilities for Na-phonolitic melts.

In order to model the degassing path at Erebus in *f-X* space, we performed experiments of (i) H_2O solubility and (ii) partitioning of Cl between a hydrous fluid phase and the melt (expressed as $D^{fl/melt}_{Cl}$). The starting material was anorthoclase phonolitic lava from Erebus (ERE 13-29 Dec 05). Experiments were carried out in the pressure range of 250-10 MPa and at a temperature of 1000 °C. Our results for H_2O solubility are in good agreement with previous studies on similar melt composition [2] and can be interpolated by the following law:

$$H_2O\ (wt\%) = 0.182 * f_{H2O}\ (MPa)^{0.677}$$

Our results for Cl partitioning indicate a more complex behavior. We found that $D^{fl/melt}_{Cl}$ varies between 6.0 and 1.7 from 250 to 100 MPa, and increases again from 50 MPa up 10.2 at 10 MPa. This variable trend with ascent supports the idea proposed by Shinohara [3] of a heterogeneous chloride system with respect to decompression, with NaCl stable at high pressure and HCl stable from 100-50 MPa and to lower pressures still. Separating our experimental data into low and high pressure ranges, we propose a fugacity-based model of equilibrium degassing for Cl [4] and discuss our preliminary results.

[1] Oppenheimer & Kyle (2008) *J. Volcanol. Geotherm. Res.* **177**, 743-754. [2] Schmidt & Behrens (2008) *Chem. Geol.* **256**, 259-268. [3] Shinohara (2009) *Chem. Geol.* **263**, 51-59. [4] Burgisser *et al.* (2008) *J. Geophys. Res.* **113**, B12204.

https://doi.org/10.1180/S0026461X00006502 Published online by Cambridge University Press

High temporal resolution $\delta^{18}O$ and $\delta^{13}C$ heterogeneity in a *Porites lobata* coral skeleton

N. ALLISON[1], A.A. FINCH[1]* AND EIMF[2]

[1]Department of Earth Sciences, University of St. Andrews, Fife KY16 9AL, UK (*correspondence: aaf1@st-and.ac.uk)
[2]NERC Ion Microprobe Facility, University of Edinburgh, Edinburgh EH9 3JW, UK

$\delta^{18}O$ and $\delta^{13}C$ were determined at high spatial resolution (beam diameter ~ 30μm) by secondary ion mass spectrometry (SIMS) across ~1 year of a modern *Porites lobata* coral skeleton from Hawaii. All analyses were made on coral fasciculi (which make up the bulk of the skeleton) and not centres of calcification. Our data indicate that skeletal $\delta^{18}O$ and $\delta^{13}C$ are dominated by weekly-monthly oscillations (of >2‰ and >5‰ respectively) which far exceed the annual seasonal signal. These variations do not reflect seawater temperature or composition.

The dissolved inorganic carbon (DIC) pool available for calcification is derived from seawater or from molecular CO_2, which can diffuse from the coral tissue into the calcification site. Variations in the $\delta^{18}O$ of the DIC pool may reflect the source of DIC (seawater or molecular CO_2), calcification site pH (affecting the proportions of DIC formed via hydration and hydroxylation of molecular CO_2 and the proportion of HCO_3^- derived from seawater DIC that is converted to CO_3^{2-}) and DIC residence time at the calcification site (influencing the extent to which oxygen isotopic equilibrium with the surrounding water is obtained). DIC pool $\delta^{13}C$ is also affected by DIC source and calcification site pH (affecting DIC speciation). However carbon isotopic equilibrium at the calcification site is reached in < 20s, before any significant uncatalysed oxygen isotopic equilibration has occurred. The $\delta^{13}C$ of the molecular CO_2 component of the DIC pool is affected by the balance of photosynthesis and respiration and the amounts, types and $\delta^{13}C$ of material respired in the coral tissues.

We do not observe significant correlations between skeletal $\delta^{18}O$ and $\delta^{13}C$ in either the original or detrended datasets. Furthermore, neither $\delta^{18}O$ or $\delta^{13}C$ correlates with calcification site pH, estimated from previous SIMS measurements of skeletal $\delta^{11}B$. Our data suggest that the $\delta^{18}O$ and $\delta^{13}C$ composition of the DIC pool is affected by multiple independent influences at this time scale.

Highly depleted melt inclusions in olivine from Shatsky Rise

R.ALMEEV[1]*, M. PORTNYAGIN[2], T. WENGORSCH[1], T. SANO[3], J.H. NATLAND[4] AND D. GARBE-SCHÖNBERG[5]

[1]Institut of Mineralogy, Leibniz University of Hannover, Germany, (r.almeev@mineralogie.uni-hannover.de)
[2]IFM-GEOMAR, Kiel, Germany
[3]National Museum of Nature and Science, Tokyo, Japan
[4]Rosenstiel School of Marine and Atmospheric Science University of Miami, USA
[5]Institute of Earth Sciences, Kiel University, Germany

Shatsky Rise east of Japan is a unique oceanic plateau with characteristics of both “plume head” and non-plume origin [1-3] which was cored during IODP Expedition 324 in 2009. Igneous rocks sampled at four sites are variably altered pillows and massive lava flows of olivine phyric and plagioclase-clinopyroxene microphyric basalts. On-board geochemical data [4] show that the basalts are broadly MORB-like, similar to those from the Ontong Java Plateau (OJP) and likely originating from a slightly enriched MORB-like source.

We report here the first results of geochemical study of olivine-hosted melt inclusions from moderately altered olivine-phyric basalts cored at the Site U1349 (Ori massif, Sample 324U1349-12R4/37-39). Melt inclusions and olivines were analyzed for major elements by electron microprobe and for trace elements by LA-ICPMS. Olivine phenocrysts range in composition from Fo81 to Fo87 (NiO up to 0.4 wt%) and contain small glassy (<20 μm in size) and relatively large partly crystallized (30-60 μm) inclusions. Before analyses, partly crystallized inclusions were homogenized in internally heated pressure vessel at 200 MPa and 1210 °C and 1280 °C and subsequently quenched after 5 and 20 minutes, respectively. Melt inclusions obtained after both heating treatments and corrected for post-entrapment re-equilibration with host olivine have primitive, broadly MORB-like compositions and highly depleted trace element patterns compared to NMORB and the Kroenke-type basalts (OJP) with respect to Ba, Th, Nb, Ta, LREE, Sr, Zr and Hf (e.g., La_N/Yb_N = 0.2-0.4 in inclusions vs. ~0.7 in NMORB). The presence of highly depleted melts trapped in olivine suggests strong geochemical heterogeneity of the Shatsky Rise mantle sources ranged from less to significantly more depleted than average DMM.

[1] Duncan & Richards (1991) *Rev. Geophys* **29**, 31–50.
[2] Sager *et al.* (1999) *J. Geoph. Res.* **104** (B4), 7557–7576.
[3] Fougler (2007) *Spec. Pap. Geol. Soc. Am.*, **430**, 1-28.
[4] Sager *et al.* (2010) Proc. IODP, **324**: Tokyo.

https://doi.org/10.1180/S0026461X00006502 Published online by Cambridge University Press

Recent cessation of Nile discharge affecting the geochemistry of SE Mediterranean inner shelf sediments

A. ALMOGI-LABIN[1]*, A. SANDLER[1] AND B. HERUT[2]

[1]Geological Survey of Israel, 30 Malkhe Israel, Jerusalem 95501, Israel (*correspondence: almogi@gsi.gov.il)
[2]Israel Oceanographic & Limnolological Research, Tel Shikmona, Haifa 31080, Israel

Climatic-control variations of Nile River discharge to the SE Mediterranean were suggested to play a major role in changing the geochemical characteristics of deep water sediments [1]. During the last century a series of dams were built on the Nile and since the operation of the Aswan High Dam (AHD), in the mid 60th of the last century, late summer floods carrying fine sediments and nutrients stopped entering the Mediterranean. This affected directly the 30 to 50 m silt belt off the Israeli coast, an integral part of the Nile littoral cell. Grain-size, major and trace elements and Sr isotopes were used for assessing the effect of the shut down of Nile discharge on a series of short cores taken along a S-N transect at ~40 m water depth. Chronology was based on ^{210}Pb dating. Grain size sharply increased since the operation of the AHD together with a two fold increase in $CaCO_3$ content accompanied by a distinct increase in Ba/Al ratio. TOC content decreased from ~1.0 wt.% to less than 0.3 wt.% at core tops and δ^{13}Corg decreased by ~3.5‰ (from -19.5 to -23‰) reflecting apparently a distinct drop in nutrient input and major reduction in primary productivity. ^{87}Sr/^{86}Sr value, around 0.7065, determined in the <63μm size fraction of the insoluble material, indicate mainly a basaltic lithological source originating apparently from the Ethiopian highlands and transported by the Blue Nile and Atbara via the Nile River towards the Mediterranean.

The sediments of the Israeli inner shelf, located distally within the Nile littoral cell, responded directly and rapidly to Nile River discharge cessation. This may indicate that distal inner shelf parts of large deltaic systems document faithfully extreme aridity episodes that might occur at the headwaters of large river systems, including that of the Nile River.

[1] Box *et al* (2011), *Quat. Sci. Rev.* **30**, 431–442.

The FeS/H_2S system - A model for a primitive DMSO reductase

T. ALPERMANN[1,2], Z. QI[1], W. POPPITZ[1] AND W. WEIGAND[1]*

[1]Institute for Inorganic and Analytical Chemistry, FSU Jena, August-Bebel-Str.2, 07743 Jena, Germany (*correspondence: wolfgang.weigand@uni-jena.de);
[2]now at: Federal Institute for Geosciences and Natural Resources, Stilleweg 2, 30655 Hannover, Germany (Theodor.Alpermann@bgr.de)

Within the Iron-Sulfur-World hypothesis, the development of an autotrophic surface metabolism based on the reduction of CO_2 and catalytic action at iron sulphide surfaces is proposed. The required redox energy for the metabolic reaction pathways is provided by the thermodynamically favoured but kinetically inhibited reaction

$FeS + H_2S \rightarrow FeS_2 + H_2$ ($\Delta_R G°$= -38 kJ/mol, pH 6.5) [1].

The reducing power accompanied by catalytic activity of the FeS/H_2S system could be demonstrated in several studies, e.g. dinitrogen N_2 could be reduced to NH_3 [2]. Another intriguing model compound for the investigation of the reducing power of the FeS/H_2S system is DMSO. In nature, the reduction of DMSO by the enzyme *DMSO reductase* in marine phytoplankton is relevant to the global climate due to the release of major amounts of DMS into the oceanic atmosphere. There, DMS acts as an important source of cloud condensation nuclei.

Our study aimed at investigating the capability of the FeS/H_2S system to reduce dimethyl sulfoxide (DMSO) to dimethyl sulphide (DMS) under geologically mild conditions (1 bar, 90°C). Experiments were carried out under strictly anaerobic conditions in glass vessels and the amount of produced DMS was quantified *via* gas chromatography. The FeS/H_2S system indeed reduces equimolar amounts of DMSO selectively to DMS with yields of up to 60% within seven days. Hence, the FeS/H_2S system can be regarded as a model of a primordial *DMSO reductase* supporting the idea of its relevance for the origin of a first metabolism.

[1] Wächtershäuser (1992) *Prog. Biophys. molec. Biol.* **58**, 85-201. [2] Dörr *et al.* (2003) *Angew. Chem. Int. Ed.* **42**, 1540-1543.

https://doi.org/10.1180/S0026461X00006502 Published online by Cambridge University Press

Numerical simulation of alteration patterns induced by sequestration of CO_2 in a carbonate-hosted saline aquifer

P. ALT-EPPING AND L.W. DIAMOND

Institute of Geological Sciences, RWI-Group, University of Bern, Baltzerstrasse 3, CH-3012 Bern, Switzerland, (alt-epping@geo.unibe.ch)

We run reactive transport simulations to understand the transient chemical processes that occur in a carbonate-dominated aquifer during and after the injection of CO_2. The model, its design and its initial and bounding physico-chemical conditions, are patterned after the Upper Muschelkalk-Gipskeuper aquifer-seal pair in the Molasse Basin in Northern Switzerland. Chemical processes are controlled by the dynamics of the CO_2 plume. Supercritical CO_2 is more buoyant than the brine. Consequently, the CO_2 plume tends to rise and spread laterally when it encounters the overlying Gipskeuper seal. Over time $CO_{2,sc}$ dissolves into the brine, causing the density of the brine to increase. The denser brine tends to sink, initiating density driven convection. Depending on the permeability of the aquifer, sinking of the CO_2-enriched brine may occur in a complex finger-like pattern. The dissolution of CO_2 into the brine entails a lowering of the *pH* and hence the dissolution of the primary carbonate mineralogy. Because the brine remains buffered at local equilibrium with the carbonates, the dynamics of the CO_2 plume and the CO_2-enriched brine is reflected by the mineral alteration pattern. Although the drop in *pH* is associated with carbonate dissolution, the *pH* recovers in certain regions of the aquifer faster than in others, thus leading to a complex pattern of carbonate dissolution and reprecipitation. This evolving pattern of carbonate dissolution/reprecipitation implies that chemical constituents that are initially incorporated in or that coexist with primary carbonate minerals may be released into the fluid, then later removed from the fluid by reprecipitation when conditions have changed. Our simulations allow us to assess the release of solid constitutents from the primary mineralogy into the brine as CO_2 injection procedes.

The increase in reservoir pressure during injection, the dynamics of the CO_2 plume and the perturbation of chemical conditions in the reservoir will initiate mass transfer across the aquifer-seal interface and initiate chemical reactions on either side of the interface. We explore the extent of species mobilization and transfer across the reservoir/seal interface, identify the type of reactions that occur as well as their implications for the tightness of the caprock.

Sensitivity to deliberate seeding of marine clouds – Observations and modeling

K. ALTERSKJÆR AND J.E. KRISTJÁNSSON*

Department of Geosciences, University of Oslo, Norway (*correspondence: jegill@geo.uio.no)

Sea salt seeding of marine clouds to increase their albedo is a proposed technique to counteract or slow global warming [1]. In this study, we first investigate the susceptibility of marine clouds to sea salt injections, using observational data of cloud droplet number concentration (CDNC), cloud optical depth, and liquid cloud fraction from the MODIS (Moderate Resolution Imaging Spectroradiometer) instruments on board the Aqua and Terra satellites. We then compare the derived susceptibility function to a corresponding estimate from the Norwegian Earth System Model (NorESM). Results compare well between simulations and observations, showing that stratocumulus regions off the west coast of the major continents along with large regions in the Pacific and the Indian oceans are sensitive.

We then carry out sensitivity experiments with a uniform increase of 10^{-9} kg m^{-2} s^{-1} of 0.13 μm radius sea salt over ocean, in alignment with earlier studies [2]. The increased sea salt concentrations and the resulting change in marine cloud properties lead to a globally averaged forcing of -5.9 Wm^{-2} at the top of the atmosphere, more than cancelling a doubling of CO_2. The forcing is large in areas found to be sensitive by using the susceptibility function, confirming its usefulness as an indicator of where to inject sea salt. When the same sea salt mass is injected in the form of much smaller sea salt particles of 0.022 μm radius, a quite different result is found. These particles are too small to activate as CCN, but they provide a large surface area for sulphuric acid gas to condense on, thereby greatly suppressing the formation of sulphate particles. Therefore the overall CCN concentration is reduced, and the globally averaged forcing is positive.

[1] Salter (2008): *Phil. Trans. R. Soc. A*, **366**, 3989-4006.
[2] Latham (2008): *Phil.Trans. R. Soc.A*, **366**, 3969-3987.

https://doi.org/10.1180/S0026461X00006502 Published online by Cambridge University Press

Abiotic synthesis of methane from biomolecules under ambient conditions

FREDERIK ALTHOFF[1] AND FRANK KEPPLER[2]

[1]Max-Planck-Institute for Chemistry, Joh.-Joachim-Becher-Weg 27, 55128 Mainz; (Frederik.althoff@mpic.de)
[2]Max-Planck-Institute for Chemistry, Joh.-Joachim-Becher-Weg 27, 55128 Mainz; (frank.keppler@mpic.de)

The formation of methane can be classified in biotic and abiotic reactions. While biotic methanogenesis is related to anaerobic microorganisms, abiotic methane formation requires high pressure and/or temperature. Such conditions can be found for instance during biomass burning or serpentinisation of olivine, under hydrothermal conditions in the deep ocean or below tectonic plates [1].

The bio available substances ascorbic acid, iron and hydrogen peroxide were used in aqueous solution to perform an abiotic methane formation under ambient conditions [2]. In a further step to this reaction other important biomolecules were added which are known from methylation reaction in biosystems, e.g. methionine, or expose a possible methane precursor methyl groups, such as choline or leucine.

Furthermore, the reaction was carried out using different iron species, such as Fe^{2+}, Fe^{3+}, ferrihydrite and other iron hydroxides.

Methionine was found to produce the highest amount of methane. Stable isotope analysis in combination with ^{13}C labelling of methionine confirmed the assumption of sulphur bond methyl group as methane precursor. Moreover, a linear increase of the generated methane with the amount of added methionine could be found.

The investigation of the iron species basically showed a conversion to methane, however, methane formation is significantly higher using iron minerals in comparison to free Fe ions. By analysing the remaining products within the solution a reaction scheme was created.

The results of these experiments show the possibility of an abiotic aerobe methane formation using biomolecules under ambient conditions.

[1] Sherwood Lollar *et al*. (2002), *Nature* **416**, 522-524. [2] Althoff *et al*. (2010), *Chemosphere* **80**, 286-292.

The correlation between iodide sorption capacity and microbial enzyme activity in soils

S. AMACHI[1]* AND Y. MURAMATSU[2]

[1]Chiba Univ., 648 Matsudo, Matsudo-shi, Chiba 271-8510, Japan (*corespondence: amachi@faculty.chiba-u.jp)
[2]Gakushuin Univ. Mejiro 1-5-1, Toshima-ku, Tokyo 171-8588, Japan (yasuyuki.muramatsu@gakushuin.ac.jp)

Iodide (I^-) sorption on soils is strongly inhibited by autoclaving, reducing agents, common enzyme inhibitors (NaN_3 and KCN), and anaerobic incubation of soils. These suggest that the sorption of iodide is influenced by the soil redox potentials, and that microbial oxidation of iodide might play a role in the process. Recently, we found that bacterial iodide-oxidizing enzyme is a laccase-like enzyme, since it oxidized not only iodide but also phenolic compounds such as ABTS, syringaldazine and 2,6-dimethoxy phenol. Laccases are copper-containing enzymes that are secreted into soils by soil fungi and bacteria.

To understand possible participation of microbial enzymes in iodide sorption, we examined the correlation of iodide sorption rate with laccase activity in several soils. Laccase activity was assayed colorimetrically with ABTS as a substrate. As have been observed in iodide sorption, laccase activity in soils was also inhibited by autoclaving, reducing agents, enzyme inhibitors, and anaerobic incubation. The calculated iodide sorption rate [$(1-C/C_0)$/h/g dry soils]and laccase activity (Unit/g dry soils) showed significant positive correlation. Furthermore, addition of bacterial iodide-oxidizing enzyme to autoclaved soil allowed it to adsorb iodide again. From these results, it is possible that iodide in soils is oxidized by laccase (or laccase-like enzyme) to I_2 or HIO, and that these oxidized iodine species are incorporated into soil organic matters.

https://doi.org/10.1180/S0026461X00006502 Published online by Cambridge University Press

Quantification of CO_2 dissolved in silicate glasses and melts using Raman spectroscopy: Implications for geodynamics

JULIEN AMALBERTI[1,2], DANIEL R. NEUVILLE[2]*, PHILIPPE SARDA[1], NICOLAS SATOR[3] AND BERTRAND GUILLOT[3]

[1]Université Paris Sud 11 - UMR IDES 8148, Orsay
[2]CNRS-IPGP, 1 rue Jussieu, 75005 Paris, (neuville@ipgp.fr)
[3]LPTL, CNRS-Université de Paris 6, 4 place Jussieu, 75005 Paris

Understanding Earth degassing is fundamental in global studies of our planet history, as well as in studies of its recent climate. Degassing occurs mainly at Mean Ocean Ridges via exsolution of CO2 vesicles in ascending tholeiite magma, and probably begins at some 30 km under the ridge. Therefore, a precise knowledge of how carbon solubility varies during ascent from the source region is mandatory, a process for which the effect of pressure remains poorly known. A pressure increase induces melt compression, known to diminish argon dissolution with respect to Henry's law at pressures above ~10 kbar, but this effect is poorly documented for carbon where things are complicated by the transformation of CO_2 into carbonate ion, CO_3^{2-}. Early experimental investigations on carbon solubility in various silicate melts up to ~20-30kbar have shown that Henry's law is not followed at high pressures.

We have performed an experimental study of C dissolution in basaltic melts using high-pressure facility in Clermont-Ferrand (France). Analysis of dissolved C was performed using a micro-Raman spectroscopy. Dissolved carbon appears as clear bands due to carbonate ions (an intense peak at ~ 1100 cm^{-1} and a doublet in the 1350-1600 cm^{-1} region), molecular CO_2 being not detectable. Calibration of Raman spectroscopy for quantitative analysis was done by preparing standards at atmospheric pressure and analyzing them using a stable isotope mass spectrometer. The results show that carbon concentration increases steadily with increasing pressure, a behavior consistent with (rare) previous studies on basaltic melts. We also have performed molecular dynamics simulations to investigate the dissolution of CO_2 in a silicate melt. The calculated solubility is consistent with the data, which help understanding how pressure acts on fluid and melt, and yield insight into the details of how CO_2 and CO_3^{2-} interact with the melt network. However, the fact that the carbon solubility in a MORB is continuously increasing with pressure is somewhat surprising, and will be discussed.

This work has shown that

- Raman spectroscopy can be used to quantify C content in natural samples
- The C solubility measured in basaltic melt exhibits a behavior with pressure different from that exhibited by rare gases.
- Our results have important implications concerning the history of the atmosphere degassing and structure of the mantle.

Microbial community structures in shallow-sea, deep-sea, and terrestrial hydrothermal systems

JAN P. AMEND[1], D'ARCY R. MEYER-DOMBARD[2] AND MATT SCHRENK[3]

[1]Washingon University in St. Louis, (amend@wustl.edu)
[2]University of Illinois at Chicago, (drmd@uic.edu)
[3]East Carolina University, (schrenkm@ecu.edu)

The shallow-sea vent fluids and beach sediments at Vulcano Island (Italy) have yielded more culturable hyperthermophiles than any other hydrothermal system—marine or terrestrial. A seemingly insignificant hot spring in Yellowstone National Park (USA) was touted as harboring "remarkable" archaeal and bacterial diversity [1,2]. But how similar are the microbial community structures between sites? And can we quantitatively link the variability between sites to geographical isolation or geochemical parameters such as pH; temperature; pressure; salinity; or oxygen, sulfide, hydrogen, and organic carbon concentrations. In addition, do shallow-sea, deep-sea, and terrestrial hydrothermal systems share a significant number of taxa? And how do the microbial community compositions in these three fundamentally different types of high temperature ecosystems correlate with a wide range of geographical and geochemical parameters?

Our preliminary data analysis of ~1200 archaeal 16S rRNA gene sequences (assigned to ~300 operational taxonomic units (OTUs) with >90% similarity) from 5 terrestrial, 6 shallow-sea, and 17 deep-sea hydrothermal systems shows that ~85% of the OTUs are unique to one of the three types of hydrothermal systems. Only 2% are shared between 'terrestrial' and 'deep-sea' and between 'terrestrial' and 'shallow-sea'; 11% are shared between 'deep-sea' and shallow-sea'. Only 1 OTU (or 0.3%) of those investigated was found in all three types of systems—this was a sequence related to the Thermoproteales, an order of obligately or facultatively anaerobic hyperthermophiles known for carrying out sulfur respiration both chemolithotrophically (with H_2) or heterotrophically. A dendogram of sequences binned by sample showed a clear clustering of the terrestrial, the shallow-sea, and the deep-sea systems. Within the deep-sea systems, the samples from sediments, chimneys, vent fluids, and in situ colonization systems clustered separately. We hypothesize that multivariate analyses of geochemical and microbiological datasets can be used to identify major geobiological patterns and putative environmental causes.

[1] Barns *et al*., (1994). PNAS 91:1609. [2] Hugenholtz *et al*., (1998). J. Bact. **180**:366.

https://doi.org/10.1180/S0026461X00006502 Published online by Cambridge University Press

Ferrous iron diffusion in ferro-periclase across the spin transition – A DFT study

M. W. AMMANN*, J. P. BRODHOLT AND D. P. DOBSON

Earth Sciences, University College London, Gower Street, London, WC1E 6BT, UK
(*correspondence: m.ammann@ucl.ac.uk)

Diffusion is believed to control the viscosity of lower mantle minerals. While diffusion-experiments are limited to conditions of the shallow lower mantle, *ab initio* methods allow us to calculate absolute diffusion rates at any pressure and temperature [1,2]. The effect of the spin-transition in ferro-periclase on rheology is currently unknown.

We here present results of density-functional-theory calculations on absolute diffusion rates of high- and low-spin ferrous iron in ferro-periclase. The diffusivity of high- and low-spin iron depends on the physical conditions (pressure and temperature), iron concentration and the value of the chosen Hubbard U. We find that low-spin iron swaps back to high-spin during migration, such that the difference between high- and low-spin migration enthalpies only depends on the energy-difference of the ground-states.

We compared our absolute diffusion rates with experimental data of magnesium-iron interdiffusion in ferro-periclase at temperatures between 1873 K and 2273 K and at pressures ranging from 7 GPa to 35 GPa. All our diffusion rates are in excellent agreement with all the available experimental data.

Our results show that throughout the Earth's lower mantle, iron diffuses at a similar rate as magnesium. Thus, the spin transition of ferrous iron has no significant impact on the rheology of ferro-periclase in the Earth's lower mantle, and ferro-periclase remains much weaker than perovskite throughout. We conclude, therefore, that ferro-periclase can only control the viscosity of the mantle in regions where it becomes interconnected, such as areas of high strain around slabs or near plumes. At much higher pressures, such as in Super-Earths, low-spin iron diffusion is expected to become much slower than magnesium, making ferro-periclase more viscous than pure periclase.

[1] Ammann, Brodholt & Dobson, (2010), *Reviews in Mineralogy and Geochemistry* **71**, 201-224. [2] Ammann, Brodholt, Wookey & Dobson (2010), *Nature* **466**, 462-465. [3] Ammann, Brodholt, & Dobson (2011) *Earth Planet. Sc. Lett.* **302**, 393-402.

Chromium isotopes in the world's oceans: Potential tracers of redox environments

K. AMOR[1]*, S.J.G. GALER[2], P. ANDERSSON[3] AND D. PORCELLI[1]

[1]Dept. of Earth Sci., University of Oxford, Oxford, UK (*correspondence: kena@earth.ox.ac.uk)
[2]Max-Planck-Institut for Chemistry, Geochemistry Dept., Mainz, Germany
[3]Laboratory for Isotope Geology, Swedish Museum of Natural History, Stockholm, Sweden

We have developed a method for extracting and separating chromium (Cr) from a seawater matrix for isotope analysis using TIMS. We investigated a variety of ion exchange resins and co-precipitators to determine the optimal extraction method. Reported abundances of total Cr in seawater range from ~70 – 500ng/kg, depending upon seawater oxicity, water depth and proximity to continental land masses. A 500ml sample size permits ~10 duplicate analyses on TIMS which requires a minimum of 10ng of Cr. The reagent blanks are <2ng Cr and yields are high. Cr has four naturally occurring stable isotopes and therefore lends itself to double spiking for improved precision. We use a well constrained and optimized double spike of ^{50}Cr and ^{54}Cr [1].

Data will be presented on the distribution of Cr in major ocean basins, and the extent of isotope fractionation will be compared in oxic/anoxic waters, deep waters, and shelves. Building a global map of marine, Cr isotopes will facilitate a better understanding of the global geochemical and biogeochemical chromium cycle. Speciation analysis of seawater Cr is at odds with theoretical models and thermodynamic data. Both the trivalent and hexavalent ions ($Cr(H_2O)_4(OH)_2^+$ and CrO_4^{2-}) should be present in seawater in solubility equilibrium with the atmosphere, with a predominance of the +6 species. Observational analysis suggests that the system is in disequilibrium suggesting active cycling of Cr species [2]. The two naturally occurring oxidation states of chromium, +3 and +6, have distinct chemical properties and behaviour, with the potential for partitioning and isotopic fractionation between different reservoirs. Cr isotope fractionation in groundwater, of up to 6‰, have been attributed to redox changes [3].

[1] Galer (2007), *Geochim. Cosmochim. Acta,* **71** (15S), A303. [2] Elderfield, (1970) *EPSL*, **9,** 10-16 [3] Ellis *et al.*, (2002), *Science*, **295**, 2060.

https://doi.org/10.1180/S0026461X00006502 Published online by Cambridge University Press

The stable isotope composition of chlorine in hyperarid soils

R. AMUNDSON[1]*, J.D. BARNES[2] S. EWING[3], A. HEIMSATH[4] AND G. CHONG[5]

[1]ESPM, Univ. of Calf., Berkeley, CA 94720, USA (*corresponding author: earthy@berkeley.edu)
[2]Geol. Sci, Univ. of Texas, Austin, TX 78712, USA
[3]Land Res. and Env. Sci., Montana State Univ., Bozeman, MT, USA 59717
[4]Earth and Space Expl., Ariz. State Univ., Tempe, AZ 85287, USA
[5]Dept. de Ciencias Geol., Univ. Catolica del Norte, Antrofagasta, Chile

Halite (NaCl) is a water soluble mineral found in soils of the driest regions of Earth, and only modest attention has been given to the hydrological processes that distribute this salt vertically in soil profiles. The recent application of stable Cl isotope analyses to soils (Bao *et al*., 2008) set in motion the opportunity to use Cl isotopes to examine these processes. Here, we compare previously published depth profiles of Cl and Cl isotopes in Antarctica to new data on soils from the Atacama Desert in Chile. We first show, using previously published S and O isotope data for sulfates in both deserts, that downward migration of water and sulfate is the primary mechanism responsible for the depth profiles of these salts, and the S and O isotopes within them. In contrast, we found quite different Cl and Cl isotope profiles between the two deserts. For Antarctic soils with an ice layer near the soil surface, the Cl concentrations increase with decreasing soil depth, while the ratio of $^{37}Cl/^{35}Cl$ increases. Based on previous field observations by others, we found that thermally driven upward movement of brine during the winter, described by an advection/diffusion model, at least qualitatively mimics the observed profiles. In contrast, in the Atacama Desert where rare but relatively large rains drive Cl downward through the profiles, Cl concentrations increased with depth while $^{37}Cl/^{35}Cl$ ratios declined. The depth trends in Cl isotopes were more closely explained by a Rayleigh-like model of downward fluid flow. The isotope profiles, and our modeling, reveal the similarities and differences between these two very arid regions on Earth, and provide additional tools to interpret the direction of fluid flow from Cl profiles on Mars.

Bao H., Barnes J.D., Sharp Z.D., and Marchant D.R. (2008) Two chloride sources in soils of the McMurdo Dry Valleys, Antarctica. *Journal of Geophysical Research* 113(D03301)

Research on geochemistry model of Nanhe W-Mo-Cu deposit in southwest section of Qinzhou-Hangzhou metallogenic belt

AN YAN-FEI[1,2]*, ZHOU YONG-ZHANG[1,2], L.V. WEN-CHAO[1,2], TAN XIN[1,2], CHEN QING[1,2], BAI MING-LIANG[1,2] AND ZHANG YAN[1,2]

[1]Guangdong Provincial Key Lab. of Geological Process and Mineral Resource Survey, 510275 China (*correspondence: anyanfei0557@163.com)
[2]Department of Earth Science, Sun Yat-sen University, 510275 China

Nanhe W-Mo-Cu Deposit, lying in the zone between granite rock and layer, located at southwest limb of Zhongdong-Liangjiang Synclinorium southwest, southwest section of Qingzhou-Hangzhou Metallogenic Belt [1-3]. Its tectonic evolution experienced two stages: Continent-island arc collision and amalgamation in Caledonian and platform cracking in yanshanian [4-6]. Ore bodies occur in the zone of Caledonian mix granite, N-E shovel fault [7]. Ore analysis of W-Mo-Cu-Pb element demonstrated that: primary tungsten enriched in amphibolite. Either tungsten or molybdenum ore is mainly enriched in the weathering zone of basic volcanic rocks and Surrounding strata. It also tell us that the content of tungsten and molybdenum elements in layer is as 4-8 times high as rock mass; while the scale in granite mass is higher than the other rock mass. In addition, the content of Cu from the layer to mass present M-type and has a certain correlation with W.

1. Ore bodies are located in the volcanic layers of Cambrian and may be mineralized Paleozoic 2. W-Mo deposit must be Sedimento-Reformed Deposits and its Distribution under strict control of the basic volcanic rocks.3. Cu deposit should be porphyry copper deposits and copper comes mainly from the melting process of granitic rocks.4. Fault activity provide access for the mineralization and magmatic action provide energy and drive。

[1] Yang M G *et al*. (2009) *Geology in China* **36**, 528-543. [2] Ji X (1993) *Journal of Sun Yat-sen University* **32**, 85-94. [3] Shu L S *et al*. (2008) *Geological Bulletin Of China* **27**, 1581-1593. [4] Hu R Z *et al*. (2007) *Mineral Deposits*. **26**, 139-152. [5] Zhou Y Z (2010) report in meeting [6] Mao J W *et al*. (2009) *Geological Review* **55**: 347-354. [7] Bureau Of Guangdong Geology (1987) The Prospecting Report of Nanhe W-Mo deposit [8] Bureau Of Guangdong Geology (1987) 1:50000 report of tangpeng regional geological survey

https://doi.org/10.1180/S0026461X00006502 Published online by Cambridge University Press

Linking geochemistry and texture of mine tailings and soils to the evolution of plant community in a contaminated copper-sulphide mining area

HOSSAIN M. ANAWAR* AND M. C. FREITAS

Instituto Tecnológico e Nuclear, URSN, E.N. 10, 2686-953 Sacavém, Portugal (*anawar4@hotmail.com)

The adverse physicochemical properties and toxic elemental contamination of mine tailings generally inhibit the plant growth in the mining area. Some other adverse factors like absence of topsoil, drought, surface mobility, compaction, absence of soil-forming fine materials, soil acidity and shortage of organic matter as well as its associated essential nutrients dwarf the spontaneous growth of the diversified plant species in mining affected lands. Therefore, this study made a survey on plant community development at the abandoned São Domingos copper-sulfide mining area in order to understand the relationship of geochemistry and texture of tailings and soils with development of plant community. The results found several communities of plant species dominating in the area depending on geochemistry, mining contamination, soil texture, soil development and distance from the mining activities. The succession of plant communities shows that the plant communities of low height and biomass and bush-type (shrub), mainly *Erica australis*, *Lavandula stoechas*, *Cistus* genus, *Rumex induratus*, *Daphne gnidium*, *Juncus scirpoides*, and *Genista hirsuta* are grown in the mine waste dumps, slags, colluvium, gossan waste, and tailings contaminated lands with thin soil cover, slopes, ditches and acid mine drainage (landscape one). The poor vegetation coverage is clearly noticeable in the severely affected areas that are vulnerable to degradation and aerial dispersion. By contrast, the upland, contaminated to variable degrees (landscape two) just adjacent to the landscape one has good alluvial soil development like loam, and higher vegetation cover. The plant communities are taller, tree-type, and of higher biomass, namely *Eucalyptus globulus*, *Pinus pinaster*, *Pistacia terebinthus*, and *Pteridium aquilinum* etc. The *Erica australis*, *Lavandula stoechas or luisieri*, and *Cistus ladanifer* are found to variable extents in both landscapes. The *Erica australis* is spontaneously grown in the acidic sulfide mining soils; and this species is very specific plant in São Domingos mining area (Anawar *et al*., 2011). The overall results indicate that the geochemistry and contamination levels of mining activities, soil texture, soil development and landscapes are the species-limiting factors for plant community development and vegetation coverage in the mining area. Although the high concentrations of toxic trace elements (e.g., As, Sb, Cr, Hg, Pb and Zn) and low pH values (soil acidity) are important factors for limiting the plant growth, however, soil texture and good soil development with enriched nutrients can present the high vegetation coverage in the mining contaminated lands and pave a biotechnology-based solution of land reclamation.

Whither the whiff?

A.D. ANBAR[1,2]*, B. KENDALL[1], C.T. REINHARD[3] AND T.W. LYONS[3]

[1]School of Earth & Space Exploration, Arizona State University, Tempe, AZ 85287, USA (*correspondence: anbar@asu.edu)

[2]Department of Chemistry & Biochemistry, Arizona State University, Tempe, AZ 85287, USA

[3]Department of Earth Sciences, University of California, Riverside, CA 92521, USA

Improved understanding of the rock record indicates that the Great Oxidation Event was the culmination of an extended period of complex redox evolution and biogeochemical change rather than a singular event. We review data emerging from the sedimentary rock record about the timing and tempo of this transition and preview frontiers of investigation.

Attention has focused in particular on high-resolution, multi-proxy analyses of latest Archean black shales in drill cores from the Hamersley Basin in Western Australia, and from the Griqualand West Basin in South Africa. These analyses yielded multiple lines of evidence suggestive of photosynthetic O_2 production at 2.6 – 2.5 Ga, including: (1) patterns of Mo and Re enrichment and Mo and U isotope variations indicating the presence of these redox-sensitive metals in mildly-oxygenated contemporaneous water columns; (2) a shift in S isotopes interpreted as revealing the onset of an oxidative S cycle; (3) ^{15}N enrichments that record the operation of an aerobic N cycle, including nitrification and denitrification; (4) sedimentary Fe speciation and $\delta^{56}Fe$ data documenting anoxic and sulfidic (euxinic) conditions at mid-depths, most likely arising from enhanced oxidative weathering of sulfides, and a redox-stratified water column; and (5) a shift in sterane/hopane ratios suggestive of a transition in microbial ecology to greater participation by O_2-dependent eukaryotes. Alternative interpretations are possible for some of these observations, but collectively, consistent with other studies, they indicate a "whiff" of O_2 in the late Archean environment.

The data prompt new questions. How high did pO_2 rise? Was O_2 persistent in the environment, or do the data represent a transient event? If transient, was this one of many such episodes? Can similar evidence be found in the earlier Archean record? These questions are the focus of ongoing investigations.

https://doi.org/10.1180/S0026461X00006502 Published online by Cambridge University Press

A magma plumbing system probed by the Grænavatn Porphyritic Group, East Iceland

CHRISTINA B. ANDERSEN[1,2]*, MORTEN S. RIISHUUS[1] AND CHRISTIAN TEGNER[2]

[1]Nordic Volcanological Center, Institute of Earth Sciences, University of Iceland, Sturlugata 7, 101 Reykjavik, Iceland (*correspondence: bomberg@hi.is)
[2]Department of Earth Sciences, University of Aarhus, 8000 Aarhus, Denmark

Neogene plagioclase ultraphyric basalts (PUBs) from East Iceland hold up to 45% macrocrysts that may lend clues to a fossil crustal plumbing system. The ~10 Ma old Grænavatn Porphyritic Group consists of 3-10 PUB lava flows and attain maximum thickness (~90m) west of Reyðarfjörður. It is a regional marker horizon, traceable for >50km along strike, but tapers out to the north, south and up-dip to the east. Modal proportions of plagioclase macrocrysts vary both vertically and laterally within single lava flows. Petrographic observations and crystal size distribution have identified three plagioclase populations; (1) single, zoned euhedral macrocrysts (~5mm) with overgrowth rims, (2) unzoned, anhedral glomerophyric macrocrysts (4-10mm) in clusters up to 3cm, and (3) lath-shaped microlites in the groundmass. Macrocryst cores (An75-85) are more primitive than groundmass microliths (An55-65), and therefore in disequilibrium with the host melt. Detailed textural and chemical mapping of zoned macrocrysts reveals complex histories with resorption, overgrowth and stages with entrapment of melt inclusions. Chemical traverses display oscillatory, continuous normal and reverse zoning. Further, we observe discontinuous reverse zoning (ΔAn4-5) that could suggest decompression of ~10km. These PUBs may enable us to examine the structure of a crustal plumbing system potentially involving events of magma ponding, rapid decompression, mixing, recharge and assimilation.

U-series disequilibria during soil weathering

M.B. ANDERSEN[1]*, D. VANCE[1], A.R. KEECH[1], J. RICKLI[1] AND G. HUDSON[2]

[1]Bristol Isotope Group, School of Earth Sciences, University of Bristol, Wills Memorial Building, BS8 1RJ, UK (*correspondence: morten.andersen@bris.ac.uk)
[2]Macaulay Institute, Aberdeen, AB15 8QH, Scotland

The weathering of continental rocks influences long-term atmospheric CO_2 and thus climate. In addition, the riverine transport of weathering products to the ocean partially controls marine geochemical budgets. U-series isotopes have long been recognised for their capability to provide time-scales of weathering processes, as well as the nature of the linkage between chemical weathering and physical denuation. However, to fully exploit the potential of the U-series chronometer in weathering studies, an improved understanding of the chemical behaviour and properties of the U-series nuclides in the weathering regime is required.

We have analysed a Scottish soil chronosequence (soil ages from 0.1-13 ka) [1] for ($^{234}U/^{238}U$), ($^{230}Th/^{238}U$) ($^{238}U/^{232}Th$) and ($^{230}Th/^{232}Th$) activity ratios to investigate the behaviour of the U-series nuclides during progressive weathering. All the bulk soil profiles studied show U-series isotopic disequilibrium, including the C-horizons. In the bulk soil samples a clear trend in ($^{234}U/^{238}U$) is observed, with values above unity for the younger soils (up to 1.3), declining towards unity with time. A corresponding trend is observed in the ($^{230}Th/^{238}U$), with values below unity (down to 0.7) for the younger soils, and increasing with older ages (up to 1.3). These observations suggest that there are two competing processes that dominate: (1) U addition to the bulk soil and; (2) soil leaching. The U added is characterised by a high ($^{234}U/^{238}U$), corresponding to the composition measured in local streams (1.3-2.0). This added U is likely to be from perculating groundwaters that adsorbs to soil surfaces. However, with time this U pool declines, likely to be related to changes in the chemical adsorption properties of the soils. The decline in ($^{234}U/^{238}U$) is combined with leaching of the soil, preferentially releasing more U than Th, due to the higher mobility of U than Th.

The U-series data from the soil chronosequences shows the importance of physio-chemical processes during weathering, which affects element and isotope redristibution during weathering. These have to be quantified in studies using the U-series chronometer to constrain time-scales of weathering.

[1] Bain *et al*. (1993) *Geoderma* **57**, 275-293

https://doi.org/10.1180/S0026461X00006502 Published online by Cambridge University Press

Monitoring beam-induced radiolysis effects on transition metal complexes in hydrothermal fluids

A.J. ANDERSON[1], R.A. MAYANOVIC[2], M.R. FRANK[3] AND S. PASCARELLI[4]

[1]Department of Earth Sciences, St. Francis Xavier University, Antigonish, Nova Scotia, Canada (aanderso@stfx.ca)
[2]Department of Physics, Astronomy & Material Science, Missouri State University, Springfield, Missouri, USA (RobertMayanovic@missouristate.edu)
[3]Department of Geology and Environmental Geosciences, Northern Illinois University, DeKalb, Illinois, USA (mfrank@niu.edu)
[4]European Synchrotron Radiation Facility, Grenoble, France (sakura@esrf.fr)

The irradiation of aqueous solutions with high brilliance synchrotron x-rays causes the decomposition of water molecules and the formation of transient species such as $H^{\bullet}$, $^{\bullet}OH$, H^{+}, OH^{-} and hydrated electrons, e_{aq}^{-}. These radiolysis products may react rapidly with solutes to modify aqueous speciation. In order to study the effects of beam-induced radiolysis on transition metal-bearing hydrothermal fluids, the structure of Cu and Fe chlorocomplexes was monitored using time-resolved x-ray absorption spectra.

XANES data were obtained at beamline ID-20-C at the Advanced Photon Source, Argonne National Laboratory, from synthetic fluid inclusions of known composition, and from solutions in hydrothermal diamond anvil cells (HDAC) up to 600 ºC. *In situ* energy-dispersive x-ray absorption spectroscopic (ED-XAS) measurements were also made on Fe^{2+} chloride solutions at beam line ID24 at the European Synchrotron Radiation Facility. The ED-XAS spectra were measured at 100 intervals with 1 s time resolution followed by 30 or 60 intervals with 60 s time resolution. Our results indicate that Fe^{2+} ions are oxidized or reduced, depending upon the pressure – temperature conditions of the aqueous fluid. Extended irradiation at 500 ºC resulted in the formation of Fe and Cu nanoparticles.

A single x-ray absorption spectrum acquired over a period of several minutes using a scanning monochromator may measure beam-induced modifications produced during the scan. Such artefacts of radiolysis may be minimized or eliminated by analyzing hydrothermal fluids in a flow-through system or by using ED-XAS to reduce the exposure time to synchrotron x-rays.

Portable Rb-Sr geochronology

F.S. ANDERSON*, K. NOWICKI AND T. WHITAKER

Southwest Research Institute, 1050 Walnut, Suite 300, Boulder, CO 80302 (anderson@boulder.swri.edu, knowicki@ boulder.swri.edu, whitaker@boulder.swri.edu)

We have produced a preliminary, low precision, 12-point Rubidium-Strontium (Rb-Sr) geochronology measurement of the Boulder Creek Granite using a laser desorption resonance ionization mass spectrometer (LDRIMS) capable of being miniaturized into a portable unit. Our current prototype can measure the isotope ratio of lab standards with 10 ppm net Sr or Rb to a precision of ±0.1% (1σ), with a sensitivity of $1{:}10^{10}$ in <15 minutes/point. Using the 1) known Rb-Sr ratios and modal mineralogy from Martian and lunar samples, and 2) LDRIMS precision & accuracy, we have numerically modeled the age error for 100-1000 points and determined that uncertainties <±50 Ma are possible [1]. The ability to make in-situ lunar and Martian radiometric measurements with uncertainties <±50 Ma would significantly improve geologic interpretation of these complex surfaces and potentially constrain impactor flux throughout the solar system.

Preliminary results from the Elephant Butte Boulder Creek Granite (BCG_EB) are compared with TIMS Rb-Sr dates of 1700±40 m.y. from 19 whole rock samples [2]. With careful choice of the statistical binning technique, an identifiable isochron, with an MSWD of 2, can be produced (Fig. 1). The age error of ±870 m.y. is consistent with our analytical models for 12 measurements at ±0.4% precision. If expanded to 100-1000 measurements, our statistical models show that this will improve to <50-100 m.y. values [1]. We have also identified and corrected a resonance effect causing the ~15% fractionation offset of $^{87}Sr/^{86}Sr$ observed in Fig. 1.

Ongoing work will improve precision, increase the number of spot measurements, and produce a portable demonstration instrument.

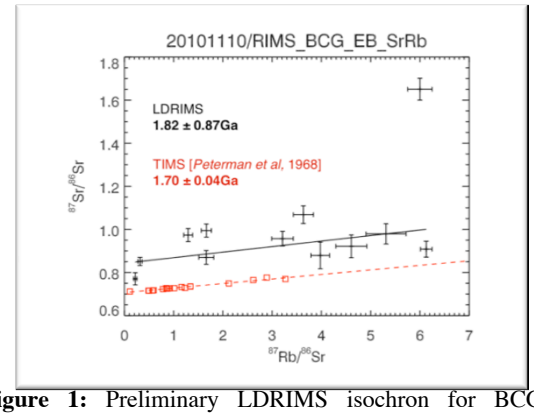

Figure 1: Preliminary LDRIMS isochron for BCG_EB (MSWD 2) is consistent with TIMS results. The age error can be reduced further by making hundreds to thousands of measurements.

[1] *Anderson and Nowicki*, LPSC, abs# 1979, 2010. [2] *Peterman et al*, JGR, 73, 2277, 1968.

https://doi.org/10.1180/S0026461X00006502 Published online by Cambridge University Press

Trace element geochemistry of micas by laser ablation ICP-MS in the Moose II lithium-tantalum pegmatite deposit, NWT

M.O. ANDERSON[1]*, D. LENTZ[1], C. MCFARLANE[1] AND H. FALCK[2]

[1]Department of Geology, University of New Brunswick, Fredericton, NB, Canada, E3B 5A3 (*correspondence: m5r5u@unb.ca; dlentz@unb.ca, crmm@unb.ca)

[2]Northwest Territories Geoscience Office, PO Box 1500, 4601-B 52 Avenue, Yellowknife, NT, Canada, X1A 2R3 (hendrik_falck@gov.nt.ca)

The Moose II zoned LCT-type pegmatite is located ~115 km east-southeast of Yellowknife, NWT, Canada, and measures 430 m long and up to 61 m wide. This deposit is a historical producer of lithium and tantalum (1946 – 1954).

Fractionation trends of micas have often been studied as petrogenetic indicators of pegmatite evolution. This study uses laser ablation ICP-MS to explore the fractionation patterns, mechanisms for emplacement, and processes leading to mineralization (e.g., Van Lichtervelde *et al*. [2]). Preliminary results indicate that the Moose II pegmatite has highly evolved compositions, typical of advanced fractionation. This is complemented by analyses of 24 muscovite mineral separates by ICP-MS and XRF, and is comparable to regional studies of muscovite in the Faulkner Lake pegmatites series [2].

	Faulkner Lake Series [2]			Moose II Pegmatite		
	Avg	**Range**	**n**	**Avg**	**Range**	**n**
Li_2O	0.032	0.018-0.052	14	0.039	0.017-0.073	24
Rb	5560	2380-10200	14	1955	720-4350	24
Cs	127	40-310	14	83	24-233	24
Be	19	11-25	14	30	21-47	24
Sn	-	-	-	249	100-437	24
Nb	92	40-170	8	77	32-156	24
Ta	124	78-207	8	13	2-74	24
Nb/Ta	0.8	0.4-1.4	8	8.9	1.9-18.5	24
K/Rb	15.9	7.1-322	14	2.8	0.9-6.3	24

Table 1: Compositional characteristics of muscovite mineral separates for the Faulkner Lake pegmatite series and the Moose II pegmatite (ICP-MS & XRF). Elements – ppm, oxides – wt.%.

[1] Van Lichtervelde *et al*. (2008) *Contrib Mineral Petrol* **155**, 791-806. [2] Wise (1987) Ph.D Thesis, 368 p.

Was Atlantic deepwater flow reversed during the Last Glacial Maximum?

ROBERT F. ANDERSON[1]*, MARTIN Q. FLEISHER [1], RAINER GERSONDE[2] AND GERHARD KUHN[2]

[1]Lamont-Doherty Earth Observatory of Columbia University, Palisades, NY, 10964 USA (*correspondence: boba@ldeo.columbia.edu)

[2]Alfred Wegener Institue for Polar and Marine Research, Bremerhaven, Germany (Rainer.Gersonde@awi.de)

Negre *et al*. [1] inferred northward flow of deep water in the Atlantic Ocean during the Last Glacial Maximum (LGM) based on the north-south gradient in sedimentary $^{231}Pa/^{230}Th$ ratios. The southern end member record of Negre *et al*. was derived from core MD02-2594 in the SE Atlantic (34° 43' S, 17° 20' E; 2,440 m).

New results will be presented from core PS2498-1 in the SW Atlantic (44.1533°S, 14.2283°W; 3783m) that exibit a pattern of sedimentary $^{231}Pa/^{230}Th$ ratios opposite of that in MD02-2594. Whereas $^{231}Pa/^{230}Th$ ratios increase from ~0.045 in the LGM to ~0.07 in the Holocene in MD02-2594, they decrease from ~0.10 in the LGM to ~0.055 during the Holocene in PS2498-1.

Sedimentary $^{231}Pa/^{230}Th$ ratios in PS2498-1 are highly correlated with the opal content of the sediments. Furthermore, the relationship between sedimentary $^{231}Pa/^{230}Th$ ratios and opal content (and with opal flux) in PS2498-1 is continuous with the relationship exhibited in TN057-13-PC4, from a site south of the Antarctic Polar Front in a region of greater average opal abundance.

Based on the observed uniform relationship between sedimentary $^{231}Pa/^{230}Th$ ratios and opal, we conclude that the abundance of opal is the master variable regulating sedimentary $^{231}Pa/^{230}Th$ ratios in the South Atlantic. This is consistent with the global data from sediment traps showing a strong correlation between particulate $^{231}Pa/^{230}Th$ ratios and the opal content of particles [2], reflecting the high affinity of Pa for sorption to opal. Finally, we further conclude that sedimentary $^{231}Pa/^{230}Th$ ratios cannot be used to infer the direction of deepwater flow in the past without a level of control on the spatial and temporal variability of opal flux that is beyond the present capabilities of the field of paleoceanography.

[1] Negre *et al*. (2010) *Nature* **468**, 84-88. [2] Chase *et al*. (2002) *Earth. Planet. Sci. Lett*. **204**, 215-229.

https://doi.org/10.1180/S0026461X00006502 Published online by Cambridge University Press

Deep ocean carbonate chemistry on millennial to Milankovitch time scales

ROBERT F. ANDERSON* AND MARTIN Q. FLEISHER

Lamont-Doherty Earth Observatory of Columbia University, Palisades, NY, 10964 USA
(*correspondence: boba@ldeo.columbia.edu)

Deep ocean carbonate ion concentration is intimately linked to ocean processes that regulate atmospheric CO_2 over glacial time scales. Well dated records of $CaCO_3$ preservation in deep-sea sediments provide valuable clues about these processes.

Building upon previous studies of $CaCO_3$ preservation in Cape Basin sediments [1, 2], we find that ^{230}Th-normalized fluxes of $CaCO_3$ are well correlated with the abundance of $CaCO_3$ during the last glacial period (LGP), alowing us to use the entire record of ODP-1089 $CaCO_3$ content [1] to infer changes in deep water carbonate ion concentration.

During the LGP, peaks in $CaCO_3$ preservation exhibit features that are reminescant of warm intervals in Antarctic ice cores. Initially we linked increased $CaCO_3$ preservation to ventilation of deep waters via the Southern Ocean, which increased during Antarctic warm periods [3]. However, precise dating of Cape Basin sediments revealed that $CaCO_3$ preservation peaks are associated with vigorous North Atlantic Deep Water (NADW) formation following the Antarctic warm periods rather than by ventilation from the Southern Ocean during these warm periods [2]. Thus, the link between deepwater formation and atmspheric CO_2 is complicated by the complementary impacts of ventilation at opposeite ends of the earth.

Millennial scale features in the $CaCO_3$ record of the Cape Basin are also observed in North Pacific sediments during the LGP, indicating the widespread impact of NADW formation on deepwater carbonate ion concentration.

Finally, we also find an intriguing correlation over longer time scales to suggest that precession forcing [4] and millennial events share some common impacts on deep water carbonate ion via NADW formation.

[1] Hodell *et al*. (2001) *Earth. Planet. Sci. Lett*. **192**, 109-124. [2] Barker *et al*. (2010) *Nature Geosci*. **3**, 567-571. [3] Anderson *et al*. (2009) *Science* **323**, 1443-1448. [4] Lisiecki *et al*. (2008) *Nature* **456**, 85-88.

How acidic is water on calcite?

M.P. ANDERSSON AND S.L.S. STIPP

Nano-Science Center, Department of Chemistry, University of Copenhagen, Denmark
(*correspondence ma@nano.ku.dk)

Mineral dissolution and precipitation take place primarily on undercoordinated sites on the solid surface, in particular kink sites. Most theoretical studies are performed using molecular mechanics assuming that only water is present at the surface. We have used density functional theory in combination with the COSMO-RS implicit solvent model to calculate pK_a values of water on various sites on a calcite surface. The mineral surfaces were modelled by 80 atom clusters and we have checked convergence of the pK_a values with respect to both cluster size and number of relaxed surface atoms. For kink sites, we found that water is acidic with a pK_a value as low as 3.5. At equilibrium, kink sites are thus covered with hydroxyl ion and water. Our results are relevant for future theoretical studies of dissolution and precipitation of minerals, where the correct equilibrium structure should be modelled.

We also calculated the pKa values for ethanol adsorbed on terrace, step and kink sites on calcite and compared the free energies of adsorption of ethanol and water. Ethanol was found to bind stronger than water on the {10.4} terrace and on the obtuse step, equally strongly on the acute step, whereas on kink sites, water (in the form of hydroxyl ions) binds more strongly than ethanol (in the form of ethoxide). This is consistent with recent experimental data using atomic force microscopy showing that ethanol hinders recrystallization on the {10.4} terrace.

https://doi.org/10.1180/S0026461X00006502 Published online by Cambridge University Press

Relationship between palaeoclimate and diagenesis intensity in sediments from transitional environments: The Galician Rías (NW Spain)

A. ANDRADE, B. RUBIO*, D. REY, P. ÁLVAREZ-IGLESIAS, A.M. BERNABEU AND F. VILAS

Research group GEOMA. Departamento de Geociencias Marinas y Ordenación del Territorio, Universidad de Vigo, Vigo Spain (*correspondence: brubio@uvigo.es)

Sediments of coastal areas such as the Galician Rías Baixas (NW Iberian Peninsula), where land and sea interdigitate, are a valuable source of information, since their high sedimentation rates (3-6 mm yr^{-1}) [1] facilitate studies of high resolution. In addition, their position under the influence of both land and sea leads to their exhibiting patterns of interaction between both environments that can help discriminate among local, regional and global climate processes. The Galician coast is one of the regions of the world with most intense coastal upwelling. This, together with continental inputs makes the organic matter contents of sediments from the Rias Baixas to be very high [2], which favour intense diagenetic processes. The intensity of these processes is not only controlled by the organic matter concentrations but also by the relative proportion of oceanic (labile) and terrestrial (refractory) organic matter. Changes in early diagenesis can throw light on the degree of oceanic influence in the Ría, and hence on changes in the circulation and ventilation of its water masses and/or the climate on shore.

In this study on sediment cores taken in the outer Ría de Muros, the combined use of textural analysis, magnetic properties ($\varkappa$, ARM/SIRM, MDF) and geochemical parameters (total concentrations of diagenetically stable and mobile elements in sediment and pore water) allowed the identification of a current redox front and two palaeosedimentary redox fronts. These fronts originated during periods of high marine/terrestrial organic matter ratio (as inferred from the TOC/TN ratio and $\delta^{13}C$). The chronological framework established by ^{14}C dating allowed correlating these fronts to known periods of increased upwelling and reduced continental input due to colder, drier climates in the northwestern Iberian Peninsula, namely the Little Ice Age, the Dark Ages, and the first cold period of the Upper Holocene.

[1] Álvarez-Iglesias, Quintana, Rubio & Pérez-Arlucea (2007) *Journal of Environmental Radioactivity* **98** (3), 229-250 [2] Vilas, Bernabeu & Méndez (2005) *Journal of Marine Systems* **54**, 261-276.

Melting properties of chondritic mantle to the core-mantle boundary

D. ANDRAULT[1], G. LO NIGRO[1], N. BOLFAN-CASANOVA[1], M.A. BOUHIFD[1], G. GARBARINO[2], M. MEZOUAR[2]

[1]Université Blaise Pascal, Clermont-Ferrand, France
[2]European Synchrotron Radiation Facility, Grenoble, France

A large proportion of our planet has experienced melting in the course of its accretion history. In the modern Earth, partial melting in the lowermost mantle is also suggested based on seismic observations of ultra-low velocity zones. The melting properties of the deep mantle thus has major consequences for the existence and survival of chemical heterogeneities in the Earth mantle and, more generally, for our knowledge of mantle dynamics.

Melting curves and Fe partition coefficient have been investigated in a chondritic-mantle material using the laser-heated diamond anvil cell (LH-DAC) at P-T conditions corresponding to the entire Earth's lower mantle. Two different *in situ* synchrotron radiation techniques have been used to infer melting properties *in situ*; X-ray diffraction and X-ray fluorescence spectroscopy.

At core-mantle boundary pressure (135 GPa), the chondritic-mantle solidus and liquidus reach 4150 (±150) K and 4725 (±150) K, respectively. These temperatures are significantly higher than most of estimations of the mantle geotherm. Therefore, partial melting in the D"-layer most certainly indicates chemical heterogeneities with high concentration of fusible elements.

Our observations of a high liquidus as well as a large temperature gap between solidus and liquidus temperatures have important implications for the properties of the magma ocean during accretion. Not only complete melting of the lower mantle would require excessively high temperatures, but also, partial melting should take place over a much larger depth interval than previously thought.

Finally, we provide distribution maps of elements (Ca and Fe) and phases (Mg-Pv, liquid) in our samples which have encountered partially molten at the lower mantle P-T conditions. The Fe partitioning coefficients extracted from these maps show a large preference of Fe for the liquid phase. This behavior is compatible with the production of high density liquids, which can be related to sinking down of liquid phases.

https://doi.org/10.1180/S0026461X00006502 Published online by Cambridge University Press

Aerosol-cloud-precipitation interactions in the climate system

M.O. ANDREAE

Max Planck Institute for Chemistry, Mainz, Germany

Aerosols serve as cloud condensation nuclei (CCN) and thus have a substantial effect on cloud properties. Increased aerosol concentrations resulting from anthropogenic pollution lead to higher cloud droplet concentrations, but smaller droplet sizes. This in turn affects the physical processes inside clouds that lead to the initiation of precipitation. Depending on a number of factors, including aerosol composition, atmospheric stability and cloud water content, increasing CCN concentrations may either decrease or increase rainfall. In convective clouds, early rain formation is suppressed, which makes more water and energy available to rise higher in the atmosphere and form ice particles. This may invigorate the dynamics of convection, encourage the formation of hail and lightning, and enhance the transport of materials to the upper troposphere. In order to understand and quantify the effects of air pollution on climate, and precipitation in particular, knowledge of natural abundance and characteristics of aerosols is as essential as the observation of perturbed conditions. I will present recent advances in the conceptual understanding of aerosol-precipitation interactions, as well as measurements on pristine and polluted aerosol characteristics.

Iron speciation in serpentine during oceanic-type serpentinization

MURIEL ANDREANI[1], MANUEL MUNOZ[2], C. MARCAILLOU[2] AND A. DELACOUR[3]

[1]Laboratoire de Géologie de Lyon, ENS - Université Lyon 1, (*correspondance: muriel.andreani@univ-lyon1.fr)
[2]Institut des Sciences de la Terre, Université Grenoble 1, France. (manuel.munoz@ujf-grenoble.fr)
[3]Géosciences Environnement Toulouse, Université Toulouse 3, France. (adelie.delacour@get.obs-mip.fr)

Serpentinisation of ultramafic rocks at mid-ocean ridges is now well known to generate high amounts of H_2, CH_4 and to support novel biological communities. The abiotic production of hydrogen is attributed to the reduction of H_2O during oxidation of the ferrous component of primary minerals. The amount of hydrogen and hydrocarbons formed abiotically is thus directly linked to the amount and state of iron incorporated into product minerals, mainly magnetite and serpentine. However, magnetite is classically the only Fe^{3+}-carrier considered for estimating bulk H_2 fluxes. This is mainly due to the scarce and scattered data on the iron redox state in serpentine minerals and its unknown relationship with both magnetite abundance and serpentinization degree.

To address these questions, we have realized punctual μ-XANES analyses at the iron K-edge (ID24, ESRF) of serpentine minerals in thin sections. Rock samples from 4 different localities (Mid-Atlantic Ridge and Pindos ophiolite) have been selected for their various degrees of serpentinisation and magnetite content.

The results show that Fe^{3+} is abundant in oceanic-type serpentine: it can represent up to 100% of the total iron in the structure but typically tends to 60-65% for sample showing more that 60% of serpentinization. Whole rock chemical analyses and petrographic characterization of the samples allowed us to establish that the Fe^{3+}/Fe^{Tot} in serpentine evolve non-linearly with the local degree of serpentinization. The Fe^{3+} is more rapidly incorporated in serpentine during the first half of reaction, especially if magnetite is rare. This demonstrates the involvement of serpentine formation on natural H_2 production. We have estimated that at least 10% of the H_2 produced is related to serpentine (MARK) and that this value easily attain 30% (Pindos) or even 70% locally in some samples from Logatchev. Thus, evaluation of the raw H_2 production during serpentinization must take into account the Fe^{3+} incorporated in serpentine which is site-dependent. This also opens new perspective on the role of serpentine minerals on the redox state in subduction zones where the oceanic crust is recycled into the earth mantle.

https://doi.org/10.1180/S0026461X00006502 Published online by Cambridge University Press

Magama composition and crystallization conditions of the rare-metal granites from Khaldzan-Buregtei massif of peralkaline rare-metal igneous rocks

I.A. ANDREEVA*

Institute of Geology of Ore Deposits, Petrography, Mineralogy and Geochemistry Ras, Staromonetny, 35, 119017, Moscow, Russia (*correspondence: andreeva@igem.ru)

New data are obtained on the mineralogical and chemical (major, trace, and volatile components) composition of melt inclusions in quartz from rare-metal granitoids in the Khaldzan-Buregtei Massif, Mongolia. The composition of melt inclusions was estimated with the use of an electron microprobe and ion probe.

The phases identified in the crystalline inclusions are tuhualite, albite, potassic feldspar, sphene, fluorite, zircon, gittinsite, pyrochlore, parisite and yttrocerite, and fluorite.

Melt inclusions in quartz are fully recrystallized, and their daughter minerals compose fine-grained aggregate of quartz, potassic feldspar, riebeckite, polylithionite, fluorite, zirconosilicate, and REE fluorcarbonate. We homogenized the melt inclusions in an autoclave at temperatures of 850 and 950ºC and a pressure of 3 kbar. The chemical composition of the homogeneous glasses was proved to be generally close to the composition of the rare-metal granites, including the concentrations of such components as SiO_2, FeO, MgO, Na_2O, and K_2O. The melts were characterized by high ZrO_2 concentrations (2-3 wt %). The F, H_2O, and CO_2 concentrations in the melts are 1.3-4 wt %, 1-3.4 wt %, and 1.56 wt %, respectively. The glasses of the melt inclusions are depleted in Ba and Sr and enriched in Be, Rb, Y, Nb, Hf, Th, and REE.

Our data indicate that the rare-metal granites were produced by a melt saturated with several trace elements and REE, which is consistent with the geochemical specifics of the rocks themselves. The melts were residual liquids that accumulated in the upper parts of the magma chamber after the fractionation of the alkaline granite magma, reached saturation with many ore components, first of all, Zr, Nb, and REE, and thus became ore-bearing magmas. The specifics of the rare-metal mineralization was predetermined by the high alkalinity of the melt (the agpaitic coefficient = 1.4) and the effects of fluorine and carbon dioxide, which resulted in the crystallization of such rare-metal phases as zircon, zirconosilicates, and REE fluorcarbonates.

Detrital monazite dating and trace-element compositions analysis by XRF-MilliProbe: Implication to provenance study within Ukrainian terrain

A.A. ANDREIEV [1], A.V. ANDREIEV [2], O.V. ZINCHENKO [2]

[1]Ukrainian State Geological Research Institute (UkrSGRI), Kyiv, Avtozavoskaya, 78 (*correspondence:geotech@ukr.net)

[2]Faculty of Geology, Taras Shevchenko National University of Kyiv, Ukraine (andreev@univ.kiev.ua)

Over 2000 detrital monazite grains from Devonian, Paleogene, Neogene, Quaternary sediments of Ukraine have been analysed by XRF Milliprobe for Th, U, Pb, Sr, Y, that as well has been used for Th-U total Pb dating of the monazites.

To apply these analytical and evaluated data for provenance investigation the distribution of above elements in monazites from the set of crystalline rocks of Ukrainian Shield (East European Craton) and Eastern Carpathians has been inferred using XRF measurements. Statistically proved analytical data have allowed distinguishing specific compositional features of monazite derived from (A) alkaline igneous rocks and carbonatites (low contents of Th, U, Y.); (B) granulites and charnockites (increased Th, Sr); (C) metamorphic rocks of amphibolite grade, granites and pegmatites (increased U, Y). The diagram in U/Th*Y/Th – Sr/Y coordinates represents above discrimination in graphic plot. In particular such regularities show systematic sensibility of monazite composition to P-T condition of host rock formation.

The generalized sources of detrital monazites seperated from the sediments within Ukrainian terrain were suggested by implication of the both geochemical and age criteria. Evidently the source of Archean-Proterozoic detrital monazite (>1500 Ma) are crystalline rocks of Ukrainian Shield. For these detrital “old” monazites the rock sources of (B) group prevail (≈2/3 of total amount) whereas ≈1/3 derived from the rocks of (C) group. The Precambrian rocks of (A) group yield insignificant part of the “old” detrital monazites in the studied sediments. Neoproterozoic-Palaeozoic ‘young’ (1100-400 Ma) population of detrital monazite apparently represents product of erosion of acid metamorphic rocks of relatively low grade, which have no direct analogues within Ukrainian Shields. Source area for this population could be Neoproterozoic terrains of EEC margin including ancient rocks of Marmarosh massive (Eastern Carpathians).

https://doi.org/10.1180/S0026461X00006502 Published online by Cambridge University Press

The effect of diffusion on P-T conditions inferred by cation-exchange thermobarometry

A.L. ANDREWS*, Z.R. WANG, E.W. BOLTON, AND J.O. ECKERT JR

Yale University, New Haven, CT, 06520, USA
(*correspondence: alexandra.l.andrews@gmail.com)

Mantle xenoliths are used to infer geothermal gradients of the sub-continental lithospheric mantle through cation exchange thermobarometry. This method assumes that cations reach thermodynamic equilibrium at depth and maintain this state during their ascent to Earth's surface. Analyses of the chemical compositions of coexisting minerals suggest that this assumption is not always valid due to diffusion and re-equilibration. Our observations include: 1) element diffusion profiles in minerals; 2) hotter and deeper P-T conditions calculated for the rims of some mineral assemblages than P-T calculations for the cores; 3) more scattered P-T conditions at higher pressures and temperatures. We examined a suite of garnet peridotites from the Kaapvaal craton (Kimberley, South Africa). Rock sections containing garnet, cpx, opx, and olivine were mounted and measured for their major element compositions at Yale University using the JEOL JXA-8530F field emission gun electron microprobe. P-T conditions calculated for these samples using BKN [1] thermobarometry vary from 930–1240°C, 39–52 kbar. More interestingly, zoning is evident in garnet grains with radii varying from 400–1550 μm. This zoning produces P-T differences of 22–144°C and 1.5–6.3 kbar between rims and cores. A multi-component diffusion model was formulated for $Ca^{2+}/Mg^{2+}/Fe^{2+}$ exchange across garnet, cpx, opx, and olivine assemblages as well as Cr^{3+}/Al^{3+} exchange between garnet and cpx. Modeling results are checked against the observed diffusion profiles. Our model suggests that P-T conditions recorded in these mantle minerals depend on the cooling rate, crystal grain size, and geothermal gradient, which might not be the same as the linear regressed line through all calculated P-T conditions.

[1] Brey and Kohler (1990) *J. Petrol.* **31**, 1353-1378.

Insight into effects of elevated CO_2 and soil nutrient levels on biological weathering at the mesocosm scale

M.Y. ANDREWS[1]*, J.R. LEAKE[1], S.A. BANWART[2] AND D.J. BEERLING[1]

[1]Department of Animal and Plant Sciences, University of Sheffield, Western Bank, Sheffield, S10 2TN, UK
(*correspondence: m.y.andrews@sheffield.ac.uk)
[2]Cell-Mineral Research Centre, Kroto Research Institute, North Campus, University of Sheffield, Broad Lane, Sheffield, S3 7HQ, UK

The evolutionary development of large vascular land plants in the Paleozoic is hypothesized to have enhanced weathering of Ca and Mg silicate minerals. This plant-centric view overlooks the fact that plants and their associated mycorrhizal fungi co-evolved. Many weathering processes usually ascribed to plants may actually be driven by the combined activities of roots and mycorrhizal fungi. Here we present initial results from a novel mesocosm-scale laboratory experiment designed to allow investigation of plant-driven carbon flux and mineral weathering at different soil depths, and under ambient (400 ppm) and elevated (1500 ppm) atmospheric CO_2.

Sequoia sempervirens (arbuscular mycorrhizal, AM) and *Pinus sylvestris* (ectomycorrhizal, EM) were studied in two experiments as part of the larger biological weathering project. Each long term (7-13 months) experiment was conducted under similar environmental conditions with the exception of the "soil" substrate in which the trees were grown. One experiment used an organic-poor, low nutrient sand:perlite 50:50 (vol:vol) mix whilst the other used an organic-rich sand:compost (50:50 vol:vol) mixture.

Both species responded differently to elevated CO_2 conditions when grown in organic-poor or -rich substrates. After $^{14}CO_2$ pulse-labeling, the observed carbon flux timing and magnitude were significantly different for both species in the sand:compost study relative to the sand:perlite study. Additionally, the peak carbon flux under elevated CO_2 in the sand:compost system lagged by several hours relative to plants grown under ambient CO_2. Total root biomass was increased under elevated CO_2 in the nutrient poor substrate, but much less so under higher nutrient conditions. Ongoing analyses will elucidate how these disparate responses to elevated CO_2 may affect mycorrhizal biomass and mineral weathering in the mesocosm systems.

https://doi.org/10.1180/S0026461X00006502 Published online by Cambridge University Press

Tilts without tears – Structure and elasticity of feldspars

R.J. ANGEL

Virginia Tech Crystallography Laboratory, Department of Geosciences, Virginia Tech, Blacksburg, VA 24060, USA. (rangel@vt.edu)

Framework structures such as feldspars and perovskites typically respond to changes in pressure, temperature and the extra-framework cations by the tilting of the strongly-bonded polyhedra, with little change in the geometry of the individual polyhedra. In the perovskites, the complex tilt patterns can be decomposed in to a combination of six fundamental tilts [1] that have been shown to act as the order parameters that relate the structural evolution of perovskites to their thermodynamic and elastic properties [2]. Tilts are therefore the appropriate fundamental description for the evolution of framework structures.

By contrast, structural variation in feldspars has only briefly been described in terms of tilts [3], and instead work for the last 3.5 decades has focussed on the variation of the T-O-T angles despite these showing very few or no systematic correlations with thermodynamic properties. The complexity and low-symmetry of the feldspar framework, which means that the tilts are not symmetry-breaking and are also difficult to model, is probably the reason for this neglect of tilting. In this contribution I will describe the decomposition of the variation of the feldspar structure in to the four fundamental tilts that were previously defined by Megaw [3], and the construction of an exact rigid-body model of the framework that can be used to show how the various tilts change the unit-cell parameters. This model explains the unit-cell parameter variations seen in real feldspars, and the extreme anisotropy of the response of the feldspar structure to changes in temperature, pressure and extra-framework cation. The success of this analysis offers the opportunity to develop a structure-based model for the thermodynamic and geochemical properties of feldspars in general.

[1] Glazer (1972) *Acta Cryst* **B28**, 3384-3392. [2] e.g. Carpenter *et al*. (2005) *Phys Rev B* **72**, 024118; Wang & Angel (2011) *Acta Cryst B,* in press. [3] Megaw (1974) in "The Feldspars", eds Mackenzie & Zussman.

Available-phosphate oxygen isotopes point to extracellular equilibration

ALON ANGERT*, SHUNIT MAZEH, AND TAL WEINER

The Institute of Earth Sciences, The Hebrew University of Jerusalem, Israel (*correspondence: angert@huji.ac.il)

The oxygen stable isotopes in phosphate which is rapidly available for biological uptake can be used as a tracer for phosphorus cycling. Using this tracer in the ocean and in soils requires good understanding of the processes that control it. Here we present the first survey of available (resin-extractable) inorganic δ^{18}Op, based on a method we have recently developed [1]. This survey took place across natural and experimental rainfall gradients, and across soil formed on sedimentary and igneous rocks. In addition, we also analyzed the soil total (HCl-extractable) inorganic δ^{18}Op. The available-P values were in the range of 14.5-21.2‰ (Fig. 1).

Figure 1: Range of concentrations and $\delta^{18}O_P$ at five sites, with annual rain fall varying between 90-780mm/y. A site with igneous bedrock is marked by triangles.

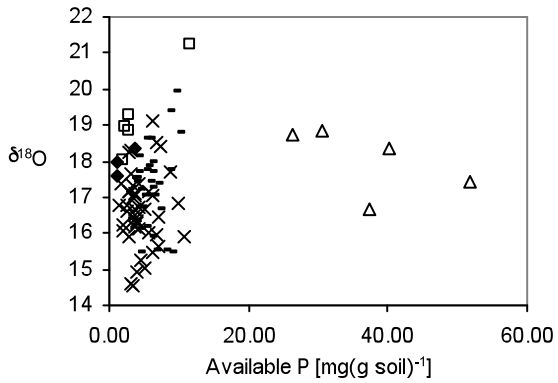

The observed available-P δ^{18}Op values are considerably higher than the values we calculated (based on [2]) for extracellular mineralization of organic phosphate. However, these values are close to the value expected for enzymatic mediated phosphate equilibration with soil water. Evidence for equilibration was also reported in ocean studies, and was usually attributed to fast microbial recycling. However, we argue that microbial recycling can explain equilibration only if inorganic-phosphate excretion overwhelms other fluxes in the system. As a result, we conclude that the equilibration can be better explained by activity of extracellular pyrophosphatase.

[1] Weiner *et al*. (2011) *RCM* **25**, 624–628. [2] Liang & Blake (2009) *GCA* **70**, 3957-3969.

https://doi.org/10.1180/S0026461X00006502 Published online by Cambridge University Press

Magma emplacement durations and rates and the dynamics of magmatism and volcanism

C. ANNEN[1]*, J. BLUNDY[1], L. CARICCHI[1], T. MENAND[2], M. DE SAINT-BLANQUAT[3], A. SCHÖPA[1] AND R.S.J. SPARKS[1]

[1]University of Bristol, Queen's Rd, Bristol BS8 1RJ, UK (*corrrespondence: catherine.annen@bristol.ac.uk) (jon.blundy@bristol.ac.uk, l.caricchi @bristol.ac.uk, anne.schopa@bristol.ac.uk, steve.sparks@bristol.ac.uk)

[2]LMV, 5 rue Kessler, 63038 Clermont-Ferrand Cedex, France (t.menand@opgc.univ-bpclermont.fr)

[3]Observatoire Midi-Pyrénées, 14 av. Edouard-Belin, 31400 Toulouse, France (michel.desaintblanquat@get.obs-mip.fr)

Protracted emplacement durations for large laccoliths, plutons and batholiths have been infered from radiometric dating. Analysis of conduit fluxes, short crystal residence times inferred from diffusion chronometry and field evidences all support a model of incremental emplacement of igneous bodies where discrete pulses are interrupted by periods of inactivity. According to this model, at least two rates of magma intrusion can be defined: the short-term emplacement rate of an individual pulse and the long-term emplacement rate of the entire igneous body.

Long-term emplacement rates, which may vary over time, control the thermal state of the igneous body and crust. The mechanical ability of the crust to accommodate pulses of magma depends on its thermal state and on short-term emplacement rates. Magma emplacement at high rates and frequency in a thermally imature and thus rheologicaly brittle crust results in fracturing and eruption, whereas magma storage is favoured on longer timescales in a thermally mature crust[1]. Intrusive/eruptive ratios depend on both short and long-term rates and vary over time in a given magmatic system. The growth of large magma chambers where large-scale convection and magma mixing can happen is only possible for a restricted range of emplacement rates.

At deep crustal levels, incremental magma emplacement implies that different timescales control differentiation. Cooling of rapidly emplaced pulses results in the generation of silicic melts on a short timescale, but the magma reservoir as a whole heats up, remelts and possibly assimilates crust on a much longer timescale.

A global understanding of magma dynamics requires dating tools that can discriminate between different processes and identify the different timescales involved.

[1] Jellinek & de Paolo (2003) *Bulletin of Volcanology* **65**, 363-381

The reaction products during the preparation of granites for the trace elements analysis by ICP-MS

J. ANOSHKINA AND O. BUHAROVA

Tomsk State University, Lenin avenu 36, 634050 Tomsk, Russia, (*correspondence: julia-seversk@mail.ru)

At present time an essential part of geochemical researches is detection of accompanying elements in different rock and mineral types and analysis of their distribution mechanisms. Last years the main analytical technique for that is ICP-MS. The main problem is sample preparation of geological matrixes. Today there are quite many schemes decomposing of these samples, but most of them are multistep, labor- and time-consuming. Microwave decomposition systems are usually used for intensification of the sample preparation. A serious difficulty for acid revelation is provoked by high-Si magmatic rocks, particularly granites. For the ICP-MS method it is necessary to transform sample to the solution completely, but the granite decomposing can't be always done integrally by using mentioned above schemes. Therefore we've been tried to detect undecomposed fraction at each stage of chemical sample preparation. For that purpose generated sediments were selected, dried and analyzed using scaning electron microscopy with energy dispersive and wave dispersive X-ray microanalysis methods after each revelation step. Sample SG-3 was used for the experiment. Samples decomposed in 3 stages: HF:HNO_3 (5:1) – HCl - HNO_3.

Supernatant liquid was analyzed by ICP-MS method. During the experiment it was revealed that a full decomposing of matrix was accompanied by generation of insoluble residue of Al, Ca, REE fluoride at the first stage. Then fluoride of REE transform to the solution on next stages. But at that on the surface of new growth residue ($0{,}01Na_2O \times 0{,}05(Mg,Fe)O \times 0{,}05Al_2O_3 \times 0{,}09SiO_2 \times 0{,}13K_2O \times 1{,}17F$; $0.03Na_2O \times 0.1MgO \times 0.13Al_2O_3 \cdot \times 1.4F$) take place fractional sorption and defective inclusions of Ta, Nb, Zr, Y, La, Ce,.

The scheme of chemical preparation of rock samples was change on the base of our recently received data. In this case the main aim of more careful methodics was a reduction of part of modified solid phases on the first stage of resolution. The sample with weight about 0.1 gram was dissolved in the complex HF – HCl – HNO_3 for three stages of acid solutions and was controlled in the open system. As the result of this scheme of sample preparation, the content of initial potassium-bearing solid phase was altered to that of ($0{,}01K_2O \times 0.08(Mg,Fe)O \times 0.08Al_2O_3 \times 1.01F$). The following resolution was defined an increase of trace element concentrations in the supernatant liquid.

The study was funded by the Russian Ministry of Education and Science.

https://doi.org/10.1180/S0026461X00006502 Published online by Cambridge University Press

Nanometer to centimeter scale analysis and modeling of pore structures in geologic CO_2 storage formations and caprocks

LAWRENCE M. ANOVITZ[1], LUKAS VLCEK[1], GERNOT ROTHER[1] AND DAVID R. COLE[2]*

[1]Oak Ridge National Lab., Oak Ridge, TN, USA 37831
[2]The Ohio State University, Columbus, OH, USA 43210
(*correspondence - cole.618@osu.edu)

The microstructure and evolution of pore space in rocks is a critically important factor controlling fluid flow. The size, distribution and connectivity of these confined geometries dictate how fluids migrate into and through these micro- and nano-environments, wet and react with the solid. (Ultra)small-angle neutron scattering and autocorrelations derived from BSE imaging provide a method of quantifying pore structures in a statistically significant manner from the nanometer to the centimeter scale. These methods were used to characterize the pore features of a variety of potential CO_2 geological storage formations such as the shallow buried quartz arenites from the St. Peter Sandstone and the deeper Mt. Simon quartz arenite in Ohio as well as the Eau Claire shale and mudrocks from the Cranfield MS CO_2 injection test. For example, analyses of experimental and natural samples of St. Peter sandstone show total porosity correlates with changes in pores structure including pore size ratios, surface fractal dimensions, and lacunarity. These new data suggest that microporosity is more prevalent in nominally coarse-grained sandstone and may play a much more important role than previously thought in fluid/rock interactions. The preliminary results from shale and mudrocks indicate there are dramatic differences not only in terms of total micro- to nano-porosity, but also in terms of pore surface fractal (roughness) and mass fractal (pore distributions) dimensions as well as size distributions. Information from imaging and scattering data can also be used to constrain computer-generated, random, three-dimensional porous structures. The results integrate various sources of experimental information and are statistically compatible with the real rock. This allows a more detailed multiscale analysis of structural correlations in the material.

Acknowledgements. Support for this work comes from the US Department of Energy through the ORNL project "Structures and Dynamics of Earth Materials, Interfaces and Reactions" (FWP ERKCC72) under contract DE-AC05-00OR22725 to Oak Ridge National Laboratory, managed and operated by UT-Battelle, LLC.

Iron oxides in copper mining environments: Transformation and reactivity

J. ANTELO[1]*, S. FIOL[2], R. LOPEZ[2], D. GONDAR[2] AND F. ARCE[2]

[1]Dept. Soil Science and Agricultural Chemistry. University of Santiago de Compostela. 15782 Santiago de Compostela. Spain (*correspondence: juan.antelo@usc.es)
[2]Dept. Physical Chemistry. University of Santiago de Compostela. 15782 Santiago de Compostela. Spain

The formation, transformation and surface chemistry of iron mineral oxides is of geological significance in surface waters polluted with acid mine drainage (AMD). Geochemical behaviour of these iron oxides controls the availability and mobility of contaminants in these highly polluted systems. The acidic pH values, together with the presence of high amounts of sulphate, will favour the formation of schwertmannite which is a metastable iron oxide that will be transformed to goethite under oxic conditions [1]. However, in copper mining environments co-precipitation of iron and copper ions is expected and therefore the surface chemistry of the iron oxides present in these systems may be different. AMD precipitates have been found to be very effective scavengers of contaminants, although changes in the AMD conditions may result in the release of metals or other contaminants to surface waters.

Several iron oxide samples have been prepared in the presence of high concentrations of sulphate and different copper concentrations ir order to simulate copper-rich mining environments. Long-term transformation experiments were conducted in order to study the mineral oxide stability and surface chemical changes produced over a fitteen months period. Schwertmannite particles are found to be formed initially, but throughout the experiment a release of sulphate, iron and copper ions was observed at the more acidic pH values, which lead to the formation of goethite-like particles. Reactivity of the different mineral phases against arsenate shows that the major adsorption capacity is found in the initial schwertmannite-like particles and arsenate mobility increases in the more stable iron mineral phases that are formed during the transformation experiment.

[1] Bingham, Schwertmann, Traina, Winland & Wolf (1996), *Geochim. Cosmochim. Acta* **60**, 2111-2121.

https://doi.org/10.1180/S0026461X00006502 Published online by Cambridge University Press

Mechanics of bacterial sulfate reduction deduced from sulfur and oxygen isotopes in pore fluid sulfate

GILAD ANTLER[1]*, ALEXANDRA V. TURCHYN[2], VICTORIA RENNIE[2], BARAK HERUT[3] AND ORIT SIVAN[1]

[1]Department of Geological and Environmental Sciences, Ben Gurion University, Beer Sheva 84105, Israel.
[2]Department of Earth Sciences, University of Cambridge, Cambridge CB2 3EQ, UK.
[3]Israel Oceanographic and Limnological Research, National Institute of Oceanography, Haifa 31080, Israel.

Bacterial sulfate reduction (BSR) is responsible for the majority of organic matter oxidation in marine sediments and therefore is a key player in the global carbon cycle. The biochemical pathway of sulfate reduction occurs in several reversible steps; each of these steps has an associated isotope fractionation. The ratio between the forward and backward fluxes at each step, the relationship of the individual fluxes to the overall rate of BSR and the resultant expressed sulfur and oxygen isotope fractionation during BSR in natural environments remains enigmatic. The aim of this study is to further our understanding of BSR through analysis and subsequent modelling of sulfur and oxygen isotopes in pore fluid sulfate from ODP-acquired deep sea sediments, the shallow Eastern Mediterranean, and the Yarqon estuary (Israel). Our data demonstrates a correlation between the net rate of BSR and the slope of the relative evolution of oxygen and sulfur isotopes ($\delta^{18}O_{(SO4)}$ vs. $\delta^{34}S_{(SO4)}$) in the residual sulfate pool. We combine these results with literature data to show that this correlation scales over many orders of magnitude (for rate of BSR). Our model, combined with previously published pure culture data [1], suggests that the critical parameter for the relative evolution of oxygen and sulfur isotopes during BSR in natural environments is the rate of intracellular sulfite oxidation. We find that the lower the net rate of BSR, the steeper the slope ($\delta^{18}O_{(SO4)}$ vs. $\delta^{34}S_{(SO4)}$) and the more intense sulfite oxidation.

[1] Mangalo *et al*. (2008) *Geochim.Cosmochim.Acta* **72**, 1513-1520.

Geochemical constrains on Lower Ordovician magmatism at the Central Iberian Zone (Central Portugal)

I.M.H.R. ANTUNES[1]*, A.M.R. NEIVA[2]* AND M.M.V.G. SILVA[2]*

[1]Polytechnic Institute of Castelo Branco, 6001-919 Castelo Branco, Portugal (imantunes@ipcb.pt) * Geoscience Centre, University of Coimbra
[2]Department of Earth Sciences, Univ. Coimbra, 3000-272 Coimbra, Portugal (neiva@dct.uc.pt; mmvsilva@dct.uc.pt)

The Central Iberian Zone (CIZ) of the Iberian Massif contains important magmatic bodies, most of them of Variscan age, emplaced during and after the ductile deformation Variscan phases. Ordovician magmatism has been considered rare in the CIZ, however recent geochronological data indicate a Lower Ordovician emplacement age for granitic rocks.

The Oledo pluton has an Early Ordovician emplacement age of 479 - 480 Ma, obtained by ID-TIMS U-Pb ages, on zircon and monazite crystals. This pluton is exposed over an area of about 260 km^2 and intruded the Cambrian schist-metagreywacke complex, which consists of alternating metapelites and metagraywackes with metaconglomerate and marble intercalations. It contains four distinct and contemporaneous granodioritic to granitic phases (GrA-GrD) derived from different magmatic sources.

The pluton shows local deformation and magmatic flow structures probably related to the Caledonian and Variscan deformation events. Granodiorite GrA is the most deformed granitic rock with shear zones and deformation at the border. Granodiorites GrA and GrC contain fine-grained biotite tonalite (TME) and granodiorite microgranular enclaves (GME), which are darker and richer in mafic minerals than the host granodiorites. The geological, mineralogical, geochemical and isotopic (Nd, Sr and O) data indicate that TME and GME and host GrA are of I- type and were related by fractional crystallization process. Least-square analysis of major elements and modelling of trace elements support that GME and host GrA are derived from the TME magma by fractional crystallization of plagioclase, grunerite, biotite and ilmenite from the TME magma. Granodiorite GrB is of hybrid origin. Most variation diagrams for whole-rocks and biotites from GME and host granodiorite GrC show linear trends. Major and trace elements modelling suggest that they result from mixing of relatively primitive granodiorite magma with a magma derived from crustal melting. TME corresponds to globules of a more mafic relatively primitive magma. Granite GrD is of S-type and represents another pulse of magma.

https://doi.org/10.1180/S0026461X00006502 Published online by Cambridge University Press

Shale to soil: Geochemistry and clay mineral transformations

R.H. APRIL*, S. LEMON AND D. KELLER

Geology Department, Colgate Univ., Hamilton, NY 13346, USA (*correspondence: rapril@colgate.edu)

We are studying the weathering characteristics of Clinton group (middle Silurian) shales as part of a larger climate transect study to better understand chemical weathering and soil formation in the Critical Zone. Our research site (Roger's Glen, NY) is the northernmost of six satellite sites - extending from Puerto Rico to New York State – tied to a larger ongoing study of shale weathering at the Shale Hills Critical Zone Observatory in Pennsylvania, USA.

The shales at our site comprise the Sauquoit and Willowvale Formations, green-gray calcareous shales and mudstones containing the clay minerals illite and chlorite. The area was glaciated and soils have developed over the past ~14,000 years on till rich in shale fragments. Illite is resistant to weathering and persists in the soil profile, but chlorite weathers to vermiculite, likely through a mixed-layer chlorite-vermiculite intermediate. Vermiculite in the upper part of the soil profile contains hydroxy-aluminum interlayers, as determined by the gradual collapse of the clay interlayer structure with K-saturation and heat treatments.

Both exchangeable cations and bulk soil chemistry show interesting trends down profile suggesting that a weathering front has developed. Exchangeable Ca and Mg, especially, show sharp increases in the uppermost and lowermost soil horizons where the influence of organic matter decay in the former and shale decomposition in the latter account for these trends. Similar increases in Ca and Mg at depth are apparent in the bulk chemistry (see figure below). Soil pH increases from 4.3 at the top of the profile to 8.1 at depth near where the soil-bedrock interface occurs. Tau plots show depletion of base cations and accumulation of Fe and Al in B-horizons as weathering proceeds down-profile.

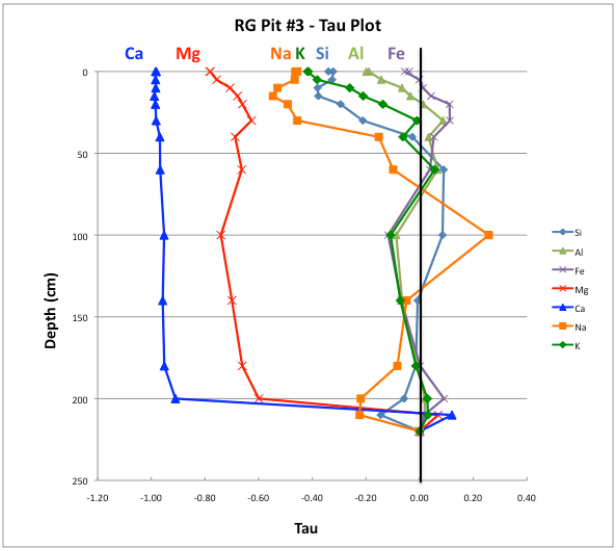

An empirical approach to estimate melting temperature and its pressure dependence of some rocks of Oman ophiolite suite

SAYYADUL ARAFIN*, RAM N. SINGH AND ABRAHAM K. GEORGE

Physics Department, College of Science, Sultan Qaboos University, Box:36, Al – Khoudh 123, Oman (*correspondence: sayfin@squ.edu.om)

Pressure Dependence of Melting temperature

We have derived an empirical relation to determine melting temperature, T_m and its pressure dependence. Seismic p- and s-wave velocities and density data [1] were used as inputs to compute Debye temperature, Θ_D which forms the important ingredient of the empirical relation. We have applied the formalism to estimate T_m and its pressure dependence for harzburgite and gabbro rocks of Oman ophiolite suite respectively.

Discussion of Results

At room temperature and atmospheric pressure, the computed values of Θ_D are found to be 694K and 547K, and those of T_m are 1532K and 1132K for harzburgite and gabbro, respectively. A comparison of the pressure dependence of T_m obtained from the empirical approach with those from Lindemann and Simon's formula will be made after we complete the full analysis.

[1] Christensen N.I.and Smewing J.D., (1981) Geology and the seismic structure of the Northern section of the Oman ophiolite, *J Geophys Res*, **86**, 2545 – 2555.

https://doi.org/10.1180/S0026461X00006502 Published online by Cambridge University Press

Ultrahigh-pressure podiform chromitites as a possible deep recycled material

S. ARAI [1]*, A.H. AHMED[2] AND M. MIURA[1]

[1]Department of Earth Sciences, Kanazawa Univ., Kanazawa 920-1192, Japan (* correspondence: ultrasa@kenroku.kanazawa-u.ac.jp, mimk1214@stu.kanazawa-u.ac.jp)

[2]Faculty of Earth Sciences, King Abdulaziz Univ., Jedda, Saudi Arabia (ahmh2@yahoo.com)

Ultrahigh-Pressure (UHP) Chromitites

Podiform chromitites, which appear in the Moho transition zone to upper mantle of ophiolites, have been considerd to be of origin of low-pressure almost *in-situ* magmatic cumulates [1]. The dicoveries of diamond and other UHP minerals (e.g., Robinson *et al*., 2004) from chromitites of Tibet seriously requires us to reconsider the origin(s) of podiform chromitites. Various features of the UHP chromities can be explained by recycling of the ordinary low-P chromitites (Fig. 1).

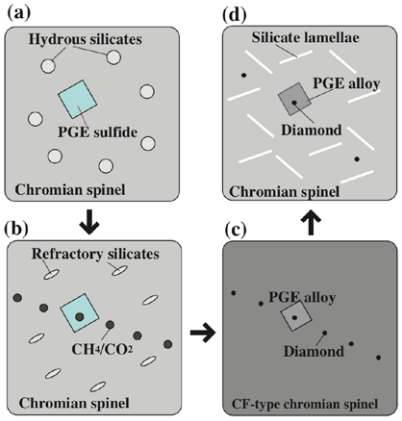

Figure 1: UHP signatures formed by deep recycling of low-P chromitites (Arai, 2010).

Chromitites from the Oman Ophiolite

Only concordant chromities, which we examined at Wadi Hilti, the Oman ophiolite, have some UHP-like signatures, e.g., pyroxene lamellae in spinel (Fig. 1d). Discordant ones show features of low-P magmatic generation (Fig. 1a). The former possibly have a deep recycling origin.

[1] Arai & Yurimoto (1994) *Econ. Geol.* **89**, 1279-1288. [2] Robonson *et al*. (2004) *Geol. Soc. Spec. Pub.* **28**, 551-560. [3] Arai (2010) *J. Mineral. Petrol. Sci.* **105**, 280-285.

Time variation of He and Ar isotopic compositions in the Earth's atmosphere

YUKO ARAKAWA AND JUN-ICHI MATSUDA

Departmen of Earth and Speace Science, Graduate School of Science, Osaka University, Toyonaka, Osaka 560-0043, Japan

It is very important to study the origin and evolution of the Earth's atmosphere. Noble gas isotopes could be useful tools to trace the degassing history of the Earth. In this study, we have examined the time variation of helium and argon isotopic ratios in the Earth's atmospehere using our previous models on matnle degassing [1, 2, 3].

We thought that the Earth was initially uniform in isotopic compostions of noble gases but was divided into three separate reservoris and that individual elements were carried by mass flow between reservoirs. The mass flow has decreased exponetially as a function of time. The details of the calculation and the isotopic ratios of He and Ar in the mantel are given in our previous papers [2, 3].

Our calculation for the terrestrial air shows that the $^{40}Ar/^{36}Ar$ ratio increased rapidly after the formation of the Earth and has been almost identical to the present value of 295.5 for the last 1 b.y. For the $^{3}He/^{4}He$ ratio calculation, we need to consider the escape of helium into the space. We put the escape terms for ^{3}He and ^{4}He amounts in air estimated from the present atmopheric He budget. In this case, we get a good agreement for the ^{3}He amount in the present air, but can not calculate the present ^{4}He content without a very low escape rate of ^{4}He. In our previous models [2, 3], we assumed that al the noble gases transferred into the continental crust remained there. However, if we assume that all the helium in the continental crust is released to the air as the helium is a tiny element, our calculation shows that both ^{3}He and ^{4}He concentrations (and, therefore, $^{3}He/^{4}He$ ratio) agree very well with the modern-day observed values. The calculated time variation of the $^{3}He/^{4}He$ ratio shows that the $^{3}He/^{4}He$ ratio in air is also constant since 0.1 b.y.

Thus we conclude that the detection of modern-day atmospheric ratio of He and Ar in the ancient terrestrial samples younger than 0.1 b.y. is not always due to the contamination by the modern-day atmosphere.

[1] Matsuda and Marty (1995) *Geophys. Res. Lett.*, **22**, 1937-1940. [2] Kamijo *et al*. (1998) *Geochim. Cosmochim. Acta*, **62**, 2311-2321. [3] Seta *et al*. (2001) *Earth Planet. Sci. Lett.*, **188**., 211-219.

https://doi.org/10.1180/S0026461X00006502 Published online by Cambridge University Press

Acid-base fractionation in the model Cl-bearing granite

L.Y. ARANOVICH[1,2]*AND M.A. NOVIKOVA[1,2]

[1]Institute of Geology of Ore Deposits RAS, 119017 Moscow, Russia (*correspondence: lyaranov@igem.ru)
[2]Institute of Experimental Mineralogy RAS, 142432 Cherogolovka, Russia (nov@iem.ac.ru)

Existing experimental data indicate rather limited chlorine solubility in felsic melts [1]. On the other hand, melting temperature of the model haplogranite in presence of concentrated alkali halide solutions is significantly higher than in pure water, and, for a constant salt concentration increases with increasing pressure [2]. Taken together, these data show that any granite melts containing even small amount of dissolved Cl (of about n*10-1 wt.%) should liberate a very concentrated brine at the early, high-temperature stages of decompression/cooling induced crystallization. With continuing crystallization fluid in equilibrium with granite melt must evolve towards pure water. We have made melting experiments at 800oC and 2 kbar total pressure on the model granite composition Ab69Qtz31 in presence of aqueous NaCl solutions ranging in concentration from XNaCl = 0.2-0.02. The experiments have shown that quench pH of the solution equilibrated with the melt depends strongly on the solution salinity: the quench pH of the most concentrated solution was about 9, while that of the least concentrated one-about 2. Acidic nature of the dilute salt solutions in equilibrium with granite melt was discovered some 40 years ago [3], whereas the very high pH values of the concentrated solutions are reported for the first time. The nature of the acid solutions is well understood as being due to hydrolysis reaction of the type: 2NaCl(fl) + H2O(fl) = Na2O(m) + 2HCl(fl) (1), where fl and m denote fluid and melt phase, correspondingly. The exact reason for the high quench pH observed in concentrated solutions remains as yet unknown, we suggest it results from dissolution of Al2O3 in the course of schematic reaction: 0.5Al2O3(m) + 3NaCl(fl) + 1.5H2O (fl) = AlCl3(fl) + 3NaOH(fl). In any event, the pH variations in alkali solutions liberated from an evolving granite melt must cause significant changes in the magmatic fluid transport properties in respect to various ore metals. This effect is demonstrated in the experiments on partitioning of W and Pb between the model melt and solutions of variable NaCl concentration.

[1] Webster & De Vivo (2002) *Amer. Mineral.* **87**, 1046–1061. [2] Aranovich & Newton (1996) *Contrib. Mineral. Petrol.* **125**, 200-212. [3] Holland (1972) *Econ. Geol.* **67**, 281-301.

Trace metal and Mo isotope systematics in petroleum fluids

COREY ARCHER[1], TIM ELLIOTT[1], SANDER VAN DEN BOORN[2], RICCARDO AVANZINELLI[3], AND PIM VAN BERGEN[4]

[1]Bristol Isotope Group, School of Earth Sciences, University of Bristol, BS8 1RJ, UK (c.archer@bristol.ac.uk)
[2]Shell Projects and Technology, Rijswijk, The Netherlands
[3]Dipartimento di Scienze della Terra - Università degli Studi di Firenze, Firenze, Italy
[4]Shell Upstream International Europe, Aberdeen, UK

The presence of trace metals in oils has long been of interest for both their detrimental and beneficial effects during hydrocarbon exploration. For example, elevated levels of trace metals can cause problems during downstream refining processes due to catalyst poisoning. In contrast, the diagnostic potential of trace metals incorporated in fluids and host rocks has been successfully applied in various fingerprinting studies. The majority of work to date has focussed on the two most abundant metals found in oils, vanadium (V) and nickel (Ni), which have been used as tools in correlation and fingerprinting, and provide information on redox conditions during source rock deposition.

Here we focus on the molybdenum (Mo) isotope system, well known to display bi-polar redox chemistry [1], and thus providing a potentially valuable new tool to exploit in petroleum systems' studies. We have developed techniques for the determination of Mo isotopes in hydrocarbon (HC) fluids. Mo is extracted from its complex organic fluid matrix, through high pressure ashing, which renders the complete decomposition of the HC fluid, allowing the Mo to be purified via conventional ion-exchange methods [2]. Preliminary data from replicate samples suggest a precision of better than 0.1‰ in $\delta^{98/95}$Mo. We combine the Mo isotope data with more conventional elemental fingerprinting, as determined through isotope dilution HR-ICPMS analysis with a new multi-element spike. This method allows greater accuracy and precision than has been previously possible, both being better than 10%.

Samples display variably positive $\delta^{98/95}$Mo ratios, ranging from +0.4‰ to +1.7‰, within the range of sediments deposited under variably reducing conditions [3]. We will further explore the relationship between oil Mo isotope composition and its source rock, as well as biodegradation and maturation processes.

[1] Erikson, B.E. and Helz, G.R. (2000). *Geochim. Cosmochim. Acta* **64**, 1149-1158. [2] Archer, C. and Vance, D. (2009). *Nature Geosci.* **1**, 597-600. [3] Siebert C, *et al* (2006). *EPSL* **241**, 723-733

https://doi.org/10.1180/S0026461X00006502 Published online by Cambridge University Press

Ion association in hydrothermal systems: Strontium chloride, hydroxide and acetate to 350 ºC and 20 MPa

H. ARCIS,[1] G. ZIMMERMAN[2] AND P. TREMAINE[1]

[1]University of Guelph, Guelph, Ontario, Canada
[2] University of Bloomsburg, Bloomsburg, Pennsylvania, USA

The ion association constants of Sr^{2+} with common ligands under hydrothermal conditions are needed to model the geochemistry of naturally occurring radioactive materials ("NORM") [1] and the chemistry of Generation IV super-critical water nuclear reactor designs [2]. Moreover, because of its favourable solubility, Sr^{2+} is an attractive model system for predicting the thermodynamic properties of M^{2+} transition metals. This paper reports the first conductivity study of aqueous $SrCl_2$ and $Sr(OH)_2$ from 25 to 350 °C, using a novel high-precision flow-through AC electrical conductance instrument [3,4] at concentrations from $5{\cdot}10^{-5}$ to 0.2 mol·L^{-1}.

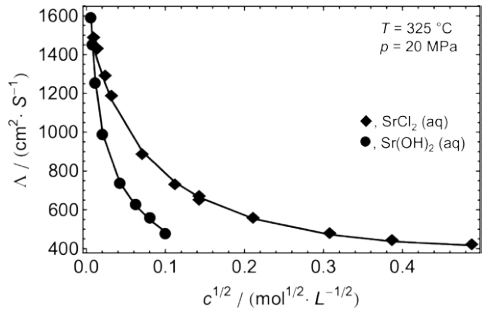

Figure 1: Molar conductivity Λ of aqueous $SrCl_2$ and $Sr(OH)_2$ *vs*. concentration *c* at 325 °C and 20 MPa.

Formation constants were determined from Λ vs *c* using the TBBK model [3,4]. The values for $Sr(OH)^+$ and $Sr(OH)_2^0$ are greater than those for $SrCl^+$ and $SrCl_2^0$ ion pairs, and both neutral species are significant above 10^{-3} mol·L^{-1} at 350 °C. Similar data have been obtained for the complexes of Sr^{2+} with acetate, $Sr(Ac)^+$ and $Sr(Ac)_2^0$ up to 275 °C at 20 MPa. The limiting molar conductivities can be used to estimate ionic mobilities and diffusion under hydrothermal conditions.

[1] Hinrichsen C. (1998) *Corrosion* **98**, Paper 98061. [2] Guzonas *et al*. (2009) *Power Plant Chem*. **11**, 284-291. [3] Hnedkovsky *et al*. (2005), *J. Phys. Chem. B* **109**, 9034-9046. [4] Mendez De Leo, *et al*. (2005) *J. Phys. Chem. B* **109**, 14243-14250.

Modes of mantle flow and He travel in the northern Lau Basin

R.J. ARCULUS*, O. NEBEL, F.E. JENNER, J.A. MAVROGENES AND N. DYRIW

Research School of Earth Sciences, ANU,Australia
(*correspondence: richard.arculus@anu.edu.au)

High $^3He/^4He$ has been documented in dredged volcanic glasses from the Rochambeau Rifts (RR) and North West Lau Spreading Centre (NWLSC) in the northwestern Lau Basin, plausibly related to southerly ingress of the Samoan Plume into the mantle wedge underlying this rapidly opening backarc basin[1]. The Central Lau Spreading Centre (CLSC), offset south of the NWLSC by the right-lateral Peggy Ridge Transform Fault, has MORB-like $^3He/^4He$, suggesting the Ridge exerts control on asthenospheric mantle as well as fracturing the lithosphere. The relative fertility of the mantle supplying the actively extending rifts and spreading centres increases from south to north (CLSC through NWLSC to RR). In terms of elevated Fe8, the RR define a new, hot, fertile, global backarc basin end-member, with strongly elevated Hf*/Hf and Dy/Yb, consistent with a garnet-bearing residue during melt generation. Both RR and NWLSC show a positive correlation between Fe8 and $^3He/^4He$. Hf-Nd isotopic covariations provide additional constraints on the nature of mantle sources involved (SOPITA, Samoan plume, Pacific) and ingress of high $^3He/^4He$ material; RR samples with high $^3He/^4He$ have low ε_{Hf} and ε_{Nd} plausibly resulting from a Samoan-SOPITA mantle mix. However, high $^3He/^4He$ samples of the NWLSC show no mixing with Samoan-type Nd and Hf. It appears plume invasion is restricted to sub-RR. The Pacific mantle signature is prominent beneath the NWLSC but disappears south of the PR towards the CLSC being replaced by SOPITA-type mantle. Decoupling of $^3He/^4He$ with Nd and Hf may indicate flow of He in a plume-derived volatile phase.

[1] Lupton, J.E. *et al*. (2009) *Geophysical Research Letters* **36**, L17313, doi:10.1029/2009GL039468.

https://doi.org/10.1180/S0026461X00006502 Published online by Cambridge University Press

Methane solubility under reduced conditions in a haplobasaltic liquid, applicable to degassing of magma ocean

P. ARDIA [1]*, A.C. WITHERS[1], M.M. HIRSCHMANN[1] AND R.L. HERVIG[2]

[1]University of Minnesota, Dept. of Earth Sciences, 108 Pillsbury Hall, Minneapolis, MN 55455 (*correspondance: pardia@umn.edu);
[2]Arizona State University, School of Earth and Space Exploration, Tempe, AZ 85287, USA

Oxygen fugacity (fO_2) may have a critical influence on the solubility of volatiles in silicate liquids, which in turn influences fluxes of volatiles from planetary interiors to their atmospheres. Carbon dissolves in oxidized basic melts as carbonate but under reduced conditions is limited by precipitation as graphite or diamond. At conditions where melt is in equilibrium with Fe alloy, the carbonate solubility will not exceed few ppm [1], limiting volcanogenic transport of C to the atmosphere. Therefore, dissolved C-H species may dominate C solubility and transport at low fO_2 [2][3].

We investigated the solubility of C-O-H fluid in a haplobasaltic melt ($Di_{40}An_{42}Ab_{18}$), adding C as $Si_5C_{12}H_{36}$+ H_2O to produce SiO_2+CH_4+H_2 and H_2O. Experiments were performed at 0.7, 1.5, 2.0 and 3.0 GPa at 1400°C and the fO_2 was buffered using a double Pt-capsule technique, where the external buffer (e.b.) fixed the fH_2 by transport across a H-permeable Pt barrier, and the internal buffer (i.b.) set the fO_2 of the silicate charge. We used three buffer combinations: 1) e.b. with Fe-FeO-Fe_3C-H_2O and i.b. with graphite; 2) e.b. with Fe-FeO-H_2O and i.b. Si^0, 3) e.b. with Ni-NiO-H_2O and i.b. Si^0. We examined resulting glasses by optical and SEM microscopy to establish equilibrium coexistence of the melt with a fluid phase and verified glass compositions with EMPA. Dissolved volatile species were identified by microRaman spectroscopy and OH and C concentrations were quantified by FTIR and SIMS, respectively. Results show that C dissolves as methane together with OH and H_2 in equilibrium with a volatile phase composed chiefly of CH_4 and H_2. At IW to IW-2 (buffer 1) the dissolved C increases linearly with pressure from 70 ppm at 0.7 GPa to 360 ppm at 3.0 GPa. Methane may therefore be the dominant C species outgassed from reduced planetary mantles.

[1] Hirschmann and Withers 2008, *EPSL* **270**, 147-155. [2] Mysen *et al*., 2009, *GCA* **73**, 1696-1710. [3] Kadik *et al*., 2010, *Geochemistry Int*. **48**, 953-960

Mobilization of Pb from weathered shots at a firing range in Athens, Greece

A. ARGYRAKI[1]*, A. GODELITSAS[1], N. PETRAKAKI[1], J.M. ASTILLEROS[2] AND A. KARAGEORGIS[3]

[1]University of Athens, 15784 Zographou, Athens, Greece (*correspondance argyraki@geol.uoa.gr)
[2]Univ. Complutense Madrid, E-2804 Madrid, Spain
[3]HCMR, PO Box 712 Anavyssos, Greece

The dispersion and accumulation of Pb and other heavy metals in soil depends on their source as well as interactions between the soil solution and mineral components, resulting in dissolution and precipitation of new solid phases which incorporate the metals. This research focused on mobilization of Pb from shots exposed to weathering within a recreational area in Athens, Greece. Parts of the study area were used in the past as firing ranges. Lead in surface soil was measured by AAS after dissolution with aqua regia and concentration values reached a maximum of 2400 mg g^{-1} with a median of 114 mg g^{-1}. Samples were subsequently collected from two vertical soil profiles located close to the areas with the highest measured Pb concentrations and analyzed by XRF in order to produce Pb profiles up to a depth of 0.5 m and investigate the downwards migration of Pb. The analytical results were interpreted in conjuction with XRD data and SEM observations on soil samples. An abrupt, ten-fold decrease of Pb soil content was observed within the upper 10 cm at both profiles. The fate of metallic Pb in soil was further studied through two experiments. The first, involved burial of unused Pb shots in uncontaminated soil at the wider area of the studied site which lithologically consists of carbonate and ophiolite rock. After a period of 4 months the shots were removed from soil. Study by SEM confirmed the formation of hydrocerussite crystals on their surface. The second experiment involved in-situ AFM in contact mode to directly monitor changes in surface microtopography of metallic Pb reacting with an aqueous solution of CO_2 at pH = 4. Data from this experiment indicated a rapid growth of Pb hydroxycarbonate phase from about 7 min to about 11 min from exposure.

In conclusion, the combination of chemical analyses and microscopic techniques contributed to the understanding of Pb mobilization process during weathering of Pb shots. This includes rapid formation of Pb carbonate phases on the surface of shots and their subsequent dissolution under surface soil conditions. Lead starts migrating downwards and is effectively immobilized through formation of secondary Pb hydroxycarbonate phases within the upper 10 cm of soil.

https://doi.org/10.1180/S0026461X00006502 Published online by Cambridge University Press

Processes and timescales of magma evolution prior to the Campanian Ignimbrite eruption (Campi Flegrei, Italy)

ILENIA ARIENZO*[1], ARND HEUMANN[2], GERHARD WÖRNER[2], LUCIA CIVETTA[1,3], ROBERTO MORETTI[1,4] AND GIOVANNI ORSI[1]

[1]Istituto Nazionale di Geofisica e Vulcanologia, sezione di Napoli Osservatorio Vesuviano, Via Diocleziano 328, Napoli, Italy (*correspondence:ilenia.arienzo@ov.ingv.it)
[2]GZG, Abteilung Geochemie, Goldschmidtstr. 1, 37077 Göttingen, Germany
[3]Dipartimento di Scienze Fisiche, Università di Napoli "Federico II", Monte S. Angelo, Napoli, Italy
[4]Dipartimento di Ingegneria Civile, Seconda Università di Napoli, Aversa, Caserta, Italy

The Campi Flegrei caldera collapsed 39 ka in the Neapolitan area (southern Italy) after the Campanian Ignimbrite eruption. This eruption, recognized as the largest and the most cataclysmic volcanic event in the Mediterranean area over the past 200 ka, extruded not less than 300 km^3 of trachytic magma. Controversy exists over the timescales required to assemble a such large volume of silicic melt and thus whether large magmatic reservoirs can actually persist below active volcanic systems over prolonged periods of time. Uranium-series analyses have been performed on Campanian Ignimbrite whole-rocks, glass matrixes and separated minerals. The compositionally most evolved sample which is most radiogenic with respect to Sr isotopes records a reference age of 71 ka. By contrast, U-Th internal isochrones of the three compositionally least evolved samples give identical initial Th isotope ratios and yield consistent ages predating the eruption by up to 6.4 ka. Therefore the time preceding this large caldera-forming eruption during which the large volume of Campanian Ignimbrite magma assembled and mixed is 6.4 ± 2.1 ka.

The highest Pb and Nd isotopic ratios and $^{230}Th/^{232}Th$ activity ratios together with the oldest reference age of the most evolved samples suggest the existence of a resident magma body possibly related to a magmatic system that is known to have fed earlier magmatic activity in the Campi Flegrei area. Conversely, the younger age of the least evolved and least radiogenic magma dates the crystallization/differentiation event of a chemically and isotopically new magma batch entering the reservoir of the resident magma some few thousand years before the cataclysmic eruption. The progress of crystallization yielded high-water contents (up to 6-7 wt%), thus producing an overpressurized gas cap. The onset of the eruption tapped this cap, with consequent depressurization and fast volume decrease that facilitated or even drove the caldera collapse, and allowed the water-rich magma to be discharged during the pyroclastic current phase.

Bahamian speleothems reveal increased aridity associated with Heinrich events

M.M. ARIENZO[1]*, P.K. SWART[1], K. BROAD[1], A.C. CLEMENT[1], A. EISENHAUER[2] AND B. KAKUK[3]

[1]RSMAS, University of Miami, Miami FL 33149, USA (*correspondence: marienzo@rsmas.miami.edu) (pswart@rsmas.miami.edu, kbroad@rsmas.miami.edu, aclement@rsmas.miami.edu)
[2]IFM-GEOMAR, Kiel, Germany (aeisenhauer@ifm-geomar.de)
[3]Bahamas Underground, Marsh Harbor, Abaco, Bahamas

During the last glacial period there is substantial evidence for global millennial scale variability in climate, dominated by Heinrich events and Dansgaard-Oeschger events. Heinrich events have been well documented in the ice core records, deep-sea sediment records and speleothems. These records document that Heinrich events are global and abrupt climate change events. Recent studies across Africa and Asia indicate that drying throughout the tropics of both hemispheres occurred during Heinrich event 1 [1]. Geochemical analysis of stalagmites from the Bahamas further support a more arid climate associated with Heinrich events in the subtropical Atlantic.

In this study, currently submerged speleothems have been collected at depths ranging from 10-40 meters below sea level. These stalagmites formed when sea level was lower than at present and the cave was subaerially exposed. The stalagmites were dated using U/Th methodologies and analyzed for stable carbon and oxygen isotopes at a resolution of 20 um (approximately one sample every 2 years). In the subtropics, it has been demonstrated that higher volume rainfall events generally leads to a depleted $\delta^{18}O$ and $\delta^{13}C$ signal, whereas heavier $\delta^{18}O$ and $\delta^{13}C$ values are attributed to lower amounts of rainfall. The geochemical results reveal a significant isotopic excursion associated with Heinrich events. The change across Heinrich events 1-4 averages about 4 ‰ for C and 2 ‰ for O. These changes were all from positive to more negative values. These results support a rapid shift from an arid to a much wetter climate in the Bahamas associated with Heinrich events. Based on our preliminary age analysis, these changes occurred over a period of approximately 50 years. These records provide a unique opportunity to study climate variations at a fine resolution and may better define the role of the sub-tropics in forcing climate change.

[1] Stager *et al.*, (2011) *Science*, **331**, 1299-1302.

https://doi.org/10.1180/S0026461X00006502 Published online by Cambridge University Press

Geochemical features of the Aladag Fe-Cu-Zn-Pb skarn deposit (Ezine/Canakkale-North West Turkey)

F. ARIK[1]* AND Ü. AYDIN[2]

[1]Selcuk University, Geological Engineering Department, Konya, Turkey (*correspondence: fetullah42@hotmail.com)
[2]General Directorate of Mineral Research & Exploration, Ankara, Turkey (umitaydin77@gmail.com)

Aladag skarn zone located 8 km southwest of Ezine County (Çanakkale-Turkey). The basement of the study area is formed by recrystallized limestones of the Middle-Late Permian Bozalan Formation. Cretaceous Denizgoren Ophiolites thrusted over the Bozalan Formation. Upper Oligocene-Lower Miocene Hallaclar Volcanics consist of andesite, basalt, rhyolite and pyroclastic rocks cover the other units. Also Upper Oligocene-Lower Miocene Kestanbol Pluton cuts the older units and represented by mainly quartz-monzonite, monzonite, monzodiorite porphyry, syenite porphyry and quartz-syenite porphyry. Lower-Middle Miocene Ezine Volcanics composed of pyroxene-andesite and trachyte [1,2].

Skarn type mineralization was developed between the Bozalan Formation and Kestanbol pluton depending on the intrusion of the pluton at the north of Aladag. Endoskarn and exoskarn zones developed in the skarn zone. Some Ca-Mg silicate together with Fe, Cu, Pb, Zn oxide and sulphide minerals were developed in the skarn zone [1, 2]. (Fig. 1).

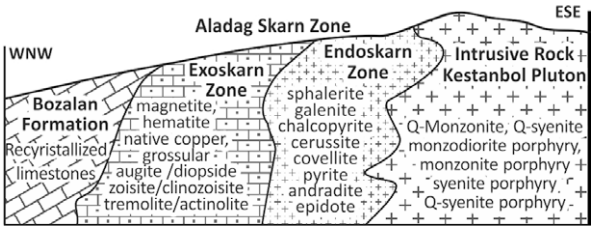

Figure 1. Schematic cross-section of Aladag skarn zone

Endoskarn zone is rich in Pb-Zn-Cu and the amounts of SiO_2, Al_2O_3, Fe_2O_3, Cu, Pb, Zn and Ag are 41.77%, 4.28%, 15.93%, 3.53%, 4.5%, 4.83% and 34 ppm respectively.

Exoskarn zone is rich in Fe and Fe_2O_3, SiO_2, Al_2O_3, MgO, CaO, Cu, Pb, Zn and Ag amounts are 66.75%, 14.85%, 1.37%, 4.34% and 8.63%, 112 ppm, 162 ppm, 213 ppm and 0.4 ppm respectively. There are significant increase in the amounts of Ca and Mg from intrusion rocks to wall-rocks in the skarn zone.

[1] Arik and Aydin, (2010), *Selcuk Univ. Sci. Res. Fund. Projects,* **97p**, [2] Arik and Aydin (2011), *Sci. Res. Essays*, **6(3)**, 592-606.

In situ secondary hydrocarbon cracking in a carbonate reservoir

S. ARKADAKSKIY[1]* B. ROSTRON[2] R. WIERZBICKI[3] AND V. ZRAL[3]

[1]Isobrine Solutions 4-341, 10230 Jasper Ave., Edmonton, T5J4P6, Canada (*correspondence: serguey@isobrine.com)
[2]University of Alberta, EAS, Edmonton, T6G2E3, Canada
[3]EnCana 1800, 855-2nd St. SW Calgary, T2P2S5, Canada

The Jean Marie member of the Redknife Formation in NE British Columbia, Canada is an Upper Devonian gas-rich (approx. 10 TCF) limestone zone, 15 to 100 m thick, lying unconformably on top of the Fort Simpson Formation and covered by the Redknife Fm. shale. The Jean Marie member is a low-permeability reservoir with dissolution related porosity and permeability locally enhanced by secondary dolomitization and fracturing. The reservoir is severely underpressured and of low water saturation. Carbon stable isotope analysis of natural gases has been used to assist hydrocarbon production from the reservoir. Here we present results from a $\delta^{13}C$ study of Jean Marie gases.

Natural gases in the Jean Marie exhibit significant compositional and $\delta^{13}C$ heterogeneity. Dry gases of reversed $\delta^{13}C_{C1}$ and $\delta^{13}C_{C2}$ compositions, lower $\delta^{13}C_{C2}$, and high C_2/C_3+ ratios are located in lower pressured NW domains of the study area, whereas C_2+ -richer gases of "normal" $\delta^{13}C$ compositions are produced to the SE. That trend is accompanied by increasing production pressures and gas condensate production. Geochemical data reveal limited gas mixing and significant reservoir compartmentalization. The $\delta^{13}C$ compositions and the low H_2S and CO_2 contents of the isotopically "reversed" gases indicate that these are not related to secondary processes such as sulphate reduction or microbial oxidation. Instead, the compositions of these gases are consistent with secondary cracking of hydrocarbons (SCH). The presence of pyrobitumen in the Jean Marie reservoir and the lack of liquid hydrocarbons in domains occupied with "reversed" gases both suggest that SHC occurred *in situ*. That challenges current models, which infer that the Jean Marie reservoir was charged first with oil and then with dry gas, both generated in the deeper, organic-rich Muskwa Formation. Instead, we propose that most natural gas in Jean Marie today was generated by secondary cracking of Muskwa oil and/or wet gas, and that late migration of dry Muskwa gas to Jean Marie was insignificant. SCH was more intense in the deeper western parts of Jean Marie where it produced dryer isotopically "reversed" gases. This study has important implications for the timing of migration and generation/destruction of hydrocarbons in the Jean Marie and similar carbonate reservoirs worldwide.

https://doi.org/10.1180/S0026461X00006502 Published online by Cambridge University Press

TAPP: Retrograde Mg-perovskite from subducted lithosphere?

L.S. ARMSTRONG* AND M.J. WALTER[1]

Department of Earth Sciences, University of Bristol, Queens Road, Bristol, BS8 1RJ, United Kingdom.
(*correspondence: L.Armstrong@bristol.ac.uk)

A phase with a tetragonal structure and compositional similarities to garnet was discovered as inclusions in diamonds over a decade ago, and given the acronym TAPP (Tetragonal-Almandine-Pyrope-Phase) [1]. TAPP has no known stability field, having never been synthesized in high P-T experiments, but a narrow stability region near the base of the transition zone has been postulated on the basis of associated inclusions [2]. Crystallographic arguments support the possibility that TAPP may be a retrograde phase formed when a higher pressure mineral was trapped in diamond then subjected to lower P-T conditions during ascent through the transition zone or upper mantle [3]. Here we propose that single-phase TAPP inclusions originated as Mg-perovskite (Mg-Pv) formed in deeply subducted mafic lithosphere.

Rare $MgSiO_3$ inclusions found in ultradeep diamonds are considered to represent former Mg-Pv, and their compositions generally match well with Mg-Pv formed in high P-T experiments on ultramafic bulk compositions (Fig.1). Likewise, the bulk compositions of TAPP inclusions match well with the trivalent-cation enriched Mg-Pv that forms in experiments on mafic compositions; Ti-rich TAPP inclusions are nearly exact matches to Mg-Pv expected to form in subducted MORB. REE abundances measured in a TAPP inclusion [4] also closely match those found in Mg-Pv inclusions [5]. Preliminary diamond anvil cell experiments on an average TAPP composition indicate formation of nearly phase-pure Mg-Pv at lower mantle conditions.

Figure 1

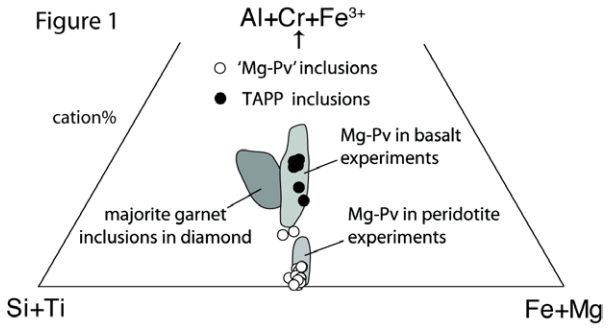

[1] Harris *et al*. (1997) *Nature* **387** 486-488. [2] Hutchison *et al*. (2001) *Contrib. Min. Pet*. **142** 119-126. [3] Finger & Conrad (2000) *Am. Min*. **85** 1804-1807. [4] Bulanova *et al*. (2010) *Contrib. Min. Pet*. **160** 489-510. [5] Harte *et al*., (1990) *Geochem. Soc. S. Pub*, 1999: p. 125-153.

Metal-silicate partitioning of iodine at high pressures and temperatures: Implications for the Earth's core

ROSALIND M.G. ARMYTAGE[1], ANDREW P. JEPHCOAT [1,2], M. ALI BOUHIFD[3,1] AND DONALD PORCELLI[1]

[1]Department of Earth Sciences, University of Oxford, South Parks Rd, Oxford OX1 3AN, UK.
(*correspondence: rosa@earth.ox.ac.uk)
[2]DIAMOND Light Source, Diamond House, Chilton, Didcot, OX11 0DE, UK
[3]Laboratoire Magmas et Volcans, Université Blaise Pascal, 5 rue Kessler, Clermont-Ferrand 63038, France

The two major causes for the difference in elemental concentrations between the silicate Earth and primitive undifferentiated chondritic silicate material are volatility and/or partitioning in the Earth's core. Compositional models of the Earth [1,2,3] suggest that the depletion of some of the halogens in the Bulk Silicate Earth (BSE) are greater than can be explained by their volatility. The calculations indicate that up to 85% of the Earth's iodine could reside in the core but to date there is no published high-pressure liquid-metal, liquid-silicate partitioining experimental data for iodine to test this idea.

We present the first results for metal silicate partitioning behaviour of iodine. Candidate CI-like glass mixtures of silicate and iron (+iron alloy) were heated in a Laser Heated Diamond Anvil Cell (LHDAC) at pressures between 2-20GPa and at ~3000 K. No pressure dependence of the partition coefficient, $D_{\text{liquid-metal liquid-silicate}}$ was observed within this range, but the composition of the metal phase was shown to have an effect. When the dominantly iron liquid was alloyed with Ni, S, O and Si there was an increase in iodine solubility in the metal. Iodine exhibited siderophile behaviour over all the PT conditions with D_I = 1.22 ±0.73 (2 s.d.) (Fe metal) and D_I = 4.40±1.36 (2 s.d.) (Fe-alloy). In conjunction with a "best estimate" concentration for iodine in the bulk silicate Earth (BSE), it is calculated that the core could be a significant reservoir for iodine, depending on the model for separation.

The implications of iodine's siderophile behaviour are considered with regards to the decay system ^{129}I –^{129}Xe ($T_{1/2}$ = 15.7Myr). As it is thought the core would have formed while ^{129}I was still extant, preliminary modelling has been carried out to assess the core's radiogenic ^{129}Xe budget and the effect this may have on mantle xenon reservoirs and closure ages.

[1] Kargel & Lewis (1993), *Icarus* **105**, 1-25 [2] McDonough & Sun (1995), *Chemical Geology* **120**, 223-253 [3] McDonough (2003), *Treatise on Geochimstry*, 547-568

https://doi.org/10.1180/S0026461X00006502 Published online by Cambridge University Press

Ore metals from the subcontinental lithospheric mantle?

NICHOLAS ARNDT

ISTerre, UMR5275 CNRS, Université Joseph Forier, 38400 Grenoble, France (arndt@ujf-grenoble.fr)

The hypothesis that the metals in some ore deposits come from the base of the lithosphere arises because we know very little about the composition of this part of the mantle. It could conceivably be enriched in certain metals, and if so, these metals could conceivably be transported to the surface in magmas or other fluids and there become concentrated in ore bodies. There is very little substance to the model, and many arguments against it. The lithosphere is by definition the coldest part of the mantle and it only melts under special conditions. The normal product is a low-degree melt - an alkaline, Si-undersaturated magma of the type that, with rare exceptions, contains few metallic ore deposits. Some gold deposits may be associated with lamprophyres that could have come from the lithosphere, but a direct genetic association has not been demonstrated. In regions of continent rifting, the lower parts of the lithosphere may well up and melt, but metallic ore deposits are rare in continental rift zones. Major magmatic ore deposits form from high-volume, high-flux magmas that result from high-degree melting in large volumes of mantle. The normal source of such magmas is in deeper, hotter parts of the mantle – the asthenosphere or a mantle plume. If melting is to occur in the lithosphere, rather than in the hotter parts of the mantle, the melting point of the lithosphere must be drastically reduced by the presence of volatiles. There is little evidence, however, that the host magmas of ore deposits were unusually rich in water or CO_2. Magmas from a sub-lithospheric source will interact with wall rocks as they pass through the lithospheric mantle and they may pick up some metals through this interaction. However, there is ample geological and geochemical evidence that the origin of most magmatic deposits involves crustal contamination of asthenosphere- or plume-derived magmas at shallow levels of the continental crust of magmas and that the major source of the ore metals is the asthenosphere or the plume.

Unexpected changes in aggregation and mineralogy of goethite during the reduction of nitroaromatics

WILLIAM A. ARNOLD[1]*, R. LEE PENN[2] KIRSTEN MOORE[1], TRAM AHN DO[2] AND AMANDA M. STEMIG[2]

[1]Department of Civil Engineering, University of Minnesota, 500 Pillsbury Dr. SE, Minneapolis, MN 55455, USA (*correspondence: arnol032@umn.edu, moor0561@umn.edu)

[2]Department of Chemistry, University of Minnesota, 207 Pleasant St. SE, Minneapolis, MN 55455, USA (rleepenn@umn.edu; doxxx042@umn.edu; stemi002@umn.edu)

When studying the reduction of nitroaromatic compounds by ferrous iron in the presence of goethite, it is routine to use batch reactors. The ferrous iron and goethite are equilibrated in a pH-buffered solution, and the reaction is initiated by introducing a target contaminant in a cosolvent. These experiments have taught us much about the reactivity of nitroaromatic compounds in systems containing reduced iron, but there are two assumptions made in these systems. First, it is assumed that the particle size/surface area/aggregation state is constant. Second, it is assumed that the mineral phase composition does not change during the course of the reaction. We have previously shown that the particle size is not constant during such reactions [1]. Our results here reveal further limitations in the above assumptions.

Stable particle sizes are observed via dynamic light scattering (DLS) when goethite nanorods are suspended in a solution buffered with 3-(N-morpholino)propanesulfonic acid. Upon injection of a methanolic stock of 4-chloro-nitrobenzene, DLS measurements show rapid aggregation of the particles. Results to date suggest that the combination of cosolvent and contaminant lead to the agglomeration. This finding suggests that the method used to introduce the contaminant, including the presence of a cosolvent, may influence the measured reaction rate of the contaminant. These effects are beyond those caused by the buffer itself [2].

Results tracking the kinetics of trifluralin (a nitroaromatic herbicide) reduction in the presence of ferrous iron and goethite nanorods show suprising changes in particle agglomeration as well as phase composition of the solids. These results reveal a reaction system that is more dynamic that previously envisioned.

[1] Chun *et al*. (2006) *Environ. Sci. Technol*. **40**, 3299-3304.
[2] Danielsen *et al*. (2005) *Environ. Sci. Technol*. **39**, 756-763.

https://doi.org/10.1180/S0026461X00006502 Published online by Cambridge University Press

Optical properties, size distribution and composition of aerosol particles in the urban area of Sao Paulo

PAULO ARTAXO[1], JOHN BACKMAN[2], LUCIANA RIZZO[3], FABIO JORGE[1] AND MARKKU KULMALA[2]

[1]Institute of Physics, University of São Paulo, Brazil (artaxo@if.usp.br)
[2] Division of Atmospheric Sciences, Department of Physics, University of Helsinki, Finland.
[3] Department of Exact and Earth Sciences, Federal University of Sao Paulo, Diadema, Brazil.

The megacity of São Paulo with its 19 million people and 7 millions cars is a challenge from the point of view of air pollution. High levels of PM10, black carbon and ozone and the peculiar situation of the large scale use of ethanol fuel makes it a special case. Little is known about the impact of ethanol on air quality and human health and the increase of ethanol as vehicle fuel is rising worldwide An experiment was designed to physico-chemical properties of aerosols in São Paulo, as well as their optical properties. Aerosol size distribution is being measured with a Helsinki University SMPS and a GRIMM OPC. Optical properties are being meeasured with a TSI Nephelometer and a MAPPF absorption photometer. An CIMEL sunphotometer from the AERONET network measure the aerosol optical depth.

The measured total particle concentration typically varies between 10,000 and 30,000 cm-3 being the lowest late in the night and highest around noon and frequently exceeding 50,000 cm-3. Clear diurnal patterns in aerosol optical properties were observed ranging between 21 and 64 Mm-1 for light scattering coefficients (σSP) and between 12 and 33 Mm-1 for light absorption coefficients (σAP). The diurnal patterns measured at the site show peaks in light absorption and scattering coefficients during morning rush hours where the single-scattering albedo (ω0) is at its lowest. Surface mean diameters can be seen growing from the minimum at noon to late into the night which can also be seen from the size dependent Angstrom exponents calculated from the light scattering coefficients. During the first month a total of seven new particle formation events were observed with growth rates ranging from 9 to 25 nm h-1. During these events the condensation sink, vapour abundance explaining the growth, and vapour production rates were calculated. Interestingly enough there were also events were condensed vapours were evaporating from the condensed phase thus shrinking the size of the particles in all sizes. Aerosol optical thickness were relativelly small at 0.1-0.3 at 500 nm, indicating low boundary layer height.

Evolution of the cratonic lithosphere inferred from lithospheric mantle heterogeneity: A geophysical perspective

IRINA M. ARTEMIEVA

IGG, University of Copenhagen, Denamrk, (irina@geo.ku.dk)

Large-scale geohysical models indicate a significant lateral heterogeneity of the cratonic lithosphere. In contrast to xenolith data, which suggest little variation in lithospheric thickness in the cratons, significant lateral variations in lithospheric thickness are seen in global thermal [1] and seismic tomography models [e.g. 2, 3]. These variations reflect the cumulative effect of the processes of lithosphere formation and its later reworking by tectonic and mantle processes, and thus provide information on the preservation style of the lithospheric mantle. Thermal [1] and seismic tomography models [2, 3] of lithospheric thickness, complemented by a global 1 deg x 1 deg database for tectono-thermal ages for the continental crust [4], are used to calculate (i) the volume of the preserved continental lithosphere of different ages within the individual cratons, (ii) a global model of lithosphere preservation since the Archean. In accord with independent estimates of the growth rate of juvenile crust [5], three major peaks in lithosphere preservation rate can be recognized globally. However, the amplitude at 2.1-1.7 Ga is at least double of that at the peaks at ca. 2.7-2.6 Ga and 1.3-1.1 Ga, and significant differences both in the time and in the amplitude of the peaks exist between different cratons [6].

Extracting non-thermal signal from seismic tomography models allows for distinguishing compositional variations in the cratonic lithosphere, which also reflect the cumulative effect of varios processes related to lithosphere formation and its later reworking [7]. Compositional seismic velocity variations in the lithospheric mantle show strong qualitative correlation with its tectono-thermal ages and with regional variations in the lithospheric thickness. Their amplitude, however, varies both laterally and vertically, reflecting either a peripheral growth of the cratons in Proterozoic or their peripheral metasomatic reworking in the post-Archean time.

[1] Artemieva & Mooney (2001), *JGR 106*, **16387-16414.**
[2] Grand (2002), *Phil. Trans. R. Soc. London 360,* 2475-91.
[3] Shapiro & Ritzwoller (2002), *Geophys. J. Int. 151*, 1–18.
[4] Artemieva (2006), *Tectonophysics 416*, 245-277.
[5] Condie & Aster (2010), *Precambr. Res. 180,* 227-236.
[6]Artemieva (2011), *Cambridge University Press*, 824 pp.
[7] Artemieva (2009), *Lithos 109*, 23-46.

https://doi.org/10.1180/S0026461X00006502 Published online by Cambridge University Press

Modeling the dissolution and growth of whole mineral grains

ROLF S. ARVIDSON* AND ANDREAS LUTTGE

[1]Department of Earth Science MS-126, Rice University, Houston TX 77005, USA
(*correspondence: rsa4046@rice.edu, aluttge@rice.edu)

The reactivity of crystal surfaces reflects the distribution and interaction of kinks, steps, and defect-related sites. During the dissolution of whole mineral grains (e.g., Fig. 1), substantial changes are commonly observed along discontinuities such as grain edges, twin boundaries, and other complex macro-features [1]. We wish to understand the evolution of these changes during the dissolution and growth of the entire crystal, and how they relate to the integrated flux of material from the particle. We examine this general kinetic problem through a series of Monte Carlo models, beginning with simulations of dissolution and growth using a simple cubic Kossel crystal, and culminating in virtual experiments involving complex crystal structures. We can use these simulations to explore a variety of problems, including (1) the contribution of these features to the integrated rate as a function of crystal diameter, (2) how processes such as uptake and release at kink sites are coordinated with diffusive transport, (3) whether the changes observed during dissolution are reversible under growth conditions, (4) how the mean and variance of the reaction rate at these edge sites compare to those on interior terraces as a function of defect density, and (5) the implications for the behavior and properties of poly-crystalline grains and nano-particles.

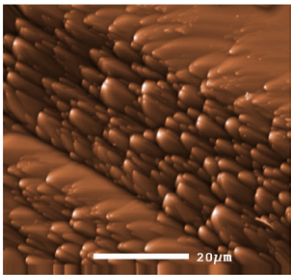

Fig. 1. Etching of face edges of dolomite [2].

[1] Zhang & Luttge (2009) *Geochim. Cosmochim. Acta* **73**, 6757–6770. [2] Arvidson & Mackenzie (1999) *Amer. J. Sci.* **99**, 257–288.

Paleozoic tholeiite magmatism in the Kola Province, Russia: Relations with alkaline magmatism

A.A. ARZAMASTSEV AND L.V. ARZAMASTSEVA

Geological Institute KSC RAS, Apatity, Russia
(arzamas@geoksc.apatity.ru)

The Kola alkaline province, formed in the northeastern part of the Fennoscandian Shield include Khibina and Lovozero plutons, carbonatite intrusions, and numerous alkaline dikes, as well as remnants of subalkaline and alkaline extrusives. The discovered manifestations of tholeiite magmatism in the region are represented by dolerite dikes forming three swarms: Pechenga, the Barents Sea coast, and the East Kola. $^{40}Ar/^{39}Ar$ geochronology obtained for 5 dolerite dikes, together with Sm–Nd mineral isochron data yield a 405-385 Ma time span of tholeiitic magmatism in Kola part of the Fennoscandian Shield. In the Sm–Nd system, the εNd(T) values (+0.9...+5.4) are close to those for alkaline rocks of the province. They testify that the tholeiite melts originated from sources with a significant share of a depleted mantle component. Trace elements characteristics suggest that the Paleozoic dolerites belong to a group of continental plateau basalts.

The finding of the Devonian tholeiites leads to the need to define their position in the general evolution model of Paleozoic magmatism, and, first of all, to define their relationships with alkaline melts. Analysis of the spatial distribution of the Paleozoic dolerite dykes shows that they are located on the periphery of the area of predominant development of alkaline intrusions and alkaline dike swarms. The set of geochronological data shows that the main manifestations of alkaline magmatism occurred in the period of 380-360 Ma. The initial melts of the Paleozoic alkaline intrusions corresponded to olivine melanephelinite, which was generated under the conditions of garnet lherzolite facies. According to the above mentioned materials, we suggest that the tholeiites correspond to the initial phase of the Paleozoic plume-lithosphere interaction, during which the occurrence of tholeiite melts in the peripheral zone of the plume was the result of partial melting of the mantle substrate under the conditions of spinel lherzolite facies. During the subsequent development of the process of plume–lithosphere interaction, the deep mantle areas corresponding to the conditions of garnet lherzolite facies were in the zone of melting. The partial melting of these lherzolites under the conditions of mantle metasomatism led to the formation of melanephelinite melts, the basis of formation of the Paleozoic Kola alkaline province.

https://doi.org/10.1180/S0026461X00006502 Published online by Cambridge University Press

Crystallization kinetics of alkali feldspar in trachytic melts of Phlegraean Fields (Napoli, Italy)

F. ARZILLI[1]*, M.R. CARROLL[1] AND M. PIOCHI[2]

[1]University of Camerino, via Gentile III da Varano, Camerino, (MC) Italy (*correspondence: fabio.arzilli@unicam.it; michael.carroll@unicam.it)

[2]INGV-OV, via Diocleziano 328, Napoli (NA), Italy

The aim of this study is to quantify crystallization kinetics of trachytic melts and eruption dynamics of phlegraean volcanoes. In particular, studying the growth rate (G_L), through cooling experiments, of alkali feldspar and their crystal size distribution (CSD), is possible to constrain residence time of magma in magma-chamber and into the conduit during the eruption.

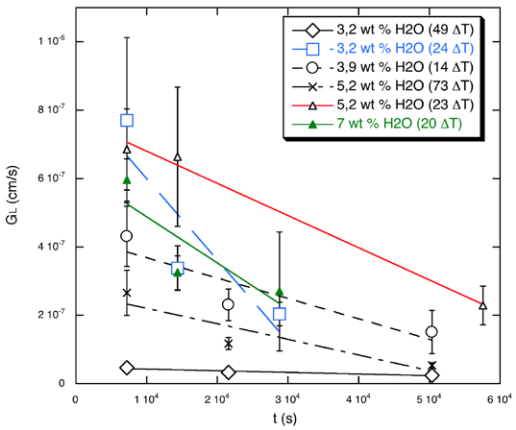

Figure 1: Relation between the growth rate (G_L) and the experimental time (t).

Discussion of Results

The order of magnitude of alkali feldspar growth rate obtained from cooling experiments varies between 10^{-7} and 10^{-8} cm/s (Fig. 1). This difference in order of magnitude depends on percentage of H_2O dissolved in the melt and degree of undercooling ($\Delta T = T_{liquidus} - T_{experimental}$) [1] (Swanson, 1977). Moreover, this difference implies significant variations of the ascent time. CSD studies on Monte Nuovo products carried out by Piochi *et al*. [2] to investigate magma dynamics in syn- eruptive conditions combined with G_L values obtained in this experimental work suggest ascent times between 2 days and several hours.

[1] Swanson (1977) *Am. Min.* **62**, 966-978; [2] Piochi *et al*. (2005) *Bull. Volcanol.* **67**, 663–678.

Molybdenum isotopes as oceanic paleoredox proxy of the Paleoproterozoic Shunga event

D. ASAEL[1]*, O. ROUXEL[2], C. REINHARD[3], T. LYONS[3] AND L. KUMP[4]

[1]Université de Brest, IUEM, UMR 6538, 29280 Plouzané, France (*correspondence: dan.asael@univ-brest.fr)

[2]IFREMER, Département Géosciences Marines, 29280 Plouzané, France (orouxel@univ-brest.fr)

[3]Department of Earth Sciences, University of California, Riverside, CA 92521-0423 USA

[4]Department of Geosciences, Penn State University, University Park, PA 16802 USA

Molybdenum (Mo) isotopes in ancient organic-rich black shales may directly reflect the contemporaneous seawater Mo isotope compositions and can thus be used as an oceanic paleoredox proxy. We measured Mo isotope composition and Fe speciation of black shales from the 2.0 Ga Zaonega Formation from the Eastern Fennoscandian Shield (ICDP FarDeep project, [1]). The studied section contains thick units of Paleoproterozoic C_{org}-rich sediments (up to 99% C) that represent a giant, petrified oil field, including petroleum source rocks and black shales. Samples were measured by MC-ICP-MS (Neptune), and data were corrected using double-spike iterations (using ^{97}Mo and ^{100}Mo). Mo isotope ratios are reported relative to our internal lab standard SPEX, where $\delta^{98/95}Mo_{SPEX} = \delta^{98/95}Mo_{NIST3137} - 0.37‰$.

Overall, the studied section shows relatively small Mo isotope variations, averaging $\delta^{98/95}Mo = 0.79 \pm 0.29$ ‰. Using Fe speciation ($Fe_{Py}/Fe_{HR} > 0.8$ and $Fe_{HR}/Fe_T > 0.38$), euxinic conditions were identified for several samples in the upper part of the section which also shows higher Mo concentrations. These samples show slightly higher $\delta^{98/95}Mo$ values of 0.88 ± 0.28 ‰, and are considered to represent contemporaneous seawater due to quantitative Mo removal to the sediment. Simple oceanic mass balance of the Mo isotope system shows that euxinic sinks dominated the Mo removal from the oceans and controlled the isotopic composition of seawater.

At this time, after the GOE, increasing oxygen levels in the atmosphere amplified the delivery of dissolved Mo to the oceans. However, the oceans were apparently dominated by anoxic, ferruginous/euxinic conditions with an oxic sink smaller than that suggested by [2] at 2.5 Ga.

[1] Melezhik *et al*. (2004) *Ore Geology Reviews* **24**, 135-154.
[2] Duan *et al*. (2011) *Geochimica et Cosmochimica Acta* **74**, 6655-6668.

https://doi.org/10.1180/S0026461X00006502 Published online by Cambridge University Press

The elasticity change of Na-contained silica according to the post-stishovite phase transition in the Earth's lower mantle

Y. ASAHARA[1]*, K. HIROSE[2,3], Y. OHISHI[4], N. HIRAO[4], H. OZAWA[3] AND M. MURAKAMI[5]

[1]Osaka university, Toyonaka 560-0043, Japan (*correspondence: asaharay@anvil.ess.sci.osaka-u.ac.jp)
[2]Tokyo institute of technology, Tokyo 152-8551, Japan
[3] JAMSTEC, 2-15, Kanagawa, 237-0061, Japan
[4]JASRI/SPring8, Hyogo 679-5198, Japan
[5]Tohoku university, Sendai 980-8578, Japan

Introduction

Stishovite is considered to be an important constituent of subducted oceanic basalts and sediments in the Earth's deep interior. It has the tetragonal rutile structure and transforms to an orthorhombic $CaCl_2$ structure at around 60 GPa in the pure SiO_2 system. Acccording to theoretical models, the phase transition is trigged by the lattice instability of a soft transverse acoustic mode associated with the shear elastic constant and it has been suggested that this elastic softning could relate to several distinctive seismic strucures in the Earth's lower mantle (e.g., [1], [2]). This possibility was denyed by the phase study of pure SiO_2 at high pressure and high temperature [3], however, natural stishovite in subducted basalts and sediments may contain several impuritities, such as Al, Mg, and Na. Therefore, the effect of impurities on the phase transition and elastic properties of stishovite should be clarified. In this study, we investigated elastic properties of sodium contained stishovite by simultaneous measurements of acoustic velocity and X-ray diffraction across the post-stishovite phase transition at room temperature.

Results

Simultaneous measurements of Brillouin scattering and X-ray diffraction on polysrystalline stishovite with 3 wt.% sodium as impurity were conducted at room temperature and the pressure range of 0-70 GPa using a combined system of Brillouin scattering and synchrotron X-ray diffraction at SPring-8/BL10XU, Japan [4]. The phase transition from rutile-structure to $CaCl_2$-structure was observed at around 35GPa with X-ray diffracton and a dipping of transversal velocity was also observed at the transion pressure.

[1] Karki *et al*. (1997) *GRL* **24**, 3269-3272. [2] Kaneshima & Helfrich (1999) *Science* 283, 1888-1891 [3] Ono *et al*. (2002) *EPSL* **197**, 187-192. [4] Ohishi *et al*. (2008) *HPR* **28**, 163-173.

Effects of fluorine on the solubility of Nb, Ta, Zr and Hf in highly fluxed water saturated haplogranitic melts

A. ASERI[1] AND R.L. LINNEN[2]

[1]Department of Earth and Environmental Sciences, University of Waterloo, (aaseri@uwaterloo.ca)
[2]Department of Earth Sciences, University of Western Ontario, (rlinnen@uwo.ca)

The effect of fluorine on the solubility of $MnNb_2O_6$, $MnTa_2O_6$, $ZrSiO_4$ and $HfSiO_4$ was determined for highly fluxed, water-saturated haplogranitic melts at 800 °C and 2000 bars. The melts correspond to the projection of the granite minimum to the intersection of the Ab-Or tieline in the Q-Ab-Or system ($Ab_{72}Or_{28}$) and also contain 1.1, 1.7 and 2.02 wt % of Li_2O, P_2O_5 and B_2O_3, respectively, Up to 6 wt% fluorine was added as AgF in order to keep the ASI of the melt constant. The nominal ASI of the melt is close to 1, so that if Li is considered to be an alkali element, the melts are alkaline. The experiments were conducted using cold seal pressure vessels with water as a pressure medium.

The solubility products $[MnO]*[Nb_2O_5]$ and $[MnO]*[Ta_2O_5]$ are nearly independent of F content, approximately $17x10^{-4}$ and $70x10^{-4}$ mol^2/kg^2, respectively, although there may be a weak negative dependence on F. These data are in agreement with [1] conducted on Li-B-free and P-poor melts. By contrast, there is a positive dependence of zircon and hafnon solubility, which increase from 0.25 wt% ZrO_2 and 0.85 wt% HfO_2 for melts with 0 wt % F to 0.38 wt% ZrO_2 and 1.16 wt% HfO_2 for melts with 6 wt % F, in agreement with [2]. However, the overall conclusion is that fluorine is less important than previously thought for the control on the behaviour of high field strength elements in highly evolved granitic melts.

[1] Fiege *et al*., (2011), *Lithos* **122**, 165-174 [2] Keppler, (1993), *Contrib. Mineral. Petrol*. **114**, 479-488.

https://doi.org/10.1180/S0026461X00006502 Published online by Cambridge University Press

Origin of craton mantle layering according to PT reconstruction

I.V. ASHCHEPKOV[1], D.A. IONOV[2], T. NTAFLOS[2]
H. DOWNES[4] AND S.V. PALESSKY[1]

[1]IGM SB RAS, Novosibirsk, Russia, (garnet@igm.nsc.ru)
[2]University de Lyon, France (dmitri.ionov@univ-st-etienne.fr)
[3]University of Vienna, Austria, (ntaflot9@univie.ac.at)
[4]University of London, G.Britain, (h.downes@ucl.ac.uk)

Reconstruction of PTXF conditions of SCLM for Ykutian [1,2] and ~70 worldwide kimbelites show high heating of Proterozoic mantle, lower heating stage to the mantle of the northern continentswith sicker SCLM in comparison with post Gondwana ones. The layering -7-12 horizons correlates with superplume events. The thransects for Siberia, Baltica, marginal N America and S Africa show motley inclined SCLM, in central parts prevail horizontal. Three traps for the melts: oxidized in- the 75-65, carbonatite- 45-40, and water-bearing basaltic- 20-30 kbar [3] are marked by pyroxenites [4]. Melt and diapiric upvelling from these levels in off-craton and rifting settings were basificated, reduced and rifted in superplume periods. Models of SCLM formation: the nucleation of restite from mantle diapirs; joining of exhousted or island-arc type blocks; the low angle subduction of submelted plates under superplumes; broken, folded high angle plates joined to the continental margins. Fluid/melt flows in the continent margins metasomitized SCLM [5]. Protokimbelites refertillized low part of mantle section in two steps–carbonatite/kimberlite and with H_2O bearing melts as evidenced by geochemical features of pyroxenes and garnets RBRF 11-05-00060a;11-05-91060-PICSa.

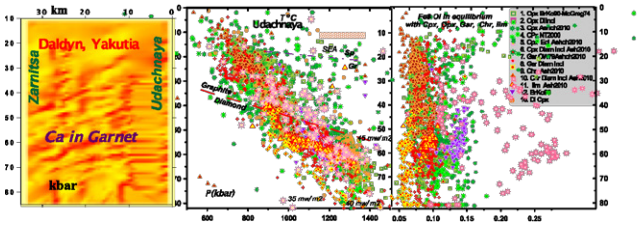

[1] Ashchepkov ea (2010) *Tectonophysics*. **485**; [2] Sobolev, (1974) *AGU, Washington, DC;* [3] Tappe *ea*. (2008) *GCA* **72 ;** [4] Pokhienko ea *al*. (1999) **7IKC**,Nixon's v. [5] Ionov *et al*. (2010) *J. Petrol*. **51**,

The melting curve of MgO from shock temperature experiments

P. D. ASIMOW* AND O. V. FAT'YANOV

Division of Geological and Planetary Sciences, California Institute of Technology, Pasadena CA 91125, USA (*correspondence: asimow@gps.caltech.edu)

MgO is a major constituent of the lower mantle and its melting curve is an essential anchor point for understanding crystallization of magma oceans or melting at the core-mantle boundary. Despite the apparent simplicity of this material, its melting curve remains highly uncertain. The laser-heated DAC-based melting curve of [1], extrapolated to 135 GPa, is 1000 K below any of the published theoretical curves [2-6], which themselves range over nearly 2500 K. A recent study of the MgO-FeO binary loop supports a very steep liquidus [7]. To resolve this issue we determined shock temperature on single-crystal MgO pre-heated to 1850 K before impact. Our data are calibrated against a standard irradiance lamp and the known shock temperatures of NaCl and MgO shocked from 300 K and are corrected for shock-front reflectivity. Melting should manifest as a drop in shock T with increasing pressure and shock T lower than expected for solid periclase in the shock state. Our experiments reach 9000 K at 250 GPa and remain solid in the shock state. This rules out the melting curve of [1] and probably [2], but we have only a lower bound on the melting curve at this time. Experiments with initial temperature up to 2350 K are in progress.

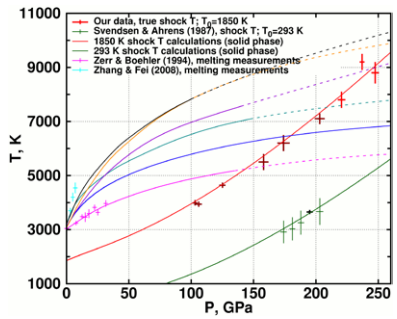

A very high melting temperature of MgO implies minimum melts of the lower mantle that are silicate- and FeO-rich and a significant ferropericlase liquidus field.

[1] Zerr & Boehler (1994) *Nature* 371, 506-508. [2] Strachan *et al*. (1999) *Phys. Rev. B* **60**, 15084-15093. [3] Belonoshko & Dubrovinksy (1996) *Geochim. et Cosmochim. Acta* **60**, 1645-1656. [4] Cohen & Gong (1994) *Phys. Rev. B* **50**, 12301-12311. [5]. Cohen & Weitz (1998) in *Properties of Earth and Planetary Materials at High Pressure and Temperature*, M.H. Manghnani & T. Yagi. p. 185-196. [6]. Liu *et al*. (2006) *Phys. Lett. A* **353**, 221-225. [7]. Zhang & Fei (2008) *Geophys. Res. Lett*. **35**, L13302.

https://doi.org/10.1180/S0026461X00006502 Published online by Cambridge University Press

^{39}Ar-^{40}Ar dating on plagioclases of metabasic and metagranitic rocks in the Yoncayolu metamorphics, NE Turkey

Z. ASLAN[1]* M.A. GUCER[2] AND M. ARSLAN[3]

[1]Dept. of Geol. Eng., Balıkesir Univ., 10145, Balıkesir, Turkey (*correspondence: zaslan@balikesir.edu.tr)
[2]Dept. of Geol. Eng., Gümüşhane Univ., 29100, Gümüşhane, Turkey (maligucer@gmail.com)
[3]Dept. of Geol. Eng., Karadeniz Tech. Univ., 61080, Trabzon, Turkey (marslan@ktu.edu.tr)

Low grade Yoncayolu (Erzincan, NE Turkey) metamorphics are overlined tectonically by ophiolitic units. The metamorphics are composed of widespread schists and metabasics, rare metagranitic rocks and calc-schists. All of these are represented by greenschist facies P-T conditions, with mineral assemblages of sericite, chlorite, illite, quartz, calcite, albite, epidote and rare muscovite in schists, and quartz, chlorite, albite, hornblende, epidote, clinozoisite and tremolite in metabasics.

Detailed mineralogical and petrographical studies are carried out on five metabasic and metagranitic samples to find out protolithic mineralogy and texture. Of these, metagranitic sample is a coarse-grained and contain anhedral quartz, plagioclase, aggregates of epidote, clinozoisite, and minor chlorite. The texture of the rock shows some evidence of minor cementation and annealing. Metabasic sample is fine-grained, sparsely phyric, consisting predominantly of altered (mainly sericitized, sometimes completely destroyed) plagioclase and hornblende. Hornblende occurs as part of the matrix, and the anhedral grains are intergrown with the plagioclase.

Metagranitic and metabasic samples were suitable for relict plagioclase separation and ^{39}Ar-^{40}Ar dating. Plagioclase of metagranitic sample (M16) yielded an age spectrum with two steps plateau characterized by 71% of ^{39}Ar and age value of 60.7±4.9 Ma, and plagioclase of metabasic sample (M32) yielded age spectrum with two steps plateau characterized by 56% of ^{39}Ar and age value of 94.1±3.3 Ma. Plagioclase plateau ages obtained from metabasic and metagranitic samples correspond Lower Cretaceous and Lower Palaeocene time, respectively. Hence the ^{39}Ar-^{40}Ar dating can be assumed as the crystallization ages of plagioclases, the metamorphism time and exhumation history of the low grade Yoncayolu metamorphics should have been later than Cretaceous-Palaeocene (?) time.

Fast iron sulfide oxidation in a region of land uplift and artificial drainage

M.E. ÅSTRÖM[1]*, A. BOMAN[2] AND S. FRÖJDÖ[3]

[1]Kalmar University, School of natural sciences, SE-39182 Kalmar, Sweden (*correspondence: mats.astrom@lnu.se)
[2] Luleå University of Technology, Department of Civil, Environmental and Natural Resources Engineering, SE-97187 Luleå, Sweden (anton.boman@ltu.se)
[3] Abo Akademi University, Department of Geology, FI-20500 Åbo, Finland (soren.frojdo@abo.fi)

Postglacial isostatic uplift (currently up to 1 meter per 100 years) has brought large areas of land above the sea level in low-lying coastal areas of northern Europe. These exposed land masses are to a significant part covered by thick marine sediments, characterised by unusually high concentrations of fine-grained metastable iron sulfides (up to 1%) in an aluminosilicate clay-silt matrix [1, 2].

When drained for agricultural purposes, these sediments rapidly develop into acidic (acid sulfate) soils and release an abundance of metals (Mn, Al, Ni, Zn, Co, Be, Ln) into drains, despite the cold climate with frozen ground and a thick snow cover for about half of the year [3, 4]. We suggest that microbially mediated oxidation of the metastable iron sulfides initiate the soil ripening process, leading to a fast decrease in pH which favours further pyrite oxidation and silicate weathering.

The farmers are worried and the environment – including surface waters and down-stream sediments – is acidified and contaminated. There is thus an urgent need to increase the understanding of this on-going landscape-wide acidification process, in which the preservation and oxidation and toxic-metal content of the metastable iron sulfides is a key parameter.

[1] Boman et al (2008) *Chemical Geology* **255**, 68-77. [2] Boman et al (2010) *Geochimica et Cosmochimica Acta* **74**, 1268-1281. [3] Åström et al (2000) *Environmental Science and Technology* **34**, 1182-1188. [4] Sundström et al (2002) *Environmental Science and Technology* **36**, 4269-4272.

https://doi.org/10.1180/S0026461X00006502 Published online by Cambridge University Press

The *Exxon Valdez*, BP MC 252, and other oil spills: What we learned about petroleum biodegradation and bioremediation

RONALD M. ATLAS

Dept. of Biology, University of Louisville, Louisville KY, 40292 USA (Correspondence: r.atlas@louisville.edu)

The oil spills from the *Exxon Valdez* oil spill in Prince William Sound, Alaska, the Gulf of Mexico (GOM) oil spill from the Deepwater Horizon MC 252 well accident and several other major spills highlight the role of microorganisms in oil weathering and the mitigation of environmental impact. Bioremediation employing fertilizer addition was used to accelerate rates of *Exxon Valdez* oil biodegradation. Rates of oil degradation were a function of the ratio of nitrogen/biodegradable oil and time. Bioremediation increased the rate of polycyclic-aromatic-hydrocarbon degradation by a factor of 2, and of aliphatic hydrocarbons by a factor of 5. Most of the oil has been eliminated from Alaskan shorelines, but some small patches of sequestered subsurface oil residue still remain 20 years after the spill where there is limited water flow. There is ongoing debate as to whether to leave the buried oil residues in place or whether to attempt to supply oxygen and nutrients in an effort to stimulate biodegradation today. The BP MC252 spill was in deep water. Physical and chemical dispersion of the MC252 oil released into the Gulf of Mexico between April 20 and July 15, 2010 resulted in a cloud of fine droplets at approximately 1100-1200 meters that generally moved in a southwesterly direction while larger droplets moved to the surface and formed slicks. During the release (April-July), concentrations of TPAH attenuated rapidly with distance from the release point (the wellhead). Reductions in concentrations as the oil moved away from the wellhead were accompanied by a decreasing ratio of C17/pristane and C18/phytane and degradation of PAHs based on ratios to the conserved hopane. The half lives for hydrocarbons in the deep sea cloud of oil was estimated to be only a few days, while oil in the surface was biodegraded more slowly.

Organic matter mineralization and trace element post-depositional redistribution in Western Siberia thermokarst lakes

S. AUDRY[1]*, O.S. POKROVSKY[1], L.S. SHIROKOVA[1], AND S.N. KIRPOTIN[2]

[1]Université de Toulouse, GET, 14 Av, Edouard Belin, F-31400 Toulouse, France (*correspondence: stephane.audry@get.obs-mip.fr)

[2]Tomsk State University, 36, Lenina Prospekt, Tomsk, 634050, Russia

This study was based on high-resolution sampling of sediments and their porewaters from three thermokarst lakes representing different stages of ecosystem maturity development located within the Nadym-Pur interfluve of the Western Siberia plain. Up to present time, the lake sediments of this region remain unexplored regarding their biogeochemical behavior. The aim was to document the early diagenesic processes to assess their impact on the organic carbon previously sequestrated in the underlying permafrost, and the post-depositional redistribution of trace elements (TE) and their impact on the water column.

Mineralization of organic matter (OM) in the sediments proceeded under anoxic conditions in all the three lakes. In the course of the ecosystem maturity development, a shift in OM mineralization pathways was evidenced with Fe- and Mn-oxyhydroxides (FMO) representing the main terminal electron acceptors in the early diagenetic reactions for the most mature stage. This shift was promoted by the diagenetic consumption of nitrate and sulfate and their gradual depletion in the water column due to progressively decreasing peat lixiviation occurring at the lake's borders. Early diagenesis was responsible for TE post-depositional redistribution. TE were mobilized from host phases (OM and FMO) and partly sequestered in the sediment in the form of authigenic Fe-sulfides. Arsenic and Sb cycling was also closely linked to that of OM and FMO. Shallow diagenetic enrichment of particulate Sb was observed in the less mature stages. As a result of authigenic sulfide precipitation, the sediments of the early stage of lake maturation were a sink for water column Cu, Zn, Cd, Pb and Sb. In contrast, all sediments were a source of dissolved Co, Ni and As to the water column. However, the concentrations of these TE remained low in the bottom waters, indicating that sorption processes on Fe-bounding particles and/or large-size colloids could mitigate the impact of post-depositional redistribution of toxic elements on the water column.

https://doi.org/10.1180/S0026461X00006502 Published online by Cambridge University Press

C- and S-transfer in subduction zones: Insights from diamonds

S. AULBACH[1,2], T. STACHEL[1], L.M. HEAMAN[1], R.A. CREASER[1], E. THOMASSOT[3] AND S.B. SHIREY[4]

[1]University of Alberta, Edmonton AB Canada
[2]Goethe-Universität, Frankfurt Germany, (s.aulbach@em.uni-frankfurt.de)
[3]Carnegie Institution-DTM, Washington, DC USA
[4]CRPG-CNRS, Nancy France

The formation of eclogitic and pyroxenitic diamonds may occur during subduction-related redox reactions. Sulphide-bearing diamonds and diamondiferous xenoliths from the central Slave craton (Diavik and Ekati pipes) are used to trace the mobility of C and S up the slab and mantle wedge.

There, eclogitic diamond formed along fluid conduits ca 1.85 Ga ago, penecontemporaneously with subduction beneath the western craton margin and with eclogitisation of basaltic protoliths. The radiogenic initial $^{187}Os/^{188}Os$ of the eclogitic sulfide inclusions is consistent with diamond formation in matured, high Re/Os oceanic basaltic crust. This may indicate that S in the inclusions was derived in situ, which is supported by fractionated S isotopes of eclogitic sulphide inclusions. Mantle-like $\delta^{13}C$ of associated diamonds suggests derivation of the carbon from reducing serpentinised oceanic mantle, which dehydrates at a depth consistent with diamond formation.

Subducting oceanic crust may release silicic melts that react with mantle wedge peridotite to form pyroxenite. A low-temperature pyroxenite xenolith has an age and initial $^{187}Os/^{188}Os$ that is identical to eclogitic inclusions in diamond, indicating that it inherited its radiogenic initial Os and S from oxidising slab-derived melt. Formation at shallow depth near the graphite-diamond transition and presence of an oxidised mantle wedge prohibits enough reduction to allow diamond formation from the slab melt and may explain why this lithology is rarely represented amongst diamonds from the central Slave craton.

A distinct group of sulphide inclusions in diamond, with Ni content similar to peridotitic inclusions, but 20 x lower Os contents have very unradiogenic Os but yield a Re-Os isochron age of 1.70±0.26 Ga, within error of the age of accretion at the craton margin. We suggest the diamonds formed through interaction of reducing Os-poor fluids with oxidising wedge mantle that was dragged down to the depth of serpentinite dehydration. The fluids may have remained reducing by extraction along conduits armoured by a reaction assemblage. They facilitated isotopic rehomogenisation of part of the mantle wedge, but did not add Os to the source. $\delta^{13}C$ will be measured soon to determine the carbon source.

Efficient analysis of seawater thorium and protactinium

M.E. AURO[1]*, L.F. ROBINSON[1,2], R. ANDERSON[3], M. FLEISHER[3] AND M.A. SAITO[1]

[1]Woods Hole Oceanographic Institution, Woods Hole, MA 02543 USA (*correspondence: mauro@whoi.edu); (msaito@whoi.edu)
[2]University of Bristol, BS8 1RJ, Bristol UK (lrobinson@whoi.edu)
[3]Lamont-Doherty Earth Observatory, Palisades, NY 10964 USA (boba@ldeo.columbia.edu; martyq@ldeo.columbia.edu)

With the advent of GEOTRACES, the requirement to analyse large numbers of seawater samples for ^{232}Th, ^{230}Th and ^{231}Pa has become more widespread. During the international intercalibration exercise we encountered unexpected difficulties with recovery and contamination of these isotopes, especially ^{232}Th. Multiple experiments were executed to identify the source of these issues. Two particular problems were (a) frits in columns supplied by Biorad contain isotope-binding surfactants and (b) new batches of Biorad AG1x-8 resin release more than 100pg of ^{232}Th after standard column cleaning. To improve yield (to 90%) and blanks (to 5pg ^{232}Th) we implemented a range of improvements including switching to Eichrom anion exchange resin and Environmental Express columns. In addition, we used Eichrom pre-filter resin to remove organics and prevent clogging during sample analysis. All Th samples were analysed on a Neptune multi-collector using peak hopping of ^{230}Th and ^{229}Th on the central SEM, with either ^{232}Th, ^{236}U (or both) used to monitor for beam intensity. We used two in-house laboratory standards to check for machine reproducibility, and the GEOTRACES intercalibration standard to check for accuracy. Over a one year period the 2 stdev reproducibility on the standard ^{232}Th concentration was 2.8% including all analyses, and 2% once contamination and yield issues had been resolved.

We apply the improved method to seawater samples in depth profiles collected from stations close to Bermuda and from 12.5S in the S. Atlantic (CoFeMUG cruise) and compare those data to published water column data. Apart from the very bottom waters and surface waters, both of which have elevated values, BATS samples average 79 pg/kg ^{232}Th. The ^{232}Th concentration in the S. Atlantic is higher throughout the water column with an average value of 195 pg/kg. In both cases ^{230}Th increases with depth, with the rate of increase greater in the S. Atlantic as expected from published water column profiles.

https://doi.org/10.1180/S0026461X00006502 Published online by Cambridge University Press

Geochemistry and mineralogical composition of the airborne particles of sand dunes and dust storms settled in Iraq and their environmental impact

SALIH MUHAMMAD AWADH

Earth Sciences Department, College of Science, University of Baghdad, Baghdad, Iraq. (Salihauad2000@yahoo.com)

Introduction

Five dust storms that are blown in 2008 and sand dunes disseminated in the Western Desert of Iraq are sampled. This work is going to discuss the origin of dust that blow on Iraq, and their environmental impacts.

Results

The enrichment of SiO_2/Al_2O_3 by mechanical and chemical processes produces quartz arenites (Orthoquartzites) [1]. Heavy minerals in dust storm and sand dunes formed 2.3% and 6.6% respectively. Clay appears to be domennanted (Figure 1).

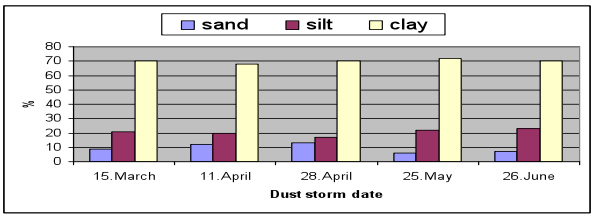

Figure 1: Average distribution of grain sizes in dust storm samples.

Conclusions

The Sahara of North Africa, lands in Saudi Arabia going to desertification. They provided 7 million tons of clayey dust during 8 dipping temperature 6ºC.

[1] Obiefuna, G.I. and Orazulike, D.M (2011) *Research Journal of Environmental and Earth Sciences* **3**(2): 95-102.

Reduction of carbon tetrachloride by organo-green rust

K.B. AYALA-LUIS, NICOLA G.A. COOPER*, C.B. KOCH AND H.C.B. HANSEN

Dept. Basic Sciences and Environment, University of Copenhagen, Thorvaldsensvej 40, DK-1871 Frederiksberg C., Denmark (*correspondence: ngac@life.ku.dk)

Layered Fe^{II}–Fe^{III} hydroxide salts (green rusts, GR) are redox reactive materials that are formed in anoxic soils and sediments and when iron corrodes. GRs are powerful reductants of environmental pollutants [1, 2]. GR intercalated with surfactants (organo-GR) is a new type of reactive hydrophobic material that has been recently synthesized in laboratory scale [3]. Due to the presence of structural Fe^{II} and a hydrophobic interlayer, organo-GRs are expected to react preferentially with non polar contaminants. Hence, the reductive properties of the novel organo-GRs were examinated against carbon tetrachloride (CT).

In the present work, we demonstrate that organo-GR can directly reduce carbon tetrachloride into less harmful non-chlorinated compounds (*in casu* carbon monoxide and formate). Chloroform (CF) was also formed as a minor end product (< 5%). Reduction of CT with other iron (hydr)oxides than GR formed mainly chloroform and other less chlorinated compounds [4]. The formation of less chlorinated compounds proceeds via hydrogen abstraction of trichloromethyl radicals ($\bullet CCl_3$) and/or protonation of the trichloromethyl carbanion ($:CCl_3^-$) following the hydrogenolysis pathway. The hydrophobic interlayer of organo-GRs may stabilize both the radical and the carbanion, sheltering them from proton donors and directing the reactions towards the formation of carbon monoxide and formate. Analyses of chloride in the reactions confirm the complete dechlorination of CT. These findings suggest that organo-GRs are promising reactants for remediation of groundwater and soil contaminated by chlorinated solvents.

[1] Hansen *et al*. (1996) *Environ. Sci. Technol*. **30**, 2053-2056. [2] Erbs *et al*. (1999) *Environ. Sci. Technol*. **33**, 307-311. [3] Ayala-Luis *et al*. (2010) *Appl. Clay Sci*. **50**, 512-519. [4] Mccormick *et al*. (2004) *Environ. Sci. Technol*. **38**, 1045-1053.

https://doi.org/10.1180/S0026461X00006502 Published online by Cambridge University Press

Geochemical and Sr-Nd isotopic characteristics of the calc-alkaline volcanic rocks from Borçka (Artvin): Implications for genesis of Tertiary magmatism in the Eastern Pontides (NE Turkey)

E. AYDINÇAKIR[1]* AND C. ŞEN[2]

[1]Dept Geol Engn., Gümüşhane Univ.,TR-29100 Gümüşhane, Turkey (*correspondence:aydincakir61@gmail.com)
[2]Dept Geol Engn, Karadeniz Tech Univ., TR-61080 Trabzon, Turkey (csen@ktu.edu.tr)

Whole-rock geochemistry and Sr-Nd isotopic data are reported for the Tertiary Borçka (Artvin) volcanics in the eastern Pontide orogenic belt (NE Turkey). Borçka (Artvin) volcanics were made of two groups that comprise of basalt-basaltic andesite-basaltic trachyandesite (Group A) and andesite-trachyandesite (Group B). The Group A contains plagioclase (An_{31-93}), clinopyroxene ($Wo_{38-48}En_{38-44}Fs_{8-17}$), hornblende ($Mg^{\#}$=0.57-0.72) phenocrysts and titanomagnetite microphenocrysts, whereas the Group B rocks include plagioclase (An_{52-93}), clinopyroxene, hornblende ($Mg^{\#}$=0.64-0.71) phenocrysts and titanomagnetite and apatite microphenocrysts with porphyritic, microlitic porphyritic, hyalo-microlitic porphyritic, fluidal and cumulophiritic textures.

Petrochemically, the volcanic rocks show calc-alkaline character with their medium K contents. They are enriched in LREE and LILE, with pronounced depletion of HFSE. The chondrite-normalized REE patterns (La_N/Lu_N=1-7) show low to medium enrichment, indicating similar sources for the rock suite. Textural features and calculated pressures based on the Cpx-barometer in each series indicate that the calc-alkaline magma equilibrated at shallow crustal depths under a pressure of about 2-7 kbar and approximating a crystallization depth of 5-18 km.

The Borçka (Artvin) volcanics are slightly depleted in isotopic composition. $^{87}Sr/^{86}Sr$ values vary between 0.70423 and 0.70511 while $^{143}Nd/^{144}Nd$ values change between 0.51266 and 0.51288. Sr-Nd isotopic ratios imply that the rocks derived from depleted mantle source in their origin. The increasing values of SiO_2 (wt.%), Sr (ppm) and $(1/Sr)x10^3$ ppm^{-1} versus $(^{87}Sr/^{86}Sr)_I$ values reveal fractional crystallisation (FC) rather than assimilation (AFC) in their evolution.

Low molybdenum isotope compositions in euxinic Sapropel S1

I. AZRIELI[1]*, A. MATTHEWS[1], M. BAR-MATTHEWS[2], A. ALMOGI -LABIN[2], D. VANCE[3], C. ARCHER[3] AND N. TEUTSCH[2]

[1]Institute of Earth Sciences, Hebrew University of Jerusalem, Israel (*correspondence: irit.azrieli@mail.huji.ac.il)
[2]Geological Survey of Israel, Jerusalem, 95501 Israel
[3]Bristol Isotope Group, School of Earth Sciences, University of Bristol, UK

Molybdenum isotopes are a powerful proxy for paleoredox conditions in organic-rich sediments. Here, we apply this isotopic system to a Holocene S1 sapropel layer sampled at 2550m depth in the Eastern Mediterranean Sea (ODP core 967D). Our study utilizes the isotopic systems of Mo and Fe, together with geochemical tracers (Ba/Al, Fe_T/Al, Mn/Al, S) to explore the relationship between the sapropel formation conditions and the Mo paleoredox proxy.

Euxinic (sulphidic) bottom water conditions during the sapropel formation are supported by Fe isotopic composition, which shows negative correlations between $\delta^{57}Fe$ and Fe_T/Al and S wt%. This is consistent with the benthic Fe shuttle model whereby Fe is exported from the oxic shelf to the deep euxinic basin[1]. The Mo paleoredox model for highly sulphidic restricted marine systems envisages organic-rich sediments acquiring Mo isotope signatures of sea water ($\delta^{98}Mo$ = 2.3‰) due to the quantitative removal of Mo from the sulphidic water column. This scenario is not realized in the 967D profile, which shows a decrease in $\delta^{98}Mo$ values from *ca* 0‰ in the pre-sapropel sediment to negative values of -0.8‰ within the sapropel, before gradually rising to values of 0 to 0.4‰ in the overlying post-sapropel sediment. Negative linear correlations between $\delta^{98}Mo$ values and Fe_T/Al, Ba/Al, Mo/Al and S indicate that maximum euxinic conditions are associated with the lowest Mo isotopic compositions.

The low $\delta^{98}Mo$ values are potentially compatible with sulphidization of Mo in mildly sulphidic euxinic conditions [2,3]. Nevertheless, increasing euxinia should lead to positive correlations between $\delta^{98}Mo$ and the geochemical proxies. Thus, additional factors such as open system conditions for Mo uptake may be required to explain the full workings of the Mo paleoredox proxy.

[1] Lyons *et al* (2009), *Annu. Rev. Earth Planet. Sci.* **37**, 507-534. [2] Neubert *et al* (2008), *Geology* **36**, 775-778. [3] Dahl *et al* (2009), *GCA* **74**, 144-163.

https://doi.org/10.1180/S0026461X00006502 Published online by Cambridge University Press

High-resolution, ultra-trace and major element chemical stratigraphy of a new Paleoproterozoic weathering profile

M.G. BABECHUK* AND B.S. KAMBER

Laurentian University, Sudbury, ON, Canada
(*correspondance: mbabechuk@gmail.com)

Paleosols contain information about ancient atmospheric and climate conditions, as well as the secular change in supply of nutrients to the ocean. A newly exposed, ~5 meters deep 1.85 Ga weathering profile is described. It developed on pillowed metabasalt (Flin Flon, Manitoba, Canada) and was sampled (~120 samples) and analyzed at much higher spatial resolution (>50 samples) than previous such profiles for ultra-trace, major element, and ferrous iron.

Consistent with previous studies on nearby paleosol exposures [1,2], the examined weathering profile is characterized by a spectacularly preserved, coherent upward Fe enrichment, accompanied by loss of Fe^{2+} and the development of a positive Ce anomaly, implying weathering in an oxic atmsophere. The new, high-precision trace element data collected reveal enrichment of several alkali (Cs, Rb, in addition to K, Na) and alkaline earth (Be, Sr, Ba) elements upward towards the paleosol contact with overlying sandstone. By contrast, the HFSE remained largely immobile in the profile which is evident through the highly consistent Zr/Hf, Th/Nb, and Nb/Ta ratios.

This presentation will discuss the distinction of original chemical features preserved in the profile, for example those inherited from the separate pillow basalt flows, versus those superimposed by weathering, water table fluctuation and possible extraneous sediment input.

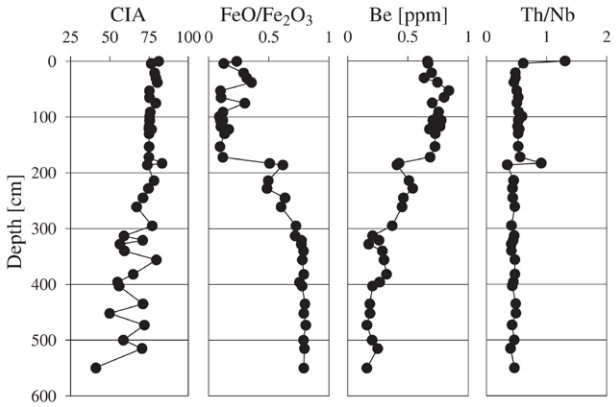

[1] Holland *et al*. (1989) *Am. J. Sci*. **289**, 362-389. [2] Pan & Stauffer (2000) *Am. Mineral*. **85**, 898-911.

The volcanic-plutonic connection

O. BACHMANN[1], C. DEERING[1], J. DUFEK[2] AND C. HUBER[2]

[1]Departement of Earth and Space Sciences, University of Washington, Seattle, USA
[2]School of Earth and Atmospheric Sciences, Georgia Institute of Technology, Atlanta, USA

The broad similarities in age and compositonal range found in plutonic and volcanic exposures from a given magmatic province clearly indicate that these rocks types are closely related genetically. However, to which extent plutons (particularly the ones with intermediate to silicic compositions) are former magma reservoirs that have lost melt remains controversial. Recent work using both geochemical and physical modeling provides new avenues to explore these issues that are fundamental to our understanding of crustal evolution. First, mechanical constraints on rates of crystal-liquid separation indicate that most chemical differentiation is likely to occur within an melt extraction window located between 50 and 80 vol% crystals across the whole range of magma composition (from mafic to silicic). This extraction window will lead to compositional gaps in extracted liquids, as observed in numerous volcanic series around the world. In contrast, plutonic exposures will span a range of compositions that will vary continously as a function of how much melt was lost at a given location. Trace element modelling suggest that variable degrees of crystal accumulations are common in all plutonic sequences, including in intermediate to silicic compositions (tonalites - granodiorites). We also report erupted crystal cumulates, excavated from shallow magma chambers during large explosive eruptions. Such findings, alongside with thermal models of magma-crust interaction, suggest that crystal fractionation occurring by melt extraction in mush zones, and accompanied by a limited amount of crustal assimilation, is the dominant differentiation process in the Earth's crust. In this framework, volcanic rocks mostly represent liquids extracted from different reservoirs while plutons typically correspond to the left-overs crystal mushes that have been periodically stripped from a fraction of their interstitial melts.

https://doi.org/10.1180/S0026461X00006502 Published online by Cambridge University Press

Enhancing the accuracy of the environmental monitoring systems in mining areas

CALIN BACIU, DAN COSTIN*, CRISTIAN POP AND LAURA LAZAR

Babes-Bolyai University, Faculty of Environmental Science and Engineering, Fantanele 30, 400294 Cluj-Napoca, Romania (correspondence: dan_fl_costin@yahoo.com)

Mining operations generally have a significant impact on the environment. Traditional monitoring by periodically performing field measurements, sampling, and lab analyses is laborious, costly, and not always reproducible and reliable. Abundant series of monitoring data may be obtained by installing continuous measuring devices in selected points. In most of the mining areas, the number of such monitoring points is rather limited. The data series provided by such systems are usually interpreted as averages of the measured parameters for a certain area. Very often, this is not the case, either due to the limited representativity of the selected points, or because of the high dynamic of the environmental parameters. The environmental issues related to mining have become an ever increasing concern all over the world, with a direct impact on the prices of commodities, as opening a new mine is getting more and more difficult. A cost-effective and precise monitoring system is essential in the management of the environmental problems. Providing accurate monitoring data may also increase the confidence and acceptance of the communities and other stakeholders towards the mining activity. New methods and tools are needed for accomplishing this goal.

The EU-funded project ImpactMin (www.impactmin.eu) develops a combination of satellite remote sensing and aerial lightweight measurements for obtaining new methods of environmental monitoring in mining areas. Four test-sites were selected for calibrating and demonstrating the new toolset. Rosia Montana test-site (Romania) has a particular position in this context, as the cumulated impact of almost 2,000 years of gold mining can be observed. Currently the mine is inactive, the operations ceased in 2006 due to economic reasons. A new mining project is proposed on the same location, intending to implement a large scale open pit operation. The newly developed monitoring methods may represent an important contribution to the proper definition of the environmental baseline conditions, should the mining operations re-start.

Acknowledgements: The present work was financially supported by the FP7-ENV-2009-1 project 244166 – ImpactMin.

Distribution of rare elements in mineral-forming environments of rare-metal granites

E.V. BADANINA[1], A.Y. BORISOVA[2], R. THOMAS[3] AND L.F. SYRITSO[1]

[1]St.Petersburg State University, St.Petersburg, Russia (elena_badanina@mail.ru)

[2]University of Toulouse III – CNRS – IRD – OMP, France (borisova@lmtg.obs-mip.fr)

[3]German Research Centre for Geosciences GFZ Potsdam, Germany

The composition of melt and its evolution in space and time is traced at formation of ore-bearing Li-F granites and them sub-effusive analogs (ongonites, rhyolites, felsit-porphyries) from Orlovka, Etyka and Sherlovaja Gora in Transbaikalia (Russia) on the basis of melt inclusions study in quartz [1]. It is established that process of fractional crystallization is not the unique mechanism of concentration of LILE (Li, Rb, Cs) and HFSE (Nb, Ta, Zr, REE, W, Sn). A role of various mechanisms of concentration (fractionation, liquid immiscibility, metasomatism) estimate by calculation of distribution coefficients and saturation degree of melt for ore minerals. Contrast behavior of various rare elements is established at different stages of melt evolution [1]. High concentration of Li, B, Ta, Zn are found out in hydrosaline and fluid inclusions of Orlovka [2]. High concentration of some rare elements are found out in fluid inclusions (FI) in quartz from Sn-bearing rhyolites of Sherlovaya Gora by LA-ICP-MS. So, the Sn concentration varies from 1864 to 5879 ppm that explains formation of large tin deposit with finely dispersed cassiterite at a hydrothermal stage. High concentration of Zr in a fluid (to 1,5 wt %) from ultrapotassic felsite-porphyriy explains the formation here saturation zones of fine crystalline zircon in a topaz from famous a topaz-aquamarine greisen of Sherlovaya Gora and confirms probability of its crystallization at a hydrothermal stage. High uranium concentration in melt of rhyolites (up to 42 ppm U) exceed those in rhyolites of a Streltsovsky deposit. Sharp increase of U in FI up to 116 ppm unequivocally testifies to a potential role of rhyolites in genesis of uranium deposits of Transbaikalia that closes discussion about a source of uranium for them.

[1] Badanina *et al*. (2010) *Petrology*. **18**. 139-167. [2] Thomas *et al*. (2009) *Min Petrol*. **96**. 129-140.

https://doi.org/10.1180/S0026461X00006502 Published online by Cambridge University Press

Orbital scale alkenone based CO_2 records across the Pliocene intensification of Northern hemisphere glaciation

M.P.S. BADGER[1]*, G.C. BOWLER[1], C. DAVIS[2], A.C. HULL[1], M.D.A. POTTS[2], D.N. SCHMIDT[2] AND R.D. PANCOST[1]

[1]Organic Geochemistry Unit, School of Chemistry, University of Bristol, Cantock's Close, BS8 1TS, U.K. (*correspondance: marcus.badger@bristol.ac.uk, gb6139@bristol.ac.uk, ah7523@bristol.ac.uk, R.D.Pancost@bristol.ac.uk)

[2]Department of Earth Sciences, University of Bristol, Wills Memorial Building, Queen's Road, BS8 1RJ, U.K. (cd9861@bristol.ac.uk, mp0702@bristol.ac.uk, D.Schmidt@bristol.ac.uk)

The most informative analogues for future anthropgenic climate change are likely to be those with boundary conditions similar to today. The late Pliocene is the most recent time in earth history with elevated global temperatures and CO_2 estimated to be similar to that anticipated by the end of this century [1, 2, 3]. Furthermore, Pliocene continental positions and vegetation distributions are thought to be broadly similar to today. Consequently the IPCC fourth assessment report highlighted the Pliocene as an important time period for further study. Recently our understanding of Pliocene CO_2 and temperature has improved, with publication of multiple records from alkenone and boron isotope reconstructions for CO_2 [2, 3], and Mg/Ca, $U^{K'}_{37}$ and TEX_{86} reconstructions for sea surface temperature. However, none of the published CO_2 records have sufficient temporal resolution to resolve orbital scale variations in CO_2, or to determine the relationship between the apparent reduction in atmospheric CO_2 and the intensification of northern hemisphere glaciation. Here we present new high resolution records of CO_2 and temperature from ODP Site 999 over the critical interval from 3.3 to 2.6 Ma using alkenone palaeobarometry and the $U^{K'}_{37}$ and TEX_{86} palaeothermometers. By combining these with a full analysis of the biotic response to changing conditions and reconstructing haptophyte cell sizes [4], critical for the alkenone palaeobarometer, we present well constrained, coupled records of the response of the climate system to changing CO_2.

[1] Haywood *et al*., (2000) *Geology* **28**, 1063-1066. [2] Seki *et al*., (2010) *EPSL*. **292**, 201-211. [3] Pagani, *et al*., (2009) *Nature Geoscience*. **3**, 27-30. [4] Henderiks & Pagani, (2007) *Paleoceanography*. **22**, 1-12.

A multidisciplinary study of core composition

JAMES BADRO

Institut de Physique du Globe de Paris, France. (badro@ipgp.fr)

Planetary cores form as a results of the major chemical differentiation even on a terrestrial planet; the melting of accretionary building blocks (dust, meteorites, planetesimals, protoplanets) leads to a separation of the metal from the silicate, ensued by a gravitationally-driven segregation of a dense metal-rich core at the centre of the planet, with the lighter buoyant silicates remaining on top. The process of core formation determines the composition of this deep reservoir, and leaves an imprint on the residual bulk silicate Earth.

Matching geophysical observables (seismically determined radial density and velocity profiles) and geochemical observables (siderophile trace-element concentration in the upper mantle, and through modelling in the bulk silicate Earth) with experimental and theoretical data provides a robust way to estimate both the present day composition of the core as well as the conditions under which it formed. Adding observational constraints, both from geophysics (gradients, anisotropy) and geochemistry (isotopic and trace-element fractionation) will help to continually improve the models and beyond that, define and refine the paradigm of core formation.

We will present the results obtained through (i) the study of phase equilibrium under extreme conditions in the laser-heated diamond anvil cell, (ii) the study of outer-core density and seismic velocity from first principles calculations, and (iii) the study of inner-core elasticity from experimental mineral physics. We will interpret these results in order to devise compositional models consistent with the observations, and to formulate scenarios for core formation.

https://doi.org/10.1180/S0026461X00006502 Published online by Cambridge University Press

Boundary depth of aragonite saturation during 10 years around Okinawa and East China Sea

D-Y. BAEK[1], H. FUJIMURA[1]*, T. OOMORI[1], T. HIGUCHI[2], B.E. CASARETO[2] AND Y. SUZUKI[2]

[1]Univ. of the Ryukyus, 1 Senbaru, Nishihara, Okinawa 903-0213, Japan (*correspondance: fujimura@sci.u-ryukyu.ac.jp)

[2]Shizuoka Univ., 836 Ohya, Suruga-ku, Shizuoka-shi, Shizuoka 422-8529, Japan

Introduction

Since industrial evolution, anthropogenic activities have been releasing CO_2 by fossil fuels combustion. Ocean absorbs about 2.0 Gt of CO_2 every year and act as a sink for atmospheric CO_2 [1]. However CO_2 dissolved into seawater lower the ocean pH and CO_3^{2-} concentration. About 0.1 pH unit has already been decreased since industrial evolution. Lower pH have influences on marine organisms especially on growth of calcareous foraminifera and corals as one of the problem in "ocean acidification". Because lower CO_3^{2-} caused lower aragonite saturation of $CaCO_3$, saturated boundary in the ocean is predicted to be shallower in the future. In this study, we investigated carbonate system by taking vertical profiles around Okinawa and East China Sea to find the shift of the boundary depth over the past 10 years.

Materials and Methods

Seawater samples were taken from East China Sea and adjacent sea around Okinawa Island, Japan at scientific survey of T/S *Nagasaki-maru* in 2000 to 2010. Parameters related to carbonate system were measured on total alkalinity (ATT05, Kimoto), total inorganic carbon (CM5012, UIC), pH and salinity (PortaSal8410A, Guildline). Aragonite saturation of $CaCO_3$ (Ω) was estimated from a calculation of carbonate chemical equilibrium in seawater samples taken at each depth of vertical profile.

Results and Discussion

The boundary depth at which aragonite saturation shows below a saturation level (i.e. Ω=1) were 537±36 m from a surface (averaged value during 2000-2002). This boundary depth was shifted to 513 m during 10 years. Although this value was within the range of uncertainties, the shift indicated that the intrusion of the anthropogenic CO_2 caused lower CO_3^{2-} and hence shallower depth of the saturation boundary.

[1] Takahashi *et al*. (2002) *Deep-Sea Res. II* **49**, 1601-1622.

Study of geochemical reaction of rocks the under the supercritical CO_2-rock-groundwater system

KYOUNGBAE BAEK*, HYUNMIN KANG, JINYOUNG PARK AND MINHEE LEE

Department of Environmental Geosciences, Pukyong National University, Namgu, Busan, 608-737, Korea (*darkbkb@naver.com)

Laboratory scale experiments to quantify the geochemical reaction in the supercritical CO_2-rock-groundwater system for CO_2 sequestration sites were performed in the high-pressurized cell. Seven types of rocks were cut into 1 cm x 1 cm x 0.3 cm size sections. Polished rock sections (granite, basalt, andesite, gneiss, limestone, sandstone and mudstone) and groundwater of 100 ml were reacted with supercritical CO_2 in the cell, maintaining the sequestration condition (100 bar and 50 °C). The gaseous CO_2 (99.99 % of purity) was injected into the cell and the high pressure condition was applied inside of the cell by using the periodic high pressure pump and the back pressure regulator. The temperature of the cell was maintained at 50 °C by using an oven. Each rock section was reacted with the supercritical CO_2 and groundwater for 10, 30 and 60days.

Before the experiment, the rock dried at 100 ℃ for a day and accurately weighed. After the reaction, the rock dried and reweighed to investigate the loss of minerals by dissolution. The alteration of pH was measured to compare before/after reaction. Rock surface was observed by using a reflecting microscope. Selected three minerals for each rock and three locations of each mineral on the rock surface were randomly selected for the image analysis of Scanning Probe Microscope (SPM). The average roughness value of those locations was measured to investigate the transmutation of rock surface compared to that before reaction. ICP-OES analysis was conducted to measure the major element concentrations dissolved in solution of the high pressure cell. SEM/EDS analysis was also performed to identify the precipitates in high pressure cell after the reaction.

Results of the experiment in the supercritical CO_2-rock-groundwater reaction showed that the concentration of cations in solution increased and the pH of solution decreased after the reaction. The average roughness value of the mineral surface in the rocks increased after 30 days. From the analysis of SEM/EDS, the interstitial spaces of rock surface could be infilled by secondary minerals, resulting in the change of void spaces (porosity) in the rock.

https://doi.org/10.1180/S0026461X00006502 Published online by Cambridge University Press

Controls on isotope and trace element systematics of slope facies Ediacaran carbonates, Yangtze Platform (South China)

W. BAERO*, H. BECKER AND U. WIECHERT

Institut für Geologische Wissenschaften, Freie Universität Berlin, Malteserstr. 74-100, 12249 Berlin, (*correspondence: wbaero@zedat.fu-berlin.de)

Trace element, Sr, C and O isotopic compositions of Ediacaran carbonates are used to assess the likely role of diagenetic processes and alteration by lokal fluid flow, relative to primary seawater derived signatures. The samples are from the slope facies Panmen section (Songtao, Guizhou) of the Yangtze Platform, South China. The section comprises the Ediacaran Doushantuo (DS) and Liuchapo Formations. At this section, carbonate bearing lithologies are restricted to the DS members I (cap carbonates in contact with Marinoan diamictites), III (dolostones and limestones) and IV (organic rich carbonate layers and carbonate concretions in black shales). Most of DS II appears to be missing from this section. Carbonates show variable negative $\delta^{18}O$ (-6 to -14) and $\delta^{13}C_{carb}$ (-2 to -10) values similar to DS I and III sediments at sections representing shallow water conditions. Acetic acid leachets of carbonates display decreasing $^{87}Sr/^{86}Sr$ upsection from high and variable values in DS I (0.722-0.717) to lower values in DS III (0.716-0.713). Ce/Ce* are near 1, with a few values significantly higher. The uppermost samples of DS IV show Ce/Ce* = 0.5 at $\delta^{13}C_{carb}$ of -1. Some of the extreme values in $\delta^{18}O$ are coupled with positive Ce (Ce/Ce* = 1.22) and Eu (Eu/Eu* = 1.33) anomalies, and particularly high $^{87}Sr/^{86}Sr$. Carbonate concretions in black shales of DS IV have extremely negative $\delta^{18}O$ but display normal $\delta^{13}C$, slightly neg. to no Ce/Ce* and strongly pos. Eu/Eu*. $^{87}Sr/^{86}Sr$ in the concretions are the lowest measured in the section (0.709), similar to values obtained for DS IV from shallow platform settings [1]. Most $^{87}Sr/^{86}Sr$ values of the section are substantially higher than seawater values during this time (0.708-0,709, [1]). High values of $^{87}Sr/^{86}Sr$, Ce/Ce* or negative $\delta^{18}O$ do not correlate with the amount of detrital material in the carbonates. Hence, we interprete high $^{87}Sr/^{86}Sr$ and Sr/Mn and the occasional presence of positive Ce anomalies to reflect recrystallization and interaction with reducing fluids that have interacted with silicate and organic material (and occasionally Fe-Mn oxides?) during the postdepositional evolution of the basin. The influence of these processes on $\delta^{13}C_{carb}$ is sometimes visible, but appears to be at the 1 ‰ level or less.

[1] Sawaki *et al*. (2010) – *Precambr. Res*. **176**, 46-64.

Fluid-rock interaction during eclogitisation: Evidence from HP metamorphic rocks from Sulawesi, Indonesia

R. BAESE* AND V. SCHENK

SFB 574: Volatiles and Fluids in Subduction Zones, Christian-Albrechts-University, 24118 Kiel, Germany (*correspondence: rb@min.uni-kiel.de)

Fluid-rock interactions within subduction zones are important for understanding recycling processes and magma generation at convergent margins that is triggered by fluid infiltration from the subducting slab. The aim of this study is to determine the composition of fluids liberated during eclogitisation reactions. The samples are high-pressure (HP) rocks from the Bantimala Complex in Sulawesi (Indonesia) that is part of the Cretaceous accretionary complex distributed all over Indonesia [1]. The eclogites are forming veins and vein networks within blueschists. The peak P-T-conditions are about 2.0-2.5 GPa and 450-550 °C. Trace element analyses of a relatively Cr-rich eclogite-blueschist pair reveal a pronounced depletion of fluid-mobile elements in the eclogite. Mass balance calculations show that the rock lost more than 80% of the REE during the fluid induced eclogitisation along the vein. The LILE (Cs, Ba, Rb, Sr), except K, are also depleted with up to 80%. In case of the HFSE (Pb, Zr, Hf, Ti, Nb) there is no depletion, and Zr, Hf and Ti are even enriched in the vein. Major element concentrations were not strongly affected by the dehydration process during eclogite formation. From these observations we deduce that the fluid produced during the blueschist-to-eclogite transformation in the veins should be enriched in the LILE and REE. The concentrations of the HFSE, Fe and Ni should be relativly low in the fluid, because these elements were incorporated in the vein minerals. These results are in agreement with those of a previous study by John *et al*. [2], who concluded that the mobilised elements during eclogitisation are those believed to be contained in slab fluids that trigger partial melting in the mantle wedge.

[1] Parkinson *et al*. (1998) *The Island Arc* **7**, 184-200. [2] John *et al*. (2008) *Lithos* **103**, 1-24.

https://doi.org/10.1180/S0026461X00006502 Published online by Cambridge University Press

Many-body effects in XPS and chemical bonding

P.S. BAGUS[1]*, C.J. NELIN[2], H.-J. FREUND[3] AND E.S. ILTON[4]

[1]Chemistry, University of North Texas, Denton, TX 76203-5017, USA (*correspondence: bagus@unt.edu)
[2]C. J. Nelin Consulting, Austin, Texas 78730, USA
[3]Fritz-Haber-Institut der Max-Planck-Gesellschaft, Faradayweg 4-6, D-14195 Berlin, Germany
[4]Pacific Northwest National Laboratory, 902 Battelle Blvd., P.O. Box 999, Richland, Washington 99352, USA

A major goal with x-ray photoelectron spectroscopy (XPS) is to derive both the character of chemical bonding and valence states from the spectra. Ionic compounds, especially oxides, often have complex and intense satellite features that arise from a combination of inter-atomic and intra-atomic many-body effects that can reflect both bonding and oxidation state. [1] While multiplet splittings arise dominantly from the open-shell structure within the ionized atom, [2] inter-atomic many-body effects may also make important contributions to the satellite structure. [1] Although these inter-atomic effects have been studied extensively, a quantitative and definitive connection between the relative energies and intensities of the satellites on the one hand and both the extent of covalent bonding and oxidation state on the other, has not been established. In the present work, we consider two oxides, UO_3 and CeO_2, where the metal cations are closed shell, which increases the importance of inter-atomic relative to intra-atomic many body effects. The CeO_2 satellites are intense while the UO_3 satellites are weak. We have established relations between the satellite energies and intensities with the extent of the covalent bonding. This theoretical information has been obtained using relativistic many-body molecular orbital wavefunctions. With these wavefunctions, the covalent character of the orbitals arises naturally. This work is an important step toward inferring material properties of interest to both geochemistry and more generally chemistry from the XPS satellite structure. This research was supported, in part, by the Geosciences Research Program, Office of Basic Energy Sciences, U. S. Department of Energy (DOE) and Geosciences Research Program, Office and, in part, by the German Science Foundation (DFG).

[1] Bagus *et al. (2010) Chem.* Phys. Lett. **487**, 237-240. [2] Bagus & Ilton, (2006) *Phys. Rev. B* **73**, 155110.

Whole rock and mineral composition constraints on the genesis of the giant Hongge Fe-Ti-V oxide deposit in the ELIP, SW China

Z.-J. BAI[1], H. ZHONG[1,*], C. LI[2], W.-G. ZHU[1] AND G.-W. XU[1]

[1]SKLODG, Institute of Geochemistry, CAS, Guiyang 550002, China (* correspondence: zhonghong@vip.gyig.ac.cn)
[2]Department of Geological Sciences, Indiana Univ., Indiana 47405, USA

The Hongge giant Fe-Ti-V oxide ore deposit, related to a plume activity (~260 Ma), is hosted in a layered intrusion located in the central part of the Emeishan Large Igneous Province (ELIP), SW China. Most of the economic Fe-Ti-V oxide ore layers occur within the middle clinopyroxenite zone of the intrusion. Opinions on the origin of the oxides vary from oxide-silicate liquid immiscibility to accumulation of titanomagnetite crystallizing from a basaltic magma.

Our new results favor the crystallization model. The occurrence of multiple Fe-Ti oxide layers within a single cyclic unit and the repetitive appearance of sulfide, olivine and Cr-rich magnetite in the base of each cyclic unit suggest that multiple pulses of magma was involved in the formation of the Hongge Fe-Ti-V oxide deposit. Magnetite and coexisting olivine in the Hongge deposit have much higher MgO contents than those in other oxide deposits associated with large layered intrusions in the world, underscoring the importance of relatively primitive parental magma and relatively early saturation of titanomagnetite in the magma in the formation of the giant Fe-Ti-V oxide deposits in the ELIP.

Phase equilibrium constraints suggest that the Hongge parental magma is similar to that of some most primitive Emeishan high-Ti basalts. Depletion of incompatible trace elements in the oxide ores and associated rocks in the intrusion as compared to the coeval high-Ti basalts suggest that not all the magma involved in development of the Hongge intrusion has been retained. We propose that this intrusion was a magma conduit and that some of the liquid was lost to the peripheral sills, shallower intrusions or lavas.

https://doi.org/10.1180/S0026461X00006502 Published online by Cambridge University Press

2D geochemical-thermomechanical modelling of Pb, Hf, Sr and Nd isotopes evolution in intra-ocean subduction zones

B. BAITSCH GHIRARDELLO[1] , K. NIKOLAEVA[2], O. JAGOUTZ[3] AND T.V GERYA[1]

[1]Geophysical Institute, ETHZ, Switzerland
[2]Faculty of Earth and Life Sciences, VU Amsterdam
[3]Dept. of Earth, Atmospheric, and Planetary Sciences, MIT, Cambridge, MA, USA

Isotopes behave differently in different processes involved in a subduction zone such as slab dehydration, mantle wedge hydration and partial melting. Therefore, they are indicative of when and where different processes are active. The aim of this study is to extend the 2D coupled petrological–thermomechanical numerical model (I2ELVIS) of intra–oceanic subduction processes to include a treatment of isotopic signatures. With this extension we hope to gain more insights into the recycling system within the mantle wedge and are able to visualize the interaction between slab components and the depleted mantle. This will allow us to draw conclusions form isotopic signatures in arc lavas about the involved chemical processes.

A chemical contamination of slab components with wedge peridotite leads to specified signatures in arc magmas. Two slab components play a key role in this contamination: first, the altered oceanic basalt crust, and second its thin layer of sediment (e.g. Poli & Schmidt, 2002). Based on these results and the well known enrichment of LILE, Pb, U, and Th as well as the decrease of HFSE, Nd and Hf in island arcs in respect to the N-MORB, we focus on a limited number of elements (Pb, Hf, Sr and Nd) for our numerical model.

Our first results show that combination of finite differences and marker in cell techniques allows successful coupling of thermomechanical evolution of subduction with mobilisation, transport and radioactive decay of isotopes. Preliminary modelling results reconcile well with observations. Particularly, our models predict a significant increase of Strontium and Lead and a slight increase of Hafnium and Neodymium in the newly formed magmatic arc crust relative to the depleted mantle (DMM), which is comparable with data from the literature. In addition, our model confirmed the evidence for slab derived fluid /melt in the newly formed crust.

Pyromorphite formation from natural and surfactant-modified montmorillonite adsorbed lead

T. BAJDA[1]*, A. FIGUŁA[1], M. MANECKI[1] AND T. MARCHLEWSKI[2]

[1]Dept. of Geology, Geophysics and Environmental Protection, AGH University of Science and Technology, Krakow, Poland (*bajda@geol.agh.edu.pl)
[2]Dept. of Geological Sciences, Miami University, Oxford, Ohio, USA

The objective of this study was to evaluate potential application of natural and surfactant-modified montmorillonite for sorption of Pb^{2+} and subsequent pyromorphite formation by the reaction of Pb-adsorbed smectite with aqueous PO_4 of various concentrations. Amine hexadecyltrimethylammonium bromide (HDTMA-Br) in the amounts of 2.0 Cation Exchange Capacity (CEC) of the clay was used to obtain surfactant-modified organo-smectite.

The reaction of Pb-adsorbed natural montmorillonite with aqueous solutions containing PO_4 and Cl ions results in the decrease in phosphate concentration associated with the formation of a new phase – pyromorphite $Pb_5(PO_4)_3Cl$. Precipitation of brom-pyromorphite $Pb_5(PO_4)_3Br$ is observed when surfactant is used for modification of montmorillonite.

Pyromorphite precipitates homogenously in the solution but crystals generally cover the surface of smectite (Fig. 1a). High concentration of K and Ca cations leads to a high desorption of Pb and formation of very fine crystals. On the other hand, low concentrations of cations results in the formation of larger crystals.

When PO_4 was sorbed on Pb–surfactant-modified smectite, formation of brom-pyromorphite $Pb_5(PO_4)_3Br$ was noted in the reaction products. Pyromorphite forms crystals on the surface of a surfactant-modified smectite (Fig. 1b). We gratefully acknowledge support of the MNiSW through grant N N525 461236.

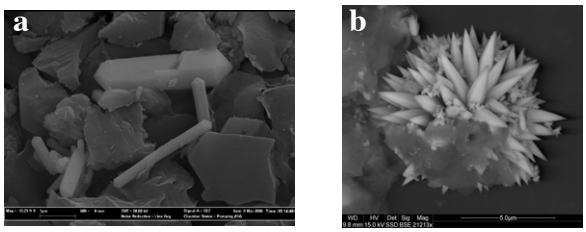

Figure 1: SEM microphotographs of (a) chlor-pyromorphite formed in the reaction of aqueous PO_4 and Pb-adsorbed montmorillonite, and (b) brom-pyromorphite formed in the reaction of aqueous PO_4 and Pb–surfactant-modified montmorillonite.

https://doi.org/10.1180/S0026461X00006502 Published online by Cambridge University Press

The influence of contaminant load on microbial ecology in a sandstone aquifer

K. BAKER[1,2], R. EDYVEAN[2], S. THORNTON[3], S. BANWART[2,3], J. SCHOLES[2] AND S. ROLFE[2]*

[1]School of Earth and Environment, University of Leeds, UK
[2]Cell-Mineral Research Centre, Kroto Research Institute, University of Sheffield, UK (*correspondence: s.rolfe@shef.ac.uk)
[3]Groundwater Protection and Restoration Group, University of Sheffield, UK

Due to widespread organic contamination derived from past industrial processes, microorganisms are becoming ever more important for the maintenance of potable groundwater supplies, as they have the ability to degrade organic contaminants *in situ*. Furthermore, the syntrophic relationships in mixed microbial communities found attached to geological surfaces results in an enhanced capability to degrade elevated levels of organic contaminants, making them integral to the natural bioremediation of contaminants [1]. Microbial biodegradation is also a sustainable alternative to costly and invasive engineering-based remediation techniques. However, contaminant toxicity can have a marked influence on microbial community structure and diversity [2], ultimately affecting the *in situ* biodegradation potential.

In this work, studies were conducted to investigate the effects of contaminant load on the indigenous microbial communities in a phenol-contaminated aquifer in the UK. Using denaturing gradient gel electrophoresis and pyrosequencing, groundwater (planktonic) microbial communities were profiled across the contaminant gradient, and compared to the attached communities formed on surrogate geological substrata incubated in the aquifer under the same hydrochemical conditions. Microbial community structure and function was found to be strongly influenced by contaminant load and groundwater hydrochemistry. Also, *in situ* microbial attachment studies reveal that the attached and planktonic communities differ markedly. These results are important for understanding the distribution and formation of microbial communities in contaminated environments and subsurface ecosystems, and lead to a better understanding of the function and limitations on *in situ* biodegradation processes in the Earth's Critical Zone.

[1] Davey and O'Toole. (2000), *Microbiol. Mol. Biol. Rev.*, **64**(4), 847-867. [2] Spence *et al.* (2001), *J. of Cont. Hydrol*, **53**, 285-304.

A new ore mineral assemblages from the Shilu iron-polymetallic deposit, Hainan Island, South China

N. BAKUN-CZUBAROW[1]*, S.Z. MIKULSKI[2], D. XU[3], D. KUSY[1] AND ZH. WANG[3]

[1]Institute of Geological Sciences, Polish Academy of Sciences, Warsaw, Poland (*correspondence: nbakun@twarda.pan.pl; dkusy@twarda.pan.pl);
[2]Polish Geological Institute – National Research Institute, Warsaw, Poland (stanislaw.mikulski@pgi.gov.pl)
[3]Guangzhou Institute of Geochemistry, Chinese Academy of Sciences, Guangzhou, China (xuderu@gig.ac.cn)

The famous Shilu iron-polymetallic ore deposit located in western Hainan Island, South China, occurs within Meso-Neoproterozoic, low-grade metamorphosed volcanoclastic sediments and carbonates. The Shilu deposit is considered to be a structurally reworked as well as hydrothermally altered and enriched ore deposit of Banded Iron Formation type. The deposit is very important iron producer from magnetite and hematite ores [1]. In our work we focused on the polymetallic sulfide mineralization, that is younger than iron oxide ores [2] and, in places, overprinted them. For the research we have chosen from the Shilu deposit several samples of sulfide ores from the Beiyi mine and its close vicinity. We have performed detailed ore microscopic studies as well as electrone microprobe analyses using CAMECA SX 100 equipped with EDS and WDS systems. In the studied samples pyrrhotite, chalcopyrite and Co-bearing pyrite (up to 11 wt% Co) dominated among ore sulfides. These ore minerals occur in quartz or calc-silicate rocks, either as disseminated grains, sometimes in veinlets, or in aggregates, that may form massive ores. Pyrrhotite and chalcopyrite may contain numerous solid inclusions, overgrowths and intergrowths of subordinate sulfides (sphalerite, galena), sulfosalts (glaucodot, costibite, cobaltite, arsenopyrite, ullmannite), sulfospinels (siegenite) and cassiterite, that belong to the minerals crystallizing at medium to low temperatures. Among these minerals siegenite and Co-bravoite dominate. Tiny crystals (10-20 μm in size) of Bi-minerals (matildite, cosalite) are also present. Moreover, in association with barite, calcite and chlorite, Ag-Hg amalgamate and cinnabar can occur. The results of our study point to the multistage medium- to low- temperature hydrothermal precipitation of ore sulfides that overprinted the Fe-oxide ores. We believe, our results will serve for better understanding of metallogenic processes in the Shilu iron-polymetallic deposit.

[1] Xu *et al.* (2011) *Ore Geol. Rev.* in press. [2] Bakun-Czubarow *et al.* (2010) *Acta Univ. Szeged., Acta Min.* **6,** 452.

https://doi.org/10.1180/S0026461X00006502 Published online by Cambridge University Press

Biogeochemistry and stable isotope investigation of acid mine drainage associated with abandoned Pb-Zn mine in Balya, Turkey

NURGUL BALCI[1]*, NEVIN KARAGULER[2], M. SEREF SONMEZ[3] AND EROL SARI[4]

[1]Department of Geological Engineering, ITU, Turkey (*correspondence:ncelik@itu.edu.tr)
[2]Department of Molecular Biology and Genetics, ITU, Turkey (karaguler@itu.edu.tr)
[3]Department of Metallurgy and Materials Engineering, ITU, Turkey (ssonmez@itu.edu.tr)
[4]Institute of Marine Science and Management, Istanbul University, Turkey (erolsari@istanbul.edu.tr)

The abandoned Pb-Zn mine in Balya Region contains mainly galena, sphalerite, pyrite, chalcopyrite, and arsenopyrite. The mine tailings and smelting waste rocks produce significant amount of acidity and heavy metals. We used laboratory and field approaches to elucidate oxidation mechanisms of galena, sphalerite and pyrite in the region. The biological and abiotic oxidation experiments with galena, sphalerite and pyrite under various conditions (pH (2-4), (4-25 ºC) conditions were carried for the laboratory studies. Sediment and water samples were collected from the mine sites. Areas of the mine flooded by water have acidic pH (3) and high concentrations of metals (Pb, Zn, Cu, Fe, Co, Cd and As). In acidic, Fe-rich waters, oxidation of Fe^{2+} after exposure to air is microbially catalyzed and follows zero-order kinetics (range of 0.92 to 1.5 mmol L^{-1} h^{-1}). Biological oxidation experiments with galena and sphalerite at 25 ºC showed high oxidation rate compared to chemical –control and suboptimal temperature (4, 10ºC) experiments. *A. thioxidans* was still active even under 4ºC although the oxidation rate of galena and sphalerite were significantly lower compared to 25ºC. Oxidation of pyrite with or without bacteria did not show significant reaction rate. The S isotopic composition of dissolved sulfate collected from the mine areas closely reflect sphalerite and galena values rather than pyrite. The $\varepsilon^{18}O_{SO4\text{-}H2O}$ values of 8.0 ± 0.2 ‰ and 7.8 ± 0.1 ‰ obtained from the field measurements is consistent with the values calculated from biological oxidation of galena and sphalerite experiments relative to pyrite experiments ($\varepsilon^{18}O_{SO4\text{-}H2O}$ values of 0.0 to 4.0 ‰) [1] . A clear distinction exits among the $\varepsilon^{18}O_{SO4\text{-}H2O}$ values produced during pyrite and sphalerite experiments may help to determine the source of acidity.

[1].Balci *et al*. (2007) *Geochimica Cosmochim. Acta* **71**, 3796-3811

Cosmogenic ^{21}Ne production systematics in quartz inferred from a 25-meter sandstone core

G. BALCO[1]*, D.L. SHUSTER[1], P-H. BLARD[2], L. ZIMMERMANN[2] AND J.O.H. STONE[3]

[1]Berkeley Geochronology Center, 2455 Ridge Rd., Berkeley CA 94550 USA (*correspondence: balcs@bgc.org)
[2]CRPG-CNRS-Université de Lorraine, 15 rue Notre Dame des Pauvres, 54501 Vandoeuvre-lès-Nancy, France
[3]Earth and Space Sciences, University of Washington, Seattle WA 98195-1310 USA

We measured ^{20}Ne, ^{21}Ne, and ^{22}Ne concentrations in quartz in a 25-meter sandstone core collected at Beacon Heights, Antarctic Dry Valleys, as part of the CRONUS-Earth project. ^{21}Ne concentrations computed as excess over atmospheric Ne are shown below. We intercalibrated measurements at BGC and CRPG by exchanging standards. A systematic difference between the two labs, most likely due to the effect of different sample preparation schemes on ^{21}Ne produced from alpha implantation at grain edges, is evident in deep samples. These data, with corresponding U and Th concentrations, permit resolution of the ^{21}Ne inventory into trapped, cosmogenic, and nucleogenic components, and thus estimates of ^{21}Ne production rates due to spallation and muon interactions.

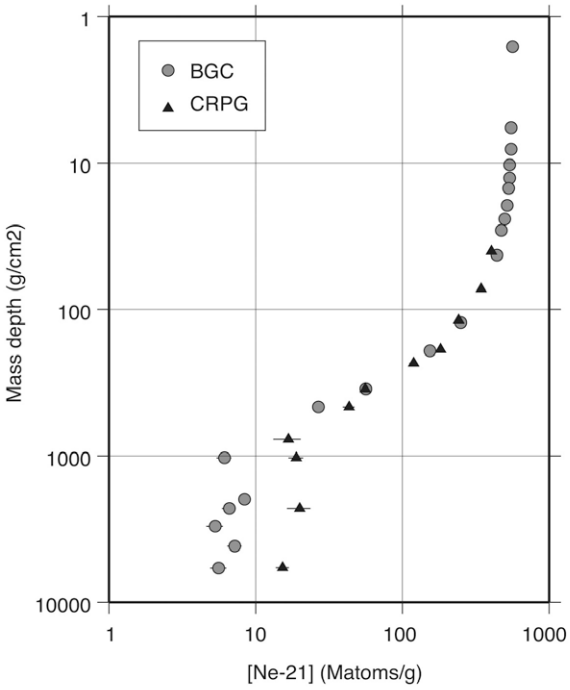

https://doi.org/10.1180/S0026461X00006502 Published online by Cambridge University Press

A 3D snapshot from granitic system: Tourmaline nodules and their bearing on the granite evolution

D. BALEN* AND Z. PETRINEC

University of Zagreb, Faculty of Science, Croatia
(*correspondence: drbalen@geol.pmf.hr)

Peraluminous granites generated during the Late Cretaceous evolution of the LP-HT zone in the Adria-Europe plate boundary setting host tourmaline nodules. These tourmaline-bearing bodies from the Moslavačka Gora (MG), Croatia show great similarity with leucogranitic veins and can be described as compact spherical to ovoid aggregates (cm to dm in diameter) with a fine-grained (grain size 1-2 mm) core (slightly alkali-deficient dravite to schorl tourmaline (#Fe 0.40-0.66) + quartz + albite + K-feldspar ± muscovite) enveloped by a leucocratic halo (quartz + K-feldspar + oligoclase An_{11-21} ± muscovite). When observed in 2D sections solely, the isolated nature of tourmaline nodules can be easily mistaken with similar 2D cross-section of a leucogranitic vein. For that reason tourmaline nodules' spatial distribution inside the host, shape and internal structure of individual bodies have been reconstructed and visualized through destructive serial sectioning tomography with physical resolution of 3.5 mm (serial cutting) or 0.35 mm (serial lapping) between individual planes. Obtained 3D reconstructions of rock volumes containing tourmaline nodules showed that they are indeed isolated spherical bodies dispersed inside the granitic host and not vein formations. The two structural units of a nodule, core and halo, are clearly distinguishable in 3D and show sharp contacts to each other but also to the granitic host.

The morphology, peculiar texture, distribution and origin of tourmaline nodules inside granite can be most suitably explained through the emplacement mechanism and crystallization setting of the host granite at upper crustal level (at MG locality calculated approx. depth of 5-6 km, T=720 °C). During emplacement, decompression and arising immiscibility leads to melt unmixing and production of two different melt phases: "normal" granitic and B-rich one. Prominent depolymerization of B-rich melt, followed by density and viscosity decrease together with lowering of liquidus and solidus temperatures, leads to physical separation of a buoyant B- and fluid-rich phase in form of distinct B-rich bubbles or pockets, which coalesce in order to decrease surface tension. Such isolated volumes now contain necessary concentration of boron and other elements needed for tourmaline growth and become precursors for the future solidified tourmaline nodules.

Noble gases and halogens in the MORB-source mantle: Recycled?

C.J. BALLENTINE*[1], R. BURGESS[1], B. WESTON[1], D. CHAVRIT[1], H. SUMINO[2] AND D.A.H. TEAGLE[3],

[1]SEAES, The University of Manchester, Manchester, U.K. (*chris.ballentine@manchester.ac.uk)
[2]GCRC, University of Tokyo, Tokyo 113-0033, Japan
[3]NOC, University of Southampton, Southampton, U.K.

Powerful information from the extinct ^{129}I and ^{244}Pu systems is derived from the distribution of the daughter ^{129}Xe and ^{136}Xe between terrestrial reservoirs. Because of its simplicity, the conclusion that the Earth was open to Xe loss until ~80Ma after the Earth accreted, for example, is unequivocal. The $^{129}Xe/^{130}Xe$ ratio in the atmosphere, mantle and any primordial volatile rich mantle reservoir will then be determined by the ^{129}I (and ^{244}Pu)/Xe ratio in that reservoir and any subsequent interactions between reservoirs. The Earth's atmosphere, for example, has a lower $^{129}Xe/^{130}Xe$ than the convecting mantle. While there has been an exceptional concentration of the halogens at the Earth's surface compared to other incompatible elements (>90% BSE) [1], this is balanced by the atmosphere's high relative Xe concentration.

In the simplest (reference) model we can make the key assumption that the closure of the respective mantle reservoirs is the same as the atmosphere closure time of 80Ma. In the case where 80% of the convecting mantle Xe is recycled air [2], we calculate the iodine concentration, required to provide the convecting mantle ^{129}Xe excess caused by ^{129}I decay to be $[I]_{model}$ ~0.14ppb I. We then predict one of three cases when comparing $[I]_{observed}$ with $[I]_{model}$: 1) They will be in close agreement, in which case we can consider the convecting mantle to be closed with respect to the I/Xe system; 2) $[I]_{observed}$ will be lower than $[I]_{model}$, which then requires either an earlier closure age of the reservoir or significant net loss of I from the system after ^{129}I has ceased to be active; or 3) $[I]_{observed}$ will be greater than $[I]_{model}$ due to a net excess of dead iodine being added to the system. Current convecting mantle I concentration estimates, based on MORB, range from <0.7 ppb to orders of magnitude higher [3] and point towards the latter, consistent with recent observation of noble gas and halogen subduction to at least 100km depth [4]. Iodine determination of the MORB (and OIB) source remains a critical objective for future work.

[1] Burgess *et al*., (2002) *EPSL* **197**, 193-203. [2] Holland & Ballentine (2006) *Nature* **441**, 186-191. [3] Aiuppa *et al*., (2009) *Chemical Geology* **263,** 1-18. [4] Sumino *et al*. (2010) *EPSL* **294**, 163-172

https://doi.org/10.1180/S0026461X00006502 Published online by Cambridge University Press

Late volatile addition to Earth

C. BALLHAUS[1]*, V. LAURENZ[1], R. FONSECA[1], C. MÜNKER[2], F. ALBARÈDE[3], A. ROHRBACH[4], M.W. SCHMIDT[4], K.P JOCHUM[5], B. STOLL[5], U. WEIS[5] AND H. HELMY[6]

[1]Steinmann Institut, Universität Bonn, Germany (*correspondence: ballhaus@uni-bonn.de)
[2]Universität zu Köln, Germany
[3]Ecole Normale Supérieure de Lyon, France
[4]ETH Zürich, Switzerland
[5]Max Planck Institut für Chemie, Mainz, Germany
[6]Minia University, 61519 Minia, Egypt

It is known for some time that relative to CI chondrite, Earth's mantle is depleted in elements more volatile than Mg and Si. Early workers attributed this to volatile loss from Earth's mantle during accretion. In recent years, however, consensus has been emerging that the opposite may be true: that the inventories of the Earth's mantle in moderately and highly volatile elements and compounds, including Earth's hydrosphere and atmosphere, may be late additions, to a silicate earth initially far more refractory than the present-day upper mantle.

We report metal-silicate experiments at 1 to 5 GPa over a temperature range from 1773 to 2573K to quantify how selected refractory and volatile elements may have partitioned between silicate and Fe metal melt. We study the partitioning of two refractory elements (i.e. W and Cr) and four elements (i.e. Pb, Cd, Sn, Se) from the volatile inventory of the Earth's mantle. Except for Se, all elements regardless of volatility become more siderophile with increasing temperature, reflecting the effect of thermal reduction. By correlating measured metal/silicate partition coefficients with the relative abundances of these elements in the mantle, the physical state of the mantle can reconstructed when the respective element abundances were established; W and Cr at magma ocean conditions around 2550K, and Pb, Cd, Sn, and Se to a mantle that must have been largely crystalline at the time of volatile addition, with core melt segregation inactive.

The experiments provide independent support for a latter-day volatile addition. Had Pb, Cd, Sn, and Se been present at magma ocean conditions, they would have been seriously depleted in abundance relative to the abundances in lithophile volatiles with similar condensation temperatures, far more than observed; Pb by up to two orders of magnitude relative to its present-day mantle concentration. Our Ds confirm that a large proportion of the volatile element inventory of Earth's mantle, including its water content, was part of a late volatile component, most likely material from the asteroid belt and added to a relatively cool mantle, at a time when core formation was completed. There is little basis to assume that the apparent Pb deficit in the silicate Earth is to be sought in the core. Rather, the $^{238}U/^{204}Pb$ ratio (μ) of Earth's mantle reflects late addition of Pb, to a highly refractory proto-mantle seriously depleted in volatiles. A late (post-core) addition of Pb via a CI-type impactor, to a refractory mantle highly depleted in lead, may also be key to solving the first lead paradox.

Surface characterization of biotite from a mesh bag field study

Z. BALOGH-BRUNSTAD[1,*,2], L. SACCONE[3], M.M. SMITS[4], C. BERNER[5], H. WALLANDER[5], T. J. MCMASTER[3] AND S.L.S. STIPP[2]

[1]Hartwick College, Oneonta, NY, 13820 USA (*correspondence: balogh_brunz@hartwick.edu)
[2]NanoGeoScience, Nano-Science Center, Dept. of Chemistry,University of Copenhagen, Denmark
[3]H.H. Wills Physics Laboratory, University of Bristol, UK
[4]Environmental Biology, Hasselt University, Belgium
[5]Microbial Ecology, Lund University, Sweden

Direct fungal-mineral contact has been proposed to play an important role in soil mineral dissolution. Indeed, nanoscale observations in controlled laboratory settings have demonstrated both physical and chemical interactions with biotite at the scale of the individual fungal hyphae [1, 2]. We incubated biotite flakes in the soil, to test if similar fungal-mineral interactions could be observed in the field. The biotite was incubated in spruce forest soils for two years at three sites with serpentinite, leucogranite and amphibolite bedrocks and contrasting tree nutrient status. Mineral surfaces were examined with scanning electron microscopy and atomic force microscopy. Ectomycorrhizal biomass was determined by Ergosterol analyses.

Microscopy revealed patchy biofilms on the biotite surfaces (19 to 44%) with the highest values found at the low Mg site (leucogranite). Direct hyphal attachment was only 3 to 5% with the lowest values found at the low Mg site, which was supported by the the lowest Ergosterol concentrations at this site. We saw shallow channels, similar to hyphae in size and branching pattern on most of the flakes (Figure 1a). The channels widened with time, probably from dissolution, and at each "pulse," the channel deepened in the direction of growth (Figure 1b). We propose that this morphology reflects the pulsive growth of the hyphal tip, inducing shear stress to the top T-O-T biotite layers.

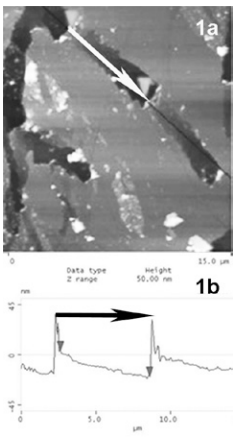

These observations support the laboratory results that fungal hyphae exercise both chemical dissolution and physical force at the hyphal-mineral interface.

[1] Balogh-Brunstad *et al.* (2008) *Biogeochem.* **88**, 153–167.
[2] Bonneville *et al.* (2009) *Geology* **37**, 615-618.

https://doi.org/10.1180/S0026461X00006502 Published online by Cambridge University Press

Cloud condensation nuclei concentrations and actual supersaturations in real clouds

U. BALTENSPERGER, Z. JURÁNYI, E. HAMMER, M. GYSEL, N. BUKOWIECKI AND E. WEINGARTNER

Laboratory of Atmospheric Chemistry, Paul Scherrer Institut, 5232 Villigen PSI, Switzerland

The number of cloud condensation nuclei (CCN) at a given supersaturation has an important influence on cloud properties and is therefore crucial for a better quantification of the indirect aerosol effect on climate. Only in recent years, CCN data have become available from different sites in a systematic manner. We have measured the CCN number concentration continuously at the high alpine site Jungfraujoch (3580 m asl) continuoulsy for several years, in the framework of the Global Atmosphere Watch (GAW) programme of the World Meteorological Organization [1], and perfomed a closure with other aerosol variables measured simultaneously at the same site [2]. We show that the critical dry diameter, above which the aerosols activate as CCN, does not show a distinct seasonal cycle, nor substantial variability, indicating that aerosol hygroscopicity stays fairly stable throughout the year. Therefore, the CCN number concentration at this site can be reliably predicted from the time-resolved particle number size distributions with approximate knowledge of the time averaged chemical composition.

Since the Jungfraujoch is within clouds about 40% of the time this site provides the possibility to compare the measured CCN number concentrations with the activation that occurs in the real clouds. For this purpose, two different inlets were used: A total inlet, heated to 25°C was used to evaporate cloud droplets and ice crystals and to sample both their residual (previously activated and/or nucleated) particles and the interstitial (non-activated) particles. A second, interstitial inlet was equipped with a cyclone to remove cloud particles and sample only the non-activated aerosol particles (smaller than 2 μm). A comparison of the size distributions behind these two inlets allows to retrieve the activation diameter in the real cloud [3]. Together with the measured CCN spectra this provides the maximum supersaturation the cloud experienced in the vicinity of the Jungfraujoch.

[1] Jurányi *et al*. (2011) *J. Geophys. Res*. 115, doi:10.1029/2010JD015199. [2] Jurányi *et al*. (2010) *Atmos. Chem. Phys*. **10**, 7891-7906. [3] Verheggen *et al*. (2007) *J. Geophys. Res*. **112**, D23202, doi:10.1029/2007/JD008714.

An animal model (sheep) for Fe, Cu and Zn isotopes cycling in the body

VINCENT BALTER[1]* AND ANTOINE ZAZZO[2]

[1]UMR 5276 Laboratoire de Géologie de Lyon, Ecole Normale Suéprieure de Lyon, BP7000, 69342 Lyon Cedex 07, FRANCE (*Vincent.Balter@ens-lyon.fr)

[2]UMR 7209 Archéozoologie, Archéobotanique, Muséum National d'Histoire Naturelle, 55 Rue Buffon, F-75231, Paris cedex 05, FRANCE (zazzo@mnhn.fr)

Iron, copper and zinc are three essential metals for life. The concentration of these metals is regulated by the metabolism to reach body requirements, but almost nothing is known about the variations of the stable isotopes in the body. This could bring new insights on the metabolism of the metals, but the mapping of the isotopic variability in normal conditions is necessary prior to any applications for the study of metal metabolic disorders. Here, we report Fe and Cu isotope compositions (δ^{56}Fe and δ^{65}Cu) and concentrations in various organs of sheep raised experimentally with constant diet (δ^{56}Fe and δ^{65}Cu ≈ 0‰). Iron isotope compositions range from about -4‰ to -1‰ (muscle and liver/kidney, respectively), and copper isotope compositions range from -1.5‰ to +1.5‰ (liver and kidney, respectively), therefore covering almost the geological variability. The variability of the Fe and Cu isotope compositions is higher than for Zn (-0.6‰ to +0.6‰, [1]), suggesting that biologically-induced metals isotope fractionations depend more on redox conditions than on ligand coordination. Contrary to humans [2], the Fe and Cu isotope compositions are similar in serum and red blood cells. The isotopic cycling of the metals in the body is discussed using mixing equations and box modeling.

[1] Balter *et al*. (2010) *Rapid Comm. Mass Spectrom*. **24**, 605-612. [2] Albarède *et al*. (Submitted) *Metallomics*

https://doi.org/10.1180/S0026461X00006502 Published online by Cambridge University Press

Particulate trace metals and dust particles in the subtropical Atlantic

W. BALZER*, W. BARKMANN AND H. DIERSSEN

University of Bremen, FB 2, 28334 Bremen, Germany
(*correspondence: balzer@mch.uni-bremen.de)

During the expedition Meteor M81/1 in the subtropical Atlantic Ocean (GEOTRACES Cruise A11; February/March 2010) particulate trace metals were sampled (by using *in situ*-pumps) to study (i) the fate of dust particles in the water column, (ii) its impact on the vertical distribution of particulate trace metals and (iii) to investigate the interaction between trace elements in solution and in the particulate phase.

The cruise track from the Canary Islands to the Brasil basin followed an approximate gradient from high to low dust input. While mineral dust and aerosol deposition is the most important source of trace elements in the open subtropical Atlantic, the surface distribution of particulate trace metals is also affected by the biotic productivity and the rate of organic matter sedimentation which tends to remove the mineral particles from the surface ocean and also decreases along the cruise track.

There is evidence to suggest that the small dust particles do not sink by themselves but that they are removed from the mixed layer by forming aggregates with sticky organic particles. These aggregates might be large enough to leave the surface ocean rapidly, sink, disaggregate, re-aggregate, etc., thus producing an observable vertical distribution of e.g. particulate Al (taken as a proxy for dust particles).

For this assemblage of processes acting on the distribution of suspended dust particles (including aggregation between organic and mineral particles, disaggregation and joint sinking) a model has been developed. The simulated concentration profiles of refractory trace metals (of suspended dust particles) are strongly related to the rate of atmospheric dust deposition and show a similar pattern as in the observed vertical concentration profiles.

Below the surface mixed layer, the different particulate trace metals exhibit extreme differences in the vertical distribution depending on the major form of their particulate transport: the concentration of the more refractory metals in inorganic entities (e.g. Al, Fe, Mn) tend to be constant or even increase with depth, while the nutrient-type elements (e.g. Cd, Ni) being associated with organic particles exhibit dramatic decreases of the concentration with depth in the deep sea. The results for the different elements are compared with those from a similar cruise in 1997 to evaluate interannual variability.

Petrogenesis of monotonous dacitic Taapaca Volcanic Complex, N. Chile

M. BANASZAK*AND G. WÖRNER

University of Göttingen, Geoscience Centre Göttingen, Goldschmidtstr. 1, 37077 Göttingen, Germany
(*correspondence: mbanasz@gwdg.de)

Taapaca Volcanic Complex (TVC) located in the Andean Central Volcanic Zone (18°S) generated monotonous high porphyric dacites (61-65.5 wt.% SiO_2) during its main eruptive history ~1 Ma [1]. Taapaca dacites show textural and mineralogical characteristics similar to the Fish Canyon Tuff [2], including sanidine megacrysts, lack of pyroxene and presence of mafic inclusions.

The occurrence of sanidine megacrysts up to 12 cm in length in intermediate volcanic rocks is a unique feature. All Taapaca sanidine show similar growth patterns, pronounced Ba-zoning, and invariable incompatible trace element contents as well as Sr- and O- isotopic compositions. Chemical characteristics of the sanidine, enclosed plagioclase, and magnesiohornblende compositions suggest crystallization in a closed-system at 700-770°C and 1.0-3.4 kbar. Microphyric basalt andesitic inclusions (52-54 wt.% SiO_2) in Taapaca dacite show a uniform mineral assemblage of plagioclase, magnesiohastingsite and Fe-Ti oxide with varying proportions of incorporated felsic components. The mafic inclusions represent compositionally two kinds of parental magma reported from neigbouring Parinacota Volcano [3], differing significantly in Sr and Ba contents, FeO^*/TiO_2 and REE patterns. Estimated P-T conditions from magnesiohastingsite composition reveal 900-1020°C and 2-8 kbar. Taapaca dacites reveal both P-T ranges obtained from two coexisting amphibole and plagioclase populations.

The composition of the dacites and compositionally diverse hybrid mafic inclusions form an array of distinct mixing lines, which converge to one rhyodacitic composition. The composition of the dacites indicates mixing between an evolved sanidine-bearing end-member composition of ~68 wt.% SiO_2 and a range of basaltic andesites in the constant ratio of 3:1. Neither basaltic andesite nor rhyodacite erupt as end-member compositions at Taapaca Volcano. Following reactivation, the uniform dacitic composition of TVC sugessts steady-state magma throughput, and a uniform volume-ratio between remobilized resident rhyodacite crystal mush and variable mafic input.

[1] Clavero *et al*. (2004) *J. Geol. Soc., London* **161**, 603-618.
[2] Bachmann *et al*. (2002) *J. of Pet*. **43**, no. 8, 1469-1503.
[3] Hora *et al*. (2009) *EPSL* **285**, 75-86.

https://doi.org/10.1180/S0026461X00006502 Published online by Cambridge University Press

Spectroscopic study of influence of silica on the stability of actinide(IV) colloids at near-neutral pH

D. BANERJEE[1,2]*, S. WEISS[1], H. ZAENKER[1], A.C. SCHEINOST[1,2] AND C. HENNIG[1,2]

[1]Institute of Radiochemistry, Helmholtz-Zentrum Dresden-Rossendorf, 01314 Dresden, Germany
[2]The Rossendorf Beamline at ESRF, B.P. 220, 38043 Grenoble, France (*correspondence: banerjee@esrf.fr)

The migration of tetravalent actinides in natural waters occurs predominantly as sorption complexes at the surface of colloidal particles like clay, but also by the formation of actinide oxyhydroxide colloids ($MO_n(OH)_{4-2n}\cdot mH_2O$ where M = Th or U [1]). Colloid-facilitated migration of plutonium has also been documented in subsurface groundwater conditions [2]. In a recent study it was observed that the stability of U(IV) and Th(IV) oxyhydroxide colloids is dramatically enhanced by the presence of silica [3]. In this study we investigate the influence of silica on the formation and stability of U and Th colloids at near-neutral pH conditions, which might have important environmental implications due to the ubiquitous nature of silica in aquifers and surface waters.

U and Th colloids with varying U/Si and Th/Si ratios were synthesized and characterized using a range of spectroscopic and microscopic techniques. TEM and XRD measurements indicated that the structure of thorium/silica colloids is highly amorphous, which is clearly different from the ordered actinide(IV) oxyhydroxide colloids which are stable at pH < 3 but agglomerate and precipitate at near neutral pH within minutes. Comparison of O 1s X-ray photoelectron spectra (XPS) of actinide(IV)-silica and actinide(IV)-oxyhydroxide colloids revealed that two types of oxygen bonds (oxo and hydroxo) occur in presence of silica, which may explain the high degree of structural disorder. Moreover, the presence of O-Si bonds at near-neutral pH values suggest that silica is able to stabilize such colloids through modification of the structure by replacing the An-O(H)-An bonds of the oxyhydroxide structure with An-O(H)-Si bonds and consequently influencing the surface charge. These observations are consistent with X-ray absorption spectroscopy (XAS) data which demonstrate higher An-Si interaction and lower An-An interaction with increasing silica content in these colloids.

[1] Rothe *et al*. (2002) *Inorg. Chem.* **41**, 249-258. [2] Kersting *et al*. (1999) *Nature* **397**, 56-59. [3] Dreissig *et al*. (2011) *GCA* **75**, 352-367.

Sorption and redox behavior of neptunium on Opalinus clay and Callovo–Oxfordian argillite

N. L. BANIK*, C.M. MARQUARDT, D. SCHILD, J. ROTHE AND T. SCHÄFER

Karlsruhe Institute of Technology (KIT), Institute for Nuclear Waste Disposal (INE),D-76344 Eggenstein-Leopoldshafen, Karlsruhe, Germany (*correspondence: nidhu.banik@kit.edu, christian.marquardt@kit.edu, dieter.schild@kit.edu, joerg.rothe@kit.edu, thorsten.schaefer@kit.edu)

Clay stone is considered as a potential host rock for a high level deep nuclear waste repository. The Opalinus clay (OPA) and the Callovo-Oxfordian argillites (COx) are being investigated as candidate host rock formation at the underground research laboratory in Mont-Terri (Switzerland) and at Bure (France), respectively. The migration behavior of Np is strongly influenced by the oxidizing and reducing conditions of the geological environment. The understanding of Np sorption and diffusion mechanisms in argillaceous rocks is necessary for the safety assessments of a nuclear waste repository.

The objective of the present work is to use Kd values determined by batch experiments for transport modeling, and to gain understanding in underlying coupled redox and sorption phenomena. The batch sorption experiments of Np(V) on OPA (pH 7.6) and COx (pH 7.2) are performed at four different solid to liquid ratios, S/L (10, 20, 50, 200), in artificial pore water under argon atmosphere (<1 ppm O_2) with 1% CO_2 conditions, at Np concentrations between 3.0×10^{-4} and 1.0×10^{-8} M and with contact times up to 1 year. Np redox speciation in clay suspension is followed at low Np concentration by TTA extraction and capillary electrophoresis coupled to ICP-MS and at high Np concentration by UV-Vis, XAFS, and XPS spectroscopy.

Np(V) sorption increases with increasing sorbent amounts (S/L ratio) and with increasing contact time. More than 80 % of Np sorbed on the clay rocks within 4 months. The preliminary Kd values are calculated to 1.03 mL/g for OPA and 0.85 mL/g for COx (S/L ratio: 20) after 4 months contact time. In concentration series at 10^{-4} M, Np was identified on the clay in the form of Np(V) by XAFS and XPS spectroscopy after 1 week contact time, whereas in solution Np(V) is detected by TTA extraction and UV-Vis spectroscopy. At $<10^{7}$ M, Np(V) is found in solution by TTA extraction after 1 week contact time, while after 4 months Np(IV)/Np(V) mixtures are analyzed. The obtained results will be presented.

https://doi.org/10.1180/S0026461X00006502 Published online by Cambridge University Press

Sulfate mineral solubilities in Na-Ca-Cl brines

JONATHAN BANKS AND SIMONA REGENSPURG SIMONA

Helmholtz-Centre Potsdam, German Research Centre for Geosciences (GFZ) Potsdam, Germany (*jbanks@gfz-potsdam.de)

Geothermal brines produced from deep sedimentary basins show a strong tendency to produce mineral precipitants (scales) during operation of a power plant. Measured SO_4^{2-} concentrations (up to 3 mM) in the fluid at the Groß Schönebeck (GrSk) *in situ* geothermal laboratory, Germany suggest that sulfate-bearing minerals may be significant scale forming phases. Of particular concern are the behavior of (1) Ba^{2+} and Sr^{2+} in the high salinity (up to 5 M Cl^-) Na-Ca-Cl fluid, and (2) the overall equilibrium concentration of SO_4^{2-} that subsequently controls the mass of $CaSO_4 \cdot xH_2O$ precipitation. In order to predict the estimated amount and nature of these scales, we have both modeled and experimentally determined mineral solubilities in synthetic GrSk brines under proposed plant operating conditions (15 bar, 70°C – 150°C).

Modelling was performed using the PHREEQc Quintessa database, with anhydrite ($CaSO_4$), barite ($BaSO_4$), and celestite ($SrSO_4$) as the equilibrium phases. Experiments were performed using a "flooding method," in which a deliberately oversaturated concentration of SO_4^{2-} was injected into a Na-Ba-Ca-Sr- Cl brine filled pressure vessel. While there is general agreement between the PHREEQc and experimental results, some significant differences do exist. PHREEQc over-estimates the amount of barite precipitation by up to three orders of magnitude and underestimates the amount of celestine precipitation by up to one order of magnitude. In total, both PHREEQc and experimental results predict between 10^1 and 10^4 grams of total sulfate mineral precipitation per m^3 of produced fluid, depending on the conditions and total available SO_4^{2-} .

Microbial cycling of sulfur in the aphotic zone a meromictic lake

B. DYLAN BANNON[1], SHUHEI ONO[2], STEFANIE P. TEMPLER[3] AND TANJA BOSAK[4]

[1]EAPS MIT, Cambridge MA 02139, (bannon@mit.edu)
[2]EAPS MIT, Cambridge MA 02139, (sono@mit.edu)
[3]Emmy Group, Ostermundingen, Switzerland, (stefanie.templer@emmi.ch)
[4]EAPS MIT, Cambridge MA 02139, (tbosak@mit.edu)

Fayetteville Green Lake (FYG) is a meromictic euxinic lake characterized by large differences in the composition of sulfur isotopes of sulfides and sulfates ($\delta^{34}_{\text{sulfate-sulfide}}$ of 56-57.5‰) [1]. Similar $\delta^{34}_{\text{sulfate-sulfide}}$ values are commonly thought to involve microbial sulfate reduction (MSR) coupled with microbial disproportionation of sulfur (MSD). Because our recent study suggests that MSR limited by the availability and quality of organic compounds can produce similar $\delta^{34}_{\text{sulfate-sulfide}}$ in the absence of MSD, here we study molecular, metabolic and physiological diversity of microbes from the sulfidic water column and the bottom sediments of FYG.

Enrichment cultures confirm the presence of S-disproportionating microbes in the sediments and the water column. Preliminary most probable number counts (MPNs) suggest that these organisms may be as abundant in sediments as sulfate reducing microbes. The MPNs also indicate a marked increase with depth of organisms that are able to couple sulfate reduction to the oxidation of acetate. Isolated microbes from the lake bottom sediments include at least two phylogenetically distinct organisms that can disproportionate S.

Preliminary studies suggest that microbes in the bottom sediments of FGL can metabolize recalcitrant organic substrates, reduce sulfate and disproportionate S. Further physiological, metabolic and isotopic analyses of enrichment cultures and isolates, as well as molecular comparisons of the diversity of dissimilatory sulfate reductase genes (*dsrAB*) and 16s rDNA genes in the water column and the sediments are in progress.

[1] Deevey, Nakai, Stuiver (1963) *Science* **139**, 407-408.

https://doi.org/10.1180/S0026461X00006502 Published online by Cambridge University Press

The landscape change of salt and alkaline land in semi-arid district before and after flooding

CHUNHONG BAO[1,2] LINSHU XU[2] YUNJUN WU[3] AND SHUWEN ZHANG[4]

[1] Hunan Agricultural University, Changsha 410128, China (Email:baoch159@163.com)
[2]College of Urban and Environmental Sciences, Northeast Normal University, Changchun 130024, China
[3]The Land and Resources Deportment of Hunan Province, Changsha 410007, China
[4]China Graduate School of Chinese Academy of Sciences, Beijing 100049, China

This paper adopted relief map and TM, SAR image, impaling the image disposal technology of Remote Sensing and the space analysis technology of Geography Information System, and combining landscape ecology theory to analyze the effect of flooding before and after 1998 on soil salinization. The analysis includes several aspects such as quantiy, spatial distribution and landscape distribution of salt and alkaline land in Zhenlai county. The results show that the sun-acreage of saline-alkali land in Zhenlai Counly in creased by 13929.5hm2 after the flood. The connectivity and integrity of saline-alkali land increased as well. Furthermore, the center of Gravity of saline-alkali offset from west to east 1.57km. The offset of the flooded area is 1.53km, and that of the non-flooded area is 3.68km. The offset distance, flooding has the effect to slow up the offset of the saline-alkali land. By contrasting the change ratio of unit area of saline-alkali land between flooding zone and no-flooding zone , it is found that the change ratio of all kind of saline-alkali land in flooding zone is higher than that in no-flooding zone at large. For example, the ratio of heavy grade of saline-alkali land in flooding zone is 5 times of that in no-flooding zone. The ratio of moderate grade saline-alkali land in flooding zone is 4.5 times of that in no-flooding zone. The ratio of gentleness grade saline-alkali land in flooding zone is 1.1 times of that in no-flooding zone. It is conculuded that the flooding has the effect to promote the extension of saline-alkali land in half arid district after the flooding. Though studying the integrity and average area of the saline-alkali patch of the landscape distribution, the landscape distribution of the saline-alkali land in the flooded area is obviously different from the non-flooded area. At the same time, the degree of salinization is higher in the flooded area than that in the non-flooded area after the flooding. The flooding push forward the speed and speed of the saliniztion in the half arid district where the terrain is low-lying and level of groundwater is higher.

Paleoproterozoic crustal growth in West Africa: Archean or modern tectonics?

L. BARATOUX[1], J. GANNE[1], M.W. JESSELL[1], S. NABA[2], AND V. METELKA[134]

[1]IRD, GET, 14 Ave E. Belin, 31400 Toulouse, France (*correspondence: lenka.baratoux@get.obs-mip.fr)
[2]Dépt. de Géologie, Univ. de Ouagadougou, Burkina Faso
[3]Institute of Geology and Paleontology, Charles University, Albertov 6, Praha 2, 12843, Czech Republic
[4]Czech Geological Survey, Klárov 3, 11821, Praha 1, CR

The Paleoproterozoic granite-greenstone terrains of the West African Craton represent the key area to study the transition from the Archean so-called “vertical” tectonics towards the modern “plate” tectonics. Our study was focused on structural evolution, geochemistry and metamorphism of the eastern and western Burkina Faso and eastern Senegal.

Geochemical data suggest that the greenstone (GS) belts, composed of tholeiitic basalts/gabbros and voluminous calc-alkaline intermediate sequences, originated in the volcanic arc setting at ~2.2 Ga. Presence of subduction zones is furthemore supported by the cold metamorphic gradient in some of the metasediments found in the eastern Burkina Faso. Compared to the Archean terrains, the proportion of komatiites and ultramafic rocks is extremely low, which suggests only limited mantle plume activity.

The calc-alkaline tonalite-trondjemite-granodiorite magmas, associated with the subduction zones, as well as younger granitoids were syntectonically emplaced into the greenstone belts during a long period from 2.18 to 2.10 Ga. No structures indicative of “sagduction” of greenstones into granitoids were found in the study area. Structural analysis of three GS belts in western Burkina Faso shows that the regional scale geometry is controlled by the rheologically strong mafic and intermediate volcanic rocks, which form up to 400 km long synforms. The granitoids are syntectonically emplaced into the presumptive antiforms between the belts.

Some of the granitoid intrusions induced a thermal overprint of the pre-existing cold metamorphic gradient in the tectonically burried greenstone belts. This is recorded as isobaric heating of Barrovian-like assemblages of garnet, straurolite and kyanite bearing micaschists. Decompressional cooling documented by the growth of sillimanite and cordierite is consistent with tectonic exhumation from the depth of at least 18 km to the depths of 4-6 km.

To conclude, our data point to the existence of subduction and collisional zone settings, which operated in a modified way compared to the present-day analogues.

https://doi.org/10.1180/S0026461X00006502 Published online by Cambridge University Press

Past fire reconstructions in ice core through the determination of specific molecular markers

CARLO BARBANTE[1,2]

[1]University of Venice, Department of Environmental Science, Calle Larga S. Marta, 2137, I-30123 Venice, Italy
[2]IDPA-CNR, Calle Larga S. Marta, 2137, I-30123 Venice, Italy

The reconstruction of the chemical composition of aerosol during the past is important for understanding the organic component contribution of biomass burning emissions to the atmosphere and complements existing data on the signatures of direct organic emissions from biomass sources. Compounds from biomass burning include monosaccharide anhydrides (MAs), and the most important tracer compound among them is levoglucosan. This is a specific molecular tracer utilized for the assessment of particulate matter composition from biomass burning in the atmosphere because it cannot be generated by non-combustive processes or by non-wood combustion. Molecular markers such as levoglucosan are important tools in tracking the transport of particles produced by biomass burning.

In order to the current concentrations of levoglucosan in the atmosphere in prespective, it is important to quantify the fluxes of this compound during the past by examining environmental archives such as snow and ice cores. Polar ice core studies have extensively documented large changes in the content of aerosol constituents such as ionic species, dust, trace elements, and organic compounds during the late Quaternary period.

The study of past fire activity using ice core records opens regions of the world where no paleofire data previously exited. Polar and low-latitude, high-altitude ice cores provide data for regions which are not represented in the global charcoal database. The available temporal resolution matches that of the ice core, with the longest temporal resolution being that of the EPICA Dome C ice core that extends back approximately eight glacial cycles. The spatial resolution of chemical markers in ice cores depends on the location of the core itself. Low-latitude ice cores primarily reflect regional climate parameters, while polar ice cores reflect a global signal. Here, we present levoglucosan flux measured across the past 600,000 years in the EPICA Dome C ice core (75°06'S, 123°21'E, 3233 masl) ice core, during the past 4000 years in the Kilimanjaro (3°04.6'S; 37°21.2'E, 5893 masl) ice core, and the applicability for determining levoglucosan in the NEEM, Greenland (77°27' N; 51°3'W, 2454 masl) ice core.

Short term environmental reconstruction from rich CO_2-spring deposits (Massif Central, France)

F. BARBECOT[1]*, B. GHALEB[2], E. GIBERT[1] AND A. NORET[1]

[1]Université Paris-Sud, Laboratoire IDES, UMR8148, Orsay, F-91405, France (*correspondance: florent.barbecot@u-psud.fr)
[2]GEOTOP, Université du Québec À Montréal, BP 8888, suc. Centre ville, Montréal, QC, H2V 3W8, Canada

Our work focuses on the understanding of the hydrogeochemical processes related to carbo-gaseous springs relation with recent environmental changes (0-20 yr), including evolution of recharge areas and fluxes for surrounding aquifers. A 80-cm sequence has been cored from carbonated travertines in order to document recent environmental fluctuations (0-20 yr) and the related geochemical parameters that control isotopic signatures of modern carbonate deposits [1]. The core was drilled on a flat zone approximately located 200-m under the emerging spring in the Limagne Plain (French Massif Central). Sediments consist of indurated carbonate, ideal for the reconstruction of hydrological fluctuations at very high resolution as they are fine, laminated deposits. Samples were taken every 1 to 2 cm according to the induration degree of the core.

The chronology of these finely laminated deposits has been determined through $^{210}Pb/^{226}Ra$ radiometric method [2,3]. Deposits accumulation rate is of 5.5 cm/yr excepted for events at 30 cm and 60 cm depth that display gaps of carbonates accumulation. Those events correlate precisely with two historical main heat waves, 2003 and 1998 [4], that confirms the indirect records of both the recharge decrease and the drying-up of the springs.

While solid carbonates precipitating along the surface flowpath originate from water with a nearly constant ^{18}O composition, highlighting the inertia of the system that gives rise to the springs, the ^{13}C signatures of those carbonates have likely registered past meteorological conditions [4]. Moreover, this environmental record offers a significant correlation between ^{13}C signal and the East Atlantic Pattern of the North Atlantic Oscillation. Higher mean temperatures can be identified by an enriched ^{13}C content, because of prominent fractionating geochemical processes involved, such as degassing and carbonate precipitation.

[1] Assayag *et al*. (2009) *Energy Procedia*, 2361–2366. [2] Condomines & Rihs (2006) *EPSL* **250**, 4-10. [3] Condomines *et al*. (1999) *CRAS Serie II*-A **328**-1, 23-28. [4] METEO FRANCE Data.

https://doi.org/10.1180/S0026461X00006502 Published online by Cambridge University Press

REE behaviour in acid mine drainage conditions in the Ríos Tinto and Odiel (Iberian Pyrite Belt, SW Spain)

L. BARBERO[1], M. OLÍAS[2], A. HIERRO[3], M. CASAS-RUIZ[4] AND J.P. BOLÍVAR[3]

[1]Dpto. CC de la Tierra, Universidad de Cádiz, Spain. (luis.barbero@uca.es)
[2]Dpto Geodinámica y Paleontología, Universidad de Huelva, Spain
[3]Dpto Física Aplicada, Universidad de Huelva, Spain
[4]Dpto Física Aplicada, Universidad de Cádiz, Spain

The Ríos Tinto and Odiel constitues one of the most extreme cases of acid mine drainage in the word and they are considered as the origin of one of the most important heavy metal discharge to the world's oceans.

In the Odiel river, the uppermost waters are clean and show geochemical parameters (pH, C, TDS, ORP, etc) typical of non-contaminated waters. The Río Tinto river shows acidic conditions from the headwaters down to the discharge into the sea. Total disolved REE contents in both rivers increases suddenly at pH values below 2.5 reaching values as high as 16000 μg/L, being lower than 1000 mg/L at pH higher than 2.5. Most enriched NASC-normalized REE patterns in Río Tinto show a negative Eu anomaly, this being progressively reduced as waters are diluted downstream and element precipitation or coprecipitation occurs. In the Río Odiel this slight negative Eu anomaly is mantained downstream which suggest that this feature is a proxy of the succesive AMD inputs. This Eu negative anomaly indicate that REE pattern are inherited from the massive sulfide or the waste rock. Another characteristic of the REE patterns of the Rios Tinto and Odiel is a MREE enrichment typical of waters related to AMD. Hypothesis to explain this include: acid leaching/dissolution of MREE-bearing amorphous iron oxyhydroxides [1]; fractionation by surface/solution reactions between MREE-enriched minerals and acid waters [2]; stabilization and coagulation by colloidal material [3]; combined action of different mechanisms [4]. To these, the possibility of disolving minerals with contrasting REE fractionation patterns should be considered.

[1] Johannesson and Zhou, 1999. [2] .Sholkovitz, 1995. [3] Elderfield *et al*., 1990. [4] Perez López *et al*., 2010.

Geochemical profiles to study the last deglaciation and its impact on rivers

EDOUARD BARD

CEREGE, College de France, Aix-Marseille University, CNRS, IRD, Technopole de l'Arbois BP 80, 13545 Aix-en-Provence Cedex 04, France (*correspondence: bard@cerege.fr)

The last deglaciation is fascinating for climatologists as it allows to study first-order climate changes that accompanied the retreat of the large Laurentide and Fennoscandian ice-sheets [1, 3]. Between 21000 and 6000 years before present, the climate system experienced a complete reorganization of all its compartments, e.g. atmosphere, oceans, lakes and rivers together with their associated ecosystems and biogeochemical cycles.

Linking records of the last deglaciation on land and in oceans requires accurate dating and comparison of different geological archives. A complementary way is to measure geochemical tracers of terrestrial and marine origins in the very same sediments raised in coastal environments.

Paleoclimate records at a particular location witness the successive phases of the last deglaciation. These various events, pauses and accelerations, have been known for many years (famous events such as Heinrich #1, Bolling, MWP1A, Allerod, Younger Dryas…), but it is only recently that geochemistry has provided analytical techniques allowing to produce high-resolution time series of various proxies based on elemental ratios (e.g. [2, 8]), organic compounds (e.g. [4, 5]) or stable and radiogenic isotopes measured in different sediment fractions: detrital, biogenic, authigenic phases or even interstitial waters (e.g. [6]).

To illustrate this growing research field, I will review what we know about deglacial sea level based on tropical corals and then go on to consider the associated changes in a few selected records from coastal zones, past river mouths or marginal seas (e.g. [4-9]). The aim is to illustrate the complex linkage between sea level rise, paleoclimatic changes and the reactivation of rivers during the last deglaciation.

[1] Bard E, Hamelin B, Delanghe-Sabatier D. (2010) *Science* **327**, 1235. [2] Böning P, Bard E, Rose E. (2007) *G-cubed* **8**(5). [3] Deschamps P, Durand N, Bard E, Hamelin B, Camoin G, Thomas AL, Henderson GM, Okuno J, Yokoyama Y. (2009) *Geophys. Res. Abst.* **11**. [4] Ménot G, Bard E. (2010) *GCA* **74**, 1537. [5] Ménot G, Bard E, Rostek F, Weijers JWH, Hopmans EC, Schouten S, Sinninghe Damsté JS. (2006) *Science 313*, 1623. [6] Soulet G, Delaygue G, Vallet-Coulomb C, Böttcher ME, Sonzogni C, Lericolais G, Bard E. (2010) *EPSL* **296**, 57. [7] Soulet G, Ménot G, Lericolais G, Bard E. (2011) *Quat. Sci. Rev.* [8] Soulet G, Ménot G, Garreta V, Rostek F, Lericolais G, Zaragosi S, Bard E. (2011) *EPSL*. [9] Vidal L, Ménot G, Joly C, Bruneton H, Rostek F, Cagatay N, Major C, Bard E. (2010) *Paleoceanography* **25**.

https://doi.org/10.1180/S0026461X00006502 Published online by Cambridge University Press

Redox reaction of pyrite with Se

FABRIZIO BARDELLI[1]*, MINGLIANG KANG[1,2], ANTOINE GEHIN[1] AND LAURENT CHARLET[1]

[1]ISTerre, Maison de Geosciences, 38041 Grenoble, France (*correspondence: fabrizio.bardelli@gmail.com)

[2]Chinese Academy of Sciences, Guangzhou, 510640, China

The radioactive isotope ^{79}Se with a half-life of 2.95×10^5 years, is presently considered as the key mobile fission product for the disposal of spent fuel and high-level radioactive waste [1]. Its solubility largely depends on redox conditions: Se(IV) and Se(VI) prevail as very mobile aqueous oxyanions, while the oxidation states 0, -I, and -II are solids with low solubility [2]. Due to the weak adsorption of Se(IV) and Se(VI) on natural minerals, and in particular on granite or claystone minerals, chemical reduction is considered to be the most effective way to immobilize ^{79}Se.

On the other hand, pyrite (FeS_2) is the most frequent sulfide mineral and is also present in geological barriers of nuclear waste repositories [3]. Its strong reducing capacity and its stability under anoxic condition make it a good candidate for the immobilization of redox-sensitive radionuclides, like ^{79}Se. Many works have focused on the identification of the reduced form of selenium when reacted with pyrite, but reported conflicting results [4,5,6]. Therefore we report a systematic where we investigate the effects of the reaction of Se(IV) and Se(VI) with pyrite in several different experimental conditions.

Experiments where conducted at ph 5.05, 5.65, 6.1, 7.0, and 8.5, reaction times of 7, 24, 36, and 48 days, and, at pH 7.0 and 8.5, with and without the addition of extra Fe^{2+} (10^{-4} mol/l). ICP-OES measurements where used to monitor the iron and Se concentrations and showed a decreasing trend of Se and increasing iron as a function of time. XAFS spectroscopy was used to unravel the selenium speciation. At pH 5.05 and 5.65 Se(0) was found to be the main reaction product, while at pH > 5.65, in addition to Se(0), XANES suggested the formation of iron selenides (Se -I or –II), in an amount which increased with the reaction time. The presence of iron selenides is further supported by Mössbauer spectroscopy clearly showing two different environments for Fe^{2+} in pyrite reacted with Se.

The results carried out in this study suggest that pyrite can significantly attenuate the mobility of ^{79}Se through chemical reduction.

[1] Chen *et al.* (1999) *J. Nucl. Mater.* **275**, 81-94. [2] Scheinost and Charlet (2008) *Environ. Sci. & Technol.* **42**, 1984-1989. [3] Beaucaire *et al.* (2000) *Appl Geochem.* **15**, 667-686. [4] Breynaert *et al.* (2008) *Environ Sci & Technol.* **42**, 3595-3601. [5] Naveau *et al.* (2007) *Environ Sci & Technol.* **41**, 5376-5382. [6] Liu *et al.* (2008) *Radiochim. Acta* **96**, 473-479.

Analysis of methanogen communities

LARRY BARESI

California State University, Northridge, CA 91330 USA (correspondence: larry.baresi@csun.edu)

Methanogens are an exciting group of microorganisms that live under conditions that are of interest to many engineers. They have been found to be active in coals, shales, and other carbon rich environments acting as both the final hydrogen and carbon sink producing methane as the final product. Physiological, molecular biology, biochemical, genetic, and ecological studies of these organisms can play a key role in optimizing their use. I will discuss the role of both past and present techniques such as DGGE/TGGE, 16s sequencing, bioinformatics, and metagenomics in expanding our understanding of this group and their associated organisms. I will also discuss how these new advances in our knowledge base can be used for the development of more effective biodegradation processes.

https://doi.org/10.1180/S0026461X00006502 Published online by Cambridge University Press

Speciation and dynamics of biologically reduced U(IV) in the Old Rifle, CO, aquifer

J.R. BARGAR[1]*, J.E. STUBBS[2], E.I. SUVOROVA[3], K.H. WILLIAMS[4], K.M. CAMPBELL[5], J.S. LEZAMA-PACHECO[1], J.M. CERRATO[6], M.A. STYLO[3], D.S. ALESSI[3], S.M. WEBB[1], R. BERNIER-LATMANI[3], D.E. GIAMMAR[6], J.A. DAVIS[4], P. FOX[4] AND P.E. LONG[7]

[1]Stanford Synchrotron Radiaion Lightsource, SLAC National Accelerator Laboratory, Menlo Park, CA, 94025, USA (*correspondence: bargar@slac.stanford.edu)
[2]University of Chicago, Chicago, IL 60637, USA
[3]Ecole Polytechnique Fédérale de Lausanne, Lausanne, CH-1015, Switzerland
[4]K.H. Williams, Lawrence Berkeley National Laboratory, Berkeley, CA, 94720, USA
[5]US Geological Survey, Boulder, CO, 80303, USA
[6]Washington University, St. Louis, MO 63130, USA
[7]Pacific Northwest National Laboratory, Richland, WA 99352, USA

The chemical and physical forms of U(IV), as well as the biogeochemical processes by which they form and transform, profoundly influence the behavior of uranium in reduced sediments. Obtaining this information for sediments biostimulated *in situ*, *i.e.*, in the field, has been one of the most important and difficult scientific challenges in the field of uranium bioremediation. We have used in-well columns to obtain direct access to sediment U(IV) species, evolving microbial communities, and trace and major ion groundwater constituents in the Old Rifle, CO (USA) aquifer. Sediments were examined using x-ray and electron microscopy (XRM and SEM/TEM), x-ray absorption spectroscopy (XAS), and chemical digestions. EXAFS analysis showed that U(IV) occurred predominantly or exclusively as monomeric U(IV) complexes under both metal- and sulfate-reducing conditions, and was associated with biomass or Fe sulfides. Intriguingly, U(IV) was bonded to oxygen atoms, even when associated with iron sulfides. A fraction of these monomeric complexes transformed into uraninite in the aquifer over a subsequent 12 month period. This work establishes the importance of monomeric U(IV) complexes in subsurface sediments at the Old Rifle site and provides a conceptual framework in which previously observed U(IV) reduction products can be related. These experiments also establish that U(IV) species are dynamic in aquifers and can undergo non-oxidative transformation reactions. These new results have imortant implications for uranium reactive transport models and remediation technologies.

Influence of citric acid, EDTA and fulvic acid on U(VI) sorption onto kaolinite

M. BARGER* AND C.M. KORETSKY

Department of Geosciences, Western Michigan University, Kalamazoo, MI 49008, USA (*correspondence: michelle.l.barger@wmich.edu)

Batch sorption experiments were used to investigate U(VI) sorption on kaolinite (2 g/L KGa-1b) as a function of pH (3-10), ionic strength (0.001 - 0.1 M $NaNO_3$), pCO_2 (0-5%), U(VI) (10^{-6} - 10^{-4} M U) and organic acid (10^{-4} and10^{-2} M citric acid, 10^{-4} - 10^{-2} M EDTA, and 10 - 20 mg/L fulvic acid). Ligand sorption on kaolinite was also assessed in the absence of U(VI).

In the absence of ligands, U(VI) sorption on kaolinite increases from pH 3 to ~7, plateaus at nearly 100% between pH ~7 - 8.5, and decreases at pH > 8.5. Ionic strength has little effect on U(VI) sorption. Thus, at circumneutral pH, kaolinite could have a strong influence on U(VI) mobility in natural systems. Compared to atmospheric conditions, U(VI) sorption under 0 pCO_2 is slightly enhanced from pH 3 – 7, and unchanged from pH of 7-10, likely due to strong aqueous U(VI)-OH^- complexes. However, with increased pCO_2, up to 5%, U(VI) sorption diminishes significantly between pH 5-10, due to formation of U(VI)-carbonate aqueous complexes.

Addition of 10^{-4} or 10^{-2} M citric acid results in decreased U(VI) sorption at all pH values, with up to 50 or 90% reduction in U(VI) sorbed, respectively. Similarly, addition of 10^{-4} -10^{-2} M EDTA yields a decrease in sorption of up to ~70% compared to organic-free experiments. TOC analyses of citric acid and EDTA sorption on kaolinite in the presence or absence of U(VI) demonstrate that less than 10% of either ligand is sorbed to the solid surface. Thus, ternary complex formation at the kaolinite surface is unlikely to occur. Instead, U(VI) binds preferentially to organic acids as aqueous complexes. Addition of 10 or 20 mg/L fulvic acid causes an increase in sorption from pH 3 to ~5 respectively, and a decrease from pH ~5 to 10. Up to 40% of 10 mg/L fulvic acid or 20% of 20 mg/L fulvic acid sorbs on kaolinite at low pH, with the amount adsorbed linearly decreasing to ~10% at pH 10. Fulvic acid complexation at the kaolinite surface results in enhanced U(VI) sorption at low pH, likely due to the formation of ligand bridges. However, at high pH, U(VI) sorption is suppressed, presumably due to formation of strong aqueous U(VI)-fulvic acid complexes.

These data suggest that U(VI) sorption on kaolinite could be significant at circumneutral pH, but that organic acids may significantly retard or enhance U(VI) mobility. The data are currently being used to develop surface complexation model parameters describing U(VI) sorption to kaolinite.

https://doi.org/10.1180/S0026461X00006502 Published online by Cambridge University Press

Mantle lithologies from minor elements in olivine: Cape Verde

A.K. BARKER[1], P.M. HOLM[2] AND V.R. TROLL[1]

[1]CEMPEG, Dept. of Earth Sciences, Uppsala University, (Abigail.Barker@geo.uu.se)
[2]Dept. of Geography & Geology, University of Copenhagen.

The Cape Verde Archipelago is known to display source heterogeneity on a 100-200 km scale, with different isotopic domains sampled in the northern islands (mixed HIMU and DMM), compared with the southern islands (mixed EM1 and HIMU). Detailed temporal studies of lavas from Santo Antão and Santiago, representing the northern and southern islands respectively, have shown that the EM1 and DMM components have uniform composition with time, whereas the HIMU component shows a synchronous decrease in $^{208}Pb/^{204}Pb$ with time throughout the Cape Verde Archipelago.

We present minor element data for primitive olivines (Fo>75%), to unravel the mantle lithologies associated with the isotopic heterogeneity in the Cape Verde archipelago.

Lavas from Santiago with low $^{206}Pb/^{204}Pb$ (18.8) and positive Δ8/4, are associated with EM1. They have olivines with Ca = 990-2040 ppm, Mn/FeO = 90-150 and Ni*FeO/MgO = 480-750. Lavas from Santiago with high $^{206}Pb/^{204}Pb$ (19.4), associated with HIMU, have Ca = 2100-2600 ppm, Mn/FeO = 106-120 and Ni*FeO/MgO = 500-640 in olivines from the old volcanics. The Ca and Mn/FeO decrease and Ni*FeO/MgO increases with time from the old volcanics to the intermediate and young volcanics.

Lavas from Santo Antão with $^{206}Pb/^{204}Pb$ of 19.2 sample local DMM and have olivines with Ca = 1900-2750 ppm, Mn/FeO = 95-110 and Ni*FeO/MgO = 305-580. Lavas from Santo Antão with $^{206}Pb/^{204}Pb$ of 19.9, representing the HIMU component, have Ca = 2100-2650 ppm, Mn/FeO = 106-116 and Ni*FeO/MgO = 540-660 in the old volcanics and lower Ca, Mn/FeO and higher Ni*FeO/MgO in the young volcanics.

The DMM of Santo Antão is peridotitic in nature, whereas the EM1 and HIMU components are sourced from mixed peridotite-pyroxenite mantle lithologies. The uniformity of the DMM and EM1 components with time shown by the isotope heteorgeneity is also reflected in the mantle lithologies, i.e. dominantly peridotitic DMM and constant proportions of peridotite and pyroxenite in the EM1 source. However, the changes in $^{208}Pb/^{204}Pb$ of the HIMU component with time observed throughout the Cape Verde archipelago are also reflected by increasing proportions of pyroxenite in the source shown by minor elements in olivine. We will present modelling results of the proportions of peridotite and pyroxenite in the EM1 and HIMU sources with time.

Phosphate dissolution/precipitation controls on isotopic compositions of continental assimilants

J.E. BARKMAN[1]*, J.G. BRYCE[1], E.B. WATSON[2], J. BLICHERT-TOFT[3], E.F. BAXTER[4] AND S.A. BOWRING[5]

[1]UNH Earth Sciences, Durham NH, USA (*correspondence: julie.barkman@unh.edu)
[2]RPI Earth & Environmental Sciences, Troy, NY, USA
[3]Ecole Normale Supérieure de Lyon, Lyon, France
[4]Boston University Earth Sciences, Boston, MA, USA
[5]EAPS, MIT, Cambridge, MA, USA

Partial melting and assimilation of lower and often ancient crustal rocks contribute to the chemical and petrologic evolution of continental magmas. In the past three decades, geochemical models have used isotopes and elemental abundances to improve the parameterization of thermal and mass transfer within the crust. Recent advances in microanalytical techniques have enabled the documentation of subtle isotopic and trace element variations at high spatial and temporal resolutions, allowing testing of assimilation models. Still, interpreting the geological implications of these chemical variations remains challenging, primarily due to the lack of experiments that can be used to parameterize the isotopic signatures of crustal anatexis products in existing assimilation models. Though experiments and theoretical treatments have improved the potential to assess Sr and Nd isotopic signatures of partial crustal melts, parameterization of Pb and Hf continue to be problematic. This has remained an issue because the isotopic signatures of Pb and Hf, two elements with many promising microanalytical applications, are strongly controlled by accessory phases.

To address these issues, we carried out isotopic measurements on partial melts generated experimentally at 900°C, 1 GPa by partially melting a 1.7 Ga two-mica granite. Resulting melts were rhyodacitic in composition (SiO_2 ~ 71 wt%), with elemental and isotopic measurements suggesting that with <10% melting, the Pb and Hf isotopic systems are in disequilibrium with their whole rock. Uranogenic ($^{206}Pb/^{204}Pb$ ~ 23) and thorogenic ($^{208}Pb/^{204}Pb$ ~ 47) Pb signatures and extraordinarily radiogenic Hf (ε_{Hf} ~ +250) suggest the melt isotopic systematics are strongly influenced by contributions from phosphates. This extremely radiogenic Hf, coupled with sluggish Hf diffusion and predictions from solubility models, provides support for the notion that ongoing dissolution and reprecipitation reactions of phosphates may play an important role in effectively redistributing radiogenic signatures of accessory phases through the melt.

https://doi.org/10.1180/S0026461X00006502 Published online by Cambridge University Press

The first multiple sulfur isotope evidence for a 2.9 Ga Mesoarchean sulfate reservoir

M.E. BARLEY[1]*, S.D. GOLDING[2], G.J. HEGGIE[1] AND M.L. FIORENTINI[1]

[1]School of Earth and Environment, The University of Western Australia, Crawley, Western Australia, 6009, Australia (correspondence: mark.barley@uwa.edu.au)
[2]School of Earth Sciences, The University of Queensland, Brisbane, Queensland. Australia

The relationship between the evolution of Earth's atmosphere and hydrosphere during the Archean are important and mass-independent fractionation (MIF) of multipe sulfur isotopes caused by ultrviolet photolysis of atmospheric SO_2 is a key contribution to this when the atmosphere was oxygen poor and ocean was sulfur poor. In particular understanding why there are significant variations in the degrees of mass independent fractionation during the Archean and why it was lowest in the Mesoarchean (from 3.3 to 2.8 Ga) is important. This had been suggested to be a result of an early rise of oxygen. However, more recent studies show there is no clear evidence that oxygen rose then and the strongest Mesoarchean $\Delta^{33}S$ MIF values ranged from -0.13 to 1.31 between 2.96 Ga and 2.9 Ga [1] that coincide with volcanic events during this period that erupted volcanic gasses to the atmosphere for development of MIF and the most abundant Mesoarchean sulfur. Because prior to 2.7 Ga there is a limited rock record and most samples analysed from the Mesoarchean are from continental margin sedimentary ocean basins, the lack of significant negative $\Delta^{33}S$ values has provided no evidence for oceanic sulfate during this period. However, the ~2.9 Ga Lake Johnston Greenstone belt in the Yigarn Craton is a marine rift with submarine volcanic rocks (basalts, felsic volcanics and komatiites) shales and banded iron formations (BIFs) with a significant amount of low temperature volcanogenic massive sulfides (VMS) and the Maggie Hays komatiite-hosted Ni sulfide deposit. The $\Delta^{33}S$ values we recently obtained from this belt range from -1.7 to 0.1 providing the first strong negative $\Delta^{33}S$ data from the Mesoarchean consistent with inorganic sulfate reduction similar to that observed in the Neoarchean VMS, komatiite-hosted Ni sulfides and BIFs. This provides evidence for a Mesoarchean sulfate reservoir linked to a subaerial volcanic plume and oceanic volcanic island eruptions.

[1] Farquar *et al*. (2007) *Nature* **449**, 706-709.

An isotopic perspective on mass bias and matrix effects in MC-ICP-MS

JANE BARLING AND DOMINIQUE WEIS

PCIGR, EOS, University of British Columbia, Vancouver, BC V6T 1Z4, Canada (jbarling@eos.ubc.ca)

Precise and accurate correction for instrumental mass bias is required to achieve the level of precision and accuracy needed for isotope ratio measurements by multi-collector inductively coupled plasma mass spectrometry (MC-ICP-MS). However, instrumental mass bias and the causes of its variation are not well constrained. With the excellent internal precision of isotope ratio measurements by MC-ICP-MS, we can investigate mass bias variation at an isotopic as opposed to elemental level in order to shed light on the processes underlying mass bias variation in the plasma. For this study we measured the spatial variation of Pb and Tl isotope ratios in dry plasma and their response to the presence of matrix.

Mass dependent radial variation of Pb isotope ratios indicates that lighter isotopes show greater dispersion from the axis of the plasma than heavier isotopes, in agreement with elemental observations by ICP-MS [1]. Axial variations in Pb and Tl isotope ratios show that isotopic signal maxima (I_{max}) are distributed in a mass dependent manner (Pb I_{max} separation: 3.47±2.07μm/amu), with I_{max} for heavier isotopes closer to the load coil than I_{max} for lighter ones; the reverse of the elemental mass dependence observed in ICP-MS [2]. This difference in mass dependent behaviour may be due to processes in the interface related to, for example, the high acceration potentials (4-10kV) used in MC-ICP-MS.

Addition of a low first ionization potential (1.IP) element to the plasma promotes ionization of Pb and Tl closer to the load coil, whereas a high 1.IP element results in ionization further from the load coil. Elements with low second ionization potential and those forming refractory oxides may also promote ionization further from the load coil. In addition to shifting the position of Pb and Tl I_{max}, the presence of matrix also reduces run-to-run variations in the mass dependent separation of isotope I_{max} (Pb I_{max} separation: 3.50 ± 0.54μm/amu). This reduced variability in mass dependent isotope separation under matrix-loaded conditions may provide an explanation for improved accuracy and external reproducibilty of dry plasma Pb isotope ratio measurements in the presence of a common matrix [3].

[1] Dziewatkoski *et al*. (1996) *Anal. Chem*. **68**, 1101-1109. [2] Vanhaecke *et al*. (1993) *JAAS* **8**, 433-438. [3] Barling & Weis (2008) *JAAS* **23**, 1017-1025

https://doi.org/10.1180/S0026461X00006502 Published online by Cambridge University Press

1500 yr cyclicity during mid- Holocene in the Eastern Mediterranean

M. BAR-MATTHEWS* AND A. AYALON

Geological Survey of Israel, Jerusalem, Israel (*correspondence:matthews@gsi.gov.il, ayalon@gsi.gov.il)

High-resolution (~3 to 20 years) speleothems records from the Eastern Mediterranean (EM) during mid-Holocene (7.0 to 4.0 ka) reveals 4 important patterens: a) ~1500 years cyclicity; b) correlation between half a cycle and archeological time framework; c) "dogtooth" pattren representing fast ~50-100 years increase in rainfall followed by gradual drying over a longer period of ~100-500 years. The structure of these changes resembles the structure the D-O events d) rapid climate changes (RCC) lasting 20-50 years [Fig. 1]. It is not clear what controls the 1500 years cycle (Bond cycles) and the so called "D-O events" that are clearly recognized during mid-Holocene speleothems in mid latitudes, the EM.

Interestingly each half cycle is associated with cultural-technological tranzitions, suggesting that these tranzitions follow long term climate trends (~400-800 years) rather than a response to RCC. Two of the tranzitions occur at the peak of the wettest period: the tranzitions from Mid- to Late Chalcolithic and from the Early Bronze II to III at 6.55-6.45ka and 4.8-4.7ka respectively, when annual precipitation increased by up to ~30% relative to present. The end of the Chalcolithic period and the transition from Early Bronze IV to the end of the Mid Bronze age occurred after of a long drying trend at 5.7-5.6ka and at 4.2-4.05ka respectively when precipitation dropped by ~30% relative to present.

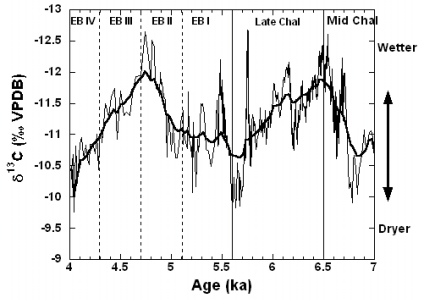

Figure 1: carbon isotopic composition showing the 1500 y cyclicity, D-O type events, RCC and the archeological time framework.

Li isotope compositions of Hawaiian post-shield lavas

ELSPETH M. BARNES, DOMINIQUE WEIS AND DIANE HANANO

Pacific Centre for Isotopic and Geochemical Research, University of British Columbia, Vancouver, BC V6T 1Z4 Canada (dweis@eos.ubc.ca)

Hawaiian post-shield lavas show more depleted geochemical signatures than their shield equivalents and the difference is attributed to material in the plume source, where the very enriched trace element concentrations in post-shield lavas clearly indicate that the source material is not MORB. We investigated Li isotope compositions in a series of well-characterized post-shield samples [1] to explain the origin of these geochemical characteristics and assess the potential contribution of recycled oceanic crust in post-shield lava.

Hualalai volcano δ^7Li values range between 1.91±1.00 (2SD) and 3.53±0.53‰, Mauna Kea samples show the smallest range, 3.39±0.89 to 4.93±1.92‰, contrasting with δ^7Li from the oldest sampled volcano, Kohala, which shows the broadest range, 1.97±0.35 to 4.04±0.44‰. For comparison, a 1993 tholeiitic sample from Kilauea volcano has δ^7Li of 3.72±1.29‰, while a Koolau Makapuu sample shows a relatively heavy δ^7Li value at about 4.5‰. In contrast to other isotopic ratios (e.g., ^{208}Pb/^{204}Pb), Kilauea and Koolau do not appear to represent compositional end-members of Hawaiian compositions in the Li isotope system.

Li isotope signatures of the studied post-shield lavas tend to be 'light' relative to shield lavas (δ^7Li 3.45 to 5.7‰; Mauna Loa and Mauna Kea)[2] and correlate positively with Nd, Hf and Pb isotope signatures, and negatively with Sr isotopes, possibly defining the history of the source material.

Our results indicate that the youngest post-shield lava sampled (Hualalai) has some of the 'lightest' δ^7Li values. Hualalai Volcano also has some of the lowest radiogenic Pb ratios that may derive from ancient recycled oceanic lithosphere and sediments that have geochemically evolved in the presence of low U/Pb during subduction dehydration processes in the upper mantle. We suggest that these dehydration processes may have driven ^{7}Li off in the fluid from the residual slab resulting in an isotopically 'light' Li signature in the plume source material [3].

[1] Hanano *et al*. (2010) *Geochem. Geophys. Geosyst.* **11**, doi:10.1029/2009GC002782. [2] Chan & Frey (2003) *Geochem. Geophys. Geosyst.* **4**, doi:10.1029/2002GC000365. [3] Elliott *et al*. (2006) *Nature* **443**, 565-568.

https://doi.org/10.1180/S0026461X00006502 Published online by Cambridge University Press

Chlorine chemistry of altered oceanic crust

J.D. BARNES*

Department of Geological Sciences, Jackson School of Geosciences, University of Texas at Austin, Austin, TX, 78712, USA (jdbarnes@jsg.utexas.edu)

Chlorine strongly partitions into aqueous fluids, thereby making Cl and its stable isotopes (^{37}Cl and ^{35}Cl) powerful tracers of fluid-rock interaction, including interaction between oceanic lithosphere and hydrothermal fluids. Although altered oceanic crust (AOC) is considered to be a major Cl reservoir estimated to subduct ~2.5-3 x 10^{12} g of Cl worldwide each year [1, 2], work on the Cl chemistry of AOC is surprising limited. Here I present new Cl concentration and isotopic data for AOC from seven DSDP/ODP/IODP drill sites (801C, 735B, 894F/G, 504B, 1256D, 417A/D/418A, 332A/B), greatly expanding the previous data set.

Chlorine concentration and δ^{37}Cl values of AOC are heterogeneous among and within individual drill sites. Cl concentrations range from <0.01 to 0.09 wt% (n = 26) and δ^{37}Cl values range from -0.8 to +1.5‰ (error < ± 0.2‰) vs. SMOC (Standard Mean Ocean Chloride) (n = 20). These data greatly expand the range of previously reported AOC δ^{37}Cl values (-1.6 to -0.9‰; n = 3; Hole 504B; [3]). Neither Cl concentration nor isotopic composition is correlated with tectonic setting or crustal age. The Cl concentration decreases with depth in ODP Hole 735B from the SW Indian Ridge from 0.09 wt% at the top of the hole to <0.01 wt% at depth. A similar pattern is seen for δ^{37}Cl values ranging from -0.6 to +1.5‰ with the most positive values located near the top of the hole. The high Cl concentrations and δ^{37}Cl values are correlated with increased hydrothermal alteration (increased amphibole abundance) near the top of the hole. However, this trend is not consistent among all the holes implying that Cl chemistry is influenced by a variety of factors. Detailed future petrography and additional geochemical work will further test the correlation between Cl concentration and isotopic composition and mineralogy, as well as, examine the role of water-rock ratios, deformation, and temperature of hydrothermal alteration. These data can ultimately be used to reevaluate mass balance calculations improving our understanding of subduction recycling.

[1] Ito *et al*. (1983) *GCA* **47**, 1613-1624. [2] Jarrard (2003) *Geochem., Geophy., Geosys*. **4**, doi:10.1029/2002GC000392. [3] Bonifacie *et al*. (2007) *Chem. Geol*. **242**, 187-201.

Is the platinum in the Bushveld complex derived from the lithospheric mantle ?

SARAH-JANE BARNES[1], WOLFGAND D. MAIER[2] AND EDWARD A. CURL[3]

[1]Universite du Quebec a Chicoutimi, G7H 2B1, Canada (sjbarnes@uqac.ca)
[2]University of Oulu, Finland, (wolfgang.maier@oulu.fi)
[3]Monash University, Australia, (edcurl@yahoo.com)

The Bushveld Complex of South Africa contains ~ 80 % of the world's Pt and almost half of its Pd resources in the form of three large ore deposits, the Merensky Reef, the UG-2 reef and the Platreef. Two questions arise a) were the magmas that formed the Bushveld Complex pariticularily Pt- and Pd-rich? and b) what is the origin of these magmas? In order to consider these questions we have estimated the compositon of the Bushveld magmas based on 40 new whole rock analyses of quench textured rocks from the margins of the intrusion.

Broadly speaking, there are two types of magmas present, a Mg-rich basaltic andesite and a tholeiitc basalt. Both of these magmas are enriched in large ion lithophile elemnts, light rare earth elements and in Pb. Both magmas have negative Ta, Nb, P and Ti anonmalies. The PGE contents of both magmas are similar to primary basalts and they do not appear to be enriched in PGE, except for Pt. The Pt/Pd ratio and Pt/Ti ratios are 1.5 to 2 times that of most basalts.

It is possible to model the lithophile element composition of the two magma types by up to ~ 50 % crustal contamination of komatiitic basalt or picrite. This conclusion is supported by Sr, Nd and oxgen isotopic work. However, the Pt contents of the model magmas and the Pt/Pd and Pt/Ti ratios are much lower than those observed. An alternative is to suggest that the Bushveld magmas formed by parital melting of the metasomatised lithosphere. But, modeling using Kaapvaal mantle xenoliths compositions and MELTS shows that this magma would be too Al_2O_3 rich and SiO_2 poor.

Two possible solutions to this are: a) the melts formed by zone refining melting of the lithosphere (to attain usually high Pt concentrations) followed by contamination with crustal melts; OR b) the current estimate of primitive upper mantle with a Pt/Pd of 1 is incorrect and it should be closer to 2, in which case mixing of a plume derived magma with continental crust melts approximates the composition of the Bushveld magmas

https://doi.org/10.1180/S0026461X00006502 Published online by Cambridge University Press

Microprospecting for platinum group minerals by X-ray fluorescence mapping using the Maia detector

STEPHEN J. BARNES[1], BELINDA GODEL[1] AND CHRISTOPHER G. RYAN[2]

[1]CSIRO Earth Science and Resource Engineerin Perth Western Australia (steve.barnes@csiro.au)
[2]CSIRO Earth Science and Resource Engineering Clayton Victoria

X-ray fluorescence microprobe mapping (XFM) has been used to locate micron-sized grains of platinum group element minerals in mantle nodules, komatiites and nickel sulfide ores using the Maia massively paralleled detector on the XFM beamline at the Australian Synchrotron [1]. The technique enables whole thin sections to be mapped at a pixel resolution of 2 microns, producing images up to 80 Mpixels in a few hours.

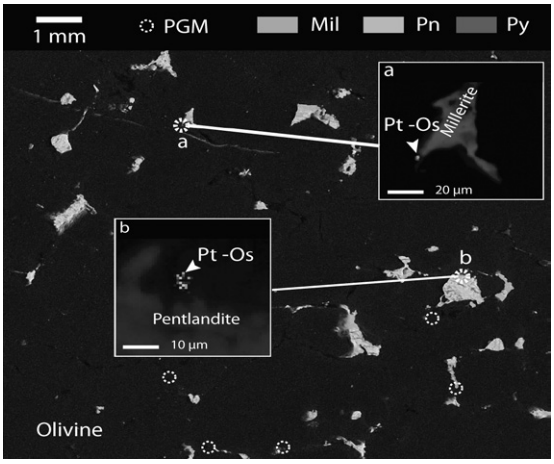

Figure 1. XFM image of sulfide-bearing dunite, Betheno, WA. Mil = millerite, Pn pentlandite, Py pyrite.

The example presented in Fig 1. shows one quarter of a standard thin section of a disseminated sulfide bearing fresh komatiitic dunite [2] containing 16 ppb Pt. XFM mapping revealed presence of 7 distinct PGM grains, only one of which had been located in a previous SEM search. This follows from the capability of the XFM method to detect buried grains within the 100 micron thickness of the section. PGMs are commonly found close to, but not in direct contact with, base metal sulfide globules.

[1] Ryan C.G. *et al*. (2010) *Nuclear Instruments & Methods in Physics Research Section A* **619**, 37-43. [2] Barnes *et al*. (2011) *Australian Journal of Earth Sciences*, in press.

Chalcophile elements in magmas and magmatic sulfide deposits: Can we see the mantle signals?

STEPHEN J. BARNES[1], MARCO L. FIORENTINI[2] AND WOLFGANG D. MAIER[3]

[1]CSIRO Perth Western Australia (steve.barnes@csiro.au)
[2]University of Western Australia Perth
[3]University of Oulu, Finland

Magmatic sulfide deposits are associated with a very wide variety of magma compositions from komatiites to andesites, spanning ranges of more than an order of magnitude in Ni content and three orders of magnitude in platinum group elements. Similar ranges are seen in sulfide ore tenors.

Late Archaean komatiites[1,2] show a strong consistency in PGE and Ni contents implying lack of S saturation except in the immediate environment of ore formation, and a broad homogeneity of deep mantle plume sources after 3 Ga.

Three trends are evident in post-Archaean basalts: source sulfide control, resulting in Pt and Pd depletion at high Mg#; cotectic sulfide fractionation, resulting in steady decrease in Pt and Pd with decreasing Mg#; and catastrophic depletion due to bulk crustal S assimilation [1]. Mantle signals are overprinted and difficult to discern in the latter two trends.

Basalts show very wide variability, and fall under a near-universal envelope of maximum Pt and Pd contents when normalised to moderately incompatible elements such as Ti. This maximum is lower than that for komatiites, implying either that all post-Archaean mantle sources are Pt-Pd depleted compared with Archaean plume sources, or that there is a universal global control owing to retention of sulfide in source mantle. However, source sulfide should produce a larger depletion, as seen in the Pt and Pd signal in primitive MORB and OIB. Within post-Archaean mafic magmas, only the Bushveld Complex sills stand out as being unusually PGE enriched, and even then the signal is only evident as a twofold enrichment in Pt [3]. Otherwise the Bushveld magmas appear to fall on extensions of the komatiite trends.

Iridium, Ru and Os are decoupled from Pt and Pd in basalts and komatiites, and show evidence for control by solubilities of Ir-rich phases [4]. This greatly limits the ability to read mantle abundances from magma compositions, and may have implications for Os iotope signals.

[1] Fiorentini *et al* (2010) *Journal of Petrology*, **52**, 83-112. [2] Fiorentini *et al* (2010) *Economic Geology*, **105**, 795-823. [3] Sarah Barnes *et al*. (2010) *Economic Geology* **105**, 1491-1512. [4] Barnes and Fiorentini (2008) *Chemical Geology* **257**, 44-58.

https://doi.org/10.1180/S0026461X00006502 Published online by Cambridge University Press

Volcanic, solar activity, and atmospheric circulation influences on cosmogenic 10Be fallout at Vostok and Concordia (Antarctica) over the last 60 years

M. BARONI[1], E. BARD[1], J.-R. PETIT[2], O. MAGAND[2] AND D. BOURLES[1]

[1]CEREGE, Aix-Marseille University, CNRS, IRD & College de France, Technopole de l'Arbois BP 80, 13545 Aix-en-Provence Cedex 04, France (baroni@cerege.fr)

[2]Laboratoire de Glaciologie et de Géophysique de l'Environnement (CNRS-UJF 5183), 38402 Saint-Martin-d'Hères, France

The cosmogenic nuclide beryllium 10 (10Be), recovered from ice cores, is often used to study solar activity on long timescales. However, the 10Be signal is also influenced by factors other than the Sun. In order to identify and quantify various contributions to the 10Be signal, two Antarctic snow records from the Vostok and Concordia sites spanning the last 60 years were studied at a sub-annual resolution. Three factors that contribute to the 10Be signal were identified. First, in both records, a significant period of approximately 11 years, that can be associated with the modulation of 10Be production by solar activity, was detected. Then, peaks in 10Be concentrations during the time of the stratospheric volcanic eruptions of the Agung (in 1963) and the Pinatubo (in 1991), respectively, were observed. The data indicate that stratospheric volcanic eruptions can impact 10Be transport and deposition. Also, an interannual variability of ~4yrs was determined in both 10Be records. As with species of marine origin, this 4yrs variability is interpreted as a tropospheric signal that could be associated with atmospheric circulation inherited from the coupled Southern Ocean ocean-atmosphere system. The results presented, here, from sites within the high Antarctic plateau open perspectives for ice cores dating over the last few centuries, as well as for the reconstruction of past solar activity in relation to climate.

Characterization of Anaerobic Methane Oxidation in Lake Kinneret (Israel)

ITAY BAR-OR[1], ORIT SIVAN[1], ADLER MICHAL[1], ARIEL KUSHMARO[2], ANN PEARSON[3], WERNER ECKERT[4]

[1]Department of Geological and Environmental Sciences, Ben-Gurion University of the Negev, Beer Sheva, Israel. (barorit@bgu.ac.il, oritsi@bgu.ac.il, sela@bgu.ac.il)

[2]Department of Biotechnology Engineering, Ben-Gurion University of the Negev, Israel, arielkus@bgu.ac.il.

[3]Department of Earth and Planetary Sciences, Harvard University, Cambridge, MA 02138, USA, (pearson@eps.harvard.edu).

[4]Israel Oceanographic and Limnological Research, The Yigal Allon Laboratory, Tiberias , Israel, (Werner@ocean.org.il)

In this study we show biogeochemical evidence for anaerobic oxidation of methane (AOM) in deep lake sediments and demonstrate that this AOM is likely driven by iron reduction. This is by producing porewater chemical and isotope profiles from Lake Kinneret (Sea of Galilee, Israel), together with incubation experiments, lipid analysis and molecular microbiology methods, including PCR, cloning and sequencing of archaea and bacteria.

Porewater profiles of methane and the stable carbon isotopes of the total lipid and methane indicate a sink for methane below the depths at which nitrate and sulfate are completely exhausted and the zone of methanogenesis. At that depths Fe(II) showed an increase, and iron isotopes decrease, suggesting that Fe(III) is the probable terminal electron acceptor. Based on these results incubation experiments of sediment cores and slurries were conducted to verify and quantify the rate of this process and its key parameters. This is by using amorphic ferric oxide and labelled methane. The results strengthened the iron dependent AOM hypothesis, and the obtained AOM rates were about 10% of the production rates. Analyses of the community structure and diversity of bacteria and archaea along the sediment gradients showed indeed the appearance of involved bacterial methanogens and methanotrophs in the deep sediment.

https://doi.org/10.1180/S0026461X00006502 Published online by Cambridge University Press

Gaseous mercury in soils over deeply buried sulfide deposits

F.C.D. BARROS[1,2], J. ENZWEILER[2]*, O.A.B. LICHT[3], Z. CASTILHOS[4] AND P.C. ARAUJO[4]

[1]University of Campinas/Votorantim Metais – Brazil, (fernanda.barros@vmetais.com.br)
[2]University of Campinas, P.O. Box 6152, CEP13083-970, Brazil, (*correspondence:jacinta@ige.unicamp.br)
[3] MINEROPAR - Serviço Geológico do Paraná - Brazil, (otavio@mineropar.pr.gov.br)
[4]Centro de Tecnologia Mineral (CETEM) - Brazil, (zcastilhos@cetem.gov.br; paraujo@cetem.gov.br)

The measurement of gaseous mercury in soils over a deep (~90 m) zinc sulfide mineralization was used to evaluate its potential as a mineral exploration technique. The Zn-Pb Santa Maria deposit (Camaquã Basin, RS, Brazil) contains sphalerite and galena as main ore minerals and up to 7 μg/g Hg. Holes at depths of 30 cm and 50 cm were made at preselected sample locations on three soil transects, two of them over the ore body. The Hg in soil pore gas was measured during 30 s, after inserting the hose of a portable Hg analyser in the hole and air purging. The concentrations of Hg in soil pore gas samples were typically low (< 5 ng/L) but significantly higher values were measured in the deeper holes, i.e., up to 18 ng/L. The higher Hg concentrations marked the position of the ore body. Total Hg in soil samples attained 40 ng/g, which also coincides with the mineralization, while median value was 21 ng/g.

Application of DSC and NMR to study the soil organic matter in the Atacama desert

N. BARROS, S. FEIJOO, J.A. RODRIGUEZ-AÑON, J. PROUPIN, M. VILLANUEVA AND J. SALGADO

Dept. Applied Physics. University of Santiago de Compostela. Spain. (nieves.barros@usc.es)

The study of the organic matter in desert soils makes necessary the development of sensitive methods to detect low percentages of SOM.Differential scanning calorimetry (DSC), together with ^{13}C CPMAS and 2D liquid H NMR was applied to study the SOM composition and structure of different mineral soils collected in the Atacama desert. DSC was very sensitive to study the SOM of those samples in base on their thermal properties. SOM combustion was detected in the DSC curves at C percentages up to 0.5 %. Most of them showed two well defined combustion peaks at temperatures atributed to carbohydrates and aromatic compounds.The heat of combustion obtained by the direct integral of those curves were directly correlated with the C and OM percentages of the soils as found in soils rich in organic matter content. The normalization of the heat of combustion to the OM content of the samples indicated different OM composition in the soils from Atacama. ^{13}C CPMAS NMR spectra indicated the existence of carbohydrates and aromatic compounds too.The aromatic compounds could be assigned to phenols derived from lignin. 2D liquid H NMR showed predominance of the aliphatic compounds when these soils are treated with chloroform.Most of the aliphatic C detected is attributed to Acetyl C and Methyl C in lipids or/and suberin. Nevertheless, the aliphatic fraction of the organic matter was not detected by the DSC and ^{13}C CPMAS NMR. Application of the three methods gives accurate information about the OM composition in these soils. It seems the carbohydrates and aromatic compounds are the main constituents in these mineral soils. Aliphatic C takes part of the general OM composition too but at lower percentages and it is necessary the specific extraction to be detected.

https://doi.org/10.1180/S0026461X00006502 Published online by Cambridge University Press

Stalagmite reconstruction of Moroccan climate from geographically spaced records

J.J. BARROTT[1]*, C.C. DAY[1], R.N.E. BARTON[2], A. BOUZOUGGAR[3] AND G.M. HENDERSON[1]

[1]Department of Earth Sciences, University of Oxford, UK, (*correspondence: julia.barrott@earth.ox.ac.uk)
[2]Institute of Archaeology, University of Oxford, UK (nick.barton@arch.ox.ac.uk)
[3]Institut National des Sciences de l'Archaéologie et du Patrimoine (abouzouggar@yahoo.fr)

Located at the boundary between Mediterranean and Saharan climates and within the southern limit of the North Atlantic storm tracks, Morocco is strategically placed for studying glacial to sub-millennial timescale shifting of climate boundaries. There is a specific lack, however, of high-resolution terrestrial records with high-precision, absolute chronology. Consequently, climate variation arising from interplay between climate systems is poorly understood and IPCC (2007) predictions of rainfall are presently uncertain. Precisely-dated, high-resolution, records of palaeoclimate linked with Morocco's extensive, rich archaeological records will also provide valuable insight into the potential effects of rapid climate change on pre-historic communities.

This study provides high-resolution and precisely dated U/Th records from speleothems discretely sampled from six caves in three sites (Ghar Cahal on the NW Mediterranean coast [5°3 W, 35°5 N]; 3 caves near Ouarzazate close to [7°3 W, 30°2 N]; and 2 caves in the SE close to Errachidia [4°2 W, 32°0 N]). Continuous growth and more negative $\delta^{18}O$ values in northern Morocco concurrent with abundant speleothem growth in the currently arid area south of the Atlas mountains suggests overall wetter conditions during the mid-Holocene and allow assessment of the pattern of rainfall and air-masses. We investigate the temporal and spatial relationships between these sites and compare them with existing records from the Holocene Climatic Optimum period, and with archaeological records in the region.

Comparison of oil sands process waters and natural water using Fourier transform ion cyclotron resonance mass spectrometry

MARK P. BARROW[1]*, JOHN V. HEADLEY[2], KERRY M. PERU[2], BRIAN FAHLMAN[2], RICHARD A. FRANK[3] AND L. MARK HEWITT[3]

[1]Department of Chemistry, University of Warwick, Coventry, CV4 7AL, United Kingdom (*correspondance: M.P.Barrow@warwick.ac.uk)
[2]Water Science and Technology Division, Environment Canada, Saskatoon, Canada
[3]Water Science and Technology Division, Environment Canada, Burlington, Canada

As the demand for petroleum has continued to rise, it has become necessary to increasingly turn to previously non-viable sources of oil, such as the oil sands in the Athabasca region of Canada. Using an alkaline hot water extraction process, the bitumen can be extracted from the oil sands prior to being upgraded to synthetic oil. Approximately three barrels of fresh water are required during the process to produce one barrel of synthetic oil. The exploitation of the Athabasca oil sands is therefore placing a burden upon the aquatic ecosystem in particular.

Fourier transform ion cyclotron resonance (FTICR) mass spectrometry has played a key role in the advent of the field of "petroleomics." The inherent ultra-high resolving power and mass accuracy is unrivalled within mass spectrometry, making the technique highly-suitable for the analysis of complex mixtures.

A 12 T Bruker solariX FTICR has been used to characterize a range of samples from the Athabasca region of Canada. The samples originate from natural water sources, such as rivers and lakes, and industrial sources, such as tailings ponds. High field FTICR mass spectrometry affords the ability to characterize the thousands of components present within the samples, which create characteristic signatures. Subsequent usage of principal component analysis (PCA) has demonstrated that these profiles can be used to determine the origins of samples, including distinguishing between industrial sources. There is potential for FTICR mass spectrometry to delineate between naturally-occurring profiles and anthropogenic sources.

https://doi.org/10.1180/S0026461X00006502 Published online by Cambridge University Press

Stable isotope (C-N) and noble gas (Ne-Ar) evidence for recycled plume components at the CIR

P.H. BARRY*[1], D.R. HILTON[1], E. FÜRI[1], B. J. MURTON[2], C. HEMOND[3] AND J. DYMENT[4]

[1]Geosciences Research Division, Scripps Institution of Oceanography, UCSD, La Jolla, California 92093, USA (*correspondence: pbarry@ucsd.edu)
[2] University of Southampton, Southampton Oceanography Centre, European Way, Southampton SO14 3ZH, UK
[3] UMR 6538 Domaines oceaniques IUEM Place Nicolas Copernic, Plouzane, 29280, France
[4] UMR-CNRS 7097, Institut de Physique du Globe de Paris, 4 Place Jussieu, 75005 Paris, France

We present new CO_2 ($\delta^{13}C$), N_2 ($\delta^{15}N$) and Ne-Ar isotope results on basaltic glasses of the Central Indian Ridge (CIR) (~17 – 21°S). Our aim is to assess whether the Réunion plume component evident along the CIR [1] also reveals a recycled contribution in the stable isotope and noble gas systematics. Positive $\delta^{15}N$ are attributed to post-Archean subduction whereas low $\delta^{15}N$ are associated with Archean recycling [2].

Nitrogen isotopes ($\delta^{15}N$) range from +3 to -3‰ (n=10) and overlap with positive $\delta^{15}N$ anomalies previously observed in Réunion xenoliths [3]. C-isotopes (n=17) range from -4 to -20‰ vs. PDB with the majority of samples falling in the MORB range. Equilibrium degassing models suggest that C-source characteristics may extend to -2.5‰. $^{20}Ne/^{22}Ne$ values range from 9.8 to 11.3 and when extrapolated to solar (Ne-B) values, $^{21}Ne/^{22}Ne$ ratios are ~0.049. $^{40}Ar/^{36}Ar$ ratios range from 298 up to 8413 with the highest $^{20}Ne/^{22}Ne$ value occurring in the highest $^{40}Ar/^{36}Ar$ sample. Notably, positive $\delta^{15}N$ samples display Ne and Ar only slightly higher than air-values, whereas negative $\delta^{15}N$ samples display distinct primordial Ne. $\delta^{15}N$ shows no correlation with $^{4}He/^{40}Ar^*$ [1] indicating $\delta^{15}N$ values are independent of degassing effects.

Taken together, the N-Ne-Ar results suggest multiple recycled components in CIR basalts, including Archean (low $\delta^{15}N$) and post-Archean (high $\delta^{15}N$) components, both of which are potentially integrated into the Réunion plume. Conversely, CO_2 results retain close to canonical MORB-like signatures, suggesting that either the source CO_2 is masked by external processes (e.g. - degassing and/or crustal contamination) or that CO_2 in the (upper and lower) mantle is homogenized to the extent that we cannot differentiate between the various reservoirs.

[1] Füri *et al*. (2011) *JGR* **116**. [2] Marty *et al*. (2003) *EPSL* **206**. [3] Fischer *et al*. (2005) *GRL* **32**.

The influence of F, P and B content on pegmatitic melt viscosity

A. BARTELS[1], J. KNIPPING[1], H. BEHRENS[1], F. HOLTZ[1] AND B.C. SCHMIDT[2]

[1]Institute for Mineralogy, Leibniz University of Hannover, Germany, (a.bartels@mineralogie.uni-hannover.de)
[2]Experimentelle und Angewandte Mineralogie, GZG, Georg-August Universität Göttingen, Germany

The key property governing dynamics in strongly depolymerized partially melted systems is the melt viscosity. To test the individual influences of elements like F, P and B on melt viscosity of pegmatitic water-bearing systems a starting glass was prepared from a mixture of SiO_2, Al_2O_3, Na_2CO_3, and K_2CO_3. This starting composition (67.73wt% SiO_2, 20.20wt% Al_2O_3, 7.80wt% Na_2O and 4.27wt% K_2O) was then doped with different amounts of F (up to 4.8 wt%), P_2O_5 (up to 4 wt%) and B_2O_3 (up to 0.93wt%).

The viscosity of hydrous melts (1 to 6 wt% H_2O) was determined in internally heated gas pressure vessels using the falling sphere method (low viscosity range) in the temperature range 1173 - 1573 K at 200 MPa and 300 MPa. In the low temperature range the viscosity was determined between 580 and 880 K at ambient pressure using the micropenetration technique.

The results demonstrate that the viscosity decreases with the addition of F at all investigated temperatures. This viscosity decrease is more pronounced at low temperature and at low water content. The viscosity of pegmatitic melts containing ~ 6 wt% H_2O and 4.8 wt% F is 225 Pa·s at 1273 K. This value is about 1 log unit higher than that of complex pegmatitic melts containing F, B, P and Li [1]. Thus, although we confirm that F is clearly a fluxing agent, additional elements and their mutual interaction play a crucial role in the viscosity of natural pegmatite melts.

Our results indicate that phosphorus may not play a major role in viscous flow. In comparison to F the effect of P_2O_5 on melt viscosity is much lower (0.5 log units compared to 1.5 log units at 1373 K, 2.5 wt% H_2O), and in water-rich samples (~6 wt% H_2O) no significant effect of P_2O_5 has been detected. Additional experiments with variation of B_2O_3 content are in progress to determine wether this component will significantly influence melt viscosities in highly fluxed water rich systems.

[1] Bartels A., Vetere F., Holtz F., Behrens H., Linnen RL Viscosity of flux-rich pegmatitic melts. *Contrib Mineral Petrol*, in press

https://doi.org/10.1180/S0026461X00006502 Published online by Cambridge University Press

The cause of high Nb/Ta in K-rich lavas from the Sunda arc system

A.R. BARTH[1,2], M. KIRCHENBAUR[1,2], S. KÖNIG[1,2], S. SCHUTH[3], A. LUGUET[2], A. IDRUS[4] AND C. MÜNKER[1]

[1]Institut für Geologie und Mineralogie, Universität zu Köln, Germany (anne.barth@uni-koeln.de)
[2]Steinmann-Institut, Rheinische-Friedrich-Wilhelms-Universität Bonn, Germany
[3]Institut für Mineralogie, Universität Hannover, Germany
[4]Department of Geological Engineering, Gadjah Mada University, Yogyakarta, Indonesia

The overall depletion of many terrestrial silicate reservoirs in Nb has been explained in some studies by the existence of superchondritic Nb/Ta reservoirs in either the core or mantle (e. g. [1–2]). As one example, K-rich lavas from the Sunda arc, Indonesia, have been invoked to tap such a high Nb/Ta reservoir, a hybridised mantle [3]. In order to elucidate the petrogenetic processes active beneath the Sunda arc and the causes for the apparently high Nb/Ta in some of these lavas, we determined major and trace element concentrations, Sr-Nd-Hf-Pb isotope compositions, and HFSE concentrations via isotope dilution by MC-ICP-MS on a representative set of 18 mafic samples, covering along and across arc sections from Krakatau to Lombok.

Similar Pb isotope compositions of all lavas, and mixing arrays of the Sunda arc lavas in εNd vs. $^{87}Sr/^{86}Sr$ space (εNd +1.3 to +5.6, $^{87}Sr/^{86}Sr$ 0.7040–0.7059) with local ocean floor sediments are in agreement with previous studies on the Sunda arc, suggesting a significant overprint of the mantle sources by fluids derived from subducted sediments. In contrast, the particularly K-rich back-arc lavas (e. g., Muriah volcano) do not lie on this mixing array (εNd -1.3 to +2.2, $Sr/^{86}Sr$ 0.7042–0.7046), and are the only ones exhibiting superchondritic Nb/Ta (18–25), attributed to slab melt overprint. However, other Sunda arc rocks yield sub-chondritic Nb/Ta (13–18).

In accord with previous studies [3–5], the incompatible trace element inventory of Indonesian high-K lavas can therefore be attributed to partial melts derived from rutile-bearing mafic oceanic crust with a thick cover of sediment. The more fluid-dominated trace element enrichment in the sources of the other Sunda arc lavas is also related to subducted sediments, resulting in distinct trace element and isotope compositions.

[1] Wade & Wood (2001), *Nature* **409**, 75–78. [2] Münker *et al*. (2003), *Science* **301**, 84–87. [3] Stolz *et al*. (1996), *Geology* **24**, 587–590. [4] Münker *et al*. (2004), *EPSL* **224**, 275–293. [5] König & Schuth (2011), *EPSL* **301**, 265–274.

Karst versus sandstone and anthropogenic influences on small rivers of the Franconian Alb

J.A.C. BARTH*, M. MADER, R. VAN GELDERN, I. SCHREITER, P. ZIMMERMANN, T. TÜRK AND P. SCHULTE

GeoZentrum Nordbayern, Friedrich-Alexander Universität Erlangen-Nürnberg, 91094 Erlangen, Germany (*correspondence: barth@geol.uni-erlangen.de)

The small rivers Wiesent, Schwabach, Pegnitz and Regnitz drain the area of the Franconian Alb in Southern Germany, a typical karst terrain. Therefore the chemistry of the rivers should trace limestone weathering as the principal influence on river water composition. However, also urban influences by the city agglomeration of Nuremberg and signals of siliciclastic rock weathering may become more important in their lowland regions. Such changes of influence may best be studied in small rivers (< 52 $m^3 s^{-1}$ for the Regnitz and < 12 $m^3 s^{-1}$ for its tributaries) with major element and stable isotope analyses of dissolved organic and inorganic carbon. For instance, CO_2 partial pressures in the Wiesent River headwaters were up to 50 times higher than those in the atmosphere (> 21000 ppmV) and exceeded values found in African tropical rivers. For the Wiesent, such high pCO_2 values originate from soils and groundwater as they primarily occur in the groundwater-dominated source region. These waters are also characterized by carbon isotope signals of the dissolved inorganic carbon ($\delta^{13}C_{DIC}$) that are more negative than –14 per mil versus the VPDB standard. This deviates from typical values found in limestone weathering areas and indicates influences of CO_2 from recycled C3 plant material. These first data from the Wiesent indicate that weathering is not limited by CO_2. However, high pCO_2 values reduced rapidly towards values around 2500 ppmV over the course of the river due to degassing. In addition, lower reachers of the Wiesent showed dilutions in ion contents that may be related to increasing influences of sandstone weathering. First results of the other rivers studied showed mainly $\delta^{13}C_{DIC}$ signals of limestone weathering with values ranging around –12 permille and confirmed that carbonate weathering is the major control in these rivers. Influences of within-river turnover of dissolved organic carbon (DOC) may be revealed by simultaneous concentration and carbon isotope analyses.

https://doi.org/10.1180/S0026461X00006502 Published online by Cambridge University Press

Melting in the deep crust: Message from melt inclusions in peritectic garnet from migmatites

O. BARTOLI[1]*, B. CESARE[2], S. POLI[3], R.J. BODNAR[4], M.L. FREZZOTTI[5], A. ACOSTA-VIGIL[6] AND S. MELI[1]

[1]Dipartimento di Scienze della Terra, Univ. Parma, Italy (*correspondence: omar.bartoli@libero.it)
[2]Dipartimento di Geoscienze, Univ. Padova, Italy
[3]Laboratory of experimental petrology, Univ. Milano, Italy
[4]Fluids research laboratory, Virginia Tech, VA, USA
[5]Dipartimento di Scienze della Terra, Univ. Siena, Italy
[6]Instituto Andaluz de Ciencias de la Tierra, CSIC, Univ. Granada, Spain

S-type granites and leucosomes in migmatites provide information on the composition of crustal anatectic melts. However, their reliability as witnesses of primary anatectic melts has been questioned by several lines of evidence. Previously, the composition of the melt produced during crustal anatexis has been assumed from glass obtained in equilibrium melting experiments of crustal rocks. However, Cesare *et al*. [1, 2] have shown that peritectic minerals in migmatites can trap droplets of melt, that were formed by incongruent melting reactions during crustal anatexis.

We performed for the first time an experimental and analytical study of melt inclusions (MI) within peritectic garnets, using the metasedimentary migmatites from Ronda (S Spain). These garnets contain primary 2-10 μm MI that range from totally glassy to fully crystallized (*nanogranite*, [1]). Raman spectroscopy has documented the presence of liquid H_2O-filled micro-pores in nanogranites. Piston cylinder remelting experiments led to the rehomogenization of crystalline MI at conditions (700 °C, 500 MPa) close to those inferred for anatexis. Remelted MI have a peraluminous, granitic composition with high (up to 7.5 wt %) H_2O content; they overlap the composition of glassy MI, but differ from the composition of leucosomes in the host rock. Some CO_2 bubbles are present after remelting experiments, suggesting fluid present, $a_{H2O} < 1$ conditions, in agreement with graphite occurrence in the protolith. Our study identifies the natural anatectic melt composition and fluid regime at the onset of crustal melting, otherwise unknown. Hence, MI in migmatites represent a unique tool for the *in situ* characterization of anatexis in its early stages, and provide the only means of determining the volatile fluid content of anatectic melts.

[1] Cesare *et al*. (2009) *Geology*, **37**, 627-630. [2] Cesare *et al*. (2011) *JVirtExpl*, **40**, paper 2.

Lime lumps in gothic joint mortars from Kruszwica (Central Poland): An insight into the lime production

W. BARTZ[1]* AND M. RUDY[2]

[1]University of Wroclaw, Cybulskiego 30, 50-205 Wroclaw, Poland (correspondence:wojciech.bartz@ing.uni.wroc.pl)
[2] Nicholaus Copernicus University, Sienkiewicza 30/32, 87-100 Torun, Poland

In this study we present the complete characterization of joint mortars from the 'Mouse Tower'. The tower is a remnant of a gothic castle, erected in mid-14th century by King Casimir the Great.

All mortars comprise a calcitic binder (micrite) and a fine- to medium-grained inert aggregate, dominated by a detrital quartz. Smaller or larger binder-related particles, so called 'lime lumps' could be found in the micritic matrix. The inner part of these lime lumps is typically composed mainly of calcite crystal and aggregates of minerals rich in CaO and/or SiO_2, identified by means of SEM-EDX as wollastonite, silica (identified as cristobalite by means of XRD), belite (C_2S), minerals with a composition close to the melilite group (gehlenite-åkermanite) and less common rankinite. The core of lime lump is rimmed by a thin zone composed of micrite and unidentified amorphous silicates.

As suggested by different authors, the presence of lime lumps is attributed to low water/quick lime ratios for slaking, rapid slaking, slaking with excess of water, or technologies based on the nonseasoning of lime. However, in our particular case the lime lumps should be considered as overburnt lumps, formed due to local increase of the temperature above mean in the kiln.

The chemical analysis revealed that the percentages of acid soluble SiO_2, which indicates the existence of hydraulicity, reach very low values. The cementation index (C.I. <0.13) classifies the joint mortars as non-hydraulic. The volume of hydraulic phases (i.e. belite) is very small, they are enclosed in the almost impermable structure, thus their presence had no impact on the hydraulic properties of whole mortar.

On the basis of our studies, we conclude the joint mortar was poorly homogenized, non-hydraulic lime, derived presumably from the calcination of impure limestone rich in clay and silt, possibly the lacustrine chalk. Deposits of this material, very common in post-glacial lakes of northern Poland, occur in the Gopło Lake, situated in the nearest vicinity of the tower.

https://doi.org/10.1180/S0026461X00006502 Published online by Cambridge University Press

U-Pb zircon ages of the Alto Paranaíba and Juína kimberlitic provinces, Brazil

M. BASEI[1]*, D. SVISERO[1], W. IWANUCH[2] AND K. SATO[1]

[1]Instituto de Geociencias, USP-Brasil
(*correspondence : baseimas@usp.br)
[2]Faculdade de Geologia, UERJ, RJ, Brasil

This work presents a set of zircon U/Pb ages of kimberlitic and akin rocks of the Alto Paranaíba (Minas Gerais – Goiás) and Juína (Mato Grosso – Rondonia) provinces. The Alto Paranaíba province is composed of hundreds of Cretaceous bodies intrusive in the southwestern border of the São Francisco Craton. The Juína Province is in the NW portion of the Mato Grosso State.

Ten zircon concentrates from APP corresponding to the Mata da Corda Group conglomerate and 74 zircon concentrates from intrusive bodies of kimberlitic affiliation of the Coromandel region were studied. Sixteen fractions corresponding to nine intrusive bodies yield $^{206}Pb/^{238}U$ ages around 87.36 ± 0.75 Ma Two younger bodies yielded ages around 80 Ma. Ten analyses corresponding to three kimberlitic bodies of the Juína Province present older $^{206}Pb/^{238}U$ ages of 93.69 ± 0.43 Ma. Whole-rock isotopic studies (Sr, Nd and Pb) suggest that the Alto Paranaíba Province kimberlitic-type rocks show signatures distinct from those that characterize the South-African bodies. The whole-rock Sm-Nd age of 850 Ma is similar to the zircon U-Pb ages of most of the juvenile granites that characterize the initial phases of the Goiás magmatic arc. It is possible that this value indicates the time of an important mantle melting associated with the Neoproterozoic subduction process that led to the generation of the arc. This frozen lithospheric mantle coupled to the base of the São Francisco Craton would be the source of the Cretaceous kimberlites of the Alto Paranaíba Province.

Seepage of subsurface brines into a major lake system using Ra and stable isotopes of oxygen and hydrogen: A case study from Lake Huron

M. BASKARAN[1]*, T. NOVELL[1], S. RUBERG[2], B.A. BIDDANDA[3], T. JOHENGEN[4], N. HAWLEY[2] AND V. KLUMP[5]

[1]Department of Geology, Wayne State University, Detroit, USA (*correspondence: Baskaran@wayne.edu).
[2]GLERL, NOAA, Ann Arbor, USA
[3]Grand-Valley State Univ., Muskegon,USA
[4]CILER, University of Michigan, Ann Arbor, USA
[5]University of Wisconsin, Madison, USA

Exchanges of water between major reservoirs such as groundwater and lake water that are common can alter the biogeochemical cycling of chemical species and thereby affect relevant ecosystems. Recently discovered sinkhole vents in Lake Huron were found to discharge highly anoxic, reducing, high-sulfate and -chloride waters with strinkingly different chemical signatures.

We collected and analyzed a suite of water samples from three sinkhole vents and adjoining waters from Lake Huron for $\delta^{18}O$, δD, $^{223,224,226,228}Ra$ and a suite geochemical ancilliary parameters. Our results show: i) Ra concentrations in the vent waters are 1 to 2 orders of magntidue higher than that of the lake water; ii) A plot of δD vs $\delta^{18}O$ show considerable deviation from the Global Meteoric Water Line indicating mixing of different water masses that have undergone different evaporation cyles; and iii) The variations in the $^{223}Ra/^{226}Ra$ and $^{224}Ra/^{228}Ra$ activity ratios in the vent waters is related to the time-scales involved in the vertical movement of the vent waters. We also have modeled the variations in the Ra activity ratios in the vent waters to obtain time scales of transport from the source waters to the place where the vent water is discharged.

https://doi.org/10.1180/S0026461X00006502 Published online by Cambridge University Press

Comparing carbon isotopic signatures between meteorites and terrestrial mantle samples: Need for reassessment of carbon composition of Earth's mantle

S.BASU[1]*, S. MIKHAIL[1,2], A.P. JONES[1] AND A.B. VERCHOVSKY[2]

[1]Department of Earth Sciences, University College London (*correspondence: sudeshnabg@yahoo.com, s.mikhail@ucl.ac.uk, adrian.jones@ucl.ac.uk)
[2]PSSRI Open University, Milton Keynes (A.Verchovsky@open.ac.uk)

Carbon isotopic composition of Earth's mantle is supposed to be -5‰ based on mean values obtained from bulk measurements of oceanic basalts, carbonatites, diamonds and other terrestrial samples [1]. This value is the most significant assumption made in order to understand how carbon is cycled between the surface and interior of the Earth. But there are specific localities that exhibit different mean values, bimodality and outliers [2].

However, the value of -5‰ may not be representative of the entire mantle. Carbon compositions in the terrestrial mantle samples show considerable variations like E-chondrites, the fundamental building blocks of Earth [3]. The carbon composition of Earth does not coincide with the Martian mantle value of -20 ‰ although both the planets should have started with similar initial compositions [4]. Carbon can form various stable compounds in the mantle governed by different oxygen fugacity, and fractionation in isotopic composition is likely to occur under high pressure-temperature conditions [5]. It becomes important to reassess the mantle compositions of Earth, particularly since Si-rich carbide-bearing diamonds from great mantle depths (> 1100 km) is now available [6]. Following preliminary combustion investigations for carbon and nitrogen, measurements of carbon isotopic compositions of these Jagersfontein diamonds and inclusions at high resolution by NanoSIMS are underway.

[1] Deines (2002) *Earth Sci. Rev.* **58,** 247-258. [2] Cartigny (2005) *Elements* **1,** 79-84. [3] Javoy *et al.* (2010) *EPSL* **293**, 259-268. [4] Grady *et al.* (2004*) Int. J. Of Astrobiology* **3(2),** 117-124. [5] Mikhail *et al.* (2010) *AGU Fall Meeting* abstract No: U21A-0001 . [6] Jones *et al.* (2008) *9th Int. Kimberlite Conference* Extended Abstract No: 9IKC-00360.

Measurements of ocean derived aerosol off the coast of California

T.S. BATES[1]*, P.K. QUINN[1], A. FROSSARD[2], L.M. RUSSELL[2], J. HAKALA[3], D.J. KIEBER[4] AND W.C. KEENE[5]

[1]NOAA PMEL, 7600 Sand Point Way NE, Seattle, WA 98115, USA (*correspondence: tim.bates@noaa.gov, patricia.k.quinn@noaa.gov)
[2]University of California, San Diego, CA, USA (afrossar@ucsd.edu, lmrussell@ucsd.edu)
[3]University of Helsinki, Helsinki, Finland (jani.hakala@helsinki.fi)
[4]State University of New York, Syracuse, NY, USA (djkieber@esf.edu)
[5]University of Virginia, Charlottesvile, VA, USA (wck@virginia.edu)

The oceans are a major source of aerosol number and mass to the atmosphere. Over the remote oceans, coarse-mode sea-salt particles dominate aerosol light scattering. Recent measurements suggest that direct emissions of ocean-derived particles also control the aerosol number concentration and thus the aerosol cloud condensation nuclei concentration. Measurements of atmospheric aerosols over the ocean include particles directly emitted from the ocean and particles produced by gas phase reactions in the atmosphere, making it difficult to distinguish between the two sources. Here we report recent measurements of particles directly emitted from the ocean using a newly developed *in situ* particle generator/sampler (SeaSweep). Bubbles were generated 1 m below the ocean surface alongside the research vessel *Atlantis* off the coast of California and swept into a hood/vacuum hose to feed a suite of instruments on board the ship measuring aerosol physical, chemical, optical, and cloud nucleating properties.

The number size distribution of the directly emitted (nascent) particles had a dominant mode at 55-60nm (dry diameter) and a secondary mode at 200-300nm. The aerosol was not volatile at 230°C. This temperature rules out ammonium sulfate and nitrate as significant components of the nascent aerosol but does not distinguish between particulate organic matter and sea salt. The organic component of the nascent aerosol volatilized at a temperature between 230 and 600°C. The nascent aerosol was not enriched in Ca, K, or Mg above that found in surface seawater. The submicrometer organic aerosol was primary composed of carbohydrates based on FTIR analysis. The nascent organic aerosol concentration did not increase in regions of higher surface seawater chlorophyll.

https://doi.org/10.1180/S0026461X00006502 Published online by Cambridge University Press

Geophysical and geochemical data used to infer origin and evolution of natural CO_2 in Italy

A. BATTANI, E. BROSSE AND C. LOISELET

IFPEN, Paris, France

CO_2-degassing is well documented throughout the whole Italian peninsula and previous studies based on geochemistry of gases have already shown the existence of different CO_2 sources, (Minissale *et al*., 1997) ranging from deep mantle-derived CO_2 related to volcanism, to more "crustal" sources", that are less documented. Italian Peninsula is characterized by a high R/Ra gradient increasing from the North to the South. Geochemical ratios (R/Ra and $CO_2/^3He$) fit quite closely to a mixing curve between a mantle-derived end member (in the south) and a crustal end member in the North.

The high R/Ra ratio recorded in Southern Italy is easily related to Calabria slab mantle wedge processes.
Concerning the central Italian volcanism, the R/Ra ratio reaches 4, indicating a strong influence of mantle-derived helium, with an important continental/ crustal contribution.

Geochemical (elemental and isotopic ratios) and seismological (P-wave tomography and SKS splitting) data support the existence of a large window in the Adrian plate underneath the southern Apennines. The influence of the slab mantle wedge is not observed here. However, window appears at the northern lateral Calabria slab edges allowing mantle inflow induced by the Calabria retrograde motion (Gasparini *et al*.,2002; Faccenna *et al*., 2005; 2007).

In the North-Central part of Apennines, the reported helium isotopic ratios point to a general prevalence of crustal influence (typical crustal values estimated around 0,02 and 0,05 Ra). A significant component of mantle-derived helium is only found in the geothermal areas of Larderello (Northern Italy) where a large thermal anomaly is present at depth. (Cloetingh *et al*., 2010). By combining geophysical and geological observations we propose to explain this local anomalous ratio by a local asthenospheric upwelling, probably associated with lithospheric delamination, or slab break off processes.

Using this approach, we provide a new insight on the origin of CO_2, and we propose a strong relationship between diagenesis and/or metamorphic processes associated with subduction dynamics, rather than thermal decomposition of carbonates.

Mussel shells as archives of geogenic and anthropogenic dissolved REE

M. BAU[1], G. MERSCHEL[1,2], S. KULAKSIZ[1], K. SCHMIDT[1], M. BRENNER[3], S. BALAN[1,4] AND A. KOSCHINSKY[1]

[1]Earth & Space Sciences, Jacobs University, Campus Ring 1, 28759 Bremen, Germany; (m.bau@jacobs-university.de)
[2]Environment and Resource Management, Free University, 1081 HV Amsterdam, Netherlands
[3]IMARE - Institute for Marine Resources GmbH, Klußmannstr. 1, 27570 Bremerhaven, Germany
[4]Environmental Science, Policy, and Management, UC Berkeley, 137 Mulford Hall, Berkeley, CA 94720, USA

Mussel shells may be used to evaluate trace element bioavailability, as the carbonate shell precipitates from the mussel's internal extrapallial fluid and not from external ambient water. We determined the REE distribution in shells of marine hydrothermal *Bathymodiolus* and littoral *Mytilus edulis* and of freshwater *Corbicula fluminea* mussels, and in the respective ambient river or seawater. Marine *Bathymodiolus* and *Mytilus edulis* shells reflect the presence and absence, resp, of positive Eu anomalies in their ambient waters, suggesting that positive Eu anomalies in mussel shells might be used to detect hidden or fossil high-temperature hydrothermal vent sites, thus helping exploration of VMS deposits [1]. Water from the Weser and Rhine rivers both display anthropogenic positive Gd anomalies that result from input of Gd used in MRI contrast agents, and the lower reaches of the Rhine River also show large an-thropogenic positive La anomalies [2]. While this La anomaly also occurs in *Corbicula* shells from the Rhine River, neither shells from the Rhine nor from the Weser River show a Gd anomaly. This demonstrates that in contrast to anthropogenic La, the Gd complexes used as MRI contrast agents are not bioavailable, which is further evidence of their conservative behaviour.

[1] Bau, M., Balan, S., Schmidt, K., Koschinsky, A. (2010) *Earth Planet. Sci. Lett.*, **299**, 310–316. [2] Kulaksiz, S. & Bau, M. (2011) *Environment International*, **37**, 973-979

https://doi.org/10.1180/S0026461X00006502 Published online by Cambridge University Press

Analysis of δD and $\delta^{18}O$ in clay minerals for reconstructing paleoenvironmental parameters

K. BAUER[1,2]*, T.W. VENNEMANN[1] AND A. MULCH[2]

[1]Institut de Minéralogie et Géochimie, Université de Lausanne, Switzerland (*correspondence: kbauer@unil.ch)
[2]Institut für Geowissenschaften, Johann Wolfgang Goethe-Universität Frankfurt am Main, Germany

Clay minerals in Molasse sediments are potential proxies for the stable isotope composition of Neogene paleowaters in the circum-Alpine region. To use this proxy requires the formation of clay minerals in weathering zones in equilibrium with ambient surface waters and no post-formational diagenetic nor low-grade metamorphic exchange with the fluid phase. Knowledge of the water-mineral fractionation factors at temperatures of formation permits an estimation of the isotopic composition of the paleowaters and allows to reconstruct paleoaltitude, paleoclimate and paleotopography.

The isotope analysis of clay minerals, however, proves to be a challenging task. In particular members of the smectite family are highly hygroscopic, leading to potentially falsified results of the isotope measurements if the adsorbed water is not removed. A number of tests and experiments were conducted in order to validate the most accurate as well as economical procedure of sample preparation. While $\delta^{18}O$ values are readily analyzed using a CO_2 laser fluorination line, the adsorbed water fraction may pose problems for the hydrogen isotope analyses using the TC/EA method. Prior to H-isotope analyses, it proves advantageous to evacuate the samples at elevated temperatures before rapidly transferrring them to the TC/EA for measurements. Additional analytical methods including XRD, TGA, SEM, and studies of organic matter within the sample material have been applied for actual samples as well as for standard materials in order to evaluate the effects of sample treatment on final measured values. The results were also cross-checked through an inter-laboratory comparison of the results obtained.

Once established, this modified preparation technique will be applied to clay mineral separates from stratigraphically distinct Molasse sediment horizons, as well to samples from recent soil profiles in the Swiss Alps, and bentonites from volcanic ash layers in Switzerland. The present results from Molasse clay minerals are in agreement with proxies of changes in paleoclimate from marine sediments and also with related isotope studies on material from high-Alpine fault zones of similar age.

Which emission sector is winning the mitigation competition when direct, indirect and semi-direct effects are investigated seperately?

SUSANNE E. BAUER[1] AND SURABI MENON[2]

[1]Columbia University and NASA Goddard Institute for Space Studies, New York NY, (sb2273@columbia.edu)
[2]Lawrence Berkeley National Laboratory, Berkeley CA, (smenon@lnbl.gov)

Attention has been drawn to black carbon aerosols, as a target for short-term mitigation of climate warming. Regulating soot emissions could, as a short-term action, potentially buy time by slowing global warming until regulations for long-lived greenhouse gases are set in place. The scientific community debates the impacts of such mitigation measures, and mitigation modelling studies show incoherent answers. One of the main reasons for the disagreement are semi-direct aerosol effects, that are neglected in some studies and included and dominating the overall results in others. In this study we apply the GISS/MATRIX model, a global climate model including detailed aerosol microphysics, to understand the single contributions of aerosol forcings and feedbacks. The study goes beyond black carbon mitigation by investigating the whole suite of aerosol sources and sectors of the CMIP5 emission data sets.

Our study finds a regionally divers picture. For example aerosol-cloud effects over the United States lead to reduced cloudiness through semi-direct effects and increased cloudiness by the indirect effect and the reversed phenomena is simulated over Europe. This response will be explained by the chemical composition of the emission mix in the different regions and its impact on black carbon coatings. The most promising emission mitigation sectors differ greatly between geographically regions and even among industrialized countries.

https://doi.org/10.1180/S0026461X00006502 Published online by Cambridge University Press

D_2O as tracer to study diffusion processes through the quartz crystal

M. BAUMGARTNER, G. DOPPLER AND R.J. BAKKER

University of Leoben, 8700 Leoben, Austria
(*correspondence: miriam.baumgartner@unileoben.ac.at)

Laboratory synthesised fluid inclusions in natural quartz are used to study diffusion processes of H_2O and D_2O molecules through the quartz crystal. Feedstock of re-equilibration experiments are pure H_2O inclusions synthesised at 600°C and 337 MPa which correspond to a molar volume of 25 cm^3/mole of the liquid phase. Those inclusions are exposed to a D_2O fluid at equal experimental conditions. Due to the concentration gradient (chemical potential) diffusion is induced and fluid exchange between the "pore fluid" and the fluid inclusions is expected. D_2O is used for re-equilibration experiments because it is easily identified in the inclusions due the increase of the melting temperature of ice (pure D_2O at +3.8 °C) and its typical Raman spectrum between 2200 – 2800 cm^{-1}. After five days of re-equilibration the inclusions shapes are strongly modified and ice melting temperatures up to +1.8 °C are observed, which corresponds to about 47 mass% D_2O. In addition, Raman spectra taken from those inclusions reveal high amounts of D_2O (see Figure below). Nevertheless, the concentration of D_2O vary significantly and inclusions with low and high contents can be found. This variation is mainly caused by the position of the inclusion in the quartz sample (3-dimensional distance from the quartz surface) and the total volume of the inclusion itself. In addition structural effects, like nano cracks and crystal defects affect the fluid flow through the quartz crystal.

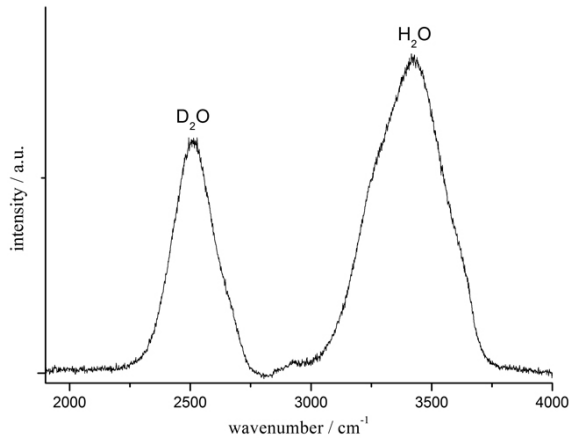

Figure 1: Raman spectrum of a fluid mixture of H_2O and D_2O measured in an inclusion after re-equilibration.

Microbially induced corrosion of depleted uranium metal in oxic soil

A.C. BAXTER[1,2] S. SHAW[3] M.N GARDNER[1] AND I.P. THOMPSON[4]

[1]Department of Earth Sciences, University of Oxford, UK
[2]AWE, Aldermaston, UK
[3]School of Earth and Environment, University of Leeds, UK
[4]Department of Engineering, University of Oxford, UK

To determine the enviomental impact of corroding depleted uranium (DU) munitions in oxic soils, fundamental information regarding the mechanisms and kinetics of DU breakdown are required. In particular, the key geochemical and microbiological factors which control the rate of corrosion. Previously, a study was conducted on DU metal pieces left *in situ* in two soil types (quartz rich dune sand and organic rich clay) for ≈8 years [1]. This concluded that a significant biological repsonse, e.g. oxalate production, was instigated from the indigenous microbes in response to the DU corroding in the soil, suggesting that microbes may have a significant influence on DU breakdown.

To detemine the microbial impact on the corrosion of DU metal, microcosm experiments were set up containing DU metal piece in a slurry containing either sterile soil or soil with the intact indigenous microbial communities.

After 5 months *in situ* corrosion had only occured in the microcosms containing the viable indigenous microbes (Figure 1).

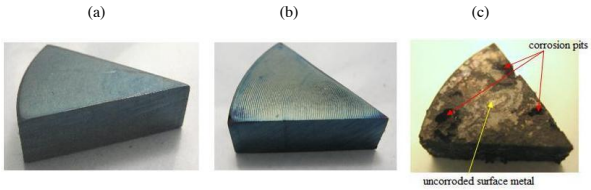

Figure 1: Digital photograph of the DU metal pieces (a) before addition to the microcosms, and after 5 months in situ in (b) sterile soil and (c) soil with viable indigenous microbial communities.

Imaging the DU metal pieces showed considerable pitting corrosion had occured on the surface. Within these pits bubble-like structures were observed which may have been caused by hydrogen generation at the metal surface. Fluorescent staining of the DU metal demonstrated diverse microbial communities had colonised within the corrosion pits.

[1] S. Shaw, *et al*. (2007) Geochemical and microbiological controls on the corrosion and transport of depleted uranium in soil. *Geochim. Cosmochim. Acta* **71**(15) A925

https://doi.org/10.1180/S0026461X00006502 Published online by Cambridge University Press

Causes of pulsed mineral growth during metamorphism

ETHAN F. BAXTER*[1,2], MARK J. CADDICK[2], ALAN B. THOMPSON[2], BESIM DRAGOVIC[1], ANTHONY D. POLLINGTON[1,3] AND JAY J. AGUE[4]

[1]Boston University, Department of Earth Science, Boston MA, 02215, USA (*correspondence: efb@bu.edu)
[2]ETH Zurich, Institute for Geochemistry and Petrology, 8006 Zurich, Switzerland
[3]University of Wisconsin, Department of Geoscience, Madison, WI, 53706, USA
[4]Yale University, Department of Geology & Geophysics, New Haven, CT, 06520-8109, USA

A growing set of observations suggests that metamorphic processes and conditions frequently are pulsed or episodic in nature rather than steady and long-lived. We recognize a "pulse" as any process, condition, or manifestation thereof that persists or dramatically accelerates for a brief period of time (relative to the general timescale of background tectonic/geologic forcing). Such pulses may include some or all of the following, which may not always be genetically linked: increased temperature, fluid influx, magmatism, and deformation, any of which may also promote mineral growth (and thus potentially be recorded therein).

Mineral growth pulses can have different causes. We describe three end-member possibilities here. First, rapid changes in *P* or *T* can drive more rapid mineral growth by quickly moving rocks through sets of reaction isopleths requiring compositional or modal change. Thermal pulses require mechanisms for rapid heating followed by focused heat dissipation, not possible via conductive heat transfer alone. For example, advective heat flow, provided by migrating syn-orogenic magmas and/or related fluids can contribute to thermal pulses. Or, rapid changes in P (and T) may accompany deformation during vertical motion in shear zones or thrusts. Second, steadily changing *P* and *T* can also produce pulsed mineral growth if reaction isopleths become closely (and/or orthogonally) spaced along portions of the *P-T* path. Third, a kinetic trigger (such as the introduction of a catalyzing fluid, which itself may be related to a pulse of dehydration or deformation) can permit a thermodynamically overstepped reaction to suddenly activate. Using vividly documented examples of mineral growth pulses [1,2] and thermal pulses [3], we explore different pulses, their possible causes, and the likely extent of their interactions.

[1] Pollington & Baxter (2010) *EPSL* **293**, 63-71. [2] Dragovic *et al*. (2011) *Goldschmidt Conference, Prague*. [3] Ague & Baxter (2007) *EPSL* **261**, 500-516.

A global distribution map for Nd isotopes in European watersheds

G. BAYON*, S. TOUCANNE*, N. FRESLON AND E. PONZEVERA

Département Géosciences Marines, IFREMER, Plouzané, France (* correspondence : gbayon@ifremer.fr; stoucann@ifremer.fr)

The Nd isotopic composition of the detrital fraction of a sediment provides information on the geographical provenance of that material. Aplication of the ε_{Nd} proxy to sedimentary records can be used to deduce sediment input variations, and hence to constrain fluctuations in transport mechanism.

In this study, we have compiled literature data for Nd isotopes in river sediments from all over Europe. This compilation was completed by analysing an extensive series of fine-grained sediments collected from various european rivers, estuaries, upper continental shelves and endorheic basins. For each sediment, the obtained ε_{Nd} value was taken as representative of the corresponding drainage basin signature. The result of this work is a global distribution map for Nd isotopes in european watersheds, which covers about 70% of the continent.

Based upon this map, we will discuss on the potential of using Nd isotopes for adressing some of the key issues related to the Late Quaternary environmental history of Europe.

https://doi.org/10.1180/S0026461X00006502 Published online by Cambridge University Press

Zinc and cadmium behavior in low-density fluids

E.F. BAZARKINA[1]*, G.S. POKROVSKI[2], N.N. AKINFIEV[1] AND A.V. ZOTOV[1]

[1]IGEM RAS, 119017 Moscow Russia (*correspondence: elenabaz@igem.ru)
[2]GET, Géoscience, Environnement Toulouse , 31400 Toulouse, France

Low-density fluids and vapors (density ≤ 0.5-0.3 g/cm^3) are ubiquitous in the Earth crust from moderate depth (vapor-brine immiscibity) to the surface (volcanic degassing). Quantitative understanding the transport capacity of such fluids for metals is, however, weak owing to both experimental difficulties and imperfections of classical thermodynamic models (e.g., HKF) when applied to the low-density aqueous phase. Our study is aimed at quantifying the transport of Zn and Cd, typical base metals, in such phases. We combined solubility measurements of ZnO and CdO in H_2O and H_2O-NaCl-HCl fluids and vapors and Zn and Cd vapor-liquid partitioning experiments in water-salt systems across a wide range of temperature, pressure and density (T = 350-450°C, P = 150-600 bar, d = 0.01-0.5 g/cm^3) with physical-chemical modeling.

Results reveal significant differences in the behavior of Zn versus Cd in low-density fluids in the presence of chloride. For example, the Cd/Zn ratio in the H_2O-NaCl-HCl vapor in equilibrium with CdO and ZnO increases with increasing Cl content, which demonstrates a stronger stability of Cd-Cl complexes compared with their Zn analogs. Our thermodynamic model [1] allow accurate description of the obtained solubility data using the neutral chloride and hydroxide species of Zn and Cd. These findings in homogenous fluids are in agreement with our data in dense aqueous solution [2], and vapor-liquid distribution measurements, which demonstrate that although both Zn and Cd partition in favor of the dense Cl-rich brine, vapor-liquid partition coefficients ($K = m_{vapor}/m_{liquid}$) for Cd are much lower than for Zn (e.g., log K ~ -5.5 and -3.3 at 450°C/280 bar for Cd and Zn, respectively). The different stabilities of Cd- and Zn-Cl complexes may play a key role in Cd fractionation by low density fluids, and explain the elevated Cd/Zn ratios in volcanic gases compared to the mean Earth crust value.

[1] Akinfiev and Diamond (2003) *GCA* **67,** 613–627. [2] Bazarkina *et al*. (2010) *Chem. Geol*. **276**, 1-17.

Reactive transport modelling of natural carbon sequestration in ultramafic tailings

S.A. BEA[1,2], K.U. MAYER[1], S.A. WILSON[1,3] AND G.M. DIPPLE[1]

[1]Department of Earth and Ocean Sciences, University of British Columbia, 6339 Stores Road, V6T 1Z4, Vancouver, BC, Canada.
[2]now at: Earth Sciences Division, Lawrence Berkeley National Laboratory, Berkeley, CA, USA (sabea@lbl.gov)
[3] now at: Department of Geological Sciences, Indiana University, Bloomington, IN, USA

Anthropogenic CO_2 is naturally sequestered in ultramafic mine tailings as a result of the weathering of serpentine minerals [$Mg_3Si_2O_5(OH)_4$] and brucite, and subsequent mineralization of CO_2 in hydrated magnesium carbonates such as hydromagnesite, $Mg_5(CO_3)_4(OH)_2{\cdot}4H_2O$ [1]. Understanding the CO_2 trapping mechanisms is key to evaluating the capacity of such tailings for carbon sequestration.

Natural CO_2 sequestration in ultramafic tailings at a mine site near Mount Keith, Australia is assessed with a modified version of the process-based reactive transport code MIN3P [2]. The model formulation includes energy and vapor transport fully coupled with fluid conservation in the aqueous phase and geochemical reactions. Atmospheric boundary conditions accounting for the effect of climate variations are also included. Kinetic dissolution of chrysotile, dissolution-precipitation of brucite [$Mg(OH)_2$] and primary carbonates [i.e. calcite, $CaCO_3$; dolomite, $MgCa(CO_3)_2$; magnesite, $MgCO_3$] as well as the formation of hydromagnesite, halite (NaCl), gypsum ($CaSO_4{\cdot}2H_2O$), blödite ($Na_2Mg(SO_4)_2{\cdot}4H_2O$) and epsomite ($MgSO_4{\cdot}7H_2O$) are considered.

Simulation results at ten years are consistent with field observations. Precipitation of hydromagnesite is predicted, and is mainly controlled by the dissolution of chrysotile (the source of Mg) and the equilibrium with the CO_2(g) ingressing from the atmosphere. The predicted rate for CO_2 entrapment in these tailings is 1.2 kg m^{-2} year^{-1}. Modeling results suggest that this rate is sensitive to CO_2 fluxes through the mineral waste and may be enhanced by several mechanisms, for instance by atmospheric pumping.

[1] Wilson, S. A., Dipple, G. M., Power, I. M., Thom, J. M., Anderson, R. G., Raudsepp, M., Gabites, J. E., Southam, G., (2009). *Economic Geology*, **104**, 95–112. [2] Mayer, K. U., Frind, E. O., Blowes, D. W., (2002). *Water Resources Research*, **38**, 1174.

https://doi.org/10.1180/S0026461X00006502 Published online by Cambridge University Press

Distribution and activity of iron-oxidizing microorganisms in acidic geothermal environments

J.P. BEAM[1], H.C. BERNSTEIN[2], M.A. KOZUBAL[1], R. P. CARLSON[2] AND W.P. INSKEEP[1]*

[1]Department of Land Resources and Environmental Sciences and Thermal Biology Institute, Montana State University, Bozeman, MT 59717, USA (*correspondence: jacob.beam@msu.montana.edu, binskeep@montana.edu)

[2]Department of Chemical and Biological Engineering and Center for Biofilm Engineering, Montana State University, Bozeman, MT 59717, USA

Iron oxide mats of acidic geothermal springs in Norris Geyser Basin, Yellowstone National Park are inhabited by numerous deeply-rooted members of the domain *Archaea*. Microorganisms of the order Sulfolobales (e.g., *Metallosphaera yellowstonensis* and other novel phylotypes) have previously been shown to be important community members and are likely responsible for the oxidation of Fe(II) and subsequent formation of Fe(III)-oxide mats. Iron-oxidizing microorganisms are hypothesized to thrive in more oxic regions of Fe(III)-oxide mats and are likely most abundant at the water/mat interface where oxygen concentrations are high relative to deeper mat positions. The current study investigated the relationship among vertical distribution of specific microorganisms, mRNA transcript levels of genes involved in Fe(II)-oxidation, and corresponding oxygen gradients measured *in situ*.

Quantitative PCR primers designed around specific phylotypes were used to determine the vertical distrbution of organisms within the Fe(III)-oxide mats. Similarly, mRNA transcripts of genes, thought to be important in Fe(II)-oxidation (i.e., Fe-specific heme copper oxidases), were amplified with primers designed for various Fe(II)-oxidizing microbial populations.

Results suggest that the spatial distribution of aerobic Fe(II)-oxidizing microbial populations correspond with measured oxygen gradients. Specifically, Fe(II)-oxidizing microorganisms become less abundant at depths below ~600 µm corresponding to depths where dissolved oxygen concentrations approach detection. Transcripts of genes (mRNA) previously shown to be involved in Fe(II)-oxidation are well represented in the top 600 µm-layer. This study highlights the important linkage among hydrodynamics, oxygen in-gassing and diffusion, and the spatial location of active Fe(II)-oxidizing microorganisms (and associated transcription of specific genes) in the biomineralization of Fe(III)-oxide phases in acidic geothermal environments.

Residence time analysis of metal-desorption and mineral-dissolution kinetics using a Damkohler approach

LINDSAY BEARUP[1], ALEXIS NAVARRE-SITCHLER[2], REED MAXWELL[3] AND JOHN MCCRAY[1]

[1]Hydrologic Science and Engineering, Colorado School of Mines, Golden CO; (lindsaybearup@gmail.com)

[2]Environmental Science and Engineering Division, Colorado School of Mines, Golden CO

[3]Department of Geology and Geological Engineering, Colorado School of Mines, Golden CO

Understanding processes that control coupled reaction and transport in contaminated and natural systems is important for predicting the behavior of metals. Mineral dissolution and metal desorption are two important processes that govern metal behavior. Reactive transport studies often assume that desorption occurs instantaneously and therefore apply thermodynamic equilibrium models, or that mineral dissolution is so slow that it is not relevant. This study investigates groundwater time scales where kinetic metal desorption and/or mineral dissolution are important mechanisms for accurate modeling of metal fate and transport. Compiled desorption reaction times for metal and metalloid rate constants show large variations, spanning over six orders of magnitude. Mineral dissolution rate constants span over thirteen orders of magnitude and overlap with the range of desorption rate constants.

The Damkohler number was used to calculate residence times where kinetic formulations for dissolution and desorption may be more accurate representations of metals behavior. According to this method, metal desorption kinetics are influential at residence times from a few days to ~ 2 years. For longer residence times, metal desorption should behave according to equilibrium desorption models. In constrast, kinetic mineral dissolution should be considered over nearly all residence times and length scales relevant to groundwater modeling. Groundwater models with residence times of minutes up to ~600 days should potentially consider both metal desorption and mineral dissolution rates, with greater residence times exhibiting equilibrium behavior and shorter residences resulting in negligible change in metal concentrations. Ultimately, this Damkohler analysis provides constraints on relevant metal release mechanisms for models of metal fate and transport, such as those used in the fields of carbon sequestration and acid mine drainage. Additionally, the results can be used in experimental design to determine the setup required to measure the desired variable, i.e. kinetic or equilibrium characteristics.

https://doi.org/10.1180/S0026461X00006502 Published online by Cambridge University Press

Fe kinetics of marine particle uptake and desorption determined from laboratory experiments

ANNA BECK* AND JESS ADKINS

Caltech, Geological and Planetary Sciences, Pasadena, CA 91125 (*correspondance: abeck@caltech.edu)

Particle residence times in the ocean are short enough for the adsorption and desorption of Fe(III) from marine particles to control the dissolved [Fe] profile. Previous laboratory experiments measured Fe(III) uptake rates using radiotracers under simulated natural conditions and in the presence of various particles. However, since at least 99.9% of dissolved Fe(III) in the ocean is bound to organic ligands, we carried out similar laboratory experiments with Fe(III) bound to desferryoxamine B, a naturally occurring siderophore, and used ^{54}Fe as a tracer.

We find the adsorption of ^{54}Fe onto a fresh, labile iron oxide (ferrihydrite) to be first order dependent on particle concentration and has a rate of -0.17 (±0.05) pmol Fe/(mg particle)/day. Experiments with ferrihydrite concentrations of less than 200 mg/L reach steady state after 100+ days, a time period two orders of magnitude larger than particle residence times in the water column, underscoring the significance of the adsorption kinetics on the profile of [Fe]. The uptake of ^{54}Fe onto clay (montmorillonite) has a very fast (<10 min) initial uptake followed by a slower, possibly first order, absorption that are both dependent on particle concentration. In stark contrast to clay and ferrihydrite, there is insignificant absorption of ^{54}Fe onto 3 other types of marine particles—stable iron oxide (goethite), opal (pulverized diatoms), and carbonate shells (forams). In desorption experiments, we find that 1) all particle types reach steady state in 1 week or less, and 2) the uptake mechanism onto ferrihydrite is irreversible. Fe cycling models currently lack these differences in particle preference and their respective rates.

Reconciling abundances of highly siderophile elements and major volatiles in the silicate and near-surface Earth

H. BECKER[1]* AND M. FISCHER-GÖDDE[2]

[1]Institut für Geologische Wissenschaften, Freie Universität Berlin, Malteserstrasse 74-100, D-12249 Berlin, Germany (*correspondence: hbecker@zedat.fu-berlin.de)

[2]Institut für Planetologie, Universität Münster, Wilhelm-Klemm-Strasse 10, D-48149 Münster, Germany

Ratios of highly siderophile element (HSE) abundances permit to distinguish between different classes of chondrites and may help in tracing the presence and evolution of differentiated metal and the differentiation of planetary crusts and mantles. The HSE can also play an important role in constraining the origin of the more abundant highly volatile elements in the terrestrial planets, in particular, if both groups of elements were added after core formation and the magma ocean stage. Recent constraints from peridotites and komatiites suggest that the relative abundances of Ru and Pd in the silicate Earth are suprachondritic. In contrast, other HSE show chondritic relative abundances, with Re/Os and Rh/Ir more similar to ratios in ordinary or enstatite rather than carbonaceous chondrites. HSE abundances and geochronological data for pre-3.8 Ga lunar impact rocks indicate that at least two ≥4.2 Ga old meteoritic components occur widely dispersed across the lunar nearside: a somewhat volatile element depleted (carbonaceous?) chondritic component in granulitic impactites and in some impact melt rocks, and a differentiated metal component, similar to some IVA iron meteorite compositions. The Earth may have accreted similar materials after 4.5 Ga, however, much larger quantities would be necessary to explain the HSE abundances in the Earth's mantle. Late accretion of 80-85 % of a slightly volatile depleted carbonaceous chondrite composition and 15-20 % of differentiated metal reproduces integrated abundances of the HSE, S, H, C and N in the silicate Earth + atmo- and hydrosphere, remarkably well, and would be consistent with the isotopic composition of S, H, C and N. Small discrepancies in abundances may reflect poorly known partition coefficients (Rh) and volatile loss (N). Reqired HSE abundances in the metal are equivalent to abundances in liquid metal that has fractionated 40-60% solid metal in the core of a ~2000 km diameter protoplanet. In order to prevent segregation of metal into the Earth's core, the bulk of this material should have accreted some time after the giant impact and solidification of the terrestrial magma ocean.

https://doi.org/10.1180/S0026461X00006502 Published online by Cambridge University Press

Atomistic approaches to determine redox reaction mechanisms of U, Np, and Pu on mineral surfaces

U. BECKER, L. SHULLER, D. RENOCK AND R. EWING

University of Michigan, Department of Geological Sciences, 2534 CC Little, Ann Arbor, MI 48109

The rich redox chemistries of U, Np, and Pu control the chemical and physical properties of nuclear materials at different stages in the nuclear fuel cycle from extraction to disposal. The redox chemistry of the actinides can be predicted based on the Eh-pH conditions; however, adsorption to mineral surfaces and redox reactions on the surface are impacted by the physicochemical properties of the mineral surface itself.

In recent studies, our research groups as well as others have been challenging the traditional way redox processes are being treated in the near-surface environment. One example that has been studied is the complicated interplay between uranyl complexes, sulfide/oxide surfaces, and organic and inorganic reductants. Our findings indicate that, despite many decades of research, the key controls of surface-mediated mechanisms and, hence, the rates of environmentally-important redox processes are still poorly understood. There are a number of reasons for this: 1) these processes almost always involve a complex series of elementary reactions, each involving the transfer of one electron at a time, 2) it can be unwieldy to resolve the influence of individual environmental parameters (pH, pe, pO2, concentration of other oxidants and reductants, other ions in solution, temperature, etc.) in rate experiments, 3) it can be challenging to differentiate rate constants for heterogeneous (surface) processes and homogeneous (solution) processes in order to assess the catalytic effects of the surface itself, and 4) rate-limiting processes such as spin transitions have been widely ignored so far. Our calculations address fundamental questions with regard to many different redox systems: Does the mineral surface directly participate in the redox event or indirectly participate by acting as a heterogeneous catalyst or an electron shuttling device for the transport of charge (and/or spin) between co-adsorbates.

Methane formation in abandoned coal mines: Role of acetogens and acetoclastic *Methanosarcinales*

S. BECKMANN[1]*, T. LÜDERS[2], M.KRÜGER[3], F. VON NETZER[2], B. ENGELEN[1] AND H. CYPIONKA[1]

[1]ICBM, Univ. of Oldenburg, Oldenburg D-26129, Germany (*correspondence: s.beckmann@icbm.de)
[2]IGOE, Helmholtz Zentrum Munich, D-85764, Germany
[3]BGR, Geomicrobiology, Hannover D-30655, Germany

Mine gas has come into the focus of the power industry and is being used increasingly for heat and power production. Worldwide, about 7% of the annual methane emissions originate from coal mining. In abandoned coal mines, stable carbon and hydrogen isotopic signatures of methane indicate a mixed thermogenic and biogenic origin. While thermogenic methane is a remainder of geological processes, biogenic formation is still going on [1]. Besides hard coal, possible sources for methane are large amounts of mine timber left behind after the end of mining.

In two abandoned coal mines in Germany, methanogenic archaea are responsible for the production of substantial amounts of methane [2]. The mines are characterised by low O_2 concentrations at high humidity and fungal mats mainly on the mine timber. We analysed active methanogens as well as the active bacteria involved in the trophic network by stable isotope probing (DNA-SIP). Therefore, the ^{13}C-labeled precursors of methane (acetate and H_2+CO_2) were fed to liquid cultures from hard coal and mine timber. Directed by the methane production kinetics, samples for DNA-SIP coupled to subsequent quantitative PCR and DGGE analyses were taken from long term incubations over 6 months. Surprisingly, the formation of ^{13}C-methane was linked to acetoclastic methanogenesis in both, the ^{13}C-acetate and H_2+$^{13}CO_2$-amended cultures of coal and timber. H_2+$^{13}CO_2$ was mainly used by acetogens related to *Pelobacter acetylenicus* and *Clostridium* species. Active methanogens, closely affiliated to *Methanosarcina barkeri*, utilized the readily available acetate rather than the thermodynamically more favourable hydrogen. Thus, the methanogenic microbial community appears highly adapted to the environment where acetate is a much more prominent intermediate than H_2.

[1] Thielemann *et al*. (2004) *Organic Geochemistry* **35**, 1537-1549. [1] Krüger *et al*. (2008) *Geomicrobiology Journal* **25**, 315-321. [2] Beckmann *et a*l. (2011) *Geomicrobiology Journal* **28**(4). [3] Beckmann *et al*. (2011) *Applied and Environmental Microbiology* doi:10.1128/AEM.02818-10.

https://doi.org/10.1180/S0026461X00006502 Published online by Cambridge University Press

PGE reference material heterogeneity – Estimating minimum analytical mass

L. PAUL BÉDARD[1], KIM H. ESBENSEN[2] AND SARAH-JANE BARNES[3]

[1]Sciences de la Terre, Université du Québec à Chicoutimi, Chicoutimi, Qc Canada; (pbedard@uqac.ca)
[2]Geological Survey of Denmark and Groenland, Copenhagen, Denmark; (ke@geus.dk)
[3]Sciences de la Terre, Université du Québec à Chicoutimi, Chicoutimi, Qc Canada; (sjbarnes@uqac.ca)

Very small analytical masses (mg to ng) are dictated by modern analytical instruments, either because of their high sensitivity, analytical protocols or because of the small sampling volume of micro-beam techniques. But small sample masses can create problems when trace elements are major constituent in some minerals (e.g. PGE as PGM) and are irregularly distributed in samples or reference materials. Accidental inclusion or exclusion could change the spatial concentration realised simply due to spatial heterogeneity issues [1,2]. Such effects influence mass balance calculation and element budgets. Recommended minimum mass for reference materials is generally determined by analysing smaller sample mass until variance become unacceptable. Is there a way to determine minimum sample mass directly related to RM heterogeneity? And is it identical for all analytes, or unique for each analyte, in each sample? In order to systematically investigate these questions, pressed-pellets of PGE-bearing reference materials (CHR-Bkg, CHR-Pt+, MASS-1, MASS-3, WMS-1, WMS-1a) were analysed with an EDAX EAGLE III micro-XRF. Approximately 10 000 contiguous measurements were made with a beam of 50 μm covering a total area of about 25 mm^2. Up to 25 analytes were measured including precious metals. Reproducibility was determined by analyzing the same location 1 000 times. In order to express the empirical heterogeneity, Angle Measure Technique (AMT) was employed [2]. The AMT transform describe the elemental map complexity as a function of geometrical scale from local to global. AMT provides a quantitative measure of the empirical heterogeneity for each element, RM, or analytical sample. From such results a minimum analytical mass for each analyte is proposed to ensure that analytical results are representative all the way down to the scale of RM fields-of-view. The proposed technique offers the advantage of defining the *effective* minimum mass for each analyte with better elemental sensitivity by allowing for a more meaningful estimation of the *global* minimum analytical mass.

[1] Savard, Barnes & Meisel (2010) *Geostandards and Geoanalytical Research* **34**, 281-291. [2] Huang & Esbensen (2000) *Chemometrics and Intelligent Laboratory Systems* **54**, 1-19.

Groundwater flow impacts on sediment biogeochemistry: A multivariate statistical approach

J. BEER[1]*, C. NEUMANN [1], J.H. FLECKENSTEIN[2], S. PEIFFER[1], AND C. BLODAU[3]

[1]Department of Hydrology, University of Bayreuth, Germany (*correspondence julia.beer@uni-bayreuth.de)
[2]Department of Hydrogeology, Helmholtzzentrum für Umweltforschung, Leipzig, Germany
[3]Department of Environmental Geology, University of Guelph, Kanada

Lakes in (former) mining areas are strongly affected by Pyrite oxidation leading to high loads of iron and sulfur and the acidification of local waterbodies. Whereas the groundwater surrounding such lakes is mostly only weakly acidic, the pH of acidic mine lakes (AML) often lies below about 3 due to iron oxidation and subsequent Schwertmannite precipitation. It has been described that advective and diffusive flow through AML sediments affect the distribution of solutes and the biogeochemical driver pH in such sediments (e.g. Beer *et al*., 2009).

To study the influence of groundwater – lake water – exchange on sediment biogeochemistry, we measured exchange rates along with sediment composition at 19 sites at an anthropogenic AML near Lauchhammer, Germany.

The pattern of the exchange rates was temporally and spatially heterogenous. Groundwater inflow dominated in the northern part of the lake and often exfiltration of acidic lake water was measured in the southern part.

To analyze the effects on the sediment, we cut sampled sediment cores according to color and textur into 3-5 layers and measured pH, sulfate reduction, contents of reduced sufur species and carbonate, etc., and analyzed the results by multivariate statistical analysis. E.g. using cluster analysis, samples were grouped into 7 clusters which showed two different spatial patterns: 1) vertically, samples representing “fresh” sediment were observed in upper layers whereas “older” sediment samples were present at depth 2) clusters combining samples with higher biogeochemical activity and higher amounts of e.g. reduced iron sulfur species, and thus trapped acidity, prevail in the northern part of the lake. This second cluster could be related to the predominance of groundwater inflow in this part of the lake.

[1] Beer *et al*. (2009), *Geochimica et Cosmochimica Acta* **73** (13, Suppl. S), A102 (Goldschmidt 2009)

https://doi.org/10.1180/S0026461X00006502 Published online by Cambridge University Press

Water content and OH speciation in natural Fe-bearing pyroxenes

K. BEGAUDEAU[1], Y. MORIZET[2] AND J-C.C. MERCIER[1]

[1]LIENSs, University of La Rochelle, La Rochelle, France
[2]LPGN, University of Nantes, Nantes, France
(*correspondence: yann.morizet@univ-nantes.fr)

H in NAMs plays a crucial role on the physical and chemical properties of the Earth's mantle [1]. FTIR and NMR analyses were used to measure H contents and constrain OH dissolution mechanisms for natural Fe-bearing pyroxenes of 40 mantle xenoliths brought up by alkaline basalts magmas. Crystal chemistry was analyzed by EMPA. Equilibrium P-T conditions were determined by a new geothermobarometer developped yielding T°C=644-1151 and P(GPa)=0.85-2.7. Polarized FTIR spectra display the main absorption bands in OH species region. H_2O estimates [2] range between 38-450 ppm H_2O for cpx and 19-184 ppm H_2O for opx. Cpx/Opx partionning coefficients range to 0.6-3.7. H_2O variations seem correlated to fO_2, P, T and crystals chemistry allowing us development of geohygrometers.

^{1}H, ^{27}Al, ^{29}Si MAS NMR were also carried out with different magnetic fields. ^{1}H spectra are not exploitable because of paramagnetic components [3]. Their influences on the change of NMR spectral features are tested with mixtures of kaolinite + magnetite. ^{29}Si and ^{27}Al spectra are slightly affected. Tests on pyroxenes show an Al species distinction. Additional data reveals H proximity around Al species confirming relationships described by FTIR [4]. Thus, the use of both spectroscopic methods opens new perspectives for mineralogy and geochemistry of mantle's peridotites.

[1] Bell & Rossman (1992) *Science* ***255***, 1391–1397 [2] Libowitsky & Rossman (1997) *Am.Min* ***82***, 1111-1115 [3] Stebbing *et al* (2009) *Am. Min* **94**, 626-629 [4] Stalder (2004) *Eur. Journal of Min* ***16***, 703-711.

Decarboxylation of fatty acids during petrogenesis: Qualitative and quantitative analyses of bitumen NSOs by FTICR-MS

F. BEHAR[1], E. SALMON[2], A.W. KAMGA[2] AND P.G. HATCHER[2]*

[1]IFP Energies Nouvelles, 1-4 avenue de Bois Préau, Rueil-Malmaison 92500, France. (Francoise.BEHAR@ifpenergiesnouvelles.fr)
[2]Department of Chemistry and Biochemistry, Old Dominion University, Norfolk, VA 23529. (esalmon@odu.edu, akamga@odu.edu, *correspondence: phatcher@odu.edu)

The NSO compounds generated during the artificial maturation of kerogen from Green River Formation were collected by successive *n*-pentane and dichloromethane (DCM) extractions and analyzed using electrospray ionization Fourier transform ion cyclotron resonance mass spectrometry (ESI-FTICR-MS). Compounds containing only CHO elements in their make-up are dominant in each spectrum and are comprised mostly of the series $C_nH_{2n}O_2$, $C_nH_{2n-2}O_2$, $C_nH_{2n-2}O_4$, and $C_nH_{2n-10}O_2$ which all correspond to carboxylic acid-containing compounds. By calibrating the FTICR-MS with internal standard, it was possible to assign a response factor for the carboxylic acids and consequently get better quantification of the total carboxylic acids content. This response factor is invariant in the carbon number range of C_{20} to C_{40}. Also, after calibration, the carboxylic acid yield remains dominant among the other peaks detected by FTICR-MS. The same quantitative strategy was used for determining the response factor of the alcohols and dicarboxylic acids in order to determine the quantitative proportions of these functional groups in the NSOs.

Results clearly demonstrate that hydrocarbon generation from kerogen is mainly attributed to decarboxylation of the NSOs compounds. Moreover, there is a strong qualitative and quantitative relationship between the hydrocarbon distributions and the fatty acid distributions. For example, the carbon preference index for hydrocarbons matches exactly that observed for the fatty acids.

https://doi.org/10.1180/S0026461X00006502 Published online by Cambridge University Press

Combined WAXS/XAFS measurements for studying the reaction of S(-II) with lepidocrocite

T. BEHRENDS[1], K. HELLIGE[2], M. SILVEIRA[3] AND S. PEIFFER[2]

[1]Utrecht University, Faculty of Geosciences, NL-3508 TA Utrecht, The Netherlands (behrends@geo.uu.nl)
[2]Department of Hydrology, University of Bayreuth, D-95440 Bayreuth, Germany
[3]Katholieke Universiteit Leuven, DUBBLE beamline, ESRF, 38043 Grenoble, France

The reaction of sulfide (S-II) with iron oxides is an important process linking the redox cycles of iron and sulfur in many subsurface environments. Here, we studied the reductive dissolution of lepidocrocite (γ-FeOOH) by S(-II) in batch reactors at constant pH. A combination of wide angle X-ray scattering (WAXS) and X-ray absorption spectroscopy (XAS) at the Fe K-edge (about 7.1 keV) was used to follow on line the progress of the reaction.

Addition of Na_2S solution to the lepidocrocite suspension led to a fast decrease in intensity of the characteristic lepidocrocite diffraction peaks. This change in the WAXS signal was larger than expected from the stoichiometric amount of consumed lepidocrocite and indicates that the long range order of the crystals was profoundly disturbed upon the attack of sulfide.

Principle component analysis of all collected XANES spectra revealed that the combination of two spectra is sufficient to reproduce the major features of all spectra. The two components can be attributed to the spectrum of Fe(III) in lepidocrocite and to that of Fe(II) tetrahedrally coordinated with S. The stoichiometry of the reaction regarding the consumption of H^+ and S(-II) per reacted Fe(III) was derived from relating the change in XANES spectra to the amount of acid, which was added during the experiment, and to the different amounts of initially added sulfide, respectively.

Analyses of EXAFS spectra demonstrated that mackinawite was not the product of the reaction, while mackinawite was shown to form when Na_2S solution was added to Fe^{2+} solution under the experimental conditions.

These observations suggest, that the reaction of lepidocrocite with S(-II) does not follow a surface controlled mechanism in which the release of Fe(II) from the surface is required for the reaction to proceed. An alternative mechanisms will be presented and the differences between observed and expected stoichiometric coefficients will be discussed.

Lithospheric control on geochemical composition of the Louisville Seamount Chain

CHRISTOPH BEIER[1], MARCEL REGELOUS[1], JOHN MAHONEY[2], LOŸC VANDERKLUYSEN[2] AND KARSTEN HAASE[1]

[1]GeoZentrum Nordbayern, Universität Erlangen-Nürnberg, Schloßgarten 5, D-91054 Erlangen, Germany. (Christoph.Beier@gzn.uni-erlangen.de)
[2]Department of Geology and Geophysics, University of Hawai'i Mānoa, 1680 East-West Road, Honolulu, HI 96822, USA

Chemical changes with time in lavas erupted on long-lived seamount chains can be used to test models for the origin of intraplate magmatism and examine the effect of sub-seamount lithosphere on volcanism. Major and trace element and Sr, Nd, and Pb isotope data for lavas from 12 seamounts along the westernmost 1500 km of the Louisville Seamount Chain (LSC) in the SW Pacific show that magmatism was compositionally remarkably uniform between 80 and 40 Ma. All 56 samples analysed are alkalic or transitional; most are basalts. The youngest lavas from a given seamount tend to have the least enriched incompatible element compositions. Unlike Hawaiian volcanoes, Louisville volcanoes appear not to pass through a tholeiitic shield-building stage. The oldest Louisville seamounts formed close to the Osbourn Trough fossil spreading centre, but there is no obvious effect on the composition of LSC lavas. Nor do Osbourn Trough MORB contain any contribution from Louisville mantle, which suggests that spreading at the Osbourn Trough ceased well before the construction of Osbourn Guyot at 79 Ma. Lavas from volcanoes in the central part of the LSC are more variable and extend to more enriched compositions. These volcanoes tend to be smaller and more widely spaced, and were underlain by the oldest, thickest oceanic lithosphere. Smaller degrees of melting of heterogeneous mantle may explain the more variable compositions of these volcanoes.

https://doi.org/10.1180/S0026461X00006502 Published online by Cambridge University Press

On carbonatization fronts in serpentinite: Implications for *in situ* CO_2 storage

A. BEINLICH[1,2,*], O. PLÜMPER[1], J. HÖVELMANN[1], H. AUSTRHEIM[1,2] AND B. JAMTVEIT[1]

[1]Physics of Geological Processes (PGP) University of Oslo, Norway (*correspondence: andreas.beinlich@fys.uio.no)
[2]Department of Earth Sciences, University of Oslo, Norway

In situ storage of CO_2 in ultramafic rocks is considered as a promising strategy to counteract global warming. In order to identify positive and negative feedback mechansims for the reaction, examination of natural analogues is essential. Here we present observations from a massively carbonatized serpentinite complex in northern Norway. The investigated area is comprised of several ultramafic fragments of a dismembered ophiolite complex. Individual fragments are hydrothermally altered to varying degrees resulting in coexisting serpentinite, ophicarbonate, soapstone, and listvenite. Generally, reaction fronts between the soapstone and the serpentinite presursor are extremely sharp and can be traced for hundreds of meters. Locally, soapstone forms m-wide reaction halos around talc veins that cross-cut the serpentinite. The reaction fronts are defined by the complete replacement of the former antigorite by talc and magnesite. Where present, listvenite is spatially related to soapstone and cross-cut by abundant subparallel quartz-magnesite veins. The vein minerals exhibit a homogeneous O-isotopic composition and indicate a formation temperature of ~ 300 ˚C. The corresponding isotopic signature of the fluid ($\delta^{13}C_{PDB}$ = 2.2(5)‰; $\delta^{18}O_{SMOW}$ = 7.8(1)‰) suggests an interaction with crustal rocks and devolatilization of associated carbonates as a possible source for the CO_2. Assuming that during alteration temperature differences between directly adjacent soapstone and listvenite units are insignificant, thermodynamic phase stability modeling suggests that the conversion of serpentinite to listvenite requires a higher PCO_2 than that of conversion to soapstone.

In situ carbon storage schemes should aim to convert peridotite to listvenite as the complete inventory of divalent metal cations would be incorporated into the carbonates. However, our observations show that listvenite is distinctly less frequent than soapstone, implying that a high PCO_2 was not maintained during the natural alteration. Furthermore, alteration with a lower PCO_2 developed sharp fronts between the reacted and unreacted rocks, indicating that the carbonatization reaction ceased abruptly before completion.

Oxygen overshoot and recovery during the Early Paleoproterozoic

A. BEKKER[1]* AND H. D. HOLLAND[2]

[1]Department of Geological Sciences, University of Manitoba, Winnipeg, MB R3T 2N2, Canada (*correspondence: bekker@cc.umanitoba.ca)
[2]Department of Earth and Environmental Science, University of Pennsylvania, Philadelphia, PA 19104 USA

During the Lomagundi Event, >2.22 to 2.06 Ga, marine carbonates recorded the largest and longest positive carbon isotope excursion, the earliest extensive marine sulfate evaporites were deposited, and the average Fe_2O_3/FeO ratio of shales increased dramatically. At the end of the Lomagundi Event, the first economic sedimentary phosphorites were deposited, and the carbon isotope values of marine carbonates returned to ~0‰ VPDB. Thereafter marine sulfate evaporites and phosphorites again became scarce, while the average Fe_2O_3/FeO ratio of shales decreased to intermediate values between those of the Archean and Lomagundi-age shales. We propose that the large isotopic and chemical excursions during the Lomagundi Event were caused by a positive feedback between the rise of atmospheric O_2 level, the weathering of sulfides in pre-2.3 Ga sedimentary rocks, and the flux of phosphate to the oceans. The rise in the terrestrial phosphate flux led to an increase in the burial rate of organic carbon and a major transfer of oxygen from the carbon to the sulfur cycle.

The end of the Lomagundi Event was probably caused by a decrease in the terrestrial phosphate flux related to the weathering of low-pyrite sediments that were deposited during the Lomagundi Event. The rate of deposition of organic matter and burial rate of sulfate evaporites decreased, the isotopic and chemical excesses of the Lomagundi Event were eliminated, and the ocean-atmosphere system entered the period frequently called the Boring Billion.

https://doi.org/10.1180/S0026461X00006502 Published online by Cambridge University Press

Chloride degassing and its effects on the evolution of magmatic redox state

AARON S. BELL[1], ADAM SIMON[2] AND JAMES D. WEBSTER[1]

[1]Department of Earth and Planetary Science, American Museum of Natural History. New York, NY. USA (abell@amnh.org)

[2] Department of Geoscience, UNLV, Las Vegas, NV. USA

Magmatic fO_2 is a parameter that plays an important role in ferromagnesian and sulfide phase equilibria, the speciation of redox sensitive volatiles, and the physical properties of silicate liquids. We have performed redox controlled experiments to investigate iron partitioning behavior between a coexisting chloride rich volatile phase and silicate liquid. The results of these experiments suggest that volatiles with relatively modest chloride contents may contain several wt % Fe as a chloride species. These experimentally generated data suggest that the degassing of chloride rich volatiles may reduce the concentration of the FeO component of the melt. Notably, the preferential scavenging of ferrous iron from the melt must increase the $Fe^{3+}/\sum Fe$, consequently causing the fO_2 residual degassed melt to also increase.

These data support a model wherein the degassing of a chloride-rich volatile phase may significantly increase the oxidation state of the residual melt. Model calculations indicate that the magnitude of the induced oxidation ranges from 0.5 to 1.0 log unit; where this value depends on the partition coefficient value and the volatile phase-melt ratio used in the calculation. The oxidation of magmas during degassing and ascent may have marked effects on the identity and composition of the hypersolidus phase assemblage. Most saliently, this oxidizing effect may be manifested in sulfide saturated arc magmas as the destabilization of coexisting immiscible sulfide liquids or crystalline magmatic suflides. Such an iron scavenging based oxidation process has important implications for the remobilization of sulfide bound chalcophile metals as well as the petrologic interpretation of compositional zoning patterns in crystallizing ferromagnesian phases.

Carbonatites and Pb isotopes – Insights into terrestrial evolution

K. BELL

Earth Sciences, Carleton University, Ottawa, Ont. K1S 2W8, Canada (kib@magma.ca)

Information concerning the depleted mantle has come from studies of oceanic basalts but these cover only a small amount of geological time, at best back to a few hundred million years. Carbonatites, however, ranging in age from 3.0 Ga through to the present, provide a means of monitoring the secular evolution of the sub-continental mantle. Initial Pb isotopic ratios in carbonatites and alkaline complex rocks from the Canadian and Fennoscandian Shields appear to trace the evolution of “depleted” subcontinental mantle over the past 2.7 Ga. $^{87}Sr/^{86}Sr$ and $^{206}Pb/^{204}Pb$ ratios from Archean carbonatites from Canada tend to cluster closely around model “bulk silicate Earth” values in isotope correlation diagrams suggesting a mantle not yet depleted. A marked depletion event >3.0 Ga indicated by the Sm-Nd and Lu-Hf systems indicates sampling of considerably older, depleted mantle sources. Mantle differentiation processes appear to have changed in some fundamental way around 3 Ga with extraction of sialic crust. The similarity in isotopic compositions of young carbonatites (<100 Ma) to some OIB components (FOZO, HIMU, EM1) with little or no involvement with DMM suggests similar sources, and sub-lithospheric, deep-seated magmatism. Analogues to present day mantle components are not recognized in Archean carbonatites. Binary mixing of mantle sources (e.g. HIMU and EM1 for many young carbonatites) can be traced back to at least 1900 Ma.

https://doi.org/10.1180/S0026461X00006502 Published online by Cambridge University Press

Dissolution rate of bunsenite (NiO) in acid solution to 130°C

A. BELLEFLEUR[1], M. BACHET[1], P. BENEZETH[2] AND J. SCHOTT[2]

[1]EDF R&D, Site des Renardières, Avenue des Renardières, Ecuelles 77818 Moret Sur Loing Cedex (alexandre.bellefleur@edf.fr ; martin.bachet@edf.fr)
[2]GET, 14 Avenue Edouard Belin, 31400 Toulouse (benezeth@get.obs-mip.fr ; jacques.schott@get.obs-mip.fr)

Rates of proton-promoted dissolution of bunsenite (NiO) were measured from 50 to 130°C in hydrochloric acid solutions (pH 3 and 4.5) in a titanium mixed flow reactor. Measurements were also realized at 25°C with the stationary pH method [1] to confirm data from literature [2]. Pure bunsenite powder (Alfa Aesar Puratronic, Lot n°23430) was used for dissolution rate measurements, after beeing calcinated for 2*20 h at 1000°C in air. To avoid plug up of the outlet filter by fine particles, the powder was not directly introduced in the titanium reactor but in a specifically designed cell with walls made of a porous membrane. Measured bunsenite dissolution rate at 25°C are $2.4\pm0.3.10^{-10}$ and $7.5\pm0.6.10^{-11}$ mol.m^{-2}.s^{-1} at pH 3 and 4.5, respectively. Apparent activation energies for dissolution rate (25-130°C) are equal to 59.7±5.3 kJ.mol^{-1} and 32.9±2.4 kJmol^{-1} at pH 3 and 4.5, respectively. Bunsenite proton-promoted dissolution rate can be expressed as $R_H=k_H\{>NiOH_2^+\}^n$ where, k_H, $\{>NiOH_2^+\}$ and n stand for the dissolution rate constant, the concentration of protonated surface sites and the order of reaction with respect to adsorbed protons, respectively [3]. A two pK, one site surface speciation model which assumes a constant capacitance of the electric double layer was used to calculate $\{>NiOH_2^+\}$ as a function of pH and temperature. The variation of the apparent activation energy with pH can be explained by the contribution of the enthalpy of protonation of surface sites to the dissolution reaction ([4], [5]). However, the variation in dissolution rate observed between pH 3 and 4.5 is not compatible with the surface protonation constant of $10^{8.17}$ from [2], suggesting a lower constant for the powder studied here. Therefore, more work on surface properties of NiO is foreseen.

[1] Westrich H. *et al* (1992) *Am. J. Sci.* **293**, 869. [2] Ludwig C. and Casey W. (1996) *J. Colloid Interface Sci.* **178**, 176-185. [3] Furrer G. and Stumm (1986) *Geochim. Cosmochim. Acta* **50**, 1847. [4] Schott J. *et al* (2009) *Rev. Mineral. Geochem.* **70**, 207. [5] Casey W.H. and Sposito G. (1992) *Geochim. Cosmochim. Acta* **56**, 3825.

Experimental studies on cesium retardation on Brazilian crystalline rocks: Petrography, porosity and distribution coefficients

J.B. BELLINE[1]*, M. SIITARI-KAUPPI[2], M. KELOKASKI[2], P. SARDINI[3], M.E.B. GOMES[4] AND M.L.L. FORMOSO[1]

[1]Post-Graduate Program in Geosciences. IG/UFRGS. Brazil. (*correspondence: jean.belline@ufrgs.br)
[2]Laboratory of Radiochemistry. Univ. of Helsinki. Finland
[3]Laboratory HydrASA. Univ. of Poitiers. France
[4]Dep. of Mineralogy and Petrology.IG/UFRGS.Brazil

Cesium is an important radionuclide in the waste from the nuclear power plant [1,2]. The diffusion and sorption of cesium into rock is important to the safety of the radiowaste disposal. The mechanisms of sorption onto the minerals are important mechanisms to predict migration rates in the host rocks [3, 4]. The low porosity of granites is considered to prevent the radionuclides migration from repository site to the biosphere. This work discusses ^{134}Cs diffusion in three brazilian granites of São Sepé Complex Granitic, Rio Grande do Sul, Brazil, in the laboratory conditions. One sample comes from an outcrop and the two others (fresh and altered) are borecores from Camaquã mine. The porosities and densities of the each sample were measured by a water saturation method (pycnometry and water immersion techniques [5]). The porosity was measured also by C-14-PMMA autoradiographic method [6, 7]. Batch experiments and in diffusion test were made on crushed rock samples with several size fractions and blocks having volumes of about 8cm^3, respectively, to obtain the distribution coefficients (K_d values) of cesium-134 and diffusion paths from ^{134}Cs autoradiographs.

[1] Milnes (1985)."*Geology Radwaste*".[2] Cornell.(1993) *J. of Rad. Nuc. Chem.* **171(2)**, 483-500.[3] . Tsukamoto and Ohe (1991) *Chem.Geol.***90**, 31-44. [4] Langmuir (1997) *Aqueous Environmental Geochemistry*.[5] Melnyk and Skeet.(1986) Can. L. Earth Sci. **23** 1068-1074.[6] Hellmuth and Siitari-Kauppi. (1990) *STUK-B-VALO*. **63**. [7] Siitari-kauppi.(2002) *Thesis*. Univ. of Helsinki. Finland..

https://doi.org/10.1180/S0026461X00006502 Published online by Cambridge University Press

Short residence time and fast transport of fine-grain detritus – From ^{7}Be in settled dust in the Judean desert

R. BELMAKER[1,2], B. LAZAR[1], M. STEIN[2] AND J. BEER[3]

[1]The Institute of Earth Sciences, Hebrew University of Jerusalem, Givat-Ram Campus, Jerusalem 91904, Israel; (reuven.belmaker@mail.huji.ac.il)

[2]Geological Survey of Israel, 30 Malkhe Israel St,. Jerusalem 95501, Israel; (motistein@gsi.gov.il)

[3]Swiss Federal Institute of Environmental Science and Technology (EAWAG), Uberlandstrasse 133, CH-8600, Dübendorf, Switzerland; (Juerg.Beer@eawag.ch)

The short-lived cosmogenic isotope ^{7}Be ($t_{1/2}$=53.3 d) was measured in dust collected from dust traps placed in the Judean Desert. This enabled us to: (a) Determine the ^{7}Be dry deposition flux in the Dead Sea region; (b) Estimate the residence time of dust in the Dead Sea drainage basin and (c) Estimate the recycled component of the long-lived cosmogenic isotope ^{10}Be ($t_{1/2}$=1.39·10^{6} y) of Judean desert dust. These estimations constrain the rate of transport of fine detritus material that is washed from the marginal terraces of the Dead Sea basin into the lakes that occupied the basin during the late Quaternary. The data show that: (a) the ^{7}Be flux in the Dead Sea regions is 2.0±0.6×10^{4} atoms·cm^{-2}·y^{-1} during summer and winter months and 5.3±0.7×10^{4} atoms·cm^{-2}·y^{-1} during fall months; (b) the residence time of dust in the drainage basin is less than one year and (c) the recycled ^{10}Be component in Judean desert dust is small. It appears that the inventory of ^{7}Be in dust settled in the Dead Sea drainage basin increases as a function of time and does not reach steady state. Thus, ^{10}Be may be used for reconstructing paleo-flood frequency and dust transport

Behaviour of dissolved silica (adsorption and coprecipitation) in the presence of calcite

D.A. BELOVA[1]*, O.N. KARASEVA[2], L.Z. LAKSHTANOV[2] AND S.L.S. STIPP[1]

[1]Nano-Science Center, Department of Chemistry, University of Copenhagen, Denmark. (*correspondence: db@nano.ku.dk)

[2]Institute of Experimental Mineralogy RAS, Chernogolovka, Russia (leonid@iem.ac.ru).

The replacement of carbonate minerals in sediments by silica is common during carbonate rock diagenesis. Silica, as well as organic material and clays, can be one of the inhibitors of chalk (>95% calcite) recrystallization process [1]. However, the mechanism of selective substitution of carbonate sediments by silica and the influence of different factors on silica uptake by adsorption and coprecipitation with calcite are still not clear. In this work, we studied the interaction between dissolved silica and calcite under a variety of experimental conditions to estimate the role of SiO_2 in chalk diagenesis.

The experiments were performed at 25 ºC, different CO_2 partial pressures (pCO_2=1 atm, pCO_2=$10^{-3.5}$ atm and no access to CO_2) and various SiO_2 concentrations ($\leq$ 2 mM). In monomeric silica solutions, no SiO_2 removal by adsorption was observed. The uptake of SiO_2 correlates with the amount of silica polymers and has its maximum value at basic pH, where some polysilicates are present.

Coprecipitation experiments were carried out by the constant addition method. The silica partition coefficient was calculated to be less than 1 and found to be dependent on calcite precipitation rate. The results of coprecipitation studies support that of adsorption experiments and also show that only insignificant amount of silica can be coprecipitated with calcite (maximum SiO_2 uptake is 4.8 μmol g^{-1}). This value increases with increasing dissolved silica concentration, increasing pH and the amount of silica polymers. Using the data from the adsorption study, namely, that polysilicic acid depolymerizes at the calcite surface, we can suggest two models for solid solution formation during coprecipitation.

We can conclude that interaction between dissolved SiO_2 at concentrations below the saturation with respect to amorphous silica and calcite is very weak and depends on adsorption of silica polymers.

[1] Baker *et al*. (1980) *Marine Geology* **38**, 185-203

https://doi.org/10.1180/S0026461X00006502 Published online by Cambridge University Press

The volatile content of subduction zone melts and fluids

A. BÉNARD[1]*, D.A. IONOV[1], N. SHIMIZU[2] AND P.Y. PLECHOV[3]

[1]Univ. J. Monnet, St Etienne & UMR6524-CNRS, France (*correspondence: antoine.benard@univ-st-etienne.fr)
[2]Woods Hole Oceanographic Institution, Woods Hole, USA
[3]Moscow State University, Moscow, Russia

Harzburgite xenoliths from the andesitic Avacha volcano (Kamchatka, Russia) contain two types of spinel-hosted melt inclusions: (a) high-T inclusions (homogenized at 1200°C) containing opx±cpx+glass and (b) low-T inclusions (homogenized at 900°C) containing amph±sulf+glass. Homogeneous glass in the high-T inclusions is similar in major element composition to basaltic andesite experimentally produced by high-degree, hydrous melting of peridotite [1]. Homogeneous glass in the low-T inclusions is silica oversaturated, Al- and Ca-rich, enriched in $LREE_N$ and $LILE_N$ relative to $MREE_N$-$HREE_N$; it displays a strong slab-related chemical overprint. The xenoliths also contain melt pockets originating from local, fluid-assisted melting, produced shortly before the entrapment of the xenoliths.

We analyzed the volatile content of melt inclusions and pockets by Secondary-Ion Mass Spectrometry (SIMS) with Cameca IMS 1280. Most inclusions contain much more CO_2 and H_2O than predicted by saturation curves for these species in silicate melt at 600 bar, implying that the melt entrapment occurred at mantle depth. High-T inclusions have 0.20±0.02 wt.% CO_2, 2.05±0.01 wt.% H_2O and 130±1 ppm S. Low-T inclusions display a wide range of CO_2 (0.01-0.57±0.01 wt.%) and H_2O (0.86-7.45±0.02 wt.%). The abundances of CO_2 and H_2O are positively correlated. The low-T inclusions define also an F-enrichment trend (from 50 to 672±5 ppm) with less variable Cl (540-759±14 ppm) and are strongly enriched in S (up to 0.59 wt.%). Glass in the melt pockets has the lowest CO_2 and H_2O contents (respectively ≤0.03±0.01 and ≤1.58±0.02 wt.%). The $\delta^{34}S$ range of +7.0 to +11.0‰ (±0.6‰, 2σ) in the melt inclusions indicates the presence of heavy oxidized sulfur, likely with surface provenance [2].

The results suggest and/or confirm that (1) the high-T inclusions trapped a mantle-derived primary melt, (2) the low-T inclusions are produced by polybaric entrapment of fluid-rich, hydrous melts in the lithospheric mantle; and provide the first "in situ" evidence for volatile recycling in the lithospheric mantle above a subducting slab.

[1] Grove *et al*. (2003) *CMP* **145**, 515-533. [2] Shimizu, N. *et al*. (2010) *GCA* **74** (S1), A953.

Laser-induced photo-luminescence spectroscopies: Probes for sulfide crystal-chemistry

A. BÉNARD[1]*, T. OLIVIER[2], B.N. MOINE[1], D.A. IONOV[1], L.-S. DOUCET[1] AND M. BOYET[3]

[1]Univ. J. Monnet & UMR6524-CNRS, St Etienne, France (*correspondence: antoine.benard@univ-st-etienne.fr)
[2]Centre de Microscopie Confocale et Multiphotonique, Univ. J. Monnet, St Etienne, France
[3]Univ. B. Pascal & UMR6524-CNRS, Clermont-Ferrand, France

We combine Two-Photon Fluorescence (TPF), Confocal Laser Scanning Microscopy (CLSM) and Confocal Laser-Induced Luminescence (LIL) to acquire 2-D and 3-D-resolved luminescence emission spectra from transition metal- and (Ca, REE)-bearing mantle-derived and meteoritic (enstatite chondrite) sulfides. The latter include primary condensates and high-degree metamorphic crystals. A wide range of excitation λ (442-800 nm) is tested; Raman micro-spectrometry adds qualitative constraints on sulfide crystallinity. Despite the small amount of luminescence emitted by the sulfides, TPF and CLSM are sensitive enough to perform 3-D imaging with a resolution of ~0.5 μm laterally and ~5 μm axially, in particular using Near Infra-Red (NIR) femtosecond excitation (TPF). Versatile concofal microscopes allow to scan collected luminescence with a 20 nm spectral window to record spectra of roughly 10 x 10 μm regions of interest.

All sulfides emit a characteristic band at 710 nm under TPF NIR radiation that can be related to the sulfur 3sσ state [1]; its increased sharpness may be due to higher crystallinity degree. Pyrrhotite has a continuous emission along a broad λ range (400-710 nm) that allows to distinguish it both from lower temperature, NiAs-type monosulfide polymorphs with two individualized Gaussian-shaped bands (centered at 460 and 650 nm) and troïlite (one major band at 710 nm). We seek to identify *4d*- and *5d*-metal monosulfide heterogeneities (PtS and PdS clusters) with the super-resolution of the TPF.

Under a 633 nm LIL excitation, CaS emits the 710 nm band characteristic of sulfur while below 442 nm, the *4f* and *5d*-derived levels of $^{VI}Ce^{3+}$ are excited with the appearance of the $\Gamma_8(^2T_{2g}) \rightarrow {}^2F(\Gamma_7, \Gamma_8(^2F_{5/2}); \Gamma_6, \Gamma_7, \Gamma_8(^2F_{7/2}))$ transitions. With the use of point charge crystal-field modelling at constant Ce valency, we infer a direct correlation of the *5d* orbitals (t_{2g}-e_g set) splitting parameter Δ_0 to the CaS lattice spacing, controlling in turn Ce partitioning. We investigate REE fluorescence mapping with the TPF super-resolution.

[1] Raybaud *et al*. (1998) *JPCM* **9**, 11085-11106.

https://doi.org/10.1180/S0026461X00006502 Published online by Cambridge University Press

On the radiogenic ^{40}Ca anomaly in seawater and limestone

MICHAEL L. BENDER* AND JOHN A. HIGGINS

Department of Geoscience, Princeton University, Princeton, NJ 08544, USA
(*correspondence: bender@princeton.edu)

Caro *et al*. [1] estimate that the silicate upper continental crust has a radiogenic ^{40}Ca anomaly of 2.5 epsilon units from ^{40}K decay. Surprisingly, Caro *et al*. show that epsilon ^{40}Ca of seawater and limestone is indistinguishable from the mantle value (epsilon ^{40}Ca~0, since the mantle has low K/Ca), with an uncertainty of about ± 0.3 units. To balance the modern oceanic ^{40}Ca budget, they suggest that the riverine flux of radiogenic crustal Ca is balanced by a small nonradiogenic flux from high-temperature hydrothermal processes at mid-ocean ridges, and a larger flux of nonradiogenic calcium from low-temperature hydrothermal systems on ridge flanks. If correct, waters in ridge flank hydrothermal systems must play a major role in the chemical mass balance of the oceans.

We discuss 3 factors that, without invoking ridge flank exchange, help explain the enigma that limestone and seawater Ca are much less radiogenic than the silicate crust. First, radiogenic ^{40}Ca is diluted into the large mass of limestone. Second, the time-averaged hydrothermal flux would be twice the present value if it scaled with past heat production. Third, nonradiogenic hydrothermal Ca would have been retained in the limestone and (via metamorphism) in the silicate crust; it would be recycled by subsequent weathering, thereby lowering epsilon ^{40}Ca in rivers. These three factors together can account for about two-thirds of the difference between the estimated ^{40}Ca anomaly of the silicate continental crust and the nonradiogenic Ca composition of seawater and limestone.

[1] Caro, Papanastastassiou & Wasserburg (2010), *Earth and Planetary Science Letters* **296**, 124-132.

Limited early continents from the chemistry of Eoarchean rocks

VICKIE C. BENNETT[1] AND ALLEN P. NUTMAN[2]

[1]Research School of Earth Sciences, The Australian National University, Canberra, Australia (vickie.bennett@anu.au)
[2]School of Earth and Environmental Sciences, University of Wollongong, NSW, Australia (allen.nutman@gmail.com)

Continuing and fundamental questions in Earth history focus on the timing and mechanisms of early continent formation. These questions take on additional significance in consideration of potential early life habitats and early tectonic regimes. Key approaches used to argue for, and against, massive early continents, have centered on the signatures of long-lived isotopic systems, i.e. initial εNd and εHf, preserved in the oldest rocks. For example, positive deviations from bulk silicate Earth compositions have been equated with massive early crust formation. Such interpretations contain the assumption that continental crust has been the primary complement to the depleted mantle throughout Earth history. However, using an expanded ^{142}Nd,^{143}Nd,^{176}Hf database derived from Eoarchean rocks worldwide we demonstrate that Nd and Hf isotopic data do not record the distinctive correlations observed in younger granitic terranes; these correlations are generated in the mantle by long term crust extraction. Furthermore, positive ^{142}Nd anomalies (relative to modern terrestrial compositions) measured in some Eoarchean rocks require extremely early (4.53 Ga - 4.4 Ga) Sm/Nd fractionation. Overall, neither Sm-Nd or Lu-Hf fractionation in the >3.7 Ga mantle can be linked to continental crust extraction.

Other types of observations from ancient rocks further support the case for limited crustal volumes. Eoarchean rocks are now recognised in 8 gneiss complexes worldwide. In each area, the oldest felsic rocks (ca. 3.7-4.0 Ga) are typically tonalites, with no evidence of pre-existing crust in the form of inherited zircon grains with older U-Pb ages. Where data are available, the initial εNd and εHf values range from chondritic to positive and δ^{18}O isotopic compositions are mantle-like; thus there is no chemical evidence for reworking of older components. In contrast, younger (≤3.65 Ga) granites (*sensu stricto)* often contain inherited zircons whose U-Pb ages match the oldest crust in each region; initial εNd and εHf values become more negative with decreasing rock age, reflecting incorporation of older felsic components. We consider that, at present, there is no compelling evidence for the existence of extensive early continents, prior to ~3.65 Ga.

https://doi.org/10.1180/S0026461X00006502 Published online by Cambridge University Press

An experimentalist call to theoreticians about XANES spectra theoretical simulation at the C K-edge, Ca and Fe $L_{2,3}$ edges

KARIM BENZERARA[1], OLIVIER BEYSSAC[1], MATTHIEU GALVEZ[1], SYLVAIN BERNARD[2] AND JULIE COSMIDIS[1]

[1]Institut de Minéralogie et de Physique des Milieux Condensés, UMR7590, CNRS, UPMC & IPGP, 4 Place Jussieu, 75005 Paris, France

[2]LMCM, UMR 7202, MNHN & CNRS, 61 rue Buffon, 75005 Paris, France

Scanning transmission x-ray microscopy (STXM) is increasingly used in geobiology and more generally in Earth sciences [1-5]. It is a transmission microscopy providing images with 25-nm spatial resolution and a x-ray absorption near-edge structure (XANES) spectrum for each pixel of this image. The few beamlines that are available worldwide (e.g., 11.0.2 at the ALS or 10ID-1 at the CLS) give the opportunity to scan over a large energy range (e.g. 70-2200 eV) with high energy resolution enabling the study of elements such as C, N, O, Mg (using K-edges), or P, Ca, Fe or As (using L-edges). XANES spectra coupled with high spatial resolution can thus provide unique information on the speciation of diverse elements which is a 1st order interest for a variety of applications. However, very often, the use of the spectroscopic information is limited to a fingerprinting approach. We believe that theoretical developments would help retrieving significantly more information from these spectra. Here we will review some of the experimental work that we have done over the last few years in order to identify some key needs that we have and that might be adressed by theoreticians. In particular, we will discuss the use of XANES spectroscopy at the C K-edge to study the chemical composition and structure of organic carbon in (ancient) rocks and mention the implications for the study of metamorphism and/or search for ancient traces of life. Absorption variations due to linear dichroism in particular will be presented. The use of XANES spectroscopy at the Fe $L_{2,3}$ edges and difficulties to retrieve Fe redox state values will be adressed.

[1] Lepot *et al*. (2009) *Geochim. Cosmochim. Acta* 73, 6579-6599. [2] Bernard *et al*. (2010) *Carbon* 48, 2506-2516. [3] Carlut, *et al*. (2010), J. Geophys. Res. 115, G00G11. [4] Benzerara *et al*. (2011) *Ultramicroscopy*, in press. [5] Miot *et al*. (2009) *Geobiology* 7, 373-384.

Arsenic contamination of groundwater in Vietnam: Delta-wide survey and 3D geospatial modelling

M. BERG[1]*, L.H.E. WINKEL[1], P.T.K. TRANG[2], V.M. LAN[2], C. STENGEL[1], M. AMINI[1], N.T. HA[3], AND P.H. VIET[2]

[1]Eawag, Swiss Federal Institute of Aquatic Science and Technology, 8600 Dübendorf, Switzerland (*correspondence: Michael.Berg@eawag.ch)

[2]Centre for Environmental Technology and Sustainable Development (CETASD), Hanoi, Vietnam.

[3]Centre for Water Resources Monitoring and Forecast (CWRMF), Hanoi, Vietnam.

Arsenic contamination of shallow groundwater is among the biggest health threats in the developing world. The Red River Delta was recognized to be affected in 1998, but the spatial extension remained unknown [1]. Here we present the results of a groundwater survey of the entire Red River Delta combined with a unique probability model based on 3-dimensional (3D) Quaternary geology. Our investigations reveal that ~7 million delta inhabitants use groundwater that contains unsafe levels of As, Mn, Se, and Ba.

Global and sub-continental arsenic risk maps based on surface geology were recently shown to be a successful tool to initiate mitigation measures [2,3]. For the Red River delta we now established a 3D model based on stratigraphy of Quaternary geology, which visualizes As hot-spots at depths and identifies safe regions for drinking water production.

This 3D model further reveiled anomalities of As enrichment in the aquifers. Particularly in the Hanoi area, depth-resolved probabilities and As concentrations indicate drawdown of As-enriched water from Holocene aquifers to naturally As-safe Pleistocene aquifers, most likely as a result of more than 100 years of groundwater abstraction. Vertical As migration induced by large-scale pumping from deep aquifers has been discussed to occur elsewhere, but has never been shown to occur at the scale seen here. The present situation in the Red River Delta is hence a warning for other As-affected regions where groundwater is extensively pumped from uncontaminated aquifers.

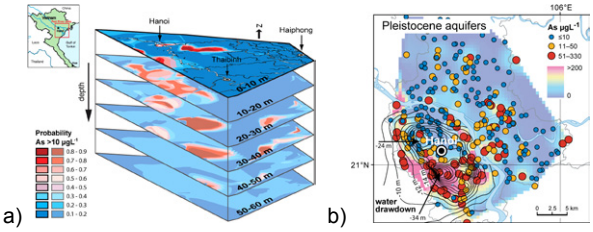

Figure 1: a) As risk map (3D), Red River Delta. b) As levels in the Pleistocene aquifers, and water drawdown in Hanoi [4].

[1] Berg *et al*. (2001) *Environ. Sci. Technol*. **35**, 2621-2626. [2] Winkel *et al*. (2008) *Nature Geosci*. **1**, 536-542. [3] Amini *et al*. (2008) *Eviron. Sci. Technol*. **42**, 3669-3675. [4] Winkel *et al*. (2011) *Proc. Natl. Acad. Sci. USA*. **108**, 1246-1251.

https://doi.org/10.1180/S0026461X00006502 Published online by Cambridge University Press

Volatile release from crustal-xenolith during subvolcanic magma transport

S. BERG[1]*, V. R. TROLL[1,2], H. ANNERSTEN[1], C. FREDA[2], L. MANCINI[3], L. BLYTHE[1], E. MUÑOZ JOLIS[1] AND A. BARKER[1]

[1]Department of Earth Sciences, Uppsala University, Villavägen 16, 752 36 Uppsala, Sweden (*correspondance: e.sylviaberg@gmail.com)
[2]Istituto Nazionale di Geofisica e Vulcanologia, Rome, Italy
[3]SYRMEP Group, Sincrotrone Trieste, Basovizza, Italy

Magma-crust interaction in magma reservoirs and conduits is a crucial process during magma evolution and ascent. This interaction is recorded by crustal xenoliths that frequently show partial melting, inflation and disintegration textures. Frothy xenoliths are widespread in volcanic deposits from all types of geological settings and indicate crustal gas liberation. To unravel the observed phenomena of frothy xenolith formation we experimentally simulated the behaviour of crustal lithologies in volcanic conduits. We subjected various sandstones to elevated temperature (from 810 to 916 °C) and pressure (from 100 MPa to 160 MPa) in closed-system autoclaves. Experimental conditions were held constant for 24h up to 5 days, then controlled decompression simulated xenolith ascent. Pressure release was a function of temperature decline in our setup. Temperature lapse rate proceeded exponentially; the first 20 minutes experienced an enhanced decline of 24-20°C/min, whereafter 6-8 hours of slow cooling followed towards room temperature. The experimental xenoliths have been analysed by synchrotron X-ray μ-CT at a resolution of 3.4 – 9 microns/pixel. This method permits visualisation and quantification of internal vesicle volumes, -networks and -connectivity in 3D.

Experimental products closely reproduced the textures of natural frothy xenoliths in 3D and define an evolutionary sequence from partial melting to gas exsolution and bubble nucleation that eventually leads to the development of three-dimensional bubble networks. The lithology proved decisive for degassing behaviour and ensuing bubble nucleation during decompression. Increased volatile content (chiefly water) and amount of relict crystals in the partial melt promote bubble nucleation and subsequent bubble coalescence to form interconnected bubble networks. This, in turn, enables efficient gas liberation. Our results attest to significant potential of even very common crustal rock types to liberate volatiles and develop interconnected bubble networks upon heating and decompression. Volatile input from xenoliths may therefore considerably affect explosive eruptive behaviour, and our experiments offer a detailed mechanism of how such crustal volatile liberation is accomplished.

Cr-isotopes and REE variations in a laterite profile: Implication for redox processes and element mobility during weathering

ALFONS BERGER AND ROBERT FREI

University Copenhagen, Denmark (*correspondence: ab@geo.ku.dk)

The isotope composition of redox sensitive elements are a powerful tool to reconstruct transport of elements depending on their oxidation state. One major application is the study of element transfer from weathering to redeposition. However, the understanding of the "output" during weathering requires insights to processes during erosion and soil development. In this context, the mineralogy and oxidate state of certain elements in weathering profile are key informations.

We will give some insights into a modern laterite profile of Madagascar. The profile is taken in an quarry near RN7 south of Antisrabe, including bed rock, saprolith and top soil. The fresh rock are a Panafrican tonalite. The sample site is characterized by minor topography and groundwater flow is controlled by small rivers. The fresh rock is dominated by two feldspars, quartz, biotite, hornblende, ilmenite, magnetite, apatite, allanite and chevkinite. Weathering starts along cracks and is accompined by change mineralogy and major elements abundances. Trace element concentrations and Pb isotopes indicate no or only minor solid mass transport. The profile reflects an *in situ* weathering profile with a water level horizon above the saprolith. The water flow horizon includes a change in Ce concentrations related to deposition of ceriate. This is most likely related to insolvable Ce(IV) in this part of the profile. In contrast, transformation during weathering from allanite/chevkinite to rhabdophane did not change the REE whole rock pattern. Cr is strongly depleted in the soil and in the saprolith and reflects mobilization of Cr by oxidation to the hexavalent state. This change of oxidation change is corroborated by fractionated Cr isotopes in the saprolith (δ^{53} Cr -0.4 – -0.5‰), relative to the δ^{53}Cr value of ~0.15‰ of the tonalite

The different behaviour of the redox sensitive elements Ce and Cr is either related to the redox potential of the elements and/or is kinetically controlled by the respective host minerals. The REE´s are predominantly hosted by accessory minerals (chevkinite, allanite, apatite), whereas Cr are incorporated rock forming silicates and oxides. Comparison of Ce anamolies and Cr isotopes provide important insights to the behaviour of these elements during weathering and consequently to the relative concentrations in the solvent.

https://doi.org/10.1180/S0026461X00006502 Published online by Cambridge University Press

Hydrothermal synthesis of cubanite under conditions relevant to the CI-chondrite parent body

E. L. BERGER*[1], D. S. LAURETTA[1] AND L. P. KELLER[2]

[1]Lunar & Planetary Laboratory, Tucson, AZ 85721 (*correspondence: elberger@lpl.arizona.edu)
[2]NASA Johnson Space Center, Houston, TX 77573

The low temperature form of $CuFe_2S_3$, cubanite, has been identified in the CI chondrites and in samples returned from Comet Wild 2 by the Stardust Mission [1]. We report the first synthesis of this mineral under aqueous conditions consistent with predictions for the CI-chondrite parent body.

An aqueous system can be described as the interplay between pH, temperature, oxygen and sulfur fugacities [2]. We form cubanite at 150 and 200ºC (fig. 1) by controlling oxygen fugacity (fO_2), pH and T. Oxygen isotope measurements and modeling of aqueous conditions on asteroidal bodies [3, and ref. therein] predict: T of 20-150ºC, pH of 7-10 and log $fO_2 > 10^{-55}$ -10^{-70}.

EMPA and FIB-TEM techniques are used to determine composition and crystal structure.

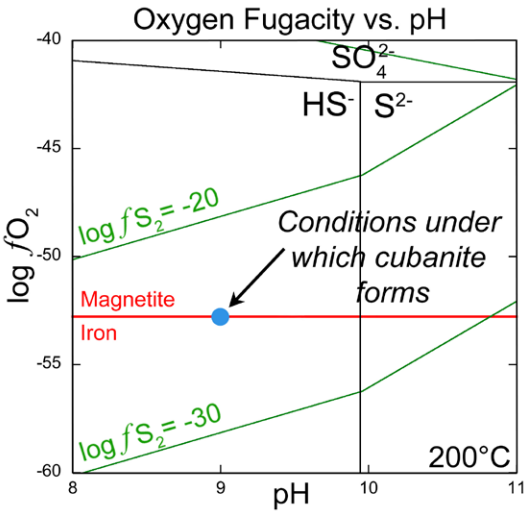

Figure 1: Oxygen fugacity vs. pH for an aqueous system containing 0.025M S. Major S species (aq), lines of constant sulfur fugacity and the iron-magnetite buffer are indicated.

[1] Berger *et al*. (2011) *GCA* doi:10.1016/j.gca.2011.03.026. [2] Barnes and Kullerud (1961) *Econ. Geol*. **56**, 648-688. [3] Brearley (2006) in *MESS-II*, 587-624.

Fluoride patterns in a boreal stream influenced by bedrock and hydrology

T. BERGER*, P. PELTOLA, H. DRAKE AND M. ÅSTRÖM

Department of Natural Sciences, Linnaeus Univ., Kalmar, Sweden (*correspondence: tobias.berger@lnu.se)

The spatial and temporal variation of fluoride in the Kärrsvik catchment (27 km^2) in SE Sweden has been monitored monthly for up to 6 years (2002 - 2009). The bedrock is characterized by 1.8 Ga old granite to quartz monzodiorite. However, in the lower reaches the F-rich, 1.45 Ga old, Götemar granite crops out.

Fluoride increased significantly at this intrusion and showed a strong negative relationship with flow, ranging between 0.6 and 4.2 mg L^{-1} (median 1.04 mg L^{-1}). In the upper reaches the concentrations were lower, <0.20 - 0.85 mg L^{-1} (median ~0.4 mg L^{-1}). The spatial concentration pattern of fluoride in well waters was concordant with that of the surface waters within the catchment.

On a continental scale, European streams (n=808, 25 countries) have median fluoride concentrations of 0.1 mg L^{-1} [1]. The Kärrsvik catchment is therefore an area with anomalous fluoride concentrations. Stream waters can be major sources of drinking water and the World Health Organization guideline value is set to 1.5 mg L^{-1}.

The fluoride pattern can be explained by three main sources associated with weathering processes in the lower reaches of the catchment: 1, glacial deposits partially enriched in weathering products from the Götemar granite, 2, larger input of baseflow water (longer interaction time with F-bearing minerals) and 3, intrusion-related fractures strongly enriched in fluorite.

Detailed studies of near-surface groundwaters in the region will further increase the understanding of the dynamics of this element in these kinds of environments.

[1] Salminen *et al*. (2005) *Geochemical Atlas of Europe. Part 2*, 161-162.

https://doi.org/10.1180/S0026461X00006502 Published online by Cambridge University Press

Early Neoproterozoic arc magmatism along the northwestern margin of the Yangtze craton and its connection with the South China Block evolution during the Rodinia assembly

W. BERKANA[1,2] ,W-L. LING[1,2]*, X-F. QIU[1,2] AND S-S. LU [1,2]

[1]State Key Laboratory of Geological Process and Mineral Resources, China University of Geosciences, Wuhan 430074, P R China (lingwenli2008@126.com)

[2]Faculty of Earth Sciences, China University of Geosciences, Wuhan 430074, P R China (wafaberkana@yahoo.fr)

The South China Block (SCB) comprises the Yangtze craton and the Cathysian block, welded during ~1.0-0.95 Ga. Neoproterozoic igneous activities of ~830-750 Ma are widely recorded in the SCB. However, their origin and tectonic setting have long been debated, resulted in competing models for the correlation of the SCB with Rodinia supercontinent.

The Wangcang igneous complex occurs along the northwestern Yangtze craton, which has long been regarded as early Precambrian basement. Our present study reveals that both the intrusive and volcanic suites were formed at ~880 Ma. The mafic rocks show tholeiitic geochemistry with initial ε_{Nd} values of +2.1 to +7.7, whereas the felsic samples are calc-alkaline series with a ε_{Nd} range of -2.1 to +4.7. These suites are suggested to have an arc magmatic origin, and their intensive deformation and high metamorphism occurred during ~880-820 Ma.

Integrating with proofs such as Nd isotope stratigraphic studies of the Yangtze craton, we suggest that the Yangtze craton had experienced a continent growth during the Rodinia assembly by microcontinent merging before the SCB unification. This study was supported by National Nature Science Foundation of China (Grants 40873017, 40673025).

The advantage of the use of Focused Ion Beam technique to specify the mantle fluid inclusions

M. BERKESI[1]*, T. GUZMICS[1], C. SZABÓ[1] AND J. DUBESSY[2]

[1]Lithosphere Fluid Research Lab, Institute of Geography and Earth Sciences, Eötvös University Budapest, 1117 Pázmány Péter sétány 1/C, Budapest, Hungary (correspondence: martaberkesi@caesar.elte.hu)

[2]UMR G2R and CREGU, Nancy University, BP-70239, 54506-Vandœuvre-les Nancy Cedex, Nancy (France) (jean.dubessy@g2r.uhp-nancy.fr)

The Focused Ion Beam (FIB) coupled with scanning electron microscopy (SEM) technique has became one of the most promising tools for many geochemical studies in the last decade [1].

It is known that within the fluid inclusions solids (referred to as daughter phases) may crystallize as a result of cooling and/or reaction with their host mineral. If the volume proportions of the daughter phases are not known, the fluid composition determined can be misinterpreted. However, *in situ* measurement of the daughter phases can be complicated and ambiguous with conventional techniques because of their size and/or composition. In this study we report our results using FIB-SEM technique on investigation of daughter phases in orthopyroxene-hosted fluid inclusions in mantle xenoliths from the Pannonian Basin (Hungary).

Solid phases such as magnesite and quartz have been found within the fluid inclusions. They have a size between 200 – 2000 nm occurring as cluster on some parts of the inclusion walls. In addition, S-bearing solid phase (probably sulfide) has also been identified. One of the most interesting feature observed was a thin film covering the wall of the studied fluid inclusions. This film has a feature that is typical for the volcanic glasses, containing numerous spherical-shaped holes (vesicles) on the surface as a result of the exsolution of volatiles. It is to emphasize that previous works on fluid inclusions have already proposed the presence of the glass film on the wall [2] in mantle fluid inclusions, however, in this work the glass film has been found *in situ*.

The acquired results of this study contribute to 1) quantification of the bulk fluid composition and 2) better understanding the mechanisms of the post-entrapment processes in fluid inclusions entrapped at lithopheric mantle condition.

[1] Wirth (2009) *Chem Geol* **261**, 217-229. [2] Hidas *et al.* (2010) *Chem Geol* **274**, 1-18.

https://doi.org/10.1180/S0026461X00006502 Published online by Cambridge University Press

Can we use variations in volatile concentrations in volcanic glass to study degassing?

KIM BERLO[1], DAVID PYLE[1], JENNI BARCLAY[2], TAMSIN MATHER[1] AND HUGH TUFFEN[3]

[1]Department of Earth Sciences, University of Oxford, Oxford, UK. (kim_berlo@inbox.com, David.Pyle@earth.ox.ac.uk, Tamsin.Mather@earth.ox.ac.uk)
[2]School of Environmental Sciences, University of East Anglia, Norwich, UK. (J.Barclay@uea.ac.uk)
[3] Lancaster Environment Centre, Lancaster University, Lancaster, UK. (h.tuffen@lancaster.ac.uk)

Decompression of volatile rich magma results in the exsolution of a separate gas phase. Major volatile species, H_2O, CO_2, SO_2, as well as many minor volatile species, $PbCl_2$, $ZnCl_2$, Hg, AsS etc, will be partitioned between the gas and the melt phase. However, the rate of magma ascent and eruption does not always allow for the equilibrium distribution between gas and melt of such species to be reached. Instead elements are quenched in transition towards an equilibrium that constantly changes as the magma ascends. Volatile elements can thus display diffusive profiles towards gas escape features, such as bubbles, tubes or fractures. This exploratory study aims to map out the extent of heterogeneity in rhyolitic glasses. Samples with different gas pathways, bubbles, fractures, channels and tuffisite veins have been selected and will be mapped for H_2O and selected trace metals (Cu, Zn, Bi, Pb) using synchrotron FTIR and XRF. The results of this study will allow us assess the extent to which volcanic gases can be in equilibrium with a melt shortly before eruption.

Calcium isotopes in lunar crust

K. BERMINGHAM[1], T. MAGNA[1,2], N. GUSSONE[1] AND K. MEZGER[3]

[1]Universität Münster, Germany
[2]Czech Geological Survey, Prague, Czech Republic
[3]Universität Bern, Switzerland

Calcium isotope compositions were determined in lunar crustal rocks in order to quantify possible mass-dependent (MDF) and mass-independent (MIF) isotope fractionation. Anorthosites show ~0.4‰ variation in $\delta^{44/40}$Ca; pristine anorthosite 60025 has an identical value to previous reports [1] but appears to be slightly heavier than the other anorthosites ($\delta^{44/40}$Ca=0.65–0.91‰) which may reflect a larger proportion of isotopically heavy olivine. Norite 77215 has $\delta^{44/40}$Ca=1.06‰, which is identical to pristine terrestrial mantle rocks [2] and likely represents a mixture between isotopically light plagioclase and heavy orthopyroxene. In general, anorthosites and norite mimic the range of terrestrial and Martian basalts [2–4] as well as lunar low-Ti and high-Ti lithologies [4]. The $\delta^{44/40}$Ca uniformity of lunar crust and mantle-derived rocks is dissimilar to the Ca systematics of major terrestrial reservoirs with predominantly light Ca isotope signature in continental crust and may suggest cessation of magmatic activity early in the lunar history without further material exchange with deeper parts of the Moon. A tight negative correlation of $\delta^{44/40}$Ca with K contents could reflect either the chemical development of the magma ocean or a collateral effect of immiscibility between Ca and K feldspars. However, only a detailed experimental investigation could provide tight constraints on the role of plagioclase in lunar Ca budget. This may be particularly important for the Moon considering that, in contrast to the Earth where >99% Ca budget is dominated by mantle, lunar crust is a significant Ca repository and hosts ~11% of the total lunar Ca. New data for lunar mare basalts coupled with data for anorthosites could help constrain the lunar Ca evolution in the context of lunar magma ocean crystallization.

The MIF effects are indiscernible for individual Ca isotopes in all investigated lunar rocks in this study. This is in agreement with previous findings for some Solar System material [5–7]. In particular, lack of resolvable MIF variations in lunar samples may imply Ca isotope homogeneity on the planetary scale.

[1] Farkaš *et al*. (2010) *LPSC* **41**, #2266; [2] Amini *et al*. (2009) *GGR* **33**, 231-247; [3] Huang *et al*. (2010) *EPSL* **292**, 337-344; [4] Simon & DePaolo (2010) *EPSL* **289**, 457-466; [5] Huang *et al*. (2010) *LPSC* **41**, #1379; [6] Moynier *et al*. (2010) *ApJ* **718**, L7-L13; [7] Simon *et al*. (2009) *ApJ* **702**, 707-715

https://doi.org/10.1180/S0026461X00006502 Published online by Cambridge University Press

Nanoscale study of the mineralogical and geochemical evolution of black shales with increasing maturity

S. BERNARD[1,*], B. HORSFIELD[2], H-M. SCHULZ[2], A. SCHREIBER[2], R. WIRTH[2] AND N. SHERWOOD[3]

[1]LMCM, MNHN, CNRS, Paris, France (sbernard@mnhn.fr)
[2]Deutches GeoForschungsZentrum GFZ, Potsdam, Germany (horsf@gfz-potsdam.de, schulzhm@gfz-potsdam.de, schreiber@gfz-potsdam.de, wirth@gfz-potsdam.de)
[3]CSIRO, North Ryde, Australia (Neil.Sherwood@csiro.au)

Gaseous hydrocarbon generation processes occur within gas shales as a response to increases in thermal maturation. While efforts have been directed at unravelling the resource potential of these unconventional systems [1], their spatial variability in chemistry and structure is still poorly understood at the sub-micrometer scale. For instance, intra-particle nanoporosity has been documented within overmature gas shale samples but has not yet been attributed to any specific organic macromolecule [2]. Here, we have characterized samples of the Lower Toarcian Posidonia Shale from northern Germany at varying stages of thermal maturation using a combination of compositional organic geochemistry and spectromicroscopy techniques, including synchrotron-based scanning transmission X-ray microscopy (STXM). We document geochemical and mineralogical heterogeneities down to the nanometer scale within the investigated samples at all levels of thermal maturity [3,4].

In particular, authigenic albite crystals containing nanometric halite inclusions have been documented within the investigated mature and overmature samples. The presence of such tracers of palaeobrine-carbonate interactions supports a maturation scenario for the Lower Toarcian Posidonia Shale intimately related to ascending brine fluids. In addition, various types of asphaltene- and NSO-rich bitumen have been detected within the same samples, very likely genetically derived from thermally degraded organic precursors. Furthermore, the organic macromolecules displaying intra-particle nanoporosity have been identified as pyrobitumen residues, such nanoporosity likely resulting from the formation of gaseous hydrocarbons. By providing *in situ* insights into the fate of bitumen and pyrobitumen as a response to the thermal evolution of the macromolecular structure of kerogen, the results reported here constitute an important step towards better constraining hydrocarbon generation processes during natural gas shale maturation.

[1] Jarvie *et al*. (2007), *AAPG* **91**, 475-499. [2] Loucks *et al*. (2009), *J. Sediment. Res*. **79**, 848-861. [3] Bernard *et al*. (2010), *Chemie der Erde - Geochemistry* **70(S3)**, 119-133. [4] Bernard *et al*., *Marine and Petroleum Geology*, in review.

Does the electron transfer process determine the product of U(VI) reduction?

RIZLAN BERNIER-LATMANI[1], DANIEL S. ALESSI[1], HARISH VEERAMANI[1], JONATHAN O. SHARP[1], ELENA DALLA VECCHIA[1], ELENA I. SUVOROVA[1], JOANNE E. STUBBS[2], JUAN S. LEZAMA-PACHECO[3] AND JOHN R. BARGAR[3]

[1]École Polytechnique Fédérale de Lausanne, Lausanne, Switzerland (*correspondence: rizlan.bernier-latmani@epfl.ch)
[2]University of Chicago, Chicago, IL 60637, USA
[3]Stanford Synchotron Radiation Lightsource, Menlo Park, CA 94025, USA

The bioremediation of uranium-contaminated sites is based on the amendment of an electron donor to stimulate microbial activity. Typically, Fe(III) and U(VI) serve as electron acceptors for microorganisms with the former supporting microbial growth. However, this biostimulation process may generate competing mechanisms of uranium bioreduction. While direct enzymatic reduction of U(VI) by microbes is a possible route of immobilization of U(IV), Fe(II) produced by the reduction of Fe(III) also is thermodynamically capable of abiotically reducing U(VI).

Here we investigate the question of whether different U(IV) products are expected from these various U(VI) reduction processes. Specifically, we consider the reduction of U(VI) via direct enzymatic reduction by both Gram-positive and Gram-negative bacteria, via abiotic reduction by Fe(II)-bearing minerals as well as through a potential combination of these direct and indirect processes in sediment columns.

The results indicate that geochemical conditions dictate the product of U(VI) reduction. For example, the same microorganism produced a monomeric sorbed U(IV) complex in the presence of particular solutes but nanoparticles of the mineral uraninite in their absence. A phosphate-reacted magnetite (Fe_3O_4) suspension produced a similar monomeric U(IV) product while unreacted magnetite produced uraninite. Finally, in studying U(VI) reduction in sediments, both laboratory and field-run columns yielded non-uraninite U(IV), suggesting that *in situ* geochemical conditions favor monomeric U(IV) formation.

This work shows that, while the kinetics of U(VI) reduction have been shown to depend on the reduction mechanism, the end-product of the reduction is largely determined by the geochemical conditions under which the reduction–biotic or abiotic- takes place.

https://doi.org/10.1180/S0026461X00006502 Published online by Cambridge University Press

Solubility of fluorine and chlorine in nominally anhydrous mantle minerals: Implications for mantle metasomatism and arc magmas

D. BERNINI[1], D. DOLEJŠ[1,2], N. DE KOKER[1], A. AUDÉTAT[1], H. KEPPLER[1] AND M. WIEDENBECK[3]

[1]Bayerisches Geoinstitut, University of Bayreuth, 95440 Bayreuth, Germany
[2]Institute of Petrology and Structural Geology, Charles University, 12843 Praha 2, Czech Republic
[3]Deutsches GeoForschungsZentrum, 14473 Potsdam, Germany

Subduction fluxes and recycling of halogens are important for interpreting the fate of halogen budget of altered subducting slab, availability of ligands for complexing in aqueous fluids, origin of high-pressure brines, and volatile signatures of arc magmas. We investigated solubilities of fluorine and chlorine in forsterite, enstatite and pyrope, and halogen partitioning between aqueous fluids and these minerals by piston-cylinder experiments at 1100 °C and 2.6 GPa. The chlorine solubility in forsterite, enstatite and pyrope is very low, 0.2-0.9 ppm, and it is independent of the fluid salinity (0.3-40 wt. % Cl). The fluorine solubility is 16-31 ppm in enstatite and 24-52 ppm in pyrope, also independent of fluid salinity. Forsterite dissolves 246-267 ppm up to a fluid salinity of 1.6 wt. % F. At higher fluorine contents in the system, forsterite is replaced by the minerals of the humite group. The fluid-mineral partition coefficients are 10^1-10^3 for fluorine and 10^3-10^6 for chlorine. The latter values are approximately three orders of magnitude higher than those for hydroxyl partitioning suggesting a gradual increase in the fluid salinity during fluid percolation through the mantle wedge. Energetics of fluorine incorporation in forsterite and the forsterite-humite chemical equilibria in the system Mg_2SiO_4-MgF_2 were further explored by first principles computations. The fluorine solubility in forsterite strongly increases with temperature, from 0.01 ppm F at 500 K up to 0.33 wt. % F at 1900 K and 0 GPa. By contrast, the effect of pressure on the fluorine solubility is very small, producing a decrease by a factor of two to three at 12 GPa. Consequently, partition coefficients of fluorine between forsterite and aqueous fluid (or silicate melt) are expected to increase with increasing temperature and decreasing pressure. When fluids or melts pass through the mantle wedge, fluorine will most efficiently be stored in the high-temperature portions of the wedge, promoting mantle metasomatism beneath the arc, and it will be released when the metasomatized mantle is advected to colder regions or to higher pressures.

Diffusion and microbial consumption of oxygen in an acidic geothermal iron-oxide mat

H C. BERNSTEIN[1], J. P. BEAM[2], R. P. CARLSON[1] AND W.P. INSKEEP[2]*

[1]Department of Chemical and Biological Engineering, Montana State University, Bozeman, MT 59717, USA (*correspondence:hans.bernstein@biofilm.montana.edu,binskeep@montana.edu)
[2]Department of Land Resources and Environmental Sciences, Montana State University, Bozeman, MT 59717, USA

The role of dissolved oxygen as a primary electron acceptor for microbially mediated iron oxidation was investigated within the primary flow path of an acidic geothermal spring in Norris Geyser Basin, Yellowstone National Park. Previous data has suggested that Fe(II)-oxidizing microbial populations (e.g., Metallosphaera yellowstonensis and potentially other novel members of the domain Archaea) represent the primary-producers within these microbial communities. Consequently, the availability of oxygen is hypothesized to limit microbial Fe(II)-oxidation and primary-productivity in this system. In situ measurements of oxygen profiles were obtained perpendicular to the direction of convective flow across the aqueous phase-Fe(III)-oxide interface using oxygen microsensors. Dissolved oxygen concentrations drop below detection by ~ 600 μm into the Fe(III)-oxide mat, indicating reactive oxygen consumption and defined spatial gradients. Evaluation of the oxygen flux across the liquid-mat boundary showed that convection was negligible compared to diffusive transport in the mat. Reaction-diffusion models were evaluated assuming both zero and first-order reaction kinetics. The in situ measurements and models suggest that the rate of oxygen consumption exceeds the rate of diffusion. Thus, microbially mediated Fe(II)-oxidation in this system is likely limited by oxygen diffusion, resulting in an active surface layer of Fe(III)-oxide biomineralization.

https://doi.org/10.1180/S0026461X00006502 Published online by Cambridge University Press

Quantitative mapping of the oxidation state of iron in mantle garnet

A.J. BERRY[1]*, G.M. YAXLEY[2], B.J. HANGER[2], A.B. WOODLAND[3], M.D. DE JONGE[4], D.L. HOWARD[4] AND D. PATERSON[4]

[1]Department of Earth Science and Engineering, Imperial College London, South Kensington, SW7 2AZ, UK (*correspondence: a.berry@imperial.ac.uk)
[2]Research School of Earth Sciences, Australian National University, Canberra, ACT 0200, Australia
[3]Institut für Geowissenschaften, Universität Frankfurt, Frankfurt am Main, D60438, Germany
[4]Australian Synchrotron, Clayton, VIC 3168, Australia

The garnet structure can accommodate both Fe^{2+} and Fe^{3+} and $Fe^{3+}/\Sigma Fe$ of garnets in garnet peridotite can be used to determine the oxygen fugacity (fO_2) of the cratonic lithosphere. This is important as an indicator of diamond (versus carbonate) stability. Post-formation metasomatic processes in the upper mantle, or during transport in kimberlites, may impose high fO_2s that result in diamond breakdown or resorption. Such events will usually be recorded by the coexisting garnet.

$Fe^{3+}/\Sigma Fe$ of garnets has traditionally been determined by Mössbauer spectroscopy of powdered samples. This lacks spatial resolution and the data for each measurement take several days to acquire. X-ray absorption near edge structure (XANES) spectroscopy is now commonly being used to determine $Fe^{3+}/\Sigma Fe$, is capable of micron spatial resolution and spectra can be recorded in ~15 minutes. We have recently reported a new method for quantifying $Fe^{3+}/\Sigma Fe$ from the XANES spectra of mantle garnets with an accuracy and precision comparable to Mössbauer spectroscopy [1].

XANES spectra were recorded in fluorescence mode from garnets prepared as either polished thin sections or electron probe mounts. A calibration curve relating the XANES spectra to $Fe^{3+}/\Sigma Fe$ of mantle garnets previously analysed by Mössbauer spectroscopy allowed garnet unknowns to be quantified. By recording the fluorescence intensity at a small number of energies as a function of position $Fe^{3+}/\Sigma Fe$ maps could be produced. It is possible to quantitatively map the oxidation state of Fe with a spatial resolution and acquisition time comparable to elemental mapping using the electron microprobe. This allows zonation of $Fe^{3+}/\Sigma Fe$ due to metasomatic processes to be identified.

[1] Berry *et al*. (2010) *Chem. Geol*. **278**, 31-37.

Carbonation of Steel Slag I

ELEANOR J. BERRYMAN[1]*, ANTHONY E. WILLIAMS-JONES[1], ARTASCHES A. MIGDISOV[1] AND SIEGER VAN DER LAAN[2]

[1]Department of Earth and Planetary Sciences, McGill University, Montreal, Quebec, Canada *(berryman.eleanor@gmail.com)
[2]Tata Steel RD&T, Ceramics Research Centre, IJmuiden, The Netherlands

Mineral carbonation provides a durable and environmentally inert method of sequestering CO_2 emissions. Larnite (Ca_2SiO_4), a major constituent of steel slag, is highly reactive with aqueous CO_2 [1]. Consequently, carbonation of steel slag offers an opportunity to reduce CO_2 emissions while recycling an industrial by-product. This study investigates the reactions taking place during the dissolution and carbonation of steel slag, and is part of a larger study designed to determine the conditions under which conversion of larnite and other calcium silicates to calcite is optimized.

Experiments were conducted on 2 – 3 mm diameter steel slag grains supplied by Tata Steel RD&T. A H_2O-CO_2 fluid mixture (XCO_2 = 0.05) was pumped through a flow-through reactor containing these grains. Temperature ranged from 120°C to 200°C, the pressure was 250 bar and the flow rate was 3.00 mL/min. The duration of experiments varied from 3 to 7 days.

The slag grains reacted to form Ca-carbonate and –phosphate phases upon contact with the CO_2-saturated fluid. These phases subsequently dissolved, forming a porous aluminium and iron oxide framework around the edges of the grains. The compositions of the reacted fluid reflect the observed dissolution of Ca-bearing phases and the buffering of Si by the formation of quartz. These results are in good agreement with predictions from thermodynamic calculations, indicating that the system achieved local equilibrium.

[1] Santos et al. (2009) *Journal of Hazardous Materials* **168**, 1397-1403.

https://doi.org/10.1180/S0026461X00006502 Published online by Cambridge University Press

Effect of CO_2-enriched fluid on three argillite type caprocks

G. BERTHE[1,2]*, S. SAVOYE[3], C.WITTEBROODT[1] AND J.-L. MICHELOT[2]

[1]IRSN, DEI/SARG/LR2S,92260 Fontenay-aux-Roses, France (*correspondence: guillaume.berthe@cea.fr)
[2]IDES,CNRS-Université Paris-Sud F-91405 Orsay, France
[3]CEA, DEN/DANS/L3MR, F-91191 Gif-sur-Yvette, France

The sequestration of CO_2 under impervious caprocks as argillite is proposed to reduce the greenhouse effect. CO_2 impact on the containment properties of argillite has to be assessed, as performed by [1] on Upper Toarcian rocks from Tounemire site (France). In the current study, we widened the approach to two other levels from Tournemire (Lower Toarcian and Domerian), displaying distinct carbonate contents (30% and 8%, resp.).

^{36}Cl, HTO, Br^- and D_2O were used as tracers in through-diffusion experiments carried out with and without CO_2-enriched fluids. The through-diffusion technique consists in imposing a concentration gradient of the tracer between the two faces of the sample. For the cells simulating an acidic fluid attack, dissolved CO_2 was injected inside the upstream reservoir. Chemistry evolution was also monitored in the up and downstream reservoirs.

Tracer data analyses indicated a degradation of the containment properties of the samples, increasing from the Paper Shale (unaffected) up to the Toarcian (Fig.1)

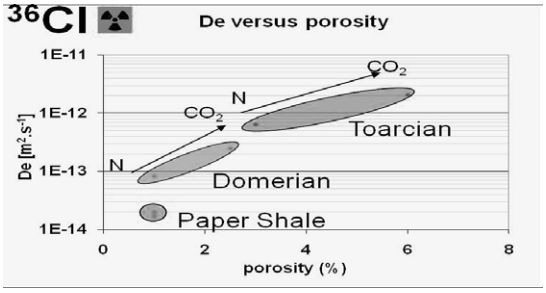

Figure 1: evolution of the diffusive parameters for the 3 levels

Such a difference can be accounted for by the distinct kinetics for achieving the chemical equilibrium regarding carbonates as shown by [Ca2+], [Mg2+] and alkalinity monitoring. This demonstrates the role played by the initial petrophysical properties of the rocks, in addition to their carbonate content.

[1] Berthe *et.al*. (2011) *Energy Procedia* **4**, 5314-5319.

On the use of nucleation barriers in numerical simulation of water-rock interactions

P. BERTIER*, C. WEBER AND H. STANJEK

Clay and Interface Mineralogy, RWTH-Aachen University, Bunsenstrasse 8, D-52072 Aachen Germany, (*correspondence: Pieter.Bertier@cim.rwth-aachen.de)

Numerical simulations of water-rock interactions in diagenetic or CO_2 sequestration systems generally predict mineral alteration processes that are considerably faster than those observed in experiments or diagenetic environments. This has been attributed to several reasons, among which the common disregard for nucleation of precipitating mineral phases in such models.

The effect of the implementation of nucleation barriers was evaluated on a kinetic reaction path model of sandstone diagenesis. Critical levels of supersaturation required for precipitation, based on literature data of formation water compositions, substantially slow down reaction kinetics due to their feedback on the dissolution rates of the minerals supplying the component species of the precipitating phase.

The implementation of nucleation barriers and rates based on classical nucleation theory have a similar effect, but often predict unrealistically high levels of supersaturation. One of the crucial parameters in classical nucleation theory is the mineral-water interface tension. Literature data on mineral-water interface tension is scarce and ambiguous. Different methods for measuring or calculating interface tensions produce very different results.

A methodology, based on capillary rise in powder beds as described by Washburn's equation, was developed for quantifying mineral water interface tensions under conditions typical of diagenetic systems. The interface tensions of several common rock forming minerals were determined. Application of these new data in the classical nucleation theory based kinetic reaction path model results in more realistic levels of supersaturation.

https://doi.org/10.1180/S0026461X00006502 Published online by Cambridge University Press

Interactions between precipitation and sea surface temperature in Northern Chilean Patagonia during the Late Holocene

S. BERTRAND[1,2,*], K. HUGHEN[2], J. SEPÚLVEDA[3] AND S. PANTOJA[4]

[1]Renard Centre of Marine Geology, University of Ghent, Ghent, Belgium (* correspondence: sbertrand@whoi.edu or sebastien.bertrand@ugent.be)
[2] Woods Hole Oceanographic Institution, Woods Hole, MA, USA
[3] Massachusetts Institute of Technology, MA, USA
[4] COPAS, University of Concepción, Concepción, Chile

The climate of Chilean Patagonia is highly influenced by the Southern Westerlies, which control the intensity and latitudinal distribution of precipitation in the Southern Andes. In austral summer, the Westerly Wind Belt (WWB) is restricted to the high latitudes (> 47°S). It expands northward in winter, which results in a strong seasonal signal in precipitation between ~47 and ~30°S. In addition, the area is characterized by a steep latitudinal Sea Surface Temperature (SST) gradient, which reflects the regional influence of the Antarctic Circumpolar Current (ACC). Here, we present a new precipitation proxy record from the Chilean fjords at 45°S, and we compare our results with regional SST records to assess the ocean-continent interactions in Chilean Patagonia during the last 2 millennia. Our precipitation record is based on a high-resolution inorganic geochemical analysis of a 2m long sediment core from Quitralco fjord (45°S), using ICP-AES and XRF core scanning techniques. Since our coring site is located in front of a small river that drains the Patagonian Andes (Rio Pelu), it is particularly sensitive to changes in river discharge, and therefore precipitation. Our data demonstrates a significant increase in Fe/Al and Ti/Al between ~700 and ~50 cal. yr BP, which corresponds to a decrease in mean sediment grain-size from ~30 to ~20 μm. This shift is interpreted as a decrease in the energy of river sediment discharge, which most likely reflects a decrease in seasonal floods. The comparison of our precipitation record with published SST records from the region demonstrates that lower (higher) SSTs are systematically coeval with a decrease (increase) in seasonal floods in the Patagonian Andes. The decrease in seasonal floods at 700-50 cal. yr. BP corresponds to a SST decrease of ~1°C. We argue that the synchronicity of changes in precipitation and SST during the last two millennia likely reflects concomitant migration of the zonal systems, i.e., the WWB and the ACC.

Evolution of the macromolecular structure of biopolymers during pyrolysis: A C-XANES study

O. BEYSSAC[1], S. BERNARD[2], K. BENZERARA[1] AND G.E. BROWN JR.[3]

[1]IMPMC, UPMC, CNRS, Paris, France (Olivier.Beyssac@impmc.jussieu.fr, Karim.Benzerara@impmc.jussieu.fr)
[2]LMCM, MNHN, CNRS, Paris, France (sbernard@mnhn.fr)
[3]SAGG, DGES, Stanford University, Stanford, USA (Gordon@pangea.stanford.edu)

Identifying traces of life in ancient rocks can be challenging as they may have experienced significant structural and chemical transformations during diagenesis and metamorphism. Natural organic matter may indeed evolve during fossilization processes and hence lose all chemical and textural information relative to its original precursor. Recently, advanced spectromicroscopy techniques have allowed evidencing that morphological, textural and chemical bio-signatures might be preserved in some contexts despite intense metamorphism [1,2], notably depending on the chemical nature of the organic precursor [3]. Synchrotron-based techniques are thus increasingly used to *in situ* characterize natural kerogens and study fossilization processes although standard data sets are still only scarcely available [4,5]. Therefore, information obtained from these recently developed techniques remains barely exploited.

Here, we have investigated the evolution of reference organic biocompounds more or less resistant to biodegradation (e.g. sporopollenin, lignin and cellulose) heat-treated at different temperatures up to 1000°C at ambient pressure using X-ray absorption near edge structure (XANES) spectroscopy at the Carbon K-edge. In addition to evidencing the differential evolutions of these precursors during carbonification and early steps of graphitization, quantitative information extracted from our results provide a calibration for the spectroscopic evolution of reference biocompounds with increasing temperatures. By providing new insights into the thermal evolution of the macromolecular structure of reference biopolymers, the present results constitute a new step towards better constraining the fate of natural organic matter during burial.

[1] Schiffbauer *et al*. (2007), *Astrobiology* **7(4),** 684-704. [2] Bernard *et al*. (2007), *EPSL* **262**, 257-272. [3] Bernard *et al*. (2010), *GCA* **74**, 5054-5068. [4] Solomon *et al*. (2009), *Soil Sci. Soc. Am. J*. **73**, 1817-1830. [5] Bernard *et al*. (2010), *Carbon* **48**, 2506-2516.

https://doi.org/10.1180/S0026461X00006502 Published online by Cambridge University Press

Seasonal shifts in concentration, age, and lability of carbon exported from the Greenland ice sheet (GrIS)

M.P. BHATIA[1]*, S.B. DAS[2], M.A. CHARETTE[3], L. XU[3], AND E.B. KUJAWINSKI[3]

[1]MIT-WHOI Joint Program, Woods Hole Oceanographic Institution (WHOI), Woods Hole MA, 02543 (*correspondence: mayab@mit.edu)
[2]Department of Geology and Geophysics, WHOI, Woods Hole MA, 02543 (sdas@whoi.edu)
[3]Department of Marine Chemistry and Geochemistry, WHOI, Woods Hole MA, 02543 (mcharette@whoi.edu, lxu@whoi.edu, ekujawinski@whoi.edu)

Active microbial communities at the base of glaciers and ice sheets provide a mechanism for (a) subglacial organic carbon metabolism on various timescales, and (b) the present-day export of labile carbon to downstream ecosystems. Prior studies point towards the importance of both these processes in modulating carbon cycling. Here we describe for the first time the bulk-level carbon composition of meltwater draining the GrIS. We investigate the dissolved (DOC) and particulate organic carbon (POC) concentration, age, and lability in the subglacial discharge throughout the summer. The early season discharge contains higher organic carbon concentrations, and exports younger DOC (~ 2 kyr ^{14}C age) compared to the peak season discharge, where the concentrations are lower and the age is older (~ 4 kyr ^{14}C age). Conversely, the age of the exported POC (~ 2.5 kyr ^{14}C age) does not change throughout the meltseason. We hypothesize that overwinter subglacial microbial processes shift the type of DOC exported, and use the dissolved ion loads in the discharge to explore this idea. These results illustrate (1) that chemically-distinct organic carbon pools are accessed by seasonally-evolving hydrology and (2) that the GrIS may deliver labile, old carbon to the North Atlantic Ocean.

Sr-Nd isotopic studies of Narcondam Volcanics, India: Constraints on Andaman-Indonesian arc magmatism

RAJNEESH BHUTANI*[1], R.S. SMITHA[1], JYOTIRANJAN S. RAY[2], HETU C. SHETH[3], S. BALAKRISHNAN[1], ALOK KUMAR[2] AND NEERAJ AWASTHI[2]

[1]Department of Earth Sciences, Pondicherry University, Puducherry-605014, India (*rbhutani@gmail.com)
[2]Geosciences Division, Physical Research Laboratory, Navrangpura, Ahmedabad-380009, India
[3]Department of Earth Sciences, Indian Institute of Technology Bombay, Powai, Mumbai-400076, India

Narcondam island, part of Andaman group of islands of India is a dormant volcano of Andaman-Indonesia island arc related to oblique subduction of Indian plate beneath the SE Asian plate.

Unlike the active Barren Island volcano of Andaman arc, which erupts basaltic to basaltic-andesite lavas, Narcondam samples, studied during the present study, range from basaltic-andesites to dacites with majority of them plotting in andesitic field of Total Alkali Silica (TAS) classification diagram.

Origin of andesitic lavas has been explained variably, ranging from models of hydrous melting of mantle-wedge to models of mixing of basaltic magma with rhyolitic magma at shallower depths [1].

Narcondam andesites show mineral textures, such as resorbed rims of plagioclase phenocrysts, Na rich layers sandwitched between Ca rich layers of plagioclase crystals and at least two generations of phenocrysts, indicating compositional changes in magma not related to fractional crystallization. Presence of rhyolitic glass inclusions, and olivine and quartz crystals together are reported from Narcondam samples in an earlier study [2]. It is therefore suggested that andesitic lavas are not primary melt but probably resulted from mixing of basaltic and rhyolitic magmas.

Sr and Nd isotope ratios are used to quantify the mixing and it appears that andesites of Narcondam and also other andesitic volcanoes of Sunda arc may have resulted from variable but small inputs of sediments (<5%) to the mixed magma which has 70 to 80% contribution from Barren Island type basaltic melt and 15-20% of rhyolitic melt similar to that erupted in Sunda arc elsewhere [3].

[1] Kent et. al. (2010) *Nature Geoscience* **3**, 632-636. [2] Pal et. al. (2007) *Journal Volcno. Geotherm. Res.* **168**, 93-113. [3] Turner and Foden (2001) *Contrib. Min. Pet.*, **142**, 43-57.

https://doi.org/10.1180/S0026461X00006502 Published online by Cambridge University Press

U-Pb cassiterite dating by LA-ICPMS and a precise mineralization age for the superlarge Furong tin deposit, Hunan Province, Southern China

XIANWU BI[1], HU RUIZHONG[1], LI HUIMIN[2], DONG SHAOHUA[1,3], CHEN YOUWEI[1] AND PENG JIANTANG[1]

[1]State Key Laboratory of Ore Deposit Geochemistry, Institute of Geochemistry, Chinese Academy of Sciences, Guiyang, China (bixianwu@vip.gyig.ac.cn)

[2]Tianjin Institute of Geology and Mineral Resources, Tianjin, 300170, China

[3]Graduate School of Chinese Academy of Sciences, Beijing 100039, P.R. China

Cassiterite is an important tin mineral in the W-Sn deposit. Furthermore, it is also a common accessory in a variety of deposits, and the successful use of cassiterite as a geochronometer would resolve many genetic questions. The direct dating of cassiterite with U–Pb and Pb–Pb methods was initially attempted by Gulson and Jones. In recent years, the U–Pb isotope data on cassiterite from tin deposits using TIMS were reported and the potential of cassiterite as a geochronometer for directly dating hydrothermal mineralization was evaluated. This study aims to directly date the U-Pb age on cassiterites from the Furong tin deposit using LA-MC-ICPMS techniques, to validate the utilization of cassiterites for precise dating of ore formation.

The Furong deposit is a newly-discovered superlarge tin deposit in the central Nanling district, South China. In this study, cassiterite from the Furong tin deposit has been successfully dated by LA-MC-ICPMS and it is the first report of the U–Pb isotope dates on cassiterite using LA-MC-ICPMS. In situ analysis of two cassiterites (WCP2-1 and WCP2-2), yield U–Pb isochron age of 155.8±1.6Ma (MSWD=20). This U–Pb age from the cassiterites in skarn type ores which is the main type ore in Furong tin deposit, yielded indistinguishable mineralization ages with U–Pb isochron age of 160.0±5.5Ma (MSWD=1.74) by TIMS and published Ar–Ar dating on hydrothermal muscovite, hornblende and phlogopite from greisen type tin ore and skarn-type ores, reveal the main stage age of Furong tin mineralization was around 155Ma. The dates obtained in this study indicated that the cassiterites with high content U are the potential directly dating minerals.

This work was supported jointly by the National Basic Research Program of China (2007CB411404)

[1] Gulson BL, Jones MT (1992) Geology 20:355–358 [2] Yuan SD, Peng JT, Hu RZ, Li HM, Shen NP, Zhang DL (2008) Miner Deposita. 43:375–382

Investigation of atmospheric nitrate and ammonium and their impact on air quality and climate in GMI

HUISHENG BIAN[1,2], STEVE STEENROD[1,2], MIAN CHIN[3] AND JOSE RODRIGUEZ[3]

[1]Goddard Earth Sciences and Technology Center, University of Maryland, Baltimore County, Baltimore, Maryland, USA

[2]Also at Atmospheric Chemistry and Dynamics Branch, NASA Goddard Space Flight Center, Greenbelt, Maryland, USA

[3]Atmospheric Chemistry and Dynamics Branch, NASA Goddard Space Flight Center, Greenbelt, Maryland, USA

The capability to simulate nitrate and ammonium aerosols has been developed in NASA GMI model by implementing a thermodynamic equilibrium model that treats gas and aerosol multiphase chemical equilibrium reactions in a SO_4-NO_3-NH_4-H_2O system. Nitrate and ammonium can influence air quality and ecosystems substantially, and their importance will be increasing in the future due to the predicted increase of nitrogen emissions. An immediate outcome from the work is the possibility to improve tropospheric O_3 simulation. Currently, the model treats HNO_3 solely as a gas phase tracer. This semi-volatile species now partitions between gas and aerosol phases, and the tracer in each phase is subject to different chemical and physical processes. A preliminary analysis has been conducted by comparing results simulated with and without new nitrate package and by comparing model results with the ground station observations from CASTNET and EMEP.

https://doi.org/10.1180/S0026461X00006502 Published online by Cambridge University Press

High resolution minor and trace element study on mussel shells from coastal region of Tatoosh Island, Washington, USA

NANXI BIAN[1]*, PAMELA MARTIN[1], CATHERINE PFISTER[2], AND ALBERT COLMAN[1]

[1]Department of Geophysical Sciences, University of Chicago, Chicago, IL, USA (*correspondence: nanxibian@uchicago.edu

[2]Department of Ecology and Evolution, University of Chicago, Chicago, IL, USA

The successively deposited calcium carbonate layers and annual growth bands in mollusk shells could offer high resolution archives of the environmental conditions the mollusk has experienced during its life. Previous studies have shown that the elemental composition of mollusk shells is related to environmental parameters[1, 2, 3].

Here, we present high resolution data of a suite of minor/trace element/Ca ratios collected from shells of mussel species, *Mytilus californianus*, using laser ablation sector field inductively coupled plasma mass spectrometry (LA-ICP-MS) as well as an ICP-MS solution based method. The mussel shells were ~10 years of age and were collected live in 2009 and 2010 from Tatoosh Island, Washington, USA, where instrumental data of various enviromental parameters over the last decade are available. We also analyzed several shells present in middens on Tatoosh Island. Radio-carbon dating data of these mussels show they lived ~1000 years ago; shell banding suggests individual ages of ~12 years. Age models were constructed using annual banding, a growth model and high resolution stable isotope composition ($\delta^{18}O$) of the shell.

Our preliminary results show that several of a suite of trace elements exhibit promising correlation with nutrient concentration and oxygen level in the sea water, and could serve as proxies for coastal geochemical cycling and a means to probe rapid changes documented in seawater chemistry at this site[4]. Data for a suite of element/Ca ratios from different transects on the same shell generally show good reproducibility. Element/Ca data from midden shells and modern shells show different ranges of variation suggesting that there have been significant differences in geochemical cycling in this coastal environment over the last 1000 years.

[1] Dodd (1965) *GCA*, **29**, 385-398. [2] Klein *et al*. (1996) *Geology*, **24**, 415–418. [3] Putten *et al*. (2000) *GCA*, **64**, 997-1011. [4] Wootton *et al*. (2008) *PNAS*, **105**, 18848-18853.

Carbonate rocks from fluid and gas expulsion sites of the Green Canyon, Gulf of Mexico: Analysis and interpretation

YOUYAN BIAN[1,3], HONGPENG TONG[1,3], DONG FENG[1,2], HARRY H. ROBERTS[2] AND DUOFU CHEN[1]*

[1]Key Laboratory of Marginal Sea Geology, Guangzhou Institute of Geochemistry, CAS, Guangzhou 510640, China (*correspondence: cdf@gig.ac.cn)

[2]Coastal Studies Institute, Louisiana State University, Baton Rouge, LA 70803, USA

[3]Graduate University of the Chinese Academy of Sciences, Beijing 100049, China

Cold hydrocarbon seepage is a frequently observed phenomenon in marine settings worldwide. Authigenic carbonates from hydrocarbon seeps are unique archives of past seepage and associated environmental parameters. Carbonate rocks were collected from fluid and gas expulsion sites of Green Canyon lease block 140 (GC 140) at 260 m water depth on the Gulf of Mexico continental slope during Johnson-Sea-Link dive 2591 in 1989. The carbonate rocks occur as blocks, crusts, and nodular masses incorporated in carbonate breccias. Most carbonates are composed of aragonite and high-Mg calcite as determined from X-ray diffraction. However, one sample was found to have compositoon of nearly 100% dolomite. Petrographically, high Mg-calcite peloidal matrix and acicular to botryoidal aragonitic void-filling cements are the most frequent associations. The carbon isotopic compositions of the carbonates ($\delta^{13}C_{Car}$) range from –36.5‰ to +4.9‰ V-PDB, indicating complex carbon sources that include ^{13}C-depleted methane, seawater CO_2, and ^{13}C-enriched residual CO_2 from methanogenesis. A similarly large variability in $\delta^{18}O_{Car}$ values (+1.6‰ to +5.5‰ V-PDB) demonstrates the geochemical complexity of the studied area. The considerable range of mineralogical and isotopic variations of the studied cold seep carbonate suggests that local controls on the fluid and gas flux, types of the local hydrocarbon reservoir may play an important role in determining carbonate mineralogy and isotope geochemistry. In addtion, the ^{14}C ages of bivalve shells incorporated in the carbonate matrix will be used to determine the timing and duration of fluid seepage in order to provide preliminary insight into probable factors governing seepage processes at the studied site.

Acknowledgements: The work was partially supported by the NSFC (40725011 and U0733003) and Chinese Academy of Sciences (KZCX2-YW-GJ03).

https://doi.org/10.1180/S0026461X00006502 Published online by Cambridge University Press

Pb-Hf-Nd isotopic decoupling in peridotite xenoliths from Mega (Ethiopia): Insights into the multistage evolution of the East African Lithosphere

G. BIANCHINI[1,2]*, J.G. BRYCE [3], J. BLICHERT-TOFT[4], L. BECCALUVA[1] AND C. NATALI[1],

[1]Università di Ferrara, Ferrara, Italy (bncglc@unife.it)
[2] CNR - Istituto di Geoscienze e Georisorse, Pisa, Italy
[3]UNH Earth Sciences, Durham NH, USA
[4]Ecole Normale Supérieure de Lyon, Lyon, France

New Hf and Pb isotopic data from clinopyroxenes from East African Rift (EAR) mantle xenoliths (Mega, Sidamo region, southern Ethiopia), coupled with recently published Nd isotope and trace element compositions, provide compelling evidence for multiple episodes of mantle depletion and metasomatic enrichment. Radiogenic values (ε_{Nd} up to +22.5 and ε_{Hf} up to +1076) suggest mantle domains currently located beneath the Main Ethiopian Rift suffered extreme melting regimes, possibly in the presence of residual (majorite?) garnet, effectively fractionating Sm/Nd, Lu/Hf and Nd-Hf systematics. Positively correlating Lu/Hf and $^{176}Hf/^{177}Hf$ provide an apparent ingrowth of 1.96 Ga, close to the CHUR model age of the most radiogenic sample (1.95 Ga, consistent with other local records of Proterozoic melting events). Pb isotopes are clearly decoupled from the Nd-Hf systematics, displaying $^{206}Pb/^{204}Pb$ up to 20.1, $^{207}Pb/^{204}Pb$ up to 15.70, and $^{208}Pb/^{204}Pb$ up to 39.8. These data suggest vigorous convection cells, possibly triggered as a far field dynamic consequence of the Afar plume impingement, preferentially occurred beneath this site, where important lithospheric discontinuities exist between the Archean/Early Proterozoic Tanzanian craton and the Late Proterozoic Panafrican mobile belt. Such deep mantle dynamics may contribute to stabilizing distinct EM1 and HIMU metasomatic components in the EAR lithospheric mantle.

Early Archean crust of the Ukrainian Shield – Evidence from detrital zircons

E. BIBIKOVA, L. SHUMLYANSKYY, C.J. HAWKESWORTH, S. CLAESSON, C. STOREY, B. DHUIME AND A. FEDOTOVA

Data on continental sediments remain the basis for many models for the generation and evolution of the crust [1]. Detrital zircons from old metasedimentary rocks can provide valuable contributions to the knowledge of the Early Earth crust. We have studied geochronologically (U-Pb, zircons, Sm-Nd) and geochemically (Hf-isotopes and REE) detrital zircons from two greenstone structures in the Azov domain, Ukrainian Shield. U-Pb isotopes of zircons from five samples of mica schists from the Soroki and Fedorof greenstone belts were analysed on ion microprobe NORDSIM at the Swedish Museum of Natural History, focusing mainly on cores identified by CL. The data include a group of ages in the range 3.5-3.6 Ga, and some zircon cores older than 3.7 Ga.

The REE patterns of metasediments and zircons are similar to those of TTG Archaean rocks [1]. Lu-Hf isotopic system was studied by La ICP-MS at University of Bristol [2] at the same spots inside zircons where the most concordant ages were obtained. In our interpretation of Hf isotope data, we follow the model proposed by [3]. The majority of granites have isotope signatures that preclude direct mantle genesis, rather we constrain the $^{176}Lu/^{177}Hf$ ratio of the crustal material that was initially extracted from the mantle to be 0.22-0.25, typical for mafic magmas. In such interpretation, the age of this crust will be about 4.2 Ga. The model age of zircons in metasediments derived from the TTG rocks with low ≤ 0.01 $^{176}Lu/^{177}Hf$ ratio, is 3.8-3.6 Ga.

Sm-Nd model ages of 3.3-3.4 Ga and εNd (T) for the analysed samples are in a good agreement with the zircon data. Our new results indicate that Eo and Paleoarchean crust in the Azov domain was widely distributed.

[1] Taylor & McLennan (1985) *The continental crust*. Oxford, Blackwell, 312 p. [2] Dhuime *et al*. (2007) *Precamb. Res* **155**, 24-46. [3] Pietranik *et al*. (2008) *Geology* **36**, 875-878.

https://doi.org/10.1180/S0026461X00006502 Published online by Cambridge University Press

Geological carbon storage: Geochemical processes

MIKE BICKLE

Dept. Earth Sciences, University of Cambridge, Downing St., Cambridge CB2 3EQ, UK (mb72@esc.cam.ac.uk)

Modelling the complex physical and chemical processes that govern retention of CO_2 in geological reservoirs over long time scales present some interesting challenges, although not perhaps as challenging as coping with the consequences of unabated CO_2 emissions.

CO_2 may be held in geological formations by structural, capillary, dissolution and mineralisation trapping. CO_2 or CO_2-charged brines may corrode reservoir minerals and caprocks. Remote imaging of CO_2 reservoirs, such as at Sleipner [1,2], captures the complex physical behaviour of CO_2 but is unable to completely explain this behaviour or resolve all potential trapping and escape mechanisms. Direct sampling of field small-scale injection experiments offers the best chance to do this [3]. Estimates of capillary trapping can be made by analysis of isotope spikes [4]. Dissolution trapping will be enhanced by the complexities of the flow processes and sampling of brines will be essential to monitor this. Prediction of the reaction rates between CO_2-charged brines and reservoir minerals or caprocks is even more difficult. Observations on geological analogue sites have recovered the rates of the sluggish reactions between silicate minerals and brines [5]. Curiously the much more rapid rates of dissolution of carbonate, evaporite and oxy-hydroxide minerals in field conditions seen in small scale injection experiments [6] are poorly known. These reactions may also release contaminants.

Modelling of fluid-mineral interactions currently uses averaged fluid properties in pseudo- 1 dimensional models [e.g. 7]. It is not clear if this is an appropriate way to approximate the complex flow paths. What is needed is a method for inverting geochemical data to constrain the key attributes of flow heterogeneities.

[1] Bickle *et al*., (2007), *EPSL* **255**, 164–176. [2] Boait *et al*., (2011), *Energy Procedia* **4**, 3254–3261. [3] Freifeld *et al*., (2009), *Energy Procedia* **1**, 2277–2284. [4] Zhang *et al*., (2011), *Int. J. Greenhouse Gas Control* **5**, 88–98. [5] Kampman *et al*., (2009), *EPSL* **284**, 473-488. [6] Kharaka *et al*., (2006), *Geology* **34**, 577-580. [7] Xu *et al*., (2010), *Chemical Geology* **271**, 153–164.

A bond-valence view of interfacial structure and reactivity

B. R. BICKMORE*

Geological Sciences, Brigham Young University, Provo, UT 84602, USA
(*correspondence: barry_bickmore@byu.edu)

Studies of interfacial structures will be most useful in cases where we can relate structure to reactivity. However, a quantitative structure-activity relationship (QSAR) requires that structural information be couched in terms that are easily translatable into energy. The bond-valence model (BVM) [1] has proven fairly effective for this purpose, and it has been used to formulate a number of QSARs, including the MUSIC model for predicting surface functional group acidity on oxide surfaces [2]. Such BVM-based QSARs have had varying success, but they are typically applicable under a fairly restricted set of conditions [3].

It is not readily apparent when QSARs like MUSIC should work or fail, however, because nobody has yet worked out a full BVM-based accounting of the relationship between molecular structure and energy. E.g., the most commonly used aspect of the BVM involves summing bond valences calculated from the lengths of bonds to counter-ions surrounding a central ion. The valence sum is then compared to an ideal value, and the difference is taken to be indicative of some aspect of structural energy. But this does not account for directionality in bonding or interactions between co-ions.

We are currently using some lesser-known aspects of the BVM, including vectorial bond valence (VBV) sums [4] and "effective valence" between co-ions [1], combined with some concepts borrowed from the Valence Shell Electron Pair Repulsion (VSEPR) model of molecular geometry, to create a more complete BVM-based model of structure-energy relationships. By analyzing oxide crystal structures and *ab initio* molecular dynamics simulations of aqueous solutions, we have shown that ideal VBV sums have a fairly straightforward relationship with bond character and coordination number. VBV sums also exhibit a strong relationship with deviations from ideal valence sums.

In addition, we will be applying such analyses to simulated interfacial structures to see how our indicators of "structural energy" vary with distance from the interface, salinity, etc. Such information could then be related to double layer theory.

[1] Brown (2002) *The Chemical Bond in Inorganic Chemistry*, Oxford. [2] Hiemstra *et al*. (1996) *J. Coll. Int. Sci*. **184**, 680-692. [3] Bickmore *et al*. (2004) *GCA* **68**, 2025-2042. [4] Harvey *et al*. (2006) *Acta Cryst*. **B62**, 1038-1042.

https://doi.org/10.1180/S0026461X00006502 Published online by Cambridge University Press

Mineral and whole-rock chemical properties of pyroxenites in the peridotites of the Kop Ultramafics, NE Turkey

Ö. BILICI * AND H. KOLAYLI

Department of Geological Engineering, Karadeniz Technical University, 61080-Trabzon, Turkey
(*correspondence: ocubil@hotmail.com)

The Kop ultramafic unit in NE Turkey is one of the largest Alpine type peridotites. Petrographic and field studies in the ultramafic unit indicate that there are widespread two main rock types as harzburgites and dunites. In addition to these, pyroxenites are also locally observed and associated with peridotites.

Pyroxenites crop out as veins/dykes in varying size within peridotites [1]. Orthopyroxenites (>500 m^2) cover larger area than clinopyroxenites (between 10 to 100 m^2) and websterites (<1 m^2). Clinopyroxenites and orthopyroxenites exhibit dyke-like body in dunites and harzburgite, respectively. Websterites are only observed as veins in harzburgitic zone. Orthopyroxenites show coarse grained texture whereas clinopyroxenite and websterites have porphyritic texture. Clinopyroxenites and websterites contain variable amounts of olivine, spinel and magnetite.

Both whole-rock and pyroxene mineral chemistry data of the pyroxenites are characterized by low contents of Al, Na, K, Ta, Zr, Hf, Ti and REE, high Mg-numbers and LILE enrichment relative to less incompatible elements. The mineral and petrochemical data suggest that clinopyroxenites and websterites from the pyroxenites have not been directly crystallized from primary magma(s) derived by partial melting of depleted mantle. Whole-rock and pyroxene compositions of orthopyroxenites are similar to those of ultra-depleted mantle-derived pyroxenites, whereas cliopyroxenites and websterites have very close chemical features to those of pyroxenites in suprasubduction zone mantle.

[1] Bilici (2010) *Karadeniz Technical University, MSc thesis,* 76pp.

In situ dating and investigation of remarkably depleted –27.3‰ SMOW "Slushball" Earth zircons

I. BINDEMAN[1], J. VAZQUEZ[2], A. SCHMITT[3], J. EILER[4], N. SEREBRYAKOV[5] AND D. EVANS[6]

[1]Geol Sci, U. Oregon, Eugene OR; (bindeman@uoregon.edu)
[2]USGS, Menlo Park, Ca;
[3]ESS, UCLA, Los Angeles, Ca;
[4]GPS, Caltech, Pasadena, Ca;
[5]IGEM-RAS, Moscow, Russia;
[6]Geol & Geophys., Yale Univ., New Haven, CT

Paleoproterozoic amphibolites and gneisses - that are remarkably depleted in ^{18}O are found in the Belomorian Belt in Karelia, Russia [1,2]. We mapped their extent to exceed 200x20km and affect metamorphosed mafic intrusions (est. ~2.4 Ga intrusion age) and host 2.6Ga gneisses found in this 1.9 Ga collisional belt. $\delta^{18}O$ values of –7 to –27.3‰ characterize minerals and rocks from several of these localities; some of these rocks are also remarkably depleted with respect to δD (-212 to –235‰ amphiboles). All have typical terrestrial $\Delta^{17}O$ values of 0‰. Based on previous paleogeographic reconstructions, we attribute the origin of these exotic O and H isotope compositions to the hydrothermal alteration associated with subglacial rifting during the Paleoproterozoic panglobal ice ages, but discuss additional possibilities: extremely low-$\delta^{18}O$ Paleo- proterozoic sea water, and excursion of Karelia to polar latitudes. Given that at high-T hydrothermal exchange equilibrium $\Delta^{18}O$(rock-water) is close to zero, but water-rock interaction is rarely 100% efficient, the lowest measured $\delta^{18}O$ value in silicates likely gives the upper $\delta^{18}O$ bound for the altering meteoric fluid; we thus continues our quest to find the lowest $\delta^{18}O$ material such as a mineral assemblage or a tiny zircon fragment that would provide record of $\delta^{18}O_{water}$.

Zircons in these rocks have survived metamorphism and record normal $\delta^{18}O$ cores and extremely low $\delta^{18}O$ rims (down to $\delta^{18}O_{SMOW}$ = 27.3 ‰). The rims are in oxygen isotope exchange equilibrium with host metamorphic assemblages at each locality. We present data from the ongoing investigation of these zircons using large radius ion microprobes for *in situ* U-Pb ages and $\delta^{18}O$ values, ion microprobe profiling using a ~1 μm gallium beam, and NanoSIMS isotope mapping of the zircon with 23 to 34‰ and sharp (~3-5 μm) isotope gradients.

[1] Bindeman *et al*. (2010) *Geology*, **38**, 631. [2] Bindeman, Serebryakov, (2011) EPSL, doi:10.1016/j.epsl.2011.03.031

https://doi.org/10.1180/S0026461X00006502 Published online by Cambridge University Press

High-precision Mg isotope measurements of inner solar system materials by HR-MC-ICPMS

M. BIZZARRO*, C. PATON, M. SCHILLER, K. LARSEN AND D. ULFBECK

Center for Star and Planet Formation, Natural History Museum, University of Copenhagen, Øster Voldgade 5–7, 1350, Copenhagen, Denmark (*correspondence: bizzarro@snm.ku.dk)

Magnesium has three naturally occurring isotopes - ^{24}Mg, ^{25}Mg and ^{26}Mg - with relative abundances of 79%, 10% and 11%, respectively. Variations in the isotopic composition of Mg can potentially occur in solar system materials through a number of processes including (*1*) stellar nucleosynthesis, (*2*) the former presence and decay of the ^{26}Al nuclide (half-life ~0.73 Myr) and (*3*) mass-dependent isotopic fractionation during high temperature processes such as partial evaporation and condensation as well as from low-temperature fluid/ rock interactions. Thus, studying the potential variability of ^{26}Mg/^{24}Mg and ^{25}Mg/^{24}Mg ratios in solar system solids can be used to infer genetic relationships between early solar system reservoirs and terrestrial planets.

We have developed novel methods for the chemical purification of Mg from silicate rocks, and high-precision analysis of Mg-isotopes by high-resolution multiple collector inductively coupled plasma source mass spectrometry (HR-MC-ICPMS) [1]. Based on the repeated analyses of international rock standards of variable matrices, we show that it is possible to routinely analyze the Mg-isotope composition of silicate materials with an external reproducibility of 2.5 and 20 ppm for the μ^{26}Mg* and μ^{25}Mg values, respectively (μ notation is the per 10^6 deviation from the DSM-3 reference material).

Using these techniques, we have analyzed to unprecedented precision the Mg-isotope composition of a strategically-selected suite of inner solar system materials, including calcium-aluminium-rich inclusions and amoeboid olivine aggregates from the reduced Efremovka CV chondrite as well as bulk chondrite meteorites and meteorite samples originating from differentiated asteroids. These new data provide important constraints regarding the relative and absolute Mg-isotope composition of bulk inner solar system planetary reservoirs, the distribution of ^{26}Al in the solar protoplanetary disk, and the mechanism and timescale of asteroidal differentiation in the young solar system.

[1] Bizzarro, M. *et al*. (2011) *JAAS* **26**, 565-577

Electrochemically-driven lithium isotopic fractionation

JAY BLACK[1]*, EMILIE PERRE[2], GRANT UMEDA[2], BRUCE DUNN[2], WILLIAM F. MCDONOUGH[3] AND ABBY KAVNER[1,4]

[1]IGPP
[2]Department of Materials Science and Engineering,
[3]ESS, University of California, Los Angeles, CA 90095 (*jayblack@ucla.edu, gumeda@yahoo.com, bdunn@ucla.edu, akavner@ucla.edu)
[4]Department of Geology, University of Maryland, College Park, MD 20742 (mcdonoug@umd.edu)

Lithium is a mobile element, with a high diffusion coefficient, and a large difference in solution diffusivities for the two stable isotopes, ^{6}Li and ^{7}Li [1], making it an ideal element for studying isotopic fractionation during electro-deposition processes. Rates of mass-transport and deposition can be dialed-in using experimental electrochemical techniques to study the competing isotopic fractionation effects of reduction/precipitation and diffusion. Previous experiments measured the equilibrium fractionation between Li metal and Li^+ in a propylene carbonate (PC) solvent [2], and large fractionations (up to -30 per-mil in ^{7}Li/^{6}Li) were observed between electrodeposited Li and stock solutions [3]. The magnitude of fractionation was largest closest to the equilibrium reduction potential, and decreased as the thermodynamic driving force (and thus deposition rate) was increased (Fig. 1) [3]. Two hypotheses for this trend are 1) mass-transport-limited supply of Li to the reactive interface resulted in an attenuated isotopic signature, and 2) the observed changing isotopic signature is an intrinsic rate-dependent kinetic effect. These competing hypotheses will be directly tested in models and experiments of temperature-depenedent isotopic fractionation during Li electrodeposition.

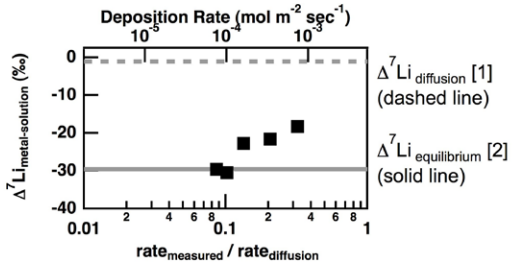

Figure 1. Lithium isotope composition of metal samples electroplated from 1M Li(PC) solutions, squares [3].

[1] Richter *et al*. (2006), *GCA* **70**, 277-289. [2] Singh *et al*. (1972), *J. Chem. Phys*. **56**, 1855-1862. [3] Black *et al*. (2009), *J. Am. Chem. Soc*. **131**, 9904-9905.

https://doi.org/10.1180/S0026461X00006502 Published online by Cambridge University Press

A long-term record of continental lithosphere exhumation via U-Pb thermochronology of the lower crust

TERRENCE BLACKBURN[1]*, SAMUEL BOWRING[1], TAYLOR PERRON[1], KEVIN MAHAN[2] AND FRANCIS DUDAS[1]

[1]EAPS, MIT, Cambridge, MA, USA (*correspondance: terrence@mit.edu)
[2]Dept of Geol. Sci., Univ. of CU Boulder, CO, USA

Exposures of cratonic lithosphere (shields) are generally characterized by low long-term erosion and sediment accumulation. Seismic tomography and mantle xenolith studies of cratons reveal keels of seismically fast and relatively buoyant and viscous mantle; physical properties intimately linked with their long-term stability and topographic expression. Missing from these observations is a long-term record (>1000 Ma) of continental exhumation/burial that can be used to quantity the forces operating within these ancient regions. The exhumation or burial of the continent surface has a direct effect on the rate of heat loss within the lithosphere. By reconstructing the thermal history for the lithosphere using thermochronologic techniques, the magnitude of burial and exhumation through time can be estimated. Here we demonstrate how a long-term record of lithosphere exhumation or burial can be reconstructed using U-Pb thermochronology on lower crustal xenoliths. The U-Pb system is sensitive to cooling at temperatures of ~400-650 °C, corresponding to lower crustal depths of 20-50 km. Integration of this thermochronologic record with thermal models for the stable lithosphere allows one to reconstruct the magnitude of surface exhumation/burial during long-term cooling of the continents. In Montana, USA, lower crustal samples record extreme slow cooling consistent with low exhumation rates (<0.01 km/Ma) over time scales billions of years. Constraining the magnitude and variation of lithosphere exhumation over a billion years or more provides the opportunity to understand the degree of thermal and mechanical coupling between continental lithosphere and the underlying convecting mantle in the deep geologic past.

Are noble gases in the sediment pore water of Lake Van promising proxies for paleoclimate conditions?

R. BLÄTTLER[1], Y. TOMONAGA[1]*, M.S. BRENNWALD[1], O. KWIECIEN[1], R. KIPFER[1,2], AND THE PALEOVAN SCIENTIFIC PARTY

[1]Eawag, Swiss Federal Institute of Aquatic Science and Technology, CH-8600 Dübendorf, Switzerland (*correspondence: tomonaga@eawag.ch)
[2]Institute of Geochemistry and Petrology, Swiss Federal Institute of Technology (ETH), CH-8092 Zurich, Switzerland

As noble gases are chemically inert, they are ideal tracers to study physical processes in water bodies. The noble-gas partitioning between the atmosphere and the respective water body occurs according to Henry's Law, which is mainly controlled by the temperature and salinity of the exchanging water phase. Therefore, atmospheric noble gases (He, Ne, Ar, Kr, and Xe) have been successfully used in the past to reconstruct the physical conditions in aquatic systems such as groundwater, lakes, and oceans.

Several decades ago, noble gases in the pore water of unconsolidated sediments have been proposed as proxies for the reconstruction of environmental conditions in lakes and oceans. During sedimentation, a certain volume of the water overlying the sediment/water interface is trapped in the pore space of the growing sediment column. If the noble-gas diffusion within the pore water is sufficiently attenuated, the sediment column can conserve noble-gas concentrations over long time scales. However, only recently analytical methods allowing robust and reliable determination of noble-gas concentrations in the sediment pore water have been developed and improved. In Lake Issyk-Kul, a large closed-basin lake in central Asia, atmospheric noble gases in sediment pore water have been successfully applied for the first time as proxies for paleoclimate conditions.

In this study we present concentration profiles measured in the sediment column of Lake Van (Turkey). Lake Van is one of the largest terminal lakes and the largest soda lake on Earth. The lake is known to react very sensitively to changes in the local climate conditions.

We interpret the measured noble-gas concentrations in terms of possible changes in the physical conditions of the water body of the lake (i.e., changes in temperature and salinity). In particular we discuss the potential of noble gases as proxies for paleoclimate reconstruction considering the ongoing ICDP deep drilling project PALEOVAN (http://www.icdp-online.org).

https://doi.org/10.1180/S0026461X00006502 Published online by Cambridge University Press

First-principles simulation of arsenate adsorption on the (1 $\bar{1}$2) surface of hematite

M. BLANCHARD*, G. MORIN, M. LAZZERI, E. BALAN AND F. MAURI

MPMC, Univ. Paris VI, CNRS, IRD, Univ. Paris VII, IPGP, 4 Place Jussieu, 75252 Paris Cedex 05, France (*correspondence: marc.blanchard@impmc.upmc.fr, guillaume.morin@impmc.upmc.fr, michele.lazzeri@impmc.upmc.fr, etienne.balan@impmc.upmc.fr, francesco.mauri@impmc.upmc.fr)

Recent experimental studies [1, 2] revealed an unprecedented bimodal distribution of arsenate at the hematite (1 $\bar{1}$2) surface, with a simultaneous adsorption of inner-sphere and outer-sphere complexes. In the present study, first-principles calculations based on density functional theory were performed to make a detailed analysis of the structural and electronic properties of these inner-sphere and outer-sphere adsorption complexes on two hydroxylated terminations of the hematite (1 $\bar{1}$2) surface. For bidentate corner-sharing complexes, the most-stable adsorption configurations display interatomic distances in excellent agreement with EXAFS-derived data (i.e. As-Fe distances of ~3.3 Å). Our calculations also suggest that edge-sharing bidentate complexes can also form on clean (1 $\bar{1}$2) hematite surfaces and do not necessarily need step edges. These edge-sharing complexes would display two As-Fe distances at about 2.85 and 3.45 Å, instead of the unique short As-Fe contribution that is usually considered. For outer-sphere complexes, the most favorable adsorption configurations indicate the stabilization of the arsenate molecule by strong hydrogen bonds as well as the involvement of electrostatic forces. It is therefore essential to include these outer-sphere complexes in the thermodynamic models used to understand the arsenic fate in the environment.

[1] Catalano *et al*. (2007) *GCA* **71**, 1883-1897. [2] Catalano *et al*. (2008) *GCA* **72**, 1986-2004.

Response of vegetation and erosion dynamics to changes in precipitation in the Nile River drainage basin during the African Humid Period

CECILE L. BLANCHET[12], JANNE LORENZEN[3], RIK TJALLINGII[2], STEFAN SCHOUTEN[2] AND MARTIN FRANK[1]

[1]IFM-GEOMAR at the University of Kiel, Whischhofstrasse 1-3, 24148 Kiel, Germany
[2]NIOZ Royal Netherlands Institute for Sea Research, Landsdiep 4, 1797 SZ 't Horntje, The Netherlands
[3]University of Kiel, Ludewig-Meyn-Strasse 14, 24118 Kiel

During the mid-Holocene, the gradual decrease in summer insolation induced a decrease in monsoon strength and subsequent aridification of northern Africa. However, the timing of environmental and climatic responses to this slow orbital forcing is still being debated, with studies reporting either a gradual or an abrupt termination of the African Humid Period (AHP).

Here we use 6 m-long sediment core P362/2-33 that was retrieved at 700 m water-depth on the Nile deep-sea fan. Detailed ^{14}C dating shows that the core covers the last 9,500 years, with laminated sediments being deposited at very high rates (up to 600 cm/ka) during the AHP. These sediments allow to investigate the linkages and feedbacks between climate, vegetation and erosion dynamics at millennial to seasonal resolution. The variations in sediment and fresh-water input, as well as sediment provenance and vegetation changes are monitored using a combination of inorganic and organic geochemical proxies (major and trace elements ratios, $\delta^{18}O$ and $\delta^{13}C$ of planktonic foraminifera, radiogenic isotope compositions of sediments, foraminifera and seawater-derived ferromanganese coatings, and abundance and isotope composition of specific biomarker lipids). Massive amounts of fresh water and sediments were delivered by the Nile River to the deep-sea fan between 9.5 and 8 ka, as indicated by high sedimentation rates, high titanium/calcium ratios and sea-water εNd values similar to the Nile River. This time interval was also characterised by the dominance of C4 grasses and soil development, as indicated by heavier $\delta^{13}C$ values for higher plants n-alkanes and elevated concentrations in soil biomarker. A first rapid decrease in fresh-water and sediment delivery was recorded around 8.5 ka in sea-water εNd and sedimentation rate followed by a gradual decrease between 8 and 4 ka identified in all proxies. The transition from C4- to C3-dominated environment occurred between 8 and 6 ka, and might reflect the aridification of the Sahara, with n-alkanes mainly originating from southern sources after 6 ka. Sediment source tracing by mean of their radiogenic isotope composition is being processed.

https://doi.org/10.1180/S0026461X00006502 Published online by Cambridge University Press

A new calibration site for cosmogenic ^{3}He production rate in the Central Altiplano

PIERRE-HENRI BLARD AND JÉRÔME LAVÉ

CRPG-CNRS, Université de Lorraine, Vandoeuvre-lès-Nancy, France. (blard@crpg.cnrs-nancy.fr)

It is critical to refine the accuracy and precision of the *in situ* cosmogenic dating tool, especially for establishing reliable glacial chronologies that can be compared to other paleoclimatic records. Indeed, the fiability of this chronometer is highly dependent on the accuracy of the spatial and time dependent correcting factors. Potential bias are particulary important for the high altitude tropical area. There is thus a crucial need of well-dated calibration sites allowing to establish robust regional production rates.

We present here a new calibration site for cosmogenic ^{3}He that is located in the tropical Altiplano (20°S, 68°W), on the southern flank of the Tunupa volcano, in the vicinity of the Salar de Uyuni at ~3800 m. The calibration site consists in a fluvio-glacial outwash that has the remarkable characteristic to be stratigraphically bracketed by two successive lacustrine shorelines. These shorelines are well-dated by ^{14}C and U-series dating [1,2], allowing to define an absolute age of 15.1±0.3 ka for the outwash deposition. We sampled 10 andesitic boulders on this site and analyzed the cosmogenic ^{3}He contents in the pyroxenes phenocrysts. The measured ^{3}He concentrations are characterized by a very low scatter: 9 samples agree within analytical uncertainties, suggesting that pre-deposition or post-deposition processes dit not produce any detectable bias. If the nucleogenic contribution from ^{6}Li capture is lower than 2% (as measured in similar samples on the same volcano [3]), these clustered data will allow defining a new reference value for the local production rates of ^{3}He with a precision better than 5% (1σ).

[1] Sylvestre *et al*., 1999, *Quat. Res*., **51**, 54:66. [2] Placzek *et al*., 2006, *G.S.A. Bull*., **118**, 515:532. [3] Blard *et al*., 2009, *Quat. Sci. Rev*., **28**, 3414:3427.

Changes in global weathering indicated by the Ca-isotope record of Oceanic Anoxic Events 1a and 2

C.L. BLÄTTLER[1]*, H.C. JENKYNS[1], L.M. REYNARD[2] AND G.M. HENDERSON[1]

[1]Department of Earth Sciences, University of Oxford, South Parks Road, Oxford OX1 3AN, U.K. (*correspondence: Clara.Blattler@earth.ox.ac.uk)

[2]Research Laboratory for Archaeology and the History of Art, University of Oxford, South Parks Road, Oxford OX1 3QY, U.K.

Oceanic Anoxic Events (OAEs) are huge perturbations to climate that offer an opportunity to observe the response of the Earth system to large and abrupt changes in the carbon cycle. Calcium-isotope ratios ($\delta^{44/42}$Ca) were measured by MC-ICPMS in carbonate-rich sedimentary sections deposited during OAE1a (Early Aptian) and OAE2 (Cenomanian–Turonian). A negative excursion in $\delta^{44/42}$Ca of ~0.20‰ is observed in two sections spanning OAE1a from Resolution Guyot (Mid-Pacific Mountains) and Coppitella (Gargano, Italy); a negative excursion of ~0.10‰ is observed in two sections spanning OAE2 from the English Chalk (at Eastbourne and South Ferriby, UK).

These Ca-isotope excursions occur at the same stratigraphic level as the C-isotope excursions that define the anoxic events, but they do not correlate with lithological changes or evidence for carbonate dissolution in the sections. Diagenetic and temperature effects on the Ca-isotope trends are discounted, leaving changes in global seawater composition as the most probable explanation for the change in $\delta^{44/42}$Ca in the carbonate records.

An oceanic box model with coupled Sr- and Ca-isotope systems indicates that a global weathering increase is likely the dominant driver of transient excursions in Ca-isotope ratios. Contributions from hydrothermal activity and carbonate dissolution are likely to be too small and short-lived to generate the observed changes in the oceanic Ca-isotope composition. A modelled increase in weathering flux, on the order of three times the modern flux, combined with increased hydrothermal activity due to formation of the Ontong-Java Plateau (OAE1a) and Caribbean Plateau (OAE2), can produce trends in both Ca- and Sr-isotope ratios that match the signals recorded in the carbonate sections. These data are the first major-element records of a weathering response to Oceanic Anoxic Events.

https://doi.org/10.1180/S0026461X00006502 Published online by Cambridge University Press

Aerobic methanotrophs drive the formation of a seasonal anoxic benthic nepheloid layer in a monomictic lake

H.J.R. BLEES[1]*, H. NIEMANN[1], C.B. WENK[1], J. ZOPFI[2], C.J. SCHUBERT[3], M.L. VERONESI[4] AND M.F. LEHMANN[1]

[1]Institute of Environmental Geosciences, University of Basel, Switzerland (*correspondence: jan.blees@unibas.ch)
[2]Laboratory of Microbiology, Institute of Biology, University of Neuchâtel, Switzerland
[3]Swiss Federal Institute of Aquatic Science and Technology (EAWAG), Kastanienbaum, Switzerland
[4]Institute of Earth Sciences, University of Applied Sciences of Southern Switzerland, Canobbio-Lugano, Switzerland

Monomictic lakes experience thermal stratification throughout most of the warmer seasons. Often this leads to seasonal bottom water anoxia, particularly if monomixis is paired with eutrophic conditions. The southern extension of Lake Lugano is a warm, monomictic basin with bottom water anoxia, and formation of a dense benthic nepheloid layer (BNL) during summer and fall. A sharp redox gradient marks the upper boundary of the BNL, which extends to up to 15m from the sediment into the water column. Previous work has revealed that the bulk organic matter in the BNL is strongly depleted in ^{13}C ($\delta^{13}C < -60‰$), indicating that the BNL in the Lake Lugano South Basin is largely composed of methanotrophic bacteria. In this study we present radio-label rate measurement and compound specific C isotope data that confirm i) high rates of aerobic methane oxidation (MOx) at the redoxcline (i.e. just above the BNL) and ii) the dominance of bacterial methanotrophic biomass in the BNL of Lake Lugano's southern basin. MOx is restricted to a narrow zone at the top of the BNL reaching maximum rates of up to 1.8 μM/day. MOx activity leads to the formation of a sharp CH_4 concentration gradient (80 μM at 92 m; 100 nM at 82 m). The C kinetic isotope effect of methane consumption is strongly suppressed at the community level (ε = -2.4‰), highlighting the near perfect methane sink at the oxycline, where > 99.9% of the CH_4 diffusing from the sediment is oxidised. Fatty acids (FAs) indicative of type I aerobic methanotrophs are depleted in ^{13}C ($\delta^{13}C$ = -65 to -80‰) and are the dominant lipids in the FA fraction. In addition, preliminary molecular analysis of the microbial community provides further evidence that the formation of the BNL is driven by aerobic methanotrophs rather than by resuspension of sediments or accumulation of organic matter from the epilimnion, as is often observed in other lakes. Prior to water column mixing, these methanotrophs greatly limit the emission of accumulated methane to the atmosphere.

Hf isotope evidence for depleted and enriched reservoirs in the Hadean

J. BLICHERT-TOFT* AND F. ALBARÈDE

Ecole Normale Supérieure, 69007 Lyon, France (*correspondence: jblicher@ens-lyon.fr)

Chase and Patchett [1] and Galer and Goldstein [2] argued for the existence of a hidden enriched reservoir in the early mantle, a perspective that has since received strong support from Hf isotope [3] and ^{142}Nd [4] evidence. The geochemistry of the earliest magmatic minerals is critical in this context. The Jack Hills zircons (JHZ) have been analyzed for Pb and Hf isotopes by several groups using either *in situ* [5-7] or solution chemistry [5,8,9] techniques. The data support the presence of normal continental crust at 4.1±0.1 Ga, with Hf model ages and inferred Lu/Hf characteristics further suggesting a 4.35 Ga protocrust formed from KREEPy upper mantle [7,9]. Whereas all studies find the same predominantly enriched signature indicating apparently massive crustal recycling and reworking during the Hadean and the Archean, only the solution chemistry studies [5,9] see evidence for a depleted reservoir in the Hadean mantle. Statistical analysis of the *in situ* data sets strongly suggests that zircons with the most radiogenic Hf were mistaken for analytical artifacts such that the high-ε_{Hf} end of the distribution became unduly trimmed. We therefore conclude that, although the JHZ protolith seems to have been largely enriched, it also contained undifferentiated and depleted components. Hf and Nd isotopes in komatiites [10] likewise suggest that the Archean and Hadean mantle comprised long-term depleted sources, identical in terms of time-integrated lithophile trace element characteristics to the Early Depleted Reservoir [11] deduced from $^{146,147}Sm$-$^{142,143}Nd$ and Lu-Hf isotope studies of modern mantle material and chondrites. The uppermost KREEPy mantle likely held enough radioactive elements and water to have outlasted the crystallization of the magma ocean for 100s of Ma. If embedded within and between magma ocean cumulates and a thin hydrous lithosphere, such material may have jump-started early plate tectonics.

[1] Chase & Patchett (1988) *EPSL* **91**, 66-72. [2] Galer & Goldstein (1991) *Geochim. Cosmochim. Acta* **55**, 227-239. [3] Blichert-Toft & Albarède (1997) *EPSL* **148**, 243-258. [4] Boyet & Carlson (2005) *Science* **309**, 576-581. [5] Harrison *et al.* (2005) *Science* **310**, 1947-1950. [6] Harrison *et al.* (2008) *EPSL* **268**, 476-486. [7] Kemp *et al.* (2010) *EPSL* **296**, 45-56. [8] Amelin *et al.* (1999) *Nature* **399**, 252-255. [9] Blichert-Toft & Albarède (2008) *EPSL* **265**, 686-702. [10] Blichert-Toft & Puchtel (2010) *EPSL* **297**, 598-606. [11] Boyet & Carlson (2006) *EPSL* **250**, 254-268.

https://doi.org/10.1180/S0026461X00006502 Published online by Cambridge University Press

Towards a resolution of the timing of Martian magmatism: Diffusion study of Hf in clinopyroxene and geochronological implications

E. BLOCH AND J. GANGULY*

Dept. of Geoscience, Univ. of Arizona, Tucson, AZ, 85721, USA (*correspondence: ganguly@email.arizona.edu)

The igneous crystallization age of the Shergottite suite of Martian meteorites has been a subject of considerable debate. While ^{147}Sm-^{143}Nd and ^{176}Lu-^{176}Hf mineral isochrons yield relatively young ages of ~150-225 Ma, ^{206}Pb-^{207}Pb ages from the same samples exceed 4.0 Ga. It has been proposed that the ^{206}Pb-^{207}Pb dates reflect the true crystallization age of the Shergottites and that the ^{147}Sm-^{143}Nd and ^{176}Lu-^{176}Hf "isochrons" represent either a mixing line with phosphate-hosted material or reflect the effect of thermal resetting at ~200 Ma [1,2]. Alternatively, it has been argued that the ^{206}Pb-^{207}Pb array is simply a mixing line arising from contamination by modern terrestrial Pb [3].

Lapen *et al*. [4] argued against the "mixing hypothesis" for younger Lu-Hf age on the basis of lack of correlation between ε(Hf) and 1/[Hf] of the samples defining Lu-Hf "isochron". In order to test the alternative hypothesis of thermal resetting via diffusion of Hf, we have determined the diffusion kinetic properties of Hf^{4+} in clinopyroxene, which is the primary host mineral of Hf. To evaluate thermal resetting due to a shock event, we assume a maximum estimate of post-shock temperature of ~1000°C. Using the average clinopyroxene radius (r) in the Shergottite RBT-04262 (0.5 mm), our diffusion data yield ~210 kyr as the time required for diffusive re-equilibration of Hf isotopes, which precludes resetting within a shock-heated and -ejected material. We have also addressed the problem of extended heating during a non-ejection impact event (or other thermal perturbation) by measuring and modeling Cr diffusion profiles in olivine in RBT-04262. Using Cr diffusion from [6], we obtain a time scale of ~1 year at the peak temperature of 1150 °C [7]. This leads to a vlue of Dt/r^2 of ~$3x10^{-5}$ for Hf in clinopryoxene, which precludes any significant diffusive resetting of Lu-Hf chronometer for the sample [8].

[1] Bouvier *et al*. (2005) *EPSL* **240**, 221-233. [2] Bouvier *et al*. (2008) EPSL **266**, 105-124. [3] Shafer *et al*. (2010) *GCA* **74**, 7307-7328. [4] Lapen *et al*. 92008) *LPSC* XXXIX [5] Stöffler *et al*. (1991) *GCA* **55**, 3845-3867. [6] Ito and Ganguly {2006) *GCA* **70**, 709-809 [7] Mikouchi *et al*. (2008) LPSC XXXIX [8] Crank (1975) Mathematics of Diffusion

What defines a saline aquifer for CO_2 injection?

MADALYN S. BLONDES* AND MARGO D. CORUM

U.S. Geological Survey, 12201 Sunrise Valley Dr., Reston, VA 20192, USA (*correspondence: mblondes@usgs.gov, mcorum@usgs.gov)

The U.S. Geological Survey is currently assessing potential CO_2 subsurface storage formations in the United States. The U.S. Environmental Protection Agency requires that any U.S. CO_2 sequestration assessment or project avoid subsurface formations containing potential drinking water. The Underground Injection Control Program (UIC) for Class VI (CO_2 storage) wells protects fresh water, defined as water with a total dissolved solids (TDS) concentration < 10,000 mg/L. However, the UIC does not define how the limit must be interpreted statisically or spatially to determine potential storage formations. For example, if one analysis has a TDS concentration > 10,000 mg/L, is the entire formation considered a saline aquifer? Could a saline water analysis from a previous injection well in the same reservoir then be cited as evidence of a saline formation available for CO_2 injection? Other possibilities include using a median or mean within uncertainty for a water chemistry dataset. Though site-specific hydrogeological studies would be required before injection to predict CO_2 migration to aquifers, the concern is whether fresh water aquifers could be defined as saline based on existing subsurace water quality data.

For example, the Mesaverde Formation in the Southwestern Wyoming Province is a known aquifer with fresh water near the surface and saline water at depth. Using multiple water quality databases that cover the Rocky Mountain region, we find n = 789 independent analyses with non-null reported TDS concentrations between 72 and 249,838 mg/L at depths > 1 km. Whereas the mean TDS concentration is "saline" (13,240 ± 17,191 (1σ) mg/L), the median concentration is "fresh" (9,482 mg/L).

Since the scale of a sequestration project is not across an entire basin, we can also provide a spatial definition of salinity. If we see a region with suitably saline data, how far from those wells can we assume the formation is saline? Though this is a complex hydrogeologic problem, our interest is simply to define whether a potential storage region is "saline" or "fresh." Using 1-D Darcy flow (neglecting convection and dispersion) for a range of applicable reservoir properties and time-scales, we model length scales of saline water flux. These results then define the radial distance from a saline data region that could be considered saline at the time-scales relevant to long-term CO_2 storage.

https://doi.org/10.1180/S0026461X00006502 Published online by Cambridge University Press

Effects of sodium borohydride reduction and dioxygen concentration on the photochemical properties of humic substances

NEIL V. BLOUGH*[,1], KELLI GOLANOSKI[1], YI ZHANG[1], AND ROSSANA DEL VECCHIO[1,2]

[1]Department of Chemistry and Biochemistry University of Maryland College Park MD United States (*correspondence: neilb@umd.edu)

[2]Earth System Science Interdisciplinary Center University of Maryland College Park MD United States

Previous results have demonstrated that the reduction with sodium borohydride of Suwannee River humic and fulvic acids, a commercial lignin, and a series of solid phase C18 extracts from fresh, estuarine, coastal and offshore waters of the middle Atlantic bight produces a preferential loss of long wavelength (visible) absorption and enhanced, blue-shifted emission [1], consistent with a previously proposed electronic interaction model [2,3]. Here the effects of this reduction on the photosensitized oxidation of 2,4,6-trimethylphenol (TMP) and on the photoproduction of hydrogen peroxide is examined. For unreduced samples, the initial rate of TMP loss (R_{TMP}) increased with decreasing [O_2] concentration over the range from 1.2 mM to ~ 50 μM; below [O_2]~50 μM , R_{TMP} decreased precipitously, with no observable loss under N_2. Borohydride reduction substantial reduced R_{TMP} at all [O_2]. These results are consistent with the (aromatic ketone) triplet sensititization model of Canonica and co-workers [4,5]. In contrast, borohydride reduction only slightly decreased the intial rates of hydrogen peroxide production and similar dependencies of the initial rates on [O_2] were observed with both reduced and unreduced samples. Preliminary work, however, indicates interesting differences in peroxide yields between these samples under conditions in which they are first irradiated under N_2 followed by the introduction of O_2 at increasing delay times.

[1] Ma *et al*. (2010) *Environ. Sci. Technol*. **44**, 5395-5402. [2] Del Vecchio and Blough (2004) *Env. Sci. Tech*. **38**, 3885. [3] Boyle *et al*. (2009) *Environ. Sci. Technol*. **43**, 2262-2268. [4] Canonica *et al*. (1995) *Environ. Sci. Technol*. **29**, 1882. [5] Canonica *et al*. (2000) *J. Phys. Chem. A* **104**, 1226-1232.

Amendment of mill tailings for *in situ* treatment of mine drainage

D.W. BLOWES[1], M.B.J. LINDSAY[1], A.H.M. HULSHOF[1], C.J. PTACEK[1], P.D. CONDON[1] AND W.D. GOULD[2]

[1]Dept. Earth and Environ. Sci. Univ. Waterloo., ON, Canada, N2L 3G1 (blowes@uwaterloo.ca; matt.lindsay@uwaterloo.ca; ptacek@uwaterloo.ca)

[2] CANMET - Mining and Mineral Sciences Laboratories Ottawa, ON,K1A 0G1 (dgould@nrcan.gc.ca)

Field studies conducted at two mill-tailings impoundments suggest that amendment of sulfide-rich tailings with small masses of organic carbon has the potential to provide passive treatment of pore water through microbially-mediated sulfate reduction, metal-sulfide precipitation and alkalinity production. At the Kidd Creek Metallurgical Site, Timmins, Ontario, fine-grained mill tailings containing 15 – 20 wt. % sulfide minerals and 8 wt.% carbonates, were amended with 20 vol. % organic carbon in the form of pulp and paper sludge or wood chips. At the Greens Creek Mine, Alaska, mill tailings containing 34 wt. % pyrite were amended with 5 or 10 vol. % organic carbon as varied mixtures of peat, spent brewing grain and municipal biosolids. Increased populations of sulfate-reducing bacteria (up to 10^6 cells g^{-1}), and increased alkalinity concentrations were observed at both sites. These changes were accompanied by decreases in pore-water concentrations of SO_4, Zn and other metals as a function of time and relative to control cells. Mineralogical investigations indicate the precipitation of secondary Fe-S and Zn-S phases. However, increases in dissolved Fe and As concentrations were observed near the onset of the Greens Creek field experiments. Combined, these experiments demonstrate the potential for tailings drainage management using organic carbon amendments, but also indicate that care must be taken to limit the inadvertent release of dissolved constituents due to the reductive dissolution of Fe(III) and SO_4–bearing phases.

https://doi.org/10.1180/S0026461X00006502 Published online by Cambridge University Press

Cell permeability/senescence controls the reduction rate of iodate to iodide in marine phytoplankton

K. BLUHM[1], P. CROOT[2], K. WUTTIG[3] AND K. LOCHTE[4]

[1] IFM-GEOMAR, Kiel, Germany (kbluhm@ifm-geomar.de)
[2] Plymouth Marine Laboratory, Plymouth, United Kingdom (pecr@pml.ac.uk)
[3] IFM-GEOMAR, Kiel, Germany (kwuttig@ifm-geomar.de)
[4] AWI-Bremerhaven, Germany (Karin.Lochte@awi.de)

The role of marine organisms in the redox cycling of iodine in the ocean is not well understood presently. Previous studies have suggested that phytoplankton play an important role in the biogeochemical cycling of iodine, and were responsible for the appearance of the non thermodynamically favoured species iodide in the euphotic zone. A key question that arises however is how this reduction occurs; Is it driven by primary production, via direct biologically mediated uptake, or alternatively is it driven chemically by redox reactions related to the passive release of reduced substances from the decay of biological materials?

To directly address this question we have recently performed laboratory experiments and field measurements (Tropical Atlantic and Pacific, Southern Ocean) for this purpose. In culture experiments, including a variety of phytoplankton taxa (diatoms, dinoflagellates and prymnesiophytes), we observed changes in the speciation of iodine over the course of an experiment indicating the apparent ability to reduce iodate to iodide. Production rates were found to be species specific and not related to biomass. In all but one species tested the iodide production commenced in the stationary growth phase and peaked in the senescent phase of the algae. This indicates that iodide production is connected to cell senescence and suggests that iodate reduction results from increased cell permeability. We hypothesize that this is due to subsequent reactions of iodate with reduced sulphur species exuded from the cell. Combined with our field observations we suggest that cell senescence and other related processes that cause cell breakage (e.g. grazing, viral lysis) are responsible for the production of iodide.

Our data additionally suggest that the iodine redox cycle is completed via biological processes also. We observed that an experimentally induced shift from senescence back to the exponential growth phase resulted in a decline in the iodide concentrations, suggesting reoxidation back to iodate. Our new data help to provide a more complete picture of iodine cycling in the ocean.

Fault zone stability in cap rocks affected by CO_2

J. BLUME[1], J. D. ECKHARDT[4], H. G. STOSCH[1], TH. NEUMANN[2], K. BALTHASAR[3], TH. MUTSCHLER[3] AND TH. TRIANTAFYLLIDIS[3]

[1]Institute of Applied Geosciences,
[2]Institute of Mineralogy and Geochemistry,
[3]Institute of Soil Mechanics and Rock Mechanics,
[4]Laboratories for Materials Testing and Research, KIT, 76131 Karlsruhe, Germany (jennifer.blume@kit.edu)

A safe geological storage of CO_2 requires a better understanding of alteration processes in cap rock formations as a function of temperature, pressure, fluid and cap rock mineralogical composition. Alterations in the cap rock can influence the tightness and the stability of a storage site. With regard to fault zones it may lead to increases or decreases of permeability due to solution with widening of flow paths or precipitation with self-healing effects. Increased permeability and consequently leakage might also change the stress field and the rock mechanical properties.

To investigate these relationships, an experimental setup was designed within the BMBF-funded GEOTECHNOLOGIEN joint project CO_2SEALS, to study experiment-related shear planes in natural rock samples, the changes in the mineralogical and rock mechanical properties and their interactions.

Annular shear planes were produced within samples of several pelictic reference rocks by a punching process. The punched samples were installed in newly developed reaction vessels, in which they were continuously percolated with a CO_2-saturated NaCl-brine at a constant pressure (5 bar) and different constant temperatures (45 to 100°C). By varing temperature and reaction time (up to 24 months) it was expected to extract reaction rates from the experiments and also study the extent of alteration.

Results of the experiments with duration up to 6 months show that interactions between CO_2-saturated brine and cap rock are most visible at temperatures >75°C. Changes in the chemical composition of the effluent and in the solid phase show, that beside carbonate dissolution and precipitation, which is the dominant short term process, silicate alteration must have occured also. Thin-layer shear tests at high pressures up to 40 MPa normal stress on powder samples (before and after reaction with CO_2) will be carried out to characterise the change of the geomechanical properties due to alterations.

https://doi.org/10.1180/S0026461X00006502 Published online by Cambridge University Press

Geothermobarometric results at the northern tip of Antarctic Batholith: Tectonic implications

H. BOBADILLA[1]*, M. CALDERÓN[2] AND F. HERVÉ[1]

[1]Departamento de Geología, Universidad de Chile. Plaza Ercilla 803. Santiago, Chile. (*correspondence: hbobadil@ing.uchile.cl)
[2]SERNAGEOMIN. Av. Santa María 104. Santiago, Chile. (mccaldera@gmail.com)

The geological relationships between the Antarctic Peninsula (AP) and South America (SA) have been the subject of sustained study in recent decades. However, there are many problems unsolved yet [1]. This work provides new information that could be used to compare and relate the magmatic and tectonic processes occurring at the northern end of AP and southern tip of SA.

Using EPMA analysis in diorites from the northern Antarctic Batholith, we have determined the composition of a selected group of minerals. Knowing the compositions of amphiboles, we have estimated the temperature (T) and pressure (P) at which they crystallized, according to several geothermobarometers [2, 3].

The results indicate that minerals are not homogeneous, but most are zoned. Particularly for amphiboles, the difference of crystallization T for the many zones could reach 200ºC. These results are interpreted as crystallization in, at least, three stages.

The crystallization T and P of amphiboles in their many zones are revealed and, by extension, an approximation for the T-P crystallization conditions of the plutons. Using a preliminary approximation of lithostatic pressure we propose a specific range of depths of intrusion; they all have been emplaced at upper crust (less than 10-15 kms). Using SHRIMP zircon U-Pb crystallization ages, exhumation rates have been inferred. They seem to rise up since Eocene to Miocene in almost ten times.

[1] Hervé, Miller & Pimpirev (2006), *Antarctica: Contributions to global earth sciences*, 217-227. [2] Otten (1984), *Contrib Mineral Petrol* **86**, 189-199. [3] Schmidt (1992), *Contrib Mineral Petrol* **110**, 304-310.

Boron, lithium and nitrogen isotope geochemistry of K- and NH_4-rich illite/smectite clays in fossil hydrothermal systems

I. BOBOS[1] AND L. B. WILLIAMS[2]

[1]Centre of Geology, University of Porto, 4169-007 Porto, Portugal (ibobos@fc.up.pt)
[2]SESE, Arizona State University, Tempe, Arizona 84287-1404, USA (Lynda.Williams@asu.edu)

Boron (B), lithium (Li) and nitrogen (N) transported by hydrothermal fluids may be incorporated into illite – smectite (I/S), as progressive illitization of smectite occurs [1]. Two illitic size fractions (<0.2μm; 0.2 – 2.0μm), distinct in age and composition, were selected corresponding to K-I/NH_4-I mixtures and to a continuous conversion series of smectite to NH_4-I via interstratified structures.

The $\delta^{11}B$ (‰) values range from -5.1 to -5.5‰ in the K-I/NH_4-I mixed phase samples and from -12.6 to -22.4‰ in the mixed-layered NH_4-I-S. The δ^7Li values measured in K-I/NH_4-I mixed phase ranges from +5 to +12.8‰ and in NH_4-I-S samples ranges from -0.5 to -12.3‰. Lower Li concentrations around few ppm were measured, whereas the B concentrations range from 400 to 1457 ppm. The $\delta^{15}N$ measurements in K-I/NH_4-I clays show a mean value of +5.4‰ and in NH_4-I-S series range from +4.8 to +14.6‰. Nitrogen contents range from 0.15 to 1.2 wt.%.

The results obtained have important implications for understanding sources of fluids cycling through subduction zones. The $\delta^{11}B$, δ^7Li and $\delta^{15}N$ values obtained on NH_4-I-S indicate two different fluids, one very high in B and N, confirming a contribution from sedimentary organic matter. The $\delta^{11}B$ and δ^7Li composition of fluids that produced older K-I/NH_4-I clays fits best with a magmatic source. The isotopically light composition of these trace elements provides an important contribution to subducted sediments in volcanic arcs.

[1] Williams, L.B., and Hervig, R.L. (2005) *Geochim. Cosmochim. Acta* **69**: 24: 5705-5716.

https://doi.org/10.1180/S0026461X00006502 Published online by Cambridge University Press

Na-bearing majoritic garnets in the system $Mg_3Al_2Si_5O_{12}$–$Na_2MgSi_5O_{12}$ at 11–20 GPa: Solid solutions and structural peculiarities

A.V. BOBROV[1]*, A.M. DYMSHITS[1], L. BINDI[2], K.D. LITASOV[3], A.F. SHATSKIY[3], E. OHTANI[3] AND YU.A. LITVIN[4]

[1]Geological Faculty, Moscow State University, Moscow, Russia (*correspondence: archi3@yandex.ru)
[2]Museo di Storia Naturale, Sezione di Mineralogia, Università di Firenze, Firenze, Italy
[3]Department of Earth and Planetary Materials Science, Tohoku University, Sendai, Japan
[4]Institute of Experimental Mineralogy, Chernogolovka, Russia

The phase with composition $Na_2MgSi_5O_{12}$ (Na-majorite), end-member of sodium-rich majoritic garnet [1], was synthesized and garnet/pyroxene *PT* phase boundary was determined in multi-anvil experiments at 11–20 GPa and 1500–2100 °C. Na-majorite was obtained at 16 GPa and 1500°C; its stability spreads to the high-temperature region with pressure (1900 °C at 17 GPa and 2100 °C at 19.5 GPa) [2]. Single-crystal study of Na-majorite provided evidence for its tetragonal symmetry, space group $I4_1/acd$, and cell parameters a = 11.3966(6), c = 11.3369(5) Å and V = 1472.5(1) Å^3 [3]. Experiments at 18 GPa and 1600 °C on the pyrope ($Mg_3Al_2Si_3O_{12}$)–Na-majorite join allowed us to study mixing peculiarities for sodium-rich majoritic garnet. The study demonstrated that the transition from cubic to tetragonal symmetry is observed for the starting composition with ~80 mol % $Na_2MgSi_5O_{12}$, which is consistent with the similar change of the structure in the pyrope–majorite ($Mg_4Si_4O_{12}$) system [4]. Significant Na-majorite solubility in pyrope, as well as findings of natural garnets with high Na concentrations (>1 wt % Na_2O) allow us to consider Na-bearing majoritic garnet as a phase accumulating sodium in the deep upper mantle and transition zone. Successful synthesis of the Na-majorite end-member and study of its structure are of key importance for obtaining of thermodynamic constants for this phase, which together with the computer modeling will allow us to suggest the new version of thermobarometer for mineral assemblages containing Na-bearing majoritic garnet.

Support: RFBR (09-05-00027), MD (534.2011.5).

[1] Bobrov *et al*. (2008) *CMP* **156,** 243-257. [2] Dymshits *et al*. (2010) *Dokaldy Earth Sci*. **434,** 1263-1266. [3] Bindi *et al*. (2011) *Am. Mineral*. **96,** 447-450. [4] Parise *et al*. (1996) *Geophys. Res. Lett*. **23,** 3799-3802.

Application of the Linkam TS1400 X-Y heating stage to melt inclusion studies

R.J. BODNAR[1]*, R. ESPOSITO[1], R. KLEBESZ[1,2], Y.I. KLYUKIN[1,3], D. MONCADA[1] AND A. DOHERTY[1,2,4]

[1]Virginia Polytechnic Institute & State University, Department of Geosciences, Blacksburg, VA, USA (*correspondence: rjb@vt.edu)
[2]Università di Napoli Federico II, Dipartimento di Scienze della Terra, Naples, Italy
[3]Institute of Geology and Geochemistry of UB, RAS, Yekaterinburg, Russia
[4]Università degli Studi di Messina, Dipartimento Elementi e Ambiente, Messina, Italy

One of the major limitations in studying melt inclusions in natural samples has been the lack of availability of easy-to-use microscope-mounted heating stages that allow the user to heat the inclusion while it is being observed and to quench the sample rapidly to maintain a homogeneous glass and to avoid reequilibration during cooling.

The recently introduced Linkam TS 1400 X-Y stage has been tested and found to produce satisfactory results for many types of melt inclusions. Several experiments have been performed on recrystallized melt inclusions (MI) contained in olivine and sanidine phenocrysts from eruptions at Campi Flegrei, Italy, and in clinopyeoxene from the Sarno eruption at Monte Somma-Vesuvius Italy. During the heating experiment, a constant flow of argon gas was introduced into the sample chamber at a flow rate of 0.5 ±5% liter/min. During heating the temperature is easily controlled and the heating rate can be adjusted during the heating experiment. In all cases, it was possible to homogenize the MI and, importantly, to quench the melt to a glass after homogenization. In one experiment, the sample was heated to 1340°C. At that temperature, the field of view became a darkish-red and it was difficult to observe the behavior of the MI. At lower temperatures the optics were excellent. The quality of the optics during heating appears to be dependent on the sample characteristics, with samples containing matrix glass being most problematic.

In most of the experiments, the MI were homogenized completely (crystals + bubbles) and remained homogeneous during quenching to room temperature to produce a glass. In one case, the MI was heated to 1340°C and the solids all melted but the bubble did not dissolve back into the melt. When the MI was quenched, the single bubble remained in the MI and grew larger during cooling. The bubble in this MI may represent a trapped vapor bubble (i.e., the MI trapped a volatile-saturated melt plus a vapor bubble) and thus the bubble should not be expected to dissolve back into melt.

https://doi.org/10.1180/S0026461X00006502 Published online by Cambridge University Press

Tracing the late Paleozoic to early Mesozoic crustal evolution of coastal Southern Peru

F. BOEKHOUT [1]*, R. SPIKINGS [1], M. CHIARADIA [1], T. SEMPERE[2], A. ULIANOV [3] AND A. GERDES U. SCHALTEGGER[1]

[1]Earth and Environmental Sciences, University of Geneva, Switzerland (*correspondence : Flora.Boekhout@unige.ch)
[2]IRD et GET, Toulouse, France
[3]University of Lausanne, Switzerland
[4]Goethe University, Frankfurt am Main, Germany

Subduction related magmatism along the Andean margin started as early as 550 Ma ago. Previous studies reveal a complex magmatic history from the late Paleozoic to the early Mesozoic that involved contributions from both mantle and crust.

This study aims to trace crustal growth and recycling through time along the South Peruvian margin with U-Pb laser ablation ICPMS dating on (Jurassic) plutonic and (Carboniferous – Jurassic) detrital zircons combined with a LA-MC-ICPMS Hf isotope study. This margin is especially suited for this type of study as no evidence is know of terrane accretion along this part of the margin since the Ordovician.

Our ages on detrital and plutonic zircons confirm periods of subduction related magmatism in the Ordovician, Permo-Carboniferous, and late Triassic-Jurassic, but also show periods of magmatic quiescence in the early Triassic and late Devonian.

A combination of Hf, Sr, Nd and Pb isotopes on the Jurassic plutonic rocks will be employed to quantify the relative contributions of mantle and crust to the melts formed along this part of the Andean margin. Additionally, Hf isotopes on detrital zircons will reveal periods of recycling and juvenile input. Preliminary results point towards crustal recycling as the dominant process of crustal evolution along the south Peruvian Andean margin between Carboniferous and Jurassic.

Aerosols, chemistry and the onset and evolution of fog layers

R. BOERS*

Royal Netherlands Meteorological Institute (KNMI) De Bilt, Netherlands (*correspondence: reinout.boers@knmi.nl)

In Western Europe, the occurrence of fog is on the decline since the 1980's. A reduction in the emission of anthropogenic aerosols due to increasingly strict regulatory measures and technological improvements on car and industrial exhaust seems a plausible reason for this decline. However, the onset and evolution of fog is the result of an interplay between a number of complex meteorological and aerosol – chemical factors. Here we model the evolution of fog and its sensitivity to atmospheric cooling rate, variation in aerosol size parameters and the aerosol chemical hygroscopicity parameter. First conclusions from these simulations can be summarized as follows:

1) Below RH=100% the three most important parameters controlling the visibility are the hygroscopicity parameter ($\varkappa$), the total number of aerosols and the relative humidity (RH) itself. For moderate to high values of $\varkappa$ (>0.4) and aerosol concentration typical for continental conditions (2000 - 4000 cm^{-3}), visibility can easily be reduced to below 1 km so that the meteorological condition for the occurrence of fog is satisfied, even though RH < 100%.

2) When RH > 100% and particle activation occurs, the parameter $\varkappa$ rapidly loses it significance in determining visibility. Rather it is the radiative cooling rate that exerts control over the value of visibility. The physical interpretation is that only a few particles (typically less than 150 cm^{-3}) are activated no matter what the value of $\varkappa$ is. Since these few particles grow rapidly upon activation they become increasingly more important in contributing to the reduction in visibility in the fog as the cooling progresses, so that the original sensitivity of visibility to $\varkappa$ when RH was still below 100% is quickly lost.

In atmospheres with RH<100% improved visibility may have been caused by reduced numbers of aerosols. However, for RH = 99% a reduction of $\varkappa$ from 0.9 to 0.5 yields an improvement of visibility from 1 to 2 km. Further work will be necessary to investigate whether changes in emission sources and land usage combined with possible changes in the relative humidity are contributing factors in explaining improved visibilities in the last three decades.

https://doi.org/10.1180/S0026461X00006502 Published online by Cambridge University Press

Structural distortion of $MgSiO_3$ perovskite and the influence of Fe and Al at pressures of the Earth's lower mantle

T. BOFFA BALLARAN[1], A. KURNOSOV[1], K. GLAZYRIN[1], M. MERLINI[2,3], M. HANFLAND[3] AND D.J. FROST[1]

[1]Bayerisches Geoinstitut, Universität Bayreuth, 95447 Bayreuth, Germany.

[2]Dipartimento di Scienze della Terra, Università degli Studi di Milano, Via Botticelli 23, 20133 Milano, Italy.

[3]ESRF - European Synchrotron Radiation Facility, 6 rue Jules Horowitz, BP 220, 38043 Grenoble, France.

The $MgSiO_3$ perovskite-type structure is considered the dominant phase in the Earth's lower mantle. As such a detailed understanding of its elastic properties and density as well as how such properties are affected by chemical substitutions are of great importance to mineral physics, seismology and geodynamics. Many studies have reported the compressibility of $MgSiO_3$ perovskite with or without additional element (mainly Fe and Al) substitution [1, 2, 3]. It has also been proposed that changes in the spin state of Fe at high-pressures may influence the compressibility of perovskite [4, 5]. Little is known, however, about the structural state of perovskite at very high pressures. Such knowledge is essential not only for constraining its physical-properties at lower mantle conditions, but also for understanding the structural instability leading to the perovskite to post-perovskite phase transition, which may cause complex seismic signatures within the D'' layer.

We have studied three single-crystals of $MgSiO_3$ with the end-member composition and containing either Fe^{2+} or Fe^{3+} and Al by means of X-ray diffraction at the ID09 beam line of the European Synchrotron Radiation Facility. Intensity data have been collected up to 90 GPa at room temperature with diamond anvil cells loaded with He as pressure transmitting medium and ruby chips as pressure calibrants. All perovskites display with increasing pressure only a small increase of the octahedral tilting, but undergo major octahedral distortions, which are more pronounced in the Fe^{3+}, Al-bearing perovskite. No evident structural changes associated with the Fe spin transition have been observed.

[1] Fiquet *et al*. (1998) *Phys Earth Planet Int* **105**, 21-31. [2] Walter *et al*. (2006) *Earth Planet Sci Letters* **248**, 77-89. [3] Andrault *et al*. (2007) *Earth Planet Sci Letters* **263**, 167-179. [4] Li *et al*. (2005) *Earth Planet Sci Letters* **240**, 529-536. [5] Catalli *et al*. (2010) *Earth Planet Sci Letters* **289**, 68-75.

Modelling the aqueous Al^{3+} System using Density Functional Theory

S. BOGATKO[1]*, E. CAUËT[2] AND P. GEERLINGS[1]

[1] Eenheid Algemene Chemie, Vrije Universiteit Brussel (VUB), Faculteit Wetenschappen, Pleinlaan 2, 1050 Brussels, Belgium (* sbogatko@vub.ac.be, pgeerlin@vub.ac.be)

[2] Service de Chimie Quantique et Photophysique CP 160/09, Université Libre de Bruxelles, 50 Av. F.D. Roosevelt, B-1050 Bruxelles, Belgium (ecauet@ulb.ac.be)

We have shown (1) that the speciation of aqueous Al^{3+} is well described over a wide range of solution pH by Density Functional Theory calculations on gas phase $Al(OH)_x(H_2O)_y^{(3-x)+}$ clusters embedded in a continuum solvent. Cluster geometry, electronic structure and Gibbs Free Energies all display similar trends suggesting increased acidity as the coordination number decreases. These results are in complete agreement with the observed cooperativity of Al^{3+} hydrolysis products (2).

Extending our model (3) to include coordination by an F^- counterion shows that this ligand coordinates the Al^{3+} cation in a similar way to the OH^- ligands thus inducing important changes in $AlF(OH)_x(H_2O)_Y^{(2-x)+}$ complexes in the direction of increased acidity, in agreement with the observed elevated acidity of natural waters in which AlF^{2+} species occur (4). Furthermore, in light of recent NMR observations (5) of a fast proton-coupled water exchange mechanism on Al^{3+} aqueous complexes, we suggest this mechanism is also present in the aqueous AlF^{2+} system.

Finally, a large array of $Al_2(OH)_x(H_2O)_y^{(6-x)+}$ aqua/hydroxo Al^{3+} dimer species have been investigated. Our results suggest that many species are possible and their stability may be understood in terms of the number of coordinating water and hydroxide ligands and the hydroxide bridging geometry. This novel approach thus provides a revealing picture of the extremely complex aqueous Al^{3+} environment and may thus be of great use to the geochemical and environmental chemistry communities.

[1] Bogatko *et al*. (2010) *J. Phys. Chem. A* 114, 7791. [2] Martin (1991) *J. Inorg. Biochem*. 44, 141. [3] Bogatko *et al*. *J. Phys. Chem. C*, **DOI**: 10.1021/jp112076r. [4] Seip *et al*. (1984) Water, Air, Soil Pollut. 23, 81. [5] Swaddle *et al*. (2005) Science, 308, 1450.

https://doi.org/10.1180/S0026461X00006502 Published online by Cambridge University Press

Element behavior in technogenic systems and methods of mine waste treatment

A.A. BOGUSH [1]*, E.V. LAZAREVA[1], V.G. VORONIN [2], O.G. GALKOVA [1] AND N.V. ISHUK [1]

[1]Institute of geology and mineralogy SB RAS, Koptyug Pr. 3, Novosibirsk 630090, Russia (*coresspondence: annakhol@gmail.com)

[2]Planeta-Ra Ltd., Lazurnay str. 4/3, Novosibirsk 630133, Russia

A huge amount of waste has accumulated in the world during the last century as a result of industrial activity. Research of element migration in technogenic systems and their accumulation on geochemical barriers is the important fundamental problem of the environmental geochemistry. The purpose was to describe migration, distribution, and redistribution of heavy metals by the example of the old tailings of the Lead Zinc Concentration Plant and Ursk tailings of the Gold Concentration Plant (Kemerovo region, Russia). The waste products of the ore mining and processing industry can be oxidized by atmospheric oxygen and microbial activity, forming acid mine drainage (AMD), with high concentrations of SO_4^{2-}, Fe, Zn, Cu, Cd, Pb, and other elements. The result obtained about element species in the sulfide tailings and the bottom sediments, using modified sequential extraction procedure, explain the main features of element migration and redeposition. In the mine waste and technogenic bottom deposits, there is vertical and horizontal substance transformation with formation of following geochemical barriers: 1) the evaporative barrier where secondary species of element, especially water-soluble, are redeposited; 2) the lithological barrier (Hardpan) which reduce migration of elements, pore water and pore gases such as O_2 and CO_2; 3) complex organic-mineral barrier on which heavy metals coprecipitate/sorb with/on iron oxy-hydroxides, organic matter and clay minerals. On the basis of the sulfide waste investigation, environmentally safe and cost-effective ways of liquid and solid waste treatment have been developing using natural (peat, clay, limestone, etc) and modified materials (peat-humic agent, organic-mineral complex, etc.), for example: 1) complex organic-mineral geochemical barriers for binding and long-term retention of pollutants; 2) methods of acid rock drainage treatment; 3) methods of solid waste conservation; 4) prevention of eolian transportation of tailings particles; 5) new method of metal extraction from acid mine drainage. This research was supported by the RFBR (grant 03-05-64529 and 06-05-65007).

Reconstruction of the Atlantic circulation back to the last interglacial by a combined proxy approach

E. BÖHM[1]*, J. LIPPOLD[1], S. WEYER[2], M. GUTJAHR[3] AND A. MANGINI[1]

[1]Heidelberger Akademie der Wissenschaften, Im Neuenheimer Feld 229, 69120 Heidelberg, Germany (*correspondence: eboehm@iup.uni-heidelberg.de)

[2]Inst. für Mineralogie, Universität Hannover, Callinstr. 3, 30167 Hannover, Germany

[3]Dept. of Earth Sciences, University of Bristol, Wills Memorial Building, Queen's Rd., Bristol BS8 1RJ, UK

The Atlantic Meridional Overturning Circulation (AMOC) plays an important role in the global climate system, due to the transport of heat and carbon. Theoretical studies and measured data suggest that the AMOC underwent different circulation modes and the transitions between these modes can be triggered by variations of freshwater runoff into the North Atlantic [1, 2, 3].

The purpose of this project is to trace these transitions by creating a high resolution data set of ε_{Nd} and $^{231}Pa/^{230}Th$ for the last interglacial (Eemian) and the following glacial. ε_{Nd} gives information about the water mass provenance, signal $^{231}Pa/^{230}Th$ serves for reconstruction of AMOC export. Thus, the combination of $^{231}Pa/^{230}Th$ and ε_{Nd} from deep sea sediments is a promising tool to derive the past paleoceanography.

First measurements of ε_{Nd} have been accomplished for the time range from 60 to 154 ka with a temporal resolution of in average 3 ka. The data display the presence of Southern Source Water during MIS 6 to MIS 6.4 and indicates an active deep water formation in the North Atlantic at the beginning of the Eemian Interglacial (MIS 5.5). The transition between these two different modes in AMOC is marked by a distinct drop in the ε_{Nd} values (-11.5 to -14). This is consistent with ε_{Nd} results obtained from the same core [4] and from a neighbouring core [5] at the transition from MIS 2 to MIS 1.1. The similar temporal behaviour of ε_{Nd} during Termination I and II implies recurring millennial-scaled identical processes converting the AMOC from a Glacial mode into an Interglacial mode.

[1] Rahmstorf (2002), *Nature* **419**, 207-214. [2] Rickaby and Elderfield (2005), *G*^{3} **6**, Q05001. [3] McManus *et al*. (2004), *Nature* **428**, 834-837. [4] Gutjahr and Lippold (2011), *Paleoceanography*, submitted. [5] Roberts *et al*. (2010), *Science*, **327**, 75-78.

https://doi.org/10.1180/S0026461X00006502 Published online by Cambridge University Press

Calcium isotope fractionation during dolomite formation

FLORIAN BÖHM[1]*, ANTON EISENHAUER[1], JAN FIETZKE[1], SVENJA RAUSCH[2], ANDREAS KLÜGEL[2] AND WOLFGANG BACH[2]

[1]IFM-GEOMAR, Kiel, Germany (*fboehm@ifm.geomar.de)
[2]Geoscience Department, University of Bremen, Germany

Dolomite is an important component of the global calcium cycle, being a source of Ca to the oceans [1]. Calcium released to the oceans by dolomitization of chalk and limestones can potentially be quantified using marine Ca isotope records [2]. However, little is known about Ca isotope fractionation and the Ca isotopic composition of dolomitic rocks. Theoretical calculations point to a -2 ‰ depletion in $\delta^{44/40}$Ca of dolomite relative to calcite at 25°C [3]. Ordovician dolostones interbedded with limestones were reported to be depleted in $\delta^{44/40}$Ca by -0.6 ‰ relative to the limestones [4].

We have investigated dolomites from an ODP core (Site 183-1140) drilled at the Northern Kerguelen Plateau (46.3°S 68.5°E, 2394 mbsl). The core penetrated 235 m of nannofossil ooze and chalk of early Oligocene to middle Miocene age, and 88 m of pillow basalts forming the basement for the sediments. The basalts erupted at about 34 Ma (latest Eocene) [5]. An interbedded chalk layer was found in the basalt, about 40 m below the top of the basement. The chalk was partly dolomitized at the contact with the basalt.

We measured oxygen, carbon, calcium and radiogenic strontium isotopes of bulk chalk and dolomite samples. The $^{87}Sr/^{86}Sr$ ratios indicate an age of dolomitization of about 10 Ma (late Miocene). Dolomitization obviously occurred about 20 Ma after eruption of the basalts, in a deep burial setting. Oxygen isotope values of chalk and dolomite demonstrate that dolomitization occurred at slightly elevated temperatures (10-20°C). The calcium isotopes of the dolomite are enriched in $\delta^{44/40}$Ca by about +0.5 ‰ compared to the chalk. This is in contrast to the depletion of $\delta^{44/40}$Ca in dolomite reported in the literature. On the other hand, dolomite veins in ocean crust basalts (DSDP/ODP Sites 37-332 and 129-801) are depleted in $\delta^{44/40}$Ca compared to calcite veins of similar age. Fluid composition, diagenetic history and kinetic isotope fractionation have to be considered when interpreting Ca isotope values of dolomite.

[1] Berner, (2004) *Amer. J. Sci.*, **304**, 438-453. [2] Heuser *et al.*, (2005), *Paleoceanography*, **20**, doi:10.1029/2004PA001048. [3] Rustad *et al.*, (2010), *GCA*, **74**, 6301-6323. [4] Holmden, (2009), *Chem. Geol.*, **268**, 180-188. [5] Frey *et al.*, (2003) *Proc. ODP Sci. Res.*, **183**

Hydroxyl group reactivity at FeOOH/gas and FeOOH/water interfaces

JEAN-FRANÇOIS BOILY

Department of Chemistry, Umeå University, Sweden
(correspondence: jean-francois.boily@chem.umu.se)

Reactions involving mineral surfaces and their surrounding environments play important roles in atmospheric and geochemical processes. Knowledge of the types, distributions and orientations of reaction centers on minerals with different surface structures is notably essential for molecular-scale resolution of mineral/gas and mineral/water interactions.

This work is focused on properties of hydroxyl functional groups of important crystal planes of FeOOH minerals exposed to vacuum, gaseous as well as liquid water. Molecular dynamics simulations were carried out to identify hydrogen bonding patterns and calculate their properties in these different systems. These efforts formed the basis of an interpretative framework to our Fourier transform infrared measurements of α-, β-, and γ-FeOOH particles (Fig. 1). These measurements, which were limited to gaseous systems, were used to extract spectroscopic signatures for distinct isolate and hydrogen-bonded hydroxyl groups.

Our combined computational and experimental efforts are helping categorize different crystallographic terminations of FeOOH minerals on the basis of their site distributions, hydrogen bonding patterns and reactivity towards water.

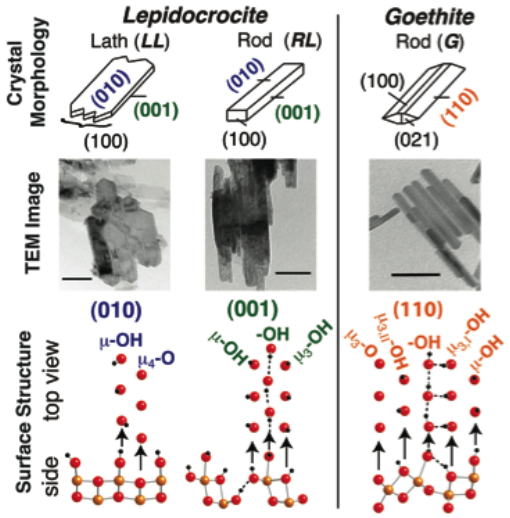

Figure 1: Morphology, TEM imaging (scale bar = 50 nm) and surface structures in three types of particle used for this work.

https://doi.org/10.1180/S0026461X00006502 Published online by Cambridge University Press

Trace elements in sediments of lakes in the Warta river basin

IZABELA BOJAKOWSKA*, TOMASZ GLIWICZ AND JAROSŁAW KUCHARZYK

Polish Geological Institute-National Research Institute, Warsaw, Poland (izabela.bojakowska@pgi.gov.pl)

The Warta River catchment (length 808.2 km), occupies an area of 54 529 km^2. The northern part of the catchment area covered by the Vistulian glaciation deposits, characterized by high abundance of lakes, while the southern part of the basin is practically without lakes.

The lake sediment samples taken from 5cm surface layer from profundal zone of 207 lakes, were analyzed for the content of As, Ba, Cd, Co, Cr, Cu, Mn, Mo, Ni, Pb, Sn, Sr, Ti, V, Zn, Al, Ca, Fe, K, Mg, Na, P and S using ICP-OES method after digestion in aqua regia. From solid samples the Hg content was measured by AAS method and C_{org}. was determined using coulometric method.

Geometric mean contents in the sediment were for: Ag - <0.5 mg/kg, Ba - 96 mg/kg, Cd - 0.5 mg/kg, Co - 2 mg/kg, Cr - 7 mg/kg, Hg - 0.10 mg/kg, Cu - 13mg/kg, Ni - 7 mg/kg, Sr - 148 mg/kg, V - 11 mg/kg and Zn - 72 mg/kg. Sediments of most of the studied lakes are characterized by low contents of trace elements, similar to the geochemical background values. Markedly increased levels of Cd, Cu, Hg, Pb, Sr and Zn were recorded in the sediments of several lakes located within the cities or their boundaries, e.g. Lakes Człuchów, Trzesiecko, Wierzysko and lakes which are used as places of recreation (e.g. Lake Jasień) and their maximum contents were for: Cd - 7.0 mg/kg, Cr - 135 mg/kg, Pb – 153 mg/kg, Zn – 1413 mg/kg, Hg - 1.163 mg/kg. High levels of Cu (579 mg/kg), Ba and Sr were detected in lake sediments, whose waters are included in the cooling system power plants Pątnów and Konin (among them Lake Goławskie and Licheńskie). Warta basin lake sediments compared to sediments of lakes, created on postglacial sediments associated with other glaciations show significantly higher contents Ba, Sr and Ca, and lower contents of Cr, Pb, Zn and Fe. Sediments from lakes of the Warta catchment are also characterized by lower contents of Ni and V as compared to the sediments of lakes of the Pomeranian phase of the Vistulian glaciation.

The presence of high amounts of Cd, Cu, Hg, Pb and Zn in sediments of some lakes in the basin of the Warta is linked to anthropogenic factors (the functioning of cities, recreation, industry). The differentiation has been observed in the contents of trace elements in sediments of lakes situated on postglacial deposits associated with various glaciations.

Submarine groundwater discharge, the subterranean estuary and climate change: *Quo vadis*?

H. BOKUNIEWICZ

School of Marine and Atmospheric Sciences, Stony Brook University, Stony Brook, New York 11794-5000 U.S.A.

The elusive role of submarine groundwater discharge (SGD), and groundwater in general, to global geochemical budgets has special importance in models of climate change. Conversely, geochemical fluxes *via* SGD can be expected to be altered significantly by a change in global climate. Our understanding is distilled from multifaceted case studies. Over the past several decades, the study of SGD has matured from being a fairly interesting novelty studied at a handful of sites before 1985; to a previously unrecognized nutrient source to coastal waters recognized in 45 studies at 39 sites worldwide by 2000 [1]; to a recognizably ubiquitous phenomenon of global importance investigated in over 300 studies and 160 sites, and counting, worldwide today. SGD is often, but not necessarily, confined to the shoreline and it is typically many times greater than the flow of terrestrial, fresh groundwater under the shoreline (i.e. the underflow). In special cases, other drivers might be considered, geothermal gradients, osmotic pressures and consolidation. Deciding its role in global geochemical budgets is, of course, compounded by variations in scale and geology. Nevertheless, issues, such as the flux of carbon, need to be addressed on the largest possible scale. Better distribution of sampling sites is warranted not only to better define current geochemical budgets, but also to anticipate future alterations. Research at sites in high latitudes, in arid environments and around oceanic islands are to be encouraged.

[1] Taniguchi, M., *et al*. (2002) *Hydrological Processes* **16**: 2115- 2129

https://doi.org/10.1180/S0026461X00006502 Published online by Cambridge University Press

Kinetics of coupled Fe(II)-catalysed ferrihydrite transformation and U(VI) reduction

D.D. BOLAND[1], R.N. COLLINS[1,2], C.J. GLOVER[3], T.E. PAYNE[1,2] AND T.D. WAITE[1,*]

[1]School of Civil and Environmental Engineering, The University of New South Wales, Sydney, NSW 2052, Australia. (*correspondance: d.waite@unsw.edu.au)
[2]Institute for Environmental Research, Australian Nuclear Science and Technology Organisation, Locked Bag 2001, Kirrawee DC, NSW 2232, Australia.
[3]X-ray Absorption Spectroscopy Beamline, Australian Synchrotron Company Ltd, 800 Blackburn Rd, Clayton, VIC 3168, Australia.

The Fe(II) accelerated transformation of ferrihydrite to more crystalline Fe(III) oxides such as goethite has implications for the environmental mobility of uranium and other toxic elements. In this study we used X-ray absorption spectroscopy (XAS) on samples obtained from both batch and real time experiments to measure the kinetics of ferrihydrite transformation to goethite and U(VI) reduction across a range of Fe(II) concentrations.

Linear combination fitting of Fe K-edge Extended X-ray Absorption Fine Structure (EXAFS) and U L(III)-edge X-ray Absorption Near Edge Structure data revealed similar time scales of ferrihydrite transformation and U(VI) reduction to U(V) for each treatment, inversely proportional to Fe(II) concentration. The higher rate of U(VI) reduction by Fe(II) on pure goethite than the ferrihydrite/goethite system suggested that it is the associated enhanced rate of goethite formation, rather than the higher Fe(II) itself that causes faster U reduction. The use of quick-scanning XAS, which allowed the collection of Fe K-edge EXAFS spectral data to k = 15 $Å^{-1}$ in < 1 minute for the real time experiments, provided improvements in experimental efficiency.

As predicted by calculations using the Nersnt equation and solubility products of the relevant Fe(III) oxides, the oxidation-reduction potential of the systems also declined on time scales similar to the transformation of ferrihydrite to goethite, further providing evidence for the strong reducing power of Fe(II) associated with goethite and that the presence of goethite is necessary for U(VI) to be reduced.

The effect of Sb(V) on the transformation of ferrihydrite to goethite, hematite, and feroxyhyte

R.M. BOLANZ[1], J. MAJZLAN[1] AND S. ACKERMANN[2]

[1]Inst. of Geosciences, Friedrich-Schiller-University Jena, Germany (ralph.bolanz@uni-jena.de)
[2]SGS INSTITUT FRESENIUS GmbH, Kölliken, Switzerland

Antimony is released into the environment in some natural and man-induced processes. [1]. Yet, its impact on the transformation processes of heavy metal-adsorbing minerals remains poorly understood. In acid-mine drainage systems and shooting ranges, the adsorption of antimony by iron oxides such as ferrihydrite can play a major role. The poorly crystalline 2-line ferrihydrite represents one of the most common Fe oxides in these settings and can transform to goethite (α-FeOOH) or hematite (α-Fe_2O_3) with time [2]. The rate of transformation depends on the pH, temperature, and on the ions and molecules present during the transformation process [3]. This study focuses on the transformation of synthetic ferrihydrite to crystalline iron oxides in the presence of Sb(V). Transformations were carried out for 1-16 days at 70 ºC and at pH 4, 7 and 12, with different concentrations of Sb(V) (0.00, 0.23, 0.75, 2.25 and 6.00 mM Sb). Samples taken from aqueous suspensions were washed, dried, and characterized by X-ray diffraction (XRD) and atomic absorption spectroscopy (AAS). At pH 12, goethite (Sb concentrations up to 3.7 mg Sb/g) is favored and the transformation is completed after one day. Only a concentration of 6 mM Sb retarded the transformation, where even after 8 days only 50 % of the ferrihydrite was transformed into goethite. Transformations at pH 7 led to a mixture of 75 % hematite and 25 % goethite (4.3 mg Sb/g). However, at concentrations of 6 mM Sb, feroxyhyte (δ-FeOOH) (9.1 mg Sb/g) was favored instead. At pH 4, hematite (32.3 mg Sb/g) was favored except for concentrations of 6 mM Sb, were again feroxyhyte (141.1 mg Sb/g) occurred. We assume that increased Sb concentrations favor feroxyhyte and indicate the incorporation of Sb into the structure of feroxyhyte.

[1] Filella *et al*. (2007) *Earth-Sci Rev* **80**, 195-217. [2] Cudennec & Lecerf (2006) *J Solid State Chem* **179**, 716-722. [3] Cornell (1987) *Pflanzenern Bodenk* **150**, 304-307.

https://doi.org/10.1180/S0026461X00006502 Published online by Cambridge University Press

Mineralogy and petrogenesis of the precambrian basement rocks, around Ede, Southwestern Nigeria

A.T. BOLARINWA[1], M.T. JIMOH[2] AND O.O. ODUSI[3]

[1]Department of Geology, University of Ibadan.
[2]Department of Earth Sciences, Ladoke Akintola University of Technology, Ogbomosho.
(*correspondence:jimohmustapha@yahoo.com)
[3]United Geophysical Nigeria Limited, Lagos.

Basement rocks around Ede southwestern Nigeria consist of Banded migmatite-gneiss, pegmatites, Amphibolites and lenses of charnockites. Petrographic studies revealed that the gneisses are composed of 50% quartz, 20% plagioclase. The pegmatite is made up of 50% quartz, 25% microcline, 20% muscovite and 5% microperthite.

The study is aimed at showing the compositional features, petrogenesis and tectonic setting of the rocks mentioned above by analysing the whole rock and trace element chemistry of the various rock types present.

Ten representative samples of the pegmatites and banded gneisses in the study area were collected and analysed for major, trace and rare earth elements. Geochemical analyses reflected the highest average SiO_2 value (72.43%) for the pegmatites while the lowest average SiO_2 content (62.48%) was obtained for the banded migmatite-gneiss. Mean Al_2O_3, Fe_2O_3, MnO, CaO and MgO are higher in the banded migmatite-gneiss than in the pegmatites. However mean Na_2O and K_2O values are higher in the pegmatites than in the banded gneisses.

Average bivariate plots indicates that the precursors of the gneisses are sedimentary while that of the pegmatites are igneous. Mode of occurrences involving partial melting seems to be compatible with the high Zr contents from the result of the trace element analytical data.

Geochemical discriminant diagrams show the rocks to have originated in a continental environment whose tectonic setting is similar to an active continental margin and a continental island arc. Geochemical studies and plots also indicate trends comparable to those typical of the calc-alkaline plutonic suites. Abundances and variations of major and trace elements suggest that part of the protoliths of the rocks are of sedimentary origin with an evolution involving partial melting and subsequent contamination by the plutonic episodes of the Pan African orogeny.

Ferric iron and water incorporation in wadsleyite under hydrous and oxidizing conditions

NATHALIE BOLFAN-CASANOVA[1], MANUEL MUÑOZ[2], CATHERINE MCCAMMON[3], E. DELOULE[4], ANAIS FÉROT[1], SYLVIE DEMOUCHY[5], LYDÉRIC FRANCE[5], DENIS ANDRAULT[1] AND SAKURA PASCARELLI[6]

[1]Laboratoire Magmas et Volcans, Université Blaise Pascal, France (N.Bolfan@opgc.univ-bpclermont.fr)
[2] ISTER, Grenoble, France
[3]Bayerisches Geoinstitut, Bayreuth, Germany
[4]CRPG, Nancy, France
[5]Géosciences Montpellier, France
[6]ESRF, Grenoble, France

Wadsleyite is the most hydrous nominally anhydrous mineral of the mantle transition zone (410-510 km depth). It also has a high affinity for trivalent cations such as Fe^{3+}. However the relationships between ferric iron and hydrogen incorporations in this mineral are unknown.

We conducted experiments at ~13 GPa and 1400°C, under oxidizing and hydrous conditions. The recovered samples were studied using micro-XANES (X-ray Absorption Near Edge Structure) to determine the ferric iron contents in polyphasic samples and SIMS (Secondary Ion Mass Spectrometry) to determine the water concentrations. XANES analyses show that ferric iron content increases with increasing total iron content, and reaches a maximum of 45 mol% of the total iron. The use of infrared spectroscopy highlights a new protonation scheme in wadsleyite, with most of the protons associated with the high frequency band near 3600 cm^{-1}. SIMS analyses show that water contents in wadsleyite vary from 0.5 to 0.7 wt% H_2O. Hydrogen content in wadsleyite is negatively correlated with ferric iron content. The divalent cations (i.e., $Mg^{2+} + Fe^{2+}$) and the Si content in wadsleyite decrease with increasing Fe^{3+} content, evidencing an incorporation mechanism via substitution into the metal sites with charge compensation by metal and Si vacancies.

These results bring new constraints on the contents of Fe^{3+} and H^+ defects in relation with the chemical environment. Such information is important in order to interprete electrical conductivity of wadsleyite in terms of hydrogen content.

https://doi.org/10.1180/S0026461X00006502 Published online by Cambridge University Press

Preliminary estimates on magma storage conditions of the Heise volcanic field, Snake River Plain

T. BOLTE[1]*, M. ERDMANN[1], B.P. NASH[2], H.E. CATHEY[2], R. ALMEEV[1] AND F. HOLTZ[1],

[1]Institute of Mineralogy, Leibniz University of Hannover, Germany (*t.bolte@mineralogie.uni-hannover.de)
[2]Department of Geology and Geophysics, University of Utah, Salt Lake City, UT, USA,

Tuffs and ignimbrites of the Heise and the Yellowstone Plateau eruptive centers, representing the silicic magmatism of the Snake River Plain – Yellowstone volcanic province, were studied to evaluate pre-eruptive storage conditions prevailing in rhyolitic magma chambers. We performed petrographic study of Blacktail Creek Tuff (6.62Ma), Tuff of Wolverine Creek (5.59Ma) and Kilgore Tuff (4.45Ma) of the Heise and the Huckleberry Ridge Tuff (2.05Ma) of the Yellowstone eruptive centers. Mineral and glass shard compositions obtained by electron microprobe were used to estimate temperatures, redox conditions and relative melt water contents.

In general, the set of mineral phases observed in studied rhyolites is similar to that of observed in BJR eruptive center [1] and are: Pl, ± Fsp, ± Cpx, ± Pig, Mt, ± Ilm, ± Qtz,± Fa, apatite and zircon. QUILF thermometry calculations performed on low- and high-Ca pyroxene pairs yield the ranges of temperatures between 818 and 830°C for Heise and 905 and 930°C for Huckleberry Ridge rhyolites. The ilmenite-magnetite oxybarometer yields oxygen fugacity values to be about QFM, which is in a good agreement with previous data [2]. The water contents of the natural rhyolitic melts, which are below 2 wt%, were only roughly estimated by projecting glass shard compositions on the ternary Qz – Ab – Or diagram with eutectic and cotectic compositions experimentally determined at hydrous conditions in the range of 50MPa to 1000MPa.

Our temperature estimates obtained for younger centers together with previously determined relatively high temperatures for Bruneau Jarbidge eruptive center (~11Ma, 905 – 980°C, [1]) suggest the change of pre-eruptive temperatures in rhyolitic magma bodies along the track of Yellowstone hotspot.

The study of melt inclusions hosted in plagioclase and fayalite is still in progress and will be presented in addition to mineral thermometry data.

[1] Cathey & Nash (2004) *J. Petrology* **45**, 27-58. [2] Honjo & Bonnichsen (1992). *Bull. of Volcanology* **54**(3): 220-237

Numerical modelling for peridotite phase melting trends in the SiO_2-Al_2O_3-FeO-MgO-CaO system at 2 GPa

C. BONADIMAN AND M. COLTORTI

Department of Eath Sciences, University of Ferrara, Italy. (bdc@unife.it)

The partial melting is the mechanism that better explain the variability of the major refractory lithophile elements (RLE) of the upper mantle rocks through time and space. Several numerical and experimental models (e.g.: Hirshmann *et al*., 1998; Herzberg, 2004 Niu, 2004) are available to simulate major element depletion trends using whole rock but no particular attention has been devoted to the compositional evolution of the single minerals. On the basis of various primitive chemical composition of the mantle (PM) and using the experimental results of Herzberg (2004) at 2.0 GPa, various melting trends which constrain the composition of the four mineral phases in the peridotite system, are calculated. This accounts for the 98.59 wt% of the upper mantle composition (SiO_2-Al_2O_3-FeO-MgO-CaO) with spinel as the aluminium phase admitted for these bulk compositions. A mass balance calculation has been applied to find the theoretical compositions of ol, cpx, cpx and sp at various degrees of partial melting. The modelling was constrained by i) mineral compositions adjusted in order to account for the properly formula units and ii) the experimental and theoretical intermineral Fe/Mg and Al partition coefficients. An iterative calculation varying the modal contents of the peridotite phases where applied to minimize the differences between calculated and whole rock compositions experimentally determined at various melting degrees. The starting point for each phase depends on the chosen whole rock PM composition and on the modal percentage that minimize the residuum. The several melting trajectories may account for a multiplicity of mantle occurrences where bulk rock analyses are not available. This model provides a new tool for unravelling the melting processes occurring within the Earth's mantle.

[1] Niu, Y. 2004, *J. Petrol*. **45**, 2423-2458. [2] Herzberg, C. 2004, *J. Petrol*. **45**, 2507-2530. [3] Hirshmann *et al*., 1998, *GCA **62**, 883-902*.

https://doi.org/10.1180/S0026461X00006502 Published online by Cambridge University Press

Sorption of Hg(II) by nanocrystalline mackinawite (tetragonal FeS)

SHARON BONE[1]*, KIDEOK KWON[2], JOHN BARGAR[3] AND GARRISON SPOSITO[1]

[1]Environmental Science, Policy and Management, UC Berkeley (*correspondance: shbone@berkeley.edu) (gsposito@berkeley.edu)
[2]Earth Sciences Division, Lawrence Berkeley National Laboratory (kkwon@lbl.gov)
[3]Molecular Environmental & Interface Science, Stanford Synchrotron Radiation Light Source (bargar@slac.stanford.edu)

Mercury is transformed to the biomagnifying species monomethyl mercury by sulphate reducing bacteria in anoxic sediments. The iron sulphide mineral, mackinawite ($FeS_{(s)}$), can limit Hg(II) bioavailability by sequestering Hg in the solid phase or by reducing it to volatile Hg (0). We use a combination of extended X-ray absorption fine structure (EXAFS) spectroscopy, density functional theory (DFT) geometry optimization and X-ray diffraction (XRD) to examine the speciation of Hg sorbed by $FeS_{(s)}$ as a function of Hg concentration, pH, and reaction time. Analysis of the Hg L_{III}-edge EXAFS spectra indicates that Hg exists in multiple coordination environments upon sorption by $FeS_{(s)}$, including a metacinnabar ($HgS_{(s)}$)-like phase and a component that we have tentatively identified as surface bound Hg. We use DFT geometry optimization to clarify the coordination environment of the putative surface complex and our preliminary results indicate that Fe-bound Hg is energetically favoured relative to S- bound Hg, as we had previously hypothesized. Lastly, Hg L_{III}-edge EXAFS spectra indicate Hg (0) forms in the presence of $FeS_{(s)}$, while spectroscopic and diffraction analysis of $FeS_{(s)}$ leads us to hypothesize that Hg(II) reduction results in the formation of surface-bound Fe^{III}. This research demonstrates that Hg(II) interacts with $FeS_{(s)}$ through multiple mechanisms, leading to the production of both sorbed and volatile Hg species, which vary in their reactivity and bioavailability in Hg-polluted sulphidic waters.

Inhibited water diffusion and inhomogeneities in glassy atmospheric aerosol proxies

D.L. BONES[1], D.M. LIENHARD[1,2], U.K. KRIEGER[2] AND J.P. REID[1]

[1]School of Chemistry, University of Bristol, Bristol, BS8 1TS, United Kingdom
[2]Institute for Atmospheric and Climate Science, ETH Zürich, Zürich, Switzerland

Atmospheric aerosol particles are typically complex mixtures of organic and inorganic species with correspondingly complex behaviours in changing humidity regimes. We investigate the formation of glassy or highly viscous phases in aqueous sugar aerosols such as sucrose and levoglucosan and aerosols of mixtures of sugars and inorganic compounds. It has recently been recognised that many aerosols exist as highly viscous solutions or as amorphous glasses, rather than a crystalline state, over a wide range of relative humidities (Virtanen, *et al*. 2010).

We use optical tweezers to trap single aerosol particles, exploiting subtle changes in the Raman spectra to deduce the size changes due to water uptake and evaporation from aqueous particles exposed to varying RH. We compare the experimental data with a kinetic model of diffusional limited size change.

Changes in size are dramatically hindered at low RH, with time scales approaching 10000s, for both increasing and decreasing RH regimes. The shift in resonance modes suggests initial formation of a layer of water on the surface of the glassy particle and subsequent establishment of a steep concentration gradient within.

[1] Virtanen A. *et al*., (2010) *Nature*, **467**, 824– 827.

https://doi.org/10.1180/S0026461X00006502 Published online by Cambridge University Press

Tracing the geographical origin of beefs based on carbon and oxygen isotopes

Y.S. BONG, K.S. LEE* AND W.J. SHIN

Korea Basic Science Institute, Ochang Center, Chungbuk 363-883, Korea (*correspondence: kslee@kbsi.re.kr)

To distinguish the country of origin of beefs that are currently sold in Korean market, a comparative analysis was conducted to examine carbon and oxygen isotopic compositions of beefs imported (from the USA, Mexico, Australia and New Zealand) and domestically produced beef. The result of the carbon isotope analysis showed good distinction between Korean beef and beef imported from the USA, Mexico and New Zealand. Based on carbon isotope values, it was difficult to distinguish between beef produced in Korea and beef imported from Australia, but these origins were easily distinguishable from oxygen isotope values. The oxygen isotope values reflect differences in consumed waters of the animal [1,2], according to the latitude of the country in which the beef was produced [3]. Such a result can be utilized to identify the origin of beef samples.

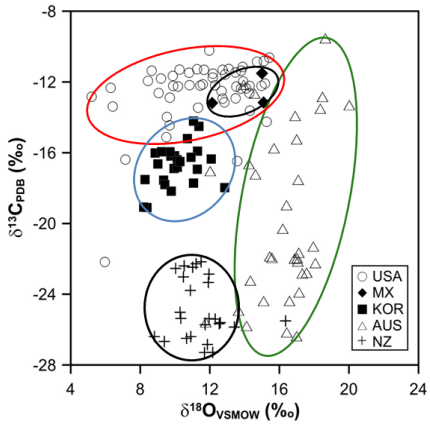

Figure 1: Cross plot of $\delta^{13}C$ and $\delta^{18}O$ values obtained from dry material from beefs produced in several countries.

[1] Franke *et al*. (2005) *Eur. Food Res. Technol*. **221**, 493-503.
[2] Kelly *et al*. (2005) *Trends food Sci. Technol*. **16**, 555-567.
[3] Nakashita *et al*. (2008) *Anal. Chim. Acta* **617**, 148- 152.

Rare earth elements fractionation as proxies of unconformity uranium deposit mineralized fluids

J. BONHOURE AND O. POURRET

HydrISE, LaSalle Beauvais, 60026 Beauvais cedex, France (jessica.bonhoure@lasalle-beauvais.fr)

To better understand the formation of uranium deposits, rare earth elements (REE) and particularly REE compositon of oxides is a powerful tool. Indeed, REE fractionation occurs in uranium oxide [1] by substitution with U and REEs are poorly affected by post-crystallization events [2]. In such a case, REE should provide information on the temperature and redox conditions during deposition, pH and complexing ion concentrations of mineralizing fluids.

We herein document the case of the Athabasca Basin unconformity type, for which REE patterns show a MREE enrichment during incorporation as free species in U oxide for a pH between 3 and 5 [3]. In order to understand the speciation of the mineralized fluid, REE speciation in three multi-ligand solutions (reduced seawater, groundwater and F-rich groundwater) was calculated using PHREEQ-C and Nagra/PSI data base [4], which was modified to include well-accepted infinite-dilution (from 25 to 200°C) of inorganic species. Results from 25 to 200 °C show that at 3<pH<5 (i) in the reduced seawater lanthanides exists; (ii) in the groundwater, lanthanides occur as sulfate and fluoride complexes and free ionic species displaying a MREE enrichment; (iii) in the F-enriched groundwater, lanthanides occurs as free ionic species (HREE enriched) and complexed with fluoride (LREE enriched). Eventually, U oxides patterns are comparable with results of REE speciation in groundwater and LREE ratio indicates a deposition temperature between 125 and 150°C.

[1] Janeczek & Ewing, (1991) *J Nucl Mat* **185,** 66-77 [2] Fryer & Taylor, (1987) *Chem Geol* **63,** 101-108 [3] Kister *et al*. (2005) *Eur J Mineral* **17**, 325-342 [4] Hummel *et al*. (2002) Nagra/PSI Chemical Thermodynamic Data Base 01/01. Universal Publishers, Parkland.

https://doi.org/10.1180/S0026461X00006502 Published online by Cambridge University Press

Calibration and applications of the dolomite clumped isotope thermometer to high temperatures

MAGALI BONIFACIE[1]*, JOHN M. FERRY[2], JUSKE HORITA[3], CRISOGONO VASCONCELOS[4], BEN H. PASSEY[2] AND JOHN M. EILER[5]

[1]Institut de Physique du Globe de Paris, France (*correspondence: bonifaci@ipgp.fr)
[2]Johns Hopkins University, MD, USA
[3]Texas Tech University, Lubbock, TX, USA
[4]ETH, Zurich, Switzerland
[5]California Institute of Technology, Pasadena, CA, USA

Carbonate clumped isotope paleothermometry is based on the temperature-dependent formation of $^{13}C^{18}O^{16}O_2^{2-}$ ion groups within solid carbonate minerals. This thermometer has now been calibrated for various synthetic and natural biogenic and abiogenic minerals (calcite, aragonite and carbonate-apatites [e.g., 1, 2]) at temperatures below ~ 50°C. Here we extend the use of the carbonate clumped isotope thermometer to shallow crustal environments by determining the Δ_{47} values of CO_2 extracted from natural and synthetic dolomites grown at know temperatures from 25 to 350ºC. The experimental temperature dependance is not linear in the Δ_{47} vs T^{-2} plot and resembles the predicted theoretical temperature dependence, both in shape and absolute value [3]. These data for synthetic dolomites overlap the previous calibrations for inorganic calcite and some forms of biogenic carbonates between 25 and 50°C, and are consistent with a single trend that also intersects data for synthetic calcite equilibrated at 1200°C. These observations suggest that a single temperature dependant relationship reasonably approximates the calibration for both phases. Data from a variety of slowly-cooled (i.e., over geological timescales) natural marbles and rapid (i.e., laboratory timescales) heating experiments provide insights into the kinetics of solid-state ^{13}C-^{18}O bond reordering in carbonates and its closure temperature. More generally, our new calibration and constraints on high-temperature kinetics have implications for the application of this technique to burial and metamorphic processes. These issues will be illustrated through estimates of the thermal history and oxygen isotopic compositions and abundances of pore fluids for several suites of late Neoproterozoic carbonates [e.g., 4].

[1] Ghosh *et al*. (2006) *GCA* **70**, 1439-1456. [2] Tripati *et al*. (2010) *GCA* 74, 569 [3] Guo *et al*., (2009) *GCA* **73** 7203 [4] Bristow *et al*., (2011) *Nature*, in press

Seasonal and tidal variations of dissolved thallium in coastal waters

P. BÖNING*, M. BECK, B. SCHNETGER AND H.-J. BRUMSACK

Institute for Chemistry and Biology of the Marine Environment, University of Oldenburg, Germany (*correspondence: p.boening@icbm.de)

Little is known on the distribution and behaviour of Thallium (Tl) in oceanic and coastal waters, perhaps due to its very low concentration level (8-20 ng L^{-1} or 40-90 pmol L^{-1}). Thallium is as highly toxic as Hg and Cd and is involved in redox reactions, which makes it an interesting candidate for the study of environmental processes.

Here we present a method for the rapid and reliable determination of dissolved Tl in sea water using sector field inductively coupled mass spectrometry (SF-ICPMS) without any preparation except 10 times dilution. Our method is suitable for the measurement of large time series of sea water samples [1]. Precision is 7 % RSD except for samples below the quantification limit (0.3 ng L^{-1}). Validation was done using the standards CASS-4 and NASS-5. For both CASS-4 and NASS-5 (salinity of 30.5) we calculated a concentration of about 11 ng L^{-1} assuming a Tl concentration of 14±2 ng L^{-1} at a salinity of 35±1. For CASS-4 we measured 10.6±0.7 ng L^{-1}, for NASS-5 10.3±0.8 ng L^{-1}[1], the latter of which is close to the value of 9.37±0.02 ng L^{-1} determined by isotope dilution-ICPMS by Nielsen *et al*. [2].

We applied our method to surface waters from the Jade Bay (an embayment of the Wadden Sea in NW Germany) [1]. Sampling was done hourly for 48 h during January, April, July and November 2010 at a fixed station located close to tidal flats, with a subsequent offshore transect. Pore waters were taken from sediments close to the fixed station.

In general, the results of all transect measurements (9-12 ng Tl L^{-1}) indicated conservative mixing since Tl varied with salinity. The time-series at the fixed station, however, yielded Tl concentrations of 6-11 ng L^{-1}, which only in part correspond to determined salinities. Hence, the distinct tidal variations in the concentration of dissolved Tl are rather explained by changes in the contribution of pore waters low in Tl (below the quantification limit).

[1] Böning, P and Schnetger, B. (submitted) [2] Nielsen, S. G. *et al*. (2004) *Chem. Geol*. **204**, 109-124.

https://doi.org/10.1180/S0026461X00006502 Published online by Cambridge University Press

Vegetation and climate: The potential role of terpene emissions and aerosol particle formation on local climate conditions

BORIS BONN

WG Aerosol and Environmental Sciences, Institute for Atmospheric and Environmental Sciences, J.W. Goethe University, D-60438 Frankfurt/Main, Germany, (bonn@iau.uni-frankfurt.de)

Any ecosystem and its individual biogenic species survive at specific climate conditions such as temperature, water supply, nutrients and chemical stress factors. In order to take measures to buffer extremes several possible pathways have been suggested. One of these include the emission of terpenes, their influence at ambient oxidant levels as well as in new aerosol particle formation. In this talk the role of individual mono- and sesquiterpenes will be discussed in a broader context emphasizing the ability of coniferous forests to compete with deciduous invaders in the context of changing climate conditions. The presentation is started with unraveling of new particle formation induced by organic volatile compounds conducted at three different scales, i.e. from gas-phase smog chamber studies via plant chamber to ecosystem smog chamber investigations. I will present a detailed understanding of the particle formation process taking into account the mixture of different mono- and sesquiterpenes emitted and their reactivity with ozone and OH. Both are essential for understanding since they limit the formation process at different steps via production of different large radicals. Since isoprene produces too small radicals any addition of isoprene attributed to changing environmental conditions leads to serious consequences on feedback processes and climate cooling. In this context I discuss the effect of a) deciduous emissions such as isoprene and b) of anthropogenic emissions such as of NO on the intensity of new particle formation. My presentation is then finalized by drawing conclusions on potential radiation and climate effects.

Chromium isotopes as an indicator of redox conditions in the Cryogenian shallow oceans

P. BONNAND[1]*, I.J. PARKINSON[1], R.H. JAMES[2] AND I.J. FAIRCHILD[3]

[1]Dept. of Earth and Environmental Sciences, The Open University, Walton Hall, Milton Keynes, MK7 6AA, UK (*correspondence: p.bonnand@open.ac.uk)

[2]National Oceanography Centre, University of Southampton European way, Southampton SO14 3ZH, UK

[3]University of Birmingham, Edgbaston, Birmingham B15 2TT, UK

Variations in atmospheric oxygen concentrations and the oxygenation level of the oceans during the geological past have been widely studied over the last 30 years [1]. A large increase in atmospheric O_2 during the Neoproterozoic has been postulated and is probably associated with a change in the redox condition of the oceans which enabled the explosion of life on Earth. Several models have been proposed, which have attempted to determine oceanic redox conditions during this Era [2]. The deeper oceans during the Neoproterozoic are generally believed to be anoxic until the end of the Ediacaran Period. However, little is known about redox conditions in the shallow oceans during the Neoproterozoic.

This study aims to determine the variation in redox conditions in the Cryogenian shallow oceans using REE chemistry and Cr isotopes in carbonate rocks. Chromium is a redox-sensitive element and its isotopes are fractionated during redox reactions [3]. Cryogenian carbonates from the Scottish Dalradian and the Greenland Eleanore Bay Supergroups are characterised by the lack of a Ce anomaly and positive $\delta^{53}Cr$ values. The lack of a Ce anomaly in ancient carbonates has been interpreted to reflect anoxic conditions [4]. However, these samples do record positive $\delta^{53}Cr$ values which are similar to modern and Phanerozoic carbonates [5]. These heavy $\delta^{53}Cr$ are interpreted to reflect oxidative weathering and the presence of sufficient O_2 to produce Cr(VI). These Cr isotopes data indicate that the shallow oceans during the Cryogenian was not anoxic and modelling suggests either dysoxic or suboxic conditions.

[1] Holland (2006), *FTRS*, **361**, 903-915; [2] Li *et al*. (2010) *Science*, **328**, 80-83.; [3] Ellis *et al*. (2002) *Science*, **295**, 2060-2062; [4] Kamber and Webb (2001), *GCA*, **65**, 2509-2525; [5] Bonnand *et al*. (2011), *JAAS*, **26**, 528-535.

https://doi.org/10.1180/S0026461X00006502 Published online by Cambridge University Press

Terrigenous input and microcharcoal changes in the Gulf of Papua during the last 60 kyrs

N. BONNET*, T. DE GARIDEL-THORON, G. MENOT, L. BEAUFORT, N. BUCHET AND E. BARD

CEREGE, Univ. Aix-Marseille, CNRS, IRD & College de France, Technopole de l'Arbois BP 80, 13545 Aix-en-Provence Cedex 04 (*correspondence: bonnet@cerege.fr)

The last glacial cycle is characterized by abrupt climate changes at high latitudes. Less documented at low latitudes, they seem to strongly impact the hydrological cycle, and therefore the amount of burnable vegetation. In Melanesia, though records of the aborigine's first migrations are scarce, it is established that human settlement occurred during the last glacial. To unravel the human impact on the fire regimes from the natural hydrological variability, we reconstruct microcharcoals and records of terrigenous inputs in a sediment core (MD97-2134) in the Gulf of Papua. We use MicroCharcoals Morphotypes (MCM) and BIT index, as respective indices of the types of burnt vegetation (woodland or grassland) and of terrigenous inputs. We assume that past terrigenous inputs in the Gulf of Papua respond to precipitations changes over the mainland which also control the frequency and intensity of fires.

The most striking feature of these records is the abrupt change in the MCM record at about 47 ka BP. Prior this change, from 60 ka BP to 47 ka BP, the BIT and MCM indexes are correlated, which suggests a direct forcing of droughts on the burnt vegetation. After 47 ka BP, each proxy shows a different dynamics: the elongation of microcharcoals decreases abruptly, whereas the BIT index still records high frequency oscillation until 31 ka BP. We interpret this abrupt decoupling of terrigenous and microcharcoal records as likely influenced by anthropogenic fires related to aboriginal practices consecutively of the first migration wave.

The MCM record further shows an increase during the early Holocene, indicating an increase in the proportion of bush/forest fires ratio. This increase might be due to the development of agriculture over Papua New Guinea, though the reduced frequency of El Niño Southern Oscillation events might have also contributed to this event.

Fungi accelerate mineral weathering via a synergy of mechanical and chemical attacks

S. BONNEVILLE[1,2]*, D.J. MORGAN[2], A.W. BRAY[2], A. BROWN[3], A. SCHMALENBERGER[4], S. BANWART[5] AND L.G. BENNING[2]

[1]Department of Earth Sciences and Environment, Free University of Brussels, BE (*s.bonneville@ulb.ac.be)
[2]School of Earth and Environment, University of Leeds, UK.
[3]Institut for Materials Research, University of Leeds, UK
[4]Department of Life Sciences, University of Limerick, IE
[5]Kroto Research Institute, University of Sheffield, UK

Rock weathering, through net transfer of atmospheric carbon into the Earth's crust, is the main climatic feedback over geological timescales. So far, the role of plant roots and, in particular, the ability of their symbiotic fungi (mycorrhiza) to accelerate mineral weathering remains debated. Mycorrhiza grow preferentially around, and on the surface of nutrient-rich minerals, making such mineral-fungi contact zones potential hot-spot of alteration in soils. However, because of their microscopic nature (only ~ 5 μm wide but up 1 mm long) and their tendency to strongly adhere to mineral substrates, an *in situ* quantification of the interfacial alteration rates by hypha on minerals has never been achieved.

Here, an ectomycorrhiza (*Paxillus involutus*) grown symbiotically with a pine tree (*Pinus sylvestris*) in the presence of freshly-cleaved biotite under humid, yet undersaturated, conditions typical of soils. A sequence of interfacial alteration cross-sections was sampled via FIB (Focussed Ion Beam) ion-milling along a single, surface-bound hypha. Elemental depth-profiles of Si, O, Fe, Al, Mg and K measured by high-resolution electron micro-spectroscopy (STEM-EDS) across these interfaces showed significant elemental transfer (for Fe, Mg, Al and K) from the mineral substrate into the hypha. A quantitative model based on solid-state diffusion was developed and hyphal interfacial alteration rates were derived from these profiles. When compared *consistently* with abiotic dissolution rates measured in batch and flow-through reactors (i.e., same substrate - biotite (001) basal plane-, pH and temperature), the results reveal that the surface bound-fungi were between 3.5 to 30 times faster to alter the basal plane of biotite. The remarkable capacity of surface-bound fungi to degrade biotite is not ascribed to hyphal acidification or organic acid exudation, but rather to the mechanical strain that these micro-organisms exert, simultaneously to chemical alteration, on the mineral substrate over which they grow [1].

[1] Bonneville *et al*. *Geology* (2009), **37**: 615-618.

https://doi.org/10.1180/S0026461X00006502 Published online by Cambridge University Press

Palaeomag-dating of Kupferschiefer ore at Sangerhausen, Germany – An epigenetic, Late Jurassic age for stratabound Cu-mineralization

G. BORG[1]*, S. WALTHER[1], K. KAWASAKI[2] AND D. SYMONS[2]

[1]Petrology and Economic Geology Research Unit, Institute for Geosciences, Martin Luther University, Halle-Wittenberg (*correspondence gregor.borg@geo.uni-halle.de)

[2]Department of Earth and Environmental Sciences, University of Windsor, Windsor, Ontario, Canada, N9B3P4 (dsymons@uwindsor.ca)

Palaeomagnetic Dating of Mineralization

We have carried out paleomagnetic and rock magnetic measurements on 205 specimens from 15 underground sites from the abandoned Sangerhausen Mining District, Germany. Cu-mineralization is richest in Upper Permian (258±2 Ma) Kupferschiefer black marly shale (9 sites), extending into footwall sandstones (3 sites) and hanging wall carbonates (2 sites). ChRM directions were isolated for all sites using detailed alternating field and thermal step demag-netization. The site mean ChRM directions from the mine stratigraphic section yield a negative fold test that indicates that the ChRM post-dates Triassic to Jurassic fault block tilting of the strata.

Discussion of Results

The mean of all site mean directions gives a Late Jurassic paleopole at 149±3 Ma on the APWP for Europe [1]. This is significantly different (>>99% confidence) from a previous, hematite-alteration- derived paleopole [2] that initially gave an age of 254±6 Ma but cannot be maintained any longer. Our Late Jurassic, i.e. epigenetic, age for the ChRM in the black shale-hosted Kupferschiefer Cu-Pb-Zn ores at Sangerhausen correlates with crustal extension that formed the nearby North German Basin north of the Harz Mountains. This event reactivated major NW-SE striking faults and - arguably - major (ore)fluid pulses, associated with such fault movement. Spatial coincidence of major ore zones with intersections of NW-SE faults and fertile basement rocks additionally support our late, epigenetic metallogenetic model.

[1] Besse & Courtillot (2002) *J Geophys Res* **107**, 1-31. [2] Jowett *et al* (1987) *J Geophys Res* **92**, 581-598.

$\delta^{13}C_{carbonate}$ chemostratigraphy of the Carrapateira Outlier (Lower Kimmeridgian), Southern Portugal

M. BORGES[1]*[,2], R. GOOGHUE[3], P. FERNANDES[1], Z. PEREIRA[2], V. MATOS[1] AND B. RODRIGUES[1]

[1]CIMA, University of Algarve, 8005-139 Faro, Portugal, (*correspondence: marisa.borges@lneg.pt)

[2]LNEG, 4466-901 S. Mamede de Infesta, Portugal, (zelia.pereira@lneg.pt)

[3]Department of Geology, Trinity College Dublin, Ireland (goodhuer@tcd.ie)

The Carrapateira Outlier (CO) located 20 km north of Sagres is formed by Upper Triassic to Kimmeridgian sediments. The studied section is located at Três Angras bay and consists of approximately 50 m of limestones interbedded with marls, assigned to the Early Kimmeridgian based on corals, foraminifera and dinoflagellate cysts. The uppermost limestone beds are rich in macrofossils with well-preserved corals in life position. To compile $\delta^{13}C$ chemostratigraphy for this section, sixty five bulk carbonate samples were studied.

The $\delta^{13}C$ values vary gradually throughout the succession showing a baseline with a general decreasing trend up section, ranging from 1,59‰ to -0.68‰. However, the $\delta^{13}C$ curve indicates two main negative $\delta^{13}C$ excursions, the first related to a coarse grained interval with a minimum value of -1.38‰ and a second excursion with a minimum value of -3,10‰, immediately below the bioclastic rich beds of the top of the section. In general, the decreasing baseline trend agrees with the global $\delta^{13}C$ curve for the Kimmeridgian in the Tethyan Realm, where the CO was located. The two negative excursions are tentatively related to regional perturbations in the carbon cycle. Hence, both are interpreted as a result of large input of ^{12}C to the basin as a result from regressive pulses as suggested by the sedimentological and palynofacies analysis studied.

Acknowledgments: This study was sponsored by FCT (PhD grant SFRH/BD/48534/2008).

https://doi.org/10.1180/S0026461X00006502 Published online by Cambridge University Press

Pyroxenites in peridotites from External Liguride ophiolites (Italy): Insights on small scale heterogeneities in MORB mantle

G. BORGHINI[1,2], E. RAMPONE[1], A. ZANETTI[3], C. CLASS[2], A. CIPRIANI[2], A.W. HOFMANN[2,4] AND S.L. GOLDSTEIN[2]

[1]DIPTERIS, Università di Genova, Corso Europa 26, 16132 Genova, Italy
[2]Lamont-Doherty Earth Observatory, Palisades NY 10964, USA
[3]CNR-Istituto di Geoscienze e Georisorse, Sezione di Pavia, via Ferrata 1, I-27100 Pavia, Italy
[4]Max Planck Institute for Chemistry, P.O. Box 3060, 55020 Mainz, Germany

The occurrence of mafic layers in peridotites constitutes an important compositional heterogeneity in the mantle, and their role in mantle melting and basalt generation is currently debated. We present field, chemical and isotopic data on pyroxenites and host peridotites from the western peridotite massifs of the External Liguride ophiolitic Units (Northern Apennines, Italy). Pyroxenites (mostly spinel-websterites) occur as cm-thick bands (up to 12 cm) parallel to the tectonite mantle foliation, and ,together with the peridotites, they are partially recrystallized at plagioclase-facies conditions. Whole-rock and mineral compositions are extremely heterogeneous, covering almost the entire compositional range of worldwide lithospheric pyroxenites (Mg# = 74-88, Al_2O_3 = 10-17 wt%, CaO = 7-20 wt%). The pyroxenite chemistry reflects high-pressure magma segregation of tholeiitic melts dominated by clinopyroxene crystallization. A multi-step, sequential leaching procedure on clinopyroxene separates enables us to remove partial contamination and provides reliable Sr isotope data. The Sr and Nd compositions of clinopyroxenes from pyroxenites and peridotites fall in the typical range of normal MORB ($^{87}Sr/^{86}Sr$ =0.7023-0.7029; $^{143}Nd/^{144}Nd$ =0.5134-0.5128). Internal Sm-Nd isochrons on plagioclase-clinopyroxene pairs from two pyroxenites yield ages of 183±14 Ma and 177±12 Ma for the low-P mantle exhumation. On a slightly larger spatial scale, chemical and isotopic profiles through the pyroxenite-peridotite boundaries indicate cm-scale modification of the wall-rock peridotite, presumably related to emplacement of the pyroxenites. This suggests that deep melt intrusion can locally modify the host peridotites and introduce small scale compositional heterogeneity in a MORB mantle.

Heating organoclays: Does it affect their potential to interact with organic compounds in aqueous environment?

M. BORISOVER[1]*, S. YARIV[2], N. BUKHANOVSKY[1] AND I. LAPIDES[2]

[1]The Institute of Soil, Water and Environmental Sciences,The Volcani Center, ARO, Bet Dagan, Israel (*correspondence: vwmichel@volcani.agri.gov.il)
[2]Institute of Chemistry, The Hebrew University of Jerusalem, Edmund Y. Safra Campus, Jerusalem, Israel

By replacing inorganic exchangeable cations in clay minerals with organic cations, hydrophilic mineral/water interfaces may be converted to organoclay interfaces of variable and controlled lipophilicity. This paper summarizes the data on aqueous sorption of a series of organic compounds on organoclays preheated at different temperatures [1]. Sorptive properties of thermally treated organoclays are of interest since: (1) they can shed light on mechanisms of organic compound - organoclay interactions; (2) the thermal treatment is considered as a tool to regenerate organoclays after their use in different environmental applications; (3) thermally treated organoclays can provide a model for examining such important environmental issue, as fire-affected soils. Thus, organoclays were (*i*) prepared from the Na-montmorillonite rich bentonite with a series of quaternary ammonium salts and freeze-dried, (*ii*) heated during two hours in air at different temperatures, from 150 ^{0}C to 420 ^{0}C, and (*iii*) characterized by C/N, FTIR, XRD, TG-DTG and surface area analyses. Mild preheating of organoclays at 150 ^{0}C was not associated with chemical changes in the sorbent structure but was able to enhance interactions with organic compounds present in water. The extent of this enhancement reflected the different abilities of organic sorbates to compete with water molecules for sorption sites on organoclays. This observation supported the earlier idea that the partial, incomplete hydration of preheated organoclays can be a reason of increased organic sorbate – organoclay interactions [2,3]. Yet, there is no clear understanding why this rehydration of preheated organoclays is partial. When organoclays were heated at higher temperatures, the significant changes in the organoclay chemistry did not result in the remarkable loss of the organoclay sorptive potential towards organic compounds present in aqueous solution.

[1] Borisover *et al*. (2011) *Appl. Clay Sci*. (in submission).
[2] Borisover *et al*. (2010) *Appl. Surf. Sci*. **256**, 5539-5544.
[3] Borisover *et al*. (2010) *Adsorption* **16**, 223–232.

https://doi.org/10.1180/S0026461X00006502 Published online by Cambridge University Press

Uranium, thorium and REE in macrofungi from pristine and polluted sites

JAN BOROVIČKA[1,2]*, JAROSLAVA KUBROVÁ[3], JAN ROHOVEC[1] AND ZDENĚK ŘANDA[2]

[1]Institute of Geology, v.v.i., Academy of Sciences of the Czech Republic, Rozvojová 269, CZ-165 00 Prague 6 (*correspondence: borovicka@gli.cas.cz)
[2]Nuclear Physics Institute, v.v.i., Academy of Sciences of the Czech Republic, Řež 130, CZ-250 68 Řež near Prague
[3]Institute of Environmental Studies, Faculty of Science, Charles University, Benátská 2, CZ-128 01 Prague 2

In recent years, interest in the biogeochemical roles of fungi in the environment has increased rapidly. Part of this research involves studying the ability of macrofungi to accumulate trace elements in fruit-bodies. Available data on some elements are rather scant or even equivocal. Specifically, ambiguous data have been reported for U, Th and REE. Since recent studies highlighted the possible role of fungi in the environmental biogeochemistry of U (Fomina *et al*. 2007, Env. Microbiol. 9: 1696-1710), there is an obvious need for more knowledge of macrofungal ability to accumulate U.

We have determined concentrations of U, Th and REE (HR-ICP-MS) in a representative set of macrofungi from unpolluted sites with differing bedrock geochemistry. Analytical results are supported by use of certified reference materials and the reliability of the determination of U was verified by epithermal neutron activation analysis (ENAA).

It appears that some data recently published on these elements are erroneous, in part because of use of an inappropriate analytical method; and in part because of apparent contamination by soil particles resulting in elevated levels of Th and REE. Macrofungi from unpolluted areas, in general, did not accumulate high levels of the investigated metals. Concentrations of U and Th were generally below 30 and 125 ng g^{-1} (dry weight), respectively. Concentrations of REE in macrofungi did not exceed 360 ng g^{-1} and their distribution more or less followed the trend observed in post-Archean shales and loess.

Concentrations of U in macrofungi from mine tailings and U-polluted forest plantations in the former Příbram mining district (Central Bohemia, Czech Republic) were significantly elevated but rather low; the highest values were in lower units of μg g^{-1}.

This research was supported by the Grant Agency of Charles University (project 3010) and the Czech Science Foundation (project P504/11/0484).

The roentgenoluminescence of feldspars from granitoids of the Kolyvan'-Tomsk folded belt as a typomorphic character

N.N. BOROZNOVSKAYA, T.S. NEBERA, S.I. KONOVALENKO, A. BAYOVA AND O. ZHEREBETSKAYA

Tomsk State University, Tomsk, Russia

Basic luminogens within the earth's crust, 92 % of which is formed of silicates, are defects in silicon-aluminum-oxygen tetrahedron (O^-) and isomorphic admixtures instead of K, Na, Ca, Mg, Al, Si (Tl^+, Pb^{2+}, Mn^{2+}, Fe^{3+}, Cr^{3+} and rare earths). L of O^- defects may be regarded as background. Its intensity is often determined by presence of decay structures and cooling rate. L of impurity defects in the earth's crust minerals depends on formation conditions (depth, crystallization temperature and cooling rate). The study has been carried out on the roentgenoluminescence spectra in the wavelength optical range (250-900 nm) in common potash feldspars (CPFS) and plagioclases from granitoids of the Kolyvan'-Tomsk folded belt (KTFB). Feldspars (FS) from all rock diversities of the Kolyvanskiy, Barlakskiy, Obskoy and Novosibirskiy massifs situated in the western part of KTFB nearby the Novosibirsk Trough have been the object of the investigation. The cause and effect relationship has been ascertained between the composition, structural ordering, crystallochemical characteristics and luminescence of the feldspars under consideration. The RL spectra of the Barlakskiy, Obskoy and Kolyvanskiy feldspar massifs are of similar character and result from the slow cooling in the conditions between the average and hypabyssal depths. The peculiarities of the RL spectra of the FS granitoids of the Novosibirskiy massif suggest the quick cooling of these rocks in the conditions of shallow depths or of the tectonically active zone (in the zone of crush). The dominating and extremely intensive RL of Fe^{3+} in the rocks of all massifs is frequently indicative of the existence of the hyperalkaline silicate melt for all objects under consideration. The presence of the Tl^+ RL with the maximum of 285 nm is the distinctive property of leucogranites from the Kolyvanskiy and Barlakskiy massifs, suggests the presence of the rare metal mineralization and is applicable as a typomorphic character. *These researches have been supported by the Ministry of Education and Science of Russia*.

Putative Cryogenian ciliates from Mongolia

TANJA BOSAK[1], FRANCIS MACDONALD[2], DANIEL G. LAHR[3] AND EMILY D. MATYS[4]

[1]EAPS MIT, Cambridge MA 02139, tbosak@mit.edu
[2]EPS, Harvard University, MA 02138, fmacdon@fas.harvard.edu
[3]Graduate Program in Organismic and Evolutionary Biology, UMass Amherst, MA 01003, daniel.lahr@gmail.com
[4]EAPS MIT, Cambridge MA 02139, ematys@mit.edu

Major lineages of modern eukaryotes, represented primarily by microscopic taxa, are thought to have originated during the Neoproterozoic. However, microfossils older than 635 Ma rarely bear unambiguous relationships to modern microscopic eukaryotes.

Here we report exceptionally preserved 715-635 million year old eukaryotic tests in limestone strata of Mongolia. These structures are most abundantly preserved within rhythmite and ribbonite strata that record a large negative anomaly in $\delta^{13}C$ of both carbonate and organic matter.

The ~100 μm long organic-rich three-dimensional tests have flask-like shapes, constricted necks, distinct and often thickened collars. The test walls are flexible, composed of densely packed alveolar structures and stainable by dyes that react with polysaccharides. The combined morphological and ultrastructural properties of the Cryogenian tests are remarkably similar to the lorica of modern group of planktonic ciliates, tintinnids.

The presence of putative tintinnids in the pre-635 Ma strata places an upper bound on the divergence of ciliates, marks the increasing diversity of phagotrophic eukaryotes during this time and suggests a reorganization of Cryogenian foodwebs. The advent of planktonic organisms forming recalcitrant organic or mineral-rich tests may have increased export and burial fraction of organic carbon, driving an increase in atmospheric oxygen and the subsequent radiation of metazoans.

Origin and signficance of basic and ultrabasic outcrops from northeastern algeria (Edough massif)

D. BOSCH[1], D. HAMMOR[2], O. BRUGUIE[1], R. CABY[1], AND M. MECHATI[2]

[1]University Montpellier 2, Place Eugene Bataillon 34095, Cedex 05, France (bosch@gm.univ-montp2.fr)
[2]Université Badji-Mokhtar, BP12, El-Hadjar, Annaba 23 000, Algeria

The Maghrebian, Betics and Apenninic chains outcrop around the mediterranean basin and constitute dismembered fragments of the Alpine orogen. Conflicting geodynamic models have been proposed in order to explain the different paleogeographic settings from which these fragments derived. Crust-mantle interactions following subduction of Jurassic oceanic crust and collision-related tectonic events of Eocene age in relation to the northward motion of Africa have been demonstrated by numerous works. The incorporation of mafic/ultramafic rocks into the basement is evidenced in various peri-mediterranean areas, in particular at c. 22 Ma. This work is focused on the basic and ultrabasic rocks from the easternmost internal part of the Maghrebides. An extensive petrological and geochemical study has been performed on three distinct outcrops, i.e. Bou Maiza gabbros, amphibolites from La voile Noire and Sidi Mohamed peridotites. Peridotites display a primitive character (Mg number >85), but slightly enriched trace elements patterns (1 to 10 times CHUR) characterized by negative Nb anomalies and flat to slightly LREE-depleted patterns. Associated isotopic constraints suggest a possible continental contamination of the peridotites by the surrounding gneisses. These ultrabasic rocks are interpreted as parts of the lithospheric mantle incorporated into the continental crust during a late Burdigalian extensional event that opened the Algerian basin. The Bou Maiza gabbros and La Voile Noire amphibolites show complementary trace elements spectra suggesting derivation from a common MORB source reservoir, but without filiation with the Sidi Mohamed peridotites. Such affinities suggest they represent a fragment of the Neothetys lithosphere obducted onto the North African margin during Miocene times.

https://doi.org/10.1180/S0026461X00006502 Published online by Cambridge University Press

Natural analogue of CO_2 mineral sequestration: The Tuscan magnesite deposits

C. BOSCHI[1], L. DALLAI[1], A. DINI[1] AND G. RUGGIERI[2]

[1]Istituto di Geoscienze e Georisorse, CNR, Pisa, Italy
[2]Istituto di Geoscienze e Georisorse, CNR, Firenze, Italy

The magnesite deposit of Malentrata (Tuscany, Italy) was derived from silicification–carbonation of Ligurian serpentinites embedded in pelite-carbonate formations, and represents a natural analogue of *in situ* CO_2 mineral sequestration. Serpentinites were transformed to a brownish friable mineral assemblage of opal, chromian montmorillonite, Fe-rich magnesite and minor iron sulfides and oxides. The serpentinite alteration was accompanied by the formation of magnesite and dolomite veinlets, and large magnesite–dolomite veins along major tectonic structures. The major veins are characterized by the following crystallization sequence: i) early magnesite, ii) green and late pale-brown dolomite cementing the early brecciated magnesite vein infill, and iii) late quartz, chalcedony and opal. The observed mineral assemblage is indicative of low temperature hydrothermal alteration driven by Si- and CO_2-rich fluids under relatively low pH conditions. Geochemical data along transects from carbonated host rocks to carbonate-silica veins suggest a marked variation of fluid composition through the main stages of precipitation. Dolomites are more enriched in Cr, Sr, Y, U and REE with respect to magnesites. Magnesites are the most REE-depleted, whereas green dolomites show quite flat enriched patterns approaching the pattern of sedimentary formations. $\delta^{18}O$ of magnesites range from 23 to 32‰, and $\delta^{13}C$ from -2 to 0‰. Both dolomite types are depleted in $\delta^{18}O$ with respect to magnesite, especially late pale-brown dolomite. $\delta^{13}C$ of dolomites is similar to magnesite with slightly lower values in green dolomites. It seems to be conceivable that fluids first interacted with serpentinites precipitating magnesite. After the magnesite precipitation, fluids interacted with the sedimentary formations, becoming progressively enriched in calcium and REEs, and depleted in $\delta^{18}O$ due to the partial equilibration with the pelite portion. At this stage dolomite precipitation recorded geochemical variations of fluids. Malentrata deposit lies at the periphery of Larderello geothermal field and it highlights the near surface local interaction between low temperature fluids and serpentinite bodies in favourable tectonic conditions.

Deciphering arsenic sources in surface waters and the role of bacterial oxidation

A. BOSSY[1]*, C. GROSBOIS[2], C. JOULIAN[3], F. BATTAGLIA-BRUNET[3] AND A. COURTIN-NOMADE[1]

[1]EA GRESE, Limoges Univ., 87060 Limoges, France (*correspondence: angelique.bossy@etu-unilim.fr)
[2]UMR 6113 CNRS ISTO, Tours Univ., 37000 Tours, France
[3]Process and Environment Division, BRGM, 45060 Orléans, France

In a geochemical anomaly in As, different potential As contributions to stream waters, such as groundwaters, runoff and As-bearing phase weathering present within the soils were studied with a high sampling frequency. It allowed deciphering the contribution of each compartment to As contamination of surface waters. The role of indigenous bacteria in As oxidation state in ground- and surface waters was also studied in laboratory.

In the soil profile, total As concentrations indicated depletion (1500 to 385 $mg.kg^{-1}$) during pedogenesis relative to a mineralogical evolution of As-bearing phases upwards the soil profile: from arsenates (Ba-rich pharmacosiderite: 14-26 wt.% As) to Fe-oxyhydroxides (ferrihydrite-like: 4-16 wt.% As; ferrihydrite-type, hematite and goethite: <3 wt.% As). Conversely, an increase of dissolved As concentrations (15-52 $\mu g.L^{-1}$) was observed in soil solutions.

In stream waters, As concentrations (7.5 to 69.4 $\mu g.L^{-1}$) were attributed to several inputs: (i) runoff and soil solutions, (ii) waters from former adits (97-120 $\mu g.L^{-1}$ As), (iii) wetland and groundwaters (up to 169 and 215 $\mu g.L^{-1}$ As, respectively). The latter inputs were characterized by dissolved As(III) during low flow period which was rapidly oxidized, suggesting the contribution of bacterial oxidation.

Bacterial As oxidation tests showed a decrease of dissolved As(III) concentrations in stream and wetland waters (-17% and -41%, respectively). In groundwaters, a stronger decline for dissolved As(III) (-95% in 15 h) was observed, then followed by an As(III) release (+51%), suggesting the presence of As(V)-respiring bacteria. The study of the As(III)-oxidizing bacterial community (PCR-DGGE method on *aoxB* genes, a genetic marker of these bacteria), showed a divergence in the community structure between (i) surface and wetland waters, and (ii) groundwaters, probably due to variable As concentrations, redox conditions and bacteria number.

https://doi.org/10.1180/S0026461X00006502 Published online by Cambridge University Press

The effect of Cl on the solubilty of Au and Pd in andesitic melts

R.E. BOTCHARNIKOV[1]*, R.L. LINNEN[2], M. GUILLONG[3], F. HOLTZ[1] AND V.S. KAMENETSKY[3]

[1]Institut für Mineralogie, Leibniz Universität Hannover, Callinstr. 3, D-30167, Hannover, Germany (*r.botcharnikov@mineralogie.uni-hannover.de)
[2]Department of Earth Sciences, BGS 1000B University of Western Ontario, London, ON, N5A 5B7 Canada
[3]ARC Centre of Excellence in Ore Deposits, University of Tasmania, Hobart, Tasmania, 7001 Australia

Chlorine is considered as an important agent responsible for the mobilization and transport of metals in magmatic systems associated with porhyry ore mineralization and with late-stage metal-rich horizons of large igneous intrusions. In the former case, the considerable role of Cl is confirmed by the observation that fluid inclusions associated with porphyry ores are often composed of low-salinity aqueous vapor and high-salinity brines, whereas in the later case it is believed that the mobility of metals in different horizons of layered intrusions might have been controlled by the general process of chromatographic separation of metals during migration and evolution of Cl-enriched fluids. Since at given magmatic conditions the mobility and transport of metals by exsolving Cl-bearing fluid phase(s) is presumably dependent on chemical potential of metal components complexing with Cl in silicate melt, quantitative experimental data on metal solubility in melts and melt-fluid partitioning are required.

Here we report the results of experiments on the solubility of Au and Pd in andesitic melts equilibrated with $Au_{80}Pd_{20}$ capsule material at 1200°C, oxidizing conditions (FMQ+3) and pressures in the range from 50 to 500 MPa as a function of Cl content in the system. Due to non-ideality of mixing in Cl-bearing fluids, the investigated systems are characterized by coexistence of andesitic melts with vapor, vapor+brine, brine, or supercritical single-phase fluid, depending on the bulk Cl content and P. The obtained data show that an addition of Cl to the system increases significantly the solubility of both metals in the silicate melt at all investigated pressures, in particular in melts coexisting with brine or supercritical fluid. The concentration of Au increases from 1-2 upto 40-50 μg/g, whereas the concentration of Pd increases from 0.1 to 20 μg/g with increasing Cl content of the melt from 0 to 2.5 wt%. Since the calculated activity coefficients of Au and Pd in the $Au_{80}Pd_{20}$ capsule are both close to 0.7, the solubility values of pure metals should be slightly higher. The results clearly show that Cl can indeed control on the mobility of Au and Pd in natural magmas.

The transformation of ACC to vaterite; An *in situ* SAXS/WAXS study

P. BOTS[1]*, J.D. RODRIGUEZ-BLANCO[1], T. RONCAL-HERRERO[1,2], S. SHAW[1] AND L.G. BENNING[1]

[1]School of Earth and Environment, University of Leeds, LS2 9JT, United Kingdom (*eepbo@see.leeds.ac.uk)
[2]Department of Geosciences, University of Oslo, PB 1047, Blindern, Oslo, Norway.

Vaterite (μ-$CaCO_3$) is rarely observed in natural systems, as it is thermodynamically unstable with respect to calcite and aragonite [1]. However, some organisms produce and stabilize vaterite as biominerals [2]. At high supersaturation vaterite forms via a nanoparticulate, poorly-ordered and metastable precursor, amorphous calcium carbonate (ACC). In the pure system, ACC transforms to vaterite within minutes, and subsequently to calcite [3]. The detailed mechanisms of the ACC to vaterite transformation are however still lacking due to the fast kinetics of this first step of crystallization. In this study we demonstrate the use of *in situ* time-resolved synchrotron-based Small- and Wide-angle X-ray Scattering (SAXS/WAXS) combined with off-line characterization to quantify the kinetics and crystallization mechanisms of vaterite at fast time scales.

The SAXS/WAXS data collected at 1 second / frame for up to 32 minutes, revealed that the ACC to vaterite transformation occurs in 3 stages. The initial stage (0-2 min) was governed by ACC precipitation and growth (to Ø ~ 38 nm). During this stage ~70 % of the total vaterite (Ø ~ 10 nm) formed via spherulitic growth at the expence of the metastable ACC [4]. The end of the spherulitic growth (at 2 min) was concomitant with a drop in supersaturation below the limit for spherulitic growth of vaterite (SI≈1.4 [4]). During the 2nd stage (2-7 min), remnant ACC lead to a further increase of the amount of vaterite (~30 %) due to ACC dissolution and vaterite nanocrystal reprecipitation. During this stage the vaterite crystallite size increased from ~10 to ~35 nm. Finally during the 3rd stage (> 7 min), no *de nuovo* precipitation of vaterite occurred, however the vaterite crystallite size continued to increase reaching ~60 nm at the end of the experiment (32 min). This increase in crystallite size was solely governed by Ostwald Ripening.

[1] Plummer L.N. and Busenberg E. (1982) *GCA* **46**, 1011-1040. [2] Lowenstam (1981), *Science* **211**, 1126-1131, [3] Rodriguez-Blanco, J.D. *et al* (2011) *Nanoscale* **3**, 265-271, [4] Andreassen, J.P. (2005) *J. Cryst. Growth* **274**, 256-264.

https://doi.org/10.1180/S0026461X00006502 Published online by Cambridge University Press

Understanding late accretion on the Earth, Moon, and Mars

W.F. BOTTKE[1], R.J. WALKER[2], J.M.D. DAY[3], D. NESVORNY[1] AND L. ELKINS-TANTON[4]

[1]Southwest Research Institute & NASA Lunar Science Institute, Boulder, CO, USA (bottke@boulder.swri.edu)
[2]Dept. of Geology, University of Maryland, College Park, MD 20742, USA
[3]Geosciences Research Division, Scripps Inst. Oceanography, La Jolla, CA 92093 USA
[4]MIT, Cambridge MA 02139 USA.

Highly siderophile elements (HSE) have low-pressure metal-silicate partition coefficients that are high [$>10^4$]. It is assumed the silicate portions of rocky planetary bodies with metallic cores are effectively stripped of HSE immediately following primary accretion and final core segregation. Accordingly, the 'giant impact' on Earth that formed the Moon should have cleansed HSE from the mantles of both worlds.

Curiously, the Earth and Moon (and Mars) have disparate, yet elevated HSE abundances. We argue late accretion may provide a solution, provided that ≥ 0.5% Earth masses of broadly chondritic planetesimals reaches Earth's mantle, and that ~10 and ~1,200 times less mass go to Mars and the Moon, respectively [1]. Our models show that leftover planetesimal populations dominated by massive projectiles can explain these additions, with our inferred size distribution matching those derived from the inner asteroid belt, ancient martian impact basins and planetary accretion models. The largest late terrestrial impactors, at 2,500-3,000 km in diameter, potentially modified Earth's obliquity by ~10°, while those for the Moon, at ~250-300 km, may have delivered water to its mantle.

To keep the iron core from such a large projectile sequestered in Earth's mantle, HSE delivery there may involve a "hit and almost run" collision. Here most of the projectile's core (and HSE) plows through the target mantle and emerges on the other side in a highly-fragmented state. The debris then evolves into a long spiral-arm-like structure that rains down across the target. These events may allow massive impactors to deliver large quantities of HSE, but in a manner akin to small body accretion that optimizes emulsification into the upper mantle. This potentially explains why mantle peridotites have similar HSE abundances and how the iron in the projectile's core became oxidized.

[1] Bottke *et al*. (2010) *Science* **330**, 1527-1530.

Direct Injection Nebulization with MC-ICP-MS: Performances and prospects

J. BOUCHEZ*[1,2], P. LOUVAT[1], G. PARIS[2,3], J. GAILLARDET[2] AND J. MOUREAU[2]

[1]IPG Paris (UMR CNRS 7154), Université Paris Diderot, 1 rue Jussieu, 75252 Paris Cedex 05, France
[2]GFZ, Telegrafenberg, Potsdam, Germany (*correspondence: bouchez@gfz-potsdam.de)
[3]CalTech, Pasadena CA 91125, USA

The advent of MC-ICP-MS during the last decade has considerably improved isotope ratio measurements in terms of accuracy, precision, reproducibility and rate of sample throughput. Nevertheless, the search continues for more efficient, more stable, more sensitive and cleaner introduction systems. This is particularly true for (1) "sticky" elements displaying long washout times (2) volatile elements whose sensitivity cannot be improved by desolvation systems.

Boron belongs to both categories. Recent development of the d-DIHEN [1] (demountable Direct Injection High Efficiency Nebulizer) allows for faster and more precise determination of boron isotope ratio by MC-ICP-MS [2]. The principle of direct injection is to place a long quartz nebulizer in the plasma torch, spraying the sample directly into the plasma.

Using d-DIHEN along with Neptune MC-ICP-MS, sensitivity of 10 V/ppm (at an uptake rate of 30 μL/min) are obtained, with washout times of 2 to 3 minutes to reach background levels of less than 1 ‰ of the previous sample signal. Recent automation using a SC sampler and the FAST system (ESI) allows for systematic triplicate measurements of each sample, thereby improving the reproducibility to less than 0.2‰ (2 S.D.) in most cases. Performances obtained with the improved interface pumping capacity along with a Teflon spray chamber will also be presented for comparison.

Li isotope measurements with d-DIHEN yield reproducibilities similar to the ones obtained with the APEX desolvation system (ESI), despite a lower sensitivity and rounder peak shape, while allowing for faster measurements because of shorter washout times.

At this level of precision, drastic intensity matching between standards and samples appears to be highly critical, and has to be within 5%. Forthcoming improvements seem to lie in even more drastic chemical purification procedures.

[1] Westphal, Kahen, Rutkowski, Acon & Montaser (2004) *Spectrochimica Acta* **59,** 353-368. [2] Louvat, Bouchez & Paris (2011) *Geostandards and Geoanalytical Research* **35**, 75-88.

https://doi.org/10.1180/S0026461X00006502 Published online by Cambridge University Press

Experimental investigation of the stability of Fe-rich carbonates in the lower mantle

E. BOULARD[1], N. MENGUY[1], A.L. AUZENDE[1], K. BENZERARA[1], H. BUREAU[1], D. ANTONANGELI[1], A. CORGNE[1,2], G. MORARD[1], J. SIEBERT[1], J.P. PERRILLAT[3,4], F. GUYOT[1] AND G. FIQUET[1]

[1]Institut de Minéralogie et de Physique des Milieux Condensés, Paris, France
[2]Institut de Recherche en Astrophysique et Planétologie, Toulouse, France.
[3]European Synchrotron Radiation Facility, Grenoble, France
[4]Université de Lyon 1, Villeurbanne, France

Carbonates are the main C-bearing minerals that are transported deep in the Earth's mantle via subduction of the oceanic lithosphere [1]. The fate of carbonates at mantle conditions plays a key role in the deep carbon cycle. Decarbonation, melting or reduction of carbonates will affect the extent and the way carbon is recycled into the deep Earth.

High-pressure high-temperature experiments were carried out up to 105 GPa and 2850 K on oxide assemblages of (Mg,Fe)O + CO_2. The presence of $Fe^{(II)}$ in starting materials induces redox reactions from which $Fe^{(II)}$ is oxidized and a part of the carbon is reduced. This leads to an assemblage of magnetite, diamonds, and carbonates or, pressure depending, their newly discovered $Fe^{(III)}$-bearing high-pressure polymorphs based on a silicate-like chemistry with tetrahedrally coordinated carbon [2]. Our results show the possibility for carbon to be recycled in the lowermost mantle and provide evidence of a possible coexistence of reduced and oxidized carbon at lower mantle conditions.

[1] Sleep, N. H., and K. Zahnle (2001) *J. Geophys. Res.-Planets* **106**(E1), 1373-1399. [2] Boulard *et al*. (2011) *PNAS*, **108**, 5184-5187.

Advances in high precision Ca isotope ratio measurements using TIMS

CLAUDIA BOUMAN*, DIETMAR TUTTAS, MICHAEL DEERBERG AND JOHANNES SCHWIETERS

Thermo Fisher Scientific, Hanna-Kunath-Str. 11, 28199 Bremen, Germany.
(*correspondence: claudia.bouman@thermofisher.com)

Ca isotopes are used in various disciplines within Earth Sciences, e.g. paleoceanography, geochronology and biogeochemistry. Precise and reproducible measurements of Ca isotopes are among the most challenging measurements within TIMS. Most important factors influencing the precision and reproducibility are sample loading, choice of double spike, instrumental mass fractionation and mass spectrometer performance. Advances in mass spectrometry have been made with the introduction of the TRITON *Plus*.

The TRITON *Plus* has innovative features that enable high precision Ca isotope ratio measurements for all Ca isotope ratios. First of all, the TRITON *Plus* enables simultaneous collection of 40Ca up to 48Ca without zoom due to the extended mass dispersion. Also, the instrument can house different ohmic resistors (10^{10}, 10^{11} and 10^{12} Ohm). This is especially useful for isotope systems with a large dynamic range, such as Ca, where the abundance of the major isotope is almost 97%. If smaller samples are analysed, the low-noise 10^{12} Ohm amplifiers are advantageous, since they show up to a factor of 3 improvement in signal/noise ratio over the standard 10^{11} Ohm current amplifiers.

In this contribution, we present basic performance features for the TRITON *Plus* with regard to Ca isotope ratio measurements, as well as precision and reproducibility for different sample sizes.

https://doi.org/10.1180/S0026461X00006502 Published online by Cambridge University Press

Alteration of oil by gas: Experiments in fused silica capillary capsules

J. BOURDET[1]*, P.J. EADINGTON[1], R.C. BURRUSS[2] AND I.-M. CHOU[2]

[1]CSIRO, CESRE, 26 Dick Perry Ave., Kensington, 6151, WA, Australia (*julien.bourdet@csiro.au)
[2]US Geological Survey, 956 National Center, Reston, VA 20192, USA

Reservoir case studies showed that the fluorescence of oil inclusion assemblages of current or palaeo-gas zone has patterns that are not seen in zones that have only been invaded by oil [1, 2]. It is suspected that a fraction of the oil is retained in the pores when oil is drained by gas and that molecules from this residual oil partionned in gas.

To attempt to reproduce the alteration of oil by gas, or gas-washing, we sealed small amounts of crude oil (59º, 42º or 33º API) and excess pure gas (methane, ethane, propane) in fused silica capillary capsules (FSCCs, [3]), with and without water. The UV-visible fluorescence spectra of oil phase(s) enclosed within the FSCCs were measured at temperatures of 20 to 100 ºC, and Raman and FT-IR spectra of the gas and oil phases were measured at 20ºC. With ethane and propane, the 33°API oil formed a new immiscible fluorescent liquid phase with fluorescence that is more blue than the initial oil, which became more yellow or disappeared or more blue when semi-solid residues formed. No or less solid residues formed in FSCCs without added water. Experiments with 59°and 42° API oil do not show immiscible hydrocarbon liquids. The fluorescence of those crude oils displays a yellow shift in presence of gas. Solid residues are minor.

We interpret for the residual oil (1) the decrease of fluorescence at short wavelengths (red-shift) as due to partitioning of low molecular weight aromatic molecules into the new immiscible liquid phase and/or vapour phase; (2) the decrease of fluorescence response at long wavelengths (blue-shift) as due to loss of high molecular weight aromatics by precipitation of solid residues; (3) the increase of fluorescence response at short wavelengths (blue-shift) as due to desorption of aromatics and resins from asphaltene. Water has effects on the precipitation of semi-solid residue and stability of oil phase in the lowest API gravity oil.

These results are consistent with the attributes of oil inclusions trapped in palaeo-oil zones that were displaced by gas and support the concept of gas-washing of residual oil.

[1] Eadington *et al*. (2008) *Geochim. Cosmochim. Acta* **72**, A236. [2] Bourdet *et al*. (2010) *Geochim. Cosmochim. Acta* **74**, A109. [3] Chou *et al*. (2008) *Geochim. Cosmochim. Acta* **72**, 5217-5231.

Conditions of metal-silicate segregration in the parent bodies of iron meteorites

BERNARD BOURDON

Laboratoire de Géologie de Lyon, CNRS, UMR 5276, Ecole Normale Supérieure de Lyon, France

While there has been extensive work on the conditions of core formation on Earth, little work has focused on the conditions of core formation in the parent bodies of iron meteorites. A major obstacle to addressing this question is that the bulk compositions of the parent bodies are unknown and the iron meteorites do not represent directly the metallic liquid that segregated from silicates. Rather the iron meteorite compositions reflect various degrees of crystallization and fractionation of metallic iron. In some cases, there can be more than one liquid making the modelling more difficult.

By making the assumption that the bulk composition of the parent bodies was chondritic for the refractory siderophile elements, one can obtain a rough estimate of the size of the core and then estimate the corresponding oxygen fugacity of the parent body. In addition, using experimental determinations of the partition coefficients between metal and silicate, one can reconstruct the temperature and pressure conditions of metal-silicate segregation for various parent bodies. Using this approach, one can also estimate the abundance of volatile siderophile elements in the parent bodies of magmatic iron meteorites.

Due to the large number of assumptions made in this modelling, one can only obtain estimates for the oxygen fugacities, pressures and temperatures during core formation of the iron meteorite meteoroids. In the case of the IIIAB meteorites, the oxygen fugacity is close to IW-1.1 while it is IW-0.8 for the IVA magmatic iron parent body, which confirms the more oxidized nature of these parent bodies compared with the Earth (IW-2). In the case of the IVA irons, the best match is obtained for a volatile depleted bulk composition and the conditions of metal segregation has to be less than 1 GPa with a temperature ranging between 1600 and 1800 K. The siderophile element abundance of IIIAB requires a slightly higher temperature range and similarly low pressure.

https://doi.org/10.1180/S0026461X00006502 Published online by Cambridge University Press

Molecular dynamics simulations of the electrical double layer on smectite clay surfaces

IAN C. BOURG AND GARRISON SPOSITO

Earth Sciences Division, Lawrence Berkeley National Lab, Berkeley, CA, USA (*correspondence: icbourg@lbl.gov)

We report new molecular dynamics (MD) simulation results elucidating the structure of the electrical double layer (EDL) on smectite surfaces contacting mixed NaCl-$CaCl_2$ electrolyte solutions in the range of concentrations relevant to pore waters in ocean sediments and in geologic repositories for CO_2 or high-level radioactive waste (0.34 to 1.83 mol_c dm^{-3}). Our simulations used methodologies known to correctly describe the structure and diffusion coefficients of water and solutes in smectite interlayer nanopores [1]. Our results confirm the existence of three distinct ion adsorption planes (0-, β-, and d-planes), often assumed in EDL models [2,3], but with two important qualifications: (1) the location of the β-, and d-planes are independent of ionic strength or ion type and (2) "indifferent electrolyte" ions can occupy all three planes. Charge inversion occurred in the diffuse ion swarm because of the affinity of the clay surface for $CaCl^+$ ion pairs. Therefore, at concentrations ≥ 0.34 mol_c dm^{-3}, properties arising from long-range electrostatics at interfaces (electrophoresis, electro-osmosis, co-ion exclusion, colloidal aggregation) will not be correctly predicted by most EDL models. Co-ion exclusion, typically neglected by surface speciation models, balanced a large part of the clay mineral structural charge in the more concentrated solutions. Water molecules and ions diffused relatively rapidly even in the first statistical water monolayer, contradicting reports of rigid "ice-like" structure for water on clay mineral surfaces.

[1] Bourg & Sposito (2010) *Environ. Sci. Technol.* **44**, 2085.
[2] Sverjensky (2006) *Geochim. Cosmochim. Acta* **70**, 2427.
[3] Goldberg *et al.* (2007) *Vadose Zone J.* **6**, 407.

Quantifying weathering and erosion rates using cosmogenic nuclides.

D.L. BOURLES, R. BRAUCHER AND L. SIAME

CEREGE, UMR 6635 CNRS-Aix-Marseille Université, BP 80, 13545 Aix-en-Provence Cedex 4, France

Quantifying chemical weathering and physical erosion rates, whose sum corresponds to denudation rates, is of great importance across a wide range of environmental science disciplines Until recently, this has nevertheless been difficult over millenial timescales. Accumulating within mineral grains exposed to cosmic ray secondary particles in the uppermost few meters of the Earth's surface, *in situ*-produced cosmogenic have provided opportunities to quantify on such timescales not only the mineral grains exposure duration near the surface, but also the rates of the processes bringing them to the surface and removing them from above it.

Corresponding to their build-up in the suitable mineral over thousands of years, the cosmogenic nulide concentrations measured in rocks, sediments or soils are relatively insensitive to short-term fluctuations and thus allow quantifying natural, long-term weathering and erosion rates. More, they permit to evidence landscapes that are not at natural steady state because affected by natural hazards (landslides) or by anthropogenic activities. Cosmogenic nuclides thus provide reliable methods to measure long-term average denudation rates in a wide range of settings and to point out any perturbations that may have disturbed them.

Through the presentation of pertinent case studies from notably Brasil, Taïwan and Africa, the following general types of denudation-related problems will be addressed: (i) denudation rates from rock surface samples; (ii) denudation rates from vertically mixed continental sediments; (iii) spatially averaged denudation rates.

https://doi.org/10.1180/S0026461X00006502 Published online by Cambridge University Press

Magma recharge and eruption processes at Volcán Llaima (Andean Southern Volcanic Zone, 38.7°S)

C. BOUVET DE MAISONNEUVE[1]*, M.A. DUNGAN[1], O. BACHMANN[2] AND F. COSTA[3]

[1]Earth Science Section, University of Geneva, 1205 Geneva, Switzerland (*correspondence: caroline.bouvet@unige.ch)
[2]Earth and Space Sciences, University of Washington, Seattle, WA 98195-1310
[3]Earth Observatory of Singapore, Nanyang Technological University, Singapore 639798

Volcán Llaima (38.7°S) is one of the most active volcanoes in Chile with over 50 eruptions since 1640. Periods of eruptive activity are generally characterized by a combination of violent Strombolian explosions and voluminous lava flows. A previous study based on whole-rock, mineral, and olivine-hosted melt inclusion compositions of basaltic-andesitic magma erupted during three different episodes revealed shallow magma storage (2-3 km depth) as mush (>50 vol% crystals) in multiple dike-like reservoirs. Further characterization of the olivine compositions and comparison of the lava and tephra yield information on magma recharge time scales and eruption triggering. Multi-element zoning patterns (Fe, Mg, Mn, Ca, Ni, Cr, Ti, Co, Sc, V, Y, Al, P) were measured by LA-ICP-MS in olivine crystals from tephra. Coherence in the zoning patterns between various traverses and crystals from the same eruption allow us to reliably identify multiple magma replenishment events and the time scales at which they occur. Most elements record the latest recharge event, which took place between 100 and 600 days before eruption, while others (e.g. V, Ti, and Sc) also preserve compositional oscillations in the crystal core which we interpret as older recharge events. Comparison of the lava and tephra reveal higher crystallinities (~50 vol% vs. ~30 vol%) and a greater fraction of more evolved (mush-derived) crystals in the lava than in the tephra. This suggests that shifts in eruptive style at Volcán Llaima are strongly affected by the ratio of volatile-rich magma recharge to resident mush. When this ratio is low, the crystallinity of the erupted magma is high, which implies that (1) the resistance to flow is large, and (2) a permeable volatile network is achieved early, thereby promoting volatile-loss and diminishing the magma buoyancy. When the fraction of recharge magma is large, the crystallinity of erupted magma is lower and bubbles will tend to couple with the magma, entraining it rapidly toward the surface and producing a Strombolian eruption.

The first 10 million years of the Solar System

A. BOUVIER

Arizona State University, School of Earth and Space Exploration, Tempe, AZ 85287, USA (correspondence: audrey.bouvier@asu.edu)

The initial conditions of the solar nebula and subsequent formation and evolution of the protoplanetary disk can be constrained using chronological and isotopic studies of meteorites and samples returned from space missions. Chronology of early Solar System processes at a sub-My resolution is based on the long-lived U-Pb and short-lived (e.g., ^{26}Al-^{26}Mg) radiogenic systems. The precision of isotopic dating has dramatically increased over the last decade with the development of new mass spectrometry techniques. The accuracy, nevertheless, relies on knowledge of the initial composition, the distribution of the isotope pairs throughout the nebula, possible late additions, and disturbances during planetary processes. The degree of heterogeneity of the solar nebula can be evaluated from isotopic variations found for some elements (e.g., Nd, Ni) in chondritic and differentiated meteorites. Recently, U isotopic variations measured in CAIs [1] revealed the presence of ^{247}Cm in the early Solar System and consequently required the adjustment of previous U-Pb dates. For example, the U-Pb and Al-Mg chronologies of the formation of CAIs relative to chondrules are important constraints for the lifetime of the protoplanetary disk but are discordant [e.g., 2,3]. This brings into question the use of some meteoritic samples as reference materials, and reinforces the need for high-precision U-Pb isotopic studies of planetary materials.

The presence of short-lived radionuclides (SLR) has implications for the astrophysical environment of the Solar System. It is essential to determine the initial abundances and distribution of SLR in the Solar System to understand their origin and transfer within the nebula and possibly the protoplanetary disk. In particular, the source(s) of ^{26}Al and ^{60}Fe in the Solar System need to be constrained more tightly. As the major initial radiogenic heat sources, these two isotopes played a crucial role in the formation and evolution of habitable planetary worlds. I will discuss the most recent advances in the chronology of primitive and differentiated meteoritic objects using the U-Pb and extinct radioactivities and how they affect our models for Solar System formation and planetary evolution.

[1] Brennecka *et al*. (2010), *Science* **327**, 449-451. [2] Amelin *et al*. (2010), *Earth Planet. Sci. Lett*. **300**, 343-350. [3] Bouvier and Wadhwa (2010), *Nature Geosci*. **3**, 637-641.

https://doi.org/10.1180/S0026461X00006502 Published online by Cambridge University Press

The formation of the angritic crust

A. BOUVIER*, G.A. BRENNECKA, M.E. SANBORN AND M. WADHWA

Arizona State University, School of Earth and Space Exploration, Tempe, AZ, 87287-1404, USA. (*correspondence: audrey.bouvier@asu.edu)

Angrites are a small group of basaltic meteorites which record the early stages of planetary formation and differentiation [1]. They are comprised of two main textural subgroups reflecting different cooling and metamorphic histories: fine-grained 'quenched' angrites (e.g., D'Orbigny), and coarse-grained 'plutonic' angrites (e.g., Angra dos Reis) [1]. The recently recovered angrite Northwest Africa (NWA) 6291 is suggested to be paired with NWA 2999; both have larger modal abundances of metal and spinel compared to other angrites [2, 3]. NWA 6291 contains fine- (FG) and coarser-grained (CG) lithologies comprised of pyroxene, anorthite, olivine, and spinel.

We measured trace element abundances and the $^{238}U/^{235}U$ ratio in a whole-rock (WR) sample of NWA 6291 (WR1, washed in 0.05M HCl). We processed 7 acid-washed WR powders prepared from the FG and CG lithologies and 3 pyroxene separates from the CG lithology of NWA 6291 for Pb isotopic analysis. The weak leachates (L_{1-3}) and all Pb column matrices of subsequent leachates (L_{4-8}) and residues (R) were recombined respectively for U separation and isotopic analysis. Analytical details are provided in [4,5]. The REE pattern is LREE-depleted (La/Yb_N=0.6), with HREE abundances at ~4×CI. The Th/U is ~3.5. The $^{238}U/^{235}U$ =137.754 for WR1, =137.785 for the recombined L_{1-3}, and =137.744 for the recombined L_{4-8} and R (±0.026, 2SD); these values are similar to those for other angrites [6].

The Pb-Pb internal isochron age of NWA 6291 (calculated using its measured $^{238}U/^{235}U$) is 4560.1 ±1.1 Ma (MSWD=2), identical to that of NWA 2999 [7] using $^{238}U/^{235}U$ =137.75. The incompatible element depletion in both these angrites relative to other quenched and plutonic angrites is attributed to lack of phosphate. Their similarities confirm their pairing and suggest a new angritic subgroup, while their ages indicate that crust formation on the angrite parent body began ~5 Ma after CAI formation, and continued for a period of ~6 Ma thereafter [4,7,8].

[1] Mittlefehldt *et al*. (2002) *MAPS* **37**, 345-369. [2] Gellissen *et al*. (2007) *LPSC* **38**, A#1612. [3] Connolly *et al*. (2006) *MAPS* **41**, 1383-1418. [4] Bouvier & Wadhwa (2010) *Nature Geosc*. **3**, 637-641. [5] Bouvier *et al*. (2011) *LPSC* **42**, A#2747. [6] Brennecka & Wadhwa (this conference). [7] Amelin & Irving (2007) *Work. Chron. Met. & Early Solar Syst*., A#4061. [8] Amelin (2008) *GCA* **72**, 221-232.

Interaction of small organic molecules with the calcite surface

N. BOVET*, M. YANG, M.P. ANDERSSON AND S.L.S. STIPP

Nano-Science Center, Department of Chemistry, University of Copenhagen, Denmark (*correspondence: bovet@nano.ku.dk)

Calcite ($CaCO_3$) is one of the most abundant salts in the Earth's crust. Its surface behaviour in the presence of liquids and gases controls its dissolution, precipitation, adsorption and desorption. To help understand these complicated phenomena, a fundamental understanding of surface/gas interaction is required.

In this work, we investigated the molecular interaction of small organic molecules with the {10.4} surface of calcite. X-ray photoelectron spectroscopy (XPS), a surface sensitive technique that allows quantitative and qualitative investigation of surfaces, and simulations using molecular dynamics (MD) and density functional theory (DFT) were applied to determine the geometry, coverage and bond strength of ethane, ethanol, t-butanol, carbon dioxide, acetic acid and glucose molecules on calcite.

A series of pristine calcite {10.4} surfaces, prepared by cleavage in vacuum, were examined with XPS while gases were leaked into the experimental chamber. We used the high resolution carbon 1s signal, which has significant energy shifts, to observe coverage of the organic molecules. We also measured the temperature of desorption for each species to estimate its bonding strength.

The results show that CO_2 molecules form the weakest bond with calcite, with a desorption temperature of –130 °C. Glucose forms the strongest bond among the molecules studied and does not desorb even at 560 °C. We also observed that all the molecules formed a compact layer on the surface, except ethane, which does not adsorb at all in our experimental conditions, exhibiting no affinity with calcite. The MD and DFT calculations parallel the experimental results, indicating that CO_2, alcohols and acetic acid form a well ordered monolayer on calcite.

We are using the information about the bonding of simple molecules on calcite to interpret interaction of more complex organic molecules, such as those that play a role in biomineralisation, adsorbing from solution and inhibiting calcite growth and recrystallisation.

https://doi.org/10.1180/S0026461X00006502 Published online by Cambridge University Press

Mineralogy and geochemistry of a potential CO_2 sequestration reservoir and seal system, Illinois Basin, USA

B.B. BOWEN[1]*, T. LOVELL[1], R. NEUFELDER[1], J. RUPP[2], J. BROPHY[3] AND R. LAHANN[2]

[1]Department of Earth and Atmospheric Sciences, Purdue University, West Lafayette, IN 47907 (*correspondence: bbowen@purdue.edu)
[2]Indiana Geological Survey, Bloomington, IN 47405
[3]Department of Geological Sciences, Indiana University, Bloomington, IN 47405

Increasing atmospheric CO_2 concentrations have resulted in numerous studies into methodolgies for sequestering antropogenic CO_2 in the subsurface. Demonstrations of geologic CO_2 sequestration in the Illinois Basin are targeted at the basal Cambrian Mount Simon Sandstone as the potenital reservoir and the overlying Eau Claire Formation as the primary seal. Characterizing the mineralogy and geochemistry of these formations is an essential step towards predicting how these units will perform as a storage reservoir and seal respectively. Ongoing investigations are focused on characterizing the mineralogical and geochemical composition of these formations utilizing core analysis, microscopy, x-ray diffraction, reflectance spectroscopy, stable isotope geochemsitry and major and trace element whole rock geochemical analysis. Minerals identified in the Mount Simon Sandstone include monocyrstalline and polycrystalline quartz, k-feldspar, illite, kaolinite, goethite, hematite, and calcite with minor zircon, muscovite, and biotite. The amount and spatial context of the mineral phases vary with depth and across the basin. Some of the minerals, such as k-feldspar and the iron oxides, occur as overgrowths and grain coatings, putting them directly in contact with pore-fluids. Principle mineral phases identified in the Eau Claire Formation include: quartz, k-feldspar, plagioclase feldspar, illite, glauconite, dolomite, ankerite, calcite, chlorite, pyrite, goethite, and hematite. The suite of minerals identified in both of these units includes both detrital grains and multiple generations of authigenic precipitates that suggest a burial history that has included multiple episodes of fluid-rock interactions. Detailed analysis of the geochemistry of specific mineral phases (e.g., stable isotopes, trace elements, etc.) can be used to determine the nature of the fluids that have interacted with these rocks in the past. These analyses help to constrain the role of fluids in the evolution of these formations, the current reactivity of the minerals present, and the potential changes that could occur with the introduction of CO_2 into the pore fluids.

Impacts and feedbacks: Are the PETM and Eocene hyperthermals relevant to future global change?

GABRIEL J. BOWEN

Purdue University, West Lafayette, IN 47907, USA (*correspondence: gabe@purdue.edu)

After more than two decades of study, significant uncertainty remains regarding the causes and mechanisms underlying Early Paleogene transient “hyperthermal” climate events such as the Paleocene-Eocene thermal maximum and Eocene Thermal Maximum-2. Despite a lack of consensus on key details such as the trigger for these events and sources of carbon to the ocean and atmosphere, these events are frequently invoked as being among the paleoclimate case studies most relevant to understanding our climate future. Given all the uncertainty, it’s fair to ask whether our current level of understanding of these events really has relevance to the study of the anthropogenic climate era.

I will make the case that by focusing on the impacts and feedbacks associated with Eocene hyperthermal events researchers have been able to demonstrate several key patterns that are of relevance to informing and testing models of future anthropogenic climate change. The foundation for this inference is the unequivocal result, supported most strongly by records of widespread deep-sea carbonate dissolution, that the PETM and other hyperthermals are distinguished first and foremost by the massive addition of CO_2 to the exogenic carbon cycle. Despite uncertainties regarding the source and amount of this CO_2, we can view the subsequent sequence of events for any hyperthermal as a realization of CO_2-driven global change.

Important impacts and feedbacks associated with hyperthermals have been identified in at least four different systems. First, observations have largely supported existing models for the centennial-to-millennial-scale dynamics of the carbon cycle in response to massive CO_2 release. Second, estimates of pCO_2 change have been used to suggest high equilibrium climate sensitivity relative to most IPCC models. Third, there is increasing evidence for continental-scale water cycle change that is broadly consistent with the predictions of global climate models. Fourth, to the degree it has been studied these events have been demonstrated to have widespread, if not always deleterious, impacts on the biota. Although many details remain to be resolved, our current state of knowledge of Early Paleogene hyperthermals enables tests, and should support refinement, of models for anthropogenic global change.

https://doi.org/10.1180/S0026461X00006502 Published online by Cambridge University Press

IsoMAP: A web-GIS workspace for modeling isotope ratios in the environment

GABRIEL J. BOWEN[1], JASON B. WEST[2], LAN ZHAO[1], CHRIS C. MILLER[1], TONGLIN ZHANG[1], ZHONGFANG LIU[1], HYOJEONG LEE[1], AND AJAY B. KALANGI[1]

[1]Purdue University, West Lafayette, IN 47907, USA (*correspondence: gabe@purdue.edu)
[2]Texas A&M University, College Station, TX 77843, USA

Researchers have amassed a vast quantity of data on the stable H and O isotope ratios of environmental waters during the past 6 decades, and these data have supported the development of numerous paleoenvironmental, paleoecological, and paleoclimatic proxies. As new analytical instrumentation supports the gathering of water isotope data at increasing rates, these measurements promise to spawn new approaches to studying our contemporary environment. A key element in the development and interpretation of H and O isotope-based applications is the development of models for water isotope data to describe and predict relationships between these parameters and environmental variables.

In order to support widespread access to large water isotope databases and facilitate modeling of water isotopes and their propagation into hydrological and biological systems we have developed a web-GIS workspace called IsoMAP (Isoscape Modeling, Analysis and Prediction; http://isomap.org). IsoMAP consists of a set of Graphical User Interface that runs within the user's internet browser, server-side databases that host and serve isotopic and climatic monitoring data and GIS layers, and codes supporting the development and use of statistical and process-based models for environmental isotope ratio variation. Working through the GUI, users can select data and specify model parameterizations, submit and manage jobs, and visualize, download, or publish output including statistical descriptions of models and map predictions of the geographic variation in environmental isotope ratios.

Potential and demonstrated applications of the current version of IsoMAP include quantification of water isotope/climate relationships for different regions and time periods, evaluation of the stability or difference in isotope/climate relationships among regions and times, calibration of H- and O-isotope based proxies, and interpretation of H and O isotope data from biological and geological materials as a geographic source tracer. Future updates will provide additional functionality such as forward-modeling of H and O isotopes in plant leaf water and biological compounds.

Tracking the evolution of phase changes in ilmenites in microbial fossilization experiments: Understanding the role of microbes in diagenesis

D.M. BOWER[1], A. KYONO[2] AND A. STEELE[1]

[1]Geophysical Laboratory, Carnegie Institution of Washington,Washington, D.C., 20015, (dbower@ciw.edu.asteele@ciw.edu)
[2]Division of Earth Evolution Sciences, University of Tsukuba, Tsukuba, Ibaraki 305-8572, Japan, (kyono@geol.tsukuba.ac.jp)

Ilmenite and related Fe-,Ti-oxides are ubiquitous components of beach sands and sedimentary rocks [1]. In many ancient sedimentary rocks, "fossil" microstructures that are used as biosignatures often contain mineral assemblages dominated by these metal oxides, and in some cases, are preserved along with trace amounts of graphitic carbon [2,3]. Passive microbial biomineralization occurs in a wide range of natural environments, and can dictate the types of minerals that precipitate [4]. Furthermore, complicated histories and atmospheric inputs also influence much of the mineralic makeup of the rocks present today. Thus, the assemblages in these rocks may not be the same as what was originally formed in the newly lithified sediments billions of years ago. To constrain the effects of microbial processes on diagenesis, phase changes in natural ilmenites (Fe_3TiO_4) were observed in the presence of microbes amd compared to those without microbes under laboratory controlled conditions of increasing temperatures. To identify the mineral phases in these samples, micro Raman spectroscopy, SEM, and XRD were used. Collectively, the results show a correlation bewteen Fe- and Ti-oxide phase changes and the presence of microbes under early diagenetic conditions (T<70ºC), where the precipitation of maghemite (γFe_2O_3) and magnetite (Fe_3O_4) starts to occur on the ilmenite surface. The preliminary results presented here are part of an ongoing collaborative study to understand the role of biological processes in diagenesis. In the process, mineralic biosignatures can be established as we continue to perfect analytical instrument techniques for future planetary life exploration missions.

[1] Morad & Aldahan (1982) *Journal of Sedimentary Petrology*, **52**, 1295-1305. [2] Noffke *et al*. (2008) *Geobiology*,**6**, 5-20. [3] Schelbe *et al*. (2004) *Advances in Space Research*, **33**, 1268-1273. [4] Konhauser (1998) *Earth Science reviews*, **43**, 91-121.

https://doi.org/10.1180/S0026461X00006502 Published online by Cambridge University Press

Alkali metal and H_2O dynamics at clay-water interfaces: Lessons from NMR

GEOFFREY M. BOWERS*,[1] JARED WESLEY SINGER[2] AND R. JAMES KIRKPATRICK[3]

[1]Departments of Chemistry and Materials Engineering, Alfred University, 1 Saxon Drive, Alfred, NY, 14802. (*correspondence: bowers@alfred.edu)
[2]Department of Materials Engineering, Alfred University, 1 Saxon Drive, Alfred, NY, 14802. (jws4@alfred.edu)
[3]College of Natural Science, Michigan State University, East Lansing, MI, 48824. (rjkirk@msu.edu)

Many geochemical processes are highly dependent on the fundamental molecular-scale structure and dynamics of ions and H_2O at solid-water interfaces. We present here a detailed description of the behavior of alkali metal cations and H_2O in the interlayers and on external surfaces of smectite/H_2O pastes based on variable temperature nuclear magnetic resonance (VT NMR) spectroscopy.

Our new and previously published data show that alkali metal cations occupy multiple distinct binding environments in natural hectorite and that dynamic averaging of these sites is intimately linked to the dynamics of free and confined H_2O from -80°C to 50°C. For hectorite, K^+ and Cs^+ occupy two cation sites (likely 12-coordinate and 9-coordinate interlayer environments) that undergo rapid exchange above -20°C and -50°C, respectively [1, 2]. Companion ^2H NMR shows that exchange between K^+ environments is linked to the onset of diffusional exchange among confined and free H_2O populations [1]. Recent variable temperature ^{23}Na NMR data at 9.4 T and 21.1 T reveal two Na^+ sites in hectorite with distinct quadrupolar couplings. These two sites experience distinct dynamic behaviors (and no evidence of direct two-site exchange) that appear more strongly linked with the dynamics of specifically free H_2O. The dynamics of confined H_2O in the Na- and K-hectorites appear to be quite similar at temperatures < -20°C and reflect a combination of fast C2 symmetry jumps and exchange among positions in the ion hydration shell. Above -20°C there is diffusional exchange between confined and free H_2O populations for the Na- and K-hectorites. Differences in the residual ^2H quadrupolar splitting at these temperatures are likely due to differences in cation hydration energies and whether the cations prefer inner- or outer-sphere interactions with the clay surface.

[1] Bowers, Bish, and Kirkpatrick (2008), *J. Phys. Chem. C*, **112**, 6430-6438. [2] Weiss, Kirkpatrick, and Altaner (1990), *Geochim. Cosmochim. Acta*, **54**, 1655-1669.

Isotopically-zoned zircons: Records of fluid/melt flow in the lower crust, Kapuskasing Uplift

J.R. BOWMAN[1]*, D.E. MOSER [2], J.W. VALLEY[3], J.L. WOODEN[4], N.T. KITA[3] AND F.K. MAZDAB[5]

[1]Dept. of Geology and Geophysics, Univ. of Utah, Salt Lake City, UT, 84112, USA (*corr: john.bowman@utah.edu)
[2]Dept. of Earth Sciences, Univ. of Western Ontario, London, Ontario, CAN N6A 5B7, (desmond.moser@uwo.ca)
[3]WiscSIMS, Dept. of Geoscience, Univ. of Wisconsin, Madison, WI, 53706, USA
[4]U.S.G.S.-Stanford Ion Probe Laboratory, Stanford, CA, 94305, USA
[5]Dept. of Geosciences, Univ. of Arizona, Tucson, AZ 85721, USA

Ion microprobe (SHRIMP and CAMECA 1280) analyses document primary isotopic (Pb, O) and trace element zoning in zircon from lower crustal paragneiss in the granulite zone of the Kapuskasing Uplift, Archean Superior Province. Older and low-$\delta^{18}O$ (5.1 to 7.1‰) igneous cores are overgrown by metamorphic zircon rims (2.66±0.01 to 2.58±0.01 Ga in age) which have significantly higher but variable $\delta^{18}O$ values (8.4 to 10.4‰). Several individual rims are zoned, with $\delta^{18}O$ decreasing outward from >10‰ to values as low as 8.4‰ at rim edges. Rims fall into two geochemically distinct groups: Type 1 rims have lower $\delta^{18}O$ (8.4 to 9.4‰), higher Th/U (0.1 ave.) and lower U/Yb (6.9 ave.). Type 2 rims have higher $\delta^{18}O$ (9.4 to 10.4‰), lower Th/U (0.025 ave) and higher U/Yb (20 ave.). Garnets separated from leucosome and melanosome in this paragneiss have significantly different $\delta^{18}O$ values of 9.2 and 9.9‰ (laser fluorination), respectively. These $\delta^{18}O$ values are similar to the average $\delta^{18}O$ values of the type 1 and 2 zircon rims; this similarity suggests that type 1 and type 2 rims are equilibrated with the leucosome and melanosome domains, respectively. The $\delta^{18}O$ data indicate that the leucosome domain is not in isotopic equilibrium with the rock matrix, which supports leucosome formation by infiltration of lower $\delta^{18}O$ fluid/melt rather than by *in situ* partial melting.

In mafic gneiss adjacent to this paragneiss, metamorphic zircons (2.67±0.01 to 2.56±0.01 Ga) have variable $\delta^{18}O$ values from 7.6 to 11.3‰. A number of zircon rims are markedly zoned, with $\delta^{18}O$ values ranging from 11.1‰ down to values as low as 7.6‰ at rim edges. These variations in $\delta^{18}O(Zrc)$, coupled with some cases of disquilibium fractionation between zircon and garnet (up to 1.1‰), record multiple fluid/melt infiltration events involved in the geochemical evolution of this section of the deep crust.

https://doi.org/10.1180/S0026461X00006502 Published online by Cambridge University Press

Uranium dynamics in biostimulated field-site sediments: Spatial distribution and formation of non-uraninite U(IV) phases

MAXIM I. BOYANOV[1]*, EDWARD J. O'LOUGHLIN[1], KELLY SKINNER[1], BHOOPESH MISHRA[1], SHELLY D. KELLY[2], WEI-MIN WU[3], CRAIG CRIDDLE[3], MARCELLA MUELLER[4], TONIA MELHORN[4], DAVID WATSON[4], SCOTT BROOKS[4] AND KENNETH M. KEMNER[1]

[1]Molecular Environmental Science Group, Biosciences Division, Argonne National Laboratory, Argonne, IL 60439, USA (*email: mboyanov@anl.gov)
[2]EXAFS analysis, 719 Crestview Dr., Bolingbrook, IL 60440
[3]Department of Civil and Environmental Engineering, Stanford University, Stanford, CA 94305-4020
[4]Oak Ridge National Laboratory, Oak Ridge, TN 37831

The fate of U released in the environment is determined by a complex array of complexation, adsorption, redox, and precipitation reactions. Reduction of soluble U^{VI} species to U^{IV} by direct or indirect bacterial activity often results in the precipitation of $U^{IV}O_2$ (uraninite) and has been explored as an immobilization strategy for subsurface U plumes. We will present results from a three year experiment in which the biogeochemical conditions in U-contaminated groundwater and sediments from a field site at Oak Ridge National Laboratory (U.S.A.) were allowed to evolve in diffusion limited reactors under iron- and sulfate-reducing conditions. The reactors were amended with ethanol at the water-sediment interface, mimicking the injection of electron donor during *in situ* subsurface remediation by biostimulation. Synchrotron x-ray absorption spectroscopy (XANES and EXAFS) was used to track *in situ* the spatial distribution, valence state, and speciation of U and Fe in the reduction zone propagating into the sediment, in parallel with measurements of solution phase [SO_4], [U], [ethanol], and pH. Results show rapid initial reduction of Fe^{III} and U^{VI} in the sediment near the interface, as well as redistribution of U^{VI} in the areas ahead of the reduction front. Sulfate removal from the solution phase and U^{VI} reduction throughout the sediment continued for two years. EXAFS spectroscopy demonstrated that U^{IV} in the reduced sediment was present as a non-uraninite U^{IV} species, similar to the non-uraninite U^{IV} species detected in sediment samples collected from the injection wells during field-scale biostimulation campaings at Oak Ridge National Laboratory. The immobilization of U^{IV} as a non-uraninite species in natural settings has important implications for the post-remediation stability of U plumes.

Sulfur speciation in lunar apatite

J.W. BOYCE[1,2]*, C. MA[1], J.M. EILER[1], Y. LIU[3], E. STOLPER[1] AND L.A. TAYLOR[3]

[1]Division of Geological & Planetary Sciences, Caltech, Pasadena, CA 91125 (*jwboyce@alum.mit.edu)
[2]Department of Earth & Space Sci., UCLA
[3]Department of Earth & Planetary Sci., Univ. of Tennessee

Apatite incorporates several volatile elements (including S, as SO_4^{2-}) and can provide a record of magmatic volatile evolution. Recent measurements of volatiles in apatite from Apollo sample 14053.241 revealed 300-450 ppm S. Although many lunar melts have sufficient S for sulfide saturation, the observed S content of lunar apatite is surprising because lunar samples (especially 14053) are highly reduced (≤ IW) and are thus expected to contain little SO_4^{2-}. One possibility is that there are micro-environments in late-stage lunar melts that are more oxidized than one would infer from conditions recorded by other components of these rocks. Alternatively, it may be that S^{2-} substitutes for F+Cl+OH in lunar apatite: S^{2-}–bearing apatite has been synthesized, but to our knowledge has not been observed in nature.

The Kα X-ray wavelength can be used to determine the relative amounts of S^{2-} and SO_4^{2-} in lunar apatite. Analyses were conducted at Caltech (JEOL 8200 with a 15 kV, 300nA, 15μm defocused beam, at 30 s/step, using PET crystals), referenced to FeS_2, $CaSO_4$, and SO_4^{2-}-rich Durango apatite.

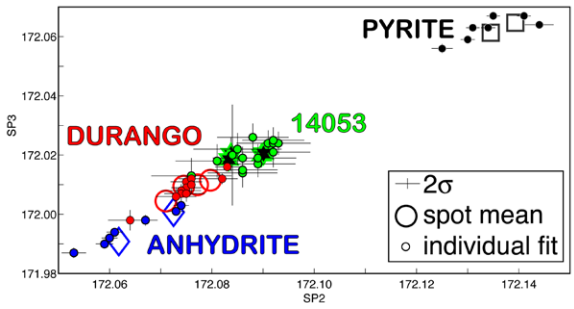

Figure 1: S Kα peak position (L-value) for two spectrometers.

The Kα peak of S in 14053 apatite is consistently shifted toward sulfide relative to both anhydrite (Δ = 29-44%) and Durango apatite (Δ = 19-24%; presumably containing all sulfur as sulfate) standards. This may indicate the first observation of a sulfide component in natural apatite. However, large uncertainties and apparent matrix effects (offset between anhydrite and Durango apatite) demand more data. Nevertheless, taking these data at face value indicates that lunar apatite includes both a S^{2-} and SO_4^{2-} component, in sub-equal proportions. The apparent SO_4^{2-} component in lunar apatite may indicate the presence of SO_4^{2-} in the late-stage lunar melt from which this apatite crystallized.

https://doi.org/10.1180/S0026461X00006502 Published online by Cambridge University Press

Lead and lead isotopes in the Atlantic and Indian Ocean: GEOTRACES data

E. BOYLE[1], Y. ECHEGOYEN-SANZ[1], K. FORNACE[1], J.-M. LEE[1], T. GAMO[2], H. OBATA[2] AND K. NORISUYE[3]

[1]Massachusetts Institute of Technology, Earth, Atm. & Planet. Sci., (eaboyle@mit.edu)
[2]University of Tokyo, Atm. & Ocean Research Institute, (gamo@aori.u-tokyo.ac.jp, obata@aori.u-tokyo.ac.jp)
[3]Kyoto University, Insitute for Chemical Research, (knorisue@inter3.kuicr.kyoto-u.ac.jp)

We will present data on the evolving anthropogenic Pb penetration into the Atlantic and Indian Oceans. In the North Atlantic Ocean, a few sites have multidecadal (Bermuda) and decadal data that show lead decreasing in the upper ocean in response to the phaseout of leaded gasoline; the decrease at depth depends on the ventilation time as shown by anthropogenic transient tracers (although Pb has been entering the deep Atlantic for at least the past 2 centuries, much longer than bomb nuclides and fluoro-compounds). The Atlantic Pb isotopic composition evolves as U.S. dominance is displaced by European Pb gas dominance; the southern Atlantic shows a distinct surface isotope composition. We will show a 10-station section in the Atlantic western boundary from 32degN to 25degS that shows N. Hemisphere Pb penetrating the S. Hemisphere dominantly with the Labrador Sea Water with some from the lower NADW. We will also show the Pb isotopic composition of these waters, including for the first time data on the scarce isotope Pb-204. We will also show a section of 8 stations from Lisbon to the Cape Verde Islands collected on the first US GEOTRACES North Atlantic Transect (2010). In the subtropics, the temporal Pb decrease due to Pb gas phaseout is reflected in this new data as compared to data from 1989 and 1999. In the tropical North Atlantic, thermocline Pb is low (<35 pmol/kg) reflecting the limited ventilation of this "shadow zone", but shows a maximum at about 700m depth. We have data from 11 stations from the Japanese Indian Ocean GEOTRACES cruise, from the Bay of Bengal and Arabian Sea into the Antarctic (18degN to 65degS). In response to later industrialization and a two-decade lag of Pb gas phaseout (and limited convection), anthropogenic Pb is higher in the surface waters of the Indian Ocean (40-80 pmol/kg) than in the present-day North Atlantic and North Pacific (20-30 pmol/kg), although Pb has not penetrated as deeply in the Indian Ocean (with little occurring below about 2000m, and some of the deep waters having extremely low Pb (~3 pmol/kg).

Modelling of hydrogeochemical processes in groundwaters of the North German Basin (NGB)

ELKE BOZAU AND WOLFGANG VAN BERK

TU Clausthal, Hydrogeologie, Leibnizstraße 10, D-38678 Clausthal-Zellerfeld (elke.bozau@tu-clausthal.de)

Modelling and forecasting quantitative hydrogeochemical changes in highly mineralised groundwaters is still a challenge. The extraction of deep groundwater for geothermal energy production from the NGB is affected by the precipitation of certain minerals, e.g. sulphates (Ba, Ca, Sr), carbonates (Ca, Fe), and silicate phases (SiO_2). These scalings often disturb the continuous production of geothermal energy and should be avoided in the technical sytems.

Groundwaters in deep aquifers of the NGB are dominated by Na^+ and Cl^-, or Na^+, Ca^{2+}, and Cl^-. The amount of total dissolved solids ranges from 100 to 300 g/l and increases with depth and temperature. Compared to surface groundwaters the deep groundwaters are enriched in a broad range of elements, including trace elements such as Ba, Pb, Sr, and Zn, and contain high amounts of dissolved gases (N_2, CO_2, H_2S, and CH_4).

An extended hydrogeochemical thermodynamic database for the well known and commonly used software PHREEQC has been developed to predict possible mineral precipitations during the use of highly mineralised groundwaters for geothermal energy production. Temperature (up to 200°C) and pressure (up to 500 bar) adaptations of the equilibrium constants were necessary. Pitzer parameters for the calculation of activity coefficients in waters of high ionic strength and solubility equilibria among gaseous and aqueous species of N_2, CH_4, and H_2S had to be implemented into the database.

In order to validate the implemented parameters the modelled mineral solubilities have been compared to experimental data gathered from the literature. First modelling results confirm the experimental data for the solubility of the minerals quartz, barite, anhydrite and calcite. However, there are problems with the solubility of several minerals at higher temperatures. Hence, evaluation and improvement of the thermodynamic database will be an ongoing process.

Acknowledgements. The presented data are results of the project "gebo" (Geothermal energy and high performance drilling research) financed by the Ministry of Science and Culture of the State of Lower Saxony and the company Baker Hughes.

https://doi.org/10.1180/S0026461X00006502 Published online by Cambridge University Press

An attempt to set the relation between chemical composition and microbiological activity in AMD reservoirs in the Łęknica region (the Muskau Arch, western Poland)

P. BOŻĘCKI AND G. RZEPA

Dept. of Mineralogy, Petrography and Geochemistry, Faculty of Geology, Geophysics and Environmental Protection, AGH - University of Science and Technology, Krakow, Poland (pbozecki@geol.agh.edu.pl)

The Muskau Arc is a large horseshoe-shaped glaciotectonic belt formed mainly during the Mid Polish Glaciation. Lignite deposits containing pyrite were excavated there to the early seventies. The abandoned mining areas were filled with acidic water, forming so-called "anthropogenic lakeland".

The aim of this study is to assess the impact of weather conditions and biological activity of selected microorganisms on the variability of chemical composition of acid mine drainage reservoirs. Water was sampled over one year period (from July 2009 to September 2010) from 11 selected locations. Water and ambient temperature, pH, Eh, EC, color, turbidity were determined in the field and samples were taken for major cations, anions and trace elements. In addition, 5 locations for microbiological research have been selected. These part consisted of qualitative determination of bacterial and fungal microflora in the waters with particular attention to microorganisms involved in the processes of iron transformation.

The results of the study show that most of the measured parameters have not only time but also spatial variability. The time variability results from seasonal changes in ambient condition as well as extreme weather events such as spring thaw and summer floods. One of the reasons for spatial variability is the variability in sources of water for distinct reservoirs. The results also show a positive correlation between :

- population size of *Acidithiobacillus ferrooxidans* bacteria and the concentration of such components as Fe and SO_4^{2-}.
- concentration of such components as Ca^{2+} and SO_4^{2-}, which may indicate that concentration level of these ions is closely linked with precipitation and dissolution of gypsum processes

This work was supported by MNiSW (project No. 0700/B/P01/2009/37) and AGH-UST (research project no. 11.11.140.158).

Sulfur isotope composition of the Bagirkacdere lead-zinc deposit, Biga Peninsula, Turkey

G. BOZKAYA

Cumhuriyet University, Department of Geological Engineering TR58140 Sivas, Turkey (gbozkaya@cumhuriyet.edu.tr)

Bagirkacdere lead-zinc deposit is one of the important deposits which are being mined on the Biga Peninsula. The vein type deposits are hosted by Triassic metamorphic rocks (Nilufer Unit of Karakaya Complex; [1]). The vein zones were emplaced within the meta-sedimentary rocks (phyllite, schist and marble) and are mainly concordant and partly discordant to foliation and/or schistosity planes. The mineralized zones contain galena, sphalerite, chalcopyrite, pyrite, marcasite, covellite, and specular hematite as ore minerals, with quartz and calcite as gangue minerals.

The $\delta^{34}S_{VCDT}$ values of galena range from -2.2 to 0.6 (average -1.07) ‰. The $\delta^{34}S_{VCDT}$ values of H_2S in equilibrium with sulphide minerals were estimated to be in the range of 2.4 to 0.14 ‰ (average 1.05‰) by evaluating the minimum and maximum $\delta^{34}S$ values of galena. For the calculation of $\delta^{34}S_{VCDT}$ values of H_2S, the average temperature of the hydrothermal fluids during the sulphide mineralization episode was assumed as 250 °C, which is obtained from the homogenization temperature measurements during fluid-inclusion studies, and the equations suggested by Li & Liu [2] was used. The $\delta^{34}S$ values of both sulphide and H_2S, which are close to 0‰, suggest a sulphur reservoir dominated by magmatic origin.

In addition, $\delta^{18}O$ and the δD data of the fluids, trapped quartz crystals, indicate that the hydrothermal fluids were completely originated from meteoric water [3]. The combined fluid inclusion and stable isotope data indicate that the reduced sulphur, depositing the sulphide minerals, was leached by heated meteoric waters during circulation within the igneous basement rocks.

[1] Bingöl, E., *et al*. (1973). *Mineral Research and Exploration Institute of Turkey (MTA) Publications*, 70–77. [2] Li, Y. & Liu, J. (2006). *Geochimica et Cosmochimica Acta,* **70**, 1789-1795. [3] Bozkaya, G.& Aydin, N. (2011). Cumhuriyet University Research Project. M-382.

https://doi.org/10.1180/S0026461X00006502 Published online by Cambridge University Press

Demir Kapija ophiolite: A snapshot of subduction initiation within a back-arc

M. BOŽOVIĆ[1], D. PRELEVIĆ[1], R.L. ROMER[2] AND M. BARTH[1]

[1]Uni Mainz, Mainz, Germany (bozovic@uni-mainz.de, prelevic@uni-mainz, barthm@uni-mainz.de)
[2]GFZ, Potsdam, Germany (romer@gfz-potsdam.de)

The Demir Kapija ophiolitic complex (Macedonia-FYROM) includes a mafic volcanic sequence (pillow lavas, diabases, and gabbros) that was intruded by intermediate to felsic and adakite-like rocks in an island arc setting.

The mafic volcanic sequence of the ophiolite complex formed in intra-oceanic back-arc setting. They are characterized by slightly increased LILE/HFSE, flat REE patterns, and radiogenic $^{143}Nd/^{144}Nd$ (up to 0.51272) and high TiO_2 contents, which reflect Pl+Ol+Cpx fractionation. The fractionation pattern between TiO_2 and MgO indicates that Ti saturation was reached and Ti-magnetite fractionated.

The intermediate to felsic and adakite-like intrusions are spatially and temporally closely related. The adakite-like volcanics show most of the features of typical adakites, i.e., low HREE, high Sr/Y, high LILE and LREE of whole-rock samples, as well as clinopyroxene major and trace element composition that are typical for adakite. The very high Th/La, Th/Yb and Ba/Yb ratios and the reduced $^{143}Nd/^{144}Nd$ values (around 0.51245) reflect contributions of sedimentary material to the mantle source of these melts. In analogy to adakites, these rocks are thought to be the product of slab melting in an unusually hot subduction zone. The intermediate to felsic volcanics show a broad range of SiO_2 content (51-75%) and more radiogenic Nd isotopic compositions than the adakite-like rocks. Their genesis is related to magma mixing of two different components; one is mantle derived, while the other one is a product of melting of an arc crust. The geochemistry of these rocks indicates that the melting of sedimentary rocks contributed to a variable extent to the source of these magmas.

During the Mid-Jurassic, opening of the short-lived Demir Kapija back-arc basin was initiated by slab roll back of the Western Vardar Ocean. Intra-oceanic subduction began within the collapsing ridge. As the subduced oceanic crust was young and hot, the thermal regime was favourable for slab melting and the formation of adakite-like rocks. Thus, the adakite-like rocks and the intermediate to felsic intrusions are related to the switch from an extensional to a compressional regime.

Testing crustal deformation and erosion-tectonic feedback models in the easternmost Himalaya using palaeo-Brahmaputra deposits

L. BRACCIALI[1,2,*], R.R. PARRISH[1], Y. NAJMAN[2] AND M.S.A. HORSTWOOD[1]

[1]NERC Isotope Geosciences Laboratory, British Geological Survey, Keyworth , Nottingham NG12 5GG, UK (*correspondence: laur@bgs.ac.uk)
[2]Lancaster Environment Centre, Lancaster University, Lancaster, LA1 4YQ, UK

Strain, uplift and exhumation of the Earth's surface impact on, and are impacted by, fluvial drainage evolution. An investigation of the latter therefore provides a key to understanding crustal deformation processes and erosion-tectonic-climate interactions. In the Himalaya, the unusual fluvial drainage configuration of the eastern syntaxial region has been interpreted either as distorted drainage resulting from crustal shortening (due to India-Asia convergence) and lateral extrusion of crustal material, or as the result of river capture events tectonically-induced by surface uplift. Determining if and when the Brahmaputra river captured the Yarlung Tsangpo is crucial to testing these models of crustal deformation. In addition, rapid fluvial incision potentially resulted in sufficient erosion by focused weakening of the crust, that deep seated ductile rocks were induced to flow upwards and be rapidly exhumed in the syntaxial region, providing a viable example of erosion-tectonic coupling. The first arrival of detritus carried by the Yarlung Tsangpo (draining the Jurassic-Paleogene Trans-Himalayan arc of the Asian plate) in the Neogene deposits of the palaeo-Brahmputra river in Bangladesh (that prior to capture would have drained the southern Himalayan slopes composed only of Precambrian-Palaeozoic Indian crust) should date the capture event, while input from the eastern syntaxis can be identified by the appearance of very young (<10 Ma) and rapidly exhumed mineral grains.

To address the river capture and the erosion-tectonic coupling hypotheses, U-Pb LA-MC-ICP-MS dating of detrital zircon grains (from palaeo-Brahmputra sediments as well as sands from modern rivers draining the Trans-Himalaya and Himalayan southern slopes) is integrated with microtextural analysis in a revised approach to the use of detrital zircon data as applied to provenance studies. In this ongoing multi-technique study, zircon data are complemented by the novel application of U-Pb dating to rutile detrital grains as well as by Ar-Ar dating of detrital white mica and zircon fission-track thermochronology.

https://doi.org/10.1180/S0026461X00006502 Published online by Cambridge University Press

Molecular tools for understanding biomarker compounds

ALEXANDER S. BRADLEY[1]* ANN PEARSON [2] AND CHRISTOPHER J. MARX [1]

[1]Department of Organismic and Evolutionary Biology, Harvard Univeristy, Cambridge MA 02138 USA (*correspondence: bradley@fas.harvard.edu)
[2]Department of Earth and Planetary Sciences, Harvard University, Cambridge MA 02138 USA

Hopanoids are pentacyclic triterpenoids found in some bacteria and widely used as organic geochemical proxies. A confident interpretation of this record requires an understanding of the function and distribution of these compounds among bacterial taxa. Recent analytical developments allowing the rapid identification of hopanoid structures [1] have made large strides towards this end. We complement this approach by performing three types of experiments: i) genetic experiments in a model organism (*Methylobacterium*) to identify genes involved in the synthesis of hopanoid side chains; ii) physiological experiments to understand the function of hopanoids, iii) replicate experimental evolution in the laboratory to understand how an organism might acquire adaptations to compensate for the absence of hopanoids.

Our studies have yielded results that have consquences for geochemical interpretation. By constructing genetic mutants, we have found that adenosylhopane is an intermediate in the synthesis of composite hopanoids in *Methylobacterium*, and this likely holds in all hopanoid-producing bacteria. This compound has previously been interpreted as a marker of terrestrial input to marine sediments [2], and this can be evaluated in light of our new understanding.

We have also found that the disruption of genes involved in hopanoid biosynthesis in *Methylobacterium* causes growth defects. The growth defect is particularly severe in a strain of *Methylobacterium* in which we disrupted hopanoid synthesis Experimental evolution of this strain in the laboratory has allowed this strain to overcome some of this defect. Other mutants, which can make hopanoid backbones but lack the ability to make either composite hopanoids or A-ring methylated hopanoids, have less-severe but still detectable growth defects. Examination of these phenotypes may cast light on the function of these molecules, which can be used to interpret the geochemical record.

[1] Talbot, Rohmer & Farrimond (2007), *Rapid Comm. Mass. Spec.* **21**: 1-13. [2] Cooke, Talbot & Wagner (2008), *Org. Geochem.* **39**:965-971

Effect of different vegetation cover on throughfall chemistry

M. BRADOVÁ[1]*, V. TEJNECKÝ[1], L. BORŮVKA[1], K. NĚMEČEK[1], J. ZENÁHLÍKOVÁ[2] AND O. DRÁBEK[1]

[1]Department of Soil Science and Soil Protection, Faculty of Agrobiology, Food and Natural Resources, Czech University of Life Sciences in Prague, CZ-165 21 Prague 6 – Suchdol, Czech Republic (*correspondence: bradova@af.czu.cz)
[2]Department of Silviculture, Faculty of Forestry and Wood Sciences; Czech University of Life Sciences in Prague, CZ-165 21 Prague 6 – Suchdol, Czech Republic (zenahlikova@fld.czu.cz)

The monitoring of throughfall at the forest ground is a widely accepted approach for the estimation of trace-substance input in different forest types and in different regions [1, 2]. This study is focused on the evaluation of quantity of materials incoming into forest soil affected by acidification process under spruce forest (*Picea abies (L.) Karst)* and under beech forest (*Fagus sylvatica L.),* and describing the fluctuation of elements in precipitation within the monitoring period. Precipitation samples were collected at monthly intervals from April to October during the years 2008 - 2010 in the Jizera Mountains. Precipitation samples were quantified and analyzed for selected components (NO_3^-, SO_4^{2-}, Cl^-, F^-) and total amount of Na, Ca, K, and Mg. pH and conductivity of precipitation were measured. Statistical analyses like simple and multiple regression and correlation and multifactorial analysis of variance were used. Results of this work showed the elements, which flow into the soil under beech forest and under spruce forest, their preference transport way and amount of them.

[1] Likens & Bormann (1995) *Biogeochemistry of a forest ecosystem*. 159 p. 2nd ed. Springer-Verlag, New York. [2] Puhe & Ulrich (2001) *Global Climate Change and Human Impacts on Forest Ecosystems*. Springer-Verlag, Berlin.

https://doi.org/10.1180/S0026461X00006502 Published online by Cambridge University Press

Using opal and organic carbon as proxies for migration of the North African monsoon

L.I. BRADTMILLER[1]*, M.B. AWALT[1], D. MCGEE[2] AND P.E. DEMENOCAL[2]

[1]Macalester College, Saint Paul, MN, 55406, USA (*correspondence: lbradtmi@macalester.edu)
[2]Lamont-Doherty Earth Observatory of Columbia University, Palisades, NY, 10964, USA

Marine and terrestrial records from northern Africa have greatly enhanced our understanding of both the causes and effects of climate change in the geologic past. Specifically, proxy records of changes in paleoproductivity yield information about upwelling strength, and therefore trade wind strength along the North African margin. Changes in wind strength, in turn, have been shown to correlate with changes in the relative aridity of the Sahel: periods of increased precipitation in the past were periods of weaker trade winds and decreased upwelling, and vice verse.

Records of opal flux over the past 18kyr illustrate the inverse relationship between precipitation and marine productivity, as periods of greater opal flux (increased wind-driven upwelling) correspond to periods of increased terrigenous flux (increased wind-borne dust flux). Paleoceanographic records have identified the African Humid Period (AHP; ~11 – 5.5 kyr) as a period of low dust flux and decreased opal flux consistent with a northerly shift in the ITCZ, increased precipitation and reduced upwelling. However, our current understanding of the causes and effects of the AHP is limited by the lack of upwelling/productivity data along a north-south transect of the African margin, as well as by a general lack of high-resolution data.

Here we present opal and organic carbon (C_{org}) records from a north-south transect of marine sediment cores on the northwest African margin. We observe decreased fluxes of opal and C_{org} in all cores at the onset of the AHP, although the magnitude of this response varies greatly from core to core. At the end of the AHP, opal and C_{org} fluxes increase, albeit not to pre-AHP levels. During both transitions the magnitude of flux change is greatest in the southernmost cores, which are closest to the region of maximum upwelling in the modern ocean. Current age models suggest that decreased fluxes of opal and C_{org} occur first in the southernmost core at the onset of the AHP, consistent with the hypothesis that these changes represent a northward shift in the ITCZ.

Chemical evolution of MORB: New insights from old crust

P.A. BRANDL*, M. REGELOUS AND K.M. HAASE

GeoZentrum Nordbayern, Universität Erlangen-Nürnberg, Schlossgarten 5, 91054 Erlangen, Germany (*correspondence: philipp.brandl@gzn.uni-erlangen.de)

The chemistry of mid-ocean ridge basalt (MORB) is studied almost exclusively using samples dredged from active spreading ridges. However, flows erupted at the ridge axis itself eventually make up the lowermost part of the extrusive section, and may not be representative of the entire oceanic crust. In contrast, samples drilled from old oceanic crust will include flows erupted both on- and off-axis, and also can be used to determine whether changes in MORB composition occur over the lifetime of an ocean basin. Despite this, few detailed studies of ancient MORB have been carried out.

We have analysed major element compositions of more than 400 fresh volcanic glasses from 35 DSDP-ODP drillsites in the Atlantic and Pacific, which range in age from 10 to 170 Ma. Trace element analyses of the same samples using LA-ICPMS are in progress.

In contrast to some previous studies, we find no significant difference in fractionation-corrected major element composition of Mesozoic and zero-age MORB in either the Pacific or the Atlantic. There is no indication that EMORB are concentrated in the upper parts of the oceanic crust, as would be expected if they were preferentially erupted off-axis. Instead, the youngest lavas (upper 100m) at a given drillsite tend to have relatively homogenous compositions, which could be explained if larger-volume flows flow further from the axis. If this is the case, then sampling MORB only from active spreading ridge axes may not give an entirely accurate picture of the average composition of the oceanic crust. It also means that direct comparison of lavas from slow- and fast-spreading ridges, which differ in axial topography and average flow volumes, will not be straightforward.

https://doi.org/10.1180/S0026461X00006502 Published online by Cambridge University Press

Quantifying rates and mechanisms of shale weathering across a continental-scale climosequence

SUSAN L. BRANTLEY, ASHLEE DERE AND TIMOTHY WHITE

The Pennsylvania State University, University Park, PA 16802; (*correspondence: sxb7@psu.edu)

Both ecosystems and humans are dependent on soil for nutrient and water cycling as well as food, making the loss of soil a major issue facing humanity. However, the rate at which soil forms has not been well quantified. To investigate rates of soil formation as a function of climate, a latitudinal climosequence of forested sites has been established in North America and Wales. The climosequence is bounded by a cold/wet end member in Wales and a warm/wet end member in Puerto Rico. In between, temperature and rainfall increase as sites extend south through New York, Pennsylvania, Virginia, Tennessee and Alabama. All sites, except Puerto Rico, are underlain by an organic-poor, iron-rich (Silurian-age) shale, providing a constant parent material from which soil is forming. Puerto Rico is located on chemically similar, but younger, shale. Soil sampling and geochemical analyses were completed similarly at all sites to allow direct comparisons and modelling of shale weathering. Independent Be^{10} estimates of erosion rates for a few locations along the transect are used to estimate residence times. Initial results show soil depth increases as a function of temperature, with shallow (~30 cm) profiles in Wales and Pennsylvania varying up to 630 cm deep in Puerto Rico. Depletion profiles of Na, a proxy for feldspar dissolution, are less than 20 % depleted at the surface in Wales and Pennsylvania, 50-60% depleted in Virginia and Tennessee, and 100% depleted at the surface in Puerto Rico. Using estimated soil residence times, apparent activation energies for Na depletion were calculated using different assumptions to range from 15-19 kcal mol^{-1}, values that are slightly higher than those reported for Na plagioclase dissolution in the laboratory. Overall, data collected from soils across the transect will promote a better understanding of how climate changes can impact soil formation rates.

CAPRAM mechanism development: Evaluation of prediction methods for aqueous phase rate constants and model results

P. BRÄUER[1]*, C. MOUCHEL-VALLON[2], A. TILGNER[1], B. AUMONT[2] AND H. HERRMANN[1]

[1] Leibniz-Institut für Troposphärenforschung, Permoserstr. 15, D-04318 Leipzig, Germany. (*correspondence: braeuer@tropos.de)

[2]LISA, UMR CNRS 7583, Universités Paris Est Créteil et Diderot, IPSL, 61 Av. du G[al] de Gaulle, 94010 Créteil cedex, France. (bernard.aumont@lisa.u-pec.fr)

Organic compounds are ubiquitos in the tropospheric multiphase system. With either large biogenic and athropogenic sources they play an important role and have thus become a major research topic within the last decades.

Modelling can provide a useful tool to explore the chemical and microphysical processes in the troposphere. However, detailed oxidation mechanisms exist mainly in the gas phase while they are very limited in the aqueous phase. Current studies aim to expand the aqueous phase mechanism CAPRAM 3.0i, which is the currently most comprehensive chemistry mechanism with 777 reactions and 380 species. However, the oxidation scheme is still incomplete for C3 and C4 organic chemistry and higher organics are missing at all.

The huge amount of organic species relevant in the troposphere makes it impossible to determine all the needed kinetic data experimentally. Therefore, estimation methods become necessary. Besides the construction of an up-to-date database of about 600 experimentally determined reaction rate constants of OH and NO_3 radicals with organics, estimation methods for the prediction of missing data have been evaluated. The evaluation led to a new oxidation schemes for C3 organic compounds added to the existing CAPRAM 3.0i mechanism. Furthermore, branching ratios were introduced for already prescribed OH reactions with organics. Model runs have been performed with the multiphase mechanism MCMv3.1 and the extended CAPRAM version for a meteorological scenario with non-permanent clouds under remote and urban conditions.

The addition of new C3 organic compounds led to the modified concentration profiles of many organic and inorganic species. For example, acid production is enhanced although contrations are still lower than measured in the field due to the missing implementation of the oxidation of higher organics. The introduction of branched OH attack to organics let to further refined results.

https://doi.org/10.1180/S0026461X00006502 Published online by Cambridge University Press

Bioavailability and toxicity of metals in an estuary contaminated by acid mine drainage

C.B. BRAUNGARDT[1]*, C. MONEY[2] AND E.P. ACHTERBERG[3]

[1]University of Plymouth, SoGEES, PL4 8AA, UK (*correspondence: cbraungardt@plymouth.ac.uk)
[2]AstraZeneca, Brixham TQ5 8BA, UK
[3]University of Southampton, NOC, SO14 3ZH, UK

Motivated by the need for a better understanding of the human impact on ecosystems (Water Framework Directive), we combined a bioassay (*Crassostrea gigas* larva) with high temporal resolution *in situ* metal speciation measurements to assess the temporal variability, biological availability and toxicity of dissolved metals in an estuary affected by historic (tin streaming) and contemporary (acid mine drainage) metal sources. Voltammetric *in situ* Profilers were deployed in the estuary for a tidal cycle to determine Cd and Cu species ('dynamic') in a size range (<4 nm) highly relevant for uptake by organisms [1]. Oyster larvae were exposed to discrete samples taken at regular intervals during the survey.

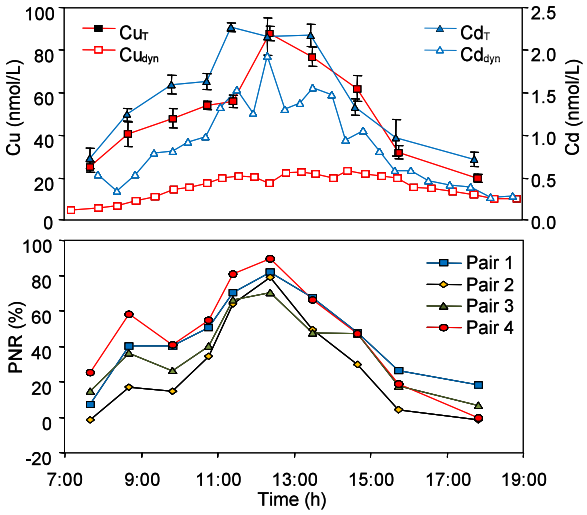

Figure 1: Dynamic (Cu_{dyn}, Cd_{dyn}) and total (Cu_T, Cd_T) metal concentrations and percent net response (PNR) of oyster larva.

Oyster larva responded to the highest dynamic Cu and Cd concentrations with maximum abnormal development (71-90% (Fig.1). Synergistic toxicity and model calculations suggest that bioavailable metal concentrations in this estuary are likely to severely compromise the ecosystem structure [2].

[1] Buffle, Tercier-Waeber (2005) TRAC **24**, 172-191. [2] Rivera-Duarte *et al*. (2005) ES&T **39**, 1542-1546.

Biotite dissolution: The effect of organic ligands and pH

A.W. BRAY[1]*, S. BONNEVILLE[1,2], D. WOLFF-BOENISCH[3] AND L.G. BENNING[1]

[1]School of Earth and Environment, University of Leeds, Leeds, UK (*correspondence: a.bray@leeds.ac.uk)
[2]Département des Sciences de la Terre, Université Libre de Bruxelles, Brussels, Belgium
[3]Institute of Earth Sciences, University of Iceland, Reykjavik, Iceland

Traditionally mineral weathering studies are based on abiotic and, more recently, dissolution in the presence of living organisms. However, for biotite, a key nutrient bearing mineral (i.e., K), the piece of the puzzle linking abiotic [1] and biotic [2] dissolution rates - the effect of organic ligands - is still missing. Here we fill this gap via biotite dissolution experiments conducted with various organic ligands typical in soils or groundwaters to better quantify the full range of processes affecting rock weathing and soil formation.

Batch (pH = 2, 4, 6, 12 hrs) and flow-through (pH = 3.3 and 6, 96 hrs) experiments were carried out at 25°C with biotite with and without oxalic and citric acids and desferrioxamine-b (DFO-B) or a mixture of these. Aqueous Si, Al, Mg, K and Fe concentrations, analysed by UV-VIS, AAS, or ICP-MS, BET surface area and EMPA compositional analyses, were used to derive rate constants.

Our results show that the presence of organic ligands can enhance the dissolution rate of biotite by up to 2 orders of magnitude (Fig. 1). The degree of enhancement of the ligand promoted dissolution, compared to the abiotic dissolution, increases with increasing pH due primarily to the speciation and extent of surface complexation of the organic ligands.

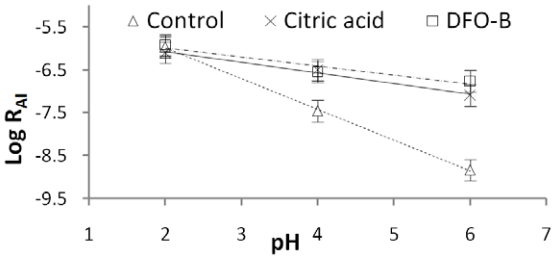

Figure 1. Log R_{Al}($mol_{(biotite)}$ m^{-2} h^{-1}) vs pH from the batch dissolution experiments (control = no organics). Rates were calculated from elemental release data (here Al) and normalised to the EMPA derived biotite stoichiometry.

[1] Malmström and Banwart (1997) *GCA* **61**, 2779-2799 [2] Bonneville *et al*. (2009) *Geology* **37,** 615-618

https://doi.org/10.1180/S0026461X00006502 Published online by Cambridge University Press

Toward calibrating the paleosol carbonate CO_2 barometer for paleoVertisols

D.O. BREECKER[1], L.A. MICHEL[2], J. YOON[1], J.S. MINTZ[2], S.G. DRIESE[2] AND L.C. NORDT[2]

[1]Department of Geological Sciences, The University of Texas at Austin, 1 University Station C1100, Austin, TX 78712
[2]Department of Geology, Baylor University, One Bear Place 397354, Waco, TX 76798 USA
*Correspondance: breecker@jsg.utexas.edu

The concentration of CO_2 ($[CO_2]$) in soils during soil calcite formation must be known in order to accurately calculate ancient atmospheric $[CO_2]$ using the paleosol carbonate CO_2 barometer [1]. The average *S(z)* value ($S(z) = [CO_2]_{soil} - [CO_2]_{atmosphere}$) appropriate in the barometer has recently been estimated at 0.25% [2]. In the present study, we measured soil $[CO_2]$ in modern Vertisols (high shrink/swell clay content soils) in order to test the value of 0.25% and help calibrate the barometer for paleoVertisols which are commonly used to reconstruct ancient atmospheric $[CO_2]$.

We installed 7 soil gas wells in the Bkss horizon of modern Vertisols in a C_4 grassland at the USDA Riesel Watershed in Riesel, TX, USA. Soil $[CO_2]$ was measured in soil gas samples withdrawn from the wells on a monthly basis. The resulting time series currently extends from January 2010 through March 2011. Soil $[CO_2]$ varied seasonally and interannually during the period of study, reaching a maximum of 9.3% in June 2010 and a minimum of 0.13% in February 2011. Soil $[CO_2]$ was above 1% at every site during the winter of 2009/2010 when the soil was water-saturated and was below 1% at every site during the winter of 2010/2011 when the soil was dry and cracked. Soil $[CO_2]$ decreased rapidly from maximum values (~3-9%) in June 2010 to values as low as 0.2% in August 2010 as the soil warmed, dried and cracked. Without indpendent evidence for the timing of calcite formation, we cannot yet confidently quantify *S(z)* values appropriate for the barometer. However, the decrease of *S(z)* values below 0.25% during the summer when soil calcite is thought to form is consistent with the conclusions drawn by [2]. Our data suggest that soil $[CO_2]$ is strongly decoupled from temperature in Vertisols and is controlled by soil moisture and the opening and closing of soil cracks which act as gas transport conduits. Preservation of foraminifera skeletons from parent material in this soil suggest that calcite dissolution/reprecipitation is limited, even under seasonal changes in soil pCO_2 that span orders of magnitude.

[1] Cerling (1991), *American Journal of Science* **291**, 377-400. [2] Breecker, Sharp & McFadden (2010) *PNAS* **107**, 576-580.

Hydraulic-hydrochemical modelling of a geothermal reservoir in Indonesia

MAREN BREHME*, SIMONA REGENSPURG AND GÜNTER ZIMMERMANN

Helmholtz-Centre Potsdam, German Research Centre for Geosciences (GFZ), International Centre for Geothermal Research, Telegrafenberg, 14473 Potsdam, Germany (*correspondence: brehme@gfz-potsdam.de; regens@gfz-potsdam.de; zimm@gfz-potsdam.de)

The purpose of this study is to explain the hydraulic and hydrochemical connection between different surface and subsurface reservoirs at a geothermal site in Indonesia. By using an integrated model to determine hydraulic pathways through porous media as well as fault structures and connecting it to a chemical transport model, the effect of geology on the hydrochemical characteristics should be explained. The numerical simulator OpenGeoSys is used for modelling the thermo-hydraulic situation. Results will eventually be combined with hydrochemical PHREEQC calculations.

In November 2010 a geothermal plant has been visited and available hydraulic, geological, and hydrochemical properties were reviewed. Additionally, water samples from production wells, hot springs, and a lake have been taken and analysed. Physicochemical parameters were measured *in situ*.

At the investigated site three different fluid containing reservoirs have been identified at various depths with temperatures between 250 and 350 °C, which show each different hydrochemical characteristics: The deepest reservoir (2300 m) with a moderate pH of 5 is marked by silicium (Si) concentrations up to 350 mg/L and high chloride (Cl) concentrations of 430 mg/L The fluid in the most shallow (1000 m) reservoir above is highly acidic (pH 1). Still higher Cl (1550 mg/L), Si (1600 mg/L), and sulphate concentrations (460 mg/L) appear in this reservoir. Acid water (pH 2.6) was also observed in a nearby lake indicating a hydraulic connection to that reservoir. PHREEQC-calculations show an oversaturation of several minerals such as alunite, silicates e.g. kaolinite, Ca-montmorillonite, and quartz at temperatures between 25 and 45 °C. Therefore silicate mineral precipitation upon fluid cooling can be expected to occur in the wells, pipes or the reservoir, which would harm the plant components or even damage the reservoir in the long term.

Apparently three aspects are challenging for the model build-up: (I) a three level-reservoir with the connected acidic lake; (II) the oversaturation of silicates upon cooling; (III) the change in composition over time.

https://doi.org/10.1180/S0026461X00006502 Published online by Cambridge University Press

How small-volume basaltic magmatic systems develop: A case study from Jeju, Korea

MARCO BRENNA[1]*, SHANE J. CRONIN[1], IAN E. M. SMITH[2], ROLAND MAAS[3] AND YOUNG KWAN SOHN[4]

[1]Volcanic Risk Solutions, Massey University, Palmerston North, New Zealand, (*correspondance: m.brenna@massey.ac.nz)
[2]School of Environment, University of Auckland, Auckland, New Zealand
[3]School of Earth Sciences, The University of Melbourne, Parkville, Australia
[4]Dep. of Earth and Environmental Sciences, Gyeongsang National University, Jinju, Republic of Korea

Jeju is a volcanic field active since c. 1.8 Ma ago. Eruptive activity began with dispersed, basaltic, monogenetic, volcanism. Continuing monogenetic volcanism was later joined by more voluminous, alkali and sub-alkalic, evolved lava effusion events building a central composite edifice. Samples from older (>0.7 Ma) and younger (<0.2 Ma) monogenetic centres were analysed for whole-rock major elements, trace elements and Sr-Nd-Pb isotopic compositions. Early monogenetic centres are depleted in MgO, Cr and Ni reflecting considerable olivine fractionation. By contrast, younger monogenetic magmas fractionated clinopyroxene + olivine at deeper levels. Isotopes show little variation across the suite, but the younger monogenetic centres have generally lower $^{87}Sr/^{86}Sr$ and $^{208}Pb/^{204}Pb$ and higher $^{143}Nd/^{144}Nd$ than the older centres and sub-alkali lavas. Major and trace element and isotope data suggest a common, shallower source for older monogenetic magmas and sub-alkali lavas, in contrast to a deeper source for younger monogenetic magmas. We propose that mantle melting was initiated near the garnet to spinel transition at a depth of near 2.5 GPa, followed by extension of the melting zone to 3-3.5 GPa, with a concomitant increase in the volume of melt derived from the shallower part of the system to produce sub-alkali magmas, possibly related to accelerated heat transfer resulting from deepening of the melting zone, and/or increased mantle upwelling. A classical mantle plume model for Jeju is not viable due to physical constraints; however decompression melting is still responsible for magmatic activity in the area. Uplift of mantle blocks under Jeju occurred due to lubrication by shear zones created during the opening of the Sea of Japan/East Sea c. 15 Ma ago, and reactivated during rotation of the direction of subduction of the Philippine Sea plate c. 2 Ma ago. This is the first attempt to directly link subduction processes and intraplate volcanism on Jeju.

Volume control on magmatic evolution and eruption style transition, Jeju, Korea

MARCO BRENNA[1]*, SHANE J. CRONIN[1], IAN E. M. SMITH[2] AND YOUNG KWAN SOHN[3]

[1]Volcanic Risk Solutions, Massey University, Palmerston North, New Zealand, (*correspondance: m.brenna@massey.ac.nz)
[2]School of Environment, University of Auckland, Auckland, New Zealand
[3]Dep. of Earth and Environmental Sciences, Gyeongsang National University, Jinju, Republic of Korea

Jeju is a volcanic field active over the last c. 1.8 Ma. Eruptive activity began with dispersed, basaltic, monogenetic, volcanism. Continuing monogenetic volcanism was later joined by more voluminous, alkali and sub-alkali lava effusion events building a central composite edifice. From three deep cores (400-500 m) through the main edifice flanks, lava samples were analysed for major, trace-element and Sr-Nd-Pb isotope compositions. The low-volume monogenetic volcanoes erupted mainly primitive alkali basalts, whereas the larger-volume lavas have chemical variability spanning alkali basalt to trachyte compositions. The oldest erupted lavas form part of a high-Al alkali suite and evolved to Sanbangsan trachytes (SiO_2 c. 62 wt%). The topmost lavas show less Al_2O_3 enrichment and MgO depletion and hence form a low-Al alkali suite, which evolved to the Hallasan trachytes (SiO_2 c. 66 wt%). The similarities in the chemical evolution trends between low- and large volume magmas suggests similar magma sources and analogous crystal fractionation processes. This implies that the volume and proportions of parent melt was the dominating factor in determining the eventual course of magmatic activity. Based on the chemical trends, the proportions of partial melts must have increased in the middle and later stages of Jeju Island's formation. This may relate to increased uplift of mantle domains (or increased mantle convection) beneath the island, leading to accelerated decompression melting, compared to the early stages of activity. This resulted in the construction of the central composite edifice. Mantle upwelling was greater in the core of the system, resulting in the larger volume lava outpourings, compared the lower supply in distal parts of the field, resulting in low-volume monogenetic activity. These results have implications for hazard forecasting in monogenetic volcanic fields, with a first conclusion being that eruptions situated in the centre of the field may give rise to larger volume lava outpourings compared to those at the outer margins.

https://doi.org/10.1180/S0026461X00006502 Published online by Cambridge University Press

$^{238}U/^{235}U$ ratios of angrites: Adjusting absolute ages of anchors

G.A. BRENNECKA* AND M. WADHWA

School of Earth & Space Exploration, Arizona State Uni., Tempe, AZ (*correspondence: brennecka@asu.edu)

The use of short-lived chronometers is critical to our understanding of the high-resolution time sequence of events in the early Solar System. To map relative ages from short-lived systems onto the absolute time scale, they are "anchored" to the Pb-Pb ages of appropriate meteoritic materials. Previously reported high precision Pb-Pb dates of the basaltic angrite meteorites, some of which have been used extensively as anchors [1-2], have assumed a $^{238}U/^{235}U$ ratio (=137.88). However, the $^{238}U/^{235}U$ ratio has recently been shown to be variable in Solar System materials [3-6], requiring the reevaluation of these previously reported Pb-Pb ages. An adjustment to the Pb-Pb age of an anchor would consequently require a corresponding correction to the calculated "model" ages for any other meteoritic materials dated using that anchor and an extinct chronometer, such as the ^{26}Al-^{26}Mg, ^{53}Mn-^{53}Cr, or ^{182}Hf-^{182}W chronometers.

Here we report U isotope compositions of several angrites. Specifically, $^{238}U/^{235}U$ ratios were measured in whole-rock (WR) samples of the D'Orbigny, NWA 4801, NWA 4590, and NWA 6291 angrites. Additionally, phosphate separates from Angra dos Reis, pyroxene separates from D'Orbigny, and the leachate and residue from a separate acid-washed WR fraction of NWA 6291 were also measured. For D'Orbigny, two WR fractions and the pyroxene mineral separate yield identical (within 2SD errors) U isotope compositions. From these measurements, a $^{238}U/^{235}U$ ratio of 137.776±0.026 is determined, corresponding to a corrected Pb-Pb age of 4563.34±0.30 Ma (using the age previously reported by [2]). Furthermore, the $^{238}U/^{235}U$ ratios determined for WR samples of the angrites NWA 4590 (137.757±0.026), NWA 4801 (137.763±0.026), NWA 6291 (137.754±0.026), as well as for the phosphate separates of Angra dos Reis (137.791±0.042) are also identical (within 2SD errors) to those determined for D'Orbigny. Therefore, there is no detectable variation in the $^{238}U/^{235}U$ ratios measured in the angrite WR samples and mineral separates. This indicates that the angrite parent body was homogenous (at our current level of precision) in terms of its $^{238}U/^{235}U$ composition.

[1] Amelin & Irving (2007) *Work. on Chron. of Met.* #4061. [2] Amelin (2008) *GCA* **72**, 221-232 [3] Brennecka *et al.* (2010) *Science* **327**, 449-451 [4] Brennecka *et al.* (2010) LPSC #2117 [5] Amelin *et al.* (2010) *EPSL* **300**, 343-350 [6] Amelin *et al* (2011) LPSC #1682

Simultaneous analysis of dissolved noble gases, SF_6 and CFCs in water

M.S. BRENNWALD[1]*, M. HOFER[1], AND R. KIPFER[1,2]

[1]Eawag, Swiss Federal Institute of Aquatic Science and Technology, Dübendorf, Switzerland (*correspondence: matthias.brennwald@eawag.ch)

[2]Institute of Geochemistry and Petrology, Swiss Federal Institute of Technology (ETH), Zurich, Switzerland

Dissolved atmospheric noble gases, sulfur hexafluoride (SF_6) and chlorofluorocarbons (CFCs) are widely used as (transient) environmental tracers in water bodies. The concentrations of these trace gases in the water are determined by their partial pressure in the air, the gas equilibration at the water surface, the (partial) dissolution of air bubbles entrapped in the water ("excess air"), and the mixing within the water body.

In contrast to the noble gases, the partial pressures of SF_6 and CFCs in the atmosphere have increased strongly during the recent decades, e.g. due to release from industrial appliances. The SF_6 and CFC concentrations therefore contain direct information on the time when the water was last in contact with the atmosphere (water age), which is highly useful to study the mixing and deep-water formation in surface waters, the transport and mixing dynamics in groundwaters, and the geochemical origin and fate of other solutes and gases in aquatic environments (e.g. oxygen, methane, nutrients or contaminants).

For reliable water dating with SF_6 and CFCs, the relative gas contributions from air/water equilibration at the water surface and the formation of excess air to the total SF_6 and CFC concentrations in the water need to be quantified. However, the information required to disentangle these two components from each other is usually poorly constrained from the data available from the conventional analytical techniques.

A way forward to address this issue is to derive the required information from the noble-gas concentrations in the water. However, the analysis of SF_6, CFCs and noble gases in water usually involves the use of separate instruments and techniques in different and highly specialized laboratories. We therefore developed a new method and apparatus for the simultaneous analysis of He, Ne, Ar, Kr, Xe, SF_6, CFC-11, CFC-12, CFC-113, N_2 and O_2 in a single water sample. The apparatus is constructed using only standard and commercially available components. The method is based on vacuum extraction of the dissolved gases from the water. The sample gases are then separated into three fractions. He and Ne is quantified by static mass spectrometry, the remaining gases are quantified by gas chromatography.

https://doi.org/10.1180/S0026461X00006502 Published online by Cambridge University Press

U-Th-Ba elemental fractionation during partial melting of crustal xenoliths and its implications for U-series disequilibria in continental arc rocks

RAUL BRENS*[1] AND ROSEMARY HICKEY-VARGAS[2]

[1]Earth & Environment, Florida International University, Miami, FL, USA. (*correspondence: RaulJr00@hotmail.com)
[2]Earth & Environment, Florida International University, Miami, FL, USA. (hickey@fiu.edu)

Understanding U-series isotopic disequilibria of partially melted crust is integral for determining the effect crustal assimilation has on the U-series signature of magmas. The U-series isotopes are too low in abundance to determine by any microbeam technique. Therefore, in this work, U, Th and Ba (as a proxy for Ra) elemental abundances were gathered on the quenched glass in partially melted crustal xenoliths of granitic composition using microbeam techniques. The crustal xenoliths, which are from basaltic volcano Mirador in Chile, are old (Miocene), and can be assumed to be at secular equilibrium, whereas melting occurred during eruption of Mirador in 1979. Any recent fractionation of U from Th or Th from Ra (Ba) by partial melting will result in isotopic disequilibrium. A comparison of the ratios Ba/Th and U/Th in the partial melts with those of the whole rock reveal how much fractionation has occurred during partial melting.

An EPMA was used to locate and analyze glass pockets in the samples, through BSE images. Laser ablation ICP-MS was used to analyze U, Th and Ba in the quenched partial melts and solution ICP-MS was used for the whole rocks.

The SiO_2 content in measured glass samples was between 54% and 75%, Al_2O_3 (13% - 27%), K_2O (0.2% to 7%). Measured Ba/Th (glass/whole rock) are between 0.2 to 51 and Th/U (glass/whole rock) range from 0.3 to 7, with the majority Ba/Th between 1 to 51 and Th/U 0.3 to 1. Different ratios of U, Th and Ba compared to the whole rock substantiate fractionation via partial melting. Thus, assimilation of partial melts of crust can play a role on U-series isotopic disequilibria, which is commonly observed in continental arc magmas. Accessory minerals show variable effects as 'restite', with allanite having a large Th excess and zircon having U excess, these are foremost accessory minerals responsible for the fractionation. Potential U-series disequilibria impacts on magma through melt extraction from country rock or incomplete homogenization during assimilation is discussed.

Mineralizing fluids of the barite-fluorite mineralization at the S edge of the Thuringian Basin, Germany

M. BREY[1], J. MAJZLAN[1], R.J. BAKKER[2] AND W. PROCHASKA[2]

[1]Friedrich-Schiller Universität, Institut für Geowissenschaften, Burgweg 11, D-07749, Jena, Germany (maria.brey@uni-jena.de)
[2] Department Applied Geosciences and Geophysics, Montanuniversity, 8700 Leoben, Austria

Numerous small deposits and occurrences of barite-fluorite mineralization are developed along the southern edge of Thuringian sedimentary basin. It is a series of Upper Permian and Triassic strata (Zechstein, followed by Buntsandstein, Muschelkalk, and Keuper). The Tertiary tectonic activity uplifted the marginal portions of the today's basin where the pre-Permian rock complexes are exposed. The studied mineralization consists mostly of barite, calcite, dolomite, and locally quartz for Kamsdorf and mostly of barite and fluorite in Trusetal and Gehren. The primary fluid inclusions in barite from Kamsdorf show a wide range of salinities between 8-22 wt% $CaCl_2$ eq, the primary inclusions in fluorite from Gehren and Trusetal have about 24 to 27 eq wt% $CaCl_2$ eq. Th measurements range between 85°C to 160°C in barite and between 80°C to 130°C in fluorite. Chemical analysis of fluids extracted from fluid inclusions in fluorite and barite show compositions dominated by Na and Ca. The Cl/Br ratio in the fluorite samples is 260-340 and in barite between 150-240, always lower than in seawater (650). Raman analyses of the vapor phase inside an inclusion suggest traces of N_2 in fluorite and CH_4 in barite. Fluorite samples were analysed for rare-earth elements and two types of REE distribution patterns were found. Type 1 is characterized by high amount of light REE without any Ce anomaly and a steep decrease towards Lu. Type 2 has significantly lesser amount of LREE, a weak Tb/Dy anomaly, and a depletion in HREE. The most fluorite samples belong to the type 2.

The paragenesis of the primary minerals and the physical-chemical properties of the fluids can be explained by large-scale fluid circulation and mixing at the edge of the Thuringian basin and the adjacent Variscan crystalline basement, mostly likely during the late Mesozoic.

This work is a part of INFLUINS, a research project funded by the German Federal Ministry of Education and Research (BMBF) whose financial assistance is gratefully acknowledged.

https://doi.org/10.1180/S0026461X00006502 Published online by Cambridge University Press

Integrating multi-scale experiments and modeling to couple biotic weathering at nano and global scales

JONATHAN W. BRIDGE*[1], LYLA L. TAYLOR[2], STEVEN A. BANWART[1] AND THE WEATHERING SCIENCE CONSORTIUM TEAM[1]

[1]Kroto Research Institute, The University of Sheffield, Sheffield, UK (*correspondence: j.bridge@sheffield.ac.uk)
[2]Department of Animal and Plant Sciences, The University of Sheffield, UK.

Soil mycorrhizal fungi act through chemical interactions at nanometer scale to dissolve minerals and transport weathering products to plant symbionts through metre scale mycelial networks [1]. Soil development occurs at regional scale over millenia (ka) and coupling between ecological, geological and atmospheric systems is apparent over evolutionary (Ma) timescales [2]. We hypothesise that biologically-driven weathering reactions at molecular scale persist through scale transitions to exert strong controls on soil formation and atmospheric CO_2 evolution that occur over much larger temporal and spatial scales.

To test this we have applied an integrated suite of observations at scales from nanometre to decimetre using common minerals, fungi and physical and chemical conditions. Our experiment results demonstrate that fungal hyphae-grain contact leads directly to mass loss from mineral grains over time [3]. Cell exudates and nanoscale cell-mineral interaction forces progressively modify mineral surfaces and alter the pore microenvironment, conditioning subsequent biotic and abiotic weathering mechanisms. Crucially, these processes are directed by mycorrhiza towards minerals which yield the best nutrient supply for plants [1].

Here, we describe the development of numerical models for key nano-scale weathering processes coupled to stochastic, agent-based simulations of hyphal growth at the micron to cm scales which permit quantitative analysis of the dynamic interactions between plant carbon energy supply and soil mineral weathering rates, mediated by mycorrhizal fungi. These profile-scale data are aggregated in a continental scale process-based model [2,4] and tested for representation of the global carbon cycle at evolutionary timescales by comparing with proxy data for paleoenvironmental conditions [5].

[1] Leake *et al*. (2008) *Mineral. Mag*. **72**, 85–89. [2] Taylor *et al*. (2009) *Geobiology* **7**, 171–191. [3] Bonneville (2009) *Geology* **37**, 615–618. [4] Taylor *et al*. (2010) *Geochim. Cosmochim. Acta* **74** (12) A1032. [5] Berner (2006) *Geochim. Cosmochim. Acta*, **70** (23), 5653-5664.

Strontium incorporation into carbonate granules secreted by earthworms

LOREDANA BRINZA[1]*, J. FRED W. MOSSELMANS[1], PAUL F. SCHOFIELD[2], PAUL D. QUINN[1] AND MARK E. HODSON[3]

[1]Diamond Light Source, UK, (Loredana.Brinza@diamond.ac.uk)
[2]Natural History Museum, London, UK, (pfs@nhm.ac.uk)
[3]University of Reading, Reading, UK, (m.e.hodson@reading.ac.uk)

Earthworms secrete significant quantities of calcium carbonate in the form of granules (0.5mg $CaCO_3$/g worm/day), which can also contain other metals depending on the soil content (Pb, Mn, Mg). This may affect metal bio-availability and impact upon element bio-geo-cycling. We have examined Sr incorporation into the granules produced by earthworm *Lumbricus terrestris* cultivated in Sr containing soil. These granules contained up to 3.5% Sr with a positive correlation between Sr concentration in pore water and Sr in the granules. Sr-μXRF maps of the granules show Sr enrichment within the outer region of the granules. These both suggest that the mechanism of Sr incorporation is either adsorption onto or co-precipitation during granule growth.

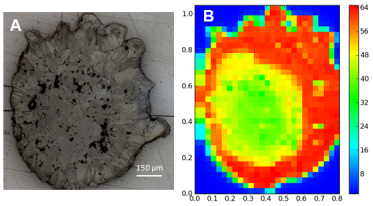

Figure 1. Slice of a calcium carbonate granule produced by ***Lumbricus terrestris*** incorporating 1.2% strontium: (A) Zeiss microscope image; (B) Sr-μXRF map: axis are in mm and the colour bar indicates: blue - low Sr and red - high Sr.

Analysis of Ca-μXANES and Sr-μEXAFS suggests that most Sr substitutes for Ca in the rhombohedral calcite structure rather than producing the orthorhombic carbonates. The results significantly improve our understanding of Sr sequestration within bio-synthesized carbonate granules in the context of its biogeochemical cycle. In terms of earthworm tolerance to Sr, earthworms showed significant mortality at soil bulk concentrations above 1000ppm.

https://doi.org/10.1180/S0026461X00006502 Published online by Cambridge University Press

Evaluation of surface complexation parameters for Eu^{3+} on muscovite and orthoclase

S.M. BRITZ[1]*, U. NOSECK[1], V. BRENDLER[2] AND M. STOCKMANN[2]

[1]GRS Braunschweig, D-38122 Braunschweig, Germany (*correspondence: susan.britz@grs.de)

[2]Helmholtz-Zentrum Dresden-Rossendorf, D-01328 Dresden, Germany

Sorption on mineral surfaces of sediments is an important retardation process for radionuclides to be considered in safety assessments for radioactive waste repositories.

This study deals with sediments of the overburden at Gorleben site that are mainly composed of tertiary and quaternary sands and clays [1]. A bottom-up approach is chosen to describe the sorption of Eu^{3+} (as homologue for trivalent actinides) on each single mineral phase of a representative sediment. Orthoclase and muscovite are important constituents of the sediment significantly contributing to the overall distribution coefficient.

The scope of the study is the assessment of surface complexation parameters by applying the geochemical speciation model PhreeqC, Version 2.17 which is coupled with the parameter-estimation code UCODE_2005. Since relevant data were missing for the sediment constituents orthoclase and muscovite batch experiments are performed for the parameter estimation. Establishing solid/liquid ratios of 1/20 and 1/80 the minerals are suspended in 0.01 M $NaClO_4$. Subsequently pH values ranging between 6 and 9 are employed in the suspensions over a period of several weeks. Eu^{3+} concentrations of 10^{-5} M, 10^{-6} M, 10^{-7} M, and 10^{-8} M are applied, whereat a chemical equilibrium between Eu^{3+} and the mineral is reached within 24 h.

PhreeqC and UCODE are used to acquire protolysis constants via a diffuse double layer model from measured titration curves. In the second step the basic required parameters, i.e. logK-values for selected surface reactions, the surface site density, and the specific surface area are iteratively determined by fitting the experimental data.

To simulate Eu-sorption on a representative sediment (10% muscovite, 10% orthoclase, 80% quartz) the derived surface complexation model is applied to a corresponding experimental data-set. Results show good reproduction of the data, hence, backing up a robust parameter set.

[1] Klinge *et al.* (2002) *Geologie und Hydrogeologie des Deckgebirges über dem Salzstock Gorleben*, Z. angew. Geol. **2**, 7-15.

Molecular fossils and the late rise of eukaryotes and oxygenic photosynthesis

JOCHEN J. BROCKS

Research School of Earth Sciences, The Australian National University, Canberra ACT 0200, Australia.

Hydrocarbon biomarkers are the molecular fossils of natural products such as lipids and pigments. They can yield a wealth of information about early microbial ecosystems and are particularly valuable when preserved in > 1 billion-year-old (Ga) sedimentary rocks where conventional fossils are often lacking. Therefore, in 1999, the detection of traces of biomarkers in 2.5 to 2.7 Ga shales from Western Australia [1, 2] was celebrated as a breakthrough. The discovery, which was later confirmed by several independent studies, led to far-reaching conclusions about the early evolution of oxygenic photosynthesis [2] and ancestral eukaryotes [1]. However, here we present new data based on the carbon isotopic composition of solidified hydrocarbons [3] and the spatial distribution of liquid hydrocarbons within the original 2.5 and 2.7 Ga shales [4] that demonstrate that the molecules must have entered the rocks much later in Earth's history and therefore provide no information about the Archean (>2.5 Ga) biosphere or environment.

The elimination of the Archean biomarker data has immense implications for our understanding of Earth's early biosphere. 2α-methylhopanes have been interpreted as evidence for the existence of cyanobacteria at 2.7 Ga, about ~300 million years before the atmosphere became mildly oxygenated in the Great Oxidation Event (GOE; between 2.45 and 2.32 Ga). Now, the oldest direct fossil evidence for cyanobacteria reverts back to 2.15 Ga, and the most ancient robust sign for oxygenic photosynthesis becomes the GOE itself. Moreover, the presence of steranes has been interpreted as evidence for the existence of ancestral eukaryotes at 2.7 Ga. However, without the steranes, the oldest fossil evidence for the domain falls into the range ~1.78-1.68 Ga. Recognition that the biomarkers from Archean rocks are not of Archean age renders permissive hypotheses about a late evolution of oxygenic photosynthesis, and an anoxygenic phototrophic origin of the vast deposits of Archean banded iron formation.

[1] Brocks *et al.* (1999) *Science* **285**, 1033-1036. [2] Summons *et al.* (1999) *Nature* **400**, 554-557. [3] Rasmussen *et al.* (2008) *Nature* **455**, 1101 - 1104. [4] Brocks (2011) *Geochim. Cosmochim. Acta, in press.*

https://doi.org/10.1180/S0026461X00006502 Published online by Cambridge University Press

Palaeoclimate record from groundwater of the Great Artesian Basin, Australia

LISA BRÖDER[1]*, ROLAND PURTSCHERT[2], ANDREW LOVE[3], SIMON FULTON[4], DANIEL WOHLING[5] AND WERNER AESCHBACH-HERTIG[1]

[1]Institute of Environmental Physics, Heidelberg University, Heidelberg, Germany (*correspondence: Lisa.Broeder@iup.uni-heidelberg.de)
[2]Climate and Environmental Physics, Physics Institute, University of Bern, Bern, Switzerland
[3]Flinders University and NCGRT, Adelaide, Australia
[4]NRETAS, Northern Territory, Australia
[5]DFW, South Australian Government, Australia

The Great Artesian Basin (GAB) is one of the largest artesian groundwater basins in the world, underlying more than one-fifth of the Australian continent. The water is stored in a multi-layered confined aquifer system. Earlier studies using different dating methods showed a wide range of water ages up to more than 400 000 years [1,2]. As the GAB aquifers constitute the major water source in this semi-arid to arid region their careful management is of great importance.

Study area of this project is the western margin of the GAB as part of the project "Allocating water and maintaining springs in the Great Artesian Basin" of the Australian National Water Commission. We aim to obtain a full record of palaeoclimate data over the last 30 kyr by analysing groundwater samples for dissolved noble gases and stable isotopes. Noble gas studies have proven to be a valuable tool for determining palaeotemperatures all over the world [3]. By examining the excess air component estimations of palaeohumidity can be made [4].

^{3}He, ^{4}He, Ne, Ar, Kr and Xe concentrations are measured using mass spectrometry. For dating mainly ^{14}C and ^{4}He, in some cases other radioisotopes, will be used. Radiogenic ^{4}He concentrations increase with distance along presumed flow lines. First results for noble gas temperatures of recent groundwaters correspond well to the mean annual air temperature in the study area (21.7°C).

[1] Collon, P. *et al*. (2000) E*arth and Planetary Science Letters* **182**, 103-113. [2] Lehmann, B.E. *et al*. (2003) *Earth and Planetary Science Letters* **211**, 237-250. [3] Kipfer, R. *et al*. (2002) *Reviews in Mineralogy & Geochemistry* **47**. [4] Aeschbach-Hertig, W. *et al*. (2002). *Study of Environmental Change Using Isotope Techniques,* Vienna, IAEA, C&S Papers Series, Vol. 13/P: 174-183.

The rapid emplacement of the Val Fredda Complex, Adamello batholith, N. Italy

C.A. BRODERICK[1]*, U. SCHALTEGGER[1], D. GÜNTHER[2] AND P. BRACK[3]

[1]University of Geneva, Earth Sciences, Switzerland (*corresponence: Cindy.Broderick@unige.ch)
[2]ETH Zürich, D-CHAB, Lab of Inorg Chem, Switzerland
[3]ETH Zürich, Earth Sciences, Switzerland

Recent advances in U-Pb zircon geochronology have revealed the complexities of pluton construction, by multiple injections on 10-100 ka to Ma timescales [1, 2]. Using high precision U-Pb dating we are potentially able to determine timescales of magma generation, crystallization and emplacement within the crust. The potential exists to better understand magma forming processes with detailed high precision U-Pb dating and trace element analyses of zircon and titanite, combined with Hf isotope analysis of zircon.

The focus of this study is on the Val Fredda Complex (VFC) in the southern tip of the Adamello batholith, N. Italy. The VFC shows complex relationships among mafic melts that were injected into solidifying felsic magmas. Single zircon crystals, from the VFC, have been dated using CA-ID-TIMS, employing the ET2535 tracer solution for maximum precision and accuracy. The mafic units have apparent autocrystic zircons that indicate growth over a duration of 100 ka, with the majority of zircons crystallizing near the solidus, as indicated by ^{206}Pb/^{238}U zircon and titanite dates, both with permil uncertainties. Data from the VFC felsic units show more complex zircon populations, including xenocrystic, antecrystic and autocrystic zircons. Trace element ratios such as Y/Hf aide in our distinctions between autocrystic and antecrystic zircons. These felsic units have apparent autocrystic zircon growth over 100 to 200 ka, with zircons crystallizing near the solidus during the last 20 to 50 ka as indicated by titanite dates. Our data suggest that the oldest autocrystic zircon could be used to approximate the injection of the respective magma pulses into the host rock, whereas the youngest zircon and titanite could be used to approximate (final?) solidification. It appears that the five units from the VFC were injected into the crust between 42.58 Ma and 42.52 Ma and achieved the final solid state between 42.48 Ma and 42.42 Ma.

[1] Michel *et al*. (2008), *Geol*. **36** : 459-462. [2] Schaltegger *et al*. (2009) *EPSL* **286**: 208-218

https://doi.org/10.1180/S0026461X00006502 Published online by Cambridge University Press

Sr isotope ratios determination by LA-MC-ICPMS in Rb rich samples: Online separation of Rb by electrothermal aerosol heating

R. BROGIOLI, L. DORTA, B. HATTENDORF AND D. GÜNTHER

Laboratory of Inorganic Chemistry, ETH Zurich, Wolfgang-Paulistrasse 10, 8093, Zürich, Switzerland

Rb/Sr geochronology using LA-ICPMS has successfully been demonstrated for solid samples where the Rb/Sr concentration ratio is lower than 0.02 [1] and 0.14 [2]. For samples with higher Rb content, the determination of Sr isotope ratios remains challenging because mathematical correction of the isobaric interference from ^{87}Rb leads to increased uncertainties in the results. Using electrothermal vaporization (ETV)-ICPMS, a method has been conceived by Rowland *et al*. [3] in order to selectively pre-vaporize Rb from a reference potassium feldspar sample (NIST SRM607) making the measurement of Sr isotope ratios possible for samples where the Rb/Sr ratio can be as high as 8.

In an earlier study we could demostrate that heating laser generated aerosols from a silicate glass reference material (NIST SRM610, Rb/Sr ~1) with a commercially available ETV unit (Perkin Elmer, HGA 600MS) to about 2000 °C, enables the reduction of the signal intensity of Rb by 99%, while the signal intensities for Sr remain practically unaffected [4]. The approach has now been used for Sr isotope ratios measuerments in NIST SRM 610 (Rb/Sr = 1), USGS BCR2G (Rb/Sr = 0.14) and $Li_2B_4O_7$ fused disks of NIST SRM607 (Rb/Sr = 8) using multicollector ICPMS coupled to the LA-ETV setup. The combination of electrothermal vaporization for interferences suppression and laser ablation for spatially resolved sampling of solids is expected to broaden the range of applications for Rb/Sr –geochonology since both, isotope ratios and elemental concentrations, can principally be determined under highly similar conditions when using either sequential LA-ICPMS approaches or a split-flow prior to ETV configuration with MC-ICPMS and single collector ICPMS operating in parallel [5].

[1] Ramos *et* al. (2004) *Chem. Geol.* **211**, 135-158. [2] Jackson *et* al. (2006) *Earth Planet. SC Lett.* **245**, 260-277. [3] Rowlan *et* al. (2008) *J. Anal. Atom. Spectrom.* **23**,167-172. [4] Brogioli *et* al. (2011) *Anal. Bioanal. Chem.* **399**, 2201-2209, [5] Yuan *et* al. (2008) *Chem. Geol.* **247**, 100-118.

Bioreduction of biotite and chlorite: Effects on mineral reactivity

D.R. BROOKSHAW*, R.A.D. PATTRICK, J.R. LLOYD AND D.J. VAUGHAN

School of Earth, Atmospheric and Environmental Sciences, and Williamson Research Centre for Molecular Environmental Science, University of Manchester, Manchester, M13 9PL, UK (*correspondence: diana.brookshaw@postgrad.manchester.ac.uk)

Interactions with mineral phases can dictate the mobility of contaminants in the subsurface. Electron transfer processes in particular have the potential to reduce redox-sensitive metals (including radionuclides) so as to form much less soluble and less mobile phases. This work concerns investigating the role that microorganisms can play in such electron-transfer processes, examining interactions involving two key phyllosilicates found in the sub-surface.

Biotite and chlorite are sheet silicate minerals containing both ferric and ferrous iron in their octahedral layers. The redox reactivity of these minerals when fresh, and after undergoing bioreduction, was studied. The model Fe(III)-reducing microorganism *Shewanella oneidensis* MR-1 was used in anaerobic batch experiments where reduction of structural iron was stimulated by addition of an electron donor. The bioreduced mineral was collected and washed before use in redox reactivity experiments.

Ferrous iron assays using the ferrozine method show that *S. oneidensis* MR-1 is able to reduce the bioavailable Fe(III) in both minerals, both in the presence and absence of an artificial electron shuttle and humic analogue (AQDS). Chromate (Cr(VI)) was used as a redox probe to explore mineral reactivity. Unaltered biotite and chlorite reduced up to ~15% of 1mM Cr(VI), compared to 82.8% for the bioreduced biotite, and 91.6% for the bioreduced chlorite. This demonstrates the importance of bioreduction in metal cycling, with the mineral surfaces conditioned to reduce the metals in solution. The amount of reduction suggests that the processes involve more than just the available Fe(II) surface atoms. Surface analysis (XPS) combined with XAS are being used to detemine the biologically induced mineralogical changes that are driving the reduction process.

The work is being extended to radionuclides, and the reduction of technetium (^{99}Tc). It is anticipated that the amount of reduction will be similar to that of Cr(VI) as Tc reduction is also a three-electron transformation (Tc(VII) to Tc(IV)).

https://doi.org/10.1180/S0026461X00006502 Published online by Cambridge University Press

Geochemistry and tectonic setting of Una-Una volcano, Sulawesi, Indonesia

S. BROOM-FENDLEY*, M.F. THIRLWALL, M.A. COTTAM AND R. HALL

SE Asia Research Group, Department of Earth Sciences, Royal Holloway University of London, Egham, Surrey TW20 OEX, UK (*correspondence: s.broom.fendley@gmail.com)

Una-Una is an isolated volcano in Gorontalo Bay, North Sulawesi situated in a complex tectonic setting. Previously, Una-Una has been linked to southward subduction of the Celebes Sea under the North Arm of Sulawesi or northward subduction linked to collision in East Sulawesi. These hypotheses have problems with the apparent depth to the Benioff zone and amount of continental underthrusting.

We present new geochemical and Sr, Nd & Pb isotope analyses of volcanic rocks from Una-Una (<~100 Ka) and the nearby Togian islands (~2 Ma). These are both alkaline or high-K calc-alkaline trachytes with elevated Sr, Pb and LILE and depleted HREE, Nb and Ta. Sr and Nd isotopes plot in the enriched quadrant on a Sr-Nd diagram and $^{207}Pb/^{204}Pb$ show a steep trajectory extending from Indian Ocean MORB. The isotopic trends and similar geochemistry indicate that the rocks are genetically related and have similar continental derived components. The elevated isotopic values require an ancient continental contribution to the source. Mixing trends between Sr and Nd isotopes show that contamination is not likely to have come from Celebes Sea sediment compositions and Indian Ocean pelagic sediment is more likely. Contamination could have occurred during Eocene-Early Miocene subduction of Indian Ocean lithosphere. Una-Una is not above a subducted slab, and is at least 200 km above any projected subduction zone. The age of volcanic rocks from the Togian Islands rule out subduction at the North Sulawesi trench as the slab would not have been deep enough.

We propose that Una-Una and the Togian Islands are the product of young extension of Gorontalo Bay due to slab roll-back. This provides a mechanism for upwelling of a pre-metasomatised mantle.

Assessing calcium isotopes as a dietary proxy for terrestrial vertebrates

J. BROSKA[1], T. TÜTKEN[2]*, S.J.G. GALER[3], P. HELD[1] AND K.W. ALT[1]

[1]Institut für Anthropologie, Johannes Gutenberg-Universität Mainz, 5099 Mainz, Germany

[2]Steinmann-Institut, Rheinische Friedrich-Wilhelms-Universität Bonn, Poppelsdorfer Schloß, 53115 Bonn, Germany (*correspondence: tuetken@uni-bonn.de)

[3]Max-Planck-Institut für Chemie, Abteilung Biogeochemie, Postfach 3060, 55020 Mainz, Germany

Vertebrates ingest calcium along with their diet, and during biomineralization the light calcium isotopes are preferentially enriched in the bioapatite of bones and teeth. Therefore, $\delta^{44/42}Ca$ should decrease systematically along a food chain, and display a trophic level effect (TLE). Since calcium isotope signatures of bones and teeth seem robust against strong diagenetic alteration, $\delta^{44/42}Ca$ is a promising proxy for reconstructing both past diets of extinct vertebrates and fossil food webs.

However, in order to be able to use $\delta^{44/42}Ca$ to elucidate the diet of extinct animals, a better understanding of $\delta^{44/42}Ca$ and TLE in modern ecosystems is paramount. With this in mind, we analysed $\delta^{44/42}Ca$ in more than 40 bones of 19 extant mammals with a broad range of well-characterized diets from savannah ecosystems in Africa. The Ca isotope data were obtained by TIMS using a ^{43}Ca-^{46}Ca double spike at MPI. Additional, established proxies for diet and trophic level such as $\delta^{13}C$ and $\delta^{15}N$ of collagen were also analyzed on the same specimens for comparison and to assess dietary differences and trophic level relationships.

A large variability in $\delta^{44/42}Ca$ was observed within each trophic level. Browsers and grazers, and some of the frugivores, had similar $\delta^{44/42}Ca$ values. A significant TLE difference in $\delta^{44/42}Ca$ of –0.36 was found to exist between herbivores (–0.53 ± 0.32‰) and carnivores (–0.89 ± 0.18‰). This TLE difference is smaller than the –0.65 that has been reported thus far, but appears to vary between different areas and geological substrates.

Carnivores with high amounts of bone consumption, such as leopards and hyenas, display the lowest $\delta^{44/42}Ca$, down to –1.2‰ (hyenas). In contrast, ant-eating insectivores, such as the aardvark and aardwolf, have the highest bone $\delta^{44/42}Ca$ (+0.03±0.27‰) observed for extant vertebrates thus far, being significantly higher than found for both herbivores and carnivores. Thus, $\delta^{44/42}Ca$ may potentially be a useful indicator of insectivory in fossil vertebrates.

Combining $\delta^{44/42}Ca$ with $\delta^{13}C$ and $\delta^{15}N$ allows us to refine our interpretation of diet of foodwebs significantly in extant and extinct vertebrates.

https://doi.org/10.1180/S0026461X00006502 Published online by Cambridge University Press

Effect of differentiation on Fe oxidation in arc basalts

MARYJO BROUNCE[1,2], KATHERINE A. KELLEY[1] AND ELIZABETH COTTRELL[2]

[1]Graduate School of Oceanography, University of Rhode Island, 215 S. Ferry Road Narragansett, RI 02882 USA
[2]National Museum of Natural History, Smithsonian Institution, Washington DC 20560, USA

The role of crustal differentiation processes in creating or modifying the relatively oxidized condition of arc basalts relative to mid ocean ridge basalts (MORB) is not well constrained. We present the first combined data set for major elements, dissolved volatile concentrations and $Fe^{3+}/\Sigma Fe$ ratios (determined by μ-XANES) in olivine-hosted basaltic glass inclusions from four Mariana arc volcanoes in order to examine how Fe oxidation varies with extent of fractional crystallization, degassing and contributions from the slab to the arc mantle source.

Glass inclusions span a variety of compositions and are consistent with multi-phase crystallization and degassing. A strong trend in Fe reduction accompanies magmatic degassing and inclusions with the highest MgO (>6.5 wt%) are consistently the most oxidized ($Fe^{3+}/\Sigma Fe>0.235$). The reduction trend suggests that redox exchange may occur during SO_2 degassing that redistributes e^- in the residual magma ($S^{2-}_{melt} \rightarrow S^{4+}_{vapor} + 6e^-$). We show that the high $Fe^{3+}/\Sigma Fe$ observed here cannot be created through extensive multi-phase fractionation (olv ± cpx ± plag) of a MORB-like primary melt ($Fe^{3+}/\Sigma Fe=0.16$ [1]). These observations support the hypothesis that the elevated $Fe^{3+}/\Sigma Fe$ of arc and back-arc basalts are due to differences in the source mantle. Primary melt compositions were reconstructed by restoring the most mafic inclusion compositions to equilibrium with Fo_{90}. A strong positive correlation exists between $Fe^{3+}/\Sigma Fe_{Fo90}$ and H_2O_{Fo90}, suggesting that slab derived fluids may contain an oxidized signature that contributes significantly to the oxidation state of basalts erupted at the Mariana arc.

[1] Cottrell and Kelley, *EPSL*, (2011).

Simultaneous reaction and creep in the KCl-KBr-H_2O system

J. BROUWER* AND A. PUTNIS

Institut für Mineralogie, Westf. Wilhelms Univ. Münster Corrensstr. 24, 48149 Münster , Germany
(* correspondence: J.Brouwer@uni-muenster.de)

As early as 1983 [1] it has been suggested that dissolution-precipitation creep rates may be affected by chemical reaction. However, for a long time research has focused mainly on creep of single phase mineral aggregates in order to understand the physics of stress-driven dissolution-precipitation creep [2,3,4]. More recent research has shown that background ions in solution may significantly effect surface kinetics and solubility both negatively and positively [5]. We present experiments on simultaneous reaction and dissolution precipitation creep in the system KBr, KCl, K(Br,Cl), H_2O.

When KBr and KCl are reacted in the presence of an aqueous fluid at room temperature a solid solution $K(Br_x, Cl_{1-x})$ will form. Creep rates of KBr and KCl in their respective aqueous solutions are compared with those of KBr and KCl in the solution of the other endmember, and with creep rates of mixtures of KBr and KCl in an aqueous solution that is in equilibrium with the solid solution that will form when reaction has gone to completion. These results provide in insight the complex combination of effects that reaction has on deformation, including changes in solid volume due to solubility differences between parent and product phases, changes in grain size and material properties, and changes in kinetics.

[1] Rutter (1983) *J. Geol. Soc.* **140**, 725-740. [2] Raj (1982) *JGR* **87**, 4731-4739. [3] Spiers and Schutjens (1990) in *Deformation Processes in Minerals, Ceramics and Rocks*, ed. Barber and Meredith, London, 334-353. [4] Gratier *et al.* (2009) *JGR – Solid Earth* **114**, B03403. [5] Zhang *et al.* (2011) *Geofluids* **11**, 108-122.

https://doi.org/10.1180/S0026461X00006502 Published online by Cambridge University Press

Redox reactions on mineral surfaces: Spectroscopic and imaging studies at the molecular level

GORDON E. BROWN, JR.[1,2,3]*, GUILLAUME MORIN[4], GEORGES ONA-NGUEMA[4], FARID JUILLOT[4], YUHENG WANG[4], DIK FANDEUR[4], KARIM BENZERARA[4], GEORGES CALAS[4], YINGGE WANG[1], JU YOUNG HA[1], SARP KAYA[2], TOM KENDELEWICZ[1], ALFRED M. SPORMANN[3], AND ANDERS NILSSON[2]

[1]Dept. of Geological & Environmental Sciences, Stanford University, Stanford, CA 94305-2115, USA (*gordon.brown@stanford.edu)

[2]Stanford Synchrotron Radiation Lightsource, SLAC National Accelerator Laboratory, Menlo Park, CA, USA.

[3]Dept. of Chemical Engineering, Stanford University, Stanford, CA, USA.

[4]Institut de Minéralogie et de Physique des Milieux Condensés (IMPMC), UPMC; Université Paris 7; CNRS; 4, Place Jussieu, 75252 Paris Cedex 05, France.

Electron transfer at mineral-water and mineral-microbe interfaces is a major biogeochemical process that can result in transformation of redox-sensitive minerals and adsorbed pollutant ions, capture (through adsorption and precipitation reactions) or release (through reductive transformation of the sorbent and desorption of surface complexes) of pollutant species, and major controls on element cycling. Over the past decade, a growing number of spectroscopic and imaging studies of the products of electron transfer reactions in model mineral-water systems have advanced our understanding of these reactions and their kinetics in the laboratory. Here, we will review a number of these studies, including abiotic reduction of As(V), Cr(VI), and Se(VI) on metal oxide surfaces, photocatalyzed As(III) oxidation on kaolinite and anatase surfaces, the role of reactive oxygen species and Fe^{2+} on the oxidation kinetics of As(III) on iron oxides, microbially mediated redox reactions of arsenic at iron oxide-water interfaces, and the role of exopolysaccharides in the reduction of nanoparticulate hematite by *Shewanella oneidensis* MR-1, and microbially mediated oxidation of metal sulfides. We will also present the results of several studies of complex environmental samples that illustrate the effects of electron transfer reactions in natural settings, including chromium reduction by magnetite, the effect of electrically insulating coatings on the Cr(VI) to Cr(III) reduction at the magnetite-water interface, Cr(III) oxidation by Mn-oxides, and arsenic redox reactions, including As(III,V) biomineral formation in an acid mine drainage environment.

Interfacial area measurements for robust models of multiphase flow in porous media

KENDRA I. BROWN[1], DORTHE WILDENSCHILD[1], WILLIAM G. GRAY[2] AND CASS T. MILLER[2]

[1]School of Chem/Bio/Env Eng, Oregon State University, Corvallis, OR 97331; (brownke@engr.orst.edu, dorthe@engr.oregonstate.edu)

[2]Dept of Env Science and Engineering, University of North Carolina, Chapel Hill, NC; (graywg@unc.edu, casey_miller@unc.edu)

Understanding the physics of natural flow systems that include *three* immiscible fluid phases in porous media is important to applications such as remediation of NAPL from the vadose zone, oil and gas recovery, and CO_2 sequestration.

Flow and transport in such systems are strongly influenced by the presence of fluid-fluid interfaces. Theoretical work based on conservation laws and the second law of thermodynamics has demonstrated the advantage of a different approach to modeling multiphase flow, accounting not only for traditional variables such as saturation and porosity, but that also incorporate specific interfacial areas, specific common curve lengths, and average curvatures, that are measures of the morphology and topology of the phase distributions.

This research expands previous work on two-fluid-phase systems to three-fluid-phase systems, and the particular focus is the generation of a pore-scale experimental data set that expresses the dependency of capillary pressures in the system on two saturations, as well as interfacial areas per volume. Synchrotron-based X-ray computed microtomography (CMT) is used to generate high-resolution images during drainage and imbibition, which are analyzed to measure the saturations and interfacial areas, and to calculate capillary pressures via meniscus curvature.

https://doi.org/10.1180/S0026461X00006502 Published online by Cambridge University Press

Magnetic properties of ilmenite-hematite containing magnetite nano-crystals

SARAH J. BROWNLEE*[1], JOSHUA M. FEINBERG[2], TAKESHI KASAMA[3] RICHARD J. HARRISON[4], GARY R. SCOTT[5] AND PAUL R. RENNE[5]

[1]Earth Research Institute, University of California, Santa Barbara, 6832 Ellison Hall, Santa Barbara, CA 93106-3060

[2]Institute for Rock Magnetism, University of Minnesota, 310 Pillsbury Drive SE, Minneapolis, MN 55455

[3]Center for Electron Nanoscopy, Technical University of Denmark, DK-2800 Kongens Lyngby, Denmark

[4]University of Cambridge, Department of Earth Sciences, Downing Street, Cambridge, CB2 3EQ

[5]Berkeley Geochronology Center, 2455 Ridge Road, Berkeley, CA 94709

This study investigates changes in the rock magnetic properties of single crystals of ilmenite-hematite from the Ecstall pluton containing nm-sized magnetite crystals that formed as a result of reheating by the adjacent Quottoon plutonic complex. Measurements of hysteresis properties, low temperature remanence, room temperature IRM acquisition, and observations from magnetic force microscopy (MFM) and off-axis electron holography show that samples fall into 3 groups, which are defined by the presence of mineral microstructures documented in *Brownlee et al*. [2010], which are in turn related to distance from the Quottoon plutonic complex. Ilmenite-hematite grains from the two groups closest to the Quottoon plutonic complex contain nm-sized magnetite crystals within hematite and ilmenite lamellae. Reheating of the Ecstall pluton led to an increase in coercivity and overall magnetic intensity, as well as the development of mixed phase hysteresis. Though the potential for lamellar magnetism exists in all of these samples, off-axis electron holography results indicate that the magnetic signal is dominated by magnetite precipitates at intermediate distances from the Quottoon plutonic complex. Increased single grain coercivity may reflect further development of exsolution lamellae at very close distances to the Quottoon plutonic complex. These results indicate that reheating had a profound affect on the overall magnetic properties of the Ecstall pluton through the growth and modification of Fe-Ti oxide microstructures.

Fate of an Eocene HT metamorphic complex in a forearc location

E. BRUAND[1]*, D. GASSER[2] AND K. STUEWE[3]

[1]SEES, University of Portsmouth, Portsmouth PO1 3QL, UK (*correspondence: emilie.bruand@port.ac.uk)

[2]Department of Geosciences, University of Oslo, 0316 Oslo, Norway (deta.gasser@geo.uio.no)

[3]Department of Earth Sciences, Karl-Franzens Universität, 8010 Graz, Austria (kurt.stuewe@uni-graz.at)

The Chugach and St Elias mountains in southern Alaska are a peculiar and interesting region from many geological aspects. For example, this area encloses a high temperature Eocene complex (CMC) developed in a Late Cretaceous accretionary prism: such a high-thermal regime is uncommon in a subduction setting during the Phanerozoic. In addition, this investigated area is also currently the focus of intense research related to the coupling of surface processes (glacial erosion) and tectonics, since fast Neogene exhumation rates have been observed in areas of intense glaciation [1]. Therefore, in order to understand links between crustal thermal evolution, metamorphism, deformation and erosion in this area, it is crucial to obtain a detailed description of its PTdt-evolution through time. For this purpose, aspects of metamorphic petrology, geochemistry, structural geology and geochronology are combined and presented in this contribution to develop a crustal scale geodynamic model of this region.

The CMC is more than 300 km long, made up of metasediments associated with an amphibolite layer in its southern part. Detailed petrological work across several parts of this complex permits to discuss the uncommon presence of such a HT complex in a forearc location. Results highlight a pressure gradient from north to south and an interesting behaviour of the southern amphibolite belt that make up the suture between the CMC and the outboard accreted terrane. In addition, our dataset including detailed structural geology and geochronology suggests that fast burial and exhumation rates in this region do not only occur in the Neogene but also during the Eocene. Our new results assess that exhumation from depths of >20 km in parts of the complex were accompanied by erosion at the surface. Our data set documents a complex deformational and thermal history including accretion of sediments, subsequent vertical flattening leading to compressed isotherms, followed by dextral transpression, exhumation and erosion within a short time period of ca. 10-15 Ma.

[1] Enkelmann *et al*. (2009) *Nature Geoscience* **5**, 360-363

https://doi.org/10.1180/S0026461X00006502 Published online by Cambridge University Press

Experimental quantification of plagioclase CSD during decompression of hydrous rhyodacite

C. BRUGGER-SCHORR AND J. HAMMER*

Dept. GG, Univ. Hawaii, 1680 East-West Rd., Honolulu, HI, 96822, USA (*correspondence jhammer@hawaii.edu)

Few experimental studies [1,2] constrain the link between crystal size distributions (CSDs) and known chemical, thermal, or barometric histories. We determine CSDs of plagioclase forming during decompression experiments on hydrous rhyodacite magma. Samples were annealed at 130 MPa, subjected to continuous decompression at either 2 MPa hr^{-1} or 0.5 MPa hr^{-1}, and then quenched at ~20 MPa intervals to provide snapshots of the system along the decompression path [3]. Crystal nucleation and growth rates derived from CSDs using standard assumptions are compared with values obtained using 2D measurements of the largest crystals (L_{max} methods) as well as bulk crystal populations (batch methods). The characteristic growth rate in the rapidly decompressed series is approximately five times faster than the growth rate in the slowly decompressed series. Because crystal growth rate depends on decompression rate, CSDs are incapable of revealing decompression timescales or magma ascent rates without independent knowledge of crystal growth rate.

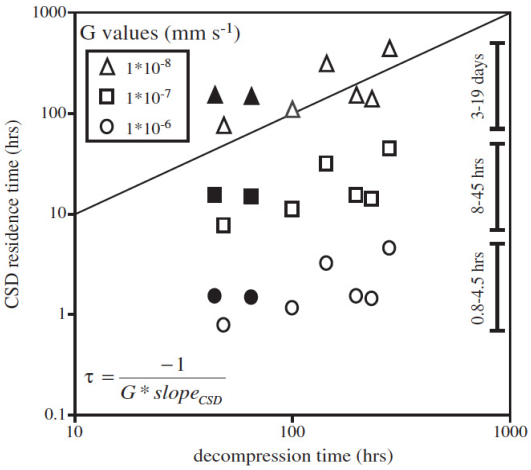

Figure 1: Residence time is computed using three published values of plagioclase growth rate. Only independent knowledge of G permits recovery of actual crystallization interval (1:1 line).

[1] Zieg and Lofgren (2006), *J Volcanol Geotherm Res* **154**, 74-88. [2] Pupier *et al*. (2008) *Contrib Mineral Petrol* **155**, 555-570. [3] Brugger and Hammer (2010) *J Petrol* **51**, 1941-1965.

Composition of Hippopotamid enamel: Paleoenvironmental reconstruction and enamel formation

G.E. BRÜGMANN,[1]*, J. KRAUSE[2], T.C. BRACHERT[3], O. KULLMER[4], I. SSEMMANDA[5] AND D.F. MERTZ [1]

[1]Institut für Geowissenschaften, Johannes Gutenberg-Universität Mainz, 55099 Mainz, Germany (*correspondence: bruegmag@uni-mainz.de)

[2]Max-Planck-Institut für Chemie, Joh.-Joachim-Becher-Weg 27, 55128 Mainz, Germany

[3]Institut für Geophysik und Geologie, Talstraße 35, Universität Leipzig, 04103 Leipzig, Germany

[4]Forschungsinstitut und Naturmuseum Senckenberg, Senckenberganlage 25, 60325 Frankfurt, Germany

[5]Geology Department, Makerere University, P.O. Box 7062, Uganda

Bioapatite in mammalian teeth is readily preserved in continental sediments and represents an important archive for environmental reconstructions. Here we present electron microprobe data for fossil and modern molar enamel of Hippopotamids from different ecosystems in Eastern Africa, representing modern and fossil lacustrine (Lake Kikorongo, Lake Albert, and Lake Malawi) and modern fluvial environments of the Nile River system.

Fossil enamel from the saline Lake Kikorongo has a much higher MgO/Na_2O ratio (~1.11) than from the Neogene fossils of Lake Albert (MgO/Na_2O~0.4), which was a large fresh water lake. Similarly, the MgO/Na_2O ratio in modern enamel from the White Nile River (~0.36), which passes through several saline zones, is higher than that from the Blue Nile River (MgO/Na_2O~0.22). Thus, MgO/Na_2O is suggested be a fingerprint for environments where river and lake water have suffered strong evaporation.

Linear regression analysis reveals very tight physiological control on the MgO, Na_2O and Cl variations (R^2: 0.6-0.84) despite large concentration variations (40% to 300%) along sections perpendicular to the enamel-dentin junction (EDJ). MgO and Na_2O decrease from the EDJ towards the outer enamel rim, whereas Cl displays the opposite variation. Nevertheless, there are co-linear relationships among these elements which can be interpreted as binary mixing lines. Enamel crystallites precipitating during amelogenesis equilibrate with a continuously evolving fluid. During this process Na_2O and MgO behave incompatibly whereas Cl is incompatible to hydroxyapatite. This results in the formation of MgO, and Na_2O-rich, but Cl-poor bioapatite near the EDJ and MgO- and Na_2O-poor, but Cl-rich bioapatite at the outer enamel rim.

https://doi.org/10.1180/S0026461X00006502 Published online by Cambridge University Press

The relationship between $\Delta^{14}C$ and $\delta^{13}C$ of DIC in the LGM Ocean

S.P. BRYAN[1]*, S.J. LEHMAN[2] AND T.M. MARCHITTO[2]

[1]Dept. of Marine Chemistry & Geochemistry, Woods Hole Oceanographic Institution, Woods Hole, MA 02543, USA (*correspondance: sbryan@whoi.edu)
[2]Dept. of Geological Sciences & INSTAAR, University of Colorado, Boulder, CO 80303, USA (scott.lehman@colorado.edu, tom.marchitto@colorado.edu)

Reconstructed atmospheric radiocarbon activities ($\Delta^{14}C$) during the last glacial period were higher than can be explained by ^{14}C production rates, seemingly requiring reduced ventiliation of the glacial deep ocean relative to the preindustrial ocean. Estimates of glacial deep ocean $\Delta^{14}C$ generally support this prediction; though large uncertainites exist in deep ocean paleo-$\Delta^{14}C$ reconstructions due to the paucity of records, generally low sedimentation rates in the deep ocean, bioturbative mixing of foraminifera of differing ages, and uncertain surface reservoir ages. Due to these uncertainties there is currently no consensus regarding the spatial extent or the degree of ^{14}C depletion in the glacial deep ocean. The lack of a strong decrease in $\delta^{13}C$ in the glacial deep Pacific Ocean has been used as an argument against the existance of a large ^{14}C-depleted water mass. However, the distributions of ^{14}C and ^{13}C of dissolved inorganic carbon are not strictly analogous. For example, in the modern ocean, differences in the depths of organic carbon remineralization vs water mass aging cause the slope of the relationship between $\delta^{13}C$ and $\Delta^{14}C$ to increase with water depth.

We explore the relationship between $\delta^{13}C$ and $\Delta^{14}C$ during the Last Glacial Maximum (~19-23 kyr BP) using a global compilation of published measurements. Despite the uncertainties listed above, there is credible evidence that deep waters in the North Atlantic, Southern Ocean and Eastern Equatorial Pacific were depleted in ^{14}C during the LGM. The decrease in deep Pacific $\Delta^{14}C$ with little associated change in $\delta^{13}C$ is equivalent to a steepening of the $\delta^{13}C$ - $\Delta^{14}C$ relationship. We suggest that this steepening may be explained by reduced organic carbon remineralization rates in the glacial deep Pacific and/or changes in preformed $\delta^{13}C$ and $\Delta^{14}C$ values. We discuss the evidence for such changes and the implications for reconstruction of the glacial ocean carbon cyle.

Rollback-enhanced decompression melting of a volatile-rich mantle: The ancient lavas of Mt. Etna

J.G. BRYCE[1]*, D. GRAHAM[2], J. BLICHERT-TOFT[3], B.B. HANAN[4], S. MILLER[1], J. BARKMAN[1], F.J. SPERA[5] AND G.R. TILTON[5]

[1]UNH Earth Sciences, Durham NH, USA (*julie.bryce@unh.edu, correspondence)
[2]COAS, Oregon State University, Corvallis, OR, USA
[3]Ecole Normale Supérieure de Lyon, Lyon, France
[4]SDSU Geological Sciences, San Diego, CA, USA
[5]UCSB Earth Sciences, Santa Barbara, CA, USA

Mount Etna, Europe's largest and most active volcano, sits above a complicated tectonic setting near the intersection of the Tyrhennian, African and Ionian plates. Geophysical evidence suggests that the large volumes of mafic lavas at Etna and the neighboring Hyblean plateau are due to enhanced melting caused by perturbations in mantle convection associated with the oversteepened Ionian slab. Here, we present new Sr-Nd-Hf-Pb data on ancient Etna basalts. We use these data, together with new major/trace element and literature data, to constrain the source lithologies responsible for early Etnean magmatism. Our sample suite includes basal tholeiites followed (at ~ 200 ka) by lavas of dominantly transitional and alkaline compositions. Major and trace element trends within the tholeiitic and alkaline series can separately be modeled by fractional crystallization, but processing through crustal magma bodies cannot satisfactorily explain the links between these two compositional series. Isotopic data are distinctive between the two groups, with the tholeiitic lavas bearing less radiogenic Sr ($^{87}Sr/^{86}Sr < 0.7032$) and Pb ($^{206}Pb/^{204}Pb < \sim 19.6$, $^{208}Pb/^{204}Pb < \sim 39.3$) when compared to the alkaline lavas ($^{206}Pb/^{204}Pb \sim 20$, $^{208}Pb/^{204}Pb > \sim 39.5$). Nd and Hf isotopic signatures define narrower ranges, with shifts of < 2 ε units across this compositional boundary and markedly more radiogenic compositions than modern Etna lavas. We interpret the isotopic data to signify mixtures of MORB mantle and enriched mantle (defined as where MORB and OIB mantle compositions generally intersect). Major element modeling using compositions of the most magnesian basalts from early Etna lavas, as well as those from the associated Hyblean plateau, indicates that these lavas represent melting from relatively fusible lithologies (volatile-rich peridotites and pyroxenites) with lower solidi than ambient asthenospheric mantle. The prevalence of fusible lithologies coupled with enhanced convection due to the unique tectonic setting, gives rise to the voluminous volcanism in the Etna /Hyblean region.

https://doi.org/10.1180/S0026461X00006502 Published online by Cambridge University Press

Thermodynamics of long-term metastable magnesium (chloro) hydroxo carbonates at 25°C

C. BUBE, M. ALTMAIER, V. METZ, D. SCHILD, B. KIENZLER AND V. NECK

Institute for Nuclear Waste Disposal (INE), Karlsruhe Institute of Technology, Herrmann-von-Helmholtz-Platz, 76344 Eggenstein-Leopoldshafen (bube@kit.edu, marcus.altmaier@kit.edu, volker.metz@kit.edu, dieter.schild@kit.edu, bernhard.kienzler@kit.edu)

The thermodynamics of magnesium (chloro) hydroxo carbonate phases is important to assess the geochemical conditions in carbonate-containing magnesium chloride-rich solutions for nuclear waste disposal scenarios in rock salt. Though Magnesite ($MgCO_3$) is known to be the thermodynamically stable solid in the Mg-Cl-HCO_3-CO_3-H-OH-H_2O system at room temperature, long-term metastable carbonates are observed to control the solution chemistry (Hydromagnesite ($Mg_5(CO_3)_4(OH)_2$:$4H_2O$) and Chlorartinite (Mg_2CO_3OHCl:$3H_2O$)). In the present study we focus on determining the phase transition between Hydromagnesite and Chlorartinite in order to estimate the equilibrium constant for Chlorartinite, which has not been reported so far.

Batch experiments with $MgCl_2$ solutions (0.25 to 4.5 M $MgCl_2$) and 0.05 M Na_2CO_3 are conducted over >3 years in Ar glove boxes. The pH_c ($-\log(m_{H+})$) is monitored with time and the respective precipitates are analysed with different methods (Raman, XRD, SEM-EDS, XPS). The equilibrium constant for Chlorartinite is calculated based on the equilibrium at the Hydromagnesite and Chlorartinite phase transition $Mg_5(OH)_2(CO_3)_4$:$4H_2O(s) + 3Mg^{2+} + 4Cl^- + 10H_2O(l) \Leftrightarrow 4Mg_2(OH)CO_3Cl$:$3H_2O(s) + 2H^+$. Calculations are done using the known $MgCl_2$-concentration, the measured pH_c and published solubility constants of Hydromagnesite. Under the given conditions, stability of Hydromagnesite is observed in solutions of less than 2.5 M $MgCl_2$, while Chlorartinite is found to exist in solutions with $MgCl_2$ concentrations higher than 3.2 M $MgCl_2$. In the intermediate solution of 2.8 M $MgCl_2$, both solid phases are detected with the analytical methods. Assuming a phase transition between 2.5 M and 3.2 M $MgCl_2$, the equilibrium constant for Chlorartinite is calculated as $\log K_{CA} = 13.15 \pm 0.36$ for reaction $Mg_2(OH)CO_3Cl$:$3H_2O(s) + 2\,H^+ \Leftrightarrow 2\,Mg^{2+} + HCO_3^- + Cl^- + 4\,H_2O(l)$, using the Pitzer approach for activity corrections. This equilibrium constant together with literature data allows for a comprehensive thermodynamic description of the system Mg-Cl-HCO_3-CO_3-H-OH-H_2O at room temperature.

Fluids in the upper continental crust

KURT BUCHER

Mineralogy Geochemistry, University of Freiburg, Germany (bucher@uni-freiburg.de)

The brittle upper continental crust consists predominantly of granite and gneiss. Fractures form an interconnected network of water conducting structures with an appreciable permeability also providing substantial fluid saturated fracture porosity.

The chemical composition of fluids in the fracture porosity of granite and gneiss changes with depth. Near the surface Ca-Na-HCO_3 waters dominate. With increasing depth water contains increasing amounts of alkalis and sulphate and grade into chloride-rich waters at greater depth. Total dissolved solids (TDS) of 10^5 mg L^{-1} are common at 5 km depth in most basement rocks. All reported deep fluids from the upper crust contain predominantly NaCl and $CaCl_2$. The brines vary from NaCl-rich in granites to $CaCl_2$-rich in mafic reservoir rocks such as amphibolites and gabbros.

In regions of the crust with strong topography, fluid flow is important and recharge water may have flushed the basement efficiently thereby removing old brine components from the granites.

Water samples from the new Gotthard Rail Base Tunnel of the Alps, from Norwegian road tunnels, from Korean granites and other localities represent this type of basement fluid. Analyzed fluids from up to 2.5 km depth differ from basement fluids from areas with less extreme topography in the following ways. Such waters have relatively low TDS of some 100 mg L^{-1} and are typically of the Na_2CO_3-Na_2SO_4 type. pH tends to be high and varies from 9 to more than 10. Low Ca and ultra-low Mg of such waters result from efficient deposition of secondary Ca-Mg-minerals as coatings on fracture walls. Reduction of CO_2 to amorphous carbon or further to CH_4 provides the oxidation capacity for sulphate production from primary rock sulphides. Ferrous iron silicate minerals (e.g. biotite) are oxidized to ferric oxides and hydroxides (e.g. hematite). Evidence for this mechanism is the presence carbon in sheared, water conducting granite and measurable quantities of methane in fracture water. Extreme local variations of redox conditions are reflected by the presence of pyrrhotite and other sulphides in a fracture system and anhydrite in nearby fractures of the same granite.

https://doi.org/10.1180/S0026461X00006502 Published online by Cambridge University Press

Geochemical signature of rocks of the neo-archean ultramafite-mafite mass in the Dzhugdzhur-Stanovoy Superterrane (the South-Eastern rim of the North-Asian craton)

I.V. BUCHKO[1]* AND S.D. VELIKOSLAVINSKY[2]

[1]Institute of Geology and Nature Management, Blagoveshchensk, Relochny, 1, Russia, (*correspondence: inna@ascnet.ru)
[2]Institute of Precambrian Geology and Geochronology, St.Petersburg, Russia

The first geochemical and geochronological data were obtained for the Neoarchean rhythmically stratified ultramafite-mafite massif in the Dzhugdzhur-Stanovoy superterrane of the south-eastern rim of the North-Asian craton.

The main petrochemical peculiarities of ultramafites and pyroxenites of the mass are the moderate increase in TiO_2 and FeO* contents at practically constant Al_2O_3, at a decrease of magnesia content from the earliest occurrences to the later ones. At the same time an increase in SiO_2, Al_2O_3 is typical for gabbro-anorthosites in the process of crystallization at a decrease of Mg# which is characteristic of high aluminiferous basalts. The duality of the petrochemical trends and the results of modeling suggest that crystallization of the rhythmically stratified ultramafites and gabbro-anorthosites occurred from two different melts corresponding in composition to pyrites and high aluminiferous basalts, respectively.

The conformity of spectra of REE and minor elements distribution are present. This lets us to conclude that the fusion of the both melts occurred from a single source that was close to Al non-depleted pycritoid in the intermediate magmatic chamber. It may be assumed that this ultramafite-mafite massif is an example of Arcean pycritoid magmatism.

The age of this massif is preliminary estimated as ~2.6 Ma (LA-ICP-MS method).

This study was supported by FEB RAS (Gr.No 09-II-SB-08-007).

Age relations, mineral-chemical and isotopic investigations on basaltic gem stone zircons from Eastern Germany

JÖRG BÜCHNER [1]*, OLAF TIETZ [1], WOLFGANG SEIFERT[2], AXEL GERDES[3] AND ULF LINNEMANN[4]

[1]Senckenberg Museum für Naturkunde Görlitz, D-02806 Görlitz, Germany (*correspondence: joerg.buechner@senckenberg.de)
[2]GFZ Potsdam, D-14473 Potsdam, Germany
[3]Geozentrum der Universität Frankfurt, D-60438 Frankfurt a. M., Germany
[4]Senckenberg Naturhistorische Sammlungen Dresden, D-01109 Dresden, Germany

In alkali basaltic rocks scarcely appear accessory minerals such as zircon and corundum. The origin of these mostly gem stone like mega-crystals is unknown and discussed controversial. Host magmas of the zircon mega-crystals are normally SiO_2 undersaturated (basanites and nephelinites).

In several localities we could observe some zircon mega-crystals and in a quarry in Saxony (eastern Germany) we collected about 40 crystals up to 15 mm in size *in situ* from the basanitic rock [1]. Zircons occur in agglutinates of lower crater facies of a scoria cone. The related lava flows are almost free of zircons and their Zr contents reaches up to 900 ppm [2]. There is a good correlation between Ar/Ar data of the basanites (30 to 31 Ma) and the zircon U/Pb data which show ages about 30.5 Ma.

First investigations indicate two different alkaline sources for zircons which origin possibly from syenitic, phonolitic or trachytic melts. This is evidenced by zircon-typology, mineral chemistry and analyses of mineral inclusions [3]. Preliminary *in situ* Hf-isotopic analyses of zircons indicate an origin from the lithospheric mantle.

The crystals show an intensive magmatic corrosion in alkalibasaltic rocks (including nephelinites), whereas zircons out of phonolites are mostly euhedral. Zircons in basaltic rocks have more or less evolved reaction rims, composed mostly of baddeyleit. Zr-contents in the rims of clinopyroxene phenocrystals decreases rapidly with the distance from the zircon inclusions. This indicates late entrainment of zircon crystals into the basanitic melt.

The age data of the zircons in relation to that of the host rocks as well as the mineral chemical and isotopic data imply a cogenetic development of both.

[1] Tietz & Büchner (2007) *ZdGG* **158**, 201-206. [2] Büchner *et al*. (2006) *Z. geol. Wiss*. **34**, 121-141. [3] Seifert *et al*. (2008) *N. Jb. Mineral., Abh*. **184**, 299-313.

https://doi.org/10.1180/S0026461X00006502 Published online by Cambridge University Press

Petit spot-like volcanoes exposed in Costa Rica

D.M. BUCHS[1]*, S. PILET[1], P.O. BAUMGARTNER[1], M. COSCA[2], K. FLORES[1] AND A. BANDINI[1]

[1]IGP/IMG, University of Lausanne, Switzerland (correspondence: dbuchs@ifm-geomar.de)
[2]US Geological Survey, USA

The study of volcanism in the ocean is fundamental to better understand the dynamics of the Earth mantle and plate tectonics. However, our understanding of this volcanism is limited by difficulties to access the roots of ocean volcanoes and the ocean floor. Recent results in Panama shown that exposed accreted volcanoes can provide another way of understanding volcanism in the oceans [1].

Petit spot volcanoes found on the subducting plate off Japan are considered to reflect volcanism in response to plate flexure [2]. However, petit spot volcanoes are very small and it remains unclear if they are a common feature on the ocean floor; documenting new occurrences of petit spot volcanoes is a key multidisciplinary issue. We recognize here ancient petit spot-like volcanoes accreted in Costa Rica based on new geochemical, geological, ^{40}Ar-^{39}Ar, and biochronologic data.

Petit spot-like volcanoes acccreted in Costa Rica consists of tectonic stacks of volcano-sedimentary material that includes vesiculated pillow lavas, volcanic breccias and thick radiolarite beds. Igneous sills compositionnally similar to the lavas are common in the radiolarite beds. Major and trace element contents of the igneous rocks indicate an alkalic, moderately fractionated composition, and support very low degrees of partial melting in the garnet stability field. Normalized trace element patterns are very similar to those of petit spot volcanoes in Japan, and distinct from those of typical OIB, MORB and off-axis seamounts.

Step-heating ^{40}Ar-^{39}Ar dating on co-magmatic amphiboles gave two ~175 Ma ages of formation for the petit spot-like volcanoes in Costa Rica. Tectonostratigraphic and biochronologic data clearly document a ~110 Ma age of accretion, and indicate that the volcanoes did not formed close to a subduction zone or a mid-ocean ridge. Therefore, we propose that petit spot-like volcanoes may represent a ubiquitous feature on the ocean floor, which can form far from mid-ocean ridges and subduction zones. Possibly, petit spot-like volcanoes exposed in Costa Rica reflect tectonically-induced leaking of melts pre-existing at the base of the lithosphere.

[1] Buchs *et al*. (2011) *Geology* **39,** 335-338. [2] Hirano *et al*. (2006) *Science* **313**, 1426-1428.

Cross calibration of a Pb Multi Ion Counting array on TIMS

NADINE BUCHS, DIETMAR TUTTAS AND CLAUDIA BOUMAN*

Thermo Fisher Scientific, Hanna-Kunath-Str. 11, 28199 Bremen, Germany. (*correspondence: claudia.bouman@thermofisher.com)

Multicollector instruments using arrays of Faraday detectors are the first choice for high precision isotope ratio measurements. With decreasing sample sizes, the noise level of the Faraday detectors becomes the limiting factor for high precision isotope ratio measurements. The new TRITON *Plus* TIMS provides Multi Ion Counting with up to eight ion counters in addition to its variable multicollector array of nine Faraday cups. Classical large scale SEMs can be combined with the newly introduced compact discrete dynode electron multipliers (CDDs). The performance of these small electron multipliers is directly comparable to the classical large-scale SEMs. Both show identical stability and linearity. Also dynamic range and noise characteristics are equal for both ion counter types.

In case of Faraday detectors, precise cross calibration is guaranteed by the gain calibration and baseline measurements. In a Multi Ion Counting array, individual yield factors must be taken into account, but the stability of the yield factors needs to be assessed as well to obtain ultimate precision for isotope ratio measurements.

This study presents two strategies for precise cross calibation of all ion counting channels. The first one includes a calibration up-front; the second strategy involved an in-run calibration to control yield drift. Experiments were done on a TRITON *Plus* setup with four ion counting detectors to collect ^{204}Pb, ^{206}Pb, ^{207}Pb and ^{208}Pb. Internal correction for mass fractionation was done using ^{208}Pb/^{206}Pb.

https://doi.org/10.1180/S0026461X00006502 Published online by Cambridge University Press

Probing the Toba super-eruption: Oxygen isotope geochemistry of zoned quartz phenocrysts

D.A. BUDD[1]*, V.R. TROLL[1,4], E.M. JOLIS[1], F.M. DEEGAN[1], V.C. SMITH[2], M.J. WHITEHOUSE[3], C. FREDA[4], C. HARRIS[5] AND D.R. HILTON[6]

[1]Dept. of Earth Sci., CEMPEG, Uppsala University, Sweden (*correspondence: david.budd.0339@student.uu.se)
[2]Research Lab. for Archaeology, University of Oxford, UK
[3]Swedish Museum of Natural History, Stockholm, Sweden
[4]Istituto Nazionale di Geofisica e Vulcanologia, Roma, Italy
[5]Dept. Geol. Sci, University of Cape Town, South Africa
[6]Scripps Institute of Oceanography, UCSD, California, USA

The Toba caldera located in Sumatra (Indonesia) is the source of the largest volcanic eruption in the Quaternary [1]. We present oxygen isotope data for a suite of zoned quartz phenocrysts (n=8) erupted as part of the Young Toba Tuff (YTT), an eruption event of approximately 2800 km^3 some 75 ka ago [1, 2]. Oxygen isotope data has been obtained by SIMS (n=92) in combination with cathodoluminescence (CL) imaging in order to establish the role of shallow level processes such as magmatic fractionation, magma-crust interaction and crystal recycling occurring in the Toba magmatic system. The CL images exhibit defined patterns of magmatic zoning which broadly coincide with fluctuations in $\delta^{18}O$ values in the quartz crystals, allowing correlation of textural and compositional data. Measured $\delta^{18}O_{quartz}$ values range from 6.7 ‰ to 9.4 ‰, independent of position on crystal core or rim. Values for $\delta^{18}O_{magma}$ have been calculated from quartz phenocrysts (assuming $\Delta_{quartz\text{-}magma}$ is 0.7 ‰ at magmatic temperatures). The lowest magma value is 6.0 ‰, apparently reflecting a primitive isotopic signal [3]. The maximum calculated magma value is 8.7 ‰ and the average is 7.2 ‰, indicating multiple sources to the Toba system including a significant crustal component. These new data allow us to unravel the heterogeneous magmatic system at Toba volcano, involving an evolved but dominantly magmatic melt and crustal partial melts reflected in elevated $\delta^{18}O$ crystal zones. Several crystals, however, show gradually lower values towards the rims pointing to either input from a less evolved magma or, more likely, a low-$\delta^{18}O$ contaminant from the shallow volcanic edifice. The crystals therefore record a complex and heterogeneous origin of the YTT magma, comprising an evolved igneous component and several substantial crustal contributions to finally assemble the massive volume of the Toba eruption.

[1] Rose & Chesner (1987) *Geology* **15,** 913-917. [2] Aldiss & Ghazali (1984) *J Geol. Soc. London* **141,** 487-500. [3] Taylor & Sheppard (1986) *Rev. Min.* **16,** 227-271.

Microbial diversity and physiology of Alberta coal seams

K. BUDWILL[1]* AND S.P. KOZIEL[2]

[1]Alberta Innovates – Technology Futures, Edmonton, AB T6N 1E4, Canada (*correspondence: Karen.Budwill@albertainnovates.ca)
[2]Alberta Innovates – Technology Futures, Vegreville, AB T9C 1T4, Canada (Susan.Koziel@albertainnovates.ca)

We have begun to map, using 16S pyrosequenicng and traditional enrichment culturing techniques, the microbial diversity and metabolic activities of coal from different Alberta coal zones. Results have implications for optimizing the bioconversion of coal to methane and other products.

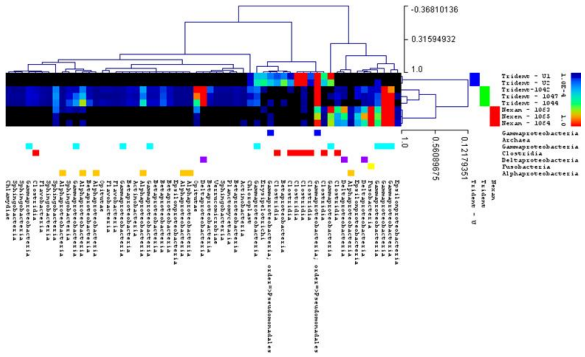

Figure 1: Hierarchical clustering tree (Linear Models for Microarray data significant taxons analysis) of 3 well sites from Mannville coal formation, Alberta.

Culture	μmol CH_4/mL culture
Coal + Tryptone	42.9
Tryptone only	11.7
Coal only	0

Table 1: CH_4 and CO_2 production at 55 days incubation in methanogenic cultures amended with 5 g coal and/or 0.05 g/mL tryptone.

Cluster analysis of microbial DNA sequences shows distinct microbial communities exist in Alberta coal deposits. The geochemical environment (e.g. salinity) likely influences community composition. Anaerobic culturing of the coal with 0.05 g/ml tryptone resulted in significant methane production and sequence reads related to *Methanobacter* increasing up to 30% from less than 1% of the total sequences detected in uncultured coal. GC-MS analysis of culture fluids provides evidence the microbial community uses coal as a carbon substrate in the presence of the nutrient.

https://doi.org/10.1180/S0026461X00006502 Published online by Cambridge University Press

Dynamics and evolution of the Earth's core and lowermost mantle

BRUCE BUFFETT

Earth and Planetary Science, University of California, Berkeley, CA 94720 USA (bbuffett@berkeley.edu)

Transport properties control many processes in the deep Earth. For example, the geodynamo is crucially dependent on electrical conductivity in the core. A typical estimate at relevant pressure and temperature is $5x10^5$ S m^{-1}, although this value is probably uncertain by a factor of two. At first glance a higher electrical conductivity might be expected to enhance the geodynamo. However, a higher electrical conductivity also implies a higher thermal conductivity, which suppresses the geodynamo. According to the Wiedemann-Franz law, an electrical conductivity of $5x10^5$ S m^{-1} corresponds to a thermal conductivity of 50 W K^{-1} m^{-1} at 4000 K. Approximately 8 TW of heat is carried by conduction toward the core-mantle boundary when the core is well mixed (i.e. adiabatic). This conductive transport represents a large fraction of the total core heat flow, suggesting that the transport due to convection is relatively small. Even modest changes in thermal conductivity can substantially alter the vigor of thermal convection. Present uncertainties in thermal conductivity permit widely varying estimates for the power available to drive the geodynamo.

Mass transport across the core-mantle boundary can also affect the dynamics and evolution of the core. Chemical disequilibrium between the core and mantle inevitably drives a flux of mass across the boundary, but the rate of transfer is limited by diffusion. Recent suggestions that the core is undersaturated in O and/or Si implies a flux of light elements into the core. Downward diffusion through the liquid core can produce a stratified layer 50 to 70 km thick if the flux of light elements from the mantle is sufficiently large. Dynamical arguments suggest that the residence time of material at the base of the mantle is 40 to 80 Ma. Steep chemical gradients in the mantle can drive a large mass flux, especially in the presence of partial melt or an interconnected ferropericlase phase. Local depletion of Si by transfer to the core would likely promote interconnection as the volume fraction of ferropericlase increases. Alternatively, a randomly oriented post-perovskite phase could permit a large flux. On the other hand, a large volume fraction of silicate perovskite at the boundary would likely suppress mass transfer. Differences in the mineralogy could have important implications for both the composition and dynamics of the core.

Net redistribution of ^{137}Cs over Australia

E.N. BUI AND A. CHAPPELL

CSIRO Land and Water, GPO Box 1666 Canberra, ACT 2601, Australia. (elisabeth.bui@csiro.au, adrian.chappell@csiro.au)

Cesium-137 (^{137}Cs), a radionuclide by-product of atomic testing, is a stratigraphic marker specific to the period of above-ground nuclear tests (1950s-70s), used to trace the movement of surficial material in terrestrial landscapes [1]. Its half-life is short (30.2 y) and its utility as a tracer will be of limited duration. We show here that its geographic pattern can shed valuable insight into contemporary geomorphic processes. We use geostatistics and estimates of net ^{137}Cs redistribution relative to a baseline reference fallout level to quantify and map topsoil erosion over Australia between 1950 and 1990. We show that net soil loss occurs in the main cultivated areas along the coastal regions of Western Australia, South Australia, Victoria, New South Wales, and Queensland. The most eroded area is in the Pilbara region of Western Australia, with median erosion rates > 6 t ha^{-1} yr^{-1}. The coincidence of net gain areas with eolian deposition in southeastern Australia suggests that the map is identifying wind-borne transport patterns. Eolian deposition in the Wet Tropics World Heritage Area supports the theory that dust is a major source of nutrients on ancient highly weathered soils where rainforests grow [2]. The potential for eolian deposition over the Wet Tropics is evident from an animation of MODIS imagery from the late September 2009 dust storm across Australia. However this is the first time that dust deposition over NE Australia has been substantiated.

[1] Zapata (2002) *Handbook for the assessment of soil erosion and sedimentation using environmental radionuclides*. Kluwer Academic Publishers, 219 pp. [2] Chadwick *et al*. (1999) *Nature* **397**, 491-497.

https://doi.org/10.1180/S0026461X00006502 Published online by Cambridge University Press

The first stepwise crushing data on C, N and Ar isotopic and elemental ratios in Guli carbonatites

A.I. BUIKIN[1], A.B. VERCHOVSKY[2], V.A. GRINENKO[1] AND L.N. KOGARKO[1]

[1]Vernadsky Institute of Russian Academy of Sciences, Moscow, Russia (bouikine@mail.ru)
[2]The Open University, Milton Keynes, UK

To get insight into the fluid regime evolution during formation of Guli massif (Maymecha-Kotuy magmatic complex, Syberia) carbonatites we have studied C, N and Ar isotopic and elemental ratios in foure carbonatite samples by stepwise crushing method. Mineral separates representing different formation stages of the massif have been selected for the investigation: two early calcites (Cal) and a late stage dolomite (Dol) and siderite (Sid).

The early calcites are characterized by significantly lower CO_2 content and lower $\delta^{13}C$ values than the late Dol and Sid (-14.1, -13.6‰ and -9.0, -10.5‰ in average respectively). Fractionation during melt degassing (when system is closing) could lead to a higher CO_2 content with higher $\delta^{13}C$ values in the late minerals. But the results on C, N and Ar elemental compositions in the fluid inclusions have shown that C/N and C/Ar ratios also dramatically increase from the early to the late samples (C/N: from 7 in Cal to 210 in Sid and 2100 in Dol; C/Ar ; from 870 in Cal to 12300 in Sid and 159000 in Dol), which could not be caused by a simple magmatic fractionation. An additional source of CO_2 could appear at the late stages of the fluid-magmatic evolution of the massif. The data on C, N and Ar concentration variations in crushing steps support this assumption: well-defined correlations between concentrations of these elements in fluid inclusions are observed in the early Cal (i.e. all gases in the inclusions have the same elemental composition and concequently the same source). For the late Sid and Dol the situation is different: when N and Ar concentrations decrease with crushing steps, the C concentration is increasing, suggesting different sources for (N+Ar) and for most of CO_2. Moreover, $^{40}Ar/^{36}Ar$ ratios in early and late samples are quite different: 3680 in Cal and 657 and 549 in Sid and Dol, respectively. This suggests the air-like argon component to be dominated in fluids during formation of the late minerals. Thus, relationships between C, N and Ar concentrations as well as differences in C and Ar isotopic compositions in fluid inclusions of the early and late carbonatites suggest that at the late stages of Guli massif carbonatites formation an additional CO_2 source with havier carbon and atmosphere-like Ar have contributed to the system.

Support: RFBR grant No 09-05-00678a.

The expansion of metal stable isotope biogeochemistry into biomedicine

T.D. BULLEN* AND M-N. CROTEAU

US Geological Survey, Menlo Park, CA 94025, USA (*correspondence: tdbullen@usgs.gov, mcroteau@usgs.gov)

Numerous metals are essential nutrients for human health, while others are toxic even at extremely low concentrations in body fluids and tissues. Moreover, a variety of metals and most recently nanometer-sized metals are increasingly being used as components of diagnostic and therapeutic agents to study or treat diseases and metabolic disorders as well as for drug and gene delivery, tissue engineering and pathogen detection. Several of the metals studied in the field of biomedicine, including Li, Ca, Fe, Cr, Zn, Cu, Mo, Ni, Cd and Hg, have variable stable isotope composition in natural materials which can now be measured accurately. Application of stable isotope tracing techniques normally used to study biogeochemical systems could be invaluable to biomedical research. Metal stable isotopes can be used to understand processes such as metal transfer among body pools, and may uniquely identify the fate of toxic metals delivered to the body in different forms such as nanoparticles or aerosols. Initial work has focused on Ca and Fe stable isotope variations in humans, reflecting the importance of bone mineral balance and blood chemistry to human health as well as the advanced state of analytical techniques for the determination of Ca and Fe stable isotope compositions.

Both natural abundance and enriched stable isotopes can be used to provide increased understanding of metabolic processes and pathways at a mechanistic level. Natural abundance stable isotope variations between ingested and excreted metals may prove useful for determining the onset of and recovery from metabolic disorder or disruption of homeostasis. Enriched stable isotopes may be particularly useful for studying processes involving metals in the body, since only very small quantities of enriched tracer are needed in the exposure media in order to create a signal in body tissues and fluids above background levels. Carefully crafted laboratory experiments with lower trophic level organisms will help guide the application of these tools to biomedicine. Coupled with continual advances in mass spectrometry, expansion of metal stable isotope biogeochemistry into the field of biomedicine will be an exceptional research opportunity for the coming years. Involving experts from the medical and other professions in this work and learning their “language” will be essential for success.

https://doi.org/10.1180/S0026461X00006502 Published online by Cambridge University Press

Vertical distribution of Fe and S species in anoxic water column of Pavin Lake (France): Electrochemical evidence for nanoparticulate FeS

E. BURA-NAKIĆ[1]*, I. CIGLENEČKI[1] AND E. VIOLLIER[2]

[1]Ruđer Bošković Institute, Bijenička 54, 10 000 Zagreb, Croatia (*correspondence: ebnakic@irb.hr, irena@irb.hr)
[2]Université Paris Diderot – IPGP-UMR CNRS, Cas Courrier 7052, 75205 Paris Cedex 13, France (viollier@ipgp.jussieu.fr)

Recently it has been shown that anodic oxidation of Hg by FeS at around -0.45 V can be used as an analytical protocol for electrochemical determination of FeS nanoparticules in natural waters [1]. The proposed protocol was tested on anoxic samples of Pavin Lake (France) where anodic waves were observed at -0.45 V (vs. Ag/AgCl); these correspond to an electrochemical transformation of particulate and/or nanoparticulate FeS to HgS.

A vertical profile of S(-II) obtained by voltammetric measurements showed that through the whole Pavin Lake monimolimnion layer a majority (~70 %) of S(-II) is in the form of FeS nanoparticulates. Concentrations of dissolved Fe(II) in the Pavin Lake monimolimnion layer are extremly high (up to the 1 mM) supporting our previous conclusion that Fe(II) is controling the speciation and distribution of S(-II) between dissolved and particulate phases [2,3]. At the oxia-anoxia boundary (from 61 to the 64 m), electrochemical measurements indicate presence of colloidal Fe(III) and /or Fe(III) organic species [2].

Thermodynamic calculations predict precipitation of FeS with log Ks value between -3.6 and -3.8 in the Pavin Lake monimolimnion layer. In the upper part of monimolimnion layer most probably precipitation of greigite is proceeding.
It was shown that modification of an Hg electrode with surface formed FeS has significant influence on the voltammetric Fe(II) determination, since cathodic reduction of Fe(II) in such conditions is occuring both on bare (-1.4 V) and on FeS modified Hg surfaces (-1.1 V)[1]; Fe(II) may be underdetermined when only the -1.4 V peak is measured.

This research was suported by COGITO and UKF grant 62/10.

[1] Bura-Nakić *et al*. (2011), *Electroanalysis*, in press. [2] Bura-Nakić *et al*. (2009), *Chem. Geol*. **266**, 311-317. [3] Viollier *et al*. (1997), *Chem. Geol*. **142**, 225-241.

Inverse modelling of gas chemistry measurements

ALAIN BURGISSER, MARINA ALLETTI AND CLIVE OPPENHEIMER

ISTO-CNRS, 1A rue de la Férolerie, 45071 Orléans, France (burgisse@cnrs-orleans.fr; marina.alletti@cnrs-orleans.fr, co200@cam.ac.uk)

We illustrate the inverse modelling of gas chemistry measurements by using gas compositional data for both quiescent and explosive emissions from the lava lake at Erebus volcano, Antarctica. The multi-component degassing model used needs calibration with experimental data in order to partition correctly the volatile species between their gaseous and dissolved forms. Solubility experiments were made on phonolite lava from the lake for H_2O, and data from the literature were reformatted to obtain the fugacity-based solubilities of CO_2 and S.

The degassing model is based on the hypothesis that the gas phase is buffering the system and controls the balance of volatile species. Two types of calculations are performed, depending on whether the measured gas was in equilibrium with the surrounding melt at the lake surface (case 1), or was emitted in isolation from the lava contained in the lake (case 2). The inversion procedure starts by calculating the equilibrium composition of all the species assumed to coexist at atmospheric pressure. This is not straightforward, as the species that are best measured at the vent and those best constrained in the model do not always match. At Erebus, such discrepancy occurs for H_2S, which is simulated but not measured, and OCS, which is measured but not simulated. Compression is then performed by assuming mass conservation of the volatile elements, either applied to the mixture of melt and gas (case 1), or only to the gas (case 2).

Model results are projections at higher pressures (up to 3 kbar) of the gas composition measured at the surface. At Erebus, we find that the difference between the gas emitted explosively and that emitted passively can be explained by a common source situated at depths corresponding to as little as 300 bars pressure. While quiescent, the lake is either degassing in fully open system, or by the means of a convective system restricted between the surface and depths equivalent to 60 to 300 bars. Additional constraints on the magmatic system are obtained by comparing the simulated melt volatile contents with those measured in melt inclusions. We will discuss the limitations of the main model assumptions (chemical equilibrium, gas buffering of the redox state, and temperature effects).

https://doi.org/10.1180/S0026461X00006502 Published online by Cambridge University Press

Electrical resistivity imaging of a deep coal mine discharge

W. BURGOS[1]*, M. FITZGERALD[2], L. LARSON[1], L. HERWEHE[2], K. SINGHA[2], AND M. GOOSEFF[1]

[1]Dept. Civil Environ. Eng., Pennsylvania State University, University Park, PA 16802, USA (*correspondence: wdb3@psu.edu, lnl5053@psu.edu, mng2@psu.edu)

[2]Dept. of Geosciences, Pennsylvania State University, University Park, PA 16802, USA (mxf218@psu.edu, lmh5193@psu.edu, ksingha@psu.edu)

The biogeochemistry of iron cycling in acidic environments is quite complex where aerobic surface sediments and anaerobic subsurface sediments are often separated by only a steep redox gradient. The hydrodynamic conditions in these systems affect geochemical conditions that in turn affect microbial community structure. Hydrodynamic conditions can be observed directly at the surface, however, identification of e.g. areas of "fast" vs. "slow" flow are more difficult in the subsurface. To characterize flow paths and hyporheic exchange in the surface and shallow groundwater at an acid mine drainage (AMD) site, we used electrical resistivity imaging (ERI) at a stream emanating from a large abandoned deep coal mine in Cambria County, Pennsylvania. Because of the high conductivity (2,000 μS/cm) of the emergent AMD, we added clean fresh water (30 μS/cm) as a tracer to visualize the spatial and temporal distribution of the hyporheic exchange. Two-dimensional imaging of stream-groundwater exchange was collected from three locations in the study reach using three electrode transects across the stream. We were able to identify the location and spatial extent of a large artesian spring of AMD that contributed significant flow to the stream. Concurrent measurements of in-stream and in-well water chemistry were in good agreement with the inverted models of electrical resistivity. We believe this is the first report of a dilution tracer coupled with ERI for 2-D imaging of hyporheic extent in an acidic stream environment.

Uranium valence cycling with iron-rich phyllosilicates

W. BURGOS[1]*, F. LUAN[1], M. BOYANOV[2], K. KEMNER[2] AND H. DONG[3]

[1]Dept. Civil Environ. Eng., Pennsylvania State University, University Park, PA 16802, USA (*correspondence: wdb3@psu.edu, ful6@psu.edu)

[2]Biosciences Division, Argonne National Laboratory, Argonne, IL 60439, USA (mboyanov@anl.gov, kemner@anl.gov)

[3]Dept. Geology, Miami University, Miami, OH 45056, USA (dongh@muohio.edu)

Iron-bearing phyllosilicate minerals are widely distributed in soils and sediments and often account for about half of the iron in soil. These minerals help establish the physical/hydrogeological conditions of subsurface redox transition zones because of their small size and limited hydraulic conductivity, and disproportionately buffer the redox conditions through the transition zone because they provide a large solid-phase reservoir of Fe(III)/Fe(II) (e.g., they are less susceptible to reductive dissolution as compared to oxides). We previously demonstrated that metal-reducing bacteria preferentially reduce soluble U(VI) over structural-Fe(III) in phyllosilicates; uraninite ($U^{IV}O_2(s)$) is rapidly reoxidized by phyllosilicate-Fe(III) (allowing U to serve as an electron shuttle); but at some thermodynamic endpoint, corresponding to an elevated concentration of structural Fe(II), phyllosilicate-Fe(III) can no longer oxidize uraninite. To better characterize this thermodynamic endpoint we conducted a series of abiotic experiments with synthetic uraninite and specimen phyllosilicate minerals, and with synthetic uraninite and clay-sized fractions from sediments collected from redox transition zones. We conducted these experiments using the unaltered clays (highest Fe(III) contents) and chemically-reduced clays (incremental increases in Fe(II) contents) to evaluate both kinetic and thermodynamic behaviour of their reactions with uraninite. Identical experiments were conducted where uraninite was replaced with non-sorbing, colorimetric redox indicators to quantify the reduction potential of the clays. Reaction products were characterized by U L_{III}-edge and Fe K-edge EXAFS spectroscopy and by TEM-electron energy loss spectroscopy.

https://doi.org/10.1180/S0026461X00006502 Published online by Cambridge University Press

Mixing of radiocarbon from high latitude oceans through the atmosphere and ocean during the last deglaciation: Results from Iceland and the Drake Passage

ANDREA BURKE[1,2]*, LAURA F. ROBINSON[2] AND NICKY J. WHITE[3]

[1]MIT/WHOI Joint Program (*correspondence: aburke@whoi.edu)
[2]Woods Hole Oceanographic Institution, 360 Woods Hole Rd. Woods Hole, MA. 02543 USA.
[3]Bullard Laboratories, Madingley Rise, Madingley Road, Cambridge, CB3 0EZ, UK

Radiocarbon is a sensitive tracer of carbon cycle processes over the last ~40 kyr. We present new radiocarbon reconstructions from U-Th dated deep-sea corals from the Reykjanes Ridge off Iceland. These results are compared to radiocarbon reconstructions from deep-sea corals in the Southern Ocean and published radiocarbon records from benthic foraminifera to further our understanding of the transfer of carbon between different reservoirs during the last glacial period and deglaciation.

Our dataset from Iceland comes from solitary and colonial corals collected by dredge from water depths ranging between 770 to 1680 m. U-Th ages of these corals range from modern to 40 ka. During the last glacial period at ~35 ka, radiocarbon reconstructed at 1680 m water depth was ~100‰ more depleted from the contemporaneous atmosphere than it is today. However at the Bolling-Allerod and throughout the Holocene these sites were better ventilated, with radiocarbon offsets from the contemporaneous atmosphere similar to those observed in this region today (~70‰).

Radiocarbon reconstructions from Iceland and the Southern Ocean do not show extreme radiocarbon depletions of the magnitude oberved in some intermediate-depth deglacial records (e.g. [1]). A comparison of $\Delta^{14}C$ records to other proxy data suggests that these large depletions cannot be explained by a common water mass (e.g. Antarctic Intermediate Water), since mixing of this water mass would dissipate any extremely depleted radiocarbon signature. However, the radiocarbon depletions that we do observe throughout the glacial ocean are large enough to explain the atmospheric drop in $\Delta^{14}C$ over the 'Mystery Interval' if we allow some direct transfer of carbon from the deep ocean to the atmosphere, such as through the Southern Ocean.

[1] Marchitto *et al*. (2007) *Science* **316**, 1456-1459.

Speciation of contaminant metals in red mud from Ajka, Hungary

I.T. BURKE[1]*, W.M. MAYES[2], C.L. PEACOCK[1], A.P BROWN[4], A.P. JARVIS[3] AND K. GRUIZ[5]

[1]Sch. Earth & Environ. and [4]Sch. Process, Environ. & Materials Eng., University of Leeds, UK (*correspondence: I.T.Burke@leeds.ac.uk)
[2]Centre for Environ. & Mar. Sci., University of Hull, UK.
[3]Sch. Civil Eng. & Geosci., Newcastle University, UK.
[5]Dept Appl. Biotechnol. & Food Sci., University of Technology and Economics, Budapest, Hungary.

The catastrophic failure of the sludge dam at the Ajkai Timfoldgyar Zrt alumina plant in Hungary on the 4th October 2010 resulted in the release of 700000 m^3 of caustic metalliferous red mud. Red mud leachate is hyperalkaline (pH 13) and has elevated concentrations of metals and metalloids such as Al (1000 ppm) As, V, and Mo (4 - 6 ppm). The red mud itself has elevated concentrations of As, V, Cr, Co, Ni and U (100-1000 ppm). These contaminants persist in water and sediment samples for up to 100 km downstream of the source. The long term effects of the red mud spill on the environment remain largely unknown, especially with respect to the behaviour of the toxic elements present. Here we describe the results of experiments using sequential extraction, electron microscopy and X-ray absorption spectroscopy techniques to characterise the occurrence of metal(loids) within the red mud.

SEM and TEM analysis of red mud material sampled from the dyke breach at Ajka was composed primarily of 10-100 nm haematite particles occurring as 100-700 nm aggregates and 1-4 μm sodium aluminosilicate particles. Transported samples also contain 10-40 μm silt particles, presumably entrained from local soils and sediments. In EDS analysis Cr, Ti, Al, Si, and Mn were associated with aggregates of nano-crystalline (~ 5 nm) haematite. Discrete 2-10 nm Ce-rich particles were also present. At Ajka, acid dosing and gypsum addition were extensively used to lower pH and precipitate soluble Al, As, V and Mo. Sequential extractions performed on transported red mud deposits determined that 70-90 % As and V are present in residual hard-to-leach phases. The remaining 10-30 %, however, occurred in weak acid / hydroxylamine HCl leached phases, which may represent the presence of freshly precipitated metal(loid) containing phases. XAS analysis of red mud samples and leachate precipitates focused on determining As and V speciation in both the labile and refractory phases present. This baseline information will help in predicting the likely environmental mobility, fate and the long term hazards from metal(loid) contamination associated with the spill.

https://doi.org/10.1180/S0026461X00006502 Published online by Cambridge University Press

Nucleosynthetic Mo and W isotope anomalies in Murchison leachates

C. BURKHARDT[1]*, T. KLEINE[2], N. DAUPHAS[3], F. OBERLI[1] AND R. WIELER[1]

[1]Institute of Geochemistry and Petrology, ETH Zurich, CH-8092 Zurich (*correspondence: burkhardt@erdw.ethz.ch)
[2]Institute for Planetology, University of Muenster, D-48149 Muenster
[3]Origins Laboratory, The University of Chicago, IL 60637, USA

Nucleosynthetic isotope anomalies at the bulk meteorite scale exist for several elements (e.g., Ti, Mo, Ru) and most likely reflect incomplete mixing of diverse presolar components in the solar nebula [e.g. 1]. These isotope heterogeneities contrast with uniform and terrestrial isotope composition for other elements (e.g., Hf, W, Os [2]). Constraining why planetary-scale nucleo-synthetic isotope anomalies exist for some elements but not for others can provide clues to understanding the early evolution of the solar nebula. To address this important issue we obtained Mo and W isotope data for acid leachates of the Murchison chondrite. About 16 g of Murchison was sequentially digested using acids of increasing strengths. Aliquots of these leachates were previously analysed for Os isotopes [3]. Here, in addition, the acid-resistant residue was completely digested after fusion with a laser.

The Mo and W isotope data, obtained by MC-ICP-MS at ETH Zurich, reveal large anomalies that correlate with each other as expected from nucleosynthetic theory [4] and can be accounted for by variable amounts of s-process Mo and W. A regression of ^{182}Hf-decay corrected W data in ε^{182}W-ε^{186}W space yields an initial ε^{182}W consistent with the solar system initial value [5]. The Mo and W anomalies do not correlate with Os isotope anomalies reported for the same samples [3], indicating that Mo and W are hosted in different carriers than Os. This can explain why planetary-scale isotope anomalies exist for Mo but not for Os. Furthermore, the well-correlated Mo and W isotope anomalies in the Murchison leachates combined with the observation that planetary-scale isotope anomalies exist for Mo but not for W suggests that Mo and W are hosted in distinct but chemically similar carriers. The different patterns of planetary-scale nucleo-synthetic anomalies thus seem to reflect the presence of distinct generations of presolar dust that have been homogenized to different degrees.

[1] Dauphas *et al*. (2002) *Astrophys. J.* **565**, 640-644. [2] Yokoyama *et al*. (2007) *EPSL* **259**, 567-580 [3] Reisberg *et al*. (2009) *EPSL* **277**, 334–344. [4] Arlandini *et al*. (1999) *Astrophys. J.* **525**, 886-900. [5] Burkhardt *et al*. (2008) *Geochim. Cosmochim. Acta* **72**, 6177-6197.

Oxygen fugacity-dependence of zircon-melt trace element partitioning

A.D. BURNHAM[1,2]* AND A.J. BERRY[1,2]

[1]Department of Earth Science and Engineering, Imperial College London, SW7 2AZ, UK (correspondence: a.burnham08@imperial.ac.uk)
[2]Department of Mineralogy, Natural History Museum, London, SW7 5BD, UK.

A common feature of terrestrial igneous zircons is a marked excess of Ce over La and Pr, and a deficit of Eu relative to Sm and Gd. This Ce anomaly is attributed to the presence of Ce^{4+}, and this Eu anomaly attributed to the presence of Eu^{2+}; all other REE occur exclusively as M^{3+}. Therefore, the magnitude of these anomalies may record the oxygen fugacity (fO_2) at which the magma crystallised. It is often unclear, however, whether the Eu anomaly reflects directly the Eu oxidation state ratio of the melt from which the zircon crystallised, or whether the Eu content of the melt was depleted by fractional crystallisation of plagioclase (or other Eu^{2+}-bearing minerals) prior to zircon growth. The present study presents the first systematic data on the dependence of zircon-melt REE partitioning on fO_2.

Synthetic zircons were grown at 1 atmosphere from a flux-free melt of 'natural' composition, over a range of 14 log units in fO_2 (IW-4 to QFM+6). The resulting crystals were characterised by cathodoluminescence and analysed by secondary ion mass spectrometry (SIMS) and laser ablation ICP-MS for P, Sc, Ti, Y, REE, Hf, Th and U.

Increasing fO_2 results in the Ce and Eu anomalies becoming more and less pronounced, respectively. There is a narrow fO_2 range over which both anomalies were observed; however the two anomalies do not covary in the same manner as natural samples. Therefore, either partitioning depends strongly on temperature and/or melt composition, or most natural samples suffer removal of Eu from the system before zircon saturation. The Ce and Eu data will be combined with direct determinations by XANES (X-ray absorption near edge structure) spectroscopy of the effects of fO_2, temperature and melt composition on the redox state ratios of Ce and Eu.

The partitioning of Sc, Y, other REE and Hf is fO_2-independent, as expected. The presence of P in the melt does not affect partitioning. Ti partitioning remains constant, indicating that Ti^{3+} (likely to represent 10-20% of Ti at the most reduced conditions studied) shows similar partitioning behaviour to Ti^{4+}. The U/Th ratio of zircon varies systematically over more than one order of magnitude with fO_2.

https://doi.org/10.1180/S0026461X00006502 Published online by Cambridge University Press

Mantle controls on the geochemistry of Kīlauea lavas erupted over the last millennium

D.H. BURNS[1], A.J PIETRUSZKA[1], M.D. NORMAN[2], J.P. MARSKE[3], M.O. GARCIA[3] AND J.M. RHODES[4]

[11]Department of Geological Sciences, San Diego State University, San Diego, CA 92182-1020, USA
[2]Research School of Earth Sciences, Australian National University, Canberra ACT 0200, Australia
[3]Department of Geology and Geophysics, University of Hawaii, Honolulu, HI 96822, USA
[4]Department of Geology and Geography, University of Massachusetts, Amherst, MA 01003, USA

Lavas from Kīlauea Volcano display rapid geochemical variations on a time scale of decades to centuries. The wall of Kīlauea Caldera at Uwekahuna Bluff exposes a 135-m thick sequence of recent prehistoric lavas (erupted mostly between AD 900-1400) and tephra from an explosive eruptive sequence at the volcano's summit (the Uwekahuna Ash). This stratigraphic section allows us to re-create a detailed temporal record of the mantle controls on the geochemical evolution of Kilauea lavas erupted over the last millennium. Previously [1], we analyzed the Pb, Sr, and Nd isotope ratios and major-element abundances of a series of 24 successive lava flows from the upper portion of Uwekahuna Bluff. The $^{206}Pb/^{204}Pb$ and $^{87}Sr/^{86}Sr$ ratios of these lavas were found to converge with prehistroic Mauna Loa lavas of the same age. This observation was attributed to the rapid passage of a small-scale compositional heterogeneity through the melting regions of both volcanoes. Here we present a detailed geochemical study (major- and trace-element abundances, and Pb, Sr, and Nd isotope ratios) of four glass separates from the Uwekahuna Ash and the remaining 38 lavas exposed lower in the Uwekahuna Bluff, along with trace-element abundances for the upper 24 lava flows from Uwekahuna Bluff. These prehistoric lavas and glasses display a small, but systematic, temporal variation in ratios of highly over moderately incompatible trace elements (e.g. La/Yb) that correlates with fluctuations in the Pb and Sr isotope ratios. These correlations suggests that the lithology of the mantle source controls the degree of partial melting at Kīlauea. The origin of these differences in source lithology will be explored using the major- and trace-element abundances of the lavas.

[1] Marske *et al*. (2007) *EPSL* **259,** 34-50.

Mechanisms of deep crustal subduction and exhumation: Insights from numerical modelling

EVGUENI BUROV

ISTEP, UMR 7193 UPMC-CNRS, Case 129, T46-00 e2, University of Pierre et Marie Curie, 4 Place Jussieu, 75252 Paris (evgenii.burov@upmc.fr)

The dynamic processes leading to syn-convergent crustal subduction and consequent exhumation of high pressure low and high temperature rocks in continental collision zones remain poorly understood. Using results of thermo-mechanical thermodynamically coupled numerical models, we here discuss different possible mechanisms of crustal subduction and exhumation. To reach that goal, oceanic subduction-continental subduction and collision is modelled using a forward viscous-elastic-plastic thermo-mechanical models and synthetic petrology models allowing to trace P-T-t paths, generated out of numerical simulations, and compare them with natural P-T-t paths. Different collision scenarios, as function of the convergence rate and thermo-rheological profile are also discussed. It is shown that crustal subduction may occur only at very specific conditions in terms of crustal rheology, structure, subduction rate and thermal regime. It is also noteworthy that the models predict strong variations in the exhumation rates during the subduction-collision stage, and indicate that UHP rocks are likely to be exhumed at the earlier stages of continental subduction. Several additional mechanisms related to strain localization due to strain softening, metamorphic reactions, heat dissipation and fluids are also discussed. A particular attention is paid to the role of surface processes, sedimentary content and inherited structures. The experiments also show that the dynamic pressure in the subduction channel is unlikely to deviate by more than ± 10% from the lithostatic approximation. The models are applied to a number of regions such as the Alpes, Zagros and Hymalaya showing each time a significant difference in the mechanisms of subduction and exhumation.

https://doi.org/10.1180/S0026461X00006502 Published online by Cambridge University Press

GEO-CARS: 3-D, chemically selective imaging of fluid inclusions with multimodal nonlinear optical microscopy

R.C. BURRUSS[1]*, A.D. SLEPKOV[2], A.F. PEGORARO[2] AND A. STOLOW[2]

[1]USGS, Reston, VA 20191 USA, (*correspondence: burruss@usgs.gov)
[2]National Research Council of Canada, Ottawa, Ontario, Canada (Aaron.Slepkov@nrc-cnrc.gc.ca; Adrian.Pegoraro@nrc-cnrc.gc.ca; Albert.Stolow@nrc-cnrc.gc.ca)

3-D images and spectra of methane-rich fluid inclusions have been recorded for the first time with coherent anti-Stokes Raman scattering (CARS) and associated nonlinear optical methods (second harmonic generation, SHG, and two-photon excitation fluorescence, TPEF). Laser scanning confocal microscopy (LSCM) with CARS was developed for biomedical imaging of lipids [1] (based on C-H stretching vibration) suggesting that we could image CH_4 in fluid inclusions. The CARS microscope uses a single ultrafast laser source that simultaneously generates additional nonlinear imaging modes (SHG and TPEF) [1]. All three signals are generated in the same focal volume and collected on separate detectors, creating high-resolution 3-D images with complimentary information such as evidence of aromatic hydrocarbons (TPEF) and sub-micrometer crystallographic disorder and internal surfaces in host minerals (SHG), in addition to the chemically-specific Raman spectral information from CARS at 2100 to 4500 cm^{-1}.

CARS images and spectra of CH_4-rich inclusions in sedimentary, igneous, and metamorphic rocks provide new information on methane in the crust. 3-D images of CH_4 and water clearly identify aqueous inclusions with CH_4-rich vapour bubbles that coexist with one-phase CH_4-rich inclusions. In crude oil inclusions, CARS spectra of CH_4 are clearly separated from fluorescence emission of the oil, allowing us to record, for the first time, the pressure sensitive peak position of CH_4 [2] in oil inclusions for input to PVT models of oil migration. Healed microfractures are visible in SHG allowing identification of distinct generations of CH_4-rich inclusions associated with specific fracture orientations. Some CH_4-rich inclusions in metamorphic and igneous rocks show TPEF signals that indicate the presence of aromatic hydrocarbons associated with CH_4. We believe this work demonstrates the broad potential of multimodal nonlinear optical microscopy and spectroscopy to provide new insight to the geochemistry of carbon in the crust and upper mantle.

[1] Pegoraro *et al*. (2010) *App. Phys.* **49**, F10-F17. [2] Lu, *et al*. (2007) *GCA* **71**, 3969-3978.

The role of microbial sulfidogenesis in shaping iron-sulfur-arsenic interactions within floodplain soils

EDWARD D. BURTON*, SCOTT G. JOHNSTON AND RICHARD T. BUSH

Southern Cross GeoScience, Southern Cross University, Australia; (*correspondence: ed.burton@scu.edu.au)

Introduction and objectives

Dissimilatory SO_4^{2-}-reducing bacteria play a key role in shaping the biogeochemical behaviour of Fe and As in floodplain wetland soils. These bacteria gain metabolic energy by coupling the anaerobic oxidation of organic C or H_2 with the reduction of SO_4^{2-}. This results in the generation of sulfide, which can interact via a series of often competing and complex reactions with both Fe and As. Here we discuss our recent research aimed at unraveling the role of microbial sulfidogenesis in shaping Fe-S-As interactions within flooded soils. More specifically, we examine how the onset of sulfate-reduction in floodplain soils can drive transformations in Fe mineralogy and cause associated changes in As mobility.

Methodological approach

To address this issue, we have employed a multi-scale approach spanning (1) field-scale investigations that include an essential integration of hydrological, geomorphological and geochemical observations, (2) a series of controlled advective-flow experiments with a pure culture of a sulfate-reducing bacteria (*Desulfovibrio vulgaris*) and (3) relatively simple batch-type incubations with a natural assemblage of anaerobic microorganisms.

Results and discussion

Aqueous sulfide is a powerful and facile reductant of Fe(III) that can drive the rapid reductive dissolution of poorly ordered ferric (hydr)oxides, such as ferrihydrite and schwertmannite. In the case of these poorly-ordered phases, the resulting production of Fe(II) can drive rapid formation of goethite – an Fe mineralogical transformation that appears to significantly retard As mobility. Under strongly sulfidogenic conditions, magnetite formation occurs preferentially along with the accumulation of Fe sulfide minerals.

Whilst sulfidogenesis initially causes pH-dependent release of Fe(II), sulfidogenesis can eventually sequester Fe via the the precipitation of Fe sulfide minerals. These minerals include mackinawite, greigite and pyrite – which appear to exhibit vastly contrasting affinities for As. Hence, the effect that Fe sulfide accumulation has on As mobility within floodplain soils is heavily dependent on Fe sulfide mineralisation rates.

https://doi.org/10.1180/S0026461X00006502 Published online by Cambridge University Press

Ancient lead trapped in the Earth's upper mantle

KEVIN W. BURTON[1,2], BENEDCITE CENKI-TOK[1,3], FATIMA MOKADEM[1,2], JASON HARVEY[1,4] AND IAN J. PARKINSON[1]

[1]Department of Earth and Environmental Sciences, The Open University, Walton Hall, Milton Keynes, MK7 6AA, UK.
[2]Department of Earth Sciences, University of Oxford, South Parks Road, Oxford OX1 3AN, UK.
[3]Géosciences Montpellier, UMR 5243 - CC 60, Université Montpellier 2, Place E. Bataillon, 34095 Montpellier cedex 5, France.
[4]School of Earth & Environment, University of Leeds, Leeds LS2 9JT, UK.

The isotope compostion of lead (Pb) the Earth's upper mantle (sampled by oceanic basalts) is far too radiogenic for evolution from chondritic (primitive solar system) material over 4.57 billion years, the so called 'Pb paradox' [1]. Loss of Pb to the core [2] or arrival in a late veneer [3], have both been proposed as mechanisms to account for this imbalance. Alternatively, recent Pb isotope data for orogenic peridotites suggests that such rocks could serve as a complentary reservoir of unradiogenic Pb [4]. However, orogenic peridotites may not be representative of the asthenopshere underlying present-day mid-ocean ridges, furthermore, it is unclear why such material is not sampled by oceanic basalts.

Here we show that sulphides trapped as inclusions in silicate minerals in abyssal peridotites from the North Atlantic ocean (ODP Leg 209; Site 1274A) preserve extremely unradiogenic Pb isotope compositions, some corresponding to an age of ca 1.8 billion years. These ages are indistinguishable from those preserved by Os isotopes in sulphides from the same abyssal peridotites [5], and demonstrate that both Pb and Os isotopes preserve an unequivocal record of ancient melt depletion in the sub-oceanic mantle. Therefore, at least, some of the Pb in the Earth's mantle is unradiogenic and complements the composition of oceanic basalts. That these sulphides contribute little of their Pb to the isotope composition of oceanic basalts may be due either to their entrapment in host silicate phases or else that they are generally present in refractory domains in the mantle that are little sampled by later melting events.

[1] Allègre, C.J. *Earth Planet. Sci. lett.* **5**, 261-269 (1969). [2] Vollmer, R. *Nature* **270**, 144-147 (1977). [3] Albarède, F. *Nature* **461**, 1227-1233 (2009). [4] Malaviarachchi, S. *et al.*, *Nature Geosc.* **1**, 859-863 (2008). [5] Harvey, J. *et al. Earth Planet. Sci. lett.* **244**, 606-621 (2006).

Fe isotope cycling in ferruginous and anoxic Lake Pavin (France) from water column to sediment

V. BUSIGNY[1], N. PLANAVSKY[2], D. JÉZÉQUEL[1], P. LOUVAT[1], G. MICHARD[1], E. VIOLLIER[1] AND T. LYONS[2]

[1]IPGP, 1 rue jussieu, 75005 Paris, France; (busigny@ipgp.fr)
[2]Earth Sciences, Univ. of California Riverside, USA

Fe isotopes are an emerging biogeochemical paleoproxy that can improve our understanding of the Fe cycle in early Earth's ocean and early microbial evolution. Sediments deposited during the Precambrian record a large range of δ^{56}Fe values, with an exceptional negative excursion (down to -3.5‰) between 2.9 and 2.3 Ga, a transition period believed to be marked by stratified redox ocean basins. The origin of this negative excursion is still debated but may be linked to a unique period of water column Fe cycling or a time of enhanced microbial Fe reduction in Fe-rich sediments.

Lake Pavin is a unique stratified aquatic system characterized by permanent anoxic and ferruginous deep water (from 60 to 92 m depth) topped by oxic shallow water (from 0 to 60 m), and can thus be regarded as a modern analog for Archean ocean. In the present work, we have studied Lake Pavin Fe isotope cycling along a profile in the water column down to the sediment in order to bring new insights into the record of ancient rocks. Four sediment cores were drilled and analyzed: (1) in the oxic zone, (2) at the oxic-anoxic boundary, (3) under the peak of H_2S production from SO_4^{2-} reduction and (4) at the bottom of the lake. In the water column, dissolved Fe concentration increases with depth from 2 μM at the oxic-anoxic boundary to 1200 μM at the lake bottom, with δ^{56}Fe increase from -1.67 to +0.31‰. The very negative δ^{56}Fe of the oxic-anoxic boundary reflects the residue of Fe oxidation and precipitation. The δ^{56}Fe increase with depth is interpreted as a coupling between (1) diffusion of Fe enriched in heavy isotopes from the bottom of the lake towards the oxic-anoxic boundary and (2) a combination of Fe reduction of downgoing Fe(III) particles and ferrous-ferric Fe interations. Analyses of bulk sediment show δ^{56}Fe values close to the purported detrital source (i.e. basalts with δ^{56}Fe ~ 0.20‰). In contrast, Fe sequential extraction in sediments shows a significant variation in δ^{56}Fe. Iron isotope mass balance calculation in both water column and pore waters of the sediment cores indicate that Fe isotope variability in iron sulfides reflects mostly Fe chemistry in the water column rather than isotopic fractionation during diagenetic processes or sulfide precipitation in the sediment.

https://doi.org/10.1180/S0026461X00006502 Published online by Cambridge University Press

Long-term versus short-term weathering fluxes in contrasting lithologies at the Luquillo Critical Zone Observatory, Puerto Rico

H.L. BUSS[1,2]*, A.F. WHITE[1], A.E. BLUM[3], M.S. SCHULZ[1] AND D. VIVIT[1]

[1]U.S. Geological Survey, Menlo Park, CA 94025, USA
[2]Department of Earth Sciences, University of Bristol, Bristol, BS8 1RJ, UK (*correspondence: h.buss@bristol.ac.uk)
[3]U.S. Geological Survey, Boulder, CO 80303, USA

(Bio)geochemical and physical weathering processes in tropical watersheds produce most of the solutes and sediments discharged to the oceans. Thus, relative to their area, tropical systems are disproportionately important in terms of weathering, erosion, and global CO_2 cycles. In addition to influencing stream and ocean chemistry and sediment loads, weathering processes exert control over chemical transport in soils and regolith (e.g., saprolite), soil and saprolite formation rates, mineral nutrient availability, and microbial growth rates. Currently, the volcaniclastic Río Mameyes watershed is being investigated as a comparison to the nearby, well-studied, granitic Río Icacos watershed in order to better understand the influence of lithology on weathering processes, weathering fluxes, and mineral nutrient availability.

Both watersheds are located in the Luquillo Critical Zone Observatory in Northeastern Puerto Rico and are characterized by similar humid, tropical climate; high annual rainfall, high year-round temperatures, tropical montane vegetation, and high relief. In both watersheds, thick (37+ m in places) saprolites blanket the ridges, but the majority of the chemical weathering occurs at the bedrock-saprolite interface. Long-term weathering fluxes are calculated from mass losses in the weathering profiles between the bedrock and the saprolite and from the age of the regolith surface (determined by cosmogenic nuclides or U-Th disequilibria). Short-term weathering fluxes are calculated from solute chemistries and infiltration rates and can be compared to watershed flux rates. Comparison of these three calculations for each watershed can be used to identify the changes in weathering regime and environment over time. Comparison of the two different watersheds demonstrates the influence of lithology on weathering fluxes on different timescales.

Defining a landscape for microbial electron transfer to extracellular minerals

JULEA N. BUTT[1]*, ANDREW J. GATES[1], SOPHIE J. MARRITT[1], MARCUS EDWARDS[1], THOMAS A. CLARKE[1], LIANG SHI[2], JAMES K. FREDRICKSON[2], JOHN M. ZACHARA[2] AND DAVID J. RICHARDSON[2]

[1]School of Chemistry and School of Biological Sciences, University of East Anglia, Norwich NR4 7TJ, United Kingdom (*correspondence: j.butt@uea.ac.uk)
[2]Biological Sciences Division, Pacific Northwest National Laboratory, Richland, WA, USA

The respiratory reduction of extracellular minerals poses a considerable challenge to microbes. Redox events associated with generating proton motive force across the inner membrane to drive ATP synthesis must be coupled to transfer of electrons to the extracellular matrix. In *Shewanella* multi-heme cytochromes support this translocation of electrons. The tetraheme containing protein CymA moves electrons from inner membrane quinols to the periplasm. Porin wrapped decaheme cytochromes provide a conduit for electron transfer across the outer membrane while additional cytochromes interface with the extracellular matrix. The redox activity of each of these cytochromes spans a distinct window of potential. Consequently when present together these cytochromes can provide both a reservoir to accommodate electrons arriving from quinol oxidation at the inner membrane and a variable driving force for delivering electrons to extracellular minerals.

https://doi.org/10.1180/S0026461X00006502 Published online by Cambridge University Press

Coevolution of early animals and environment

N. J. BUTTERFIELD

Department of Earth Sciences, University of Cambridge, Cambridge, UK CB2 3EQ (njb1005@cam.ac.uk)

Large scale coevolution of organisms and environment is conventionally viewed from the bottom up – with microbially driven biogeochemical cycles providing the ecological oportunity, and larger, more physiologically constrained organisms rapidly evolving in response. Nowhere has this approach been more popularly applied than in oxygen-limitation hypotheses aimed at the seemingly delayed appearance of large and/or predatory animals. In this presentation I consider the nature of biological/environmental coevolution through the Proterozoic-Phanerozoic transition.

There is no question that planetary environments and biogeochemical cycling changed dramatically through the the Ediacaran and early Cambrian, an interval also marked by the first significant appearance of macroscopic organisms in the fossil record. More significantly, fundamental shifts in the the composition and evolutionary dynamics of contemporaneous microfossils attests to the genuine absence of eumetazoans prior to the Ediacaran. If oxygen availability was a first-order constraint on animal evolution, then the critical threshold was crossed in the early Ediacaran. Evidence for earlier oxygen limitation comes from geochemical proxies for deep-water anoxia, though it is notable that these same signatures extend into early Palaeozoic strata – while evidence of significant surface water oxygenation extends well back into the Neoproterozoic.

Such geochemical expression is difficult to reconcile with oxygen limitation hypotheses – particularly in light of the modest oxygen demand of most animals, and the conspicuous monophyly of the Metazoa. As such, the delayed appearance of eumetazoans is more convincingly ascribed to the extraordinary complexity of gene regulatory networks underlying organ-grade multicellularity; i.e., internal rather than external constraints. Once these developmental schemes were established, however, they opened up a new universe of ecological, evolutionary and biogeochemical phenomena, ranging from bioturbation and faecal pellets to the coevolutionary forcing of biomineralization, large body size, eukaryotic dominated phytoplankton and fundamental shifts in oceanic structure. Unlike the exclusively bottom-up microbial world of the pre-Ediacaran, the Phanerozoic biosphere must also be viewed from the top down – with animals playing a key role in the construction and definition of environments.

Influence of secondary organic aerosols (SOA) on "Bromine Explosion" in smog-chamber experiments

J. BUXMANN[2]*, N. BALZER[1], J. OFNER[1], U. PLATT[2] AND C. ZETZSCH[1]

[1]Atmospheric Chemistry Research Laboratory, BayCEER, University of Bayreuth, Germany

[2]Institute of Environmental Physics, University of Heidelberg, Germany

(*correspondence: joelle.buxmann@iup.uni-heidelberg.de)

It is assumed that SOA slow down the catalytic bromine release via "Bromine Explosion" (auto catalytic release of reactive bromine from salt surfaces). Based on this theory a new experimental setup was developed, in which a substrate NaCl/NaBr=300:1 mixture was placed on a teflon pan located in an aerosol smog-chamber [1]. Direct observation of BrO is possible using an active Differential Optical Absorption Spectroscopy (DOAS) instrument [2] in combination with a multi-reflection cell. SOA was formed during the ozone-initiated oxidation of α-pinene, catechol and guaiacol, respectively [3].

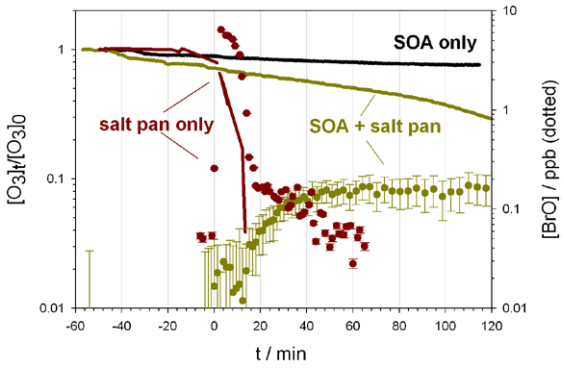

Figure 1: Time profile of O_3(lines) and BrO(dotted) during experiments with different initial composition: with salt pan as halogen source (red), with SOA only (black) and with both (green). At t=0 the solar simulator was switched on.

The experiments showed that the presence of SOA modifies the kinetics of halogen cycles in the gas phase: With salt pan only a complete ozone depletion was observed within first 10 minutes due to "Bromine Explosion" with up to 6ppb BrO. With salt pan and SOA the BrO formation showed a delay and its maximum mixing ratio of 150 ppt was one order of magnitude lower than without SOA.

[1] Siekmann 2008), PhD-thesis, University of Bayreuth [2] Platt and Stutz (2008) Volume. ISBN 978-3-540-21193-*Springer-Verlag Berlin Heidelberg* [3] Ofner *et al*. (2011) *Atmos. Chem. Phys*., **11**, 1-15.

https://doi.org/10.1180/S0026461X00006502 Published online by Cambridge University Press

Dissolved organic carbon and soil respiration release in undisturbed columns from SE Spain

A. BÜYÜKKILIÇ YANARDAĞ*, M. GÓMEZ-GARRIDO, M. D. ESTÉVEZ RODRÍGUEZ, I. H. YANARDAĞ AND A. FAZ CANO

Universidad Politécnica de Cartagena, Agrarian Science and Technology Department Research Group: Sustainable Use, Management and Reclamation of Soil and Water, Murcia/España (*correspondence: ab16@alu.upct.es)

When pig slurries (PS) are applied to agricultural fields at different rate, large amounts of carbon can be introduced into soils. Better knowledge land application of pig slurry is important to know influence on carbon in leaching experiment. This study assessed the leaching potential of carbon cycle after an intensive farm pig manure at rates of control, single, triple doses are applied and investigated 'how is the relation between leaching of dissolved organic carbon (DOC) and soil respiration in the laboratory leaching experiment in silty loam soil?'.

Leaching was carried out weekly using distilled water to simulate the monthly rainfall events in the study area. Experiment was carried out for 12 weeks rainfall. Soil solutions and CO_2 were analyzed in each week. The results showed that; DOC are changed between 1.1 and 24.3 ppm, DIC are changed 20.5 and 47.8 ppm, NT are changed 2.3 and 55.9 ppm. during leaching experiment. Soil respiration varied between 10 and 150 mg C-CO_2 kg^{-1} soil h^{-1} in the control, between 10 and 250 mg C-CO_2 kg^{-1} soil h^{-1} in single plots, between 10 and 450 mg C-CO_2 kg^{-1} soil h^{-1} in triple plots.

Dissolved Organic and Inorganic Carbon, Dissolved Nitrogen, are effected temperature, and pH in the leaching system. pH is a more important factor for DOC leaching than temperature. Soil respiration is not significantly affected by pig manure application even during the four weeks, which is found balance and hold C in the soil with application. In single doses plots, respiration values are strongly correlated with time and also this dose is the agronomic rate of N-requirement (170 kg N/ha/yr) [1]. Finally, single application doses to silty loam soils have positive effect on carbon to the atmosphere and ground water.

[1] Directive 91/676/EEC (1991), *Concerning the protection of waters against pollution caused by nitrates from agricultural sources*. Ofic. J.L 375, 31.12. European Union, Brussels.

Inorganic and organic occurences from diagenesis of the Güvenç formation shales in the Adana basin, Turkey

A. BUYUKUTKU[1]* AND M. ALBAYRAK[2]

[1]Ankara University Engineering Faculty, Department of Geological Engineering, 06100 Besevler, Ankara, Turkey (*correspondence: butku@eng.ankara.edu.tr)

[2]General Directorate of Mineral Research and Exploration, Sogutozu, Ankara, Turkey (mustafa_albayrak@hotmail.com)

In the study, shale diagenesis of Güvenç Formation in Adana Basin was determined on the surface samples. Güvenç shales consist of organic matter (% 0.3-0.4) for hydrocarbon formation. X-Ray Diffractometer, Scanning Electron microscope equipped with an energy dispersive analyzer were used for detailed mineralogical, microstructural and elemental analysis for shale diagenesis. Fourier transform infra red spectroscopy (FTIR) was used for organic sample origin in the Güvenç Shales.

Diagenesis in the shales principally involves the progressive development of various types of cements in the following order: Calcite and feldspar formation, mixed layer smectite-illite and smectite-chlorite authigenesis, illite, chlorite authigenesis, quartz.

The C-H peak at 860 cm^{-1} shows the occurrence of aromatic groups (Fig. 1).

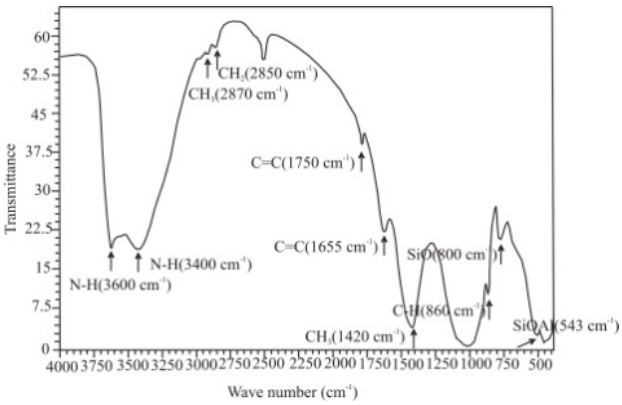

Figure 1: FTIR spectrum of the sample

https://doi.org/10.1180/S0026461X00006502 Published online by Cambridge University Press

Gallium oxide solubility in vapor and indicators of heterogeneous fluid filtration

A.YU. BYCHKOV, S.YU. NEKRASOV, I.YU. NIKOLAEVA AND S.S. MATVEEVA

Moscow State Universiy, Moscow,Russia (bychkov@geol.msu.ru)

The solubility of gallium and aluminum oxides in gas phase in the system Ga_2O_3 (Al_2O_3)-HCl-H2O was studied at 200-350ºC and pressure up to saturated vapor. The concentration of gallium increases with the increasing of HCl pressure. The formulae of gallium gaseous specie was determined as $GaOHCl_2$. The constant of gallium oxide solubility reaction was calculated at 200, 250, 300 and 350ºC. The concentration of aluminum in gas phase is insignificant in the same conditions. The possibility of gallium transportation in gas phase with small quantity of Al allow to separate this elements in hydrothermal processes with gas phase. The Ga/Al ratio can be used as the indicator of gas phase separation and condensation. The separation of gas and liquid phases was determined on greisen deposits by carbon isotope fractionation of carbon dioxide in fluid inclusion. The important feature of both ore mains is heterogenization and boiling of ore-forming fluids. Greisen ore bodies are formed as a result of strongly focused fluid flow in the T-P gradient fields. Gas and liquid phase separation specifies the vertical zonality of quartz type veins. The gas phase with the high gallium concentration is separated from a flow of liquid phase. Liquid phase react with the granites forming greisen metasomatites. Condensation of the gas phase in upper parts of massive produces the increasing of Ga/Al ratio in muscovite 3-5 times more, then in granites and bottom part of vein (from $2 \bullet 10^{-4}$ to $8 \bullet 10^{-4}$ mass ratio). The muscovite type veins has no separation between gas and liquid due to there thickness and small pressure gradient. There is no difference in Ga/Al ratio in muscovite from this veins. The Spokoinoe deposit is classified by mineralized dome type. The heterogenization of fluid occurs in H_2O-CO_2 system for water phase and carbon dioxide with temperature decreasing. Two-phase flow is separated in granite, forming greisen metosomatites. The Ga/Al ratio in rock increase up to 3 times to the upper part of metasomatitic zone. The Ga/Al ratio in muscovite can be applied for other hydrothermal systems for geochemical indicator of gas phase separation and condensation zone determination.

Geochemical evidence for lithosphere delamination beneath the central Rio Grande rift

B.L. BYERLY* AND J.C. LASSITER

Geological Sciences Department, University of Texas at Austin, Austin, TX, USA (* correspondence: benbyerly@utexas.edu)

Seismic studies have shown a low-velocity zone in the mantle that extends up to the Moho (~40km) beneath the central Rio Grande rift (RGR). Gao *et al*. [1] interpreted the low velocity zone to be the result of delamination of the original (≥100km thick) Proterozoic lithosphere and replacement with hot asthenosphere. However, hydration or melt infiltration of the lithosphere could also produce the observed low wave speeds. We have examined the geochemical signatures of spinel peridotite xenoliths hosted in alkalic basalts erupted near Elephant Butte, NM, USA in the central RGR in order to determine their chemical affinity (old continental lithosphere or young asthenosphere), and thereby test the delamination hypothesis.

Peridotite xenoliths from Elephant Butte can be divided into two distinct groups. One group is commonly fine grained and displays foliation. These are relatively fertile (3.5-4.5 wt.% Al_2O_3), have depleted Sr- and Nd-isotope signatures (e.g. $^{87}Sr/^{86}Sr \approx 0.7018$-$0.7025$), $^{187}Os/^{188}Os$ ranging from 0.124-0.130, and are LREE depleted with flat M-HREE. These signatures are similar to fertile abyssal peridotites, thought to represent the convecting upper mantle. In contrast, the other group are coarser grained, more refractory (~1.5wt. % Al_2O_3), display LREE enrichment, unradiogenic $^{187}Os/^{188}Os$ (~0.120), radiogenic $^{87}Sr/^{86}Sr$ (0.7041-0.7043) and lower modal abundance of CPX. These signatures are characteristic of Proterozoic SCLM. Two-phase pyroxene geothermometry of xenoliths from Elephant Butte shows no significant difference in temperature (~1000°C) between the two groups. Based on a local heat flow of 90mW/m^2 these temperatures correspond to a depth of ~45km.

The fertile xenoliths most likely represent convecting asthenospheric mantle that has recently replaced the lithosphere. The refractory xenoliths represent Proterozoic lithosphere which has undergone varying degrees of ancient melt depletion and metasomatism. This indicates that lavas from Elephant Butte are sampling the lithosphere asthenosphere boundary which lies at ~45km depth and that significant thinning of the lithosphere has occurred, consistent with the delamination hypothesis of Gao *et al*. [1].

[1] Gao *et al*. (2004) *J Geophys Res* **109**, B03305.

https://doi.org/10.1180/S0026461X00006502 Published online by Cambridge University Press

Using bacteria to produce tailored magnetic nanoparticles

J.M. BYRNE[1]*, V.S. COKER[1], N.D. TELLING[2], G. VAN DER LAAN[1,3], D. J. VAUGHAN[1], R.A.D. PATTRICK[1] AND J.R. LLOYD[1]

[1]SEAES, Williamson Research Centre for Molecular Environmental Science, University of Manchester, M13 9PL, UK (*correspondence: James.Byrne@postgrad.manchester.ac.uk)

[2]Institute for Science & Technology in Medicine, Keele University, Stoke-on-Trent ST4 7QB, UK

[3]Diamond Light Source, Didcot, Oxfordshire OX11 0DE, UK

Magnetic iron oxide nanoparticles of the form $M_xFe_{3-x}O_4$ (M = Co, Zn, Cr, Mn etc.) are useful for a wide range of applications including targeted cancer therapies, remediation of contaminated ground waters and data storage devices. Many current production processes use chemical and mechanical methods which often use toxic reagents and are expensive. This work presents an alternative biotechnological approach, harnessing the reductive capabilities of the subsurface Fe(III) reducing bacterium *Geobacter sulfurreducens* which yields relatively large quantities of magnetite nanoparticles at ambient temperatures.

The intrinsic magnetism and small size of the nanoparticles are paramount to their commercial use, and must be optimised during production for specific applications. In this study, the incorporation of dopants including zinc and cobalt into the structure of the biomagnetite nanoparticles was studied, and changes in the magnetic and structural properties of the resulting iron oxide minerals quantified. We demonstrated a significant increase in the magnetic moment of the particles at 5K and room temperature by doping with relatively low quantities of zinc, whilst cobalt induced large increases in coercivity. The inclusion of dopants also significantly affected the size of the nanoparticle crystals, with decreases from ~20nm to 8nm observed as dopant concentration increased.

Analytical methods including x-ray absorption, (XAS and XMCD), SQUID magnetometry and Mössbauer spectroscopy were used to provide important information about the mineral structure and indications of where in the crystal the dopants were incorporated, i.e. tetrahedral or octahedral components of the magnetite. Such techniques are vital to better understand how to improve bioproduction methods in order to maximize the potential of biogenic nanoparticles.

https://doi.org/10.1180/S0026461X00006502 Published online by Cambridge University Press

Low-temperature Pt–Pd mineralisation: Examples from Brazil

A.R. CABRAL[1]*, B. LEHMANN[1] AND M. BRAUNS[2]

[1]Mineral Deposits, TU Clausthal, 38678 Clausthal-Zellerfeld, Germany
(*correspondence: alexandre.cabral@tu-clausthal.de)
[2]Curt-Engelhorn-Zentrum Archäometrie, 68159 Mannheim, Germany

Hematite-bearing Au–Pd mineralisation in Brazil commonly has a platiniferous component [1, 2]. Examples are Hg-bearing hongshiite, PtCu, and Pt_2HgSe_3, both from Itabira, Minas Gerais. These minerals occur in specular hematite-rich veins that cross-cut the ~0.6-Ga Brasiliano tectonic foliation of the host rock (itabirite). This vein mineralisation is called 'jacutinga'. The presence of barite in hongshiite and Na/K–Na/Li fluid–mineral geothermometers indicate that oxidising brines of evaporitic origin were instrumental to the Au–Pd–Pt mineralisation at a maximum temperature of about 350°C [3].

Platiniferous alluvia are found in the quartzitic domains of the Palaeo-Mesoproterozoic southern Serra do Espinhaço, Minas Gerais, north of Itabira. Alluvial palladiferous gold and specular hematite point to 'jacutinga'-like veins in the quartzite country rock in the Córrego Bom Sucesso area. We found high Pd/Ag ratios (~4–3700) in the alluvial palladiferous gold. Such ratios are thermodynamically restricted to very oxidising brines [4]. In addition, Córrego Bom Sucesso is famous for its botryoidal Pt–Pd aggregates, reaching several millimetres across, which formed within the alluvium [1, 2, 5].

In northern Brazil, Au–Pd–Pt bonanza mineralisation triggered the gold rush that made Serra Pelada known worldwide. The near-surface mineralisation is hosted by weakly metamorphosed metasedimentary rocks of supposedly Neoarchaean age, but the bonanza ore is coeval with a Mn–Ba oxide, which has a Late Cretaceous $^{40}Ar/^{39}Ar$ age [6]. Fluid-inclusion microthermometric data from quartz and the mineral assemblage of Mn–Ba oxide and fine-grained specular hematite give evidence for very oxidising brines at temperatures between ~100 and 170°C.

[1] Hussak (1904) *Sitz.-Ber. math.-naturwiss. Kl. Kais. Akad. Wiss.* **113**, 379-466. [2] Cabral *et al.* (2009) *Econ. Geol.* **104**, 1265-1276. [3] Lüders *et al.* (2005) *Miner. Deposita* **40**, 289-306. [4] Gammons *et al.* (1993) *Geochim. Cosmochim. Acta* **57**, 2469-2479. [5] Cabral *et al.* (2011) *Chem. Geol.* **281**, 125-132. [6] Cabral *et al.* (2011) *Econ. Geol.* **106**, 119-125.

Iodine fingerprints biogenic fixation of platinum and palladium

A.R. CABRAL[1]*, M. RADTKE[2], F. MUNNIK[3], B. LEHMANN[1], U. REINHOLZ[2], H. RIESEMEIER[2], M. TUPINAMBÁ[4] AND R. KWITKO-RIBEIRO[5]

[1]Mineral Deposits, TU Clausthal, 38678 Clausthal-Zellerfeld, Germany
(*correspondence: alexandre.cabral@tu-clausthal.de)
[2]BAM Federal Institute for Materials Research and Testing, 12489 Berlin, Germany
[3]Institute of Ion Beam Physics and Materials Research, HZDR, P.O. Box 510119, 01314 Dresden, Germany
[4]Faculdade de Geologia, UERJ, 20550-050 Rio Janeiro-RJ, Brazil
[4]Centro de Desenvolvimento Mineral, VALE, Caixa Postal 09, 33030-970 Santa Luzia-MG, Brazil

Botryoidal aggregates of platinum (Pt) and palladium (Pd) from an alluvial deposit (Córrego Bom Sucesso) in Serro, Minas Gerais, Brazil, were likely the sample material from which Wollaston [1] isolated and identified Pd for the first time [2]. We recovered millimetre-sized botryoidal and rod-shaped grains of Pt and Pd from the alluvial deposit. Their arborescent morphologies indicate that the Pt–Pd aggregates formed *in situ* within the alluvium [2]. We carried out synchrotron radiation-induced X-ray fluorescence (SR-XRF) spectrometry on the Pt–Pd aggregates to determine iodine. We found high concentrations of iodine, in the range from 10 to ~120 μg/g [3]. Iodine is a strongly biophile element [4], which is enriched in peatlands by microbial activity [5]. Its high concentration in the Pt–Pd nuggets suggests that microbial activity took place during precious-metal fixation in the aqueous alluvial milieu. The Pt–Pd nuggets have an average thallium/selenium ratio of about 0.08, a value close to that for fluvial waters, suggesting that Pt and Pd were fixed from highly dilute solutions within the alluvium [6]. Inorganic and biogenic processes, i.e. electrochemical metal accretion [7] and bioreduction, are thought to have contributed to the growth of biogenic Pt–Pd nanoparticles that formed on organic templates such as humified plant remains.

[1] Wollaston (1809) *Phil. Trans.* **99**, 189-194. [2] Hussak (1906) *Z. prakt. Geol.* **14**, 284-93. [3] Cabral *et al.* (2011) *Chem. Geol.* **281**, 125-132. [4] Goldschmidt (1958) Geochemistry. Oxford University Press. [5] Keppler *et al.* (2004) *Environ. Chem. Lett.* **1**, 219-223. [6] Cabral *et al.* (2009) *Econ. Geol.* **104**, 1265-1276. [7] Cabral *et al.* (2009) *Eur. J. Mineral.* **21**, 811-816.

https://doi.org/10.1180/S0026461X00006502 Published online by Cambridge University Press

Volatile and trace element abundances in HIMU melt inclusions

R.A. CABRAL[1]*, M.G. JACKSON[1], E.F. ROSE-KOGA[2], J.M.D. DAY[3] AND N. SHIMIZU[4]

[1]Department of Earth Sciences, Boston University, Boston, MA 02215, USA (*correspondence: racabral@bu.edu)
[2]Laboratoire Magmas et Volcans, Universite Blaise Pascal, CNRS, UMR 6524, IRD, R 163, Clermont-Ferrand, France
[3]Scripps Institution of Oceanography, La Jolla, CA 92037, USA
[4]Woods Hole Institute of Oceanography, Woods Hole, MA 02543, USA

Water distribution within the mantle influences magma chemistry and evolution, location and extent of melting, and volcanism over geological time. During subduction, oceanic crust has been suggested to transport significant quantities of water and other volatiles to post-arc depths [1]. Despite the important control water has over mantle characteristics and behavior, the amount of water that is retained within the descending slab is poorly constrained [2, 3].

One possible method for constraining the amount of surviving volatiles is to examine oceanic hotspot lavas that are thought to sample melts of subducted oceanic crust. It is hypothesized that subducted material can be returned to the shallow mantle in areas of mantle upwelling, where it is partially melted and erupted during hotspot volcanism. Lavas from Mangaia represent the HIMU (high-μ, or high $^{238}U/^{204}Pb$) mantle end member, which contains geochemical signatures associated with recycled oceanic crust.

Earlier work on olivine-hosted melt inclusions from Mangaia found the inclusions to host volatile-rich phases (e.g., amphibole, phlogopite, apatite, and carbonatite [4]), an observation that is consistent with Mangaian melt inclusions being volatile-rich. High volatile abundances, coupled with major- and trace-element compositions in melt inclusions that are consistent with HIMU source derivation, may indicate that subducted oceanic crust has retained a significant amount of water [1]. This would imply that dehydration during subduction of oceanic crust is not an efficient process.

Here, we will place new constraints on deep cycling of volatiles into the mantle through examination of olivine-hosted melt inclusions, and we will present the first ever volatiles data on HIMU end member glasses.

[1] Hacker (2008) *G3* **9**, doi:10.1029/2007GC001707. [2] Hilton *et al*. (2002) *Rev.Miner* **47**, 319-370. [3] Wallace (2005) *Volcan.Geotherm.Res*. **140**, 217-240. [4] Saal et. al. (1998) *Science* **282**, 1481-1484.

Mineralogy of stream sediments and soils of Santiago Island, Cape Verde

M.M.S. CABRAL PINTO[1,2]*, M.M.V. SILVA[2], R. HERNANDEZ[1] AND E.A. FERREIRA DA SILVA[1]

[1]Geobiotec Center, University of Aveiro, Portugal
[2]Geociences Center, University of Coimbra, Portugal (*marinacp@ci.uc.pt)

Santiago Island covers an area of 991 km^2 and is characterized by a rough relief. (up to 1392 m) and valleys with almost vertical slopes and large flat areas in the coastal zones. The climate is semi-arid, with torrential rains. The lavas occupy most of the island, the pyroclasts are subordinated and the quaternary sedimentary cover occurs in small areas. The mineralogical composition of the 70 stream sediments and 70 soil samples, collected from all geological formations of the island, was studied in the < 2mm fraction. The samples are dominated by primary silicate minerals, such as feldspar (15.0 to 35.4 %), pyroxene (7.8 to 37.4 %) and olivine (0.0 to 9.0 %), reflecting the mineralogical signature of the igneous rocks that support the island. Quartz, phyllosilicates (smectite, kaolinite, mica/illite), calcite, hematite, leucite, apatite, nepheline, magnetite, titanomagnetite, ilmenite, chromite, garnet, zeolites, siderite, opal, barite, titanite, zircon, halite, aragonite, dolomite, brucite larnite and chlorite were also identified. Higher proportion of feldspar and pyroxene were detected on stream sediments (27.3 % and 25.6 %, respectively), than the soils (24.1 % and 17.0 %, respectively). The soils have higher relative proportion of quartz (24.5 %), phyllosilicates (16.1 %), calcite (2.8 %) and hematite (9.6 %) than stream sediments (12.2 %, 14.5 %, 0.8 % and 9.0 %, respectively). These differences are due to pedogenetic processes and wind-transported materials that affect the soils. Soil and stream sediments that cover formations affected by intense weathering are enriched in phyllosilicates and hematite and impoverished in pyroxene and olivine.

https://doi.org/10.1180/S0026461X00006502 Published online by Cambridge University Press

Contrasting mechanisms for two pulses of garnet growth at Stillup Tal, Tauern Window, Austria

MARK J. CADDICK[1], ETHAN F. BAXTER[1,2] AND ANTHONY D. POLLINGTON[2,3]

[1]ETH Zürich, 8092 Zürich, Switzerland
[2]Boston University, Boston MA, 02215, USA
[3]University of Wisconsin, Madison, WI, 53706, USA

Growth of *ca*. 110 cm^3 sub-spherical garnet crystals in a shear zone in the Austrian Tauern Window required *ca*. 7.5 Myrs, with the vast majority of this growth occurring in two distinct pulses [1]. These pulses are characterised by growth rates at least 5 times higher than the 'ambient' rate experienced during the *ca*. 2 Myr inter-pulse hiatus, and during the final stages of crystal growth. Here we explore possible mechanisms for such short crystal growth bursts, testing their viability in terms of an Alpine history, and using the available constraints to calibrate an exhumation velocity.

The first growth pulse occurred early in the preserved garnet history (inner 2 cm diameter of the crystal core) and is well resolved to no more than a few hundred thousand years duration (likely much less). A thermodynamically constrained garnet growth model [2] and a complex suite of mineral inclusions suggest that this records growth over a relatively limited range of P and T, at > 35 km depth and temperatures several 10s of degrees above the garnet-in reaction. A sharp Mn decrease within this growth phase likely reflects Rayleigh fractionation, but otherwise both garnet composition and its mineral inclusion assemblage are effectively constant. This supports the hypothesis that a kinetic trigger initiated and accelerated garnet growth at this time, with a distinct network of radiating fluid inclusions (absent outside the crystal core) attesting to fluid abundance [1].

A second phase of accelerated growth is more poorly resolved to no more than 1.5 million years (again, probably much less). Characteristic changes in all measured divalent cations imply that both this rapid crystal overgrowth and the slowly-grown crystal segment that preceeded it grew during *ca*. 5 kbars decompression and 50-100 ˚C heating. Results are consistent with equilibrium growth along a *P-T* trajectory that traversed fields of relatively constant mineral assemblage and then intersected a set of mineral reactions that accelerated garnet growth. Both slow garnet growth *after* the first pulse and rapid growth in the second pulse are thus possible without recourse to additional kinetic mechanisms or substantial increases in heating or decompression rate.

[1] Pollington & Baxter (2010) *EPSL*. **293**. 63-71. [2] Caddick *et al*. (2010) *J. Pet*. **51**. 2327-2347.

The characteristics of organic matter adsorbed on clay minerals and its significance in carbon cycling

CAI JINGGONG[1]*, JI JUNFENG[2], LU LONGFEI[1], DING FEI[1] AND CAI YUANFENG[2]

[1]State key laboratory of marine geology, Shanghai, 200092, China (*correspondence: jgcai@tongji.edu.cn)
[2]State Key Laboratory of Mineral Deposits Research, Nanjing; 210093,china

The protection of organic matter (OM) via adsorption on clay minerals is well recognized in recent years, however, the quantity and occurrence of OM adsorbed on different kinds of clay minerals may be not the same. As a result, smectite and illite were selected to synthetize with OM which are positive (HDTMA), negative (SDS) and neutral (0p-10) OM in various CEC. The amount, stability and occurrence of OM combined with different kinds of clay minerals were studied and their evolution distinction in the carbon cycling was discussed as well.

The result shows that the total organic carbon (TOC) absorbed on both the smectite and illite is 5-20%, and increasing with the CEC. Moreover, the TOC of positive OM absorbed on the smectie or illite is higher than the other kinds of OM. After 6 months at room temperature, the TOC absorbed on semectite decreases slightly(5-20%), whereas the TOC absorbed on illite decreases sharply to less than 2%. In a programming heating experiment, the TOC of smectite-complexes was 7% at the temperature of 300°C, and decreased to 2% as the temperature up to 500°C; however, the TOC of illite-complexes decreased to below 2% at 100°C. These results suggest that the stability of the complexes combined with smectite and illite is distinctively different. The diagnostic peaks of the smectite-complexes, including the d001 reflection peak on XRD, the methyl vibration peak and water vibration peak on IR, were changed in a programming heating, which indicate that the OM was not simply absorbed on the surface of smectite but also into the interlayer space. However, the diagnostic peaks of the illite-complexes on XRD and IR were changed slightly, which indicate that the OM was simply absorbed on the surface of illite. The different occurrences of OM associated with smectite and illite must determine the fate of OM in the evolution, which is significant in carbon cycling study.

This research was supported by the NSFC (Grants 40872089 and 41072089) and the State Key Lab. of Marine Geology Fund,Tongji University (MG200902).

https://doi.org/10.1180/S0026461X00006502 Published online by Cambridge University Press

Contaminant transport modeling in the candidate VLLW disposal site

CAI XINGQI, WANG YONGLI* AND DUO TIANHUI

[1]Department of Geochemistry, Chengdu University of Technology, Sichuan Province (*correspondence: wangyl@cdut.edu.cn, tsaiseven@sina.com, dth4358@126.com)

This paper takes advantage of MODFLOW software to simulate the groundwater pollutant(Sr) migration in the candidate VLLW disposal site in the Tea ditch and its nearby living quarters.

Simulation results show that, when the VLLW are dumped in landfills, there's no significantly impact on the environment and the residents living quarters in the south in 200 years. Meanwhile, we also simulate the condition once this disposal site leakage occurs. And this suggests, after the leakage 5 years, Besides pollutant concentration observation Well-3 (OW3) not observed in obvious pollutants, the rest two were observed a evident value of the pollutant concentration, since then, pollutants spread to the whole proluvial fan gradually, there's no doubt that it has a significant influence on the proluvial fan and the resident nearby.

Alteration of arsenopyrite in sulphruic acid

YUANFEGN CAI[12] AND XIAOXIAO HU[2]

[1]State Key Laboratory of Mineral Deposits Research, Dept. of Earth Sciences, Nanjing University, Nanjing, China
[2]Scool of Earth Sciences and Engineering, Nanjing University, Nanjing, China (caiyf@nju.edu.cn)

Arsenic contaminants gives the huge threaten on humanbeings health and life.

A massive asenopyrite sample was cut into small pieces of cube with the size of about 3 mm to have a reference shape and size when studying the leaching process. The leaching is lasting one month at the temperature of 100, 150, 200, 250 and 300 ºC in sulphric acid with the concentration of 1, 0.1 and 0.001M. The arsenopyrite cube and acid was enclosed in a tefelon tube and wraped with steel vessel. Each cube was measured in size and weight previous and after the leaching process. Then, the cube relicit was cut into sections and was used to carry out morphological observation under both petrographical microscope and Scanned Electron Microscope (SEM), surficial chemical element identification with the use of X-ray Photoelectron Spectroscopy (XPS). And the liquid lechate was tested by ICP-AES.

Results show that the size of cube keeps almost same but the weight decrease with increase of the concetration of sulphruic acid. It suggests that some element was leached out from the arsenopyrite. The majority of arsenic is present in the liquid leachate. The XPS measurement from both surface and profile shows the signal of As disappeared or weakened after the leaching process by XPS, while its signal increased with the in crease of etching time when depth profile scan is carried out. The morphological obervations gives the fact that the leaching starts from the outmost surface of cube or the edge of cracks, large quantities of pores present in the product area, the boundary of product and arsenopyrite is distinct and sharp, no buffer area is present, and the relicit keeps the shape of cube.

Our study shows that the leaching process of arsenopyrite is controled by the coupled dissolution-precipitation process. The As ion was leaching out and the new product, most probable arsenic oxide, precipitated on the surface of cube or along the cracks. This may suggest that the contamination of suface water and groundwater from weathering of arsenopyrite or arsenic pyrite or other arsenic mineral is main geological cause, And it will bring the huge threaten to the crops, habitants and long tern side-effect to the biosphere.

Acknowledgements: This work was financially supported by the NSFC project (40872035)

https://doi.org/10.1180/S0026461X00006502 Published online by Cambridge University Press

Molecular scale origin of nuclear waste glass properties

G. CALAS[1], L. CORMIER[1], J.M. DELAYE[2], L. GALOISY[1], P. JOLLIVET[2] AND S. PEUGET[2]

[1]Institut de Minéralogie et de Physique des Milieux Condensés, UPMC; Université Paris 7; CNRS; 4, Place Jussieu, 75 Paris, France (georges.calas@impmc.upmc.fr)
[2]CEA Valrhô-Marcoule, DEN/DTCD/SECM, BP17171, 30207 Bagnols-sur-Cèze cedex, France (jean-marc.delaye@cea.fr)

Assessing the long-term behavior of nuclear waste glasses implies predict their performance, and more precisely their evolution under irradiation and during interaction with water. Structure-property relationships depending on the local and medium-range structure of borosilicate glasses of nuclear interest [1] exemplify structural features rationalizing properties observed during glass elaboration or under forcing conditions (alteration, irradiation). Structural data are correlated with numerical simulations to determine the local structure of glasses, with a special attention to the interplay between glass components [2]. During alteration, some elements, such as Fe, change coordination, as other such as Zr only change coordination in under-saturated conditions. This may explain the chemical dependence of the initial alteration rate and the transition to the residual regime, illustrating the molecular-scale processes during glass-to-gel transformation [3]. Determining molecular scale processes helps in the exploration of new compositions of nuclear glasses [4].

Under irradiation, various structural effects are observed, including coordination change, ion migration or disorder effects. These studies show that glasses with a simplified composition do not show the same behavior as more realistic glasses. Molecular dynamics (MD) simulations provide complementary information on elastic effects [5]. Recent direct evidence for B-coordination change under external irradiation, together with structural models derived from MD, sheds light on the structural mechanisms at the origin of radiation-induced modifications of glass properties, emphasizing the importance of the thermal regime in the cascade core. Molecular scale view of nuclear glasses provides a unifying view of the processes that define the properties of this important class of materials.

[1] G. Calas *et al*. (1982) *C. R. Chimie* **5**, 831–843. [2] L. Cormier *et al*. (2000) *Phys. Rev. B* **61**, 14495-14499. [3] E. Pelegrin *et al*. (2010) *J. Non Cryst. Solids* **356**, 2497-2508. [4] B. Bergeron *et al*. (2010) *J. Non Cryst. Solids* **356**, 2315-2322. [5] G. Bureau *et al*. (2008) *Nucl. Instr. Meth. Phys. B* **266**, 2707-2710.

Occurrences of nickel in different host phases of a laterite deposit: An example from Berong, Philippines

M.Y. CALIBO*, C.A. ARCILLA, R.M. ONG, M.L.G. TEJADA AND J.P. RAFOLS

National Institute of Geological Sciences, University of the Philippines – Diliman, Quezon City, 1101 Philippines (*correspondence: merylyc@gmail.com)

Despite being globally widespread and relatively easy to mine, nickel laterite ores prove to be difficult to process. Beneficiation of Ni and other economically extractable elements along with it, greatly depends on the mixture of the feed material (silicate phases and oxide phases) which, in turn, is dependent on the mineralogy of the raw ore. The type(s), concentration and consumption of acid to be used in dissolution are controlled by the percentages of both gangue and host minerals trapping the Ni, whether by sorption or isomorphous substitution. A modified selective sequential extraction was designed to recover Ni from from its various host phases to optimize the beneficiation process using samples from different zones in a nickel laterite deposit in Berong, Palawan. This deposit is defined by, from top to bottom, an iron oxide-hydroxide zone, a transition zone made up of serpentine and iron oxides, a nickel-enriched serpentine zone, and a nickel-depleted serpentine zone, based on mineralogy and geochemistry. The occurrence of Ni as adsorbed and exchangeable cations, in carbonates, in amorphous iron oxides, within the structure of crystalline iron oxides and hydroxides, and in residual silicate layers within each of the zones was determined. Qualitative analysis of nickel in iron oxides, serpentine and talc using electron-probe microanalyzer supports the results of the extraction experiment. In limonite zones, dominated by goethite and other secondary iron oxides, > 90% of the total nickel reside in the crystal structure of Fe oxides. In the iron oxide – magnesium silicate transition horizon and in the nickel-enriched saprolite zone, respectively, > 80% and an average of 77% of the nickel are distributed in Fe oxides and within the octahedral layers of serpentine. The remaining Ni ions not taken up by these crystalline minerals are mostly associated with amorphous Fe oxides. An EPMA image, depicting relative abundance of Ni, Mg, and Fe in a section of weathered bedrock, implies that Ni is more closely associated with Fe than with Mg. An industrially significant output of this research is the finding that residual silicates, which take an enormous amount of acid to dissolve, need not be dissolved in order to optimize the beneficiation of nickel.

https://doi.org/10.1180/S0026461X00006502 Published online by Cambridge University Press

Geochemistry of eastern North American CAMP diabase dykes

S. CALLEGARO[1]*, A. MARZOLI[1], H. BERTRAND[2], L. REISBERG[3], M. CHIARADIA[4] AND G. BELLIENI[1]

[1]University of Padua, Department of Geosciences, Italy (*correspondence: sara.callegaro@unipd.it, andrea.marzoli@unipd.it, giuliano.bellieni@unipd.it)
[2]Laboratoire de Géologie de Lyon, UMR-CNRS 5570, Lyon, (herve.bertrand@ens-lyon.fr)
[3]CRPG (CNRS UPR2300), Université de Lorraine, France (reisberg@crpg.cnrs-nancy.fr)
[4]Université de Genève, Switzerland (Massimo.Chiaradia@unige.ch).

Swarms of diabase dykes and a few sills of the Central Atlantic magmatic province (CAMP) intruded the Piedmont area of the Appalachians and the coastal plains of eastern North America (ENA) between 202 and 195 Ma [1]. Based on field observations, an age progression can be defined from NW- to N- and NE-oriented dykes. The basaltic dykes are Mg, Cr-, and Ni-rich, which may only in part reflect accumulation of mafic minerals. Incompatible trace element contents are fairly homogeneous and generally low, e.g. La_{Ch}/Yb_{Ch} (0.54-2.39), typical of melts issued from a quite depleted shallow mantle-source. The incompatible trace element contents are not correlated with isotopic compositions of ENA dykes, which display a considerable spread in initial isotopic signatures, i.e. $^{87}Sr/^{86}Sr_{200Ma}$ (0.7043-0.7088), εNd_{200Ma} (-6.8-+2.1) and $^{206}Pb/^{204}Pb_{200Ma}$ (17.41–18.61). Pb isotopic compositions plot above the NHRL, at positive Δ7/4 (10-17) and Δ8/4 (19-73). Generally low $^{188}Os/^{187}Os_{200Ma}$ ratios (0.127–0.144), which argue for negligible amounts of crustal contamination, coupled with the large range of Sr-Nd-Pb isotopic compositions, suggest generation from a strongly heterogeneous mantle source, probably metasomatized lithosphere. The alternative, a deep enriched mantle source, is unlikely because the crystallization temperatures calculated [2] for high-Fo (up to Fo_{89}) olivines (ca. 1350 °C) are not supportive of a very hot (i.e. mantle-plume) origin (see also [3]). Considering the isotopic compositions of ENA lava flows, some dykes may have fed eruptions chemically similar to the Newark Preakness and Hook Mt. flows, i.e. the youngest flows from the Newark Supergroup basins, whereas none of the analyzed basaltic dykes yields geochemical compositions similar to the slightly older Orange Mt. basaltic flows.

[1] Nomade S. *et al*. (2006) *Paleo3* **244**, 326-344. [2] Putirka K. (2008) *Rev. Mineral*. **69**, 61-120. [3] Herzberg C. (2009), *Nature,* **458**, 619-623.

Productivity and circulation changes during the last deglaciation from biomarkers and Nd isotopes

E. CALVO[1]*, L.D. PENA[2], C. PELEJERO[3] AND I. CACHO[4]

[1]Institut de Ciències del Mar, CSIC, Pg. Marítim de la Barceloneta 37-49, Barcelona, Spain (*correspondence: calvo@icm.csic.es)
[2]Lamont-Doherty Earth Observatory of Columbia University, 61 Route 9W, Palisades, NY 10964, USA
[3]ICREA and Institut de Ciències del Mar, CSIC, Pg. Marítim de la Barceloneta 37-49, Barcelona, Spain
[4]GRC Geociències Marines, Dept. d'Estratig., Paleontol. i Geociències Marines, Universitat de Barcelona, Spain

The Eastern Equatorial Pacific (EEP) is thought to have exerted a strong control over glacial/interglacial CO_2 variations through its link to circulation and nutrient-related changes in the Southern Ocean. Changes in phytoplankton productivity and composition associated with increases in equatorial upwelling intensity and influence of Si-rich waters of Sub-Antarctic origin have been recently detected in ODP Site 1240 (0º 01.31'N, 86º 27.76'W; 2,921 mbsl) [1]. However, these changes do not seem to have been crucial in controlling atmospheric CO_2, as they took place during the deglaciation, when atmospheric CO_2 concentrations had already started to rise. New results from Nd isotopes in foraminifera shells of *Neogloboquadrina dutertrei* from the same intervals corroborate this interpretation. *N. dutertrei* preferentially dwells in the lower thermocline, at the core of the Equatorial Undercurrent (EUC). Therefore, changes in the Nd-isotopic composition of these foraminifera will reflect the composition of the EUC, which, in turn, reflects changes in the advection of Sub-Antarctic Mode Water and Antarctic Intermediate Water and the composition of the Southern Ocean end-member. Our evidence indicates that diatoms outcompeted coccolithophores at times when the influence of Si-rich Southern Ocean intermediate waters was greatest as recorded by low ε_{Nd} values (-2.8). This shift from calcareous to non-calcareous phytoplankton would cause a lowering in atmospheric CO_2 through a reduced carbonate pump, as hypothesized by the Silicic Acid Leakage Hypothesis. However, the concomitant intensification of Antarctic upwelling brought large quantities of deep CO_2-rich waters to the ocean surface. This process very likely dominated any biologically mediated CO_2 sequestration, and probably accounts for most of the deglacial rise in atmospheric CO_2.

[1] Calvo, E., *et al*. (2011), *Proceedings of the National Academy of Sciences* **108** (14), 5537-5541.

https://doi.org/10.1180/S0026461X00006502 Published online by Cambridge University Press

Nickel isotopes, BIFs and the Archean oceans

V. CAMERON[1]*, D. VANCE[1] AND S. POULTON[2]

[1]BIG, Dept. of Earth Sciences, University of Bristol, Bristol BS8 1RJ, UK (*correspondence: glxvc@bristol.ac.uk)
[2]School of Civil Engineering & Geosciences, Newcastle University, Newcastle upon Tyne NE1 7RU, UK

Trace metal isotopes provide vital clues to the Earth's biogeochemical evolution. Key to these efforts is the development and application of new isotopic systems of bioessential elements important to specific organisms or metabolisms or, as recorders of changing environmental conditions through time. Nickel (Ni) is primarily restricted to microorganisms and metabolisms that might have evolved in a much different Archean environment [1-3]. Methanogens and their particular metabolism, methanogenesis, purportedly fit the criteria for an ancient origin of evolution and many studies have shown the absolute requirement that these microorganisms have for Ni.

Recently, we published the first measurements of nickel stable isotopes from abiotic terrestrial materials and pure cultures of methanogens [4]. Terrestrial samples representing the mantle and crust displayed very little isotopic variability (average δ^{60}Ni of 0.15 ± 0.24‰, 2σ). In contrast, Ni isotopes were significantly fractionated by pure cultures of methanogens. The largest fractionation, δ^{60}Ni of -1.46 ± 0.08‰, was achieved by a methanogenic hyperthermophile. Our data suggest the biological cycling of Ni may be an important contributor of Ni isotopic variations in the rock record. Furthermore, biological fractionation of Ni has the potential to be a powerful new biomarker particularly in regards to the nature and impact of early life.

We have started evaluating our new Ni isotopic tool by applying it to the measurement of Ni stable isotopes in banded iron formations (BIFs). In order to characterize the Ni isotopic composition of the geochemical and biological environment of the primitive Earth, it is essential to first understand the state and changing conditions of the Archean oceans. Such information recorded within BIFs and other terrestrial materials is necessary to support our continued efforts to establish Ni stable isotopes as a functional and detectable biosignature.

[1] Bapteste *et al*. (2005) *Archaea* **1,** 353-363. [2] Fraústo da Silva & Williams (2001) in *The Biological Chemistry of the Elements: The Inorganic Chemistry of Life* (Oxford University Press, Oxford), pp. 436-449. [3] Tice & Lowe (2006) *Earth Sci Rev* **76,** 259-300. [4] Cameron *et al*. (2009) *Proc Natl Acad Sci USA* **106,** 10944-10948.

The weathering of platinum from nuggets and platinum immobilisation by *Cupriavidus metallidurans*

G. CAMPBELL[1], F. REITH[2], L. MACLEAN[3] AND G. SOUTHAM[1]*

[1]Department of Earth Sciences, The University of Western Ontario, London, ON Canada N6A 5B7 (*correspondence: gsoutham@uwo.ca)
[2]School of Earth and Environmental Sciences, The University of Adelaide, CSIRO Land and Water, Waite Laboratories, Urrbrae, South Australia, Australia
[3]Canadian Light Source Inc., 101 Perimeter Road, Saskatoon, SK Canada S7N 0X4

Platinum nuggets, collected from a platiniferous and auriferous site near Fifield, New South Wales, Australia were examined to evaluate mineral dissolution-precipitation processes occurring at the nugget–'soil solution' interface. Nuggets possessed striations indicating mechanical transport with the soil environment and micrometer-scale dissolution pits corresponding to regions possessing soil materials (quartz, clays and organics) and acicular, iron oxides suggesting an oxidising weathering environment. The occurrence of 100 nm-scale, cubic minerals at the soil solution interface and comparably sized cubic dissolution 'pits' suggest that platinum weathering occurs via preferential dissolution of the 'bulk' platinum nugget (an Fe-Pt alloy). Examination of these cubic minerals using scanning electron microscopy in secondary electron and back-scattered electron (BSE) imaging modes, and using energy dispersive spectroscopy indicated that they are enriched with copper (i.e., a Cu-Pt alloy). Growth of platinum nuggets via secondary platinum mineral formation was not observed. *Cupriavidus metallidurans* cultures reacted with 0.5 and 5 mM platinum (IV) chloride, immobilised platinum from solution rapidly i.e., within minutes. EXAFS/XANES analysis of these reaction systems demonstrated that most of the Pt(IV) chloride complex was reduced to Pt(II) and that platinum binding shifted from chloride to primarily, amino functional groups. Using transmission electron microscopy, *C. metallidurans* was also found to precipitate nm-scale colloidal platinum when exposed to 5 mM platinum (IV) chloride; the formation of these colloids occurred within the bacterial cell envelope. Understanding the biogeochemistry of platinum, in particular weathering and formation of colloids has important implications within geologic settings, i.e., for platinum dispersal in relation to exploration geochemistry programs.

https://doi.org/10.1180/S0026461X00006502 Published online by Cambridge University Press

Kinetic modeling of microbial Fe(II) oxidation, Fe(III) hydrolysis, and mineral precipitation in acid waters

K.M. CAMPBELL* AND D.K. NORDSTROM

U.S. Geological Survey, Boulder, Colorado, 80303, USA
(*correspondence: kcampbell@usgs.gov)

Acidophilic Fe(II)-oxidizing microorganisms are widespread in acidic mine-impacted waters and are the primary drivers for Fe(II) oxidation at low pH. The resulting changes in Fe chemistry have profound effects on trace element redox cycling and mobility in the environment. Sorption, precipitation, or redox activity of Fe(III)-containing mineral phases control the mobilization or sequestration of metal(loids) of concern in natural waters. Although Fe(II) oxidation is microbially-mediated, biogeochemical predictions for an acidic, Fe(II)-rich natural water require a coupled biotic-abiotic process model.

We present experimental and model results from a series of batch experiments conducted at four initial Fe(II) concentrations (10, 50, 100, and 159 mM), three initial pH values (2.0, 2.5, and 3.0), and inoculated with a pure strain of *Acidithiobacillus ferroxidans* isolated from acid rock drainage near a molybdenum mine. The pH, aqueous Fe(III), Fe(II), direct cell counts, and solid phase precipitates were monitored over the course of the experiments. For all inital Fe(II) concentrations except 10 mM, the pH increased initially, due to the acid-consuming stoichiometry of Fe(II) oxidation, but then decreased due to the combined effects of Fe(III) hydrolysis and precipitation of schwertmanite ($Fe_8O_8(OH)_6SO_4$) and/or jarosite ($KFe_3(SO_4)_2(OH)_6$). The Fe(III) concentration in the 10 mM Fe experiments was too low to precipitate jarosite, and only an increase in pH from Fe(II) oxidation was observed. The amount of pH increase due to Fe(II) oxidation was greatest at an initial pH of 2 for all initial Fe concentrations. The final pH in all bottles at 50 mM, 100 mM, and 159 mM Fe was very similar (pH 2), regardless of inital pH, because of equliibrium with mineral precipitates, primarily jarosite. Since the decrease in pH was due to both hydrolysis and precipitation, the kinetics of Fe(III) hydrolysis were measured in a separate experiment. PHREEQC, a geochemical model with the ability to incorporate multiple kinetic expressions, was used to simulate the experimental results by including kinetic expressions for microbial Fe(II) oxidation, Fe(III) hydrolysis, and jarosite precipitation. In addition, we compared various proposed kinetic formulations for microbial Fe(II) oxidation from the literature to our experimental results.

C, Sr isotopes in cap carbonate and and *Ce anomaly* in BIFs of Jucurutu Formation, Seridó Belt, NE, Brazil

M.S. CAMPOS[1], A.N. SIAL[1]*, C. GAUCHER[2], V.P. FERREIRA[1], ROBERT FREI[3], R.C. NASCIMENTO[4] AND M.M. PIMENTEL[5]

[1]NEG-LABISE, Dept. Geol. UFPE, Recife, 50670-000, Brazil (*correspondence: sial@ufpe.br)
[2]Facultad de Ciencias, Universidad. de la Republica, Montevideo,Uruguay (gaucher@chasque.com)
[3]Univ. Fundação do Amazonas, Manaus, Brazil
[4]Inst. Geography and Geol., Univ. Copenhagen, Denmark
[5]Inst. Geoc., Univ. Fed. Rio G. do Sul, Porto Alegre, Brazil

BIFs associated with Neoproterozoic glaciations are an important pillar of the Snowball Earth hypothesis and are regarded as accumulation of Fe^{+2} in ice-capped anoxic ocean. BIFs at Jucurutu (Mina do Bonito), Florânea (Cabeço da Mina) and São Mamede (Riacho Fundo) towns, Seridó Belt (itabirite and Fe ores, amphibole-itabirite, and tremolite schist) are overlain by Jucurutu marbles. Micro-drilled carbonate samples from the Jucurutu Formation exhibit $\delta^{13}C$ values as low as -12‰ in the first meter, followed by mantle values (-6 to -4‰) and then by positive values up section (+4 to +10‰). Surprisingly, $\delta^{13}C$ values for carbonates that overlie itabirites at Riacho Fundo and at Cabeço da Mina are all positive. Perhaps, the difference of C isotope behavior between basal carbonates at Mina do Bonito (negative), and Riacho Fundo and Cabeço da Mina (positive) reflect, perhaps, topographic control during deposition.

C-isotope stratigraphy for carbonates of the Jucurutu Formation support their deposition as cap carbonate. Negative $\delta^{13}C$ values are followed upsection by positive values. Sr isotope ratio for Jucurutu carbonates (~0.7074) approach Sr isotope ratios for Sturtian II cap carbonates (e.g. Maiberg, Pedro Leopoldo, Mirassol D´Oeste among others) between 740 and 635 Ma.

Negative Ce anomaly values (<0.10) result from Ce depletion or fractionation with metallic oxides, therefore, it indicates oxidizing conditions of the ocean water [1]. On the other hand, positive values (>0.10) reflect anoxic conditions of the ocean water. The values of Ce/Ce* in the BIFs vary from 0.54 to 2.46, indicating extremely anoxic environment, which seems to support the hypothesis of deposition of BIFs in an ocean capped by ice.

[1] Kato *et al*. (1996). *Journal Southeast Asian Earth Sci*. **14** 161–164.

https://doi.org/10.1180/S0026461X00006502 Published online by Cambridge University Press

Kaolinite as a sorbent for As natural contamination

B. CAMPREDON, C. HUREL AND N. MARMIER

LRSAE – Sci. Fac., University of Nice Sophia Antipolis, Parc Valrose, 28 avenue Valrose, 06108 Nice cedex 2 France

The geological formation of the Mercantour basin is made of metamorphic rocks, granite, Permian argillite and sedimentary rocks, which can provide high arsenic concentrations in the riverine waters. In the Var (South of France) watershead high arsenic input were measured, and were attributed to the dissolution of the metamorphic rocks form the old massifs of Mercantour. This natural contamination may affect the geological environments, since the sediments are the main sinks of pollutants. When the environmental conditions are changed (hydrologic conditions, flow variation, pH, redox potential, etc.) the sediments can act as a source of contamination. In this study, kaolinite (a clayey material) was chosen as a potential binding agent for trapping the local excess of As. This adsorbent material was chosen on the basis of his natural occurrence in the studied watershead ecosystem.

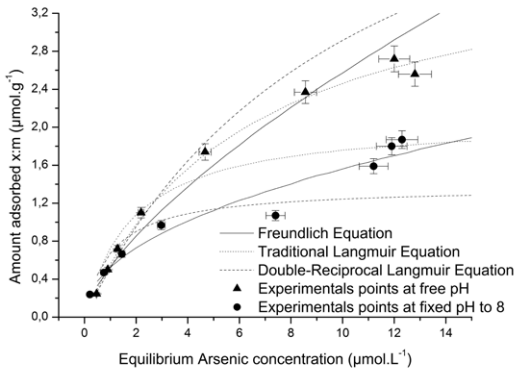

Figure 1: As adsorption on Kaolinite in $NaNO_3$ 0.1M and 13.3μM initial As concentration.

Adsorption of As on kaolinite was studied in various electrolytic conditions (concentration and composition), various solid to liquid ratios and various pH conditions (figure 1). The results were modeled considering empirical models and mechanistic models (surface complexation).

Changes in organic aerosol composition with aging inferred from aerosol mass spectra

M.R. CANAGARATNA[1,*], N.L. NG[1], J.L. JIMENEZ[2], P.S. CHHABRA[3], J.H. SEINFELD[3] AND D.R. WORSNOP[1]

[1]Aerodyne Research, Inc, Billerica, MA, USA (*correspondence: mrcana@aerodyne.com, ng@aerodyne.com, worsnop@aerodyne.com)

[2]CIRES & Department of Chemistry and Biochemistry, University of Colorado, Boulder, CO, USA (jose.jimenez@colorado.edu)

[3]Department of Chemical Engineering, California, Institute of Technology, Pasadena, CA, USA, (puneet@caltech.edu, seinfeld@caltech.edu)

The Aerosol Mass Spectrometer (AMS) provides real-time quantitative mass concentrations of non-refractory species in ambient aerosols. Factor analysis of ambient AMS organic aerosols (OA) spectra has been used to characterize the evolution of OA composition due to photochemical processing. A large database of ambient OA components has been analyzed with the "triangle" plot [1], in which f_{44}, ratio of m/z 44 (mostly CO_2^+ from acid-derived groups) to total signal in the component mass spectrum, is plotted against f_{43} (mostly $C_2H_3O^+$ from non-acid oxygenates). Examination of ambient oxidized organic aerosol (OOA) components in the triangle plot indicates that the relative acid group content and similarity of OA components increase with aging. A new parameterization of the H:C of OA components in term of f_{43} allows for further transformation of this data into the Van Krevelen diagram (H:C vs. O:C) [2]. Ambient OOA components also map out a triangular space in Van Krevelen diagram, showing a range of H:C at lower oxidization which decreases with increasing oxidation. The average slope (ΔH:C/ ΔO:C) that describes the transformation between the less and more aged OOA components is ~-0.5. This slope is consistent with the additions of both acid *and* alcohol functional groups without fragmentation, and/or the addition of acid groups with C-C bond breakage. The importance of acid formation in OOA evolution is consistent with increasing f_{44} in the triangle plot with photochemical age. The simple triangle and Van Krevelen plots for laboratory SOA formed in chamber experiments are also investigated.

[1] Ng, N. L., *et al*. (2010) *Atmos. Chem. Phys*., **10**, 4625-4641. [2] Heald, C. L., *et al*. (2010), *Geophys. Res. Lett*., **37**, L08803.

https://doi.org/10.1180/S0026461X00006502 Published online by Cambridge University Press

The many flavors of oxygen-minimum zones past and present

DONALD E. CANFIELD

NordCEE and Institute of Biology, University of Southern Denmark, University of Southern Denmark, Campus vej 55, 5230 Odense M, Denmark

Oxygen-deficient oxygen minimum zones (OMZs) are concentrated today in only a few regions of the global ocean. They are truly anoxic and despite their limited areal extent, they are sites of globally-significant rates of nitrogen loss as N_2 gas. While this loss was traditionally ascribed to canonical heterotrophic denitrification, recent work has demonstrated that most nitrogen loss is, instead, channeled through the anammox (anaerobic ammonia oxidation) process. Active nitrogen cycling was thought to inhibit sulfate reduction, explaining the lack of sulfide into these oxygen-free waters. New results show, by contrast, that these waters likely support an active, but cryptic, sulfur cycle, where sulfide produced by sulfate reduction is actively oxidized through nitrate reduction. Metagenomic results confirm the presence of microbial sulfur-cycling communities, and through their activities, these organisms may contribute to significant amounts of organic matter mineralization in OMZ water and to the ammonia driving anammox. Accumulating evidence suggests that in the past, oxygen minimum zones supported chemistry quite different from those found today. Many instances of both sulfidic and ferrugenous OMZs, extending well into the Precambrian, have now been described. We are still challenged to understand the circumstances responsible for the development of these different styles of OMZ water chemistry. However, the different flavors of OMZs through time must reflect the evolving chemistry of the coupled ocean-atmosphere system through time, and how this has controlled the variable expression of the different microbial populations known to inhabit OMZs today.

The alteration and the fluid inclusion characteristics of the Çavdır (Burdur) copper mineralization, SW Turkey

Z. CANSU[1]* AND H. EMRE[1]

Istanbul University, Department of Geological Engineering, 34230, Istanbul, Turkey
(*correspondence: zynporu@istanbul.edu.tr)

Çavdır (Burdur) copper mineralization, located in southwestern Turkey, occurs in the gabbros of the Lycian Allochthon. The mining district has a few meter wide vein systems that contain malachite±azurite, plus minor chalcopyrite, bornite, iron minerals such as goethite, hematite and magnetite in quartz gangue. The strike of major ore-bearing veins is N 30º to 45º E that are nearly paralel to the major fault in the study area. The veins are accompanied by extensive alteration.

Qualitative clay analysis were made to define alteration minerals and kaolinite, smectite, illite, zeolite, chlorite group minerals, cristobalite were determined by X-Ray Diffractometer method.

Microthermometric measurements were done on fluid inclusions of the quartz gangue. Fluid inclusions are two phased L+V (liquid+vapour) and NaCl-H_2O in system. Mean homogenization temperature is measured as 283ºC, the mean salinity is calculated from the equation %NaCl= [(-1,78x Tm_{ice})-(0,0442xTm_{ice}^2)-(0,000557xTm_{ice}^3)] [1] as %8 NaCl equivalent and the mean density is found as 0,82 gr/cm^3 by plotting % NaCl equivalent versus Th (ºC) [2].

These alteration and microthermometric datas connote an epithermal system. In the light of the acquired datas, it is suggested that the mineralization occurred in the effect of tectonic control and the heated ground water by the crust tickening (because of the emplacement of the Lycian thrust sheets) and geothermal gradient mobilized copper minerals from parental rocks.

[1] Bodnar (1993) *Geochemica et Cosmochimica Acta* **57**, 683-684. [2] Wilkinson (2001) *Lithos* **55,** 229-272.

https://doi.org/10.1180/S0026461X00006502 Published online by Cambridge University Press

Zircon U-Pb chronology and geochemistry of Late Paleozoic-Early Mesozoic intrusive rocks in eastern segment of the northern margin of the North China Craton, NE China and its tectonic implications

H.H. CAO, W.L. XU *, F.P. PEI AND F. WANG

College of Earth Sciences, Jilin University, Changchun 130061, China (caohua9871@163.com; (*correspondence: xuwl@jlu.edu.cn)

Chronological and geochemical data of Late Paleozoic-Early Mesozoic igneous rocks in the Kaiyuan-Panshi area, NE China, provide insights for the Late Paleozoic-Early Mesozoic tectonic evolution in the eastern segment of the northern margin of the North China Craton (NCC). LA-ICP-MS zircon U-Pb dating results indicate that the Late Paleozoic-Early Mesozoic magmatisms can be subdivided into three stages, i.e., the middle Permian (~270 Ma), the late Permian-early Triassic (259~249 Ma), and the late Triassic (~222 Ma).

The middle Permian magmatisms consist chiefly of garnet-bearing monzogranites. Their SiO_2-high and Al-rich geochemical feature suggest that they could have formed under a setting of crustal thickening.

The late Permian-early Triassic intrusive rocks are composed mainly of the gabbro, monzodiorite, monzonite, monzogranite, and syenogranite. Chemically, they belong to a calc-alkaline series and are characterized by enrichment in LILEs and depletion in HFSEs and P. Combined with the contemporaneous high-Mg andesites in the adjacent area, we propose that they could have formed under an active continental margin setting.

The late Triassic igneous rocks are composed of pyroxene-peridotites and olivine-pyroxenite with cumulate texture. Combined with the existence of coeval A-type granites and mafic-ultramafic rocks in the adjacent area, it is suggested that they could form under an extensional environment.

Taken together, we propose that the collision and subduction between the continent (NCC) and the island arc could happen in eastern segment of northern margin of the North China Craton from the middle Permian to early Triassic, and that a post-orogenic extension environment occurred in the study area in the late Trassic.

This research was financially supported by research grants from the Natural Science Foundation of China (Grant 41072038) and the Geological Survey of China (Grants 1212010611806 and 1212010070301).

Difference of organic matter in the Early Cambrian Ni-Mo-bearing black rock series in the Zunyi city of South China: Implications for the origin of the deposits

JIAN CAO*, CHUNHUA SHI, KAI HU, SHANCHU HAN, LIZENG BIAN AND SUPING YAO

State Key Laboratory for Mineral Deposits Research (Nanjing University); School of Earth Sciences and Engineering, Nanjing University, Nanjing, 210093 (*correspondence: jcao@nju.edu.cn)

The Ni-Mo polymetallic mineral deposits in the Zunyi city of South China is likely the most representative case of such deposits worldwide, and thus have received large research attentions during recent years. The issue is disputable as the origin of the deposits has been reported to be of sea water or hydrothermal sources. In this work, we mainly reported the difference of organic matter between the metallic and non-metallic intervals, and further addressed the origin of the deposits.

Analytical results from petrography, organic and elemental geochemistry showed that biogenic and organic matters occur widely both in the metallic and in the non-metallic intervals, indicating important effects on the formation of the deposits. The matters vary in abundance, type and maturation between the metallic and non-metallic intervals. For example, the organic matter abundance and maturity of the metallic interval are both the highest in the section. In addition, a special organic matter in elliptical shape was only observed in the metallic interval. The mineral element may be sourced either from sea water or from hydrothermal water. In particular, the sea water and hydrothermal water may be the dominant source for Mo and Ni, respectively. The mineralization of Mo and Ni is relatively early and late, respectively. Based on these results, a new mineralization model was tentatively established.

https://doi.org/10.1180/S0026461X00006502 Published online by Cambridge University Press

Geochronology and geochemistry of Xingdi No. 1 intrusion in Kuluketage, NW China: Tectonic implication for Xingdi mafic-ultramafic rock belt

XIAOFENG CAO[1,2], XIANG GAO[1], XINBIAO LÜ[1,2]*, YUEGAO LIU[1], SHENTAI LIU[1] AND CHAO CHEN[1]

[1]Faculty of Earth Resources, China University of Geosciences, Wuhan 430074, China (*correspondence:Lvxb_01@163.com; cao079@qq.com)

[2]State Key Laboratory of Geological Processes and Mineral Resources, China University of Geosciences, Wuhan 430074, China

The Xingdi No. 1 mafic-ultramfic intrusion is the largest in the Xingdi mafic-ultramafic belt with an exposed area of ca. 20 km^2 and intruded into the Paleoproterozoic basement. Gabbro is the major rock type and there is minor olivine pyroxenite. Sm-Nd geochronometry of the gabbro gives an isochron age of 761.2±31.2 Ma. It is the same with the intrusion age of Xingdi No. 2 pluton (760±6 Ma). The gabbro is systematically enriched in large ion lithosphere elements (LILE), light rare earth elements (LREE) and depleted in high field strength elements (HFSE) and heavy rare earth elements (HREE). The studied rocks are characterized by low whole-rock and mineral $\varepsilon Nd_{(t)}$ values (–7.8 to –7.1) and elevated $(^{87}Sr/^{86}Sr)_i$ values (0.7066–0.7073). These geochemical characteristics, together with the presence of the abundant hornblende, biotite, bladed biotite enclosed in amphibole, and crescent-shaped Paleoproterozoic wall-rock enclosed within the intrusion are key features of magma mixing in the source or assimilation during its emplacement. The rocks have Zr/Y ratio of 3.81–13, which fall in the area of within-plate basalt area. As the Xingdi No. 1 and No. 2 plutons formed at the same period and display similar geochemical characteristics, we propose that they formed within the same tectonic setting and derived from the same origin, but No.1 experienced higher extent of evolution and contamination. On the basis of previous studies, the Neoproterozoic tectonic and magmatic events in Kuluketage comprise syn-collisional granite around TC (ca. 1.0–0.9 Ga), post-collisional K-rich granite and alkaline mafic-ultramafic intrusions (ca. 830–800 Ma) and rifting-related mafic-ultramafic plutons, dykes and bimodal volcanic rocks (ca. 774–744 Ma).

This work is founded by 305 Project of State Science and Technology Support Program (Grant No. 2007BAB25B04).

CO_2 sequestration in deep aquifers: Insights into future hazards from a natural analog (Campi Flegrei, Italy)

R. CAPOBIANCO[1]*, R. ESPOSITO[1], R.J. BODNAR[1], G. CHIODINI[2] AND J.D. RIMSTIDT[1]

[1]Virginia Tech, Blacksburg, VA 24061, USA (*correspondence: rcapobi@vt.edu)

[2]Istituto Nazionale di Geofisica e Vulcanologia, sezione di Napoli, Osservatoria Vesuviano, 80124 Napoli, Itally

Among the major challenges facing the world today are climate changes and the alteration of Earth's surface geochemistry that are occurring as the result of release of anthropogenic CO_2 into the environment. Geologic sequestration of CO_2 in deep aquifers is an approach to reducing CO_2 emissions to the atmosphere that has recieved much attention recently [1]. The largest of the sequestration projects currently underway, the In Salah Project (Algeria) injects approximately 1 Mt of CO_2 per year [2]. A large coal-fired powerplant emits over an order of magnitude more CO_2 than this; for example, the Scherer plant (GA, US) emitted about 25 Mt in 2010 [3].

Campi Flegrei is a natural analog for large-scale CO_2 sequestration in confined saline aquifers. At Campi Flegrei active magmatism at depth is releasing large amounts of CO_2 that migrate upward into a confined saline aquifer at depths of about 2-3 km. Campi Flegrei is estimated to have injected 63 Mt of H_2O and CO_2 during the crisis of 1982-1984, corresponding to a total volume increase of $5.7*10^7$ m^3 or $2.85*10^7$ m^3/y [4]. This is similar to the volume ($2.4*10^7$ m^3) that would be occupied by the annual CO_2 emissions from the Scherer plant at the T&P conditions of interest in a geologic sequestration scenario. We predict that large-scale sequestration of CO_2 as a supercitical phase will have consequences similar to those observed at Campi Flegrei – seismic activity, bradyseism, and release of CO_2 rich fluids from the aquifer to the surface. These effects may be mitigated to some extent through careful management of the reservoir during and following injection.

[1] Benson & Cole (2008) *Elements* **4**(5), 325-331. [2] Michel *et al*. (2010) *International Journal of Greenhouse Gas Control* **4**(4), 659-667. [3] Environmental Protection Agency (2011), 2010 *Coal Unit Characteristics*. [4] Lima *et al*. (2009). [4] *Earth-Science Review* **97**(1-4), 44-58.

https://doi.org/10.1180/S0026461X00006502 Published online by Cambridge University Press

VSI study of biotite dissolution at acidic pH and 25-50˚C

C. CAPPELLI[1]*, J. CAMA[2], F.J. HUERTAS [1]

[1]Instituto Andaluz de Ciencias de la Tierra (IACT), CSIC-UGR, Avenida Fuentenueva s/n., 18002 Granada, Spain (*correspondence: chiaracappelli@ugr.es)

[2]Institute of Environmental Assessment and Water Research (IDAEA), CSIC, Jordi Girona 18-26, 08034 Barcelona, Catalonia, Spain

Generally, the dissolution rates of the phyllosilicates that comprise the mica group (e.g. muscovite, biotite and flogopite) were obtained from experiments in which ground powders were used, and the calculated rates were normalised either to total or edge surface area, derived from BET measurements. Using the vertical scanning interferometry (VSI) technique we attempt to compute biotite dissolution rates from quantifying surface normal retreat of the cleavage (001) surface at pH 1 and 25, 40 and 50 ºC. The advantage of these measurements is that allows us to obtain biotite dissolution rates from mineral surface retreat, and thus avoiding the need to normalize the dissolution rates with externally measured surface areas.

Single biotite fragments of approximately 100 mm^2 were placed in 250 mL of 0.1 M HNO_3 solution (pH 1) and 25, 40 and 50 ºC for almost two weeks. During this time span the cleavage surface was examined by VSI after 4, 7 and 13 days. On the one hand, dissolution features were observed on the cleavage surface, and on the other hand, the dissolution rates were computed from surface retreat compared to a non-reacted reference surface.

The calculated biotite dissolution rates, with an average error of ~10 %, were 2.5×10^{-8}, 1.1×10^{-8} and 0.3×10^{-8} mol m^{-2} s^{-1} at 50, 40 and 25 ºC, respectively, which are higher than those calculated from the total mineral surface area, although rates normalized to total surface area may have little relevance for micas, since reactive sites probably are concentrated on edge surface [1]. VSI examinations of the reacted cleavage surface show that biotite dissolution was controlled by preferential surface edge dissolution.

The calculated activation energy of the biotite dissolution at pH 1 from the rates obtained at 25, 40 and 50 ºC is 14.35 kcal mol^{-1} (R^2 = 0.997), which is similar to that of biotite dissolution at very acidic pH [2].

[1] Kalinowski & Schweda (1996) *GCA* **60**, 367-385 [2] McMaster *et al*. (2008) *MinMag* **72**, 115-120

Spin transition in Fe-bearing perovskite: Implications for the lower mantle

RAZVAN CARACAS

CNRS, ENS Lyon, UMR5276, Lyon, Frence

Using lattice dynamical calculations based on density functional perturbation theory we are able to disentangle a part of the complex phase diagram and spin behavior of the $(Mg,Fe)SiO_3$ perovskite (pv). To do this we investigate the dynamic stability of Pbnm $FeSiO_3$ pv and show the existence of unstable phonon modes. We track the eigen-displacements of the phonons modes to find low-spin and intermediate spin states. On solid-state physical basis we explore a set of hypothetical structures with various spin configurations and considerably lower enthalpy than the parent orthorhombic Pbnm structure. We show that the spin evolves along a high-spin to mixed high- and intermediate spin to low-spin transition sequence. We also analyze the thermal behavior of both high-spin and low-spin phases and we discuss a first thermal phase diagram.

We show that the elastic moduli and the bulk seismic wave velocities are weakly affected by the spin transition. However, the intrinsic differences in seismic anisotropy between the high-spin and low-spin phases of Fe-bearing pv coupled with lattice preferred orientation that can develop during mantle flow lead to distinct seismic signatures between the top and the bottom of the lower mantle [1]. These signatures are detectable by seismic observations and they need to be taken into account in tomographic studies of the Earth's lower mantle.

Finally, we find that the electronic gap widens during crossover to the low-spin phase. This has a direct influence on the electircal conductivity and agrees qualitatively with in situ measurements [2].

[1] Caracas, Mainprice, and Thomas (2010) *Geophys. Res. Lett.* **37**, L13309. [2] K. Ohta, *et al*. (2008) *Science* **320**, 89.

https://doi.org/10.1180/S0026461X00006502 Published online by Cambridge University Press

Fe-rich stalactites from Libiola mine: Mineralogical and geochemical features

C. CARBONE[1]*, E. DINELLI[2], P. MARESCOTTI[1] AND G. LUCCHETTI[1]

[1]DIP.TE.RIS, University of Genova, Corso Europa, 26, Italy (*corrrespondence: carbone@dipteris.unige.it)
[2]Dip. di Scienze della Terra e Geologico-Ambientali, Alma Mater Studiorum - Università di Bologna, Italy

The aim of this work is to characterize the mineralogy of different-shaped Fe-rich stalactites as well as to investigate the physico-chemical parameters of the associated mine and drip waters. The mineralogy has been investigated by means of reflected and transmitted light microscopy, XRPD, SEM-EDS, EPMA-WDS, and TEM-EDS analyses. Mine and drip waters have been sampled for chemical analyses. Water temperature, electrical conductivity, alkalinity by acidimetric titration, pH, and Eh were determined in the field during sampling. In the laboratory, waters have been analyzed for: Mg, and Ca by AAS, Na and K by AES Cl, SO_4^{2-}, and NO^{3-} by ion-chromatography, Si, Fe, minor and trace elements by ICP-OES. Three different types of stalactites were distinguished on the basis of their morphology: 1) "soda straw"-, 2) "deflected"-, and 3) "coned shaped"-stalactites. Mineralogical results showed that all the samples are characterized by poorly crystalline Fe-rich phases associated to goethite with different degree of crystallinity. Nevertheless, there are significant differences either in their texture and chemistry. The "soda straw" stalactites are enriched in Cu and Zn and evidenced botroydal to mammellonar textures; the "deflected" stalactites are enriched in Ni and showed concentric layering characterized by sheaves of radiating fibers; the "coned shaped" stalactites are enriched in Cu, Zn and Ni and evidenced a concentric layering maked by the alternance of botroydal/mammellonar and fibrous-radiating textures. Geochemical investigations evidenced that the composition and physico-chemical parameters of mine and drip waters are in any case different from the other AMD occurrences in the mining area [1, 2]. All water samples contain Cu, Ni, and Zn to appreciable levels, and the physico-chemical conditions are consistent with stability of ferrihydrite, which however tends to transform to goethite upon ageing. Few of the mine waters plot close to the metastability field of schwertmannite.

[1] Dinelli & Tateo F (2002) *Appl. Geochem,* **17**, 1081–1092.
[2] Marini *et al.* (2003) *Geochem J.* **37**, 199–216.

1998-2010 more than ten years of soil CO_2 flux measurement at Solfatara of Pozzuoli (Campi Flegrei, Italy)

C. CARDELLINI[1]*, G. CHIODINI[2], S. CALIRO[2], D. GRANIERI[3], R. AVINO[2], F. FRONDINI[1].

[1]Università di Perugia, Perugia, Italy (*correspondece: geochem@unipg.it)
[2]INGV sez. Napoli, Napoli, Italy
[3]INGV sez. Pisa, Pisa, Italy

With a flux of deeply derived fluids of ~5000 t/d and an energetic release of ~100 MW Solfatara of Pozzuoli is one of the largest studied volcanic-hydrothermal system of the world. Since 1998, CO_2 flux surveys where performed using the accumulation chamber method: i) over a large area, including the volcanic apparatus and its surroundings, ii) at fixed points inside the crater and ii) by two automatic stations. The monitoring of CO_2 fluxes allowed to recognize both "long-term" and "short-term" variations in the degassing of the Solfatara system. The main "long-term" CO_2 flux variation consisted in the expansion of the area interested by anomalous soil CO_2 degassing which doubled since 2003. This variation mainly occurred external to the Solfatara cone in correspondence of a major fault system NE-SW oriented and was correlated with the occurrence in 2000 of relatively deep, LP seismic events, which were interpreted as the indicator of the opening of an easy-ascent pathway for the transfer of magmatic fluids towards the shallower domain hosting the hydrothermal system. The input of these magmatic fluids has been highlighted by the changes in the chemical and isotopic compositions of fumarolic fluids. "Short-term" variations of CO_2 flux were recorded by both automatic stations and at fixed measurement points. A marked peak of the mean CO_2 fluxes of fix points inside the crater occurred in 2000, probably connected with the 2000 seismic crises. In 2006 an evident anomaly was registered outside the crater. This anomaly was interpreted as due to shallow permeability changes along the NW–SE fault, induced by an earthquake swarm of October 2006. The physical feasibility of the interpretations of these variations was assessed by physical-numerical simulations of the gas along a "faulted" hydrothermal system. The relevant changes observed at Campi Flegrei since 2000 have to be taken in to consideration for the interpretation of the behaviour of this dangerous volcano.

https://doi.org/10.1180/S0026461X00006502 Published online by Cambridge University Press

Tectonic controls for high magmatic fluxes within continental arcs: The Jurassic and Paleogene magmatic record of the Sierra Nevada de Santa Marta, northern Colombia

A. CARDONA[1,2], V. VALENCIA[3], G. BAYONA[2], C. MONTES[1,2], M. DUCEA[4], J.F. DUQUE[5] AND J. VERVOORT[3]

[1]Smithsonian Tropical Research Institute, Panamá, Panamá. (*correspondence: cardonaa@si.edu)
[2]Corporación Geológica Ares, Bogotá, Colombia.
[3]School of Earth & Environmental Sciences, Washington State University, Pullman, USA.
[4]Department of Geosciences, University of Arizona, Tucson, USA.
[5]Centro de Geociéncias, Universidad Autónoma de México, Queretaro, México.

Magmatic fluxes in continental arcs have shown to include major flare-ups episodes during their evolution. These episodes reflect catastrophic events which may be connected to major plate tectonic reorganizations. U-Pb zircon crystallization from plutonic rocks (30 U-Pb LA-ICP-MS) and detrital zircons (ca. 2000 U-Pb LA-ICP-MS detrital zircon analysis) from northern Colombia have revealed the existence of two major continental magmatic flare ups in the Middle Jurassic (ca. 190-180 Ma) and the Paleogene (60-45 Ma). Their tectonostratigraphic relations suggest that these two episodes are related to different periods of subduction initation along the Pacific margin of South America. The older is related to an extensional type subduction formed after the break-up of Pangea, whereas the younger Paleogene reflect subduction initiation after arc- continent collision in the Late Cretaceous. These tectonic correlations suggests that the early episodes of subduction in continental margins are responsible for the compositional modification of significant segments of the continental crust.

Pre-eruptive history and longevity of felsic magma in Iceland illuminated by *in situ* U-Th dating and trace-element analysis of zircon from historical eruptions

T.L. CARLEY[1]*, C.F. MILLER[1] AND J.L. WOODEN[2]

[1]Vanderbilt U., Dept. of Earth and Environmental Sciences, Nashville, TN, USA (*correspondence: tamara.l.carley@vanderbilt.edu, calvin.miller@vanderbilt.edu)
[2]Stanford U. USGS-SUMAC SHRIMP Lab, Stanford, CA, USA (jwooden@stanford.edu)

We are investigating zircons from silicic volcanic rocks from recent (primarily historical) eruptions in different tectonic regions of Iceland: Torfajokull ~7500 and ~3100 BP and 871 and 1477 AD (rift-tip); Hekla 1104 AD (transitional to rift); and Oraefajokull 1362 AD (off-rift). Precise knowledge of these eruption ages, combined with relatively high precision U-Th disequilibrium ages of zircon (*in situ* SHRIMP-RG) that date crystal growth, permit us to elucidate longevity of and processes within these felsic magma systems. While zircon age distributions from individual eruptions are variable, all display evidence for extensive growth that predates eruptions by >10 k.y. Seventy percent of Hekla and Torfajokull ages are older than 10 ka, with 60% of model ages falling at 10-30 ka and reaching a maximum of 50 ka. The predominance of older ages, the general paucity of <10 ka ages, and observation of near-eruption age crystallization of major phases (e.g., Torfajokull [1]) suggests that these zircons experienced a history separate from that of magma in which they erupted. Zircon morphology (presence of rounded centers and grain boundaries), compositional zoning (core-to-rim complexities in Ti, Hf concentrations) and U-Th ages together point to growth at relatively low temperatures, subsequent storage in a subvolcanic, silicic mush or recently solidified rock, and entrainment by the hotter erupting magma. While Oraefajokull zircons are dominantly <10 ka, grain morphology and trace-element zoning suggest a similarly complex history. The erupted materials were likely ascending magmas that entrained a pre-existing zircon cargo.

[1] Zellmer *et al*. (2008) *EPSL* **269**, 387-397

https://doi.org/10.1180/S0026461X00006502 Published online by Cambridge University Press

Alkalic magmas and the diversity of mantle compositional variation

RICHARD W. CARLSON

Department of Terrestrial Magnetism, Carnegie Institution of Washington, 5241 Broad Branch Road, NW, Washington, DC 20015 USA, (rcarlson@ciw.edu)

As very small degree melts, mafic-alkalic magmas are sensitive tracers of small-scale compositional heterogeneity in the mantle. Some alkalic magmas contain trace element and isotopic signatures indicative of sources dominated by components derived from subducted sediments. Excellent examples of this end member are the alkalic magmas of Italy. In the north, mantle sources for these magmas contain tens of percent subducted sediment whereas in the south, the sources are just overprinted by small volume fluids released from the subducting plate. Many mafic-alkalic and carbonatitic magmas, however, have isotopic compositions that overlap values seen in intraplate oceanic basalts. Along with key OIB-like trace element ratios (e.g. Ce/Pb, Th/Ta) this suggests that these magmas simply represent very low degree (<1%) melts of "normal" mantle. Within this group, there are examples of regional isotopic differences that suggest lithospheric sources. For example, group I kimberlites from South Africa have εNd > +4 whereas similar composition kimberlites from Brazil have εNd < -4. The isotopic compositions of these kimberlite groups, however, also overlap the range seen in slightly older regionally-associated flood basalts, the Karoo and Parana, respectively. This may suggest sources in lithospheric mantle that was metasomatized by melts from compositionally distinct sublithospheric mantle. Mafic-alkalic magmas from Montana have OIB-like trace element characteristics, but extreme isotopic compositions (e.g. εNd often < -15) indicating source metasomatism some 1.8 Ga prior to the Cenozoic magmatism. Low $^{187}Os/^{188}Os$ in potassic ultramafic magmas (kimberlites, katungites, meimechites) point to peridotitic sources whereas more radiogenic Os in Na-rich varieties (e.g. kamafugites, nephelinites) suggest pyroxene-rich sources. Mafic-alkalic magmas appear most commonly in "thermally-limited" settings where melting cannot proceed to high enough degrees to make basalt. Such settings include areas where adiabatic ascent is inhibited by thick lithospheres (cratons, early stages of continental rifting), marginal to plumes in the early and late stage of ocean island formation, the final stages of a dying subduction zone, or in areas of rigid lithosphere where heating can only be accomplished by conduction from below. This marginal melting regime enhances the contribution from easily fusible metasomatic components in the source if they are present.

Implications of a non-chondritic primitive mantle for chemical geodynamics

RICHARD W. CARLSON[1] AND MATTHEW G. JACKSON[2]

[1]Department of Terrestrial Magnetism, Carnegie Institution of Washington, 5241 Broad Branch Road, NW, Washington, DC 20015 USA, (rcarlson@ciw.edu)

[2]Department of Earth Sciences, Boston University, 675 Commonwealth Ave. Boston, MA 02215 USA, (jacksonm@bu.edu)

Among the compositional components identified in the mantle, most attention has been devoted to those components produced by continental and oceanic crust production and recycling. "Primitive mantle" appears in most models of mantle compositional variation, but usually in the abstract sense in that few, if any, samples of oceanic basalt have all the characteristics expected for a melt of the model primitive mantle that is assumed to have chondritic relative abundances of the refractory lithophile elements. For example, the high $^{3}He/^{4}He$ component may sample a reservoir preserving primitive mantle noble gas characteristics, but at the same time generally has positive εNd and often has Pb isotopic composition plotting well to the right of the Geochron. PREMA, for "prevalent mantle" was coined by Zindler and Hart (1986) early in the investigation of mantle isotopic variation as the most common isotopic component seen not only in ocean island basalts but in both continental and oceanic large igneous provinces and as a component in many intraoceanic island arc lavas. This component largely vanished from the discussion of mantle compositional variation in part because its origin was unclear – it could not be primitive mantle because it did not have chondritic Nd or Hf isotopic composition and it might just be some "most likely" mixture between depleted mantle and enriched recycled components. The elevated $^{142}Nd/^{144}Nd$ of all post-Hadean igneous rocks on Earth, however, suggests that primitive mantle has Nd, and by inference Sr and Hf, isotopic compositions in the realm of what traditionally has been called depleted mantle. We use the trace element characteristics of Baffin Island and Ontong-Java lavas that have isotopic compositions closest to those expected for the non-chrondritic primitive mantle to examine how this reservoir was produced early in Earth history. We also explore the consequences of a non-chondritic primitive mantle for such issues as the relative fraction of DMM and PREMA in the current mantle and the role of the primitive mantle in the origin of the massive volcanism associated with large igneous provinces.

https://doi.org/10.1180/S0026461X00006502 Published online by Cambridge University Press

In silico, physiological, and proteomic cost-benefit analysis of resource-limited microbial growth

ROSS P. CARLSON*, REED L. TAFFS AND JAMES FOLSOM,

Deparment of Chemical and Biological Engineering, Montana State University, Bozeman, 59717 USA, (rossc@erc.montana.edu)

Evolutionary selection has produced fit microbes with robust and often redundant metabolic network functionality. Maintaining and regulating network redundancy represents a substantial resource burden especially in nutrient limited environments and therefore needs to be off set by fitness advantages. A genome enabled *in silico* methodology was developed and experimentally tested which quantifies molecular-level, resource allocation tradeoff strategies that permit competitive cellular functioning under a continuum of nutrient availabilities. The approach decomposed a metabolic network into a complete listing of non-divisible, mathematically-defined biochemical pathways which were then used to identify all potential strategies for investing limiting resources like iron and nitrogen into the genome encoded metabolic machinery. The tabulated enzymatic resource investment requirements for each distinct biochemical pathway were examined in concert with the pathway's efficiency at converting substrate into biomass. The analysis identified the most competitive molecular-level tradeoffs between pathway resource requirements and metabolic efficiency; allocating limiting resources to perform one function well came at the cost of performing another metabolic function well. *In silico* predictions were evaluated experimentally using physiological and proteomic data collected from iron- or nitrogen-limited *Escherichia coli* chemostat cultures. Experimental chemostat data was consistent with *in silico* theory and illustrated that under iron- and nitrogen-limited conditions *E. coli* regulates its metabolism to invest the limiting resource competitively at the cost of optimal biomass yields on electron donor. The study highlights a fundamental evolutionary and metabolic design paradigm for competitive network structure and control.

Solubility as a determinant of rates of intergranular diffusion in metamorphic rocks

W.D. CARLSON

Department of Geological Sciences, University of Texas at Austin, Austin TX 78712 USA (wcarlson@mail.utexas.edu)

Rates of intergranular diffusion in metamorphic rocks are principally determined not by temperature, but instead by the properties of the intergranular medium, particularly those properties that govern the solubility of the diffusing species.

Quantitative comparison of length scales and time scales for metamorphic reaction in natural examples reveals extremely large variations in rates of intergranular diffusion for Al among systems with different H_2O activities. For instance, at 600 °C the effective diffusion coefficient for Al ($m^2 \cdot sec^{-1}$) is $10^{-18.8}$ in fluid-saturated systems, $10^{-22.5}$ in hydrous-but-fluid-undersaturated systems, and $10^{-25.4}$ in anhydrous systems. Thus even at constant temperature, Al diffusivities can range across 6 to 7 orders of magnitude depending on the character of the intergranular medium.

In fluid-saturated systems, garnet zoning—which monitors the length scale of chemical equilibration during growth—shows that intergranular solubilities controlled by characteristics of the fluid itself (H_2O/CO_2 ratios, availability of ligands for complexation, pH) can exert greater influence on diffusivities than temperature. As a case in point, the nature of compositional zoning in garnet from Harpswell Neck, Maine, varies markedly from cores to rims. For Mn, Fe, and Mg, many crystals have irregular, patchy distributions in their cores that give way to smooth, concentric zoning in their outer rims. In contrast, zoning of Ca and Y is comparatively smooth and concentric throughout these crystals. Rims of all crystals share equivalent concentrations of all elements. Raman spectrometry of fluid inclusions demonstrates that growth of garnet cores took place in the presence of a CO_2-rich fluid, whereas growth of garnet rims took place in the presence of an H_2O-rich fluid. Thus the patterns of garnet zoning imply that low solubility for Mn, Fe, and Mg and high solubility for Ca and Y in a CO_2-rich fluid restricted the length-scales of equilibration for the former and expanded them for the latter during the growth of garnet cores; transition to an aqueous fluid with relatively high solubility for all elements then led to rock-wide equilibration for all during growth of garnet rims. Differential solubility of cations in fluids of variable composition is therefore a fundamental control on rates and scales of intergranular diffusion.

https://doi.org/10.1180/S0026461X00006502 Published online by Cambridge University Press

Structural changing control of potassium saturated smectite at high pressures and high temperatures: Application for subduction zones

L.C. CARNIEL, R.V. CONCEIÇÃO AND N.DANI

Geoscience Institute, UFRGS, Porto Alegre – RS, Brazil. (larissa.colombo@ufrgs.br rommulo.conceicao@ufrgs.br norberto.dani@ufrgs.br)

The lithospheric mantle is characterized by pressure ranges from ~ 2.0 and ~ 7.7 GPa and a specific mineralogy and composition. This region can be re-hydrated and re-enriched in incompatible elements (eg. potassium) through subduction processes that bring pelagic material, composed of clay minerals and other phyllosilicates, into these regions. These minerals act as carriers of water and incompatible elements, re-enriching the lithospheric mantle as they are destabilized. Then, simulating conditions of high pressure and temperature in potassium enriched smectite would help to check the stability field of this mineral and its transformations during the process of subduction. This research focuses on the construction of a phase diagram of smectite, previously saturated with potassium at different temperatures and pressures. We performed experiments in smectite under pressures between 2.5 and 4.0 GPa and at different temperatures (400°C to 700°C). From our results, we conclude that at 2.5 GPa pressure, which is about 75 km depth in the mantle, the clay mineral transform into a new phase at 500° C that correspond to the illite. At higher pressures, we conclude that at 4.0 GPa pressure, equivalent to 120 km depth, the same transformation occurs at 400°C. Such results aid new information to understand the dehydration of pelagic sediments in a process of subduction, and the mobility of some incompatible elements in such tectonic setting.

Elasticity and anelasticity of relaxor ferroelectrics

M.A. CARPENTER[1]*, J.F.J. BRYSON[1], E.H. KISI[2], S.M. FARNSWORTH[2] AND G. CATALAN[3]

[1]Dept. of Earth Sciences, Downing St., Cambridge CB2 3EQ (*correspondence: mc43@esc.cam.ac.uk)

[2]School of Engineering, The University of Newcastle, Callaghan NSW 2308, Australia

[3]Campus Universitat Autònoma de Barcelona, ICREA, Bellaterra 08193 Spain

The elastic behaviour of ferroelectric and relaxor ferroelectric materials makes an interesting contrast with that observed in association with ferroelastic phase transitions in minerals, though the same basic principles apply. Softening of the bulk and shear moduli of polycrystalline samples occurs in the high temperature structure as a consequence of dynamical effects, there are marked elastic anomalies associated with the phase transition, and anelastic losses arise due to mobile transformation microstructures. Distinctive features of relaxor ferroelectric perovskites are frequency-dependent softening and acoustic losses associated with freezing of polar nanoregions (PNR's), together with a large degree of softening of shear elastic constants due to condensation of static PNR's in the stability field of the paraelectric phase. The latter occurs ahead of the transition to a long range ordered ferroelectric structure. These distinctive features have been investigated by Resonant Ultrasound Spectroscopy (RUS) measurements of polycrystalline $Pb(Mg_{1/3}Nb_{2/3})O_3$ (PMN) and single crystals of $0.955Pb(Zn_{1/3}Nb_{2/3})O_3$-$0.045PbTiO_3$ (PZN-PT). In PMN the pattern of the elastic compliance as a function of temperature mirrors the real part of the dielectric constant and the inverse mechanical quality factor mirrors tanδ, showing that a key aspect of PNR formation is the development of local strain fields. In PZN-PT, there is a large difference in the shear elastic constants between poled and unpoled crystals in the stability fields of the rhombohedral and tetragonal phases and well into the stability field of the cubic phase. This signifies that the PNR's themselves develop a stable microstructure which can be polarised and which gives rise to acoustic losses in much the same way as a conventional ferroelectric microstructure. Central to all this behaviour, as with other types of phase transitions, including order/disorder, displacive, magnetic transitions and changes in spin state, is the coupling of strain with some primary order parameter or with microstructure.

https://doi.org/10.1180/S0026461X00006502 Published online by Cambridge University Press

Evaluating sources and transport of zinc and cadmium and their complexing ligands in the Atlantic and Pacific Oceans

G. CARRASCO[1]*, L.A. DUFFAUT-ESPINOSA[2], P.L. MORTON[3] AND J.R. DONAT[4]

[1]Earth, Atmos. and Planet. Sciences Dept., MIT, Cambridge, MA, USA. (*correspondence: gcarrasc@mit.edu)
[2]Electrical and Computer Engineering Dept., Johns Hopkins University, Baltimore, MD, USA. (lduffaut@jhu.edu)
[3]Earth, Ocean and Atmos. Sciences Dept., Florida State University, Tallahassee, FL, USA. (pmorton@fsu.edu)
[4]Chemistry and Biochemistry Dept., Old Dominion University, Norfolk, VA, USA. (jdonat@odu.edu)

Introduction and Methods

Using Anodic Stripping Voltammetry [1], the complexation and chemical speciation of Zn and Cd has been determined in the water column in the Western North Pacific, the Equatorial South Atlantic as well as in the Elizabeth River and the Chesapeake Bay waters and benthos. Using a novel mathematical interpretative tool (Titration Data Interpreter) that allows for precise, non-biased ligand parameter optimization of the Gerringa linearization [2], the speciation of these two metals data was calculated.

Discussion

The results obtained in these oceanic regions indicate marginal seas and other pointed sources provide both metals and strong ligands, combining riverine, terrestrial, marine and anthropogenic matter, as recent literature suggests [3-7]. The ligands are transported and decay with time along water masses in both Atlantic and Pacific Oceans, implying connections to ligands produced the water formation regions [3,7,8] and from estuarine origin. A consortium of strong ligands complexes these two metals, affecting their chemical speciation in surface, intermediate and deep waters. The ramifications of this phenomenon on the close and remote upwelling of potentially limiting concentrations of bioavailable Zn and Cd will be discussed.

[1] Bruland (1989) *Limnol. Ocean.* **34**, 269-285. [2] Gerringa *et al.* (1995) *Mar. Chem.* **48,** 131-142. [3] Nishioka *et al.* (2007) *J. Geophys. Res.* **112**, C10012. [4] Vangriesheim *et al.* (2009) *DSR-II* doi:10.1016/j.dsr2.2009.04.002 [5] Lam & Bishop (2008) *Geophys. Res. Lett.* **35**, LO7608. [6] Hernes & Benner (2002) *DSR-I* **49,** 2119-2132. [7] Baars & Croot (2011) *DSR-II* doi:10.1016/j.dsr2.2011.02.003. [8] Ellwood & van den Berg (2000) *PMar. Chem.* **68,** 295-306.

Amino sugar and amino acid degradation and transformation in two lakes with different redox state

D. CARSTENS[1,2]*, K.E. KÖLLNER[1,2], H. BÜRGMANN[1] AND C.J. SCHUBERT[1]

[1]Swiss Federal Institute for Aquatic Science and Technology (Eawag), 6047 Kastanienbaum, Switzerland (*correspondence: doerte.carstens@eawag.ch)
[2]Institute of Biogeochemistry and Pollutant Dynamics, ETH Zürich, 8092 Zürich, Switzerland

Transformation and degradation processes of organic matter in aquatic systems play a key role in the global carbon cycle. Although lakes seem to store carbon efficiently, little is known about organic matter degradation in these systems. In order to study the fate of organic nitrogen compounds in lacustrine systems under different redox conditions, Lake Brienz (oligotroph, fully oxic) and Lake Zug (eutrophic, stratified oxic/anoxic) were investigated. Profiles of particulate amino sugar and amino acid concentrations were measured in the water column of both lakes as well as in the first centimeters of the sediments by gas chromatography. Decreasing carbon normalized amino sugar yields with increasing water depth indicated enhanced degradation of amino sugars compared to the bulk organic matter in both lakes. Under oxic conditions the degradation was more pronounced. The amino sugar composition of the particulate organic matter revealed a replacement of planktonic biomass by heterotrophic mircoorganisms from the upper water layers towards the lake bottom. The contribution of bacteria to the organic carbon was estimated using the amino sugar muramic acid, which is unique to bacteria as part of their cell wall. In the oligotrophic lake 0.8-11% of the organic carbon derived from bacteria and in the eutrophic lake this contribution was 0.3-5%. These findings underline that bacteria are not only drivers of organic matter degradation in lacustrine systems but also a significant source of organic matter themselves.

https://doi.org/10.1180/S0026461X00006502 Published online by Cambridge University Press

On the mass independent fractionations of O, Hg, Si, Mg and Cd during open-system evaporation or thermal decomposition

P. CARTIGNY[1]*, J.M. EILER[2], P. AGRINIER[1] AND N. ASSAYAG[1]

[1]Stable Isotope Laboratory of IPG-Paris, France. (*correspondence : cartigny@ipgp.fr)
[2]Division of Geological and Planetary Sciences, California Institute of Technology, Pasadena, CA 91125, USA.

Many experiments in which an element or a mineral is evaporated or thermally decomposed under vacuum are known to consistently display unexpected behaviors. These include too low rates of evaporation, smaller (i.e. closer to 1) than predicted fractionation factors, and an inconsistent behavior of the stable isotope ratios of a given element (i.e. mass-independent fractionation). This applies to many elements including O, Hg, Si, Mg and Cd.

We present interpretations for a series of earlier observations, including experiments by Miller *et al*. (2002) in which mass-independent O isotope fractionations are produced during thermal decomposition of carbonates [1], and the finding of Estrade *et al*. (2009) showing an unexpected slope in a plot of Δ^{199}Hg vs Δ^{201}Hg (close to 1.2 instead of 2.4) during open-system evaporation of Hg [2].

These and related results can be explained if a fraction (usually a few to several tens of percent) of the evaporated compounds actually forms (or re-equilibrate) under conditions of isotope equilibrium, the remaining fraction obeying kinetic fractionation of its stable isotopes. This is the mixing of the that results in the appearance of mass-independence, rather than the action of a novel isotope effect having non-cannonical mass law.

[1] Miller M.F. *et al*. (2002) *PNAS* **99**, 10988–10993. [2] Estrade N. *et al*. (2009) *Geochim. Cosmochim. Acta* **73**, 2693-2711.

Howardite noble gases as indicators of asteroid surface processing

J.A. CARTWRIGHT[1], D.W. MITTLEFEHLDT[2], J.S HERRIN[2] AND U. OTT[1]

[1]Max Planck Institut für Chemie, J.-J.-Becher-Weg 27, 55128 Mainz, Germany (julia.cartwright@mpic.de)
[2]NASA/Johnson Space Centre, Houston, Texas, USA.

Introduction and Research Objective:

The HED (Howardite, Eucrite and Diogenite) group meteorites likely originate from the Asteroid 4 Vesta [1] - one of two asteroid targets of NASA's Dawn mission [2]. Whilst Howardites are polymict breccias of eucritic and diogenitic material that often contain "regolithic" petrological features, neither their exact regolithic nature nor their formation processes are well defined [3-4]. As the Solar Wind (SW) noble gas component is implanted onto surfaces of solar system bodies, noble gas analyses of Howardites provides a key indicator of regolithic origin. In addition to SW, previous work by [5] suggested that restricted Ni (300-1200 μg/g) and Al_2O_3 (8-9 wt%) contents may indicate an ancient well-mixed regolith. Our research combines petrological, compositional and noble gas analyses to help improve understanding of asteroid regolith formation processes, which will play an intergral part in the interpretation of Dawn mission data.

Methodology:

Following compositional and petrological analyses [4,6], we developed a regolith grading scheme for our sample set of 30 Howardites and polymict Eucrites [4]. In order to test the regolith indicators suggested by [5], our 8 selected samples exhibited a range of Ni, Al_2O_3 contents and regolithic grades. Noble gas analyses were performed using furnace step-heating on our MAP 215-50 noble gas mass spectrometer.

Discussion of Results:

Of our 8 howardites, only 3 showed evidence of SW noble gases (e.g approaching $^{20}Ne/^{22}Ne \sim 13.75$, $^{21}Ne/^{22}Ne \sim 0.033$ [7]). As these samples display low regolithic grades and a range of Ni and Al_2O_3 contents, so far we are unable to find any correlation between these indicators and "regolithic" origin. These results have a number of implications for both Howardite and Vesta formation, and may suggest complex surface stratigraphies and surface-gardening processes.

[1] Drake M.J. (2001) *MAPS* **36**:501-513. [2] Rayman, M.D. *et al*. (2006) *Acta Astronautica* **58**:605-616. [3] Mittlefehldt, D.W. *et al*. (1998) *Rev. Min*. **36**: 4.1-4.195. [4] Cartwright, J.A. *et al*. (2011) *LPSC XLII* (abs. # 2655). [5] Warren, P.H. *et al*. (2009) *GCA* **73**:5918-5943. [6] Mittlefehldt, D.W. *et al*. (2010) *LPSC XLI* (abs. #2655). [7] Grimberg, A. *et al*. (2008) *GCA* **72**:626-645.

https://doi.org/10.1180/S0026461X00006502 Published online by Cambridge University Press

Magnetic susceptibility of sands from a river beach for forensic applications

Á. CARVALHO[1], H. RIBEIRO[1], A. GUEDES[1,2], H. SANT'OVAIA[1,2], I. ABREU[1,3] AND F. NORONHA[1,2]*

[1]Centro de Geologia da Universidade do Porto (CGUP), Portugal

[2]Departamento de Geociências, Ambiente e Ordenamento do Território da Faculdade de Ciências da Universidade do Porto, Portugal

[3]Departamento de Biologia da Faculdade de Ciências da Universidade do Porto, Portugal (*fmnoronh@fc.up.pt)

Soil studies are often undertaken in forensic investigation because its particles are normally tranferred to the surfaces in contact with them, providing important information. Soil is composed by organic and inorganic materials and its history is reflected in its bio-physicochemical characteristics, including low-field magnetic susceptibility (MS). MS is defined as the ratio of the material magnetization (per unit mass) to the weak external magnetic field, and in soils, it is directly proportional to the quantity, composition and grain size of minerals in the sample (which can be diamagnetic, paramagnetic or ferromagnetic species).

In order to investigate the variability of this property in Areinho, a fluvial river beach in Porto region (Northern Portugal), twenty four samples were collected along a transect perpendicular to the river side and prepared for magnetic susceptibility analysis. MS was measured on 1g of dry bulk samples, applying them an external magnetic field of 300 A/m, and a Kappabridge model KLY4S of Agico balance equipped with the Sumean software was used. Before each measurement the equipment was calibrated. The MS of Areinho sands is low with values ranging between $0.68x10^{-8}m^3/Kg$ and $18.09x10^{-8}m^3/Kg$ which is an agreement with its mineralogical composition. All measurement results were reproducible. From this study we conclude that MS protocol is suitable for the analysis of sands with the advantage of being fast and non-destructive.

Acknowledgements: The first author benefits from a PhD scholarship (SFRH/BD/61460/2009) funded by Fundação da Ciência e Tecnologia (QREN-POPH-Type 4.1-Advanced Training, subsidized by the European Social Fund and national funds MCTES). The authors acknowledge the funding of FCT - POCI 2010 to CGUP.

Radionuclides in uranium milling tailings and environment remediation

F.P. CARVALHO, J.M. OLIVEIRA AND M.MALTA

Instituto Tecnológico e Nuclear, E.N. 10, 2686-953 Sacavém, Portugal (carvalho@itn.pt)

The environmental and public health risks posed by legacy uranium mine sites and milling tailings in Portugal was assessed in order to allow for decision making regarding environmental remediation and for radiological protection measures of the population.

Most of old uranium mine sites did not pose noticeable ionizing radiation and contamination risks to the environment and population, especially the sites operated as open pits and without *in situ* chemical operations. The mines where *in situ* ore leaching with sulfuric acid was operated and the ore milling tailings are the sites with higher ambient radioactivity and contamination with radioactive and stable metals [1]. Over some waste piles the radiation dose attained 30 mSv y^{-1}, higher than the annual limit for members of the public, 1 mSv y^{-1}. Confinement and coverage of these uranium waste piles was necessary and allowed for reducing radon exhalation, dispersal of radioactive materials in soils, and abatement of surface runoff and radionuclide leaching with acid drainage. *in situ* formation of H_2SO_4 in waste piles still generates radioactive leachates in underground mines and in milling tailings that require continued treatment. Irrigation of agriculture plots in the mine areas with mine drainage and water from contaminated wells is the main pathway to transfer radionuclides, especially ^{226}Ra, into locally grown vegetables and into the food chain [1,2].

Milling tailings with high radioactivity must be confined to reduce dispersion of radionuclides and exposure of biota and the public. Water from rivers that received past discharges of acid mine drainage have contaminated sediments that may require removal. Mine drainage and underground waters in the area of former mines shall be monitored to avoid exposure of the public to acid, metals and radionuclides. Withouth suitable monitoring and abatement measures, radiological exposure of members of the public may be many times about radiation exposure legal limits.

[1] FP Carvalho, J M Oliveira, I Lopes, A Batista, *J Environ Radioactivity* **98**(2007)*:298-31*. [2] FP Carvalho, JM Oliveira, M Malta, *J Radional Nuc Chemistry* **281** (2009)*:479-484*.

https://doi.org/10.1180/S0026461X00006502 Published online by Cambridge University Press

Geochemistry of groundwater from Graciosa Island (Azores): A contribution to the hydrothermal system conceptual model

M.R. CARVALHO[1], P.M. CARREIRA[2], J.M. MARQUES[3], G. CAPASSO[4], F. GRASSA[4] AND J.C. NUNES[5]

[1]Universidade de Lisboa, Faculdade de Ciências, Depart. Geologia/CeGUL, Portugal
[2]Instituto Tectonológico e Nuclear, Lisboa, Portugal
[3]Instituto Superior Técnico, Lisboa, Portugal
[4]Istituto Nazionale di Geofisica e Vulcanologia, Sezione di Palermo, Palermo, Italy
[5]Universidade dos Açores & INOVA Inst., Azores, Portugal

Graciosa island is located in the Azores Archipelago, along the so-called Terceira Rift, a major tectonic structure that makes the NE boundary of the Azores Plateau. In general terms, it includes a basaltic plataform on the NW and a silicic poligenetic volcano with caldera on the SE, the Graciosa Caldera Volcano. This volcano has produced significant tephra falls, pyroclastic flows, lahars, and lava flows, both of basaltic s.l. and trachitic s.l. composition.

The hydrothermal system shows fumarolic emissions inside the volcano caldera and thermal springs located along the shoreline. This system is exploitated in a thermal building through shallow and deep (110 m) boreholes, near the coast.

In Graciosa two types of Na-Cl groundwater systems can be identified: 1) a cold one emerging at springs and exploited by wells for public water supply, and 2) a hydrothermal system with temperatures around 40-44 ºC. The cold groundwaters have pH higher than 7 and different degree of mineralization, according to the proximity to the sea. The thermal waters show mixing with seawater, pH varying between 6.20 and 6.94, 166 mg/L of SiO_2, and significant concentration of metals, such as Mn, Fe, Co, Ni, Cu and Zn. The thermal water mineralization varies strongly, showing EC from 8.87 mS/cm (shallow water) to 47.4 mS/cm (deeper water). The higher mineralized water is rich in CO_2(g), with 2130 mg/L of total dissolved CO_2. Geothermometers application reveals aquifer temperature ≈ 167 ºC and immature/mixed waters, not reaching complete equilibrium with reservoir rock.

The geochemistry of the thermal waters indicates the occurrence of seawater/host rock interaction processes at high temperature and slightly acid conditions, favored by CO_2(g) input, and a different degrees of mixing with cold and shallow groundwaters.

Geochemistry of S-type granitic rocks from the Valongo area (Northern Portugal)

P.C.S. CARVALHO[1]*, A.M.R. NEIVA[1], M.M.V.G. SILVA[1] AND F. CORFU[2]

[1]Geoscience Centre and Department of Earth Sciences, University of Coimbra, 3000-272 Coimbra, Portugal (*correspondence: paulacscarvalho@gmail.com)
[2]Department of Geosciences, University of Oslo, PB1047 Blindern, N-0316, Norway

Variscan peraluminous granitic rocks crop out at the eastern limb of the Valongo anticline, located about 18 km at east of Oporto, in the Dúrico - Beirão region, northern Portugal and Central Iberian Zone of the Iberian Massif.

The medium- to coarse-grained porphyritic biotite>muscovite granite (G1) intruded Ordovician and Silurian metasediments and produced a contact metamorphic aureole. The medium-grained porphyritic biotite ≈ muscovite granodiorite (G2) intruded the earlier granite and the contact is by faulting. The fine-grained porphyritic biotite>muscovite granodiorite (G3) intruded the other two granitic rocks. Granite G1 and granodiorite G2 are late-D3, whereas granodiorite G3 is post-D3. The U-Pb ages for zircon and monazite, obtained by ID-TIMS, are 309.6±1.0 Ma for G1, 307.0 ± 3.2 Ma for G2 and 305.1± 0.4 Ma for G3 and 587 Ma for inherited zircon cores from G2 and G3. Variation diagrams show that G3 has higher TiO_2, total FeO, MgO, CaO, Zr, Ba, Th, Ce contents and lower SiO_2, Li, Rb contents than G1 and they define independent trends. G2 is not related to G1. Granite G1 and granodiorite G3 have similar $(^{87}Sr/^{86}Sr)_i$ of 0.7085, εNd_T -6.64 (G1) and -6.92 (G3) and $\delta^{18}O$ 11.36 ‰ (G1) and 10.90 ‰ (G3). Therefore, they are derived by partial melting of the same metasedimentary materials, containing Neoproterozoic detritus, but G3 results from a higher degree of partial melting than G1. Granodiorite G2 results from a distinct granitic magma and is derived by partial melting of metasedimentary materials containing Neoproterozoic detritus, as it has $(^{87}Sr/^{86}Sr)_{307}$ of 0.7080, εNd_{307} of -7.06 and $\delta^{18}O$ of 11.31 ‰. The three granitic rocks are of S-type.

https://doi.org/10.1180/S0026461X00006502 Published online by Cambridge University Press

Systematic variations in argon diffusion in feldspars

W.S. CASSATA[12], P.R. RENNE[12] AND D.L. SHUSTER[12]

[1]Berkeley Geochronology Center, USA
[2]University of California, Berkeley, USA

Feldspars are commonly used in $^{40}Ar/^{39}Ar$ studies to constrain the thermal evolution of meteorites, mountain belts, intrusive magmatic bodies, and a host of other Earth and planetary processes. Although the kinetics of Ar diffusion in K-feldspars have been extensively researched, comparably little work has been published on plagioclase feldspars, despite their being the primary host of potassium in most chondritic, lunar, and Martian meteorites and many terrestrial igneous bodies. Similarly, little is known of the potential effects of composition and structural state on Ar diffusion kinetics, or the extent to which diffusion might be anisotropic.

In this study, ~100 step-heating diffusion experiments were conducted on feldspars that range in composition from nearly pure orthoclase to nearly pure anorthite, with the bulk of the samples being plagioclase feldspars. These experiments reveal systematic variations in diffusive behavior that appear to be closely related to composition and microstructure. For example, plagioclase crystals having compositions between An_{50} and An_{90} typically yield Arrhenius arrays with pronounced upward curvature between 600 and 800 °C, the opposite of that commonly observed on Arrhenius plots from K-feldspars inferred to have multiple diffusion domains. Plagioclase crystals with compositions $<An_{50}$ yield linear Arrhenius arrays that give way to downward curvature between 600 and 1000 °C, where the temperatures at which linearity ceases appear to depend on the composition of the sample and the heating schedule. Brecciated and microstructurally complex plagioclase crystals exhibit Arrhenius arrays consistent with multiple diffusion domains. Preliminary experiments on cleavage flakes indicate that diffusion may be faster in the [001] crystallographic direction than [010], and additional experiments are underway to confirm this finding. Activation energies for plagioclase and K-feldspars span a large range, from ~160-300 kJ/mole.

Arrhenius plots for Ar diffusion in plagioclase appear to reflect a confluence of intrinsic diffusion kinetics and structural ordering-disordering that occurs during prolonged step-heating. These data indicate that Ar diffusivity is intimately related to composition and microstructure in plagioclase. As such, there is no broadly applicable set of diffusion parameters that can be utilized in thermal modeling. Sample-specific data are required.

Tracking the magmatic evolution of an island arc volcano: Insights from a high-precision Pb isotope record of Montserrat, Lesser Antilles

M. CASSIDY*, R.N. TAYLOR, M.J. PALMER AND J. TROFIMOVS

National Oceanography Centre, Southampton, University of Southampton, Waterfront Campus, European Way, Southampton SO14 3ZH
(*correspondance:m.cassidy@soton.ac.uk)

It is rare to have a chance to examine the magmatic evolution of an island arc volcano over a period of millions of years. The volcanic succession exposed on Montserrat provides such an opportunity, extending from the 2 Ma andesites of the Silver Hills complex through to the youngest dome collapse of the Soufrière Hills volcano (February 2010). In this study we present new trace element, Sr, Nd and high-precision double spike Pb isotope data taken through Montserrat's time sequence. As well as from subaerial locations, we have collected samples from marine sediment cores, as significant volumes of pyroclastic material have ended up in the Caribbean Sea.

Each of Montserrat's volcanic groups; South Soufrière Hills (SSH), Soufrière Hills, Centre Hills and Silver Hills, can be clearly discriminated using trace element and isotopic parameters. Furthermore, the SSH can be divided into two suites: A and B, combining trace elements and Pb isotopes.

The trends in trace elements and isotopes suggest some variability in fluid and sediment addition over time. The SSH in particular has a greater slab fluid signature as indicated by elevated Pb/Ce, but less sediment addition than the other volcanic centres. $^{206/204}Pb$ against $\Delta 7/4$ and $\Delta 8/4$ diagrams show that Montserrat falls along two differing trends, one defined by the SSH volcanic region and the second trend defined by the other volcanic regions on Montserrat (Silver Hills, Centre Hills and Soufrière Hills). Furthermore, the SSH volcanic centre differs noticeably in trace elements and isotope ratios. This demonstrates that the source which generated the SSH magmas is different to the source of the other volcanics on Montserrat. Both isotopic trends point to an enriched mantle source underneath Montserrat. Samples from the current period of activity will be discussed including the presence of mafic enclaves within the current eruption.

https://doi.org/10.1180/S0026461X00006502 Published online by Cambridge University Press

Metamorphic and geodynamic evolution of the high-grade units of Mundão – Sátão (Northern Portugal)

P. CASTRO[1], T. BENTO DOS SANTOS[1,2]*, C. MEIRELES[1], A.J.D. SEQUEIRA[1] AND N. FERREIRA[1]

[1]LNEG – Laboratório Nacional de Energia e Geologia, Portugal (*correspondence: telmo.santos@lneg.pt)
[2]Centro de Geologia, Universidade de Lisboa, Portugal

The Mundão – Sátão sector (N Portugal) is composed of syn- to post-D_3 Hercynian granitoids and by pre-Ordovician metasediments, belonging to the Schist – Greywacke Complex of the Iberian Central Zone. The metasediments comprise two low-grade sequences (chlorite to biotite zones), Ponte Chinchela and Nelas Units, separated by the exotic high-grade tectonometamorphic sequence of the Casinha Derrubada Unit (CDU) [1] that includes three tectonic slices separated by thrusts, from bottom to top: a) micaschists and mylonites with sillimanite; b) mylonites with porphyroclastic staurolite; and c) biotitic micaschists with garnet.

The CDU is a MP metamorphic sequence associated with the establishment of the metamorphic peak during D_2. Late retrograde evolution is evidenced by prismatic andalusite pseudomorphs after porphyroclastic staurolite, and andalusite + biotite coronas around staurolite rims. These textural evidence are coeval with the reorientation of staurolite prismatic crystals from sub-horizontal to sub-vertical and late incipient migmatization by decompression and crossing of the granite wet solidus curve during D_3 exhumation phase.

The observed petrological/geochemical features and the paragenetic evolution of the CDU high-grade rocks imply that this area is not a typical contact metamorphic sequence [2] or a complete Barrovian-type sequence arround an anatectic dome [3]. The new data points out the existence of net-tectonic control on the emplacement of the high-grade rocks at this sector and that the CDU is an incomplete Barrovian-type sequence from MT to HT, subsequently exhumed onto a low-grade metamorphic sequence. The evidence suggest that the tectonometamorphic evolution of the CDU rocks is consistent with a clockwise P-T-t path, involving: 1) a metamorphic peak at T ~ 600 – 700 ºC and P ~ 6 – 7 kbar; 2) significant decompression to 2 – 3 kbar; 3) rapid cooling as the result of thermal readjustment to higher crustal levels.

[1] Ferreira *et al*. (2009) *Carta Geol. Portugal (Folha 17-A)*, LNEG. [2] Esteves (2006) *Unpub. MSc Thesis*, Univ. Aveiro, 113. [3] Valle Aguado *et al*. (2010) *e-Terra*, **16**, 9, 1-4.

Surface transformations and element cycling resulting from interfacial Fe(II)-Fe(III) self exchange

J.G. CATALANO[1]*, A.J. FRIERDICH[1], Y. LUO[1,2], P. FENTER[3], C. PARK[4] AND K. M. ROSSO[5]

[1]Earth & Planetary Sciences, Washington Univ., St. Louis, MO 63130 USA (*correspondence: catalano@wustl.edu)
[2]Energy, Environmental, and Chemical Engineering, Washington Univ., St. Louis, MO 63130, USA
[3]Chemical Sciences and Engineering Division, Argonne National Laboratory, Argonne, IL 60439 USA
[4]HPCAT, Carnegie Institution of Washington, Argonne, IL 60439 USA
[5]Chemical & Materials Sciences Division, Pacific Northwest National Laboratory, Richland, WA 99352 USA

Biogeochemical iron cycling induces coupled electron transfer and atom exchange between aqueous Fe(II) and Fe(III) oxide surfaces [1-4]. Our recent work [5] has explored the molecular-scale structural transformations of hematite surfaces that result from this process. Under both acidic (pH 3) and neutral (pH 7) conditions Fe(II) induces layer-by-layer dissolution or growth of the hematite (110) and (012) surfaces. In contrast, the hematite (001) surface develops a <1 nm-thick discontinuous film that displays structural relaxations different from the underlying surface. This demonstrates that Fe(II) activates localized growth and dissolution independent of macroscopic Fe(II) adsorption.

We have further explored the effect of this process on the fate of the structurally-compatible trace element Ni. For both hematite and goethite we observe that aqueous Fe(II) induces the incorporation of adsorbed Ni into the iron oxide structure. In addition, pre-incoporated Ni is released into solution by Fe(II). The rates of release and incoporation are orders of magnitude slower than the rate of macroscopic Fe(II) adsorption but comparable to iron isotope equilibration [3]. We propose that Fe(II) catalyzes a thermodynamically-controlled redistribution of Ni among the mineral bulk, mineral surface, and aqueous solution. This work has implications for the validity of proxies for ocean composition on the early Earth and micronutrient and contaminant availability in soil, sedimentary, and aquatic systems.

[1] Williams & Scherer (2004) *Environ. Sci. Technol.* **38**, 4782-4790. [2] Yanina & Rosso (2008) *Science* **320**, 218-222. [3] Handler *et al*. (2009) *Environ. Sci. Technol.* **43**, 1102-1107. [4] Rosso *et al*. (2010) *Environ. Sci. Technol.* **44**, 61-67. [5] Catalano *et al*. (2010) *Geochim. Cosmochim. Acta* **74**, 1498-1512.

https://doi.org/10.1180/S0026461X00006502 Published online by Cambridge University Press

Reworked Hadean crust in the ca. 3780 Ma Nuvvuagittuq supracrustal belt

N.L. CATES[1], S.J. MOJZSIS[1], K. ZIEGLER[2] AND A.K. SCHMITT[2]

[1]Dept. of Geological Sciences, University of Colorado, Boulder, CO 80309-0399 USA (cates@colorado.edu)
[2]Dept. of Earth and Space Sciences, University of California, Los Angeles, CA 90095-1567 USA

Variably deformed amphibolites and granitoid gneisses of the Nuvvuagittuq supracrustal belt (NSB) preserve lower $^{142}Nd/^{144}Nd$ ratios than the terrestrial standard. Expressed as negative $\varepsilon^{142}Nd$ values, the amphibolites also show a slight positive correlation in Sm/Nd. Combined ^{142}Nd and ^{147}Sm-^{143}Nd data were used [1] to produce a ca. 4280 Ma isochron; this could make the NSB amphibolites the oldest preserved terrestrial rocks by about 300 Myr. Alternatively, the $^{142}Nd/^{144}Nd$ signal may be inherited from crustal recycling of remnant ancient mafic lithosphere and hence it would have no bearing on the crystallization ages of the amphibolites.

Here we report U-Pb ages for detrital igneous zircons with rhythmically zoned rounded cores and later metamorphic overgrowths, extracted from NSB fuchsitic quartzites. We show that they are statistically indistinguishable from other ~ 3800 Ma zircon ages obtained for transecting felsic gneisses [2, 3]. The zircon-bearing fuchsitic quartzites show: i) Elevated whole-rock Cr (>150 ppm) contents, and rounded chromites with mantling Cr-muscovite, inconsitent with orthogneiss compositions; ii) Enriched $LREE_{CN}$ and mantle-normalized multi-element compositions inconsistent with NSB chemical sediments (BIFs), but nearly identical to quartz-biotite schists (metaconglomerates) which also host mass-independently fractionated sulfur isotopes; iii) Major and trace elements, including elevated REE, Nb and Ti contents that are neither compatible with a silicification origin of NSB amphibolites, nor with hydrothermal quartz veinings; and iv) Oxygen isotopes consonant with a sedimentary origin.

It is thus improbable that amphibolites of the NSB represent relict genuine Hadean mafic crust captured in a supracrustal belt that can be no older than 3780 Myr. Comparison of detrital and igneous zircon ages from multiple lithologies in the NSB show that its initial development took place in under 20 Myr in the Eoarchean. However, our results do underscore the notion that recycling of volumetrically significant relict Hadean mafic crust continued to play a role in Eoarchean crustal processes, in accord with data in [1].

[1] O'Neil *et al*. (2008) *Science* **321**, 1828-1831. [2] Cates & Mojzsis (2007) *EPSL* **255** 9-21. [3] Cates & Mojzsis (2009) *Chem. Geol*. **261** 98-113.

Colloidal control on the distribution of major and trace elements in a small mountain stream (Malaval catchment, Massif Central, France)

C. CATROUILLET[1], C. DE BARDON DE SEGONZAC[1], O. POURRET[1] AND M. STEINMANN[2]

[1]HydrISE, LaSalle Beauvais, 60026 Beauvais cedex, France (olivier.pourret@lasalle-beauvais.fr)
[2]UMR 6249 Chrono-Environnement, Univ. Franche-Comté, 25030 Besançon cedex, France (marc.steinmann@univ-fcomte.fr)

Organic and/or inorganic colloids play a major role in the mobilization and speciation of trace elements in river waters. Environmental physicochemical parameters (pH, Eh, T, ionic strength…) are the controlling factors of colloidal mobilization. Ultrafiltration experiments using small ultracentrifugal filter devices were performed at different pore size cut-offs (30 kDa, 10 kDa and 3 kDa) to study the colloidal control on partitioning of major and trace elements in stream water [1]. Six sites were sampled in the Malaval stream catchment from upstream to downstream (Massif Central, France [2]) during two sampling campaigns (September 2009 and June 2010) and analyzed for major and trace elements, and organic carbon. In addition to evolution with distance, the modification of the colloidal pool by water mixing at two confluences of the Malaval stream with tributaries was also studied.

The main results of the present study are the following: most elements behave coherently through time and their speciation evolves with distance from source. Based on principal component analysis and hierarchical ascendant classification performed on the whole ultrafiltration dataset, three groups of elements with a specific chemical behavior can be distinguished: (i) a dissolved group (Na, Mg, Si, K, Ca, Rb, Sr), (ii) a reactive group (Al, Fe, Y, Pb, Cu, Ni, As, U, Zr) and (iii) an intermediate group (Co). In addition to this statistical approach one trace element of each group (Sr, Co and Nd) has been studied in more detail on ultrafiltrated sample fractions (0.2 μg/L, 30 kDa, 10 kDa and 3 kDa). The results suggest that (i) the alkalines and alkaline earths are present as dissolved species, whereas (ii) rare earth elements and some metallic elements are bound to colloidal material. However, (iii) a few elements, like cobalt, have an ambivalent behavior: in some samples they behave like the first group and in others like the second group.

[1] Pourret *et al*. (2007) *App. Geochem*. **22**, 1568-1582 [2] Steinmann & Stille (2008) *Chem. Geol*. **254**, 1-18.

https://doi.org/10.1180/S0026461X00006502 Published online by Cambridge University Press

Effects of Laschamp excursion on cosmogenic isotope production

A. CAUQUOIN[1]*, J. JOUZEL[1] AND G. M. RAISBECK[1,2]

[1]IPSL / LSCE, UMR CEA-CNRS-UVSQ, CEA Saclay, 91191 Gif-sur-Yvette, France
(*correspondence: alexandre.cauquoin@lsce.ipsl.fr, jean.jouzel@lsce.ipsl.fr)
[2]Centre de Spectrométrie Nucléaire et de Spectrométrie de Masse, IN2P3-CNRS-Université de Paris-Sud, Bât. 108, 91405 Orsay, France (raisbeck@csnsm.in2p3.fr)

The Laschamp excursion is a period of reduced geomagnetic field intensity occurring 40.7 ± 1.0 ky ago [3] During this period, cosmogenic isotope production was affected not only directly by the reduced magnetic field, but also due to an increased sensitivity to solar activity. The latter occurs because a larger fraction of the lower energy interstellar galactic cosmic ray particles, normally excluded by the magnetic field, is able to reach the earth's atmosphere when the geomagnetic field is reduced. The overall result is a period of increased cosmogenic isotope (^{10}Be,^{14}C) production having considerable structure.

The aim of this study is to estimate, using high resolution (decadal) profiles of ^{10}Be in ice cores from both Antarctica and Greenland as a proxy for production, input into a 10-box carbon cycle model, the expected influence of the Laschamp event on the concentration of ^{14}C in the atmosphere between 37.5 and 45.5 ky BP.

Several cases were tested, from modern carbon cycle (pre-industrial) to severely reduced surface-deep ocean exchange flux [1]. We find that the atmospheric Δ^{14}C due to increased production during this period varies from 180 to 300 ‰. This is considerably smaller than the ~500 ‰ modelled by Hoffmann *et al*. [2] between 44-41 ky, which they attribute mainly to increased production. We believe the main difference is their use of an inadequate approximation for production as a function of geomagnetic field intensity. Hoffmann *et al*. also deduced an ~500 ‰ increase in atmospheric Δ^{14}C from measurements in stalagmites. If such an increase did indeed occur, we conclude that a substantial fraction must have resulted from a redistribution of the carbon cycle.

[1] K. Hughen *et al*. (2006) *Quat. Sci. Rev*. **25**, 3216-3227. [2] D. L. Hoffmann (2010) *Earth Planet. Sci. Lett*. **289**, 1–10. [3] B. Singer *et al*. (2009) *Earth Planet. Sci. Lett*. **288**, 80-88.

Environmental geochemistry of nickel in stream sediments in Pernambuco State, Brazil

R. CAVALCANTE, E. A. M. LIMA, M. FRANZEN AND S. S. COSTA

CPRM - Geological Survey of Brazil
(correspondence*: rogerio.cavalcante@cprm.gov.br, enjolras.lima@cprm.gov.br; melissa.franzen@cprm.gov.br)

The studied area covers the whole Pernambuco State, where they were collected 1162 samples of stream sediments to nickel (Ni). Analyses for environmental geochemistry have been achieved by the concentration ratios of metal and the average content in Brazilian standards [1].

The drainage sediments were analyzed by ICP-MS in fractions <80 mesh. Statistical analysis of dispersion of data obtained and toxicological reference [1] provided level above which the Ni may be considered anomalous.

The study shows Ni contents below the background, and environmentally consistent with the average (18 ppm) below which is not predictable adverse effects on biota. With the exception, there are three main areas with few values exceeding the limit proposed by [1]: (i) western 40-75 ppm Ni; (ii) center 43-54 ppm Ni; e (iii) east 50-80 ppm. The above data may correspond to normal values, backgrounds rocks of the area and may not represent anthropogenic pollution.

[1] CONAMA 2004. Resol. Nº 344/2004. Web page: http://www.mma.gov.br

https://doi.org/10.1180/S0026461X00006502 Published online by Cambridge University Press

Laboratory studies into sea-spray chemical speciation in plankton-enriched sea-water

D. CEBURNIS[1]*, J. OVADNEVAITE[1], M. ZACHARIAS[2], J. BIALEK[1], S. CONNAN[2], M. RINALDI[3], C. MONAHAN[1], M.C. FACCHINI[3], H. BERRESHEIM[1], D.B. STENGEL[2] AND C.D. O'DOWD[1]

[1]School of Physics and Center for Climate and Air Pollution Studies, Ryan Institute, National University of Ireland Galway, Galway, Ireland. (*correspondence: darius.ceburnis@nuigalway.ie)

[2]Botany and Plant Science, School of Natural Sciences, Ryan Institute, National University of Ireland Galway, Galway, Ireland.

[3]Institute of Atmospheric Sciences and Climate, National Research Council, Bologna, 20129, Italy.

Marine aerosol enrichment by biogenic organic matter (OM) has been linked to phytoplankton activity [1], thus having a strong seasonal impact on both the Earth's albedo and climate. In addition to a seasonal cycle, sea-spray generation and its enrichment with OM is a very dynamic process producing regular OM plumes over N.E. Atlantic [2]. Plankton-enriched seawater contains a complex mixture of dissolved and particulate organic carbon components (POC and DOC) producing both water soluble and insoluble organic aerosol species [3, 4]; this warrants detailed laboratory studies aimed at establishing a link between observed ambient aerosol OM and its very primary form.

Laboratory studies using the microalgal species *Emiliania huxleyi*, *Leptocylindrus danicus* and *Cylindrotheca closterium* were performed using on-line and off-line analytical techniques, a sea spray production chamber and an ageing chamber with day-light and ozone. Under controlled conditions a sea spray highly enriched in OM was produced with levels similar to Facchini *et al*. [3]. HR-ToF-AMS, ^{1}HNMR and HTDMA techniques confirmed OM composition of highly hydrocarbon-like, water insoluble OM characteristic of unsaturated lipids exhibiting low hygroscopic growth factor. Freshly produced OM, while largely insoluble, was far less oxidised (less sugars) than the OM reported by Facchini *et al*. [3]. Processing with light and ozone continued to support primary origin of ambient OM.

[1] O'Dowd, C.D., *et al*. (2004) *Nature* **431,** 676-680. [2] Ovadnevaite, J., *et al*. (2011) *Geophys. Res. Lett.* **38**(2), L02807. [3] Facchini, M.C., *et al*. (2008) *Geophys. Res. Lett.* **35**(17), L17814. [4] Russell, L.M., *et al*. (2010) *P. Natl. Acad. Sci. USA* **107**(15), 6652-6657.

Mineralogy and geochemistry of zeolites of pyroclastic deposits in Northwestern of Tuzgölü Basin (Turkey)

MUAZZEZ ÇELIK KARAKAYA* AND NECATI KARAKAYA

Selçuk Universitesi Muh.-Mim. Fakültesi Jeoloji Müh. Böl. Konya, 42079, Türkiye (mzzclk@hotmail.com)

The Early Miocene volcanic rocks in the Kulu (Konya)-Haymana (Ankara) area were classified as andesitic-dacitic lavas and pyroclastics, and in some cases as trachytic and trachyandesitic. The zeolitic tuff layers are interbedded with bentonite layers and rarely silica lenses or thin layers. Plagioclase crystals, glass shards, and volcanic rock fragments altered to zeolites and smectite in tuff of the volcanic rocks. Clinoptilolite/heulandite, erionite/offlerite, analcime, and chabazite and rarely phillipsite and mordenite occur with other authigenic minerals, e.g. Fe- and Mg-rich smectite, K-feldspar. Gypsum, calcite, dolomite, and hexahydrite were also found in the some altered tuffs and clay layers. The zeolite minerals grow up as crypto- to microcrystalline aggregates after dissolved glass fragments in cavities and represent most of the matrix in the altered tuffs.

Nine K-feldspar, twelve plagioclase and sixty nine zeolite minerals were analyzed by microprobe. Zeolite analyses were made on single crystal and crystal clusters of heulandite, clinoptilolite, erionite, and chabazite. The structural formulae of the feldspar were calculated as $(Si_{2.98}Al_{1.03})(K_{0.67}Na_{0.27}Ca_{0.01})$ and $(Si_{2.67}Al_{1.31})(K_{0.05}Na_{0.60}Ca_{0.28})$, respectively, and the zeolite minerals as $[(Si_{28.7}Al_{7.3})(Mg_{1.5}Ca_{0.9}Sr_{0.1})(K_{1.0}Na_{1.3})]$, $[(Si_{29.6}Al_{6.4}Fe_{0.1})(Mg_{1.0}Ca_{1.0}Sr_{0.1})(K_{0.8}Na_{0.9})]$, $[(Si_{28.3}Al_{8.2})(Mg_{1.7}Ca_{0.3}Sr_{0.1})(K_{2.0}Na_{1.2})]$, and $(Si_{9.88}Al_{2.18}Fe_{0.01})(Mg_{0.2}Ca_{0.6}Sr_{0.03})(K_{0.3}Na_{0.17})]$, respectively. Clinoptilolites are mostly high-silica Ca-rich heulandites having intermediate composition between heulandites and clinoptilolites. Si/Al ratios of heulandites (3.70-4.20) and clinoptilolites (4.30-5.30) are similar to heulandite group minerals and their divalent/monovalent cation ratios range from 0.41 to 5.75 and 0.44 to 3.6, respectively. The structural (Na+K) content is higher than that of (Ca+Ba+Sr) in all heulandite group minerals and erionites. Mean Si/Al ratio of erionites is 3.40 and divalent/monovalent cation ratios are between 0.42 and 1.25. Zeolite minerals, e.g. analcime, chabazite, erionite, and phillipsite, and saline minerals such as gypsum, calcite, dolomite and hexahydrite were precipitated in a closed alkaline and saline environment. High proportions of alkali cations would indicate that highly alkaline pH values are likely in pore water in the tuff.

https://doi.org/10.1180/S0026461X00006502 Published online by Cambridge University Press

Acid gases speciation in H_2S-CO_2-Portland Cement-H_2O system

J. CENTENO

PDVSA Intevep, Los Teques, Venezuela,
(*correspondence: centenojs@pdvsa.com)

This study presents the interactions of H_2S and CO_2 with the cementitious material used in the oil wells construction to determine the speciation of these chemicals in a closed system conditions at high temperatures and pressures. Using a charge balance was possible to determine the mass of each of the species involved in the chemical balance of the system and make the corresponding mass balance. H_2S and CO_2 are aggressive agents and their action against the cementitious material is influenced by the characteristics of cement, porosity, permeability, type of hydration products, partial pressure of CO_2 and H_2S, temperature and composition of formation water, in particular is important to consider the salinity. The CO_2 attack is preferential on portlandite [Ca $(OH)_2$] present in cement and its initial impact is minimal on calcium silicates; deteriorates the outer surface of cement and migrates through the matrix affecting its internal structure. Chemical attack of samples was performed in a closed system under high temperature and pressure (ATAP), with known concentrations of CO_2 and H_2S, establishing conditions under which is progressively increased aggressiveness of the attack (approximately up to 38 atm CO_2 16 atm H_2S). Each test series includes the following time intervals: 20, 40, 80 days. The mass balance allowed calculating the concentrations of sulfide (HS^-) and bicarbonate (HCO_3^-), according to the following expressions:

$$[HS^-] = pH_2S10^{-7}\left(2[Ca^{2+}]+[Na^+]+[K^+]-2[SO_4^{2-}]\right)$$

$$[HCO_3^-] = 2[Ca^{2+}]+[Na^+]+[K^+]-[HS^-]-2[SO_4^{2-}]$$

The main conclusion suggests an inhibitory effect of CO_2 on the solubility of H_2S.

Lignin decomposition in paddy soils as affected by redox conditions

C. CERLI[1]*, Q. LIU[2], A. HANKE[1], K. KAISER[3] AND K. KALBITZ[1]

[1]Institute of Biodiversity and Ecosystem Dynamics, Earth Surface Science, University of Amsterdam, 1098 XH Amsterdam, The Netherlands (*correspondence: c.cerli@uva.nl; a.hanke@uva.nl, k.kalbitz@uva.nl)

[2]Institute of Soil Science, Chinese Academy of Sciences, 210008 Nanjing, China (qliu@issas.ac.cn)

[3]Soil Sciences, Martin Luther University Halle-Wittenberg, 06120 Halle (Saale), Germany (klaus.kaiser@landw.uni-halle.de)

In submerged soils, lignin constitutes a major portion of the total organic matter (OM) because of hampered degradation under anoxic conditions. Paddy soils management involves alternating redox cycles with periodic changes in soil solution chemistry and microbial metabolism. Such an environment might promote both degradation and preservation of lignin, affecting the overall composition and reactivity of total and dissolved OM.

We sampled two soils either subjected to cycles of anoxic (rice growing period) and oxic (harvest and growth of other crops) conditions since 700 and 2000 years. We incubated suspended Ap material, sampled from the two paddy plus two corresponding non-paddy control soils under oxic and anoxic condition, for 3 months, interrupted by a short period of three weeks (from day 21 to day 43) with reversed redox conditions. At each sampling time (day 2, 21, 42, 63, 84), we determined lignin-derived phenols (by CuO oxidation) as well as phospholipids fatty acids contents and composition. We aimed to highlight changes in lignin decomposition as related to changes in microbial community composition.

In well-established paddy soils relative short (3 weeks) changes in redox conditions had no effect on lignin decomposition or oxidation state. Also, lignin was not altered during oxic incubation. Since fungi represented only small portion of the microbial biomass in the studied soils, they were obviously not capable to cause much degradation, even under favourable conditions. On the contrary, 3 months of anoxic conditions resulted in a decrease in lignin-derived phenols. This decrease was likely not a result of degradation but of (partial) dissolution and/or pH-induced changes of the surface properties of Fe and Mn hydrous oxides causing the release of mineral-associated lignin-derived phenols. Thus, we speculate, that oxidised lignin fragments produced during the (oxic) dry period do not remain in the soils but leach with water drainage during the flooding period.

https://doi.org/10.1180/S0026461X00006502 Published online by Cambridge University Press

Model calculations of scale forming minerals of high enthalpy geothermal waters in Turkey

ZIYA CETINER[1] AND YONGLIANG XIONG[2]

[1]Canakkale 18 Mart University, Department of Geological Engineering, 17010, Canakkale, Turkey (ziyac@comu.edu.tr)
[2]1404 North Country Club Circle, Carlsbad, New Mexico, USA (yongliangxiong@yahoo.com)

Located on the active Alpine-Himalayan Orogenic Belt, Turkey's geological and neo-tectonic evolution had been dominated with active faults and volcanisms which are the leading causes of substantial geothermal resources. Such resources are widespread throughout the country and are indentified with three distinctive geothermal regions based on their tectonic settings. Of which, high enthalpy resources, suitable for geothermal power production, are mainly located in the western part of the country along the major graben and associated fault systems. These include Denizli-Kızıldere (242°C), Aydın-Germencik (232°C), Manisa-Kavaklıdere (213°C), Aydın-Pamukören (187°C), Canakkale-Tuzla (175°C), Aydın-Salvatlı (171°C) and Kütahya-Simav (162°C) [1]. Low and moderate enthalpy sources exist in the Middle and Eastern Turkey along North Anatolian Fault Zone because of volcanism and fault formations.

The total geothermal potential in Turkey is estimated to be about 31,500 MWt. Most of the geothermal development in Turkey has been initiated by MTA (General Directorate of Mineral Research and Exploration of) since 1962. A law allowing geothermal sources discovered by the MTA to be used by commercial organizations was introduced in 2007. Moreover, legislation concerning renewable energy was brought in at the end of 2010. These new laws have led to increased efforts to explore profitable geothermal electricity and to use the heat directly.

In this study, geochemistry of the medium to high enthalpy geothermal waters suitable for electrical energy production has been critically reviewed and the solubilities of potential scale-forming minerals including silica polymorphs and carbonates at various temperatures have been calculated by using EQ3/6, for determining the optimum operation conditions in power generation.

[1] Mertoglu O. *et al*. (2010). *Proceedings World Geothermal Congress*. Bali, Indonesia, 25-29 April 2010.

Geochemical tracing of water-rock interactions in the Ringelbach granitic research catchment (Vosges, France)

F. CHABAUX , T. SCHAFFHAUSER, B. FRITZ, B. AMBROISE AND P. STILLE

LHYGES, Université de Strasbourg/EOST, CNRS, France (fchabaux@unistra.fr)

For constraining the nature of water-rock interactions occuring within granitic watersheds a geochemical and isotopic (Sr, U) study of all springs within the Ringelbach granitic research catchment (Vosges, France) has been undertaken, following the approach classically developped in the Lab [1]. This study also includes the analysis of water samples collected in two 150-m deep boreholes, which permit the evaluation of (a) water flux and composition in the deeper part of the watershed and (b) deep weathering processes within the granitic bedrock. At the scale of a single spring, important geochemical variations are observed over the year. Such variations cannot be accounted for by a simple mixing scenario of rainwater contributing in variable quantities to the chemical composition of these waters. For each considered spring, the geochemical variations have to be interpreted as the contribution of two different weathering fluxes with changing intensities over the hydrological cycle. At the scale of a same slope a systematic geochemical variation of the spring waters is observed according to their emercgence altitude along this slope. These chemical changes affect both the elementary and U activity ratios but not the Sr isotope ratios. This indicates that geochemical variations are not simply controlled by mixing processes between waters having interacted with different lithologies. Furthermore, geochemical variations observed in subsuface waters (springs) cannot be explained by a contribution of deep waters (boreholes). All together these data suggest that the main parameter explaining geochemical variations of water samples collected within the Ringelbach catchment is the water pathway of the waters within the watershed. Modeling approaches confirm and constrain the importance of this parameter in the control of geochemical characteristics of surface waters (Schaffhauser *et al*., this issue).

[1] S. Durand, F. Chabaux, S. Rihs, P, Duringer, P. Elsass (2005), *Chem. Geol*., **220**, 1-19; [2] M.L. Bagard, F. Chabaux, Oleg S. Pokrovsky, J. Viers, Anatoly S. Prokushkin, P. Stille, S. Rihs, A.D. Schmitt, B. Dupré (2011) *GCA*, DOI: 10.1016/j.gca.2011.03.04.

https://doi.org/10.1180/S0026461X00006502 Published online by Cambridge University Press

Biogeochemical characterization of Mercury (Hg)-contaminated sediments at the Bunikasih Gold mine, West Java Province, Indonesia

SITI KHODIJAH CHAERUN[1,2]*, SAKINAH HASNI[1], EDY SANWANI[3] AND D. BARRIE JOHNSON[4]

[1]Laboratory of Mining Biotechnology and Enironmental Bioengineering, School of Lifesciences and Technology, Institut Teknologi Bandung, Ganesha 10, Bandung 40132, West Java, Indonesia (*correspondence: skchaerun@gmail.com)
[2]Centre for Life Sciences, Institut Teknologi Bandung
[3]Department of Metallurgical Engineering, Faculty of Mining and Petroleum Engineering, Institut Teknologi Bandung
[4]School of Biological Sciences, Bangor University, UK

The objective of this study was to investigate the biogeochemical characteristics of mercury (Hg)-contaminated sediments at the Bunikasih Gold Mine, West Java Province, Indonesia in order to provide a basic and initial description of biogeochemically sediments at this contaminated site for bioremediation purposes. Sediments contained elevated total Hg concentrations of 28 – 61 ppm. XRD analysis revealed the presence of quartz and berlinite minerals, indicating that mercury contained in sediments was not in mineral form of mercury but in other form. SEM-EDS analysis indicated the presence of Si (30 – 44%), Al (0.6 – 8%), O (45 – 51%), and C (3.5 – 7%). Ten heterotrophic bacteria that were resistant to $HgCl_2$ (25 ~ 550 ppm) were isolated from the Hg-contaminated sediments. 16S rRNA gene sequence analysis identified the bacteria as strains of *Pseudomonas koreensis*, *Pseudomonas putida*, *Pseudomonas fulva, Stenotrophomonas maltophilia* and *Aeromonas sobria*.

The findings of this study provide evidence of heterotrophic bacteria associated with Hg-contaminated sediments as well as provide the first information of phylogenetically-diverse Hg-resistant bacteria in the Hg-polluted sites of Indonesia. Such information may prove highly useful for developing in situ bioremediation of Hg-contaminated sites in Indonesia.

This work was supported by a grant from HIBAH DIKTI DIPAH ITB 2010, Indonesia

Interactions of Eu(III) and Cm(III) with celestite and strontianite: Precipitation kinetics and uptake mechanisms characterisation

A. CHAGNEAU[1,2], K. HOLLIDAY[1], M. SCHMIDT[1], T. STUMPF[1] AND T. SCHÄFER[1,2]

[1]Karlsruhe Institute of Technology (KIT), Institute for Nuclear Waste Disposal (INE), D-76344 Eggenstein-Leopoldshafen, Karlsruhe, Germany
[2] Freie Universität Berlin, Institute of Geological Sciences, Hydrogeology Group, 12249 Berlin, Germany

The present work focuses on the characterization of lanthanides and actinides interactions with celestite ($SrSO_4$) and strontianite ($SrCO_3$). Precipitation kinetics studies of the minerals were performed in batch type and mixed-flow reactors experiments, in presence and absence of Eu(III) and Cm(III) in solution. It is shown that the presence of Eu(III) and Cm(III) as trace elements (up to 4.5×10^{-4} mol L^{-1}) have no effect on the precipitation rates, which are dependant on the initial saturation index.

TRLFS analyses shown a clear incorporation of the Eu(III) and Cm(III) into the mineral structures, with a minor surface component for the strontium sulfate. Similar studies were earlier performed on aragonite, calcite ($CaCO_3$) and gypsum ($CaSO_4$) in the same experimental conditions. Incorporation was observed for aragonite and only surface complexation for the calcium sulfate, while both mechanisms were observed for calcite. Therefore, the ligand strength was expected to play an important role in the uptake mechanisms. The present work focused on two minerals isostructural with aragonite, demonstrating the importance of the lattice parameters in the uptake mechanisms as well. Moreover, the presence of Eu(III) and Cm(III) as incorporated species has no effect on these lattice parameters.

The Eu(III) and Cm(III) affinity coefficients for the $SrSO_4$ and $SrCO_3$ structure as well as the strontianite and celestite precipitation rates as a function of the oversaturation (SI) were determined. This information is prerequisite to develop a reactive transport model able to predict the behavior of these elements in a porous media under chemical perturbation.

https://doi.org/10.1180/S0026461X00006502 Published online by Cambridge University Press

Enhanced growth of *Acidovorax delafieldii* 2AN during nitrate-dependent Fe(II) oxidation in continuous-flow systems

A. CHAKRABORTY[1], J. SCHIEBER[2], E.E. RODEN[3] AND F.W. PICARDAL[1]*

[1]School of Public and Environmental Affairs, Indiana University, Bloomington, IN 47405 USA (*correspondence: picardal@indiana.edu)
[2]Department of Geological Sciences, Indiana University, Bloomington, IN 47405 USA
[3]Department of Geology and Geophysics, University of Wisconsin, Madison, WI 53706 USA

It is not clear if microbial, NO_3^- -dependent, Fe(II) oxidation (NDFO) is energetically beneficial to cells or if it is primarily a fortuitous, side-reaction, involving both abiotic and enzymatic reactions during heterotrophic growth. Although recent batch experiments by others have suggested that NDFO may provide an energetic benefit through a mixotrophic physiology, it is not known if long-term growth yields can be enhanced by Fe(II) oxidation, and if this enhancement can be realized at environmentally relevant Fe^{2+}, NO_3^-, and organic C concentrations. *Acidovorax delafieldii* 2AN was incubated anoxically in batch reactors using a bicarbonate-buffered, artificial groundwater medium containing 5-6 mM nitrate, 8-9 mM Fe(II) and 1.5 mM acetate. A novel, continuous-flow culture system was also used to evaluate growth on low concentrations of substrates, e.g. 100 μM nitrate, 20 μM acetate and 50-250 μM Fe(II).

In batch reactors, almost 90% of the Fe(II) was oxidized with concomitant reduction of NO_3^- and complete consumption of acetate. However, cells became encrusted with Fe(III) (oxy)-hydroxides, lost motility and formed aggregates. Encrusted cells could neither oxidize more Fe(II) nor utilize further additions of acetate. In batch experiments using chelated iron [Fe(II)-EDTA], aggregated and encrusted cells were not produced and further additions of acetate and Fe(II) could be oxidized. This suggests that the cell encrustations prevent substrate entry into the cell or otherwise render cells physiologically inactive. In the continuous-flow system, the growth yield of *A. delafieldii* 2AN was always greater in the presence of Fe(II) than in its absence and ESEM examination showed that encrustation was minimized. This suggests that cell encrustations may be an artifact of the high concentrations of Fe(II) and NO_3^- used in batch cultures. Our results provide evidence that, under environmentally relevant concentrations of Fe(II) and NO_3^- , NDFO can enhance growth without the formation of cell encrustations that may limit viability in batch culture.

Kimberlites, flood basalts and mantle plumes: New insights from the Deccan Large Igneous Province

N.V. CHALAPATHI RAO[1,2]* AND B. LEHMANN[2]

[1]Centre of Advanced Study in Geology, Banaras Hindu University, Varanasi-221005, India (*correspondence: nvcr100@gmail.com)
[2]Mineral Resources, Technical University of Clausthal, Adolph-Römer-Straße 2A, 38678 Clausthal-Zellerfeld, Germany (lehmann@min.tu-clausthal.de)

A temporal and spatial relationship between small-volume, volatile-rich and highly potassic continental melt fractions, such as kimberlites and related rocks, and large-volume continental flood basalts exists in several Large Igneous Provinces (LIPs). Many of these LIPs are also widely regarded as products of mantle plume-lithosphere interactions. The small-volume melts either immediately pre-date or post-date or even are co-eval with the main flood basalt event. The overlap of ages between the flood basalts and the kimberlites very likely reflects a cause and effect relationship via mantle plumes.

Recently discovered end-Cretaceous diamondiferous kimberlites (orangeites) in the Bastar craton of central India which are synchronous with the flood basalts, carbonatites, lamprophyres and alkaline rocks of the Deccan LIP provide an opportunity to re-evaluate the role of mantle plume-lithosphere interactions in the generation of these disparate magmas. The geographical zonation of the kimberlite-lamprophyre-carbonatite-alkaline rock spectrum in the Deccan LIP is inferred to reflect variable thickness of the pre-Deccan Indian lithosphere with a thinner lithosphere along the known rift zones of northwestern and western India and a thickened lithosphere underlying the Bastar craton of central India. This heterogeneity is thought to have controlled the volume of melt generation and melt ascent, as well as the ultimate alkaline magma type.

These findings are supported by the regional lithospheric thickness map, generated from converting seismic shear wave velocities into temperature profiles, which depicts that the present-day lithosphere beneath the Bastar craton is thicker than that in western and NW India where the centre of the Deccan plume-head was located. Thermal weakening of the sub-Bastar craton due to mantle plume-lithosphere interaction at the end-Cretaceous resulting in a thin-spot is suggested to have controlled the Deccan-related mafic dyke emplacement in the Bastar craton

https://doi.org/10.1180/S0026461X00006502 Published online by Cambridge University Press

A new *Gallionellales* isolate: A model system for comparative studies of Fe-oxidizer physiology and biomineralization

CLARA S. CHAN*, SEAN T. KREPSKI AND GAURAV SAINI

Dept. of Geological Sciences, University of Delaware, Newark, DE 19716 (*correspondence: cschan@udel.edu)

The Fe-depositing bacterium *Gallionella ferruginea* was first described in the early 19th century based in part on its twisted ribbon-like stalk, which has since been widely used in its identification. In 1993, Hallbeck *et al*. [1] reported the 16S rRNA sequence of a stalk-forming isolate. Recently, researchers have isolated several Fe-oxidizing bacteria (FeOB) related to *Gallionella*; however, none produce biomineral structures that typically comprise Fe microbial mats, so we have made relatively little progress characterizing and linking FeOB physiology, biomineralization, and mat formation. Towards these goals, we have isolated a novel stalk-forming FeOB, strain R-1, from a freshwater Fe seep in Delaware, USA. R-1 is a neutrophilic, obligate Fe-oxidizing Betaproteobacterium. Despite strong morphological similarity to *G. ferruginea* [1], this isolate shares only 93.6% 16S rRNA gene sequence similarity. It is more similar (94.0-94.4%) to *Sideroxydans* isolates [2,3], which do not produce morphologically-distinct minerals. Its phylogenetic distance from other *Gallionellales*, especially its distance from *G. ferruginea* shows the high diversity of FeOB in this order.

R-1 is remarkably similar to the marine Zetaproteobacterial Fe-oxidizer *Mariprofundus ferrooxydans* PV-1, presenting an opportunity for comparative study. Both organisms are obligate FeOB isolated from Fe mats. R-1 oxidizes ~1-2x10^{-14} mol Fe/cell, comparable to PV-1 (0.9x10^{-14} mol Fe/cell). Like PV-1, R-1 cells are relatively Fe-free, with a fibrillar, ribbon-like Fe and polysaccharide-rich stalk, binding multiple lectins. We postulate that the R-1 stalk plays similar roles to that of PV-1, especially as a mechanism for removing Fe(III) waste from the cell [4]. TEM studies have shown that cell surface structure differs from PV-1, which may imply different surface chemistry. We have been investigating surface characteristics by atomic force microscopy, electrophoretic mobility, hydrophobicity tests, and probing by charged nanoparticles. Results to date suggest that both R-1 and PV-1 surfaces have near-neutral charge, which helps explain how cells avoid encrustation.

[1] Hallbeck *et al*. (1993) *J. Gen. Microbiol*. **139**: 1531-5. [2] Emerson and Moyer (1997) *Appl. Env. Microbiol*. **63**: 4784-92. [3] Lüdecke *et al*. (2010) *Env. Microbiol*. **12**: 2814-25. [4] Chan *et al*. (2011) *ISME J*. **5**:717-27.

Evaluation of relationships used to model sea surface iodide concentrations

R.J. CHANCE[1]*, A.R. BAKER[1], L.J. CARPENTER[2] AND T. JICKELLS[1]

[1]School of Environmental Sciences, University of East Anglia, UK (*correspondence: r.chance@uea.ac.uk)

[2]Department of Chemistry, University of York, YO10 5DD, UK

Sea-to-air exchange supplies reactive iodine to the atmosphere, where it contributes to tropospheric ozone depletion and particle formation, and allows the dispersal of radioactive iodine discharges. A major contributor to this process is the reaction of ozone with iodide at the air-sea interface. Sea surface iodide concentrations range from 5 to 200 nM, varying with latitude and proximity to the coast; the controls on this distribution are not well understood. Recent attempts to quantify the contribution of the ozone–iodide reaction to large scale ozone deposition [1,2] have modelled sea surface iodide concentrations using observed relationships between iodide and nitrate [3] or chlorophyll [4].

Here, we present new iodide measurements from the tropical eastern Atlantic and the Southern Ocean, incorporate these into a preliminary global surface iodide climatology and use this to evaluate the two different modelling approaches. We find that neither model was able to fully explain the observed global iodide distribution. We propose the compilation of a global iodide climatology which can be used to rigorously test models and new hypotheses concerning the marine biogeochemical cycle of iodine. If spatial resolution is sufficient, such a database might also be used directly in modelling studies.

[1] Ganzeveld *et al*. (2009), *Glob. Biogeochem. Cyc*. **23**, GB4021. [2] Oh *et al*. (2008), *Atmos. Environ*. **42**, 4453-4466. [3] Campos, Sanders & Jickells (1999), *Mar. Chem*. **65**, 167-175. [4] Rebello, Herms & Wagener (1990), *Mar. Chem*. **29**, 77-93.

https://doi.org/10.1180/S0026461X00006502 Published online by Cambridge University Press

Carcass Island: A new site for the observation of Southern South American dust in the western Falkland Islands

R.J. CHANCE AND A.R. BAKER*

School of Environmental Sciences, University of East Anglia, UK (*correspondence: alex.baker@uea.ac.uk)

Dust originating in Southern South America (SSA) is probably the largest source of mineral matter and its associated trace elements to the remote South Atlantic and Atlantic sector of the Southern Ocean. Antarctic ice core records show very large variations in dust supply over glacial – interglacial timescales, which may be related to changes in atmospheric pCO_2 and temperature proxies.

Our understanding of the current strength and transport of SSA dust sources is very poor however, partly because persistent cloud cover makes remote sensing observations in the region difficult, but also due to a lack of observations of surface level dust concentrations along transport pathways.

In September 2010 we established a new site for the collection of SSA dust on Carcass Island (51°15'S, 60°35'W) in the western Falkland Islands, as part of the UK contribution to the GEOTRACES programme. Weekly aerosol samples were collected at the site between September 2010 and April 2011, using a high-volume sampler under the control of a wind sector monitor ("clean" sector 220-310 degrees, relative to true north). The collector was mounted at the top of a short (~3m) aluminium scaffolding tower near the crest of a small ridge approximately 400m from the shore. The nearest settlement is >3km downwind of the site. During site visits rain samples were also collected either at the aerosol site or settlement.

Samples will be analysed for their soluble and total trace metal content and major ions (including macronutrient) chemistry. We intend to operate the site in future years.

This contribution will describe the Carcass Island site in detail and we hope to be able to present preliminary results from the first year of sampling.

High-pressure Mössbauer Spectroscopic study of Lohawat (Howardite) meteorite up to 9GPa

USHA CHANDRA[1], POOJA SHARMA[1] AND G.PARTHASARATHY[2]

[1]High Pressure Physics Lab., Department of Physics, University of Rajasthan,Jaipur 302055 ; (chandrausha@hotmail.com)

[2]National GeoPhysical Research Institute(CSIR), Uppal Road, Hyderabad 500606 (gpsarathy@ngri.res.in)

The effect of high-pressure on Lohawat(Howardite) Meteorite which fell at Lohawat village in Jodhpur was studied using Mössbauer spectroscopic technique with diamond anvil cell and 4:1 methanol:ethanol mixture as hydrostatic pressure medium[1]. The main minerals detected in the meteorite were orthopyroxenes and plagioclase with little amount of olivine. Ambient Mössbauer study showed ferrosilite with Fe^{2+} in two inequivalent octahedral sites M1 and M2 [2]. Both the sites behave differently under pressure.At 2.8 GPa, a sudden decrease in Mössbauer parameters (quadrupole splitting and isomer shift) indicate transformation of high spin Fe^{2+} to low spin configuration. The trend of decrement continues up to 5.6 GPa where isomer shift reaches a low of -0.14 mm/s . Further increase in pressure reverses the trend and at 8.4 GPa the value becomes +0.05mm/s. The observation of low spin Fe^{2+} configuration in pyroxene is unusual , not observed in terrestrial samples. Such a behaviour resembles post-peovskite character which occurs at ~ 120 GPa [3]. The presence of low spin Fe^{2+} phase at low pressure of ~ 2GPa indicates the defects generated in the system under shock impact. The results thus obtained are also supported by high pressure electrical resistivity measurements.

We acknowledge CSIR, New Delhi; PLANEX (ISRO), Ahmedabad for Financial support and Prof. R.P.Tripathi for providing the meteorite sample.

[1] Chandra U., Ind. J. (2007) *Pure & Appl. Phys.*.**45** 790.
[2] Tripathi R.P. *et al*. (2000) *Meter. & Planet. Sc*. **35** 201.
[3] McCammon *et al*. (2010) *PEPI* **180** 215.

https://doi.org/10.1180/S0026461X00006502 Published online by Cambridge University Press

Phosphorus in olivine from Italian potassium-rich lavas

S.R. CHANEVA*, I.K. NIKOGOSIAN, M.J. VAN BERGEN AND P.R.D. MASON

Department of Earth Sciences, Utrecht University, the Netherlands
(*correspondence: simonachaneva@gmail.com; iniki@geo.uu.nl; vbergen@geo.uu.nl; mason@geo.uu.nl)

Phosphorus in igneous olivine is promising as a petrogenetic proxy and as a sensitive indicator of crystal growth histories [1,2]. To explore its applicability in solving outstanding issues concerning Italian K-rich magmatism, we analyzed a collection of well characterized forsterite-rich olivines, along with their Mg-rich melt inclusions (MI) for P contents. The wide compositional range of the basaltic samples (from high to low-K) and the regional coverage of volcanic centres (between the Roman Province and Vulture) enabled us to detect variations in magmagenetic conditions that control the behaviour of phosphorus.

Phosphorus concentrations in the olivines were determined by EPMA (15kV, 100nA, extended counting times) and by LA-ICPMS, along with standard major and trace element analyses that included homogenized MI. Intra-crystal variations were explored in rim-to-rim traverses by EPMA, following a procedure optimized for P. Detection limits were 40±20 ppm for both techniques, based on the analyses of a series of reference materials. The measured olivines cover an overall range in P between 40 and 230 ppm, despite their consistent forsterite-rich nature (Fo>87). The olivines from the medium to low-K series (M-LKS) contain less P (<70 ppm, except for Campi Flegrei where <230ppm was found) than those from the high-K series (HKS) which reach a maximum of 130 ppm. Corresponding MI from M-LKS and HKS samples contain up to 0.7 and 1.9 wt.% P_2O_5, respectively.

The P contents in olivine tend to increase with K_2O and P_2O_5 contents in the melt, and show regional systematics, suggesting that they signal variations in mantle source composition and/or mode of melt extraction. On the other hand, some M-LKS melts with similar P contents crystallized olivines with significantly different contents, indicating that P in the melt may not be the only control of uptake by olivines. Additional factors to be considered include growth rate [1] and coupled substitutions (e.g., with Al, Cr, Ti). Also, profiles in selected olivines show P depleted zones around MI, which questions the supposed immobility of P in olivine.

[1] Brunet & Chazot (2001) *Chem. Geol.* **176**, 51-72. [2] Milman-Barris *et al.* (2008) *CMP,* **155**, 739-765

High-precision age for the Haifanggou Formation and its implications for the coevolution of plants and atmospheric CO_2

SU-CHIN CHANG*[1], HAICHUN ZHANG[2], SIDNEY R. HEMMING[3,4], GARY T. MESKO[3] AND YAN FANG[2]

[1]Dept. of Earth Sciences, The University of Hong Kong, Hong Kong (*correspondence: suchin@hku.hk)
[2]State Key Laboratory of Palaeobiology and Stratigraphy, Nanjing Institute of Geology and Palaeontology, Chinese Academy of Sciences, Nanjing, China
[3]LDEO, Columbia University, NY, USA
[4]Dept. of Earth & Environmental Sciences, Columbia University, NY, USA

Atmospheric CO_2 levels have fluctuated greatly during the Phanerozoic [1]. Although many organic and inorganic factors affected atmospheric CO_2 levels, plants have played an important role in CO_2 fluctuations. Recently, most paleobotanists accept an Early Cretaceous origin for angiosperms and support that angiosperms underwent a rapid ecological radiation in middle-late Cretaceous [2]. Because high concentrations of Cretaceous atmospheric CO_2 underwent a long-term decline, several hypotheses suggested that the origin and radiation of angiosperms and atmospheric CO_2 levels are closely related [3].

The recent discovery of *Schmeissneria* from the middle part of the Jurassic Haifanggou Formation provided evidence that the origin of angiosperms could predate the Early Cretaceous [4]. Because previously reported ages for the Haifanggou Formation are scattered and the uncertainties of these ages were fairly large, our on-going work aims to establish high-precision $^{40}Ar/^{39}Ar$ ages for volcanic ashes from the Haifanggou Formation.

Our preliminary results indicate that *Schmeissneria* is older than 160 Ma. The age results will provide a robust geochronological calibration for the oldest angiosperm and will improve our knowledge of the link between atmospheric CO_2 and the rise and the radiation of angiosperms.

[1] Berner *et al.* (2001) *American Journal of Science* **301**, 182-204. [2] Friis *et al.* (2005) *Current Opinion in Plant Biology* **8**, 5-12. [3] Beerling (1994) *Philosophical Transactions of the Royal Society, London* ***B*****346**, 421-432. [4] Wang *et al.* (2006) *Progess in Natural Science* **16**, 222-230.

https://doi.org/10.1180/S0026461X00006502 Published online by Cambridge University Press

Characteristic elements and lead isotope of Kaempferia Galangal from Yangchun, Guangdong, China

X.Y. CHANG[1,2], S.M. FU[1], N. CHEN[1], H. LIU[1], H.Y. ZHANG[1], Q.H. WU[1], X.F. ZHAO[1] AND B.Q. ZHU[2]

[1]School of Environmental Science and Engineering, Guangzhou University, Guangzhou 510006, Guangdong China; (*correspondence: changxy@gzhu.edu.cn)

[2]Guangzhou Institute of Geochemistry, Chinese Academy of Science, Guangzhou 510640, Guangdong China;

Products of designations of origin was used to describe a product originating in that specific place, region, or country, if the quality or characteristics of which were essentially or exclusively due to a particular elements geochemical factors, and the production, processing and preparation of which took place in the defined specific place, region, or country [1-3].

Select products of designations of origin Kaempferia Galangal from YangChun, Guangdong Province, China. The plants and soil profile samples were collected and the element content, element speciation, and lead isotope ratio were determined. Through the multivariate statistical analysis to ascertain the characteristic elements and multielement group, and provide evidence for establishing the elements- isotope fingerprints of product identification system. Fourteen trace elements in soil and galangal samples were measured to explore the feasibility of characteristic elements as the fingerprinting marker of products of origin. The results showed that there was a significant correlation between the contents of trace elements in soil and galangal. Trace elements yield a good inheritance between soil and galangal. Mg, Mn, Zn, Sb, Fe, Cu and Sr were the characteristic elements of Galangal by weight analysis. The geochemical tracer method could be used in research the effect of regional geochemical background on the products of origin.

Lead isotope ratios analysis result showed that the sources of lead in the soil profile and Galangal was very stable, lead isotope ratios of Galangal was very close to the distribution characteristics of soil region. $^{206}Pb/^{208}Pb$ -$^{206}Pb/^{207}Pb$ showed significant correlation further proves the product with soil were homology. Lead isotope could be used as the criterion of fingerprint identification of products of designations of origin.

[1] Rosman *et al*. (1998) *Environmental Research* **78,** 161-167. [2] Paul & Trevor (2007) *Geology* **28**, 627-630. [3] Chang *et al*. (2011) *Chinese Journal of Geochemistry* **30,** 138-144.

The project was supported by NSFC(40772201).

Weathering fluxes from time series sampling of the Irrawaddy and Salween Rivers

HAZEL CHAPMAN[1]*, MIKE BICKLE [1], SAN HLA THAW[2] AND HRIN NEI THIAM[2]

[1]Earth Sciences, University of Cambridge, Downing St. Cambridge CB2 3EQ, UK (*hjc1000@cam.ac.uk)

[2]Department of Meteorology & Hydrology, 50 Kaba-Aye Pogoda Rd, Mayangon 11061, Yangon, Myanmar

The Irrawaddy and Salween rivers in Myanmar Burma have water fluxes ~70% of the Ganges-Brahmaputra river system. Together these systems are thought to deliver about half the dissolved load from the tectonically active Himalayan-Tibetan orogen [1]. Previously very little data was available on the dissolved load and isotopic compositions of these rivers.

Here we present time series data of 171 samples collected fortnightly at intervals throughout 2005 to 2007 from the Irrawaddy and Salween at locations near the river mouths, the Irrawaddy at Myitkyina, the Chindwin, a major tributary of the Irrawaddy and a set of 28 small tributaries which rise in the flood plain of the Irrawaddy between Yangon and Mandalay. The samples have been analysed for major cation, anion, Sr and $^{87}Sr/^{86}Sr$ ratios. The new data indicates that the Irrawaddy has an average Na concentration only a third of the widely quoted single published analysis [2].

The catchment of the Salween extends across the Shan Plateau in Myanmar through the Eastern syntaxis of the Himalayas and into Tibet. The Irrawaddy flows over the Cretaceous and Tertiary magmatic and metamorphic rocks exposed along the western margin of the Shan Plateau and the Cretaceous to Neogene Indo-Burma ranges. The chemistry of the waters reflects these differences with the $^{87}Sr/^{86}Sr$ compositions of the Salween and Upper Irrawaddy (between 0.713 and 0.718) significantly higher than the downstream Irrawaddy (0.709 to 0.711) and the Chindwin (0.708 to 0.710). The Irrawaddy and the Chindwin exhibit lower $^{87}Sr/^{86}Sr$ and Na/Ca ratios during and immediately post-monsoon, interpreted to reflect higher weathering of carbonate at high flow (c.f. [3]). The Salween exhibits higher $^{87}Sr/^{86}Sr$ ratios but lower Na/Ca ratios during the monsoon, interpreted to reflect higher inputs from the upper parts of the catchment in the Himalayas.

[1] Robinson et al., (2007) *Journal of Geology* **115**, 629–640. [2] Meybeck & Ragu, (1997), UNEP (United Nations Environment Programme) *GEMS*, 245 pp. [3] Tipper et al., (2006) *Geochim. Cosmochim. Acta*. **70**, 2737–2754.

https://doi.org/10.1180/S0026461X00006502 Published online by Cambridge University Press

Complexation studies of EDTA with ^{99}Tc analogue rhenium

PAUL M. CHAPMAN, CLAIRE L. CORKHILL AND MARÍA ROMERO-GONZÁLEZ

Cell-Mineral Research Centre, Kroto Research Institute, The University of Sheffield, S3 7HQ, UK
(*correspondence: pmchapman2@sheffield.ac.uk)

Technetium-99 (^{99}Tc) is one of the important waste products formed during the nuclear fuel cycle. In oxidising conditions, ^{99}Tc exists as the highly mobile pertechnetate anion ($Tc(VII)O_4^-$), which has widespread environmental implications. When present in anoxic environments and in the presence of reducing species, it is expected that an insoluble solid oxide, $Tc(IV)O_2$, will form. Complexation of Tc(IV) with man-made and naturally occurring ligands is expected to increase environmental mobility.

The purpose of this investigation was to use a novel technique, Raman spectroscopy, to determine the complexation of rhenium, a non-radioactive analogue for ^{99}Tc, with ethylenediaminetetraacetic acid (EDTA) under oxic and anoxic conditions. EDTA is a common nuclear waste co-contaminant and has functional groups representative of much larger natural organic molecules.

In oxic and anoxic conditions, perrhenate ($Re(VII)O_4^-$) and EDTA were combined with HCl to attain pH values of 3.7, 6.5 and 10.3. Raman spectroscopy showed that the EDTA and perrhenate remained unchanged (e.g. 971cm^{-1} peak characteristic of the Re-O bond in a perrhenate anion was observed) at all pH values, indicating that no complexation had occurred.

Under highly acidic (pH 0.6) and anoxic conditions, *in situ* reduction of Re(VII) in the presence of EDTA resulted in an orange-yellow colour solution and a UV-VIS peak at 450nm, indicative of the formation of a Re(IV)-complex. Changes in the Raman spectrum of this solution also indicated complexation shifts of a CN stretch (to 1112cm^{-1}) and a COO^- vibration (to 1332cm^{-1}). Other Raman bands of the Re-EDTA complexes were also investigated for complexation shifts and binding mode information.

It has been shown that rhenium complexes to EDTA by *in situ* ligand reduction under very low pH conditions. Binding through the carboxylate and nitrogen groups of a tetradentate EDTA ligand to a mono-oxorhenium core is proposed. It is hypothesised that ^{99}Tc could complex under less harsh conditions in presence of ligands, which would prevent the formation of the precipitate $Tc(IV)O_2$ and hence increase the environmental mobility of ^{99}Tc.

H_2-rich fluids issued from the Kulo Lasi volcano, a new active hydrothermal field recently discovered in the South-West Pacific

J.L. CHARLOU*, J.P. DONVAL, C. KONN, V. GUYADER, Y. FOUQUET AND THE SCIENTIFIC PARTIES

Ifremer c/Brest, Laboratoire de Géochimie et Métallogénie, BP70, 29280, Plouzané
(*correspondance: charlou@ifremer.fr)

A lot of Back-arc basins (Fidji, Lau, Manus,…) investigated in the last 20 years revealed an intense hydrothermal activity. A new active vent field was recently discovered off-shore the Futuna island in an unexplored area during a French cruise (September 2010) from hydrothermal anomalies detected in the seawater column. High-temperature fluids were collected by the submersible Nautile from active vents located on a volcano (Kulo Lasi caldeira). The fluids exhibit temperatures of 343°C, pH of 2.36, low H_2S content (1-3 mM), variability in chlorinity (485 to 735 mM) and are enriched in Mg and SO_4. Mixing lines of elements vs Mg clearly reveal three types of fluids, all controlled by phase separation. Mg and SO_4 data in fluids also show a magmatic influence. Silica measurements show that the reaction zone is at a relatively low depth (~700 m). The fluids are poor in H_2S and CH_4 but enriched in CO_2 and H_2 and also contain a lot of organic compounds (see Konn *et al*., this meeting). The enrichment in CO_2 is explained by magmatic degassing from arc-magmas very rich in CO_2 compared to ridge-magmas, as previously shown in many active sites in back-arc basins. The generation of H_2 is explained by cristallization of the ascending magmatic basalt and by interaction of hot lava with seawater possible during the hydrothermal circulation. The Kulo Lasi fluids are compared to other fluids previously studied in various back-arc basins.

https://doi.org/10.1180/S0026461X00006502 Published online by Cambridge University Press

Oxygen dynamic in the Eastern South Pacific OMZ

JOSE CHARPENTIER[1]* AND OSCAR PIZARRO[2]

[1]Oceanographic center for the Eastern-South Pacific, COPAS, University of Concepción, Casilla 160-C, Concepcion, Chile (*correspondence: jcharpentier@profc.udec.cl)
[2]Department of Geophysics, Faculty of Physical and Mathematical Sciences, University of Concepción, Casilla 160-C, Concepcion, Chile (orpa@profc.udec.cl)

The eastern South Pacific holds one of the largest and most intense oxygen minimum zones (OMZ) of the world. This region also sustains a very high productivity and a unique ecosystem constrained by low oxygen concentration. To analyze the temporal evolution of the OMZ and relevant processes related to its biogeochemistry a monthly, ship-based, oceanographic time series have been maintained over the continental shelf off central Chile (~36.5º S) since 2002 [1]. During the last 2 years moored instruments have been added to this initiative including an ADCP to measure currents in the water column, and sensors of temperature and oxygen. Additionally several oceanic glider sections have been carried out along the same region.

Dissolved oxygen over the continental shelf is very low (typically lees than 0.5 mL L^{-1}) immediately below the mixing layer. Its temporal variability shows a marked seasonal pattern, mainly driven by upwelling events that predominate during austral spring-summer. The mechanism by which upwelling drives mid-water anoxia is not well known, but is greatly related to the supply of fresh nutrients to the photic zone, and to the advection of low-oxygen water from the north. Winter oxygen concentrations are usually larger in the water column and are related to downwelling events and to the increasing of fresh water discharge. These phenomena related to the dissolved oxygen variability off central Chile are discussed in this work based on observational evidences.

Data from moored instruments shows an interesting pattern that suggests upwelling (and downwelling) events affect oxygen concentration in "pulses" that occur in a temporal scale of days. Oxygen budget for the upper and lower layer of the water column shows that biological oxygen production in the mixed layer during spring-summer is almost equilibrated by biological oxygen consumption. Preliminary modeling results of the oxygen dynamics are also discussed.

[1] Ulloa, O. and S. Pantoja (2009) *Deep Sea Research Part II:* **56** 987-991 [2] Paulmier, A., D. Ruiz-Pino, V. Garçon, and L. Farías (2006) *Geophysical Research Letters* **33** L20601, doi:10.1029/2006GL026801

What real constraints do cherts bring on precambrian surface temperatures?

MARC CHAUSSIDON[1] , PHILIPPE LACH[2], FRANCOIS ROBERT[3], MARIE CHRISTINE BOIRON[3] AND BEATRICE LUAIS[1]

[1]CRPG-CNRS, Nancy Université, BP 20, 54501 Vandoeuvre-lès-Nancy, France (*correspondence: chocho@crpg.cnrs-nancy.fr).
[2]LMCM-CNRS-MNHN, 61 rue Buffon, 75231 Paris Cedex 5, France.
[3]G2R-CNRS, Nancy Université, Boulevard des Aiguillettes, B.P. 70239, 54506 Vandoeuvre-lès-Nancy, France

The extent of surface temperature change during the Precambrian is one of the key questions for the evolution of the Earth and the development of life. Solar physics dictates that the luminosity of the Sun was 25-30‰ lower than today in the early archean [1, 2]. Archean surface temperatures above the freezing point of water, as indicated by marine sediments of that age, were likely the result of enhanced concentration of greenhouse gases and/or decrease in Earth albedo or both [3, 4]. The low $\delta^{18}O$ values discovered in archean cherts of presumably marine sedimentary origin can be interpreted as reflecting very high surface temperatures 55-85°C during this period [5 and refs therein]. Contradictory lower temperatures have been infered from cherts and from thermodynamic stability fields of other minerals [6, 4]. Studies of Si isotopic compositions of cherts [7] and of micrometer scale distribution of $\delta^{18}O$ and $\delta^{30}Si$ values [8] allow to add independant constraints on seawater temperature and to define quantitative criteria to assess the origin of cherts (sedimentary or not) and the preservation of their isotopic signature. In addition it allows to propose a way to correct the inferred seawater temperature from isotopic fractionation taking place during the formation of chert upon diagenesis. Germanium concentrations (the partitioning of Ge between quartz and fluid is temperature dependant) in precambrian cherts show a range from ≈ 0.1 to ≈10 ppm (this study) which adds potentially another dimension to constrain the silica cycle and seawater temperatures in the precambrian.

[1] Gough D. O. (1981) *Sol. Phys.* **74**, 21-34. [2] Minton D. A. and Malhotra R. (2007) *Ap. J.* **660**, 1700-1706. [3] Kasting J. F. (1993) *Science* **259**, 920-926. [4] Rosing M. T. *et al.* 2010) *Nature* **464**, 744-747. [5] Knauth L. P. (2005) *Paleo3* **219**, 53-69. [6] Hren M. T. (2009) *Nature* **462**, 205-208. [7] Robert F. and Chaussidon M. (2006) *Nature* **443**, 969-972. [8] Marin J. *et al.* (2010) *Geochim. Cosmochim. Acta* **74**, 116-130. [8] Marin-Carbonne J. *et al.* in prep.

https://doi.org/10.1180/S0026461X00006502 Published online by Cambridge University Press

Ion microprobe high precision measurements of oxygen and magnesium isotopic compositions in extraterrestrial materials

MARC CHAUSSIDON AND CLAIRE ROLLION-BARD

CRPG-CNRS, Nancy Université, BP 20, 54501 Vandoeuvre-lès-Nancy, France
(*correspondence: chocho@crpg.cnrs-nancy.fr).

Two key isotope systems in cosmochemistry are oxygen isotopes (non mass dependent oxygen isotope variations, i.e. $\Delta^{17}O$, are ubiquitous in meteorites, especially in the high temperature components of chondrites) and Mg isotopes (^{26}Mg radiogenic excesses, i.e. $\delta^{26}Mg^*$, are due to the *in situ* decay of short-lived ^{26}Al with a half life of 0.73 Myr). Because of the presence of Al/Mg variations and of mineralogical variations in chondrites at the micrometer scale, ion microprobe is the only technique which offers the appropriate spatial resolution to unravel the $\Delta^{17}O$ and $\delta^{26}Mg^*$ systematic.

Recent developments using multicollectors ims 1270 and ims 1280 HR2 large radius Cameca ion microprobes allow to reach a precision (2 sigma error) better than 0.01 ‰ for $\delta^{26}Mg^*$ and better than 0.04‰ for $\Delta^{17}O$, for sputtered volumes of 20μm diameter and less than 1μm depth (in Mg-rich silicates and oxides).

Such high precisions transform the "traditional" O and Mg isotopes into "new" isotopic systems in meteorites. In the case of ^{26}Al for instance, the homogeneity of the distribution of ^{26}Al (which is a prerequisite to its use as a precise chronometer) can be quantified for the first time by comparing chondrules to the solar system Mg isotopic growth curve [1]. ^{26}Al model ages can be calculated in chondrules or in Al-free phases from their Mg isotopic composition [2]. These model ages in Mg-rich olivines from type I chondrules can be compared to high precision $\Delta^{17}O$ values to identify the origin of the olivines and to test whether they could be fragments of the mantles of planetesimals which differentiated very early in the disk [3].

[1] Villeneuve J., Chaussidon M., Libourel G. (2009) *Science* **325**, 985-988. [2] Villeneuve J., Chaussidon M., Libourel G. (2011) *Earth Planet. Sci. Lett.* **301**, 107-116. [3] Libourel G., Chaussidon M. (2011) *Earth Planet. Sci. Lett.* **301**, 9-21.

Average Nd-Hf isotopic compositions and model age of the upper continental crust

C. CHAUVEL[1], M. GARCON[1], N.T. ARNDT[1], S. GALLET[2] AND B.M. JAHN[2]

[1]ISTerre, BP 53, 38041 Grenoble Cedex 9, France
[2]Institute of Earth Sciences, Academia Sinica, Taipei, Taiwan

Establishing the average chemical and isotopic composition of the upper continental crust as well as its model age is difficult due to the diversity in compositions and ages of this major Earth reservoir. Estimates exist for major and trace elements as well as for some isotopic systems, but not for the Nd-Hf isotopic couple. In 1999, Vervoort *et al.* [1] defined the Nd-Hf "crustal array" and showed that Nd and Hf are correlated in crustal rocks of various ages and origins, but they could not define an average value.

Here we estimate the average composition of upper continental crust using two complementary types of sedimentary materials: (1) loess because they represent well-mixed materials from large areas of upper continental crust; (2) beach placers because they concentrate heavy and resistant minerals such as zircon and monazite. We determined the Hf and Nd isotopic compositions on samples from various locations in Western Europe, Tajikistan, China, Argentina, Africa, USA and Australia.

The loess have remarkably uniform Nd and Hf isotopic compositions and the average value plots on the "mantle array" within the field of crustal materials. Placers have more variable compositions linked to the age of the drained area. Indeed, samples from Europe, South Africa, Eastern Australia and USA have compositions comparable to the loess, but the Western Australian placers have significantly less radiogenic values due to the presence of Archean terranes in the source area.

Combining the constraints provided by the loess and the placers, we suggest that the following Nd and Hf characteristics: $\varepsilon_{Nd} = -10.3 \pm 1.2$ and $\varepsilon_{Hf} = -13.8 \pm 4.2$. The corresponding model age is 1.75 Ga, a value in the young side of other estimates.

[1] Vervoort *et al.* (1999) *EPSL* **168**, 79-99.

https://doi.org/10.1180/S0026461X00006502 Published online by Cambridge University Press

Mobility of rare earth elements during igneous rocks weathering and associated stream water transport (Malaval catchment, Massif Central, France)

L. CHAUX[1], T. ROUTIER[1], O. POURRET[1], M. STEINMANN[2] AND S. BONTEMPS[2]

[1]HydrISE, LaSalle Beauvais, 60026 Beauvais cedex, France (olivier.pourret@lasalle-beauvais.fr)

[2] UMR 6249 Chrono-Environnement, Univ. Franche-Comté, 25030 Besançon cedex, France

Rock alteration occurs within the critical zone at the interface between atmosphere, biosphere, hydrosphere and lithosphere. It is a major process within the global bio-geochemical cycle and contributes also to the evolution of landscapes. Chemical weathering dissolves partially or completely bedrock minerals to form weathering profiles, and dissolved ions are transported by surface and underground runoff to the oceans. In order to establish a link between the distribution patterns of the rare earth elements (REE) in stream water and bedrock, a detailed alteration study of the granitic, gneissic and basaltic bedrocks of a small mountain catchment was realized (Malaval catchment, Massif Central, France).

The mineralogy of fresh and weathered samples was determined by microscopy and XRD. Major and trace elements were determined by ICP-AES and ICP-MS. A comparison between the REE patterns of the more altered horizons of each profile and the < 0.22 μm water fraction of the Malaval stream has been realized in order to determine the influence of the different bedrocks on stream water chemistry [1]. Results suggest similar alteration mechanisms for granite and gneiss, which is mainly controlled by the dissolution of plagioclase leading to losses of Na_2O, CaO, SiO_2 and Al_2O_3. Mobilization of K_2O can be related to fracturing of K-feldpar, whereas the evolution of the REE patterns is mainly controlled by the distribution of zircon. In the alteration profiles on basalt, olivine is the first mineral to be altered into orange oxides leading to a mobilization of MgO. The transformation of plagioclase into clays is accompanied by losses of Na_2O and CaO. Lowered iron concentrations can be related to fracturing of pyroxene. A comparison between the REE patterns of the most altered horizons of the different weathering profiles suggests that water chemistry of the adjacent Malaval stream is mainly controlled by basalt weathering. In order to confirm this finding, sequential leachings have been performed on basalt samples and compared with stream water.

[1] Steinmann & Stille (2008) *Chem. Geol.* **254**, 1-18.

Spatial and temporal variability of fluid and gas chemical composition at the Lucky Strike hydrothermal vent site (Mid-Atlantic Ridge)

V. CHAVAGNAC, C. BOULART, C. MONNIN AND A. CASTILLO

Geosciences Environement Toulouse, 14 Avenue Edouard Belin, 31400 Toulouse, FRANCE (valerie.chavagnac@get.obs-mip.fr)

Numerous acidic submarine hydrothermal sites have been discovered, sampled and studied along the Mid-Atlantic ridge between 14ºN and 38ºN near the Azores hot spot. Most hydrothermal systems lie on basaltic substratum and only a few of them on ultramafic rock substratum. The Lucky Strike hydrothermal field was discovered in 1992 during the joint US-French FAZAR expedition on a volcanic segment at 37º50'N at 1700m water depth. The high-temperature hydrothermal fluids (up to 328ºC) have been collected in 1993 and 1994. The chemical composition of fluid and gas emitted at this site indicate variable chlorinities lower than seawater, low hydrogen sulfide, low metal concentrations and high gas contents. The distinct chemical end-members argue for a significant geographic control of the venting system and fluid chemistry is strongly affected by phase separation at depth.

The Lucky Strike hydrothermal field was visited during the BATHYLUCK and MOMARSAT cruises in 2009 and 2010, respectively, in order to assess the spatial and temporal variability of the hydrothermal fluid and gas chemical composition. Numerous fluid discharges on the western side the lava lake were collected as limited chemical were acquired thus far. A maximum temperature of 340ºC was measured at South Crystal. Based on the distribution of element concentrations, fluid chemistry is strongly affected by phase separation at depth as well as the geographic control of fluid plumbing system. Our results indicate that 3 different fluids are feeding the Lucky Strike field (1: Eiffel Tower, Montségur; 2: White Castle, Isabel, Cypress; 3: Y3, Nuno, Crystal, South Crystal, Sintra). The concentrations of CH_4 and CO_2 have increased since 1994 at Eiffel Tower, Sintra, Montségur and Y3, while the N_2 concentrations have all decreased significantly. The H_2 concentrations have stayed stable at Eiffel tower while increasing at Y3 but decreasing at Montségur. CH_4 is generated by water-rock interaction by Fischer-Tropsch caalysis of CO_2 reduction.

https://doi.org/10.1180/S0026461X00006502 Published online by Cambridge University Press

The noble gas and halogen composition of the hydrated oceanic crust

D. CHAVRIT[1]*, R. BURGESS[1], C. BALLENTINE[1], B. WESTON[1] AND D. TEAGLE[2]

[1]S.E.A.E.S, The University of Manchester, Manchester, UK (*correspondence: deborah.chavrit@manchester.ac.uk)
[2]National Oceanography Centre, University of Southampton, Southampton, UK

Mantle heavy noble gases have a remarkable similarity to those found in marine pore fluids [1,2]. This implies a significant contribution of these gases into the mantle recycled through subduction zones. In order to better constrain the quantity and character of noble gases available for subduction, we are reassing the major host phases of noble gases in pre-subducted material.

We have acquired, from different ODP sites, a sample suite that is representative of the altered oceanic crust. Noble gas (He, Ne, Ar, Kr and Xe) isotopes and abundances are being determined using crushing release measured with an upgraded VG5400 mass spectrometer.

Preliminary results from four altered basalts (ODP sites 504B and 1256D in the Southeast Pacific Ocean, respectively 5.9 and 15 Ma) show Ne to Xe isotopically identical to air. $^{3}He/^{4}He$ ratios are uniform at 6.82±0.42 (R/Ra). Heavy noble gas elemental ratios fall within a narrow range, with $^{130}Xe/^{36}Ar$ and $^{84}Kr/^{36}Ar$ ratios varying between seawater values and values enriched in Xe and Kr and indistinguishable from mantle values [1]. The range of $^{130}Xe/^{84}Kr$, varying by up to a factor 2.5, suggests that different trapping or fixation sites could control such compositions.

This is supported by an observed correlation of increase of the $^{132}Xe/^{36}Ar$ ratio relatively to $^{84}Kr/^{36}Ar$ with crushing step in the same sample, which does not seem related to air contamination. This could be representative of the different phases retaining different amounts of heavy nobles gases.

These measurements will be extended to include halogen determinations which are tracers of marine pore fluids and seawater interaction [2]. Analysing noble gases and halogens in basalts characterized by different alteration patterns and in gabbros and sediments will allow the identification of the noble gas host phases, as well as the controls of the seawater noble gases interaction with the oceanic crust.

[1] Holland & Ballentine (2006), *Nature* **441**, 186-191. [2] Sumino *et al*. (2010), *EPSL* **294**, 163-172.

Experimental constraints on magmatic wolframite

X. CHE[123], R.L. LINNEN[23] AND R.C. WANG[1]

[1]School of Earth Sciences and Engineering, Nanjing University, (xdche.nju@gmail.com)
[2]Dept. Earth Sciences, University of Western Ontario
[3]Dept. Earth & Enviromental Sci., Univ. of Waterloo

Wolframite is normally a hydrothermal mineral but at the Yaogangxian tungsten deposit, Hunan, China it also occurs as an apparent magmatic phase disseminated in a medium-grained two-mica granite. The magmatic wolframites are tabular crystals, hundreds of μm long, in planar contact with with magmatic K-feldspar and quartz. The major elements of magmatic wolframite are similar to hydrothermal crystals in quartz veins from the main zone of mineralization at the deposit. However, Zr, Nb, Ta and Mo are more abundant in magmatic wolframites compared to hydrothermal varieties.

The solubilities of synthetic hubnerite ($MnWO_4$) in flux-rich water saturated haplogranitic melts have been determined at 850° to 700°C and 2000 bars in order to test the magmatic hypothesis. The melts contain 1.1, 1.7 and 2.02 wt % of Li_2O, P_2O_5 and B_2O_3, respectively. Up to 6 wt% fluorine was added as AgF; the ASI of the melt is close to 1, but if Li is considered to be an alkali element, the melts are alkaline. Hubnerite solubility is weakly dependent on F. At 800°C the solubility products for hubnerite (*K*sp) range from $38x10^{-4}$ mol^2/kg^2 for a 0 wt% F melt to $69x10^{-4}$ mol^2/kg^2 for a 6 wt% F melt. Hubnerite solublity is strongly temperature dependent. *K*sp for a 6 wt% F melt decreases from $162x10^{-4}$ mol^2/kg^2 at 850°C to $17x10^{-4}$ mol^2/kg^2 at 700ºC. Another potential control on hubnerite solubility is $f_{O2.}$ The *K*sp is $38x10^{-4}$ mol^2/kg^2 at an f_{O2} near Ni-NiO, $53x10^{-4}$ mol^2/kg^2 using a Co filler rod and $69x10^{-4}$ mol^2/kg^2 using Ti filler rod (see [1] for approximate f_{O2} values). The weak variation of solubility with f_{O2} implies that the predominant oxidation state of W in the melts is +6, even at reduced conditions.

The above experimental solubilities are too high to support the magmatic wolframite hypothesis, however the melts in these experiments are alkaline and solubilities are lower in subaluminous compositions [2]. Because of the strong temperature dependence, magmatic wolframite may nevertheless occur in nature, but the melts should have crystallized at a low temperature and be subalkaline to peraluminous in composition.

[1] Matthews *et al*. (2003), *Amer. Mineral*. **88**, 701-707. [2] Linnen and Cuney, (2005), *Geol. Assoc. Can Short Course* Vol. **17**, 45-67.

https://doi.org/10.1180/S0026461X00006502 Published online by Cambridge University Press

Silica coatings on young Hawaiian basalts: Constraints on formation mechanism from silicon isotopes

S.M. CHEMTOB[1]*, J.A. HUROWITZ[2], Y. GUAN[1], K. ZIEGLER[3], J. M. EILER[1] AND G.R. ROSSMAN[1]

[1]California Institute of Technology, Pasadena, CA 91125 (*chemtob@gps.caltech.edu)
[2] Jet Propulsion Lab, Caltech;
[3] UCLA, Los Angeles, CA

Young basalts from Kilauea, on the big island of Hawai'i, frequently feature visually striking, white, orange and blue coatings, consisting of a 10-50 μm layer of amorphous silica, capped, in some cases, by a ~1 μm layer of Fe-Ti oxide [1]. The coatings provide an opportunity to study the early onset of acid-sulfate weathering, a process common to many volcanic environments. Silicon isotopes fractionate with the precipitation of clays and opaline silica, and have been demonstrated to be an indicator of weathering intensity [2,3]. Here we report *in situ* measurements of δ^{30}Si of the silica coatings and their implications for coating formation.

The analyzed coated basalt was collected from 1997 overflow lavas at the rim of the Pu'u O'o cone. The sample was mounted in cross section. Analyses were conducted on a Cameca 7f-Geo ion microprobe with a O^- primary beam (~30 μm spot) and two Faraday cups. The silica coating was measured against the Rose Quartz standard (RSQ). We tested whether the coating's amorphous structure introduced a matrix effect by analyzing quartz and fused glass of the same composition (Ge214). Measurements of those materials were the same within error, so although we have not ruled out other relevant matrix effects (e.g. water content), we accept RSQ as a viable standard for analyzing amorphous silica.

The silica coating was determined to have δ^{30}Si = -1.8 ± 1.0‰ (2σ). Hawaiian basalts have δ^{30}Si ≅ -0.5‰ [2], so the silica coatings are ~1‰ lighter than the substrate. The sign of this fractionation is consistent with previously reported values for secondary silica [2-4], and implies that, although the silica coatings have a residual/leaching morphology [1], Si was mobile during coating formation. Basalt dissolved in acidic solution, then a fraction of aqueous Si precipitated as amorphous silica; the remaining dissolved Si (tens of percent) was lost from the system. Ongoing work includes confirmation of the SIMS analysis by ICP-MS and replication of observed coating morphologies and isotopic properties in flow-through alteration experiments.

[1] Chemtob *et al*. (2010), *JGR* **115**, 2009JE003473. [2] Ziegler *et al*. (2005), *GCA* **69**, 4597-4610. [3] Georg *et al*. (2007), *EPSL* **261**, 476-490. [4] Douthitt (1982) *GCA* **46**, 1449-1458.

Origin of the late Mesozoic high-Mg diorites from the North China Craton: Petrological and Os isotopic constraints

B. CHEN*[1,2], C. WANG[2], A.K. LIU[2] AND L. GAO[2]

[1]College of Geology & Prospecting Engineering Program, Xinjiang University, Urumqi 830046, China (*correspondence: binchen@pku.edu.cn)
[2]School of Earth and Space Sciences, Peking University, Beijing 100871, China

The Mesozoic Tietongou & Jinling high-Mg dioritic plutons from the north China craton contain plagioclase (45-55%), hornblende (20-40%), Cpx (10%) and minor Opx, olivine, biotite, quartz, and accessory sphene, magnetite and apatite. The diorites (SiO_2 = 52-63%) show high MgO (9.2-3.5%), Sr (470-980 ppm), Ni (15-157 ppm), Cr (35-416 ppm) and Co (20-35 ppm), with I_{Sr} = 0.7052-0.7083 and $\varepsilon_{Nd}(t)$ = -4.5 to -15. The contradictory geochemical features of the high Sr and high compatible Ni, Co and Cr are reminiscent of the sanukitoids of late Archean times.

Traditionally, the Tietongou and Jinling high-Mg dioritic plutons were suggested by most workers to have originated from partial melting of the eclogitized Archean mafic lower crust delaminated to mantle depths due to crustal thickening, followed by interaction of the resultant dioritic melts with mantle peridotites during magma ascent, during which the melts gained additional MgO. However, our petrological and Os isotopic data suggest that the dioritic plutons formed from a process of magma mixing between basaltic magma and granitic crustal melt formed due to underplating of the basaltic magma in the lower crust. In this model, no crustal thickening and delamination of the lower mafic crust is required. Main arguments are as below. (1) Plagioclase shows compositional and textural disequilibrium, as revealed by the eroded calcic core (An_{78-60}) surrounded sharply by a mantle with much lower An contents (38-16), which is typical of magma mixing between mafic and felsic magmas. (2) Hornblende shows complex compositional zoning, with low TiO_2 zones (0.8%) surrounded by high TiO_2 zones (2.7%), suggesting an input of high temperature basaltic magma during magma evolution. This agrees with the complicated compositional zoning of Cpx. Opx is always rimmed by Cpx, indicating a reaction relationship. This, along with the presence of millimeter-scale relict aggregates of olivine + Opx, suggests that the dioritic plutons are actually mixture of melts plus xenoliths. (3) The dioritic plutons have Os isotopic ratios in the range 0.33-1.22. If the dioritic plutons were formed by interaction of the melts from the delaminated Archean lower crust with mantle rocks, the required proportions of the latter would be unreasonably high (30-85%). The Os isotopic data can be reasonably explained by our magma mixing model: the majority of the dioritic plutons were basaltic magma from an enriched mantle source, which mixed with subordinate crustal melts (9-35%) in the lower crust.

https://doi.org/10.1180/S0026461X00006502 Published online by Cambridge University Press

Hydrothermal circulation and post-obduction hydration & carbonation of oceanic lithosphere - $^{87}Sr/^{86}Sr$ and oxygen isotopic study of Oman ophiolite

C. CHEN*, C. ANDRONICOS, L.M. CATHLES AND W.M. WHITE

Department of Earth and Atmospheric Sciences, Cornell University, Ithaca, NY 14853
(*correspondance: cc839@cornell.edu)

We report whole-rock isotopic analyses on 33 samples collected from Nakhl, Sumail and Wadi-Tayin nappes of Oman ophiolite, sampling a transect from upper gabbros to the Moho Transition Zone. $^{87}Sr/^{86}Sr$ and $\delta^{18}O$ varied as follows: (1) upper gabbros: $^{87}Sr/^{86}Sr$ 0.7032~0.7080, $\delta^{18}O$ 2.4~6.3; (2) middle gabbros: $^{87}Sr/^{86}Sr$ 0.7031~0.7060, $\delta^{18}O$ 5.3~6.1; (3) lower gabbros: $^{87}Sr/^{86}Sr$ 0.7031~0.7064, $\delta^{18}O$ 3.4~6.7; (4) Moho peridotites and carbonates, $^{87}Sr/^{86}Sr$ 0.7035 ~ 0.7086, $\delta^{18}O$ 2.95 ~ 30.57. These data together with petrographic studies confirmed that the entire ophiolite section below sheeted dikes was subjected to >300°C hydrothermal alteration during its formation and that locally temperatures exceeded 500°C. High $\delta^{18}O$ and $^{87}Sr/^{86}Sr$ in excess of Cretaceous seawater (0.7079) clearly show that serpentinization and carbonation of the ophiolite have also occurred post-obduction. Four out of five samples with $^{87}Sr/^{86}Sr > 0.7079$ are from Moho Transition Zone: two samples magnesite rocks with $\delta^{18}O$ ~30, the other two are serpentinites with $\delta^{18}O > 7$. One tiger gabbro has $^{87}Sr/^{86}Sr$ of 0.7080 and $\delta^{18}O$ of 2.4. Leaching experiments show that the radiogenic Sr is not restricted to carbonate vein minerals. Thus original isotopic information is easily overprinted by the late stage processes if the peridotites are entirely altered into serpentinites or carbonates. On the other hand, gabbros, which have cracks filled with carbonates but not fully altered, can preserve hydrothermal alteration information during formation.

Atoll garnet in the Yukahe UHP eclogite: Evidence for melt/fluid activity during the eclogitic facies metamorphism

D.L. CHEN, L. LIU AND X.M. LIU

State key Laboratory of Continental Dynamics, NW Univ., Xi'an, 710069, PR China. (dlchen@nwu.edu.cn)

The typical mineral assemblage of the Yukahe eclogite from the North Qaidam in NW China is Grt+Omp+Phen+Rt+Coe. Garnets in the eclogite show two shapes of normal porphyroblast garnet and atoll texture garnet. In which, the normal garnet cores contain mineral inclusions of Pl, Amp, Ap, Zoi, Ep and Qz, and change into Omp, Phen and Rt in the mantles, the rims are clean with few inclusion. EMP analyses revealed a compositional zoning with a bell-shaped decrease of Spe and a bowl-shaped increase of Pyr content towards the rim and a small decrease of Pyr in the outmost rims. The atoll garnets commonly consist of a euhedral ring and a island/peninsula core of garnet, eclogite facies multiphase solid inclusions of Omp, Phen, Grt, Rt and Qz filled between the core and the ring. In a few cases the garnet core is totally missing and filled with a single Phen. The island cores contain the same mineral inclusions as those of in the normal garnet cores; the garnet rings, like the rims of the normal garnet, are clean without any inclusions. A successive compositional zoning with Spe content decrease and Pyr content increase were revealed from the core to the ring, similar to that of the normal garnets. Omp and Phen occur in the matrix and within the atoll have almost the same composition. EBSD analyses demonstrate that the island/ peninsula garnet cores or fractions inside atolls have crystallographic orientations identical to that of the atoll rings. LA-ICP-MS analyses indicate that Omps in both the matrix or within the atoll display the same REE patterns with a peak in MREEs and a pronounced depletion in both LREEs and HREEs. Whereas, the rings of the atoll garnet, ralitive to the core, show a distinct enrichment in MREEs and a visible depletion in HREEs. The mineral assemblage and their composition within atoll garnet are as same as that of the peak metamorphism of the Yukahe eclogite except for Coe, combined with the existing geochemical and chronological studies of leucosomes interbeded with the UHP eclogite body, it suggests that atoll garnets in the Yukahe eclogite formed under eclogite facies conditions during almost the peak metamorphism. It provides good evidence for melt/fluid activity during UHP metamorphism.

https://doi.org/10.1180/S0026461X00006502 Published online by Cambridge University Press

Provenance of early sedimentary sequences in the Tethyan Yunnan, SW China: Age and Hf isotope of early Archean zircons

F. CHEN [1], B.-X. LIU [1], S.-Q. LI [1] AND W. SIEBEL [2]

[1]CAS Key Laboratory of Crust-Mantle Materials and Environments, University of Science and Technology of China, Hefei 230026, China

[2]Institut für Geowissenschaften, Universität Tübingen, 72074 Tübingen, Germany

This study presents U-Pb ages and Hf isotopic composition of detrital zircons from Cambrian to Ordovician sedimentary rocks exposed in the Tethyan belt of western Yunnan, SW China. This orogenic belt belongs to the eastern Tethyan belt in SW Asia. It is composed of several micro-continents or continental block of different affinities.

The early Paleozoic sedimentary rocks, collected from the Baoshan block, contain detrital zircons of different crystallization ages ranging from about 3800 Ma to 550 Ma ($^{207}Pb/^{206}Pb$ age), but mostly clustering around 1.0 Ga and 2.4 Ga. About 10% zircon grains yield $^{207}Pb/^{206}Pb$ ages older than 3.0 Ga Ma, indicating significant sedimentary source(s) of early Precambrian crustal material. Initial εHf values of the detrital zircons vary from -34 to +15, while TDM values of zircons, calculated from Lu-Hf isotopic composition, range from about 1.0 Ga to 4.0 Ga with peaks around 1.8 Ga and 2.8-3.0 Ga. Their Nd isotopic composition of whole-rocks (TDM values from 1.8 Ga to 2.5 Ga) also imply significant put-in of old crustal material.

The Baoshan block is considered as the northern part of the Sibumasu microcontinent in the eastern Tethyan orogenic belt. From the analytical results of detrital zircons above, we propose that the sedimentary sources of the early Paleozoic sequences in the western Yunnan originated from Archean and Paleoproterozoic terrains most likely in India and NW Australia.

A study of the column bioleaching of Xianshan uranium ore

GONGXIN CHEN [1,2]*, JINHUI LIU [1] AND ZHANGXUE SUN [1]

[1]East China Institute of Technology , Fuzhou 344000 , China (*correspondence: gxchen@ecit.edu.cn)

[2]China University of Geosciences, Beijing 100083 , China

The samples of uranium ore were obtained from the U mine at Xianshan, Jinagxi Province (China). Quantitative chemical analysis showed that the uranium ore had a mediate carbonate content (CO_2~1.42%), that pyrite was the most important sulphur mineralization (~1.43%) and that the principal components were silicates. The most common uranium mineralization in the vein, pitchblende, appears as UO_2. The particle size of the ore is less than 10mm. Acidithiobacillus ferrooxidans, Leptospirillum ferrooxidans and Acidithiobacillus thiooxidans isolated from the mine waters of the Xianshan uriamium depoist were used in this bioleaching experiment.

The column was made of PVC with 300cm heigh and 80cm diameter. Once the column was fully charged, it was irrigated with 20g/L H_2SO_4 about 20 days to reach the correct degree of acidity, after which the inoculum was introduced and irrigation continued until the end of the experiment. Sample volumes of liquid were extracted periodically and the pH and redox potential (Eh) were measured. The U_30_8, Fe_{Total}, and Fe^{2+} content were also analyzed.

Mixed bacteria play an important role in the leaching process. In 120 days, the recovery of pyrite leaching is about 70%, and of uranium is up to 90%. Acid consumption is very low, about 6.8%. Results also show that U leaching and pyrite leaching are closely related during bioleaching. With the increase of pyrite leaching recovery, uranium leaching recivery is also increased. Due to some pyrite in U mine, biological leaching have good benefit to extract U from the ore compared with those traditional leachings such as heap leaching with acid and stirring tank leaching with MnO_2.

This study is financially supported by Foundation of Jiangxi Educational Committee for Youths (GJJ11155).

https://doi.org/10.1180/S0026461X00006502 Published online by Cambridge University Press

Precise determination of the Ca isotopic compositions by thermoionization mass spectromery

H.-W. CHEN[1]*, J.-C. CHEN[1], J.J. SHEN[1], D.-C. LEE[1] AND T. LEE[12]

[1]Institute of Earth Sciences, Academia Sinica, Taipei, Taiwan, ROC (*correspondence: haart@earth.sinica.edu.tw)
[2]Institute of Astronomy and Astrophysics, Academia Sinica, Taipei, Taiwan, ROC

High precision Ca isotopic measurements have been set up using the thermo ionization mass spectrometry (TIMS). With the improved sample loading technique, it is possible to sustain a Ca ion current of 1.5~3nA for more than an hour for high precision Ca isotopic measurements. Using this procedure, typical analytical precision (2σ) for $^{40}Ca/^{44}Ca$, $^{43}Ca/^{44}Ca$, $^{46}Ca/^{44}Ca$, and $^{48}Ca/^{44}Ca$ are 1.6, 0.31, 7.5, and 0.68 epsilon (ε; in parts per 10^4), respectively, after normalizing to $^{42}Ca/^{44}Ca = 0.31221$ [1]. Four separate runs are usually taken for individual sample to ensure the reproducibility of the isotopic measurements, and the analytical uncertainty (2σ) can be further reduced to 0.87, 0.13, 4.6, and 0.42ε for $^{40}Ca/^{44}Ca$, $^{43}Ca/^{44}Ca$, $^{46}Ca/^{44}Ca$, and $^{48}Ca/^{44}Ca$, respectively, if the data of all four runs are combined. With the improved analytical precision, in particular for the less abundant ^{43}Ca and ^{48}Ca, it is possible to re-examine the Ca isotopic heterogeneity in terrestrial and meteoritic materials, and to explore the preserved non-linear stellar nucleosynthetic signatures in meteorites and homogenization process in the early solar system.

[1] Russell *et al*. (1978) *GCA* **42**, 1075-1090.

Interaction of NOM and NZVI: Implication for NZVI's toxicity and reactivity in the environment

JIAWEI CHEN[1,2]*, ZONGMING XIU[2], GREGORY V. LOWRY[3] AND PEDRO J. J. ALVAREZ[2]*

[1]State Key Laboratory of Geological Process and Mineral Resources, China University of Geosciences, Beijing 100083, China (*correspondence:chenjiawei@cugb.edu.cn)
[2]Dept. of Civil & Environmental Engrg., Rice University, Houston, TX 77005, USA
[3]Dept. of Civil & Environmental Engrg., Carnegie Mellon University, Pittsburgh, PA 15213, USA

Nano-scale zero-valent iron (NZVI) particles are increasingly used to remediate aquifers contaminated with hazardous oxidized pollutants such as trichloroethylene (TCE). However, the high reduction potential of NZVI can result in toxicity to indigenous bacteria and hinder their participation in the cleanup process. Here, we report on the mitigation of the bactericidal activity of NZVI towards gram-negative *Escherichia coli* and gram-positive *Bacillus subtilis* in the presence of Suwannee River humic acids (SRHA), which were used as a model for natural organic matter (NOM). *B. subtilis* was more tolerant to NZVI (1 g/L) than *E. coli* in aerobic bicarbonate-buffered medium. SRHA (10 mg/L) significantly mitigated toxicity, and survival rates increased to similar levels observed for controls not exposed to NZVI. TEM images showed that the surface of NZVI and E. coli was surrounded by a visible floccus. This decreased the zeta potential of NZVI from -30 to -45 mV and apparently exerted electrosteric hindrance to minimize direct contact with bacteria, which mitigated toxicity. H_2 production during anaerobic NZVI corrosion was not significantly hindered by SHRA ($p > 0.05$), However, NZVI reactivity towards TCE (20 mg/L), assessed by the first-order dechlorination rate coefficient, decreased by 23% (from 0.0178 ± 0.0007 h^{-1} to 0.0137 ± 0.0004 h^{-1}). These results suggest that the presence of NOM offers a tradeoff for NZVI-based remediation, with higher potential for concurrent or sequential bioremediation at the expense of partially inhibited abiotic reactivity with the target contaminant [1].

This study was sponsored by the USEPA (R833326), the Fundamental Research Funds for the Central Universities (2010ZD14, 2010ZD13), National Program of Control and Treatment of Water Pollution (2009ZX07424-002), Program for New Century Excellent Talents in University (NCET-07-0769), and China Geological Survey (Ke [2011]-01-66-07).

[1] Chen *et al*. (2011) *Water Research* **45**, 1995-2001.

Research on pretreatment of highly concentrated dye-printing wastewater using surplus sludge together with powder ash

JINGYING CHEN

Department of Civil and Environmental Engineering, East China Institute of Technolog, Fuzhou344000, China (cjy006@163.com)

The pretreatment craft is extremely essential in the processing of dye-printing waste water. Using surplus sludge together with the powder ash as the flocculants to pretreat highly concentrated dye-printing wastewater, which leads to the remarkable reduction of the discharge monitoring index in the wastewater — chroma, the suspended solid and the chemical oxygen demand.[1]

This article has conducted the experimental study uses surplus sludge together with the powder ash as the flocculants to pretreatment highly concentrated dye-printing waste water. The results show that through control the volume ratio of the surplus sludge and coal ash, static time and so on, when the volume ratio is the dye-printing waste water/Surplus sludge/coal ash =60: 1: 8, and the static time between 20 ~ 40 minutes, there is a remarkable reduction of the discharge monitoring index in the waste water–chroma and the chemical oxygen demand. The finding provides the experiment basis for reducing the consequent biochemical treatment loads effectively reducing the running cost for highly concentrated dye-printing waste water disposal exploring the industrialized technical designing direction and the way on using the waste to deal with the waste.

[1] Zheng Z, Xu J , Sun Y Y, *et al*. Synthesis and chiroptical properties of optically active polymer liquid crystals containing azobenzene chromophores [J]. *Poly Science*, 2006, **44** (10) : 3210- 3219.

Mass-dependent fractionation and mass-independent fractionation of Hg isotopes in aqueous environment

JIUBIN CHEN[1,2], HOLGER HINTELMANN[2] AND XINBIN FENG[1]

[1]State Key laboratory of Environmental Geochemistry, Institute of Geochemistry, Chinese Academy of Sciences, 46 Guanshui Road, Guiyang, GuiZhou 550002, China

[2]Chemistry Department, Trent University, 1600 West Bank Drive, Peterborough, Ontario, K9J7B8, Canada

Preliminary studies have demonstrated both mass-dependent fractionation (MDF) and mass-independent fractionation (MIF) of Hg isotopes in the environment (1) and the potential for their application in biochemistry and geochemistry. However, the majority of previous work has focused either on developing reliable MC-ICP-MS measurements or on monitoring isotopic variation of Hg in solid samples and in Hg-enriched synthetic solutions. Little has been reported for Hg isotope geochemistry in natural aqueous environment because of the very low Hg concentrations (several ng/L).

Precipitation samples and water samples from different aquatic systems (remote lakes, contaminated rivers, groundwater) were analyzed for Hg isotopic composition after pre-concentration using a new pre-concentration method (2). The results displayed evident MDF and MIF of Hg isotopes in natural aqueous environment. All samples displayed a total δ^{202}Hg variation of 2.42‰ (-1.68‰ to 0.74‰), with lower values for precipitation and lake waters and higher values for contaminated river waters. Unlike waters from contaminated rivers, precipitation samples displayed positive MIF of odd Hg isotopes, contrast to the predicted result from previous studies. Moreover, our results confirmed the observation of MIF of odd Hg isotopes (^{200}Hg) in precipitation samples (3), implying that the (atmospheric) process introducing the MIF for even Hg isotopes may be different from that producing MIF of odd isotopes in the aqueous environment. More research is required to fully understand the behavior of Hg isotopes in the hydrosphere.

[1] Bergquist, B. *Sci*. 2007; [2] Chen J-B. *JAAS,* 2010**;** [3] Gratz, L. *EST* 2010.

https://doi.org/10.1180/S0026461X00006502 Published online by Cambridge University Press

The evidences of the Initial broken for the Shangdan Ocean: Geochronology and geochemistry of the Muqitan Formation, in North Qinling

JUN-LU CHEN, XUE-YI XU, HONG-LIANG WANG AND PING LI

Xi'an Center of Geological Survey(Xi'an Institute of Geology and Mineral Resource), CGS, Xi'an, Shaanxi 710054, China

The Muqitan ophiolitic mélange found within the Muqitan Formation near Muqitan region, the North Qinling Orogen. They mainly consist of amphibolite with minor meta-gabbro and meta-chert. Zircon LA-ICP-MS U-Pb dating yields an age of 762.5±4.6Ma for the amphibolites, interpreted as crystallization time, The amphibolites are characterized by low TiO_2 (0.57%~2.16%), relatively low K_2O/Na_2O ratios (0.06~0.55) and moderate-high Mg# (45.3~68.7). They are geochemically similar to low-Ti tholeiites. The Muqitan amphibolites have low REE contents, with differentiated LREE/HREE patterns and no Eu anomalies on the chondrite-normalized REE diagram, analogies to E-MORB. The amphibolites display an enrich elements Rb, Ba,Th, and La pattern, low ($^{87}Sr/^{86}Sr$)i ratios of 0.7038 to 0.7040 and high εNd(t) values of +4.1 to +6.9, suggesting a mantle origin, similar in composition to FOZO-like source. Their (Th/Nb)N, Nb/La and Ba/La ratio features indicate that these amphibolite have been experienced varying degrees of crustal contamination. All these data, combined with the regional geological features demonstrate that the Muqitan amphibolites are interpreted as remnants of the Shangdan ancient oceanic crust that would have formed during the inception of the oceanic open at ca. 762.5 ±4.6Ma.

Acknowledgment: This study was supported by the National Natural Science Foundation of China (Grant No. 40972150)

Deposition and remobilization of oxidized multiwalled carbon nanotubes on silica surfaces: Implications for environmental fate and transport

KAI LOON CHEN* AND PENG YI

Department of Geography and Environmental Engineering, Johns Hopkins University, Baltimore, Maryland 21218 (*correspondence: kailoon.chen@jhu.edu, peng.yi@jhu.edu)

Carbon nanotubes (CNTs) are increasingly used in commercial and industrial applications because of their superior mechanical and electronic properties. With CNT-containing products already available in the market, it is inevitable that some CNTs will be released into natural aquatic systems. In order to predict the fate and transport of CNTs in surface water and groundwater systems, it is important to understand the interaction between CNTs and natural surfaces. In this study, we investigate the deposition and remobilization of oxidized multiwalled carbon nanotubes (MWNTs) on silica surfaces with a quartz crystal microbalance with dissipation monitoring (QCM-D). The distributions of oxygen-containing surface functional groups for two MWNTs are determined using X-ray photoelectron spectroscopy in conjunction with vapor phase chemical derivatization. Deposition kinetics of lowly oxidized MWNTs (LO-MWNTs) and highly oxidized MWNTs (HO-MWNTs) are compared in monovalent (NaCl) and divalent ($CaCl_2$) electrolytes. HO-MWNTs are found to be more stable to deposition than LO-MWNTs in the presence of NaCl. However, in the presence of $CaCl_2$, the attachment efficiency profiles of both MWNTs are comparable, which is possibly due to Ca^{2+} cations having a higher affinity to form complexes with adjacent carboxyl groups on HO-MWNTs than with isolated carboxyl groups on LO-MWNTs. Additionally, the deposited MWNTs can be released from silica surfaces when they are rinsed with low ionic strength solutions, indicating that the deposition of MWNTs is not always irreversible. The degree of nanotube release is observed to be dependent on the ionic strength and pH of rinsing solutions.

https://doi.org/10.1180/S0026461X00006502 Published online by Cambridge University Press

DIE model and compensation method applied in through-casing resistivity measurement

CHEN QING

CEEE of Huazhong University of Science and Technology, 430074Wuhan, China

Double-Injection-Electrodes (DIE) model and its compensation arithmetic method has been proven to be very useful for eliminating the errors caused by electrode-scale mechanical tolerances in formation resistivity measurement through metal case. In this paper, we found that even minor casing joint or casing corrosion may deteriorate the measurement accuracy. Based on theoretical analysis and self-adaptive goal oriented hp-Finite Element (FE) simulations, the compensation effects of DIE model were estimated. The calculated results from DIE model are always close to the real formation resistivity no matter the metal casing is ideal or not. Meanwhile, large errors occur in Single-Injection-Electrode (SIE) model, where the calculated formation resistivity may provide negative numbers when casing joint or casing corrosion exists. The Double-Injection-Electrode (DIE) model is predicted to have good compensation effects to many non-ideal situations with uneven metal casing besides electrode-scale mechanical tolerances.

Timing of dehydration melting and fluid flow during continental subduction-zone metamorphism in the Dabie orogen

REN-XU CHEN* AND YONG-FEI ZHENG

School of Earth and Space Sciences, University of Science and Technology of China, Hefei 230026, China (chenrx@ustc.edu.cn)

Dehydration melting of UHP metamorphic rocks and the possible presence of supercritical fluid during continental subduction-zone metamorphism has been revealed by microscale observations of petrology and geochemistry. However, a direct geochronologic constraint on partial melting and fluid supercriticality is still lacking. This study reports for the first time the outcrop-scale occurrence of migmatite-like structure within UHP eclogite in the Dabie orogen. Leucocratic veins and their host rocks were investigated by means of petrology and zirconology. Metamorphically grown zircons from the veins yield consistent U-Pb ages of 215±4 to 218±4 Ma; zircon trace elements indicate that they crystallized in the presence of garnet or amphibole. Ti-in-zircon and Zr-in-rutile thermometers gave variable temperatures from 537 to 758°C. Thus the veining occurred in the stage of transition from HP eclogite-facies to amphibolite-facies retrogression during exhumation of the deeply subducted continental crust. On the other hand, based on the paragenesis and trace element composition of vein minerals, vein-forming fluids are mainly composed of SiO_2 + Al_2O_3 + CaO + K_2O + FeO + MgO + H_2O and enriched in LREE, HREE, HFSE, LILE, and Pb, Th and U. The enrichment of HREE and HFSE suggests that the fluids have very high capacity of dissolving water-insoluble elements, pointing to the possible presence of supercritical fluid. While the supercritical fluid is stable in the UHP regime, it would separate into a hydrous melt and an aqueous fluid during the decompression exhumation into the HP eclogite facies. As a consequence, the vein minerals rich in the trace elements would precipitate as a product of phase separation. Thus, the dehydration melting of UHP metamorphic rocks is considered as the prerequisite for local formation of supercritical fluid in the UHP regime, whereas the phase separation of supercritical fluid during the exhumation is suggested as the basic cause for differential partition of trace elements between rock-forming and accessory minerals in the veins. Therefore, the zircon U-Pb dates on the leucocratic veins provide a temporal constraint on the lower limit of local melting during the continental collision.

https://doi.org/10.1180/S0026461X00006502 Published online by Cambridge University Press

Fungal spore contributions to subtropical aerosol particles

S.-H. CHEN AND G. ENGLING*

Department of Biomedical Engineering and Environmental Sciences, National Tsing Hua University, Hsinchu 300, Taiwan (*correspondence: guenter@mx.nthu.edu.tw)

Primary Biological Aerosol Particles (PBAPs), as derived from pollen, fungi, bacteria, viruses, algae, and plant fragments, have recently been shown to contribute sizeable portions of atmospheric particulate matter (PM) on global scale, specifically in coarse mode particles [1, 2]. Fungal spores in particular constitute an important type of PBAPs [3, 4]. A new method for estimating PBAP contributions was introduced by Bauer and coworkers by utilizing molecular source tracers, i.e., the polyols arabitol and mannitol [5]. While conversion factors from ambient tracer concentrations to fungal spore mass have been determined for a continental location in Europe [4, 5], there are no reports to date regarding the tracer characteristics of different types of fungal spores in other areas and specifically in Asia.

Our recent investigations have shown that fungal spore content in coarse PM can be rather high in tropical regions with contributions up to 26% of organic carbon and up to 18% of PM_{10} [6]. Ambient conditions, such as temperature and moisture, influence biological activity, including fungal spore release rates. Moreover, fungi species in different locations likely have varying polyol content. Therefore, it is crucial to determine the absolute and relative abundance of individual polyol tracers in different fungi species (i.e., source samples), as well as the concentrations of these tracers in ambient PM as a function of environmental conditions.

In order to address these open questions, size-resolved PM samples were collected at various sites across Taiwan, including coastal, urban, rural and high-altitude sites. In addition, various types of fungi were cultured. The polyol tracers arabitol and mannitol, along with other carbonaceous species, were quantified in the ambient and source samples by high-performance anion exchange chromatography (HPAEC). New insights into the size-dependent composition of fungal spore tracers in subtropical PM and in specific fungi species will be presented here.

[1] Jaenicke *et al*. (2007) *Env*. *Chem*. **4**, 217-220. [2] Heald & Spracklen (2009) *Geophys*. *Res*. *Lett*. **36**, L09806 [3] Elbert *et al*. (2007) *Atmos*. *Chem*. *Phys*. **7**, 4569-4588. [4] Bauer *et al*. (2008) *Atmos*. *Env*. **42**, 5542-5549. [5] Bauer *et al*. (2008) Atmos. Env. **42**, 588-593. [6] Zhang *et al*. (2010) *Env*. *Res*. *Let*. **5**.

Hf-Nd isotope variations of late Cenozoic Arctic intermediate water reflect continental weathering

TIAN-YU CHEN[1], MARTIN FRANK[1] AND ROBERT F. SPIELHAGEN[1,2]

[1]IFM-GEOMAR, Leibniz Institute for Marine Sciences, Wischhofstrasse 1-3, 24148 Kiel, Germany (tchen@ifm-geomar.de; mfrank@ifm-geomar.de; rspielhagen@ifm-geomar.de)

[2]Academy of Sciences, Humanities and Literature, 55131 Mainz, Germany

The late Cenozoic glaciation history of the Arctic is important for understanding the global climate system and feedback mechanisms. However, such information from the Arctic basin itself is limited. The combined Hf-Nd isotope composition of past seawater in high latitudes has been suggested as a proxy for changes in intensity and regime of continental weathering due to fractionation processses as a function of weathering regime.Enhanced physical weathering during glaciations is expected to cause a more congruent release of Hf weathered from continental rocks. So far, there are, however, no records from the Arctic basin. We extracted combined seawater-derived Nd-Hf isotope compositions from the authigenic Fe-Mn oxyhydroxide fraction of two sediment cores recovered on Lomonosov Ridge (PS2185, ACEX), in order to reconstruct weathering regime and past circulation.

We produced ε_{Nd} (~-10.5) and ε_{Hf} (~0.4) signatures of AIW from the core-top sediments, which agree well with previously reported values directly determined on nearby water samples of AIW. Over time, Hf isotopes have in general become less radiogenic since 16 Ma, which is not observed for Nd isotopes. Similar to Nd isotopes, clear glacial-interglacial variations of Hf isotopic compositions were also observed in the late Quaternary, with more radiogenic Hf isotope signatures in glacial stages and less radiogenic Hf isotope compositions during interglacial stages. Unlike Nd isotope compositions of AIW, which are at present dominated by current inputs from the North Atlantic, Hf isotope signatures of AIW are apparently more influenced by input from local shelf sediments and surrounding rivers. Our interpretation for the long term Hf isotopic evolution is that they reflect progressively more congruent weathering of rocks of the continents surrounding the Arctic Ocean, associated with stepwise cooling of the Northern hemisphere. Glacial-interglacial variations of Hf isotopes also seem to have been controlled by the variable weathering regime as a function of climate and temperature changes.

https://doi.org/10.1180/S0026461X00006502 Published online by Cambridge University Press

(U-Th)/He geochronological evidence for rapid uplift of Tianshan orogenic belt since Miocene

CHEN WEN[1]*, SUN JINGBO[1], JI HONGWEI[2,1], LI JIE[2,1], YIN JIYUAN[1], GONG JUNFENG[1] AND LIU XINYU[1]

[1]Laboratory of Isotope Geology, Institute of Geology, CAGS, Beijing, 100037 China (*correspondence: chenwenf@vip.sina.com)

[2]China University of Geosciences (Beijing), Beijing, 100083 China

The Tianshan orogenic belt, lying across Central Asia, is an important part of the Central Asian Orogenic Belt, which formed by the continental collision between Siberia and Tarim plate in Late Paleozoic. Since Cenozoic, strong compression caused by the collision between Indian and European plates has led to intense uplift of pre-Mesozoic terrains in Tianshan Area. Analysis of growth strata and regional geological studies show that rapid uplift of the Tianshan in Late Cenozoic occurred younger than 10-7Ma, of which the existence of extremely thick Quaternary molasse sediments indicates that the uplift and denudation in a relatively high tectonic position occurred younger than 3Ma, paradoxically, most of the thermochronology data gained from the FT (Fission Track) is >20Ma [1], lack of data which is <7Ma.

Non-dilution ^{4}He content measurement technique is developed in the Helix MC multi-collector mass spectrometer in our laboratory [2], as well as the establishment of the (U-Th)/He dating experimental procedure. Apatite in granite、gabbro sampled from Tianshan orogenic belt are dated by (U-Th)/He method, obtained a series of ages around 5Ma-10Ma, which provide geochronological evidence for a rapid uplift event in Late Miocene-Pliocene in Tianshan orogenic belt.

Acknowledgements: This work was supported by the Science and Technology Research Project of China (No.: 2007CB411306; 200911043-13; 1212011120293)

[1] Hendrix *et al*. (1994), *Geology*, **22**:487-490. [2] Chen *et al*. (2010), *Mineral Deposit*, **29**(S):821-822.

Redox evolution of the late Neoproterozoic to early Cambrian ocean on Yangtze platform, China

X. CHEN[1,2]*, D. VANCE[2], H.-F. LING[1], C. ARCHER[2], G.A. SHIELDS-ZHOU[3] AND L.M. OCH[3]

[1]Department of Earth Sciences, Nanjing University, Nanjing 210093, China (*correspondence: imchenxi@gmail.com)

[2]Bristol Isotope Group, School of Earth Sciences, University of Bristol, Bristol BS8 1RJ, UK

[3]Department of Earth Sciences, University College London, London WC1E 6BT, UK

The late Neoproterozoic-early Cambrian interval (663-521 Ma) witnessed a critical transition in the surficial Earth system. Although it is still debated whether physical or biological factors controlled this transition, the redox state of the atmosphere and ocean are generally considered to be a key factor in the cause and effect relationships. Here we present data for several redox tracers, including Mo isotope compositions, Fe speciation and Mo/TOC ratios in the organic-rich shales/carbonates from the Yangtze platform, Southern China.

The results suggest a key evolutionary transition either side of ca. 580-551 Ma. Between 663 and 580 Ma, Fe speciation data give high Fe_{HR}/Fe_T (> 0.38) with relatively low Fe_{Py}/Fe_{HR} (< 0.7). Both Mo concentrations and Mo/TOC ratios are low. δ^{98}Mo values are not far from the modern dissolved riverine input value of 0.7. Between ca. 551 and 521 Ma, Fe speciation begins to show more variation. Unprecedented enrichment of Mo also emerges as a characteristic of sediment and the range of δ^{98}Mo values show an extended range of variation.

The data suggest a still low atmosphere O_2 level during the early stage, resulting in low input of Mo and sulfate to the ocean. Sulfate deficiency and/or low productivity in the ocean induced ferruginous anoxia. Due to a low proportion of Mo output via the oxic sink and quantitative removal to sediments, no obvious fractionation of Mo was recorded. But a pronounced oxidation event initiated after (at least) ca. 551 Ma. Elevated atmosphere O_2 level and sulfate input to the ocean may have resulted in expansion of euxinic, suboxic, and oxic environments. Moreover, expansion of the ocean Mo reservoir also stimulated greater fractionation of Mo in anoxic/suboxic environments. δ^{98}Mo in euxinic sediments reached the modern value after ca. 530 Ma, marking the epilogue of this profound redox transition in the ocean, and coincident with the immediately following peak of metazoan radiation. This study is supported by NSFC grant 40872025.

Metasomatic pyroxenites and peridotites in the mantle wedge: Tracing the high Nb/Ta reservoir

Y. CHEN, K. YE, S. GUO AND J.B. LIU

State Key Laboratory of Lithospheric Evolution, Institute of Geology and Geopgysics, Chinese Academy of Sciences, P.O. Box 9825, Beijing 100029, China (*correspondence: chenyi@mail.iggcas.ac.cn)

The Nb/Ta ratios in most silicate earth reservoirs are generally subchondritic (< 19.6±0.6), and thus a 'hidden' high Nb/Ta ratio reservoir is expected in the deep Silicate Earth. The core of the Earth [1] and the deep recycled eclogites [2] have been regarded as the candidates of the high Nb/Ta reservoirs. However, high-pressure experiments demonstrate that the melts/fluids released from the HP-UHP eclogite commonly have higher Nb/Ta ratios than the residue rutile-bearing eclogites [3-5]. Such melts and fluids with high HFSE and Nb/Ta ratios are expected to penetrate into the cold mantle wedge just above the subduction slab and result in significant metasomatism. However, the Nb/Ta ratios in the metasomatic cold mantle wedge are still unclear.

A relevant case study is represented by a mafic-ultramafic complex in Maowu, Dabieshan UHP belt, eastern China. It is mainly composed of orthopyroxenite and garnet orthopyroxenite, with minor garnet clinopyroxenite, garnet websterite, harzburgite and dunite. The Maowu pyroxenites are formed by interactions of refractory mantle wedge harzburgite or dunite with slab-derived fluid. Most of these metasomatic pyroxenites and peridotites contain Ti-clinohumite, which is the major Ti-Nb-Ta-bearing mineral in these rocks. The Ti-clinohumite is formed by the interaction between protolith olivine and a UHP (~5.5 GPa, 800 ºC) slab-derived fluid rich in Ti, Nb and Ta. The whole-rock Nb/Ta ratios in most fresh metasomatic pyroxenites and peridotites are superchondritic (20-28), however, the unmetasomatic harzburgite and dunite still have subchondritic Nb/Ta ratios (13-17). The Nb/Ta ratios in the Ti-clinohumite are similar to those of the whole rock. The superchondritic Nb/Ta ratios in the Maowu metasomatic pyroxenites and peridotites indicate that the cold metasomatic mantle wedge just above the subduction slab may be the potential "hidden" superchondritic Nb/Ta reservoir in the Silicate Earth.

[1] Wade & Wood (2001), *Nature* **409**, 75-78. [2] Rudnick *et al*. (2000), *Science* **287**, 278-281. [3] Foley *et al*. (2000), *GCA* **64**, 933-938. [4] Rapp *et al*. (2003), *Nature* **425**, 605-609. [5] Schmidt *et al*. (2004) *EPSL* **226**, 415-432.

Metamorphic growth and recrystallization of zircons in negative $\delta^{18}O$ metamorphic rocks: A combined study of U-Pb dating, trace elements, and O-Hf isotopes

YI-XIANG CHEN, YONG-FEI ZHENG AND REN-XU CHEN

School of Earth and Space Sciences, University of Science and Technology of China, Hefei 230026, China (cyxz@mail.ustc.edu.cn)

A combined *in situ* SIMS and LA-(MC)-ICPMS study incorporating of U-Pb dating, trace elements, O-Hf isotopes was conducted on zircons from ultrahigh-pressure metamorphic rocks at Qinglongshan in the Sulu orogen, China. The results indicate that many zircons are actually different proportions of mixtures between residual cores and metamorphic overgrowths, with contrasts in $\delta^{18}O$ values, U-Pb ages, Th/U ratios and REE patterns. Generally, residual cores have U-Pb ages of middle Neoproterozoic, positive $\delta^{18}O$ values, high Th/U and $^{176}Lu/^{177}Hf$ ratios, high REE contents, and type magmatic REE patterns. They crystallized from positive $\delta^{18}O$ magmas in the middle Neoproterozoic. In contrast, newly grown domains show concordant Triassic U-Pb ages, negative $\delta^{18}O$ values, low Th/U and $^{176}Lu/^{177}Hf$ ratios, low REE contents, and REE patterns typical of metamorphic growth. The domains grew from negative $\delta^{18}O$ fluids that were produced by metamorphic dehydration of high-T glacial meltwater altered rocks. The large $\delta^{18}O$ variations between grains and intragrain domains indicate varying degrees of O isotope exchange between the residual cores and the negative $\delta^{18}O$ metamorphic fluids. Protolith magmatic zircons underwent three types of metamorphic recrystallization, with extents of modification depending on accessibility of the negative $\delta^{18}O$ fluids. Solid-state recrystallization still maintains the positive $\delta^{18}O$ values and other features of magmatic zircon except some extent of lowering in U-Pb ages. Dissolution recrystallization results in strongly negative $\delta^{18}O$ values, almost complete resetting of U-Pb ages and partial redistribution of REE systems. Replacement recrystallization causes variable negative $\delta^{18}O$ values, partial resetting of REE, and the U-Pb and Lu-Hf isotope systems. Therefore, this combined *in situ* study not only places robust constraints on genesis of metamorphic zircons, but also allows discrimination between the different types of zircons in eclogite-facies metamorphic rocks.

https://doi.org/10.1180/S0026461X00006502 Published online by Cambridge University Press

Stability of engineered nanoparticles under various environmental conditions: Measurements and modeling

YONGSHENG CHEN, WEN ZHANG, KUNGANG LI

School of Civil and Environmental Engineering, Georgia Institute of Technology, Atlanta, Georgia, 30332 (yongsheng.chen@ce.gatech.edu)

To better understand and predict the environmental fate of engineered nanoparticles (ENPs) and their biological effects, characterization of their aqueous stability (e.g., aggregation and ion release) is important. In this study, we investigated and developed models to describe aqueous behaviors of serval selected ENPs. The ENPs include CeO_2, Ag, and quantum dots (QDs), which have broad commercial applications and toxicological relevance. The primary physicochemical properties of ENPs (i.e., morphology, size distribution and surface potential) were characterized by transmission electron microscopy (TEM), atomic force microscopy (AFM), dynamic light scattering (DLS), and zeta potential instrument. The aqueous stability was evaluated by studying the aggregation kinetics under different levels of salt, natural organic matter (NOM) and temperature by time resolved-dynamic light scattering (TR-DLS). Extended Derjaguin–Landau–Verwey–Overbeek (EDLVO) theory and the attachment efficiency (or inverse stability ratio) were both used to interpret the aggregation mechnisms. Moreover, we developed models by combining EDLVO with Arrhenius equation or von Smoluchowski's population balance equation to describe aggregation kinetics of ENPs. Particularly, the model derived from EDLVO and Arrhenius equation was also used to simulate the Ag^+ release kinetics and the influences of particle size, concentration, dissolved oxygen, and other environmental factors (e.g., temperature) on ion release kinetics. Finally, we investigated the oxidative dissolution of QDs under irradiation of ultravoliet (UV) light at 254 nm.. The effects of irradiation intensity, dissolved oxygen (DO), temperature, and surface coating on the dissolution kinetics of QDs were systematically investigated. Our results showed that the possible mechanism of the oxidative dissolution of QDs involved the formation of reactive oxidative species (ROS) on the surface of QDs under UV irradiation, and ROS may further oxidize the core-shell compositions of QDs and subsequently release the metal ions (Cd^{2+}, Se^{2+}, and Zn^{2+}). The knowledge gained from this study proivdes insight information about aqueous stability of ENPs, which lays out groundwork toward a better understanding of environmental impacts of ENPs.

Quantification non-linear flow and transport in fractures based on boundary layer theory and MIM

Z. CHEN, H. N. LI AND R. Z. LI

School of Resources and Environmental Engineering, Hefei University of Technology, Hefei, 230009, China (czhfut@gmail.com)

Solute transport in fractures or fractured media becomes a big issue in CO_2 geological sequestration, groundwater reservoir finding, oil exploiting, nuclear waste disposal and many other fields[1-4]. More and more attentions were drawn on solute transport in single rough fracture. Among which, Fickian Law is believed to be the "right" form of governing law, however, extensive evidences such as "early arrival" and "the long tail" show non-Fickian transport [5-6].

The roughness of the fracture and the non-linear flow were considered to be two important reasons for non-Fickian transport [7]. Application of boundary layer theory in describing the flow condition in fracture seems to be a choice in non-Fickian explanation by Qian *et al*. [8]. A viscous boundary layer existed near fracture wall and the flow velocity changed rapidly. A low velocity zone (or zero velocity in cavities caused by roughness) and a fast velocity zone exist based on boundary layer theory. As a simplification of the boundary layer dispersion problem in single rough fracture, the mobile-immobile (MIM) model may be applicable. MIM approah assign a mobile domain and a immobile domain for the transport. The mobile domain was used to approximate the region near the symmetry of the fracture and the immobile domain used in low velocity zone.

By fitting the experimental data of solute breakthrough curve (BTC) through a single rough fracture using MIM we found that MIM did an excellent work. The early arrival of peak value can be explained by the dispersion in fast velocity zone and the long tailing phenomenon can be explained by the delayed transport in low or zero velocity zone. Further work can be carried out on finding the relationship between the thickness of boundary layer and mobile water fraction coefficient in MIM.

[1] Zhou *et al*. (2004) *Int. J. Rock Mech. Min. Sci*. **41**:402. [2] Luo *et al*.(2006) *Geochim.Cosmochim. Acta* **70**: 376-376. [3] Qian *et al*. (2006) *Hydrogeol. J*. **14**: 1192-1205. [4] Qian *et al*. (2009) *Hydrogeol. J.* **17** (7): 1749-1760. [5] Qian *et al*. (2005) *J. Hydrol.* **311**: 134-142. [6] Luo *et al*.(2009) *Geochim.Cosmochim. Acta* **73**: 802-802. [7] Qian *et al*.(2007) *J. Hydrol.* **339**: 206-219. [8] Qian *et al*. (2011) *J. Hydrol.* **399**: 246-254.

https://doi.org/10.1180/S0026461X00006502 Published online by Cambridge University Press

Influence of sedimentary gas bubble ebullition on interfacial transport in permeable marine sands

C.H. CHENG AND M. HUETTEL*

Earth, Ocean, and Atmos. Science Dept., Florida State University, Tallahassee, FL, USA
(*correspondence: mhuettel@fsu.edu, chc09@fsu.edu)

In the uppermost centimeter of shallow, permeable sediments, photosynthesis by microalgae causes oxygen supersaturation, leading to the formation of oxygen bubbles. Ebullition is one of several processes that affect circulation and exchange of water into and out of the sediment, yet is not well understood. It occurs when these gas bubbles are released due to growth in size or waves and tide-induced pressure oscillations, and may enhance the release or exchange of solutes. In sandy, coarse-grained sediments bubbles occur mostly as small inconspicuous interstitial bubbles, in contrast to larger formations of free methane gas in deeper layers of muddy sediments. Laboratory ebullition experiments utilizing inert dye showed the effects of the sediment depth of ebullition and the volume of sediment affected by the bubble flow. Compared to sediment cores, where diffusion was the sole transport mechanism for the dye, flux in the ebullition experiments was enhanced 5-23 fold. Analyses of the sediment cores revealed a distinct pattern of pore water flow as a result of ebullition, where circulation that was effective in vertical and horizontal mixing of pore fluids. In field experiments using bromide as intert tracer, bubble ebullition caused an enhancement of pore water exchange and thus benthic pelagic coupling.

Water table fluctuations with soil temperature changes in a laboratory experiment

DONG-HUI CHENG

School of Environmental Sciences and Engineering, Chang′an University, Xi′an 710054, China (chdhbsh@chd.edu.cn)

A New Observation about Water Table Fluctuation

A phenomenon of the diurnal water table fluctuations with soil temperature changes was derived from a laboratory experiment on soil (eolian sand) evaporation. The water table rise with the soil temperature increase in daytime and it declined with the soil temperature decrease in nighttime. In 10-day time scale, the water table also exhibited the same variations with temperature changes. The influence of temperature on diurnal water table fluctuation was considered ignorable and only exhibited in long-term changes in previous studies [1,2]. However, our experiment results showed it is notable.

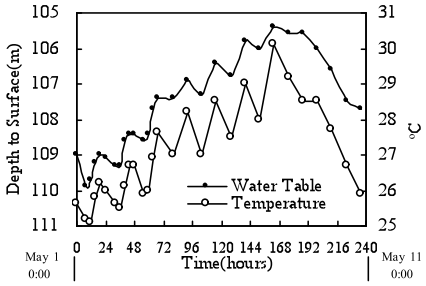

Figure 1: Water table fluctuations with soil tempeture changes

Discussions of Results

In our experiment, the groundwater evaporation was not effect on the water level due to the depth to water table (about 1.1 m) was much less than the extinction depth of water evaporation in the eolian sand media (about 0.5 m), as well as the barometric pressure change. Traditionally the water table fluctuations due to temperature changes were interpreted using the Muskat equation [3,4]. However, it only reasonable to explain the water tables rise due to temperature rise. The Influence of temperature on the soil capillary pressure of soi is probably main factor for water table fluctuation. a completely discussion of these results will be presented in the conference.

[1] Loheide (2005) *Water Resour. Res.* **41**, W07030 doi:10.1029/2005WR003942. [2] Hare *et al.* (1997) *Ground Water* **35**, 667-671. [3] Constantz (1994) *Water Resour. Res.* **30**, 3253-3264D. [4] Meyer (1960) *J. Geo. Res* **65**, 1747-1752 .

https://doi.org/10.1180/S0026461X00006502 Published online by Cambridge University Press

Erosion rate of yellow soil on pine hill in the Three Gorges reservior region using ^{137}Cs Technique

J. CHENG [1,2], Y. SHUANG[1,2]*, Z.Y. JIANG[1,2] AND H. LI[1,2]

[1]Chongqing Key Laboratory of Exogenic Minerallization and Mine Environment, Chongqing Institute of Geology and Mineral Resources, Chongqing 400042, China (*correspondence: shy0124@yahoo.com.cn)

[2]Chongqing Research Center of State Key Laboratory of Coal Resources and Safe Mining 400042, China

Soil erosion and degradation, as one of the major environmental problems man is confronted with, is becoming a hot spot in the study of soil and environmental Science. In recent years, radio-isotope tracer in soil erosion studies has become one of the hottest research topics in the field of soil Science. This research presents the ^{137}Cs tracer in the soil erosion rates in the Three Gorge Reservoir Region in Chongqing.

Two yellow soil profile samples which formed by the weathering of quartz sandstone of the Upper Triassic Xujiahe Fm were collected from the pine hill. Simplified mass balance model established by Zhang *et al* [1] is applied to overestimate the soil erosion rates.^{137}Cs of Section A (sits on upper section of the hill, with an incline of about 15 degrees) is mainly gathered in middle section (4-10cm). The ^{137}Cs inventories of the section is estimated to be 1099.8 Bq/m^2. The soil erosion rate on this section is 1009.92 t/km^2.a, in concordance with the result of Dong *et al* (2006)[2].

As to section B (sits on middle to lower section of the hill, with an incline of about 15 degrees), ^{137}Cs is mainly gathered in surface soil (2-6cm). The ^{137}Cs inventories and soil erosion rate values are 2139.8 Bq/m^2 and -190.937 t/km^2.a respectively, indicating slight accumulation happened before.

Combined with some previous results[2], it may be deduced that the soil erosion rates of this area might have little relationship to the soil type and soil forming rocks, but were greatly affected by topography, soil utilization way and vegetation.

This research project was financially supported by the Argo-geologic Survey in Zhong county Project from Chongqing Administration of Land, Resources and Housing.

[1] Zhang *et al*. (1990) *Hydro. Sci*. **35**, 243-252. [2] Dong *et al*. (2006) *J. Soil and Water Conserv*. **20**, 1-5.

Alteration of biochemical pools assemblage induced in *A. variabilis* by TiO_2 nanomaterials exposure

C. CHERCHI AND A.Z. GU*

Dept. of Civil and Environmental Enginering, Northeastern University, Boston, MA 02115 (*correspondence: april@coe.neu.edu)

In this study Fourier Transformed Infrared spectroscopy and Transmission Electron Microscopy were used to evaluate the ecotoxic impact of TiO_2 nanomaterials to the cellular reorganization of macromolecules in the nitrogen-fixing cyanobacteria *A. variabilis*. The increase in occurrence and intracellular levels of cyanophycin grana proteins (CGPs, Figure 1) reveal changes in the dynamics of cellular nitrogen storage and metabolism. The results also showed characteristic temporal re-allocation patterns after short and long-term exposure of the predominant chemical markers (lipids, nucleic acids, carbohydrates and proteins) with nTiO_2 dose-dependent trends.

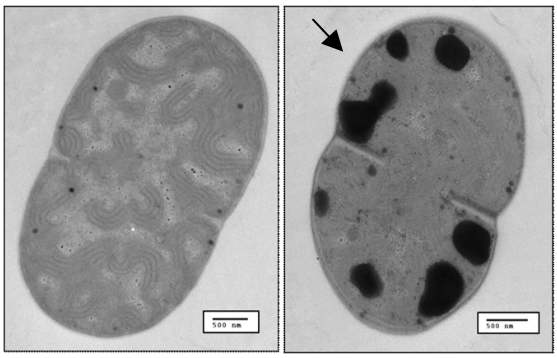

Figure 1: CGPs formation after cell exposure to nTiO_2 (right) compared to control (left).

In conclusion, this study reveals important insights into the metabolic strategies implemented by cyanobacteria under nTiO_2 exposure and anticipates at larger scale the impact on important biogeochemical processes, such as nitrogen cycle, and ecological food web dynamics.

https://doi.org/10.1180/S0026461X00006502 Published online by Cambridge University Press

Natural water contamination under chromite deposit mining

E.V. CHERKASOVA AND B.N. RYZHENKO

Vernadsky Institute of Geochemistry and Analytical Chemistry RAS, Moscow, Russia (ryzhenko@geokhi.ru)

For any chromite mining site there is a problem of ore waste burial. In our opinion for Aganozerskoe deposit (Russia, Kareliy) there are two possibilities for waste burial: to keep waste wet with water on the land surface or to put it in the nearest water reservoir (pool, lake). According to [1] the main factors which determine dissolution of minerals and migration of aqueous species are the following: (a) weight ratio of rock to water (R/W), (b) partial pressure of O_2 and CO_2 in the site atmosphere, (c) chemical and mineralogical compositions of the site rock, (d) temperature-pressure conditions of the water-rock system under study. Using these conclusions and computer simulation technique of water-rock systems the chemical reactions which are occurred between the rock minerals and water have been modeled to estimate the groundwater contamination.

The computer model of water - serpentinised ultramafic rock - atmosphere system that has been constructed is based on groundwater and rock chemical compositions of Aganozeskoe deposit. The system under consideration consists of H-O-Si-Al-Ca-Mg-Na-K-Ti-P-Mn-Cl-S-C-Cr-Zn-Ni-Co-V. The simulation code is HCh [2, 3]. The modeling shows that keeping waste wet on the land surface under the atmosphere oxygen access to the chromite ore and ore waste stores will result in chromite oxidation and aqueous chromium species migration in environment. The burial of ore waste in water pool decreases the influence of oxidizing dissolution of chromite. But it is necessary to keep the pool water isolated from landscape lakes. According to [4] the rate of oxidizing dissolution of chromite might be experimentally measured.

[1] *Крайнов С.Р., Рыженко Б.Н., Швец В.М* М.: Наука, 2004. [2] *Шваров Ю.В*. Геохимия. 1999. № 6. С. 646-652. [3] *Шваров Ю.В*. Геохимия. 2008. № 8. С. 890-897. [4] *Oze C.J.-P*. Ph.D.Thesis. Stanford University. 2003

Lead isotope composition variations in sulfides from hydrothermal fields of the Mid-Atlantic Ridge: High-precision MC-ICP-MS isotope data

I.V. CHERNYSHEV, N.S. BORTNIKOV AND A.V. CHUGAEV[1]

IGEM RAS, Moscow, Russia (cher@igem.ru)

The high-precision MC-ICP-MS method of Pb-isotope analysis (±0.03%) with mass-bias correction to $^{205}Tl/^{203}Tl$ isotope ratio [1, 2 and others] have been applied for study of sulfides from 4 hydrothermal fields (HFs) in the southern part (12°58'–16°38' N) of Mid-Atlantic Ridge (MAR) spreading zone: Ashadze, Semenov, Logachev, and Krasnov.

Sulfide Pb-isotope ratios variation scale in the four studied HFs have been estimated: 0.04–0.09% for $^{206}Pb/^{204}Pb$, 0.02–0.04% for $^{207}Pb/^{204}Pb$, and 0.04–0.07% for $^{208}Pb/^{204}Pb$, while analytical error was ±0.03%. These variations are lower by a factor of 3–4 than was evident from the data previously obtained for HFs in MAR and Pacific Ocean by traditional TIMS, which are characterized by precision ±0.1-0.2%. Using high-precision MC-ICP-MS method we did not reveal dependence of the Pb-isotope composition on the type of HFs sulfide mineral and total Pb concentration in it.

The results provide the following regularities [3]. (1) At small (close to 0.03%) variations of the Pb-isotope composition of sulfides from individual HF, the latter differ significantly from each other by all isotope ratios. (2) Sulfides of HFs related to serpentinized peridotites have more radiogenic Pb-isotope composition by all isotopes (^{206}Pb, ^{207}Pb, and ^{208}Pb) in comparison to HFs occurring on tholeiitic basalts. (3) On the evolutionary Pb-Pb isotope diagrams the Pb-isotope compositions of HFs sulfides discretely plot in the area of MAR basalts and are located exactly along the NHRL. The Pb-isotope characteristics of sulfides from MAR HFs permit participation of two mantle sources of Pb (DMM and HIMU) in their formation with prevalence of the first of them. Sulfides of MAR HFs are similar to MORB by the total range of the Pb-isotope composition; because of this, the data obtained do not contradict the idea that hydrothermal solutions and then sulfides inherit the Pb-isotope composition from underlying rock series. As above represented data show convective cells provide exceptional homogenization of Pb isotope composition for individual HFs.

[1] Rehkamper, Halliday (1998) *Intern. J. Mass Spec. Ion Proc* **58**, 123–133. [2] Chernyshev *et al*. (2007) *Geochem. Int.* **45**, 1065-1076. [3] Chernyshev *et al*. (2011) *Doklady Earth Sciences* **437**, 507–512.

https://doi.org/10.1180/S0026461X00006502 Published online by Cambridge University Press

U-Pb and Th-Pb dating of apatite by LA-ICPMS

DAVID M. CHEW[1]*, PAUL J. SYLVESTER[2] AND MIKE N. TUBRETT[2]

[1]Department of Geology, Trinity College Dublin, Dublin 2, Ireland. (correspondance*: chewd@tcd.ie)
[2]Department of Earth Sciences and Inco Innovation Centre, Memorial University, St. John's, Newfoundland, A1B 3X5 Canada (psylvester@mun.ca, mtubrett@mun.ca)

Apatite is a common U- and Th-bearing accessory mineral in igneous, sedimentary and metamorphic rocks and ore systems. However, low U, Th and radiogenic Pb concentrations, elevated common Pb and the lack of a U-Th-Pb apatite standard remain significant challenges in dating apatite by LA-ICPMS.

This study has determined U-Pb and Th-Pb ages for seven apatite occurrences (Durango, Emerald Lake, Kovdor, Mineville, Mudtank, Otter Lake and Slyudyanka) by LA-ICPMS [1]. Analytical procedures involved rastering a 10µm spot over a 40×40µm square to a depth of 10µm using a Geolas 193nm ArF excimer laser coupled to a Thermo ElementXR single-collector ICPMS. These raster conditions minimized laser-induced inter-element fractionation which was corrected for using the back-calculated intercept of the time-resolved signal. A Tl–U–Bi–Np tracer solution was aspirated with the sample into the plasma to correct for instrument mass bias. External standards (Plešovice and 91500 zircon, NIST SRM 610 and 612 silicate glasses and STDP5 phosphate glass) along with Kovdor apatite were analysed to monitor U-Pb, Th-Pb and Pb-Pb ratios.

Common Pb correction employed the ^{207}Pb method, and also a ^{208}Pb correction method for samples with low Th/U. The ^{207}Pb and ^{208}Pb corrections employed either the initial Pb isotopic composition where known or the Stacey and Kramers model. No ^{204}Pb correction was undertaken because of ^{204}Pb interference by ^{204}Hg in the argon gas supply.

Age calculations used a weighted average of the common Pb-corrected ages and Tera-Wasserburg Concordia intercept age (both unanchored and anchored through common Pb). The samples yield ages consistent with independent estimates of the U-Pb apatite age, which demonstrates the suitability of the analytical protocol employed. Weighted mean age uncertainties are as low as 1-2% for U- and/or Th-rich Palaeozoic-Neoproterozoic samples [1].

[1] Chew *et al*. (2011) *Chem. Geol*. **280**, 200–216.

Aqueous CO_2 solutions at silica surfaces and confined environments

ARIEL A. CHIALVO[1], LUKAS VLCEK[1] AND DAVID R. COLE[2]

[1]Oak Ridge National Laboratory, Oak Ridge, TN 37631, U.S.A. (chialvoaa@ornl.gov)
[2]Ohio State University, Columbus, OH 43210, U.S.A.

The CO_2 capture and sequestration in geological reservoirs have been considered as a potential approach to mitigate its release into the atmosphere and reduce its contribution to the greenhouse effect on climate change. The feasibility and safety of this process for long-term storage of CO_2 depends on the low hydraulic permeability of the caprock and its ability to hold the aqueous fluid in its porous structure, *i.e*., its interfacial and confinement properties.

Interfacial and confined fluids exhibit microstructural, dynamical, and thermophysical behavior that differ dramatically from their bulk counterparts. The immediate consequence is the inherent inability of current modeling approaches to capture the actual (aqueous-caprock) fluid-solid and fluid-fluid interfacial mechanisms underlying the geological CO_2 sequestration.

Here we present a molecular-based study of the microstructural and dynamical behavior of CO_2-aqueous solutions at silica surfaces and under extreme confinement, to address fundamental issues, including (a) how the degree of surface hydrophobicity affects the interfacial structure, (b) how the overlapping of interfacial structures affects the confined fluid composition (relative solubility), and (c) how to account for the effect of medium polarization on the species solubilities.

Toward those goals we developed (i) a synergistic approach to calibrate the CO_2-H_2O interactions for the accurate and simultaneous prediction of the compositions of the two phases in liquid (water_rich)-liquid (CO_2_rich) equilibrium at realistic well conditions [1]; and (ii) we applied a molecular dynamics protocol that allows the simultaneous study of the behavior of the aqueous system at interfaces and within confinement between silica surfaces, while the fluid remains in equilibrium with its own bulk at isobaric-isothermal conditions.

[1] L. Vlcek, *et al*., "Optimized Unlike-pair Interactions for Water-Carbon Dioxide Mixtures described by the SPC/E and EPM2 Models" *Journals of Physical Chemistry B*. In press

Acknowledgements. Support for this work comes from the US Department of Energy through the LBNL "Center for Nanoscale Control of Geologic CO_2" (FWP ERKCC67) under contract DE-AC05-00OR22725 to Oak Ridge National Laboratory, managed and operated by UT-Battelle, LLC.

https://doi.org/10.1180/S0026461X00006502 Published online by Cambridge University Press

Carbon-isotope and Mercury Stratigraphies of the Frecheirinha Formation cap carbonate, Northeastern Brazil

L. CHIGLINO[1], A.SIAL[1] AND C. GAUCHER[3]

[1]NEG-LABISE, Departamento de Geologia, Universidade Federal de Pernambuco, Recife, Brazil (Sial@ufpe.br, leticia@ufpe.br)

[2]Facultad de Ciencias, Universidad de La República, Montevideo, Uruguay (gaucher@chasque.com)

The Frecheirinha Formation is a carbonate unit of the Ubajara Group in the the Middle Coreaú Domain, state of Ceará, Brazil. This formation is composed of basal marls followed by limestone-dolostones rhythmites and by stromatolitic limestone in the top. It overlies red to purple slates and, locally, itabirites of the Caiçaras Formation. The C-isotope pathway for the Frecheirinha Formation with negative $\delta^{13}C$~-6 ‰values in the base and positive values up to 3.7 ‰ in the top of the formation is compatible with pathways for cap carbonates elsewhere. On the contrary to other studied cap carbonates in northeastern Brazil (e.g. Sergipano and Seridó Belts and Rio Pardo Basin), no $\delta^{13}C$ value > + 3.7‰ has been recorded in the Frecheirinha Formation, and this raises the possibility of an Ediacaran age for this carbonate sequence. A preliminary Hg survey with carbonate samples from the Freicherinha Formation was carried out, aiming to use Hg as a proxy of volcanism intensity and CO_2 buildup during a possible snowball event. Typically, Hg contents have been analyzed only form basal marls and that show negative $\delta^{13}C$ values ~ -6‰. In this way, only carbonates deposited at the earliest stages of the aftermath of glacial events were analyzed. The highest mercury contents were over 10 times higher than background values (<1nng^{-1}).This suggest that CO_2 in the basal portion of this carbonate formation is mostly mantle-derived, transferred to the atmosphere by volcanism. The only age available for the Frecheirinha Formation (0.61 Ga) is based on poor Rb-Sr isochron for clay fractions of the Caiçara Formation [1]. The Mucambo pluton intruded these carbonates at 0.54 Ga [2]. These carbonates show $^{87}Sr/^{86}Sr$ values ~ 0.7075 which do not allow an unambiguous age assignment. Similar Sr-isotope values and associated itabirites without glacial features occur in the Ediacaran Arroyo del Soldado Group of Uruguay.

[1] Sial *et al*. (2003). IX Brazilian Geochemical Congress. Belém, Pará: 410-411. [2] Sial *et al*. (2000), *Annals of the Braz. Academy of Science,* **72**: 539-558.

Compound-specific stable isotope analysis of amino acids as a novel tool for ecological food web study

Y. CHIKARAISHI, N.O. OGAWA, Y. TAKANO, M. TSUCHIYA AND N. OHKOUCHI

Institute of Biogeosciences, Japan Agency for Marine-Earth Science and Technology (ychikaraishi@jamstec.go.jp)

Knowledge of the trophic position (TP) of organisms in food webs allows understanding of biomass flow and trophic linkages in complex networks of ecosystems. Compound-specific stable isotope analysis (CSIA) of amino acids is a novel method with that enables TP estimates of organisms in food webs [1-4]. This approach is based on contrasting isotopic fractionation during metabolic processes between two common amino acids: glutamic acid (Glu) shows significant ^{15}N-enrichment of +8.0‰ during reactions (transamination, deamination) that cleaves the carbon-nitrogen bond, whereas phenylalanine (Phe) shows little change in $\delta^{15}N$ values (by +0.4‰) during conversion to tyrosine that neither forms nor cleaves the carbon-nitrogen bond [3]. In the previous studies [3,4] we established based a number of natural and laboratory grown organisms a general equation for estimating the TP of organisms by CSIA of amino acids:

$$TP = [(\delta^{15}N_{Glu} - \delta^{15}N_{Phe} + \beta)/7.6\ ] + 1$$

where β represents the isotopic difference between Glu and Phe in primary producers (–3.4‰ for aquatic cyanobacteria and algae, +8.4‰ for terrestrial C3, and –0.4‰ for terrestrial C4 plants). In the presentation, we briefly review this amino acid method and then show its application to various natural organisms in aquatic marine and freshwater as well as terrestrial food webs.

[1] McClelland & Montoya (2002) *Ecology* **83**, 2173-2180. [2] Popp *et al*. (2007) In *Stable isotopes as indicators of ecological change*. Academic Press. pp 173-190. [3] Chikaraishi *et al*. (2009) *Limnol. Oceanogr.: Meth* 7, 740-750. [4] Chikaraishi *et al*. (2010) *In Earth, Life, and Isotopes*. Kyoto University press. pp. 37-51.

https://doi.org/10.1180/S0026461X00006502 Published online by Cambridge University Press

Self-assembly in natural organic matter: Lipid and amphiphilic components

G. CHILOM, J. SHORE AND J. A. RICE*

Dept. Chemistry & Biochemistrry, South Dakota State University, Brookings, SD 57007, USA (gabriela.chilom@sdstate.edu, jay.shore@sdstate.edu, *correspondence: james.rice@sdstate.edu)

Recent work has demonstrated that natural organic matter (NOM) in soils and sediments has a hierarchical or "structure within a structure" architecture [1,2]. The first-order structure results from the self-assembly of amphiphilic and lipid components to form a nanostructured composite material. The second-order structure is formed by the self-assembly of this composite with additional but nonamphiphilic components. The objective of this study is to investigate the dependence of NOM self-assembly on the concentration and nature of components in the first-order level of organization, which is assumed to initiate and control the final NOM structure. Composite materials isolated from four different environmental samples were analyzed by differential scanning calorimetry and multidimensional solid-state NMR spectroscopy. Variation of the excess heat capacity and the mobility and domain structures of composite materials with their composition was used to assess structural organization of these materials.

[1] Chilom & Rice (2009) *Langmuir* **25**, 9012-9015. [2] Chilom *et al*. (2009) *Org. Geochem.* **40**, 455-460.

Emplacement of passive margin sediments into deep crustal hot zones of continental arcs: Interplay of tectonic and magmatic thickening in the formation of continental crust

E. J. CHIN[1], C.-T. LEE[1], D. L. TOLLSTRUP[2], L.-W. XIE[2], J. B. WIMPENNY[2] AND Q.-Z. YIN[2]

[1]Rice University, Houston, TX USA (ejc5@rice.edu)
[2]University of California, Davis, CA, USA

Both magmatic and tectonic processes cause thickening of continental arc lithosphere. In western USA, increased Farallon-North American plate convergence during the Cretaceous was accompanied by lithospheric thickening due to enhanced magmatism and tectonic shortening. Here, we use lower crustal metaquartzite (80% SiO_2) xenoliths in late Miocene basalts in the central Sierra Nevada Batholith, California to constrain how arc lithosphere thickens and matures. The xenoliths are equigranular in texture and contain >50% qtz, ~10% gt, <40% pl, trace TiO_2, Al_2SiO_5, and biot. High qtz mode, abundant detrital zircons, and oriented graphites suggest a supracrustal sedimentary protolith. However, last equilibration T using TitaniQ are 700-800°C. Thermodynamic modelling shows that coexistence of gt and pl for these bulk compositions limits equilibration P's to 0.6-1.6 GPa with GASP barometer giving 0.9-1.3 GPa. These P-T constraints indicate equilibration of the metaquartzites within a hot lower crust (18-45 km). All zircons have discordant U-Pb with variable upper intercept ages (1.7, 2.7, 3.3 Ga; consistent with Hf model ages) and common lower intercept age (100 Ma). Collectively, the above indicate that protoliths of the metaquartzites were Proterozoic to Paleozoic passive margin sediments of N. American affinity and that they were transported to lower crustal depths at ~100 Ma during the peak of Cretaceous arc magmatism. Underthrusting of N. American lithosphere beneath the arc could have transported these sediments to high P, but underthrusting alone cannot explain the xenoliths' high final temperatures. An extra heat source, imparted by deep lithosphere magmatic "hot" zones, is needed. Our results thus suggest a complex interplay between tectonics and magmatism that drives vertical growth and compositional evolution of continental arcs. Despite the common view that magmatic differentiation drives lower crust to become mafic and upper crust felsic, underthrusting can introduce felsic rocks into lower crust. Local density, rheologic and seismic inversions are thus expected.

https://doi.org/10.1180/S0026461X00006502 Published online by Cambridge University Press

Multi-decadal change of atmospheric aerosols and their effect on surface radiation

MIAN CHIN[1]*, THOMAS DIEHL[1,2], DAVID STREETS[3], MARTIN WILD[4], YUN QIAN[5], HONGBIN YU[1,6], QIAN TAN[1,2], HUISHENG BIAN[1,2] AND WEIGUO WANG[7]

[1]NASA Goddard Space Flight Center, Greenbelt, Maryland, 20771, USA (*correspondence: mian.chin@nasa.gov)
[2]University of Maryland Baltimore County, Baltimore, Maryland, USA
[3]Argonne National Laboratory, Chicago, Illinois, USA
[4]ETH, Zurich, Switzerland
[5]Pacific Northwest National Laboratory, Redland, Washington, USA
[6]University of Maryland College Park, College Park, Maryland, USA
[7]NOAA NCEP, Camp Springs, Maryland, USA

We present an investigation on multi-decadal changes of atmospheric aerosols and their effects on surface radiation using a global chemistry transport model along with the near-term to long-term data records. We focus on a 28-year time period of satellite era from 1980 to 2007, during which a suite of aerosol data from satellite observations, ground-based measurements, and intensive field experiments have become available. We analyze the long-term global and regional aerosol trends and their relationship to the changes of aerosol and precursor emissions and assess the role aerosols play in the multi-decadal change of solar radiation reaching the surface (known as "dimming" or "brightening") at different regions of the world, including the major anthropogenic source regions (North America, Europe, Asia) that have been experiencing considerable changes of emissions, dust and biomass burning regions that have large interannual variabilities, downwind regions that are directly affected by the changes in the source area, and remote regions that are considered to representing "background" conditions.

Oxygen optodes as fast sensors for eddy correlation measurements in aquatic systems

LINDSAY CHIPMAN[1], MARKUS HUETTEL[1]*, PETER BERG[2], VOLKER MEYER[3], INGO KLIMANT[4], RONNIE GLUD[5,6] AND FRANK WENZHOEFER[3,7]

[1]Department of Earth, Ocean, and Atmospheric Science, Florida State Univ., Tallahassee, FL 32303, USA (lec05d@fsu.edu, *correspondence: mhuettel@fsu.edu)
[2]Department of Environmental Science, University of Virginia, Charlottesville, VA, USA (pb8n@virginia.edu)
[3]Max Plank Institute for Marine Microbiology, Bremen, Germany (vmeyer@mpi-bremen.de, fwenzhoe@bremen.de)
[4]Graz University of Technology, Graz, Austria (klimant@tugraz.at)
[5]Institue of Biology, University of Southern Denmark, Odense, Denmark (rnglud@biology.sdu.dk)
[6]Scottish Association for Marine Science, Dunstaffnage Marine Laboratory, PA37 1QA, Dunbeg, Scotland
[7]HGF MPG Research Group Deep Sea Ecology and Technology, AWI-Bremerhaven, Germany

The aquatic eddy-correlation technique can be used to non-invasively determine the oxygen flux across the sediment-water interface by analyzing the covariance of vertical flow and oxygen concentration in a small measuring volume above the seabed. The method requires fast sensors that can follow the rapid changes in flow and the oxygen transported by this flow. In this paper, we demonstrate the suitability of fast optical oxygen sensors (optodes), in place of the traditionally used electrodes. Optodes have the advantage over electrodes of being less susceptible to signal drift, more durable under field conditions, less expensive, and repairable. Comparisons of the response times of optodes and electrodes to rapid oxygen changes showed that the optimized optodes had a slightly longer response time (164 ± 70 ms) than the microelectrodes (151 ± 60 ms) but were fast enough to capture the oxygen fluctuations that are relevant for the eddy correlation flux calculations. Side by side comparisons of benthic oxygen fluxes collected with both electrode-based and optode-based eddy correlation instruments in freshwater and marine environments showed good agreement between the measured fluxes. Over a 4 h mid-day measuring period, short term (15min) oxygen fluxes in the spring-fed Wakulla River (Florida) fluctuated between 52 and 401 mmol m^{-2} d^{-1} (average 165 ± 67 mmol m^{-2} d^{-1}), revealing the importance of local light and flow variations on the benthic oxygen exchange.

https://doi.org/10.1180/S0026461X00006502 Published online by Cambridge University Press

Oxidation of FeS by $Fe^{3+}_{(aq)}$

P. CHIRITA[1]* AND M.L. SCHLEGEL[2]

[1]University of Craiova, Calea Bucuresti 107I, Craiova Romania (*correspondence: paulxchirita@gmail.com)
[2]CEA, DEN/DANS/DPC/SCP/Laboratory for the Reactivity of Surfaces and Interfaces, F-91191 Gif-sur-Yvette, France (michel.schlegel@cea.fr)

The oxidative dissolution of iron monosulfides (FeS) releases toxic elements, such as heavy metals and arsenic, in natural solutions [1]. Also, partial oxidation of sulfur from FeS minerals produces sulfur-bearing compounds which may alter the redox properties of natural media [2]. Hence, it is important to understand the reactions between FeS minerals and oxidative solutions.

In this work we examine the kinetics and mechanism of oxidative dissolution of synthetic FeS in presence of $Fe^{3+}_{(aq)}$ by monitoring the pH, Eh and total dissolved Fe concentration ($[Fe]_{total}$) of oxidant solutions during their contact with FeS that lasted 4 hours. Note that concentrations of dissolved sulfur were too low to be reliably quantified. The experiments were performed in acidic media ($2 \leq pH \leq 3$), 25 ºC and $[Fe^{3+}_{(aq)}]$ spanning the $[10^{-4}; 10^{-3}]$ mol L^{-1} range.

The experimental data indicate that Fe^{3+} was removed from the solution at pH>2. A progressive increase in pH values and an Eh decrease within 4 h of reaction time were also observed. The reaction order of FeS oxidation with respect to $[H^+]$ is estimated to 0.65 at initial pH 3.0, and increases up to 1.0, when initial pH decreases [3], indicating that $[H^+]$ is an important parameter of FeS oxidation. In contrast, ferric iron concentration has only a small effect on FeS oxidative dissolution rate in studied $[Fe^{3+}_{(aq)}]$ range.

Taking into consideration present findings it can be stated that mechanism of FeS oxidation starts with the protonation of mineral surface [2]. Thereafter, the adsorbed protons accelerate Fe^{2+} release [3]. Finally, $Fe^{3+}_{(aq)}$ may adsorb at the surface and oxidize the sulfur moieties to insoluble species, presumable polysulfide ($S_n^{2-}{}_{(s)}$) and elementar sulfur ($S^0_{(s)}$).

The authors greatly appreciate support from IFA-CEA Program (Project C1-04).

[1] Thomas *et al*. (1998) *Geochim. Cosmochim. Acta* **62** 1555-1565. [2] Chirita *et al*. (2008) *J. Colloid Interface Sci*. **321**, 84–95. [3] Chirita and Descostes (2006) *J. Colloid Interface Sci*. **299** 260-269.

Two competing processes in petrogenesis of basaltic magma conduits

SOFYA CHISTYAKOVA* AND RAIS LATYPOV

Department of Geosciences, University of Oulu, Oulu, FI-90014, Finland
(*correspondence: sofya.chistyakova@oulu.fi)

A recent geochemical study of dolerite dykes from many regions of the world has revealed that small dolerite dykes (<50 cm wide) representing shallow parts of basaltic magma conduits are remarkably zoned [1-5]. The zonation is compositionally anomalous since compatible and incompatible components behave in a manner inconsistent with predictions of fractional crystallization of basaltic magma. Here we put forward a novel concept interpreting the anomalous compositional trends in dolerite dykes as a result of competition between two petrogenetic processes with opposite effects on dyke composition. These are (a) the filling of dykes with magmas that become increasing more evolved with time and (b) *in situ* cumulate growth of these inflowing magmas against dyke sidewalls. The first process makes inward-solidifying rocks geochemically more evolved whereas the second process more primitive. The combined operation of these two competing processes results in intricate chemical profiles of dykes. Geochemical modelling indicates that all the observed patterns in distribution of compatible and incompatible elements in small dolerite dykes can be reproduced by variations in the relative contribution of these two petrogenetic processes. One important implication of this study is that compositional zonation of small dolerite dykes is indicative of an effective magma fractionation along sidewalls of the deeper parts of basaltic magma conduits.

[1] Chistyakova & Latypov (2009a) *Geol. Mag*. **146**, 485-496. [2] Chistyakova & Latypov (2009b) *Lithos* **112**, 382-396. [3] Chistyakova & Latypov (2010) *Geol. Mag*. **147**, 1-12. [4] Chistyakova & Latypov (2011a) (Ed.) Srivastava, Keys for Geodynamic Interpretation, p. 569-581. [5] Chistyakova & Latypov (2011b) (Ed.) Srivastava, Keys for Geodynamic Interpretation, p. 583-601.

https://doi.org/10.1180/S0026461X00006502 Published online by Cambridge University Press

Zircon U-Pb and Hf isotopic constraints on the magmatic and tectonic evolution in Iran

HAN-YI CHIU[1]*, SUN-LIN CHUNG[1], MOHAMMAD H. ZARRINKOUB[2], I-JHEN LIN[1], HSIAO-MING YANG[1], CHING-HUA LO[1], HAO-YANG LEE[1], KWAN-NANG PANG[1], SEYYED S. MOHAMMADI[2] AND MOHAMMAD M. KHATIB[2]

[1]Department of Geosciences, National Taiwan University, Taipei, Taiwan (*correspondence: hychiu@ntu.edu.tw, sunlin@ntu.edu.tw)
[2]Department of Geology, Birjand University, Birjand, Iran

This study reports new zircon LA-ICPMS U-Pb ages and Hf isotope compositions, coupled with whole-rock Ar-Ar age data and geochemical analyses, for magmatic rocks of Cenozoic age from the Urumieh-Dokhtar magmatic arc (UDMA) in Iran. The UDMA has been divided into three parts by latitude of ~35°N and ~31°N in this study. The northwestern UDMA show two distinct age periods: (1) the older period of 53-27 Ma exhibits zircon $\varepsilon_{Hf}(T)$ values from +11.8 to +1.8; and (2) the younger period of <11 Ma exhibits zircon $\varepsilon_{Hf}(T)$ values from +12.8 to +5.9 and reveals the same formation time as the collision-related volcanism in eastern Anatolia proposed by Keskin [1]. The central and southeastern parts of UDMA yield ages of 51-16 Ma with zircon $\varepsilon_{Hf}(T)$ values from +12.8 to -1.3 and ages of 45-5 Ma with zircon $\varepsilon_{Hf}(T)$ values from +15.7 to +1.1, respectively. The overall zircon $\varepsilon_{Hf}(T)$ values implicate that at least three significant episodes of mantle input occurred in the middle Eocene (~40 Ma), the early Oligocene (~30 Ma) and the late Miocene (~10 Ma). Zircons from the youngest magmatic rocks in central UDMA, however, show much negative $\varepsilon_{Hf}(T)$ values from +8.1 to -1.1, suggesting contamination of crustal materials has played an important role in the middle Miocene magmatism in this region. Furthermore, the pre-collisional, calc-alkaline magmatism in the UDMA appears to cease southeastward, that implies the diachronous collision occurred between Arabia and Eurasia and started in Armenia and northwestern Iran.

[1] Keskin (2007) *Geol. Soc. Amer. Spec. Paper* **430**, 693-722.

Optimization of a low-background liquid scintillation counter for the determination of ^{222}Rn and Uranium isotope in ground water

S.Y. CHO, K.Y. LEE, Y.Y. YOON AND K.S. KO

KIGAM, Daejeon 305-350, Korea (sycho@kigam.re.kr, kylee@kigam.re.kr, yyoon@kigam.re.kr, kyungsok@kigam.re.kr)

An analytical method for the measurement of the ^{222}Rn and Uranium isotope in water sample by liquid scintillation counting technique using LKB Wallac Quantulus 1220 liquid scintillation counter(LSC) equipped with pulse shape analyzer(PSA). We have optimized the pulse-discrimination capabilities of the detector to achieve the best α/β separation and the lowest detection limits possible. LSC was calibrated using the optimization of PSA with ^{241}Am and ^{90}Sr/^{90}Y as well as ^{226}Ra. The optimum PSA level for the measurement of ^{222}Rn was 100 when measuring a sample containing 8 ml water and 12 ml of Optiphase HiSafe™ 3 scintillation cocktail. By the analysis of ^{226}Ra standard, ^{222}Rn counting efficiency and precision were found to be 91.6 ± 3.6% and 2%, respectively. Detection limits of ^{222}Rn for 5 hours counting were counted to be 0.11 Bq/L.

A solvent extraction method was used for the measurement of uranium isotope in ground water samples. The effect of solution volume was not significant, the error being less than 5% for solutions ranged from 100 to 1000 mL at pH 2. The uranium extraction efficiency was found to be the maximum at pH 2 while the pH was varied from 0.5 to 10. We dispersed 20 mL of liquid scintillation for both solvent extraction and alpha/beta discrimination in one liter of water at pH 2. The extraction efficiency of uranium isotopes was near 96% according to the NIST standard. Using the method, the lower detection limit for uranium was determined to be 0.018 Bq/L, with the counting time of 300 min. The results of this study were also compared to those obtained by the conventional ICP-MS measurement. It is demonstrated that the suggested method is valuable to determine the optimum extraction and measurement conditions for uranium in ground water

The analytical method obtained from this work was also applied to the determination of ^{222}Rn and uranium isotopes in some ground water samples.

https://doi.org/10.1180/S0026461X00006502 Published online by Cambridge University Press

Hydrothermal copper mineralization in the Gyeongnam mineralized district, Korea

SANG-HOON CHOI

Chungbuk National Univ., Cheongju, Chungbuk, 361-763 Korea (cshoon@chungbuk.ac.kr)

Copper mineralization in the Gyeongnam district, which is located within the Cretaceous Gyeongsang basin, mainly occurs in hydrothermal polymetallic quartz and/or carbonate veins. These veins are all related to the Cretaceous Chindong granite. Generally, successive polymetallic ore mineralization in the district shows a simplified mineralogy progressing through: Fe-W-Mo, Cu, (Cu-)Zn-Pb with sulfosalts, and/or ferric mineralization. The early Gyeongnam hydrothermal system is characterized by high-salinity brine and/or CO_2-rich fluids. The vein mineralization initiated at high temperature (≈550℃) from fluids with high salinity (up to about 60 equiv. wt. % NaCl or NaCl+KCl) derived mainly from the granite source and/or CO_2-rich fluid by fluid unmixing coupled with boiling. The oxygen isotope data ($\delta^{18}O_{water}$ = 8.9 to 4.7‰ for the early mineralization) suggest that early hydrothermal fluids in the Gyeongnam hydrothermal system likely represent magmatic and/or meteoric water whose isotopic composition was controlled by exchange with a large volume of igneous (and metamorphic or sedimentary) rocks at near-magmatic temperatures. In the waning portion of the vein mineralization, the high-temperature, high-salinity fluids gave way to progressively cooler, more dilute fluids (down to ≈150℃ and ≈1 equiv. wt. % NaCl). There is a systematic decrease in calculated $\delta^{18}O_{water}$ values with decreasing temperature in the Gyeongnam hydrothermal system (from 5.0 to -9.9 ‰). These trends are interpreted to indicate progressive mixing of high-salinity, magmatic hydrothermal fluids with cooler and less saline meteoric groundwater. Equilibrium thermodynamic data combined with mineral paragenesis, and fiuid inclusion and isotope data indicate that copper minerals precipitated mainly within a temperature range of 350° to 250°C. During early copper mineralization at 350°C, significant amounts of copper (10^3 to 10^2 ppm) could be dissolved in weakly acid NaCl solutions. For late mineralization at 250°C, about 10^0 to 10^{-1} ppm copper could be dissolved. Equilibrium thermodynamic interpretation indicates that the copper in the Gyeongnam hydrothermal system could have been transported mainly as a chloride complex and the copper precipitation occurred as a result of cooling accompanied by changes in the geochemical environments (fs_2, fo_2, pH, etc.) resulting in decrease of solubility of copper chloride complexes.

Mineralogy and Geochemistry of the Yangyang IOA deposit, South Korea

SEON-GYU CHOI[1]*, JIEUN SEO[1], JUNG-WOO PARK[2], DONG WOO KIM[1]

[1]Department of Earth and Environmental Sciences, Korea University, Seoul 136-701, Korea (*correspondence: seongyu@korea.ac.kr, still4@korea.ac.kr, heskool@korea.ac.kr)

[2]Research School of Earth Sciences, Australian National University, Canberra ACT 0200, Australia (jung.park@anu.edu.au)

The Yangyang deposit is characterized by the occurrence of a distinctive type of iron oxide apatite (IOA) deposit such as a Kiruna-type deposit. Occurrence in iron mineralization is concordant to discordant layered, lenticular or massive, magnetite-biotite, magnetite-actinolite, and magnetite-apatite-biotite-pyrite ores, which are hosted by a stratum of metamorphosed subvolcanic-sedimentary unit enclosed within Paleoproterozoic gneiss complexes. The phosphorous content in the apatite-rich magnetite ore varies up to ca. 7.38 wt. % P_2O_5. However, the iron ores have about 40 to 90 wt. % Fe_2O_3 with significantly low titanium content (< 0.57 wt. % TiO_2) and V content (< 404 ppm V).

The dominant mineral constituents consist of magnetite, actinolite, biotite and fluorapatite with subordinate amounts of scapolite, albite, diopsidic pyroxene, pyrite and carbonates. Titanite, allanite, monazite and fluorite are distinctively found in a mineral accessory assemblage. Apatite grains contain Th-poor monazite, magnetite, and sulfide inclusions commonly, and exhibit patchy zoning in concentrations of REE and some trace elements such as Si, S, V, Zr, Y, Pb, Th, and U, suggesting that apatite undergoes hydrothermal overprint as observed in other IOA deposits of Kiruna area, Sweden, and Bafq district, Iran. Sulfides clearly overprint the oxide stage assemblages and consist of minor pyrite ± chaclcopyrite. Low Ti, V, Cr, Co and Ni contents in magnetite indicate that these magnetites are not magmatic origin (i.e., nelsonite). The halite-bearing fluid inclusion in apatite shows an evolving hydrothermal system from saline fluids. REE-rich fluorapatite and titanite in the Yangyang ore mean ages of 198±13 Ma and 226.1±5.3 Ma, respectively (U-Pb LA-ICPMS ages). The Yangyang iron deposit has been precipitated from iron oxide-volatile-rich magmatic-hydrothermal fluids, which is derived from slightly alkaline magma.

https://doi.org/10.1180/S0026461X00006502 Published online by Cambridge University Press

Lu-Hf and Sm-Nd isotope systematics of Korean spinel peridotites: A case for Nd-Hf decoupling

SUNG HI CHOI[1,*] AND SAMUEL B. MUKASA[2]

[1]Department of Geology and Earth Environmental Sciences, Chungnam National University, Daejeon 305-764, S. Korea (*correspondence: chois@cnu.ac.kr)
[2]Department of Earth Sciences, University of New Hampshire, Durham, NH 03824 (sam.mukasa@unh.edu)

We have determined the Hf and Nd isotopic compositions of spinel peridotite xenoliths in alkali basalts from Baengnyeong (BR) and Jeju (JJ) islands, South Korea, in order to constrain the timing of melt depletion events. Equilibration temperatures estimated by two pyroxene thermometry range from 780 to 950ºC, and 960 to 1010ºC for BR and JJ peridotites, respectively. The BR peridotite clinopyroxenes are characterized by extremely radiogenic Hf in association with isotopically less extreme Nd, resulting in strong Nd-Hf decoupling compared to the mantle array. This is in stark contrast to the observation of well-correlated isotopic compositions of Hf and Nd in the JJ peridotite clinopyroxenes, plotting along the Nd-Hf mantle array. The Hf abundances and isotopic compositions of the BR clinopyroxenes were less affected by relatively recent secondary enrichments that overprinted the LREE abundances and Nd isotopes, which caused decoupling of Nd-Hf isotopes. In the case of JJ peridotites, the Nd-Hf isotopic compositions are considered to have been re-equilibrated, probably because of efficient diffusion at relatively higher temperature than the BR peridotites.

Lu-Hf tie lines for clinopyroxene and orthopyroxene from four of the Korean peridotites have negative slopes on the Lu-Hf isochron diagram, yielding negative ages. This is interpreted as indicating recent isotopic exchange of orthopyroxene by reaction with metasomatic agents having low $^{176}Hf/^{177}Hf$ components. Secondary overprinting in orthopyroxene was facilitated by the fact that this mineral has considerably lower Hf concentrations than does the co-located clinopyroxene. BR lherzolite clinopyroxenes yield a Lu-Hf isochron age of 1.9 ± 0.1 Ga, which is independently supported by a model Os age (T_{RD}) of 1.8 Ga on a refractory BR peridotite. We interpret this age range to mark the time of stabilization of the mantle section beneath this area by major melt extraction. This Proterozoic melt removal coincided in time with widespread ca. 2.1 to 1.8 Ga tectonothermal events documented throughout the Korean peninsula.

Kinetics and mechanism of antigorite dehydration: Implications for subduction zone seismicity

M. CHOLLET[1], I. DANIEL[1], K. T. KOGA[2], G. MORARD[3] AND B. VAN DE MOORTÈLE[1]

[1]Université Lyon 1, ENS de Lyon, CNRS, UMR 5276, Laboratoire de Géologie de Lyon, France (isabelle.daniel@univ-lyon1.fr)
[2]Laboratoire Magmas et Volcans, UMR CNRS 6524, IRD – M163, Université Blaise Pascal Clermont-Ferrand, France
[3]MARUM, Center for Marine Environmental Sciences, Bremen, Germany
[3]Institut de Minéralogie et de Physique des Milieux Condensés, Paris, France

Properties of serpentine minerals are thought to influence the occurrence and location of intermediate-depth seismicity in subduction zones, which is often characterized by two dipping planes separated by ca. 30 km defining a double seismic zone. The seismicity of the lower plane is believed to be provoked by the dehydration of serpentine since the experimentally determined stability limit for antigorite matches hypocenters location. This requires that the fluid produced by dehydration is released much faster than the typical time-scale of ductile deformation mechanisms. Here we measured the kinetics of antigorite dehydration *in situ* at high pressure and high temperature by time resolved synchrotron X-ray diffraction in a closed system. Antigorite dehydrates in two steps. During step (1) it partially breaks down into olivine and a hydrous phyllosilicate closely related to the 10Å phase. The modal abundance of the intermediate assemblage is described by 66 wt% antigorite, 19 wt% olivine, 12 wt% 10Å phase. During step (2) at higher temperature, the remaining antigorite and the 10Å phase fully dehydrate. From the analysis of reaction progress data, we determined that the major release of aqueous fluid occurs during step (2) at a fast rate of 10^{-4} $m^3_{fluid}.m^{-3}_{rock}.s^{-1}$. This exceeds by orders of magnitude the typical time scale of deformation by ductile mechanisms of any mineral or rock in the subducting slab or in the overlying mantle wedge. These results suggest that the fast dehydration of antigorite may well trigger the seismicity at intermediate depth in subduction zones.

[1] Chollet *et al*. (2011) *Journal of Geophysical Research*, **116**, B04203.

https://doi.org/10.1180/S0026461X00006502 Published online by Cambridge University Press

Distribution characteristics of Pt, Pd, and related traffic elements in dusts from Seoul, Korea

H.T. CHON[1]*, M. SAGER[2] AND H.Y.LEE[3]

[1]Department of Energy Resources Engineering, Seoul National University, Seoul 151-744, Korea (*correspondence: chon@snu.ac.kr)
[2]Austrian Agency for Health and Food Safety, A-1226 Vienna, Austria
[3]Korea Institute of Geosciences and Mineral Resources, Daejeon 305-350, Korea

The emission level and pollution characteristics of platinum (Pt) in dust, soils, and tree barks collected from Seoul metropolitan city was published for the first time in Korea (Lee and Chon, 2006). The previous study confirmed that an important source of Pt in roadside environment is automobile catalytic converter, and that it indicates a tendency to increase Pt levels in road dusts along with traffic volume. The study also suggested that not only traffic volume but also driving style have a great influence on Pt levels in road dusts.

In this study previous dust samples and some new collected dusts from Seoul were reanalyzed to determine Pt, Pd, and some traffic metal elements by ICP-MS and ICP-OES. The concentration levels of Pt and Pd were in the range of 0 – 444 (median 76) ng/g and 172 – 1,215 (median 609) ng/g, respectively, and remarkably high concentration of Pd and Pt in dust was found in the heavy traffic areas . Palladium also shows similar distribution trend with Pt that remarkably high concentration of Pd and Pt in dust was found in the heavy traffic areas. Distribution trend of some traffic elements such as Pb, Cr, Cu, Ni, Mo, Bi is also similar to that of Pt showing relatively high correlations (higher than r = 0.50) with Pt and Pd. Road dusts with high Pt and Pd levels were enriched in traffic related elements compared with road dusts from control suburb areas.

Geologic carbon-sulfur co-sequestration: Experimental investigation of a natural analogue, Madison Limestone, SW Wyoming USA

C. CHOPPING[1] AND J. KASZUBA[1,2]

[1]Department of Geology and Geophysics, University of Wyoming, Laramie, Wyoming 82071, USA (cchopp@uwyo.edu, john.kaszuba@uwyo.edu)
[2]School of Energy Recources, University of Wyoming, Laramie, Wyoming 82071, USA

SO_2 is a common impurity in effluent gasses of coal-fired power plants. Co-sequestering SO_2 and CO_2 can eliminate the need for pure CO_2 separations and related parasitic energy costs. For 50 million years, the Mississippian Madison Limestone in SW Wyoming has naturally contained a mixture of CO_2 (66%-95%), H_2S (5%) and other gases as well as sulfur complexes (SO_4^{2-} and HS^-) and minerals (anhydrite, pyrite, and native sulfur). These products of SO_2 disproportionation provide the opportunity to evaluate how a carbon-sulfur co-sequestration scenario evolves.

Hydrothermal experiments performed at 250 bars, 110°C evaluated brine-rock±supercritical CO_2 reactions between a Na-Cl-SO_4^{2-} brine (I=0.52 mol/Kg, 80 mmol/Kg SO_4^{2-}) and two different synthetic rock types (Do-Cc-Anh-Py and Do-Cc-Py). After CO_2 injection, dissolved CO_2 concentrations increased from 1.0 mmol/Kg to 1.1 mol/Kg. In situ pH decreased from approximately 7.5 to 4.8. Ca^{2+} and Mg^{2+} concentrations initially increased, but subsequent anhydrite precipitation decreased Ca^{2+} and SO_4^{2-} concentrations in both experiments. Fe^{2+} and Mn^{2+} metal mobilization increased from below detectable limits to 0.06 mmol/Kg in both experiments. Calcite dissolution, as evidenced by mineral pitting and etching, and anhydrite mineralization in the experiments are consistent with petrologic observations of Madison Limestone core. Ca^{2+} from dissolving calcite and dolomite reacts with SO_4^{2-} provided by SO_2 disproportionation to precipitate anhydrite. Anhydrite precipitation provides a mineral trap for sulfur, but may also clog available pore space.

https://doi.org/10.1180/S0026461X00006502 Published online by Cambridge University Press

Bio-inorganic interfaces in the critical zone

J. CHOROVER

Department of Soil, Water and Environmental Science, University of Arizona, Tucson, AZ 85721 (chorover@cals.arizona.edu)

At the particle scale, critical zone biogeochemical interfaces are heterogeneous and patchy. Patchiness results from the wide range in mutual affinities among primary bio-geo-chemical components that are continuously influent to terrestrial weathering systems (water, minerals, solutes, gases, cells). In addition, hydrologic events shift the disequilibrium state, generating short time-scale surface reactions, colloidal dynamics, and biotic/abiotic transformations that are superimposed on (and constrained by) long-term weathering history. A corollary is that the structure and reactivity of bio-inorganic interfaces are a function of the sequence of perturbations acting on the porous medium over an integrated soil residence time.

The complexity of critical zone systems raises challenging research questions that highlight the need to unravel these couplings and feedbacks: What products form when biochemical and geochemical components react in pore waters? How stable are these products to further biogeochemical transformation and how do they influence the evolution of interfacial structure in particles, aggregates, and porous media? How does this "architecture" dictate surface reactions and the bioaccessibility of carbon and/or contaminants? How does interfacial reactivity change over time and environment to control larger system (e.g., catchment) response?

These questions can be addressed by combining tools of analytical biogeochemistry with those of hydrology, geomorphology and ecology in bench-, meso- and field-scale experiments. One goal is to elucidate molecular- and pore-scale components and processes that are active contributors to observed meso- and field-scale phenomena (e.g., metalloid stabilization, carbon sequestration, catena structure formation, catchment hydrochemical response). Such studies require multi-faceted, interdisciplinary measurements in common systems and locations. Examples are presented from ongoing studies conducted at three scales (1) biomolecule-mineral surface reactions in aqueous suspensions, (2) metal(loid) transformation in phytostabilized tailings mesocosms, and (3) biogeochemical weathering fluxes in semi-arid catchments of the southwestern US.

Geochemical position of Pb, Zn and Cd in soils near a mine/smelter: Effects of land use, type of contamination and distance from pollution source

VLADISLAV CHRASTNÝ[1], ALEŠ VANĚK[2], MICHAEL KOMÁREK[3] AND MARTIN NOVÁK[1],

[1]Czech Geological Survey, Geologická 6, 152 00 Praha 5, Czech Republic

[2]Department of Soil Science and Soil Protection, Czech University of Life Sciences Prague, Kamýcká 129, 165 21 Praha 6, Czech Republic

[3]Department of Agro-Environmental Chemistry and Plant Nutrition, Czech University of Life Sciences Prague, Kamýcká 129, 165 21 Praha 6, Czech Republic

Contaminated agriculture and forest soil samples with mining and smelting related pollutants were collected in the Pb-Zn-Ag mining area near Olkusz, Upper Silesia to (i) compare the chemical speciation of metals in meadow and forest soils situated at the same distance from the point source of pollution (paired sampling design), (ii) to evaluate the relationship between the distance from the polluter and the retention of the metals in the soil, and (iii) to assess the effect of deposited fly ash vs. dumped mining/smelting waste on the mobility of metals in the soil. The smelting emissions intensively contaminated mainly the upper soil horizons, while the deposition of processing waste resulted in a contamination of the deeper parts of soil profiles. The maximum concentrations of Pb, Zn and Cd were detected in a forest soil profile near the smelter and reached about 25 g kg^{-1}, 20 g kg^{-1} and 200 mg kg^{-1} for Pb, Zn and Cd, respectively. Forest soils are much more affected than agriculture soils. However agriculture soils suffer from the downward metal migration more than the forest soils. Metal mobility ranges in the studied forest soils are as follows: Pb>Zn≈Cd for relatively circum-neutral soil pH (near the smelter), Cd>Zn>Pb for acidic soils (further from the smelter). The mobilization of Pb, Zn and Cd in soils depends on the persistence of the metal-containing particles in the atmosphere, and consequently on the mineralogical transformation controlled by the soil pH. Under relatively comparable pH conditions, the main soil properties influencing metal migration are total organic carbon (TOC) and cation exchange capacity (CEC).

https://doi.org/10.1180/S0026461X00006502 Published online by Cambridge University Press

Multi-isotopic constraints on contamination history, contaminant migration and structure of the F-Area acidic plume, Savannah River Site

JOHN N. CHRISTENSEN[1]*, MILES E. DENHAM[2], MARK E. CONRAD[1], MARKUS BILL[1] AND JIAMIN WAN[1]

[1]Lawrence Berkely National Lab., Berkeley, CA, USA (*correspondance: jnchristensen@lbl.gov) (msconrad@lbl.gov; mbill@lbl.gov; jwan@lbl.gov)
[2]Savannah River Natl. Lab., Aiken, SC, USA (miles.denham@srnl.doe.gov)

Seepage basins in the F-Area of the Savannah River Site were used from 1955 to 1989 for the disposal of low-level radioactive acidic (ave. pH ~2.9) waste solutions from site operations involving irradiated uranium and other materials used in the production of radionuclides. These disposal activities resulted in a persistent acidic groundwater plume (pH as low as 3.2) beneath the F-Area including contaminants such as ^{3}H, HNO_3, ^{90}Sr, ^{129}I and U that has impinged on surface water about 600 m from the basins. After cessation of disposal in 1989, the basins were capped in 1991. Since then, remediation consisted of a pump-and-treat system that was recently replaced by *in situ* treatment using a funnel-and-gate system with injection of alkaline solutions to neutralize pH.

In order to delineate the history of contamination and the current mobility and fate of contaminants in F-Area groundwater, we have undertaken a study of variations in the isotopic compositions of U ($^{234}U/^{238}U$, $^{235}U/^{238}U$, $^{236}U/^{238}U$), Sr ($^{87}Sr/^{86}Sr$), Nd ($^{143}Nd/^{144}Nd$) water ($\delta^{18}O$, δD) and nitrate ($\delta^{15}N$, $\delta^{18}O$) within the contaminant plume. The chemical and isotopic variations in the plume all delineate upper (0-15ft below water table) and lower (15-35 ft) zones within the upper aquifer. Together, the data suggest that the lower zone represents the effects of seepage from the basins during operation, while the upper zone represents mostly meteoric water contaminated by infiltration through the sub-basin vadose zone since closure/capping. Through U isotopic analysis, we have been able to detect recent migration as the plume expands laterally, with the greatest extent of U contamination near the top of the aquifer but decreasing with depth. Comparing the U isotopic compositions of groundwater samples collected within the plume two years apart tracks the migration of U from up-gradient portions of the plume. Nd isotopic compositions indicate that REE concentrations were controlled by progressive interaction between acid solutions and natural trace minerals in the sediments. Nitrate has an isotopic signature of processed waste, but no sign of nitrate bioreduction within the plume.

Vertical distribution of ^{236}U in the western equatorial Atlantic Ocean

M. CHRISTL[1]*, J. LACHNER[1], C. VOCKENHUBER[1], M. RUTGERS V. D. LOEFF[2], O. LECHTENFELD[2] AND I. STIMAC[2]

[1]Laboratory of Ion Beam Physics, ETH-Zurich, Switzerland, (*correspondence: mchristl@phys.ethz.ch)
[2]Alfred Wegener Institute, 27570 Bremerhaven, Germany

During the Pelagia Geotraces cruise PE321 in summer 2010 two depth profiles of ^{236}U were sampled in the western equatorial Atlantic Ocean (WEA) and subsequently analyzed at ETH Zurich using low energy accelerator mass spectrometry (AMS). These data represent the first ^{236}U-measurements in the open Atlantic Ocean.

^{236}U is almost exclusively produced by neutron capture on ^{235}U. While the natural background of $^{236}U/^{238}U$ is estimated to be in the 10^{-12} - 10^{-14} range anthropogenic $^{236}U/^{238}U$ ratios are much higher. For example, it can be estimated that as a consequence of the atmospheric nuclear bomb explosions about 1-2 tons of ^{236}U were blown into the atmosphere. Mixed with the upper few hundred meters of the Ocean this would result in $^{236}U/^{238}U$ ratios in the 10^{-9} range. Although the expected signal dynamics of $^{236}U/^{238}U$ in the environment is very large, currently only AMS-systems have the capability for a fast and quasi background free detection of $^{236}U/^{238}U$ ratios significantly below 10^{-9}.

At stations 39 and 40 of the PE321 cruise two depth profiles were sampled for ^{236}U (25 m. 2500 m, and 4250 m). The $^{236}U/^{238}U$ ratios decrease from about 10^{-9} at the surface down to about 10^{-10} in the Antarctic Bottom Water (AABW). The advective contribution of anthropogenic ^{236}U from the North Sea (from nuclear reprocessing plants) seems unlikely at this location. The most likely explanation for the elevated ratios in the AABW is the transport and the subsequent release of particle bound ^{236}U from the biologically active surface waters. Extrapolating from the calculated ^{236}U-inventories a total input of 1.5 - 2 tons of ^{236}U can be estimated for the global fallout. The inventory calculations are consistent with global fallout as the sole source for ^{236}U at the WEA. However, simple box model results show that very high U-export rates from the surface layer to the deep sea (>50 ng cm^{-2} yr^{-1}) would be necessary to reproduce the measured concentration profile.

Furthermore, a close correlation of salinity and ^{236}U was found, which is much steeper than the relation with natural U-isotopes in the open ocean. This indicates that, in contrast to natural U, ^{236}U has not yet reached steady state. Our results indicate that ^{236}U might have a large potential as a new conservative and transient tracer in Oceanography.

https://doi.org/10.1180/S0026461X00006502 Published online by Cambridge University Press

Sr isotopes ($\delta^{88/86}$Sr and ^{87}Sr/^{86}Sr) in cold seep environment of Niger and Nile Delta Fans

NAN-CHIN CHU*[1], EMMANUEL PONZEVERA[1], EMMANUEL FAVREAU[1], GERMAIN BAYON[1] AND YVES FOUQUET[1]

[1]IFREMER, BP70, Plouzané, 29280, France (*correspondence: nchu@ifremer.fr; eponzevera@ifremer.fr; gbayon@ifremer.fr; fouquet@ifremer.fr)

In cold seep areas, carbonates form as a result of the anaerobic oxidation of methane, which increases alkalinity in pore waters. Upon formation, cold seep carbonates incorporate dissolved alkali earth elements, such as Ca and Sr. The Ca and Sr isotopic compositions of authigenic carbonates and associated pore waters can hence provide information into fluid sources and biogeochemical processes at cold seeps. Over the last decades, radiogenic ^{87}Sr/^{86}Sr ratios in sediment interstitial fluids have been used for identifying deep fluid sources in seepage areas. However, recent studies have demonstrated that significant fractionation of stable Sr isotopes can occur in marine carbonates, which led to a revisited view of the oceanic budget [1].

Here, we report paired ^{87}Sr/^{86}Sr and $\delta^{88/86}$Sr values on a series of authigenic carbonate crusts and associated pore waters from fluid seepage areas of the Niger and Nile deep-sea fans. Sr isotopes were measured on a Neptune MC-ICP-MS using Zr for mass bias correction to acquire simutaneously radiogenic and stable (^{87}Sr/^{86}Sr and $\delta^{88/86}$Sr) values [2, 3]. Our results indicate that $\delta^{88/86}$Sr values for most carbonate samples exhibit very small fractionation relative to seawater or pore water signatures, contrary to biogenic carbonates that shows a 0.1‰/amu lower than seawater [1]. Exceptions are found for a few samples collected from mud volcano settings, which are characterized by distinctively low ^{87}Sr/^{86}Sr and $\delta^{88/86}$Sr values. We will discuss the Sr isotope systematics in comparison with other proxies.

[1] Krabbenhöft (2010) *GCA*, **74**, 4097-4109. [2] Ohno and Hirata (2007) *Anal. Sci.*, **23**, 1275-1280. [3] Yang *et al.* (2008) *JAAS*, **23**, 1269-1274.

What role did methane seeps play in the formation of the Doushantuo cap carbonate?

XUELEI CHU[1]*, JING HUANG[2] AND T.W. LYONS[3]

[1]Institute of Geology and Geophysics, CAS, Beijing 100029, China (*Correspondance: xlchu@mail.iggcas.ac.cn)
[2]Institute of Geology and Geophysics, CAS, Beijing 100029, China (jhuang@mail.iggcas.ac.cn)
[3]Dept. of Earth Sciences, Univ. of California, Riverside, CA 92521, USA (timothyl@ucr.edu)

Extremely negative $\delta^{13}C_{carb}$ values, less than -30‰, have been reported for the cap carbonate of the Ediacaran Doushantuo Formation (ca. 635 Ma) and used to support the hypothesis that methane hydrate destabilization contributed significantly to formation of the enigmatic cap carbonate and negative carbon isotope anomalies following Neoproterozoic ice ages (1, 2). Here, we show distinct differences between the methane-related carbonate and bulk cap carbonate.

Negative $\delta^{13}C_{carb}$ values of <-30‰ obtained from isopachous cements and recrystallized carbonate crusts have been found only in the Yangtze Gorges area (YGA), South China. These microsamples were reported from secondary, pore-filling carbonate minerals tied to methane seep activity, rather than reflecting the bulk composition of the cap carbonate. We investigated the Doushantuo cap carbonate at three localities, the Jiulongwan (inner-shelf, YGA), Zhongling (outer-shelf), and Long'e (basin) sections, and find that the $\delta^{13}C$ and $\delta^{18}O$ values for the cap vary from -2‰ to -10‰ and -5‰ to -12‰, respectively, and show a postive $\delta^{13}C$-$\delta^{18}O$ correlation, with a negative trend from the shallow to deep sites. Interestingly, all the microsampled $\delta^{13}C$ and $\delta^{18}O$ data from the methane-seep sections in the YGA (1, 2) show two distinct trends in the $\delta^{13}C$-$\delta^{18}O$ cross-plot, a positive correlation the same as the bulk cap carbonate and negative correlation attributed to methane oxidation. Similar to the Upper-Cretaceous Tepee Buttes in Colorado (3), the latter shows a nice relationship from early to late diagenetic carbonate phases – starting with very light, methane-dominated carbon.

We conclude that the methane-related carbonate can be distinguished clearly from the bulk Doushantuo cap carbonate by coupled C and O isotopes.

This research is funded by the Ministry of Science and Technology of China (Grant 2011CB808805)

[1] Jiang *et al.* (2003) *Nature* **426**, 822-826. [2] Wang *et al.* (2008) *Geology* **36**, 347-350. [3] Kauffman *et al.* (1996) *Geology* **24**, 799-802.

https://doi.org/10.1180/S0026461X00006502 Published online by Cambridge University Press

Multi-scale modelling of ions and water diffusion in clays

S.V. CHURAKOV

Paul, Scherrer Institute, Villigen-PSI, CH-5232, Switzerland (sergey.churakov@psi.ch)

Materials with low hydraulic permeability such as clays are major components in engineered and natural barriers for waste disposal sites. Migration of ions and water through such barrier systems over safety relevant times are predicted solving diffusion equation on continuum scale. Natural clay, however are highly heterogeneous in terms of porosity and mineralogical composition. These heterogeneities are manifested at different scales and consequently have strong influence on diffusion of solutes. To fully understand the mechanism of ion transport in clays the solute migration has to be addressed using complementary simulations and measurements capable of resolving the transport and chemical phenomena on different scales.

In clays, up to 50-70% of fluid accessible pore space is attributed to the interlayer and the diffuse double-layer porosity where solution properties, namely the mobility of ions and water, are strongly influenced by mineral surfaces. The transport through such nanopores is readily addressed by molecular simulations. At the sub-micrometer scale the individual interlayers are interconnected thought the macrospores. Molecular simulations with explicit solvent approach are not feasible at this scale anymore. Instead pore scale stochastic approaches are used to assess the influence of pore geometry and topology on the effective diffusion coefficient of the sample. Finally, state-of-the-art X-ray tomography measurements can provide 3D mineral distribution in a sample non-destructively at a resolution down to few micrometers. These data are directly used in transport simulations to reveal the consequences of mineralogical and textural heterogeneities in clays and their influence on the effective transport parameters of clay samples. Such a multi-scale treatment of transport phenomena using complementary modelling and measurement techniques is a necessary condition for accurate and reliable prediction of radionuclides migration over geological space and time domains.

Two step up-scaling of molecular diffusion coefficients in clays

S.V. CHURAKOV[1]*, TH. GIMMI[1,2] AND M TYAGI[1]

[1]Paul, Scherrer Institute, CH-5232 Villigen-PSI, Switzerland (*correspondence: sergey.churakov@psi.ch)

[2]University of Bern, CH-3012 Bern, Switzerland

Mass transport in rocks with low hydraulic conductivity such as clays originates from Brownian motion of molecules and ions in the solution and their interaction with the surface of the minerals. Up-scaling these molecular phenomena to the continuum scale, which is required for large-scale and long-time predictions, is particularly challenging because the considered scales differ by orders of magnitude. To address the up-scaling problem we developed a two-step simulation approach which enables us to derive macroscopic diffusion coefficients of water and ions for continuum equations from pore scale molecular diffusion coefficients [1]. Our starting point for the up-scaling procedure is local pore diffusion coefficients derived from molecular dynamics simulations for specific local environments, such as the interlayer or edge regions of clay particles. We then assign these local diffusion coefficients to different types of porosity of a model clay structure and obtain the structure-averaged effective diffusion coefficient of the sample by random walk simulations. Our model clay rock is composed of compacted grains of clay minerals. The space between the grain boundaries forms micro-pores. To generate such structures, a kinetic Monte Carlo method is employed on a grid to obtain closely packed grains of desired shapes, sizes and orientations. By varying the composition and geometrical properties of the clay model we have investigated the effects of mineralogical heterogeneities and of anion exclusion on the diffusion coefficients measured in laboratory experiments. Our up-scaling concept is general and can be used for up-scaling molecular diffusion coefficients for porous materials with almost arbitrarily complex structures.

[1] Churakov & Gimmi, (2011) *J. Phys. Chem. C* **115**, 6703-6714.

https://doi.org/10.1180/S0026461X00006502 Published online by Cambridge University Press

Geochemical study Soltanieh Formation limestone deposits to determine the primary mineralogy and the mineralogical processes of limestone (SW Urmia)

ALIASGHAR CIABEGHODSI

Urmia University-Faculty of Sciences-Department of Geology-Po.Box:57153-165 Urmia-Iran (a.siabeghodsy@urmia.ac.ir)

Soltanieh Formation deposits in the south west of Urmia mainly carbonate rocks and shale alternation is made. Soltanieh Formation calcareous rocks mainly influenced meteoric diagenetic an open system are located. According to the distribution main and secondary elements and isotopes of oxygen and carbon range of calcareous deposits formation Soltanieh comparable Gordon Limestone of Tasmania with the mercenaries and the mineralogical composition is aragonite. Mineralogical composition of aragonite limestone Neoproterozoic other parts of the world already has been confirmed by other researchers [1]. These studies indicate that the limestone, such as Gordon Limestone of Tasmania, Meteoric affected processes are located. Soltanieh Formation limestone samples of oxygen and carbon isotope values are light to light? 13 °C (mean (-4.57 ‰ VPDB Soltanieh formation in the samples due to the severe effect is diagenesis meteoric. Changes in Sr/Mn indicates high dissolution rate This is limestone. temperature of the limestone formation based on the heaviest isotope of oxygen (equivalent to ‰ 83/5-) and? w sea water (equivalent to 1 ± 3 -), respectively 23 and 31 °C has been calculated.

[1] Fairchild & Spiro (1987) *Sedimentology* **34**, 973-989.

Europium structural role in silicate glasses

M.R. CICCONI[1]*, G. GIULI[1], E. PARIS[1], W. ERTEL-INGRISCH[2], D.B. DINGWELL[2] AND P. ULMER[3]

[1] School of Science and Technology – Geology Division, University of Camerino, I (*correspondence: mariarita.cicconi@unicam.it)
[2]Dept. of Earth and Environmental Sci., LMU München, D
[3]Institut f. Mineralogie und Petrographie, ETH Zürich, CH

Rare Earth Elements (REE) have demonstrated to be important geochemical indicators; in fact, the distribution of REE in igneous rocks are frequently used to constrain the mineralogy of the source materials, the degree to which magma composition has been modified by crystal fractionation, and to identify the mineral phases removed from the magma during differentiation. Moreover, the Eu redox ratio can be used to constrain the formation conditions within a very large range of oxygen fugacity down to few log units below the Fe/FeO buffer. The $Eu^{+2}/(Eu^{+2} + Eu^{+3})$ ratio is therefore very useful in the study of meteoritic material and in studying planetary evolution. A complete understanding of transition and REE elements is important for the geochemical and petrological interpretations of magmatic processes and partition properties between melt and crystals. To this aim, synthetic silicate glasses corresponding to compositions relevant for the Earth sciences were used to study the dependence of the redox states of Eu on the bulk melt composition and at different values of oxygen fugacity (from air to IW-2). The samples have been analyzed via Eu LIII-edge X-ray Absorption Spectroscopy (XAS) to study the Eu oxidation states and local environments. Eu LIII-edge XANES peak analysis allowed the quantitative assessment of Eu redox ratio. XANES spectra vary systematically with composition and with f_{O2} (log $f_{O2} \sim 0$ to –11.6) indicating changes in the Eu oxidation state. The intensity of the shoulders on the absorption edges were quantified and used to determine $Eu^{+2}/(Eu^{+2} + Eu^{+3})$ ratio. Moreover, the local environment of Eu was determined by EXAFS (Extended X-ray Absorption Fine Structure) analyses, highlighting the different Eu behaviour as function of the f_{O2}. This work has clearly demonstrated that for a better interpretation of the Eu anomalies observed in rocks and minerals, which are often used to constrain magmatic evolutions of igneous regions, the melt composition and the redox condition must be taken into consideration.

https://doi.org/10.1180/S0026461X00006502 Published online by Cambridge University Press

Nanoparticles in aqueous environments: Electrochemical, nanogravimetric, STM and AFM studies

I. CIGLENEČKI[1]*, E. BURA-NAKIĆ[1], M. MARGUŠ[1], I. MILANOVIĆ[1], N. BATINA[2], A. AVALOS-PEREZ[2] AND D. KRZNARIĆ[1]

[1]Ruđer Bošković Institute, Bijenička 54, 10 000 Zagreb, Croatia (*correspondence: irena@irb.hr)

[2]Laboratorio de Nanotecnología e Ingeniería Molecular, Área de Electroquímica, Depto. Qiumica, UAM-I, Mexico City, Mexico.

Electrochemical and piezo-nanogravimetric (EQCM) studies in combination with atomic force and scanning tunneling microscopy (AFM,STM) have been used for characterization and determination of chalcogenide nanoparticles in model solutions and natural samples. Different electrode surfaces (Hg and Au) were used to give more details relating to attachment, adsorption, deposition and interaction between selected nanoparticles and functionalized electrode surfaces.

Mercury electrodes preconcentrate some metal sulfide nanoparticles effectively, enabling their detection at submicromolar concentrations. Voltammetrically active metal sulfides are accumulated on Hg electrode surfaces by two mechanisms: a) adsorption of nanoparticles to an electrode where they undergo reduction at -0.9 to -1.35 V (vs. Ag/AgCl), and b) formation directly at the Hg electrode surface in supersaturated metal sulfide solutions; the latter produces an analytical artifact [1]. In the case of FeS nanoparticles, anodic oxidation of Hg by FeS at around -0.45 V is the operating mechanism for their determination in aqueous solution [2].

By following changes in resonance frequency accompanied with some changes in current produced during oxido-reduction processes, it is possible to characterize physico-chemical properties and to calculate the mass of nanoparticles deposited on the Au surface over a broad range of environmentaly relevant solution characteristics, including variation in ionic strength, composition and particle sizes. Particle deposition mechanisms are studied in relation to variations of particle charge, particle size and applied electrode potential, all with the aim to improve and develop new analytical methods for fast, selective, qualitative and quantitative nanoparticle characterization in natural waters.

This research was suported by UKF grant 62/10.

[1] Bura-Nakić *et al*. (2007), *Anal. Chim. Acta* **594**, 44-51. [2] Bura-Nakić *et al*. (2011), *Electroanalysis,* in press.

The largest deposit of strategic REE, Bayan Obo, geological situation and environmental hazards

HANA CIHLAROVA[1], JINDRICH KYNICKY[1], XU CHENG[2], WENLEI SONG[2], ANTON CHAKMOURADIAN[3] AND KATARINA REGUIR[3]

[1]Mendel University in Brno, 613 00 Brno, Czech Republic; (xcihlaro@seznam.cz)

[2]Chinese academy of sciences, China (xucheng1999@hotmail.com)

[3]University of Manitoba, Winnipeg, Manitoba, Canada (chakhmou@cc.umanitoba.ca)

Bayan Obo Fe-Nb-REE super large deposit in Inner Mongolia is the main source of REE in the world and makes China the monopolist producer of these strategic elements. A typical feature of the Bayan Obo super large deposit is the presence of polymetalic Fe-Nb-REE mineralization in 3 different ores - disseminated, banded and massive. The principal REE bearing minerals are bastnaesite [(Ce,La,Nd)(CO_3)F] followed by monazite [(Ce,La,Nd)PO_4] in disseminated and banded ores. Magnetite and hematite are the dominant Fe-ore minerals in massive ores. Mining process in grassland and ore processing in Baotou bring several environmental hazards. Actual risk assessment is contaminated dust by Th and heavy metals, and it´s transporting by sand storms to X00 km in main direction to SE (Peking capital). Leaching of old-mined ore is responsible for contamination of soil and ground water collectors by heavy metals and radioactive thorium (bastnaesite and monazite ores contain up to 0,5% ThO_2). The harm to environment of the past is mainly ore processing causing dominantly water contamination. Presently the ore processing is ecologically and economically well-developed under supervision of Baotou Institute of rare earth elements.

https://doi.org/10.1180/S0026461X00006502 Published online by Cambridge University Press

Structural aspects and surface reactivity of aluminous ferrihydrite precipitates

A.C. CISMASU [1]* F.M. MICHEL[1,2] J.F. STEBBINS[1], C.M. LEVARD[1] AND G.E. BROWN JR[1,2].

[1]Dept. of Geological & Environmental Sciences, Stanford University, Stanford, CA 94305-2115, USA (*correspondence: cismasu@stanford.edu)

[2]Stanford Synchrotron Radiation Lightsource, SLAC National Accelerator Laboratory, Menlo Park, CA 94025, USA

Ferrihydrite (Fh), a hydrated, nanoparticulate, high surface area, reactive Fe-oxide, impacts the mobility of inorganic and organic pollutants through sorption reactions in a variety of natural environments. Aluminous Fh is common in nature primarily because of the natural abundance of Al. However, few studies have dealt with Al-Fh, and thorough structural analyses of this phase are lacking. The mode of association of Al with Fh may vary from true chemical substitution, to surface precipitation, to formation of a mixture of two (or more) individual nanoscale phases. This may have a considerable effect on the composition and/or structure of Fh nanoparticle surfaces, and thus on their surface reactivity and their interaction with pollutant species.

Here we used a variety of laboratory (TEM, NMR), and synchrotron-based techniques (X-ray total scattering and PDF analysis, scanning transmission x-ray microscopy) to characterize two Al-Fh series synthesized at variable precipitation rates in the presence of 5 to 40 mol % Al. We find that roughly 25 mol % Al is incorporated in Fh, regardless of the synthesis method we used. Phase separation (formation of Al-hydroxides, e.g., gibbsite) was most significant at Al concentrations above 30 mol % Al. However, Al-hydroxide phases were also detected in samples of lower Al content (as low as 15 mol % Al), particularly in the slowly precipitated series; this finding may be a result of the kinetics of co-precipitation. Furthermore, it appears that the amount of Al incorporated in Fh is not affected by the synthesis method and is more likely controlled by the accumulated strain caused by Al in the Fh lattice. Finally, the surface reactivity of selected Al-Fh samples was investigated by Zn-adsoprtion experiments, which indicate a slight decrease in overall Zn adsorption in comparison to pure Fh. Our results provide an in-depth look at the structure and surface of Al-Fh, as well as insights about the interaction between Al and Fe during co-precipitation.

Re-partitioning of Fe and Cu during the oxidation and acidification of acid sulfate soil materials

S.R. CLAFF[1,2]*, E.D. BURTON[1], L.A. SULLIVAN[1] AND R.T. BUSH[1]

[1]Southern Cross GeoScience, Southern Cross University, Lismore, NSW, Australia (*correspondence salirian.claff@scu.edu.au)

[2]CRC CARE, University of South Australia, Mawson Lakes, SA 5095, Australia

Drainage and excavation of coastal lowlands for agricultural and urban development often results in the oxidation of underlying Fe-rich sulfidic sediments. Exposure and subsequent dissolution of these sulfide minerals creates acidity in the form of sulfuric acid and ferrous Fe [1]. The coupled processes of oxidation and acidification result in the release and re-partitioning of Fe and associated trace metals from stable, reduced mineral phases to more mobile, oxidised forms. Elevated metal concentrations are commonly associated with the drainage waters of these landscapes [2]

We followed the partitioning changes to Fe and Cu during the short-term oxidation and acidification of two acid sulfate soil materials. The “labile”, “acid-soluble”, “organic”, “crystalline oxide”, pyritic” and “residual” metal pools were measured sequentially [3].

Initially Fe and Cu were stored in the “pyritic”, “acid-soluble” and “residual” metal fractions. The “residual” fraction measured changed little during the 90-day oxidation experiment, indicating that it was not a major source for Fe and Cu to more mobile fractions during short-term oxidation events. The “pyritic” fraction, however, is dominated by minerals which undergo oxidative dissolution when exposed to atmospheric oxygen. Major re-partitioning of Fe and Cu was expected and observed - metals initially associated with the “pyritic” fraction were re-distributed to more environmentally available fractions i.e. the “acid-soluble” and “labile” fractions. The “acid-soluble” fraction was a major source of metals both initially and as oxidation progressed. The shift to “labile” and thus leachable metal pools did not occur until conditions of extreme acidification (i.e. pH <4) were reached.

As the “labile” fraction poses the most immediate environmental hazard, managing soil acidity will be the most effective means for reducing Fe and Cu mobility in acid sulfate soils.

[1] Sundström and Åström (2006) *Bor. Environ. Res.* **11**, 275-281[2] Nordmyr *et al.* (2008) *Est. Coast. Shelf Sci.* **76**, 141-152 [3] Claff *et al.* (2010) *Geoderma* **155**, 224-230.

https://doi.org/10.1180/S0026461X00006502 Published online by Cambridge University Press

Non-invasive geophysical imaging for characterization of engineered *in situ* radionuclide precipitation

BOYCE CLARK[1]*, JEFF GILLOW[2], PAUL PRESTON[3], BERNIE ILGNER[1] AND SCOTT MORIE[4]

[1]ARCADIS U.S., Inc., Baton Rouge, LA 70816, USA (*correspondence: boyce.clark@arcadis-us.com);
[2]Highlands Ranch, CO 80129, USA (jeff.gillow@arcadis-us.com);
[3]Knoxville, TN 37934 (paul.preston@arcadis-us.com, bernie.ilgner@arcadis-us.com)
[4]Nuclear Fuel Services, Erwin, Tennessee 37650 (csmorie@nuclearfuelservices.com)

Stabilization of aqueous-phase uranium can be achieved through injection of degradable organic carbon to create anaerobic conditions. Uranium is soluble under aerobic conditions, exhibiting complex geochemistry and persistence in these environments. Under anaerobic conditions, uranium reductively precipitates to the insoluble uraninite mineral phase. Under these conditions, oxidized iron minerals are transformed to reduced iron minerals such as iron sulfide. Under aerobic conditions, the reduced iron minerals provide stability to the uraninite by acting as a redox buffer and physical encapsulant. Formation of these reduced iron sulfide minerals can be engineered through the injection of soluble iron and sulfate along with degradable organic carbon. At Nuclear Fuel Services in Erwin, TN, localized areas of the facility with low concentrations of uranium in groundwater are being treated with in-situ reductive precipitation of uranium and engineered precipitation of reduced iron sulfide minerals.

In order to non-invasively characterize the treatment zone, time-domain induced polarization (IP), a surface geophysical technique capable of locating iron and sulfide minerals based on their chargeability was used to guide a drilling program. Based on the IP imaging, soil cores were obtained. The cores were analyzed using advanced mineralogical characterization methods including scanning electron microscopy, energy dispersive x-ray spectroscopy, microprobe x-ray fluorescence, and x-ray absorption spectroscopy to evaluate the elemental association and valence state of uranium, sulfur, and iron. The results of this comprehensive characterization indicates that targeted phases are forming in the soil as a result of treatment. This presentation will discuss the soil characterization, coupled with non-invasive geophysical characterization and strategy for the in-situ engineered precipitation of soluble uranium through creation of reactive mineral phases.

Combustion aerosol over marine stratus: Long range transport, subsidence and aerosol-cloud interactions over the South East Pacific

A. CLARKE[1]*, S. FREITAG[1], J. SNIDER[2], J. KAZIL[3,4], G. FEINGOLD[4], T. CAMPOS[5] AND V. BREKHOVSKIKH[1]

[1]University of Hawaii, Honolulu, HI, USA (*correspondence: tclarke@soest.hawaii.edu)
[2]University of Wyoming, Laramie, WY, USA
[3]CIRES, University of Colorado, Boulder, CO, USA
[4]NOAA, Earth System Res. Lab., Boulder, CO, USA
[5]NCAR, Boulder, CO, USA

The worlds largest stratus deck over the South East Pacific (SEP) was a study target for the VOCALS (http://www.eol.ucar.edu/projects/vocals/) experiment in October 2008. Aerosol-cloud interactions were one major goal of several ship and aircraft studies including results from 14 flights of the NCAR C-130 aircraft reported here. Each flight covered about a 1000 km range with multiple profiles and legs below, in and above the Sc deck.

Strong aerosol sources along the coast of Chile were expected and found to influence cloud condensation nuclei (CCN) in coastal clouds. However; “rivers” of elevated CO, black carbon (BC) associated with combustion aerosol effective as CCN at <0.3%S were also common in subsiding FT air overlying the extensive Sc deck for over 1000km offshore. This subsidence, linked to the Hadley circulation, brought in aerosol from sources over the western Pacific as well as South America. Observed entrainment of this aerosol was linked to cloud related turbulence. When present, this combustion aerosol increased available CCN and decreased effective radius compared to clouds in “clean” MBL air advected from the South Pacific. We hypothesize that this entrainment can help buffer MBL clouds over the SEP against depletion of CCN by drizzle. This may delay transition of closed cell to open cell convection, potentially leading to increased lifetimes of Sc clouds that entrain such aerosol.

https://doi.org/10.1180/S0026461X00006502 Published online by Cambridge University Press

The structure and topology of cytochromes involved in outer membrane electron transport

T.A. CLARKE[1]*, M.J. EDWARDS[1], A.M. HEMMINGS[1], A. HALL[1], G. WHITE[1], A. GATES[1], J.N. BUTT[1], L. SHI[2], J. FREDRICKSON[2], J. ZACHARA[2] AND D.J. RICHARDSON[1]

[1]Centre for Molecular and Structural Biochemistry, School of Biological Sciences, Univ. of East Anglia, Norwich, UK (*correspondence : tom.clarke@uea.ac.uk)
[2]Pacific Northwest National Laboratory, Richland, WA, USA

Characterisation of Outer Membrane Cytochromes.

Extracellular mineral respiration is dependent on the correct expressionof an outer membrane porin-cytochrome complex, where a large transmembrane porin mediates direct electron transfer between a small decaheme periplasmic cytochrome and an extracellular decaheme cytochromeon the cell surface. [1] Over 30 % of the *Shewanella oneidensis* surface is covered with these outer membrane cytochromes and it has been shown that there are multiple members of the outer membrane cytochrome family are capable of interacting with a broad range of mineral oxides [2,3].

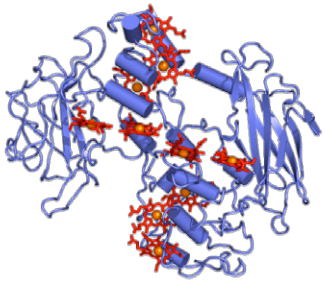

Figure 1: Structure of MtrF, a decaheme outer membrane cytochrome involved in mediating electron transport between *S. oneidensis* and extracellular mineral.

We have resolved the crystal struture of one of these outer membrane cytochrome, shown in figure 1, and this has revealed that these proteins comprise a c-type cytochrome core flanked by two β-barrel domains [4]. This structure provides a base for understanding how these systems interact with both the outer membrane and the extracellular enviroment.

[1] Hartshorne *et al*. (2009) *P.N.A.S.***106**, 22169-74 [2] Lower *et al*. (2007) *Appl. Env. Microbiol*. **75,** 2931-2935 [3] Shi *et al*. (2009) *Env. Microbiol. Reports* **1,** 220-7. [4] Clarke *et al*. (2011) *P.N.A.S. Accepted for publication*.

Plate- versus plume-driven processes – South Atlantic DUPAL revisited

C. CLASS[1]* AND A. P. LE ROEX[2]

[1]Lamont-Doerty Earth Observatory, Palisades, NY10964, USA (*correspondence: class@ldeo.columbia.edu)
[2]University of Cape Town, Rondebosch, 7701, South Africa

The DUPAL anomaly in the South Atlantic is present in intra-plate volcanism associated with the Tristan-Gough, Discovery and Shona plumes, and along adjacent sections of the southern Mid-Atlantic Ridge. Its origin has been variably attributed to either plate-driven processes introducing continental material into the shallow mantle, or plume-driven processes sampling sources in the lower mantle, which cannot be distinguished based on geochemical arguments alone. Here we present an integration of geochemical arguments and dynamic considerations and test the following hypotheses:

(1) South American origin – Previous geochemical evidence suggests that the DUPAL originates from the South American sub-continental lithospheric mantle (SCLM), possibly thermally eroded by the Tristan plume head. However, our mass balance calculation shows that an unrealistic volume of SCLM would be needed for the contamination of thousands of cubic km of upper mantle in a direction unsupported by any obvious mantle flow regime.

(2) South African origin - A mantle flow field induced by the African Superplume has been inferred previously from seismic anisostropy, suggesting mantle flow from beneath Africa and possible contamination of the S Atlantic upper mantle with African plate material. However: (i) off-craton SCLM and lower crustal samples provide no evidence in support of thermally eroded or tectonically detached African plate material being the origin of the S Atlantic DUPAL anomaly [1]. (ii) Erosion of the base of the Kaapvaal craton by the Superplume-related mantle flow is not supported by available constraints on the composition of the Kaapvaal SCLM [1]. In addition, volcanism from upper mantle melting anomalies at Vema and 7 degree Seamount do not support an overall contamination of the S Atlantic shallow mantle [1].

(3) Deep origin – A deep, plume-related origin of the S Atlantic DUPAL is supported by the spatial extent of the anomaly in S Atlantic MORB adjacent to DUPAL plumes. Mixing systematics are consistent with the different plumes showing plume-ridge interaction as a function of distance to the ridge. Extreme isotopic heterogeneity of the S Atlantic DUPAL source is indicated from plume trail samples of the DUPAL plumes. Similarities and differences to Indian and Pacific Ocean DUPAL anomalies are explored.

[1] Class & le Roex (2011) *EPSL* **305**, 92-102.

https://doi.org/10.1180/S0026461X00006502 Published online by Cambridge University Press

Ecological impact of submarine groundwater discharge in a Mediterranean lagoon: Correlations between radon, radium and nitrate in the Mar Menor, Murcia, Spain

CHRISTELLE CLAUDE[1], PAUL BAUDRON*[23], ADRIANO MAYER[1], JAVIER GILABERT [4], DAVID MARTINEZ VICENTE[2] , OLIVIER RADAKOVITCH[1], CHRISTIAN LEDUC[3], JOSE LUIS GARCIA AROSTEGUI[5], AND FRANCICO CABEZAS CALVO-RUBIO[2]

[1]CEREGE, Europôle de l'Arbois, 13545 Aix-en-Provence, France, (claude@cerege.fr)
[2]F-IEA, Complejo de Espinardo, C\ Nacional 301, 30100 Murcia, Spain, (paul.baudron@baudron.com)
[3]G-EAU, BP 5095, 34196 Montpellier cedex 5, France, (Christian.Leduc@ird.fr)
[4]Department of Chemical & Environmental Engineering, Technical University of Cartagena (UPCT), Alfonso XIII, 52, E30203, Cartagena, Spain, (javier.gilabert@upct.es)
[5]IGME, Avenida Miguel de Cervantes, 45, 30009 Murcia, Spain, (j.arostegui@igme.es)

Since 15 years numerous works have shown the influence of submarine groundwater discharge (SGD) on the water budget of lagoons, bays or open coastal areas [1]. In particular the high concentrations in nutrients of discharging groundwater may result in very productive ecosystems [2]. A radon-radium study was coupled with nutrients in semi-arid South-Eastern Spain. Mar Menor lagoon (135 km^2) is bordered by a Quaternary sedimentary aquifer extending over 1200 km^2. ^{222}Rn and ^{224}Ra activities in groundwaters along the coast range between 2200 to 17500 and 16 to 120 Bq/m^3 respectively. In the lagoon, ^{222}Rn and ^{224}Ra activities varied from 10 to 100 and 4 to 8 Bq/m^3 respectively. The increase of both nuclides is localized and synchronous with a peak in NO_3^- and chlorophyll, revealing groundwater input. In the same area, changes observed in coastal vegetation could be related. Further measurements will refine the SGD flux to Mar Menor and its ecological impact.

[1] Moore W. S. (1996), *Nature* **380**, 612-614. [2] Laroche, J., Nuzzi, R., Waters, R., Wyman, K., Falkowski, P.G., and Wallace, D.W.R. (1997), *Global Change Biology* **3**, 397-410.

Uranium-series mobility during spheroidal weathering of 300 kyrs old basalt (La Réunion Island)

CHRISTELLE CLAUDE[1], JEAN-DOMINIQUE MEUNIER*[1], DAOUDA TRAORE[2], FRANÇOIS CHABAUX[3], BRUNO HAMELIN[1] AND FABRICE COLIN[2]

[1]CEREGE, Europôle de l'Arbois, 13545 Aix-en-Provence, France, (claude@cerege.fr)
[2]IRD, Anse Vata, BP A5, 98848 Nouméa Cedex, New Calédonia, (fcolin.noumea@gmail.com)
[3]Laboratoire d'Hydrologie et de Géochimie de Strasbourg EOST, 1 rue Blessig , 67084 Strasbourg cedex, (fchabaux@unistra.fr)

Spheroidal weathering (also named corestone-shell systems hereafter called CSS) is a common form of chemical weathering affecting many types of rocks [1]. The spheroidal structures are good models for studying weathering budget because the volume of shell rocks during weathering is conservative [2]. The CSS constitute therefore an open system for mobile elements such the major cations and silica that are leached out of the units. Conversely, they also can be seen as a closed system relative to poorly mobile elements such as Ti, Al or Fe which are only displaced from the core to the outer shell. During chemical weathering processes, natural radionuclides from the uranium series are either mobile or refractory and this differentiated behavior disturbs the status of radioactive secular equilibrium characterizing geological formations. Consequent radioactive ^{234}U-^{238}U-^{230}Th disequilibria can be used as a tool to estimate rate of soil formation on a time scale of circa 1 Ma. Here we combine mineralogical observations, geochemistry of major and trace elements to Sr isotopes and U-series as an attempt to constraint the rate of spheroidal weathering of a basaltic flow dated at 292 ±10 ka from la Reunion Island. U-transport model shows a remobilization process occurring on a time-scale of ca 250 ka. $^{87}Sr/^{86}Sr$ variations are small (0.7042 - 0.7050). Highly mobile Sr is leached out in 1500 yrs only. Sr fluxes are 1 order of magnitude higher than steady state conditions [3] suggesting that weathering rates could be higher during the first stages of alteration.

[1] Ollier, C.D., (1971), *Earth Sci. Rev.* **7**, 127-141. [2] Patino, L.C., Velbel, M.A., Price, J.R., Wade, J.A., (2003). *Chem. Geol.* **202**, 343-364. [3] Rad, S.D., Allègre, C.J., Louvat, P., (2007), *Earth Planet Sci. Lett.* **262**, 109-124.

https://doi.org/10.1180/S0026461X00006502 Published online by Cambridge University Press

Evolving isotopic fluxes to Asian marginal seas controlled by Monsoon strength since the Last Glacial Maximum

PETER D. CLIFT, DENGKE HU AND DAVID LIMMER

School of Geosciences, University of Aberdeen, Aberdeen, AB24 3UE, UK

The intensity of the Asian monsoon is expected to have a major impact on the strength of erosion and chemical weathering in continental river basins. Because these processes are linked to solar insolation there should be major variations in the chemical flux to the ocean on millennial timescales. To test this hypothesis we have examined the erosional response of rivers in different parts of Asia to monsoonal changes since 14 ka. ODP Site 1144 in the South China Sea shows little provenance variation, but a major changes in Sr isotope composition, clay mineralogy, clastic mass accumulation rates and Ti/Ca values. We interpret this to reflect erosion of Pleistocene fluvial terraces in Taiwan and from the exposed Taiwan Strait during early Holocene monsoon intensification. The isotope and chemical proxy pulse lasts from 11 to 8 ka, considerably shorter than the period of strong summer monsoon derived from speleothem records. Assuming these latter to be robust rainfall proxies we suggest that the fall in weathering intensity after 10 ka reflects decline in the erosion of the terraces onshore as the valleys are emptied and the Taiwan Strait was drowned by rising sealevel. In the Pearl River estuary itself we see a clear but different signal. Here $^{87}Sr/^{86}Sr$ values rise after 9 ka and only begin to fall again after 6 ka, reaching minimum values at 3.5 to 1.0 ka. If Sr isotopes are controlled by weathering then the response appears to lag monsoon intensity by ~2 k.y. A major increase in $^{87}Sr/^{86}Sr$ after 1.0 ka and the large mis-match between modern river sediments and the Holocene delta suggests major changes in erosion patterns, probably caused by the expansion of farming. Further west in the Indus delta Nd and Sr isotopes change quickly during from 14 to 9 ka as the monsoon intensifies, likely driven by changing patterns of erosion as the location of heaviest rains migrates. In the offshore shallow delta rising $^{87}Sr/^{86}Sr$ values during the early Holocene also suggest stronger chemical weathering. The effect is strongest in the early Holocene, but does not reduce after the weakening of the monsoon after ~5 ka. We suggest that reworking of older more weathered material from the flood plain at that time buffers the flux to the ocean. Although a wetter monsoon might be expected to drive more chemical weathering we find that on millennial timescales reworking of material formed during drier glacial times is often the source of the most weathered materials.

H isotopes in lavas from Loihi and Pitcairn: Primitive or recycled water?

M. CLOG*, C. AUBAUD AND P. CARTIGNY

Laboratoire de Géochimie des Isotopes Stables, IPGP, UMR7154, 1 rue Jussieu, 75005 Paris, France (*corresponding author, clog@ipgp.fr)

Hotspots sample mantle domains distinct from mid-ocean ridge systems. The source of hotspot lavas has been shown to contain recycled, subducted materials but also primitive material as seen from noble gases isotopic compositions. Water contents are higher in OIBs than in MORB but due to divergent H_2O/Ce and δD measured on different hotspots, there is presently no consensus on either the origin of water in hotspot lavas or even if there still is juvenile water in their sources. Lavas from Loihi seamount and Pitcairn both contain EM-1-type material and have primitive neon isotopic compositions, pointing at a mixing between recycled and primitive components in the mantle, and making the comparison of H systematics between the two hotspots key to shed light on the potential existence of primitive water. 7 samples from Loihi and 17 from the active zone of the Pitcairn hotspot were analysed in this study. Water concentrations measured by manometry range from 0.4 to 0.9% for Loihi and 0.5 to 1.2% for Pitcairn, while δD range respectively from -72 to -65‰ and -53 to -36‰. All but one sample from Loihi are unaffected by degassing, and the H_2O content variations are mainly due to variations of partial melting and crystal fractionnation. The δD of the 6 other samples are very homogenenous (-67.9±1.5‰). For the Pitcairn samples, initial water concentrations and isotopic compositions are calculated using the concentrations and δD of water in the vesicles, assuming closed-system degassing for water.

In Pitcairn samples, the results are compatible with a two-components mixing, one D- (δD>-40‰) and water-rich (H_2O/Ce>150), and the other D- (δD<-45‰) and water-poor (H_2O/Ce<125). The water-rich samples are also those richest in incompatible trace elements. Previous studies [1,2] have shown that in samples from Pitcairn, the ones most affected by the EM-1 component have primitive neon isotopic composition and are also richer in incompatible elements. The contrasted δD between the two hot-spots suggests that the component bearing primitive Ne is water-poor, and, thus, that water in Pitcairn comes from recycling processes.

[1] Honda and Woodhead (2005), *EPSL* **236**, 597-612 [3] Eisele *et al* (2002), *EPSL* **196**, 197-212.

https://doi.org/10.1180/S0026461X00006502 Published online by Cambridge University Press

Zn mobility during oceanic crust alteration inferred by its isotopic composition

C. CLOQUET[1]*, J. CARIGNAN[1,2] AND C. FRANCE-LANORD[1]

[1]CRPG/CNRS, BP 20, 54501, Vandoeuvre-lès-Nancy, France (*correspondance: cloquet@crpg.cnrs-nancy.fr)
[2]Takuvik, CNRS-ULaval, Québec, G1V 0A6, Canada

In the last 10 years, with the multiplication of MC-ICP-MS, our knowledge of the transition metal isotope geochemistry has been expanded. Among the studied elements, Zn became a useful tracer in biological systems and to trace anthropogenic activities [1,2]. However, Zn geochemical behaviour still suffers from lack of information and remains not well characterised.

In this work, we studied volcaniclastic sediment and basalts from ODP Leg 129, Sites 800 & 802A, located in the northern Pigafetta Basin near the HIMU Seamount and in the center of the East Mariana Basin. The two sites were drilled for about 500 m through sediment sequence largely constituted of volcaniclastic sediments. Calcium and Sr contents and Sr isotopes already demonstrated the role of diagenetic reactions in these cores. The aim of the study was to investigate the mobility of Zn during various reactions occurring in these cores like alteration, diffusion and diagenetic processes in real samples.

After Zn isolation from the matrix, the isotopic composition was measured by MC-ICP-MS. All the results are expressed relative to IRMM 3702 which presents a δ^{66}Zn of +0.3‰ compared to JMC_{lyon}. The δ^{66}Zn total range is from 0.1 to 0.6‰ for the two cores, the highest value being found at the top of the core. Both cores present a similar behaviour with a mean value around 0.3‰ reflecting their relative homogeneity in the volcaniclastic sediments. The value obtained for the basalt is also around 0.3‰ which is higher than values reported so far for fresh basalts (0‰). Zn isotopes do not fully follow Sr isotopes behaviour. However, a trend of the Zn isotopic composition to the light value from the top to the bottom of the core is observed. Such a variation can be interpreted in term of interaction between the sea water and the sediments from one part and between hydrothermal fluids and sediments from an other part.

[1] Weiss *et al*. (2005) *New Phyto*. **165**, 703-710. [2] Cloquet *et al*. (2006) *Environ*. *Sci*. *Technol*. **40**, 6594-6600.

Calcium isotope fractionation during plant growth under limiting and non-limiting nutrient supply

F. COBERT[1], A.-D. SCHMITT[2], P. BOURGEADE[2], F. LABOLLE[3], P.-M. BADOT[2], F. CHABAUX[1] AND P. STILLE[1]

[1]Laboratoire d'Hydrologie et de Géochimie de Strasbourg; Université de Strasbourg/EOST, CNRS; 67000 Strasbourg, France.
[2]Université de Franche-Comté et CNRS-UMR 6249, Chrono-environnement, 25030 Besançon Cedex, France.
[3]Université de Strasbourg, Institut de Zoologie et de Biologie générale, 67000 Strasbourg, France.

Hydroponic experiments have been performed to identify the co-occurring geochemical and biological processes affecting Ca isotopic compositions within plants. Four experiments have been conducted combining two Ca concentrations (5 and 60 ppm) and two pHs (4 and 6). Another experiment was performed with limiting Ca nutrient supply at 5 ppm Ca and pH=6. All the experiments have been achieved on bean plants in order to have access to a complete growth cycle in a short duration. Several organs (root, stem, leaf, reproductive) were sampled at two different growth stages (10 days and 6 weeks of culture).

Our results show, in agreement with previously published field studies [1, 2, 3,4], that all the bean organs are enriched in the light ^{40}Ca isotope compared to the nutritive solution. Moreover, Ca concentrations and pH influence Ca isotopic composition within plant organs. We identified three fractionation levels. The first one occurs during the uptake of the nutrient elements by the lateral roots. The second one takes place during the long distance transport of Ca, from roots to shoots. The third one takes place during formation of reproductive organs. The experiment with limited Ca supply shows a ^{44}Ca enrichment in solution through time; the plants seem to establish an isotopic equilibrium with the nutrient solution.

The data confirm the potential of the Ca isotopic system for tracing biological fractionations in ecosystems.

[1] Wiegand *et al*., (2005). *Geophys*. *Res*. *Lett*., **32**, L11404. [2] Page *et al*., (2008). *Biogeochemistry*, **88**, 1-13. [3] Cenki-Tok *et al*,. (2009). *GCA*, **73**, 2215-2228. [4] Holmden and Bélanger (2010). *GCA*, **74**, 995-1015.

https://doi.org/10.1180/S0026461X00006502 Published online by Cambridge University Press

Gold scavenging by liquid bismuth melts

A. B. COCKERTON* AND A. G. TOMKINS

School of Geosciences, Monash University, PO Box 28E, Victoria 3800, Australia
(*correspondence: amy.cockerton@monash.edu)

Bismuth is associated with gold in several different types of ore deposits. It has a melting temperature of only 271°C and therefore, when bismuth becomes saturated in a hydrothermal fluid at temperatures above this, it will precipitate from the fluid, not as a solid, but as a liquid. This liquid bismuth can subsequently continue to interact with and be transported by the hydrothermal fluid. Numeric modelling has shown that gold concentrations become several orders of magnitude higher in a bismuth melt versus the corresponding Bi-absent hydrothermal fluid, supporting the theory that a bismuth melt can scavenge and concentrate gold and other metallic ions from the hydrothermal fluid [1]. This theory is known as the Liquid Bismuth Collector Model (LBCM) [2].

We have investigated the bismuth-rich Stormont gold prospect in north-western Tasmania, to test the LBCM. Conditions at Stormont have been found to be favourable for bismuth to have precipitated as liquid with mineralisation temperatures between 400-500°C. In situ evidence for gold-scavenging by liquid bismuth is observed in the close textural relationship between native gold and bismuth. Zoned andradite crystals suggest hydrothermal fluid composition fluctuations, which may have contributed to zone refinement within the prospect. Liquid bismuth can sequester gold from undersaturated fluids [1]. Therefore, a zone refining process can potentially operate in a system where repeatedly infiltrating undersaturated fluids, controlled by favourable structures, can dissolve gold not attached to bismuth and then re-precipitate it where bismuth is concentrated. This leads to enhanced correlation between the two elements.

[1] Tooth *et al*. (2008), *Geology* **36**, 815-818. [2] Douglas *et al*. (2000), *15th Australian Geological Convention*, 135.

Revealing the hidden signature of biomacromolecules in ancient organic fossils

G.D. CODY[1], R.M. HAZEN[1], S.N. GUPTA[2] AND A.L.D. KILKOYNE[3]

[1]Geophysical Laboratory, Carnegie Institution of Washington, Washington DC 20015 USA (gcody@ciw.edu)
[2]Indian Institute of Science Education and Research, India
[3]Advanced Light Source, Lawrence Berkeley Laboratory, Berkely, CA, USA

The organic fossil record of eukaryotic organisms reaches back to the dawn of the Paleozoic. In the case of the arthropod fossil record, the preserved organic residue is derived from arthropod's exterior cuticle, the rigid exoskeleton characteristic of all members of the Arthropod phylum. In modern arthorpods, the exocuticle is composed of a nanocomposite of chitin and structural protein with very exterior region also containing fatty acids. The conventional geochemical view holds that the biopolymer chitin and structural protein is not preserved in ancient fossils as they are readily degradable through microbial chitinolysis and proteolysis and otherwise susceptible to destruction during diagenesis. Recently, however, we showed that a clear molecular signature of relict chitin-protein complex is preserved in a Middle Pennsylvanian (310 Ma) scorpion cuticle and a Silurian (417 Ma) eurypterid cuticle via analysis with carbon, nitrogen and oxygen X-ray Absorption Near Edge Structure (C-, N-, and O-XANES) spectro-microscopy [1]. The application of high-resolution X-ray microscopy employing functional group derived absorption contrast reveals the complex laminar variation in major biomolecule concentration across modern scorpion cuticle; XANES spectra highlight the presence of the characteristic functional groups of the chitin-protein complex. Modification of this complex is evident via changes in organic functional groups. Both fossil cuticles contain considerable aliphatic carbon relative to modern cuticle. In both cases, however, the concentration of vestige chitin-protein complex is high, 59 and 53 % in the fossil scorpion and eurypterid, respectively. We have recently used the Scanning Transmission X-ray Microscope (STXM) at beam line 5.3.2 at the Advanced Light Source to analyze the preserved organic cuticle of a Cambrian (507 Ma) trilobite from the Wheeler Shale. The thin section was prepared using a focused ion-beam mill. We detect very high N/C and O/C consistent with preservation of abundant, albeit altered, remnants of chitin/protein complex.

[1] Cody *et al*. (2011) *Geology* **39**, 255-258.

https://doi.org/10.1180/S0026461X00006502 Published online by Cambridge University Press

Large weakening in monsoonal rainfalls over western India during the Younger Dryas

ANTOINE COGEZ[1]*, LAURE MEYNADIER[1], CLAUDE ALLÈGRE[1] AND FRANCK BASSINOT[2]

[1]Equipe de Géochimie et Cosmochimie, Institut de Physique du Globe de Paris, Sorbonne Paris Cité, Univ Paris Diderot, UMR 7154 CNRS, F-75005 Paris, France (*correspondence: cogez@ipgp.fr)

[2]Laboratoire des Sciences du Climat et de l'Environnement, CEA, CNRS, Gif sur Yvette, France

We studied the monsoonal rainfalls evolution since 30 kyrs over western India, using neodymium isotopes (εNd) in sediment cores. Since neodymium isotopes are not fractionated by physico-chemical processes, they are an excellent tracer of mixing in seawater between different continental sources weathered by rainfalls. Using this technique Gourlan *et al*. (2010) already found that Ganges and Brahmaputra discharge was 3 times stronger during interglacial than during glacial times. To test such a result for the Western Gaths in India where the precipitations are among the strongest in this area, we measured εNd since 30 kyrs in 5 oceanic cores, one in the middle of the Arabian Sea, two along the Western Indian Coast and two south of India, on the Maldives Plateau. The carbonate phase and Mn coatings around foraminiferae were leached using acetic acid; we also measured εNd in the detrital fraction of the sediment because it carries the signature of the sources. Dating was performed using $\delta^{18}O$ in planktonic foraminiferae from the same cores and three or four radiocarbon dates per cores.

Both signals from the cores located along the Western Gaths display a large positive peak synchronous with the Younger Dryas (YD) event, 12 kyrs ago. Using a first order mixing model we estimate that local precipitations could have been up to 5 times weaker during this period. Moreover the recovery to Holocene rain level could have been much more longer than the onset. To our knowledge this is the first time that εNd records display a dependency of monsoon rain on YD event. This clearly show that monsoon regime was controlled by Northern Hemisphere climate regime. Large amplitude differences are seen when comparing εNd to $\delta^{18}O$ in planktonic foraminiferae.

The three other cores display a pattern characteristic of the deglaciation (decreasing εNd since the Last Glacial Maximum) without the trace of YD and rather correlated with the $\delta^{18}O$ records. We surmise that those patterns are imprinted by Himalaya where ice covering has a large influence on the precipitations and sediments discharge.

Early Ordovician volcanism in Eucísia and Mateus areas, Central Iberian Zone, northern Portugal

C.J.M. COKE[1], R.J.S. TEIXEIRA[1], M.E.P. GOMES[1], F. CORFU[2] AND A. RUBIO ORDÓÑEZ[3]

[1]Department of Geology, UTAD, Apartado 1013, 5001-801 Vila Real, Portugal (ccoke@utad.pt, rteixeir@utad.pt, mgomes@utad.pt)

[2]Dep. of Geosciences, Univ. of Oslo, PO Box 1047 Blindern, N-0316 Oslo, Norway (fernando.corfu@geo.uio.no)

[3]Dep. of Geology, Univ. of Oviedo, C/ Jesús Arias de Velasco, 33005 Oviedo, Spain (arubio@geol.uniovi.es)

The Eucísia (Alfândega da Fé) and Mateus (Vila Real) areas are located in the Central Iberian Zone, a segment of the northern Gondwana margin which underwent a long Variscan geodynamic evolution. Lithostratigraphically both areas are characterized by a predominance of Precambrian to Cambrian metasedimentary rocks and by the transgressive nature of the Ordovician formations. Continental rifting on the platform of northern Gondwana began around the Middle Cambrian, and opening of the Rheic ocean took place near the Ordovician-Cambrian boundary. In the Eucísia and Mateus areas there is evidence of extensional volcanism related to these events, contemporaneous with a transient inversion, known as the Sardic phase. At Eucísia the Ordovician Armorican Quartzite Formation hosts a < 40 cm thick ash-fall tuff bed, which is mainly composed by muscovite and small amounts of quartz. At Mateus, a subvolcanic porphyritic rock occurs in a 3 m thick vein cutting Precambrian-Cambrian schists. The phenocrysts consist of euhedral/ovoidal plagioclase and microcline and rounded bluish quartz. The groundmass is dark, fine grained and contains quartz, feldspars, muscovite, rare biotite and graphite (identified by XRD). The mineralogical and textural features of this vein resemble those of the augen gneisses from the Ollo de Sapo Formation in Sanabria (Spain), except for a lower degree of deformation/recrystallization. The tuff and the porphyry are both alkali-calcic, peraluminous (ASI ≈ 1.75 – 2.91) and classified as rhyolites in the R_1-R_2 diagram. They show moderate REE contents ($\Sigma \approx 78.3 – 182.6$), $(La/Lu)_N$ values between 11.78 and 12.06, weak negative Eu anomalies ($Eu/Eu^* \approx 0.45 – 0.52$) and REE patterns typical of peraluminous granites. Both rocks have a high content of zircon xenocrysts, but also some magmatic zircon prisms which were dated by U-Pb (ID-TIMS) yielding concordia ages that indicate crystallization in the Early Ordovician: the ash-fall tuff from Eucísia at 482.1 ± 1.5 Ma and the rhyolite porphyry from Mateus at 478.0 ± 1.7 Ma.

https://doi.org/10.1180/S0026461X00006502 Published online by Cambridge University Press

Bioengineering nano-magnetite for contaminant clean-up

V.S. COKER[1]*, D. CREAN[2,1], R.S. CUTTING[1], N.D. TELLING[3], J.M. BYRNE[1], R.A.D. PATTRICK[1], G. VAN DER LAAN[4,1], D.J. VAUGHAN[1] AND J.R. LLOYD[1]

[1]SEAES, University of Manchester, M13 9PL, UK (*correspondence: vicky.coker@manchester.ac.uk)
[2]Department of Materials Science & Engineering, University of Sheffield, S1 3JD, UK
[3]Institute for Science & Technology in Medicine, Keele University, Stoke-on-Trent ST4 7QB, UK
[4]Diamond Light Source, Didcot, Oxfordshire OX11 0DE, UK

The engineering of novel materials is a key development in the challenge of remediating toxic metals and radionuclides in the subsurface. Our work focuses on utilising nano-scale magnetite, synthesised through the bioreduction of ferrihydrite by *Geobacter sulfurreducens* at ambient temperatures. In order to increase the activity and longevity of this substrate in key reactions, including chromium(VI) and toxic organics reduction, the surface of the nano-magnetite is functionalised by a precious metal catalyst, nano-palladium, in a simple, one-step process, aided by the organic residue on the iron mineral surface derived from the bacterial culture [1].

Pd-functionalised nanomagnetite has been tested in the remediation of Cr(IV) in batch and continous-flow column experiments and in hollow-fibre membrane units. Conditions in the column studies were varied to take into account key environmental parameters including oxic, anoxic, and a nitrate co-contamination. An electron donor, sodium formate, was supplied in the influent leading to a substantial increase in the removal capacity of the Pd-magnetite. In addition, the columns containing both Pd-biomagnetite and formate were found to maintain an 80 % removal beyond 300 hours, whereas without formate complete breakthrough occurred at 60 hours. We hypothesise that oxidation of formate in these experiments is coupled to recharge of the nanocatalyst surface by the Pd, maintaining the reductive power of the system.

Cr(III) formed was associated strongly with the biomagnetite, and XMCD studies suggest that the Cr(III) replaces Fe in the magnetite lattice, effectively 'locking-up' the Cr, as seen previously [2]. This novel system could provide effective and sustained immobilisation of contaminants, far outreaching the reductive capacity of non-functionalised magnetite.

[1] Coker *et al*. (2010) *ACS Nano* **4**, 2577-2584. [2] Cutting *et al*. (2010) *Environ. Sci. Technol*. **44,** 2577-2584.

PGE contents and spinel compositions of different podiform chromitites in the Eastern Anatolia complex, Turkey

A.R. ÇOLAKOGLU[1]*, K. GÜNAY[1] AND H.M. PRICHARD[2]

[1]Yüzüncü Yıl University, Department of Geological Engineering, Zeve Campus, TR-65080 Van, Turkey (*correspondence:arc.geologist@yyu.edu.tr, kurtulusgunay@yyu.edu.tr)
[2]School of Earth and Ocean Sciences, Cardiff University, Main College, Cardiff, CF10 3AT, United Kingdom (hazelprichard@googlemail.com)

This study presents mineralogy, PGE contents and spinel compositions of four different podiform chromitite localities in the east of Turkey. The ophiolitic rocks are observed as relatively large tectonic units in the Eastern Anatolian Accretionary Complex [1]. Chromite texture are observed as massive, nodular and dissemine-banded type. The highest value (390 ppb) of ΣPGE are obtained from milonitic shear zone chromitites with an average ~290 ppb. Os, Ir and Ru show relatively enrichment, compare to Pt, Pd and Rh elements. This enrichment are consistent with other chromitite deposits in Turkey. Chromite grains contain inclusion of mafic silicates (olivine, amphibole and clinopyroxene), sulphides (etc. millerite, heazlewoodite, awaruite, chalcopyrite, godlevskite, orcelite) and euhedral Laurites. The chromite compositions of different localities ore exhibit characteristic of different tectonic setting. The high Cr# and low TiO_2 content of spinel from the eastern Anatolia chromitites possibly has genetic linkage with a boninite melt generated by high degrees of partial melting and the others are formed in island arc setting towards to back arc basin [2, 3].

[1] Sengör *et al*. (2008) *Earth Science Rev*. **90**, 1-48. [2] Kamanetsky *et al*. (2001) *Journal of Petrology* **42,** 655-671. [3] Zhou *et al*. (1998) *Geochimica et Cosmochimica Acta*, **62**, 677–688.

https://doi.org/10.1180/S0026461X00006502 Published online by Cambridge University Press

Aerosol spatial scales in observations and models: Implications for the aerosol direct effect

PETER R. COLARCO*

Atmospheric Chemistry and Dynamics Branch, NASA GSFC, Greenbelt, MD 20771, USA
(*correspondence: Peter.R.Colarco@nasa.gov)

Consideration of variability in aerosol spatial and temporal distributions are prime concerns in developing sampling strategies for future satellite missions. Previous studies suggest homogeneity in tropospheric aerosol spatial distributions at scales of about 200 km. These studies, however, did not have access to the extensive global data sets of aerosols from the past decade of EOS observations, and so their conclusions on aerosol spatial scales must be viewed as tentative. In the first part of this study we evaluate what the global distribution of aerosol optical depth looks for different spatial sampling strategies. We sample MODIS observations at their native swath width, along a satellite-subpoint track like what the APS would have observed, and at an intermediate swath width similar to what MISR observes. We investigate the convergence of the aerosol optical depth statistics for all cases. In the second part of this study we employ these sampling strategies on the results of the NASA GEOS-5 global aerosol model to investigate the implications for computed aerosol direct radiative forcing.

Missed connection: Ignimbrite seeking plutonic relationship

DREW S. COLEMAN*, RYAN D. MILLS AND MICHAEL J. TAPPA

Department of Geological Sciences, University of North Carolina, Chapel Hill, NC 27599-3315
(*correspondence dcoleman@unc.edu)

New U-Pb zircon geochronologic data for rocks from the Southern Rocky Mountain volcanic field demonstrate a distinct disconnect between the timing of ignimbrite eruption and plutonism. In both the Questa and Aetna calderas, only discontinous dikes yield the same ages as ignimbrites. The dominant volume of exposed plutonic rocks was assembled either before or after the ignimbrite events.

Geochronology for rocks in the Questa and Aetna calderas demonstrate that the largest exposed plutons (the Rio Hondo and Mt. Princeton, respectively) were assembled incrementally. Data for the Rio Hondo pluton indicate a magma accumulation rate of 0.0003 km^3yr^{-1} for the exposed portion of the pluton. Data for the Mt. Princeton pluton indicate an accumulation rate of 0.0009 km^3yr^{-1}. Both rates are comparable to rates published for other plutons, and orders of magnitude too slow to accumulate large eruptible magma volumes. Extrapolation of the accumulation rate for the Rio Hondo pluton over the 8.5 m.y. history of the volcanic field yields an estimated volume of plutonic rocks comparable to the volume under the field indicated by geophysical studies. We propose that the bulk of the plutonic rocks beneath the volcanic center accumulated during periods of low volcanic effusivity (the waxing and waning stages of caldera formation), and that most of the magma generated during caldera formation erupted. Furthermore, because the oldest portion of the Rio Hondo pluton is the granitic cap exposed beneath a gently dipping roof contact, the roof granite cannot be a silicic liquid fractionated from the deeper (younger) portions of the pluton. Instead, the data suggest that the variation in composition of the pluton is inherited from the lower crustal source. We suggest that if magma flux is high enough, zoned ignimbrites can be formed by evolution of the melt compositions being generated at the source. Thus eliminating the “need” for large shallow magma chambers and plutons in support of ignimbrite evolution.

If the intrusive equivalents to the ignimbrites are limited to dikes, and the plutonic rocks crystallized over the history of the fields, then the plutonic record of the ignimbrite stage of caldera formation is sparse. This predicts that the plutonic record will be dominated by waxing and waning stage magmatism, and the volcanic record will be dominated by ignimbrite stage magmatism.

https://doi.org/10.1180/S0026461X00006502 Published online by Cambridge University Press

Investigating the effects of hydrologic fluctuations on organic sulfur speciation in boreal peatlands

J.K. COLEMAN WASIK[1,2]*, B.M. TONER[3], D.R. ENGSTROM[2], P.E. DREVNICK[4] AND M.A MARCUS[5]

[1]Water Resources Science Graduate Program, University of Minnesota, St. Paul, MN 55108, USA (*correspondence: jcoleman@smm.org)

[2]St. Croix Watershed Research Station, Marine on St. Croix, MN 55047, USA

[3]Department of Soil, Water, and Climate, University of Minnesota , St. Paul, MN 55108, USA

[4]Centre Eau Terre Environment, Québec (Québec) G1K 9A9, Canada

[5]Advanced Light Source, Lawrence Berkeley National Laboratory, Berkeley, CA 94720, USA

Sulfur has a complex biogeochemical cycle in peatlands due to its chemical reactivity, wide range of oxidation states, and importance to bacterial metabolism [1]. In sulfur-limited systems sulfate plays a synergistic role in the production of monomethylmercury (MeHg), the bioaccumulative form of mercury [2]. Therefore an understanding of how sulfate is incorporated into and released from peat soils may improve prediction of MeHg production within, and export from, peatlands. Climatic variability can cause large changes in oxidation- reduction potentials within peatlands by influencing the position of the water table. Wetlands are often considered to be sinks in the landscape for sulfate because sulfate inputs to saturated systems are readily consumed by sulfate-reducing bacteria. However, following droughts wetlands have been found to be significant sources of sulfate to downstream aquatic ecosystems [3].

This research compared sulfur speciation in peat from a boreal peatland during and after an historic drought in northern Minnesota. Greater than 95% of sulfur in each peat sample was in an organic form making traditional, wet-chemical sulfur fractionation methods uninformative about a large portion of the total sulfur pool. As an alternative, sulfur speciation in peat was measured at the micron scale by X-ray fluorescence mapping at six incident energies spanning the sulfur 1s absorption edge. Composite maps were fit with reference spectra. X-ray absorption spectroscopy is being used to verify sulfur speciation maps. At naturally occurring sulfur levels, we are able to obtain high quality data. Our goal is to develop a data analysis protocol providing quantitative, spatially resolved sulfur speciation.

[1] Urban *et al*. (1989) *Biogeochem* **7**, 81-109. [2] Gilmour *et al*. (1992) *Environ. Sci. Technol*. **26**, 2281-2287. [3] Eimers *et al*. (2007) *Environ. Monit. Assess*. **127**, 399-407.

Magma degassing timescales from vesicle size distribution and bubble composition heterogeneity in MORB glasses

A. COLIN, P. BURNARD AND B. MARTY

CRPG-CNRS, 15 rue Notre Dame des Pauvres, 54500 Vandoeuvre-lès-Nancy, France

Vesicle size distributions (VSD), the number of bubbles of a given size plotted against the size interval are classically used to model the growth rate of vesicles by assuming continuous vesicle nucleation and growth (as for crystal size distributions [1]). However, VSD data in MORB samples are sparse, due to the difficulty in making representative measurements in low vesicle density samples. Here, we use direct 3D images in order to calculate vesicle sizes and their distributions.

The images were obtained by X-ray microtomography (resolution of 5μm or less) of small pieces (some mm^3) of glassy pillow lava rims sampled along the mid-Atlantic ridge and the East Pacific Rise. The observed trends allow us to discuss several key issues such as the duration of the vesicle-magma segregation and the link between magma initial volatile content and the vesicle growth rate. Atlantic MORBs and Icleandic glass samples show VSDs that have a distinct kink in the VSD at 100 – 200 μm micron vesicles, showing that there are (at least) two different episodes of vesicle generation: smaller vesicles result from decompression during the final stages of eruption while larger bubbles likely represent magma chamber processes. Vesicle-poor samples such as those from the East Pacific Rise tend to only have a single episode of vesicle generation.

In order to constrain these degassing processes, the trapped glass vesicles were subsequently opened by laser ablation and their volatile contents (He, Ar, CO_2) analysed vesicle by vesicle. The different vesicles preserved in the final glass nucleated at different stages in the magma history, and thus preserve more or less degassed stages of the magmatic volatile evolution. In some samples, the analysed vesicles have homogeneous compositions, while other samples show systematic inter bubble variations consistent with a solubility-controlled Rayleigh distillation. There is no evidence for kinetic fractionation of volatiles in the majority of our samples. These key observations allow the degassing mechanisms to be modeled, as well as the timescales involved in the preservation of such millimetric heterogeneities.

[1] Marsh, B. D. (1988) *Contrib. to Mineralogy and Petrology* **99**, 277-291

https://doi.org/10.1180/S0026461X00006502 Published online by Cambridge University Press

Generation of HIMU and EM-1 reservoirs by CO_2-fluxed lower mantle melting: Implications for OIBs, kimberlites and carbonatites

K.D. COLLERSON[1,2]*, Q. WILLIAMS[3], A.E. EWART[1] AND D. MURPHY[4]

[1]Earth Sciences, Univ. Queensland, Brisbane, Qld, 4072, Australia (*correspondence:k.collerson@uq.edu.au)
[2]Murrumbo Rare Metals Ltd. Box 1271, New Farm, Qld, 4005, Australia
[3]Earth and Planetary Sciences, UCSC, Santa Cruz, California, 95064, U.S.A
[4]Biogeosciences, QUT, Brisbane, Qld, 4000, Australia

A New Paradigm

P/D isotope ratios of enriched mantle (EM) and high-μ (HIMU) reservoirs sampled by OIBs, CFBs, kimberlites and carbonatites are produced by CO_2-fluxed lower mantle (LM) melting [1]. Our model resolves the long-standing conjecture regarding the formation of HIMU and EM.

Modelling and Implications

Using measured or inferred partition coefficients, we show that U/Pb, Rb/Sr, Sm/Nd, Lu/Hf, and Re/Os ratios of EM are associated with C-rich melts while residues evolve to HIMU [1]. LM melting occurs in thermochemical upwellings by carbonate suppression of the liquidus. End-members originate in domains isolated from whole mantle convection. Melts with > 1% CO_2 and residues are variably buoyant allowing spatial separation of EM and HIMU. HIMU is a refractory residue with long LM residence time and thus it evolves to extreme isotopic compositions. EM is a melt that reacts with ambient mantle and does not produce such extreme isotope ratios. Entrainment in plumes transports EM and HIMU domains at different ascent rates to magmagenetic zones at the top of the LM and in the transition zone.

HIMU does not involve hydrothermally altered oceanic crust, and EM does not require entrainment of continent-derived sediment. Generating EM and HIMU by a single melting process from pristine mantle explains the presence of primitive rare gas end-member isotope ratios in mantle plume magmas as well as constraints of the Pb isotope paradoxes. Carbon in the deep mantle clearly plays an important role in Earth's geochemical evolution. Kimberlites, carbonatites and OIBs all preserve an isotopic record of their LM pedigree.

[1] Collerson *et al.*, (2010) *PEPI*, **181**, 112-131.

Ferric iron geometry and coordination during hydrolysis and ferrihydrite precipitation

R.N. COLLINS[1,2,*], A.L. ROSE[3], C.J. GLOVER[4], D.D. BOLAND[1], T.E. PAYNE[1,2] AND T.D. WAITE[1]

[1]School of Civil and Environmental Engineering, The University of New South Wales, Sydney, NSW 2052, Australia. (richard.collins@unsw.edu.au)
[2]Institute for Environmental Research, Australian Nuclear Science and Technology Organisation, Locked Bag 2001, Kirrawee DC, NSW 2232, Australia.
[3]Southern Cross Geoscience, Southern Cross University, PO Box 157, Lismore, NSW 2480, Australia.
[4]X-ray Absorption Spectroscopy Beamline, Australian Synchrotron Company Ltd, 800 Blackburn Rd, Clayton, VIC 3168, Australia.

Definitive structural characterisation of ferrihydrite has challenged scientists primarily due to its nanosized particles and inherent long-range structural disorder which challenges analytical methodology (and modelling) typically employed to determine the structure of minerals. Here we report on the application of a synchrotron quick-scanning X-ray absorption spectroscopy (XAS) approach, which allows the collection of Extended X-ray Absorption Fine Structure (EXAFS) spectral data to k = 15 $Å^{-1}$ in < 1 minute, to obtain unparalleled iron K-edge data on the hydrolysis of $Fe^{III}(H_2O)_6$ and ferrihydrite precipitation.

Modelling of the pre-edge and EXAFS data: 1) supports theoretical studies which have suggested the existence of a monomeric penta-coordinated Fe^{III} hydrolysis species and; 2) corroborates recently proposed structural models of ferrihydrite that contain tetrahedral Fe^{III}. Modelling results indicate that ferrihydrite consists of 15 to 25 % tetrahedral Fe^{III} and suggest that this geometry must be included in any comprehensive structural model of ferrihydrite and, furthermore, should be considered when evaluating the reactivity, stability and other structure-property relationships of this mineral.

https://doi.org/10.1180/S0026461X00006502 Published online by Cambridge University Press

Microbial uptake and methylation of dissolved elemental mercury

MATTHEW COLOMBO*, TAMAR BARKAY, JOHN R. REINFELDER AND NATHAN YEE

School of Environmental and Biological Sciences, Rutgers University, New Brunswick, NJ, USA (*correspondence: mcolombo@eden.rutgers.edu)

Introduction

Mercury [Hg] bioaccumulation in fish is critically dependent on the conversion of inorganic Hg to methylmercury [MeHg]. In aquatic ecosystems, Hg is primarily methlyated by anaerobic sulfate- and iron-reducing bacteria. These microbes are known to methylate mercuric Hg [Hg^{2+}] to form MeHg. The formation of dissolved elemental mercury [$Hg^0_{(aq)}$] is thought to limit the concentration of Hg available for methylation. However, the uptake and transformation of Hg^0 by anaerobic bacteria has never been tested. Here, we conducted experiments to determine if the sulfate-reducing bacterium *Desulfovibrio desulfuricans* ND132 and the iron-reducing bacterium *Geobacter sulfurreducens* PCA can produce MeHg when provided with $Hg^0_{(aq)}$ as their sole mercury source.

Materials and Methods

Strains PCA and ND132 were grown to exponential phase and subsequently exposed to a constant source of $Hg^0_{(aq)}$ under strict anaerobic conditions. Heat-killed cells (80°C for 30 min), bacterial exudates (growing culture passed through a 0.2 µm filter), and sterile medium were incubated under identical conditions. Samples were acidified and frozen for MeHg analysis and purged with N_2 gas at ~800 mL/min to remove all volatile $Hg^0_{(aq)}$ prior to total Hg analysis.

Results and Discussion

After ~24 h of exposure to $Hg^0_{(aq)}$, strains PCA and ND132 converted $Hg^0_{(aq)}$ to non-purgeable total Hg at rates of ~30 µg/L/d and ~1500 µg/L/d, respectively. Control experiments conducted with heat-killed cells, bacterial exudates, or sterile medium could not account for the Hg retention, suggesting an active role by the microorganisms. When provided with $Hg^0_{(aq)}$ as the sole mercury source, strains PCA and ND132 produced MeHg at rates of ~0.2 µg/L/d and ~0.3 µg/L/d, respectively. These experimental results indicate that iron-reducing and sulfate-reducing bacteria are able to uptake and methylate elemental Hg. The implications of this process in the terrestrial mercury biogeochemical cycle will be discussed.

An integrated approach to estimate the U and Th content of the Central Apennines continental crust

M. COLTORTI[1], R. BORASO[1], F. MANTOVANI[1,2], M. MORSILLI[1], G. FIORENTINI[1,2] AND G. RUSCIADELLI[3]

[1]Earth Sciences Department, University of Ferrara
[2]Physics Department, University of Ferrara
[3]INFN, Ferrara Section
[4]Earth Sciences Department, University of Chieti

A study for estimating the Th and U content of Central Italy continental crust was undertaken for evaluating the geo-neutrino flux, which is currently measured through Borexino experiment at LNGS (Laboratori Nazionale Gran Sasso). Three main layers were identified: Sedimentary Cover, Upper Crust and Lower Crust, only the first one outcropping in the Gran Sasso area. Sampling of the other two layers was performed in the Valsugana area and in the Ivrea-Verbano zone, assuming rock abundances and composition of the south Alpine basement fairly homogeneous.

U and Th abundances of the main lithotypes belonging to the Mesozoic and Cenozoic were grouped into four main "Reservoirs" based on similar paleogeographic conditions and mineralogy. Irrespective of magmatic or metamorphic origin Upper and Lower Crust lithotypes were also subdivided into a mafic and an acid reservoir, with comparable U and Th abundances. Based on geological and geophysical properties, relative abundances of the various reservoirs were calculated and used to obtain the weighted U and Th abundances for each of the three geological layers. Using the available seismic profile as well as the stratigraphic records from a number of exploration wells, a 3D modelling was developed over an area of 2°x2° centered at LNGS. This allows to determine the volume of the various geological layers and eventually integrate the Th and U contents of the whole crust beneath LNGS.

On this base the local contribution to the geo-neutrino flux was calculated and added to the contribution given by the rest of the world. This new calculation predicts a geoneutrino signal at Borexino detector about 4 TNU lower than that previously obtained based on general, worldwide assumptions. The considerable thickness of the sedimentary rocks, mainly represented by U- and Th-poor carbonate, is responsible for the difference. These results suggest that worldwide average of continental crust cannot be extrapolated to young terrains without taking into account composition and thickness of lithotypes within the Sedimentary Cover.

https://doi.org/10.1180/S0026461X00006502 Published online by Cambridge University Press

U-Pb perovskite ages of kimberlites from the Rosário do Sul cluster: Southern Brazil

R.V. CONCEIÇÃO[1], C. LENZ[2], C.A.S. PROVENZANO[3], A. SANDER[3] AND F.V. SILVEIRA[3]

[1]UFRGS-Brazil; (rommulo.conceicao@ufrgs.br)
[2]UFS-Brazil, (crislenz@yahoo.com.br)
[3]CPRM-Brazil, (carlos.provenzano@cprm.gov.br; andrea.sander@cprm.gov.br; fvsilveira@gmail.com)

The age of the Rosário do Sul kimberlitic magma is first presented here. The Rosário do Sul kimberlitic cluster is located in the southwestern part of the Rio Grande do Sul state (Southernmost Brazil). This cluster is composed of many pipes, dikes and sills intruding the Paraná Basin sedimentary rocks. The Rosário do Sul kimberlites are composed of macrocrystals and fenocrystals of olivine in a fine grained matrix which consist of serpentine, phlogopite, carbonate, spinel, perovskite, apatite and zircon. Xenoliths of peridotitic rocks of variable sizes were found (1 mm to 5 cm) immersed in the matrix. The dating of the kimberlite has been conducted using perovskite, which is found in the matrix and do not show any inheritance records, which relates it to a primary magmatic origin. *In situ* LA-ICP-MS analyses were performed at the Isotopic Laboratory at UFRGS in a Neptune equipment. Zircon standard GJ-01 was used, due to the absence of perovskite standart in the LGI. The laser was set up to produce a 30 μ diameter spots with a ~0.5 mJ/pulse output energy. The data reduction was performed using an Excel spreadsheet program from the University of Brasília, Brazil. The ages were plotted in a Concordia Diagram, which yield lower intercept U-Pb ages of 128 ± 5 Ma (MSWD of 3.4). This age is very close to that of the Parana Flood Basalts, which is assumed as ~130 Ma. Such new data suggest a very complex and heterogeneous mantle and the occurrence of a great geothermal variation underneath South America, on the region of Parana Flood Basalts.

Contrasting roles of continental and oceanic arcs in the growth of continents

K.C. CONDIE[1]* AND A. KROENER[2]

[1]Dept of Earth & Environmental Science, New Mexico Tech, Socorro, NM 87801 USA (*correspondence: kcondie@nmt.edu)
[2]Institut für Geowissenschaften, Universität Mainz, 55099 Mainz, Germany (kroener@uni-mainz.de)

Oceanic arcs (OAs) are commonly cited as the primary building blocks of continents, yet there are many lines of evidence that continental arcs (CAs) are more important in this regard. Modern OAs are mostly subducted and lithosphere buoyancy considerations show that OAs with crust <20 km thick should completely subduct. Analysis of terranes indicates that <10% of post-Archean accretionary orogens comprise accreted OAs, whereas CAs comprise 40-80%.

OA felsic igneous rocks are depleted in incompatible elements compared to upper continental crust (UC) and have lower La/Yb and Sr/Y ratios, whereas those produced in CAs are similar in composition to UC. Nd and Hf isotopic ratios suggest that accretionary orogens comprise 40-65% juvenile crustal components and that >50% of these components are produced in CAs.

These observations present a paradox: older continental crust is necessary for the production of new continental crust. As indicated by Th/Yb, Nb/Yb, and Nb/Yin greenstone volcanics, CAs did not become widespread until after the late Archean. Prior to 2.5 Ga, OAs may have been more difficult to subduct due to a hotter mantle, and together with oceanic plateaus, they may have contributed to the construction of Archean continents. After this time, however, the production site of continental crust shifted to CAs, and most OAs were subducted.

https://doi.org/10.1180/S0026461X00006502 Published online by Cambridge University Press

Synthetic 'age solutions' reference materials for U-Th geochronology

DANIEL J. CONDON[1], GIDEON HENDERSON[2], DAVID A. RICHARDS[3] AND JON WOODHEAD[4],

[1]NERC Isotope Geoscience Laboratory, British Geological Survey, UK
[2]Department of Earth Science, Oxford University, UK
[3]School of Geographical Sciences, University of Bristol, UK
[4]School of Earth Sciences, University of Melbourne, Australia

Over the past 15 years there has been considerable improvement in our ability to measure U and Th isotope ratios and concentrations resulting in a reduction of U-Th age uncertainties by an order of magnitude (age uncertainties are now as low as 0.1%). The accuracy of these dates is dominated by (1) the U/Th tracer calibration; (2) mass spectrometry, (3) various corrections applied, and (4) 'constants' used in the age calculation (secular equlibrium and decay constants, the $^{235}U/^{238}U$ value of natural U etc.). Some of these parameters can be considered as 'systematic' (i.e., decay constant uncertainties) and others either contain a random component or are systematic but 'laboratory' specific (such as tracer calibration).

At present inter-laboratory agreement and intra-laboratory long-term external reproducibility of U-Th Isotope Dilution Isotope Ratio Mass Spectrometry data is assessed through analyses of natural cabonate 'standards'. Though powdered carbonates standard zircons are ideal for assessing the total system (dissolution, purification via anion echange chemistry and mass-spectrometry), these are limited in supply and not widley avaibalbe limiting their use for asessing inter-laboratory agreement. Here we outline a proposal and the initial steps taken for the development the development and calibration of a series of synthetic U-Th 'age solutions' prepared by mixing different amounts of high-purity mono-isotopic solutions (^{234}U, ^{230}Th etc.) in proportions that mimic commonly analysed materials (e.g., a last-interglacial speleothem) so that their analyses closely replicates the analytical protocols employed on normal samples. We believe these solutions will augment natural carbonate standards as a means of interlaboratory comparsion and assessment of long-term external reproducibility, and as such are intended for community use and will be made available. The intercalibration project is part of a broader community effort that has developed out of the PALSEA and EARTHTIME initiatives.

Measuring the isotopic composition of small (<5 ng) U samples by MC-ICP-MS

J.N. CONNELLY AND M. BIZZARRO

Centre for Star and Planet Formation, State Natural History Museum of Denmark, Øster Voldade 5-7, 1350 Copenhagn K, Denmark.

Pb-Pb ages have been based on Pb isotopic measurements while assuming that the $^{238}U/^{235}U$ ratio is constant at 137.88. Using a second-generation multi-collector inductively coupled plasma mass spectrometer (MC-ICP-MS), [1] has documented 3400 ppm variability in the $^{238}U/^{235}U$ ratios of calcium-aluminum-rich inclusions (CAI) in chondrites [1], corresponding to a 5 Myr deviation in calculated Pb-Pb ages. This makes clear the need to measure the U isotopic composition of all meteorites and their components when determining their Pb-Pb ages. The challenge lay in developing analytical protocols to measure the isotopic composition of typically small samples of U (<5 ng) sufficiently precisely to be useful in constraining events that occurred in the first 10 million years of the solar system. With 100 ppm uncertainty corresponding to 0.15 Myr, we must achieve less then 200 ppm uncertainty on $^{238}U/^{235}U$ ratios. We have developed a three stage chemistry starting with Eichrom's UTEVA resin followed by two progressively smaller anion columns that effectively isolates U from the sample matrix elements. U is measured using an Aridus II desolvating nebulizer on a ThermoFisher Neptune with the Jet Cone Interface, a configuration that delivers ~2500 V of signal per 1 ppm concentration of U. Running with an uptake rate of 0.15 ml/min, we analyze 5 ng for a total acquisition time of 15 min with a ^{235}U intensity of ~40 mV. Fractionation correction for the measured $^{238}U/^{235}U$ ratio is controlled by the simultaneous measurement of the synthetic equal-atom ^{233}U-^{236}U tracer IRMM 3636 that was added to samples before dissolution. Blank correction is determined by bracketing runs (of equal time as unknown runs) of the 2% HNO_3 used to dissolve samples. CRM 112a spiked with IRMM 3636 is run as a bracketing standard to monitor within run stability. Using these methods, we are able to routinely determine the isotopic composition of small (<5 ng) amounts of U separated from terrestrial rock standards and doped meteoritic matrices to better than 200 ppm precision and external reproducibility. Analyzing meteorites and their components, we have investigated the $^{238}U/^{235}U$ variability of the inner solar system.

[1] Brennecka *et al*. (2010) *Science* **327**, 449-451.

https://doi.org/10.1180/S0026461X00006502 Published online by Cambridge University Press

Isotopic evidence for microbial oxidation of dissolved methane in the Gulf of Mexico oil spill deep plume

M.E. CONRAD*, M. BILL, W.T. STRINGFELLOW, S.E. BORGLIN, O.U. MASON, E.A. DUBINSKY, Y.M. PICENO, J.L. FORTNEY, L.M. TOM, K.L. CHAVARRIA, R. LAMENDELLA, D.C. JOYNER, K. WETMORE, J. KUEHL, R. MACKELPRANG, C. WU, J. LIM, F. REID AND T.C. HAZEN

Earth Sciences Division, E.O. Lawrence Berkeley National Laboratory, Berkeley, CA 94720
(*correspondence: MSConrad@lbl.gov)

The blowout of BP's Macondo well and subsequent sinking of the Deepwater Horizon drilling platform on April 20, 2010 led to one of the largest oil spills in history. By the time the well was capped on July 12, 2010, ~4.9 million barrels of oil are estimated to have leaked into the Gulf of Mexico. Accompanying this spill was the development of a deep plume of dispersed oil and dissolved gases at a depth of 1100-1200 mbsl that was detected at distances of up to 35 km from the wellhead. The $\delta^{13}C$ values of dissolved hydrocarbon gases (C1-C5) and BTEX compounds in 77 samples collected from in and around the deep plume between May 28, 2010 and August 24, 2010 were analyzed to track the fate and potential biodegradation of those compounds. C2 to C5 gases and BTEX compounds were only high enough for $\delta^{13}C$ analyses in samples collected before mid-June. The $\delta^{13}C$ values of these compounds remained within ±2‰ of $\delta^{13}C$ values of samples from the Macondo well. CH_4 concentrations in early plume samples (collected before mid-June) were as high as 300 μM, but dropped off significantly in later samples. The $\delta^{13}C$ of CH_4 in the early samples were between -57‰ and -59‰ compared to an average $\delta^{13}C$ value of -58‰ for samples from the Macondo reservoir. After mid-June, CH_4 from some of the samples had higher $\delta^{13}C$ values. The last two CH_4 samples with measurable $\delta^{13}C$ values were collected during early August, 3 weeks after the well was capped and had $\delta^{13}C$ values of -44‰ and -23‰. For a fractionation factor of 0.984 for microbial oxidation of CH_4, those values indicate 60% and 90% oxidation of the methane, respectively. These samples coincided with drops in the dissolved oxygen concentrations in the water column of ~1.5 mM also suggesting increased aerobic microbial activity. In addition, the $\delta^{13}C$ values of bacterial phospholipids extracted from a single sample were lower than normal background biomass, suggesting that the bacteria were consuming CH_4 and other hydrocarbons with lower $\delta^{13}C$ values than the background organic matter.

Dynamics of the Pliocene East Antarctic Ice Sheet revealed by isotopes in marine sediments

C. COOK[1]*, T. VAN DE FLIERDT[1], T. WILLIAMS[2], S. HEMMING[2] AND E.L. PIERCE[2]

[1]Imperial College London, London, UK, SW7 2AZ (*correspondance: c.cook09@imperial.ac.uk)
[2]LDEO, Palisades, NY 10964-1000 USA

Our understanding of the dynamics of the East Antarctic Ice Sheet (EAIS) during the climatically warm early Pliocene, and the transition to the cooler, but more variable late Pliocene, is limited. Integrated isotope analyses of detrital marine sediments from ODP Site 1165 (64°22-77S, 67°13-14E), Prydz Bay, East Antarctica, offer novel insights into the evolution of the East Antarctic Ice Sheet, and reveal the controls on sediment composition in a glacial environment. Here we investigate the $^{40}Ar/^{39}Ar$ ages of hornblende grains from ice-rafted detritus (IRD) (>150μm) and neodymium and strontium isotope fingerprints of detrital marine sediments (<63μm).

Early Pliocene sediments, deposited between 5.0 and 3.5 Ma, are dominated by hornblende IRD grains typical of the local Prydz Bay region ($^{40}Ar/^{39}Ar$ ages of ~500 Ma). However, fine-grained (<63 μm) material exhibits εNd values of -14, untypical of modern marine sediments in this area (εNd: -17 to -19). The source of these higher εNd values could be either the nearby Mawson coast (εNd: ~-15- to -14) or the distal Wilkes Land margin (-12.3 to -14.8), with sediments carried by bottom currents. Strontium isotopes, however, are more radiogenic than expected, an observation that could either be due to sedimentary sorting, continental weathering, or subtle shifts in provenance affecting Rb/Sr rations. Conversely, Late Pliocene sediments with depositional ages of 3.3 to 2.8 Ma display an increase in distally sourced Wilkes Land IRD ($^{40}Ar/^{39}Ar$ ages of 1100-1300 Ma). The IRD provenance signal is positively correlated to detrital $^{87}Sr/^{86}Sr$ and εNd signatures in the fine fraction of the same samples, indicating an increasing amount of material derived from the distal Wilkes Land margin (εNd: -12.3 to -14.8; $^{87}Sr/^{86}Sr$: 0.730-0.735). Our results imply that ice rafting played an important control on sediment composition in the late Pliocene, possibly related to the growth of the EAIS in a cooler Late Pliocene climate.

Overall, the radiogenic isotope composition of Pliocene detrital sediments in the Southern Ocean reflects changing environmental conditions as well as sedimentary processes. Interpretation of such data can provide a valuable framework for the interpretation of ice sheet instability events along the Antarctic continental margin.

https://doi.org/10.1180/S0026461X00006502 Published online by Cambridge University Press

Systematic tapping of independent magma chambers during the 1 Ma Kidnappers supereruption

G.F. COOPER*, C.J.N. WILSON AND J.A. BAKER

SGEES, Victoria University, PO Box 600, Wellington, NZ
(*correspondence: george.cooper@vuw.ac.nz)

The 1.0 Ma Kidnappers eruption (~1200 km^3 bulk volume) from Mangakino volcanic centre produced the largest phreatomagmatic fall deposit in New Zealand, followed by the most widespread ignimbrite on Earth [1]. Samples collected through a proximal 4.0 m section of the Kidnappers fall deposit, representing the first 60-70 % of erupted material, reveal multiple, independent magma chambers of comparable size were tapped during the eruption. Evidence for this includes the following: (i) Major and trace element chemistries of individual matrix glass shards define three glass populations (types A, B and C), which display a systematic change through the fall deposit. (ii) Plagioclase, hornblende and Fe-Ti oxide compositions show bimodal distributions, corresponding to type A and B glass compositions, with a minor tail corresponding to C. (iii) Type B glass shards and biotite first appear at the same level in the fall deposit suggesting the later tapping of a biotite-bearing magma. (iv) Compositional gaps between glass types A and B imply that no mixing between these magmas occurred.

Parallel covariant trends in glass trace element chemistry indicate at least two independent magmas (A, B) underwent a parallel evolution with respect to crystallizing plagioclase and zircon. Temperature and pressure estimates from hornblende and Fe-Ti oxide equilibria from each magma type show that the two magma chambers were similar and therefore adjacent, not vertically stacked, in the crust. Hornblende temperature and pressure estimates from magmas A and B range from 770 to 860°C and 90 to 220 MPa corresponding to magma chamber depths of *ca*. 4 to 8 km. Hornblende pressure estimates coupled with *in situ* trace element fingerprinting imply that a horizontal stratification was also present in both of the A and B magma chambers. Pumice glass analyses from the subsequent ignimbrite display a broader compositional range than the fall deposits indicating the discharge of magma(s) that are not represented earlier in the eruption. This work has implications for understanding the dynamics of large (‘super‘) volcanic events and how such large volumes of silicic magmas are generated, stored and erupted.

[1] Wilson *et al*. (1995), *Nature* **378**, 605-607.

Distinguishing between open and closed system magma differentiation at arc volcanoes by combining U-series and elemental systematics

L.B. COOPER[12]*, O. REUBI[1], M. DUNGAN[2], B. BOURDON[3] AND C.H. LANGMUIR[4]

[1]Inst. of Geochemistry and Petrology., ETH Zurich, Switzerland
(correspondence: lauren.cooper@erdw.ethz.ch)
[2]Sect. of Earth Sciences, Univ. of Geneva, Switzerland
[3]Ecole Normale Supérieure de Lyon and CNRS, France
[4]Dept. of Earth and Planetary Sciences, Harvard Univ., USA

Constraining crustal assimilation in volcanic arcs is important because crustal components can be added during both mantle melting and magma ascent. Reubi *et al*. [1] present evidence for up to 10-15% assimilation of crust at Volcán Llaima (38.7°S), Chilean Southern Volcanic Zone, resulting in a diminution of U-series excesses from mantle signatures towards U-rich plutonic endmembers on the equiline. These trends strongly correlate with trace element indices of contamination over 51-57 wt% SiO_2. Llaima is now a very well-characterized volcano with respect to U-series activity ratios (U-Th-Ra-Pa), with 28 historic samples selected from >180 on the basis of major and trace elements. These data will be used to model differences in magma evolution in seven historic eruptive episodes (1640-2009).

In order to evaluate along-arc variations in crustal contributions, we have analyzed five selected samples from nearby Volcán Lonquimay (30 km NE of Llaima, 38.4°). Major and trace element variations over 52-63 wt% SiO_2 provide much less evidence for open-system processes than that recorded by the more contaminated Llaima samples (Rb/Zr=0.12-0.31 at Llaima versus 0.14-0.17 at Lonq.). U-series activity ratios for Lonquimay are constant and overlap with the least contaminated Llaima samples. And, simple equilibrium phenocryst assemblages in the Lonquimay lavas suggest that magma evolution is controlled almost exclusively by closed-system crystal fractionation. The cause of the Llaima/Lonquimay contrast remains unclear. Llaima is larger and more active than Lonquimay, perhaps leading to a higher efficiency of assimilation.

With the further constraints provided by U-series, greater quantitiative understanding of the extent and causes of crustal contamination will become possible. Much of the earlier data from southern Chile may need to be re-evaluated. More U-series studies are currently underway at Nevados de Chillán (36.8°), Antuco (37.3°), Villarrica (39.5°), and Osorno (41°).

[1] O. Reubi *et al*. (2011) *Earth Planet Sci Lett* **303**, 37-47.

https://doi.org/10.1180/S0026461X00006502 Published online by Cambridge University Press

U-Pb geochronology of the Southern Scandinavian Caledonides: The Mesoproterozoic Espedalen anorthosite-gabbro-norite massif and associated rocks

F. CORFU[1] AND M. HEIM[2]

[1]University of Oslo, Dept. Geosciences PB 1047 Blindern, N-0316 Oslo, fernando.corfu@geo.uio.no
[2]The Norwegian University of Life Sciences (UMB), PB 5003, N-1432 Aas, (michael.heim@umb.no)

Exactly 100 years ago V.M. Goldschmidt completed his PhD thesis on contact metamorphism in the Oslo Graben, and shifted attention to the Caledonian mountains and their problems concerning tectonics, metamorphism and magmatism. Based on these studies, in 1916 he provided a detailed description of the two main plutonic suites that occur in the nappes, the anorthosite-charnockite series and the contrasting opdalite-trondhjemite series. He outlined the main features of the rocks and discussed many of the fundamental question concerning these suites, their relationships, ages, origin and processes controlling their formation. Interestingly, and in spite of the enormous progress in many fields, many of the problems discussed in his paper remain relevant and unsolved today, a century later. In our present study we deal with an anorthosite massif and associated rocks in the eastern-most part of the Jotunheimen mountains investigated by Goldschmidt. One basic question concerns the relationship between these rocks and the major other anorthositic domains in the Jotunheimen and Bergen regions, and the relationships between the various members of the suite including the out of order sequence of crystallization of anorthosite and other mafic to intermediate rocks. Zircon found in coarse grained noritic anorthosite in Espedalen indicates an age of about 1520 Ma, similar to, or slightly younger than those for tonalite and granite in the supposed metamorphous sub-volcanic complex at the interface with tectonically underlying psammitic rocks. Zircons from a lamprophyre dyke yields an age of 1514 Ma. The U-Pb data also record partial disturbances during the Sveconorwegian orogeny, a feature typical of most rocks of the Jotun Nappe Complex. The age of 1520 Ma for the Espedalen massif shows that this intrusion is clearly distinct from the Sveconorwegian anorthosite (ca. 965 - 970 Ma) in the Jotun and Lindås nappes. The 1500 Ma event correlates instead with the very intense activity that build much of the south-Norwegian crust, thus supporting a provenance of the nappe from southern Baltica.

Nuclear imaging of ^{99m}Tc transport and immobilisation through porous media

CLAIRE L. CORKHILL[1]*, JONATHAN W. BRIDGE[1], PHILIP HILLEL[2], CLAIRE UTTON[3], NEIL C.HYATT[3], STEVEN A. BANWART[1] AND MARIA ROMERO-GONZALEZ[1]

[1]Kroto Research Institute, Department of Civil and Structural Engineering, University of Sheffield, S3 7HQ, UK. (*corresponding author: c.corkhill@sheffield.ac.uk)
[2]Department of Nuclear Medicine, Hallamshire Hospital, Sheffield, S10 2JF, UK
[3]Department of Materials Science and Engineering, University of Sheffield, S1 3JD, UK

^{99}Tc is a β-emitting radioactive fission product of ^{235}U, formed in nuclear reactors. Its long half life ($2.1x10^5$ years) and high environmental mobility in oxic conditions as the pertechnetate anion ($Tc(VII)O_4$) presents a major challenge to nuclear waste disposal strategies.

We demonstrate non-invasive quantitative imaging of the transport of ^{99m}Tc, a γ-emitting metastable isomer of ^{99}Tc commonly used in medical imaging. Transport of this radionuclide was measured during co-advection through quartz sand and various cementitious materials commonly used in nuclear waste strategies, including crushed ordinary portland cement (OPC), OPC combined with blast furnace slag (BFS) or pulversised fly ash (PFA), and Nirex Reference Vault Backfill material. Pulse-input experiments of approximately 25MBq ^{99m}Tc were conducted under saturated conditions and at a constant flow of 0.33ml/min. Dynamic gamma imaging was conducted every 30s for 2 hours.

Relative changes in mass distribution of ^{99m}Tc over time were quantified by spatial moments analysis of the resulting plume. ^{99m}Tc advected through quartz sand and crushed OPC demonstrated typical conservative behaviour, while transport through BFS- and PFA-containing cements produced a significant reduction in colloid centre of mass transport velocity over time. We propose that this is likely due to reduction of ^{99m}Tc by active reducing agents such as Fe and S in the cementitious material. Concurrent batch experiments using ^{99}Tc demonstrated the relatively irreversible sorption of Tc to these materials.

Gamma camera imaging has proven an effective tool for helping to understand the factors which control the migration of radionuclides for surface, near-surface and deep geological disposal of nuclear waste.

https://doi.org/10.1180/S0026461X00006502 Published online by Cambridge University Press

Pedogenesis and stabilization of soil organic carbon in a charcoal production plot

JEAN-THOMAS CORNELIS*, BRIEUC HARDY, BRUNO DELVAUX AND JOSEPH DUFEY

Earth and Life Institute – Environmental Sciences, Université catholique de Louvain, Louvain-la-Neuve, Belgium (*correspondence: jean-thomas.cornelis@uclouvain.be)

Charcoal addition to soil has the potential to improve physical, chemical and biological functions of soil [1], while being used as a potential long-term sink for atmospheric CO_2 due to the intrinsic recalcitrance of aromatic components [2]. Our hypothesis is that production process and addition of charcoal in soil can influence the pedogenic processes governing the soil capacity to stabilize organic carbon (OC).

The experimental site is located in an oak forest in the loessic silt belt of Belgium. The well-drained and acidic (pH 3.8-4.3) soil is classified as a Luvisol with an argic horizon occurring at 30 cm depth. We carried out the mineralogical and physico-chemical analysis (i) in an ancient charcoal production plot (1750-1870), and (ii) in the reference forest soil. Moreover, we analyzed the content of labile and stable (mineral-protected and recalcitrant) OC in charcoal-enriched, organo-mineral (Ah), eluvial (E) and argic (Bt) horizons.

The soil-pH increases by 0.6-0.8 units and the base saturation is until eight fold higher after the addition of charcoal. In the eluvial E horizon just below the charcoal accumulation, we observe a slight decrease of the content of amorphous and crystalline iron oxides, which provide reactive hydroxylated surfaces for OC associations. The mass of stable OC per unit area in the soil below the ancient charcoal production plot is significantly higher (13.9 $kg.m^{-2}$) than in the reference Luvisol (5.8 $kg.m^{-2}$). Charcoal, as residues of slow pyrolysis, strongly increases the sequestration of C in soil through (i) intrinsic recalcitrance and (ii) charcoal-organo-mineral interactions. Indeed, the part of humified, dissolved or colloidal OC released from charcoal and stabilized upon silicates and oxy-hydroxydes is not negligible (5.6 $kg.m^{-2}$). Finally, the pedological modifications induced by the charcoal production process do not significantly influence the stable OC stock. Therefore, the addition of charcoal will lead to higher C sequestration in topsoil without affecting the subsoil capacity to stabilize OC.

[1] Glaser B., Lehmann J. & Zech (2002) *Biology and Fertility of Soils* **35**, 219-230. [2] Baldock J. & Smernik R. (2002) *Organic Geochemistry* **33**, 1093-1109.

Spectral Gamma-ray applications to marine organic-rich sediments of the Lower Jurassic of Portugal

G.G. CORREIA[1]*, L.V. DUARTE[1], A.C. PEREIRA[1], R.L. SILVA[1] AND J.G. MENDONÇA FILHO[2]

[1]Universidade de Coimbra, Departamento de Ciências da Terra and IMAR-CMA, 3000-272 Coimbra, Portugal (*correspondence: gil.correia@gmail.com)

[2]IGEO and LAFO, Universidade Federal do Rio Janeiro, 21949-900 Rio de Janeiro, Brazil

This study is based on a high-resolution gamma ray analysis, performed on the hemipelagic Lower Jurassic organic-rich unis of the Lusitanian Basin (Portugal). This time interval, namely the Late SinemurianPliensbachian, is recognized as one of the most important potential oil source rock in Portugal [1].

Supported by more than 1000 gamma-ray measurements from outcrop and laboratory, the obtained data (total GR, Th, U and K) were correlated with several mineralogical (by X-Ray diffraction) and geochemical parameters, such as total organic carbon (TOC), insoluble residue (IR) and sulfur. From our results, and similarly to other case studies [2], we emphasize the relation between U and TOC, whose maximum value reaches 20%. A fair to good correlation is generally observed between these two variables (Fig. 1), however other lithological and geochemical (e.g. IR) parameters of the organic-rich facies may determine some variations.

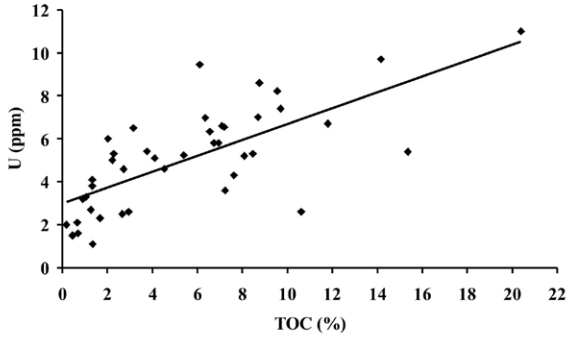

Figure 1: U/TOC correlation of the studied Lower Jurassic samples, with the U values obtained in laboratory.

This work has been financially supported by project PTDC/CTE-GIX/098968/2008 (FCT - Portugal).

[1] Duarte *et al*. (2010), *Geologica Acta* **8** (3), 325-340. [2] Luning & Kolonic (2003), *Journal of Petroleum Geology* **26**, 153-174.

https://doi.org/10.1180/S0026461X00006502 Published online by Cambridge University Press

Deglaciation pattern during the Late-Glacial / Holocene transition in the Southern French Alps. Chronological data from the Clarée Valley (Durance catchment, S. France)

ETIENNE COSSART[1], DIDIER BOURLES[2], REGIS BRAUCHER[2], MONIQUE FORT[3], ROMAIN PERRIER[3] AND LIONEL SIAME[2]

[1]Université Paris 1 Panthéon-Sorbonne, UMR Prodig 8586 – CNRS, 2 rue Valette, F-75005 Paris, etienne.cossart@univ-paris1.fr
[2]UMR CEREGE 6635 – CNRS, Plateau de l'Arbois, F-13100 Aix en Provence
[3]Université Paris Diderot (Paris 7), UMR Prodig 8586 – CNRS, 2 rue Valette, F-75005 Paris

The Southern French Alps, characterized by many climatic influences, remain a scientific problem for palaeo-environmental studies. Indeed, the lack of chronological benchmarks hitherto hampered the definition of sequences of glacier variations since the Last Glacial Maximum (LGM), even if a scenario was established in the Ubaye valley. This scenario was then considered as a regional model by many geomorphologists, but this valley is not necessarily representative of the entire region. We focus here on the upper part of the Durance watershed because it corresponds to the accumulation zone of the main glacier of the Southern French Alps during the LGM. Thanks to extensive fieldwork and geomorphic mapping of remnants of past glaciations, and thanks to new chronological data (about 35 cosmic ray exposure –CRE– ages) we propose the first absolute scenario established in the very upper part of the catchment. To assess CRE ages, we sampled glacially-polished surfaces, in order to assess both the retreat of the front and the thinning rate of the glacial tongue. We also paid attention to morainic ridges and glacio-fluvial remnants. The results show that cirque glaciation began only at the beginning of the Holocene, and that thick valley glaciers still occupied the upper valleys during the Late-Glacial period, until the Younger Dryas stadial. The disappearance of the tongue occurred rapidly, between Younger Dryas and Preboreal sequences due to both ELA rise and a topographic threshold effect. Finally, this scenario appears to be well in accordance with new data obtained in other parts of the Alps.

The composition of the Earth's outer core from first principles

ALEXANDER S. CÔTÉ[1,2], JOHN P. BRODHOLT[1] AND JAMES BADRO[2]

[1]Dept. of Earth Sciences, University College London, U.K.
[2]Institut de Physique du Globe de Paris, France.

The exact composition of the Earth's core remains an unanswered question. Published models for the outer core allow a mixture of several coexisting light elements (Si, S, O, C), and many arguments have been put forward over the years for and against each of those elements.

In this study we performed *ab initio* molecular dynamics calculations on liquid Fe and liquid Fe-(Si,S,C,O) mixtures at different P and T conditions of the Earth's outer core in order to attempt to constrain the light-element concentration based on densities and bulk sound velocities. By fitting equations of state to our P-V data, we were able to obtain density and velocity vs. concentration profiles for each iron-light-element liquid alloy; this allowed us to estimate the density for different outer core compositions found in the literature and compare them with seismic models such as PREM and AK135. We find that the density of liquid Fe containing 4% of Ni (no light elements) is approximately 7% denser than the core. Incorporating light element increases the bulk sound velocity while decreasing density. We also find that many of the published compositional models for the outer core result in densities lower than the seismological models. This indicates that the light element concentrations predicted in those models are slightly overestimated. Our data agree with an O-rich outer core (up to 6.3wt. %), and we find that large amounts (more than 3 wt. %) of Si cannot be incorporated in the outer core.

https://doi.org/10.1180/S0026461X00006502 Published online by Cambridge University Press

Zn isotope fractionation in the soil-plant system (a pot experiment)

E. COUDER[1]*, T. DROUET[2], B. DELVAUX[1], C. MAERSCHALK[3], C. MEEUS[3] AND N. MATTIELLI[3]

[1]Earth and Life Institute – Environmental Sciences – Science Soil, Université catholique de Louvain, Croix du Sud, 2/10, 1348 Louvain-la-Neuve, Belgium (*correspondence: Eleonore.Couder@uclouvain.be)
[2]Laboratoire d'Ecologie végétale et Biogéochimie, Université Libre de Bruxelles, 1050 Brussels, Belgium
[3]Département des Sciences de la Terre et de l'Environnement, Université Libre de Bruxelles, 1050 Brussels, Belgium

Zinc isotopes constitute a precious tool to trace metal sources and better understand the cycling of this micronutriment in the environment. The aim of the present study is to investigate the Zn isotope fractionation for evaluating the interaction between plant species and soil types, in order to better characterize Zn migration through the soil-plant system.

Three contrasted soils, originating from a zone with intense metallurgical activites in Belgium, have been used for the culture experiment conducted in controlled conditions: a calcareous soil ($\delta^{66}Zn_{bulk\ soil}$ = +0.06‰) and an acid shale-derived soil ($\delta^{66}Zn_{bulk\ soil}$ = +0.08‰) both essentially feeded by aerial fallouts, and a slag heap-derived soil ($\delta^{66}Zn_{bulk\ soil}$ = +0.37‰). Two plant species have been chosen: a dicot species (rape) and a monocot species (ryegrass). The Zn isotopic compositions have been measured in roots ($\delta^{66}Zn$ = +0.01 to +0.43‰) and in shoots ($\delta^{66}Zn$ = -0.23 to +0.28‰).

The results show that (a) the Zn isotopic compositions of all materials reflect the Zn isotopic signatures of the main Zn inputs (aerial fallouts *vs* smelter-slag residues); (b) light Zn isotopes are preferentially accumulated in shoots; (c) the magnitude of Zn fractionation during Zn transport from roots to shoots appears to be related to the cation exchange capacity of roots (CECR) and the water use efficiency (WUE). The plant species affects the Zn signature in plant parts through the density of negative charges in the roots, *i.e*. CECR being larger for the dicot species implies a larger Zn isotope fractionation between shoots et roots. In addition, the WUE might regulate a form of isotopic selection by controlling the efficiency of Zn adsorption on cell walls.

In the soil-plant system, enrichment in light Zn isotopes is favoured into the plants. As Zn is subsequently recycled to the soils through dead plant material return, the plant cover plays a key role on Zn fractionation in soils.

Early fossilization process of cyanobacteria in modern microbialites

ESTELLE COURADEAU[1,2], KARIM BENZERARA[1], EMMANUELLE GERARD[2], IMENE ESTEVE[1], DAVID MOREIRA[3] AND PURIFICACION LOPEZ-GARCIA[3]

[1]IMPMC, UMR 7590, UPMC, IPGP & CNRS 4 place Jussieu, Paris, France (estelle.couradeau@impm.upmc.fr)
[2]Géobiosphère actuelle et primitive UMR 7154, IPGP, UPD & CNRS, 1 rue Cuvier , Paris, France
[3]Ecologie, Systématique et Evolution, UMR 8079 CNRS & Université Paris-Sud, France (puri.lopez@u-psud.fr)

Most extant life diversity is microbial. Despite so, microbes are rarely described in the rock record. Part of the problem comes from the difficulty to identify microfossils unambiguously, since they can be morphologically confused with abiotic biomorphs [1]. Therefore, identifying traces that can be diagnostic of microbial fossils is crucial. To contribute to this aim, we studied the ongoing fossilization of cyanobacterial cells in modern microbialites from Alchichica Lake (Mexico). Alchichica Lake is a Mg-rich hyperalkaline crater lake (pH 8.9) containing living stromatolites composed of aragonite [$CaCO_3$] and hydromagnesite [$Mg_5(CO_3)4(OH)_2 \bullet 4(H_2O)$] [2]. Cyanobacteria comprise most of the microbialite biomass. Scanning electron microscopy coupled with confocal laser scanning microscopy were used to co-localize cyanobacterial cells and associated minerals. These observations showed that cells from the order Pleurocapsale become specifically encrusted within aragonite with an apparent preservation of cell ultrastructures. Early fossilization gradients from living to totally encrusted cells span distances of a few hundred micrometers. Cells with increasing levels of encrustation where observed down to the nm-scale by transmission electron microscopy performed on Focused Ion Beam (FIB) ultrathin (<100 nm) foils. Two types of aragonite crystals differing by their morphology were seen within and outside cells. Synchrotron-based scanning transmission x-ray microscopy (STXM) analyses at the C and N K-edges [3] were performed on the same FIB foils. They provide information on the evolution of carbon and nitrogen speciation along this early fossilization gradient. We propose a model of the early fossilization process of these cyanobacteria and their associated organic molecules.

[1] Garcia-Ruiz JM & al. (2003) *Science* **302**:1194-7.[2] Kaźmierczak J & al (2011) *Facies* **2011**:1-28.[3] Bernard S & al. (2010) *GCA* **74**:5054-68.

https://doi.org/10.1180/S0026461X00006502 Published online by Cambridge University Press

Solid speciation of As, Pb and Sb-rich anthropogenic residues

A. COURTIN-NOMADE[1]*, O. RAKOTOARISOA[1], H. BRIL[1], M. KUNZ[2] AND N. TAMURA[2]

[1]University of Limoges, GRESE Laboratory, FST, 123, avenue A. Thomas, 87060 Limoges Cedex, France (*alexandra.courtin@unilim.fr)

[2]Advanced Light Source, Lawrence Berkeley National Lab, 1 Cyclotron Rd, Berkeley, CA 94720, USA

We studied As, Pb and Sb solid speciation to better understand the geochemical pathways and mobility of these potentially toxic elements, which are released upon weathering of mining and industrial waste products. Such studies are indispensible to understand soil and water contaminations and to propose remediation solutions. Studied samples are mining residues (mill tailings and slags) from the French Massif Central, generated by former activities over a century (1830 to 1970). They were collected at two different mining districts: Pontgibaud, which was one of the largest production site for Ag and Pb (c.a. 50'000 t Pb) and Brioude-Massiac, which produced around 40'000 t of Sb (second largest nationwide production). Samples were also studied to compare the evolution of industrial processes and to test the variations in Pb or Sb retention.

Mining residues from the two locations show elevated concentrations in As, Pb and Sb, up to 0.16%, 6.6% and 1.1% respectively. However spatially concentrated accumulations of As (up to 11 wt.%), Pb (up to 70 wt%) and Sb (up to 28 wt.%) are also observed. The mineralogical characterization of the products with such contents is essential for the modeling of the geochemical processes controlling the toxicity of these elements. Arsenic, Pb and Sb have only been detected in secondary products resulting from oxidation of Pb or Sb-rich sulfides (galena, stibnite and berthierite) but only few relics of primary sulfides have been observed. Synchrotron X-ray microdiffraction (beamline 12.3.2, Advanced Light Source, USA) and micro-Raman investigations indicate that Sb forms complex mixing phases with goethite and/or lepidocrocite. Antimony is also trapped by jarosite suggesting a substitution of $Fe^{3+}$by Sb^{5+} (up to 3% Sb). Antimony is present as oxides, stibiconite $SbSb_2O_6(OH)$ and associated with Fe, and possibly Mn (oxy-)hydroxides within solid phases of highly heterogenous compositions. Arsenic is also typically associated to iron (oxy-)hydroxides presenting various cristallinity. Main Pb host phases are sulfates (e.g., anglesite $Pb(SO_4)$, beudantite $Pb(Fe_{2.54}A_{1.46})(As_{1.07}O_4)(S_{0.93}O_4)(OH)_6$) but Pb is also associated to complex mixing of silicates and Fe oxides.

S isotopes distinguish two S pulses at terrestrial Cretaceous-Paleogene boundary sections

M.L. COUSINEAU[1]*, F. THERRIEN[2], T. MARUOKA[3], B.A. WING[4] AND D. FORTIN[1]

[1]Earth Sciences, University of Ottawa, Ottawa, Ontario, Canada (*correspondence: mlcousineau@uottawa.ca)

[2]Royal Tyrell Museum of Palaeontology, Drumheller, Alberta, Canada (francois.therrien@ab.gov.ca)

[3]Integrative & Environmental Sciences, University of Tsukuba, Ibaraki, Japan (maruoka@ies.life.tsukuba.ac.jp)

[4]Earth and Planetary Sciences, McGill University, Montréal, Québec, Canada (boswell.wing@mcgill.ca)

The Cretaceous-Palaeogene (K-Pg) boundary marks a major biotic turnover in Earth's history that may have resulted, at least in part, from a massive bolide impact.

Two of the northernmost occurrences of the K-Pg boundary in terrestrial sediments have been positively identified on the Knudsen's *T. rex* Ranch in the Scollard Formation of south-central Alberta, Canada. We conducted a high-resolution (2-cm intervals) study of bulk sulfur isotopes and sulfur content across a ~50-cm stratigraphic interval spanning the K-Pg boundary, representing a time interval of ~500 Ka.

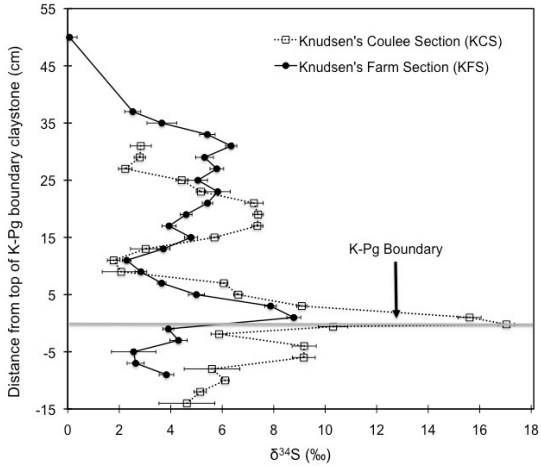

Figure 1: $\delta^{34}S$ profiles at the Knudsen's *T. rex* Ranch

Positive $\delta^{34}S$ excursions at both sites reveal a pulse of ^{34}S-enriched sulfur at the boundary, likely originating as oceanic sulfate and evaporite target rocks. Post-boundary $\delta^{34}S$ excursions may reflect injection of volcanically-derived sulfate aerosols; at least one peak (KFS) is contemporaneous with a major phase of Deccan trap volcanism. Analyses of minor S isotopes (^{33}S, ^{36}S) offer the possibility to validate our interpretation of the origins of the boundary and post-boundary S injections into the freshwater environment.

https://doi.org/10.1180/S0026461X00006502 Published online by Cambridge University Press

Copper and zinc isotope fractionation during their interaction with phototrophic biofilm

A. COUTAUD[1,2]*, O.S. POKROVKSY[1], J.L. ROLS[2], J. VIERS[1] AND L. TEN-HAGE[2]

[1]GET, CNRS/UPS, 14 av Edouard Belin, 31400 Toulouse, France (*correspondence: aude.coutaud@get.obs-mip.fr)
[2]EcoLab, CNRS/UPS, 118 rte de Narbonne, 31062 Toulouse cedex 9, France

In geochemistry, the study of the interactions between trace metals (TM) and aquatic microorganisms is limited essentially by the characterisation of surface's interactions for short exposure time and for uptake experiments for selected monospecific groups of algae and bacteria. The originality of our work is to combine the study of Cu and Zn isotope fractionation with biological characterisation of phototrophic biofilms during long incubation times in order to allow for the integration of an ecological dimension.

Towards this goal, batch and open flux experiments including trace metals (TM) sorption, incorporation and extracellular release were performed on mature biofilm having a cyanobacterial dominance. Moreover, the impact of temporary drying on metal release from biofilm was studied. Anothers experiments were performed in Taylor Couette reactor to study the relation between a biofilm growth cycle and the degree of stable isotope fractionation during metal uptake.

Results show that in batch reactor, the pattern of metal isotope fractionation is dramatically different between Zn and Cu. There is an accumulation of heavy Zn isotope in the biofilm during the first 96 hours with an average isostopic shift close to 0,3 ± 0,1 ‰. In contrast, the copper interacting with biofilm during 48 hrs is enriched in light isotopes (approx 0,16 ± 0,07 ‰) but later this trend is reversed bringing to enrichment the biomass in heavy isotope. The observed difference may be linked to (i) the different toxicity of metal with Cu being more toxic than Zn and (ii) the difference of physicochemical properties of metal interaction reactions: internalization of copper is faster than that of Zn and only Cu could undergo redox reaction within the biofilm matrix and inside the cells.

Our results provide firm basis for establishing the link between metal complexes structure and toxicity and the degree of stable isotope fractionation that can be used for tracing biological processes in natural waters.

Montalto Formation: A Middle Cambrian to basal Ordovician sequence in Dúrico-Beirã area (Northern Portugal)

H. COUTO

Universidade do Porto, Faculdade de Ciências, DGAOT, Centro de Geologia, Rua do Campo Alegre 687, 4169-007 Porto, Portugal (hcouto@fc.up.pt)

Montalto Formation [1] occur in Dúrico-Beirã area (northern Portugal) in Central-Iberian Zone. It's formed by three lithologic associations. The Lower lithologic association is mainly composed of grey and violet slates with intercalations of altered volcanic acid rocks and exhalites. The Intermediate lithologic association is composed by alternating sequences of slate, quartzite, and subordinate wacke. The Upper lithologic association is mainly composed of conglomerates usually clasto-suported with minor pelite, siltite, quartz arenite and wacke intercalations. Some conglomerates are well calibrated dominantly bearing quartz clasts usually elongated and orientated. Other conglomerates occurring to the top of the sequence are polygenic, poorly calibrated with clasts of varied nature (quartz, schist, black quartzite) intersperse with pelitic or quarztic layers evidencing a more superficial facies, probably continental. Dykes of diabase are particularly frequent in this lithologic association. This formation overlies the Terramonte Formation [1], a thick flyschoïd sequence, showing some turbiditic characters being equivalent to Desejosa Formation defined in Douro Group (Lower Cambrian to Middle Cambrian) [2]. Montalto Formation underlies a lithologic association mainly composed of conglomerates, quartz-arenites, minor pelites and wakes interbeded with volcanic rocks exhibiting bimodal composition (volcanoclastic rocks of rhyolitic affinities and basic volcanic rocks) that evidence a continental rifting [3] of probably Tremadocian age. To the top the Armorican quartzites occur (Floian). So, an age between Middle Cambrian and basal Ordovician (Tremadoc) is proposed to Montalto Formation. This contrast to a Floian age proposed by some authors [4] when correlating Montalto Formation to Vale de Bojas Formation and Eucísia Formation (Trás-os-Montes). These last formations can be correlated to the volcano-sedimentary sequence of probable Tremadocian age [3].

[1] Couto, H. (1993) Phd thesis. 607pp. Faculdade de Ciências da Universidade do Porto. [2] Sousa, B., 1984. *Cuadernos Geologia Ibérica, Madrid*, **9**: 9-36. [3] Couto H. & Lourenço, A. 2008. *33rd International Geological Congress Oslo, Norway*. SES-07 Dynamics of sedimentary basins. Abstract CD-Rom. [4] Sá, A. *et al*. 2006. *Ibérica,. VII Congresso Nacional de Geologia,* Évora, **2,** 621-624.

https://doi.org/10.1180/S0026461X00006502 Published online by Cambridge University Press

Late Ordovician to Lower Silurian transition in Valongo Anticline (Northern Portugal): Evidences of an erosional unconformity previous to the Silurian sea level rise

H. COUTO AND A. LOURENÇO[1,2]

[1]Universidade do Porto, Faculdade de Ciências, DGAOT, Centro de Geologia, Rua do Campo Alegre 687, 4169-007 Porto, Portugal. (hcouto@fc.up.pt)

[2]Universidade do Porto, Reitoria, Centro de Geologia, Praça Gomes Teixeira, 4099-002 Porto, Portugal. (aafonso@reit.up.pt)

This work discusses the transition of Ordovician to Silurian in Valongo Anticline. This structure is an antiform related with the Variscan orogeny, located in the Centro Iberian Zone (Northern Portugal). The Sobrido Formation representing the Hirnantian glacial deposits was recently revised [1] evidencing the presence of ice-contact deposits.

The transition between Upper Ordovician and Lower Silurian strata is variable. Transitional sections locally record a ferruginous level and black basal quartzites. These quartzites seems equivalent to Vale da Ursa Formation [2] of Central Portugal (Dornes). They are followed by black-shales or dark grey schist turning to light grey and purple with pyrophillite and bearing Middle to Upper Llandovery graptolites [3] with intercalations of centimetric cherty or quartzitic layers. The presence of a ferruginous level and the fact that sometimes quartzites are lenticular or absent evidences a minimum glacio-eustatic sea-level. The quartzites are interpreted to record scour, a lag, and the development of an erosional unconformity before the Silurian sea level rise. This is in agreement with what has been advocated by other authors [4] that consider the sea levels reached a minimum during the glaciation near the Ordovician-Silurian boundary before a further significant rise took place during the Llandovery. Black shales were controlled by the early Silurian palaeorelief as suggested for the Lower Silurian "hot shales" in North Africa and Arabia [5]. This model can explain why often in Valongo Anticline, the Lower Silurian black-shales or dark grey schist occur in the middle of Hirnantian diamictites.

[1] Couto & Lourenço (2011), *Cuadernos del Museo Geominero* (in press). [2] Cooper (1980), Phd thesis, Sheffield University, England. [3] Romariz (1962), *Revista Faculdade Ciências de Lisboa, 2ªSér. C*,**10** (2) 115-312.[4] Servais *et al*. (2009) *GSA Today* **19** (4) 4-10. [5] Lünning *et al*. (2000), *Earth Science Reviews* **49**, 121–200.

Psychrophilic methanogens: A possible solution to more cost-effective anaerobic wastewater treatment

JILLIAN M. COUTO, GAVIN COLLINS AND WILLIAM T. SLOAN

School of Engineering, University of Glasgow, Glasgow UK, G12 8QQ

Wastewater treatment facilities are a rich source of methane gas, an effective renewable energy source. Methane is produced anaerobically by mesophilic or thermophilic microbial communities and thus currently requires a net input of energy to heat waste treatment facilities, reducing the cost-effectiveness of this process. Our aim is to investigate the potential of psychrophilic microbes to produce methane, hence reducing the need for this net input of energy. To do this we have designed a functional screen of metagenomes harvested from cold temperature environments, specifically arctic soils and cold-adapted agricultural waste sludge, which will be scanned for novel functional candidate genes. This screen entails scanning thousands of genes for their ability to be activated in an anaerobic and cold environment when exposed to intermediary metabolites produced during methanogenesis. Similar to a previous design (Uchiyama *et al*, 2005) [1], genes within our metagenomic library, housed in e-coli, will produce a fluorescence signal when activated by these metabolites. This is detected in a high throughput manner using fluorescence activated cell sorting technology. Once isolated, these candidates will then be further characterized and tested for use within a bioreactor system, with the ultimate goal of producing methane at cold temperatures.

[1] Uchiyama, Abe, Ikemura & Watanabe (2005), *Nature Biotechnology* **23**, 88-93.

https://doi.org/10.1180/S0026461X00006502 Published online by Cambridge University Press

Geochemical behavior of (thio)arsenates with Fe-minerals

R.M. COUTURE[1,*], D. WALLSCHLÄGER[2], K. MITCHELL[1] AND P. VAN CAPPELLEN[1]

[1]Earth and Environmental Sciences, University of Waterloo, Waterloo, Canada (*correspondence: r.couture@uwaterloo.ca)
[2]Environmental and Resources Studies, Trent University, Peterborough, Canada

Under microbially-mediated sulfate (SO_4) reducing conditions, the mobility of arsenic (As) in iron (Fe) rich sediments is influenced by the transformations of Fe minerals and changes in aqueous As speciation. Hence, to predict As mobility in complex biogeochemical systems, the sorption of aqueous As species to various Fe mineral phases should be fully understood. However, despite the accumulating evidence that thioarsenates dominate As speciation under a variety of environmental conditions, their sorption behaviour in sediments is poorly known. We used batch experiments to measure sorption of six individual As species in suspensions of 2-lines ferrihydrite (2L-Fh), hematite, goethite, mackinawite ($FeS_{m(s)}$) and pyrite. The table below shows the results for $FeS_{m(s)}$ and 2L-Fh. As can be seen, there are marked differences in the partition coefficients of the different soluble As species.

	$FeS_{m(s)}$	2L-Fh
Arsenate	5	1600
Arsenite	3	50
Mono-thioarsenate	0.1	12
Di-thioarsenate	310	70
Tri-thioarsenate	0.2	150
Tetra-thioarsenate	1.5	120

Table: Partition coefficients (K_d; L g^{-1}) for As sorption to selected Fe-minerals at pH 7 and ionic strength = 0.05M.

We also used flow-through reactors (FTRs) to look at the formation and sequestration of thioarsenates in Fe-rich and Fe-poor lake sediments run under SO_4 reducing conditions. The FTRs where supplied with either soluble arsenate or soluble arsenite. We monitored SO_4, total sulfide, zero-valent sulfur, Fe as well as pH and E_h in the outflow of the FTRs. The results indicate that arsenate is first reduced to arsenite, which is then sulfidized to thioarsenates. Thioarsenates only dominated As speciation in the FTR outflow of the Fe-rich sediments. In addition, As was released as mono-thioarsenate, in line with the observation that mono-thioarsenate is the least strongly bound to Fe-minerals (see Table). These preliminary observations are currently being used to improve existing reactive-transport models for the fate of As under sulfate reducing conditions.

Metatranscriptomics of the green sulfur bacteria in a meromictic Swiss lake (Lago di Cadagno)

R.P. COX[1,2*], K. HABICHT[1,3], M. MILLER[2], N. STORELLI[4,5], M. TONOLLA[4,5] AND N.-U. FRIGAARD[6]

[1]NordCEE, [2]Dept. Biochem. Mol. Biol., [3]Inst. Biol., Univ. of Southern Denmark, 5230 Odense M, Denmark (*correspondance: r.p.cox@bmb.sdu.dk)
[4] Dept. Plant Biol., Univ. Geneva, Switzerland
[5] Inst. Microbiol., Canton Ticino, Bellinzona, Switzerland
[6] Dept. Biol. Univ. Copenhagen, 3000 Helsingør, Denmark

Lake Cadagno in the Swiss Alps is a potential modern analog of the early ocean. The lake is permanently stratified with anoxic water containing sulfate (1.5 - 2.0 mM) and sulfide below the chemocline. The sulfidic water column contains high concentrations of phototrophic sulfur bacteria (peak concentrations more than 250 μg/L BChl *e*). We have previously shown that the bacterial community in this layer is dominated by the green sulfur bacterium *Chlorobium clathratiforme* (up to 70% of recovered bacterial 16S rRNA gene sequences in a clone library [1]. Several lines of molecular sequence evidence suggest that this population is clonal and has replaced the previously dominant purple sulfur bacteria over the last decade [1]. This feature makes the lake a highly suitable site for metatranscriptomic studies of natural populations.

Samples were collected at the top of the chemocline during the day (1) and at night (2) and at a depth where light intensity precludes active photosynthesis (3). The mRNA was converted to cDNA and subjected to high-throughput sequencing. As expected from previous results [1,2] a high proportion of the sequences could be matched to the genome of *Chlorobium clathratiforme* BU-1 which was isolated from a lake in Southern Germany. There were relatively small differences in the normalised transcript levels between the 3 samples. The highest transcript levels were observed for the major protein of the light-harvesting chlorosomes, *csmA*, and the gas vesicle protein *gvpA*.

[1] Gregersen *et al*. (2009) *FEMS Microbiol. Ecol*. **70**, 30-41.
[2] Habicht *et al* (2011) *Environ. Microbiol*. **13**, 203-21

https://doi.org/10.1180/S0026461X00006502 Published online by Cambridge University Press

Molecular modelling of carbon dioxide adsorption in zeolites

J.C. CRABTREE*[1], S.C. PARKER[2] AND J.A. PURTON[3]

[1]Doctoral Training Centre in Sustainable Chemical Technologies, University of Bath, BA2 7AY (*correspondence: j.c.crabtree@bath.ac.uk)
[2]Department of Chemistry, University of Bath, BA2 7AY
[3]Daresbury Laboratory, Daresbury, Warrington, WA4 4AD

There is growing concern about the dangers of climate change. The majority opinion is that a major cause is the emission of greenhouse gases such as carbon dioxide (CO_2). Adsorption and separation of CO_2 is therefore a key area of research. Silicate materials are a promising class of material for the adsorption of CO_2 [1][2]. Natural and synthetic zeolites have been chosen as the initial focus of this computational study. They present a good model system as they are microporous and there is experimental data for comparison with simulations.

The computational methods use interatomic potentials to describe the interactions between atoms. Energy minimisation is used to find the most stable configurations of the zeolites. Molecular dynamics is used to study the diffusion of CO_2 in the zeolites while Grand Canonical Monte Carlo (GCMC) simulations are used to generate adsorption isotherms. Zeolites have been modelled in the siliceous form and as aluminosilicates with counter-ions. The main counter-ion that has been considered is Na^+, but the models are being extended to cope with others including K^+, Li^+ and Ca^+.

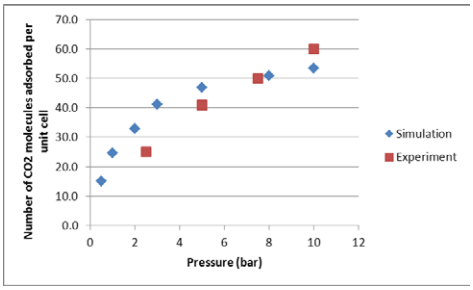

Figure 1: adsorption isotherm of CO_2 in siliceous faujasite, comparing simulations to experimental data [3]

The results gained in this work so far correlate well with experimental data and the work is currently being extended to cover a wide range of other structures and materials to find a good selective adsorbent for CO_2.

[1] Choi *et al*. (2009) *ChemSusChem* **2** 796-854. [2] Wang *et al*. (2011) *Energy Environ*. Sci **4** 42-55. [3] Maurin *et al*. (2005) J. *Phys*. *Chem*. B **109** 16084-16091

Fe and C isotopes in BIF carbonates: Evidence for authigenic formation and microbial Fe respiration

P.R. CRADDOCK AND N. DAUPHAS

Origins Laboratory, Dept of the Geophysical Sciences, The University of Chicago (craddock@uchicago.edu)

We report here iron ($\delta^{56}Fe$, vs. IRMM-014 [1]) and carbon isotopic ($\delta^{13}C$, vs. V-PDB) compositions of Fe-rich and Fe-poor carbonates in two Banded Iron-Formatios (BIF): the ~2.5 Ga Hamersley Basin, Australia and ~3.8 Ga Isua Supracrustal Belt (ISB), Greenland [2]. In the Hamersley Basin, Fe-rich carbonates (in the iron-formation) have $\delta^{56}Fe$ ranging widely from -1.0 to +1.2 ‰ (mean ~ 0 ‰), different from that of Fe-poor carbonates (platform dolomites) that have $\delta^{56}Fe$ lighter than -0.5 ‰. The $\delta^{13}C$ of the same Fe-rich carbonates (-8 to -16 ‰) are also distinct to those of Fe-poor carbonates (~ 0 ‰) [3]. The Fe and C isotope compositions are inconsistent with formation of Fe-rich carbonate in the iron-formation in isotope equilibrium with seawater, and instead reflect an authigenic origin via oxidation of organic carbon coupled to near-complete reduction of ferric precursors (e.g., ferrihydrite) in marine sediments [2,4]:

$$2Fe_2O_3{\cdot}3H_2O + CH_2O + 7H^+ \rightarrow 4Fe^{2+} + HCO_3^- + 10H_2O.$$

Organic carbon oxidation and ferric Fe reduction likely occurred rapidly following primary deposition at the seafloor, but the Fe and C isotope compositions of Fe-rich carbonates indicate that chemical exchange between pore waters and seawater was far from complete. Most likely, the reaction was mediated by heterotrophic microbes via dissimilatory Fe reduction; thus the Fe and C isotope data record evidence for evolution of microbial Fe respitation by ~2.5 Ga. Further, the authigenic formation of Fe-rich carbonate in the iron-formation implies no constraint on the pCO_2 of the overlying Archean ocean and atmosphere as suggested by [5; also see 6]. Coupled Fe and C isotopic signatures of Fe-rich meta-carbonates from the ISB are similar to those of known chemical sedimentary origin from Hamersley Basin [2,7,8]. By analogy, Fe-rich metacarbonates appear to have formed as chemical sediments and preserve isotope evidence that is consistent with the evolution of Fe catabolims by 3.8 Ga.

[1] Dauphas N. *et al*. (2009) *Chem*. *Geol*. **267**, 175-184. [2] Craddock P.R. & Dauphas N. (2011) *EPSL*, **303**, 121-132. [3] Becker R.H. & Clayton R.N. (1972) *GCA, **36***, 577-595. [4] Heimann A. *et al*. (2010) *EPSL*, **294**, 8-18. [5] Rosing, M.T. *et al*. (2010) *Nature*, **464**, 744-747. [6] Dauphas N. & Kasting J. (2011) *Nature, in press*. [7] Dauphas N. *et al*. (2004) *Science*, **306**, 2077-2080. [8] Dauphas N. *et al*. (2007) *GCA*, **71**, 4745-4770.

https://doi.org/10.1180/S0026461X00006502 Published online by Cambridge University Press

Electrolyte adsorption to goethite-water interfaces

LOUISE J. CRISCENTI AND DAVID HART

Sandia National Laboratories, Albuquerque, NM 87185, USA (*correspondence: ljcrisc@sandia.gov)

Adsorption onto goethite surfaces is a critical process influencing trace metal migration in the environment. This study investigates interfacial water structure and the adsorption of electrolyte anions and cations on different goethite surfaces to develop a better appreciation of the local environments that favour trace metal adsorption. The impact of different electrolytes (e.g., NaCl, Na_2SO_4, Na_2SeO_3) over a range of concentrations on water structure and surface loading will be presented.

Two goethite surfaces, the (100) and (101) surfaces as defined in the Pnma space group are under investigation. The (100) surface has three types of surface sites (5-fold Fe, Fe_2O_IH, Fe_3O_{II}) and the (101) surface has four types of sites ($Fe_1O_{II}H$, $Fe_2O_{II}H$, Fe_3O_{II}, and Fe_3O_IH). To date, molecular dynamics (MD) simulations have been performed to investigate the impact of 1M – 5M NaCl concentrations on interfacial water structure and surface loading. Each surface slab contains 192 Fe atoms and is protonated to create a neutral slab. The density of the bulk solution is maintaned at 1.0 g/L regardless of salt concentration. A Leonard-Jones wall is imposed at both the top and bottom of the simulation cell. A natural surface of water is allowed to form at the top of the cell through an NPT simulation. Then, a vacuum gap three times the cell height is added to prevent interactions between periodic cells in the Z direction. Production runs were performed using the NVT ensemble at 298K for10 ns.

Water layers at the (100) surface exhibit more structure and more hydrogen bonding with surface hydroxyl groups than at the (101) surface. Na^+ adsorbs as inner-sphere complex to both surfaces; Cl^- adsorbs as an outer-sphere complex. From atomic density profiles, the introduction of 5M NaCl does not change the overall interfacial water structure, reinforcing previous MD studies that also suggest that the electric double layer is dominantly formed by interfacial water structure rather than ions at the surface.

This research is supported by the U.S. Department of Energy, Office of Basic Energy Sciences, Division of Chemical Sciences, Geosciences, and Biosciences. Sandia is a multiprogram laboratory operated by Sandia Corporation, a Lockheed Martin Company, for the United States Department of Energy's National Nuclear Security Administration under contract DE-AC04-94AL85000.

Deglacial NW Atlantic ventilation from paired deep-water coral radiocarbon and Nd isotopes

KIRSTY C. CROCKET[1]*, TINA VAN DE FLIERDT[1], LAURA F. ROBINSON[2] AND JESS F. ADKINS[3]

[1]Earth Science and Engineering, Imperial College London, London SW7 2AZ, UK. (*k.crocket@imperial.ac.uk).

[2]Department of Earth Sciences, University of Bristol, Bristol BS8 1RJ, UK.

[3]GPS, Californian Institute of Technology, 1200 E. California Blvd., Pasadena, CA 91125, USA

Sequestration of carbon in the deep ocean during glacials and its subsequent release during deglaciation undoubtedly play a role in glacial/interglacial variation of atmospheric CO_2, although concrete evidence of the ocean's role has yet to be established. One route of investigation is to determine ocean ventilation rates. To do so requires combining dynamic tracer data, such as radiocarbon, with a conservative tracer to identify the water masses involved and their mixing ratios.

We describe the use of deep sea corals as an archive material providing same-sample U/Th ages, radiocarbon data and conservative water mass tracer data in the form of Nd isotope compositions. The majority of corals in this study are deglacial in age and span a water depth of 1000 to 2600 m in the NW Atlantic, where changes in the water column structure were pronounced across the last glacial/interglacial cycle [1]. Additional coral samples are located in the NE Atlantic and the northernmost parts of the North Atlantic to provide a broader picture of change.

This study builds on existing coral work, which has identified radiocarbon age reversals within single specimens [2] and rapid changes in radiocarbon content of the NW Atlantic water column [1]. By pairing the Nd isotope data to the radiocarbon data, we are able to identify the water masses present in the NW Atlantic during the deglaciation, the extent of mixing between these, and ultimately to translate the radiocarbon data into ocean ventilation rates.

[1] L.F. Robinson, *et al*. (2005), *Science* **310**, 1469-1473.
[2] J.F. Adkins, *et al*. (1998), *Science* **280**, 725-728.

https://doi.org/10.1180/S0026461X00006502 Published online by Cambridge University Press

Sinking Titanic (Ti^{IV}) – Insights into the speciation and distribution of Titanium in the Atlantic Ocean

P. CROOT[1], A. DAMMSHÄUSER[2] AND M. HELLER[3]

[1] Plymouth Marine Laboratory, Plymouth, United Kingdom (pecr@pml.ac.uk)
[2] IFM-Geomar, Kiel, Germany (adammshaeuser@ifm-geomar.de)
[3] IFM-Geomar, Kiel, Germany (mheller@ifm-geomar.de)

Titanium is a major component of the continental crust but is found in very low concentrations (< 300 pM) in seawater due to the strong hydrolysis of titanic (Ti^{IV}) and/or titanyl (TiO^{2+}) ions resulting in the formation of the poorly soluble TiO_2 (or $TiO(OH)_2$). The reduced form of Ti, titanous (Ti^{III}), is a strong reducing agent and is subsquently rapidly reoxidized to Ti^{IV} under all but the strongest reducing conditions.

There is no known biological enzyme that utilizes titanium and no organism has been found to require it for growth. However in recent years, research has been focused on Ti-complexes as potential anti-cancer drugs and in the utilization of Ti^{IV} to form nano-structures by the same enzymes that diatoms use to construct their silicate shells. Other recent developments include the common useage of Ti as a bio-inert substrate in the body and the increasing use of nanoparticle TiO_2 in a range of products. This increased exposure to Ti in our daily lives has new investigations into the biochemistry of Ti and revealed the potential for Ti competition for strong Fe(III) binding sites in organisms (e.g. transferrin).

To investigate the biogeochemistry of Ti in the ocean we recently developed a new sea-going voltammetric technique capable of rapidly measuring pM dissolved Ti, and we have applied this to work on a number of cruises in the Atlantic, including the preliminary German GEOTRACES cruise of 2005 and the IPY GEOTRACES Zero-Drake cruise in the Atlantic sector of the Southern Ocean. In this presentation we will outline our new findings on the speciation of dissolved Ti in the ocean, focusing on the evidence, or lack of it, for the existence of titanium-organic complexes in seawater. Finally we will show the distribution of dissolved Ti throughout the water column in the Atlantic ocean and comment on its potential for use as a tracer of dust input similar to Al and Fe.

Gas Phase Low Volatility Organic Compounds (LVOCs): Measurements from chambers, planes and automobiles

E.S. CROSS[1]*, K.E. DAUMIT[1], J.F. HUNTER[1], A.J. CARRASQUILLO[1], A.G. SAPPOK[1], V. WONG[1] S. HERNDON[2], J.T. JAYNE[2], D.R. WORSNOP[2] AND J.H. KROLL[1]

[1]Massachusetts Institute of Technology, Cambridge, MA 02139 USA
[2]Aerodyne Research Inc., Billerica, MA 01822 USA

Gas phase low volatilty organic compounds (LVOCs) comprise an atmospherically important, largely *unmeasured* class of organic species in the atmosphere. LVOCs consist of intermediate volatility organic compounds (IVOCs; *i.e.* C_{13}-C_{20} *n*-alkanes) and semivolatile organic compunds (SVOCs; *i.e.* C_{21}-C_{32} *n*-alkanes). Atmospheric oxidation of gas phase LVOCs results in the formation of secondary organic aerosol (SOA) which in turn has direct implications for climate and human health. The rates and the chemical properties of LVOC emissions and oxidation products (in the gas phase and particle phase) are poorly characterized and not accurately parameterized in atmospheric chemistry models.

This paper will provide an overview of experimental results obtained with a novel technique called the Total Gas Phase Organics (TGO) instrument that provides a volatility-resolved, quantitative measure of gas phase LVOCs (and LVOC oxidation products) in the atmosphere. Experimental results from instrument characterization studies, chamber oxidation studies, and LVOC emissions characterization studies (including a medium duty diesel engine and the NASA DC-8 aircraft engine) will be presented. The capability of the TGO instrument for tracking total gas phase carbon during a chamber oxidation experiment will be discussed.

https://doi.org/10.1180/S0026461X00006502 Published online by Cambridge University Press

New juvenile glass chemistry from Colli Albani, Italy and its use in understanding petrogenesis

JO CROSS[1]*, VICTORIA SMITH[2], GUIDO GIORDANO[3], JULIE ROBERGE[4], EMMA TOMLINSON[1] AND MARTIN MENZIES[1]

[1]Department of Earth Sciences, Royal Holloway University of London, Egham Hill, Egham, Surrey, TW20 0EX (*j.k.cross@es.rhul.ac.uk)
[2]RLAHA, University of Oxford, Dyson Perrins building, South Parks Road, Oxford OX1 3QY, UK
[3]Dipartimento di Scienze Geologiche, Università di Roma TRE - L.go S. Murialdo 1, 00146 Roma, Italy
[4]Departamento de Geoquímica, Instituto de Geología, Universidad Nacional Autónoma de México, Ciudad Universitaria, Coyoacán D.F. 04510, Mexico

Colli Albani is a quiescent caldera complex located within the Roman Comagmatic Province, Italy. The recent Via dei Laghi phreatomagmatic eruptions led to the formation of nested maars. The largest is Lago Albano (ca 70-20ka) which has erupted at least seven times. The highly explosive nature of the eruptions from Colli Albani and contrasting alkali-rich, silica under-saturated magma compositions has resulted in several contrasting petrogenetic models [1].

Results are presented from a petrological and geochemical study of the Lago Albano deposits. Juvenile clasts in the deposits display evidence for mingling of different melt fractions. The juvenile (magmatic) fragments from explosive (base surge and fall deposits) and effusive (lava flows) episodes provide an opportunity to constrain the temporal magmatic and volatile history of the system. New WDS-EPMA and LA-ICPMS data for interstitial glass in magmatic cumulates (pre-eruptive), and melt within juvenile clasts (syn-eruptive) reveal extreme sub-volcanic fractionation generating distinct magma compositions (K-rich foidites).

[1] Conticelli *et al*. (2010), *IAVCEI Sp Pub*

Oxidative weathering fractionates chromium isotopes

S.A. CROWE[1*], L.N. DØSSING[2], L.C.W. MACLEAN[3], R. FREI[2], D.A. FOWLE[4], A. MUCCI[5] AND D.E. CANFIELD[1]

[1]Institute of Biology, Univ. of Southern Denmark and Nordic Center for Earth Evolution, Odense, Denmark (sacrowe@biology.sdu.dk)
[2] Dept. of Geography and Geology, Univ. of Copenhagen and Nordic Center for Earth Evolution Copenhagen, Denmark
[3]Canadian Light Source, Saskatoon, Canada
[4]Dept. of Geology, Univ. of Kansas, Lawrence, USA
[5]Dept. of Earth and Planetary Sciences, McGill Univ., Montreal, Canada

Cr isotopes hold great promise for use as a paleoredox proxy, but the processes that induce Cr isotope fractionation remain speculative. The reduction of Cr(VI) favours the light Cr isotope, causing residual Cr(VI) to become progressively heavier [1], but we do not know if fractionation accompanies the oxidation of Cr(III) to Cr(VI). We present Cr isotope ratio measurements of a lateritic soil profile from Indonesia. Our measurements reveal that the Cr isotopic composition of the soil becomes progressively lighter with increased weathering up the profile. The uppermost unit, the topsoil, possesses the lightest composition, $\delta^{53}Cr = -1.19 \pm 0.25$ ‰ ($\delta^{53}Cr = 1000 \times [(^{53}Cr/^{52}Cr)_{sample}/(^{53}Cr/^{52}Cr)_{SRM979})-1]$), whereas the unaltered peridotite bedrock has Cr isotope ratios consistent with mantle-derived igneous rocks [2]. Our measurements demonstrate the preferential retention of light Cr in the soil and the release of heavy Cr(VI) to runoff, supporting the hypothesis that the marine Cr isotope record tracks the oxygenation of the atmosphere through geological time [3].

[1] Ellis, Johnson, & Bullen (2002) *Science* **295**, 2060-2062. [2] Schoenberg *et al*. (2008) *Chem. Geol*. **249**, 294-306. [3] Frei *et al*. (2009) *Nature* **461**, 250-254.

https://doi.org/10.1180/S0026461X00006502 Published online by Cambridge University Press

Magmatic processes leading to explosive mafic eruptions of Volcán de Colima, Mexico

JULIA CRUMMY[1]*, IVAN SAVOV[1], DAN MORGAN[1], CARLOS NAVARRO[2], MARJORIE WILSON[1] AND SUE LOUGHLIN[3]

[1]University of Leeds, Leeds, LS2 9JT, UK (*correspondence: j.crummy@see.leeds.ac.uk, I.Savov@leeds.ac.uk, D.J.Morgan@leeds.ac.uk, B.M.Wilson@leeds.ac.uk)

[2]Colima Volcano Observatory, University of Colima, Colima, Mexico (naoc@ucol.mx)

[3] British Geological Survey, Murchison House, Edinburgh, EH3 3LA, UK (sclou@bgs.ac.uk)

We present new geochemical and petrological data for the Holocene tephra deposits of Volcán de Colima. Historically, the volcano is characterised by mostly effusive andesitic lava flows and frequent Vulcanian-style explosions (up to 11 times per day in 2010), producing steam and ash clouds reaching heights of several km. Explosive basaltic-andesitic Plinian eruptions at Colima have occurred throughout the Holocene. The last such event was the 1913 eruption which produced an ash column 23km in height, and pyroclastic flows which travelled 15km from the vent. Ash was reported in the town of Saltillo 725km away. The 1913 eruption lava and ash samples contain magmatic water contents of up to 6.3 wt.%.

Deposits representing highly-explosive activity at Volcán de Colima reveal a tantalising story of magma evolution over a 30,000 year period [1]. We report results concerning the 4,400 and 4,700 yrs B.P. eruptions, which represent the felsic and mafic end-member magma, and show that Plinian-style explosions can occur at Colima over a range of compositions from basaltic-andesite to high-silica andesite, all with a common, high H_2O content of over 4.3 wt.% H_2O.

SEM, EPMA and CSD analyses support the bulk rock dataset and reveal a complex crystallisation history of the 4,400 and 4,700 yrs B.P. magmas. However, Sr isotope analyses indicate a well-established feeder system with little change in $^{87/86}Sr$ ratios (0.703459 - 0.703735, n=61) over >12,000 years.

At Volcán de Colima, high-MgO magmas (5.61 wt.%) are H_2O rich, implying little mixing and/or very fast ascent rates from source to surface.

[1] Luhr *et al* 2010, *Journal of Volcanology & Geothermal Research*, v. **197**, p. 1-32

U and Sr isotopic variations at a deep underground laboratory, Homestake Mine, SD

M.F. CRUZ[1]*, K. MAHER[1], N. OLSEN[1], T. JONES[2], M. CONRAD[3] AND E. SONNENTHAL[3]

[1]GES Dept., Stanford University, Stanford, CA 94305, USA (*correspondence: mfcruz@stanford.edu, kmaher@stanford.edu)

[2]South Dakota School of Mines, Rapid City, SD 57701, USA (tessaj@gmail.com)

[3]Lawrence Berkeley National Lab, Berkeley, CA 94720, USA (msconrad@lbl.gov, elsonnenthal@lbl.gov)

The U and Sr isotopic composition of groundwater in fracture-dominated flow systems can potentially provide a useful means of quantifying fluid flow, reaction rates and/or the extent of exchange with the bulk matrix. The Deep Underground Science & Engineering Laboratory (DUSEL) at the former Homestake gold mine in South Dakota provides a unique opportunity to assess the behavior of U and Sr isotopes in a fracture-dominated environment. The folded and fractured metapelites are low-permeability with flow localized in fractures and shear zones. Samples from depths up to 5000 ft below the surface were analyzed for major and trace elements, $\delta^{18}O$, δD, $^{87}Sr/^{86}Sr$ and ($^{234}U/^{238}U$),.

The ($^{234}U/^{238}U$) values of waters at the site is 2.99 at the surface, then increases to 3.24 at 800 ft depth, then decreases gradually to 1.94 at 4,850 ft depth. We interpret the initial increase to alpha-recoil enrichment of ^{234}U, while the subsequent decrease suggests that as temperature increases with depth, mineral dissolution dominates. This is consistent with $^{87}Sr/^{86}Sr$ values, which increase with depth from 0.71 to 0.77, approaching the bulk-rock value of 0.76 to 0.8, again suggesting increased reactivity. By coupling Sr and U isotopes with field and geochemical data investigations at DUSEL can provide further insights as to the isotopic exchange processes during fracture-dominated water-rock interactions.

https://doi.org/10.1180/S0026461X00006502 Published online by Cambridge University Press

Geochemistry of the Artic Loki's Castle hydrothermal vent products

M.I. CRUZ[1], A.S. DIAS[1], J.M.R.S. RELVAS[1], C. CARVALHO[1], RITA FONSECA[2], R.B.-PEDERSEN[3] AND F.J.A.S. BARRIGA[1]

[1]Creminer/LA-ISR, Geology Department, University of Lisbon, Portugal (corresponding author: micruz@fc.ul.pt)
[2]Creminer/LA-ISR, Geosciences Dep., Univ. Évora, Portugal
[3]Centre for Geobiology, Department of Earth Science, University of Bergen, Norway

Loki's Castle is the northernmost hydrothermal vent field known to date in the Arctic Ocean [1]. It is located in the junction between the Monhs and Knipovich Ridge, an ultra-slow spreading center at a rate of 17mm/year [2]. ROV-collected samples of chimney fragments and their surrounding deposits revealed to be mostly composed of sphalerite, chalcopyrite, pyrite and anhydrite, their maximum metal contents for Fe 31wt%, for Zn 5.4wt% and for Cu >1wt%. The surrounding sediments contain a significant hydrothermal component, denounced by high metal contents that average 4.6 wt% Fe, 100 ppm Zn and 33 ppm Cu. Sediments from the same area collected at depth by gravity cores show equally high average metal contents; although the Cu and Zn enrichment may be more prominent in particular layers reaching 446 ppm Zn and 128 ppm Cu. The REE sediment patterns mimic those of the North American Shale Composite [3]. Major and trace element geochemistry of the less altered volcanic rock fragments collected near the vent field allows their classification as tholeiitic basalts.

[1] Pedersen, R.B., *et al*., (2010) Discovery of a black smoker vent field and vent fauna at the Arctic Mid-Ocean Ridge. *Nat Commun*,. **1**(8): p. 126. [2] Peive, A.A. and N.P. Chamov, (2008) Basic tectonic features of the Knipovich Ridge (North Atlantic) and its neotectonic evolution *Geotectonics*,. **42** (Number 1): p. 7. [3] Gromet, L.P., *et al*., (1984) The "North American shale composite": Its compilation, major and trace element characteristics. *Geochimica et Cosmochimica Acta*, **48**: p. 2469-2482.

Metamorphic reaction rates from diffusion of Nb in rutile

ALICIA M. CRUZ-URIBE[1], MAUREEN D. FEINEMAN[1] AND THOMAS ZACK[2]

[1]The Pennsylvania State University, State College, PA 16802, USA (amc472@psu.edu, mdf12@psu.edu)
[2]Institut für Geowissenschaften, Universität Mainz, Becher Weg 21, 55128 Mainz, Germany (zack@uni-mainz.de)

Determining the timescales over which metamorphic reactions occur has long been an important and difficult question to answer. Here we examine rutile replacement by titanite in a migmatized garnet amphibolite from Catalina Island, CA, and compare the data to results from an amphibolitized eclogite from Tromsø, Norway. We estimate the timescales and rates of the rutile-to-titanite reaction by fitting models of Nb back-diffusion during titanite replacement to measured Nb profiles in rutile.

Trace element concentrations in rutile and titanite were determined by LA-ICP-MS for grains from Catalina. Niobium profiles across two rutile grains show clear evidence for Nb back-diffusion into rutile during titanite growth at the grain boundary (from 2280 to 3050 ppm over 350 μm). The same feature was reported and modeled by Lucassen *et al*. [1] for Nb and Zr in a 7 mm rutile from Tromsø. Zr-in-titanite thermometry suggests 740-770°C for Catalina and 650-730°C for Tromsø. New experimentally-determined diffusion coefficients for Nb in rutile (R. Dohmen, pers. comm.) were used to model Nb diffusion in the Catalina rutile, and to revisit the Tromsø sample in light of the new diffusion data.

A simple 1-D moving interface diffusion model yields reaction front velocities, which were converted to rates using the distance the boundary had moved relative to the pre-reaction rutile surface. Reaction rates of 0.2–2.0 x 10^{-6} a^{-1} were determined for Catalina, and 0.03–4.99 x 10^{-8} a^{-1} for Tromsø. Reaction rates were then normalized to the surface area of the rate-limiting mineral per unit of rock (Rnet, g/cm^2/a). Normalized reaction rates for Catalina are 0.18–1.42 x 10^{-5} g/cm^2/a and for Tromsø are 0.04–5.82 x 10^{-7} g/cm^2/a, which suggests 2-3 orders of magnitude difference in Rnet over ~120°C change in temperature for the rutile-titanite reaction. Reaction rates for the Tromso sample are consistent with those previously determined for regional metamorphism, whereas the Catalina reaction rates fall between those reported for regional and contact metamorphic settings [2]. This observation is consistent with the presence of free fluid or melt during subduction-related metamorphism.

[1] Lucassen *et al*. (2010) *Cont. Min. Pet.* **160**, 279-295. [2] Baxter (2003) *Geol. Soc. Lon. Spec. Pub.* **220**, 183-202.

https://doi.org/10.1180/S0026461X00006502 Published online by Cambridge University Press

Geological characteristics and genesis discovery of native copper in East Tian Mountain, Xinjiang, P.R. China

CUI BIN, HE ZHIJUN AND ZHAO LEI

China University of Geosciences , Beijing, 100083
(cuibin76@163.com, zhaolie51yh@yahoo.com.cn)

The Dongtianshan copper is a type of mineralization belt newly found by work in recent years. The copper from Shilipo, Dongtianshan is found in maroon basaltic tuff. Through analysis of the geochemical characteristics show the formation of Dongtianshan copper relates to the mineralization of the mantle plumes.

The main elements of two mineral occurrences are of the similar content characteristics. The K_2O and Na_2O content in Shilipo is apparently lower than that of Heilongfeng, but is similar to that of Bingdao volcanic rocks. Compared the copper-bearing basalt with Bingdao basalt, the MgO content of Dongtianshan basalt is relatively low, in the range of 3.06%-3.61% while the MgO content of Bingdao basalt is 7.53%-12.24%. To the alkali content, the Bingdao basalt has high Na_2O, but no high K_2O

The copper-bearing basalt from Dongttanshan shows the LR/ HR of 11.29×10^{-6} and 11.58×10^{-6},a little higher than the values of Bingdao basalt. However, the content values of the MREE and HREE have not much difference between Dongtianshan basalt and Bingdao basalt and show the relatively strong comparability. The Emeishan basalt with the LR/HR of 41.21×10^{-6}. In the curve ofn, Emeishan basalt presents the right-inclined shape of LREE slight concentration. The REE partition pattern of Cu-bearing basalt from Dongtianshan has the fairly strong comparability with the REE partition curve of the Bingdao basalt related to mantle plumes, reflecting the characteristics of the mantle magma.

It is considered that the copper-bearing basalt of Dongtianshan is from mantle sources and possesses the similar characteristics to the mantle plumes.

[1] Kutina J. (1996). The role of mantle-rooted structural discontinuities in concentration of meatals. *Global Tectonics and Metallogeny*, **5**:79-102.

Water pollution treatment of chinese highway tunnel construction

CUI GUANGYAO[1]*, WANG MINGNIAN[1], LU JUNFU[2] , ZHANG WEIQING[1] AND WANG WEIJIA[1]

[1]School of Civil Engineering, Southwest Jiaotong University, Chengdu, 610031, China
(*correspondence: cyao456@163.com)
[2]State Key Laboratory of Geohazard Prevention and Geoenvironment Protection, Chengdu University of Technology, Chengdu, 610059, China

The damage to water environment in highway tunnel construction is mainly manifested in two aspects: the destruction of groundwater system in the tunnel area and wastewater pollution generated in the process of highway tunnel construction. The steady-state of groundwater system in the tunnel area must be destroyed in the process of highway tunnel construction, and the highway tunnel will become the natural channel discharging underground water. The waste water generated in the process of highway tunnel construction will also pollute groundwater system in the tunnel area and damage surrounding environment.

Water pollution treatment mainly focus on the six aspects: (1) construction and domestic garbage must be stacked centrally; (2) the domestic sewage can be discharged only after it is disposed; (3) the settling ponds should be build in the tunnel area; (4) the storehouse storing grease must be make anti-seepage treatment; (5) mechanic waste oil should be recycle or carefully dispose; (6) the management of chemical grout must be strengthen.

Taking the route that can develop continuously is the inevitable choice of 21 centuries China. To the sustainable development, the water environmental protection is of critical importance. The highway tunnel construction and water environmental protection go hand in hand only if we must consider the characteristic of the highway tunnel to perfect construction technology and take corresponding water environmental protection countermeasure.

[1] CUI GUANG-YAO (2010) *Geochimica et Cosmochimica Acta*, **74**(12), Supplement 1: A199. [2] Xu WL, Zhang JQ(2010) *Geochimica et Cosmochimica Acta,* **74**(12), Supplement 1: A1162. [3] Ren Y, Hu Z.Z, Yang X (2008) *Chinese Journal of Underground Space and Engineering*, **4**(2):365-373.

https://doi.org/10.1180/S0026461X00006502 Published online by Cambridge University Press

Re-Os geochronology of lacustrine organic-rich sedimentary rocks: Systematics and implications

V.M. CUMMING[1]*, D. SELBY[1] AND P. LILLIS[2]

[1]Earth Sciences Department, Durham University, DH1 3LE, UK (*correspondence: v.m.cumming@durham.ac.uk)
[2]U.S. Geological Survey. Box 25046, MS977, Denver Federal Center, Denver, Colorado 80225, USA

The Re-Os geochronometer is widely utilised to determine precise depositional ages of marine organic-rich sedimentary rocks (ORS). However, Re-Os systematics have not been fully evaluated in lacustrine ORS. Lacustrine sedimentary rocks provide an invaluable archive of continental geological processes responding to tectonic, climatic and magmatic influences. The lack of marine biostratigraphic constraints in lacustrine sedimentary rocks means that correlation to global geological phenomena requires accurate and precise geochronological frameworks.

Here we apply the Re-Os geochronometer to the Eocene Green River Formation (GRF), the world's largest succession of lacustrine ORS representing a classic model of lacustrine deposition. We present two precise Re-Os ages of 48.5 ± 0.6 Ma and 49.2 ± 1.0 Ma from the Uinta basin that are in excellent agreement with Ar/Ar and U/Pb dates of interbedded tuffs within the GRF. An additional Re-Os age of 47.8 ± 9.9 Ma has a higher uncertainty attributed to a smaller spread in $^{187}Re/^{188}Os$ ratios. This third age is from a section suggested to have been deposited in the deepest lake setting. It possesses higher TOC that exhibits more significant correlation with Re, Os and trace elements than the sections which yield precise ages. The redox sensitive trace elements are used to assess Re-Os systematics in lacustrine ORS and suggest deposition from an oxic-dysoxic water column.

In addition to geochronology, the initial $^{187}Os/^{188}Os$ (Os_i) of the GRF (~1.4-1.5) has implications for the understanding of global ocean Os fluctuations. The Os_i is similar to continental runoff today (~1.54), suggesting that the $^{187}Os/^{188}Os$ of continental runoff into the ocean has not changed since the Eocene. Global ocean $^{187}Os/^{188}Os$ has evolved from ~0.56 during the Eocene to a modern day value of 1.06. This study suggests that global ocean Os evolution has been driven by a decrease of unradiogenic Os flux rather than an increase in radiogenic Os from continental runoff.

Geochemical and isotopic insights into the development of a large caldera-forming eruption, Atitlan Caldera, Guatemala

HEATHER S. CUNNINGHAM*

Department of Geoscience, University of Wisconsin at Madison, 1215 W Dayton St, Madison, WI 53706 USA, (*correspondence: hcunningham@geology.wisc.edu)

How do large volumes of rhyolitic magma accumulate prior to the eruption of large caldera-forming eruptions? Rhyolitic magmas are proposed to originate either from rhyolitic pods that are the result of rapid differentiation, through assimilation of crustal melts, or a combination of the two. High magma flux rates are required to sustain an eruptable crystal-melt reservoir. These issues are evaluated at Atitlan Caldera, Guatemala where eruption of the ~300 km^3 Los Chocoyos rhyolitic ignimbrite and air fall occurred at 84 ka. Eruption of a compositionally zoned ignimbrite recorded the presence of rhyodacite and high silica rhyolite in the proportions of 1:4. The rhyodacite displays trace element ratios similar to the basaltic andesite enclaves found in early Los Chocoyos fall deposits, as well as, stratocone lavas erupted around the caldera boundary before and after the Los Chocoyos. In particular, the rhyodacite displays higher Sr/Y, La/Yb and Ce/Y than the high silica rhyolites. Generation of rhyolitic magmas by exclusive melting of old granitic crust is inconsistent with trace element models and Sr isotopic data. Sr isotopes for the rhyodacite and high silica rhyolite are slightly elevated from the mafic enclave and unlike the Sr isotope ratios for the more evolved granite. The rhyodacite can be modeled to form via batch partial melting of the mafic enclave, assumed to reflect the least differentiated end member, with garnet in the residuum. The high silica rhyolite can be modeled from 70% fractional crystallization of the basaltic andesite and 15% assimilation of 15.2 Ma granitic pluton exposed along the caldera boundary. Thus, partial melting and differentiation of basaltic andesite stalled in the crustal plumbing system with minor addition of granitic crustal melts can account for the formation of rhyolitic magmas at Atitlan Caldera. Thermal models project that a flux rate of 10^{-2} km^3/yr is required to provide enough heat to form large volume rhyolitic eruptions. Stratocone eruption rates of basaltic andesite at Atitlan Caldera since the Los Chocoyos are 4 x 10^{-3} km^3/yr. Assuming a 3:1 intrusive:extrusive ratio, current magma flux rates at Atitlan Caldera are at least 1.2 x 10^{-2} km/yr and able to sustain the formation of large volume rhyolitic magmas.

https://doi.org/10.1180/S0026461X00006502 Published online by Cambridge University Press

Understanding biological control and environmental influence – unlocking the secrets of biomineralisation

MAGGIE CUSACK

School of Geographical & Earth Sciences, University of Glasgow, G12 8QQ, UK

In the natural world of biominerals elegant, functional structures are produced from the most basic of resources. Vertebrates have skeletons made from calcium phosphate (apatite) while invertebrates tend to assemble mineral structures from silica or calcium carbonate. Although the ingredients are simple, the control of how these fundamental building blocks are put together is very much under the control of biological processes. Understanding this biological control and its rôle in the formation of biominerals has implications in a number of diverse areas. Understanding the biomineralisation process will provide a much more accurate interpretation of the climate information stored within marine biominerals, e.g. brachiopods and corals. An exploration of the biological control exerted in biomineral formation in several phyla provides the context for the consideration of the recording of environmental information.

C, O and H isotope compositions of the Wilmott and Yungul 'carbonatites' and the associated fluorites in the Speewah Dome, Kimberley Region, Australia

GY. CZUPPON[1]*, L.G. GWALANI[2], A. DEMÉNY[1], R. RAMSAY[2], K. ROGERS[2], A. EVES[2] AND CS. SZABÓ[3]

[1] Inst. for Geochemical Research, Hung. Acad. Sci., Budaorsi ut 45, Budapest, 1112, Hungary (*correspondence: czuppon@geochem.hu, demeny@geochem.hu)

[2] Speewah Metals, 22/77 Allendale Square, St Georges Terrace, Perth, WA6000, Australia (lgwlani@gmail.com, ramsay@iinet.net.au, karogers@bigpoint.net.at, fridgelizard@gmail.com)

[3] LRG, Dept. of Petrology and Geochemistry, Inst. of Geog. and Earth Sci., Eötvös University, Pázmány 1/C, Budapest 1117, Hungary (cszabo@elte.hu)

The Yungul and newly discovered Wilmott 'carbonatites' (carbonate-cemented breccias and carbonate veins), as well as the associated fluorite veins are located on the eastern margin of the Kimberley Block (NW Australia). The C and O isotope compositions of Wilmott carbonatites show a distinct negative trend different from that observed for Yungul 'carbonatites', in which the $\delta^{13}C$ and $\delta^{18}O$ values form a positive trend and has been explained by high-temperature rock-fluid interaction and H_2O degassing. However, the observed $\delta^{13}C$ shift in Wilmott 'carbonatites' requires additional processes such as CO_2 and H_2O degassing. Inclusion-hosted H_2O contents (determined by vacuum crushing) range from 250 to 1300 ppm for Yungul, whereas the Wilmott 'carbonatites' yielded H_2O contents between 250 and 510 ppm. The H isotope compositions determined for inclusion-hosted H_2O show a large range for Yungul 'carbonatites' (from -83‰ to -24‰) with the Wilmott rocks at the lower end (from -85‰ to -60‰). δD-H_2O variations in both 'carbonatites' indicate an open system in which the H_2O degassing took place at relatively high temperature (>400°C). The associated fluorite veins are characterized by high H_2O contents (600-2300ppm) with relatively high δD values (between -30‰ and -17‰) forming a positive linear trend related to close system evolution. The fluorite and 'carbonatite' trends converge to the same isotopic composition, thus, although the fluid regimes were likely different for fluorites and 'carbonatites' (i.e. open – closed systems), the ultimate origin of the fluids could be the same.

https://doi.org/10.1180/S0026461X00006502 Published online by Cambridge University Press

Microbial life associated with low temperature alteration of ultramafic rocks in the Leka ophiolite complex

FRIDA LISE DAAE[2], INGUNN THORSETH[1], HÅKON DAHLE[2], STEFFEN LETH JØRGENSEN[2] AND ROLF B. PEDERSEN[1]

[1]Centre for Geobiology/Department of Earth Science, Allegaten 41, 5007 Bergen, Norway (*correspondance: frida.daae@bio.uib.no, Ingunn.Thorseth@geo.uib.no)

[2]Centre for Geobiology/Department of Biology, Allegaten 41, 5007 Bergen, Norway

The Leka Ophiolite Complex (Mid-Norway) is a unique location for sampling oceanic crust and mantle lithologies. To examine peridotite-hosted subsurface microbial communities we have drill-sampled a dunite unit that is located close to ancient crust-mantle boundary. Samples were taken of mineralised fractures as well as of ground water produced by a 50 m deep borehole. Microbial community analyses were done by 16S rRNA gene sequence amplification clone library constructions. The morphological diversity was examined by electron microscopy. Enumeration of *Archaea* and *Bacteria* were done with fluorescent microscopy and real time polymerase chain reaction.

Different microbial communities were observed in the groundwater, the fracture fillings and the surface water. The groundwater, having a pH of 9.1, was dominated by close relatives of putative hydrogen oxidizing beta Proteobacteria suggesting that microbial communities at Leka are largely driven by hydrogen possibly produced by low temperature water-rock reactions. The microbial communities in the mineralised fractures are dominated by close relatives of heterotrophic hydrocarbon-degraders, but close relatives of hydrogen-, manganese-, and iron-oxidizers were also present.

Metal-silicate mixing during impact-driven planet accretion – Implications for the age of the Moon

T.W. DAHL[1] AND D.J. STEVENSON[2]

[1]NordCEE and Univ. of Southern Denmark, 5230 Odense, Denmark

[2]Division of Geological and Planetary Science, Caltech, Pasadena, CA 91125, USA,

The final accretion of planet Earth involved giant collisions between protoplanets (>1000km radius) with the Moon forming as a result of one of these impacts. At this stage both bodies had differentiated into a metallic core surrounded by a silicate mantle. During the Moon-forming impact nearly all metal sank into the Earth's core. We have investigated to which extent large self-gravitating iron cores can mix with surrounding silicate as they sink through the Earth's mantle. This allows us to evaluate how incomplete metal-silicate equilibration during core formation influences the short-lived chronometer, Hf-W, used to infer the age of the Moon.

We have established fluid dynamical models of turbulent mixing in fully liquid systems to constrain the degree of iron-silicate mixing. Erosion of sinking cores driven by Rayleigh-Taylor instability does lead to mixing, but only 1-20% of Earth's core would emulsify and equilibrate with the silicate mantle during Earth's entire accretion process. The initial speed and obliquity of impact is of little importance, but the size and shape of the sinking core matters. We evaluate the mixing potential for shear instabilities where silicate entrainment across vertical walls leads to mixing. The turbulent structure indicates that vortices remain at the largest scale and do not cascade down to centimeter length scales where diffusion operates and isotopes can equilibrate.

Because most of the impacting metal plunge directly through the silicate mantle, and the fraction of impacting metal that mix within diffusion distance from silicate is small, giant impacts have limited effect on siderophile depletion during core formation. On a global scale residual ^{182}W from early core formation processes is left behind in the mantle and this source of ^{182}W generates a higher ε_W excess compared to what is expected in early models for ^{182}W evolution in the silicate Earth. Hence, the Moon forming impact must have occurred >30 Myrs after CAI formation. Furthermore, we find that a single giant impact has limited ability to reset the Hf-W system and that ε_W is more sensitive to early core formation processes than to radiogenic ingrowth after the giant impact [1].

[1] Dahl T.W. & Stevenson D. J (2010) *EPSL* **295**, 177-186.

https://doi.org/10.1180/S0026461X00006502 Published online by Cambridge University Press

Effects of mining on groundwater quality in Gaft Chromite Mine, Iran

B. DAHRAZMA[1]*, M. KHARGHANI[2] AND M. AKHIANI[2]

[1]Shahrood University of Technology, Shahrood 3619995161, Iran
(*correspondence: behnaz_dahrazma@shahroodut.ac.ir)
[2]Islamic Azad University – Shahrood Branch, Shahrood, Iran.

Effluent from chromite mines due to extraction activities into aquatic systems is an environmental issue [1, 2]. To investigate the effects of chromite extraction on the groundwater quality in Gaft Chromite Mine, water samples were taken from the mine area.

Due to basic condition of the tunnel effluent (pH=9.74), solubility of most ions decreased [3, 4] and thus EC, total hardness, and concentration of ions in tunnel effluent were similar to the upstream groundwater as well as groundwater in the mine site [Fig.1]. In other words, mining activities had no adverse effect on the water quality of the region although it slightly increased the concentration of Cr (VI) in the groundwater in the mine site. The concentrations of Cr (IV) in water samples were 0.04, 0.04, 0.06 and 0.02 (all in mg/L) in upstream and downstream groundwater, groundwater in the mine site, and tunnel effluent respectively. Because of the geochemical condition downstream of the mine [5], the reduction in the pH of downstream groundwater (pH=8.13), the concentration of bicarbonate, chloride, calcium, magnesium, and sodium ions as well as the total hardness and EC in downstream groundwater (4 Km far) were increased.

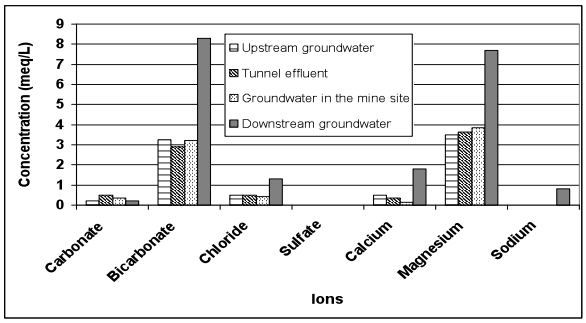

Figure 1: Concentration of ions in water samples.

[1] Seralathan Kamala-Kannan *et al*. (2008) *Chemosphere* **71** 1233-1240. [2] Aradhi K. Krishna *et al*. (2009) *Journal of Hazardus Material* **167** 366-373. [3] Takeno (2005) *Geological Survey of Japan Rep. No. 419*. [4] Ratnakar Dhakate and V. S. Singh (2008) *Journal of Geography and Regional Planning* **4** 058-067. [5]Vatanpoor (2005) *Gaft Mine Comprehensive Exploration*.

Zircon Hf-O isotope evidence for crust-mantle interaction during continental deep subduction

LI-QUN DAI, ZI-FU ZHAO AND YONG-FEI ZHENG

School of Earth and Space Sciences, Univisity of Science and Technology of China, Hefei 230026, China (lqdai@mail.ustc.edu.cn)

In situ SIMS zircon U-Pb dating and O isotope analysis as well as LA-(MC)-ICPMS zircon U-Pb dating and Lu-Hf isotope analysis were carried out for postcollisional mafic-ultramafic rocks in the Dabie orogen, China. The zircon U-Pb dating gives consistent ages of 126±1 to 131±1 Ma for magma crystallization. Survival of residual zircon cores is identified by CL imaging and U-Pb dating, yielding ages of 697±10 and 770±11 Ma that agree with protolith ages of UHP metaigneous rocks in the orogen. Zircon Hf-O isotope compositions show systematic variations that can be categorized into three groups. Group I has the lowest $\delta^{18}O$ values of 2.0 to 2.9‰ but the highest $\varepsilon_{Hf}(t)$ values of -6.3 to 1.1 with the youngest Hf model ages of 1.1 to 1.6 Ga. Group II displays intermediate $\delta^{18}O$ values of 4.0 to 5.1‰ and $\varepsilon_{Hf}(t)$ values of -29.0 to -9.9 with Hf model ages of 1.8 to 3.0 Ga. Group III exhibits the highest $\delta^{18}O$ values of 5.2 to 7.3‰ but the lowest $\varepsilon_{Hf}(t)$ values of -33.7 to -18.2 with the oldest Hf model ages of 2.3 to 3.3 Ga. The three groups of Hf-O isotope compositions correspond to a three-layer Hf-O isotope structure in the subducted continental crust, suggesting its involvement in the mantle source. Along with existing data for whole-rock Sr-Nd isotopes and trace elements, it appears that the mantle source for the postcollisional mafic-ultramafic rocks is characterized by fertile lithochemistry, the continental crust-like signature of trace elements, the heterogeneous enrichment of radiogenic isotopes, the differential incorporation of supracrustal materials, and the variable concentrations of water. Clearly, such a source is neither the asthenospheric mantle nor the refractory subcontinental lithospheric mantle (SCLM). It is a kind of orogenic SCLM that would be generated by reaction of the overlying SCLM peridotite with hydrous silicate melts derived from the different layers of subducted continental crust. Therefore, the postcollisional mafic-ultramafic rocks provide a petrological record of crust-mantle interation during the continental deep subduction. Melt-peridotite reaction is hypothesized to take place in the Triassic to generate the mantle source of pyroxenite and hornblendite, which underwent partial melting in the Early Cretaceous to cause the mafic-ultramafic magmatism.

https://doi.org/10.1180/S0026461X00006502 Published online by Cambridge University Press

The Biodegradation of [omim][PF_6] with activated sludge in anoxic conditions

N. DAI[1,2,3], F.-J. ZHANG[2], J.S. WANG[1,3], Y.G. TENG[1,3] AND J. CHEN[4]

[1]College of Water Sci., BNU, Beijing, China (daining54@163.com)
[2]College of Environ. and Res., Jilin University, Changchun, China
[3]Eng. Res. Center of Groundwater Pollu. Control and Remed., ME, Beijing, China
[4]Key Lab. Rare Earth Chem. and Phys., Changchun Institute of Appl. Chem., CAS, Changchun, China

Many Ionic Liquids have significant solubility in water, which can result in the potential problems with degradation or persistence in environment. Biodegradation is the microbial breakdown of chemical compounds, such as Ionic Liquids. Compared to chemical or physical methods, it seems to be more environmentally friendly. This study focuses on the biodegradation efficiency and the pathways of [omim][PF_6] under anoxic conditions. Biodegradation efficiency of [omim][PF_6] under anoxic conditions was studied by acclimatizing the activated sludge with the UASB reactor. The proposal of possible metabolic pathways of $[omim]^+$ in anoxic conditions was analyzed by identification of the breakdown products using GC-MS. The biodegradation experiments were also performed under aerobic conditions. It suggests faster flow enhanced the contact frequency of [omim][PF_6] and microbe, but was not conducive to the removal rate with the increase of run-time. The results showed that the [omim][PF_6] removal efficiency reached the highest as the flow velocity of UASB was 0.75 $mL{\cdot}min^{-1}$ in this study. The molecular weights of the main degradation products were 83, 155, 102, 170 and 109, respectively. It is predicted that there were 3 main pathways for anoxic biodegradation of $[omim]^+$, which were different from the aerobic process because of the different electron acceptor. Similar to the aerobic process, N—C bond ruptured first, but the metabolism of $[omim]^+$ did not appear to undergo oxidation reactions but reduction reactions in anoxic conditions. The toxicity of the breakdown products was reduced under anoxic conditions according to their polarities and EC_{50} in references.

Acknowledgements: This research was financially supported the National Science & Technology Pillar Program during the Eleventh Five-Year Plan of China (2009BADC2B01-01)

Controls on and effects of surface ocean oxygenation prior to the Great Oxidation

STUART DAINES*, JAMES CLARK AND TIM LENTON

School of Environmental Sciences, University of East Anglia, UK (*correspondence: s.daines@uea.ac.uk)

Multiple lines of evidence suggest that organisms that produced free oxygen had evolved by ~2.7Ga, while geochemical evidence shows pervasive oxygenation of ocean margins prior to the Great Oxidation Event (GOE) at 2.4Ga [1]. However, given the likely heterogeneous spatial distribution of environments supporting oxygen-producing ecosystems, it is unclear whether oxygen production would have resulted in a significant flux to the atmosphere, or remained a local phenomenom restricted to “oxygen oases” in the surface ocean or mat-based environments. Here we use a combination of ocean GCM and box-model coupled atmosphere-ocean-ecosystem studies, in combination with constraints from proxy data, to investigate: (i) factors controlling the prevalence of surface ocean oxygenation prior to the GOE, (ii) the (local) geochemical signature of early oxygenic photosynthesis in different environments (i.e., restricted to shelf seas, or widespread in the surface ocean), and (iii) the likely impacts on atmospheric oxygen, including constraints on the relative timing of the evolution of oxygen photosynthesis relative to the GOE.

As an initial geochemical diagnostic for spatial structure we focus on factors controlling the production of isotopically light organic carbon via methane recycling. We show that oxygenation of the surface ocean could have been widespread in upwelling regions, that consumption of oxygen in the surface ocean increases stability of a low atmospheric pO_2 state, and that aerobic methanotrophy in open environments produces only relatively small changes in $\delta^{13}C$ insufficient to explain the excursions seen at ~2.7Ga [2] which would then require a different mechanism and most likely restricted environments.

[1] Kendall, Reinhard, Lyons, Kaufman, Poulton, Anbar (2010) *Nature Geosci*. **3**, 647-652. [2] Eigenbrode & Freeman (2006), *PNAS* **103**, 15759-64.

https://doi.org/10.1180/S0026461X00006502 Published online by Cambridge University Press

Chemical and isotopic composition of Lower Vindhyan organic rich sediments: Role of chemical alteration and grain size distribution

TARUN K. DALAI

Department of Earth Sciences, Indian Institute of Science Education and Research-Kolkata, Mohanpur, West Bengal 741252, INDIA (dalai@iiserkol.ac.in)

Several grey and black shales samples from the Lower Vindhyan section in the Central India have been collected. The samples have been chosen to represent various degrees of chemical alteration; those collected from the surface are extensively weathered whereas those collected from deeper in the mine cuts are relatively fresh. These samples have been analyzed for major ion composition, C_{org} and $\delta^{13}C$ of bulk organic matter.

The major ion compositions indicate influence of both chemical alteration and grain size distributions driven by mineralogical sorting. Abundances of bulk organic content (C_{org}) show significant positive correlation with Na/Al and an inverse correlation with K/Na. In contrast, C_{org} exhibits a weak positive correlation with Si/Al. Together, these observations indicate that organic carbon content in these samples are controlled by various degrees of chemical alteration and that the influence of grain size distributions and mineraological sorting may be rather weak. It is unclear to what extent the original relationship between the grain size and C_{org} has been lost by chemical alteration.

Carbon isotpic composition ($\delta^{13}C$) of bulk organic matter shows a significant positive correlation with ($1/C_{org}$). A first order interpreation of this trend is that relatively fresh organic matter is characterized by more negative $\delta^{13}C$ values whereas less negative $\delta^{13}C$ values represent organic matter that are altered by exchanging carbon with the weathering solution. Our results are in contrast to those observed by Van Os *et al*. [1]. Abundances of specific organic compounds, a suite of trace elements and grain size distributions would be measured to better understand the role of chemical alteration, grain size distributions and specific organic compounds in influencing the abundances of metals, organic carbon and carbon isotope composition of organic mater of these organic rich sediments.

[1] Van Os *et al*. (1996) *Aquatic Geochemistry* **1,** 303-312.

XPS heating with mass spectrometry: Tackling chalk, coccolith and calcite surfaces

K.N. DALBY*, N. BOVET AND S.L.S. STIPP

Nano-Science Center, Department of Chemistry, University of Copenhagen, Denmark (*kdalby@nano.ku.dk)

Chalk hosts significant quantities of the North Sea oil and biogenic calcite ($CaCO_3$) is a major component of the chalk. The biogenic calcite is in the form of coccoliths, precipitated by some species of single-celled marine algae. To understand the complex recrystallisation behavior of natural chalk, abiogenic calcite is often used as a model system. Abiogenic calcite is also used as a proxy for chalk during surface reactivity studies[1].

In this study to examine similarirties and differences between the biogenic and abiogenic calcite surfaces, we used X-ray photoelectron spectoscopy (XPS), coupled with an *in situ* residual gas analyzer (RGA), to examine natural chalk, cultured coccoliths and natural abiogenic calcite (Iceland Spar). We characterised, compared and contrasted the surface of the natural and model systems before, during and after heating to 500 ºC. The samples were heated to mimic reservoir conditions and to investigate the kinetics of the decarbonation reaction.

High resolution carbon 1s (C 1s) XPS spectra of the samples show differences in the surface composition. All samples display C-C bonds at 285.0 and CO_3 bonds at 290.1 eV. In addition, the chalk and coccoliths show evidence of C-OH (287.0 eV) and COOH (289.0 eV) compounds coating the surfaces. The ratio of all four C contributions is variable between the various samples of chalk and coccoliths. These coatings could prevent recrystallisation and dissolution of ancient coccoliths in chalk.

During heating to 500 ºC, both H_2O and CO_2 are released by all samples. The abiogenic calcite contains water-rich inclusions and these 'explode' during heating, producing spikes in the mass spectrometer data. No evidence of inclusions exist in the chalk or coccolith samples, which release H_2O and CO_2 at a more constant rate. During the heating experiments, the C-OH and COOH coatings are removed from the surfaces of the coccoliths and chalk, and the surface composition becomes more similar to the abiogenic calcite. Ongoing work will examine sample reactivity, including dissolution rates of chalk and coccolith surfaces before and after heating.

[1] Bovet *et al*. (2011) *This Issue*.

https://doi.org/10.1180/S0026461X00006502 Published online by Cambridge University Press

A Late Triassic major negative $\delta^{13}C$ spike linked to Wrangellia LIP: The Carnian Pluvial Event revealed

J. DAL CORSO[1]*, P. MIETTO[1], R.J. NEWTON[2], R.D. PANCOST[3], N. PRETO[1], G. ROGHI[4] AND P.B. WIGNALL[2]

[1]Dipartimento di Geoscienze, Università degli Studi di Padova, via Gradenigo 6, 35131, Padova, Italy (*correspondence: jacopo.dalcorso@unipd.it).
[2]School of Earth and Environments, University of Leeds, Woodhouse Lane, LS2 1JT, Leeds, UK.
[3]Organic Geochemistry Unit, School of Chemistry, University of Bristol, BS8 1TS, Bristol, UK.
[4]Istituto di Geoscienze e Georisorse, CNR, via Gradenigo 6, 35131, Padova, Italy.

During the Carnian (Late Triassic) a major climatic and biotic change is known, namely the Carnian Pluvial Event (CPE) [1]. This event is characterized by more humid conditions testified by hygrophytic palynological assemblages and palaeosols typical of humid climates; the crisis of rimmed carbonate platforms, a rise of the CCD and the increase of siliciclastic input across the western Tethyan realm; high extinction rates among ammonoids, crinoids, bryozoans and conodonts [2] and the first occurrences of dinosaurs and calcareous nannoplankton [3]. The CPE is similar in age to the eruption of Wrangellia large igneous province (LIP) [3], an oceanic plateau outcropping in western North America. Here we report an abrupt negative $\delta^{13}C$ shift at the onset of the CPE: high and low molecular weight n-alkanes, isoprenoid lipids and total organic carbon (TOC) show a sharp 2‰ - 4‰ negative carbon isotope excursion (CIE) that testify for a rapid injection of ^{12}C into the atmosphere-ocean system. This CIE occurs at the end of a ~3‰ long term Ladinian-Carnian positive CIE previously explained with organic carbon sequestration by coal swamps after the end-Permian mass extinction [4]. We propose that this CIE was caused by an injection of light C by the Wrangellia volcanism into the reservoirs of the exogenic C-cycle with strong consequences for climate and biota.

[1] Simms & Ruffel (1989) *Geology* **17,** 265-268. [2] Rigo *et al*. (2007) *Palaeogeogr. Palaeocl. Palaeoecol*. **246,** 188-205. [3] Furin *et al*. (2006) *Geology* **34,** 1009-1012. [4] Korte *et al*. (2005) *Palaeogeogr. Palaeocl. Palaeoecol*. **226,** 287-306.

Widespread evidence for heterogeneous accretion of the terrestrial planets and planetisimals

C.W. DALE[1]*, K.W. BURTON[2], D.G. PEARSON[1,3], AND R. GREENWOOD[4]

[1]Dept. of Earth Sciences, Durham University, DH1 3LE, UK (correspondence: christopher.dale@durham.ac.uk)
[2]Dept. of Earth Sciences, Oxford University, OX1 3PR, UK
[3]Dept. for Earth & Atmos Sci, University of Alberta, Edmonton, Canada
[4]PSSRI, Open University, Milton Keynes, UK

The abundance and relative proportion of highly siderophile elements (HSEs) in Earth's mantle deviate from those predicted by low-pressure equilibrium partitioning between metal and silicate during formation of the core. For many elements, high-pressure equilibration in a deep molten silicate layer (or 'magma ocean') may account for this discrepancy [1], but some highly siderophile element abundances demand the late addition, a 'late veneer', of extraterrestrial material (i.e. heterogeneous accretion) after core formation was complete [2]. Siderophile elements in smaller asteroidal bodies will not be affected by high-pressure metal-silicate equilibration and so, with highly efficient core formation [3] and if a 'late veneer' is absent, significant differences in the proportions of HSEs can be anticipated.

Here we present new HSE abundance and $^{187}Os/^{188}Os$ isotope data for basaltic meteorites, the HEDs (howardites, eucrites and diogenites thought to sample the asteroid 4 Vesta), anomalous eucrites (considered to be from distinct Vesta-like parent bodies) angrites and aubrites (from unidentified parent bodies) and SNCs (thought to be from Mars). Our data, taken with those for lunar rocks [4], demonstrate that these igneous meteorites all formed from mantle sources that possessed chondritic (i.e. primitive solar system) elemental and isotope compositions, indicating that late accretion is not unique to Earth, but is a common feature of differentiated planets and asteroidal bodies. Variations in the total HSE abundance suggest that the proportion of 'late veneer' added is a simple consequence of the size of each body (cross-section and/or gravitational-attraction), and may account for the volatile element budget, and the oxidation-state of Earth, Mars, the Moon and Vesta.

[1] Righter *et al*. (2008) *Nature Geosci*. **1**, 321-323. [2] Brenan & McDonough (2009), *Nature Geosci*. **2**, 798-801. [3] Greenwood *et al*. (2005) *Nature* **435**, 916-918. [4] Day *et al*. (2007) *Science* **315**, 217-219

https://doi.org/10.1180/S0026461X00006502 Published online by Cambridge University Press

Transport of endocrine disruptive compounds in Hawaiian soils

MATTEO D'ALESSIO[1,2], JOSEPH LICHWA[2], MICHAL SNEHOTA[3] AND CHITTARANJAN RAY[1,2]*

[1]Department of Civil Environmental Enegineering, University of Hawaii at Manoa, Honolulu, HI, 96822, USA (*correspondence: cray@hawaii.edu)
[2]Water Resources Research Center, Hawaii
[3]Czech Technical University in Prague, Czech Republic

The release of endocrine distruptive compounds (EDCs) into the environment is of increasing concern due to their impact on freshwater organisms, ecosystem sustainability and human health. Several studies have emphasized that extended exposure to low concentration of some hormones can alter the endocrine and reproductive systems of aquatic animals. This study was conducted to investigate the transport behavior of two natural EDCs (17 beta estradiol, E2 and estrone, E1) in several Hawaiian soils under different experimental conditions. Soils collected in Hawaii showed higher cotent of mineral oxides, such as iron and manganese oxides compared to most soils in the continental US. Batch sorption and column leaching experiments were used to better understand the fate of both chemicals.

During batch experiments, equilibrium conditions were reached within 12 hours. In all soils having E2 only, its loss occurred due to sorption and degradation. Microbial degradation was inhibited using sodium azide. 100 mg/L azide alone did not completely stop degradation of E2. It was unclear whether this loss was due to microbes or partially due to abiotic mechanisms.

Column experiments showed that with E2 only, E1 was constantly present, showing the degradation of E2 to E1 despite the addition of a sodium azide. For different soils (5 total), breakthrough curves (BTC) of E1 and E2 appeared after the BTC of bromide, suggesting the presence of sorption process during the transport of estrogens through the soil matrix. Facilitated transport was mostly observed in presence of volcanic ash soil. The presence of recycled water enhanced the transport of estrogens in all the different soils. Early appearance of peaks, long tails and complete recovery (mass balance) of both estrogens was more pronounced in transport studies involving the recycled water. Non-equilibrium conditions were observed during the study, especially in presence of undisturbed soil when flow interruption occurred. These conditions were mostly related to the presence of macropores in the soil. Macropores were able to reduce the contact time between soils and estrogens, facilitating their transport.

The oxygen isotopic composition of xenoliths from Tallante (Southern Spain): Evidence for crust recycling into the mantle

L. DALLAI[1] * AND G. BIANCHINI[1,2]

[1]CNR - Istituto di Geoscienze e Georisorse, Pisa, Italy (*correspondence: dallai@igg.cnr.it)
[2]Dipartimento di Scienze della Terra, Università di Ferrara, Ferrara, Italy

Mantle xenoliths from Tallante (Betic Cordillera, Spain) include samples recording a peculiar distinct style of metasomatism that induced orthopyroxene, plagioclase, phlogopite and amphibole crystallization and generated "hydrous" opx-rich mantle domains. The latter are locally crosscut by felsic veinlets containing plagioclase and orthopyroxene ± quartz ± phlogopite ± amphibole. The observed parageneses and available Sr-Nd-Hf isotopic data suggest that metasomatic agents were related to recycling of crust components within the mantle, plausibly in connection with subduction processes occurred during the Cenozoic Betic orogenic cycle.

In this study we investigated representative samples of composite xenoliths consisting of peridotite crosscut by felsic veins (varying in size from centimetric to millimetric) and unveined peridotites, measuring the $^{18}O/^{16}O$ ratios of the constituent minerals by laser fluorination. Results show that the narrow O-isotope compositional "typical" of mantle rocks, and the limited oxygen isotope fractionation at mantle temperatures, make oxygen isotopes a powerful tool for identifying recycled crustal material in the mantle. Orthopyroxene and plagioclase of the centimetric vein show $\delta^{18}O$ values of +9.8 and +10.6‰, respectively, whereas clinopyroxene of the surrounding peridotite country rock has $\delta^{18}O$= +6.2‰. Plagioclase of two distinct millimetric felsic veins show $\delta^{18}O$ of 7.6 and 7.3‰. The $\delta^{18}O$ values significantly higher than typical mantle ones provide insights to the genesis of the Cenozoic subduction-related magmas of the Betic region that include silica-oversaturated calcalkaline (s.l.) and lamproite products, possibly resolving source vs. shallow level crustal contamination of the magmatic rocks. Moreover, the different O-isotope composition recorded in veinlets characterized by different thickness could provide insights into diffusion-assisted O-isotope requilibration of mantle rocks, thus constraining the time for "crust digestion" into the mantle.

https://doi.org/10.1180/S0026461X00006502 Published online by Cambridge University Press

How do plant emissions affect atmospheric nanoparticle formation?

MIIKKA DAL MASO[1,2], THOMAS F.MENTEL[2], ASTRID KIENDLER-SCHARR[2], EINHARDT KLEIST[2], RALF TILLMANN[2], MIKKO SIPILÄ[1], TUUKKA PETÄJÄ[1], JANI HAKALA[1], LI LIAO[1], KATRIANNE LEHTIPALO[1], MARKKU KULMALA[1] AND DOUGLAS WORSNOP[1]

[1]Department of Physics, University of Helsinki, PO Box 48, 00014, Helsinki, Finland, miikka.dal@helsinki.fi
[2] Institut für Chemie und Dynamik der Geosphäre (ICG), Forschungszentrum Jülich, 52425 Jülich, Germany

Non- and semivolatile compounds, produced by the oxidation of atmospheric trace gases that are emitted by human and biological activity, can undergo a phase transition and enter the atmospheric aerosol phase, either onto existing particles or forming new nanosized condensation nuclei. The most likely candidates of precursors of aerosol number-producing vapors are sulphur dioxide and plant-originated volatile organic compounds.

Currently, the controlling mechanism of tropospheric nanopartile formation is still an open question. Field and laboratory measurements have clearly indicated a strong correlation between observed sulphuric acid – a product of SO_2 oxidation – and nanoparticle concentrations and formation rates (eg. [1]). On the other hand, observed seasonality and comparisons with plant VOC emission strengths show that aerosol formation is also correlated with biogenic organic oxidation. Laboratory studies with real plant emissions have shown a clear dependence of aerosol formation on the VOC emission strength and also the chemical mixture ([2, 3]), thereby ruling out the possibility that nanoparticle formation by nucleation would be completely independent of organic compounds.

We investigated the formation of nanosized condensation nuclei (nano-CN) from sulphuric acid and plant emissions in the Jülich Plant Chamber setup. We performed a series of experiments using boreal forest tree emissions at levels commonly found in the boreal boundary layer.

We found that while the variation of the VOC concentration had a strong inpact on the gas phase chemistry and also the hydroxyl radical and sulphuric acid levels, the changes in particle formation rates were not explainable by sulphuric acid concentration variations alone, but the particle formation process is directly influenced by the plant emissions.

[1] Riipinen *et al*., (2007). [2] Mentel *et al*., (2009). [3] Kiendler-Scharr *et al*., (2009).

Estimating mantle temperature from a global comparison of seismic models and the petrology of mid-ocean-ridge basalts

COLLEEN A. DALTON*[1], ALLISON GALE[2] AND CHARLES H. LANGMUIR[2]

[1]Earth Sciences, Boston University, 675 Commonweath Ave., Boston, MA 02215 USA (*correspondence: dalton@bu.edu)
[2]Earth and Planetary Sciences, Harvard University, 20 Oxford St., Cambridge, MA, 02138 USA; (agale@fas.harvard.edu; langmuir@eps.harvard.edu)

Inferring mantle temperature and composition is one of the primary applications of seismic tomography. Mantle temperature and composition also strongly influence the petrology of mid-ocean-ridge basalts (MORBs) erupted on the seafloor. It is therefore reasonable to hypothesize that a relationship exists between seismological and petrological data. We have investigated whether such a relationship does exist using global seismic models and a new and expanded global compilation of MORB major-element chemistry. Petrological data obtained from PetDB form the core of our geochemical database, which is augmented by unpublished analyses and Iceland samples from GEOROC. We correct all measured values to 8% MgO and determine the mean composition for 231 individual ridge segments. We compare the petrological data (ridge depth, Na8, Fe8, etc.) with global mantle models of shear-wave speed, attenuation, and transition-zone topography. Ridge depth and wave speeds at 200-400 km depth are correlated globally, suggesting that the same factors that control ridge depth and crustal thickness also influence seismic velocity. For several ridges, anti-correlation between ridge depth and depth to the 410-km discontinuity is seen, in particular the Southwest Indian Ridge and the Mid-Atlantic Ridge. The comparisons also reveal correlation between Na8 and shear-wave speed at 200-300 km globally. Comparison of the petrological data and mantle seismic models provides an opportunity to understand the connection between temperature and composition at depth and the processes occurring at the surface.

https://doi.org/10.1180/S0026461X00006502 Published online by Cambridge University Press

Xenoliths reveal lower crustal deformation and metamorphism with no obvious surface expression

J.S. DALY[1]*, R. VAN DEN BERG[2], M.J. WHITEHOUSE[3], AND H. O'ROURKE[1]

[1]UCD School of Geological Sciences, University College Dublin, Belfield, Dublin 4, Ireland (*correspondence: stephen.daly@ucd.ie)
[2] Barberton Mines (Pan African Resources), Consort Section, Mpumalanga, South Africa
[3]Swedish Museum of Natural History, Stockholm, Sweden

Lower crustal xenoliths afford an opportunity to investigate the crustal architecture in 3D and to test whether deformational and metamorphic events in the lower crust are coupled to those known from outcrop studies.

Within the Iapetus Suture Zone (ISZ) in Ireland, where Laurentia and Avalonia collided obliquely during the c. 420 Ma Caledonian Orogeny, Carboniferous magmatism has transported granulite-facies lower crustal xenoliths at several localities. The xenoliths are predominantly metasedimentary and on seismic and geochemical grounds provide a near-perfect match with present-day lower crust [1, 2]. Thermobarometry indicates original depths of c. 22-33 km, and temperatures in the range 700 - 900 °C [1]. Ion microprobe U-Pb zircon dating of syn-tectonic granitic leucosomes in metasedimentary xenoliths indicates at least three discrete high-grade metamorphic events (382 ± 2 Ma, 373 ± 3 Ma and 360 ± 3 Ma), all younger than Caledonian. The oldest corresponds to an episode of Middle Devonian volcanism and may be related to syn-sedimentary extension. However, the younger events have no deformational or thermal effects known at outcrop. They demonstrate that ductile deformation and melting took place c. 25 km below the surface without significant surface expression suggesting significant mechanical and thermal decoupling of the lower and upper crust.

[1] Van den Berg *et al*. (2005) *Tectonophysics* **407**, 81-99. [2] Hauser *et al*. (2008) *Geophysical Journal International* **175**, 1254-1272.

Pt-bearing metabasites from the East Sayan (Russia): Composition and origin

B.B. DAMDINOV

Geological Institute SB RAS, Ulan-Ude, Russia (damdinov@gin.bscnet.ru)

Glaucophane-bearing metabasites in the East Sayan are known as Okinsky blueschist belt. In one of the small massifs PGE mineralization was established. This massif is presented by latitudinal strike body, which contained by greenschist strata. Basic and ultrabasic rocks are altered to amphibolites, epidote-actinolite-amphibolic rocks and serpentinites, which most fractured and rich by asbestos veinlets. Further small pyroxenite bodies, gabbro and lherzolite relics are detected. Amphiboles are presented by three varieties. At first has a dark-green to light-brown color diagnosed as ferrichermakite, at second has light-blue color – vinchite, ferribarruasite, at third presenting as violet-color margin is a magnoriebeckite. From the center to outside direction Na-content increases whereas Ca and Al contents are decrease. PGE is concentrated by extensive zones of pyrite-magnetite mineralized amphibolites and sulfidized garnet-diopside-chloritic rodingites. Ore minerals are presented by magnetite with rare ilmenite relics, hematite, rutile, cassiterite and sulfides which form single areas and presented by pyrite, chalcopyrite, zigenite, arsenopyrite, sphalerite, galena. Noble metal minerals are native gold, mercurian gold, Cu-bearing gold. Platinum-Group element (PGE) minerals are presented by sperrylite. Concentrations of noble metals in ores attain to Au – up to 1.47 ppm, Pt – up to 5.2 ppm, Pd – up to 0.55 ppm. Obtained P-T conditions of metabasite formation correspond to P>8 kbar, T – 250 - 300°C are indicate it's formation in the subduction zone or accretion wedge. Island-arc complexes are characterized by mercury and tin deposit presence, where ore-forming elements are entered from mantle fluids. These fluids also contain noble metal, incoming by the mantle ultrabasic rocks partial melting.

https://doi.org/10.1180/S0026461X00006502 Published online by Cambridge University Press

The pecularities of Khasurta massif rocks formation on the melt inclusion study (Angaro-Vitim batholith, Western Transbaikalia)

L.B. DAMDINOVA AND B.TS. TSYRENOV

Geological Institute SB RAS, Ulan-Ude, Russia
(ludamdinova@mail.ru, tsyrenov@mail.ru)

The Khasurta pluton (about 900 km^2) presents early phase of the Angara-Vitim batholith formation. On the south this pluton is overlapped by Mesozoic and Cenozoic deposits of the Udinskaya intermontane trough, on the north it is limited by a regional break, and on the east and west it intrudes Proterozoic - Early Cambrian volcano-terrigenous and terrigene-carbonaceous sediments. As a whole the pluton is in discordant contact with surrounding rocks.

The pluton's interior is not homogenous and consists of monzonitic and granosyenitic rocks. As a rule surrounding carbonaceous rocks are substituted by scarns in contact with the pluton.

Zircon grains were selected from monzonites. Zircon grain sizes of - up to 1 mm in length, they often form intergrowths. Small crystals (200 - 600 microns) have a zircon habit, and a light pink color.

Melt inclusions in zircon grains from monzonites were studied. A composition of ungomogenized melt inclusions was analysed using the electron microscope (LEO 1430 VP), have been identified: quartz, K feldspar, plagioclase, apatite, muscovite.

Six experiments each with a duration of about 1-3 hours at different temperatures (800-1000°C) were carried out (inclusions size – 4-10 μm). Using an electron microscope the composition of the three homogenized inclusions has been studied. Its composition is more acidic as compared with monzonite and has increased Na, K content.

Thus, based on these results we conclude that Khgasurta massif rock crystallisation temperature was more than 920°C. Monzonites are represent acid ("sienitic") magmas cumulates. High Na and K content permit to suggest monzonite affiliation to the shoshonitic series.

Study was supported by Lavrentievsky grant SB RAS.

Radiochemical analysis of environmental radioactivity for surveillance and characterization

HAIJUN DANG*, HAITAO ZHANG AND XIAOWEI YI

Northwest Institute of Nuclear Technology, Xi'an, China
(*correspondence: harryhjdang@163.com)

Great changes have been achieved in the world politics and economics with the development of nuclear science and technology. However, many problems in the sustainable developing of society and potential risks to the ecology have been also aroused by radioactive pollution. To assess the risk of radionuclides in environment, not only the total amount but also the biogeochemical behavior, the origin and the diffusion (migration) path of these radioactive pollutants in environment need to know. For this purpose, radiochemical analytical methods are keys to characterization of radioactivity.

Since 1990s, inductively coupled plasma mass spectrometry (ICP-MS) has been widely used for monitoring trace radionuclide and identifying the source terms for different environment samples, including soil, underground water, plants and air [1]. In our laboratory, different analytical methods based on ICP-MS measurement and radiochemical separation have been developed to monitor and characterize radionuclides in environment. This work aims to summarize the newly developed analytical methods using UTEVA extraction chromatography combined with ICP-MS for monitoring transuranium nuclides in soil [2] and a direct aerosol measurement attempt with ICP-MS for determining the radionuclide concentration in air [3]. Meanwhile, the result of an environmental radioactivity investigation will be presented to show the bioavailability of radionuclides of different origin [4], as well as the radioactivity transfer from soil to plant. In addition, the developed methods to identify nuclear materials by isotopic signature and age determination have also been well shown with satisfactory result [5]. However, tackle for very low level contamination and for deliberately mixed material is still a challenge to work on.

[1] Yang Haiyou & Yu Shui (2008), *J Chinese Mass Spectr* **29**(3), 172-184. [2] Yi Xiaowei *et al*. (2010), *J Nucl. Radiochem* **32**(1), 22-26. [3] Su, Yong Yang *et al*. (2011), *Internat J Environ Analyl Chem* **91**(5), 473 – 483. [4] Shi Yanmei *et al*. (2007), *J Nucl. Radiochem* **29**(4), 248-252. [5] Hai-Tao Zhang, *et al*. (2008), *Radiochimica Acta* **96**(6), 327-331.

https://doi.org/10.1180/S0026461X00006502 Published online by Cambridge University Press

High-pressure microbiology in the synchrotron light

I. DANIEL[1], A. PICARD[2,3], D. TESTEMALE[4] AND J.-L. HAZEMANN[3]

[1]Université Lyon 1, ENS de Lyon, CNRS, UMR 5276, Laboratoire de Géologie de Lyon, France (isabelle.daniel@univ-lyon1.fr)
[2]Max Planck Insitute for Marine Microbiology, Biogeochemistry Department, Bremen, Germany
[3]MARUM, Center for Marine Environmental Sciences, Bremen, Germany
[4]Institut Néel, Département MCMF, Grenoble, France

The Earth's subsurface is characterized by hostile conditions for life in terms of temperature, pressure and nutrient availability. Although our current view of the biosphere extension is restricted to shallow geological depths, deep life may enconter pressures of hundreds MPa. As an important microbial energetic process, dissimilatory metal reduction needed to be investigated as a function of pressure.

We measured the effects of pressure on the reduction of Se(IV) and Fe(III) to Se(0) and Fe(II), respectively by the bacterial model Shewanella oneidensis MR-1. This strain is a mesophilic and piezosensitive counterpart of psychrophilic and piezophilic Shewanella representatives that have been frequently isolated from deep-sea environments. Kinetics and yields of Se(IV) and Fe(III) reduction were monitored *in situ* by X-ray Absorption Spectroscopy (XAS) in an autoclave optimized for *in situ* XAS measurements [1]. Most measurements were performed at the BM30B beamline of the European Synchrotron Radiation Facility (ESRF, Grenoble, France). Early measurements on the reduction of Se(IV) were also performed in diamond anvil cell at the ID22 beamline of the ESRF.

Metal reduction occurs in cultures of MR-1 at pressures in excess of 100 MPa. This shows that the metabolic activity of a microbe, despite being piezosensitive, extends far beyond its pressure limits for growth here at 50 MPa. Consequently, considering only the ability to grow in the conditions of the deep subsurface as a proof of metabolic activity may lead to an underestimation of the impact of the biosphere in deep environments. Although the exact experimental conditions do not mimic complex subsurface environments, we show here that the metabolic activity of a surface microbe potentially brought to the deep subsurface can affect significantly biogeochemical cycles as those of selenium, but more importantly those of iron and carbon.

[1] Picard *et al*. (2011) *Geobiology*, **9**, 196-204.

Subduction factory unroofed: Modern submarine magmatism in the North Fiji Basin, Southwest Pacifc

LEONID DANYUSHEVSKY AND TREVOR FALLOON

CODES CeO and School of Earth Sciences, University of Tasmania, PB 79, Hoibart, TAS 7001, Australia (*correspondence l.dan@utas.edu.au, Trevor.Falloon@utas.edu.au)

An extensional setting at the southern termination of the North Fiji Backarc Basin (southwest Pacific), which occurs in response to westward roll-back of the Vanuatu trench and eastward roll-back of the Tonga trench, allows subduction-related magmas to reach the surface (seafloor) with only a minimal extent of both fractionation and crustal contamination, thus providing a unique insight into magma generation processes with the subduction factory.

Volcanic rocks collected within this are during the SS10/2004, SS08/2006 and SS03/2009 voyages of the R/V "Southern Surveyor" reveal a large spectrum of subduction-related magma compositions from backarc basin basalts to boninites, calc-alkaline basalts and high-Mg adakites. All magma series have very primitive, high MgO endmembers, which contain abundant high-magnesian olivine phenocrysts (Fo 92-94) formed during the earliest stages of melt evolution.

The data reveal that melts produced due to adiabatic decompression of the mantle wedge play an important role in magma genesis. Within the studied area, a number of such melts can be identified which differ in both the extent of the contribution of the subduction-derived components, and the extent of depletion of the mantle source. Also abundant are melts produced by melting of the basaltic component of the subducted oceanic crust, which extensively re-equilibrate with the surrounding mantle during their accent to the surface. These melts are also characterised by a range of compositions, range from low-Si, high-Mg to high-Si, high-Mg adakites.

There is clear petrographic and geochemical evidence for extensive mixing between high-Mg adakitic and backarc basin magmas in this area, which results in formation of primitive magmas with typical calc-alkaline and boninitic affinities. Our results suggest that in less extensional settings, where unfractionated magmas rarely reach the surface, the role of this mixing in the genesis of typical calc-alkaline magmas may be more difficult to identify, however it may play an important role in subduction-related magma genesis in general.

https://doi.org/10.1180/S0026461X00006502 Published online by Cambridge University Press

Application of the correspondence analysis to determine anomalous elements and samples

F. DARABI GHOLESTAN[1]*, R. GHAVAMI- RIABI[1] AND H. ASADI-HARONI[2]

[1] Mining, Petrolum and Geophysics Faculty, Shahrood Univ. of Tech, 7 Tir square, Danshgh Bolv. (*Corresponding author: farshad_darabi@yahoo.com)

[2]Mining Engineering Dept., Isfahan Univ. of Tech., Khomani shahr Bolv.

Determination of the anomaly elements and samples

Based on the soil lithogeochemistry samples were taken from a probable porphyritic Cu-Au mineralized area, the mineralized elements and anomalous samples were identified [1,2,3]. For this propose, a correspondence analysis was done on a matrix of 29 elements (columns) and 149 samples (rows) from the study area. According to the correspondence analysis, a final matrix of 28 factors or variables (columns) and 29+149 labels (rows), which includes of elements and sample numbers, was calculated. The cross plots of two variables (Fig. 1 A and B) from the final matrix were confirmed Au and Cu as anomaly elements and numbers 40, 74, 22 and 84 as anomalous samples.

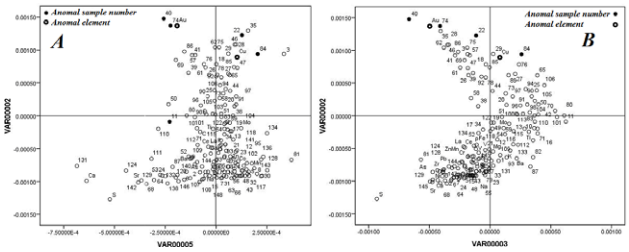

Figure 1: Correspondence analysis for identification of the anomalous element and samples

Conclusion

Identiification of the anomaly sample numbers and anomaly elements could be possible by using the correspondence analysis. The combination of this method and anomaly separation method could separate the high potential eara for follow up exploration program.

[1] Davis, J.C. (2002), John Wiley & Sons, 646 pp. [2] Greenacre, M.J. (2007), Boca [3] Abdi, H. (2007), Thousand Oaks (CA).

Large-area input, inventories, and transport of ^{129}I and ^{127}I in Germany

A. DARAOUI, M. SCHWINGER AND B. RIEBE

Inst. f. Radioökologie u. Strahlenschutz, Leibniz Universität Hannover, Germany (riebe@irs.uni-hannover.de)

The environmental abundance of ^{129}I has been changed substantially, mainly as a consequence of the ^{129}I releases from European reprocessing plants. The stable ^{127}I and the long-lived ^{129}I exhibit massive disequilibria in all biotic and abiotic compartments of the environment in Western Europe. Measurements of ^{127}I and ^{129}I in some German soils revealed ^{129}I/^{127}I ratios of 10^{-7} to 10^{-10} [1, 2], whereas the ^{129}I/^{127}I ratio in a pre-nuclear Russian soil was found to be 5.7 x 10^{-12} [3]. Iodine from wet and dry precipitation is accumulated in soils, transported by surface waters, infiltrates groundwater, and makes its way through the biosphere. Many of the ecological pathways of iodine are still unknown.

The goal of this project is to investigate the continuous atmospheric input via dry and wet deposition, the inventories in the pedosphere and the output by river waters of ^{129}I and ^{127}I in entire Germany.

To this end, aerosol filter samples from 4 locations will be analysed, as well as precipitation samples from 10 locations, and surface water samples from 15 locations along the major rivers in Germany. Sampling is supported by DWD (German Meteorological Service), BfG (Federal Institute for Hydrology), PTB (Federal Metrology Institute), and BfS (Federal Office for Radiation Protection). Additionally, sampling of different soil types at various locations in Germany, down to a depth of 50 cm, is in progress.

Deposition rates, deposition densities and transport rates will be calculated using inductivity coupled plasma mass spectrometry (ICP-MS) and accelator mass spectrometry (AMS) as analytical tools. First results from the two-year sampling, which startet in March 2011, will be shown. A sufficiently dense grid of sampling points will allow a nation-wide mapping of the atmospheric input, the accumulation in soils, and the transport with surface waters back to the sea. Based on these data, a model will be established describing the different pathways of iodine isotopes in the environment.

[1] Ernst *et al*. (2003) *Kerntechnik* **68**(4), 155–167. [2] Daraoui *et al*. (2011) to be submitted to *J. Environ. Rad* [3] Szidat *et al*. (2000) *Nucl. Instr. Meth. Phys. Res. B* **172**, 699–710.

https://doi.org/10.1180/S0026461X00006502 Published online by Cambridge University Press

Formation of Platinum-Group Minerals from an evolving sulfide liquid at Sudbury, Canada

S.A.S. DARE[1]*, S.-J. BARNES[1], H.M. PRICHARD[2] AND P.C. FISHER[2]

[1]L'Université du Québec à Chicoutimi, Québec, Canada, G7H 2B1 (*correspondence : sasdare@hotmail.com)
[2]Cardiff University, Wales, U.K., CF10 3AT

Chalcophile and platinum-group elements (PGE) are collected by a magmatic sulfide liquid and form PGE (± Ni-Cu) deposits. Early-crystallizing monosulfide solid solution (MSS) concentrates Os, Ir, Ru and Rh (IPGE) and the residual liquid concentrates Cu, Pt, Pd, Ag, As, Bi, Te, and Sn. It is important to determine the host phases of the PGE, which are sulfide minerals and/or platinum-group minerals (PGM), in order to understand the petrogenesis of the deposit and to improve PGE extraction. Previous work shows that PGM form by:
1) exsolution from base metal sulfides, 2) crystallization from the residual Cu-rich liquid and/or a late-stage immiscible melt and 3) remobilization during metamorphism or by hydrothermal fluids.

We have investigated the origin of PGM from Sudbury Ni-Cu-PGE deposits by combining a PGM study with whole-rock data and laser ablation-ICP-MS analysis of the sulfides. We found that a large proportion of the PGE are hosted in As-, Bi-, Te- and Sn-rich PGM, which formed over a wide range of temperatures during the evolution of the sulfide deposit. The amount of As in the initial sulfide melt, which varied according to the As content of the assimilated country rocks, was critical in determining whether As-PGM (IrAsS, RhAsS ± $PtAs_2$) crystallized early (1200-900°C) from the sulfide liquid togther with MSS. An As-rich sulfide melt crystallizes sulfarsenides so that the co-existing MSS is depleted in Ir and Rh whereas an As-poor sulfide melt does not crystallize sulfarsenides and the IPGE remain in MSS. The amount of Bi, Te and Sn increases during sulfide fractionation so that the following Pt-Pd-minerals crystallized from the residual liquid. Solitary grains of Pd_2Sn and PtSn crystallized early (1300-800°C) from the Cu-rich sulfide liquid whereas an un-named Pt(Sn,Bi)Te phase together with numerous Pt-Pd-Bi-Te-Ag minerals crystallized as composite grains from micro-droplets of an immiscible late-stage melt (1000-600°C). The small amount of Pt, Pd, Bi and Te, which partitioned into MSS, later exsolved (< 600°C) as laths of $(PtPd)(BiTe)^2$ and PdBiTe and were remobilized during greenschist metamorphism.

Probable Mars atmospheric changes by the proposed terraforming process with silicon utilizing organisms

SATADAL DAS

Peerless Hospital & B. K. Roy Research Centre, Kolkata, India. (drsatdas@hotmail.com)

The silicon utilizing organisms particularly diatoms are well known to tolerate different stress as evidenced in studies on past mass extinctions on Earth and also in artificial laboratory conditions. Thus these organisms may be utilized in terraforming suitable solar system objects and such proposals have already been given for Mars and the Moon [1] and further proposals are likely to be placed for Venus, Callisto, Europa, Ganymede, Enceladus and Titan in near future. In Mars, after initiation of such a terraforming process, by application of these organisms on the surface among basalts, clays, ice etc, a target oxygen level of 150 m bar in the atmosphere may reach within 500 years, with expected significant increase in nitrogen to 300 m bar and decline of carbon dioxide to as low as 10 m bar. As most solar radiations usually reach the surface of Mars, these organisms are expected to grow even at a low temperature in a surface pressure of 6-7 m bar. High carbon dioxide levels will affect the growth, fluorescence, pigmentation and carbonic anhydrase activity of these organisms with involvement of chlorophyll a, chlorophyll c and fucoxanthin. Presence of diverse genes is essential for proper terraforming process with organisms, mainly for efficient management of C and N. Thus a set of such organisms may be chosen for initial terraforming process according to gene library matching. Iron present on Mars surface has also a pivotal role in controlling carbon uptake by these organisms and regulating atmospheric partial pressure of carbon dioxide. Finally atmospheric erosion and escape processes particularly solar wind ion or proton and magnetospheric-plasma-driven sweeping may alter the expected values to some extent.

[1] Das (2010), *Lunar settlements*, Ed Benaroya, CRC press, 679-692.

https://doi.org/10.1180/S0026461X00006502 Published online by Cambridge University Press

Silicate melting in the Earth's deep upper mantle caused by C-O-H volatiles

R. DASGUPTA[1]*, K. TSUNO[1], A. C. WITHERS[2] AND A. MALLIK[1]

[1]Dept. of Earth Science, Rice University, Houston, TX (*correspondence: Rajdeep.Dasgupta@rice.edu)
[2]Dept. of Geology & Geophysics, University of Minnesota, Minneapolis, MN

The onset of silicate melting in the Earth's upper mantle influences the thermal evolution of the planet, geochemical differentiation of the interior, flux of key volatiles to the exosphere, and geophysical properties of the mantle. Although the first initiation of melting beneath mid oceanic ridges likely produces dry carbonatite melt as deep as ~350 km, owing to vanishingly small volume (~0.03%), its effect on geochemical and geophysical properties of the mantle is unclear. Geophysical data, however, suggest possible presence of partial melts to depths exceeding 200 km. Silicate melts have better prospects in this respect owing to higher viscosities and densities; however, they are not thought to be generated at depths approaching or in excess of 200 km. Here we present experiments in natural peridotite+CO_2 systems over 2 to 5 GPa and constrain the location and the slope of the onset of silicate melting (melts with ≤25 wt.% CO_2) in a carbonated mantle. We show that the P-T slope of transition from carbonate to silicate melt is steeper than the solidus of volatile-free peridotite owing to diminishing non-ideality of mixing between carbonate and silicate melt components as a function of pressure. This causes carbonated silicate melting of dry peridotite beneath ridges to commence as deep as ~230 km. Taking into account 50-200 ppm water in the nominally anhydrous mantle and its effect on freezing point depression, the onset of silicate melting for a sub-ridge mantle with ~100 ppm CO_2 becomes as deep as ~260-300 km. Deep carbonated silicate melting can deplete the mantle from its water storage capacity, to match the depleted mantle water content beneath ridges. Deep onset of silicate melting also restricts the stability of carbonatite in the Earth's deep upper mantle and the inventory of carbon and other highly incompatible elements at ridges becomes almost entirely controlled by flux of deep, wet carbonated silicate melts.

Finally, deeper transition from carbonatite to carbonated silicate melts causes the melt CO_2 to be diluted at greater depths than previously modeled. This causes graphite to carbonated melt transition depth beneath continents to be deeper than recent estimates.

SHRIMP U-Pb geochronology of Neoproterozoic Rio Una sequence, NE Brazil, and the Rodinia break-up

*A.F. DA SILVA FILHO[1], I.P. GUIMARAES[1] AND R.A. ARMSTRONG[2]

[1]Universidade Federal de Pernambuco, Departamento de Geologia, Recife, Brazil, (*correspondence:afsf@ufpe.br)
[2]Australian National University, RSES, Canberra, Australia, (richard.armstrong@anu.edu)

The amalgamation of Gondwana resulted from the fragmentation of Rodinia and the reassembly of the cratonic blocks during the Neoproterozoic. The Borborema Province is the western part of a major Brasiliano belt that extends from Brazil through NW Africa in pre-drift reconstructions. This province results from the convergence and collision among the West African, Congo-São Francisco, and Amazonia land masses about 600 Ma. The Rio Una Sequence is located within the PEAL Domain of the Borborema Province. It is comprised by 3 units. We are presenting U-Pb dating of the unit 1.This unit comprises migmatized metapelites with peraluminous mesossome (andaluzite-, cordierite-, garnet-bearing biotite gneisses), with quartzites intercalations. The studied sample was collected near one of these intercalations. The analyzed sample shows zircon grains with length ranging from 80μm up to 200μm. They are elongate to rounded zircons, with aspect ratio ranging from 1:1 to 2:1. They usually show oscillatory zoning, and in some case a narrow metamorphic overgrowth. The $^{232}Th/^{238}U$ ratio of almost all analysed grains ranges from 0.20 to 2.16, suggesting that they come from an igneous protolith, or from a recycled igneous rock. The U-Pb data with less than 5% discordance cluster mostly in the intervals 850-1100 Ma and 1800-2100 Ma. The data points that the unit 1 show a maximum depositional age of 854Ma. The age of this sequence is coeval with the age attributed to the beginning of the Rodinia break-up.

https://doi.org/10.1180/S0026461X00006502 Published online by Cambridge University Press

Mechanisms of copper immobilization by bacteria during precipitation of iron oxides

C.J. DAUGHNEY[1]*, P. J. SWEDLUND[2] AND M. MOREAU-FOURNIER[1]

[1]GNS Science, Lower Hutt, New Zealand (*correspondance: c.daughney@gns.cri.nz)
[2]University of Auckland, Auckland, New Zealand

This project focuses on interactions between bacteria and iron oxides, and the effects of such interactions on the behaviour of dissolved copper ions. Laboratory experiments were performed to track the fate of dissolved copper and iron during the gradual, incremental oxidation of dissolved Fe(II) and precipitation of iron oxide in the presence of *Anoxybacillus flavithermus* cells. The experimental data reveal significant and complex controls on copper immobilization, related to progressive changes in 1) ratio of copper to dissolved Fe(II) concentration, inferred to result from competition for bacterial sorption sites; 2) ratio of precipitated iron oxide to bacteria, inferred to result from desorption of Fe(II) initally associated with the bacterial surface; and 3) reaction time, inferred to result from increasing quantities of biogenic dissolved organic matter. Surface complexation models are developed to describe the experimental data. This study demonstrates that the immobilization of metal cations in bacteria-bearing settings should not be examined independently of progressive oxidation, hydrolysis and precipitation of iron.

Mars as a planetary oligarch

NICOLAS DAUPHAS[1] AND ALI POURMAND[1,2]

[1]Origins Laboratory, Department of the Geophysical Sciences and Enrico Fermi Institute, The University of Chicago, Chicago IL 60637, USA (dauphas@uchicago.edu).
[2]RSMAS, Division of Marine Geology and Geophysics, University of Miami, Miami, FL 33149, USA.

There is considerable uncertainty as to how and when Mars formed [1,2]. In particular, its small mass compared to Earth and Venus is difficult to explain and some have suggested that Mars could be a stranded planetary embryo (also called an oligarch) that escaped collision and merging with other embryos [3]. A diagnostic parameter to assess this idea is its accretion time, which can be calculated using ^{182}Hf-^{182}W systematics of martian meteorites [2,4]. Unfortunately, the Hf/W ratio of the martian mantle is very uncertain, resulting in model age estimates that range between 0 to 15 My after solar system birth. To better constrain the Hf/W ratio of the martian mantle, we have measured the concentrations of Lu, Hf, U, Th by isotope dilution, as well as ^{176}Hf/^{177}Hf isotopic ratios of 43 chondrites from all major groups of chondrites [the methodology is described in ref. 5].

We estimate the Hf/W atomic ratio of the martian mantle to be 3.51±0.45 . Using this Hf/W ratio, the measured value of $\varepsilon^{182}W_{Mars\ mantle}$=+2.6 [2,4] can only be reproduced with an accretion timescale of ~2 Myr [6]. This is consistent with a stranded planetary embryo origin for Mars. Objects formed in the first few million years of the formation of the solar system would have incorporated enough ^{26}Al to melt. We thus demonstrate that a magma ocean powered by ^{26}Al-decay must have been present on early Mars. This changes our perspective on the formation of our planet as we have now identified a sample of the embryonic material that the Earth was made of. For example, Earth may have inherited its missing Xe problem [7] from a Mars-like precursor.

[1] Dauphas N. & Chaussidon (2011) AREPS 39, in press (doi:10.1146/annurev-earth-040610-133428). [2] Nimmo F. and Kleine T. (2007) *Icarus* **191**, 497. [3] Wetherill G.W. (1991) *LPS XXII*, 1495. [4] Foley C.N. *et al*. (2005) *GCA* **69**, 4557. [5] Pourmand A. and Dauphas N. (2010) *Talanta* **81**, 741. [6] Dauphas N. & Pourmand A. (2011) Nature, in press (doi:10.1038/nature10077). [7] Dauphas N. (2003) *Icarus* **165**, 326.

https://doi.org/10.1180/S0026461X00006502 Published online by Cambridge University Press

Linking solution composition and surface topography to the rate and mechanisms of diopside dissolution

D. DAVAL[1]*, G. D. SALDI[1], R. HELLMANN[2] AND K. G. KNAUSS[1]

[1]ESD, LBNL, Berkeley, CA 94720, USA (*correspondence: ddaval@lbl.gov)
[2]ISTerre, CNRS/UJF, 38041, Grenoble, France

Whereas the dissolution rate of silicate minerals has been extensively studied at far-from-equilibrium conditions, extrapolating such rates over a broad range of solution composition has proven challenging. Regarding diopside, recent studies [1, 2] suggested that below 125 °C, an unexpected drop of the rate occurred for Gibbs free energies of reaction (ΔG_r) as low as –76 kJ.mol^{-1}, with severe consequences on our ability to predict the rate of complex processes such as carbonation reactions [2].

The mechanism responsible for such a drop remains unclear and therefore needs to be deciphered. An examination of our previous data [2] led us to envisage that two different, non-exclusive aspects were worth investigating: (i) the possible passivating ability of interfacial, nm-thick Si-rich layers developed on weathered silicate surface, and (ii) the stop of etch pits formation on crystal surface, which were found to be responsible for drops of olivine [3] and albite [4] dissolution rates, respectively.

Our ongoing experiments aim at better constraining these two mechanisms, and determining in turn whether one of them could explain the above-mentioned drop of diopside dissolution rate. Classical flow-through experiments with controlled SiO_2(aq) concentrations are combined with both *ex situ* AFM measurements and *in situ* monitoring of the topography of the dissolving surface of diopside in a hydrothermal AFM flow-cell (e.g. [5]). By investigating the dissolution of several cleavages, we will show how these latter techniques represent a powerful tool for studying the anisotropy of diopside dissolution, and determining which face ultimately controls its dissolution rate. An attempt to link these observations to macroscopic determination of diopside dissolution rates as a function of fluid composition will be discussed.

[1] Dixit & Carroll (2007) *Geochem. T*, **8,** 1-14. [2] Daval *et al.* (2010) *Geochim. Cosmochim. Ac.*, **74,** 2615-2633. [3] Daval *et al.* (2011) *Chem. Geol.*, **284,** 193-209. [4] Arvidson & Luttge (2010) *Chem. Geol.*, **269,** 79-88. [5] Saldi *et al.* (2009) *Geochim. Cosmochim. Ac.*, **73,** 5646-5657.

Zone of Anomalous Mantle

A.W. DAVIES AND R. DAVIES

Talmora Diamond Inc. 6 Willowood Ct, Toronto M2J2M3 Canada (rayal.davies@sympatico.ca)

The most striking characteristic of both the Siberian and Slave diamond fields is their linear distribution. The concept of the "Corridor of Hope" was introduced [1] to refer to a northwest trend that appears to have controlled the emplacement of the most significantly diamondiferous kimberlites of the Slave craton. With displaced northern [2, 3] and southern extensions the corridor is 2300 km long.

The Siberian diamond fields have a linear distribution over 1000 km with one offset. The linear is described [4] as a "Zone of Anomalous Mantle" and mantle xenoliths and xenocrysts [5] show that Hartsburgite makes up a significant part of the lower mantle beneath 190-240 km thick lithospheric Archean terrane to the south but is missing beneath 125 km thick lithospheric Proterozoic terrane to the north.

Helmstaedt [6] proposed a model for the Slave craton in which Paleoproterozoic lithosphere has underplated Mesoarchean lithosphere beneath the corridor and the upper edge of the underplating Proterozoic is 270 km west of the corridor and controls the geometry of the corridor. Significantly Mirny is 250 km NW of the Akitkan Proterozoic fold belt and there is evidence [7] for a Proterozoic fold belt 250 km east of the Alakit/Daldyn/Muna diamond fields.

A modified 2.0-0.8 Ga reconstruction of the Proterozoic Supercontinent [8] has the Siberian "Zone of Anomalous Mantle" lined up with the N American corridor.

Conclusion

Proterozoic lithosphere underplated an Archean craton (Siberia & N America) on its Pacific ocean side that resulted in a single zone of anomalous mantle. Except where the zone was cut by the Aekit Proterozoic orogenic belt that separated, thinned and destroyed the base of the adjoining Siberian and N American (Alaska North Slope) cratons, it is extremely favourable for hosting diamondiferous kimberlites.

[1] Schiller (2003) *Res. World. Mag.*, **1**, No.3, 28-30. [2] Darnley Bay Res. (2003) Web site. Sum. Rpt. 5. [3] Davies *et al.* (2011) Poster, Diam. Sch. 2011. [4] Kaminsky *et al.* (1995) *J. of Geochem. Expl.*, **53**, 167–182. [5] Griffin *et al.* (1999) *Tect.phys.*, **310**, 1-35. [6] Helmstaedt (2009) *9IKC Proc.*, 1055-1068. [7] Poudjom Djomani *et al.* (2003) *Geochem. Geophys. Geosyst.*, **4**, No.7, 1066. [8] Rosen (2002) *Rus. J. of Earth Sci.*, **4**, No.2, 103–119.

https://doi.org/10.1180/S0026461X00006502 Published online by Cambridge University Press

Dynamical constraints on mantle reservoirs through time

G. F. DAVIES

Research School of Earth Sciences, Australian National University, Canberra ACT 0200, Australia (Geoff.Davies@anu.edu.au)

It is now generally accepted that Earth formed hot, due particularly to a giant, moon-forming impact late in accretion. A resulting magma ocean probably cooled on a geologically short timescale, and may not have left a strongly differentiated mantle, due to vigorous internal mixing, except possibly in the D" region. Loss of excess initial mantle heat would have taken ~0.5 Gyr. Core cooling is controlled by mantle plumes and may always have been slow. Plume activity may have been 2-8 times stronger during the Hadean and early Archean.

The Earth's surface would have cooled early, soon after the last giant impact (~4.45 Ga?). An active mantle would be expected to produce mafic crust at a substantial rate, and this may have tended to founder episodically, possibly in large bodies. Conceivably some of these persist in D".

Gravitational settling of foundered or subducted mafic crust could have left the upper mantle strongly depleted, explaining isotopic evidence of stronger early depletion of incompatible elements. This upper mantle would produce only a thin mafic crust, which would facilitate an early start to plate tectonics and efficient cooling of the mantle.

A 'basalt barrier' may have formed within the transition zone, yielding a cool upper mantle and a hot lower mantle. Episodic breakdown and overturn of this stratified mantle during the first 1-2 Gyr could have volcanically resurfaced much of the planet.

An accumulation of denser mafic material in D" probably formed early. This persists strongly to the present, though it might not be able to form now. It could retain a record of major melting events from throughout Earth history.

No other mantle stratification is plausible at present. A putative thick layer in the lower mantle should produce mantle plumes several times stronger than what is observed, so it is unlikely.

Lithologic heterogeneity of the mantle probably formed early from foundering differentiated material. Much of the mantle complement of incompatible elements may be carried in hybrid pyroxenite, formed by reaction of melt from mafic inclusions with surrounding peridotite. Noble gases plausibly persist from the early Earth in this material, and the present mantle complement of incompatibles may be 2-3 times previous estimates, whose assumptions make them lower bounds.

Dynamical geochemistry

G.F. DAVIES

Research School of Earth Sciences, Australian National University, Canberra ACT 0200, Australia (Geoff.Davies@anu.edu.au)

Despite progress in reconciling important aspects of mantle chemistry with dynamics, mass balances of key elements and observations of noble gases have remained enigmatic. Resolution may follow from taking fuller account of the lithological heterogeneity of the mantle [1].

The Hofmann-White-Christensen reconciliation of refractory trace elements and their isotopes with the dynamical mantle has been strengthened by work over the past decade. The apparent age of lead isotopes and the broad refractory-element differences among and between ocean island basalts (OIBs) and mid-ocean ridge basalts (MORBs) can now be quantitatively accounted for with some assurance.

Noble gases may reside in a so-called *hybrid pyroxenite* assemblage that is the result of melt from fusible pods reacting with surrounding refractory peridotite and refreezing. Hybrid pyroxenite that rises off-axis may not remelt and erupt at MORs, so its volatile constituents would recirculate within the mantle. Hybrid pyroxenite is likely to be denser than average mantle, and thus some would tend to settle in the D" zone at the base of the mantle, along with some old subducted oceanic crust. Residence times in D" are longer, so the hybrid pyroxenite there would be less degassed. Plumes would sample both the degassed, enriched old oceanic crust and the gassy, moderately enriched hybrid pyroxenite and deliver them to OIBs. This model can account quantitatively for the main He, Ne and Ar isotopic observations, and for the poor correlation of unradiogenic gases with refractory-element enrichment in OIBs.

The difficulty with mass balances can be traced to the common inference that the MORB source is strongly depleted of incompatible elements. However conventional estimates focus on an ill-defined "depleted" mantle component while neglecting less common enriched components. Recent estimates have also been tied to the composition of peridotites, but these probably do not reflect the full complement of incompatible elements in the heterogeneous mantle. New estimates that account for enriched mantle components can satisfy mass balance requirements, although some additional uncertainties apply to argon. The result is that the MORB source is depleted by only about a factor of 2, relative to the primitive Earth.

[1] G. F. Davies, (2011) *Dynamical geochemistry of the mantle, Solid Earth Discuss.*, **3**, 249-333, www.solid-earth-discuss.net/3/249/2011/

https://doi.org/10.1180/S0026461X00006502 Published online by Cambridge University Press

Approaching the final frontier in lateral resolution for isotopic and chemical analysis with CHILI

A.M. DAVIS[1,2,3]*, T. STEPHAN[1,2], M.J. PELLIN[1,2,3,4], M.R. SAVINA[1,4], I.V. VERYOVKIN[1,4], R. YOKOCHI[1,2], R. TRAPPITSCH[1,2], N. LIU[1,2], A.J. KING[1,2]

[1]Chicago Center for Cosmochemistry
[2]Dept. of Geophysical Sciences, Univ. of Chicago, Chicago, IL 60637 (*correspondence: a-davis@uchicago.edu)
[3]Enrico Fermi Inst., Univ. of Chicago, Chicago, IL 60637
[4]Materials Science Div., Argonne National Laboratory, Argonne, IL 60439

There is a clear need for improvements in lateral resolution and sensitivity beyond what is available with current state-of-the-art secondary ion mass spectrometry (SIMS) instruments. SIMS lateral resolution has reached ~50 nm and useful yields are at most a few percent. We are completing construction of CHILI (the CHicago Instrument for Laser Ionization), a resonant ionization mass spectrometry (RIMS) nanobeam instrument designed for isotopic and chemical analysis at the few-nm scale with a useful yield of 35–50% [1]. CHILI is equipped with a COBRA-FIB high resolution liquid metal ion gun (LMIG) and an e⁻CLIPSE Plus field emission electron gun from Orsay Physics, each of which can be focused to <4 nm. The electron gun will be used for secondary electron imaging, as the built-in optical microscope is diffraction-limited to ~0.5 μm. A piezoelectric stage capable of reproducible nm-scale motions and equipped with a sample holder that will accept a wide variety of sample mounts is operational. The flight tube for the time-of-flight mass spectrometer mounted vertically above the sample chamber; this assembly is mounted in the center of an H-shaped laser table equipped with active vibration cancellation devices. The table has been demonstrated to have a vertical vibrational amplitude of less than 0.2 nm. Resonant ionization will be done with six Ti:sapphire tunable solid state lasers pumped with three 40W Nd:YLF lasers, which will allow two to three elements to be analyzed simultaneously. Ion detection in existing RIMS instruments [2,3] is done with a microchannel plate with a single anode. Isotope ratio precision is limited by counting statistics, as no more than one ion of the most abundant isotope of an element can be counted for each pulse. CHILI will initially be equipped with such a detector, but we are developing a multianode detector to significantly improve the count-rate capability.

[1] Stephan *et al*. (2011) *LPS* **42**, #1995. [2] Savina *et al*. (2003) *GCA* **67**, 3215. [3] Veryovkin *et al*. (2008) *LPS* **39**, #2396.

Partitioning of first-row transition elements between peridotite and melt

FRED A. DAVIS[1]*, MUNIR HUMAYUN[2], MARC M. HIRSCHMANN[1] AND RUPERT S. COOPER[1]

[1]Dept. Of Earth Sciences, Univ. Of Minnesota, Minneapolis, MN 55455, USA (*correspondence: davis957@umn.edu)
[2]Dept. of Earth, Ocean, & Atmospheric Science, and National High Magnetic Field Laboratory, Florida State University, Tallahassee, FL 32310-4100, USA

To constrain possible lithologies in source regions of OIB [1-3], we experimentally determined partitioning of first-row transition elements (FRTE), Ga, and Ge between minerals in garnet peridotite and near-solidus partial melt at 3 GPa using LA-ICP-MS. K_D^{Mn-Fe} between peridotite and melt is ~1, so low-degree partial melts of peridotite inherit Fe/Mn of their source, similar to the results of previous studies [1]. K_D^{Zn-Fe} between peridotite and melt is 0.80, lower than previously determined from intermineral partitioning in natural peridotites (0.85-1) [3], primarily due to a lower measured K_D^{Zn-Fe} for opx (0.77 rather than 0.96). Most peridotite xenoliths have $(Zn/Fe)*10^4$ from 4-12 [4], thus partial melts of peridotite may have $(Zn/Fe)*10^4$ ratios as great as 15. Most primitive OIB have $(Zn/Fe)*10^4$ from 10-15 [4], so derivation from a peridotite source can only be ruled out for a very few OIB lavas based solely on Zn/Fe. A fertile peridotite with 0.2 wt.% TiO_2 can generate a near-solidus melt with ~3.3% TiO_2. OIB with >3.3% TiO_2 require a non-peridotite or metasomatized source.

D_{Sc}	D_{Ti}	D_V	D_{Cr}	D_{Mn}
0.86	0.062	0.65	4.1	0.81
D_{Fe}	D_{Co}	D_{Zn}	D_{Ga}	D_{Ge}
0.81	1.8	0.65	0.15	0.71

Table 1: Bulk perid./melt partition coefficients averaged from four experiments (assumed mineral mode: 60.8% olivine, 7.7% opx, 22.6% cpx, 8.9% garnet).

[1] Humayun *et al*. (2004) *Science* **306**, 91-94. [2] Sobolev *et al*. (2005) *Nature* **434**, 590-597. [3] Le Roux *et al*. (2010) *Geochim Cosmochi. Acta* **74**, 2779-2796. [4] GEOROC database (http://georoc.mpch-mainz.gwdg.de/georoc/, accessed: 4/13/2011).

https://doi.org/10.1180/S0026461X00006502 Published online by Cambridge University Press

A coupled ion exchange, surface complexation, calcite dissolution, and mass transfer model to describe uranium(VI) desorption and reactive transport at the Rifle (USA) field site

J.A. DAVIS[1]*, M. HAY[2], P.M. FOX[1] AND K. WILLIAMS[1]

[1]Lawrence Berkeley National Laboratory, Berkeley, CA, 94720, USA (*correspondence: jadavis@lbl.gov)
[2]U. S. Geological Survey, Menlo Park, CA 94025, USA (mbhay@usgs.gov)

Predicting uranium mobility in the subsurface requires detailed knowledge of geochemical processes controlling the sorption dynamics of U(VI). This is a particular challenge in cases where aqueous solution conditions are highly variable. Desorption of U(VI) from mineral surfaces is strongly dependent on aqueous chemistry (e.g., pH, HCO_3 and Ca concentrations). Further, kinetic processes such as intragranular diffusion affecting U(VI) desorption equilibrium may become increasingly important under conditions where changing solution chemistry causes relatively steep U(VI) concentration gradients.

In this research we have quantified the effects of aquifer sediment properties on the transport dynamics of U(VI) under variable chemical conditions and developed a reactive transport model that can be applied to field settings. An ion exchange model was calibrated first in experiments conducted with the aquifer sediment <2 mm fraction with calcite removed. This was then applied in combination with a surface complexation model to describe U(VI) transport in laboratory columns. Chemical conditions within the columns were varied through the injection of influent solutions with differing pH, bicarbonate, and major ion concentrations. Initial conditions within the columns were impacted by slow calcite dissolution. Stopflow events during column elution demonstrated U(VI) desorption was not at local equilibrium, and U(VI) elution data were used to calibrate a distributed rate mass transfer model for U(VI) desorption, at flow rates and alkalinity concentrations relevant to the Rifle site. Oversaturation with respect to calcite was observed in this column experiment and in the Rifle aquifer. In a column experiment with high influent bicarbonate, calcite oversaturation exceeded one order of magnitude, suggesting calcite nucleation and precipitation and U(VI) co-precipitation within the column. The model was successfully applied to describe field injection experiments after correction for local surface sediment properties (surface area, ion exchange capacity, and initial adsorbed U(VI)).

Geochemistry of granites from magmatic-metamorphic complex of Boein-Miandasht, Sanandaj-Sirjan Zone, Iran

A.R. DAVOUDIAN[1]*, N. SHABANIAN[1] AND F. PANAHDAR[2]

[1]Faculty of Natural Resources and Earth Sciences, Shahrekord University, Shahrekord, Iran (*correspondence: alireza.davoudian@gmail.com)
[2]Islamic Azad University- Khorasgan Branch, Isfahan, Iran

Geological Setting and sample description

The granitic plutons crop out the north of the Boein – Miandasht city: they intruded into the metamorphic rocks. Various ages have been assigned to the metamorphic complex: Precambrian [1], Paleozoic and Mesozoic [2]. Metamorphic rocks in the study area comprise phyllite, mica schist, amphibolite, marble and meta-rhyolite with minor quartzite. Alkali granite is the major rock type in the plutons. It is composed of quartz, K- feldspar, plagioclase, biotite, amphibole, epidote, allanite, zircon, sphene, magnetite, tourmaline and apatite.

Discussion and Results

The granites have contents of SiO_2, ranging from 68.7 to 73.3%. They have high alkalis, with K_2O= 2.3 to 5.01% and Na_2O =3.75 to 5.0%, but low Fe_2O_3 (0.8 - 1.7%), FeO (1.1-1.9%), MnO (<0.1%), MgO (0.4-0.7%), CaO (0.9-1.8%), TiO_2 (0.3-0.5%) and P_2O_5 (0.1-0.2%). Al_2O_3 ranges from 13.8% to 14.9%.

Similarly the trace element compositions exhibit significant variations, particularly in the case of Rb (146.7–212.8 ppm), Y (32.1–40.2 ppm), Sr (65.3–153.0 ppm), Ba (400–633ppm), Ga (18.0-20.0 ppm) and high field-strength elements (HFSE) (Nb: 15.6–27.4 ppm; Ta: 1.5– 2.4ppm; Zr: 184.3–346.0 ppm; Hf: 5.2–10.1 ppm). The granites displays the characteristics of A-type grnitoids. According to a geochemical classification scheme for granitoids, proposed by Frost *et al*. [3], the granitic rocks belong to ferroan, alkali-calcic, mildly peraluminous granites. The plot of Zr + Nb + Ce + Y vs. 10000*Ga/Al suggest an A-type to fractionated granites character for the rocks. The granites show A2 field on ternary diagrams from Eby [4].

[1] Thiele *et al*. (1968) *G.S.I*. [2] Mohajjel *et al*. (2003) *J. Asian Earth Sci*. **21**, 397-412. [3] Frost *et al*.(2001) *J. of Petrology* **42**, 2033–2048. [4] Eby (1992) *Geol*. **20**, 641–644.

https://doi.org/10.1180/S0026461X00006502 Published online by Cambridge University Press

Molecular characterization of archaeal lipids across a hypersaline gradient

K.S. DAWSON*, K.H. FREEMAN AND J.L. MACALADY

Dept. of Geosciences, Pennsylvania State Univ., University Park, PA 16802, USA
(*correspondence: katsdawson@psu.edu)

Four halophilic archaeal strains, *H. utahensis, N. pharaonis, H. sulfurifontis* and *H. gomorrense*, were grown at a range of salinities (10-30% NaCl, (w/v)). These strains represent four archaeal genera and have a range of salinity optima. Molecular analysis of membrane lipids in each strain by GC-MS revealed structures consistent with saturated, unsaturated and polyunsaturated dialkyl glycerol diethers (DGDs) of both phytanyl (C_{20}) and sesterpanyl (C_{25}) isoprenoid chains. In addition, we observed three trends: (1) the percentage of unsaturated DGDs increased with increasing NaCl concentration in the growth medium; (2) strains with a higher optimal NaCl concentration had a higher percentage of unsaturated DGDs; and (3) $C_{25\text{-}20}$ DGDs occurred in the two strains with higher optimal NaCl concentrations, *N. pharaonsis* and *H. utahensis*. The strong linear correlation between optimal growth salinity and the amount of unsaturated DGDs (Fig. 1) suggests that the degree of membrane lipid unsaturation is an important adaptation to specific salinity niches in archaeal halophiles. In addition, in three of the four halophile strains we tested, the fraction of unsaturated DGDs increased above a salinity threshold or in response to increasing salinity in the growth medium. Thus, halophilic archaea may regulate membrane lipid unsaturation in response to environmental salinity changes regardless of their salinity optima.

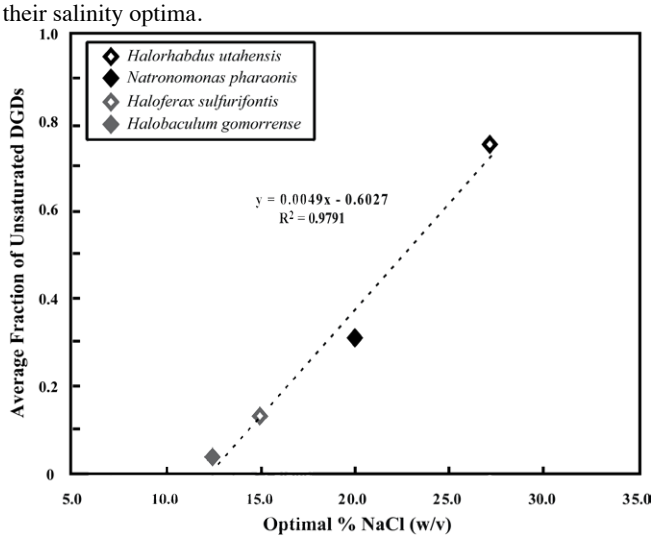

Figure 1: Average fraction of unsaturated DGDs versus optimal % NaCl (w/v) for four halophilic archaeal strains.

O and Ca isotopes in calcite grown under cave-analogue conditions

C.C. DAY[1]*, L.M. REYNARD[2], M.D. POINTING[1], C.L. BLÄTTLER[1] AND G.M. HENDERSON[1]

[1]Department of Earth Sciences, University of Oxford, UK, (*correspondence: chris.day@earth.ox.ac.uk)
[2]Institute of Archaeology, University of Oxford, UK

Speleothem oxygen isotopes and growth rates are valuable proxies for reconstructing climate history. However, oxygen isotopes and growth rate are controlled by diverse environmental variables (including the climatically important variables rainfall and temperature) and there is a paucity of laboratory experiments to quantify the influence of these variables on speleothem chemistry. Quantitative data from such studies would dramatically improve our ability to reconstruct palaeoclimate from stalagmites.

We have completed a new series of carbonate growth-experiments in karst-analogue conditions in the laboratory [1,4]. The setup closely mimics natural processes (e.g. precipitation driven by CO_2-degassing, low ionic strength solution, thin solution film) but with a tight control on growth conditions (temperature, pCO_2, drip rate, calcite saturation index and the composition of the initial solution).

We derive a relationship between growth mass, temperature and drip rate, whilst in a more qualitative sense we observe a wider diameter of calcite growth with increased drip rate. $\delta^{18}O$ results show that speleothem growth from fast dripping, cold settings are most favourable for palaeoclimate work. $\delta^{18}O$ and $\delta^{44/42}Ca$ provide important insight into the mechanisms of stable isotope fractionation in speleothems, which we discuss in the context of surface entrapment controlling Ca and O isotopic fractionation [2, 3].
Collectively, these experiments therefore provide a more robust understanding of the way that stalagmite carbonate responds to climatically important environmental variables.

[1] Day C.C. and Henderson G.M., *Geochim. Cosmochim. Acta* in review. [2] DePaolo D.J. (2011), *Geochim. Cosmochim. Acta* **75**, 1039-1056 [3] Dietzel *et al.* (2009), *Chem. Geol.* **268**, 107-115 [4] Reynard. L.M. *et al. Geochim. Cosmochim. Acta* in press

https://doi.org/10.1180/S0026461X00006502 Published online by Cambridge University Press

^{186}Os-^{187}Os and highly siderophile element abundance systematics of Earth's upper mantle

J.M.D. DAY[1,2], J.M. WARREN[3] AND R.J. WALKER[2]

[1]Geosci. Res. Div., Scripps Institution of Oceanography, La Jolla, CA 92093-0244 (jmdday@ucsd.edu)
[2]Dept. Geol., Univ. Maryland, College Park, MD 20742
[3]Dept. Geol. Env. Sci., Stanford University, CA 94305

Osmium isotope and highly siderophile element (HSE) abundance systematics of abyssal peridotites may provide new constraints for interpreting isotopic and elemental signatures preserved in terrestrial lavas, as well as for deciphering melt depletion and recycling in the convecting mantle. Here we report new high-precision ^{186,187}Os/^{188}Os isotope and HSE abundance data for bulk samples of abyssal peridotites from the Arctic (Gakkel), Indian (central [CIR] and southwest [SWIR]), and Atlantic (Kane) ridges.

Peridotites from the global suite range from relatively fresh to serpentinized harzburgites and lherzolites, with no systematic variation observed for HSE abundances or ^{186,187}Os/^{188}Os with alteration. Average HSE abundances of different ridge segments are broadly similar (0.007±2 × CI-chondrite). The HSE are in approximately chondritic-relative abundances, although all ridges studied have supra-chondritic Ru/Ir (Kane = 1.4±0.2; Gakkel = 1.6±0.6; SWIR = 1.5±0.3; CIR = 1.4±0.1), similar to estimates for primitive upper mantle (PUM). Unlike PUM, there is no systematic supra-chondritic Pd/Os in SWIR, CIR, or the majority of Gakkel peridotites. There is greater HSE abundance variability in ultra-slow spreading Gakkel, versus Indian or Atlantic peridotites. Abyssal peridotites analyzed in this study have ^{187}Os/^{188}Os ratios ranging from 0.1217 to 0.1587. The ^{186}Os/^{188}Os of SWIR peridotites (0.1198385±4), which were affected by the Bouvet hotspot at ~20Ma, are, on average, higher than for CIR (0.1198360±5), Kane (0.1198353±7 [1]), and Gakkel peridotites (0.1198332±6). SWIR show a general positive correlation for ^{187}Os/^{188}Os-^{186}Os/^{188}Os, but no other correlations are observed between these ratios in the dataset. If CIR, Kane and Gakkel peridotites are representive of convecting upper mantle, then this reservoir has evolved with a long-term Pt/Os that is well within the range of chondrites. In contrast, SWIR peridotites derive from a mantle source with higher Pt/Os. If SWIR ^{186}Os/^{188}Os values relate to high time-integrated Pt/Os, how this signature is transferred from the hotspot to the peridotites is unclear. Lack of correlation between Pt/Os and ^{186}Os/^{188}Os for the suites suggests abyssal peridotites do not record absolute and relative abundances of the HSE in the convecting upper mantle with high fidelity.

Metasomatism beneath the Kerguelen Plateau associated with heterogeneous mantle plume

V. DEBAILLE[1]*, G. HUBLET[1], N. MATTIELLI[1] AND D. WEIS[2]

[1]DSTE, Université Libre de Bruxelles, Brussels, Belgium. (*correspondence: vinciane.debaille@ulb.ac.be)
[2]PCIGR, University of British Columbia, Vancouver, Canada

The Kerguelen Plateau, in the Southern part of the Indian Ocean, represents the second largest igneous province on Earth. Its main emerging feature is the Kerguelen Archipelago, located in the Northern part of the plateau (NKP). Basic and ultrabasic xenoliths are commonly found disseminated within alkaline lava series, especially in the Southern and South-East part of the archipelago. The xenoliths were formed in PT conditions generally comprised between 0.75 to 1.6 GPa and 880 to 1010°C, corresponding to lithospheric conditions [1]. The xenoliths thus provide a unique opportunity to understand the processes that occurred during the construction of the NKP.

While there is no evidence for contamination of the xenoliths from their host lavas during their ascent, the xenoliths are metasomatized, as showed by the presence of both silicate and carbonate melt inclusions [2], and enrichment in incompatible trace elements [1]. In light of the comparable isotopic signatures for the Kerguelen alkaline volcanism and the xenoliths, the origin of this metasomatism, both silicate and carbonatitic-silicate melts, seems related to the Kerguelen Mantle Plume itself [3]. Using various types of xenoliths, we show here that (i) the metasomatism event is ~40 million years old, corresponding to the onset of the interaction between the South-East Indian Ridge and the Kerguelen mantle plume [4], and (ii) the two metasomatic melts can be distinguished using both trace element and isotope ratios. As such, xenoliths metasomatized by carbonatitic-silicate melts have $(Sm/Yb)_N$ > 1, and ^{206}Pb/^{204}Pb < 18.200. Using Nd, Hf and Pb isotope ratios, xenoliths metasomatized by carbonatitic-silicate melts show a stronger affinity with the EM-I component, while the one metasomatized by silicate melts are closer of the EM-II component. This suggests that the carbonatitic-silicate and silicate melts do not initially originate from a homogeneous source that later separated due to immiscibility at shallow depths between silicate and carbonatitic melts, but instead reflect the heterogeneity of the Kerguelen mantle plume.

[1] Grégoire *et al*. 1994 *Nature* **367**, 360-363. [2] Schiano *et al*. 1994 *Earth Planet. Sci. Lett*. **123**, 167-178. [3] Mattielli *et al*. 1999 *J. Petrol*. **40**, 1721-1744. [4] Doucet *et al*. 2002 *J. Petrol*. **43**, 1341-1366.

https://doi.org/10.1180/S0026461X00006502 Published online by Cambridge University Press

Borosilicate glass alteration driven by magnesium carbonates

M. DEBURE[1,2], P. FRUGIER[1], L. DE WINDT[2] AND S. GIN[1]

[1]CEA Marcoule, DTCD/SECM/LCLT, BP 17171, 30207 Bagnols-sur-Cèze Cedex, France (mathieu.debure@cea.fr; pierre.frugier@cea.fr)
[2]Geosciences Dept., Mines-ParisTech, 35 Rue St-Honoré, 77305 Fontainebleau, France (laurent.de_windt@mines-paristech.fr)

Multi solid interactions: experiment and modeling

Geochemical modeling of glass and silicate mineral alteration is a major challenge for understanding natural processes in the earth sciences (e.g. chemical compositions of natural waters and oceans...). In confined media, solids reactivity quickly controls solution compositions. The alteration of a simplified synthetic glass, representative of the French reference nuclear glass in the presence of a simple Mg-bearing phase is a key step towards the understanding of the interactions between nuclear glass and nearfield materials in geological repository. Indeed, magnesium in solution is one of the elements known to potentially enhance glass alteration. In a first study, hydromagnesite was chosen as the simplest and as the most reactive Mg bearing carbonate.

Experiments were performed in closed system at 90°C and characterized by SEM, XRD and TofSIMS. They revealed that glass alteration is enhanced in presence of hydromagnesite at 90°C.

Geochemical modeling was performed using the GRAAL model [1] implemented within the CHESS/HYTEC reactive transport code. The model was efficient enough for quantifying the amount of present solids, the pH and the elements concentration with time whatever the glass/hydromagnesite ratio.

Future experimental and modeling work will concern more representative solids, like dolomite and smectites.

[1] P. Frugier *et al*., (2009) *Journal of Nuclear Materials* **392** 552-567.

Carbonation of forsterite and serpentine: Modeling the optimum conditions in terms of pH and temperature

JULIEN DECLERCQ AND ERIC OELKERS

14 Av. Edouard Belin 31400 Toulouse, France; (declercq@get.obs-mip.fr, oelkers@get.obs-mip.fr)

Carbonation of forsterite into magnesite and quartz following the reaction:

$$Mg_2SiO_4 + 2CO_2 \rightarrow 2MgCO_3 + SiO_2$$

has been assumed in a plethora of studies. However the consumption of metals by the formation of secondary phases has been overlooked.

In this study we intent to shed some light and define the conditions of successful carbonation experiments and industrial CO_2 mineralization projects in terms of pH and temperature. In order to minimize the precipitation of secondary phases we have mapped out the thermodynamic stability of magnesite relative to mineral phases like antigorite and brucite from 25 to 200°C, a pH ranging from 4 to 8 and 10 bars of CO_2 and performed both closed system batch simulations and kinetic simulation of the carbonation of forsterite and serpentine using the kinetics expressions and data available in the literature.

The results illustrate several important constrains on the formation of magnesite or serpentine. A key role in the reaction process is played by the temperature, due to the lowering reaction rates below 100°C where both magnesite and quartz fail to precipitate;whereas at temperatures greater than 200°C the overall forsterite to magnesite reaction is thermodynamically unstable. Furthermore, the pH effect cannot be ignored, as at pH below 4 the magnesite is extremely soluble and will not precipitate whereas at pH above 9 brucite is becoming the dominant precipitating phase, thus it is unlikely that carbonation will occur.

https://doi.org/10.1180/S0026461X00006502 Published online by Cambridge University Press

SIMS U-Pb ages for heterogenite from Katanga (DRC): Implications for the genesis of Co-U deposits in Shinkolobwe

S. DECRÉE[1]*, É. DELOULE[2], T. DE PUTTER[1], S. DEWAELE[1], F. MEES[1] AND C. MARIGNAC[3]

[1]Royal Museum for Central Africa, B-3080 Tervuren, Belgium (*correspondence: sophie.decree@africamuseum.be)
[2]CRPG/CNRS, F-54501 Nancy, France
[3]UMR-G2R CREGU & Ecole des Mines de Nancy, Nancy, France

Heterogenite (CoOOH) deposits are the most abundant Co ore in the Katanga Copperbelt (DRCongo), which hosts world-class Co deposits accounting for ~50% of the world's reserves [1]. Most of the heterogenite deposits occur in the upper oxidized zone of the primary deposits, and were formed during a Mio-Pliocene major uplift and weathering episode [2]. However, U-rich heterogenite, present in deeper zones of several deposits, may have a different origin and age.

Assuming that U in this heterogenite is in the UO_2 form, we attempted to obtain *in situ* U-Pb ages for heterogenite samples from Shinkolobwe, using a Cameca IMS 1270 ion microprobe, with settings comparable to those used for standard U-Pb age measurements on uraninite. These analyses yield two distinct Neoproterozoic ages, recorded by the upper intercept of the concordia lines: 680.9 ± 7.4 Ma and 823.2 ± 2.2 Ma. In both cases, the lower intercepts provide imprecise near-zero ages indicating recent (or continuous) Pb loss from the heterogenite.

At the present stage of knowledge, the 823 Ma date cannot easily be related to a known oxidizing event in the area. It is, however, reasonably close to the 816 ± 62 Ma Re-Os age obtained for Zambian primary sulfides [3]. The 681 Ma date could correspond to the Nguba karstification/weathering event described for the area [4]. If our age is meaningful, heterogenite could have formed in a period of superficial weathering, during the formation of the Katanga basin. This supergene event would, however, be contemporaneous with significant precipitation/reconcentration of uraninite, since the oldest uraninite age obtained for the Shinkolobwe deposits (at 652.3 ± 7.3 Ma) overlaps with ages for heterogenite in $^{207}Pb/^{206}Pb$ age density diagrams.

At this stage, the present study does not allow a full understanding of the timing and conditions of Co and U mineralization in Katanga. The results, however, indicate the importance of acquiring additional ages for heterogenite-uraninite deposits in order to understand the genesis of these giant Co-Cu-U ore deposits.

[1] USGS (2009) *Mineral Commodity Summaries 2009*, p. 195. [2] Decrée *et al*. (2010) *Min. Dep*. **45**, 621-629. [3] Selley *et al*. (2005) *Econ. Geol*. **100th anniversary volume**, 965-1000. [4] Buffard (1993) *Karstologia* **21**, 51-55.

Chemical limits of trace elements in pyrite

ARTUR P. DEDITIUS[1], STEPHEN E. KESLER[2], MARTIN REICH[3,4], SATOSHI UTSUNOMIYA[5] AND RODNEY C. EWING[2]

[1]Institute of Appplied Geosciences, Graz University of Technology, Rechbauerstrasse 12, 8010 Graz, Austria
[2]Department of Geological Sciences, University of Michigan, 1100 N. University Ave., Ann Arbor, MI, USA
[3]Department of Geology, Universidad de Chile, Santiago, Chile
[4]Andean Geothermal Center of Excellence, Universidad de Chile, Santiago, Chile
[5]Department of Chemistry, Kyushu University, Hakozaki 6-10-1, Fukuoka-Shi, 812-8581, Japan

Pyrite in magmatic-hydrothermal settings contains significant concentrations of trace elements of economic and environmental importance, including Ag, As, Au, Bi, Cd, Co, Cu, Hg, Ni, Pb, Sb, Se, Te, Tl and Zn, which reflect the availability (solubility) of these elements in their parent hudrothermal solution. A review of our own and published analyses (including EMPA, SIMS, LA-ICP-MS, PIXE and HRTEM) of pyrite from Carlin-type, epithermal, and orogenic gold deposits reveals positive correlations for Sb-Pb-Bi, Au-Ag-Te, and Cu-Ag-Sb in all samples. Element-element ratios for most analyzed pyrites are: Au/Ag – 0.8-1.1, Au/Te – 0.8 to 1.0, Au/Sb – 0.7 to 1.1, Te/Pb – <1.1, Sb/Pb – 0.9-1.1, Sb/Cu – <1.0, Ag/Pb – 0.8-1.1, Bi/Pb – 1.0-0.7, and Bi/Sb – 0.7-1.1 in all types of deposits. Silver is enriched with respect to Te in low-T deposits, which have relatively high Ag/Te ratios of 1.0-1.2. Previous work has shown that As facilitates the incorporation of Au into pyrite via structural distortion and charge imbalance and that the Au content of pyrite is related to its As content such that the maximum Au content is $C_{Au} = 0.02C_{As} + 4 \cdot 10^{-5}$. Pyrite with Au-As contents above this maximum contain nano-inclusions of Au. These relations apply to epithermal and Carlin-type deposits, which form at relatively low temperatures. Au-As relations in pyrites from orogenic gold and skarn deposits, which form at higher temperatures, show similar relations but with smaller amounts of Au for any specfic As content, suggesting that the solubility of Au in pyrite (as a function of As) decreases with increasing temperature. Arsenic also appears to facilitate incorporation of Ag, Te, Sb, Bi and Hg into the pyrite structure in the same mode as for gold, although analyses are not sufficient to establish specific solubility limits. Samples with contents of these elements that exceed the apparent solubility limits contain nanoparticulate sulfides and sulfosalts in distorted, polycrystalline areas of pyrite.

https://doi.org/10.1180/S0026461X00006502 Published online by Cambridge University Press

Boron isotope systematics during magma-carbonate interaction

F.M. DEEGAN[1], E.M. JOLIS[1], V.R. TROLL[1,2], C. FREDA[2] AND M.J. WHITEHOUSE[3]

[1]Dept. Earth Sci. (CEMPEG), Uppsala University, Uppsala, Sweden. (Frances.Deegan@geo.uu.se)
[2]Istituto Nazionale di Geofisica e Vulcanologia, Rome, Italy
[3]Swedish Museum of Natural History, Stockholm, Sweden

Carbonate assimilation is increasingly recognised as an important process affecting the compositional evolution of magma and its inherent ability to erupt explosively due to release of carbonate-derived CO_2 [e.g., 1, 2, 3]. In order to gain insights into this process, we performed short time-scale carbonate dissolution experiments in silicate melt using natural starting materials from Merapi and Vesuvius volcanoes at magmatic pressure and temperature [1, 4]. The experiments enable us to resolve in detail the timescales, textures and chemical features of carbonate assimilation. Three compositionally distinct glass domains have been defined: i) Ca-normal glass, similar in composition to the starting material; ii) Ca-rich, contaminated glass; and iii) a diffusional glass interface between the Ca-normal and Ca-rich glass. Here we present new boron isotope data for the experimental products obtained by SIMS. The glasses show distinct and systematic variation in their $\delta^{11}B$ values. The contaminated regions generally show extremely negative $\delta^{11}B$ values (down to -41 ‰) relative to fresh arc volcanics (-7 to +7 ‰ [5]). Considering that carbonates have $\delta^{11}B$ values of +9 to +26 [6], the data can not be explained by simple mixing processes between the end-members alone. This implies that the $\delta^{11}B$ of the original contaminant was drastically modified before being incorporated into the melt, which can be explained by B isotope fractionation during early degassing of the carbonate. Our preliminary results are the first of their kind and provide well constrained insights into the behaviour of boron upon degassing of carbonate. This in turn has implications for both late stage contamination in dangerous volcanic systems and deep subduction zone processes, where B is frequently employed as a tracer of crustal recycling.

[1] Chadwick *et al*. (2007) *J. Petrol*. **48**, 1793-1812. [2] Deegan *et al*. (2010) *J. Petrol*. **51**, 1027-1051. [3] Freda *et al*. (2010) *Bull. Volcanol*. DOI: 10.1007/s00445-010-0406-3 [4] Jolis *et al*. (2011) *Min. Mag*., this volume. [5] Leeman & Sisson (1996) *Rev. Min*. **33**, 645-707 [6] Ishikawa & Nakamura (1993) *Earth Planet Sci. Lett*. **117**, 567-580.

Alteration of nitrogen isotopic signatures during phytoplankton degradation

A. DEEK[1]* , M. F. LEHMANN[1] AND C. J. SCHUBERT[2]

[1]University of Basel, Insitute of Environmental Geosciences, Bernoullilstr. 30, CH-4056 Basel, Switzerland (*correspondence: astrid.deek@unibas.ch)
[2] Eawag, SURF, CH-6047 Kastanienbaum, Switzerland

Stable nitrogen isotope ratios in sediments are widely used in paleoenvironmental studies to reconstruct past biogeochemical conditions and processes in the water column. Previous investigations have revealed that both the decay of sinking particulate organic matter in the water column and early diagenesis of deposited organic matter within sediments are associated with significant bulk N isotope effects that can mask primary isotope signals.

To study the mechanisms that underly the alteration of N isotope signals by bacterial degradation, we conducted a series of oxic and anoxic incubation experiments that mimic the decay of organic matter in nature. We used closed system experiments containing defined algae/sediment mixtures (*Chlorella vulgaris*), suspended in oxic or anoxic water from Lake Lugano, and inoculated with a natural consortia of bacteria. In order to assess N isotope partitioning during simulated organic matter decay, we monitored the N-isotope changes in specific organic (amino acids, amino sugars) and inorganic compounds (NH_4^+, NO_3^-) in both the particulate and dissolved fractions.

We will present initial data in the light of organic compound selectivity, kinetic isotope fractionation associated with degradation of specific organic components, and the effect of bacterial biosynthesis on bulk N isotope composition during early diagenesis.

https://doi.org/10.1180/S0026461X00006502 Published online by Cambridge University Press

Age and geochemical characteristics of the Malayer plutonic complex, West of Iran

R. DEEVSALAR[1*] AND V. AHADNEJAD[2]

[1]Tarbiat Modares University, Tehran, Iran (*Deevsalar@gmail.com)
[2]Payame Noor University, Tehran 19395-4697, Iran (v.ahadnejad@gmail.com)

The Malayer plutonic rocks (48° 35'-48° 54' E and 34° 03'-34° 20' N) are located in Sanandaj-Sirjan zone. The plutonic rocks in this region were attributed to active continental margin, and subduction of Neotethys under Iraninan micro-continet. Based on field observations and petrographic studies, this region can be divided into three major parts: Granitic, Granodioritic and Gabrodioritic. The isotopic studies have been shown that initial Sr ratios range from 0.70797 to 0.71087, $\varepsilon_{Nd(t)}$ from -2.3 to -4.9 and T_{DM} from 955 to 1.33 Ga. The $^{87}Sr/^{86}Sr_{(i)}$ and $\varepsilon_{Nd(t)}$ of the Malayer rocks are consistent with lower crust and oceanic sediments signatures. All felsic and intermediate samples regardless of their ages have a negative $\varepsilon_{Nd(t)}$ values and plot close together in $\varepsilon_{Nd(t)}$ vs $^{87}Sr/^{86}Sr(i)$ diagram and mid-Proterozoic depleted-mantle model ages, which shows a genetic link between them. These isotopic signatures, coupled with the presence of inherited zircon with Proterozoic and Paleozoic ages, suggest that these rocks are the products of crustal melting and crust-mantle interaction during arc magmatism along the active margin of Iranian micro-continet in the Middle-Jurassic. U-Pb dating for this rocks yielded data between 162 Ma and 187 Ma (Middle-Jurassic). With respect to similar state in adjacent regions of MPC in SSZ, has been suggested that in Middle Jurassic had been occurred extreme plutonism. Based on different geochemical evidences such as discordant variation pattern for some major and trace elements between felsic to intermediate rocks and mafic rocks to enclaves and from mafic to felsic rocks, high potassium calk-alkaline character of granitc rocks, enrichment of LILEs in comparison with HFSEs, constant variation of compatible elements such as V, Ni, and Cr in the differentiated phases, negative anomaly of Nb and Ta, and En negative anomaly, the main processes in formation of granitic are magmatic differentiation associated with crustal contamination and with respect to equivalent age of granite and diorite that indicate the contemporaneity of the granitic and basaltic magmas, magma mingling or mixing for diorites and magmatic enclaves. Negative anomaly of Eu, non-concordant REEs variations, low enrichment of LREEs in mafic rocks imply to plagioclase differentiation due to partial melting process. These may indicate partial melting of ultramafic source as responsible for generating of mafic rocks.

Origin and isotope composition of the radium content in highly saline fluids

D. DEGERING* AND M. KÖHLER

VKTA Kernverfahrenstechnik und Analytik Dresden, P.O. Box 510119, D-01314 Dresden, Germany (*correspondence: detlev.degering@vkta.de)

The occurrence of highly saline fluids is characteristic for several facilities in deep geothermal energy. These brines contain inter alia enhanced contents of the radium isotopes ^{226}Ra, ^{228}Ra and ^{224}Ra. Activity concentrations up to 50 Bq l^{-1} were observed for geothermal systems in Germany. Radium isotopes are accumulated in scales of the $Ba/SrSO_4$ type resulting in specific activities > 500 $Bq{\cdot}g^{-1}$ [1]. Such levels of natural radioactivity demand for the application of radiation protection meausures in the plant.

This phenomenon is not only limited to hydrothermal systems. Deep waters from rock aquifers can show salinities > 100 $g{\cdot}l^{-1}$, thus enhanced geothermal system (EGS) plants may also be faced with this problem.

Otherwise, the concentrations and the isotope ratios of these three radium isotopes with quite different half-lifes in the order of days until 10^3 years allow conclusions about origin and transport characteristics of the geothermal brines.

A detailed investigation of the radium release at the rock/fluid interface is necessary for the description of the source term of radium isotopes in hydrothermal brines. The α-recoil during the decay of the thorium precursors in the decay chains ($^{230}Th \rightarrow ^{226}Ra$, $^{232}Th \rightarrow ^{228}Ra$, $^{228}Th \rightarrow ^{224}Ra$) is considered as the dominating process in comparison to selective solution. Based on a range calculation for the recoil nuclei by the SRIM code [2], a model was developed that predicts the concentration of each radium isotope in the fluid. The crucial parameters according to this model are the U/Th-contents of the source material and its specific surface.

The model was tested on the well investigated aquifer system of the deep geothermal plant at Neustadt-Glewe, Germany. A good agreement between modelling and analytical results was obtained.

The radium concentration can be predicted for any aquifer type if its composition and structure are sufficiently known. Otherwise, the model may serve as a tool for clarifying the source of saline waters in hardrock systems.

[1] Degering, Köhler and Hielscher (2011), submitted to *Z. Geol. Wiss*. [2] Ziegler and Biersack (2006), *TRIM/SRIM, Version 2006.01*, www.srim.org

https://doi.org/10.1180/S0026461X00006502 Published online by Cambridge University Press

Correlations between Hf, O and trace element concentrations in zircon from rhyolitic rocks (NE German Basin)

E. DEJA[1]*, A. PIETRANIK[1], J. KIERCZAK[1], R. MILKE[2] AND C. BREITKREUZ[3]

[1]University of Wrocław, Institute of Geological Sciences, Poland; (elka_deja@yahoo.com)
[2]Freie Universität Berlin; (milke@zedat.fu-berlin.de)
[3]TU Bergakademie Freiberg, Germany; (cbreit@geo.tu-freiberg.de)

Hundreds of deep hydrocarbon exploration wells exposed the Late Paleozoic volcanic province in NE Germany, which covers the area 500 by 800 km^2 and comprises rhyolites (ca. 70%), andesites and basalts (ca. 30%) [1]. SHRIMP zircon emplacement ages of volcanic rocks in NE Germany range from 303 to 290 Ma with the major peak of the volcanic activity being 299 - 295 Ma [2,3].

The range of εHf and $\delta^{18}O$ values in these magmatic zircons in the three sites investigated have been modelled by simple assimilation - fractional crystallization processes of mantle derived magma contaminated by sediments with model ages of ca. 2.1 Ga.

Trace element composition of zircons do not correlate with the isotopic composition, but zircons from the least contaminated sample have different chemical characteristic to that of zircons from more contaminated samples. For example distribution of Hf is bimodal in the least contaminated sample, whereas Hf has intermediate values in the more contaminated ones. The implication is that the least contaminated sample contains zircons from various sources recording different stages of fractional crystallization, whereas more contaminated samples contain one population of zircons, probably crystallized from the surrounding magma.

Acknowledgements: The study was funded by the grant Iuventus Plus from the Polish Ministry of Science to AP.

[1] Benek *et al*. (1996) *Tectonophysics* **266**, 379–404. [2] Breitkreuz & Kennedy (1999) *Tectonophysics* **302**, 307–326. [3] Breikreuz *et al*. (2007) *Geol.Soc.Am - SP* **423**, 173-190.

Melts in the deep mantle: Insights from first principles molecular dynamics

NICO DE KOKER[1], LARS STIXRUDE[2] AND BIJAYA KARKI[3]

[1]Bayerisches Geoinstitut, Bayreuth, Germany, (nico.dekoker@uni-bayreuth.de)
[2]University College London, UK
[3]Louisiana State University, Baton Rouge, USA

As the primary medium through which planetary differentiation occurs, silicate melts are a key entity in the study of the thermal and chemical evolution of Earth. Over the past few years we have used first-principles molecular dynamics simulations to investigate the liquid state physics of the magnesio-, calsio- and aluminosilicate melts at pressure and temperature conditions relevant to the entire mantle. First-principles methods characterize bonding directly in terms of the electronic charge density computed via density functional theory, and is equally robust at ambient and extreme pressure and temperature conditions. This allows accurate predictions of the physics of melts at extreme conditions to be made.

Liquid state diffusion and thermodynamics have been investigated in detail, with special attention to dependence on pressure, temperature and composition. Comparison to corresponding changes in liquid structure enables us to understand thermodynamic and diffusive behavior in a detailed atomistic context. Our results provide a rigorous test for a new fundamental thermodynamic relation for melts, which we derived to accurately describe liquid state thermodynamics. The relation is unique in that it accounts for electronic free energy contributions and displays the correct limiting behavior at extreme volume and temperature, capturing the thermodynamics of liquid-vapor coexistence.

Our work has allowed for deeper insight into the evolution of terrestrial planets, including the thermal state and mode of crystallization of magma oceans, the possible presence of melt in the deep earth, and their relative buoyancy. This insight in turn acts as a guide for questions to be addressed in the future, as first-principles simulations of systems of larger numbers of atoms and complex chemical compositions representative of natural systems become feasible.

https://doi.org/10.1180/S0026461X00006502 Published online by Cambridge University Press

Ab initio study on lattice thermal conductivity of minerals

HARUHIKO DEKURA[1]*, TAKU TSUCHIYA[2] AND JUN TSUCHIYA[1]

[1]Senior Research Fellow Center, Ehime University, 2-5 Bunkyo-cho, Matsuyama, Ehime 790-8577, Japan (*correspondence: dekura@sci.ehime-u.ac.jp)
[2]Geodynamics Research Center, Ehime University, 2-5 Bunkyo-cho, Matsuyama, Ehime 790-8577, Japan

Thermal transport property of materials under pressure and temperature is of importance for understanding the dynamics of the solid Earth and the thermal history. However, both experimental and theoretical determinations of the thermal conductivity still remain technically challenging particularly at the deep mantle condition.

Recent progress in *ab initio* computational method based on the density functional theory (DFT) is making it possible to examine the transport phenomena including the lattice thermal conduction. The intrinsic bulk thermal conduction of insulator is essentially caused by lattice anharmonicity owing to phonon-phonon interaction. Determination of the anharmonic coupling constant is therefore the key to predicting the thermal transport property. Earlier theoretical works calculated the lattice thermal conductivity of MgO with *ab initio* molecular dynamics (MD) simulation or direct evaluation of the anharmonic force constants [1,2]. However, in these approaches, the simulation cell size could often be insufficient for accurate description of the long wavelength phonon scattering. As an alternative approach, the anharmonic coupling strength between phonon modes can be more efficiently and more accurately evaluated within the density functional perturbation theory (DFPT). In this approach, the higher-order force tensors are calculated based on the perturbative scheme taking care only of the primitive cell. We developed a technique for calculation of the phonon linewidh to obtain the phonon lifetime. Then the lattice thermal conductivity is evaluated combining with additional harmonic-level properties. In this presentation, we show the decay process of phonons and the lattice thermal conductivity of MgO and some typical minerals as a test for the applicability of our technique.

Research supported by Senior Research Fellow Center, Ehime University.

[1] Nico de Koker, Phys. Rev. Lett. 103, 125902, 2009; [2] X. Tang and J. Dong, Proc. Natl. Acad. Sci. U.S.A. 107, 4539, 2010).

Modelling of long-term diffusion-reaction in the Callovo-Oxfordian clay for radioactive waste confinement

M. DELALANDE[1], B. FRITZ[1], A. CLEMENT[1] AND N. MICHAU[2]

[1]LHYGES, Université de Strasbourg/EOST, CNRS, France (correspondence: delalande@unistra.fr)
[2]ANDRA, 1/7 rue Jean Monnet, F-92298 Châtenay-Malabry Cedex, France (nicolas.michau@andra.fr)

One of the French options for the final disposal of high-level radioactive waste is a deep geological repository into the Callovo-Oxfordian formation (COX, Haute-Marne, Meuse, France). In this concept, COX clay associated with compacted bentonite, or not, may constitute the barrier system. In such systems, the interactions between groundwater and clays, as well as between the corrosion products of steel overpacks and clays under the influence of temperature elevation, may modify the chemical and physical properties of the selected clay buffers. Clay material has a low permeability, and consequently molecular diffusion is the main mechanism of mass transport in a clay barrier. The system is modeled in reducing conditions using the KIRMAT code (KInetic Reactions and MAss Transport). The software has been developed [1] from the single-reaction path model KINDIS [2] generated from the purely thermodynamic code DISSOL [3, 4].

This study is focused on the possible feedback effects of geochemical reactions on the transport properties (porosity and diffusion) of COX clay. The results of modeling obtained after 10,000 years of simulated mass transport-reaction are compared to the previous studies on an engineer pure bentonite barrier [5, 6, 7, 8, 9]. The mineralogical modifications of clays in contact with the geological interacting fluid, and with Fe^{2+} and OH^- ions provided by the corrosion of the steel overpacks as well as the evolution of porosity and molecular diffusion will be discussed.

[1] Gérard *et al*. (1998) *J. Contam. Hydro*. **30**, 201–216. [2] Madé *et al*. (1994) *Computers & Geosci*. **20(9)**, 1347-1363. [3] Fritz (1975) *Sci. Géol., Mémoires* **41**, 152p. [4] Fritz (1981) *Sci. Géol., Mémoires* **65**, 197p. [5] Montes-H *et al*. (2005) *App. Clay Sci*. **30**, 181–198. [6] Montes-H *et al*. (2005) *App. Clay Sci*. **29**, 155–171. [7] Montes –H *et al*. (2005) *App. Geochem*. **20**, 409–422. [8] Bildstein *et al*. (2006) *Phys. & Chem. Earth* **31**, 618–625. [9] Marty *et al*. (2010) *App. Clay Sci*. **47(1-2)**, 82-90.

https://doi.org/10.1180/S0026461X00006502 Published online by Cambridge University Press

Mediterranean sapropel formation; Preservation and palaeoceanography

GERT J. DE LANGE[1], C. SLOMP[1], D. CRUDELI[2], C. CORSELLI[2], M. SPERANZA PRINCIPATO[3], ELISABETTA ERBA[3], J. THOMSON[4,] AND A. REITZ[5]

[1]Geosciences-Utrecht, NL; (gdelange@geo.uu.nl)
[2]University bicocca Milano, IT
[3]Universita degli Studi di Milano, IT

Precession-related deposition of eastern Mediterraneran sapropels are associated with humid climate conditions. The last of such 'humid periods' occurred from 10.4 to 5.7 kyr ^{14}C ago, simultaneous with the sustained wet period in the circum Mediterranean area. The end of this humid period coincides with a high peak of MnO_2. This peak in all 30 studied cores occurs in response to a relatively abrupt re-ventilation event at 5.7 kyr. Subsequently, oxygen continued to progressively move downward into the sapropel sediment thus removing organic C.and organic biomarkers. Such removal mechanism seriously affects the traditional interpretation based on palaeoproxies.

From a detailed study of the mechanisms of formation of sapropel S1 across the eastern Mediterranean basin as a function of time and water depth, we demonstrate that surface waters had a reduced salinity and concomitantly that the deep (> 1.8 km) eastern Mediterranean Sea was devoid of oxygen during 4,000 years of S1 formation. This has resulted in a differential basin-wide preservation of S1 determined by water depth, as a result of different ventilation/climate-related redox conditions above and below 1.8 km. Climate-induced stratification of the ocean may thus contribute to enhanced preservation of organic matter, ie to formation of sapropels (and potentially black shales)

Production flux of sea-spray aerosol

GERRIT DE LEEUW[1,2,3], EDGAR L ANDREAS[4], MAGDALENA D. ANGUELOVA[5], C. W. FAIRALL[6], ERNIE R. LEWIS[7], COLIN O'DOWD[8], MICHAEL SCHULZ[9] AND STEPHEN E. SCHWARTZ[7]

[1]Finnish Meteorological Institute, Climate Change Unit, Helsinki, Finland, (Gerrit.Leeuw@fmi.fi)
[2]Univ. of Helsinki, Department of Physics, Helsinki, Finland
[3]TNO Env. and Geosci., Utrecht, The Netherlands
[4]NorthWest Research Associates, Inc. (Seattle Division), Lebanon, NH 03766, USA
[5]Naval Research Laboratory, Washington, DC 20375, USA
[6]NOAA/ESRL, Boulder, CO 80305, USA
[7]Brookhaven National Laboratory, Upton, NY 11973, USA
[8]National Uni. of Ireland Galway, Ireland
[9]Norwegian Met. Inst., Gaustadsalleen 21, NO - 0349 Oslo

Knowledge of the size- and composition-dependent production flux of primary sea-spray aerosol (SSA) particles and its dependence on environmental variables is required for modeling cloud microphysical properties and aerosol radiative influences, interpreting measurements of particulate matter in coastal areas and its relation to air quality, and evaluating rates of uptake and reactions of gases in sea-spray drops. The current status of the knowledge on the primary SSA production flux, mainly for particles with r_{80} (equilibrium radius at 80% relative humidity) less than 1 μm, has recently been reviewed by de Leeuw et al. (2011). These authors discussed the production of sea-spray particles and its dependence on controlling factors which have been investigated in laboratory studies that have examined the dependences on water temperature, salinity, and the presence of organics, and in field measurements with micrometeorological techniques that use newly developed fast optical particle sizers. Extensive measurements show that water-insoluble organic matter contributes substantially to the composition of SSA particles with r_{80} < 0.25 μm and in locations with high biological activity can be the dominant constituent. Order-of-magnitude variation remains in estimates of the size-dependent production flux per white area, the quantity central to formulations of the production flux based on the whitecap method. This variation indicates that the production flux may depend on quantities, such as the volume flux of air bubbles to the surface, that are not accounted for in current models. Variation in estimates of the whitecap fraction as a function of wind speed contributes additional, comparable uncertainty to production flux estimates.

de Leeuw et al. (2011) conclude that despite the many gains in understanding in recent years, the uncertainty in the SSA production flux remains sufficiently great that present knowledge of this quantity cannot usefully constrain the representation of emissions of SSA in chemical transport models or climate models that include aerosols. As a consequence it is not yet possible to improve the modeling of these emissions much beyond the current state of affairs which shows nearly two orders of magnitude spread in current estimates of global annual SSA emissions.

https://doi.org/10.1180/S0026461X00006502 Published online by Cambridge University Press

On the morphology and chemistry of (micro)fossils: Matches, mismatches and kerogen formation

JAN W. DE LEEUW[1,2]

[1]NIOZ Royal Netherlands Institute for Sea Research, P.O. Box 59, 1790 AB Den Burg-Texel, The Netherlands. (jan.de.leeuw@nioz.nl)

[2]Utrecht University, Depts of Earth Sciences and Biology, Budapestlaan 4, 3584 CD Utrecht, The Netherlands.

The far greater part of organic matter on Earth is present in sediments and consists of high molecular weight, insoluble constituents collectively known as kerogen. To improve our understanding of the origin, chemistry and fate of this kerogen, morphologically well preserved organic (micro)fossils and their extant counterparts are studied assuming that the preservation of such fossils is a consequence of the resistance towards (bio)degradation of the organic constituents they are made of.

Many investigations of well-preserved (micro)fossils and laboratory experiments with their extant counterparts using pyrolytic, chemical and spectroscopic analytical approaches do indeed indicate that biopolymers such as algaenan in algae, cutan in plant cuticles and lignin in wood are resistent towards diagenesis and may thus be responsible for excellent fossil preservation.

However, this “match” of preserved biochemistry and morphology is not always encountered. In many well-preserved fossil algal cells and plant cuticles and their extant counterparts these resistant biomacromolecules, algaenan and cutan resp., are completely absent. Recent studies seem to indicate that the excellent preservation of such fossils is due to a gradual replacement of originally present labile bio(macro)molecules by newly formed highly resistant geomacromolecules without significant morphological changes, a “mismatch” between biochemistry and morphology. In particular studies of sporopollenin in extant and fossil macro- and microspores indicate that pre- or post depositional exposure of organic entities to oxygen triggers oxidative cross linking of “nearby” low molecular weight (poly)unsaturated membrane lipids resulting in resistant, mainly aliphatic geopolymers partly or completely replacing the original biopolymers.

This kind of (micro)fossil studies is crucial to unravel the molecular structure of kerogen and, consequently, to understand the molecular chemistry of fossil fuel genesis.

Origin of karstic dissolution voids in Jurassic shallow marine carbonates at SW of Ankara, (Turkey)

ARIF DELIKAN AND HÜKMÜ ORHAN

Selçuk Üniv. Müh. Mim. Fak. Jeoloji Müh. Bölümü Konya, Türkiye (adeli@selcuk.edu.tr, horhan@selcuk.edu.tr)

Jurassic rocks cropping out at the southwest of Ankara (Turkey) rest unconformably on the basement rocks commonly as microbial deposits but also as detrital sediments. Karstification occurs in shallow marine biomicrite bearing sponge spicules as well as in microbial carbonates. Most of the cavities in the carbonates developed when they were carried to subaerial conditions as a result of sea level changes and, also by tectonic activities. Karstic voids are irregular in shape and disconnected. Their fillings are initiated with more than one crystallization phase of low-magnesian calcite with different colors [1]. Following this coating crystallization phase, the remaining voids were filled by different type of sediments. These infilling sediments are generally laminated, pink, or in different color.

They are vadose silts in varying size, but in some cases, comprises grains derived from host rocks. Compared to others, some karstic cavities are large. They were interpreted as being formed following fracturings in relation with tectonic activities. These cavities commonly were filled by marine sediments. Being coated by calcite crystals implies that these cavities were inundated by marine water having adequate condition for calcite crystallization before filling by marine sediments. Lamination of fine filling sediments is commonly parallel to the parent rocks. But fillings of cavities in a 12 cm thick layer have laminated sets which are neither parallel to each other nor to the bedding of parent rocks. This shows that the basement of the basin was not stabile and, was tilted differently in time.

[1] Jimenez de Cisneros, C., Mas, J.R. and Vera, J.A, (1991) *Sedimentary Geology* **73** 191-208.

https://doi.org/10.1180/S0026461X00006502 Published online by Cambridge University Press

Potentiality and limits of applying DSC and TG to complex systems: Direct and indirect information

MARIA TERESA DELL'ABATE

CRA-RPS, Via della Navicella 2, 00184 Rome, Italy (mariateresa.dellabate@entecra.it)

The relationships between agriculture and environmental quality find a key issue in the study of the processes enhancing organic matter stability in soil, in order to increase C sink and mitigate the effects of global change. Various and different approaches are possible, due to the complexity and heterogeneity of the soil system where SOM chemical composition and its architecture are widely interdependent within the soil matrix. In recent years the application of thermal analysis to the study of soil organic matter has found a renewed interest, mainly due to the possibility to obtain quantitative estimation of organic matter within the soil mineral matrix, possibly without chemical extraction. In addition, the dynamic measure conditions obtained through the thermal scans give the theoretical possibility to deduce the kinetics of the thermally induced processes. Different patterns of thermal stability are shown by different biomasses, compost or soils. However, it could be misleading to assimilate the time based output of DSC and TG measures to the kinetics of the processes occurring in soil, thus the concepts of organic matter stability or lability or recalcitrance needs to be better defined according to appropriate definition of the reference context.

In the presentation, the comparison between information obtainable from compost or soil analysis will help us to highlight potentiality and limits in applying DSC and TG to complex systems in order to move from a qualitative approach to a better definition of thermal and biochemical stability indexes. Finally, an open question should be discussed: can we forecast or imagine to include information on thermal behaviour of SOM within an ecological approach to the soil system?

Sorption of metals on a novel synthesized Mn (oxy)hydroxide

L. DELLA PUPPA[1], M. KOMÁREK[2] AND F. BORDAS[1]

[1]Faculté des Sciences et Techniques, Université de Limoges, 123 Avenue Albert Thomas, 87060 Limoges Cedex, France (loic.della@etu.unilim.fr)

[2]Czech University of Life Sciences Prague, Kamycka 129, 165 21 Prague 6, Czech Republic

Novel synthetic manganese (oxy)hydroxide

A novel synthetic manganese (oxy)hydroxide is synthetized using the modified protocol of Ching *et al*. [1], wich is commonly used for the preparation of birnessite. This (oxy)hydroxide is studied as a possible chemical stabilizing agent for metals in contaminated soils. Its stability in deionized water and the sorption of Cu and Pb are studied.

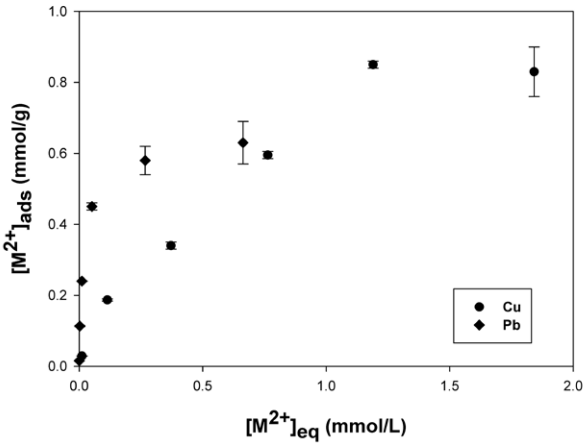

Figure 1: Adsorption isotherms of Cu and Pb on the Mn (oxy)hydroxide at pH 4

Results

The dissolution of the Mn (oxy)hydroxide in water reaches 12 and 1 mmol/g for solid/liquid ratios of 1/500 and 1/10, respectively and indicates that the phase could be fairly stable in soils. The Langmuir isotherm parameters calculated show that the maximum adsorbed quantity of Cu and Pb reach 1.3 and 0.6 mmol/g. The sorption parameters of the Mn (oxy)hydroxide were compared to those of birnessite at pH 4, which reached 1.1 and 1.4 mmol/g for Cu and Pb, respectively. Birnessite thus adsorb better Pb than the synthesized phase, but for praticial use as a chemical stabilizant, our Mn (oxy)hydroxide could be promising due to its easy synthetisation.

[1] Ching *et al*. (1997) *Inorg. Chem*. **36,** 883-890.

https://doi.org/10.1180/S0026461X00006502 Published online by Cambridge University Press

Impact of authigenic particles on phosphate and trace metal budgets of anoxic basins

O. DELLWIG[1], T. LEIPE[1], C. MÄRZ[2], M. GLOCKZIN[1], K. HÄUSLER[1], M. MOROS[1], F. POLLEHNE[1], B. SCHNETGER[3], M.E. BÖTTCHER[1] AND H.-J. BRUMSACK[3]

[1]Leibniz Institute for Baltic Sea Research, Rostock, Germany, (olaf.dellwig@io-warnemuende.de)
[2]Newcastle University, Newcastle upon Tyne, UK
[3]Institute for Chemistry and Biology of the Marine Environment, University of Oldenburg, Germany

Intense element cycling causes steep gradient of nutrients and redox-sensitive trace metals at pelagic redoxclines; the transition zone separating oxygenated surface waters from sulphidic bottom waters. Besides well-known Mn-oxides, SEM-EDX inspection of authigenic particles from the redoxcline of the Black and Baltic Seas evidence existence of postulated Fe-phosphates as well as mixed phases comprising Mn, Fe, and P as a new solid species (Mn-Fe-P shuttle). Throughout the redoxcline, these minerals show a general succession with maximum abundance of Mn-oxides above the redoxcline followed by mixed phases and almost pure Fe-phosphates within and below the redoxcline. Morphological similarities and molar Fe/P ratios suggest the formation of irregular Fe-oxyhydroxo coatings on sinking MnO_x particles followed by immediate adsorption of phosphate. Despite oxidation by O_2, batch-type experiments using biogenic Mn-oxides demonstrate the efficient potential of Fe^{2+} oxidation by sinking MnO_x particles. When entering sulfidic waters MnO_x is further reduced, thus causing an increasing relative abundance of Fe-phosphate.We suggest a conceptual model for the Mn-Fe-P shuttle at pelagic redoxclines, which affects phosphate transport throughout the water column and thus impacts primary production at least over longer time scales. This Mn-Fe-P-shuttle likely played an important role for the cycling of P in ancient ocean basins, e.g., during certain periods of Cretaceous black shale formation and should be considered in future modelling approaches dealing with stratified ecosystems. Furthermore, this shuttle influences the cycles of certain trace metals via scavenging. High-resolution determination of trace metals in sapropelic sediments from the Gotland Basin (Baltic Sea) will be compared with the elemental composition of authigenic particles from the water column in order to assess preferential enrichments in the sedimentary record.

Li content and isotopic distributions in granulite of Kerguelen plateau

E. DELOULE[1], J. INGRIN[2], Q.-K. XIA[3] AND M. GRÉGOIRE[4]

[1]CRPG-CNRS, BP20, 54500 Vandoeuvre les Nancy, France. (deloule@crpg.cnrs-nancy.fr)
[2] UMR CNRS 8207, Univ. Lille 1, 59655 Villeneuve d'Ascq, France. (jannick.ingrin@univ-lille1.fr)
[3]CAS Key Lab. of crust-mantle materials and environment, USTC, 230026, Hefei, China. (qkxia@ustc.edu.cn)
[4]GET, UMR CNRS 5563, OMP, Univ. Toulouse III, 31400, Toulouse, France. (gregoire@get.obs-mip.fr)

Kerguelen basalts contain abundant mantle xenoliths, including mantle peridotites and deep magmatic segregates equilibrated in the granulite facies [1]. Lithium chemical and isotopic distribution were measured in two-pyroxene granulites, in order to define their signature and describe the Li behavior during the lower crust formation processes. Li content and isotopic composition were measured in using the Cameca IMS 1270 Ion probe at CRPG, with reference Cpx and Opx with compositions close from those of the samples.

The studied xenoliths display close mineralogical compositions, bearing Mg81-92 Al-diopside, Mg-78-93 enstatite and labradorite or bytownite. Spinel and garnet are observed in 2 of them, and they all are type II xenoliths [1,2]. On the whole rock scale the Li contents range from 1,5 up to 9 ppm, with Li content decreasing from Cpx to Opx with a ratio Opx/Cpx of 0.8-0.9 and a ratio Plag/Cpx of 0.2-1. At the grain scale, Li displays a homogeneous distribution, at the exception of depleted or enriched Cpx rims. Only the more Li depleted sample display heterogeneous Li distribution in both Cpx and Opx.

The δ^7Li values measured on Cpx and Opx range between +4 and +14, with most of the values between +5 and +8. The cpx depleted or enriched rims display δ^7Li values associated to Li diffusion. Only the Li poor xenolith display δ^7Li values scattered on a large range, from -9 to +14. A general observation is that Cpx display rather slightly higher δ^7Li values than Opx, and those values are more scattered in Opx than in Cpx. The δ^7Li values for Plag are in progress and will be presented, but could not affect a lot the Li isotope budget, are most of Li is beard by Opx and Cpx.

The bulk value for these granulite samples is in agreement with a direct derivation from the mantle (5-8 ppm, δ^7Li≈+5). But their Li content is lower than expected for the lower continental crust [3], suggesting that Li in the lower continental crust is not mainly derived from the mantle.

[1] Gregoire *et al*. (1998) *Contrib Mineral Petrol* **133**, 259-283. [2] Gregoire (1994) PhD thesis. [3] Rudnick and Gao (2004) *Treatise on Geochemistry* **3**, 1-64.

https://doi.org/10.1180/S0026461X00006502 Published online by Cambridge University Press

Contrasting silicon and magnesium isotope fractionation with clay mineralogy in volcanic soil weathering sequences, Guadeloupe

B. DELVAUX [1], S. OPFERGELT[1,2], R.B. GEORG [3], Y-M. CABIDOCHE [4], K.W. BURTON [2] AND A.N. HALLIDAY [2]

[1]Earth and Life Institute, Université catholique de Louvain, Louvain-la-Neuve, Belgium (sophie.opfergelt@uclouvain.be)
[2]Department of Earth Sciences, University of Oxford, Oxford, United Kingdom
[3]Trent University, Water Quality Centre, Peterborough, Ontario, Canada
[4]INRA, UR 135 Agropedoclimat Zone Caraibe Environm & Agro, Petit Bourg, Guadeloupe

The weathering of continental silicate rocks influences global climate by consuming atmospheric CO_2. Magnesium and Si stable isotopes are used as weathering proxies in soils and rivers, but the impact of the mineralogy of secondary phases on isotope fractionation remains unexplored so far. Here, we investigate variations in δ^{26}Mg vs. DSM-3 and δ^{30}Si vs. NBS28 in bulk soils and clay fractions relative to their parental andesite in two soil weathering sequences (Guadeloupe) that were formed in contrasting climatic conditions. The Western slope of La Soufrière volcano (dry conditions) presents a soil sequence Andosol - Cambisol - Vertisol with formation of smectite, whereas the Eastern slope (high rainfall) presents Andosol - Nitisol - Ferralsol with formation of kaolinite.

For Mg isotopes, clay fractions (δ^{26}Mg -0.41 to -0.10‰) were isotopically heavier than the andesite (δ^{26}Mg -0.47‰), supporting a preferential incorporation of heavy Mg isotopes in secondary Mg-bearing clay minerals. The clay fractions on the Eastern slope were progressively heavier with increasing weathering degree, -in contrast to the Western slope were clay fractions were progressively lighter with increasing weathering degree and with increasing exchangeable Mg associated with smectite. For Si isotopes, clay fractions were lighter than the parental material, and progressively lighter with increasing weathering degree. More importantly, larger Si isotope fractionation was associated with the formation of kaolinite (δ^{30}Si -1.95 to -1.32‰) than with the formation of smectite (δ^{30}Si -1.05 to -0.94‰) relative to the parental andesite (δ^{30}Si -0.37‰). Our results highlight that a similar parental andesite exposed to different climatic conditions can generate contrasting Mg and Si isotope fractionations in secondary phases, which offers great potential for paleo-reconstruction of soil environments.

Impact of reductants on the optical properties of Humic Substances (HS)

ROSSANA DEL VECCHIO*[,1,2] LYNNE HEIGHTON[1], KELLI GOLANOSKI[1] AND NEIL V. BLOUGH[1]

[1]Department of Chemistry and Biochemistry University of Maryland, College Park, MD United States
[2]Earth System Science Interdisciplinary Center, University of Maryland, College Park, MD United States (*correspondence:rossdv@umd.edu)

Our previous results have shown that the reduction with sodium borohydride of Suwannee River humic and fulvic acids, a commercial lignin, and a series of solid phase C18 extracts from fresh, estuarine, coastal and offshore waters of the middle Atlantic bight produces a preferential loss of long wavelength (visible) absorption and enhanced, blue-shifted emission [1]. These results are consistent with and interpreted within a previously proposed charge transfer model [2, 3]. Here we extend this work to other reducing agents (such as cyanoborohydride and sodium dithionite) and other humic substances (from aquatic and soil environments) to investigate the impact of other reductants on the optical properties of humic substances and attempt to assess the relative importance of quinones and ketones to the optical properties of these materials. Preliminary results indicate that a) borohydride reduces all HS examined independent of their source as determined by UV/Vis and fluorescence; b) cyanoborohydride did not reduce any of the HS examined to a significant extent; c) dithionite appears to reduce HS but to a much smaller extent that borohydride. Ongoing work aims to extend this work to more HS and model quinones/ketones and to quantify the loss of absorption with respect to dithionite consumed.

[1] Ma *et al*. (2010) *Environ. Sci. Technol.* **44**, 5395-5402. [2] Del Vecchio and Blough (2004) *Environ. Sci. Technol.* **38**, 3885-3891. [3] Boyle *et al*. (2009) *Environ. Sci. Technol.* **43**, 2262-2268.

https://doi.org/10.1180/S0026461X00006502 Published online by Cambridge University Press

δ^{30}Si and Ge/Si changes in BIFs along the Archaean

C. DELVIGNE*[1,2], D. CARDINAL[2,3], A. HOFMANN[4] AND L. ANDRÉ[1,2]

[1]Department of Earth Sciences and Environment, Université Libre de Bruxelles, Brussels, Belgium (*correspondance: cdelvign@ulb.ac.be)
[2]Department of Geology and Mineralogy, Royal Museum of Central Africa, Tervuren, Belgium
[3]LOCEAN, University Pierre and Marie Curie, Paris, France
[4]Department of Geology, University of Johannesburg, South Africa

The Precambrian ocean underwent a long-term cooling as inferred by oxygen isotopes and recently corroborated by an increase in δ^{30}Si values [1]. However, this was questioned because both primary and secondary cherts were considered. To get new insights to the Archaean ocean evolution, we coupled δ^{30}Si and Ge/Si ratios in Banded Iron Formations (BIFs) spanning a large time scale (from 3.8 to 2.46Ga). Trends in Si-rich mesobands of BIFs confirm an increase of δ^{30}Si values from ~-2.1‰ (3.8Ga, [2]) to ~-1.1‰ (2.46Ga) with a simultaneous decrease in Ge/Si ratios from ~29.1μmol/mol (3.8Ga, [3]) to 2.7μmol/mol (2.46Ga). We suggest they both reflect a decrease of high-T hydrothermal inputs to oceans through time. As high-T hydrothermal fluids display high Ge/Si ratios, a decrease in hydrothermal inputs would lower the oceanic Ge/Si ratio as well as it would have contributed to cool the ocean. The maintenance of an Early Archaean high-T ocean would prevent significant direct silica precipitation from the ocean and its gradual cooling would have facilitated direct silica-rich precipitation that may have led the oceans towards heavier δ^{30}Si signatures.

[1] Robert and Chaussidon (2006) *Nature* **443**, 969-972.
[2] André *et al*. (2006) *Earth Planet. Sci. Lett*. **245**, 162-173.
[3] Frei and Polat (2007) *Earth Planet. Sci. Lett*. **253**, 266-281.

A warming-cooling cycle between 3.8 and 3.2 ky BP: Correlations of speleothem and bivalve compositions with ice core records

A. DEMÉNY[1]*, G. SCHÖLL-BARNA[1], Z. SIKLÓSY[1], G. SERLEGI[2], P. SÜMEGI[3] AND M. BONDÁR[2]

[1]Institute for Geochemical Research, Hungarian Academy of Sciences, H-1112 Budaörsi út 45, Hungary (*correspondence: demeny@geochem.hu)
[2]Archaeological Institute, Hungarian Academy of Sciences, H-1014 Budapest, Úri str 49, Hungary
[3]Department of Geology and Paleontology, University of Szeged, H-6722 Szeged, Egyetem str 2, Hungary

Climate conditions during the Holocene were relatively stable compared to the entire Quaternary, so that only minor fluctuations are detectable – for example – in the stable isotope records of ice cores. On the other hand, climate fluctuation events have been detected in Europe by geological and geochemical records interpreted to reflect temperature and/or humidity changes, sometimes in contradiction with each other. In this study freshwater bivalve shells (*Unio* sp.) were collected from Bronze age archaeological excavations around Lake Balaton (Central-Western Hungary) spanning the period of about 3 to 4 ky BP and their stable C and O isotope compositions were measured in order to investigate lake evolution processes in this period of time. The data indicate warmer/dryer conditions around 3.7 ky BP, bracketed by relatively cooler and/or wetter environments. These observations seemed to be in contradiction with earlier results that lead us to compare the geochemical data from bivalve shells with speleothem records of the region as well as with the GISP2 ice core oxygen isotope data. H, C and O isotope compositions and trace element data (e.g., Mg/Sr ratios, P concentrations) in stalagmites can be correlated with the bivalve shell data, indicating warming around 3.8-3.6 ky BP associated with lower humidity during summer (elevated winter/summer precipitation ratio), followed by an ~300 year long cool phase with summer-dominated precipitation. Good agreements between different paleoclimate records indicate that the warming-cooling events affected a large region from the North Atlantic at least to Central Europe. Temperature and humidity variations inferred from the data suggest that the North Atlantic Oscillation was a major governing factor in climate changes during the Bronze Age.

https://doi.org/10.1180/S0026461X00006502 Published online by Cambridge University Press

Structure and relative stability of hydrous and anhydrous Ca-Mg carbonates from first-principle calculations

R. DEMICHELIS*, P. RAITERI AND J. D. GALE

Department of Chemistry, Faculty of Science and Engineering, Curtin University, GPO Box U1987, Perth, WA 6845, Australia
(*correspondence: raffaella@ivec.org)

Calcium and magnesium carbonates play an important role in the chemistry of the hydrosphere, lithosphere, atmosphere and biosphere. From a technological point of view, the precipitation of carbonates in industrial and domestic environments represents a problem in terms of process efficiency and maintenance costs.

The crystallisation and growth mechanisms of these compounds, as well as their structure and relative stability, are still a matter for investigation. In particular, relatively little data is available for the hydrated phases, due to limited natural occurrence and low stability. However, they may well play a role during the crystallisation and growth mechanism of the anhydrous phases (included Ca-Mg carbonate solid solutions) and in CO_2 sequestration, especially at low temperature [1-5]. Information regarding the formation of mixed calcium-magnesium carbonates is also pertinent to understanding the dolomite problem.

A comprehensive *ab initio* structural and thermodynamic study of calcium-magnesium carbonates and their hydrates will be presented. The good agreement between calculated and available experimental data attests to the validity of the applied computational approaches, namely Density Functional Theory in the present study.

[1] Nebel *et al*. (2008) *Inorg. Chem.* **47**, 7874-7879. [2] Tang *et al*. (2009) *J. Appl. Cryst.* **42**, 225-233. [3] De Angelis *et al*. (2007) *Amer. Mineral.* **92**, 510-517. [4] Vágvölgyi *et al*. (2008) *J. Therm. Anal. Calorim.* **94**, 523-528. [5] Davies *et al*. (1977) *Chem. Geol.* **19**, 187-214.

Nucleation of amorphous calcium carbonate: A combined theoretical and experimental perspective

R. DEMICHELIS[1], P. RAITERI[1]*, J. D. GALE[1], D. GEBAUER[2] AND D. QUIGLEY[3]

[1]Nanochemistry Research Institute, Department of Chemistry, Curtin University, PO Box U1987, Perth, WA 6845, Australia. (*correspondence: p.raiteri@curtin.edu.au)
[2]Department of Chemistry, University of Konstanz, Universitätsstrasse 10, Box 714, D-78457 Konstanz, Germany
[3]Department of Physics and Centre for Scientific Computing, University of Warwick, Gibbet Hill Road, Coventry CV4 7AL, UK

The nature of the nucleation of amorphous calcium carbonate is examined in the light of both recent experimental [1,2] and theoretical [3] results. While experiment demonstrates the existence of stable pre-nucleation clusters, followed by a nucleation event, computer simulations suggest that the free energy of adding ion pairs to amorphous calcium carbonate is exothermic regardless of size, which may indicate the absence of a barrier. How these two different sets of observations can be reconciled will be examined in this work through the use of molecular dynamics simulations of pre-nucleation calcium carbonate solutions.

In this presentation we will explore the use of computer simulation methods to try to unravel the complexities of the nucleation and growth processes for calcium carbonate. Central to this is the development of a force field that is accurately calibrated against experimental free energies [3] since failure to do so can result in qualitative errors for interfacial properties. Based on this we have explored the stability of ACC versus crystalline nanoparticles while accounting for the variable water content in the amorphous structure [4]. In the light of this, and new experimental results, we propose a model to explain the non-classical aspects of the nucleation mechanisms of calcium carbonate, the origins for which can be traced back to the interfacial properties.

[1] D. Gebauer *et al*. (2010), *Angew. Chem. Int. Ed.* 49, 8889. [2] D. Gebauer *et al*. (2008), *Science*, **322**, 1819. [3] P. Raiteri *et al*. (2010), *J. Phys. Chem. C*, **114**, 5997. [4] P. Raiteri and J.D. Gale (2010), *J. Am. Chem. Soc.*, **132**, 17623.

https://doi.org/10.1180/S0026461X00006502 Published online by Cambridge University Press

S in CAMP and Paranà-Etendeka CFBs

A. DE MIN[1], S. CALLEGARO[2], D. BAKER[3] AND A MARZOLI[2]*

[1]Università di Trieste, Italy (*correspondence: demin@univ.trieste.it)
[2]Università di Padova, Italy (sara.callegaro@unipd.it; andrea.marzoli@unipd.it)
[3]McGill University, Canada (don.baker@mcgill.ca)

Synchrony of continental flood basalts (CFB) and significant Phanerozoic mass extinction events may suggest a trigger effect of large scale basaltic eruptions on the global climate and environment, mainly due to intense emissions of volcanic gases such as SO_2 and CO_2 [1]. However, this interpretation is based on poorly constrained gas contents of the basalts and on even less well known gas emission rates. Here we investigate the S content of basalts of two of the largest CFB provinces: the Central Atlantic magmatic province (CAMP) and the Paranà-Etendeka (PE). Notably, while the CAMP is synchronous with and possibly triggered the end-Triassic extinction [2], PE basalts had a very minor effect on the early Cretaceous biosphere [3].

Melt inclusions in CAMP basalt olivines yield S contents (electron microprobe analyses) comparable to those found in Deccan basalts [1], whereas S in matrix glass is close to detection limit, suggesting that degassing during the eruption was almost complete.

As an alternative approach, we measure S (and Cl) contents (synchrotrone analyses) also in phenocrysts from CAMP and PE basalts and extrapolate the magmatic S content through newly established crystal/melt partition coefficients. These results illuminate the difference which seem to exist between the two CFB provinces and contribute to our understanding of their different environmental impacts.

[1] Self S. *et al*. (2008), *Science* **319**, 1654-1657. [2] Cirilli S. *et al*. (2009), *EPSL* **286**, 514-525. [3] Wignall P. (2001), *Earth. S. Rev* **53**, 1-33.

Mineral chemistry and fluid inclusion characteristics of the Kabadüz Ore Veins (Ordu, NE-Turkey)

Y. DEMIR[1], M.B. SADıKLAR[2], I. UYSAL[2], A. CERIANI[3], AND N. HANILÇI[4]

[1]Gümüşhane Uni., Dep. of Geol., Gümüşhane, Turkey, (ydemir78@hotmail.com)
[2]KTU, Dep. of Geol., 61000 Trabzon, Turkey
[3]Pavia Uni., Dep. of Geol., Pavia, Italy
[4]Istanbul Uni., Dep. of Geol., Istanbul, Turkey

Hydrothermal vein type deposits of Kabadüz region (Ordu, NE-Turkey), are located in the Upper Cretaceous andesitic-basaltic rocks and formed in fault zones of the NW-SE directions. The primary mineral paragenesis of the ore veins are composed of pyrite, chalcopyrite, sphalerite, galena and tetrahedrite-tennantite with quartz and lesser amount calcite and barite as a gangue mineral. Petrographical studies suggest that ore veins in the region have similar mineral paragenesis, succession and textural properties.

Pyrite contains up to 0.95 wt% Zn, and 0.60 wt% As, chalcopyrite contains up to 0.86 wt% Zn and 0.14 wt% Au. Sphalerite is poor in Fe and contains up to 0.35 wt% Mn, 2.18 wt% Cu, and 0.89 wt% Cd. Tetrahedrite and tennantite are also poor in Fe content (up to 1.56 wt%). Different phases from the each different veins are found to be similar in composition. Lower Ni and Co content of the pyrites and Zn/Cd ratio of the sphalerites suggest that hydrothermal solutions related to the acidic type magmatic activity.

Homogenisation temperature (Th) and salinity data vary between 180-436.1 ºC and, 0.4-14.7 % NaCl, at the fluid inclusions of sphalerite and quartz. On the basis of first melting temperatures, $CaCl_2$, $MgCl_2$ and $FeCl_2$ were dominant at the higher Th, whereas NaCl and KCI at the lower Th conditions. Salinity content of the inclusions imply that hydrothermal solutions related to the magmatic sources. On the other hand well defined positive correlation between Th and salinity indicate that meteoric water involved in the hydrothermal solutions. In addition to petrographical studies, mineral chemistry analyses and fluid inclusion properties indicate that ore veins in the region have occured same or similar ore formation conditions.

https://doi.org/10.1180/S0026461X00006502 Published online by Cambridge University Press

Water weakening in dunite: Highlights from torsion experiments

S. DEMOUCHY[1]*, L.N. HANSEN[2], M.E. ZIMMERMAN[2], A. TOMMASI[1], F. BAROU[1], D.L. KOHLSTEDT[2]

[1]Geoscience Montpellier, Université Montpellier 2 & CNRS, Montpellier 34095, France (*correspondence: sdemouchy@um2.fr).

[2]Dept. Geology and Geophysics, University of Minnesota, Minneapolis, MN 55455, USA.

We have performed torsional deformation experiments on pre-hydrogenated fined-grain olivine aggregates using an innovative assembly to estimate water-weakening in mantle rocks at high shear strains. San Carlos olivine powder was cold-pressed, then 45 μL of water was added, and the sample was subsequently hot-pressed at 1523 K and 300 MPa for 3 h, producing aggregates with average grain sizes of 7 or 15 microns. Deformation experiments were performed in a high-resolution gas-medium apparatus equipped with a torsional actuator under a confining pressure of 300 MPa, a temperature of 1473 K, and constant shear strain rates of 1.4 x 10^{-4} to 8 x 10^{-5} s^{-1}.

Peak shear stresses ranged from 150 MPa to 195 MPa, values slightly weaker than determined in previous torsion experiments on dry fined-grain dunites with equivalent grain sizes, shear strain rates, and finite strains. Textures and microstructures of the starting material and deformed specimens were fully characterized by scanning electron microscopy and by electron backscatter diffraction. All deformed aggregates show a shape preferred orientation marking a foliation and lineation, grain size reduction, and a well-developed olivine crystal preferred orientation consistent with deformation by dislocation creep with dominant activation of the (010)[100] slip system. The hydrogen concentration in olivine aggregates was determined with unpolarized Fourier transform infrared spectroscopy. Analyses of the spectra indicate that the hydrogen concentration of the olivine might be limited and show a potential contamination by water-rich inclusion or intergranular material. These torsion experiments on hydrogenated fined-grain dunite provide new insights into the water weakening phenomenon observed in various nominally anhydrous minerals.

A missing process in the Eastern margin of Tibetan Plateau from multi-system thermochronology and its implication for late Cretaceous tectonic change from the Paleo-Tethyan to Neo-Tethyan regime

BIN DENG[1] AND SHUGEN LIU[2]

[1]State Key Laboratory of Oil and Gas Reservoir Geology and Exploitation in Sichuan Province,China (dengbin3000@163.com)

[2]State Key Laboratory of Oil and Gas Reservoir Geology and Exploitation in Sichuan Province (lsg@cdut.edu.cn)

Due to be lack of structural and sedimentary records to constrain the Jurassic-to-Cretaceous evolution, a missing process was here in Eastern margin of Tibetan Plateau. Given that all radioisotopic systems are subject to disturbance and resetting at different temperatures, we can restore the cooling process or emplacement of rock using different minerals or radioisotopic systems, which we call multi-system thermo-chronology. Based on the analysis of 125 thermochronology ages (e.g., U/Pb, Ar/Ar, Rb/Sr, FT, U-Th/He) of igneous rocks from the eastern margin of Tibet in the Yidun Arc, Yadjiang Deprssion and Songpan-Garze Fold Belt, we reconstruct the emplacement process of different granites using the multisystem thermochronology approach, to decipher the process.

At mid-to-late Indosinian, the initial emplacement age and depth of granites distinctly decrease from north to south, followed by a long slow cooling process in mid-to-upper crust during Yanshanian indicating a long period of thermal stability and tectonic quiescence. Those reflect the control of Paleotethyan tectonic setting. Whereas, between early and late Cretaceous, there was widespread granite emplacement and uplift-related cooling on the eastern margin of Tibetan again, with the declining tendency of magmatic activity and tectogenesis from south to north due to far-field effects of Lhasa-Qiangtang collision. In addition, the granites in north do not have an obvious emplacement process. Which reflect the control of Neotethyan tectonic setting. Correspondingly, as a sedimentary respose to the change of tectonic regime, there is an obvious change on depositional contact in adjoint basins from Late Cretaceous to Neogene. That is from a southward decreasing angularity of the unconformity in early to a northward decreasing angularity in later. Thus, the eastern margin of Tibet is thought to have experienced an important late Cretaceous (about 100Ma) tectonic change from the Paleo-Tethyan regime to Neo-Tethyan regime.

https://doi.org/10.1180/S0026461X00006502 Published online by Cambridge University Press

The applications of x-ray fluorescence analysis in the resource assessment of Dashui Gold deposit in Gansu, China

HUI DENG[1], JIANGSU ZHANG[2], XIUHONG PENG[3,4]*, HAI YANG[3] AND CHENGSHI QING[3]

[1]State Key Lab. of Geohazard Prevention and Geoenvironment Protection, Chengdu University of Technology
[2]Third Geology and Mineral Resources Exploration Academy of Gansu Province, China (*correspondence:pengxhh@cdut.edu.cn)
[3]Geochemistry Dep., Chengdu Univ. of Technology China
[4]Key Lab. of Nuclear Techniques in Geosciences, China

X-ray Fluorescence Analysis Technique is fast, nondestructive and portable for measuring in the field. It has been widely used in ore exploration and prospect such as searching and delineating mineralization anomalies, and looking for concealed ore, etc.

Dashui Gold Deposit in Maqu, Gansu, which was found in west Qinling mountain area, is a type of gold deposits with unique mineralization. The mineralization intensity was closely related to the silicification and hematitization. Recent years because of mining of the gold deposit, the ore-prospecting results are descending with mineral resource crisis. Therefore applying the X-ray Fluorescence Analysis in Dashui Gold Deposit will serve for locating mineralization, dividing ore bearing strata and delineating the prospecting target area promptly.

On the basis of geochemical exploration and actual situation of the deposit, the representative 3530m, 3605m and 3645m middle sections of exploration line 72 of Dashui Gold Deposit were selected for measuring. The measuring device is CIT-3000SMP. The design spacing is 3m, and the measuring time is 120 seconds per point. Five limestone and six diorite porphyrite samples with chemical analysis results had been used to fit standard curves respectively, do multi-element measurement, delineate the beneficial occurrence areas of gold and quickly access the location and distributional pattern of the geochemical halos of the gold mine. The results indicate that:

The measuring results of Au, As, Cu, Fe, Mn, Sr, Zr, Mo, Sb, Ag and Zn, etc. are good, they all reflect the fluorescence anomaly. The anomalies of Au, Cu, As, Fe and so on appear obviously in the known ore bodies. They concomitantly appear with a high anomaly coincide degree. One first-grade prospective area (the anomaly contrast is more than 2.5 times) with excellent potential has been delineated. The width is 10-24m, and the controlling length is 250m. It is like the lens with a wilder bottom than the top, and the long axis is parallel to the existed ore body Au2.The second-grade prospective area (the anomaly contrast is from 1.5-2.5 times) with good potential is also lenticular. Its controlling width is about 10m. The length is 80m.

Effect of Carbon, Sulfur and Silicon on Iron melting at high pressure: Implications for composition and evolution of the terrestrial planet cores

L. DENG[1,2]*, Y. FEI[1], X. LIU[2] AND A. SHAHAR[1]

[1]Geophysical Laboratory, Carnegie Institution of Washington, 5251 Broad Branch Road, NW, Washington, DC 20015, USA (*correspondence: ldeng@ciw.edu)
[2]The Key Laboratory of Orogenic Belts and Crustal Evolution, Ministry of Education of China; School of Earth and Space Sciences, Peking University, Beijing 100871, China

High-pressure Fe-S-C and Fe-S-Si-C melting experiments, with a reasonable abundance of carbon, sulfur and silicon in the terrestrial planet cores, have been conducted to investigate how melting relations and crystallization sequences change with pressure and bulk composition. The results were used to understand the composition and evolution of the terrestrial planet cores.

For $Fe_{84.69}C_{4.35}S_{7.85}$, the first crystallized phase is Fe_3C at 5 GPa and Fe_7C_3 at 10-20 GPa. For $Fe_{84.87}C_{2.08}S_{11.41}$, Fe_3C is the stable carbide at subsolidus temperature at 5-15 GPa. For $Fe_{86.36}C_{0.96}S_{10.31}$ and $Fe_{85.71}C_{0.33}S_{11.86}$, the first crystallized phase is metallic Fe instead of iron carbide at 5-10 GPa. It is observed that the cotectic curve between Fe and Fe_3C moves toward the iron-rich direction with pressure increasing from 5 to 10 GPa in the Fe-C-S system. If this tendency persists to the Earth's present pressure condition, only a small amount of carbon is needed to form an iron carbide solid inner core.

Experiments on $Fe_{82.95}C_{0.66}S_{13.7}Si_{2.89}$ show even a small amount of C significantly lowers the closure pressure of the miscibility gap. Given an Earth's core containing a significant amount of S and moderate Si and with small amount of C, no compositional stratification is expected for Earth's Fe-S-C-Si core, although it may occur during early melting events. It is observed that S preferentially partitions into molten iron while significant amount of Si enters the solid phase with temperature decrease. Meanwhile, the C concentration in the liquid and solid iron metal changes little with temperature variations. If S, C and Si partitioning behaviour between molten iron and solid iron metal with temperature are expected to be the same under Earth's present core pressure condition, the solid inner core should be iron dominated with dissolved Si. On the other hand, the liquid outer core will be S rich and Si poor. Moderate carbon will be evenly present in both solid and liquid iron metallic core.

Based on our melting data in a multi-component system, no layered liquid core should exist in Venus and Mars, because of their high core pressures. On the other hand, Mercury, which has an estimated CMB pressure of ~7 GPa, may have a layered liquid outer core due to immiscible liquids (one is S rich and one is Si rich) and a solid Fe-Si inner core.

https://doi.org/10.1180/S0026461X00006502 Published online by Cambridge University Press

Confocal Raman spectroscopic characteristic of pseudoleucite in alkaline intrusive rocks: Central Anatolia, Turkey

K. DENIZ* AND Y.K. KADIOGLU

Ankara Univ., Dept., of Geol., Eng., & YEBIM Ankara, Turkey (*correspondence: kdeniz@eng.ankara.edu.tr)

Pseudoleucite is one of the main mineral of the silica undersaturated rocks of alkaline rocks of Central Anatolian Crystalline Complex. The pseudoleucite comprises aggregates of K-feldspar and nepheline preserving orginal crystal forms of leucite. Confocal Raman spectroscopic studies reveal that the leucite has been replaced by disordered K-feldspar with a structural state intermediate between orthoclase and nepheline form in spheluritic texture under the microscope (Figure 1). The pseudoleucites are inferred to have grown of crystallization of leucite at high temperature and pressure then transformed to orthoclase with less amount of nepheline through reaction with sodium-rich fluids and PH_2O at low pressure and temperature in proportion to previous original formation of the leucite in the same system.

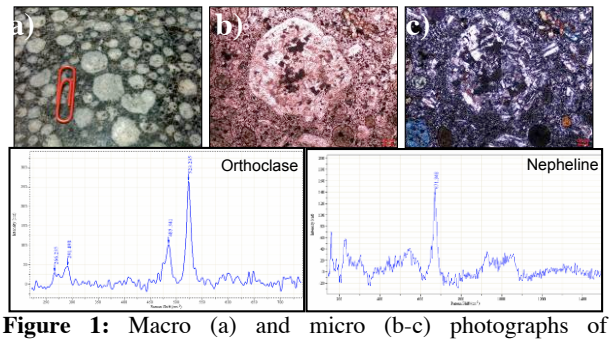

Figure 1: Macro (a) and micro (b-c) photographs of pseudoleucite and CR Spectrums of orthoclase and nepheline

Discussion and Results

Compositional zoning in primary and late-stage minerals indicates complex, multi-stage crystallization and replacement histories. Late stage fluids of alkaline magma, rich in F, Cl, CO_2 and H_2O, reacted with primary minerals to form complex intergrowths of minerals such as pseudoleucite, cancrinite, fluorite, V-bearing magnetite, F-bearing garnet and Na-augite. Early crystallization of apatite and titanite controlled the compatible behavior of P and Ti, respectively.

The formation of melanite and uvarovite garnet also affected the behavior of Ti, Cr as well as Zr, Hf and the heavy rare-earth elements in these rocks. The innovator crystalization of leucite, cause to intergrowths of K-feldspar and nepheline at the late stage of fractionation.

Global asssesments of linkages between air quality and climate

F. DENTENER

European Commission, Joint Research Center, Ispra, Italy. (frank.dentener@jrc.ec.europa.eu)

Aerosols are among the most important contributors to air quality problems, and are also active constituents of the climate system. Unfortunately, there are large scale differences between global climate models and urban-to-regional scale air quality models, which prevented consistent and extensive scientific analysis of air quality and climate impacts. In addition, since air pollution and greenhouse gas mitigation policies were often developed independently, a policy driver to the integrate these urban-to-global scales was missing. This situation is changing- global models are increasing resolution, and regional models are expanding model domains. Global model analysis are used for air quality analysis, and regional models are use for regional climate assessments. The co-benefits for air quality are increasingly important aspects of climate policies, while targetted air quality policies may help to prevent rapid climate change on the decadal time scales.

In this overview talk, I will present results from the international HTAP (Hemispheric Transport of Air Pollution) assessment, with a focus on the role of contintal transport versus 'local' emissions of aerosols and precursors, discuss re-analysis efforts to understand the interaction between changing climate and air quality in the past decades, and the describe the current understanding of the health and climate effects of these aerosols on the global scale. I further present the implications and insights derived from various air pollution/climate scenarios resulting from recent assessments (GEA, RCP, etc).

https://doi.org/10.1180/S0026461X00006502 Published online by Cambridge University Press

Influence of solute-solvent interactions on mass discrimination during chemical diffusion

D.J. DEPAOLO[1,2]*, J.M. WATKINS[2] AND F.J. RYERSON[3]

[1]Lawrence Berkeley National Lab, Berkeley, CA 94720, USA (*correspondence: depaolo@eps.berkeley.edu)
[2]University of California-Berkeley, Berkeley, CA 94720, USA
[3]Lawrence Livermore National Lab, Livermore, CA 94550, USA

Chemical diffusion in molten silicates and aqueous solutions leads to stable isotope variations in nature because chemical diffusivities are mass dependent. For diffusion in liquids, there is no general theory that relates cation diffusivity to mass, but mass discrimination during diffusion must be affected by the nature of cation-solvent interactions.

To investigate the relationship between liquid structure and cation diffusion, we measured Ca and Mg isotope diffusivities in silicate liquids using diffusion couples of natural and synthetic compositions. In all experiments, the initial isotopic composition is uniform and each isotope diffuses in the same direction down a substantial concentration gradient, enriching the Ca- or Mg-poor liquids in the lighter isotope by an amount dependent on: (1) the initial concentration contrast between liquids, (2) the relative chemical diffusivities of isotopes, and (3) the efficiency of isotopic exchange or self diffusion superimposed on chemical diffusion. Results from these experiments, in combination with results from natural volcanic liquids, show clearly that the efficiency of isotope separation (E) is systematically related to the solvent-normalized diffusivity - the ratio of the diffusivity of the cation (D_{cation}) to the diffusivity of silicon (D_{Si}).

We present an idealized quantitative model to explain the relationship between E and D_{cation}/D_{Si}. The model views cation diffusion as a combination of two (or possibly more) distinct mechanisms of transport: “free” cations that site-hop among aluminosilicate structures, and “bound” cations that translate or rotate with aluminosilicate structures in the melt. We assume that the rate of exchange between free and bound cations is infinitely fast to maintain local equilibrium. In this model, the observed or net diffusivity and its mass dependence are determined by the relative abundance (K) of free versus bound cations in the liquid. This conceptualization provides a framework for describing mass discrimination in complex liquid systems and for understanding the role of diffusion in contributing to stable isotope variations in minerals.

Bimodal volcanism of the Northern frames of the Eastern link of the Mongolian-Okhotsk orogenic belt (Russia)

INNA DERBEKO

Institute of Geology and Nature Management FEB RAS, Blagoveshchensk, Russia, (derbeko@mail.ru)

In the Southern frames of Eastern link of Mongol-Okhotsk orogenic belt (MOOB), in the end of early Cretaceous (119 - 97 Ma), a bimodal volcano-plutonic complex was formed. It correlated by a whole number of parameters with bimodal formations of the Western link of the belt [1]. The formations in the Northern frames of the Eastern link of MOOB, that are analogical by the age and petrochemical characteristics, are separated. There are insignificant differences in geochemical characteristics (Fig.1). There are also diversities by isotopic parameters $^{87}Sr/^{86}Sr$ =0.70592-0.70620, by $\varepsilon Nd_{(T)}$ = (-11.77) – (-12.20) and T_{Nd}(DM-2st)=1901-1937 Ma [2]. Along Southern and Northern borders of the Eastern flank of MOOB the bimodal volcano-plutonic complexes were formed during 119-97 Ma. Their geochemical characteristics show that they were formed in the situation of convergence borders of the platforms (collision of North-Asian and North-Chinese continents).

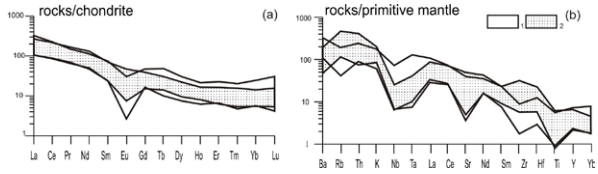

Figure 1: Geochemical characteristics of the rocks of the bimodal complexes framing MOOB: 1 – Northern, 2 – Southern. Concentrations of the rear elements in the Compositions of chondrite C1 and primitive mantel are brought according to the data (Sun, McDonough, 1989).

[1] Derbeko (2010) *GCA*. **74**. Iss. 11. Suppl. 1. A225. [2] Stricha & Rodionov (2006) *Doklady Akademii Nauk*. **406**. P. 375-379.

https://doi.org/10.1180/S0026461X00006502 Published online by Cambridge University Press

The insoluble organic matter in carbonaceous meteorites

S. DERENNE[1] AND F. ROBERT[2]

[1]BioEMCo, CNRS-UPMC, Paris, France (sylvie.derenne@upmc.fr)
[2]LEME, MNHN-CNRS, Paris, France (robert@mnhn.fr)

Carbonaceous meteorites are the most primitive objects of the solar system. They exhibit significant carbon contents mostly occuring as insoluble organic matter (IOM). IOM might be the first OM available on early Earth for life and should provide information on solar system history. It is therefore esential to decipher the chemical structure of IOM.

IOM was isolated from the Murchison meteorite using successive water and solvent extractions and acid treatments (HCl, HF). Its chemical structure was investigated through a combination of various spectroscopic methods (Fourier tranform infra-red, solid-state ^{13}C and ^{15}N NMR, electron paramagnetic resonance, X-ray absorption near-edge spectroscopy), chemical (RuO_4 oxidation) and thermal (pyrolysis) degradations and high resolution transmission electron microscopy. The use of these complementary analytical tools yielded key information on the IOM structure at a molecular level and led to 11 quantitative parameters. A statistical model was therefore proposed for this molecular structure, fitting with these 11 parameters.

Moreover, deuterium isotope abundance was determined in individual compounds released through RuO_4 oxidation and pyrolysis pointing to 3 types of H (aromatic, benzylic and aliphatic) with different D enrichment related to the C-H bond strength. This was further confirmed by laboratory experiments. We therefore propose that the IOM formed in a D-poor environment and was then transported and further enriched through exchange in a D-rich medium. EPR studies also revealed that free radicals were the hosts of extreme D enrichments revealed through nanoSIMS.

These results are difficult to reconcile with the usual interpretation according to which high D/H ratios represent survivals of interstellar grains. More likely, the deuterium-enrichment process took place after the formation of organic grains characterized by low D/H ratios, through an isotopic exchange-reaction with D-rich gaseous molecules, such as H_2D^+ or HD_2^+. This exchange reaction most likely took place in the diffuse outer regions of the protoplanetary disk around the young Sun.

Element transport and mineral replacement reactions during alkali contact metamorphism

I.T. DERREY*, M.A.W. MARKS AND G. MARKL

Eberhard Karls Universität Tübingen, Wilhelmstraße 56, 72072 Tübingen, Germany (*correspondence: insa-theresa.derrey@student.uni-tuebingen.de)

To study element transport in crustal rocks, high concentration gradients are favorable, as they are present along the margins of peralkaline rocks intruded into common crustal rocks. The 1.16 Ga peralkaline Ilímaussaq intrusion in SW-Greenland is characterized by its high alkali as well as high LILE, HFSE and volatile content. It intruded at the contact between the granitic Julianehåb batholith and a volcano-sedimentary succession [1].

We took 19 samples along a 1 km long profile from the contact of the Ilímaussaq intrusion into the adjacent granite. Accounting for the exponential character of diffusive processes, we chose a close spacing between samples near the contact with increasing distances further away from the intrusion.

Significant contact alteration, accompanied by growth of new minerals (aegirine, arfvedsonite) has been previously reported [2] and can be observed in the field up to a distance of 40 m away from the contact. This is confirmed by stable isotopic data of Li and B [3, 4], supporting diffusive alteration of the contact rocks.

Our whole rock analyses reveal an influence of the alkaline fluids released by the Ilímaussaq complex on the host granite up to ca. 200 m by elevated contents of e.g. Na, Ca and P as well as depletion in Si and K. In addition, batches of eutectic quartz-feldspar intergrowths in the granite up to ca. 10 m from the contact imply partial melting of the granite.

Among the mineral replacement reactions the growth of amphibole and pyroxene at the expense of biotite as well as the replacement of perthitic alkalifeldspar by almost pure albite are most obvious. To get a full insight on replacement reactions and changes in mineral chemistry along the profile, microprobe analyses will be carried out.

[1] Poulsen (1964) *Rapp. Grønl. Geol. Unders.* **2**, 16. [2] Ferguson (1964) *Bull. Grønl. Geol. Unders.* **39**, 82. [3] Marks *et al.* (2007) *Chem. Geol.* **246**, 207–230. [4] Kaliwoda *et al.* (in press) *Lithos*, 14.

https://doi.org/10.1180/S0026461X00006502 Published online by Cambridge University Press

Reconciling multiple constraints on late Cenozoic erosion and weathering fluxes: Can we do it?

LOUIS A. DERRY

Dept. of Earth & Atmospheric Sciences, Cornell University, Ithaca NY USA 14853; (derry@cornell.edu)

Records of geochemical tracers in late Cenozoic marine sediments show large changes, the causes of which have been the subject of intense interest in the geoscience community. Intensive tracers include $^{87}Sr/^{86}Sr$, $^{187}Os/^{188}Os$, $\delta^{18}O$, $\delta^{13}C$, $^{44}Ca/^{42}Ca$, $^{26}Mg/^{24}Mg$ $\delta^{11}B$, Ge/Si, $\delta^{30}Si$ and $^{10}Be/^{9}Be$. Information from these tracers needs to be integrated with elemental mass balance constraints such as Mg/Ca in forams, sediment accumulation rates, changes in the CCD, and reconstructions of pCO_2. To date, a quantitative and self-consistent scenario that successfully integrates this diverse and increasingly detailed set of observations has been elusive. All of the isotopic tracers are subject to provenance effects, i..e. values can vary as a function of source, and the mix of sources changes in time. The stable isotope tracers are additionally subject to fractionation at the source via changes in weathering processes and/or biological cycling. They can be further impacted by fractionation during incorporation into sediment archives.

Studies at the small watershed scale suggest that several of the tracers ($^{87}Sr/^{86}Sr$, $^{26}Mg/^{24}Mg$, Ge/Si, $\delta^{30}Si$) can be used to identfy particular mineral weathering reactions and/or identify the effects of biocycling. Integrating this information over larger spatial and temporal scales is not straigtforward. Biocycling effects can be important over short time scales but their impact is reduced over time scales much longer than the residence time of the tracer in regolith-soil-plant system.

Recycling of the sedimentary mass is a major source of the erosional flux, and can be particularly significant for tracers significantly stored in carbonate rocks, as these are nearly quantitatively recycled during erosion. While the late Cenozoic shift in $\delta^{13}C$ has received relatively little attention comparted to some other tracers, a decrease in $\delta^{13}C_{sw}$ beginning in the mid–Miocene is consistent with both a proportional and absolute increase in the weathering flux of carbonates. A mid-Miocene acceleration in sediment recycling appears at least consistent with most of the available constraints from other tracers of weathering and erosion, and a model can be used to make testable predictions for other tracer systems. Since each system is individually underconstrained, a quantitative approach that attempts to satisfy multiple tracer records is necessary.

Spatial vegetation patterns, catastrophic shifts and desertification in arid ecosystems under land use and climate regimes

PETER C. DE RUITER[1] AND SONIA KEFI[2]

[1]Land Dynamics of Wageningen University (NL); (Peter.deRuiter@wur.nl)

[2]Institut des Sciences de l'Evolution, CNRS UMR 5554 Montpellier, France

Desertification currently affects the livelihood of more than 200 million people. A primary aim of the international community is to stop desertification to enhance agricultural productivity and combat hunger of many millions of people. Desertification, especially the shift of productive semi-deserts into non-productive full-deserts, can have a 'sudden' or 'catastrophic' character, indicating the existence of critical transitions over 'thresholds' or 'tipping points'

These catastrophic events result from the interplay between two different ecological interactions among the plants making up the vegetation in semi-desert ecosystems. The first is facilitation, where plants support each other in terms of collectively attracting water and nutrients and provide the soil with organic matter compounds. Facilitation acts at relatively small spatial scales. Second, there is competition between plants for the same resources (water, nutrients), but then on a relatively large spatial scale. The process of facilitation helps plants to survive, together, under harsh conditions. Such survival under harsh conditions requires though a critical vegetation biomass, below which the plants cannot adequately acquire the necessary resources. Similarly, when conditions becomes gradually harsher (e.g. less resources, higher grazing intensity), then at a critical point, the vegetation cannot attract enough resources anymore to survive and the ecosystem will collapse into a non-vegetation bare soil desert ecosystem.

We will present the outcome of a study in which spatial explicit models that simulate desertification is combined with field observations on semi-deserts under various land use and climate regimes. The results showed that particular non-random patterns in the spatial distribution of the vegetation are indicative the proximity of a critical threshold. The model results closely resembled the patterns that were observed in the field trials.

[1] Rietkerk, M., Dekker S.C., de Ruiter P.C., van de Koppel J. (2004). Self-Organised Patchiness and catastrophic shifts in Ecosystems. *Science* **305**: 1926-1929 [2] Kéfi S., Rietkerk M., Alados C.L., Pueyo Y., Papanastasis V.P., ElAich A., de Ruiter P.C. (2007) Spatial vegetation patterns and imminent desertification in Mediterranean arid ecosystems. *Nature* **449**: 213-217.

https://doi.org/10.1180/S0026461X00006502 Published online by Cambridge University Press

Bacterial cells can biosorb and accelerate the transport of heavy metals mixtures in soils

AURELIEN DESAUNAY AND JEAN M.F. MARTINS

LTHE-CNRS-Univ. Grenoble I (UMR 5564), Domaine Universitaire BP 53, 38041 Grenoble Cedex 9, France; (jean.martins@hmg.inpg.fr)

Recent field observations have demonstrated that supposedly poorly mobile metals can be detected at long distances from their source, highlighting the importance of poorly predicted transport processes. The fast mobilisation of metals by the colloidal and mobile fraction of soils and in particular biotic colloids (bacteria, algae, fungi, virus, etc.), is now identified as an important secondary transport process that can lead, under specifc conditions, to accelerated and potentially dominant pollutant transfer towards aquifers. In order to better understand the role of the bacterial compartment of soils to metal leaching, we conducted a coupled study under static and dynamic conditions. Firstly we evaluated Zn and Cd metal biosorption onto active or inactive Gram negative bacteria (*Escherichia coli* and *Cupriavidus metallidurans* CH34) by characterizing the sub-cellular distribution of the metals through a cell disruption approach. The quantification of Zn and Cd in extracellular, membrane and cytoplasm compartments of the cells permitted to show that metals are unequally distributed between the three cell compartments and also between the two bacteria. Surprizingly, metals internalization appeared to be the dominant accumulation process of metals (high cytoplasm contents). The physiological state of the cells was also shown to be important in metal management by the bacteria, since metal accumulation in active cells was reduced due to enhanced efflux and/or EPS production mechanisms. These results suggest bacteria can internalize important amounts of heavy metals and also that adsorption onto cell surface is only a first step in metal management by bacteria. The so-determined thermo-dynamic reactivity constants were used to fit metal breakthrough curves performed in natural sand columns. The transport experiments of bacterial cells, metals or mixtures of bacteria and/or metals performed in the second part of the study, demonstrated that bacteria are able to accelerate the *in situ* mobilization of Cd and Zn retained in natural sand columns. This transport process was shown to be dominant upon aqueous transport and was correctly fitted using a combined transfer and geochemical modeling approach. Altogether, these results showed that, under specific conditions, heavy metal transport by bacterial cells can dominate aqueous transport processes in soils.

Silicon stable isotope constraints on the global oceanic Si cycle

G. F. DE SOUZA[1]*, B. C. REYNOLDS[1] AND B. BOURDON[1,2]

[1]ETH Zurich, Institute of Geochemistry and Petrology, Zurich, Switzerland (*correspondence: desouza@erdw.ethz.ch)
[2]École Normale Supérieure de Lyon and CNRS, France

The global oceanic distribution of nutrients such as silicon (Si) governs the distribution and magnitude of primary productivity in the sea, and thus the strength of the ocean's biological carbon pump. These nutrient distributions are the combined result of biological and physical processes that interact over a range of temporal and spatial scales. Information on the stable isotope composition of dissolved nutrients can be employed to deconvolve the processes contributing to the observed oceanic tracer field, potentially allowing the identification of nutrient sources and/or the relevant biological–physical cycling processes.

We will present a dataset of the stable Si isotope composition of dissolved silicon (expressed as δ^{30}Si) from three major oceanic regions: the Atlantic, the Southern Ocean and the South Pacific, including samples collected as part of the GEOTRACES programme. This high-precision dataset has been produced by a single laboratory, allowing a more robust assessment of intra- and inter-basin gradients than has been previously possible.

The coherence of the δ^{30}Si distribution in the deep Atlantic is a testament to the strength of δ^{30}Si as a tracer of the modern oceanic Si cycle. Values of δ^{30}Si vary systematically with Si concentration, from +1.7‰ and higher in the Si-poor deep subpolar North Atlantic to values of +1.2‰ in the deep South Atlantic, associated with the mixing of water masses of Nordic and North Atlantic origin with Si-rich bottom waters from the Southern Ocean. The North Atlantic most likely owes its high-δ^{30}Si signature to the input of ^{30}Si-enriched silicic acid through the upper return path of the meridional overturning circulation (MOC), indicating that the basin-scale δ^{30}Si gradient in the deep Atlantic is dominantly controlled by the interaction of biological Si utilisation with subsurface watermass formation in the Southern Ocean, and subsequent Si transport by the MOC.

In our presentation, we will extend our analysis of oceanic δ^{30}Si in the MOC context to the global ocean, including the interpretation of our dataset in the framework of geochemical box models of the ocean.

https://doi.org/10.1180/S0026461X00006502 Published online by Cambridge University Press

Use of stable (HOCN) and radiogenic (Sr) isotopes to determine the geographic provenance and traceability of artisanal cheeses of Quebec, Canada

S. DESROCHERS*, R. K. STEVENSON, J-F. HÉLIE, AND A. POIRIER

GEOTOP et, Science de la Terre et de l'Atmosphère, Université du Québec à Montréal, P.O. Box 8888, Station Centre-Ville, Montreal, Qc, Canada, H3C 3P8 (*correspondence: desrochers.steph@gmail.com)

Introduction

Analysis of stable isotopes has often been used to determine the traceability of different food products [1] The light stable isotope ratios in dairy products such as cheese can provide information for tracing geographical origin.[4] The province of Quebec is Canada's largest cheese producer and artisanal cheeses are becoming a larger part of this market. In this context, we selected artisanal cheeses from six different regions of the province of Quebec to study the applicability of light stables isotopes and radiogenic isotope (Sr) ratios as descriminants to provide geographic traceability.

Sampling method and results

The cheese samples were analysed for light stable isotope ratios (HOCN) which are mainly influenced by altitude, distance from the sea, use of fertilizer, rainfall, food type, temperature, longitude and latitude [2,3,6]. The Sr isotope analyses are indicative of the geology of the type of substrate of the grazing areas [5]. Prelininary results yeild $^{87}Sr/^{86}Sr$ ratios that vary from 0.71084 to 0.71347. These values reflect soils composed largely of galcial tills derived from either the Canadian shield or Appalachain Orogen. Stable isotope δD values vary beteween -103.06‰ to -55.74‰, and $\delta^{18}O$ between -17.99‰ to -7.54‰. In addition, samples of the food, water, soil and raw milk will also be analysed to determine if enrichment or depletion of the different stable isotope ratios occurs during the manufacture of milk and during the conversion of milk to cheese.

[1] Kelly, Heaton & Hoogewerff (2005) *Food Science and Technology* **16**, 555-567. [2] Mariotti *et al* (1981) *Plant soil,* **62**, 413-430. [3] Moser & Rauert (1980) Berlin: Bornträger. [4] Pillonel & al (2002) *Lebensm. Wiss. u. Technol.* **36**, 615-623. [5] Rossmann *et al* (2000) *European Food and Research Technology,* **211**, 32-40. [6] Smith & Epstein (1971) *Plant physiology*, **47**, 380-384.

Indian Ocean monsoon dynamics recorded in a speleothem from Socotra, Yemen

D. DE VLEESCHOUWER[1], M.VAN RAMPELBERGH[1], PH. CLAEYS[1], H.CHENG[2], S.VERHEYDEN[1] AND E. KEPPENS[1]*

[1]Earth System Science, Vrije Universiteit Brussel, Pleinlaan 2, B-1050 Brussels, Belgium (*correspondence: ekeppens@vub.ac.be),

[2]Geology and Geophysics, University of Minnesota, 100 Union St SE Minneapolis, MN 55455, USA

On the arid Indian Ocean Socotra Island (12º30'36" 53º55'12"), the Intertropical Convergence Zone (ITCZ) induces a bimodal distribution of the precipitations. Rain falls only as the northward migrating ITCZ passes in May-June and as it returns southward from September to December. The watershed effect of the 1540m-high SW/NE oriented Haggeher Mountains forces precipitations to concentrate on the windward side of the range [1]. Multi-proxy analyses ($\delta^{18}O$, $\delta^{13}C$ & greyscale) are carried out at high resolution (500μm = time-scale ~3 years) on two stalagmites collected in the eastern part of the island: STM1 from the Hoq Cave and STM5 from Casecas cave, 6 km away. Based on TIMS U/Th-dating they resp. cover the last 6000 years and the last 1000 years. Spectral analysis of the obtained records reveals an important ~205-years component in STM1. Comparing the ∂18O & ∂13C records with a reconstruction of solar activity [2] indicates that for most of the last 6000 years periods of lower precipitation and less vegetation are associated with periods of high solar activity. Periods of low solar activity induce more precipitations and higher vegetation abundance. In Oman, solar activity is positively related with the intensity of the rainy seasons because of changes in the latitudinal position of the ITCZ and the convective activity [3]. The Socotra results independently confirm this hypothesis and refine it by identifying the 205-years "De Vries / Suess" sunspot cycle as the dominant forcing cycle for the Indian Monsoon Dynamics on a centennial scale.

[1] Scholte, P., De Geest, P., (2010) *Journal of Arid Environments* **74**, 1507; [2] Steinhilber, *et al*., (2009) *Geophysical Research Letters* **36**, 1; [3] Fleitmann *et al*. (2007) *Quaternary Science Reviews* **26**, 170.

https://doi.org/10.1180/S0026461X00006502 Published online by Cambridge University Press

Evolution of crust in the Dharwar craton: The Nd isotopic evidence

SUKANTA DEY

Department of Applied Geology, Indian School of Mines, Dhanbad – 826004, India (geodeys@gmail.com)

The western and eastern Dharwar cratons (WDC and EDC) show appreciably different crustal evolution patterns as recorded by 333 whole-rock Nd isotopic data (including 34 unpublished data of the author). Both the cratons exhibit evidence of Palaeoarchaean crust (Fig. 1) whose rock record is either destroyed by later crustal reworking or awating to be discovered. In EDC 3-2.7 Ga is the most significant crust extraction period, whereas in WDC crust was extracted in two dominant episodes i.e. 3.5-3.2 and 3-2.9 Ga. Some komatiites and mafic volcanics of the older episode have considerably higher εNd values (>4.5) indicating that at least parts of the contemporary mantle was extremely depleted possibly due to extraction of crust during some earlier event(s). Younger mantle-derived rocks in the WDC (especially the 2.9 Ga mafic volcanics) do not show evidence of such extremely depleted mantle. This requires immediate refertilization of the mantle below WDC after the older episode of crust formation (~3.2 Ga). The Neoarchaean period in the WDC is characterized by some juvenile addition of crust and extensive crustal recycling during 2.7-2.6 Ga. For EDC contrasting source characteristics of contemporary mantle-derived Neoarchaean rocks (extremely depleted to chrondritic mantle) suggests juxtaposition of unrelated terranes by accretionary processes. The terminal Neoarchaean in EDC is characterized by granitoid formation from metasomatized mantle wedge as well as widespread crustal recycling.

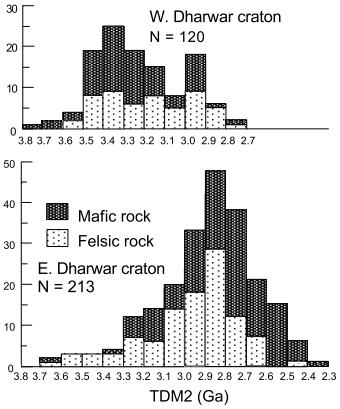

Figure 1: Distribution of depleted mantle model ages in the eastern and western Dharwar cratons.

Isothermal, kinetic and mechanism studies of uranium biosorption by *Aspergillus niger* from aqueous solutions

R. DHANKHAR* AND A. HOODA

Department of Environmental Sciences, M.D.U, Rohtak, INDIA (*correspondence: dhankhar.r@rediffmail.com)

Biosorption have emerged as an alternative technology for heavy metal and radionuclide removal from ground water contaminated due to mining sources [1, 2]. In light of this, present study has been carried out to investigate the biosorption potential of *Aspergillus niger* for removal of uranium form aqueous solution. Some concerned results are shown in Fig. 1.

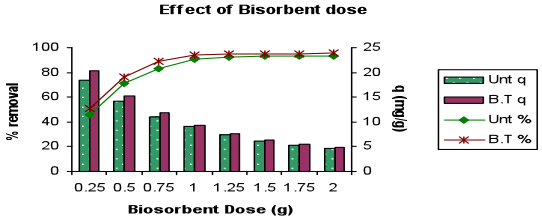

Figure 1: Effect of Biosorbent dose on biosorption of U (VI) on non-living *A. niger* biomass.

Discussion of Results

Uranium uptake at pH 5 and 100 μm particle size, Adsorbent dose of 10g/L and initial metal concentration of 100mg/L. Maximum uptake of 9.21 mg/g was observed after the Contact time of 75 minutes. Equilibrium data fitted well to Langmuir model and Uptake kinetic followed pseudo-second order model. Base treatment was found to enhance the metal removal ability of untreated biomass. The mechanism of process was gained by FTIR and SEM. IR spectra analysis revealed that Carbonyl and amino groups have played important role in U (VI) biosorption.The results are well in concordance with some earlier findings in that concern [3, 4].

[1] Crini (2006) *Biores Technol*. **97**, 1061–85.
[2] Vijayaraghavan *et al*. (2008) *Dyes Pigm*. **76**, 726–32.
[3] D. Humelnicu *et al*. (2011) *Journal of Hazardous Materials* **185**, 447-455. [4] Wang *et al*. (2010) *Journal of Environmental Radioactivity* **xxx**, 1-5.

https://doi.org/10.1180/S0026461X00006502 Published online by Cambridge University Press

Growth and reworking of Gondwana through time

B. DHUIME[1,2]*, C.J. HAWKESWORTH[1], P.A. CAWOOD[1], C.D. STOREY[3] AND K.N. SIRCOMBE[4]

[1]Department of Earth Sciences, University of St. Andrews, North Street, St. Andrews KY16 9AL, UK (*correspondence: b.dhuime@bristol.ac.uk)
[2]Department of Earth Sciences, University of Bristol, Wills Memorial Building, Queens Road, Bristol BS8 1RJ, UK
[3]School of Earth and Environmental Sciences, University of Portsmouth, Portsmouth PO1 3QL, UK
[4]Minerals Division Geoscience Australia PO Box 278 Canberra, ACT 2601 Australia

The timing of continental crust generation is dependent on the nature of the rock record. Juvenile igneous rocks from various continental segments usually show marked age peaks suggesting episodic growth [e.g. 1]; and fine-grained sediments, which provide an average of their igneous source terranes, provide smooth curves of crust generation [e.g. 2], which are more consistent with the continuous nature of crust formation at the level of destructive plate margins. Thus there are long-standing questions over (i) whether the age peaks of juvenile rocks are representative, or merely artefacts of selective preservation [3], and (ii) the extent to which the processes and rates of crust generation and recycling have varied with time.

We present an integrated U-Pb, Hf and O isotopes study on zircons from sedimentary deposits along ~2000 km of the eastern Australian coastline. The data establish that continental growth of Gondwana is continuous, with a significant inflection point in the rate of generation at around 3 Ga. This point marks the transition between (i) very rapid generation of continental crust in the first ~1.5 Ga of Earth history and (ii) lower volumes of preserved crust towards the present day. Such a fundamental change in the way the continental crust was generated and preserved can be linked to the onset of 'modern' plate tectonics, which may have been active since at least 3.1 Ga [4]. This is also consistent with the formation of Hadean/Early Archean crust in a tectonic environment different from modern plate tectonics [5].

[1] Condie (1998) *Earth Planet. Sci. Lett.* **163**, 97-108. [2] Allègre & Rousseau (1984) *Earth Planet. Sci. Lett.* **67**, 19-34. [3] Hawkesworth *et al.* (2009) *Science* **323**, 49-50. [4] Cawood *et al.* (2006) *GSA Today* **16**, 4-11. [5] Kemp *et al.* (2010) *Earth Planet. Sci. Lett.* **296**, 45-56.

Soil closure ages from meteoric ^{10}Be, McMurdo Dry Valleys, Antarctica

W.W. DICKINSON[1]*, M. SCHILLER[2], B.G. DITCHBURN[3], I.J. GRAHAM[3] AND A. ZONDERVAN[3]

[1]Antarctic Research Ctr., Victoria University, Wellington, NZ (*correspondence: Warren.Dickinson@vuw.ac.nz)
[2]Centre for Star and Planet Formation, University of Copenhagen, Copenhagen, DK-1350, Denmark
[3]GNS Science, PO Box 30368, Lower Hutt, New Zealand

Understanding Neogene polar climate in the McMurdo Dry Valleys relies largely on evidence from landscape evolution, glacial modelling and stratigraphy. We provide new evidence from meteoric ^{10}Be for the onset of frozen, hyper-arid conditions in Dry Valley soils. A simple decay model for the co-occurrence of ^{10}Be and illuviated clay in two adjacent profiles indicates the clays were actively migrating down from the surface in a warmer climate until the system froze between 6 and 9 Ma. The model also suggests denudation rates of 0.02–0.06 m Myr^{-1} since closure. These data provide an independent test to glacial-stratigraphic evidence used to determine Antarctic paleoclimate.

Clays bound with meteoric ^{10}Be are prevalent in many Dry Valley soils to depths of over 4 m. These particles, which are now frozen in place, were illuviated by percolating water from the surface, during a previous 'wet period'. We use two adjacent profiles to take advantage of the ^{10}Be clock and determine when ^{10}Be was sealed or closed off from the surface. The two-profile method allows elimination of several variables and hence, calculation of how long ^{10}Be has been in the soil since freezing or closure. By sampling soils at a variety of altitudes and locations, we may build up a better picture of the transformation from sub-polar to polar conditions in the Dry Valleys.

https://doi.org/10.1180/S0026461X00006502 Published online by Cambridge University Press

Ocean oxygenation during the PETM: Mo isotope data from the Arctic and Tethyan Oceans

A.J. DICKSON[1]*, A.S. COHEN[1], A.L. COE[1], Y. GAVRILOV[2] AND E. SHCHERBININA[2]

[1]Department of earth and Environmental Sciences, The Open University, Milton Keynes, MK7 6AA, U.K. (*correspondance: a.dickson@open.ac.uk)

[2]Geological Institute of the Russian Academy of Sciences, Pyzhevsky 7, Moscow 119017, Russia.

Evidence for ocean deoxygenation during past intervals of global warming can help to set observations of expanding oxygen minimum zones in the moderns oceans into a longer term geological context. The molybdenum (Mo) isotope composition of the hydrogenous Mo in marine sediments that accumulated in euxinic settings can preserve the seawater Mo-isotope composition, which in turn reflects the balance between oxic, anoxic, and euxinic sinks in the global ocean. As such, it can be used to determine the extent of de-oxygenated waters in past oceans when the local depositional environment is well characterised. We present new Mo isotope data of samples from Arctic Ocean IODP Site 302 and from continental shelf sites on the northern Tethyan margin (Guru-Fatima and Kheu River) that accumulated during the Paleocene-Eocene Thermal Maximum (PETM) ~56 Ma ago. The PETM is characterised by a global C-isotope excursion (CIE) caused by the introduction of a large amount of isotopically depleted carbon into the earth-ocean-atmosphere system, which in turn caused global temperatures to rise by 5-8ºC.

Mo isotope data from IODP Site 302 broadly mirror the organic carbon isotope excursion recorded in the same sample suite, with near uniform values of 2.1 ‰ during the peak of the CIE and lower values during the late Paleocene and during the PETM recovery interval. Samples that accumulated during the peak of the CIE were deposited under locally euxinic conditions, demonstrated by trace element data measured in the same samples and also by comparision to published organic geochemical data. Their Mo-isotope values consequently record the seawater value at this time, which was only ~0.2 ‰ lower than modern seawater (~2.3 ‰). This finding suggests that (1) once euxinia in the Arctic Ocean is accounted for, global ocean anoxia was not widespread during the PETM and (2) the Arctic ocean was unrestricted during the PETM. In contrast, preliminary Mo isotope data from the northern Tethys Ocean suggest a slight expansion of ocean anoxia at the onset of the CIE, an interval that is missing within the Arctic core.

Hydrogen sorption by synthetic montmorillonites and clayrock at high temperature

MATHILDE DIDIER[1,2,3], FABRIZIO BARDELLI[2], ERIC GIFFAUT[1] AND LAURENT CHARLET[2]

[1]ANDRA, Châtenay-Malabry, France

[2]ISTerre, University Joseph Fourier, Grenoble, France

[3]CEA/LITEN/DTNM/LCSN, Grenoble, France

Hydrogen is more and more studied as a future energy carrier due to its availability and its energy capacity. The montmorillonite clay minerals are recognized as good hydrogen adsorbents [1] due to their large specific surface area and their wide range of porosity. In addition to this application, a clayrock has been considered as a host rock for French nuclear waste and particularly the Callovo-Oxfordian (COx), principally constituted by smectite and illite clays. Regarding nuclear waste repository, hydrogen gas is expected to develop from the anaerobic corrosion processes of the waste containers after the disposal closure. It is therefore of fundamental importance to study the fate of the hydrogen gas produced in the system, in terms of reactivity and integrity of the surrounding claystone layer.

This study aims at investigating hydrogen sorption on different types of synthetic montmorillonites and COx clayrock using gas chromatography and Sievert technology. Two-month long experiments were carried out at 90°C (the maximum temperature in the waste repository site) with dried or saturated clays. The hydrogen partial pressure varies from 0.1 to 0.45 bars.

Dried experiments show a sorption of hydrogen amount of 0.13 wt%. Experiments with saturated clays highlight a decrease of headspace hydrogen pressure (the figure below) as a function of time for a COx powder in NaCl aqueous solution taking into account the dissolved hydrogen. Sievert technology using high pressure of pure hydrogen gas (up to 80 bars) at 90°C shows a maximum sorption of 0.20 wt% for synthetic montmorillonite and 0.16 wt% for COx sample.

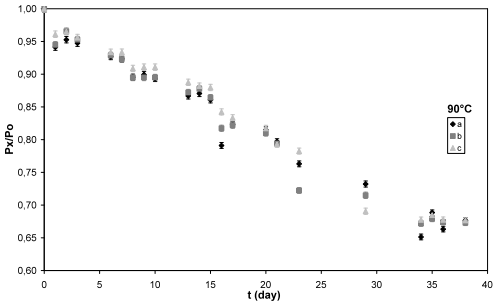

Figure 1: Evolution of hydrogen relative pressure with time for clay fraction of a COx sample at T = 90°C

[1] Gil, A. *et al*. (2009) *International Journal of Hydrogen Energy*, **34**, 8611-8615,

https://doi.org/10.1180/S0026461X00006502 Published online by Cambridge University Press

The effect of size on nanoparticle dissolution rate

TAMARA DIEDRICH[1]*, JACQUES SCHOTT[1], ERIC OELKERS[1], AGNIESZKA DYBOWSKA[2] AND EUGENIA VALSAMI-JONES[2]

[1]GET-Université de Toulouse-CNRS-IRD-OMP, 14 Avenue Edouard Belin, 31400 Toulouse, France, (*correspondence: tdiedric@gmail.com)
[2]Department of Mineralogy, Natural History Museum, Cromwell Road, London, SW7 5BD, U.K.

The dissolution rate of nanoparticles affects both their persistence in the environment and the release rate of their metal content, and, hence, can control their toxicity. While previous studies concluded that nanoparticles dissolve faster than their bulk analogs, contradictory evidence suggests that nanoparticles dissolve more slowly. Furthermore, insufficient characterization of the nanoparticulate samples and the solution chemistry in past studies obscures the relationship between particle size, surface area, and dissolution rate. There is a critical need for additional studies, using well-characterized nanoparticles and reactive solutions, to develop a model of nanoparticle dissolution rate.

Dissolution rates are a function of both the distance from equilibrium (providing the driving force for dissolution) and a dissolution rate constant (reflecting the dissolution mechanism and the strength of bonds critical to maintain the structure). The current study takes the approach of studying dissolution rates at far-from-equilibrium conditions to quantify the effect of particle size on the dissolution rate constant, isolating any potential kinetic effect of particle size from the well-established effect of particle size on solubility.

Multiple samples of both nanotalc and amorphous silica nanospheres were synthesized, ranging in size from approximately 20 to 200 nm. Samples were characterized by XRD, SEM, TEM, dynamic light scattering, and gas adsorption. Flow-through experiments were performed at far-from equilibrium conditions with pH from 2-10. Batch experiments were performed at both far-from and approaching equilibrium.

Preliminary interpretation of these data suggests that any effect of size on dissolution kinetics is minor. Thus, as the dissolution rate constant appears to be size independent (within experimental error), the dissolution rate of nanoparticles as a function of size and departure from equilibrium can be modeled by using classical kinetic rate laws and taking account of the effect of size on solubility.

Marine redox conditions and sulfur cycling during the deposition of the 2.3 Ga Timeball Hill Formation

D. DIEKRUP[1]*, A.J. KAUFMAN[2], B. KENDALL[3] AND H. STRAUSS[1]

[1]WWU Münster, Institut für Geologie und Paläontologie, Corrensstr. 24, 48149 Münster, Germany (*correspondence: daviddiekrup@uni-muenster.de)
[2]Department of Geology and the Earth System Science Interdisciplinary Center, University of Maryland, College Park, MD 20742, USA
[3]School of Earth and Space Exploration, Arizona State University, Tempe, Arizona 85287, USA

Rhenium and Molybdenum concentrations in shales and sulfur isotopes in disulfides and organic matter provide new insights in the development of the ocean-atmosphere system during the deposition of the 2.3 Ga Timeball Hill Formation, South Africa. Relatively low enrichment factors (relative to average crustal abundances) of Mo between 0.1 and 2.4 and high Re enrichment factors between 1.1 and 25.0 can be distinguished. Marginal concentrations of Mo correlate with the highest enrichments of Re, and appear to be coupled to the most negative $\delta^{34}S$ values (down to -30 ‰ against V-CDT in disulfides) and highest concentrations of organic bound sulfur.

High Re concentrations over wide parts of the stratigraphy argue for a deposition under anoxic but, as indicated by low Mo concentrations, not for euxinic deepwater conditions. Pyrite from these stratigraphic levels show the lowest $\delta^{34}S$ values, thus high isotopic fractionation, which suggests the establishment of an oceanic sulfate pool. The absence of large Mo and Re enrichments in the middle parts of Lower and Upper Timeball Hill shales indicate potentially oxic oceanic conditions. These samples show high $\delta^{34}S$ values in disulfides which could indicate a low sulfate flux to the oceans.

These observations lead to the conclusion that the water column was constantly non-euxinic at 2.3 Ga. The intensity of continental weathering and the subsequent delivery of nutrients to the oceans was variable and a consequence of the fluctuations of the atmospheric oxygen content.

https://doi.org/10.1180/S0026461X00006502 Published online by Cambridge University Press

Structural incorporation of selenium in iron sulfides

A. DIENER* AND T. NEUMANN

Institut für Mineralogie und Geochemie, Karlsruher Institut für Technologie, Adenauerring 20b, 76131 Karlsruhe, Germany (*correspondence: alexander.diener@kit.edu)

One of the key issues regarding the disposal of high-level nuclear waste in deep geological formations is related to the long term safety of a waste repository. Different performance assessment calculations for such repositories show a domination of ^{79}Se radionuclide with regard to the total exposure to the biosphere in the period of 10^4-10^6 years after disposal. Selenium is often associated with sulfides such as pyrite, a frequent minor constituent of host rocks and bentonite backfills considered for radioactive waste disposal. In this study, we investigated the incorporation of Se(-II) and Se(+IV) into pyrite.

The syntheses occurred via direct precipitation in batch and as coatings on natural pyrite in mixed flow reactor (MFR) experiments under anoxic conditions for Se-concentrations in the solutions up to 10^{-3} molL^{-1}. Furthermore, a high temperature synthesis by chemical vapor transport enabled the synthesis of Se-doted pyrite for single-crystals with a size up to 1 cm.

The mineralogical analyses by SEM and XRD reveal the syntheses of pure phases. Neither achavalite (FeSe), nor ferroselite ($FeSe_2$) were detected. The average of Se-uptake in 34 samples in batch experiments has been 98% and in MFR syntheses 99.5%, indicating a high potential for the retention of selenium by pyrite.

XAFS investigations have been performed at synchrotron light facility ANKA, Karlsruhe. These analyses and additional XPS measurements point out a reduced valence state of Se by initially dissolved Se(-II) and Se(IV) coprecipitated in pyrite and mackinawite. Curve progression and k-edge values [1,2] for selenide doted mackinawite (E_0: 12655.3 eV) in batch experiments imply a valence state of Se(-II) and for selenide doted pyrite (E_0: 12656.9 eV ± 0.3) in batch experiments a valence state of Se(-I), while the k-edge value of Se(0) as reference is higher (E_0: 12658.0 eV).

XAFS analysis on the coatings from MFR-syntheses, performed under slightly supersaturated conditions, indicate a coprecipitation of Se(-II) and Se(IV) predominantly as Se(0). With regard to batch experiments, these results indicate a substitution of sulfur with selenide just for high supersaturated solutions. In selenide doted mackinawite via direct precipitation in batch experiments occured a substitution of S with Se in an achavalite-type compound. As well, S is substituted by Se in selenide doted pyrite, ending in a FeSSe compound which could be best described by a slightly distorted pyrite structure.

[1] Charlet *et al*. (2007) *Geochim. Cosmochim. Acta* **71**, 5731–5749. [2] Scheinost *et al*. (2008) *J. of Contam. Hydr*. **102**, 228-245.

Geochemical expression of buried iron-oxide Copper Gold mineralisation within physical and chemical interfaces of the deep cover at the Hillside Prospect, South Australia

B.J. DIETMAN AND S.M. HILL

Deep Exploration Technologies Cooperative Research Centre, School of Earth & Environmental Sciences, University of Adelaide, SA 5005 Australia

Iron-Oxide Copper Gold (IOCG) mineralisation is an economically important mineral system in Australia, and includes the enormous Olympic Dam resource. Relative to its economic significance, however, little is known about the regolith geochemical expression of IOCG mineralisation, and therefore geochemistry has been under-utilised within the exploration for further deeply (10s-100s metres) buried deposits. This study shows that the weathered and transported cover overlying buried mineralisation can host systematic geochemical expressions of buried IOCG mineralisation.

The Hillside Prospect is 100 km northwest of Adelaide within the southern end of the IOCG prospective, eastern Gawler Craton. Mineralisation here is associated with N-S trending structures of the Pine Point Fault Zone.

Surface (soil) geochemistry results have shown locally elevated Cu-Au concentrations overlying buried mineralisation. The processes and associations with the underlying mineralisation and parts of the 10s-100s m deep cover in between the mineralisation and the soil are poorly constrained. Coastal cliffs in the area expose buried mineralisation at 10s of metres depth and the overlying saprolite, palaeodrainage, marine and aeolian sediments. Multi-element geochemical characterisation of these profiles shows variations in the chemical parametres associated with physical interfaces (e.g. unconformities and sediment lithologies) and chemical interfaces (e.g. palaeo- and contemporary redox boundaries, watertables) that provide strong expression and contrast within the cover for settings laterally proximal or distill to mineralisation. Many of the chemical interfaces are associated with supergene halos that are organised into locally enriched and differentiated U, Au and Cu zones flanking mineralisation. Whilst redox conditions and secondary iron oxide hosts provide important constraints on this geochemical expression, the secondary carbonate minerals and deep-rooted plant biogeochemical processes are also important.

https://doi.org/10.1180/S0026461X00006502 Published online by Cambridge University Press

Os isotopes in detrital Os alloys from the Rhine and evidence for a 1.2-1.3 Ga global? mantle melting event

ARJAN H. DIJKSTRA[1,*], CHRIS W. DALE[2], DMITRY S. SERGEEV[3], ZELIMIR GABELICA[4] AND ALAIN DEVILLIERS

[1]Centre for Research in Earth Sciences, University of Plymouth, UK (*arjan.dijkstra@plymouth.ac.uk)
[2]Department of Earth Sciences, Durham University, UK
[3]Institute of Mineralogy and Geochemistry, University of Lausanne, Switzerland
[4]ENSCMu, Université de Haute-Alsace, Mulhouse, France

Osmium isotope 'dating' of large populations of mantle-derived osmium-bearing alloys provides a key test for the idea of episodic crustal growth linked to global mantle melting events in Earth history [1]. Os alloys are formed within the mantle during high-degree melting, and their $^{187}Os/^{188}Os$ isotopic ratio can be used to date their formation.

Over 200 detrital Os alloys from placer gold occurrences in the Rhine between Basel and Frankfurt were obtained by gold washing techniques and hand-picking from gold separates. These 20-300 μm detrital Os alloys are derived from outcrops of ultramafic rocks in the Alps, which include blocks of mantle rocks with Tethyan affinity such as the Totalp Massif, and ultramafic lenses of unknown (Precambrian?) age in the Gotthard and Aar Massifs. Another source may be the Molasse of the Alpine foreland basin. $^{187}Os/^{188}Os$ isotope ratios were measured by LA-MC-ICPMS, to determine Re-depletion ages that should constrain the ages of melting in the mantle source rocks. The data show distinct age peaks at 0.5 and 1.2-1.3 Ga.

The 1.2-1.3 Mesoproterozoic age peak recorded by the Rhine Os alloy population does also occur in Os alloy age distributions of other ophiolites worldwide, generally as a subsidiary peak [1]. We show that the Mesoproterozoic age is also prevalent in Re-depletion age distributions of whole rock samples of refractory mantle xenoliths from ocean islands, and whole-rock samples of anomalously depleted abyssal peridotites from modern oceans, *e.g.,* from the 15-20 Fracture Zone (MAR) and Macquarie Island [2]. Therefore, analysis of Re-depletion ages from mantle rocks worldwide collectively point to a Mesoproterozoic, 1.2-1.3 Ga high-degree mantle melting event of global significance. This event may be related to a slab-avalanche or whole-mantle overturn event in Mesoproterozoic times.

[1] Pearson *et al*. (2007) *Nature* **449**, 202-205. [2] Dijkstra *et al*. (2010) *J. Petrology* **51**, 469-493

Adsorption of a textile dye (Acid Red 88) by montmorillonitic clay: Estimation of equilibrium, kinetic and thermodynamic parameters

S. DIKMEN[1*], B. ERSOY[2] AND A. GUNAY[3]

[1]Dept. of Physics, Anadolu Univ., Eskisehir, 26470, Turkey (*correspondence: sdikmen@anadolu.edu.tr)
[2]Dept. of Chem. and Materials Eng., King Abdulaziz Univ., Jeddah, 21589, Saudi Arabia. (bersoy@aku.edu.tr)
[3]Istanbul Metropolitan Municipality, Waste Management Directorate, Sisli, Istanbul (ahmetgunay2@gmail.com)

Introduction

Textile dyes are one group of the pollutants and the presence of dyes in the aquatic environment has been of great concern because of their potential health hazards associated with the carcinogenic, mutagenic, allergenic and toxic natures as well as negatively effects on the photosynthetic activity in aquatic life [1].

Method

The adsorption of AR88 onto montmorillonite was studied with variation in the parameters of pH, contact time, adsorbent and dye concentrations, and temperature to estimate the equilibrium, kinetic parameters and thermodynamic [2].

Kinetic models including pseudo-second-order, pseudo-nth-order, Bangham and double-exponential models were selected to follow the adsorption process. Kinetic parameters such as the rate constants, the equilibrium adsorption capacities and the related correlation coefficients, for each kinetic model were calculated and discussed. Thermodynamic parameters such as activation energy (Ea), Gibbs free energy (ΔG^o), enthalpy (ΔH^o) and entropy (ΔS^o) were also evaluated.

Discussion of Results

The dynamic data were fitted well the pseudo-nth-order kinetic model and also followed double-exponential function, the pseudo-second-order and Bangham Model, respectively.

The adsorption data obtained were well described by the Langmuir isotherm model. The maximum adsorption capacity was found to be 588 mgg^{-1} from the Langmuir isotherm model at 20 ºC. The negative value of change in Gibbs free energy indicates that the adsorption is spontaneous. The results show that montmorillonitic clay could be employed as low-cost material for the removal of acid dyes from textile effluents.

[1] Akar *et al*., (2008) *Bioresource Tech*. **99**, 3057-3065. [2] Günay *et al*., (2007) *J. Hazard. Mater*.**146(1,2),** 362-371.

https://doi.org/10.1180/S0026461X00006502 Published online by Cambridge University Press

Geochemical and tectonic fingerprinting of ophiolites

Y. DILEK[1]* AND H. FURNES[2]

[1]Department of Geology, Miami University, Oxford, OH 45056, USA (*correspondence: dileky@muohio.edu)
[2]Department of Earth Science & Centre for Geobiology, University of Bergen, Bergen 5007, Norway

We present a new classification of ophiolites, incorporating the diversity in their structural architecture and geochemical signatures that result from the variations in petrological, geochemical and tectonic processes during formation in different geodynamic settings. We define ophiolites as suites of temporally & spatially associated ultramafic to felsic rocks related to separate melting episodes & processes of magmatic differentiation in particular tectonic environments. Their geochemical characteristics, internal structure and thickness vary with spreading rate, proximity to plumes or trenches, mantle temperature, mantle fertility, and the availability of fluids. Subduction-related ophiolites include *suprasubduction zone* and *volcanic arc* types, whose evolution is governed by slab dehydration and accompanying metasomatism of the mantle, melting of the subducting sediments and repeated episodes of partial melting of metasomatized peridotites. Subduction-unrelated ophiolites include *continental-margin*, *mid-ocean ridge* (*plume-proximal, plume-distal and trench-distal*), and *plume-type* (*plume-proximal ridge* and *oceanic plateau*) ophiolites that generally have MORB compositions. Subduction-related ophiolites develop during the closure of ocean basins, whereas subduction-unrelated types evolve during rift-drift and sea-floor spreading. Geochemical and tectonic fingerprinting of Phanerozoic ophiolites within the framework of this new ophiolite classification is an effective tool for identification of the geodynamic settings of oceanic crust formation in Earth history that in turn helps us deduce the processes by which these oceanic rocks were incorporated into continental margins. We apply this new ophiolite classification to Precambrian greenstone belts as a conceptual framework to examine potential vestiges of Proterozoic and Archean oceanic lithosphere.

Protection of organic matter by clay minerals in source rocks revealed by biomarker analysis

DING FEI* AND CAI JINGONG

State key laboratory of marine geology, Shanghai, 200092, China (*correspondence: dingf2007@163.com)

Several mechanisms have been proposed in description the accumulation and preservation of organic matter(OM) in sediments, and the adsorption of clay minerals is concerned as an important way. It is significant that these different occurrences of OM studies with the biomarker information obtained from an source rock. The 10 source rock samples, an depth interval from 1294 to 3357 m from Shayejie formation in Dongying depression of China, were collected. The clay size fraction (<2μm) were isolated by sedimentary approach after the dispersion of the source rock by ultrasonic and deionized water. Both the clay size fraction and bulk source rocks were extracted by dichloromethane, and GC/MS was applied.

The normalized amount of the extractable organic matter (EOM) is higher in clay size fraction than it in the whole rock, 0.56mg/g and 0.37mg/g respectively, although the composition are similar between them. This suggestes that EOM mainly occurred as combined with clay size fraction in source rocks. The biomarker data show that there is no notable difference on characteristics of OM associated with clay fraction and in the whole rock. However, the differences between clay size fraction and whole rock show that the weak degradation of OM combined with clay fraction occur no matter caused by micro-organisms or thermalism, which could be demonstrated by the relative abundance of alkanes and isopreiods (Pr/nC_{17} and Ph/nC_{18} ratios are 1.44 and 1.54 in mean for the whole rock while 1.33 and 1.2 in mean for clay size fraction) and the ratios of maturity parameters(such as C_{31}22S/S+R ratios are 0.46 and 0.41 in average respectivelly, C_{29} ααα 20S/20(S+R) ratios are 0.18 and 0.14 in average respectively, for the whole rock and clay size fraction). In addition, the information acquired from biomarker of the whole rock may be obscured for the variety occurrences of OM in the whole rock, which should be caution.

This research was supported by the National Natural Science Foundation of China(Grants 40872089 and 41072089) and the State Key Lab. of Marine Geology Fund, Tongji University (MG200902).

https://doi.org/10.1180/S0026461X00006502 Published online by Cambridge University Press

Application of the field seismic data in superficial structure study for Wenshui Area

L. DING, S.G. HE AND E.G. GAO*

Institute of Disaster Prevention Science & Technology, Yanjiao, 101601, Beijing, China
(*correspondence: grg@ustc.edu.cn)

The Wenshui area is located in middle-west of Shanxi Province in north China, where plenty of coal resources are mined. In recent years, a large amount of seismic exploration work with the aim at coal recources has been done in the area successively. Based on the foundation of seismic exploration data, this study focuses on the superficial structure of sedimentary basin in the Wenshui area.

A 3D seismic data acquisition had been done in the Wenshui area. Seismic exploration lines are little longer than the field survey profile to cover all the possible coal resources area. In order to obtain the superficial structure of the area, seismic data processing had been done. And it can be summarized concisely into the following steps [1]: (1) carefully checked the positions of field shot-receiver pairs to obtain accurate localities; (2) calculated the static corrections in details; (3) eliminated bad shots, bad courses and abnormal amplitudes; (4) selected appropriate deconvolution parameters; (5) made accurate velocity analysis and got residual static corrections through stacking; (6) carried out the post stack processing and precise migration.

The result shows that there is a large syncline structure in the centre of the region, suggesting long-term tectonic push influenced Wenshui area since Triassic. This crustal deformation was accompanied with rock cracking in both coal sills and their wall rocks, which could lead to potential danger to the deep exploitation for coal mines.

This study is supported by Teacher Foundation of China Earthquake Administration (No: 20090112)

[1] Zhang Z. J., *et al* (2004), *Chinese J . Geophys*. (in Chinese), 469-474.

Silicon isotope composition of chert in carbonate rocks, as an indicator of paleo-environmental variation in ocean

TIPING DING [1,2], JIANFEI GAO [1,2] AND SHIHONG TIAN [1,2]

[1]Institute of Mineral Resources, CAGS, Beijing, China
[2]Key Laboratory of Isotope Geology, CAGS, Beijing, China

An investigation on the silicon isotope variation of chert bands and nodules in carbonate sedimentary formation from early Proterozoic to Mesozoic is undertaken in this study to study the temporal variation of the environmental conditions of the ocean.

The cherts in carbonate formation of Proterozoic period show large variation on their silicon isotope compositions. The δ^{30}Si values of chert from early Proterozoic Futuo Group vary from 0.1‰ to 1.3‰, with an average of 0.76‰, whilst those from middle Proterozoic Changcheng Group vary from 1.1‰ to 3.4‰, with an average of 2.09‰. The chert from late Proterozoic strata has lowest δ^{30}Si values, varying from 0.0‰ to 0.9‰ and with an average of 0.36‰.

The cherts in carbonate formation of Palaeozoic and Mesozoic periods show smaller δ^{30}Si variation than for Proterozoic. The chert of early Palaeozoic shows δ^{30}Si values from -0.6‰ to 1.7‰, averaging 0.70‰. Similarly, the chert of late Palaeozoic shows δ^{30}Si values from -0.4‰ to 1.7‰, averaging 0.61‰. Furthermore, the chert of Mesozoic shows δ^{30}Si between -0.3‰ and 1.1‰, averaging 0.55‰.

The positive δ^{30}Si values observed in all cherts in the carbonate formation from Proterozoic to Mesozoic indicate that the ocean has positive δ^{30}Si value since early Proterozoic period. This may be caused by the increase of biological activities, which generate silicon isotope fractionation while reduce the silicon content in the ocean water. The higher and more variable silicon isotope compositions of Proterozoic chert may reflect the significant change of environment conditions (temperature and Si content) in ocean from Archean to Proterozoic.

https://doi.org/10.1180/S0026461X00006502 Published online by Cambridge University Press

Volatiles and viscosity

D.B. DINGWELL

Earth and Environment, LMU – University of Munich, Theresienstr. 41/III, 80333 Muenchen, Germany

The physical properties of magmatic melts are notably influenced by the presence of dissolved volatiles. The influence of volatiles on the PVT-equation-of-state of silicate melts is slowly being mapped out in terms of the molar volume and its temperature- and pressure derivatives. The influence on transport properties is , to date, better constrained, and indeed the effects are even more dramatic for some volatiles. In both cases a wide range of complementary experimental techniques are being applied and it is often the case that proxy methods for property determinations yield results where direct determination is experimentally hindered.

Perhaps the most exhaustively investigated example of the influence of volatiles on properties is the case of the influence of water on viscosity. Its extensive investigation in the past 20 years contains many examples of experimental foresight and advance, as well as a number of pitfalls. Using this example, together with the allied determinations of transport properties in melts, a sketch of the state-of-the-art will be attempted.

An example of fluid immiscibility during the subvolcanic emplacement of a boron-rich acidic melt: The Capo Bianco aplite (Elba Island, Italy)

ANDREA DINI

Istituto di Geoscienze e Georisorse - CNR, Pisa, Italy

Very unusual melts rich in boron and other volatile and rare elements are produced during partial melting of continental crust as well as by differentiation of granitoid plutons. Commonly these melts crystallize at plutonic depths producing typical coarse-grained rocks (pegmatites) that are industrial sources for rare elements (e.g. Ta, Li). Sometimes, such melts produce intrusive bodies showing a fine grained microgranite-aplite texture. In both cases the final equigranular isotropic texture reached by these rocks masks the original structure of magma (e.g. presence of early phenocrysts) and the eventual dynamic patterns experienced during transfer and emplacement of magma.

The Capo Bianco aplite sill (Elba Island, Italy) was emplaced at shallow depth (≈ 2.6 km) in the Late Miocene, recording very peculiar petrographic (layered and oriented texture) and geochemical features that recall a fluid immiscibility process between silica-rich and boron-rich melts. The rapid crystallization of the peraluminous, boron-rich Capo Bianco aplite allowed the preservation of the original structure of the acidic magma with a small percentage of early, millimetric phenocrysts (quartz, K-feldspar, oligoclase, muscovite) into a very fine-grained quartz-feldspatic groundmass. The groundmass also hosts a large number of spherical-ellipsoidal tourmaline orbicules ranging in size between few mm up to 15 cm. The tourmaline orbicules are made up by fibrous-radiating schorl-elbaite needles and quartz. Their textural relationships with the host, internal textural and chemical-isotopic features suggest that they represent an early character of the magma and excludes their formation by late- to post-magmatic processes. This observation coupled with geochemical composition of the rock and available experimental data on silicatic melts/glasses indicate that tourmaline orbicules can represent the product of rapid crystallization of boron-rich silicate melt bubbles earlier separated from the acidic magma before the final emplacement. Capo Bianco aplite can thus be regarded as a serendipitous occurrence of a boron-rich magma that escaped the source region and stopped/crystallized in a subvolcanic setting, just at the right depth for maintaining a snapshot of the silicate-liquids immiscibility processes and the emplacement dynamic.

https://doi.org/10.1180/S0026461X00006502 Published online by Cambridge University Press

Coupling isotope labeling with compound specific stable isotope analysis of microbial biomarkers

MICHELA DIPPOLD[1,2], CAROLIN APOSTEL[1], LEOPOLD SAUHEITL[2,3], BRUNO GLASER[2,4] AND YAKOV KUZYAKOV[1,5]

[1]Departement of Agroecosystem Research, University of Bayreuth: (midipp@gmx.de)
[2]Soil Physics Section, Uiversity of Bayreuth
[3]Institute of Soil Science, Leibniz-University, Hannover
[4]Soil Biogeochemistry, Martin-Luther-University, Halle-Wittenberg
[5]Department of Soil Science of Temperate and Boreal Ecosystems, Georg-August-University of Göttingen

The vast number of high molecular substances in soil and their specific degradation pathways all end up in a reasonable small number of low molecular substances (LMWOS). Thus, the transformation and fate of LMWOS is one of the most important processes in biogeochemical cycles. These transformations are mainly controlled by microbial utilization and thus coupling the fate of LMWOS with their use by microbes is one of the tasks in the elucidation of C transformations and cycles.

Therefore we performed field experiments including application of dual-labeled and uniformly or position-specifically labeled amino acids. The microbial utilization was measured by means of ^{13}C- and ^{15}N-analysis of microbial biomass with the chloroform-fumigation-extraction method. A more specific look on the utilization of individual amino acids or C positions by distinct microbial groups was gained by the ^{13}C-PLFA approach.

Comparison of ^{13}C- and ^{15}N-incorporation revealed, that for a well N-supplied microbial community (C:N~6) of a grassland ecosystem appr. 50% of the amino acid N is mineralized by the microbes, whereas the remaining amino acids were incorporated into the microbial biomass. Incorporation of amino acid C into microbial biomass was highest for osmotrophic, prokaryotic groups. Position-specific labeling showed that highly oxidized groups are preferentially degraded, whereas more reduced C positions showed higher incorporation into the microbial biomass.

Our results show, that the combination of labelling with compound specific isotope analysis of microbial biomarkers opens a new way to investigate the microbial transformations of LMWOS in soil. Especially investigating the utilization of individual C atoms by microbial groups allows conclusions about the mechanisms and kinetics of microbial substrate utilization and the interactions between these groups. This will improve our understanding of soil carbon fluxes.

Control of biomineral formation during microbial Fe(III) reduction by local Fe^{2+} gradients – A multiscale approach

U. DIPPON*, C. SCHMIDT, M. OBST, A. PIEPENBROCK AND A. KAPPLER*

Geomicrobiology, University of Tuebingen, 72076 Tuebingen, Germany (*correspondence: urs.dippon@uni-tuebingen.de, *correspondence: andreas.kappler@uni-tuebingen.de)

The identity of minerals formed as a consequence of microbial iron(III) reduction is a function of geochemical conditions and microbial metabolic activity. While geochemical conditions set a thermodynamic framework for biomineralization, the microbial cells can influence the mineralization product by providing templates for mineral nucleation, localization of mineral precipitation, production of electron shuttles and changing the rate of Fe(III) reduction. Local Fe(II):Fe(III) ratios are known to be a key parameter for the transformation of Fe(III) minerals such as ferrihydrite to either dissolved Fe^{2+}, Fe(II) minerals (siderite), Fe(II)/Fe(III) minerals (green rust or magnetite) or other Fe(III) minerals (goethite).

We showed that under identical total concentrations of Fe(III) minerals, the geometry of the experimental setup significantly affected the local geochemistry, iron reduction rates and mineralogy of the reduction products in experiments with the iron-reducing strain *Shewanella oneidensis* MR-1. In these setups, the bacteria reduced 2.5 to 15 mM ferrihydrite with lactate as electron donor in glass tubes that were stored either horizontally or vertically.

In all setups with >7.5 mM ferrihydrite, magnetite formation was observed probably due to a high Fe(III):Fe(II) ratio present during ferrihydrite reduction. At lower concentrations of ferrihydrite, no magnetite but rather dissolved Fe^{2+} and/or siderite were formed in horizontally incubated tubes. However, in vertically incubated tubes magnetite was formed even at ferrihydrite concentrations as low as 2.5 mM. Probably ferrihydrite accumulation at the bottom of vertically incubated culture tubes also led to high Fe(III):Fe(II) ratios allowing magnetite to form. A multiscale approach combining bulk analysis with high resolution geochemical measurements and confocal laser scanning microscopy allowed us to characterize the microenvironments, localize cells at the mineral-solution interface and correlate geochemical data to mineral identification by XRD and Mössbauer spectroscopy.

https://doi.org/10.1180/S0026461X00006502 Published online by Cambridge University Press

Molecular microstratigraphy via laser-desorption ionization Fourier-transform ion cyclotron resonance mass spectrometry (LDI-FT-ICR-MS)

THORSTEN DITTMAR[1]*, SAMUEL ABIVEN[2], JUTTA NIGGEMANN[1] AND JENS FUCHSER[3]

[1]Max Planck Research Group for Marine Geochemistry, University of Oldenburg, Germany, (*correspondence: tdittmar@mpi-bremen.de; jniggema@mpi-bremen.de)

[2]University of Zurich, Soil Science and Biogeography, Switzerland (samuel.abiven@geo.uzh.ch)

[3]Bruker Daltonics, Bremen, Germany (Jens.Fuchser@bdal.de)

Ultrahigh-resolution mass spectrometry via the Fourier-transform ion cyclotron resonance technique (FT-ICR-MS) offers fundamentally new insights into the molecular world of natural waters. Oceans and freshwater systems are among the most complex molecular mixtures on Earth, containing ten-thousands if not millions of different compounds, collectively known as dissolved organic matter (DOM). With help of FT-ICR-MS, DOM can now be appreciated in its full molecular complexity, and a holistic geo-metabolomic approach is in sight that will allow a mechanistic understanding of element cycles in the ocean. In sediments and soils similar progress has been hampered by limited capabilities for the ionization of organic matter from solid samples for FT-ICR-MS analysis. In the life sciences, different laser-desorption ionization techniques (LDI) coupled to FT-ICR-MS are established tools for the molecular characterization of metabolites in organic tissues. Recently, this technique was extended for two-dimensional imaging of organic tissues allowing the identification of specific metabolites on a micrometer spatial scale. Objective of our study was to apply LDI-FT-ICR-MS for the molecular imaging of sediments. We obtained detailed molecular fingerprints of finely layered marine sediments, spatially resolved on a 50 micrometer scale. These first molecular images of marine sediments illustrate the enormous potential of LDI-FT-ICR-MS for the geosciences. Instead of targeting a small number of specific biomarkers, molecular formulae of hundreds to thousands of individual compounds are simultaneously obtained. Micrometer-scale stratification can be resolved on an extremely small amount of sample which is otherwise not accessible to molecular analysis.

Origin of iron layer in sediment of Lake Superior: Abiotic vs. biotic

M. DITTRICH[1], J. GORDON[1], B. RAOOF[1], A. CHESNYUK[1], S. QUAZI[1], R. SHEN[1], J. BOLLMANN[2], S. KATSEV[3] AND R. FULTHORPE[1]

[1]Department of Physical and Environmental Sciences, University of Toronto Scarborough, 1265 Military Trail, Toronto, Canada, M1C 1A4, (*correspondence: mdittrich@utsc.utoronto.ca)

[2]Department of Earth Sciences, University of Toronto, 22 Russel St, Toronto, Canada, M5S 3B1, (bollman@utoronto.ca)

[3]Large Lakes Observatory 2205 East 5th Street, Duluth, MN 55812, (skatsev@d.umn.edu)

In spite of being the largest by surface and one of the most oligotrophic fresh water bodies in the world, Lake Superior is rather a blank spot on the map of modern Geochemistry and Geomicrobiology. Although the limnological puzzles of Lake Superior are increasingly attracting scientists [1], very little is known about the sediments and their associated microflora. In this study we investigated geochemical and microbiological processes that may lead to the formation of a two cm thick iron layer about 10 cm below the sediment surface. Sediment cores from two stations (EM, 230m water depth and ED, 310m water depth) in East Basin were used. We monitored oxygen and pH depth profiles with microsensors, porewater and sediment solid matter were analyzed for nutrient and metal contents. The total cell count was determined using DAPI. DNA was extracted from the sediment samples and 16S ribosonal RNA amplicons were analyzed with denaturing gradient gel electrophoresis (DGGE).

The cluster analysis performed on the DGGE fingerprint revealed that there is no distinct microbial community in the iron layer, infact the bacterial community of the iron layer was 97% similar to that of adjacent layers. The scanning electron microscope (SEM) images from the iron layer 10-12cm show filament like structures that was encrusted with spheres ca. 20 nm in diameter (Figure 1A,B).

A B

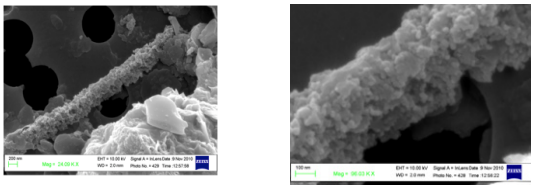

Figure 1. SEM images of filament like structure in the iron layer (A). Filament or tube covered was with spheres (B).

[1] Steiner R. (2011) *Inland Water* **1**, 29-46.

https://doi.org/10.1180/S0026461X00006502 Published online by Cambridge University Press

Gallium in bauxite deposits

TH. DITTRICH*, TH. SEIFERT AND J. GUTZMER

Department of Mineralogy, TU Bergakademie Freiberg, Brennhausgasse 14, D-09596, Freiberg, Germany (*correspondence: Thomas.Dittrich@mineral.tu-freiberg.de Thomas.Seifert@mineral.tu-freiberg.de, Jens.Gutzmer@mineral.tu-freiberg.de)

Gallium is consumed in rapidly increasing amounts by high technology applications. The annual primary production of Ga in 2009 of 111t is set to increase twentyfold by 2030 [1,5]. However, Ga is the sixteenth most common element in the Earth's crust (16ppm) and thus is much more common than metals like Cu, Zn, Ag or Cu. Despite of its relative abundance, Ga minerals are very rare and no distinct ore deposits from which gallium could be exploited as major product are known. This is attributed to the close geochemical affinity of Ga to Al resulting in Ga to substitute easily in rock-forming Al silicates (e.g., feldspar, nepheline).

Currently, almost all Ga is extracted as byproduct during beneficiation of bauxite. Ga occurs in bauxite in concentrations of <10-160ppm (Ø50ppm) [4, 5]. Based on the data of bauxite reserves and resources given by the USGS (2010) [5] and Bogatyrev & Zhukov (2009) [2] and under the assumption of an average Ga content of 50ppm, the geologically available Ga quantities in bauxites are estimated as 1.355Mt and between 2.75—3.75Mt Ga, respectively. The majority of bauxite deposits form by intensive chemical weathering of Al-rich lithologies During this process Ga behaves immobile much like Al, and is incorporated into Al-bearing minerals (e.g. gibbsite, kaolinite).

[1] Angerer *et al*. (2009) ISI p 383. [2] Bogatryrev & Zhukov (2009) *Geol Ore Deposit* **51**, 379-396. [3] Meyer *et al*. (2002) *Ore Geol Rev* **20**, 27-54. [4] Mordberg *et al*. (2001) *MinMag* **65**, 81-101. [5] USGS (2010) *Min. Commodity Summaries*.

Crustal growth in the North China Craton at ~2.5 Ga: Evidence from *in situ* zircon U-Pb dating, Hf isotopes and whole-rock geochemistry of the Dengfeng complex

CHUNRONG DIWU[1]*, YONG SUN[1], ANLIN GUO[1], HONGLIANG WANG[2] AND XIAOMING LIU[1]

[1]State Key Laboratory of Continental Dynamics, Department of Geology, Northwest University, Xi'an, 710069, China (*correspondence: diwuchunrong@163.com)

[2]Xi'an Institute of Geology and Mineral Resource, Xi'an 710054, China

The Dengfeng complex situated on the southern margin of the North China Craton (NCC) belongs to the southern portion of the Trans-North China Orogen. This late Neoarchean (~2.5 Ga) terrane is important to understand the formation and evolution of NCC during this period. The Dengfeng complex is well exposed in the Junzhao region and comprises two distinct lithologic units: supracrustal assemblage and plutonic rocks. LA-ICPMS magmatic zircon U–Pb dating shows that the complex formed within the range of 2547~2504 Ma. The available Hf isotope data indicate that the majority of ca. 2.5 Ga zircons from the Dengfeng complex give high $\varepsilon_{Hf}(t)$ values close to the initial Hf isotope ratios of the contemporaneous depleted mantle. These indicate that the rocks in the Dengfeng represent juvenile crust. The TTG gneisses in the Dengfeng complex display low Mg# (41-48), MgO (<2 wt%), Cr (6-14 ppm), Ni (9-22 ppm) contents and low Nb/Ta ratio (6-12), which are interpreted to have been produced by the partial melting of a flatly subducted slab. The metadiorites of the Dengfeng complex are typically characterized by high $Mg^{\#}$ (59-69), MgO (3.5-6.6 wt %), Ni (82-130 ppm) and Cr (148-237 ppm) abundances, elevated Sr (1759-1927 ppm) and Ba (1742-2289 ppm) concentrations, and high LREE (La_N=38-487). Such geochemical features are similar to Archean sanukitoids. A two-stage model is applied here to explain the genesis of metadiorites of Dengfeng complex: (1) firstly, the mantle is metasomatized either by melts or by aqueous fluids from a subducted slab; (2) then, sanukitoid magmas were produced by partial melting of the hybridized mantle. Furthermore, the amphibolites of supracrustal rocks have a mixture of MORB- and arc-like geochemical affinities, suggesting the development of a back-arc in the southern part of the NCC at ca. 2.5 Ga. The contemporary late Neoarchean TTGs, sanukitoids and MORB-back arc association may represent a late Neoarchean tectonic mélange, implying for a Neoarchean subduction-accretion process and the modern-style plate tectonics processes probably initiated in the southern NCC by 2.5 Ga.

https://doi.org/10.1180/S0026461X00006502 Published online by Cambridge University Press

Molecular iodine emission rates from *Laminaria digitata* as a function of algal part, irradiance and temperature

S. DIXNEUF[1,2], A.A. RUTH[1,2], U. NITSCHKE[3] AND D.B. STENGEL[3]

[1]Department of Physics, University College Cork, Ireland
[2]Environmental Research Institute, University College Cork, Ireland
[3]Botany and Plant Science, School of Natural Sciences, Ryan Institute for Environmental, Marine and Energy Research, National University of Ireland Galway, Galway, Ireland

Sea-to-air biogenic iodine fluxes play a key role in the global and local environmental iodine cycles, particularly in coastal areas where kelp beds are exposed to air during spring tides. The general knowledge of the marine sources and mechanisms of (elemental) iodine emission, either as molecular I_2 or volatile iodo-carbons, is still very limited.

Here time-resolved flux measurements of I_2 emitted by the brown macroalga *Laminaria digitata*, probably the strongest iodine accumulator amongst living organisms, were achieved by applying incoherent-broadband cavity-enhanced absorption spectroscopy (IBBCEAS) [1,2]. I_2 emission rates of three different (air-exposed) thallus parts of *L. digitata*, i.e. the distal blade, the meristematic area, and the stipe, were investigated under low-light and dark conditions [3]. Furthermore, impacts of light intensity and temperature on the I_2 emission rates were investigated for blades. Overall I_2 emissions were highly variable, but the release from stipes was ten times higher than that from meristematic areas and distal blades. Increased irradiances and temperatures resulted in higher I_2 emissions, indicating the importance of I_2 in algal stress responses. The results suggest that I_2 emission may be considered an indicator of the physiological status of the alga, and that iodine might have a multifunctional role in *L. digitata*.

[1] Fiedler *et al*. (2003) *Chem. Phys. Lett*. **371**, 284–294. [2] Dixneuf *et al*. (2009) *Atmos. Chem. Phys*. **9**, 823-829. [3] Nitschke *et al*. (2011) *Planta* **233**, 737-748.

Computational studies of actinide clusters and hydrolysis reactions

DAVID A. DIXON*[,1,2], VIRGIL E. JACKSON[1], MONICA VASILIU[1], STEPHEN WALKER[1], JESSICA DUKE[1], RYAN FLAMERICH[1], KARAH KNOPE[2] AND LYNDA SODERHOLM[2]

[1]Department of Chemistry, The University of Alabama, Shelby Hall, Box 870336, Tuscaloosa Al 35487-0336. (*correspondence: dadixon@bama.ua.edu)
[2]Chemical Sciences and Engineering Division, Argonne National Laboratory, Argonne, IL 60439

Advances in theory, algorithms, software, and computer architectures, have made it possible to begin to calculate reliably the thermodynamics for geochemical processes in solution. There is a need to develop a fundamental understanding of actinide-aggregate formation under conditions that promote hydrolysis. We are developing the scientific basis for a molecular-level understanding of nanoaggregate species in terms of their structures, stabilities, formation reactions, and surface reactivities, particularly the formation of colloidal particles containing heavy elements. In addition, this research will help us to meet the need to develop new separations strategies for next generation nuclear fuels that are better able to remove stable metal aggregates without the need for extreme solution conditions. Our focus is on the initial aqueous reactions including olation and oxolation as well as the acidity of metal ions in solution. For the +2 metal aquo ions, it is possible to predict the size of the first solvation shell by predicting the correct pK_a in terms of experiment. Positive ions with a charge > +2 require more solvent shells in order to predict the pK_a reliably. We have studied a wide range of oxolaton and olation reactions of +2 cations and the type of reaction that dominates in terms of the thermodynamics is dependent on the cation size, the size of the first solvation shell, and the electronic structure of the ion. The structures of $(ThO_2)_n$ nanoclusters have been studied and compared to the analogous transition metal nanoclusters. Calcuations of the hydrolysis reactions of the nanoclusters provide for the first time an estimate of the physisorption and dissociative chemisortion energies of H_2O on the ThO_2 surface. The electronic structure of nanoparticles containing a Th_6O_8 core will be discussed including predicitions of particle acidity and proton location. These particles are of interst as they contain a Th_6O_8 core embedded in an anion shell. There is good agrement between theory and experiment for the structures of the clusters.

This work is supported by the U.S. DOE, OBES, Chemical Sciences under contract DE-AC02-06CH11357.

https://doi.org/10.1180/S0026461X00006502 Published online by Cambridge University Press

Speed limits to soil weathering and CO_2 withdrawal

JEAN L. DIXON AND FRIEDHELM VON BLANCKENBURG

GFZ German Research Centre for Geosciences, Potsdam, Germany (jeannie@gfz-potsdam.de, fvb@gfz-potsdam.de)

Weathering fluxes in soil-mantled landscapes are capped by a global maximum that has important implications for Earth's long term climate. We identify the empirical, statistical and theoretical limits to climate, weathering and uplift feedbacks using a new global compilation of long term, soil-based denudation and weathering rates from cosmogenic nuclides and short term, river-based sediment and dissolved loads. Weathering accelerates by the increased exposure of minerals to erosion, and recently it was suggested that 50% of the global CO_2 withdrawal occurs in the worlds active mountain belts [1]. The observation that chemical weathering rates and physical erosion rates are tightly correlated has vindicated this hypothesis. But this relationship is predominantly valid for soil-mantled landscapes, and not rapidly uplifting mountain belts. We show that the rate of soil production obeys a global 'speed limit' of 270 t km^{-2} y^{-1}, and the associated soil weathering flux a limit of 135 t km^{-2} y^{-1}, corresponding to denudation and weathering rates of 100 and 50 mm ky^{-1}, respectively. Erosion rates may far exceed the soil speed limit, and are typically associated with landscapes of high relief and hillslope gradients [2]. There, erosion is governed by mass wasting processes typical of non-soil-covered landscapes in active mountains [3]. Yet chemical weathering rates from dissolved loads of rapidly eroding mountain rivers suggest that these landscapes also obey or fall below the limit of weathering observed for soils. Considering that such mountain belts are a small component of the continental land surface, we quantify that even if weathering fluxes in such areas were higher than today, they would represent a minor contribution to global CO_2 withdrawal. Therefore, Earth's long term climate sees little drawdown and more drawbacks from uplifting areas where denudation drives above the soil speed limit.

[1] Hilley and Porder (2008) *Proc Nat Acad Sci* **105**, 16855-16859. [2] Montgomery and Brandon (2002) *Earth Planet Sci Lett* **201**, 481-489. [3] Dibiase *et al.* (2010) *Earth Planet Sci Lett* **289**, 134-144.

Why do earthworms synthesize ACC?

P. DIZ[1] , C.L. GIL[1], J. MENDEZ[3], M.J.I. BRIONES[2] AND L.G. DUPORT[1]

[1]Dept. Geociencias Marinas. Universidad de Vigo, 36310 Vigo, Spain

[2]Dept. Ecología y Biología Animal. Universidad de Vigo, 36310 Vigo, Spain

[3]CACTI. Universidad de Vigo, 36310 Vigo, Spain

From the early work by Darwin [1] several hypotheses have been proposed to answer this question, namely pH buffering of the blood and the ingested plant material, respiratory functions, egg formation or simply spurious mineralization.

In this study we investigated the microstructural transformations which take place during the carbonate formation inside the calciferous gland of the earthworm species *Lumbricus friendi* Cognetti. We firstly identified the presence of ACC [2] by FTIR and then we followed the different evolution stages of calcium carbonate in the precursor fluid previous to the formation of to the solid phases by performing *in situ* XRD experiments.

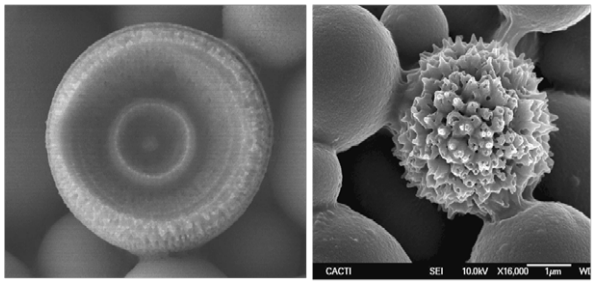

Figure 1. Two transformation stages from ACC to crystalline phases in earthworm's spherulites.

The results presented here shown that the formation of crystalline polymorphs of calcium carbonate in earthworms is preceded by the precipitation of ACC in a process that seems to follow a truly biomineralization mechanism, controlled by the organism. The high solubility is beneficial for temporal storage of calcium carbonate ions which could then get dissolved and used elsewhere according to the organism's requirements. Stabilisation of ACC seems to be achieved thanks to the presence of macromolecular constituents in the organic matrix, which also could be selectively used to promote the elimination of carbonate excess by nuclei induction of the crystalline phases and thus providing an efficient mechanism for Ca^{+2} control in the intracellular fluids.

[1] Darwin, C., (1881). John Murray, London [2] Gago-Duport *et al*. (2008) *J. Structural Biology*, **162**, 3, 422-435.

https://doi.org/10.1180/S0026461X00006502 Published online by Cambridge University Press

Toxicity of silver nanoparticles to environmental microbial consortia

JAN DOBIAS[1], ALESSANDRA COSTANZA[2], ELENA I. SUVOROVA[1], MASSIMO TROTTA[3] AND RIZLAN BERNIER-LATMANI[1]*

[1]Environmental Microbiology Laboratory, EPFL – Ecole Polytechnique Fédérale de Lausanne, 1015 Lausanne, Switzerland. (*correspondence: rizlan.bernier-latmani@epfl.ch)
[2]Università degli Studi di Bari Aldo Moro, 70121 Bari, Italy.
[3]Department of Chemistry, University of Bari, 70126 Bari, Italy.

Nanomaterials, particularly silver nanoparticles (AgNPs), are present in a large number of consumer goods due to their strong antimicrobial properties. Their extensive use raises concerns as to their release to the environment and their potential toxicity to aquatic microbiota.

The mechanism of AgNPs toxicity remains elusive and may include direct inhibition by the nanoparticulate form and/or indirect toxicity via soluble silver released from AgNPs. Additionally, numerous studies have attempted to unravel the role of AgNP size and coating in bacterial toxicity response but there remains a large gap in our understanding of the impact of basic AgNP characteristics on their toxicity.

Here we report on a systematic study of AgNP toxicity towards two pure cultures -*Escherichia coli* and *Bacillus subtilis*- and a microbial community from lake Geneva. We studied the effect of size (5nm, 10nm, 20nm, 50nm and 100nm) and that of surface coating (polyvinylpyrrolidone, tannic acid, citric acid and carbonate) on toxicity.

The AgNPs were obtained commercially and extensively characterized by electron microscopy (EM), dynamic light sacttering, zeta potential and the release of silver ions quantified by inductively coupled plasma mass spectrometry. The impact of AgNPs (0 to 1mg/L) on growth was monitored by optical density at 600nm, by colony formation for pure cultures and by measuring protein concentration and monitoring the microbial diversity of the community for the consortia. Additionally, the spatial relationship of AgNPs and cells was assayed by EM imaging of resin-embedded cells. The environmental relevance of the experimental conditions was ensured by growing cultures in artificial lake water.

Results to date show little toxicity to laboratory strains with *E. coli* being more sensitive than *B. subtilis* and size being a less important factor than surface coating. The systematic approach of this study –where AgNP size distribution is narrow and the geochemical conditions and microorganisms environmentally relevant- may be helpful to policy makers aiming at regulating the use of AgNPs in consumer goods.

VESPERS XRF and Laue Diffraction mapping of Carlin-type auriferous arsenian pyrite

A. DOBOSZ[1]*, G.R. OLIVO[1] AND A.R. PRATT[2]

[1]Department of Geological Sciences, Queen's University, Kingston, Ontario, K7L 3N6, Canada (*correspondence: 6ad2@queensu.ca)
[2]CANMET Mining and Mineral Sciences Laboratories, Natural Resources Canada, 555 Booth St, Ottawa, Ontario, K1A 0G1, Canada (Allen.Pratt@NRCan-RNCan.gc.ca)

Carlin-type gold deposits produce 8% of the world gold, and the main ore is auriferous pyrite commonly associated with various trace elements (Ag, As, Au, Cu, Hg, Ni, S, Sb, Se, Te, Tl and Zn). Their compositions have been investigated using electron-microprobe (EMP) and dynamic Secondary Ion Mass Spectrometry (SIMS), which indicates that gold and related trace elements occur in complex, micrometer-size irregular zones or overgrowths within single grains. The development of VESPERS (Very powerful Elemental and Structural Probe Employing Radiation from a Synchrotron) allows for non-destructive elemental mapping and crystal structure determination through XRF and Laue diffraction (LD). This methodology was applied in selected auriferous pyrite grains that were previously investigated using EMP and SIMS to advance our understanding of the relationship between the abundance of trace-elements and crystal structure.

The VESPERS elemental mapping results are consistent with those obtained by SIMS and EMP; however it offers the advantage of mapping a wide range of elements and the collection of LD patterns simultaneously and non-destructively. The elements that have adequate peak resolutions are Au (L series) and As, S, Fe, Ni, Cu (K series). Elements with peak overlap that have not yet been resolved include Ag, Sb, Te, Tl and Zn. Synchrotron LD data was collected along selected domains and the crystal structures are being interpreted.

https://doi.org/10.1180/S0026461X00006502 Published online by Cambridge University Press

Fluids nature at peak of ultrahigh-pressure metamorphism in deep subduction zones – Evidence from diamonds

L. Dobrzhinetskaya[1]*, R. Wirth[2], H.W. Green[1] and H. Sumino[3]

[1]University of California, Riverside, CA 92521, USA (*correspondence: larissa@ucr.edu)
[2]GeoForschungsZentrum, D-14473, Potsdam, Germany
[3]The University of Tokyo, Tokyo, Japan

Role of fluid circulating in deep subduction channels was/is a subject of many outstanding geochemical and numerical modelling studies. One of the intriguing processes is a fluid-rock interaction during subduction of the continental slab because the latter is characterized by contrast chemistry in comparison with the surrounding mantle and its fluids. Diamond due to its chemical inertness is the only mineral which contains "unchanged" fluids that was trapped during its crystallization at the peak of UHP metamorphism. We have demonstrated earlier with FIB-TEM studies that many diamonds from the UHPM terranes of Kazakhstan and Germany preserved intact C-O-H fluid inclusions [1]. This fluid responsible for diamond crystallization contains traces of both crustal and mantle components: Al, K, Ca, Mg, Fe, Si, Ti, V, Zn, Co, Fe F, Cl, S [1]. We have recently found more evidence to support crust-mantle origin of the fluids penetrating continental slabs in the deep subduction channels. This derives from a new finding of the polycrystalline diamonds included in zircons from Erzgebirge quartz-feldspathic gneisses containing remnants of fluid available for their compositional evaluation with EDAX spectrometry. The diamonds consist of 5-15 crystals of 0.3-5 micron size with a typical "zig-zag" grain boundaries and triangle voids filled with a C-O-H fluid with traces of Al, Co, F, V, Zn, Si, Cl, S, Ca, Mg, Fe, K in different combination. Such observations emphasize that diamonds from UHPM terranes have a similar nature of crystallization – from a fluid originated from a mixed crust-mantle geochemical reservoir. Moreover, the Kokchetav diamonds $^3He/^4He$ ratios are similar to those known for OIB setting [2]. Sumino *et al*. have suggested an interaction of the subducted continental slab with the deep mantle plume at the depth of the diamond stability filed. Therefore, the fluids penetrated continental slabs in deep subduction channels at peak of UHPM might originate from crust – mantle – deep mantle plume reservoirs.

[1] Dobrzhinetskaya *et al*. (2007) *PNAS* **104,** 9128-9132. [2] Sumino *et al*. (2011) *EPSL* (in press)

Kinetics of the reaction perovskite + ferropericlase = ringwoodite

David Dobson[1], James Badro[2], Anders Meibom[3] and Elisabetta Mariani[4]

[1]UCL, UK, (d.dobson@ucl.ac.uk)
[2]IPGP Paris, France.
[3]MNHN, Paris, France
[4]University of Liverpool, UK

The kinetics of solid-state disproportionation reactions can be strongly assymetric due to the different diffusive length scales of disproportionation versus recombination. Transport of material from the lower mantle into the transition zone requires the reaction of perovskite (pv) plus ferropericlase (fp) to produce ringwoodite (rw); this reaction is diffusive on the grain-length scale and hence might allow a significantly wide region where metastable phases exist. We present experiments to investigate the kinetics of this reaction. We have assumed that the transformation from pv to majorite (mj) is fast (being diffusive at the unit-cell length scale) and hence performed coupled reaction experiments of MgO with $(Mg,Al)(Al,Si)O_3$ mj at a pressure of 20 GPa (in the rw and mj stability fields) at temperatures of 1773 to 2123 K. The reaction is, as expected, mediated by diffusion of chemical components through the growing rw layer, with growth rate of the layer being linear with t^2. Rw grows with strong topotactic relations to the MgO which would, on completion of the reaction, result in single (or twinned) crystals of rw replacing the MgO grains. However, the kinetics of the reaction is further complicated by the incompatibility of aluminium in rw. As the rw layer grows, a double-diffusive instability develops with the rw-mj interface becoming fingered to maximise the surface area from which to diffuse aluminium into the garnet. The mean grain-size of regions with this texture is ~2 micrometres, which shows little coarsening due to zenner pinning. Reaction continues until all of the MgO is replaced leaving fine-grained reaction rims between these rw regions and the remaining excess $(Mg,Al)(Al,Si)O_3$ garnet. Two ways to estimate the grain size of the lower mantle might arise from this:

1. Seismological estimates of the thickness of the 670-km discontinuity are consistent with the equilibrium reaction. This means that the width of the region where the metastable mj + fp = rw reaction occurs is below seismological resolution.

2. The reaction texture might (occasionally) survive in porphyroclastic mantle xenoliths.

Both these estimates are consistent with a maximum lower-mantle grain size of about 1 cm.

https://doi.org/10.1180/S0026461X00006502 Published online by Cambridge University Press

Mid and heavy REE in carbonatites at Lofdal, Namibia

V.N. DO CABO[1], F. WALL[2], M.A. SITNIKOVA[3], R. ELLMIES[1,3], F. HENJES-KUNST[3], A. GERDES[4] AND H. DOWNES[5]

[1]Geological Survey of Namibia, Ministry of Mines and Energy, Windhoek, Namibia
[2]Camborne School of Mines, University of Exeter, UK (*correspondence f.wall@exeter.ac.uk)
[3]BGR, Federal Institute for Geosciences and Natural Resources, Hannover, Germany
[4]Goethe-University Frankfurt, Frankfurt, Germany
[5]Birkbeck University of London, London, UK

Carbonatites provide most of the World's rare earth elements (REE) but are characteristically enriched in the light REE with low contents of the more highly sought after mid and heavy REE. The Lofdal carbonatite complex, 35 km NW of Khorixas, Namibia, is an exception in that it contains hundreds of carbonatite dykes, some of which are mid and heavy REE-enriched, containing up to 3% xenotime-(Y) in dolomite-ankerite and ferruginous calcite carbonatite. Gd and Dy are the most abundant lanthanides in the xenotime-(Y). ThO_2 content is the main environmental problem with REE deposits and at Lofdal, there is up to 1 wt% ThO_2 in magmatic xenotime-(Y) and usually lower, about 0.3 wt%ThO_2, in hydrothermal xenotime-(Y). However, many rocks contain Th silicate. The hydrothermal xenotime-(Y) occurs in shear zones and associated calcite has a high $^{87}Sr/^{86}Sr$ ratio of 0.70804, $\delta^{13}C$ (‰V-PDB) of -3.66 and $\delta^{18}O$ (‰V-SMOW) =18. The xenotime-(Y) at Lofdal is the same age as the main carbonatite (765 ±16 Ma) and thus later metamorphic alteration can be ruled out. However, together with the presence of xenotime-(Y) in albitised country rocks and carbonatite-free shear zones, there is good evidence that most of the xenotime-(Y) formed from a carbonatite-related hydrothermal system circulating around the dykes.

Magmatic processes during the formation of Monte dei Porri Volcano, Island of Salina, Aeolian Islands, Italy

A. DOHERTY[123], B. DE VIVO[3], R. BODNAR[1], H. BELKIN[4] AND A. MESSINA[2].

[1]Fluids Research Laboratory, Virginia Tech (VT), Blacksburg, USA (angdoh@vt.edu)
[2]Dipartimento di Scienze degli Alimenti e dell'Ambiente, Università di Messina, Italy
[3]Dipartimento di Scienza della Terra, Università di Napoli Federico II), Italy
[4]United States Geological Survey, Reston, VA, USA

The island of Salina is the second largest of the Aeolian Islands, the subaerial expression of the Aeolian Magmatic Arc, located in the Tyrrhenian Sea, southern Italy. Salina lies in the centre of the arc and exhibits the widest variation in geochemical composition across all the Aeolian Islands, ranging from high-alumina basaltic to dacitic lava flows to rhyolitic pumiceous tephras erupted from 6 volcanic centres.

The Monte dei Porri volcanic eruptions were the last cone building events on the island occurring between 67ka and 13ka and occurred after 60ka of repose. The units consist of basaltic-andesite to dacite lavas, interlayered with unconsolidated tephras consisting of juvenile scoria fragments, entrained lithics and rhyolitic pumices. Phenocryst assembleges consist of calcic plagioclase (often with oscillatory zoning), clinopyroxene (augite), olivine and titanium-iron oxides ± orthopyroxene (often zoned), K-feldspar and quartz. Melt inclusions are a ubiquitous feature of all units and appear to be recrystallized in the lavas and occur as both recrystallized and glassy inclusions with and without vapour bubbles in the tephras. Rare primary fluid inclusion assemblages are also present in the tephras.

Raman spectroscopy of the glassy melt inclusions of the tephras reveals the presence of volatiles in the melt inclusion glass in the form of H_2O. CO_2 was not found in the glass or the vapour bubbles. Geothermometry based on plagioclase-liquid and clinopyroxene-liquid models indicates crystallisation temperatures of ~1200°C for feldspars and ~1050°C for clinopyroxene phenocrysts.

Petrographic analysis suggests the mixing of one or more magmas with different compositions played an important role in the evolution of the magmatic system.

https://doi.org/10.1180/S0026461X00006502 Published online by Cambridge University Press

A predictive thermodynamic model for element partitioning between plagioclase and melt

RALF DOHMEN[1] AND JON BLUNDY[2]

[1]Ruhr-University Bochum, Germany (ralf.dohmen@rub.de)
[2]University of Bristol, UK (jon.blundy@bristol.ac.uk)

There are various attempts in the literature to infer from the chemical zoning in plagioclase phenocrysts the magma evolution [1] and to determine magma residence times of plagioclases from diffusion modelling [2]. Both methods rely on accurate knowledge of partitioning coefficients between plagioclase and melt, D_i, and their dependencies on thermodynamic parameters and chemical composition. Based on a regular mixing model and numerical fitting of numerous experimental data [3] derived an equation for Sr and Ba of the form, $RT \ln D_i = A_i{*}X_{An} + B_i$. In a more recent work [4] the same relation was also used for various other elements to fit experimental pl-melt partitioning data. However, there is no a priori justification to use this relation also for other elements than Ba and Sr.

Here we present a new predictive model for the element partitioning between the metal site in plagioclase and melt. We have used the Brice model [5] to fit simultaneously the experimental data of 115 partitioning experiments, including those of [4] and unpublished data (partially published in [5]). The dependency of D_i on X_{An} is dominated by lattice strain effects and is related to the linear dependence of the optimum ionic radius r_0 on the anorthite content. Once the relevant parameters of the Brice model, r_0 and the Young's modulus of the site, are calibrated, the partitioning data can be corrected to isolate their T dependence. The inferred T dependence of the divalent cations and monovalent cations is perfectly consistent with available data for the free energy of fusion for anorthite and albite, respectively. The effect of the melt chemistry cannot be ignored in general but is minor compared to the lattice strain effects in most cases.

The major implication of this new model is that D_i becomes less sensitive to X_{An} and more sensitive to T than predicted by the relations of, e.g., [3] and [4]. This can be explained by the implicit relationship of X_{An} and T in most partitioning experiments.

[1] Blundy and Shimizu (1991) *Earth Planet Sci Lett*, **102**, 178-197; [2] Costa *et al* (2003) *Geochim Cosmochim Acta*, **67**, 2189-2200; [3] Blundy and Wood (1991) *Geochim Cosmochim Acta*, **55**, 193-209; [4] Bindeman *et al* (1998) *Geochim Cosmochim Acta*, **62**, 1175-1193; [5] Blundy and Wood (1994) *Nature*, **372**, 452-454.

Sr-Nd-Hf-Pb isotope systematics of the Oyu Tolgoi Cu-Au deposit (Mongolia)

A. DOLGOPOLOVA[1]*, R. SELTMANN[1], R. ARMSTRONG[1], E. BELOUSOVA[2] AND R. PANKHURST[3]

[1]NHM, Department of Mineralogy, CERCAMS, London SW7 5BD, UK (*correspondence: allad@nhm.ac.uk)
[2]GEMOC, Macquarie University, NSW, 2109 AUSTRALIA (elena.belousova@mq.edu.au)
[3]BGS, Keyworth, Nottingham NG12 5GG, UK (rjpankhurst@gmail.com)

New Sr-Nd, Hf and Pb isotope data are presented for a representative suite of 21 samples of plutonic and volcanic rocks (D_3 to C_1) from the giant Oyu Tolgoi porphyry Cu-Au district in the South Gobi, Mongolia.

Sr-Nd isotopes (whole-rock) show a restricted range of initial compositions, with εNd varying from +2.1 to +7.4 and ($^{87}Sr/^{86}Sr$)t predominantly between 0.7035 and 0.7045 reflecting formation from a relatively uniform juvenile lithophile-depleted source.

Hf isotopes (zircon) exhibit a range of -4.5 to +13.6 (**Fig. 1**). Felsic rocks show predominantly (apart from one sample) a juvenile mantle-derived signature whereas volcanic rocks exhibit some mixing with evolved crustal sources.

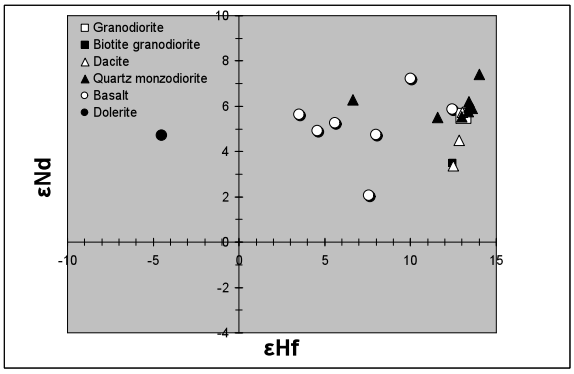

Figure 1: Hf and Nd isotopes for the Oyu Tolgoi deposit.

Pb isotopes (whole-rock) indicate a rather preserved array of isotopic compositions such as $^{206}Pb/^{204}Pb$ 17.773-19.058, $^{207}Pb/^{204}Pb$ 15.445-15.544 and $^{208}Pb/^{204}Pb$ 37.456-38.489. These are in full agreement with Sr-Nd-Hf isotopes indicating presence of a mantle component. Several samples show contributions from a MORB-related source.

All four isotopic systems hint that magmas from which the large Oyu Tolgoi porphyry system was generated, originated predominantly from juvenile material within the subduction-related setting of the Gurvan-Saikhan terrane.

https://doi.org/10.1180/S0026461X00006502 Published online by Cambridge University Press

Biogeochemical sustainability of semi-natural ecosystem

V.V. DOLIN

Institute for Environmental Geochemistry, 34-a, Palladin av., 03680 Kyiv, Ukraine (vdolin@i.com.ua)

The research is based on the novelty balance approach to the migration of artificial matter between biotic levels of an ecosystem and inanimate matter. *The Geochemical transition factor (GTF)* that represents the quantity of substance accumulated by plants from the area unit has been utilized for balance calculations. The temporal dinamics of GTF, permiting to asses the intensity of *biogeochemical flux,* suggested as volume of substance transferring during the time unit through the area unit of conditioned interface between abiotic and biotic levels.

In meadow ecosystem the only 10^{-5}–10^{-3} part of artificial contaminants is involved to biogeochemical cycling. The conciderably greater part accumulates in living matter of forest ecosystem: up to 50% of ^{14}C (Fig. 1), 10% of ^{3}H, 20% of ^{90}Sr, 13% of ^{137}Cs, 3% of ^{241}Am, 6% of Zn, 1% of Al and Ni, and less than 1% of Fe, Mn, and Cu. Artificial radionuclides and heavy metals are strongly accumulated in bottom deposits of aqueous ecosystem: anomalies of contamiation are closely localized to the pollution source. Accumulation of ^{14}C by micelium from irradiateted graphite is 50-100 times less than from sucrose solution in check experiment.

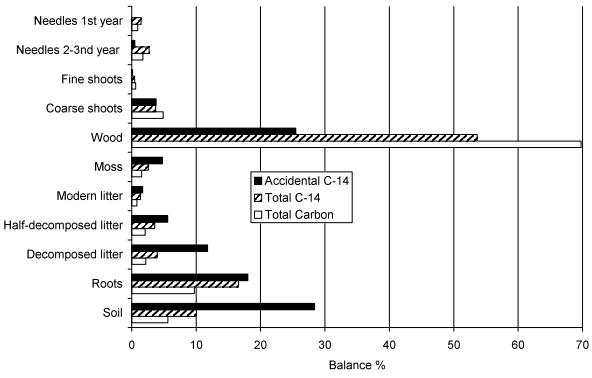

Figure 1. Distrubution of Carbon isotopes in pine ecosystem

The insignificant part of artificial matter involved to biogeochemical cycling determines the environmental capacity to contamination. Experience of geoecological investigations gives rise to conclusion about comparative sustainability of ecosystems in spite of the catastrophic increase of artificial loading.

Compact representation of complex organic aerosol processes

M.M. DONAHUE

Center for Atmospheric Particle Studies, Carnegie Mellon University, Pittsburgh, PA 15213, USA

Myriad organic compounds constitute organic aerosol (OA), tightly interconnecting multiphase chemistry, phase partitioning equilibria, and mass-transfer dynamics. Representations range from bare-minimum simplicity (e.g. emitting 12.5% of all terpenes as non-volatile, non-reactive, water-soluble organic aerosol) to maximal complexity (explicitly representing the multiphase chemistry and phase partitioning of millions of compounds). We favor a middle ground, grouping organic compounds in a property-based space that is directly tied to both vial physical properties as well as observable characteristics of ambient and lab-generated organic particles. This is the volatility basis set.

The first incarnation followed a single property – volatility – expressed in terms of a saturation mass concentration and typically lumping compounds into bins separated by factors of 10 in a logarithmic space. The 1D-VBS can precisely describe ideal phase partitioning over as many orders of magnitue as the number of bins. It can thus span the complete range of volatility relevant to atmospheric organics with 9 or so model compounds. It can also be used to fit chamber and dilution data to empirically constrain the volatility distribution of complex processes. It fosters insight into chemical evolution by forcing a mass balance. However, the single dimension suffers when confronted with non-ideal solutions as well as complex chemistry.

We have now added a second dimension, representing the oxidation of organics, to form a 2D-VBS. Oxidation state of bulk aerosol can be directly measured with advanced mass spectroscopy, and of course individual molecules can be located in this space as well. Oxidation in the atmosphere is irreversible, while volatility goes through a minimum as oxidation progresses. These fundamental behaviors are readily captured in the 2D-VBS.

As an illustration and test of OA evolution, a large team conducted the Multiple Chamber Aerosol Chemical Aging Study (MUCHACHAS) in 2008-2010 to observe the effects of OH radical "aging" on biogenic secondary organic aerosol (SOA). The effects were dramatic. They varied in different chambers, but a 2D-VBS model of the chemistry and chamber characteristics captures this variation using a predictive, previously published description of OA aging chemistry, showing that OA mass can double with aging. This aging chemistry must be included in transport models.

https://doi.org/10.1180/S0026461X00006502 Published online by Cambridge University Press

Copper and zinc isotope composition of China and India dust sources

SHUOFEI DONG[1], D.J.WEISS[1,2], J. NAJORKA[2], M. FERRAT[1], B. SPIRO[2], Y. SUN[3], S. GUPTA[1] AND R. SINHA[4]

[1]Imperial College London, London, SW7 2AZ, UK
[2]The Natural History Museum, London, SW7 5BD, UK
[3]Institute of Earth Environment CAS, Xi'an, China
[4]IIT-Kanpur, 208016 (UP), India

Copper (Cu) and zinc (Zn) play key roles in aquatic ecosystems. Zinc is an essential trace element limiting the biological productivity in the open ocean and Cu is potentially toxic to phytoplankton. Work to date suggests that the stable isotope systems of these metals can improve our understanding of their aqueous chemistry and behaviour in the marine environment. Significant spatial variability in isotopic ratios was found between and within ocean basins.

At present, one of the major gaps in knowledge is the characteristics of the isotopic composition of Zn and Cu of terrestrial sources into the marine ecosystem, in particular atmospheric deposition, which is the major source of trace elements to the remote open ocean.

Here we present the first characteristics of the Cu and Zn isotope compositions of the major dust sources in China and India, and discuss the findings with respect to (i) the dominant controls (mineralogy size fractions and Enrichment Factor), and (ii) their implication for the application to marine studies, focussing on the North East Pacific Ocean (NEPO).

a) We observe significant Cu and Zn isotopic variations between bulk samples from Chinese dust, Chinese Loess, and Indian dust (error in 2SD), i.e., Chinese deserts (Taklamakan, Badain Jaran, and Tengger): $\delta^{65}Cu_{NIST976}$= 0.06±0.11‰ (n=10), $\delta^{66}Zn_{Lyon}$= 0.19±0.19‰ (n=10); Chinese loess: $\delta^{65}Cu_{NIST976}$= 0.27±0.19‰ (n=12), $\delta^{66}Zn_{Lyon}$= 0.41±0.17‰ (n=15); Thar Desert (India): $\delta^{65}Cu_{NIST976}$= 0.48±0.12‰ (n=4), $\delta^{66}Zn_{Lyon}$= 0.49±0.22‰ (n=5). b) Cu isotope values seem to be negatively correlated with the abundance of the clay mineral illite at 95% CI R^2 = 0.74, (n=10). c) The $\delta^{65}Cu_{NIST976}$ and $\delta^{66}Zn_{Lyon}$ values differ among the various size fractions of Chinese deserts by up to 0.97 ‰ (Tengger Desert) and 0.35 ‰ (Taklamakan Desert), respectively. This implies that bulk isotopic signatures might be misleading for the characterization of dust. d) Enrichment factors (EF) of the dust range between 0.48 (Thar Desert) and 1.86 (Taklamakan Desert) for Cu and between 0.40 (Chinese loess) and 0.70 (Tengger Desert) for Zn, suggesting that the lower EF values, the heavier the isotope signature of the dust. e) The isotope signature of long range transport Chinese dust (≤5 μm) input to the NEPO area has values of $\delta^{65}Cu_{NIST976}$ = 0.16±0.19‰ and $\delta^{66}Zn_{Lyon}$ = 0.29±0.24‰, which are lower for Cu and similar of Zn relative to the isotope signatures of dust input estimated in pervious studied of NEPO surface waters.

Multiple magma inputs and sulfur sources in the development of the BIC intrusion, Northern Michigan, Midcontinent Rift system

KELLIE DONOGHUE* AND EDWARD RIPLEY

Indiana University, Bloomington, IN 47408 (*correspondence: Kdonoghu@indiana.edu, Ripley@indiana.edu)

The BIC intrusion is located in the Marquette-Baraga dike swarm in the Upper Peninsula of Michigan, and is associated with magmatism related to the development of the ~1.1Ga Midcontinent Rift System. The intrusion is currently being evaluated for the presence of economically viable sulfide-rich Ni- Cu-(PGE) mineralization. Rio Tinto's Eagle deposit is located 43 km to the west within the same dike system; the geometric form of the BIC intrusion, however, is distinctly different from those of the intrusions found in the vicinity of the Eagle deposit. The BIC intrusion is funnel-shaped with basal peridotite overlain by clinopyroxenite and gabbro. Sulfide minerals (pyrrhotite, chalcopyrite, pentlandite) are found in all of the units units but massive sulfide mineralization is restricted to the base of the peridotite unit. Country rocks are composed of siltstones and shales that are sulfide-bearing themselves. A smaller satellite intrusion is referred to as Little BIC, which is composed of peridotites with both massive and semi-massive (net-textured) mineralization.

Sulfide distribution in the BIC intrusion is variable, suggesting that multiple pulses of sulfide-saturated magma were involved in its genesis. $\delta^{34}S$ values of sulfide minerals throughout the intrusion fall within a narrow range of -2 to +2‰. $\delta^{34}S$ values of the sedimentary country rocks show a much wider range of -6 to +20‰. The massive sulphides in Little BIC have the same narrow range of $\delta^{34}S$ values as in BIC, but semi-massive sulphides are considerably higher (~+6‰) and clearly signify a large component of crustally derived sulfur. The BIC system conforms to a growing body of evidence for the importance of multiple sulfur sources in conduit-related Ni-Cu-(PGE) occurrences. We are currently evaluating the possibility that different processes for the attainment of sulfide saturation (e.g. fractional crystallization versus sulfur assimilation) are responsible for the sharp difference in $\delta^{34}S$ values between semi-massive sulfides at Little BIC and other sulfide occurrences in the system.

https://doi.org/10.1180/S0026461X00006502 Published online by Cambridge University Press

Do fluid inclusions preserve their initial composition? Experimental studies of H_2O diffusion through quartz

G. DOPPLER*, M. BAUMGARTNER AND R.J. BAKKER

University of Leoben, 8700 Leoben, Austria
(*correspondence: gerald.doppler@unileoben.ac.at)

The main focus of our diffusion studies lies on experimental works on synthetic and natural fluid inclusions (FI) in well selected quartz crystals. A major point of our investigations is to perform re-equilibration experiments with synthetic FI which are composed of water-related species, such as H_2O, D_2O and $H_2{}^{18}O$, at known P-T conditions and specific molar volumes of the liquid phase. Due to the possibility of post-entrapment compositional and density changes of FI, the analyses of fluid properties have to be performed with particular attention. To comply with this requirement we work on molecules with different properties, e.g. different melting points of H_2O and D_2O (melting points: 0 °C H_2O vs. +3.8 °C D_2O) to achieve better quantitative insights on the diffusion rates. Re-equilibration experiments are carried out at high experimental temperatures and pressures (max. 700 °C and 1 GPa). We design our recent experimental work to test the behaviour of aqueous FI in quartz under conditions of different pressure and different water fugacity. We expect a movement of the water-related species within the quartz lattice. Re-equilibration processes are not yet fully understood, therefore further investigations are required to characterize all aspects of post-entrapment changes in FI. Additionally we are able to determine changes in the shape of the synthesised inclusions (morphological changes) interrelated with the location (depth) of the inclusions within the quartz crystal. First results leed to the assumption that the size, the shape (Fig. 1) and the location directly correlate. This unambiguously correlates with the measured changes in the fluid-phases composition of the primary synthesised FI.

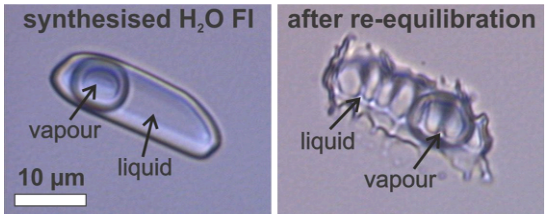

Figure 1: Photomicrograph of a FI in quartz after 19 days of re-equilibration. Pressure: 337 MPa; Temperature: 600 °C (left), 400 °C (right).

Host rocks of Santa Eulalia Plutonic Complex (Southern Portugal): A preliminary study

A. DÓRIA*, M.A.RIBEIRO, H. SANT'OVAIA AND F. FERNANDES

Centro Geologia, Faculdade de Ciências, Univ. Porto R. Campo Alegre, 4169-007 Porto, Portugal
(*correspondence: adoria@fc.up.pt)

The Santa Eulália Plutonic Complex (SEPC) is a calcalkaline granitic body that occupies an area of 400 km^2 and is located in the Variscan Iberian sector. SEPC is considered as late-Variscan because it cross-cuts the regional variscan structures, namely a major NW-SE shear zone in the contact between the two axial geotectonic zones of the iberian varican belt. The host rocks of the plutonic complex are composed by metamorphic formations from Upper Proterozoic to Lower Paleozoic. In the NE-sector of the shear zone a metasedimentary Ediacaran unit (Série Negra) outcrops, composed by metasedimentary siliciclastic rocks, including some black cherts. In the SW-sector of the shear zone, a low-grade metasedimentary and metavolcanic unit involving quartz-pelitic, carbonated and volcanic rocks, correspond to the Early Cambrian sequence.

In the western sector of SEPC, several metasedimentary enclaves are present mainly with pelitic and carbonated composition. These enclaves show internal structure and lithological diversity consistent with the external metasedimentary units and, due to the thermal effect, have intense metamorphic recrystallization. One of the enclaves near the NW border of SEPC, marble, calc-silicated rocks and acid porphyritic rocks were studied, including petrography, mineral and whole-rock chemistry. The calc-silicated and the porphyritic rocks show similar Eu-nomaly, Eu/Eu* respectively 0.86 and 0.88. However, the fractionation of LREE and HREE is quite different: in porphyritic rocks $(La/Sm)_n$ = 6.59, $(Gd/Yb)_n$ = 2.13, $(La/Yb)_n$ =28.9 and ∑REE = 233.51, while in calc-silicated rocks $(La/Sm)_n$ = 1.66, $(Gd/Yb)_n$ = 1.38, $(La/Yb)_n$ =3.04 and ∑REE = 181.63. The marble has a higher negative Eu-anomaly, with Eu/Eu*=0.57 and $(La/Sm)_n$ = 3.15, $(Gd/Yb)_n$ = 1.62, $(La/Yb)_n$ =7.87 and ∑REE = 17.31. These preliminary geochemical data indicate that all these lithologies derived from a continental crustal source.

This work has been financially supported by PTDC/CTE-GIX/099447/2008 (FCT-Portugal, COMPETE/FEDER).

https://doi.org/10.1180/S0026461X00006502 Published online by Cambridge University Press

Synoptic approaches to scale CH_4 flux in boreal landscapes

P. DÖRSCH[1]*, H. LANGE[2], B. THOMAS[3], H. SILJANEN[4], S. JENSEN[5] AND L. BAKKEN[1]

[1]Norwegian University of Life Sciences, 1432 Ås, Norway (*correspondance: peter.doersch@umb.no)
[2]Norwegian Forest and Landscape Institute, 1431 Ås, Norway
[3]Leibniz Center for Agricultural Landscape Research, D-15374 Müncheberg
[4]University of Eastern Finland, Kuopio, Finland
[5]University of Bergen, Norway

Boreal wetlands are an important source of atmospheric methane (CH_4) and susceptible to future climate change. Typically, boreal wetlands form microtopes embedded in complex landscapes, posing a challenge to scaling CH_4 source strength to greater areas. Here we report on an analysis of air borne (LiDAR, hyperspectral scanning) and ground based (chamber measurements, molecular analysis) approaches to characterize and scale CH_4 fluxes in a highly stratified mountainous landscape in Southern Norway (60º22' N 9º39'E, 510-750 m, 3ºC, 850 mm). We investigated relationships between peat depth, porewater CH_4 concentrations and CH_4 emission fluxes and found a significant correlation between CH_4 pore water concentration and VNIR reflectance spectra. Spectral separation was further tested in predefined vegetation/wetland types. We used molecular markers and *in vitro* CH_4 uptake kinetics to infer the abundance and activity of type I and type II methanotrophs in different landscape units. Synoptic approaches to scale CH_4 flux in heterogeneous landscape by means of molecular and biophysical signatures will be discussed.

Investigation of the precision and accuracy of isotope ratio measurements for atmospheric sampling for laser ablation multi collector-ICPMS

LADINA DORTA, ROBERT KOVACS, JOACHIM KOCH AND DETLEF GÜNTHER*

ETH Zürich, Laboratory for inorganic Chemistry, Zurich, Switzerland (*correspondence: guenther@inorg.chem.ethz.ch)

Laser ablation ICPMS is a powerful method for solid sample measurements. The sample size is however limited by the ablation cell size. Many efforts were made in developing ablation cells with different volumes and shapes for large samples. However the coupling of a gas exchange device (GED) [1] to the ICPMS allows to get rid of the ablation cell. The laser ablation process takes place in air environment. The aerosol is sucked into the GED by a membrane pump through a tube located directly at the ablation site. In the GED, the air is exchanged to Argon. The aerosol is then transported to the ICP in an Argon atmosphere. The figures of merit for atmospheric laser ablation were determined and similar accuracies as for conventional laser ablation were reported [2].

Laser ablation coupled to a multi collector-ICPMS (MC-ICPMS) allows precise isotopic information of a sample, used for e.g. age determination. These samples are mostly archeological and do not always fit into an ablation cell. The isotope ratio determination with LA-GED-MC-ICPMS would therefore be a method of choice for large and precious samples.

The precision and the accuracy of the atmospheric sampling for isotope ratio measurements were investigated with a Ti-Sapphire based femtosecond laser (Legend, Coherent Inc., Santa Clara (CA), USA) coupled to a gas exchange device and a Nu Plasma (Nu Instruments, Wrexham, UK). The measurements were done on pure lead, galena, brass and zircon. Even if a loss in sensitivity is observed, similar precision and accuracy were obtained comparing the atmospheric ablation with the conventional laser ablation set up.

[1] Nishiguchi K., Utani K., Fujimori E. (2008), *J. Anal. At. Spectrom.* **23**, 1125-1129. [2] Kovacs R., Nishiguchi K., Utani K., Günther D. (2010), *J. Anal. At. Spectrom.* **25**, 142-147.

https://doi.org/10.1180/S0026461X00006502 Published online by Cambridge University Press

Inception! Quantifing U-series disequilibria during the early stages of granite alteration

ANTHONY DOSSETO[1] AND CLIFFORD S. RIEBE[2]

[1]GeoQuEST Research Centre, School of Earth and Environmental Sciences, University of Wollongong, Wollongong, NSW, Australia. (tonyd@uow.edu.au)
[2]Dept. Geology & Geophysics, University of Wyoming, Laramie, WY, USA. (criebe@uwyo.edu)

Quantifying the balance between soil production from saprolite and regolith production from bedrock is crucial to assessing soil sustainability over human timescales, quantifying how landscapes evolve over millenia, and understanding weathering-related feedbacks in Earth's long-term climate evolution. Uranium-series isotopes have recently emerged as a tool for constraining rates of soil production from saprolite and regolith production from bedrock (e.g. [1-4]). To date, U-series work on weathering has focused mostly on samples in which the inception of weathering occurred at depth beneath a mantle of similarly weathered material. In this work, we focus on a bare rock ridge, using U-series isotopes to constrain weathering rates during the early stages of granite alteration. The goal is improved understanding of the pronounced dicotomy of bare and soil mantled rock on the slopes of the Sierra Nevada Batholith (California). Cores ~30cm long were drilled in a granitic ridge: one core was collected under a thin regolith cover, probably wind-blown material, in a small depression and shows evidences of relatively extensive weathering. This core is of special interest for addressing the role of a regolith cover in promoting weathering of the underlying bedrock. Another core was collected in nearby almost pristine bedrock but showing some evidences of weathering. Uranium and thorium isotope composition of samples taken along these cores will shed light on the mobility of chemical elements and the rates of granite weathering during the early stages of water-rock interaction.

[1] O. Dequincey *et al*., (2002) *Geochim. Cosmochim. Acta* **66**, 1197. [2] A. Dosseto, S. P. Turner, J. Chappell (2008), *Earth and Planetary Science Letters* **274**, 359. [3] A. Dosseto, H. L. Buss, P. O. Suresh (2011), *Appl. Geochem.* **in press**,. [4] E. Pelt *et al*., (2008) *Earth and Planetary Science Letters* **276**, 98.

Contrasting mantle signatures along the Mid-Atlantic Ridge (10-50°N)

LAURE DOSSO[1]*, CEDRIC HAMELIN[2], BARRY HANAN[3], MATTHEW THIRLWALL[4] AND SERGEI SILANTIEV[5]

[1]CNRS, UMR 6538, IFREMER, 29280 Plouzané, France (*correspondence: laure.dosso@univ-brest.fr)
[2]IPGP, 1 rue Jussieu, 75252 Paris CEDEX 05, France (hamelin@ipgp.fr)
[3]Department of Geological Sciences, SDSU, San Diego, California 92182-1020, USA (barry.hanan@geology.sdsu.edu)
[4]Department of Geology, Royal Holloway University of London, Egham, Surrey TW20 0EX, United Kingdom (m.thirlwall@es.rhul.ac.uk)
[5]Vernadsky Institute of Geochemistry, Moscow 117975, Russia (silantyev@geokhi.ru)

The description of mantle geochemical heterogeneities contributes to the understanding of time and length scales of mantle convection. Using trace element and Sr-Nd-Pb isotopic ratios, the geochemical structure of the northern mid-atlantic ridge between 10 and 50°N has long been described with major anomalous zones at the latitudes of 14°-15°N, 38-39°N and 42-43°N. New Hf isotopic data from basaltic samples along this 10-50°N section of the ridge (shown as solid symbols in figure below, open symbols indicate published values) combined with Sr or Nd isotopes reveal clear contrasting geochemical signatures of different sections of the ridge. It emphasizes the heterogeneous character of the depleted mantle source of MORB, as previously reported and discussed with Sr isotopes in [1] and brings a new perspective on the mantle dynamics in the region.

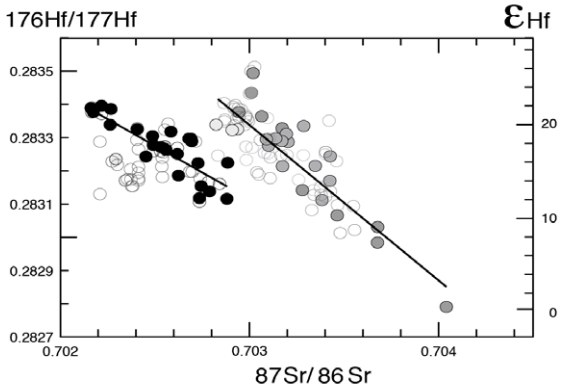

[1] Dosso *et al*. (1999), *Earth Planet. Sci. Lett*. **170**, 269-286.

https://doi.org/10.1180/S0026461X00006502 Published online by Cambridge University Press

Os isotope and PGE data on the age and evolution of lithospheric mantle in the central Siberian craton

L.S. DOUCET[1]*, D.A. IONOV[1], R.W. CARLSON[2], A.V. GOLOVIN[3] AND I.V. ASHCHEPKOV[3]

[1]Univ. J. Monnet & CNRS-UMR6524, St Etienne 42023, France (*correspondence: luc.serge.doucet@univ-st-etienne.fr)
[2]DTM-CIW, Washington D.C. 20015, USA
[3]Inst. Geology & Mineralogy, Novosibirsk 630090, Russia

The Siberian craton was assembled 1.8-2.1 Ga ago from terrains containing components as old as 2.4-3.5 Ga [1]. To better constrain the age of the lithospheric mantle in the central craton and its relationship to the events that formed or assembled the overlying crust, we present new whole-rock Re-Os and PGE data on 31 fresh (LOI <1%) spinel and garnet peridotite xenoliths from the Udachnaya kimberlite [2]. 18 out of 24 refractory (0.1-1.2% Al_2O_3) rocks in this study contain 1-10 ppb Os. They mostly yield T_{RD} ages from 1.5 to 2.3 Ga (average 1.8 Ga). The T_{RD} ages do not correlate with P-T estimates (<2.5-6.8 GPa; 760-1330°C), hence depth. These peridotites are depleted in Pd, less commonly in Pt relative to Os-Ir-Ru, with the strongest Pt-Pd depletions in cpx-free spinel peridotites, likely reflecting the lower compatibility of Pt and Pd in residues of melting. Six refractory peridotites have low Os (≤0.5 ppb), high Re/Os and yield low (0.7-1.6 Ga) or meaningless T_{RD} ages. Cpx- and gar-rich peridotites (1.4-4.0% Al_2O_3; likely re-fertilised) with Os >1 ppb have eruption-age-corrected $^{187}Os/^{188}Os$ = 0.120-0.124; some show high Pt/Ir and Pd/Ir indicating Pt-Pd mobility during melt metasomatism.

Overall, Re-Os ages in Udachnaya peridotites are Paleoproterozoic (including 7 out of 8 samples from earlier work [3]), coeval with final rather than early stages of craton formation. Older ages have been reported on megacrystalline dunites (3 out of 5 in [3]), eclogites [4] or inclusions in diamonds [5] that cannot be abundant in the mantle. Thus, long-lived, thick, cold, diamond-bearing lithospheric keels may be generated in the Proterozoic as well as in the Archean.

[1] Rosen (2002) *Russ. J. Earth Sci.* **59**, 103-119. [2] Ionov *et al.* (2010) *J. Petrol* **51**, 2177-2210. [3] Pearson *et al.* (1995) *GCA* **59**, 959-977. [4] Pearson *et al.* (1995) *Nature* **374**, 711-713. [5] Pearson *et al.* (1999) *GCA* **63**, 703-711.

Permafrost active layer dynamics inferred from major element geochemical signatures in six Arctic Alaskan rivers

T.A. DOUGLAS[1], A.D. JACOBSON[2], J.W. MCCLELLAND[3], A.J. BARKER[1], M.S. KHOSH[3] AND G.O. LEHN[2]

[1]U.S. Army Cold Regions Research and Engineering Laboratory Fort Wainwright, Alaska 99703; (thomas.a.douglas@usace.army.mil; ajbarker3@gmail.com)
[2]Northwestern University Evanston, Illinois 60208; (adj@earth.northwestern.edu; greg@earth.northwestern.edu)
[3]University of Texas, Port Aransas, Texas 78373 (jimm@mail.utexas.edu; mattkhosh@mail.utexas.edu)

Arctic climate warming is expected to degrade permafrost and affect watershed hydrogeology and biogeochemistry. Increasing temperatures could lead to the downward migration of the seasonally thawed (active) layer into previously frozen soil. This could create a unique weathering signal in surface waters during late summer and early fall when the active layer is at its deepest extent. The response of permafrost to climate warming may not lead to a simple, homogeneous increase in active layer depths. Ice lenses, peat layers, and heterogeneous soil ice (water) contents will respond differently to warming. Our study was initiated to determine whether geochemical tracers can provide a proxy for these active layer dynamics in Arctic watersheds.

We collected up to 65 surface water samples from six Arctic Alaskan rivers from melt to freeze-up in 2009 and 2010. Watershed areas range from 1.6 to 610 km^2. Two rivers were underlain by organic rich permafrost, two rivers drained mountainous bedrock, and two rivers were underlain by both bedrock and organic rich permafrost.

We measured the major ion geochemistry of the water samples. For most of the rivers, Na, Ca, Mg, and SO_4 concentrations are lower during melt runoff and steadily increase throughout the summer into the fall. Potassium values are greatest in early melt waters and then decrease through the summer into the fall. Nitrate concentrations increase steadily in the late fall in bedrock dominated streams, suggesting a decrease in N assimilation rates in the bedrock soils during late summer and fall. Our results suggest river chemistry is driven by flow paths that deepen from surface to mineral soils as the melt season progresses.

https://doi.org/10.1180/S0026461X00006502 Published online by Cambridge University Press

Comparative planetology – What are the factors controlling the nature of terrestrial planetary crusts?

H. DOWNES

Department of Earth and Planetary Sciences, Birkbeck University of London, Malet Street, London WC1E 7HX United Kingdom (h.downes@ucl.ac.uk).

Size, composition, or location?

Within the Solar System, rocky bodies (planets, moons, asteroids) have a variety of sizes and crustal compositions. A common view is that "there are more variables than planets" [1], whereas others insist that the only significant factor controlling planetary evolution is the size of the body [2]. Consideration of pairs of similar sized planetary bodies (e.g., Earth/Venus; Moon/Mercury; Moon/Io, Callisto/Ganymede) suggests that two other factors are also important.

Firstly, the composition of the body controls much of its evolution, including the nature of its crust (both primary and present-day). Whether the mantle of the body is Fe-rich (e.g. Moon, Mars) or Mg-rich (Earth, Venus, Mercury) controls the compositions of erupted basalts but, more importantly, can lead to plagioclase flotation in a magma ocean under anhydrous conditions. Presence of volatiles, particularly water, to the mantle inhibits formation of an anorthositic crust [3]. Water also lowers the solidus of basalts, which can then partially melt to produce magmas of intermediate compositions which are too buoyant to subduct, leading to formation of a silicic continental-type crust. Significantly, this process does not require the operation of plate tectonics but only requires the melting of hydrated basaltic material, as is demonstrated by the Archean TTG crust of the Earth. Secondly, the location of the planetary body is an important factor, as seen in the dichotomy between Ganymede and Callisto in which the proximity to Jupiter governed the amount of impact-related heating [4] and later tidal heating, or in the contrasting magmatic histories of the Moon and Io.

Based on the three main factors, predictions can be made regarding the nature of crusts that are likely to be formed on planetary bodies of different sizes and bulk compositions, and this can then be extended to a consideration of specific locations of planets or moons (e.g. proximity to a gas giant; inside/outside the stability zone of surface liquid water etc).

[1] Taylor SR & McLennan SM (2008) *Planetary Crusts*. Cambridge. [2] Albarède F and Blichert-Toft J (2007) *Comptes Rendus Géoscience*, **339**, 917-927. [3] Brown S & Elkins-Tanton L (2009) *EPSL* **286,** 446-455. [4] Barr A & Canup R (2010) *Nature Geosciences* **3**, 164-167.

The oxidation state of Ti in synthetic and meteoritic hibonite

P.M. DOYLE[1,2]*, A.J. BERRY[1,2], P.F. SCHOFIELD[2], J.F.W. MOSSELMANS[3], A.D. SMITH[4], A. SCHOLL[5] AND A.T. YOUNG[5]

[1]Imperial College, London, UK (*correspondence: p.doyle07@imperial.ac.uk)
[2]Natural History Museum, London, UK
[3]Diamond Light Source, Oxfordshire, UK
[4]STFC Daresbury Laboratory, Daresbury, UK
[5]Advanced Light Source, Lawrence Berkeley National Lab, Berkeley, CA, USA

Hibonite ($CaAl_{12}O_{19}$) is a Ti-bearing mineral found in calcium aluminium inclusions (CAIs) and is thought to be the second mineral to condense from a solar composition gas [1]. As such, the crystal chemistry of hibonite could provide insight into the conditions of the early Solar System. Ti may occur as Ti^{3+} under reducing conditions, with up to 23% of the Ti in meteoritic hibonite previously reported as Ti^{3+} [2].

We have used X-ray spectromicroscopy (XANES, XPEEM) to determine Ti^{3+}/Ti^{4+} ratios for a range of meteoritic hibonites, with spatial resolutions between 3 μm and 100 nm. We aim to use this information to investigate if hibonite grains record temporal variations in oxygen fugacity in the early Solar Nebula.

Ti-bearing hibonite samples were prepared at 1400 °C under oxidising and reducing atmospheres using a $CO\text{-}CO_2$ gas mixing furnace in order to produce a sample series with 0-100% $Ti^{3+}/\Sigma Ti$ (where $\Sigma Ti = Ti^{3+}+Ti^{4+}$). Neutron powder diffraction data was used to determine the site occupancy of Ti^{3+} and Ti^{4+} in the sample suite. Ti K- and L-edge spectra were recorded for these samples and meteoritic hibonite (c/o A. Bischoff and S. Rout). Spectral features that vary as a function of Ti^{3+}/Ti^{4+} in the synthetic hibonite series were identified.

The resulting calibration curve was used to determine Ti^{3+}/Ti^{4+} ratios for the meteoritic hibonite grains. The results show that blue hibonite from CAIs in the unique Acfer094 meteorite and greeny-blue hibonite from a CAI in the El Djouf001 CR meteorite have up to 10% $Ti^{3+}/\Sigma Ti$, and colourless hibonite grains from the Hughes030 and NWA2446 R-type meteorites have less than 3% $Ti^{3+}/\Sigma Ti$. Additionally, there is evidence that there may be a degree of core-to-rim variation of the $Ti^{3+}/\Sigma Ti$ ratio within some hibonite grains.

[1] Lodders (2003) *Astrophys. J* **591**, 1220-1247; [2] Beckett *et al*. (1988) *GCA* **52**, 1479-1495.

https://doi.org/10.1180/S0026461X00006502 Published online by Cambridge University Press

Accelerating garnet growth and related dehydration at blueschist-facies conditions, Sifnos, Greece

BESIM DRAGOVIC*[1], ETHAN F. BAXTER[1,2] AND MARK J. CADDICK[2]

[1]Boston University, Department of Earth Science, Boston MA, 02215, USA

[2]ETH Zurich, Institute for Geochemistry and Petrology, 8006 Zurich, Switzerland

While subduction is considered to be a gradual process, consisting of steadily changing pressures and temperatures, metamorphic reactions and mineral growth during subduction may, in some cases, be episodic, or pulsed. Whether the net transformation and accompanying dehydration of subducting material occurs steadily, or in one or more bursts, has important implications for subduction zone petrology and geodynamics.

Here, microdrilling based on major element zoning contours as determined by electron microprobe mapping, from a 4.9-cm diameter garnet in a quartzofeldspathic gneiss from Sifnos, Greece, in the Attic-Cycladic Blueschist Belt, provides information on the rate of mineral growth during metamorphism. Ten concentric growth zones were sampled from the garnet for Sm-Nd geochronology using ID-TIMS. After acid cleansing of mineral inclusions, many of the garnet zones contained very low (0.02 ppm) Nd concentrations, yielding very low sample sizes (~1.5 ng Nd) but very high $^{147}Sm/^{144}Nd$ (3.4 to 9.8) indicating success in the removal of adverse inclusion effects. These samples were analyzed using a NdO+ with Ta_2O_5 activator method. Garnet-matrix isochron ages reveal that growth spanned at least 7.3 ± 3.3Ma from onset in the core at 52.7 ± 3.3Ma to cessation at the rim just after 45.44 ± 0.21 Ma. Over this timespan, the garnet growth rate accelerated significantly. The innermost 1 cm of garnet (radially) grew at an average rate of ca. 0.9 cm^3/Ma, whereas the outermost 0.9 cm grew within just a few 100,000s of years at a growth rate of ca. 100 cm^3/Ma. This is an acceleration factor of at least ~ 2 orders of magnitude.

Rapidly accelerating garnet growth may occur due to gradually changing P and T, if the PT trajectory crosses closely spaced reaction isopleths. Or, the dehydration of subducted material can provide a synergistic kinetic trigger - a catalyzing fluid - further accelerating garnet growth, and thus water release. Thermodynamic analysis of the garnet forming dehydration reactions and P-T trajectories, can help elucidate the causes and consequences of this acceleration in the net reaction rate.

Microbial mobilization of arsenic from soil of the Mokrsko gold deposit, Czech Republic

P. DRAHOTA[1]*, A. REDLICH[2], L. FALTEISEK[3], J. ROHOVEC[4] AND I. ČEPIČKA[3]

[1]Institute of Geochemistry, Mineralogy and Mineral Resources, Charles University, Prague, Czech Republic (*correspondence: drahota@natur.cuni.cz)

[2]Department of Physical and Macromolecular Chemistry, Charles University, Prague, Czech Republic

[3]Department of Zoology, Charles University, Prague, Czech Republic

[4]Institute of Geology, AS CR v.v.i., Prague, Czech Republic

Arsenic mobilization from soil is an issue of concern, as aquatic arsenic can migrate into pristine areas, endangering aquatic organisms and people. Such mobilization in the Mokrsko gold deposit distributes nearly 1.4 kg ha^{-1} $year^{-1}$ of arsenic throughout naturally contaminated soil [1]. To gain an understanding of possible biological mechanisms contributing to this transport, mobilization of solid-phase arsenic was investigated in Mokrsko soil microcosms.

Anaerobic microcosms catalyzed rapid release of arsenic from soil containing arsenic-rich goethite, pharmacosiderite and arseniosiderite, mobilizing 33±6% of the total arsenic. Sterilization prevented this transformation. Highly positive correlation between the extracted amounts of arsenic and iron from soil under anaerobic condition implied that microbial reductive dissolution of iron oxides and iron arsenates is responsible for the arsenic release. Sequential extraction analyses designed to determine the arsenic fractionation before and after incubation experiments supported massive dissolution of amorphous and crystalline iron phases in oxalate fractions (65% reduction). The isolation technique enabled the characterization of nine arsenate–resistant bacteria, mostly related to facultative anaerobic genera *Bacillus* and *Pseudomonas*, which are using arsenate for respiration [2]. However, the link between arsenic reduction/mobilization and the isolated strains is missing and will be completed soon.

Preliminary observations indicate that a direct microbial arsenic-mobilizing activity exist in the soil, isolated strains are well known arsenic-transforming agents, and thus suggest that dissimilatory arsenic reduction may contribute to arsenic flux from anoxic condition of the Mokrsko gold deposit.

[1] Drahota *et al*. (2006) *Sci. Total Environ*. **372**, 306-316. [2] Freikowski *et al*. (2010) *Appl. Microbiol. Biotechnol*. **88**, 1363-1371.

https://doi.org/10.1180/S0026461X00006502 Published online by Cambridge University Press

Geochemical correlations of low-temperature calcite and groundwater in subsurface granite fractures

H. DRAKE[1]*, E.-L. TULLBORG[2] AND M. ÅSTRÖM[1]

[1]School of Natural Science, Linnaeus University, SE-391 82 Kalmar, Sweden
(*correspondence: henrik.drake@lnu.se)
[2]Terralogica AB, Box 4140, SE-443 14 Gråbo, Sweden

Studies of calcite precipitated in bedrock fractures can reveal past groundwater conditions (e.g. [1]). Studies of low-temperature fracture calcite in Proterozoic or Archaean crystalline rocks are, however, very limited, mainly because this calcite usually is very fine-grained or forms rims on older, much more abundant, hydrothermal calcite and is thus difficult to distinguish. Knowledge of chemical characteristics and the correlation with groundwater chemistry is thus scarce for low-temperature calcite in these settings.

In the Proterozoic rock setting at Laxemar, SE Sweden, Quaternary glaciations and related marine transgressions and land uplift, have favoured calcite formation in the bedrock fractures due to repeated introduction and mixing of different waters [2]. We have sampled very fine-grained euhedral low-temperature calcite from these fractures from drill cores (~50 samples, down to 1 km depth) and analysed them for trace elements (using ICP-MS, LA-ICP-MS, WDS) and $\delta^{13}C$, $\delta^{18}O$, $^{87}Sr/^{86}Sr$, following detailed SEM-studies (e.g. CL) of crystal zonations. Existing groundwater data from the same borehole sections [2] enabled detailed direct calcite-groundwater comparison in terms of both geochemistry and isotopic ratios, e.g. depth-variations. Thereby we tested the utilisation of low-temperature fracture calcite in terms of understanding the groundwater history, also giving input to the understanding of trace element incorporation into calcite in natural systems.

Calcite $^{87}Sr/^{86}Sr$-ratios correlated with the groundwater in all sections and ~50% of the sections showed $\delta^{18}O$ calcite-groundwater equilibria at ambient temperatures, which suggests potential scattered recent precipitation, e.g. indicated for intruding marine and meteoric water. Calcite isotope signatures also differ considerably from Proterozoic and Paleozoic calcite [3]. The calcite generally showed Me/Ca depth trends consistent with the groundwater for Mn, Mg and Sr. However, only Mn incorporation was in the range expected from experiments [4], which shows the difficulty of applying experimental data onto natural systems, and that $^{87}Sr/^{86}Sr$, $\delta^{18}O$, and Mn are the most representative proxies for low-temperature calcite-groundwater interaction.

[1] Tullborg *et al*. (2008) *Appl Geochem* **23**,1881–1897. [2] Laaksoharju *et al*. (2009) *SKB report* **R-08-93**. [3] Drake & Tullborg (2009) *Appl Geochem* **23**, 715-732. [4] Curti (1999) *Appl Geochem* **14**, 433-445.

Recent and fossil chemosynthetic endosymbioses

ANNE DREIER[1,2]*, MARTIN BLUMENBERG[2], MARCO TAVIANI[3], LORENA STANNEK[1] AND MICHAEL HOPPERT[1,2]

[1] Institute of Microbiology and Genetics, University of Goettingen, Grisebachstr. 8, 37077 Goettingen, Germany
(*correspondence: adreier1@gwdg.de)
[2] Courant Centre Geobiology, University of Goettingen, Goldschmidtstr. 3, 37077 Goettingen, Germany
[3]ISMAR-CNR, Via Gobetti 101, 40129 Bologna, Italy

Metazoans with chemosynthetic endosymbionts are widespread in marine habitats and respective endosymbioses are known from seven recent animal phyla. However, very little is known about endosymbioses in fossil settings and, hence, ecological significance as well as evolution of endosymbioses in earth history. In the presented project, we investigate the ancient and recent bivalve fauna living at marine sedimentary oxic/anoxic interfaces. Two bivalve species collected from the same benthic environment a Mediterranean lagoon- were studied in detail. The diet of *Loripes lacteus* is based on thiotrophic gill symbionts. *Venerupis aureus* is a filter feeding bivalve without symbionts. Analysis of 16S rDNA and fluorescence-*in situ* -hybridisation confirmed the presence of symbionts in *Loripes* gill tissue. In addition, the presence of one key enzyme of sulfur oxidation (APS-reductase) could be detected by immunofluorescence.

In search of biosignatures associated with thiotrophic chemosymbionts that could also be detected in fossil bivalves, we analysed the isotopic composition of shell lipids ($\delta^{13}C$) and the shell matrix protein conchiolin ($\delta^{13}C$, $\delta^{15}N$, $\delta^{34}S$). In recent shells and in gill tissue the stable isotopic ratio of carbon is more depleted in the thiotrophic *Loripes*: e.g., $\delta^{13}C_{lipid(18:1FA)}$ -32.2‰, $\delta^{13}C_{conchiolin}$ -25.4‰ than in the filterfeeding *Venerupis*: $\delta^{13}C_{lipid(18:1FA)}$ -28.2‰, $\Delta^{13}C_{conchiolin}$ -21.8‰. The isotopic ratios of nitrogen and sulfur are also more depleted in the chemosynthetic *Loripes* ($\delta^{15}N_{conchiolin}$ +3‰, $\delta^{34}S_{conchiolin}$ -18.5‰ in contrast to filter feeding *Venerupis*: $\delta^{15}N_{conchiolin}$ +10.1‰, $\delta^{34}S_{conchiolin}$ +13.6‰). Our results give evidence for a major influence of sulfide-oxidizing symbionts on the isotopic composition of organic matter of the host bivalve and are compared with respective data from fossil samples.

https://doi.org/10.1180/S0026461X00006502 Published online by Cambridge University Press

Stable isotopes of snow precipitation at Concordia station (East Antarctica)

G. DREOSSI[1], B. STENNI[1]*, M. BRAIDA[1], C. SCARCHILLI[2], M. VALT[3], A. CAGNATI[3], M. FREZZOTTI[2], M. BONAZZA[1], L. GENONI[1], D. FROSINI[4], D. KARLICEK[1] AND R. UDISTI[4]

[1]Department of Geosciences, University of Trieste, Italy (*correspondence: stenni@units.it)
[2]ENEA, Roma, Italy
[3]ARPA Veneto, Italy
[4]Department of Chemistry, University of Florence, Italy

The main key factors controlling the oxygen and hydrogen isotope composition of present-day Antarctic precipitation are mainly related to the condensation temperature of the precipitation and the origin of the moisture [1]. In order to calibrate the isotopic tool a multiyear survey from 2006 to 2010 has been carried out in the inland plateau site of Dome C (75°06'S 123°21'E; 3233 m; T=-54.5°C; snow acc. rate 25 kg m^{-2} yr^{-1}) in East Antarctica.

Here we present $\delta^{18}O$, δD and deuterium excess (d) data obtained from daily snow depositions. Observations of deposition amount, shape and size of crystals were also determined. The isotopic data will be also studied as function of synoptic meteorological conditions, using ECMWF re-analyses data and back trajectory models. Preliminary data suggest a good correlation between $\delta D/\delta^{18}O$ and temperature, both in anti-phase with d at seasonal scale (Fig. 1).

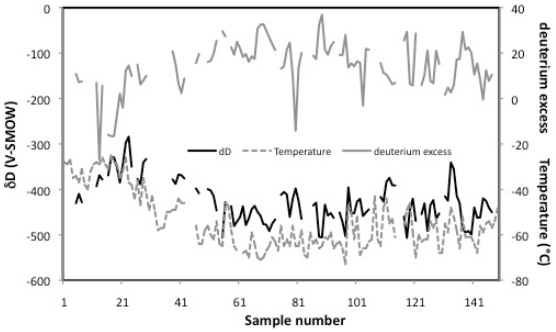

Figure 1: δD, temperature and d data of DC precipitation.

[1] Masson-Delmotte *et al*. (2008) *J. Clim*. **21**, 3359-3387.

Computational approaches to hydrothermal fluid-rock interaction on nanometer to kilometer scales

THOMAS DRIESNER

ETH Zurich, Institute of Geochemistry and Petrology, Clausiusstrasse 25, 8092 Zurich, Switzerland (thomas.driesner@erdw.ethz.ch)

Fluid-rock interaction in hydrothermal systems plays a central role in processes such as the formation of ore deposits, geothermal energy production, and global element cycles. A quantitative understanding of fluid-rock interaction requires looking at vastly different length (nm to km) and time (ps to Ma) scales. Chemical thermodynamics provides the framework that links the scales and computational approaches are essential for both improving thermodynamic models and applying them in the modeling of natural processes.

In spite of decades of research, a universal model of the thermodynamics of fluids at high temperature, pressure and salinity is still lacking, which hampers our ability to quantitatively model fluid-rock interaction in systems such as mid-ocean ridge hydrothermal convection or magmatic-hydrothermal ore formation. Existing equations of state are based on physical concepts that do not reflect the molecular interactions in fluids under those conditions. Hence, molecular simulation has become increasingly popular to better understand the nm-scale physics of hydrothermal fluids. In particular, short-range solute-solvent and solute-solute interactions such as solvation and ion pairing are studied since they are not captured by the most common semi-empirical activity models. While many new insights have been gained from molecular simulation, incorporating them into equations of state is still in its infancy.

On the application side, reactive transport computations combine chemical speciation and fluid transport codes to study the progression of fluid-rock reaction fronts in permeable media on macroscopic scales. These tools have so far only rarely been applied in a hydrothermal context, partly for the reasons outlined above, and partly because most of the available codes are restricted to groundwater flow equations that do not adequately describe the flow of compressible and/or boiling hydrothermal fluids. With the recent revival of research on geothermal systems, new codes are emerging that utilize advanced hydrothermal fluid flow codes that can also simulate flow in complex, "realistic" geometries of fractured geological media. First results indicate that correctly representing geometries is key to understand the causes of heterogeneity in evolving fluid-rock interaction.

https://doi.org/10.1180/S0026461X00006502 Published online by Cambridge University Press

A meso-scale laboratory study of stable isotope variations during uranium bioremediation

J.L. DRUHAN[1]*, C.I. STEEFEL[2], M.E. CONRAD[2] AND D.J. DEPAOLO[1,2]

[1]Department of Earth and Planetary Science, University of California Berkeley, Berkeley CA 94720 (*correspondence: jennydruhan@berkeley.edu)
[2]Earth Sciences Division, Lawrence Berkeley National Laboratory, Berkeley CA 94720

We present results from a large-scale column experiment designed to bridge the gap between the field scale and small columns and advance our understanding of the isotopic signatures of biostimulation geochemistry. Stable isotope variations of major elements such as C, Ca and S can identify processes unobservable in concentration data alone but an understanding of these isotope systems must first be developed under controlled biostimulation conditions.

A 1m long, 10cm diameter column was packed with sediment from the saturated zone of the Rifle Integrated Field-Scale Subsurface Research Challenge (IFRC) site in western Colorado. The pore velocity of the column experiment was matched to that of the field, thus providing a direct representation of the first meter down-gradient of the *in situ* uranium bioremediation injection gallery while ensuring steady flow and boundary conditions. Side-ports along the length of the column provided <20cm sampling resolution, while inert tracers and electron donor were added to the injection solution.

This study has generated an extensive isotopic and biogeochemical reactive transport dataset and provides an unprecendented opportunity to constrain carbon, calcium and sulfur isotopic dynamics. Results include:
1) δ^2H and $\delta^{18}O$ breakthrough curves yielding a starting porosity of 0.38 decreasing to 0.30 over 42 days.
2) $\delta^{13}C$-labeled acetate allows tracking of carbon originating from electron donor consumption throughout the system.
3) $\delta^{44}Ca$ variations in the fluid phase identify two primary controls on Ca: precipitation of carbonates and ion exchange between the fluid and sediment.
4) A $\delta^{34}S$ fractionation factor of 12‰ between SO_4^{2-} and HS^- in comparison with a Rayleigh model α of 10‰ indicates variation in α values across the flow path.

These observations are a direct result of the improved spatial and temporal sampling resolution afforded by the experimental design and allow new insight into the highly reactive zone adjacent to contaminant remediation injection wells.

Redox front variability and phosphorus flux across the sediment-water interface

G.K. DRUSCHEL[1], L.G. SMITH[1], N. SHUFELT[1], M.C. WATZIN[2], A.R. PEARCE AND D.M. RIZZO[3]

[1]Department of Geology, University of Vermont. 180 Colchester Ave., Burlington, VT 05405. (Gregory.Druschel@uvm.edu)
[2]Rubenstein School of the Environment and Natural Resources, University of Vermont.
[3]School of Engineering, University of Vermont.

Phosphorus mobility across the sediment-water interface (SWI) in Missisquoi Bay, a shallow (<15m) bay in Lake Champlain, is largely controlled by redox changes exhibiting diel and seasonal variability that can significantly impact nutrient fluxes and associated cyanobacterial activity. In these iron rich (4-5% w/w total Fe) sediments, reactive P (RP) is strongly correlated to reactive Fe, indicating the mobility of a large portion (30-40%) of the P pool in the sediment is associated with iron oxyhydroxide minerals. We investigated changes in sediments, sediment porewaters, and the overlying water column chemistry and microbiology over three consecutive seasons with detailed monitoring of diel changes at the SWI at each sampling time. Sediment cores were profiled using voltammetric electrodes to characterize porewater redox chemistry (O_2, Mn^{2+}, Fe^{2+}, Fe^{3+}, HS^-, $FeS_{(aq)}$). Core profiles show redox conditions become more reducing as the season progresses, with the most strongly reducing conditions present during peak bloom conditions. Redox conditions measured continually over 24-hour periods using *in situ* voltammetric electrodes positioned at the SWI showed significant changes in redox conditions over diel cycles. Cluster analysis of the data using self-organized mapping techniques indicate redox chemistry across the SWI is a significant controlling component of the system that influences cyanbacterial blooms.

As P fluxes are sensitive to a thin layer of iron oxyhydroxides at the sediment surface, changes in redox chemistry at the SWI significantly impact nutrient flux between the sediment porewaters and the overlying water column. Mesocosm experiments utilizing Missisquoi Bay sediments are underway to characterize phosphorus fluxes between the sediments and water column under different redox conitions at the SWI. Preliminary results indicate that both the direction and intensity of P flux across the SWI are dependent on the redox front position and the frequency of how often the redox front sweeps across the SWI.

https://doi.org/10.1180/S0026461X00006502 Published online by Cambridge University Press

Behaviour of Tc(VII) in aqueous solutions in the presence of iron oxides and microorganisms

R. DRUTEIKIENĖ[1]*, B. LUKŠIENĖ[1], D. PEČIULYTE[2] AND BALTRŪNAS[1]

[1]Center for Physical Sciences and Technology, Vilnius, Lithuania (*correspondence: ruta@ar.fi.lt)
[2]Institute of Botany of Nature Research Vilnius, Lithuania (dalia.peciulyte@botanika.lt)

This study investigates the redox behaviour of Tc(VII) in a heterogeneous system containing hematite and magnetite with emphasis on transformation of oxidation state through microbial-mediated processes under oxic conditions. Results showed that after a short exposure period under alkalini conditions (pH 8-9) more then 75% of TcO_4^- were associated with Fe(II) oxide particles and removed from solution. The removal of Tc from solution may be controlled by reduction of Tc(VII) to Tc(IV) by biogenic Fe(II). Under these circumstances no pronounced effect of the sorption of technetium onto Fe(III) oxide was determined. Sorption of Tc onto hematite is achieved because of presence of specific microorganisms. Results of the combined effect of microorganisms and iron-bearing minerals on Tc (VII) sorption peculiarities have shown that bacteria *Arthrobacter globiformis* and *Cellulomonas cellulan*s did not have any influence on Tc sorption onto hematite, while micromicete *Fusarium oxysporum* altered sorption to approximately 85% compared to that in the system without microorganisms. Presence of microorganisms *Penicillium* sp., *Rhodococcus* sp and *Streptomyces* sp. in the tested system induced Tc sorption onto hematite up to 71-82%.

The research has received funding from the European Union's European Atomic Energy Community's (Euratom) Seventh Framework Programme FP7/2007-2011 under grant agreement n° 212287 (RECOSYproject) and from Lithuanian Agency for Science, Innovation and Technology (Grant No 31V-6)

Iron oxides of soils from Cenozoic basalts weathering in eastern China: Relationship with climate change

KAI DU[1], YANG CHEN[1]*, XIAOYONG LONG[1,2], HUI LI[1] AND JUNFENG JI[1],

[1]Institute of Surfacial Geochemistry, School of Earth Science and Engineering, Nanjing University, 210093, China (*correspondence: chenyang@nju.edu.cn)
[2]School of Geographic Science, Southwest University, 400715, China

The Cenozoic basalts are widely distributed from Heilongjiang to Hainan provinces in eastern China, which provide the unique climatic conditions to study basalts weathering. The five soil sequences developed from basalt bedrocks in eastern China were studied, along climate gradient ranging from 200 (Inner Mongolia) to 2,000 mm (Hainan) mean annual precipitation. Magnetic properties, chemical analyses and diffuse reflectance were measured to characterize the iron oxides in soils, since iron oxides are common weathering products and sensitive to response to climate change. Results show that content of free iron oxide, magnetic susceptibility, frequency dependence susceptibility and redness index of surface soil samples are all positively related to MAP, with lowest value in Inner Mongolia samples and highest in Hainan samples. Especially, the content of free iron oxide increases by almost 10 times ranging from 0.5 % to 5.5 % wt. According to similar chemical composition of basalt bedrocks, it can be concluded that climate took most effect on Cenozoic basalt weathering. Further studies are necessary to extract more credible and sensitive indicators like element ratios and mineral index.

This study is funded by the NSF of China (Grant No. 41021002) and China Geological Survey.

https://doi.org/10.1180/S0026461X00006502 Published online by Cambridge University Press

Mineral variation induced by CO_2 injection in saline aquifer

S.H. DU[1,2], X.S. SU[1,2]* AND X.X. GU[1,2]

[1]College of Environment and Resources, Jilin Univ. Changchun, China,
[2]Key Laboratory of Groundwater Resources and Environment, Ministry of Education, Jilin Univ., Changchun, China (yoko_sh@yeah.net, *correpondence: suxiaosi@163.com, 40617997@qq.com)

Conceptual modelling

A reactive transport model with TOUGHREACT [1] for the carbon dioxide sequestration into appropriate deep saline aquifer with a depth of 1200m has been involved in this study. Considering storage conditions, a 1D homogeneous conceptual storage formation with a thickness of 50m is constructed, the salt is 1 mol/L, and T is 50℃, carbon dioxide was injected with a speed of 100kg/s through the central injection well, which lasted for 10a, and the complex geochemical reaction occurs between carbon dioxide and minerals afterward could be known with the model.

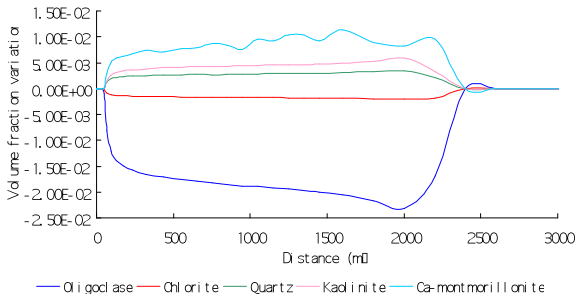

Figure 1: Mineral variation at 1000a after CO_2 injection

Considering the long term of mineral reaction, the minerals fractions variation at 1000a after the CO_2 injection have been detected from the reaction transport model, and the results represented as Figure 1. From the figure we can see that, the injected CO_2 influencing area has reached 2500m. Dissolution and precipitation occur with different extent ascribe to the distances and minerals. According to the simulation model, there are obvious volume variations of oligoclase, chlorite and illite because of mineral precipitation, and there are obvious volume variations of Calcite, Ca-montmorillonite, quartz, kaolinite, siderite and albite because of mineral dissolution, these are similar with the study results of other studies [2].

[1] Xu T. *et al* (2006), *Computer & Geosciences*, **32**, 145-165.
[2] Zhang W. *et al* (2009), *International Journal of Greenhouse Gas Control*, **3**, 161-180.

Translocation and fractionation of Rare Earth Elements in intensely weathered lateritic profiles in Western Australia

X. DU[1,2]*, A.W. RATE[1] AND M. GEE[1]

[1]School of Earth and Environment, The University of Western Australia, Crawley, 6009, WA, Australia (*correspondence: dux01@student.uwa.edu.au)
[2]School of Environmental Studies, China University of Geosciences, 430074, Wuhan, China

Three intensely weathered lateritic profiles (GE, MQ I, II) developed on granite with dolerite dykes in Western Australia were studied to investigate the translocation, fractionation and geochemical pathways of rare earth elements (REE) during intense weathering and lateritization. The study has relevance for geochemistry, pedogenesis and environmental chemistry research, and mineral exploration of REE which is one of the most important strategic resources in the world. Geochemical mass balances were calculated based on bulk geochemical compositions. REE-bearing minerals in parent rocks and regolith samples were identified by synchrotron X-ray powder diffraction (SXRD) and scanning electron microscopy with energy dispersive spectroscopy (SEM-EDS).

In all three profiles, chondrite normalized REE distributions confirmed that the regolith was developed from granite. High deficiency of REE in the weathered residue indicated strong depletion, except in soils of horizon A in MQ profiles. In MQ profiles, the REE patterns normalized to parent rock represented two layers: accumulation in the upper part of profiles and depletion at the lower part, indicating the regolith below 0.6m depth in MQ I and 1.1m depth in MQ II were weathered *in-situ*. The source of REE accumulation in surface soil in MQ profiles was unclear, possibly representing biogeochemical recycling. In the GE profile, regolith samples showed great loss of total REE, up to 95 % in the mottled clay (10m deep), followed by ferricrete (83%loss, 3.5m deep).

Depletion of LREE is greater than HREE in all three profiles, except saprolite. In GE profile, a strong linear relationship of (LREE)/(HREE) ratio normalized by parent granite with pH suggested the fractionation of REE in GE profile was controlled by pH. In MQ profile II, main REE-bearing accessory minerals of the parent granite included allanite, fluocerite and epidote. In the weathered regolith, the small grain size of phosphate phases (<20 μm) were surrounded by clay matrix. The geochemical composition and mineralogy of the regolith indicated REE fractionation intensified during advanced weathering.

https://doi.org/10.1180/S0026461X00006502 Published online by Cambridge University Press

Using *ab initio* potential to predict thermodynamic properties of fluids and minerals

ZHENHAO DUAN, Z.G. ZHANG, R. SUN AND C. ZHANG

Key Laboratory of the Earth's Deep Interior, Institute of Geology and Geophysics, Chinese Academy of Sciences, Beijing 100029

Macroscopic thermodynamic properties (PVT properties, phase behavior, chemical potential, speciation reactions, enthalpy etc.) of fluids are determined by intermolecular, and to a less extent, intramolecular interactions, which are functions of molecular distances and angles. Here we present our two studies to demonstrate how to predict the thermodynamic properties through molecular level study.

(1) Using ab initio calculated molecular potentials of thousands of different configurations, predicting multi-phase equilibria of methane hydrate, liquid and vapor phases under conditions of different temperature, pressure, salinilty and pore sizes. Comparison with the experimental data shows that this model can accurately predict the equilibrium *p-T* condition of CH_4 hydrate in seawater and porous media with high accuracy.

(2) Based on molecular interaction potential for pure H_2O and CO_2 and the ab initio potential surface across CO_2–H_2O molecules, we carried out more than one thousand molecular dynamics simulations of the PVTx properties of the mixtures in the TP range from 673.15 to 2573.15 K up to 10.0 GPa. Comparison with extensive experimental PVTx data indicates that the simulated results generally agree with experimental data within 2% in density, equivalent to experimental uncertainty.

[1] Sun and Duan (2007), *Chemical Geology* **244** , 248 [2] Duan and Zhang (2006) *Geochim. Cosmochim. Acta* **70**, 2311-2324. [3] Duan and Sun (2006) *American Mineralogists,* **V91** ,pp1346-1354[4] Zhang and Duan (2005) *J. Chem. Phys*.**122**, 214507.

Rock-Eval pyrolysis of the Água de Madeiros Formation (Lower Jurassic) from the Lusitanian Basin, Portugal

L.V. DUARTE [1]*, J.G. MENDONÇA FILHO[2], R.L. SILVA[1] AND L.C.V. OLIVEIRA[3]

[1]Universidade de Coimbra, DCT and IMAR-CMA, 3000-272 Coimbra, Portugal (*correspondence: lduarte@dct.uc.pt)
[2]LAFO, UFRJ, 21949-900, Rio de Janeiro, Brazil
[3]Universidade Petrobras, Rio de Janeiro, Brazil

The Lower Jurassic hemipelagic series in the Lusitanian Basin constitutes one of the most important intervals regarding the occurrence of potential hydrocarbon source-rocks in Portugal [1]. One of these units is the Água de Madeiros Formation (Upper Sinemurian to lowermost Pliensbachian), which is composed by organic-rich marl–limestone alternations with several black-shale horizons [2].

Based on the study of this unit in its type locality (S. Pedro de Moel area), about 58 m thick, we present in this work a high-resolution organic geochemical analysis centered in Rock-Eval pyrolysis. Total organic carbon (TOC), determined in more than 170 samples and covering the whole succession, shows a large variation and reaches up to 22 wt.%. A great part of the 78 analyzed samples by pyrolysis present S2 values above 10 mg HC/g rock, reaching a maximum of 78.1 mg HC/g rock. Moreover, these high S2 values are correlative with the highest recorded values of the Hydrogen Index, that shows an average around 400 mg HC/g TOC (maximum of 637 mg HC/g TOC).

Despite these interesting geochemical indicators in terms of good source-rock potential, thermal maturity of the Água de Madeiros Formation in the studied reference section is low (clearly immature), as suggested by T_{max} values always below 437 ºC.

This work is a contribution to project PTDC/CTE-GIX/098968/2008 (FCT-Portugal, COMPETE/FEDER).

[1] Oliveira *et al*. (2006) *Boletim de Geociências da Petrobras* **14** (2), 207-234. [2] Duarte *et al*. (2010) *Geol Acta* **8**, 325-340.

https://doi.org/10.1180/S0026461X00006502 Published online by Cambridge University Press

CO_2 degassing and groundwater mixing in the Navajo aquifer, Green River, Utah

BENOÎT DUBACQ[1]*, NIKO KAMPMAN[1], NELLY ASSAYAG[1,2], MAX WIGLEY[1] AND MIKE BICKLE[1]

[1]University of Cambridge, Dept. Earth Sciences, Downing Street, Cambridge, CB2 3EQ, United Kingdom (*correspondence: bd298@cam.ac.uk)
[2]IPGP, Sorbonne-Paris-Cité University, 75252 Paris, France

Natural subsurface CO_2 accumulations provide a unique opportunity to understand the long-term fate of anthropogenic CO_2 injected into geological reservoirs. Key parameters include the impact of CO_2 dissolution on reservoir pH and subsequent mineral dissolution / recrystallization processes. Cold-water geysers driven by the degassing of CO_2-saturated fluids in Crystal Geyser, Green River, Utah, allow direct sampling of the underlying CO_2-rich Navajo aquifer. Liquid and gaseous phases have been synchronously sampled during and between geysers eruptions; both water and gas samples have been analyzed for carbon isotopic composition. Water samples have also been analyzed for major and trace elements. The fluid composition changes systematically through the course of an eruption. This reflects mixing of fluid from a deep CO_2-charged aquifer into the shallow Navajo aquifer on the time-scale of eruptions, driven by the pressure perturbation induced by geysering. The evolution of CO_2 degassing has been reconstructed using thermodynamic modelling of the solubility of CO_2 and aqueous phase speciation coupled with a Rayleigh distillation model to reproduce the observed trends in $\delta^{13}C$ of gases and dissolved inorganic content of the waters. Results suggest that the Navajo aquifer at depth is under-saturated in CO_2. Degassing is estimated to initiate about 120 meters below the surface, when the fluid rises in the pipe. The pH at depth is calculated to be ~5.35, which is 1.35 pH unit lower than its surface value.

Ce-rich layers in manganese micronodules of the Brasil Basin

A. DUBININ*, T. USPENSKAYA, V. SVAL'NOV AND T. DEMIDOVA

PP Shirshov Institute of Oceanology RAS, 117997 Moscow, Russia, (*correspondence: dubinin@ocean.ru)

Manganese micronodules (MN) were selected from miopelagic clays of Brasil basin (Atlantic Ocean) to investigate the evolution of their chemical composition depending on the size fraction. We studied bulk MN composition in size fraction: 1000-500, 500-250, 250-100 и 100-50 μm at site 1536 (24º01.1' W, 22º17.6' S, depth 5500 m (depth in core 420-430 cm).

Mn and Fe contents are changed from 23.6 to 31% and from 4.0 to 12.2% respectively. The ratio of Mn/Fe is initially increased from 3.5 to 5.8 and then it is decreased to 2.5 with the increase of MN size fraction.

Changes in iron content resulted in the similar variation in contents of phosphorus, Co, Li, Be, V, Tl, Y, Th, U and rare earth elements.The value of cerium anomaly is decreased from 5.1 to 4 and then it is increased to 14 with the increase of the MN size fraction.

To understand the variations of trace element composition between separate size fractions we analyzed the polished sections of MN by X-ray microanalysis on a scanning electron microscope JEOL JSM-6480LV.

Phase 1 with high manganese and nickel contents and the ratio of Mn/Fe = 9.6 is most widely represented. It is not-layered, enriched in clay material, captured during its formation from the associated sediment. It was formed during early diagenesis and grew at relatively high rate.

Phase 2 is thin-layered, Mn/Fe = 3.2. Phase 1 overlaps unconformably phase 2. It represents the first generation of MN.

Phase 3 is layered, Mn/Fe = 2.1, discontinuous layers of Ce enriched oxyhydroxide phase are contained between their layers.

Enriched in cerium phase 4 is found as the island chains of the substance between the layers of phase 3 and contains an average of about 8% of cerium. It has the lowest Mn/Fe = 1.6 and high Ti and P contents.

Variations in micronodule composition can be explained by influence of two processes – hydrogenous-diagenetic (phases 2-4) and diagenetic (phase 1).

https://doi.org/10.1180/S0026461X00006502 Published online by Cambridge University Press

X-ray spectroscopic constraints on complexing of high-field-strength elements in subduction zone aqueous fluids

J. DUBRAIL[1], M. WILKE[1], C. SCHMIDT[1], K. APPEL[2], S. PASCARELLI[3], K. KAVSHINA[3] AND C.E. MANNING[4]

[1]Deutsches GeoForschungsZentrum (GFZ), Potsdam, Germany (julien@gfz-postdam.de)
[2]Deutsches Elektron Synchrotron, Hamburg, Germany
[3]European Synchrotron Radiation Facility, Grenoble, France
[4]University of California Los Angeles, UCLA, USA

Magmatic rocks related to subduction zones commonly display element patterns characterized by depletion of high-field-strength elements (HFSE, i.e., Ti, Zr, Hf, Nb and Ta). The depletion may be due to low solubility in the aqueous fluids that are involved in the processes at subduction zones. The geochemical budget of HFSE is largely controlled by accessory phases such as zircon. Therefore, knowledge is needed on solubility and stability of these phases. Fluid composition should be one of the most important parameters because it can strongly affect complexing of HFSE in aqueous fluids. Complexing with alkalies and silica dissolved in the fluid has been suggested as an efficient mechanism to promote HFSE mobility [1,2]. However, direct evidence on the HFSE speciation in fluids at subduction zone conditions is lacking.

Experimental information on HFSE complexation was obtained for aqueous fluids with HCl, NaOH, $Na_2Si_3O_7$ (NS3), or $Na_2Si_3O_7$ + 1 or 5 wt% Al_2O_3, equilibrated with zircon or hafnon in hydrothermal diamond-anvil cells at *T* up to 750 ˚C and *P* up to 1 GPa. On these fluids, XANES and EXAFS spectra were collected *in situ* at *P* and *T* at beamlines ID 24 and ID 26 (ESRF). For NS3 ± Al_2O_3 solutions, measured XANES and EXAFS at the Zr-K and Hf-L_3 edges indicated complexes with 6 oxygens in the first shell. The XANES simulated with FEFF9 [3] based on a $Na_2ZrSi_4O_{11}$ cluster (as in vlasovite) is in good qualitative agreement with measured spectra. In contrast, 7 oxygens are indicated in the NaOH solution. For HCl solutions, a spectrum simulated for a $(Zr,Hf)O_4Cl_3$ cluster reproduced qualitatively the features of the experimental spectra. Our results confirm that alkalies and silica dissolved in aqueous fluids may efficiently transport HFSE in the fluids emanating from the subducting slab.

[1] Manning (2004), *Earth Planet. Sci. Lett.* **223**, 1-16. [2] Manning *et al.* (2008), *Earth Planet. Sci. Lett.* **272**, 730-737. [3] Rehr & Albers (2000), *Reviews of Modern Physics* **72**, 621-654.

High pressure geochemistry in laser-heated diamond anvil cells with synchrotron light

L. DUBROVINSKY[1,*], K. GLAZYRIN[1], C. MCCAMMON[1], A. KANTOR[1], N. DUBROVINSKAIA[2], V. PRAKAPENKA[3], M. MERLINI[4,5], M. HANFLAND[5], A. CUMAKOV[5] AND S. PASCARELLI[45]

[1]Bayerisches Geoinstitut, Bayreuth, Germany (*correspondence: leonid.dubrovinsky@uni-bayreuth.de)
[2]Laboratory of Crystallography, Bayreuth University, Bayreuth, Germany
[3]GSECARS, APS, The University of Chicago, USA
[4]Dipartimento di Scienze della Terra, Universita degli Studi di Milano, Milano, Italy
[5]ESRF, Grenoble, France

A major goal in the geosciences is to understand (and predict) how the Earth works, which requires a detailed knowledge of how the mineral phases which make up the Earth behave under high pressure and high temperature conditions. Geochemistry of deep Earth interiors is particularly concern with phase transitions and crystalchemistry of silicates and oxides, oxidation and electronic state of elements (first of all iron), and elements partitioning between major lower mantle phases. We demonstrate that combination of laser-hated diamond anvil cell technique and modern synchrotron facilities (high resolution angle dispersive X-ray diffraction, XANES, nuclear inelastic scattering (NIS), and nuclear forward scattering(NFS)) make possible *in situ* studies pressure and temperature dependence of chemical and physical properties of minerals. Particularly, accurate single crystal diffraction studies of iron bearing silicate perovskite and ferropericlase extended to 100 GPa and over 2500 K and, together with NFS, NIS, and XANES data revel crystalchemistry of iron at conditions of Earth lower mantle.

https://doi.org/10.1180/S0026461X00006502 Published online by Cambridge University Press

Potential source variation in Munro komatiites: Fred's and Theo's Flows, Ontario, Canada

C. DUCHEMIN[1]*, C. CHAUVEL[2], V. DEBAILLE[1], N. ARNDT[2] AND N. MATTIELLI[1]

[1]Dept. of Earth and Environmental Sciences, Université Libre de Bruxelles, Brussels, Belgium (*correspondence : cduchemi@ulb.ac.be)

[2]ISTerre, UMR5275 CNRS, Université Joseph Fourier, 38041 Grenoble, France

Munro-type komatiites, also called Al-undepleted komatiites, are volcanic ultramafic rocks characterized by a high MgO content (>18 wt%), and near-chondritic ratios of Al_20_3/TiO_2 and $(Gd/Yb)_n$.

We present new data of trace element concentrations, measured in two thick, differentiated flows, both Archean (2.7Ga) in age, located in the Munro Township in the Abitibi greenstone belt. Fred's Flow has komatiitic affinity. It differentiated from a parental magma with about 20% MgO into a series of upper spinifex lavas, a central gabbroic unit and lower olivine-dominated cumulates. Theo's flow has an Fe-rich tholeiitic affinity. It differentiated from a less-magnesian picritic parental magma into a central gabbro and underlying pyroxene-rich cumulates. The goal of this geochemical study is to better understand the petrogenetic relationship of those two flows.

The results reveal notable differences in REE pattern between the samples. Eight Fred's Flow units are characterized by moderate to strong depletion in LREE ($0.55 \leq (La/Sm)_n \leq 0.99$) and relatively flat HREE patterns ($0.88 \leq (Gd/Yb)_n \leq 1.20$), whereas seven Theo's Flow units have a convex pattern with ($0.83 \leq (La/Sm)_n \leq 1.24$) and ($1.34 \leq (Gd/Yb)_n \leq 1.63$). Elements such as Ba, Cs, Sr and Eu were mobile during metamorphism and/or hydrothermal alteration.

As a whole Theo's Flow is more enriched in trace elements than Fred's Flow and its HREE are depleted, indicating that garnet was residual during partial melting. Together with the Fe-rich composition, this may reflect a lower degree of melting and/or a more enriched source, perhaps one with a high eclogite component. Fred's Flow magmas probably formed by fractional melting of a hotter peridotitic source.

Multiscale melt extraction in the lower crust and upper mantle

JOSEF DUFEK AND CHRISTIAN HUBER

School of Earth and Atmospheric Sciences, Georgia Institute of Technology, Atlanta GA 30332, USA.

The dynamics associated with melt extraction, including both the movement of melt and the much slower deformation of the solid residue, involves motion on a range of scales. Ultimately melt separation occurs on the crystal scale, while consequent solid deformation occurs on scales of 10s to 100s of kilometers. In order to examine both the solid-state instabilities and melt extraction in detail, we have adopted a multi-scale modeling approach. Crystal scale melt extraction under different amounts of mantle anisotropy is calculated using a lattice Boltzmann method, and a parameterized permeability based on numerous calculations is then incorporated into a multiphase thermal and dynamic model to study the location, timing and flux of melt separating from the crystalline solid. We apply this approach to examine the residence time and extraction rates of melt in lower crustal MASH zones and examine the consequences of foundering of dense crustal roots.

The foundering of dense, mafic residual material from the base of the crust and lithosphere into the underlying mantle has been proposed to explain the long-term chemical evolution of continental crust. Such density instabilities generate solid-state dynamics in the upper mantle surrounding the downwelling material and the return flow of the surrounding mantle. Upwelling regions may generate melting and perturb the flux of magma reaching the base of the crust. We find that large-scale mantle stresses create anisotropy in the permeability structure of the mantle that focuses melt in roughly annular regions surrounding downwelling material. The extent of melting is a function of the degree hydration of the mantle, with the most hydrated conditions resulting in a factor of 3-4 times estimates of background arc melt flux. When the presence of a slab is considered, melt flux is focused preferentially several kilometers toward the backarc region, leaving a magmatic shadow immediately below the downwelling flow.

https://doi.org/10.1180/S0026461X00006502 Published online by Cambridge University Press

Sorption and interfacial redox of Sn(II) under anoxic conditions: Magnetite vs. anatase

S. DULNEE[1]*, D. BANERJEE. [1,2] A. ROSSBERG[1,2] AND A.C. SCHEINOST [1,2]

[1]Institute of Radiochemistry, Helmholtz Zentrum Dresden Rossendorf, D-01314, Germany (*correspondance s.dulnee@hzdr.de)

[2]The Rossendorf Beamline at ESRF, F-38043 Grenoble, France

The long-lived fission product ^{126}Sn is of substantial interest in the context of nuclear waste deposition in deep underground repositories. However, the redox state (di- or tetravalent) under the expected anoxic conditions is still a matter of debate. We therefore investigated the stability of Sn(II) in the presence of a highly redox-reactive mineral, magnetite ($Fe^{II}Fe^{III}_2O_4$), in comparison to a non-redox-reactive, anatase (TiO_2).

Sorption experiments were performed at < 2 ppm O_2, and redox state and local structure was monitored over time by X-ray absorption spectroscopy (XAS).

We found a rapid (< 30 min) oxidation of Sn(II) to Sn(IV) in the presence of magnetite. Although solubility calculation predicted the precipitation of SnO_2, the local structure determined by XAS showed two Sn-Fe distances of about 3.15 and 3.60 Å in line with edge and corner sharing arrangements between octahedrally coordinated Sn(IV) and the magnetite surface, indicative of inner-sphere complexation. The structure of the complex remained largely unchanged up to an equilibration time of 1 month.

After 30 min reaction with anatase, Sn(II) was conserved. However, even with the redox-inert anatase, Sn(II) oxidized to Sn(IV) over time, forming an Sn(IV) inner-sphere complex with Sn-Ti distances at 3.24 and 3.53 Å. Therefore, our results clearly indicate that Sn(IV) is the most relevant oxidation state to be considered even under reducing conditions, and that inner-sphere complexation is a relevant retention mechanism.

Evidence of lime-CO_2 evolution and priming effect of agricultural liming

WILFREDO DUMALE, JR.[1,2]*, TSUYOSHI MIYAZAKI[2] KENTA HIRAI[2], TAKU NISHIMURA[2] AND HIROMI IMOTO[2]

[1]Department of Plant Science, Nueva Vizcaya State University, Bayombong, 3700 Nueva Vizcaya, Philippines (*correspondence: dumalewajr@soil.en.a.u-tokyo.ac.jp)

[2]Department of Biological and Environmental Engineering, University of Tokyo, 1–1–1 Yayoi, Bunkyo-ku, Tokyo 113-8657 Japan (amiyat@soil.en.a.u-tokyo.ac.jp, hirai@soil.en.a.u-tokyo.ac.jp, takun@soil.en.a.u-tokyo.ac.jp, imojin@soil.en.a.u-tokyo.ac.jp)

Agricultural liming contributes significantly to atmospheric CO_2 emission from soils [1] and enhances the turnover of soil organic matter (SOC), termed priming effect (PE) [2]. We believe that these impacts of liming acid soils should be factored in our existing soil organic matter (SOM) models but data on magnitude of lime-contributed CO_2 and priming effect in a wide range of global acid soils are still few.

Using two acid soils in Japan: (1) an acidic Kuroboku Andisol from Tanashi, Tokyo Prefecture (35°44' N, 139°32' E), and (2) Kunigami Mahji Ultisol of Nakijin, Okinawa Prefecture (26°38' N, 127°58' E), we employed a unique methodology to separate and quantify lime-contributed ($^{13}CO_2$), and SOC-originated ($^{12}CO_2$) CO_2-C evolution using $Ca^{13}CO_3$ (^{13}C 99%) as lime and tracer.

Our experimental data have confirmed that (1) lime contributes heavily to CO_2 evolution, and (2) liming acid soils increases SOC turnover. On the average, lime-CO_2 was 76.84% (Kuroboku Andisol) and 66.36% (Kunigami Mahji Ultisol) of overall CO_2 emission after 36 days, indicating that the mineralization of lime-carbonates is the major source of CO_2 emission from acid soils during agricultural liming. The calculated PE of lime (Kuroboku Andisol, 51.97-114.95%; Kunigami Mahji Ultisol, 10.13-35.61%) was entirely ^{12}C turnover of stable SOC since the soil microbial biomass (SMBC), a labile SOC pool, was suppressed by liming in our experiment.

Liming can influence the magnitude of CO_2 evolution from agricultural ecosystems considering global extent of acid soils and current volume of lime utilization. The measured PE of liming in SOC is large and can significantly alter atmospheric CO_2 evolution from agricultural ecosystems.

[1] Biasi *et al*. (2008) *Soil Biol. Biochem*., **40**, 2660–2669. [2] Kuzyakov *et al*. (2000) *Soil Biol. Biochem*., **32 (11-12),** 1485–1498.

https://doi.org/10.1180/S0026461X00006502 Published online by Cambridge University Press

Co-evolution of clay-sized organic and mineral constituents during initial soil formation

A. DÜMIG[1]*, R. SMITTENBERG[2] AND I. KÖGEL-KNABNER[1]

[1]Lehrstuhl für Bodenkunde, Technische Universität München, D-85350 Freising-Weihenstephan, Germany (*correspondence: duemig@wzw.tum.de)

[2]Geologisches Institut, ETH Zürich, CH-8092 Zürich, Switzerland

Clay fractions from a soil chronosequence (Switzerland) after retreat of the Damma glacier (15, 75 and 120 yrs) and from mature soils outside the proglacial area (> 700 yrs) were used to elucidate the evolution of organo-mineral assoziations during initial soil formation.

The chemistry of clay-bound organic matter was assessed by ^{13}C NMR spectroscopy and the contents of amino acids and neutral sugar monomers were determined by acid hydrolysis. The mineral phase was characterized by X-ray diffraction, oxalate extraction, N_2 adsorption, and cation exchange capacity at pH 7 (CEC_{pH7}), before and after H_2O_2 treatment.

The OC loading of the clay fractions strongly increased within about 100 yrs of soil formation. This resulted in decreasing specific surface area (SSA) of the mineral phase and increasing CEC_{pH7} which is in line with XRD analysis as no significant transformations of clay minerals were detected. The SSA of H_2O_2-treated clay fractions were strongly related to oxalate soluble Fe (Fe_o) and a strong correlation was found between increasing contents of Fe_o and OC with soil age.

Clay-bound OC of the 15-year-old soils was of refractory nature owing to high proportions of carboxyl C and aromatic C which may be ascribed to inherited OC. With increasing age (75 and 120 yrs), the relative proportions of carboxyl and aromatic C decreased. This was mainly associated with increasing O-alkyl C proportions, whereas accumulation of alkyl C is detected only in the mature soils. These findings are in line with the amounts of carbohydrates which were predominantly derived from microbial input. Proteins accumulated to a similar extent as carbohydrates and H_2O_2 resistant OM showed very low C/N ratios.

The formation of organo-mineral associations starts with the sorption of microbial-derived proteinaceous compounds and carbohydrates on mineral surfaces which are mainly provided by ferrihydrite. The sequential accumulation of different organic compounds and the large OC loadings point to layering of OM during the evolution of clay fractions.

Composition of error in LA-ICP-MS U/Pb geochronology: Lessons from the processing of standard measurement series performed in ten laboratories

I. DUNKL[1]*, R. TOLOSANA-DELGADO[2] AND H. VON EYNATTEN[1]

[1] Sedimentology & Environmental Geology, Geoscience Center, University of Göttingen, D-37077 Göttingen, Germany (*correspondence: istvan.dunkl@geo.uni-goettingen.de)

[2] Maritime Engineering Laboratory, Technical University of Catalonia, Barcelona, Spain (raimon.tolosana@upc.edu)

We have studied the error propagation and the composition of the error of the calculated U/Pb ages of standards measured in ten laboratories by laser ICP-MS technique. These laboratories used different mass spectrometers, laser cells and instrumental settings. The data reduction was performed by several alternative methods e.g. using Arithmetic Mean of Ratios (AMoR), Ratio of Means (RoMa), Median and regression methods and the residual errors of these procedures were compared. The effect of outlier rejection using the standard 2-sigma method and an iterative outlier-testing method was also studied.

Beyond the classical measures of the precision of the age like concordance we performed several experiments to express the scatter of the data obtained by the the laser ablation.

The so called Extra Poissonal Error is recommended for the optimization of the dwell times of the analytes.

The ratio of the mean and the Tzero intercept (of regression) gives a more robust measure for the fractionation than the ratio of the means of first half / second half of the ablation signal.

The influence of the drift through a measurement session was also studied.

The calculations were performed by the UranOS software: www.sediment.uni-goettingen.de/staff/dunkl/software/

https://doi.org/10.1180/S0026461X00006502 Published online by Cambridge University Press

Rapid expansions in biological metal utilization

CHRISTOPHER L. DUPONT

J. Craig Venter Institute, San Diego, CA 92121.
(cdupont@jcvi.org)

The fundamental chemistry of trace elements dictates the molecular speciation and reactivity both within cells and the environment at large. Using protein structure and comparative genomics, we elucidate several major influences this chemistry has had upon biology. All of life exhibits the same proteome size-dependent scaling for the numberof metal-binding proteins within a proteome. This fundamental evolutionary constant shows that the selection of one element occurs at the exclusion of another, with the eschewal of Fe for Zn and Ca being a defining feature of eukaryotic proteomes. Remarkably, most of known metalloezymes evolved during two transitional eras. First, development of protein structures for metal homeostasis coincided with the emergence of metal-using proteins, which predominantly bound metals abundant in the Archean ocean. Potentially, this promoted the diversification of emerging lineages of Archaea and Bacteria through the establishment of biogeochemical cycles. In a later expansion, over 75% of known Zn binding structures evolve at the same time as the Eukaryotic superkingdom emerged. These Zn-binding proteins are fundamental to eukaryotic cellular biology, while the localization to the nucleus indicates that they are diagnostic features of this superkingdom. Zn bioavailability may have been a limiting factor in eukaryotic evolution. In both scenarios, the newly evolved metalloezymes would drastically change cell biology and by extension, geochemistry.

The role of extracellular organic matter (EOM) in the nucleation and growth of microbial carbonates

CHRISTOPHE DUPRAZ

Center for Integrative Geosciences, Marine Sciences,
University of Connecticut, Storrs, CT 06269, USA.
(Christophe.dupraz@uconn.edu)

Microbes are key players in the global carbon cycle, where they influence the balance between the organic and inorganic carbon. Microbial populations can be organized in microbial mats, which can be defined as organosedimentary biofilms that exhibit tight coupling of element cycles. Complex interactions between mat microbes and their surrounding environment can result in the precipitation of carbonate minerals (i.e., microbialite). This process refers as 'organomineralization *sensu lato*', which differs from 'biomineralization' (*e.g.*, in shells and bones) by lacking genetic control on the mineral product. Organomineralization can be: (1) *active*, when microbial metabolic reactions are responsible for the precipitation (*"biologically-induced" mineralization*) or (2) *passive*, when mineralization within a microbial organic matrix is environmentally driven (*e.g.*, through degassing or desiccation) (*"biologically-influenced" mineralization*). Two tightly coupled components that control carbonate organomineralization *s.l.*: (1) the alkalinity engine and 2) the extracellular organic matter (EOM), which is ultimately the location of mineral nucleation.

The EOM is composed of two main carbon pools: the high molecular weight extracellular polymeric substances (EPS) and the low molecular weight organic carbon compounds (LMW-OC). Both pools play a critical role in carbonate precipitation by providing Ca^{2+} and CO_3^{2-} as well as a nucleation template for mineral growth. EOM contains several negatively charged functional groups, which, depending on the pH, can be deprotonated (each group has unique pK value(s)) and, thus, bind cations. This binding capacity can deplete the surrounding environment of cations (e.g., Ca^{2+}, Mg^{2+}) and, thus, inhibits carbonate precipitation. Therefore, organomineralization is only possible if the inhibition potential is reduced through (1) oversaturation of the EOM binding capacity or (2) EOM degradation.

Studying microbe-mineral interactions, particularly the role of EOM in carbonate formation, is essential in the investigation of early life (e.g., definition of biosignature), especially at the interface between the biotic and prebiotic worlds, where newly formed organic matter could have strongly influenced the nucleation and growth of minerals, notably carbonate.

https://doi.org/10.1180/S0026461X00006502 Published online by Cambridge University Press

Advances in the understanding of atmospheric impacts of volcanic ash emissions since Eyjafjallajokull 2010

A.J. DURANT*[1,2,3] AND A.J. PRATA[1]

[1]Norwegian Institute for Air Research, P.O. Box 100, NO-2027 Kjeller, Norway (*correspondence: adu@nilu.no)
[2]Centre for Atmospheric Science, Department of Chemistry, University of Cambridge, UK
[3]Geological and Mining Engineering and Sciences, Michigan Technological University, USA

Volcanic emissions contain a mixture of gases, and aerosol and silicate ash particles [1]. Volcanic aerosol injected high into the stratosphere may impact atmospheric chemical cycles, or interact with solar and terrestrial radiation and influence climate. Airborne ash and sulphate aerosol in the troposphere, in contrast, has shorter-lived atmospheric and climatic impact. The eruption of Eyjafjallajokull in April and May 2010 brought the atmospheric impacts of volcanic ash emissions to global attention through prolonged grounding of commercial aircraft and subsequent impact on the global economy. In response, the research community engaged across disciplines at an unprecidented scale to provide information, often in real-time, on eruption source parameters, airborne ash characteristics and fallout. One year on from the eruption, we investigate what new knowledge on the impacts of volcanic ash emissions has emerged.

Measurements of ash in the Eyjafjallajokull volcanic cloud from surface [2] and aircraft-mounted instruments [3], and satellite-based sensors combined with modelling [4] tracked the evolution of the ash emissions and provided sometimes contrasting indications of spatial variation in airborne ash concentration. Satellite measurements suggest highly heterogeneous structures with pockets of highly concentrated ash; in contrast the ground-based lidar network suggest low concentrations and highly dispersed ash layers, while airborne measurements suggest concentrations no greater than 1 mgm^{-3} in thin layers [3]. Ash aggregation, while not generally included in ash transport and dispersion models, played an important role in the sedimentation of fine ash generated by the eruption [5]. Finally, it is clear, post-analysis, that there is a need for assiduousness when applying standard atmospheric measurement techniques to the study of volcanic ash clouds.

[1] Durant *et al*. (2010) *Elements* **6**, 235-240. [2] Wiegner *et al*. (2011) *Phys. Chem. Earth*, In Press. [3] Schumann *et al*. (2011) *Atmos. Chem. Phys.* **11**(5), 2245-2279. [4] Stohl *et al*. (2011) *Atmos. Chem. Phys. Discuss*. **11**, 5541-5588. [5] Loughlin (2010) *www.bgs.ac.uk/research/highlights/IcelandAshParticles.html*

The geochemical characteristics of beach sediments of the Finike Gulf (Southwest Turkey)

E.S. DURMUS,.[1,2]*, M. ERGIN[1], Z. KARAKAS[1], K. SOZERI[1], B. ESER-DOGDU[1] AND Z. ONAL[1].

[1]Ankara University, Department of Geological Engineering, 06100, Tandoğan, Ankara
[2]Mahatma Gandi Caddesi No:33/1 GOP,Ankara (*correspondence: elifseda_d@hotmail.com)

In the Finike Gulf (SW-Turkey), geochemical characteristics of modern beach sediments were studied to determine their possible economical potential with respect to marine placer deposits and related depositional, transportation and provenance factors. This study was supported by the the Scientific Research Projects Office of the Ankara University. The study comprised geomorphological field observations, sediment sampling and laboratory analysis (i.e., grain size, multielement composition, total heavy minerals). Within this context, in September 2009, large number of modern-surface sediment samples were collected from the foreshore and backshore sub-environments of the beaches of the Finike Gulf.

Sand with varying proportions is the dominant grain size in beach sediments, Element composition of sediment samples was mostly comparable with that of average earth's crustal rocks. However, relatively higher concentrations were measured for Ni (up to 451 ppm) and Cr (2548 ppm). These values can be related to the presence and wide occurrences of ophiolitic rocks (known as "Antalya Nappes") on the coastal hinterland [1]. The study is still going on.

[1] Ergin *et al*. (2007) *Marine Geology* **240**, 185–196.

https://doi.org/10.1180/S0026461X00006502 Published online by Cambridge University Press

Facies and petrochemical characteristics of the Tertiary aged Tekkeköy (Samsun) area volcanics, NE Turkey

T. DURSUN* AND M. ARSLAN

Department of Geological Engineering, Karadeniz Technical University, 61080-Trabzon, Turkey
(*correspondence: tugbadursun61@gmail.com)

Tertiary volcanics crops out widespreadly in the eastern Pontide, NE Turkey. Of these, the Tekkeköy (Samsun) area volcanics in a E-W trending shallow marine basin lie along the Black Sea coast in the western part of the Eastern Pontide Tertiary Volcanic Province (EPTVP) [1]. The volcanic facieses are dominantly basaltic pyroclastics, less basaltic lava flows, dykes and trachytic dome. The basaltic rocks contain plagioclase, augite and rare olivine with porphyric, microlitic porphyritic, intergranular and locally cumulophyric textures. Trachytic rocks are composed of plagioclase, sanidine, hornblende and biotite with trachytic texture.

Petrochemically, the volcanics can be classified as basalt, trachybasalt, basaltic-andesite, basaltic trachyandesite and trachyte, and exhibit mildly alkaline to subalkaline with medium- to high-K in character. Major oxides and trace elements versus SiO_2 variations show negative correlation for Al_2O_3, Fe_2O_3*, CaO, TiO_2, P_2O_5, MnO, MgO, Co and V whereas positive correlation for K_2O, Na_2O, Rb, Ba and Zr, most of which can be explained by fractionation of cpx+Fe-Ti oxide in mafic rocks, and hornblende +apatite+Fe-Ti oxide in felsic rocks. Besides increase in U and Th with increasing SiO_2 from mafic to felsic rocks may be regarded to small amount of crustal assimilation. N–MORB normalized trace elements patterns show enrichment in LILE (Sr, K, Rb, Ba) and depletion in HFSE (Th, Ce, Zr, Ti, Y) with negative Ta-Nb anomaly, suggesting a subduction and/or crustal contamination signature The chondrite–normalized REE patterns of mafic to felsic samples are similar to each other revealing a common parental source magma (s) for the volcanics. The REE patterns have also concave in shape with marked light REE enrichment and heavy REE depletion, implying effect of significant cpx and hornblende controlled fractionation during the evolution of the volcanics. Facies and petrochemical features of the Tekkeköy volcanics suggest that they may evolved from parental magma (s) derived from an enriched lithospheric mantle source, and correlate others of collisional-post collisional volcanics in the EPTVP.

[1] Arslan, M. (2003) *Geology and Mining Potential of Eastern Black Sea Region Symp. Proc., Trabzon,* 103-105.

B-bearing fluids: Caught in the act

B.L. DUTROW*[1], D.J. HENRY [1], C.W. GABLE[2], B.J. TRAVIS[2] AND C.T. FOSTER JR[3]

[1]Department of Geology & Geophysics, Louisiana State Univ., Baton Rouge, LA 70803;
(*correspondence: dutrow@lsu.edu)
[2]Earth & Env. Sciences, Los Alamos National Lab, Los Alamos, NM 87545
[3]Dept. Geosciences, Univ. Iowa, Iowa City, IA 52242

Fluid flow in the Earth's crust can be tracked, in part, by minerals that require a fluid-mobile element for formation. Tourmaline is nature's boron recorder. In many metamorphic systems, tourmaline growth reflects availability of boron-bearing fluids to the rocks. Such fluids can be internally derived, primarily from the progressive release of B during metamorphic breakdown reactions e.g., clays and micas. Alternatively, B-bearing fluids can be externally derived and infiltrate the metamorphic rocks e.g., from an associated pluton, if there exist sufficient chemical gradients, porosity and permeability.

During metamorphism, tourmaline (tur) formation records both types of fluid involvement. For example, internal fluids carrying B are marked by discrete stages of tourmaline growth, typically as overgrowths on a detrital tur core. Progressive growth zones are marked by distinct changes in mineral chemistry and decreases in compositional variability at the *+c* and *-c* axes. Externally derived fluids may be recognized by development of tourmaline-rich zones adjacent to igneous intrusions. In contrast, B infiltration may leave a more subtle trace such as the development of tourmaline-rich muscovite pseudomorphs after staurolite. Here tur records the infiltration of B-bearing magmatic fluids during high-grade metamorphism. Irreversible mineral-texture modeling combined with thermodynamic properties of the aqueous ions suggest that infiltration develops near the peak of contact metamorphism after sillimanite begins to form.

Computational heat and mass transport modeling of fluid evolution from a crystallizing pluton approximates timing as well as the timescales over which infiltration likely occurs during prograde metamorphism. For a 30km by 3km sheet-like granitoid intruded into host rocks with sufficient permeability to allow fluid flow, peak temperatures occur in about 500ky. By this time, host rocks have largely dehydrated, fluid pressures are insufficient to fracture the rock and provide pathways for flow, and the pluton has largely crystallized and released its fluid. Consequently, tourmaline growth and B movement must occur within this time frame. Tourmaline growth and dissolution provide a powerful signature of B cycling and transfer via fluids in the crust.

https://doi.org/10.1180/S0026461X00006502 Published online by Cambridge University Press

The evolving landscape of U-series sea level chronologies

ANDREA DUTTON

Department of Geological Sciences, University of Florida, Gainesville, FL 32611, USA (*correspondence: adutton@ufl.edu)

Several factors have contributed to the recent movement within the U-series dating community to promote more consistent practices that will ultimately produce more robust chronologies both within and between individual laboratories. First, instrumental and methodological advances have greatly increased the precision of the U-series technique. One consequence of this improved analytical capability is the amplification of the impact of interlaboratory differences in standardization techniques. Second, publication of revised decay constants for ^{230}Th and ^{234}U as well as inconsistent adoption of these constants across the community have led to issues in the appropriate comparison to and conversion of legacy data. This becomes a problem when new data are contextualized with regional or global datasets generated with different decay constants, and requires the availability of raw data and standardization procedures that have not always been routinely published. Third, there has been an increasing demand for more precise constraints on both the absolute and relative timing of past sea level changes to provide empirical constraints on future sea level behavior. This pressure comes from both within and beyond the scientific community, and routinely encourages scientists to push their interpretations to the very limits prescribed by the data.

All of these issues play into the ongoing debate about the appropriate identification, interpretation, and handling of data from corals that have been compromised by open-system behavior. It is increasingly apparent that modeled open-system ages versus screened closed-system ages lead to notable discrepancies in chronologies of past sea level change. This debate is compounded by the recognition that uranium isotope (^{234}U/^{238}U) ratios of seawater may have varied significantly over the last glacial cycle. Understanding this variability, and its cause, are critical to both the modeled open-system and closed-system approaches to building chronologies of sea level change.

These considerations will be addressed in the context of amalgamating and integrating disparate datasets of sea level change during the last interglacial. This analysis provides impetus to establish more consistency in the analysis, reporting, and treatment of U-series data that will pave the way to advancing our understanding of ice sheet dynamics.

Multiscale modeling of ionic transport in charged clays

M. DUVAIL[1,2]*, D. COELHO[2], S. BÉKRI[3] AND B. ROTENBERG[1]

[1]CNRS and UPMC-Paris6, Laboratoire PECSA UMR 7195, 4 place Jussieu, F-75005 Paris, France (*correspondence: magali.duvail@upmc.fr)

[2]Andra, 1 – 7 rue Jean Monnet, F-92298 Châtenay-Malabry, France

[3]IFP Energies nouvelles, 1 et 4 avenue du Bois-Préau, F-92852 Reuil-Malmaison, France

Modeling the solute transport through a pore network in clays is a crucial issue in better understanding its macroscopic transfer processes. Indeed, although the microscopic (sub-nanometer scale) and macroscopic (multi-microns scale) transport properties in such materials are now well known, a lack remains between these two scales.

This study aims at developing a model representing as accurately as possible the main macroscopic properties of a clay sample. In our model, the material is represented by a pore network in which each pore is connected to an other by a channel.

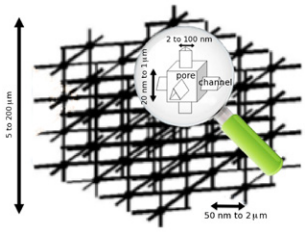

Figure 1: Zoom on an unit cell of the Pore Network Model lattice.

A Lattice-Electrokinetics scheme [1,2] is used to model the microscopic transport properties through the interporal channels (nm scale). Then macroscopic properties (µm scale) are calculated from the microscopic ones using a Pore Network Model (PNM) [3]. Indeed, the calculation of the macroscopic transport properties through a pore and channel network using PNM requires a good understanding of the microscopic ion transport processes (at the channel scale), that depend on the pore and channel properties. Thus, the key question we address here is "How do the transport properties depend on these pore and channel properties?"

[1] B. Rotenberg *et al*. (2008) *Europhysics Letters* **83**, 34004-6. [2] B. Rotenberg *et al*. (2010) *Faraday Discussions* **144**, 223-243. [3] S. Bekri *et al*. (2002) *Developments in Water Science* **47**, 1115-1122.

https://doi.org/10.1180/S0026461X00006502 Published online by Cambridge University Press

The effect of sodium fluoride on soil microbial activity during organic matter decomposition – A calorimetric approach

J.E. DZIEJOWSKI

Department of Chemistry, University of Warmia and Mazury, 10-957 Olsztyn, Poland (dziejo@uwm.edu.pl)

Results and Discussion

Soils exposed to intensive emissions from phosphoric fertilizers and aluminum industries or other fluoride sources have high fluoride concentrations [1]. Fluorides found in soil can affect its microbial activity which can be measured using calorimetric methods [2]. Soil samples were collected at the Agricultural Station of the University. During successive experiments, at 0; 0.05; 0.1; 0.25 and 0.55 % fluoride content and 1 mg glucose in 1g of soil changes in microbial activity were investigated by the calorimetric method. Soil moisture corresponded to 60 % of the maximum water-holding capacity. The changes in the rate of heat production, peak time, total heat effects and the apparent rate constant parameters were used to characterize the glucose biodegradation processes in soil. Sodium fluoride introduced into the soil in the amount corresponding to 0.25 and 0.55 % of fluoride ions decreased the rate of glucose biodegradation. The total heat effects of the studied processes were higher in the presence of fluorides in comparison with soil samples containing no sodium fluoride. The obtained results suggest that despite the reduced rate of glucose biodegradation in the presence of higher doses of sodium fluoride, this compound contributes to an increase in the bioavailability of soil organic substrate for microbial decomposition,

[1] Ozsvath (2009) Fluoride and environmental health: a review. *Rev. Environ. Sci. Biotechnol.* **8**, 59-79. [2] Barros *at al.* (2007) Calorimetry and soil. *Thermochim.* Acta **458**, 11-17. 50.

https://doi.org/10.1180/S0026461X00006502 Published online by Cambridge University Press

Effect of climate change-driven sea water intrusion on the mobilisation of Tc(VI) from reduced sub-surface sediments

J. EAGLING*, P. WORSFOLD, G. O'SULLIVAN AND M. KEITH- ROACH

BEACh Group, University of Plymouth, Plymouth, PL4 8AA , UK (correspondence: jane.eagling@plymouth.ac.uk)

Nuclear fuel cycle operations have resulted in a significant legacy of contaminated land that requires long term management or remediation. Future sea level rise predictions suggest that nuclear facilties situated in coastal locations will become threatened in terms of seawater intrusion. Increased pore water salinity coupled with any influx of oxygenated seawater may impact on the stability of radionuclides associated with sub-surface sediments. Of particular concern is the high yield, redox sensitive fission product ^{99}Tc which, under reducing conditions, accumulates in sediments as hydrous Tc(IV)n.H_2O phases.

In this work Tc (1 μM) was reduced and sorbed with sediments under anaerobic conditions**.** Although nitrate has been reported to inhibit Tc reduction, in this study extensive sorption of Tc (87%) was observed during nitrate reduction. Tc reduction increased to 98% with the onset of Fe reduction.

Mobilisation of Tc(IV) from initially nitrate- and iron-reducing sediments into groundwater and seawater was then studied using batch and column experiments. Batch results showed that Tc was oxidised prior to mobilisation in groundwater and seawater. Limited release into degassed seawater suggested that the formation of soluble Tc(IV) carbonate or colloidal species was not significant. Release of Tc from the initially nitrate- and iron-reducing sediments into groundwater was broadly similar, with 36-48% mobilised after 90 days. In contrast, the initial redox status of the sediments had a marked effect on Tc mobilisation into seawater. Significantly less Tc was released from sediments with ingrowth of Fe(II) (17 ± 2%) compared with the nitrate-reducing sediments (45 ± 7%). These results suggest that Fe(II) phases are able to hinder Tc reoxidation and release into seawater. In column experiments a near instantaneous pulse (4-7%) of Tc was mobilised, followed by a slower sustained release that continued for the duration of the month long experiments, resulting in > 90% Tc release.

Reduced sediments may therefore act as a secondary source of Tc to marine environments during sea level rise-driven intrusion. Mobilisation occurs primarily via reoxidation whilst changes in pore water salinity alone appear unlikely to increase the rate and extent of Tc release.

Mercury and enstatite chondrite origins by equilibrium condensation from chondritic-IDP enriched vapor

D.S. EBEL[1,2]* AND C.M.O'D. ALEXANDER[3]

[1]Department of Earth and Planetary Science, American Museum of Natural History, Central Park W. at 79th St., New York, NY 10024, USA (*correspondence: debel@amnh.org)

[2]Lamont-Doherty Earth Observatory of Columbia University, New York.

[3]Dept. of Terrestrial Magnetism, Carnegie Institution of Washington, 5241 Broad Branch Rd., Washington, DC 20015 USA

Mercury's core is at least 60% of its mass, compared to Earth's ~32%. The origin of Mercury's anomalous core and low FeO surface mineralogy [1] are outstanding questions in planetary science. If Mercury accreted primarily from a local annulus of precursor solids [2], then Mercury's composition may result from chemical controls on equilibrium partitioning of Fe and Si between those solids and coexisting vapor. High temperatures and enrichment in solid condensates or 'dust', relative to H-rich vapor, are likely conditions near the midplane of the inner solar protoplanetary disk. FeO-rich silicate liquids similar to the liquids quenched in ferromagnesian chondrules are thermodynamically stable in oxygen-rich systems that are highly enriched in a dust of CI-chondrite composition [3]. However, the solids surviving into the orbit of Mercury's accretion zone were probably more similar to FeO-poor, anhydrous, ice-free and organic-rich chondritic (interplanetary) dust particles (C-IDPs) [4]. Chemical systems enriched in C-IDP dust can produce condensates with atomic Fe/Si 50% above chondritic [5] for conservative estimates of C-IDP composition and enrichments of up to 1000x. These Fe/Si ratios approach that estimated for bulk Mercury. Stable minerals are FeO-poor, and include CaS and MgS. These reduced species are also found in enstatite chondrites. Disk gradients in volatile compositions of planetary and asteroidal precursors may at least partially explain Murcury's anomalous composition, as well as some meteorite parent body compositions. This model predicts low Ca/Al, and very low FeO content of Mercury's surface rocks.

[1] Robinson & Taylor (2001) *Meteor & Planet Sci* **36**, 841-847. [2] Drake & Righter (2002) *Nature* **416**, 39-44. [3] Ebel (2006) In: Lauretta & McSween (Eds.), *Meteorites and the Early Solar System II*, U. AZ, pp. 253-277. [4] Messenger *et al*. (2003) *Science* **300**, 105-108. [5] Lodders (2003) *Ap.J.* **591**, 1220-1247.

https://doi.org/10.1180/S0026461X00006502 Published online by Cambridge University Press

Geochemical and mineralogical studies on the Fe-Mn deposits of Dehbid area, Fars province, South Iran

S. EBRAHIMI AND Z. MOOSAVI TEKYEH

School of Mining, Petroleum and Geophysics Engineering, Shahrood University, Shahrood, Iran, (ebrahimisusan@gmail.com)
School of Chemistry, Shahrood University, Shahrood, Iran

The Dehbid Fe-Mn deposits are located at about 260 Km of northeast of Shiraz (Fars Province), in the Sanandaj- Sirjan metamorphic zone. The deposits are hosted by shale and limestone of the Lower Devonian and thick massive limestone of the Middle and Upper Devonian. The studied area is affected by two metamorphism phases, therefore, the sequence of limestone and shale sediments in the Devonian have been transformed to garnet mica schist - amphibolites and marble.

The main ore bodies are accommodated as lenticular and vein, which are concordant to the host rock bedding. Some 5 veins have been mapped in the area; they are classified in two groups with 2-8m wide, and 20-850m long. Mineralogical studies show that the ores are including magnetite, hematite, goethite, pyrite, pyrolusite, and psilomelane. Gangue minerals include quartz and carbonate. The values of the Fe_2O_3 and MnO vary between 30 to 80 wt% and 2-13 wt%, respectively. Co/Ni ratios in the hydrothermal iron deposits are between 0.2-7 and in the Dehbid area the ratio ranges 0.1 to 3.6 that characterizes hydrothermal origin of magnetite.

Geology, petrography and sedimentology aspects indicate the Fe- Mn prospect of the Dehbid which is a strataband type deposit. Moreover, giving the influence of volcanic phase occurred in the lower Devonian and the combined geochemical evidences; the origin of the materials is considered distal Sedimentary- Exhalative.

Chemocline oscillations in the Black Sea documented by sedimentary iron isotopes and trace metal patterns

S. ECKERT[1]*, B. SCHNETGER[1], H. FRÖLLJE[1], S. SEVERMANN[2], C. MONTOYA-PINO[3], S. WEYER[4], J. KÖSTER[1], H. ARZ[5] AND H.-J. BRUMSACK[1]

[1]ICBM, Universität Oldenburg, 26111 Oldenburg, Germany (*correspondence: s.eckert@uni-oldenburg.de)
[2]Institute of Marine and Coastal Science, Rutgers University, NJ-08901 New Brunswick, USA
[3]Institut für Geowissenschaften, Universität Frankfurt, 60431 Frankfurt a. M., Germany
[4]Institut für Mineralogie, Leibniz Universität Hannover, 30167 Hannover, Germany
[5]IOW, 18119 Rostock, Germany

The reconstruction of chemocline fluctuations in the Black Sea basin using sediment archives is challenging. Thus a reliable and ubiquitous proxy is required, which can be applied to samples independent of their location and water depth in the basin. Recently sedimentary Fe/Al ratios combined with $\delta^{56}Fe$ values served as a promising proxy for redox interface fluctuations in marine settings. Elevated Fe/Al ratios coupled with low $\delta^{56}Fe$ values in Black Sea sediments document periods when significant transfer of isotopically light reactive Fe from the shelf to the euxinic basin occurred. The suboxic chemocline, impinging margin sediments allows the lateral transport of Fe^{II}_{aq} across the deep basin. However, to date no published dataset provides high-resolution Fe/Al records of sediment cores from different sampling locations across the Black Sea. Here we show major/trace element data from seven sediment cores sampled at millimeter scale from key locations throughout the entire Black Sea. Synthetic depth profiles were generated by merging the single cores. Furthermore, selected cores were analyzed for $\delta^{13}C$, $\delta^{56}Fe$, $\delta^{97}Mo$, $\delta^{238}U$, and isorenieratene derivatives.

Our results show two distinctive peaks in the vertical distribution of Fe/Al accompanied by lower $\delta^{56}Fe$: 1) at the boundary of lithological Units II to III (marine ingression), and 2) in the centre of sapropelic Unit II. The same geochemical signatures reappear throughout Unit I. Our results point towards repetitive chemocline fluctuations owing to changes in the proportion of marine and riverine input into the Black Sea. The rise of the chemocline results from higher input of marine waters, while increased riverine input presumably lowers the redox interface. These results compare quite well with the Eemian sapropel (MIS 5e). Geochemical data from this second sapropel also document a dramatic change from limnic to marine conditions.

https://doi.org/10.1180/S0026461X00006502 Published online by Cambridge University Press

Synchrotron rapid scanning X-ray fluorescence of soft-tissue fossils

N.P. EDWARDS[1]*, H. BARDEN[1], P.L. MANNING[1], W.I. SELLERS[2], B.E. VAN DONGEN[1], U. BERGMANN[3] AND R.A. WOGELIUS[1]*

[1]University of Manchester, School of Earth, Atmospheric and Environmental Sciences, Manchester, M13 9PL, UK (*correspondence: nicholas.edwards@postgrad.manchester.ac.uk, roy.wogelius@manchester.ac.uk)

[2]University of Manchester, Faculty of Life Sciences, Manchester, M13 9PT, UK

[3]SLAC National Accelerator Laboratory, Linac Coherent Light Source, Menlo Park, CA, 94025, USA

Many geochemical and biological analytical techniques have been employed in the identification and quantification of soft-tissues in the fossil record. However, almost all of these techniques require destructive sampling and are unable to provide high resolution, large scale, spatially resolved chemical information from fossil material. Synchrotron rapid scanning x-ray fluorescence (SRS-XRF) developed at the Stanford Synchrotron Radiation Lightsource (SSRL), non-destructively provides highly sensitive, *in situ* and large scale 2D elemental maps at rapid scanning times (~30 secs/cm^2) and reveals the distribution of elements present in concentrations below the detection limits of many conventional geochemical techniques. Furthermore, we have uniquely combined x-ray absorption near edge spectroscopy with XRF rapid scanning, to produce maps showing only organic sulfur species. Our recent multi-technique study of fossilised reptile skin (~50 Mya), employing SRS-XRF, Fourier Transform Infrared (FTIR) spectroscopy and Pyrolysis-Gas Chromatography Mass Spectrometry, strongly suggests that remnants of the living organism's original chemistry (protein compounds) are preserved. Additionally, a new taphonomic model has been proposed to explain the survival of these compounds, involving ternary complexation between organic molecules, trace metals and silicate surfaces.

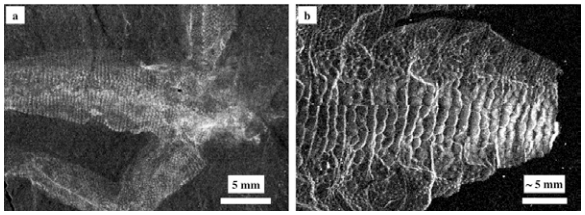

Figure 1: Trace metal loading in a) fossil and b) extant reptile skin.

Fractionation of Cl and Br isotopes during precipitation of salts from their saturated solutions

H.G.M. EGGENKAMP[1]*, M. BONIFACIE[2], M. ADER[2] AND P. AGRINIER[2]

[1]Centro de Petrologia e Geoquímica, Instituto Superior Técnico, 1049-001 Lisboa, Portugal (*correspondence: hermanus.eggenkamp@ist.utl.pt)

[2]Institut de Physique du Globe de Paris, 75005 Paris, France

We determined Cl and Br isotope fractionation of LiCl, NH_4Cl, CsCl, $CaCl_2$, $SrCl_2$, $BaCl_2$, $FeCl_3$, LiBr, NH_4Br, $MgBr_2$, $CaBr_2$ and $SrBr_2$ between their saturated solutions and first precipitating salts at 23 °C. Considering previous data for NaCl, KCl and $MgCl_2$ [1] and NaBr and KBr [2] we now have isotope fractionation estimates for common halogen components in marine and terrestrial salt deposits.

$10^3\ln\alpha$ for most salts is relatively modest (i.e., a few tenths of a per mil), although clear variations, both positive and negative, are observed.

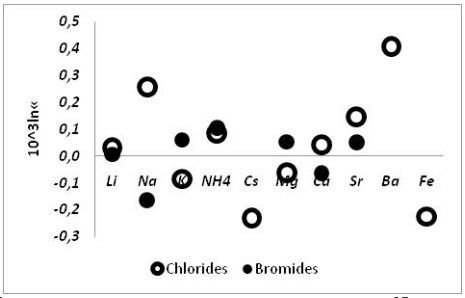

$10^3\ln\alpha$ corresponds to the difference in $\delta^{37}Cl$ and $\delta^{81}Br$ between solution and precipitate.

The results obtained in this study can be used to predict Cl and Br isotope fractionation during salt formation in various marine and terrestrial salt deposits. These data can be related to $\delta^{37}Cl$ data obtained from evaporites which show that different salts have different $10^3\ln\alpha$ [1] [3].

The observation that $10^3\ln\alpha$ for Cl and Br salts from different elements have different amplitudes and signs might account for the different behaviour of Cl and Br isotopes in natural samples, which show a non-ideal correlation [4] [5].

[1] Eggenkamp *et al.* (1995), *GCA* **59**, 5169-5175. [2] Eggenkamp (1995) EUG VIII Conf., *Terra Nova* **7**, Abs. Supp. **1**, 331. [3] Eastoe *et al.* (2007) *Appl. Geochem.* **22**, 575-588. [4] Eggenkamp & Coleman (2000) *Chem. Geol.* **167**, 393-402. [5] Shouakar-Stash *et al.* (2005) *Anal. Chem.* **77**, 4027-4033

https://doi.org/10.1180/S0026461X00006502 Published online by Cambridge University Press

From seconds to millennia: Weathering and erosion of the highly dynamic soils of Alpine areas

M. EGLI[1]* AND C. ALEWELL[2]

[1]Department of Geography, University of Zurich, Winterthurerstrasse 190, 8057 Zurich, Switzerland (*correspondance: markus.egli@geo.uzh.ch)
[2]Institute of Environmental Geosciences, University of Basel, Bernoullistrasse 3, 4056 Basel, Switzerland (christine.alewell@unibas.ch)

Alpine areas are very fragile ecosystems and are strongly sensitive to changing environmental conditions (such as climate warming and land-use change). Soil erosion in the Alps is a well-recognized problem and its temporal scale varies from seconds to millennia. It is identified as a priority for action within the EU (European Union) soil protocol of the Alpine Convention. Steep slopes, extreme climate, fragile soils and the often intensive use of agricultural land characterise the environment of the Alps. There are several approaches to estimating erosion rates in these areas such as modelling using the Universal Soil Loss Equation or empirical determinations using radiogenic isotopes such as Cs or Be or even stable isotopes ($\delta^{13}C$). Recent results show that heavy-rainfall events as well as erosion processes during wintertime and early spring have a considerable influence on the erosion rates. This explains the often-observed failure of common erosion models for alpine areas - the measured rates are too low. The counter-part to erosion is weathering, keeping the sensitive process of soil formation in balance. Weathering in cold regions has often focused on the notion of 'cold'. As a result of this approach, the process focus has been that mechanical processes predominate and that chemical weathering is temperature-inhibited, often to the point of non-occurrence or extremely slow. Recent investigations show that in cryic, ice-free environments, chemical weathering can be a very active process leading to substantial leaching of chemical components and the formation of secondary weathering products (such as clay minerals). Contrary to popular belief, weathering in cold Alpine regions, including chemical weathering, is not strictly temperature-limited but is rather limited by moisture availability. As a consequence of warming, additional areas will become ice-free in high Alpine areas and subject to weathering, soil formation and erosion. Obvious soil changes must be excepted in proglacial areas and at low- to mid altitude sites. Concepts of weathering mechanisms, erosion processes and an overview of recent results from Alpine regions will be presented.

Tracing molecular proxy signals from biological source to sedimentary sink

T. I. EGLINTON[1,2]*, V. GALY[2], X. FENG[1], B. VOSS[2], B. PEUCKER-EHRENBRINK[2], C. PONTON[2], L. GIOSAN[2], E. SCHEFUSS[3], D. MONTLUCON[1], P. DOUGLAS[4], M. PAGANI[4], Y. WU[5] AND N. DRENZEK[6]

[1]ETH Zürich, Zürich, CH-8092 Switzerland (*correspondence: timothy.eglinton@erdw.ethz.ch)
[2]Woods Hole Oceanographic Inst., Woods Hole, MA 02543, USA
[3]Univ. Bremen, Bremen, D-28359, Germany
[4]Yale Univ., New Haven, CT 06520, USA
[5]East China Normal Univ., Shanghai, 200062, P. R. China
[6]Schlumberger-Doll Research, Cambridge, MA 02139, USA

The abundances, distributions, and isotopic signatures of biomarker compounds preserved in aquatic sediments are increasingly being used to derive a diverse array of paleoenvironmental and paleoclimatic information. With analytical advances and development of streamlined methodological approaches, there is growing emphasis on biomarker-based reconstructions of past climate at high temporal resolution, and as part of multi-proxy investigations. Crucial to the accurate interpretation of such records is a robust understanding of the provenance of these molecular signals, as well as the timescales associated with signal transfer from biological source to sedimentary sink. While there is often an implicit assumption that the delivery of these signals to the sedimentary archive is virtually instantaneous. there is growing evidence from biomarker-specific ^{14}C measurements that transport may take several hundred to several thousand years. In the case of markers of vascular plant vegetation, storage in soils and at other locations within terrestrial drainage basins may induce significant temporal lags, while in the marine environment episodes of sediment resuspension and redistribution prior to burial have also been inferred to create significant temporal offsets in sedimentary records. The magnitude of such temporal lags may also vary as a function of climate, potentially yielding complex age relationships between proxy records through time. This presentation will describe studies using molecular isotopic ($\Delta^{14}C$, $\delta^{13}C$, δD) measurements that seek to explore the interplay between biomarker provenance and signal transmission times in the context of drainage basin properties and past climate variability. The results will be discussed in terms of implications for interpretation of biomarker records and carbon cycling on the continents.

https://doi.org/10.1180/S0026461X00006502 Published online by Cambridge University Press

Changes in silicate utilization and upwelling intensity off Peru since the LGM – Insights from silicon and neodymium isotopes

CLAUDIA EHLERT*, PATRICIA GRASSE AND MARTIN FRANK

IFM-GEOMAR, Wischhofstr. 1-3, 24148 Kiel, Germany (*correspondence: cehlert@ifm-geomar.de)

The Peruvian coastal upwelling area is characterized by one of the most pronounced Oxygen Minimum Zones in the world's ocean. Oxygen concentrations in the water column are controlled by consumption through decomposition of organic matter versus ventilation via ocean circulation. Surface bioproductivity which is dominated by diatoms building their frustules from dissolved silicic acid is a function of both nutrient supply and upwelling intensity. The utilization of silicic acid is reflected by its stable silicon isotope composition ($\delta^{30}Si$). The lighter isotopes are preferentially incorporated into the diatom frustules leaving the ambient seawater enriched in the heavier isotopes. Thus $\delta^{30}Si$ values directly mirror silicate availability and the amount of newly supplied silicate with upwelled waters.

Today, the upwelling is strongest near the coast between 10-15°S. There, fractionation is lowest ($\delta^{30}Si$ = 2‰ for surface water and 1‰ for diatoms, respectively) because the permanent re-supply of nutrients prevents a high degree of fractionation. Outside the main upwelling zone fractionation is higher (up to 2.8‰ in the water and 1.8‰ in the diatoms) indicating slightly increased limitation of silicic acid.

A downcore record from 12°S documents that the main upwelling region has been highly dynamic since the LGM. Biogenic opal concentrations range from 2-31wt%. Accordingly the diatom $\delta^{30}Si$ data range from 0.4-1.6‰. During the deglacial and early Holocene the $\delta^{30}Si$ was overall lower than during the late Holocene but much more variable indicating a more dynamic regime. For the late Holocene the low range in $\delta^{30}Si$ indicate constant upwelling. Low $\delta^{30}Si$ during the early Holocene would require surface water with $\delta^{30}Si$ ~1.7‰. Today, no surface waters in the area show such low values. Radiogenic Nd isotopes will be applied to address possible changes in source water, either freshwater runoff from the hinterland or enhanced contributions from the south.

For the entire record low $\delta^{30}Si$ values correspond to low biogenic opal concentrations. The opposite would be the case if silicic acid utilization had been the only driving factor of the $\delta^{30}Si$ variability. Instead, limitation by other nutrients, e.g. phosphate, during phases of low productivity is more likely.

Strontium and sulfur isotopes in celestite from Likak deposit, SW Iran

F. EHYA[1]*, B. SHAKOURI[2], M.R. ESPAHBOD[2] AND H. ASGARIYAN[2]

[1]Department of geology, Islamic Azad University-Behbahan Branch, Behbahan, Iran (*correspondence: ehya@behbahaniau.ac.ir)

[2]Department of geology, Islamic Azad University-North Tehran Branch, Tehran, Iran

Celestite mineralization in Likak deposit is hosted by Lower to Middle Miocene Gachsaran evaporitic formation. An epigenetic mode of formation via replacement of pre–existing gypsum and anhydrite by later celestite was previously proposed for mineralization [1].

In order to determine the origin of strontium and sulfur for celestite mineralization, 6 samples of the mineral from various outcrops of the orebody were collected for isotopic analyses (2 samples for strontium and 4 for sulfur isotopes). The isotopic analyses were performed by Actlabs (Activation Laboratories Ltd., Canada) using a Triton Multi–collector Mass Spectrometer for strontium, and a VG 602 Isotope Ratio Mass Spectrometer for sulfur isotopes.

Strontium isotopic ratios ($^{87}Sr/^{86}Sr$) are 0.708768 and 0.708829 for analyzed samples. These ratios match well with values reported by McArthur and Howarth [2] for Miocene seawater and indicate that Sr was originated from seawater. The celestite samples display $\delta^{34}S$ values falling in the range of 25.7–27.8. Sulfur isotopic ratios indicate higher $\delta^{34}S$ values in analyzed samples than those of Miocene seawater [3]. These higher values were probably resulted by bacterial reduction of sulfate [4–6].

Since celestite mineralization has an epigenetic origin, it can be suggested that precursors of the mineralizing fluids were probably produced by evaporation of seawater in a coastal marine setting. As these brines entered into underlying sediments, they leached considerable amounts of Sr from host sediments. Once these Sr–enriched fluids discharged back up into overlying beds containing gypsum and anhydrite, replacement of the beds by celestite were occurred [7].

[1] Ehya (1997) *Msc. Thesis, Shiraz Univ.* [2] McArthur & Howarth (2004) *Camb. Univ. press*, 96-105. [3] Paytan *et al.* (1998) *Science* 282, 1459-1462. [4] Halas & Mioduchowski (1978) *Ann. Univ. Mariae Curie-Sklodowska* **33**, 115-130. [5] Kesler & Jones (1981) *Chem. Geol.* **31**, 211-224. [6] Taberner *et al.* (2002) *Sedimentology* **49**, 171–190. [7] Hanor (2004) *Jour. Sed.* Res. 74, 168-175.

https://doi.org/10.1180/S0026461X00006502 Published online by Cambridge University Press

Formation of barite chimneys in hydrothermal systems

B. EICKMANN[1]*, M.P ETERS[2], H. STRAUSS[3], I.H. THORSETH[1] AND R.B. PEDERSEN[1]

[1]Centre for Geobiology and Department of Earth Science, University of Bergen, 5007 Bergen, Norway (*correspondance: Benjamin.Eickmann@geo.uib.no)
[2]Department of Geology, University of Maryland, College Park, Maryland 20742, USA
[3]Institut für Geologie und Paläontologie, Universität Münster, 48149 Münster, Germany

Two recently discovered hydrothermal systems at the slow-spreading Arctic Mid-Ocean Ridge system, the Jan Mayen (JMVF) and the Loki's Castle vent fields (LCVF) contain barite chimneys of variable composition. Both hydrothermal systems consists of two active vent sites, which is confirmed by elevated hydrogen sulphide concentrations and discharge of high-temperature fluids, reaching 270°C in the JMVF and 317°C in the LCVF.

In contrast to the high-temperature vent sites, areas of diffuse venting with emanating clear fluids at slightly elevated temperatures (~20°C) have been found to harbour numerous barite chimneys. The barite chimneys in the JMVF are composed of barite, silica and abundant iron, zinc and lead-sulphide minerals, with pyrite representing the dominant sulphides. In contrast, the barite chimneys of the LCVF consist mainly of pure barite with lesser amounts of sulphide minerals.

In additon to oxygen isotopes, this study presents the first multiple sulphur isotope data on barite chimneys in hydrothermal systems. $\delta^{34}S_{sulphate}$ and $\delta^{18}O_{sulphate}$ values of the JMVF barite chimneys are lower than $\delta^{34}S$ of seawater sulphate and $\delta^{34}S$ values of extracted sulphides point to a magmatic source. This indicates that these barite chimneys have been precipitated from a mixture of seawater and hydrothermal fluids. $\delta^{34}S_{sulphate}$ and $\delta^{18}O_{sulphate}$ values for the barite chimneys in the LCVF are higher than $\delta^{34}S$ values for contemporaneous seawater, and show remarkable differences between the surface and the interior. The highest $\delta^{34}S_{sulphate}$ values have been found in the chimney interior, reaching $\delta^{34}S_{sulphate}$ values up to +34.9‰. Negative $\Delta^{33}S_{sulphate}$ values in combination with positive $\delta^{34}S_{sulphate}$ and $\delta^{18}O_{sulphate}$ values strongly point to biological sulfate reduction processes, most likely in the sub surface of the LCVF. The presence of filaments within the chimneys (revealed by SEM) and the finding of framboidal pyite in barite chimneys and underlying sediments in the LCVF indicates that biologic processes caused the observed sulfur and oxygen isotope fractionation.

Sorption of lanthanide ions to mineral surfaces monitored by luminescence spectroscopy techniques

S. EIDNER, K. BRENNENSTUHL, S. ZILM-GRAMCKOW AND M.U. KUMKE*

University of Potsdam, Institute of Chemistry (Physical Chemistry), Karl-Liebknecht-Straße 24-25, D-14476 Potsdam-Golm, Germany (*correspondence: Kumke@uni-potsdam.de)

The distribution of metal ions in the environment is a crucial issue which needs fundamental understanding of the processes involved, e.g., for predicting the safety of repositories for radioactive or chemotoxic waste. In general, the distribution of metal ions is governed by processes like adsorption, desorption, and/or incorporation into inorganic or organic phases, respectively, precipitation from and transport in the aqueous phase. The toxicity of metal ions is not only reflected by its appearance in an environmental compartment, but is determined by its chemical speciation. Therefore, experimental techniques are utile, which allow to monitor the presence and chemical environment of a metal ion at the same time.

The sorption of lanthanide ions on mineral phases, like kaolinite, was investigated by luminescence techniques. As lanthanide ions Europium(III) and Terbium(III) were used because of their outstanding luminescence properties. The influence of salinity and/or the presence of potentially complexing agents on the lanthanide ion's sorption (strength, etc.) was further investigated. As complexing agents low molecular weight organic substances (LMWOS), such as formic and acetic acid, but also potentially chelating agents, like hydroxy propionic acids, were used. Such LMWOS had been identified as constituents of Kerogen isolated from clay minerals and may here distinctly determine the speciation of metal ions. From the luminescence characteristics of the lanthanide ions conclusions concerning their coordination were deduced. Going down to cryogenic temperatures allowed to distinguish between different complex species. Taking advantage of the inter-lanthanide energy transfer made it possible to calculate averaged distances (in the Å to nm range, which extends the observable interionic distance range beyond the first coordination sphere) between sorbed lanthanide ions. Combining the results of the different luminescence techniques deepens the understanding of metal ion sorption on mineral phases, which is a key aspect for understanding transport phenomena of ions (e.g., actinides) in host rock formations.

https://doi.org/10.1180/S0026461X00006502 Published online by Cambridge University Press

The suitability of ^{236}U as an ocean tracer

R. EIGL[1]*, G. WALLNER[1], M. SRNCIK[1], P. STEIER[2] AND S. WINKLER[2]

[1]Institut für Anorganisch Chemie, University of Vienna (*correspondance: rosmarie_eigl@yahoo.de)
[2]Isotopenforschung, University of Vienna, 1090 Wien Austria (peter.steier@unvie.ac.at) (stephan.winkler@univie.ac.at)

^{236}U is probably the second most abundant anthropogenic radionuclide (above 10^6 kg produced so far [1]). While previous measurements could identify ^{236}U only in the vicinity of known contaminated sites (Chernobyl, Sellafield, etc.), our measurements are evolving into a consistent picture of the dispersion of anthropogenic ^{236}U. This led to the insight that ^{236}U is a component of the global fallout from nuclaer weapons testing and was produced via the $^{238}U(n, 3n)^{236}U$ reaction [2].

^{236}U has a well defined source function, is conservative in sea water (residence time approximately 500000 years) and has a sufficiently long half-life (23 Ma) to assure complete mixing in the ocean. The expected natural level below 10^{-13} is negligible compared to the measured anthropogenic ratios. ^{236}U is thus suitable as a tracer for the study of ocean dynamics on a global scale and may in some respects even outperform some more established isotopes.

We analyzed sea water samples from places around the world: the Atlantic ocean ($^{236}U/U = (1.9\pm0.6)\times10^{-9}$), the Pacific ocean ($^{236}U/U = (5.2\pm0.5)\times10^{-9}$), the Black Sea ($^{236}U/U = (3.6\pm0.5)\times10^{-9}$) and the Irish Sea ($^{236}U/U = (2.0\pm0.02)\times10^{-6}$). The measured isotopic ratios coincide with established values for contamination by global fallout, except from Irish Sea water, which was clearly influenced by the Sellafield reprocessing plant.

[1] Steier (2008) *Nucl. Instr. and Meth.* B **266** 2246-2250. [2] Sakaguchi (2009) *Science of the Total Environment* **407** 4238-4242.

An absolute reference frame for clumped isotope thermometry

JOHN M. EILER[1], KATE DENNIS[2], HAGIT P. AFFEK[3], BEN PASSEY[4] AND DAN SCHRAG[2]

[1]California Institute of Technology, (eiler@gps.caltech.edu)
[2]Harvard University; (kdennis@fas.harvard.edu)
[3]Yale University; (hagit.affek@yale.edu)
[4]Johns Hopkins University, (bhpassey@jhu.edu)

Analysis of multiply substituted isotopologues of molecules ('clumped isotope geochemistry') presents special challenges to both precision and accuracy. Previous discussions have focused on mass spectrometric precision for these rare species and intralaboratory reference frames. This discipline has spread, demanding interlaboratory standardization. We present a four-laboratory study of the calibration of mass-47 anomalies (Δ_{47} values) in CO_2 (especially extracted from carbonate). We consider: instrument linearity, source fragmentation/recombination reactions (which vary between mass spectrometers and with time and instrument settings), and differences in methods, materials and conditions for sample preparation. We address these problems by developing a method for standardizing Δ_{47} measurements to an absolute reference frame based on theoretical predictions of the abundances of multiply-substituted isotopologues of gaseous CO_2 that has reached a thermodynamic equilibrium at a known temperature. By analyzing CO_2 gases that have been subjected to established laboratory procedures known to promote isotopic equilibration (i.e., heated gases and water-equilibrated CO_2), and by reference to the statistical thermodynamic predictions of equilibrium isotopic distributions, it is possible to construct an empirical transfer function that can then be applied to CO_2 samples with unknown Δ_{47} values. This reference frame may be unique in that it is based on thermodynamic equilibrium, rather than the isotopic composition of an arbitrary reference material. We describe the protocol necessary to construct such a reference frame, the method for converting gases with unknown clumped isotope compositions to this frame, and suggest a protocol for ensuring that reported Δ_{47} values can be compared among different laboratories, independent of laboratory-specific analytical or methodological artefacts. Application of this approach to measurements of CO_2 extracted from several carbonate reference materials results in interlaboratory agreement on their Δ_{47} values to within est. ±0.01 ‰, 1σ. Finally, we present a revised paleotemperature scale that applies when using the absolute reference frame described here, as opposed to the previous paleotemperature equation based on data from a single laboratory. More generally, this study presents a model for how interlaboratory standardization might be approached for other 'clumped isotope' measurements.

https://doi.org/10.1180/S0026461X00006502 Published online by Cambridge University Press

Strontium isotope fractionation and its application in Earth system sciences

A. EISENHAUER*, F. BÖHM[1], H. VOLLSTAEDT, A. KRABBENHÖFT, V. LIEBETRTAU, J. FIETZKE[1], B. KISAKÜREK[1] AND J. EREZ[2]

[1]Leibniz Institute of Marine Sciences, IFM-GEOMAR, Kiel, 24148, Germany (*correspondance: aeisenhauer@ifm-geomar.de)

[2]Institute of Earth Sciences, The Hebrew University of Jerusalem, 91904, Israel

Taking strontium (Sr) isotope fractionation into account allows the independent and simultaneous determination of paired Sr ratios ($^{87}Sr/^{86}Sr$*, $\delta^{88/86}Sr$) in silicate and carbonate material. Following this approach the Sr isotope composition of seawater ($\delta^{88/86}Sr_{seawater}$: ~0.39 ‰) and marine carbonates ($\delta^{88/86}Sr_{carbonates}$: ~0.15 – 0.25 ‰) differ as a function of local environmental parameters and physiological processes which possibly qualifies Sr isotope fractionation as a new proxy in marine geochemistry. This approach extends the well-established application of the radiogenic Sr ($^{87}Sr/^{86}Sr$) by an additional dimension and also allows for simultaneous calculation of Sr input and output fluxes of the ocean using complete Sr isotope budget equations. In addition, Sr isotope fractionation is a new isotope tool for the study of organic and inorganic $CaCO_3$ precipitation mechanisms being sensitive to the precipitation rate at least for calcite.

Recent results indicate that the $\delta^{88/86}Sr$ value of seawater is controlled by the balance between input and output of shelf-carbonates. In periods of shelf carbonate exposure this input dominates that of Sr originating from silicate weathering. In this regard taking the long residence time (2.5 Ma) and Sr concentration in seawater into account it can be understood why modern and Quaternary corals show about the same $\delta^{88/86}Sr$ value in the order of ~0.2‰. Latter observation qualifies Sr isotope fractionation in marine carbonates as a temperature proxy tool as long as a solid and sensitive temperature-$\delta^{88/86}Sr$ calibrations can be established.

On Phanerocoic timescales $\delta^{88/86}Sr_{seawater}$ follows the general distribution of “calcite seas” and “aragonite seas”, implying a control mechanism by $Mg/Ca_{seawater}$ ratios and further global spreading rates. On shorter timescales in the order of the residence time of Sr in the ocean we observe a strong relationship between the abundance of marine calcifiers and the $\delta^{88/86}Sr_{seawater}$ values providing the opportunity to study the disturbances of the ocean carbon budget during mass-extension events as shown for the Ordovician/Silurian and Permian/Triassic boundary, respectively.

Observational constraints on the water and volatile content of planet-forming regions of circumstellar disks

J.A. EISNER

University of Arizona, Steward Observatory, 933 N. Cherry Ave., Tucson, AZ 85721, USA; (jeisner@email.arizona.edu)

Models of the protosolar nebula suggest that the Earth formed in an environment too hot for water or volatiles to exist in solid form. Because the Earth is known to possess these elements, investigators posit that they were delivered after the Earth formed by comets, asteroids, hydrated dust grains, or a combination of these mechanisms. Planets in habitable zones around other stars—of which we now have several examples—would require similar mechanisms for water and volatile delivery.

Understanding water delivery to the Earth is a crucial part of the story of our origins. Protoplanetary disks around young stars offer a window through which we can view processes that presumably occurred in our solar system billions of years ago. Study of these disks also illuminates the physical processes by which habitable planets may form elsewhere in the Galaxy.

Recent advances in spectroscopic capabilities both in space and on the ground enable probes of warm water vapor and volatile material across a range of excitation conditions. I will review observations of protoplanetary disks that reveal the spatial distribution, temperature, and column density of gas-phase water and volatile material in 'terrestrial' regions. The presence of these molecules in warm, inner disk regions implies transport from cooler regions at larger stellocentric radii, and presents observational constraints on models for water and volatile delivery to terrestrial planets.

https://doi.org/10.1180/S0026461X00006502 Published online by Cambridge University Press

Geoenvironmental factors evaluate the underground waters in the eastern desert of Egypt

ELSAYED AHMED EL GAMMAL

National Authority for Remote Sensing and Space Science-Cairo, Egypt (egammal@hotmail.com)

New areas of utilization had to be developed within the desert area where the underground water reservoir could be used. Therefore, selection of good localities for drilling new water wells suitable for human use and how to use the present water wells is very important in any planning and development. The aim of this paper is to ultimate the benefits of the water wells and delineate their risk. And intends to contribute in developing a suitable methodology for the founding good new water wells. In this study, we proposed the following geoenvironmental factors to ultimate the water wells availability and quality; i) Impact of the surrounded (host) rocks and the type of aquifer sediments. ii) Impact of mining and quarirs activities and mineralized body in the drained basin. iii) Impact of well´s situation in site of water flow in it's drained basin. Eastern Desert of Egypt occupies more than 230, 000 km^2. Hundred important water wells had selected in Eastern Desert to investigate the impact of suggested geoenvironmental factors. There are 96 gold mines in Eastern Desert, in spite of gold mining activities started in the Pre-Dynastic period of the Egyptian history (4000yearsBC) and continued up to the recent years. Besides ochre (iron oxides) and several Pb-Zn mines.

New geomorphological and drainage basin maps for Eastern Desert had been prepared using Landsat ETM images and revise the published geological and topographic maps. Correlation between the published chemical analyses of the underground water for 82 wells on one side and the host rock forming minerals, mining activities, position in the drained basin and the type of the aquifer on the other side.

Elements, when leached from mining wastes are concentrated in certain parts of a drainage basin by flash flood. And contaminate the underground water with elements both from the ore body and mining activities such as Pb, Zn, Cu, and Fe and dissolved materials are high content in these wells. The alkaline water found at the footslopes of syenite mountaines. Abundance from clay minerals in underground water found at granite and syenite terrain as a result of weathering of feldspars. This study monitored that the underground water analyses reflected the rock forming minerals and mining activities in it's surroundings. The aquifer type has considerable significance. There are good water from several wells regarding to these factors. This article elucidates that the proposed impact of the mentioned geoenvironmental factors is actually, the first attempt in the study of the subject in Egypt. Therefore, it is strongly advisable to perform an geoenvironmental impact assessment before starting any drilling for new water wells and before use the present wells and have to put in data base.

Gold and platinum group mineral at Bleïda Far West, Anti-Atlas, Morocco

M. EL GHORFI[1], L. MAACHA[1], A. EN-NACIRI[1] AND T. OBERTHÜR[2]

[1]Managem, Twin Center, Tour A, Angle Bd Zerktouni et Massira Khadra, Casablanca, Morocco

[2]BGR, Stilleweg 2, 30655 Hannover, Germany

The Bou Azzer-El Graara inlier in the Anti-Atlas is well known for its Co-As deposits with gold as a by-product, and the abandoned Bleïda Cu deposit. Recent prospecting by Reminex led to the discovery of a significant gold-palladium mineralization some 7 km NW of the former Bleïda copper mine (-6.5173038, 30.3923419).

At Bleïda Far West, Au-Pd mineralization is hosted by hydrothermally altered amphibolites and chlorite schists. The mineralization occurs in a 7 by 5 km wide corridor, and is associated with intense silicification and numerous, narrow, quartz-dominated, carbonate-bearing veins. Close to surface, the mineralization is hosted in weathered, soft, clayey and powdery material rich in Mn- and Fe-oxides/hydroxides with visible gold.

The pristine mineralization is virtually sulfide-free. Gold (grains up to 400 μm in diameter) is associated with hematite, quartz, calcite, barite, epidote and chlorite. Individual gold grains and grains within individual samples are usually chemically homogeneous. The composition of gold analysed by EPMA (n = 82) ranges from 79 to 93 wt.% Au, 6 to 19 wt.% Ag, and 0.5 to 7 wt.% Pd. The gold grains are intergrown with a distinct suite of PGM, namely mertieite-I [$Pd_{5+x}(Sb,As)_{2-x}$], keithconnite [$Pd_{20}Te_7$], palladseite [$Pd_{17}Se_{15}$], and sperrylite [$PtAs_2$].

A genetic model on the genesis of the Bleida FW mineralization must bear in mind that the gold is associated with hematite and barite, not with sulfides. The combined geochemical and mineralogical evidence so far suggests a relatively low-temperature hydrothermal origin of the gold from oxidizing fluids, related to syn-tectonic quartz-diorite intrusions, or other, still imprecisely known events.

https://doi.org/10.1180/S0026461X00006502 Published online by Cambridge University Press

Secondary crustal effects on MORB composition at the Kolbeinsey Ridge

L.J. ELKINS*[1], K.W.W. SIMS[2], J. PRYTULAK[3], N. MATTIELLI[4], T. ELLIOTT[5], N. DUNBAR[6], J. BLICHERT-TOFT[7], C. DEVEY[8], D. MERTZ[8], J.-G. SCHILLING[10] AND M. MURRELL[11]

[1]Bryn Mawr College, Bryn Mawr, PA 19010 USA (*correspondence: lelkins@brynmawr.edu)
[2]Univ. of Wyoming, Laramie, WY 82071 USA (ksims7@uwyo.edu)
[3]Oxford University, Oxford, UK (julie.prytulak@earth.ox.ac.uk)
[4]Université de Bruxelles, Brussels, Belgium (nmattiel@ulb.ac.be)
[5]University of Bristol, Bristol, UK (tim.elliott@bristol.ac.uk)
[6]New Mexico Tech, Socorro, NM 87801 USA (nelia@nmt.edu)
[7]ENS de Lyon, Lyon, FR (jblicher@ens-lyon.fr)
[8]GEOMAR, Kiel, Germany (cdevey@ifm-geomar.de)
[9]Universitaet Mainz, Mainz, Germany (mertz@uni-mainz.de)
[10]Univ. Rhode Island, Narragansett, RI 02882 USA (jgs@gso.uri.edu)
[11]LANL, Los Alamos, NM 87545 USA (mmurrell@lanl.gov)

We present results for the systematic crustal alteration of basalts from the shallow, slow-spreading Kolbeinsey Ridge (67°05'-70°26'N). Age-constrained Kolbeinsey lavas are isotopically depleted (e.g. $^{87}Sr/^{86}Sr$ = 0.70272-0.70301) with ($^{230}Th/^{238}U$) = 0.95-1.30, low U (≥11ppb), and low Th (≥33ppb). The basalts have a narrow range of ($^{230}Th/^{232}Th$) ratios (1.20-1.32) over a large range in ($^{238}U/^{232}Th$) (0.94-1.32), producing a horizontal array on a ($^{230}Th/^{232}Th$) vs. ($^{238}U/^{232}Th$) diagram. However, we observe that the range of ($^{230}Th/^{238}U$) (0.96-1.30) is inversely and nearly linearly correlated with ($^{234}U/^{238}U$), reflecting shallow crustal alteration of the basalts. Variations in U and Th concentrations and Cl/K_2O ratios are not systematic, indicating a combination of crustal alteration mechanisms. For example, samples with elevated Cl/K_2O ratios but no elevated ($^{234}U/^{238}U$) ratios have likely experienced the addition of subsurface brines with low oxidation states and, thus, low U solubilities; the addition of those fluids is not expected to systematically affect the U isotope composition of the basalts. $^{87}Sr/^{86}Sr$ and ($^{234}U/^{238}U$) isotope variations, on the other hand, support the systematic addition of material from hydrothermally altered crustal rocks to the basalts.

Unaltered Kolbeinsey lavas have high ($^{230}Th/^{238}U$) values (≥1.2), which are consistent with melting in the presence of garnet and with production of thick ocean crust by large degrees of melting.

Fractionation of Li and Mg isotopes in mantle derived materials– Promise, perils and progress

T. ELLIOTT[1], P. POGGE VON STRANDMANN[1], Y.-J. LAI[1], S. KASEMANN[2], D. IONOV[3], E. TAKAZAWA[4], H. MARSHALL[5], K. GALLAGHER[6] AND R. DOHMEN[7]

[1]Bristol Isotope Group, School of Earth Sciences, University of Bristol, BS8 1RJ, U.K.
[2]Fachbereich Geowissenschaften der Universität Bremen, D-28334, Bremen, Germany
[3]Université de Lyon, UJM St. Etienne & UMR6524-CNRS "Magmas et Volcans", 42023 St. Etienne, France.
[4]Dept. of Geology, Niigata Univeristy, 950-2181, Japan
[5]Dept. of Geology & Geophysics, WHOI, MA 02543, USA
[6]Géosciences, Université de Rennes 1, France
[7]Institut für Geologie, Ruhr Universität Bochum, Germany

Li and Mg provide an intersting pair of elements with which to explore the process that influence high temperature fractionation of cationic species in geological environments. There are large relative mass-differences between the isotopes of Li (17%) and Mg (8%) that should should promote discernible fractionations. Both elements are hosted in major lattice sites in common mantle minerals and so the energetics of exchange between different minerals can be reasonably well understood. Neither show multiple valences over mantle conditions, that can dominate fractionation behaviour. The value of understanding the processes that lead to their high temperature fractionations, aside from intrinsic curiosity, is that signatures related to processes of planetary differentiation and recycling may be discerned over later magmatic influences

The importance of diffusion in isotopic fractionation in the Li system has been highlighted in a number of earlier studies. Our new *in situ* studies re-emphasise the complexity and magnitude of fractionations that can occur by late-stage diffusion. Moreover, we show that Mg isotopic variations in bulk xenoliths co-vary with those of Li. Again diffusion is implicated although it is not obvious what drives the ingress of Mg. We suggest it may be related to volatile loss *en route* to surface. In samples uninfluenced by diffusive fractination, as identified from unzoned, mineral Li isotope profiles, natural fractionation factors can be gleaned from analyses of co-existing bulk minerals. Clinopyroxenes are heavier in both Li and Mg systems, as predicted in the latter by computational studies of equilibrium partitioning. More experimental data could yield better constraints over a wider range of conditions.

https://doi.org/10.1180/S0026461X00006502 Published online by Cambridge University Press

Widespread synchronous volcanism on the Snake River Plain

B. ELLIS[1]*, J.A. WOLFF[1], D. MARK[2] AND I. BINDEMAN[3]

[1]SEES, Washington State Uni., Pullman, WA, 99164, USA (*correspondance: ben.ellis@wsu.edu)
[2]SUERC, East Kilbride, G75 0QF, Scotland, UK
[3]Geological Sciences, Uni. of Oregon, Eugene, OR, USA

Rhyolitic volcanism in the central Snake River Plain (SRP) represents the early history of the Yellowstone hotspot. An ignimbrite flare-up has been recognised in the SRP between 11.7 and 10.2 Ma [1] during which >75% of the total volume of ~20,000 km^3 of high temperature rhyolitic magma was erupted. Ignimbrites of the central SRP are almost identical in field appearance being intensely welded with an anhydrous mineral assemblage, so geochemical methods are required to distinguish between magma batches. Here, we combine field constraints, mineral and glass compositions, stable isotopes, and new high precision $^{40}Ar/^{39}Ar$ geochronology to fingerprint magma batches and investigate the timing and distribution of volcanism during the flare-up. Our results indicate that five similar but subtly different magmas were erupted and deposited to both the north and south of the plain beginning with Brown's Bench 4 (11.59 ± 0.081 Ma, n=31, 2σ) and ending with the Tuff of Fir Grove (11.14 ± 0.13 Ma, n=19, 2σ). Magma batches may be distinguished by the presence of multiple compositional populations of both pigeonite (Mg# 9-17) and augite (Mg# 8-22) and variation in ilmenite compositions. All five ignimbrites exhibit the characteristic depletion in $\delta^{18}O$ observed in the central SRP with feldspar values between 1.96 and 2.97‰.

The widely dispersed (>100 km E-W) and geographically limited nature of some of the ignimbrites suggests they were erupted from different sources currently buried beneath younger basalts within the SRP. These results suggest that the currently accepted model of discrete 'eruptive centres' requires reconsideration. The high precision geochronology shows that during the flare-up ignimbrite-forming eruptions were occurring in the central SRP at a frequency more than 7 times that of the present Yellowstone volcanic field and 5 times that of the Heise eruptive centre. We propose that the opening of the western Snake River Plain graben, itself exploiting a pre-existing crustal weakness illustrated by the Vale fault zone directly to the NW, caused lithospheric thinning and resulted in the increased eruptive frequency.

[1] Bonnichsen *et al*. (2008) *Bull. Volc*. **70**,315-342.

Geochemical alteration of fracture geometry during leakage of CO_2

B.R. ELLIS[1], C.A. PETERS[1]*, J.P. FITTS[2], G.S. BROMHAL[3], D.L. MCINTYRE[3] AND R.P. WARZINSKI[3]

[1]Dept. of Civil & Environmental Engineering, Princeton University, Princeton, NJ 08544 (*correspondance: cap@princeton.edu)
[2]Environmental Sciences Department, Brookhaven National Laboratory, Upton, NY 11973
[3]U.S. DOE National Energy Technology Laboratory, Morgantown, WV 26507 and Pittsburgh, PA 15236

A series of three flow-through experiments were performed on artificially fractured caprock samples to investigate fracture evolution during simulated leakage of CO_2-acidified brine. The core samples are from the Amherstburg limestone, which is the caprock for a CO_2 storage demonstration project in northern Michigan, USA.

The evolution of fracture aperture was monitored in real time using X-ray computed tomography (CT). Before and after the experiment, 3-D reconstructions of the fracture structure, aperture and surface roughness were examined at higher resolution via micro X-ray CT. The cores were then sectioned and examined with scanning electron microscopy, X-ray flourescence and micro X-ray diffraction.

Although all three samples were of nearly identical mineralogical composition, the brine flow rates, initial brine compositions, and initial fracture permeabilities differed across the three samples. These differences in flow conditions and fluid composition generated different degrees of fracture deterioration. The first run resulted in substantial erosion of the fracture surface, while the second run had a decrease in fracture permeability that may be attributed to mineral precipitaion along the fracture.

Spectroscopic analysis of the samples after CO_2-brine flow demonstrated preferential calcite dissolution. Mineral spatial heterogeneity coupled with the preferential dissolution of calcite led to non-uniform degradation along the fracture and an increase in surface roughness. In areas where calcite is intermixed with dolomite and other silicate minerals the dissolution of calcite leads to the formation of a degraded zone along the fracture boundary, resulting in a smaller increase in fracture aperture.

The potential mineral precipitation found in the second run is in stark contrast to the rapid mineral dissolution found in the first and suggests a complex interplay of mineral spatial heterogeneity, brine composition, and flow conditions controlling caprock fracture evolution. Results from this study will be we used to frame a discussion on how flow through caprock fractures may be influenced by geochemical alteration of fracture geometry.

https://doi.org/10.1180/S0026461X00006502 Published online by Cambridge University Press

Deglacial southern ocean ventilation history from a benthic foraminiferal $\delta^{13}C$ Transect

AURORA C. ELMORE[1], ELIZABETH L. SIKES[2], MEA S. COOK[3], BENEDETTO SCHIRALDI[2] AND THOMAS GUILDERSON[4]

[1]Marine Science Center, University of New England, Biddeford, ME (*correspondence: aelmore@une.edu)
[2]Institute of Marine and Coastal Sciences, Rutgers University, New Brunswick, NJ
[3]Geosciences Dept. Williams College, Williamstown, MA
[4]Lawrence Livermore National Labs, Livermore, CA

Abrupt climate changes during the last deglaciation are associated with corresponding changes in Southern Ocean overturning circulation and ventilation, particularly during the Antarctic Cold Reversal (ACR). Herein, we present high-resolution, mono-specific (*P. wuellerstorfi*), benthic foraminiferal $\delta^{13}C$ records from a depth transect of cores to reconstruct ventilation changes in the New Zealand region of the Southern Ocean. The cores span depths of; 600m (RR0503 87TC/87JPC), 1200m (RR0503 79JPC), 1600m (RR0503 83TC/83JPC), 2045m (H214;), 2500m (RR0503 125JPC), and 3800m (RR0503 41JPC). Age control is based on tephrastratigraphy, and additionaly constrained by $\delta^{18}O$.

During the last glacial period, the difference in $\delta^{13}C$ values ($\Delta\delta^{13}C$) between 600 and 3800m, is ~1.7‰, significantly higher than during the Holocene (~0.7‰), implying reduced glacial ventilation. In the early deglaciation, $\delta^{13}C$ increased at deep sites, suggesting increasing ventilation. Glacial $\delta^{13}C$ values at 1200m lie evenly between the values of the deeper sites (1600 – 3800m) and the shallowest core (600m), suggesting a distinct glacial intemediate water mass. During the ACR, $\delta^{13}C$ at 1200m increased and converged with values at 600m, suggesting that a single water mass to bathed 600 – 1200m. Following the ACR, $\delta^{13}C$ values at 1200m again become distinct from the shallow and deep sites and the $\delta^{13}C$ in the deeper cores increases rapidly (by ~0.5‰), reducing the $\Delta\delta^{13}C$ to ~1.0‰ post-ACR.

These results indicate a step-wise change in stratification and ventilation across the ACR boundary, suggesting the ACR had both a short term and enduring impact on shallow interior ventilation in the Southern Pacific.

Characterisation of the transfer and biodegradation of chloroacetamide herbicides in lab-scale wetlands

O.F. ELSAYED[1], E. MAILLARD[1], S. VUILLEUMIER[2] AND G. IMFELD[1]*

[1]Laboratory of Hydrology and Geochemistry of Strasbourg (LHyGeS), UMR 7517, University of Strasbourg - CNRS (*correspondence: imfeld@unistra.fr)
[2]Department of Microbiology, Genomics, and the Environment (GMGM), UMR 7156, University of Strasbourg - CNRS (vuilleumier@unistra.fr)

Chloroacetamide herbicides are extensively used in the USA and in Europe for the control of annual grasses and broad-leaved weeds in a variety of crops including maize, sugar beet and sunflower. The major dissipation route for metolachlor, alachlor and acetochlor herbicides appears to be microbially-mediated degradation in soil ecosystems. However, detailed knowledge about their transfer, mitigation and biodegradation in wetland systems is scarce. Here, we examine the transfer and attenuation of metolachlor, acetochlor and alachlor in wetland systems, mainly focusing on their *in situ* biodegradation under different conditions and the characterisation of the microorganisms involved. In order to reach an integrated understanding of chloroacetamides attenuation processes, our investigations will include two different scales. The mesocosm scale experiment will examine the transport and biogeochemical changes under field-like conditions, whereas the microcosm experiment will involve aerobic and anaerobic enrichment cultures set-up in a sediment extract medium and a minimal medium. The biogeochemical dynamics of the lab-scale wetland systems will be characterised using hydrochemical, biomolecular and compound-specific isotope analyses (CSIA). Changes in herbicide concentrations, their enantiomeric ratios and some of their degradation products will be assessed over the flow path and over time. In parallel, changes in the structure of the microbial communities present in lab-scale wetlands will be characterised using PCR-T-RFLP analysis. CSIA methods will be developed to characterise the biodegradation of chloroacetamide herbicides during their transfer in wetland systems.

https://doi.org/10.1180/S0026461X00006502 Published online by Cambridge University Press

Formation of layered Fe(II)-Al(III) hydroxides during reaction of Fe(II) with γ-Al_2O_3 and montmorillonite

EVERT J. ELZINGA

Rutgers University, Department of Earth & Environmental Sciences, 101 Warren Street, Newark NJ 07102

The biogeochemical cycling of iron in aqueous geochemical environments is intimately linked to the cycling of carbon, nitrogen, phosphorus and sulfur, and strongly impacts the solubility and speciation of trace metal and metalloids in these systems. In riparian zones, reductive dissolution of Fe(III)-(oxyhydr)oxides mediated by soil microbes leads to a buildup of high concentrations of dissolved Fe(II) in soil solution and concurrent release of sorbed contaminants. The fate of released Fe(II) is at least partially controlled by sorptive interactions with Al-oxides and phyllosilicates minerals in the soil matrix. Here, X-ray absorption spectroscopic evidence is presented for the formation of Fe(II)-Al(III)-layered double hydroxide phases during reaction of Fe(II) with Al-oxide and montmorillonite clay. These phases form fast (on time scales < 24 h) and are therefore expected to be a major sink for Fe(II) released during reductive dissolution of Fe(III)-oxides. In addition, owing to small particle size, layered structure, and high Fe(II) content, these phases are likely to be highly reactive towards redox-active contaminants such as Cr(VI), and may control retention of divalent metals such as Ni(II) and Zn(II) through adsorption and coprecipitation reactions. The research presented here characterizes formation of these phases in relation to observed macroscopic uptake trends of Fe(II) as a function of Fe(II) concentration, pH and reaction time.

Cycling of nitrogen in the Namibian coastal upwelling system – The stable isotope view

KAY-CHRISTIAN EMEIS[1], BIRGIT NAGEL[1] AND NIKO LAHAJNAR[2]

[1]Institute of Coastal Research, Helmholtz Center Geesthacht, Max-Planck-Str. 1, 21502 Geesthacht, Germany (Kay.emeis@zmaw.de, Birgit.nagel@hzg.de)

[2]KlimaCampus, Bundesstr. 55, 20146 Hamburg, Germany (Niko.lahajnar@zmaw.de)

Nitrogen is a key element in regulating biological processes in the ocean, and the history of the nitrogen cycle under past conditions on Earth is of high relevance for paleoceanographic and paleoclimate studies. The ratio of the two stable N-isotopes ($^{15}N/^{14}N$; expressed as $\delta^{15}N$ versus air N_2) preserved in sediments is commonly assumed to reflect the isotopic composition of N-sources, or the extent of assimilation by phytoplankton. But although $\delta^{15}N$ is widely appreciated as one of few available proxies to reconstruct marine nutrient cycles in the geological past, there are several biases on the $\delta^{15}N$ of sedimentary records. Here we explore the dynamics of nitrogen isotopic composition in several compartments of reactive nitrogen in a depositional setting characterized by extreme gradients in $\delta^{15}N$ of nitrate, suspended matter and surface sediments – the coastal upwelling area offshore Namibia. The gradient observed in $\delta^{15}N$ of surface sediments mirrors the state of oxygen depletion in the water in contact with sediments, as well as changes in source nitrate, in water-column denitrification, in particle advection along the shelf break, and in dominant upwelling mode (coastal versus shelf break upwelling). Based on data of nitrate $\delta^{15}N$ and $\delta^{18}O$ in several seasonal sampling campaigns, we attempt to isolate possible diagenetic effects by determining $\delta^{15}N$ of suspensions and surface sediments in conjunction with indicators of organic matter quality (i.e., the degradation index of amino acids, C-normalized amino acid concentrations) in the pronounced oxygen gradient of the region. Besides sharpening the $\delta^{15}N$ as a proxy for the geological past, the data also allow us to examine some basic biogeochemical concepts underlying nutrient stoichiometry in the ocean. This is important in light of the expected increasing importance of upwelling processes for the supply of nutrients to the surface ocean.

https://doi.org/10.1180/S0026461X00006502 Published online by Cambridge University Press

Noble gas isotope fractionation during air-sea exchange: A tracer for mechanisms that determine N_2/Ar ratios in the ocean

STEVEN EMERSON[1]*, KEVIN TEMPEST[1] AND ROBERTA HAMME[2]

[1]School of Oceanography, University of Washington, Seattle, WA, 98195 (*correspondence: emerson@u.washington.edu; ket5@u.washington.edu)

[2]School of Earth and Ocean Sciences, University of Victoria, Victoria, BC, V8W 3V6 (rhamme@uvic.ca)

Our observations indicate that the N_2/Ar ratio in the world's ocean increases from near equilibrium with the atmosphere at the surface to ~ 1.5 % supersaturation at depth (~ 1000 m) and the values in deep waters increase from the Atlantic to Pacific Ocean by ~ 0.5 %. The reason for the increase is a combination of air-sea exchange during formation of subsurface waters and denitrification below the euphotic zone. In order to separate these two processes one must understand bubble processes that occur during gas exchange. The change in gas ratios is more strongly influenced by small bubbles that totally collapse than larger bubbles that exchange gases across the bubble-water interface.

The isotope ratios of argon (^{40}Ar/^{36}Ar) and neon (^{22}Ne/^{20}Ne) are sensitive to the mechanisms of bubble processes because kinetic isotope fractionation caused by molecular diffusion coefficient differences is a tracer for the bubble exchange mechanism. We have determined the kinetic isotope fractionation factor during gas exchange for argon and neon in laboratory experiments to be – 3.3 ± 0.3 ‰ and – 6.7 ± 0.3 ‰ respectively. These values agree to within the estimated error of theoretical calculations [1] if one assumes the gas exchange process is proportional to the square root of the molecular diffusion coefficients. Using the measured fractionation factors in a gas exchange model [2] to determine the sensitivity of argon and neon isotope ratios to bubble processes suggests that neon isotopes might be a useful tracer for determining the importance of the bubble exchange mechanism. The changes, however, are small—on the order of 0.1-0.2 ‰ -- and to our knowledge, highly accurate neon isotope ratios in seawater are yet to be determined.

[1] Bourg & Sposito (2008) *Geochem. Cosmochim. Acta.* **72** 2237-2247. [2] *Stanley et al.* (2009) *Jour. Geophys. Res.* **114**, C11020, doi:1029/2009JC005396.

Rock alteration and element transfer during formation of U deposits related to Na-metasomatites in the Ukrainian Shield

A. EMETZ [1]*, M. CUNEY [2], J. MERCADIER [2], V. MYKHAYLOV[3] AND N. NAZARCHUK [3]

[1]IGMOF NAS of Ukraine, Kiev-124, 34 Palladina St. (*correspondence: alexander_emetz@yahoo.com)

[2]UHP, B.P.23, 54501 Vandoeuvre-Les-Nancy, France (michel.cuney@g2r.uhp-nancy.fr)

[3]TS KNU, Kiev-022, 90 Vasylkivska St. (taw@bigmir.net)

The Central Ukraine U Province is situated in the Ingul Megablock and along its eastern border in Kryvy Rig – Kremenchug syncline zone of the Ukrainian Shield. The Province includes about 20 U deposits and numerous U showings hosted by Palaeoproterozoic metamorphic and magmatic complexes. Two of these deposits (the Zhovta Richka and Pervomayske deposits) already have been exchaused but four U-deposits in the altered granitic rocks (Vatutynske, Novokostantynivka, Michurynske and Central deposits) are currently operated. Rock samples were selected in underground mines and from drillcores, were examined for mineral paragenesises using optical microscopy and after agate mortar crushing were analysed for major and trace elements with ICP-AES/-MS techniques (CNRS, Nancy, France). Element transfer was estimated using simply binary and/or isocon diagrams [1]. Multistaging of metasomatic alteration of the host rocks (dominantly granites and migmatites) provided sequential changing of mineral paragnesyses from earlier to later mineral paragenesises. The earliest alteration represents successive transformation of the host granitoids into chloritized granites and episyenites, which were progressively dequartzified and eventually transformed into aegirine and aegirine-reibeckite albitites due to progressive K-Na exchange between hydrothermal solution and the rocks. Na, V, Ca and Sr were the most prominent extrinsic elements introducing in the host rocks during this stage of the alteration whereas Si, K and Rb were ejected. Next stage of hydrothermal activity provided carbonate metasomatism with partial leaching of the albitites and crystallization of garnet, epidote, calcite, magnetite and either Mg-amphyboles or phlogopite mineralization with reverse depletion in Na. Na, Si, V, Ba and P were transferred out of the albitite bodies but U, K, Rb, Ca, Sr, Mg, U, Mn, Zr, Hf and Co were added.

[1] Grant (1986) *Econ. Geol.* **81**, 1976-1982.

https://doi.org/10.1180/S0026461X00006502 Published online by Cambridge University Press

Impact of interfacial free energy on weathering rates

SIMON EMMANUEL[1]*AND JAY J. AGUE[2]

[1]Institute of Earth Sciences, The Hebrew University of Jerusalem, Edmond J. Safra Campus, Givat Ram, Jerusalem, 91904 Israel (*correspondence: simonem@cc.huji.ac.il)

[2] Department of Geology and Geophysics, Yale University, P.O. Box 208109, New Haven, CT 06520-8109 USA and Yale Peabody Museum of Natural History, Yale University, New Haven, CT 06511, USA (jay.ague@yale.edu)

The natural weathering rates of primary minerals can be orders of magnitude lower than the rates of mineral dissolution found in laboratory experiments. As primary dissolution rates are thought to be determined by the rate of secondary mineral precipitation, understanding the factors controlling precipitation rates could be the key to resolving this apparent discrepancy. Using model calculations we demonstrate that the effects of interfacial energy in systems close to equilibrium, and which possess a large number of micron and nanometer scale crystals, can have a critical impact on net mineral precipitation rates [1]. Net rates can be much lower than those predicted by standard kinetic formulations; moreover, when the proportion of small crystals is high enough, net dissolution can dominate even when the system is supersaturated with respect to large crystals. Importantly, secondary minerals that form from the incongruent dissolution of primary phases are often submicron in size, and field conditions are often far closer to equilibrium than those typically encountered in laboratory experiments. Thus, we propose that standard rate models - which do not account for interfacial energy effects in small crystals - may be unsuitable to describe reaction rates in weathering systems.

[1] Emmanuel and Ague (2011) *Chem. Geol.*, **282**, 11-18.

Metalliferous organic-rich black shales: Where do the metals come from?

POUL EMSBO* AND GEORGE BREIT

USGS, MS 973, Federal Center, Denver, CO, 80225 (*correspondence: pemsbo@usgs.gov)

The amount of metal contained in a metalliferous black shale (MBS) can rival or surpass any ore deposit. Currently anomalous metal and carbon contents of these shales are thought to be controlled solely by ordinary oceanographic processes. Elevated metal and carbon contents of these shales are considered to reflect anoxic, high productivity conditions that optimize extraction of metals from normal seawater.

This explanation is challenged by the lack of modern analogs of ancient MBS. Despite intense study, modern euxinic environments of high productivity fail to form sediments with comparable metal enrichments. Moreover, mass balance constraints that consider the total mass and recharge of metal to the ocean, ocean circulation, and sedimentation rate suggest that typical seawater may not be an adequate source for the mass of metal in some MBS.

An alternative metal supply is apparent in the fluids that form, synsedimentary exhalative (sedex) deposits. The metal supplied by the discharge of these hydrothermal fluids into ocean basins can be shown to surpass global riverine fluxes. The metal mass in a sedex deposit requires discharge of 1000's of km^3 of warm saline fluid over a periods of 10's ky. The large volume would have impacted ocean chemistry far beyond the extent of the deposit.

A genetic link between MBS and sedex deposits is reinfored by their common occurrence in age correlative strata. Although this temporal relationship has been previously ascribed to euxinic conditions necessary to form sedex deposits, the sedex fluids may, themselves, have enhanced or caused euxinic conditions.

An overlooked aspect of sedex systems is the flux of nutrients (i.e. NH_4, reduced C, trace metals, Ba, Si) added to the oceans by the ore fluids that may exceed the entire modern riverine flux. Such fertilization would undoubtedly promote massive increase in bioproductivity and spur basin-wide anoxic/euxinic conditions. Overall, the enormous flux of nutrients and metals delivered to the ocean by sedex systems may provide a plausible explanation for the enigmatic metal-rich end members of MBS.

https://doi.org/10.1180/S0026461X00006502 Published online by Cambridge University Press

Cationic polymerization of isoprene on cloudwater droplets

SHINICHI ENAMI, HIMANSHU MISHRA, MICHAEL R. HOFFMANN AND AGUSTÍN J. COLUSSI

California Institute of Technology, Pasadena 91125 USA

We show that gas-phase isoprene is readily protonated ans subsequently polymerized by collision with liquid microjets surface of mildly acidic water (1 < pH < 4) within ~10 ms. Kinetic isotope effects for the products formation were determined to reach up to 7, showing the direct evidence that the observed phenomena are due to a truly interfacial reactions initiated by proton on water. Since such reactions only occur at superacidic condition in homogeneous bulk media (e.g., pH < -1) or in pure gas phase, the surface of ambient atmospheric aerosol particles will behave as an unusual catalyst for reactive uptake of global gaseous unsaturated hydrocarbons.

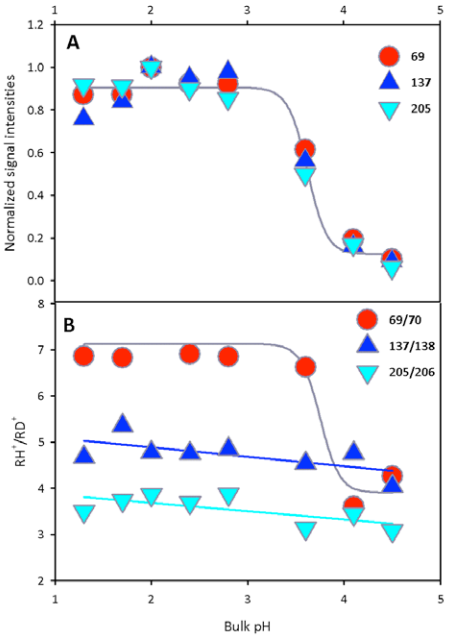

Figure 1: **A**: Signals $IsoH^+$ (m/z = 69), $(Iso)_2H^+$ (137), and $(Iso)_3H^+$ (205) from protonation/polymerization of isoprene produced on H_2O:D_2O (50/50 = vol/vol) microjets exposed to 88 ppmv isoprene(g) for ~10 μs as a function of bulk pH. **B**: Kinetic isotope effects (KIE) for the products of isoprene (g) on H_2O:D_2O (50/50 = vol/vol) microjets exposed to 88 ppmv isoprene (g) as a function of bulk pH. All experiments in 1 atm N_2(g) at 293 K.

Testing the use of detrital rutile to investigate HP/UHP rocks

FLORENTINA C. ENEA[1]*, JEANETTE TAYLOR[2], CRAIG D. STOREY[1], HORST MARSCHALL[3] AND M. K-SCHMOLKE[4]

[1]University of Portsmouth, SEES Burnaby Building, Portsmouth, PO1 3QL, UK (*corespondence: florentina.enea@port.ac.uk).

[2]Bristol University, SES, Wills Memorial Building, Queen's Road, BRISTOL BS8 1RJ, UK

[3]Woods Hole Oceanographic Institution Woods Hole, MA 02543, USA

[4] Universität Potsdam, Institut für Geowissenschaften, Karl-Liebknecht-Straße 24-25, 14476 Golm, Germany

Accessory rutile generally is the main host of Ti in HP/UHP metamorphic rocks. It is also a major carrier of HFSE, providing a potential tracer of contrasting tectonic processes. For example, the Zr-in-rutile geothermometer has now been widely and successfully applied to HP rocks, And Cr/Nb ratios have been used to distinguish between different bulk composition of the host rock. Moreover, rutile is a robust mineral in sedimentary environments and is common as an accessory phase in sandstones. Therefore, its potential as a detrital tracer of HP metamorphism is high. Metamafic and metapelitic rocks from two case studies located in Syros, Greece and the Western Alps, both settings displaying HP/UHP conditions, have been sampled together with sediments that resulted from the erosion of these rocks in beach and river catchments. The geochemical correlation of rutile between source rocks and sediments is assessed based on its HFSE budget.

This study aims to establish geochemical signatures of rutile that are characteristic for detrital grains sourced from HP/UHP rocks formed in subduction zones. The Zr-in-rutile thermometer [1, 2] provides peak metamorphic temperatures for the investigated samples that are coherent with published peak temperatures for the respective metamorphic sequences. In addition, the calculated temperatures are independent of the source rock lithologies, i.e., the presence or absence of quartz. The T histograms for the Western Alps indicate a low-T peak, suggesting the blueschists, eclogites and Dora Maira rocks are dominant, and not the high-T Ivrea rocks, as expected. Cr/Nb ratios have been employed successfully and *in situ* analysis fall strictly into the mafic (for Syros) and pelitic (for the Western Alps) source rock fields [3, 4, 5].

[1] Zack *et al* (2004b) *CMP* **148**, 471–488. [2] Watson *et al* (2006) *CMP* **151**, 413–433. [3] Zack *et al* (2002) *Chem. Geo.*, **184**, 97-122. [4] Zack *et al*. (2004a), *Sed. Geo*, **171**, 37-58. [5] Meinhold (2010) *E-S Rev*. **102**, 1–28 .

https://doi.org/10.1180/S0026461X00006502 Published online by Cambridge University Press

Characterizing sources of airborne mineral dust, in Iraq

J.P. ENGELBRECHT[1] AND R.K.M. JAYANTY[2]

[1]Desert Research Institute, 2215 Raggio Parkway, Reno, NV 89512, USA (*correspondence: johann@dri.edu)
[2]RTI International, 3040 East Cornwallis Road, Research Triangle Park, NC 27709, USA (rkmj@rti.org)

The purpose of the Enhanced Particulate Matter Surveillance Program (EPMSP) was to provide scientifically founded information on the chemical and physical properties of airborne mineral dust and other particulates sampled in the Middle East. Aerosol [1, 2] and bulk soil [3] samples were collected during a period of approximately one year at 15 Middle East sites – including Djibouti, Afghanistan, Qatar, United Arab Emirates, Iraq, and Kuwait.. Collocated low volume particulate samplers, one each for the total suspended (TSP), less than 10 μm in aerodynamic diameter (PM_{10}) and less than 2.5 μm in aerodynamic diameter ($PM_{2.5}$) particulates were deployed at each of the sites and operated on a "1 in 6 day" sampling schedule. The filters were chemically analyzed for their elemental and ion contents, as well as for their elemental (EC) and and organic carbon (OC) fractions.

This presentation reports on the data mining of chemical results - by applying Principal Components Analysis (PCA) and Positive Matrix Factorization (PMF) to chemical data from Teflon membrane and quartz fiber filter sets collected at six sites in Iraq (Balad, Baghdad, Tallil, Tikrit, Taji and Al Asad).

From the PMF modelled results it is evident that there are substantial differences in mineral dust compositions amongst the six Iraq sites and between the PM_{10} and the $PM_{2.5}$ size fractions. This is related to dissimilarities in the local geology and soil types, as well as different particle size distributions. Although regional mineral dust sources are similar for all six sites, the aerosols at the height of the sampler inlets are substantially modified by local dust representative of the local soils at or close to the sampling sites, exacerbated by dust from agricultural activities, roads, and other local dust sources.

[1] Engelbrecht *et al*. (2009a) *Inhalation Toxicology* **21**, 297-326. [2] Engelbrecht & Derbyshire (2010) *Elements* **6**, 241-246. [3] Engelbrecht *et al*. (2009b) *Inhalation Toxicology* **21**, 327-336.

Allanite petrochronology in high-pressure rocks

M. ENGI[1]*, D. REGIS[1], J. DARLING[1], B. CENKI-TOK[1,2] AND D. RUBATTO[3]

[1]Dept. of Geological Sciences, University of Bern (*correspondence: engi@geo.unibe.ch)
[2]Geosciences Montpellier, University of Montpellier
[3]School of Earth Sciences, Australian Nat. Univ., Canberra

Allanite is a REE- and Th-rich epidote widespread in greenschist to eclogite facies rocks. Its prograde mineral reactions commonly produce distinct growth zones, which can be directly related to PT-conditions. In favorable cases, Th-U-Pb isotope analysis (by LA-ICP-MS or ion microprobe) allows such growth zones to be dated.

Improved LA-ICP-MS analysis (line raster laser ablation, ^{204}Pb-based common lead correction) yields accurate Th-Pb and U-Pb ages with no need for matrix-matched standardisation. The analytical errors imply realistic 2σ-age uncertainties of ~1%.

A multicomponent solution model formulated for allanite was tentatively calibrated, based on the limited experimental data available as well as select natural phase relations. Phase diagrams calculated for a range of typical compositions comply with mineral reaction sequences and established PT-wisdom from various metamorphic systems. The stability limits obtained confirm that allanite is very useful for blue-schist and eclogite facies rocks. Computed REE-partitioning with other REE-phases agrees reasonable well with distribution coefficients observed in high-pressure samples.

Several case studies in LT-eclogite facies metagranitic and -sedimentary samples from the Sesia Zone (Western Alps, Italy) are presented. These demonstrate the potential power of allanite petrochronometry [e.g. 1], but also indicate limits and possible pitfalls: Detailed petrography is needed to define which stages and PT-conditions are dated, and microstructural observations should be integrated where possible. It is critical to obtain REE-patterns for each allanite growth zone and to characterize all mineral inclusions. Common lead contents can be so high as to make dating unrealistic.

Allanite recystallisation behaviour is not well understood, and relics (e.g. igneous cores) commonly occur. Microchemical characteristics (Th/U, Sr) help to distinguish their origin. In relatively dry lithologies, the robust mechanical properties of allanite can preclude recrystallisation, even in high strain shear zones. By contrast, allanite has excellent potential as a chronometer for mylonites, where hydrous fluid commonly leads to recystallisation even at T as low as 400°C.

[1] *Rubatto et al*. (2011) *Nature Geosci*., 10.1038/NGEO1124

https://doi.org/10.1180/S0026461X00006502 Published online by Cambridge University Press

Modeled response in radiative properties of shallow convective clouds due to perturbations in meteorological state variables and atmospheric aerosol loading

ANDERS ENGSTRÖM AND ANNICA M. L. EKMAN

Department of Meteorology, Stockholm University, SE-106 91 Stockholm, Sweden (anderse@misu.su.se)

In order to quantify aerosol indirect effects in observational data it is necessary to minimize the impact from other cloud-controlling variables. The vast amount of meteorological data from operational atmospheric analysis data (or re-analysis data) combined with retrieved aerosol characteristics from satellite, provides and opportunity to compare cloud properties under similar meteorological conditions but with a different aerosol signature. However, even when keeping meteorological variations at a minimum with respect to a mean atmospheric state, the sensitivity of clouds to small perturbations around this mean state is not well known [1]. Hence small variations in meteorology may correlate both spatially and temporally with small variations in the aerosol concentration which could explain a certain fraction of the observed relationship between aerosols and clouds.

The aim of the present study is to 1) identify the sensitivity of cloud fraction and cloud albedo to small perturbations in meteorological conditions and compare this to the sensitivity induced by increasing aerosol number concentrations and 2) estimate the range of variability in observational data of meteorological variables permitted to determine a clear and unambiguous signal in cloud fraction and cloud albedo due to aerosols. A cloud-resolving model is used to simulate a large ensemble of isolated shallow convective clouds where the vertical profiles of zonal wind, temperature and water vapor mixing ratio as well as initial profiles of accumulation and Aitken mode aerosols are perturbed.

[1] Stevens and Feingold (2009) *Nature* **461,** 607–613.

Hydrothermal Co-Ni mineralization, associated with serpentinized peridotites: Bou Azzer, Morocco

A. ENNACIRI[1]* , L. MAACHA[2], L. BARBANSON[3], W.D.MAIER[4]

[1]Managem, Twin Center, Tour A, Angle Bd Zerktouni et Massira Khadra, Casablanca, Morocco (*correspondence : ennaciri@managem-ona.com)
[2]Managem (maacha@managem-ona.com)
[3]ISTO, Université d'Orléans, CNRS, France (luc.barbanson@univ-orleans.fr)
[4]WD Maier, University of Oulu, Oulu 90014, Finland

The Co, As (Ni, Ag, Au) ores of the Bou Azzer district comprise an unusual type of vein-style deposit, associated with mantle peridotites of a Neoproterozoic ophiolite. Two types of Co-rich mineralization are exploited: (1) Veins located at the contact between sepentinites and wall rocks; (2) Veins in dioritic wall rocks, extending up to 400m from the serpentinites. From early to late, the mineral succession in both types is : (1) Ni-arsenides (rammelsbergite, para-rammelsbergite); (2) Co-arsenides (safflorite, skutterudite), in some cases with native gold; (3) Fe-Arsenides (löllingite); (4) sulfoarsenides (gersdorffite, cobaltite, arsenopyrite); (5) sulfides and sulfosalts (chalcopyrite, sphalerite, terahedrite, tennatite), in some cases with native bismuth and silver; (6) chlorite with molybdenite with minor brannerite and late native gold. The gang minerals are essentially quartz, calcite and dolomite. Fluid inclusion studies indicate complex brines belonging to the system (Na, Ca, K, Ba, Cl). Equivalent weight salinity ranges from 34. 5 wt. % and 40. 5 wt. %. Homogenization temperatures range from 225 °C to 195°C. Co and Ni are proposed to have been leached from the serpentinites. However, the origin of the arsenic is poorly constrained. Derivation from the mantle rocks would imply very high fluid-rock ratios. Alternatively, As could be derived from crustal rocks underlying the ophiolite.

https://doi.org/10.1180/S0026461X00006502 Published online by Cambridge University Press

Comparison of mercury bioacumulation within a trophic-web for pristine and anthropogenically contaminated aquatic ecosystems

V.N. EPOV[1]*, M.V. PASTUKHOV[2], V. PERROT[1], S. HUSTED[3], V.I. ALIEVA[2], D. AMOUROUX[1], V.I. GREBENSHCHIKOVA[2] AND O.F.X. DONARD[1]

[1]LCABIE, IPREM, CNRS-UPPA-UMR-5254, 64053, Pau, France (*correspondance: vladimir.epov@univ-pau.fr)
[2]LGM, Institute of Geochemistry SB RAS, 640033, Irkutsk, Russia (mpast@igc.irk.ru)
[3]Faculty of Life Sciences, University of Copenhagen, DK-1871, Copenhagen, Denmark (shu@life.ku.dk)

Lake Baikal-Angara River aquatic ecosystem includes natural basin of Lake Baikal (LB) with more than 360 inflow rivers, and few artificial basins such as Irkutsk, Bratsk and Ust'-Ilimsk Water-Reservoirs located downstream the only outflow Angara River. The main anthropogenic sources of Hg in the region were two chemical industrial factories "*Usol'ekhimprom*" and "*Sayanskkhimplast*", located on the shore of the Bratsk Water-Reservoir (BWR). Anthropogenic utilization of mercury is a global health issue due to its high degree of mobility, toxicity and bioaccumulation of methylmercury through the food-web.

Sediments, water, zoo- and phyto-plankton, different trophic level of fish and seal samples have been studied for Hg speciation and Hg stable isotopes (Table). Also main ecological parameter and carbon/nitrogen stable isotopes were charactarised for biological samples. Stable isotope Hg signature of LB plankton, fish and seal tissues showed positive correlation of δ^{202}Hg with trophic level. The comparison of the results obtained for contaminated and pristine sites suggests that Hg isotopic signature reveals both MeHg pathways in aquatic environments and trophic bioaccumulation routes.

Sample	$[Hg]_{tot}$	δ^{202}Hg	Δ^{199}Hg	%MeHg
Seal-muscle	300	+1.84‰	5.03‰	82.9‰
Perch(LB)	163	-0.48‰	1.14‰	95.1‰
Roach(LB)	58.6	-0.61‰	0.58‰	96.0‰
Plankton(LB)	2.1	-0.90‰	1.53‰	15.7‰
Pike(BWR)	3270	-0.18‰	0.04‰	90.6%
Perch(BWR)	1195	-0.26‰	0.52‰	92.0‰
Roach(BWR)	388	-0.17‰	1.19‰	94.2‰
Plankton(BWR)	3.6	-0.37‰	1.28‰	51.5‰

Table: Summarised total Hg (ng g^{-1}), MeHg content and isotope composition of Hg in some trophic web samples.

ICP-MS determination of trace elements in marine biological samples: Comparison of sample preparation procedures and selected digestion methods

E.N. EPOVA, J. CASTRO GEORGI AND O.F.X. DONARD

LCABIE, UPPA-CNRS-UMR 5254 IPREM, Hélioparc, 64053 Pau, France

Marine biological samples (oysters, mussels, fish) can be used as bio-indicators to control the industrial pollution for the quality of aquatic environments and to investigate the toxicological impact for the different food chains. These samples with high sensitivity to toxic compounds in the surrounding water ecosystems are easily accessible resources that can be used for analysis.

Presented here is a comparison of two most used sample pretreatment techniques such as freeze-drying and fresh-freeze from the perspective of analytical efficiency and practical convenience of procedures applied to the processing of a considerable amount of samples. The concentrations of 20 elements in standard reference materials (SRMs) and different marine biological samples are studied and compared with previously published data. Validation of the pretreatment techniques are perform using several SRMs of oyster, fish and mussel tissues (1566b, 2977, TORT 2 and DORM 2) which display different matrix properties and large number of certified elements.

https://doi.org/10.1180/S0026461X00006502 Published online by Cambridge University Press

Lead cycling in forested catchments: Trends in input-output mass balances over 12 years of easing industrial pollution

LUCIE ERBANOVA, LEONA ZEMANOVA*, MARTIN NOVAK AND DANIELA FOTTOVA

Czech Geological Survey, Geologicka 6, 152 00 Prague 5, Czech Republic
(*correspondence: leona.zemanova@seznam.cz)

In Central Europe, forested headwater catchments are an important source of drinking water. In the second half of the 20th century, extensive coal mining and burning, along with chemical industry, metal smelting and traffic contributed to high emissions of a number of environmentally relevant elements. Lead (Pb) entering ecosystems via wet and dry deposition originated from all these sources. The highest anthropogenic emissions of Pb occurred in the mid 1980s, and a considerable decrease in Pb emissions has been observed over the past 25 years. The fate of lead and its potential release to stream water has been studied in 11 small spruce-forested catchments in the Czech Republic. Here we compare Pb input-output mass balances for the hydrological years 1996 and 2008, i.e., for periods of time 12 years apart. Atmospheric input via spruce canopy throughfall was monitored monthly. In clearings, two rain/snow collectors were installed per site. Stream discharge was sampled once a month near a gauging station. The calculated catchment-level Pb inputs have been vegetation-type weighted. In 1996, catchments situated in the more industrialized north of the country showed high Pb deposition rates of 25 to 50 g Pb ha^{-1} yr^{-1}. Catchment situated in the less polluted south of the country showed lower Pb deposition rates of less than 17 g Pb ha^{-1} yr^{-1}. Lead export via stream discharge formed less than 20 % of the input at most sites across the country. Only two sites in the industrial north (Krkonose and Orlicke Mts.) exhibited a higher proportion of exported Pb, relative to contemporary input (32 to 60 %). Overall, most of the anthropogenic Pb entering the ecosystems remained immobilized within the biomass and soils. Twelve years later, in 2008, atmospheric Pb depositions into all catchments significantly decreased, averaging 11 g Pb ha^{-1} yr^{-1}. The amount of exported Pb, and the proportion of exported Pb, relative to contemporary atmospheric input, decreased in comparison with 1996. In 2008, the annual Pb export was less than 2 g ha^{-1} yr^{-1} at 8 out of 11 sites. Our data show that, with easing atmospheric pollution, less Pb is exported from the catchments, even though the total amount of Pb that had accumulated since the beginning of the Industrial Revolution (1860) was sizeable.

Biomineralization and seawater dynamics in foraminifera studied with the fluorescent dye Calcein

J. EREZ[1]*, Y. LEVENSON[1] AND A. ALMOGI-LABIN[2]

[1]Institute of Earth Sciences, The Hebrew University of Jerusalem, Jerusalem 91904, Israel (*correspondence: erez@vms.huji.ac.il)
[2]Geological Survey of Israel, 30 Malkhe Israel, Jerusalem, 95501, Israel

The calcite shells of foraminifera which accumulate on the ocean floor are an important component of the global carbon cycle. These shells provide highly valuable paleoceanographic information based on their trace elements and stable isotopes. Understanding their biomineralization is therefore an essential goal both for ocean acidification studies and for obtaining new and reliable paleoceanographic information. Recently we showed that perforate foraminifera precipitate their calcite directly from seawater vacuoles [1, 2]. Here we describe the uptake and release dynamics of seawater in the benthic foraminifera *Amphistegina lobifera* and *A. lessoni* using pulse-chase experiments with the membrane impermeable fluorescent dye Calcein. Three different reservoirs of seawater stored in vacuoles were found with residence times of ~ 20 min., ~ 6 hr and ~ 10 days. The internal volume of seawater is large and it is recycled fast enough to provide Ca^{2+} and CO_3^{2-} for the normal calcification process. At low salinities Calcein released during the chase is higher then in normal salinity by a factor of 2. This may be part of the osmotic regulation mechanism in these giant cells. Calcein is incorporated into the shells in direct proportion to calcification measured by weight increase or by alkalinity depletion. The distribution coefficient of Calcein in the shells is very low in the order of 10^{-4}. It increases significantly with salinity and with calcification rate and using Rayleigh type fractionation model we calulate that higher fraction of the calcification reservoir is utilized at optimal conditions. These observations provide the foundations for a realistic model to describe the behavior of stable isotopes and trace elements in the modified seawater calcification reservoir in foraminifera. Furthermore, it explains the sensitivity of foraminifera to ocean acidification.

[1] Erez, J., (2003), *Reviews in Mineralogy and Geochemistry* **54:**115-149. [2] Bentov S., Erez, J and Brownlee, C. (2009), *PNAS* **106(51)** 21500-21504

https://doi.org/10.1180/S0026461X00006502 Published online by Cambridge University Press

Using lead isotopes in marine barite to understand intermediate water dynamics

A.M. ERHARDT[12] AND A. PAYTAN[2]

[1]Department of Geological and Environmental Sciences, Stanford University, Stanford, CA 94305 (*correspondence: erhardt@stanford.edu)
[2]Institute of Marine Sciences, University of California Santa Cruz, Santa Cruz, CA 95064 (apaytan@ucsc.edu)

Lead isotopes in marine barite hold the potential to provide insight into changes in intermediate water circulation. Marine barite forms at intermediate water depths and incorporates Pb into the crystal structure at ~2ppm. As a result, the isotopic composition of Pb in marine barite represents the ratios of dissolved Pb in intermediate water. The ability of marine barite to document this elusive water mass makes this new proxy a powerful tool in understanding intermediate water dynamics.

Since anthropogenic pollution has irrevocably altered Pb concentrations and isotope ratios in the present day ocean, calibration of Pb proxies relies on a survey of Holocene sources. We will present results from marine barite separated from several cores in the equatorial Pacific. The ferromanganese grain coatings and detrital fractions for many of these samples will also be presented. By analyzing these three fractions from the same sample, we show that marine barite is recording a unique signature. This implies that the Pb in intermediate water is different that that of deep water or the bulk detrial fraction, potentially allowing us to deconstruct dust and circulation based Pb sources.

Additional work documenting potential source regions for intermediate water lead will be presented. Preliminary box modeling work will be shown to help resolve these source questions and illustrate the unique utility of this emerging proxy.

Geochronological and thermochronological evolution of the southern Gaoligongshan metamorphic belt, Yunnan (China)

S. EROĞLU[1], W. SIEBEL[1], M. DANIŠIK[2], J. PFÄNDER[3] AND F. CHEN[4]

[1]University of Tübingen, Germany
[2]University of Waikato, Hamilton, New Zealand
[3]Technical University of Freiberg, Germany
[4]University of Science and Technology of China, Hefei, China

The Gaoligongshan metamorphic belt is located east of the Eastern Himalayan Syntaxis (EHS) and plays a key role in the evolution of southeastern Tibet. Here, we present geochronological data of orthogneisses and mylonites that pertain to the evolution, cooling and exhumation history of this mountain range. Zircon U/Pb dating allow us to distinguish between at least four different magmatic events at about ~486 Ma, ~282 Ma, ~136 Ma and ~76 Ma. Similar ages have been reported for ortho-derivative rocks of the adjacent Tengchong and the Baoshan blocks and suggest that the southern Gaoligongshan is composed of rocks orginally belonging to the Lhasa and the Sibumasu terrane derived rocks. Late Eocene to Early Miocene U-Pb zircon and Rb/Sr muscovite ages are coeval with the onset of lateral crustal displacement along major shear zones in Eastern Tibet and Indochina and post-collision volcanic activity in Western Yunnan. Main phase of crustal rotation in the Tengchong and Baoshan blocks and mylonitization along the Gaoligongshan shear zone started during the Miocene, between 19 and 12 Ma (Rb/Sr biotite and Ar/Ar mica ages). The final stage of exhumation of the Gaoligongshan is revealed by apatite FT and apatite (U-Th-Sm)/He thermochronology, with ages between 8 and 5 Ma, which was presumably triggered by crustal root delamination and backarc extensional processes as a consequence of the Andaman sea floor spreading.

Based on our results, we propose that the tectonometamorphic evolution of the Gaoligongshan was the result of Tibetan extrusion and escape tectonics around the EHS, the southeastward movement of Indochina and backarc-extensional effects of the Andaman seafloor spreading, which makes it to a junction point between Tibet Plateau and Indochina.

https://doi.org/10.1180/S0026461X00006502 Published online by Cambridge University Press

Building stone potential of the Eastern Black Sea Region, NE Turkey

HAKAN ERSOY, BÜLENT YALÇINALP AND MEHMET ARSLAN

Karadeniz Technical University, Department of Geology, 61080, Trabzon, Turkey, (ersoy@ktu.edu.tr, arslan@ktu.edu.tr, bulent@ktu.edu.tr)

Turkey is located in the orogenic belt of the Alpin-Himalayan that has the world's richest natural stone formations. The country has rich marble and limestone formations on the one hand, travertine and onyx formations on the other hand. More than 500 natural stone sites, 800 factories operating in the sector and 90 % of the sites are located in the western Anatolia, mainly in Aegean and Marmara Region of Turkey. In all parts of Turkey, mainly Marmara and Aegean Region, there are good quality natural stone reserves. Although the eastern Black Sea region has limited number of natural stone variety it has a considerable number of natural stone reserves mainly granites. Total natural stone reserves are about 450 million tons and operated reserves were about one percent of this. However, there are more than 30 important natural stone sites in operation in the region. The reserve of the natural stones is about 13 million tons. The most important carbonate bearing marbles are travertines with the reserves of about 1.6 million meters cubes in total carbonate natural stones. In this study carbonate bearing natural stone potential of the eastern Black Sea region was revealed and their geological and geomechanical properties were investigated in terms of marbling sector.

Do melt inclusions record the pre-eruptive volatile content of magmas?

R. ESPOSITO* AND R. J. BODNAR

Virginia Polytechnic Institute & State University, Department of Geosciences, Blacksburg, VA, USA (*correspondence: rosario@vt.edu)

In the last several decades the number of publications describing the use of melt inclusions (MI) to determine the pre-eruptive volatile contents of magmas has increased significantly. However, in most MI studies, the volatile contents of the MI within a single sample or even within a single phenocryst vary widely, and it is often not possible to assess the reliability of the data. In order for MI to provide reliable information concerning the pre-eruptive volatile content, the MI must obey Roedder's (Sorby's) Rules. Namely, the MI must have trapped a single homogeneous melt phase, the volume of the MI must remain constant after trapping, and nothing can be added or lost from the MI after trapping. The adherence to Roedder's Rules is tested by examining two or more melt inclusions from a Melt Inclusion Assemblage (MIA), representing a group of MI that were all trapped at the same time. If all of the MI in the assemblage show the same room temperature phase relations and the same composition, then it is highly likely that the MI in the assemblage obey Roedder's Rules.

In this study, the volatile contents of MI from well-characterized MIAs hosted in phenocrysts from White Island (New Zealand) and from Solchiaro (Italy) were analyzed by Secondary Ion Mass Spectrometry (SIMS). In some MIA, abundances of all of the volatiles (H_2O, F, Cl, CO_2 and S) were consistent in all MI within the MIA. In other MIAs, CO_2 and S abundances showed wide variation, with CO_2 most often showing large variability within an MIA. The reason for the wide range in CO_2 content is unknown, but could reflect small-scale heterogeneities in the melt during inclusion trapping or varying degrees of post-entrapment crystallization for MI in the MIA.

https://doi.org/10.1180/S0026461X00006502 Published online by Cambridge University Press

Mercury isotope fractionation during bio-accumulation in lichens

N. ESTRADE[1], J. CARIGNAN[1,2]* AND C. CLOQUET[1]

[1]CRPG/CNRS, BP 20, 54501, Vandoeuvre-lès-Nancy, France (nicolas.estrade@yahoo.fr)
[2]Takuvik, CNRS-ULaval, Québec, G1V 0A6, Canada (*correspondance: jean.carignan@takuvik.ulaval.ca)

Recently, mercury (Hg) isotope mass-independent fractionation (MIF) were reported in various lichens [1] and interpreted as the evidence for the atmospheric Hg to be a complementary reservoir to aquatic Hg [2] with respect to $\Delta^{199\text{-}201}$Hg. Recent data from the literature on more "direct" samples for atmospheric Hg [3, 4] suggest small Hg MIF, even slightly positive $\Delta^{199\text{-}201}$Hg, in contrast to significant negative $\Delta^{199\text{-}201}$Hg values measured in lichens. This raised the question of the integrity of Hg isotopes measured in lichens relative to atmospheric matter, with the possibility of MIF during bio-accumulation.

A large amount of lichen tufts (*Evernia Prunastri*) was retrieved from trees in a small forest south of Nancy (France), rinsed with distilled water and dried at room temperature for a few days. Aliquots of bulk samples (1 g) were plunged into solutions (50 ml) containing various amounts of dissolved elements to simulate rain water. Lichens and solutions were in contact between 1 and 60 minutes (n=6).

Mass balance for Hg was calculated using Hg in lichens and Hg in the remaining solutions. Both were very similar suggesting that all Hg lost from the solution was pumped out by lichens (no wall adsorption). The δ^{202}Hg measured in lichens changed from -3.5‰ (initial value) to -0.5‰, interpreted as a progressive adsorption of solution Hg (0‰). However, Hg in the remaining solution shifted its δ^{202}Hg up to +1.5‰, decreasing with time, suggesting kinetic fractionation occurred when adsorption started. Isotopic equilibrium was not reached after 60% of total solution Hg was adsorbed by lichen ($\Delta^{xx}Hg_{sol\text{-}lichen} \leq 1‰$).

Some lichens were exposed to sunlight (6 to 10 weeks) after being in contact with the NIST 3133 Hg, increasing their [Hg] variously from 0.15 to 18 µg/g. In all cases, no significant MIF were measured in both light exposed and non-exposed lichens, suggesting that bio-accumulation of Hg(II) by lichen do not result in MIF.

[1] Carignan et al. (2009) *Environ. Sci. Technol.* **43**, 5660-5664. [2] Bergquist & Blum (2007) Science **318**, 417-420. [3] Gratz et al. (2010) *Environ. Sci. Technol.* **44**, 7764-7770. [4] Sherman et al. (2010) *Nature Geosci.* **3**, 173-177.

Effect of initial Al concentration, pH and silicic acid on the formation and stability of tridecameric Al polymer

M. ETOU*, S. HAGIWARA, T. SAITO, Y. OKAUE AND T. YOKOYAMA

Department of Chemistry, Faculty of Science, Kyushu University, 6-10-1, Hakozaki, Fukuoka, Japan 812-8581 (*correspondence: mayumie@mole.kyushu-u.ac.jp)

Tridecameric Al polymer (the Keggin-type Al_{13} polycation)

Al^{3+} and its hydrolytic species which elute from soil due to the soil acidification have strongly toxic effect to palnt and living organisms. In Al^{3+} hydrolytic specis, tridecameric Al polymer (Keggin type Al_{13} polycation, $[AlO_4Al_{12}(OH)_{24}(H_2O)_{12}]^{7+}$) show the strongest toxicity. Surprisingly, Hunter and Ross detected Al_{13} in organic horizon of forested Spodsol in USA [1]. Much attention has been paid to the formation conditions of Al_{13}. According to the equilibrium calculation, at the total Al concentration of 10^{-5} mol/dm^3(M) which is the concentration level of soil solution, the occurrence of Al_{13} is sufficiently considered [2]. However, the detection of Al_{13} species such a low Al concentration is extremely difficult. Therefore, in this study, we developed the detection method of Al_{13} by ^{27}Al MAS NMR after adsorption onto chelate resin from solution with various Al concentration. Furthermore, we also studied the stability of Al_{13} on the solid surface and elution of Al species from solid surface and the effect of silicic acid to the formation and stability of Al_{13}.

When Al_{13} is formed in the soil environment, it is possible to adsorb on the surface of microbes and humic substances. In this study, the chelate resin was used as a model compound of the surface of microbes and humic substances because of similarity of functional group. For the concentration limit for the formation of Al_{13}, we could detect Al_{13} species after the adsorption onto chelate resin above 10^{-4} M. The pH range where Al_{13} can form in solution is very narrow [3], however, we also revealed that when Al_{13} adsorbed onto the resin, the pH range where it can exist clearly expanded. When the silicic acid coexisted in initial solution, the formation of Al_{13} distinguishably retarded.

[1] D. Hunter and D. S Ross, (1991) *Science* **251**, 1056. [2] G. Furrer *et al*., (1992) *Geochem. Cosmochim. Acta* **56**, 3831. [3] A. Etou *et al*., (2009) *J. Colloid Interface Sci.* **337**, 606.

https://doi.org/10.1180/S0026461X00006502 Published online by Cambridge University Press

Stability and transformation of Pb smelter fly ash in soils

V. ETTLER[1*], M. MIHALJEVIC[1] AND O. SEBEK[2]

[1]Institute of Geochemistry, Mineralogy and Mineral Resources, Faculty of Science, Charles University in Prague, Albertov 6, 128 43 Prague 2, Czech Republic (*correspondence: ettler@natur.cuni.cz)

[2]Laboratories of the Geological Institutes, Faculty of Science, Charles University in Prague, Albertov 6, 128 43 Prague 2, Czech Republic

Soils represent an important sink for metals released into the environment by anthropogenic activities. Emissions from non-ferrous metal smelters are responsible for extremely high concentrations of metals in adjacent soils related to the deposition of the fly ash particles during periods of the filtering inefficiency in the smelter flue-gas cleaning system [1, 2, 3].

To understand the dynamics and fate of smelter-derived contamination, we studied the reactivity of secondary Pb smelter fly ash in acidic soils. The polyamide bags (mesh 1 μm, 2 x 4 cm) were loaded with 0.5 g of fly ash and sealed by welding. Testing bags were placed in contrasting soils in two experiments: (i) a short-term (21-day) laboratory pot experiment with soil pore-water monitoring (Rhizon suction cups) and (ii) a long-term (1-year) *in situ* experiment in soils developed under different vegetation cover (spruce, beech, meadow). After each experiment, the bags were weighted to determine the mass loss and the weathered fly ash was studied by XRD and TEM/EDS. The total concentrations of metals, their chemical fractionation and Pb isotopic composition were determined in soils by the combination of ICP techniques.

More than 60% of fly ash was dissolved during the experiment, especially in organic soil horizons and secondary anglesite ($PbSO_4$) formed as a stable alteration product [1, 2]. A significant increase in the metal concentrations in the soils was observed during the experiment, especially in the litter and organic horizons: Cd (248 x), Pb (15 x), Zn (1.8 x). Cadmium was the most mobile element in the pots and soil profiles, being strongly released into the soil water and bound mostly in the labile soil fractions. A significant shift in the Pb isotopic values towards the fly ash signature ($^{206}Pb/^{207}Pb$ =1.16) confirmed the effect of smelter-induced contamination on metal dispersion, binding and mobility in soils.

[1] Ettler et al. (2005) *Chemosphere* **58**, 1449-1459. [2] Ettler *et al*. (2008) *ES&T* **42**, 7878-7884. [3] Ettler *et al*. (2009) *J. Hazard. Mater*. **170**, 1264-1268.

Treatment of rural effluents by infiltration percolation process using sand-clay fortified by pebbles

SAIFEDDINE ETURKI[1]*, NACEUR JEDIDI[1] AND HAMED BEN DHIA[2].

[1]Wastewater treatment laboratory ,Water research and technologies Center, Borj Cedria technopole , BP 273 Soliman 8020, Tunisia (*correspondence : turkisaifeddine@yahoo.fr)

[2]Water, Energy and Environnement Laboratory, National School of Engineers of Sfax, Road of Soukra, 3038 Sfax Tunisia

Low-cost and high-performance decentralized wastewater treatments system for rural application in developing nations necessitated this study. The grain size and mineralogy of the sand filter constituting the infiltration bed, is of course one of the key elements and is the main subject of this article. In the other hand, clay samples collected from north eastern Tunisia were characterized by studying the mineralogical and geochemical composition and prove her great potential to fix pollutants. Performance efficiency studies were conducted to determine the best combination ratio of sand-clay/pebbles. Sand-clay (mixture contain 90% sand 10% of clay in weight) fortified with pebbles in the ratio 3:1 gave the optimum water purification and appropriate permeability for the infiltration percolation system. The effects of continued usage on the performance efficiency of the fortified column were studied and the results showed a decrease of Nitrogen, BOD, COD and Bacteria.

https://doi.org/10.1180/S0026461X00006502 Published online by Cambridge University Press

A possible evidence of urbanization effect on the light precipitation in the mid-Korean peninsula

S.-H. EUN[1], B.-G. KIM[1,*], S.-H. CHAE[1,2] AND J.-C. PARK[3]

[1]Department of Atmospheric Environment Sciences, Gangneung-Wonju National University (*Correspondence: bgk@gwnu.ac.kr)

[2]Applied Meteorology Research Laboratory, National Institute of Meteorological Research

[3]College of Engineering, Gangneung-Wonju National University

The continuous urbanization by a rapid economic growth and a steady increase in population could affect the meteorology in the downstream region [1]. This study presents the associated analysis of long-term (1972~2007) precipitation trends in the mid-Korean peninsula and the WRF model simulation for a golden day (2009/2/11). The mid-Korean peninsula has very favorable geographic characteristics for the study of urbanization effect on the cloud and precipitation in the downstream region such that seoul metropolitan area is located in the west, with relatively flat area in the east, and the big mountains along the east coast. The analysis stations consist of the urban region (Seoul, Incheon, Suwon), its downwind region (Chuncheon, Wonju, Hongcheon), and the mountainous region (Daegwallyeong). The trend of population, as a surrogate of urbanization, continues to increase. The category of precipitation amount (PA) is divided by the intensity such as light precipitation for PA≤1 mm d^{-1}, intermediate for 1 mm d^{-1}<PA≤10 mm d^{-1}, and heavy for PA>10 mm d^{-1}, respectively.

During the long-term period, PA and PF (precipitation frequency) in the downwind region of urban area significantly increased for the westerly and light precipitation case only, while PA and PF in the mountainous region decreased. Especially the enhancement ratio of PA and PF for the downwind area vs. urban area remarkably increased, implying the possible urbanization effect on the downwind precipitation. In addition, the WRF simulation applied for a golden day demonstrates the enhanced convergence and its associated updraft in the downwind area (about 60 km from the urban), leading to an increase in the cloud mixing ratio.

This study was supported by Basic Science Research Program through the National Research Foundation of Korea (2010-0211, 2009-0085533).

[1] Alpert *et al*. (2008*) J. Appl. Meteor. and Climat*. **47**, 933-943.

Polysaccharide fractionation of soil organic matter due to reaction with ferrihydrite

K. EUSTERHUES*[1], J. NEIDHARDT[1], T. RENNERT[1], I. KÖGEL-KNABNER[2] AND K.U. TOTSCHE[1]

[1]Institut für Geowissenschaften, Friedrich-Schiller-Universität Jena, Germany (*correspondence: karin.eusterhues@uni-jena.de)

[2]Lehrstuhl für Bodenkunde, Technische Universität München, Germany

Ferrihydrite, a poorly crystalline Fe oxyhydroxide, is known to be highly reactive towards soil organic matter (OM) and may play an important role in its long-term stabilization. To investigate composition and maximum OM loading of ferrihydrite-OM associations, we performed adsorption and coprecipitation experiments at pH 4.5 using the water-extractable OM of a Podzol forest-floor layer. The reaction products were studied by ^{13}C CPMAS NMR, FTIR and analysis of hydrolyzable neutral polysaccharides. To better understand the behavior of polysaccharides, adsorption and coprecipitation experiments were also done with glucose, galactose and glucuronic acid.

Adsorption and coprecipitation of the forest-floor extract yielded similar maximum loadings of 195 and 170 mg C g^{-1} ferrihydrite. Relative to the original forest-floor extract, the ferrihydrite-associated OM was enriched in polysaccharides, but depleted in aliphatic C and carbonyl C, especially when adsorption took place. Moreover, mannose and glucose were bound preferentially to ferrihydrite, while fucose, arabinose, xylose and galactose remained in the supernatant. This fractionation of sugar monomers was more pronounced during coprecipitation. Experiments with synthetic sugar monomers resulted in relatively low maximum loadings of ~15 and ~25 mg C g^{-1} for glucose and galactose, whereas glucuronic acid produced a maximum loading of 72 mg C g^{-1}. Signals of ferrihydrite-associated glucose and galactose were hardly detectable by FTIR, whereas spectra of ferrihydrite-associated glucuronic acid closely resembled that of the ferrihydrite-associated forest-floor extract.

We conclude that the observed preferential association of polysaccharides from natural OM with ferrihydrite is not caused by direct interaction of the neutral polysaccharides' hydroxyls. Instead of that, we assume that (i) the dominant adsorption mechanism is outer-sphere complexation of carboxyls on the ferrihydrite surface and (ii) the enrichment of glucose and mannose in the ferrihydrite-associated OM may be explained by a preferential association of these monomers with carboxyl-rich compounds.

https://doi.org/10.1180/S0026461X00006502 Published online by Cambridge University Press

An Eocene analogue for the future oceanic response to increased CO_2 – Existence of a tropical thermostat?

DAVID B. J. EVANS[1]*, WOLFGANG MÜLLER[1], JONATHAN A. TODD[2] AND WILLEM RENEMA[3]

[1]Royal Holloway Univeristy of London, Egham, UK (*correspondence: david.evans.2007@live.rhul.ac.uk)
[2]Natural History Museum, London, UK
[3]Naturalis, Leiden, The Netherlands

Future anthropogenic-induced atmospheric greenhouse gas increase is expected to result in a globally warmer Earth. Whilst this will likely result in an increase of high-latitude sea surface temperatures (SST), the future response of the tropical oceans is uncertain. It has been suggested [1] that a tropical 'thermostat' regulates low-latitude surface ocean temperatures. The mid-Eocene was characterised by higher atmospheric greenhouse gas concentrations [2] and therefore may provide a suitable analogue with which to test the thermostat hypothesis. However, there is disagreement between different palaeo-temperature proxies and recent climate models, with some suggesting considerably warmer Eocene SST.

We present new Eocene tropical ocean surface temperature data from central Java, based on a calibration of the relationship between test Mg/Ca and temperature in large benthic foraminifera. This is the first time such material has been used for palaeo-temperature reconstructions, including appropriate corrections for both changes in the ionic composition of seawater over geological time and corresponding D_{Mg} variation. Large benthic foraminifera were chosen over their more routinely studied planktic relatives because they are longer lived and therefore facilitate both annual and seasonal temperature reconstruction. This is important because it is now recognised that seasonality is a key component of climate change [3].

Our results, measured by laser-ablation plasma mass spectrometry, indicate Eocene southeast Asia tropical SST broadly similar to today. These data, backed by a compilation of $\delta^{18}O$-derived temperatures from well-preserved planktic foraminifera, support the existence of a tropical thermostat. Moreover, comparison with higher palaeo-latitude LBF from the Hampshire Basin (UK) provides further evidence that oceanic latitudinal temperature gradients were greatly reduced when compared to the present day.

[1] Kleypas *et al*. (2008) *Geophys. Res. Lett*. **35**. [2] Demicco *et al*. (2003) *Geology* **31**: 793-6. [3] Denton *et al*. (2005) *Quat. Sci. Rev*. **24**: 1159-82.

What can equilibrium thermodynamics tell us about metasomatic alteration?

K.A. EVANS

Department of Applied Geology, Curtin University, GPO Box U1987, Bentley, WA6845, Australia. (K.evans@curtin.edu.au)

In metamorphic petrology, equilibrium thermodynamics is often used to help us interpret metamorphic evolution of rocks that, we can reasonably assume, evolved close to thermodynamic equilibrium, with a relatively fixed bulk composition, except for volatiles, and under conditions where pressure and temperature are controlling intensive variables.

In rocks that have been significantly affected by metasomatic alteration, these assumptions are, in many cases, no longer reasonable. The nature of a metasomatic rock means that chemical potential variables are likely to have been fixed during their formation, rather than bulk composition variables. Metasomatic processes can also happen quickly, so the assumption of thermodynamic equilibrium on all but the shortest length scales might be faulty. Further, the changes in volume may be sufficient that it might be appropriate to consider volume, rather than pressure as a controlling variable.

Such observations are not new, but they are worth revisiting in the light of the massive recent improvements in imaging and analytical techniques that have led to renewed appreciation of the importance of processes such as dissolution-precipitation, and an increased understanding of the mechanics of metasomatic alteration.

Here, methods to improve the conceptual models and quantification of metasomatism, are discussed. These include judicious use of the phase rule, appropriate choices of conjugate variables, and methods to assess the lengthscales over which thermodynamic equilibrium may have applied. These methods are discussed with reference to metasomatic alteration of BIF-derived iron ore and serpentinisation of ultramafic rocks.

https://doi.org/10.1180/S0026461X00006502 Published online by Cambridge University Press

The relationship between subduction zone redox budget and arc magma fertility

K.A. EVANS[1] AND A. G. TOMKINS[2]

[1]Department of Applied Geology, Curtin University, GPO Box U1987, Bentley, WA6845, Australia. (K.evans@curtin.edu.au)
[2]School of Geosciences, P.O. Box 28E, Monash University, Vic. 3800, Australia. (Andy.tomkins@monash.edu.au)

A number of lines of evidence point to a causal link between oxidised slab-derived fluids, oxidised sub-arc mantle, and the formation of economic concentrations of metals such as Cu and Au that require oxidised magmas. However, trace element evidence from V/Sc ratios suggests that sub-arc mantle is no more oxidised than mantle elsewhere.

A simple analytical model is applied to constrain the evolution of sub-arc mantle oxidation state as a function of redox-budget fluxes from the subducting slab. Influential variables include the solubility of Fe^{3+} and SO_4^{2-} in slab-derived fluids, the geometry of the infiltration of slab-derived fluids in sub-arc mantle, the coupling between slab-derived and arc-output redox budgets, and the concentration of redox-buffering elements such as Fe and S in the sub-arc mantle.

Plausible Archean and Proterozoic redox budget fluxes would not have created oxidised sub-arc mantle. Phanerozoic redox budget fluxes, on the other hand, which are dominated by the sulfate component, could have increased sub-arc fO_2 by up to three $\log_{10}$ units. The results are generally consistent with the proposed elevated fO_2 for sub-arc mantle but do not explain V/Sc results.

Increases in sub-arc mantle fO_2 are favoured by focussed fluid infiltration and magma generation, weak coupling between slab and arc-output redox budgets, and restricted redox-buffering in the sub-arc mantle. Fertile arc segments for ore deposits associated with oxidised magmas require fluid chemistry and pressure-temperature gradients that enhance Fe^{3+} and SO_4^{2-} solubility in aqueous and silica-rich fluids, tectonic stress regimes that favour focussed transfer of components into the sub-arc mantle, and a relatively weak redox buffer for the sub-arc mantle. The paucity of Cu and Au deposits associated with oxidised magmas in the Precambrian may be explained as a consequence of a lack of subducted oxidised material, rather than simply as a consequence of preservation potential. Additionally, the reduced nature of subducted material in the Precambrian may have caused S and metal enrichment in the sub-arc mantle.

Coffinitization of uraninite – A review and discussion of observations on different scales

L.Z. EVINS[1]* AND K.A. JENSEN[2]

[1]SKB, Blekholmstorget 30, 101 24 Stockholm, Sweden (*lena.z.evins@skb.se)
[2] NRCWE, Lersø Parkallé 105, DK-2100 København Ø, Denmark (kaj@nrcwe.dk)

Coffinite ($USiO_4 \bullet nH_2O$) is a common secondary mineral in uranium ores, observed to replace uraninite in reponse to alteration of uraninite in a reducing environment [1]. This process is often referred to as coffinitization. However, it has proven difficult to synthesize coffinite in the laboratory, and in nature, coffinite is commonly very finegrained, resulting in a lack of experimental data concerning thermodynamic properties for coffinite [2,3]. As is noted by [2], the there are natural, coarse-grained coffinite crystals available from the Grants uranium region. However, it is also observed by [4] that there exists intermediate solid solutions in the system thorite–xenotime–zircon–coffinite and that in natural samples, moderate to strong deviation from perfect stoichiometry is commonplace.

In a recent attempt to synthesize coffinite [3], aqueous U was added to a Si-rich solution under controlled conditions to form a green gel subsequently heated for a few days in condition-controlled autoclave. This produced coffinite but only as a nanocrystalline mixture between coffinite and UO_2. Another experiment investigated the hydrothermal alteration of pellets of UO_2 in groundwater spiked with $CaCl_2$, $NaHCO_3$ and Na_2SiO_3[5]. At the end of the experiment (180 °C, c. 40 days, reducing environment) about 25% of the pellet surface was covered with a phase with a U:Si element ratio of 1:1. However, it was not possible to identify this material as coffinite by XRD.

In spite of these experimental difficulties, coffinite is a widespread alteration product of uraninite. This review aims to elucidate the spatial relationships between coffinite and uraninite as seen on different scales with different methods. The mechanism of uraninite alteration in natural, reducing, Si-rich environments is discussed and some new arguments put forward, involving the effect of impurities, defects, and grain size. Coffinitization is discussed in terms of solid-fluid interaction.

[1] Janeczek, Ewing (1992) *J. Nucl. Mat.* **190**, 157-173. [2] Deditius (2008) *Chem. Geol.* **251** 33–49 [3] Pointeau et al. (2009) *J.Nucl. Mat.* **393** 449–458 [4] Förster (2006) *Lithos* **88** ,35– 55 [5] Amme (2005) *J. Nucl. Mat.* **341**, 209–223.

https://doi.org/10.1180/S0026461X00006502 Published online by Cambridge University Press

Tin substitution in chalcopyrite and sphalerite from hydrothermal sulfides

C. EVRARD*[1], N. MOUSSA[1,2], Y. FOUQUET[1] AND E. RINNERT[3]

[1]Laboratoire de géochimie et métallogénie, Ifremer Centre de Brest, BP 70, 29820 Plouzané, France (*correspondence: catherine.evrard@ifremer.fr)
[2]UMR6538 Domaines Océaniques, UBO-IUEM, Place Nicolas Copernic, 29280 Plouzané, France
[3]Service Interface et Capteurs, Ifremer Centre de Brest, BP 70, 29820 Plouzané, France

Unusual tin concentrations (500-2000ppm) were measured in sulfides from the Logatchev hydrothermal field. This hydrothermal site is located on the Mid-Atlantic Ridge, at a depth of 3000 m in an ultramafic environment. The fluid temperature was measured between 300 and 350°C at the exit of the chimneys.

Tin is usually not present in marine sulfides, but detailed microprobe and SEM analyses and element mapping showed a specific distribution for this metal. High tin concentration, are mostly in sphalerite (3 to 5%wt) and chalcopyrite (1 to 2%wt) from the hot part of the chimneys. The highest concentrations, up to 6%wt, are located at the replacement front of chalcopyrite and sphalerite.

Raman spectroscopy studies exclude the presence of tin minerals, like stannite, kesterite or cassiterite, and prove that tin is substituted in the lattice of sphalerite or of chalcopyrite.

The variation of the fluid composition, the temperature and the pressure induces the evolution of the chimney and changes in its mineral composition. These changes, linked to substitution, create different types of minerals with different valence, like $Cu^{+}Fe^{3+}S^{2-}_{2}$ and $Cu^{2+}Fe^{2+}S^{2-}_{2}$ for chalcopyrite.

Fe^{2+} is oxided in Fe^{3+} at high temperature in spite of the oxygen free environment[1] and enhance the tin substitution with the reaction: $2Fe^{3+} <-> Sn^{4+}Fe^{2+}$ [2].

[1] Di Benedetto (2005), *Phys Chem Minerals* **31**, 683-690.
[2] Kase (1987), *Canadian Mineralogist* **25**, 9-13.

Interesting finds in Norilsk copper-nickel sulfide ores

T.L. EVSTIGNEEVA

IGEM RAS, 35, Staromonetny, 119017, Moscow, Russia

Norilsk ores contain a unique set of ore minerals among which the minerals of platinum metals have a significant place. Nowadays more than 100 PGM are described in Noril'sk ores. Along with PGM the wide range of the rare minerals, considered unusual to deposits of similar type, is discovered in these ores. During detailed research using SEM+EDD some new data about PGM paragenesis, associated ore minerals, and unexpected mineral finds are obtained.

An investigation of massive copper rich sulfide ores with chalcopyrite group minerals (talnakhite, mooihoekite, putoranite) has shown, that fine-filiform band of cooper sulfides, $Cu_2S/Cu_{2-x}S$, are often observed along PGM and sulfide mineral boundaries. The thickness of these bands generally does not exceed 0.n microns (n~ 2-5). It could be the reason for some copper "surplus" in PGM composition.

Such observation could also explain the stoichiometry deviation observed on occasion in chalcopyrite group minerals. So, some sample compositions are enriched in Cu. It causes to "strange" formula with higher Cu apfu.

Beside sulfides (i.e. Ni_{ss}) among interesting minerals discovered recently in Cu-Ni-sulfide ores it possible to mention just a few: submicro- and nano-dimentional segregations of thorium , uranium and REE minerals - thorite, uranothorianite, Th-monacite, etc. The grain size of these minerals does not exceed a fraction of a micron. They are found in pyrrhotite ores, Oktyabrsky mine. It is neccesary to note that in Taïmyr peninsula there is an uranium manifestation, named Kamenskoje. Now it is difficult to understand if there is any association of this manifestation with Cu-Fe-Ni-PGE deposits of Noril'sk region. But the finding of Pd-minerals in natural reactor Oklo, in U-bearing black shales, and some other information about "coexisting" PGE and U (Th) in nature allow one to discusse some genetic problems.

https://doi.org/10.1180/S0026461X00006502 Published online by Cambridge University Press

Insights into lower crustal evolution from Hf isotope and Zr thermometry data for rutile

T.A. EWING*, D. RUBATTO AND J. HERMANN

Research School of Earth Sciences, A.N.U., Canberra, Australia (*correspondence: tanya.ewing@anu.edu.au)

Chemical and isotopic analysis of minerals previously resident deep in the crust provides critical information towards understanding the formation, evolution and differentiation of the continental crust. Rutile is an accessory mineral in many lower crustal metapelites and is an appealing target for such studies, but its full potential has not yet been exploited. While the ability to measure Hf isotopes in rutile has been demonstrated [1], an understanding of the behaviour of this system in rutile at high temperatures is lacking. Hf isotope information for this mineral can be combined with temperatures determined by Zr-in-rutile thermometry.

In this study, the classic lower crustal section of the Ivrea-Verbano Zone (IVZ), Italy, was used as a natural laboratory in which to explore the behaviour of the Hf isotope and Zr thermometry systems in rutile at high temperatures. Zr-in-rutile thermometry for a suite of granulite facies metapelites from the IVZ records high temperatures related to peak metamorphic conditions, as well as resetting of the Zr-in-rutile thermometer in some grains. Rutile from metapelite slivers incorporated into the underplating Mafic Complex record heating to temperatures in excess of 1000 ºC during emplacement of the gabbro. Zr-in-rutile is the only thermometer to record this extreme thermal overprint, which is not recorded by Ti-in-zircon or Fe-Mg thermometry.

Hf isotope data for the same suite of metapelites demonstrate that rutile preserves a robust record of Hf isotope composition, even under conditions of high temperature metamorphism and partial melting. The results also demonstrate that in metapelites that have experienced the highest temperatures, zircon dissolution plays an important role in determining the Hf isotope composition of subsequently-formed phases. This observation has profound implications for the interpretation of Hf isotope data for all minerals in both metamorphic and magmatic systems. When complete dissolution of zircon occurs, rutile is shown to become the main host of Zr and Hf in these samples, and controls the Zr/Hf of residue and melt.

The new results demonstrate the valuable contribution that chemical and isotopic analysis of rutile can make to constraining the evolution of the lower crust.

[1] Ewing *et al*. (2011) *Chem. Geol*. **281**, 72-82.

https://doi.org/10.1180/S0026461X00006502 Published online by Cambridge University Press

New *Thiomonas* and *Bordetella* strains involved in iron oxidation at a slightly acidic, heavy metal contaminated creek

M. FABISCH*, F. BEULIG, D. M. AKOB, AND K. KÜSEL

Friedrich Schiller University Jena, 07743 Jena, Germany
(*correspondence: maria.fabisch@uni-jena.de)

Legacy uranium mining in the area of Ronneburg, Germany, resulted in heavy metal contamination of small creeks. Iron rich creek sediments cover a wide pH range from extremely acidic (pH 2.7) over moderately acidic (pH 4.4) to slightly acidic (pH 6.3). In this study, we i) characterized the biogeochemistry of creek sites with different pHs, ii) studied bacterial communities in creek sediments and iii) isolated iron oxidizing bacteria (FeOB) at slightly acidic pH. Sediments were highly contaminated with up to 403 μg g^{-1} (dry wt) Zn, 201 μg g^{-1} (dry wt) Cu, and 165 μg g^{-1} (dry wt) Ni, and with smaller concentrations of up to 4.4 μg g^{-1} (dry wt) Cd. Oxic and anoxic *in vitro* sediment incubations revealed iron oxidation and reduction rates of same magnitude, indicating active iron cycling for all creek sediments regardless of pH. Members of the *Betaproteobacteria* dominated microbial communities in sediments as shown by 16S rRNA gene cloning and sequencing. High fractions of clones showed ≥97% sequence similarity to reported FeOB or iron reducers (FeRB), e.g., *Gallionella ferruginea* and *Ferritrophicum radicicola* (FeOB) or *Rhodoferax ferrireducens* and *Geobacter argillaceus* (FeRB), especially in a RNA-derived clone library from slightly acidic creek sediment (pH 6.3). Three novel FeOB strains, *Thiomonas* sp. strain FB-6 and FB-Cd and *Bordetella petrii* strain FB-8, were isolated from this sediment under lithoautotrophic, microoxic, pH 5.5 conditions. Due to its high similarity to one RNA-derived clone from this study, FB-6 is likely involved in active iron oxidation in creek sediment. Preliminary work indicated heavy metal tolerance and metabolic versatility for the 3 isolates. Future studies will investigate the mechanisms of metal attenuation by these novel FeOB under slightly acidic pH.

Source apportionment of atmospheric organic aerosol by nuclear magnetic resonance (NMR) spectroscopy: Results from EUCAARI project

M.C. FACCHINI[1], E. FINESSI[1], S. DECESARI[1], M. PAGLIONE[1], R. HILLAMO[2], T. RAATIKAINEN[2], C.D. O'DOWD[3], A. KIENDLER-SCHARR[4] AND D.R. WORSNOP[5]

[1]National Research Council (CNR), Institute of Atmospheric Sciences and Climate (ISAC), Bologna, Italy (mc.facchini@isac.cnr.it, +39-051-6399563);
[2]Finnish Meteorological Institute, Air Quality Research, Helsinki, Finland;
[3]National University of Ireland (ECI), Galway, Ireland;
[4]Forschungzentrum Jülich (ICG), Germany;
[5]Aerodyne Research, Inc., Billerica, MA, USA

Submicron aerosol samples were collected in nine EUCAARI IOPs site and analysed by means of proton-Nuclear Magnetic Resonance (^{1}H-NMR) spectroscopy with aim of organic aerosol characterization and source apportionment.. Analogously to more established methodologies employing mass spectrometric techniques, we exploit factor analysis of spectra for the identification of a small number of recurrent chemical classes.

Factor analysis of NMR spectral datasets is already widely used for the analysis of complex organic matrices in several scientific fields, from pharmaceutics to food and medical chemistry. Deconvolution of main spectral profiles within each time series of ^{1}H-NMR spectra of submicron aerosol samples was conducted using non-negative factor analysis techniques, such as PMF, NMF and MCR.

Some recurrent profiles were identified in different IOPs of EUCAARI project and their contribution to the total mass of OA were quantified. The results of this statistical analysis were compared to those of existing methodologies of factor analysis applied to atmospheric aerosol spectroscopic datasets (AMS) collected in the same period for each measurement campaign.

Our findings indicate that factor analysis applied to NMR atmospheric datasets can efficiently complement AMS in lumping the complex oxidized organic mixtures into chemical classes characterized by specific sources or ageing states. More specifically, NMR spectroscopy provides a better discrimination between aromatic and aliphatic structures, which is critical for the quantification of biomass burning products, and for the discrimination between biogenic and anthropogenic SOA.

https://doi.org/10.1180/S0026461X00006502 Published online by Cambridge University Press

Is microbial degradation of heavy hydrocarbons a major source of methane in CBM reservoirs? Evidence from Australia

M. FAIZ[1]*, A. MURPHY[1], D. MIDGLEY[2] AND P. HENDRY[2]

[1]Origin Energy (Resources) Ltd., Brisbane, Qld, Australia (*correspondence: mohinudeen.faiz@originenergy.com.au)
[2]CSIRO Food and Nutritional Sciences, North Ryde, NSW, Australia

It is proposed that it is a misnomer that humic coals (Type III organic matter enriched in vitrinite and inertinite) predominantly generate methane, whereas Type I and Type II organic matter (enriched in liptinite) generate wet gases. Data from deep bituminous coals in Bowen, Surat, Galilee and Sydney basins of Australia indicate that humic coals containing only minor amounts of liptinite can generate significant amounts (>30%) of heavy hydrocarbons (Figure 1). However, subsequent to basin uplift most of the ethane and heavier hydrocarbons in shallow coals appear to be degraded to methane by microbal activity. In addition to alteration of wet gases, microorganisms can also degrade other organic components of coal including aromatics and secondary bitumens occluded in the coal matrix. In deeper, low permeability coals where microbial activity is not prevalent thermogenically generated heavy hydrocarbons appears to be well preserved.

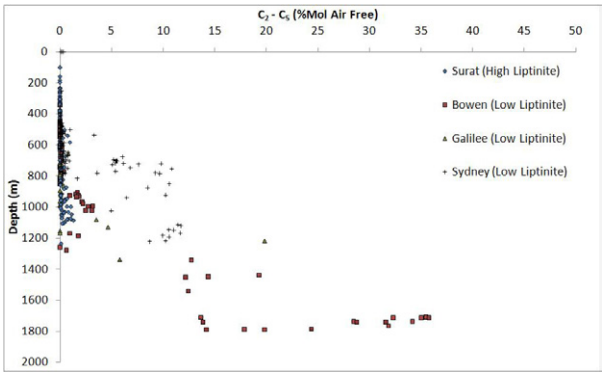

Figure 1: Coalbed gas wetness ($C_2 - C_5$) versus depth.

Microbiological studies including 16SrDNA analyses of coal and associated water samples from the Bowen and Surat basins have enabled the identification of bacteria and archaea capabale of degrading aliphatics and aromatics in coal to produce lighter hydrocabons including methane. The most prevalent bacterial phyla include the Proteobacteria and the Firmicutes and most commonly observed methanogen families include Methanobacteriaceae and Methanosarcinaceae.

Assessment of pore fluid pressure history in basin-centered gas accumulations using fluid inclusions

A. FALL[1]*, P. EICHHUBL[1], R. J. BODNAR[2] AND S.E. LAUBACH[1]

[1]Bureau of Economic Geology, The University of Texas at Austin, Austin, TX 78713, USA (*correspondence: andras.fall@beg.utexas.edu)
[2]Department of Geosciences, Virginia Tech, Blacksburg, VA 24061, USA

Continuous gas charge of low-permeability tight-gas sandstones creates a dynamic system where pore pressure increases locally and temporarily to near lithostatic pressures, and fractures the rocks. Methane concentrations of aqueous fluid inclusions trapped in crack-seal fracture cements can be used as proxy to determine the pore pressure variations in these systems. The natural fracture network creates pathways that allow upward gas migration to form a continuous gas-saturation interval in the absence of a top seal in the deep-central parts of sedimentary basins. The Piceance Basin, Colorado, has been considered a basin-centered gas accumulation. This model contrasts with models of low-permeability reservoirs where gas accumulates in conventional traps. To test these models, we determined the temperature, pressure, and fluid composition history during fracture opening in Mesaverde Group sandstones of the Piceance Basin based on fluid inclusion microthermometry and Raman microspectrometry. Homogenization temperature of aqueous fluid inclusions record systematic temperature trends from ~140 to 185°C and to 158°C over time. In contrast, we observe oscillating pore fluid pressures ranging from ~55 to ~110 MPa over time. We interpret the oscillating pressure record to indicate migration of gas in high pressure cells that move upward by natural hydraulic fracturing. Repeated passage of high pressure cells result in cyclic fracture opening and sealing. Comparison of microthermometry data with burial models suggests that gas generation, migration of high pressure cells, and natural hydraulic fracturing lasted for ~33 m.y. in the Piceance Basin.

https://doi.org/10.1180/S0026461X00006502 Published online by Cambridge University Press

Gold ore-forming fluids and metallogeny in the Zhaoyuan-Laizhou concentration region of Jiaodong peninsula, Eastern China

HONG-RUI FAN, FANG-FANG HU, XIAO-HUI JIANG, KUI-FENG YANG AND TING-GUANG LAN

Key Laboratory of Mineral Resources, Institute of Geology and Geophysics, Chinese Academy of Sciences, P.O. Box 9825, Beijing 100029, China (fanhr@mail.igcas.ac.cn)

Zhaoyuan-Laizhou gold concentration region in the Jiaodong Peninsula of Eastern China is currently the most important gold producer in China. Several world-class gold deposits (>100 t gold) have been discovered in the region. There are two main types of gold deposits, namely quartz vein-style (Linglong type) and fault-zone hosted disseminated/stockwork-style (Jiaojia type).

Detailed fluid inclsuion studies have been carried out in the Linglong and Jiaojia type deposits in the region. Three types of fluid inclusions have been distinguished from quartz in gold lodes: (A) H_2O-CO_2 inclusions, (B) CO_2-H_2O±CH_4 inclusions, and (C) aqueous H_2O inclusions. The pre-gold H_2O-CO_2 fluid inclusions occur isolated in samples of the early milk-white quartz and are assumed to have been trapped during crystallization of the earliest quartz. Fluid inclusions associated with gold mineralization contain mostly CO_2-H_2O-NaCl±CH_4 fluids, and occur isolated, and sometimes in healed fractures particularly in smoke-grey quartz with variable CO_2 and CH_4 contents. There are similar changes of molar volumes of H_2O-CO_2 and CO_2-H_2O±CH_4 inclusions with 50 - 70 cm^3/mole from the depsoits. Estimated fluid trapping pressures of pre-gold and gold-stage are 1.0 - 3.5 kbar and 0.7 - 2.5 kbar, respectively. The pressure is tending towards depression along with fluid evolution.

Obtained Rb-Sr and Ar-Ar isochron ages from the Zhaoyuan-Laizhou gold concentration region give gold mineralization time around 120 Ma. Gold deposits in the region are formed in the same mineralizing-geodynamic circumstance, and related with Mesozoic tectonic transition in the eastern North China craton.

This work was financially supported by Natural Science Foundation of China (40625010) and the Crisis Mines Continued Resources Exploration Project of China Geological Survey (20089930).

Genesis of carbonatite from Hannuoba and Yangyuan, North China

QICHENG FAN, JIANLI SUI, XINGXXNG DU AND YONGWEI ZHAO

Institute of Geology, China Earthquake Administration, Beijing100029, China (fqc@ies.ac.cn)

Most of the mantle-derived magmas are silicate melt, with very few others, such as carbonate magmas. However these rare carbonate magmas tell quite different but important stories on mantle evolution. Here we report a new case of mantle-derived carbonate magma found in the Cenozoic basalts in Hannuoba and Yangyuan, North China. The carbonate melts occur in small veins, which cut through the basalts and mantle peridotite xenoliths. The carbonatite veins are mainly dominated by calcite (>90%), with a little amount of mantle minerals, e.g. olivine, clinopyroxene, orthopyroxene and spinel. The xenoliths are altered by the carbonate melt, and their colors changed from originally yellow or green to purplish brown-amarance, with grayish white network stringers of carbonatite cut through. Whole rock chemical compositions reveal that the carbonatite veins have low rare earth elements (ΣREE =8.7-13.7×10^{-6}) and trace elements, with slightly enriched LREE patterns. Stable isotopes of C and O in the carbonatite veins are $\delta^{13}C$=-11.2~-12.3‰ and $\delta^{18}O$=22.6~22.8‰, respectively. Only a few fresh samples from Hannuoba have mantle carbonatite C and O isotopic ratios ($\delta^{13}C$ = -5.7~-7.3‰ , $\delta^{18}O$ = 8.5~10.1‰), while most samples show significant characteristics of weathering. Radioactive isotopes of Sr, Nd, Pb are $^{87}Sr/^{86}Sr$= 0.7078-0.7079, $^{143}Nd/^{144}Nd$=0.5129, $^{206}Pb/^{204}Pb$=18.0, $^{207}Pb/^{204}Pb$=15.5, $^{208}Pb/^{204}Pb$=38.0, respectively. ε_{Nd} of two samples in Hannuoba vary in 5.3-5.5, and reveal their DM mantle origin. The carbonatite indicate that they have the same origin of depleted mantle as the basalt, but weathering after magma eruption modifies the carbonatite.

Supported by NSFC 40772038

https://doi.org/10.1180/S0026461X00006502 Published online by Cambridge University Press

Biosynthesis of sterols and wax esters by *Euglena* of acid mine drainage biofilms: Implications for eukaryotic evolution and the early Earth

JIASONG FANG[1,2], SHAMIK DASGUPTA[2], SANDRA S. BRAKE[3], STEPHEN T. HASIOTIS[4] AND LI ZHANG[5]

[1]Department of Natural Sciences, Hawaii Pacific University, Kaneohe, HI 96744, USA; (jfang@hpu.edu)
[2]School of Ocean and Earth Sciences, Tongji University, Shanghai, China; (jsfang@tongji.edu.cn)
[3]Department of Geology, Iowa State University, Ames, IA 50011, USA; (samik2403@gmail.com)
[4]Department of Earth and Environmental Systems, Indian State University, Terre Haute, IN 47809, USA; (Sandra.Brake@indstate.edu)
[5]Department of Geology, University of Kansas, Lawrence, KS 66045, USA; (hasiotis@ku.edu)
[6]State Key Laboratory of Geological Processes and Mineral Resources, Faculty of Earth Sciences, China University of Geosciences, Wuhan, China; (lizhang@cug.edu.cn)

Acid mine drainage (AMD) environments are potential analogs for Earth's primordial environment. We studied biofilms of an AMD system (pH 2.0-3.5) in western Indiana, USA. Biofilms, either floating or attached to the bottom of the AMD flow channel, are formed by the acidophilic, microeukaryote *Euglena mutabilis*. Lipid analysis of benthic and floating biofilms revealed the dominance of photosynthetic organisms, *Euglena mutabilis*, as indicated by the detection of abundant phytadiene, phytol, phytanol, polyunsaturated *n*-alkenes, polyunsaturated fatty acids, short-chain (C_{25-32}) wax esters (WE), ergosterol, and tocopherols. The WE were probably synthesized in mitochondria under anaerobic conditions, whereas the sterols (ergosterol and ergosta-7,22-dien-3β-ol) were likely synthesized in the cytosol in the presence of molecular oxygen by the acidophilic, photosynthetic microeukaryotes *Euglena*. The dual aerobic and anaerobic biosynthetic pathways may be the biochemical relics of the anaerobic past of the Earth. Given that the oxygenation of the oceans is a relatively recent event (i.e., ~580 Ma ago), ca 1 billion years after eukaryotes arose, the conserved compartmentalization of *Euglena* biosynthetic machinery may have allowed early eukaryotes to survive and diversify early on Earth, when the oceans were anoxic and sulfidic, and despite their evolution, they preserved this physiology. Wax esters and their diagenetic products (short-chain *n*-alkanes and alkanoic acids) may be the molecular biosignatures of these organisms in the geologic record.

Unconstrained fluxes to the ocean: Calcium isotopes in dust-producing regions

MATTHEW S. FANTLE[1], HEATHER TOLLERUD[1], ANTON EISENHAUER[2] AND CHRIS HOLMDEN[3]

[1]Geoscience Dept., Penn State, University Park, PA 16802
[2]Leibniz Institute of Marine Science, IFM-GEOMAR, Wischhofstr. 1-3, 24148 Kiel, Germany
[3]Dept. Geological Sciences, 114 Science Place, Univ. Saskatchewan, Saskatoon, SK, S7N 5E2

Though mineral dust can be an important input to the ocean over geologic time scales, little is known about its Ca isotopic composition (delta44/40Ca). This study measures the Ca isotopic composition of sediments from an active dust source in the western U.S. (Black Rock Desert, NV). We present geochemical, mineralogical, and isotopic data from 22 sediments collected from the upper 0.5 cm of the playa. Isotope data for sequential water & 0.5 N HCl leaches and leached residues are presented. Lithium metaborate fusions of bulk sediments reveal Ca concentrations between 0.28 and 40 wt.% (median: 6.8 wt.%), an 80% enrichment relative to upper continental crust. XRD data indicates calcite concentrations of 2–32%, with most samples containing 7–14%. Water leaches generally sample <1% of total Ca, while acid leaches sample >60%. Water leaches are, on average, +0.33±0.16‰ (1SD) heavier than acid leaches; the degree of fractionation varies (Δ_{w-a} = ~0-0.6‰) and appears to depend only on the fraction of Ca in the acid-soluble fraction. Acid leaches are, on average, -0.45±0.07‰ (bulk Earth scale), similar to the delta44/40Ca of modern nannofossil ooze (-0.4‰) and modern rivers (-0.41±0.08‰; Tipper *et al*., 2010).

Dust-derived Ca is an important mass flux to constrain. Assuming a modern mineral dust flux of ~10^3 Tg/yr to the global ocean (e.g., Duce and Tindale, 1991) and a calcite concentration <10%, the inferred Ca mass flux to the ocean is <100 Tg/a. This flux is comparable to the mass flux of Ca delivered by rivers to the modern ocean (~550 Tg/yr). The implication of this work is that the "mobile" fraction of playa-derived dust (water- & acid-soluble pools) is not fractionated relative to riverine input to the ocean. If, however, the acid-soluble fraction is not readily released into the water column, the water-soluble fraction (which can be significantly heavier) is the appropriate flux to consider when discussing atmospheric inputs of Ca to the ocean. During transport, calcite dissolution can be inhibited by high pHs (>8) generated when soluble Na-carbonates dissolve in aerosols. Such pHs are seen in modern systems close to dust sources (e.g., the Mediterranean), where the bulk of dust is deposited.

https://doi.org/10.1180/S0026461X00006502 Published online by Cambridge University Press

Isotope constraints on the biogeochemical cycling of calcium (Ca) in a base-poor forest ecosystem

JURAJ FARKAŠ[1], ADRIEN DÉJEANT[2], MARTIN NOVÁK[1] AND STEIN B. JACOBSEN[3]

[1]Department of Geochemistry, Czech Geological Survey, Geologická 6, 152 00 Prague 5, Czech Republic
[2]Institut de Physique du Globe de Paris (IPGP), École Normale Supériere, Université Paris Diderot, France
[3]Department of Earth and Planetary Sciences, Harvard University, 20 Oxford Street, Cambridge, MA, USA

We studied the biogeochemical cycling of Ca in an old-growth forest at Wachusett Mountain, which feeds the Nashua River Watershed located in central Massachusetts, the northeastern USA. The forest grows on naturally base-poor soils (i.e. Ca and Mg depleted) developed on the granodioritic bedrock of Precambrian age. Trees are thought to obtain dissolved Ca mainly from an easily accessible soil-water reservoir termed the 'exchangeable cation pool'. The status of Ca reserves in this soil pool is sensitive to anthropogenic soil acidification and excessive timber harvesting. Our study shows that in the base-poor forest at Wachusett Mountain the 'exchangeable Ca pool' of mineral soils has a unique isotope signature that is significantly enriched in radiogenic ^{40}Ca due to the dissolution of K-rich silicate minerals such as biotite. In contrast, samples of local vegetation (i.e. woody tissues of red oak) show no detectable excess of the radiogenic ^{40}Ca, thus challenging a prevalent belief that the 'exchangeable cation pool' of mineral soils plays an important role as the source of Ca in forest nutrition. This study shows that base-poor forests are able to bypass the 'exchangeable Ca pool' in mineral soils, and still meet their nutritional needs, thus being largely independent of the rock-derived nutrient sources. Consequently, the growth of base-poor forests must rely primarily on alternative Ca sources, which do not show the radiogenic ^{40}Ca excess. Such sources of Ca may include (i) atmospheric deposition [1, 2], (ii) recycling of the forest-floor organic matter, and/or (iii) the fungal-mediated dissolution of apatite [3]. Finally, we will also discuss temporal variations in the Ca isotope composition of a tree-ring record from a 260-year old red oak collected at our study site.

[1] Holmden & Bélanger (2010) *Geochimica et Cosmochimica Acta*. **74**, pp. 995-1015; [2] Kennedy *et al*. (2002) *Proceedings of the National Academy of Sciences* **99**, pp. 9639-9644; [3] Blum *et al*. (2002) *Nature* **417**, pp. 729-731.

Rapid climate change during marine isotope stage 5-4 glacial inception in the subpolar North Atlantic

ELIZABETH J. FARMER* AND MARK R. CHAPMAN

School of Environmental Sciences, University of East Anglia, Norwich, UK. (*correspondence: e.farmer@uea.ac.uk)

Previous work from North Atlantic core NEAP 18K highlighted the occurrence of a number of previously unrecognised ice rafting events occurring not only during periods of greatest ice volume, but also during periods of ice sheet growth and decay. Ice core records highlight two events (Dansgaard-Oeschger (DO) events 19 and 20) during the transition between MIS 5 and 4 as the largest events in the last 100 ka, with temperature shifts in excess of 10°C over a matter of decades.

In the present work, the new record from NEAP 17K is presented. A neighbouring core to NEAP 18K, this core has a higher accumulation rate through the MIS 5/4 period, and, like NEAP 18K, is in a key region for monitoring the movements of the polar front and changes in the surface to deep ocean connectivity and potential for NADW production over glacial-interglacial time scales

Two rapid shifts in faunal assemblage are clearly evident during the transition. SST estimates indicate temperature shifts in the order of 8°C. These oscillations correlate with DO events 19 and 20, and are preceded by small ice rafting events, C19 and C20, coincident with a freshening of the surface waters. Benthic stable isotope data provide stratigraphic control and allow us to examine the relative strength of North Atlantic Deep Water production. Mg/Ca records separate the response of the surface and subsurface water masses and provide an intriguing alternative temperature record.

These records support the ice core proxies in suggesting that this interval was a period of extreme and rapid climatic change in the North Atlantic. The linkage between the surface and deep ocean, and the parallels in the Greenland ice cores, would indicate that these events were not local to Greenland alone but were felt across the North Atlantic region and are associated with a significant reorganisation of North Atlantic circulation.

https://doi.org/10.1180/S0026461X00006502 Published online by Cambridge University Press

Development of a micro-interdigitated electrode array for use in high precision TIMS-based isotope ratio determinations

G. L. FARMER* AND E.P. VERPLANCK

Dept. of Geological Sciences and CIRES, University of Colorado, Boulder, CO 80309, USA; (*correspondence: farmer@colorado.edu)

Thermal ionization mass spectrometry (TIMS) remains the method of choice for high precision Pb isotopic measurements, but "silica gel" techniques used to generated thermalized Pb ions have ionization efficiciencies of only 10% at best. To improve Pb ionization efficiencies from liquid glass ion emitters and ultimately the precision of U-Pb age determinations we are using electrochemical techniques to increase Pb ionization efficiencies *in situ* in liquid glasses. Our initial work demonstrated that Pb-doped high temperature (~1,300ºC) liquid glass can serve as the electrolyte in an electrochemical cell and that Pb metal atoms prevalent in the glass under vacuum conditions can be oxidized to Pb^+ by the application of ~1V across Pt wire electrodes. To take advantage of this ionization mechanism, we are developing a micro-interdigitated electrode array (IDA) for use as an "electrochemical" ion source. This array consists of a "comb" structure of interleaved tungsten electrode "fingers" sputtered onto a pure silicon wafer. The array fabrication process includes spinning photoresist on an oxidized 275µ thick silicon wafer and exposing the wafer to UV light through a photomask. The DC sputter deposition system applies a 1µ layer of tungsten to the wafer. A photoresist liftoff procedure removes most of the metal layer, leaving the IDA structures on the wafer. The electrode lengths and widths range from 100-200µ and 10-200µ, respectively. There are 1-14 pairs of these electrodes on each IDA, with gap widths of 10-15µ. Our initial results reveal that a Pb-doped silica suspension can be dried and melted on the IDA surface by a metal ribbon resistive heater placed in contact with the electrically non-conducting silicon wafer substrate of the IDA. Our next step will be to install the IDA and heater ribbon in a Finnigan-MAT 261 TIMS, and to connect the assembly to a specially-designed potentiostat that will allow the IDA to float at 10KV while a differential voltage from 0.1 to 10V is applied across the IDA electrodes. This work is currently in progress.

Potential for manganese oxidation in shallow groundwater induced by water table fluctuation

C. E. FARNSWORTH[1,2], A. VOEGELIN[1] AND J. G. HERING[1,3,4]*

[1]Eawag, Swiss Federal Institute of Aquatic Science & Technology, Dübendorf, Switzerland CH-8600 (*correspondence: janet.hering@eawag.ch)

[2]Division of Engineering and Applied Science, California Institute of Technology, Pasadena, CA USA 91125

[3]Institute for Biogeochemistry and Pollutant Dynamics, ETH, Zürich, Switzerland

[4]École Polytechnique Fédérale de Lausanne, School of Architecture, Civil, & Environmental Engineering, Lausanne, Switzerland

On-off cycles of production wells, especially in bank filtration settings, cause oscillations in the local water table, which can entrap significant amounts of dissolved oxygen (DO) in the shallow groundwater. Although attempts to quantify air entrapment and transport in groundwater are ongoing, less attention has been paid to the potential geochemical reactions initiated by DO introduction to low-DO groundwater.

The potential for DO introduced in this manner to oxidize manganese (Mn), mediated by the obligate aerobe *Pseudomonas putida* GB-1, was tested in a column of quartz sand with anoxic influent solution and 1.3-m water table changes every 30-50 h. The frequency and amplitude of the oscillations simulated those of a bank filtration site in Berlin, Germany. After a period of filter ripening in the column, 100 µM Mn was rapidly removed during periods of low water table and high dissolved oxygen concentrations. The accumulation of Mn in the column was confirmed by XRF analysis of the sand at the conclusion of the study, and both measured net oxidation rates and XAS-derived speciation suggest microbial oxidation as the dominant process. The addition of Zn, which inhibited GB-1 Mn oxidation but not its growth, interrupted the Mn removal process, but Mn removal recovered within one water table fluctuation. Thus transient DO conditions could support Mn oxidation, and the conditions under which this process could be relevant in shallow groundwater in alluvial sediments will be presented.

https://doi.org/10.1180/S0026461X00006502 Published online by Cambridge University Press

Redox and early Earth's sulfur cycle

JAMES FARQUHAR[1], MARK CLAIRE[2], SHAWN DOMAGAL-GOLDMAN[3], BRIAN HARMS[1], SIMON W. POULTON[4]* AND AUBREY L. ZERKLE[4,1]

[1]Department of Geology and ESSIC, Univ. Maryland, USA
[2]Virtual Planetary Laboratory, University of Washington, Seattle, WA, USA
[3]NASA Headquarters, Washington, D.C., USA
[4]School of Civil Engineering and Geosciences, Newcastle University, UK (*correspondence: s.w.poulton@ncl.ac.uk)

It has been a little over 10 years since it was recognized that mass-independent sulfur isotope signatures in the Archean and earliest Paleoproterozoic rock record provided information about the redox state of Earth's surface environments. As the dataset has grown, new features of the record have emerged, including the recognition of a relatively clear change in the magnitude of $\Delta^{33}S$ that defines the range of variation between the Eo-Paleoarchean, the Mesoarchean, and the Neoarchean [1], a change in the symmetry of this signal about the origin for this same interval [(maximum positive $\Delta^{33}S$)/(maximum negative $\Delta^{33}S$)] [2], and changes in the relationship between $\Delta^{36}S$ and $\Delta^{33}S$ that are corelated with the age and stratigraphy of the measured samples (e.g., [3,4]). It also appears that the the mean value of $\Delta^{33}S$ (and $\Delta^{36}S$) for different parts of the Archean varies, which bears on the issue of whether the available samples can be used to close the sulfur cycle.

Our work over the past few years has focused on understanding these and other aspects of the sulfur cycle, and also on connections between the implied causes of MIF-S and the sources/sinks in the sulfur cycle, and their collective implications for the evolution of the redox state of the Archean and Paleoproterozoic atmosphere and oceans. The picture that emerges appears to call for a change in the cycling of sulfur extending from the Eoarchean, through the Paleo- and Mesoarchean, and into the Neoarchean. The record implies significant changes in structure of the sulfur cycle pathways – specifically related to the role of those for reduction and reoxidation of sulfur compounds. These data, sulfur cycle models, and the basis for these assertions will be discussed.

[1] Ohmoto, *et al*., (2006) *Nature*, **442**, 908-911. [2] Halevy, *et al*., *Science*, **329**, 204-207. [3] Kaufman, *et al*., (2007) *Science*, **317**, 1900-1903. [4] Farquhar, *et al*., (2007) *Nature*, **449**, 706-U5.

Evidence for subduction history recorded by mineral inclusions in high-grade metamorphics of the Modanubian zone, central Europe

SHAH WALI FARYAD, ONDREJ LEXA, MARTIN RACEK, DAVID DOLEJŠ AND RADIM JEDLIČKA

Institute of Petrology and Structural Geology, Charles University Prague, Albertov 6, Prague 2, Czech Republic

Felsic granulites with lenses of eclogites and garnet peridotites in the Variscan orogen of central Europe contain various mineral inclusions that can be used to reconstruct their early prograde metamorphic history. Ultrahigh-pressure conditions for some of these rocks were deduced by conventional geothermobarometry and from inclusions of microdiamonds. These rocks are usually interpreted to be exhumed from lower crust or upper mantle by crustal thickening followed by extrusion to middle crustal levels.

We investigated mono- and polyphase mineral inclusions and their replacement products in garnets from granulites and mantle peridotites. Inclusions of Cr-rich spinel were commonly encountered in garnet or in pyroxene enclosed by garnet. In clino- and orthopyroxene, garnet form by destabilization and exsolution of Al-Tschermak end-member during pressure increase and/or temperature increase. In addition, garnet grains from pyroxenites and eclogites contains inclusions of omphacite and a variety of single- or multiphase inclusions, which consist of combinations of sodic-calcic amphibole, alkali feldspar, phlogopite, chlorite, and carbonate. The inclusions have negative crystal shapes and their mineral assemblages and composition may point to crystallization in the presence of chlorine-bearing aqueous fluid(s). These features suggest (re)crystallization of mantle peridotites and pyroxenites during pervasive fluid percolation probably driven by slab dehydration and decarbonation during subduction. Eclogite-facies prograde history is independently supported by the presence omphacite and phengite in garnet, respectively.

https://doi.org/10.1180/S0026461X00006502 Published online by Cambridge University Press

Relation between cobalt fractionation and its accumulation in metallophytes from South of Central Africa

M.P. FAUCON[1,2]*, G. COLLINET[3], P. JITARU[2], N. VERBRUGGEN[4], M. SHUTCHA[5], G. MAHY[6], P. MEERTS[1] AND O. POURRET[2]

[1]Laboratoire d'Ecologie Végétale, Univ. Libre Bruxelles, 1050 Bruxelles, Belgium
[2]HydrISE, LaSalle Beauvais, 60026 Beauvais cedex, France (michel-pierre.faucon@lasalle-beauvais.fr)
[3]Laboratory of Geopedology, Gembloux Agricultural Univ., 5030 Gembloux, Belgium
[4]Laboratoire de Physiologie et de Génétique Moléculaire des Plantes, Univ. Libre Bruxelles, 1050 Bruxelles, Belgium
[5]Univ. Lubumbashi, Facultés des Sciences Agronomiques, Lubumbashi, Democratic Republic of Congo
[6]Laboratory of Ecology, Gembloux Agricultural Univ., 5030 Gembloux, Belgium

Metallophytes are plants that mostly occur on metal-rich soils. Some metallophytes grow particularly on soils contaminated by Co, especially in South of Central Africa. *Crepidorhopalon perennis* and *C. tenuis* show a variable ability to accumulate Co in shoots, which can be explained both by synergistic and antagonistic interactions among several trace metals [1]. In fact, Co accumulation in shoots is favoured by high Co concentrations and hampered by high concentrations of Fe and Mn in soils [2].

In this study, we focus on Co fractionation in soil in order to explain the large variation in Co accumulation in *Crepidorhopalon perennis* and *C. tenuis* species, and also the interactions among various trace metals. Organic matter, pH as well as total (using the mixture HF-HCl-$HClO_4$) and extractable (acetate-EDTA 1 mol/L, pH=4.25) concentrations of Mn, Cu, Co, Fe, Ca, Mg and Zn, were measured. Cobalt fractionation was furthermore modelled using Windermere Humic Aqueous Model (WHAM 6) [3]. Positive correlation between sum of organic and free Co concentrations estimated by WHAM 6 and concentrations of extractable (acetate-EDTA) Co was found. Furthermore, fractionation modelling shows a strong affinity of Mn-oxides for Co, which can explain the lower Co levels in the plants grown on Mn-rich soils. The high Mn and Fe status of Cu-Co soil in South of Central Africa may actually exert a protective effect against the toxic effects of Co.

[1] Faucon *et al*. (2007) *Plant Soil* **301**, 29-36. [2] Faucon *et al*. (2009) *Plant Soil* **317**, 201–212. [3] Lofts & Tipping (1998) *GCA* **62**, 2609-2625.

Bioavailability of tungsten in soils and tailings of mining areas with distinctive paragenesis (Northern Portugal)

PAULO FAVAS[1,3], JOÃO PRATAS[2,3] AND ELISA GOMES[1,3]

[1]Dep. of Geology, UTAD, Ap.1013, 5000-801 Vila Real, Portugal (pjcf@utad.pt)
[2]Dep. of Earth Sciences, University of Coimbra, Largo Marquês de Pombal, 3001-401 Coimbra, Portugal
[3]Geosciences Center, University of Coimbra

This paper compares five mining areas of Northern Portugal with distinctive paragenesis (Ervedosa Mine with cassiterite and diverse sulphides; Rio de Frades Mine and Regoufe Mine with wolframite, scheelite, cassiterite and sulphides; Adoria Mine with volframite, cassiterite and sulphides; and Tarouca Mine with scheelite, cassiterite and sulphides) for bioavailable levels of tungsten in soils and the resulting bioaccumulate levels in six species of plants (*Erica arborea* L., *Halimium umbellatum* (L.) Spach, *Pinus pinaster* Aiton, *Pteridium aquilinum* (L.) Kuhn, *Pterospartum tridentatum* (L.) Willk. e *Quercus faginea* Lam.).

The mechanisms relating to the mobility and bioavailability of this metal have been explored using sequential chemical extraction techniques. The procedure adopted in this study allows the separation of the water-soluble fraction, so the extracted chemical elements must be considered highly bioavailable because they are easily mobilised. The elements extracted from the so-called exchangeable fractions, which in this study were leached through the use of NH_4 OAc, are an important part of the potentially available elements and can be considered as an estimate of bioavailability.

Tungsten appears to be relatively immobile in most studied sites, but soils of Tarouca mine show significant increases in bioavailable fraction.

The soils of the Tarouca mine area stand out by their higher content of W in the bioavailable fraction. Probably as a result of easier fragmentation and dissolution of scheelite, compared to wolframite. This is reflected in the bioaccumulated concentrations in the tissues of the studied species at this site. It's in the samples of Tarouca mine that occur higher bioaccumulated levels of W than all five mines. This exemplifies the importance of soil mineralogy, controlling the biogeochemical distribution of elements.

https://doi.org/10.1180/S0026461X00006502 Published online by Cambridge University Press

The characteristics of three different subduction zones in Iranian plateau

ARDALAN FAZELVALIPOUR

Member of Young Researchers club, Islamic Azad University Mashhad Branch- Iran, (dra_fv@yahoo.com)

Iranian plateau is a tectonically young complex region resulting from collision of Arabian Plate with Eurasia. Existence of three different subduction zones within different geographical parts provides different tectonic and geodynamic characteristics with the plateau. In this study, we use surface wave tomography method to image S-velocity structure of upper mantle and Moho depth variations across the Iranian plateau. Our results show that there is a clear evidence for subducting of Arabian plate beneath central Iran across the Zagros collisional zone in south-west Iran. Active subduction still occurs to the southeast of Iran where the oceanic part of Arabian plate is being subducted beneath Makran coast. The oceanic crust of South Caspian Basin is being westward under thrusting under Talesh and Alborz mountains in northern part of Iran.

To image *S*-velocity structure of upper mantle and Moho depth variations of Iranian plateau ,we apply surface wave tomography based on Partitioned Waveform Inversion (PWI) method(Nolet, 1990). PWI method consists of two steps: in the first step, 1-D average S-velocity model and average Moho depth is determined for each event-station propagation path using nonlinear waveform inversion. The results are given based on absolute S-velocity variations with depth for the given path. Then, 1-D S-velocity models obtained in the previous step, are firstly reformulated (normalized) with respect to a common background model and are secondly combined using a damped linear inversion algorithm to image 3-D S-velocity perturbations and Moho depth variations for the studied area. Depending on epicentral distances and quality of the data, the selected time window for waveform-fitting in the first step is started from beginning of S phases (for $\Delta \leq 30^{o}$) or SS (for $\Delta \leq 70^{o}$) to end of fundamental mode of surface waves. This indicates that only those phases with turning point in the upper-mantle are included in the inversion. Synthetic seismograms are constructed by mode-summation using the first 30 modes of Ray leigh waves, with phase velocitiesbetween2 and 10 km/s.

The efficiency of PWI method strongly depends on path coverage of waveforms in the studied region (Fig. 1). Our dataset consist of Z-component of broadband seismograms from events with a magnitude between 5.5 and 7.7 recorded by one temporary array and two permanent networks Of nearly 3000 seismograms originally analysised, we have fitted 974 waveforms from 47 events and 39 stations (Fig. 2) which result in 11688 linear constraints on upper-mantle S-velocity structure and Moho depth for the studied area

The damped linear inversion of the constraints derived from waveform fittings yields a 3-DS-velocity model and Moho map across Iranian plateau. In the following sections, we explain the results.

Diamond record of metasomatism

Y. FEDORTCHOUK[1]* AND Z. ZHANG[1,2]

[1]Dalhousie University, Halifax, Nova Scotia, B3H4J1, Canada (*correspondence: yana@dal.ca, Zhang.Zhihai@dal.ca)

[2]China University of Geosciences, Wuhan, 430074, China

The majority of diamond population from a kimberlite carry surface features developed during accent in kimberlite magma. However, a small proportion of each diamond population shows other resorption styles reflecting diamond-dissolution events prior to the kimberlite emplacement. In order to better understand the nature of diamond-destructive fluids (or melts) in the mantle we focused this study on the latter group. Detailed study of diamond morphologies, nitrogen content and aggregation, and internal structure using cathodoluminesence images was done for micro-diamonds from four kimberlite pipes from the Ekati Mine, Canada.

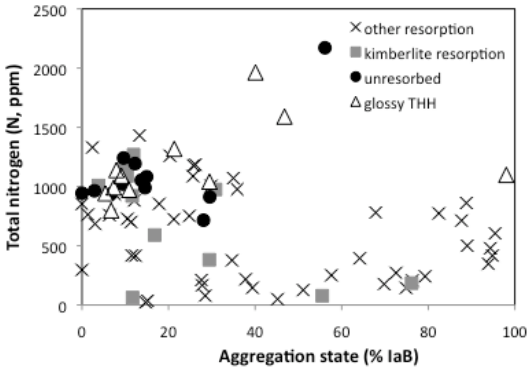

Figure 1: Nitrogen data for morphological groups.

We defined four groups: 1) unresorbed octahedral diamonds and those with “kimberlitic” resorption features; 2) stones with deep hexagonal and trigonal etch pits; 3) several types of step-faced crystals; 4) other surface features different from the “kimberlite-induced” resorption. A correlation between the resorption style and nitrogen content and aggregation state of diamonds determined by Fourier Transform Infrared analyses (Fig. 1) indicates similar thermal /crystallization history of diamonds with similar resorption style. Comparison to the products of high-pressure experiments [2] suggests diamond interaction with water-rich fluids in the mantle source. Further work will refine diamond grouping. The conditions of these resorption events will be constrained through diamond dissolution experiments.

[1] Fedortchouk *et al* (2010) *EPSL* **298**, 549-559. [2] Khokhryakov & Pal'yanov (2010). *Amer. Miner.*, **95(10),** 1508-1514.

https://doi.org/10.1180/S0026461X00006502 Published online by Cambridge University Press

Fluids at continental margins: What we can learn from ^{129}I results

UDO FEHN

Dept. of Earth and Environmental Sciences, U. Rochester, Rochester, NY, 14627, USA (ufehn@ur.rochester.edu)

The close association of iodine with organic material and the presence of the long-lived radio-isotope ^{129}I ($T_{1/2}$ = 15.7 Ma) make this isotope system an interesting tracer for fluid movements at continental margins. The system was applied to studies of volcanic fluids associated with subduction zones [1] as well as to methane-rich fluids at passive [2] and active margins [3]. Volcanic fluids are characterized by iodine concentrations close to 10 μM, i.e. only moderatly higher than in seawater (0.4 μM) and by CO_2 as their dominant carbon species. Results for volcanic fluids show ^{129}I/I ratios which are site-dependent and are consistent with derivation from subducting marine sediments. In contrast, fluids associated with gas hydrates or emanating from mud volcanoes along continental margins are enriched in iodine by factors of 500 or more compared to seawater and are dominated by the presence of CH_4. ^{129}I/I ratios in these methane-rich fluids predominantly fall into a narrow range between 200 and 400x10^{-15}, regardless of site or age of subducting slab present in active margins. Because the ^{129}I results show neither relation to the age of the host sediments nor to the ages of subducting slabs or other tectonic features, a significant proportion of iodine in the fluids in these locations probably is derived from sources in the upper plates of active margins. More specifically, the iodine age distribution suggests that organic sources of Eocene age or older have contributed to the iodine present in these fluids. These sources are found in the deeper sections of passive margins and in the continental parts of subduction zones. The ^{129}I/I results demonstrate that different processes are active in fore arc and main arc areas: volcanic fluids in the main arcs show the recycling of volatiles from subducting marine sediments but fluids in fore arc areas are predominantly derived from sources in upper plates, i.e. the terrestrial parts of continental margins.

[1] Fehn, Snyder & Egeberg (2000) *Science* **289**, 2332-2335. [2] Snyder & Fehn (2002) *Geochim. Cosmochim. Acta* **66**, 3827-3838. [3] Lu, Tomaru & Fehn (2008) *Earth Planet. Sci. Lett.* **267**, 654-665

Silicon self-diffusion in forsterite, revisited

H. FEI[1]*, T. KATSURA[1], S. CHAKRABORTY[2], R. DOHMEN[2], C. HEGODA[3], D. YAMAZAKI[3], M. WIEDENBECK[4], H. YURIMOTO[5], S. SHCHEKA[1], K. POLLOK[1] AND A. AUDÉTAT[1]

[1]BGI, Univ. Bayreuth, D95440, Bayreuth, Germany (*correspondence: hongzhan.fei@uni-bayreuth.de)
[2]Inst. Geo.Min. Geophy., Ruhr-Univ. Bochum, D44780, Bochum, Germany
[3]ISEI, Okayama Univ., 6820193, Misasa, Tottori, Japan
[4]GFZ Potsdam, D14473 Potsdam, Germany
[5]Dept. Nat. His. Sci., Hokkaido Univ., 0600810, Sapporo, Japan

The plastic deformation of minerals in the mantle is believed to be controlled by diffusion. Si is the slowest diffusion species in most mantle minerals, and therefore expected to limit the creep rates [1]. Jaoul *et al*. [2] measured the Si self-diffusion coefficient (D_{Si}) in forsterite (*Fo*) at ambient pressure, showing log[D_{Si} *(m^2/s)*]= -22.1 at 1600 K. Such a value is approximately 3 orders of magnitude lower than that expected from the deformation experiments [3]. Moreover, measurement of D_{Si} at high pressures [4] showed very high D_{Si}, i.e., logD_{Si} = -19.8 at 1600 K. In order to solve these discrepancies, we revisited D_{Si} in *Fo* in this study.

Fo crystals were polished in colloidal silica solution, deposited with 300-500 nm of ^{29}Si enriched Mg_2SiO_4 films coverd by 100 nm of ZrO_2 films. They were annealed at 1600 K and 0, 1 and 8 GPa for diffusion. The diffusion profiles were obtained by SIMS.

Surface roughness is a serious error source for SIMS analysis. Although the roughness just after deposition was less than 10 nm, that after annealing become as large as 250-300 nm. Hence, the samples were polished again in colloidal silica solution after diffusion. The final roughness was thus reduced to be less than 50 nm.

logD_{Si} was determined to be -19.3±0.5 at 0 GPa and 1600 K in this study, which is 2.8 orders of magnitude higher than that by Jaoul *et al*. [2]. Their low D_{Si} could be obtained due to the bad contact of the coating layer with the host. The present D_{Si} is consistent with the high dislocation climb rates in deformation experiments. Our data also indicates a small activation volume as 3.0×10^{-6} m^3/mol.

[1] Shimojuku *et al*. (2009), EPSL **284**, 103-112. [2] Jaoul *et al*. (1981), Anelasticity in the Earth, Geodyn. **4**, 95-100 [3] Kohlstedt (2006), Rev. in Min. & Geochem. **62**, 377-396. [4] C. Hegoda (2009), Ms thesis, Okayama Univ.

https://doi.org/10.1180/S0026461X00006502 Published online by Cambridge University Press

Efficient carbon leaching in silicate through fluid/melt migration and implications for diamond formation

YINGWEI FEI[1]*, CHI ZHANG[1] AND RENBIAO TAO[1,2]

[1]Geophysical Laboratory, Carnegie Institution of Washington, 5251 Broad Branch Road, NW, Washington, DC 20015, USA (*correspondence: fei@gl.ciw.edu)

[2]School of Earth and Space Sciences, Peking University, Beijing 100871, China

Natural diamond forms in silicate metrix at depths great than 150 km. Carbon concentration in the mantle is very low and there must be an efficient process to concentrate carbon to form diamond. Carbon-bearing fluids and carbonates are considered to be the major carbon sources for diamond formation, and their migration in silicate rocks at high pressure and temperature could provide important clues for understanding the mechanism of carbon enrichment during diamond formation.

Fluid and melt migrations in the mantle are droven by tempertaure/pressure and chemical gradients and gravity. High-pressure experiments in silicate-fluid and silicate-carbonate systems were performed to examine migrations of C-saturated fluid and carbonate melt in silicate matrix. We start with homogeneous mixture of amorphous carbon and silicate minerals (olivine or pyroxene). With presence of fluids, we observed efficient separation of graphite/diamond from its matrix and it concentrated at the end of the capsule. We further examined the effect of thermal gradient and gravity on the separation by a multiple-capsule techniqued.

Carbon can exist in its reduced (e.g., elemental C and CH_4) or oxidized (e.g., CO_2 and CO_3^{2+}) forms. Redox reaction plays an crucial role in diamond formation process. It is important to determine if carbon enrichment is more efficient in its reduced form than in its oxidized form. We examine the CO_2-rich melt distribution in solid silicate phase by SEM imaging and 3D tomography. The carbon enrichment through oxidized melt is not as efficient as in the form of elemental carbon, indicating that efficient diamond growth may require reduction of carbon to its reduced form first.

Upper crustal overprinting of lower crustal processes at Maipo Volcano (34˚10'S), Southern Volcanic Zone

MAUREEN D. FEINEMAN[1], DANA DREW[1], TIMOTHY MURRAY[1] AND PATRICIA SRUOGA[2]

[1]Pennsylvania State University, University Park, PA 16802, USA (mdf12@psu.edu, dld5066@psu.edu, ttm5055@psu.edu)

[2]CONICET-SEGEMAR, Av. J. A. Roca 651, Buenos Aires, 1067 ABB, Argentina (patysruoga@gmail.com)

The Diamante Caldera – Maipo Volcanic Complex is situated in the northernmost part of the Andean Southern Volcanic Zone (SVZ), upon ~50 km thick continental crust. Receiver function data suggest magma stalling at the base of this thickened crust in the northern SVZ [1], which is consistent with along-arc trace element variations that show increasing evidence for equilibration with garnet in basalts and basaltic andesites erupted to the northern end of the SVZ [2]. In a suite of basaltic andesite to dacite lavas sampled at Maipo, we observe clear evidence of assimilation and fractional crystallzation (AFC) processes in the upper crust, overprinted upon the lower crustal, presumably garnet-equilibrated trace element signature. The basaltic andesites are characterized by Sr/Y = 35-40, Eu/Eu* >0.85, $^{87}Sr/^{86}Sr$ = 0.7045-0.7050, and $^{144}Nd/^{143}Nd$ = ~0.5126. These chemical characteristics reflect a significant lower crustal input relative to basalts and basaltic andesites from the central and southern portions of the SVZ, which sit upon much thinner crust and are characterized by Sr/Y = 15-30, Eu/Eu* ≈ 1, $^{87}Sr/^{86}Sr$ = ~0.7040, and $^{144}Nd/^{143}Nd$ = ~0.5129 [3]. The Maipo data show continuous geochemical trends from the basaltic andesites to the dacites, which are characterized by Sr/Y = 14-24, Eu/Eu* ≈ 0.50-0.75, $^{87}Sr/^{86}Sr$ = 0.7054-0.7057, and $^{144}Nd/^{143}Nd$ = ~0.5125. These dacites are consistent with differentiation from the basaltic andesites by AFC with a plagioclase-rich crystallizing assemblage in an upper crustal magma chamber. Constant Gd/Yb (2.5-3.1) in the lavas may reflect a buffering effect of amphibole during differentiation, although it is rarely observed in the phenocryst assemblage. The high Sr/Y in the more primitive magmas, which suggests garnet fractionation at depth, has been erased in the more evolved magmas. Thus we note that the absence of high Sr/Y in intermediate arc magmas does not necessarily indicate that the magma did not interact with garnet at depth.

[1] Gilbert *et al*., (2006) *GJI* **165**, 383-398. [2] Hildreth and Moorbath, (1988) *CMP* **98**, 455-489. [3] Hickey *et al*. (1986) *JGR* **91**, 5963-5983

https://doi.org/10.1180/S0026461X00006502 Published online by Cambridge University Press

Metastable phase equilibria of the quaternary system KCl + K_2CO_3 + K_2SO_4 + H_2O at 273.15 K

S. FENG[1,2], Y. ZENG*[1,2], Z. L. CUI[1] AND X. D. YU[1]

[1]College of Materials and Chemistry & Chemical Engineering, Chengdu University of Technology, Chengdu 610059, P. R. China;

[2]Mineral Resources Chemistry Key Laboratory of Sichuan Higher Education Institutions, Chengdu 610059, P. R. China (*correspondence: zengyster@gmail.com)

The Zabuye salt lake, located in Tibet, is famous for its high concentration of lithium, potassium and borate. During the process of natural evaporation, metastable phenomena existed in different degree. The metastable phase diagrams are the basis of comprehensive utilization of saline lake brine. In this paper, the solubility of the system was measured at 273.15 K using an isothermal evaporation method.

Figure 1 is the metastable phase diagram of the system at 273.15 K. The diagram consists of three crystallization fields corresponding to single salts $K_2CO_3 \cdot 3/2H_2O$, KCl and K_2SO_4, respectively. There are three univariant curves corresponding to curves AE, BE and CE, indicating the cosaturation of two salts. Invariant point E is saturated with salts $K_2CO_3 \cdot 3/2H_2O$, KCl and K_2SO_4. The crystallization field of K_2SO_4 is the largest, and the crystallization field of K_2CO_3 is the smallest. These results indicate that salt K_2SO_4 is easy to be saturated and crystallized from the aqueouse solution coexisting with sulphate, chloride and carbonate of potassium.

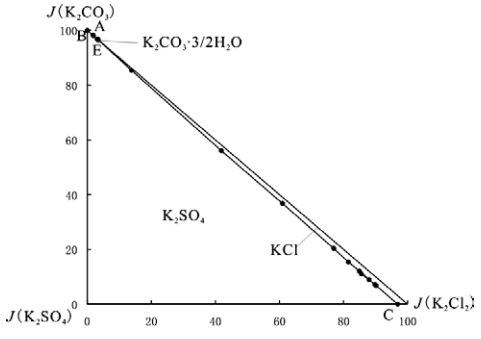

Figure 1. Metastable phase diagram of the quaternary system $K^+//Cl^-$, CO_3^{2-}, SO_4^{2-}-H_2O at 273.15 K

The authors acknowledge the support of the Program for New Century Excellent Talents in University (NCET-08-0900) and the National Nature Science Foundation of China (No. 40673050).

Comparing the fate of lignin in dissolved and particulate organic matter of Ganges–Brahmaputra river system

XIAOJUAN FENG[1]*, VALIER GALY[2], DANIEL B. MONTLUCON[3] AND TIMOTHY I. EGLINTON[4]

[1] Geological Institute, ETH Zurich, Switzerland & Dept. of Marine Chemistry & Geochemistry (MC&G), Woods Hole Oceanographic Institution (WHOI), Woods Hole, MA, USA (*correspondence: xfeng@erdw.ethz.ch)

[2] Dept. of MC&G, WHOI, Woods Hole, MA, USA (vgaly@whoi.edu)

[3] Geological Institute, ETH Zurich, Switzerland & Dept. of MC&G, WHOI, Woods Hole, MA, USA (daniel.montlucon@erdw.ethz.ch)

[4] Geological Institute, ETH Zurich, Switzerland & Dept. of MC&G, WHOI, Woods Hole, MA, USA (timothy.eglinton@erdw.ethz.ch)

Rivers deliver huge amounts of terrestrial organic carbon (OC) into oceans in both dissolved and particulate form. The fate of dissolved organic matter (DOM) and particulate organic matter (POM) may vary due to different degradation pathways and physical protection mechanisms. Determining the composition and residence time of DOM and POM during riverine transport is crucial for understanding the role of terrestrial OC in global carbon cycling. As a uniquely terrestrial biomarker, lignin serves as an effective tracer of vascular plant OM in river DOM and POM. While it has been established that lignin is a prominent component of POM and is widely dispersed by rivers, much less is known about the fate of lignin in the dissolved form. Here we investigate the abundance and composition of lignin-derived phenols in the DOM and POM from the Ganges-Brahmaputra river system. Lignin phenols were liberated from POM collected on filters and from DOM collected on C_{18} solid-phase cartridges using the CuO oxidation method. We compared the abundance, composition, and degradation stage of lignin phenols to assess lignin fractionation and degradation in the dissolved and particulate phases during the land-river transport. Furthermore, we collected large-volume samples of riverine DOM and POM in order to isolate sufficient quantities of lignin phenols by high pressure liquid chromatography for compound-specific radiocarbon and stable carbon isotopic analysis. The radiocarbon age of dissolved lignin versus lignin in sedimentary particles provides insights on the fate and transport of terrestrial organic matter within fluvial systems.

https://doi.org/10.1180/S0026461X00006502 Published online by Cambridge University Press

Provenance study of Swahili metals using lead isotopic analysis

T.R. FENN[1]*, D.J. KILLICK[1] AND J. RUIZ[2]

[1]Sch. of Anthropology, Univ. of Arizona, Tucson, AZ 85721, USA (*correspondence: tfenn@email.arizona.edu)
[2]Dept. of Geosciences, Univ. of Arizona, Tucson, AZ 85721

East Africa and Indian Ocean Trade

This research examines the provenance of non-ferrous metals found at East African Swahili sites dating from the late 1st and early 2nd millennium AD. Previous archaeological work on the Swahili Coast documented evidence of long-distance Indian Ocean maritime trade including imported objects from the Middle East, India and China [1, 2, 3]. Recent research has also examined the movement of specific commodities (e.g., ceramics, glass beads) from various regions of the Indian Ocean to the East African coast [4, 5].

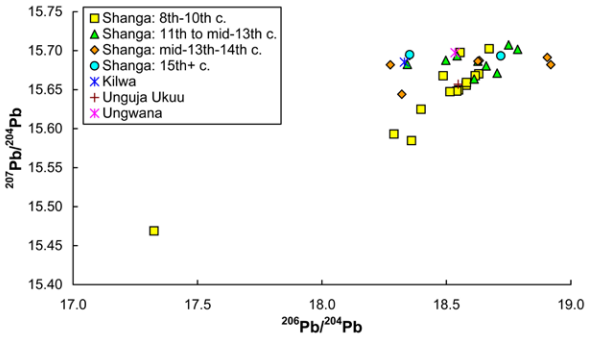

Figure 1: Lead isotopic ratios of non-ferrous metals from the Swahili sites of Shanga, Kilwa, Unguja Ukuu and Ungwana.

Metals Trade to the Swahili Coast

Very little research has been made on the movement of metals to the East Africa coast [6, 7]. The current research conducted elemental composition and lead isotopic analyses of more then 30 non-ferrous objects and has identified several different source regions supplied metal to the Swahili coast. Results indicate that Iran likely was a major source, but that metals also came from the Arabian Peninsula and China, but that none appear to have originated from India.

[1] Horton (1996) *Shanga*. [2] Chittick (1974), *Kilwa*. [3] Abungu (1998), *Transformations in Africa*, 204-218. [4] Kennet (2004), *Sasanian and Islamic pottery from Ras al-Khaimah*. [5] Dussubieux *et al*. (2008), *Archaeometry* **50**, 797-821. [6] Kusimba *et al*. (1994), *Society, Culture, and Technology in Africa*, 63-77. [7] Horton (1988), *Antiquity* **62**, 11-23.

Cation adsorption at the muscovite-electrolyte solution interface

P. FENTER[1]*, S.S. LEE[1], M. SCHMIDT[1], L. SODERHOLM[1], R.E. WILSON[1], C. PARK[2], K.L. NAGY[3] AND N.C. STURCHIO[3]

[1]CSE Division, Argonne National Laboratory, Argonne IL 60439 (*correspondence: Fenter@anl.gov)
[2] HP-CAT, Geophysical Laboratory, Carnegie Institution of Washington, Argonne, IL 60439,
[3]Dept. of Earth and Environmental Sciences, MC-186, University of Illinois at Chicago, Chicago IL 60607.

The interaction of ions with charged mineral surfaces is central to many geochemical processes, including the transport and bioavailability of dissolved species. The muscovite (001)-electrolyte interface is apparently simple, with a fixed lattice charge of the muscovite located below the surface and without under-coordinated surface oxygen sites that would lead to a strong pH dependent surface charge. Yet, we find that the adsorption structure of cations at this interfaces is unexpectedly complex.

Previously, we found that Rb^+ adsorbs in the ditrigonal site as an inner-sphere (IS) species, while Sr^{2+} adsorbs as both IS and outer-sphere (OS) species [1]. A systematic study of a range of divalent cations has shown that there exists a third adsorbed species, an extended OS species (OS_{ext}), and the partitioning between these three species is controlled by the cation hydration enthalpy [2]. Ongoing work has extended these observations to other multivalent ions (Y^{3+}, Th^{4+}) whose adsorption structure can be understood in the same context as that observed for divalent ions.

We have also explored the role of competitive adsorption to influence the distribution of adsorbed cations. Specifically we have found that the partitioning of cations between IS, OS and OS_{ext} species can change with the introduction of competing cations. Furthermore, the introduction of natural organic matter (in the form of dissolved fulvic acid) can dramatically alter the adsorbed cation distribution which is controlled by a balance between cation hydration, cation organophillicity, and cation-mineral interactions.

This work was supported by DOE/BES Geoscience Research Program (ANL and UIC) as well as the National Science Foundation (UIC). The Th results were supported by DOE OBER, NSF and EPA.

[1] C. Park *et al*. *Physical Review Letters*, **97**, 016101(1-4) (2006). [2] S. S. Lee *et al*., *Langmuir Letters*, **26**(22) 16647-16651 (2010).

https://doi.org/10.1180/S0026461X00006502 Published online by Cambridge University Press

Bioavailability of metals in a creek environment in Mumbai, India

LINA FERNANDES AND G. N. NAYAK

Department of Marine Sciences, Goa University-403206

A sediment core collected from Thane creek (north-east of Mumbai) in India was studied, with an aim to assess the degree of sediment contamination and bioavailability of metals. The concentration and chemical distribution of elements (Al, Fe, Cu, Cr, Mn, Co, Pb, Ni, Zn) along with speciation of selected metals was determined to know the extent to which selected elements were bioavailable and also to differentiate the anthropogenic metals from those of natural origin.

Geoaccumulation index computed for the studied elements, show Cu, Pb and Cr are moderately polluted. In accordance with these results, sequential extraction was carried out, to identify if Pb, Cr and Cu in the different sediment phases are bioavailable. From the results, for Cu, the order of percentage contribution is Residual (F5) >Fe-Mn oxides (F3)>organic/sulphide (F4)>carbonates (F2) >Exchangeable (F1), for Cr it is F5>F4>F3>F2>F1 which clearly indicates that, these metals are primarily immobile and have or bear the least bioavailability. For Pb it appears to be F5>F3>F4>F1>F2. Metals, especially of anthropogenic input, are expected to associate with the first four fractions and metals found in the residual fraction are considered to be of natural occurrence derived from the parent rock. For Pb, the percentage of the first two fractions (F1 & F2) are high when compared to first two fractions of Cu and Cr. F1 and F2 are very important from an ecotoxicological point of view because these are the fractions that are readily bioavailable to organisms that ingest sediments and hence can pose a health threat to the aquatic environment.

Use of CO_2/H_2O IRGA-based evolved gas analysis during thermal analysis of soil organic matter

JOSÉ M. FERNÁNDEZ[1], JOSEPH M. CRAINE [2] AND ALAIN F. PLANTE[1]

[1]Dept. of Earth and Environmental Science, Univ. of Pennsylvania, PA-19104, USA. (*correspondence: joseman@sas.upenn.edu, aplante@sas.upenn.edu)

[2]Div. of Biology, Kansas State Univ. KS-66506, USA (jcraine@ksu.edu)

Despite the increasing use of thermal analysis to characterize soil organic matter (SOM) in recent years, the exothermic region that represents the temperature range in which SOM is oxidized has not yet been equivocally defined.

In this study, surface soils from 28 sites across North America, ranging from Alaska to Puerto Rico, were analyzed in an oxidizing atmosphere (synthetic air, 30 mL min^{-1}) with a simultaneous thermal analyzer (thermogravimetry and scanning differential calorimetry) coupled to an infrared gas analyzer (IRGA) to measure CO_2 and H_2O gases evolved from thermal reactions.

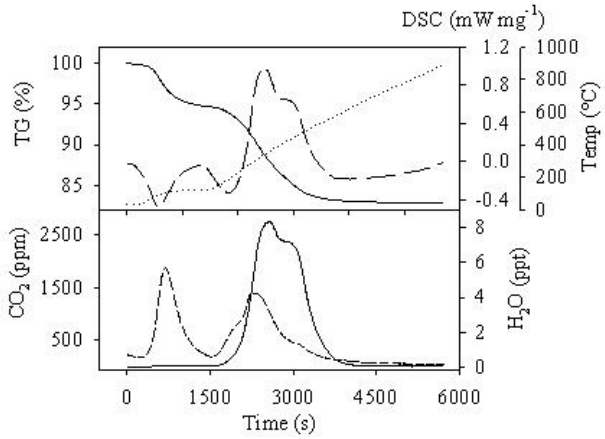

Figure 1: a) DSC (mW mg^{-1}), TG (%) and temperature (°C) of thermal analysis of a bulk soil sample, and **b)** evolved CO_2 (ppm) and H_2O (ppt) measured by IRGA.

Evolved CO_2 gas analysis suggests the onset temperature of the exothermic region was 256 ± 18 °C, though CO_2 evolution typically began near 125 °C. The endset temperature was typically 537 ± 36 °C, but varied widely due to the presence of pyrogenic C or carbonates. Defining the exothermic region is essential to characterizing SOM using thermal analysis.

https://doi.org/10.1180/S0026461X00006502 Published online by Cambridge University Press

Determining the influence of the mineral matrix on thermal analysis of soil organic matter in bulk samples

JOSÉ M. FERNÁNDEZ[1]*, CRAIG RASMUSSEN[2] AND ALAIN F. PLANTE[1]

[1]Dept. of Earth and Environmental Science, Univ. of Pennsylvania, PA-19104, USA. (*correspondence: joseman@sas.upenn.edu, aplante@sas.upenn.edu)
[2]Dept. of Soil, Water and Environmental Science, Univ. of Arizona, AZ- 85721, USA. (crasmuss@cals.arizona.edu)

Thermal analysis has the potential to analyze the quality continuum of soil organic matter (SOM) in a quick and inexpensive way, most importantly without pre-treatment of the sample [1]. However, many soil mineral components also exhibit diverse thermal effects. There are different reactions related with the soil mineral matrix (e.g., clay dehydration) that could interfere in the interpretation of thermogravimetry (TG) and differential scanning calorimetry (DSC) results, affecting both weight loss and energy flux measurements, and leading to an over- or underestimation of parameters initially assigned to the thermal oxidation of soil organic matter [2].

To study the effect of the mineral matrix on thermal properties of SOM, five forest soils from conifer ecosystems of the western U.S. with different mineralogy but similar clay to organic C ratios were selected. One aliquot of each soil was treated with HF (10%) to remove minerals, while a second aliquot was treated with NaOCl (6%) to remove organic matter. Bulk soil, HF-treated and NaOCl-treated samples were then analyzed using a simultaneous thermal analyzer under: i) an oxidizing atmosphere (synthetic air, 30 mL min^{-1}) to assess the combustion characteristics of the organic material, and ii) an inert atmosphere (N_2, 30 mL min^{-1}) that suppresses combustion but allows the observation of other thermal reactions. All samples were re-run after each analysis to establish a baseline thermal signature.

Results obtained allowed for quantification of the influence of the mineral matrix on different parameters estimated for the thermal decomposition of SOM in bulk soil samples, and support the hypothesis that on a per-mass basis, the thermal reactions of organic matter are significantly greater than those of the mineral fraction. Thus, only a moderate concentration of SOM is necessary for the mineral phase to have a negligible effects on the DSC signal of bulk soil.

[1] Plante *et al*. (2009) *Geoderma* **153**, 1-10. [2] Rovira & Vallejo (2000) *Commun Soil Sci Plant Anal* **31**, 81-100

Modelling of a bentonite column experiment with CrunchFlow including new clay-specific transport features

R. FERNÁNDEZ[1]*, U. K. MÄDER[2] AND C. I. STEEFEL[3]

[1]Departamento de Geología y Geoquímica, Facultad de Ciencias, Universidad Autónoma de Madrid, Campus de Cantoblanco, 28049. Madrid, Spain (*correspondence: raul.fernandez@uam.es)
[2]Institut für Geologie, Universität Bern, Batzerstrasse 1-3, CH-3012 Bern, Switzerland (urs.maeder@geo.unibe.ch)
[3]Earth Sciences Division, Lawrence Berkeley National Laboratory, One Cyclotron Road, M.S. 90-1116 Berkeley, CA 94720 USA (CISteefel@lbl.gov)

The porosity concept in bentonite has become an important issue since bentonite is foreseen as a confining and buffer material in high level radioactive waste repositories. The mechanisms associated to transport in the bentonite barrier play a critical role to characterize the chemical and mineralogical evolution of the repository near field.

As a consequence of the interest generated in the last years on this topic, the geochemical code CrunchFlow [1] has been recently implemented to take into account an explicit diffuse layer model associated to charged surfaces in clay systems.

A multi-component advective-diffusive ion transport experiment performed for 304 days at laboratory scale with a cylindrical column of a compacted MX-80 saturated bentonite was proposed as a benchmark experiment to test the new features in CrunchFlow. An artificial saline solution was infiltrated from one column end and the outflow solution was collected in syringes at the other end.

The Cl^- evolution in the experiment and the breakthrough of a non-reactive tracer were used to constrain the microporosity (diffuse layer) and macroporosity (free water) volume fractions and the transport parameters (advective flow rate and specific diffusion coefficients of aqueous species).

The chemical and mineralogical behaviour observed in the experimental system is rather complex. However, the model shows good agreement with the experimental results and demonstrates the relevance of the partition of the pore water in sub-volumes with different characteristics.

[1] Steefel (2009) CrunchFlow. Software for Modeling Multicomponent Reactive Flow and Transport. User's manual. Earth Sciences Division. Berkeley, CA. 91 pp.

https://doi.org/10.1180/S0026461X00006502 Published online by Cambridge University Press

Geochemical partitioning and mineral speciation of Zn in naturally metal-enriched soils of SW Spain

J.C. FERNANDEZ-CALIANI[1]*, I. GIRALDEZ[2], M.B. RIVERA[1] AND C. BARBA-BRIOSO[1]

[1]Dept. Geology, University of Huelva, Spain (*correspondence: caliani@uhu.es)

[2]Dept. Chemistry and Materials Science, University of Huelva, Spain

Some soils of the Sierra de Aracena (SW Spain) have been naturally highly enriched in Zn, and other metals, by intensive supergene alteration of sulphide-bearing parent rocks. The soils are mineralogically composed of illite, vermiculite, kaolinite, quartz, feldspars with minor hematite, and have a near neutral reaction (pH: 6.6-6.9).

Results from the BCR sequential extraction procedure modified by using focused ultrasound [1] showed that the vast majority of Zn was present in the residual immobile fraction of soils (F4, Table 1). The exchangeable fraction of Zn, assessed by single extraction with $MgCl_2$ and NH_4AcO, was found to be virtually negligible (< 1%). A SEM-EDS analysis hinted that Zn is hosted mainly in the crystal lattice of vermiculite (up to 0.37 pfu).

These findings conclusively indicated that potential mobility of Zn should remain low under the present soil conditions.

Samples	**FH-4a**	**FH-5a**
Total concentration in soil	7680	5540
Sequential extraction (in triplicate)		
F1 (HOAc 0.11 M, 7 min)	195±4	295±11
F2 ($NH_2OH.HCl$ 0.1 M, pH 2, 7 min)	572±23	610±21
F3 (H_2O_2 8.8 M, 2 min, 85° C + NH_4Ac O 1M, pH 2, 6 min)	254±30	265±19
F4 (HF+HNO_3+HCl digestion)	7032±75	4797±93
Total (Σ F1+F2+F3+F4)	8053	5967
Single extractions (in triplicate)		
$MgCl_2$ 1 M, 1 h	26.4±2.3	59.6±5.3
NH_4AcO 1M, 1 h	11.5±0.5	21.4±1.2

Table 1: Concentrations of Zn in soil samples and extract solutions, as determined by ICP-OES. All values are reported in mg kg^{-1}

[1] Pérez-Cid *et al*. (1998) *Anal Chim Acta* **360**, 35-41

An experimental study on the role of the tetrahedral SO_4^{2-}, CrO_4^{2-} and SeO_4^{2-} anions in the $CaCO_3$ polymorphism

ÁGELES FERNÁNDEZ-GONZÁLEZ[1,*], LURDES FERNÁNDEZ-DÍAZ[2], NURIA SÁNCHEZ-PASTOR[2] AND MANUEL PRIETO[1]

[1]Department of Geology, Universidad de Oviedo, Spain. (*correspondence: mafernan@geol.uniovi.es)

[2]Department of Crystallography and Mineralogy, Universidad Compltense, Madrid, Spain.

Crystallization in the $CaCO_3$–H_2O system is major topic, in a wide variety of disciplines, from geology and geochemistry to biomineralization and industrial crystallization. Although calcite is its most stable polymorph under Earth's surface conditions, $CaCO_3$ can precipitate as three different crystalline forms: vaterite, aragonite and calcite. Moreover, a number of hydrated and amorphous phases with different water contents can also precipitate. The nucleation and growth of metastable $CaCO_3$ polymorphs is commonly related to the predominance of kinetic factors over thermodynamic properties. The presence of different foreign ions in the fluid during $CaCO_3$ crystallization can also promote the formation of metastable phases. The possible incorporation of foreign ions into the structure of the different polymorphs would change their energetic properties and because the free energy of $CaCO_3$ polymorphs is relatively close, any modification of their energetic properties could determine stability crossovers that would affect the polymorph selection at nucleation and the development of transformations between polymorphs. Therefore, when foreign ions are present in the crystallization medium, both kinetic and thermodynamic factors have to be considered to understand the formation of $CaCO_3$. Recent studies have shown that tetrahedral anions like sulfate, chromate or selenate are among the most influential in the crystallization of $CaCO_3$, contributing to the stabilization of amorphous calcium carbonate in biogenic systems [1] or vaterite [2] in inorganic systems. We present here experimental results that illustrate the influence of some tetrahedral anions on the crystallization of $CaCO_3$ from aqueous solutions. These results include examples of unexpected polymorph formation and transformation pathways that carry the pass by of polymorphs.

[1] Gal A., Weiner S. & Addadi L. (2010*), J. Am Chem. Soc.* **132**, 13208-13211. [2] Fernández-Díaz L., Fernández-González A. & Prieto M. (2010), *Geochim. Cosmochim. Acta* **74** 6064-6076.

https://doi.org/10.1180/S0026461X00006502 Published online by Cambridge University Press

Water structure and hydration properties of imogolite nanotubes

A. FERNANDEZ-MARTINEZ[1], G.J. CUELLO[2], I.C. BOURG[1], M.R. JOHNSON[1], G.A. WAYCHUNAS[1], G. SPOSITO[1] AND L. CHARLET[3]

[1]Geochemistry Dept. Earth Sciences Division, Lawrence Berkeley National Laboratory, Berkeley, USA
[2]Institut Laue-Langevin, BP 153, Grenoble, France
[3]Environmental Geochemistry Group, LGIT-UJF, Grenoble, France.

Imogolite is a nanotubular aluminosilicate present in the clay fraction of volcanic soils. It has high specific surface areas (~500 m^2/g) and is one of the few minerals reactive towards both anions and cations under the same soil physico-chemical conditions, properties which make it an important constituent of the soils where it is present. However, precise determinations of imogolite structure and geochemical reactivity have been hindered by its nano-crystalline character. Structural analyses, until now, were restricted to standard X-ray and electron diffraction techniques, the diffraction peaks being used mainly as fingerprints for the identification of the mineral in soils. In this work, we present a detailed structural characterization of the structure of synthetic imogolite using high-energy X-ray diffraction (HEXRD), neutron diffraction with isotopic substitution (NDIS), transmission electron microscopy (TEM), and molecular dynamics (MD) simulation methods.

Theoretical and experimental investigations of the structure of water at the imogolite – water interface revealed the presence of highly structured water shells both at the surface and inside the nanotubes. We used these structural inputs to develop a geochemical multi-site complexation (MUSIC) model of the acidity of surface Al_2-OH groups on the external surface of imogolite and compared this to the acidity of similar sites on the equivalent (but planar) surface of gibbsite. This comparison yielded insights into the influence of surface curvature on mineral reactivity. Our MD simulations also probed the energetics of water adsorption and revealed that the external surface of imogolite is more hydrophobic than that of gibbsite. Ongoing work involving the use of inelastic neutron scattering also will be presented and discussed.

Anisotropy of magnetic susceptibility of Triassic Red Beds, Central Portugal

C. FERREIRA[1], C. GOMES[2]* AND H. SANT'OVAIA[3]

[1]DCT, Universidade de Coimbra, Portugal
[2]*CGUC, DCT, Universidade de Coimbra, Portugal (*correspondence: romualdo@dct.uc.pt
[3]Centro de Geologia da U. Porto, DGAOT, FCUP, Porto, Portugal.

Three sites in the Conraria and Castelo Viegas Formations, belonging to the "Silves Group" of Upper Triassic age, in the Coimbra region, central Portugal, were studied using the Anisotropy of Magnetic Susceptibility (AMS) methodology. The Conraria Formation is the lower unit and has mean thickness of 160 ± 15 m. The Castelo Viegas Formation is thicker (170-190 m) and the sediments are generally coarser and lighter than the sediments of the Conraria formation. The main goal of this study is to compare the AMS of the of the Conraria Formation, site A, with the two levels from the Castelo Viegas Formation, sites B and C. Site B is on a lower stratigrafic position than site C. AMS were carried out on 99 samples, 45 from site A, 10 from site B and 34 from site C. The magnetic susceptibility ranges between 40.6 and 239.7 x 10^{-6} SI in site A, between 64.4 and 100.0 x 10^{-6} SI in site C and between 51.5 and 58.4 x 10^{-6} SI in site B. Magnetic anisotropy (described by the parameter (kmax/kmin-1) x100) ranges between 0.4 and 8.3% in A, from 0.7 to 0.8 % in site C and between 2.3 and 3.0% in site B. The AMS ellipsoid is dominantly oblate in A and in site B, however site C present both oblate and prolate AMS ellipsoids. AMS fabric show different patterns in the studied sites: NW-SE subhorizontal magnetic foliations associated with subhorizontal N-S trending magnetic lineations in site A; N-S subvertical magnetic foliations associated to N-S trending magnetic lineations in site B; and scattered AMS ellipsoid axes in site C due to its lower anisotropy. Our results show that sites A and site C have higher magnetic susceptibility than site B which is related with mineralogical composition. Sites A and B have a magnetic foliation that probably underlines a primary sedimentary fabric however this foliation has tilted in site C. The N-S magnetic lineation probably materializes the paleocurrents. The general parallelism of the magnetic fabric with bedding indicates a composite fabric between a primary sedimentary fabric and an early tectonic event as is attested by the magnetic anisotropy of Conraria formation and site B of Castelo Viegas Formation.

https://doi.org/10.1180/S0026461X00006502 Published online by Cambridge University Press

Highly felsic peraluminous granitoids in the Borborema province, northeastern Brazil

V.P. FERREIRA[1], A.N. SIAL[1], M.A. PARADA[2] AND A.J. TOSELLI[3]

[1]NEG-LABISE, Dept. Geol. UFPE, Recife, Brazil (*correspondence valderez@ufpe.br)
[2] University of Chile, Santiago, Chile
[3]University of Tucuman, Tucuman, Argentina

Only few Neoproterozoic peraluminous granitoids occur in the oriental Borborema province, northeastern Brazil. Among these peraluminous granitoids are the two-mica Chã Grande (CHG), the two-mica Mamanguape (MAMA) that locally presents almandine, and the Ouro Branco (OBR) with three facies (two mica, tourmaline muscovite, and garnet muscovite) granitoids. The granitoids present A/CNK > 1.1, are silica-rich (70-76%, with narrower variation within individual pluton), have Rb/Sr >>2 and their chemistry form overlapping trends in most major oxide variation diagrams. Chondrite-normalized REE patterns are fractionated with variable negative Eu anomaly, both increasing from the CHG through OBR and MAMA. In a normative Qz-Or-Ab diagram, CHG compositions cluster about a minimum-melt composition typical of water-saturated granite system. Compositions of the other plutons form a spread suggestive of variable water activity, and distinct source compositions, with a trend from the field of orthoclase to the quartz-orthoclase cotectic for the MAMA, and a trend next to the albite-orthoclase cotectic to the minimum melt point for the OBR. Major- and trace-element compositions suggest that the OBR and MAMA granitoids formed by vapor-absent muscovite melting of felsic pelites and greywackes, respectively. The CHG granitoid was produced by vapor-saturated muscovite melting of greywackes. The granitoids present strongly negative $\varepsilon Nd_{0.6Ga}$ values (-12.8 – 16.6), and very high initial $^{87}Sr/^{86}Sr$ ratios (0.720-0.729), and Nd model ages Archean to Paleoproterozoic (3.1 to 2.3 Ga), the oldest T_{DM} already found in the Borborema province. These granitoids resemble Himalayan-type peraluminous collision-related leucogranites.

Atmospheric lead deposition in ombrotrophic peat bogs of Southern Poland

BARBARA FIAŁKIEWICZ-KOZIEŁ[1]*, NADINE MATTIELLI[2] AND NATHALIE FAGEL[3]

[1]Department of Biogeography and Paleoecology, Institute of Geoinformation and Geoecology, Adam Mickiewicz University, Poznań, Poland. (*basiafk@amu.edu.pl)
[2]Unité de recherche: "Isotopes : Pétrologie et Environnement", Département des Sciences de la Terre et de l'Environnement, CP 160/02, Université Libre de Bruxelles, Avenue FD. Roosevelt 50, 1050 Bruxelles, Belgium
[3]Department of Geology, AGEs Argiles, Géochimie et Environnements sédimentaires, Université de Liège, Allée du 6 août, B18, 4000 Liège, Belgium

The aim of this study was to differentiate anthropogenic *vs*. natural sources of lead in cores from two ombrotrophic peat bogs, located in Southern Poland. Total lead concentrations were measured by (ICP-AES) after HF-HNO_3-HCl digestion. Stable lead isotopes were measured by (MC-ICP-MS). A detailed age model was constructed using both ^{210}Pb and ^{14}C measurements.

The main results show a record of *ca*. 2000 years of variations in lead concentration and isotopic compositions. In the lowest part of the cores (IIthBC to IVth AD) the $^{206}Pb/^{207}Pb$ ratio equals 1.187. Historically it is a period of Celts and Przeworska culture. Lead isotope ratios point to possible impact of both cultures on the peat bogs. From Vth to VIth century AD, the $^{206}Pb/^{207}Pb$ ratio averages 1.192, reflecting that the Pb supplied to the bog is mainly originated from natural sources (*i.e*. erosion). Then, from the IXth to the XVIIth century AD, the $^{206}Pb/^{207}Pb$ ratio ranges from 1.176 to 1.179, which is in good agreement with Polish galena and coal from Eastern countries. A dramatic increase in lead accumulation rates during the 1920-1930's, it may reflect the higher metal demand for the armament industry, the influence of coal combustion and the latter use of leaded gasoline.

https://doi.org/10.1180/S0026461X00006502 Published online by Cambridge University Press

Partitioning of S(-Cl) and S-isotopes between fluid and andesitic melt

A. FIEGE[1]*, H. BEHRENS[1], C. MANDEVILLE[2] AND N. SHIMIZU[3]

[1]Institute for Mineralogy, Leibniz University Hannover, GER (*correspondence: a.fiege@mineralogie.uni-hannover.de)
[2]US Geological Survey, Reston, USA
[3]Woods Hole Oceanographic Institution, Woods Hole, USA

Isothermal decompression experiments were conducted at ~1030°C in IHPV. A hydrous S-(Cl-)bearing silicate melt with a composition close to Krakatau andesite was used as starting material. Pressure was released continiously from 400 MPa to 70 MPa using a novel type of automatic high-pressure valve. Decompression rates range from slow (~0.0005 MPa/s) to very fast (~0.1 MPa/s) and oxygen fugacity (fO_2) ranges from QFM+0.5 to QFM+3.5. The samples were directly quenched after decompression or further annealed for 1 to 48.5 h at final conditions. The partitioning coefficient of S between aqueous fluid and andesitic melt ($D_s^{fl/m}$) was determined by measuring S, Cl (EMP) and H_2O (FTIR) in the quenched glasses and subsequent mass balance calculations. SIMS was used to determine the isotopic abundance of sulfur ($\delta^{34}S_{melt}$) in the glasses. A suite of silicate standards with known $\delta^{34}S$ was used for SIMS calibration. XANES at ANKAs SUL-X beamline (Germany) was conducted to evaluate the sufur speciation in the experimental products.

For directly quenched samples, $D_s^{fl/m}$ was observed to increase significantly at QFM+0.5 from 59 ± 17 to 252 ± 103 with decreasing decompression rate (~0.1 MPa/s to ~0.0007 MPa/s). Upon further annaeling (1 to 48.5 h), at QFM+3.5 $D_s^{fl/m}$ decreases from 337 ± 124 to 24 ± 1. In addition, the molar $(S/Cl)_{fluid}$ ratio increases exponentially with increasing $(S/Cl)_{melt}$ at QFM+1.8. XANES measurements may have revealed significant amounts of H_2S in fluid inclusions at $fO_2 \leq$QFM+1.2 while at $fO_2 \geq$QFM+1.8 predominantly SO_2 seems to be present. Preliminary SIMS data indicates a major influence of fO_2 on fluid/melt fractionation of S isotopes upon degassing. $\delta^{34}S_{melt}$ decreases by 3.2-5.4 ‰ at QFM+1.2 and increases by 2.1-3.1 ‰ at QFM+3.5 if ~90% of the S in the melt is released. Thus, the isotopic fractionation is slightly larger than predicted by the model of de Hoog *et al*. [1] but in agreement with the data of Mandeville *et al*. [2] for oxidizing conditions. Hence, combining S and Cl data in volcanic gases with *in situ* sulfur isotope analyses might become a powerful tracer to forecast volcanic eruptions in near future.

[1] de Hoog, J.C.M., *et al*. (2001), *EPSL* **189**, 237-252. [2] Mandeville, C.W. *et al*. (2009), *GCA* **73**, 2978-3012

Rapid dyke emplacement as an eruption trigger Dabbahu Volcano, Ethiopia

LORRAINE FIELD, KATE SAUNDERS* AND JON BLUNDY

Department of Earth Science, University of Bristol, Wills Memorial Building, Queens Road, bristol, BS8 1RJ. (Lorraine.Field@bristol.ac.uk,* Kate.Saunders@bristol.ac.uk, Jon.Blundy@bristol.ac.uk)

Dabbahu is a quaternary, central volcano situated at the northern end of the Manda Hararo rift segment in the Afar region of Ethiopia. Magmatic rift segments have formed over the past ~3 Ma as faulting and volcanism have focused into localised regions [1]. In 2005 a small rhyolitic ash eruption and extrusion of a small pumice dome from the Da'Ure vent on the northern flanks of Dabbahu coincided with the largest dyke opening event ever measured [2].

Olivine crystals from an early 65 kyr basaltic flow at Dabbahu are composed dominantly of Mg-rich cores (700-1000 μm) with narrow (10-50 μm) Fe-rich rims. The timescale since the intrusion of this new magma batch and eruption was investigated by diffusion modelling of multiple elements (Fe-Mg, Mn, Ni and Ca) in four crystals. Olivine crystals were forward modelled from an initially homogenous composition using a semi-infinate open boundary, finite difference model for Fe-Mg, Mn and Ni, and where possible Ca. Co-existing clinopyroxene crystals indicate a magmatic temparature of ~1176°C. Calculated timescales from Fe-Mg (0.75-8.92 days), Mn (1.27 -4.05 days) and Ni (0.94-8.11 days) are all similar to each other, demonstrating the strength of this method and the short residence times of these crystals in the final magma after the growth of the Fe-rich rims.

Elevated seismicity associated with the 2005 dyke intrusion at Dabbahu volcano persisted for only 4.5 days before moving south [2]. These timescales are comparable to those obtained from olivine profiles in the > 65 kyr Dabbuhu eruption. We infer that the olivine crystals preserve an early record of dyke intrusion, during the initial shield building episode of Dabbahu volcano, similar to the 2005 event.

[1] Barberi and Varet, (1977), *GSA bulletin* **88**:1251-1266. [2] Wright, Ebinger, Biggs, Ayele, Yirgu, Keir & Stork (2006), *Nature* **442**:291-29.

https://doi.org/10.1180/S0026461X00006502 Published online by Cambridge University Press

Cloud-aerosol interactions in operational NWP: Presently simple, but the future is complicated

P.R. FIELD*, J. WILKINSON, B. SHIPWAY AND A. HILL

Met Office, Fitzroy Road, Exeter, EX1 3PB, UK
(*corresponence: paul.field@metoffice.gov.uk)

Met Office high resolution (dx=1.5, 4.0 km) operational forecasts over the UK and the wider North Atlantic (dx=12km) now couple a simple aerosol tracer to the warm cloud microphysics representation. The first part of the talk will review the performance of this implementation and briefly consider the effects on fog. More complex aerosol representations are now available within the MetOffice model and the second part of the talk will introduce our progress in coupling a new multimoment, multispecies microphysics to such representations. Our eventual goal is to determine what level of complexity is required in the representation of cloud-aerosol interactions to deliver improvements in NWP.

Determination of $\delta^{11}B$ ratios in marine biogenic carbonates via LA-MC-ICP-MS

J. FIETZKE[1]*, F. RAGAZZOLA[1], A. HEINEMANN[1], I. TAUBNER[1], F. BÖHM[1], J. EREZ[2], T.H. HANSTEEN[1] AND A. EISENHAUER[1]

[1]Leibniz Institute of Marine Sciences, IFM-GEOMAR, Kiel, 24148, Germany (* jfietzke@ifm-geomar.de)
[2]Institute of Earth Sciences, The Hebrew University of Jerusalem, 91904, Israel

A new in-situ method using LA-MC-ICP-MS for the determination of stable boron isotope ratios ($\delta^{11}B$) in carbonates was developed and recently published.[1] Data were acquired via a standard sample standard bracketing procedure typically providing a reproducibilty of 0.5 ‰ (SD) for samples containing 35 ppm of boron. A single ablation interval consumed about 5 μg of the sample corresponding to about 0.2 ng of boron.

The major analytical finding was the similar instrumental fractionation behaviour of carbonates, silicates and sea salt with respect to boron isotopes. As no matrix induced offset was detectable between these distinct materials we propose the use of NIST glasses as internal standards for boron isotope ratio measurements via LA-MC-ICP-MS. This finding overcomes the problem of a missing matrix matched carbonate standard for in-situ boron isotope studies.

As a first test application a set of coral samples from a culturing experiment was analysed. $\delta^{11}B$ values range from 19.5 – 25 ‰ depending on the pH of the water used in the particular treatment being in good agreement with the results of earlier studies. Further results from cultured marine calcifiers (e.g. bivalves and coralline red algae) will be presented.

[1] Fietzke *et al*. (2010) *J. Anal. At. Spectrom.* **25**, 1953-1957, doi: 10.1039/c0ja00036a

https://doi.org/10.1180/S0026461X00006502 Published online by Cambridge University Press

The geographic and stratigraphic record of Ordovician $\delta^{13}C_{carb}$ in outcrops and the subsurface of Anticosti Island, Canada

DAVID A. FIKE[1], DAVID S. JONES[1,2] AND WOODWARD W. FISCHER[3]

[1]Department of Earth & Planetary Sciences, Washington University, CB 1169, 1 Brookings Dr., St. Louis, MO 63130, USA. (dfike@levee.wustl.edu)
[2]Geology Department, Amherst College, Amherst, MA 01002, USA. (djones@amherst.edu)
[3]Division of Geological and Planetary Sciences, California Institute of Technology, MC 100-23, Pasadena, CA, 91125, USA. (wfischer@caltech.edu)

The Ordovician Period contains both an interval of intense biodiversification as well as one of the largest mass extinctions of the Phanerozoic. The latter, in particular, is associated with an interval of widespread glaciation across the southern supercontinent of Gondwana, together with the global Hirnantian $\delta^{13}C_{carb}$ positive excursion. Here we analyze the mixed carbonate-siliciclastic facies found in outcrops across Anticosti Island, Canada. These data allow us to generate a record of geographic and stratigraphic variability in Late Ordovician $\delta^{13}C_{carb}$ across Anticosti Island during this important interval of Earth history. High-resolution paired $\delta^{13}C_{carb}$ and $\delta^{13}C_{org}$ data both record the +4‰ Hirnantian positive isotope excursion and provide an independent measure of time for stratigraphic correlation [1]. Discontinuities in the isotope record at key lithologic transitions vary as a function of geographic location across the island, providing the foundation for a diachronous model of the deposition of the Hirnantian strata. Moving into the subsurface, we examine the record of Late Ordovician strata preserved in cores and well cuttings from multiple borehole locations across Anticosti island. These data reveal the presence of multiple $\delta^{13}C_{carb}$ excursions throughout the > 1 km of Late Ordovician strata in the subsurface, providing multiple new points for generating stratigraphic correlations across Anticosti Island and between other Late Ordovician locales.

[1] Jones, D. S., Fike, D. A., Finnegan, S., Fischer, W. W., Schrag, D., and McCay, D., 2011. Terminal Ordovician carbon isotope stratigraphy and glacioeustatic sea–level change across Anticosti Island (Québec, Canada). *Geological Society of America Bulletin* **in press**, doi:10.1130/B30323.1.

Antimony in the environment: The facts – or maybe not

M. FILELLA

Institute F.-A. Forel, University of Geneva, Route de Suisse 10, CH-1290 Versoix, Switzerland (montserrat.filella@unige.ch)

Antimony belongs to group 15 of the periodic table of the elements, along with N, P, As and Bi. It is ubiquitous throughout the environment as a result of natural processes and human activities and it has no known function in living organisms. After a long history of neglect as an element of environmental relevance, Sb attracted increasing public attention in the mid 1990s following a series of claims that it was involved in Sudden Infant Death Syndrome. It has remained a focus of considerable scientific research since that time and a substantial number of papers have now been published on the element and its behaviour in the natural environment.

However, a critical analysis of existing information, its sources, and the methods applied to obtain it [1-8], shows that, aside from a few well-established facts, many key aspects of the environmental chemistry of Sb remain poorly understood. Unfortunately, gaps in knowledge are too often hidden by a strong tendency to blindly reproduce some 'well-known' facts and references without looking them up or tracking down additional, more updated information. Well-focussed research, building on thorough knowledge of what is already known, will undoubtedly shorten the path towards a better understanding of Sb behaviour in environmental and biological systems. With this aim, this communication will discuss critical areas identified in [4], with special emphasis on the update of low temperature equilibrium and solubility data [9-11] and the description of antimony interactions with potential natural binders. Implications for the interpretation of existing ecotoxicity data and the prediction of the fate of antimony in water and soils will be critically presented.

[1] Filella *et al*. (2002) *Earth-Sci. Rev*. **57**, 125-176. [2] Filella *et al*. (2002) *Earth-Sci. Rev*. **59**, 265-285. [3] Filella *et al*. (2007) *Earth-Sci. Rev*. **80**, 195-217. [4] Filella *et al*. (2009) *Env. Chem*. **6**, 95-105. [5] Filella (2010) *Met. Ions Life Sci*. **7**, 267-301. [6] Belzile *et al*. (2011) *Crit. Rev. Env. Sci. Technol*. **41**, 1-65. [7] Filella (2011) *Earth-Sci. Rev*. doi: 10.1016/jearscirev.2011.04.002 [8] Filella *et al*. (2011) *Crit. Rev. Env. Sci. Technol*. (in press). [9] Filella *et al*. (2003) *Geochim. Cosmochim. Acta* **67**, 4013-4031. [10] Filella *et al*. (2005) *J. Environ. Monit*. **7**, 1226-1237. [11] Diemar *et al*. (2009) *Pure Appl. Chem*. **81**, 1547-1553.

Selenide retention by mackinawite: A multi-edge XAS approach

N. FINCK[1]*, K. DARDENNE[1] AND D. BOSBACH[2]

[1]Institute for Nuclear Waste Disposal (INE), Karlsruhe Institute of Technology (KIT), P.O. Box 3640, D-76021 Karlsruhe (*correspondence: nicolas.finck@kit.edu).
[2]Institute for Energy and Climate Research, Safety Research and Reactor Technology (IEF-6), Nuclear Waste Management, Forschungszentrum Jülich GmbH, D-52425 Jülich.

The fission product ^{79}Se ($T_{1/2} > 10^6$ a) is of concern for the safe disposal of High Level nuclear Wastes (HLW). The chemistry of selenium resembles that of sulfur, and the Se solubility is controled by its oxidation state. Ubiquitous in nature, iron sulfides are believed to control the *in situ* redox potential of most rock formations envisaged for the disposal of HLW. Under HLW repository relevant (reducing) conditions, Se may occur in low oxidation states. Robust structural data for selenide (Se(-II)) binding to mackinawite were obtained by collecting multi-edge XAS data.

Disordered mackinawite (FeS_{am}) was precipitated in the presence of Se(-II) (SeMack). XAS data were collected at the S, Fe and Se K-edge for SeMack, at the S and Fe K-edge for pure FeS_{am} and at the Fe and Se K-edge for FeSe. For each sample, the data were fit at all edges simultaneously. The (compelling) formation of a FeSe-like phase in SeMack is ruled out from the absence of detected neighboring Se atom in the Se first shell. In contrast, the detection of Fe neighbors at ~2.38 Å and higher distances S backscatterers strongly points to Se located in a FeS-like environment. Separately, selenide ions were contacted with pre-existing FeS_{am} in suspension (Se/FeS). Analysis of the Fe and Se K-edge XAS data reveals the presence of different crystal-chemical enviroments. The detection of Se neighbors in the Se first coordination sphere points to the presence of Se(0). The (compelling) presence of selenium in a FeSe-like environment is ruled out by the absence of higher distance Se backscatterer. In contrast, part of retained Se may be located in an environment close to that of SeMack. The presence of Se in a reduced form (0, -II) in SeMack and Se/FeS will ensure a low mobility in the near field of HLW disposal sites.

This multi-edge XAS approach places high confidence in the molecular scale process understanding of selenide binding to mackinawite.

Osmium, carbon and trace element investigations into archaeological material

A.J. FINLAY[1], J. MCCOMISH[2], R. BATES[3], D. SELBY[1]

[1]Department of Earth Sciences, Durham University, Durham, DH1 3LE, U.K. (a.j.finlay@durham.ac.uk)
[2]York Archaeological Trust for Excavation and Research Limited, 47 Aldwark, York, YO1 7BX, U.K.
[3]Department of Earth Sciences, University of St Andrews, North Street, St Andrews, Fife, KY16 9AL, U.K.

We present initial results from two studies investigating how the utilisation of Osmium (Os) and Carbon (C) isotope analysis as well as trace element geochemistry can be used to provide information on the source and manufacture of archaeological artifacts.

The first study comprises Os and C isotope analysis of drillings from an iron cannon from the pinnace Swann recovered off the Isle of Mull (Scotland). Os isotope analysis of the cannon provides a radiogenic $^{187}Os/^{188}Os$ ratio (0.825 ± 0.032) which has not been reset during casting. Therefore the $^{187}Os/^{188}Os$ ratio may be applied to identify the source of the ore. Furthermore the $\delta^{13}C$ ratio of the cannon (-30.3 ‰) is similar to charcoal and may reflect the use of charcoal as a reducing agent in the manufacturing of the cannon.

The second study (incorporating trace element and Os isotopic analysis of source clay, fired souce clay and Roman ceramic building material (CBM)) was undertaken to test how trace elements can be utilised to identify the centres of manufacture of tile. Aliquots of raw clay and fired clay as well as CBM samples from York (U.K.) and Carpow (Fife, U.K.) roman fortresses are geochemically indistinguishable, yet are distinct from the published literature. Therefore we believe that trace element geochemistry can be used to identify the centre of construction of CBM and so further understand trade networks within the roman world. Re-Os isotopic analysis of the CBM samples to further aid protolith identification is ongoing. Initial results show that the CBM contains Re and Os abundances similar to average upper continental crust, however, the $^{187}Os/^{188}Os$ ratio is very radiogenic (4.8 ± 0.8) and so may be useful in geochemically isolating CBM manufactured from different sources.

These studies demonstrate how combining isotopic and trace elemnt analysis can further our understanding of the source and manufacture of a wide range of archaeological material.

https://doi.org/10.1180/S0026461X00006502 Published online by Cambridge University Press

Paleohydrological communication between Baksa Gneiss and overlying Carboniferous sediments

KRISZTIÁN FINTOR

Univ. of Szeged, H-6701, P.O. Box 651, Hungary (efkrisz@gmail.com)

The investigated area the Baksa Gneiss Complex (BC) and its overlying Téseny Sandstone formation (TS) are located at the SW part of the Pannonian Basin near to the low and medium level nuclear waste disposal site (Mórágy Granite Formation) of Hungary. Quartz-carbonate veins of the BC and TS were analyzed by fluid inclusion micothermometry and stable isotope geochemistry in order to reveal the paleohydrological relationship between them.

Veins show rather similar features. In BC qtz→dol→cal1→cal2 is characteristic while in TS qtz→dolC→dolMn→dolFe sequence is typical. Results of microthermometry are also very similar. Quartz phases contain aqueous inclusions exhibiting H_2O-NaCl-$CaCl_2$ model composition. Calculated salinity varies within 20-25 wt% NaCl and 1-7 wt% $CaCl_2$, while T_h values are within 50-130 °C range. Primary inclusions in dol and dolC phases show H_2O-NaCl-$CaCl_2$ composition and high salinity is presumable from low T_m(Ice) data (-20 – -25 °C). T_h values are in a 90-180 °C range. Fluid captured in dolFe phase exhibiting different character with H_2O-NaCl composition and low 2.5 -5 wt% eq. NaCl salinity, T_h values are in a short 80-110 °C range.

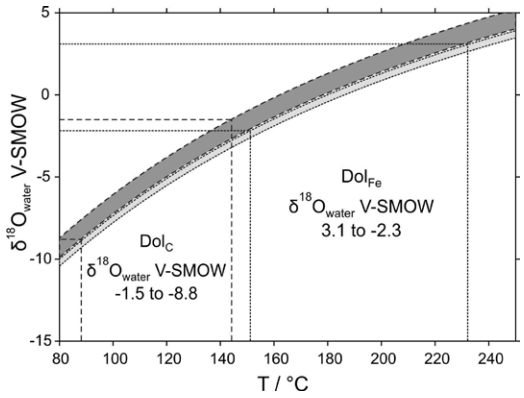

Figure 1. $\delta^{18}O$ signatures of pore fluids

The calculated $\delta^{18}O$ signature of the mineralizing fluid (Fig. 1.) (dolC: 3.1 – -2.3 $\delta^{18}O$ V-SMOW; dolFe: -8.8 – -1.5 $\delta^{18}O$ V-SMOW) together with fluid chemistry indicating paleohydrological communication between crystalline basement and sedimentary cover.

Evidence of water degassing in Archean Komatiites

M.L. FIORENTINI,[1], S.W. BERESFORD[1], W.E. STONE[2] AND E. DELOULE[3]

[1]Centre for Exploration Targeting, School of Earth and Environment, University of Western Australia
[2] Metals Exploration Division, North American Palladium Ltd., Toronto, Canada
[3]CPRG, CNRS, Vandoevre Les Nancy, France

Komatiites are ancient volcanic rocks, mostly over 2.7 billion years old, which formed through >30% partial melting of the mantle [1]. Establishing the volatile content of komatiites is crucial to constraining the thermal evolution of the Early Earth and its primordial atmosphere. The Agnew-Wiluna greenstone belt of Western Australia contains three co-genetic komatiite units that 1) display laterally variable volcanological features, including thick cumulates and spinifex-textured units, and 2) were emplaced as both lava flows and intrusions at various locations. 500m-thick komatiite sills contain widespread occurrence of hydromagmatic amphibole in orthocumulate- and mesocumulate-textured rocks, which contain ca. 40-50 wt% MgO and ≤3 wt% TiO_2. Conversely, komatiite flows do not contain any volatile-bearing mineral phases: ~150 meter-thick flows only contain vesicles, amygdales and segregation structures, whereas <5-10 meter-thick flows lack any textural and petrographic evidence of primary volatile contents.

Existing models on the thermal evolution of the Early Earth are mainly based on data from komatiite flows rather than intrusions [1]. In the Agnew-Wiluna greenstone belt, we hypothesize that the original volatile content of the flows was lost, but that of the sills was partially retained. Accordingly, evidence from komatiite flows in the Agnew-Wiluna greenstone belt does not necessarily reflect the total volatile content of parental komatiite magmas, because the flows, irrespective of their initial water content, have degassed upon emplacement and crystallization. Therefore, we suggest that evidence from komatiite intrusions worldwide should be considered along side with data from lava flows to evaluate the thermal architecture of the Early Earth and the complex chemo-physical zonation that occurred at the interface between water and seafloor in the primordial oceans.

[1] Arndt, N. T., Barnes, S. J. and Lesher, C. M. (2008). *Komatiite*. Cambridge: Cambridge University Press.

https://doi.org/10.1180/S0026461X00006502 Published online by Cambridge University Press

Melting of peridotite to 140 GPa

G. FIQUET[1]*, A.L. AUZENDE[1], J. SIEBERT[1], A. CORGNE[2], H. BUREAU[1], H. OZAWA[3] AND G. GARBARINO[4]

[1] IMPMC , UMR CNRS 7590, Université Pierre et Marie Curie, IPG Paris, 75252 Paris cedex 05, France (*correspondence: guillaume.fiquet@upmc.fr)
[2] Observatoire Midi-Pyrénées, CNRS, Université Paul Sabatier, 31400 Toulouse, France
[3] Earth and Planetary Sciences, Tokyo Institute of Technology, Tokyo, Japan
[4] European Synchrotron Radiation Facility, 38043 Grenoble cedex, France

Melting phase relations and major elements partitioning have been determined for a fertile peridotite (KLB-1) between 36 and 140 GPa. The experiments were conducted in diamond-anvil cells at the high-pressure beamline ID27 of the European Synchrotron Radiation Facility (ESRF) so as to use clear in situ melting criterion and to determine phase relationships from X-ray diffraction. Focused ion beam (FIB) sections of the recovered diamond-anvil cell samples were further investigated at the nano-scale by scanning and analytical transmission electron microscopy to check melting/crystallization sequences as well as variations of phase composition with temperature and pressure. Our results show that Mg-perovskite is the liquidus phase above 50 GPa, whereas ferropericlase is the solidus phase. Our results also yield strong constraints on the solidus curve of the lower mantle, which is measured at 4180 ± 150 K at core mantle boundary pressure. Since this value matches estimated mantle geotherms, molten regions may exist at the base of the present-day mantle. Melting phase relations and element partitioning data show that the produced liquids could be dense and host many incompatible elements at the base of the mantle. Such a melt could indeed segregate from the crystalline solids and accumulate at the core mantle boundary over time as fertile material passes through the boundary layer. Incompatible elements might accumulate in such a partial melt, and further add excess heat production to the melt piles at the base of the mantle. The data also allow us to constrain the way the putative magma ocean would have crystallized. The change in melting phase relations observed between 40 and 60 GPa indicates that a perovskite rich layer may be created in the mid-lower mantle during crystallization of this magma ocean whereas dense liquids having both a higher iron content and a higher oxide/perovskite content could sink to the core mantle boundary.

GIS based spatial distribution mapping for surface waters in Solaklı Basin (Trabzon, Turkey)

ARZU FIRAT ERSOY[1], FATMA GULTEKIN[1], ESRA HATIPOGLU[1] AND SECIL CELEP[2]

[1]Karadeniz Technical University, Engineering Faculty, Geological Engineering Department, 61080, Trabzon, Turkey (fatma@ktu.edu.tr, firat@ktu.edu.tr, hatipogluesra@gmail.com)
[2]Provincial Directorate Disaster and Emergency Management 53000, Rize, Turkey

Shortage of clean ground water to satisfy the need for drinking-potable water of increasing human population is one of the most significant problems encountered in today's world. On the other hand, surface water is contaminated due to lack of sufficient conservation. This study aims at revealing the current status of surface and groundwater in Solaklı (Trabzon) Basin by means of physical and chemical investigation. Quality assessment parameters are determined at 33 points in the basin with 2 points selected for groundwater and 31 points selected for surface water quality assessment. A Geographical Information System (GIS) tool was used to construct thematic maps for surface water quality in the Solaklı Basin. Water chemistry data were integrated and overall picture about the spatial variation in the surface water quality of Solaklı Basin was defined. While the amounts of the chemical components found in natural waters basins in don't vary considerably throughout the basin, amounts of pollutant parameters such as NO_2, NO_3 and PO_4 increase depending on the discharge of settlement areas. Surface waters in Solaklı basin are classified as high quality for many parameters according to criteria designated in Inland Surface Water Classification. Surface waters are classified as polluted water in terms of the Cu and NO_2^- values. Amounts of Mn and Ni in the Solaklı basin groundwater using as potable water for Of Town are found to be above Turkish Drinking Water Standards.

https://doi.org/10.1180/S0026461X00006502 Published online by Cambridge University Press

Integrating multivariate statistical analysis for geochemical assessment of groundwater quality in Gümüşhacıköy Plain (Amasya, Turkey)

ARZU FIRAT ERSOY, ESRA HATIPOGLU* AND FATMA GULTEKIN

Karadeniz Technical University, Depaertment of Geological Engineering, 61080, Trabzon, Turkey (*correspondence: hatipogluesra@gmail.com)

Groundwater is the main source for drinking water, agricultural and the industrial sector, the demand for water has increased over the years and led to water scarcity in all over the world. In the Gümüşhacıköy Basement, in the mid-northern part of the Turkey, agriculture is the most important mainstay and this area includes the most important agricultural areas of Turkey. The groundwater is extracted by wells drilled in the alluvium of the Gümüşhacıköy Plain to meet municipal, industrial and especially agricultural requirements. Factor analyses technique is useful in the analysis of groundwater data corresponding to large number of variables. Principal Component Analysis (PCA) performed on correlation matrix of the raw data in which a water sample is described by 15 physical and chemical parameters for 38 samples. The PCA produced 4 for significant component that explained 78 % of the cumulative variance. Piper and Chadha graphical methods were used to identify geochemical facies of groundwater samples and geochemical processes occurring in the study area. The water is mainly of Ca-Na-HCO_3 type.

Retention of colloids at rough rock surfaces

CORNELIUS FISCHER[1,2] GOPALA K. DARBHA[1] ALEXANDER MICHLER[1] AND THORSTEN SCHÄFER[3]

[1]GZG, Georg-August-Universität Göttingen, Germany; (cornelius.fischer@geo.uni-goettingen.de)
[2]Department of Earth Science, Rice University, Houston, TX, USA
[3]Inst. f. Nukleare Entsorgung, KIT, Karlsruhe, Germany

The retention of colloidal particles at mineral and rock surfaces is of fundamental importance for numerous processes, including trace metal and contaminant mobility, wastewater treatment, or diagenetic and weathering reactions. In nature, particle attachment conditions are often electrostatically unfavourable due to the pH-dependent mineral surface charge. In such cases, surface roughness of the collector surfaces may play an important role in governing the retention efficiency.

In this study, we compare the retention of colloids (polystyrene latex colloids [d = 1 μm] and hematite colloids [d = 0.95 μm]) at rough single mineral surfaces (quartz, albite, K-feldspar, biotite) and surfaces of mineral aggregates (Granodiorite from Grimsel test site, Switzerland). Surface roughness variations are in a range of 0.05 to 3 μm. Experiments were repeated under defined ionic strength variations. Particle retention experiments were performed at pH = 5.

Vertical Scanning Interferometry (VSI) was applied for characterization of surface topography, quantification of surface roughness, as well as quantification of colloid deposition. This method provides a large field-of-view that is sufficient to detect common inhomogeneities at mineral surfaces and to quantify their lateral extent. Application of so-called *converged* roughness parameters enabled the quantification of roughness differences at irregular surfaces.

A positive correlation between colloidal deposition flux (*Sh*) and surface roughness (*Rq*) of single mineral samples was observed for retention under unfavourable consitions. For granodiorite surface samples, however, the observed particle retention was tenfold higher. The experiments showed the quantitative and predictable impact of intergranular porosity as well as roughness variations caused by mineral aggregates on the retention of colloids.

https://doi.org/10.1180/S0026461X00006502 Published online by Cambridge University Press

Long-term CO_2-exposure experiments – Mineralogical results and reactive geochemical modeling

SEBASTIAN FISCHER[1,2] AND AXEL LIEBSCHER[1]

[1]Helmholtz Centre Potsdam, GFZ German Research Centre for Geosciences, Centre for CO_2 Storage
[2]Technical University of Berlin, Faculty VI, Working Group Mineralogy-Petrology

Rock core samples of the Upper Triassic Stuttgart Formation (saline aquifer) from the Ketzin pilot CO_2 storage site were exposed to pure CO_2 and synthetic reservoir brine at simulated reservoir P-T conditions (5 MPa, 40 °C). Autoklave reactors were opened and samples were taken after 15, 21, 24 and 40 months, respectively. The samples were then analysed mineralogically and geochemically and compared to baseline data of untreated samples. Rietveld refined XRD data show no significant trends for the studied intervals. On freshly broken rock fragments of the CO_2-treated samples, corrosion textures were found on plagioclase, K-feldspar and anhydrite surfaces. BSE images of the respective twin samples show (intensified) alterations of feldspar minerals. EMPA data display a change in the mineral chemistry of plagioclase, namely a preferred occurrence of sodium-rich endmember compositions after CO_2 exposure. Inorganic fluid data show, besides others, highly increased calcium, potassium and sulfate concentrations [1]. The experimental observations were reproduced using the reactive geochemical modeling code PHREEQC.

The mineralogical-chemical measurements imply preferred dissolution of calcium out of plagioclase (albitization) next to dissolution of K-feldspar and anhydrite. Due to the heterogenic character of the Stuttgart Formation, which formed in a fluvial environment [2], it is often difficult to distinguish between natural variability and CO_2-related changes. Additional profound evaluation is needed to interconnect the indicated changes during the experiments and to better understand CO_2-brine-rock interaction occurring within the Ketzin reservoir.

[1] Wandrey, *et al*. (2011). Monitoring petrophysical, mineralogical, geochemical and microbiological effects of CO_2 exposure – Results of long-term experiments under in situ condition. *Energy Procedia* **4**, 3644-3650, doi: 10.1016/j.egypro.2011.02.295. [2] Förster *et al*. (2006). Baseline characterization of the CO_2SINK geological storage site at Ketzin, Germany. *Environ Geoscience*, **13**, 3, 145-161.

A dynamic Archean sulfur cycle

W.W. FISCHER[1], D.A. FIKE[2], Y. GUAN[1], J.M. EILER[1], J.L. KIRSCHVINK[1] AND T.D. RAUB[1]

[1]California Insitute of Technology, Pasadena, CA, USA (wfischer@caltech.edu)
[2]Washington University, St. Louis, MO, USA (dfike@levee.wustl.edu)

Many aspects of the Earth's early sulfur cycle, from the origin of mass anomalous fractionations to the scale and degree of biological involvement, remain poorly understood. We have been studying the nature of multiple sulfur isotope (^{32}S, ^{33}S, and ^{34}S) signals using a novel combination of scanning high-resolution low-temperature superconductivity SQUID microscopy and secondary ion mass spectrometry (SIMS) techniques in a suite of samples from distal slope and basinal environments adjacent to a major Late Archean-age (~2.6-2.52 Ga) carbonate platform. Coupled with petrography, these techniques allow us to interrogate, at the same microscopic scale, the complex history of mineralization in samples containing diverse sulfide-bearing mineral components. Because of a general lack of Archean sulfate minerals, we focused our analyses on early diagenetic pyrite nodules, precipitated in surface sediments. This allows us to assay fractionations by controlling for isotope mass balance.

These rocks record meaningful differences in sulfur isotopic composition at microscopic scales. We observe large gradients in $\Delta^{33}S$ (> 5‰) over short length scales, pointing to substantial environmental heterogeneity and dynamic mixing of sulfur pools. Petrography and magnetic imaging demonstrate that these mass anomalous fractionations were clearly acquired prior to burial and compaction. We also commonly observed large radial $\delta^{34}S$ gradients (> 20‰) in nodules, from low values near their centers, increasing to heavier values near their rims. These observations imply that microbial sulfate reduction was a conspicuous metabolism during organic diagenesis in environments with particularly high rates of organic carbon delivery.

https://doi.org/10.1180/S0026461X00006502 Published online by Cambridge University Press

Age and nature of meteoritic components on the Moon

M. FISCHER-GÖDDE[1,2]* AND H. BECKER[2]

[1]Institut für Planetologie, Westfälische Wilhelms-Universität Münster
(*correspondence: m.fischer-goedde@uni-muenster.de)
[2]Institut für Geologische Wissenschaften, Freie Universität Berlin, Germany

Osmium isotopes and highly siderophile elements (HSE: Re, Os, Ir, Ru, Pt, Rh, Pd, Au) in ancient lunar impact rocks provide further constraints on ages and compositions of meteoritic materials accreted to the early Earth-Moon system. We report the first Re-Os isochron age on a lunar impact melt rock from Apollo 16 (67935, 4.21±0.13 Ga). The Re-Os age together with recent age data underscores the significance of pre 4.0 Ga basin forming impacts on the Moon. The new HSE data will be discussed along with previous precise data sets to identify specific impactor compositions and to evaluate mixing processes in ancient lunar impact rocks. Granulites from Apollo 16 and 17 (67915, 67955, 79215) display HSE ratios and $^{187}Os/^{188}Os$ largely similar to volatile element depleted carbonaceous chondrites. Apollo 16 impact melt rocks 60315 and 67935 show strongly fractionated HSE compositions with subchondritic Os/Ir, chondritic Re/Ir, and suprachondritic $^{187}Os/^{188}Os$, Ru/Ir, Pt/Ir, Rh/Ir, Pd/Ir and Au/Ir, similar to some IVA iron meteorites. Slightly suprachondritic ratios of $^{187}Os/^{188}Os$, Ru/Ir, Pt/Ir, Pd/Ir observed for Apollo 14 sample 14310 are similar to ratios observed for other Apollo 14 and and Apollo 17 poikilitic impact melt rocks. The Re-Os age of 4.2 Ga obtained on 67935 in combination with a previously reported Sm-Nd recrystallization age of 4.2 Ga for 67955, support previous notions that significant contributions of meteoritic material were supplied to the lunar surface before the 3.9-3.8 Ga basin forming era. Similar ages, but different HSE compositions of the meteoritic components in 67935 (iron meteorite-like) and 67955 (carbonaceous chondrite-like) indicate two different impact events on the Moon at ≥4.2 Ga. The occurence of granulites with similar composition at Apollo 15, 16 and 17, and the iron meteorite signature at Apollo 14, 15 and 16 suggests a wide dispersal of these compositions over the lunar nearside. Following this reasoning, the slightly subchondritic Os/Ir and slightly suprachondritic $^{187}Os/^{188}Os$, Ru/Ir, Pt/Ir and Pd/Ir of poikilitic Apollo 17 and Apollo 14 impact melt rocks may be explained by mixing 80-95% of a carbonaceous chondrite-like HSE end-member composition as indicated by the granulitic impact rocks (e.g. 67955) with 5-20% of a fractionated iron meteorite-like impactor composition as inferred from 67935 and 60315.

Silicon isotope evidence against an Enstatite Chondrite Earth

CAROLINE FITOUSSI*[1,2] AND BERNARD BOURDON[1,2]

[1]Laboratoire de Géologie de Lyon, Ecole Normale Supérieure de Lyon and UCBL, CNRS, France
(*correspondence: caroline.fitoussi@ens-lyon.fr)
[2]Institute of Geochemistry and Petrology, ETH Zurich, Switzerland

Enstatite chondrites are undifferentiated meteorites which formed at particularly reducing conditions as testified by the presence of Si in the metal phase. Enstatite chondrites are striking in having terrestrial compositions for several isotope systems such as O, Cr, Ti, and several others. Javoy *et al*. [1] interpreted these similarities as evidence for the Earth to be made of these chondrites. Silicon is particularly difficult to reconcile with this interpretation since it requires 28 wt% Si to be incorporated into the core which is way above the maximum Si core content (~7wt%). To get around this problem, a layered model with a Si-enriched hidden reservoir was proposed [1].

The silicon isotope compositions of enstatite chondrites and aubrites were measured on the MC-ICPMS Nu1700 at ETH Zurich. Bulk meteorites and separate enstatite minerals of the same meteorite were analyzed. The heaviest Si isotope composition was measured in an enstatite separate of an EH3 chondrite and gave $\delta^{30}Si$=-0.38 ± 0.03‰. Even in an extreme scenario of Earth's core formation in which (i) the accreting material is assumed to have a composition $\delta^{30}Si_{sil}$=-0.38‰ for its silicate phase (which is unlikely given that most bodies experienced thermal metamorphism or even metal-silicate differentiation, which would both give a lighter $\delta^{30}Si_{sil}$ ([2]; this study)) and (ii) there is no equilibration between metal and silicate during core merging of an impactor with the proto-Earth's core (e.g. [3]) (which is also unlikely given that it was shown that more than 36% of equilibration is necessary to account for both siderophile element abundances in the Earth's mantle and Hf-W data [4]), the resulting $\delta^{30}Si_{BSE}$ would never exceed -0.38‰. This is significantly lighter than the now agreed Si isotope composition of the Bulk Silicate Earth (BSE) $\delta^{30}Si_{BSE}$=-0.28‰ ± 0.03‰ [2; 5-6]. Therefore, while being quite intriguing meteorites from their similarities with the Earth, enstatite chondrites or aubrites cannot have been the material accreting the Earth.

[1] Javoy *et al*., *EPSL*, 2010; [2] Ziegler *et al*., *EPSL*, 2010; [3] Canup, *EPSL*, 2004; [4] Rudge *et al*., *Nature Geosci*., 2010; [5] Fitoussi *et al*., EPSL, 2009; [6] Savage *et al*., *EPSL*, 2010.

https://doi.org/10.1180/S0026461X00006502 Published online by Cambridge University Press

Apatite fission track and (U-Th)/He dating in the world's youngest UHP terrane: The Woodlark rift of southeastern Papuan New Guinea

P.G. FITZGERALD[1]*, S.L. BALDWIN[1], S.R. MILLER[1], T.A. LITTLE[2], L.E. WEBB[3], J.R. METCALF[1] AND S.E. PERRY[1]

[1]Syracuse University, Syracuse, NY 13244, USA (*corrspondence: pgfitzge@syr.edu)
[2]Victoria Univ., Wellington 6040, New Zealand
[3]Univ. of Vermont, Burlington, VT 05405, USA

Seafloor spreading in the Woodlark Basin of southeastern Papua New Guinea was underway by ~6 Ma and propagated westwards via stepwise spreading nucleation. Just west of the active seafloor spreading tip, extensional gneiss domes form topographic highs of the D'Entrecasteaux Islands (DEI) within the central portion of the Woodlark rift. Since ~8 Ma, HP and UHP rocks were exhumed rapidly from depths of up to ~100 km. Low-temperature thermochronology (apatite fission track (AFT) and apatite (U-Th)/He dating (AHe)) is used to constrain the late-stage exhumation histories in the DEI and conjugate rift margins of the Woodlark Basin. AFT ages generally decrease from ~8 Ma at Misima Island in the east, to between ~1.5 and 0.5 Ma in the DEI. AHe minimun ages similarly decrease to the west, from ~6 Ma at Misima Island to between 2.0 and 0.3 Ma within the DEI with ages youngest on Goodenough Island, the western-most DEI.

Higher temperature thermochronometers and exposure at the Earth's surface provide boundary constraints within which to interpret AFT and AHe results. Detailed age trends are difficult to establish due to the young age and low uranium concentrations resulting in few fission tracks plus small yields of radiogenic ^{4}He. ^{4}He concentrations in these recently and rapidly exhumed samples are often near background levels, and consequently difficult to accurately measure, making some ages unreliable and significantly increasing single grain age variation. We compare AFT ages and AHe ages to higher precision ^{40}Ar/^{39}Ar ages (e.g., biotite, K-feldspar) from the same samples in order to judge their reliability and reproducibility. Single grain AHe age variation is large with no apparent variation with respect to [eU], therefore the RDAMM model is not applicable in this case. In the absence of variable [eU] control, minimum single grain AHe ages are reliably closer to the "real" AHe ages, and it is these ages that show the westward younging pattern. Lithology also plays a strong role in the relative signal size; for example, higher [eU] from pegmatitic apatites give reliable ages whereas lower [eU] from a muscovite granite yields unreliable ages.

Dissolved iron partioning between soluble and colloidal fractions in the tropical North Atlantic Ocean

J.N. FITZSIMMONS AND E.A. BOYLE

Mass. Institute of Technology, E25-615, Cambridge MA 02139 (jessfitz@mit.edu)

Dissolved iron distribution and size partitioning were investigated in the tropical North Atlantic Ocean. "Dissolved Fe" (dFe, 0.4µm filtered) was collected along a 27-station transect to 1000m; "soluble Fe" (sFe, 0.02µm filtered) was collected at seven of those stations including one full depth station to 4370m at the transect's deepest point. "Colloidal Fe" (cFe) was defined as the difference between dFe and sFe. In the seven stations where Fe size partitioning was monitored, surface dFe ranged from 0.46 to 1.10nM and was dominated by cFe in all samples but one, averaging 81% (±7) of the surface dFe at these six stations. This reinforces the hypothesis that dust-derived dFe is preferentially distributed into the colloidal size fraction. At the two westernmost sites, a transition towards more subtropical gyre-like characteristics was observed (pycnocline extended to ~400m), and cFe maintained low values throughout the pycnocline (28±9%). sFe, in contrast, was relatively constant with depth directly below the pycnocline, averaging 0.51±0.04nM and 0.37±0.05nM between 500-1000m at the two western stations. From mid-basin to the eastern stations an oxygen minimum zone develops, and across the five stations where Fe size partitioning was monitored oxygen concentrations at 500m decreased from west to east from 105 to 48µmol/kg, increasing to 63µmol/kg at the easternmost station near the African continent. At the same time, there was a shift in the sFe distribution from fairly constant sFe with depth in the west/mid-basin to a strikingly regular peak in sFe at 500m in the OMZ of 0.70±0.01nM in the four eastern stations. In the OMZ, cFe was also high, contributing ~45% of the dFe at 500m. This OMZ peak in sFe was in contrast to the constant sFe profiles observed by Bergquist *et al*. [2] in the same OMZ, although their profile was on the western edge of the OMZ with lowest oxygen concentrations of only 100µmol/kg. Finally, North Atlantic Deep Water was seen in the deep profile from 1500-4370m. Average dFe was 0.79±0.06nM, slightly higher than the deep ocean value further north observed by Wu *et al*. [1] and further west and North by Bergquist *et al*. [2]. sFe was constant at 0.30±0.01nM throughout the NADW, occupying ~38% of the dFe present.

[1] Wu *et al*. (2001) *Science* **293**: 847. [2] Bergquist *et al*. (2007) *GCA* **71**:2960.

https://doi.org/10.1180/S0026461X00006502 Published online by Cambridge University Press

Megadroughts at the dawn of Islam recorded in a stalagmite from Northern Oman

D. FLEITMANN[1]*, R.S. BRADLEY[2], S.J. BURNS[2], M. MUDELSEE[3], H. CHENG[4,5], L.R. EDWARDS[4], A. MANGINI[6] AND A. MATTER[1]

[1]Institute of Geological Sciences and Oeschger Centre for Climate Change Research, University of Bern, Bern, Switzerland (*correspondence: fleitmann@geo.unibe.ch)
[2]Climate System Research Center and Department of Geosciences, University of Massachusetts, Amherst, USA.
[3]Climate Risk Analysis, Hannover, Germany
[4]Department of Geology and Geophysics, University of Minnesota, USA.
[5]Institute of Global Environmental Change, X'an Jiaotng University, Shaanxi, China.
[6]Heidelberg Academy of Sciences, Heidelberg, Germany.

To date, the late Holocene climatic history of Oman and the entire Arabian Peninsula is poorly understood due to the lack of well dated and highly resolved paleoclimate records. In order to fill this gap of knowledge an actively growing stalagmite (specimen H12) was collected from Hoti Cave located in northern Oman. Total annual rainfall in this area varies between 50 and 255 mm yr^{-1}, with more than 65% of total annual rainfall occurring between December and March. The chronology of stalagmite H12 is based on 24 Th-U ages, which indicate that H12 grew continuously during the last 2650 years. The H12 oxygen isotope record ($\delta^{18}O$) is based on 1345 measurements corresponding to a temporal resolution of around 2 years. The comparison of the H12 $\delta^{18}O$ record with meteorological data reveals that $\delta^{18}O$ values reflect the amount of precipitation.

The H12 $\delta^{18}O$ time series shows distinct centennial- to decadal-scale changes in the amount of precipitation. The most striking feature of the H12 isotope profile is a series of severe droughts between A.D. 500 and A.D. 1000, the most severe perennial drought is centred at around A.D. 530. During this time South Arabia experienced a series of profound societal changes, such as the collapse of the Himyarite Kingdom which was the dominant state in Arabia. Our stalagmite $\delta^{18}O$ time series from Northern Oman seems to support the hypothesis that the collapse of the 1500-year-old South Arabian civilizations and transition from the pre-Islamic to the Islamic era in the 6th and early 7th century A.D. may have been triggered by reoccurring severe droughts.

The role of siderophores and biofilm formation in phosphate acquisition and Pb release from pyromorphite by *Pseudomonas mendocina* bacterium

JUSTYNA FLIS[1,2]*, CAROLYN A. DEHNER[3], JENNIFER L. DUBOIS[3], MACIEJ MANECKI[1] AND PATRICIA A. MAURICE[2]

[1]Dept. of Mineralogy, Petrography and Geochemistry, AGH-University of Science and Technology, 30-059 Krakow, Poland, (*correspondence: flisjustyna@tlen.pl)
[2]Dept. of Civil Engineering and Geological Sciences, University of Notre Dame, Notre Dame, IN, 46556 USA
[3]Dept. of Chemistry and Biochemistry, University of Notre Dame, Notre Dame, IN 46556 USA

The phosphate-ammendment immobilization is recommended to be one Best Management Practice (BMP) to treat Pb contaminated soils. (USEPA, 2005). In this method the highly insoluble mineral pyromorphite (PY), $Pb_5(PO_4)_3Cl$ is formed. Despite the extreme insolubility of pyromorphite ($logK_{sp}$=-79.6), Pb has remained unexpectedly mobile at a number of remediated soils (SERDP 2008). The activity of the soil oragnisms is a potential cause of the secondary excesive pyromorphite dissolution and several mechanism that can play a role were identified.

In order to investigate the role of siderophores and biofilm formation by soil bacteria in Pb and P release from PY, two sets of the batch microbial growth experiments were carried out: 1 – bacteria were grown in a direct contact with the mineral surface; 2 – the access to mineral surface was limited to the bacteria by a use of dialyse membrane. In both experiments, the siderophore-producing *P. mendocina* bacterium and an engineered mutant of the species incapable of producing and releasing siderophores were used. P was the limiting nutrient and the synthesized crystals of pyromorphite were the sole source of phosphates in the experimental media. Both, the siderophore-producing wild type and the mutant were able to obtain P from PY. However, the association or attachment of the bacteria to the mineral surface appeared to be important for P acquisition. The OD of the bacterial suspension was two times lower when the microbial – mineral contact was limited. Pb release from PY was substantially greater in the presence of the siderophore-producing wild type than the siderophore(-) mutant and when the bacteria were capable to attach to the PY surface. This substantiates the role of siderophores and biofilm formation by bacteria in Pb remobilization from PY.

This work was supported by the research projects: N N307 101535 and N N307 771540, and the Fulbright Poland Advanced Research Grant.

https://doi.org/10.1180/S0026461X00006502 Published online by Cambridge University Press

Diffusion induced by pressure gradients in natural garnets

D. FLOESS*, L. BAUMGARTNER AND Y. PODLADCHIKOV

Faculty of Geosciences – University of Lausanne, CH
(*correspondence: david.floess@unil.ch)

Recently, we proposed that diffusion relaxation of major elements in garnet induces pressure gradients within the crystal [1]. This is based on the fact that the molar volumes of the garnet end-members vary roughly by 10%. Consequently, the re-equilibration of a zoned garnet by diffusion will produce pressure gradients due to the elastic (nearly isochoric) response of the crystal. Diffusion experiments [2], which show apparent uphill diffusion, were used to argue that such pressure gradients do exist and that ductile accommodation of volume changes only occured in the experiments at the highest temperature (1250 °C). We examined HP garnets with coesite inclusions in order to investigate the significance of this process for natural environments.

Whiteschists from the Dora Maira Massive in the Western Alps underwent eclogite facies metamorphism (3.3-4.3 GPa, 720-780 °C) during the Alpine event at 35Ma [3]. Coesite included in garnet ($py_{0.96}gr_{0.02}alm_{0.02}$) during the HP stage was partially transformed to quartz during the subsequent, rapid exhumation (from 3.5 to 1 GPa within 2 Ma [4]). Coesite is preserved by maintaining a high pressure on the inclusion wall due to the large volume change of the phase transition. The surface of the host garnet experiences a lower pressure controlled by the exhumation *P-T* path. This pressure difference should induce a diffusion of major elements in the garnet surrounding the inclusion. Element distribution maps show well-defined Fe-rich, Ca-poor halos surrounding the coesite-inclusions. The observed diffusion profiles are in agreement with predictions, assuming a positive ΔP around the inclusions. The measured diffusion lengths (40-150 μm) agree with simple diffusion models using published diffusion coefficients.

Thus, understanding the effect of pressure gradients on diffusion and, alternatively, the generation of pressure due to relaxation of chemical gradients by diffusion, is crucial for interpreting *P-T-t* paths of zoned minerals correctly.

[1] Baumgartner *et al*. (2010), *GSA meeting Denver*. [2] Vielzeuf & Saúl (2010), *CMP* 1-20. [3] Compagnoni & Rolfo (2003), *UHP Metamorphism - EMU notes 5*. [4] Rubatto & Hermann (2001), *Geology* **29**, 3-6.

Interaction of particulate pollution and precipitation

A.I. FLOSSMANN AND W. WOBROCK[12]

[1]Clermont Université, Université Blaise Pascal, Laboratoire de Météorologie Physique, F-63000 Clermont-Ferrand, France
[2]CNRS, INSU, UMR 6016, LaMP, F-63177 Aubière, France

In the litterature, numerous studies regarding a possible reduction of precipitation as a result of anthropogenic pollution have been published. A scientific review of the aerosol pollution impact on precipitation can be found in [1].

Often, these results were obtained by modelling exercises in an individual cloud using a simple dynamical framework. We have studied extensively the validity of the simple “air parcel” type assumption, in focussing on the particular role of supersaturation in a bin resolved microphysics model and a 3-D dynamics of an entire cloud. We could confirm a strong dependancy of the results on the dynamic framework used.

The results of parcel model studies seemed to indicate that increasing particulate pollution and decreasing solubility suppresses rain formation. In individual and short time cloud simulations this behaviour was confirmed in our 3D model studies. However, we could identify an important amount of particle processing by repeated super- and subsaturation cycles.

Thus, taking into account entire cloud fields over longer periods of time yields the strong spatial and temporal variability of the results with isolated regions of inverse correlation of the effects. Even though in general the expected behaviour was found, after several hours of simulation, the integrated precipitation of the more polluted cases caught up. This suggests that a changing pollution will affect the spatial and temporal pattern of precipitation, but will probably not reduce the overall long term precipitation amount which might be entirely governed by the moisture state of the atmosphere [2].

[1] Levin, Z., and W.R. Cotton (Eds.) (2009), Springer, 386pp.
[2] Flossmann, A. I. and W. Wobrock (2010) *Atmos. Res.* **97** , 4, 478-497

https://doi.org/10.1180/S0026461X00006502 Published online by Cambridge University Press

Pre-biotic organic matter from comets and asteroids

GEORGE J. FLYNN[1] AND SUE WIRICK[2]

[1]Dept. Of physics, SUNY-Plattsburgh, 101 Broad St., Plattsburgh, NY 12901 USA (george.flynn@plattsburgh.edu)
[2]CARS, University of Chicago, Chicago IL 60637 USA (swirick@bnl.gov)

Anders (1989) suggested interplanetary dust particles (IDPs), ~5 to 50 μm in size, delivered a layer of organic-rich material from asteroids and comets to the surface of the early Earth and proposed this organic matter may have been important for the origin of life. Recent modeling by Nesvorny and Jenniskens (2010) suggests >85% of the interplanetary dust results from fragmentation of Jupiter-family comets like 81P/Wild 2, sampled by NASA's Stardust spacecraft, and 26P/Grigg-Skjellerup, the target of a short stratospheric dust collection coinciding with the Earth's crossing of the dust steam from a recent outburst on that comet. Analyses of organic matter in Wild 2 samples was further complicated by organic contamination in the aerogel. Nonetheless, volatile aliphatic hydrocarbon, co-located with the particle tracks, but distributed out to several track diameters, was seen in some Wild 2 tracks by infrared spectral mapping. In addition, using carbon x-ray absorption near-edge structure spectroscopy, we detected several spectrally distinct C=C and C=O bearing organic phases spatially associated with surviving Wild 2 particles. We also analyzed particles from the Grigg-Skjellerup timed collection. These were collected from the stratosphere after relatively gentle deceleration, better preserving indigenous organic matter than for the Wild 2 particles. We found a diversity of mineralogies and elemental compositions and abundant organic matter, identified by detection of the aliphatic C-H_2 and C-H_3 functional groups, in particles from the Grigg-Skjellerup timed collection. The organic/silicate ratio in both the Wild 2 impactors and the particles from the Grigg-Skjellerup timed collection is significantly larger than in carbonaceous chondrite meteorites, which have reflection spectra very similar to C-type asteroids, the most common type of asteroid in the outer-half of the main-belt. This indicates both direct delivery by cometary impacts (Chyba *et al*., 1990) and accretion of cometary IDPs (Anders, 1989) contributed significant quantities of organic matter, including aliphatic hydrocarbons (C-H_2 and C-H_3), C=C (most likely C-rings), and C=O, to the surface of the early Earth. Further analysis should determine the abundance and speciation of N in this organic matter.

Fe isotopes and the contrasting petrogenesis of A-, I and S-type granite

J. FODEN[1], P. SOSSI[1,2] AND G. HALVERSON[3]

[1]School of Earth and Environmental Sciences, University of Adelaide, Adelaide, SA 5000, Australia
[2]Department of Earth and Planetary Sciences, McGill University, 3450 University Street, Montreal, Quebec, H3A 2A7, Canada
[3]Now at RSES , ANU Canberra

Our study of closed to oxygen differentiation of a tholeiitic dolerite sill [1], from mafic dolerite parent through to highly differentiated felsic granophyre, shows strong fractionation of the isotopic composition of iron with a strong positive correlation of δFe^{57} with $Fe^{3+}/\Sigma Fe$. Both initially rise during fractionation controlled by ferrous iron bearing phases (pyroxenes) and then fall abruptly after magnetite saturation is reached. This is consistent with the model of Dauphas *et al* [2] that assumes $\Delta^{57}_{Fe3+\,-\,Fe2+}$ =0.45‰.

Our new data from a range S-, I- and A-type (ferroan) granites from the Cambrian Delamerian orogen in South Australia [3] yields similar results to Dauphas and Freydier [4] and shows that the A-types have very heavy δFe^{57} values (0.3-0.45) whereas the I- and S-types tend to be less fractionated and lighter. These results suggest the ferroan A-types result from protracted closed magma chamber fractionation with delayed magnetite saturation. This is also consistent with their depletion in compatible elements (Mg, Ni and Cr) and enrichment in incompatibles (REE, U, Th). S- and I-types are generated at least in part by crustal partial melting, where the persistent buffering by restitic residual minerals and early magnetite or Fe^{3+}-rich biotite saturation prevents iron isotope fractionation.

[1] Sossi, Foden & Halverson, (2011) *EPSL* (in press). [2] Dauphas *et al*. (2009) *EPSL* **288**, 255-267. [3] Foden *et al*., (2002) *J.Geol Soc*, **159**, 601-621. Dauphas and Freydier Chem. Geol. **222** 132–147.

https://doi.org/10.1180/S0026461X00006502 Published online by Cambridge University Press

Exploring the mobility of actinyl ions in the biogeosphere: A spectroscopic and theoretical study of U(VI) complexes with organic phosphate groups

HARALD FOERSTENDORF[1]*, SATORU TSUSHIMA[1], SEBASTIAN BRÜNING[2] AND BO LI[1]

[1]Helmholtz-Zentrum Dresden-Rossendorf, Institute of Radiochemistry, Dresden, Germany (*correspondence: foersten@hzdr.de)
[2]University of Applied Science, Dresden, Germany

The high affinity of uranyl(VI) ions to distinct functional groups of biomolecules is considered to contribute decisively to the migration behaviour of these metal ions in the biogeosphere [1]. In particular, organic phosphate groups are predestined to form actinide complexes at a physiologically relevant pH level [2]. Because the phosphorylated sites of biomolecules often represent a key role in their proper physiological function, the study on the complexation is of great significance.

In this work, U(VI) complexes of phosphorylated amino acids, namely p-serine and p-tyrosine, were investigated by vibrational spectroscopy serving as model compounds for more complex systems. The spectra obtained demonstrate the high affinity of the actinyl ion to phosphate groups. Contributions from the carboxyl and amino groups to the U(VI) complexes can be neglected.

These results are compared with spectra obtained from our recent investigation with a naturally occurring highly phosphorylated protein, phosvitin [3]. The spectral homologies confirm the suggestion that U(VI) is preferentially bound by organic phosphate groups under physiologically relevant conditions.

The derivation of molecular structures from vibrational spectra can be supported by theoretical approaches, such as density functional theory (DFT) calculations. A series of calculations was performed to reproduce the vibrational spectral data focusing on the frequency range of the vibrational modes of the phosphate groups. A comparison with the experimental data provides additional structural information on a molecular level.

[1] Van Horn, J. D. *et al*. (2006) *Coord. Chem. Rev*. **250**, 765-775. [2] Barkleit, A. *et al*. (2008) *Dalton Trans*., 2879-2886. [3] Li, B. *et al*. (2010) *J. Inorg. Biochem*. **104**, 718-725.

Linking early atmospheric composition to volcanic degassing from a reduced mantle

STEPHEN F. FOLEY[1] AND MIKHAIL I. EREMETS[2]

[1] Geocycles Research Centre and Institute for Geosciences, University of Mainz, 55099 Mainz, Germany.
[2]Geocycles Research Centre and Max Planck Institute for Chemistry, Postfach 3060, 55020 Mainz, Germany.

The composition and chemical evolution of the atmosphere is inextricably linked to volcanic degassing, and so to the oxidation state of the upper mantle and long-term recycling of surface material into the mantle. Early warming of the Earth may be explained by a thick, N_2-rich atmosphere [1], but how the atmosphere came to be so N_2-rich has not been explained. Most information on the oxidation state of the mantle comes from oxygen barometry on mantle rocks, but with a bias in favour of continental mantle lithosphere, especially garnet peridotites. Cratonic mantle peridotites mostly formed in the late Archean, and information on their oxidation state is overprinted by the oxidizing effects of later melt infiltration. Correcting for this and the effect of pressure leads to the conclusion that the early mantle was more reduced than modern asthenosphere [2]. In reducing conditions, the speciation of carbon and nitrogen differs from modern conditions. Carbon occurs as CH_4 rather than CO_2 at mantle pressures, and nitrogen dissolves in melts as NH_2^- or NH_3 rather than N_2. The consequences for volatile solubilities in melts of the mantle are immense: the solubility of reduced carbon is <0.2 wt% in contrast to >20 wt% for CO_2 [3], whereas nitrogen solubility is 3-4 times higher in reducing conditions [4]. This means that early degassing was dominated by N_2 and H_2O, whereas CO_2 degassing first became important later in Earth history. Later loss of nitrogen from the atmosphere may have occurred by loss to space in the absence of a strong dynamo before 3.4 Ga [5] or by return to the mantle in subduction zones. Here, the mantle inventory of nitrogen in solid form may be higher than previously thought, as shown by the stability of solid polymeric nitrogen at lower mantle pressures [6,7].

[1] Goldblatt *et al*. (2009), *Nat Geosci* **2**, 891-896 [2] Foley (2011), *J. Petrol.* **52**, 10.1093/petrology/egq061 [3] Taylor & Green (1987), *Geochem. Soc Spec. Publ.* **1**, 121-138 [4] Mysen *et al*. (2008), *Am. Mineral.* **93**, 1760-1770 [5] Tarduno *et al*. (2010), *Science* **327**, 2138-1240 [6] Eremets *et al*. (2001) *Nature* **411**, 170-174 [7] Eremets *et al*. (2004), *Nature Materials* **3**, 558-563.

https://doi.org/10.1180/S0026461X00006502 Published online by Cambridge University Press

Chemical analysis of Saharan dust in marine aerosols

K.W. FOMBA*, K. MÜLLER, T. GNAUK AND H. HERRMANN.

Leibniz-Institut für Troposphärenforschung, Permoserstr. 15, 04318 Leipzig, Germany
(*correspondence: Fomba@tropos.de)

The interaction between the ocean and the atmosphere is very important in understanding various factors that control the global climate. Amongst others, mineral dust deposition onto the oceans plays a vital role. Understanding the influence of mineral dust onto the ocean requires adequate information about its chemical composition.

The chemical composition of marine aerosols at the Cape Verde Atmospheric Observatory has been analyzed. The data were collected during six intensive field campaigns and continuous measurements from January 2007 until date. For the collection of samples, a high volume DIGITEL DHA-80 sampler (PM_{10}-inlet) was routinely operated throughout the year in a 72 h- sampling period collecting particles on 150 mm quartz fiber filters. In addition, a five-stage BERNER impactor with a PM_{10} cutoff (0.05-10 μm size range) was used to collect size-resolved samples. The samples were analyzed for ions, OC/EC and trace metals.

Our observations show both Saharan dust and marine influenced air masses. Air masses with Saharan dust storms contained significant amounts trace metals and organic carbon compared to marine air masses. Dust events were observed mostly during the winter months of the year. During the events, the contribution of sea salt to the total PM_{10} mass was found to be low. The sea salt and Saharan dust in the particle were found in the coarse mode fractions while the organics and non sea salt components were observed mostly in the submicron fraction.

Significant differences were observed in the trace metal composition (especially iron) between days of Saharan dust outbreak (about 4.2 Fe, 3.4 Ca, 0.3 Ti, and 0.1 Mn $\mu g/m^3$) and days without (less than 1.0 ng/m^3), confirming that the Sahara desert is an important source of trace minerals in this region of the tropical Northern Atlantic. Typically, ions contributed about 55 % to the PM_{10} mass but decreased to a minimum of about 7% during dust episodes. OC and EC were found in very low concentrations except during dust events where the concentration increase by about a factor of five due to the influence of air masses from the African continent.

Timescale of quartzarenite xenoliths assimilation by trachybasaltic melt: Case of 2001 Etna eruption

I.S. FOMIN* AND P.YU. PLECHOV

Lomonosov Moscow State University, Russia
(*correspondence: fomin@web.ru, pavel@web.ru)

Lavas of Etna 2001 eruption contain abudant quartzarenite xenoliths.

According to [1] and [2] we can suppose, that xenolith's source is located between 0 and 3 km b.s.l. Seismic data and direct observation [3] give us 12-19 days for magma to go through this layer and to stream out of vent. Reaction rims between xenolithes and host rock have width up to 300-500 μm, which give us time of interaction as 12-19 days ([4],[5]).

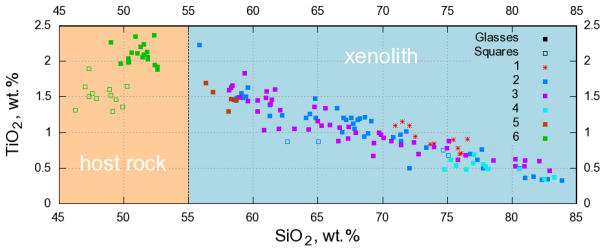

Figure 1: TiO_2 content in xenolithes (1 – inner parts; 2 – cracks in xenolith's surface with host rock groundmass penetration; 3 –near edge; 4 – near neogenic quartz dendrites) and host rock (5 - mingled zone near xenolith; 6 – outside xenolith). Filled squares for glass, open squares for square analyses.

A sample plot for compositions of glasses and whole-rock squares inside and outside xenoliths is presented on Fig.1. Analyses for host rock give us single clouds of compositions for all elements. We suppose, that 0-200 μm mingled zone is insignificant. In xenoliths we estimated good linear mixing trend. Sharp border between two mediums give us significant gap in SiO_2 content.

We conclude, that influence of assimilation on melt composition is insignificant in comparison with crystal differentiation.

[1] Cristofolini *et al*. (1979) *Boll. Soc. Geol. Ital*. **98**, 239-247. [2] Bonforte *et al*. (2009) *Tectonophys*. **471**, 78-86. [3] Viccaro *et al*. (2008) *Per. Min*. **77**, 21-42. [4] Donaldson (1985) *MinMag* **49**, 683-693. [5] Watson (1982) *Cont. Min. Petr*. **80**, 73-87.

https://doi.org/10.1180/S0026461X00006502 Published online by Cambridge University Press

Experimental constraints on the development of Os isotopic heterogeneity in the Earth's mantle

RÁUL O. C. FONSECA*, AMBRE LUGUET, CHRIS BALLHAUS AND FLORIAN POHL

Steinmann Institut, Universität Bonn, Germany (*correspondence: raul.fonseca@uni-bonn.de)

Owing to differences in compatibility between Re and Os, the decay of ^{187}Re to ^{187}Os is an exceptional tracer of melting in the Earth's upper mantle. There is a wide consensus that the mantle displays Os isotopic heterogeneity at the grain scale, which is exemplified by large variations of ^{187}Os/^{188}Os in oceanic basalts. The decoupling of the Re-Os isotopic system during partial melting of the mantle, is thought to be associated with alloy/sulfide equilibrium at high temperature. Alloys remain at the source and develop non-radiogenic Os isotopic ratios, as they have very low Re/Os. On the other hand, sulfides have high Re/Os and develop more radiogenic ^{187}Os/^{188}Os over time. However, not much is understood on the timing and conditions at which the de-coupling of the Re-Os isotope system takes place. Alloy model ages calculated using Os isotopes can be as old as 4.1Ga. The relative long-lived nature of these alloys implies that these phases are extraordinarily resilient to isotopic re-equilibration despite being hosted by mantle lithologies. Sulfides on the other hand, are broadly younger than alloys and are vulnerable to low-T metasomatic re-equilibration.

In order to provide constraints on the high-T stability of Os-rich alloys, we have carried out piston-cylinder experiments where variable proportions of Re, Os and Ir were equilibrated with FeS at temperatures ranging between ~1800 and ~2000K and constant pressure (15 kbar). Experiments were carried out in closed graphite capsules, with oxygen fugacity buffered near the C-CO redox buffer. Results show that Re, Os and Ir form an almost complete solid solution in the alloy at temperatures exceeding 1900K. At T lower than 1900K, a miscibility gap develops in the Re-Os-Ir-Fe-S and run products consist of a Re-rich sulfide melt, an OsIrFe alloy and a discrete Re alloy phase. We also show, that depending on the initial proportions of Re, Os and Ir in the charge, alloy-sulfide pairs will develop different ^{187}Os/^{188}Os over time.

Our results preclude equilibration of Os-rich alloys in the mantle at temperatures exceeding 1900K, as alloys would be richer in Re, which is not the case for natural alloy compositions. Furthermore, we show that alloys have to be isolated from mantle sulfides for up to several billion years, with implications to our understanding of mantle convection.

The fate of sorbed contaminants during the biogeochemical cycling of iron in natural environments

D. FORTIN

Dept, Earth Sciences, University of Ottawa, 140 Louis Pasteur, Ottawa, ON, Canada, K1N 1J6, (dfortin@uottawa.ca)

Bacteriogenic iron oxides (BIOS) naturally occur in a wide range of environments, including wetlands, hydrothermal sea vents and hot springs. BIOS are essentially composed of neutrophilic iron-oxidizing bacteria and poorly ordered iron oxides, such as ferrihydrite. Given their high surface reactivity and surface area, they have been shown to be efficient sorbents of aqueous contaminants. The present study investigates the redox stability of naturally occurring BIOS and the fate of their sorb contaminants (As and Sr). Results indicate that BIOS samples (composed of ferrihydrite and smaller amounts of lepidocrocite and goethite) from a wetland area and gold mine tailings undergo rapid microbial reduction in the presence of a well known iron-reducing bacterium (i.e., *Schewanella putrefaciens*CN32). In fact, the reduction rates observed for the various BIOS samples far exceed those of synthetic iron oxides (ferrihydrite). The results also show that the presence of sorbed Sr and As (present as outer-sphere and inner-sphere complexes, respectively) stabilizes BIOS during microbial reduction by blocking reactive sites onto the iron oxides. Finally, the fate of Sr and As during reduction mirrors that of Fe(II), suggesting that all sorbed contaminants are likely sorbed onto the iron oxides.

https://doi.org/10.1180/S0026461X00006502 Published online by Cambridge University Press

Optimization and application of engineered nanocrystalline iron oxides (nMAG) for uranium analysis in environmental samples

JOHN D. FORTNER

Department of Energy, Environmental and Chemical Engineering, Washington University in St. Louis, Brauer Hall, Campus Box 1180, One Brookings Drive, St. Louis, Missouri 63130, (jfortner@seas.edu)

Here, we demonstrate optimization and application of engineered, monodispersed, nanoscale iron oxide particles (termed nMAG) as concentration/seperating agents for uranium analysis in aqueous samples. Taking advantage of favorable sorption chemistries, sorbed uranium (as uranyl species) can reach >25% by weight associated with nanoscale magnetite particles (12 nm) which are surface stabilized with an oleic acid bilayer. Because these materials exhibit strong, permanent magnetic properties, they can be selectively removed from complex samples using magnetic fields resulting in high (uranium) concentration factors. Furthermore, as these materials are surface stabilized and monodispersed, dense and extremely thin films can be formed minimizing the self-absorption of α-particle emission from uranium isotopes. Taken together, engineered material features enhance uranyl detection (via α-counting) by over 1000 times when compared to a commercial available, aggregated, "nanoscale" iron oxide.

The relationship between ice volume, CO_2 and climate in the Middle Miocene

GAVIN L. FOSTER[1]*, CAROLINE H. LEAR[2] AND JAMES W.B. RAE[3]

[1]School of Ocean and Earth Science, National Oceanography Centre, Southampton, Southampton, (*correspondence: gavin.foster@noc.ston.ac.uk)

[2]School of Ocean and Earth Sciences, Cardiff University, Cardiff, LearC@cardiff.ac.uk

[3]Bristol Isotope Group, Department of Earth Sciences, University of Bristol, Bristol, James.Rae@bristol.ac.uk

The global cooling from the early Cenozoic ice-free world (~50 Ma) to today's bipolar icehouse world has long been ascribed to declining levels of CO_2 [1]. This overall cooling trend is recorded by a ~4 ‰ increase in deepwater benthic foraminiferal $\delta^{18}O$ values, which reflects both a ~12 °C cooling of bottom waters, and the formation of Earth's continental ice caps. Roughly half of this signal (a ~2 ‰ increase in benthic foraminiferal $\delta^{18}O$) occurs between the Miocene Climatic Optimum (~16 Ma; MCO) and today, including a ~1 ‰ step marking the Middle Miocene Climate Transition (MMCT) at ~14.5 Ma. The MMCT is thought to coincide with the expansion of the Antarctic ice sheet, changes in ocean circulation patterns, and a ~50 m lowering of global sea level. Although most pCO_2 reconstructions display an overall decline through the early Cenozoic, there is little agreement between them for this crucial period and estimates of pCO_2 during the middle Miocene are either higher (stomatal index [2]), lower (boron isotopes in foraminifera [3]), or around the same [4] as the pre-industrial. This has led to suggestions that either existing proxy records are flawed, or climate and pCO_2 have been decoupled for some portions of Earth's history [4] with uncertain implications for the prediction of future climate change. Here we use boron isotopes in planktonic foraminifera to show that the MCO was associated with elevated pCO_2 and that drawdown from this maximum was related to orbitally-paced organic carbon burial during the MMCT. Contrary to previous studies (e.g. [4]) our new boron based pCO_2 record therefore reaffirms the link between CO_2, climate and the cyrosphere for this important part of the Cenozoic.

[1] Berner *et al*. (1983) *Am. J. Sci*., **283**, 641-683. [2] Kürschner, *et al*. (2008) *PNAS*, **105**, 440-453. [3] Pearson & Palmer (2000) *Nature*, **406**, 695 - 699. [4] Pagani *et al*. (1999) *Science*, *285*, 876-879.

https://doi.org/10.1180/S0026461X00006502 Published online by Cambridge University Press

Quantifying ocean acidification during the Palaeogene hyperthermals

L.C. FOSTER [1]*, D.N. SCHMIDT[1], A. RIDGWELL[2] , E. THOMAS[3], C.D. COATH[1], R. HINTON[4] AND T.B. SCOTT[5]

[1]University of Bristol, Department Earth Sciences, BS8 1RJ, Bristol, UK, (*correspondence: l.c.foster@bristol.ac.uk, D.Schmidt@bristol.ac.uk)
[2]School of Geographical Sciences, University of Bristol, BS8 1SS, UK (andy@seao2.org)
[3]Department of Geology & Geophysics, Yale University CT 06520-8109, USA (ellen.thomas@yale.edu)
[4]Grant Institute, The King's Buildings, West Mains Road, Edinburgh EH9 3JW, UK (Richard.Hinton@ed.ac.uk)
[5]Interface Analysis Centre, University of Bristol, BS2 8BS UK (T.B.Scott@bristol.ac.uk)

Palaeogene hyperthermals are associated with rapid negative Carbon Isotope Excursions (CIE) and global warming and hence may provide an analogue for future ocean acidification. We present $\delta^{11}B$ (pH), Mg/Ca (temperature), B/Ca (carbonate ion concentration) and wall thickness data from the benthic foraminifer *Oridorsalis umbonatus* to study the extent of the change in the carbonate system and the calcification response. In addition, we present Electron Backscatter data to assess preservation and diagenetic alteration.

Our study examines both the temporal and geographical response of ocean acidification during Palaeogene hyperthermals. For the former we present data from Walvis Ridge (1262, paleodepth 3500 m) for three proposed paleo-ocean acidification events: Early Late Palaeocene Event (ELPE), Paleocene-Eocene Thermal Maximum (PETM) and ELMO (59- 53 Ma). These events differ in the extent of carbonate dissolution and thus allow us to study the relative changes in ocean carbonate chemistry. We also present a detailed study of the PETM across a range of sites on Exmouth Plateau (762), Kerguelen Plateau (1135) and a shallower site on Walvis Ridge (1263, paleodepth 1500 m) to determine the global response.

Spatial and temporal tritium variability at Vostok station

E. FOURRE[1]*, P. JEAN-BAPTISTE[1], J.R. PETIT[2], V. LIPENKOV[3], R. WINKLER[1] AND A. LANDAIS[1]

[1]LSCE, CEA-Saclay, 91191 Gif-sur-Yvette, France (*correspondence : Elise.Fourre@lsce.ipsl.fr)
[2]LGGE, CNRS-UJF, 38402 St Martin d'Hères, France
[3]Arctic and Antarctic Research Institute, 199397 St Petersburg, Russia

Tritium (^3H) concentration was measured in snow deposited at the Vostok station (East Antarctica) from two snow pits covering the period mid-50s to 2006 and 2008 respectively. At Vostok, ^3H concentrations are relatively high: low vapour pressure and almost no snowfall make this site specially sensitive to stratospheric inputs highly enriched in tritium. In the upper part of both pits, the post-bomb tritium record shows interannual variability.

As shown in the figure below, the records versus depth are affected by spatial distorsion, although the two pits are only distant of a few hundreds of meters. This can be attributed to redistribution of snow by wind, formation of dunes at different scales, locally different densification processes, etc..., as reported for instance by Ekaykin *et al*. (2002) for δD and $\delta^{18}O$.

However, despite this stratigraphic noise, a similar cyclic interannual pattern can be identified on both pits. This suggests that tritium can be used as a tracer of the relative contribution of stratospheric and tropospheric moisture to the snow deposition.

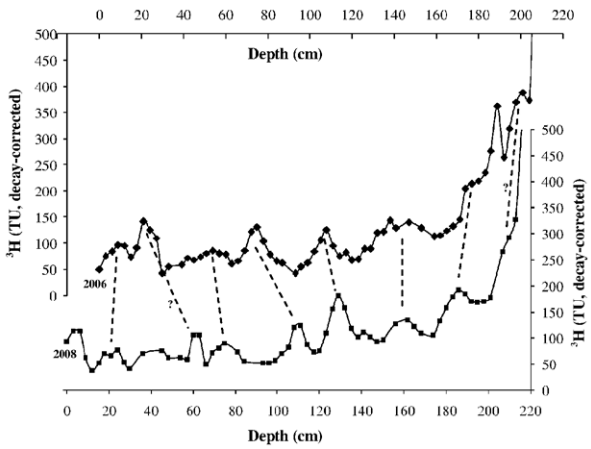

[1] Ekaykin *et al*. (2002) *Ann of Glaciology* **35** 181-186

https://doi.org/10.1180/S0026461X00006502 Published online by Cambridge University Press

Ca fluxes linked to particles exchange with seawater during Himalayan erosion

CHRISTIAN FRANCE-LANORD[1], MAARTEN LUPKER[1], BRUNO LARTIGES[2] AND JÉRÔME GAILLARDET[3]

[1]CRPG-CNRS, Université de Lorraine, Vandoeuvre Nancy, France
[2]GET-OMP, Université Paul Sabatier, Toulouse, France
[3]Institut de physique du Globe de Paris (IPGP), France

Silicate weathering as a long term sink for atmospheric CO_2 must be coupled to carbonate precitation and burial. At the global scale, this process is hampered if the alkalinity exported by rivers is derived from alkaline silicates as no Ca (or Mg) is then supplied to the ocean to precipitated carbonates. One process to compensate for alkaline cation flux is the adsorbed cation exchange at the Contient-Ocean transition. In the river system, the dominant dissolved species, Ca^{++} is also the main adsorbed cation on the sediment load. Upon transfer in seawater, Ca^{++} is potentially exchanged for seawater Na^{+}, leading to a yet unacounted Ca flux [ref].

We atempt to evaluate this process on the Ganga-Brahmaputra rivers (G-B) which generate ca. 10% of the global river particles flux to the oceans. In addition, the Himalayan crust mostly delivers alkaline silicates to weathering. We measured Cation Exchange Capacity (CEC) on modern river sediments sampled in the Bangladesh delta. Measured CEC are strongly dependant on the grain size and mineralogical composition of the sediments. It varies between 15 meq/100g for clay rich sediment and 1 for coarse quartz rich sediment. This CEC is primarly bounded to Ca^{++} (85%) and Mg^{++} (12%) with minor proportions of K^{+} and Na^{+}.

Assuming conservatively a G-B sediment flux of 1×10^{9} t/yr and an average composition for the sediment with Al/Si = 0.23; this leads to a maximum of $\approx 2.5\times10^{10}$ moles of exchangeable Ca. Assuming a complete efficiency of Ca-Na exchange in seawater, this corresponds to ca. 20% of the present dissolved flux of silicate derived Na. CEC of Himalayan sediments is therefore largely insufficient to strenghthen the long term CO_2 uptake through alkaline silicate weathering in the Himalayan basin. The fate of Himalayan silicate alkalinity is therefore more likely to be involved in reverse weathering reactions with no net effect as sink for atmospheric CO_2.

This conclusion is likely generalisable to other large Asian rivers. On the contrary, rivers draining volcanic terranes may generate higher CEC given their sedimentological characteristics.

[1] Sayles & Mangelsdorf (1977) *GCA*, **41**: 951-960

Molecular fossils and organic proxies evidencing the facial evolution of the Lower Miocene Sokolov basin, Eger Graben

J. FRANCU[1]*, D. MÁCOVÁ[1], I. SÝKOROVÁ[2], M. HAVELCOVÁ[2], B. KŘÍBEK[3], K. MARTÍNEK[4] AND P. ROJÍK[5]

[1]Czech Geological Survey, Leitnerova 22, CZ-65869 Brno (*correspondence: juraj.francu@geology.cz, daniela.macova@geology.cz)
[2]Inst. of Rock Structure and Mechanics, CAS, Praha (sykorova@irsm.cas.cz, havelcova@irsm.cas.cz)
[3]Czech Geological Survey, Geologická 6, 152 00 Prague 5, Czech Republic (bohdan.kribek@geology.cz)
[4]Institute of Geology and palaeontology, Charles University, Prague, Czech Republic (karel@natur.cuni.cz)
[5]Sokolovská uhelná JSC, Staré náměstí 69, 356 01 Sokolov, Czech Republic (rojik@suas.cz)

The Eger Graben deposits provide a geochemical archive covering Early to Middle Miocene fluvial to lacustrine environments. Proxy data based on bulk rock pyrolysis and molecular fossils provide evidence of a series of sedimentary events and climatic perturbations.

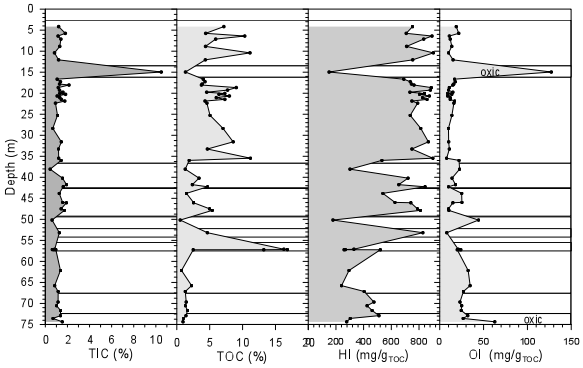

Figure 1. Total inorganic and organic carbon (TIC, TOC), hydrogen index (HI), and oxygen index (OI) in the DP-333 profile – clay interval starting above the coal seams.

Sudden flooding terminated the coal deposition. Aquatic plants and later algae became the major biological producer of organic matter. 6 epizodic drops of lake level were associated with drying, partial oxidation and formation of semifusinite. Analogical phases of palaeo-environmental evolution manifested by proxy data were identified in Sokolov and other Miocene basins.

This study was supported by the Czech Ggrant Agency (GAČR 205/08/1087).

https://doi.org/10.1180/S0026461X00006502 Published online by Cambridge University Press

The influence of local cation-distribution on the magnetic properties in ilmenite-rich α-Fe_2O_3-$FeTiO_3$ systems

CATHRINE FRANDSEN* AND STEEN MØRUP

Technical University of Denmark, Department of Physics, Building 307, DK-2800 Kongens Lyngby, Denmark (*correspondance: fraca@fysik.dtu.dk)

The ilmenite-hematite (xFeTiO$_3$ – (1-x)Fe$_2$O$_3$) system has attracted significant attention because of its complex magnetic properties. Both ilmenite (FeTiO$_3$) and hematite (α-Fe$_2$O$_3$) are antiferromagnetic, but intermediate compositions can be strongly ferrimagnetic [1] and finely exsolved structures of hematite and ilmenite are found to have a magnetization larger than expected [2].The system is of significant interest as a source of natural remnant magnetism on the Earth, the Moon and Mars [2].

Here, we compile some recent Mössbauer studies of ilmenite-rich samples with different degree of local Fe^{3+}-ordering, ranging from a disordered cation distribution in a ball milled ilmenite [3], to Fe^{3+} in nanometer-sized hematite clusters in rapidly cooled ilmenite-rich samples [4], to nano- to micrometer-sized hematite lamellae exsolved in a slowly cooled natural sample of hemoilmenite [5]. We discuss the influence of the local cation ordering on the magnetic properties of the (xFeTiO$_3$ – (1-x)Fe$_2$O$_3$) system.

In the ball milled ilmenite-rich sample, the cations are disordered, and this has a large influence on the magnetic hyperfine interaction, but the Néel temperature is essentially not affected [3]. Nanometer-sized hematite clusters within an ilmenite-like matrix of rapidly-cooled samples show ferrimagnetic behaviour due to superexchange coupling with Fe^{2+} in ilmenite [4]. In the natural sample, high-field Mössbauer measurements indicate the presence of a minor ferrimagnetic hematite component [5].

[1]T. Nagate (1953), *Nature* **172**, 850. [2] P. Robinson, R.J. Harrison, S.A. McEnroe, and R.B. Hargraves (2002), *Nature* **418**, 517. [3] S. Mørup, H. K. Rasmussen, and C. Frandsen, in preparation.[4] C. Frandsen, B.P. Burton, H.K. Rasmussen, S.A. McEnroe, and S. Mørup (2010), *Phys. Rev. B* **81**, 224423. [5] C. Frandsen, S. Mørup, S.A. McEnroe, P. Robinson, and F. Langenhorst (2007), *Geophys. Res. Lett.* **34**, L07306.

Secular depletions in highly siderophile elements recorded in >3.6 Ga komatiites

E.A. FRANK[1]*, W.D. MAIER[2] AND S.J. MOJZSIS[1]

[1]University of Colorado, Department of Geological Sciences & Center for Lunar Origin and Evolution (CLOE), NASA Lunar Science Institute, Boulder, CO 80309-0399, USA (*correspondence: elizabeth.frank@colorado.edu)

[2]University of Oulu, Linnanmaa, 90014 Oulu, Finland

Plume-derived extrusive ultramafic rocks of peridotitic composition (komatiites) - and their metamorphic equivalents - can be used to probe changes in highly siderophile element (HSE) abundances for the komatiite source (mid- to lower mantle). These rocks appear to show a time-dependent depletion trend (see figure) in HSE abundances from Neoarchean to Paleoarchean samples [1]. In the figure, the solid line denotes the modern peridotite Pt concentration, while the dashed line shows the mean abundance for the oldest three analyzed komatiites.

HSEs should have strongly partitioned into the core during differentiation, but they show a higher than expected mantle abundances. This conundrum has led to the proposal that a "Late Veneer" (LV) delivered ~1% of Earth's mass after core closure [2], although this explanation is contested [3, cf. 4]. Recent modeling [5] shows that it is dynamically feasible for a ~2700-km diameter impactor to have delivered 1% of Earth's current mass as an LV after the Moon-forming impact. Assuming CI compositions, such an event is enough to explain the observed HSE enhancement. Some evidence also exists for LVs on the Moon and Mars in lunar basalts and SNC meteorites [6, 7]. While Mars' abundances are roughly equivalent to Earth's, the Moon is apparently ~1000× less enhanced for uncertain reasons.

We report new data from >3.6 Ga komatiitic rocks that exhibit a low HSE abundance. If Earth experienced an LV, it likely occurred between Moon formation and solidification of the first continental crust (pre-4.4. Ga). We postulate that the LV polluted the upper mantle with suspended platinoid elements that became progressively mixed. Additional samples in the data gap between 2.9 and 3.2 Ga will be measured for their HSE abundance to determine whether they too follow the postulated mixing trend.

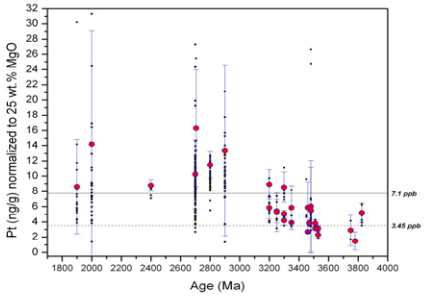

[1] Maier *et al.* (2009) *Nature* **460**, 620-623. [2] Chou (1978) *Proc. Lunar Planet. Sci. Conf.* IX, 219–230. [3] Righter *et al.* (2008) *Nature Geoscience* **1**, 321-323. [4] Holzheid *et al.* (2000) *Nature* **406**, 396-399. [5] Bottke *et al.* (2010) *Science* **330**, 1527-1530. [6] Day *et al.* (2007) *Science* **315**, 217. [7] Jones *et al.* (2003) *Chem. Geol.* **196**, 21.

https://doi.org/10.1180/S0026461X00006502 Published online by Cambridge University Press

Distribution of neodymium isotopes in Eastern Equatorial Pacific seawater

MARTIN FRANK[1]*, PATRICIA GRASSE[1], TORBEN STICHEL[1,2] AND LOTHAR STRAMMA[1]

[1]IFM-GEOMAR, Wischhofstr. 1-3, 24148 Kiel, Germany (*correspondence: mfrank@ifm-geomar.de)

[2]SOEST, University of Hawaii 1680 East-West Rd, Honolulu, HI 96822, USA

The Rare Earth Element (REE) neodymium (Nd) is introduced into seawater through continental weathering and exchange with the continental shelves. Due to its intermediate oceanic residence time and the fact that it is independent of biological fractionation it is a powerful chemical water mass proxy and can also be applied for the reconstruction of past ocean circulation. For its reliable use a precise knowledge of the present-day distribution and input mechanisms is required. Over the last years, a large number of Nd isotope data have been produced for Atlantic seawater but only very few data are available for the Pacific Ocean.

In this study we present the first dissolved Nd isotope data for the Eastern Equatorial Pacific (EEP), where one of the globally largest Oxygen Minimum Zones (OMZ) is located. Samples were recovered along several zonal and meridional sections during "FS Meteor" cruises M77/3 and M77/4 in 2009. Surface waters in the study area show a wide isotopic range (ε_{Nd}= -8 to ε_{Nd}= +3), due to contributions from land accompanied by leaching of particles and shelf sediments. Near surface circulation in the EEP is controlled by the complex Peru-Chile Current System and intense coastal upwelling. These water masses originate from the western and central Pacific, such as the Equatorial Undercurrent, which is the main feeder of the Peruvian Upwelling. This current, which enters the system near the equator is characterized by highly radiogenic isotope values (ε_{Nd}= -1.8), significantly different from less radiogenic subsurface currents stemming from the south, as well as from central and northern Pacific areas (ε_{Nd}= -4). Deep and bottom waters at the southernmost stations (14°S) of the study area (ε_{Nd}= -7) are clearly influenced by less radiogenic water masses originating from the Southern Ocean. Towards the equator, the bottom waters show a trend towards more radiogenic values (ε_{Nd}= -2). In addition, the REE patterns of the same seawater samples were analyzed to better understand the input mechanisms (potential release from reducing sediments within the OMZ) and vertical exchange processes (biological productivity) in this highly dynamic system.

Formation of nanoparticles with stereochemical effects using the polyphenol-pseudoboehmite complexation

MARTINA FRANKE

Department of Soil Science, University of Trier, D-54296 Trier, Germany (s6mafran@uni-trier.de)

Stereochemical effects were observed by the formation of organominerally nanoparticles using the system of polyphenol-pseudoboehmite. In this study, four types of phenolic compound, being pyrocatechol, resorcin, pyrogallol and guaiacol, were used for the preparation of four types of organomineral complexes. The complexes were synthesized by adsorption in a gas-solid phase at 50 °C in the presence of atmospheric pressure for a period of 60 days in total darkness. Subsequently, a comparative structure analysis was conducted from pseudoboehmite and polyphenol-pseudoboehmite complexes by using methods of VNIR spectroradiometry and Fourier transform infrared (FTIR) spectrometry. The complexation took place at surface level between OH atoms of pseudoboehmite and the functional groups of polyphenol due to the elimination of H_2O. However, the growth of nanoparticles was dependent on stereochemical effects, based on the constitution, configuration and conformation of molecules.

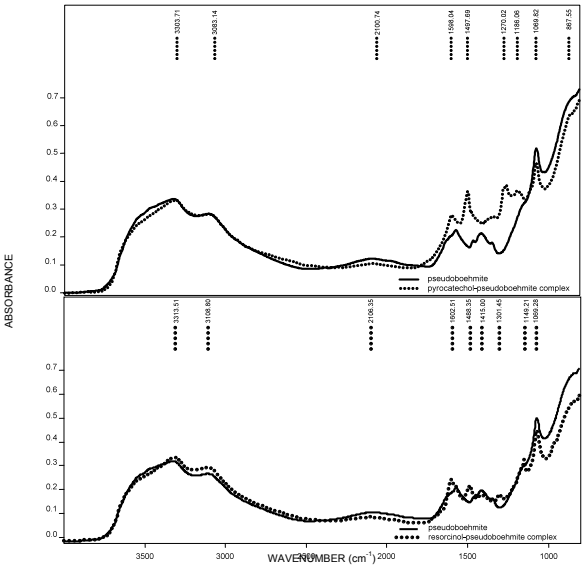

[1] Franke M (2002), diploma thesis, University of Trier, 187.

https://doi.org/10.1180/S0026461X00006502 Published online by Cambridge University Press

Geochemical mapping of phosphorus in drainage sediments of Pernambuco State, Brazil

M. FRANZEN*, E.A.M. LIMA AND R. CAVALCANTE

Geological Survey of Brazil (CPRM) –
(*correspondence: melissa.franzen@cprm.gov.br;
enjolras.lima@cprm.gov.br;
rogerio.cavalcante@cprm.gov.br)

Phosphorus (P) is an essential element for life as primary nutrient. Their presence and availability in soils is essential, however, when available in excess in the water, may be responsible for the eutrophication of water bodies.

Analytical results of P in sediments from drainage obtained at the Multipurpose Geochemistry Project in Pernambuco State, executed by the Geological Survey of Brazil (CPRM), were used to produce the geochemical mapping of low density.

Were analyzed by ICP-OES sediments in fractions <80 mesh. Statistical analysis of dispersion of data obtained provided thresholds above which the levels of P may be considered anomalous. The geochemical maps combine statistical distribution of the percentiles (25%, 50% and 75%) to levels of toxicological and crustal reference, resulting in products that serve both for environmental purposes regarding the delineation of prospective areas.

The regional geochemical mapping confirmed areas of known occurrences, as the phosphorite mineralization of the Pernambuco-Paraíba Basin and the mining district of Sumé, and also highlights some areas within the State of likely prospective potential. These are located mainly over the Meso-Neoproterozoic complexes and predominantly in falt zones, where the paragenesis and tectonic setting suggest the possibility of lenticular bodies of carbonatite [1], although these are not yet mapped.

The hypothesis suggests potential to prospective studies of detail, since the anthropogenic contamination is unlikely because of the semi-arid climate does not favor the accumulation of organic matter and the agricultural activity is limited.

[1] LAPIN *et al*. (1999) *RBG* **29**, 483-490.

Chiral interactions of amino acids in a hydrated vermiculite clay

DONALD G. FRASER, NEAL T. SKIPPER, MARTIN V. SMALLEY AND H. CHRISTOPHER GREENWELL[1234]

[1]Department of Earth Sciences, University of Oxford, Parks Road, Oxford OX1 3PR, UK
[2]Department of Physics & Astronomy, University College London, Gower Street, London WC1E 6BT, UK
[3]Department of Physics, University of York, Heslington, York YO10 5DD, UK
[4]Department of Chemistry, Durham University, South Road, Durham DH1 3LE, UK

Recent work suggests a link between chiral asymmetry in the amino acid iso-valine extracted from the Murchison meteorite and the extent of hydrous alteration.

We present the results of neutron scattering experiments on an exchanged, 1-dimensionally ordered n-propyl ammonium vermiculite clay. The vermiculite gel has a (001) d-spacing of order 5nm at the temperature and concentration of the experiments and the d-spacing responds sensitively to changes in concentration, temperature and electronic environment. The data show that isothermal addition of D-histidine or L-histidine solutions produces shifts in the d-spacing that are different for each enantiomer. This chiral specificity is of interest for the question of whether clays could have played an important role in the origin of biohomochirality.

https://doi.org/10.1180/S0026461X00006502 Published online by Cambridge University Press

Biogeochemical redox transformations of pertechnetate ($^{99}TcO_4^-$)

J.K. FREDRICKSON[1], J.-H. LEE[1], A.E. PLYMALE[1], A.C. DOHNALKOVA[1], S.M. HEALD[2], T. PERETYAZHKO[1], J.P. MCKINLEY[1], AND J.M. ZACHARA[1]

[1]Pacific Northwest National Laboratory, Richland, WA, USA
[2]Argonne National Laboratory, Advanced Photon Source, Argonne, IL, USA

Technetium-99 is an important risk-driving radioactive subsurface contaminant at the U.S. Department of Energy (DOE)'s Hanford Site in southeastern Washington State. The monovalent anion $Tc(VII)O_4^-$ (pertechnetate) is subject to subsurface migration but Tc is considerably less soluble in its most reduced form, $Tc(IV)O_2$. Reduction can be catalyzed directly by a range of anaerobic microorganisms but also indirectly by products of microbial metabolism including ferrous iron and sulfide. We have investigated Tc(VII) reduction reactions in Hanford subsurface sediments and in well-defined model systems that include metal-reducing microorganisms and Fe-bearing minerals to explore speciation effects on reaction rates and Tc endproducts. In Hanford sediments collected from anoxic regions of the subsurface or oxic sediments subjected to microbial reduction, 2×10^{-5} M (20 μM) aqueous Tc(VII) was reduced to below the detection limit (3.98×10^{-9} M) over times ranging from days to months. The rate and extent of reduction was dependent on sediment source, Fe(II) speciation, and sulfide concentration. X-ray microprobe analyses, including fluorescence mapping, elemental multichannel analysis, and micro-diffraction, were used to deduce Tc speciation and mineralogic association in the various sediments. In bioreduced Hanford formation sediments Tc(IV) was associated with phyllosilicates (mica), as indicated by associated Fe and Rb (analogous to K) signals. X-ray absorption spectroscopy (XAS) revealed the presence of $Tc(IV)O_2$ and Fe(III)- associated Tc(IV). Tc(VII) was also reduced by sediment-associated biogenic sulfide; Tc-S bonding at the nearest coordination environment around absorber Tc atom was revealed by XAS. These results indicate that Fe(II) associated with Hanford subsurface sediments can be a facile reductant of $Tc(VII)O_4^-$ and that the rate of reduction and nature of Tc end product is a function of Fe(II) speciation. These results have implications for far-field ^{99}Tc migration at Hanford where groundwater flow paths traverse Fe(II)-bearing sediments that can reduce Tc(VII) to relatively insoluble Tc(IV) phases.

High CO_2 concentrations negatively affect methanogenesis and sulphate reduction in gas fields of the North German Plain

J. FRERICHS[1]*, C. GNIESE[2], A. SCHULTZ[3], H.-H. RICHNOW[3], D. KOCK[1] AND M. KRÜGER[1]

[1]BGR, Hannover, Germany
(*correspondence: Janin.Frerichs@bgr.de)
[2]TUBAF, Freiberg, Germany
[3]UFZ, Leipzig, Germany

In consequence of their global warming potential, large-scale solutions are needed to reduce the emissions of greenhouse gases like CO_2 or CH_4. The carbon capture and storage offers one option to reduce CO_2 emissions. Favorable CO_2 storage sites are depleted gas and oil fields. Our study is focusing on the direct influence of high CO_2 concentrations on the autochthonous microbial population and environmental parameters at such sites. The studied reservoir formation is operated by Gaz de France Suez E&P DEUTSCHLAND GmbH. The conditions in the reservoir around two production wells differ in various geochemical and microbiological parameters (Ehinger *et al*. 2009). Based on these results our study included cultivation and molecular-biological approaches. The two wells differed in the indigenous and inducible (with substrate addition) microbial activity. The addition of methanol to fluids of both wells induced biogenic methane production only in well A. Fluids of well B showed induced sulphide production after addition of hydrogen and CO_2. Results from molecular biological analysis of original fluids supported the activity profile for both sites. The abundance of archaeal 16S rDNA and *mrcA* was several magnitudes higher in fluids of site A whereas site B was dominated by *Bacteria*. Incubations with high carbon dioxide concentrations showed a significant decrease of methane and sulphide production with increasing CO_2 levels. In a second step actively growing methanogenic and sulphate-reducing enrichments from the reservoir fluids were incubated under in situ pressure and temperature with high CO_2 levels. First experiments indicated that the microorganisms survived short termed incubation although the respiratory activity was not detectable. From this experiment viability rates of micro-organisms together with molecular analysis of community changes were investigated. At the end, these experiments will provide information about biogeochemical and micro-biological changes during and after the storage of CO_2 and their potential impacts on reservoir geology, storage capacity, and long-term stability.

https://doi.org/10.1180/S0026461X00006502 Published online by Cambridge University Press

Oxide surfaces: Geometric and electronic structure

H.-J. FREUND

Faradayweg 4-6, 14195 Berlin, Germany,
(freund@fhi-berlin.mpg.de)

Single crystalline oxide surfaces have been prepared by physical vapour deposition on suited metal single crystals. The geometric structures of surfaces have been characterized by a number of techniques, including STM and NC-AFM as well as LEED, and LEEM. The electronic structure has been studied using photoelectron spectroscopy NEXAFS as well as EPR, and augmented by FTIR. In this talk a number of specific examples including iron oxides, ceria, vanadia, and MgO are discussed. The study of water on those surfaces has been investigated.

Felsic magma generation in the oceanic crust: A geochemical study of Pacific Antarctic Rise lavas

SARAH FREUND, KARSTEN M. HAASE, CHRISTOPH BEIER AND MARCEL REGELOUS[1]

GeoZentrum Nordbayern, Friedrich-Alexander-Universität Erlangen-Nürnberg, Erlangen, Germany
(Sarah.Freund@gzn.uni-erlangen.de)

Glassy lavas from the Pacific Antarctic Rise show variable SiO_2 contents between 49 and 68 wt.% and range from basalts to dacites. The trace element compositions range from depleted to slightly enriched mid-ocean ridge basalts whereas the evolved lavas are more enriched in most incompatible elements but show negative anomalies of Ba, Nb Sr, Ti and positive anomalies of Rb, U, Zr and Hf compared with the basalts. In terms of major elements the lavas lie on typical tholeiitic fractionation trends. The evolved lavas show the same trends as the basalts in Nd and Pb isotope space while there is a deviation towards higher Sr isotope ratios at a given Nd isotope ratio. The evolved glasses tend toward anomalously low $\delta^{18}O$ values and show increasing Cl content with increasing SiO_2. These isotopic and chemical variations likely reflect assimilation of hydrothermally altered crustal rocks. Because light $\delta^{18}O$ values occur only in the lower part of the oceanic crust (> 1 km bsf) the assimilation and fractional crystallization processes probably occurred at the lower boundary of the sheeted dikes. Crustal partial melting yielding dacite magma and mixing of these melts with basalts can be ruled out based on trace element ratios and major element distributions. The petrogenesis of the evolved magmas has been modeled quantitatively using MELTS [1] and EC-RAFC [2]. We conclude that AFC processes lead to the formation of evolved magmas beneath the PAR with trace element similarities to the continental crust.

[1] Ghiorso, S. & Sack, R.O. (1995), *Contrib Mineral Petrol,* (1995) **119**:197-212. [2] Bohrson, W.A. & Spera, F.J. (2007), *Geochemistry Geophysics Geosystems,* Vol. **8**, Technical Brief.

https://doi.org/10.1180/S0026461X00006502 Published online by Cambridge University Press

Measuring annual variation of soil air composition focusing on the effect of oxygen depletion on noble gas partial pressures

F. FREUNDT, T. SCHNEIDER AND W. AESCHBACH-HERTIG*

Institute of Environmental Physics, Heidelberg University, 69120 Heidelberg, Germany (*correspondence: aeschbach@iup.uni-heidelberg.de)

While it is known that the partial pressures of soil air components like oxygen, carbon dioxide and nitrous oxides show fluctuations on both temporal and spatial scales [1] primarily caused by microbiologic activities in the soil, the use of dissolved noble gases as a climate proxy utilizes the basic assumption that the ground air equilibrating with water during recharge is of atmospheric composition with regard to noble gases [2].

This assumption has been questioned to account for lower than expected noble gas temperatures, suggesting an enrichment of noble gas partial pressures in ground air caused by removal of CO_2 (produced by oxygen depletion) due to its high solubility [3].

To test this proposition, two permanent sampling sites were built in clay dominated soil, allowing for sampling of ground air in regular intervals and depths up to 6 meters. The locations were chosen based on preliminary data by T. Schneider [4] indicating the possibility of high oxygen depletion. O_2 and CO_2 concentrations were measured on site while the noble gases helium, argon, neon, krypton and xenon were measured using mass spectrometry.

Preliminary noble gas data from the first four months of sampling indicate no deviation of noble gas partial pressures from atmospheric values, suggesting that the proposed oxygen depletion model cannot be supported by actual data from the sampled clay soils. Further data extending the record to ten months (August to May) will be presented.

[1] Amundson & Davidson (1990) *J Geochem Explor* **38**, 13-41. [2] Aeschbach-Hertig *et al*. (1999) *Water Resour. Res.*. **35**, 2779-2792. [3] Castro *et al*. (2007) *Earth Planet. Sci. Lett.* **257**, 170-187. [4] Schneider (2010) *University of Heidelberg, master thesis*.

Molybdenum isotopes as a novel tracer for subduction components in the Mariana arc

HEYE FREYMUTH*, TIM ELLIOTT AND MATTHIAS WILLBOLD

Bristol Isotope Group, University of Bristol, Wills Memorial Building, Queen's Road, Bristol BS8 1RJ (*correspondence: glxhf@bristol.ac.uk)

At least two different slab-derived components have been proposed to be present in arc volcanoes: a sediment component and a component derived from altered mafic oceanic crust. Despite a widely held belief of the involvement of these components in the genesis of arc volcanoes [1,2] the unambiguous identification of these components and discrimination of their chemical signatures from residual phase mineralogy remains difficult. We propose stable molybdenum isotopes as a novel tracer for subduction components in arc magmas.

Molybdenum has seven stable isotopes, which have been shown to fractionate during the incorporation of dissolved Mo into oceanic sediments. Under oxic conditions, Mo slowly adsorbs to particles in the sediment, a process that is particularly efficient when Fe-Mn oxides are present. The adsorption of Mo is associated with isotopic fractionations from $\delta^{97/95}Mo_{seawater} \approx 1.8$ ‰ to $\delta^{97/95}Mo_{oxic\text{-}sediments} < 0$ ‰. Under anoxic conditions, Mo is quantitatively removed from the water column and sediments with a heavy isotopic composition are produced [3,4].

We measured Mo isotopes on basalts from the Mariana arc as well as representative samples of subducting sediments from ODP sites 800, 801 and 802 using a double-spike technique [5]. The sediments are light in their isotopic composition with $\delta^{97/95}Mo_{sediments} < 0$ ‰, consistent with the incorporation of Mo into the sediment under oxic conditions. The arc basalts are enriched in Mo relative to Pr, an element with similar degree of incompatibility during mantle melting. The Mo isotopes in the arc basalts correlate well with Mo/Pr, Ba/La and Ce/Pb ratios, with samples containing a larger sediment component [6] also having the lowest $\delta^{97/95}$Mo. Less incompatible element enriched samples are isotopically heavy and their $\delta^{97/95}$Mo exceeds the range of ocean island basalts and continental material. They presumably trace a fluid derived from deeper parts of the subducted lithosphere.

[1] Plank & Langmuir (1998) *Chem. Geol.* **145,** 325–394. [2] Plank (2004) *J.Petrology,* **5**, 921–944. [3] Anbar & Rouxel (2007), *Ann. Rev. Earth Planet. Sci.*, **35**, 717–746. [4] Siebert *et al*. (2003) *EPSL* **211**, 159–171. [5] Archer *et al*. (2008) *Nature Geosc.*, **1**, 597-600. [6] Elliott *et al*. (1997) *JGR*, **102**, 14,991-15,019.

https://doi.org/10.1180/S0026461X00006502 Published online by Cambridge University Press

Selenium uptake in otoliths from cold-water fish species captured downstream from coal mining

LISA A. FRIEDRICH[1]*, NORMAN M. HALDEN[2] AND VINCE P. PALACE[1]

[1]Department of Fisheries and Oceans Canada, Winnipeg, Manitoba, Canada R3T 2N6 (*correspondance: lisa.friedrich@dfo-mpo.gc.ca, vince.palace@dfo-mpo.gc.ca)

[2]Department of Geological Sciences, University of Manitoba, Winnipeg, Manitoba, Canada R3T 2N2 (nm_halden@umanitoba.ca)

Establishing the exposure histories of wild fish to trace element contaminants within an aqueous environment is often difficult for fish species with large home ranges. Chemical analyses of muscle or visceral tissues can provide information on recent exposure, but depuration, metabolic transformation, and tissue redistributions preclude temporal resolution. Otoliths, the calcified structures in the inner ear of teleost fish, are considered to be metabolically stable and therefore may serve as continuous recorders of exposure to trace elements in the environment. Otoliths are composed of layers of aragonite in a protein matrix deposited annually throughout the lifetime of the fish, thus providing a time scale. Both the inorganic portion and protein matrix have the capacity to incorporate a wide range of trace elements, and, as such, otoliths may be used to determine a fish's history of contaminant exposure in the wild.

Otoliths from three cold water fish species from Elk River, British Columbia, Canada were examined to delineate any selenium (Se) contamination signatures contained therein relating to adjacent coal mining activity. The Elk River watershed contains elevated levels of Se owing to naturally occurring seleniferous host rock surrounding coal deposits, as well as five coal mining operations that mobilize Se from exposed host rock into the watershed. Selenium concentrations in otolith primordia tended to be low, indicating that these fish emerged in low Se areas, and moved into areas of increased Se later in life. Individuals captured from the same area had varying Se exposure profiles, indicating the fish do not move *en masse* into and out of high-Se areas. Year-to-year variability of Se exposure patterns within an otolith suggests inconsistent utilization of high- and low-Se areas by the individual. The contrasting exposure profiles for these fish, which have home ranges of tens of kilometres, indicate that soft tissue concentrations would not necessarily reflect the relative abundance of Se in their environments.

Fe(II)-induced trace element release from crystalline iron oxides

A.J. FRIERDICH* AND J.G. CATALANO

Earth & Planetary Sci., Washington Univ., St. Louis, MO 63130, USA (*correspondence: frierdich@wustl.edu)

Interfacial electron transfer and atom exchange (ET-AE) between aqueous Fe(II) and Fe(III) oxides induces surface transformations resulting from spatially separated growth and dissolution processes [1-4]. Redox-active elements are known to experience speciation changes during Fe(II)-Fe(III) ET-AE but the fate of redox-inactive elements remains poorly understood. We have recently shown [5] that aqueous Fe(II) can catalyze Ni(II) cycling through goethite and hematite by inducing adsorbed Ni to become incorporated into the mineral and pre-incorporated Ni to be released to solution. Here we examine the kinetics of Ni(II) and Zn(II) release from Ni(II)- and Zn(II)-substituted goethite and hematite when these minerals are exposed to aqueous Fe(II) solutions.

Ni and Zn release follows a 2nd order kinetic rate law and occur on a different timescale than Fe(II) adsorption but on a similar timescale as Fe isotope exhchange for goethite [2]. This suggests that the mechanism for release is not related to displacement of surface associated Ni but rather occurs during the Fe(II)-Fe(III) ET-AE process. The concentration of Fe(II) and pH strongly influence the quantity and rate of metal release. The type of metal substituent also affects reactivity; Zn release is more pronounced from hematite vs. goethite whereas the opposite trend occurs for the Ni systems. Sequential batch experiments (i.e., periodic fluid replacement to remove products while the solid remains for further reaction) display greater total Ni and Zn release than observed in single batch experiments (cf. 28% vs 9% of Ni released from goethite), demonstrating that the aqueous metal concentration is a negative feedback on release. Incorporated redox-active trivalent metals [Mn(III) and Co(III)] exhibit similar release to solution, suggesting that their release is coupled to reduction and that they may cause net Fe(II) oxidation. Our results illustrate a previously unrecognized role of Fe(II) on the release of trace elements from iron oxide minerals. Such reactions may liberate essential trace elements or cause enhanced mobility of contaminants in natural environments and engineered systems.

[1] Catalano *et al*. (2010) *Geochim. Cosmochim. Acta* **74**, 1498-1512. [2] Handler *et al*. (2009) *Environ. Sci. Technol.* **43**, 1102-1107. [3] Rosso *et al*. (2010) *Environ. Sci. Technol.* **44**, 61-67. [4] Yanina & Rosso (2008) *Science* **320**, 218–222. [5] Catalano *et al*. (2011) *Min. Mag*., this volume.

https://doi.org/10.1180/S0026461X00006502 Published online by Cambridge University Press

Potential products of fluid-rock interactions in the Soultz-sous-Forêts Enhanced Geothermal System

B. FRITZ[1]*, A. BALDEYROU-BAILLY[1], AND O. VIDAL[2]

[1]LHYGES, Université de Strasbourg/EOST, CNRS, France (corresponding author : bfritz@unistra.fr)
[2]ISTerre, Université J. Fourier, CNRS, Grenoble, France

A geochemical modelling approach of fluid-rock interactions has been applied to the potential water-rock interaction processes in the Enhanced Geothermal System (EGS) of Soultz-sous-Forêts (France) [1,2,3] which started in 2008. The aim of the study was to detect the possible risks of minerals precipitation in the circulation loop in the temperature range between 200°C at depth (5km) and 60°C in the surface power system before re-injection, in conditions reproducing those of the industrial exploitation of the site.

The major result of the simulations highlights the role of carbonates as possible products of the thermal fluids particularly in the low temperature part of the thermal loop and on short term. In the reservoir rock-forming silicates may be partially dissolved by the reinjection of fluids leading to the long term formation of clay minerals in the porosity of the rock. The modelling approach has been combined with an experimental approach of water-rock interaction under a strong thermal gradient which confirms the dynamics of silicates in these temperature conditions and with this type of saline fluid (TDS about 100g/l).

The formation of clay minerals (illites and / or chlorites) may modify the porosity and the permeability of the granitic reservoir during future exploitation.

[1] A. Baldeyrou-Bailly, F. Surma and B. Fritz (2004), *Geol. Soc. Special publ.* **236**, 355-367. [2] B. Fritz, E. Jacquot, B. Jacquemont, A. Baldeyrou-Bailly, M. Rosener, O. Vidal (2010) *CR Geoscience*, **342**, 653-667. [3] B. Fritz and A. Gérard (2010) *CR Geoscience*, **342**, 493-501,

Composition, structure and shape of *in situ* precipitated Fe-oxide nanoparticles from a soil effluent

A. FRITZSCHE*, A.K. WIECZOREK, T. RENNERT, M. HÄNDEL AND K.U. TOTSCHE

Institute of Earth Sciences, Friedrich Schiller University of Jena, Burgweg 11, 07749 Jena, Germany (*correspondence: a.fritzsche@uni-jena.de)

Iron oxides are generally highly reactive. In nanoparticulate form, the reactivity of Fe oxides and their mobility in the aqueous phase is even increased. Thus, dispersed Fe-oxide nanoparticles are considered as key reactive components for biogeochemical processes that involve Fe. However, the majority of related investigations is based on synthetic Fe-oxide nanoparticles, the composition and properties of which may not reflect those of Fe-oxide nanoparticles actually occurring in nature.

In this study, soil columns were filled with material from a topsoil horizon. The soil columns were operated in duplicate under water-saturated conditions with a low ionic influent. The activity of soil microorganisms led to anoxic conditions and thus the reductive dissolution of pedogenic Fe oxides and the accumulation of Fe^{2+} in the column effluent. The effluent was re-aerated after its discharge resulting in the oxidation of Fe^{2+} and the precipitation of Fe oxides. The effluent was dialysed to separate the Fe oxides from non-particulate compounds.

X-ray diffraction and Mössbauer spectroscopy revealed the formation of short-range ordered ferrihydrite (Fh). Its crystallisation was probably disturbed by dissolved organic matter and inorganic species (e.g. As, Si) that associated with Fh. Fourier transform infrared spectroscopy pointed to mainly polysaccharides, aliphatics and carboxyls as available organic compounds to associate with the Fh particles. The aggregation intensity decreased in response to decreasing effluent ionic strengths. Dynamic light scattering revealed aggregate sizes from 50 nm to 500 nm, which was confirmed by atomic force microscopy and scanning electron microscopy. The latter approaches consistently revealed the coexistence of bulky and to a lesser extent linear-aligned nanoaggregates. Both aggregate types exhibited similar mechanical and physical properties and were composed of smaller particles (~ 10 nm).

This study demonstrated the reproducible stabilisation of nanoaprticulate Fh also in complex solutions like effluents from soil. Such near-natural nanoparticles represent eligible specimen to investigate the fate and effect of nanoparticulate Fe oxides in the (soil) environment.

https://doi.org/10.1180/S0026461X00006502 Published online by Cambridge University Press

Strontium isotope fractionation in scleractinian corals

N. FRUCHTER*[1], F. BÖHM[1], A. EISENHAUER[1], M. DIETZEL[2], A. KRABBENHÖFT[1], A. NIEDERMAYR[2], S. REYNAUD[3], B. LAZAR[4] AND M. STEIN[5]

[1]Leibniz Institute of Marine Sciences, IFM-GEOMAR, Kiel, Germany. (*nfruchter@ifm-geomar.de)
[2]Institute of Applied Geosciences, Graz University of Technology, Graz, Austria.
[3]Centre Scientifique de Monaco, Principality of Monaco.
[4]Institute of Earth Sciences The Hebrew University of Jerusalem, Israel.
[5]Geological Survery of Israel, Jerusalem, Israel.

Preferentially lighter strontium isotopes ($\delta^{88/86}Sr_{carbonates}$(NBS987) ~0.15 to 0.25 ‰) are taken up from seawater ($\delta^{88/86}Sr_{seawater}$: ~0.39 ‰) by marine calcifiers during calcium carbonate precipitation. A temperature sensitivity of Sr isotope fractionation has been reported [1,2,3]. However the published results are discrepant and enigmatic.

In order to shed light into the temperature dependency of strontium isotope fractionation, we conducted inorganic precipitation experiments of aragonite, and investigated cultured and natural modern corals. The aim of the study is to enhance our understanding of strontium isotope fractionation mechanisms for biocalcification of corals and for the applicability of $\delta^{88/86}Sr$ as a temperature proxy. Strontium isotope distribution was measured by TIMS using the double spike method [4]. In addition to strontium isotope analyses we determined elemental ratios like Sr/Ca.

Preliminary results indicate seasonal $\delta^{88/86}Sr$ variations in modern corals which are positively correlated with the Sr/Ca ratios and hence, inversly correlated with temperature. The seasonal amplitude in the Sr/Ca ratios is 0.43 mmol/mol and corresponds to a temperature variation of ~7°C. The seasonal variation in $\delta^{88/86}Sr$ in the same coral is 0.04‰. The positive correlation between $\delta^{88/86}Sr$ and Sr/Ca is not in accordance with the Rayleigh distillation model for Sr/Ca ratios in corals that was proposed by Gaetani *et al*. [4].

[1] Fietzke & Eisenhauer (2006) *Geochem. Geophys. Geosys.* **7**. [2] Rüggeberg *et al*. (2008) *Earth Plan. Sci. Lett*. **269**, 569-574. [3] Krabbenhöft *et al*. (2011) *Geophy. Res. Abs.* EGU2011-6277-8. [4] Krabbenhöft *et al*. (2009) *J. Anal. Atom.Spectrom*. **24**, 1267-1271. [5] Gaetani *et al*. (2011) *Geochim. Cosmochim. Acta* **75**, 920-932.

Modeling glass alteration layers

P. FRUGIER*, S. GIN, N. RAJMOHAN AND M DEBURE

CEA Marcoule, DTCD/SECM/LCLT, BP 17171, 30207 Bagnols-sur-Cèze Cedex, France, (*correspondence: pierre.frugier@cea.fr, stephane.gin@cea.fr, nrmohan_2000@yahoo.com , mathieu.debure@cea.fr)

Glasses major constituents interact chemically within the amorphous layers resulting from glass alteration in water. These interactions determine the composition, the dissolution kinetic and the apparent solubility of the amorphous layers as well as their potential passivating properties with respect to the underlying glass. The knowledge of these interactions is required to predict concentrations in solution, pH and eventually glass alteration rates. However, these amorphous layers are complex solids resulting both from initial glass structure and recondensation processes, constantly reorganizing as solution composition changes. Identifiying the main phenomenologies is required for modeling the amorphous layers with a number of parameters consistent with experimentaly accessible data and geochemical modeling tools. These phenomenologies were translated in modeling hypothesis which are part of a model called GRAAL [1,2].

GRAAL model is implemented within a geochemistry and transport code called HYTEC [3]. Therefore, it can account for the thickness and composition of the amorphous layer whatever the time and position in space of a glass under alteration. Chemical description whithin GRAAL has been recently improved thanks to 24 experiments relative to six simple glasses containing Si, B, Na, Ca, Al and Zr, altered for months at four different neutral to alkaline pH [4]. Ten new modeling hypothesis were done for describing these six elements chemical interactions in the amorphous layer. One example: orthosilicic acid activity in solution is significantly lower than amorphous silica solubility only if enough aluminum is also available. Therefore a silica-aluminum rich end-member is taken into account to model the amorphous layer whereas Ca, Na, B and even Zr interactions with Si can be neglected to account for Si activity in solutions (in our experimental conditions at least).

We aim here at sharing both the success and limits of GRAAL model fundamental hypothesis and we will try to demonstrate the usfullness of the approach.

[1] Frugier P. *et al*. (2008) *J. Nucl. Mater*. **380**, 8–21. [2] Frugier P. *et al*. (2009) *J. Nucl. Mater*. **392**, 552–567. [3] van der Lee *et al*. (2003) *Computers and Geosciences* **29**, 265-275. [4] Rajmohan N *et al*. (2010) *Chemical Geology* **279**, 106-119

https://doi.org/10.1180/S0026461X00006502 Published online by Cambridge University Press

Phase equilibria constraints on the magma evolution of basanite-phonolite series of the Cumbre Vieja volcano (La Palma, Canary Islands)

P. FUCHS[1]*, R. ALMEEV[1] AND A. KLÜGEL[2]

[1]Institute of Mineralogy, Leibniz University Hannover, Germany (*p.fuchs@mineralogie.uni-hannover.de)
[2]Geosciences Department, University of Bremen, Germany

Eruptive products of the recent Cumbre Vieja volcano (La Palma oceanic island) cover a large spectrum of alkali-rich rocks ranging from basanites to phonolites. Current model of Cumbre Vieja plumbing system is based on cpx-barometry and xenoliths and includes three major intervals of magma stagnation and fractionation at mantle and crustal depths (430–780MPa, 180-420MPa and <150MPa) [1]. However, the relative influence of different thermodynamic parameters on stability fields of minerals is still unknown. We present first results of our experimental project aimed at evaluating p-T-aH_2O-fO_2 conditions in the course of basanite-tephrite-phonolite magma differentiation.

As a prerequisite study for these experiments phase equilibria simulations were conducted for a highly magnesian sample of Cumbre Vieja volcano (12.7 wt% MgO) utilizing the MELTs model [2]. Calculations were performed using solid phase fractionation mode, at QFM+1 oxygen buffer, in the pressure interval from 100 to 800 MPa (including both isobaric and polybaric simulations), and with various H_2O contents in parental melt (2-6 wt%). Good agreement between residual melt compositions and natural liquid lines of descent (LLD) were obtained only for the stage of "basanite to tephrite" magma evolution by crystallization of 25-30% ol+sp and subsequent ol+cpx+sp at pressures between 400 and 800 MPa and hydrous conditions. This stage is characterized by strong MgO depletion at nearly constant SiO_2 contents and proceeds until an inflection point at 5 wt% MgO (tephritic melt). Subsequently CaO, FeO and TiO_2 start to decrease and SiO_2 increases up to 58 wt% until the magma reaches phonolitic compositions. This strong change in melt composition is explained by appearance of kaersutite on the liquidus of tephritic melts, which has been so far impossible to reproduce in MELTs mainly due to the lack of kaersutite crystallization model. Thus, the conditions of kaersutite crystallization are crucial to understand the evolution of La Palma magmas from tephrite to phonolites. This problem is prioritized in our ongoing experimental investigations.

[1] Klügel *et al*. (2005) *EPSL* **236**, *211-226*. [2] Ghiorso & Sack (1995) *CMP* **119**, *197-212*.

The transport of gold in petroleum: An experimental study

S. FUCHS*, A. MIGDISOV AND A.E. WILLIAMS-JONES

Department of Earth and Planetary Sciences, McGill University, Montreal, QC, H3A 2A7, Canada (*Correspondence: sebastian.fuchs@mail.mcgill.ca)

Although there is a close spatial association between gold and organic matter in intracratonic basins such as the Witwatersrand (South Africa), the role of the organic matter in the ore-forming process is not understood. One hypothesis is that the organic matter aids in the deposition of remobilized gold by reducing gold-bearing hydrothermal fluids. Another is that the organic matter represents hydrocarbon liquids, which acted as agents of gold transport. In the case of the Witwatersrand, the latter hypothesis would be consistent with the observation that organic-rich shales, which could have acted as source rocks, are present in the basin, that during burial these rocks passed through the thermal window for oil generation (90°C-160°C) and that structures (thrusts) and porous rocks (sandstones and conglomerates) were present, thereby facilitating hydrocarbon migration.

We report here the results of a study designed to determine the solubility of gold in crude oil and its refined fractions. The experiments were conducted in titanium alloy autoclaves at temperatures in the range 100°C to 300°C for 7-10 days. At the end of an experiment, the quenched oil was sampled. Gold that may have condensed on the walls of the autoclave was dissolved in aqua regia after heating the autoclave to 400°C. This washing solution and the crude oil were analysed using neutron activation to determine the solubility of gold in the crude oil. The results of these experiments show that gold solubility in crude oil reaches a maximum of 39ppb to 48ppb at 250°C. Below and above this temperature, the solubility of gold is significantly lower. Concentrations of gold in the refined fractions (distillates and residua) were significantly lower than in the crude oil. In the residual fractions, gold reached a maximum concentration at 150° (8 ppb), whereas in the distillates the maximum concentration occurred at 300°C (27 ppb). As large aromatic molecules were likely degraded during the refining process and the solubility of gold was low in all the refined fractions, we consider it likely that these molecules exercise an important control on gold solubility. The concentrations of gold in crude oil measured in this study are similar to or higher than those of epithermal ore-forming fluids, suggesting that petroleum can act as an agent for the transport of gold in environments such as the Witwatersrand basin

https://doi.org/10.1180/S0026461X00006502 Published online by Cambridge University Press

On the hygroscopic behaviour of marine particles enriched with biogenic nanogels

E. FUENTES[1], H. COE[1], D. GREEN[2] AND G. MCFIGGANS[1]*

[1]Center for Atmospheric Science, SEAES, University of Manchester, M13 9PL, UK (*correspondence: g.mcfiggans@manchester.ac.uk)

[2]Scottish Association for Marine Science, Oban, UK

The present study investigates the effect of nanogel organic matter <0.2 μm exuded by marine biota on the organic enrichment and hygroscopic behaviour of the submicron primary marine aerosol. This investigation is based on the laboratory generation of primary aerosol from seawater enriched with biogenic organic matter released by laboratory-grown algal cultures [1].

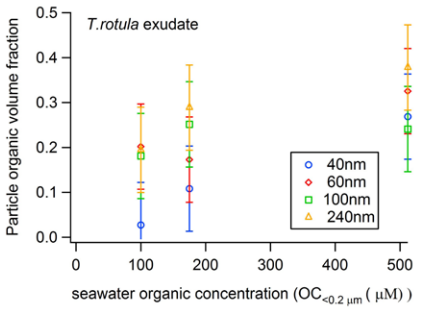

Figure 1. Particle organic volume fraction as a function of seawater organic concentration (OC<0.2 μm).

The primary particles organic fraction was found to correlate with the seawater organic concentration, with values on the order of 5–37% for seawater organic content between 175-512 μM. The particle organic fractions were found to be lower than those reported in atmospheric measurements [2] and no saturation in the particles organic composition was observed even for unrealistically high seawater organic content [3]. Because of the effect of the organic matter, the hygroscopic growth and cloud condensation nuclei activity of the organics-enriched particles were reduced in a 5–24% with respect to the organics-free primary marine aerosol.

[1] Fuentes *et al*. (2010) *Atmos. Meas. Tech.,* **3**, 141-162.
[2] O'Dowd *et al*. (2008) *Geophys. Res. Lett*., **35,** L01801.
[3] Fuentes *et al*. (2011) *Atmos. Chem. Phys.*, **11**, 2585-2602.

Prediction of coral reef calcification in Sesoko Island by ocean acidification

H. FUJIMURA[1]*, A. AOYAMA[1], T. OOMORI[1], T. HIGUCHI[2], B.E. CASARETO[2] AND Y. SUZUKI[2]

[1]Univ. of the Ryukyus, 1 Senbaru, Nishihara, Okinawa 903-0213, Japan (*correspondance: fujimura@sci.u-ryukyu.ac.jp)

[2]Shizuoka Univ., 836 Ohya, Suruga-ku, Shizuoka-shi, Shizuoka 422-8529, Japan

Carbon dioxide has been increasing rapidly by fossil fuel combustion since industrial revolution, causing various global climate changes. Anthropogenic CO_2 induces lower pH in the ocean which is known as an "oceanic acidification". Lower pH level causes the decrease in the calcification rates of many calcifying marine organisms such as shellfish and coral. While many studies have been investigated on the influence of pH to individual marine species, the effects of oceanic acidification on the natural coral reef have not been elucidated. We present relationship between calcification rates and seawater CO_2 concentration (PCO_2) in Sesoko coral reef, Okinawa, Japan and predict the time when the calcifying environment in coral reef will turn to the dissolution with respect to $CaCO_3$.

We had continuously monitored the reef water PCO_2 (LI840A, Li-cor), total alkalinity (Alk-01, Kimoto), water current (Compact-EM, Alcec) and depth (U20, Onset) at Sesoko coral reef since October 2010. Outer reef water samples were taken about every few months to obtain the oceanic values. Alkalinity depletion method was applied to calculate the community metabolism under the natural water flow condition.

Calcification rate increased during daytime and decreased at night. However we observed no dissolution at Sesoko coral reef. Threshold of PCO_2 value at which $CaCO_3$ production turns to dissolution was calculated to be 945 ppm. This value was similar to the results derived from Molokai reef flat of Hawaii [1].

[1] Yates *et al*. (2006) *Biogeosciences* **3**, 357-369.

https://doi.org/10.1180/S0026461X00006502 Published online by Cambridge University Press

Search for nucleosynthetic tellurium isotopic anomalies in meteorites by N-TIMS

Y. FUKAMI AND T. YOKOYAMA

Department of Earth and Planetary Sciences, Tokyo Institute of Technology, 2-12-1 Ookayama, Meguro, Tokyo 152-8551, Japan (fukami.y.aa@m.titech.ac.jp)

Tellurium is one of the promising elements for the study of nucleosynthetic isotope anomalies recorded in meteorites. Tellurium has eight stable nuclides, of which ^{120}Te is produced by the p-process, $^{122, 123, 124}$Te by the s-process, and $^{128, 130}$Te by the r-process. ^{125}Te and ^{126}Te are produced by both the r- and s-processes. The isotopic composition of Te is also affected by short-lived ^{126}Sn – ^{126}Te decay system ($T_{1/2}$ ~ 234 kyr) [1]. The ^{126}Sn is generated only by the r-process, and ^{126}Te excesses in meteorites would provide a smoking gun evidence for the injection of freshly synthesized nuclides by supernovae into the molecular cloud, which presumably triggered the formation of the solar system [2]. It has been reported that presolar diamonds from Allende (CV3) have large nucleosynthetic isotope anomalies of r-process Te isotopes [3,4], whereas bulk chondrites, iron meteorites and terrestrial samples have a uniform Te isotopic composition [5]. Small potential nucleosynthetic Te isotope anomalies in Allende CAIs have been reported, however, the possibility of analytical artifacts is not excluded [6].

It is considered that samples which potentially have nucleosysthetic anomalies (e.g. presolar grains) contain subnanograms of Te. In this study, we developed a precise Te isotope measurement technique using subnanograms of Te by applying a Negative Thermal Ionization Mass Spectrometry (N-TIMS) with secondary electron multiplier. We achieved ~14‰ for δ^{120}Te/^{124}Te, ~3‰ for $\delta^{123, 125}$ Te/^{124}Te, ~5‰ for δ^{126}Te/^{124}Te, ~7‰ for δ^{128}Te/^{124}Te, and ~10‰ for δ^{130}Te/^{124}Te as the external reproducivility (2S.D.) when 200 pg of Te was used. This analytical method will be applied to acid resistant fractions of primitive chondrites that are enriched in various types of presolar grain in order to identify whether nanodiamonds and other presolar phases have Tellurium isotopic anomalies.

[1] Oberli *et al*. (1999) *Int. J. Mass. Spectrom*. **184**, 145-152. [2] Cameron *et al*. (1977) *Icarus*. **30**, 447-461. [3] Richter *et al*. (1998) *Nature*. **391**, 261-263. [4] Maas *et al*. (2001) *Meteorit. Planet. Sci*. **36**, 846-858. [5] Fehr *et al*. (2005) *GCA*. **69**, 5099-5112. [6] Fehr *et al*. (2009) *Meteorit. Planet. Sci*. **44**, 971-984.

The Ag, Fe, and Zn isotopic compositions of Ag-Au ore deposits in Japan

M. FUKUYAMA[1]*, D-C. LEE[1] AND S-C. YANG[2]

[1]Institute of Earth Sciences, Academia Sinica, Taipei 11529, Taiwan(*correspondence: mayuko@earth.sinica.edu.tw)
[2]National Taiwan University, Taipei 11677, Taiwan

Recent MC-ICPMS studies have been able to improve the analytical precision to resolve sub-per mil differences in Ag isotopic compositions. This has led to the discovery of Ag isotopic variation in native Ag ore deposits, which have been attributed to mass dependent stable isotopic fractionations during natural chemical processing [1]. This suggests that Ag isotope may be a useful tracer for the studies of the origin and chemical evolution of ore deposits.

We have investigated the Ag isotopic variations for a series of Ag-Au ore deposits in Japan in order to better constrain the formation and evolution of these ore deposits. These include the Au-Ag epithermal vein type deposits, Pb-Zn vein type deposits, polymatallic vein type deposits, and Kuroko type deposits, while Ag occurs as either native or sulfide minerals in these deposits. The $\varepsilon^{107/109}$Ag data vary from -7.1 to 1.5 relative to the NIST SRM 978a, while both the lowest and highest Ag isotopic data were obtained from the Kuroko type deposits. These deposits have similar geological signature, yet they exhibit the largest Ag isotopic variations among the samples included in this study. Most of samples include a suite of Ag hosted minerals, however, no significant variation of εAg was found among these minerals. Further study is required to understand the causes for Ag isotopic variation in these ore deposits. Consequently, we have started to measure Zn and Fe isotopes to evaluate the effect of other potential factors, e.g., redox condition, pH and temperature, to the Ag isotopes in these ore deposits.

[1] Hauri *et al*. (2000) *Lunar Planet. Sci*. **31**, 1812.

https://doi.org/10.1180/S0026461X00006502 Published online by Cambridge University Press

Redox transformations of Cu in periodically flooded soils

B. FULDA[1]*, A. VOEGELIN[2] AND R. KRETZSCHMAR[1]

[1]Insitute of Biogeochemistry and Pollutant Dynamics, ETH Zurich, Switzerland
(*correspondence: beate.fulda@env.ethz.ch)
[2]Eawag, Swiss Federal Institute of Aquatic Science and Technology, Duebendorf, Switzerland

Copper is an essential nutrient, but due to its high toxicity for microorganisms also of concern as soil contaminant. Cu(II) dominates in oxic soils and strongly binds to natural organic matter (NOM). In redox-dynamic environments such as wetland soils, however, periodic flooding and soil reduction may lead to the transformation of Cu(II) to Cu(I) or even Cu(0) [1] and may thereby strongly affect the solubility and mobility of soil Cu. Sulfate reducing conditions during soil flooding may lead to the precipitation of Cu sulfide minerals [1]. However, the soft metal cation Cu^{+} probably also exhibits a high affinity to reduced organosulfur compounds, as it is known for other soft metal cations [2].

In a laboratory batch incubation experiment with paddy soil, we therefore investigated changes in the oxidation state and speciation of Cu over a soil reduction-reoxidation cycle as a function of the molar ratio between reducible sulfate and soil Cu (sulfate/Cu 0.1; 0.4; 1.2). Cu K-edge EXAFS data suggested that, after oxic equilibration, spiked Cu(II) mainly adsorbed as Cu(II) to soil organic matter and minerals. During the first few days of soil reduction, a large fraction of soil Cu became reduced to Cu(I) that was complexed by organic thiol groups (based on EXAFS and wet chemical data), and a small fraction was reduced to metallic Cu. During further reduction over 40 days of flooding, Cu was completely transformed to Cu sulfide at high initial sulfate/soil Cu ratio, whereas the Cu(0) fraction increased at low initial sulfate/soil Cu ratio. This difference in Cu speciation during soil flooding also affected Cu speciation after subsequent reoxidation. Whereas metallic Cu was rapidly oxidized to adsorbed Cu(II), a significant part of the S-coordinated Cu(I) remained stable over 14 days of aeration. Our data suggest that metallic Cu may control Cu solubility during soil reduction, especially in sulfate-limited soil. Our data also support the hypothesis that reduction of Cu^{2+} to the much softer chalcophile cation Cu^{+} prior to sulfate reduction may induce a shift in Cu-complexation from O/N- to reduced S-functional groups of organic matter.

[1] Weber *et al*. (2009) *Nature Geoscience*, **2**, 267-271. [2] Karlsson *et al*. (2005) *Environ. Sci. Technol*. **39**, 3048-3055.

Coenzyme F430, understanding methanotrophy in methane rich environments

JAMES M. FULTON [1,2], LAURENCE R. BIRD[1] AND KATHERINE H. FREEMAN [1]*

[1]Dept. of Geosciences, Pennsylvania State University, University Park, PA 16802, USA
(*correspondence: khf4@psu.edu)
[2] Marine Chemistry and Geochemistry Department, Woods Hole Oceanographic Inst., Woods Hole, MA 02543, USA

Large amounts of methane are oxidized by communities of methanotrophic archaea and sulphate reducing bacteria, preventing this potent greenhouse gas from reaching the atmosphere [1,2,3]. Methyl-coenzyme M reductase, an enzyme traditionally associated with methanogenesis, has recently been linked also to the anaerobic oxidation of methane [3]. Cofactor F430 is a tetrapyrrole nickel complex contained within the active site of methyl-coenzyme M and appears to be used in both methanogenesis and methanotrophy [3, 4]. Here we present a new approach for purifying F430 from natural samples and determining its stable isotopic composition (^{15}N and ^{13}C). F430 is isolated using multi-dimensional preparatory and high-performance chromatographic separations. Compound identity and purity are confirmed using molar C:N ratios, light absorbance and MS^{n} detection and fragmentation of F430 isolated from pure cultures of *Methanosarcina acetivorans*. C isotope analyses using nano-EA/IRMS [5] of natural samples are challenged by the presence of co-eluting non-tetrapyrrole structures. Our efforts to date document evidence for F430 in environmental samples, enrichment cultures as well as pure cultures of *Methanosarcina acetivorans*. The identification of F430 in environmental samples potentially provides evidence for anaerobic methane oxidation in a low oxygen environment via the reversal of the enzymes involved in methanogenesis.

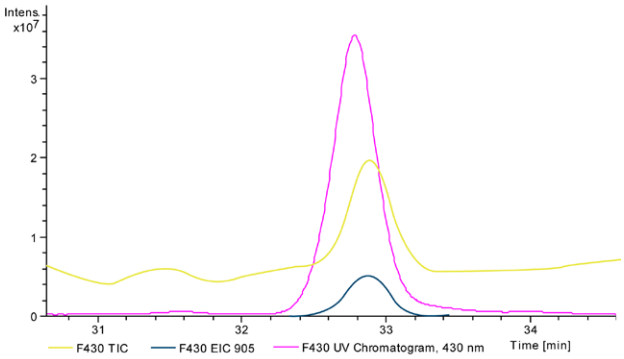

Figure 1: F430 is identified in samples based on adsorption in the 430 nm wavelength and the 905 ion

[1] Orphan (2001) *Science* **293** 5529 484 [2] Orphan (2008) Geobiology **6** 4 376 [3] Scheller (2010) *Nature* **465** 7298 606 [4]Mayr (2008) *Journal Of The American Chemical Soc*. **130** 32 10758 [5] Polissar (2009) *Analytical Chemistry*. **81** 755

https://doi.org/10.1180/S0026461X00006502 Published online by Cambridge University Press

An experimental study of minettes and associated mica-clinopyroxenite xenoliths from the Milk River area, Southern Alberta, Canada

S.P. FUNK* AND R.W. LUTH

C. M. Scarfe Laboratory of Experimental Petrology, Department of Earth & Atmospheric Sciences, University of Alberta, Edmonton, AB, Canada (*correspondence: sfunk@ualberta.ca)

Because of their hydrous nature, lamprophyres provide unique insights into the cycling of water into and out of the Earth's interior. Lamprophyres from southern Alberta, Canada, were studied by Buhlmann *et al*. [1], who suggested they were derived from a mantle source containing mica, clinopyroxene, and olivine. The present experiments were conducted using a piston-cylinder apparatus at conditions appropriate for the Earth's upper mantle (~1.5 - 2.5 GPa, ~1200°C - 1400°C). A multiple saturation point of olivine and orthopyroxene was found at ~2.0 GPa and ~1350°C. This result was unexpected because partial melting of refractory harzburgite should not yield lamprophyric magmas [2]. We suggest that during ascent the minette magma chemically re-equilibrated with harzburgitic wall-rock [3]. These experiments show that these minettes are not primary.

We also conducted a set of melting experiments on three chemically distinct cognate xenoliths to determine their solidus temperatures at 1.5 - 2.5 GPa, and to characterize the glass composition. The near-solidus melts have striking similarities to madupitic lamproites studied by Barton & Hamilton [4] from the Leucite Hills, Wyoming. They hypothesized that madupitic magmas could be the product of partial melting of mica-pyroxenite. The present experiments confirm this hypothesis.

[1] Buhlmann *et al*. (2000) *Can. J. Earth Sci*. **37**, 1629-1650. [2] Parman & Grove (2004) *J. Geophys. Res*. **109**, 1-20. [3] Foley (1992) *Lithos* **28**, 435-453. [4] Barton & Hamilton (1979) *Contrib. Mineral. Petrol*. **69**, 133-142.

Origin and flux of lunar (micro-) impactors: Constraints from N-Ar analyses of single Luna 24 grains

E. FÜRI[1]*, B. MARTY[1] AND S.S. ASSONOV[2]

[1]CRPG/CNRS, BP20, 54501 Vandoeuvre-les-Nancy, France (*correspondence: efueri@crpg.cnrs-nancy.fr)
[2]Universität zu Köln, 50674 Köln, Germany

The $^{15}N/^{14}N$ ratio of N trapped in the lunar regolith varies by ~300 ‰, which has been attributed to either a) a secular increase of the N isotope composition of solar wind (SW) [1], or b) varying mixing proportions between solar N and non-solar N sources that are enriched in ^{15}N [2, 3]. In light of the recent Genesis findings, which revealed that modern SW N is isotopically light [4, 5], we use in this study the approach of single grain analyses to re-evaluate the provenance of N in Luna 24 soils. Our new N-Ar data, together with previous results from the Apollo sites, allow us to place limits on the proportion of solar and non-solar N trapped in lunar regolith, as well as on the recent flux of planetary material to the Moon's surface.

Single Luna 24 grains with $^{40}Ar/^{36}Ar$ ratios < 1 have $\delta^{15}N$ values between -54.5 and +123.3 ‰ relative to air. Thus, low-antiquity lunar soils record both positive and negative $\delta^{15}N$ signatures, and the secular increase of the $\delta^{15}N$ value [1] is no longer apparent when the Luna and Apollo data are combined. Instead, the N isotope signatures, corrected for cosmogenic ^{15}N, are consistent with binary mixing between SW N ($\delta^{15}N_{SW} \approx$ -407 ‰ [5]) and a non-solar N component with a $\delta^{15}N$ value of +100 to +150 ‰.

Micrometeorites and interplanetary dust particles, which dominate the current flux of extraterrestrial matter on Earth, match well the required characteristics of the non-solar component present in the lunar regolith. In contrast, a possible cometary contribution to the non-solar N flux is constrained to be ≤ 8 to 15 %, assuming a $\delta^{15}N$ value of +900 ‰ for cometary material [6]. Based on the observed mixing ratio of solar to planetary N, we estimate the flux of micro-impactors to be (2.2 to 6.2) × 10^3 tons yr^{-1} at the lunar surface. Thus, assuming a water content of ~10 wt%, characterizing carbonaceous chondrites [7], micro-impactors may deliver up to ~600 tons of water per year to the Moon.

[1] Kerridge (1975) *Science* **245**, 162-164. [2] Wieler *et al*. (1999) *EPSL* **167**, 47-60. [3] Hashizume *et al*. (2002) *EPSL* **202**, 201-216. [4] Marty *et al*. (2010) *GCA* **74**, 340-355. [5] Marty *et al*. (2011), *LSPC* **XXXII**, #1870. [6] Bockelée-Morvan *et al*. (2008) *ApJ* **679**, L49-L52. [7] Kerridge (1985) *GCA* **49**, 1707-1714.

https://doi.org/10.1180/S0026461X00006502 Published online by Cambridge University Press

Chemical compound classes supporting microbial methanogenesis in coal

A. FURMANN[1], A. SCHIMMELMANN[1], S. C. BRASSELL[1], M. MASTALERZ[2] AND F. PICARDAL[3]*

[1]Department of Geological Sciences, Indiana Univ., Bloomington, IN 47405, USA
[2]Indiana Geological Survey, Bloomington, IN 47405, USA
[3]School of Public and Environmental Affairs, Indiana Univ., Bloomington IN 47405, USA
(*correspondence: picardal@indiana.edu)

Microbial generation of coalbed methane (CBM) occurs in numerous basins worldwide. This study aims to identify specific classes of chemical compounds in coals from the Illinois Basin in southwestern Indiana that are degraded during methanogenesis. Springfield (SPR) coal is rich in vitrinite and Lower Block Coal (LBC) coal has greater liptinite and inertinite contributions. Anaerobic bioreactors contained a mineral-salts medium, operationally-defined coal extracts and a microbial inoculum obtained anoxically via filtration of formation water from a CBM-producing well. Our experiments investigated methanogenesis and concurrent degradation of organic matter (OM) using H_2O-, CH_3OH-, and CH_2Cl_2-soluble fractions of extractable OM from coal as the sole carbon source. This approach allowed us to trace specific molecular changes in the OM during methanogenesis. GC/MS and FTIR techniques were employed to compare the molecular composition of the initial organic extracts with their biodegraded residues.

Periodic GC-FID methane measurements over several months revealed greater CH_4 generation in reactors containing extracts from SPR coal, and slightly more CH_4 produced from CH_3OH-extracts than from CH_2Cl_2 (DCM) extracts. Inoculated controls containing H_2:CO_2 or acetate instead of coal extracts showed significant methanogenesis indicating that a viable inoculum was used in all reactors. GC/MS characterization of organic extracts enabled assessment of the occurrence and distribution of constituent *n*-alkanes, acyclic isoprenoid alkanes, hopanes in higher abundance than steranes, methylphenanthrenes, phenanthrene, anthracene, fluoranthene, and pyrene in the non-polar fraction, as well as carboxylic acids in the polar fraction. FTIR results showed higher aromaticity and presence of longer aliphatic chains in DCM extracts than in methanol extracts. The expected greater biodegradability of lower-MW compounds with lesser aromaticity might explain greater CH_4 production in the reactors containing methanol extracts. Continued analysis through June 2011 is expected to result in diagnostic changes in molecular composition, most likely affecting *n*-alkanes and possibly some aromatics.

Different types of Precambrian ophiolites

H. FURNES[1], Y. DILEK[2] AND M. DE WIT[3]

[1]Dept. of Earth Science & Centre for Geobiology, Univ. of Bergen, Norway
(*correspondence: harald.furnes@geo.uib.no)
[2]Dept. of Geology, Miami Univ., Oxford, Ohio, USA
[3]AEON & Dept. of Geological Sciences, Univ. of Cape Town, South Africa

Phanerozoic ophiolites are classified into subduction-related and unrelated types based on their tectonic and geochemical association with palaeo-subduction zones [1]. These two main types are further subdivided into several subtypes that exhibit different crustal architecture and igneous stratigraphy, with or without a sheeted dike complex. The geochemistry of the lavas and/or dikes of the two main types show pronounced differences in the concentration of elements that are sensitive to subduction processes (Cs, Pb, Rb, K, Ba, Th, U and LREE), and thus define contrasting patterns with respect to element-element -, element ratio -, and multi-element diagrams. We apply this new ophiolite classification to some of the well-preserved Precambrian greenstone belts, ranging in age from ca. 2.0 – 3.8 Ga. The metabasalts of the Isua (Greenland) and Barberton (South Africa) greenstone belts, 3.8 and 3.5 Ga, respectively, show geochemical signatures comparable with those of the best-documented Phanerozoic suprasubduction-zone ophiolites. The 2.7 Ga Wawa greenstone belt (Superior Province, Canada) and the 1.95 Ga Jormua Complex (Finland), on the other hand, display subduction-unrelated geochemical patterns, and are classified as plume- and continental margin type ophiolites, respectively. This approach to identifying Precambrian ophiolites with their distinct geochemical and tectonic fingerprints can be used effectively to decipher the geodynamic setting of the formation of ancient oceanic crust during the geological evolution of the greenstone belts.

[1] Dilek & Furnes (2011) *GSA Bull* **123**, 387-411.

https://doi.org/10.1180/S0026461X00006502 Published online by Cambridge University Press

Arsenic distribution in an unconformity related hydrothermal vein system

TOBIAS FUßWINKEL[1], THOMAS WENZEL[1], THOMAS WAGNER[2], MARKUS WÄLLE[2] AND JOACHIM LORENZ[3]

[1]Department of Geosciences, University of Tübingen, Wilhelmstr. 56, D-72072 Tübingen, Germany (tobias.fusswinkel@uni-tuebingen.de)
[2]Institute of Geochemistry and Petrology, ETH Zurich, Clausiusstr. 25, CH-8092 Zürich, Switzerland
[3]Graslitzer Straße 5, D-63791 Karlstein am Main, Germany

Many active geothermal systems discharge large amounts of arsenic, contributing significantly to geogenic arsenic contamination. This study aims at a better understanding of the physicochemical controls that favor transport or fixation of arsenic in geothermal environments. The unconformity related hydrothermal vein system at Sailauf (Germany) provides a well suited natural field laboratory, with As enriched mineral assemblages exposed immediately below the Permian unconformity. Hydrothermal minerals of the rhyolite hosted veins comprise mainly Ca-Mn carbonates, which are intergrown with braunite, hematite, hausmannite and manganite. Arsenate minerals are present as late vug fillings, intergrown with late stage carbonates, and fracture fillings of native arsenic. The textural features suggest a significant mobility of As in the hydrothermal fluids, in particular during late-stage low-temperature fluid-mineral reactions.

As a first step towards a quantitative As budget of the system, we determined the distribution of arsenic and other trace elements in cogenetic gangue and ore minerals by combination of EPMA and LA-ICPMS. The work is complemented by fluid inclusion studies that involve As analysis by LA-ICPMS of single fluid inclusions. While early primary calcites are virtually devoid of As, cogenetic main stage braunites were found to contain arsenic in oscillatory zoning patterns. Concentrations range from 100 ppm in the As-poor to 6000 ppm within the As rich growth zones. Primary tabular hematite exhibits variable As contents of 100 to 1000 ppm, whereas late stage carbonates can have as much as 1000 ppm As. The trace element distribution, in conjunction with fluid inclusion and stable isotope data, will be used as input for geochemical modeling of the As mineralization processes. The modeling will look at the competing effects of precipitation of As phases as a consequence of fluid boiling or mixing processes, and As incorporation into oxide minerals controlled by surface complexation.

Irreducible uncertainty in estimates of silicate mineral weathering rates

M.N. FUTTER[1]*, J. KLAMINDER[2], R.W. LUCAS[3] AND S.J. KÖHLER[1]*

[1]Swedish University of Agricultural Sciences, SE750 07 Uppsala, SE (*correspondence: martyn.futter@slu.se)
[2]Umeå University, SE90187 Umeå. SE
[3]Swedish University of Agricultural Sciences, SE90183 Umeå SE

The notion that precise estimates of silicate mineral weathering rates are possible is a key assumption behind many environmental policies. Earlier, we showed that an ensemble of published silicate mineral weathering rate estimates was insufficiently precise to evaluate sustainability of forest harvest at a single site [1]. Here, we extend this analysis with a comprehensive dataset from 82 different sites on 3 continents where 3 or more published weathering rate estimates were available. The range (max/min) of published weathering rate estimates at a single site (below) had a median value of 6 and a maximum of 52.

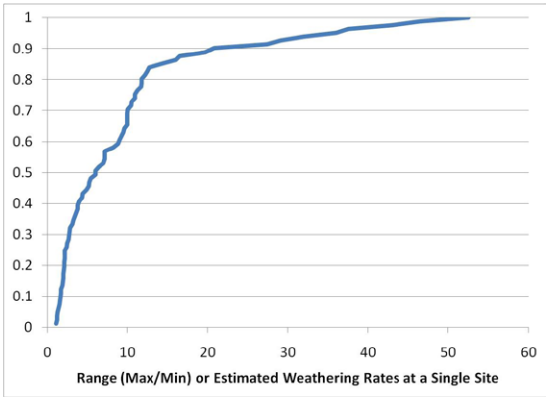

Figure 1: Cumulative distribution plot of range (max/min) or published weathering rate estimates for single sites.

While the weathering rate uncertainty can be partitioned into model structural, weathering zone depth, parameter and data terms, there is an irreducible factor of 2 uncertainty in rate estimates. Failure to consider this uncertainty can have profound consequences for critical load estimates, sustainable forest harvesting or assessing the feasibility of geo-engineering projects for climate change mitigation.

[1] Klaminder *et al*. (2011) *For. Ecol. & Mgmt*. **261** 1-9.

https://doi.org/10.1180/S0026461X00006502 Published online by Cambridge University Press

Siderite in Archaean banded iron formations - A sensor for CO_2 partial pressures of ancient atmospheres?

F.M. GÄB[1]*, C. BALLHAUS[1] AND J. SIEMENS[2]

[1]Steinmann Institut, Universität Bonn, Germany (*correspondence: fgaeb@uni-bonn.de)

[2]Institute for Crop Science and Resource Conservation-Soil Science, Universität Bonn, Germany

It has been around for some time that siderite in Archaean BIFs can serve as a CO_2 sensor for Archaean atmospheric compositions [1], according to

Fe^{2+} (aq) + $3H_2O$ + CO_2 (atm) = $FeCO_3$ (siderite) + $2H_3O^+$ (aq).

This equilibrium is seemingly shifted to the right as the CO_2 partial pressure (pCO_2) of the atmosphere rises, triggering the precipitation of marine carbonates including siderite if there is sufficient Fe^{2+} (aq) dissolved in seawater. In reality, rising pCO_2 causes the H_3O^+ activity to increase (ocean acidification), lowering the CO_3^{2-}/HCO_3^- activity ratio in water until carbonate minerals become unstable. Hence, the above equilibrium is metastable and unviable to describe natural atmosphere-seawater interactions, contrary to assertions by Ohmoto *et al*. [1]. We are equilibrating natural and artificial seawater at 25°C with oxidized N_2-O_2-CO_2 and reduced N_2-CH_4-H_2-CO_2 atmospheres with variable pCO_2 ranging from $< 10^{-5}$ to 1 atm. Up to a pCO_2 of ~ 0.05 atm, the carbonate alkalinity of seawater is independent of pCO_2 as predicted by thermodynamics, however, when pCO_2 increases above 0.07 atm (pH < 6.5) carbonate alkalinities gradually decline and carbonate minerals become unstable. Carbonate minerals find ideal conditions when the pCO_2 of the atmosphere is at its minimum and the CO_3^{2-}/HCO_3^- activity ratio in seawater at its maximum (i.e. high weathering rates, low atmospheric pCO_2). When the $pCO_2 < 2*10^{-4}$ atm (< 200 ppm CO_2 in the gas phase), natural seawater at 25°C spontaneously precipitates aragonite in the form of micro-ooides. The precipitation of siderite in Fe^{2+}-doped seawater equilibrated with a reduced atmosphere is impossible, so long as the water contains the current marine Ca^{2+} concentrations. In an artificial, NaCl-$NaHCO_3$-$FeCl_2$-bearing, Ca^{2+}-free seawater proxy (100 ppm Fe^{2+}, carbonate alkalinity 4000 μmol kg^{-1}), falling pCO_2 causes the precipitation of an amorphous blue-green phase that we tentatively identify as ferrous-ferric carbonate hydrate. Precipitation of that phases lowers the carbonate alkalinity by around 40 percent. That phase may qualify as precursur to siderite and could be an important primary inorganic precipitate from an Fe^{2+}-bearing, sulfate-poor, reduced Archaean ocean in exchange equilibrium with a reduced CH_4-bearing, CO_2-poor atmosphere. We conclude that siderite is not likely to be a primary precipitate from Archaean seawater. We further conclude that potential precursor phases to siderite (i.e. amorphous Fe-carbonate-hydrates) are most stable at maximum CO_3^{2-}/HCO_3^- activity ratios in the water, hence are favoured at atmospheric compositions poor in CO_2.

[1] Ohmoto H., Wanatabe Y, Kumazawa K. (2004) *Nature* **429**, 395-399.

Growth rate effect on oxygen isotope fractionation between calcite and fluid: *In situ* data

R.I. GABITOV *, A.K. SCHMITT[1], E.B. WATSON[2], K.D. MCKEEGAN[1] AND T.M. HARRISON [1]

[1]University of California, Los Angeles, CA, 90095, USA (*correspondence: gabitr@ucla.edu)

[2]Rensselaer Polytechnic Institute, Troy, NY, 12180, USA

The oxygen-18 content of carbonates (expressed as $\delta^{18}O$) is widely used in paleoclimatology, yet it is clear from comparison between experimental and natural carbonates that isotopic equilibrium is not always achieved. This observation underscores the importance of exploring possible effects of growth rate on isotopic fractionation, which is the focus of this study.

In situ Secondary Ion Mass Spectrometry (SIMS) analyses of $\delta^{18}O$ were performed on single crystals of experimentally grown calcite at an external reproducibility of 0.25 ‰ (1σ). Growth rate (V) variations within crystals grown isothermally (at 15, 20, 22, and 25°C) were monitored by sequentially spiking calcite-precipitating fluids with rare earth element (REE) dopants. The REE were analyzed with SIMS at spots matching those where $\delta^{18}O$ was determined. REE patterns reveal concentric domains of calcite growth. The growth rate of calcite generally decreases with time - i.e., crystal rims advanced at slower rates than cores. The compositions of $\delta^{18}O$ in bulk calcites and experimental fluids were measured by Fisons Optima and Finnigan MAT 251 mass spectrometers, respectively. The average of SIMS $\delta^{18}O$ values agrees with bulk $\delta^{18}O$ determined by conventional mass spectrometry within analytical uncertainty. The fractionation factor ($\alpha^{18}O$) decreases by 0.8±0.08 ‰ with increasing V (0.12–16 μm/day) at 25°C. If the core is included at an estimated V>30 μm/day, a total range of 1.7 ‰ is observed at 25°C. A maximum difference of 3 ‰ was observed between the rim and core of the calcite crystal grown at 15°C.

Our results provide the first *in situ* evidence that ^{18}O may be depleted in the near-surface region of calcite relative to the bulk crystal lattice, consistent with the surface entrapment model [1]. As predicted, this effect increases with decreasing temperature. Therefore, knowledge of crystal growth rates needs to be accounted for when using $\delta^{18}O$ in natural carbonates as a proxy for sea-water temperature.

[1] Watson (2004) *Geochim. Cosmochim. Acta*, **68**, 1473–1488.

https://doi.org/10.1180/S0026461X00006502 Published online by Cambridge University Press

Post-entrapment changes to H_2O and CO_2 in olivine-hosted melt inclusions

GLENN GAETANI[1]*, JULIE O'LEARY[1,2] AND NOBUMICHI SHIMIZU[1]

[1]Geology & Geophysics, Woods Hole Oceanographic Institution, Woods Hole MA 02543 USA (*correspondence: ggaetani@whoi.edu)
[2]ExxonMobil Production Company, Houston TX 77067

Olivine-hosted melt inclusions are an important source of data on magmatic volatiles. The strength of the olivine protects inclusions from decompression and degassing during ascent and eruption, preserving pre-eruptive volatiles. However, inferring mantle volatiles requires that melt inclusions remain closed systems from the time of entrapment. We used a combination of experiments and modelling to investigate the potential for post-entrapment modification of H_2O and CO_2. Our results demonstrate that proton diffusion re-equilibrates H_2O in a matter of hours, but that a significant flux of C through the host olivine is unlikely. However, H_2O changes can affect CO_2 through the formation of vapor bubbles within the inclusion. The combination of diffusive re-equilibration and vapor bubble formation significantly affect degassing paths and entrapment pressures inferred from the volatile content of melt inclusions.

Effects of diffusive re-equilibration were assessed using hydration and dehydration experiments performed on natural inclusion-bearing olivines. All run products were analyzed for major elements by electron microprobe and for H_2O and D/H ratio by SIMS. The oxidation state of Fe was determined by μ-XANES. Our results demonstrate that proton diffusion is extremely efficient at modifying the concentration of H_2O in melt inclusions. These changes do not affect the fugacity of oxygen within the inclusion, which is controlled by the creation or destruction of metal vacancies that diffuse through the olivine at rates comparable to protons.

Initially vapor-saturated inclusions are driven toward undersaturation by the loss of H_2O, so that the concentration of CO_2 is not significantly effected. This produces melt inclusions with variable CO_2 at constant H_2O, resulting in an apparent open-system degassing path. Conversely, the addition of H_2O to melt inclusions, as during magma mixing, drives inclusions toward vapor oversaturation, leading to the production of CO_2-rich vapor bubbles. Therefore, the addition of H_2O will cause melt inclusions to evolve along an isobaric CO_2 degassing path, leading to significant changes in both H_2O and CO_2.

Causes and consequences of Zn, Fe and S isotope fractionation in a large hydrothermal system: The Navan orebody, Ireland

D. GAGNEVIN[1], A.J. BOYCE[2], C.D. BARRIE[2], J.F. MENUGE[1]* AND R.J. BLAKEMAN[3]

[1]School of Geological Sciences, University College Dublin, Belfield, Dublin 4, Ireland (*correspondence: j.f.menuge@ucd.ie)
[2]SUERC, East Kilbride, Glasgow G75 0QF, Scotland
[3]Boliden Tara Mines Limited, Navan, County Meath, Ireland

This study investigates the extent, causes and consequences of Zn and Fe isotope fractionation within the world-class Irish-type Navan Zn-Pb orebody, Ireland. Layered sphalerite (ZnS) has been targeted for isotopic analyses. Using samples of growth-layered sphalerite, as well as bulk Zn ore concentrates and potential source rocks, we are able to examine processes of fractionation ranging from millimeter to kilometer scales.

Large variations in $\delta^{66}Zn$ (of 0.55‰), $\delta^{56}Fe$ (of 2‰) and $\delta^{34}S$ (of 28‰) have been measured in microdrilled sphalerite. Significantly, the range of $\delta^{66}Zn$ (0.33‰) and $\delta^{56}Fe$ (0.95‰) across 3 mm of sphalerite colloform growth banding represents a substantial fraction of the range exhibited by common terrestrial rocks. Moreover, $\delta^{66}Zn$ and $\delta^{56}Fe$ display a well-defined positive correlation and both also correlate with $\delta^{34}S$; S isotope compositions have previously been proven to monitor the extent of mixing between shallow, metal-poor, surface brines and deep, metal-rich, hydrothermal fluids in Irish-type deposits. The observed relationships represent the interplay between kinetic Zn and Fe isotope fractionation during sphalerite precipitation, and mixing of S between hydrothermal fluids and bacteriogenic brines.

Concentrate data clearly show that relatively high $\delta^{56}Fe$ and $\delta^{66}Zn$ dominate the overall system, and that lower $\delta^{56}Fe$ and $\delta^{66}Zn$ found associated with hydrothermal sulphide are a minor component of the overall deposit signature. Basement rock $\delta^{66}Zn$ data confirm that the basement is isotopically not homogenous, nor homogenised in the hydrothermal system.

Our data suggest that incoming pulses of metal-rich hydrothermal fluid triggered sulphide mineralisation, and that rapid precipitation of sphalerite from hydrothermal fluids will strongly fractionate Zn and Fe isotopes at very short time and length scales, thereby limiting the use of Fe and Zn isotopes as exploration tools. However, Zn and Fe isotopes in sulphides appear to be powerful tools to assess and decipher the physical and chemical processes responsible for the genesis of ore bodies.

https://doi.org/10.1180/S0026461X00006502 Published online by Cambridge University Press

Minor elements in layered sphalerite record fluid origin in the giant Navan Zn-Pb orebody, Ireland

D. GAGNEVIN[1]*, J.F. MENUGE[1], A. KRONZ[2], C.D. BARRIE[3] AND A.J. BOYCE[3]

[1]UCD School of Geological Sciences, University College Dublin, Belfield, Dublin 4, Ireland (*correspondence: damien.gagnevin@ucd.ie)
[2]Georg-August-Universität Göttingen, Germany
[3]S.U.E.R.C, East Kilbride, Glasgow, Scotland

This study aims to test whether the chemistry of sphalerite in the world-class, Irish-type, Navan ore deposit may help to decipher the nature and origin of the ore-forming fluids. Detailed electron microprobe traverses were carried out across colloform and other growth-layered sphalerite, on samples that were previously analysed for Zn, Fe and S isotopes (Gagnevin *et al*., Goldschmidt 2011). In particular, the S isotope data enabled us to distinguish between samples that precipitated from hydrothermal, metal-bearing fluids or from cooler, bacteriogenic, sulphide-bearing fluids.

On the hand sample scale, Cd and Fe discriminate between the two fluid sources (Fig. 1); Cd, Sb, and to a lesser extent Cu, are enriched in sphalerite precipitated from hydrothermal fluids ($\delta^{34}S > 0$), while Fe and As are enriched in sphalerite precipitated from bacteriogenic fluids ($\delta^{34}S < 0$), suggesting that sphalerite chemistry is a good guide to fluid origin.

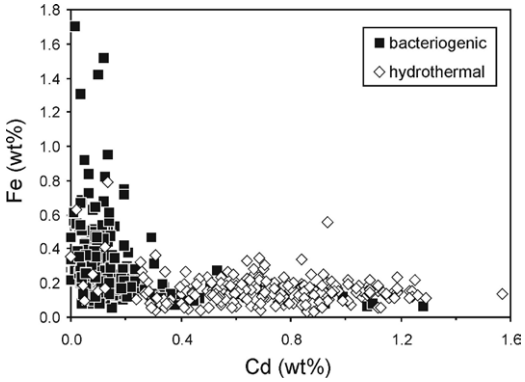

Figure 1: Cd vs Fe concentrations of layered sphalerite investigated in this study.

Frequent large (up to order of magnitude) elemental variations between successive sphalerite layers, whether colloform or not, indicate repeated influxes of hydrothermal fluids, with probable control also from kinetic effects and substitution mechanisms. Moreover, we show that sphalerite texture is sometimes, but usually not, correlated with sphalerite chemical composition.

Calcium isotopes during coral biomineralization

A.C. GAGNON[1,2]*, D.J. DEPAOLO[1], J.F. ADKINS[3] AND J.J. DE YOREO[2]

[1]Earth Sciences Division, Lawrence Berkeley National Lab, USA (*correspondence: acgagnon@lbl.gov)
[2]Molecular Foundry, Lawrence Berkeley National Lab, USA
[3] Geological and Planetary Sciences, Caltech, USA

A mechanistic understanding of biomineralization promises to separate biological and environmental signals in skeletal carbonates, improving the interpretation of paleoproxies. Towards this goal, we measure calcium isotope ratios of micromilled samples from modern scleractinian deep-sea coral, testing two questions in coral biomineralization. Is amorphous calcium carbonate (ACC) an important precursor during skeletal nucleation? Can reservoir effects (Rayleigh models) explain the biologically controlled variability of non-traditional stable isotopes.

Centers of calcification (COCs) are morphologically and compositionally distinct regions of the coral skeleton associated with nucleation. To test if an ACC precursor phase can explain the geochemistry of COCs, we compare the calcium isotope ratios of COCs to synthetic ACC. The $\delta^{44}Ca$ of COCs are similar to the surrounding skeleton and to inorganically precipitated aragonite, but are fractionated significantly more than inorganic ACC ($\Delta^{44}Ca_{COC\text{-}seawater} = -1.0 \pm 0.1$ ‰ while $\Delta^{44}Ca_{ACC\text{-}solution} < -0.2$ ‰). If ACC is involved in skeletal nucleation, then the distinct calcium isotope signature of this phase is lost during subsequent phase transformation. As calcium is the major cation in aragonite, this presumably means the minor and trace element composition of an ACC phase would be altered as well, and suggests that ACC is unlikely to explain the compositional anomalies associated with COCs in coral.

Even when grown under constant environmental conditions, metal/calcium ratios in deep-sea coral vary by more than 5 %. This variability can be explained by skeletal precipitation from closed batches of seawater or a more general steady-state reservoir effect where seawater transport to the site of calcification balances precipitation. Both models make similar predictions regarding calcium isotopes, higher skeletal Sr/Ca ratios should correlate with lighter $\delta^{44}Ca$. We observe this predicted trend in preliminary results from micromilled samples, suggesting that in addition to metal/calcium ratios, reservoir effect models of coral biomineralization may also explain the variability of some isotope systems. Analysis of coral from a range of conditions will test if we can recover biomineralization corrected records of seawater isotope ratios and environmental conditions.

https://doi.org/10.1180/S0026461X00006502 Published online by Cambridge University Press

Volcanic gases and redox biogeochemistry at the Archean-Proterozoic transition

FABRICE GAILLARD[1], BRUNO SCAILLET[1] AND NICHOLAS T. ARNDT[2]

[1]Institut des Sciences de la Terre d'Orléans, CNRS-INSU/Université d'Orléans, 45071, Orléans, France
[2]ISTerre, Université Joseph Fourier de Grenoble, CNRS, 38400, Saint Martin d'Hères, France.

A major crust-forming event at 2.7 Ga preceded a major change in the chemistry of surface waters on ancient Earth. Formation of a permanently oxygenated atmosphere at 2.45 Ga dramatically affected redox processes in the exosphere, as recorded in the ancient sulphur biogeochemical cycle. The emergence of oxygenic cyanobacteria and changes in composition of volcanic gases are possible triggers of the rise of atmospheric oxygen, but the sequence of these events and the evidence for such changes are debated. In particular, robust geochemical data indicates that the oxidation state of volcanic rocks and their source regions has remained constant since 3.5 Ga.

Using thermodynamic calculations simulating gas-melt equilibria during magma ascent, we show that change in the average pressure of volcanic degassing due to a global decrease in sea level accompanying the growth of the continental crust provides a simple yet robust explanation: Archean volcanic degassing was mostly submarine, occurring under water pressures of 10-100 bar and producing gases with H_2S/SO_2 >1, with low sulphur content. In contrast emergence of the continents in the late Archean led to widespread subaerial volcanism that yielded gases much richer in S and dominated by SO_2. The transition from H_2S dominated gases at elevated pressure of degassing to SO_2 dominated ones at atmospheric pressure is redox-compensated by a strong H_2 enrichment in the gas.

Archean and early Proterozoic sulphur biogeochemical cycles can be explained by a change in composition of volcanic gases that is unrelated to a change in magmatic source processes but most likely caused by geodynamic and eustatic modifications. The resulting changes in volcanic gas compositions must have impacted on the oxygenation of the atmosphere.

The subduction weathering factory

J. GAILLARDET*, P. LOUVAT*, C. DESSERT AND E. LAJEUNESSE

Institut de Physique du Globe de Paris, UMR 7451, Sorbonne Paris Cité. 75238 PARIS Cedex 05

About 30% of the global consumption of atmospheric CO_2 is due to the weathering reactions involving volcanic rocks. Therefore, volcanic settings are essential to consider both in terms of fluxes and mechanisms of chemical weathering. However few studies have focused on the weathering of volcanic arc islands although it is a key geodynamical setting, for example for the production of continental crust. Most of the degassing of deep CO_2 occurs in subduction zones and subducion volcanism is particularly rich in volatiles, such as sulfuric or chlorhydric acids that are major suppliers of acidity to the earth's surface.

The synthesis of available data on river chemistry in volvanic arc setting and new data from our group on the rivers of lesser Antilles show that the chemical denudation rates are amongst the highest on earth. They range from 10 t/km^2/yr to 700 t/km^2/yr in the most active regions.

Two dominant mechanisms appear to play the major roles in the subduction zone factory. The first is hydrothermal activity, the second is water runoff; the former being linked to the latter though the water cycle. Hydrothermal activity produces high temperatures and additional acidity in the form of sulfuric, chlohydric and carbonic acids. Runoff values are generaly associated to high precipitation regimes, due to the orographic effect. The orographic effect is temperature-dependent based on the Clausius-Clapeyron relationship.

Due to these two main mechanisms, subduction weathering factory transforms the rocks into sediments at a very high rate and is responsible for high CO_2 consumption rates. Our study suggests that chemical denudation is a significant fraction of the total erosion rate of volcanic arcs and that total erosion rates are in the order of the long-term magnatic eruptive rates.

https://doi.org/10.1180/S0026461X00006502 Published online by Cambridge University Press

On the peculiarities of Australian and Venezuelan pink diamonds: Influence of the geologic settings

E. GAILLOU[1,2], J.E. POST[1] AND J.E. BUTLER[3]

[1]Department of Mineral Sciences, Smithsonian Institution, Washington, DC 20560, USA.
[2]Department of Terrestial Magnetism, Carnegie Institute, Washington DC 20015, USA.
[3]Chemistry Division, Naval Research Laboratory, Washington DC 20375, USA.

Pink diamonds have a heterogeneous color that typically is restricted to lamellae formed by plastic deformation oriented along {111}. Pink diamonds from Argyle in Australia and from Santa Elena in Venezuela show distinct visual and spectroscopic features compared to diamonds from other localities. Their pink color is prominent and has a banded pattern, sometimes wavy, interlaced with smaller bands of colorless areas. The birefringence indicates that the plastic deformation is located mostly inside the colorless areas for Argyle and Santa Elena diamonds, and inside the pink areas for other diamonds. Cathodoluminescence (CL) images show that plastic deformation features cut across the growth patterns of the diamonds. They quench partially the CL in colorless areas, while the pink areas retain growth sectors, as delineated in CL images by H3 and N3 centers. For other pink diamonds, the colored lamellae contain H3 and 405.5 nm centers. It is possible that for Argyle and Santa Elena diamonds, a pre-existing pink color was partially quenched during a later episode of plastic deformation. Conversely, diamonds from other localities apparently acquired their pink color from a later stage of plastic deformation. The geological settings of diamonds from Argyle in Australia and Santa Elena in Venezuela are similar, forming underneath Proterozoic cratons (and not the typical Archean cratons), that experienced high thermal events in their early histories.

Potential for widespread microbial liberation of structurally-coordinated iron from common clay minerals in marine sediments

ROBERT R. GAINES[1], JOHNSON TRANG[1], SAMUEL SCOTT[1], E.J. CRANE[1], MARIA PROKOPENKO[2] AND WILLIAM M. BERELSON[2]

[1]Pomona College, Claremont, CA, 91711, (robert.gaines@pomona.edu; jt012007@mymail.pomona.edu; sws1@hi.is; ej.crane@pomona.edu)
[2]University of Southern California, Los Angeles, CA, 90089, (prokopen@usc.edu; berelson@usc.edu)

Clay minerals are the most abundant materials found at the surface of earth and they are the primary constituents of marine sediments. Iron, a limiting nutrient in many marine settings, is a common constituent of clay minerals. Recent *in vitro* experimental evidence has shown that lab cultures of Fe-reducing bacteria are able to utilize structurally-bound Fe from the crystal lattice of nontronite, an uncommon and particularly Fe-rich smectitie (>12wt.%). Reduction of structurally-coordinated Fe results in liberation of Fe(II) to solution, where it is available for other biotic processes, and the transformation of smectite to illite. However, it has remained unclear: 1. whether or Fe-reducers are able to access structurally coordinated Fe found in low wt.% in common clay minerals; 2. if naturally occuring populations of Fe-reducers are able to reduce structurally coordinated Fe as some lab strains are; and 3. if this process is significant in the marine Fe-cycle. In order to address these questions, we combined *in vitro* experiments using a suite of clay minerals with iron contents ranging from low (0.8 wt.%) to high (13.9 wt.%) with high-resolution analyses of sediment cores from the Santa Monica Basin, a location noted for a high benthic flux of Fe(II) from the sediments. Experimental evidence clearly indicates that, under *in vitro* conditions, Fe(III) bound in common clay minerals is available for reduction by the lab strain *Shewanella oneidensis* MR-1 as well as by naturally-occuring consortia of Fe-reducers cultured from the San Pedro and Santa Monica Basins. Analyses of sediment cores suggest that structural Fe bound in illite-smectite mixed layer clays (~3.0wt.%) of the Santa Monica Basin is bioavailable. Depth of smectite-illite conversion (<20cm) suggests that Fe may be liberated on the timescale of decades to ~200 years, contributing to the flux of Fe(II) from the sediments. Our findings suggest that common clay minerals may represent a large and previously unrecognized pool of bioavailable Fe in the world ocean that contributes significantly to biogeochemical cycling of Fe and C.

https://doi.org/10.1180/S0026461X00006502 Published online by Cambridge University Press

Experimental studies on CO_2 sequestration in basaltic rocks with a plug flow reactor

I. GALECZKA*, D. WOLFF-BOENISCH, AND S. R. GISLASON

Institute of Earth Sciences, University of Iceland, Sturlugata 7, 101 Reykjavik, Iceland (*img3@hi.is)

Mineral trapping in silicate rocks is considered the most stable strategy of CO_2 storage. Conceptual model of CO_2 mineral fixation in Iceland assumes that acidic carbonated waters injected into basaltic rocks will initially cause rock dissolution and release of divalent cations such as Ca^{2+}, Mg^{2+} and Fe^{2+}. As reactions progress, these elements will combine with CO_3^{2-} and precipitate as carbonates due to increasing pH [1]. A large scale experiment with a plug flow reactor imitating chemical and physical conditions within the basaltic rocks after CO_2 injection, gives an opportunity to study the rate of basaltic rock dissolution and solid replacement reactions under controlled CO_2 conditions. The experimental set-up makes it possible to follow changes in pH, Eh and chemical composition of the fluid on different levels along the flow path within the column. Characterization and quantification of secondary minerals (carbonates and clays) enables determination of molar volume and porosity changes with time. Data obtained from experiment will be used in reactive transport models to elucidate the advance of reaction fronts, forecast porosity changes followed by estimation of upper limit CO_2 injected into a given geological formation.

Experimental set-up consists of 7 titanium compartments assembled into a 2.5 m long pipe (5.4 cm OD x 5 cm ID), corresponding to a volume of ~ 5 dm^3. The column is filled with basaltic glass grains, of known chemical composition and surface characteristic (45-100 μm size fraction). CO_2 saturated water will be pumped under 75 bar pressure through the column. This contribution will present first preliminary results from this column experiment.

[1] Gislason *et al*. (2010) *JGGC*, **4**, 537-545

Stable Sr isotopes in seawater

S.J.G. GALER*, A. KRABBENHÖFT, W. ABOUCHAMI, G. BORNGÄSSER AND H. FELDMANN

Max-Planck-Institut für Chemie, Postfach 3060, 55020 Mainz, Germany (*steve.galer@mpic.de)

Early work on dissolved Sr in GEOSECS ocean profiles from the Atlantic and Pacific showed Sr/salt variations with depth, providing evidence for depletion of dissolved Sr in surface waters [1]. This depletion was attributed to uptake of Sr from surface waters by acantharians, whose skeleton is made of celestite ($SrSO_4$), which subsequently dissolves at depth, thus exerting a control on strontium cycling in the water column [2].

We explore the potential of stable Sr isotopes as a tracer of such nutrient-like behaviour in seawater. We have analysed surface seawater samples and a depth profile collected in the Southern Ocean during GEOTRACES cruise ANT-XXIV-3 along the Greenwich Meridian, as well as the NASS-4 standard and a deep-water North Atlantic sample. The Sr isotope data were obtained using a ^{84}Sr-^{87}Sr double spike by TIMS at MPI. Measured $\delta^{44/42}Ca$ obtained on the same samples are effectively homogeneous with an average value of 0.83 ± 0.04‰ (total range) relative to SRM 915a.

The $^{87}Sr/^{86}Sr$ of both surface water and depth profile samples gave a consistent value of 0.709176±8 (range) relative to 0.710250±7 (2SD) for SRM 987. The $^{88}Sr/^{86}Sr$ ratios, expressed as $\delta^{88/86}Sr$, show little variation in the deep waters, averaging 0.35±0.02‰. In contrast, surface waters show subtle variations along the transect (0.33±0.02‰) just within error of that in deep waters. The Southern Ocean compositions tend to be isotopically slightly lighter, overall, than those of the Atlantic further north (0.36±0.02‰), and as measured for IAPSO seawater [3, 4].

These preliminary data suggest that constancy of $\delta^{88/86}Sr$ in seawater cannot be assumed a priori. Any variations thus far appear to lie on the edge of the analytical precision. Nevertheless, mapping the ocean $\delta^{88/86}Sr$ distribution appears to be an important task, and may help elucidate the internal biological cycling of strontium in the water column.

[1] Brass & Turekian (1974) *EPSL* **23**, 141-148. [2] Bernstein *et al*. (1987) *Science* **237**, 1490-1494. [3] Fietzke & Eisenhauer (2006) *G³* **7**, DOI: 10,1029/2006GC001243. [4] Krabbenhöft *et al*. (2009) *JAAS* **29**, 1267-1271.

https://doi.org/10.1180/S0026461X00006502 Published online by Cambridge University Press

Continuum model for diffusive transport in the electrical double layer and clay interlamellæ

J.M. GALINDEZ[1]*, C.I .STEEFEL[1] AND U. MAEDER[2]

[1]Lawrence Berkeley National Laboratory, One Cyclotron Road, Berkeley, CA 94720, USA (*correspondence: JMGalindez@lbl.gov)
[2]Universität Bern, Switzerland (urs.maeder@geo.unibe.ch)

A continuum model for diffusive transport in the electrical double layer and the interlamellar space in clays is presented. The model makes use of a Donnan equilibrium assumption to calculate explicitly the composition of the diffuse double layer given an arbitrary bulk solution composition. In this approach, rather than solving the Poisson-Boltzmann equation explicitly, an average electrostatic potential corresponding to the double layer is computed. In the model, the double layer balances the charge of the mineral surface, which may be fixed charge (as in the case of ion exchange) or dynamically computed charge using a surface complexation model. In the case of clay interlamellæ, the charge of the clay is fixed and the ions occupying the space are treated as part of a double layer that may or may not be overlapping. Diffusive transport is handled with the Nernst-Planck equation, with accounting for the local immobile charge of the mineral surface. The approach allows for modeling of anion exclusion in clay-rich materials, as well as ion exchange within clay interlamellæ and edges.

Based on the same theoretical foundations as the single-type porosity model developed by Birgersson and Karnland [1], this continuum model provides identical predictions as long as the entire pore space is assumed to be occupied by the electrical double diffuse layer as, e.g., in highly compacted clays. These predictions were in turn validated by comparison with diffusion experiments conducted by Van Loon *et al*. [2]. The present work also explores the limitations of a discrete two-type porosity model in reproducing the actual continuous distribution of ion concentrations over the pore space as obtained with analytical expressions for very simple cases involving a pore space confined between two parallel electrically charged walls and saturated with a binary salt.

[1] Birgersson & Karnland (2009) *Geochim. Cosmochim. Acta* **73**, 1908-1923. [2] Van Loon, Glaus & Müller (2007) *Appl. Geochem.* **22**, 2356-2552.

Geochemistry of nickel isotopes in ferromanganese crusts

L.GALL[1]*, H.M. WILLIAMS[2], C. SIEBERT[1] AND A.N. HALLIDAY[1]

[1]Department of Earth Sciences, University of Oxford, Oxford, OX1 3AN, UK (*correspondence: louiseg@earth.ox.ac.uk)
[2]Department of Earth Sciences, University of Durham, Durham, DH1 3LE, UK

The stable isotope behavior of nickel (Ni) has not been studied as intensively as those of other transition metals (e.g. Fe and Mo), even though Ni is ubiquitous in many geological environments and a bioessential trace metal, for example in the production of methane by methanogens [1]. In this study we have measured the mass-dependent isotope composition of Ni ($\delta^{60/58}$Ni, relative to Ni SRM 986) in a variety of terrestrial samples by MC-ICPMS [2]).

Our results demonstrate that there are significant variations in $\delta^{60/58}$Ni in nature (-0.5 – 2.5‰). The Ni isotopic composition of 8 samples of igneous and mantle rocks is effectively homogeneous, with only small variations (<0.2‰) between different rock types. In contrast we find that ferromanganese crusts are much heavier. We analysed surface scrapings from 20 hydrogenetic crusts, including samples from all major ocean basins. The average $\delta^{60/58}$Ni value for these crusts is +1.65‰ with a variation of ±0.4‰.

There is no systematic variation with geographical position, water depth, or Ni concentration. However, given the residence time of Ni in the oceans (10,000 yr [3]), Ni isotope variations in ferromanganese crusts might reflect extreme local effects, such as differences in isotopic composition of source materials, input from hydrothermal vents, and fractionation during removal of Ni from seawater and adsorption. Further studies are needed to identify the specific processes. However, our data clearly demonstrate mass dependent fractionation of Ni isotopes in the marine environment.

[1] Cameron *et al*. (2009) *PNAS* **106**, 10944-10948. [2] Gall, Williams, Siebert, and Halliday (2011, *in prep*). [3] Sclater *et al*. (1976) *Earth Planet. Sci. Lett*. **31**, 119-128.

https://doi.org/10.1180/S0026461X00006502 Published online by Cambridge University Press

The Prestige oil spill after a decade: Evaluation of remediation strategies and the role of bioremediation.

J.R. GALLEGO[1]*, A.I. PELÁEZ[1], J. SÁNCHEZ[1], M.J. GCÍA- MTNEZ[2], J.E. ORTIZ[2], T. TORRES[2] AND J.F. LLAMAS[2]

[1]Environmental Biotechnology and Geochemistry Group. University of Oviedo. C/Gonzalo Gut. S/N, 33600-Mieres (Asturias), Spain. (*correspondence: jgallego@uniovi.es)
[2]ETSMinas, Universidad Politécnica de Madrid. C/Ríos Rosas, 21-28003 Madrid, Spain.

In 2002, the Atlantic and Cantabrian shorelines of Spain were affected by the Prestige heavy fuel oil spill. Initially the fuel was physically removed in rocky areas by means of hot pressurized water washing and similar procedures, whereas in sandy beaches other machinery was used. However, bioremediation was also considered given that the destructive effects of the hot pressurized water on the biota, the difficulties to collect oily waste, and other questions related with the grain-size of the sediments affected and the strong fuel adhesion in the shore rocks [1, 2, 3].

Our research carried out several studies all along the coasts in which natural attenuation, biostimulation and bioaugmentation techniques were tested in pilot and full-scale experiments for remediating oil-coated sands, gravels, pebbles, cobbles and boulders. Microbiological control and normalization by means of non-degradable chemical biomarkers were made to monitor these procedures. To improve bioremediation yields, novel *in situ* fresh-water irrigation and on-site techniques were developed, following similar strategies than those habitually used in soil remediation. The results obtained underscored the utility of these innovative designs to be used as an alternative to the limited effectiveness of the application of oleophilic fertilizers, clearly limited by the recalcitrance and by the reduced bioavailability of resin and asphaltene fractions. As a conclusion, long-term strategies for the bioremediation of other spillages with similar characteristics are suggested.

[1] Gallego *et al.* (2006) *Org Geochem.* **37**, 1869-1884. [2] Gallego *et al.* (2007) *Env Eng Sci.* **24**, 493-504. [3] Alonso-Gutiérrez *et al.* (2009) *App Env Microbiol.* **75**, 3407- 3418.

Evidence of Fe-oxide clusters in obsidians

L. GALOISY, G. CALAS AND N. MENGUY

Institut de Minéralogie et de Physique des Milieux Condensés (IMPMC), UPMC; Université Paris 7; CNRS; 4, Place Jussieu, 75252 Paris Cedex 05, France. (Laurence.galoisy@impmc.upmc.fr)

Iron has long been known to play an important role in determining the properties of natural magmatic liquids. The determination of the sites occupied by ferrous and ferric cations in natural glasses may provide information on the physico-chemical conditions prevailing at the magmatic stage as well as on the cooling conditions of the magma. We discuss the spectroscopic data obtained on the Fe environment in calc-alkaline rhyolitic glasses (obsidians) from various localities, at the light of transmission electron microscopic observations. Fe^{2+} and Fe^{3+} ions partly occur within the glass structure, as indicated by XANES [1], EPR and optical absorption spectroscopy (OAS). OAS reveals that some Fe^{2+} occurs in a regular octahedral site, an unusual environment in glasses.

The presence of Fe-oxide nano-clusters, suspected from previous EPR spectroscopy data, is confirmed by variable-temperature OAS in all the obsidians investigated. Specific absorption bands, assigned to Fe-Fe and Fe-Ti intervalence charge transfers (IVCT), are characterized by a spectacular intensity enhancement at low temperature (10K). This thermally-activated behavior shows an activation energy similar to that observed for IVCT in various minerals. The evidence of specific Fe^{2+} sites and of IVCT processes, indicate the presence of Fe-oxide clusters. These clusters, showing a local re-arrangement around Fe, are related to the cooling history of the glass, as they are not found in synthetic glasses [2]. They may be also precursors of the amorphous and crystalline Fe-oxides (Ti-magnetite and magnetite), 5-10 nm large, evidenced using TEM. The existence of these clusters and their nature seem to be related to the conditions of formation of the investigated obsidians and they may obscure the information brought by these glasses about its magmatic history.

[1] L. Galoisy *et al.* (2001) *Chem. Geol.* **174**, 307–319. [2] C. Weigel *et al.* (2008) *Phys. Rev.* B **78**, 064202.

https://doi.org/10.1180/S0026461X00006502 Published online by Cambridge University Press

Looking for PON in fluviatile and marine sediments: Insights from nitrogen isotopic compositions

A. GALY[1,*], R. G. HILTON[2], N. HOVIUS[1], J. SMITH[1] AND R. B. SPARKES[1]

[1]Department of Earth Sciences, University of Cambridge, Downing Street, Cambridge CB2 3EQ, UK (*correspondance: albert00@esc.cam.ac.uk)

[2]Department of Geography, Durham University, Science Laboratories, South Road, Durham, DH1 3LE, UK

Processes involved in the cycling of organic matter can be preserved in sediments and recent studies have unravelled the importance of the erosion of the continents to the global organic carbon transfer [1-3]. The significance of such transfer to the biogeochemical cycles of other chemical elements associated to the organic matter (H, N, O, P, S, …) is, however, hampered by the small (<1%) abundance of particulate organic carbon in sediments transported by river in active margins and the occurrence of inorganic phases. This is particularly the case when N is considered since nitrate particulate deposition and ammonium in phyllosilicate can both be present in sediments. Here, we present case studies from modern systems investigating soil and river sediments from Taiwan and the Swiss Alps with modern marine clastic sediments from Taiwan and their Cenozoic analogue from the foreland basins of the Alps and the Pyrenees. Sediments have been decarbonated using hydrochloric acid and the decarbonatation process can have a significant impact on the N-isotopic composition, depending on how well lithified the sediments are. However, variations in the isotopic composition of bulk soils and common plant species are correlated in the tropical mountain forest of Taiwan. This suggests that the physical erosion of fixed-N in organic debris can be significant for the N cycle in vegetated active mountains belts. It also suggests an accurate quantification of the particulate organic nitrogen (PON) in these types of material [4]. The offset of ~4 permil between soil PON and standing biomass PON can be a powerful tool to distinguish erosional regimes where the erosion of the vegetation is insignificant (Swiss Alps) or not (Taiwan).

[1] Galy *et al*. (2007) *Nature,* **450**: 407-410, doi:10.1038/nature06273 [2] Hilton *et al*. (2008) *Nature Geosci,* **1**: 759-762, doi:10.1038/ngeo333 [3] Hilton *et al*. (2011) *Geology,* **39**: 71-74, doi:10.1130/G31352.1 [4] Hilton *et al*. (2010) *Geochim.Cosmochim. Acta,* **74**: 3164-3181, doi:10.1016/j.gca.2010.03.004

Speciation of trace elements in Strengbach soil solutions by ultrafiltration

S. GANGLOFF*, P. STILLE AND F. CHABAUX

LHYGES – UMR7517 1rue Blessig – 67084 Strasbourg, France (* sgangloff@unistra.fr, pstille@unistra.fr, francois.chabaux@eost.u-strasbg.fr)

This study deals with colloidal phases of soil solutions collected in the Strengbach watershed (OHGE). These solutions carry the chemical elements in the first meter of soil. The sampling has been performed below spruce at different depths (-5cm, -10cm, -30cm and -60cm) of a brown acidic to ochreous podzolic soil with help of lysimetric plates. The colloidal phase has been studied by frontal filtrations (1μm, 0,45μm and 0,22μm) and tangential ultra-filtrations (300kDa, 30kDa, 10kDa and 5kDa). Then, the initial solution, the different permeates and retentates have been analyzed for major, trace element and Dissolved Organic Carbon (DOC) concentrations.

The study elucidates the behavior of the different chemical elements in the various colloidal fractions separated from the soil solutions. The retention rate, derived during the ultra-filtration experiment, allows determining the proportion of each element in different forms, i.e. proportions in dissolved form and in the different colloidal fractions. The comparison of each element with DOC indicates that only some of the elements are correlated with DOC. Among the latter, it is possible to distinguish two elemental groups showing different behaviors: those correlated only with DOC and those correlated with DOC and another secondary phase such as iron oxy-hydroxides. The mass balance of the ultra-filtrations showed that in the >1μm filtrates some elements (REE, PO_4^{3-}, Pb, Fe, Al) occur as precipitates, as colloids or as dissolved phase. The precipitates contain among others secondary minerals fluorencite and pyromorphite. The formation of these minerals occurs below 5 cm depth.

The ultra-filtrations of samples taken at different depths of the soil profile indicate that the chemical compositions of the colloidal fractions change in function of depth. Such depth variations may point to indicate the occurrence of different levels of colloid formation in these soil solutions.

https://doi.org/10.1180/S0026461X00006502 Published online by Cambridge University Press

Climate-carbon cycle feedback during glacial cycles

A. GANOPOLSKI[1]*, V. BROVKIN[2], R. CALOV[1], D. ARCHER[3] AND G. MUNHOVEN[4]

[1]PIK, Potsdam, 14412, Germany (*correspondence: andrey@pik-potsdam.de)
[2]MPI-M, Hamburg, Germany (victor.brovkin@zmaw.de)
[3]University of Chicago, Chicago, 60637, IL, USA (d-archer@uchicago.edu)
[4]University of Liège, B-4000 Liège, Belgium (guy.munhoven@ulg.ac.be)

Paleoclimate records reveal a close link between global ice volume and atmospheric CO_2 concentration, at least, through the last 800,000 years. Despite many efforts over the last two decades, mechanisms of glacial-interglacial CO_2 variability and its role for the glacial cycles remain elusive. Here using the Earth system model of intermediate complexity CLIMBER-2 which includes all major components of the Earth system – atmosphere, ocean, land surface, ice sheets, terrestrial biota, eolian dust and marine biogeochemistry – we performed simulations of the last glacial cycles employing variations in the Earth's orbital parameters as the only prescribed climatic forcing.

In the experiments with constant CO_2 concentration, temporal dynamics of the simulated glacial cycles strongly depend on the CO_2 level. For CO_2 concentrations about and above preindustrial one, the model simulates only short glacial cycles with precessional and obliquity frequencies. However, for lower CO_2 concentrations the model simulates long glacial cycles with dominant 100 kyr periodicity. Simulated glacial cycles agreed favorably with paleoclimate reconstructions, but their amplitude is underestimated compared to those of the simulations with time-dependent CO_2 concentration. These results confirm that the positive climate-carbon cycle feedback plays an important role in amplification of long glacial cycles. Experiments with fully interactive CO_2 shed some light on the mechanism of climate-carbon cycle feedback during glacial cycles. Forced by orbital variations only, the model is able to reproduce the main features of CO_2 changes: the 40 ppmv CO_2 drop during glacial inception, the minimum concentration at the last glacial maximum being 80 ppmv lower than the Holocene value, and the relatively abrupt CO_2 rise during the deglaciation. The main drivers of atmospheric CO_2 evolve with time: changes in sea surface temperature and volume of bottom water of southern origin exert CO_2 control during glacial inception and deglaciation, while changes in carbonate chemistry and marine biology are dominant during the first and second parts of the glacial cycles, respectively.

Evaluation of marine primary organic aerosol emission schemes

BRETT GANTT*, MATTHEW JOHNSON AND NICHOLAS MESKHIDZE

North Carolina State Unverisity, Raleigh, NC, USA (*correspondence: bdgantt@ncsu.edu)

In the last decade, there has been an increase in research concerning primary organic aerosol (POA) emissions from the ocean. Global source of ocean-emitted POA has been shown to be comparable to primary organic carbon particles emitted from combustion [1] and are sometimes found in concentrations more typical of organic aerosols in urban areas [2]. Due to their importance, several attempts have been made to better quantify the emission rate of marine POA for use in air quality and global climate models. In this work, we present results from the chemical transport model GEOS-Chem in which five distinct emissions schemes [1, 3, 4, 5, 6] of marine POA are implemented using a consistent sea spray function and chlorophyll-a concentrations ([Chl-*a*]). Model simulations are evaluated against long- and short-term observations collected in multiple coastal sites.

Calculations show that these schemes emit marine POA at different magnitudes and have distinct temporal/spatial distributions. Three of the emission schemes [3, 4, 5] are strongly tied to the wind speed dependence of the sea spray function and to a much lesser extent the [Chl-*a*]. On the other hand, the Spracklen *et al*. [1] emission scheme is primarily driven by [Chl-*a*] and is insensitive to surface wind speed. Between these two extremes is the Gantt *et al*. [6] scheme, which is affected by both wind speed and [Chl-*a*].

Preliminary results show that the emission schemes with strong wind speed dependence overpredicted concentrations in the winter relative to the summer at sites in the Northern Atlantic and Southern Ocean [7, 8]. The high organic concentration episode at Mace Head [2] was not reproduced well by any scheme, although the emissions with wind speed dependence outperformed the emissions based solely on [Chl-*a*]. This study shows that large uncertainty in marine POA emissions exists and requires further evaluation.

[1] Spracklen *et al*. (2008), *Geophys. Res. Lett.*, **35**, L12811. [2] Ovadnevaite *et al*., (2011), *Geophys. Res. Lett.,* **38**, L02807. [3] Vignati *et al*. (2010), *Atmos. Environ.*, **44**, 670–677. [4] Fuentes *et al*. (2010), *Atmos. Chem. Phys*., **10**, 9295–9317. [5] Long *et al*. (2011), *Atmos. Chem. Phys.,* **11**, 1203–1216. [6] Gantt *et al*. (2011), *Atmos. Chem. Phys. Discuss.,* **11**, 10525-10555. [7] Yoon *et al*. (2007), *J. Geophys. Res.*, **112**, D04206. [8] Scaire *et al*. (2009), *J. Geophys. Res.*, **114**, D15302.

https://doi.org/10.1180/S0026461X00006502 Published online by Cambridge University Press

Mechanism of water–rock interaction of alkaline leaching uranium in Shihongtan deposit

B. GAO[1,2] * AND Z. X. SUN[1,2]

[1]School of Civil and Environmental Engineering, East China Institute of Technology, Fuzhou 344000, China (*correspondence: gaobai2007@sohu.com)

[2]Key Laboratory of Radioactive Geology and Exploration Technology Fundamental Science for National Defense Fuzhou, Jiangxi, 344000, China

The saturation index of sulphate and carbonate in groundwater of Shihongtan uranium deposit in Xinjiang has been calculated by geochemical model PHREEQC (table 1).

Calcite	Dolomite	Anhydrite	Gypsum	Uraninite
0.75	1.44	0.04	0.30	-6.34
-1.30	-2.76	-0.81	-0.60	-2.76
0.00	-0.17	-0.77	-0.56	-3.71
-0.23	-0.49	-1.56	-1.35	-5.69
-0.51	-0.37	-0.97	-0.66	-3.15

Table 1: The calculated results of saturation index of mineral.

The results indicate that mining of the deposit is a difficult task by traditional acid or alkaline *in situ* leaching. Experimental researches of laboratory and field show that mining the uranium deposit is possible because of avoidance of precipitation of calcium sulphate and calcium carbonate in the aquifer, if the total dissolved solides of groundwater were diluted less than 3.45 g/L[1]. The uranium leaching is controlled by species of uranium mineral with study of electron probe. The uranium associated with kaolin or in between the grains of minerals is easier to be leached out than those associated pyrite or encompassed by the minerals[2]. Experimental researches show that more time of leaching, higher content of Ca^{2+} in recovery solution because of calcic mineral dissolution in uranium ora and wall rock. The precipitation jam of calcium carbonate during *in situ* leaching will come into being because of reducing the liminal value of HCO_3^- content.

The study was supported by the project of the National Natural Science Foundation of China(40872165) and Science Bureau of Jiangxi Province (2009AF00100).

[1]Gaobai (2010) *Uranium mining and Metallurgy* **29** , 61-65. [2] Gaobai (2009) *China University of Geosciences*, 45-46.

Geochemical characteristics of trace elements of sandstone-type uranium deposits in the Ordos Basin

E.G. GAO, S.G. HE* AND S.C. SUN

Institute of Disaster Prevention Science & Technology, Yanjiao 101601, Beijing, China (grg@ustc.edu.cn)

The Ordos basin is the second largest sedimentary basins in China, as called Shan-Gan-Ning basin, and its main body area is 2.5×10^5 square kilometers. The Yimeng Uplift in the north, the Weibei Uplift in the south, the West Fold and Fault Belt in the west, and the Western Shanxi Flexure Belt in the east form a particular structure pattern. The Ordos basin is enriched with many energy resources and deposits [1-3], therefore, it has profound scientific sense and industrial value. Recent exploitation indicates that the sandstone-type uranium minmeralization has economic value in this basin [4], it becomes the hotspot in the uranium exploration in China.

High precision ICP-MS was hired to study trace elements and REE from sandstone-type uranium deposit in the Ordos Basin, Northwestern China. We focus on the mechanism of uranium enrichments so that to present basis for further exploration. Results of total REE ranges from 30.3 to 713.4μg/g, REE distribution patterns of the sandstone-type uranium samples is light REE enriched and high REE depleted. Our study shows that high Y abundance and abnormity of Eu between 0.70~1.92. results show that U abundances are 0.73~150μg/g showing strong correlation between U enrichments and the related elements such as Ti, V, Zr, Mo and Au. In addition, thorium enrichments in most samples are correlated with ΣREE with some accordance of former study [5,6].

This study is supported by Teacher Foundation of China Earthquake Administration(No: 20090112)

[1]Ye, J.R. and Lu, M.D. (1997) *J. Petrol. Geol.*, **20**, 347-362. [2] Liu, S.F. (1998) *J. Asian Earth Sci.,* **16**, 369-383. [3]Yang, X.Y. *et al.* (2009) *Inter. Geol. Rev.*, **51,** 422-455. [4] Xie, A.G. *et al.* (2003). *Acta Petrol. Sinca,* **24,** 18-29. [5] Ling, M.X. (2006). *Chinese J. Geochem.,* **25,** 354-364. [6] Zhu, X.Y. *et al.* (2003) *Geology & Geochemistry,* **31,** 39-45.

https://doi.org/10.1180/S0026461X00006502 Published online by Cambridge University Press

Extensive N-loss from permeable Wadden Sea sediments due to aerobic denitrification

H. GAO, A. KHALILI, D. DE BEER, G. LAVIK AND M.M.M. KUYPERS*

Max Planck Institute for Marine Microbiology, 28359 Bremen, Germany
(*correspondence: mkuypers@mpi-bremen.de)

The role of permeable sediments in the oceanic N-budget is poorly understood. In this study, nitrogen (N) loss rates were determined in permeable sediments of the Wadden Sea using a combination of stable N isotopes, microsensor measurements and model simulation approaches. Results indicate that permeable Janssand sediments are characterized by some of the highest denitrification rates in the marine environment. Moreover, several lines of evidence showed that denitrification occured under oxic conditions. N loss rates generally showed little temporal and spatial variation (207 ± 30 μmol m^{-2} h^{-1}) over the three field campaigns conducted in autumn 2006 and spring and summer 2007. Utilizing an extensive time series of nutrient concentrations and current velocities obtained from a continuous monitoring station, NO_x^- flux into the sediment was modeled over a full annual cycle. Modeled NO_x^- fluxes were sufficiently high to support the experimentally derived N-loss rates. Combining the measured rates with the modeled results, an annual N-removal rate of 745 ± 109 mmol N m^{-2} y^{-1} was estimated for permeable sediments of the Wadden Sea. This rate agrees well with previous N loss estimates for the Wadden Sea based on N budget calculations. Our results indicate that permeable sediments, accounting for 58- 70 % of the continental shelf area, are an important N-sink and their contribution to the global N-loss budget should be reevaluated.

Applications of laser microprobe analysis for silicon and oxygen isotopes (Fujian, China)

J.F. GAO AND T.P. DING

The Key Laboratory of Metallogeny and Mineral Assessment, Institute of Mineral Resources; Chinese Academy of Geological Sciences, Beijing 100037, China.
(correspondence: tony_and_mary@126.com)

The O and Si isotope compositions of minerals from the miarolitic cavity granite and pegmatite in Yunxiao county, Fujian province are measured by using conventional method and laser probe analytic method for determining their material sources and forming conditions. The results are listed in the Table 1.

Sample	$\delta^{18}O_{V\text{-}SMOW}$ (‰)			$\delta^{30}Si_{NBS\text{-}28}$ (‰)		
	Q	Fs	Gar*	Q	Fs	Gar*
Gr-01	7.6	6.4		-0.1	-0.1	
Gr-02	8.0	5.6		-0.3	0.0	
Peg-01	7.7	6.3	3.3, 3.3	-0.2	-0.2	-1.8, -1.9
Peg-02	7.4	5.6	3.1, 3.6	-0.5	-0.3	-1.8, -2.2
Peg-03	7.7	6.0	3.4	-0.4	0.2	-2.0

Table 1 : The results of oxygen and silicon isotope compositions
*minerals were analyzed by using laser probe isotope analytic method. Q-quartz; Fs-feldspar; Gar-garnet.

The O and Si isotope compositions of quartz and feldspar from the pegmatite are very similar to those of the granite, indicating that they have the same magma source.

From the oxygen isotope fractionation between quartz and feldspar, a temperature of 461°C is obtained for the granite, indicating that the granite may be subjected some extend of water-rock interaction after crystallization. This is consistent with the extensive development of pegmatite miarolitic cavity in granite. From the oxygen isotope fractionation between quartz and feldspar, a temperature range between 505°C and 532°C is obtained for pegmatite, indicating that fluid temperature was more than 500°C when the pegmatite was formed.

The silicon and oxygen isotopic ratios of garnet were both significantly lower than those of coexisting quartz and feldspar in miarolitic cavity, indicating that parallel silicon and oxygen isotopic fractionations are present between garnet and quartz (and feldspar), although the extent of silicon isotopic fractionation is smaller that those of oxygen isotope fractionation.

https://doi.org/10.1180/S0026461X00006502 Published online by Cambridge University Press

Quasi-simultaneous observation of currents, salinity and nutrients in the Changjiang plume on the tidal timescale

L. GAO* AND D.J. LI

State Key Laboratory of Estuarine and Coastal Research, East China Normal University, 3663 North Zhongshan Road, Shanghai 200062, China
(*correspondence: lgao@sklec.ecnu.edu.cn)

During both the spring- and the neap-tide periods of November 2005, quasi-simultaneous observations were carried out by six boats over 26 h at 12 stations in the Changjiang plume. The simultaneous observations provided the actual distribution isopleths of salinity and nutrients that displayed considerable intra-tidal variations at surface, especially in the southeastern section of the study area (Figure 1). The lack of synopticity in sampling might lead to large discrepancies of the interpolated contours of salinity from the actual distribution isopleths. No clear flood-ebb asymmetry of salinity stratification was observed; whereas at inner stations, surface-to-bottom bulk velocity difference always tended to be greater during the ebb fraction of a semidiurnal cycle. At a given station, the weaker neap tides commonly induced stronger salinity stratification, less intra-tidal variability of salinity and nutrients, and less intrusion of bottom saltwater. Nutrients showed more nonconservative behaviors during the neap tides, presumably as a result of the prolonged residence time of seawater and decreased suspended particulate matter levels than during the spring tides.

This study was jointly funded by Ministry of Science and Technology of China (2010Cb951203), Shanghai Municipality (10JC1404400) and State Key Laboratory of Estuarine and Coastal Research of China (2009KYYW03).

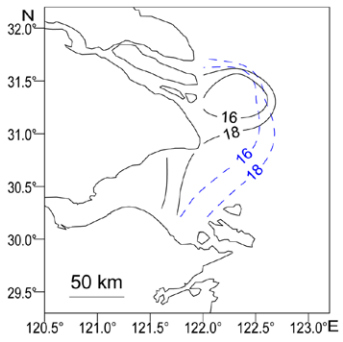

Figure 1: Comparison between the snapshot distribution isopleths of salinity at surface on the two occasions of 12:00 (solid black lines) and 18:00 on November 2 (dashed blue lines) during the spring-tide survey. The two occasions are roughly regarded as the peak high- and peak low-tide phases for the entire survey region.

Study on endocrine disrupting chemicals removal features in pingshantou waterplant of Huainan City, China

LIANGMIN GAO* AND GUIRONG SU

School of Earth and Environment, An Hui University of Science and Technology, Huainan 232001, China
(*correspondence: gaolmin@163.com)

Using a method for solid-phase extraction concentrated and high performance liquid chromatography analysis, detected the EDC_S content of different water treatment process in pingshantou waterplan of Huainan city, researched the distribution characteristics and removal efficiency of EDC_S in different water treatment process. The research results are as follows: DMP and DEP could be removed by rate of 100%, but BBPDBP, EE_2, E_1, BPA and NP were detected in different water treatment process, the detection rate was 100%. While the content of DMP, BBP, DBP, BPA increased in water treatment process. The content of BBP, DBP, EE_2, BPA increased after pipe delivering. Conclusions: Conventional drinking water treatment process of EDC_S removal is very limited; There are no rule to follow with EDC_S in coagulation-sedimentation and chlorination process, the reasons may be: degradation products and secondary pollution were produced in processing process, which caused the content of BBP, DBP elevated in coagulation-sedimentation and chlorination process; And several byproducts of BPA and NP were found in chlorination. In addition, the impact of pollution substances exudated from conveying water pipe on EDC_S should not be ignored.

https://doi.org/10.1180/S0026461X00006502 Published online by Cambridge University Press

Fluorescence spectrum characteristic of the extractable humus in soil from Shannan developed area

LIANGMIN GAO*AND QINQIN ZHANG

School of Earth and Environment, An Hui University of Science and technology, Huainan 232001, China (*correspondence: gaolmin@163.com)

Humus is a kind of amorphous, brown or brownish black, hydrophilic, acidic, polydispersed organic matter and more dispersed widely in soil, sediment, and water (such as lakes, rivers, oceans and groundwater, etc.). It is not only a major source of soil nutrients but also has a significant impact to physical, chemical and biological properties of soil, it is one of the indicators of soil fertility.

Contents of extracted humus in soil planted with different crops were determined, and the fluorescence spectra features of extracted humus in the same sampling point in different soil layers were analyzed. The results showed that contents of extracted humus in soil planted with different crops are different, there is no obvious rule. For different soil layers of the same sampling point, the distribution of extracted humus is not the same, mostly show that: the surface (0~20cm)> the middle (40~60cm)> the lower (80~100cm). The excited state fluorescence spectra of extracted humus in soil of different land types have similar fluorescence characteristics, peak obvious presents in about 390nm and 455nm. The fluorescence emission spectra are all broadband peak without obvious features. emission wavelength is about 500nm.The stimulate spectra of extractable humus in cotton soils has two distinct peaks around 445nm and 460nm, with the deepening of soil the two peaks separate more obviously. And extractable humus in surface layer, middle layer and lower layer has inspired fluorescence peak in 503nm, 498nm and 492nm in turn, peak type is moderate, and along with the increase of soil depth, fluorescence intensity greatly increase.

Geochemical and U-Pb age constraints on the occurrence of polygenetic titanites in UHP metagranite in the Dabie orogen

X.-Y. GAO[1]*, Y.-F. ZHENG[1], Y.-X. CHEN[1] AND J.L. GUO[2]

[1]CAS Key Laboratory of Crust-Mantle Materials and Environments, School of Earth and Space Sciences, University of Science and Technology of China, Hefei 230026, China (*correspondence: gaoying@ustc.edu.cn)

[2]State Key Laboratory of Geological Processes and Mineral Resources, China University of Geosciences, Wuhan 430074, China

Accessory minerals such as zircon and titanite are common in continental subduction-zone metamorphic rocks, and time and process of their formation can be dated by the U-Pb method and geochemical tracers. This is a great advantage to identify their genesis with respect to the origin of host rocks. Magmatic titanite was identified in the core of a few titanite grains with the overgrown rim of metamorphic titanite in UHP metagranite in the Dabie orogen. LA-ICPMS U-Pb dating gave Neoproterozoic ages for the magmatic titanite but Triassic ages for the metamorphic titanite. The magmatic and metamorphic titanites are clearly distincted by differences in petrological and geochemical compositions. The magmatic titanite occurs as residual cores that show bright BSE, the presence of allanite and quartz inclusions, low contents of CaO, Al_2O_3 and TiO_2 but high contents of Fe_2O_3 and MgO. In trace elements, the magmatic titanite exhibits high REE and HFSE contents, distinctly negative Eu anomalies with flat MREE-HREE patterns, and high Th/U ratios. In contrast, the metamorphic titanite occurs as rims and grains of homogeneously dark BSE that contain inclusions of epidote, quartz, K-feldspar, rutile, biotite and phengite, and have relatively high contents of CaO, Al_2O_3 and TiO_2, but low contents of Fe_2O_3 and MgO, and relatively low REE and HFSE contents, slightly negative Eu anomalies with HREE depletion relative to MREE, and low Th/U ratios. The Zr-in-titanite thermometry yields 727 to 877°C at 0.5 to 1.0 GPa for the magmatic titanite, and 729 to 870°C at 1.5 to 2.0 GPa for the metamorphic titanite. The Neoproterozoic U-Pb chronometric system of magmatic titanite survived the Triassic continental subduction-zone HP-UHP metamorphism. This suggests a relatively high closure temperature of >800°C for the titanite U-Pb system. The metamorphic titanite is principally a product of retrograde metamorphism during decompression exhumation at the transition from HP eclogite-facies to amphibolite-facies. Therefore, titanite holds a great potential to petrology and geochemistry of continental subduction-zone processes.

https://doi.org/10.1180/S0026461X00006502 Published online by Cambridge University Press

Effect of phosphate fertilizer on the mobility of arsenic in fairdpur soil, central Bangladesh

X.B. GAO[1], Y.X. WANG[1]*, Q.H. HU[2] AND T. MA[1]

[1]School of Environmental Studies and MOE Laboratory of Biogeology and Environmental Geology, China University of Geosciences, Wuhan, 430074 P. R. China (Xubo.gao.cug@gmail.com; *correspondence: YX.Wang@cug.edu.cn; Tengma@cug.edu.cn)

[2]Department of Earth and Environmental Science, The University of Texas at Arlington, Arlington, TX 76010 (maxhu@uta.edu)

Effects of long term using of phosphate fertilizer on the mobilization of arsenic from soils have been seldom studied. In this study, the effects were investigated by column experiments using surface soil samples collected from fairdpur, central Bangladesh, an area with high arsenic presence in groundwater. A solution of 160 mg/L $Ca(NO_3)_2$ was first applied to the fully-saturate columns packed with soils to establish the stable As concentration in the effluent, and followed by leaching with phosphate fertilizer solution (represented with 10 mg/L Na_2HPO_4). An increase in the arsenic concentration in the effluent was observed after the $Ca(NO_3)_2$ input solution was replaced with either Na_2HPO_4 solutions. Dissolution of soluble arsenic-bearing minerals in the sediment with a rapid release of As, major cations, Fe, Mn, and Si was observed in the first hour. During the leaching period, there is no significant increase of As(III)/As(V) ratios in the effluent due to the oxic conditions in the experiment. Desorption of As from oxyhydroxide sorbents by phosphate is one of the major factors responsible for the elevated As concentration observed in the effluent [1, 2]. During the leaching periods of Na_2HPO_4, sodium mole percentage, as well as Na^+/Ca^{2+} and Na^+/Mg^{2+} ratios, of the effluent increased, probably due to aggregate breakdown, colloidal dispersion and mobilization in the columns, while an increase in Fe and Mn contents of the effluent may result from the release of particulate Fe and Mn oxyhydroxides. In addition, complexation of particulate arsenic with Fe/Mn oxyhydroxides may account for a significant portion of the enhanced arsenic concentration in the effluent.

[1] Gao et al. (2011) *Journal of Environmental Science & Health, Part A* **46**, 471-479. [2] Wang et al. (2009) *Applied Geochemistry* **24,** 641-649.

LA-ICP-MS zircon U-Pb geochronology of granites and its geological implication in the Baiganhu W-Sn deposit, NW China

YONG-BAO GAO[1,2]*, WEN-YUAN LI[1] AND ZHAO-WEI ZHANG[1,2]

[1]Xi'an Center of Geological Survery, CGS, Xi'an, Shaanxi 710054, China

[2]Chang'an University, Xi'an, Shaanxi 710054, China (*correspondence: gaoyongbao2006@126.com)

Baiganhu W-Sn deposit is a new found large W-Sn deposit in Qimantge, NW China, and W-Sn mineralization is closely related to the tonalite and monzonite granite, both of which belong to S-type granites. However, because of lacking of precise isotopic dating, the metallogenic epoch of Baiganhu W-Sn deposit is disputed. This paper provides the LA-ICP-MS zircon U-Pb isotopic dating result of the tonalite (BKN-01) and monzonite granite (BKN-03) from the Baiganhu deposit and discusses its geological significance. The CL images of zircons in the granites show most of the zircons present the typical characteristics of magmatic zircons with zoning structures.The LA-ICP-MS Zircon U-Pb isotopic dating show that the weighted mean $^{206}Pb/^{238}U$ ages of tonalite and monzonite granite are 429.5±3.2 Ma (MSWD = 0.0026), and 430.5±1.2 Ma (MSWD = 0.0111) respectively. Both of the ages are concordant (Fig.1), and they can represent the petrogenic ages of the granites. Therefore, this paper proposed that the S-type granites in Caledonian period, which were formed by the melting of sedimentary strata, are closely related with forming of W-Sn in Baiganhu depsoit. These findings are of great significance in further research on the formation environment of Baiganhu W-Sn deposit, and guiding the ore prospecting directions.

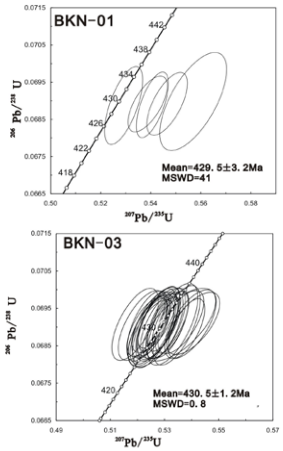

Figure 1: U-Pb concordia diagram of zircons of granites in the Baiganhu W-Sn deposit, Qimantage, NW China.

This study was supported by China Geological Survey project (No. 1212010911032, 1212011121088 and 1212011121092)

https://doi.org/10.1180/S0026461X00006502 Published online by Cambridge University Press

Geochemistry, paleoenvironment and timing of Lower Aptian organic rich beds of Paja Formation (Eastern Cordillera, Colombia)

TATIANA GAONA-NARVAEZ[1]*, FLORENTIN J.-M.R. MAURRASSE[1], FERNANDO ETAYO-SERNA[2] AND CARRIE REBENACK[1]

[1]Dept. of Earth and Env., Florida Int. Univ. 11200 S.W. 8th Street, Miami, FL 33199, USA (*correspondence: tgaon001@fiu.edu; maurrass@fiu.edu, crebe001@fiu.edu)
[2] Inst. Colombiano de Geología y Minería, INGEOMINAS, Diagonal 53 # 34-53, Bogotá, Colombia (fetayos@gmail.com)

Lower Aptian organic-rich marine sediments are interpreted with respect to anoxic episode, "Oceanic Anoxic Event 1a" (OAE-1a), coeval with $\delta^{13}C$ segments C3 to C6, of duration between 1.0 and 1.3 MA [1,2].

A 115m section of the Lower Aptian Arcillolitas Abigarradas Member of the Paja Fm at Villa de Leiva (Tunja-Villa de Leiva road) includes a prominent 4m-thick interval of black shale 10 meters below the base of the lowest Upper Aptian (Gargasian) *Dufrenoyia sanctorum-Stoyanowiceras treffryanus* ammonite assemblage zone [3]. Similarly, at the Curití Quarry (San Gil-Curití road), a 12m section includes 8m-thick organic-rich shale at the base of the Paja Fm, which overlies Barremian-age carbonate ramp deposits of the Rosablanca Fm. The base of the Paja Fm yielded reworked and phosphatized middle Barremian to lowest Aptian ammonites: *Pulchellia*, *Gerhardtia*, *Toxancycloceras*, *Karsteniceras* and *Prodeshayesites*. High-resolution analyses of these sections, including TIC (wt% $CaCO_3$), TOC (wt% C), and stable carbon isotope values ($\delta^{13}C_{org}$), characterize the stratigraphic relationship of these organic-rich levels of the Paja Fm and OAE-1a.

At Villa de Leiva, the organic-rich interval includes laminae associated with gypsum, pyritic concretions, absence of bioturbation and benthic fossils, and yielded increased TOC values (1.17% to 5.33%). These sediments accumulated under anoxic conditions in a subtidal, hypersaline environment [4]. C- isotope data show $\delta^{13}C_{org}$ values from -19.79‰ to -24.65‰. At Curití, the organic-rich sediments are devoid of benthic fossils and bioturbation, and TOC values are up to 8.4%, also indicative of oxygen-depleted conditions. C- isotope data yielded $\delta^{13}C_{org}$ values between -22.05‰ and -20.47‰. In both sections the range of $\delta^{13}C_{org}$ values, and the trend of the $\delta^{13}C_{org}$ curve are compatible with the Lower Aptian interval C7 [1, 2]. Therefore, both organic-rich intervals of the Paja Fm are subsequent to OAE-1a, which is known to occur between isotopic levels C3 and C6.

[1] Menegatti et al. (1998) *Paleoceano*. **13**, 530-545. [2] Li, Y-X. et al. (2008) *Earth Planet. Sci. Lett.* **271**, 88-100. [3] Etayo-Serna (1979) *Pub. Geol. Esp., INGEOMINAS* **2**, 186 pp. [4] Forero & Sarmiento (1985) *Pub. Geol. Esp., INGEOMINAS* **16**, XVII.1-XVII.16.

Beach placer, a proxy for the average Nd-Hf isotopic composition of a continental area

M. GARCON*, C. CHAUVEL AND S. BUREAU

ISTerre, BP 53, 38041 Grenoble Cedex 9, France (*correspondence: marion.garcon@ujf-grenoble.fr)

Beach placer deposits concentrate detrital heavy minerals which are the erosion products of large areas of continental crust. Here, we report the first analyses of Nd-Hf isotopic ratios and trace element concentrations that we measured in a beach placer from Camargue, France and in its pure mineral separates. Both the bulk composition of the placer and those of its pure mineral separates were determined. We also report mineral proportions obtained using observations under a binocular microscope and X-ray microfluorescence cartography.

Our results indicate that monazite totally controls the placer Nd isotopic composition (ε_{Nd} = -9.3) while zircon dominates its Hf isotopes (ε_{Hf} = -13.0) even though both mineral phases represent only a small proportion of the heavy mineral assemblage (3.5 and 10% respectively). We demonstrate that the Camargue placer provides a good estimate of the average Nd and Hf isotopic composition of the continental area drained by the Rhone River in western Europe ($\varepsilon_{Nd} \approx$ -9 and ε_{Hf} = -13). Using these values, we calculate two-stages model ages and show that almost all the placer minerals are derived from Proterozoic crustal protoliths. This provides valuable information on the history of the continental crust drained by the Rhone River. In particular, it suggests that little juvenile crust was created during the recent geological events that formed the Alps and the Massif Central, the two main massifs from which the placer minerals originate.

More generally, we propose that similar measurements made on other worldwide beach placer deposits could provide estimates of the present-day Nd and Hf isotopic composition of large continental areas, values that are difficult to obtain due to the well-known heterogeneity of continental material but are essential to model the growth of continental crust through Earth history or to model the impact of crustal material when recycled into the mantle.

https://doi.org/10.1180/S0026461X00006502 Published online by Cambridge University Press

Analysis of geochemical "twins" Al/Ga and Si/Ge in rock-forming silicate minerals in granitoides using LA-ICP-MS

N. GARDENOVÁ[1]*, V. KANICKÝ[1], K. BREITER[2], AND T. VACULOVIČ[1]

[1]Department of Analytical Chemistry, Faculty of Science, Masaryk University, Brno, Czech Republic (*correspondence: 369148@mail.muni.cz)
[2]Institute of Geology, Academy of Science ČR, Praha

The aim of this study is to determine ratios of Al/Ga and Si/Ge in natural silicate minerals from different types of granitoids from Bohemian massif and compare these ratios with elemental ratios commonly used in geochemistry like K/Rb, Nb/Ta and Zr/Hf. All these ratios represent (i) different source lithology (metasedimentary or metaigneous rocks, subduced slab, metasomatised lover crust) of granitic melts, (ii) evolution via fractional crystallisation, mixing, reaction with fluid atc., (iii) ability of particular crystal lattice of rock-forming minerals to preferentially accommodate Ga or Ge.

The presented results was obtained using three different methods – pneumatic nebulization with inductively coupled plasma mass spectrometry (PN-ICP-MS), laser ablation with ICP-MS (LA-ICP-MS) and electron probe microanalysis (EPMA). PN-ICP-MS was used for determination of whole content of the rock samples after fusion with $LiBO_2$. LA-ICP-MS and EPMA was used for local microanalysis of individual grains of silicate minerals.

The first results show that of Al/Ga-ratio in analyzed rock is relatively stable (Al/100Ga ~5-15), whereas Si/100Ge-ratio during fractionation increased: in the Třebíč pluton from about 80 in amphibole-biotite durbachites to 250-300 in late biotite durbachites, in orthogneisses from about 230 in biotite otrhogneisses to about 380 in some of two-mica facies, in the Melechov pluton from about 150 in the Lipnice facies do about 400 in the Melechov facies. In the Podlesí granite system, the Ge- and Ga-contents are influenced by greisenisation: namely the Ga is during hydrothermal processes mobile and its content remarkably decreases (Al/Ga-ratio increase).

Laser-ablation analyses of individual silicate minerals from the Cínovec borehole showed, that Ga is preferentially concentrated namely in mica (zinnwaldite and protolithionite), and more in albite than in associated K-feldspar. Ge is namely concentrated in mica. Contents of both Ga and Ge in quartz are lower than their detection limits.

Production of superoxide and hydrogen peroxide on photolysis of natural organic matter

S. GARG[1], A.L. ROSE[1,2] AND T.D. WAITE[1]*

[1]School of Civil and Environmental Engineering, The University of New South Wales, Sydney, NSW 2052, Australia (d.waite@unsw.edu.au)
[2]Southern Cross Geoscience, Southern Cross University, Lismore, NSW 2480, Australia

Irradiation of Suwannee River fulvic acid (SRFA) at pH 8.1 with simulated sunlight resulted in production of nanomolar concentrations of superoxide and hydrogen peroxide. Analysis of the results obtained confirmed that SRFA contains a redox-active chromophore which reduced oxygen to yield superoxide upon photoexcitation. Hydrogen peroxide was generated exclusively via uncatalysed disproportionation of superoxide produced in this way.

Superoxide decayed through both uncatalysed disproportionation and an oxidative pathway that did not result in hydrogen peroxide production, whereas hydrogen peroxide did not undergo further reaction to any discernible extent over the one-hour duration of irradiation. Singlet oxygen did not contribute substantially to production of superoxide or hydrogen peroxide, but was found to play a critical role in controlling the mechanism and associated rate of superoxide decay in the irradiated solution.

A kinetic model based on these observations is presented which provides an excellent description of the experimental results and is also consistent with observations from a wide range of other studies investigating various aspects of SRFA redox chemistry and photochemistry.

https://doi.org/10.1180/S0026461X00006502 Published online by Cambridge University Press

Dissolution of gold in hydrochloric acid

D. GARIJO* AND N. SHIKAZONO

Graduate School of Science and Technology, Keio University, Yokohama, 223-8522, Japan (*correspondence: garijodiego@gmail.com, sikazono@applc.keio.ac.jp)

The purpose of this work is to study hydrochloric acid as an alternative to cyanide for the dissolution of gold in the mining industry. The use of cyanide is controversial due to its toxicity. With hydrochloric acid the process would be safer for the environment and workers. J. D. Clemens showed that hydrogen gas can pass through Teflon at high temperature [1]. When dissolving gold in hydrochloric acid, several reactions should be taken into account:

$$Au + H^+ + 2Cl^- \rightarrow AuCl_2^- + 1/2H_2$$
$$Au + 3H^+ + 4Cl^- \rightarrow AuCl_4^- + 3/2H_2$$
$$Au + 4H^+ + 4Cl^- \rightarrow HAuCl_4 + 3/2H_2$$

The removal of H_2 in the system should quicken the process by forcing these reactions to proceed from left to right. Research by Nakata using Teflon vessels showed high gold concentrations compared to previous studies [2]. This is supposed to be due to degassing of H_2 from the system.

A proper combination of parameters will determine if the process is possible and economically viable. By now, it has been found that area of the gold particles, concentration of hydrocloric acid, temperature and time are the most relevant variables. The presence of amorphous phase can determine the speed of dissolution in short time intervals. The manufacturing process, apart from creating amorphous phase as a result of mechanochemical reactions, may inject energy into the surface. If this energy is heterogeneously distributed, activated zones could be preferentially dissolved. Regarding the recycling of gold alloys, composition can be important. The nature of the vessel (Teflon, or other non-permeable) is not important when the experiment is very short (less than ten days).

[1] J. D. Clemens *et al*., Teflon as a Hydrogen Diffusion Membrane: Applications in Hydrothermal Experiments, *Hydrothermal Experimental Techniques,* 121-140, eds. G.C. Ulmer and H.L. Barnes, John Wiley and Sons, New York. [2] N. Shikazono *et al*. , Dissolution of Gold in Hydrochloric Acid Solution at 150°C, *Hiyoshi Review of Natural Science Keio University* No.11 (1992), 1-4

Colloidal arsenic distribution and speciation in mine soils

F. GARRIDO[1], F. LABORDA[3], E. BOLEA[3] M. HELMHART[1] P. O'DAY[2] AND S. SERRANO[1]

[1]Institute for Agricultural Sciences (CSIC), Madrid (Spain)
[2]University of California, Merced, CA 95343 USA
[3]Institute of Environmental Sciences, University of Zaragoza, Zaragoza (Spain)

Arsenic associated with colloidal particles is an important vector for As migration in contaminated soils. Using Asymmetric-Flow Field-Flow Fractionation (AsFlFFF) coupled to an inductively coupled plasma-mass spectrometer (ICP-MS), we determined the As distribution as a funtion of the particle size of the colloidal fraction of soils samples. The samples were collected from stained preferential flow paths and bulk soil samples, impacted by a mine waste. Physical and chemical properties of the colloids were also determined using X-ray-difraction, SEM and TEM. Arsenic and Fe speciation in the colloidal fraction was characterized using X-ray absorption (XAS) spectroscopy techniques.

Preliminary results indicated that more than 47% of the As mobilized in the preferential flow paths (70.5 mg/L) was associated with the colloidal fraction of the soil. Instead, 5% (2 mg/L) of the mobile As in the bulk samples of the soil was colloidal As. Common to both samples, a similar fractogram (1-1000 nm) was obtained for As, Fe and Al, suggesting an association of As with Fe and/or Al colloidal particles. As XAS analysis of the colloidal fractions (>10 nm) of the soil samples, indicated As adsorption on ferryhidrite as the main As-colloid retention mechanism. The presence of Fe-oxyhydroxides in addition to phyllosilicates was also showed by Fe X-ray absorption analisys. These results show the important role of Fe-oxyhydroxides as nanovectors of colloidal As in preferential flow paths and bulk samples of a contaminanted soil.

https://doi.org/10.1180/S0026461X00006502 Published online by Cambridge University Press

Platinum group minerals (PGM) from chromitites of Kytlym Uralian-Alaskan type complex (Russia)

G. GARUTI[1]*, F. ZACCARINI[1] AND E.V. PUSHKAREV[2]

[1]University of Leoben, Dept. Appl. Geol. Sci. Geophysics, Leoben, Austria (*correspondence: giorgio.garuti@unileoben.ac.at)

[2]Ural Division of Russian Academy of Sciences, Inst. Geol. Geoch., Ekaterinburgniversity of Leoben, Russia

Several PGM have been found in two different types of chromitites associated with the Kytlym Uralian–Alaskan type complex (Northern Urals, Russia). Type-1 chromitite forms small schlieren or pods irregularly distributed in dunite, whereas the type-2 occurs as thin layers within amphibole-rich clinopyroxenite veins (Butyrin-veins) cutting across the dunite. Type 2 chromitite is enriched in Fe^{3+} and Ti compared to type 1. The concentration of IPGE (Os+Ir+Ru) decreases from 408-580 ppb in type-1 to 293 ppm in type-2. The latter also distinguishes for a much higher PPGE (Rh+Pt+Pd) content (22679 ppb) compared with type-1 (4776-10836 ppb), showing a Pd-Ir ratio of 151 in front of 0.6 in type-1. Alloys in the Pt-Fe-Ni system (isoferroplatinum tetraferroplatinum and ferronickelplatinum), erlichmanite, cuprorhodiste and osmium occur as primary polygonal inclusions in type-1chromitite. Tulameenite is exclusively located along cracks in contact with secondary ferrian chromite, magnetite and chlorite, or constitutes the metasomatic replacement of primary Pt alloys. In contrast, the PGM assemblage of type-2 chromitite consists of Pd, Hg, Pt and Cu alloys (mainly potarite and Cu-rich potarite) and Pt-Fe-Cu with minor unnamed compounds of Rh-Te-Hg, Pt-Fe-Pd and Pd-Fe-Cu-S. With the exception of few Pt-Fe alloys that occur enclosed in fresh chromite, most of these PGM occur as irregular grains in the contact between chromite and silicates (clinopyroxene and amphibole), usually associated with pentlandite and pyrrhotite. Type-1 PGM precipitated in the high-temperature magmatic stage prior to or concomitant with chromite crystallization, under variable condition of S and O fugacities as well as Fe activity. Only tulameenite formed during low temperature, hydrothermal process. The composition and paragenetic assemblage indicates that PGM in type-2 chromitite derived from a more evolved melt (high Pd-Ir ratio) characterized by the activity of high-temperature fluids enriched in Hg, Te and Cu. The origin of this melt, i) last-stage fractionation of the same melt that generated the type-1 chromitite, or ii) fluid-rich melt derived from an external source, is still open to question.

Comparison of biomass used in Polish power-plants with other types of biomass

R. GASEK[1]*, W. WILCZYŃSKA-MICHALIK[1] AND M. MICHALIK[2]

[1]Institute of Geography, Pedagogical University, ul. Podchorążych 2, 30-058 Kraków, Poland (*correspondence: rgasek@ap.krakow.pl; wmichali@up.krakow.pl)

[2]Institute of Geological Sciences, Jagiellonian University, ul. Oleandry 2a, 30-063 Kraków, Poland (marek.michalik@uj.edu.pl)

The aim of this study is to compare general characteristics of biomass used in energy production in Poland with other biomass types. We analyzed wood and woody biomass, agricultural straw, and agricultural biomass.

Moisture content (as-received and air dried) is, respectively, within ranges of 5.4-26.2wt% and 1.2-1.6wt%. Ash yield (dry basis, 550ºC) varies from 0.8 to 10.6wt%. Volatile matter (dry basis) content is between 72.3-84.8wt%.

The C content in biomass is within the range 49.04-54.51wt% (daf – dry, ash-free basis); O content calculated by difference varies in the interval 37.32-43.26wt% (daf); H within the range of 5.58-6.35wt% (daf); N content is from 0.29-2.93wt% (daf); S content varies from 0.01 to 0.23wt% (daf). The Cl content measured in dry material varies from 0.017-0.253wt%.

Negative correlation between VM(db) and ash content (db) is evident; less pronounced negative correlation exists between O and C. Positive correlation between N and Cl content can be noted. Correlations between major elements (e.g. Ca, Mg, K, Fe) are week or absent.

Comparison of studied samples of biomass with published data (e.g. [1]) indicates that values of moisture, volatile matter content and ash yield are within relatively narrow range. Ash yield is relatively low in studied samples and volatile matter values are relatively high. The C content is relatively low in comparison with other types ob biomass. Oxygen content is rather high. The S, N and Cl contents are relatively low.

[1] Vassilev *et al*. (2010) *Fuel* **89**, 913-933.

https://doi.org/10.1180/S0026461X00006502 Published online by Cambridge University Press

Changes in Neogene Himalayan erosion regime: Input of Pb and Nd isotopes into the Indian Ocean

J.C. GATTACCECA[1]*, A. GALY[1], A. M. PIOTROWSKI[1] AND M. FRANK[2]

[1]Dept. of Earth Sciences, University of Cambridge, CB2 EEQ Cambridge, UK (*correspondence: jcg54@cam.ac.uk)
[2]Leibniz Institute of Marine Sciences (IFM-GEOMAR), Wischhofstraße 1-3, 24148 Kiel, Germany

Pb- and Nd- isotopic time-series from the authigenic fraction of Central Indian Ocean sediments have been interpreted as responding to changes in the relative amount of Himalayan erosion during the Cenozoic [1,2]. Detrital records of Nd- and Sr- isotopes from the Bengal deep-sea fan suggest a source of sediment dominated by the High Himalaya Series (HHS) for the last 20 Ma [3,4]. Associated variations of Pb-isotopes are not known, and a more precise reconstruction is hampered by the lack of information about temporal changes in the isotopic composition of detrital Pb and Nd carried by rivers draining the Himalayas.

We present new Pb- and Nd-isotope time series, together with rare earth elements, from the bulk detrital and silt-sized fractions as well as the authigenic fraction of deep-sea sediment over the last 20 Ma from Ocean Drilling Program Sites 717 and 718 on the Bengal fan, along with Pb- and Nd-isotopic compositions of the bedloads of Himalayan rivers.

The oldest bulk detrital and silt-sized fraction samples (7-17 Ma) show similar and relatively uniform Pb- and Nd-isotopic compositions characteristic of a stable input from the HHS. The youngest samples (<1Ma) show the same uniformity with a shift towards more radiogenic values, implying a greater contribution of the Lesser Himalaya Series. However, over the Pliocene (1-7 Ma), strongly marked shifts in both isotopes are observed, along with a decoupling between the bulk detrital and silt-sized fractions.

These results imply a strong variability in the erosion and weathering regime of the Himalaya over the Neogene, and we will discuss them in the context of tectonic and climatic changes. We will discuss as well the implications of these changes for the interpretation of the deep water evolution of these isotope systems in the Central Indian Ocean.

[1] Frank et O'Nions (1998) *EPSL* **158**, 121-130 [2] Gourlan *et al*. (2010) *Quaternary Sci*. **29**, 2484-2498 [3] Derry and France-Lanord (1996) *EPSL* **142**, 59-74 [4] Galy *et al*. (2010) *EPSL* **290**, 474-480

Black Reef and Witwatersrand Gold fingerprint, South Africa

C GAUERT[1]*, D BATCHELOR[2], S FUCHS[1,3] AND G KLOESS[3]

[1]Univ. of the Free State, RSA (*correspondence: Gauertcdk@ufs.ac.za)
[2]Karlsruhe Inst. f. Technologie, Inst. f. Synchrotronstrahlung
[3]Inst f. Mat Sc. & Crystal, University of Leipzig, Germany

The origin of the gold, the Uranium and the PGEs in the basal conglomerate of the palaeoproterozoic Black Reef Formation (BR) of the Transvaal Supergroup in South Africa is debated because of the economic significance of this gold ore body. The geochemical trace element fingerprint of the Gold is used to unravel the origin of the Black Reef Gold. Based on EMP, LA-ICP-MS and SR-µ-XRF measurements Black Reef and Witwatersrand (WR) gold can be distinguished by means of their different degree of true fineness, and the Hg, Cu, Fe, S, Ti and Ni trace element content. Among the elements which are correlatible with gold, Sn, Sb, Pd, and Pt, possibly in combination with Mn, Se, Pb, and Ir appear to be the most effective element distinction of gold sources due to their moderate iterative variation.

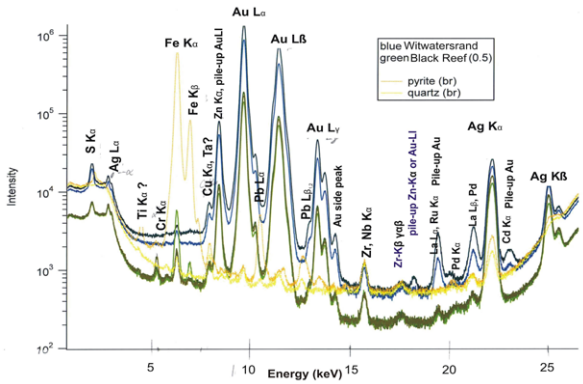

Figure 1: Synchrotron micro-XRF spectrum of BR and WR Gold, and pyrite and quartz at 30 keV energy.

The very similar heavy mineral content argues in favour of a reworked WR gold origin of the BR gold. Against a WR origin argues concretionary pyrite as major component and the less frequently occurring Ni-Co-Fe-sulpharsenides in the Witwatersrand reefs, however its frequent appearance in BR.

The Gold in the BR at Consolidated Modderfontein Au Mine on the East Rand has a lower fineness, lower Hg and Cu content compared to WR gold, whereas Fe, S, Ti and Ni concentrations are higher. Compositions of WR gold from different localities, as well as greenstone-hosted gold will be used in the debate of an alternative source area for the BR gold from the East and West Rand areas.

https://doi.org/10.1180/S0026461X00006502 Published online by Cambridge University Press

Characterization of nanoparticulate arsenic in waters draining abandoned gold mine tailings

A.G. GAULT[1]*, M.B. PARSONS[2] AND H.E. JAMIESON[1]

[1]Department of Geological Sciences and Geological Engineering, Queen's University, Kingston, Ontario, K7L 3N6, Canada (*correspondance: gault@geol.queensu.ca)
[2]Natural Resources Canada, Geological Survey of Canada (Atlantic), 1 Challenger Drive, Dartmouth, Nova Scotia B2Y 4A2, Canada

Waters draining abandoned gold mine sites often contain elevated concentrations of As, however, relatively few studies have attempted to distinguish between colloidal As and truly dissolved As. This distinction is important since it impacts the mobility, bioavailability, and toxicity of As. We collected surface waters draining abandoned gold mine tailings in Nova Scotia, Canada and sequentially filtered them through standard 450 nm pore size filters followed by stirred cell ultrafiltration through 10 nm polycarbonate membranes. Arsenic concentrations in the <450 nm fraction, traditionally termed "dissolved", ranged from 0.2 – 1.6 mg/L. Colloids, operationally defined here as suspended solids of 10 to 450 nm diameter, accounted for 5 – 56% of this As. SEM inspection of the 10 nm filters indicated that Fe and Ca were commonly associated with As-bearing nanoparticles. This was corroborated by synchrotron-based μXRF mapping which revealed that As was closely correlated with Fe, and to a lesser extent Ca. Multiple μXANES analyses indicated that arsenate was the dominant form of nanoparticulate As, with minor amounts of arsenite. These analyses showed no evidence for As-bearing sulfides, implying that arsenopyrite, the original mineralogical host of As prior to mining, was not a significant contributor to colloidal As. Synchrotron-based μXRD examination was hampered by the limited sample mass collected on the filter; however, akaganeite was found to be associated with As hotspots identified by μXRF mapping. Taken together, these preliminary data suggest the primary nanoparticulate vectors of As are secondary mineral assemblages such as hydrous (Ca-)Fe arsenates and Fe oxyhydroxides, previously shown to be major As-rich phases within the near-surface, weathered tailings at these historical gold mine sites [1].

[1] Walker *et al*. (2009) *Can. Mineral*. **47**, 533-556.

Cadmium isotopic composition in cultured marine phytoplankton

M. GAULT-RINGOLD[1,2]*, R. STRZEPEK[1,3], C. H. STIRLING[1,2], R. D. FREW[1] AND K. A. HUNTER[1]

[1]Dept. of Chemistry, Univ. of Otago, Dunedin, New Zealand (*correspondence: melaniegr@chemistry.otago.ac.nz)
[2]Center for Trace Element Analysis, Dunedin, New Zealand
[3]NIWA, Dunedin, New Zealand

Cadmium (Cd) has been used as a marine paleo-nutrient proxy [1] despite its complex and poorly understood biogeochemical cycling in the oceans. The past five years have seen an increasing interest in the stable isotopic composition of Cd in the marine enviroment as this information has the potential to be used as a tracer for the physical and biological controls of Cd cycling in the oceans and its use as a micronutrient. It has also been suggested that Cd isotopes themselves may be a reliable paleoproxy for primary productivity [2].

Both iron (Fe) and zinc (Zn) have been shown to influence the uptake of Cd in both cultured and natural phytoplankton populations [3]. Phytoplankton utilize Cd in the place of Zn for the enzyme carbonic anhydrase (CA) with some species expressing a Cd-specific CA enzyme when grown under Zn-limiting conditions [4].

Using multiple-collector inductively coupled plasma mass spectrometry (MC-ICPMS) combined with double spiking techniques, significant 0.1%-level isotopic fractionation of Cd in seawater has been demonstrated and attributed to biological uptake [5]. Using these techniques, we examined the Cd isotopic fractionation associated with biological uptake in cultured marine phytoplankton under varying Fe and Zn-limiting conditions.

These experiments confirm that there is an isotopic fractionation associated with biological uptake of Cd, leaving the residual medium isotopically heavy. Fractionation factors calculated, assuming a Rayleigh distillation model, for these cultures demonstrate that Zn-limitation is influential in the resulting Cd isotopic compositions.

The importance of Zn bioavailibility on Cd isotopic composition implies that the biogeochemical cycling of Cd in the oceans is complex, which calls into question the potential application of Cd stable isotopes as a paleonutrient proxy.

[1] Elderfield and Rickaby (2000) *Nature* **405**, 305-310. [2] Abouchami *et al*. (2011) *EPSL* In Press. [3] Frew *et al*. (2001) *Deep-Sea Res. Part II* **48**, 2467-2481. [4] Lane *et al*. (2005) *Nature* **435**, 42-42. [5] Ripperger *et al*. (2007) *EPSL* **261**, 670–684.

https://doi.org/10.1180/S0026461X00006502 Published online by Cambridge University Press

Water-rock interaction at the Theistareykir geothermal field in NE-Iceland

BJARNI GAUTASON[1]* AND KARLIS MUEHLENBACHS[2]

[1]Iceland GeoSurvey & Univ. of Akureyri, P.O. Box 30, 602 Akureyri, Iceland (*correspondence: bg@isor.is)
[2]University of Alberta, Edmonton AB, T6G-2E3, Canada (karlis.muehlenbachs@ualberta.ca)

The Theistareykir volcanic system constitutes the western most part of the Northern Volcanic Zone (NVZ) in Iceland. Unlike its nearest neighbor to the east, the Krafla system, it does not have a well developed caldera structure. However, near the center of the system there are sporadic outcrops of siliceous rocks.

Bæjarfjall is a sub-glacial tuya located centrally in the system. On its northern slopes extensive acid sulfate alteration provides evidence for a vigorous geothermal system. To date six deep (≈ 2 to 3 km) exploration wells have been drilled in the area. Cuttings from the wells record extensive alteration of the bedrock with epidote-chlorite (T ≥ 240°C) and amphibole-epidote (T ≥ 290°C) facies metamorphism recorded at relatively shallow depths. Temperature logging and modelling shows that the geothermal gradient in the area follows the boiling point curve in the uppermost 2.5 km.

We have separated cuttings from selected depths in well ThG-1, taking care to obtain only cuttings of the dominant lithology from each of the selected depth intervals. These cuttings have been analyzed for their $^{18}O/^{16}O$ ratios. The $\delta^{18}O$ values of the rocks range from -4.0 to -10,2 (‰ SMOW) recording extensive exchange with meteoric derived hydrothermal fluid and very high time-integrated water-rock ratios. A general trend of decreasing $\delta^{18}O$ with depth is observed. From the data gathered to date it appears that most depleted rock occur close to presently active aquifers. More surprising however, is the depleted character ($\delta^{18}O$ < -8.0 ‰SMOW) of apparently unaltered (basaltic) intrusives.

The overall characteristics of the profile ($\delta^{18}O$ vs. depth) is similar to that obtained previously from the Krafla hydrothermal system [2].

[1] Gautason *et al*. (2010) *World Geoth. Congress Proceed*., **1136**, 5 pp. [3] Hattori & Muehlenbachs (1982) *J. Geophys. Res*. **87,** 6559-6565.

Magnesite growth inhibition by organic ligands: Complexation and adsorption

Q. GAUTIER[1,*], P. BÉNÉZETH[1], G. JORDAN[2], U-N. BERNINGER[2] AND J. SCHOTT[1]

[1] Géosciences et Environnement Toulouse (GET), CNRS, UMR 5563, 14 Avenue Edouard Belin, 31400 Toulouse, France (*correspondence: quentin.gautier@get.obs-mip.fr)
[2] Dept. f. Geo- u. Umweltwissenschaften, Ludwig-Maximilians-Universität, 80333 München, Germany

Magnesite is object of scientific attention due to its potential for long-term CO_2 sequestration. Organic ligands are widespread in natural environments, and because of their promoting effect on Mg-containing silicates dissolution, it has recently been suggested that some carboxylate ligands could be used to enhance *ex situ* mineral carbonation [1]. However, the influence of such organic ligands on magnesite precipitation still needs to be elucidated.

We performed macroscopic and microscopic crystal growth experiments using mixed-flow reactors (MFR) and Hydrothermal Atomic Force Microscopy (HAFM) at temperatures between 80 and 150°C and slightly alkaline conditions. Three model ligands were investigated for their different chemical and structural properties: oxalate, citrate and EDTA.

MFR experiments showed that at concentrations above 0.01 mM, the investigated ligands inhibited magnesite growth. Inhibition is positively correlated with the complexation of Mg^{2+} by the ligands. Furthermore, by precisely calculating saturation states, we show that citrate causes a reduction of the kinetic rate constant of magnesite growth: for instance, citrate concentrations as low as 0.2 mM induce a 4-fold decrease of the rate constant, an effect that is not observed for oxalate. These results point towards different surface effects of the ligands.

HAFM observations showed that all three ligands interacted with steps on the magnesite surface, and modified the shape of growth islands. Measurements of step advancement rates suggest that citrate strongly inhibits growth at acute steps, which has been suggested to control magnesite growth at similar conditions [2].

Therefore at the investigated conditions, inhibition of magnesite growth by organic ligands appears to be a consequence of both Mg^{2+} complexation decreasing solution saturation, and specific interactions of the ligands at the magnesite surface. The results help to assess a potential use of organic ligands for mineral carbonation purposes and may improve our understanding of the long-term fate of CO_2 in ligands-containing storage sites.

[1] Krevor S.C.M., Lackner K.S. (2011) *IJGGC*, in press. [2] Saldi G.D., Jordan G., Schott J. & Oelkers E. (2009) *GCA* **73**, 5646-5657.

https://doi.org/10.1180/S0026461X00006502 Published online by Cambridge University Press

Magnetic susceptibility of Zafarghand granitoidic pluton

NEGAR GAVANJI*, M. SADEGHIAN AND S. SHEKARI

Shahrood University of Technology, Shahrood, Iran
(*correspondence: g.negar20@yahoo.com)

Zafarghand granitoidic pluton (ZGP) is located in the 160 km of NE Isfahan. This pluton is one of the granitoidic pluton of Orumieh Dokhtar structural zone and its lithological composition range includes: gabbro, diorite, granodiorite and granite.. Eocene volcanic and volcano sedimentary are host rocks. This pluton investigated in the light of Anisotropy of Magnetic Susceptibility (AMS) method. 1008 samples were gotten from 123 stations in ZGP. Based on some criterias, magnetic parameters of these samples have been measured in the magnetic lab of Shahrood University of technology by MFK1-FA kappabridge machine. The measured mean magnetic susceptibility (Km in μSI) of the different rock groups are as follows: Gabbros (38120), diorites (26558), granodiorites (16922) and granites (9885). Based on these values gabbros and diorites have higher magnetic susceptibility [F.1].

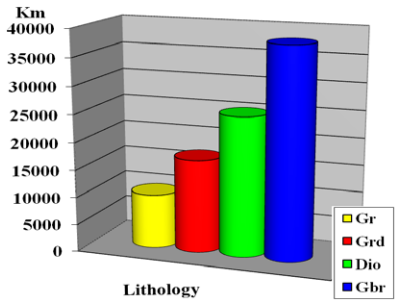

Figure 1: Km- Lithology diagram

This characteristic confirmed by the presence of magnetite in polished sections, thermal magnetic diagrams and Geochemistry analyze. Km values which they are more than (500 μSI) indicate that studied granitoidic rocks are ferromagnetic and correlate with I-type granitoids [1, 2].

[1] Tarling D.H. *et al* (1993) Chapman & Hall, London 217. [2] Bouchez, J.L. (1997) Kluver, Dordrecht, 95-112.

Highly siderophile element and Os isotope systematics of pyroxenite layers from the Lanzo peridotite body (Northern Italy)

T. GAWRONSKI* AND H. BECKER

Institut für Geologische Wissenschaften, Freie Universität Berlin, Malteserstrasse 74- 100, D-12249 Berlin, Germany
(*correspondence: gawronsk@zedat.fu-berlin.de)

Mantle pyroxenites are believed to represent a minor constituent of the Earth's mantle, but may yield insight into the origin, modification and transport of mafic magma. Mantle sources enriched in pyroxenite have been suggested as explanation for coupled suprachondritic ^{187}Os-^{186}Os signatures in some mantle plume sources [1, 2].

The spinel and plagioclase facies Lanzo peridotite body includes layers of spinel-and plagioclase-bearing websterite, clinopyroxenites and orthopyroxenites up to several dm in thickness. Abundances of highly siderophile elements (HSE) in the pyroxenites display no correlation with Al_2O_3, CaO and Na_2O. Concentrations of Os, Ir, and Ru range from 1 to 0.01 x values in peridotites. Aluminum rich clinopyroxenites show enrichment of Pt, Pd, Au and Re over Os, Ir, and Rh, and initial γ_{Os} (200 Ma) of +25 to +150. Concentrations of Pt, Pd, Au and Re in such samples are only occasionally higher than estimates for primitive mantle values. Aluminum poor websterites are less depleted in Os, Ir, Ru, Rh and display less enrichment of incompatible HSE, with γ_{Os} (200 Ma) of -2 to +43, reflecting a smaller contribution from melt enriched in incompatible HSE. HSE ratios in the pyroxenites range from sub- to suprachondritic (Os/Ir:0.40-1.66, Ru/Ir:0.26-3.70, Rh/Ir:0.23-0.55, Pt/Ir:1.03-26.48, Pd/Ir:0.79-42.92, Au/Ir:0.02-3.75, Re/Ir:0.15-2.67, Pt/ Re:1.96-151.30). Two samples (out of 12) with unusual composition display Pt/Re high enough to develop coupled suprachondritic ^{186}Os-^{187}Os with time as reported for some picrites and komatiites [2].

With the exception of 3 samples, most pyroxenites are correlated in a Re-Os isochron diagram and yield an errorchron date of 1136±120 Ma (^{187}Os/^{188}Os$_i$ = 0.13±0.01). This date is considerable older than the emplacement during the early Mesocoic (200 Ma) but coincides with a Sm-Nd model age of 1200 Ma for the southern Lanzo peridotite body [3].

[1] Luguet *et al*. (2008), *Science* **319**, 453-456. [2] Brandon and Walker (2005), *EPSL* **232**, 211-235. [3] Bodinier *et al*. (1991), *Journal of Petrology- Special Lherzolites Issue*, 191-210.

https://doi.org/10.1180/S0026461X00006502 Published online by Cambridge University Press

Spatial distribution of erosion rates in small Tahitian catchment (10km^2), from cosmogenic ^{3}He in olivine

ERIC GAYER[1], FENGYIN YE[2] AND SUJOY MUKHOPADHYAY[3]

[1]Institut de Physique du Globe de Paris, Sorbonne Paris Cité, UMR 7154 CNRS, 75005 Paris, France (egayer@ipgp.fr)
[2]Université de Polynésie Française, GEPASUD, Tahiti.
[3]Harvard University, Cambridge, 02138 MA, USA.

Understanding mechanisms that modify landscapes is essential for risk assessment in tropical islands. Such an understanding requires quantification of the rates at which landscapes respond to tectonic and climatic signals. Because measurements of long-term erosion rates are critical for understanding landform evolution, the use of cosmogenic isotopes in river sediments to estimate average erosion rates of drainage areas has grown rapidly in recent years.

In this study we present measurements of cosmogenic ^{3}He concentrations ([^{3}He$_c$]) in olivine grains from Tahitian river sediments (French Society Island) to predict the spatial pattern of erosion rates in the drainage area [1].

The olivine-rich sands come from 3 locations along the Matatia River, on the west part of Tahiti (catchment mouth, intermediate and upstream positions). He concentrations and isotopic ratios have been measured in 3 samples of olivine grains (1-2 mm) each weighing ~500 mg. The [^{3}He$_c$] has been calculated using: (i) the ^{3}He/^{4}He ratio measured by crushing and (ii) the ^{3}He and ^{4}He concentrations measured by melting the resulting powder.

Initial results indicate (i) an average erosion rate of 0.39±0.19 mm/yr upstream of the catchment mouth, and (ii) an average erosion rate of 0.0078±0.0007 mm/yr for the upstream sub-basin. The erosion rate at the intermediate position is too high to accumulate measurable amounts of ^{3}He$_c$.

The observed variation of erosion rates along the drainage area could be related to different erosional processes (landslides vs. soil creep), or can represent the erosion rates of different sub-basins (main stream vs. tributary). The measured erosion rates at the different locations allow us to invert for the spatial distribution of the erosion rates through nonlinear slope- and curvature-dependent erosion rates. This approach also enables us to constraint the form of parameterized erosion laws.

[1] Gayer, Mukhopadhyay and Meade (2008) *Earth Planet. Sci. Lett.* **266**, 303-315.

Melting conditions with PRIMELT: Examples and future work

ESTEBAN GAZEL[1], CLAUDE HERZBERG[2] AND PAUL ASIMOW[3]

[1]Lamont-Doherty Earth Observatory, (egazel@ldeo.columbia.edu)
[2]Rutgers University, (herzberg@rci.rutgers.edu)
[3]California Institute of Technology, (asimow@gps.caltech.edu)

Determination of the magmatic melting conditions in the mantle is important for understanding the origin of intraplate magmas. The major element composition of primary magmas can provide such information, but there are important limitations. Of these, the best known is fractional crystallization. Other factors are source lithology variations and volatile content. PRIMELT2 [1] was introduced to calculate primary magma composition, but is restricted to primitive lavas that only crystallized olivine. It was calibrated from experiments on fertile mantle peridotite, and provides a mass balance primary magma. It calculates primary magma composition, melt fraction for accumulated fractional and batch melting, mantle potential temperature, olivine phenocryst composition, and warns the user of potentially compromising effects of source lithology variations and CO_2 content.

PRIMELT2 was used to evaluated variations in mantle potential temperature of OIB (ocean islands) [1] and to compare OIB to Large Igneous Provinces (LIPS) [2]. Results show that mantle plumes for LIPS were hotter and melted more extensively than plumes of modern OIB. Petrological solutions obtained from back-arc alkaline lavas from the Central American Volcanic Front yield T_p estimates within expected ambient mantle (1350-1400°C) [3]. These results indicate that PRIMELT2 is applicable for melting in a variety of tectonic environments. Work in progress will test the effects of alteration and simulate a decompression melting path.

[1] Herzberg & Asimow (2008) G3 **9**, Q09001. [2] Herzberg & Gazel, (2009) Nature **458,** 619-622. [3] Gazel *et al*., (2011) Lithos **121,** 117–134

https://doi.org/10.1180/S0026461X00006502 Published online by Cambridge University Press

How geochemical proxies provide quantifiable evidence of climate shifts over the last 25,000 years

GEOFFREY GEBBIE

Department of Physical Oceanography, Woods Hole Oceanographic Institution, MS #29, Woods Hole, MA 02543 USA (ggebbie@whoi.edu)

Some of the best, but still limited, evidence for large climate shifts, including the end of the Last Ice Age, comes in the form of geochemical proxies preserved in seafloor sediments. The proxy data is actually recording oceanic tracer distributions, which in turn, depend upon the sea surface and the atmosphere in a complicated way. In the terminology of inverse methods, the "observation step" must be modelled as well; that is, the process that translates the physical variables of the ocean into a proxy signal must be explicitly (i.e., mathematically) stated. In many cases, this process is calcification in foraminifera, and empirical relationships are used here as the model of this step. In cases where the observation or proxy step is oversimplified in the model, a whole range of plausible solutions can be excluded without good reason.

While it is clearly of interest to estimate past rates of ocean circulation from geochemical proxies, an inverse method is used to show that the seafloor proxies from the Last Glacial Maximum inform us primarily about shifts in the water-mass configuration. In this particular example, I show that the geochemical proxies, $\delta^{18}O$, $\delta^{13}C$, and Cd/Ca ratio, give quantifiable evidence for a shift in the pathways of the interior ocean, not just changes in surface boundary conditions. Given this information, estimates of the rate of overturning circulation in the Atlantic are revisited, but significant uncertainties remain in the inverse estimate of this particular quantity.

Selenium reduction by pyrite: pH effect and Mossbauer study

ANTOINE GEHIN[1], MINGLIANG KANG[1,2], JEAN-MARC GRENECHE[3] AND LAURENT CHARLET[1]

[1] Environmental Geochemistry Group, ISTerre, Maison des Geosciences, 38041 Grenoble, France (*correspondence: antoine.gehin@obs.ujf-grenoble.fr)

[2] Guangzhou Institute of Geochemistry, Chinese Academy of Sciences, Guangzhou, 510640, P.R.China

[3]Condensed Matter Physics Laboratory, IRIM2F, University of Maine, 72085 Le Mans, France

The radioactive isotope ^{79}Se is presently considered as the key mobile fission product for the disposal of spent fuel (SF) and high-level radioactive waste (HLW). Its solubility is largely controlled by oxidation state. Due to the weak adsorption of Se(IV) and Se(VI) on natural minerals, specially on granite and clay minerals, chemical reduction is considered to be the most effective way to immobilize ^{79}Se [1,2].

On the other hand, pyrite is the most frequent sulfide mineral and is also present in geological barriers of nuclear waste repositories [3].

Therefore, we investigate the interaction between pyrite and Se(IV) from pH 5.05 to 8.5. After 1 month, solution analyses show that Se(IV) concentration decreases under the detection limit and suggest that Se(IV) is involved in redox reactions with FeS_2

We focus specially on the behavior of iron species in the immobilization of Selenium. Mossbauer spectroscopy performed on the solid at different pH shows clearly significant iron environment modifications, and thus it suggests particularly the precipitation of new solid phases included Fe and Se, like FeSe or $FeSe_2$.

These resulsts are confirmed by XAFS spectroscopy used to unravel the selenium speciation., and microscopy analysis (SEM and TEM).

[1] Chen *et al*. (1999) *J. Nucl. Mater*. **275**, 81-94. [2] Scheinost *et al*. (2008) *Environ Sci & Technol*. **42**, 1984-1989. [3] Beaucaire *et al*. (2000) *Appl Geochem*. **15**: 667-686.

https://doi.org/10.1180/S0026461X00006502 Published online by Cambridge University Press

U-Pb ages and Hf isotopes of detrital zircons from miogeoclinal strata of western North America

GEORGE GEHRELS AND MARK PECHA

Department of Geosciences, University of Arizona, Tucson AZ 85721 USA (ggehrels@gmail.com)

U-Pb ages and Hf isotope signatures have been determined from 32 samples of Neoproterozoic, Paleozoic, and lower Mesozoic miogeoclinal strata from western North America. Samples have been collected along five transects in eastern Alaska, northern British Columbia, southern British Columbia, Utah-Nevada, and northern Mexico. Detrital zircon grains from these samples were analyzed for U-Pb by ID-TIMS in the mid-90's to generate a spatial-temporal reference for the ages of grains that accumulated along the western edge of North America. We have recently re-analyzed these samples by CL-based LA-MC-ICPMS to determine more robust U-Pb age distributions (~200 grains/sample) as well as complementary Hf isotope signatures (~50 grains/sample).

U-Pb ages from these samples match well with the ages determined by ID-TIMS, and in most cases resemble the ages of nearby basement rocks. Hf isotope signatures for these detrital grains reveal a fascinating history of crustal genesis and recycling. In southern regions, primary age groups are 1.0-1.2, ~1.4, and 1.6-1.8 Ga, which matches the ages of bedrock terranes in the region. Hf signatures of these grains record generation of juvernile crust at 1.6-1.8 Ga, followed by recycling of this crust during younger magmatism. Central transects contain these same age groups, plus a significant Late Archean contribution. Hf data suggest formation of juvenile crust during Late Archean time, with significant recycling of this crust during 1.6-2.2 Ga magmatism. Little juvenile crust is recorded between 1.6 and 1.8 Ga, whereas, surprisingly, 1.0-1.2 and ~1.4 Ga zircons are considerably more juvenile than coeval grains to the south. Northern transects record protracted magmatism from 3.6 Ga to 300 Ma. Some juvenile crust of early Paleozoic, Early Proterozoic, and Late Archean age is represented, but most grains have Hf compositions that lie between observed 1.8-2.0 and 2.5-2.8 Ga evolution bands. This presumably reflects homogeneous mixing of 1.8-2.0 and 2.5-2.8 Ga crust, rather than recycling of 2.0-2.3 Ga juvenile crust, as the 2.0-2.3 Ga grains present are not juvenile.

Actinium-227 in the Atlantic sector of the Southern Ocean: New results from Bonus-Goodhope and UK Geotraces

WALTER GEIBERT[1]*, ALAN HSIEH[2], CLAUDIA HANFLAND[3], ELISABET VERDENY[4], PERE MASQUE[4], GIDEON HENDERSON[2]

[1]School of GeoSciences, University of Edinburgh, West Mains Road, Edinburgh EH9 3JW, UK (*correspondence: walter.geibert@ed.ac.uk)

[2]Department of Earth Sciences, University of Oxford, UK

[3]Alfred Wegener Institute for Polar and Marine Research, Bremerhaven, Germany

[4]Institut de Ciència i Tecnologia Ambientals - Departament de Física, Universitat Autònoma de Barcelona, Spain

Actinium-227 is a naturally occurring radionuclide, which is released from marine sediments, in particular deep-sea sediments. With a half-life of 21.77 years, it is an excellent indicator of vertical mixing in the deep-sea, and a tracer for upwelling of deep water masses. Therefore, it has potential to be used to quantify fluxes of micronutrients from the deep-sea.

Here, we present new data from the Southern Ocean that were obtained during the UK Geotraces cruise and the Bonus-Goodhope cruise in the South Atlantic. We characterise the main water masses in the Atlantic sector of the Southern Ocean, and discuss to which extent the Ac data can be expected to remain constant over time within water masses.

We also compare results that were obtained by direct alphaspectrometric analyses (Bonus-Goodhope) to indirect measurements by radium delayed coincidence counting (RaDeCC) and discuss the differences of the methods.

If a general input function for Ac from marine sediments could developed, ^{227}Ac could be used to validate deep ocean circulation and mixing in models, analogue to the application of ^{3}H or chlorofluorocarbon as tracers for surface water masses. New depth profiles from the UK Geotraces cruise promise to give new estimates of ^{227}Ac flux from the deep sea, and bring the implementation of ^{227}Ac in models closer.

https://doi.org/10.1180/S0026461X00006502 Published online by Cambridge University Press

Si-isotope fractionation during silica precipitation: An experimental approach

S. GEILERT[1]*, M.J. VAN BERGEN[1] AND P.Z. VROON[2]

[1]Department of Earth Science, Utrecht University, the Netherlands (*correspondence: geilert@geo.uu.nl)
[2]Faculty of Earth and Life Sciences, Vrije Universiteit Amsterdam, the Netherlands

Interpretations of silicon isotope compositions of natural silica deposits suffer from poor constraints on the isotopic fractionation behaviour during precipitation of the silica from a saturated solution. We tested an experimental setup to explore the conditions under which equilibrium precipitation of amorphous silica would occur in the 10-60°C temperature range using flow-through reactors. The objective is to constrain magnitudes and sign of silicon isotope fractionation, the degree of temperature dependence and the sensitivity to non-equilibrium conditions.

Stock solutions, prepared from amorphous silica powder and brought to saturation at 90°C, were forced to pass flow-through reactors, seeded with ca. 200 mg of silica powder with known surface area at well-controlled flow-rates. Precipitation was induced by placing the reactors in a water-bath at the desired temperature. According to a comprehensive set of test runs, our experimental set-up enables us to achieve equilibrium during controlled silica precipitation in the reactors, provided that conditions are carefully tuned. Factors with a strong influence included the applied flow-rate, pH, specific surface area and degree of supersaturation.

Silicon isotope measurements ($^{30}Si/^{28}Si$ and $^{29}Si/^{28}Si$), carried out on input and output solutions using a Finnigan Neptune MC-ICPMS, presented insight into the sign and magnitude of isotopic fractionation. Preliminary results for runs where equilibrium was secured demonstrated that, under these experimental conditions, $\delta^{30}Si$ values for SiO_2 remaining in solution were up to 0.5‰ lower relative to the input solution, implying discrimination against the uptake of the lighter isotopes in the solid. The fractionation increased with decreasing temperature.

The observed direction is opposite to what is often seen in natural solid-fluid systems, indicating that equilibrium versus non-equilibrium conditions during precipitation might be a critical factor in the use of Si isotopes as a proxy.

The rusty sink: Impact of Iron on the sedimentary organic biomarker record

YVES GÉLINAS[1]*, KARINE LALONDE[1], LUC TREMBLAY[2], ANJA MORITZ[1] AND ANDREW BARBER[1]

[1]Chemistry and Biochemistry, Concordia Univ., Montreal (QC), Canada, H4B 1R6 (*correspondence: ygelinas@alcor.concordia.ca)
[2]Chimie et Biochimie, Univ. Moncton, Moncton (NB), Canada, E1A 3E9 (luc.tremblay@umoncton.ca)

The biogeochemical cycles of iron (Fe) and organic carbon (OC) are strongly linked, each element exerting some degree of control over the other. In the oceans, organic ligands control the concentration of dissolved Fe in the water column. In soils, Fe and OC concentrations are typically correlated, suggesting that they are closely associated. Nevertheless, until now, the role of Fe in the preservation of sedimentary OC has not been clearly established. We recently determined that 20 to 40% of the total OC in marine and freshwater sediments is closely associated to solid reactive Fe phases (operationally defined as the solid iron phases that are reductively dissolved with sodium dithionite). In young and mature sediments, solid reactive Fe phases do not provide sufficient surface area for chemisorption of OC onto Fe oxides. Alternatively, high OC:Fe ratios reflect the existence of largely organic Fe-OC macromolecular structures (through chelation and co-precipitation), attached only minimally to the surface of clay mineral grains. The organic matter in these Fe-OM chelates is 'glued' together by iron ions or nanophases of iron oxide crystals. We also found isotopic and elemental fractionation between Fe–associated OC and the rest of the sedimentary OC pool, with ^{13}C and nitrogen-enriched OC preferentially bound to Fe, and suggesting biochemical fractionation. The presence of iron and the interactions between iron and organic matter also affect the recovery of a broad range of organic biomarkers from sediments. In this communication, we will present and discuss the impact of iron on the recovery of amino, lipid and lignin biomarkers as well as on the environmental message obtained through biomarker analysis. Alternative methods that circumvent the effects will also be presented.

https://doi.org/10.1180/S0026461X00006502 Published online by Cambridge University Press

T and fO_2 guided, gas phase mediated Na and K exchange between silicate melt drops

M. GELLISSEN[1,2], A. HOLZHEID[1], PH. KEGLER[1] AND H. PALME[2]

[1]Univ. Kiel, Inst. f. Geowissenschaften; (mgellissen@web.de)
[2]Forschungsinstitut und Naturmuseum Senckenberg, Frankfurt a.M.

The overall depletion of volatile lithophile elements in the mantles of the terrestrial planets along with nearly unfractionated Mn/Na ratios [1] as well as the varying abundances of Na and K relative to Si in meteorites and even individual chondrules [2] leads to the question of the nature of the depletion process (evaporation or incomplete condensation). As our early experiments showed little or no loss from Na and K bearing minerals we focussed on evaporation from siliceous melts with different fractions of Al, Na, K and partly Fe, Ti and Mn.

We used 11 synthetic silicates with a molar Si/(Al+Na+K) ratio of 3/1, varying Al/alkali and Na/K ratios and NBO/T from 0 to 0.67. Each run contained samples of different composition. Also a Si, Fe, Ti and Mn bearing mixture enriched with Na and K was used. Samples' weights were about 4 mg. Time series were done in 1 atm CO/CO_2 gas mixing furnaces from 1000 to 1550 °C and log fO_2 from air to IW-2. Sample mounting was by Pt wire loop technique [3].

Under all experimental conditions Na and K are lost from high Na, K samples and gained by low Na, K samples, with all samples reaching an approximately constant level after several hours. The process is faster with increasing temperature and decreasing oxygen fugacity. The Na concentration at the converging point decreases with increasing gas flux, but is independent of Al concentration in the starting composition, despite variations from 0 to 26 wt % Al_2O_3. The effect for K is less pronounced.

Na and K contents are controlled by the Na and K vapor pressures in the furnace, which again is determined mainly by the gas flow in the furnace and by the total amount of alkalis released by heating. The lesser dependence of the K concentration from the gas flux is a hint to a faster kinetic behavior compared to the Na. More experiments with varying gas flow rates are in progress.

[1] Palme & O'Neill (2003) Treatise on Geochemistry (eds. Turekian, Holland), Vol 2, The Mantle and the Core (ed. Carlson). [2] Jones *et al*. (2005) in: Chondrites and the Protoplanetary Disk ASP Conference Series, **341:** 251-281. [3] Donaldson *et al*. (1975) *Am. Min*., **60**: 324-326.

Petrology of the Middle Eocene sub-volcanic association of Western Pontides

S. CAN GENÇ[1], FATMA GÜLMEZ[1], MEHMET KESKIN[2], OKAN TÜYSÜZ[3] AND TURGAY IŞSEVEN[4]

[1]ITU Dept of Geology 34469 Istanbul, Turkey (*correspondance: scangenc@itu.edu.tr)
[2]IU Dept. of Geology Istanbul, Turkey;
[3]ITU Inst. of Eurasian Earth Sci., 34469 Istanbul, Turkey;
[4]ITU Dept. of Geophysics 34469 Istanbul, Turkey;

The Middle Eocene (49.3±2 – 38.1±1.9 Ma) magmatic rocks (MEMR) form an east-west trending belt along the northern Turkey. They rest unconformably on the pre-Middle Eocene units. Here, we present geological and petrological data from the western part of this belt, between Armutlu Peninsula and the Almacık Mountains. These rocks forming a "sub-volcanic association" are represented by the basic to intermediate volcanic rocks, dikes and coeval granitic rocks. The volcanic rocks of the MEMR form a continuous trend from basalt to dacite. Granitic rocks comprise granite, granodiorite and tonalities. Both the volcanic and the granitic rocks display medium-K subalkaline affinity, and CA trend with rare tholeiitic lava samples. They display significant enrichment in LIL elements, and slightly enrichment in LREE. There are apparent impoverishments in Ta and N, in N-MORB normalized spider diagrams. Initial Sr and Nd isotopic values for the volcanic rocks of the MEMR are ($^{87}Sr/^{86}Sr_i$: 0.703976-0.706441) and ($^{143}Nd/^{144}Nd_i$: 0.512856-0.512601), respectively. From these data and combined ƐNd(T) (-1.55 - +5.38), Pb and ^{18}O (8.5-13) isotopic values, we conclude that the magma produced the MEMR was hybrid in composition, including depleted mantle and crustal components. AFC processes played an important role for the genesis of magma. According to these geochemical features, MEMR displays close similarity to the subduction-related magmas. In the light of geological and petrological findings, we conclude that the MEMR was produced in a post-collisional setting, and we favour the slab breakoff model that provides a better explanation for the generation of the MEMR.

https://doi.org/10.1180/S0026461X00006502 Published online by Cambridge University Press

Redox reactions of Fe^{II-III} oxyhydroxycarbonate minerals in gleysols, fougèrite, trébeurdenite and mössbauerite, and water denitrification

J.-M. R. GÉNIN[1]*, O. GUÉRIN[2], E. KUZMANN[3] AND C. RUBY[1]

[1]Institut Jean Barriol, Université Henri Poincaré, ESSTIN, 2 rue J. Lamour, F54500, Vandoeuvre-lès-Nancy, France (*correspondence: jean-marie.genin@esstin.uhp-nancy.fr)
[2]Laboratoire de Géomorphologie, Ecole Pratique des Hautes Etudes, 15 bd de la mer, F35800, Dinard, France
[3]Department of Chemistry, Eötvös Lorand University, Pazmany Peter setany, H1117, Budapest, Hungary

Colour change from bluish-green to ochre in gleysols is due to redox reactions within Fe^{II-III} oxyhydroxycarbonate, related to a green rust Fe^{II-III} double layered hydroxide of general formula $Fe^{II}_{6(1-x)}\ Fe^{III}_{6x}\ (OH)_{2(7-3x)}\ O_{2(3x-1)}\ CO_3\ 3H_2O$. Minerals are named (i) fougérite for $Fe^{II}_4\ Fe^{III}_2\ (OH)_{12}\ CO_3 \bullet 3H_2O$ green rust Fe^{II-III} hydroxycarbonate (ii) trébeurdenite for $Fe^{II}_2\ Fe^{III}_4\ (OH)_{10}\ O_2\ CO_3 \bullet 3H_2O$ Fe^{II-III} oxyhydroxy- carbonate (iii) mössbauerite for $Fe^{III}_6\ (OH)_8\ O_4\ CO_3 \bullet 3H_2O$ ferric oxyhydroxycarbonate at definite x values of 0.33, 0.67 and 1, respectively; the exceptional redox flexibility comes from toptotactic reactions as shown by XRD and TEM; the relative trivalent cation average ratio x extends from 0.33 to 1 by mixing minerals as shown by Mössbauer spectra (Fig. 1).

Figure not supplied.

Figure 1: Mössbauer spectra measured at 78 K of samples vs x (***a***) fougèrite; (***b***) trébeurdenite (***c***) mössbauerite

In samples extracted out of waterlogged gleys in a water table (Fougères), x varies between 0.33 and 0.67 by mixing fougèrite with trébeurdenite, whereas in those extracted from the schorre of a maritime marsh (Trébeurden), x varies between 0.67 and 1 by mixing trébeurdenite and mössbauerite, due to partial oxidation of the gley at low tide. This redox flexibility is responsible for water denitrification in water tables combined with anaerobic bacterial reduction.

Plume-ridge interaction: Constraints on melting dynamics from the Azores and Iceland

F.S. GENSKE[1,2]*, C. BEIER[1,2], S.P. TURNER[1], K.M. HAASE[2] AND B.F. SCHAEFER[1]

[1]GEMOC, Department of Earth and Planetary Sciences, Macquarie University, Sydney NSW 2109, Australia (*correspondence: felix.genske@mq.edu.au)
[2]GeoZentrum Nordbayern, Universität Erlangen-Nürnberg, Schloßgarten 5, D-91054 Erlangen, Germany

Ocean Island Basalts (OIB) erupted in the vincinity of Mid-Ocean Ridges (MOR) provide important information on melting processes, melt movement and composition of the Earth´s mantle. In particular the major element, trace element and Sr-Nd-Pb isotope ratios allow for constraints on the distinct melting behaviour of enriched and depleted mantle sources, their along and across axis distribution and potential changes in melting depth and melting temperatures.

While the flow of melts into the Mid-Atlantic Ridge (MAR) in the Azores and Iceland has been the subject of several studies, both plumes exhibit active volcanism on the western side of the Mid-Atlantic Ridge away from the proposed plume locality. Such off-axis volcanism beneath the North-American plate is comparable for the two OIB settings in terms of trace element and isotopic source composition relative to the main plume centre. Incompatible trace element ratios of Nb/Zr, Ta/Hf and La/Sm are elevated by similar factors in the off-axis (western) lavas when compared to the lavas from the plume centre. We compare the melting dynamics (i.e. P-T conditions of basalt generation) underneath the Snaefelsness peninsula (Iceland) with those underneath Flores and Corvo islands (Azores); both examples of unusual off-axis and "off-plume" magmatism.

We demonstrate that Iceland and the Azores exhibit comparable excess temperatures, but that melting underneath the western Azores islands is initiated deeper. The sources in the Azores are more enriched and degrees of partial melting are slightly lower than compared to Snaefellsness. This implies that for both cases melting dynamics are largely controlled by the geochemical composition of the source and possibly lithosphere thickness rather than upwelling rate. The differences between eastern and western (i.e. plume related vs. "off-plume") sources may reflect different proportions of enriched melts during binary mixing with depleted MORB mantle (DMM) sources.

https://doi.org/10.1180/S0026461X00006502 Published online by Cambridge University Press

Weathering of black shales and Re-Os isotope systematics

S. GEORGIEV[1,2]*, H. STEIN[2,1], J. HANNAH[2,1], B. BINGEN[1,2], V. HATLØ[3], E. REIN[3], S. PIASECKI[4], H. WEISS[5] AND G. XU[2,1]

[1]Geological Survey of Norway, 7491 Trondheim, Norway
[2]AIRIE Program, Colorado State University, USA
(*correspondence: georgiev@colostate.edu)
[3]Statoil ASA, 5254 Sandsli, Norway
[4]Geological Survey of Denmark and Greenland (GEUS)
[5]SINTEF Petroleum Research, 7465 Trondheim, Norway

Late Permian organic-rich shales from the Ravnefjeld Fm in East Greenland yield a precise isochron from drill core samples, but scattered data from outcrop samples. Using Re-Os isochroneity as a gauge to distinguish fresh undisturbed shale from macroscopically fresh but chemically altered shale, we explore additional geochemical parameters that evidence subtle weathering and oxidation of shale.

Systematic differences between weathered and fresh samples are used to characterize and quantify the effect of weathering on shale chemistry. Weathering oxidizes organic matter (OM) and sulfides (mainly pyrite framboids <6 μm on average), sometimes imperceptibly. The kerogen oxygen content (approximated by the S3 parameter of Rock-Eval pyrolysis) is a more consistent proxy for weathering than major or trace element compositions. Comparison with time equivalent fresh shale from the mid-Norwegian shelf reveals that shale weathering is best detected and characterized by the combined use of Rock-Eval indices for oxidation of OM and sulfur content data that document oxidation of pyrite. Based on this example, we present a sampling strategy to optimize the potential for accurate and precise Re-Os geochronology.

Correlations among trace metals, total organic carbon and total sulfur show that both Re and Os are concentrated in OM rather than sulfides. While both Re and Os are mobile during weathering, isotopic disturbance may occur through several contrasting mechanisms depending on local factors from the outcrop to the mm-scale. Depending on the type of isotopic disturbance, weathered shales may yield erroneously younger or erroneously older model ages.

Late Permian shales in this study have exceptionally high Re/Os ratios that lead to rapidly increasing $^{187}Os/^{188}Os$ with time. Mass balance shows that recent (or Cenozoic) weathering of such shales may influence the Os isotopic composition of seawater much more strongly than weathering of typical Phanerozic shales; the effect will be comparable to weathering of Precambrian shales.

Funded by Norwegian Research Council Award 180015/S30.

Modeling the effects of fertilization and pH on dissolved inorganic phosphorus in soils

F. GERARD[1], N. DEVAU[1], E. LE CADRE[2] AND P. HINSINGER[1]

[1]INRA, UMR 1222 Eco&Sols, Montpellier, France
[2]Supagro, UMR 1222 Eco&Sols, Montpellier, France

We used a set of mechanistic (macro-scale) adsorption models within the framework of the component additive approach in an attempt to determine the effect of repeated massive application of inorganic P fertilizer on the processes controlling the concentration of dissolved inorganic phosphorus (DIP) in soils. We studied a Luvisol with markedly different total concentrations of inorganic P as the result of different P fertilizer history (i.e. massive or no application for 40 years). Soil pH was made to vary from acid to alkaline.

Satisfactory results were obtained using generic values for model parameters and soil-specific ones, which were either determined directly by measurements or estimated from the literature. We showed that adsorption largely controlled the variations of DIP concentration and that, because of kinetic constraints, minor precipitation of Ca-phosphates may have occurred under alkaline conditions, particularly in the P-fertilized treatment. The adsorption of Ca^{2+} onto soil minerals promoted adsorption of phosphates through electrostatic interactions. The intensity of this mechanism was high under neutral to alkaline conditions. The variation in DIP concentration with pH can be related to changes in the contribution of the various soil minerals to P adsorption.

https://doi.org/10.1180/S0026461X00006502 Published online by Cambridge University Press

Advances in analyses of radiogenic isotope by LA-MC-ICPMS: The importance of mass bias and interference correction

A. GERDES

Institut für Geowissenschaften, Goethe University Frankfurt, Altenhoeferallee 1, D-60438 Frankfurt am Main (gerdes@em.uni-frankfurt.de)

Isotope analysis by laser ablation sector-field ICP mass spectrometry (LA-SF-ICPMS) becomes increasingly important to study magmatic, metamorphic, and sedimentary processes. The information gained can be, for instance, crucial for a better understanding of the timing and genesis of magmatic and sedimentary rocks, the formation of ore deposits, and the evolution of the continental crust. Due to disturbance of the isotope system by alteration and partial recrystallization the initial isotope composition is often preserved only in single growth domains of minerals.

Developments in LA-SF-ICPMS over the last years make it now possible to analysis precisely the isotopic composition of Sr, Nd, Hf, and U-Th-Pb with a spatial resolution of down to 30 to 5μm, depending on elemental concentration. Hence, a very sensitive detection system coupled to powerful Laser with short wave length and high resolution imaging system is crucial for this type of analyses.

Beside high background (e.g., gas blank), matrix effects, and mass bias correction, the precision and accuracy of these isotope analyses often strongly suffers from isobaric and molecular interferences on the relevant masses. Although these interferences in question can be usually monitored simultaneously on a different mass, the interference correction is hampered by prediction of the mass discrimination behaviour of this isotope pair.

Data will be shown that the discrimination of the lighter isotopes in the plasma interface of the ICP-MS is dependent on element and on the matrix. With examples from the different isotope system, analytical protocols will be discussed to overcome this problem. The results of recent studies performed in our lab demonstrate that LA-MC-ICPMS analyses of $^{87}Sr/^{86}Sr$ (e.g., plagioclase, titanite, apatite, monazite, xenotime, pyrochlor, perovskite), $^{143}Nd/^{144}Nd$ (e.g., titanite, monazite, apatite, pyrochlor, perovskite, garnet) and $^{176}Hf/^{177}Hf$ (e.g., zircon, zirconolite, baddeleyite) isotopes can be precise and accurate to about 0.01% or better, despite of 10 to >50% interference on the relevant isotope ratio. Providing that between different phases the range in the mother-daughter isotope ratio is sufficient large enough, it is even possible to obtain geologically meaningful isochrones in the Rb-Sr and Sm-Nd system by LA-MC-ICPMS analyses.

Geochemical signatures of thermochemical sulfate reduction – Ketones and sulphur species

S. GERMEROTT[1], C. OSTERTAG-HENNING[2] AND H. BEHRENS[1]

[1]Institute for Mineraloy, Leibniz University of Hannover, Callinstr. 3, 30167 Hannover, Germany (*correspondence: s.germerott@mineralogie.uni-hannover.de)

[2]Federal Institute for Geosciences and Natural Resources, Stilleweg 2, 30655 Hannover, Germany

Thermochemical sulfate reduction (TSR) is defined as the abiological, thermally-driven reduction of sulfate with H_2S and CO_2 as major reaction products. The reaction can proceed at temperatures above 120°C when sulfate as well as reducing agents, such as e.g. hydrocarbons or ferrous iron, are present. In spite of its great importance for hydrocarbon reservoir alteration and sulfide ore formation, the TSR process is not adequately understood. In this study we present findings from laboratory experiments that lead to an improved description of the geochemical signature of TSR and thus to a better understanding of TSR reaction mechanisms. A major goal was to identify key chemical compounds that play an important role during TSR.

Experiments were performed in sealed gold capsules, at 300°C and 350°C, 350 bar, for a duration of 24 - 336 h. A redox-mineral buffer, consisting of pyrite (FeS_2), pyrrhotite (FeS) and magnetite (Fe_3O_4) was used to constrain the redox conditions during the experiments. Na_2SO_4, dissolved in water, was used as sulphate source and C_8H_{18} as model hydrocarbon (= reducing agent). Furthermore, the influence of elemental sulphur on the TSR reaction was investigated. After the experiments the products were analyzed by different gas chromatographic techniques. In addition to CO_2 and hydrocarbons, we focused on the analysis of ketones and organosulphur compounds.

In general, a higher reaction rate was found at 350°C compared to 300°C. Concurrent processes in the degradation of octane under the experimental P-T conditions comprise cracking and TSR reactions. A pronounced influence of TSR was indicated by the formation of CO_2, ketones, aromatics and organosulphur compounds. The experiments with elemental sulphur showed the highest yields of TSR products. The analytical data suggest that the oxidation of carbon proceeds via one or more intermediate reaction steps with metastable oxygenated or sulfurized compounds, e.g. the formation of ketones.

https://doi.org/10.1180/S0026461X00006502 Published online by Cambridge University Press

Subcrustal CO_2 flux measurement in the Hranice hydrothermal Karst

MILAN GERŠL[1]*, EVA GERŠLOVÁ[1], DUŠAN HYPR[2] AND VLADIMÍR KOLEJKA[1]

[1]Czech Geological Surwey, Brno branch, Leitnerova 22, 679 36 Brno (* correspondence: milan.gersl@geology.cz)
[2]Czech Speleological Society, 6-18 tartaros, Brno

In the Hranice Karst (Czech Republic) the term thermomineral karst was introduced to the international literature [1]. This active thermal karst is developed in the sequence of Paleozoic limestones as a result of deep influx of thermal water charged with subcrustal carbon dioxide (CO_2). Gas origin is also supported by helium isotopic ratio in water-gas mixture [2]. The carbon dioxide concentration in Zbrašov aragonite cave atmosphere reflects seasonal temperature variation and is well documented and described for the last 30 years [3].

Measurement techniques

CO_2 flux measurement was performed in 2009–2010 using accumulation chamber equipped with infrared analyzer in the Hranice field area. CO_2 flux was measured in the Zbrašov aragonite cave system during the summer 2010. The cave atmosphere was suck out to get permanent flow of CO_2. This status was hold for 6:27 hours. Chemical and isotopic composition of selected gas samples were determined in the laboratory by gas chromatography / mass spectrometry.

The average CO_2 concentration was 2.529% and flux ranged from 74 to 125 $g.m^{-2}.d^{-1}$ reflecting venting of subcrustal CO_2 in the Hranice area. In the Zbrašov aragonite cave the CO_2 concentration in the atmosphere varies from 0 to 85% with measured constant flux of 32894,45 $g.m^{-2}.d^{-}1$.

[1] Kunský, J. (1957): Thermomineral karst and caves of Zbrašov, Northern Moravia. - *Sbor. Čs. Spol. Zeměpis*., 62, 4, 306-351. Praha. [2] Meyberg, M., Rinne, B. (1995): Messung des $^3He/^4He$-Isotopenverhaltnisses im Hranicka Propast (Tschechische Republik). – *Die Höhle, Zeitschrift für Karst- und Höhlenkunde*, **46**(1), 5-8. Wien. [3] Geršl, M., Hladil, J., Hypr, D., Stepišnik, U. (2004): Variability of carbon dioxide concentrations in Zbrašov Aragonite Caves and its assessment on the base of nine-year monitoring research. – *3. nár. speleolog. kongres*, 8.-10. 10. 2004 Sloup, 15-19. Kuřim.

Ophiolites of the Kuznetzky Alatau Ridge (SW Siberia) as a possible ancient crust fragments of the Paleoasian Ocean

I.F. GERTNER* AND T.S. KRASNOVA

Tomsk State University, Lenin avenu 36, 634050 Tomsk, Russia, (*correspondence: labspm@ggf.tsu.ru)

An assessment of initial stages of the Paleoasian Ocean opening is still a matter of researcher's argument. Besides it assumes a quite long time interval which, according to the geodynamic reconstructions within Altay-Sayan folded area, ranging from 700 to 1000 Ma. One of the reasons for doubts about geochronology evaluation of the ophiolitic suite fragments is isotopic data absence for the rocks with ultrabasic and basic composition which are oceanic crust and lithospheric mantle standard.

Ophiolites of the Kuznetsky Alatau Ridge trace an ancient suture zone formed as a result of the collision of few arc island terrains on the active margin of Siberian continent during the Late Cambrian and Early Ordovichian time (530-480 Ma). Their absolute ages was recently estimated by the Sm-Nd mineral isochron for the amphibolite (694±43 Ma) and results of U-Pb dating of zircons from the plagioriolite spaitly associated with ocean basalts (544±8Ma). According to regional geological conclusions the real temporal range of ophiolite forming is about 500 Ma (from Early Cambrian to Late Riphean time). Our data of Sm and Nd isotopes for the whole rocks of mantle hyperbasites and ultramafic-mafic rocks are close to ancient boundary of these rocks.

The Sm-Nd isochron based on the three whole rock samples of harzburgite, chromitite and dunite has a slope corresponding to the age 947±51 Ma at MSWD = 1.18. But the 6-point regression line based on the whole rocks magmatic peridotites and gabbroides of toleitic series is a more reliable. Its slope corresponds to the age 943±39 Ma at MSWD = 0.966. In particular the restitic ultrabasites correspond to the characteristics of the strongly depleted backarc basin -type mantle substrate. Their model age calculation with using modern depleted mantle model certainly suggests a younger initial substrate. For the "restitic" ultrabasites T (DM) values range from 760 to 866 Ma, whereas for "magmatic" rocks these values corresponds to the real isochron age of 945-1000 Ma. These data confirm a possible geochemical heterogeneity of ultramafic-mafic complexes in the suture zone of the thrust-folded systems.

The study was funded by Russian Ministry of Education and Science.

https://doi.org/10.1180/S0026461X00006502 Published online by Cambridge University Press

Mantle heterogeneities beneath Laguna Timone volcano, Pali Aike volcanic field, Southern Chile

F. GERVASONI[1]*, R.V. CONCEIÇÃO[1], T.L.R. JALOWITZKI[1] AND Y. ORIHASHI[2]

[1]Geoscience Institute, UFRGS, Porto Alegre - RS, Brazil (*correspondence: fernanda.gervasoni@ufrgs.br)
[2]Earthquake Research Institute, The University of Tokyo, Tokyo, Japan (oripachi@eri.u-tokyo.ac.jp)

Laguna Timone(52°01'39"S, 70°12'53W), inactive Quaternary volcano in Pali Aike volcanic field [1], southernChile, host large mantle xenoliths from the lithosphere. They are characterized by spinel-lherzolite, garnet-spinel-lherzolite, garnet-lherzolite, garnet-harzburgite, glimmerite (PM18-3) and some xenoliths are phlogopite- and/or pargasite-bearing, which suggest their origin in mantle deeper source and a metasomatism. Geochemical data show #Mg between 88 to 91 and major elements depletion compared to primitive mantle (PM) [2]. Rare earth elements (REE), normalized to PM, suggests four: Group 1 has light REE depletion and heavy REE enrichment (Ce_N/Yb_N= 0.12-0.43); Group 2 has LREE enrichment and HREE depletion (Ce_N/Yb_N=2.07-15.3); Group 3 have middle REE enrichment and depletion (Ce_N/Yb_N= 0.96-0.98), and Group 4 have similar values between LREE and HREE (Ce_N/Yb_N= 0.78- 1.68). All samples are more enriched in Ta than Nb, and are strongly depleted in Y; Zr and Hf are enriched in most samples. The Sr and Rb are depleted while Ba is enriched. Spider diagrams show anomalies in some samples such as Nb, Ta, Zr and Hf high enrichment in sample PM18-3. Calculations with no-modal batch melting model shows that Laguna Timone xenoliths have suffered ~20% of melt. The Rb-Sr, Sm-Nd and Pb-Pb isotopes analysis are under progress. Laguna Timone xenoliths came from a deep source in the Patagonian mantle and suffered several thermal multi- stage, indicated by mineralogic evidence (garnet-lherzolite to spinel-lherzolite transitions phases) and a modal metasomatism (phlogopite and pargasite).

[1] Stern *et al* (1999), *Lithos* ***48***, 217–235. [2] Sun & McDonough (1989), *Geol. Society* **42**, 313-345.

Geodynamic regimes of continental crust growth and lithosphere reworking in subduction zones

TARAS GERYA

Institute of Geophysics, Swiss Federal Institute of Technology, Sonneggstrasse 5, 8092 Zurich, Switzerland, (taras.gerya@erdw.ethz.ch)

It is widely accepted that new continental crust can grow in subduction zones. Indeed, physical-chemical controls and dynamics of crustal addition remain partly enigmatic. Based on numerical models we identify the following geodynamic regimes of subduction, crustal growth and lithospheric reworking which may potentially form on Earth: (1) stable subduction, (2) retreating subduction with a focused backarc spreading center, (3) retreating subduction with distributed intra-arc extension, (4) advancing subduction with thickening overriding plate. Transitions between these different regimes are mainly caused by the concurrence of rheological weakening effects of (1) aqueous fluids percolating from the subducting slab into the mantle wedge and (2) melts propagating from the partially molten areas formed in the mantle wedge toward the surface. The aqueous fluids mainly affect the forearc region. Strong fluid-related weakening promotes plate decoupling and reduces subduction drag and thus results in stacking of sediments in the accretion prism. In contrast, reduced weakening by fluids results in strong coupling of the plates and leads to advancing collision-like subduction with enhanced subduction erosion. Thickening of the overriding plate and sedimentary plumes in the mantle wedge are the consequences. On the other hand, melts, extracted from the hot regions above the slab, rheologically weaken the lithosphere below the arc which thus controls overriding plate extension and shortening. Strong rheological weakening by melts in combination with weak plate coupling triggers retreating subduction with a pronounced backarc spreading center. Also, weakening of the arc by melts extracted from sedimentary plumes, generate weak channels through which these structures may be emplaced into subarc crust. If there is insufficient melt-related weakening, plumes cannot ascend but extend horizontally and thus underplate the lithosphere. Models with notable melt- and fluid-related weakening often predict existence of hot, rheologically weak asthenospheric window in the bottom of the arc that allows for potential relamination of positively buoyant subducted rocks to the crust and recycling of dense magmatic residue back into the mantle.

https://doi.org/10.1180/S0026461X00006502 Published online by Cambridge University Press

Time constraint on Brunhes-Matuyama inversion inferred by U-Series disequilibrium

B. GHALEB[1], C. FALGUÈRES[2], J.P. POZZI[3], L. ROUSSEAU[2], J. CARLUT[4] AND L. BOUDAD[5]

[1]GEOTOP, Université du Québec À Montréal, BP 8888, suc. Centre ville, Montréal, QC, H2V 3W8, Canada
[2]Département de Préhistoire MNHN, UMR7194 CNRS, 1 rue René-Panhard, 75013 Paris , France
[3]Ecole Normale Supérieure, Géologie, UMR8538, 24 rue Lhomond, 75231 Paris, France
[4]IPGP, UMR7154, 1 rue Jussieu 75238, Paris, France.
[5]Université Moulay-Ismaël, BP 141, Errachidia, Maroc.

In southwestern Morocco (northern Sahara border) hydrothermal travertine deposits ($CaCO_3$) occurred covering several km^2 with a thickness up to 15m. The main interest in dating such deposits is that travertine formations are generally regarded as remnants of Quaternary humid phases. A continuous core of 12 m mainly consisting of pure $CaCO_3$ alternating with detrital layers of clay was sub-sampled for U-series dating (pure $CaCO_3$) and for magnetic properties in layers rich in detritus. The magnetic record results indicated two main features: 1) normal polarity inclinations with a mean value around 40° is found for all measured samples from surface until 9.03 meter deep and 2) at 9.05 meters deep, reverse polarity inclinations abruptly appear with a mean inclination value around –40°. This polarity inversion was attributed to the Brunhes-Matuyama transition.

U-series dating indicates that samples from the top of the core up to 5.6 m yield ages ($^{230}Th/^{234}U$), ($^{234}U/^{238}U$) compatible with statigraphy ranging between 500 ka and present-day. On the other hand, all samples below the depth of 5.6 m indicate infinite ages implying that secular radioactive equilibrium is reached from this depth down. However, samples above 5.6 m that yielded finite ages allowed us to calculate an initial $(^{234}U/^{238}U)_0$ value for the hydrothermal fluid from which the $CaCO_3$ was precipitated. This calculation was also carried on samples collected in outcrop or section near the coring site that gave calculable ages. Compiling these initial values, the frequency histogram of $(^{234}U/^{238}U)_0$ shows an almost unimodal distribution with a mean value of 5 ± 0.5 for all samples (< 500 ka). Assuming this value constant before 500 ka, we calculated the time needed for the $(^{234}U/^{238}U)_0$ of samples to reach the measured one for the samples older than 500 ka. The decay of ^{234}U excess depends on its half-life (245.2 ± 0.49 ka) and may allow to date up to 10^6 y. We find an age of 800 ± 50 ka for samples located at depth between 8 and 10 m. This age is in agreement, though less precise, than the age of Brunhes-Matuyama transition of 780 ka.

Two easy methods in evaluation of an exploration data set

R. GHAVAMI- RIABI[1]*, R. KHALO-KAKAI[1] AND H. ASADI-HARONI[2]

[1]Mining, Petrolum and Geophysics Faculty, Shahrood Univ. of Tech, 7 Tir square, Danshgh Bolv.
(*correspondence: rghavami2 @yahoo.com)
[2]Mining Engineering Dept., Isfahan Univ. of Tech., Khomani shahr Bolv.

Mineralized factors and data

There are two type of statistical analyses for an easy and rapidly evaluation of an exploration data set. It is possible to evaluate and separate the mineralized and pathfinder elements in an exploration data set by using the discrimination and correspondence analyses [1,2,3]. The results of the two method confirm each other for a data set in the study area (Fig. 1 A and B) [4]. The data will be separated into a few sub-populations, if there are a few source of variation in the concentrations (Fig. 1-A). The anomalous sample numbers could distinguish by using correspondence analysis (Fig.1-B).

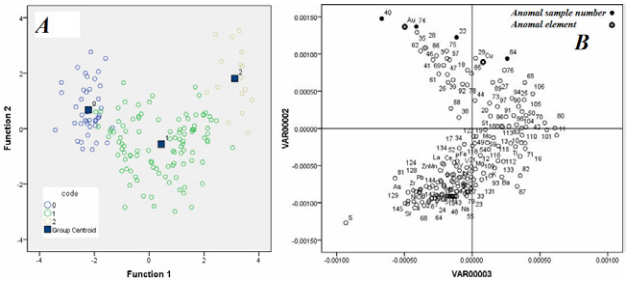

Figure 1: Discrimination (A) and correspondence (B) analysis of an exploration data set

Conclusion

It is important to identify the source of anomaly in a data set, paragentic parameters, and separation of the highly and relatively anomalous data in an exploration or envirnomental evaluation. These aims could be accessable by using discriminationa nd correspondence analyses togetther.

[1] Davis, J.C. (2002), John Wiley & Sons, 646 pp. [2] Greenacre, M.J. (2007), Boca [3] Peh, Z. & Halamić, J (2010), *J. Geo. Expl.*, **107**, 30-38. [4] www.statsoft.com/textbook/stathome.html

https://doi.org/10.1180/S0026461X00006502 Published online by Cambridge University Press

Arsenite oxidation by indigenous bacteria in the Bengal Delta Plain Aquifers (West Bengal, India)

DEVANITA GHOSH[1], JOYANTO ROUTH[2]* AND PUNYASLOKE BHADURY[1]

[1]Dept of Biological Sciences, IISER Kolkata, Mohanpur - 741252, Nadia, West Bengal, India

[2]Dept. of Earth Sciences, IISER Kolkata, Mohanpur - 741252, Nadia, West Bengal, India

(*correspondence: joyanto.routh@iiserkol.ac.in)

Microbial oxidation of arsenite occur in numerous phylogenetically distinct microorganisms, which play a role in As cycling by converting arsenite to the more strongly sorbing, less mobile, and toxic arsenate species[1].

We are studying biogeochemical processes associated with As cycling in Barbakpur village, Rahamatpur block, West Bengal – a region severely affected by high (up to 1 mg/l) As concentrations in groundwater. Water and sediment samples were collected to isolate microorganisms oxidizing arsenite. A new set of primers was designed based on amino acid alignments of several published arsenite oxidase subunit B (*AroB*) genes [2]. Besides, eubacterial 16S rRNA primers were also used to study the microbial communities. *AroB*-like sequences were detected in three wells. Molecular phylogeny based on *AroB* and 16S rRNA sequences reveal the presence of diverse bacterial groups. In addition, ongoing geochemical studies focus on characterizing the organic matter in sediments, which sustain these heterotrophs, arsenite speciation, and trace metal analyses [3].

[1] Evelyne Lebrun (2003) *Mol. Biol. Evol.* **20** (5):686–693. [2] William P. Inskeep (2007) *Environmental Microbiology* **9** (4), 934–943. [3] Joyanto Routh *et al* (2011) *Applied Geochemistry* **26** (4), 505-515.

Stability of phase D at high pressure and temperature: Implications for the role of fluids in the deep mantle

SUJOY GHOSH AND MAX W. SCHMIDT

Institute of Geochemistry and Petrology, ETH Zurich, Switzerland (sujoy.ghosh@erdw.ethz.ch)

Water is transported into the Earth's interior via hydrous phases in descending slabs. Numerous high-pressure studies have clarified that several dense hydrous magnesium silicates (DHMS) are stable at mantle conditions in model compositions [1, 2]. These phases act as water carriers in the subducting slab and may play a critical role in water cycling in the Earth's history and partial melting in the deep mantle. Among these DHMS, phase D is the DHMS phase hosting water in the lower part of the transition zone (where slab may travel along the upper/lower mantle boundary) carrying H_2O from the upper to the lower mantle.

In the present study, we report data on the melting phase relations of phase D and of phase D + olivine + enstatite in (i) MgO-SiO_2-H_2O system (ii) with Al_2O_3 and (iii) with Al_2O_3 + FeO added in proportions appropriate for the mantle. Stochiometric oxide mixtures of brucite and quartz of phase D composition were used as starting material. Multianvil experiments were carried out at pressures between 22 and 24 GPa at temperatures between 1000 and 1800 ºC using 10/3.5 pressure assembly.

Our data show that phase D decomposes to MgSi-ilmenite + stishovite + melt or MgSi-perovskite + stishovite + melt and indicate that phase D can be stable along a slab geotherm up to the base of the upper mantle for a range of H_2O contents. Melt compositions are strongly magnesian with Mg:Si ratio of 1.5-5.2. Furthermore, mass balance calculation of the phase D composition experiments (with Al, Fe) compostion suggests that melts can contain ~ 34 wt% H_2O which fits well with EPMA analysis. The data are used to determine the stabilty of phase D, the proportions of melt formed during melting, the composition of the partial melts and the variation in the melt composition at different pressure temperature conditions. Upon thermal relaxation (to adiabatic temperatures)of a slab travelling along the 660 km discontinuity, phase D would melt releasing a H_2O-rich magnesian melt from the slab. At present experiments at 32 GPa are under way to constrain the P-T slope of the melting.

[1] Shieh, S. R., Mao, H. K., Hemley, R. J., Ming, L. C., 2000. *EPSL* **177**, 65-80. [2] Frost, D. J., Fei, Y., 1998. *JGR* **103**, 7463-7474

https://doi.org/10.1180/S0026461X00006502 Published online by Cambridge University Press

Impact of groundwater composition and diffusive transport limitations on uraninite stability

D.E. GIAMMAR[1]*, J.M. CERRATO[1], C.J. BARROWS[1], Z. WANG[1], V. MEHTA[1], J.S.-LEZAMA-PACHECO[2] AND J.R. BARGAR[2]

[1]Department of Energy, Environmental and Chemical Engineering, Washington University, St. Louis, MO 63130, USA (*correspondence: giammar@wustl.edu)
[2]Stanford Synchrotron Radiaion Lightsource, SLAC National Accelerator Laboratory, CA, USA

The long-term stability of biogenic uraninite in sediments and groundwater are important to the performance of *in situ* bioremediation strategies for uranium-contaminated sites. Stability is influenced by subsurface biogeochemistry, structure and composition of uraninite (UO_2), and coupling with pore scale transport processes. Laboratory measurements of UO_2 dissolution rates under well-mixed and diffusion-limited regimes were integrated with direct characterization of the solid phase to investigate the effects of groundwater cations on UO_2 stability.

Groundwater contains abundant ions that can moderate U release from biogenic uraninite. Experiments were performed with Ca^{2+} and Zn^{2+} as model non-redox active groundwater cations with differing affinities for adsorption to metal oxides. Calcium only slightly inhibited UO_2 dissolution, but zinc had a much greater inhibitory effect. Complementary sorption experiments verified that Zn^{2+} adsorbed more strongly than Ca^{2+} to the uraninite surface. The inhibition of dissolution by the cations is orders of magnitude stronger for oxic conditions than for anoxic conditions, which suggests that the adsorbing or surface-precipitating cation is acting to block the access of oxygen to the UO_2 surface or inhibit the electron transfer from the UO_2 to a soluble oxidant. The molecular-scale structure around calcium and zinc species present at UO_2 –water interfaces were determined using X-ray absorption spectroscopy.

To examine UO_2 dissolution under diffusion-limited conditions, experiments separated the reacting UO_2 from the bulk solution by placing it in a tube covered with a membrane that allowed diffusive exchange of solutes. Slower net release rates of uranium from the tubes were caused by modest diffusive limitations to oxygen transfer to the UO_2. Experiments were performed in both simple aqueous solutions and synthetic groundwaters to further explore the role of groundwater cations on the dissolution process.

Cu speciation in coastal waters using a vibrating gold microwire electrode

K. B. GIBBON-WALSH, P. SALAÜN AND C.M.G. VAN DEN BERG*

Marine Electrochemistry, School of Environmental Sciences, University of Liverpool, Liverpool, L69 3GP, UK (*correspondence: vandenberg@liv.ac.uk)

Cu speciation by pseudopolarography

Pseudopolarography (PP) was developed and optimised for use on a vibrating gold microwire electrode with the intention of developing a more sensitive technique for the speciation of Cu in seawater, with potential for in-situ application. The method was optimised and a desorption potential and conditioning sequence improved the electrodes reproducibility. Model ligands, including glutathione and other well characterised ligands[1] were studied in order to estimate the strength and class of Cu complexing ligands in Liverpool Bay.

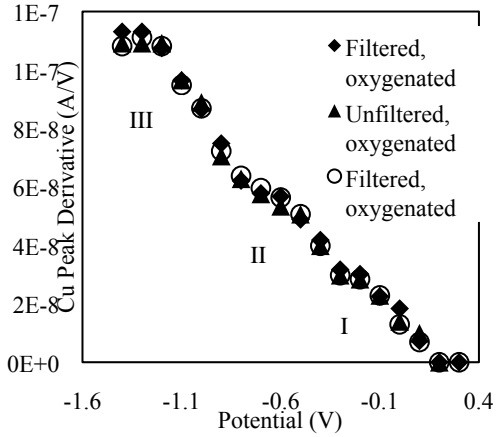

Figure 1: On-board PP analysis in oxygenated coastal sea water (Liverpool Bay)

Cu pseudopolarograms performed on-site, in coastal sea water from Liverpool Bay always show a succession of waves (Fig 1.). The most positive wave corresponds to free+labile Cu complexes while wave II and III represents more strongly bound complexes. Only minor variations were observed between filtered/unfiltered sample and oxygen is not an interference highlighting the potential of the technique to be used in-situ.

[1] Croot *et al*. (1999) *Marine Chemistry* **67,** 219-232.

https://doi.org/10.1180/S0026461X00006502 Published online by Cambridge University Press

Quantifying biotic responses to past abrupt climate change: Thresholds and sensitivities

S.J. GIBBS[1]*, K.M. EDGAR[1,2], P.R. BOWN[3], S.A. O'DEA[1], A. SLUIJS[4], B.H. MURPHY[5] AND J.C. ZACHOS[5]

[1]School of Ocean and Earth Sciences, National Oceanography Centre, Southampton, SO14 3ZH, UK (*correspondence: sxg@noc.soton.ac.uk)

[2]School of Earth and Ocean Sciences, Cardiff University, CF10 3AT, UK.

[3]Department of Earth Sciences, University College London WC1E 6BT, UK.

[4]Biomarine Sciences, Institute of Environmental Biology, Utrecht University. The Netherlands.

[5]Department of Earth and Planetary Sciences, University of California, Santa Cruz, CA 95064, USA.

Paleogene hyperthermals represent transient global warming events associated with massive carbon injection into the ocean-atmosphere system. Because the rate and magnitude of carbon release varied between the events, they are natural experiments ideal for exploring the relationship between carbon cycle perturbations, climate change and biotic response. Here we investigate how we can quantifiably compare biotic responses to events of differing magnitudes and environmental character, to utilise the wealth of high-resolution microfossil data emerging across a range of climate change scenarios. We quantify marine biotic variability through several hyperthermals from 56 to 40 million years ago, using records of evolutionary turnover and assemblage variance. Microfossil records from the biologically and functionally distinct plankton groups show a linear relationship between assemblage variability and the magnitude of carbon cycle perturbation during the various hyperthermals. These Paleogene plankton data show threshold behavior and scaled response to environmental changes associated with carbon cycle perturbations reflecting behaviour likely inherent in planktonic ecosystems and may suggest future biotic response may scale at least in a similar way to the hyperthermals.

Experimental investigation of the differentiation of iron-rich peralkaline magma

CHRISTOPHER GIEHL*, RAINER BABIEL, STEPHAN REICHE, MICHAEL MARKS AND MARCUS NOWAK

Institute for Geosciences, Eberhard-Karls-University, 72074 Tuebingen, Germany (*correspondence: christopher.giehl@uni-tuebingen.de)

In this study we investigate the magmatic differentiation of peralkaline Fe-rich phonolitic melts. These are highly evolved compositions ((Na+K)/Al ratios >1) and are believed to be differentiated from mantle-derived alkali basaltic and nephelinitic sources. The studied composition (FeO_{tot} = 11.6 wt%, #Fe = 0.98, (Na+K)/Al = 1.46) resembles a dyke rock, which is a potential source magma for parts of the Ilímaussaq peralkaline nepheline syenite complex, South Greenland [1].

However, the liquid line of descent of such Fe-rich phonolitic compositions is not well understood because of a lack of experimental data. Therefore, we performed crystallization experiments with synthetic glass as starting material at 1 kbar and 950 to 750°C. We used hydrothermal rapid quench vessels and covered a wide range of water activities and oxygen fugacities using gold capsules and graphite-lined gold capsules. To achieve near-equilibrium conditions, run times of 4 hours were sufficient for H_2O-saturated experiments, in nominally anhydrous experiments run times of 3 weeks were necessary. H_2O-saturated experiments reproduce only parts of the observed early magmatic phases of the dyke rock (sp + cpx). In contrast, under nominally anhydrous and more reducing conditions, the complete early magmatic phase assemblage of the dyke rock (sp, cpx, ol, afs, ne) and an alkali-rich residual melt ((Na+K)/Al = 1.65) was successfully reproduced at and below 850°C. Experiments already conducted were carried out using an equilibrium crystallization approach. Upcoming experiments will simulate fractional crystallization using multi-step differentiation to elucidate the complex differentiation process due to the unusually large temperature interval of crystallization suggested for such magma compositions.

[1] Marks & Markl (2003) *MinMag* **67**, 893-919.

https://doi.org/10.1180/S0026461X00006502 Published online by Cambridge University Press

Dust particles in brochoalveolar lavage fluids from coal miners in Quang Ninh province, Viet Nam

R. GIERÉ*, T.B. HOÀNG-HÒA AND K.P. SEDLAZECK

Albert-Ludwigs-Universität, 79104 Freiburg, Germany
(*correspondence: giere@uni-freiburg.de)

Inhalation is the most important pathway for airborne particles into the human body. The pulmonary system provides an efficient filtering mechanism, which retains most of the coarse particles in the nasal and oral cavities. The fine-particle fraction (≤2.5 μm aerodynamic diameter) penetrates deeper into the respiratory tract and reaches the alveolar region. Here, the particles remain for long periods of time and interact with lung fluid and tissue. The deepest part of the lungs, thus, acts a special type of active sampler for atmospheric dust. The deposited particles can be studied in tissue samples or in brochoalveolar lavage (BAL) fluids.

This investigation aims at characterizing mineralogically and chemically the particles in BAL fluids, which were retrieved from coal miners in the Quang Ninh province, northern Viet Nam. The BAL fluids were filtered to recover the solid fraction, which was dried and studied by X-ray diffraction (XRD). The main mineral component is halite, an artefact from the sterile saline solution (0.9 wt% NaCl, heated to 37 ºC) used during the lung lavages. One of the samples also contains thenardite (Na_2SO_4) and gibbsite ($Al(OH)_3$).

To remove halite, all samples were rinsed repeatedly with deionized water, filtered and dried, and then subject to further investigations. These residues contain the following main components (in wt%): C = 3.3-4.8; Al = 1.7-7.4; Si = 24-94; and Fe = 0.7-1.2. Minor amounts of Na, Mg, S, K, Ca, Cr, Zn, Cd, Ba and Pb are also present, whereas Ni, Cu, As, and Sb were not detected.

XRD analysis of the washed residues revealed that they contain primarily quartz and gibbsite. We are currently using scanning electron microscopy, combined with energy-dispersive X-ray spectroscopy (SEM-EDX), to collect quantitative data on the mineralogical composition of these residues. So far, we have detected the following additional phases: clay minerals, Cr-Fe(Ni)-alloys, K-feldspar, Fe-sulfides, Fe-oxides/hydroxides, gypsum, calcite, dolomite, fly ash spheres, and coal particles. One of the residues also contains Mg-silicates, indicating that the coal miner may have worked in a silicate mine in the past.

Through BAL analysis it is thus possible to deduce the occupational exposure of subjects. This technique could also be applied to humans living in areas with high levels of particulate pollution to identify the main particle sources.

Origin of the differences in redox reactivity of iron (oxyhydr)oxides revealed by time-resolved spectroscopy

B. GILBERT[1]*, J. E. KATZ[2], X. ZHANG[3], K. ATTENKOFER[3], C. FRANDSEN[4], PIOTR ZARZYCKI[5], KEVIN M. ROSSO[5], R. W. FALCONE[1] AND G. A. WAYCHUNAS[1]

[1]Lawrence Berkeley National Laboratory, Berkeley CA USA. (*correspondence: bgilbert@lbl.gov)
[2]Denison University, OH USA.
[3]Argonne National Laboratory, Argonne, IL USA.
[4]Department of Physics, Technical University of Denmark
[5]Pacific Northwest National Laboratory, USA.

The redox chemistry of nanoscale transition metal oxides, hydroxides and oxyhydroxides is of central importance to broad areas of the Earth sciences, including soil and marine biogeochemistry, contaminant remediation, and paleoclimate records. Iron-bearing phases are the most important redox-active minerals in nature and the complex chemistry of these materials exemplifies the challenges in understanding solid phase redox reactions. For example, following the exposure of ferric iron (Fe^{3+}) (oxyhydr)oxides to reducing agents, interfacial electron transfer (ET) can lead to several transformation pathways including release of soluble ferrous iron (Fe^{2+}) (dissolution), formation of alternative ferric or mixed valence phases (transformation), or particle growth. Understanding and predicting such redox processes will require the application of time-resolved methods capable of observing the intermediate species that control reaction path.

We have applied an optical-pump–X-ray-probe method with subnanosecond time resolution to study the fate of ferrous iron sites formed by electron injection at the surface of three phases of ferric iron (oxyhydr)oxides. We used this approach, combined with conventional kinetics studies, to distinguish the timescales for the elementary redox processes occuring during the reductive dissolution of 6-line ferrihydrite, maghemite and hematite nanoparticles. For each phase we quantified the rates of Fe-to-Fe electron hopping, the rates of interfacial electron transfer, the lifetime of kinetic electron trapping within the nanoparticles, and the rates of the full reaction including ferrous iron release into solution. Comparison of these rates which span from the nanosecond to the second scale reveal new insights into the electronic and structural factors controling the redox reactivity of these phases.

https://doi.org/10.1180/S0026461X00006502 Published online by Cambridge University Press

Mapping the amorphous-to-crystalline transitions in $CaCO_3$ biominerals with 20-nm resolution

P.U.P.A. GILBERT

Departments of Physics and Chemistry, University of Wisconsin, Madison, WI 53706, USA (pupa@physics.wisc.edu)

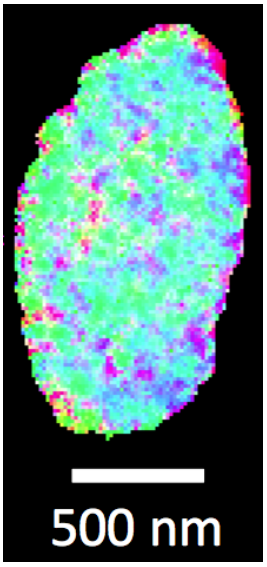

One of the most fascinating aspects of calcite biominerals are their intricate and curved morphologies, quite different from the normal rhombohedral crystal habit of geologic calcite. These morphologies are achieved via amorphous precursor mineral phases [1]. In this talk we will show that in sea urchin larval spicules two distinct phase transitions occur, 1→2 and 2→3 [2]. The 1→2 transition is regulated by inhibiting proteins, while the 2→3 is thermodynamically driven, and occurs spontaneously [3].

Figure 1: Cross-section of a 48-h sea urchin larval spicule, caught in the act of transforming from ACC (type 1 = red, type 2 = green) to crystalline calcite (type 3 = blue), and with imaged XANES-PEEM spectromicro-scopy.

[1] Y Politi, RA Metzler, M Abrecht, B Gilbert, FH Wilt, I Sagi, L Addadi, S Weiner, and PUPA Gilbert. (2008) Mechanism of transformation of amorphous calcium carbonate into calcite in the sea urchin larval spicule. *Procs. Natl. Acad. Sci. USA* **105**, 17362-17366. [2] AV Radha, TZ Forbes, CE Killian, PUPA Gilbert, and A Navrotsky. (2010) Transformation and crystallization energetics of synthetic and biogenic amorphous calcium carbonate. *Procs. Natl. Acad. Sci. USA* **107**, 16438–16443. [3] YUT Gong, CE Killian, IC Olson, NP Appathurai, RA Metzler, AL Amasino, FH Wilt, PUPA Gilbert. Phase Transitions in Sea Urchin Larval Spicules. In preparation.

Natural and artifical noble gases as tracers of injected CO_2 migration within a deep reservoir

STUART GILFILLAN[1]*, R. STUART HASZELDINE[1], ROBERT POREDA[2] AND SUSAN HOVORKA[3]

[1]Scottish Carbon Capture and Storage, University of Edinburgh, UK. (*correspondence: stuart.gilfillan@ed.ac.uk)

[2]Department of Earth and Environmental Sciences, University of Rochester, New York, USA.

[3]Gulf Coast Carbon Center, Bureau of Economic Geology, University of Texas at Austin, Texas, USA.

CO_2 capture and subsequent geological storage of CO_2 is gaining momentum as a means of economically abating anthropogenic CO_2 emissions from point sources. For the technology to be universally deployed it is essential that a robust, reliable and inexpensive means to trace the migration of CO_2 within the subsurface exists. Monitoring during injection will increase confidence that the site characteristics were correctly determined and met. Furthermore, should migration and subsequent surface leakage occur, the ability to track origin and ownership of CO_2 at near and ground surface will be critical for remediation purposes.

As an analogue for tracing CO_2 migration within an engineered storage site, this presentation will examine both natural and artificially injected noble gases at the SECARB early project at Cranfield in MS, USA. Natural CO_2 rich in mantle derived noble gases was injected into a portion of the reservoir via a deep injection well and samples were collected via U-tube sampling equipment from two nearby observation wells. Additionally, two separate injections of artificial Kr and Xe tracers injected with the CO_2 were undertaken.

Noble gases are conservative tracers within the subsurface, proving to be invaluable in determining both the origin of CO_2 and how it is stored in natural CO_2 reservoirs [1,2]. This presentation will compare measurements of the natural $^3He/^4He$, $CO_2/^3He$, ^3He, ^4He, Ne and Ar concentrations within the reservoir prior to CO_2 breakthrough with those after CO_2 arrival at the observation wells. We show that a component of the He fingerprint observed in the injected CO_2 can be clearly traced in both observation wells. Additionally, we see a clear spike in Kr and Xe concentrations following CO_2 break through. Our results show that CO_2 can be traced within a storage site using noble gases, illustrating significant potential for monitoring CO_2 migration in future engineered storage sites.

[1] Gilfillan *et al.*, (2008) *GCA* **72**, p.1174-1198. DOI:10.1016/j.gca.2007.10.009 [2] Gilfillan *et al.*, (2009) *Nature*, **458**, p.614-618. DOI:10.1038/nature07852

https://doi.org/10.1180/S0026461X00006502 Published online by Cambridge University Press

Tracing mantle enrichments into oceanic crust and hydrothermal systems, Juan de Fuca Ridge

JAMES GILL

Earth and Planetary Science Dept., UCSC, Santa Cruz CA 95064 USA (jgill@pmc.ucsc.edu)

High-precision Pb isotopes have become useful in discovering segment-scale (<100 km) heterogeneity in MORB sources. Here I describe how this heterogeneity co-varies with other isotopes and with major and trace elements within a 10-km long "4th order" segmentation of the axial magma chamber at the Endeavour segment of the Juan de Fuca Ridge, and how this heterogeneity is passed on to hydrothermal systems. Basalts in the one km-wide axial valley at Endeavour are characterized by large (3 to 4-fold) variations in their K/Ti, Zr/Nb, and La/Yb ratios at 7-8% MgO. Variations in Sr, Nd, and Hf isotopes are small (<0.0001) but correlate with the element ratios. Variations in Pb isotopes are larger ($^{206}Pb/^{204}Pb$ = 18.4-18.9) and therefore more useful. Pb correlations lie below the NHRL. $^{206}Pb/^{204}Pb$ correlates best with HFSE-enrichment, especially Nb. That correlation differs from what is seen along the southern JdFR and EPR, and defines a type of mantle enrichment specific to the northernmost JdFR. This enriched mantle only began to be tapped within the last ~30 Ka. Qualitatively, I attribute the enrichment to a young pyroxenitic source with a lower solidus than the surrounding perodotite, and with "C"-type isotopic characteristics. The Pb in the vigorous hydrothermal systems at Endeavour is entirely basalt-sourced, without evidence of sediment, which leaves the anomalously high CH_4 and NH_3 in the hydrothermal fluids unexplained. Preliminary results indicate differences in Pb isotopes between hydrothermal fields a few km apart. This may help to map their recharge zones and the integrated architecture of the basaltic crust.

Kinetics of free radical formation at mineral-water interfaces

C. GIL-LOZANO *[1], A.F. DAVILA [2], A.G. FAIREN[2] AND L.G. DUPORT[1]

[1]Universidad de Vigo. 36200 Vigo. Spain. (*correspondence: karolina_gil@uvigo.es)
[2]SETI Institute, Mountain View, CA 94043, USA.

The formation of free radicals on sulphide and silicate mineral surfaces [1,2] is a relevant topic due to its great importance in the treatment of mine wastes, geomedicine and, more recently, as an hypothetic oxidation pathway on Mars and Early Earth [3]. Although the atomic mechanisms involved in mineral surface reactions are relatively well understood, the kinetics pathways as well as the time extent of these reactions in natural environments have not yet been well characterized.

In this work, the kinetics of H_2O_2 generation at mineral–water interface was monitored with real time microlectrode measurements. Experiments were performed under continuous stirring by using aqueous slurries of pyrite, antigorite, olivine, and glauconite, as sample probes, in both oxic and anoxic conditions

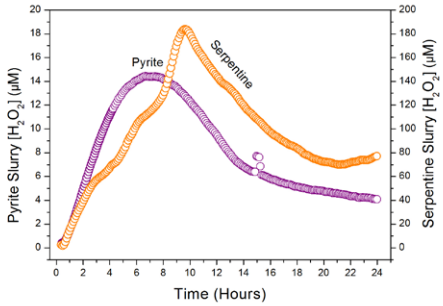

Figure 1. Kinetic of H_2O_2 formation from pyrite and serpentine slurries in water, under anoxic conditions.

Our experimental results show that, under oxic conditions, peroxide formation takes place very fast at the initial stages of the process with a significant consumption of $O_2(g)$, whereas, under anoxic condition, the rate of H_2O_2 generation proceeds more slowly, giving rise to the formation of $O_2(g)$ as a by-product and, thus indicating the presence of different reaction mechanisms. Preliminary kinetics models based on the experimentally determined constants, coupled with surface complexation calculations, will also be presented.

[1] Borda et al. (2003) *Geochim. et Cosmochim. Acta* **67**, 935-939. [2] Gournis et al. (2002) *Phys. Chem. Miner* **29**, 155-158. [3] Davila et al (2008) *EPSL* **272**, 456–463.

https://doi.org/10.1180/S0026461X00006502 Published online by Cambridge University Press

Evaluation of thermodynamic data and activity coefficient models for the geochemical modeling of CO_2 storage systems

M.J. GIMENO*, P. ACERO, V. GUTIÉRREZ, L.F. AUQUÉ, M.P. ASTA AND J. GÓMEZ

Earth Sciences Dpt., University of Zaragoza, Spain (*correspondence: mjgimeno@unizar.es, patriace@unizar.es, vane_rodrigo@hotmail.com, lauque@unizar.es, mpasta@unizar.es, jgomez@unizar.es)

The selection of adequate CO_2 geological storage systems and the evaluation of their storage capacity and behavior rely largely on geochemical modeling, whose results are strongly dependent on the selection of appropriate thermodynamic data and approaches.

In this study, two groups of geochemical calculations were carried out to gain insight into the influence of those issues. In the first group of calculations, the saturation state of several dilute groundwaters with respect to different mineral phases potentially relevant in geologícal storages for CO_2 was assessed by using different geochemical codes and thermodynamic databases. For the second group of calculations, the geochemical evolution in the direct vicinity of a hypotethical well during the dessication caused by the injection of supercritical CO_2 into two types of saline aquifers was simulated with the assistance of the PHREEQC code (Parkhurst and Appelo, [1]) by using two different databases and approaches for the calculation of activity coefficients included with the code: (1) the Wateq4f.dat database with an ionic association approach, and (2) an improved version of the pitzer.dat database with the specific ion interaction approach developed by Pitzer [2].

In the calculations for the dilute groundwaters, signifficant differences in the saturation indexes are only obtained for minerals for which varieties with different cristalinity are included in the databases (remarkably for dolomite). For the modelling exercises focused on the evolution of saline waters, the main differences between the results obtained by the two model approaches described above, are mainly related to the order and dessication degree at which different mineral phases precipitate and to the amounts of precipitated minerals throughout the simulations.

[1] Parkhurst and Appelo (1999) *Water Resources Research Investigations Report* **99**-4259. [2] Pitzer (1973) *J. Phys. Chem.*, **77**, 268–277.

Age and origin of alkaline lavas from Tore-Madeira Rise: Interactions between complex lithosphere motion and multi-components source

J. GIRARDEAU[1], R. MERLE[2]*, A. MARZOLI[2] AND M. CHIARADIA[3]

[1]Université de Nantes, 2 rue de la Housssinère, 44322 Nantes, France (Jacques.Girardeau@univ-nantes.fr)

[2]Università di Padova, via Gradenigo 6, 35100 Padova, Italia (*correspondence: renaud.merle@unipd.it; andrea.marzoli@unipd.it)

[3]Université de Genève, 13 rue des Maraîchers, 1205 Genève, Switzerland (Massimo.Chiaradia@unige.ch)

The Tore-Madeira Rise (TMR) is an alignment of seamounts of 1000×50 km oriented SSW-NNE, extending from the Tore seamount, located 300 km west of Lisbon, to the archipelago of Madeira. Here, we document the petrology, geochemistry and isotopic characteristics of TMR lavas from 22 dredging sites, located on 13 seamounts and 5 localities on Tore seamounts. The exclusive occurrence of alkaline lavas (mafic and differentiated) substantiates the importance of alkaline magmatism in the TMR edification. The dredged basalts display typical OIB-like incompatible elements and REE characteristics similar to those observed in Madeira basalts. Reliable $^{40}Ar/^{39}Ar$ and U/Pb ages suggest five magmatic phases on the TMR and surrounding areas that can be related to the motion of the Iberian plate. No specific isotopic characteristics can relate to a given magmatic phase. Regardless of their age, the Pb isotopic compositions of the basaltic rocks plot below the NHRL, in the field of the Madeira archipelago lavas while the differentiated lavas display a trend from this field toward high $^{207}Pb/^{204}Pb$ which is interpreted as a contamination by the sub-continental lithospheric mantle (SCLM) of the Iberian margin. This precludes the involvement of two distinct mantle plumes (Canary and Madeira) in the genesis of the TMR lavas, as previously suggested. The isotopic composition of the basaltic lavas requires at least three distinct components. The main isotopic characteristics are related to a mixture between a depleted asthenosphere-like mantle and a HIMU-like component. The contribution of an EMI-like component is also required in particular to explain the isotopic characteristics of the Seine-Isabelle-Godzilla seamounts. Considering the position of these seamounts close to the southern branch of the Azores-Gibraltar Fracture zone, we interpret this EMI-like component as due to a sliver of SCLM trapped in the asthenosphere. However, this SCLM is distinct to those involved in the genesis of the differentiated samples.

https://doi.org/10.1180/S0026461X00006502 Published online by Cambridge University Press

Insights into marine microbial communities that couple anaerobic biogeochemical cycles to remote oxidants

PETER R. GIRGUIS[1]*, PENGFEI SONG[2] AND MARK NIELSEN[2]

[1]Harvard University, 16 Divinity Avenue Room 3085, Cambridge, MA 02138 (* correspondence: pgirguis@oeb.harvard.edu)
[2]Harvard University, 16 Divinity Avenue Room 3092, Cambridge, MA 02138

Extracellular electron transfer (EET) is a process whereby microbes shuttle electrons outside the cell, and access solid-phase oxidants as well as spatially remote oxidants. EET has been well-studied in cultivated microbes, e.g., heterotrophic iron-reducing δ-proteobacteria. The relevance of EET in nature, however, and its impact on biogeochemical cycles remains poorly constrained. Anaerobic marine sediments host microbial communities that are involved in numerous biogeochemical cycles, and those capable of EET would have access to solid-phase as well as remote oxidants. Here we present the first comprehensive data on the population structure and functional potential of marine bacteria associated with EET. These communities were recovered from two systems: the anode of a bioelectrochemical system (BES) deployed in marine sediments *in situ*, and a BES deployed in high temperature hydrothermal vents. These communities were dominated by distinct groups of Proteobacteria and Fusobacteria. Metagenomic analyses and geochemical considerations suggest that they are participating in a complex sulfur cycle that includes the recycling of sulfur among oxidizers, reducers and disproportionators. Unexpectedly, these analyses revealed numerous other physiological capacities. These data suggest that microbial EET is likely more widespread than previously considered, and the functional potential of these communities requires us to reconsider the canonical view of anaerobic sediment biogeochemistry. If these microbial metabolisms are coupled to remote oxidants such as oxygen and nitrate via EET, the biogeochemical cycling of these elements will likely be more vigorous than previously recognized (as these reactions become more thermodynamically favorable). The findings presented herein provide a plausible explanation for some previously observed elevated rates of recalcitrant carbon degradation, and underscores the need for further investigation into the relevance of EET to global biogeochemical cycles.

Aerobic hydrogen oxidation by a chemolithotrophic *Beggiatoa* strain

A.-C. GIRNTH* AND H.N. SCHULZ-VOGT

Max Planck Institut for Marine Microbiology, Celsiusstraße 1, 28357 Bremen, Germany
(*correspondence: acgirnth@mpi-bremen.de)

Hydrogen oxidation in oxic/anoxic gradients

Transition zones between oxic and anoxic environments are primary habitats for aerobic hydrogen oxidizers. In sulfidic sediments, filamentous bacteria of the genus *Beggiatoa* thrive within this narrow horizon and feature fine-tuned chemotactic responses to keep track of the interface. So far, only anaerobic hydrogen oxidation coupled to reduction of stored sulfur has been shown for a heterotrophic *Beggiatoa* strain [1]. Here we demonstrate aerobic hydrogen oxidation by the chemolithoautotrophic strain *Beggiatoa* 35Flor grown in a mineral medium featuring artificial oxygen, sulfide and hydrogen gradients.

Beggiatoa 35Flor uses hydrogen as an accessory electron donor

In the presence of hydrogen, *Beggiatoa* 35Flor mats exhibit higher oxygen consumption once the sulfide flux decreases, as indicated by a shorter distance of the mats to the air/agar interface. Microsensor profiles show that low hydrogen fluxes are continually and fully oxidized within the oxic region of the *Beggiatoa* mat. Higher hydrogen fluxes have initially a more pronounced influence on the mat position, but oxidation ceases after a few days for a yet not determinable reason. A gene encoding for the large subunit of a hydrogen uptake hydrogenase was retrieved from strain 35Flor. Supply with fixed nitrogen compounds does not impair the hydrogen-oxidizing capacity of this nitrogen-fixing strain, suggesting that the hydrogenase is regulated independently of the nitrogenase. This result indicates that hydrogen is used as an electron donor and not merely oxidized for energy recycling. All attempts to grow the strain 35Flor with hydrogen as the only electron donor failed so far.

Our findings show that the strain *Beggiatoa* 35Flor is capable of aerobic hydrogen oxidation when grown in gradient medium imitating its natural habitat. However, hydrogen appears to serve only as an accessory electron donor since growth on hydrogen alone could not be achieved.

[1] Schmidt *et al.* (1987), *J. Bacteriol.* **169**, 5466-5472.

https://doi.org/10.1180/S0026461X00006502 Published online by Cambridge University Press

The ash that closed Europe's airspace: Part I, grains size distribution of the Eyjafjallajökull ash and soluble salt coatings

S.R. GISLASON[1]*, E.S. EIRIKSDOTTIR[1], H.A. ALFREDSSON[1], N. OSKARSSON[1], B. SIGFUSSON[3], G. LARSEN[1], T. HASSENKAM[2], S. NEDEL[2], N. BOVET[2], C.P. HEM [2], Z.I. BALOGH [2], K. DIDERIKSEN[2] AND S.L.S. STIPP[2]

[1]Institute of Earth Sciences, University of Iceland, Reykjavik, Iceland; (sigrg@raunvis.hi.is)
[2]Nano-Science Centre, Department of Chemistry, University of Copenhagen, Denmark; (stipp@nano.ku.dk)
[3]Reykjavik Energy, Iceland.

On 14 April 2010, when magma from the Eyjafjallajökull volcano intruded glacier-meltwater, an explosive phreato-magmatic eruption sent unusually fine-grained ash into the jet stream. It quickly dispersed over Europe. Reported airplane encounters with ash have caused sand blasted windows and melting of particles inside jet engines, causing them to fail. Therefore, air traffic was grounded for several days. Concerns also arose about health risks from fallout, because ash can transport acids as well as toxic compounds. Most studies on ash are made on post-eruptive material that have mixed with other atmospheric particles and suffered exposure to water as rain or fog, which would alter surface composition. In this study, a unique set of dry ash samples was collected during the explosive eruption and compared with fresh ash with the same bulk composition from a later more typical magmatic event, when meltwater did not have access to the magma.[1]

Up to 70 mass % of the phreato-magmatic ash particles, collected 50 km from the source, was <60 μm in diameter, 22% was <10 μm and 11% was ≤ 4.4 μm. The finest grain size was found in the centre of the plume. The magmatic ash was coarser and its surface area was an order of magnitude smaller than for the explosive ash. The relative concentration of surface salts was significantly lower on the explosive ash than the magmatic ash, because less volatile compounds were available to condense on the surfaces when water and steam were present. Instead, they dissolved in the meltwater and were transported as solutes in the ensuing floodwaters. The surface salts dissolved rapidly when exposed to experimental and natural waters, releasing pollutants and nutrients. Some of the salts further enhanced bulk dissolution of the ash.

This paper is the first of a two part presentation, where the second part, by Susan Stipp, focuses on the characteristics of the nanoparticles.

[1] Gislason S.R. *et al*. (2011), *PNAS,* **108,** 7307-7312.

The effect of time and climate on volcanic soil formation

S.R. GISLASON[1], E.S. EIRIKSDOTTIR[1], H.A. ALFREDSSON[1], B. SIGFUSSON[2], M.T. JONES[1] AND E.H. OELKERS[3],

[1]Institute of Earth Sciences, University of Iceland, Reykjavik, Iceland; (sigrg@raunvis.hi.is)
[2]Reykjavik Energy, Iceland.
[3]GET-Université de Toulouse-CNRS-IRD-OMP, 14 Avenue Edouard Belin, 31400 Toulouse, France

Andosols, soils derived from volcanic material, cover about 1.9% of the terrestrial surface and store about 4.9% of the Earth's carbon [1]. Andosols cover most of the volcanic islands on Earth. These soils are fertile, most of the islands are heavily populated and much of the river suspended matter delivered to the ocean stems from these islands. To a great extent, the sol is formed from air borne volcanic ash, preventing nutrient depletions with time, but making it prone to mechanical erosion.

In the days, weeks and months after deposition of air borne volcanic ash, nutrients and pollution will migrate into the soil at elevated rates. This is caused by soluble metal and proton salts coating the volcanic ash that dissolve orders of magnitude faster than the bulk volcanic ash that is mostly glass. Between these periodic fluxes of dissolved elements, weathering and erosion rates are primarily governed by climate, lithology, average rock age, topography and vegetation cover. A detailed study of catchements in NE Ieeland shows that for each degree of temperature increase the runoff, mechanical weathering flux, and chemical weathering fluxes in these catchments have been found to increase from 6 to 16%, 8 to 30%, and 4 to 14% respectively, depending on the catchment [2]. These results demonstrate a significant feedback between climate and Earth surface weathering on the timescale of years to millions of years [3], and suggest that weathering rates are currently increasing with time due to global warming.

[1] Eswaran *et al*. (1993) *Soil Science Society of America Journal* **57,** 192–194. [2] Gislason *et al*. (2009) *Earth Planet. Sci. Lett*. **277,** 213–222. [3] Gislason *et al*. (2006) *Geology,* **34**, 49-52.

https://doi.org/10.1180/S0026461X00006502 Published online by Cambridge University Press

Effect of alkali content and Fe oxidation state on the S oxidation state and solubility in rhyolitic glasses

G. GIULI[1]*, E. PARIS[1], R. ALONSO MORI[2], P. GLATZEL[2], M.R. CICCONI[1], B. SCAILLET[3] AND S.G. EECKHOUT[2]

[1]School of Science and Technology, Geology division, University of Camerino, ITALY

[2]European Synchrotron Radiation Facility (ESRF), Grenoble, France

[3]Inst. de Sciences de la Terre D'Orleans, UMR, CNRS-UO, Orleans, France

The Fe oxidation state, coordination geometry and <Fe-O> distances have been determined by Fe K-edge XANES and EXAFS for a set of sulphur bearing silicate glasses of rhyolite composition in the aim of determining: 1) the effect of bulk composition on the iron oxidation state and local structural environment;2) the effect of Fe oxidation state on sulphur behaviour in the corresponding magmas/melts. Glass compositions have been chosen so as to represent S- Cl-F bearing rhyolitic magmas with low to high alkali content. These glasses have been equilibrated at a range of different oxygen fugacity conditions typical of magmatic conditions and ranging from –15.4 to –10.75 log units (at 800 °C, 1.5 kbar). Comparison of the pre-edge peak data with those of Fe model compounds allowed to determine the Fe oxidation state and coordination number for all the glasses analysed. The $Fe^{3+}/(Fe^{3+} + Fe^{2+})$ ratio varies from 0.25 to 0.80 (±0.05) in the glasses studied. Moreover, pre-edge peak data clearly indicate that Fe^{3+} can be present in [4] and/or [5] coordination according to the alkali content of the glass, whereas Fe^{2+} is present in [5] coordination units for these compositions. The presence of minor amounts of [6] coordinated Fe cannot be ruled out by XANES data alone. EXAFS derived Fe-O distance in the most oxidised sample (Fe-O=1.85 Å) indicates that Fe^{3+} is in tetrahedral coordination. For these glass compositions, going from reducing to oxidising condition results in higher fraction of network forming $[4]Fe^{3+}$, thus increasing the polymerisation of the tetrahedral network.Alkali content has been found to have a very strongly effect on the Fe oxidation state: at a given oxygen fugacity, Fe oxidation state increase noticeably with increasing alkali content. A direct proportionality has been found between the S^{2-}/Fe^{2+} molar fractions. As Fe oxidation state is known to affect the solubility of S^{2-} species in silicate melts, Alkali content is expected to play a major role together with oxygen fugacity in the S geochemical behaviour in silicate magmas.

[1] Giuli, G. *et al*. (2002) *Geochim. Cosmochim. Acta*, **66**, 4347- 4353. [2] Giuli, G. *et al*. (2011) *American mineral*., **96**, 631-636

Redox dynamics resulting from chemical and physical fluxes in surficial permeable sediments

B.T. GLAZER[1]*, J. FRAM[1,2], J.L. MURPHY[1], K. FOGAREN[1] AND F. J. SANSONE[1]

[1]University of Hawaii, Department of Oceanography, 1000 Pope Rd., Honolulu, HI 96822; (*correspondance: glazer@hawaii.edu)

[2]College of Oceanic and Atmospheric Sciences, Oregon State University, 104 COAS Administration Bldg

The upper layers of nearshore permeable sediments are dynamic, active sites of intense redox cycling. Previous research and our preliminary results indicate that vertical redox oscillations in these sediments can be driven by biogeochemical or physical variability, or by episodic events such as severe storms and their associated terrestrial runoff. Further, it can be assumed that each of these forcings operate on different and distinctive time and vertical scales. The current work focuses on central goals of calculating the fluxes of redox-sensitive chemical species in surficial permeable coastal sediments, and understanding the transformations within the highly responsive "zone of reactivity" in the upper centimeters of these sediments.

We have made extended deployments of a custom physical and chemical sensor package in nearshore permeable sediments, as part of a cabled seafloor observatory. Instrumentation includes a multi-channel high-resolution miniature thermistor chain, an in situ electrochemical analyzer (ISEA-III, AIS Inc.), a profiling micromanipulator, oxygen optrodes (Aanderaa), independent temperature loggers (RBR), and a seafloor visualization system, all integrated into the existing physcial sensor network observatory (Kilo Nalu Nearshore Reef Observatory, Oahu, Hawaii, USA). Here, we describe on-going work aimed at: (i) improving our understanding of the interaction between these active, carbon recycling sediments and the overlying water column; (ii) examining in detail the temporal and spatial variability of key redox-reactive chemical species; (iii) quantifying the relative contributions of benthic photosynthesis, sand ripple position, currents and waves to redox oscillations; and (iv) integrating fine-scale chemical measurements with porewater velocity modeling to calculate biogeochemical fluxes.

https://doi.org/10.1180/S0026461X00006502 Published online by Cambridge University Press

Mercury stable isotopic variations in Arctic Ocean pelagic sediment

JAMES D. GLEASON[1], JOEL D. BLUM[1], TED C. MOORE[1], LEONID POLYAK[2] AND MARTIN JAKOBSSON[3]

[1] University of Michigan, Dept. of Geological Sciences, Ann Arbor, MI 48109, USA (*correspondence: jdgleaso@umich.edu)
[2] Ohio State University, Byrd Polar Research Center, Columbus, OH 43210, USA (polyak.1@osu.edu)
[3] Stockholm University, Dept. of Geology and Geochemistry, Stockholm, Sweden (martin.jakobsson@geo.su.se)

Mercury isotopic compositions were measured in 14 samples of Arctic Ocean pelagic sediment from three sites: Lomonosov Ridge, Yermak Plateau and Mendeleev Ridge. Holocene-age sediment from 4 piston cores shows highly negative and variable mass dependent isotopic fractionation (δ^{202}Hg = -1.06 to -2.98; +/-0.15‰). Surface sediment at two localities (Lomonosov Ridge and Yermak Plateau) shows small deviations from mass dependence recorded as Δ^{201}Hg = -0.11 to -0.14 (+/-0.10‰). In piston core 96/12-1pc (Lomonosov Ridge; 1003 m water depth; 87°05.9'N; 144°46.4'E), δ^{202}Hg appears to decrease with depth in the core from surface (δ^{202}Hg = -2.22) down to MIS 5.3 (~100 ka; 2 meters depth; δ^{202}Hg = -2.98). Mercury concentrations (~3 ppb to 114 ppb) are not well correlated with Hg isotopic composition, and neither of these parameters appears to be correlated with the Mn-rich/Mn-poor cyclic banding in core 96/12-1pc, which is thought to record variations in Quaternary ventilation and/or ice conditions of the Arctic Ocean. Overall, the sediment Hg isotopic compositions likely reflect a variable provenance signal of mixed terrestrial and atmospheric Hg reservoirs supplying the Arctic Ocean. The enhanced negative Δ^{201}Hg signature in the modern Arctic sediments could be due to the influence of anthropogenic Hg from coal combustion, or from enhanced photochemical reduction and loss of Hg from modern Arctic surface waters due to reduced sea-ice cover.

Sulfate reduction and microbial abundance in saline, alkaline Lake Van (Turkey)

CLEMENS GLOMBITZA*, JENS KALLMEYER AND PALEOVAN SCIENTIFIC PARTY

University of Potsdam, Institute of Earth and Environmental Sciences, Karl-Liebknecht-Str. 24, 14476 Potsdam, Germany
(*correspondance: clemens.glombitza@geo.uni-potsdam.de)

Lake Van is the fourth lagest terminal lake in the world. It is located on the Eastern Anatolia High Plateau (Turkey) and surrounded by two semi-active vulcanos (Nemruth Dagi and Syphan Dagi). Evaporation processes, chemical weathering of vulcanic rocks and hydrothermal activity have created an environment of extreme alkalinity (155 m eql^{-1}, pH 9.81) and salinity (21.4 ‰) [1]. Kempe and Degens [2] proposed an ancient Ocean with high alkalinity, a high pH and low Ca and Mg concentrations, analogous to modern soda lakes like Lake Van. This theory was and still is discussed controversly, e.g. Hardie [3] suggested that the post-Hadean ocean was never a soda ocean but instead a neutral-halide ocean. Recently, Shibuya *et al*. reportet evidence for high alkaline fluids in an Archean subseafloor hydrothermal system resultling in reactive mixing zones between alkaline fluids and neutral seawater [4]. A detailed study of the currently ongoing microbial processes in Lake Van may provide the information necessary to interpret the signals from fossil ecosystems. Independent from the different opinions about early Ocean chemistry, this study explores an ecosystem that deviates considerably from typical freshwater or marine systems with regard to porewater chemistry and biogeochemical processes.

We here report the first results from microbiological investigations (porewater chemistry, cell abundance and sulfate reduction rates) in samples from two sites (Northern Basin and Ahlat Ridge) at Lake Van, retrieved during the ICDP drilling campaing in summer 2010. Although located in relatively close proximity (7 km) sulfate reduction rates reveal unexpected differences between the two sites, indicating a high sensitivity of microbial activity to changes in hydrological conditions and organic matter input. Overall cell abundances deviate considerably from what is commonly observed in marine sediments.

[1] Kempe *et al*. (1991), *Nature* **349**, 605-608. [2] Kempe and Degens (1985), *Chem. Geol*. **53**, 95-108. [3] Hardie (2003), *Geology* **31**, 785-788. [4] Shibuya *et al*. (2010) *Precambrian Res*. **182**, 230-238.

https://doi.org/10.1180/S0026461X00006502 Published online by Cambridge University Press

Land use control of groundwater chemistry in the Pyosun Watershed, Jeju Island, Korea

YOUNG-HWA GO[1], SEONG-TAEK YUN[1]*, KYUNG-GOO KANG[2], BERNHARD MAYER[3], KYOUNG-HO KIM[1] AND HAE-NAM HYUN[4]

[1]Department of Earth and Environmental Sciences, Korea University, Seoul 136-701, South Korea (*correspondence: styun@korea.ac.kr)
[2]Jeju Special Self-Governing Province Development Corporation, Korea
[3]Department of Geoscience, University of Calgary, Calgary, Alberta, Canada T2N1N4
[4]Department of Bioscience and Industry, Jeju National Universityi, Jeju 690-756, South Korea

As groundwater from basaltic aquifers is a unique source of water supply in the volcanic Jeju Island, Korea, a better understanding of the current status of groundwater is important for a sustainable future water supply. For this study of the Pyosun Watershed located at the southeastern part of the island, we collected 90 groundwater samples from 45 existing wells and 41 soil water samples using porous cups installed at various depths at two sites. Hydrochemically, well groundwater was dominantly of the Na(-Mg-Ca)-HCO_3(-Cl) type, while soil water varied between Na(-Mg-Ca)-Cl-HCO_3(-SO_4) type at an upgradient forested area to a Na(-Mg-Ca)-Cl type at a downgradient agricultural (orchard) area. Most ions in groundwater, especially NO_3, Cl, SO_4, Na, Ca and Mg, increased in concentrations in aquifers at low altitudes (about <150 m a.s.l.) where land use is dominated by orchards and rural developments. Nitrate concentrations of groundwater ranged from 0.4 to 23.3 mg/L (median 4.7 mg/L). The results of a Principal Component Analysis (PCA) of hydrochemical data indicates that two major processes (i.e., anthropogenic contamination and water-rock interaction) control the groundwater chemistry. Water-rock interactions were dominated by silicate weathering (as indicated by the increases of HCO_3 and silica) with minor ion exchange and sorption. Combined with hydrochemical data, nitrogen and oxygen isotopes of groundwater nitrate (n=43) showed the systematic change of major nitrate sources, from nitrification in soil organic matter at upgradient forested and grassland areas to chemical fertilizers at the orchard areas to minor contributions of manure and sewage-derived nitrate at low altitudes. Thus, careful control of fertilizer use is highly recommended for a sustainable management of future groundwater quality in the Pyosun Watershed.

Hydrochemical characteristics of Bigadiç (Balikesir) geothermal area, Turkey

GÜLER GÖÇMEZ[1] AND ERDOĞAN ÖLMEZ[2]

[1]Department of Geology Engineering, Selcuk University, (gulergoçmez@selcuk.edu.tr)
[2]Directorate of Mineral Research and Exploration of Turkey (erdogan_olmez@yahoo.com)

The study area is located in 57 km southwesthern of Balıkesir, West Anatolia, Turkey. The stratigraphy of the area is characterized by the presence of ophiolites of Mesozoic basement, covered by Tertiary aged Dedetepe Formation (riodacite, dacite, tuff, agglomerate) and Quaternary covers. Major visible tectonic lines that control fluid flow in region is represented by faults approximately trending in N-NE direction; it determined the main morphological structure of the region.

The chemical composition of water discharges clearly shows that the Bigadiç geothermal system produces similar types of fluids having travelled distinctly different pats. A plume of high HCO_3 and SO_4 waters feeds discharge area, bordered by two strike slip faults. EC values of hot and mineral water in region are range between 2100 and 3040 μS/cm, temperature is between 24 and 98 ºC, total mineralization ranges from 2646 to 3537 mg/l, and pH values range from 6.4 to 8.3 and show generally the acidic character. Four wells in region were opened (HK-1; T=47 ºC and Q=0.5 l/s: HK-2; T=98 ºC and Q=60 ºC: HK-3; T=98 ºC and Q=40 l/s; HK-4; T=94 ºC and Q=10 l/s) to use in balneological purposes, space and greenhouse heating.

The hot and mineral waters have “Rav waters” properties according to Giggenbach diagramme. The reservuar rock temperature is calculated due to geothermometers as 100 to 110 ºC. The hot and mineral water is classified as B-F-Na-HCO_3-SO_4 according to AIH. High content of boron in fluids produced from the geothermal system throughout the volcanic environment, thought to be associated with extentional tectonics and volcanic hosted rocks leachings from the Bigadiç area appear to repr. All of these extentional type discharges from the Bigadiç area appear to represent geothermal fluids most directly derived from an environment dominated by riolitic/andesitic magmatism.

https://doi.org/10.1180/S0026461X00006502 Published online by Cambridge University Press

Recent advances in first principles based modeling and simulations of the physics and chemistry of large, complex atomistic systems

WILLIAM A. GODDARD, III

Charles and Mary Ferkel Professor of Chemistry, Materials Science, and Applied Physics Director, Materials and Process Simulation Center (MSC) California Institute of Technology (139-74) Pasadena, CA 91125

Advances in theoretical chemistry, computational chemistry, materials science, physics, and supercomputers are making it practical to consider first principles (de novo) predictions and simulations of the atomistic level physics and chemistry of complex systems and processes in the Chemical, Biological, and Materials Sciences. Our approach is to build a hierarchy of models each based on the results of more fundamental methods but coarsened to make practical the consideration of much larger length and time scales. Connecting this multi-paradigm multi-scale hierarchy back to quantum mechanics enables the application of first principles to the coarse levels essential for practical simulations of complex systems.

We will highlight some recent advances in multi-paradigm multi-scale methodology selected from: · The ReaxFF reactive force field for prediction of reactive processes in complex systems · The eFF method for electron dynamics of highly excited complex systems · PBE-lg and XYGJ-OS quantum mechanics methods for accurate intermolecular interactionsat modest cost ·The 2PT method for fast accurate calculations of entropy from molecular dynamics that we will illustrate with recent applications to Energy, Catalysis, Nanotechnology, and Materials selected from:

Applications of Multiparadigm, Multiscale Methodologies to high velocity impact ·EOS and phase transitions of materials from 2PT analysis of ReaxFF-lg reactive dynamics simulations Spin-coupling and superexchange in ferroelectrics ·Mechanism of superconductivity in cuprates; strategies for increased Tc ·Copper-Indium-Gallium-Selenide (CIGS)/CdS photovoltaics ·Hydration and hydrolysis processes in concrete (Ettringite) Functionalizing MOF, COF, ZIF Materials for storage and partitioning of H_2, CO_2, CH_4 ·Mechanisms of fuel cell catalysts including the oxygen reduction reaction ·Solid acid, Solid oxide, alkaline, and ceramic electrolytes ·simulations of transport in dye synthesized photovoltaics including electrodes, ionic liquid,and reluctant · New anodes and electrolytes for Li batteries · ReaxFF-Monte Carlo methods for resolving partial occupations from Rietveld analyses into supercells with whole atoms; application to Mixed metal oxide catalysts for ammoxidation of propane

Characterization of Saharan dust from red rain precipitated over Athens, Greece

A. GODELITSAS[1]*, P. NASTOS[1], T.J. MERTZIMEKIS[1], K. TOLI[1], A. DOUVALIS[2] AND R. SIMON[3]

[1]University of Athens, Greece (*correspondence: agodel@geol.uoa.gr)
[2]University of Ioannina, Greece
[3]ANKA Synchrotron Facility, KIT, Germany

Aeolian transport of Saharan dust influences significantly the rain acidity and furthermore the climate of the Mediterranean, causing among others, intense “red (or mud) rain” and even “red snow” episodes. During these episodes geological material from Sahara is deposited to the aquatic, terrestrial and urban environment [e.g. 1-3]. The Saharan dust samples were collected on membrane filters after intense “red rain” episodes over Athens megacity, Greece. Initial characterization by means of XRD, SEM-EDS and laser micro-Raman showed quartz, calcite and dolomite as major phases as well as phyllosilicates (mostly clays), rutile, zircon and goethite as minor constituents [4]. Preliminary analyses of metals using bulk XRF indicated Fe, Sr, Mn, Zn, Pb, Cr, Ni and Cu whereas gamma-ray spectroscopic measurements showed very low natural radioactivity and absence of human-produced nuclides. Detailed Synchrotron micro-XRF studies proved the presence of very hazardous elements, such as Pb and As, which had not been located on the samples by preliminary conventional investigation using SEM-EDS. It was also confirmed that many trace elements are intercorrelated (e.g. Fe-Mn-V-Cu) in other minor phases, of potential anthropogenic origin, hosted into the carbonate-silicate matrix. Subsequent Mössbauer spectroscopic study showed abundant Fe^{3+}-containing constituents and less Fe^{2+} phases. Moreover, sequential leaching experiments, using appropriate acids and ICP-MS analyses, revealed a high percentage of extractable Fe (and also Zn, Mn and Pb) due to carbonate phases comprising ~60% of the material. The above data can be important [see e.g. 5] for the geoavailability and bioavailability of aerosol-derived useful and harmful metals in southern Greece and generally in the entire semi-closed low-nutrient / low-chlorophyll marine ecosystem of eastern Mediterranean.

[1] Loÿe-Pilot M.D. *et al*. (1986) *Nature*, **321**, 427. [2] Avila A. *et al*. (1997) *J. Geophys. Res.*, 102/D18, 21977. [3] Papastefanou C. *et al*. (2001) *J. Env. Radioactivity*, **55**, 109. [4] P. Nastos *et al*. (2008), *Abstracts of 26th Eur. Conf. of SEGH, Athens*. [5] Journet E. (2009) *Nature Geosci*., **2**, 317.

https://doi.org/10.1180/S0026461X00006502 Published online by Cambridge University Press

Isotope fractionation due to temperature gradients: Molecular dynamics simulation

GAURAV GOEL[1,2], DANIEL J. LACKS[2], JAMES A. VAN ORMAN[1,2], CRAIG C. LUNDSTROM[3], CHARLES E. LESHER[4]

[1]Department of Geological Sciences, Case Western Reserve University, Cleveland, OH 44106
[2]Department of Chemical Engineering, Case Western Reserve University, Cleveland, OH 44106
[3]Department of Geology, University of Illinois, Urbana, IL 61801
[4]Department of Geology, University of California, Davis, CA 95616

Experimental studies show that large isotope fractionation can occur along temperature gradients in silicate melts [1-3]. This thermally induced isotope fractionation can be much larger than the equilibrium fractionation between minerals and melts, In particular, lighter isotopes are found to be enriched in the hotter regions, and heavier isotopes are enriched in the colder regions of experimental charges, with the magnitude of the fractionation depending on the type of atom. The effect may be important in places such as at the edges of magma chambers and in other regions with sustained thermal gradients.

We have carried out molecular dynamics simulations to determine the factors that control the thermal fractionation of isotopes. The simulations are run for magnesium silicate melts (50-70% SiO_2), with non-equilibrium molecular dynamics techniques used to produce the temperature gradient. The results of the simulations are in good agreement with experimental observations [e.g. 2, 3], both in terms of the absolute magnitude of the fractionation and the relative magnitudes for different types of atoms.

The simulations are carried out as a function of pressure, to predict the behavior under conditions deep inside the earth, which experiments have not yet addressed. Increasing pressure change the magnitude of the isotope fractionation per temperature change for atoms that form part of the network structure (Si, O), but its effects are insignificant for atoms that are not part of the network (Mg).

[1] T. K. Kyser, C. E. Lesher and D. Walker (1998), *Contrib. Mineral. Petrol.* **133**, 373-381; [2] F. M. Richter, et. al. (2008), *Geochim. Cosmochim. Acta* 206-220; [3] F. Huang, P. Chakraborty, C. C. Lundstrom, C. Holmden, J. J. G. Glessner, S.W. Kieffer, C. E. Lesher (2010), *Nature* **464**, 396-400.

Pb and Zn distribution in stalagmites

J. GÖTTLICHER[1]*, S. MARKS[2], R. SIMON[1], R. STEININGER[1] A. PLATTE [3] AND S. NIGGEMANN[4]

[1]Karlsruhe Institute of Technology, Institute for Synchrotron Radiation, Eggenstein-Leopoldshafen, Germany (*correspondence: joerg.goettlicher@iss.fzk.de)
[2]Münster, Germany
[3]Letmathe, Germany
[3]Dechenhöhle, Letmathe, Germany

The impact of atmospheric emission on carstwaters and carst bedrocks is investigated by analyzing speleothems (here: stalagmites of $CaCO_3$) for metals that have been set free during the early years of industrialization. Letmathe in the Sauerland (one of the low mountain ranges in Germany) was chosen as a suitable area because two caves (Dechenhöhle and Hüttenbläser) are located in the main wind direction about 1 km away from a Pb and Zn smelter operating from 1862 to 1925. Additionally, slices from beech trees (≈155-165 y old) close to the cave were available for measuring their metal contents. Evidence for airborne Pb and Zn in this area came from analyses of gypsum encrustations at a nearby rock formation [1] and from deer antlers [2].

The young zone of the stalagmites is grey colored compared to the beige inner and therefore older part. X-ray fluorescence (XRF) spectra of the stalagmites measured at the SUL-X and FLUO beamline of the synchrotron radiation source ANKA show discrete peaks for Pb and Zn in the gray zone, highest contents at the boundary grey/beige and almost no Pb and Zn in beige zone. Pb and Zn are partly correlated. XRF spectra of beech trees exhibit a few spikes of Pb but they are not concentrated in the older part as expected. Zn is represented by a large number of peaks of different heights and frequencies with time. In both types of samples (stalagmite, wood) a discrete occurrence of Pb and Zn have been found rather than a homogeneous elevation during the time when atmospheric emission was most intensive. For the stalagmites the Pb and Zn pattern could be explained by particular entry or by enrichments at grain boundaries of crystallites which has to be proven. For the nature of metal distribution in trees no explanation has been found so far

We thank ANKA for beamtime in the projects ENV-163 and ENV-186, and the forest officials of Letmathe for providing us slices of trees.

[1] Richter D.K. *et al.* (1997) *Speläologisches Jahrbuch – Verein für Höhlenkunde in Westfalen 1995/1996, Iserlohn*, **49**, 49-60; [2] Kierdorf, H.; Kierdorf, U. (2000) *Z. Jagdwiss.* **46**, 270-278.

https://doi.org/10.1180/S0026461X00006502 Published online by Cambridge University Press

Plant impoundments as habitats for methanogenesis in tropical rainforest canopies

S. GOFFREDI[1]* AND W. USSLER III[2]

[1]Occidental College, Los Angeles, CA 90041, USA (*correspondence: sgoffredi@oxy.edu)
[2]Monterey Bay Aquarium Research Institute, Moss Landing, CA 95039, USA (methane@mbari.org)

Tropical epiphytes within the family Bromeliaceae possess foliage arranged in compact rosettes capable of retaining water. This creates an unusual environment suspended in the rainforest canopy; acidic and anaerobic, with decomposition of impounded material. Archaeal communities within the tanks were dominated by methanogens (~90% of archaeal ribotypes) and community structure, although variable, was generally dominated by the hydrogenotropic *Methanoregula*, with *Methanocella*, a specific clade of the acetoclastic *Methanosaeta*, rice cluster II, and *Methanosarcina* also present. Close relatives were recovered previously from peat bog, acidic fens, and anoxic rice fields, all areas of similarly high organic content and low pH. All tanks (n = 63, comprised of 6 plant species, sampled over a two year period) showed presence of methanogens, as long as they exceeded ~22 cm in plant height or ~7 cm tank depth. Soil was negative for methanogens (n=8), except in one case, in which the dominant methanogen, related to *Methanosarcina*, was different from nearby bromeliads. Archaeal methyl coenzyme M reductase A copy numbers correlated with both plant height and light levels, suggesting that these environmental parameters affect conditions for methanogenesis. Methane-specific isotopes ranged from -45 to -63‰, and direct methane production rates, comparable to emissions measured for pasture and peat bogs, were measured in microcosm experiments. These results suggest that bromeliad-associated archaeal communities may play an important role in the cycling of carbon in tropical forests.

Osmium isotopic tracing of atmospheric emissions from an aluminum smelter

J. GOGOT*[1], A. POIRIER[1] AND A. BOULLEMANT[2]

[1]GEOTOP-UQAM, CP. 8888, Succ. Centre-ville, Montréal, Qc, Canada. H3C 3P8 (*correspondence: julien.gogot@gmail.com, poirier.andre@uqam.ca)
[2]RIO TINTO ALCAN, CRDA, 1955 bld Mellon CP 1250, Jonquiere (QC), G7S 4K8, Canada (amiel.boullemant@riotinto.com)

In this study, we use osmium (Os) isotopes as a tracer of the environmental footprint of an aluminum smelter in Saguenay (Canada). This prebaked technology smelter transforms alumina (extracted from bauxite) in primary aluminum via carbon anodes. These latter are almost entirely consumed during the electrolytic process and are emitted as CO2 when reducing Al_2O_3 to Al(l). Such large gas emissions entrain inevitably some particulate matter (dust) at the stacks, despite gas and dust scrubbers demonstrate a more than 99.5% efficiency.

Heavy metals found in atmospheric emissions from this type of industry may have an isotopic composition significantly different from the local natural environment. The results of isotopic analysis of a sample of anode have revealed the presence of very radiogenic Os ($^{187}Os/^{188}Os$= 2.393 $\pm$ 0.005) compared to typical eroding continental crust (~1.2) and to usual anthropogenic sources (0.1-0.2). This suggested that Os might be a good candidate to follow a smelter's environmental impact. The main objective of this study is to determine the isotopic composition of real emissions from an aluminum smelter for metals of geochemical interest (variable isotopic composition) and compare them with the natural surrounding environment.

During this meeting, we present Os results for a wide range of analyzed samples: carbonaceous material (anode); filters of emissions from the plant; samples of soils and sediment collected in the surrounding environment of the plant; and sedimentary sequence including pre-anthropogenic levels to characterize the natural background.

https://doi.org/10.1180/S0026461X00006502 Published online by Cambridge University Press

Insights into short-term changes in local and global seawater redox conditions during Cretaceous OAE 2

T. GOLDBERG[1]*, S.W. POULTON[2], T. WAGNER[2] AND M. REHKAMPER[1]

[1]Imperial College London, SW7 2AZ London, UK, (*correspondence: t.goldberg@imperial.ac.uk)
[2]Newcastle University, NE1 7RU, Newcastle upon Tyne, UK

The mid Cretaceous was a time of extreme greenhouse conditions. Related to this were a series of major black shale deposition events associated with global perturbations of the carbon cycle (ocean anoxic events; OAEs). These units potentially document periods of rapid climate change where the redox state of the Cretaceous ocean repeatedly fluctuated between oxic, anoxic and euxinic depositional conditions, linked to orbital-driven natural processes. Understanding these short-term cycles is essential for improving our knowledge of how future rapid climate warming may affect ocean chemistry.

Global seawater $\delta^{98/95}$Mo is reflected in euxinic environments, and differs accordingly to the extent of oxic and anoxic sinks [1]. To recognise short-term changes and relationships in the local, regional, and global redox state of seawater, high-resolution (millennial – centennial) Fe, S and redox sensitive trace elements (Mo, V, U, Cr) were paired with Mo isotopes ($\delta^{98/95}$Mo). The study site was a low latitude Palaeo-North Altantic shelf region, deposited ~ 94 Ma ago.

In terms of local conditions, iron-sulphur systematics and biomarker evidence point to a predominantly sulphidic water column with short, periodic intervals of ferruginous conditions. Severe trace element depletion is mainly connected to sulphidic intervals, whereas ferruginous intervals show elemental recovery via continental input. A steady Mo isotopic composition is identified during local euxinia, indicating a reduction of the oceanic oxic sinks during OAE 2. During ferruginous conditions $\delta^{98/95}$Mo is affected by regional Mo uptake mechanisms. Conspicuous is an ~10-15 ky decrease in $\delta^{98/95}$Mo during euxinic deposition, coinciding with the peak of the positive carbon isotope excursion. This could be indicative of a massive increase in the spatial extent of ocean anoxia/euxinia in the Cretaceous oceans.

[1] Anbar & Rouxel (2007) *Annu. Rev. Earth Planet. Sci.* **304**, 87-90.

Clouds and the Faint Young Sun Paradox

COLIN GOLDBLATT[1] AND KEVIN J. ZAHNLE[2]

[1]Astronomy Department, University of Washington, Seattle, WA 98195, USA (cgoldbla@uw.edu)
[2]Space Science and Astrobiology Division, NASA Ames Research Center, Moffett Field, CA 94035, USA (kevin.j.zahnle@nasa.gov)

We investigate the role which clouds could play in resolving the Faint Young Sun Paradox (FYSP). Lower solar luminosity in the past means that less energy was absorbed on Earth (a forcing of $-50 Wm^{-2}$ during the late Archean), but geological evidence points to the Earth having been at least as warm as it is today, with only very occasional glaciations. We perform radiative calculations on a single global mean atmospheric column. We select a nominal set of three layered, randomly overlapping clouds, which are both consistent with observed cloud climatologies and reproduced the observed global mean energy budget of Earth. By varying the fraction, thickness, height and particle size of these clouds we conduct a wide exploration of how changed clouds could affect climate, thus constraining how clouds could contribute to resolving the FYSP. Low clouds reflect sunlight but have little greenhouse effect. Removing them entirely gives a forcing of $+25 Wm^{-2}$ whilst more modest reduction in their efficacy gives a forcing of +10 to $+15 Wm^{-2}$. For high clouds, the greenhouse effect dominates. It is possible to generate $+50 Wm^{-2}$ forcing from enhancing these, but this requires making them 3.5 times thicker and 14K colder than the standard high cloud in our nominal set and expanding their coverage to 100% of the sky. Such changes are not credible. More plausible changes would generate no more than $+15 Wm^{-2}$ forcing. Thus neither fewer low clouds nor more high clouds an provide enough forcing to resolve the FYSP. Decreased surface albedo can contribute no more than $+5 Wm^{-2}$ forcing. Some models which have been applied to the FYSP do not include clouds at all. These overestimate the forcing due to increased CO_2 by 20 to 25% when pCO_2 is 0.01 to 0.1 bar [1, 2].

[1] Goldblatt and Zahnle, *Clim. Past*, **7**, 203-220, 2001, doi:10.5194/cp-7-203-2011. [2] Goldblatt and Zahnle, *Nature*, in press, 2011, doi:10.1038/nature09961.

https://doi.org/10.1180/S0026461X00006502 Published online by Cambridge University Press

Scaling of critical zone processes in the Praire Pothole region, USA

MARTIN GOLDHABER[1]*, CHRISTOPHER MILLS, JEAN MORRISON AND CRAIG STRICKER

[1]USGS, Denver, CO, USA, (*correspondence; mgold@usgs.gov, cmills @usgs.gov, jmorrison@usgs.gov, cstricker@usgs.gov)

The Prairie Pothole Region, which occupies 750,000 km^2 of the north central U.S. and south central Canada is one of the most important ecosystems in North America. It contains millions of small wetlands underlain by glacial till that are internally drained within discrete, km-scale basins. We studied the geochemistry of soils, sediments, wetland water, and groundwater in the 92 hectare Cottonwood Lakes (CWL) area of North Dakota. The CWL area includes upland groundwater recharge wetlands with compositions similar to rainwater (TDS 150 mg/l), and a discharge wetland at a local topographic low only 200m from the recharge wetlands. Oxygenated water interacting with pyrite in surficial glacial till has oxidized the till to depths >10 m. Coupled fluid flow and chemical reaction modeling shows that this oxidation process has taken $>10^3$ years. The resulting SO_4^{2-}-enriched fluids have migrated from upland recharge areas and accumulated in the discharge wetland which has >2500mg/l SO_4^{2-}. The drastic variability in recharge and discharge wetland chemistry is reflected by fauna and flora. Sulfur isotope data support the conclusion that isotopically light pyrite, origionally from marine shale (mean $\delta^{34}S_{SO4}$ =-16‰) is the source of groundwater sulfate ($\delta^{34}S_{SO4}$=-7.5 to -15.9‰). Heavier $\delta^{34}S_{SO4}$ values within discharge wetlands (maximum +4‰) is evidence that bacteria are reducing SO_4^{2-} to sulfide, a process that drives the precipitation of high Mg calcite.

Our evaluation of literature data on water compositions of 178 wetlands throughout a 10^3 km^2 area surrounding the study site document that oxidation of pyrite and formation of SO_4^{2-} enriched wetlands has occurred over a large area in North Dakota.

Oxygen isotope variations in the Allende CV3 meteorite

A. GOLDMANN[1,2], A. PACK[2], M. GELLISSEN[3], N. ALBRECHT[2], J. ZIPFEL[4] AND H. PALME[4]

[1]Leibniz-Universität Hannover;
[2]Georg-August-Universität Göttingen;
[3]Christian-Albrechts-Universität Kiel;
[4]Senckenberg Forschungsinstitut und Naturmuseum, Frankfurt

Introduction

The Allende (CV3) carbonaceous chondrite consists of mm-sized chondrules, fine-grained matrix, Ca- and Al-rich inclusions (CAIs), dark inclusions (DI) and amoeboid olivine aggregates (AOA). Various components of the Allende meteorite fall on a mixing line in the $\delta^{17}O$ vs. $\delta^{18}O$ space [1].

In this study, we investigate isotope variations of small bulk samples (~0.3 – 1.1 g) and compare the variations with chemical data of the same aliquots.

Samples and Measurement techniques

37 of 39 samples of a 22.5 mm^2 large and 4 mm thick slice of the meteorite were analyzed. One sample (C4) contained a macroscopically visibly CAI, one (F3) a large DI. Oxygen isotopes were analyzed in Göttingen using IR laser fluorination in combination with GC-irmMS using a MAT 253 gas source mass spectrometer. The $\Delta^{17}O$ is calculated relative to the rocks- and minerals-defined TFL (N > 700) with a slope of $\beta = 0.5151 \pm 0.0007$ (1σ) and an intercept of $\gamma = -0.0014 \pm 0.008$ (1σ). The accuracy and precision of a single isotope analysis is ~0.15 ‰ and $\delta^{18}O$ and ±0.04 ‰ in $\Delta^{17}O$.

The chemical analyses were obtained by XRF in Cologne.

Results

The O-isotope data fall on the AML. The $\Delta^{17}O_{TFL}$ shows a spread from –4.6 ‰ to –2.3 ‰. The lower limit is marked by sample C4 (CAI) and the upper limit by the DI in sample F3. Excluding these 2 samples, a spread in $\Delta^{17}O$ of –4.1 to –3.0 ‰ is observed. For the remainig samples, no correlation between chemical composition (e.g. Al content) and $\Delta^{17}O$ is observed. The Al_2O_3 concentrations range from 2.6 – 4.3 wt.%, with constant Ca/Al-ratios..

Discussion

A correlation between $\Delta^{17}O$ and chemistry is expected if variations in Al (and other refractory elements) is caused by addition of CAI-like material. Such a correlation is not observed. This suggests the existence of an oxygen component, independent of the chemical variability. Implications with respect of the correlation between O- and Cr-isotopes [3] will be discussed.

[1] Clayton, R.N. *et al*. (1977) *EPSL*, **34**: 209-224 [2] Young & Russell (1998) *Science*, **282**: 452-455. [3] Trinquier *et al*. (2007) *ApJ*, **655**: 1179-1185.

https://doi.org/10.1180/S0026461X00006502 Published online by Cambridge University Press

Nanoparticles of X-ray amorphous mineralogical substances

YE.A. GOLUBEV

Institute of Geology, Syktyvkar, 167982, Russia
(golubev@geo.komisc.ru)

Representations about the particular ultradisperse structural state of x-ray amorphous mineralogical substances (mineraloids), distinct from atomic-molecular are developed [1-4]. For mineraloids it are find out and in details described submicro-nanoscale structures of natural solid bitumens, fossil resins, of some inorganic metacolloids by HRTEM, STM, AFM, SEM. This has allowed revealing various species of superstructural orderings in mineraloids, to define its mechanisms, to allocate key value of influence of the heating factor for the sizes nanoparticles in organic mineraloids.

Results of studying submicro-nanoscale structures and mechanisms of their ordering are important for modifying technological properties of natural substances, making of geomaterials. Special interest cause mineraloids with periodically-ordered nanoscale structures like noble opal has aroused. The similar regular structures are characteristic for a row organic and inorganic mineraloids.

[1] Golubev (2005) *Journal of Crystal Growth* **275**, e2357-e2360. [2] Golubev, Kovaleva, Yushkin (2008) *Fuel* **87**, 32-38. [3] Golubev (2009) *Doklady Earth Sciences* **425,** 429-431. [4] Golubev, Kovaleva (2010) *Russian Journal of Chemistry*, **2**. 103-109.

Statistical evaluation of the Holocene climate parameters in the NE of European Russia (from palynological data)

YU.V. GOLUBEVA* AND YE.A. GOLUBEV

Institute of Geology, Komi Science Centre, Ural Division of RAS, 167982 Syktyvkar, Russia,
(*correspondence: bratushchak@geo.komisc.ru)

In the given work present paleoclimatic investigation included palynological and statistical analyses, radiocarbon dating of the Holocene lake, alluvial (oxbow lake) and swamp sediments in middle and northern taiga subzones of the Komi Republic. On the basis of cores of four boreholes and fourteen outcrops, synchronous spectra correlation and Holocene separation were accomplished [1].

Mean annual and July temperatures were estimated by zonal method of the Holocene paleoclimates reconstruction [2], based on palynological assemblages for characteristics of environmental changes during the interval. It has been established that the sediments accumulated during the Preboreal–Subatlantic interval, when repeated climatic changes occurred.

To determine the main trends of paleoclimate changes climatic curves have been drawn. The curves show deviations of the mean annual and July temperatures during the Holocene from their current values. For this purpose, the statistical weight of mean temperature values are taken into account in paleoclimatic curves approximating, as the temperature ranges in certain intervals of the Holocene vary considerably.

According to the palynological data and statistical analyses three periods with warmer climatic conditions (Early Boreal, Middle Subboreal and Late Atlantic) were estimated. It is established, that climatic optimum have developed at the end of the Atlantic period to what distribution of the most thermophilic tree species (oak, elm, hazel and maple) and the highest temperatures testifies. The Atlantic period is characterized by mean July temperature on 2.5–3.5 °C and mean annual temperature on 2–3 °C warmer, than at the present time. The Boreal and Subboreal temperature maxima had the subordinated value. Thus, from the Preboreal period the increase tendency of temperatures up to the maximal values at the end of the Atlantic period is observed. Then reduction of temperatures to the present has followed.

This research was supported by grant by the Program of Presidium RAS n. 14.

[1] Golubeva (2008) *Lithosphere*. **2**. 124-132. [2] Savina & Khotinsky (1982) Evolution of the environment at the USSR territory during Late Pleistocene and Holocene 244 p.

https://doi.org/10.1180/S0026461X00006502 Published online by Cambridge University Press

Stability of Cu adsorbed onto clay surfaces: An experimental and computational study

MÁRIO A. GONÇALVES[1], DAVID MARTINS[1] AND STEPHEN C. PARKER[2]

[1]Departamento de Geologia and CREMINER/LA-ISR, Faculdade de Ciências U. Lisboa, Lisboa, Portugal (mgoncalves@fc.ul.pt, dmmartins@fc.ul.pt)
[2]Department of Chemistry, University of Bath, Bath BA2 7AY, United Kingdom (s.c.parker@bath.ac.uk)

The stability of adsorbed metals onto mineral surfaces is an essential property in controlling their ultimate fate in the environment. This study addresses this problem with the analysis of batch and flow-through (kinetic) experiments using Cu and illite, complemented with ab-initio and molecular dynamics studies. Experiments were performed at pH 4.5 to 6.5, and 10^{-4}M – 10^{-3}M ionic strength.

Batch and kinetic experiments gave consistent results on total adsorbed Cu per gram of adsorbent: 6.4 – 9.1 × 10^{-5} mol/g for pH 4.5, and 9.0 – 13.0 × 10^{-5} mol/g for pH 5.5. Results follow a Langmuir-type adsorption isotherm, but at pH 6.5 surface Cu precipitation occurs.

Desoprtion rates were measured with the results from flow-through experiments, and ranged between 1.0 – 2.4 × 10^{-10} mol/m^2/min. The amount of desorbed Cu ranged between 6 and 54% of the total adsorbed Cu. These results indicate that Cu surface stability is favoured for high pH/low ionic strength solutions, also lending support on the Eigen-Wilkins-Werner mechanism [1]. Metal adsorption on edge surface sites of clays is shown by spectroscopic studies [2].

We are also investigating the edge surface sites further by calculating the different modes of adsorption of Cu complexes at edge sites and comparing them to adsorption on (001) surface using atomistic simulation techniques. Initially, the static simulation code METADISE [3] was used to explore the structure and the stability of the different surface cuts for the (010), (100), and (-110) edge surfaces of an idealised pyrophyllite structure. Inner and outer-sphere Cu complexes are currently being optimised using DFT within the VASP code [4] to aid in the interpretation of the experimental results.

Contribution of Project KADRWaste PTDC/CTE-GEX/82678/2006 funded by FCT (Portugal).

[1] Sposito, G. (2004), *The Surface Chemistry of Natural Particles*, OUP. [2] Morton *et al*. (2001), GCA **65**, 2709-2722. [3] Watson *et al*. (1996), *J. Chem. Soc. Farad. Trans*,. **92**, 433-438. [4] Kresse & Furthmuller (1996), *Phys. Rev. B*, **54**, 11169-11186.

Redox state of lithospheric mantle in central Siberian craton: A Mössbauer study of peridotite xenoliths from the Udachnaya kimberlite

A.G. GONCHAROV[1,2]*, D.A. IONOV[2], L.-S. DOUCET[2] AND I.V. ASHCHEPKOV[3]

[1]IPGG RAS, Saint-Petersburg, Russia (
*correspondence: ag.goncharov@ipgg.ru)
[2]Université J. Monnet, Saint-Etienne 42023, France
[3]Inst. Geology & Mineralogy, Novosibirsk 630090, Russia

Redox state in a vertical profile of lithospheric mantle in central Siberian craton (Russia) was determined based on peridotite xenoliths from the 360 My old Udachnaya kimberlite. Equilibration temperatures (*T*) and pressures (*P*) for garnet peridotites are 860-1340°C [1]; P values for spinel peridotites were estimated from *T* (760-965°C) projections to a conductive geotherm defined by the gar peridotites. Mössbauer spectroscopy was used to obtain $Fe^{3+}/\Sigma Fe$ ratios in garnet from 15 samples (9–23%) and spinel from 7 samples (6-22%). Oxygen fugacity (f_{O2}) was calculated using oxygen thermobarometry. The f_{O2} decreases with pressure, hence depth. Low-T samples (750-1000°C; *P* = 2.6-5.3 GPa) yield f_{O2} *(ΔFMQ)* = (0.0) to (-1.8) log units whereas high-T (1200-1350°C; 5.4-6.8 GPa) samples have f_{O2} *(ΔFMQ)* = (-2.4) to (-3.1) log units. The low-T peridotites overlap the graphite and carbonate stability fields; the high-T gar peridotites plot in the diamond stability field. Speciation of hypothetical C-O-H fluids coexisting with the rocks was assessed from the T, P and f_{O2} data. Fluids for the high-T, hence the deepest, samples mainly consist of methane and water indicating that these "craton roots" are not likely to contain partial melts because of high T's of peridotite solidus in the presence of reduced C-H compounds.

[1] Ionov *et al*. (2010) *J. Petrology* **51**: 2177-2210

https://doi.org/10.1180/S0026461X00006502 Published online by Cambridge University Press

Influence of thiol-containing ligands for the aggregation and dissolution of metallic silver nanomaterials

ANDREAS P. GONDIKAS[1], BRIAN REINSCH[2], GREG LOWRY[2] AND HEILEEN HSU-KIM*[1]

[1]Duke University, Civil and Env. Eng., Durham, NC, USA (*correspondence: hsukim@duke.edu)
[2]Carnegie Mellon University, Civil and Env. Eng., PA, USA

The environmental fate and mobility of metallic nanoparticles (NPs) in natural waters will be strongly influenced by reactions between the particle surfaces and metal-binding organic ligands that are prevalent in natural waters. Thiol- containing organics are known to dominate the speciation of soft-sphere metals such as ionic silver (Ag^+) in the environment [1]. Furthermore, the type and reactivity of the synthetic coating that is used during the synthesis of the nanomaterials will be a key factor controlling interactions with thiol-containing organic ligands. The objective of this work was to examine how thiols can modify particle surfaces and their reactivity during aggregation and dissolution of the nanoparticles. We studied zero valent silver (Ag) NPs with two types of coatings: citrate (CIT) and polyvinylpyrollidone (PVP). Our studies involved cysteine (CYS) and N-acetyl-cysteine (NAC), two low molecular weight thiol ligands that we utilized as analogues for the natural organics that are expected to bind dissolved Ag^+ in the aquatic environment.

Aggregation and dissolution experiments with CIT- and PVP-coated Ag NPs demonstrated that thiol-containing ligands increased aggregation rates of the particles, depending on solution ionic strength and type of thiol. The increase in aggregation was greater for the PVP-coated Ag NPs relative to the CIT-coated NPs. The addition of cysteine to Ag NP suspensions also increased the dissolved Ag concentration. These results indicated that cysteine was simultaneously sorbing to the Ag NPs and promoting their dissolution, resulting in surface modifications that increased aggregation rates. These results were supported by silver L-III-edge and sulfur K-edge X-ray absorption spectroscopy measurements that showed oxidation of the silver and the formation of Ag(+I)-CYS bonds for Ag NPs that were exposed to CYS.

Overall, our study highlights the importance of the coating and Ag^+-binding organic ligands for modifying the surface of silver nanomaterials in environmental settings. Sorption of natural organics alters the aggregation and solubility of the nanomaterials, and ultimately, will influence their persistence in the environment.

[1] Smith *et al*. (2002) *Comparative Biochemistry and Physiology Part C* **133**, 65-74

The isotope evidence of ore-forming materials of the Erdaogou gold deposit in Beipiao Liaoning deriving from magmatic rocks mixed by the crust and mantle source

GONGLI[1] , MAGUANG[1]*, ZHANG GUIPING[2] AND CHEN KUI KUI[1]

Henan Polytechnic University, Heana 454001, China (*correspondence: maguang5678@163.com)
[2]China Geological Library, Beijing, 100083

The isotope characteristic value is one of most effective methods recognized to solve petrogenetic question. Because of its tracing function, more and more geologists home and abroad pay attention to it in recent years.

Initial ratio of strontium isotope ($^{87}Sr/^{86}Sr$) varied greatly in Mesozoic volcanic rock in western of Liaoning area (basalt is 0.70474~0.70875, andesite is 0.70496~0.70595, trachyte-andesite is 0.70496~0.70595, dacite is 0.7076, liparite is 0.7081~0.7199) (Wanglaichun,1985); but initial ratio of strontium isotope in Duimiangou rock-mass is between the range of 0.704~0.708, indicated that the granitic magma coming from the upper mantle, and was contaminated by Si-Al layer of crust. The strontium isotopes ($^{87}Sr/^{86}Sr$) <0.710 and $\delta^{18}O$ <10 ‰, it is in line with the characteristics features of crust and mantle source.

From the figure of lead isotope ^{206}Pb / ^{204}Pb -^{207}Pb / ^{204}Pb in main alteration and mineralization rock (figure 1), we can see: a great number of the sample points of lead isotope fall within a wide range of the upper mantle and crust line, this reflects that lead in mineralization fluid comes from the magmatic rock of a mantle-crust mix, but majored in crust origin.

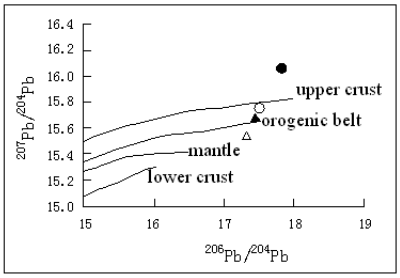

Figure 1: The Graphic of lead isotope ^{206}Pb / ^{204}Pb -^{207}Pb / ^{204}Pb in main alteration and mineralization rock

https://doi.org/10.1180/S0026461X00006502 Published online by Cambridge University Press

Mantle-to-surface magma dynamics at Mauna Loa and Kīlauea, Hawai'i

H.M. GONNERMANN[1]*, M. POLAND[2], J.H. FOSTER[3], B. BROOKS[3], C.J. WOLFE[3,4] AND A. MIKLIUS[2]

[1]Department of Earth Science, Rice University, Houston, TX 77005 (*correspondence: helge@rice.edu)
[2]U.S. Geological Survey, Hawai'ian Volcano Observatory, Hawai'i National Park, HI 96718
[3]Department of Geology and Geophysics, SOEST, University of Hawai'i, Honolulu, HI 96822
[3]Department of Terrestrial Magnetism, Carnegie Institution of Washington, Washington, DC 20015

In 2002 Mauna Loa Volcano, Hawai'i, began a nearly decade long period of inflation. Almost simultaneously, inflation and heightened activity occurred at neighboring Kīlauea Volcano. We address the question if and how both volcanoes are dynamically linked.

We model asthenospheric and crustal magma flow and pressure using a numerical model that integrates kinematic models of volcano deformation with a lumped parameter flow model. The model is constrainted by continuous global position system (GPS) measurements of deformation at both volcanoes. The past decade of summit deformation at Kīlauea and at Mauna Loa can both be explained by coupling crustal magma flow and storage to a common permeable asthenospheric melt zone beneth both volcanoes. Each volcano's shallow crustal magma system is connected to the asthenospheric melt zone by a lithospheric magma plumbing system through which changes in magma pressure can be transmitted. Consequently, pore pressure diffusion within the porous zone produces a dynamical linkage between both volcanoes and increased activity at one volcano may or may not be correlated with activity at its neighbor, depending on the interplay between deep and shallow magmatic processes.

A characteristic pore pressure diffusion time between both volcanoes of approximately ½ year explains the time-delayed onset of inflation at Mauna Loa relative to Kīlauea during 2002. Moreover, magma flow paths within the asthenospheric melt zone capture compositionally distinct magma from different parts of the asthenospheric melt source over long periods of time, consistent with geochemical observations. Because the time required for melt flow within the porous layer between both volcanoes is about three orders of magnitude slower than pore pressure diffusion. Consequently, significant redistribution of melt by porous flow requires time scales of 100s to 1,000s of years, so that decadal changes in surface activity are unlikely to affect long-term trends in magma geochemistry.

Oxidation of Fe(II) in natural waters at high nutrient concentration

ARIDANE G. GONZÁLEZ, J. MAGDALENA SANTANA-CASIANO*, NORMA PÉREZ AND MELCHOR GONZÁLEZ-DÁVILA

Departamento de Química, Facultad de Ciencias del Mar, Universidad de Las Palmas de Gran Canaria, Campus de Tafira, 35017 Las Palmas, Spain

The Fe(II) oxidation kinetic was studied in seawater enriched with nutrients as a function of pH (7.2-8.2), temperature (5-35ºC) and salinity (10-36.72) and compared with seawater media. The effect of nitrate ($0\text{-}1.77\cdot10^{-3}$ M), phosphate ($0\text{-}5.80\cdot10^{-5}$ M) and silicate ($0\text{-}2.84\cdot10^{-4}$ M) was studied at pH 8.0 and 25ºC. The Fe(II) oxidation is faster when a high nutrient concentration is present, decreasing the $t_{1/2}$ and compromising the permanence of Fe(II) in nutrient rich waters. The most important nutrient affecting the oxidation rate is silicate. A kinetic model was applied to the experimental results in order to follow the speciation of each Fe(II) species and to compute the fractional contribution to the overall rate constant as a function of pH. The speciation was controlled by Fe^{2+} from pH 6 to 7.9 and $FeCl^{+}$ from pH 6 to 7.6. $FeH_3SiO_4^{+}$ was the most important species for pH higher than 7.6, when the concentration of total silicate was 1.41 10^{-4} M. The $Fe(OH)^{+}$ controlled the kinetic process at pH lower than 8.1, while the $Fe(OH)_2$ began to control the oxidation rate constant at higher pH values.

https://doi.org/10.1180/S0026461X00006502 Published online by Cambridge University Press

Microbial induced mineralization in Co-rich ferromanganese crusts from the Scotia Sea

F.J. GONZÁLEZ[1]*, L. SOMOZA[1], A. MALDONADO[2], T. TORRES[3] AND J.E. ORTIZ[3]

[1]Geological Survey of Spain (IGME). Madrid, Spain (*correspondence: fj.gonzalez@igme.es)
[2]Inst. Andaluz Ciencias Tierra, (IACT: CSIC/UG). Spain
[3]Lab. Estratigrafía Biomolecular (LEB/UPM). Madrid, Spain

Co-rich ferromanganese crusts were collected at 2000-2500 m water depth in oceanic ridges and seamounts from the Scotia Sea during the SCAN-2004 and SCAN-2008 oceanographic cruises. Fe-Mn crusts form botryoidally pavements up to 50 mm thick on tholeiitic oceanic basalts.

According to data of X-ray diffraction and petrographic observations the crusts are essentially composed by poorly crystalline feruginous-vernadite (δ-MnO_2), and goethite and detrital quartz and phyllosilicates as accessory minerals. The Mn/Fe ratio in bulk samples is 1.1, indicating precipitation from cold ambient of seawater onto hard rock substrates. All the studied Fe-Mn crusts concentrate strategic elements (Co, Ni, Tl, REE or PGE) several orders of magnitude above the mean concentration in the Earth´s crust.

Fe-Mn crusts occur as fine laminated manganese oxides structures. SEM imagings reveal abundant like-microbe tubular sheaths (less than 1μm in diameter and 10-200μm long). These textural features can be due to the Mn-biomineralization action of chemolithoautotrophic microorganisms (*Leptothrix* spp.?, *Metallogenium*?). We interpret these filaments as fossilised bacteria (mineralised biofilms) according to their morphology, size ranges and textural features of colonial associations, similar to modern bacteria. They could be easily formed by action of Mn-oxidizing bacteria forming sheaths stained by vernadite, precipitated within extracellular structures. EDX-SEM and Electron Microprobe analyses show the chemical composition of fossilised bacterial biofilms with enrichments in strategic elements with respect to the bulk sample: 22.6% Mn, 22.4% Fe, 1.6% Ti or 1.5% Co and also 7.6% C and 6.8% F. Biomarkers like n-alkanes (n-C_{18}) and nitrogen compounds, detected by GC-MS analysis, could be related to the bacterial mineralization. These findings suggest a link between the microbial and the mineralization. The microbes could have played a critical role in the accumulation of metals through sorptive, catalytic and oxidative processes forming Fe-Mn crust deposits with economic potential. It also remarks the high scavenging efficiency of vernadite for remediation or recovery of trace metal contamination.

Arsenic biomineral formation leads to partial encrustation of thermoacidophilic archaea

P. GONZALEZ*, J. WEIJMA AND C.J.N. BUISMAN

Wageningen University, Sub-dept. of Environmental Technology.Bornse Weilanden 9, 6708 WG Wageningen, The Netherlands,P.O. Box 17, 6700 AA Wageningen (*correspondence: paulaa.gonzalezcontreras@wur.nl)

Acidophilic iron oxidizing *Sulfolobales* spp. mediate the formation of jarosite nanoprecipitates and bioscorodite precursors [1]. In batch experiments, scorodite biomineral formation by *Sulfolobales* spp. was induced at a pH of 1 and 75°C [2]. At these conditions, we observed formation of precursors (nuclei) of scorodite on the cell surface. This suggests that the mechanism of scorodite formation begins with the sorption of ferric iron and arsenate onto the cell surface, followed by the formation of ferric arsenate nuclei from the adsorbed metal species. By growth of the nuclei and ageing of the precipitates, scorodite crystals were formed on the cell surface, which led to a partial encrustation of the cells. In the absence of arsenic , jarosite precipitates were found on the cell surface, but this did not result in encrustation.

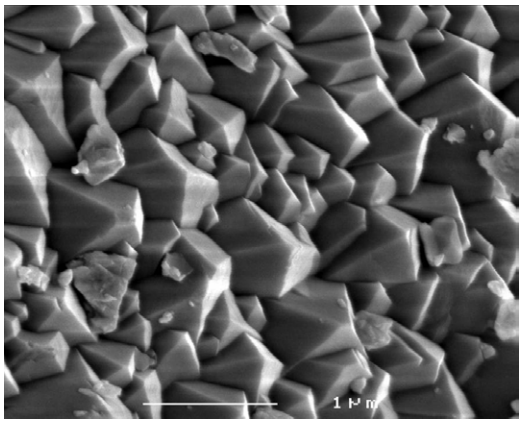

Figure 1. SEM photograph of the biomineralized scorodite by *Sulfolobales*. Photograph with 30000 magnification and SE detection at 3.5 KV.

[1] Gonzalez *et al*. (2010) *Environ. Science & Tech*. [2] Gonzalez *et al*. (submitted). *Geochimica Cosmo. Acta*.

https://doi.org/10.1180/S0026461X00006502 Published online by Cambridge University Press

Weathering intensity in the Mesoproterozoic and modern large-river systems: A comparative study in the Belt-Purcell supergroup

I. GONZÁLEZ-ÁLVAREZ[1,2]* AND R. KERRICH[2]

[1]CSIRO, Australian Resources Research Centre, Earth Science and Resource Engineering, Kensington, WA 6151, Australia,
(*correspondence: i.gonzalez.alvarez@gmail.com)
[2]Department of Geological Sciences, The University of Saskatchewan, 114 Science Place, Saskatoon SK, S7N 5E2

River systems are the main contributors of continental siliciclastic sediments to ocean basins, and potentially preserve a record of weathering conditions across the catchment areas. Proterozoic rivers have been viewed as mostly braided systems due to the lack of influence of rooted vegetation that produces fast channel lateral migration, high run-off rates, and low bank stability. Many large-scale Proterozoic siliciclastic basins are preserved, formed by river systems up to pan-continental scale. However, their significance as archives of continental weathering intensity remains under explored.

This study evaluates secular weathering variations for the Mesoproterozoic based on the Chemical Index of Alteration (CIA), accounting for post-depositional K addition and specifically for siliciclastic units of the Belt-Purcell Supergroup (BPS). BPS CIA values throughout the succesion span 60-85, averaging ~70. These values could be linked to CO_2 emissions from magmatism accompanying rifting of Columbia at ~1.4 Ga. The new data, along with K-corrected CIA data from the literature, could be interpreted as recording a rising trend from ~50 at ~2.5 Ga to ~75 at 1.6 Ga, a low of 50 at ~1.5 Ga, and ~50-60 from 1.4 Ga to 1.0 Ga. However, CIA link to global geodynamic events remains challenging due to scarcity and lack of space-time resolution of data sets.

BPS CIA values of ~70, are commensurate with modern large river systems such as the Orinoco, Nile and Amazon rivers. The Appekunny and Grinnell formations (Lower BPS succesion) display two intense weathering periods (~80±5) equivalent to humid-dry tropical conditions in modern rivers such as the Orinoco, Parana, Mekong and Amazon rivers, with a arid-template climate period in between.

This study suggests that BPS CIA values reflect a more aggressive chemical weathering, since Proterozoic rivers had less sediment residence time due to lack of vegetation cover, and therefore, faster transport time than their modern counterparts. To achieve high CIA values in shorter periods of time without vegetation cover, higher chemical weathering conditions need to be invoked.

Geodynamic implications of >1 Ga Re-Os model ages in PGM from the Dobromirtsi Ultramafic Massif, Central Rhodope, Bulgaria

J.M. GONZÁLEZ-JIMÉNEZ[1] W.L. GRIFFIN[1], F. GERVILLA[2], T. KERESTEDJIAN[3], S.Y O´REILLY[1] AND N.J. PEARSON[1]

[1] GEMOC ARC National Key Centre, Sydney, Australia. (jose.gonzalez@mq.edu.au.; bill.griffin@mq.edu.au; sue.oreilly@mq.edu.au; npearson@mq.edu.au).
[2] Dpt. Mineralogy & Petrology, University of Granada, Spain. (gervilla@ugr.es).
[3]Geological Institute, Bulgarian Academy of Sciences, Bulgaria. (thomas@geology.bas.bg).

The Dobromirtsi Ultramafic Massif is a relic of meta-ophiolitic mantle, located in the Central Rhodope Dome in southern Bulgaria. The ultramafics have been trust over Paleozoic (470-450 Ma; [3]) para-gneisses and are unconformably covered by Tertiary volcano-sedimentary rocks. The massif consits of strongly metamorphosed (greenschist to amphibolite facies) harzburgite and dunite, containing several chromititite pods, and cross cut by pyroxenite veins [2].

Os-rich laurite $(Ru,Os)S_2$ ± Os-Ir alloys ± pentlandite constitute the PGM assemblage in unaltered chromite. In altered zones, Os-poor partially desulfurized laurite, sometimes replaced by Ru-rich base-metal sulfides + Os-Ir alloys is the common assemblage [1].

In situ Re-Os analyses reveal that unaltered laurite has a small spread in T_{RD} (300-600 Ma). In contrast, 11 out of 36 of the altered grains yield T_{MA} (and T_{RD}) model ages > 1Ga and up to 2.2 Ga ($^{187}Os/^{188}Os$ = 0.1124- 0.1206; average = 0.1173 ± 0.003; 2σ). These unradiogenic Os signatures requiere a mantle source that underwent differentiation processes in the Proterozoic; we suggest tha this source lies in the ultramafic rocks surronding the chromitites and that hydrothermal fluids sequester this signature when it infiltrate the peritotite. The referred source would correspond to the sub-continental mantle beneath Gondwanaland. To the best of our knowledge, this is the first Os-isotope evidence of Gondwanaland terrains in Central Rhodope, as has been argued but not proved by Cherneva & Georgieva [4].

[1] González-Jiménez, J.M., *et al*. (2010). *Resources Geology*. **60**, 4, 315-334; [2] Gonzalez-Jiménez, J.M., *et al*. (2009). *Geologica Acta*. **4**, 413-427; [3] Ovcharova, M. (2004). PhD Thesis. In Bulgarian; [4] Cherneva, M. & Georgieva (2005). *Lithos*. **82**, 149-168.

https://doi.org/10.1180/S0026461X00006502 Published online by Cambridge University Press

Multiphase magmatic history of the Oman-UAE ophiolite

K.M. GOODENOUGH[1]*, M.T. STYLES[2], R.J. THOMAS[2], D.I. SCHOFIELD[3], Q.G. CROWLEY[4] AND I.L. MILLAR[2]

[1]British Geological Survey (BGS), West Mains Road, Edinburgh EH9 3LA (*correspondence: kmgo@bgs.ac.uk)
[2]BGS, Keyworth, Nottingham, NG12 5GG
[3]BGS, Columbus House, Tongwynlais, Cardiff, CF15 7NE
[4]Dept. Of Geology, Trinity College, Dublin 2, Ireland

The Oman-United Arab Emirates (UAE) ophiolite is the largest ophiolite complex in the world. The majority of the ophiolite lies in Oman, but it has a northerly extension into the UAE. This has been mapped and studied in detail by the BGS since 2002, funded by the UAE's Ministry of Energy.

The Oman-UAE ophiolite was traditionally interpreted as a classic mid ocean-ridge ophiolite, but more recently it has been recognised that a second, voluminous phase of magmatism is superimposed upon the early MORB-like ophiolite sequence. In the UAE, our field mapping has shown that this later magmatic phase forms extensive intrusions including large gabbro plutons, tonalite bodies and mafic dyke swarms throughout the crustal sequence and the mantle transition zone. The later magmatism has been dated at 96.4 to 95.2 Ma [1], coeval with similar magmatism in the Oman sector of the ophiolite [2]. The age of the early magmatism is not yet known.

Petrology and mineralogy of the early magmatic phase are consistent with formation at a spreading ridge, but the magmas of the later phase were more hydrous. Dykes and lavas from the early magmatic phase have MORB-like geochemistry, whereas those from the later magmatic phase show geochemical features of subduction-related magmatism, such as lower Ti/V and Zr/Y. Whole-rock Pb isotope data also distinguish the two phases, and support a supra-subduction zone setting for the later phase.

The youngest, volumetrically minor magmatism, recorded in the UAE sector of the ophiolite as localised mafic dykes, has geochemical and isotopic signatures more like those of ocean island basalts, and may be associated with an extensional, post-obduction event. This magmatism is tentatively dated at about 91 Ma.

[1] Goodenough, K M *et al*. (2010). Architecture of the Oman-UAE ophiolite: evidence for a multi-phase magmatic history. *Arab. J. Geosci*. **3**, 439-458. [2] Warren, C J *et al*. (2005). Dating the geologic history of Oman's Semail ophiolite: insights from U-Pb geochronology. *Contrib. Min. Pet*. **150**, 403-422.

Vadose zone controls on weathering intensity and depth: Observations from granitic and basaltic saprolites

B.W. GOODFELLOW[1]*, G.E. HILLEY[1], O.A. CHADWICK[2], M.S. SCHULZ[3] AND E. SHELEF[1]

[1]Department of Geological and Environmental Sciences, 450 Serra Mall, Stanford University, Stanford, CA 94131, USA. (hilley@stanford.edu; shelef@stanford.edu; *correspondence: bgood@stanford.edu)
[2]Department of Geography, University of California Santa Barbara, CA 93106, USA (oac@geog.ucsb.edu)
[3]US Geological Survey, 345 Middlefield Rd. MS-420, Menlo Park, CA 94025, USA (mschulz@usgs.gov)

An investigation of vadose zone weathering processes has been undertaken on saprolites developed in Californian granitoids and Hawaiian basalts. Granitoid observations have been made across a drying gradient (declining precipitation, increasing temperature), from the coast inland to the Sierra Nevada foothills. Observations of basalt weathering have been made across strong precipitation/hydrological gradients on Kauai and Hawaii and along a chronosequence of weathering profiles developed on lava flows ranging from ~10–40 ka on Hawaii to >4 Ma on Kauai.

Results indicate strong climatic control, through infiltration, on the depth and intensity of weathering in both lithologies. Dry, lower infiltration sites display only thin saprolites, strongly influenced by rock texture. At wet, higher infiltration, sites, the vadose zone is comprehensively altered to saprock and saprolite. In both granitoids and basalt, vadose zone and weathering depth appear to be governed by local base level. This is demonstrated by weathering to just above sea level, sharp contrasts between unweathered bedrock in perennial streams and weathered rock on adjacent slopes, and the presence of deep saprolites on steep slopes.

In addition, laboratory analyses of granitoids indicate that vadose zone hydrology exerts a fundamental control on the effective operation and relative dominance of the key weathering reactions. In zones of matrix permeability, oxidation of Fe-bearing phases comprehensively disaggregates the rock but results in minor mass loss and clay mineral formation. Conversely, the higher transient flow rates that characterize zones of fracture permeability result in plagioclase hydrolysis, significant mass losses and accompanying clay mineral formation. A variable hydrological regime may also contribute to high partial pressures of O_2 in vadose zone pore waters and pore spaces, thereby enhancing the oxidative environment and predisposing grussic saprolite formation in granitoids.

https://doi.org/10.1180/S0026461X00006502 Published online by Cambridge University Press

Mn/Cr systematics in carbonaceous chondrites: Mineral isochrons versus stepwise dissolution

C. GÖPEL[1]*, J.- L. BIRCK[1] AND B. ZANDA[2]

[1]IPGP- Géochimie et Cosmochimie, 1 Rue Jussieu, 75238 Paris Cedex 05, France (*correspondance: gopel@ipgp.fr)
[2]MNHN & CNRS, 61 rue Buffon, 75005 Paris, France

The Mn/Cr isotope systematics of meteorites holds a double information: the ^{53}Cr-^{53}Mn system may be used for dating while ^{54}Cr isotope systematics yields information on the mixing of nucleosynthetically distinct components of the solar system. We present Mn/Cr data on two recently discovered carbonaceous meteorites. Sequential dissolution steps of bulk rock powder were performed but also for the first time for carbonaceous meteorites the Mn/Cr systematics were measured on separated minerals.

Tafassasset is equilibrated and recrystallized. Its minerals are metal, olivine, low Ca pyroxene, feldspar with accessory chromite and phosphate. Tafassasset's classification as a CR chondrite or a primitive achondrite is still debated [1, 2]. Chromite, olivine and bulk rock define an isochron whose slope corresponds to ^{53}M/^{55}Mn= 3.07 x10^{-6} and $\varepsilon^{53}Cr_i$ = 0.07 translating into an absolute age of 4563.4 ±0.4 x10^6 y using the LEW Cliff 86010 anchor [3]. With the exception of the first leaching step, all dissolution steps fall on a linear array. The age obtained by this procedure, 4563.6 ±1.3 x10^{6}y, is identical to the age of the mineral isochron. All samples exhibit an excess of ^{54}Cr= 1.37ε which allows us to consider Tafassasset as a metamorphosed CR chondrite.

Paris is the less altered CM chondrite known to date with affinities to CO chondrites. It contains more chondrules, refractory inclusions and metal but less matrix than the others. Forsterite, fayalite, a separate of fine-grained material attached to chondrules (presumably FGR) and an aliquot of the bulk rock were analyzed for Mn/Cr systematics. All samples fall on a line with a slope of ^{53}M/^{55}Mn = 5.582 x10^{-6} and $^{53}Cr_i$ = -0.179. This slope corresponds to an age of 4566.54 ± 0.55 x10^{6}y based on the LEW Cliff 86010 anchor [3]. All mineral fractions as well as the bulk rock of Paris exhibit a positive ^{54}Cr anomaly. In contrast, the sequential dissolution pattern is similar to that of Murchison.

The ^{54}Cr values of both meteorites fall on the correlation line that has been established between ^{54}Cr and Δ^{17}O for carbonaceous chondrites [5]. In conclusion, the ^{53}Cr and ^{54}Cr isotope systems represent an efficient tool to decipher the origin and classification of meteorites.

[1] Bourot-Denise *et al*. (2002) *LPSC* **33**, #1611. [2] Zipfel *et al*. (2002) *MAPS* **37**, A155. [4] Amelin (2008) *GCA* **72**, 221-223. [5] Trinquier *et al*. (2006) *Astr. J.* **655**,1 179-1185.

Intra-cratonic lithospheric deformations — Heterogeneities, faulting and Rayleigh-Tylor instabilities

WERONIKA GORCZYK[1], BRUCE HOBBS[1], GUIZHI ZHU[2], KLAUS GESSNER[2] AND ALISON ORD[2]

[1]School of Earth and Environment, The University of Western Australia, Perth, Australia.
[2]Dept. of Geosciences, ETH-Zurich, Switzerland.

The seismological structure of the Earth's lithosphere is identified to be strongly heterogeneous in terms of thermal and rheological properties. Lithospheric discontinuities are thought to be long lived and are mostly correlated with major tectonic boundaries that commonly have been reactivated and are subsequently the foci of magma intrusion and major mineralization. The occurrence of such variations may be caused for instance by amalgamation of micro-continents such as is thought to be characteristic of the Yilgarn, Western Australia or parts of South Africa.

This paper explores the control that 3D lithospheric heterogeneity exerts on the thermal and chemical evolution during deformation subsequent to the development of the heterogeneity, as well as periodicity and lateral distribution of phenomena such as Rayleigh-Taylor instabilities and fluid transport from the mantle through the crust. Exploration of the parameters controlling the 3D distribution of focusing mechanisms is crucial for understanding the distribution of major ore deposits along main structures. Empirical observations in Kalgoorlie area (Western Australia, Yilgran craton) show that spacing of major gold deposits is approximately 30km along major lithospheric heterogeneities. This spatial distribution may result from periodic development of Rayleigh-Taylor instabilities along the contact zone, which results in fluid transfer in areas where delamination has occurred. From numerical experiments it appears that the yield strength of the weak zone is one important parameter controlling the spatial distribution of deformation

Above the site of localised delamination of the mantle lithosphere, a series of deep crustal faults develop that may extend into the upper mantle. These deep structures can act as the pathways for mantle derived CO_2 ± H_2O fluids and alkaline igneous complexes.

https://doi.org/10.1180/S0026461X00006502 Published online by Cambridge University Press

Geochemical features of the fluvial plain sediments from the riverbank profiles of the metallogenic area of Eastern Serbia– Ecological significance

V. GORDANIC[1]*, M. VIDOVIC[1], D. JOVANOVIC[2] AND A. CIRIC[2]

[1]The University of Belgrade, IHTM, Dep. Ecol., Serbia (corresp:gordanicv@gmail.com; mivibgd@yahoo.com)
[2]Geological Institute of Serbia, Belgrade, Serbia (dramar@sezampro.rs; abciric@eunet.rs)

During the geochemical mapping of the Eastern Serbia region (in scale 1:1.000.000) samples from the river bank profiles of the drainage areas of several rivers were gathered. Samples (181) were taken from the A-horizons, overbank sediments and stream sediments of the different localities (56). Geochemical features of the area are preserved in the investigated river bank profiles. Significant Cu and Au deposits and smaller deposits of U, Fe and W exist in the area. The anomaly concentrations of the same metals are noted in the investigated river bank sediments.

Well preserved geochemical inscription in the river bank profiles is in good correlation with metallogenic features of this part of the Carpatho-Balkan geochemical province. Sampling network is adjusted to the hydrographical features and mapping scale. The most interesting results are presented in the table 1.

locality	level	**Pb**	**Zn**	**Cu**	**Au**	**Sb**
Mali Timok	A	160	357	1610	0.20	7
	OB	311	1065	3500	0.22	15
	S	148	984	5444	0.25	8
	level	**As**	**Cd**	**Cr**	**V**	**U**
Mali Timok	A	20	3.0	60	140	-
	OB	65	2.1	40	30	3.5
	S	20	5.1	20	60	-

A= A-horizon; OB=overbank sediment); S =stream sediment

The results of gamma spectrometric analyses for ^{238}U, ^{232}Th and ^{40}K reflect radiation burden of selected localities.

Geochemical inscription from the river bank profiles are significant for geochemical prospecting and for rmineral raw material exploration, as well as for definition of anomalous concentrations areas of toxic and other elements.

This work has been financed by the Ministry of Science and Technology of the Rep. of Serbia, project OI 176018.

[1] Ottesen *et al*. (1989) *J. Geochem. Expl*. **32**, 257-277.

Partial melting and its role in elemental recycling: Insight from Pamir metasedimentary xenoliths

S.M. GORDON[1]*, P. KELEMEN[2], B.R. HACKER[3], P. LUFFI[4] AND L. RATSCHBACHER[5]

[1]Geological Sciences, University of Nevada, Reno, NV 89557, USA (*correspondence: staciag@unr.edu)
[2]Lamont-Doherty Earth Observatory, Columbia University, Palisades, NY, 10964, USA
[3]Earth Research Institute, University of California, Santa Barbara, CA, 93106, USA
[4]Earth Science, Rice University, Houston, TX 77005, USA
[5]Geowissenschaften, Technische Universitat Bergakademie, Freiberg, D-09599 Freiberg, Germany

Elemental recycling during subduction has played a key role in the geochemical evolution of the Earth, with recycling efficiencies as high as >75–80% for some elements (e.g., Th). Tracking the fluids and/or melts responsible for recycling, and understanding the *P-T* conditions at which recycling occurs, are more difficult as access to these conditions is limited to experiments. Crustal xenoliths erupted in Tajikistan record temperatures ranging from 875–1100 ºC at pressures of 19–29 kbar. Garnet–kyanite–sanidine gneisses have a meta-sedimentary protolith and represent dehydration-melting residua based on their bulk composition trend of Al_2O_3 > (CaO + K_2O + Na_2O) and that micas are only found as inclusions within garnet and kyanite. Because the metasedimentary xenoliths record a range of temperatures and reached conditions at which melting occurred, they are key samples to investigate the conditions at which recycling occurs. A LA-ICP-MS was used to measure the trace-element composition of all major and minor phases to determine where the key trace elements (e.g., Th, Sr) are stored at different temperatures. Here we highlight three of the samples that range in attaining maximum temperature from 875 ºC to 1000 ºC. In all samples, sanidine contains the large-ion lithophile elements, garnet the heavy rare-earth elements, rutile hosts Nb and Ta, and zircon contains Zr and Hf. In the granulite-facies (plagioclase-stable) gneiss, plagioclase stores Sr but less Ba and Rb, whereas sanidine stores Ba and Rb at all temperatures and Sr at high temperatures. The bulk compositions of the samples indicate that Th, La, and Ba were not depleted until temperatures >900 ºC, even though all three samples appear to have experienced melting. Thus, melting does not seem to have been directly responsible for the depletion, as only the high-*T* samples show depletion. Instead, high-temperature fluids most likely facilitated the recycling of elements from the subducted crustal material.

https://doi.org/10.1180/S0026461X00006502 Published online by Cambridge University Press

Redox conditions in infiltration basins of a large scale soil aquifer treatment (SAT) of effluent

O. GOREN[1]*, I. GAVRIELI[1], A. BURG[1], I. NEGEV[2], J. GUTTMAN[2], T. KRAITZER[2], H. CHIKUREL[2], W. KLOPPMANN[3], C. GUERROT[3] AND M. PETTENATI[3]

[1]Geological Survey of Israel, Jerusalem, Israel (*correspondence: orly.goren@gsi.gov.il)
[2]Mekorot National Water Company, Tel Aviv, Israel
[3]BRGM, Water Department, Orléans, France

Soil Aquifer Treatment (SAT) is considered to be an efficient and reliable effluent tertiary treatment system, in which the vadose zone and the aquifer serve as mechanical, geochemical and biological filters. In the SAT system of the Shafdan reclamation plant, Israel, large volumes of secondary effluent (about 130 million m^3 annually) are recharged into the Costal Plain Aquifer and are recovered for irrigation after residence time of a few months in the aquifer.

A severe degradation of the reclaimed water quality occurs due to a sharp increase of the Mn concentrations. This enrichement is the result of sedimentary Mn-oxides reduction under suboxic conditions within the aquifer. Such conditions prevail in the aquifer due to the intensive organic matter oxidation and nitrification that take place in the upper part of the vadoze zone and consume the dissolved oxygen from the recharged effluent [1].

The present work focuses on the redox reactions that occur in the infiltration basins as well as in the upper few meters below the basins, and aims to determine their sensitivity to different conditions, such as sunlight, temperature and recharge regime.

The preliminary results point to diurnal changes in the intensity of different redox reactions in the basins which have a significant impact on the redox conditions of the infiltrating effluents. The dissolved oxygen (DO) increases during the day to over-saturation values and decreases during night to under-saturation due to net photosynthesis and respiration, respectively. Unlike the DO, the dissolved organic carbon (DOC) in the effluents is quite stable during the 24-hour period. Moreover, the DOC concentrations in the water in the upper one meter of the vadose zone are higher than those in the basin. This implies that significant part of DOC oxidation takes place downward in the vadose zone. A combination of nitrogen mass balance and isotopic composition of oxygen and nitrogen in nitrates point to nitrogen removal by both NH_3 volatilization and denitrification.

[1] Oren *et al*. (2007) *Environ. Sci. Technol*. **41**: 766-772.

An electrochemical approach to determine the redox properties of iron-bearing clay minerals

CHRISTOPHER A. GORSKI[1], MICHAEL SANDER[2], MICHAEL AESCHBACHER[2], LAURA E. KLÜPFEL[1] AND THOMAS B. HOFSTETTER[1,2]

[1]Swiss Federal Institute of Aquatic Science and Technology, Dübendorf, Switzerland
[2]Institute of Biogeochemistry and Pollutant Dynamics (IBP), Swiss Federal Institute of Technology, ETH Zurich, Switzerland

Clay minerals often contain redox-active structural iron (Fe) that can participate in electron transfer reactions with several environmental constituents, including bacteria, biological nutrients, and pollutants. Despite significant work, the electron accepting/donating capacities and Fe^{2+}/Fe^{3+} reduction potential(s) remain difficult to access due to the lack of reactivity between clay minerals and electrodes.

In the current study, we have overcome this challenge by using organic electron transfer mediator compounds that rapidly react with both the clay mineral and the working electrode. Our approach uses chronoculometry, where a fixed potential is applied (E) to the working electrode in a solution containing the mediator. The current (I) is then monitored after the addition of a known amount of clay mineral to quantify the number of electrons transferred. Electrochemical studies were complemented by batch experiments, where a solution of mediator at a set potential (E) is spiked with an alloquot of smectite and the change in potential is measured over time.

For these experiments, we have used an Fe-rich model clay mineral (ferruginous smectite, SWa-1). Highly reducing (E = -0.64 V, SHE) and highly oxidizing (E = +0.61 V, SHE) potentials led to the complete reduction and oxidation of the structural Fe of the smactite, respectively. At intermediate potentials, the Fe^{2+}/Fe^{3+} ratio has been measured as a function of E, pH, and the reduction/re-oxidation cycles of the smectite. We find that the redox properties of structural Fe cannot be described by a single standard reduction potential (E^o); instead, the properties can be explained by either capacitor-like behavior or a distribution of local structures of octahedrally bound Fe with distinct $E°$ values. Addtionally, the reduction/re-oxidation cycles of the smecite appears to strongly influence the Fe(II)/Fe(III) versus E relationship and the electron accepting/donating capabilites during Fe reduction and oxidation. The outcome of our study will help to address the biogeochemical implications of Fe redox reaction involving clay minerals.

https://doi.org/10.1180/S0026461X00006502 Published online by Cambridge University Press

Forensic analysis of surface fallout from low yield surface nuclear tests

RICHARD C. GOSTIC*, KIM B. KNIGHT, GREG SPRIGGS AND IAN HUTCHEON

Lawrence Livermore National Laboratory, Livermore, CA 94551, USA (*correspondance: gostic2@llnl.gov)

Five decades after the last US atmospheric test, fallout samples from low yield surface and near surface events are being re-examined for their forensic value using a combination of radiometric (counting) and mass spectrometry based techniques. Preliminary data from these studies indicate that soil samples collected along historical fallout plumes contain easily accessible information about key components of each test such as fuel isotopics and the elemental composition of structural components.

The distribution of fuel, activation product and fission product signatures as a function of soil grain size and distance from ground zero has been found to be nearly uniform among larger grain sizes of fallout soil (> 0.1 mm). Anthropogenic glasses extracted from the fallout soil samples constitute <5% of the bulk soil mass, yet contain >50% of the total activity. Order of magnitude increases in the concentrations of actinides such as ^{235}U or ^{239}Pu are observed in the glass relative to the soil. By gamma spectroscopy ^{235}U concentrations are estimated to be >60 μg/g and ^{239}Pu concentrations >20 μg/g in glasses recovered from two different tests. Preliminary analysis of the U bearing glasses by ICP-MS indicates a fuel with a minimum enrichment of 84% ^{235}U. Analysis of the stable isotope signal from ICP-MS measurements shows that Be is present in the glass at concentrations 4 times higher then the bulk soil, and that Cr, Co and Mo are present in the U bearing glasses at 3-20 times the bulk soil concentration.

These results demonstrate that fallout from low yield surface nuclear tests collected as surface deposits long after the detonation contains valuable information about device characteristics. This information is relevant to characterizing historical activities from surface based nuclear test programs and is applicable to nuclear forensics research. This work performed under the auspices of the U.S. Department of Energy by Lawrence Livermore National Laboratory under Contract DE-AC52-07NA27344. LLNL-ABS-480552

Rapid esterifications for compound-specific stable isotope analysis of fatty acids

A.S. GOTO AND T. KORENAGA

Department of Applied Chemistry, Tokyo Metropolitan University, Tokyo 192-0397, Japan (*correspondence: akigoto@tmu.ac.jp)

Fatty acids are frequently found as abundant lipid molecules in biological and geological samples, and therefore have been employed as biomarkers in a number of studies particularly for organic geochemistry. However, to reduce polarity and enhance volatility of fatty acids, and resultingly to improve the shape and resolution of fatty acid peaks on gas chromatograms, derivatization such as esterification or silylation are generally required for identification and quantification as well as compound-specific stable isotope analysis (CSIA) of fatty acids.

Here we evaluate methyl (MCF) and ethyl chloroformate (ECF) derivatizations as a rapid and simple esterification for CSIA of fatty acids. These derivatizations are generally prepared with an admixture of MCF/H_2O/methanol/pyridine or ECF/H_2O/ethanol/pyridine at room temperature for 5 min (Fig. 1). In this study, we used 0.1M HCl aq., H_2O, 0.1M NaOH aq., or organic alcohol (methanol or ethanol) instead of H_2O to evaluate the efficiency of derivatization.

For both MCF and ECF derivatizations, fatty acids are esterified very rapidly (within 5 min) even at room temperature, and accuracy of the carbon isotope measurements is always less than 0.3‰ (1σ). Although the yield of derivatives would depend on the chemical constituents and pH of derivative reagents as well as on the carbon-chain length of fatty acids, quantitative esterification is observed by using ECF/ethanol/pyridine (2/60/5, v/v). Thus we conclude that these derivatizations are potentially suitable as a rapid and simple esterification tool for CSIA of fatty acids.

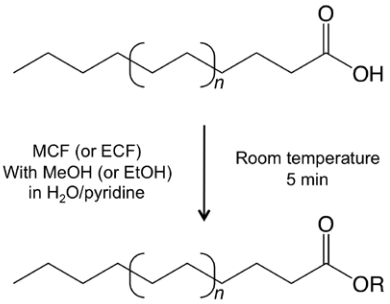

Figure 1: MCF or ECF derivatization of fatty acids.

https://doi.org/10.1180/S0026461X00006502 Published online by Cambridge University Press

U-Pb zircon geochronological, geochemical and Sr-Nd-Hf isotopic studies of granitoids in Muzhaerte River, Southwest Tianshan UHP belt (NW China), and their tectonic implications

L.L. GOU AND L.F. ZHANG*

The Key Laboratory of Orogenic Belt and Crustal Evolution, MOE; School of Earth and Space Sciences, Peking University, Beijing 100871, China
(*correspondence: Lfzhang@pku.edu.cn)

Two granitic intrusions, Changawuzi and Alasan plutons, in Muzhaerte River of Southwest Tianshan UHP belt (NW China) were studied, with the purposes of determining their ages, petrogenesis and implications for the evolution of South Tianshan orogenic belt. A SHRIMP zircon $^{206}Pb/^{238}U$ age of 333±3 Ma was obtained for the Changawuzi pluton and LA-ICP-MS zircon U-Pb dating gave three $^{206}Pb/^{238}U$ ages of 296±4 Ma, 292±2 Ma and 287±8 Ma for the Alasan pluton respectively. The Changawuzi pluton is formed in a continental marginal setting by fractional crystallization from the partial melting of juvenile mafic continental marginal arc rocks, which later assimilated ancient continental crustal material to the extent of 10-15% during emplacement as suggested by the Sr-Nd isotope mixing modelling. The elemental and Sr-Nd-Hf isotopic geochemical studies indicate that the Alasan pluton was the products of fractional crystallization of magma, which were generated by partial melting of mixture of crustal juvenile medium-to-high K intermediate-to-basaltic rocks and 10-30% ancient continental crustal material. As the closure of paleo-South Tianshan ocean (319 Ma), the lithospheric tearing with localized upwelling of asthenosphere occurred at the beginning of slab breakoff because of the localized deformation. This induced the syn-collision magmatisms (317-301 Ma) in the Middle Tianshan terrane. Afterwards, the extensive upwelling of hot asthenosphere induced the partial melting of the crust and formation of voluminous granitic rocks in the early Permian (300-270 Ma) in the South Tianshan orogenic belt. These results imply successive stages of late subduction and closure of paleo-South Tianshan ocean, as well as the collision and post-collision between Tarim plate and Yili-Central Tianshan block happened in Late Paleozoic period.

Geochemical composition of recent sediments and subrecent variability of the last 500 years for the SW Adriatic Sea and the Gulf of Taranto (Southern Italy)

M-L.S. GOUDEAU *AND G.J. DE LANGE

Department of Earth Sciences–Geochemistry, Faculty of Geosciences, Utrecht University, Utrecht, Netherlands
P.O. Box 80.021 3508 TA Utrecht
(*correspondence: m-l.goudeau@geo.uu.nl)

Previous studies from the Gallipoli shelf, Gulf of Taranto, S. Italy, indicate that continuous sedimentation at high accumulation rates and low bioturbation [1] permit high-resolution paleoclimate studies. Measurements of carbonate contents, thermolumuniscens, oxygen and carbon isotopes, [2,3] and reconstructed sea surface temperatures [4] display cyclic frequencies similar to those known for solar cycles. Origin and processes related to these patterns, however, remain unclear. To study these cycles in more detail, a multi-proxy approach is needed to reconstruct e.g. changes in run-off, and productivity in the past. The Gulf of Taranto however is located in a coastal area, influenced by rivers, ocean currents, and eolian dust sources, affecting the geochemical composition of the in situ sediments [5-8]. Assessing input and geochemical fingerprints of all different sources to the Gulf of Taranto in the present system, will permit changes in these sources to be reconstructed. Here, we present details and interpretation for a compositional study of core top samples from the S. Adriatic and the Gulf of Taranto and terrestrial samples from the Italian Adriatic coastal area. Results are then used to reconstruct e.g. run off in the Gulf of Taranto for the last 500 years.

[1] Cini Castagnoli *et al*., (2002) [2,3] Cini Castagnoli *et al*., (1996), and (2002). [4] Versteeg, (2007). [5] Frigani *et al*., (2005). [6] Tankere, (2000); [7] Tesi *et al*., (2007) [8] Rossini, (1996).

https://doi.org/10.1180/S0026461X00006502 Published online by Cambridge University Press

Isotopic variations in mafic volcanic rocks from the western branch of the East African Rift

D. GRAHAM*[1], T. FURMAN[2], J. BLICHERT-TOFT[3], J. LUPTON[4], C. EBINGER[5] AND N. ROGERS[6]

[1]College of Oceanic & Atmospheric Sciences, Oregon State University, Corvallis, OR 97331, USA (*correspondence: dgraham@coas.oregonstate.edu)
[2]Department of Gesciences, Pennsylvania State University, University Park, PA 16802, USA
[3]Laboratoire de Géologie de Lyon, Ecole Normale Superieure de Lyon, 69007 Lyon, France
[4]NOAA/PMEL, Hatfield Marine Science Center, Newport, OR 97365, USA
[5]Department of Earth and Environmental Sciences, University of Rochester, Rochester, NY 14627, USA
[6]Department of Earth Sciences, Open University, Milton Keynes, MK7 6AA, UK

Isotopic variations in lavas from regions of low tectonic extension, such as the western branch of the East African Rift (EAR), can be used to probe regional variability in the underlying continental lithospheric mantle. Volcanic rocks from the western branch of the EAR are isotopically among the most extreme young samples on Earth. Pb, Hf, Nd and Sr isotope compositions for mafic, undersaturated alkalic lavas from Rungwe, Kivu, Virunga and Toro-Ankole all show large variations over short lateral distances, indicating extensive isotopic heterogeneity in the continental lithospheric mantle source for these lavas, mostly due to ancient metasomatism associated with African orogenic events. Trends in the isotopic data show a convergence near values of $^{206}Pb/^{204}Pb$=18.9-19.2,$^{207}Pb/^{204}Pb$=15.63-15.67, $^{208}Pb/^{204}Pb$=39.3-39.7, ε_{Nd}=0, ε_{Hf}=3 and $^{87}Sr/^{86}Sr$=0.705. The isotopic variation within each volcanic province extends away from these values to distinct compositions. In contrast, $^{3}He/^{4}He$ within each province shows a restricted range; 7.5-9.0, 5.0-6.5, 6.7-7.5 and 5.6-6.8 R_A for Rungwe, Kivu, Virunga and Toro-Ankole, respectively. There is no evidence for the presence of high $^{3}He/^{4}He$ plume material such as that beneath the Ethiopian Rift and Afar. The convergence of the Pb-Hf-Nd-Sr isotopes suggests that primary magma is derived from a common mantle source beneath the western branch of the EAR, such as the lithosphere/asthenosphere boundary. In contrast, the distinct isotopic variations within each volcanic region represent the shallower, provincial characteristics of the underlying lithosphere and crust.

Electron shuttle production by *Shewanella oneidensis*

JEFFREY A. GRALNICK* AND NICHOLAS J. KOTLOSKI

Department of Microbiology and BioTechnology Institute, University of Minnesota, St. Paul, MN, USA, (*correspondence: gralnick@umn.edu)

Extracellular Respiration

Many dissimilatory metal reducing bacteria have evolved mechanisms to transfer electrons from the cytoplasmic membrane quinone pool to insoluble substrates (e.g. oxide minerals and electrodes) located beyond their outer membranes [1, 2]. *Shewanella oneidensis* strain MR-1 is the best understood model system for extracellular respiration. While biochemical evidence supports a direct mechanism for electron transfer to insoluble substrates, there is also strong physiological evidence for electron shuttling [3, 4]. Flavins (riboflavin and flavin mononucleotide (FMN)) were identified as the primary electron shuttle compounds produced by *Shewanella*. Our work seeks to define the contribution of electron shuttles to the reduction of insoluble substrates by *S. oneidensis* and understand the molecular mechanism underlying the production and processing of flavin shuttles produced by these bacteria.

Discussion of Results

We designed a mutagenesis screen in *S. oneidensis* to isolate strains that no longer accumulated flavins in culture supernatants. This work led to the identification of UshA, a 5'-nucelotidase involved in the processing of periplasmic flavin adenine dinucleotide (FAD) to FMN and adenosine monophosphate [5]. Strains defective in *ushA* accumulated FAD in culture supernatants instead of FMN or riboflavin. We repeated our mutagenesis screen in an *ushA* deletion mutant background to identify additional components involved in electron shuttle processing and secretion. This secondary screen identified mutants defective in flavin export and in regulation of flavin secretion. Here, we present the characterization of the two new components related to electron shuttle export by *S. oneidensis*. We have generated the first strain of *S. oneidensis* that is fully defective in electron shuttle secretion, allowing us to conclude that electron shuttling accounts for ~75% of the electron transfer activity to insoluble substrates. Moreover, electron shuttling mutants have no defect in respiration of soluble organic electron acceptors or chelated iron.

[1] Lovley *et al*. (2004) *Adv Microb Physiol* **49**, 219-86. [2] Shi *et al*. (2007) *Mol Microbiol* **65**, 12-20. [3] Marsili *et al*. (2008) *PNAS* **105**, 3968-73. [4] von Canstein *et al*. (2008) *Appl Enviorn Microbiol* **74**, 615-23. [5] Covington *et al*. (2010) *Mol Microbiol* **78**, 519-32.

https://doi.org/10.1180/S0026461X00006502 Published online by Cambridge University Press

Deciphering mafic and felsic lunar magmatic events: Insight from zircon

M.L. GRANGE[1]*, A.A. NEMCHIN[1], N. TIMMS[1], R.T. PIDGEON[1] AND C. MEYER[2]

[1]Dept. of Applied Geology, Curtin University, GPO Box 1987, Perth, Western Australia 6845. (*correspondence: m.grange@curtin.edu.au)

[2]NASA Johnson Space Center, Houston, TX 77058, USA.

Microstructural studies of zircon grains from lunar breccia samples, combining high resolution imaging together with in-situ U-Th-Pb analyses, has allowed us to distinguish primary zircon, formed by igneous crystallisation in plutonic rocks, and secondary, impact-related, features in zircon grains. Dating of these grains can be used to identify multiple igneous and impact events. For example, a single impact melt breccia from the Apollo 17 landing site contains grains that record more than 3 igneous events in addition to 3 distinct impact events, indicating that the region sampled by this breccia probably significantly exceeds the area of the landing site. As a result, the study of primary zircon ages in the available samples can be used to investigate the temporal distribution of plutonic magmatism on the Moon, even though these samples were collected from the relatively small areas covered by the lunar landing missions.

The study of primary zircons containing inclusions of rock-forming minerals or zircons preserved in lithic clasts found in lunar breccias also provides an opportunity to place temporal constraints on the different types of plutonic magmatism on the Moon. U and Th concentrations of these zircon grains vary systematically allowing clear separation of zircons formed in mafic rocks, such as anorthosite, norite, and gabbro-norite, from those formed in felsic rocks (i.e. granophyre and felsite). This chemical variation can be used to determine plutonic hosts of zircon grains found as mineral clasts in the breccia samples and as loose grains in lunar soils, expanding significantly the number of zircons with known origin.

A comparison of ages of zircons originating from mafic and felsic host rocks suggests a possible age difference between these two chemical rock groups. If confirmed by further analyses this would indicate that the two current explanations for the formation of felsic rocks on the Moon, (i) as residual melt left after extreme fractionation of basaltic magma or (ii) as a result of liquid immiscibility during late stages of fractionation of basaltic melts, are incorrect. Both mechanisms imply close temporal relationships between mafic and felsic rocks, which does not appear to be supported by the available U-Pb ages.

Silicon isotopes as a tracer for silicate utilization in the Peruvian upwelling

PATRICIA GRASSE*, CLAUDIA EHLERT, LOTHAR STRAMMA, EVGENIYA RYABENKO, JASMIN FRANZ AND MARTIN FRANK

IFM-GEOMAR, Wischhofstr. 1-3, 24148 Kiel, Germany (*correspondance: pgrasse@ifm-geomar.de)

Natural stable isotopes are a powerful tool in marine sciences to investigate biological processes, such as present and past nutrient utilization. In this study we present the first dissolved silicon isotope data in the upwelling area off Peru, where one of the world's largest Oxygen Minimum Zones (OMZ) is located. Samples were recovered during "FS Meteor" cruises M77/3 and M77/4 in 2009. Silicic acid is the most important component required for the growth of diatoms, which dominate the primary productivity in this region. Stable silicon (Si) isotopes are fractionated during diatom growth in that the lighter isotopes are preferentially incorporated into diatom frustules with a fractionation factor of -1.1‰. The Si isotope composition of dissolved silicic acid of the corresponding surface waters is therefore left isotopically heavier. The silicon isotope composition, $^{30}Si/^{28}Si$ is given relative to a reference standard (NBS28) and expressed in the $\delta^{30}Si$ notation. Dissolved Si isotope signatures of seawater provide a measure for the degree of utilization of silicic acid but are also influenced by water mass mixing. Surface waters on the shelf off Peru are mainly fed by the Peru Chile Undercurrent ($\delta^{30}Si$=1.5‰), which consists of water masses ultimately originating from the western and Central Pacific. In areas and during phases of intense upwelling the fractionation of Si isotopes was observed to be weaker due to upwelling driven supply of less fractionated Si ($\delta^{30}Si$=1.8‰) from water depths of 50 to 150m, whereas under weak upwelling conditions the surface waters are heavier ($\delta^{30}Si$=2.8‰) due to more complete utilization of the available dissolved silicic acid. The distribution of the dissolved silicon isotope compositions correlates strongly with particulate biogenic silicate (opal) concentrations in that the highest opal concentrations in surface waters on the shelf reflect the lowest $\delta^{30}Si$ values thus the strongest upwelling intensity. The most extreme $\delta^{30}Si$ values in surface waters ($\delta^{30}Si$=3.2‰) are observed offshore where silicic acid is limited. Furthermore we compare $\delta^{30}Si$ data with the dissolved nitrogen isotope distribution, which, in addition to nitrate utilization, is also influenced by denitrification and annamox processes in the OMZ. Combined silicon and nitrogen isotope compositions can thus help to disentangle different fractionation processes within the nitrogen cycle.

https://doi.org/10.1180/S0026461X00006502 Published online by Cambridge University Press

Chemical modification of airborne mineral dust

VICKI H. GRASSIAN

Department of Chemistry, University of Iowa, Iowa City, IA 52246, USA (vicki-grassian@uiowa.edu)

Introduction

Mineral dust aerosol, i.e. suspended soil particles, can impact a wide range of global processes including the chemistry of the Earth's atmosphere and the Earth's climate. Atmospheric processing of mineral dust through heterogeneous chemical and photochemical reactions will modify the properties of the dust particle and thus alter how these particles impact global processes [1-3].

Approach

Using a combined approach of applying state-of-the-art surface sensitive probes, aerosol instrumentation and reactivity studies provides for an understanding of reactions on dust particles and how these reactions can alter the global impacts of mineral dust aerosol. These laboratory studies can provide a conceptual framework from which to understand the details of chemical processes that modify the properties of mineral dust aerosol as these particles are transported through the atmosphere [4].

Discussion of Results

The importance of mineralogy, the link between interfacial chemistry and climate and the specificity of mineral dust aerosol chemistry will be discussed. Examples will be shown that clearly provide evidence to show that mineral dust modifies the chemical balance of the atmosphere through heterogeneous reactions and that heterogeneous reactions modifies the physicochemical properties of mineral dust particles.

[1] Usher *et al*. (2003) *Chem. Rev.* **103**, 4883-4940. [2] Cwiertny *et al*. (2008) Ann. Rev. Phys. Chem. *59*, 27-51 [3] Gasso *et al*. (2010) *Elements* **6**, 247-253. [4] Hatch and Grassian (2008) *J. Env. Mon.* **10**, 919 – 934.

Stable isotopes of organics and inorganics of Aptian lacustrine sediments in North-Eastern Brazil

R. GRATZER[1]*, V.H. NEUMANN[2], W. VORTISCH[1], D. ROCHA[2] AND A. BECHTEL[1]

[1]Montanuniversität Leoben, 8700 Leoben, Austria, (*correspondence: gratzer@unileoben.ac.at)

[2]Universidade Federal de Pernambuco, Recife, Brazil (neumann@ufpe.br, dunaldson@msn.com)

The Jatobá Basin is located in the Pernambuco-Alagoas massif, NE Brazil. The elliptical basin, orientated NE-SW, is characterized by a semi-graben structure with tilted blocks toward NW direction. The analysed section [1] consists of shales, marls, sandstones, limestones and dolostones.

Stable isotope analysis was carried out on carbonates and organic matter. TOC content varies from 0.5-13 wt%, Hydrogen and Oxygen Indecies from 6 to 715 and 4 to 44 respectively. The organic matter is immature (R_o % 0.28) and is represented by kerogen Type I in the lower section. In the upper section it is modified by the addition of terrestrial organic matter. A ~3 m thick clay-rich shale seperates the the sections.

	Lower section	Upper section
$\delta^{13}C$ Carbonates	-8.72 to -3.65	-3.57 to +2.47
$\delta^{18}O$ Carbonates	-8.09 to -4.98	-8.67 to -4.11
$\delta^{13}C$ Pr + Ph	-28.25 to -31.66	-31.66 to -30.28
$\delta^{13}C$ C_{29} Steranes	-26.39 to -30.12	-30.12 to -28.08
$\delta^{13}C$ C_{30} Hopanes	-27.40 to -32.96	n.d.

Table 1: Variation and trends in $\delta^{13}C_{PDB}$ ‰ and $\delta^{18}O_{PDB}$ ‰ of carbonates and $\delta^{13}C_{PDB}$ ‰ organic compounds.

$\delta^{18}O$ of carbonate minerals (Table 1) indicates fresh water conditions throughout the sediment column. In the deepest part of the lower section dolomite occures together with high TOC contents. Here $\delta^{13}C$ suggests intense microbial activity during carbonate formation. In contrast, $\delta^{13}C$ shift to more positive values in the upper part, indicating less microbial influence. The upward trend of organic $\delta^{13}C$ is towards lighter values in the lower section and heavier values in the upper section (see Table 1). This is interpreted as the result of changing environmental conditions and enhanced terrigeneous organic matter input.

[1] Vortisch *et al*. (2011). *MinMag*, this volume.

https://doi.org/10.1180/S0026461X00006502 Published online by Cambridge University Press

Hydrogeochemical survey of CO_2 geological leakage using noble gases: Application to the Furnas Caldera (Azores, Portugal)

C. GREAU[1,2]*, M. MOREIRA[1], P. AGRINIER[1], V. LAGNEAU[2], H. SCHNEIDER[3], P. MADUREIRA[4] AND L. RUZIE[1]

[1]Institut de Pysique du Globe de Paris (IPGP), 1 rue Jussieu, 75005 Paris, France (*correspondence : greau@ipgp.fr)
[2]École des Mines de Paris, Centre de Géosciences, 35, rue Saint Honoré, Fontainebleau, 77305 Cedex, France
[3]EDF R&D, Site des Renardières, Route de Sens, Écuelles, Moret-sur-Loing, 77818 Cedex, France
[4]Universidade de Évora, Centro de Geofísica de Évora, Departamento de Geociências, 8 Rua Romão Ramalho, 59, 7000-671 Évora, Portugal

Significant natural CO_2 emissions have been measured across the caldera of Furnas (São Miguel Island, Azores) allowing us to consider the area as a CO_2 leakage analogue.

During two field trips, we have collected twenty springs in purpose to measure CO_2 contents (Dissolved Inorganic Carbon and $\delta^{13}C$) and noble gas isotopic compositions (He and Ne) and for seventeen water samples, major ions chemistry. The corrected $^3He/^4He$ ratios (normalized to air ratio R_A) range from 1.46 to 5.17, the carbon contents (DIC) range from 0.57 to 41,41 mmol/l and most of the waters have a $\delta^{13}C$ about -4 ‰.

With field observations and waters chemistry, we have characterized seven different types of water springs through the caldera, resulting from various mixing rates between three sources : soil equilibrated meteoritic water, gas emanations (CO_2, He…) from a magmatic intrusion and hydrothemal waters coming from a shallow depth aquifer. Saturation indexes and geothermometers indicate a trachytic aquifer at a temperature of about 145°C.

In order to confirm that noble gases are good tracers of CO_2 leakage, we are building a first mixing model using noble gases and carbon isotopes and a second one based on major ions chemistry with CHESS hydrochemical modelling software. Preliminary mixing models seem to be consistent thus confirming that noble gases can be used as tracors of CO_2 leakage.

Comparison of Diviner Lunar Radiometer Observations of Apollo sites and Apollo soils measured in simulated Lunar environment

B.T. GREENHAGEN[1]*, I.R. THOMAS[2], N.E. BOWLES[2], C.C. ALLEN[3], K.L. DONALDSON HANNA[4], E.J. FOOTE[5], AND D.A. PAIGE[5]

[1]JPL, Caltech, Pasadena, CA 91109, USA (*correspondence: Benjamin.T.Greenhagen@jpl.nassa.gov)
[2]Univ. of Oxford, Oxford, OX1 3PU, UK
[3]NASA Johnson Space Center, Houston, TX 77058, USA
[4]Brown Univ., Providence, RI 02912, USA
[5]Univ. of California, Los Angeles, CA 90095, USA

The Diviner Lunar Radiometer (Diviner), onboard NASA's Lunar Reconnaissance Orbiter, has made the first direct global measurements of lunar silicate mineralogy using multispectral thermal emission mapping [1]. Diviner has three spectral channels near 8 μm designed to characterize the Christiansen feature (mid-infrared emissivity maximum) [2], which systematically shifts to shorter wavelengths with increasing silicate polymerization [e.g. 3,4].

Only laboratory experiments conducted in simulated lunar environment (SLE) are directly comparable to Diviner data. The Lunar Thermal Environment Simulator at University of Oxford's Atmospheric, Oceanic, and Planetary Physics Laboratory is uniquely capable of measuring thermal emission of samples in SLE [5]. In the lunar environment, large thermal gradients develop in the top few hundred microns of the surface, driven by the difference in the solar and thermal skin depths (i.e. the surface is heated to greater depth than the infrared emitting layer). The thermal gradients generally result in a significant enhancement of Christiansen feature spectral contrast and significant decreases in Reststrahlen Bands spectral contrast.

Diviner observations include all six Apollo sites at approximately 200 m spatial resolution. Spectral differences between the Apollo sites caused by composition and space weathering are apparent in Diviner data [1]. Since the compositions of Apollo soils are known, the Apollo sites are important calibration points for the Diviner dataset. This presentation will include the first comparison of Diviner observations of Apollo sites and spectra of Apollo soils measured in SLE.

[1] Greenhagen *et al*. (2010) *Science* **329**, 1510. [2] Paige *et al*. (2010) *SSR* **150**, 125. [3] Logan *et al*. (1973) *JGR* **78**, 4983. [4] Salisbury and Walter (1989) *JGR* **94 (B7)**, 9192. [5] Thomas *et al*. (2010) *LPSC* **42**, #1364.

https://doi.org/10.1180/S0026461X00006502 Published online by Cambridge University Press

Surface modifications of engineered nanoparticles and their impacts on cytotoxicity

KELVIN B. GREGORY[1,2], ZHIQIANG LI[1,2] AND GREGORY V. LOWRY [1,2]

[1]Carnegie Mellon University, Civil and Environmental Engineering, Pittsburgh, PA, 15213, USA
[2]Center for Environmental Implications of Nanotechnology

The interactions of engineered nanoparticles (ENP) with the natural environment will have a deterministic affect on their fate and transport, yet the impacts of environmental tansformations of ENP are poorly understood. For example, previous work in our laboratory demonstrated that bare particles of nanosized zero-valent iron exhibited toxicity towards bacterial cells at concentrations as low as a few mg/L, yet oxidation of the iron surfaces or the presence of natural or engineered coatings may eliminate the toxic effects of NZVI. We examined the impact of surface transformations on the bacterial toxicity of ENP through the application of natural and/or engineered coatings on the particles. We selected particles with different mechanisms of expressing cytotoxicity; 1) NZVI- requires direct contact with cells, 2) TiO_2- produces reactive oxygen species, and 3) AgNP- produce toxic metal cations. Our findings show that both natural and engineered surface coatings on NP may greatly reduce or eliminate the cytotoxicity of NP. However, the ability and mechanism of interference with toxicity is dependent on both the type of particle well as the coating. While engineered coatings of NZVI induced electrostatic or electrosteric repulsion between the NP and cell that prevented toxicity, in the case of TiO_2, the natural organic matter coatings scavenged reactive oxygen species. Interestingly, engineered polyaspartate coatings did not prevent the toxicity of TiO_2. The coating of AgNP with engineered and natural polymers has little impact on toxicity, but oxidation of the surface through sufidation greatly reduced toxicity. Our studies imply that surface modifications may be engineered to minimize cytotoxicity and that the potential for detrimental impacts of ENP in the environment is lessened by coatings on which arise in natural systems.

Physical versus chemical non-equilibrium model for simulating U(VI) adsorption

JANEK GRESKOWIAK[1,2,*], MICHAEL B. HAY[3], HENNING PROMMER[2], CHONGXUAN LIU[4], VINCENT E. A. POST[5], RUI MA[6], CHUNMIAO ZHENG[6], JAMES A. DAVIS[3] AND JOHN M. ZACHARA[4]

[1]University of Oldenburg, 26111 Oldenburg, Germany (*correspondence: janek.greskowiak@uni-oldenburg.de)
[2]CSIRO Land and Water, Wembley, Australia
[3]USGS, Menlo Park, USA
[4]Pacific Northwest National Laboratory, Richland, USA
[5]Flinders University, Adelaide, Australia
[6]University of Alabama, Alabama, USA

Surface complexation reactions and diffusional mass-transfer between mobile pore water and immobile water associated with the intra-grain pores have been found to play an important role for the overall U(VI) transport behaviour in the US DOE Hanford 300A aquifer. Several laboratory- and field-scale scenario simulations have been carried out to investigate the behaviour of two alternative model approaches for the simulation of coupled intra-grain diffusion and surface complexation of U(VI) under dynamic groundwater flow and hydrochemical conditions.

The physical non-equilibrium approach explicitly calculates aqueous speciation and surface complexation in the intra-grain pore spaces as instantaneous recations and simulates the diffusional mass-exchange between the mobile and immobile domains by a set of multiple 1^{st}-order rates. The chemical non-equilibrium approach approximates the diffusion-limited surface complexation by a multiple 1^{st}-order kinetic reactions, which makes it computationally efficient compared to the physical non-equilibrium approach. While for linear sorption scenarios the two model approaches are equivalent, they show differences when the sorption process becomes non-linear, for example as a result of surface complexation reactions under varying hydrochemical conditions.

Under the Hanford 300A field scale hydrological and hydrochemical conditions, the two model approaches predicted largely similar U plume behaviour. In contrast, simulated U(VI) mass discharge into the Columbia River that is adjacent to the 300A was noticeably higher in the physical model due to a higher degree of non-equilibrium in the plume fringe located at the river-groundwater interface. However, compared to other effects, such as that of calcite dissolution on U(VI) mass discharge, the choice of the non-equilibrium model approach appeared to be less important.

https://doi.org/10.1180/S0026461X00006502 Published online by Cambridge University Press

Experimentally determined standard properties for $MgSO_4 \cdot 4H_2O$ (starkeyite) and $MgSO_4 \cdot 3H_2O$; A revised internally consistent thermodynamic dataset for magnesium sulfate hydrates

K.-D. GREVEL[1,2]*, J. MAJZLAN[1], A. BENISEK[3], E. DACHS[3], M. STEIGER[4], A. D. FORTES[5] AND B. MARLER[2]

[1]Inst. of Geosciences, Friedrich-Schiller University, Jena, Germany (*correspondence: Klaus-Dieter.Grevel@rub.de)
[2]Inst. for Geology, Mineralogy and Geophysics, Ruhr-University, Bochum, Germany
[3]Dept. of Materialscience & Physics, Mineralogy Division, University Salzburg, Austria
[4]Dept. of Chemistry, University of Hamburg, Germany
[5]Dept. of Earth Science, University College London, UK

A number of different hydrated forms of $MgSO_4 \cdot nH_2O$ ($1 \le n \le 11$) are known to exist on Earth and also on Mars. Recently, the enthalpies of formation from the elements ($\Delta_f H^0_{298}$) of kieserite ($n = 1$), sanderite ($n = 2$), hexahydrite ($n = 6$), and epsomite ($n = 7$) were measured [1]. Now, we have obtained $\Delta_f H^0_{298}$ of synthetic $MgSO_4 \cdot 3H_2O$ and $MgSO_4 \cdot 4H_2O$ (starkeyite) by solution calorimetry in water at $T = 298.15$ K. The resulting values are –2210.3 ± 1.3 and –2498.7 ± 1.1 $kJmol^{-1}$ for the trihydrate and starkeyite, respectively.

The standard entropy of starkeyite was derived from low-temperature heat capacity measurements using a PPMS® system [2] in the temperature range 5 K < T < 300 K resulting in S^0_{298} (starkeyite) = 254.5 ± 2.0 $J \cdot K^{-1} mol^{-1}$.

Additionally, DSC measurements with a Perkin Elmer Diamond DSC in the temperature range 280 K < T < 295 K were performed to check the reproducibility of the PPMS® measurements around ambient temperature.

All Mg sulfate hydrates change their hydration state in response to the local temperature and humidity conditions. Based on recently reported equilibrium relative humidities [3] and the new standard properties described above, the internally consistent thermodynamic database for the $MgSO_4 \cdot nH_2O$ system [1] was refined.

[1] Grevel, K.-D., Majzlan, J., (2009) *Geochim. Cosmochim. Acta* **73**, 6805-6815. [2] Dachs, E., Bertoldi, C., (2005) *Eur. J. Mineral.* **17**, 251-261. [3] Steiger, M., Linnow, K., Erhardt, D., Rohde, M., (2011) *Geochim. Cosmochim. Acta* accepted.

Ore deposits and the SCLM

W.L GRIFFIN[1]*, G. BEGG[1,2], SUZANNE Y. O'REILLY[1], AND N.J. PEARSON[1]

[1]GEMOC/CCFS, Earth and Planetary Sciences, Macquarie Univ., NSW 2109 Australia (*correspondence: bill.griffin@mq.edu.au)
[2]Minerals Targeting Intl., 26/17 Prowse st., W. Perth 6005, Australia (graham@mineralstargetting.com.au)

The single largest influence on the formation of Earth's ore deposits has been the generation of the Archean subcontinental lithospheric mantle (SCLM). Geological and geochemical evidence suggests that subduction-like processes, and the progressive depletion of the convecting mantle, began at least 3.8-4.0 Ga ago, but there are few large ore deposits older than ca 3 Ga. Re-Os data suggest that the formation of the Archean cratonic SCLM began ca 3.5 Ga ago, and reached a peak around 3 Ga. This primitive SCLM was much more depleted than is commonly recognised; it was essentially a magnesian dunite, the residue after large-scale extraction of crustal material from rising plumes/mantle overturns. Since its formation it has been progressively refertilised by fluids and melts from the asthenosphere and subducting slabs. At present ≥70% of continental crust is underlain by Archean-aged SCLM. The coming of the SCLM has had major effects on the types of ore deposits and their distribution in space and time. (1) *Preservation:* The Archean SCLM is buoyant relative to the asthenosphere and resists subduction, giving its overlying crust a "life raft"; the more fertile SCLM beneath younger terrains is denser, and can be delaminated and recycled, leaving its overlying crust unprotected from the convecting mantle. Ore deposits generated in juvenile arcs, some continental arcs and rifted-margin basins thus are unlikely to survive subsequent orogenies. (2) *Lithospheric architecture*; the deep roots of old continents focus fluid flow toward their margins, and act as physical guides for plume melting. (3) *A durable metasomatic reservoir*; the refertilisation of the ancient SCLM has built up the concentrations of metals, which can be tapped by ascending magmas. There are many komatiites, but those fertile in Ni-Cu-PGEs are limited to ages <2.9 Ga, and lie along ancient craton margins. Kimberlites may be generated by low-degree melting of SCLM, but only those that intersect previously metasomatised SCLM during their ascent will carry many diamonds. (4) *New ore-forming environments*. The coming of the SCLM provided tectonic settings that did not previously exist, allowing the generation of new types of ore deposit: large foreland basins (banded iron formations), craton margins (Ni-Cu-PGE), back-arc/pericratonic basins and passive margins (granular iron formations, Pb-Zn, Mississippi Valley-type deposits).

https://doi.org/10.1180/S0026461X00006502 Published online by Cambridge University Press

The geogenic impact on groundwater composition in the Netherlands

JASPER GRIFFIOEN[12]*, SOPHIE VERMOOTEN[2] AND BAS VAN DER GRIFT [2]

[1]TNO Geological Survey of the Netherlands, Utrecht, the Netherlands (*correspondence: jasper.griffioen@tno.nl)
[2]Deltares, Utrecht, the Netherlands

The quality of groundwater is vital for both its natural function and anthropogenic use. Surprisingly, the geogenic control on groundwater composition has received little attention while the petrological composition of the rock matrix forms a major factor on groundwater composition. We have systematically investigated the geogenic control on both major groundwater composition and a series of trace elements at a national scale for the Netherlands. Several thousands of existing groundwater analyses were classified on geological formation. Additionally, the samples were grouped into 26 unique geographical regions. Regional statistics were created for all solutes of interest. An interpretation was established in terms of salinity, pH and carbonate status, redox status and nutrients. Interesting regional differences are noted within both the Pleistocene part of the Netherlands where phreatic aquifers are dominant, and the Holocene part where a reactive layer of clay and peat lies at the surface. This holds both for the major groundwater composition as well as for trace elements. These differences can partly be related to the sedimentary origin of the deposits, where marine deposits are more reactive than fluvial deposits. Upon result, the buffering capacity of marine deposits is larger but the natural contamination with arsenic, nutrients and salinity, too. This buffering capacity is monitored by an additional field and laboratory campaign, which establishes regional statistics on reaction capacities of sediment.

The crystal chemistry of (As,Sb,Bi)-bearing dumortierite

L.A. GROAT[1]*, R. JAMES EVANS [1], E.S. GREW[2] AND A. PIECZKA[3]

[1]University of British Columbia, Vancouver, British Columbia V6T 1Z4, Canada (*correspondence: lgroat@eos.ubc.ca)
[2]University of Maine, Orono, Maine 04469-5790, U.S.A
[3]University of Science and Technology, 30-059 Kraków, Poland

Dumortierite [c. $(Al,\square)Al_6(BO_3)Si_3O_{13}(O,OH)_2$] and holtite [c. $(Ta,\square,Al)Al_6(BO_3)(Si,Sb,As)_3O_{12}(O,OH,\square)_3$], are isostructural minerals found in a few granitic pegmatites. Dumortierite may contain several wt.% of Sb_2O_3, As_2O_3, Ta_2O_5, thereby blurring compositional distinctions between the two, although generally As > Sb in dumortierite. For this study we investigated the effect of minor amounts of Sb and As on the crystal structures of dumortierite samples D21 (Rats quarry, Hartmannsdorf, Saxony), D31 (Tonagh Island, Enderby Land, Antarctica) and D27 (Uval'dy Lake, Il'men Mountains, southern Urals, Chelyavinskaya Oblast', Russia). Average electron microprobe compositions for sample D21 show 2.32 wt.% As_2O_3 (0.14 atoms per formula unit) and 0.57 wt.% Sb_2O_3 (0.02 Sb apfu); for D31, 2.85 wt.% As_2O_3 (0.18 apfu) and 1.03 wt.% Sb_2O_3 (0.04 apfu); and for D27, 1.69 wt.% As_2O_3 (0.10 apfu) and 0.68 wt.% Sb_2O_3 (0.03 apfu). Analyses of samples D21 and D27 show no appreciable Ta, whereas sample D31 contains on average 1.62 wt.% Ta_2O_5 (0.04 apfu). Sample D27 also contains Bi (1.07 wt.% Bi_2O_3, 0.03 apfu).

Crystal structure refinements of single-crystal X-ray diffraction data converged to R1 values 1.92, 1.62, and 3.04% for samples D21, D31, and D27 respectively (all D27 crystals investigated were twinned in the normal fashion for dumorterite, with three twin individuals related by 120° rotation about a threefold twin axis parallel to a). For all three samples the results suggest that the As and Sb atoms are at the Sb1 and Sb2 sites, as is the case for holtite. However in the dumortierite samples the atomic displacement parameters (ADPs) associated with the atoms at these sites are unusually large, with U_{eq} Sb1 values of 0.03 Å^2, 0.02 Å^2, and 0.09 Å^2, and U_{eq} Sb2 values of 0.02 Å^2, 0.03 Å^2, and 0.06 Å^2, for samples D21, D31, and D27, respectively (for holtite these values are generally less than or equal to 0.01 Å^2). Atomic displacement parameters for the coordinating oxygen atoms are no larger than in holtite and dumortierite with no As or Sb.

The reason for the large ADPs remains under investigation but may be a function of the small amounts of As and Sb at these sites, or perhaps indicates the presence of both trivalent and pentavalent As and Sb (and perhaps Bi, or Bi^{3+} and Bi^{5+}) at the Sb1 and Sb2 positions.

https://doi.org/10.1180/S0026461X00006502 Published online by Cambridge University Press

Reconstruction of permanent thermocline temperatures in the Atlantic during Heinrich Stadial 1

J. GROENEVELD[1]*, C. M. CHIESSI[2], A. MACKENSEN[3] AND R. TIEDEMANN[3]

[1]Marum Excellence Cluster, Alfred Wegener Institute, Bremerhaven, Germany (*correspondence: Jeroen.Groeneveld@awi.de)
[2]School of Arts, Sciences, and Humanities, University of São Paulo, São Paulo, Brazil
[3]Alfred Wegener Institue for Polar and Marine Research, Bremerhaven, Germany

Changes in Atlantic Meridional Overturning Circulation (AMOC) have been modeled to lead to a global adjustment of the depth of the thermocline via the propagation of Kelvin waves, particularly in the North Atlantic with warming during AMOC slowdown. The aim of this study is to test for significant warming during AMOC shutdown by reconstructing permanent thermocline temperatures for the Deglaciation at key locations in the Atlantic. Therefore, we used Mg/Ca-paleothermometry on the deep-dwelling foraminifer *Globorotalia inflata*.

We established a new Mg/Ca-temperature calibration for *G. inflata* based on core top samples from the South Atlantic. The reconstructed apparent calcification depth for dominantly non-encrusted specimens is 350-400 m making *G. inflata* ideal to reconstruct temperature changes in the permanent thermocline.

First results from core GeoB9508-5 off northwest Africa, which is close to the boundary between the predicted thermocline warming (to the north) and cooling (to the south), show a significant warming during HS1 of ~4°C supporting the prediction of subsurface warming in the North Atlantic during AMOC slowdown. Interestingly, this warming occurs after the actual start of HS1.

Temporal dynamics of arsenic-bearing phases during the suspended transport

C. GROSBOIS[1]*, A. COURTIN-NOMADE[2], E. ROBIN[3], H. BRIL[2], N. TAMURA[4], J. SCHÄFER[5] AND G. BLANC[5]

[1]Université François Rabelais de Tours. UMR 6113 CNRS ISTO. Tours, France (*correspondence : cecile.grosbois@univ-tours.fr)
[2]Université de Limoges. EA GRESE IFR 145 GEIST. Limoges, France
[3]Université d'Orsay. LSCE, UMR CEA/CNRS 1572. Gif s/Yvette, France
[4]ALS, LBNL, Berkeley, California USA
[5]Université de Bordeaux 1. UMR 5805 CNRS EPOC. Talence, France

In a former gold mining district (Isle river basin, France), arsenic-bearing phases have been characterized in suspended particulate matter by in-situ techniques (EPMA, SEM-EDS/ACC system and synchrotron based μXRD) in order to describe the temporal dynamics of As at a particle scale during the solid transport.

The most frequent As-bearing phases but the least As-concentrated (0.10-1.58 wt% As) were aggregates of various fine clay particles (chlorite-phlogopite-kaolinite assemblage during the high flow and chlorite-illite- muscovite assemblage during the low flow). They were also associated to Fe-coatings and nano- to micro- particles of Fe oxyhydroxydes like goethite (0.18 - 0.45 wt% As, Fig. 1).

Iron and Mn oxyhydroxydes were the 2 other types of As-bearing phases (0.12-2.80 wt% As and 0.14-1.26 wt% As respectively), present as discrete particles. Their occurrence and in-situ concentrations varied throughout the hydrological cycle, according to their detrital or newly formed origins.

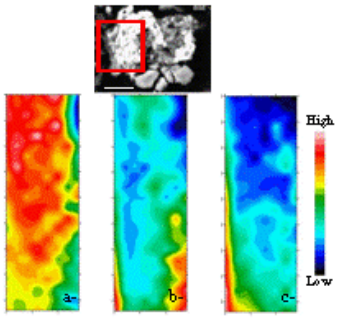

Figure 1: BSE image of a grain of Fe oxyhydroxyde associated to μ-XRD maps representing the relative abundance of a- goethite (4.18 Å), b- chlorite (7.07 Å) and c- muscovite (9.9 Å).

https://doi.org/10.1180/S0026461X00006502 Published online by Cambridge University Press

Birefringence mapping: A new *in situ* mass-loss technique for determining mineral solubilities

JULIANE GROSS[1]*, MICHAEL BURCHARD[2] AND WALTER V. MARESCH[3]

[1]Lunar and Planetary Institute, Houston TX 77058, USA (*correspondence: gross@lpi.usra.edu)
[2]Ruprecht-Karls Universität, 69120 Heidelberg, Germany
[3]Ruhr-Universität Bochum, 44801 Bochum, Germany

Data for the solubility of minerals in aqueous solutions at high pressures and temperatures are essential for our understanding of fluid properties, mass transport and growth/dissolution processes of minerals in Earth's crust and upper mantle. [e.g. 1-4].

Although a fairly extensive dataset is now available on the solubility of minerals in aqueous fluids at high pressures, most of the data above 0.5 GPa have been obtained by *ex situ* weight-loss quench methods in piston-cylinder presses [e.g. 5-7]. However, the uncertainties are generally large and difficult to quantify, because the resulting phase assemblages and product textures are characterized at post-experimental conditions. This can be problematic for the interpretation of the results if phase transitions, quench crystallization, incongruent dissolution or mechanical fragmentation occured.

We developed a new *in situ* mass-loss technique for hydrothermal diamond anvil cell experiments that uses the fact that crystals show birefringence in polarized light. Birefringence depends on the crystal's phase difference and its thickness. By measureing the phase difference at every point on a crystal, the thickness of the crystal at every such point can be determined and its surface area mapped. By multiplying the thickness of the crystal with its surface area its volume can be calculated. The mass of a crystal is then given by its volume multiplied by its density. With this method crystal masses less then a few µg can be determined

This new method combines the advantages of *ex situ* and *in situ* approaches, such as direct observation of the reaction path of the sample while circumventing their obvious disadvantages, such as quench problems.

[1] Wyllie P.J. (1979) *R.E. Krieger Pub. Co, New York*, 464 p.; [2] Manning C.E and Ingebritsen S.E. (1999) *Rev. Geophys.*, **37**, 127-150. [3] Manning C.E. (2004) *11th Proc. of Intern. Symp.*, 45-49. [4] Manning C.E. (2004) *Earth Planet. Sci. Lett.*, **223**, 1-16. [5] Manning C.E. (1994) *Geochim. Cosmochim. Acta,* **58**, 4831-483. [6] Newton R.C. and Manning C.E. (2006) *Geochim. Cosmochim. Acta,* **66**, 4165-4176. [7] Fockenberg *et al*., (2006) *Geochim. Cosmochim. Acta,* **70,** 1796-1806.

Antimony and arsenic behaviour upon microbial dissolution of mining waste

M. GRYBOS*[1], J. KIERCZAK[2], O. RAKOTOARISOA[1], A. COURTIN-NOMADE[1] AND H. BRIL[1]

[1]University of Limoges, GRESE Laboratory, FST, 123, avenue A. Thomas, 87060 Limoges Cedex, France (*correspondence: malgorzata.grybos@unilim.fr)
[2]University of Wroclaw, W. Cybulskiego 30, 50205 Wroclaw, Poland

In surface and sub-surface environment, microorganisms mediate dissolution and precipitation processes of minerals, and thus affect geochemical cycling of elements. Antimony (Sb) and arsenic (As) are considered to have comparable geochemical behavior and toxicity, both are redox sensible and toxic even at low concentrations. In natural environment, weathering of mining waste is one of the major source of contamination by metal(oid)s including Sb and As. Determination of biotic factors influencing Sb and As mobility is crutial to understand geochemical behaviour of these elements in environement.

In this study, we performed controlled incubations of mine tailings containing > 0.2% and 0.06% of Sb and As respectively under abiotic and biotic (phylogenetically divers heterotrophic bacteria) conditions to assess the role of bacteria on As and Sb release upon dissolution process. Role of microbes (biotic factor) was evaluated by comparing the amount of a given element released during biotic incubation to the amount of the same element released during abiotic incubation at the same pH value.

The results shown that all used bacteria were able to weather highly contaminanted solids. For a given pH value, the amount of released Sb and As varied between the strains and was from half-fold less to three-fold greater than under abiotic conditions. This indicates that complexing metabolites produced by bacteria play an important role in the overall dissolution process and may have accelerating or inhibiting effect on Sb and As release. Positives correlation coefficients of biotic factors between Sb and Fe ($R^2 = 1$), Ca ($R^2 = 0.58$), and Al ($R^2 = 0.999$) as well as negative correlation coefficients of biotic factors between As and Fe ($R^2 = 0.58$), Ca ($R^2 = 0.98$), and Al ($R^2 = 0.57$) sugest its different behaviour upon microbial dissolution.

In conclusion, heterotrophic bacteria influence Sb ans As geochemical pathway and mobility in environement.

https://doi.org/10.1180/S0026461X00006502 Published online by Cambridge University Press

Features of the pyrites in black shale series in Southern Anhui Province

YOUFEI GUAN[1,2], YONG ZHAN[1,2], HAIJIAO YOU[1,2], GUODONG SHI[2] AND MAOYAN MA[2]

[1]China Gezhouba Group Corporation, P.R. China (631677428@qq.com)
[2]Anhui University of Architecture, P.R. China

Black shale series in southern Anhui Province are located widely and belong to Lower Yangtze depression area, mainly developing the Sinian and Early-Middle Triassic sedimentary cover, late Yanshanian intrusions, and Indosinian-Early Yanshanian NE Jura-type folds and a series of the NE thrusting (sliding) nappe structure.

According to the crystal habit of the pyrite crystals in black shale series in southern Anhui Province, the pyrites can be divided into five crystal forms: {100} cube, {100}+{200} cube and pyritohedron combination, {111} octahedron, {210} pyritohedron and {210}+{111} pyritohedron and octahedron combination. The Co/Zn ratios of pyrites with various crystal forms are relatively low, mostly less than 0.15. The As content of the pyrite with {100} + {200} crystal form is the highest (120 ppm), and that of the pyrite with {111} crystal form is about 32 ppm on average that is many times higher than claystone's (6.6 ppm).

The Co/Zn ratios of sediments can distinguish their different sources. The Co/Zn ratio for hydrothermal origin is relative low, with value of 0.15 on average, and that in iron-manganese crust or concretion is about 2.5 in general. Therefore, the Co/Zn ratios can be used as a sensitive indicator to distinguish the source of sediments. The Co/Zn ratios of the pyrites from black shale series in southern Anhui Province suggests that the pyrites are derived from submarine hydrothermal fluid. As is an active element of hydrothermal fluid, so the As anomaly in sediments can be used as an indicator of submarine hydrothermal activity. The As values of the pyrites from black shale series in southern Anhui Province indicates that the pyrites have features of strong hydrothermal deposit.

Many studies suggest that hydrothermalism is the key for the formation of noble metal deposits in black shale series. This conclusion has been proved in Hunan-Guizhou. The pyrite's features and genesis indicate that the noble metals may enrich and even form deposit in black shale series in southern Anhui Province.

This research was financially supported by the Natural Science Foundation of Anhui Province Provincial Education Department of China (NO.KJ2010A070).

Mineral paragenesis and textural features of gneisses and amphibolites from Daday-Devrekani (Kastamonu, Turkey) Massif: Preliminary results

M.A. GUCER[1]* AND M. ARSLAN[2]

[1]Dept. of Geol. Eng., Gümüşhane Univ., 29100-Gümüşhane, Turkey (*correspondence: maligucer@gmail.com)
[2]Dept. of Geol. Eng., Karadeniz Tech. Univ., 61080-Trabzon, Turkey (marslan@ktu.edu.tr)

The Daday-Devrekani (Kastamonu, N Turkey) massif contains various metamorphic rocks ranging from Precambrian to Early Cretaceous in age [1]. NE part of the massif contains medium to high grade metamorphic rocks, called Devrekani Metamorphics [2], and divided into two sub-units; gneissic rocks of the lower parts and calcite marbles of the upper parts. In this study, gneissic and amphibolitic rocks of the massif were examined in terms of mineral assemblages and textural evidence of metamorphic P-T conditions. The gneissic rocks are biotite-hornblend, cordierite-biotite, sillimanite-biotite, sillimanite-cordierite-mica, sillimanite-garnet-mica, sillimanite-cordierite-garnet-mica, microcline-biotite, muscovite-microcline-biotite and sillimanite-garnet-cordierite-microcline-biotite gneisses. They contain quartz, K-feldspar (orthoclase, microcline), plagioclase, biotite, muscovite, sillimanite, cordierite, garnet, hornblend, sericite, Fe-Ti oxide, ±apatite, ±hematite, ±zircon, ±hercynite (?). The amphibolitic rocks contain hornblende, oligoclase-andesine, Fe-Ti oxide and ±orthoclase. The rocks exhibit grano-, lepidograno-, fibrolepidograno-, nemato-, nematograno-, lepidonemato- and porphyro- blastic textures. In some gneiss, there are pre-kinematic and syn-kinematic mineral growth, and cordierite porphyrpblasts containing sillimanite, hercynite (?) and garnet inclusions.

Possible mineral reactions in gneissic rocks are as (1) Muscovite + quartz → K-feld. + sillimanite + H_2O, (2) chlorite + muscovite (or chloritoid) + quartz → garnet + biotite + H_2O, (3) garnet + sillimanite + quartz → cordierite, (4) sillimanite + garnet → cordierite + hercynite, (5) biotite + sillimanite + plagioclase + quartz→garnet + cordierite + K-feld. + H_2O. Possible mineral reaction in amphibolites is albite + actinolite + epidote + chlorite → plagioclase (An>17) + hornblende. All these features suggest amphibolite facies P-T conditions.

[1] Boztuğ, D., and Yılmaz, O., (1995), *Geological Bulletin of Turkey,* Vol. **38**, No. 1,33-52, Ankara. [2] Yılmaz, O. and Tüysüz, O. (1984), *MTA Report* No: 7838 (unpublished), Ankara.

https://doi.org/10.1180/S0026461X00006502 Published online by Cambridge University Press

Dissolution rates of plagioclase feldspars as a function of solution composition

S. GUDBRANDSSON[1]*, D. WOLFF-BOENISCH[2], S.R. GISLASON[2] AND E. H. OELKERS[1]

[1]GET-Université de Toulouse-CNRS-IRD-OMP, 14 Avenue Edouard Belin, 31400 Toulouse, France (*correspondence: snorgud@hi.is)

[2]Institute of Earth Sciences, University of Iceland, Sturlugata 7, 101 Reykjavik, Iceland

Feldspars are the most abundant mineral in the Earth's crust and plagioclase is the most abundant of these feldspars. Plagioclase dissolution is therefore a major, and at times dominant, contributor to global weathering rates. It is therefore remarkable how little work has been performed to systematically characterize the dissolution rates of this mineral as a function its composition and the composition of the fluid phase.

Towards the improved characterization of the dissolution behaviour of the plagioclases in natural processes, the steady-state dissolution rates of 5 distinct plagioclase feldspars, spanning the compositional range from albite to anorthite, have been measured in mixed-flow reactors at 25 ºC as a function of pH from pH 2 to 11. Rates tend to exhibit a typical U-shape behaviour; rates decrease with increasing pH at acidic conditions, then increase with increasing pH at basic conditions. Similar to past work [1, 2] plagioclase dissolution rates increase with increasing An content at acidic conditions. In contrast, preliminary work suggests little effect of An content at basic pH.

Interpretation of the dissolution rates of the plagioclase feldspars is challenging because this mineral tends to consist of finely intergrown albite rich and anorthite rich phases. To address this challenge, measured rates have been interpreted assuming the dissolving plagioclase is a mechanical mixture of two distinct end-member feldspars similar to that done recently for the dissolution of crystalline basalt [3].

[1] Oxburgh, *et al*. (1994) *Geochim. Cosmochim. Acta* **58,** 661-669. [2] Oelkers & Schott (1995) *Geochim. Cosmochim. Acta* 59, 5039-5053. [3] Gudbrandsson *et al*. (2008) *Min. Mag*. **72,** 155-158.

^3H – ^3He isotopic tracer for age estimating of the ground waters (Aquifers of the Khibiny slopes, Kola Peninsula)

ANTON GUDKOV[1]*, IGOR TOLSTIKHIN[1] AND STANISLAV IVANOV[2]

[1]Russian Academy of Science, Kola Science Center, Geological Institute (*correspondence: Gantoris@rambler.ru, igor.tolstikhin@gmail.com)

[2]Russian Academy of Science, Kola Science Center, Institute of the North Industrial Ecology Problems (etostas@mail.ru)

To introduce the ^3H - ^3He method samplers of stainless steel and degassing of water, using the flow of water vapor through the capillary as a gas – carrier have been developed and made. When being pumped through the capillary almost all helium and neon (over 95%) is collected in the trap. At the same time gets not more than 0.5 grams of water (i.e. approximately 0.3% of the sample mass, Beyerle *et al*., 2000) gets in the trap. The extraction and purification processes take approximately 30 minutes. The water samples were taken from the bores located at the southern slope of the Khibiny mountains (the Kola peninsula). The picture shows the measured relations of ^3He / ^4He and ^{20}Ne / ^4He in the samples from water inlets "Centralniy" (the grey squares, the figures are numbers of the bores Kamensky *et al*., 1991) and "Klyuchevoy" (the grey circles). In these coordinates the mixture of young waters (the corresponding points, the square and the circle are located above the coordinates of the air saturated water, ASW) and the deep ancient waters (in the lower left corner of the graph, the radiogenic He is formed in enclosing rocks, and migrating from them, is accumulated in ground waters) is expressed in the straight line. Regression line extrapolation of the samples from the water inlet "Centralniy" (the black line on the graph) to the trend APB + $^3He_{TRI}$ gives ^3He / ^4He = 3, 65 × 10^{-6}. Concentration of the $^3He_{TRI}$ in the young water, $[^3He]_{TRI} = [^3He]_{MEASURED} \times \{(^3He / ^4He)_{YOUNG} - (^3He / ^4He)_{ASW}\}$ и $[^3H]_{MEASURED}$ = 30 TE gives 3H - 3He the age of 16. The intersection of the regression line and the line of accumulation of radiogenic helium (the black square in the circle) gives the parameters of ancient water, whose age is estimated as40,000 years old (Kamensky *et al*, 1991). In the case of water inlet "Klyuchevoy" ^3He / ^4He relations in ground waters are close to those in the ASW whereas ^{20}Ne / ^4He is slightly lower which indicates to an admixture of ancient waters. Supposing that these isotopic relations in ancient waters of the Khibiny southern slopes are close, one can build a line passing through the points corresponding to the ancient waters and waters from the water inlet "Klyuchevoy" (the black dotted line). Extrapolation of this line to the trend ASW + $^3He_{TRI}$ gives $(^3He / ^4He)_{YOUNG}$ = 1,65 × 10^{-6} a slightly higher value than the value of ASW.A small excess of ^{3}HeTRI along with a relatively low [3H] MOD = 12, TE correspond to the water age.

https://doi.org/10.1180/S0026461X00006502 Published online by Cambridge University Press

The use of magnetic susceptibility in forensic soils analyses

A. GUEDES*, H. RIBEIRO, H. SANT'OVAIA, A. RODRIGUES, B. VALENTIM, S. LEAL AND F. NORONHA

Centro de Geologia da Universidade do Porto e Departamento de Geociências, Ambiente e Ordenamento do Território, Faculdade de Ciências, Universidade do Porto, Rua do Campo Alegre 687, Porto, Portugal, (*correspondence: aguedes@fc.up.pt)

Magnetic parameters such as magnetic susceptibility (MS) are important in characterizing materials, and detectable quantities of magnetic and paramagnetic minerals are almost always found in soils, the magnetic susceptibility being the sum of all contributions from the forming minerals, and varying due to concentration and composition of those minerals. The MS measurements of soils at room temperature are non-destructive. Therefore, the same material is available for further analysis with any other technique. Additionally, does not require sample preparation, and can be used as a simple and fast method which may be operable in small samples. So, MS is an excellent tool for studies of soils being used as trace evidence in forensic investigations.

Magnetic susceptibility measurement methodology, discriminatory power, reproducibility and accuracy in analysis were tested on soil samples for its use in forensic applications. Seventeen soil samples were collected on several Portuguese sites surrounded by different lithologies. At each site, samples were manually collected from the surface soil with a plastic spade. The magnetic susceptibility was measured applying an external magnetic field of 300 A/m to the sample, and a Kappabridge, model KLY-4S of Agico balance equipped with the Sumean software was used. Tests were performed on each sample to establish the discriminatory power between similar and different geological and geographical origins; the measurement reproducibility within samples and along the time; the variation with sample quantity, size fractions and presentation method. Before each measurement, the equipment was calibrated, and regularly calibrated along the measurement period due to the repeated nature of the measurements carried out. Magnetic susceptibility was calculated in m^3/kg. It was observed that magnetic susceptibility can enable discrimination between soil samples, measured values are reproducible over time, and the analysis can be carried out in samples as small as 0.5 g.

This research was supported by Project PTDC/CTE-GEX/67442/2006 of FCT (Portugal).

Chemical and isotopic properties of airborne particles in industrial, urban and rural areas of the Rhine Valley

F. GUÉGUEN[1,2], P. STILLE[1], V. DIETZE[3] AND M. MILLET[2]

[1]Laboratoire d'Hydrologie et de Géochimie de Strasbourg, Université de Strasbourg/EOST, CNRS; 1 rue Blessig, F-67000 Strasbourg

[2]Equipe de Physico-Chimie de l'Atmosphère, Laboratoire des Matériaux, Surfaces et Procédés pour la Catalyse, Université de Strasbourg/ECPM, CNRS; 1 rue Blessig, F-67000 Strasbourg

[3]German Meteorological Service, Research Center Human Biometeorology; Stefan-Meier-Str.4. D-79104 Freiburg

In order to evaluate the past and actual air pollution, tree barks (biomonitoring) and airborne particulate matter (dp >2.5 μm) were collected around and within the industrial area of the cities of Strasbourg (France) and Kehl (Germany) situated on both sides of the river Rhine. Theses cities suffer from emissions of traffic and industries (steel plant, thermal power plant and waste incinerators) located in the industrial harbour.

Sr, Nd and Pb isotopic ratios measured on barks allowed to distinguish between various sources of pollution. Traffic emissions are the main contaminants in the urban areas of the cities, whereas local industrial emission plumes are distinguishable around and within the industrial harbour.

Organic and inorganic emissions were monitored during 9 months by Sigma-2 passive samplers as well as by passive air samplers with XAD-2 resin for PCB collection for actual air quality measurement in these environments. Sample sites were located in remote, rural and in urban areas, where different industrial emission plumes have been detected by tree bark biomonitoring.

Ambient aerosol collected in these different environments have similar trace element concentrations but the mass deposition rate is highest in the industrial zone. Enrichment factors (EF) $((X/Nd)/(X/Nd)_{UCC})$ are particularly high in Mn, Cr, Zn, Mo, Cd, and similar to EF measured in tree barks.

Isotopic ratios of the collected particles from different sampling sites allowed to distinguish between anthropogenic and natural sources. The dominating emission source in the industrial area is the steel plant as also demonstrated by the aerosols trace metal concentrations. Both organic and trace metal emissions are correlated, which allows the Sr and Nd isotopes to be a powerfull tool to trace the polluting sources.

https://doi.org/10.1180/S0026461X00006502 Published online by Cambridge University Press

Isotope fractionation during Fe translocation in plants grown with an artificial chelate

M. GUELKE-STELLING[1]* AND F. VON BLANCKENBURG[2]

[1]KIT, Inst. for Mineralogy and Geochemistry, D-76131 Karlsruhe (*correspondence: monika.stelling@kit.edu)
[2]GFZ Potsdam, D-14473 Potsdam (fvb@gfz-potsdam.de)

The determination of the plant-induced Fe-isotopic fractionation with multiple-collector ICP-MS is a promising tool to better quantify their role in the geochemical Fe cycle and possibly to identify the physiological mechanisms of Fe uptake and translocation in plants.

We show here that half of the entire range of Fe isotope variations detected to date on this planet (-2.5‰ in δ^{56}Fe) ocurrs when Fe is moved *within* a single plant. This finding extends that of an earlier study in which we found that strategy I plants, which rely on reduction of iron before uptake, were enriched in stable ^{54}Fe relative to ^{56}Fe when grown on soil. In contrast strategy II plants (grasses), which rely on chelation of Fe(III) by phytosiderophores before uptake, were slightly enriched in the heavier iron isotopes [1,2].

In our new study bean plants (strategy I) and oat plants (strategy II) were grown in a nutrient solution supplemented with Fe(III)-EDTA, and were harvested at three different ages. All parts of the plants during all growth stages were quantified for Fe amounts and isotope composition. Total bean plants, regardless of their age, were found to be enriched in the light iron isotopes by -1.2‰ relative to the growth solution throughout. However, during growth plants internally redistributed isotopes where young leaves increasingly accumulated the lighter isotopes whereas older leaves and the total roots were simultaneously depleted in light iron isotopes. For bean fruits, mass balance indicates that these obtain ca. 40% of their Fe from translocation within the plant (with δ^{56}Fe = -2.65‰), and 60% from the roots. Given that not all of this fruit Fe can be supplied by older leaves, the roots apoplast plays a major role as intermediate Fe store. Both apoplast Fe and tissue-bound Fe is remobilised by reduction – preferring the light Fe isotopes. In contrast, during growth of the oat plants the initial isotope ratio obtained during uptake is maintained in all organs at all growth stages, including the roots. Hence it can be assumed that both uptake and translocation of Fe in strategy II plants maintains the irons' ferric state, or that Fe is always bound to high-mass ligands, so that isotope fractionation is virtually absent in these plants.

[1] Guelke & von Blanckenburg (2007) *Env. Sc. Techn.* **41**, 1896-1901. [2] Guelke *et al.* (2010) *Chem. Geol.* **277**, 269-280.

The nitrogen isotopic composition of a Proteozoic microbial community

NUR GUENELI* AND JOCHEN J. BROCKS

Research School of Earth Sciences, The Australian National University, Canberra, A.C.T. 0200, Australia (*correspondence: nur.gueneli@anu.edu.au)

Nitrogen is an essential element for life, incorporated into fundamental components such as amino acids and DNA. The isotopes of nitrogen can be used to trace biogeochemical processes, yet, the use of this tool to reconstruct Precambrian environments is still in its infancy. Recent studies on nitrogen isotope fractionation in microorganisms [1,2] have significantly improved interpretations of paleorecords [3-5] and the use of nitrogen isotopes in combination with established biomarker techniques has now the potential to yield novel information about the succession of predominant primary producers through deep time.

The 1.64 Ga Barney Creek Formation (BCF), northern Australia, represents a marine succession deposited below wave base in the intracratonic McArthur Basin. The dolomitic shales of the BCF bear the oldest preserved, clearly indigenous molecular fossils [6]. Based on these biomarkers, the upper BCF marks a marine basin with anoxic, sulphidic, sulphate-poor and stratified waters inhabited by green and purple phototrophic sulphur bacteria (PSB) [7]. Evidence for these PSB disappears in deeper successions. However, it is currently under debate whether the lack of PSB derives from biological or thermal degradation, or a shift in ecological settings. Here, we will present ^{15}N and ^{13}C data in combination with biomarker analysis to test whether regime changes caused a shift in predominant primary producers in the McArthur Basin.

[1] Beaumont *et al.* (2000) *Org Geochem* **31**, 1075-1085. [2] Granger *et al.* (2008) *Geochim Cosmochim Ac* **74,** 1030-1040. [3] Thomazo *et al.* (2011) *Geobiology* **9**, 107-120. [4] Bauersachs *et al.* (2009) *Org Geochem* **40**, 149-157. [5] Beaumont & Robert (1999) *Precambrian Res* **96**, 63-82. [6] Summons *et al.* (1988) *Geochim Cosmochim Ac* **52**, 1747-1763. [7] Brocks *et al.* (2005) *Nature* **437**, 866-870.

https://doi.org/10.1180/S0026461X00006502 Published online by Cambridge University Press

Fluid inclusion analysis by laser ablation ICPMS: How consistent are element ratios?

MARCEL GUILLONG[1]*, THOMAS PETTKE[2] AND LEONID DANYUSHEVSKY[1]

[1]CODES, ARC Centre of Excellence in Ore Deposits, University ofTasmania, Private Bag 79, Hobart, TAS, 7001, Australia
(*correspondence: marcel.guillong@utas.edu.au)
[2]Institute of Geological Sciences, University of Bern, Baltzerstrasse 1 + 3, CH-3012 Bern, Switzerland

Analysis of fluid inclusions is a commonly used technique to obtain insights into fluid evolution and ore forming processes. Laser ablation ICPMS offers the possibility to analyse individual inclusions for a wide range of elements and certain isotope ratios, with low detection limits. Quantification of inclusion composition is commonly performed by normalising measured element signals to those of Na or Cl, which are used as internal standards, with their concentrations determined via micro thermometry.

Using a Resonetics M-50 laser probe which allows for analysis of fluid inclusion at depths up to several hundred microns, we observed that values of some element signal ratios change between shallow inclusions and deep inclusions by up to a factor of 2.5. This limits the accuracy of inclusion analysis at larger depth from the sample surface. The Cl/Na and the Pb/Na ratios were found to be affected the most. Ablating a scapolite sample with homogeneous Na, Pb and Cl concentrations showed very similar behaviour. Such strong fractionation behaviour of chlorine has not been reported to date for LA-ICPMS analysis. This may account for some of the scatter observed when analysing a series of individual fluid inclusions, as inclusions are commonly located at a range of depth below the surface. Results from two different brine assemblages will be presented and discussed.

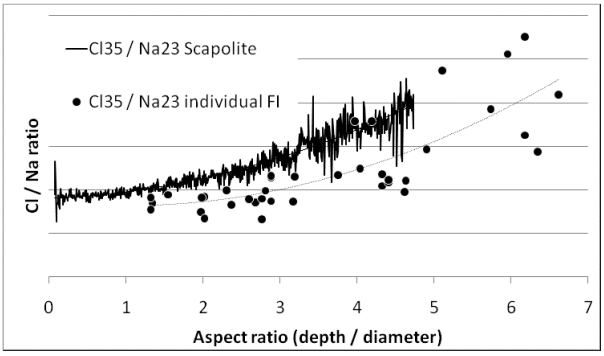

Figure 1: Aspect ratio dependent Cl/Na ratios for scapolite mineral and a fluid inclusion assemblage.

U-Pb SHRIMP and geochemical data of granitoids characterizing the evolution of shear zones in NE Brazil

I. P. GUIMARÃES[1]*, A.F. SILVA FILHO[1]; F.M.V. SILVA[2] AND R. ARMSTRONG[3]

[1]Depto de Geologia –UFPE
(*correspondence: ignez@ufpe.br)
[2]Geologia - UFPE, Petrobrás (francismiller@hotmail.com)
[3]RSES - Australian National University
(richard.armstrong@edu.edu.au)

A large volume of granitic magmatism associated with large scale shear zone and metamorphism under high-T conditions, characterize the Brasiliano/Pan African Orogeny in the Borborema Province, NE Brazil. Granitoids from two plutons and later dykes intruded along a large dextral sense E-W trending Shear Zone show distinct crystallization ages and geochemical signature. The oldest studied granitoids (U-Pb SHRIMP age of 618 ± 5 Ma), Serra de Inácio Pereira Pluton (SIPP), show high Ba (4440 to 6654 ppm) and Sr (2358 to 2962 ppm) and medium to high Zr (321 a 378 ppm), low Y (19 a 25 ppm) and Nb (14.7 to 17.0 ppm) contents. Their REE patterns are characterized by small or no negative Eu anomalies (Eu/Eu*= 0.92 – 1.15) and $(Ce/Yb)_N$ ratios ranging from 28.34 to 40.09. In contrast, the granitoids showing crystallization age of 563 ± 4 Ma, the Serra do Marinho Pluton (SMP) have low Sr (238 to 272 ppm), and high Zr (755 to 846 ppm) contents. The contents of Y (40 to 75 ppm) and Nb (9.0 to 51.0 ppm) are higher and the Ba (1660 to 1680 ppm) contents lower compared to the values recorded in the SIPP granitoids. Their REE patterns are characterized by negative Eu anomalies (Eu/Eu*= 0.39 – 0.59) and $(Ce/Yb)_N$ ratios ranging from 6.62 to 20.25. Later dykes of subvolcanic granitoids have crystallization ages of 527 ± 6 Ma and A-type geochemical signature. The SIPP granitoids are coeval with the peak of regional metamorphism and originated by melting of a paleoproterozoic source. The SMP show geochemical signature of post-collisional A-type granites and the later dykes have signature of A-type post-orogenic extension-related granitoids coeval with the deposition of small sedimentary basin.

https://doi.org/10.1180/S0026461X00006502 Published online by Cambridge University Press

Microbial diversity in Oylat Cave and their roles on biogeochemical cycling

YASEMIN GULECAL* AND MUSTAFA TEMEL

Istanbul University, Istanbul, Turkey
(*correspondence: ygulecal@istanbul.edu.tr)

The subsurface of the Earth is one of the major habitats and contains a significant proportion microbial life [1, 2]. However, our overall knowledge about the life forms and biogeochemical processes contained within it is rather scarce, mainly because of the difficulties in approaching this habitat. One relatively easy way to approach this habitat is to investigate karst terrains, which expand over ~20% of the Earth's subsurface [3]. Since caves are one of the most prominent features of karst terrain, they may serve as noteworthy entries and virtual "windows" into subsurface habitats [4]. Recent work has revealed interesting insights into the diversity and resilience of different life forms in caves may be revealed and how to recognize biosignatures for subsurface life on other planetary bodies [for example,5-6].

Our studying area which is Oylat Cave in Bursa (Turkey) has been developed at the intersection of two fault zones striking along WNW-ESE and NE-SW directions in recrystalized limestone unit of Permian-Triassic age. Clastics and carbonate sediments are in the Oylat Cave developed due to karstification. The aim of study was to investigate the microbial diversity and their roles of biogeochemical cycling.We have not only used the geochemical analyses but also genetic tools. In addition, this study reports the first microscopic investigations on the microbial communities encountered in the microbial biofilm Oylat Cave.

[1] Whitman *et al*., (1998). *Proc. Natl. Acad. Sci. USA* **95**: 6578–6583. [2] Roussel *et al*, (2008). *Science* **320**:1046 [3] Ford and Williams, (2007) *Karst Hydrogeology and Geomorp*. Wiley, New York. [4] Engel *et al*., (2009) *ISME J*. **4**(1): 98–110. [5] Boston *et al*., (2001) *Astrobiol. J*. **1**(1): 25–55. [6] Tewari *et al*., (2001) *I.C.T.P., Trieste, Italy*. Kluwer Academic, Dordrecht, pp. 251–254.

Geochronology of Cenozoic intrusive rocks of NW Anatolia: Topkaya-Eskişehir, Turkey

B. GÜLLÜ* AND Y.K. KADIOĞLU

Ankara Univ., Department of Geol., Eng., & YEBIM Ankara, Turkey (*correspondence: bgullu@ankara.edu.tr)

The intrusive rocks of Northwest Anatolia mainly exposed at Sivrihisar, Karakaya and Topkaya region of Eskisehir in Sakarya continent. Topkaya (Eskişehir) Granitoid is intruded into the metamorphic basement and obducted ophiolitic suite in the composition of granodiorite, monzogranite and cutting by felsic and mafic dykes. They have MME ranging from 1cm up to 60cm in sizes [1].

The ^{40}Ar /^{39}Ar age data reveal 44.30 ± 0.47 Ma for granodiorite of Topkaya granitoid. The isotopic ratio of granitoids and mafic dykes of the Topkaya have almost same $(^{87}Sr/^{86}Sr)_i$ and $\varepsilon_{Nd\ ratio}$ ($(^{87}Sr/^{86}Sr)_{i\text{-granodiorite}}$=0.705593-0.706133, $\varepsilon_{Nd\text{-granodiorite}}$= -0.6, -0.7; $(^{87}Sr/^{86}Sr)_{i\text{-mafic dyke}}$ =0.705677-0.705706, $\varepsilon_{Nd\ mafic\ dyke}$= -0.39, -0.4).

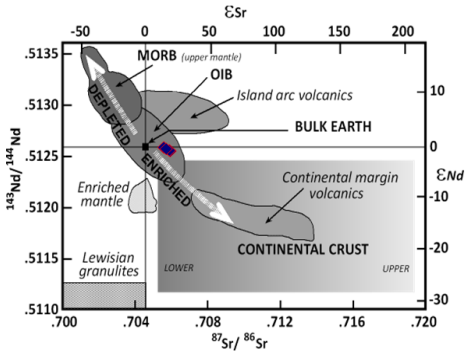

Figure 1: Isotope correlation diagram. The positions of the main tectonic environments and isotopic reservoirs taken from [2], [3], [4].

Discussion and Results

The ^{40}Ar /^{39}Ar age and geochemistry may be interpreted to reflect the time of magmatism since the level of emplacement was shallow enough such that rapid cooling would have occurred.

The granitoid exhibited initial rates $^{87}Sr/^{86}Sr$ always less to 0.708, suggesting represent I-type granites [5]. Sm-Nd data show distinct isotopic signatures, to the granitoid and mafic dykes. Both units exhibited εNd initials values clear negative, suggesting crustal contribution with mantle products in the source.

The authors wish to thank Ankara University for support BAP 09B4343016 Project.

[1] Güllü & Kadıoğlu (2010) IV. *Ulusal Jeokimya Sempozyumu* 55-56. [2] Zindler & Hart (1986) *Chemical Geodynamics* 493-571. [3] Faure (1986) PIG., **589**. [4] Rollinson (1993) UGD., **352**. [5] Chappell & White (1974) Two contrasting granite types, *Pac. Ged*. **8**, 173-4.

https://doi.org/10.1180/S0026461X00006502 Published online by Cambridge University Press

Hydrochemical properties of thermal waters in the Eastern Black Sea section

FATMA GULTEKIN*, ARZU FIRAT ERSOY AND ESRA HATIPOGLU

Karadeniz Technical University, Depaertment of Geological Engineering, 61080, Trabzon, Turkey (*correspondence: gultekinftma@hotmail.com)

The Ilıca (Artvin), Ayder and İkizdere (Rize) and Sarmaşık (Ordu) thermal waters are located Eastern Black Sea section. Thermal springs and thermal wells have temperatures ranging from 37 to 70°C. The pH values of the thermal waters change between 6.32 and 8.92. Thermal waters display various chemical compositions and high temperature waters have Na-SO_4, Na-HCO_3 and Na-Cl type. In the Ordu and Artvin area Late Cretaceous and Eocene aged volcanic rocks constitute reservoir and cap rocks. Late Cretaceous aged granite, granodiorite and monzonite rocks are reservoirs and cap rocks in the Rize geothermal system. The water-rock interaction has been investigated in this study. The thermal waters located rocks dominate region in the Gibbs Diagram. The chemistry of thermal water is controlled by weathering of minerals containing the rocks. According to chemical analysis basaltic rocks have higher Co, Sr, V, Cu, Pb, Zn, Ni and As content than granitic rocks. Especially Ilıca, İkizdere and Sarmaşık thermal waters have high As, B, Ba, Br, Fe, Li, Rb, Cs and Zn concentration. Compare with Rare Earth Elements (REE) content rocks and thermal waters La, Ce, Nd and Pr are immobile elements for Ayder and Sarmasık thermal waters. Ilıca and İkizdere thermal waters are similar to REE content.

Duofuton mafic volcanic suite at northeastern margin of the Qing-Tibet plateau: Its age, geochemistry and tectonic implications

A. GUO, X. HU, Y. GUO, C. ZHANG AND L. ZHANG

State Key Lab of Continental Dynamics/Department of Geology, Northwest University, Xian 710069, China (anlingxb@nwu.edu.cn)

Located at the northeastern margin of the Qinghai-Tibet Plateau, the Duofuton volcanics belong to a Na-rich and mafic volcanic suite. The suite has yielded an age of 96.21±2.10 Ma by the whole-rock $^{40}Ar/^{39}Ar$ method, indicating a magmatic product in early Late Cretaceous time.

The rocks are characterized by the (La/Yb_N) ratios of 6~11, ΣREE of 117, enrichment in incompatible elements. The Nb/U and Ce/Pb ratios are 30 and 17 on average, respectively.

The $^{87}Sr/^{86}Sr$ ratios of the samples are 0.7041~0.7069, $^{143}Nd/^{144}Nd$ =0.5129 ($\varepsilon_{Nd(t)} = 6$) and $\Delta^{207}Pb/^{204}Pb$ and $\Delta^{208}Pb/^{204}Pb$ =11 ~ 19 and 73~84. Coupled with high $^{87}Sr/^{86}Sr$ ratios, they show Dupal anomalies. The rocks are OIB-like in nature and their source region exhibits mixture between DM and EMII, while some samples are contaminated by continental crust. The complexity of the OIB-like rocks may have inherited from the proto- and paleo-Tethyan mantle in the region and is possibly not related to materials of eastward extrusion from the plateau. Compared with the contemporaneous volcanics in the area, it can be inferred that the mantle region below at the northeastern margin is heterogeneous. The development of the volcanic activity in the area could be triggered by the distance effect from the initial collision between the Eurasian Plate and a microcontinent in northwest Indian Plate.

https://doi.org/10.1180/S0026461X00006502 Published online by Cambridge University Press

Using Mössbauer spectra to characterize and differentiate tourmaline crystals from China

Y. GUO[1], S.Y. YANG[2]*, J.H. MIN[1], L.J. WANG[1] AND Y.B. XIA[1]

[1]School of Materials Science and Engineering, Shanghai Uni., Shanghai 200072, China,
[2]State Key Lab. of Marine Geology, Tongji Uni., Shanghai 200092, China (*correspondence: syyang@tongji.edu.cn)

Tourmaline is a valuable crystalline raw material notable for its piezoelectric and pyroelectric properties. It is also regarded as precious stones in jewlry industry. Tourmaline occurs in almost all types of geologic circumstances and coexists with numerous minerals. Consequently, chemical variation of tourmaline is tightly related with its crystal structure and physical properties which provides important constraints on the origin of tourmaline. Mössbauer spectra analysis has been playing an important role in the detailed study of isomorphic substitutions in tourmaline crystal by Fe^{2+} and Fe^{3+} and the distribution of these ions over distinct crystallographic positions. Nevertheless, the traditional researh on Mössbauer parameter of tourmaline crystals has great uncertainty in the determination of the valance states and occupation types by the expecience values.

In this contribution, the multi-statistic method of cluster analysis was used to effectively determine the Mössbauer spectra and examine microscopic structures of Fe ions in different tourmaline crystals from Guangxi, Hebei, Neimeng and Xingjiang Provinces where have much variable geologic background. The determined assignment corresponds well with previous documented results. We observed four kinds of distribution styles of iron (Fe) ion in the measured tourmaline samples, which distinctly occupy four zones in the diagram of isomer shift and quadrupole splitting. The tourmaline crystals from Guangxi, Hebei and Neimeng are characterized by similar Mössbauer spectra bearing three doublets, which correpand to Fe^{2+}(Y), Fe^{2+}(Z) and Fe^{3+}(Y) sites with two kind of valances respectively. In comparison, only two doublets appear in the Mössbauer spectrum of Xinjiang tourmaline, and the Fe ions having bivalence states occupy Fe^{2+}(Y) and have a neighborhood effect in the Y-Z site. Our study on Mössbauer spectra together with scanning electronic microprobe analysis clearly suggests these tourmaline crystals sourced from different areas have variable compositions and crystalline structures indicative of their different origins.

This work is supported by Supported by NSFC (Grant No: 60676002, 41076018) and Shanghai Municipal Education Commission, Shanghai, China (Grant No:06AZ007)

Long term aerosol trends over large global urban centres

PAWAN GUPTA[1,2]*, MAUDOOD N. KHAN[2] AND ARLINDO DA SILVA[1]

[1]NASA Goddard Space Flight Center, Greenbelt, MD, USA (*correspondence: pawan.gupta@nasa.gov)
[2]Universities Space Research Association, Huntsville, AL, USA (maudood.n.khan@nasa.gov, arlindo.dasilva@nasa.gov)

Aerosol Optical Depth (AOD) retrieved from MODIS and MISR sensors onboard EOS Terra satellite over the last decade (2001-2010) has been utilized to analyze aerosols trends over global megacities. Analysis provides an assessment of retrieval capabilities of these sensors. Level 2 data sets have been carefully analyzed over selected urban centers to understand the retrieval capabilities of these two sensors over complex urban surfaces. Areas over each urban center have been identified, where MODIS operational algorithm is unable to retrieve AOD due to limitation of dark target approach. MISR aerosol product has been used to identify dominating aerosol size distribution and type, as function of seasons. Spatial gradient in AOD within and around the city has been estimated as well. Impact of spatial and temporal averaging over long term trends will also be addressed.

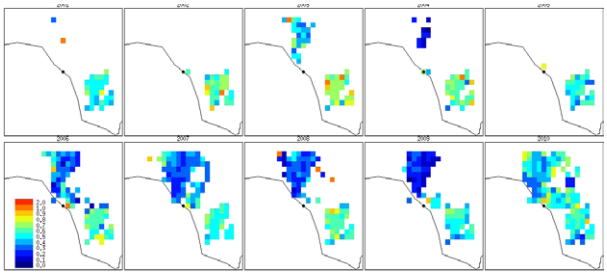

Figure 1: Annual mean aerosol optical depth from MODIS (Terra) over Karachi, Pakistan for 2001 to 2010.

https://doi.org/10.1180/S0026461X00006502 Published online by Cambridge University Press

Conduit-scale to localized degassing in ascending magmas: Insights from Cl measurements in Vesuvius 79AD pumice

L. GURIOLI[1], T. SHEA[1]*, E. HELLEBRAND[1] AND J.E. HAMMER[1]

[1] LMV, Univ. Blaise Pascal, Clermont-Fd, France
[2]SOEST, Univ. Hawaii, 1680 East-west rd., Honolulu, HI, 96822, USA (*correspondence tshea@hawaii.edu)

During the ascent and decompression of magmas that fed the 79AD eruption, melts experienced a complex vesiculation history [1]. Both textural evidence from tephra and conduit ascent modelling suggest that velocity gradients affect the ascending magma column and cause spatial variations in degassing [2]. Localized shearing is one of the dominant mechanism through which these velocity gradients can be accommodated during ascent [3]. These shear zones can enhance bubble connectivity and provide pathways for volcanic gases. Here, we present chemical evidence for spatial degassing variations at the scale of the conduit as well as at localized scale. Because Cl diffuses slower than H_2O during ascent, it records a different portion of the magma's history. Figure 1 below shows Cl increases within denser more degassed zones in 79AD pumice clasts. Through textural observations of vesicles as well as Cl and H_2O measurements within pumice glass from various phases of the 79AD eruption, we derive a general conduit model that involves the birth, development, and death of shear-zones.

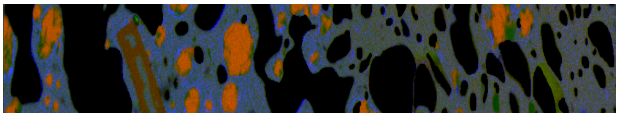

Figure 1: Compositional map (Cl=blue, K=red, Si=green) made in 79AD pumice. Cl increases towards the denser zone richer in large collapsed vesicles (left) likely due to degassing of H_2O. Image width ~ 0.5mm.

[1] Shea *et al*. (2010), *J. Volcanol. Geotherm. Res* **192**, 69-84. [2] Sable *et al*. (2006), *J. Volcanol. Geotherm. Res* **158**, 333-354. [3] Wright *et al*. (2009), *Geology* **37**, 1023-1026.

Soil source contribution estimation mation of Arsenic and Lead in atmospheric precipitaion at urban industrial area, Raipur, Central India

BALAKRISHNA GURUGUBELLI AND SHAMSH PERVEZ

School of Studies in Chemistry, Pt. Ravishankar Shukla University, Raipur, INDIA. 492010

The components and quantities of atmospheric dust fallout have been reported to be the pollution indicator of large urban areas. The multiplicity and complexity of sources of atmospheric dusts in urban regions has put forward the need of source apportionment of these sources indicating their contribution to specific environmental receptor. The study presented here is focused on investigation of soil source contribution estimates of Arsenic and lead in urban dust fallout in an urban-industrial area, Raipur, India. Source-receptor based representative sampling plan using longitudinal study design has been adopted. Source apportionment has been done using Chemical Mass Balance (CMB 8). Dominance of coal fired industries sources on arsenic levels measured at selected ambient residential receptors compared to line sources has been observed. Road-traffic has shown highest contribution of dust at indoor houses and out door-street automobile exhaust has shows highest contribution for arsenic. The results of CMB output and regression data of source-receptor dust matrices have shown comparable pattern.

https://doi.org/10.1180/S0026461X00006502 Published online by Cambridge University Press

Calcium isotopes in Martian meteorites

N. GUSSONE[1], T. MAGNA[1] AND K. MEZGER[2]

[1]Universität Münster, Germany (Nikolaus.Gussone@uni-muenster.de, tomas.magna@uni-muenster.de)
[2]Universität Bern, Switzerland (klaus.mezger@geo.unibe.ch)

Mass-dependent fractionation of Ca isotopes at high temperatures has long been considered minor; consequently, Ca isotopes have mostly been used to study low-temperature processes [1,2]. Here we report high-precision Ca isotope data for a suite of Martian meteorites revealing a $\delta^{44/40}$Ca variation of ~0.4‰ among shergottites, nakhlites, chassignites and orthopyroxenite. Calcium isotope ratios of Martian crust generally fall into the range of terrestrial basalts but tend to be slightly heavier than Earth's crust. $\delta^{44/40}$Ca exhibits no clear relationship with modal contents of olivine, plagioclase and/or pyroxene although pyroxene is the main Ca carrier in the mantle [3]. No systematic behavior is observed between individual groups of shergottites, despite the range in element depletion/enrichment, suggesting a lack of Ca isotope fractionation imparted by different degrees of melting. $\delta^{44/40}$Ca of 1.06 in orthopyroxenite ALH 84001 is in the mantle range whereas low $\delta^{44/40}$Ca in NWA 2737 may reflect the presence of carbonate minerals. Nakhlites mostly have distinctive $\delta^{44/40}$Ca similar to terrestrial plume basalts [4], supporting the derivation of nakhlites from a Martian mantle plume. Whether this difference is directly linked to the dominance of clinopyroxene (with generally lower $\delta^{44/40}$Ca) in nakhlite lavas or is an intrinsic feature of nakhlite mantle source remains to be solved. Nevertheless, Ca appears to evolve distinctively different isotope ratios in plumes and mantle rocks, providing evidence for resolved Ca isotope fractionation at magmatic temperatures.

Collectively, the new data suggest $\delta^{44/40}$Ca ~1.0–1.1 for the bulk silicate Mars. This is identical to an estimate of the Earth's upper mantle [3] and suggests broadly similar processes for mantle melting in the interiors of Mars and Earth, independent of time constraints on the activity of mantle dynamics. Unlike other stable isotope systems, the bulk Ca isotope composition of Earth and Mars differs from enstatite chondrites [5,6]. Thus, they are probably not the major building material for Earth and possibly also not for Mars.

[1] Gussone *et al*. (2006) *Geology* **34**, 625-628; [2] Heuser *et al*. (2005) *Paleoceanography* **20**, PA2013; [3] Huang *et al*. (2010) *EPSL* **292**, 337-344; [4] Amini *et al*. (2009) *GGR* **33**, 231-247; [5] Simon & DePaolo (2010) *EPSL* **289**, 457-466; [6] Simon *et al*. (2009) *ApJ* **702**, 707-715

Lead(II) sorption to soil materials – Binding heterogeneity and influence of phosphate

J.P. GUSTAFSSON[1], C. TIBERG[2], A. EDKYMISH[1] AND D.B. KLEJA[3]

[1]KTH (Royal Institute of Technology), Department of Land and Water Resources Engineering, Teknikringen 76, 100 44 Stockholm, Sweden. (gustafjp@kth.se)
[2]Swedish University of Agricultural Sciences, Department of Soil and Environment, Box 7014, 750 07 Uppsala. (Charlotta.Tiberg@slu.se)
[3]Swedish Geotechnical Institute, Kornhamnstorg 61, 111 71 Stockholm. (Dan.Berggren.Kleja@swedgeo.se)

Lead (Pb) is a common pollutant, but still the environmental behaviour of lead is incompletely known. Attempts to simulate the binding of lead(II) to soils by use of geochemical models have usually underestimated lead binding with about one order of magnitude.

Here, new evidence will be presented about some key mechanisms that can explain the failure of most previous modeling attempts. First, the adsorption of Pb^{2+} to ferrihydrite, an important Pb^{2+} sorbent in soils, is shown to be very strong, particularly at low Pb^{2+} / ferrihydrite ratios. Second, the sorption of Pb^{2+} to ferrihydrite is greatly enhanced in the presence of phosphate. The effect is stronger than that predicted by electrostatic interactions only. The mechanisms involved are being studied with spectroscopic methods.

Third, data will be presented that show that the sorption of Pb^{2+} to solid-phase organic matter, especially mor layer material, is much stronger than that of fulvic or humic acid, which are often used as model compounds for solid-phase organic matter. Apparently, Pb^{2+} is strongly bound to a non-humic organic fraction of the solid-phase organic matter, but the mechanism by which this occurs remains obscure. Taken together, these observations may explain the often observed deviation between model and reality concerning lead(II) binding.

https://doi.org/10.1180/S0026461X00006502 Published online by Cambridge University Press

Lack of a late deglacial carbonate compensation signal in the intermediate depth Amundsen Sea

M. GUTJAHR[1,2]*, D. VANCE[1], J.W.B. RAE[1], G.L. FOSTER[2], C.D. HILLENBRAND[3] AND G. KUHN[4]

[1]Bristol Isotope Group, Department of Earth Sciences, University of Bristol, Queens Road, Bristol BS8 1RJ, UK (*correspondence: marcus.gutjahr@noc.soton.ac.uk)
[2]School of Ocean and Earth Science, National Oceanography Centre, Southampton, UK
[3]British Antarctic Survey, High Cross, Madingley Road, Cambridge CB3 0ET, UK
[4]Alfred Wegener Institute for Polar and Marine Research, Am Alten Hafen 26, 27568 Bremerhaven, Germany

The Southern Ocean (SO) is an important component in deglacial ocean circulation- and climate change. Ice core-derived temperature and atmospheric pCO_2 records show a deglacial rise as early as 17.9 ka [1, 2], thereby leading Northern Hemisphere warming by about three thousand years [3]. The atmospheric CO_2 rise occurred alongside increasing bioproductivity around Antarctica, providing evidence that reinvigorated upwelling of Circumpolar Deep Water (CDW) around Antarctica led to large-scale degassing of Dissolved Inorganic Carbon (DIC) stored in the glacial deep ocean [4].

Changing CDW circulation patterns should also find their expression in variable CDW DIC/alkalinity relationships. In broad terms, the release of previously deep-sea stored DIC to the atmosphere should leave deglacial CDW more alkaline until the excess alkalinity is removed from the water column. To test this hypothesis we have measured the boron isotopic composition (expressed in $\delta^{11}B$) of calcitic scleraxonian cold-water corals sampled in intermediate water depths in the Amundsen Sea (~123°W, ~69°S, 2500 m to 1430 m water depth). We will present an assessment of the genus-specific biological fractionation (c.f. [5, 6]) alongside fossil-coral $\delta^{11}B$ values dating back to the Antarctic Cold Reversal. Our corals appear to be internally homogenous and modern samples have only slightly elevated $\delta^{11}B$ compared to that of ambient intermediate water borate ion. We find that modern and early Holocene coral display fairly constant $\delta^{11}B$ compositions, whilst deglacial coral $\delta^{11}B$ are slightly elevated. This suggesty that the deglacial evolution of the deep Southern Ocean carbonate system is more complicated than a simple degassing and carbonate compensation model may indicate.

[1] Monnin *et al*. (2001) *Science* **291**, 112-114. [2] Lemieux-Dudon *et al*. (2010) *QSR* **29**, 8-20. [3] Blunier & Brook (2001) *Science* **291**, 109-112. [4] Anderson *et al*. (2009) *Science* **323**, 1443-1448. [5] Hönisch *et al*. (2004) *GCA* **68**, 3675-3685. [6] Krief *et al*. (2010) *GCA* **74,** 4988-5001.

The emergence of metabolism: Prebiotic simulations of shallow sea hydrothermal vents

MARCELO I. GUZMAN

Department of Chemistry, University of Kentucky, Lexington, KY 40506, USA (marcelo.guzman@uky.edu)

The origin of metabolism has been one of the most challenging and intriguing issues in the origin of life research. All known carbon fixation pathways used by living organisms, including the reductive tricarboxylic acid cycle, share at least one common intermediate [1]. The implications are that 1) all carbon fixation mechanisms are linked, and 2) a prebiotic mechanism of carbon fixation should have used some of the key organic compounds that participate in central anabolism today. The prebiotic system should have implemented the core reactions involved in central metabolism abiotically and nonezymatically [2]. The model is based on sulfur-containing semiconductor minerals, *in situ* produced in a shallow sea hydrothermal vent [3]. The advantage of the model is to use free energy from sunlight photons to drive otherwise unviable reactions in the absence of enzymes using photocatalysts.

Current work examines the origin of metabolism in a simulated prebiotic shallow water hydrothermal vent. Zinc sulfide (ZnS, sphalerite) was used as a candidate mineral to jumpstart the origin of metabolism in chemoautotrophs. Photochemical reactions of simple organic compounds with carbon dioxide occur at the semiconductor interface. The experimental results show the production of C2, C3, C4, C5, and C6, intermediates of central metabolism [4]. Starting from CO_2, and by consecutive reactions, we observed formate, acetate, oxalate, glyoxylate, glycolate, lactate, pyruvate, succinate, α-ketoglutarate, and isocitrate. The mechanism provides a way to capture energy from the environment while producing carbon feedstock useful in anabolism. The results of this study suggest that central metabolites could have participated in a viable enzyme-free cycle for carbon fixation in a shallow sea hydrothermal vent, where light, sulfide minerals, carbon dioxide, and other organic compounds interacted on the prebiotic Earth to generate an autonomous chemical cycle [5].

[1] Guzman & Martin (2010) *Chem Commun* **46**, 2265. [2] Wächtershäuser (1988) *Microbiol Rev* **52**, 452. [3] Guzman & Martin (2008) *Int J Astrobiology* **7**, 271. [4] Morowitz *et al*. (2000) *Proc Natl Acad Sci USA* **97**, 7704. [5] Guzman & Martin (2009) *Astrobiology* **9**, 833.

https://doi.org/10.1180/S0026461X00006502 Published online by Cambridge University Press

Melt inclusions in coexisting perovskite, nepheline, magnetite and clinopyroxene in pyroxene melilitolite from Kerimasi Volcano, Tanzania

T. GUZMICS[1]*, R.H. MITCHELL[2], M. BERKESI[1], C. SZABÓ[1] AND R. MILKE[3]

[1]Lithosphere Fluid Research Lab, Institute of Geography and Earth Sciences, Eötvös University Budapest, 1117 Pázmány Péter sétány 1/C, Budapest, Hungary (correspondence: tibor.guzmics@gmail.com)
[2]Lakehead University, Thunder Bay, ON P7B 5E1, Canada
[3]Free University, Habelschwerdter Allee 45, 14195 Berlin, Germany

We studied melt inclusions in pyroxene melilitolite from Kerimasi volcano, Tanzania. Primary silicate melt and fluid inclusions were entrapped in perovskite, magnetite, nepheline and clinopyroxene, however, perovskite usually enclosed multiphase melt inclusions containing both silicate and carbonatite melt (Fig. 1).

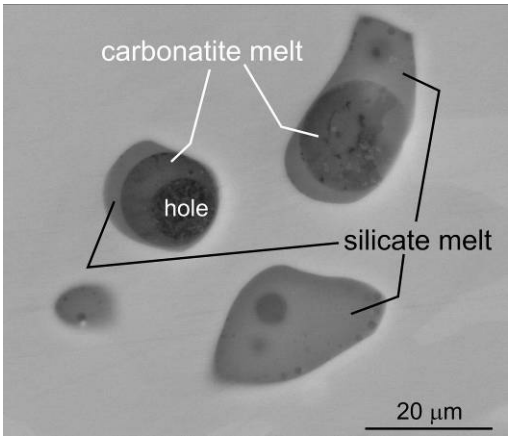

Figure 1: Quenched melt inclusions containing immiscible melts in perovskite after heating to 1050 ºC.

High temperature heating experiments on melt inclusions show minimum homogenization temperatures at 1040 ºC in clinopyroxene and at 1050 ºC in nepheline and perovskite, which correspond to actual crystallization temperature. Nevertheless, in many cases, heterogeneous entrapment of melts and fluid prevented complete homogenization of melt inclusions. We applied furnace technique in order to produce homogenous melt(s). Melt compositions indicate an earlier formation of this rock than Kerimasi calciocarbonatite.

CO_2 sequestration and hydrothermal basalt alteration at 40-250 °C

A. P. GYSI* AND A. STEFÁNSSON

Institute of Earth Sciences, University of Iceland, 101 Reykjavik, Iceland (*correspondence: apg2@hi.is)

In order to gain insight into the geochemical processes associated with CO_2 mineralization and sequestration in basalts, a series of CO_2-water-basaltic glass reaction path experiments and numerical simulations were performed at 40-250 °C and initial pCO_2 of 0-20 bar, and the water chemistry and the secondary minerals studied as a function of reaction progress.

At 40-75 °C, the addition of CO_2 changes the water-basalt reaction path considerably. At low reaction progress (pH <6.5), the pH was buffered by CO_2 ionization, consumption of protons (H^+) by the dissolving basaltic glass and proton consumption-release upon secondary mineral formation. The stable mineralogy consisted of Ca-(Mg)-Fe clays, amorphous SiO_2 and Ca-(Mg)-Fe-(Mn) carbonate (ankerite) solid solutions. The moles of carbonates and SiO_2 per moles dissolved basaltic glass was observed to increase at elevated pCO_2, whereas the amount of clays forming decreased. At high reaction progress (pH >8), the pH was buffered by the basalt alteration and secondary mineral formation and dissolved silica ionization. The stable mineral assemblages consisted of Mg-Fe clays, zeolites and Ca-Mg carbonates.

At 150-250 °C, the secondary mineral assemblages formed during the experiments where similar to those observed in natural geothermally altered basalts, and consisted of amorphous SiO_2, mixed Mg-Fe smectites/chlorite, zeolites and calcite. The amount of clays and a basaltic glass surface alteration layer increased in thickness with temperature, coating sometimes the entire basaltic glass surface. At 250 °C, the clay compositions were generally closer to chlorite and the basaltic glass completely altered after ~50 days, whereas at 150 °C a thin alteration layer was observed after ~125 days reaction time.

The dissolution of basaltic glass in CO_2-rich waters was found to be incongruent with the overall water composition and secondary mineralogy depending on pH, reaction progress and temperature. Competing reactions between clays (Ca-Fe smectites) and carbonates at low pH, and zeolites and clays (Mg-Fe smectites) and carbonates at high pH, control together the availability of Ca, Mg and Fe, playing a key role for CO_2 mineralization and sequestration into basalts [1, 2].

[1] Gysi & Stefánsson (2008) *Min. Mag.* **72**, 55-59. [2] Gysi & Stefánsson (2011) *submitted to Geochim. Cosmochim. Acta.*

https://doi.org/10.1180/S0026461X00006502 Published online by Cambridge University Press

Sediment melt flux into the melting zone of the Northernmost Tonga island arc

KARSTEN M. HAASE, MARCEL REGELOUS AND CHRISTOPH BEIER

GeoZentrum Nordbayern, Friedrich-Alexander-Universität Erlangen-Nürnberg, Erlangen, Germany (haase@gzn.uni-erlangen.de)

The lavas from the northernmost islands Tafahi and Niuatoputapu in the Tonga island arc are long known to differ in terms of composition from rocks from the central and southern volcanoes of this arc. The differences are believed to reflect either the influence of plume-type mantle from Samoa or the subduction of OIB-material from the Louisville Seamount Chain. Although the distance between the two islands is only 8 km we find significant differences between the lavas. Compared to lavas from the central Tonga arc the Tafahi-Niuatoputapu basaltic lavas have relatively high SiO_2 contents at a given MgO but are highly depleted in heavy rare earths, Ti and Zr, thus resembling boninites. This implies a highly depleted mantle wedge composition beneath the northern Tonga arc.

Radiogenic isotope variations indicate that binary mixing of different slab components occurs in the melting zones beneath each island. The Niuatoputapu lavas have slightly U-shaped REE patterns with significant negative Ce anomalies that are less pronounced in the lavas from Tafahi. The Ce anomaly probably reflects a prevailing influx of sedimentary components. Most samples also show superchondritic Nb/Ta indicating residual rutile in the sedimentary component. This component also has relatively high Pb isotope ratios and most likely represents a partial melt of subducted volcaniclastic sediments from the Louisville Seamount Chain. The sedimentary component mixes with a hydrous fluid from altered mid-ocean ridge basalts. Seismic studies show that the slab beneath the northern Tonga arc is only about 70 km deep which may lead to the prevailing influence of sediment melts relative to fluids from altered basaltic crust.

Subduction and exhumation of the UHP Western Gneiss Region: Petrology, structural geology, and LASS petrochronology

BRADLEY R. HACKER* AND ANDREW R.C. KYLANDER-CLARK

University of California, Santa Barbara, 93106-9630 (*correspondence: hacker@geol.ucsb.edu)

The Western Gneiss Region of Norway is one of Earth's two giant UHP terranes, with eclogites distributed across an area ~150 x 200 km. A new LASS petrochronology dataset of more than 200 samples now rivals structural, petrological, and $^{40}Ar/^{39}Ar$ datasets in richness and information content. The half of the WGR that is close to the foreland shows weak Caledonian deformation and preserves Precambrian Sm-Nd garnet ages, Precambrian U-Pb zircon ages, partially reset U-Pb titanite ages, 398–397 Ma U/Th-Pb monazite ages, and muscovite $^{40}Ar/^{39}Ar$ ages that decrease monotonically away from the foreland from 400 to 390 Ma.

The hinterland portion is variably deformed and preserves three distinct UHP domains that are marked by 420–400 Ma Lu-Hf and Sm-Nd eclogite ages, 418–407 Ma Sm-Nd garnet ages from HP gneiss, 425–405 Ma monazite U/Th-Pb ages from garnet-stable gneiss, 430–415 Ma U-Pb zircon ages from HP gneiss, 407–392 Ma U-Pb zircon ages from exhumation-related leucocratic intrusions, 405–394 Ma U/Th-Pb monazite ages from post-UHP gneiss, 400–398 Ma U-Pb zircon ages from post-UHP gneiss, 395–381 Ma U-Pb rutile ages, and 390–375 Ma muscovite $^{40}Ar/^{39}Ar$ ages. In general, coherence among the age gradients defined by the different isotopic systems indicates simple east-directed exhumation. In detail, however, differences among the ages within the three UHP domains indicate juxtaposition of the central and northern UHP domains against the southern UHP domain after titanite and rutile closure and prior to muscovite closure.

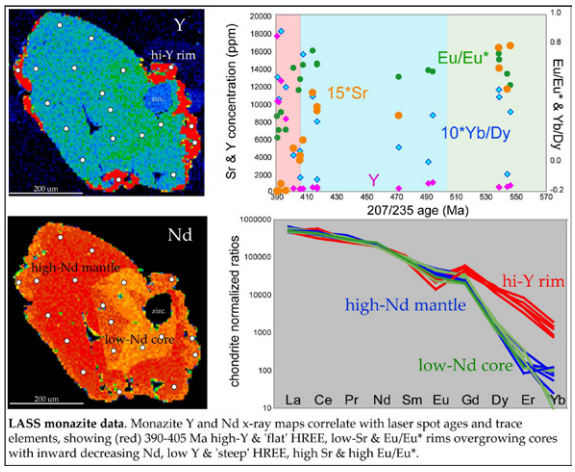

LASS monazite data. Monazite Y and Nd x-ray maps correlate with laser spot ages and trace elements, showing (red) 390-405 Ma high-Y & 'flat' HREE, low-Sr & Eu/Eu* rims overgrowing cores with inward decreasing Nd, low Y & 'steep' HREE, high Sr & high Eu/Eu*.

https://doi.org/10.1180/S0026461X00006502 Published online by Cambridge University Press

Sources and sinks of acetate in an acidic peatland

ANKE HÄDRICH[1], VERENA HEUER[2], MARTINA HERRMANN[1], KAI-UWE HINRICHS[2] AND KIRSTEN KÜSEL[1]

[1]Aquatic Geomicrobiology Group, Dept. Ecology, University of Jena, D-07743 Jena, Germany, (kirsten.kuesel@uni-jena.de)

[2]Organic Geochemistry Group, Dept. of Geosciences and MARUM Center for Marine Environmental Sciences, University of Bremen, P.O. Box 330 440, D-28334 Bremen, Germany, (vheuer@uni-bremen.de)

Acetate in anoxic environments originates from fermentation of organic matter or the reduction of CO_2 using the acetyl-CoA pathway (acetogenesis). As a key intermediate acetate is consumed by various anaerobic microorganisms which complicates unraveling its turnover in pore waters. This study aimed to i) determine proportions of acetate forming processes via stable carbon isotope analysis of acetate and ii) to identify the acetogens in an acidic fen (pH ~4.8) located in northern Bavaria, Germany. Assessing the functional *fhs* gene involved in the acetyl-CoA pathway revealed sequences of potentially novel acetogens like a phylotype related to *Eggerthella* present only in surficial soil layers. The presence of active acetogens in peat soil was suggested by ^{13}C-depleted acetate (-37‰ vs VPDB) in H_2/CO_2 supplemented microcosms compared to acetate with -14‰ vs VPDB in an unsupplemented control. Peat pore water profiles showed acetate concentrations from 0-170 μM with δ^{13}C values of -17.4‰ up to -3.4‰ vs VPDB. The ^{13}C-enrichment of acetate relative to peat TOC (-26‰ vs VPDB) suggested the predominance of sinks which are preferentially consuming ^{12}C-acetate. Depth profiles of $\delta^{13}C_{CH4}$ point towards acetoclastic methanogenesis as a sink for acetate prevailing mainly in the upper fen soil layers. Additionally, iron and sulphate reduction appeared to play a role in acetate turnover at this acidic fen.

The variability in formation water composition and the implications for CO_2 storage conditions

R.R. HAESE[1]* AND M. PREDA[2]

[1]CO2CRC and Geoscience Australia, GPO Box 378, Canberra ACT 2601, Australia (*correspondence: ralf.haese@ga.gov.au)

[2]Geological Survey of Queensland, Department of Employment, Economic Development and Innovation, Brisbane QLD, Australia (micaela.preda@deedi.qld.gov.au)

Background and motivation

The prediction of CO_2 storage conditions and safety requires a range of informtion. The emphasis of this study is the composition of formation water and its control on the long-term distribution of injected CO_2 and the different CO_2 trapping mechanisms in the reservoir. Formation water composition was compiled for basins from the USA, Canada, Norway, Germany and Australia and the data was then used to make inferences on a) the density-driven convection of fluid due to differences in the CO_2 concentration, b) CO_2 solubility (fluid trapping) and c) long-term fluid-rock reactions leading to the immobilization of CO_2 (mineral trapping).

Preliminary results

The reported formation water composition is highly variable between basins with total dissolved solid (TDS) concentrations ranging from 340 to 355,000 mg/L. The lowest TDS concentrations are in the drinking water range and are found in Australian basins, while the highst concentrations are found in formations in near proximity to salt deposits. The CO_2 solubility decreases by approximately 50% from lowest to highest TDS concentrations. The fluid density increase due to CO_2 saturation follows an exponential function with the highest density increase in freshwater. The latter leads to significantly more rapid convective mixing. The combined effect of higher solubility and more rapid convection means a more effective CO_2 trapping in the fluid and its downward transport in reservoirs with low TDS fluids. The prediction of CO_2 mineral trapping capacity is dependant on the water and mineral composition in the reservoir. Examples for differences in mineral trapping capacity with variable water and mineral composition will be given.

https://doi.org/10.1180/S0026461X00006502 Published online by Cambridge University Press

Effect of process conditions on the biological selenate reduction and selenium particle production

S.P.W. HAGEMAN*, R.D. VAN DER WEIJDEN, J. WEIJMA AND C.J.N. BUISMAN

Wageningen University, Sub-dept. of Environmental Technology. Bornse Weilanden 9, 6708 WG Wageningen, The Netherlands, P.O. Box 17, 6700 AA Wageningen (*correspondence: Simon.Hageman@wur.nl)

Objective and methods

Diverse microorganisms can reduce selenate to elemental Se. Elemental Se particle properties are determined by the Se production mechanism and kinetics. The effect of the used bacterial mixed culture, temperature, Se oxyanion and electron donor concentration on Se particle size, shape, sedimentation rate, and purity was investigated.

Experiments were performed in a pH and T controlled fed-batch system. The feed contained 25mM Se oxyanions and the electron donor was lactate or ethanol.

Results and discussion

SEM pictures of the Se precipitates showed that it was possible to affect the Se particle properties (needles to spheres) by varying process parameters.

The mechanism of Se precipitation was also investigated to determine whether the reaction is direct bio-mineralization or a combination of direct and indirect bio-mineralization. A possible two step mechanism is suggested.

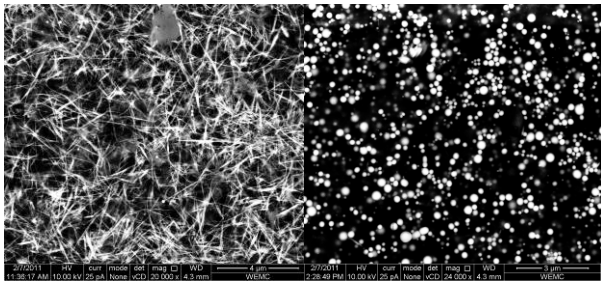

Figure 1: SEM-photos of the Se precipitates. The picture on the left shows Se needles, the scalebar in the lower right corner is 4μm. The picture on the right shows Se spheres, the scalebar in the lower right corner is 3μm.

Atomic environment of Y in silicate melts from molecular dynamics and x-ray absorption spectroscopy

V. HAIGIS*, S. SIMON, M. WILKE AND S. JAHN

German Research Centre for Geosciences, Telegrafenberg, 14473 Potsdam, Germany (*correspondence: haigis@gfz-potsdam.de)

Trace element partitioning strongly depends on major element composition of the involved phases. Whereas the influence of crystal chemistry is well described by the lattice strain model [1], the role of melt composition and structure is still poorly understood. In experiments with immiscible silicate melts, Schmidt *et al*. [2] observed partitioning of Y and rare earth elements into the more depolymerized (silica-poor) melt, where the tetrahedral network is partially destroyed. An explanation of these findings in terms of atomic-scale structure is still missing.

We performed molecular dynamics (MD) simulations to investigate the local environment of Y as a trace element in different silicate melts of the system CaO-Al_2O_3-SiO_2. The interactions between atoms were described by a new polarizable ion model which also captures many-body effects and was parametrized non-empirically, using density functional theory data as a reference. As a result, we found a systematic dependence of the atomic-scale structure around Y on melt polymerization, which can be quantified by means of the ratio of non-bridging oxygen to the network forming cations Si and Al (NBO/(Si+Al)): Upon increasing NBO/(Si+Al) from 0.0 to 1.9, the coordination of Y by O drops from 7.7 to 6.2, and the average Y-O distance decreases from 2.56Å to 2.46Å. Moreover, using the method of thermodynamic integration, we obtained first results for the exchange coefficient (ratio of partition coefficients) $D_Y^{melt1/melt2}/D_{Al}^{melt1/melt2}$ of Y and Al between two melts.

To validate our structural findings, we performed a joint theoretical and experimental study on extended x-ray absorption fine structure (EXAFS) spectra of Y in silicate melts. These spectra contain information about the coordination of Y and distances to neighbouring atoms. Traditionally, a structural model is refined until the measured spectrum is satisfactorily reproduced. However, for amorphous systems it is often difficult to make an appropriate guess for the structure, and hence we propose a converse approach. We modelled EXAFS spectra by averaging over many MD snapshots, and the agreement with experimental spectra confirms that our model faithfully reproduces the atomic-scale environment of Y.

[1] Blundy & Wood (1994), *Nature* **372**, 452-454 [2] Schmidt *et al*. (2006), *Science* **312**, 1646-1650

https://doi.org/10.1180/S0026461X00006502 Published online by Cambridge University Press

A deglacial ^{14}C budget

M.P. HAIN[1]*, D.M. SIGMAN[1] AND G.H. HAUG[2]

[1]Department of Geosciences, Guyot Hall, Princeton University, Princeton, New Jersey 08544 (*correspondence: mhain@princeton.edu)
[2]Geological Institute, Department of Earth Sciences, ETH Zürich, Zürich 8092, Switzerland

Using the simplest possible model, an ocean split into upper (32%) and deep (63%) plus biosphere/atmosphere (5%), we construct a best estimate LGM ^{14}C budget based on ocean and atmospheric $\Delta^{14}C$ measurements. This budget is consistent with the estimates for the production-based global ^{14}C inventory during the LGM. Since the inferred ^{14}C ventilation ages for the mid-depth and deep ocean are significantly older than pre-industrial, some combination of sluggish LGM ocean overturning and greater surface reservoir ages is implicated. However, this budget leaves little room for a sizable, severely ^{14}C deplete Mystery Reservoir in the deep LGM ocean.

Given this preliminary LGM budget, it is very difficult, yet possible, to explain some of the deglacial observations by simple redistribution of ^{14}C from the upper ocean into the deep ocean. Specifically, the modest deglacial $\Delta^{14}C$ decline of southern-sourced mid-depth waters [1,2] can be accounted for by rising $\Delta^{14}C$ in the deep Southern Ocean [3]. However, for the Heinrich stadial 1, most records show constant or modestly decreasing planktic-benthic $\Delta^{14}C$ difference, suggesting a decline in the absolute $\Delta^{14}C$ of the deep ocean [4-6]. If these observations collectively reflect global deep ocean $\Delta^{14}C$, then (a) an imbalance between deglacial production and decay of ^{14}C, (b) the addition of ^{14}C-dead geologic carbon, and/or (c) a substantial deepening of the thermocline are required to close the deglacial budget. These alternative mechanisms would also significantly contribute to the deglacial 190‰ decline in atmospheric $\Delta^{14}C$.

[1] De Pol-Holz *et al*. (2010) *Nature Geosc*. doi:10.1038/NGEO745. [2] Rose *et al*. (2010) *Nature* doi:10.1038/nature09288. [3] Skinner *et al*. (2010) *Science* doi:10.1126/science.1183627. [4] Robinson *et al*. (2005) *Science* doi:10.1126/science.1114832. [5] Galbraith *et al*. (2007) *Nature* doi:10.1038/nature06227. [6] Broecker *et al*. (2008) *EPSL* doi:10.1016/j.epsl.2008.07.035.

The lithium isotopic signature of carbonatites

R. HALAMA[1,2]*, W.F. MCDONOUGH[2], R.L. RUDNICK AND K. BELL

[1]SFB 574, University of Kiel, 24105 Kiel, Germany (*correspondence: rh@min.uni-kiel.de)
[2]Department of Geology, University of Maryland, College Park, MD 24072, USA
[3]Department of Earth Sciences, Carleton University, Ottawa, Canada, K1S 5B6

Carbonatites are mantle-derived intraplate magmas that provide a means of monitoring the chemical secular evolution of the Earth's mantle [e.g., 1]. Speculations that mantle-derived rocks may record secular lithium (Li) isotopic variations as Li is progressively recycled into the mantle [2] have been fueled by the diverse Li isotopic composition of subducted sediments and basaltic ocean crust. The Li isotopic composition of carbonatites reflects their mantle source because there is no, or very little, Li isotope fractionation during their differentiation [3] and partial melting. A correlation is expected between recycled materials and Li isotopic anomalies, if a) non-mantle-like Li is introduced to the mantle through subduction [2], or b) Li isotopic heterogeneities are generated kinetically in the mantle by diffusion from subducted, Li-rich materials [4]. Li isotopic compositions of Archean to Recent carbonatites from several continents (δ^7Li = +4.1±1.3; n=23) overlap the range typical for modern mantle-derived rocks (MORB and OIB) and show no variation with time [5]. If the mantle sources of carbonatites are related to subduction and recycling of oceanic lithosphere, as suggested by some studies [e.g., 6], we see no evidence for this in terms of their Li isotopes, suggesting that neither of the two conditions above hold and that one or both of the following is true: a) the bulk composition of subducted material does not deviate greatly from the average mantle value (δ^7Li = +4±2), in agreement with a bulk δ^7Li of +3.1 for a typical subducting oceanic slab [7], b) crustal Li is effectively homogenized upon subduction into the mantle [5]. Alternatively, carbonatites may derive from primitive or depleted mantle sources, which have not been influenced by crustal recycling.

[1] Bell & Blenkinsop (1987) *GCA* **51**, 291-298. [2] Elliott *et al*. (2004) *EPSL* **220**, 231-245. [3] Halama *et al*. (2007) *EPSL* **254**, 77-89. [4] Vlastélic *et al*. (2009) *EPSL* **286**, 456-466. [5] Halama *et al*. (2008) *EPSL* **265**, 726-742. [6] Nelson *et al*. (1988) *GCA* **52**, 1-17. [7] Marschall *et al*. (2007) *EPSL* **262**, 563-580.

https://doi.org/10.1180/S0026461X00006502 Published online by Cambridge University Press

Origin of vesuvianite-bearing ultramafic layers from the Raspas Complex, Ecuador

R. HALAMA[1]*, I.P. SAVOV[2], D. GARBE-SCHÖNBERG[1] AND T. TOULKERIDIS[3]

[1]SFB 574, University of Kiel, 24098 Kiel, Germany (*correspondence: rh@min.uni-kiel.de)
[2]School of Earth and Environment, University of Leeds, Leeds LS2 9JT, United Kingdom
[3]Center of Geology, Volcanology and Geodynamics, Escuela Politécnica del Ejército, Quito, Ecuador

Serpentinized ultramafic rocks from the Raspas Complex (Ecuador) are spatially associated with eclogites and high-pressure metapelites and assumed to have experienced similar peak P-T conditions (1.8-2.0 GPa at 600 °C) [1,2]. Their compositions vary from low Al_2O_3 (<1wt.%) typcial for harzburgites to high Al_2O_3 (up to 15 wt.%) and CaO (up to 16 wt.%) contents. Some of the Ca-rich ultramafic layers contain pargasitic amphibole, vesuvianite and, very rarely, relicts of Ca-rich garnet. The aim of this study is to test whether the hydrous ultramafic assemblages can provide P-T estimates that confirm, or disprove, peak P-T conditions similar to the associated eclogites. Moreover, the origin of the layers in terms of mantle processes vs. fluid influx during subduction zone metamorphism will be evaluated.

Pseudosection calculations using the THERIAK software reveal that vesuvianite has, for most compositions, a wide stability field in P-T space. However, to stabilize Ca-rich garnet in the garnet-bearing sample, temperatures in excess of 550°C are required. This points to peak P-T conditions overlapping those of the eclogites and hence a similar subduction path.

For the Ca-rich ultramafic layers, the elevated Al_2O_3 and CaO contents and correlations between Ni and MgO are similar to pyroxenite layers in orogenic ultramafic massifs [3]. Chondrite-normalized REE patterns have La_N/Yb_N ratios <1, suggesting derivation from a depleted source, similar to the Al-poor peridotites [2]. Initial Sr isotope ratios (0.7025-0.7028) also point to a depleted mantle signature without significant effects of alteration or subduction zone metasomatism. These observations, combined with up to 10x chondritic REE abundances, indicate that these ultramafic layers represent former pyroxenite layers within an orogenic peridotite massif.

[1] Gabriele *et al*. (2003) *Eur. J. Mineral.* **15**, 977-989. [2] John *et al*. (2010) *Contrib. Mineral. Petrol.* **159**, 265-284. [3] Downes (2007) *Lithos* **99**, 1-24.

En echelon volcanic chains at hotspots as probes of the deep mantle

P.S. HALL[1]*, S. HUANG[2] AND M.G. JACKSON[1]

[1]Department of Earth Sciences, Boston University, Boston, MA 02043, USA (*correspondence: phall@bu.edu)
[2]Department of Earth and Planetary Sciences, Harvard University, Cambridge, MA 02138, USA

Systematic differences have been identified in the isotopic composition of lavas from the geographically distinct Loa and Kea trend volcanoes at Hawaii, with lavas from the southern (Loa) trend having higher $^{208}Pb^*/^{206}Pb^*$ and lower ε_{Nd} than lavas from the northern (Kea) trend [1,2]. This inter-trend difference has been interpreted as reflecting geochemical zonation within the conduit of the Hawaiian plume. Here we report on the existence of similar inter-trend isotopic differences in lavas from both the Samoa and the Marquesas hotspots. As with Hawaii, both of these hotspots are located on the Pacific plate and feature volcanism organized into en echelon trends. In Samoa, lavas from the southern (Malu) trend are found to have higher $^{208}Pb^*/^{206}Pb^*$ and lower ε_{Nd} than lavas from the northern (Vai) trend. Similarly, lavas from the southern (Motu) trend in the Marquesas have higher values of $^{208}Pb^*/^{206}Pb^*$ at a given value of ε_{Nd} than lavas from the northern (Nuku) trend volcanoes. In addition, the average isotopic compositions of lavas from these three hotspots show a geographic variation on a large scale that is consistent with the inter-trend. In particular, the southernmost hotspot (Samoa) has the highest $^{208}Pb^*/^{206}Pb^*$ and lowest ε_{Nd} while the northernmost hotspot (Hawaii) has the lowest $^{208}Pb^*/^{206}Pb^*$ and the highest ε_{Nd}.

Geodynamic models have demonstrated that the azimuthal distribution of heterogeneity within the thermal boundary layer (TBL) at the base of a plume is preserved within the plume conduit itself [3]. We propose that the observed inter-trend and inter-hotspot isotopic variations reflect the large-scale distribution of heterogeneities within the TBL at the base of the mantle, from which the respective plumes originate. Comparison of the observed isotopic compositions to seismic shear-wave velocity (v_s) in the lowermost mantle [4,5] at these locations reveals that the high $^{208}Pb^*/^{206}Pb^*$, low ε_{Nd} component correlates well with the large region of low v_s known as the Pacific superplume.

[1] Abouchami *et al*. (2005) *Nature* **434**, 851-856. [2] Huang *et al*. (2005) *Geochem. Geophys. Geosyst.* **6**, Q11006. [3] Farnetani and Hofmann (2009) *Earth Planet. Sci. Lett.* **282**, 314-322. [4] Panning and Romanowicz (2006) *Geophys. J. Int.* **167**, 361-379. [5] Ritsema *et al*. (2011) *Geophys. J. Int.* **184**, 1223-1236.

https://doi.org/10.1180/S0026461X00006502 Published online by Cambridge University Press

Hydrogen, carbon, nitrogen and xenon depletion in terrestrial planets

ALEX N. HALLIDAY

Department of Earth Sciences, Oxford University, South Parks Road, Oxford, OX1 3AN, UK (alexh@earth.ox.ac.uk)

The $^{40}Ar/^{36}Ar$ of MORB, OIB and well gases can be used to calculate the degree of degassing of primordial ^{36}Ar from the total mantle as sampled, which can be shown to be >95% and was probably nearer to 99% given evidence for ^{36}Ar recycling. On this basis a minimum primordial ^{20}Ne budget of $(2\text{-}7)\times10^{13}$ kg can be calculated from upper mantle estimates assuming the lower mantle is if anything less degassed, and this is close to the atmosphere's 6×10^{13} kg. A similar calculation for Xe using upper mantle estimates yields minimum degassing of 3×10^{10} kg primary ^{130}Xe, again close to the atmosphere's 9×10^{10} kg. There is no evidence that the atmospheric pattern is fractionated relative to mantle. The primordial ^{3}He budget can be calculated in the same way and an overall composition derived for the bulk silicate Earth's noble gases (BSE = total Earth minus core). When combined with updated budgets for ^{1}H, ^{12}C, ^{14}N, Earth's composition correlates with that in chondrites. The noble gases ^{3}He, ^{20}Ne, ^{36}Ar and ^{84}Kr in particular are in chondritic proportions and provide evidence against models based on fractionated solar components. Relative to CI chondrites they are more abundant by 1 to 2 orders of magnitude than ^{1}H, ^{12}C, ^{14}N and ^{130}Xe. Normalised to CI chondrites carbon and nitrogen are the most depleted elements in the BSE. Venus and Mars display a similar primordial pattern (excluding ^{1}H and ^{3}He). This reproducible feature cannot be explained with combinations of diverse protolith materials. For example, enstatite and CI chondrites have similar relative proportions of volatiles. Therefore, it appears that there was early removal of ^{1}H, ^{12}C, ^{14}N and ^{130}Xe relative to ^{3}He, ^{20}Ne, ^{36}Ar and ^{84}Kr. The present day budgets of carbon and nitrogen in Venus and Earth are strikingly similar, and similar in C/N to the budgets in Mars and CI chondrites providing evidence that they were subsequently replenished as veneers in proportion to planetary mass. More than half of Earth's water predates this veneer assuming a CI hydrogen budget. The mechanisms for preferential removal of ^{1}H, ^{12}C, ^{14}N and ^{130}Xe are unclear. They might all be depleted by core formation. Carbon, nitrogen and xenon also form low temperature species with first ionization potentials less than that of hydrogen. Therefore, depletion and possibly also xenon isotopic fractionation may relate to ionisation from solar EUV in the inner circumstellar disk [1].

[1] Zahnle *et al*. (2007) *Space Science Reviews* **129**, 35-78.

Partitioninig of hydrogen between plagioclase and basaltic melt

M. HAMADA, M. USHIODA AND E. TAKAHASHI

Dept. Earth & Planet. Sci., Tokyo Institute of Technology, Tokyo 152-8551, Japan (hamada@geo.titech.ac.jp)

The hydrogen in nominally anhydrous minerals (NAMs) can be an indicator of H_2O in silicate melts if the partitioning behavior of hydrogen between NAMs and melts is known. Plagioclase is one of the NAMs and igneous plagioclase accommodates hydrogen as OH [1]. We will report preliminary experimental results on the partitioning of hydrogen between Ca-rich plagioclase and arc basaltic melt.

Hydrous melting experiments of basaltic magma were carried out at 350 MPa using internally-heated pressure vessel. Starting material was powdered hydrous basaltic glass (50.5% SiO_2, 18.1% Al_2O_3, 4.9% MgO) with 1 to 4 wt.% H_2O. A grain of Ca-rich plagioclase (about 1 mg, An_{95}) and 10 mg of powdered glass were sealed in a $Au_{80}Pd_{20}$ alloy capsule and kept at temperature slightly above crystallization temperature of plagioclase as a liquidus phase, in order to attain near equilibrium between plagioclase and melt. Oxygen fugacity during the experiments was estimated to be 3 log unit above Ni-NiO buffer. Experiments were terminated after 24 hours, which is long enough to attain equilibrium partitioning of hydrogen between plagioclase and melt. Concentration of H_2O in melt and concentration of OH in plagioclase was analyzed using FT-IR [2].

Linear correlation between H_2O concentration in melt and OH concentration in plagioclase is recognized. Obtained partition coefficient is ≈ 0.008 in molar basis, which is higher than the estimated partition coefficient using H_2O in dacitic melt inclusions and hydrogen in their host plagioclase, ≈ 0.004 [3]. This difference in partition coefficients between basaltic system and dacitic system may be explained by difference in crystallization temperature of plagioclase; we suggest that partition coefficient of hydrogen is higher at higher temperature. We are conducting further experiments to prove this hypothesis.

[1] Johnson & Rossman (2004) *Am. Mineral.* **89**, 586-600. [2] Johnson & Rossman (2003) *Am. Mineral.* **88**, 901-911. [3] Johnson (2005) *GCA* **69**, A743 (Goldschmidt Conference Abstracts 2005).

https://doi.org/10.1180/S0026461X00006502 Published online by Cambridge University Press

Microbial arsenic transformation associated with soda lake in Khovsgol, Mongolia

N. HAMAMURA[1]*, T. ITAI[1], N. DAMDINSUREN[2], A-L. REYSENBACH[3] AND W.P. INKEEP[4]

[1]CMES, Ehime Univ., Matsuyama, Ehime 790-8577, Japan (*correspondence: nhama@ehime-u.ac.jp)
[2]Nat. Univ. of Mongolia, Ulaanbaatar, 14201, Mongolia
[3]Portland State Univ., Portland, OR 97201, USA
[4]Montana State Univ., Bozeman, MT 59717, USA

Soda lakes are extreme habitats characterized by high pH, high salt content, and elevated concentrations of trace elements from volcanic origin. To gain insight regarding the role of microorganisms in the geochemical cycling of arsenic (As), we characterized the bacterial community associated with a soda lake in northern Mongolia. Geochemical analysis of the salt evaporites present in lakeshore soils showed elevated concentrations of Se, As, phosphate and nitrate (pH >8.5). Microbial populations present in the same samples were investigated using molecular methods (16S rRNA and functional genes involved in As transformation) and culturing approaches to isolate relevant organisms involved in As transformation. Bacterial 16S rRNA gene sequences recovered from soda lake sediments and soils were affiliated with halophilic alkaliphiles, including *Bacillus* and *Halomonas* spp. Dissimilatory arsenate reductase genes (*arrA*) were detected, and formed a distinct phylogenetic clade suggesting the presence of unique arsenate-reducing bacterial populations. Pure cultures of *Alkaliphilus*- and *Halomonas*-related organisms were obtained and both showed capabilities for As transformation. The *Halomonas*-related isolate contains a gene similar to anaerobic arsenite oxidase (*arxA*) recently identified in the haloalkaliphilic, arsenite-oxidizing *Alkalilimnicola ehrlichii* strain MLHE-1. These results demonstrate that indigenous microorganisms associated with soda lake environments are capable of As cycling and contribute to the speciation and mobility of As *in situ*.

A new depleted mantle end-member revealed by high resolution sampling along the Mid-Atlantic Ridge

CÉDRIC HAMELIN[1]*, ANTOINE BEZOS[2], LAURE DOSSO[3], JAVIER ESCARTIN[1], MATHILDE CANNAT[1] AND CATHERINE MEVEL[1]

[1]IPGP, 1 rue Jussieu, 75252 Paris cedex 05, France (*correspondence: hamelin@ipgp.fr; escartin@ipgp.fr; cannat@ipgp.fr)
[2]LPGN, UMR 6112, 2 rue de la Houssiniere, 44322 Nantes, France. (antoine.bezos@univ-nantes.fr)
[3]CNRS, UMR 6538, IFREMER, 29280 Plouzané, France (laure.dosso@univ-brest.fr)

New samples from the center of Lucky Strike segment along the Mid-Atlantic Ridge define an atypical correlation, significantly different from the mantle array. This trend is characterized by radiogenic values of $^{177}Hf/^{176}Hf$ for a given $^{143}Nd/^{144}Nd$. Similar anomalous $^{177}Hf/^{176}Hf$ data have already been reported along Mohns and Knipovich ridge [1], and near Ascension Island [2]. In order to explain this atypical signature, these studies have proposed respectively: a disequilibrium melting during garnet breakdown and an anomalous mantle source created by an ancient melting event with residual garnet. Based on our new sampling, we propose a simple petrogenetic model for Lucky Strike basalts. This model allows us to reconsider the two hypotheses for Hf isotopes anomalous values. It reveals an unusual refractory component in the mantle near the Azores.

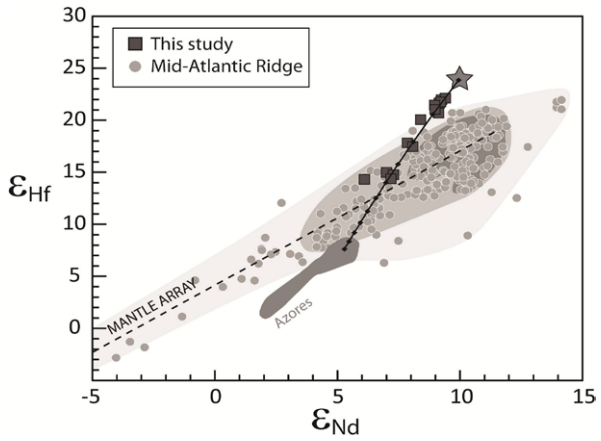

[1] Blichert-Toft *et al*. (2005), *Geochemistry Geophysics Geosystems,* **6**(1), Q01E19. [2] Paulick *et al*. (2010), *Earth and Planetary Science Letters* **296**, 299–310.

https://doi.org/10.1180/S0026461X00006502 Published online by Cambridge University Press

Developments in Noble Gas mass spectrometry

D. HAMILTON*, J.B. SCHWIETERS, D. TUTTAS, M. KRUMMAN, M. DEERBERG, N.S. LLOYD

Thermo Fisher Scientific, Hanna-Kunath-Str. 11, 28199 Bremen, Germany
(*correspondence: Doug.Hamilton@ThermoFisher.com)

Recent advances in ion optics and electronic design have added features to the new range of Noble Gas mass spectrometers from Thermo Fisher Scientific that will enable the scientific community to resolve a number of existing analytical limitations.

The first development relates to detector technology. Because instrument transmission and ion source efficiency can be very high, detector noise can be the limiting factor for ultra-small sample analysis. Faraday cup detectors are the detectors of choice for high accuracy and high precision isotope ratio measurements because of their unmatched stability and linearity and because of the electronic cross calibration network available to precisely and accurately cross calibrate the multiple Faraday detector channels against each other.

Today, most IOMS systems are equipped with current amplifiers using a 10^{11} Ohm resistor coupled to the feedback loop of a high stability and temperature-stabilized operational amplifier.

In this paper we will describe our latest investigations in Faraday cup measurements utilising 10^{12} & 10^{13} resistors for signal intensities in the range of 1 pA to 1 fA.

The second development relates to a new beam deflection technology added to the new ARGUS VI mass spectrometer that enables a fixed collector array to be given some of the properties of a mechanically adjustable array. This enables multi-dynamic multi-collector measurements to be taken utilising a fixed array thus enabling the end user to perform vital detector cross-calibrations “in run”.

Lastly we will describe early results on a new high resolution platform and the capabilities of this platform to finally deal with certain isotopic interferences in both the Argon and Neon spectra.

Martian surface geochemistry from MGS TES: Evidence of global-scale dissolution of olivine from basalts

VICTORIA E. HAMILTON[1]* AND A. DEANNE ROGERS[2]

[1]Southwest Research Institute, Boulder, CO 80302, USA; (*correspondence: hamilton@boulder.swri.edu)
[2]Stony Brook University, Stony Brook, NY 11794-2100 USA

Previous studies of MGS TES-derived major element oxides have found relatively high SiO_2 abundances, interpreted as being due to the presence of high-silica weathering phases in basaltic materials [e.g., 1]. Our derivation of major element chemistry from TES is not substantially different than that obtained in previous studies. However, we have applied new and different approaches to analyzing the data in terms of primary and secondary compositions and draw additional conclusions for the weathering history of the Martian surface.

The molar proportions of Al_2O_3, $CaO+Na_2O+K_2O$, and FeO+MgO can be indicative of weathering trends and the global TES data plot along a line that is consistent with the trend measured in Gusev crater. In Gusev, this trend is attributed to olivine dissolution at low water-to-rock ratios [e.g., 2]. On this diagram, however, the same trend also could reflect primary igneous variation, for which there is evidence on Mars [e.g., 3]; we are in the process of examining trends on regional scales to distinguish between these in TES data.

To evaluate primary igneous trends, we excluded all likely weathering phases and recalculated the bulk oxides. As a result, SiO_2 is reduced relative to prior studies, and overlaps the basaltic field on a total alkalis vs. silica classification diagram to a greater degree than shown previously. On a plot of FeO*/MgO vs. SiO_2, however, our data still largely plot in the calc-alkaline field. This suggests that the igneous phases represent: 1) a non-tholeiitic composition, 2) weathering of a tholeiitic composition that enriches the residual material in relatively higher SiO_2 phases, and/or 3) a weathered tholeiitic composition depleted in FeO relative to MgO. In the absence of evidence for abundant calc-alkaline compositions on Mars, we suggest that olivine dissolution could produce both 2 and 3 above, offering a plausible explanation for the observed trends. We are recalculating compositions with added olivine to constrain how much olivine could have been removed to produce the observed compositions.

[1] McSween *et al*. (2009) *Science*, **324**, 736-739. [2] Hurowitz *et al*. (2006) *JGR*, **111** (E02S19). [3] Rogers and Christensen (2007) *JGR*, **112** (E01003).

https://doi.org/10.1180/S0026461X00006502 Published online by Cambridge University Press

A sulfidic driver for the Late Ordovician extinction

E.U. HAMMARLUND[1,2]*, T.W. DAHL[1], D.A.T. HARPER[3], D.P.G. BOND[4], C.J. BJERRUM[5] AND D.E. CANFIELD[1]

[1]Nordic Center for Earth Evolution (NordCEE) and Institute of Biology, University of Southern Denmark, 5230 Odense M, Denmark (*correspondence: emma@biology.sdu.dk)
[2]Department of Palaeozoology, Swedish Museum of Natural History, Box 50007, 104 05 Stockholm, Sweden
[3]Natural History Museum of Denmark, Øster Voldgade 3-5, 1350 Copenhagen K, Denmark
[4]School of Earth and Environment, University of Leeds, LS2 9JT, UK
[5]Institute of Geography and Geology, Copenhagen University, Øster Voldgade 10, 1350 Copenhagen K, Denmark

The first of three major Phanerozoic extinctions occurred during the late Ordovician Hirnantian stage when 86% of marine species and up to 24% of families perished in two phases. The extinction has been linked to cooling, glaciation and transgression but the exact kill mechanism(s) remain enigmatic because the timing of events and environmental changes are unclear. We analyzed sediments from the Dobs Linn (Scotland), the Billegrav (Denmark), and the Carnic Alps (Austria). These record a positive excursion in the isotopic composition of pyrite sulfur of up to 40‰ during the early to mid-Hirnantian, with maximum $\delta^{34}S$ values close to those of modern rivers. Similar excursions have previously been noted from the Hirnantian of China. The positive $\delta^{34}S$ shift is interpreted to reflect a drop in seawater sulfate concentration promoted by enhanced pyrite burial during expanded global ocean euxinia.

We examined changes in local depositional environments during the late Ordovician extinctions using multiple redox indicators: reactive iron, molybdenum, organic nitrogen and carbon isotopes, and pyrite framboid size distributions. The emerging picture is of deep ocean euxinia, prevailing before the initiation of the first phase of Hirnantian extinction. We argue that both phases of the extinction, and especially the second, were linked to marine euxinia.

During the first phase of extinction, a sea level fall of up to 150 meters decreased shelf area and accompanying euxinia further compressed the habitable oxic zone of the upper ocean, foremost affecting nektonic species. The second phase occurred in the aftermath of the Hirnantian glaciation when ice caps retreated, leading to transgression and the invasion of shelves by deep sulfidic waters, killing mid and shallow water fauna.

Bench scale experiments modeling the effects of a phytostabilization strategy for arsenic and lead containing mine tailings in the semi-arid Southwestern United States

CORIN M. HAMMOND*, ROBERT A. ROOT, SCOTT WHITE, RAINA M. MAIER AND JON CHOROVER

Department of Soil, Water, and Environmental Science, University of Arizona, Tucson, AZ 85721, USA (*correspondance: schowalt@email.arizona.edu)

The Iron King Mine-Humboldt Smelter Site in Dewey-Humboldt, Arizona, U.S.A. is characterized by high iron oxyhydroxide content, acidic pH, and concentrations of arsenic and lead in the top 35 cm averaging about 4,010 mg kg^{-1} and 2,390 mg kg^{-1}, respectively. In the semi-arid climate, human exposure to contaminated tailings particulate matter occurs primarily by aeolian dispersion and water erosion. Consequently, the site was added to the National Priorities (*Superfund*) List by the United States Environmental Protection Agency (EPA) in 2008.

The overall research goal is to develop a cost effective phytostabilization strategy to remediate the Iron King Mine tailings by amending the tailings with compost, lime, mycorrhizal fungi, irrigation, tilling, and seed of native halotolerant plant species. ICP-MS analysis reveals variation in contaminant "solubility" (defined here as <0.2 μm diameter) as a function of dissolved organic matter (DOM) from dairy compost additions. Both arsenic and iron exhibited significant reductions in concentrations in the aqueous phase with increased DOM (Figure 1). This trend is attributed to decreased surface charge of suspended oxyhydroxide colloids with sorbed DOM enhancing flocculation. The colloids (<200 nm) were further investigated with synchrotron XAS and the arsenic species was shown to be As(V) associated with ferric hydroxides.

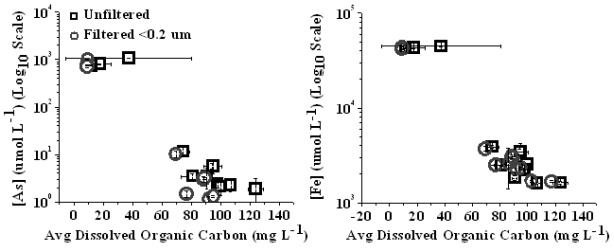

Figure 1: Arsenic (left) and iron (right) supernatant concentrations from batch experiments show similar trends with respect to dissolved organic carbon concentration.

https://doi.org/10.1180/S0026461X00006502 Published online by Cambridge University Press

The deep carbon cycle confronted to mantle electrical conductivities

TAHAR HAMMOUDA[1], FABRICE GAILLARD[2], BERTRAND GUILLOT [3], DIDIER LAPORTE[1], PASCAL TARITS[4], NICOLAS SATOR[3], MATTHIEU MICCOULAUT[3] AND SOPHIE HAUTOT[4]

[1]LMV, Clermont-Ferrand, France (t.hammouda@opgc.univ-bpclermont.fr)
[2] ISTO, Orléans, France, (gaillard@cnrs-.orleans.fr)
[3] LMPTC, Paris, France, (guillot@lptl.jussieu.fr)
[4] UBO, Brest, France, (tarits@univ-brest.fr)

The deep carbon cycle is tightly related to (i) subduction processes that injects in the mantle oxidized carbon species, (ii) deep redox processes that traps carbon as graphite or diamond, and (iii) volcanic degassing that transfers carbon form the mantle into the atmosphere. The rate at which such a transfer operates is slow with time-scale comparable to the age of the Earth if it is rate-controlled by solid state mantle convection. Carbonatite melts, however, the oxidized and molten form of mantle carbon, are likely to shortcut these slow processes provided that large scale connected paths exist at depth, and that carbonatite stability is allowed by appropriate redox conditions. Our proposal is that such channels could indeed be revealed by mantle electrical conductivity as deduced from magnetotelluric methods. This approach allows imaging the deep volatile cycling, which has so far relied essentially on petrologically-based models.

Petrologically-based models predict an increasingly reduced mantle with increasing depth, with the possibility that the asthenosphere could be saturated with metallic iron. This should prevent carbonate stability at depth exceeding 200-250 km. Water activity should also be reduced due decomposition into hydrogen. However, there is geochemical evidence for carbonate-rich melts formed at depth exceeding 250 km. This requires redox heterogenities at depth such as oxidized regions within a globally reduced mantle. Similarly, electrical mapping of the mantle images conductive regions surrounded by a globally more insulating mantle. Some conductive mantle regions appear to be spatially connected to subduction regions, which could indicate release of carbonatite at depth, due to melting of subducted carbonates. This process requires that those deep regions are oxygen-enriched and subduction of oxidized material can provide the excess oxygen. In upwelling regions (MOR), underneath volcanic zones that experience CO_2 degassing, electrically conductive zones seems to be deeply rooted suggesting that the deep mantle source regions of those volcanic emissions are more oxidized than the surrounding mantle. We will define the oxygen/carbon ratios required at such depth to reconcile high conductivity and oxidizing conditions.

Tectono-geochemistry exploration and the ore-finding discovery – A case study of the Zhaotong Zn-Pb deposit, Yunnan, China

HAN RUN-SHENG[1]*, WANG XUE-KUN[1] AND WANG FENG[2]

[1]Kunming University of Science and Technology; Southwest Institute of Geological Survey, Geological Survey Center for Non-ferrous Mineral Resources, 650093, P.R.C.; (*correspondence: hrs661@yahoo.com.cn)
[2]Yunnan Chihong Zn Ge Co., Ltd., 655011, P.R.C.

The Zhaotong Zn-Pb deposit is one of the typical deposits in northeast Yunnan rich Zn-Pb-Ge deposit district, and is located in the sagged Yunnan basin at the middle end of the Yangtze Platform. It lies in a structurally compounding position of NE-, SN- and NW-trending fault-fold belts. The ore-bodies occur in the Zaige Formation of Upper Devonian and the Baizuo Formation, which are mainly composed thick layer coarse-grained dolomite, is strictly controlled by the interstratified faults. The length of ore-body is 325 m and its depth is more than 500m, its average thickness is about 16m. The ore grade of Pb and Zn is high up to 20%-35% principally with compact lump shape. In the ores there are other elements including Ag, Ge, Cd. Mineral composition in the ores mainly includes sphalerite, galena, pyrite, ferro-calcite, calcite, dolomite and quartz. The dolomitization is widely observed in wall-rock alteration.

Based on studying the structural ore-controlling laws, M-2, M-4 and A-2, A-3, D-2, F-1 tectono-geochemical anomalies in the mining area were delineated by tectono-geochemical mapping for 1:5000, 1:2000 measuring scale. The main anomalies extend in NE-SW-trending, and superimposed anomalies of Zn-Pb-Cd-Mn-Ge-Ba and Mo-U-W element groups are significant. By the IP and TEM geophysical exploration techniques, two positioning targets were proposed. The one parallels the SW-NE-trending mineralized zone of No.1 orebody group, the other is at the depth of No.1 orebody at the southwest end, concealed orebody may extend from 95 exploration lines to 80 lines. By engineering verifying, more concealed orebodies had found. NO.1-6 orebody is one of the largest, its thickness is 15.6-54.2m, its content of Pb and Zn is 25 % - 35 %. The increase of the Pb-Zn metal reserves by near 1.0 million tones so that the deposit changes into a large-type lead-zinc deposit. This discovery is a successful example after an important breakthrough had made by tectono-geochemical exploration technology in the Huize Pb-Zn deposit.

*NSF (40863002) and Projects the Distinguishing Discipline of KUST (2008).

https://doi.org/10.1180/S0026461X00006502 Published online by Cambridge University Press

Spatio-temporal variation of total mercury concentrations in Antarctic snowpack

YEONGCHEOL HAN[1], YOUNGSOOK HUH[1], SUNGMIN HONG[2]; SOON DO HUR[3] AND HIDEAKI MOTOYAMA[4]

[1]School of Earth and Environmental Sciences, Seoul National University, Seoul, Korea (hanlove7@snu.ac.kr; yhuh@snu.ac.kr)
[2]Department of Oceanography, Inha University, Incheon, Korea (smhong@inha.ac.kr)
[3]Korea Polar Research Institute, Incheon, Korea (sdhur@kopri.re.kr)
[4]National Institute of Polar Research, Tokyo, Japan (motoyama@nipr.ac.jp)

Investigation of mercury in the shallow snowpack is helpful for interpreting its deep ice core data and for understanding the mercury dynamics in polar regions. The total mercury concentration (Hg_T) was determined in surface snow (n=44) along a ~1500 km transect from the coast to Dome Fuji in east Dronning Maud Land and from two 4-m snow pits collected during the Japanese-Swedish IPY Antarctic Expedition (Nov 2007 – Jan 2008). The Hg_T of surface snow samples were low (<0.4 – 10.8 pg g^{-1}) and exhibited spatial and/or temporal heterogeneity. However, high Hg_T above the third quartile (>1.7 pg g^{-1}) were observed only in the inner Plateau (>570 km from sea-ice, >3500 m altitude). The Hg_T in two snow pits ranged between <0.3 and 2.4 pg g^{-1} (n=160) with eposodic peaks. The average Hg sequestration rates were estmated to be 1.3±0.9 pg cm^{-2} yr^{-1} for ~52 years and 2.8±0.6 pg cm^{-2} yr^{-1} for ~36 years. These are comparable to the interglacial mercury deposition rate of ~6 pg cm^{-2} yr^{-1} recovered from the deep ice core at Dome C [1].

Our Hg_T determination may underestimate the actual amount in the snow by a factor of 2-5, since additional experiments revealed some loss of volatile mercury from snowmelt samples which had been kept frozen in the dark. Even allowing for potential underestimation, no depositional enhancement that should accompany photo-oxidation of atmospheric elemental mercury in austral mid-summer [2, 3] was observed in surface or pit snow samples. Our Hg_T values could represent the particle-bound refractory fraction that has survived post-depositional reduction within the sunlit snow layer and sequestered on the Antarctic Plateau.

[1] Jiratu *et al*. (2009) *Nat. Geosci*. **2**(7), 505-508. [2] Brooks *et al*. (2008) *Atmos. Environ*. **42**(12), 2877-2884. [3] Brooks *et al*. (2008) *Atmos. Environ*. **42**(12), 2885-2893.

Study on the geochemical characteristics of noble gasses in groundwater in Beishan, Gansu Province, China

YONG HAN[1], GUANGCAI WANG[1] AND YONGHAI GUO[2]

[1]School of Water Resources and Environmental Science, China University of Geosciences, Beijing 10083, China (hanyongzh@163.com)
[2]CNNC Beijing Research Institute of Uranium Geology, Beijing 100029, China (guoyonghai@163.net)

Beishan, located in the Nouthwest of China, has been considered as one of the candidate areas for sitting disposal repository for high level radioactive waste. Groundwater activities is one of most important concerns for such a site. A preliminary hydrogeological investigation has been conducted to understand the groundwater flow systems in the area. The methods regarding noble gases and their isotopes in groundwater were involved in the investigation in an attempt to understand the groundwater recharge, circulation and flow modes. A total of 16 gas samples in situ deaerated from groundwater and 9 groundwater samples by copper tubes were collected. Concentrations and isoptoes of noble gases were determined by mass-spectrometer VG5400.

The values of N_2/Ar range from 45.76 to 81.23 for all groundwater samples, suggesting groundwaters have close relations with atmosphere and atmospheric precipitation. This can be proved by the relationship between δD and $\delta^{18}O$ of groundwater samples, which shows all groundwaters originate from meteoric rainfall. $^3He/^4He$、$^4He/^{40}Ar$ indicate that noble gases in groundwater maily derived from atmosphere and crust with different extent of water-rock interaction and rate of water circle. The excess air in four samples exceed 100% suggesting the relatively larger recharge rate from precipitation. Based on the noble gasses in groundwater, groundwater recharge temperature was estimated by using a computing program, Noblegas [1]. In combination with the age of groundwater, the recharge temperature in the deep borehole BS02 is 5.9°C indicating colder groundwater recharge conditions. According to the analysis above and the hydrogeological conditions, five water circulation modes were generalized, such as Precipitation-Deep or Lateral Recharge, Local Precipitation Recharge-Evaporation and so on.

Supported by the Fundamental Research Funds for the Central Universities of China (No.53200959016) and NSFC project (No.40930637).

[1] Aeschbach-Hertig W, *et al*. (1999), *Water Resources Research*, **35**, 2779-2792.

https://doi.org/10.1180/S0026461X00006502 Published online by Cambridge University Press

A high-resolution, multi-isotopic study of mantle heterogeneity beneath the southeast Indian Ridge: Preliminary Pb and Hf results

B. HANAN[1]*, J. BLICHERT-TOFT[2], K. SAYIT[1], A. AGRANIER[3], C. HEMOND[3], A. BRIAIS[4], M. MAIA[3], D. GRAHAM[5] AND F. ALBARÈDE[2]

[1]San Diego State University, San Diego, CA 92182-1020, USA (*correspondence: Barry.Hanan@sdsu.edu)
[2]Ecole Normale Supérieure, 69007 Lyon, France
[3]IUEM-UMR, University of Brest, 29280 Plouzané, France
[4] CNRS-OMP, BGI, 31400 Toulouse, France
[5] COAS, Oregon State University, Corvallis, OR 97331, USA

This investigation is designed to constrain mantle melting conditions and composition at high resolution. Fresh basalt glass was recovered from ~130 localities along ~1200 km of the Southeast Indian Ridge (SEIR) axis between 89.5° and 99.3°E during the GEISEIR I expedition. From 89-96° the sampling density was 0.1 km^{-1} and for 96-99° it was 0.2 km^{-1}.

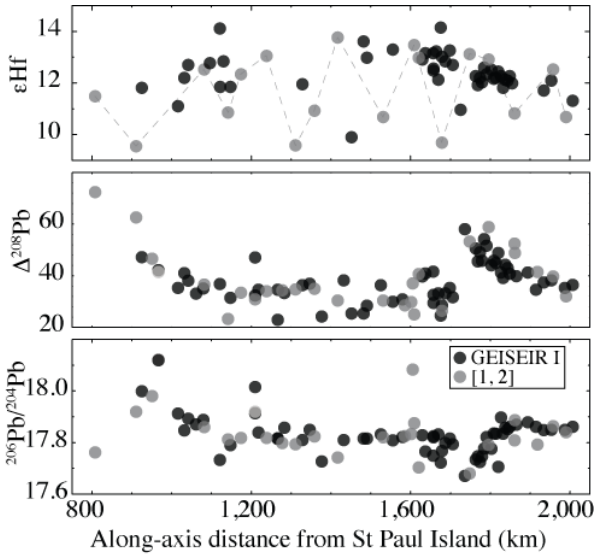

The new data are consistent with the bimodal Hf isotope distribution and presence of ancient compositional streaks along the SEIR [1]. The Pb isotope variation is highly structured, similar to [2], likely reflecting variable melting of an isotopically heterogeneous mantle.

[1] Graham *et al*. (2006), *Nature* **440**, 199-202. [2] Mahoney *et al*. (2002), *J. Petrol*. **43**, 1155-1176.

Characterization of pedogenic Mn concretions and coatings in redoximorphic soils

M. HÄNDEL*, T. RENNERT AND K.U. TOTSCHE

Institute of Earth Sciences, Friedrich Schiller University of Jena, Burgweg 11, 07749 Jena, Germany (*correspondence: matthias.haendel@uni-jena.de)

Secondary Mn minerals play an important role in many soil chemical processes such as sorption of metal ions and degradation of organic contaminants. Redoximorphic soils such as Gleysols and Stagnosols are characterized by spatially separated enrichment and depletion zones of pedogenic (hydrous) Fe and Mn oxides, which appear as a result of the periodic change between reducing and oxidizing conditions.

We investigated stagnic and gleyic subsoil horizons developed from loess, Early Triassic sandstone, calcareous gravel and Middle Jurassic loamy sediments with pH values from 3.7 to 7.3. The concretions, coatings and parts of the surrounding matrix were characterized by electron microprobe analysis and polarizing microscopy on thin sections, XRD, FTIR spectroscopy and analyzed for their total element contents and their oxalate- and dithionite-extractable fractions. Diffractograms and FTIR spectra often showed a signal overlapping of clay and Mn minerals. Nevertheless, birnessite [$Na_4Mn_{14}O_{27}$•$9H_2O$] was detected in a gleyic horizon (pH 7.3). We further assume todorokite [$(Mn^{II},Ca,Mg)Mn_3^{IV}O_7$•$H_2O$] in an acidic stagnic horizon (pH 3.7).

Backscattered electron images and EDX measurements showed that Mn phases in stagnic horizons always occur together with clay minerals in a matrix. Iron precipitates are partly present in a clay matrix like Mn phases and also as pure Fe precipitates at the edges of pores inside the concretions. Single particles cannot be discerned and are thus <500 nm. Concretions formed in Middle Jurassic sediments showed a shell-like structure, which suggests a periodic genesis. In contrast, concretions developed in stagnic horizons from sandstone were formed by the flow of the soil solution into the interior of aggregates, where Mn phases precipitated. All pedogenic Mn precipitates were enriched in Co (360 μg/g) and Ni (480 μg/g). The presence of Ni in the Mn precipitates was confirmed by EDX.

Further studies with TEM and EXAFS are required to clarify the detailed mineralogy of the Mn precipitates.

https://doi.org/10.1180/S0026461X00006502 Published online by Cambridge University Press

Evolution of a mantle wedge: Basalts from the Colville and Kermadec Ridges

M.R. HANDLER[1]*, R.J. WYSOCZANSKI[2] AND E.M.F. BURGER[1]

[1]SGEES, Victoria University of Wellington, New Zealand (*correspondence: Monica.Handler@vuw.ac.nz)
[2]NIWA, PO Box 14901, Wellington, New Zealand

The Kermadec Arc intra-oceanic arc system has been active for at least the last 17 Ma. Volcanic rocks extracted from much the same location over this period allow the composition and fluxing of the mantle wedge to be investigated over a prolonged period of subduction.

The Southern Kermadec Arc consists of the active Southern Kermadec Arc volcanic front and the Havre Trough back-arc system bound by two sub-parallel ridges, the Colville Ridge to the west and Kermadec Ridge to the east. These ridges represent the proto-Kermadec volcanic arc split by the opening of the Havre Trough at c. 6 Ma. Here, we will present the first major and trace element data, Sr and Pb isotopic data and mineral chemistries of lavas from this remnant arc and compare them with the currently active Southern Kermadec Arc and Havre Trough back arc basin.

The ridge samples comprise highly porphyritic basalts. The crystal cargoes of the ridge crest samples are dominated by plagioclase that span the compositional range observed in the modern arc, extending to very primitive compositions (An ≤ 98). By contrast, samples dredged from a knoll on the Kermadec Ridge contain abundant olivine (Fo ≤ 94; NiO ≤ 0.5 wt%) and pyroxene phenocrysts. Preliminary trace element data suggest a mantle wedge source that was less depleted than the modern wedge (e.g. N-MORB normalised HREE concentrations ~ 0.6 – 1.0), and already polluted with both fluid-mobile element enrichments (e.g. Ba/Nb = 84 – 300) and a sediment melt component (e.g. (La/Sm)N = 1-2). These data suggest that the fluid flux into the mantle wedge has been broadly similar through the life of the arc system, however the mantle wedge has become more depleted and has had less of a sediment melt component added with time.

Insights into the Galápagos plume from uranium-series isotopes of recently erupted basalts

HEATHER K. HANDLEY[1], KIM BERLO[2], CHRISTOPH BEIER[3], SIMON TURNER[1] AND ALBERTO E. SAAL[4]

[1]GEMOC, Department of Earth and Planetary Sciences, Macquarie University, Sydney, NSW 2109, Australia.
[2]Department of Earth Sciences, University of Oxford, Oxford OX1 3PR, UK.
[3]GeoZentrum Nordbayern, Universität Erlangen-Nürnberg, Schlossgarten 5, D-91054 Erlangen, Germany.
[4]Department of Geological Sciences, Brown University Providence, Rhode Island 02912, United States.

Uranium-series isotopes (^{238}U-^{230}Th-^{226}Ra-^{210}Pb), major element, trace element and Sr-Nd isotopic data are presented for recent (< 60 years old) Galápagos archipelago basalts and are interpreted in terms of chemical fractionation by magmatic processes. Volcanic rocks from all centres (Fernandina, Cerro Azul, Sierra Negra and Wolf volcano) display ^{230}Th excesses (4-15%) and steep rare earth element patterns indicative of residual garnet during partial melting of the mantle source. Rare earth element (REE) modelling suggests that only a few percent of garnet is involved. Correlation between ($^{238}U/^{232}Th$), radiogenic isotopes and Nb/Zr ratio suggests that the U/Th ratio of Galápagos volcanic rocks is primarily controlled by geochemical source variation and not fractionation during partial melting. Unexpectedly, the lowest ($^{230}Th/^{238}U$) is not observed at Fernandina (supposed centre of the plume) but at Wolf volcano on the 'periphery' of the plume. Small radium excesses are observed for all samples with ($^{226}Ra/^{230}Th$) ranging from 1.107 to 1.614. ^{226}Ra-^{230}Th disequilibria do not correlate with other U-series parent-daughter nuclide pairs or geochemical data, suggesting modification at shallow levels on timescales relevant to the half-life of ^{226}Ra (1600 years). ^{226}Ra and ^{210}Pb excesses are inconsistent with interaction of magma with cumulate material unless decoupling of ^{210}Pb (or an intermediate daughter, such as ^{222}Rn) occurs prior to modification of Ra-Th disequilibria. The intriguing correlation of $(^{210}Pb/^{226}Ra)_0$ with Nb/Zr and radiogenic isotopes requires further investigation but may suggest possible control via magmatic degassing and accumulation related to source heterogeneities.

https://doi.org/10.1180/S0026461X00006502 Published online by Cambridge University Press

The uptake of radionuclides into nanoparticulate hydroxyapatite

S. HANDLEY-SIDHU*, J. C. RENSHAW, B. STOLPE, J.R. LEAD AND L.E. MACASKIE

The University of Birmingham, Edgbaston, Birmingham B15 2TT, UK
(*correspondence: s.handley-sidhu@bham.ac.uk)

Hydroxyapatite (HAp) is a potential material for the remediation of metal contaminated waters [1, 2] and as a radionuclide waste storage material [3]. *Serratia* sp. cells bio-manufacture nanophase hydroxyapatite (Bio-HAp) from the substrates glycerol 2-phosphate and Ca^{2+} [4]. Varying the manufacturing conditions influenced Bio-HAp properties (e.g. organic content, Ca/P ratio, specific surface area (SSA), and crystallite size).

The uptake of key radionuclides was investigated: Eu^{3+} (as an analogue for trivalent actinides), U^{6+}, Sr^{2+} and Co^{2+}. All the Bio-HAp (n=10) tested in this study were more efficient than commercially available HAp. For Eu^{3+}, Co^{2+}, Sr^{2+} the main Bio-HAp properties that increased metal uptake were: decreasing crystallite size, increasing SSA and organic content. However U^{6+} uptake showed no relationship to these properties. Figure 1 shows the relationship of crystallite size and Eu^{3+} uptake (mmol per 100g).

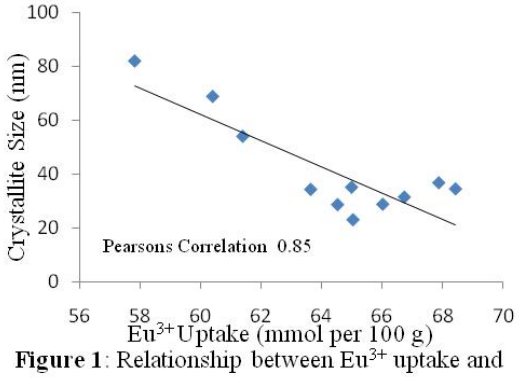

Figure 1: Relationship between Eu^{3+} uptake and crystallite size.

Overall, Bio-HAp shows promise for the remediation of aqueous metal waste especially since Bio-HAp can be synthesized for optimal metal uptake properties.

[1] Handley-Sidhu (2011) *Biotechnol. Lett.* 2011, **33**, 79-87. [2] Simon (2004) *Sci. Total Environ.* **326**, 249-256. [3] Oelkers (2008) *Elements* **4**, 113-116. [4] Thackray (2004) J. *Mater. Sci. Mater. Med.* **15**, 403-406.

Petrogenetic implications from PGE in the layered mafic Dufek intrusion and related sills of the Ferrar large igneous province, Antarctica

RICARDA HANEMANN[1], LOTHAR VIERECK-GOETTE[1] AND SAMUEL MUKASA[2]

[1]Inst. f. Geowiss., FSU Jena, Burgweg 11, 07747 Jena
[2]College of Engineering and Physical Sciences, University of New Hampshire, Durham, N.H. 03824, USA

The Jurassic Ferrar large igneous province extends in a >3000 km long, linear belt along the western margin of the East Antarctic craton and comprises numerous sills, dikes and lava flow sequences as well as the layered mafic Dufek intrusion. According to previous studies, the strikingly uniform crust-like trace element and isotope data have been interpreted to indicate a single magma source within the subcontinental lithospheric mantle characterised by crustal enrichment due to Palaeozoic subduction processes.

The goal of the present study is to further describe the petrogenesis of the Ferrar magmatic rocks by investigating the fractionation behaviour of platinum-group elements (PGE) during magmatic evolution. Therefore, we studied the stratigraphic distribution of PGE throughout both the Dufek intrusion and selected Ferrar sills from Northern Victoria Land by analysing the abundances of Ir, Ru, Rh, Pt and Pd by ID-ICP-MS after NiS-fire in about 130 rock samples.

Considering the lithological and geochemical variablity, the studied rocks also exhibit highly variable PGE compositions; PGE totals range from 4 to 138 ppb within Ferrar sills and reach up to ~800 ppb for analysed rocks from the Dufek intrusion. In general, the combined PGE are dominated by Pt and Pd with the Ir-PGE often being near or below detection limits indicating a strong fractionation between the single PGE. The samples analysed do not show clear variations of PGE as a function of stratigraphy or modal rock composition. Obviously, only Fe-Ti oxide-rich rocks from upper parts of both the sills and the Dufek intrusion exhibit significantly elevated PGE concentrations.

The PGE characteristics obtained are attributed to an extensive pre- and post-emplacement differentiation history under mainly sulphur-undersaturated conditions resulting in PGE enrichment until the onset of Fe-Ti oxide fractionation at advanced stages of low-pressure magma evolution. The inferred very low level of S-saturation during differentiation processes of the Ferrar magmas is in agreement with an origin of their primary magmas by high-degree partial melting of a refractory, sulphur-depleted subcontinental lithospheric mantle source proposed beneath this province.

https://doi.org/10.1180/S0026461X00006502 Published online by Cambridge University Press

Origin of early hydrothermal fluids associated with the Sudbury structure deduced from individual fluid inclusion Sr isotope analysis

JACOB HANLEY[1]*, FELIX OBERLI[2] AND THOMAS PETTKE[3]

[1]Saint Mary's University, Dept of Geology, Halifax, Canada, B3H3C3 (*correspondence: jacob.hanley@smu.ca)
[2]ETH Zurich, Institute of Geochemistry and Petrology, CH-8092 Zürich, Switzerland
[3]University of Bern, Institute of Geological Sciences, CH-3012 Bern, Switzerland

Early quartz-epidote-calcite-sulfide veins and stockworks in the Archean footwall of the Sudbury Igneous Complex contain inclusions of ore metal-bearing (Cu-Ag-Pt-Bi-Au) aqueous brine (Ca-Na-Cl) with high Sr and relatively low Rb bulk concentrations (4400 μg/g Sr; 110 μg/g Rb; Sr/Rb = 40; n = 18) in addition to wt% concentrations of K, Fe, Mn, Zn, Pb and Ba[1]. Inclusions were trapped in the veins at ~ 0.5 kbar; 200-250ºC[1]. We have determined initial (at 1.85 Ga[2]) $^{87}Sr/^{86}Sr$ ratios in individual brine inclusions by LA-MC-ICP-MS to constrain the source of this fluid that circulated prior to magmatic sulfide deposition.

Analyses of 62 brine inclusions yielded an average initial $^{87}Sr/^{86}Sr$ = 0.70308 ± 0.00020 (1SE). Tentatively, we suggest that the data are most consistent with this early, metalliferous hydrothermal fluid containing a significant endowment of regional Proterozoic seawater ($^{87}Sr/^{86}Sr$ = 0.70296[3]) which covered the target area at the time of impact and subsequent formation of the melt sheet. Suspected major crustal reservoirs in the area had initial $^{87}Sr/^{86}Sr$ too radiogenic to have been an exclusive source for the Sr in the inclusions; these include the gneissic country rocks hosting the veins and their associated groundwaters (initial $^{87}Sr/^{86}Sr$ = 0.71008-0.71092[3]) and magmatic fluids derived from the main igneous units of the Sudbury Igneous Complex itself (initial $^{87}Sr/^{86}Sr$ = 0.70710-0.70742[3]). However, some individual inclusions of assemblages show significant variation in composition (e.g., for 3 inclusions: initial $^{87}Sr/^{86}Sr$ ranges from 0.7018 to 0.7046). A standard deviation for all inclusions analyzed (1σ on mean) of ± 0.001540 suggests the inclusions have trapped pulses of a poorly mixed fluid involving mainly seawater, and a minor component from an additional source, either magmatic and/or groundwater. Scatter due to analytical bias is also being investigated.

[1] Hanley *et al*. (2005) *Mineral. Deposita* **40**, 237-256. [2] Krogh *et al*. (1984) *Ont.Geol.Surv. Spec. Vol.* **1**, 431-446. [3] Campos-Alvarez *et al*. (2010) *Chem. Geol.* **278**, 131-150.

Pairing Re-Os geochronology and biostratigraphy – Dating fossils

J. HANNAH*[1,2], H. STEIN[1,2], G. YANG[1] AND J. MALETZ[1]

[1]AIRIE Program, Dept Geosciences, Colorado State University, Fort Collins, CO 80523-1482, USA (*correspondence: jhannah@cnr.colostate.edu)
[2]Geological Survey of Norway, 7491 Trondheim, Norway

With hard-earned insights in sampling strategies and improvements in analytical precision, Re-Os geochronology of organic material in sedimentary rocks is now an established method for placing time pins in the stratigraphic record. Age uncertainties better than 1% are routine, and as low as 0.5% not uncommon. We are now able to address a range of questions using Re-Os geochronology where age constraints were previously lacking. For example, Re-Os shale geochronology can assist uncertain biostratigraphic correlations, and provide ages where biota are absent. We have established the timing of tectonic events in the southern Superior province with a 2695 ± 14 Ma age in a supracrustal sequence [1]. We have confirmed correlation of Anisian-Ladinian (Middle Triassic) biozones between Boreal and Tethyan terranes, where there are no common fossil assemblages and U-Pb geochronology is limited to the Tethyan realm [2]. Further work on the Boreal Triassic section (Xu *et al*., this meeting) affirms the proposed "Alternate" Triassic time scale. Similarly, tight time constraints on the Permo-Triassic extinction were previously limited to the Meishan area in Tethys. We have extended that extinction timeline to the Boreal, with remarkably precise Re-Os isochrons from opposing sides of the Norwegian Sea [3].

An obvious next step is direct dating of fossil organic remains. The Lower and Middle Ordovician sections in western Newfoundland display sequences of well-defined graptolite zones, but lack radiometric age constraints. Re-Os analysis of *Archiclimacograptus* sp., hand-picked from Table Cove Fm shales (Table Head Group) yields 11.4 ppb Re and 0.540 ppb Os. Isotopic ratios are reasonable for the proposed biostratigraphic age. Detailed age constraints from multiple graptolite horizons can delimit durations of biozones, refine the Ordovician time scale, and confirm global correlations. Ultimately, we can assign absolute ages to stratigraphic key surfaces and system tracts, reflected in environmentally sensitive graptolite assemblages, to improve precision of the sea-level curve for the Lower and Middle Ordovician.

Funded by U.S. NSF grant EAR-0844213

[1] Yang *et al*. (2009) *EPSL* **280**, 83-92. [2] Xu *et al*. (2009) *EPSL* **288**, 581-587. [3] Georgiev *et al*. (2010) *GCA* **74**:12S, A324 and Georgiev *et al*. (in review) *EPSL*.

https://doi.org/10.1180/S0026461X00006502 Published online by Cambridge University Press

The role of aluminum in ferrihydrite preservation

C.M. HANSEL

School of Engineering and Applied Sciences, Pierce Hall, Room 118, Harvard Univerisity, Cambridge, MA 02138 (hansel@seas.harvard.edu)

The poorly crystalline Fe(III) (hydr)oxide ferrihydrite is considered one of the most important sinks for (in)organic contaminants within the environment. In sedimentary environments, the oxidation of carbon and hydrogen is constrained by microbial reduction of Fe(III) (hydr)oxides, of which ferrihydrite is considered the most biologically available. Yet, pure ferrihydrite ripens rapidly to more crystalline Fe phases, such as goethite, leading to diminished sorption capacities and bioavailability. This ripening is accelerated by surface reactions between ferrihydrite and aqueous Fe(II) and can also lead to ferrihydrite conversion to magnetite at higher Fe(II) levels. While ferrihydrite within most natural systems contains high levels of adsorbed or co-precipitated cations, particularly aluminum (Al), little is known regarding the impact of these cations on the capacity for ferrihydrite to ripen to more stable Fe(III) phases or serve as an effective electron acceptor. Accordingly, we explored the impact of adsorbed and substituted Al on the microbial reduction and abiotic Fe(II)-induced secondary mineralization of ferrihydrite over a wide range of Al levels.

Here, we show that Al substituted within (6-24 mole %) or adsorbed on (0.1 to 27% Γ_{max}) ferrihydrite results in diminished microbial reduction and abiotic Fe(II)-induced secondary mineralization resulting, in both cases, in the preservation of ferrihydrite even at low Al levels. The preservation of ferrihydrite increases linearly with the amount of Al adsorbed on or co-precipitated within ferrihydrite. In fact at Al substitution levels exceeding 17 mole %, the rate of microbial Fe(III) reduction is lower for ferrihydrite than for the more crystalline (and hence considered less bioavailable) phase goethite. Furthermore, formation of magnetite is completely inhibited at Al substitution levels greater than 17 mole %, levels that are frequently observed within natural ferrihydrites. Interestingly, the secondary minerals formed upon reaction with different Fe(II) levels (0.2 and 2.0 mM) varies not only with the concentration of Al, but also the mode of Al incorporation (adsorption versus co-precipitation). These findings provide insight into the mechanisms that may be responsible for ferrihydrite preservation and low levels of secondary magnetite typically found in sedimentary environments. The findings also have large implications for constraints on carbon oxidation in sedimentary systems containing compromised ferrihydrites.

Lithium isotope perspective on the Iceland mantle plume

H.-E. HANSEN[1], T. MAGNA[2,3], J. KOŠLER[1] AND R.-B. PEDERSEN[1]

[1]University of Bergen, Norway
[2]Universität Münster, Germany
[3]Czech Geological Survey, Prague, Czech Republic

The Iceland mantle plume represents a quest of searching for the individual mantle end members as well as other components that may have contributed to the observed elemental and isotope variability. Here we present Li contents and isotope compositions in samples from two distinct volcanic centres in Iceland, Krafla and Theistarykir, that show a considerable range in Li and δ^7Li extending that reported previously [1–3]. Pristine Theistareykir basalts (MgO>7%) have consistently low Li contents and range in δ^7Li (+4.2 to +8.1‰) that mimics "depleted" lavas of [1], thought to be variously contributed by an old altered oceanic crust that underwent prior extraction of Li-rich arc magmas at convergent boundaries. Chemically evolved rocks from Krafla (MgO<2%) have similarly invariant δ^7Li pattern coupled with high Li enrichments as reported in [2]; this suggests that magmatic differentiation does not impart resolved Li isotope fractination in juvenile crust derived from plume basalts. The radiogenic Sr–Nd isotope data appear to follow bi-modal distribution akin to [1] and no influence of magmatic evolution on either Sr or Nd in Li-rich rhyolitic and dacitic magmas which may mean a rapid formation of silicic rocks from parental basalts. The new and published data show a strong negative correlation between Li and Mg which shows a significant coupled data density gap between 2 and 5% MgO and 10 and 20 ppm Li, respectively, suggesting a lack of andesitic lavas between basalts and chemically evolved dacites and rhyolites. This may have petrogenetic consequences for formation of new crustal material through magmatic differentiation of rising plume magmas.

[1] Magna *et al.* (2011) *GCA* **75**, 922-936; [2] Schuessler *et al.* (2009) *EPSL* **258**, 78-91; [3] Ryan & Kyle (2004) *Chem Geol* **212**, 125-142

https://doi.org/10.1180/S0026461X00006502 Published online by Cambridge University Press

A possible mantle plume source in the lower mantle; Evidence from Polynesian HIMU

T. HANYU[1]*, Y. TATSUMI[1], R. SENDA[1], T. MIYAZAKI[1], Q. CHANG[1], Y. HIRAHARA[1], T. TAKAHASHI[1], H. KAWABATA[1], K. SUZUKI[1], J.-I. KIMURA[1] AND S. NAKAI[2]

[1]Institute for Research on Earth Evolution, Japan Agency for Marine-Earth Science and Technology, Yokosuka 237-0061, Japan (*correspondence: hanyut@jamstec.go.jp)
[2]Earthquake Research Institute, The University of Tokyo, Bunkyo-ku, Tokyo 113-0032, Japan

One of the major issues of mantle geochemistry is to decipher heterogeneous nature of the mantle through the studies of ocean island basalts (OIBs) related with mantle plumes. In this study, we focus on OIBs from Polynesia, with unique geochemical characteristics referred to as HIMU. Combined Pb-Sr-Nd-Hf-Os-He isotope analyses using mineral separates provide reliable isotopic information of the basalt source. Coherent isotopic systematics in multi-isotope spaces defined by the HIMU basalts are best explained by recent mixing of melts derived from the HIMU reservoir and the local shallow mantle. The HIMU reservoir has high Pb isotope ratios ($^{206}Pb/^{204}Pb \geq 21.5$), low Nd isotope ratios (epsilon Nd $\leq$ +4), low Hf isotope ratios (epsilon Hf $\leq$ +3), low He isotope ratios ($^{3}He/^{4}He \leq 6$ Ra), and moderately high Os isotope ratios ($^{187}Os/^{188}Os$ = 0.14-0.15). Low $^{3}He/^{4}He$ is consistent with involving recycled materials, most probably, the oceanic crust in the source. However, moderately high Os isotope ratios suggest that the HIMU reservoir is not a recycled oceanic crust itself, but a metasomatised mantle by subducted oceanic crust-derived melt. Such the metasomatism can occur at various settings in the recycling process. These would include (a) wedge mantle metasomatism beneath subduction zones by melting of subducted slab, (b) metasomatism of the upper mantle by melting of stagnant slab, and (c) metasomatism of the lower mantle by melting of deep slab near core-mantle boundary. The parent-daughter element fractionation in Sm/Nd, Lu/Hf and U/Pb deduced from the present day Nd, Hf and Pb isotopes of the HIMU reservoir, respectively, should constrain when and where the subducted oceanic crust melted and subsequent metasomatism occurred. We demonstrate a possibility that melting of the oceanic crust in the lower mantle at 2-3 Ga leaving Mg-perovskite as the residual phase adequately fractionates these parent-daughter element ratios. If this is the case, the oceanic crust was subducted and melted to metasomatize the lower mantle to generate the HIMU reservoir.

Sorption mechanism of dilute fluorine in wastewater using aluminium hydroxide coprecipitation method

D. HARAGUCHI*, C. TOKORO AND S. OWADA

Waseda university, Tokyo 169-8555, Japan (*correspondence: d.haraguchi@suou.waseda.jp)

Hydroxide coprecipitation method is widely used in a treatment of wastewater containing dilute toxic anions. But now detail mechanism or quantitative characteristic is not well understood and also demanded. This study discussed a sorption mechanism of fluorine (F(-I)) in wastewater using aluminum hydroxide coprecipitation method by analyzing filtrates and precipitates using artificial wastewater.

Sorption mechanism of F(-I) coprecipitation with aluminium hydroxide was investigated using 4 kinds of experimental methods: (i) sorption instherm, (ii) zeta potential mesurement, (iii) XRD analysis, and (iv) FT-IR analysis. We compared between coprecipitation experimental results and simle adsorption ones in which F(-I) was just adsorbed on the sysnthized aluminum hydroxide.

Sorption isotherms of F(-I) on aluminum hydroxide exhibited a BET type isotherms and sorption densities abruptly increased when the initial F/Al molar ratio was more than 3. And zeta potential hardly changed even if sorption densities increased when the initial F/Al was more than 3. But results of XRD and FT-IR suggested that precipitates between F(-I) and Al (i.e., AlF_3 and $AlF(OH)_2$) were not formed in all cases [1]. In other words, sorption of F(-I) to aluminum hydroxide was always achieved by simple adsorption. In particular, FT-IR spectra indicated the amount of F(-I) adsorbed to Al-O bonding increased when initial F/Al was more than 3. Therefore, these results exhibited that F(-I) was adsorbed as complex ions between F(-I) and Al (i.e., AlF_3^0 and AlF_4^-) and sorption densities of F(-I) abruptly increased when initial F/Al molar ratio was more than 3. There was little to distinguish coprecipitation experimetnal results from simple adsorption ones in all kinds of experiments.

For summary, All of experimental results showed that F(-I) was adsorbed as F^- when the initial F/Al molar ratio was less than 3 whereas F(-I) was adsorbed as complex ions between F(-I) and Al (i.e., AlF_3^0 and AlF_4^-) when the initial F/Al molar ratio was more than 3.

[1] C. Stosiek, G. Scholz, S. L. M. Schroeder and E Kemnitz. (2010) *Chem. Mater.*, **22**, 2347–2356.

https://doi.org/10.1180/S0026461X00006502 Published online by Cambridge University Press

Dating crocidolite deposits using the argon-argon-method

M. HÄRING[1]*, J.A. PFÄNDER[1] AND J. GUTZMER[2]

[1]Institut für Geologie, TU Freiberg, Germany (*correspondence: maria.haering@student.tu-freiberg.de)
[2]Institut für Mineralogie, TU Freiberg, Germany

Understanding the mechanisms and geological framework of crocidolite formation is a matter of debate and often hampered by a precise knowledge of its formation age. To address this issue, we have dated a series of crocidolite (amphibole asbestos) samples from the Asbesheuwels Subgroup (Griqualand West, South Africa) using the Ar-Ar technique. At very low K-contents (0.01 – 0.20 wt% K), between 6 and 30 mg of fiber bundles were measured by laser induced step wise heating on a ARGUS noble gas mass spectrometer.

Resulting ages span a large range between 2.13 and 1.22 Ga at relatively well developed plateaus, from which some of them indicate diffusive Ar loss. The crocidolite ages therefore did not reflect a single event, but a series of post-formation thermal overprints that may have disturbed the K-Ar system. Although no closure temperature is reported for crocidolite, we assume it to be similar to other amphiboles (~500-550°C) and thus interpret the oldest age (2.13 ± 0.02 Ga) as formation age of the crocidolite deposit. This is slightly younger than the age of the banded iron formation (2.5 - 2.4 Ga). Several of our Ar-Ar ages range between 1.63 ± 0.02 and 1.87 ± 0.02 Ga (4 samples) and are most likely related to the Kheis event, during which the Congo Craton collided with the Kaapvaal Craton [1]. The youngest age preserved by one sample (1.22 ± 0.02 Ga) most likely reflects a thermal resetting during the Namaqua-Natal-orogeny at about 1.4 - 1.0 Ga [1].

In conclusion, crocidolite is a suitable phase to be dated by the Ar-Ar technique. Interpretation of ages, however, is hampered by the fact that the retentivity behavior of Argon in crocidolite during thermal overprints is unknown and that the conditions of crocidolite formation itself are poorly understood.

[1] McCarthy, T., Rubidge, B. (2005): *The Story of Earth and Life – A southern African perspective on a 4.6-billion-year journey,* Struik, Singapore.

Sr isotopic composition of manganese nodules: Recorder of Cambrian ocean

Y. HARLAVAN[1]*, M. BAR-MATTHEWS[1] AND A. MATTHEWS[2]

[1]Geological Survey of Israel, 30 Malkhe Israel St., Jerusalem 95501, Israel (*correspondence: y.harlavan@gsi.gov.il)
[2]Institute f Earth Sciences, Hebrew University of Jerusalem

The rapid increase in seawater Sr isotopic composition at the start of the Paleozoic era is attributed to the onset of intensive weathering of the Pan-African orogen. A potential recorder of this significant change is found in Cambrian Mn ores in southern Israel. However, because these ores experienced several stages of dissolution, mobilization and alteration, the timing of their formation is in dispute. Two different generations of Mn nodules (types A and B) were recognized in previous studies [1]. Sr isotope measurements reveal that Type A Mn nodules have a constant value of the $^{87}Sr/^{86}Sr$ ratio (0.7089 ± 0.0005), whereas type B Mn nodules show a wide range (0.709 to 0.716). A composite seawater Sr isotope curve [2] places the Type A Mn nodule values in the lower Cambrian period (*ca*. 550Ma), and hence reinforces their Cambrian origin. This finding agrees with field observations, metal ratios and Eh-pH calculations, which show that Type A Mn nodules formed at the sediment-water interface under oxidizing conditions [1]. In contrast, the high $^{87}Sr/^{86}Sr$ ratios of Type B nodules indicate post-deposition processes that involved radiogenic solutions. The current study indicates that Mn nodules can retain oceanic Sr isotopic ratios, even where they experience complex alteration events. It is, however, essential that the field, petrographic and mineralogical relations are determined.

[1] Bar-Matthews, M., 1987, *Israel. Geol. Mag.* **124**, 211-229.
[2] Nicholas, C. J. (1996). J. *Geol. Soc.*, **153**, 243-254.

https://doi.org/10.1180/S0026461X00006502 Published online by Cambridge University Press

Experimental high-grade alteration of zircon using alkali- and Ca-bearing solutions

DANIEL E. HARLOV[1] AND DANIEL J. DUNKLEY[2]

[1]GeoForschungsZentrum Telegrafenberg, D-14473 Potsdam Germany

[2]National Institute of Polar Research, 3-10 Midori-cho, Tachikawa-shi, Tokyo-to 190-8518 Japan

Natural alteration of zircon takes place either via partial dissolution coupled with overgrowth or via fluid-aided coupled dissolution-reprecipitation [1, 2]. Coupled dissolution-reprecipitation results in the zircon being partially to totally replaced by compositionally re-equilibrated zircon, a new mineral phase or both. In this study, fragments (50 - 200 μm) from an inclusion-free, relatively non-metamict euhedral zircon (nepheline syenite pegmatite, Seiland magmatic province, northern Norway) were experimentally reacted in 20 mg batches with a series of alkali- and Ca-bearing fluids plus 5 mg (ThO_2 + $ThSiO_2$ + SiO_2) in sealed Pt capsules at 900 °C and 1000 MPa for 6 to 11 days (piston cylinder press, CaF_2 setup, cylindrical graphite oven). Fluids included 5 mg 2 N NaOH, 5 mg 2 N KOH, 10 mg $Na_2Si_2O_5$ + 5 mg H_2O, 1 mg NaF + 5 mg H_2O, and 1 - 5 mg $Ca(OH)_2$ + 5 mg H_2O. In each experiment, the fluid reacted with the zircon. This reaction took the form of partial replacement of the zircon with compositionally altered zircon via coupled dissolution-reprecipitation plus varying amounts of overgrowth. The reacted zircon is characterized by a sharp compositional boundary between the altered and original zircon as well as, in some cases, by a micro-porosity and/or inclusions of ZrO_2 or $ThSiO_4$. SIMS analysis of the replaced zircon indicates that it is strongly enriched in Th + Si, heavily depleted in U, and heavily to moderately depleted in (Y+REE). If YPO_4 replaces (Th + Si) in the system, the altered zircon is enriched in YPO_4 and heavily depleted in Th and U. In all experiments radiogenic ^{206}Pb (3 to 5 ppm in the unaltered zircon) is strongly depleted in the altered zircon. Hf concentrations in the altered zircon retain the same value as in the original zircon. The results from these experiments indicate that zircon can be compositionally altered via alkali- and Ca-bearing fluids via coupled dissolution-reprecipitation processes under high-grade conditions and that their internal geochronometer can be reset due to the massive loss of radiogenic Pb.

[1] Geisler *et al*., (2007) *Elements* **3**, 43-50. [2] Putnis (2009) *Rev Mineral Geochem,* vol **70**, 87-124.

Pyrrhotite oxidative dissolution: A microstructural perspective by FIB-TEM and surface topometry

D. HARRIES[1]*, K. POLLOK [1] AND F. LANGENHORST [2]

[1]Bayerisches Geoinstitut, Universität Bayreuth, D-95440 Bayreuth, Germany (*correspondence: dennis.harries@uni-bayreuth.de)

[2]Institut für Geowissenschaften, Friedrich-Schiller-Universität Jena, D-07749 Jena, Germany

Pyrrhotite is non-stoichiometric iron sulfide ($Fe_{1-x}S$ with x < 0.125) and abundant in the Earth's crust. Due to variable Fe deficiency many structural variants arise from the ordering of Fe vacancies within the NiAs-based structure [1]. The resulting superstructures show different physicochemical and magnetic properties, bearing on pyrrhotite's contribution to rock magnetisation and many issues in geochemistry, petrology, and technical mineral processing (e.g., [2]). In the processing of Ni ores, pyrrhotite needs to be separated and is usually discarded to the tailings, where interaction with meteoric waters may lead to oxidation and formation of acid mine drainage.

In order to study differences in reactivity of pyrrhotite varieties, we conducted oxidative dissolution experiments on carefully polished pyrrhotite surfaces containing crystallographically coherent intergrowths of 4C- and NC-pyrrhotite (N = 4.81-4.87). The intergrowths, sharing the same crystallographic orientations, offer the possibility to eliminate the effect of crystal anisotropy, which is significant. Experiments were conducted at 30-50 °C using Fe^{3+} and H_2O_2 as oxidants in acidic solution of pH<3.0. From the reacted samples, surface cross sections in form of electron transparent lamellae were prepared using the FIB technique and studied using analytical TEM. The surface topography of the reacted pyrrhotites was recorded by vertical scanning confocal microscopy and used to deduce individual reaction rates of the intergrown pyrrhotite varieties.

Our results show, that reaction rates strongly and abruptly decrease as pH become larger than 2.65 (close to the iso-electric point [3]). At pH<2.65, NC-pyrrhotite oxidises and dissolves faster than 4C-pyrrhotite and abundant elemental sulfur precipitates. At pH>2.65, 4C-pyrrhotite reacts faster and sulfur appears to be absent. We are continuing to search for S-enriched sulfides (e.g., FeS_2) at the reaction interface by TEM, but until now, no such phases have been found.

[1] Harries *et al*. (2011) *Am. Min*. **96**, in press (DOI: 10.2138/am.2011.3644). [2] Becker *et al*. (2010) *Min. Eng*. **23**, 1045-1052. [3] Dekkers & Schoonen (1994) *GCA* **58**, 4147-4153

https://doi.org/10.1180/S0026461X00006502 Published online by Cambridge University Press

O-isotope evidence for a hydrothermally altered volcanic roof to the Bushveld Complex

CHRIS HARRIS*AND DUANE FOURIE

Dept of Geological Sciences, University of Cape Town, Rondebosch 7701, South Africa (*correspondence: chris.harris@uct.ac.za)

The preserved rocks of the Bushveld Complex are mainly plutonic, and intrusion culminated in the production of > 90 000 km^3 of granite and granophyre. We present mineral $\delta^{18}O$ values that suggest that these granitic magmas assimilated hydrothermally altered material, presumably from a once substantial volcanic edifice. In the granites and granophyres, high-temperature equilibrium O- isotope fractionations are preserved between quartz and zircon, but not between quartz and feldspar, with many samples having -ve values for $\Delta_{quartz\text{-}feldspar}$. Quartz separated from four granite samples, showed no significant difference in core and rim $\delta^{18}O$ values. These data indicate that quartz was not significantly affected by the alteration that raised feldspar $\delta^{18}O$ values. Quartz is, therefore, a reliable proxy for magma $\delta^{18}O$ values in these rocks, leading to estimates of 6.8‰ (assuming $\Delta_{quartz\text{-}magma}$ = 1.18‰), and 6.9‰ (assuming $\Delta_{quartz\text{-}magma}$ = 0.66‰) for the granites and granophyres, respectively. Similar magma $\delta^{18}O$ values (6.6‰) were obtained from zircon data, assuming $\Delta_{zircon\text{-}magma}$ = -1.3‰. The similarity in $\delta^{18}O$ value between granites and granophyres from the three major lobes of the complex suggests a common origin.

Whereas the mafic and ultramafic rocks of the Rustenburg Layered Suite (RLS) have abnormally high $\delta^{18}O$ values (7.1‰) compared to other layered intrusions, the Bushveld granites have abnormally low $\delta^{18}O$ values compared to granites worldwide. Both the RLS and the granitic rocks have similar crustal ε_{Nd} values (mean = -6.4 and -5.3, respectively). Granitic magma derived from mafic magmas similar to those that produced the RLS would have had a magma $\delta^{18}O$ value of about 7.7‰, 1‰ higher than observed. We therefore suggest that the granite magmas assimilated a significant quantity of hydrothermally altered volcanic material with low $\delta^{18}O$ value as has been postulated for Yellowstone.

Cloud processing measured with sulfur isotopes during HCCT 2010

E. HARRIS[1]*, B. SINHA[1], P. HOPPE[1], J. CROWLEY[1], S. BORRMANN[1], S. FOLEY[2], T. GNAUK[3], D. VAN PINXTEREN[3] AND H. HERRMANN[3]

[1]Max-Planck-Institut für Chemie, Becherweg 27, 55128 Mainz, Germany (*correspondence: eliza.harris@mpic.de)

[2]Institute for Geosciences, University of Mainz, Becherweg 21, 55128 Mainz, Germany

[3]Leibniz-Institute for Tropospheric Research, Permoserstrasse 15, 04318 Leipzig, Germany.

Processing of aerosol by clouds has been shown to modify the CCN spectrum, leading to important climatological effects [1, 2]. In-cloud SO_2 oxidation and uptake of sulfate play a large role in this processing, causing both mass increases and hygroscopicity changes. However, the uptake of sulfate and SO_2 is not well constrained or resolved for different particle types and sizes [3, 4].

This study uses isotopic measurements to investigate the uptake of sulfur to particles in an orographic cloud during the HCCT campaign. The campaign took place at the Schmücke mountain in Germany and used connected flow conditions between measurement sites to study the evolution of air masses due to cloud processing. The FEBUKO campaign at the same site saw in-cloud mass production of up to 0.38 μg m^{-3}, 5% of the upwind aerosol mass [5]. Upwind, downwind, cloud droplet residue and interstitial particles were collected during HCCT, as well as SO_2 and H_2SO_4 gases at upwind and downwind sites. NanoSIMS isotopic analysis was then used to constrain the formation and uptake of sulfate in the cloud.

Clear changes were seen in the isotopic composition of the samples between the different sites. Sulfuric acid was depleted in ^{34}S following the cloud. Fine particles were enriched in ^{34}S, consistent with H_2SO_4 condensation as the dominant process. Coarse droplets were also enriched in ^{34}S following the cloud, however SO_2 oxidation to sulfate appeared to be the dominant process. In two out of three measured events, SO_2 gas was enriched while coarse mineral dust sulfate was depleted in ^{34}S, showing a reaction other than aqueous oxidation by H_2O_2 or O_3 had dominated overall SO_2 removal. Laboratory studies are being carried out to identify this 'missing' in-cloud oxidation pathway.

[1] Bower *et al*. (1997) *Atmos. Environ*. **31**, 2527-2543. [2] Hegg *et al*. (2004) *Tellus* **56B**, 285-293. [3] Kasper-Giebl *et al*. (2000) *J. Atmos. Chem*. **35**, 33-46. [4] Barrie *et al*. (2001) *Tellus* **53B**, 615-645. [5] Mertes *et al*. (2005) *Atmos. Environ*. **39**, 4233-4245.

https://doi.org/10.1180/S0026461X00006502 Published online by Cambridge University Press

Accelerated carbon sequestration in mine tailings using elevated pCO_2

A.L. HARRISON*, I.M. POWER AND G.M. DIPPLE

The University of British Columbia, Vancouver, BC V6T 1Z4, Canada (*correspondence: aharriso@eos.ubc.ca)

Mineralization of atmospheric CO_2 within hydrated Mg-carbonate minerals occurs passively in ultramafic mine tailings via weathering of Mg-silicates [1]. If this process were accelerated, large mines may have the capacity to sequester millions of tonnes of CO_2 annually, providing the potential to offset the greenhouse gas emissions of mining. Recent evidence from laboratory experiments and reactive transport modelling indicates uptake of atmospheric CO_2 into solution is rate limiting [2]. An increase in CO_2 partial pressure may accelerate carbon sequestration by increasing dissolved inorganic carbon (DIC) and enhancing primary mineral dissolution due to increased acidity.

The effect of elevated pCO_2 on carbonation rate was examined experimentally to mimic process water chemistry and temperature conditions in tailings at the Mount Keith Nickel Mine (MKM), Western Australia. N_2 and CO_2 mixtures, ranging from 10% to 100% CO_2, were sparged into 3.0 L alkaline slurries containing 5% brucite [$Mg(OH)_2$]. Subsequent experiments will examine carbonation of serpentine, which is more abundant in MKM tailings but dissolves more slowly in aqueous solutions. System mass, pH, temperature and gas composition were monitored throughout the experiment. Samples were analyzed for DIC, Mg concentration, mineralogy and carbon content of solids. Nesquehonite [$MgCO_3 \cdot 3H_2O$] completely replaced brucite within 10 hours with 100% CO_2 gas and within 100 hours with 10% CO_2 gas. This corresponds to an increase in brucite carbonation rate from ~0.007 to ~0.07 g CO_2/g brucite/ hour. PHREEQC geochemical modelling using experimentally derived mineral dissolution rates indicates that serpentine dissolution would exhibit a similar acceleration at elevated pCO_2 conditions. Modelling of experimental conditions indicates that equilibrium between the gas and aqueous phases is not attained during sparging of CO_2-rich gas. Thus there is potential to further accelerate carbonation.

Brucite dissolution provided sufficient buffering capacity for carbonate mineral formation despite a significant pH shift to near neutral conditions in response to CO_2 injection. The carbonation process therefore not only sequesters CO_2, but also neutralizes process water alkalinity. At the mine scale, complete carbonation of brucite at MKM would sequester a total of 1.2 to 3 Mt CO_2.

[1] Wilson *et al*. (2009), *Econ. Geol*. **104**: 95-112. [2] Wilson *et al*. (2010), *Environ. Sci. Technol*. **44**: 9522-9529.

Jack Hills zircon Lu-Hf revisited

T.M. HARRISON AND E.A. BELL

Dept. of Earth and Space Sciences, UCLA, Los Angeles, CA 90095 USA; (tmh@oro.ucla.edu, ebell21@ucla.edu)

Our in situ Lu-Hf analyses of Hadean zircons [1,2] revealed surprising results, including the presence of unradiogenic $^{176}Hf/^{177}Hf$ close to solar system initial (Hf_o) and those with highly positive $\varepsilon_{Hf(T)}$ suggestive of their origin from a long-term depleted source. The latter population, however, was not observed in our follow-up study (or even later efforts by others). As these results have profound implications for the early history of BSE, we have revisited these issues with new in situ Lu-Hf analyses of Hadean zircons from Jack Hills (JH), Western Australia. These analyses were undertaken on an expanded suite of rocks from the region, including a paragneiss adjacent the 'Blob' granite. In situ Lu-Hf analyses using a NEPTUNE LA-ICPMS-MC confirm the presence of large negative $\varepsilon_{Hf(T)}$ deviations and re-open the possibility of significant positive deviations. Specifically, we re-analyzed zircon ANU125 11.3, earlier found to be within error of Hf_o, at multiple locations and replicated the earlier datum within uncertainty. Using currently adopted CHUR parameters, these data collectively require the source of this zircon to have separated from BSE by 4.45 Ga at the latest (assuming Lu/Hf=0) and more likely by 4.5 Ga ($^{176}Lu/^{176}Hf$=0.015). The paragneiss zircons displays uniform $^{176}Hf/^{177}Hf$ but Hadean grains contain younger domains such that matching of age to Lu-Hf systematics is less certain. If the Hadean ages and measured $^{176}Hf/^{177}Hf$ reflect closed system behaviour, then $\varepsilon_{Hf(T)}$ deviations up to +18 are possible. Alternatively, these data could be evidence for the homogenisation of zircon $^{176}Hf/^{177}Hf$ within the source rock. Focussed Lu-Hf studies of 3.9-3.5 Ga JH zircons show a general diminution of $\varepsilon_{Hf(T)}$ deviations by ~4 Ga, suggestive of vigorous continental crust-mantle re-cycling, although evidence of highly negative $\varepsilon_{Hf(T)}$ continues to 3.6 Ga. We thus infer that a geochemical reservoir resembling the modern continental crust formed by ca. 4.5 Ga, perhaps leaving a depleted signature in a sufficiently large portion of the upper mantle to be later sampled by other JH zircons. Numerous geochemical investigations of Hadean zircons reveal their origin in a continental crust-like environment. Thermo-barometric results for Jack Hills zircons and their inclusions imply low conductive heat flows suggestive of their formation under a suppressed heat flow condition. Thus the single most compelling model for their formation is also the simplest: re-working of an initially tonalitic flotation crust by a process similar to that operating at modern convergent margins.

[1, 2] Harrison *et al*., 2005, 2008,

https://doi.org/10.1180/S0026461X00006502 Published online by Cambridge University Press

The Mantle Zoo: New species, endangered species, extinct species

STAN HART

Woods Hole Oceanographic Institution, Woods Hole, MA (shart@whoi.edu)

It has been 29 years since Allegre introduced the field of Chemical Geodynamics, and 25 years since Zindler and Hart formalized the concept of geochemical mantle components, with an attendant, to some odious, concoction of acronym soup. Work on this marriage of mantle geochemistry and mantle dynamics continues unabated to this day, with many Sisyphean heroes along the way. In 1986, we had a chondritic Earth model that we believed (give or take a minor problem with oxygen), and plumes ruled the dynamics of the mantle. Today we don't know what Earth is made of, and there is a vocal (albeit misguided) faction that repudiate plumes! We know unequivocally that the mantle is chemically heterogeneous, but we do not know the scale lengths of these heterogeneities. We know unequivocally that these heterogeneities have persisted for eons (Gy); we don't know where they were formed or where they are stored.

The most accessible and well understood mantle reservoir is the upper depleted MORB mantle (DMM). Classically, this mantle was depleted by extraction of oceanic and continental crust from a "chondritic" bulk silicate Earth. In this post-Boyet and Carlson world, the complementary enriched reservoir may instead be hidden in the deepest mantle. If the Earth is non-chondritic, DMM will be an endangered species. It is widely believed that the DMM is a mixture of peridotitic and mafic lithologies; I think this is an open question.

Radiogenic Pb mantle (HIMU) was argued by Hofmann and White (1982) to be re-cycled ocean crust, and this is still the most viable of existing models. It does require some *ad hoc* chemical manipulations during subduction to satisfy the isotopic constraints (e.g. Th/U fiddling). Given 2 Gy of likely aggregate mantle strains, the mafic component in HIMU will be of small scale length (< 50 m), possibly subsumed into the dominant peridotitic lithology. This mantle species is widespread (Atlantic, Pacific and Antarctic hotspots).

Enriched mantles (EM1 and EM2) almost certainly reflect recycling of enriched continental material. This was verified spectacularly by Jackson *et al* (2007), with the report of EM2 Samoan lavas with $^{87}Sr/^{86}Sr$ up to 0.721. The lithology and scale length of EM1 and EM2 is unconstrained. EM1 is present in Atlantic, Pacific and Indian hotspots; EM2 is confined to the SW Pacific hotspots.

In 2007, FOZO was split into 2 new subspecies (A and B). Many would like to see both become extinct!

Enhanced weathering – Not only CO_2-consumption

JENS HARTMANN[1]*, PETER KÖHLER[2] AND DIETER WOLF-GLADROW[2]

[1]Institute for Biogeochemistry and Marine Chemistry, Universität Hamburg, Germany (*correspondence: geo@hattes.de)

[2]Alfred Wegener Institute, Bremerhaven, Germany

Artifically enhanced weathering at the terrestrial surface by spreading olivine powder on land is one posibillity to contribute to the drawdown of CO_2 from the atmosphere. However due to limitations it is assumed that possibly not more than 1 Gt C a^{-1} can be sequestered by this technique .[1]

Further "effects", which may contribute additionally to the CO_2-sequestration by this technique, have been less analysed, and quantified.[2] At the same time as CO_2-is bound in the water, in the form of bicarbonate or carbonate, silica is released into the aqueous system. In case the propoposed technique would be excersised to its limits, the release of dissolved silica would be a multiple of the natural dissolved silica fluxes from the terrestrial system to the river systems and thus of the land-ocean fluxes.

Dissolved silica is a beneficial nutrient to many crop species, and harvest as well as biomass of these plants are likely to increase significanlty.[3] Additional biomass of plants due to additional silica uptake could be used in strategies to recarbonize the soil-carbon pool. In addition, increased levels of dissolved silica will likely increase the biomass of silica uptaking species in limnic systems, specifically in those, which are eutrophied, and/or are characterised by low silica concentrations. Some proportion of the biomass is sedimented and stored in the river systems, like in lakes or flood plains, and it is not known how much this could be. Further, instead of the mineral olivine one could use less soluble, grinded rocks, which contain significant amounts of phosphorus. In this case P-limited ecosystems might increase their biomass and add to the CO_2-sequestration by artifically enhanced weathering.

[1] Köhler, P., Hartmann, J., Wolf-Gladrow, D. The geoengineering potential of artificially enhanced silicate weathering of olivine. *Proc. Nat. Acad. Sciences* **107**(47), 20228-20233 (2010) [2] Hartmann, J., Kempe, S. What is the global potential for CO_2 sequestration by "stimulated" weathering? *Naturwissenschaften* **95**,1159–1164 (2008) [3] Alvarez, J., Datnoff, L.E. The economic potential of silicon for integrated management and sustainable rice production. *Crop Protection* **20**(1), 43–48 (2001)

https://doi.org/10.1180/S0026461X00006502 Published online by Cambridge University Press

New approaches to analyze the preferential loss of elements from the continental crust

JENS HARTMANN *AND NILS MOOSDORF

Institute for Biogeochemistry and Marine Chemistry, Universität Hamburg, Germany (*correspondence: geo@hattes.de)

Lithological information can be combined with geochemical data to estimate differences between the terrestrial surface and the upper continental crust[1]. In addition, lithological characteristics influence the evolution of the continental crust and its differentiation because they control global chemical weathering. The preferential depletion of elements of the terrestrial surface by chemical weathering can be estimated spatially explicitly using information on lithology, climate and further Earth surface properties[2].

Application of models based on recent available geodata suggest that a large proportion of land-ocean dissolved element fluxes originate from small, highly active areas, which represent only a minor part of the Earth's surface[3]. It is found that the accurate quantification of the fluxes from these areas is crucial to explicate the influence of chemical weathering on the chemical differentiation of the upper continental crust. Specifically the estimation of land-ocean fluxes of Ca and Mg relies on adequate lithological information. To represent relevant, but small areas adequately at the global scale, new global geodata, like improved lithological maps (e.g. the global lithological map, GLiM), are needed. GLiM consists of more than one million polygons, assembled from more than 65 geological maps. In combination with recently developed weathering models it can be used to quantify the preferential loss of elements from the surface of the upper continental crust.

[1] Hartmann, J., Dürr, H. H., Moosdorf, N., Kempe, S. & Meybeck, M.. The geochemical composition of the terrestrial surface (without soils) and comparison with the upper continental crust. *Int. J. Earth Sciences,* doi: 10.1007/s00531-010-0635-x (2011). [2] Hartmann, J., Moosdorf, N.. Chemical weathering rates of silicate-dominated lithological classes and associated liberation rates of phosphorus on the Japanese Archipelago – implications for global scale analysis. *Chemical Geology,* doi: 10.1016/j.chemgeo.2010.12.004. (in press). [3] Hartmann, J., Jansen, N., Dürr, H.H., Kempe, S., Köhler, P. Global CO_2-consumption by chemical weathering: What is the contribution of highly active weathering regions? *Global Planetary Change*, **69**, 185-194 (2009)

Influence of soil shielding on local to global chemical weathering rates

JENS HARTMANN*, NILS MOOSDORF AND RONNY LAUERWALD

Institute for Biogeochemistry and Marine Chemistry, KlimaCampus, Universität Hamburg, Germany (*correspondence: geo@hattes.de)

Chemical rock weathering rates vary spatially, following lithological and hydroclimatic patterns, which have been identified as important controls on chemical weathering rates at the local to global scale. Chemical weathering rates of tropical-continental or permafrost regions can, for comparable runoff and lithological conditions, be lower than than those of island arcs with relatively young rocks and/or "young" terrestrial surfaces.

One of the factors leading to a decrease in chemical weathering rate is the shielding effect of deeply weathered soils above the bedrock [1]. Further, permafrost- or peatland-areas can shield the underlaying bedrock, leading to lower weathering rates if compared to those of island arcs like the Japanese Archipelago.

To quantify this shielding effect at the local to global scale, multi-lithological weathering-functions [2] were applied to river catchments in tropical and permafrost regions. Some of these regions were proposed to yield high chemical weathering fluxes [3].

For comparable lithologies and runoff conditions a reduction of chemical weathering rates by ~50% relative to the weathering rates of island arc regions was identified for certain soil types overlaying the bedrock (Gleysols, Histosols, and deeply weathered tropical soils like Ferrasols). A large regional variability of the reduction factor can be observed.

[1] Stallard, R.F., Edmond, J.M., (1983) Geochemistry of the Amazon 2: The influence of geology and weathering environment on the dissolved load. *Journal of Geophysical Research*, **88**, 9671-9688 (1983) [2] Hartmann, J., Moosdorf, N.. Chemical weathering rates of silicate-dominated lithological classes and associated liberation rates of phosphorus on the Japanese Archipelago – implications for global scale analysis. *Chemical Geology*, doi: 10.1016/j.chemgeo.2010.12.004. (accepted). [3] Hartmann, J., Jansen, N., Dürr, H.H., Kempe, S., Köhler, P. Global CO_2-consumption by chemical weathering: What is the contribution of highly active weathering regions? *Global Planetary Change*, **69**, 185-194 (2009)

https://doi.org/10.1180/S0026461X00006502 Published online by Cambridge University Press

Evolution of the LUSI mud volcano: Fluid chemistry and remote sensing

H.E. HARTNETT*, L. VANDERKLUYSEN AND A.B. CLARKE

Sch. of Earth & Space Exploration, Arizona State Univ., Tempe, AZ 85287 (*correspondence: h.hartnett@asu.edu)

The LUSI mud volcano near Sidoarjo in East Java, Indonesia has been erupting since May 2006. It discharged as much as 180,000 m^3/d at the peak of its activity [1, 2], destroyed thousands of homes, and displaced tens of thousands of people. The solids in the mud can be traced with some certainty to the blue-gray clays of the Upper Kalibeng formation, found 1600-1800 m beneath the LUSI main vent. The erupting fluid is a mixture of water, clay, and other minerals at near-boiling temperatures that is accompanied by venting of hot gases, primarily H_2O vapor, CO_2, and CH_4 [2]. The origin of the LUSI fluids remains a matter of speculation.

LUSI is an evolving and complex dynamic system, thus, we take a multi-disciplinary approach to assess both the fluid provenance and erpution behaviour. Our effort includes both geochemical analyses of aqueous and solid-phase components (elemetal and isotopic composition) as well as ground-based (FLIR) and satellite-based (MODIS, ASTER) thermal remote sensing data for the LUSI main-vent region. Preliminary geochemical results (IC, ICP-MS, Sr isotopes) indicate the water in the LUSI mud may have multiple sources (Fig. 1). Solid-phase analyses (XRD, ICP-MS) confirm the mud has an elemental composition and mineralogy very similar to that of the Kalibeng formation. The satellite-based thermal remote sensing data are used to calculate the radiant heat-flux from LUSI over time. We compare these estimates with ground-based flow rate and thermal flux estimates to establish and calibrate a remote-sensing proxy for mud emission rate.

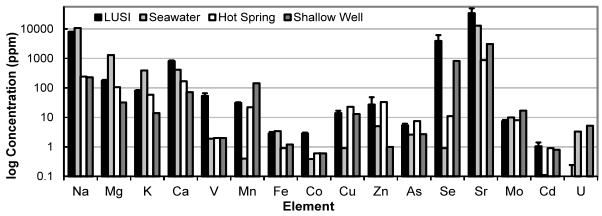

Fig. 1. Metals (ppm) in LUSI fluid (black), and a selection of potential source fluids; LUSI fluid is likely a mixture of multiple water sources that may include hydrothermal fluids.

[1] Zoporowski & Miller (2009) *Mar. Petrol. Geol.* **26**, 1879-1887. [2] Mazzini, *et al.* (2007) *EPSL* **261,** 375-388.

The leaching of arsenic and heavy metals from pyrite slags depots in the upper banks under conditions of highly dynamic groundwater-surfacewater interaction

N. HARTOG[1]*, P. VAN GAANS[1], K.-J. VERMEULEN[2] AND M. JANSEN[2]

[1]Soil and Groundwater Systems, Deltares, Utrecht, The Netherlands (*correspondence: niels.hartog@deltares.nl)
[2]Dutch Railways Foundation for Soil Remediation (SBNS), Utrecht, The Netherlands

Pyritic waste slags from mining activities in Germany were used "*free-of-charge*" in The Netherlands This occured in the 1970's to fill former clay pits in the largely unsaturated upperbank deposits within the drainage area of the river Rhine. The original clay pits in part extended down to the confined sandy aquifer beneath. The present-day groundwater flow patterns within this aquifer are highly dynamic. Variation in surface water levels, causing alternating infiltration and drainage periods, in combination with hydraulic heterogeneity are the main controls. The flow dynamics are reflected in the erratic temporal evolution in groundwater observation wells of both contaminant concentrations (arsenic and heavy metals) and main elements. While weathering of the pyritic slags is the controls the release of contaminants, secondary reaction strongly influence overall contaminant behavior. High arsenic concentrations appear to be associated with the occurrence of drainage conditions, when arsenic mobility is probably enhanced by reductive dissolution of secondary ironhydroxide precipitates at to redox and pH boundaries below the pyritic slags. Mobility of zinc and nickel is probably controlled by pH-dependent adsorption to the sediment under the carbonate-buffered conditions. Geochemical modeling using PHREEQC corroborates that the oxidation of pyrite with oxygen and subsequent pH-buffering by carbonate dissolution are the main geochemical processes. In addition, acid buffering by K-feldspar under conditons in or close to the pyrite slags seems to occur when carbonate buffer is consumed. The extent to which nickel and zinc will be transported further off site will depend in particular on the depletion of sediment acid-buffering capacity, the concentrations of zinc and nickel evolving from the pyriteslags, and the adsorption capacity for nickel and zinc in the sediment. The main control for arsenic transport will be the development of redox conditions in the pyrite slag as well as future alteration of the hydrological situation.

https://doi.org/10.1180/S0026461X00006502 Published online by Cambridge University Press

Magma evolution and the formation of a 'Daly Gap' in the volcanic and plutonic rocks of Akaroa Volcano, New Zealand

EVA HARTUNG[1], CHAD DEERING[2], BEN KENNEDY[1], ALEYSHA TRENT[1], JONATHAN GANE[1], ROSE TURNBULL[3]

[1]Geological Sciences, University of Canterbury, Christchurch, 8140, New Zealand (eva.hartung@pg.canterbury.ac.nz)
[2]Earth and Space Sciences, University of Washington, Seattle, WA 98195-1310, USA (cdeering@u.washington.edu)
[3]GNS Science, Dunedin, 9016, New Zealand

The origin of compositional gaps in volcanic deposits remains controversial. In Akaroa Volcano (9.6-8.6 Ma), New Zealand, a dramatic compositional gap exists in both eruptive and co-genetic intrusive products between basalt and trachyte, and between gabbro and syenite respectively. Previously, the formation of more evolved magmas has been ascribed to crustal melting. However, the interpretation of new major and trace element analysis from minerals and bulk-rocks coupled with the mechanics of crystal-liquid separation offers an alternative explanation that alleviates the thermal restrictions required for crustal melting models.

Major and trace element trends can be reproduced by polybaric Rayleigh fractionation from dry melts (<0.5 wt.% H_2O) at the QFM buffer in a two-stage model. In the first stage, basalt and trachybasalt are produced by separation from an olivine-pyroxene dominant primitive mush at 50-80 vol. % crystallinity near the crust-mantle boundary (10-12 kbar). In the second stage, trachyte melt is extracted from the more evolved trachybasalt mush at mid-crustal levels (3-5 kbar) after the melt has reached 50 vol.% crystallinity. The fractioned assemblage of plagioclase, clinopyroxene, olivine, magnetite and apatite is left in a cumulate residue and corresponds to mineral assemblages of ultramafic enclaves. Trace element modeling of crystal fractionation using this extraction window is consistent with the concentration measured in trachyte (= liquid) and enclaves (= cumulate residue). Similar to the compositional gap observed in the eruptive products, feldspar data also show a distinct gap between the mineral compositions of basalt and trachyte. Yet, importantly, the feldspars from co-magmatic enclaves fill the feldspar compositional gap observed between the basalt and trachyte.

The results of these models indicate that the bimodal distribution of the volcanic products formed from punctuated melt extraction within an optimal crystal fraction window of 50 – 80 % at shallow depth.

Serpentinization and subsequent metamorphism in Mid-Atlantic Ridge peridotites from Hole 1268a, ODP Leg 209: Seawater vs. hydrothermal alteration

J. HARVEY*, I.P. SAVOV AND R.J. NEWTON

School of Earth & Environment, University of Leeds, Leeds LS2 9JT, UK (*correspondence: feejh@leeds.ac.uk)

Material recovered from Hole 1268a, ODP Leg 209, comprises heavily serpentinized peridotite. Subsequent serpentine-to-talc metamorphism and accompanying Si-metasomatism has been attributed to interaction with seawater modified by hot underlying gabbroic intrusions [1]. Sulphur abundances are elevated ([S] ≤2 wt %; [2]) and $\delta^{34}S$ in peridotite-hosted sulphides from talc-metamorphosed lithologies is significantly heavier than in nearby peridotites serpentinized at low-temperatures [3]. These values are consistent with high-temperature ultramafic-hosted hydrothermal vents elsewhere on the Mid-Atlantic Ridge [4] and suggests that the influence of high-temperature fluids from the nearby Logatchev hydrothermal field may extend to a radius of at least 15 km. Using a combination of radiogenic (Sr, Nd) and stable (B, S, O) isotopes this study aims to quantify fluid-rock ratios and chemical exchange, and the relative effects of seawater and hydrothermal fluids on the chemical and mineral evolution of peridotites from Hole 1268a. Preliminary results demonstrate Sr isotope ratios that are relatively uniform throughout the length of the borehole and indistinguishable from those of seawater This suggests particularly high (>100) fluid/rock ratios and contrasts with peridotites and gabbros from other, less altered ODP-drilled Holes nearby (e.g. Hole 1275). It is expected that this will be more precisely constrained with Nd and B isotopes.

[1] Bach *et al*. (2004) *Geochem. Geophys. Geosys.* **5** doi:10.1029/2004GC000744. [2] Paulick *et al*. (2006) *Chem. Geol*. **234**. 179-210. [3] Alt *et al*. (2007) *Geochem. Geophys. Geosys*. **8**, doi:10.1029/2007 GC001617. [4] Delacour *et al*. (2009) *Geophys. Research Abst*. **11**, EGU2009-9488

https://doi.org/10.1180/S0026461X00006502 Published online by Cambridge University Press

Role of water in continental melting

P. HASALOVÁ* AND R.F. WEINBERG

School of Geosciences, Monash University, Clayton, 3800, Victoria, Australia
(*correspondence: pavlina.hasalova@monash.edu)

The Zanskar region, NW India, exposes the High Himalayan Crystalline (HHC) which is a sequence of medium- to high-grade rocks intruded by many granites. Rocks here underwent early dehydration melting that was later overprinted by water-fluxed melting producing extensive migmatites. Each event is recognizable in the field: early dehydration melting has produced leucosomes with peritectic garnet and sillimanite, in contrast to tourmaline-rich two-mica leucogranites associated with later water-fluxed melting. Potential water source here are the underlying cooler rocks that were heated and dehydrated by the thrusting of the hot rocks of the HHC. This water migrated upwards causing extensive melting of the overlying hot rocks. Water flowed into the hot system along a network of fractures. Melting took place at the fracture walls and as water diffuses a diffusion front was set up with a water content/activity gradient away from it. This gradient is preserved in the rock record as reflected in melt volumes produced and mineral composition. Garnets at the far end of the diffusion front reveal different composition and zoning pattern than garnet close to the diffusion front. Garnet close to the diffusion front reveals either no element zoning or Ca and Mg rich cores, in contrast to well preserved prograde zoning at the far end of the diffusion front. This means that rocks that underwent the same P-T history have preserved a mixed signal that is related to fluctuation in volume of water and/or water activity rather than to changes in P-T conditions. And we suggest that presence of water influnce diffusion rates in garnet.

Clay minerals deposit of Halakabad (Sabzevar- Iran)

SEYED MOHAMMAD HASHEMI

Department of Geology, Mashhad branch, Islamic Azad University, Mashad, Iran (dhashemi@mshdiau.ac.ir)

Clay minerals are expanded in south of Sabzevar. They are identified with light color in the filed. The XRD and XRF chemical and mineralogical studies on the Clay minerals indicated that their main clay minerals are Kaolinite, Illite and Dickite. Pyrophyllite is minor clay mineral. Quartz and Sanidine non clay minerals are present with clay minerals. Ratio of Al_2O_3 is about 40 per cent, it is very good for industrial minerals .Volcanic rocks are origin clay minerals. Their composition are basic to acidic. In south of Sabzevar town there is a small part of these rocks available which include volcanic and volcaniclastic rocks. Geochemical and petrographic studies showed that their compositions are generally acidic and intermediates and are of Dacite and Rhyolite and Andesite rocks type that have changed into clay minerals.

https://doi.org/10.1180/S0026461X00006502 Published online by Cambridge University Press

Meteoritic organics as a carrier of the oxygen isotope anomaly in the solar system

KO HASHIZUME[1], NAOTO TAKAHATA[2], HIROSHI NARAOKA[3] AND YUJI SANO[2]

[1]Dept. of Earth & Space Sci., Grad. School of Sci., Osaka Univ., Toyonaka, Osaka 560-0043, Japan; (kohash@ess.sci.osaka-u.ac.jp)
[2]Atmosphere and Ocean Research Institute, Univ. of Tokyo, Kashiwa, Chiba 277-8564, Japan.
[3]Dept. of Earth & Planet. Sci., Grad. School of Sci., Kyushu Univ., Fukuoka 812-8581, Japan.

It is generally accepted that Earth formed from building blocks that compose of metals, rocks, water and organics. The latter two are particularly important to characterize the surface of our planet covered by atmosphere, ocean, and lives, although their exact origins remain unresolved. The organic matter abundantly found in primitive meteorites may provide us precious clues to address this issue. Several pioneers [1-4] discovered that a tiny fraction of the meteoritic organics, opposed to the bulk of them which are likely homogenized by later planetary processes, may preserve primordial isotopic signatures acquired upon its birth in the space medium. The main target of this study is to search for the oxygen isotope anomalies among the meteoritic organics.

We report the detection of organic grains, extracted from an Antarctic carbonaceous chondrite Yamato-793495 (CR2), with the highest $^{17,18}O/^{16}O$ ratios ($\delta^{17,18}O_{SMOW}$~+500‰) [5] among all planetary materials besides the presolar grains. The isotopic composition is plotted in the O isotope diagram close to the slope-1 line, where the compositions for the planet-forming building-blocks are predicted to be plotted on, suggesting that the detected organic grain may represent one of the fundamental carriers responsible for the O isotope anomaly, i.e., the non-mass-dependent $^{17,18}O/^{16}O$ variations commonly observed among all available solid planetary materials. By the multi-isotope imaging analysis, we discovered that $^{17,18}O$ enrichments among the organics were correlated with ^{13}C enrichments. This correlation is naturally explained by the self-shielding effect of CO that occurred in a warm (>60 K) gas medium illuminated by UV light, such as the surface layer of the solar nebula.

[1] Busemann *et al*. (2006) *Science* **312**, 727-730. [2] Nakamura-Messenger *et al*. (2006) *Science* **314**, 1439-1442. [3] Floss & Stadermann (2009) *Astrophys J*. **697**, 1242-1255. [4] Remusat *et al*. (2009) *Astrophys*. *J*. **698**, 2087-2092 (2009). [5] Hashizume *et al*. (2011) *Nature Geoscience* **4**, 165-168.

Isotopic and geodynamic implications of progressive magmatism in W. Anatolia (Turkey)

A. HASOZBEK[123]

[1]New Brunswick Laboratory, SED, Argonne, IL 60439, USA (*correspondence: Altug.Hasozbek@ch.doe.gov)
[2]Institut für Geowissenschaften, Universität Tübingen, Tubingen, D-72074, Germany
[3]Technical Higher Education, Dokuz Eylul University, Torbali, Izmir, 35860 Turkey

In the Aegean region, complex geodynamic processes including subduction, continent continent collision, and back-arc extension occurred from the Eocene to the present time. In NW Anatolia (Turkey), the products of these events are widely exposed. During and after the closure of the Neo-Tethyan Ocean and progressive collision of the Tauride-Anatolide Platform with the Sakarya Continent, widespread magmatism occurred in NW Anatolia. This magmatism is manifested in a NW trending belt along the northern border of the Menderes Massif. Due to the complex geodynamic setting of this region, the exact emplacement mode of the granitoids is still a matter of debate.

In order to see whole progressive magmatic evolution of the Western Anatolia and to understand its tectono-magmatic position in the Aegean region, during and after the collision of the Anatolide-Tauride platform with the Sakarya Continent, magmatic associations from Eocene to Miocene time were examined and gathered together by detailed mapping, geochemical, isotopic and geochronological studies. According to our new results, the Eocene and Miocene granites are shallow seated bodies (4-7 km), granite-granodiorite and monzogranite in composition, and are I-type, calc-alkaline in nature. Their Sr-Nd-Pb-O isotopes are in line with derivation from lower-to middle crustal source lithology. It can be demonstrated that mantle to crustal assimilation during the magma generation played an important role. Within the emplacement natures and isotopic results of the Western Anatolian magmatic associations, considerable limitations are put forward regarding to previously suggested extensional related emplacement models. The magmatic associations in Western Anatolia were formed in two distinct separated phases; the first and the earliest phase resulted in progressive magmatism and formed the intrusive suites of the Western Anatolia during the Eocene- Miocene time long before the main extension phase started. The late phase is mostly associated with the extensional regime.

https://doi.org/10.1180/S0026461X00006502 Published online by Cambridge University Press

Tracking single coccolith dissolution with picogram resolution: Implications for CO_2 sequestration and ocean acidification

T. HASSENKAM, A. JOHNSSON, K. BECHGARRD AND S.L.S STIPP

Nano-Science Center, Department of Chemistry, Univeristy of Copenhagen, Denmark, (tue@nano.ku.dk, stipp@nano.ku.dk)

Coccoliths are micrometer scale shields made from 20 to 60 individual calcite ($CaCO_3$) crystals that are produced by some species of algae. Chalk deposits, the fossil remains of ancient algae, have remained remarkably unchanged by diagenesis. Even after 60 million years, the fossil coccolith crystals are still tiny (<1 μm), compared with inorganically produced calcite, where one day old crystals can be 10 times larger. This raises the question if the biogenic nature of coccolith calcite gives it different properties than inorganic calcite? And if so, can this protect coccoliths in CO_2 challenged oceans? By recording the changes in resonant frequency of a cantilever coccolith setup the dissolution of individual specimens, can be tracked with picogram (10^{-12} g) resolution.

The results show that the behaviour of modern and fossil coccoliths is similar and both are more stable than inorganic calcite. However, ancient and modern coccoliths, that resist dissolution in Ca-free artificial seawater at pH > 8, all dissolve when pH is 7.8 or lower. Ocean pH is predicted to fall below 7.8, by 2100, in response to rising CO_2 levels. Our results imply that at these conditions, the advantages offered by the biogenic nature of calcite will disappear, putting coccoliths on algae and in the calcareous bottom sediments at risk [1].

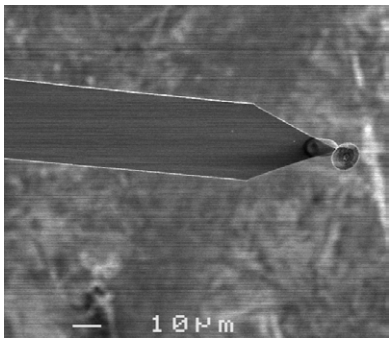

Figure 1: AFM cantilever with a single coccolith attached to the end. Mass 500 pg

[1] Hassenkam *et al*. (2011) *PNAS* **accepted**

Online preconcentration ICP-MS analysis of rare earth elements in seawater

ED HATHORNE[1]*, TORBEN STICHEL[1,2], PATRICIA GRASSE[1] AND MARTIN FRANK[1]

[1]IFM-GEOMAR, Wischhofstr. 1-3, 24148 Kiel, Germany (*correspondance: ehathorne@ifm-geomar.de)

[2]SOEST, University of Hawaii 1680 East-West Rd, Honolulu, HI 96822, USA

The rare earth elements (REEs) with their systematically varying properties are useful tracers of continental inputs, particle scavenging activity and the oxidation state of seawater. However, their generally low (~pmol/kg) concentration and fractionation potential during chemical treatment makes them difficult to measure. Here we report initial results for GEOTRACES samples obtained using an automated preconcentration system, which separates the matrix and elutes the preconcentrated sample directly into the spray chamber of an ICP-MS instrument.

The commercially available SeaFAST system (Elemental Scientific Inc.) uses a resin with ethylenediaminetriacetic acid and iminodiacetic acid functional groups to preconcentrate REEs and other metals while alkali and alkaline earth elements are washed out. Importantly, time resolved analysis of the elution peaks demonstrates that this resin does not fractionate the REEs. The technique we developed for the analysis of REEs in seawater samples loads 4 mL of undiluted, filtered and acidified (pH ~2), seawater sample onto the column. The column is flushed with water and a pH 6 buffer solution for ~10 mins to wash the matrix away before the REEs are eluted with nitric acid into the ICP-MS for measurement. Using this technique each analysis takes about 15 mins and we obtain sub ppt limits of detection (3 times the standard deviation of blank measurements). Repeated measurements of a sample from 2000 m water depth in the Southern Ocean allows the external precision of the technique to be estimated at < 10% for all REEs and < 5% for many others. Comparison of Nd concentrations with isotope dilution measurements for 30 samples shows the techniques agree within 10%. To assess the accuracy of the technique for all REEs mine water standards have been diluted with NaCl matrix and analysed as unknowns. The results for most elements agree well with values in the literature. This makes the online preconcentration ICP-MS technique advantageous for the minimal sample preparation required and the relatively small sample volume consumed. Further development of the technique is underway to ensure accurate results even for the least abundant REEs in seawater samples.

https://doi.org/10.1180/S0026461X00006502 Published online by Cambridge University Press

Mineralogical and geochemical characteristics of Emet borate basin, Kütahya, Western Anatolia, Turkey

ZEYNEP NAZLI HATIPOGLU[1] AND ABIDIN TEMEL[2]

[1]Acme Analitik Laboratuar Hizmetleri LTD. STI. 21. Cadde 108/2, 06370, Yenimahalle/ Ankara, Turkey
[2]Hacettepe Üniversitesi Müh. Fak. Jeoloji Müh. Böl. 06800, Beytepe/ Ankara Turkey

The volcanosedimentary borate deposites in Emet, Kütahya have been studied to investigate the mineralogy and geochemistry of neoformation minerals (carbonate, clay, sulphate, borate minerals). For this purpose, 193 samples collected from 4 different locations (Espey, Hisarcık open pits and two drill holes) in Emet.

XRD whole rock analyses made on all samples show that, clay, feldspar, realgar, mica, carbonate (dolomite, calcite), sulphate (glauberite, gypsum, anhydrite), opal-CT and borate (colemanite, ulexite, probertite, hydroboracite, P-veachite) are the minerals detected. XRD clay fraction analyses made on 69 samples revealed that there are illite, smectite, kaolinite and chlorite minerals. ICP major element analyses applied on smectite minerals show that the trioctaedric smectites are saponite and stevensite in composition.

At the investigation area, an increase at the amount of smectite has been discovered from northern parts (Espey) to southern parts (Hisarcık). As the dolomite minerals are absent at Espey open pit and present at two drill holes and Hisarcık open pit, the Espey area can probably be the edge of the basin. Ca-borate→ Ca-borate + Na-borate→ Na-Ca-borate + Mg-Ca-borate mineralogical zoning show that the drilling area of two drill holes which are located between Espey and Hisarcık open pits, can be the center of the basin. Especially at the borate bearing zones Sr reaches high concentrations. Samples that have higher clay contents also have higher REE contents.

Chemical heterogeneities along the South Atlantic Mid-Ocean-Ridge (5-11°S): Shallow or deep recycling of ocean crust?

F. HAUFF[1]*, K. HOERNLE[1], T.F. KOKFELT[2], K. HAASE[3], D. GARBE-SCHÖNBERG[4] AND R. WERNER[1]

[1] IFM-GEOMAR, Wischhofstr. 1-3, 24148 Kiel, Germany (*correspondence: fhauff@ifm-geomar.de)
[2]GEUS, Øster Voldgade 10, 1350 Copenhagen K, Denmark
[3] GeoZentrum Nordbayern, University of Erlangen-Nürnberg, Schlossgarten 5, 91054 Erlangen, Germany
[4]Inst. Geosciences, Christian-Albrechts-Univ., Kiel, Germany

Between 5° and 11°S, the Mid-Atlantic Ridge displays anomalous crustal thickness and geochemical compositions, thought to be related to either small scale upper mantle heterogeneities or a weak, diffuse mantle plume. We report new high precision trace element and Sr, Nd and Pb (DS) isotope data for 72 ridge axis samples and 9 off-axis seamount samples along with U–Th–Ra disequilibria data for off axis seamounts at c. 9.7°S. At least four distinct components are needed to explain the geochemical variations along the ridge: 1) a common depleted (D-MORB-like) component near and north of 4.8–7.6°S, 2) an enriched component upwelling beneath Ascension Island and the northern A1 ridge segment (segment numbers ascend from north to south), 3) an enriched component upwelling beneath the A2 ridge segment, and 4) an enriched component upwelling beneath the line of seamounts east of the A3 segment and the A3 and A4 segments. The A1 and the A3+A4 segment lavas form well-defined mixing arrays from Ascension Island and the A3 seamounts respectively to the depleted D-MORB component. We propose that the enriched components represent different packages of subducted ocean crust and/or ocean island basalt (OIB) type volcanic islands and seamounts that have either been recycled through 1) the shallow mantle, upwelling passively beneath the ridge system or 2) the deep mantle via an actively upwelling heterogeneous mantle plume that interacts with the ridge system.

https://doi.org/10.1180/S0026461X00006502 Published online by Cambridge University Press

Arsenic and tungsten in groundwaters of West Bengal, India

T. JADE HAUG[1], ANDREW NEAL[2], NINGFANG YANG[1], KATHERINE TELFEYAN[1], SAUGATA DATTA[2] AND KAREN H. JOHANNESSON[1]

[1]Department of Earth and Environmental Sciences, Tulane University, New Orleans, LA 70118, (thaug@tulane.edu, kjohanne@tulane.edu)

[2]Department of Geology, Kansas State University, Manhattan, KS 66506, (sdatta@k-state.edu)

Arsenic (As) concentrations and speciation were measured along with tungsten (W) in groundwaters from Murshidabad, West Bengal, India ($6.91 \leq pH \leq 7.54$). Total dissolved As concentrations (As_T) range from < 1 to 4622 μg kg^{-1}, and As(III) predominates in solution accounting for between 54% to >98% of As_T. W concentrations range from 0.15 to 1.1 μg kg^{-1}. The W concentrations are low compared to alkaline groundwaters (pH > 8) from Nevada, USA, where W concentrations range from 0.27 to 742 μg kg^{-1} [1, 2]. Although W correlates with As in the Nevada groundwaters ($r^2 = 0.63$, $p < 0.05$ [1]), W is not correlated with As_T or As(III) in Murshidabad groundwaters ($r^2 = 0.075$, $p > 0.2$ and $r^2 = 0.085$, $p > 0.2$, respectively). These relationships suggest that As and W biogeochemistry differ as a function of pH and redox conditions. Both W and As are strongly desorbed from mineral surface sites at high pH and under oxidizing conditions [3], which explains, in part, the relationship between these two elements in groundwaters from Nevada. Under reducing conditions and neutral pH that characterizes Murshidabad aquifers, As(III), which occurs as the uncharged $H_3AsO_3^0$ species, is more mobile than the tungstate oxyanion, WO_4^{2-}. We hypothesize that both As(III) and W are mobilized by reductive dissolution of Fe(III) oxides/oxyhydroxides, but that WO_4^{2-} is strongly re-sorbed, whereas As(III) is relatively more mobile as the uncharged, $H_3AsO_3^0$ in Murshidabad.

[1] Seiler *et al*. (2005) *Appl. Geochem*. **20**, 423. [2] Johannesson *et al*. (2000) *Aquatic Geochem*. **6**, 19. [3] Johannesson and Tang (2009) *J. Hydrol*. **378**, 13.

The volatile content of primitive Lunar volcanic glasses

E.H. HAURI[1], A.E. SAAL[2], , M.J. RUTHERFORD[2] AND J.A. VAN ORMAN[3]

[1]DTM, Carnegie Institution of Washington, (ehauri@ciw.edu)
[2]Dept Geological Sciences, Brown University
[3]Dept Geological Sciences, Case Western Reserve University

The general consensus is that the Moon formed and evolved through a single or series of catastrophic heating events in which most of the highly volatile elements, especially hydrogen, were evaporated away. That notion has changed with new reports showing evidence of indigenous water in lunar volcanic glasses [1] and in lunar apatites from mare basalts [2, 3, 4]. These results represent the best evidence for the presence of a deep source within the Moon relatively rich in volatiles. We compiled volatile data (C, H_2O, F, S, Cl) for more than 360 individual Apollo 14, 15 and 17 lunar glasses with composition ranging from very-low to high-Ti contents. The glassy volcanic spherules range in size from ~100 μm to ~ 1 mm. We measure the volatile content by SIMS using a Cameca IMS 6F and NanoSIMS at DTM, CIW. Our new SIMS detection limits (~0.13 ppm C; ~0.4 ppm H2O, ~0.05 ppm F, ~0.21 ppm S, ~ 0.04 ppm Cl) represent at least 2 orders of magnitude improvement over previous analytical techniques.

Our data support the hypothesis that there were significant differences in the initial volatile content of lunar magmas, and/or the mechanism of eruptive de-gassing was different for different eruptions. Interestingly, a general correlation was found between the volatile enrichment and the incompatible trace elements. This suggests that eruptive degassing, although extensive, did not completely erase initial differences in volatile contents between the distinct compositional groups of volcanic glasses. Our results suggest not only a much wetter Moon's interior than previously thought [1], but also suggest that the KREEP component, either through shallow assimilation by the melt or deep hybridization of the LMO cumulate, may influence the volatile composition of erupted lunar magmas.

[1] Saal, A. E. *et al*. (2008) *Nature* **454**, 192. [2] McCubbin, F.M. *et al*. (2010) *PNAS*, **107** (25), 11223. [3] Boyce, J. W. *et al*. (2010) *Nature* **466**, 466. [4] Greenwood, J. P. *et al*. (2010) P*roc. 41th LPSC* Abs 2439. [5] Hauri, E. H. *et al*. (2006) *EPSL* **248**, 715. [6] Spangler, R. *et al*. (1984), *J. Geophys. Res*. **89**, 487. Proc. 40th LPSC Abs 2374

https://doi.org/10.1180/S0026461X00006502 Published online by Cambridge University Press

Use of pyrolysis-GC/MS combined with petrographic analysis to monitor changes of organic matter in coal and biomass derived materials

MARTINA HAVELCOVÁ*, IVANA SÝKOROVÁ AND HANA TREJTNAROVÁ

Institute of Rock Structure and Mechanics AS CR,v.v.i. V Holešovičkách 41, 182 09 Prague, Czech Republic (*correspondence: havelcova@irsm.cas.cz)

Charred solid organic residues produced during biomass and fossil fuel combustion are collectively referred as black carbon (BC). BC is ubiquitous and can be found in sediments, soils, and the atmosphere [1]. Because of the important role and effect of BC materials on the environment and biogeochemical cycles, different techniques have been used to study their chemical properties and structures [2].

In this study (project IAA300460804), pyrolysis of coal and biomass was studied under varying conditions of temperature and environment. The solid products, i.e. chars, were analysed by combination of optical microscopy and pyrolysis-GC/MS methods. The elemental composition was also determined and the chemothermal oxidation method [3] was employed to determine the BC content in the samples.

The composition of chars was dependent on the used conditions and indicated that incomplete combustion leads to the formation of aromatic structures and regions. Chars prepared in oxidative atmosphere created more condensed aromatic network at lower temperatures by comparison to chars prepared in inert atmosphere. Compounds typical for the BC presence like indene, benzonitrile, naphthalene, methylnaphthalenes, fluorene were found in all chars.

The results of BC determination were in good consensus with H/C atomic ratios and reflectance values. The found relation among identified organic compounds and BC corresponds with the results for carbonaceous matter in dust and lacustrine seidments from Prague [4].

[1] Goldberg (1985) John Wiley and Sons, New York. [2] Song and Peng (2010) *J. Anal. Appl. Pyrolysis*. **87**, 129-137. [3]Gustafsson *et al*. (2001) *Global Biogeochemical Cycles* **15**, 881–890. [4] Sykorova *et al*. (2009) *Int.J. Coal Geol*. **80**, 69-86.

LTD Phase I.: Long-term real-scale diffusion experiment results

V. HAVLOVA[1]*, A. MARTIN[2], J. EIKENBERG[3] AND F. SUS[1]

[1]NRI Rez plc., Husinec-Rez 130, 250 68 Rez, Czech Rep. (*correspondence: hvl@ujv.cz)

[2]NAGRA, Hardstrasse 73, 5430 Wettingen, Switzerland

[3]Paul Scherrer Institute, 5232 Villigen PSI, Switzerland

Matrix diffusion can significantly decrease the amount of radionuclides potentially released from deep geological repository of radioactive waste. A systematic reseach approach to understanding the diffusion process was applied within Phase I of the Long Term Diffusion Project (LTD) at the Grimsel Test Site, Switzerland (GTS, www.grimsel.com).

In workpackage 1 of the LTD project, a cocktail of ^{3}H, ^{22}Na, ^{131}I and ^{134}Cs tracers was circulated in a packed-off interval in a borehole drilled 8 m into undisturbed granitic matrix in GTS and left for 26 months in the contact with the rock. Tracer solution was regurarly sampled in order to obtain the pattern of radionuclide activity decrease in the test interval. Later the borehole was overcored and the rock segments were analysed for radionuclide content.

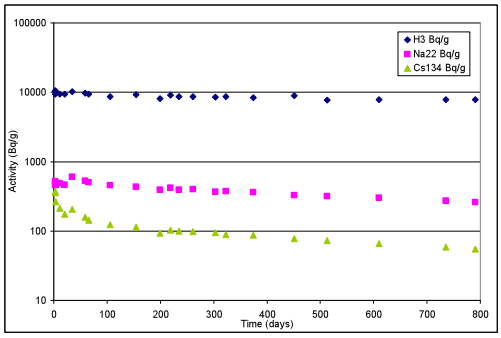

Figure 1: Radionuclide activity (Bq/g) decrease in the test interval.

The activity decrease in the circulation tank is shown in Fig. 1. ^{22}Na and ^{134}Cs were analysed in the rock samples, using γ-spectroscopy. Special care had been applied for ^{3}H analyses (modified LSC). Diffusion profiles within the rock segments clearly showed that ^{3}H had reached a distance of 17 cm from the borehole. ^{22}Na migrated up to 7 cm and ^{134}Cs up to 1.5 cm distance respectively. The results are under further evaluation.

The research was held in co-operation with NAGRA, NRI, Helsinki University, JAEA and AIST (2005-2009). NRI thanks to RAWRA and to to the Czech Ministry of Education, Youth and Sport (contract No. P05LA248) for funding.

https://doi.org/10.1180/S0026461X00006502 Published online by Cambridge University Press

The generation and evolution of the continental crust

CHRIS HAWKESWORTH[1]*, PETER CAWOOD[1] AND BRUNO DHUIME[1,2]

[1]Department of Earth Sciences, University of St. Andrews, St. Andrews KY16 9AL, UK (*correspondence: cjh21@st-andrews.ac.uk)

[2]Department of Earth Sciences, University of Bristol, Queens Road, Bristol BS8 1RJ, UK

There is increasing evidence for marked changes in the crustal record at the end of the Archaean, and that these reflect changes in both the generation and the evolution of the continental crust. The post Archaean crust has marked peaks in crystallisation ages that coincide with the development of supercontinents. These peaks appear to be an artefact of preservational bias, in that magmas generated in some tectonic settings may be preferentially preserved in the geological record, rather an indication of periods of unusually large volumes of crustal magmatism. The creation and destruction of supercontinents require some form of plate tectonics, and yet the rates of crust generation and destruction along modern subduction zones are strikingly similar.

In the Archaean, and by implication the Hadean, the continental lithosphere was thinner, mountains were more difficult to support, and perhaps there was less erosion. There is also less evidence for the development of peaks of ages globally. Material must have moved up and down in the uppermost mantle, and yet the magmatic record is different from that commonly associated with subduction. The zircon record yields little evidence for the development of depleted mantle in the Hadean, and on that basis for large volumes of continental crust. Granitic crust was generated by the remelting of mafic crust, and there is some evidence for a shift from mafic to more evolved source rocks with time. The Hadean crust appears to have had a bimodal silica distribution, as also characterizes the early Archaean rock assemblages. These at present characterise intraplate rather than plate margin settings, and yet most of the crust was generated by the end of the Archaean, and the average crust has a composition similar to that of destructive plate margin magmatism.

Hf isotopes require no subduction in the Hadean?

CHRIS HAWKESWORTH[1]*, A.I.S. KEMP[2], S.A.WILDE[3] AND J.D.VERVOORT[4]

[1]Department of Earth Sciences, University of St. Andrews, St. Andrews KY16 9AL, UK (*correspondence: cjh21@st-andrews.ac.uk)

[2] School of Earth and Environmental Science, James Cook University, Townsville, Australia

[3]The Institute of Geosciences Research, Curtin University of Technology, Perth, Australia

[4]School of Earth and Environmental Science, Washington State University, Pullman, USA

The Hf, Pb and O isotope data on results of an in situ isotopic study of 67 Jack Hills zircons (Kemp et al. 2010) are combined with Hf isotope data from zircons of the Narryer gneisses (3.65- 3.3 Ga) and from Neoarchaean granites that intrude the Jack Hills belt. The detrital zircons define a subchondritic ε_{Hf} – time array consistent with the protracted intra-crustal reworking of an enriched, dominantly mafic protolith that was extracted from primordial mantle at 4.4-4.5 Ga. There is no evidence for the existence of strongly depleted Hadean mantle, and on that basis for large volumes of continental crust. There is also no evidence for juvenile input into the parental magmas to the Jack Hills zircons.

This simple Hf isotope evolution is difficult to reconcile with modern plate tectonic processes, which generate magmas with both juvenile and reworked sources. Strongly unradiogenic Hf isotope compositions of zircons from several Archaean gneiss terranes, including the Narryer and Acasta gneisses, suggest that dominantly mafic Hadean source reservoirs were tapped by granitic magmas up to 1.8 billion years after the initial crust generation episode. This implies the presence of Hadean crust with a bimodal silica distribution, as also characterizes the early Archaean rock assemblages, but not modern arcs. It supports the notion of a long-lived and globally extensive Hadean protocrust that may have comprised the nuclei of many Archaean cratons. Such Hadean protocrust survived the postulated late heavy meteorite bombardment of the terrestrial planets at ca. 3.9 Ga and might not have endured if crust-mantle recycling processes like subduction were efficient in the Hadean.

[1] Kemp, A.I.S., Wilde, S.A., Hawkesworth, C.J., Coath, C.D., Nemchin, A., Pidgeon, R.T., Vervoort J.D. & DuFrane A. (2010) *Earth. Planet. Sci. Lett.* **296**, 45-56

https://doi.org/10.1180/S0026461X00006502 Published online by Cambridge University Press

The influence of boundary scavenging and particle composition on dissolved and buried ^{230}Th and ^{231}Pa in the subarctic North Pacific

CHRISTOPHER T. HAYES[1]*, ROBERT F. ANDERSON[1] AND RAINER GERSONDE[2]

[1]Lamont-Doherty Earth Observatory of Columbia University, Palisades, NY, 10964 USA (*correspondence: cth@ldeo.columbia.edu)
[2]Alfred Wegener Institue for Polar and Marine Research, Bremerhaven, Germany (Rainer.Gersonde@awi.de)

The well-known production rates of insoluble ^{230}Th and ^{231}Pa in seawater via decay of soluble uranium make them useful tracers of scavenging processes in the modern ocean. Additionally, their half-lives (75.7 and 32.5 kyr, respectively) and preservation in the sediment record make them attractive tools for understanding the particle flux of the late Pleistocene ocean. Yet, multiple processes affect the distribution of these radionuclides in the ocean including particle flux, particle composition, advection and eddy diffusion. Based on the available, spatially-limited, modern ocean observations, it is often unclear which factor has the primary control on a particular seawater profile or surface sediment survey. This ambiguity hinders our understanding of the behavior of other trace metals that undergo scavenging (such as the micronutrient Fe) in addition to our ability to interpret sediment ^{231}Pa/^{230}Th records which have important paleoceanographic and paleoclimtologic consequences.

New observations of ^{230}Th and ^{231}Pa in the water column and in surface sediments are presented here from the Innovative North Pacific Experiment cruise (INOPEX, Jul-Aug 2009) which crossed large gradients in particle flux and particle composition. Boundary scavenging, or preferential removal at high particle flux sites, appears to have little impact on lateral gradients in the concentrations and ratio of dissolved ^{230}Th and ^{231}Pa. As well, concentrations in surface sediments compared with those in the immediately overlaying bottom water allow calculation of pseudo-distribution coefficients for the scavenged elements and fractionation factors for the ^{231}Pa/^{230}Th ratio. These parameters in light of sediment compositions demonstrate the relative importance that the chemical composition of particulate matter plays in scavenging. A new paradigm for understanding the removal of particle-reactive elements from the ocean may need to necessarily include the differential scavenging intensities of variable particle types as well as seafloor processes, which will also be investigated here through high depth-resolution profiles of water within 200 m of the bottom.

Mineral evolution: What's next?

R.M. HAZEN[1], R.T. DOWNS[2], J. GOLDEN[2], E.S. GREW[3], M. MCMILLAN[2], J.P. RALPH[4] AND D. A. SVERJENSKY[1,5]

[1]Geophysical Laboratory, Washington, DC 20015 USA (*correspondence: rhazen@ciw.edu)
[2]University of Arizona, Tucson, AZ 85721 USA
[3]University of Maine, Orono, ME 04469 USA
[4]mindat.org, 81 Woodcote Grove Rd, Surrey CR5 2AL, UK
[5]Johns Hopkins University, Baltimore, MD 21218 USA

The central thesis of mineral evolution is that the near-surface mineralogy of terrestrial planets and moons diversifies through time owing to processes such as planetary accretion and differentiation, the evolution of igneous rocks, fluid-rock interactions, and the influences of life. Studies of mineral evolution thus seek to frame mineralogy in an historical context by focusing on temporal changes in near-surface characteristics, including mineral diversity and associations, relative abundances of mineral species, ranges of chemical and isotopic compositions, and grain sizes and morphologies [1,2]. Mineral evolution also exemplifies aspects of other complex evolving systems, in that we observe complexification (i.e., diversification) through time and each stage of mineral evolution depends on the sequence of prior stages [3]. Recent efforts in mineral evolution research have focused on first reported appearances of mineral species containing specific chemical elements, e.g., U, Be, B, Hg and Mo through time [4,5]. These studies reveal striking increases in the diversity of mineral species, notably between 2.0 to 1.7 and 0.6 to 0.2 billion years ago. Other on-going studies correlate the relative abundances of minerals to geologic conditions, with special attention on changes in clay mineralogy, both in absolute and relative terms [6]. Variations in the extent of incorporation of non-essential elements in specific minerals through time, notably redox sensitive elements, represents a third promising avenue of research, e.g., reported increased incorporation of Re and W in molybdenite (MoS_2) during the past billion years. These efforts are being facilitated by development of a Mineral Evolution Database linked to the comprehensive mindat.org platform [7].

[1] *Am. Mineral.*, 2009, **93**, 1693-1720; [2] *Elements*, 2010, **6**, 9-12; [3] *ibid.*, 43-46; [4] *Am. Mineral.*, 2009, **94**, 1293-1311; [5] *GSA Abstr. Prog.*, 2010, **42**(5), 199; [6] *ibid.*, 199; [7] *Am.Mineral.*, 2011, **96**, in press.

https://doi.org/10.1180/S0026461X00006502 Published online by Cambridge University Press

The Deepwater Horizon oil spill: Ecogenomics of the deep-sea plume

TERRY C. HAZEN

Lawrence Berkeley National Laboratory, Berkeley, CA USA (tchazen@lbl.gov)

The explosion on April 20, 2010 at the BP-leased Deepwater Horizon drilling rig in the Gulf of Mexico off the coast of Louisiana, resulted in oil and gas rising to the surface and the oil coming ashore in many parts of the Gulf, it also resulted in the dispersment of an immense oil plume 4,000 feet below the surface of the water. Despite spanning more than 600 feet in the water column and extending more than 10 miles from the wellhead, the dispersed oil plume was gone within weeks after the wellhead was capped – degraded and diluted to undetectable levels. Furthermore, this degradation took place without significant oxygen depletion. Ecogenomics enabled discovery of new and unclassified species of oil-eating bacteria that lives in the deep Gulf where oil seeps are common. Using 16s microarrays, functional gene arrays, clone libraries, lipid analysis and a variety of hydrocarbon and micronutrient analyses we were able to characterize the oil degraders. Metagenomic sequence data was obtained for the deep-water samples using the Illumina platform. In addition, single cells were sorted and sequenced for the some of the most dominant bacteria that were represented in the oil plume; namely uncultivated representatives of *Colwellia* and *Oceanospirillum*. The results provide information about the key players and processes involved in degradation of oil, with and without COREXIT, in different impacted environments in The Gulf of Mexico. This data suggests that a great potential for intrinsic bioremediation of oil plumes exists in the deep-sea and other environs in the Gulf of Mexico.

Silver nanoparticle-reactive oxygen species interactions: Application of a charging-discharging model

D. HE, A.M. JONES, S. GARG AND T.D. WAITE*

University of New South Wales, Sydney, NSW, Australia 2052 (di.he@student.unsw.edu.au, adele.jones@unsw.edu.au, s.garg@unsw.edu.au, *correspondence: d.waite@unsw.edu.au)

A complex interplay between AgNPs, Ag^+, superoxide and H_2O_2 exists with an understanding of these interactions potentially at the core of the bactericidal behavior of silver species [1-3]. This work is focused on obtaining a better understanding and, to the extent possible, quantification of the interaction between AgNPs and ROS.

The ability of these particles to catalytically decompose H_2O_2 was examined by measuring the decay of H_2O_2, the re-formation of AgNPs and the subsequent degradation of Ag^+ [4]. A kinetic model based on the concept of electron storage and subsequent discharge by AgNPs has been developed and found to adequately explain all results obtained [5-7].

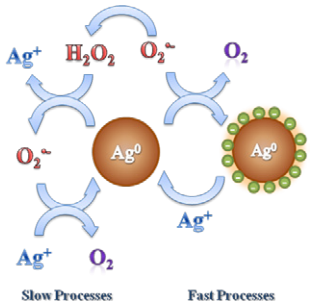

Figure 1: Schematic presentation of the action of AgNPs as electron pool in ROS reactions.

[1] Morones *et al*. (2005) *Nanotechnology* **16**, 2346. [2] Hwang *et al*. (2008) *Small* **4**, 746. [3] Kohn & Nelson (2007) *Environ. Sci. Technol.* **41**, 192. [4] Guo *et al*. (2008) *J. Photoch. Photobio. A* 193, 89. [5] Henglein (1979) *J. Phys. Chem.* **83**, 2209. [6] Henglein & Lilie (1981) *J. Am. Chem. Soc.* **103**, 1059. [7] Henglein (2001) *Langmuir* **17**, 2329.

https://doi.org/10.1180/S0026461X00006502 Published online by Cambridge University Press

Effects of water on the thermal stability of hydrocarbons and the composition and isotope characteristics of the gas products

HE KUN, ZHANG SHUICHANG AND MI JINGKUI

Research Institute of Petroleum Exploration and Development, PetroChina, Beijing 100083, China

As ubiquitous inorganic agent in subsurface, water can react with hydrocarbons [1], although no consistent opinion about the effects of water on the stability of hydrocarbons were achieved[2].

In this paper, a series of isothermal gold-tube pyrolysis experiments using *n*-C_{16} and a marine oil were conducted to study the effects of water chemistry on gas yields and isotopes. It was revealed that the interaction between water and hydrocarbons lead to a relative high content of inorganic gas products. Water showed distinct effect on the cracking of hydrocarbons at lower and higher temperature. Meanwhile, the pH and dissolved salts type and concentration can affect the reaction rate of the organic-inorganic interactions.

The ^{13}C of hydrocarbon gas, especially for CH_4 and C_2H_6, was depleted in the presence of water. An enrichment of D for CH_4 and C_3H_8 can be evidently observed in hydrous pyrolysis using H_2O and *n*-C_{16}, whereas, a reverse phenomenon occur for C_2H_6. The increase of δD for all the hydrocarbon gases with the presence of D_2O demonstrates that water has provided hydrogen for generation of hydrocarbon gas in pyrolysis. In addition, the presence of smectite and calcite carbonate can remarkably promote the gas yields. The unique surface acid of clay mineral accelerated the decomposition of D_2O and the exchange of D between water and hydrocarbon gases, though its catalytic effect on generation of gas yields was weaker than the carbonate.

[1] Seewald (2003) *Nature* **426**, 327-333. [2] Lewan (1997) *GCA* **61**, 3691-3723.

Interaction of synthetic manganite with antimony(III)

M.C. HE* AND X.Q. WANG

State Key Laboratory of Water Environment Simulation, School of Environment, Beijing Normal University, No. 19 Xinjiekouwai Street, Beijing 100875, China. (*correspondence: hemc@bnu.edu.cn)

Manganese oxides play an important role in many redox processes in the environment, such as oxidation of antimony (Sb) [1]. The kinetics of antimony transformation by synthetic manganite is examined in this study.

The kinetic experiment was carried out with a background electrolyte of 0.01 M $NaNO_3$ and 5 mM CH_3COONa at pH 4. Sb species were measured by hydride generation atomic fluorescence spectrometer (HG-AFS) (AFS 230, Haiguang Corp., Beijing).

The oxidation of Sb(III) by synthetic manganite is shown in Figure 1. Rapid uptake of Sb(III) by manganite is apparent as well as formation of Sb(V) at the initial period. Then, the Sb(V) in the solution is adsorbed by manganite and reduced gradually with the reaction time. Figure 2 shows the normalized Sb L-edge XANES spectra of reference materials ($KSb(OH)_6$ and Sb_2O_3) and the samples collected from the Sb(III)-manganite system. It is obvious from the spectra that the absorption edge of Sb(III) shift to higher energy at the Sb(V). This indicates that the adsorbed Sb species on the manganite surface is Sb(V).

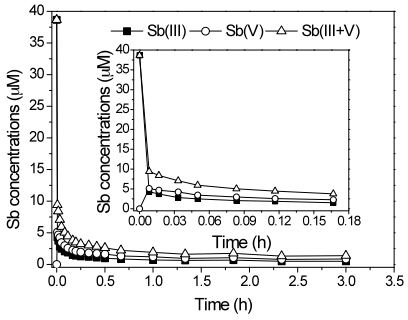

Figure 1: Speciation of dissolved Sb_{total}, Sb(III) and Sb(V) recovery during the reaction of 38.66 μM Sb(III) with synthetic manganite (0.12 g/L) as a function of time at pH 4.0.

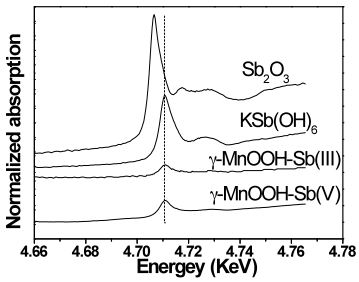

Figure 2: Normalized Sb L-edge XANES spectra

[1]Belzile *et al*. (2001) *Chem. Geol*. **174**, 379-387.

https://doi.org/10.1180/S0026461X00006502 Published online by Cambridge University Press

LA-ICP-MS chronological study of Tongka gneissic granite in Northern Gangdise, Qinghai-Tibet Plateau

SHIPING HE, CHAO WANG AND PINGYANG GU

Xi'an Institute of Geology and Mineral Resources, Xi'an 710054, Shaanxi, China (xakeyi@163.com)

The Tongka gneissic granite, which locates in Jiayuqiao Block in the northern margin of Gangdise, intruded to the high-amphibolite facies metamorphic rocks of Kaqiong Rock Group of Meso-Neoproterozoic and developed intensive plastic deformation with band fabrics and crumpled texture. The CL imagines of the zircons from Tongka gneissic granite show that the zircons well developed oscillatory zoning core and dark growth rim. Two discordant lines can be obtained by LA-ICP-MS in-situ zircon U-Pb isotopic analysis (Fig. 1). The upper intercept age of the oscillatory zoning cores is (549±18)Ma (MSWD=0.02, Points=23), with the ^{207}Pb-^{235}U weighted average age, (550±10)Ma (MSWD=0.03). However, the dark growth rims yield an upper intercept age (416±23)Ma (MSWD=0.001, Points=8), and the ^{207}Pb-^{235}U weighted average age is (416±20)Ma (MSWD=0.001). The ratios of Th/U of the cores (0.39~1.59) are generally higher that of the rims (0.32~1.29), which proves that the age (549±18)Ma represents the crystallization time of the gneissic granite, equivalent to the time of Pan-Africa Movement (600-500Ma), and the age (416±20)Ma represents the time of an intensive tectonic-thermal event in late Caledonian. This study further confirmed that the Jiayuqiao block in the northern margin of Gangdise is Pan-African basement.

This study was supported by China territorial resources survey project(No. 1212010610102).

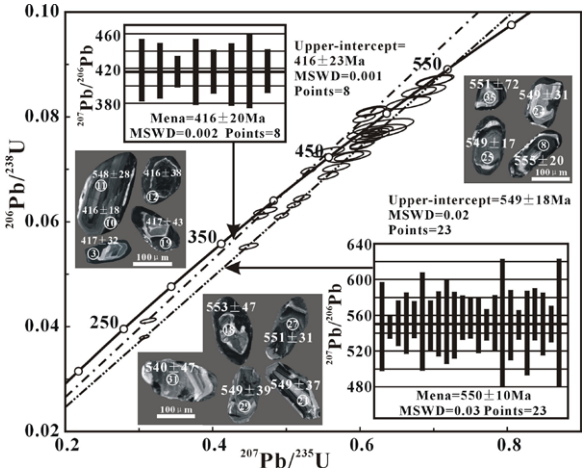

Figure 1: U-Pb concordia diagrams and CL images

Global constraints on biogenic particles

COLETTE L. HEALD[1]*, DOMINICK V. SPRACKLEN[2] AND ALEX GUENTHER[3]

[1]Department of Atmospheric Science, Colorado State University, Fort Collins, CO, USA (*correspondence: heald@atmos.colostate.edu)

[2]School of Earth and the Environment, Leeds University, Leeds, UK (d.spracklen@see.leeds.ac.uk)

[3]Atmospheric Chemistry Division, National Center for Atmospheric Research, Boulder, CO, USA (guenther@ucar.edu)

The biosphere is a source of particles and their precursors to the global atmosphere, yet the magnitude and drivers of these emissions are poorly understood. Two key classes of biogenic particles are primary biological aerosol particles (PBAP) and secondary organic aerosol (SOA) from biogenic volatile organic compounds (VOCs). In this presentation I will discuss modeling efforts and field observations of PBAP, (with a focus on fungal spores) and SOA (including biogenic VOC precursors), highlighting challenges and recent progress.

https://doi.org/10.1180/S0026461X00006502 Published online by Cambridge University Press

Short magma residence times for Kilauea Volcano based on high-precision Pb isotope ratios

D.E. HEATON[1], A.J. PIETRUSZKA[1], M.O. GARCIA[2] AND J.P. MARSKE[2]

[1]Deptartment of Geological Sciences, San Diego State University, San Diego, CA 92182-1020, USA
[2]Department of Geological Sciences, University of Hawaii, Honolulu, HI 96822, USA

We present new high-precision Pb isotopic analyses of 46 historical Kilauea summit lavas (1823-2008). These data are used here to investigate the architecture of Kilauea's summit magma storage reservoir and the characteristics of the volcano's mantle source region. These lavas exhibit a temporal trend characterized by low $^{206}Pb/^{204}Pb$ ratios in 1823, a gradual increase to a maximum in 1921, an abrupt drop to relatively constant intermediate values from 1923 to 1959, and a rapid decrease to 2008. These variations indicate that Kilauea's summit reservoir is being supplied by rapidly changing parental magma compositions derived from a mantle source that is heterogeneous on a small scale. At least three components are required to explain two distinct mixing arrays on a plot of $^{206}Pb/^{204}Pb$ vs. $^{208}Pb/^{204}Pb$, where the 19th century lavas have a low $^{206}Pb/^{204}Pb$ at a given $^{208}Pb/^{204}Pb$ compared to the 20th century lavas. Analyses of multiple lavas from several individual eruptions reveal small but significant differences in $^{206}Pb/^{204}Pb$ ratios (~0.01-0.03). For example, the extra-caldera lavas from Aug. 1971 and Jul. 1974 display significantly lower Pb isotope ratios and higher MgO contents (10 wt. %) than the intra-caldera lavas (MgO ~7-8 wt. %) from the same eruption. These distinctions appear to be spatially delineated by the rim of the volcano's summit caldera. From 1971 to 1982, the $^{206}Pb/^{204}Pb$ ratios of the lavas define two separate decreasing temporal trends. Intra-caldera lavas from 1971, 1974, 1975, Apr. 1982 and the lower MgO lavas from Sep. 1982 have consistently higher $^{206}Pb/^{204}Pb$ ratios at a given time (compared to the extra-caldera lavas and the higher MgO lavas from Sep. 1982). Magma residence-time modeling of the high $^{206}Pb/^{204}Pb$ (low MgO) and low $^{206}Pb/^{204}Pb$ (high MgO) trends suggest that the intra- and extra-caldera lavas are being supplied from two distinct magma bodies, each with a volume of ~0.2 km^3. This volume estimate is more precise and much smaller than previous estimates of a single, ~2-3 km^3 magma body based on trace element ratios. Overall, these observations suggest that Kilauea's summit reservoir has a small volume that efficiently transfers the changing compositional signals of the mantle-derived parental magmas.

The calcite–water interface and its interactions with selenium IV and VI

FRANK HEBERLING, STEPHANIE HECK AND JÖRG ROTHE

Institute for nuclear waste disposal, Karlsruhe Institute of Technology (KIT), PO-Box 3640, 76021 Karlsruhe, Germany

Due to the reactivity of its surface, calcite may play an important role for the retention of contaminants in soils, lacustrine-, marine- and aquifer environments.

Selenium is on the one hand an important nutrient. On the other hand, if a certain concentration limit is exceeded, it is toxic. The chemical toxicity is highest for the oxidized selenium IV and VI species. These are also the species expected to be the most mobile in soils and aquifers. Selenium-79, is a long lived nuclear fission product formed in nuclear power plants. It is of special concern, as it is expected be able to diffuse through the technical and geological barrier systems around nuclear waste disposals and increase the radiotoxicity of groundwater in adjacent aquifers.

At calcite equilibrium conditions, tetravalent selenium shows only very weak adsorption at the calcite surface. At pH below 9, K_D values are about 0.001. Above pH 9 no adsorption is observed. In situ grazing incidence EXAFS measurements at the calcite(104) face show no contribution to the selenium(IV) spectra that could be assigned to the calcite surface. If the calcite saturation index is increased selenium(IV) starts coprecipitating with calcite. The ordering of the coprecipitated selenite ($Se(IV)O_3^{2-}$) ions corresponding to the orientation of the calcite carbonate ions becomes visible in polarization dependent grazing incidence XANES spectra. Coprecipitation of selenite with calcite is quantified in mixed flow reactor (MFR) experiments at steady state and low supersaturation (SI~0.8) conditions. Homogeneous partition coefficients range from 1 to 10. EXAFS spectra measured on selenite doped calcite from MFR experiments show that selenite is structurally incorporated into calcite onto a slightly distorted carbonate lattice site.

Selenium(VI) shows a slightly stronger adsorption to the calcite surface. Grazing incidence EXAFS spectra, measured in situ at the calcite(104) face, show clear contributions that can be assigned to two Ca^{2+} neighbours from the calcite surface, at about 3.5 Å distance. There are two non-equivalent adsorption sites at the calcite(104) face that could explain this result. The GIXAFS data however, cannot be used to distinguish between the two.

Coprecipitation of selenium(VI) with calcite in MFR experiments was below detection limit.

https://doi.org/10.1180/S0026461X00006502 Published online by Cambridge University Press

Metal attenuation in tailings

T. HEDLUND*, L. LÖVGREN AND T. KARLSSON

Department of chemistry, Umeå University, 901 87 Umeå, Sweden (*correspondence: tomas.hedlund@chem.umu.se)

Oxidation of sulphide mineral in mine waste can result in extensive release of metals, which may escape the waste via groundwater discharge. However, the metals may also be attenuated by various processes in which metal ions are re-associated with the solid matter within the tailings. The objective of our work is to identify the minerals in mining waste that are of significance for the attenuation in short and long term perspective of heavy metals release in mine waste by quantifying the metal retardation capacity of tailings of different properties or origin.

The metal uptake capacity has been studied for Cu, As, Zn and Cd in batch and column experiments on tailings sampled in four different locations: Kristineberg, Aitik, Zinkgruvan and Boliden. In order to distinguish between adsorbed metal and precipitation of metal oxide/hydroxide, the acid neutralization capacity of the tailing was neutralized before the batch and column experiments. The elemental composition of tailings and pore-water was analysed using ICP-AES/MS. Characterization of the mineralogical composition by using Mineral Liberation Analysis and the speciation and local structure of metal ions associated with tailings was investigated using X-ray Photoelectron Spectroscopy and synchrotron based X-ray Absorption Spectroscopy.

Our result for Cu shows that there is an initial uptake likely explain by precipitation of $Cu(OH)_2$ (supported by XANES analysis) follow by a slower process involving phase transformation e.g. formation of secondary copper sulphide. The copper uptake capacity was highest, up to 50 μmol/g of tailing, for Kristineberg and Zinkgruvan. Uptake of arsenic appears to be more strongly correlated to sulphide content of tailings with an uptake capacity similar to copper for tailings with high sulphide content. For cadmium no significant uptake could be observed.

Donnan equilibrium in Na-montmorillonite from a molecular dynamics perspective – Consequences for diffusional transport

M. HEDSTRÖM*, M. BIRGERSSON AND O. KARNLAND

Clay Technology AB, Ideon Science Park, SE-223 70 Lund, Sweden (*correspondence: mh@claytech.se, mb@claytech.se, ok@claytech.se)

Bentonite clay is proposed as buffer material in several concepts of High Level Radioactive Waste repositories, and a correct description of ion diffusion in this material is of vital importance for any quantification of the chemical evolution of the repository near field.

This study investigates the importance of ion equilibrium between montmorillonite interlayer space and an external solution for the diffusional behaviour of bentonite.

We present molecular dynamics simulations of the Donnan equilibrium principle in compacted montmorillonite with three hydration layers of water in the interlayer. This draws attention to the misconception, frequently seen in the literature, stating that anions cannot enter interlayer space due to electrostatic repulsion forces, sometimes referred to as anion exclusion. However, the calculations presented here show that excess salt, i.e., both anions and cations enter interlayer space to the extent predicted by Donnan equilibrium. Thus the excess salt concentration is reduced in the interlayer in comparison to the external electrolyte but not totally excluded [1].

Taking into account that anions can and will enter the interlayer space a general theoretical framework for describing through-diffusion in montmorillonite is developed [2]. By using a single pore space, the interlayers, cations and anions are treated symmetrically as opposed to conventional multi-porosity models where anions and cations follow different pathways. The validity of the presented approach is further justified in comparisons to experimental chloride tracer diffusion data [3].

[1] Hedström & Karnland (2011) *Geochim. Cosmochim. Acta*, submitted [2] Birgersson & Karnland (2009) *Geochim. Cosmochim. Acta* **73**, 1908-1923. [3] Van Loon, Glaus & Müller (2007) *Appl. Geochem.* **22**, 2536-2552.

https://doi.org/10.1180/S0026461X00006502 Published online by Cambridge University Press

Mineral alterations due to accessory gases in the geological storage of CO_2

K. HEESCHEN*, A. RISSE, S. STADLER AND C. OSTERTAG-HENNING

Federal Institute for Geosciences and Natural Resources (BGR), D-30655 Hannover, Germany (*correspondence: Katja.Heeschen@bgr.de)

To establish reliable numerical models that depict the geochemical processes caused by the storage of CO_2 in saline aquifers it is essential to have an applicable database. This has to include thermodynamic properties and kinetic data of those gas mixtures occurring in the captured CO_2 gas stream, which will contain minor amounts of gases such as O_2, N_2, NO_x, SO_x, CO, H_2S. However, quantitative measures of the chemical alterations due to these accessory gases are scarce at relevant conditions.

The COORAL project "CO_2 Purity for Capture and Storage", concentrates on the effects of accessory gases during all four processes: capture, transport, injection and storage. At BGR it is the storage that is in focus. High-pressure-high-temperature (HPHT) experiments are carried out using unstirred batch-reactor systems ($P \leq 590$ bar; $T \leq 350$°C) to elucidate mineral and fluid alterations and quantify kinetic rates for different mineral–fluid–CO_2–co-injected gas system.

A first set of experiments using pure CO_2 and carbonates allowed testing the laboratory set-up and adjusting the modelling environment (PHREEQC). Dolomite-brine-CO_2 experiments exhibited a very good reproducibility of the increase in cation concentrations at the different stages of the experiment. Release rates for both, Mg and Ca, vary between $2*10^{-10}$ mol s^{-1} cm^{-2} at the very beginning and $4*10^{-13}$ mol s^{-1} cm^{-2} just before approaching steady state. There is a tendency towards slightly higher rates for Ca release during the first stage of the experiment.

The main target of the running experiments is set on the effects of binary gas mixtures in the system mineral–fluid–CO_2–O_2 (this contribution) and mineral–fluid–CO_2–SO_2 [1]. The mineral phase consists of carefully crushed, sorted and cleaned natural mono-minerals while the natural saline water is represented by a Na-Cl solution of 150 g/l NaCl in most cases.

[1] Risse *et al*. (2011), *MinMag*, this volume.

Comparison of land-based REE ore deposits with REE-rich marine Fe-Mn crusts and nodules

JAMES R. HEIN[1]*, TRACEY CONRAD[1] AND ANDREA KOSCHINSKY[2]

[1]USGS, Menlo Park, CA, 94025, USA (*correspondence: jhein@uss.gov)
[2]Jacobs University, Bremen, Germany (a.koschinsky@jacobs-university.de)

REEs are essential for a large variety of high-tech and green-tech applications. The global market has been supplied over the past 10 plus years, from a single source, China. China's domestic needs have meant that its export of REEs has and will continue to decrease significantly. Consequently, other land-based sources of REEs are being explored and mines developed. Deep-ocean deposits may offer a partial solution to this projected shortage, but marine deposits have not been evaluated. Here we compare data for the Clarion-Clipperton Mn Nodule Zone (CCZ) in the NE Pacific and the prime Fe-Mn crust zone (PCZ) in the central Pacific with the two largest land-based mines, Mountain Pass (MP) in USA and Bayan Obo (Obo) in China. The land-based deposits are lower tonnage deposits, but higher grade (MP $0.9x10^8$ tons at 5% total REEs as oxides (TREO); Obo, $8x10^8$ tons at 6% TREO), compared to the CCZ ($211x10^8$ tons at 0.10% TREO) and PCZ ($75x10^8$ tons at 0.3% TREO). These grades and tonnages correspond to tons of TREO of $4.9x10^7$ Obo, $0.45x10^7$ MP, $2.1x10^7$ CCZ, and $2.3x10^7$ PCZ. The land-based deposits have <1% heavy REEs, whereas the CCZ has 10% HREEs and the PCZ, 6.3% HREEs. An important environmental issue is the high Th contents in the land-based deposits (100s of ppm) in contrast to the low Th in marine deposits (mean 14 ppm CCZ; 11 ppm PCZ).

https://doi.org/10.1180/S0026461X00006502 Published online by Cambridge University Press

Stepwise C & O stable isotope shows no detectable CO_2-sequestration by cements in analogue for engineered storage

N. HEINEMANN[1]*, M. WILKINSON[1], A. E. FALLICK[2] AND R. S. HASZELDINE[1]

[1]School of Geosciences, The University of Edinburgh, The King's Buildings, West Mains Road, Edinburgh, EH9 3JW (*correspondence: n.heinemann@sms.ed.ac.uk)
[2]Scottish Universities Enviromental Research Centre, East Kilbride, G75 0QU

Geochemical models often predict a relatively rapid growth of carbonate minerals as the most secure form of long term, engineered, CO_2 storage. But validation of model-results remains difficult due to the long periods of time involved, 1000's of years. Natural analogue studies can bridge the gap between experiments and real-world storage.

The Fizzy field, a southern North Sea (UK) gas accumulation with a high natural CO_2 content (c. 50%) provides an ideal opportunity to study the long term effect of CO_2 related mineral reaction. However all such reservoirs contain 'normal' diagenetic dolomite, so that distinguishing sequestration related dolomite is a challenge. Previous petrographic work and comparison of stable carbon and oxygen isotopes from dolomite in the Fizzy field and dolomite in the Orwell field, an adjacent gas field with low CO_2 content, did not find major differences [1]. However, stable isotope measurements were only made on whole-rock samples such that internal zonations of crystals may have been masked.

We extracted CO_2 from dolomite from both the Fizzy and the Orwell gas field in a stepwise manner in order to reveal any zonation of the crystals which could be related to enhanced dolomite precipitation due to the high CO_2 concentration. The results do not match with the calculated isotopic equilibrium composition for the CO_2 which is currently present in the Fizzy field but are comparable with data from the adjacent low CO_2 Orwell field. We conclude that the dolomite present in the Fizzy field is not related to high CO_2 concentration but a product of earlier diagenetic events.

[1] Wilkinson *et al*. (2009) *Journal of Sedimentary Research* **79**, 486-494.

Investigation of organo-mineral interactions in artificial soil incubations by NanoSIMS

KATJA HEISTER[1]*, CARMEN HÖSCHEN[1], GEERTJE J. PRONK[1], CHRISTIAN POLL[2], ELLEN KANDELER[2], CARSTEN W. MÜLLER[1] AND INGRID KÖGEL-KNABNER[1]

[1]Lehrstuhl für Bodenkunde, Technische Universität München, 85350 Freising-Weihenstephan, Germany (*correspondence: heister@wzw.tum.de)
[2]Institute of Soil Science and Land Evaluation, Soil Biology, University of Hohenheim, Emil-Wolff-Str. 27, 70593 Stuttgart, Germany

Soils are complex mixtures of minerals, organic material (OM) and microorganisms. These components interact with each other, forming biogeochemical interfaces (BGIs). BGIs in soils are believed to be hot-spots where many important processes like sorption and microbial activity occur. Thus, depending on the components involved, various microhabitats for soil microorganisms are created.

In order to study the effect of mineral composition on the development of BGIs, we performed an artificial soil incubation experiment. The artificial soils are model systems, comprising of well-defined mixtures of various minerals like quartz, clay minerals and iron and aluminium hydroxide and sterilized manure as organic substrate that were inoculated with soil microorganisms and incubated over different time periods up to 18 months.

The microorganisms were active and OM turnover occurred in the soil systems. Phospholipid-derived fatty acid (PLFA) pattern showed that the initial composition of the artificial soils initiated the development of different soil microbial communities.

Selected samples after one year of incubation were investigated with nano-scale secondary ion mass spectrometry (NanoSIMS) to study BGI formation. NanoSIMS analysis demonstrated that patchy attachment of OM occurred to clay minerals. Up to now, no intact microbial cells were detected in the artificial soils using NanoSIMS, which is probably due to sample pretreatment or too low abundance of microorganisms in these samples.

Our data demonstrate that in these simple soil systems, depending on the mineralogical composition, microhabitats were created, and that NanoSIMS is a tool to visualize these hot-spots in soil at a relevant scale.

https://doi.org/10.1180/S0026461X00006502 Published online by Cambridge University Press

First high-resolution $\delta^{13}C$-records of the Early Aptian OAE 1a within the mid-latitudes of NW-Europe (Germany, Lower Saxony Basin)

M. HELDT [1]*, F.W. LUPPOLD [1], W. WEISS [1], J. MUTTERLOSE [2], U. BERNER [1] AND J. ERBACHER [1]

[1]BGR, 30655 Hannover, Germany (*correspondence: Matthias.Heldt@bgr.de)
[2]Ruhr-University Bochum, 44801 Bochum, Germany

Two mid-Cretaceous sediment cores (Hoheneggelsen 9 and Ahlum 1 cores) from the area south of Brunswick, North Germany, were investigated in detail on the base of biostratigraphy, $\delta^{13}C$-stratigraphy and geochemistry. Results suggest a latest Barremian to early Late Aptian age for the deposits. In both cores, three lithological units are recognized: a lower claystone unit including finely laminated black shale horizons ("Blättertone"), an overlying prominent black shale horizon ("Fischschiefer") and an upper marly section (*Hedbergella* marls). Isotope stratigraphy allows to subdivide the deposits into segments (C1-C7), which are used for high-resolution stratigraphy globally. These segments also allow to identify the Late Early Aptian Oceanic Anoxic Event 1a (OAE 1a). The present study represents the first high-resolution $\delta^{13}C_{carb}$ and $\delta^{13}C_{org}$ records across this event within the mid-latitudes of NW-Europe. Our results confirm that the regional sedimentary expression of the OAE 1a is the above-mentioned "Fischschiefer" horizon, a 2-3 m-thick laminated black shale layer known from NW Germany and the southern North Sea.

The main trends of the $\delta^{13}C$ isotope curves of both cores can be correlated with global curves. However, several bulk carbonate samples of the Early Aptian, including those of the OAE 1a, are considerably depleted in $\delta^{13}C$. This might be explained by authigenic carbonate formation, induced by microbial sulphate reduction and –in cases of extreme ^{12}C enrichment- also by microbial methane generation and oxidation processes. Such processes are confined to anoxic enironments. Consequently, strong ^{12}C enrichement mainly correlates with the black shales, including the "Fischschiefer" horizon (OAE 1a), which are associated with anoxic bottom water conditions. The overlying marls (*Hedbergella* marl unit), deposited under oxic seafloor conditions, show values closer to normal marine levels. The early diagenetic processes of the carbonates discussed above did not affect the $\delta^{13}C_{org}$ ratios of both cores to greater extent. These are close to normal marine levels and show variations in the range of a few permil only. Our study shows, that $\delta^{13}C_{org}$ data is better suited for stratigraphy in mid-Cretaceous anoxic sediments of the Lower Saxony Basin.

Causes and consequences of outer core compositional stratification

GEORGE HELFFRICH[1] AND SATOSHI KANESHIMA[2]

[1]Earth Sciences, University of Bristol, Bristol BS8 1RJ, UK
[2]Earth and Planetary Sciences, University of Kyushu, 6-10-1 Hakozaki, Higashi-ku, Fukuoka 812-8581, Japan

We report on a detailed investigation of the structure of the topmost outer core using seismic waves travelling across it at depths between 60-700 km. The observations are regional array recordings of between 120-200 seismograms from the same earthquake using stations in Europe and Japan. The use of arrays allows high-precision measurements of differential SmKS travel times and slownesses for multiple (m) values up to 5. The study [1] yields a well constrained velocity structure for the topmost 500 km of the outer core. The uppermost 300 km is gradationally slower than the PREM model by up to 0.3%. Applying Birch's homogeneity test to the velocity profile shows that it differs at more than the 95% confidence level from compression of a simple liquid of fixed composition. Thus the outer core is stratified in its composition.

The thickness of the layer requires the layer's bulk to be derived from the core rather than from the core-mantle boundary given known diffusivity of core liquids. Consequently, the gradient must arise from light element addition within the core, probably from the growth of the inner core. A rough material balance may be made between the density jump at the inner core boundary and the thickness of the layer. Using a core liquid velocity model in the Fe-O-S system, the velocity change requires a 3-5 wt% light element concentration increase in the topmost core. Maintaining a 300 km thick layer against convective mixing in the outer core suggests that the shallowest core is stagnant. One way to suppress convection there is by making the outermost core isothermal, suggesting that there is not a significant thermal boundary layer at the base of the mantle.

[1] Helffrich & Kaneshima (2010) *Nature* **468**, 807-810.

https://doi.org/10.1180/S0026461X00006502 Published online by Cambridge University Press

Processes affecting iron solubility in the Tropical North Atlantic

M.I. HELLER[1] AND P.L. CROOT[2]

[1]IFM-Geomar, Kiel, Germany (mheller@ifm-geomar.de)
[2]Plymouth Marine Laboratory, Plymouth, United Kingdom (pecr@pml.ac.uk)

Iron (Fe) has been clearly shown to be a limiting nutrient for phytoplankton productivity in many different oceanic regions. A critical apsect underlying iron limitation is the low solubility, under ambient seawater conditions, of solid iron phases supplied as aerosols or riverine particles to the ocean. Processes which enhance the solubility of iron in seawater, either through redox reactions or organic complexation, are key to our understanding of the biogeochemical cycling of iron and its global distribution. In this work we combine information from a recent meridional cruise through the Atlantic (PS ANT XXVI-4) with sampling performed within the SOPRAN project at the TENATSO time series site located near Cape Verde to examine processes influencing iron solubility in the Tropical North Atlantic in the region under the Saharan dust plume.

A promising indicator of iron solubility in deep waters is marine humic fluorescence (ex 320/em 420), as work in the Pacific [1] has shown strong correlations with Fe solubility and AOU. This suggests that iron solubility in deep waters is scaled to the release of iron complexing ligands from the decomposition of sinking organic matter. During ANTXXVI-4 we observed a region of intermediate waters with strong humic fluorescence consistent with observations of elevated Fe concentrations [2]. The humic fluorescence signal however is sharply attenuated in surface waters due to bleaching, suggesting that other ligands or processes are important in the euphotic zone. Our work at TENATSO suggest that iron solubility is not significantly enhanced by reactions with superoxide [3] and is controlled by the presence of non-fluorescing colloids or siderophore type ligands consistent with earlier previous work in the Mauritanian upwelling [4].

[1] Tani, H., *et al*. (2003) *Deep-Sea Research*, 50: 1063-1078. **[2]** Measures, C.I., *et al*. (2008) *Global Biogeochemical Cycles*, 22. **[3]** Heller, M.I. and P.L. Croot. (2010) *J. Geophys. Res*., 115: C12038. **[4]** Schlosser, C. and P. Croot. (2009) *Geophys. Res. Lett*., 36: L18606, doi:10.1029/2009GL038963.

Albite precipitation in mudstones – Comparison of natural and synthetic systems

HELGE HELLEVANG*, BRIT THYBERG AND JENS JAHREN

Department of Geosciences, Univ. Oslo, Pb. 1047, Blindern, Oslo, Norway. (*correspondence: helghe@geo.uio.no)

Closed system hydrothermal batch experiments on smectite (SWy-2, The Clay Minerals Society) and smectite + K-feldspar, reacted with NaCl solutions, were performed at 200 °C with each experiment runing for 2-3 weeks. The experiments show that dispersed albite readily forms from smectite in systems supersaturated with respect to albite. This compares well with observations from natural mudstones, where micro-sized authigenic albite (mAlb) is found together with authigenic 2-4 μm micro-crystalline quartz (mQtz) embedded in an illitized clay matrix (Fig. 1). The amount of authigenic mAlb formed in the natural systems are about 10-15% of the produced authigenic mQtz. The suggested reaction equation indicate that less than 2 wt % sodium and 2-3 wt % potassium is required to account for both the estimated mAlb and illite formation from smectite and K-feldspar.

The findings indicate closed system diagenesis predicted from the physical and chemical properties of fine grained siliciclastic rocks during burial, and that the source for necessary sodium, silica and aluminum for authigenic mAlb formation is smectite and K-feldspar dissolution resulting in mainly illite and quartz formation.

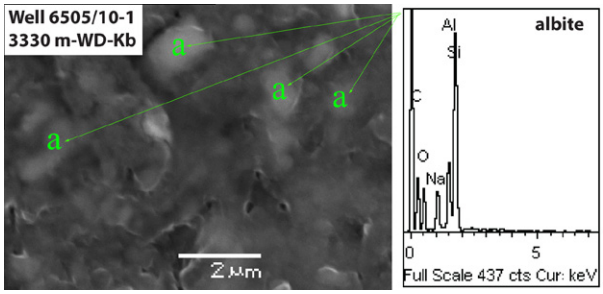

Figure 1: SEM image of natural mAlb (a) together with feldspar, quartz and clay from well 6505/10-1 sampled at 3330 m.

https://doi.org/10.1180/S0026461X00006502 Published online by Cambridge University Press

Arsenic, copper, and zinc leaching through preferential flow in mining-impacted soils

MARTIN HELMHART[1], PEGGY O'DAY[2], JAVIER GARCIA-GUINEA[3], SUSANA SERRANO[1] AND FERNANDO GARRIDO[1]

[1]Institute for Agricultural Sciences (CSIC) c. Serrano 115-dup, 28006 Madrid (Spain)
[2]School of Natural Sciences, Universtiy of California, 5200 North Lake Rd, Merced, CA 95344 (USA)
[3]National Museum of Natural Sciences (CSIC), Jose Gutierrez Abascal 2, 28006 Madrid (Spain)

The effect of preferential flow on the spatial distribution and chemical speciation of As, Cu and Zn in a metal(loid) polluted soil was studied within the river bed of a small stream that collects surface runoff from an arsenic-bearing, mainly as scrorodite (FeAsO4·2H2O), waste pile near an abandoned mine. Water flow domains, either preferential or matrix, were identified by staining techniques, a detailed soil sampling procedure, and statistical analysis. General soil properties were studied in each flow domain. In addition, total metal(loid) content and chemical distribution by means of sequential extraction procedure were done within each flow domain. Lastly, As speciation was studied by X-ray absorption spectroscopic (XAS) methods.

An upper river bed and its underlying subsoil were distinguished, and both were characterized by low pH and high As, Cu, Zn and Fe concentrations as compared to the adjacent soil. Metal(oid) concentrations were higher in the river bed than in the subsoil due to the accumulation of incoming material from the waste pile. In the river bed, higher metal(oid) concentrations were found in the preferential flow domain compared to matrix flow. Instead in the subsoil, preferential flow paths were characterized by a lower ion exchange capacity and lower Cu and Zn concentrations from acidic leaching, and higher concentrations of total organic matter attributed to high root content, compared to the soil matrix. Arsenic was mainly concentrated in the preferential flow paths as As(V). XAS analysis indicated As sorption on iron hydroxide phases as the primary retention mechanism in the subsoil, which may be a reversible process if geochemical conditions change. Preferential flow, acting as a by-pass connecting the highly contaminated river bed layer with deeper soil, has an impact on the distribution of metal(oids) at the study site and may increase the risk for groundwater contamination.

Mechanisms of light-induced flocculation of terrestrial dissolved organic matter and iron

JOHN R. HELMS[1], KLAUS SCHMIDT-ROHR[2], JINGDONG MAO[1] AND KENNETH MOPPER[1*]

[1]Department of Chemistry and Biochemistry, Old Dominion University, Norfolk, Virginia 23529 (jhelms@odu.edu; jmao@odu.edu; *correspondence: kmopper@odu.edu)
[2]Department of Chemistry, Iowa State University, Ames, Iowa 50011 (srohr@iastate.edu)

Dissolved organic matter (DOM) rich water samples from the Great Dismal Swamp (Virginia, USA) were filtered (<0.1 micron) and UV-irradiated (~290 nm lower cutoff) for 30 days. During the irradiation, particulate organic matter (POM) and particulate iron formed. Water samples before and after particle removal, as well as isolated particles, were analyzed by ultraviolet-visible absorption spectroscopy, high temperature combustion (TOC/DOC), solid-state ^{13}C nuclear magnetic resonance (NMR) spectroscopy, Fourier transform infrared (FT-IR) spectroscopy, and flame atomic absorption spectroscopy (for iron). After 30 days of UV light exposure, 7.1% of the original DOC was converted to particulate organic carbon (POC) while 75% was converted to inorganic photoproducts. Approximately 84% of the absorption in the 250-450 nm region was removed by photobleaching, while 8.3% was removed by photo-flocculation. About 87% of the iron was removed from the dissolved phase after 30 days of irradiation, but iron did not begin to flocculate until a considerable excess of DOM was removed by photodegradation and flocculation between 10 and 20 days of irradiation. These results suggest that, during the initial 10 days, there was still sufficient organic ligands present to keep iron in solution. NMR and FT-IR spectroscopies indicated that the photochemically flocculated POM is significantly more aliphatic than the irradiated DOM. Further, photo-flocculated POM was enriched in amide functional groups, while carbohydrate-like material was resistant to both photochemical degradation and flocculation. When photochemical flocculation is considered, the extent to which photochemistry may remove terrestrial DOM from the upper water column is revised upward by about 10%. Abiotic photochemical flocculation is therefore a heretofore-ignored phenomenon that significantly alters our understanding of sedimentation in humic lakes and the transport of DOM and POM in ocean margin environments such as estuaries.

https://doi.org/10.1180/S0026461X00006502 Published online by Cambridge University Press

PGE complexes at superliquidus temperature: Embryos for platinum-group minerals?

H.M. HELMY[1]*, C. BALLHAUS[2], C. WOHLGEMUTH-UEBERWASSER[3], R. WIRTH[4] AND M. TREDOUX[5]

[1]Minia University, 61519 Minia, Egypt (*correspondence: hmhelmy@yahoo.com)
[2]Steinmann Institut, Universität Bonn, Germany
[3]University of Johannesburg, PO Box 524, South Africa
[4]GFZ, Potsdam, Germany
[5]Univ of the Free State, 9300 South Africa

Even though As, Sb, Te, and Bi are mere trace elements in magmatic sulfide melts, minerals of the platinum-group elements (PGE) with these ligands are exceptionally common. Obviously, at subsolidus temperatures, there is a marked chemical preference of the PGE to bond with the chalcogenes and semimetals and form discrete arsenides, antimonides, tellurides, and bismuthinides. The question addressed here is if similar PGE-ligand preferences also exist at supersolidus and superliquidus temperature. Should such proposition be proven correct, we could argue that discrete crystalline PGE-chalcogene and PGE-semimetal phases have their chemical equivalents at superliquidus conditions in the form of PGE-As, Sb, Te, and Bi molecular associations, complexes or even poly-atomic clusters [1]. We could even go as far as proposing that the crystallization of a discrete PGE phase with a specific metal-ligand combination merely reflects the re-organization to larger units, of PGE-ligand molecules or complexes with the same PGE-ligand combination.

Experiments were carried out in an Ir-Pt-As-bearing, monosulfide (mss)-saturated Fe-Cu-S system at 950°C at minimum and maximum sulfur fugacities as bracketed by the Fe-FeS (metal-troilite) and $Fe_{1-x}S$-S_2 (mss-sulfur) equilibria. Copper was added to expand the two-phase (mss-melt) stability field such that mss grains coexisted with sulfide melt pools sufficiently large for contamination-free laser-ablation analysis. Platinum, Ir, and As were added to the sulfide matrix at the tens of ppm levels. The molecular As/PGE bulk ratios varied from 0, 1, 2, 3 and 5. In charges with high sulfur fugacity, i.e. when all As is present as cation [2], the partition coefficients of Pt, Ir and As are insensitive to the As/PGE atomic bulk ratio. At low sulfur fugacity, in contrast, when all As is dissolved as anions, the mss-sulfide melt partition coefficients of Pt and Ir decrease with increasing atomic As/Pt; DIr (mss/sulfide melt) slightly and DPt (mss/sulfide melt) sharply by almost one order of magnitude. The results can only be rationalized if PGE minerals such as $IrAs_2$ (iridarsenite) or $PtAs_2$ (sperrylite), and potentially many more discrete PGE phases with rare elements as ligands, have their equivalents at superliquidus temperature in the form of Ir-As, Pt-As etc. molecules, complexes or even poly-atomic clusters [1].

[1] Tredoux *et al.* (1995) *S Afr J Geol*, **98**, 157-167. [2] Helmy *et al.* (2010) *Geochim Cosmochim Acta,* **74**, 6174-6179.

Geochemical roles of thioanions of the heavier metals and metalloids

G. R. HELZ

Department of Chemistry and Biochemistry, University of Maryland, College Park, MD, 20742, USA (helz@umd.edu)

Where sulfide replaces oxygen in sedimentary environments, many elements' aqueous geochemistry is altered profoundly. Among first row transition metals, the primary effect is reduction (e.g. $Cr^{VI} \rightarrow Cr^{III}$, $Mn^{IV} \rightarrow Mn^{II}$, $Fe^{III} \rightarrow Fe^{II}$, $Cu^{II} \rightarrow Cu^{I}$). Secondarily (i.e. at higher sulfide concentrations), sulfide complexes can form through replacement of O, N or Cl atoms in first coordination shells of the reduction products. In contrast, for many heavier metals and metalloids, the primary effect is ligand replacement, with reduction occurring secondarily, if at all. Thus thioanions may form with trace elements in their highest oxidation states (e.g. $Re^{VII}S_4^-$ $Mo^{VI}S_4^{2-}$, $As^{V}OS_3^{3-}$, $Sb^{V}_2S_6^{2-}$). In each of these known cases, the thioanion a) is stabilized at geochemically reasonable sulfide concentrations (10^{-6} to 10^{-4} M) at near-neutral pH and b) appears not to precipitate a binary sulfide solid phase under conditions ordinarily found in nature.

Owing to experience with first-row transition metals, geochemists have tended to attribute behavior of heavier metals and metalloids in sulfidic waters to reduction rather than ligand exchange. Although the determing role of ligand exchange in Mo's behavior in sulfidic waters has become accepted over the past 15 years, belief in Re's reduction in these waters still prevails. I will present a new, ligand-exchange model for Re's response to sulfide that is analogous to that recently proposed to explain Mo behavior in euxinic waters [1]. The model can explain important features of Re's geochemistry, including its precipitation exclusive of Mo in suboxic environments and its precipitation at a nearly constant ratio to Mo in sulfidic environments.

Because thioanions can act as multidentate, sulfur-donating ligands, they may influence the geochemistry of other trace metals. Both As^{III} and Mo^{VI} thioanions are now known to form extraoridinarily stable complexes with coinage metals (Cu, Ag, Au). It can be expected that the same will eventually be demonstrated for thioanions of other elements, especially Sb and Bi.

[1] Helz, G. R.; Bura-Nakić, E.; Mikac, N.; Ciglenečki, I. (2011) *Chem. Geol.* in press.

https://doi.org/10.1180/S0026461X00006502 Published online by Cambridge University Press

Rates and mechanisms of oxygen consumption by fresh volcanic material in the marine environment

D.J. HEMBURY[1]*, M.R. PALMER[1] AND G.R. FONES[2]

[1]School of Ocean & Earth Science, University of Southampton, Southampton, SO14 3ZH, UK (*correspondence: d.hembury@noc.soton.ac.uk)
[2]School of Earth & Environmental Sciences, University of Portsmouth, Portsmouth, PO1 3QL, UK

Volcanic sediments are ubiquitous in the marine environment, to the extent that almost a quarter of the Pacific Ocean sediments are believed to be of volcanic origin. Volcanic material from explosive volcanism is fresh, fine grained and highly reactive. Although longer term alteration of volcanic material in the marine environment is relatively well studied, and has been demonstrated to make a significant contribution to the global cycling of elements, early diagenetic alteration of volcanic sediment in the marine environment is less well understood. We may, therefore, be missing an important component in our understanding of global geochemical cycles.

The ongoing eruption of Soufriere Hills, Monsterrat, West Indies, provides an excellent case study for these processes. Oxygen microelectrode profiles were measured in cores collected from around the island, 18 months after the May 2006 dome collapse event deposited approximately 115 x 10^6 m^3 of non-dense rock equivalent of material into the ocean [1]. Profiles reveal that oxygen is typically depleted to zero within 0.5 cm of the sediment water interface in volcanic deposits, compared with up to 6.5 cm in unaffected sediments. Oxidation of all available organic carbon in the volcanic sediments is only sufficient to sustain the calculated rate of oxygen consumption for c. 25 days. Hence, there must be another mechanism for oxygen consumption in these sediments. Results from laboratory flow-through experiments with the volcanic sediment indicate that consumption of the dissolved oxygen is likely driven by a coupled charged transfer reaction involving oxidation of silicate bound Fe^{II}.

[1] Trofimovs *et al*., (2011), *Bull. Volcanology,* (in press).

Intercalibration of Ar-Ar standards and samples at LDEO

SIDNEY R. HEMMING[1,2], KAORI TSUKUI[1,2], GARY T. MESKO[2], GULEED ALI[1,2], YUE CAI[12], ALEXANDER ADLER[1], SIOBHAN CAMPBELL[1], ELLEN CRAPSTER-PREGONT[1,2], CATHLEEN DOHERTY[1,2], JOEL GOMBINER[1], JOHN RUSSELL[1], JOHN TEMPLETON[1,2], MARISSA TREMBLAY[1] AND MARC VANKEUREN[1,2]

[1]Columbia University, New York, NY, (sidney@ldeo.columbia.edu)
[2]Lamont-Doherty Earth Observatory of Columbia University, 61 Rt 9W, Palisades, NY 10964

The Columbia University Spring 2011 Introduction to Geochronology and Thermochronology class is conducting an intercalibration experiment of Ar-Ar monitor standards in addition to some promising, well-behaved sanidine samples that have been analyzed multiple times in several labs. The goals are to document the intercalibration factors "R" (as defined by Renne *et al*., 1998, Chemical Geology) for the lab at Lamont-Doherty Earth Observatory and further to integrate research and education by providing a real introduction to EARTHTIME with a hands on exercise to examine the issues related to obtaining the highest quality Ar-Ar dates. This experiment will address the degree to which the Ar-Ar dates can be confidently compared between our lab and others that have reported on these samples, and will provide insights into potential sources of bias.

We have designed aluminium disks with 12 "unknown" pits, each surrounded by 4 "monitor" pits. Each unknown shares 2 of the 4 surrounding pits with an adjacent unknown. One package was irradiated for 4 hours, and another for 24 hours at the USGS TRIGA reactor in Denver, CO. Both irradiations contain several pits with Fish Canyon and Taylor Creek sanidine standards, which will result in 7 populations.

https://doi.org/10.1180/S0026461X00006502 Published online by Cambridge University Press

Central Indian Ridge versus Reunion hotspot : Do interaction processes account for on and off axis geochemical observations?

C. HEMOND[1], M. JANIN[1], B. MURTON[2] E. FÜRI[3,5], D. HILTON[3] AND J. DYMENT[4]

[1]Domaines Océaniques, IUEM, Université de Brest Plouzané, France (chhemond@univ-brest.fr)
[2]National Oceanography Centre, Southampton, UK
[3]Scripps Institution of Oceanography, La Jolla, CA, USA
[4]IPGP, Paris, France
[5]now at CRPG, Vandoeuvre lès Nancy, France.

We examine data produced on samples recovered along three cruises along the CIR axis segment supposedly involved in the interaction process, off axis along two sections up to 800ky on both sides of the axis and on several off axis volcanic features on the African plate between the CIR and the hotpsot present surface expression, La Réunion island.

Trace elements are enriched along the spreading axis from the central part of the segment and northward to the Marie-Celeste fracture zone. Enriched samples occur also symmetrically off axis as spikes along the northern section at 19°10”S with a wavelength of about 200 ky. This is not the case along the southern section at 19°30”S on which enriched samples are found only in the axial trench. All off axis ridges and seamounts are depleted in trace elements.

Isotopically, the picture is quite complex. On axis samples fall on isotope trends that are compatible with mixing material from both an heterogeneous Réunion plume and the local Indian upper mantle. Off axis samples along the northen sections fall on a similar mixing trend showing that if Cordier *et al*. (2010) were right, the enriched material is intrinsically part of the local mantle. The enriched trace element trend to the north does exist in Sr, Nd and Hf isotopes but Pb isotopes reveal that the northern most samples fall together with samples from the next northern short segment on a separate mixing line. That reveals the potential existence of a distinct local component that is not drastically different but only a bit more radiogenic in 208 at a given 206. He isotopes (Füri *et al*. 2011) revealed that some ^{3}He enriched material also exist to the North of the segment and and they attributed it to the trace of the Réunion hotspot left behing within the upper mantle.This northern Pb mixing line points to two enriched samples in Pb isotopes, one coming from the Marie Céleste fracture zone and the other from an off shore seamout built on the southern slop of the Piton de la Fournaise. They may reveal the existence of a discrete Reunion component that does not survive when melts pass through large magma plumbing and/or magma chambers but appears when small melt bacthes can be preserved.

Quantifying fluxes of metals to surface waters of the South-East Atlantic

G.M. HENDERSON[1]*, E.P. ACHTERBERG[2], A.R. BAKER[3], R. CHANCE[3], W. GEIBERT[4], W.B. HOMOKY[2], Y.-T. HSIEH[1], M.B. KLUNDER[2], M.C. LOHAN[5], P. MARTIN[2], R.A. MILLS[2], A. MILNE[5], M.R. PALMER[6], R.J. SANDERS[2], A.L. THOMAS[1], B.D. WAKE[2], E.M.S. WOODWARD[7] AND THE UK-GEOTRACES CONSORTIUM.

[1]Department of Earth Sciences, University of Oxford, Oxford, United Kingdom, (*correspondence: gideonh@earth.ox.ac.uk)
[2]National Oceanography Centre, Southampton
[3]University of East Anglia, [4]University of Edinburgh
[5]University of Plymouth
[6]National Oceanography Centre, Liverpool
[7]Plymouth Marine Laboratory

The UK-GEOTRACES Consortium aims to assess the balance of inputs of trace elements and isotopes from each of the four ocean boundaries (rivers, sediments, atmosphere, and volcanic) to the highly productive region along 40ºS in the Atlantic. Circumstances during the first UK-GEOTRACES cruise in late 2010 delayed completion of the full trans-Atlantic section, but allowed unexpected multiple occupation of key portions of the eastern third of the section, covering the Cape Basin. These multiple occupations significantly enhanced the realisation of one of the key objectives of the UK-GEOTRACES Consortium: observational quantification of the fluxes of trace metals to productive surface waters.

Vertical micro-profiler (VMP) measurements in the upper 500m of the water column provide constraints on both the vertical and off-shelf mixing of waters. Combined with measured gradients of trace elements, VMP data provide fluxes due to mixing. In the near-shelf, these can be compared with mixing derived from measurements of the Ra-isotope quartet in both surface and deeper waters.

Downward fluxes of trace elements were assessed using combined ^{234}Th and particle composition measurements, with repeat occupations allowing the commonly applied steady-state ^{234}Th approximation to be tested. Addition of trace elements from the atmosphere was also constrained by combining aerosol collection on ship, and relevant high resolution surface ocean chemistry (particularly ^{232}Th and Al concentrations).

In combination, these measurements provide an unusually firm set of constraints with which to quantify and balance the budget of trace elements, including the micronutrients, to the surface of a key open-ocean region.

https://doi.org/10.1180/S0026461X00006502 Published online by Cambridge University Press

Zinc and silicon isotope fractionation by deep-sea sponges

KATHARINE R. HENDRY[1], MORTEN B. ANDERSEN[2] AND LAURA ROBINSON[1,2]

[1]Department of Marine Chemistry and Geochemistry, Woods Hole Oceanographic Institution, Woods Hole, MA 02540, USA

[2]Department of Earth Sciences, University of Bristol, Wills Memorial Building, Queens Road, Bristol, BS8 1RJ

Dissolved Zn is an important micronutrient essential for the growth of marine phytoplankton, and exhibits a seawater depth profile similar to that of major nutrients, such as dissolved Si. Previous work has shown that diatoms Zn/Si ratios relate to the availability of free Zn^{2+} ions in surface seawater, and their Zn and Si isotopic composition relates to surface opal productivity and nutrient utilization. Conversely, the Zn/Si ratio of deep-sea sponge opaline spicules, among the earliest multicellular fossils to appear in the geological record, has been shown to related to the rain of Particulate Organic Carbon (POC). Here, we present a new calibration of sponge Si isotopes from different species and different ocean basins, showing a strong relationship between Si isotope fractionation and ambient dissolved Si concentrations. We also present new Zn concentration and isotope data from deep-sea sponges collected from the Southern Ocean. Our results highlight some species-specific differences in Zn uptake. The isotope data suggest, unlike for Si, sponges acquire some Zn from dietary sources, and some directly from seawater i.e. reflect both the dissolved and particulate pool of Zn. We discuss the consequences of these different uptake mechanisms for the use of sponge spicules as chemical palaeoenvironmental indicators.

Boron isotopes ($\delta^{11}B$) in coral: Energy budgets and pH control at the site of calcification

E. HENDY[1,2]*, T. MASS[3], I. BRICKNER[4] AND A. GENIN[5,6]

[1]School of Earth Sciences, University of Bristol, Wills Memorial Building, Queens Rd, Bristol, BS8 1RJ, UK (*correspondence: e.hendy@bristol.ac.uk)

[2]School of Biological Sciences, University of Bristol, Woodland Rd, Bristol, BS8 1UG, UK

[3]Institute of Marine and Coastal Sciences, Rutgers, The State University of New Jersey, 71 Dudley Road, New Brunswick, NJ 08901, USA

[4]Department of Zoology, Life Sciences Faculty, Tel Aviv University, Tel Aviv 69978, Israel

[5]The Interuniversity Institute for Marine Sciences, H. Steinitz Marine Biology Laboratory, P.O. Box 469, Eilat 88103, Israel

[6]Department of Ecology, Evolution, and Behavior, Life Sciences Institute, The Hebrew University of Jerusalem, Jerusalem 91904, Israel

The rate of water flow around a coral colony has a dramatic effect on diffusive boundary layer thickness and thereby colony physiology and skeletal formation. A controlled flow rate experiment was used to test whether these responses to environmental conditions influenced skeletal $\delta^{11}B$ as a measure of the pH at the site of calcification. Coral nubbins of *Pocillopora verrucosa* were grown for 2 years on stages within a reef and exposed to one of two flow regimes; flow enhanced by underwater pumps (15-20 cm s^{-1}) or reduced-flow, near stagnant conditions (~ 1 cm s^{-1}). Colonies in the enhanced-flow condition developed a more compact morphology, denser skeleton and calcified faster, in addition they had significantly higher tissue protein and chlorophyll concentrations, a higher density of zooxanthellae and higher reproductive output in terms of both quantity of oocytes and their size. We will present MC-ICPMS $\delta^{11}B$ analyses of the skeletons to explore colony control of the pH at the site of calcification and the allocation of energy resources by coral to the fundamental processes of skeletogenesis, growth, maintenance and reproduction.

https://doi.org/10.1180/S0026461X00006502 Published online by Cambridge University Press

Calibrating the boron isotope *p*H-proxy in *Globigerinoides ruber* by MC-ICPMS

MICHAEL J. HENEHAN[1]*, GAVIN L. FOSTER[1], JAMES W.B. RAE[2], JONATHAN EREZ[3], PAUL WILSON[1] AND MICHAL KUCERA[4],

[1]School of Ocean and Earth Science, National Oceanography Centre, Southampton, Southampton, UK (*correspondence: M.J.Henehan@soton.ac.uk)
[2]Bristol Isotope Group, Department of Earth Sciences, University of Bristol, Bristol, UK
[3]Earth Science Institute, The Hebrew University in Jerusalem, Jerusalem, Israel.
[4]Institute für Geowissenschaften, Eberhard-Karls Universität Tübingen, Tübigen, Germany

A key issue for reconstructing climate of the past is the need for accurate constraints on atmospheric concentration of CO_2. For timescales beyond the last 800 kyrs, further than the reach of the Antarctic ice cores, we have to rely on indirect proxy based estimates of CO_2. The boron isotope-pH proxy in foraminifera is gathering increasing momentum as a means to this end. This proxy has a firm theoretical grounding but tests of this understanding, with some recent exceptions [1], are restricted to a few culture based calibration studies (e.g. [2]). In this contribution we will present new attempts to calibrate the boron isotope pH proxy for *Globigerinoides ruber* – a surface dwelling tropical/subtropical species with symbiotic algae. We have cultured *G. ruber* at a range of pH values (8.2, 7.9, 7.6) and we will compare this data to published [3] and new core top data for this species. These data enable a determination of the pH sensitivity of $\delta^{11}B$ in *G. ruber* and provide valuable insights into the causes of "vital effects" that are known to influence the boron isotope system in planktonic foraminifera [2].

[1] Rae *et al*. (2011) *EPSL*, **302**, 403-413. [2] Sanyal *et al*. (1996) *Paleoceanography*, **11**, 513-517. [3] Foster (2008) *EPSL,* **271**, 254-266.

Comparison of XRF core scan data to conventional geochemical analyses: Usage in high resolution paleoenvironmental research

F.M. HENNEKAM* AND G.J. DE LANGE

Utrecht University, Faculty of Geosciences, Budapestlaan 4, 3508 TA, Utrecht, The Netherlands (*correspondence: hennnekam@geo.uu.nl)

Core scanning by X-ray fluorescence (XRF) is getting an increasingly common method to rapidly obtain paleo-environmental data from untreated (marine) sediments. A sediment surface is not an ideal substrate for XRF analysis; artifacts may occur relating to water content, grain size, surface roughness, water film formation, and sediment inhomogeneity. A high resolution analysis of an Eastern Mediterranean sediment core is used to get a grip on the signal-to-noise ratio of XRF core scan measurements. A suit of major elements (and elemental ratios), often used as paleoproxies, have been examined to indicate their relative correctness compared to 'real' data generated by both glass bead XRF and ICP-AES on distinct samples. Examples are shown to illustrate the consequences for the paleoproxy-interpretation.

XRF core scan data only reflects the chemical composition of a thin (few μm to hundreds of μm) layer of the sediment surface. The inhomogeneity in this surface can cause seemingly large paleoenvironmental variability. It is shown that (random) water rich spots can form underneath the Ultralene covering foil, having a substantial effect on the lighter elements with shallow response depths. This can create non-existing peaks in the XRF core-scan-produced paleoenvironmental record. Such deviations may especially occur for elemental ratios when elements are measured in different runs (e.g. other tube-voltage settings). This study promotes to verify certain high/low amplitudinal variability by means of a (destructive) conventional geochemical analysis prior to their interpretation.

https://doi.org/10.1180/S0026461X00006502 Published online by Cambridge University Press

The special case of actinide(IV) complexation by the carboxylic function of small and large organic ligands

C. HENNIG[1]*, K. TAKAO[1,2], S. TAKAO[1,3], M. MEYER[4], A. JEANSON[5], S. DAHOU[5] AND C. DEN AUWER[5]

[1]Helmholtz-Zentrum Dresden-Rossendorf, Institute of Radiochemistry, 01314 Dresden, Germany (*correspondence: hennig@esrf.fr)
[2]Department of Materials and Life Science, Seikei University, Tokyo 180-8633, Japan
[3]Bruker AXS K.K., Nano Business Unit Microanalysis Group, Kaganawa 221-0022, Japan
[4]Institut de Chimie Moléculaire de l´Université de Bourgogne, UMR 5260 du CNRS, 21078 Dijon, France
[5]CEA Marcoule, Radiochemistry and Process Department, 30207 Bagnols sur Cèze, France

Accidental release of radionuclides from mining activities, nuclear energy production, and radioactive waste storage sites requires research to predict the fate and mobility of these contaminants in the environment and more specific in organisms. To date, the interaction of actinides with biological systems is widely unkown, due to the lack of structural information on the molecular level. The aim of this presentation is to summarize recently explored coordination principles of tetravalent actinides with small carboxylic [1] and aminocarboxylic ligands as well as the interaction with proteins [2].

Tetravalent actinides form with carboxylate ligands in aqueous solutions at low pH values usually monomeric complexes. They show at the other hand a strong tendency toward hydrolysis already at low pH. As the pH reaches the onset of An(IV) hydrolysis, olation and oxolation occur as competing reactions to the carboxylate complexation. We observed under these circumstances the formation of several well-defined polynuclear species. The carboxylic group acts in such systems as a terminating ligand and stabilizes nanosized polynuclear clusters in solution and in the solid state [1]. It is important to note that this reaction prevents widely the formation of polynuclear hydrolysis species as well as the formation of An(IV) hydrous oxide colloids.

[1] Takao *et al*. (2009) *Eur. J. Inorg. Chem*. 4771-4775. [2] Jeanson *et al*. (2009) *New J. Chem*. **33**, 976-985.

Geochemistry of cold seeps - Fluid sources and systematics

CHRISTIAN HENSEN[1]*, FLORIAN SCHOLZ[1], ANJA REITZ[1], VOLKER LIEBETRAU[1], MATTHIAS HAECKEL[1], MARK SCHMIDT[1], KLAUS WALLMANN[1] AND ROLF L. ROMER[2]

[1]Leibniz Institute of Marine Sciences, IFM-GEOMAR, Kiel, Germany (*correspondance: chensen@ifm-geomar.de)
[2]Deutsches GeoForschungsZentrum, Potsdam, Germany

Emanation of fluids at cold seeps, mud volcanoes, and other types of submarine seepage structures is a typical phenomenon occurring at continental margins worldwide. They represent pathways along which volatiles and solutes are recycled from deeply buried sediments into the global ocean, and hence they may be considered as a potentially important link in global geochemical cycles.

In this contribution we present geochemical data from various geological and tectonic settings such as the Gulf of Cadiz, the convergent margin off Central America, and/or the Black Sea and provide approaches how to systemize available data sets. Clay-mineral dewatering plays a central role in terms of fluid-mobilization from greater depth, however, resulting cold seep fluids are typically very different from each other and cover a large range of geochemical signatures. This is is due to variations in control parameters such as the type and thickness of the sediment cover, thermal conditions, extension of fluid pathways, and the potential for secondary overprinting. For example, freshened fluids emanating at cold seeps off Costa Rica indicate dewatering and related geochemical reactions in subducting sediments, while fluids sampled at mud volcanoes in the Gulf of Cadiz provide evidence for a high-temperature fluid source originating in the underlying oceanic basement. The latter finding provides evidence for a hydrological connection between buried oceanic crust and the water column even at old crustal ages.

Varius geochemical tracers were proposed in the past to decipher relevant processes in the subsurface. In a recent systematic study, Scholz *et al*. [1] demonstrated the general use of Li, reflecting the temperature-dependent isotope fractionation during early diagenetic Li uptake and burial diagenetic Li release from sediments. However, additional approaches are required in order to provide robust geochmical interpretations of cold seep fluids.

[1] Scholz *et al*., (2010) *GCA*, **74**, 3459-3475.

https://doi.org/10.1180/S0026461X00006502 Published online by Cambridge University Press

On organic synthesis reactions driven by serpentinization

M. HENTSCHER[1], W. BACH[1] AND F. KLEIN[2]

[1]University of Bremen, 28359 Bremen, Germany (hentscher@uni-bremen.de, wbach@uni-bremen.de)
[2]WHOI, Woods Hole, MA 02543, USA (fklein@whoi.edu)

Moderate temperature, alkaline fluids with high amounts of hydrogen and methane issue from the seafloor in oceanic core complexes [1]. These fluids contain low molecular weight organic molecules likely related to abiotic synthesis [2,3]. The amount of dihydrogen produced during serpentinization of mantle peridotite at elevated temperatures is the driver behind forming abiotic organic carbon species. Recent models of serpentinization [e.g., 4, 5] provide insights into the quantity of hydrogen which is produced at different temperatures and water-rock-ratios from variable lithologies. Based on these models, affinites for the synthesis of organic molecules during the serpentinization process were calculated.

Methane is predicted to be the dominate organic species, but its formation is known to be kinetically sluggish [6]. Preliminary results for different serpentinization scenarios show strong affinities in the overall reaction for hydrocarbons at low temperatures. These reactions are kinetically sluggish in aqueous solutions at low temperatures, and at higher temperatures, when rates are increased, the affinities decrease because less hydrogen is available from fluid-rock equilibrium. When the affinities of the overall reactions are normalized to electrons transferred, the highest affinities are predicted for formic acid, which is indeed elevated in fluids from the Lost City vent field [3].

Mixing of 350°C hydrothermal fluid from serpentinization systems with cold seawater also creates abundant driving force for organic synthesis [7l. As the time scales of mixing much exceed those at which abiotic organic synthesis reactions proceed, these environments generate an energetically feasible habitat for microbes. Affinity calculations for these environments allow an assessment of energy availability for catabolism, which can be coupled to anabolic energy demand to characterize the uniqueness of serpentinization systems.

[1] Kelley *et al*. (2001) *Nature* **412**, 145. [2] Proskurowski *et al*. (2008) *Science* **319**, 604. [3] Lang *et al*. (2010) *GCA* **74**, 941. [4] McCollom and Bach (2009) *GCA* **73**, 856. [5] Klein *et al*. (2009) *GCA* **73**, 22, 6868. [6] Seewald *et al*. (2006) *GCA* **70**, 446. [7] Shock and Schulte (1998*) J. Geophys. Res.* **103**, 28513.

Subsurface biogeochemistry of hydrothermal flow at the Hook Ridge, Bransfield Strait

L. HEPBURN[1]*, R.A. MILLS[1], A. AQUILINA[1], J.T. COPLEY[1], A. GLOVER[2] AND P. TYLER[1]

[1]National Oceanography Centre, Southampton, SO14 3ZH, UK (*correspondence: leh204@soton.ac.uk) (ram1@soton.ac.uk, aa@noc.soton.ac.uk, jtc@noc.soton.ac.uk, pat8@noc.soton.ac.uk)
[2] Natural History Museum, London, SW7 5BD, UK (a.glover@nhm.ac.uk)

Metalliferous sediments at active hydrothermal vent sites host significant populations of free-living and symbiotic chemosynthetic microorganisms associated with benthic fauna. Reduced hydrothermal fluids flow through the sediments and interact with oxic, overlying seawater to create steep redox gradients in the subsurface biosphere. The products of these redox reactions provide a suite of electron donors and acceptors that stimulate microbial metabolism and support chemosynthetic consortia of subseafloor micro-organisms. We are yet to fully understand the impact of macro-faunal and microbial communities on the geochemical flux of C, S, Fe, Mn and other elements across redox boundaries near the sediment-water interface. Here we present the pore-fluid and solid phase geochemistry of sediments from Hook Ridge – an extensive, high-temperature, hydrothermal system in the central Bransfield Strait, Antarctica [1].

Hook Ridge hydrothermalism is characterised by areas of shimmering water and water column E_h anomalies at a depth of 1100m. Ship-board and shore-based, analyses of extracted pore-fluids demonstrate the advection of low-chlorinity (<490 mM), high-sulfide (>120 μM), high-methane (>15 μM) and Fe-rich (>545 μM) fluids through the sediments, at rates of 20-50 $cmyr^{-1}$. Downcore sulfate-methane distributions suggest the presence of anaerobic oxidation of methane (AOM) at this site. These sediments are dominated by patches of the siboglinid chemosynthetic polychaete *Sclerolinum sp*. that likely contain sulfophilic chemosynthetic symbionts [2]. Faunal, mineralogical and geochemical analyses of Hook Ridge sediments are used to constrain the distribution and impact of the biogeochemical processes occurring in this sediment-hosted hydrothermal system.

[1] Klinkhammer *et al*. (2001) *EPSL* **193**, 395-407. [2] Sahling *et al*. (2005) *Limnol. Oceanogr*. **50**, 598-606.

https://doi.org/10.1180/S0026461X00006502 Published online by Cambridge University Press

Pilot-scale barrier system for removal of nitrate in mine drainage

ROGER HERBERT[1]* AND HARRY WINBJÖRK[2]

[1]Department of Earth Sciences, Uppsala University, 752 27 Uppsala, Sweden.
(*correspondence: Roger.Herbert@geo.uu.se)
[2]LKAB, 983 34 Malmberget, Sweden

Undetonated ammonium nitrate is readily soluble in water and quickly enters into the mine water and process water at a mine site. In order to investigate the application of nitrate removal by denitrification in the cold climate of northern Sweden, a pilot-scale barrier system was constructed of sheet metal in autumn 2009 at the Malmberget iron ore mine. The barrier (9m x 2m x 1.5m) appears as an open basin with three inner dividing walls, and is filled with a reactive mixture consisting of crushed rock, sawdust, and sewage sludge. Water flows through the barrier at ca. 0.45 m^3/hour.

The chemical analyses of water flowing into and out of the barrier during 2010 indicate that the degree of nitrate removal generally lay in the range between 11 and 77% of influent nitrate concentrations. Stable isotope analyses of $\delta^{15}N$ and $\delta^{18}O$ in nitrate demonstrate an enrichment in ^{15}N and ^{18}O in nitrate as water flows through the barrier, supporting the conclusion that denitrification is responsible for nitrate removal. Ammonium concentrations in the barrier effluents are initially high, but these high levels are subsequently flushed from the barrier.

In order to increase the degree of nitrate removal by denitrification in the barrier, a reactive carbon source needs to be added to the influent waters; this will be tested during the 2011 field season.

Temporal variations in Galápagos plume-ridge interaction at the Cocos-Nazca spreading center

A. HERBRICH[1]*, K. HOERNLE[1], F. HAUFF[1], R. WERNER[1] AND D. GARBE-SCHÖNBERG[2]

[1]Leibniz Institute of Marine Sciences IFM-GEOMAR, Wischhofstrasse 1-3, 24148 Kiel, Germany
(*correspondence: aherbrich@ifm-geomar.de)
[2]Inst. Geosciences, Christian Albrechts Universität zu Kiel, Ludewig-Meyn-Strasse 10, 24118 Kiel, Germany

The major goals of cruise SO208 with the German research vessel Sonne were to investigate 1) plume-ridge interaction through time at the Cocos-Nazca spreading center (CNS) north of the Galápagos Islands by sampling across axis profiles of the seafloor and 2) off axis volcanism at the East Pacific Rise (EPR) versus far field effects of the Galápagos hotspot documented in seamounts off the coast of N Costa Rica and Nicaragua. Overall the nature of material transfer from the plume to the ridge and its large scale distribution throughout the Eastern Pacific is beeing investigated by means of major and trace element and Sr-Nd-Pb (double spike) isotope data.

The seamounts on the EPR generated part of the Cocos plate appear to originate on one hand from a depleted MORB-like source consistent with their formation near the EPR axis, while other seamounts formed through lower degrees melting of an enriched OIB source either more distant from the EPR or by intraplate volcanism. Geochemical profiles across the Western and Eastern CNS indicate the participation of two different Galápagos plume components with a change in the amount this material entering the CNS with time. While at the western profile element ratios of more to less incompatible elements show an overall decrease of a plume component, Wolf-Darwin or Northern domain [1], with increasing age, the opposite is observed at the eastern profile. The Central domain component [1] increases with increasing age of the crust in this area. These observations indicate variable flux of specific Galápagos plume components to the CNS over the past 800 000 years. Sr-Nd-Pb isotope data to verify these observations are currently being generated and will be presented at the conference.

[1] Hoernle *et al*. (2000) *Geology* **28**, 435–438

https://doi.org/10.1180/S0026461X00006502 Published online by Cambridge University Press

Discrimination of secondary organic aerosol from different sources

M.F. HERINGA[1], R. CHIRICO[1,2], S.M PLATT[1], L. PFAFFENBERGER[1], P. BARMET[1], J.G. SLOWIK[1], P.F. DECARLO[1,3], J. DOMMEN[1], A.S.H. PRÉVÔT[1] AND U. BALTENSPERGER[1]

[1]Laboratory of Atmospheric Chemistry, Paul Scherrer Institut, 5232 Villigen PSI, Switzerland

[2]now at Italian National Agency for New Technologies, Energy and Sustainable Economic Development (ENEA), UTAPRAD-DIM, Via E. Fermi 45, 00044 Frascati, Italy

[3]now at AAAS Science and Technology Policy Fellow, US EPA, Washington, DC, USA

Secondary organic aerosol (SOA) comprises a major fraction of the submicron aerosol mass [1]. It consists of thousands of different compounds, and undergoes permanent chemical evolution during the atmospheric aging process, resulting in an increasingly oxidized aerosol [2]. As a result of this, chemical features of SOA (such as unit mass spectra from aerosol mass spectrometry) become increasingly similar with increasing aging time. This is good news for modeling purposes, as the specific SOA source becomes less important for the quantification of the SOA impact e.g. on climate. However, this also means that it is difficult to perform an apportionment of the SOA to its various sources, e.g., by positive matrix factorization [3]. We have investigated SOA formation from a variety of sources, including both combustion exhaust (with either the full exhaust or only the gaseous precursors) [4, 5], as well as anthropogenic and biogenic model precursors such as trimethylbenzene and α-pinene. We characterized the formed SOA using a high resolution time-of-flight aerosol mass spectrometer. The various fragments obtained from the high-resolution spectra were tested for characteristic differences using a variety of methods. The results will be discussed along with a comparison to high-resolution aerosol mass spectra from ambient samples.

[1] Hallquist *et al*. (2009) *Atmos. Chem. Phys*. **9**, 5155-5236. [2] Jimenez *et al*. (2009) *Science* **326**, 1525-1529. [3] Lanz *et al*. (2007) *Atmos. Chem. Phys*. **7**, 1503-1522. [4] Chirico *et al*. (2010) *Atmos. Chem. Phys*. **10**, 11545-11563. [5] Heringa *et al*. (2011) *Atmos. Chem. Phys. Discuss*. **10,** 8081-8113.

How does the slab component get across the mantle wedge?

JÖRG HERMANN[1] AND CASSIAN PIRARD[2]

[1]Research School of Earth Sciences, The Australian National University, 0200 Canberra, (joerg.hermann@anu.edu.au)

[2]Department of Petrology, Vrije Universiteit Amsterdam, 1081HV Amsterdam, (cassian.pirard@falw.vu.nl)

Arc lavas are enriched in volatiles, LILE and LREE with respect to MORB. This enrichment is attributed to mantle metasomatism by a slab-derived fluid phase (slab component). There has been great progress in the last years to constrain the nature and composition of this fluid phase. The slab fluid is in disequilibrium with the mantle wedge and the way how it reacts with peridotites is crucial for understanding subduction recycling of volatiles and trace elements. In this contribution, evidence from natural rocks and experiments are presented to constrain the nature and extent of mantle wedge metasomatism by slab-derived fluids.

Contacts between felsic and ultramafic rocks in high- and ultrahigh-pressure terrains can be used as proxies for processes acting at fore-arc (50-80 km) and sub-arc depth (80-120 km), respectively. Interaction of aqueous fluids released from felsic rocks at for-arc conditions (P=10-20 kbar, T ~600°C) with peridotites leads to metasomatic rinds that are rich in talc, amphibole and phlogopite. Phlogopite sequestres most of the LILE and thus residual fluids are very dilute. At higher pressures and temperatures, interaction of hydrous melts with peridotites produces garnet and orthopyroxene and minor phlogopite and residual fluids show some enrichment of LILE and LREE.

Experiments were designed to constrain interaction of a slab-derived hydrous melt with harzburgites during porous and channel flow. The porous flow experiments produced a highly metasomatized peridotite consisting of amphibole, phlogopite, olivine, orthopyroxene and an aqueous fluid at subsolidus condition. Amphibole and phlogopite host significant amounts of LREE and LILE, respectively. The wet solidus in this metasomatised mantle wedge peridotite is at 900°C at 25 kbar and at 950°C at 35 kbar. The extent of mantle metasomatism in layered experiments, mimicking channel flow, is minimal. At the interface between the slab melt and olivine a small ~200μm wide layer of garnet-orthopyroxenite forms that shields the melt from further interaction with the olivine grains. Most importantly, no phlogopite and amphibole have been observed in all such experiments. Therefore, data from natural rocks and experiments indicate that channel flow appears to be the most efficient way to transfer trace elements from the top of the slab to the locus of partial melting in the mantle wedge.

https://doi.org/10.1180/S0026461X00006502 Published online by Cambridge University Press

Reactive fluid flow and time-integrated fluxes in an upper crustal magmatic-hydrothermal system, Krušné hory Mts., Central Europe

MATYLDA HEŘMANSKÁ* AND DAVID DOLEJŠ

Institute of Petrology and Structural Geology, Charles University, 128 43 Praha 2, Czech Republic (*correspondence: matylda.h@seznam.cz)

Advances in thermodynamic modeling of fluid-mineral interactions at elevated temperatures and pressures permit calculation of time-integrated fluid fluxes in metamorphic complexes and shear zones using inversion of mineral reaction progress and application of local equilibrium. Such estimates may, however, only provide an upper bracket on the integrated fluid flux when the incoming fluid is out of equilibrium with the host lithology. We extended the transport theory to account for effects of thermal and pressure gradients and chemical disequilibrium simultaneously, and apply it to greisen alteration in the Western Krušné hory granite pluton (central Europe). Veins and swarms of fracture-controlled greisens up to 400 m long and 800 m deep show the following spatial alteration zoning (from margin to interior): greisenized granite, muscovite-quartz greisen, topaz-quartz greisen, pure quartz greisen, and hydrothermal quartz vein. Greisen textures and distribution of relics of magmatic quartz phenocrysts suggest that greisenization was a constant-volume replacement process. We modeled set of infiltrating fluids, from 650 °C and 1 kbar (magmatic fluid phase exsolving at the solidus) to 400 °C and 500 bar (greisen formation). The corresponding time-integrated fluid fluxes vary from 10^2 to 10^6 m^3 fluid m^{-2} rock, dictated by chemical disequilibrium whereas pressure and temperature gradients have subordinate effects. Successive replacement of feldspar by muscovite and topaz under conserved volume constrains the time-integrated fluid flux to $0.2\text{-}1.0\cdot10^3$ m^3 fluid per m^2 rock. The formation of a single greisen vein with a typical volume of $0.1\text{-}5\cdot10^4$ m^3 would require $0.01\text{-}3.10^7$ m^3 aqueous fluid. For a characteristic vein length (transport distance) of 400-800 m, the plausible fluid flow rate is 10^{-10} to 10^{-9} $m.s^{-1}$. By using mass balance and an assumed 5 wt. % H_2O dissolved in a granitic magma, such amount of fluid phase would have exsolved from 5.10^5 to 3.10^8 m^3 magma or an intrusion measuring $0.8\text{-}7\cdot10^2$ m in each dimension, which is comparable with dimensions of the host granitic pluton. Our results indicate that strong alterations may be produced by integrated fluid fluxes that are by 2-3 orders of magnitude lower than those in metamorphic shear zones.

Fluid and trace element migration in subducted oceanic rocks from Ecuador

P. HERMS[1]*, T. JOHN[1,2], R. J. BAKKER[3] AND V. SCHENK[1]

[1]Institut für Geowissenschaften and SFB 574, Universität Kiel, 24098 Kiel, Germany (*correspondence:ph@min.uni-kiel.de, vs@min.uni-kiel.de)

[2]Institut für Mineralogie, Universität Münster, 48149 Münster, Germany (timm.john@uni-muenster.de)

[3]Department Applied Geosciences & Geophysics, Mineralogy & Petrology, University of Leoben, 8700 Leoben, Austria (Ronald.Bakker@mu-leoben.at)

The ophiolite association of the Raspas complex in Ecuador, representing subducted oceanic lithosphere, stands out by high-pressure zoisite veins and associated metasomatized zoisite eclogites, indicating fluid flow and element mobility at depth of about 60 km. Fluid inclusion investigations in vein zoisite and metasomatized zoisite eclogites reveal a homogeneous low-salinity fluid composition in the system H_2O-NaCl-CH_4-CO_2 which is conform with an open-system fluid infiltration derived from an external source. Deserpentinized, pseudo-spinifex textured chlorite harzburgites found within the ultramafitites of the Raspas Complex are a potential source for the external CH_4-bearing low-salinity aqueous fluid. However, the enrichment in LREE, MREE, Pb, Sr, Th, U, found in the metasomatically overprinted seafloor-altered MORB-type eclogites and in zoisite veins can be explained best by leaching of these elements from metabasites and metapelites in zones of intense fluid-rock interaction. A garnet-amphibole rock, deficient in LREE and Sr, could represent such a leached metabasite. Other LIL elements, as well as B, Th and U could be derived from metapelites. All the elements enriched in the metasomatized eclogites and zoisite veins must have been fluid mobile at eclogite-facies conditions and transported by channelized fluid flow and high fluid flux.

https://doi.org/10.1180/S0026461X00006502 Published online by Cambridge University Press

Biogeochemical characterization of contaminant Mn sequestration

ELIZABETH M. HERNDON[1]*, DAVID EISSENSTAT[2], CARMEN ENID MARTINEZ[3] AND SUSAN L. BRANTLEY[1,4]

[1]Dept. of Geosciences, Penn State University, University Park, PA, USA 16802 (*eherndon@psu.edu)
[2]Dept. of Horticulture, Penn State University
[3]Dept. of Crop and Soil Sciences, Penn State University
[4]Earth & Environ. Systems Institute, Penn State University

Manganese contamination in soils is prevalent in industrialized regions. Over the past few centuries, large quantities of Mn have been extracted from the lithosphere, emitted to the air via anthropogenic activities, and redeposited to the Earth's surface. In order to evaluate environmental impacts of Mn deposition, we must better understand the biogeochemical behaviours of Mn in soils. Vegetation can act as an element "capacitor", storing large quantities of Mn and releasing it slowly into the environment over time. Here, we quantify mass fluxes of Mn amongst soil, vegetation, and pore fluid reservoirs in field and greenhouse experiments. We find that much greater quantities of Mn are taken up by vegetation than leached into pore fluids each year, preventing Mn loss from the soil system.

Characterization of Mn-compounds in the environment is often limited by their high reactivity and poor crystallinity; however, synchrotron source radiation can be used to map the microscale distribution of Mn (X-Ray Fluorescence) and identify its chemical state (X-ray Absorption Spectroscopy) in environmental samples. We use XRF and XAS to characterize the spatial abundance and chemical forms of Mn in mineral soil, organic soil, and tree leaf samples from both the field and a controlled greenhouse experiment. XRF analysis of leaves from trees exposed to high Mn reveals that the Mn is concentrated in visible dark spots, the key indicator of Mn toxicity in vegetation. XAS results indicate that Mn is present as an organically-complexed Mn^{+3} compound in vegetation and as mixed-valence oxides ($Mn^{+3/+4}$) in organic and mineral soils. Vegetation has previously been thought to contain primarily Mn^{+2} due to the instability of the trivalent ion. The dominance of Mn^{+3} in foliage would change current perceptions of biogeochemical Mn cycling and has implications for litter decomposition, a process that often uses Mn^{+3} as a catalyst. The presence of Mn-oxides in soil organic matter is consistent with the rapid oxidation of Mn released from foliage during decomposition. High rates of Mn uptake into vegetation, combined with accumulation of solid-phase Mn in the soil, effectively increases the residence time of Mn in contaminated systems.

Simulations of glacial/interglacial cycles with simple box-models: Key triggers for deglaciations

C. HERRERO*, A. GARCÍA-OLIVARES AND J. L. PELEGRÍ

Institut de Ciències del Mar (ICM-CSIC). Pg. Marítim de la Barceloneta, 37-49, 08003 Barcelona, Spain (*correspondence: herrero@icm.csic.es)

García-Olivares *et al*. [1] have calibrated Paillard's model [2] to obtain a best fit with experimental time-series of $\delta^{18}O$ and CO_2 available for the last 800 kyr.

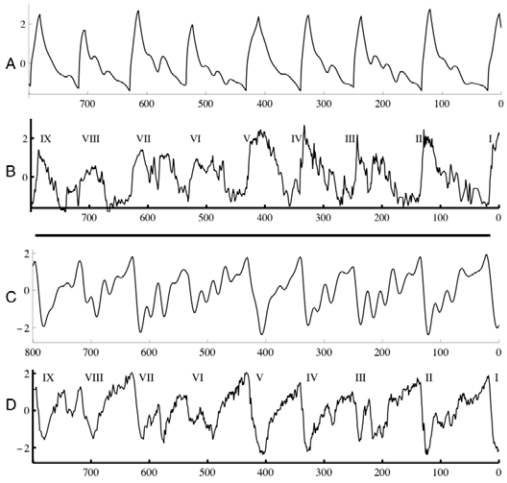

Figure 1. CO_2 predicted by the model (A) and experimental time-series [3] (B). Ice Volume V predicted by the model (C) and $\delta^{18}O$ experimental time-series [4] (D).

We discuss how the physical pump and, to some extent, the density of Antarctic deep water, may be important factors controlling the oceanic pulse that triggers deglaciations. Specifically, an increase of sea ice coverage during a glaciation may modulate the annual net heat gain of the Southern Ocean surface, and a reduction of the deep mixing rate would limit the upwelling of CO_2 enriched deep water, thus being key factors for triggering deglaciations.

[1] García-Olivares & Herrero (2011). Submitted to Scientia Marina. [2] Paillard & Parrenin (2004) *Earth Planet. Sci. Lett.* **227**, 263–271. [3] Lüthi *et al*. (2008). *Nature* **453**, 379-382. [4] Lisiecki & Raymo (2005) *Paleoceanography* **Vol. 20**, PA1003, doi:10.1029/2004PA001071.

https://doi.org/10.1180/S0026461X00006502 Published online by Cambridge University Press

Thermodynamic principles of soil organic matter decomposition in a changing world

A.M. HERRMANN[1]*, S.M. GRICE[1,2], K. RITZ[2] AND J.A. HARRIS[2]

[1]Uppsala BioCentre, Swed. Univ. Agric. Sci., 75007 Uppsala, Sweden (*correspondence: Anke.Herrmann@slu.se)
[2]School of Applied Sciences, Cranfield University, U.K.

The role of soils in governing the terrestrial carbon balance is acknowledged as being important but remains poorly understood within the context of climate change. Soils exchange energy with their surroundings and are therefore open systems thermodynamically, but little is known how energy transformations of decomposition processes are affected by temperature. Soil organic matter and the soil biomass can be conceptualised as analogous to the 'fuel' and 'biological engine' of the earth, respectively, and are pivotal in driving the belowground carbon cycle.

Thermodynamic principles of soil organic matter decomposition were evaluated by means of isothermal microcalorimetry (TAM Air, TA Instruments, Sollentuna Sweden: (i) Mineral forest soils from the Flakaliden long-term nitrogen fertilisation experiment (Sweden) were amended with a range of different substrates representing structurally simple to complex, ecologically pertinent organic matter and heat signatures were determined at temperatures between 5 and 25°C. (ii) Thermodynamic and resource-use efficiencies of the biomass were determined in arable soils which received contrasting long-term management regimes with respect to organic matter and nitrogen since 1956.

The work showed that (i) structurally labile components have higher activation energy and temperature dependence than structurally more complex organic components. This is, however, in contrast to the thermodynamic argument which suggests the opposite that reactions metabolising structurally complex, aromatic components have higher temperature dependence than reactions metabolising structurally more labile components. (ii) Microbial communities exposed to long-term stress by heavy metal and low pH were less thermodynamic efficient and showed a decrease in resource-use efficiency in comparison with conventional input regimes. Differences in efficiencies were mirrored in both the phenotypic and functional profiles of the communities.

We will present our findings illustrating the capacity of isothermal microcalorimetry to evaluate temperature dependencies of soil organic matter decomposition, associated energy transformations and thermodynamic principles in soil ecosystems.

Compositional and structural dynamics of dissolved organic matter in Taihu lake, China

NORBERT HERTKORN*[1], FENFEN ZHANG[2], PHILIPPE SCHMITT-KOPPLIN[1], AGNES FEKETE[1], ANDRAS GASPAR[1], YING WU[2] AND JING ZHANG[2]

[1]Institute of Ecological Chemistry, Helmholtz Zentrum München, German Research Center for Environmental Health, Ingolstaedter Landstrasse 1, D-85764 Neuherberg, Germany (hertkorn@helmholtz-muenchen.de)
[2]State Key Laboratory of Estuarine and Coastal Research, East China Normal University, 3663 North Zhongshan Road, 200062 Shanghai, P.R. China

Lake Tai (Taihu) near Shanghai / China experiences with a surface area of 2250 square kilometers and a remarkable average depth of only 1.9 m pronounced seasonal variance in climate conditions, biodiversity and composition of dissolved organic carbon (DOC). High resolution organic structural spectroscopy (high field NMR and FTICR mass spectrometry) revealed a remarkable seasonal variation of DOC composition and structure throughout all structural regimes which nevertheless followed the seasonal cycles. Taihu DOC showed variable contents of abiotic molecules and biosignatures; however, the time-dependent individual molecular signature of Lake Taihu DOM was likely dominated by microbial metabolism rather than abiotic chemistry. Non-target high-resolution organic structural spectroscopy offers opportunities to considerably improve the significance of future functional biodiversity studies which might lead to a novel unified perception of biodiversity and biogeochemistry.

https://doi.org/10.1180/S0026461X00006502 Published online by Cambridge University Press

Quantifying the $[Ba^{2+}]$: $\delta^{18}O_{SEAWATER}$: surface salinity relationship in the Eastern Equatorial Pacific

J.E. HERTZBERG* AND M.W. SCHMIDT

Department of Oceanography, Texas A&M University, College Station, TX 77843, USA (*correspondence: jhertzberg@ocean.tamu.edu)

Fluvial inputs to the world's oceans serve as the main source for dissolved barium in seawater. Barium desorbs from suspended clays in freshwater, making riverine water enriched in $[Ba^{2+}]$ [1, 2]. The suspended clays flocculate when riverine water mixes with seawater in estuaries, resulting in a conservative linear mixing between high $[Ba^{2+}]$, low sea surface salinity (SSS) in estuaries and low $[Ba^{2+}]$, high SSS in open ocean waters. Therefore, SSS can be estimated from dissolved barium concentrations in regions influenced by high riverine input. Furthermore, planktonic foraminifera incorporate barium into their calcium carbonate tests in proportion to seawater Ba/Ca ratios [3, 4]. Thus, foraminiferal Ba/Ca ratios from ocean sediment cores can be employed as a proxy for paleosalinity reconstructions. However, integral to the use of this proxy is the quantification of the regional seawater Ba/Ca:SSS relationship. Here, we quantify this relationship for the eastern equatorial Pacific Ocean, a location where intense seasonal rainfall and high riverine input from Central and northern South America creates the sharpest SSS gradient in the modern tropics. In October and November of 2010, surface seawater samples were collected along 85°W in a latitudinal transect from 10°N to 8°S during the RV *Melville* cruise MV1014, and analyzed for SSS, Ba/Ca ratios, and $\delta^{18}O$. For salinities < 31.4, we find a large change in Ba/Ca of 8.02 µmol/mol per salinity unit, while for salinities > 31.4 the relationship levels off at a Ba/Ca ratio of 4.5 µmol/mol. Based on the $\delta^{18}O$:SSS relationship in our samples, we also find two distinct end members of freshwater input to the region, one with a Costa Rican riverine $\delta^{18}O$ end member of -10.0‰ for salinities up to 31.4 and one with a freshwater end member of -7.2‰ dominated by freshwater precipitation for salinities > 31.4. This indicates that the Ba/Ca:SSS relationship for salinities < 31.4 is indeed driven by regional fluvial inputs. We will also present new reconstructions of regional SST and SSS based on a new set of multicores collected from the Cocos and Carnegie Ridges.

[1] Hanor & Chan (1977) *Earth Planet. Sci. Lett.* **37**, 242–250. [2] Edmond *et al.* (1978) *Neth. J. of Sea Res.* **12**, 324–328. [3] Lea & Spero (1992) *Geochim. Cosmochim. Acta* **56**, 2673–2680. [4] Hönisch *et al.* (2011) *Mar. Micropaleo.* **79**, 52–57.

REE in fossil biogenic apatite

D. HERWARTZ[1]*, T. TÜTKEN[1], KP. JOCHUM[2] AND P.M. SANDER[1]

[1]Steinmann Institut, Universität Bonn, Poppelsdorfer Schloss, 53113 Bonn, Germany

[2]Max-Planck Institut für Chemie, Becherweg 27, 55128 Mainz, Germany

Rare earth elements (REE) in fossil biogenic apatites are frequently used as palaeonevironmental proxies, because the in-vivo REE concentrations (lower ppb range) are efficiently overprinted by diagenetic post-mortem REE uptake (in the ppm range) especially in fossil bone and dentin. The post-mortem REE uptake was long assumed to be limited to the fossilisation process, were carbonate hydroxyl-apatite is transformed into a more stable fluor-apatite, organic components are degraded and the porosity is filled by secondary minerals. However, recent studies reveal that REE uptake takes place over prolonged timescales in the order of millions of years, rather than thousands of years [1,2]. Furthermore, substantial intra-bone fractionation of the REE is observed, even exceeding two orders of magnitude in $(La/Sm)_N$ and $(La/Yb)_N$ within single bone specimens [2]. These observations necessiate a deeper understanding of REE with respect to fossil bones, if this group of elements is to be used as a palaeoenvironmental proxy in the future.

We will present REE profiles measured by LA-ICPMS over individual fossil bone samples from a wide range of diagenetic settings, ranging from Lower Triassic to Holocene age. Key observations are (1) MREE are efficiently scavenged at the outer bone rim and are increasingly depleted towards the central bone; (2) negative Ce-anomalies develop with increasing distance from the outer bone rim, which have no environmental significance; and (3) positive La and superchondritic Y/Ho anomalies evolve with increasing distance from the bone rim and decrease again towards the marrow cavity. A comparison with literature data indicates that (1) fossil bones derive their REE budget from the ambient pore fluid, rather than surface waters; and (2) that individual fossil bones may have intra-bone $(La/Sm)_N$ and $(La/Yb)_N$ variability covering more than half of the range previously found in literature compilations [n = 1691; 3]. Our data implies, that HREE are generally more mobile in diagentic fluids, which is likely due to stronger complexation of HREE with carbonate ions, when compared to the LREE.

[1] Kocsis *et al.* (2010) *Geochim. Cosmochim. Acta* **74**, 6077-6092. [2] Herwartz *et al.* (2011) *Geochim. Cosmochim. Acta.* **75**, 82-105. [3] Trueman *et al.* (2006) *Geochim. Cosmochim. Acta* **70**, 4343-4355.

https://doi.org/10.1180/S0026461X00006502 Published online by Cambridge University Press

Heavy isotope fractionation in magmatic systems: The example Tl

K. HETTMANN[1]*, K. KREISSIG[2], E. SCHAUBLE[3], M. REHKÄMPER[2], M. MARKS[1] AND G. MARKL[1]

[1]Eberhard Karls Universität Tübingen, Wilhelmstrasse 56, 72072 Tübingen, Germany (*correspondence: kai.hettmann@uni-tuebingen.de)
[2]Dept. of Earth Science & Engineering, Imperial College London, SW7 2AZ London, United Kingdom
[3]University of California, Los Angeles, 595 Charles Young Drive East, Los Angeles, CA 90095-1567, USA

Variations in the isotopic composition of heavy isotopes are not expected to occur by mass-dependent fractionation in high-temperature systems, since relative mass differences are very small (e.g. < 1% for Tl) and the fractionation scales with $1/T^2$ [1]. In contrast, the mass-independent fractionation due to differences in the nuclear volume between isotopes generally increases with atomic number and scales with 1/T [2].

In this study we show that isotopic fractionation of Tl occurs in the peralklaline Ilimaussaq intrusion, southwest Greenland. We studied magmatic and hydrothermal amphiboles and astrophyllite, which is a rare amphibole-related mineral. The isotopic compostion of Tl varies systematically with increasing magmatic differentiation. The most differentiated rocks show the largest variations, which are most probably related to fluid unmixing from the late-stage magma, as shown in previous studies [3]. Late-stage magmatic and hydrothermal minerals exhibit contrasting isotopic compositions, with isotopically light Tl in the magmatic samples and heavier Tl in the hydrothermal rocks. Post-magmatic hydrothermal alteration affected a single sample and produced the heaviest observed Tl isotope composition. Overall, the rocks of the Ilimaussaq intrusion thus display a variability of 1‰ in the $^{203}Tl/^{205}Tl$ isotope ratio as a results of fractionation that occurred at temperatures of between 250 and >1000°C [4].

In addition to this study of natural samples, we will carry out ab-initio modelling of the isotopic fractionation of Tl due to mass-dependent and –independent effects to enhance the existing knowledge [5] of the importance of non-classical fractionation processes in high-temperature systems.

[1] Bigeleisen & Mayer (1947) *J. Chem. Phys.* **15**, 261. [2] Bigeleisen (1996) J. Am. Chem. Soc. **118**, 3676–3680. [3] Pfaff *et al.* (2008) *Lithos* **106**, 280-296. [4] *Markl et al.* (2001) *J. Petrol.* **42**, 2231-2257. [5] Schauble (2007) *Geochim. Cosmochim. Acta* **71**, 2170-2189.

Tracing water masses with radiogenic isotopes: Water column and Fe-Mn crust records from the eastern equatorial Pacific Ocean

L. HEUER[1]*, M. FRANK[1], A. EISENHAUER[1] AND M. CHRISTL[2]

[1]IFM-GEOMAR, Wischhofstr. 1-3, 24148 Kiel, Germany (*correspondence: lheuer@ifm-geomar.de)
[2]Laboratory of Ion Beam Physics, ETH Zurich, Switzerland

The radiogenic isotope compositions of neodymium (Nd) and lead (Pb) have been shown to be effective tracers for continental weathering inputs and in the case of Nd, due to its quasi-conservative behavior, also for present and past ocean circulation.

We present the first full water depth profiles of dissolved Nd isotopes and concentrations from the eastern equatorial Pacific. Time series of past deep water Nd and Pb isotope compositions were obtained from a Mn nodule, as well as from two Fe-Mn crusts that grew on the flank of a seamount at different water depths (4000-3500 m; 3500-3000 m). We also present a comparison of vertical and horizontal time series obtained from a discoidal Mn nodule. The ages of the crusts and the nodule were derived from $^{10}Be/^{9}Be$ chronology. Growth rates are on the order of 3-6 mm/Myr for the crusts and much higher at 24-46 mm/Myr for most of the nodule.

Nd concentrations of the unfiltered water samples range from 8 to 58 pmol/kg and show a systematic increase with water depth caused by scavenging processes. Compared with previous data the deep water concentrations at around 4000 m yield exceptionally high values greater than 50 pmol/kg.

The seawater Nd isotope compositions (εNd) vary between -5 at depth and +1 near the surface. While surface waters are primarily influenced by the weathering inputs from young volcanic rocks (radiogenic εNd signatures) the deep water signatures are influenced by admixture of Circumpolar Deep Water (unradiogenic εNd signatures), which spreads northwards into the Pacific Ocean. The deep water Nd isotope signatures at 4000 m water depth (εNd = -3.5) corresponds well to the signatures measured for surface layers on a Fe-Mn crust and a nodule from the study area. This demonstrates that the present day bottom water at this site has been dominated by modified North Pacific Deep Water rather than of less radiogenic Antarctic Bottom Water (εNd=-8).

https://doi.org/10.1180/S0026461X00006502 Published online by Cambridge University Press

Calcium isotopes in human urine under simulated microgravity conditions

A. HEUSER[1]*, P. FRINGS-MEIUTHEN[2], J. RITTWEGER[2], AND S.J.G. GALER[3]

[1]Steinmann-Institut, Universität Bonn, Bonn, Germany (*correspondence: aheuser@uni-bonn.de)
[2]Institute of Aerospace Medicine, German Aerospace Center (DLR), Köln, Germany
[3]Max-Planck-Institut für Chemie, Abteilung Biogeochemie, Postfach 3060, 55020 Mainz, Germany

Living under microgravity in space leads to a migration of bodily fluids into the upper parts of the body and mechanical unloading of the weight-bearing muscles and bones. The latter results in bone loss, which remains a key physiological issue for astronauts during long-duration space flights. Many of the physiological effects of microgravity can be simulated on Earth by a head-down-tilt bed rest (HDTBR) study, in which the head is tilted down at 6° during prolonged bed rest.

In order to evaluate the response of Ca metabolism during HDTBR, we analyzed the Ca isotopic composition of urine taken at different phases of such a study. This involved 7 test subjects, and consisted of two sessions, of 35 days each, comprising four phases: adaptation, bed rest, inpatient and outpatient regeneration.

The Ca isotopic composition of urine reflects a balance between bone loss and bone gain and/or kidney function [1]. During bone gain, blood gets enriched in heavy Ca, while during bone loss, light Ca is released from bones into the blood without further fractionation, and passes into the urine from the blood via the kidneys.

Preliminary data show that large differences of about 0.8‰ exist in the Ca isotopic composition ($\delta^{44/42}$Ca) of urine between subjects, which reflect individual Ca metabolism. The time-evolution of $\delta^{44/42}$Ca during the course of the study is similar for all subjects, however. During the adaptation phase, $\delta^{44/42}$Ca increases and reaches a peak at the beginning of the bed-rest phase. This can be explained in terms of a changed diet. During the bed rest period, $\delta^{44/42}$Ca decreases and returns to values seen at the start of this phase. This decrease indicates that loss of bone mass takes place during the bed-rest period, and persists during the early regeneration phase. Towards the end of outpatient regeneration, $\delta^{44/42}$Ca increases, returning to values at the study onset, closing the overall cycle.

This study confirms that Ca isotopes in urine are a valuable noninvasive tool for investigating Ca metabolism in humans, and presumably other vertebrates as well, whether or not the body is functioning normally or adapting to new, imposed conditions.

[1] Heuser & Eisenhauer (2010) *Bone* **46**, 889–896.

The origin of an oceanic plateau: Isotope geochemistry (Sr, Nd, Pb and Hf) of volcanic rocks from IODP Site U1347 on the Shatsky Rise (Northwest Pacific)

K. HEYDOLPH[1]*, J. GELDMACHER[2] AND K. HOERNLE[1]

[1]IFM-GEOMAR, Wischhofstr. 1-3. D-24148 Kiel, Germany, (*correspondence: kheydolph@ifm-geomar.de)
[2]Integrated Ocean Drilling Program, Texas A&M University, 1000 Discovery Drive, College Station, Texas 77845-9547 (geldmacher@iodp.tamu.edu)

The submarine Shatsky Rise plateau is a unique large igneous province (LIP) in the northwest Pacific Ocean ca. 1500 km east of Japan. It is the only large intraoceanic plateau, which formed during the Late Jurassic to Early Cretaceous at a time period with numerous reversals of the Earth's magnetic field. The magnetic reversals combined with bathymetric data allow a detailed reconstruction of the tectonic history. Accordingly the three main volcanic edifices Tamu, Ori and Shirshov massifs formed by massive volcanism during a short time span along a southwest - northeast trending, rapidly spreading triple junction. Therefore, the magnetic and bathymetric data suggest that the Shatsky Rise formed through the interaction of a mantle plume head with a ridge [1, 2].

We present new Sr-Nd-Pb and for the first time Hf isotope data from volcanic rocks of relatively fresh basaltic lava flows from the southernmost drill site U1347 on Tamu massif. Initial ^{176}Hf/^{177}Hf and ^{143}Nd/^{144}Nd isotopic compositions are fairly uniform throughout the entire hole ranging between 0.283076 to 0.283100 and 0.512909 to 0.512981 respectively, showing neither distinct MORB nor intraplate (plume) affinity. Relatively unradiogenic ^{87}Sr/^{86}Sr data ranging from 0.70276 to 0.70296 mostly overlaps with Pacific MORB like values. Combined Nd and Hf isotopic compositions form a tight cluster at the edge of the Pacific MORB field below the present-day Hf-Nd mantle array. Although initial Pb double spike $^{206/204}$Pb and $^{208/204}$Pb isotopic compositions range from 18.13 to 18.46 and 37.71 to 37.96 respectively and overlap with MORB-like compositions, they trend towards more intraplate-like values. Whereas combined initial Pb double spike $^{207/204}$Pb and $^{206/204}$Pb and Hf values form clusters within the Pacific MORB field.

[1] Nakanishi *et al*. (1999), *J Geophys. Res*. **104**, 7539-7556.
[2] Sager *et al*. (1999), *J Geophys. Res*. **104**, 7557-7576.

https://doi.org/10.1180/S0026461X00006502 Published online by Cambridge University Press

Iron isotopes and komatiites: Implications for mantle oxygen fugacity

KATE HIBBERT[1]*, HELEN M. WILLIAMS[1,2], ANDREW KERR[3] AND IGOR PUCHTEL[4]

[1]Department of Earth Sciences, University of Oxford, South Parks Road, Oxford, UK (*correspondence: kate.hibbert@bristol.ac.uk)

[2]Department of Earth Sciences, Durham University, Durham, UK

[3]School of Earth and Ocean Sciences, Cardiff University, Park Place, Cardiff, Wales

[4]Department of Geology, University of Maryland, College Park, MD 20742, USA

Due to the high degrees of partial melting involved in komatiite genesis, komatiites provide a unique insight into the mantle. We report iron isotope data for 3 exceptionally preserved komatiite localities ranging from 2.7Ga to 90Ma, which enable a study of mantle fO_2 and melting processes over this time period. Data is presented both for whole-rocks and mineral separates. Whole-rock δ^{57}Fe values range from -0.23 to 0.34‰. Olivine samples are consistently lighter than corresponding whole-rocks (δ^{57}Fe = -0.47 to -0.11‰). Pyroxene samples range from δ^{57}Fe = -0.16 to 0.41‰.

Consistent with previous findings [1] iron isotope data for all localities correlate with proxies of partial melting. The highest degree partial melts show the lightest iron isotope compositions ($\delta^{57/54}$Fe = -0.23‰). This trend is also observed for olivine separates from the same samples. Consequently no simple relationship exists between the iron isotope composition of komatiites and the bulk silicate earth (BSE) value.

Furthermore we show that whole-rock iron isotope data correlate with V/Sc and propose that this effect is not due to crystal fractionation, but rather due to oxygen fugacity. The relatively incompatible behaviour of vanadium compared to scandium demonstrates that the komatiite source is relatively oxidising. As a result we are able to show that the variations in iron isotopes measured were created by partial melting in relatively oxidising conditions. It is further shown that there is no marked difference between 90Ma and 2.7-2.4Ga komatiites suggesting little or no change in mantle fO_2 from the late Archean to the present day.

[1] Williams *et al*. (2005) *EPSL*. **235**, 435-452.

A depth transect of four 25 kyr ^{231}Pa/^{230}Th records from the Argentine Basin: Assessing southern component flow rates

B.J. HICKEY[1]*, G.M. HENDERSON[1], A.L. THOMAS[1], J.W.B RAE[1], C. CHIESSI[2] AND S. MULITZA[2]

[1]Department of Earth Sciences, University of Oxford, UK (*correspondence: benh@earth.ox.ac.uk)

[2]Department of Geosciences, University Of Bremen, Germany

We present ^{231}Pa/^{230}Th data from a suite of cores along a depth transect in the Argentine Basin, to reconstruct water mass distribution and circulation histories of southern component water masses for the last 25 kyr .

Opal and particle flux data from these cores show little correlation with ^{231}Pa/^{230}Th values meaning that changes in ^{231}Pa/^{230}Th cannot be explained by a local composition or particle flux effect and are instead likely to be reflecting changes in circulation.

A core bathed by AAIW throughout the last 25 kyrs (GeoB 2107, 1048 m), has relatively high ^{231}Pa/^{230}Th values (0.075) during the Holocene and distincly lower values (0.055) at the LGM suggesting faster AAIW transport during the last glacial. At greater depths, ^{231}Pa/^{230}Th and δ^{13}C data in core GeoB 2109 (2504 m) indicate a change in both circulation and water mass distribution on glacial-interglacial timescales, with moderate flow of AABW at the LGM being replaced by more vigorous flow of NADW during the Holocene.

On millenial timescals, ^{231}Pa/^{230}Th values in deep cores GeoB 2109 and GeoB 2112 (4010 m) indicate enhanced production of AABW during northern hemisphere stadials, when ^{231}Pa/^{230}Th records are of opposite signal between hemispheres, supporting a possible bipolar seesaw relationship in deep water formation between hemispheres. These data indicate that the ^{231}Pa/^{230}Th proxy can be used to reconstruct past flow rates of multiple water masses in the Argentine Basin and provide evidence that southern source water masses play a dynamic counterpart to NADW formation on abrupt as well as glacial-interglacial timescales.

https://doi.org/10.1180/S0026461X00006502 Published online by Cambridge University Press

Evaluating $^{238}U/^{235}U$ in U-bearing accessory minerals: Implications for U-Pb geochronology

J. HIESS*[1], D.J. CONDON[1], S.R. NOBLE[1], M.S.A. HORSTWOOD[1], N. MCLEAN[2] AND J.M. MATTINSON[3]

[1]NERC Isotope Geoscience Laboratory, BGS, Keyworth, UK (*correspondence: jies@bgs.ac.uk)
[2]EAPS, Massachusetts Institute of Technology, MA, USA
[3]DES, University of California, Santa Barbara, CA, USA

U-daughter (U-Pb, Pb-Pb, and U-series) geochronology and cosmochronology utilise the value of the present day $^{238}U/^{235}U$ ratio to calculate U/Pb and Pb/Pb isotopic dates. For decades, this value has been assumed to be invariant and equal to 137.88, but recent experiments indicate that there is potential for per mil level variation in $^{238}U/^{235}U$ in natural materials, hypothesized to be the result of redox reactions. These studies have largely focused on materials formed in low-temperature environments (e.g. speleothems, corals) and U ore deposits. At present there is no published high-precision $^{238}U/^{235}U$ data for U-bearing accessory minerals commonly used for U-Pb geochronology.

We present $^{238}U/^{235}U$ determinations (total uncertainties of ~200 ppm) for a suite of common U-bearing accessory minerals (zircon, monazite etc.), from a variety of geological environments and ages. Measurements have been made by multi-collector thermal ionization mass spectrometry (MC-TIMS) and multi-collector inductively coupled plasma mass spectrometry (MC-ICPMS), accurately correcting for mass fractionation using the IRMM 3636 ^{233}U-^{236}U double spike. These results indicate that accessory mineral $^{238}U/^{235}U$ ratios are in general lower than the 'consensus' value of 137.88 and record limited but resolvable variation.

Systematic discordance has been observed between ^{238}U-^{206}Pb and ^{235}U-^{207}Pb dates for closed-system minerals, and has been used to reassess the relative decay constants of ^{238}U and ^{235}U [1,2,3]. Our new determination of coupled $^{238}U/^{206}Pb$, $^{235}U/^{207}Pb$ and $^{238}U/^{235}U$ measurements on closed system zircons permits further refinement of $\lambda^{238}U/\lambda^{235}U$ estimates using parameters whose values and uncertainties are all traceable to SI units.

[1] Mattinson, (2000). EOS, *AGU Fall* V**61**A-02. [2] Mattinson, (2010) *Chem Geol* **275**: 186-198. [3] Schoene *et al*., (2006) *GCA* **70**: 426-445.

The impact of aerosols on radiation and climate

E.J. HIGHWOOD[1]*, C.L.RYDER[1], L. GUO[1], M. NORTHWAY[4], N. CHALMERS[1], W. MORGAN[2], G. MCMEEKING[2,3], N. STUBER[4] AND A. FERRARO[1]

[1]Department of Meteorology, University of Reading, P.O. Box 243, Reading, UK (*correspondence: e.j.highwood@reading.ac.uk)
[2]Centre for Atmospheric Science, University of Manchester, Manchester, UK
[3]Now at Colorado State University, USA
[4]Formerly at Department of Meteorology, University of Reading, UK.

Overview

Aerosols have played a major role in past climate change, and it is likely that they will continue to do so in the future. Although our understanding of the underlying physical processes has improved over recent years, the mechanisms by which they affect climate are still more uncertain than those relating to well mixed greenhouse gases. This overview talk will discuss the various ways in which atmospheric aerosols can interact with radiation thereby producing a climate forcing and initiating a climate response.

Examples used

1) The optical properties and direct effect of Saharan dust from aircraft measurements and models
2) Optical closure studies for aerosol in anthropogenically perturbed air masses and the influence of uncertainty in aerosol refractive index
3) The impact of sulphate and black carbon aerosol on the East Asian summer monsoon.
4) Mechanisms involved in the semi-direct effect of absorbing aerosols.

https://doi.org/10.1180/S0026461X00006502 Published online by Cambridge University Press

Radiolabelling of engineered nanomaterials as a tool for sensitive particle tracking

H. HILDEBRAND AND K. FRANKE

Helmholtz Centre Dresden – Rossendorf, Institute of Radiochemistry, Reactive Transport Division, Permoserstrasse 15, D-04318 Leipzig, Germany (h.hildebrand@hzdr.de, k.franke@hzdr.de)

Engineered nanoparticles (NPs) are present in a wide variety of consumer products, occasionally in significant quantities. During aging, abrasion or disposal of such products, NPs-release is likely - accompanied with effects for the environment that have to be investigated in more detail. The aim of this study is to quantify the amount of NPs (TiO_2 and Ag^0) released from composite coatings due to weathering, aging or mechanical stress and to follow the NPs along their further fate in the environment.

Generally, particle tracking may provide information on the transport behavoir of the particles in aqueous media or on their interactions with biota. Since NPs are possibly released in tiny amounts and into very complex natural systems, we suggest the radiolabelling of NPs as a tool for their very sensitive detection throughout their life cycle including complex media such as aquifer sands, soil or cells.

Within this study, a novel radiolabelling technique for TiO_2 (P 25, Evonik Degussa) and Ag^0 (Sigma-Aldrich) NPs is under development. During this labelling process, significant changes of the chemical composition and properties of the particles are avoided to the greatest possible extend.

Stability of the NPs in different media has been studied and results contribute to first estimates concerning their transport behaviour in the aquatic environment. Batch tests including sediment materials were conducted to describe interactions of Ag^0 and TiO_2 NPs with natural matrices.

Interactions of engineered NPs and natural colloids have been studied as well. Results show that natural colloids have a strong influence on stability and transport of engineered NPs under environmental conditions.

Based on these data, radiolabelling of engineered NPs may open up the chance for sensitive tracking of particles not only in environmental media but also in other complex systems.

How precisely can we date climate/ocean instabilities of the Last Interglacial?

CLAUDE HILLAIRE-MARCEL

GEOTOP-UQAM, Montreal (Qc) H3C 3P8, Canada, (hillaire-marcel.claude @uqam.ca)

We examine here how precisely climate and environmental events of the Last Interglacial (LI) can be correlated and/or dated. For example, the SPECMAP chronology, often used for correlations (e.g., through stable isotope stratigraphies) cannot be linked to any given time series without taking into consideration: i) the specific lag times of Earth system components to insolation at a given latitude, ii) feedback processes between these components. As a matter of fact, the SPECMAP chronology and the timing of changes in the paleocean mass, salinity and isotopic composition, should unavoidably be in offset up to a few thousand years. In addition, neither geochemical signatures, nor the ocean volume, respond linearly to mass transfers into the hydrosphere (ocean/glaciers). A fortiori, adding tectonics, geoidal anomalies, site specific morphological responses to relative sea-level (RSL) changes and littoral activity, one may conclude that any direct attempt at correlating "RSL records" is risky. Finally, one cannot assume an equilibrium state of the Earth and its oceans, neither any probability of a "return" to a given state (i.e., the Earth is always in a no-analogue situation). Fortunately, the LI falls within U-series time control. Most other geochronometers lack precision (OSL, fission track) or are not necessarily applicable to relevant time series ($^{40}Ar/^{39}Ar$). If analytical techniques now permit to calculate ^{230}Th-ages with a fairly high precision, a large array of intrinsic limitations still prevail. For example, closed chemical systems are rarely secured in geological samples and there is no way to assess this closure with the degree of precision required to estimate age differences of the order of $\sim 10^3$ yr. Furthermore, uncertainties in our present knowledge of the U-series decay constants already result in an age uncertainty of about ±1250 years (2σ) within MIS age ranges. Thus, one must conclude that unequivocal correlation of proxies documenting millennial frequency, climate/ocean instabilities of the last interglacial remains out of reach, but in exceptional cases and short intervals (Blake paleomagnetic event, tephra events). In a similar fashion, most processes which are critical for the understanding and modeling of the immediate future of the Earth climate/ocean system are within the error bars/stochastic noise of the paleo-records.

https://doi.org/10.1180/S0026461X00006502 Published online by Cambridge University Press

Superplume control of East Africa Rift volcanism: Helium isotope evidence from alkaline magmatism of Tanzania

D.R. HILTON[1], S.A. HALLDÓRSSON[1], P.H. BARRY[1], T.P. FISCHER[2], J.M. DE MOOR[2], C.J. RAMIREZ[3], F. MANGASINI[4] AND P. SCARSI[5]

[1]Scripps Inst. Oceanography, UCSD, La Jolla, CA, USA. (drhilton@ucsd.edu, shalldor@ucsd.edu, pbarry@ucsd.edu)
[2]Dept Earth Planet. Sci. UNM, Albuquerque, NM, USA. (fischer@unm.edu, mdemoor@unm.edu).
[3]U. Costa Rica, San Jose, Costa Rica. (carlosjru@yahoo.com)
[4]U. Dar es Salaam, DeS, Tanzania. (mangasini@udsm.ac.tz)
[5]NRC Italy, Pisa, Italy. (paolo.scarsi@gmail.com)

We present new helium isotope data on mafic crystals of lava/tephra samples from both Older and Younger Extrusives of Rungwe Volcanic Province (RVP) in southern Tanzania – the southernmost expression of Cenozoic volcanism along the East Africa Rift System (EARS). All samples are alkalic in composition and include alkali basalts, basanites, nephelinites and a picrite and trachy-basalt. We compare these samples with peridotite xenoliths from 5 localities on or close to the Archean craton in northern Tanzania.

Regarding the He results: (1) The highest measured $^3He/^4He$ ratios (~ 15 R_A) far exceed the canonical range of 8 ± 1 R_A, diagnostic of MORB-source mantle. Indeed, a total of 17 (out of 31) RVP samples have OL/CPX $^3He/^4He$ > MORB. High $^3He/^4He$ ratios are found in volcanoes of the Younger Extrusives (Ngozi, Rungwe and Kiejo) and in the Kiwira Series (Older Extrusives), and thus are widespread in time and space. (2) Remaining RVP samples fall within the range normally associated with MORB: this He component is sampled in all 6 Rungwe volcanic series. (3) All of the northern Tanzania peridotite xenoliths fall within or overlap the SCLM range (6.1 ± 0.9 R_A).

The range of $^3He/^4He$ ratios at RVP reveal a heterogeneous mantle source including a deep (plume) component. In contrast, the peridotite xenoliths sample shallow lithospheric mantle. We view the African Superplume – a huge low velocity anomaly originating near the core-mantle boundary – as the ultimate source of high $^3He/^4He$. Alkaline volcanism at RVP samples this component implying the superplume is a continental-scale feature. It provides dynamic support for topographic swells throughout the EARS and heat/mass to drive continuing magmatism.

Erosion in the Arctic: Enhanced carbon sequestration associated with high latitude warmth?

R.G. HILTON[1]*, V. GALY[2], J. GAILLARDET[3], D. CALMELS[3], D.R. GRÖCKE[4] AND C. BRYANT[5]

[1]Department of Geography, Durham University, Science Laboratories, Durham, DH1 3LE, UK (*correspondance: r.g.hilton@durham.ac.uk)
[2]Woods Hole Oceanographic Institution, Woods Hole, MA 02543, USA (vgaly@whoi.edu)
[3]Institut de Physique du Globe, 4 place Jussieu, 75252 Paris cedex 05, France (gaillardet@ipgp.fr, calmels@ipgp.fr)
[4]Department of Earth Sciences, Durham University, DH1 3LE, UK (d.r.grocke@durham.ac.uk)
[5]NERC Radiocarbon Facility, East Kilbride, Scotland, G75 OQF, UK (c.bryant@nercrcl.gla.ac.uk)

Soils at high latitudes contain ~40% of the total carbon stock in organic matter on land (~500x10^{15} gC). This region experienced large climatic fluctuations over glacial-interglacial cycles and throughout the Cenozoic, while is extremely sensitive to changes in climate predicted over the coming century. If these changes force transfer of this C back to the atmosphere, or transfer to lithospheric storage, they may induce feedbacks in the Earth System. Here we question whether erosion of this soil organic matter results in a significant transfer of particulate organic carbon (POC) by Arctic Rivers to the ocean. We have sampled the Mackenzie River, Canada, and its major tributaries shortly after freshet (ice break up floods) in June 2009, using a depth-sample approach to collect the full range of erosion products in river suspended and bed sediment. The ^{14}C-content (fraction modern, F_{mod}) and the stable carbon isotopes ($\delta^{13}C_{org}$, ‰) provide the first systematic assessment of POC source in this river. They demonstrate mixing of ^{14}C-enriched (F_{mod}>0.84) and depleted (F_{mod}<0.10) POC, consistent with input of fossil POC from bedrock and modern POC from vegetation and soils. However, $\delta^{13}C_{org}$ requires a third component with a ^{14}C-age of ~12ka (F_{mod}~0.22). This is consistent with soils formed following the retreat of ice after the Last Glacial Maximum. We estimate that the Mackenzie River is likely to have exported ~15-20x10^{15} gC of post-LGM soils to the Arctic Ocean as POC during the Holocene. This is a result of the prevailing climate, promoting high soil carbon stocks and very high erosion rates during the freshet. We propose that the erosion and transfer of soil-derived POC to the ocean by Arctic Rivers may sequester CO_2 while high-latitudes are ice-free, providing a negative feedback to climate over glacial-interglacial cycles.

https://doi.org/10.1180/S0026461X00006502 Published online by Cambridge University Press

Carbon export by erosion of biomass from a mountain belt: Controls on rates of transfer

R.G. HILTON[1], N. HOVIUS[2]*, A. GALY[2,3], M.J. HORNG[4] AND H. CHEN[5]

[1]Department of Geography, Durham University, Science Laboratories, South Road, Durham, DH1 3LE, UK (r.g.hilton@durham.ac.uk)
[2]Department of Earth Sciences, University of Cambridge, Downing Street, Cambridge CB2 3EQ, UK (*correspondance: nhovius@esc.cam.ac.uk)
[3](albert00@esc.cam.ac.uk)
[4]Water Resources Agency, Ministry of Economic Affairs, Taipei 10651, Taiwan (mjhorng@gmail.com)
[5]Department of Geoscience, National Taiwan University, Taipei 10617, Taiwan (hchen@ntu.edu.tw)

Erosion of particulate organic carbon (POC) from the continents and its delivery to the ocean by rivers is an important global carbon transfer. POC yields are highest in mountain river catchments which contribute a significant part of this flux. To understand how surface processes drive CO_2 sequestration, it is key to better constrain how POC is eroded from the terrestrial biosphere (POC_{mod}) in mountain landscapes. This necessitates river sampling over a large range of hydrological conditions and recognition that fossil POC from sedimentary rock is important in these settings[1]. Here we focus on 11 major catchments of the Central Range, Taiwan, where physical erosion is high and frequent tropical cyclones provide a large range of flow conditions. We sampled river suspended load at hydrometric gauging stations one to three times a month over two years. The fraction of non-fossil POC of the suspended load was quantified using a mixing model constrained by the stable carbon isotopes and nitrogen to organic carbon ratio (whose precision and accuracy was independently assessed using ^{14}C[1]). A general positive relationship was observed between suspended sediment and POC_{mod} yields across the mountain belt. However, four catchments with similar sediment yields over the gauged period ($20\pm2\times10^3$ t km^{-2} yr^{-1}, mean ± σ) had POC_{mod} yields which varied by a factor of ~4 (15 ± 8 tC km^{-2} yr^{-1}, mean ± σ). We can explain the general trend and variability by modelling erosion processes in mountain landscapes: bedrock landslides supply the bulk of clastic sediment and some POC_{mod}; further POC_{mod} is supplied by shallow landsliding and overland flow. Erosion of POC_{mod} is strongly controlled by climate in these catchments.

[1] Hilton *et al*. (2010) *Geochim. Cosmochim. Acta,* **74**: 3164-3181, doi:10.1016/j.gca.2010.03.004

Experimental constraints on molybdenum isotope fractionation between metal and silicate liquids

REMCO C. HIN[1]*, CHRISTOPH BURKHARDT[1], MAX W. SCHMIDT[1], BERNARD BOURDON[1,2] AND THORSTEN KLEINE[3]

[1]Institute of Geochemistry and Petrology, ETH Zurich, Switzerland (*correspondence: remco.hin@erdw.ethz.ch)
[2]Ecole Normale Supérieure de Lyon and CNRS, France
[3]Institut für Planetologie, Westfälische Wilhems-Universität Münster, Germany

So far planetary core formation conditions have been mainly constrained by element partitioning, particularly by experimental determination of distribution coefficients between metal and silicate liquids. However, driven by analytical developments fractionation of non-traditional stable isotopes has become a new tool for studies of core formation. Experimental determinations of metal-silicate liquid equilibrium Si and Fe isotope fractionation factors reveal significant effects for Si, but not for Fe [1,2].

As a siderophile and refractory element, Mo can provide additional information about conditions of core-mantle differentiation. As oxidised Mo should occur in a 4+ valence state in equilibrium with metal [3], its bond stiffness may be more similar to that of Si than to that of Fe.

To evaluate the possibility of equilibrium mass-dependent Mo isotope fractionation during metal-silicate segregation, we have designed piston cylinder experiments with a basaltic silicate composition and an iron based metal with ~8 wt% Mo. Metal and silicate phases are completely segregated by use of a centrifuging piston cylinder at ETH Zurich, such preventing analyses of mixed metal and silicate signatures. Molybdenum isotope compositions were measured using a Nu1700 MC-ICP-MS at ETH Zurich. To ensure an accurate correction of analytical mass fractionation a ^{100}Mo-^{97}Mo double spike was admixed before chemical Mo purification.

Preliminary results suggest that the equilibrium $^{98}Mo/^{95}Mo$ isotope fractionation factor between metal and silicate liquids may be -0.17±0.15‰ (2σ uncertainty) at 1350°C and 1 GPa. More analyses on reproduced experiments will have to show if this small fractionation can be confirmed, making Mo isotopes a potential tool for constraining the conditions of core formation in asteroids and terrestrial planets.

[1] Shahar *et al*. (2009) *EPSL* **288**, 228-234. [2] Poitrasson *et al*. (2009) *EPSL* **278**, 376-385. [3] Farges *et al*. (2006) *Can. Min*. **44**, 731-753.

https://doi.org/10.1180/S0026461X00006502 Published online by Cambridge University Press

Release of trace metals in soil suspensions as affected by redox potential and temperature

I. HINDERSMANN AND T. MANSFELDT

Department of Geosciences, Soil Geography/Soil Science, University of Köln, Albertus-Magnus-Platz, 50923 Köln, Germany (iris.hindersmann@uni-koeln.de)

The redox potential is a master variable for the behavior of trace (semi)metals in the soils and sediments environment. In this study we investigated the influence of redox potential and temperature on the solubility of trace metals. A humic topsoil of a floodplain soil at the river Wupper in Northrhine Westphalia, Germany, was chosen. The total amounts (aqua regia) were for Zn 903, Cu 551, Pb 354, Ni 93.5, As 35.7, Co 22.4, Sb 20.5, Cd 8.3, and Mo 6.5 mg kg^{-1}. Microcosm experiments were performed under controlled redox und temperature conditions at 500, 300 and 100 mV and at 7, 15 and 25 °C, respectively. Soil suspensions were obtained at different intervals und analyzed by ICP-MS for trace metals.

Most of the metals demonstrate an increase of concentration with lowering the redox potential. Especially Co and Mo showed a strong increase that is expressed by a high correlation between metal activity and pe+pH. Increasing the temperature resulted in a quicker decrease of the redox potential that can be explained by a higher activity of microorganisms. Only Sb revealed after a first increase a continuous decrease in its concentration. Responsible for this feature are presumably gaseous losses due to biological methylation.

Metal behavior depends among other things on the amounts of adsorbents. The most important adsorbents for Mo and Co are iron and manganese oxides. Under reducing conditions these oxides are dissolved and metals are liberated. However, for Pb, Cd, Cu, Zn, Ni and Cr other processes like complexation or pH-depending sorption are also important.

Calcium isotope fractionation in alpine plants

R.S. HINDSHAW[1,2]*, B.C. REYNOLDS[1], J.G. WIEDERHOLD[2,1], M. KICZKA[2,1], R. KRETZSCHMAR[2] AND B. BOURDON[1,3]

[1]Institute of Geochemistry and Petrology, ETH Zurich, Switzerland (*correspondence: hindshaw@erdw.ethz.ch)
[2]Institute of Biogeochemistry and Pollutant Dynamics, ETH Zurich, Switzerland
[3]ENS Lyon and CNRS, France

The presence of vegetation has a major impact on the biogeochemical cycles of many elements, through uptake, recycling and the acceleration of weathering rates. As one of the essential plant macronutrients, the biogeochemical cycle of calcium is particularly affected. Calcium uptake by plants is one of the few processes known to fractionate stable calcium isotopes, but the mechanisms of this process and the impact of vegetation on the Ca isotope ratios in runoff are poorly understood. This study aims to increase understanding of the fractionation processes during uptake and translocation within plants by analysing the calcium isotopic composition of alpine plants taken directly from a granitic, glacier forefield (BigLink CZO, Damma glacier, Switzerland).

Stable calcium isotope fractionation was measured (double-spike TIMS) in various species of alpine plants, including woody species, grasses and herbs. Analysis of plant parts (root, stem, leaf and flower samples) provided information on Ca isotope fractionation within plants. Additional seasonal sampling of leaves revealed temporal variation in leaf Ca isotopic composition.

There was significant Ca isotope fractionation between bulk soil and both root tissue ($\Delta^{44/42}Ca_{root\text{-}soil} \approx -0.40‰$) and whole plant Ca isotopic compositions. Ca isotope fractionation between roots and leaves was species dependent, with negligible fractionation between leaves and roots in some species and isotopically heavier leaves compared to roots in others. Ca isotope ratios increased with leaf age in woody species but remained constant in herbs and grasses. The large Ca isotopic difference between root tissue and bulk soil is considered to be caused by the preferential binding of isotopically-light Ca to root adsorption sites. Several factors such as presence of a woody stem, root cation exchange capacity, presence of Ca oxalate and levels of mycorrhizal infection are likely to contribute to the observed differences in whole plant Ca isotopic compositions both between and within species.

https://doi.org/10.1180/S0026461X00006502 Published online by Cambridge University Press

Development of an aqueous activity model for geothermal conditions

F.F. HINGERL[1,2]*, T. WAGNER[2], D.A. KULIK[1], G. KOSAKOWSKI[1] AND T. DRIESNER[2]

[1]Paul Scherrer Institut, Nuclear Energy and Safety Research Department, 5232 Villigen PSI, Switzerland (*correspondence: ferdinand.hingerl@psi.ch)
[2]ETH Zurich, Geochemistry and Petrology, Clausiusstrasse 25 8092 Zurich, Switzerland

Geochemical and reactive transport modeling of fluid-rock interaction in enhanced geothermal systems is a challenging task because of the high temperatures, pressures, and sometimes extreme fluid salinities. For such systems, extended thermodynamic databases and activity models are needed to accurately predict fluid-mineral equilibrium reactions. Typically, the Pitzer activity model is used for high salinity fluids. We tested the EUNIQUAC local composition model [2] as an alternative, because it needs substantially fewer fitting parameters to describe species interactions and temperature dependence. However, tailoring the model parameters of EUNIQUAC to geothermal applications requires re-fitting and extending the existing parameter space.

We developed a new tool named GEMSFIT that allows generic fitting of activity models (for aqueous electrolyte and non-electrolyte solutions) and equations of state implemented in our geochemical equilibrium solver GEM-Selektor (http://gems.web.psi.ch). GEMSFIT combines a PostgreSQL database for storing and managing the datasets with experimental measurements and interaction parameters, the parallelized genetic algorithm toolbox of MATLAB® for the parameter fitting, and an interface to the GEMS3K code (kernel of GEM-Selektor) to access activity models and perform chemical equilibrium calculations.

Our comparison revealed that the original EUNIQUAC model is less accurate than the Pitzer model. Hence, we modified the EUNIQUAC model in order to enhance its accuracy and retain its advantages. The new model called ELVIS combines an electrostatic framework developed by Helgeson and coworkers [1] with non- electrostatic concepts derived from the EUNIQUAC model [2].

ELVIS has significantly less fitting parameters than the Pitzer approach, but is comparable in terms of quality of the fit to experimental data. We believe that with the ELVIS approach, it will be possible to derive correlations and predictions for the model parameters, which is very difficult in the Pitzer framework.

[1] Helgeson, H. H., Kirkham, D. H., Flowers, G. C. (1981), *Am. J. Sc.* (**281**), 1249-1516. [2] Thomsen, K., Rasmussen, P., Gani, R. (1996), *Chem. Eng. Sc.* **51**, 3675-3683.

Rare earth elements of Precambrian-Cambrian phosphorites from the Yangtze Platform (S. China)

DOROTHEE HIPPLER AND GERHARD FRANZ

Technical University Berlin, Department of Mineralogy, Ackerstrasse 76, 13355 Berlin, Germany (dorothee.hippler@tu-berlin.de; gerhard.franz@tu-berlin.de)

The Precambrian to early Cambrian transition comprises an episode of major environmental changes which are believed to be relevant for the most prominent bioradiation in Earth's history: from an ocean in which algae and microbes were the dominant form of life to one in which significant skeleton-forming higher life spread. Concomitant with these global changes is the onset of biomineralization and widespread calcium phosphate deposition. However, so far, neither the source of phosphate for massive phosphorite, nor the formational mechanisms are known with certainty.

The investigation of the rare earth element (REE) content in phosphorites constitutes a powerful tool to obtain important information on depositional conditions, detrital influence and post-depositional alteration. The authigenic nature of most sedimentary apatites moreover helps in understanding the palaeochemistry of the primary marine environment.

Here, we present rare-earth elements of Precambrian Cambrian phosphorites form different sediment successions on the Yangtze Platform, representing the known facies belts from shelf to basinal environments. The total REE contents of all phosphorites investigated cover a wide range (37 - 1154 ppm), with two samples recording > 700 ppm, which is lower than the averages reported for geologically old phosphorites. PAAS (= Post-Archaean Average Shale) normalized REE patterns are characterized by LREE depletion and MREE enrichment. Low detrital input is indicated by low concentrations of Zr, the lacking correlation of HREE vs. Zr, and low Sc/La ratios. All phosphorites investigated yield negative Ce-anomalies, which is typical of seawater, indicating the palaeoceanic redox conditions of the primary water body. Unlike Ce, Eu does not show any marked anomaly. A positive Eu anomaly can only be reported for one phosphorite concretion, which is likely linked to the high barium content in this phosphorite. This suggests strongly reducing conditions at the time of phosphorite formation, increasing the mobility of Eu as Eu^{2+}. The high Ba content can furthermore be indicative for an increased palaeo-productivity.

https://doi.org/10.1180/S0026461X00006502 Published online by Cambridge University Press

Advances in resolution and accuracy of *in situ* determination of isotope ratios

T. HIRATA[1]*, T.D. YOKOYAMA[1], S. OKABAYASHI[1], K. MAKI[1], T. SUZUKI[2] AND Y. KON[3],

[1]Laboratory for Planetary Sciences, Kyoto University, Kitashirakawa Oiwakecho, Kyoto, 606-0582, Japan (*correspondance: hrt1@kueps.kyoto-u.ac.jp)
[2]Japan Agency for Marine-Earth Science and Technology, Yokosuka, Kanagawa, Japan.
[3]Geological Survey of Japan, Tsukuba, Ibaraki 305, Japan

It is widely recognized that the combination of the ICP-Mass spectrometry (ICP-MS) and laser ablation sample introduction technique was one of the most sensitive and versatile analytical technique for the elemental analyses of solid samples [1]. We have developed a new calibration technique for multi-element and isotopic analyses of solid samples using laser ablation-ICP-mass spectrometry coupled with a galvanometric optics. With the galvanometric optics equipped with the femtosecons laser system, two or more sample points could be ablated within very short time interval (~10 msec), and the resulting sample aerosols released from different ablation pits or different solid samples was mixed and homogenized within the sample cell or during the sample transport stages. This suggests that the addition of analytes or second internal elements can be made directly onto the solid samples. In this study, we have measured the REE abundances for two zircon samples (Nancy 91500 and Prešovice) using the standard addition calibration technique using the NIST SRM912. The resulting REE abundance data show excellent agreement with the previously reported values within the analytical uncertainties achieved in this study. Another advantage to use the galvanometric optics is the "integration" of the sample aerosol released from multiple spot. Using the integration technique, the U-Pb age of the zircon sample can be determined from separate 10 ablation pits of small ablation pit sizes (~8 μm). Finally, we would like to show the analytical capability of the newly developed laser ablation in liquid (LA) technique for elemental and isotopic analysis from small areas [2]. The combination of the ICP-mass spectrometry and the laser ablation technique including the LAL has the potential to become a significant tool for *in-situ* elemental and isotopic analysis of solid samples.

[1] Pisonero, J., Günther, D. (2008) *Mass Spectrometry Reviews,* **27**, 609-623. [2] Okabayashi *et al*. (2011) *J. Anal. At. Spectrom*. DOI: 10.1039/c0ja00200c.

The high conductivity of iron and thermal evolution of the Earth's core

K. HIROSE[1]*, H. GOMI[1], K. OHTA[1], S. LABROSSE[2] AND J. HERNLUND[3]

[1]Tokyo Institute of Technology, Tokyo 152-8551, Japan (*correspondence: kei@geo.titech.ac.jp)
[2]Ecole Normale Supérieure de Lyon, Lyon, France
[3]University of California, Berkeley, CA 94720, USA

The large amount of heat conducted down the isentropic gradient of Earth's outer core contributes nothing to driving convection or re-generation of Earth's magnetic field by dynamo action. The energy for maintaining a geodynamo for at least the past 3.5 gigayears (Gyr) must be supplied in excess of this waste heat, placing tight constraints upon the thermal evolution of the core. Here we measured the electrical resistivity of iron was measured up to 100 GPa at room temperature in a diamond-anvil cell (DAC). The resistivity of hcp-Fe strongly reduced with increasing pressure. A heating experiment was also conducted at 65 GPa in the externally-heated DAC. The observed change in the sample resistance was in good agreement with the prediction by the Bloch-Grüneisen formula, which supports the validity of this formula for hcp-Fe at high pressure. The thermal conductivity of iron is estimated from its resistivity at high pressure and temperature on the basis of the Wiedemann-Franz law. Considering the effect of light alloying element, the conductivity of the uppermost core is in the range of 90-130 W/m/K, significantly higher than previous estimates. Such high thermal conductivity implies a relatively young inner core and a large degree of secular core cooling (~1000 K). The high initial CMB temperature further suggests that a significant portion of the lower mantle would be molten in early history of the Earth [1, 2].

[1] Labrosse *et al*. (2007) *Nature*, **450**, 866-869. [2] Nomura *et al*. (2011) *Nature*, in press.

https://doi.org/10.1180/S0026461X00006502 Published online by Cambridge University Press

Deep Earth volatile cycles: From ancient to modern

MARC M. HIRSCHMANN

Dept. of Earth Sciences, University of Minnesota, Minneapolis, MN 55455 USA (mmh@umn.edu)

Earth's mantle is significant reservoir for key volatile species and exchange between the mantle and near-surface reservoirs (="exosphere") influences planetary climate and habitability as well as dynamical evolution of the interior. Volatile cycling is governed in large part through plate tectonic processes but also has significant influence on regulating the vigour of plate tectonics. Yet, it is not clear how this coupling between geodynamical and geochemical evolution arose or whether one was a prerequisite for the establishment of the other. Originally, much of Earth's volatile inventory was presumably present as a thick atmosphere, in part because volatiles were probably delivered late in the accretion history and because of the efficiency of impact degassing. The early inventory of mantle H_2O may descend from the magma ocean, in which portions of a steam atmosphere are dissolved in the magma and then precipitated with nominally anhydrous minerals. In contrast, low magmatic solubility of C-bearing species may suggest that the earliest mantle was depleted in C. Thus, the earliest Earth could have been characterized by an exosphere with low H/C and a mantle with high H/C – the reverse of the modern case in which the mantle has low H/C (as demonstrated by H/C ratios of minimally degassed oceanic basalts) and the exosphere high H/C. Thus, either some process retained carbon in the early mantle or subsequent evolution has preferentially sequestered carbon in the interior.

In this plenary review, I will consider the current state of the principal reservoirs of H and C and explore the possible key influence of magma ocean processes on the subsequent evolution of Earth's volatile cycling.

Re-Os dating and trace element characteristics of pyrite from the Lisheen Pb-Zn deposit, Ireland

DANNY HNATYSHIN[1], ROBERT A. CREASER[1] AND JAMIE J. WILKINSON [2]

[1]Department of Earth and Atmospheric Sciences, University of Alberta, Edmonton, AB T6G 2R3, Canada

[2]Department of Earth Science and Engineering, Imperial College London, South Kensington Campus, Exhibition Road, London SW7 2AZ, United Kindom

The Lisheen Mine in the Irish Midlands exploits a typical example of a carbonate-hosted base metal deposit from the district. Like the majority of the Irish Pb-Zn deposits, Lisheen is hosted by Lower Carboniferous strata, but the timing of sulfide mineralization is only poorly constrained by geochronologic methods. As such, the genetic models for this important type of sedimentary-hosted ore remain controversial, with timing constraints provided primarily by geologic relationships and, more recently, by paleomagnetic data. The widely proposed syngenetic and syndiagenetic models require that mineralization occurred around the stratigraphic age of ca. 345 Ma, but none of the available geochronological constraints gives this age. Recent paleomagnetic data from Lisheen has been interpreted to indicate post-Variscan epigenetic mineralization at ~277 Ma, much younger than previously proposed and in apparent contradiction to Variscan (~300 Ma) thrust deformation of the ores. In order to address this problem we have applied Re-Os dating to main ore-stage pyrite from different parts of the deposit. Pyrite samples from the Main Zone, Derryville Zone, and Bog Zone were found to be very variable in Re/Os ratios (300 – 10000), as well as in the trace element abundances in general. Thirty-three Re-Os analyses of pyrite from the Main Zone, Bog Zone, and the nearby Galmoy deposit yielded an age of 342 ± 5 Ma, within uncertainty of the stratigraphic age. However, data from the Derryville zone give an age of 306 ± 10 Ma with a very high initial $^{187}Os/^{188}Os$ value of 3.6, suggesting resetting. The variation within and between these isochrons were investigated using electron mircoprobe and ICPMS analysis to help understand the relationship between rhenium, various trace elements, pyrite morphology and its subsequent alteration. Based on our results it is evident that pyrite throughout Lisheen has been heavily disturbed providing a possible explanation for the scatter seen in the isochrons and a reason why the paleomagnetic age of 277 Ma does not appear to record the timing of primary sulfide mineralization.

https://doi.org/10.1180/S0026461X00006502 Published online by Cambridge University Press

Influences of pH and oxidation on the leaching potential of As, Cu, Pb and Zn from sediments through a pH_{stat}-leaching test in combination of a BCR 3-step extraction

HUU HIEU HO[1,2]*, RUDY SWENNEN[2] AND VALÉRIE CAPPUYNS[2]

[1]Vietnam Institute of Geosciences and Mineral Resources (VIGMR), Hanoi, Vietnam (*correspondence: hohuuhieu@yahoo.com)

[2]Department of Earth and Environmental Sciences, K.U. Leuven, Belgium (rudy.swennen@ees.kuleuven.be)

Since contaminated river-bed sediments in Haiphong Harbor (Vietnam) are regularly dredged and disposed on land, an understanding about the influences of key parameters such as pH and oxidation on the leachability of As, Cu, Pb and Zn is necessary for management and treatment of these dredged wastes. A 96h pH_{stat}-leaching test examining the leaching behaviors of elements at pre-set pH values (2, 4, 6, 8 (natural), 9 and 11), is performed on a freshly-collected wet sediment and a 2 month-ripened dry sediment. Additionally, a BCR 3-step extraction is also used to clarify the differences in leachability between 2 types of sediment. The results indicate that the pH-dependent leaching behavior reflects a concave curve with the lowest value at pHs 6 or 8 and the highest value at pH 2 in case of Cu, Pb and Zn, or at pH 11 in case of As. Generally, due to oxidation, the leachability of As and Zn has decreased considerably at highly-acid and highly-alkaline pHs (2–4 and 9–11) while , for Cu and Pb, it has increased at acid pHs (2–6), but decreased at highly-alkaline pHs (9–11). As shown by results of BCR 3-step extraction, for As and Zn, there is a transfer from easily-soluble exchangeable & carbonate fraction to hardly-soluble reducible fraction through oxidation. As a consequence, the smaller exchangeable & carbonate fraction in the oxidized sediment is the cause for the lower leachability of As and Zn at almost all pH values. In contrast, for Cu and Pb, there is a transfer from the oxidizable fraction to the reducible fraction. Therefore, the more important reducible fraction in the oxidized sediment contributes to the higher leachability of Cu and Pb at acid pHs (2–4) while the smaller oxidizable fraction contributes to their lower leachability at alkaline pHs (9–11) if compared with the fresh sediment.

Is TEX_{86} paleothermometry applicable in the polar regions?

S.L. HO[1]*, S. FIETZ[2], G. RUEDA[2], A. MARTINEZ-GARCIA[3], G. MOLLENHAUER[1], A. ROSELL-MELE[2], F. LAMY[1], N. RUGGIERI[1] AND R. TIEDEMANN[1]

[1]Alfred Wegener Institute, 27515 Bremerhaven, Germany; (*correspondence: Sze.Ling.Ho@awi.de)

[2]Autonomous University of Barcelona, 08193 Bellatera, Spain.

[3]Swiss Federal Institute of Technology Zürich, 8092 Zürich, Switzerland.

TEX_{86} paleothermometry [1] is an organic sea surface temperature (SST) proxy based on the archaeal glycerol dialkyl glycerol tetraethers (GDGT) lipids, which are ubiquitous in the global ocean. This relatively recent proxy potentially offers an advantage over its more established counterpart, i.e. the alkenone unsaturation index, that has limited success in the polar regions due to its absence or extremely low abundance in this realm. Furthermore, the polar regions, especially the Southern Ocean, are severely under-represented in the global TEX_{86}-SST calibration data set. Therefore, this study aims to investigate the distribution pattern of GDGTs and to evaluate the applicability of TEX_{86} paleothermometry in the polar regions. A principal component analysis (PCA) on the GDGTs data shows that the variance in the relative distribution of the GDGTs in our study region is similar to that of the global data set, suggesting that the lipids are probably contributed by a common group of source organism. However, the TEX_{86}-SST relationship in the Arctic differs substantially from that of the Southern Ocean, resulting in poor overall correlation ($r^2 = 0.06$). Meanwhile, the TEX^L_{86} [2] fares much better than TEX_{86} ($r^2 = 0.50$). Seasonality does not lead to a different TEX_{86}- and TEX^L_{86}-SST relationship, relative to that of the annual mean. Interestingly, the TEX_{86} and TEX^L_{86} are found to correlate well, if not better, with the temperature at the base of thermocline and the oxygen minimum zone. At this stage, the explanation for this finding is still elusive. Nevertheless, its implication for paleo reconstruction work could be significant. Therefore, future work shall be focused on the elucidation of the relationship of TEX_{86} with the temperature at different water depths, and the reason for the large scatter in the TEX_{86} data in the polar regions.

[1] Schouten, Hopmans, Schefuss & Sinninghe-Damsté (2002) *Earth Planetary Science Letters* 204, 265-274. [2] Kim, van der Meer, Schouten, Helmke, Willmott, Sangiorgi, Koc, Hopmans & Sinninghe-Damsté (2010) *Geochimica et Cosmochimica Acta* 74, 4639-4654.

https://doi.org/10.1180/S0026461X00006502 Published online by Cambridge University Press

Cd isotope fractionation in some phytoplankton: A novel proxy for Fe limiting status in the oceans

TUNG-YUAN HO[1]*, SHUN-CHUNG YANG[1,2,3] AND DER-CHUEN LEE[2]

[1] Research Center for Environmental Changes, Academia Sinica, Taipei, Taiwan (*tyho@gate.sinica.edu.tw)
[2]Institute of Earth Sciences, Academia Sinica, Taipei, Taiwan
[3]Department of Geosciences, National Taiwan University, Taipei, Taiwan

The concentrations of carbon dioxide and dusts in Antarctica ice cores exhibit close correlation, indicating that Fe input in the oceans may regulate carbon cycling and climate change globally. The information of bioavailable Fe status in the surface waters of the oceans may help us appreciate how carbon dioxide has been cycled on Earth. Because Fe status in seawater influences intracellular Cd composition and transport in phytoplankton, Cd isotopic fractionation in phytoplankton may serve as a useful proxy for Fe availability in oceanic surface waters. Here, we show that marine diatom take up light Cd isotopes under Fe limited condition, attributed to dominant high affinity transporter for Cd under Fe deplete condition and to dominant low affinity non-specific Fe transporter for Cd under Fe deplete condition. Our findings elucidate why Cd isotopic composition are relatively light in seawater and Fe-Mn crusts collected in the Southern Ocean, where the surface water is Fe-limited and diatom is dominant. We anticipate our study provide the basis for applying Cd isotopic composition in environmental recorders (e.g., biogenic hard parts, coral reef, Fe-Mn crusts) to re-establish Fe limiting and non-limiting status in the contemporary and ancient oceans.

Characterization of airborne dust particles in the coal mining area of Cam Pha, northern Viet Nam

T.B. HOÀNG-HÒA[1 1]*, R. GIERÉ[1], V. DIETZE[2], U. KAMINSKI[2] AND P. STILLE[3]

[1]Albert-Ludwigs-Universität, D-79104 Freiburg, Germany (*correspondence: hoahtb@gmail.com)
[2]German Meteorological Service, Research Center Human Biometeorology, Stefan-Meier-Str. 4, D-79104, Freiburg, Germany
[3]École et Observatoire des Sciences de la Terre, Université de Strasbourg, F-67084 Strasbourg, France

Cam Pha, located in Quang Ninh province, is one of the largest coal mining areas in Viet Nam (reserves ~10 Gt). This study focuses on the mineralogical and chemical characterization of airborne dust. Exposure to dust is a major challenge for the population living near the mines, especially the open-pit mines. Additional major dust sources comprise mine dumps containing the overburden, a coal-processing facility, a coal-shipping harbour, mining traffic, and various industries, including coal-fired power stations.

Coarse particles (d_p >2.5 μm) have been collected with the passive sampler device Sigma-2 on transparent adhesive collection plates for subsequent single-particle analysis by automated optical microscopy according to VDI guideline 2119 [1]. Select specimens, sampled during different meteorological conditions, were investigated further by SEM-EDX single-particle analysis and by determining their bulk chemical and isotopic composition (ICP-MS and MC-ICP-MS, respectively).

Wind directions indicate that the particles are mainly derived from the open-pit mines, consistent with bulk chemical and isotopic data ($^{87}Sr/^{86}Sr$ = 0.7278 – 0.7427; ε_{Nd} = -14.6 – -14.9; $^{206}Pb/^{207}Pb$ = 1.1789 – 1.1884), which suggest that the dust contains mostly natural materials (coal, silicate minerals from sedimentary rocks). Relative to the coal, the bulk airborne dust is enriched in Na, Mg, K, and Ca, but depleted in most other components. Element-ratio plots reveal some systematic differences between the dust samples and specimens of coal and overburden, pointing to an additional, yet unknown particle source. To verify the hypothesis of an additional dust source and to provide quantitative data on the mineralogical composition of the dust samples, we are currently optimizing the automated SEM-EDX single-particle analysis technique.

[1] VDI (1997): *VDI guideline* **2119**, part 4.

https://doi.org/10.1180/S0026461X00006502 Published online by Cambridge University Press

Naturally occurring inorganic nanoparticles: General assessment and a global budget for one of Earth's last unexplored major geochemical components

M.F. HOCHELLA, JR.[1]*, D. ARUGUETE[1,2], B. KIM[1] AND A.S. MADDEN[3]

[1]Department of Geosciences, Virginia Tech, Blacksburg, VA 24061, USA (*correspondence: hochella@vt.edu)
[2]Present address: Geobiology and Low Temperature Geochemistry, Division of Earth Sciences, National Science Foundation, 4201 Wilson Blvd., Rm. 785, Arlington, VA 22230, USA
[3]School of Geology and Geophysics, Univeristy of Oklahoma, Norman, OK 73019, USA

Naturally occurring inorganic nanoparticles have been one of the principal catalytic components of Earth throughout its history. Yet these ubiquitous materials have largely escaped our close scrutiny until very recently. They are illusive and difficult to study. They have properties that change significantly with their exact size, shape, aggregation state, and surrounding environment. It has not even been clear how they accumulate, disperse, and move around the planet, nor even for sure what their major sources and sinks are. In this project, we derive a global budget for naturally occurring inorganic nanoparticles, assessing the sources and sinks for there materials, as well as the fluxes between these compartments (atmosphere, continents, continental shelves, and open oceans). Although this worldwide natural nanomaterial budget has a great amount of uncertainty because of limited available observations and data, it still should be a valuable guide as geoscientists attempt to better understand this poorly understood, yet fundamentally important driver of many significant Earth processes and functions. In addition, these kinds of budgets provide a basis for fundamental understanding such as residence and transfer times between compartments.

Specific findings include the following: 1) The primary producer of Earth's inorganic nanoparticles is soil through terrestrial weathering processes; 2) rivers, and to a lesser extent glaciers, bring 0.1% to 0.01% of the Earth's continental nanomaterial reservoir to the continental edge/ocean margins each year; 3) only about 1.5% of this material makes it to the deep oceans due to aggregation and settling in saline ocean margins; and 4) the airborne and waterborne inputs of nanominerals and mineral nanoparticles to the open oceans are very similar.

Palaeotemperature estimation by tandem $\delta^{18}O$ measurement of calcium carbonate and gypsum hydration water

D.A. HODELL*, A.V. TURCHYN AND C.J. WISEMAN

Department of Earth Sciences, University of Cambridge, Cambridge, UK (*correspondence: dah73@cam.ac.uk)

A fundamental problem in oxygen isotope palaeothermometry is the carbonate mineral-water temperature equation is often under constrained. Both the oxygen isotope composition of the carbonate mineral and water from which it precipitated must be known to calculate temperature. Gypsum ($CaSO_4 \cdot 2H_2O$) is a hydrated mineral containing 20.9% water by weight that records the oxygen and hydrogen isotopic of the water from which it formed. If (i) isotopic equilibrium is achieved between the mother water and hydration water; (ii) the fractionation factors are known and temperature independent, and (iii) no exchange has occurred between environmental water and hydration water after deposition, then palaeotemperature can be calculated by measuring oxygen isotopes of co-occurring gypsum hydration water and biogenic carbonate. We developed a precise and accurate method for the simultaneous measurement of $\delta^{18}O$ and δD of gypsum hydration water by cavity ringdown spectroscopy using a Picarro water isotope analyzer. The fractionation factors between gypsum hydration water and mother water were re-determined to be α_{18O}= 1.004 and α_D = 0.981 and found to be temperature independent between 12 and 40ºC, in excellent agreement with previous studies. Three paired measurements of 1200-yr old gypsum and carbonate from Lake Chichancanab, Mexico, yielded a temperature of 25ºC (range 23 to 27 ºC), which is equal to mean annual temperature (MAT) today. Twenty paired measurements of ostracods and gypsum hydration water samples from Late Peten-Itza, Guatemala, yielded a mean temperature of ~19°C (range 16 to 22 ºC) for the Late Glacial period (18 to 10 ka), which is 6 to 7°C cooler than MAT today (~25 to 26ºC). When isotope values of gypsum hydration waters from both lakes are corrected for fractionation, the $\delta^{18}O$ and δD of the palaeo-lake water fall on a projection of the modern evaporative line for the region with slope of ~5, suggesting the crystal water preserves the isotopic signal of the lake water, and has not undergone isotopic exchange with sediment pore water. The method is promising for deconvolving $\delta^{18}O$ of calcite into its temperature and $\delta^{18}O_{water}$ components.

https://doi.org/10.1180/S0026461X00006502 Published online by Cambridge University Press

The Christmas Island Seamount Province, Indian Ocean: Origin of intraplate volcanism by shallow recycling of continental lithosphere?

K. HOERNLE[1]*, F. HAUFF[1], R. WERNER[1], P. VAN DEN BOGAARD[1], S. CONRAD[1], A. GIBBONS[2] AND D. MÜLLER[2]

[1]IFM-GEOMAR, Kiel, Germany
(*correspondence: khoernle@ifm-geomar.de)
[2]School of Geosciences, University of Sydney, Australia

The east-west-trending Christmas Island Seamount Province (CHRISP, 1800x600 km) in the northeastern Indian Ocean is elongated orthogonal to present-day plate motion, posing the question if a mantle plume formed this volcanic belt. Here we report the first age (Ar/Ar) and geochemical (Sr-Nd-Hf-Pb DS isotopic data) from the CHRISP seamount chain. A crude E-W age decrease from the Argo Basin (136 Ma), to the Eastern Wharton Basin (115-94 Ma) to the Vening-Meinesz seamounts (96-64 Ma) to the Cocos-Keeling seamounts (56-47 Ma) suggests spatial migration of melting. Christmas Island, however, yields much younger ages (44-4 Ma), inconsistent with an age progression. The isotopic compositions (e.g. $^{206}Pb/^{204}Pb$ = 17.3-19.3; $^{207}Pb/^{204}Pb$ = 15.49-15.67; $^{143}Nd/^{144}Nd$ = 0.51220-0.51295; $^{176}Hf/^{177}Hf$ = 0.28246-0.28319) range from enriched MORB (or "C") to very enriched mantle (EM1) type compositions more typical of continental than oceanic volcanism. Lamproitic and kimberlitic rocks from western Australia, India and other continental areas, derived from metasomatized subcontinental lithospheric mantle, could serve as the EM1 type endmembers. The morphology, ages and chemical composition of the CHRISP, combined with plate tectonic reconstructions, cannot be easily explained within the framework of the mantle plume hypotheses. We therefore propose that the seamounts are derived through the recycling of continental lithosphere (mantle ± lower crust) delaminated during the breakup of Gondwana and brought to the surface at the former spreading centers separating Argoland (western Burma), Greater India and Australia.

Mercury colloid formation in a floodplain soil

A.F. HOFACKER[1]*, A. VOEGELIN[2] AND R. KRETZSCHMAR[1]

[1]Institute of Biogeochemistry and Pollutant Dynamics, ETH Zurich, Switzerland
(*correspondence: anke.hofacker@env.ethz.ch)
[2]Eawag, Swiss Federal Institute of Aquatic Science and Technology, Dübendorf, Switzerland

Understanding the biogeochemistry of mercury (Hg) in contaminated floodplain soils is essential for predicting potential Hg release induced by soil redox fluctuations. We studied Hg in the porewater of a surface soil collected in the contaminated floodplains of the river Mulde (Germany) during 26 days of flooding in laboratory microcosms. Porewater was sampled anoxically and analyzed for dissolved and colloidal Hg and other elements. Colloids collected on filter membranes (0.025 μm) were analyzed by X-ray absorption spectroscopy (XAS) at the Hg L3-edge at 30 K.

The concentrations of colloidal Hg increased rapidly upon soil flooding, peaked at 12 μg/L at day 3, and decreased during subsequent sulfate reduction. Total Hg in the porewater was dominated by colloidal Hg over the duration of the experiment. We previously reported a similar behavior for Cu in soil from the same site [1]. The peak in colloidal Cu was shown to result from the formation of metallic Cu(0) nanoparticles associated with bacterial cells, followed by their transformation into Cu_xS colloids and the precipitation of dispersed Cu_xS nanoparticles upon sulfate reduction [1]. Hg EXAFS (extended X-ray absorption fine structure) spectra of colloids collected during the first 5 days of flooding exhibited oscillations, which indicated that Hg was incorporated in a highly crystalline structure. The spectra did not match any crystalline HgS reference, but were well described by a shell-fit based on a structural model for Hg-substituted Cu metal. This showed that colloidal Hg has formed by Hg(II) reduction and substitution of Hg(0) for Cu(0) in metallic Cu nanoparticles (molar Hg/Cu ratio ~0.002). Since metallic Cu increased to ~14% of total soil Cu within the first days of flooding [2], Hg-substituted Cu-metal likely also formed in the soil matrix. Like for Cu, subsequent sulfate reduction may have caused a transformation of Hg(0) into HgS, but colloidal concentrations were too low for Hg L3-edge XAS.

The formation of Hg-substituted Cu metal nanoparticles in soil is a novel finding with important implications for colloidal transport and volatilization of Hg in contaminated floodplains. Hg-substituted Cu metal nanoparticles may act as effective colloidal carriers for Hg release. On the other hand, incorporation of Hg(0) in Cu metal may impede the formation of volatile elemental Hg(0), which plays an important role for gaseous Hg release from contaminated floodplain soils.

[1] Weber *et al*. (2009) *Nature Geosci*. **2**, 267-271. [2] Weber *et al*. (2009) *Geochim. Cosmochim. Acta* 2009, **73**, 5513–5527.

https://doi.org/10.1180/S0026461X00006502 Published online by Cambridge University Press

Eoarchean TTG formation by melting of thickened mafic arc crust

J.E. HOFFMANN[1,2,*], T.J. NAGEL[1] AND C. MÜNKER[2]

[1]Steinmann Institut, Universität Bonn, Germany (*correspondence: hoffjoel@uni-bonn.de)
[2]Institut für Geologie und Mineralogie, Universität zu Köln, Germany

The processes leading to the formation of the earliest preserved continental crust are strongly debated. Here we present trace element and radiogenic isotope data combined with petrological and geochemical modelling that provides evidence for the formation of massive Eoarchean TTGs from southern West Greenland from mafic precursors emplaced in an arc related setting. New trace element and Hf-Nd isotope data of well preserved tholeiites from the Isua Supracrustal Belt (ISB) confirm an island-arc origin and yield decoupled Hf-Nd isotope values with near chondritic initial εHf (-0.7 to +2.5) and depleted εNd (ca. -0.1 – +4.4) [1]. The TTGs from the Itsaq Gneiss Complex (IGC; εHf = -1.1 – +1.3; εNd = -2.2– +4.1) overlap the ISB tholeiites in their Hf-Nd isotope composition and also share positive ^{142}Nd anomalies [e.g., 2] both arguing for a genetic relationship. Thermodynamic calculation of mineral assemblages in a partially molten typical ISB tholeiite using the Theriak/Domino software predicts 10-20 % of tonalite melt between 800-950 ˚C at pressures of 10-14 kbars. Calculated co-existing residues are garnet-amphibolite and amphibole/rutile-bearing eclogite. Trace element modelling of melt compositions in equilibrium with the calculated assemblages yields compositions that are very similar to those of representative juvenile Eoarchean TTGs from the IGC [3]. In contrast, melting of N-MORB at equal pressures does not produce similar trace element patterns in the TTGs, because the stability field of plagioclase is enlarged if compared to IAT residues.

New high-precision HFSE data for the best preserved Eoarchean juvenile TTGs from Greenland, in particular Nb/Ta compositions, confirm the source compositions indicated by the modeling approach, suggesting residual amphibole, ilmenite and rutile to control the HFSE budget.

Altogether, our results suggest formation of the earliest TTG components of the IGC by partial melting of thickened mafic crust with island arc affinity rather than through direct melting of the subducting slab.

[1] Hoffmann *et al*. (in review) *GCA*. [2] Bennett *et al*. (2007) *Science* **318**,1907–1910. [3] Hoffmann *et al*. (2011) *GCA*. doi:10.1016/j.gca.2011.04.027

Hydrogen sulfide reaction with natural organic matter: Implications for arsenic binding

M. HOFFMANN, C. MIKUTTA* AND R. KRETZSCHMAR

Institute of Biogeochemistry and Pollutant Dynamics, ETH Zurich, Switzerland (*correspondence: christian.mikutta@env.ethz.ch)

Natural organic matter (NOM) represents a major source and sink of sulfur (S). As part of the S-cycle, the incorporation of S into NOM has been shown to proceed via different pathways involving hydrogen sulfide (HS^-) ions [1]. Nucleophilic introduction of S into NOM can generate highly reactive S species such as thiol groups, which in turn strongly interact with soft metal cations or metalloids. In our study we tested the reactivity of NOM towards arsenite (As(III)) and arsenate (As(V)) after its equilibration with HS^- at pH 7 under anoxic conditions (pO_2 <1ppm). We hypothesized that this reaction increases the content of reduced S species in NOM and thus its ability to retain arsenic.

Natural organic matter (40-250 μm) was extracted from an oxic ombrotrophic peat bog and reacted with HS^- solutions (1-29 mmol S/mol C) at pH 7. Afterwards the sorption of arsenic to pure and HS^--reacted NOM was studied in batch experiments. The speciation of S in untreated and HS^--treated NOM was characterized by S K-edge X-ray absorption near edge structure (XANES) spectroscopy. The coordination of arsenic reacted with NOM was investigated by both As K-edge XANES and extended X-ray absorption fine structure (EXAFS) spectroscopy.

Reaction of NOM with HS^- solutions increased its S content from 1210 up to 28000 mg/kg. Sulfur K-edge XANES spectra of pure NOM revealed that S in reduced (-I to I) and intermediate (II to IV) oxidation states prevailed. Sulfur incorporation did not result in a preferential formation of reduced S species, suggesting the partial oxidation of thiol groups.

Arsenate was not retained by pure and HS^--reacted NOM. While As(III) did not sorb to pure NOM, its sorption increased linearly with S content of HS^--reacted NOM. Arsenic K-edge EXAFS spectra showed that the first coordination shell of As(III) was progressively dominated by S atoms with increasing S content of NOM.

Our results document that NOM can rapidly incorporate S under sulfate-reducing conditions. The organic S species formed are highly reactive towards potentially toxic metals and metalloids such as As(III). Our findings provide a possible explanation for recently observed As accumulations in peatlands [2].

[1] Aizenshtat, Z., *et al*. (1995), *Geochemical Transformation of Sedimentary Sulfur*, *ACS Symp. Series*, **612**, 16-37. [2] González A, Z.I., *et al*. (2006), *Environmental Science & Technology*, **40**, 6568-6574.

https://doi.org/10.1180/S0026461X00006502 Published online by Cambridge University Press

Anions dramatically enhance proton transfer across the air-water interface

MICHAEL R. HOFFMANN, HIMANSHU MISHRA, SHINICHI ENAMI, ROBERT J. NIELSEN, WILLIAM A. GODDARD III AND AGUSTÍN J. COLUSSI

California Institute of Technology, Pasadena 91125 USA

Fundamental processes in chemistry and biology are driven by proton transfer (PT) across water interfaces with hydrophobic media. However, what distinguishes PT 'on water' from conventional PT 'in water' remains unclear. Here we show that PT from gaseous nitric acid to liquid water is dramatically accelerated by non-specific anions. We found that $HNO_{3(g)}$ fails to dissociate on pure water surfaces but is fully deprotonated on 1 mM electrolytes. Quantum mechanical (QM) calculations confirm that $HNO_{3(g)}$ dissociation on pure water is unfavorable and show that anions pre-organize interfacial water, thereby setting the stage for adiabatic PT. Our findings provide direct evidence of the critical role electrostatic pre-organization plays in catalyzing proton transfers across water-hydrophobe interfaces, such as those involved in cloud acidification and enzymatic events.

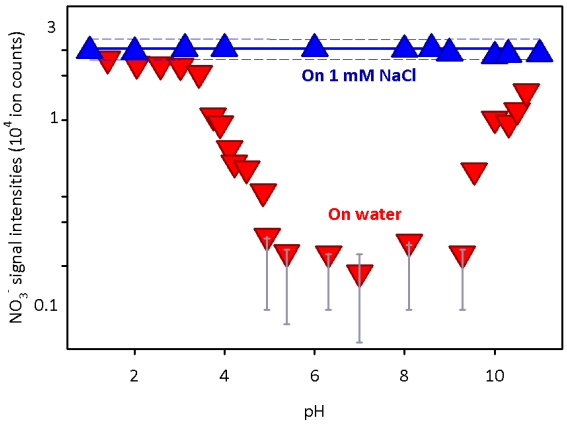

Figure 1: Electrospray ionization mass spectral nitrate (m/z = 62) signals detected on water or 1 mM NaCl microjets exposed to 0.4 ppbv gaseous nitric acid for ~ 10 μs as functions of water pH. Solid, dashed lines are a linear regression and its 95% confidence limits, respectively, to the data obtained on 1 mM NaCl. Error bars estimated from reproducibility tests. All experiments in 1 atm of $N_{2(g)}$ at 300 K.

George Tilton: Pioneer of lead isotope geochemistry

A.W. HOFMANN[1,2]

[1]Lamont-Doherty Earth Observatory, Columbia University, P.O. Box 1000, Palisades NY 10964, USA
[2]Max Planck Institute for Chemistry, Postfach 3060, 55020 Mainz, Germany (albrecht.hofmann@mpic.de)

George Tilton, who died on October 12, 2010, was one of the giants of isotope geochemistry and cosmochemistry. He is best known as the father of U-Pb dating of zircons and other minerals, a method for measuring ages of minerals and rocks that now yields uncertainties of one million years or less, for rocks and meteorites as old as 4.5 Ga. Thousands of papers have been published based on this method.

George Tilton also contributed pioneering work applying lead isotopes to measure the age of the solar system and to determine the evolution of the Earth. Later in his career, he turned his attention to the isotope geochemistry of carbonatites.

I will highlight some of George's landmark contributions and discuss the current state of some of the enduring puzzles, often called "paradox", posed by the lead isotope systematics of modern and ancient rocks. I will also discuss two basic questions that continue to engage isotope geochemists: (1) Did the U/Pb ratio of the accessible silicate Earth increase subsequent to accretion and core formation, and if so, why? (2) Why did the Th/U ratio of the accessible Earth begin with an apparently superchondritic value in Hadean time and decrease to subchondritic values subsequently? Answers to these seemingly arcane questions are fundamental to understanding the origin and global evolution of our planet.

https://doi.org/10.1180/S0026461X00006502 Published online by Cambridge University Press

Displaced helium in tilted mantle plumes

A.W. HOFMANN[1,2], C.G. FARNETANI[3], M. SPIEGELMAN[1] AND C. CLASS[1]

[1]Lamont-Doherty Earth Observatory, Columbia University, P.O. Box 1000, Palisades NY 10964, USA
[2]Max Planck Institute for Chemistry, Postfach 3060, Mainz 55020, Germany (albrecht.hofmann@mpic.de)
[3]Institut de Physique du Globe de Paris, Université Paris Diderot, Paris, France

Primordial 3He is widely thought to be a diagnostic tracer distinguishing mantle plume-related magmas from MORB-type magmas, under the assumption that the deep mantle serves as storage reservoir of primordial ^{3}He and also as source of mantle plumes. Yet on several high-^{3}He/^{4}He-hotspots, e.g. Hawaii, Galapagos, and Iceland, the maximum ^{3}He/^{4}He ratio appears to be displaced from the plume center in the direction opposite to that of inferred asthenospheric flow and/or plate motion. We model this process using the assumption that helium initially located in the center of a plume conduit is sequestered into a carbonatite melt forming in the rising plume at a depth of 400 to 600 km. The model predicts that such a carbonatite liquid will ascend rapidly and subvertically through the plume with separation velocities up to a meter per year or more. As the plume is tilted by upper-mantle flow, the carbonatite carrier of the plume helium is displaced in the upwind direction. This can explain the helium maximum at Loihi Volcano for Hawaii, at Fernandina (Galapagos), and possibly the high ^{3}He/^{4}He values on the Reykjanes Ridge. The model also predicts the declining ^{3}He/^{4}He ratios on Mauna Loa, Mauna Kea, and Haleakala, as these volcanoes age, as well as the uniformly MORB-like helium in all post-shield and rejuvenated Hawaiian lavas.

Our model is consistent with the model of Tolstikhin and Hofmann (2005), in which the storage reservoir for primordial solar helium is located in the D'' layer at the base of the mantle, from where it diffuses into the overlying actual source of the mantle plume. The base of this source layer, which subsequently forms the center of the conduit, therefore contains the highest ^{3}He/^{4}He ratio. This plume source consists of a mixture of recycled (oceanic) crustal-lithospheric material and normal depleted mantle peridotite; the radiogenic 4He derived from its local Th-U content strongly affects the ultimate ^{3}He/^{4}He ratio of a given plume.

Ion desolvation as a mechanism for kinetic isotope fractionation

A.E. HOFMANN[1]*, I.C. BOURG[1] AND D.J. DEPAOLO[1,2]

[1]Earth Sciences Division, Lawrence Berkeley National Laboratory, Berkeley, CA, USA 94720 (*correspondence: aehofmann@lbl.gov)
[2]Department of Earth & Planetary Sciences, U.C. Berkeley, Berkeley, CA, USA 94720

Kinetic processes, including mass-dependent diffusivity differences and boundary-layer reactions, have been invoked to explain non-equilibrium Ca isotopic fractionations observed in calcite precipitation from aqueous solutions [1,2]. Current available data suggest that a 1.6 ‰ kinetic fractionation between ^{44}Ca and ^{40}Ca occurs during non-biogenic calcite precipitation [2]. This fractionation cannot be attributed to isotopic diffusion in bulk liquid water, which causes a much smaller fractionation of 0.6‰ [3]. Ion desolvation—both of the crystal surface and of the cations in solution—has been implicated as a rate-limiting step in crystal growth [4,5,6,7], but, to the best of our knowledge, it has not previously been proposed as a mechanism for isotopic fractionation. Here, we carry out the first study of the isotopic mass dependence of metal cation desolvation rates.

To investigate the effect of isotopic mass on desolvation rate, we performed a series of classical molecular dynamics simulations involving one cation (Li^+, K^+, Rb^+, Mg^{2+}, Ca^{2+}, Sr^{2+}, or Ba^{2+}) and 550 water molecules in a periodically replicated cell. Simulations were performed with two prominent water models (SPC/E and TIP4P) at 278, 298, and 323K for a range of real and hypothetical masses (2-200 Da).

Our results indicate that the desolvation rates k_w of the alkali metals and at least some of the alkali earths follow an inverse power-law dependence on isotopic mass m ($k_w \propto m^{-\gamma}$). In other words, lighter isotopes exchange water molecules between their first hydration shell and the bulk liquid more quickly than heavier isotopes of the same species. Preliminary results show that the power-law exponent $\gamma \sim 0.05 \pm 0.02$ for Ca^{2+}, Ba^{2+}, Li^+, K^+, and Rb^+ at 298 K, with no clear dependence on temperature, water model, or the identity of the cation. Thus, if ion desolvation is the rate-limiting step for calcite precipitation, our preliminary results are consistent with a fractionation between ^{44}Ca and ^{40}Ca of ca. 5 ± 3 ‰.

[1] Gussone *et al*. (2003) *GCA* **67**, 1375-1382. [2] DePaolo (2011) *GCA* **75**, 1039-1056. [3] Bourg *et al*. (2010) *GCA* **74**, 2249-2256. [4] Nielsen (1984) *J. Cryst. Growth* **67**, 289-310. [5] Dove & Czank (1995) *GCA* **59**, 1907-1915. [6] Kerisit & Parker (2004) *JACS* **126**, 10152-10161. [7] Piana, Jones, & Gale (2006) *JACS* **128**, 13568-13574.

https://doi.org/10.1180/S0026461X00006502 Published online by Cambridge University Press

Geochemical evolution of lavas of the Rabaul caldera – Fractionation of Fe isotopes and HFSE ratios during fractional crystallisation

S.V. HOHL[1], S. KÖNIG[2], C. MÜNKER[2], S. SCHUTH[3] AND J. KUDUON[4]

[1]Steinmann Institut, University of Bonn, Germany
[2]Institut für Geologie und Mineralogie, University of Cologne, Germany
[3]Institut für Geographie, University of Colgne, Germany
[4]Rabaul Volcanological Observatory, Papua New Guinea

The Rabaul area, Papua New Guinea, is among the few examples worldwide, where the magmatic evolution of a single, still active system can be examined *in situ*. Our work focusses on the geochemical evolution of the Rabaul caldera system, and on differences between the two major volcanic cycles found at Rabaul.

Crystal fractionation of olivine, pyroxene and plagioclase is the most important process controlling the long-term magmatic evolution. The abscence of systematic variations in Sr-Nd-Hf isotope compositions with MgO or SiO_2 suggests that the volcanic system has been in steady state or even behaved as closed system, indicating that isotopically different materials such as crustal rocks or older basement have not been assimilated to a significant extent. Within the analytical error of ±0.4 б-units, most Fe isotope compositions of inner caldera lavas (б ^{56}Fe from 0.01 to 0.14 ‰) overlap with the mafic outer caldera samples and compositions of terrestrial basalts. Only some felsic samples show slightly lower values indicating possible fractionation of magnetite [2]. Trace element compositions of Rabaul lavas indicate that slab derived fluids control the subarc enrichment of the mantle wedge. Coupled Hf-Nd isotope compositions (εHf from +13.9 to +15.4 and εNd from +6.4 to +8.1) reveal the presence of the Indian-Australian mantle domain beneath Rabaul. High-precision HFSE data obtained by isotope dilution reveal subchondritic Nb/Ta ratios (15.5 to 18) and near chondritic Zr/Hf (40-44). Ratios of Nb/Ta tend to decrease with increasing degree of differentiation, consistent with amphibole fractionation. Likewise, a distinct increase of Zr/Hf ratios from the basaltic lavas (40) to the dacitic lavas (43-44) can be explained by fractionation of clinopyroxene or amphibole. Increasing W/Th (0.27-0.42) and decreasing Ta/W (0.73-0.49) ratios with increasing degree of differentiation indicate a higher incompatibility of W relative to Th and Ta. The overall low Ta/w and high W/Th in Rabaul lavas support previous models [3] arguing for a high mobility of W in fluid-dominated subduction systems.

[1] Shahar, A.; Young, E. and Manning, C.E. (2008): *Earth and Planetary Science Letters* **268**, 330-338. [2] König, S.; Münker, C.; Schuth, S. & Dieter Garbe-Schoenberg (2008): *Earth and Planetary Science Letters* **274** 82- 92.

Measurement of isotopes and chemistry in tunnel inflow for study of water flow in fractured rock

MILAN HOKR[1]* AND ALEŠ BALVÍN[2]

[1]Technical University of Liberec, Studentska 2, Liberec, 46117, Czech Rep (*correnpondence: milan.hokr@tul.cz)
[2]Technical University of Liberec, Studentska 2, Liberec, 46117, Czech Rep (ales.balvin@tul.cz)

We present the introductive study of the starting project of water composition monitoring in the underground springs in the tunnel through a granite massif in up to 150m depth, in Bedrichov site, northern Bohemia, Czech Republic. The work continues the recent geological and multidisciplinary research at Czech Geological Survey [1][3]. The site is specific with combination of two different excavation method in the single tunnel and quite small total inflow concentrated to main faults and few fractures.

The inflow data are available with 5 years history. Within the 8 selected inflows of different depth and different flowrate, pH and conductivity is periodically measured and samples of 2H and 18O isotopes collected in 14 days intervals from beginning of 2010, together with single sampling of tritium and standard full chemical analyses. The isotope analyses are measured in connection with GNIP and GNIR data from Uhlirska exparimental basin nearby [2].

The evaluation from first year of sampling shows small but visible tranfer of year cycle of stable isotopes to the underground. We present several hypotheses based on lumped parameters model, which are still preliminary, but we expect the potential of combining more method together with sampled depth-dependence of water geochemical parameters.

[1] Klomínský *et al* (2010), *RAWRA report*. [2] Žák *et al* (2009) *Int. J. Earth Sci*. **98**, 949-967. [3] Vogel *et al* (2010) *Vadose Zone J*. **9**, 1–8.

https://doi.org/10.1180/S0026461X00006502 Published online by Cambridge University Press

Geochemical impact of seepage from a Canadian oil sands tailings pond: A radial diffusion cell study

A. HOLDEN[1], K. U. MAYER[2] AND A. ULRICH[1]*

[1]Civil and Environmental Engineering, University of Alberta, AB, Canada (*correspondence:aulrich@ualberta.ca)
[2]Earth and Ocean Sciences, University of British Columbia, BC, Canada (umayer@eos.ubc.ca)

In Northern Alberta, Canada, the first of several oil sands tailings facilities has been constructed atop glaciofluvial outwash channels that are buried by surficial clays and till. Process-affected (PA) water from such ponds is expected to infiltrate through the low permeability sediments and affect the underlying sand channel aquifer(s). These channels are highly permeable and have the capacity to act as migration pathways, facilitating the release of tailings pond seepage into nearby surface water bodies. However, the nature and significance of this impact are not known.

In this study, radial diffusion cell experiments [1] were conducted to characterize the biogeochemical processes that control the composition of the ingressing PA seepage as it interacts with the glacial till sediments. The focus was on major ions contributing to salinization and the evolution of redox chemistry.

Following the addition of PA water into the aquitard sediment core, ion exchange led to a decrease of Na contained in the PA water and the release of pre-bound Ca, Mg and K. Elevated NO_2, NO_3 and high SO_4 concentrations were mitigated by reduction reactions – the latter in contrast with earlier findings from similar sediments [2]. Cl unexpectedly showed evidence of release from the sediments into the core reservoir, which is attributed to electrochemical migration to maintain charge neutrality.

[1] van der Kamp *et al*. (1996) *Water Resour. Res*., **32**, 1815-1822. [2] Holden *et al*. (2011) *J. Contam. Hydrol*., **119**,55-68.

Measurement of four-isotope sulfur ratios on SHRIMP-SI

PETER HOLDEN*, RICHARD ARMSTRONG, JOHN FOSTER, PETER LANC, NORM SCHRAM AND TREVOR IRELAND

Research School of Earth Sciences, The Australian National University (*correspondance: peter.holden@anu.edu.au)

The recent postulation that metabolic pathways may leave a detectable signal in the fractionation of the four sulfur isotopes (^{32}S, ^{33}S, ^{34}S & ^{36}S), potentially gives the geochemist another tool in the search for the earliest life on Earth and beyond.

However, accurate and precise measurement of the minor isotope ^{36}S presents significant analytical challenges, even for conventional gas-phase analysis. We have developed a multi-collector ion-microprobe analysis protocol that collects in-situ 4-isotope S data from both sulphates and sulphides. Valuable spatial information is maintained.

Data are acquired using a 3nA Cs^+ primary beam focussed to a 25µm spot on the target. S isotopes are detected in faraday cups, which contain slit sizes appropriate to resolve any unwanted hydride interferences. Secondary S^- beam signals are determined using our new in-house Iflex temperature and humidity controlled electrometers. Each Iflex has 3 selectable resistors ($10^{10}\Omega$, $10^{11}\Omega$, $10^{12}\Omega$) and a 27pF capacitor so that the detection system can be tuned to the appropriate beam intensity. Under such conditions pyrite targets yield approximately 2GHz ^{32}S, 16MHz ^{33}S, 88MHz ^{34}S, and 0.3MHz ^{36}S.

The low abundance ^{36}S isotope can be collected in either current or charge mode. Charge-mode detection eliminates the dead-time correction, drift in detector response and linearity issues associated with electron multipliers. In addition, response times are much faster than high ($>10^{11}\Omega$) Ohmic resistors. Experimentation suggests that charge-mode delivers superior data quality over electron multipliers down to 50kHz, and $10^{12}\Omega$ resistors up to 1 Mhz and thus neatly bridges the "gap" between conventional electrometers and ion-counting.

Provisional data yields external 2 s.d. uncertainties for $\Delta^{33}S$ and $\Delta^{36}S$ that are better than 0.3‰ and 0.5‰ respectively, which are comparable to conventional analyses, but using several orders of magnitude less material. At this level of precision, documented anomalies of 2‰ can be easily resolved making SHRIMP a viable alternative to the protracted extraction procedures necessary for gas-phase analysis.

https://doi.org/10.1180/S0026461X00006502 Published online by Cambridge University Press

Noble gases from the Precambrian Shield of Canada

G. HOLLAND[1]*, B. SHERWOOD LOLLAR[2], L. LI[2], G. LACRAMPE-COULOUME[2], G.F. SLATER[3] AND C.J. BALLENTINE[4]

[1]LEC, Lancaster University, Lancaster. LA1 4YQ. U.K. (*correspondence: g.holland@lancaster.ac.uk)
[2]Dept. of Geology, Univ. of Toronto, ON, Canada M5S 3B1
[3]SGG, McMaster Universty, Hamilton ON Canada L8S 4K1
[4]SEAES, Manchester Univ, Manchester M134 9PL. U.K.

An increased recognition of the role of subsurface microbes in the production and alteration of oil and gas deposits has sparked heated debate about the volume and extent of life in the deep subsurface. The deep terrestrial biosphere in the tectonically quiescent Precambrian Shields of Canada, Scandinavia and South Africa are dominated by radiogenic noble gases and crustal-derived carbon sources. These radiogenic gases have been used previously to calculate long residence times on the order of 10–25 million years for the deepest high-salinity fracture waters [1]. Correlations of increasing salinity with highly altered hydrogen and oxygen isotope signatures for the waters, together with increasing concentrations of radiogenic noble gases, suggest that ground waters were subject to extensive water–rock reactions over geological time in hydrogeologically isolated fracture networks [2].

We have performed noble gas analyses on 6 samples from a mine site in Ontario (ON). Results show highly radiogenic noble gas ratios for He, Ne and Ar, analogous to the anomalously high Ne signatures recently described for fracture waters in South African gold mines [3]. $^{3}He/^{4}He$ in these samples are <0.02Ra. We have found very high $^{40}Ar/^{36}Ar$ ratios (up to 44,000) the highest observed in crustal fluids and the first documented ^{129}Xe excess (~1%) that cannot be attributed to a mantle component. Elemental ratios suggest solubility controlled gas/groundwater phase partition processes have operated but Kr and Xe enrichment suggest input from sediment and / or sediment derived porewater. This sediment contribution is also required to explain the ^{129}Xe excesses. ^{129}Xe is the decay product of ^{129}I with $t_{1/2}$ = 15.7Ma implying significant closed system fluid evolution, consistent with the hydrogeologically isolated nature of the fractures.

[1] Lippmann *et al*. (2003) *GCA* **67,** 4597-4619. [2] Sherwood Lollar *et al*. (2008) *GCA* **72,** 4778-4795. [3] Lippmann *et al*. (2011) *Chem. Geol.,* In press.

Hydrothermal alteration of diatomite for the fixation of heavy metal ions

D. HÖLLEN*[1], P. GRUNERT[2], D. KLAMMER[1] AND M. DIETZEL[1]

[1]Graz University of Technology, Institute of Applied Geosciences, Rechbauerstr. 12, A-8010 Graz (*correspondence: daniel.hoellen@tugraz.at)
[2]University of Graz, Institute of Earth Sciences, Heinrichstr. 26, A-8010 Graz

The application of alterated diatomite as a hierarchically structured material for ion fixation from aqeuous solutions is based on macropores (~100 nm) from the intricate silica structure of diatomite, micropores (~0.3-0.4 nm) from neoformed zeolites and highly active surface sites from amorphous precursor phases. Such kind of materials can be obtained by hydrothermal synthesis.

A stock solution was prepared by dissolving 1 g of gibbsite (γ–$Al(OH)_3$) in 0.5 L of 1 M KOH and subsequent filtration (0.45 μm). 0.025 L of the stock solution reacted with 0.5 g diatomite (”Thiele”) in a Teflon coated autoclave at 50 to 150°C. After distinct reaction times from 6 up to 1500 h reaction products were separated from the solutions by filtration. Solutions were analysed for composition and solids for composition and structure. Ion fixation capacities of the reaction products were studied in aqueous solutions containing 0.5 mM of Cu^{2+}, Pb^{2+} and Zn^{2+} at pH 5.1 and 25°C for 72 h.

Initially, the diatoms are converted partly into spherical amorphous nanoparticles (20-200 nm). After 24 to 192 h mainly merlinoite and minor amounts of chabazite were formed. Proportions depend on temperature and reaction time. At a reaction time between 96 and 192 h a quasi steady state was reached with ≈ 30 wt.% amorphous phase, ≈ 60 wt.% merlinoite and 10 wt.% accessory phases (relictic quartz, mica as well as newly formed chabazite). The heavy metal ion fixation capacity of the pristine diatomite is low. Interestingly, the reaction product containing the amorphous precursor phase non-selectively reduced ≥ 99 % of the primarily dissolved heavy metals (specific surface area = 38 m^2/g). The final reaction products (15 m^2/g) reduced heavy metal concentrations less efficiently (~ 90 %), but selectively. Challenging tasks for the ongoing study are to tailor the reaction products with regard to metal fixation and hierarchical pore structures for waste and drinking water purification.

https://doi.org/10.1180/S0026461X00006502 Published online by Cambridge University Press

Using TRLFS to explain increased uptake of Eu^{3+} and Cm^{3+} into biologically produced apatite

KIEL HOLLIDAY*[1], STEPHANIE HANDLEY-SIDHU[2], JOANNA RENSHAW[2], LYNNE MACASKIE[2] AND THORSTEN STUMPF[3]

[1]Institut für Nukleare Entsorgung, Hermann-v.-Helmholtz-Platz 1, 76344 Eggenstein-Leopoldshafen, Germany (kiel.holliday@kit.edu)
[2]University of Birmingham, Edgbaston-Birmingham, B15 2TT, (s.handley-sidhu@bham.ac.uk)
[3]Institut für Nukleare Entsorgung, Hermann-v.-Helmholtz-Platz 1, 76344 Eggenstein-Leopoldshafen, Germany (thorsten.stumpf@kit.edu)

The long term geochemical modeling of nuclear waste in the environment requires a molecular understanding of the interaction between radioactive materials and mineral phases. Of particular importance is the adsorbtion and incorporation of trivalent actinides such as plutonium, americium and curium. In this study time-resolved laser fluorescence spectroscopy was used to probe europium and curium which have been incorporated into biologically produced apatite. Apatite produced by *Serratia* bacteria has been shown to have an increased uptake of various cations. Time resolved laser fluorescence spectroscopy was used to identify and characterize the nature of Eu^{3+}/Cm^{3+} sorption and incorporation within the mineral phase. Using site-selective excitation different interactions can be isolated. The lifetime and emission spectra were analyzed at each site that was identified. The number of hydrating waters was determined by the lifetime measurement and used to distinguish species that are sorbed to the surface from those incorporated into the bulk. Emission spectra were measured to determine the symmetry of the site being occupied by the sorbed or incorporated trivalent cation and determine the substitution for non-equivalent calcium positions. By these measurements it was determined that Eu^{3+} and Cm^{3+} are incorporating into the amorphous grain boundaries of the apatite polycrystalline material. Biologically produced apatite has smaller crystalline grains resulting in a greater amount of amorphous grain boundary within a particle as compared to synthetic or natural apatite. This greater amount of amorphous grain boundary results in an increased uptake of Eu^{3+} and Cm^{3+} and is therefore a more effective barrier to radionuclide migration.

Nitrogen isotopes and geochronology of the Musselwhite Au mine, Canada

P. HOLLINGS[1]*, C. ISAAC[1,2], J. BICZOK[3], R. MAAS[4] AND R. FRIEDMAN[5]

[1]Lakehead University, Thunder Bay, ON, Canada (*correspondence: peter.hollings@lakeheadu.ca)
[2]Centre for Exploration Targeting, University of Western Australia, Western Australia 6009
[3]Goldcorp Inc. Musselwhite Mine, P.O. Box 7500, Thunder Bay, Ontario, Canada P7B 6S8
[4]University of Melbourne, VIC 3010, Australia
[5]University of British Columbia, 6339 Stores Road, Vancouver, BC, V6T 1Z4, Canada

The Musselwhite Au mine, a large orogenic lode gold deposit hosted in amphibolite grade metamorphic rocks, is located in the ~2.98 Ga North Caribou Lake greenstone belt of the North Caribou Terrane, Superior Province, Canada. The mine has produced ~3.1 million ounces of gold and has a total reserve and measured plus indicated resource base of 2.31 million ounces as of December 31, 2010. Gold mineralization within the host iron formation is largely confined to subvertical shear zones along the steeply dipping limbs of isoclinal folds and tends to swell where these limbs transition into the crests or keels of antiformal and synformal structures.

Nitrogen isotopes in biotite from Musselwhite Mine are characterized by a $\delta^{15}N$ range from -1.3 to 11.1 per mil whereas oxygen and hydrogen isotopes of biotites from the mine range from +7.1 to +10.1 per mil for $\delta^{18}O$ and -55 to -100 per mil for δD. Biotite samples from granites and metasedimentary rocks adjacent to the deposit have a $\delta^{15}N$ range of -6.9 to +6.1 per mil.

Uranium-lead ages on zircons and monazites from intrusive rocks surrounding the mine range in age from 2875 Ma to 2670 Ma, whereas Ar-Ar ages range from 2658 to 2440 Ma. An Sm-Nd age of 2690±9 Ma for garnets that host gold mineralization is bracketed by peraluminous S-type granites with ages of 2668.3±1.6 Ma and 2715.8±1.6 Ma.

The $\delta^{15}N$, $\delta^{18}O$ and δD stable isotopic data for biotite from the mine suggests that both metamorphic and magmatic fluids played a role in the formation of the deposit. Sm-Nd ages of garnets that are coeval with mineralization suggest that the orogenic gold mineralization at the Musselwhite mine was broadly synchronous with the ~2700 Ma orogeny caused by the collision of the Oxford-Stull domain with the North Caribou Terrane ~75 km northeast of the mine. The presence of coeval S-type granites suggest that these may have played a greater role in the formation of orogenic gold deposits than has been previously recognised.

https://doi.org/10.1180/S0026461X00006502 Published online by Cambridge University Press

$\delta^{44/40}$Ca variability in modern shallow water carbonates

C. HOLMDEN[1]*, D.A. PAPANASTASSIOU[2], P. BLANCHON[3] AND S. EVANS[4]

[1]Saskatchewan Isotope Laboratory, University of Saskatchewan, Saskatoon, Canada S7N-5E2 (*correspondence: ceh933@mail.usask.ca)
[2]Science Division, Jet Propulsion Laboratory, M/S 183-335; California Institute of Technology[3], Pasadena, CA 91109
[3]Instituto de Ciencias del Mar y Limnologìa, Apartado Postal 1152, Cancún, D.F. Mexico.
[4]Department of Geosciences[5], Boise State University, 1910 University Drive, Boise, Idaho 83725-1535

Shallow water carbonates from Florida Bay, the Florida Reef Tract and the Mexican Caribbean fringing reef at Punta Maroma were studied to determine the range of Ca isotope variation among the cohort of modern carbonate producers, and to look for local scale Ca cycling effects. The total range of Ca isotope fractionation is 0.4‰ in carbonates from Punta Maroma, yielding a production weighted average $\delta^{44/40}$Ca value –1.12‰. This value compares well with bulk carbonate sediments from the Florida Reef Tract (–1.11‰) and Florida Bay, near a tidal inlet in the Florida Keys (–1.09‰). No evidence was found for the ~0.6‰ fractionation between calcite and aragonite observed in laboratory precipitation experiments.

Isotope fractionation effects are subordinate to local scale Ca cycling effects as a potential source of isotopic variability in shallow water carbonates. This is observed in the innermost restricted region of northeastern Florida Bay, where a 0.7‰ gradient of decreasing $\delta^{44/40}$Ca values in sediments and waters occurs between the coastal zone of Florida Bay and the southern mangrove fringe of the Florida Everglades. The reduction in $\delta^{44/40}$Ca values towards the Everglades in this setting is predominantly due to submarine groundwater discharge (SGD), which is characterized by low $\delta^{44/40}$Ca values, similar to marine limestone, and Ca concentrations that are higher than seawater. Mixing model calculations show that between 9 and 71% of the Ca in coastal waters with salinities ranging between 30 and 14 ppt, respectively, is from SGD and surface water runoff.

By analogy with Florida Bay, restricted circulation with contemporaneous oceans may have led to overprinting of ocean $\delta^{44/40}$Ca signatures in carbonate deposits located in near shore settings of ancient epeiric seas. If this is correct, some of the scatter in the Paleozoic portion of the Ca isotope evolution curve of Phanerozoic of oceans, which is, itself, reconstructed from analyses of brachiopods collected from the deposits of epeiric seas, may be due to local Ca cycling effects.

Diffusive fractionation of transition metals in grain boundaries

V. HOMOLOVA, E.B. WATSON AND J.B. THOMAS

Rensselaer Polytechnic Institute, 110 8th Street, Troy, NY USA (*correspondence: homolv@rpi.edu)

Grain boundaries (GBs) provide one of the most important transport pathways in metamorphic rocks. The equilibration length scale of a particular element may be dependent upon its GB diffusivity, and inter-element differences in these quantities may lead to a diffusive fractionation of elements during metamorphism. The detector particle method is one way to study GB diffusivities and consists of juxtaposing a diffusant source with a pre-synthesized matrix "rock" containing dispersed sink phases. The diffusion profile obtained by measuring diffusant concentrations in the detector (sink) particles will reflect the GB concentration of the diffusant to an extent determined by the volume percent of sink phases ($vol\%_{sink}$) and the partitioning behaviour of the diffusant between the grain boundary and the sink phase ($K_d^{prt/gb}$). To better constrain GB diffusivities, experiments and finite difference modelling were undertaken to elucidate the relationships between $vol\%_{sink}$, $K_d^{prt/gb}$, and the characteristic distance (x). Experiments involved juxtaposing a pre-synthesized quartzite matrix containing 1-3.5wt% dispersed enstatite with a source of either chromium-nickel-iron alloy, chromium oxide, or nickel metal containing 2200ppm manganese. Experiments were run in a piston cylinder apparatus at 1250°C and 1GPa for durations of 9.25-92 hours. Post-experiment analyses of the enstatite sink particles for the GB diffusants (Cr, Mn, Ni) were performed with a Cameca SX100 microprobe. In 24 hours, Cr GB diffusion length scales decrease from 0.069 to 0.019cm in experiments containing 1 to 3.5wt% sink particle, respectively, while Mn GB diffusion length scales decrease from 0.108 to 0.027cm. Due to the incompatibility of Ni in the sink particles (relative to Mn), Ni effectively experiences 0 $vol\%_{sink}$ at short diffusion distances where Mn concentrations are high. Nonetheless, Ni GB diffusion length scales decrease by ~70% (from 0.94 to 0.26cm) in experiments containing 1 and 3.5wt% sink particles, respectively. GB diffusion length scales of Cr, Mn and Ni all appear to decrease by a factor of ~4 over the range of $vol\%_{sink}$ studied here. These results are in line with finite difference modelling which also predicts a decrease in x with a decrease in spacing of the sink particles (which is equivalent to an increase in $vol\%_{sink}$). The models also predict a non-linear, inverse correlation between $K_d^{prt/gb}$ and x.

https://doi.org/10.1180/S0026461X00006502 Published online by Cambridge University Press

New data on unexpectedly high arsenic concentrations within a landfill plume in Central Massachusetts, USA

R. HON[1]*, Y. XIE[1], C. SOELLER[1], W.C. BRANDON[2] AND R.J. SIMEONE[3]

[1]Earth and Environmental Sciences, Boston College, 140 Commonwealth Ave, Chestnut Hill, MA 02467, USA (*correspondence: hon@bc.edu)

[2]U.S. EPA, Region 1, 5 Post Office Square, Suite 100, Boston, MA 02109, USA

[3]Department of the Army, Base Realignment and Closure Division, U.S. Army Garrison Fort Devens, 30 Quebec Street, Unit 100, Devens, MA 01434-4479, USA

A contaminant leachate plume, associated with a closed and capped landfill in North Central Massachusetts, USA, contains surprisingly high levels of arsenic which at several locations within the plume can reach and exceed 15,000 ppb of As in groundwater. The landfill waste material was dumped over a layer of peat of variable thickness (up to 4 m thick), originally a marshland that developed over a thick sequence of glacial lake deposits (50 to 100 ft). During the summer of 2010 a comprehensive study of the landfill area included direct-push drilling at 18 separate locations, with sampling at regular 10 ft vertical intervals. The results indicate the regions of elevated arsenic concentrations and more importantly provide a unique opportunity to delineate arsenic pathways in 3D space. The study identified an existence of unexpectedly high arsenic zone in groundwater with strong concentration gradients on each side of the zone. The zone is less than 3.5 m thick, contains As above 10,000 ppb (up to 16,000 ppb), and is positioned beneath the peat layer and above a basal till unit. Although the landfill waste can not be ruled out as potential source, one possibility for the source of As is the peat layer itself which, when covered by the waste material, may have promoted bacterial activity driven by organic carbon transported downward from landfill waste prior to capping, creating a reducing environment and remobilization of arsenic. However, the post-glacial geohydrologic evolution of the area is poorly constrained. Historically, the landfill operated as an open dump for a period of 100 years or more. Hydraulic conditions necessary to move shallow groundwater through waste to depth were eliminated by cap construction in the mid-1990's, and the hydraulic regime following capping continues to evolve.

Geological characteristics and fluid inclusions of Chagangnuoer iron ore deposit in the western Tian Shan Mountain, NW China

WEI HONG AND ZUOHENG ZHANG

MLR Key Laboratory Metallogeny and Mineral Assessment, Institute of Mineral Resources, CAGS, Beijing 100037, China (correspondence: zuoheng@hotmail.com)

Located along the southwestern margin of the Central Asia Orogenic belt, the Chinese western Tian Shan Mountain is famous for abundance of mineral resources. In recent decade, remarkable advances have been made in the iron ore exploration in the Awulela metallogenic district. Take Chagangnuoer iron ore deposit for example, which is found in the late 1960s with only 6 millions ton reserves. With careful magnetic survey in 1980s and drilling prospecting since 2004, this iron ore has become a large scale one whose reserves are more than 210 million tons. Hosted in the andesite and andesitic volcaniclastic rock of the Lower Carboniferous Dahalajunshan Formation, orebodies are controlled by NW, NWW, NEE strike faults and circular faults. This iron ore is composed of two major orebodies as FeI and FeII. FeI orebody is NE-SW strike, about 2900 meters in length, 63 meters in average thickness, and about 190 million tons reserves with thin copper layer. Wall rock alterations mainly exhibit garnetization, actinolitization, chloritization, epidotization, calcitization and so on. And marble distributes in the bottom of orebody. Ore minerals are consisted of magnetite, pyrite and chalcopyrite while gangue minerals are composed of garnet, actinolite, chlorite, epidote, tremolite, calcite *et al*.

Three kinds of fluid inclusions have been discovered in calcite, liquid-rich inclusion (75%), pure liquid inclusion (20%), and daughter (halite) inclusion (3~5%). Homogenization temperature is 290~410℃in the calcite paragenesis with garnet, whereas homogenization temperature is 120~230 ℃ in the calcite paragenesis with chlorite and epidote. According to a table describing the relationship between salinity and freezing-point depression [1], NaCl-eq salinity is 10.49~17.87%.

[1] Bodnar RJ (1993) Revised equation and stable for determining the freezing point depression of H_2O-NaCl solutions. *Geochimica et Cosmochimica Acta* **57**, 683-684.

https://doi.org/10.1180/S0026461X00006502 Published online by Cambridge University Press

Impact of biological and mineral dust aerosols on mixed-phase clouds

C. HOOSE[1]*, C. ANQUETIL-DECK[1], S.M. BURROWS[2], M. HUMMEL[1], J.E. KRISTJANSSON[3] AND O. MÖHLER[1]

[1]Karlsruhe Institute of Technology, Institute for Meteorology and Climate Research, Karlsruhe, Germany (*correspondence: corinna.hoose@kit.edu)
[2]Max Planck Institute for Chemistry, Mainz, Germany
[3]University of Oslo, Department of Geosciences, Oslo, Norway

Freezing of supercooled water droplets, at temperatures between 0 and -37°C, is facilitated by insoluble aerosols acting as ice nuclei. Numerous laboratory experiments have investigated the efficiency of aerosol particles to induce freezing. Different particle types (e.g., mineral dusts or ice nucleation active bacteria) are usually studied in isolation. Here we summarize experimental results by using the metrics of "surface site densities" [1], which allows a more quantitative comparison than if only the nucleation onset temperatures are studied. This approach accounts for the size dependency of the nucleation process, but does not consider any time dependency.

In the atmosphere, in addition to the ice nucleation efficiencies, the available surface and number concentrations at cloud altitudes of the various ice-nucleating particle types are main determinants of their contribution to cloud ice formation. The concentrations of bacteria, fungal spores, pollen and mineral dust are simulated in the global climate model CAM-Oslo [2,3], and (so far for pollen and mineral dust only) the mesoscale model COSMO-ART [4]. In the global model, ice nucleation is dominated by mineral dust due to its higher average concentrations. The mesoscale model is capable of capturing small-scale fluctuations. The implications of this variability will be investigated.

[1] Connolly *et al* (2009), *Atmos. Chem. Phys.* **9**, 2805–2824. [2] Hoose *et al* (2010), *Environ. Res. Lett.* **5**, 024009. [3] Hoose *et al* (2010), *J. Atmos. Sci.* **67**(8) 2483–2503. [4] Vogel *et al* (2009), *Atmos. Chem. Phys.* **9**, 8661–8680.

Bacterial oxidation of pyrrhotite and troilite under acidic conditions

J. HOPF[1]; K. POLLOK[1], M.F. HOCHELLA[2] JR. AND FALKO LANGENHORST[3]

[1]Bayerisches Geoinstitut, University of Bayreuth, D-95440 Bayreuth, Germany
[2]Center for NanoBioEarth, Department of Geosciences, Virginia Tech, Blacksburg, Virginia 24061, USA
[3]Institute of Geosciences, FSU Jena, D-07749 Jena, Germany

To study the influence of microorganisms on sulfide oxidation, experiments on pyrrhotite in the presence of the two acidophilic species *Acidithiobacillus ferrooxidans* (*A.f.*) and *Acidithiobacillus thiooxidans* (*A.t.*) were performed. Pyrrhotite cubes with approximate dimensions of ca. 3×3×3 mm were polished on four faces to a smooth mirror finish. The host pyrrhotite was of the NC-type and contained 1-3 μm wide, fine exsolution lamellae of troilite [1].

First, oxidation experiments with *A.f.* cells were carried out in a simple acidic medium supplemented with pyrrhotite cubes for different time intervals (1 to 40 days). A consistent abiotic experiment was performed, serving as a control. *A.f.* developed a whitish biofilm on the cubes within 40 days. The surface underneath had deep trenches, inferring a preferential dissolution of the embedded troilite lamellae. Surfaces between these trenches displayed a layered and frayed structure, indicating enhanced pyrrhotite surface dissolution. XPS results indicated that *A.f.* drastically enhanced the oxidation of Fe(II) to Fe(III) on the pyrrhotite surface, whereas the pure abiotic experiment did not show any alteration, under the given conditions.

Further oxidation experiments with both acidophilic species (*A.f.* and *A.t*) were performed similarly. *A.f.* and *A.t.* distinctly augmented the pyrrhotite oxidation and particularly enhanced troilite lamellae dissolution. Experiments with bacteria in a dialysis capsule revealed a slower increase in surface roughness compared to free cells, indicating an active involvement of bacteria in the dissolution. Troilite lamellae dissolved similarly in both biotic experiments, but not in the control. The total rate constant for pyrrhotite dissolution was lowest for the control (1.9×10^{-9} mol/(m²×s)) and highest for the *A.f.* experiment with free cells (1.4×10^{-8} mol/(m²×s)). Both bacterial strains oxidized pyrrhotite and especially the troilite phase. The bacterial cell contact to the mineral surface seemed to be irrelevant for the process, therefore a contact-independent mechanism is most likely for biotic pyrrhotite/troilite oxidation.

[1] Harries *et al.* (2011) *Am. Min.* **96**, in press (DOI: 10.2138/am.2011.3644).

https://doi.org/10.1180/S0026461X00006502 Published online by Cambridge University Press

Early thermal events of the HED parent body (4 Vesta) from eucrite zircon U-Th-Pb-Ti depth profiles

M.D. HOPKINS[1,3]*, S.J. MOJZSIS[1,3] AND W.F. BOTTKE[2,3]

[1]University of Colorado, Department of Geological Sciences, 2200 Colorado Avenue, Boulder, CO, 80309 USA (*correspondence: michelle.hopkins@colorado.edu)
[2]Southwest Research Institute, Department of Space Studies, 1050 Walnut Street, Ste. 300, Boulder, CO, 80302 USA
[3]Center for Lunar Origin & Evolution, NASA Lunar Science Institute

Meteoritic zircons provide a means to probe the thermal evolution of asteroids, but this technique has been limited due to generally low yields of small (~10μm ∅) grains in thin sections cut at random orientations and analyzed in 2-D "spot mode". Conversely, the 3-D zircon depth-profile method chemically and isotopically maps minute (sub-μm) domains within individual grains that conventional 2-D spot analyses cannot capture. We report data from coupled Ti-thermometry and U-Th-Pb profiles used to evaluate apparent crystallization temperature and composition as a function of age in zircons from the Millbillille brecciated eucrite. Crushed and sieved ~3g aliquots were separated using reagent grade methylene iodide to extract the largest zircons. Two large grains (mb1_gr1 ~40μm; mb7_gr1 ~20μm) were imaged by back-scattered electrons, and the internal distributions of U-Th-Pb-^{49}Ti (and -^{57}Fe-^{177}Hf^{++}-^{89}Y) in each zircon measured on the UCLA Cameca ims1270 ion microprobe in depth-profile mode. Results show that mb1_gr1 preserves a concordant core age of 4561±13 Ma (2σ; mswd=0.72; n=7) and a 4.5μm overgrowth at 4524±9 Ma (2σ; mswd=2.52; n=19). Sample mb7_gr1 shows one domain age of 4537±10 Ma (2σ; mswd=3.0; n=19) statistically indistinguishable from the younger mantle in zircon mb1_gr1. Core ages from mb1_gr1 correlate well with other reported crystallization ages for eucrites [1] and ^{40}Ar-^{39}Ar ages of unbrecciated eucrites [2]. Because the decay of ^{26}Al was effectively complete 5 Myr after t_0, we propose that later ~4530 Ma events that overprint ca. 4560 Ma ages were caused by shock-heating from a large impact, or burial of hot material excavated by impact. The manifestation of such a large and early impact event on a small (900km) body such as 4 Vesta should be as a subdued impact basin from the mechanical relaxation of the asteroid's crust. NASA's DAWN mission will encounter Vesta (July, 2011) and should be capable of resolving whether such an old basin is present.

[1] Bukovanska *et al*. (1997) *Journal of GEOsciences*, **42**, 20. [2] Bogard & Garrison (2003) *Meteor Planet Sci,* **38**, 669-710.

Rejuvenation of an old magmatic system at Parinacota Volcano, Chile

J.M. HORA[1]*, G. WÖRNER[1], A. KRONZ[1], M. BANASZAK[1], B.S. SINGER[2] AND C.M. JOHNSON[2]

[1]GZG Abt. Geochemie, Georg-August Universität Göttingen. Goldschmidtstraße 1, 37077 Göttingen, Germany (*correspondence: jhora@gwdg.de)
[2]Department of Geoscience, University of Wisconsin-Madison. 1215 W. Dayton St. Madison WI 53706, USA

The history of Parinacota Volcano in the Andean CVZ represents a transition between two fundamentally different modes in which magmatic reservoirs can operate: long-term crystal accumulation and storage vs. rapid throughput with minimal crustal transit times. Changes in volcanic output rate and compositional range parallel reorganization of the magma system preceding a sector collapse, after which the volcano was rapidly rebuilt [1]. ^{238}U-^{230}Th disequilibria indicate crystal ages of >120 k.y. in the pre-collapse time interval. In contrast, some post-collapse magmas have $(^{230}Th/^{238}U)_0$ eruption-age-corrected activity ratios as high as 1.33, implying that transit times from a region of garnet-residual partial melting in the lower crust to the surface were < 20 ky.

Minerals from pre-collapse highly porphyritic rhyodacite domes (eruption age 47-40 ka) do not form a linear array on an U-Th equiline diagram, but rather define a pair of wedges delineated by reference isochrons that have ages of 47.7 and 168 ka [2]. Because these are bulk crystal ages, two possible explanations are: (1) a protracted crystallization interval, during which crystals were nucleating continuously, or (2) crystal cores from a nascent pluton or crystal-rich mush zone that are older than 168 ka were subsequently overgrown with younger rims of variable thickness, resulting in average ages that in some cases approach that of eruption.

The phase assemblage present in these domes allows several geothermometers to be applied, recording different points along a pre-eruption Temperature-time path. Fe-Ti oxide equilibria yield temperatures of 792±30°C, whereas Zr-in-titanite gives temperatures that are ~85°C cooler. Because Zr diffusion in titanite is slow [3] compared to Fe-Ti oxide reequilibration, it is likely that the lower temperatures in titanite record an earlier point in T-t history. This would contradict the hypothesis of protracted monotonic cooling prior to eruption. Instead, it may indicate a re-heating event associated with recharge that remobilizes older (colder) crystals and facilitates their eruption after a long period of storage.

[1] Hora *et al* (2009) *EPSL* **285**:75-86, [2] Hora *et al*. (2010) *Geology* **38**:923-926, [3] Cherniak (2006) *CMP* **152**:639-647

https://doi.org/10.1180/S0026461X00006502 Published online by Cambridge University Press

Palladium-silver systematics in the oldest differentiated planetesimal

M.F. HORAN[1]*, R.W. CARLSON[1] AND J. BLICHERT-TOFT[2]

[1]Carnegie Institution of Washington, Dept. of Terrestrial Magnetism, Washington DC 20015, USA (*correspondence: horan@dtm.ciw.edu)
[2]Ecole Normale Supérieure de Lyon,69007, France

Combined Hf-W and Pb–Pb isotopic data and calculated cooling rates from Muonionalusta, a Group IVA iron meteorite, indicate that it accreted, differentated and cooled within 2-3 Ma after the formation of CAIs [1]. This chronology suggests that its Pd-Ag isotopic systematics hold the potential of better constraining the Solar System initial abundance of ^{107}Pd ($t_{1/2}$ = 6.5 Ma). High-Pd/Ag metal from Gibeon (also group IVA) has given ^{107}Pd/^{108}Pd = (2.40±0.05) x 10^{-5}, but interpreting this ratio as the Solar System initial has been complicated by unsupported radiogenic ^{107}Ag in associated low-Pd/Ag troilite [2,3]. By contrast, a much higher Solar System initial ^{107}Pd/^{108}Pd of (5.9±2.2) x 10^{-5} was inferred from carbonaceous chondrites [4].

Metal and troilite samples were taken from two slabs of Muonionalusta [1]. Pd and Ag concentrations, determined by isotope dilution, and Ag isotopic compositions, measured on unspiked aliquots, were analyzed using a Nu Plasma MC-ICP-MS [5]. Troilite results confirm that Muonionalusta escaped isotopic resetting by shock [1], and indicate that the Pd/Ag ratio of Muonionalusta parental materials was ≥100 times chondritic. Metal compositions represent 1-10% troilite mixed with radiogenic ^{107}Ag, implying that metal and troilite were once isotopically homogenized in a molten core with 6-12% S. Pd-Ag isotopic data from three metal pieces, however, do not lie on a single isochron, but two samples have slopes corresponding to ^{107}Pd/^{108}Pd = (2.33 ± 0.27) x 10^{-5}, within the uncertainty of Gibeon [2,3]; one metal has a slope of 1.58 x 10^{-5}, implying an age 4 Ma younger than Gibeon.

If the Solar System initial ^{107}Pd/^{108}Pd was as high as inferred for carbonaceous chondrites [4], then Muonionalusta Pd-Ag records an age of ≥ 8 Ma, inconsistent with the quick formation and cooling required by W and Pb-Pb ages. If the Pd-Ag and Pb-Pb systems closed at the same time and record the same event in Muonionalusta, then these data imply an initial Solar System ratio between 2.6 x 10^{-5} and 3.0 x 10^{-5}.

[1] Blichert-Toft J. *et al*. (2010) *EPSL* **296**, 469-480. [2] Chen J.H. and Wasserburg G.H. (1990) *GCA* **54**, 1729-1743. [3] Chen J.H. and Wasserburg G.H. (1996) *Geophysics Monograph* **95**, AGU. [4] Schönbächler M. *et al*. (2008) *GCA* **72**, 5330-5341. [5] Carlson R.W.and Hauri E.H. (2001) *GCA* **65**, 1839-1848.

Distribution and time variation of helium isotope ratios around the source region of the Iwate-Miyagi Nairiku Earthquake in 2008

KEIKA HORIGUCHI[1]*, TAKASHI NAKAYAMA[2] AND JUN-ICHI MATSUDA[1]

[1]Department of Earth and Space Science, Graduate School of Science, Osaka University, Toyonaka, Osaka 560-0043, Japan. (*correspondence: keika@ess.sci.osaka-u.ac.jp)
[2]Research Center for Prediction of Earhthquakes and Volcaic Eruptions, Graduate School of Science, Tohoku University, Sendai, Japan.

The Iwate–Miyagi Nairiku Earthquake in 2008 (M_{JMA}7.2) occurred on June 14th 2008. We monitored the time change for helium isotopic ratios before and after the earthquake, to define the behavior of the upcoming fluid around the source region. The spring water and gas samples were collected in eight localities, only a week after the earthquake [1]. We repeated the sampling over the next two years (after half a year, one year, one and a half years, two years). Compared to the data before the earthquake [2], we found 10-85% increase of ^{3}He/^{4}He ratio of hot spring gas in five hot springs after the earthquake, suggesting that the upwelling of aqueous fluid containing mantle fluid [1]. The ^{3}He/^{4}He ratios show a very large change that becomes steady after half a year and increases slowly as a whole in this region following the earthquake. In addition, in order to investigate the diurnal variation of helium isotopic ratios, hot spring water was collected every hour or every three hours for 24 hours in Yabitsu hot spring. The diurnal variation of the ^{3}He/^{4}He ratio is only about 3%. The ^{3}He/^{4}He ratios in this region show a significant change after a week, become steady after half a year, and increase slowly as a whole thereafter. This variation is much larger than the diurnal variation, indicating that a gradual upwelling of magmatic fluid still continues in this region.

[1] Horiguchi and Matsuda (2008) *Geochem. J.,* **42**, e1-e4. [2] Horiguchi *et al*. (2010) *Island Arc,* **19**, 60-70.

https://doi.org/10.1180/S0026461X00006502 Published online by Cambridge University Press

Extensive denitrification in the subsurface of the Oak Ridge Site, Tennessee

J. HORITA[1]*, M.E. CONRAD[2], N. YOSHIDA[3], M. BILL[2], J. KOSTKA[4], D.B. WATSON[5], S. BROOKS[5] AND P. JARDINE[6]

[1]Texas Tech University, Department of Geosciences, Lubbock, TX 79409-1053 (*correspondence: juske.horita@ttu.edu)
[2]Lawrence Berkeley National Laboratory, Berkeley, CA
[3]Tokyo Institute of Technology, Tokyo, Japan
[4]Georgia Institute of Technology, Atlanta, GA
[5]Oak Ridge National Laboratory, Oak Ridge, TN
[6]University of Tennessee, Knoxville, TN

The operation of a waste disposal facility on the Oak Ridge Reservation in East Tennessee has resulted in extensive subsurface contamination. Groundwater is highly contaminated near the source with U (>60 ppm), Tc (>40,000 pCi/L), nitrate (up to 40,000 ppm), and acidity (pH range of 3 to 7). Due to high groundwater nitrate concentrations at this site, nitrate is often the most abundant electron acceptor available for microbial growth in the subsurface, and denitrifying bacteria have been shown to predominate over the microbial communities. Significant quantities of gases (CO_2, CO, H_2 and CH_4) indicative of microbial activity were also detected in groundwater, including high concentrations of N_2O (up to 4% of gases) and excess N_2.

The dissolved nitrates are intimately linked to the fate of uranimum contamination via redox cycles. To quantify the relative roles of dilution, assimilatory uptake, and denitrification as mechanisms of nitrate attenuationan, an integrated hydrobiogeochemical study was conducted. The fate of nitrate and denitrification products (N_2O and N_2) were investigated by means of mass-balance and stable isotope techniques. The degree of denitrification is up to 13% or greater, and systematic variations in $\delta^{15}N$ were observed (NO_3>N_2O>excess N_2) with decreasing concentrations of dissolved nitrates. Large negative isotope fractionations were calculated during denitrification: -30's and -40's of ‰ for $\delta^{15}N$ and $\delta^{18}O$, respectively. Large isotopic variations of the intermediate N_2O, including site-specific $\delta^{15}N$ fractionation, also provide insights into extensive denitrification processes of dissolved nitrate in groundwater at the site.

Funded in part by Subsurface Biogeochemical Research Program, U.S. Department of Energy under contract DE-AC05-00OR22725, Oak Ridge National Laboratory, managed by UT-Battle, LLC.

Isotopic fractionation of cadmium into calcite

T.J. HORNER*, R.E.M. RICKABY AND G.M. HENDERSON

Dept. Earth Sciences, University of Oxford, OX1 3AN, UK (*correspondence: Tristan.Horner@earth.ox.ac.uk)

Isotopic analyses of dissolved Cd (cadmium) in surface seawater have recently shown great potential as a new proxy for disentangling phytoplankton Cd (and by inference 'nutrient') utilization from abiotic processes, such as ocean mixing. Extending this information into the past requires the signal to be captured and faithfully preserved in a suitable sedimentary archive. However, the importance of environmental factors and the controls they may have on Cd isotopic fractionation into such archives, particularly calcite, remain poorly understood.

To this end, we performed controlled inorganic $CaCO_3$ precipitation experiments in artificial seawater solutions to understand such environmental controls. We precipitated calcite under different growth rates, temperatures, salinities, and ambient [Mg^{2+}], measuring isotopic compositions using double spike MC-ICPMS.

We find that the isotopic fractionation factor for Cd into calcite, $\alpha_{Cc\text{-}Cd}$, in artificial seawater solutions is always less than unity (i.e. light isotopes of Cd preferred in the reaction product) and appears to be insensitive to the majority of environmental factors studied. The magnitude of the fractionation factor shows no response to temperature or Mg concentration; or growth rate across the ranges studied.

However, no isotopic offset was recorded between the growth solution and carbonate when precipitated from de-ionized water, in contrast to those precipitated from artificial seawater solutions. This and other observations lead us to conclude that the cause of isotopic fractionation is related to kinetic isotope effects during the largely unidirectional incorporation of Cd at the mineral surface. This process is modulated by increased ion blocking of surface sites as salinity – and therefore the concentration of impurity ions – increases.

With the isotopic constraints from our experiments, we evaluate the role of $CaCO_3$ productivity in surface waters in the modern oceanic Cd budget, comparing with phytoplankton physiological Cd utilization. We conclude that carbonates are unlikely to play a significant role in setting the Cd isotope composition of seawater, although they are likely to be a minor sedimentary sink (and thus temporal archive) because of the low solubility of $CaCO_3$-bound Cd.

https://doi.org/10.1180/S0026461X00006502 Published online by Cambridge University Press

REE abundances in CAIs from Rumuruti chondrites

M. HORSTMANN[1]*, A. BISCHOFF[1] AND J. BERNDT[2]

[1]Institut für Planetologie, WWU Münster, Germany (*correspondence: marianhorstmann@uni-muenster.de)
[2]Institut für Mineralogie, WWU Münster, Germany

Introduction

Ca,Al-rich inclusions (CAIs) are the oldest objects known in our solar system (~4.56 Ga; [1]). Recently, CAIs from Rumuruti (R) chondrites were studied in great detail [2-4] but only limited trace element data [5] exist. The latter are important to reveal information on the formation processes of individual CAIs. So far, the rare earth element (REE) abundances of 16 inclusions have been determined by LA-ICP-MS.

Samples and Analytical Techniques

Sixteen randomly selected CAIs from the R chondrites NWA 753 and 1476 as well as Dar al Gani 013 described by [2-4] were measured with a ThermoFisher Element 2 single collector ICP-MS coupled to a laser ablation (New Wave 193 nm excimer system) unit. NIST SRM-612 was used as an external standard and BCR2-G for additional verification of precision and accuracy of the analyses. Data was processed with Glitter using Ca or Mg as internal standard (EPMA data by [4]).

Results

The CAIs show REE enrichments typically between ~5 and ~30 × CI for most elements. Four inclusions were found that exhibit fractionated patterns similar to Group II [e.g., 6]. The other twelve patterns are generally flat (Groups I (2 inclusions), III (1), V (4); [e.g., 6]) with variable abundances of the most volatile REEs (Eu, Yb) or display flat patterns with negative Eu anomalies (5 inclusions). The two CAIs of Group I have almost chondritic REE abundances.

Discussion

The REE patterns can be explained by different processes, including fractional condensation and (in)complete equilibrium condensation from a gas of solar nebula composition. However, distillation might also be a mechanism to account for the depletions of the volatile elements observed.

[1] Amelin *et al*. (2002) *Science* **297**, 1678-1683. [2] Rout & Bischoff (2008) *MAPS* **43**, 1439-1464. [3] Rout *et al*. (2009) *GCA* **73**, 4264-4287. [4] Rout *et al*. (2010) *Chemie der Erde* **70**, 35-53. [5] Horstmann *et al*. (2010) *MAPS* **45**, A84. [6] Mason & Martin (1977) *Smiths. Contr. Earth Sciences* **19**, 84-95.

Employment of the nanoscaled-SIMS in soil science

C. HÖSCHEN*, K. HEISTER , C. W. MÜLLER AND I. KÖGEL-KNABNER

Lehrstuhl für Bodenkunde, Technische Universität München, 85350 Freising-Weihenstephan, Germany (*correspondence: hoeschen@wzw.tum.de)

The NanoSIMS technique is needful for investigating soils systems which are inevitable structurally heterogeneous down to submicron scale. Clay minerals, iron oxides, aluminium (hydr)oxides and charcoal are considered as major components controlling the formation of soil interfaces and aggregates which are relevant for the sorption of organic matter.

The high lateral resolution achieved with the NanoSIMS 50L instrument makes possible elemental localisation at such small spatial ranges and offers inside views into the complex elemental structural architecture of soil samples.

Allowing the simultaneous detection of up to 7 ion species by NanoSIMS it is possible to obtain information about elements characteristic for the coexistent soil constituent phases: organic matter (carbon, nitrogen, sulphur) and minerals (oxygen, silicium, aluminium, iron). Accurately measuring these organic matter-minerals associations has the need of solving isobaric mass interferences.

The good transmission at high mass resolution power of the nano-scaled SIMS technique is necessary to image processes playing an important role in soil science and taking place at small spatial scales and low concentrations in soils.

We discuss the employment of the NanoSIMS 50L instrument at TU München in soil science. We have explored the potentials of this new technique for the study of model compounds (clay minerals, iron, aluminium (hydr)oxides and charcoal) of incubated mixtures of known composition, i.e. artificial soils.

We present examples of mass interferences occuring in soil investigations solved by the NanoSIMS technique. At mass number 43 high mass interferences are occuring which are given from elements associations like $^{12}C^{31}P$, $^{27}Al^{16}O$, $^{12}C^{16}O^{15}N$, $^{30}Si^{12}C^{1}H$. Their differenciation needs an MRP of about 16000. By choosing the right beam deflection in front of the detector it is possible to measure these masses independently.

https://doi.org/10.1180/S0026461X00006502 Published online by Cambridge University Press

Zn-labeled montmorillonite RN sorption reversibility studies

P. HÖSS[1]*, L. TRUCHE[2], M. BOUBY[1], J. BRENDLÉ[3], F.M. HUBER[1,4] AND T. SCHÄFER[1,4]

[1]Institute for Nuclear Waste Disposal (INE), Karlsruhe Institute of Technology (KIT), Postfach 3640, 76021 Karlsruhe, Germany (*correspondence: p.hoess@kit.edu)
[2]G2R/UMR/CNRS, Univ. Henri Poincaré, 54500 Nancy, France
[3] Lab. Mat. Mineraux, UMR CNRS 7016, Univ. Haute Alsace, 68093 Mulhouse, France
[4] Institute of Geological Sciences, Hydrogeology Group, Freie Universität Berlin, 12249 Berlin, Germany

Compacted bentonite will be used in the context of a deep geological high level nuclear waste disposal as geo-engineered barrier and might be eroded in contact with water conducting features having low salinity (glacial melt water intrusion scenario) forming colloidal/nanoparticular phases. The potential role of these generated colloids enhancing radionuclide (RN) mobility is *inter alia* depending on the RN sorption reversibility and the colloid attachment probability.

Former laboratory batch studies on the sorption/ desorption of RN in the ternary system RN–fracture filling material (FFM)–FEBEX bentonite revealed relative high uncertainties in the measured bentonite colloid concentrations based on the ICP-MS Al signal indicative for structural Al [1,2] and the Al concentrations found in the natural Grimsel Groundwater (GGW; pH 9.6; ionic strength 1.2 mM) used as background electrolyte. The use of Zn-labeled montmorillonite, where Zn occupies the Mg positions within the octahedral layers of the clay mineral [3] is considered as a good way to circumvent these analytical drawbacks. Detailed studies on the characteristics (size, morphology and stability) of Zn-montmorillonite colloids released into GGW using ICP-MS, PCS, AFM, AsFlFFF and LIBD showed a very good agreement of their properties compared to those of the FEBEX bentonite derived montmorillonite colloids. Therefore, Zn-montmorillonite was chosen to carry out compara-tive batch type studies. We will present results of the ongoing sorption/desorption laboratory experiments in the ternary system RN (^{243}Am(III), ^{232}Th(IV), ^{242}Pu(IV), ^{237}Np(V), ^{233}U(VI) and ^{99}Tc(VII))–FFM (1-2 mm size fraction from the Grimsel Test Site (GTS, Switzerland)–Zn-montmorillonite.

[1] Schäfer *et al*. (2004) *Radiochim. Acta* **92**, 731-737. [2] Huber *et al*. (2011) *Appl. Geochem*. (in review). [3] Reinholdt *et al*. (2001) *Eur. J. Inorg. Chem*. **2001**, 2831-2841.

Lithium isotope fractionation during extreme weathering of basalt in Hainan island, South China

KEJUN HOU[12], YANHE LI[1] AND DEFANG WAN[1]

[1]MRL Key Laboratory of Metallogeny and Mineral Assessment, Institute of Mineral Resources, Chinese Academy of Geological Sciences, Beijing 100037, China; (Kejunhou@126.com)
[2]China University of Geological Sciences (Beijing), Beijing 100041 China

Many isotope systems are sensitive to weathering processes, including radiogenic isotopes like those of Sr and Nd and stable isotopes, such as those of Li and Mg. Lithium is a fluid-mobile, moderately incompatible trace element having two isotopes with ~16% relative mass difference. Like other alkali metals, lithium is present on the Earth only in the +1 valence state, so its isotopic composition is not influenced by redox reactions. Moreover, lithium is not a nutrient and does not participate in biologically mediated reactions. These characteristics make lithium isotopes potentially excellent tracers of near-surface fluid–rock reactions (Rudnick *et al*., 2004).

Lithium and Lithium isotopes of the samples from from a laterite profile developed from Neogene basalts in the northern region of Hainan Island, South China were detail measured. The results show a trend of decreasing δ^7Li with increasing weathering intensity. These observations are consistent with leaching of Lithium via Rayleigh distillation during progressive weathering. The δ^7Li was extremely low in the middle (2-3m) profile, this may indicate there has an paleo-water profile.

https://doi.org/10.1180/S0026461X00006502 Published online by Cambridge University Press

Tracer application of chemical speciation of ^{129}I in Arctic seawater

X.L. HOU[1,3]*, M.Y. LUO[1,3], Y.K. FAN[1],[3], J. P. GWYNN[2], M. KARCHER[4], A. ALDAHAN[5] AND G. POSSNERT[6]

[1]Risø National Laboratory, Technical University of Denmark, DK-4000 Roskilde, Denmark, (*correspondence: xiho@risoe.dtu.dk)

[2]Norwegian Radiation Protection Authority, Fram Centre, Tromsø, 9296, Norway

[3]Xi'an AMS center, Institue of Earth Environment, CAS and Xi'an Jiaotong University, Xi'an, China

[4]O.A.Sys – Ocean Atmosphere System GmbH, Hamburg, Germany and Alfred Wegener Institute for Polar and Marine Research, Bremerhaven, Germany

[5]Department of Earth Science, Uppsala University, SE-758 36 Uppsala, Sweden

[6]Tandem Laboratory, Uppsala University, SE-751 21 Uppsala, Sweden

Anthropogenic ^{129}I discharged from European reprocessing plants has widely dispersed in the Nordic waters including the Arctic. Due to the high solubility and long residence time of iodine in seawater, anthropogenic ^{129}I has become an ideal oceanographic tracer for investigating transport pathways and the exchange of water masses. Iodine is a redox sensitive element, existing mainly as iodide and iodate, with minor amounts of organic iodine in marine water. The chemical speciation analysis of ^{129}I in seawater can be used not only to investigate the marine geochemical cycle of iodine, but any variation in the chemistry of a particular marine system.

Depth profiles of seawater were collected from 60 locations in the Arctic in four Arctic expeditions during 2005-2008. Collected seawater samples were stored in plastic bottles without any treatment until analysis. A volume of 1 l of each sample was used for the chemical separation of iodine species. Iodide and iodate were separated using anion exchange chromatography. The separated iodine species, as well as total iodine were separated from the water matrix component and all interfering elements by solvent extraction and were then precipitated as AgI for measurement of ^{129}I by accelerator mass spectrometry. The ^{127}I of different species separated from each water sample was measured using inductively coupled plasma mass spectrometry. The analytical results on the concentrations of chemical species of ^{129}I and ^{127}I as well as ^{129}I/^{127}I ratios of different species of iodine for these water samples will be presented. The spatial variations of ^{129}I, ^{127}I and their speciation in seawater in the Arctic will be derived. Sources and transport pathways of ^{129}I in the Arctic, the transformation process of chemical species of iodine and their mechanism will be discussed.

Colloidal processes in gold transport and deposition

R M HOUGH

CSIRO Earth Science and Resource Engineering, Perth, Australia, (robert.hough@csiro.au)

New studies of gold are revealing how metallography is a key component of our understanding of the deposition of precious alloys in primary ore systems. Alluvial gold nuggets once thought to be secondary in origin have now been shown to be the erosional residue of hypogene systems, i.e. primary. A new frontier in both hypogene and supergene systems is the nano domain. In hypogene settings gold at all scales can be metallic and particulate as has been directly observed in refractory ores, or the so called "invisible gold" in pyrite and arsenopyrite. Such nanoparticulate and colloidal transport of gold is a viable mechanism of dispersing the gold during weathering of ore deposits. Deposition of supergene (secondary) gold in the regolith is a product of the dissolution of hypogene gold from the a primary deposit (hosted by sulphides or quartz), transportation in solution and then re-precipitation elsewhere in the weathering profile. The natural nanoparticulate fraction of Au in these environments probably occurred as a colloidal suspension before final deposition as metallic particles and raises the question of how common a process is this in all gold depositional settings? These gold nanoparticles, long known about in materials sciences and manufacturing have now been seen in these natural environments as pure Au nanotriangles, hexagons and spheres. The destabilisation of the colloid will produce rapid deposition of the Au, potentially through evaporation in a single drying even meaning Au deposition can be a rapid event in the critical zone. The regularly heterogeneous distribution, trace concentration and nanoparticulate grain size of metallic gold in all ore systems has made it difficult for direct observation. Yet, it is critical to be able to establish a broad view of the microstructural/microchemical residence of the actual gold in a given sample. New generation element mapping (e.g. Maia on the Australian Synchrotron) tools now allow us to 'see' this invisible gold component and detect is wider distribution for the first time and to probe its chemistry and controls on deposition. These studies have the potential to provide a new approach and view of the formation, deposition and provenance history of the metal in all gold deposits.

https://doi.org/10.1180/S0026461X00006502 Published online by Cambridge University Press

Experimental and numerical investigation of focused flow through porous media due to mineralization

J. HOUGHTON[1] AND L. URBANO[2]

[1]Environmental Science, Rhodes College, USA (houghtonj@rhodes.edu)
[2]Lamplighter Montessori School, Memphis, TN, USA (lurbano@lamplighterschool.org)

The chemical input to the world's oceans from subsurface microbial biofilms in mid-ocean ridge hydrothermal systems has been difficult to quantify due to their inaccessibility. Results from experiments in a novel flow-through experimental apparatus using non-invasive monitoring of mixing via infrared imaging coupled to a 2D solute transport model allows the evaluation of changes in permeability, hydraulic conductivity and flow velocity during mixing of two end-member fluids within porous media. Initial Tests were conducted using instantaneous precipitation of amorphous Fe(III) oxyhydroxide upon mixing NaOH (1.2M) with $FeCl_3$ (0.4M) at the range of temperatures tested (25 to 40°C), according to the reaction:

$$3NaOH + FeCl_3 = FeOOH + 3NaCl + H_2O$$

Results indicate clear alteration of fluid flow vectors after 4.3 minutes of mixing, corresponding to the precipitation of 0.059 g FeOOH and a reduction in bulk porosity of 11.6% over only 35% of the flow cell. The NaOH solution was subsequently focused through a high permeability zone at double the starting velocity as Fe(III) precipitation increasingly blocked flow until complete blockage of all fluid outflow due to mineral precipitation occurred at 8 minutes. The corresponding bulk chemistry of the outflow changed from complete titration of the NaOH solution initially, to an excess of 9.56 mM/s in the outflow at the time of clogging as the availability of $FeCl_3$ becomes limiting. This technique successfully quantifies mm-scale changes in permeability due to amorphous FeOOH, a biofilm analogue, allowing non-invasive monitoring in real-time on spatial scales relevant to microbial biofilms.

F,Cl-rich mineral assemblages from burned spoil-heaps in the Rosice-Oslavany coalfield, Czech Republic

S. HOUZAR[1]*, P. HRŠELOVÁ[2], J. CEMPÍREK[1] AND J. SEJKORA[3]

[1]Moravian Museum, Brno, Czech Republic (*correspondence: shouzar@mzm.cz)
[2]Palacký University, Olomouc, Czech Republic
[3]National Museum, Prague, Czech Republic

Unusual Si-Al deficient and F,Cl-rich oxide-sulphosilicate-sulphate mineralization was found on burned spoil-heaps at Oslavany and Zastávka in the Rosice-Oslavany coalfield, Czech Republic. The assemblage typically forms irregular, zoned nodules ~5–15 cm in size enclosed in the common pyrometamorphic material of the piles, i.e. hematite-rich clasts, paralavas and clinkers. Their cores are usually formed by fine-grained mixture of gypsum and brucite with relics of anhydrite and periclase, respectively; locally, portlandite was found. The cores are rimmed by (or intersected by veinlets of) dark gray aggregates of medium- to fine-grained mixture of gypsum, anhydrite, Mn-rich srebrodolskite (X_{Mn}~0.4), magnesioferrite, unnamed $Ca_4(Mn,Fe)_2O_7$, and F,Cl-rich silicates that commonly replace anhydrite and gypsum. Prevailing F,Cl-rich minerals are fluorellestadite and Cl-rich hydroxylellestadite (X_{Cl}≤0.25). Rarely, inclusions of subhedral crystals of Fe,Si,Cl-rich mayenite (≤3.2 apfu Fe^{3+}, ≤2.2 apfu Si, ≤4.6 apfu F+Cl) were found in ellestadite at both localities; in Oslavany, it is associated with cuspidine. In Zastávka, assemblage with fluorite and F,Cl-rich Ca-silicates (rondorfite and kumtyubeite replaced by ellestadite and bultfontainite / cuspidine-like mineral) was rarely encountered. Surface and cavities of the nodules are sometimes covered by Mg-sulfates (epsomite-kieserite) and needles of gypsum. The observed oxide-sulfosilicate-sulfate assemblage is a high-grade pyrometamorphic product of the original dolomite-anhydrite-gypsum protolith, at T_{min} > 800°C. The most probable source of F is a thermal decomposition of fluorite and micas while chlorine was most probably released from the organic matter.

Burning spoil-heaps in the Rosice-Oslavany coalfield are characterized by high-grade pyrometamorphism followed by multi-stage mineral assemblages formed at lower temperature [1]. Similar oxide-sulfosilicate-sulphate assemblages were rarely found in nature e.g. in marble xenoliths in ignimbrites [2] or tephrites [3], and also on burning coal spoil-heaps [4].

[1] Dokoupilová *et al*. (2007) *Min Mag* **71,** 443-460. [2] Galuskina *et al*. (2009) *Am Mineralogist* **94,** 1361-1370. [3] Baumgärtl and Cruse (2007) *Aufschluss* **58,** 257-400. [4] Sharygin (2010) *Proc. ICCFR (Berlin)* 162-170.

https://doi.org/10.1180/S0026461X00006502 Published online by Cambridge University Press

A novel technique for F/OH apatite series synthesis and early results on thermodynamic mixing properties of fluor-hydroxylapatite solid solutions

GUY L. HOVIS

Department of Geology & Environmental Geosciences, Lafayette College, Easton, PA 18042 USA (*correspondence: hovisguy@lafayette.edu)

Synthesis and Unit-Cell Data

We have used a novel technique, to be described at the Goldschmidt Conference, to synthesize fluorapatite from a hydroxylapatite end member. In turn, these F and OH apatite end members have been utilized to synthesize multiple intermediate compositions along the F-OH apatite join. Employing NIST 640a Si as an internal standard, X-ray powder diffraction data were collected for all series members and, with the software of Holland and Redfern [1], utilized to refine unit-cell dimensions. The resulting data for these hexagonal crystalline solutions indicate that the "a" unit-cell dimension decreases linearly across the series as fluorine content increases, while the "c" dimension is nearly constant. Unit-cell volumes are linear, or nearly so, with composition, indicating volumes of mixing that are either small or non-existent.

Solution Calorimetric Results

Heats of solution have been measured at 50 °C in 20.0 wt% HCl under isoperibolic conditions for all F-OH apatite series members. Utilizing a 50-mg sample size in all experiments, calorimetric data collected prior to the abstract deadline for this conference show enthalpies of solution that behave linearly with composition for the F-rich half of the series, while data for OH-rich compositions appear to show small negative enthalpies of mixing. Overall, calorimetric results indicate that there is no enthalpy barrier to complete mixing between the hydroxylapatite and fluorapatite end members. We anticipate completion of the calorimetric study prior to the Goldschmidt Conference, but even at this time the nearly ideal thermodynamic behaviour of both volume and enthalpy is clear. Present results extend the thermodynamic data base for the apatite system [$Ca_5(PO_4)_3$(F,Cl,OH,0.5CO_3)] to compositions beyond the F-Cl apatite binary (Hovis and Harlov [2]; Schettler, Gottschalk and Harlov [3]).

[1] Holland and Redfern (1997) *Mineralogical Magazine* **61**, 65–77. [2] Hovis and Harlov (2010) *American Mineralogist* **95**, 946-952. [3] Schettler, Gottschalk and Harlov (2011) *American Mineralogist* **96**, 138-152.

Efficient cycling of Particulate Organic Carbon through orogenic systems

N. HOVIUS[1], A. GALY[1], R.G. HILTON[2], R.B. SPARKES[1], S.-J. KAO[3], AND J. LIU[4]

[1]Department of Earth Sciences, University of Cambridge, UK. (nhovius@esc.cam.ac.uk)

[2]Department of Geography, Durham University, UK. (r.g.hilton@durham.ac.uk)

[3]Research Center for Environmental Changes, Academia Sinica, Taipei, Taiwan. (s.j.kao@gate.sinica.edu.tw)

[4]Institute of Marine Geology and Chemistry, National Sun Yat-Sen University, Kaohsiung, Taiwan.

High erosion rates on convergent margins drive a transfer of Particulate Organic Carbon (POC) from standing biomass and soils into sedimentary basins. These basins are prone to rapid tectonic recycling, entraining buried POC in mountain building, exhumation and renewed erosion. The role of mountain building in the global carbon cycle depends, in part, on the rate of remineralization of entrained or fossil POC during exhumation and erosion. We have determined the geological resilience of POC in Taiwan, a small and fast eroding mountain belt in the west Pacific rim.

The flux weighted average of POC in 11 Taiwanese comprises a mixture of ~70% fossil POC and ~30% recently photosynthesised POC from the terrestrial biosphere. Measured fossil POC yields from Taiwan ranged from about 10 to 250 tC $km^{-2}yr^{-1}$. Efficient transfer of this material involved supply of about 1.3 X 10^6 t yr^{-1} of fossil POC exhumed in Taiwan to the ocean, with <15% loss due to weathering in transit. Nearby marine sediments show a positive trend between $\Delta^{14}C_{org}$ and $\delta^{13}C_{org}$ which is consistent with a mixture of the known terrestrial input and recent marine organic carbon. This indicates that fossil and non-fossil terrestrial POC is efficiently buried offshore Taiwan.

Plio-Pleistocene marine sediments have been exhumed in the frontal ranges of west Taiwan. These sediments contain first cycle fossil POC and graphitized carbon harvested from bedrock of the Taiwan Central Range. Peak metamorphic conditions in the Taiwan orogen have been insufficient to form highly ordered graphite found in the frontal ranges. Instead, this may have originated in an older orogeny elsewhere in east Azia before entrainment in Taiwan. Presence of this graphite in recent hyperpycnal deposits off SW Taiwan suggests that POC can survive multiple cycles of burial, exhumation and erosion. Resilience of fossil organic carbon during orogenic cycling in coastal mountain belts may enhance long-term storage of carbon in Earth's lithosphere.

https://doi.org/10.1180/S0026461X00006502 Published online by Cambridge University Press

Mineralogical study of arsenic carrier in coal combustion by-products of Kyjov-Poša impoundment (Slovakia)

R. HOVORIČ[1]*, Ľ. JURKOVIČ[2] AND E. HILLER[2]

[1]Department of Mineralogy and Petrology, Comenius University, Bratislava (*correspondence: hovoric@fns.uniba.sk)
[2]Department of Geochemistry, Comenius University, Bratislava (jurkovič@fns.uniba.sk, hiller@fns.uniba.sk)

The annual production of the coal combustion by-products (hereinafter CCB's) plays widely significant role as the anthropogenic arsenic resource [1, 2].

Previous research in the Kyjov-Poša locality well identified impoundment itself as the source of numerous organic and inorganic pollutants [3, 4, 5]. Downstream aquatic system which receives CCB's storage leachate contains elevated concentration of As exceeding the maximal allowed concentration for ground water after governmental regulation 296/2005 (<0.03 mg/l, Slovak Republic).

CCB's deposit stores circa 4.25 milion tons of ash with average As content 461 mg/kg (34 samples), thus 1960 tons of As in total.

The present study clarify As pathways after brown coal burning through storage deposit into the aquatic system. Realgar and orpiment rich coal after desulfurization in high-pressure boilers create As_2O_3 (gas?) as the main As (III) carrier that precipitate on the CCB's particle surfaces in the form of arsenolite and claudetite. Moreover, it is observed that arsenic oxidation state changes from tri-valent to penta-valent form linked with arseniosiderite crystalization. Solubility of arsenolite and claudetite in water seems to be dominant controlling factor of the arsenic mobility in studied site.

[1] Henke (2009) Willey, 291-297. [2] Reinmann *et al*. (2009) *Appl Geochem* **24**, 1147-1167. [3] Hiller *et al*. (2009) *Appl Geochem* **24**, 2175–2185. [4] Hiller *et al*. (2009) *J. Hydro. Hydromech* **57**, 3, 200–211. [5] Jurkovič *et al*. (2006) *Slov. geol. mag* **12**, 1, 31–38.

Mixed-habit diamonds: Evidence of a specific mantle fluid chemistry?

D. HOWELL[1]*, W.L. GRIFFIN[1], S.Y. O'REILLY[1], C. O'NEILL[1], N. PEARSON[1], S. PIAZOLO[1], T. STACHEL[2], R. STERN[2] AND L. NASDALA[3]

[1]GEMOC, ARC National Key Centre, Macquarie University, Sydney, NSW 2109, Australia (*correspondence: daniel.howell@mq.edu.au)
[2]CCIM, Earth and Atmospheric Sciences, University of Alberta, Edmonton, AB, T6G 2E3, Canada
[3]Institute of Mineralogy and Crystallography, University of Vienna, Althanstr. 14, 1090 Wien, Austria

Mixed-habit diamonds are a relatively understudied subset of samples, considering the amount of research that has been carried out on these vessels from the mantle. They exhibit periods of growth during which they were bound by two surface forms [1]; smooth octahedral facets, along with hummocky, non-facetted "cuboid" surfaces whose mean orientation is {100} [2]. This type of diamond is commonly referred to as *star* or *centre-cross*, because the cuboid sectors have a much darker appearance due to abundant graphite inclusions (Figure 1). However, for unknown reasons, cuboid sectors do not always contain these graphite inclusions. This means that occurrence of this type of diamond is likely under-reported simply as it is not always visible.

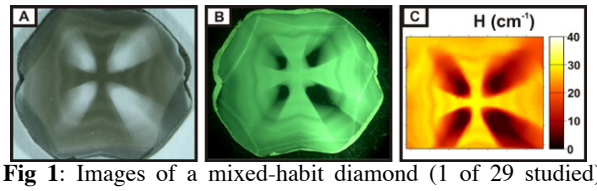

Fig 1: Images of a mixed-habit diamond (1 of 29 studied), under (A) visible light, (B) UV, & (C) IR map showing H concentration.

Mixed-habit diamonds have a number of unique characteristics (i) high nitrogen concentrations in both O and C sectors (higher in O than C), (ii) high hydrogen concentrations in the C sectors only (iii) low levels of nitrogen aggregation (iv) anomalously low platelet concentrations in the C sectors (v) vivid green CL that highlights an extremely complex growth history. We present a study that utilizes a holistic analytical approach (IR mapping, CL imaging, CL spectroscopy, SIMS C-isotope, Raman, EBSD) to identify all of these unique characteristics and understand them within the context of diamond growth. This will provide insights into the chemistry of the mantle fluids involved in this type of diamond growth.

[1] Frank (1967) *Proc. Int. Industrial Diamond Conf.*, 119-135. [2] Lang (1974) *Proc. R. Soc. Lond.*, ***A*. 340**, 233-248.

https://doi.org/10.1180/S0026461X00006502 Published online by Cambridge University Press

Tin-bearing skarns with As mineralization at the south-eastern margin of the Bohemian Massif

V. HRAZDIL*, S. HOUZAR AND J. CEMPÍREK

Moravian Museum, Brno, Czech Republic
(*correspondence: vhrazdil@mzm.cz)

Rare but geochemically significant tin mineralization occurs in calc-silicate rocks (unzoned skarns) in marbles at the south-eastern margin of the Bohemian Massif (Svratka Unit); it is locally associated with arsenic and boron mineralization. The three stage origin of the skarn assemblage commenced by high-temperature reactions in a Fe-poor system, resulting in diopside, grossularite, wollastonite and clinozoisite. During the second stage, fluid infiltration introduced Fe, Sn, As, Bi and locally also B and F in the system, producing Sn-rich titanite and malayaite, Sn-bearing andradite ($Adr_{85-90}Grs_{10-13}$; 1.2-2.4 wt.% SnO_2), löllingite, As-bearing fluorapatite (≤12.24 wt.% As_2O_5), As,B-rich vesuvianite (≤1.97 wt.% As_2O_5; ~1.96 wt.% B_2O_3), bismuth and rare nordenskiöldine and fluorite. The third, retrograde stage caused alteration of the primary phases and produced e.g. secondary cassiterite, stokesite or datolite.

The infiltration of fluids modified the system evolution to the conditions with high fO_2, $a(H_2O)$ and locally elevated a(F) and a(B). Initial tin storage in the Sn-rich titanite and the malayaite as the earliest phases of skarn evolution [cf. 1] was followed by subsequent exsolution of cassiterite from malayaite and corrosion of primary phases. Distribution of As and Sn during following contemporaneous crystallization of silicates (Sn-rich andradite, As,B-rich vesuvianite), phosphates (As-rich fluorapatite) and borates (nordenskiöldine) was constrained also by structures of individual phases rather than by the P-T-X conditions (Tmin > 300°C, elevated activity of fluids) alone. Residual As in the fluid produced löllingite.

The occurrences of tin-bearing calc-silicate rocks are spatially bound to tourmaline orthogneisses with elevated contents of tin and fluorine [2,3]. The orthogneisses were earlier suggested being a source for Sn-anomalies in surrounding metapelites [3]. The tin skarns provide new evidence for metasomatic processes during the multistage metamorphic evolution of the area in a time span between late Cambrian and Carboniferous [4].

[1] Cempírek *et al*. (2008) *Min Mag* **72,** 1293-1305. [2] Houzar *et al*. (2006) *Acta Mus Moraviae* **91,** 3-77. [3] Němec (1979) *Z geol Wiss* **7,** 1437-1447. [4] Schulmann *et al*. (2005) *Am J Sci* **305,** 407-448.

Mid-latitude continental response to falling atmospheric P_{CO2} during the Eocene-Oligocene transition

MICHAEL T. HREN, N.D. SHELDON, STEPHEN GRIMES, M. COLLINSON, J. HOOKER, M. BUGLER AND K. LOHMANN

The Eocene-Oligocene transition represents one of the most dramatic and permanent changes in global climate during the Cenozoic and was driven in part, by large-scale changes in atmospheric CO_2. Marine sediments provide a detailed record of changes in surface and deep ocean temperature and the development of the Antarctic ice-sheet during this time interval, however continental records that can be correlated to the geomagnetic polarity timescale are relatively few. As a result, there is considerable uncertainty over the magnitude and rate of continental climate response to changing CO_2 levels and the feedbacks associated with these changes. We measured the Δ_{47} of aragonite shells from freshwater gastropods in Eocene to Oligocene sediments in the Hampshire Basin, Isle of Wight, UK, to reconstruct the change in mid-latitude (~50°N) Northern Hemisphere terrestrial temperature during this critical climate transition. Isotopologue data show that growing season water temperatures decrease by more than 15°C from 34.5 to 33 Ma, corresponding to a maximum decrease in mean annual air temperature of more than 10°C. This drop in mid-latitude continental temperature occurs in tandem with a large-scale declines in atmospheric CO_2. The magnitude of this continental temperature change during a near-halving of CO_2 levels indicates a strong regional climate sensitivity for this climate transition. These data highlight the importance of understanding the relationship between the marine record and the continental realm, and spatial heterogeneity in the climate-CO_2 feedback systems.

https://doi.org/10.1180/S0026461X00006502 Published online by Cambridge University Press

Separating the sources of ^{228}Ra to the open ocean with ^{223,224,226,228}Ra measurements in Loch Etive and the South-East Atlantic

Y.-T. HSIEH[1], W. GEIBERT[2,3], P. VAN BEEK[4] AND G.M. HENDERSON[1]

[1]Department of Earth Sciences, University of Oxford, Oxford, UK (yuteh@earth.ox.ac.uk)
[2]University of Edinburgh, Edinburgh, UK
[3]Scottish Association for Marine Science, Oban, UK
[4]LEGOS, Toulouse, France

Open ocean ^{228}Ra concentrations have been suggested as a proxy to constrain SGD fluxes – an important flux of nutrients and other dissolved species to seawater which is otherwise very difficult to constrain in magnitude [1]. Using open-ocean ^{228}Ra to assess SGD fluxes relies on being able to independently estimate the global fluxes of ^{228}Ra from other sources, particularly from shelf sediments and rivers. The magnitude of these fluxes has significant uncertainty.

We have provided new constraints on these fluxes with a suite of analysis on Loch Etive, a Scottish fjord. The loch has no known or expected groundwater input, and the fjordic overturning circulation usually restricts water exchange in the inner deep basin, with renewal events resetting the system to ocean values irregularly, about every 1 to 2 years. This allows us to assess ^{228}Ra flux from typical shelf sediments to the deep water, without groundwater inputs. At the same time, riverine input is assessed by measurement of the surface layer. We report ^{224}Ra and ^{223}Ra measurements by RaDeCC, and ^{228}Ra and ^{226}Ra measurements using a newly developed MC-ICP-MS approach [2]. Water in the deep loch shows higher ^{228}Ra concentrations than surface layer due to the sedimentary input, which is used to estimate ^{228}Ra sediment flux. Ra fluxes assessed from sediments and rivers in this setting are compared with values from the literature, which helps in the interpretation of the extant ^{228}Ra open ocean dataset.

We make use of understanding from Loch Etive in interpreting new preliminary data for the Ra quartet from the UK-GEOTRACES cruise in the SE Atlantic Ocean (GA10). Surface samples and depth profiles were collected for Ra using bottle and stand-alone-pumping and allow assessment of the fluxes of Ra, and hence information about the mixing transport of other elements to the open ocean.

[1] Moore *et al*. (2008) *Nat. Geosci*. **1**, 309-311. [2] Hsieh and Henderson (2011) *J. Anal. At. Spectrom*. DOI:10.1039/C1JA10013K.

Global distributions of mineral dust properties from SeaWiFS and MODIS: From sources to sinks

N. CHRISTINA HSU*, C. BETTENHAUSEN AND A. SAYER

NASA Goddard Space Flight Center, Greenbelt, MD, USA, (*correspondence: christina.hsu@nasa.gov, corey.bettenhausen-1@nasa.gov, andrew.sayer@nasa.gov)

The impact of natural and anthropogenic sources of mineral dust has gained increasing attention from scientific communities in recent years. Indeed, these airborne dust particles, once lifted over the source regions, can be transported out of the boundary layer into the free troposphere and can travel thousands of kilometers across the oceans resulting in important biogeochemical impacts on the ecosystem. Due to the relatively short lifetime (a few hours to about a week), the distributions of these mineral dust particles vary extensively in both space and time. Consequently, satellite observations are needed over both source and sink regions for continuous temporal and spatial sampling of aerosol properties.

With the launch of SeaWiFS in 1997, Terra/MODIS in 1999, and Aqua/MODIS in 2002, high quality comprehensive aerosol climatology is becoming feasible for the first time. As a result of these unprecedented satellite data records, studies of the radiative and biogeochemical effects due to dust aerosols are now possible. In this study, we will show the comparisons of satellite retrieved aerosol optical thickness using Deep Blue algorithm with data from AERONET sunphotometers over desert and semi-desert regions as well as vegetated areas. Our results indicate reasonable agreements between these two. These new satellite products will allow scientists to determine quantitatively the aerosol properties near sources using high spatial resolution measurements from SeaWiFS and MODIS-like instruments. The multiyear satellite measurements since 1997 from SeaWiFS will be compared with those retrieved from MODIS and MISR, and will be utilized to investigate the interannual variability of source, pathway, and dust loading associated with the dust outbreaks over the entire globe. Finally, the trends observed over the last decade based upon the SeaWiFS time series in the amounts of tropospheric aerosols due to natural and anthropogenic sources (such as changes in the frequency of dust storms) will be discussed.

https://doi.org/10.1180/S0026461X00006502 Published online by Cambridge University Press

Influence of dissolved organic matter for the precipitation of nanoparticulate metal sulfides

H. HSU-KIM[1]*, A. DEONARINE[1], A.P. GONDIKAS[1], T. ZHANG[1], A. MORRIS[1], G.R. AIKEN[2], J.N. RYAN[3]

[1]Duke University, Durham, NC, USA (*correspondance: hsukim@duke.edu)
[2]U.S. Geological Survey, Boulder, CO, USA
[3]Univerisity of Colorado, Boulder, CO, USA

Metal sulfide precipitation is traditionally viewed as a process that reduces the bioavailability of contaminant metals in anaerobic settings. Our previous work has demonstrated that dissolved natural organic matter (NOM) can alter the kinetics of ZnS and HgS precipitation, resulting in the stabilization of nanoparticles in aqueous solution. The structure and composition of dissolved NOM varies widely and will control NOM interactions with metal sulfides. Furthermore, we have shown that NOM-coated nanoparticles of HgS may be bioavailable to methyating bacteria. This process depends on the "age" of those nanoparticles. The aim of this work was to investigate how the composition of NOM influences the stability of ZnS and HgS nanoparticles as they nucleate and aggregate in water with dissolved NOM. We utilized dynamic light scattering to monitor relative growth rates of metal-sulfide-NOM particles. We tested nine different NOM isolates that were derived from several different surface waters and represented a wide range of NOM composition. The NOM was observed to reduce particle growth rates, depending on solution variables such as type and concentration of NOM, monovalent electrolyte concentration, and pH. The rates of growth increased with increasing ionic strength, indicating that observed growth rates primarily represented aggregation of charged metal-S-NOM particles. Furthermore, our results indicated that stabilization of nanoparticles occurred mainly with NOM fractions of the greatest molecular weight and aromatic carbon content. Future work will utilized a combination of methodologies (photon scattering, X-ray absorption spectroscopy) to probe the mechanism of metal-sulfide-NOM polymerization during early stages of precipitation. Overall, our results highlight that nanoscale products are formed from reactions between trace metals, sulfide and NOM and that these entities may exhibit unique reactivities.

Isotope evidence for regional precipitation characteristics in the Poyang Lake Basin

HU CHUN-HUA[1,2], ZHOU WEN-BIN[1,2]*, JIANG JIAN-HUA[1,2], GUO CHUN-JING[1,2] AND ZHANG PEI[1,2]

[1]School of Environmental and Chemical Engineering, Nanchang University, Nanchang, 330031, China (*correspondence: ouyangyinghui@126.com)
[2]Key Laboratory of Lake Poyang Environment and Resource Utilization, Ministry of Education, Nanchang University, Nanchang, 330029, China

The study of hydrogen-oxygen isotopes tracing of atmospheric precipitation have been extensively used in global water circulation, water vapor source and lake palaeoenvironmental reconstruction etc, and provided significant theoretical evidence for global climate change or region research [1-2]. Region complicated geography and climatic conditions show a great effect on content of precipitation isotope in previous research with obviously different features [3]. In these work, we study isotope compositions and its change pattern of precipitation effects of water circulation in Poyang Lake Basin and its differences compared with large scale or high-altitude area rainfall isotope features.

The results show that: (1) The value of $\delta^{18}O$ and δD show significantly seasonal variability that dry season is greatly higher than wet season, which mainly affected by oceanic air mass and polar continental air mass alternatively; (2) In 2008 and 2009, precipitation line equation in Poyang Lake Basin have the regional or basin features made a greatly differences with global, coastal regions and high-altitude area, whereas being similar to low-altitude of China inland like Fuzhou and Wuhan district, also demonstrated these areas being controlled by the same type of monsoon and water vapor source of rainfall; (3) Precipitation effect in the Poyang Lake Basin is mainly controlled by southeast and southwest monsoon, but southeast monsoon has been a larger contributor.

[1] Sebastian F. M *et al*. (2010) *Earth Planet. Sci. Lett*. **292**, 212-220. [2] Araguas L *et al*. (2000) *Hydrol Process* **14**, 1341-1355. [3] Zhang X P & Yao T D. (1994), *Journal of Glaciolgy and Geocryology* **3**, 202-210.

https://doi.org/10.1180/S0026461X00006502 Published online by Cambridge University Press

Molybdenite Re-Os and zircon U-Pb dating of the Mesozoic Xingjiashan Mo-W deposit in the Jiaodong Peninsular, Eastern China

FANG-FANG HU, HONG-RUI FAN, TING-GUANG LAN AND KUI-FENG YANG

Key Laboratory of Mineral Resources, Institute of Geology and Geophysics, Chinese Academy of Sciences, P.O. Box 9825, Beijing 100029, China (huff@mail.igcas.ac.cn)

The Xingjiashan deposit, located in the Jiaodong Peninsular in eastern China, is a typical skarn-type Mo-W deposit with an average Mo grade of 0.12 wt.% and W_2O_3 grade of 0.24 wt.%. The deposit is the only Mo-W one in the famous Jiaodong gold province, and temporally and spatially associated with intermediate to fine-grained Xingfushan adamellite porphyry. Mo-W mineralization is present mainly as veins, lenses and layers that are hosted by skarn.

LA ICP-MS U–Pb zircon age determinations of Xingfushan adamellite porphyry yielded a crystallization age of 162.1±1.4 Ma. Rhenium and osmium isotopes in molybdenite from the Xingjiashan deposit are used to determine the age of mineralization. Rhenium concentrations in molybdenite samples are between 3.2 and 7.8 μg/g. Analysis of seven molybdenite samples yields an isochron age of 162.9±2.7 Ma (MSWD=0.32). The W-Mo mineralization is therefore considered to be genetically related to adamellite porphyry emplacement in the Mesozoic. A low Re content of molybdenite in the ores indicates that the metal source was a crustal system. From these geochronological data and previously presented regional geological relationships, we propose that adamellite porphyry emplacement and Mo-W mineralization in the Xingjiashan mine resulted from an early stage of the subduction of the Paleo-Pacific plate beneath the North China craton.

This work was financially supported by Natural Science Foundation of China (40625010) and the Crisis Mines Continued Resources Exploration Project of China Geological Survey (20089930).

Contamination by polycyclic aromatic hydrocarbons (PAHs) in Tianjin rivers, China

J. HU[1]*, D. LIU[2,3], Y.L. ZHANG[1,2] AND G.P. ZHANG[1]

[1]Institute of Geochemistry, Chinese Academy of Sciences, Guiyang, Guizhou, PR China
(*correspondence: hujian@vip.skleg.cn)
[2]Graduate University of Chinese Academy of Sciences, Beijing, PR China
[3]Guangzhou Institute of Geochemistry, Chinese Academy of Sciences, Guangzhou, PR China

Tianjin is one of the most important industrial areas in northern China, and suffers from severe contamination of PAHs. Many rivers are located in the northeastern and south-western area of Tianjin city. Coal combustion, vehicle emission, coking industry, and biomass burning are the major contributors to PAHs pollution in the area. To understand the contamination status and behavior of PAHs in the river system, 72 water samples were collected from 12 major rivers in January 2008, and the levels of 16 priority PAHs in water and suspended particulate matter (SPM) samples were examined.

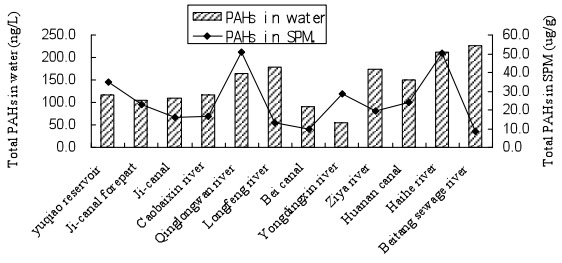

Figure 1: The contents of PAHs in water and SPM samples

The total concentrations of 16 PAHs varied from 25.1 to 131.1 ng/L in water, and from 0.13 to 213.8μg/g dry weight in SPM respectively (Fig.1). Two- to three-ring PAHs predominated in water samples of the study areas, and Nap was the most dominant. PAHs contents in SPM of the northern rivers were less polluted than those of the southern rivers. Predomination of low molecular weight PAHs suggests the relatively recent local source and coal combustion source of PAHs in the study area.

This work was supported by the National Natural Science Foundation of China (Grant No. 40703021 and 40721002).

Nucleation pathways and energetic controls during templated nucleation of calcite by MHA and MUA self-assembled monolayers

QIAONA HU[1,2]*, UDO BECKER[1], MIKE NIELSEN[2] AND JIM DE YOREO[2]

[1]University of Michigan, Dept. of Geological Sciences, Ann Arbor, MI 48105 (*correspondence: qiaona@umich.edu)
[2]Molecular Foundry, Lawrence Berkeley National Lab, Berkeley, CA 94720

Organic templates in living systems are believed to control nucleation rates and crystallographic orientations of nuclei. Self-assembled monolayers (SAMs) have been frequently used as a simple model to reproduce the function of natural templates. In particular, SAMs made of alkanethiol molecules have been demonstrated to effectively induce highly-oriented nucleation of calcium carbonate [1, 2].

Although a mechanistic understanding of templating requires knowledge of the thermodynamic and kinetic barriers, no experimental work has been done to quantify these factors. Moreover, the importance of indirect nucleation pathways via amorphous precursors during templating remains unresolved. The objective of this study is to use measurements of nucleation rates to determine the interfacial energies between template-directed calcite nuclei and 16-mercaptohexadecanoic acid (MHA) and 11-mercaptoundecanoic acid (MUA), and to determine whether nucleation occurs via the amorphous phase. The results reveal that (1) MHA and MUA both significantly reduce the effective surface energy of calcite from about 97 mJ/m2 in solution to about 45.3 and 52.7 mJ/m2 on MHA and MUA respectively, providing a thermodynamic basis for the strong capacity of MHA and MUA to promote calcite nucleation; and (2) at solute activities below the solubility limit of amorphous calcium carbonate, calcite forms directly.

[1] A. M. Travaille *et al*., (2002) *Adv. Mater*. **14**, 492. [2] Y.-J. Han, J. Aizenberg, (2003) *Angew. Chem. Int. Ed*. **42**, 3668.

Late Cenozoic history of deep water circulation in the western North Pacific: Evidence from Nd isotopes of ferromangnese crusts

RONG HU, TIAN-YU CHEN AND HONG-FEI LING *

State Key Lab for Mineral Deposits Research, School of Earth Sciences and Engineering, Nanjing University, Nanjing 210093, China (*correspondence: hfling@nju.edu.cn)

Despite the importance of deep ocean circulation in regulating the global climate, its past variations in the western North Pacific are still poorly understood. Nd isotopes of ferromanganese crusts have proven a good proxy for paleoceanic circulation changes. We obtained late Cenozoic Nd isotopic data of two ferromanganese crusts located near Mariana arc but at different water depths (MKD13: 1500m, MDD53: 2700m), and studied their implications for paleocirculation changes in this area. From early to late Miocene, Nd isotopic compositions of MDD53 remained stable. MDD53 was also characterized by the least radiogenic feature (Nd: -4.0 to -5.0) compared with crusts of similar water depths in the Miocene North Pacific. Afterward in the Pliocene Nd value of MDD53 increased sharply. In contrast, Nd isotopes of MKD13 became more and more radiogenic in the Miocene and were almost invariable afterwards. We interpret the continual increase in Nd of the shallower crust MKD13 as reflecting progressive closure of Indonesian Seaway in the Miocene, while the deep western boundary current originated from the Southern Pacific may have dominated Nd isotopes of the deeper crust MDD53 during the same time interval. The lack of Nd isotopic variation of MKD13 in the Pliocene indicates that there were no changes in Nd sources in the shallower water. Therefore the observed large shift to more radiogenic Nd isotopes of MDD53 in the Pliocene should not be caused by change in vertical input from shallower to deeper water. Instead, we suggest that the ventilation of deep southern component current along the studied water depth range (~2700m) may have evidently decreased in the early Pliocene.

This study was funded by the Chinese Association for Research of Oceanic Mineral Resources (DY-115-01-2-2) and the Education Ministry of China.

https://doi.org/10.1180/S0026461X00006502 Published online by Cambridge University Press

Noble gas isotopes of tungsten-tin polymetallic deposits in South China: Constraints on origins of ores and related granites

R.Z. HU*, X.W. BI AND G.H. JIANG

State Key Laboratory of Ore Deposit Geochemistry, Institute of Geochemistry, Chinese Academy of Sciences, Guiyang 550002, China
(*correspondence: huruizhong@vip.gyig.ac.cn)

South China is rich in tungsten-tin polymetallic deposits, and has the world's largest tungsten resources. These deposits have ages of ca.150-160 Ma, and are spatially, temporally and genetically related to granites which were previously believed to be S-type granitoids. Previous studies have significantly advanced our understanding of the ore formation. However, it has been poorly constrained whether or not mantle components were involved in the genesis of the deposits.

This study provides He and Ar isotope data of fluid inclusions in pyrite and arsenopyrite from the Yaogangxian, Furong, Shizhuyuan, Dajishan, Xianghualing, Yanbei, and Xihuashan tungsten-tin polymetallic deposits in South China. $^{3}He/^{4}He$ ratios range from 0.1 to 3.0 Ra (where Ra is the $^{3}He/^{4}He$ ratio of air = 1.39×10^{-6}). Moreover, there are excellent correlations between He and Ar isotopic compositions. The results suggest that the ore-forming fluids of the deposits are a mixture between a crustal fluid and a fluid containing mantle components. The existence of mantle noble gases in fluids, exsolved from the ore-bearing granitic magma, provides new insights about the origin of the deposits and associated granites. The hosting granites, previously considered as S-type, were actually formed by crustal melting induced by heat and volatile release from the mantle.

New insights on the origin of unresolved complex mixtures

S.Z. HU [1]*, S.F. LI [1], J.H. WANG[2], D.M. ZHANG[1] AND J. MA[1]

[1]Key Laboratory of Tectonics and Petroleum Resources (China University of Geosciences Wuhan), Ministry of Education, China (*correspondence: hushzh@cug.edu.cn, lishf@cug.edu.cn, zdm2007@cug.edu.cn)
[2]School of Marine Sciences, Sun Yat-sen University, Guangzhou, China (wangjh@gig.ac.cn)

Biodegradation results in the dissappearance of the dominant aliphatic and aromatic components of petroleum and in the development of an unresolved complex mixture(UCM), referred to as a big "hump" in GC. Many studies showed that UCM should result from the relative concentration of a complex mixture that is already present in crude oil, which arises from the removal of major resolved alkylated species by biodegradation[1-2]. However, the recent study on crude oil in Biyang depression, which carried out by 5A molecular sieve adduction and laboratory bacteria degraded experiment, suggested that UCM may be produced by biodegradation (Fig.1).

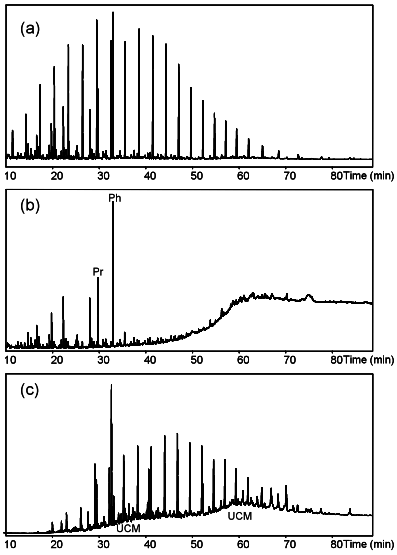

Figure 1 Gas chromatograms for : (a) SH1 crude oil; (b) non-adducted fractions for SH1 crude oil by 5A molecular sieve; (c) SH1 biodegraded oil after a 9-day laboratory experiment by a culture of aerobic bacteria isolated from a biodegraded oil in the field

[1] M.A. Gough (1990) *Nature* **334**, 648-650. [2] Ventura G T, (2008) *Org.Geo.* **39** (7),846-867.

https://doi.org/10.1180/S0026461X00006502 Published online by Cambridge University Press

Study on mineral surface reacted with water at high temperatures above 300°C

SHUMIN HU, RONGHUA ZHANG AND XUETONG ZHANG

Institute of Mineral Resources, Chinese Academy of Geological Sciences, Lab.Geochemical Kinetics. Baiwanzhuang road 26, Beijing 100037 (zrhhsm@pku.edu.cn)

Reactions at solid-water interface play an important role in a number of natural processes. Steady-state dissolution rates of pyroxene, actinolite, wollastonite, garnet and basaltic rock have been measured at temperatures (T) from 25 to 400°C and at 23-35MPa. All dissolution experiments were performed in mixed-flow reactor or packed bed reactor (with Zr metal liner). The mineral samples used in these experiments have been analyzed chemically. The compositions and structures of their surfaces are also analyzed through SEM and TEM before and after reactions. All experiments were performed at far-from-equilibrium conditions. The dissolution of silicate mineral in water, such as pyroxene, actinolite, may require the breaking of more than one metal-oxygen bond type. Different metal elements in silicate mineral behave different release rates, so that the dissolution product is often non-stoichiometric. Usually, Na, Mg, Fe, Ca dissolve faster than Si at T <300°C. In contrast, at T≥ 300°C, Si release rate is higher than other metals. For actinolite and diopside, Ca /Si release ratio at near 200°C is stoichiometric. SEM and TEM analyses of surfaces found the non-stoichiometric surface leaching-layer occurred at surface when dissolution is non-soichiometric. At T<300°C, surfaces of actinolite and pyroxene after reacted with water is a light Si-rich and little Fe (or / and Mg, Ca) deficient. In contrast, at T ≥ 300°C, the reacted surfaces are a light Fe-rich and little Si deficient. TEM study indicates that amorphous nanothin layer was found at the surface. Metal-H^+ exchange and hydration reaction at mineral surface will pass through this layer. As dissolution is non-stoichiometric, composition and structure of non-stoichiometric surface layers change with elapsed time. For instance, when basaltic rock reacted with aqueous solutions at 90°C, release rates of Ca (Mg) decrease with the elapsed time in 7 days, the rates of Si increase with the time. The surface area (m^2/g) and total pore volume (cc/g) increase with the time. Compositions of the surface vary with the time.

Note: This project is supported by the project of 2010G28, 2008ZX05001-003-006, K1006, SinoProbe-07-02-03, SinoProbe-03-01-2A.

Raman spectroscopic study of the system $NaCl$-Na_2CO_3-Na_2SO_4-H_2O: Implications for the determination of Cl^- concentration in fluid inclusions

W. HU[1]*, X. WANG[1], I.M. CHOU[2] AND Q. SUN[3]

[1]School of Earth Sciences and Engineering, Nanjing University, Nanjing, Jiangsu 210093, P.R. China (*correspondence: huwx@nju.edu.cn)

[2]954 National Center, U.S. Geological Survey, Reston, VA 20192, U.S.A.

[3]School of Earth and Space Sciences, Peking University, Beijing 100037, P.R. China

Raman spectroscopy has been demonstrated to be an efficient method for the determination of salinities in aqueous solutions [1, 2]. This study demonstrates the sensitivity of the method and the effects of other common anions, SO_4^{2-} and CO_3^{2-}, on calculated salinities.

In this study, we synthesized aqueous fluid inclusions containing various salts in fused silica capillary capsules (FSCCs) [3], and collected Raman spectra of these fluids. The OH stretching vibration bands of water between 2700 and 3900 cm^{-1} wavenumbers were fitted with PeakFit v. 4.0 using two Gaussian sub-bands at ~3220 and ~3440 cm^{-1}, which are considered to result from strong (HBS) and weak hydrogen bonds (HBW), respectively [2]. Our results show that, in Cl^- solutions, the ratio (K) between the peak height (I) to width (H) ratios of the two Gaussian sub-bands ($K = (I/H)_{HBW} / (I/H)_{HBS}$) varies with salt concentration, and that the difference in the K values between salt solution and pure water ($\Delta K = K_{salt\ solution} - K_{H_2O}$) can be used to calculate Cl^- concentration.

Our results for NaCl solutions are in good agreement with those of Sun *et al*. [2], and demonstrate that a variation of 0.5 mass % of NaCl can be easily detected. We also observed that the ΔK values increase with increasing SO_4^{2-} and CO_3^{2-} concentrations at a constant NaCl concentration, and that the effect of SO_4^{2-} is much stronger than that of CO_3^{2-}. For example, the presence of 0.05 m of CO_3^{2-} and 0.05 m of SO_4^{2-} in 0.5 m of NaCl solutions will result in the increase of 0.03 and 0.12 m in the calculated Cl^- concentrations, respectively. Therefore, the relationship between ΔK and Cl^- concentration can only be applied to Cl^- dominated solutions; otherwise, the Raman spectrometer needs to be calibrated with standards such as those prepared in FSCCs.

[1] Dubessy *et al*. (2002) *Appl. Spectrosc*. **56**, 99-106. [2] Sun *et al*. (2010) *Chem. Geol*. **272**, 55-61. [3] Chou *et al*. (2008) *Geochim. Cosmochim. Acta* **72**, 5217-5231.

https://doi.org/10.1180/S0026461X00006502 Published online by Cambridge University Press

Solubility of gold in granitic silicate melts at 850°C, 100MPa

XIAOYAN HU[1]*, XIANWU BI[1], GUOSHENG CAI[2]

[1]Institute of Geochemistry, Guiyang 550002, P.R. China (*correspondence: huxiaoyan@mails.gyig.ac.cn)
[2]Nonferrous Metal and Nuclear Industry Geological Exploration Bureau, Guiyang 550002, P.R. China

A lot of gold deposits are closely associated with intrusive igneous granites. It is curious how about the transportation of Au in the magma system, how about the gold solubility in different silicate melts and coexisting aqueous fluids. So, experiments were conducted to measure the solubility of gold in granitic silicate melts and coexisting aqueous fluids at 850°C, 100 MPa, and oxygen fugacity near NNO.

Haplogranitic gels with different compositions, distilled water, hydrochloric acid solutions with different HCl concentration were employed as starting material in the experiments. The weight ratio of the starting solid material and starting aqueous fluids are 1:1. Pure gold capsule was used as container; it also provided Au in the experiments. The temperature, pressure and run time were 850°C, 100MPa and 96 hours, respectively. Moreover, the pressure of several experiments ranged from 60 MPa to 100MPa.

The results of the experiment show that the solubility of gold in different melts is ranged from several ppm to dozens of ppm. The lowest gold solubility in silicate melt phase is 2.27ppm, in which K-rich peralkaline gels and distill water were employed as starting material. The detected gold concentration in melt phase is higher when the starting fluid is hydrochloric acid bearing. The solubility of gold in coexisting aqueous fluids is ranged from several hundred ppb to several ppm, and it increases with the content of HCl in the hydrochloric acid solutions. The contents of gold in granitic silicate melts are obviously higher than those in coexisting aqueous fluid.

The solubility of gold is also affected by the composition of the melt. Gold solubility in peralkaline silicate melts is higher than that in peraluminous silicate melts. Especially, increase of Na_2O/K_2O mole ratio in melt could increase gold solubility in melt phase. Pressure also has evident effect on gold solubility in granitic silicate melts. The solubility of gold in granitic silicate melts increases with increasing pressure.

Concluded from the experimental results, gold solubility in granitic melts is affected by the composition of the melt, the volatiles in the magma and the pressure. Gold solubility in peralkaline, especially sodium-rcih peralkaline granitic silicate melts is relative high, and this kind of granitic silicate melt could extract gold and be as an important media for gold transportation.

A discussion on ore-forming fluid sources by gas composition of inclusion and stable isotope in Qinglong Antimony deposit, Guizhou China

HU YU-ZHAO, WANG XIAO-LAN AND WANG JIN-JIN

Kunming University of Science and Technology, Kunming, 650093 (huyuzhao155@sohu.com)

Gas compositions of quartz and fluorite intergrowth with stibnite are determined as follows, H_2O-95.00 mol% (mean, n=9), CO_2 -2.36 mol%, N_2-1.429 mol%, CH_4-0.516mol%, C_2H_6 -0.444 mol%, Ar-0.146, H_2S -0.001 mol %, and O_2 not detected. In xCO_2/xCH_4-xN_2 / xCH_4chart, 4 samples fall into formation water area, and 5 into atmospheric water area. In xCH_4-xC_2H_6- xCO_2 chart, all fall into gas area.

Data determined from inclusions in authigenic quartz show that δD compositions that range from-105.8 to -128.1‰ with a mean of -114.2 (n=5). The $\delta^{18}O$ values of authigenic quartz range from 3.8 to 6.9‰ with a mean of 5.4, converted into $\delta^{18}O$ of water range from- 7.8 to -10.2‰ with a mean of -8.08. In the δD-$\delta^{18}O$ figure, the data above fall into formation water, and lie in the left inferior of formation water area in Alberta basin.

The gas compositions and their proportion of Qinglong deposit are similar to Shuangjiang CO_2 pool (approximately 100 km E) with CO_2 values of 63.81%, N_2 21.49%, CH_4 14.57%, $C_2H_6$0. 015%. In this CO_2 pool, $^3He/He$ and $^{40}Ar/^{39}Ar$ respectively with1031 and 1.28% may be explained crust-derived causes. The $\delta^{13}C$ of methane is -35.7-35.8‰ and ethane is -38.8‰ which have the characteristics of the mixture of Coal type gas and oil type gas. The δ^{13} C of CO_2 with - 4.7 ‰ may be result of pyrolysis of lots of carbonate.

The freezing point temperature of fluorite inclusions range from - 0.2 to -1.3°C, and their salinity range from 0.4 to 2.2%NaCl. So the ore-forming fluid of Qinglong antimony deposit shows certain characteristics of low salinity formation water, and light hydrocarbon comes from coal and oil field.

* Granted by the project of the Distinguishing Discipline of KUST (2008).

https://doi.org/10.1180/S0026461X00006502 Published online by Cambridge University Press

NIST SRM 610-614 matrix induced unique element fractionation in laser ablation ICP-MS at high spatial resolution analysis

Z.C. HU*, L. ZHOU, Y.S. LIU, L.S. ZHAO AND S. GAO

State Key Laboratory of Geological Processes and Mineral Resources, China University of Geosciences, Wuhan, 430074, PR China (*correspondence: zchu@vip.sina.com)

The greatest strength of the LA-ICP-MS technique is its application to microsampling in which extremely small pits are obtained. The results of this study highlight some significant different laser-induced fractionations between widely used external reference materials NIST SRM 610-614 and natural silicate reference materials (e.g., USGS reference glasses (GSE-1G, GSD-1G), MPI-DING glasses, USGS basalt glasses and zircon reference material GJ-1) at high spatial resolution analysis. For the sample matrices and analytical conditions used in this study, the laser-induced elemental fractionations for 63 selected isotopes are negligible at the spot sizes of 160-44 μm. However, the laser-induced elemental fractionations of Li, Na, Si, K, V, Cr, Mn, Fe, Co, Ni, Cu, Rb, Cs and U (with respect to Ca) increase significantly with decreasing spot sizes from 44 μm to 32 μm, 24 μm and 16 μm in these natural silicate reference materials. Unlike in these sample matrices, laser-induced elemental fractionations of these elements in NIST SRM 610-614 are unique in that they are almost not affected by the change of spot sizes from 44 to 32 to 24 μm, with only slight increase at the spot sizes of 16 μm. The much less significant laser-induced elemental fractionation in NIST SRM 61X in comparison with other natural silicate materials makes them nonideal as external reference materials at high spatial resolution analysis. Alternatively, this NIST SRM 61X-specific matrix effect for Li, Na, K, V, Cr, Mn, Fe, Co, Ni, Cu, Rb, Cs and U can be minimized by using Si for internal standardization. U and Pb in zircon GJ-1 are exceptions, which are zircon-specific.

[1] Sylvester (2008) *Mineral. Assoc. Can.*, Short Course Series **40**, 1-348. [2] Jochum *et al.* (2007) *J. Anal. At. Spectrom.* **22**, 112–121. [3] Günther *et al.* (1997) *J. Anal. At. Spectrom.* **12**, 939–944.

Single-grain muscovite Rb-Sr age of Xushan W deposit, central Jiangxi, China, and its geological implication

R.M. HUA[1]*, G.L. LI[1], X.L. WEI[2], X.D. WANG[1] AND X.E. HUANG[2]

[1]State Key Laboratory for Mineral Deposits Research, Nanjing University, Nanjing 210093, China (*correspondence: huarenmin@nju.edu.cn)

[2]Jiangxi Bureau of Nonferrous Metal Exploration, Nanchang 330001, China

The Xushan tungsten deposit in central Jiangxi province, China, comprises three types of ore-bodies, i.e. quartz vein type, skarn type, and altered granite type. Rb-Sr micro-isochron method [1] is first applied to determine the ore-forming age by using single grain of muscovite growing at the edge of the wolframite-quartz vein. Six pieces of muscovite are used for Rb-Sr isotope analysis. Result shows that the mineralization age is 147.1 ± 3.4Ma, with MSWD = 0.71. This ore-forming age is similar to many tungsten deposits in southern Jiangxi. The very high I_{Sr} value (0.849 ± 0.026) may suggest that the ore-related granite was a melting product of highly evolved and highly saturated crust material, and the ore-forming fluid had extracted the strontium of extremely high $^{87}Sr/^{86}Sr$ ratios from the granite through water-rock interaction. It also suggests that there was almost no contribution of mantle material during the formation of either ore-related granite or tungsten mineralization, which is also proven by some He-Ar isotope studies [2, 3].

[1] Li QL *et al.* (2005) *Chinese Sci Bulletin* **50**, 2861–2865. [2] Wang XD *et al.* (2010) *Chinese Sci Bulletin* **55**, 628-634 [3] Li GL *et al.* (2011) *Resource Geol* **61**, in press

https://doi.org/10.1180/S0026461X00006502 Published online by Cambridge University Press

U-series disequilibria of arc lavas revisited: Time-scales of magmatism in convergent margins

FANG HUANG[1,2]

[1]CAS Key Laboratory of Crust-Mantle Materials and Environments, School of Earth and Space Sciences, USTC, Hefei 230026. (fhuang@ustc.edu.edu)
[2]Institute for Geochemistry and Petrology, ETH Zurich, 8092 Zurich, Switzerland

U-series disequilibria have provided a unique powerful tool to constrain the processes and time-scales of magmatism in convergent margins. Preferential transfer of U and Ra relative to Th via addition of slab-derived fluid to the mantle wedge has been proposed to explain the ^{238}U and ^{226}Ra excesses observed in arc lavas (e.g., [1]). However, an in-growth melting process is required to produce ($^{231}Pa/^{235}U$)>1 in most young arc lavas and ^{230}Th excess in a significant number of samples. It is thus critical to provide a self-consistent explanation for U-series disequilibria in arc lavas.

Most arc lavas are highly differentiated. Re-visiting global arc lava data shows that U-series disequilibria are correlated with magma differentiation indices (e.g., SiO_2); Sr/Th and Ba/Th generally decreases with increasing SiO_2, showing the effect of magma differentiation at crustal depths. Most importantly, although ($^{226}Ra/^{230}Th$) is correlated with Sr/Th and Ba/Th in lavas from individual arcs, such relationship is not clearly observed in less-differentiated basaltic lavas. Therefore, current observations do not support inheritance of ^{226}Ra and ^{238}U excesses from the metasomatised mantle wedge. Instead, in-growth melting may play a more important role than previously believed. Namely, partial melting of the mantle wedge produces ^{226}Ra and ^{231}Pa excesses, and ^{238}U-^{230}Th disequilibrium in arc lavas, depending on fO_2, residual phases, thermal structure, and initial conditions of the wedge [2]. U-series disequilibria are further modified by ageing effect and assimilating old materials, resulting in the positive correlation between ($^{226}Ra/^{230}Th$) and Sr/Th in arc lavas. Such a model reconciles controversial temporal implications from different parent/daughter pairs and implies that rapid magma upwelling (<8,000 years) from the mantle to the Earth's surface is not required.

[1] Turner *et al*. (2003) *Rev. Mineral. Geochem.* **52**, 255-315.
[2] Huang *et al*. (2011) *GCA* **75**, 195-212.

Influence of microbial cells and extracellular polymeric substances on the sorption of As(V) and As(III) on Fe (hydr)oxides

J.-H. HUANG[1]*, E. J. ELZINGA[2] AND R. KRETZSCHMAR[1]

[1]Institute of Biogeochemistry and Pollutant Dynamics, ETH Zurich, Switzerland
(*correspondence: jenhow.huang@env.ethz.ch)
[2]Department of Earth & Environmental Science, Rutgers University, Newark, New Jersey, United States

Adsorption and desorption regulate the partitioning of trace elements between aqueous and solid phases in soils and sediments. Previous studies have indicated that phosphate groups in microbial extracellular polymeric substances (EPS) form inner-sphere surface complexes on Fe(III)-oxide surfaces e.g. with phosphate groups [1], suggesting the potential influence of microbial EPS on As adsorption behavior. In this study, we investigated the adsorption behavior of As(V) and As(III) on goethite, ferrihydrite and hematite under the influence of *Shewanella putrefaciens* cells and EPS, including non P-containing EPS (xanthan, alginic acid) and P-containing EPS isolated from *S. putrefaciens* CN-32. Batch experiments for determing adsorption isotherms and As(V) desorption kinetics were performed at pH 7.0 at room temperature. Additionally, an ATR-FT-IR study was performed to reveal As(V) concurrent desorption with attachment of *S. putrefaciens* cells.

Adsorption of As(III) and As(V) at solution concentrations between 0.001 and 20 μM decreased by 10-45% in the presence of 0.3 $g.L^{-1}$ EPS from *S. putrefaciens*. Addition of 0.5 g L^{-1} xanthan and alginic acid decreased As(V) and As(III) adsorption at solution concentrations between 0.6 and 6 μM by 7-66%, which is comparable with EPS from *S. putrefaciens*. Also, inactive *S. putrefaciens* cells, which were treated with paraformaldehyde, induced desorption of As(V) from Fe (hydr)oxide surfaces. ATR-FT-IR spectra evidenced the formation of inner-sphere complexes between bacterial phosphate and carboxylate groups and hematite, which may compete for Fe (hydr)oxide surface sites with As(V). At low cell density (5×10^7 cells mL^{-1}) inner-sphere coordination of carboxylate groups became less important than at high cell density (5×10^9 cells mL^{-1}). Our results indicate that the competition between As and bacterial functional groups for Fe (hydr)oxide surface sites is an important factor leading to increased mobility of As.

[1] Omoike & Chorover (2006) *Geochim. Cosmochim. Acta* **70**, 827–838. [2] Huang *et al*. (2011) *Environ. Sci. Technol.* **45**, 2804–2810.

https://doi.org/10.1180/S0026461X00006502 Published online by Cambridge University Press

Element mobility across the boundary between UHP eclogite and gneiss: Insights into supercritical fluids in continental subduction zones

JIAN HUANG[1,2]*, YILIN XIAO[1] AND GERHARD WÖRNER[2]

[1] School of Earth and Space Sciences, University of Science and Technology of China, Hefei 230026, PR China (*correspondence: jhuang01@mail.ustc.edu.cn)

[2]Geowissenschaftliches Zentrum der Universität Göttingen, Abteilung Geochemie, Goldschmidtstr. 1, 37077 Göttingen, Germany

We carried out a combined study of petrology, whole-rock major and trace elements as well as Sr-Nd-O isotopes on samples from a profile across the boundary between ultrahigh pressure (UHP) eclogite and gneiss from the Dabie orogen. The contact is characterized by the presence of amphibole-rich rocks that formed by retrogression from eclogite. Directly at the contact to the gneiss, the rock has higher concentrations in K, Al, LILEs, REEs and HFSEs, but similar SiO_2, FeOt and transitional metal element contents compared to retrogressed eclogite further away from the boundary. $\delta^{18}O$ values of the gneiss show a slight decrease, while retrogressed eclogites display a progressive increase towards the boundary. This indicates fluid-assisted O isotope exchange across the contacts of different lithologies at local scales. Mass balance calculations reveal variable but significant element mobility acrross the boundary of the mafic and felsic UHP metamorphic rocks with the following order of mobility : Ba > (K, Li, Cs, Rb, Pb)> U > Th > REE > Nb (Ta) > Zr (Hf). Amphibolite-facies retrogression of eclogites are known to have no effect on their major and trace elements [1, 2]. Also, Si-rich metasomatism from partially melted gneisses should increase the silica content of the retrogressed eclogite [2]. Therefore neither process is viable here. We thus propose that the variations observed here were caused at high pressures by supercritical fluids that were probably generated by the breakdown of phengite at P-T conditions above the second critical end-point for silicate-H_2O systems.

[1] Sassi *et al.*(2000) *CMP* **139(3)**: 298-315. [2] Zhao *et al.* (2007) *GCA* **71(21)**: 5244-5266.

Geochemical characteristics and geological significance of the basic intrusive rocks in Shifengshan copper deposit, Yimen, Yunnan, China

JIAN-GUO HUANG, RUN-SHENG HAN AND LEI WANG

Kunming University of Science and Technology; Southwest Institute of Geological Survey, Geological Survey Center for Non-ferrous Mineral Resources, Kunming 650093, P.R.C. (hjg1966@yahoo.com.cn)

Shifengshan copper deposit is the one of typical deposit which located at the Kunyang Rift of Proterozoic Yangtze oldland edge in Yimen Yunnan. It is found recently the basic intrusive rocks (sample as the gabbro in the 840m of the ore district) have presented intrusive contact connection with the surrounding rocks. it is seen chalcocitization in the edge of the gabbro.

Major elements are SiO_2 45.64-48.18×10^{-2}, Na_2O 4.66-5.20×10^{-2}, K_2O 1.06-2.56×10^{-2}, MnO 0.08-0.10×10^{-2}, characterized by high Na_2O but low MnO, the Rittmann index σ is 11.15-13.68. Trace elements present evident enrichment of K、Rb、Th, but the loss of Sr、Ta、Nb、Yb、Sc、Cr and so on, which are indicated the character of intra-continental rift basalts. ∑REE is 157.37-219.18×10^{-6}, Eu is Enrichment slightly (1.10-1.41), and it is rich in LREE(LREE/HREE=6.02-8.12, $(La/Yb)_N$ =7.99-12.70. REE distribution patterns show oblique to the HREE side and enrichment in LREE.

Based on reseach on geology. petrology and petro-geochemistry, we believe that the basic intrusive rock bodies formed in initial continental rift environment, which belong to the deep source of formation of basaltic magma, may be mixed with crustal material.

This paper was financially supported by the innovation team of ore-forming dynamics and prediction of concealed deposits, KMUST, Kunming, China (2008).

https://doi.org/10.1180/S0026461X00006502 Published online by Cambridge University Press

Research of three-dimensional engineering geology strata modeling in urban underground space

HUANG JINGLI[1,2]

[1]Geotechnical investigation and surveying institute, Changchun Institute of Technology, Changchun, China, 130000

[2]College of construction engineering, Jilin University, Changchun, China, 130000

The utility of urban underground space is a certain development trend in future. To efficient use the underground space, and to avoid of engineering accident and unnecessary resource waste, the rock and mass characteristics in strata and the distribution must be ascertained. Establishment of Three-dimensional engineering geology strata model could provide a reliable evidence for the city planning and engineering contracture.

Based on the investigation data, analysis and adjust the data according to accrual strata distribution, construct Changchun city engineering geology borehole data, then use the solids module in GMS (Groundwater Modeling System) to construct the three-dimensional engineering geology strata model of underground space in Changchun city. Analysis the cross section and vertical section of the visual three-dimensional strata, and qualitatively evaluated the engineering geology distribution characteristics of rock and mass in Changchun city.

In addition, compared to other software, GMS is convenient to draw and visualized well. The three-dimensional engineering geology strata model constructed with GMS could truly show the actual situation.

Records of sulfur isotopic composition and their significance from the Permian strata at Shangsi section of Guangyuan, Sichuan

JUNHUA HUANG, PENGWEI LI, LAISHI ZHAO, LIAN ZHOU, JUN CAO AND LIDAN LEI

State Key Laboratory of Geological Processes and Mineral Resources, China University of Geosciences, Wuhan 430074, China

By analyzing the data of TOC total sulfur and sulfur isotopic composition of carbonate-associated sulfate (CAS) and pyrites from the Permian strata at the Shangsi section of Guangyuan, Sichuan province, and based on the C-S charts and associated sulfur isotopic theory, the relationship between the variation of $\delta^{34}S_{seawater}$ and the related paleoenvironments and paleoclimate was deciphered, together with discussion of the marine sulfur cycle; The organic matter burial efficiency in different periods was analyzed by dividing the $\triangle^{34}S_{CAS\text{-}Py}$ values into different grades and mineralization of the sedimentary organic carbon by BSR was also quantified. Some information about the sedimentary environments and the diagensis of the burial organic matter in this area has been obtained.

Carbon-sulfur charts show that the concentration of sulfate in the seawater was very low during the whole Permian in this area, and is just 0.6-0.8 of the modern marine in late Permian although with a little increase and the occurrence of sulfidization in bottom waters in this period. Characteristics of high S/C ratio and $\delta^{34}S_{Py}$ in the bottom of Chihsia formation indicates late intrusion of hot sulfuric fluid , therefore, the information about the sedimentary environments and early diagenesis is uncertain.

Another negative shifts in $\delta^{34}S_{seawater}$ values occurred in middle Dalong ages, however, with a lager extent of 16.5‰. There have been many hypotheses about its mechanism, among of which the reoxidization of massive H_2S from the bottom water was the direct cause. Recent research suggests that BSR is controlled by anoxic environments, supply of organic matter and SO_4^{2-} ion as well as favorable temperature. Highest activity of BSR occurs under the condition of 20-35℃. Therefore, persistent supply of heat to the bottom water released by The “short-lived” mantle plume event (lasting 10-20Ma, Siberian volcanism envent) during this period is the necessary factor of the fierce activity of BSR. In the meanwhile, the rising of the bottom water’s temperature would accelerate the upward diffusion of H_2S and mixing of the ocean, which finally caused a large amount of H_2S accumulating and reoxidized in the surface waters.

https://doi.org/10.1180/S0026461X00006502 Published online by Cambridge University Press

Formation of a layered Fe^{III} (hydr)oxide intercalated with dodecanoate

LI-ZHI HUANG*, KARINA B. AYALA-LUIS, CHRISTIAN BENDER KOCH AND HANS CHRISTIAN B. HANSEN

Department of Basic Sciences and Environment, University of Copenhagen, Thorvaldsensvej 40, DK-1871 Frederiksberg C, Denmark (*correspondence: lizhi@life.ku.dk)

A layered Fe^{II}-Fe^{III} hydroxide (Green rust, GR) intercalated with dodecanoate has been freeze dried under anoxic conditions and then oxidized by dioxygen to produce the corresponding layered Fe^{III} (hydr)oxide dodecanoate (isomer shift: 0.5003 mm s^{-1}, quadrupole splitting: 0.7523 mm s^{-1} at 80K). The final product ($oxGR_{C12}$) contains no Fe^{III} oxide impurities, and it has the same layer structure as the GR_{C12} (see Fig. 1).

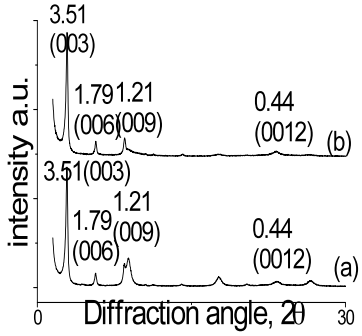

Figure 1, XRD patterns of (a) GR_{C12} (b) $oxGR_{C12}$ resulting from solid-state oxidation. (unit:nm; monochromated Co-Kα radiation (40 kV, 40 mA); randomly oriented powder sample was used.)

The average chemical composition of $oxGR_{C12}$ is $Fe^{III}_{2.8}O_{1.8}(OH)_{3.8}(C_{12})$. Mössbauer spectroscopy shows the presence of a trioctahedral Fe^{III} (hydr)oxide, and the huge variation in quadrupole splitting values of the Fe^{III} doublet reflect dramatic changes of electric field gradient due to the distortion of the octahedral sites which result from the mixture of OH^- and O^{2-} ions at the apices of Fe octahedrons. The $oxGR_{C12}$ product is stable in air and water (from pH 3 to pH 8), but it is destroyed in presence of 0.1M HCl and when dodecanoate is exchanged with carbonate. The intercalated dodecanoate stabilizes the Fe hydroxide layers and hinders transformation to Fe oxides. This is the first report describing the formation of a stable layered trioctahedral Fe^{III} (hydr)oxide.

Ab initio electronic structure of $Pu(OH)_4$: Comparison between density functional and multi-reference theories

PATRICK HUANG[1]*, MAVRIK ZAVARIN[1,2] AND ANNIE B. KERSTING[1,2]

[1]Physical & Life Sciences Directorate, Lawrence Livermore National Laboratory, Livermore CA, USA (*correspondence: huang26@llnl.gov)

[2]Glenn T. Seaborg Institute, Lawrence Livermore National Laboratory, Livermore CA, USA

Current spectroscopic techniques do not readily allow for the atomic-scale characterization of metal ions and complexes at low concentrations (i.e., < 10^{-10} M). This is problematic for highly insoluble species such as Pu(IV), where little direct information is available on its chemical behavior at environmental conditions. To this end, *ab initio* simulations are potentially useful for gaining insights into Pu complexes in aqueous environments. However, the electronic structure of actinide complexes poses difficulties. Accurate treatments of actinides often require sophisticated correlated wavefunction techniques whose cost grows rapidly with the number of electrons, and are only practical for small systems. Large-scale dynamical simulations of condensed phase phenomena typically rely on density functional theory (DFT); however, current DFT approximations for exchange-correlation (E_{xc}) can yield large errors for actinides due to the presence of localized 5*f*-electrons.

We report benchmark studies for the monomeric $Pu(OH)_4$ complex employing a range of *ab initio* techniques including single-reference approaches (unrestricted Hartree-Fock, UHF; second-order Møller-Plesset perturbation theory, MP2), multi-reference approaches (complete active space self-consistent field method, CASSCF; multi-reference perturbation theory, MRPT) and DFT. We find that single-reference methods such as MP2 provide a reasonable description of ground state geometries and energies, and an explicit inclusion of multi-reference effects involving the Pu 5*f* electrons is not essential. However, DFT with standard approximations for E_{xc} performs poorly for $Pu(OH)_4$. We explore the use of DFT+*U* as a simple way to improve on the DFT description of on-site Pu 5*f*-electron correlations. Using small hydrated cluster models, $Pu(OH)_4(H_2O)_n$, we determine an *ab initio* parameterization of DFT+*U* suitable for the aqueous phase simulation of $Pu(OH)_4$. With this DFT+*U* parameterization, we carry out periodic, *ab initio* molecular dynamics simulations of $Pu(OH)_4$ in a bulk water environment, in order to determine the aqueous solvation structure around $Pu(OH)_4$.

https://doi.org/10.1180/S0026461X00006502 Published online by Cambridge University Press

A critical look at the titanium-in-quartz (TitaniQ) thermobarometer

R. HUANG AND A. AUDÉTAT*

Bayerisches Geoinstitut, Universität Bayreuth, 95440 Bayreuth, Germany
(*correspondence: andreas.audetat@uni-bayreuth.de)

Synthetic quartz was grown in rutile-bearing $H_2O(\pm NaCl)$ fluids at 600-800 °C and 1-10 kbar by dissolution and reprecipitation of quartz in a small thermal gradient. Rapid attainment of rutile saturation is proved by the formation of rutile crystals at the contact between old quartz substrate and new quartz overgrowth. Titanium concentrations in new quartz correlate positively with the concentrations of Li and Al and depend strongly on quartz growth rate, increasing by up to a factor of 2.5 as the growth rate varied from ~4 μm/day to ~110 μm/day. Considering the composition of the most slowly grown quartz samples as most representative we obtain Ti concentrations that are about three times lower than those obtained during earlier calibrations of the TitaniQ thermobarometer [1, 2]. Our data can be fitted by the equation

$$\log \text{Ti (ppm)} = -0.27943 \cdot 10^4/T - 660.53 \cdot (P^{0.35}/T) + 5.6459$$

where T is given in Kelvin and P in kbar.

An independent test was made by analyzing igneous quartz from five intrusive and three volcanic magma systems that crystallized at known pressures (0.8–2.7 kbar) and temperatures (675–780 °C). The activity of TiO_2 was constrained from the composition of melt inclusions hosted in the analyzed quartz. Although the results depend on the model chosen to calculate $aTiO_2$, they agree much better with our calibration than with previous TitaniQ calibrations. Crystallization pressures calculated based on our calibration agree within 0.1-1.0 kbar with independent pressure estimates, whereas those calculated based on [1,2] are consistently higher by 3-9 kbar. Slight deviations between our calibration and the natural data are either due to uncertainties in the calculation of $aTiO_2$ of the natural melts or due to failure to synthesize structurally perfect quartz even at our slowest growth rates. Our findings imply that TitaniQ should not be applied to quartz grown from hydrothermal fluids, because growth rates in these environments can be very high. TitaniQ is more likely to work in igneous quartz, although the present models for TiO_2 solubility in quartz and silicate melts may still need to be refined.

[1] Wark & Watson (2006) *Contrib. Mineral. Petrol.* **152**, 743-754. [2] Thomas *et al.* (2010) *Contrib. Mineral. Petrol.* **160**, 743-759.

Hydrogen production from low temperature olivine alteration

SHANSHAN HUANG[1]* , HELGE HELLEVANG[2] AND INGUNN HINDENES THORSETH [1]

[1]Centre for Geobiology and Department of Earth Science, Univ. Bergen, Norway.
(*correspondence: shanshan.huang@geo.uib.no)
[2]Department of Geosciences, Univ. Oslo, Norway

Hydrous alteration of olivine, the main component in ultramafic rocks, has received much attention because the reducing power in the form of H_2 generated in this process is proposed to have fueled the emergence of life [1] and the present deep biosphere [2]. While most previous research was done at high temperatures (over 200ºC) [3], the upper temperature for living organisms is recorded as 122ºC. This study is thus focused on the H_2 production from olivine hydration at 80ºC, the core temperature for thermophiles and hyperthermophiles. Reactions with fluids representing the variety of composition of natural waters is studied.

Reactions with ground Fo90 were carried out in serum bottles which was deoxygenated with N_2. Headspace gas and solutions were analysed. A correlation between pH, olivine dissolution and H_2 production was established experimentally. Our data show that saline water and seawater promote H_2 production from olivine hydration compared with pure water. This is partly due to higher alkalinity in the seawater that buffers the pH. The H_2 production is found to correlate to the end pH in these systems. Geochemical modelling will be coupled to further understand the mechanism.

Olivine dissolution in water showed no passivation over 80 days. This means H_2 produced in this environment is proportional to the surface area of olivine in contact with H_2O. Experimental data also suggest high rock:water ratio and low pH promote H_2 generation.

We then tested the effects of seawater level of sulfate, nitrate and bicarbonate on H_2 production. Enhanced values of H_2 concentration was observed for sulfate- and bicarbonate-added reactions, in which sulfate-containing solution produced most H_2. The effect of nitrate addition is not obvious. The H_2 production in this set of expriments is not related to pH. The reaction mechanism is under further investigation.

[1] Russell *et al.* (2010) *Geobiology* **8**, 355-371. [2] Hellevang (2008) *Int. J. Astrobiol.* **7**, 157-167. [3] Seyfried *et al.* (2007) *Geochim. Cosmochim. Acta* **71**, 3872-3886.

https://doi.org/10.1180/S0026461X00006502 Published online by Cambridge University Press

Geochemical characteristics of natural gas reservoired in Lower Triassic Jialingjiang Formation in Naxi-Hejiang area, Southern Sichuan Basin, China

SHIPENG HUANG* AND XIAOWAN TAO

PetroChina Research Institute of Petroleum Exploration & Development, Beijing 100083, China
(*correspondence: hspsk@163.com)

Natural gases reservoired in Lower Triassic Jialingjiang Fm are mainly composed of alkanes, and the dry coefficients are more than 0.99, which indicates that the maturity of the gases is high. $\delta^{13}C_1$ values of the gas vary from -35.3‰ to -29.4‰, and $\delta^{13}C_2$ values vary from -35.1‰ to -32.1‰, $\delta^{13}C_3$ values range from -31.2‰ to -23.7‰, and the average values of $\delta^{13}C_1$, $\delta^{13}C_2$ and $\delta^{13}C_3$ are -31.3‰, -33.8‰, -29.8‰, respectively. Most of the carbon isotope series are reversed ($\delta^{13}C_1>\delta^{13}C_2<\delta^{13}C_3$). Hydrogen isotopes values of methane (δD_1) range from -140‰ to -114‰, δD_2 vary from 136‰ to -116‰, and δD_3 between -126‰ and -103‰. Gas samples with the characteristics of $\delta D_1> \delta D_2< \delta D_3$ account to 60% of the total number.

All the gas samples are of thermogenic gas based on the $C_1/C_{2+3}—\delta^{13}C_1$ correlation (correlation diagram source from [1]), and distribute between type II kerogen and type III kerogen area, indicating that gas preserved in Jialingjiang Fm was mixed, and the mixture of gases generated from two type kerogens caused the reversion of the carbon isotope series and the hydrogen isotope series. Ethane carbon isotope is often used to identify source rock's (kerogen's) type, and it is believed that carbon isotope value of ethane of the type II kerogen is less than -29‰ [2]. The gas reservoired in Jialingjiang Fm were mainly derived from type II kerogen based on the analysis of ethane carbon isotopes. Gas preserved in Low Permian Maokou Fm was studied to be generated from the carbonate strata of Lower Permian [3-4]. Gas preserved in Jialingjiang Fm is similar to the gas reservoired in the Maokou Fm in the composition of carbon isotopes, but the former is a little heavier than the latter. Gas resevoired in Jialingjiang Fm was mainly generated from type II kerogens of Lower Permian and mixed by the gas derived from type III kerogen of Upper Permian Longtan Fm.

[1] Whiticar (1999). *Chemical Geology*, **161**:291-314. [2] Dai *et al* (2004), *OG*, **35**:405-411. [3] Zhang *et al* (2007) *Chinese Science Bulletin*, **52(supp1)**:113-124. [4] Dai *et al* (2010). *Acta Petrolei Sinica*, **31**:710-717.

The phase equilibrium of ternary system Cd^{2+}, $Na^+//Cl^-$-H_2O at 298 K

HUANG YI*[1], LU DANPING[2] AND ZOU FANG[1]

[1]Department of Geochemistry, Chengdu University of Technology, Sichuan, P.R.China
[2]Trade Union, Chengdu University of Technology, Sichuan, P.R.China

Solid- Liquid Equilibrium of ternary system Cd^{2+}, $Na^+//Cl^-$-H_2O at 298 K were studied by an isothermal solution saturation method. Experimental results indicate that there are three univariant curves AE, EF and FB, two invariant point s E, F, and three crystallization fields in the quaternary system. The quaternary system has one double salt $Na_2CdCl_4{\cdot}3H_2O$. The crystallization zones of equilibrium solid phases are $CdCl_2{\cdot}H_2O$ (AEC field), $Na_2CdCl_4{\cdot}3H_2O$ (EFM field) and NaCl (BDFfield), respectively. The composition of the invariant point E is $CdCl_2{\cdot}H_2O$ and $Na_2CdCl_4{\cdot}3H_2O$ of which content was 52.70% and 4.11%, respectively. The composition of the invariant point F is $Na_2CdCl_4{\cdot}3H_2O$ and NaCl of which content was 27.92% and 14.95%, respectively. The physico-chemical properties of solution in the quaternary system show regular changes along with the increased cadmium concentration. The results indicated that $CdCl_2{\cdot}H_2O$ possessed the highest solubility among those three salts, which means a strong transfer of Cd ion and a high pollution risk of soil environment. And the solubility of NaCl would be restrained as the salts existing together.

[1] Lindsay W L, *Chemical equilibria in soils*, JohnWiley & Sons, New York, **1979**, 57. [2] Barber, S.A, *Soil Nutrient Bioavailability: A Mechanistic Approach*, John Wiley, New York, **1984**, 93.

https://doi.org/10.1180/S0026461X00006502 Published online by Cambridge University Press

Study on distribution of technetium species and influence factors in groundwater

HUANG ZHIGANG[1] AND WANG YONGLI[2]*

[1]Department of Geochemistry, Chengdu University of Technology, Sichuan Province, (darkenerge@yahoo.cn)
[2]Department of Geochemistry, Chengdu University of Technology, Sichuan Province (*wangyl@cdut.edu.cn)

Tc is a major components in high-level radioactive wastes. The species distribution of Tc is a key factor to study the transport and deposition behavior in aqueous solution. It is easy to calculate species using geochemical computer program. We have calculated the species distribution of Tc in Beishan groundwater by PHREEQC, The result shows that TcO_4^- is the main specie. Under oxidation condition , the influence of pH to the existing form of Tc is very small, mainly in the form of TcO_4^-. however, under the reducing environmental condition that pe=-3 ~ -0.5, between the range of pH=4.6 ~ 8.8, it is mainly in the form of $TcO(OH)_2$, if it is pH> 8.8, then the mainly form will be TcO_4^-.

Crystal-poor vs. crystal-rich ignimbrites: A competition between stirring and reactivation

CHRISTIAN HUBER[1], OLIVIER BACHMANN[2] AND JOSEF DUFEK[1]

[1]School of Earth and Atmospheric Sciences, Georgia Institute of Technology, Atlanta GA 30332, USA.
[2]Department of Earth and Space Sciences, University of Washington, Seattle WA 98195, USA.

Ignimbrites, providing unique windows into magma reservoirs prior to explosive volcanic eruptions, are of two main types: (1) crystal-rich dacites and (2) dominantly crystal-poor rhyolites. Crystal-rich dacites are typically homogeneous, while crystal-poor ignimbrites can display strong gradients in composition and crystallinity. This presents a conundrum as the more viscous, crystal-rich units should be less prone to mixing. Here we show that this dichotomy reflects the competition between two timescales that follow magma recharge prior to eruption: (1) a thermal reactivation timescale, that measures the time necessary to make a locked crystal mush rheologically eruptible (<50% crystals), and (2) a homogenization timescale associated with convective stirring. Using a thermo-mechanical model, we show that the reactivation timescale of locked mushes is much greater than the time necessary to homogenize reservoirs by convective stirring. Hence, crystal-rich units, which require a reactivation stage, are inevitably well stirred. In contrast, crystal-poor magmas are rheologically ready to be mobilized without reactivation and need not be thoroughly mixed upon eruption. This model provides an integrated picture of upper crustal reservoirs and has major implications for the link between shallow plutonic and volcanic rocks.

https://doi.org/10.1180/S0026461X00006502 Published online by Cambridge University Press

Optimization of thermodynamic properties and phase diagrams of P_2O_5 and CaO-P_2O_5 systems

P. HUDON* AND IN-HO JUNG

Dept. of Mining and Materials Engineering, McGill University, Montreal, QC, H3A 2B2, Canada (*correspondence: pierre.hudon@mcgill.ca)

P_2O_5 is an important oxide component in the late stage products of igneous rocks such as granites and anorthosites. More often than not, it combines with CaO and crystallizes in the form of apatite, while in volatile-free conditions, Ca-whitlockite is formed. In spite of their interest, the thermodynamic properties and phase diagrams of the P_2O_5 unary and CaO-P_2O_5 binary are not well known yet. In the case of the P_2O_5 unary, no experimental thermodynamic data are available for the liquid and the *O* and *O'* solid phases. As a result, we re-evaluated all the thermodynamic and phase diagram data of pure P_2O_5. The CaO-P_2O_5 binary was then optimized to reproduce all available thermodynamic and phase equilibrium data simultaneously in order to obtain one set of model equations for the Gibbs energies of all phases as functions of temperature and composition. Thermodynamic modeling was performed using the Modified Quasichemical Model [1-3] implemented in the FactSage software [4]. The optimized CaO-P_2O_5 binary is shown in Figure 1.

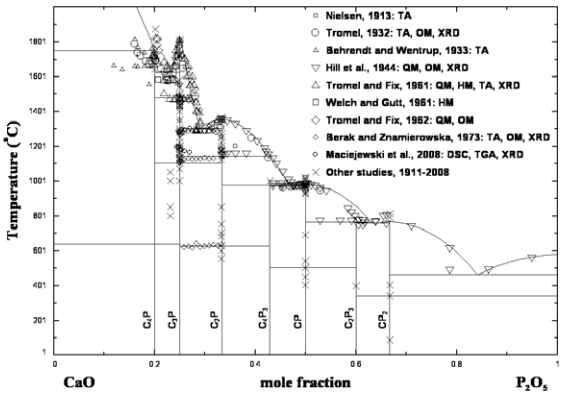

Figure 1: Optimized CaO-P_2O_5 binary.

[1] Pelton & Blander (1984) *Proc. AIME Symp. Metall. Slags Fluxes*, TMS-AIME, 281-294. [2] Pelton & Blander (1986) *Metall. Trans. B* **17** 805-815. [3] Pelton *et al.* (2000) *Metall. Mater. Trans. B* **31**, 651-660. [4] Bale *et al.* (2002) *Calphad* **26**, 189-228.

Penetration, accumulation and degradation of Deepwater Horizon oil in Florida sandy beaches

MARKUS HUETTEL[1]*, JOEL E. KOSTKA[1], OM PRAKASH[1], WILL A. OVERHOLT[1], STEFAN GREEN[1,2], GINA FREYER[1,3], ANDY CANION[1], JONATHAN DELGARDIO[1] AND NIKITA NORTON[1]

[1]Earth, Ocean, and Atmos. Science Dept., Florida State University, Tallahassee, FL, (*correspondence: mhuettel@fsu.edu)

[2]DNA Services Facility, University of Illinois at Chicago, Chicago, IL

[3]Institute of Ecology, Friedrich Schiller University, Jena, Germany

Crude oil from the Deepwater Horizon spill was washed onto sandy shores of the Northern Gulf of Mexico, and this study investigates the fate of this oil and its impact on microbial communities in oiled beach sands. Tar balls and pancake oil were deposited on the beach surface, and due to the subsequent deposition of sand layers, congealed oil and tar were embedded as deep as 75 cm in Pensacola beach sands. Dissolved, low-viscosity and dispersed oil fractions could penetrate the sand through the pore space, staining the beach surface layers. Adsorbed oil increased the cohesiveness of the sand and reduced sand permeability. Oiled sand layers contained elevated rates of potential oxygen consumption and dissolved inorganic carbon production, indicative of ongoing degradation of the sedimentary oil deposits. Twenty-four bacterial strains from 14 genera were isolated from oiled beach sands and confirmed as oil-degrading microorganisms by phenotypic characterization and phylogenetic analysis of small subunit (SSU) ribosomal RNA (rRNA) gene sequences. SSU rRNA gene copy numbers of total bacteria were approximately 10 times higher in oiled vs. clean sand. Oil contamination from the Deepwater Horizon spill had a profound impact on the abundance and community composition of indigenous bacteria in Gulf beach sands, and our evidence points to members of the *Gammaproteobacteria* (*Alcanivorax*, *Marinobacter*) and *Alphaproteobacteria* (*Rhodobacteraceae*) as key players in beach oil degradation.

https://doi.org/10.1180/S0026461X00006502 Published online by Cambridge University Press

Crystal growth history of quartz in the Ordovician Millbrig K-bentonite

W.D. HUFF* AND F.O. INANLI

University of Cincinnati, Cincinnati, OH 45221
(*correspondence: warren.huff@uc.edu)

Crystal size distribution (CSD) analysis has been applied to quartz crystals of the Ordovician Millbrig K-bentonite, which represents one of the largest known fallout ash deposits in the Phanerozoic Era, to establish crystal growth histories and conditions in the magma chamber prior to eruption. Specific CSDs of the quartz crystals of the Millbrig K-bentonite were examined to establish their growth conditions prior to the eruption. On the crystal size distribution plot, all Millbrig samples exhibit concave-down shapes in agreement with previously reported CSDs on large silicic systems [1] but in contrast to more mafic systems characterized by linear CSDs. Crystal growth mechanisms responsible for the concave down CSDs are thought to be surface-controlled crystal growth followed by a episode of textural coarsening. Although all samples follow concave-down shapes, two samples exhibit rather different CSD shapes. These findings appear to fingerprint a separate magma batch with different crystal growth conditions. These ash beds appear to be a product of a series of separate eruptions that represent separate magma layers or batches, each with slightly different crystal growth conditions.

Haynes [2] interpreted the multiple ash layers as either a product of several periods of eruptive activity or the cumulative effect of an evolving magma chamber during a single massive eruptive event. Our data support the model of several periods of eruptive activity that was closely spaced in time. The two of the eight Millbrig samples must have come from an earlier phase eruption and are part of a basal section that have not been preserved in the stratigraphic record and lacks lateral continuity in distal parts of the deposits. Therefore, the multiple ash beds in the Millbrig must have been a product of series of separate eruptions that represent separate magma layers or batches that had different crystal growth conditions.

Although conclusions on crystallization processes and the origin of deposits cannot be drawn from CSD shapes alone, it is shown here that CSDs of a fallout ash deposits can be used to fingerprint separate magma batches, provide valuable information on crystal growth rates as well as nature of the crystal growth mechanisms of quartz crystals.

[1] Bindeman (2003) *Geology* **31**, 367-370. [2] Haynes (1994) *Geol. Soc. Am Spec. Pap.* **290**, 1-80.

Photochemical transformations of carboxylates on TiO_2 and iron(III)(hydr)oxide surfaces

STEPHAN J. HUG AND PAUL BORER

Eawag, Swiss Federal Institute of Aquatic Science and Technology, CH-8600 Dübendorf, Switzerland

Colloidal iron(III)-phases play an important role in the adsorption, transport and transformation of organic and inorganic compounds. In sunlit aqueous phases, light-induced electron transfer in the bulk and on the surface of colloids can lead to photochemical oxidation, reduction and transformation of adsorbed compounds and often to dissolution of ironphases. As illumination of TiO_2 and iron(III)(hydr)oxides with UV-A light can produce oxidizing species, these solids are also of interest for water treatment and degradation of toxic compounds.

To investigate the different phototransformation pathways, we have followed photoreactions of dicarboxylates and of α-hydroxy-dicarboxylates on TiO_2 (a semiconductor known to produce OH-radicals with UV-A light) and on various iron(III)(hydr)oxides (where the photoproduced oxidizing species is not as well-defined) with in-situ ATR-FTIR measurements.

All investigated dicarboxylates adsorbed strongly to TiO_2 and to iron(III)(hydr)oxides up to circumneutral pH. Distinct changes of IR-spectra upon adsorption indicate inner-sphere coordination. On TiO_2, all dicarboxylates were quickly and completely mineralized by UV-A illumination and oxalate was formed before complete mineralization. In contrast, UV-A illumination of lepidocrocite, goethite and hematite did not lead to appreciable degradation of dicarboxylates except oxalate on the same time scale, but to transformation of α-hydroxy-dicarboxylates to oxo-carboxylates, which were further degraded only slowly.

These results suggest different photodegradation pathways. In comparison to TiO_2, OH-radicals seem not to be formed in high yield on iron(III)(hydr)oxides. Instead, photooxidation is more likely induced by direct ligand-to-metal charge transfer on the surface, or by bulk adsorption and migration of valence band holes to the surface and subsequent reaction with surface-coordinated carboxylate groups. The formed oxidants are able to readily oxidize α-hydroxy-carboxylates, but not dicarboxylates except oxalate. If generally valid, this means that iron(III)(hydr)oxides are not efficient photocatalysts for the complete mineralization of organic compounds, but that adsorbed compounds can be photo-transformed to distinct products.

https://doi.org/10.1180/S0026461X00006502 Published online by Cambridge University Press

Rare earth elements in pore waters of the Bering Sea sediments

YOUNGSOOK HUH* AND TSEREN-OCHIR SOYOL-ERDENE

School of Earth and Environmental Sciences, Seoul National University, Seoul 151-747, Korea
(*correspondence: yhuh@snu.ac.kr)

The rare earth elements (REEs) were measured in pore waters of the Bering Sea sediments using HR-ICP-MS after RE-spec column separation. Site U1345 was drilled during IODP Exp. 323 at the gateway to the Arctic Ocean to a depth of 140 mbsf. This is an area of high biological productivity and the drill site was at a water depth of 1008m in the center of modern oxygen minimum zone [1]. The pore water sampling depth resolution was 10m in Hole A (n=17) and 0.25m in Hole B (n=77).

The pore water REE concentrations were higher than sea water. Maximum concentrations were found below the sulfate-methane transition zone (6.5 mbsf) and centered at approximately 8–17 m: e.g. 790 pmol kg^{-1} Nd, 3000 pmol kg^{-1} Yb. The concentrations then decreased toward the bottom.

Shale-normalized REE patterns were HREE-enriched at all depths. This pattern has been linked to remineralization of POC and complexation of the HREE with DOC [3]. The HREE-enrichment was most extreme at the depth of maximum REE concentrations. There was a slight MREE bulge in the upper 3m. Ce anomalies were negligible throughout the depth profile.

Comparison to other chemical species (shipboard analyses of dissolved Fe, Mn, Ba, phosphate, etc.) will be presented.

[1] Takahashi *et al*. (2010) Proc. IODP, 323. [2] Wehrmann *et al*. (2010) *Chem. Geol*. in press. [3] Haley *et al*. (2004) *GCA* **68**, 1265-1279.

State-dependent chemistry of model atmospheric aerosol

A. J. HUISMAN, K. U. KRIEGER* AND TH. PETER

Institute for Atmosphere and Climate, ETH Zurich, Switzerland.
(*correspondence: ulrich.krieger@env.ethz.ch)

The chemical reactivity of aerosols is often studied by techniques such as aerosol flow tubes and environmental chambers, which are well suited to study processes with timescales of minutes to many hours. However, given the multiday longevity of aerosol in the atmosphere and the potential of aerosol to access a diffusion limited, glassy state, longer timescale studies are needed to understand the physical and chemical properties of glassy (or once-glassy) aerosols in the atmosphere.

An electrodynamic balance is used to trap a single particle of 1-10 micrometer diameter for up to a week at a time. The timescale of these experiments allows us to use atmospherically relevant oxidation conditions. The particle size and composition are nondestructively monitored as a function of relative humidity and temperature (and thus, physical state) and exposure to oxidant.

We explore the properties of binary and ternary systems (of which one component is water) including the evaporation rate and hygroscopicity of the particle. The particle is oxidized and subsequently recharacterized to discern the influence of this oxidation on e.g. the hygroscopicity. The relative humidity in the balance may be reduced to decrease water content of the sample, leading to vitrification and altered hygroscopicity, volatility, and potentially reactivity.

Results will be compared with numerical solutions of the diffusion equation providing information into the role of diffusion in limiting chemical reactivity. These results provide insight into the relationship between physical state and chemical reactivity, (including the potential of chemical processing to alter physical state or properties such as hygroscopicity) and the influence, if any, of past chemical processing on future chemical reactivity.

https://doi.org/10.1180/S0026461X00006502 Published online by Cambridge University Press

Crystal chemistry of Fe^{3+} in $(Mg,Fe)SiO_3$ perovskite and implications for lower mantle properties

DANIEL R HUMMER* AND YINGWEI FEI

Geophysical Laboratory, Carnegie Institution of Washington Washington, DC 20015 (dhummer@ciw.edu)

Recent work on Fe-bearing silicate perovskites indicates that Fe^{3+} may be an important cation in mantle perovskites, [1,2] and the behavior of Fe^{3+}-bearing perovskite therefore has important implications for the composition and dynamics of the lower mantle. In order to understand the effect of Fe^{3+} on the perovskite structure, we carried out multi-anvil syntheses of Fe^{3+}-bearing $(Mg,Fe)SiO_3$ (with and without Al) from a starting mixture of oxides, using Fe_2O_3 as the exclusive source of iron. To maintain a $Fe^{3+}/\Sigma Fe$ ratio close to 1 in the final run product, the sample capsule was surrounded by an oxidizing layer of Fe_2O_3.

Synthesis products were characterized using electron microscopy, electron microprobe, X-ray diffraction, and Mossbauer spectroscopy. Microprobe and Mossbauer measurements indicate that the synthesized perovskites contain no Fe^{2+} within detection limits, but as much as 7.4 mol% Fe^{3+}. Although evidence of Fe^{3+} in both crystallographic sites was observed in all samples, results suggest that Fe^{3+} preferentially occupies the octahedral site. The presence of Fe^{3+} in the octahedral site of $(Mg,Fe^{3+})SiO_3$ causes a substantially larger molar volume than that of $(Mg,Fe^{2+})SiO_3$ with the same Fe content (in which Fe^{2+} substitutes exclusively into the dodecahedral site). Fe^{3+} greatly increases the b/a axial ratio, potentially enhancing the seismic anisotropy of the lower mantle. Changes in the crystal chemistry of Fe^{3+}-bearing perovskite with depth may also complicate the nature of the spin transition zone, since octahedral Fe^{3+} becomes low spin at much lower pressures than does dodecahedral Fe^{3+}. [3]

[1] McCammon (1997) *Nature* **387**, 694-696. [2] Frost *et al* (2004) *Nature* **428**, 409-412. [3] Catalli *et al* (2010) *Earth Plan. Sci. Lett.* **289**, 68-75.

Agricultural impact on P and metal availability in stream sediments

SILJA V. HUND[1]*, ALYSSA E. SHIEL[2], SANDRA BROWN[1], LESLIE M. LAVKULICH[1] AND DOMINIQUE WEIS[2]

[1]SWC, Land and Food Systems, Univ. of British Columbia, Vancouver, Canada; (*correspondence: silja@interchange.ubc.ca)

[2]PCIGR, Earth and Ocean Sciences, Univ. of British Columbia, Vancouver, Canada

Intensive commercial agriculture is associated with significant applications of phosphorus fertilizers for crops and trace metals (e.g., Zn, Cu) for animal production. Excess amounts of these elements are often found in nearby aquatic systems. This is of particular concern as high P levels cause stream eutrophication. Therefore, analytical protocols are needed to assess the impact of agricultural pollution. Sequential extraction (SE) schemes have been developed to determine the availability of contaminants for aquatic systems in relation to their chemical bonding within the sediment. While most SE schemes consider P and metals separately, we provide an assessment of a SE scheme for both categories (modified after the method of Tiessen and Moir [1] for P).

Our study focused on the Sumas River watershed, an intensive agricultural region in British Columbia (Canada) strongly affected by nutrient and metal pollution. To quantify agricultural impacts, we collected river bed sediment samples from headwaters (no anthropogenic disturbance) to the intensively managed agricultural region downstream, over the length of 35 km. We examined trends in concentrations (e.g., P, Zn, Cu, and Pb) for different geochemical fractions of these stream sediments. Both concentrations and Pb isotopic compositions are used to trace natural (e.g. serpentinites present in headwater region) and anthropogenic sources, and to corroborate the utility of the SE scheme.

Our results show increasing contaminant concentrations towards downstream, e.g., from 33 to 5,479 ppm for P, from 24 to 167 ppm for Zn, from 9 to 60 ppm for Cu, and from 0.9 to 21 ppm for Pb. The most effective extractants were found to be 0.1 M NaOH (for labile P and Cu) and 1 M HCl for other metals. An increase of labile P with increasing agriculture intensity suggests that sediment source is important for contaminant availability, with anthropogenically-introduced contaminants often accumulating in more labile fractions. For sediments, the $^{206}Pb/^{207}Pb$ ratio decreases from headwaters (1.20373) to downstream (1.17631), consistent with increasing contributions of anthropogenic origin.

[1] Tiessen, H. and Moir, J. (1993), *Soil Sampling and Methods of Analysis, CSSS, Lewis Publ.*,75-86.

https://doi.org/10.1180/S0026461X00006502 Published online by Cambridge University Press

Time scales of cooling of post-plutonic picritic to dacitic dikes (Adamello-Italy)

N. HÜRLIMANN[1]*, O. MÜNTENER[1], P. ULMER[2] AND A. ULIANOV[1]

[1]Institute of Mineralogy and Geochemistry, University of Lausanne, Switzerland (*correspondence: niklaus.hurlimann@unil.ch)
[2]Institute for Mineralogy and Petrology, ETH Zürich, Switzerland

The formation of late magmatic dikes crosscutting previous plutonic voluminous bodies is a common feature. The textures of these rocks indicate similarity with volcanic rocks and general proximity to liquid compositions. The detailed study of zoning patterns of pheno- and xenocryst assemblages together with high-precision U-Pb ages allows us to get constraints on residence times and cooling rates of these magmas. Cooling rates obtained from diffusion patterns in minerals are linked to the thermal condition of the wallrock during emplacement of the dikes. Knowing the emplacement ages of the dikes and the plutonic wallrock could put constraints on cooling of the latter.

We show partially equilibrated zoning patterns of elements as Mg, Sr, and Ba in plagioclase pheno- and xenocrysts of basaltic-andesite to dacite post-plutonic dikes within the S-Adamello in Italy. Zoning patterns allow extraction of time constraints of diffusive processes under certain temperature conditions during temporary storage of magma or during ascent in dikes based on the continuity relation for the diffusive flux of these elements [1]. Hbl-Pl thermometry for the matrix and phenocrysts constrains the temperature during magma evolution. In earlier picro-basaltic to basaltic dikes Mg-Fe^{2+} interdiffusion patterns of chromite-spinel as inclusions in olivine provides further constraints on cooling rates of these magmas. Attainment of equilibrium of zoned phenocrysts for major and trace-elements was tested by analyzing the aphyric- to fine grained matrix by LA-ICP-MS, to determine actual liquid compositions.

[1] Costa, Chakraborty & Dohmen (2003), *Geochim. Cosmochim. Acta* **67**, 2189-2200.

The role of sulfur in triggering early Neoproterozoic oxygenation

M.T. HURTGEN[1], N.L. SWANSON-HYSELL[2], G.P. HALVERSON[3] AND A.C. MALOOF[2]

[1]Northwestern University, Evanston, IL 60208, USA (*correspondence: matt@earth.northwestern.edu)
[2]Princeton University, Princeton, NJ 08544, USA
[3]McGill University, Montreal, Quebec, H3A 2A7, Canada

Several lines of evidence suggest that Earth surface oxygen levels increased ~2300 million years ago [1]. While oxygen concentrations through the remainder of the Proterozoic (2500-542 million years ago) are poorly constrained, recent studies have linked an increase in the abundance of redox-sensitive elements and the difference between sulfur isotope ratios measured in sedimentary sulfate and contemporaneously deposited pyrite to a second oxygenation event ~580 million years ago—coincident with the diversification of macroscopic metazoa [2-5]. Here, we present paired sulfate and pyrite sulfur isotope data from two time-equivalent sections of the early Neoproterozoic (Tonian Period; 1000 to ~720 million years ago) Bitter Springs Formation, Australia. The $\delta^{34}S_{sulfate}$ record is obtained from anhydrite in drill core and carbonate-associated sulfate in drill core and outcrop samples. $\delta^{34}S_{sulfate}$ values are very similar between anhydrite and CAS in the drill core data set and between the drill core data and the CAS obtained from outcrop samples. These data suggest that an increase in microbial sulfide production in anoxic marine bottom waters and sediments enhanced nutrient recycling, thus sustaining elevated organic carbon burial rates and early Neoproterozoic oxidation. Our findings are consistent with evidence of eukaryotic diversification at this time [6] and suggest that oxidation of the atmosphere-ocean system occurred earlier in the Neoproterozoic than previously appreciated. These results highlight the role that sulfur plays in regulating the exogenic cycles of carbon and oxygen, particularly in low sulfate oceans of Earth's past [7].

[1] Bekker *et al*. (2004) *Nature* **427,** 117-120. [2] Fike *et al*. (2006) *Nature* **444,** 744-747. [3] Canfield *et al*. (2007) *Science* **315,** 92-94. [4] McFaddenet al. (2008) *Proc. Natl. Acad. Sci. USA* **105**, 3197-3202. [5] Scott *et al*. (2008) *Nature* **452,** 456-459. [6] Knoll *et al*. (2006) *Phil.Trans. R.Soc. B* **361,** 1023-1038. [7] Adams *et al*. (2010) *Nature Geoscience* **4**, 201-204.

https://doi.org/10.1180/S0026461X00006502 Published online by Cambridge University Press

New insights into gold transport in HCl-bearing vapour at elevated temperatures

N. C. HURTIG*, A. A. MIGDISOV AND A. E. WILLIAMS-JONES

Dept. of Earth & Planetary Sci., McGill Univ., Montréal, QC, H3A 2A7, Canada
(*correspondence: nicole.hurtig@mail.mcgill.ca)

Metal transport by vapour is an especially attractive hypothesis for explaining ore formation in shallow magmatic environments, where exsolution of fluid occurs in the stability field of vapour. Convincing evidence for the transport of high concentrations of metals by vapour in natural systems has been provided by quantitative analyses of fluid inclusions in porphyry Cu-Au deposists and associated epithermal Au-Ag deposits. Other evidence of metal transport by vapour in natural systems comes from metallic mineral deposits around high temperature fumaroles and in the pipelines from geothermal wells (scalings).

Experimental studies on metal solubility and speciation in water vapour at temperatures up to 400°C have emphasised the role of hydration in metal transport by vapour. These studies have shown that the concentrations of Ag, Au, Cu and Mo in vapour are comparable to those measured in hot fumarolic gas condensates. The high concentrations reported for fluid inclusions have not been observed experimentally. The current study was conducted for a range of fO_2 and at higher pressures than previous experimental studies, in order to approximate a little more closely the pressures of natural systems.

Experiments were carried out in batch-type Ti autoclaves at a temperature of 367°C and pressures up to 194 bars in HCl-bearing vapour. Oxygen fugacity was buffered either by the assemblage (MoO_2/MoO_3) or graphite. Gold concentrations ranged between 1.1 and 321 ppb in condensed samples of the reacted vapours. At pressures below 100 bar, gold concentration increased at a rate of 2-3 per log bar, similar to that observed previously. However, above this pressure, there was a sharp increase in the pressure dependency of gold solubility to approximately 8-14 per log bar. This suggests that at the lower pressures investigated, the hydration number was similar to that predicted by other studies, but increased sharply at higher pressure. Gold solubility increased with increasing fO_2 and was approximately one order of magnitude higher in the MoO_2/MoO_3 buffered system than in the system buffered by graphite.

Geothermobarometry of basaltic glasses from Tamu massif, Shatsky Rise oceanic plateau

A. HUSEN[1]*, R. ALMEEV[1], K. SHIMIZU[2], T. SANO[3], J.H. NATLAND[4], J. KOEPKE[1] AND F. HOLTZ[1]

[1]Institute of Mineralogy, Leibniz University of Hannover, Germany (*correspondence: a.husen@mineralogie.uni-hannover.de)
[2]IFREE, JAMSTEC, Yokosuka, Japan
[3]National Museum of Nature and Science, Tokyo, Japan
[4]Rosenstiel School of Marine and Atmospheric Science, University of Miami, USA

IODP Expedition 324 [1] recovered samples from Shatsky Rise oceanic plateau ranging from picritic basalts (15.6 wt% MgO) to more differentiated tholeiitic basalts (4.9 wt% MgO). In order to determine crustal magma chamber and magma evolution processes lava samples from several evolutionary stages should be investigated. We present results of the mineralogical study of lower MgO pillow and massive flow basalts (Site U1347). Major element glass and mineral compositions were analyzed by electron microprobe (JAMSTEC and University of Hannover). Glass H_2O and CO_2 determinations were performed by FTIR spectroscopy.

In general, basaltic glasses from Site U1347 are evolved tholeiitic basalts (5.2-6.8 wt% MgO), resembling typical EPR MORBs, located in the high-FeO and low-Al_2O_3 fields of EPR basalts. The CaO/Al_2O_3 ratios observed in U1347 basalts are amongst the highest known for all MORBs, probably indicating very low pressures of partial crystallization. H_2O contents in the glasses show MORB values, ranging from 0.18 to 0.6 wt%. CO_2 contents are usually below detection limit of the FTIR method (<50 ppm). The glass compositions and the H_2O concentrations were used to simulate conditions of multiply saturation [2]. Our calculations demonstrate that basaltic melts could have been last equilibrated with Ol-Pl-Cpx association at 1110 to 1170°C in the range of pressures between 1 atm to 3 kbar. These estimates represent the maximum values, since Ol is scarcely observed in natural Pl-Cpx-phyric lavas. The compositions of coexisting Pl and Cpx (~30 samples studied) show two compositional trends. One trend can be reproduced as a result of ideal fractional crystallization at pressures between (0.5-3 kbar). The second trend is the object for future investigations. Application of Cpx-melt and Pl-melt geothermobarometers [3] gives inconsistent results for the same samples and generally shows high P-T values using Cpx-melt (3.7-7 kbar, 1140-1220 °C) and low and negative pressure values using Pl-melt equilibria.

[1] Sager *et al*. (2010) *Proc. IODP*, 324: Tokyo. [2] Almeev *et al*. (2008) *JPet*, **49**, 25-45. [3] Putirka (2008) *Rev. Min. Geoch*. **69**: 61-120.

https://doi.org/10.1180/S0026461X00006502 Published online by Cambridge University Press

On the fate of ^{220}Rn in partially saturated media

STEPHAN HUXOL*[1], MATTHIAS S. BRENNWALD[1], EDUARD HOEHN[2] AND ROLF KIPFER[1,3]

[1]Eawag, Swiss Federal Institute of Aquatic Science and Technology, CH-8600 Dübendorf, Switzerland (*correspondence: stephan.huxol@eawag.ch)
[2]Buchserstr. 44, CH-8157 Dielsdorf, Switzerland
[3]Institute of Isotope Geology and Mineral Resources, Swiss Federal Institute of Technology Zurich (ETH)

Thoron (^{220}Rn, half-life 55.6s) is a short lived isotope of the radioactive noble gas radon (main isotope: ^{222}Rn, half-life 3.58d). While ^{222}Rn is part of the ^{238}U-decay series, ^{220}Rn originates from the ^{232}Th-decay series. As $^{220,\ 222}$Rn are produced from alpha-decay of radium isotopes, $^{220,\ 222}$Rn emanate from minerals containing their precursors $^{224,\ 226}$Ra. As a result, both radon isotopes are found in soil gas and soil-near air, ^{222}Rn also in ground water. Hence, it is expected to find also ^{220}Rn in ground water. However, ^{220}Rn could not be detected in natural aquatic environments, although ^{220}Rn in water can be measured in laboratory experiments by a tailored improved radon- and thoron-in-water detection system.

In a field experiment, $^{220,\ 222}$Rn concentrations in various depths were continously monitored in the unsaturated soil. During a rain event, the lower most sampling port was flooded by the rising groundwater table. In response to saturation, the ^{222}Rn concentrations decreased by 40-50%, but the ^{220}Rn concentrations become virtually zero. After the event, e.g. the return to partly unsaturated conditions, the ^{222}Rn concentrations increased to former levels whereby the ^{220}Rn concentrations only slightly rose to 20% of the pre-event concentration. We conclude from the different response of $^{220,\ 222}$Rn, that the release of ^{220}Rn to soil air is controlled by the soil water content, i.e. the thickness of water films around the soil grains. As the diffusion length of ^{220}Rn is about 75 times smaller than that of ^{222}Rn, most of the short lived ^{220}Rn decays within the water film, if the layer reaches a certain critical thickness. In contrast, the long lived ^{222}Rn diffuses through the water film into the soil air.

We tested this hypothesis in laboratory experiments with Mn-coated sand, that emanates ^{220}Rn. In a closed vessel, the sand was sequentially wetted while the ^{220}Rn concentration in the surrounding air was analyzed. Preliminary results show that the release of ^{220}Rn from sand to air is effectively controlled by the water content of the sand: at a critical water content, the measured ^{220}Rn concentration dropped to almost zero, adding experimental support that the release of ^{220}Rn is controlled by the available humidity in the porous media.

A new highly effective silicagel emitter for lead isotopic measurements

MAGDALENA HUYSKENS*, TSUYOSHI IIZUKA AND YURI AMELIN

Research School of Earth Sciences, Australian National University, Canberra 0200 Australia (magda.huyskens@anu.edu.au, tsuyoshi.iizuka@anu.edu.au, yuri.amelin@anu.edu.au)

In modern U-Pb-geochronology a precision as high as 0.01% can be achieved in isotopic analyses using thermal ionization mass spectrometry. One of the prerequisites for achieving this high precision was the development of a highly effective ion emitter [1], which is based on a colloidal silicagel formerly produced by the chemical company Merck. Unfortunately this silicagel is not available for purchase anymore, and another ion emitter will be needed if the emitter efficiency of colloidal silica deteriorates with time. We tested colloidal silicagels from Alpha Aesar, Nissan Chemicals and Sigma-Aldrich as possible alternatives to the established Merck emitter. The gels were tested for U and Pb blanks and the ion yield (number of ions detected divided by number of atoms loaded) depending on the SiO_2 concentration and particle size using 300 pg Pb of the Pb isotopic standard SRM-981. For the most effective emitter, we also searched for the optimal mixing proportion of silicagel and H_3PO_4.

The Pb blanks of the gels from all three companies are below 0.7 pg/g and for Sigma-Aldrich ~0.15 pg/g. The U blanks from Nissan Chemicals are between 21 and 38 pg/g and for Alfa Aesar ~0.7 pg/g, rendering these silicagels unsuitable for U analysis. The gel from Sigma-Aldrich shows low U blanks below 0.1 pg/g. We found no correlation between ionisation efficiency and the particle size of SiO_2. The most effective emitter is from Sigma-Aldrich at a concentration of 0.4%. The average ion yield for this concentration is 5.8% (n=18), higher than the average ion yield of 4.1% (n=23) of the Merck gel. The accuracy and reproducibility of the isotopic ratios of both gels are comparable (^{207}Pb/^{206}Pb = 0.914740 ± 0.000041 for Sigma-Aldrich and ^{207}Pb/^{206}Pb = 0.914735 ± 0.000048 for Merck). Fractionation factors range between 1.0005 and 1.0012. The highest ion yield for Sigma-Aldrich gel was obtained using 92 µg of H_3PO_4 and 0.004 ml of gel.

From these observations we conclude that the Sigma-Aldrich silicagel is an excellent alternative for the established Merck silicagel for Pb isotopic measurements.

[1] Gerstenberger & Haase (1997), *Chem Geol* **136**, 309-312.

https://doi.org/10.1180/S0026461X00006502 Published online by Cambridge University Press

The uraniferous groundwaters and minerals in the two-mica granite of the Daejeon area, South Korea

J. HWANG[1]* AND S.H. MOON[2]

[1]Daejeon University, Daejeon 300-716, Korea
(*correspondence: jeongha@dju.ac.kr)
[2]KIGAM, Daejeon 305-350, Korea (msh@kigam.re.kr)

Daejeon is the most worrisome area for U-contaminated groundwater in South Korea. Many workers have deep concerns about the geological environment and sources of uranium in the groundwater of the Daejeon area. The regional geology is dominated by Mesozoic two-mica granite and Paleozoic meta-sedimentary rocks composed of metamorphic black slate, mica-schist, and carbonate rock. The black slate includes low grade U ore up to 0.11%, but has not been mined. The U concentration in groundwater is high in the two-mica granite area, but the U-minerals have not yet been described. To elucidate the source of U in groundwater, the geochemistry and environmental isotopes of the groundwater, as well as the U-minerals of the source rock, are examined in this study.

The groundwater in uraniferous meta-sedimentary rocks has a very low U concentration, less than 10μg/L. Meanwhile, the maximum level of U in two-mica granite is as high as 402μg/L. The ranges in Eh values of groundwater in granite and meta-sedimentary rocks are +202~+385 mV and -50~+225 mV, respectively. Granite aquifers are mostly subject to oxidizing conditions but meta-sedimentary aquifers are subject to relatively reducing conditions. Despite the high content of U in black slate, very little U is extracted into groundwater due to the reducing environment. The ranges in the $^{87}Sr/^{86}Sr$ ratios for groundwater in granite and meta-sedimentary rocks are 0.7111~0.7201 and 0.7112~0.7620, respectively. The consistent $^{87}Sr/^{86}Sr$ ratios of groundwater in granite indicate that the aquifer has remained a closed system. The $^{87}Sr/^{86}Sr$ ratios of uraniferous groundwater are similar to those of granite in the Daejeon area. The geochemical and isotopic data indicate that the U in groundwater in this area is genetically associated with the granite and not with the U-ores in black slate.

To examine the U-minerals in granite, a gamma ray spectrometry survey was conducted and U-count anomalies were identified along the contact zone between the two-mica granite and mica-schist, and fracture-filling quartz veinlet. The U-mineralization is dominated by uraninite, coffinite, uranophane and is commonly accompanied by hydrothermal alteration. The mica schist in contact with granite include graphite and sulphide, which provide a reducing environment favorable for U deposition. The redox condition is the critical factor for the formation of U-ores and uraniferous groundwater in the Daejeon area.

The charateristics of tremolite asbestos occurred in abandoned asbestos mines in South Korea

J. HWANG, J. OH, G. PARK AND H. LEE*

Pusan National University, Busan 609-735, Korea
(*correspondence: hmlee61@hotmail.com)

Recently, asbestos health risk and mining restoration become a big issue in the abandoned asbestos mine area. Tremolite asbestos has been known as the most toxic one causing lung cancer and mesothelioma. Tremolite asbestos mines are rarely found in the world, but four mines (Sinsuk mine and Daebosuksan mine in Boryeong area, Chungcheongnam-do, Bonghyeon mine in Yeongju area, Gyeongsangbuk-do and Ewha mine in Yeongwol, Gangwon-do) were operated up to 1980's in South Korea. The geological and mineralogical informations are needed for the asbestos health risk evaluation and mine restoration. In this study, the origin and characteristics of tremolite asbestos and the property changes by weathering process were examined with ores and soils in abandoned mine areas.

All the mines are formed in metamorphic rock strata consisting of the Precambrian mica schist and gneiss. Tremolite asbestos deposits are known to be formed by hydrothermal alteration of dolomitic limestone or ultramafic rocks intercalated in the Precambrian metamorphic rock strata. Associated minerals are significantly different with different mines. Tremolite in ores and soils were analyzed with optical microscope and SEM/EDS. Tremolite asbestos fibers have the average length of 12~38μm. The aspect ratio varies significantly and have range of 7.4~19. The significant morphological difference is observed with different mines. Tremolites found in soils of mine area shows similar morphological properties with ores. The distribution in soil is limited to the transportation ranges by stream water and sediments. The properties of tremolite asbestos are not varied with weathering process and closely related to the parent rock types. In all mines, prismatic tremolites are also commonly occurred with asbestos form tremolites. Although some of asbestos form tremolites may be formed by splitting through the cleavage of prismatic tremolite, those are mainly formed by crystal growth habit regulated by the environmental condition at the time of formation.

As described above, the associated minerals and crystal morphology are significantly different among the mines in the Boryeong area and the Yeongju and Yeongwol areas. It is considered that the differences in associated minerals and crystal morphology are caused by the degree of hydrothermal alteration and parent rock type.

https://doi.org/10.1180/S0026461X00006502 Published online by Cambridge University Press

Strongly reduced gases emitted during flood magmatism and their environmental consequences

G. IACONO-MARZIANO[1]*, F. GAILLARD[1], B. SCAILLET[1], V. MARECAL[2], M. PIRRE[3], A.G. POLOZOV[4] AND N.T. ARNDT[5]

[1]ISTO, UMR 6113 CNRS-Université d'Orléans, France (*correspondence: giada.iacono@cnrs-orleans.fr)
[2]CNRM-GAME, Toulouse, France
[3]LPC2E, UMR 6115 CNRS-Université d'Orléans, France
[4]IGEM RAS, Moscow, Russia
[5]ISTerre Université de Grenoble, France

We use thermodynamic calculations to show that high-temperature interaction between basaltic magma and organic matter can profoundly affect the redox state of the magma and of the gases in equilibrium with it. Our calculations simulate the incorporation into the gas-melt system of organic compounds like CH and CH_2 and take into account S-H-O-C gaseous species at temperatures and pressures in equilibrium with a basaltic liquid. We predict that the assimilation of less than 1 wt% organic matter produces gases with very unusual compositions that are CO-dominated and have H_2O and CO_2 as minor constituents. The crystallization of graphite and native iron is also predicted as a consequence of CH or CH_2 incorporation.

We combine our calculations with existing petrological observations on the Siberian Traps to assess the relevance of this process for the emplacement of voluminous magmatic intrusions in the coaliferous sediments of the Tunguska Basin. Critical is the presence of magmatic graphite and native iron in igneous mafic rocks, which allows to constrain the minimum amount of organic matter assimilated and the composition of the produced gases. We also present an estimation of the fluxes of the exceptional CO-dominated gas emissions, which are likely to have been produced by the emplacement of the Siberian intrusions. We finally evaluate the fate of such gases during their diffusion in the atmosphere, by using a regional 3D atmospheric model coupled to a tropospheric chemistry one.

The chemistry and the environmental impact of the Romanian phosphogypsum

A.M. IANCU, ŞT. MARINCEA, D.G. DUMITRAŞ, C. GHINEŢ AND N. CĂLIN

Geological Institute of Romania,Caransebes 1st., Bucharest 012721, Romania (aurash83@yahoo.com)

The aim of this paper is the mineralogical and geochemical description of phosphogypsum from a Romanian location for an accurate assessment of its environmental impact. Phosphogypsum is a technogenic (mineralurgic) by-product from the extraction of phosphoric acid from raw phosphate ore, consisting mainly of apatite [ideal formula: $Ca_5(PO_4)_3(F, OH, Cl)$]. The extraction technology uses normally the sulfuric acid to attack the apatite mineral. The phosphogypsum contains (in weight percentages) 32% CaO, SO_3 45% and 15% water of crystallization, with approximately 8% of impurities.

The chemical composition of phosphogypsum is influenced by three factors: 1) by the type of phosphate rock (apatitic rock) used as primary material, and olso by the nature and distribution of the trace elements of the rock; 2) by the processes of manufacturing of the phosphoric acid: the extraction process of the phosphogypsum, having as an intermediar product the calcium dehidrate, leads to the formation of some phosphogips, witch have a high level of contamination than their homologue, in some compounds as: Mn_2O_3, MgO, Fe_2O_3, Al_2O_3, Na_2O, K_2O, SiO_2, P_2O_5; 3) by the dumps age or stored phosphogypsum deposits, which, due to the percolation of the meteoric wather, have the tendancy of lousing, through solubilisation, a part of some trace elements. Some of the chemical, mineralogical and radiometric characteristics of the phosphogypsum, but also its use as a primary material can directly influence its impact on the environment and also on the human health collectivises.

The main factors, that have a major impact on the environmental safety, but also on the phosphogypsum recycling, are the radioactivity, the toxic elements contents, pore water acidity, mineral's impurity, the contents in rare elements.

The pollutants emitted from the phosphogypsum dumps have a potential impact on the environment, affecting both the people and the animals. The potential pathways of human exposure to these pollutants include: the irradiation with gamma rays; the content in toxic elements; contaminated dust and other elements which can provoce the cancer; the ingestion of contaminated groundwater.

https://doi.org/10.1180/S0026461X00006502 Published online by Cambridge University Press

Reliance of the rate of dissolution of the SON68 glass on SiO_2(aq): New quantification using interferometry

JONATHAN P. ICENHOWER,*[1] CARL I. STEEFEL,[1] ANDREAS LUTTGE,[2] JOE RYAN[3] AND ERIC M. PIERCE[4]

[1]Lawrence Berkeley National Laboratory, Berkeley, CA 94720 USA (*correspondence: jpicenhower@lbl.gov, cisteefel@lbl.gov)
[2]Rice University, Houston, TX 77005 USA (aluttge@rice.edu)
[3]Pacific Northwest National Laboratory, Richland, WA 99352 USA (joe.ryan@pnl.gov)
[4]Oak Ridge National Laboratory, Oak Ridge, TN 37831 USA (pierceem@ornl.gov)

At present, one of the most vexing problems confronting experimentalists and modelers alike is how nuclear waste glasses will react long-term in the repository environment. Many of the experiments that underpin modeling efforts have been conducted at conditions that are not germane to answering these questions. One of the most important constituents in natural subsurface waters is dissolved silica [SiO_2(aq)], and efforts are underway to understand the dependence of the dissolution rate on this component. A method to determine rates accurately in solutions containing high concentrations of SiO_2(aq) is needed.

We present evidence that rates of glass dissolution can be quantified by using a Vertical Scanning Interferometer (VSI) over a range of SiO_2(aq) concentrations. Polished glass monoliths (SON68) were exposed to solutions containing 0 to 5.46×10^{-3} mol/L SiO_2(aq) at 90°C and pH = 9. Both batch (static) and flow-through reactor systems were employed. In the former, the surface area of glass to volume of solution ratio (SA/V) was kept at a low value, ensuring that the system maintained a constant chemical affinity. In the flow-through systems, the SA/V ratio was higher and the release of elements into solution was monitored to ensure steady-state values. Dissolution rates by VSI were determined by comparing the height of the reacted surface to that of a pristine reference surface, and these rates were compared against those determined by assaying the effluent solutions from the flow-through experiments. The results revealed a close correspondence between the two methods for determining rates, and both methods indicated a linear dependence of the rates upon the concentration of SiO_2(aq) in solution [$\log R = -1.37 \times 10^{-2}(Si) - 5.41$]. This linear dependence shows that the rate can be quantified at conditions pertinent to the disposal environment and that a mechanistic basis for predicting rates can be realized.

Smoke aerosol emission source analysis from satellite and airborne measurements

CHARLES ICHOKU[1]*, CHARLES GATEBE[1,2] AND RALPH KAHN[1]

[1]Climate and Radiation Branch, NASA Goddard Space Flight Center, Greenbelt, MD 20771, USA (*correspondence: Charles.Ichoku@nasa.gov)
[2]GEST, University of Maryland Baltimore County, MD, USA

Accurate estimation of smoke emission source strength from active fires is essential for modeling smoke emission fluxes, transport, atmospheric interactions, and impacts on air quality and climate. For several decades, researchers have made efforts to estimate smoke emissions from ground-based measurements, but the spatial and temporal coverage is severely limited. The rapid growth of satellite measurement capability during the last decade has provided the potential to overcome these limitations by covering the entire globe for long periods of time. However, satellite remote-sensing methods are faced with new challenges as they attempt to use instantaneous observational snapshots to address continuous and highly variable processes such as fires and their emissions. The result is that, although the satellite enables more ground to be covered, uncertainties in quantifying emissions still remain, and may be even greater, compared to the ground-based methods. One of the promising ways to address this issue is the use of airborne measurements to bridge the spatial and temporal scales between the regional-scale satellite snapshots and landscape-scale, longer-duration processes of fire behavior and emissions. The ARCTAS summer campaign that was conducted in Canada in June–July 2008 provides a unique opportunity to demonstrate this approach with regard to closely exploring improved understanding of smoke emission mechanisms by remote sensing. In this talk, we will show preliminary results of using the vertical scans of plumes from the Cloud Absorption Radiometer (CAR) instrument aboard the NASA P-3 aircraft to complement the analysis of fire radiative power (FRP) and aerosol optical depth (AOD) measurements from MODIS aboard the Terra and Aqua satellites, and near-source plume-height measurements from MISR aboard Terra, to better understand the relationships between them, and elaborate the emission rates, spatial characteristics, and injection processes of smoke particulate matter.

https://doi.org/10.1180/S0026461X00006502 Published online by Cambridge University Press

Characteristics of the Ruwai base metal-Ag skarn in Tertiary middle Kalimantan volcanic arc, Indonesia

A. IDRUS[1]*, F.M. MEYER[2], S. SINDERN[2], L.D. SETIJADJI[1] AND I.W.WARMADA[1]

[1]Department of Geological Engineering, Gadjah Mada University, Yogyakarta, Indonesia (*correspondence: arifidrus@gmail.com)
[2]Institute of Mineralogy and Economic Geology, RWTH Aachen University, Aachen, Germany

This study is dealing with geology and characteristics of mineralogy, geochemistry and physicochemical conditions of hydrothermal fluid responsible for the formation of the Ruwai skarn base metal (Pb-Zn-Cu)-Ag deposit in Tertiary middle Kalimantan volcanic arc, Indonesia. The formation of Ruwai skarn is genetically associated with calcareous rocks consisting of limestone and siltstone (derived from marl?) and controlled by NNE-SSW-trending strike slip faults and localized along N 70° E-trending thrust fault, which also acts as contact zone between sedimentary and volcanic rocks in the area. The Ruwai skarn is mineralogically characterized by prograde alteration (garnet and clino-pyroxene) and retrograde alteration (epidote, chlorite, calcite and sericite). Garnet is of andraditic composition, whereas clino-pyroxene is identified as wollastonite, diopside and hedenbergite. Both garnet and clinopyroxene show a petrographic and chemical zonation. Ore mineralization is typified by sphalerite, Ag-rich galena and chalcopyrite, which formed at the early retrograde stage. Galena is typically enriched in silver up to 0.45 w t% and bismuth of about 1 wt %. Geochemically, SiO_2 is enriched and CaO is depleted in limestone, consistent with silicic alteration (quartz and calc-silicate) and decarbonatization of the wallrock. The measured resources of the deposit are 2,297,185 tonnes at average grades of 14.98 % Zn, 6.44 % Pb, 2.49 % Cu and 370.87 g/t Ag. Ruwai skarn orebody originated at moderate temperature of 250-266 °C and low salinity of 0.3-0.5 wt.% NaCl eq. The late retrograde stage formed at low temperature of 190-220 °C and low salinity of ~0.35 wt.% NaCl eq., which was influenced by meteoric water incursion at the late stage of the Ruwai base metal-Ag skarn formation. Further exploration of the skarn extension in the prospect area should consider the structural setting, lithologic distribution and the presence of the diagnostic calc-silicate minerals.

Pressure-induced phase transitions and H-D isotope effects in portlandite

R. IIZUKA[1]*, H. KAGI[1], K. KOMATSU[1], T. YAGI[2] AND S. NAKANO[3]

[1]Geochemical Research Center, Graduate School of Science, Univ. of Tokyo, Tokyo 113-0033, JAPAN (*correspondence: riizuka@eqchem.s.u-tokyo.ac.jp)
[2]ISSP, Univ. of Tokyo, Chiba 277-8581, JAPAN
[3]NIMS, Ibaraki 305-0044, JAPAN

$Ca(OH)_2$, portlandite, has a CdI_2 type structure and is one of the simple hydrous minerals. A crystal-to-crystal phase transition ocurrs around 10 GPa at room temperature in various pressure transmitting media [1, 2]. In brucite, which has an iso-structure of portlandite, H-D isotope effect on the compressibility was found from neutron diffraction [3]. In our study, the isotope effect on the pressure-induced responses was studied in order to clarify the phase transition mechanism accompanied by the geometrical change of hydrogen bonding for neutron diffraction studies in future.

Powder samples were synthesized by hydration of CaO powders with water (or D_2O) in a Teflon lined stainless steel autoclave at 240°C for one week. The single-crystals were obtained by recrystallizing from powder. These samples were loaded in clamped DACs with a few small ruby chips. As a pressure medium, 4:1 methanol-ethanol mixture or He gas was used. IR absorption spectra were measured at the IR synchrotron radiation beamline BL43IR at SPring-8. Angular-dispersive synchrotron X-ray diffraction experiments up to 25 GPa were performed on the BL-18C beamline in the Photon Factory (PF), KEK.

No remarkable difference between $Ca(OH)_2$ and $Ca(OD)_2$ samples was found in the compression behaviors from powder XRD patterns. They were consistent with the previous studies [4-7]. The OH(OD) vibration peaks of IR spectra were split at 6-7 GPa for single-crystals in He medium. No significant difference suggesting the isotope effect was found in the phase transition pressure. The hydrostaticity was found to contribute strongly to the process of the phase transition or amorphization. This implies that neutron diffraction of portlandite needs to be carefully measured under controlled stress conditions using large-volume presses.

[1] Catalli *et al*. (2008) *GRL* **35**, L05312. [2] Ekbundit *et al* (1996) *J. Solid State Chem*. **126**, 300-307. [3] Horita *et al*. (2010) *PCM* **37**, 741–749. [4] Meade & Jeanloz (1990) *GRL* **17**, 1157–1160. [5] Nagai *et al*. (2000) *PCM* **27**, 462–466. [6] Pavese *et al*. (1997) *PCM* **24**, 85–89. [7] Xu *et al*. (2007) *J. Solid State Chem*. **180**, 1519–1525.

https://doi.org/10.1180/S0026461X00006502 Published online by Cambridge University Press

Evolution of the African continental crust from Pb-Hf-O isotope systematics of detrital zircons

TSUYOSHI IIZUKA[1,2]*, IAN H. CAMPBELL[1] AND CHARLOTTE M. ALLEN[1]

[1]RSES, ANU, Canberra ACT 0200, Australia (ian.campbell@anu.edu.au, charlotte.allen@anu.edu.au)
[2]DEPS, Uni. Tokyo, Tokyo 113-0033, Japan (*correspondence: iizuka@eps.s.u-tokyo.ac.jp)

To better understand the evolutionaly history of the African continental crust, we have determined U-Pb ages, Lu-Hf and O isotopic compositions of ca. 450 detrital zircons from the Congo, Nile, Orange, Zambezi and Niger Rivers. The U-Pb isotopic data reveal the lack of >3.2 Ga zircons in the river sands, and distinct peaks at 2.7-2.5, 2.1-1.9, 1.2-1.0 and 0.9-0.6 Ga. The εHf(t) population shows that many zircons, even those having Archean U-Pb ages, crystallized from magmas involving an older crustal component (Figure 1). The O isotopic analyses reveal that ca. 70% of the zircons have $\delta^{18}O$ values higher than 6.5 (Figure 1), indicating that reworking of supracrustal material is important in the granitoid crust formation. However, no >2.0 Ga detrital zircons have $\delta^{18}O$ values higher than 8.0, suggesting restricted contribution of mature sediment to granitoid magma genesis in the Archean and early Proterozoic. We calculated Hf isotopic model ages for the zircons to estimate the mean mantle-extraction ages of their source materials. The oldest zircon Hf model ages of ca. 3.4 Ga suggest that some crust generation had taken place by that time, and that it was subsequently reworked into <3.2 Ga granitoid crust. The Hf model age distribution of the zircons having $\delta^{18}O$ values lower than 6.5 shows a prominent peak at 1.1-0.8 Ga, implying rapid generation of the continental crust at that time.

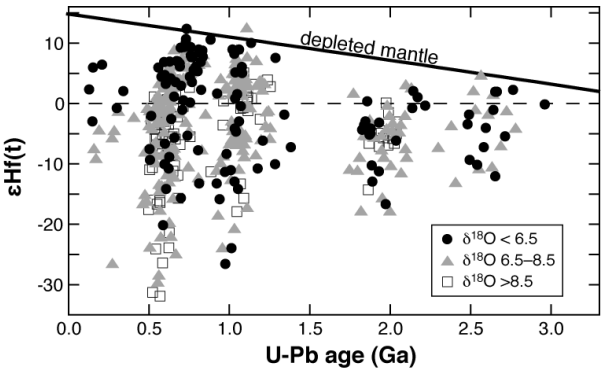

Figure 1: Plot of age vs. εHf(t) for African detrital zircons.

Biogeochemical processes in mud-volcano sediments from the Kumano forearc basin, Japan

A. IJIRI[1*], T. TOKI[2], Y.T. YAMAGUCHI[3], S. KWAGUCCI[1], S. HATTORI[4], Y. MORONO[1], U. TSUNOGAI[5], K. NAKAMURA[6], K. TAKAI[1], J. ASHI[3], F. INAGAKI[1]

[1]Japan Agency for Marine-Earth Science and Technology, Japan (*corespondence: ijiri@jamstec.go.jp)
[2]University of the Ryukyus, Japan
[3]The University of Tokyo, Japan
[4]Tokyo Institute of Technology, Japan
[5]Hokkaido University, Japan
[6]National institute of Advanced Industrial Science and Technology, Japan

Remarkable populations of microbial life have been observed in global subseafloor environments. However, it remains largely unknown if the deep-derived diapiric structure provides potential habitats for subseafloor life or not. Here, we investigated microbial communities and biogeochemical processes in mud-volcano subsurface sediments down to 20 meters from the summit, obtained from the Kumano forearc basin in the Nankai Trough during the CK09-01 D/V *Chikyu* training cruise in 2009.

Pore water extracted from the cored sediments showed significantly low chlorinity to seawater (averaged in 23% of that in seawater), indicating that dehydrate reaction of clay minerals had previously occurred in the deeply buried sedimentary layer. The cored sediments contained relatively low population of microbial cells ($<10^4$ cells/cm^3). The $\delta^{13}C$ value of dissolved inorganic carbon ($\delta^{13}C_{DIC}$) increased with the coring depth, reaching +40‰ at 3 meters below the seafloor (mbsf). The highly ^{13}C-enriched values are possibly due to strong microbial reduction of DIC to ^{12}C-enriched products. The hydrogen isotopic composition of methane (-181±2‰) and magnitude of the carbon isotopic fractionation between DIC and methane (75.6±2.8‰) bellow 3 mbsf suggest the significant contribution of hydrogenotrophic methanogenesis as the source of methane. The $\delta^{13}C$ value of acetate was appeared to increase with the sediment depth (from -41 to -22‰), synchronous to the increase of $\delta^{13}C_{DIC}$. The significant isotopic fractionation between DIC and acetate (54.0±6.9‰) indicates that the principal process producing acetate is homo-acetogenesis via the reductive acetyl-CoA pathway. Radioactive tracer experiments exhibited relatively high activities of homo-acetogenesis (14–34,900 pmol/cm^3/day) and hydrogenotrophic methanogenesis (0.6–128 pmol/cm^3/day), consistently suggesting that autotrophy plays significant biogeochemical roles in the mud-volcano subseafloor microbial ecosystem.

https://doi.org/10.1180/S0026461X00006502 Published online by Cambridge University Press

Enhanced chemical weathering during early Triassic in response to the collapse of terrestrial ecosystem after the end-Permian mass extinction

M. IKEDA*, H. SAKUMA, R. TADA AND S. TAKAHASHI

Dept. of Earth and Planetaly Science, University of Tokyo, 113-0033, Japan
(*correspondence: m_ikeda@eps.s.u-tokyo.ac.jp

The vegetation recovery after the end-Permian mass extinction was delayed by > 5 m.y. until middle Triassic. It is demonstrated that the collapse of terrestrial vegetation enhanced physical weathering during early-middle Triassic, whereas its impact on chemical weathering intensity has not been investigated. Here, we investigate the variations of chemical weathering intensity and biogenic Si flux from lower to middle Triassic pelagic siliceous sequence of the equatorial Panthalassa in Japan, whose cyclostratigraphy is well established [1, 2]. Our results suggested that the chemical weathering intensity and the biogenic Si flux during early Triassic were extremely high relative to middle Triassic and decreased during middle Triassic. Also, the calculated biogenic Si budget on pelagic Panthalassa during early and middle Triassic was several times larger than total Si budget of global ocean today [3], suggesting that pelagic siliceous sequence at equatorial Panthalassa was the major sink of oceanic Si. Hence, the changes in biogenic Si flux on pelagic Panthalassa could reflect changes in global chemical weathering intensity in time scales larger than the residence time of Si in the ocean (> 10 kyr [3]). Therefore, the increase and following decrease in chemical weathering intensity during early to middle Triassic would have been related to the collapse of terrestrial vegetation and its recovery during early Triassic.

[1] Ikeda *et al*., (2010), *Earth Planet. Sci. Lett*., **297**, 369-378. [2] Sakuma *et al*., in review *Island Arc* [3] DeMaster *et al*., (2002), *Deep-Sea Research,* **49**, 3155–3167

Trace metal concentrations and Pb isotopes of sediments from Barkley Sound, British Columbia

MARIKO IKEHATA*, ALYSSA E. SHIEL AND DOMINIQUE WEIS

PCIGR, EOS, University of British Columbia, Vancouver BC, V6T 1Z4, Canada
(*correspondence: mikehata@eos.ubc.ca)

Port Alberni is home to several industries (e.g., pulp and paper mills), responsible for releasing significant amounts of heavy metals (e.g., As, Cd, Pb and Hg) into Alberni Inlet every year [1]. Alberni Inlet may carry this metal effluent into Barkley Sound, located on the west coast of Vancouver Island, British Columbia (BC), home to economically important oyster farms. Alberni Inlet supplies freshwater to Barkley Sound and the headwaters are proximal to Port Alberni. Emissions associated with recreational boating in Barkley Sound and traffic in the lower mainland and on Vancouver Island are other potential sources of Pb pollution. We determined As, Cd and Pb metal concentrations and Pb isotopic compositions in sediment samples from Barkley Sound, collected from transects along Imperial Eagle Channel, Trevor Channel, and from Junction Passage, to assess metal contamination associated with local industries and trace the source of Pb pollution.

Metal concentrations for sediments from Barkley Sound range from 6.20 to 10.8 ppm for As, from 0.36 to 0.56 ppm for Cd, and from 4.91 to 17.5 ppm for Pb. The highest concentrations of As and Cd were observed in sediments from Junction Passage, directly downstream from Alberni outlet. In general, a decrease in Pb, As and Cd in the sediment was observed along NW-SE transects, i.e. towards the open ocean. Sediment $^{206}Pb/^{207}Pb$ ratios increase with increasing distance from Port Alberni, suggesting increasing natural contributions. The $^{206}Pb/^{207}Pb$ ratios (1.1783 to 1.1909) were primarily within the high end of the range reported for BC road dust [2], with the exception of that of sediment from the most distal site in Trevor Channel, with an isotopic composition closer to that of North Pacific sediments [3]. Our study shows that metal concentrations in Barkley Sound sediments are controlled in large part by anthropogenic activities and industrial inputs to Alberni Inlet.

[1] Environment Canada (2009) National Pollutant Release Inventory Facility (NPRI) [2] Preciado *et al*. (2007) *Water Air Soil Poll* **184**, 127-139. [3] Carpent *et al* (2010) *Gold. Conf. Absr*. 144

https://doi.org/10.1180/S0026461X00006502 Published online by Cambridge University Press

High fluctations of suspended load in a tidal influenced river mouth, west coast of India

D. ILANGOVAN

National Institute of Oceanoraphy, Goa-403206, India

Suspended load of water bodies play a major role in studies related to pollution levels, turbidity, source and sink of sediments, sediment transport, etc. Proper sampling method brings out acceptable interpretations. Many times, one time observation of suspended sediment load is considered as representative of that aqueous ecosystem. However, one time observation of suspended sediment load may be less objectionable in substantiating the interpretation of the observation when aqueous body is a land locked lake or undisturbed fresh water river system. Therefore, the present study was carried out to check the validity of one time sampling. The study involved, every 2 hours observation of suspended sediment load at surface, mid depth and at near bottom of a tidally influenced river mouth (River Dahej), at west coast of India, for 2 days. The obtained data reveal high fluctuations in the volume of suspended sediment matter. Various parameters such as flood tide, ebb tide, slack period, spring tide, neap tide, fresh water-sea water mixing, water currents, etc., must be controlling the suspended sediment matter concentration in an environment which is influenced both by marine and riverine ecosystem. This study therefore, reveals the necessity of an acceptable sampling protocol considering all the controlling parameters so that interpretations of the observations are truly representative of the conditions of the involved aqueous ecosystem.

Effect of lake sediment application on soil structure assessed by means of X-ray computed microtomography

B. ILLERHAUS[1]*, M. JOSCHKO[2], D. BARKUSKY[3], J. REINHOLD[4], G. GLEIXNER[5] AND F. GERLACH[6]

[1]BAM Bundesanstalt für Materialforschung und –prüfung, Berlin, Germany (*correspondence:bernhard.illerhaus@bam.de)
[2]Leibniz-Zentrum für Agrarlandschaftsforschung (ZALF) e. V., Inst. Für Landschaftsstoffdynamik, Müncheberg, Germany
[3]ZALF Forschungsstation Landwirtschaft, Müncheberg, Germany
[4]Stahnsdorf, Germany
[5]MPI-BGC Jena, Germany
[6]ZALF Komturei Lietzen, Germany

It is known that lake sediments applied to agricultural soils may improve soil fertility on dry sandy soils by increasing soil carbon storage and water holding capacity. In contrast, the effect of lake sediments on soil structure has not been well documented yet even though some of the documented effects must be linked to soil morphology. X-ray computed microtomography enables to characterize objects down to 50 μm or less and has recently successfully been applied to soil. The aim of this study was therefore to analyze, by means of X-ray computed microtomography, the structure of soil amended with lake sediments compared to a control.

At the long-term experimental site Lietzen in Brandenburg, lake sediments were applied to the soil after harvest at rates of 15 and 70 t/ha. At two locations within the 70 ha sized field, two undisturbed soil samples each (diameter 3.1 cm, height 4 cm) were taken from 0-4 cm soil depth. They were analysed with a 320 kV micro focus X-ray tube (spatial resolution 1/1000 of maximum sample diameter). The morphometric analysis included the determination of the overall pore volume and the local variance in the samples.

The morphological analysis showed that differences between amended and control soil were minor. In contrast, soil texture which differed strongly between the two sampling sites seemed to profoundly affect soil microstructure (pore volume, soil heterogeneity). It is assumed that the observed differences in soil structure are ultimately linked to soil texture-induced differences in soil biological activity.

The results show that more research is needed to entangle the effects of soil texture vs. management effects on soil microstructure and to identify mechanistical links between soil structure and soil biota under field conditions.

https://doi.org/10.1180/S0026461X00006502 Published online by Cambridge University Press

The Lomagundi-Jatuli $\delta^{13}C$-Event revisited

C.J. ILLING[1]*, R.E. SUMMONS[2], A.E. FALLICK[3], V.A. MELEZHIK[4] AND H. STRAUSS[1]

[1]Institut für Geologie und Paläontologie, WWU Münster, Münster, Germany (*correspondence: c.illing@uni-muenster.de)
[2]Department of Earth, Atmospheric, and Planetary Sciences, Massachusetts Institute of Technology, Cambridge, USA
[3]Scottish Universities Environmental Research Centre, Glasgow, Scotland
[4]Geological Survey of Norway (NGU), Trondheim, Norway

The Lomagundi-Jatuli Event (LJE) is characterized by a positive carbonate carbon isotope ($\delta^{13}C_{carb}$) excursion [1, 2] in the aftermath of the Great Oxidation Event (GOE). Results reported from different successions, ranging in age from 2.4 to 2.2 Ga, imply that the LJE is global in nature [3, 4, 5, 6]. Assuming that the atmospheric/ oceanic dissolved inorganic carbon pool is faithfully archived in respective carbonate rocks, this carbon isotope excursion would indicate a shift in $\delta^{13}C$ of atmospheric CO_2 of at least ~5‰ for the duration of the LJE. The most likely explanation for this strong shift in $\delta^{13}C_{carb}$ is an enhanced biological CO_2-fixation and organic carbon burial leaving the residual pool enriched in ^{13}C. However, an alternative view has recently been proposed [7].

Here, we report paired analysis of $\delta^{13}C_{carb}$ and $\delta^{13}C_{org}$ for rocks capturing the LJE. These were obtained by the Fennoscandian Arctic Russia-Drilling Early Earth Project (FAR-DEEP). Carbonates show the typical positive $\delta^{13}C_{carb}$, values. In contrast, however, the organic matter does not record a corresponding positive shift in $\delta^{13}C_{org}$. Standard isotope mass balance provides no satisfactory explanation. Hence, alternative explanations are in need!

[1]Schidlowski *et al*. (1975), *GCA* **40**, 449-455. [2] Melezhik *et al*. (1999), *Earth Sci. Rev*. **48**, 71–120. [3] Baker & Fallick (1989) *Nature* **337**, 352-354. [4] Karhu & Holland (1996), *Geology* **24**, 867-870. [5] Maheshwari *et al*. (2010), *Precambr. Res*. **182**, 274-299. [6] Tang *et al*. (2011), *Gondwana Res*. **19**, 471-481. [7] Hayes & Waldbauer (2006) Phil. Trans. Roy. Soc. B **361**, 931-950.

Coupled geochemical and foraminiferal response to environmental changes during the deposition of Upper Cretaceous oil shale in the Negev, Israel

P. ILLNER[1], S. ASHCKENAZI-POLIVODA[2], Z. BERNER[1], S. ABRAMOVICH[2], A. ALMOGI- LABIN[3] AND S. FEINSTEIN[2]

[1]Karlsruhe Institute of Technology (KIT), Institute for Mineralogy & Geochemistry, Karlsruhe, Germany (peter.illner@kit.edu)
[2]Ben Gurion University of the Negev, Beer Sheva, Israel
[3]Geological Survey of Israel, Jerusalem, Israel

The accumulation of a 40 m thick oil shale sequence during the latest Campanian marks a major change in the dynamics of the Late Cretaceous southern Tethys upwelling system. Based on the vertical distribution of foraminiferal taxa, Ashckenazi-Polivoda *et al*. [1] established a high resolution paleoenvironmental scheme, defining five planktic (P-Type) and five benthic foraminifera (B-Type) assemblages which thrived under distinct bottom-water aeration and surface water productivity conditions.

Principal component analysis of major and trace elements concentrations in the studied sequence allows distinguishing three factors. The first reflects the interplay between biogenic-carbonate (Ca, Sr) and terrigenous input (Al, Si, K, Ti, V, Fe, Ga, Nb, Ba, Pb, Th). The second mirrors the degree of bottom water oxygenation (C_{org}, S, Ni, Cu, Zn, As, Cd, Mo, U vs. Mn), while the third factor stands for conditions that promoted phosphorite deposition (P, Y, La, U). The comparison of these chemostratigraphic features with the distribution of the foraminiferal assemblage types as defined in [1] points to a strong interdependence between these geochemical and micropaleontological environmental indicators. The distribution of the planktic assemblages P-Types 1 and 4, and the benthic assemblage B-Type 4 parallels the variations in the degree of bottom water oxygenation and detrital input. P-Type 1 and 2 (high *Heterohelix*) assemblages coincide with a gradual decrease in biogenic carbonate production and a relative weak anoxic response to the increase in terrigenous input. In contrast, assemblages P-Type 4 (dominance of *Globigerinelloides*) and B-Type 4 (triserial buliminids and *Gavelinella*), limited to the base of the oil shale, are characterized by strong anoxia and high carbonate production, as reflected by scores of factors 1 and 2.

[1] Ashckenazi-Polivoda *et al*. (in press) *Palaeogeogr. Palaeoclimatol.Palaeoecol*. DOI10.1016/j.palaeo.2011.02.018

https://doi.org/10.1180/S0026461X00006502 Published online by Cambridge University Press

Mobility and bioavailability of some potentially harmful elements around an industrial contaminated environment (Estarreja, Portugal)

M. INÁCIO*, E. SILVA AND V. PEREIRA

University of Aveiro, Department of Geociences, Portugal (*correspondence: minacio@ua.pt)

Located in north central Portugal the industrial Chemical Complex of Estarreja (CQE) is composed of several chemical industries that could cause environment pollution. The most important inputs into the environment are chiefly related to past industrial activities, with the production of sulphuric acid from arsenopyrite roasting (e.g. As, Cu, Ni, Pb and Zn) and from a chloralkali plant (e.g. Hg).

The main purpose of this study was to evaluate the levels of some heavy metals and arsenic in soils and forage plants from Estarreja and from a reference site (Ouca, with no significant industry but a similar geology, pedology). These soils are sandy soils, often used as pasture and agricultural land. In Estarreja 90 topsoils and 27 forage plants were collected; in Ouca 20% of these numbers were sampled. Both soils and plants (separated into roots and green shoots) were analyzed in the same way, extraction with aqua regia and analysis by ICP/ES & MS, for 32 chemical elements. Three single extractants (water; ammonium acetate; EDTA) were used to assess the mobile and plant available fraction of some potentially harmful elements.

The first results show high levels of As and Hg in Estarreja compared to those given in the international guidelines. The maximum concentrations found in the soils are above 10.000 $mgkg^{-1}$ for As and above 100 $mgkg^{-1}$ for Hg. In green shoots, the maximum concentrations found are 255 $mgkg^{-1}$ for As and 5 $mgkg^{-1}$ for Hg. The spatial distribution of these elements shows a typical anthropogenic pattern, with the highest values near the factories and sewage outlets. It was possible to identify an area around the factories and sewage outlets where the median concentrations for As and Hg are more than 10 times higher than the median concentrations found in the reference area, which are close to the national backgrounds [1]. The EDTA was the most effective extractant for all the elements, except Zn, which was higher in the ammonium acetate extracts. However, the amounts extracted with these three extractants are low (less than 5%) for As, Hg, Pb, Cu and Zn, thus attenuating the impact of high metal contents in soils of green areas often used as pasture land and agriculture.

[1] Inácio *et al*. (2008). *Journal of Geochemical Exploration*; **98**: 22-33.

Sequestering of phosphorus during freshening of a silled marine basin; Role of manganese

J. INGRI[1], T. SUTTERASAK[2], A. WIDERLUND[3] AND S-Å. ELMING[4]

[1]Division of Applied Geology, Luleå University of Technology, S-971 87 Luleå, Sweden, (Johan.Ingri@ltu.se)

[2]Division of Ore geology and Geophysics, Luleå University of Technology, S-971 87 Luleå, Sweden, (Thongchai.Sutterasak@ltu.se)

[3]Division of Applied Geology, Luleå University of Technology, S-971 87 Luleå, Sweden, (Anders.Widerlund@ltu.se)

[4]Division of Ore geology and Geophysics, Luleå University of Technology, S-971 87 Luleå, Sweden, Sten-(Ake.Elming@ltu.se)

We have documented sediment sequestering of phosphorus in the Bothnian Bay, northern Baltic Sea, during the last 7000 years, using a paleomagnetic dating method. High resolution sampling and multi-element analyses coupled with ”absolute dating” of the sediment provides a powerful environmental record that can be used to foresee biogeochemical changes caused by climate-induced freshening of the Baltic and other silled marginal marine basins. Late Holocene freshening is pronounced in the Bothnian Bay, with a decline of surface salinity from 10-11‰ down to present day values between 1‰-3‰, consistent with the absence of a permanent halocline, and phosphorous limitation of primary production.

The P/Fe ratio in a 6-m-long piston core show distinct peaks above the time level 2500 years BP, closely related to temporal peak values for manganese, the Mn/Fe ratio and a major changes in magnetic susceptibility. We suggest that the changes in phosphorus sequestering in the core can be explained by the position of the suboxic zone at the time of deposition. A suboxic redox potential can be maintained in these layers if there is an excess of manganese that can oxidise formed sulphide in the sediment during burial. Particulate manganese maintains the suboxic redox level preventing dissolution of Fe-oxyhydroxides with associated phosphorus, at depth in the sediment. Today, the barrier between the sulfide zone and the sulfate zone is situated 0.5 m below the sediment surface. Trace metal data suggest that this zone has been located within the sediment during the whole lifetime of the core. Hence, a layer with high concentrations of Mn and Fe-oxyhydroxides, formed above the sulfide boundary, may pass through the sulfide barrier, leaving Fe-Mn oxyhydroxides in relative equilibrium below the active sulfide boundary.

https://doi.org/10.1180/S0026461X00006502 Published online by Cambridge University Press

Water content of lithospheres deduced from xenoliths: The example of Kerguelen Islands and South African craton

J. INGRIN[1], J. LIU[1,2], Q.-K. XIA[3], E. DELOULE[3] AND M. GRÉGOIRE[4].

[1]UMR CNRS 8207, Univ. Lille 1, 59655 Villeneuve d'Ascq, France. (jannick.ingrin@univ-lille1.fr)
[2]CAS Key Lab. of crust-mantle materials and environment, USTC, 230026, Hefei, China. (liujia08@mail.ustc.edu.cn, qkxia@ustc.edu.cn)
[3]CRPG-CNRS, BP20, 54500 Vandoeuvre les Nancy, France. (deloule@crpg.cnrs-nancy.fr)
[4]GET, UMR CNRS 5563, OMP, Univ. Toulouse III, 31400, Toulouse, France. (gregoire@get.obs-mip.fr)

The formation of the Kerguelen crust since 110 Ma, through magma underplating, may represent a good analogue for continental growth in oceanic environment like it was during the Archean period. The study of water content of granulite xenoliths representative of Kerguelen deep crust and related mantle xenoliths offers the opportunity to: 1) evaluate the distribution of water along the Kerguelen lithosphere; 2) compare it to the content of the older lithosphere like for instance the South African cratonic lithosphere.

We measured water content from 10 granulite xenoliths and 5 mantle xenoliths from alkali basaltic lavas erupted on Kerguelen Islands on the Northern part of the Kerguelen plateau. The xenoliths are composed of two-pyroxenes granulites with spinel or garnet [1]. The analysis of water dissolved as H-related point defects in the main anhydrous phases was done by micro-FTIR with a spot size of 50 microns, a spectral resolution of 4 cm^{-1} and with unpolarized beam following the procedure proposed by Kovacs *et al*. [2]. The water contents of pyroxenes from the granulite xenoliths (up to 180 and 330 ppm H_2O for orthopyroxenes and clinopyroxenes respectively) are significantly higher than those from the mantle xenoliths.

The Kerguelen xenoliths are less hydrous than the ones from the Kaapvaal Craton [3] suggesting that the mantle source at the origin of their formation is less hydrous than the ones at the origin of the older deep crust formed beneath South Africa or the North Chinese cratons [4].

[1] Gregoire *et al*. (2001) *Contrib Mineral Petrol* **142**, 244-259. [2] Kovacs *et al*. (2008) i**93**, 765-778. [3] Ingrin *et al*. (2010) *EGU*. [4] Yang *et al*. (2008) *JGR* doi:10.1029/2007JB005541.

Studies on annual variation of $^{14}C/^{12}C$ ratios in plant samples by AMS

A. INOUE[1*], Y. MURAMATSU[1], H. MATSUZAKI[2] AND S.YOSHIDA[3]

[1]Depertment of Chemistry, Gakushuin University, Mejiro1-5-1, Toshima, Tokyo, Japan (*correspondence: 10142005@gakushuin.ac.jp, yasuyuki.muramatsu@gakushuin.ac.jp)
[2]School of Engineering, University of Tokyo, Hongo1-3-7, Bunkyo, Tokyo, Japan
[3]National Institute of Radiological Sciences, Anagawa 4-9-1, Inage, Chiba, Japan

Carbon-14 ($T_{1/2}$; 5730yr) is one od the most impotant radionuclides produced by the reaction of cosmic ray with nitrogen in the upper atmosphere. Therefore, $^{14}C/^{12}C$ ratios in plant materials should provide information on the past atmospheric ^{14}C levels which might be related to the variation of solar activities. The ^{14}C levels in the atmosphere are also affected by the anthropogenic sources such as nuclear weapons testing and accident of nuclear facilities. In this study, we have determined $^{14}C/^{12}C$ ratios by AMS in three different plant materials, i.e. tree rings of Japanese Yaku-ceder, Japanese rice grains and tree rings of pine from Chernobyl area, for assessing the variation of atmospheric ^{14}C.

In order to know the natural variation of ^{14}C, we used tree rings of old Yaku-ceder (1139 year-old) and focused on a period between 1000-1100 A.D. As a result, we found a peak around 1050 A.D. This suggests that the solar activity was weak in this period.

Results obtained for rice grain samples (1950-2009 A.D.) showed that there was the highest peak around 1963 due to nuclear weapons testing and the values decreased gradually. Residence time of the produced ^{14}C was calculated to be about 11 years.

Tree rings of pine collected from the vicinity of Chernobyl NPP was used to assess the release of ^{14}C at the accident, which occurred in late April 1986. A peak of $^{14}C/^{12}C$ ratio clearly observed in the tree ring of 1986. However, the ratio varied widely within the tree ring. This heterogeneous distribution should be due to the short time releases (about 10 days) of ^{14}C during the accident. To examine this, we have separated early and rate wood and found that the early wood contained markedly high ^{14}C and the late wood contained low ^{14}C compared to whole ring of the same year .

https://doi.org/10.1180/S0026461X00006502 Published online by Cambridge University Press

Effects of thermal and salinity stresses on growth of aposymbiotic and symbiotic primary polyps

M. INOUE[1*], K. SHINMEN[1], H. KAWAHATA[1], T. NAKAMURA[2], A. IGUCHI[3], A. SUZUKI[4] AND K. SAKAI[3]

[1]AORI, Univ of Tokyo, Kshiwa 277-8564, Japan (*correspondence: mayuri-inoue@aori.u-tokyo.ac.jp)
[2] Univ of the Ryukyus, Nishihara, Okinawa 903-0213, Japan
[3]Sesoko Station, Univ. of the Ryukyus, Okinawa 905-0227
[4]GSJ, AIST, Tsukuba 305-8567, Japan

In order to better understand the effects of high thermal and low salinity stresses on coral calcification from the aspect of coral-algal symbiosis, aposymbiotic (lacking symbionts) and symbiotic coral primary polyps were experimentally exposed to several seawater temperatures (27 ~ 33˚C) and salinities (26 ~ 34 treatments). Calcification rates of polyp skeletons with zooxanthellate (symbiotic) were higher than those without zooxanthellate (aposymbiotic) in both the experiments even under high thermal and low salinity stresses.

Symbiotic polyps showed non-linear calcification responses to thermal stresses whereas aposymbiotic demonstrated linear increase of calcification responses according to the increase of temperature. Both aposymbiotic and symbiotic polyps showed the linear decreases of calcification rates according to the decrease of salinity. Our results suggest that future global warming may have negative impact on coral calcification at the primary polyp processing symbionts. In addition, low salinity stress, which would be caused by increase of the intensity of local floods related to future climate change, would certainly decrease coral calcification.

Peridotite xenolith inferences on the formation and evolution of the central Siberian cratonic mantle

D.A. IONOV[1], L.S. DOUCET[1*] R.W. CARLSON[2], N.P. POKHILENKO[3], A.V. GOLOVIN[3] AND I.V. ASHCHEPKOV[3]

[1]Univ. J.Monnet, CNRS-UMR6524, St Etienne 42023, France (*correspondence: dmitri.ionov@univ-st-etienne.fr)
[2]DTM-CIW, Washington D.C. 20015, USA
[2]Inst. Geology & Mineralogy, Novosibirsk 630090, Russia

Ongoing multi-disciplinary studies of large and fresh (LOI ≤1%) mantle xenoliths from the Udachnaya kimberlite in the central Siberian craton address the structure, composition and origin of cratonic lithospheric mantle. Petrographic data document successive deformation of coarse garnet peridotites (with strong crystal preferred orientation) to form: (1) olivine grains that are broken but not recrystallised, (2) porphyroclastic, (3) fluidal mosaic microstructures [1]. Extremely high sub-Moho velocities recorded in some seismic profiles in the craton may reflect strong anisotropy of foliated coarse peridotites [2]. Both sheared and coarse peridotites occur near the base of the lithosphere (≥1300°C, ~6.8 GPa). Oxygen fugacity decreases with depth. The major element composition of the majority of refractory peridotites is consistent with melt extraction at 1-5 GPa; Mg# is ≤0.929. These rocks are depleted in Pd, less commonly in Pt, relative to Os-Ir-Ru. Re-Os ages (T_{RD}) of the melt extraction residues range from 1.5 to 2.3 Ga (av. 1.8 Ga). 15-20% of coarse peridotites are enriched in opx and may have experienced silica addition in subduction settings.

The Proterozoic Re-Os T_{RD} ages of melt extraction residues from this and earlier [3] work indicate that most of the lithospheric mantle formed simultaneously with the assembly of the craton 1.8-2.1 Ga ago and is not coeval with the oldest exposed crustal rocks (2.6-3.5 Ga) [4]. More ancient mantle materials appear to come from volumetrically small terrains. The Siberian craton, and possibly other long-lived, thick, cold, diamond-bearing lithospheric domains, may have been created in the Paleoproterozoic rather than in the Archean.

[1] Ionov *et al*. (2010) *J. Petrol* **51**, 2177-2210. [2] Bascou *et al*. (2011) *EPSL* **304**, 71-84. [3] Pearson *et al*. (1995) *GCA* **59**, 959-977 [4] Rosen (2002) *Russ. J. Earth Sci*. **59**, 103-119.

https://doi.org/10.1180/S0026461X00006502 Published online by Cambridge University Press

Stacked SIMS Spectra: Unravelling ion production in geological materials

TREVOR R. IRELAND, PETER HOLDEN AND PETER LANC

Research School of Earth Sciences, The Australian National University (*correspondence: trevor.ireland@anu.edu.au)

Ion microprobe analyses rely on the production of secondary ions from solid target materials. In the material science community, complexity in ion production is noted for even simple targets comprised of only a few elements. In geological materials, complex mass spectra result from the large number of elements present and their propensity to form molecular ions. The analyses of molecular species is a cornerstone of zircon age determinations but resolution of unwanted interferences is also required.

We have developed a protocol to measure SIMS spectra under varying analytical conditions (mass resolution, energy filtering). These spectra can be stacked to allow identification of relevant species and custom built software allows individual peaks to be scrutinised. A reference lookup list means that isobars can be readily identified.

The spectra have been obtained on SHRIMP-RG, an instrument that allows mass resolution up to 20,000. A combined faraday – ion counter detection system is rapidly switched depending on count rates. Energy filtering can be changed to establish the nature of the molecular interferences based on the progressive exclusion of polyatomic intereferences with energy offset.

Thus far we have applied this technique to NIST glasses as well as minerals used for geochronology – zircon, monazite, and xenotime. For monazite, unresolved interferences in the Pb spectrum could potentially affect some analyses.

Having spectra from different matrices will also allow examination of ion production and speciation models, which will lead to a better understanding of zircon geochronology by SHRIMP.

Trans-lithospheric variations in highly siderophile elements beneath the Ontong Java Plateau

A. ISHIKAWA[1,2*], T. MARUOKA[3], C. W. DALE[4] AND D. G. PEARSON[5]

[1]The University of Tokyo, Tokyo, 153-8902, Japan (*correspondence: akr@ea.c.u-tokyo.ac.jp)
[2]IFREE, JAMSTEC, Yokosuka, 237-0061, Japan
[3]University of Tsukuba, Tsukuba, 305-8572, Japan
[4]Durham University, Durham, DH1 3LE, UK
[5]University of Alberta, Edmonton AB, T6G 2E3, Canada

We determined highly siderophile element (HSE) concentrations and sulfur contents for 70 peridotite xenoliths from Malaita, Solomon Islands, which represent virtually the entire thickness (~120 km) of oceanic lithosphere beneath the Ontong Java Plateau. The major aim is to assess whether the fertile part of the suboceanic mantle yields suprachondritic Ru/Ir and Pd/Ir ratios and hence investigate the extent of non-chondritic HSE systematics in the Earth's mantle. To date, most constraints on PUM HSE characteristics come from subcontinental mantle due to the rarity of fertile samples from ophiolites and abyssal peridotites. In contrast, our Malaita sample set includes MORB source-like spinel lherzolites representing shallow lithosphere (<85 km) and garnet lherzolites from basal lithosphere (95-120 km), likely representing a deep-plume source [1]. A further aim is to examine the formation of an intralithospheric harzburgite layer (85-95 km). A previous Re-Os study revealed that the varying degree of Os-depletion uniquely recorded in this melt-depleted layer is intimately related to the ~122 Ma plateau magma production [2].

The new HSE data demonstrate that lherzolite and harzburgite, the two principal lithologies, display contrasting HSE patterns. Regardless of *P-T,* mineralogy and alteration indices, almost all lherzolites show coherent patterns with suprachondritic Ru/Ir and Pd/Ir, but chondritic Os/Ir and Pt/Ir. This supports the widespread occurrence of PUM-like compositions in Earth's mantle. In contrast, harzburgites display HSE depletion with decreasing sulfur content, coupled with highly fractionated patterns relative to PUM and systematically decreasing HSE/Ru, most likely resulting from progressive extraction of HSE residing in sulfide. We establish an order of HSE compatibility that may place key constraints on the mechanism and condition of formation of harzburgites and their extracted magma.

[1] Ishikawa *et al*. (2004) *J. Petrol*. **45**, 2011-2044. [2] Ishikawa *et al*. (2011) *EPSL* **301**,159-170.

https://doi.org/10.1180/S0026461X00006502 Published online by Cambridge University Press

Possible high-PGE-Au silicate melt/aqueous fluid in mantle wedge: Inferred from Ni metasomatism in Avacha peridotite xenolith

SATOKO ISHIMARU[1,2]*, SHOJI ARAI[2], ANASTASSIA Y. BORISOVA[3,4] AND AKIHIRO TAMURA[2]

[1]Kumamoto Unv., Kumamoto 860-8555, Japan (*correspondence: ishimaru@sci.kumamoto-u.ac.jp)
[2]Kanazawa Univ., Kanazawa 920-1192, Japan
[3]GET-OMP, Toulouse 31400, France
[4]Geological Department, MSU, Moscow 119899, Russia

Platinum-group elements (PGE) and gold (Au) have highly siderophile features and favor to be partitioned into metals and sulfides (such as the Earth's core). Among them, IPGE (Os, Ir and Ru) are well partitioned into residues relative to PPGE (Rh, Pt and Pd) and Au during partial melting of mantle peridotite, although PGE are not mobile during low-temperature alteration processes. We found Ni-rich domains in a highly metasomatized mantle peridotite xenolith (#159) from Avacha volcano, the Kamchatka arc, composed of ordinary mantle minerals (olivine, orthopyroxene, clinopyroxene, chromian spinel, and monosulfide solid solutions; MSS) with high-Ni contents, around aggregates of clays rich in Fe, Ni and S [1]. The high-Ni, -Fe, -S clays at the center of the Ni-rich domain show varied colors under the microscope, from yellowish to brownish. Most of them fill interstitices or cracks, but some are observed as globluer inclusions in olivine (Fo_{93}). The MSS in this sample #159 rarely have quite thin hydroxide alteration rims. The Ni/(Fe + Fe) atomic ratio of the clays are varied (0-0.7) and show a good correlation with their color; when the Ni/(Fe + Ni) is low, the color of the clay is pale and yellowish. The S content of the clays also varies from below the detection to 66,000 ppm but does not show any correlation with the Ni/(Fe + Ni) ratio. Some clays have an extremely PGE- and Au-enriched feature, and the IPGE concentration is 100 times higher than the chondrite values. The presence of high-Ni halo and chemical zoning of NiO content of olivine from the center (5.3 wt%) to the outward (0.4 wt%) in the Ni-rich domain, the high-Fe, -Ni, -S clays are an alteration product of the metasomatic agent that drastically enhanced the Ni content of the surrounding minerals. We propose these clays were new type of S-rich silicate melt or silicate-bearing aqueous fluid to concentrate PGE and Au in addition to Ni and Fe within the mantle wedge.

[1] Ishimaru & Arai (2008) *CMP* **156**, 119-131.

Processes and timescale of subduction initiation and subsequent evolution of oceanic island arc

O. ISHIZUKA[12]*, K. TANI[2], M.K. REAGAN[3], K. KANAYAMA[4], S. UMINO[4], Y. HARIGANE[4,1], I. SAKAMOTO[5], Y. MIYAJIMA[5,6], M. YUASA[1] AND D.J. DUNKLEY[7]

[1]Geological Survey of Japan/AIST, Central 7, 1-1-1 Higashi, Tsukuba, Ibaraki, 305-8567, Japan (*correspondence:o-ishizuka@aist.go.jp)
[2]IFREE, JAMSTEC, 2-15 Natsushima, Yokosuka , 237-0061, Japan (kentani@jamstec.go.jp)
[3]University of Iowa, Iowa City, IA 52242, USA
[4]Kanazawa University, Kanazawa, 920-1192, Japan
[5]Tokai University, Shizuoka, 424-8610, Japan
[6]Marine Work Japan, Kanagawa, 236-0024, Japan
[7]National Institue of Polar Research, Tokyo, 190-8518, Japan

The Izu-Bonin-Mariana (IBM) forearc is thought to be an excellent location for investigating the record of subduction initiation and subsequent arc evolution [1] because of the exposure of early-arc lavas on the forearc islands. Recent dredging and diving in the IBM forearc [2, 3] have revealed a bottom to top stratigraphy of: 1) mantle peridotite, 2) gabbroic rocks, 3) a sheeted dyke complex, 4) basaltic pillow lavas (forearc basalts: FAB), 5) boninites and magnesian andesites, 6) tholeiites and calcalkaline arc lavas. This forearc stratigraphy is remarkably similar to that found in many ophiolites.

The FAB and associated diabase overlying gabbros can be regarded as a first magmatic product produced by decompression melting associated with subduction initiation. $^{40}Ar/^{39}Ar$ ages of 48-52 Ma for these basalts as well as 51.6-51.7 Ma zircon U-Pb ages for the gabbros strongly imply that subduction initiation took place at 51-52 Ma. The change to flux melting and boninitic volcanism took 2-4 m.y., and the change to flux melting in counterflowing mantle and "Normal" arc magmatism took 7-8 m.y. This evolution from subduction initiation to arc normalcy occurred nearly simultaneously along the entire length of the IBM subduction system. The contemporaneousness of IBM forearc magmatism with the major change in plate motion in Western Pacific at ca. 50 Ma suggests that the two events are intimately linked. Mesozoic rocks found in the deep Bonin forearc suggest that the overriding plate at subduction initiation consisted of Mesozoic terranes.

The similarity between the IBM forearc stratigraphy and many ophiolites supports the hypothesis that the forearc crust section that is produced at subduction initiation and is preserved in the IBM system represents an in-situ section of supra-subduction zone ophiolite.

[1] Stern & Bloomer (1992) *Geol. Soc. Am. Bull.* **104**, 1621-36. [2] Reagan *et al.* (2010) G^3, doi:10.1029/2009GC002871. [3] Ishizuka *et al.* (2011) *Earth Planet. Sci. Lett.* **306,** 229-240

https://doi.org/10.1180/S0026461X00006502 Published online by Cambridge University Press

Organic geochemical analysis of the impact of cadaver burial on soil

SOFO S. ISMAIL[1,2]*, IAN D. BULL[1] AND RICHARD P. EVERSHED[1]

[1]School of Chemistry, University of Bristol, Cantock's Close, Bristol BS8 1TS, UK (*correspondence: chssi@bri.ac.uk)
[2]Faculty of Science & Technology, Universiti Malaysia Terengganu, 21030 Kuala Terengganu, Terengganu, Malaysia

A comparative study of soil lipids collected from eleven crime scenes across Malaysia, with different post-depositional intervals (PDI) of cadavers, was conducted. A laboratory degradation study of porcine flesh in soil was also carried out in parallel. The overall premise for this work was that organic molecular components in soil will be useful in determining the provenance of a cadaver and/or calculation of its post-mortem interval (PMI).

The results from the Malaysian samples show that the concentrations of palmitic (C16:0) and stearic (C18:0) acids are higher in the cases with a low PMI, In addition, their unsaturated analogues, palmitoleic (C16:1) and oleic (C18:1) acids are also present at high concentration. The higher concentration of cholest-5-en-3β-ol (cholesterol) in the cases with low PMIs indicates that this component is most likely derived from the decomposing body. The cases with longer PDI demonstrate a large shift towards plant-derived organic material. Differences observed are presumably due to the transformation of the cadaver derived lipids and can be associated with PMI and/or PDI.

Subsequently, porcine flesh was degraded in aerobic and anaerobic soil mesocosms, representative of tropical and temperate climates, for a year. Mesocosms were sampled throughout the experiment and target analytes were chosen to provide information about both materials derived from the flesh and the response of the microbial community to its presence in the soil environment. Initial results reveal that flesh derived triacylglycerol components degrade within the first 120 days resulting in a corresponding increase in concentration of free fatty acids, i.e. palmitic and stearic acids. Similar patterns of degradation are observed under both aerobic and anaerobic conditions. Preliminary analysis of phospholipid fatty acid distributions, derived from the soils, reveals a concentration increase in the region of 180-400% for soils incubated with porcine flesh after 121 days, with a currently unidentified C18:1 fatty acid moiety becoming the dominant component in the latter samples.

[1] Ambles *et al*. (1989b) *J. Soil Sci*. **40**, 685-694. [2] Bull *et al*. (2009) *Science and Justice*, **49**, 142-149. [3] Dent *et al*. (2004) *Env. Ecology* **45**, 576–585. [4] Evershed (1993) *World Archaeology* **25**, 74-93. [5] Forbes *et al*. (2005) *For. Sci. Int*. **127**, 225-230. [6] A.A. Vass (2001) *Microbial Today*, **28**, 190-192

.

Role of acid mobilization in association of smaller particle size with higher iron solubility

AKINORI ITO

RIGC, JAMSTEC, Yokohama 236-0001, Japan (akinorii@jamstec.go.jp)

Iron (Fe) is an essential nutrient for phytoplankton. Iron-containing soil dust mobilized from arid regions supplies the majority of iron to the oceans, but primarily presents in an insoluble form. Since most aquatic organisms can take up iron only in the dissolved form, a key flux is the amount of soluble iron in terms of the biogeochemical response to atmospheric deposition. Atmospheric processing of mineral aerosols by anthropogenic pollutants may transform insoluble iron into soluble forms. We discuss the effect of the acid mobilization on a relationship between aerosol iron solubility and mineral particle size in an aerosol chemistry transport model [1]. The iron solubility from onboard cruise measurements [2, 3] over the Atlantic and Pacific Oceans in 2001 is used to evaluate the model performance in simulating soluble iron.

The association of smaller size with higher solubility as a role of the acid mobilization considerably improves the results of soluble iron in terms of ratio of fine to total particles, compared to constant iron solubility. The improvement of model-observation agreement provides strong evidence for faster iron dissolution in fine particles by anthropogenic pollutants. Accurate simulation of the ratio of fine to total aerosols of soluble iron has important implications with regards to the ocean fertilization because of a longer residence time of smaller particles, which supply nutrients to more remote ocean biome. The model reveals higher concentration of soluble iron in the coarse mode than that in the fine mode over the Southern Ocean except downwind regions of Australian dust, in contrast to the Northern Ocean. These results suggest that dust does not efficiently transport soluble iron to significant portions of the Southern Ocean. This corroborates hypothesis that phytoplankton blooms are not sustained by the supply of iron to surface waters from dust deposition in the Southern Ocean [4] except the Australian sector [5].

[1] A. Ito & Y. Feng (2010), *Atmos. Chem. Phys*. **10**, 9237-9250. [2] Y. Chen & R. L. Siefert (2003), *J. Geophys. Res*. **108**, 4774. [3] A. R. Baker *et al*. (2006), *Mar. Chem*. **98**, 43-58. [4] S. Blain *et al*. (2007), *Nature* **446**, 1070-1074. [5] E. Brévière *et al*. (2006), *Tellus* **58B**, 438-446.

https://doi.org/10.1180/S0026461X00006502 Published online by Cambridge University Press

Zircon U-Pb and FT dating on clastic dykes in the Matsukawa Geothermal field, Japan, with reference to the Quaternary Kakkonda granite

H. ITO[1]*, A. TAMURA[2], T. MORISHITA[2] AND S. ARAI[3]

[1]Central Research Institute of Electric Power Industry, Chiba 270-1194, Japan (*correspondence: ito_hisa@criepi.denken.or.jp)
[2]Frontier Science Organization, Kanazawa Univ., Ishikawa 920-1192, Japan
[3]Department of Earth Sciences, Kanazawa Univ., Ishikawa 920-1192, Japan

We have determined both U-Pb and fission-track (FT) zircon ages from Quaternary clastic dykes in the Matsukawa Geothermal field, northeast Japan [1]. Since the dykes contain granitic xenoliths, the dated zircons may have derived from granitic basements underneath. A weighted mean LA-ICP-MS U-Pb (^{238}U-^{206}Pb) age of 1.30±0.04 Ma (1σ error) and a weighted mean FT age of 1.0±0.1 Ma (1σ error) were obtained from the zircons. This indicates that if zircons are of granitic origin, the granite intruded ~1.3 Ma and cooled to ~300 ºC at ~1.0 Ma, considering closure temperatures of both the dating methods.

Adjacent to the Matsukawa geothermal area, the Quaternary Kakkonda granite with K-Ar ages of 0-0.2 Ma resides below 1.5-3 km depths. The intrusion of the Kakkonda granite is assumed to be ~1.0 Ma based on geological and geochronological evidence [2]. Therefore strong correlation is plausible between the two granites.

U-Pb zircon dating of the Kakkonda granite is now under way. We will report the dating results and the relevance of the Quaternary granite for the related geothermal systems.

Sample code	Number of grains	Dosimeter number	Dosimeter density x 10^5 cm^{-2}	Spontaneous number	Spontaneous density x 10^5 cm^{-2}	Induced number	Induced density x 10^6 cm^{-2}	P(χ^2) %	T ± 1σ Ma
SP-2	30	2270	3.487	88	1.27	2096	3.03	75	1.0 ± 0.1

Ages are calculated using ζ=142.1±5.7 (1σ error). Dosimeter glass CN-1 used.

Table 1: Zircon fission-track dating result.

[1] Hanano (2003) *Geothermics* **32**, 311-324. [2] Doi *et al.* (1998) *Geothermics* **27**, 663-690.

Two flood basalt events and contemporary granites within the same LIP: Siberian Traps case study

A.V. IVANOV[1], H. HE[2], L. YAN[2], V.V. RYABOV[3], A.Y. SHEVKO, S.V. PALESSKY AND I.V NIKOLAEVA[3]

[1]Institute of the Earth's Crust SB RAS, Irkutsk, Russia, (aivanov@crust.irk.ru)
[2]Institute of Geology and Geophysics CAS, Beijing, China, (huaiyuhe@mail.iggcas.ac.cn)
[3]Institute of Geology and Mineralogy SB RAS, Novosibirsk, (Russia, trapp@igm.nsc.ru)

Siberian Traps LIP contains effusive, intrusive and volcanoclastic rocks of variable composition from ultrabasic to acidic, though low-Ti basalts and their intrusive analogues are predominant rock types. Our new ^{40}Ar/^{39}Ar results combined with published values suggest that basaltic magmatism appeared during different periods of time (Fig. 1). Among four episodes, at least two (at the Permo-Triassic boundary and one at the Early/Middle Triassic) can be considered as flood basalt events on merit of the volume and geochemistry. Two other episodes of basaltic volcanism were probably less voluminous. U-Pb data for granites show that granites in peripheral parts of the Siberian Traps LIP were contemporaneous to the two flood basalt events, but the latest Bolgokhtokh intrusion is younger than any of basalt. Thus Siberian Traps LIP is much more complex then usually considered.

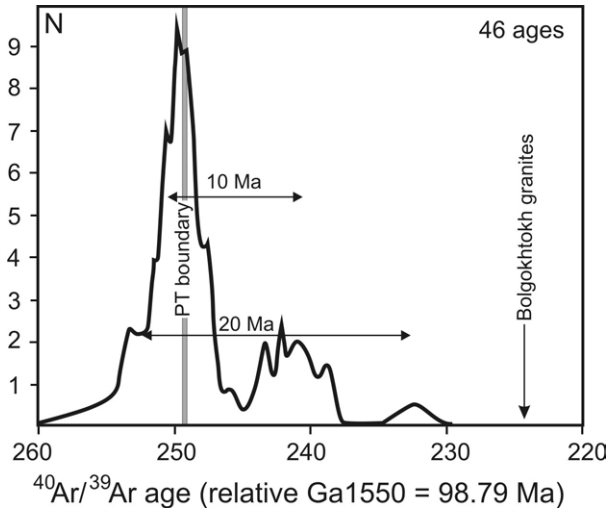

Figure 1: Probability distribution of ^{40}Ar/^{39}Ar ages.

https://doi.org/10.1180/S0026461X00006502 Published online by Cambridge University Press

Fluid processes in subduction zones and global water circulation

HIKARU IWAMORI

Tokyo Institute of Technology: (hikaru@geo.titech.ac.jp)

Water within the Earth, including OH and H in minerals, may play an important role in the planetary evolution, yet its distribution and circulation are poorly constrained. Seismic observations, e.g., those based on dense networks over the Japan arcs, suggest deep subduction of water and dehydration of the slab [1 and the refs. therein]. Geochemistry of volcanic rocks is useful for quantifying the amount and composition of slab-derived fluid, and suggests a typical range from 0.1 to 1 wt.% H_2O in the mantle wedge with regional variations according to the tectonic settings [2]. Numerical models provide a consistent view, in which fluid flow with local chemical equilibration explains the above observations [3]. In addition, these models and water solubility to minerals at high pressures [4] imply that a boundary layer with several 1000 ppm H_2O hosted by NAMs subducts to depths greater than 300 km.

The deeply subducted water, especially in the lower mantle, is not well mapped by geophysical means: seismic velocity may be influenced by major element compositions and temperature, while electrical conductivity is sensitive to the amount of water but provides a poor spatial resolution at depths [5]. Geochemistry of oceanic basalts can be used as a probe for the subducted components. Statistical analysis on the mantle isotopic variability suggests that such a component is in fact inherited in the mantle and forms geographical domains, possibly related to the extensive subduction having surrounded the supercontinents in the past, Pangea, Gondwana and Rodinia [6]. Repeated formation-breakup of supercontinents seems to be recorded in the mantle geochemistry, controlling the global material circulation.

[1] Hasegawa *et al*. (2009) *Gondwana Res*. **16**, 370-400. [2] Nakamura *et al*. (2008) *Nature Geosci*. **1**, 380-384. [3] Iwamori (2007) *Chem. Geol*. **239**, 182-198. [4] Bolfan-Casanova (2005) *Mineral. Mag*. **69**, 229–257. [5] Karato (2011) *EPSL* **301**, 413-423. [6] Iwamori *et al*. (2010) *EPSL* **229**, 339-351.

Mantle compositional variability constrained from arc and oceanic basalts

HIKARU IWAMORI

Tokyo Institute of Technology: (hikaru@geo.titech.ac.jp)

Mantle compositional variability has been extensively studied using oceanic basalts, including mid-oecan ridge basalts (MORB) and ocean island basalts (OIB), as geochemical 'messages' from the mantle [1]. However, the spatial coverage of ridges and ocean islands is insufficient for resolving even a global distribution of compositional variability (Fig.1). Here we discuss the mantle compositional variability in subduction zones that extend over a long distance comparable to mid-ocean ridges, mostly around the Pacific Ocean (Fig.1). As a result, we are able to map global geochemical domains, when combined with the mantle compositional variability obtained from MORB and OIB.

Arc basalts associated with subduction are the products of interaction between slab-derived materials and mantle wedge beneath the arcs. In order to extract the compositional variability of the mantle, influence of the subducted materials needs to be evaluated. Based on Sr, Nd and Pb isotope ratios mainly from the GEOROC and PetDB databases, and using the multivariate analyses, in particular, Independent Component Analysis, it has been found that depleted portions of the arc basalts well represent the compositions of mantle wedge that has not been fluxed by slab-derived materials. These portions lie on a compositional plane that is well defined by MORB and OIB, and can be decomposed into two independent components. Consequently, geographical domains in terms of 'anciently subducted component' ('IC2' in [2]) have been found and its implications on mantle dynamics are discussed.

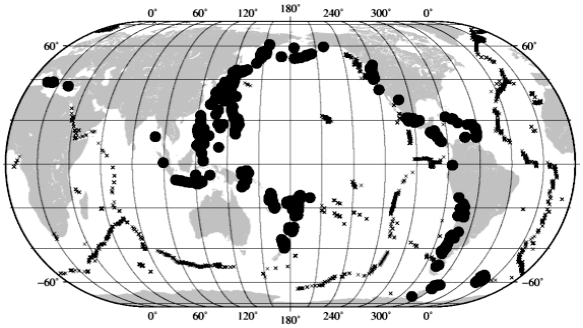

Figure 1: Distribution of oceanic basalts (small crosses) and arc basalts (solid circles) used in this study.

[1] Hofmann (1997) *Nature* **385**, 219-229. [2] Iwamori *et al*. (2010) *EPSL* **229**, 339-351.

https://doi.org/10.1180/S0026461X00006502 Published online by Cambridge University Press

$\delta^{13}C$ evidence of conodont evolution as a response to bioproduction perturbations

O.P. IZOKH

Sobolev Institute of Geology, and Mineralogy SB RAS, Novosibirsk, Russia (izokhop@gmail.com)

Usually $\delta^{13}C$ variations in marine sediments are related to the mass extinction in the Earth's past, and explained as reflection of the changes in primary bioproduction of the paleooceans, but sometimes the $\delta^{13}C$ excursion coincide with important evolutionary changes in biosphere. One of examples is radiation of polygnathid conodonts at the lower Emsian (Devonian), where negative $\delta^{13}C$ excursion (from +2 to -0.7 ‰) is aligned with the appearance of well-developed Pa element of the *Polygnathus kitabicus*, *Pol. pannonicus* and *Pol. sokolovi*.

Apart of bioproduction decrease, carbonates secondary changes also may cause negative excursion. To exclude the diagenetic nature of these isotopic signals, investigations of geochemical criteria of primary carbonate material safety (Fe/Sr and Mn/Sr) have been done. Together with the petrographic studies they are very effective for allocation of diagenetically altered samples.

All studied lower Emsian samples from Zinzilban section (Zeravshan Ridge, Kitab State Geological Reserve, Uzbekistan) are characterized by the low concentration of Fe (<100 ppm) and Mn (<22 ppm) with Sr contents from 150 to 400 ppm. Thus, Fe/Sr and Mn/Sr not exceed 0.5 and 0.07 accordingly, that evidence absence of carbonate material alteration. Also, it was controlled by petrographic studies. Thus, $\delta^{13}C$ negative excursion with high probability is a primary signal and the correlation of this event with the complication of conodont Pa element can reflect changes in their nutrition type, induced by the decreasing of the simple food.

Mo-isotopes as tracers of Cretaceous ocean anoxia

G.J. IZON[1]*, A.S. COHEN[1], A.L. COE[1], S.W. POULTON[2] AND T. WAGNER [2]

[1]Department of Earth and Environmental Sciences, The Open University, Milton Keynes, MK7 6AA, UK. (*correspondence: G.Izon@open.ac.uk)

[2]School of Civil Engineering and Geosciences, Newcastle University, Newcastle upon Tyne, NE1 7RU, UK.

Recent observations and modelling have shown that ocean warming and stagnation, driven by global climate change, may lead to widespread ocean deoxgyenation with direct impacts on marine biogeochemistry and ecosystems. Measurements of marine oxygen levels extend back no more than *c*. 50 years, whilst accurate predictions of future deoxgyenation trends are difficult and uncertain. In contrast, the geological record of past abrupt global warming events can provide insights into the entire earth system response - the mechanisms, extent, duration and consequences of - seawater deoxgyenation that are associated with CO_2-induced global warming.

The Cretaceous oceans were particularly susceptible to transient widespread deoxygenation, containing as many as 6 discrete intervals known as Ocean Anoxic Events (OAEs). Of these, OAE 1a (~120 Ma) and OAE 2 (~93 Ma) may have been global in extent and are marked by a sudden increase in organic C accumulation in conjunction with broad positive carbon isotope excursions.

We present new Mo-isotope, trace element and Fe-speciation analyses of samples from OAE 1a (the Selli event) and OAE 2 (the Bonarelli Event). Mo-isotope data can, under certain circumstances, provide quantitative estimates of how the extent of seawater anoxia may have fluctuated in the past. Our data from Gorgo a Cerbera, Italy, indicate that local conditions became progressively more reducing during OAE1a. $\delta^{98/95}Mo$ ratios show pronounced stratigraphic variations, consistent with diminished oxic sedimentation globally. Laminated sediments from Demerara Rise are enriched in redox sensitive trace metals (RSTM) throughout much of the Cenomanian. However, OAE 2 is marked by relatively low levels of RSTM consistent with the global expansion of anoxic sedimentation and the drawdown of the RSTM inventory. Our sample specific Fe-speciation data show that the water column was periodically euxinic, allowing us to use Mo-isotope data to critically test ideas on the timing, extent and duration of one of the most prounced deoxgyenation events of the Mesozoic.

https://doi.org/10.1180/S0026461X00006502 Published online by Cambridge University Press

^{129}I as atmospheric tracer

TANIA JABBAR[1], PETER STEIER[2], GABRIELE WALLNER[1], NORBERT KANDLER[1] AND CHRISTIAN KATZLBERGER[3]

[1]Department of Inorganic Chemistry, University of Vienna, Währingerstr. 42, A-1090 Vienna, Austria

[2]Vera Laboratory, Faculty of Physics – Isotope Research, University of Vienna, Währingerstr. 17, A-1090 Vienna, Austria

[3]AGES Austrian Agency for Health and Food Safety, CC Radiation Protection and Radiochemistry, Spargelfeldstr. 191, A-1226 Vienna, Austria

Iodine is an important element in oceanic, atmospheric and terrestrial systems. Atmosphere is one of the most important compartments for natural and anthropogenic changes and provides rapid response to disequilibrium. Iodine is transferred between compartments on different time scales and in different chemical forms (species). However, the dominant transfer pathway is either through the atmosphere as reactive gases (e.g. I_2, CH_2I_2, CH_2ICl, CH_3I), bound to aerosols or in the aqueous phase (i.e. rain, rivers, lakes and oceans).

^{129}I has received increased attention in recent years as unique atmospheric and environmental tracer. ^{129}I is a long lived ($T_{1/2}$ = 15.7 Ma) radionuclide whose concentration in environment has been elevated by several orders of magnitude, mainly by emission from reprocessing plants [1]. However in spite of environmental relevance, there is still little knowledge about temporal variability of the ^{129}I anthropogenic fallout over Europe. One of the main goals of this study is to trace transport path of ^{129}I released from reprocessing plants in atmosphere by measuring its concentration.

This study deals with temporal changes of iodine isotopes (^{127}I and ^{129}I) in aerosols collected within two years in Vienna, Austria (202 m a. s. l). The data shows isotopic ratios of the order of 10^{-8} to 10^{-7}. The predominant basis for the higher ratios in the aerosols appears to be upcurrent sources of ^{129}I from nuclear fuel reprocessing plant at Sellafield. Apart from this, short term variability of ^{129}I concentrations was associated with air mass transfer and wind pattern.

[1] Tania Jabbar, Peter Steier, Gabriele Wallner, Norbert Kandler & Christian Katzlberger (2011) 'AMS anaylsis of iodine-129 in aerosols from Austria' *NIMSB* (accepted).

Mineral composition of particulate matter in human lung samples from Upper Silesia (Poland) – Preliminary results

M. JABLONSKA

University of Silesia (mariola.jablonska@us.edu.pl)

The aim of this study is to compare the mineral composition of airborne particles to mineral composition of particles inhaled by humans who lived in highly urbanized and industrialized region of Upper Silesia (S Poland). The characterization of mineral particles in samples of lung tissues of 40 subjects by TEM and ASEM revealed the presence of quartz, aluminosilicates including feldspars, Ca carbonates, iron oxides, Ca sulphates, and kaolinite as major components.

All of those minerals are major mineral constituents of dust particles in Upper Silesia in addition to soot. Some of them may serve as tracers of the source of inhaled particles. For instance, barite particles in lung tissues may be related to the abundant airborne barite resulted from the combustion of the uniquelly Ba-rich Silesian coal. The lung tissues lack of Pb-particles, which are common in airborne soot particles. Their fast dissolution in lung fluids is a possible explanation of their absence in lung tissues.

Additionally, Ca-phosphates (perhaps of the apatite group) and zinc oxide were observed on rare occasions in lung tissues.

This work is supported by research project N306314439 of the Polish Ministry of Science and Higher Education.

Direct ventilation of the North Pacific did not reach 2300 m during the last glacial termination

S.L. JACCARD[1]* AND E.D. GALBRAITH[2]

[1]D-ERDW, ETHZ, Zurich, Switzerland (*correspondence: samuel.jaccard@erdw.ethz.ch)
[2]Earth and Planetary Sciences, McGill University, Montreal, Canada (eric.galbraith@mcgill.ca)

It has recently been argued that the North Pacific circulation during HS1 (18-14.6 kyr) was distinct from both the LGM and the warmer intervals that followed, with a greater formation of 'deep waters' sinking to 2500-3000 m. This intriguing conjecture appears to be inconsistent with a number of geochemical proxies measured at multiple North Pacific core sites from this depth range.

'Ventilation' involves the input of atmospherically-equilibrated waters to the ocean interior. Well-equilibrated waters have high concentrations of oxygen and relatively low concentrations of dissolved carbon dioxide. Bottom waters with high oxygen concentrations inhibit the diagenetic enrichments of some redox-sensitive trace metals in underlying sediments, while low concentrations of carbon dioxide (relative to alkalinity) produce high carbonate ion concentrations, encouraging preservation of calcium carbonate ($CaCO_3$) microfossils in sediment. Thus, poorly ventilated bottom waters are likely to show both sedimentary authigenic U enrichments and poor $CaCO_3$ preservation. Measurements at sites from the NW Pacific and in the Bering Sea show that, at 2393 m and 2209 m water depth, respectively, these twin hallmarks of poor ventilation reigned throughout the LGM and HS1, to finally disappear after ~15 ka. This sequence of change is consistent with a poorly ventilated deep ocean throughout this interval that extended from the abyss to within < 2500 m of the surface. The assembled evidence does not appear to provide an opening during the deglaciation during which the North Pacific water could have pumped oxygenated waters into the deep.

A new starting point for the mantle's geochemical reservoirs

M.G. JACKSON[1] AND R.W. CARLSON[2]

[1]Dept. Earth Sciences, Boston University, 675 Commonwealth Ave., Boston, MA 02215 (jacksonm@bu.edu)
[2]Department of Terrestrial Magnetism, Carnegie Institution of Washington, 5241 Broad Branch Road, NW, Washington, DC 20015 USA (rcarlson@ciw.edu)

The present-day terrestrial mantle, as sampled by melts that erupt at the surface, is chemically and isotopically heterogeneous. The discovery of a surviving portion of the early-formed silicate Earth that existed immediately after formation of the core—referred to as primitive mantle—would place constraints on the earliest chemical evolution of the Earth. Such a discovery would also provide a starting point to understand the origin and long-term evolution of the various geochemically-distinct mantle reservoirs that now make up Earth's interior. Earth's primitive mantle has long been thought to be compositionally similar to primitive chondrites, at least for the refractory, lithophile elements. However, the recent discovery that modern terrestrial lavas have $^{142}Nd/^{144}Nd$ ratios ~18 ppm higher than chondrites suggests that the Earth's primitive mantle has a Sm/Nd ratio that is ~5% higher than chondrites [1], and that all modern terrestrial mantle and crustal reservoirs ultimately were derived from this reservoir with superchondritic Sm/Nd. Today, the $^{143}Nd/^{144}Nd$ of the primitive (albeit non-chondritic) reservoir would be ~0.5130, a ratio that is closer to the depleted MORB mantle than to chondritic. In order to extract the continents from the non-chonditic primitive mantle, the depleted mantle reservoir must comprise > 50% of the mass of the mantle, thus extending into the lower mantle. Another implication of a non-chondritic Earth is that it provides a new reference for the composition of primitive mantle (e.g. $^{143}Nd/^{144}Nd$ = 0.5130), and reservoirs that were once considered depleted relative to chondritic (e.g. HIMU, with $^{143}Nd/^{144}Nd$ = 0.51285) are actually enriched relative to the postulated non-chondritic mantle. The observation that the most frequently-occurring $^{143}Nd/^{144}Nd$ ratio (0.5130, PREMA) in ocean island basalts (OIB), including lavas with high $^{3}He/^{4}He$, overlaps with the value suggested for a non-chondritic mantle (0.5130) suggest that large portions of the mantle sampled by OIB remain little-modified with respect to $^{143}Nd/^{144}Nd$. If the Earth's primitive mantle is not chondritic and a portion has survived in the deep Earth to the present-day, we consider the best candidate to be the mantle reservoir sampled by lavas with the highest $^{3}He/^{4}He$.

[1] Boyet and Carlson, *Science*, (2005).

https://doi.org/10.1180/S0026461X00006502 Published online by Cambridge University Press

A 'hotspot highway' in the S. Pacific

M.G. JACKSON[1]*, S.R. HART[2], J.G. KONTER[3], A.A.P. KOPPERS[4], H. STAUDIGEL[5], M.D. KURZ[2], J. BLUSZTAJN[2] AND J. SINTON[6]

[1]Dept. Earth Sciences, Boston University, 675 Commonwealth Ave., Boston, MA 02215, USA (*correspondence: jacksonm@bu.edu)
[2]Woods Hole Institute of Oceanography, Woods Hole, MA 02543, USA
[3]Dept. Geological Sciences, University of Texas at El Paso, TX 79968, USA
[4]Coll. Oceanic and Atmospheric Sciences, Oregon State University, Corvallis, OR 97331, USA
[5]Scripps Institution of Oceanography, La Jolla, CA 92037, USA
[6]Department of Geology and Geophysics, University of Hawai'i at Mānoa, Honolulu, Hawaii 96822, USA

New deep-sea dredges from the Samoan region provide evidence for three seamounts (Malulu, Papatua [PPT], Waterwitch) and one atoll (Rose) that are not geochemically related to the Samoa hotspot track. We use a plate motion model to show that three non□Samoan hot spots, currently active in the Cook□Austral Islands, are responsible for 10–40 Ma volcanism in the Samoan region. The four 'interloping' volcanoes in the Samoan region exhibit geochemical affinities with the three hot spots. All three hot spots would have left a depleted, viscous, refractory keel that is coupled to the base of the Pacific lithosphere that has been 'rafted' to the Samoan region. Without major modification of the current 'propagating lithospheric cracks' model, it is not clear how such cracks could yield melts from the refractory keel present under the Samoan lithosphere. Instead, a region of buoyantly upwelling mantle, or plume, is suggested to generate the shield stage volcanism in the Samoan region.

Another implication of the Cook-Austral interlopers in the Samoan region is that they may provide the "missing link" to what may be a third long hotspot track in the Pacific, in addition to the Hawaii and Louisville chains. The Hawaii and Louisville hotspots exhibit very different behavior at ~45-50 Ma (the Hawaiian hotspot exhibits a clear "kink", and Louisville exhibits a gradual bend), and it is important to establish a third long-lived hotspot for comparison during this critical time in Pacific tectonics. Plate reconstruction models suggest the Rurutu hotspot track—one of the three hotspots in the Cook-Austral Islands—bends at ~45 Ma and emerges from the Gilbert Islands before trending through Samoa and toward the present-day hot spot location beneath Rurutu. Deep-sea dredging the seamounts in the region predicted to be the ~45 Ma Rurutu "bend" is necessary for evaluating a genetic and temporal link to the Rurutu hotspot.

Quantitative determination and mapping of trace element concentrations in sulfide minerals using LA-ICP-MS

S.E. JACKSON[1], S. SHUTTLEWORTH[2] AND L.J. CABRI[3]

[1]Geological Survey of Canada, Ottawa, ON K1A 0E8, Canada (*correspondence: simon.jackson@nrcan.gc.ca)
[2]Photon-Machines Inc., 15030 N.E. 95th St., Redmond, WA 98052, USA (shutts@photon-machines.com)
[3]Cabri Consulting Inc., 99 Fifth Avenue, Suite 122, Ottawa, Ontario, K1S 5P5 (lcabri@sympatico.ca)

Quantitative trace-element analysis of sulfide minerals has a number of important applications, including: empirical indication of deposit setting, geo-thermometry and geo-barometry, ore paragenesis studies, indicator mineral surveys, and deportment investigations. However, progress in this field has been hindered by the lack of multi-element sulphide mineral standards for trace-element microbeam techniques and methods for mapping trace element concentration distributions in samples with complex mineralogy.

In this study, element distribution maps have been constructed from time-resolved LA-ICP-MS signal intensity data acquired during multiple, continuous parallel line ablations and lines of edge-to-edge, square spot ablations across selected areas of petrographic sections. The data were deconvoluted, calibrated and digitally combined using in-house software to generate elemental concentrations maps, which provide detailed information on spatial variations of elements within and between sulfide grains and their enclosing minerals.

Determining concentrations in mono-mineralic sampling areas was perfomed using conventional calibration protocols involving external standardization and normalization using an internal standard, performed on a (mass) scan-by-scan basis. External standardization was achieved using a multi-element synthetic pyrrhotite standard that was prepared by reaction in an evacuated quartz tube of elemental iron and sulfur doped with multi-element aqueous standards. This has been shown to be homogeneous (r. s. d. <10%) for the majority of the 30 doped elements. For complex mineralogies, both sulfide and silicate external standards were employed, together with normalization using different internal standard elements and/or concentrations for different minerals, and algorithms that automatically detected the mineral phase being analyzed.

The effect of different laser sampling strategies and algorithms for data smoothing and interpolation, and assignment of colours to element maps will be demonstrated.

https://doi.org/10.1180/S0026461X00006502 Published online by Cambridge University Press

Polycrystalline diamonds witness redox processes in the Earth's mantle

D.E. JACOB[1]*, R. WIRTH[2] AND F. ENZMANN[1]

[1]Johannes Gutenberg-Universität, D-55099 Mainz, Germany (*correspondence: jacobd@uni-mainz.de)
[2]Helmholtz Centre Potsdam, D-14473 Potsdam, Germany (wirth@gfz-potsdam.de)

Polycrystalline diamond aggregates (framesites) from the Orapa kimberlite (Botswana) contain a syngenetic micro- and nano-inclusion suite of magnetite, pyrrhotite, omphacite, garnet, rutile and C-O-H fluid in order of abundance. This suite of inclusions is distinctly different from those in fibrous diamonds, although the presence of sub-micrometer fluid inclusions provides evidence for a similarly important role of fluids in the genesis of polycrystalline diamond. High resolution μ-Computed Tomography (resolution 1.3μm per voxel) combined with Focused Ion Beam assisted Transmission Electron Microscopy reveals epigenetic replacement coatings of hematite and late stage sheet silicates around magnetites showing that magnetites are often (but not always) interstitial to the diamond and, thus, were open to late stage more oxidized overprinting. We present evidence that the primary paragenesis preceding this late stage event formed from a reduced, water-rich C-O-H fluid oversaturated in carbon upon entering the base of the subcratonic lithosphere along opening cracks. Precipitation of diamond increased the water content of the fluid, fluxing melting of surrounding rocks (eclogitic silicates, Fe-sulfides, oxides), which re-precipitated in the interstices between diamonds and as nano-inclusions. Pyrrhotite crystallization led to a rise in fO_2 in the small-scale Fe-O-S melt, which is amplified by the precipitation of diamond from the C-O-H fluid, moving the whole system towards more oxidizing conditions. Thus, fO_2 conditions were more reducing at the start of diamond precipitation and evolved towards more oxidizing conditions upon cooling and solidification. The inclusion paragenesis was generated in a local small-scale equilibrium system, and is representative only for the redox conditions towards the end of diamond precipitation. It is generally acknowledged that sulfide melts are relatively immobile in the Earth's mantle. Formation of polycrystalline diamond would require only local remobilization and small-scale transport of pre-existing material. Cratonic roots have been episodically impregnated with carbon-rich fluids - small volume melts from mantle sources as well as subducted basaltic material - since Archean times. This process leads to diamond formation at a range of spatial scales.

Diamond-graphite transformation: A NanoSIMS isotope study of diamond-graphite inclusion in zircon from the Kochetav massif

B. JACOBSEN[1]*, J. MATZEL[1], I.D. HUTCHEON[1], H.W. GREEN[2] AND L.F. DOBRZHINETSKAYA[2]

[1]Lawrence Livermore National Laboratory, CA 94550, USA (*correspondence: jacobsen5@llnl.gov)
[2]University of California, Riverside, CA 92521, USA

Diamond from ultrahigh-pressure metamorphic terrains (UHPM) is an important mineralogical indicator of deep lithospheric slab subduction (>150 km) into Earth's mantle. Details about diamond-to-graphite transition occurring during subsequent exhumation are not well understood. Because the structures of diamond and graphite are so dissimilar, it is unlikely that a direct phase transformation would occur in the graphitization process. Heating experiments at T=1500-1800°C and ambient pressure showed that diamond is replaced by disordered graphite along planes with a high concentration of dislocations.

In order to better understand the process of diamond-to-graphite transformation we measured C, and N isotopes in an inclusion, comprising graphite with a diamond core, in zircon from the Kokchetav massif, Kazakhstan. The inclusion is ~ 10 μm in diameter and consists of a ~3 μm diamond core that is surrounded by a graphite rim ~7 μm in thickness. The C and N isotopes were measured with a Cameca NanoSIMS-50. Diamond and graphite in the inclusion are isotopically indistinguishable (i.e. $\Delta^{13}C_{diamond\text{-}graphite}$ and $\Delta^{15}N_{diamond\text{-}graphite} \approx 0$). The C and N isotopic composition for the entire inclusion is $\delta^{13}C = -30 \pm 1$ ‰ and $\delta^{15}N = +0.5 \pm 3$ ‰ respectively, which is in the range of carbon of organic origin.

The distinctive geometry of the diamond-graphite inclusion – the diamond core mantled by graphite – suggests a retrogressive reaction that probably occurred due to decompression during the host rock's exhumation to the Earth's surface from depths > 120-150 km. The lack of intra-mineral isotope fractionation between diamond and graphite for both C and N isotopes suggests that the retrogressive diamond-to-graphite transformation occurred at temperatures above 500 °C and pressures less than 4 GPa. Raman spectroscopy studies of this diamond by Smith *et al*. (2011) show the presence of 1624 -1647 cm-1 bands which are close to those of disordered graphite. We thus hypothesize that during exhumation diamond was gradually replaced by graphite through an intermediate phase of disordered graphite.

https://doi.org/10.1180/S0026461X00006502 Published online by Cambridge University Press

CO_2 evasion from the Greenland Ice Sheet: A new carbon-climate feedback

ANDREW D. JACOBSON[1] AND JONG-SIK RYU[1,2]

[1]Department of Earth and Planetary Sciences, Northwestern University, USA, (adj@earth.northwestern.edu)
[2]Division of Earth and Environmental Sciences, Ochang Center, Korea Basic Science Institute, South Korea, (jsryu@kbsi.re.kr)

Rising greenhouse gas levels may increase global surface temperatures between 1 and 6°C by 2100. Even greater increases are expected for the Arctic, where sea ice reduction, organic matter decomposition in lakes and thawed permafrost, and other positive feedbacks can potentially amplify the global trend. Melting of the Greenland Ice Sheet (GIS) figures prominently in climate change predictions because it will impact albedo, sea level, and possibly, ocean circulation. However, direct carbon cycle feedbacks are poorly constrained. Here, we show that melting of the GIS yields a previously unknown flux of CO_2 that will likely increase in a warmer world. Water emerges from the Russell Glacier in West Greenland with CO_2 partial pressures (pCO_2) 3 – 10X supersaturated with respect to atmospheric equilibrium. This CO_2 likely originates from microbial respiration beneath the GIS. During downstream transport, the chemical weathering of glacial till sequesters 70% of the excess CO_2 as HCO_3 – a carbon sink on human timescales – and the remaining 30% evades to the atmosphere. Scaled to all rivers draining the GIS, the evasion flux of 0.13 Tg C/yr is small by comparison to other atmospheric CO_2 inputs; however, we hypothesize that significant increases could occur as retreat of the ice sheet margin and expansion of moulins exposes meltwater to basal ice with pCO_2 values up to 340X higher than the current atmospheric value. Worst-case model predictions yield evasion fluxes of 100 – 180 Tg C/yr by 2100 depending whether melting increases linearly or exponentially with time. These CO_2 fluxes surpass those reported for Arctic Lakes (20 Tg C/yr) and would increase by 23% those predicted for permafrost thaw (800 – 1100 Tg C/yr). Our findings suggest that Arctic climate change could have a more significant feedback on global climate than currently anticipated.

Along-arc geochemical variations in the Southern Volcanic Zone, Chile

G. JACQUES[1]*, K. HOERNLE[1,2], H. WEHRMANN[1], D. GARBE-SCHÖNBERG[3], P. VAN DEN BOGAARD[1,2], F. HAUFF[2], J. MAHLKE[2], K. SCHUMANN[2] AND L.E. LARA[4]

[1]Sonderforschungbereich 574, IFM-GEOMAR, 24148 Kiel, Germany (*correspondence: gjacques@ifm-geomar.de)
[2]IFM-GEOMAR, 24148 Kiel, Germany
[3]Institute of Geosciences of the University of Kiel, 24118 Kiel, Germany
[4]Servicio Nacional de Geología y Minería, 0104 Santiago, Chile

The origin of enriched isotopic signatures in volcanic rocks from the northern segment of the Southern Volcanic Zone (SVZ) in Chile is controversial. Hildreth and Moorbath [1] argued for crustal assimilation in the context of their MASH model. Stern [2] and recently Kay *et al*. [3], however, proposed that subduction erosion can best explain the increasing enrichment of the magmas from the Miocene to present. We present new trace element and isotope data from young olivine-bearing volcanic rocks along the volcanic front of the SVZ in Chile. We observe systematic spatial variations in Sr, Nd, Hf and Pb isotopic compositions along the arc with the northern part of the Southern Volcanic Zone (NSVZ) having the most enriched signatures. Oxygen isotope data, with one exception, show uniform compositions, close to that expected for the upper mantle. Mixing calculations using O and Sr isotope ratios suggest that the enriched signature of the NSVZ lavas is primarily acquired in the mantle, favoring the subduction erosion model. Crustal assimilation, however, could also affect the composition of these lavas.

[1] Hildreth & Moorbath, (1988) *Contrib. to Mineralogy & Petrology* **98**, 455–489. [2] Stern, C.R. (1991) *Geology* **19**, 78–81. [3] Kay *et al*. (2005) *GSA Bulletin* **117**, 67–88.

https://doi.org/10.1180/S0026461X00006502 Published online by Cambridge University Press

Role of three-dimensional mantle flow in magmatism at slab edges

MARGARETE JADAMEC[1]*, PATRICIA DURANCE[1], KEN MCLEAN[1], MAGALI BILLEN[2] AND LOUIS MORESI[1]

[1]School of Mathematical Sciences, Monash University, Clayton, Victoria, Australia 3600 (*correspondence: margarete.jadamec@monash.edu)
[2]Geology Department, University of California, Davis, CA, 95616, USA

Adakitic volcanics associated with subduction-transform plate boundaries have been identified in numerous localities, including the eastern Alaska slab edge, the Kamchatka-Aleutian plate boundary corner, the Cascadia-San Andreas transform fault juncture, and the New Hebrides trench-Hunter Ridge [1, 2]. Three-dimensional (3D) models investigating the solid state flow in the mantle due to subduction of a slab edge predict toroidal flow around the slab edge and an upward flow component, which could lead to decompression melting within several hundred kilometers outward of the slab edge as well as contribute to melting of the slab edge. However, the position of the volcanics with respect to the slab edge and associated upwelling in the mantle has only recently been tested in 3D geodynamic models [3, 4]. We use 3D numerical models to investigate the role of rheology and slab geometry on the mantle flow and its implications for anomalous arc volcanism near two slab edges: the eastern Alaska slab edge and the slab edge in the easternmost New Hebrides [3, 5]. In the eastern Alaska region the Aleutian trench terminates at a near right angle into the Fairweather-Queen Charlotte transform boundary. In the eastern New Hebrides, the subduction zone makes a nearly 90 degree arcuate turn, such that the slab edge intersects with the back arc spreading center. The models predict localized rapid mantle velocities (greater than 80 cm/yr), which may contribute to the preservation of primitive magmas that can be brought to the surface. These models do not investigate the link between melt migration and solid state flow of the mantle, which is an important and complex process, but rather aim to place a framework for interpreting how the 3D solid state flow field may influence migration patterns in subduction zones.

[1] Yogodzinski *et al*. (2001) *Nature* **409**, 500–504. [2] Durance (2009) PhD Thesis, Monash University. [3] Jadamec & Billen (2010) *Nature* **465**, 338–341. [4] Schellart (2010) *Geology* **38**, 691–694. [5] McLean (2010) Honors Thesis, Monash University.

The magnitude and composition of the delamination flux in arcs during continental crust formation

OLIVER JAGOUTZ[1] AND MAX W. SCHMIDT[2]

[1]EAPS, MIT (jagoutz@mit.edu)
[2]ETH Zürich (max.schmidt@erdw.ethz.ch)

As the bulk continental crust is not in equilibrium with a mantle assemblage significant volumes of mafic/ultramafic composition counterbalancing the andesitic bulk composition of the crust are missing. Significant volumes of such complementary compositions are exposed in the Kohistan Arc, NE Pakistan. We constrain the bulk composition of the Kohistan arc and constrain the volume and composition of rocks needed to balance the andesitic crust composition to a mantle derived melt using the cumulates exposed in Kohistan. The Kohistan bulk arc composition results very similar to global continental crust estimates indicating that modern arc activity is the dominant process that formed the (preserved) continental crust. Fitting the bulk Kohistan arc crust and the ultramafic cumulates exposed at base of the arc (dunites, wehrlites, websterites, cpx-bearing garnetites and hornblendites, and garnet gabbros) to primitive arc melts with calc-alkaline/tholeiitic, alkaline, and boninitic affinity from various island arcs demonstrates that delamination of wehrlites + garnet hornblendites ± garnet gabbros perfectly explains the evolution from a tholeiitic/calc-alkaline primitive high-Mg basalt to the continental crust. Mass balance demonstrates that volumes of delaminate similar or larger to the continental crust are required. Including these ultramafic cumulates into the estimates of mass fluxes at convergent margin significantly increases the volume of magma production rates in convergent magin setting. Compared to depleted mantle, the delaminate is enriched in Pb and low U concentrations (low mue composnent) and may compensate for the depleted mantle radiogenic lead composition.

https://doi.org/10.1180/S0026461X00006502 Published online by Cambridge University Press

Structure of CaO-Al_2O_3-SiO_2 melts studied by molecular dynamics and diffraction experiments

S. JAHN[1], V. HAIGIS[1], J.W.E. DREWITT[2], J. KOZAILY[3], A. BYTCHKOV[3] AND L. HENNET[2]

[1]GFZ German Research Centre for Geosciences, Telegrafenberg, 14473 Potsdam, Germany (jahn@gfz-potsdam.de)
[2]CNRS-CEMHTI, 45071 Orleans Cedex 2, France
[3]ILL, 38042 Grenoble Cedex 9, France

The structural characterization of multicomponent liquids is a challenging problem. From the experimental perspective, measurements need to be performed *in situ* at high temperature (and possibly high pressure). Furthermore, a single method such as x-ray or neutron diffraction, Raman or NMR spectroscopy is usually not sufficient to provide a reliable structural model. On the other hand, molecular modeling approaches using classical interatomic potentials often lack accuracy and computationally expensive first-principles simulations suffer from finite size and time effects. It appears attractive to combine the strengths of different techniques to investigate the structure of chemically complex melts and the relation between their structure and their physical or thermodynamic properties.

Calcium aluminosilicate melts and glasses are important in both geological and technological context. Here, we employ advanced classical interaction potentials that were parametrized using electronic structure calculations [1] to predict the structure of representative liquids of the CaO-Al_2O_3-SiO_2 system at ambient pressure and a temperature of 2500 K as a function of chemical composition. The quality of the simulation model is assessed by comparing the computed total static structure factors to data from x-ray and neutron diffraction experiments (e.g. [2]). In this presentation, we will focus on structural changes across the binary CaO-SiO_2 and CaO-Al_2O_3 as well as the metaluminous ($CaAl_2O_4$)-SiO_2 joins. Similar to the MgO-Al_2O_3 system [3], the average Al coordination decreases from about 4.4 in pure Al_2O_3 melt to 4.0 in Ca-rich melts. At the same time, the number of OAl_3 triclusters is reduced significantly. The distributions of Ca coordination are rather broad but they are dominated by a sixfold octahedral geometry and show a decreasing average coordination towards the Ca-rich melts. In the glass-forming region of the CaO-Al_2O_3 system, a maximum in the melt viscosity is observed well above the glass transition temperature.

[1] Jahn & Madden (2007) *Phys. Earth Planet. Int.* **162**, 129–139. [2] Drewitt *et al.* (2011) *J. Phys. Condens. Matter* **23**, 155101. [3] Jahn (2008) *Am. Mineral.* **93**, 1486–1492.

Role of microbe in the formation of illite from nontronite: Mesophilic and thermophilic bacterial reaction

DEB P. JAISI[1,2], DENNIS D. EBERL[3], HAILIANG DONG[1] AND JINWOOK KIM[4]*

[1]Department of Geology, Miami University, Oxford, OH 45056, USA
[2]Department of Plant and Soil Sciences, University of Delaware, Newark, DE 19716, USA
[3]US Geological Survey, Boulder, CO 80303, USA
[4]Department of Earth System Sciences, Yonsei University, Seoul, Korea (*correspondence: jinwook@yonsei.ac.kr)

The formation of illite through the smectite-to-illite (S-I) reaction is considered to be one of the most important mineral reactions occurring during diagenesis. In biologically catalyzed systems, however, this transformation has been suggested to be rapid and to bypass the high temperature and long-time requirements. To understand the factors that promote the S-I reaction, the present study focused on the effects of pH, temperature, solution chemistry, and aging on the S-I reaction in microbially mediated systems. Fe (III)-reduction experiments were performed in both growth and non-growth media with two types of bacteria: mesophilic (*Shewanella putrefaciens* CN32) and thermophilic (*Thermus scotoductus* SA-01). Reductive dissolution of NAu-2 was observed and the formation of illite in treatment with thermophilic SA-01 was indicated by X-ray diffraction (XRD) and high-resolution transmission electron microscopy (HRTEM). A basic pH (8.4) and high temperature (65°C) were the most favorable conditions for the formation of illite. A long incubation time was also found to enhance the formation of illite. K-nontronite (non-permanent fixation of K) was also detected and differentiated from the discrete illite in the XRD profiles. These results collectively suggested that the formation of illite associated with the biologically catalyzed smectite-to-illite reaction pathway may bypass the prolonged time and high temperature required for the S-I reaction in the absence of microbial activity.

https://doi.org/10.1180/S0026461X00006502 Published online by Cambridge University Press

Solar noble gases in Tagish Lake

T. JAKUBOSWKI[1], U. OTT[2]*,
S. HERRMANN[2] AND P.J.A. MCCAUSLAND[3]

[1]Balonowa 5/2, Wroclaw 54-129, Poland (illaenus@gmail.com)
[2]Abteilung Biogeochemie, Max-Planck-Institut für Chemie, Postfach 3020, DE-55020 Mainz, Germany (*correspondence: uli.ott@mpic.de)
[3]Department of Earth Sciences, University of Western Ontario, London, Ontario K7L 3N, Canada

Tagish Lake fell in January 2000 [1] and is an ungrouped C2 meteorite and a 'breccia at all scales' [2]. Originally two different lithologies, a carbonate-rich one and a carbonate-poor one [2] were recognized, but additional work has revealed that there are even more distinct lithologies [3-5].

Analysis of the carbonate-rich lithology by [6] found abundant primordial noble gas, but solar noble gases were absent. A similar result was obtained by [7] in the analysis of a 'whole-rock' sample. Here we report noble gas data for a carbonate-poor sample of Tagish Lake, which, besides the primordial noble gases contains abundant solar gas.

We analyzed two samples. A smaller sample (#1; 20.2 mg) was heated in three temperature steps (600, 1000, 1800 °C), while a larger sample (#2; 93.9 mg) was heated in 200 °C increments from 400 °C to 1800 °C. Results for He, Ne and Ar are summarized in the Table below. Primordial Kr and Xe were also found at typical abundance levels relative to Ar (^{36}Ar/^{84}Kr/^{132}Xe ~ 80/0.85/1).

#	^{3}He	^{4}He	^{22}Ne	20/22	21/22	^{36}Ar
1	5.99	16774	7.77	10.12	0.0851	90.3
2	8.35	22745	11.45	10.42	0.0853	96.4

Based on the presence of texturally and mineralogically distinct clasts, Nakamura *et al*. [6] concluded that the carbonate-rich lithology they studied is a breccia, however distinct from an asteroidal regolith breccia which would be characterized by the presence of solar noble gases. Our results indicate that there are other lithologies of Tagish Lake that in fact show solar wind gases. This and also the difference in cosmogenic ^{21}Ne (in 10^{-8} cc/g units: 0.46 and 0.64 in our samples vs. 0.114 in [6]) indicate that different lithologies / clasts of Tagish Lake may have experienced quite different irradiation histories.

[1] Brown *et al*. (2000) *Science* **290**, 320–325. [2] Zolensky *et al*. (2002) *MAPS* **37**, 737–761. [3] Blinova *et al*. (2009)*LPSC* **XL**, #2039. [4] DeGregorio *et al*. (2010) *MAPS* **45**, A69. [5] Izawa *et al*. (2010) *MAPS* **45**, 675–698. [6] Nakamura *et al*. (2003) *EPSL* **207**, 83–101. [7] Grady *et al*. (2001) *MAPS* **36**, A71-A72.

Investigation the use of ozonation column for phenol removal

H. JALAYERI[1]*, R. MARANDI[2] AND F. DOULATI[1]

[1]Dept of Mining, Shahrood Univ of Tech (*correspondence: hjalayeri@yahoo.com)
[2]Dept of chemical, Islamic Azad Univ, North Tehran

The phenol and this compound are highly toxic and carcinogenic. This pollutant can be observed in the effluents of many industries such as petroleum refining, coal tar distillation and coke in steel mills [1-3]. Advanced oxidation specific ozonation was considered for water treatment as the potential research interest in recent years. Ozonation has a high capacity and suitable for remove phenol. Effective factors were evaluated initial phenol concentration, pH, H_2O_2 volume and Duration ozonation. The results of ozonation were shown that the percentage removal of phenol was related to time. Increased phenol concentration decrease phenol removal rate so that maximum of the percentage removal was obtained for 100, 200 and 300 ppm phenol respectively after 20, 35 and 55 min (Figure 1). The experiments were carried out in pH of 2, 4, 7 and 9. The results were illustrated in table 1.

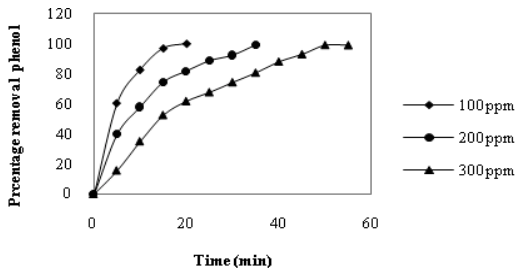

Figure 1: Effect of initial phenol concentration on removal

pH	2	4	7	9
Percentage removal 10 min (%)	55.18	65.12	70	95.3

Table 1: Effect of pH on phenol removal after 10 min

The most advantages of this study were the design of ozonation column and using a ozone diffuser that led to increase the percentage phenol removal in the shortest time possible. The optimum pH was 9 for remove phenol from wastewater and also increased H_2O_2 had little effect on removal.

[1] Moussavi *et al*. (2009*) J.Hazard. Mater*. **171**, 175–181.

https://doi.org/10.1180/S0026461X00006502 Published online by Cambridge University Press

Venting history and accumulation rates of hydrothermal sulfide, Endeavour Segment, Juan de Fuca Ridge

J.W. JAMIESON[1]*, M.D. HANNINGTON[1], D.S. KELLEY[2], D.A. CLAGUE[3] AND J.F. HOLDEN[4]

[1]U. of Ottawa, Ottawa, Canada
(*correspondence: john.jamieson@uottawa.ca)
[2]U. of Washington School of Oceanography, Seattle, USA
[3]MBARI, Moss Landing, USA
[4]U. of Massachusetts, Amherst, USA

Active hydrothermal systems on the ocean floor provide modern analogues for the formation of ancient VMS deposits. Seafloor hydrothermal processes are also an important mechanism for the transfer of heat and chemicals between the underlying crust and oceans. However, the rates at which these processes occur remain poorly constrained.

Here, we present radioisotope ages and volume estimates of hydrothermal sulfides from the Endeavour Segment, an intermediate rate ocean spreading center along the Juan de Fuca Ridge that hosts 5 active high-temperature vent fields. The ridge is currently undergoing a period of tectonic extension and volcanic quiessence. A suite of 43 sulfide samples, collected by manned submersible from the active fields and extinct/inactive sites, have been dated using ^{226}Ra/Ba ratios from hydrothermal barite that precipitates along with sulfide minerals. Radium-226 has a half-life of 1,600 years, making it an ideal chronometer for samples younger than ~20, 000 years. Results indicate that venting within the current axial valley of the Endeavour segment was initiated at least 2, 500 years ago. Venting within the Main Endeavour Field, the largest field by area, has been continuous for this period of time.

Using a GIS-based volume calculator developed at MBARI, the total volume of hydrothermal sulfide (including active and inactive/extinct structures) is determined from high-resolution bathymetry of the entire ridge segment. By combining volume data with the age of venting at Endeavour, the mass accumulation rates of sulfide can be determined at the segment scale. These results can be used to calibrate the efficiency of sulfide deposition from hydrothermal vents, and provide a time-integrated history of heat, fluid and chemical fluxes at the ridge-segment scale. The comparison of time-integrated rates with real-time estimates, based on fluid and chemical fluxes, as well as heat flow measurements, allow for an estimate of the episodicity of venting at Endeavour.

Porosity evolution, fracturing and Liesegang-banding during spheroidal weathering

BJØRN JAMTVEIT*, MAYA KOBCHENKO AND ANDERS MALTHE-SØRENSSEN[1]

Physics of Geological Processes, University of Oslo, Norway
(*correspondence: bjorn.jamtveit@geo.uio.no

A 10-meter thick andesitic sill intrusion from the Neuquen Basin, Argentina, shows spectacular examples of spheroidal weathering and Liesegang banding. The Liesegang patterns demonstrate how andesite blocks, initially cut out by a pre-weathering joint set, are subdivided by fractures forming during the spheroidal weathering process. The stresses causing fracturing originate from the growth of ferrihydrite and calcite in the pore space of the andesite, partly at the expense of original ilmenite, amphibole, and plagioclase. Fresh andesite has a porosity of ca. 8%. The porosity evolution and fracture formation during progressive weathering has been characterized in 3D by X-ray computed tomography (CT). The extent of pore filling increases with pore-size. Pores > 10^6 μm^3 are almost completely filled, whereas pores < 10^3 μm^3 are < 50% filled. More than 85% of the pore volume is comprised of pores < 10^3 μm^3, and thus the overall porosity is only slightly reduced during weathering. The fracturing associated with spheroidal weathering is caused by growth in pores comprising the largest 10% of the total porosity. We suggest that variation in growth rate with pores size is controlled by more effective transport of externally derived components to the larger pores. Models for diffusive transport in a porous rock with a pore size distribution similar to the observed will be presented, along with a fracturing model where stresses are generated by growth in pores.

https://doi.org/10.1180/S0026461X00006502 Published online by Cambridge University Press

New isotopic constraints on Amsterdam-St. Paul hotspot activity: Evidence for a deep-seated mantle plume and implications for the DUPAL anomaly origin

M. JANIN[1]*, C. HEMOND[1], M. MAIA[1], A. AGRANIER[1], K.T.M. JOHNSON[2] AND E. PONZEVERA[3]

[1]UMR Domaines Océaniques, IUEM, place Copernic, 29280 Plouzané, France (my.janin@gmail.com)
[2]School of Ocean and Earth Science and Technology, University of Hawaii, Honolulu, Hawaii 96822, USA
[3]Département Géosciences Marines, Ifremer, 29280 Plouzané, France

The Amsterdam-St Paul oceanic plateau (ASP) results from the interaction between the ASP hotspot and the Southeast Indian ridge. A volcanic chain, named the chain of the dead Poets (CDP), lies to its northward tip and is related to the hotspot intraplate activity.

The ASP plateau and CDP study reveals that ASP plume composition comes from oceanic crust and pelagic sediments recycled in the mantle through a 1.5 Ga subduction process. The ASP plateau lavas have a composition (major and trace elements and Sr-Nd-Pb-Hf isotopes) reflecting the interaction between ASP plume and the Indian MORB mantle, with some clear DUPAL input [1].

The Indian upper mantle below ASP plateau is heterogeneous and made of a depleted mantle with lower continental crust strips probably delaminated during the Gondwana break-up. The lower continental crust is one of the possible reservoirs for the DUPAL anomaly origin [2-3-4-5] and our data support it. The three endmembers involved (plume, upper mantle and lower continental crust) and their mixing in different proportions enhances an important geochemical variability in the plateau lavas.

[1] Hart, (1984) *Nature* **309**, 753–757. [2] Arndt, Goldstein, (1989) *Tectonophysics* **161**, 201–212. [3] Escrig, Capmas, Dupré, Allègre, (2004) *Nature* **431**, 59–63. [4] Hanan, Blichert-Toft, Pyle, Christie, (2004) *Nature* **432**, 91–94. [5] Meyzen, Ludden, Humler, Luais, Toplis, Mével, Storey, (2005) *Geochem. Geophys. Geosyst.* **6**, Q11K11

Development of an active mine water treatment technology by use of schwertmannite

E. JANNECK[1], D. BURGHARDT[2], E. SIMON[3], C. DAMIAN[3], M. MARTIN[1], G. SCHÖNE[4], J. MEYER[4] AND S. PEIFFER[3]

[1]GEOS Ingenieurges. mbH, 09633 Halsbrücke (e.janneck@geosfreiberg.de)
[2]TU Dresden, Institute for Groundwater Management, 01069 Dresden (diana.burghardt@tu-dresden.de)
[3]Universität Bayreuth, Department of Hydrology, 95440 Bayreuth (s.peiffer@uni-bayreuth.de)
[4]WISMUT GmbH, 09117 Chemnitz (j.meyer@wismut.de)

As a residual of microbial ferrous iron oxidation, large amounts of schwertmannite (Fe_8O_8 $(OH)_6SO_4$) were produced in a pilot plant for lignite mine water treatment in Tzschelln (Lusatia, Germany). The secondary mineral has excellent properties for removal of arsenic and other oxoanions from mine water and rapidly transforms into ferric hydroxides of high specific surface area once exposed to water containing at least some alkalinity. Therefore, the research project SURFTRAP was carried out to investigate the applicability of schwertmannite for the treatment of ground- and surface water contaminated with arsenic.

Following to fundamental, hydrochemical and structural investigations in the laboratory, a pilot scale test was performed in the bypass of an active water treatment plant for contaminated flooding water from uranium ore mining. About 25 mg Fe/L as schwertmannite were necessary to undershoot the governmental described effluent limits (0.3 mg As/L and 0.5 mg U/L). The costs of the higher demand of schwertmannite compared to the conventional $FeCl_3$ additon (10 mg Fe/L) could be compensated by a reduction of lime milk requirement of about 25%.

Furthermore, dumping experiments with arsenic-loaded schwertmannite-sludges were performed. A discontinuous irrigation scenario and a continuous groundwater equilibration scenario was investigated. After one year, no significant arsenic release was observed.

https://doi.org/10.1180/S0026461X00006502 Published online by Cambridge University Press

Pb-Sr-Nd-Hf isotope variations of megacrysts from Mesozoic Southern African kimberlites reflect mixing of HIMU melts with deep lithosphere

P.E. JANNEY[1] AND D.R. BELL[1,2]

[1]School of Earth & Space Exploration, Arizona State University, Tempe AZ 85287 (pjanney@asu.edu)
[2]Department of Chemistry and Biochemistry, Arizona State University, Tempe AZ 85287 (david.r.bell@asu.edu)

Clinopyroxene (cpx) megacrysts are abundant in southern African kimberlites and most have compositions that are not in equilibrium with normal mantle peridotite. Cpx megacrysts constitute a major part of the Cr-poor megacryst fractionation sequence. Although much of their major element variation is attributable to simple fractional crystallization, deflection of the frationation trends in many cases toward Cr- and Mg-rich compositions suggests that crystallizing megacryst parental magmas are not closed systems. We present Pb-Sr-Nd-Hf isotope data for cpx megacryst samples at regular intervals along evolution paths. The two localities we have examined in detail thus far, Pofadder and Monastery, display illuminating similarities and differences. Mg- and Cr-rich compositions dominate the cpx megacryst population at Pofadder, with only a minority of Cr-poor varieties. These megacrysts describe wide variations in all isotope systems (e.g. $^{206}Pb/^{204}Pb$ = 18.3 to 19.6) with the Cr-poor megacrysts having the most radiogenic Pb (although with lower Δ7/4 and Δ8/4), Nd and Hf isotope ratios. At Monastery, Cr-poor varieties dominate the cpx megacryst assemblage, with a small population of only moderately Cr-rich megacrysts. Here, isotope ratios display a much smaller variation (e.g. $^{206}Pb/^{204}Pb$ = 20.3 to 20.8) and encompass HIMU compositions comparable to the most extreme OIB at St. Helena. Pb becomes progressively less radiogenic as Cr# gradually drops with decreasing Mg#, and this progression continues as the evolution path is deflected toward higher Cr# and mildly increased Mg#. Our isotope data are consistent with an increasing degree of mixing between megacryst parental magmas having HIMU isotopic characteristics and deep lithospheric peridotite (having relatively unradiogenic $^{206}Pb/^{204}Pb$, Nd and Hf) with increasing magma evolution, the extent of assimilation appearing to be much greater at Pofadder than at Monastery. The nearly monotonic changes in the isotope ratios of cpx megacrysts from Cr-poor to Cr-rich compositions at these localities confirms that the two suites are petrogenetically related. Moreover, such mixing may be partly responsible for the lack of strong HIMU compositions directly observed in southern African kimberlites

Geochronological, geochemical and growth constrains of Alpine clefts from U-Th-Pb in monazite

EMILIE JANOTS[1], ALFONS BERGER[2], EDWIN GNOS[3], MARTIN WHITEHOUSE[4] AND ERIC LEWIN[1]

[1]ISTerre, Grenoble, France (*correspondence: emilie.janots@ujf-grenoble.fr)
[2]Museum of Natural History, Geneva, Switzerland
[3]University of Kopenhagen, Denmark, [4]Museum of Stockholm, Sweden

Monazite is a powerful U-Th-Pb chronometer of geological processes. Although conditions that drive its dissolution and precipitation remain unclear, monazite occasionally occurs in hydrothermal veins. Recent studies showed that hydrothermal monazite is successful to date mineralization. The originality of the present work is to evaluate if compositional and isotopic signature of monazite can record the geochemical environment and duration of rock-fluid interaction.

For this study, the selected monazite crystals satisfy two criteria: they are geologically young to ensure a Ma-resolution in age, and large enough (~mm-sized) to detect an age evolution over a grain profile. Studied monazite come from two distinct Alpine clefts from Central Alps (Griesserental and Blauberg, Switzerland). U-Th-Pb isotopic data were measured using ion microprobe.

In the two hydrothermal monazite crystals, U-Th-Pb isotopic signature gives indications about the ages, duration, fO_2 and geochemical environment (close vs open system) of the mineralization. Geochronologically, the Th-Pb age is preferred to the U-Pb age (s), because of (1) the unusually low U/Th contents, (2) significant contribution of common Pb and (3) ^{206}Pb excess in the Griesserental crystal, related to significant incorporation of ^{230}Th. Blauberg and Griesserental crystals show similar Th-Pb ages ~12 Ma, with no significant variations. However, one younger analysis point (~10 Ma) suggests possible crystallization over 2 Ma in the Blauberg crystal. Compositionnally, both crystals show unusually high Th/U values, indicating oxidizing conditions and dominant hexavalent U. Blauberg monazite is rather homogeneous displaying some sector zoning. The Griesserental crystal has a rim with higher Th/U and ^{206}Pb excess (up to 80% of the ^{206}Pb) than in its core. This zoning is coherent with a two-stage crystallisation in a closed system. While ^{230}Th was in disequilibrium with the U-series when the core precipitates, the fluid had time to reach equilibrium when the rim crystallized.

https://doi.org/10.1180/S0026461X00006502 Published online by Cambridge University Press

Nature, origin and causes of Jurassic felsic igneous activity in the Victory Glacier area (Eastern Graham Land)

V. JANOUŠEK[1,2]*, A. GERDES[3], J. ŽÁK[2,1], I. SOEJONO[1], Z. VENERA[1], V. ERBAN[1,2], O. LEXA[2,1] AND P. MIXA[1]

[1]Czech Geological Survey, Klárov 3, 118 21 Praha 1, Czech Republic (*correspondence: vojtech.janousek@geology.cz)

[2]Faculty of Science, Charles University in Prague, Albertov 6, 128 43 Praha 2, Czech Republic

[3]Institut für Geowissenschaften, Geochemie & Petrologie, Altenhöferallee 1, D-60438 Frankfurt, Germany

Geochemical signatures of felsic igneous rocks (biotite granites and rhyolite dykes) from the Victory Glacier area (eastern Graham Land, Antarctic Peninsula) are mutually indistinguishable, corresponding to high-K calc-alkaline, subaluminous to slightly peraluminous rocks. The NMORB-normalized spiderplots show strong LILE/HFSE enrichment typical of magmas generated at active continental margins or having originated by anatexis of mature continental crust. Characteristic are also fractionated chondrite-normalized REE patterns with deep negative Eu anomalies. The Sr–Nd isotopic signatures are those of fairly evolved crust ($^{87}Sr/^{86}Sr_{175}$ = 0.7084–0.7107, ε^{175}_{Nd} = -4.4 to -4.8). Taken together, the felsic rocks most likely originated from highly differentiated magmas derived by low-P (residue lacking Grt), low-T (Mnz and Zrn saturation temperatures ~770 °C) anatexis of metapsammites or orthogneisses. The widespread crustal anatexis took place within attenuated crust, as a part of the Chon Aike silicic large igneous province [1] magmatism.

New U–Pb Zrn dating shows that the Jurassic magmatic flare-up was rather short-lived (Toarcian–Aalenian). The two recognized Bt granite generations (~185/~166 Ma) both pre- and post-dated the rhyolitic volcanism (~174–179 Ma).

Field relationships indicate that the rhyolite dykes were emplaced in a biaxial extension deformation regime. The appropriate tectonic setting was either rifting accompanying mantle-plume-assisted Gondwana break-up [2] or extension behind the emerging Antarctic Peninsula arc [3]. The two scenarios do not have to be mutually exclusive, though [1, 4].

Funding by Ministry of Environment of the Czech Republic (# SPII1a9/23/07) is gratefully acknowledged.

[1] Bryan S (2007) *Episodes* **30**, 20–31. [2] Storey BC *et al*. (2001) In, *Geol. Soc. Am. Spec. Pap.* **352**, 71–80. [3] Storey BC & Alabaster T (1991) *Tectonics* **10**, 1274–1288. [4] Riley & Knight KB (2001) *Ant. Sci.* **13**, 99–110.

A physiochemical analysis of the mechanisms for transport and retention of Technetium (^{99}Tc) in unsaturated Hanford sediments

D.P. JANSIK, [1]*,2 D.M. WELLMAN[1], E.A. CORDOVA[1], D. DAGE[1] AND J. ISTOK[2]

[1]Pacific Northwest National Lab, Richland, WA 99352, USA (*correspondence: Danielle.Jansik@pnl.gov)

[2]Oregon State University, Corvallis, OR 97330, USA

The transport of technetium (^{99}Tc) is of interest due to the potential for human exposure and impact on ecosystems. Technetium has been released to the environment predominantly through nuclear fuel processing; as a result, further spreading of ^{99}Tc is a concern at DOE sites across the US. Specifically, technetium is a contaminant of concern at the Hanford Site in southeastern Washington, due to the magnitude of material that was disposed. The current body of work conducted on ^{99}Tc has provided a wealth of information regarding the redox relationships, sorption, solubility, and stability of the mineral phases [1], however little work has been conducted on the transport of technetium under vadose zone conditions.

The current conceptual model for technetium transport in the Hanford deep vadose zone is driven by two dominant hypotheses. The first component, proposes technetium movement is dominated by anisotropy and capillary forces; with the mobile technetium spreading laterally across higher conductivity saturated zones and being resisted by low saturation high conductivity zones. Within these regions technetium transport is considered highly dependent on the unsaturated hydraulic conductivity and capillary pressure. Thus, understanding saturation dependent technetium transport is critical for estimating the vertical fluxes of technetium and predictive modelling. The second premise assumes that technetium is in the form of the oxic pertechnetate species. Using an integrated testing approach we examined the mechanisms for physical and chemical retention and transport of technetium in unsaturated sediments. By employing transport and breakthrough curve analysis as well as pore water and sequential extractions, we evaluated transport behaviour, technetium mineral association, and technetium leachability with regard to pore size distribution.

[1] Artinger *et al*. 2003; Beals and Hayes, 1995; Cui and Eriksen, 1996b; Gu and Schulz, 1991; Jaisi *et al*. 2009; Keith-Roach *et al*. 2003; Kumar *et al*. 2007.

https://doi.org/10.1180/S0026461X00006502 Published online by Cambridge University Press

Pushing the limits of AMS measurements of cosmogenic radioisotopes in natural systems

M. JANZEN[1] AND A. GALINDO-URIBARRI[1,2]

[1]Department of Earth and Planetary Sciences, University of Tennessee, TN 37996, United States (mjanzen1@utk.edu)
[2]Physics Division, Oak Ridge National Laboratory, P.O. Box 2008, MS 6368, Oak Ridge, TN 37831, United States (uribarri@ornl.gov)

Pushing the detection limits of cosmogenic radioisotopes using Accelerator Mass Spectrometry (AMS) techniques will be extremely advantageous to the field of earth sciences. In the late 1970's research in earth sciences was revolutionized by the use of AMS to achieve isotopic levels many orders of magnitude lower than conventional mass spectrometers. In earth sciences AMS techniques are most commonly employed for the measurement of cosmogenic radioisotopes. These isotopes are most useful for quantifying processes at Earth's surface. At the Holifield Radioactive Ion Beam Facility (HRIBF) we have exceptional capabilities owing to the unique set up including the highest operating voltage electrostatic accelerator in the world, the 25-MV Tandem, as well as unique beam transport components and peripheral equipment. This system allows for the detection of extremely rare isotopes and effectively remove isobar interferences. Recent measurements on $^{36}Cl/Cl$ ratios within seawater samples have shown that the levels of detection can be pushed as far as 10^{-16} [1]. Recent developments of new AMS methods such as photodetachments of negative ions may allow us to push the limits even further and increase the range of radioisotopes that can be detected [2]. I will describe an on-going research program at HRIBF that includes identifying natural systems where this extra sensitivity could make a difference. Measurements at the limit of sensitivity will contribute to constrain the predictions from cosmogenic production models at Earth's surface.

[1] A. Galindo-Uribarri *et al*. (2007) *Nucl. Instr. Meth*. B **259**, 123. [2] A. Galindo-Uribarri *et al*. (2010) *Nucl. Instr. Meth*. B **268**, 834.

Linking geochemistry to microbial community structure and function in sulfidic geothermal systems of Yellowstone National Park

Z.J. JAY[1], B. PLANER-FRIEDRICH[2], D.B. RUSCH[3] AND W.P. INSKEEP[1]*

[1]Department of Land Resources & Environmental Sciences, Montana State University, Bozeman, MT 59717, USA (*correspondence: binskeep@montana.edu)
[2]University of Bayreuth, Bayreuth, Germany
[3]J. Craig Venter Institute, Rockville, MD 20850, USA

Analysis of metagenome sequence from high-temperature microbial communities in Yellowstone National Park (YNP) suggests the importance of heterotrophic, S-respiring crenarchaeal populations in sub-oxic sulfidic sediments. The primary goal of this study was to determine the role of Thermoproteales and Desulfurococcales populations in S and C cycling in these communities using both molecular and culture methods. Metagenome sequence was obtained from three sub-oxic, elemental S-dominated hot springs in YNP: Monarch Geyser (80° C, pH 4), Cistern Spr. (CS; 76° C, pH 5) and Joseph's Coat HS (JCHS; 80° C, pH 6). Major sequence assemblies from these sites resulted in nearly complete consensus genomes of *Acidilobus*, *Vulcanisaeta* and *Caldivirga*-like organisms in all sites, *Thermoproteus*/*Pyrobaculum* spp. in JCHS and CS, and two different Sulfolobales phylotypes in CS. Several enzymes and transporters involved in protein, carbohydrate, and lipid catabolism were identified. The predominant community members all contain bd-ubiquinol oxidase genes and lack any evidence for heme-copper oxidases often associated with aerobic respiration. The expression of genes involved in anaerobic respiration, including novel S reductases in the dimethylsulfoxide (DMSO) molybdopterin family, NAD(P)H:S^0 oxidoreductases, and nitric oxide reductases, was studied using RT-PCR to estimate the activity of these processes in each habitat. Results from molecular analyses of field samples were compared to controlled experiments using a *Pyrobaculum* sp. isolated from JCHS that is capable of growing anaerobically on S^0, using yeast extract as a C and energy source. This organism contains a novel DMSO reductase, highly related to gene sequences identified in the JCHS metagenome. The effect of S^0 particle size on microbial growth was evaluated in concert with the expression of novel DMSO reductases. These data provide insight regarding the structure and function of high-temperature microbial communities, and the role of specific phylotypes in S and C cycling in sub-oxic, sulfidic geothermal systems.

https://doi.org/10.1180/S0026461X00006502 Published online by Cambridge University Press

Chemical speciation of airborne mineral dust in the Middle East

R.K.M. JAYANTY[1]*, J.B. FLANAGAN[1] AND J.P. ENGELBRECHT[2]

[1]RTI International, 3040 East Cornwallis Road, Research Triangle Park, NC 27709, USA (*correspondence: rkmj@rti.org, jamesf@rti.org)
[2]Desert Research Institute, 2215 Raggio Parkway, Reno, NV 89512, USA (johann@dri.edu)

Background

On July 8, 1997, the U.S. Environmental Protection Agency (EPA) promulgated a new national ambient air quality standard (NAAQS) for particulate matter with an aerodynamic diameter less than 2.5 μm (PM2.5). In response to the new NAAQS, EPA established two networks: the larger network monitors total mass to assess compliance with the standard. The second, smaller network, the PM2.5 Chemical Speciation Network (CSN) provides data to support attainment activities, and supplies a broad-based dataset to support human health studies and other research. RTI International has provided analytical services and other support to the chemical speciation network since early 2000.

Project Description

Desert Research Institute (DRI) contracted with RTI to provide analytical services for the U.S. Army's Enhanced Particulate Matter Surveillance Program (EPMSP), which began sampling in late 2006. The primary objective of EPMSP was to gather information on the chemical and physical properties of ambient PM in the Middle East. Ambient air samples were collected over a period of approximately one year at 15 sites, which included Djibouti, Afghanistan, Qatar, United Arab Emirates, Iraq, and Kuwait. Three particulate size fractions were sampled: PM2.5, total suspended particulates (TSP), and particulate matter less than 10 μm (PM10). Teflon, nylon, and quartz filters were used for sampling, and all filters were subsequently analyzed by RTI. Analyses included: trace elements (by X-ray Fluorescence Spectroscopy), anions and cations (by ion chromatography), total mass (by gravimetry), and elemental, organic, and carbonate carbon (by Thermal-Optical Transmittance).

Discussion

Because of the high levels of mineral dust found in the deserts of the Middle East, the levels of crustal elements found in the EPMSP samples were significantly higher than in CSN samples from the U.S., which posed some analytical challenges that will be discussed in this presentation.

Trace element geochemistry of soils in fluoride-rich shallow groundwater sites in Sri Lanka

D.T. JAYAWARDANA[1]*, A. PITAWALA[2] AND H. ISHIGA[1]

[1]Shimane University, Department of Geosciences, 690-8504, Matsue, Japan (*correspondence: taranga23@yahoo.com)
[2]Peradeniya University, Department of Geology, 20400, Peradeniya, Sri Lanka

Higher groundwater fluoride is a controversial issue in dry zone of Sri Lanka. This study described the geochemistry of residual soil from higher (< 8 mg/L) and lower (< 1 mg/L) water fluoride sites in dry zone to identify possible sources for fluoride. Twenty two major and trace elements have been determined for seventy four soil samples by means of X-ray fluorescence. Results denote that soil fluoride is lower than upper continental crust and basement rocks in both higher (<411 mg/kg) and lower (<277 mg/kg) water fluoride sites. Negative linear correlation exists between fluoride in the soil and the water suggested that fluoride readily leaching to water rather than retaining in soils due to unconsolidated sandy clay loam texture. Weathering of heavy minerals such as zirconium, apatite, fluorite, monazite and garnet are the main source for the soil in high water fluoride area. Consequently, stable extent of Zr, Nb and Th and depletion of F together with CaO and P_2O_5 than basement is occurred, hence loss of CaO provides favourable condition to leach F to water. Conversely, lower water fluoride area soils show enrichment of TiO_2, Fe_2O_3, MnO, Cr, V and Sc denote the weathering of biotite, hornblende, garnet and pyroxenes in the basement. Primary minerals present in that soil is the main cause for the enrichment of those elements. Further, fluoride levels in the soil and subsequently in water show close link with magmatic differentiations along the geological formations. Thus soil geochemistry evident that meta-igneous rocks of the higher water fluoride area may have associate with a fluoride rich residual melt while lower water fluoride area associate with acidic meta-igneous rocks with concordant meta-sedimentary rocks.

https://doi.org/10.1180/S0026461X00006502 Published online by Cambridge University Press

Transfer of uranium isotopes, thorium and their decay products to edible plants

M. JEAMBRUN[1], L. POURCELOT[1], C. MERCAT[2], F. GAUTHIER-LAFAYE[3] AND B. BOULET[4]

[1]Institut de Radioprotection et de Sûreté Nucléaire, Bat 153 BP3 13115 St Paul lez Durance cedex, France (marion.jeambrun@irsn.fr , laurent.pourcelot@irsn.fr)
[2]AREVA NC, BP44 26701 Pierrelatte Cedex, France (catherine.mercat@areva.com)
[3]Université de Strasbourg, EOST, 1, rue Blessig 67000 Strasbourg, France (fgl@unistra.fr)
[4]Institut de Radioprotection et de Sûreté Nucléaire, Bat 501 Bois des Rames 91400 Orsay, France (beatrice.boulet@irsn.fr)

Some of the primordial radionuclides (uranium, thorium and their decay products) are the main source of both external and internal radiation for humans. They can be incorporated metabolically into plants and can be transferred to animals and humans via the foodchain. However, there is a lack of data concerning the Earth crust derived actinides measured in edible plants. Furthermore their main sources as well as their mechanisms of transfer are still misunderstood. Indeed, whereas radionuclides such as uranium and radium would be transferred by root uptake, others radioelements like ^{210}Po and ^{210}Pb are preferentially carried by atmospheric particles. The aim of this work is firstly to understand the differences in activity between various plants species. The appreciation of the equilibriums and the disequilibriums between radionuclides in the decay series as well as the uptake of radionuclides by roots and the inputs by the atmosphere and irrigation should be taken into account to clarify the transfer mechanisms responsible of these differences. Secondly, the objective consists in studying the variability of natural radioactivity in edible plants, according to uranium content in soils from various areas with different geological characteristic and anthropic influence like the nuclear fuel cycle which may enhance the activity in local foodstuffs.

Fluid-mobile element enrichment in mantle wedge of subduction zones

MARLON M. JEAN AND JOHN W. SHERVAIS

Geology Department, Utah State University, Logan Utah 84322-4505

Our previous work has shown that supra-subduction zone ophiolites, which form in the mantle wedge of nascent subduction zones, preserve mantle lithologies that formed in response to hydrous melting and represent the refractory residuum of that process [1-3]. In this study we document the a new algorithm for using fluid-mobile element (FME) concentrations in unaltered residual pyroxenes to calculate the composition and flux of slab-derived fluids in the mantle wedge during melting.

We use high-precision laser ablation ICP-MS analyses (Element 2 ICP-MS with 213 nm laser) of relic pyroxenes in supra-subduction zone peridotites for B, Be, Rb, Th, Ba, Li, and Pb – analyzed in conjunction with a suite of non-fluid mobile elements including the REE and high-field strength elements, which are used to assess melt extraction and melt percolation. Pyroxenes in all SSZ ophiolite samples display enrichments in the FME relative to depleted MORB mantle. In contrast, melting models based on the MREE-HREE and HFS elements show that the FME should have concentrations that are effectively zero after significant melting. We derive an alogrithm may be used to calculate the FME:

$$C_{wr,\,add}=[C_{cpx\text{-}obs}/[[D_{cpx}/(D_{bulk}-PF)]*[1-(PF/D_{bulk})]^{(1/P)}]]-[C_{0,\,wr}]$$

Where $C_{wr,\,add}$ =concentration of FME added to mantle wedge, $C_{cpx\text{-}obs}$=observed pyroxene, D_{cpx} and D_{bulk} = mineral and bulk partition coefficients, P=melt proportion, and F=melt fraction.

Melt models require enormous fractions of FME if the peridotite and fluid are 'mixed' prior to melting. However, if the calculated fluid is added continuously so that it is in equilibrium with the observed refractory pyroxenes, fluid addition models provide reasonable results.

Our results show that high concentrations of fluid-mobile elements in supra-subduction peridotites can be attributed to a flux of aqueous fluid or fluid-rich melt phase derived from the subducting slab. Further, our calculated FME-enriched source yeilds model melts with the trace element signatures of the arc volcanics.

[1] Choi *et al*. 2008 *Cont Min Pet* **155**, 551–576. [2] Choi *et al*. 2008 *Geology* **36**, 595–598. [3] Jean *et al*. 2010 *Cont Min Pet* **159**, 113–136.

https://doi.org/10.1180/S0026461X00006502 Published online by Cambridge University Press

Raman spectroscopic identification of evaporitic minerals and biomarkers using miniaturised portable devices

J. JEHLICKA[1]*, P. VITEK[1], A. OREN[2] AND H.G. M. EDWARDS[3]

[1]Institute of Geochemistry, Mineralogy and Mineral Resources, Charles University in Prague, 12843 Prague, Czech Republic (*correspondence: jehlicka@natur.cuni.cz)

[2]The Alexander Silberman Institute of Life Sciences, The Hebrew University Jerusalem 91904, Israel

[3]Centre for Astrobiology and Extremophiles Research, University of Bradford, Bradford BD71DP, UK

Raman spectroscopy for exobiological applications

It is advocated that in the frame of forthcoming probes planned within future exobiological missions on Mars, Raman spectroscopy will play an important role. It is planned to use this non-destructive tool to identify both minerals and potential organic compounds – possible biomarkers of preexisting life. In this work, minerals from four groups (halides, sulphates, carbonates and borates), examples of pigments known from bacteria, as well as selected osmotic biochemicals (betaine, ectoine), were investigated to estimate the potential of miniaturised spectrometers to work under complex Earth conditions to detect these compounds. Raman spectra were obtained outdoors using a portable Raman spectrometer (DeltaNu, Inspector Raman, excitation 785 nm). Collection specimens and reference compounds were investigated, as well as white evaporitic crusts from two dry evaporitic lakes (Bristol Lake, Owens Lake, California, U.S.A.) and saltern evaporation ponds (Eilat, Israel).

Results

Generally speaking, excellent identificaton of minerals and associated biomaterials through their Raman band positions was achieved on mineralogical specimens from collections. Good results were obtained using the portable spectrometer outdoors on native white evaporitic crusts under ambient atmospheric conditions. Shielding of the measurement area against insolation was nevertheless necessary. Although the recording of weaker Raman features was sometimes problematic, this did not compromise the precise identification of the mineral concerned. Raman spectra of investigated pigments and halophile osmotic compounds obtained permit their reliable identification as well.

Chalcophile element systematics in the North West Lau backarc basin

FRANCES E. JENNER, JOHN A. MAVROGENES*, RICHARD J. ARCULUS AND HUGH ST.C. O'NEILL

Research School of Earth Sciences, Australian National University, ACT Australia 0200 (*correspondence: john.mavrogenes@anu.edu.au)

The Lau Backarc Basin hosts numerous individual spreading centers, including the 70 km-long Northwest Lau Spreading Center (NWLSC) located ~500km west of the northern Tonga Arc volcanic front. Submarine volcanic glasses with from 9 to 2 wt.% MgO (49-62 wt.% SiO_2) were recovered from the NWLSC. These samples show no evidence of a subducted slab component. There is no indication of S loss by degassing. Fractional crystallization of olivine and clinopyroxene drives the liquid to high FeO* with decreasing MgO until the appearance of magnetite on the liquidus at ~4 wt.% MgO. S parallels FeO* but the S levels are initially below those of sulfide-saturated MORB, indicating undersaturation in sulfide. Consequently Cu, Se and Ag also initially increase with decreasing MgO. The apogee in Cu, Ag and Se contents, attributable to sulfide saturation, is at ~5.5 wt% MgO, notably earlier than the maximum in FeO* and S. Because S simply tracks FeO* at sulfide saturation, the Cu-Ag-Se trend reveals the onset of sulfide saturation better than S itself. The behaviour of Cu, Se and Ag in the basaltic to andesitic suite from the NWLSC is intermediate between MORB and oxidised backarc basin magmas; it contrasts with that from the Pual Ridge back arc basin by reaching sulfide saturation prior to the onset of magnetite fractionation. Therefore, chalcophile elements in the NWLSC are removed by continuous pyrrhotite fractionation whereas the more oxidised Pual Ridge magma fractionates to very high chalcophile element abundances before massive precipitation of Cu-Ag (and Au) sulfide at the magnetite crisis.

[1] Jenner, F. E. O'Neill, H. St. C. Arculus, R. J. Mavrogenes, J. A. (2010) *Journal of Petrology* **51**(12), 2445–2464.

https://doi.org/10.1180/S0026461X00006502 Published online by Cambridge University Press

Characterization of magma from inclusions in zircon: Apatite and biotite work well, feldspar less so

E.S. JENNINGS[1], H.R. MARSCHALL[1,2], C.J. HAWKESWORTH[3] AND C.D. STOREY[4]

[1]Department of Earth Sciences, University of Bristol, Bristol BS8 1RJ, UK (eleanor.jennings@bristol.ac.uk)
[2]Department of Geology and Geophysics, Woods Hole Oceanographic Institution, Woods Hole, Massachusetts 02543, USA (hmarschall@whoi.edu)
[3]University of St Andrews, College Gate, North Street, St Andrews KY16 9AJ, UK (chris.hawkesworth@st-andrews.ac.uk)
[4]School of Earth and Environmental Sciences, University of Portsmouth, Burnaby Road, Portsmouth PO1 3QL, UK (craig.storey@port.ac.uk)

Detrital zircon grains are frequently employed to decipher sediment provenances and crustal evolution throughout Earth history, and they provide unique evidence of Hadean crust-mantle differentiation. However, interpretation of detrital zircon is hampered by the remarkably restricted range of geochemical characteristics of zircon derived from a range of igneous source rocks. Mineral inclusions in zircon are an underexploited resource and provide valuable additional petrologic information on the condition under which zircon crystallised. Zircon grains from a range of plutonic rocks (diorite-monzonite-granite sequence) contain inclusions of apatite and mafic phases (biotite, amphibole, pyroxenes) which accurately reflect the chemical compositions of the equivalent phases in the matrix of the host rocks. Chemical characteristics of the inclusions, such as Mg/Fe ratios of mafic phases, and Sr abundances in apatite, correlate well with the compositions of the whole rocks. High concentrations of Y_2O_3 (>0.4 wt%) and low concentrations of SrO (<0.02 wt%) in apatite inclusions in zircon are diagnostic of evolved, felsic granitoid host rocks. In strong contrast, the relative abundances and compositions of plagioclase and alkali feldspar inclusions in zircon are decoupled from the composition of the whole rock, and are generally indicative of chemically evolved, granitic melts, regardless of the bulk rock composition. This is best explained by the late crystallization of zircon relative to the bulk of the feldspars.

We conclude that inclusions of apatite and mafic phases in zircon constrain the potential source rocks of detrital zircon, whereas feldspar inclusions do not. This ability to differentiate between grains from primitive and evolved sources has important applications to the interpretation of Hadean zircons.

Secular trends in granite zircon εHf–$\delta^{18}O$, Australian Tasmanides

HEEJIN JEON[1]*, IAN S WILLIAMS[1], BRUCE W CHAPPELL[2] AND VICKIE C BENNETT[1]

[1]Research School of Earth Sciences, Australian National Univ., Acton, ACT 0200, Australia (*correspondence: heejin.jeon@anu.edu.au)
[2]Department of Earth Sciences, Univ. of Wollongong, Wollongong, NSW 2522, Australia

The possible role of arc/back-arc accretionary processes in generating continental crust has recently been highlighted [1]. In this context, it has been argued that the Phanerozoic Tasmanides (~3000 x 6000 km) comprising the eastern third of the Australian continent formed during repeated opening and closing of sediment-filled back-arc basins triggered by alternating slab rollback and advances in a long-lived Cambrian to Triassic subduction system [2]. Kemp *et al*. [3] attempted to correlate additions of newly formed juvenile crust to the Tasmanide igneous rocks with the pattern of deformational/tectonic events during three orogenies (Delamerian, Lachlan, New England) using isotope signatures (whole rock Nd, zircon U/Pb, Hf and O). They proposed S-type granite emplacement in thickened crust followed by increasing juvenile contributions during back-arc rifting. The limited data set did not fully define the long-term Tasmanide isotopic trend, however, and few data represented the key Carboniferous event between the main crust forming episodes in the Lachlan (LFB) and New England (NEO) orogens.

New zircon U-Pb, Hf and O isotopic data from Carboniferous-Early Triassic granites in the LFB and NEO have been used to test the Kemp *et al*. [3] tectonic model. The I-type LFB Carboniferous granites show a trend from juvenile to more crustal (higher) $\delta^{18}O_{Zrn}$ with time, but a step from strongly to weakly positive εHf (t). Permian S-type granites of the NEO have very high, crustal $\delta^{18}O_{Zrn}$, but uniformally moderately positive εHf (t). Most analysed NEO I-type granites have moderate $\delta^{18}O_{Zrn}$, except for the oldest, in which the range of $\delta^{18}O_{Zrn}$ is similar to that in the LFB S-types. All have moderately to strongly positive εHf (t).

The zircon Hf and O isotopic compositions in the post-Devonian granites of the LFB and NEO are decoupled. Further, emplacement of the NEO S-type granites did not coincide with any recognised deformation episode. These features are not consistent with current models of arc/back-arc accretion.

[1] Cawood & Buchan (2007) *Earth Sci. Rev.* **82**, 217–256.
[2] Collins & Richards (2008) *Geology* **36**, 559–562.
[3] Kemp *et al*. (2009) *EPSL*, **284**, 455–466.

https://doi.org/10.1180/S0026461X00006502 Published online by Cambridge University Press

Lead isotopic compositions for Pb-Zn deposits in the Eastern South Korea

Y.-J. JEONG[1], C.-S. CHEONG[1], H.-J. JO[1], J.Y. CHOI[1], D.-B. SHIN[2], M.-S. HAN[3] AND J.-J. HWANG[3]

[1]Korea Basic Science Institute, Daejeon 305-333, Korea (hero0123@kbsi.re.kr)
[2]Department of Geoenvironmental Sciences, Kongju National University, Kongju 314-701, Korea
[3]Division of Conservation Science, National Research Institute of Cultural Hertage, Daejeon 305-380, Korea

In this paper, the lead isotopic compositions of galena, collected from 15 lead-zinc deposits in the eastern part of South Korea were analyzed, mainly aiming at understanding the regional variation and the geochemical evolution of Pb isotopic composition of lead-zinc deposits in Korea.

For 9 lead-zinc deposits in the Ogcheon system and the Yeongnam massif, Pb isotopic compositions of galena are ranging 18.562-19.784 for $^{206}Pb/^{204}Pb$, 15.729-15.934 for $^{207}Pb/^{204}Pb$, and 38.849-39.859 for $^{208}Pb/^{204}Pb$.

In contrast, for galena samples collected from 6 lead-zinc deposits in Gyeongsang basin, the lead isotopic composition varies in a relatively small range; those isotopic compositions of $^{206}Pb/^{204}Pb$, $^{207}Pb/^{204}Pb$ and $^{208}Pb/^{204}Pb$ are in the range of 18.265-18.441, 15.581-15.726 and 38.332-38.993, respectively, which are slightly lower than those observed in the Gyeongsang basin.

Based on our observations, it seems that lead isotopic compositions in Korea can be classified according to the tectonic boundary between the Gyeongsang basin and the Yeongnam massif. Also, it appears that Pb for lead-zinc deposits in the Ogcheon system and the Yeongnam massif seems to have been originated from upper crustal materials of old continental, because they fit well onto the general trend of lead isotopic compositions of Precambrian basement rocks in South Korea.

Ni and Cr speciation in soils formed on ultramafic rocks from Barberton Greenstone Belt (South Africa)

I. JERZYKOWSKA* AND M. MICHALIK

Jagiellonian University, Institute of Geological Sciences, Oleandry 2a, 30-063 Kraków, Poland (*correspondence: irena.jerzykowska@uj.edu.pl)

Five soil samples were collected by Jolanta Mesjasz-Przybyłowicz (from the depth of about 10 cm) near the Agnes Mine in Mpumalanga Province, the Republic of South Africa. Soils are formed on amfibole-talc shists and serpentinites of Onverwacht Group in Barberton Greenstone Belt. Soils are characterised by mean Mg/Ca ratio 4, 27 and mean pH_{H2O} value 5, 43 [1].

Soil samples and the bedrock fragments were analyzed using optical microscope, SEM EDS and X-ray diffraction. Seven-step sequential extraction (exchangeable ions, carbonates, manganese oxides, amorphous iron oxides and hydroxides, crystalline iron oxides, organic matter and sulfurs, residual fraction) was executed on 4 soil samples. Chemical composition of soils and extracts was determined using IPC MS and ICP AES.

Soils are composed mainly of amfibole, talc, serpentine, chlorite, quartz and various clay minerals. According to EDS measurements of weathered rock fragments form soils, the most important Ni and Cr bearing phases are rarely occurring Mn-oxides, Fe-oxyhydroxides and commonly occurring various phyllosilicates. Mean and maximal values are listed in Table 1.

wt.%	Phyllosilicates		Fe-oxyhydroxides		Mn-oxides	
	NiO	Cr_2O_3	NiO	Cr_2O_3	NiO	Cr_2O_3
Mean	0,12	0,21	0,43	1,76	9,69	0,05
SD	0,58	1,11	1,25	2,7	4,28	0,15
Max.	12,53	3,85	6,81	16,74	17,74	0,42

Table 1: Mean and maximal concentrations of NiO and Cr_2O_3 (wt.%; EDS results) in weathered rock fragments

Sequential extraction experiment results agree with EDS studies. About 50% of Ni and Cr are bound to residual phases which are mainly silicates. Almost 50% of Cr is accumulated in crystalline Fe-oxides. Very important Ni containing phases are crystalline and amorphous Fe-oxides (respectively 27% and 8%) and to a lesser amount Mn-oxides (5%).

[1] Mesjasz-Przybyłowicz *et al*. (2007) *Plant Soil* **293**, 61–78.

https://doi.org/10.1180/S0026461X00006502 Published online by Cambridge University Press

Changes in microbial community structure associated with dynamics in oxygen supply at the Crimean shelf of the Black Sea

GERDHARD L. JESSEN[1]*, ANNA LICHTSCHLAG[1], DAPHNE DONIS[1], FRANK WENZHÖFER[2], CARSTEN J. SCHUBERT[3], ALBAN RAMETTE[1] AND ANTJE BOETIUS[1,2]

[1]MPI for Marine Microbiology, 28359 Bremen, Germany (*correspondence: gjessen@mpi-bremen.de)
[2]HGF-MPG Joint Research Group on Deep Sea Ecology and Technology, AWI, 27515 Bremerhaven, Germany
[3]Swiss Federal Institute of Aquatic Science and Technology, Seestrasse 79, 6047 Kastanienbaum, Switzerland

Today's rapid global warming of oceans together with eutrophication appears to promote a deoxygenation of some of the world's water bodies [1, 2], which eventually leads to hypoxia and even anoxia in regions of low oxygen supplies. With less than 60 μM oxygen most animals are negatively impacted and microorganisms dominate benthic energy fluxes [3]. As a result, it can be expected that in zones with oxygen dynamics around this tipping point benthic and microbial community structure will vary considerably in space and time, with repercussions on the flux of energy and matter trough the ecosystem. Here we present effects of varying hypoxic conditions on benthic microbial communities. Sediments from a series of transects across oxic to hypoxic conditions at the Crimean shelf of the Black Sea were analysed by community fingerprinting using ARISA (Automated Ribosomal Intergenic Spacer Analysis), in order to asses the connections between oxygen supply and benthic microbial community structure.

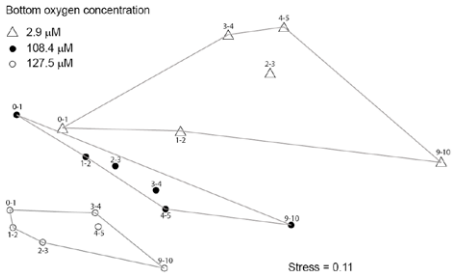

Figure 1: NMDS ordination plot (Bray-Curtis distance matrix) of ARISA profiles for the upper 10 cm layer sediment. Numbers represent each horizon sampled (cm).

Our data clearly exhibited a strong change in benthic bacterial community structure along a sampling transect including oxic, anoxic and highly dynamic hypoxic zones (Fig. 1), indicating an effect of temporal dynamics in oxygen supply at the microbial scale. This study is supported by the EU project HYPOX.

[1] Hoegh-Guldberg & Bruno (2010) *Nature* **328**, 1523–1528. [2] Zhang *et al*. (2010) *Biogeosciences* **7**, 1443–1467 [3] Díaz & Rosenberg (2008) *Science* **321**, 926–929.

Sulfur, carbon and nitrogen isotopic variation in the drinking water source of Beijing

JI HONGBING[1,2,3]*, ZHU XIANFAN[2], LI HUIYIN[2], LU FENGYUN[2] AND XING XIN[2]

[1]School of Civil and Environmental Engineering, University of Science and Technology Beijing, Beijing 100083, China (*correspondence: hongbing.ji@yahoo.com)
[2]The Key Laboratory of Metropolitan Eco-Environmental Processes, College of Resource Enviroment and Tourism, Capital Normal University, Beijing 100048, China
[3]State Key Laboratory of Environmental Geochemistry, Institute of Geochemistry, Chinese Academy of Sciences, Guiyang 550002, China

Samples of water, suspended particulate matter and sediments were collected in the drinking water source of northern Beijing and analyzed for sulphur, carbon and nitrogen isotopic compositions. The results showed that: (1) The ratios of sulphur isotope were between 4.9‰ and 10.7‰ in water samples; (2) The carbon and nitrogen isotopic ratios in suspended particulate matter were -29.34‰–-25.91‰ and -0.96‰–6.73‰ in summer, and -30.75‰–-25.75‰ and -0.83‰–9.67‰ in winter, respectively; (3) The sulphur, carbon and nitrogen isotopic ratios in surface sediments were -11.8‰–6.1‰, -27.25‰–-21.58‰ and 1.32 ‰–6.74‰, respectively. The differences of sulphur isotopic compositions in surface sediments from different sampling sites show the differences in the sources of sulphur. The suspended particulate organic matter was derived mainly from SOM-C_3 and macrophyte in summer, while it was derived from SOM-C_3 and plankton in winter. Surface sedimentary organic matters were mainly derived from SOM-C_3. Nitrogen isotopic ratios reflected the combined results of materials source and it can be used to trace some special biogeochemical processes. This study reveals that the source of organic matter has a close relationship with the situation of soil erosion in the areas.

This study was supported by the program of "One Hundred Talented People" of the CAS.

https://doi.org/10.1180/S0026461X00006502 Published online by Cambridge University Press

Research on chronology and formation mechanism of Xiaorequanzi Cu-Zn field in Tianshan Orogenic Belt, Western China

JI HONGWEI[1,2]*, SUN JINGBO[2], LI JIE[1,2], LI HUAQIN[1,3], CHEN FUWEN[3] AND CHEN WEN[2]

[1]China University of Geosciences, Beijing, 100083 China (*correspondence: jhw5566@163.com)
[2]Institute of Geology CAGS, Beijing, 100037 China
[3]Wuhan Center of Geological Survey, Wuhan, 430223 China

A large number of VHMS deposits have developed within Tianshan orogenic belt in western China, and Xiaorequanzi Cu-Zn field, consisting of several sulphide deposits, is more typical. There are three perspectives on the genesis of the deposit. First, according to the phenomena that intermediate-acid porphyry veins usually emerge near the ore body, the copper amount of porphyries is several times higher than the Clarke value of similar rocks, it is a porphyry copper deposit. Second, based on the features that the deposit occurs in the Xiaorequanzi volcanic rocks, ore body is layered and like-layered, it is a VHMS deposit. Third, on the basis of the traits that oxide ores in the surface and deep primary ores are more veins, it is volcanic hydrothermal-type deposit.

In order to identify the mineralization age and genesis of Xiaorequanzi Cu-Zn deposit, the metallogenetic and magmatic events in mining area were systematically researched by Rb-Sr isotopic geochronology. The whole-rock Rb-Sr isochron age of ore-bearing rocks, andesite, is 313Ma; the Rb-Sr isochron age of quartz fluid inclusion in copper-bearing quartz veinlets is 297Ma; the age of albite porphyry is 267Ma; the Rb-Sr isochron age of quartz fluid inclusion in stockwork copper ore, which formed in the period of magmatic hydrothermal, is 264 Ma. Isotopic dating results show that Xiaorequanzi Cu-Zn field belongs to the composite deposit, consisting of volcanic exhalation sedimentation and post-magmatic hydrothermal reworking. The mineralization should be divided into two phases: the main occurred in the late Carboniferous, 313~297Ma, which is consistent with the time of volcanic eruptions. Superimposed mineralization of the late magmatic hydrothermal occurs in the middle to late Permian, about 264Ma, which is roughly the same as the emplacement time of subvolcanic rocks in the region.

This work was supported by the Science and Technology Research Project of China (No.: 2007CB411306; 200911043-13; 1212011120293)

Mineralogic and climatic interpretations of the Late Miocene-Pliocene Red Clay Formation on the Chinese Loess Plateau

JUNFENG JI, TONG HE, LIANG ZHAO, YANG CHEN AND JUN CHEN

Institute of Surface Geochemistry, School of Earth Sciences and Engineering, Nanjing University, Nanjing 210093, China (jijunfeng@nju.edu.cn)

The closest past analog to the contemporary global warming is the Pliocene. Its climate reconstruction has been focused on continuous sedimentary records and terrestrial eolian deposits. The late Miocene-Pliocene Red Clay Formation on the Chinese Loess Plateau is among the best archives of the Pliocene paleoclimate change. In this study, we examined three classic Red Clay profiles at Lingtai, Duanjiapo and Bajiazui on the Chinese Loess Plateau with X-ray diffraction, Fourier transform infrared spectroscopy, diffuse reflectance spectrophotometer and scanning electron microscopy. Compared to the overlying Pleistocene loess-paleosol sequences, the Red Clay profiles show the following different mineralogical features: (1) carbonates are composed of both calcite and protodolomite; (2) the protodolomite are rhombic euhedral crystals growing in soil voids and coexisting with secondary calcite and palygorskite; (3) smectite is one of the dominate clay minerals; (4) the hematite/goethite (Hm/Gt) ratio varies from 0.30 to 0.52, and is much higher than that of Quaternary loess and paleosol. The occurrences of protodolomite and palygorskite as well as abundant hematite and smectite in the Red Clay sequence may indicate that it was formed under a prevailing warm and dry climate condition, which is probably a response of the inner Asia continent to the Pacific permanent El Niño and global high temperature climate in the late Miocene to Pliocene.

https://doi.org/10.1180/S0026461X00006502 Published online by Cambridge University Press

Thermodynamic study for CO_2 storage in deep saline aquifers

XIAOYAN JI[1]* AND CHEN ZHU[2]

[1]Division of Energy Engineering, Lulea University of Technology, 97187 Lulea, Sweden (*correspondence: xiaoyan.ji@ltu.se)

[2]Department of Geological Science, Indiana University, USA (chenzhu@indiana.edu)

Storage of CO_2 in deep saline aquifers is one proposed option to limit the continuing buildup of greenhouse gases in the atmosphere. To reduce the capture costs, co-injection of CO_2 and H_2S is proposed. To predict the sequestration capacity and the fate of injected gases as well as for other geochemical applications, it is necessary to study the thermodynamic properties and phase equilibria for the CO_2 sequestration-related systems at temperatures up to 200 °C and pressures up to 600 bar.

A new thermodynamic model, on the basis of statistical associating fluid theory equation of state, is developed to represent the phase equilibria and thermodynamic properties for CO_2-H_2O-NaCl, H_2S-H_2O-NaCl, and CO_2-H_2S-H_2O-NaCl systems. The parameters of pure components are obtained from the fitting of their saturated vapour pressure and liquid density data, and the cross parameters are obtained from the fitting of the phase equilibrium data of H_2S (CO_2)-H_2O-NaCl system.[1-4] With the available parameters, the phase equilibria and thermodynamic properties for CO_2-H_2S-H_2O-NaCl are predicted. The prediction shows that the solubility of the H_2S-CO_2 mixture increases with increasing pressure, decreasing concentration of NaCl and decreasing temperature. The mixture of H_2S-CO_2 is more soluble than pure H_2S under certain conditions and also more soluble than pure CO_2.

This thermodynamic model will be further implemented into a dynamic model to investigate the process of gas diffusion and dissolution in brine and the process of mineral dissolution and precipitation with dissolved CO_2 and H_2S. It is expected that the coupling of the dynamic model with the thermodynamic model will provide reliable long-term predictions pertaining to geochemical carbon sequestration, such as sequestration capacity, CO_2 leakage, the mechanics of CO_2 trapping, and environmental impacts, etc.

[1] Ji & Zhu (2010) *Energy & Fuels* **24**, 6208–6213. [2] Ji & Adidharma (2007) *Ind. Eng. Chem. Res.* **46**, 4667–4677. [3] Ji & Adidharma (2008) *Chem. Eng. Sci.* **63**, 131–140. [4] Ji, Tan, Adidharma & Radosz (2005) *Ind. Eng. Chem. Res.* **44**, 8419–8427.

Detrital zircon provenance of late Ordovician-Silurian sandstones in the Lower Yangtze foreland basin of South China

DONG JIA, HAIBIN LI, LONG WU AND YIQUAN LI

Dept. of Earth Sciences, Nanjing University, Nanjing 210093, China (djia@nju.edu.cn)

The Lower Yangtze foreland basin is situated northwest of the early Paleozoic (ca.460–400Ma) Wuyi orogenic belt in South China [1]. In this basin, the upper Neoproterozoic-Ordovician strata are composed of shelf carbonates, slop limestones as well as mudstones [2]. Significant changes of lithofacies, and depositional environment took place during latest Ordovician–Silurian, which were coincident with the timing of the Wuyi orogeny. In order to demonstrate the basin development was in response to the orogenic event, seven sandstone samples were collected from upper Ordovician and Silurian strata. U–Pb ages of 604 detrital zircon grains yield remarkable peaks at ca. 2500Ma, 1200–900Ma, 860–740Ma and 458–425 Ma. The early Paleozoic zircons (458–425 Ma) correspond to the granitic rocks within the Wuyi orogenic belt to south or southeast, suggesting exhumation of syn-orogenic rocks. Besides, the Precambrian zircons (ca. 2500Ma, 1200–900Ma, 860–740 Ma) are most likely recycled from pre-orogenic strata in the Wuyi orogenic belt due to their similarity in age distribution [2]. The predominant Neoproterzoic (860–740Ma) zircons indicate the Yangtze basement had been involved in the orogenic belt. The youngest zircons at the top of the succession yield a maximum depositional age of ca. 425 Ma.

This research was supported by the Ph.D. Programs Foundation of Ministry of Education of China (20090091110020) and National S&T Major Project of China (2008ZX 05003–001 and 2008ZX05009–001).

[1] Li Z-X *et al*. (2010) *GSA Bulletin*. **122**, 772–793. [2] Wu *et al*. (2010) *Geol. Mag*. **147**(6), 974–980.

https://doi.org/10.1180/S0026461X00006502 Published online by Cambridge University Press

A major decline of C_4 plant in the source region of the North Pacific eolian dust (Asian interior) from 12 to 9 Ma

GUODONG JIA[1,2], ZHIYANG LI[2] AND PING'AN PENG[3]

[1]State Key Laboratory of Isotope Geochemistry, Guangzhou Institute of Geochemistry, Chinese Academy of Sciences, Guangzhou 510640, China (*correspondence: jiagd@gig.ac.cn)

[2]CAS Key Laboratory of Marginal Sea Geology, Guangzhou Institute of Geochemistry, Chinese Academy of Sciences, Guangzhou 510640, China

[3]State Key Laboratory of Organic Geochemistry, Guangzhou Institute of Geochemistry, Chinese Academy of Sciences, Guangzhou 510640, China

Aeolian deposition in the central north Pacific has been well recognized to originate from arid Asian interior. However, works on terrestrial organic tracers therein are rare. In this work, higher plant leaf wax n-alkanes from ODP Site 1208 in the northwest Pacific since the middle Miocene were analyzed to explore the source region vegetation and climate changes. Both average chain length of wax n-alkanes and their accumulation rates showed a general increasing trend, consistent with the well recognized climatic drying trend of the Asian interior. The record of isotopic fractionation factor between plant and atmospheric CO_2 ($\varepsilon_{plant-CO2}$), calculated from $\delta^{13}C$ values of n-alkane and atmospheric CO_2, showed a prominent decrease from 12.4 to 9.3 Ma, and displayed a general pattern of higher values prior ~8 Ma and lower values post ~8 Ma. Although all values of $\varepsilon_{plant-CO2}$ (−18.5 to −16.8‰) were well within the range of C_3 plants, adjustment of isotopic discrimination of C_3 plants was rule out as the main cause of the observed $\varepsilon_{plant-CO2}$ variations. Therefore, relative abundances of C_3 vs. C_4 plants were invoked to interpret the $\varepsilon_{plant-CO2}$ record, and higher C_4 contributions (13.8 ± 2.0%) were inferred due to slightly warmer climate in the source region prior to ~8 Ma. The suggested major C_4 decline from 12.4 to 9.3 Ma was concurrent with evidences supporting a prominent uplift of northern Tibetan plateau [1], demonstrating close relationships of Tibetan uplift, drying and cooling climates, and vegetation changes of the Asian interior.

[1] Sun, Zhu & An (2005) *Earth & Planetary Science Letters* **235**, 641–653.

Geochemistry of the Xuanwei Group in Guizhou, Southwestern China

F. JIANG[1], Z.W. ZHANG[2] AND B.M. CHI[1]*

[1]Institute of Disaster Prevention Science & Technology, Yanjiao 101601, Beijing, China (gaodashu@126.com)

[2]State Key Laboratory of Ore Deposit Geochemistry, Institute of Geochemistry, Chinese Academy of Sciences, 46 Guanshui Road, Guiyang 550002, PR China

Introduction

According the regional geological information, the sedimentation of southwestern margin of the Yangtze plate was of platform type, its sedimentation in the Xuanwei Group was series of marine to land transformation association [1]. The Upper Permian Emeishan basalt group underlying contact with Xuanwei Group, is continental flood basalt [2], as an eruption of the Emeishan large igneous province magmatism [3]. Sedimentary environment is very useful to understand activities in the Emeishan large igneous province and geological event of great significance to the changed environmental process.

Methods and Results

Trace elements and strontium isotopes are measured of samples from the Xuanwei Group, west Guizhou, and we also collected data from publications from the Emeishan Group and its adjacent regions [1-3]. Based on analyses of petrochemistry and strontium isotopes of carbonaceous shale and sandy shale rocks, geochemical characteristics indicate that sedimentary environments show hydrothermal activity, accomanyed with normal sedimentary participation. The fluctuations in Ce anomaly represent conversion process from oxidative environment and deoxidized environment. Strontium isotopic ratios $(^{87}Sr/^{86}Sr)_{t0}$ manifesting that materials of the Xuanwei Group may be derived from Emeishan basalts mixed with marine carbonate from chemical weathering. It conclude that sedimentary sources were not only by Emeishan basalt weathering, but also causes of hot water sedimentary display.

[1] Lin J.Y. (1985) *Chin. Sci. Bull.* **12**, 929–932. [2] Song X.Y. *et al.* (2001) *Acta Geol. Sinica* **75**, 498–506. [3] Zhang Z.W. *et al.* (2010) *Chinese J. Geochem.* **29**, 355–364.

https://doi.org/10.1180/S0026461X00006502 Published online by Cambridge University Press

A 700-year record of accumulation rates at Dome A, Antarctica

S. JIANG[1], Y.S. LI[1], J.H. COLE-DAI[2] AND D.G. FERRIS[2]

[1]Polar Research Institute of China, Shanghai, China (jiangsu@pric.gov.cn)
[2]Department of Chemistry and Biochemistry, South Dakota State University, Brookings, South Dakota, USA

Dome A, located along the dividing line of East Antarctica, has the highest altitude in Antarctica. Preliminary evidence indicates that Dome A holds high potential for 'oldest ice' cores [1].

During the 21st Chinese Antarctic Research Expedition in 2004/2005 austral summer, a 109.91 m ice core (hereafter DA2005 ice core) was recovered at the site about 300 m away from the summit of Dome A. Chemical analysis of the DA2005 core has been used to construct continuous, detailed glaciochemical record. And time stratigraphic horizons from known volcanic eruptions were used for dating. Several clearly visible sulfate peaks in the top 35 m part of DA2005 were identified by comparison with common volcanic chronologies from Antarctica [2, 3]. These include the well-known volcanic events in the last millennium: Agung 1963, Krakatoa 1883, Tambora 1815 and an unknown eruption 1809, Unknown 1693, Kuwae 1453 and Unknown 1259. A mean accumulation rate was calculated according to the time stratigraphic horizons between two adjacent events and was assumued constant to date the intervening snow layers. Results show that the mean accumulation rates during different time periods are quite constant, ranging from 21.5 to 24.5 $mmH_2O{\cdot}yr^{-1}$. And the resulting dates for other volcanic events during the period of 1259-1963 A.D. are in good agreement with those in previous Antarctic ice core volcanic records. The mean accumulation rate between Agung and 1259 A.D. is 23.2 $mmH_2O{\cdot}yr^{-1}$, which is the same as the value between 1966 and 2004 A.D. measured from snow blocks collected at Dome A [4]. It seems that there is neither an indication of a change nor a trend in the accumulation rate apparent during the period of 1259-1963 A.D. which may indicate no drastic change in deposition has occurred at Dome A within this time period.

This work was supported by National Science Foundation of China grants (NSFC 40906098, 40773074, 40703019).

[1] Xiao *et al*. (2008) *Chin. Sci. Bull* **53**, 102–106. [2] Delmas *et al*. (1992) *Tellus* **44B**, 335–350. [3] Cole-Dai *et al*. (2000) *J. Geophys. Res* **105**, 24431–24441. [4] Hou *et al*. (2009) *Sci. China Ser. D-Earth Sci* **52**, 1502–1509.

Analysis of microbial molecular ecology techniques in constructed rapid infiltration system

XIN JIANG[1,2] *, MING-CHAO MA[2], JUN LI[2] AND ANHUAI LU[1]

[1]School of Earth and Space Sciences, Peking University, Beijing 100871, China (*correspondence: jiangxinmail@yahoo.com.cn)
[2]Institute of Agricultural Resources and Regional Planning, Chinese Academy of Agriculture Science, Beijing 100081, China

The microbial molecular ecology techniques, which were developed on the basis of molecular, were applied in studying the bacteria in Constructed Rapid Infiltration system (CRI). These techniques are very efficient in better describing the bacterial diversity, microbial community distribution and the relations between microbial group structure and nitrogen contamination through the analysis of microbial nucleic acid sequence fragment in CRI. The results further revealed the removal mechanism of contamination, which are essentially for the improvement of wastewater treatment in CRI.

In this study, a series of microbial molecular ecology techniques were applied in studying the bacteria in CRI. The microbial community distribution of bacteria was analyzed by PCR-DGGE qualitatively and a bacterial 16S rDNA gene clone library was constructed to analyze the bacterial diversity quantitatively. The anaerobic ammonium oxidation bacteria were proved to exist in CRI by phylogenetic analysis with a DNA sequence similarity of 97 %. The relations between microbial groups' structure and nitrogen contamination, and the removal mechanism of contamination were revealed.

https://doi.org/10.1180/S0026461X00006502 Published online by Cambridge University Press

Granularity and geochemistry of olivine in Jinchuan Ni-Cu-PGE magmatic sulfide deposit

JIAO J G[1,2], LIU M W[2], DUAN J[1] AND JU H[1]

[1]Chang'an University, Xi'an 710054, China (*correspondence: (jiangang@chd.edu.cn)

[2]Key Laboratory of Western China's Mineral Resources and Geological Engineering, Ministry of Education of P.R.C, Xi'an 710054, China

The Jinchuan Ni-Cu-PGE deposit is the third largest magmatic Ni deposit in the world, hosted by a small ultramafic intrusion in the Longshoushan terrane located in the south-western part of the North China Craton.

Granularity of olivine in the Jinchuan complex is from 1-8mm in diameter.Those olivine with 6-8mm distributes in ore-body 24, only contains disseminate sulfide; the olivine with 3-6mm still mainly lies in ore-body 24 contain partial net-texture sulfide; the olivine with 1-3mm in diameter distributes all mine, including most net-texture ore and no-sulfide rocks.

Our datum prove forsterite contents (mol. % Fo) of olivine in the Jinchuan rocks are in the range of 83.9-85.5% in pyroxene-bearing peridotite (no sulfide, olivine 1-2mm in diameter, at the surface of ore-body 2), 82-83.5% in dunite and lherzolite (mostly net-texture sulfide, olivine 1-3mm or 6-8mm in diameter, in ore-body 1, 24), and 78-81% in olivine pyroxenite (partial net-texture sulfide or no sulfide with tremolite, olivine 1-2mm in diameter, in ore-body 1, 2) (Fig.1). Little variation within one sample is observed for olivine.

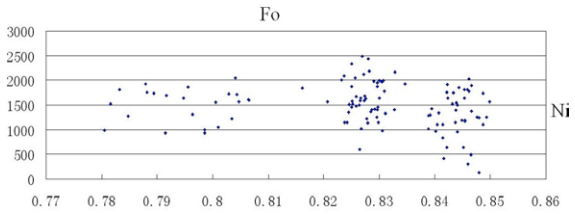

Figure 1: Compositional variations of different types of olivine from the Jinchuan rocks

So Granularity and forsterite contents of olivine have no accordant variation; Most net-texture sulfide ore holds forsterite contents from 82-83.5%, indacating the main ore-forming condition; 83.9-85% in pyroxene-bearing peridotite with no sulfide and stabilized Ni contents in olivine means olivine has partially crystalized before sulfur saturation as the decrease of temperature.Three type of forsterite contents means three types of rock-forming conditions, maybe three middle magma chambers.

This work is supported by the NSFC (grants 41072058).

An Atomic Force Microscope study of the microstructure of 'barkinite' liptobiolith

KUN JIAO[1], SUPING YAO[1]* AND KE ZHANG[1]

[1]State Key Laboratory for Mineral Deposits Research (Nanjing University), School of Earth Sciences and Engineering, Nanjing University, Nanjing 210093, China (*correspondence: spyao@nju.edu.cn)

Using Atomic Force Microscope (AFM) to observe the surface of 'barkinite' and vitrinite in nanoscale, reveal the surface microstructures of 'barkinite' and vitrinite, that is, the netlike structure of vitrinite macromolecular clusters and the fiberlike, granular, and netlike structure of 'barkinite' macromolecular clusters. With increasing maturity, the structure of 'barkinite' macromolecular clusters are fiberlike - granular - irregular netlike - netlike in sequence (Fig.1), while the structure of vitrinite macromolecular clusters change from loose, irregular network to highly orient arranged, regular network. Quantitative analysis of the structure of macromolecular cluster and arrangement in maceral by using cross - section analysis tool of Atomic Force Microscope provide a new approach to study the structure evolution of maceral molecule and hydrocarbon generation mechanism.

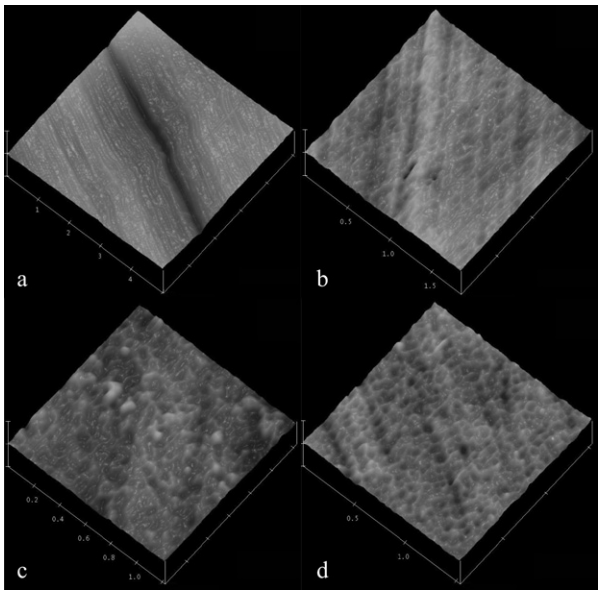

Figure 1: Microstructure evolution model of "barkinite" (a-gas coal, b-gas-fat coal, c-fat coking coal, d-anthracite)

https://doi.org/10.1180/S0026461X00006502 Published online by Cambridge University Press

Enhanced phosphorus regeneration in low oxygen marine settings: insights from modern and ancient sediments and implications for the future ocean

TOM JILBERT[1], CAROLINE P. SLOMP[1], PETER KRAAL[2], ANNE K. STEENBERGH[3] AND VIRGINIA PALASTANGA[1]

[1]Department of Earth Sciences (Geochemistry), Faculty of Geosciences, Utrecht University, P.O. Box 80.021, 3508 TA Utrecht, The Netherlands

[2]Southern Cross University, Southern Cross GeoScience, Military Road, Lismore, 2480 NSW, Australia

[3]Netherlands Institute of Ecology, Droevendaalsesteeg 10, 6708 PB Wageningen, The Netherlands

Phosphorus (P) is a key nutrient for marine productivity and its availability plays a crucial role in the development of oxygen deficiency in marine systems. Most importantly, enhanced release of phosphate from seafloor sediments under low-oxygen conditions can drive a positive feedback loop between increased productivity, oxygen depletion and marine P availability. This feedback loop helps to sustain low oxygen conditions in restricted basins such as the Baltic Sea and may have contributed to the development of large-scale oceanic anoxia and massive burial of organic matter in the Earth's past. Here, we first summarize the field evidence for enhanced regeneration of P relative to organic carbon (C) from modern and ancient sediments. We then briefly review the responsible mechanisms, including enhanced regeneration of P from organic matter under low oxygen [1], and limited retention of P in inorganic minerals. We also present the results of an experimental investigation into the bacterial controls on P regeneration. Finally, we discuss the role that enhanced regeneration of P from sediments can play at the regional and global scale. We show that enhanced regeneration of P can account for the underestimation of phosphate concentrations in existing nutrient budgets of the Baltic Sea. Using biogeochemical ocean modeling, we show that oxygen depletion in the global ocean is also highly sensitive to the rate of enhanced regeneration of P. These results underline the need for improved quantitative and mechanistic understanding of the P cycle to better understand past changes in ocean oxygenation, and to predict those which may occur in the future.

[1] Ingall, E. D. Bustin, R. M. & Van Cappellen, P. (1993) *Geochim. Cosmochim. Acta* **57**, 303–316, 1993.

Ripening processes during crystallization of natrojarosite

AMALIA JIMÉNEZ*, ANA HERNÁNDEZ, ÁNGELES FERNÁNDEZ-GONZÁLEZ AND MANUEL PRIETO

Facultad de Geología, C/ Jesús Arias de Velasco s/n, 33005, Oviedo, Spain. (*correspondence: amjimenez@uniovi.es)

The crystallization behavior of jarosite type compounds $MFe_3(SO_4)_2(OH)_6$ (M = Na^+, H_3O^+, K^+, Ag^+, NH_4^+) has received increasing attention due to the formation of these minerals in acid mine water drainage environments during the oxidation of sulphide minerals. The fact that jarosites were identified on Mars gives these minerals an additional interest as indicators of water-limited chemical weathering on that planet. Although different jarosite-type compounds have been synthetised by precipitation at temperatures close to 100°C [1], the genesis of these minerals in environmental conditions needs to be studied in depth. In this work, natrojarosite was synthesized by mixing 60 ml of $Fe_3(SO_4)_2$ (1N) and 40 ml of NaOH (1N) parent solution at 25 ± 0.1°C. Similar experiences were performed using 0.5N concentrations for both parent solutions (50:50 ratio). The experiments were carried out for specific reaction periods (1 day to 7 weeks) by keeping the solutions at constant agitation. The aging process of natrojarosite was followed by monitiring the precipitate crystallinity (X-ray diffraction), the aqueous solution composition (ICP-AES), and the pH.

Using 1N parent solutions, a low-crystallinity precipitate was obtained in the early stages of the experiments. However, as the reaction time passes by, the main XRD reflections (012, 021 and 113) of natrojarosite become more apparent and undergo a progressive decrease of widthness (FWHM) and an increase of intensity which indicate an increasing degree of crystallinity. In contrast, using 0.5N parent solutions the precipitate remained amorphous during the whole aging process. The pH values varied between 2.6 and 2.2, in all experiments. The aqueous solution exhibited a slight increase of both Fe and Na concentrations that is consistent with the development of the crystalline phase. Aqueous solution modellization (phreeqc code) evidenced higher saturation indices for hematite than for natrojarosite, which indicates that the formation of natrojarosite was governed by kinetic factors.

[1] J.E. Dutrizac & S Kaiman (1976) *Canadian Mineralogist* **14**, 151–158.

https://doi.org/10.1180/S0026461X00006502 Published online by Cambridge University Press

Comparison of different evaluation schemes and optimization of instrumental parameters for chlorine isotope analysis of organic compounds using GC-qMS

B. JIN, C. LASKOV, M. ROLLE AND S.B. HADERLEIN

Center for Applied Geosciences, University of Tübingen, Sigwartstrasse 10, D-72076 Tübingen, Germany (biao.jin@uni-tuebingen.de)

Compound specific chlorine isotope analysis is a valuable tool to detect and quantify biodegradation processes and abiotic transformation of chlorinated organic compounds in the subsurface. The new GC-qMS method avoids tedious off-line sample pretreatments and offers a quick and sensitive method for on-line determination of chlorine isotope ratios. In this study, the GC-qMS method for chlorine CSIA of chlorinated hydrocarbons was evaluated and validated. We compared the existing evaluation schemes to determine chlorine isotope ratios with newly proposed and/or modified ones. Besides, we tested the important instrumental settings such as split ratio, ionization energy and dwell times. Chlorinated ethenes were selected as model organic contaminants. Headspace sample of tetrachloroethene (PCE), trichloroethene (TCE) and cis-dichloroethene (cisDCE) at aqueous concentrations in the range of 20-500 μg/L were analyzed using GC-qMS. The results showed good precisions (relative standard deviation: 0.4‰ - 2.1‰, n=5). We also found that the precison of the GC-qMS method depends on the applied evaluation schemes, instrumental parameters and target compounds. A systematic test and evaluation of these important factors enabled us to optimize the GC-qMS technique to determine the chlorine isotope ratios of chlorinated organic contaminants.

In situ Pb and U isotope analysis of single ostracod shells from Nam Co, Tibet

K.P. JOCHUM[1]*, D. SCHOLZ[2,1], P. FRENZEL[3], G. GLEIXNER[4], F. GUENTHER[4], A. SCHWALB[5], B. STOLL[1], U. WEIS[1] AND M.O. ANDREAE[1]

[1]Max-Planck-Institut für Chemie, Postfach 3060, 55020 Mainz, Germany (*correspondence: k.jochum@mpic.de)
[2]Universität Mainz, 55128 Mainz (Germany)
[3]Universität Jena, Burgweg 11, 07749 Jena (Germany)
[4]MPI für Biogeochemie, 07701 Jena (Germany)
[5]Techn. Universität, 38106 Braunschweig (Germany)

We have developed a new LA-ICP-MS technique for combined *in situ* trace element, Pb and U isotope analysis of single ostracod shells. High spatial resolution is achieved by using spot sizes of 12 - 100 μm. We analyzed very small (ca. 0.5 mm) and thin (about 0.05 mm) shells from eight levels of a Holocene lake sediment core from Nam Co, Central Tibetan Plateau, deposited within the last 7700 a BP [1]. *In situ* measurements of ($^{234}U/^{238}U$), $^{208}Pb/^{206}Pb$ and $^{207}Pb/^{206}Pb$ yielded a precision (RSD) of about 2 % for U = 10 – 20 μg g^{-1} and 0.2 % for Pb = 10 – 40 μg g^{-1}.

Our results show identical ratios for ostracods from the same core depth indicating that they reflect the composition of the lake water. ($^{234}U/^{238}U$) and $^{208}Pb/^{206}Pb$ show significant variability with age: Ostracods from the upper core section show uniform isotope ratios (1.42 ± 0.01 and 2.134 ± 0.003, respectively). The older samples show lower and more variable isotope ratios. These findings are in agreement with investigations of the sediments [1] and suggest that the isotope ratios of the ostracod shells reflect past climate variability: reduced precipitation and runoff, low lake level and maximum salinity since ca. 800 a BP, more humid conditions and a positive precipitation/evaporation balance between 5400 and 7200 a BP [1]. The lowest ratios (($^{234}U/^{238}U$) = 1.13, $^{208}Pb/^{206}Pb$ = 2.112) are observed in a 6000 a old ostracod shell, where a high intensity of monsoonal precipitation, associated with elevated lake levels in Tibet, is recorded [1].

[1] Mügler *et al*. (2010) *J. Paleolimnol*. **43**, 625–648.

https://doi.org/10.1180/S0026461X00006502 Published online by Cambridge University Press

On the duration and rates of fluid release from a dehydrating slab

T. JOHN[1], Y. PODLADCHIKOV[2], N. GUSSONE[1], G. BEBOUT[3], R. HALAMA[4], T. MAGNA[1] AND R. KLEMD[5]

[1]Institut für Mineralogie, Universität Münster, Germany (timm.john@uni-muenster.de)
[2]Institut de Géophysique, University of Lausanne, Switzerland
[3]Lehigh University, Bethlehem, PA 18015, USA
[4]Institut für Geowissenschaften und SFB 574, Universität Kiel, Germany
[5]GeoZentrum Nordbayern, Universität Erlangen-Nürnberg, Germany

At subduction zones, seawater-altered oceanic lithosphere recycles back into the mantle, heats up during descent and releases fluids by devolatilization of hydrous minerals. Large-scale fluid flow resulting from this dehydration is implicit in recent models for the formation of arc magmas and appears to be linked to intraslab seismicity and non-volcanic tremors. However, the mechanisms as well as spatial and temporal scales of this fluid flow are only poorly known.

Exposures of veins (mineralized fractures) in oceanic lithosphere, metamorphosed at high pressures in subduction zones, provide direct evidence for fluid mobility within subducting slabs. We quantify the duration of dehydration-related fluid flow through subducting oceanic plates by investigating a high-pressure vein and its reaction selvage. Using a novel approach employing an array of radiogenic (Sr) and stable (Li, Ca) isotope data combiend with Li-diffusion and reaction kinetic modelling, we demonstrate that large amounts of fluid can be transported along major conduits over km distances in a pulse-like manner through slabs over surprisingly short time periods of ~170 to as little as ~6 years.

This indicates that even though the overall slab dehydration is a continuous process, dehydrating slabs release their fluid by short-lived, channelized fluid-flow events, involving aseismic mobile hydraulic fractures that rapidly traverse the subducting slabs. Furthermore, the time for mineral reactions to reestablish thermodynamic equilibrium in rocks along the flow pathways is estimated to be at least three times shorter than that of the overall fluid-rock interaction. This indicates that local thermodynamic equilibrium is indeed a valid assumption for understanding fluid-mediated processes at high fluid-rock ratios and sluggish reaction kinetics are negligible.

Sedimentary basin acid sulfate weathering: Its recognition and palaeo-environmental implications in the Eucla Basin, South Australia

ASHLYN JOHNSON[1]*, S.M. HILL[1], D. CHITTLEBOROUGH[2] AND D. MITCHELL[3]

[1]Deep Exploration Technologies Cooperative Research Centre. School of Earth and Environmental Sciences. University of Adelaide. SA 5005 (*correspondence: ashlyn.johnson@adelaide.edu.au)
[2]School of Earth and Environmental Sciences. University of Adelaide. SA 5005
[3]Iluka Resources Limited, 11 Dequetteville Tce, Kent Town, Adelaide, SA 5067

'Acid Sulfate weathering' broadly describes soil and regolith materials that typically had an abundance of iron sulfides that have oxidised to sulphates. This redox process as well as other processes such as ferrolysis and microbiological functions are important producers of protons and therefore acidity within the regolith. Although previous studies have tended to focus on the soil management and sediment diagenesis and weathering geochemical implications, this study considers the significance of these processes from a sedimentary basin geochemical perspective. As such, further insights into basin-hinterland palaeo-environments and controls and the stratigraphic implications for the resulting regolith materials are gained. The study basin is the Eucla Basin, which is one of the world's largest on-shore Cainozoic basins, extending across Australia's central southern continental margin.

One of the major controls on palaeo- and contemporary acid-sulphate weathering within the Eucla Basin is the setting of regional groundwater systems within the Eocene marginal marine sediments in the basin. In geochemically reduced settings, typically below the watertable, the sediments contain an abundance of pyrite, whereas where these sediments have been oxidised, typically above the watertable, the pyrite has been oxidised and sulphates (which are now widely expressed as alunite found under many playa lake beds) and iron oxides (especially hematite but also goethite) are prevalent. These processes also have a profound influence on the mobility and reorganisation of Al and Si, largely derived from clay minerals such as smectite and kaolinite. This has resulted in the formation of authigenic clays (e.g. halloysite) and phreatic silicification (ie. groundwater silcretes) hosting abundant termite bioturbation preserved in the basin's geological record. Palaeo-watertables that may be linked to eustatic, climatic and tectonic variations are now being interpreted across large parts of this basin.

https://doi.org/10.1180/S0026461X00006502 Published online by Cambridge University Press

Redox transformations of iron in extremely low pH environments: Environmental and industrial implications

D. BARRIE JOHNSON[1]*, SABRINA HEDRICH[2] AND TADAYOSHI KANAO[3]

[1]Bangor University, Bangor, LL572UW, UK (*correspondence: d.b.johnson@bangor.ac.uk)
[2]2Bangor University, Bangor, LL572UW, UK (s.hedrich@bangor.ac.uk)
[3]Okayama University, Okayama, 700-8530, Japan (tkanao@cc.okayama-u.ac.jp)

Iron is a particularly important microbial resource in extremely acidic (pH <3) environments, where it serves not only as a micronutrient, but also as a major electron donor and/or acceptor. This is due primarily to the much greater stability of ferrous iron (even in oxygen-saturated liquors) and solubility of ferric iron in extremely acidic compared to neutral pH waters. Many different species of acidophilic prokaryotes are known to either catalyze the dissimilatory oxidation of ferrous iron or the dissimilatory reduction of ferric iron, while some can do both, depending on the prevailing environmental conditions.

Measurements of specific rates of iron oxidation by acidophilic bacteria have revealed significant differences between species. In general, specialized chemolithotrophs, such as *Leptospirillum* spp., exhibit significantly faster rates than more generalist mixotrophic and heterotrophic species, such as *Sulfobacillus* spp. and *Ferrimicrobium acidiphilum*. Measurement of specific rates of dissimilatory reduction of soluble ferric iron by *Acidiphilium cryptum* str. SJH have shown that these are often much greater than values recorded for neutrophiles. Rates of reductive dissolution of ferric minerals by acidophilic bacteria appear to depend on the relative acid-solubilities of the former. Acidophilic iron-reducing bacteria appear to use the often small amounts of ferric iron in solution, thereby causing the equilibrium between mineral-phase and solution-phase iron to move in the direction of the latter. Reductive dissolution (and concommitant release of associated metals and metalloids) of a wide range of ferric iron minerals, including jarosites, schwertmannite and goethite, has been demonstrated *in vitro*.

Recent developments that harness redox transformations of iron for industrial applications include remedation of mine waters using the recently characterised species *Ferrovum myxofaciens*, and the extraction of nickel from oxidized ores by causing the reductive dissolution of goethite. The latter represents a major development in 'biomining'.

Oxygen isotope exchange between H_2O and super critical CO_2: Lab experiments and field evidence

G. JOHNSON, B. MAYER*, M. NIGHTINGALE AND M. SHEVALIER

Applied Geochemistry Group, Department of Geoscience, University of Calgary, 2500 University Drive N.W., Calgary, Alberta, Canada T2N 1N4 (*correspondence: bmayer@ucalgary.ca)

Traditionally, the application of stable isotopes in Carbon Capture and Storage (CCS) projects has focused on $\delta^{13}C$ values of CO_2 to trace the migration of injected CO_2 in the subsurface. More recently the use of $\delta^{18}O$ values of both CO_2 and reservoir fluids has been proposed as a method for quantifying *in situ* CO_2 reservoir saturations due to oxygen isotope exchange between CO_2 and H_2O and subsequent changes in $\delta^{18}O_{H2O}$ values in the presence of high concentrations of CO_2. To verify that oxygen isotope exchange between CO_2 and H_2O reaches equilibrium within days, and that $\delta^{18}O_{H2O}$ values indeed change predictably due to the presence of CO_2, a laboratory study was conducted to measure the isotope composition of H_2O, CO_2, and dissolved inorganic carbon (DIC) at representative reservoir conditions (50°C and 19 MPa) and varying CO_2 pressures. Results obtained showed that $\delta^{18}O$ values of CO_2 were on average 36.4 ± 2.2 ‰ (1σ, n = 15) higher than those of water at all pressures up to and including reservoir pressure (19 MPa), in excellent agreement with the theoretically predicted isotope enrichment factor of 35.5 ‰ for the experimental temperature of 50°C. Since the fraction of oxygen sourced from CO_2 is related to the total volumetric saturations of CO_2 and water as a fraction of the total volume of the system, we conclude that changes in $\delta^{18}O$ values of reservoir fluids can be used to calculate reservoir saturations of CO_2 in CCS settings given that the $\delta^{18}O$ values of CO_2 and water are sufficiently distinct. This was confirmed by field data obtained from eight observation wells at the Pembina Cardium CO_2 Monitoring Pilot in Alberta (Canada). Arrival of injected CO_2 caused changes in the $\delta^{18}O$ values of reservoir fluids of up to 4 ‰, as well as increasing DIC, Ca and Fe concentrations in the reservoir fluids.

https://doi.org/10.1180/S0026461X00006502 Published online by Cambridge University Press

Updated dust-iron dissolution mechanism: Effects of organic acids, photolysis, and dust mineralogy

M.S. JOHNSON AND N. MESKHIDZE

Deptartment of Marine, Earth, and Atmsospheric Sciences, North Carolina State University, Raleigh, North Carolina, USA (msjohns2@ncsu.edu, nmeskhisze@ncsu.edu)

Aeolian dust deposition to remote oceanic regions is a major atmospheric supply pathway of essential nutrients (e.g. iron (Fe) and phosoporus (P)) which have a controlling effect on marine primary productivity. The soluble/bioavailable fractions of Fe and P in mineral dust are minor at the source regions and increase during the transport. Nutrient mobilization from mineral dust is a complex process; in the atmosphere it is thought to be controlled by dust mineralogy, atmospheric chemical composition, and meteorological variables. Therefore, quantitative predictions for the formation of these important nutrients should be included in global-scale coupled biogeochemical cycle models for improved prediction of future climate.

Here, the global 3-D chemistry transport model GEOS-Chem with a state-of-the-art Fe- and P-dissolution scheme is used to generate comprehensive global datasets for nutrient concentrations and deposition (Fig. 1). The model improvements include source-specific dust-mineralogy, organic ligand-promoted Fe dissolution, the photolytic redox cycling of Fe (II)/Fe (III), and acid-based P dissolution. Preliminary results indicate that Fe bound in clay minerals and the presence of oxalate significantly increases soluble Fe production in mineral dust. Photolysis can further increase the amount of soluble Fe by converting Fe (III)-species into the more bioavaliable ferrous Fe (Fe (II)) form. Model predicted diurnal variations in Fe (II)/Fe (III) are consistent with available data.

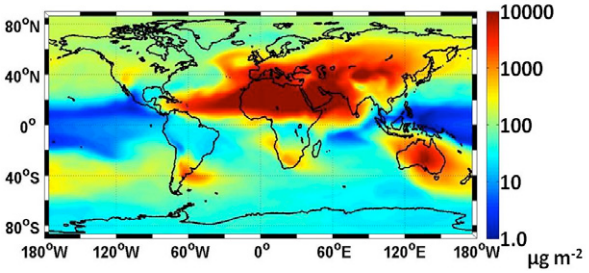

Figure 1: Model-predicted total column burden of soluble Fe (μg m^{-2}) between June-August 2009.

Adsorption of organic ligands on silicate mineral surfaces in the presence of CO_2 and water: Insight into olivine dissolution rates

NATALIE C. JOHNSON[1]*, BURT THOMAS[2], KATHERINE MAHER[3], DENNIS K. BIRD[3], ROBERT ROSENBAUER[2] AND GORDON E. BROWN, JR.[1,3,4]

[1]Department of Chemical Engineering, 381 North-South Mall, Stauffer III, Stanford University, Stanford CA 94305-2115, USA

[2]United States Geological Survey, 345 Middlefield Rd, Menlo Park CA 94025, USA

[3]Department of Geological and Environmental Sciences, 450 Serra Mall, Braun Hall Building 320, Stanford University, Stanford CA 94305-2115, USA

[4]Stanford Synchrotron Radiation Laboratory, 2575 Sand Hill Rd, Menlo Park CA 94025, USA

(*correspondence: nataliej@stanford.edu)

The dissolution of magnesium silicates releases magnesium cations (Mg^{2+}) into solution, which in the presence of dissolved carbon dioxide (CO_2) can, under certain conditions, precipitate as magnesium carbonates. This process results in the mineralization of CO_2, a safe, long-term storage strategy to control rising CO_2 concentrations in the atmosphere. However, the kinetics for these processes are slow and the mechanisms are not fully understood. Previous work by this group and others has found the dissolution rates of silicates to be enhanced by the presence of organic acids in some cases, but reduced in other cases. This study seeks to understand the factors that determine whether an organic compound acts as an activator or an inhibitor. Organic ligands may adsorb to silicate surfaces as outer-sphere complexes, likely passivating active sites and reducing dissolution rates, or as inner-sphere complexes, drawing electron density away from the mineral surface, weakening near-surface bonds, and increasing dissolution rates. The nature of the adsorbed complexes depends on mineral surface charge and ligand charge, both of which are controlled by pH. X-ray photoelectron spectroscopy has been used to examine the organic carbon adsorbed on olivine and quartz surfaces after reaction with organic acids, water, and CO_2. Initial results show additional carbon on the surfaces exposed to the organic-containing aqueous phase but none on surfaces exposed only to the supercritical CO_2-H_2O phase. Mineral surfaces exposed to both the CO_2 and H_2O phases also showed increased superficial carbon.

https://doi.org/10.1180/S0026461X00006502 Published online by Cambridge University Press

Calibrating S isotope fractionation in sulfate reducing bacteria

DAVID T. JOHNSTON[1]*, ALEXANDER S. BRADLEY[2]*, RENATA CUMMINS[1], WILLIAM D. LEAVITT[1] AND PETER R. GIRGUIS[2]

[1]Department of Earth and Planetary Sciences, Harvard University, Cambridge MA 02138 USA (*correspondence: johnston@eps.harvard.edu)
[2]Department of Organismic and Evolutionary Biology, Harvard University, Cambridge MA 02138 USA (bradley@fas.harvard.edu)

The sulfur isotopic composition of sedimentary sulfate and sulfide minerals throughout Earth history is a reflection of the activity of dissimilatory sulfate-reducing bacteria (SRB). The magnitude of the fractionation between sulfur compounds is intrepreted as a biochemical consequence of changing environmental conditions. However, quantitatively understanding the isotopic variability within the geological record requires calibrating the physiological controls on dissimilatory sulfate reduction (e.g. sulfate concentrations, relevant electron donor, etc.). We have interrogated these controls with three complementary approaches.

First, through the incorporation of recent biochemical and crystal structure data, we have rexamined the reaction network involved in dissimilatory sulfate reduction. Our revised network adequately describes previous observations, and is experimentally testable.

Second, we measured the production of intermediates in pure cultures of *D. desulfuricans* grown on sulfate/sulfite and lactate/formate. In these experiments we observe the systematic production and consumption of sulfite and thiosulfate. We have tracked the isotopic consequences of each experiment, including the measurement of the site-specific isotopic composition of thiosulfate. These data reinforce our model predictions and provide valuable constraints on the fractionations associated with thiosulfate production and consumption.

Third, we performed community scale experiments in quasi-chemostat microbial reactors to better quantify changes in fractionation in response to sulfate concentrations. Whereas the pure culture work investigates the internal cycling, the reactor work assesses the first-order controls on sulfate uptake.

Through this broad combination of experimental and conceptual approaches, we provide unprecidented insight in the operation of the sulfate reduction pathway: information that can be used to better calibrate and inform our interpretation of sulfur isotopes in the sedimentary record.

Constraining magma-carbonate interaction at Vesuvius, Italy: Insights from stable isotopes and experimental petrology

E.M. JOLIS[1], V.R. TROLL[1,2], C. HARRIS[3], C. FREDA[2], G. ORSI[2], C. SIEBE[4], L.S. BLYTHE[1], F.M. DEEGAN[1], V. MISITI[2] AND L. CIVETTA[5]

[1]Dept. Earth Sci., CEMPEG, Uppsala University, Sweden (ester.jolis@geo.uu.se)
[2]Istituto Nazionale di Geofisica e Vulcanologia, Italy
[3]Dept. of Geol. Sci., University of Cape Town, South Africa
[4] Instituto de Geofisica, UNAM, Mexico.
[5]Dip. Sci. Fis., Università 'Federico II', Napoli, Italy

At Vesuvius volcano, Italy, abundant high temperature calc-silicate (skarn) xenoliths have been found in many eruptive deposits and, provide evidence for intense interaction between magma and carbonate crust. In order to understand magma-carbonate interaction and to quantify carbonate assimilation processes, we present a combined stable isotope study of natural samples and piston cylinder de-carbonation experiments.

The sample study shows that $\delta^{18}O$ and $\delta^{13}C$ isotope values of igneous-, skarn- and carbonate rocks indicate that significant crustal contamination of Vesuvius magmas has taken place. Calc-silicate xenoliths define variable degrees of decarbonation and interaction processes between magma and crust, producing progressively more lava-like values [1].

In the experiments, we simulated the processes of carbonate assimilation under magmatic pressure and temperature conditions (0.5GPa and 1200°C) with Vesuvius magma composition and local crust as starting material. We have constructed a high-resolution time-sequence of magma-carbonate interaction in our experimental products with short but increasing dwell run-times (t_d), of 0, 60, 90 and 300 sec [2]. We observe a progressive carbonation of the host melt, and rapid liberation of large quantities of CO_2 coming from the breakdown of the enclosed carbonate. Variable degrees of carbonate assimilation and chemical mixing between carbonate and silicate melts are observed, with diffusion processes playing an important role at melt interfaces.

The combination of petrological evidences and experimental products allows insights into the processes and time-scales of magma-crust interaction and reinforces the hypotheses that carbonate assimilation is an ongoing and significant magmatic process at Mt. Vesuvius.

[1] Turi *et al*. (1976) *Contrib. Minerol. Petrol*. **55**, 1–31.
[2] Deegan *et al*. (2010) *J. Petrol* **5**, 1027–1051.

https://doi.org/10.1180/S0026461X00006502 Published online by Cambridge University Press

Irregular retreat of tropical glaciers during the Holocene

V. JOMELLI[1]*, M. KHODRI[2], V. FAVIER[3], D. BRUNSTEIN[4], M.P. LEDRU[5], P. WAGNON[6], PH. BLARD[7], JE. SICART[8], R. BRAUCHER[9], D. GRANCHER[10], D. BOURLES[11], P. BRACONNOT[1,2] AND M. VUILLE[13]

[1]LGP CNRS (jomelli@cnrs-bellevue.fr)
[2]Locean IRD (mkhodri@gmail.com)
[3]OSUG-UJ-LGGE (vifavier@gmail.com)
[4]LGP CNRS (brunstein@cnrs-bellevue.fr)
[5]ISEM IRD (ledru@ird.fr)
[6]LTHE-LGGE, IRD (wagnon@lgge.obs.ujf-grenoble.fr)
[7]CRPG CNRS (blard@crpg.cnrs-nancy.fr)
[8]LTHE IRD (sicart@ird.fr)
[9]CEREGE CNRS (braucher@cerege.fr)
[10]LGP CNRS, Meudon grancher@cnrs-bellevue.fr)
[11]CEREGE CNRS-Université (bourles@cerege.fr)
[12]IPSL/LSCE CEA (pascale.braconnot@lsce.ipsl.fr)
[13] Dept. of Atmos (mathias@atmos.albany.edu)

Causes and timing of tropical glacier fluctuations during the Holocene are poorly understood. We present a chronology for the past 11, 000 years of the Bolivian Telata glacier. We show that Telata glacier retreated irregularly. A rapid and strong melting from the maximum extent, at 10.8 ka ± 0.9, to 8.5 ka ± 0.4 ^{10}Be years was followed by a slower retreat until the Little Ice Age (LIA) while a dramatic acceleration occurred over the 20th century. A glacier-climate model and additional climate constraints indicate that annual temperatures for this region were -3.3±0.8 °C cooler at 11 ka BP and were -2.1±0.8 °C below the present value until the end of the LIA. We suggest that low-frequency warming of the eastern tropical Pacific and increased atmospheric temperature in response to enhanced austral summer insolation were the main drivers for the long-term Holocene retreat of the glacier. Future temperature projections estimate a 4°-5°C warming in the tropical Andes by 2100, a warming close to our estimate for the whole Holocene.

Mineral composition of the metallurgical slag after steel production

I. JONCZY

Silesian University of Technology, Faculty of Mining and Geology, Institute of Applied Geology, 44-100, Gliwice, Poland (iwona.jonczy@polsl.pl)

Introduction

Metallurgical slags are increasingly often used as material in production of aggregates, but there are also attempts made to recover metals from them. That is why it is important to carry out research on their mineral and chemical composition, which may deliver much valuable information during an economic exploitation of slags, e.g. connected with new phases forming in a metallurgical furnace, forms of metal occurrence in slag components and possibilities of their release from slag components and migration to the environment [1, 2].

Research results

The conducted mineralogical research of slags after steel production proves that among their phase components, apart from metal concentrations (including up to 98% Fe) and glaze, oxide and silicate phases are especially interesting because of their heterogeneous chemical composition.

Oxide phases are represented by iron oxides (magnetite, hematite, wustite), chromite, ilmenite and phases with compound chemical composition. We can recognize among them oxides Ca-Mg or Ca-Ti with elements of: Cr, Mn, Fe, Zn. A common component is also a solid solution od compounds: FeO, MgO, MnO occuring in variable quantity relations, with admixtures: V, Zn, Cr, Ti and Ca.

Among silicate phases there are distinguished, among others, pyroxenes from a series of augite, monticellites, wollastonite, dicalcium silicates (larnite). Their chemical composition is considerably diversified, and often differs from the chemical composition of the same phases forming in natural conditions. Silicate phases are also carriers of heavy metals, which may be included in their internal structures or form micro-inclusions. For instance, a considerable group consists of calcium silicates with admixtures of Ti, Cr, Mn, V, Mg and P, as well as calcium silicates and aluminosilicates Ca-Fe.

The scientific work is financed as a research project from the means allocated for science in the years 2010-2011.

[1] Kucha *et al*. (1995) *Minerlogia Polonica* **26**, 75–99.
[2] Jonczy (2009) *Mineral Resources Management* **25**, 19–34.

https://doi.org/10.1180/S0026461X00006502 Published online by Cambridge University Press

A Precambrian manganous sea?

C. JONES*, S.A. CROWE AND D.E. CANFIELD

NordCEE, Institute of Biology, Syddansk Universitet (*correspondence: carriayne@biology.sdu.dk)

Differences in the biogeochemical behavior of Fe and Mn can lead to their physical separation and a variation in the Fe:Mn ratio in sedimentary rocks. The mechanisms controlling the Fe:Mn ratios of Precambrian sedimentary rocks remain understudied. Using previously published data from the Mt. McRae shale deposit [1, 2] and the biogeochemical characteristics of Fe and Mn, we evaluate the potential controls on Fe and Mn co-deposition in this succession. We suggest that before the 'whiff' of oxygen, as recorded in the Mt. McRae shale, Fe and Mn were deposited together as carbonate minerals at a ratio reflecting their supply from hydrothermal fluids. During the 'whiff', iron likely precipitated and was sequestered in the sediments as sulfide minerals. This sulfide resulted from a global increase in the flux of sulfate to the oceans due to increased oxidative weathering on the continents [2]. We propose that this led to a global enhancement of Fe removal as Fe sulfides, preferentially enriching seawater in dissolved manganese relative to iron. In the Mt. McRae shale, we find evidence for this in the sediments deposited after the 'whiff', which exhibit a Mn enrichment relative to Fe with respect to both a hydrothermal source and continental weathering. These observations support the hypothesis of a transitional manganous ocean that punctuates intervals of ferruginous and euxinic ocean redox states [3]. We propose that enrichments of Mn relative to Fe in marine sediments deposited under anoxic conditions are a sensitive proxy for increased oxidative weathering.

[1] Anbar *et al*. (2007) *Science* **317**, 1903–1906. [2] Reinhard *et al*. (2009) *Science* **326**, 713–716. [3] Jones *et al*. (2011) *Biogeosci. Disc*. In press.

Ecological niches of Fe-oxidizing acidophiles in a coal mine discharge

D. JONES[1]*, J. BROWN[2], L. LARSON[2], D. MILLS[1], W. BURGOS[2] AND J. MACALADY[1]

[1]Dept. of Geosciences, Penn State Univ., University Park, PA 16802, USA (*correspondence: djones@psu.edu, dbm5029@psu.edu, jlm80@psu.edu)

[2]Dept. Civil Environ. Eng., Penn State Univ., University Park, PA 16802, USA (jfb213@psu.edu, lnl5053@psu.edu, wdb3@psu.edu)

Low pH iron oxidation is a promising strategy for cost effective bioremediation of acidic mine drainage (AMD). To effectively utilize the iron-oxidizing potential of naturally-occurring microbiota in AMD discharges, knowledge of the diversity, iron-oxidizing efficiency, and natural distribution of acidophilic communities is required. Here we used full-cycle rRNA analyses to describe the composition of sediment communities at Red Eyes, an AMD site in Somerset County, PA, USA. Near anoxic emergences, the dominant microbial communities are green benthic *Euglena* biofilms and associated populations of *Gamma-* and *Betaproteobacteria*. As pH and Fe^{2+} concentrations decrease downstream, the dominant iron oxidizers shift first to (i) a close relative of *Gallionella spp*., followed by (ii) *Ferrovum spp*., and finally to (iii) *Acidithiobacillus ferrooxidans*. Archaea and *Leptospirillum spp*. are less than 2% of cells.

In previous research using laboratory reactors [1], we found that normalized iron-oxidation rates were 1.5-2x faster for the *Ferrovum*-dominated communities compared to the *Acidithiobacillus*-dominated communities. We have since extended our sampling and analyses to identify environmental variables that control the distribution of these and other iron-oxidizers at Red Eyes. Overall, turnover among communities is related to changes in pH and Eh. Results so far suggest that the transition between *Ferrovum-* and *Acidithiobacillus-*dominated communities depends on iron concentration rather than pH. Ongoing analyses will further define the ecological niches of these and other important AMD populations.

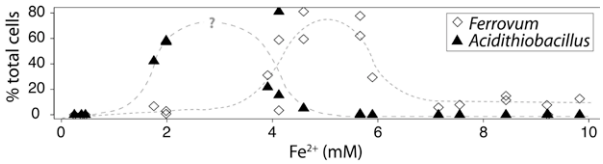

Figure 1. Fluorescence *in situ* hybridization cell counts of *Ferrovum* and *Acidithiobacillus* versus Fe^{2+} concentration.

[1] Brown *et al*. (2010) *Appl Environ Microbiol* **77**, 545–554.

https://doi.org/10.1180/S0026461X00006502 Published online by Cambridge University Press

Differential changes in Ni^{2+}, Co^{2+} and Fe^{2+} coordination in silicate melt with pressure

J. JONES[1]*, H. STC. O'NEILL[1] AND A. BERRY[2]

[1]Research School of Earth Sciences, Australian National University, Canberra, ACT 0200, Australia (*correspondence: jesse.jones@anu.edu.au)

[2]Department of Earth Science and Engineering, Imperial College London, South Kensington, UK

It is currently debated whether siderophile element abundances in the Earth's mantle reflect single-stage metal-silicate equilibration at high pressure at the base of an extensive magma ocean (homogeneous accretion), or the mixing of differentiated protoplanets each with a core formed at low pressures (heterogeneous accretion). This question has been addressed by parameterizing metal/silicate partition coefficients of siderophiles such as Ni, Co and Fe as a function of pressure, temperature and other variables, and extrapolating these parameterizations to determine P-T conditions that reconcile observed mantle abundances. Implicit in these parameterizations is that the partial molar volumes vary monotonically with pressure. XANES spectroscopy shows that the average coordination of Ni^{2+} in silicate glasses recovered from melts quenched at pressure, changes from tetrahedral to octahedral between 1 and 4 GPa, while that of Co^{2+} and Fe^{2+} remain unchanged. The effects of this transition are clearly mirrored in the distribution coefficients between iridium metal and silicate melt measured over the same range, showing that the quenched glasses reflect the liquid state at P and T. The partitioning can be modelled using different values of the partial molar volume of tetrahedral and octahedral NiO in the silicate melts. Changes in coordination environment of each siderophile in silicate melts will generally occur over different pressure intervals, preventing simple extrapolation of metal/silicate partitioning. The results enable an improved parameterization of the pressure dependence of Fe-Ni-Co partitioning, which excludes the simple single-stage magma-ocean hypothesis.

Martian magmatic volatiles recorded in olivine-bearing melt inclusions and matrix of shergottite Y-980459

J.H. JONES[1], T. USUI[1], C.M. O'D. ALEXANDER[2], J. WANG[2] AND J.I. SIMON[1]

[1]KR, NASA/JSC, Houston, TX 77058 (john.h.jones@nasa.gov)

[2]Department of Terrestrial Magnetism, Carnegie Institution of Washington, Washington DC, 20015

Martian basaltic meteorites [shergottites] contain a wealth of information about Mars. Of particular interest is the geochemical record contained in melt inclusions from the most primitive shergottite, Yamato 980459 (Y98). Using polished sections of Y98 mounted in indium to avoid volatile contamination from epoxy, our ion- and electron-microprobe study aims to constrain the volatile contents of primary Martian magmas generated by mantle melting. This record is also used to track the subsequent melt evolution of shergottite magmas. We report preliminary results for volatile abundances (H_2O, CO_2, S, Cl, F) in olivine-hosted melt inclusions (MI) and groundmass glasses (GG).

Unlike other shergottites, MIs in Y98 have remained glassy because of rapid cooling following eruption. Volatile concentrations of MI and GG in Y98 were analyzed by a Cameca ims-6f at DTM following the techniques of [1]. MIs contain distinctly higher contents of H_2O (~200 ppm) and CO_2 (600-1600 ppm) than GGs (<100 ppm H_2O and <20 ppm CO_2). In contrast, the MIs contain lower amounts of F (~15 ppm) and S (~900 ppm) than those in the GGs (~25 ppm F and 2200-3000 ppm S). Cl contents are almost constant among the MIs and GGs (~50 ppm). The CO_2 solubility in basaltic magmas suggests that the MIs were trapped at a depth of ~3 kbar. The pre-erupted magmatic water contents recorded in the Y98 MIs are ~2 orders of magnitudes lower than those proposed by the wet shergottite magma hypothesis (e.g. 1.8 % [2]), although the absolute water abundances in the MIs may have been changed by post-entrapment modifications. By using Na as an indicator of the degree of crystal fractionation (mainly olivine + pyroxene), the degree of degassing between pre-erupted (MI) and erupted (GG) Y98 melts are estimated as follows: CO_2 (~100 %) > H_2O (>80%) > Cl (50-70 %) > F (~0 %) ≈ S (~0 %, probably saturated with sulfide). Likewise, we estimate that the bulk Y98 liquid contained <30 ppm H_2O, 200-500 ppm CO_2, ~20 ppm Cl, ~5 ppm F, and ~300 ppm S.

[1] Hauri *et al*. (2002) *Chem. Geol*. **183**, 99-114. [2] McSween *et al*. (2001) *Nature* **409**, 487-490.

https://doi.org/10.1180/S0026461X00006502 Published online by Cambridge University Press

Incongruent dissolution of volcanic riverine particulate material in seawater: Consequences for global element cycling

M.T. JONES[1]*, C.R. PEARCE[2], C. JEANDEL[3] AND E.H. OELKERS[4]

[1]Institute of Earth Sciences, University of Iceland, Sturlugata 7, Reykjavik, Iceland (*correspondence: morgan@hi.is)
[2]Department of Earth and Environmental Sciences, The Open University, Walton Hall, Milton Keynes, UK
[3]LEGOS-Université de Toulouse-CNRS-IRD-OMP, 14 Avenue Edouard Belin, 31400 Toulouse, France
[4]GET-Université de Toulouse-CNRS-IRD-OMP, 14 Avenue Edouard Belin, 31400 Toulouse, France

The world's rivers transport material from the land to the oceans in dissolved form and as particulate matter. Although particulate fluxes dominate over dissolved fluxes for the majority of elements relatively little attention has been paid to the role of riverine particulate material, both in the fluxes of elements to the oceans and moderating global climate [1]. The degree to which riverine particulate matter plays a role in the compositional evolution of seawater depends on its dissolution rate after arrival in the ocean. Volcanic islands supply the most easily weathered material to the oceans and are an important component of the global suspended flux. However, the apparent dearth of original volcanic minerals in oceanic drill cores suggests that the dissolution of riverine particulate material in seawater may be an important component of land-to-ocean element fluxes.

This study measured directly the initial element release rates of riverine particulate material in seawater through a series of closed-system batch reactor experiments. Large changes to the concentrations and isotopic ratios of elements are observed in seawater when mixed with riverine particulates. Elements such as Si, Ca, Mn and Ba show marked increases in seawater concentrations, indicative of particulate dissolution. Other elements such as Li become rapidly depleted in seawater, suggesting element exchange reactions or the formation of secondary phases. Sr and Nd display comparatively little change in seawater concentrations, but have large changes in isotopic ratios. Taken together, these results demonstrate a significant role of seawater weathering of riverine particulate material to the fluxes of elements to the oceans and have important consequences for the use of isotopes as tracers of global processes.

[1] Gislason *et al*. (2006) *Geology* **34**, 49–52.

Fluid and temperature conditions in an oceanic detachment fault footwall: Insights from late-stage mineral veins (ODP Leg 304/305)

N. JÖNS[1]*, W. BACH[1], M. ROSNER[1,2,3] AND B. PLESSEN[2]

[1]Dept. of Geosciences, University of Bremen, Germany (*correspondence: njoens@uni-bremen.de)
[2]Helmholtz-Zentrum Potsdam/ GFZ, Potsdam Germany
[3]FB Geowissenschaften, Freie Universität Berlin, Germany

The Atlantis Massif is an oceanic core complex located at the Mid-Atlantic Ridge at ca. 30°N. During IODP Leg 304/305 Hole U1309D the footwall of the detachment fault, which is related to exhumation of the Massif, was drilled. It consists mainly of gabbros and troctolites, with minor amounts of basaltic and ultramafic rocks. The 1416 m long drilled section is fractured and shows a retrograde overprint recorded by granulite- to zeolite-facies mineral assemblages. Late-stage mineral veins (consisting of anhydrite, calcite, prehnite or zeolite) formed from sub-seafloor fluid-rock interactions. These veins were examined to further our understanding of the fluid regime and temperature conditions in detachment fault systems.

Abundant syn- to postkinematic calcite has low concentrations of incompatible elements (e.g. U, Sr, Li) as well as flat chondrite-normalized REE+Y pattern with a positive Eu anomaly. This indicates that the calcite precipitating fluids are similar to basalt-hosted hight-T vents and indicate no affinity to the nearby serpentinization-derived Lost City vent field. The deep origin of the fluids is highlighted by low $^{87}Sr/^{86}Sr$ (0.704 to 0.708), mantle-like $\delta^{7}Li_{LSVEC}$ (+0.8 to +9.4‰) and $\delta^{13}C_{PDB}$ (-6 to -2‰). From $\delta^{18}O$ values, minimum calcite precipitation temperatures of 150-220°C are derived.

Anhydrite and anhydrite + zeolite veins have $^{87}Sr/^{86}Sr$ values consistent with anhydrite formation from down-flowing seawater which had leached only minor amounts of Sr from the basement. The REE pattern of anhydrite veins indicate that admixed hydrothermal fluids at depth played a minor role.

Silicate minerals (prehnite, quartz, plagioclase) predominate veins in the deepest section of Hole 1309D and indicate precipitation temperatures ranging from 270 to 145°C (estimated from $\delta^{18}O$ values). They are comparatively unradiogenic in $^{87}Sr/^{86}Sr$ (0.7033-0.7046) and demonstrate (in contrast to anhydrite) enhanced intensity of reactions between infiltration seawater and basement with increasing depth.

https://doi.org/10.1180/S0026461X00006502 Published online by Cambridge University Press

Surface properties and complexation on titanium dioxide nanoparticles

C.M. JONSSON*, J. PEREZ HOLMBERG, J. GALLEGO-URREA, Z. ABBAS, E. AHLBERG, J. BERGENHOLTZ AND M. HASSELLÖV

Department of Chemistry, University of Gothenburg, SE-41296 Gothenburg, Sweden (*correspondence: caroline.jonsson@chem.gu.se)

There is an increasing amount of synthetic nanoparticles in the environment. Due to their small size, they have properties that result in higher reactivity compared with larger particles and bulk materials. Interactions that occur at the surface of nanoparticles are important for understanding and predicting nanoparticle fate and behavior, as well as characterizing the potential risks for the environment and human health.

Surfactant-free TiO_2 nanoparticles were synthesized and characterized according to [1]. Temperature during synthesis reaction, dialysis and storage was found to strongly influence the particle size and crystal structure. Potentiometric titrations were used to determine the surface charge of the particles at varying pH and ionic strength.

In order to mimic the interactions of nanoparticles with natural organic matter (NOM), surface complexation on TiO_2 was studied using model organic substances possessing carboxyl and hydroxyl groups. Results show that the adsorption of 2, 3-dihydroxybenzoic acid (2, 3-DHBA) was influenced by pH, and the amount adsorbed varied greatly with initial TiO_2 particle size. The size dependent surface complexation is investigated further in order to obtain a mechanistic understanding of the processes that occur at the molecular level when TiO_2 nanoparticles interact with NOM.

Further, the stability of TiO_2 nanoparticle dispersions in presence and absence of well-characterized macromolecules (sodium alginate, humic acid, and fulvic acid) was studied in different electrolyte environments and at varying pH. The aggregation behavior was investigated by monitoring the changes in particle size using dynamic light scattering.

[1] Abbas *et al*. (2011) *Colloids Surf. A, Physicochem. Eng. Aspects*, doi, 10.1016/j.colsurfa.2011.03.064

Stable carbon isotope chemostratigraphy and implications for global carbon cycling, Cretaceous Western interior basin

YOUNG JI JOO*, MATTHEW HURTGEN AND BRADLEY B. SAGEMAN

Department of Earth and Planetary Sciences, Northwestern University, Evanston, IL 60201, USA (*correspondence: yjoo@earth.northwestern.edu)

The Late Cretaceous provides a critical analog for the anthropogenic greenhouse world. Strata of 100 Ma±20 myr record one of the warmest times in Earth history and are characterized by high-resolution time control, global correlation of deposits from deep ocean to epicontinental seas, and a series of global scale perturbations of the land-ocean-climate system. These perturbations include major changes in carbon cycling, surface temperatures, glacial ice volumes, sea level, and marine redox conditions over geologically short intervals (10's – 100's of kyr, similar to durations predicted for an anthropogenic greenhouse forced by combustion of all fossil fuel reserves). Recent findings from the Cenomanian-Turonian Ocean Anoxic Event 2 (OAE2), one of the largest Cretaceous events, have implicated active volcanism from emplacement of the Caribbean large igneous province as a trigger. One approach to testing this hypothesis involves carbon isotopes, since a volcanically triggered OAE should leave a characteristic signal. This study reports a new Cenomanian to Campanian carbon isotope record for the central Western Interior basin linked to a carbon isotope mass balance model. Major perturbations in the isotope record, such as Mid-Cenomanian Event and OAE2, are correlated to other carbon isotope records and analyzed with a series of model experiments. The new d13C record contributes to Late Cretaceous chemostratigraphy and allows testing of the volcanic initiation hypothesis, as well as the role of regional variations in organic matter burial.

https://doi.org/10.1180/S0026461X00006502 Published online by Cambridge University Press

Speciation of trivalent metal ions at the silica/water interface studied by second harmonic generation

DAVID S. JORDAN, SARAH A. SASLOW AND FRANZ M. GEIGER

Department of Chemistry, Northwestern University, 2145 Sheridan Rd. Evanston, IL 60208 (*correspondence: geigerf@chem.northwestern.edu)

The nonlinear optical technique of second harmonic generation (SHG) is used to study the interactions of Al (III), Y (III), La (III), and Gd (III) with the fused silica/water interface. Specifically, the Eisenthal $\chi^{(3)}$ technique [1] is employed in order to quantify several thermodynamic binding parameters of these ions as a function of background electrolyte concentration. Using this highly surface specific technique, we are able to quantify binding contants, adsorption free energies, absolute number densities, and interfacial charge densities in real-time and without the use of labels. We also examine the relationship between the measured adsorption free energies and the electric double layer interfacial potential at each electrolyte concentration to elucidate the charge state and possible binding pathways for each ion at the fused silica surface.

Our results show that the binding of each trivalent ion is fully reversible under the experimental conditions employed in this study. Adsorption isotherms are measured under dynamic flow conditions and fit using the Triple Layer model. We employ an analysis that takes advantage of the additive adsorption free energy expression in which the observed free energy is modeled as a sum of the electrostatic free energy and the intrinsic chemical free energy [2]. From this analysis, we find that the Al (III) ion binds to the fused silica surface as a fully hydrated trivalent species in a bidentate geometry. In contrast, the Y (III), La (III), and Gd (III) ions are each shown to adsorb to the silica surface in a reduced valence state. Despite identical oxidation state, the extent and mode of binding varies between each ion. These SHG studies provide valuable data that can be used to predict the transport these metal ions are throughout the environment.

[1] Salafsky & Eisenthal (2000) *J. Phys. Chem. B* **104**, 7752–7755. [2] Langmuir, D. *Aqueous Environmental Geochemistry*, Prentice Hall, Upper Saddle River, NJ, 1997.

Hydrate destabilization and methane release events during last glacial episode in Bay of Bengal

R.K. JOSHI AND A.MAZUMDAR*

Geological Oceanography, National Institute of Oceanography, Donapaula, Goa, 403004, India (*correspondence: maninda@nio.org)

We report here for first time episodic methane expulsion events in the Krishna-Godavari basin, Bay of Bengal during the marine isotope stage 4 (MIS-4) and at the transition of MIS-4 and MIS-5. We have observed sharp negative carbon isopote excursions in the isotope profiles of planktonic (*G. ruber*) and benthic (*Uvigerina sp.*) foraminifera in a core MD161-8, recovered on board *Marion Dufresne* as part of our gas hydrate exploration program in 2007. Depleted carbon isotope excursions in both benthic (B_1, B_2 and B_3) and planktonic (P_4, P_5 and P_6) foraminifera suggest that the methane expulsion events not only altered the carbon stable isotopic composition of the bicarbonate pool near the sediment waters interface, but also that of the shallow water column. A significant fraction of methane gets oxidized to HCO_3^- via anaerobic methane oxidation (AMO) at or below the sediment water interface. Depletion in carbon stable isotope ratios of the dissolved inorganic carbonate (DIC) pool depends on the carbon stable isotope ratios of methane advecting from deeper layers. Reported[1] $\delta^{13}C_{CH4}$ values (-75 to -85 ‰ VPDB) and C1/C2+C3 ratios (1110 to 3354) suggest presence of biogenic hydrocarbon gases within the methanogenic zone at the site MD161-8. Carbon stable isotope ratios of infaunal benthic foraminifera like *Uvigerina sp.* may get significantly influenced by incorporation of isotopically depleted carbon as HCO_3^- in the calcitic shell during growth and considered as a potential proxy for paleo-methane seepage. On the other hand, the depleted carbon isotope excursions recorded for the corresponding planktonic foraminifera, *G. ruber,* suggests that a part of the expelled methane reached the upper mixed layer (0-25m) where aerobic methanotrophy resulted in the depletion of carbon stable isotope ratios of the DIC reservoir.

We attribute the methane emission events to destabilization of the base of gas hydrate stability zone (BGHSZ) due to shale tectonics induced focused fluid flow. Fluid released from the over-pressured mud, possibly played important role in creating fractures as well as advection of the gases in K-G basin.

[1] Mazumdar *et al.* (2009) *G-cubed* **10**, 1–15.

https://doi.org/10.1180/S0026461X00006502 Published online by Cambridge University Press

Clumped isotope measurements to reveal diagenetic histories

A.-L. JOURDAN*, C.M. JOHN AND S. DAVIS

Qatar Carbonates and Carbon Storage Research Centre (QCCSRC), Department of Earth Science & Engineering, Imperial College London, London SW7 2AZ, United Kingdom (*correspondence: a.jourdan@imperial.ac.uk)

Clumped isotope geochemistry is a growing field, and more particularly the 'carbonate clumped isotope paleothermometer' is becoming more widely applied. Isotopologues are molecules that are identical except for their isotopic composition. Clumped isotopes are isotopologues where two or more heavy isotopes are clumped together; the effects of clumping are enhanced with decreasing temperatures, the zero point energy of the system being lowered. However, calibrating clumped isotopes is still a novel and challenging field of research, and more importantly measuring isotopologues requires skills and high sensitivity mass spectrometry.

So far, clumped isotopes have been used mainly in paleoclimate research. Here, we intend to calibrate the carbonate clumped isotope paleothermometer for diagenetic material. Carbonates are reactive minerals that can easily be modified during burial and exhumation. Post-depositional diagenetic processes such as dissolution and re-precipitation of new minerals are common and result in modified mineralogical and petro-physical characteristics of the initial carbonate rock. Temperature at which those transformations occur is a fundamental parameter in diagenesis: given a known geothermal gradient and burial history, the temperature of precipitation of carbonate cements can be translated into depth and timing of the event, assuming a thermal equilibrium between the fluids and the rock. Because it is thermodynamically based, the clumped isotope paleo-thermometer is independent of the isotopic composition of the diagenetic fluid and therefore can be applied with greater confidence.

We are currently implementing the technique at Imperial College London, both in a manual and in an automatic manner. Our aim is to improve the technique in order to be able to measure smaller sample sizes of diagenetic material (such as cement and crack infills) and to lower the associated error down to ± 1°C. We are therefore running a wide range of calibrations, on calcite and dolomite, and from different synthetically precipitated carbonate materials.

Ultimately, we aim to constrain the depositional and diagenetic environments of selected outcrops in Oman in the context of a wider study on Carbon Capture and Storage.

We would like to acknowledge that the QCCSRC is funded jointly by Qatar Petroleum, Shell, and the Qatar Science & Technology Park.

A ~3.63 Ga major impact recorded by the Bunburra Rockhole anomalous basaltic achondrite

F. JOURDAN[1]*, P.A. BLAND[2], A. BOUVIER[3] AND G. BENEDIX[4]

[1]Western Australian Argon Isotope Facility, and JdL-CMS, Curtin University of Technology, GPO Box U1987, Perth, WA 6845, Australia (*correspondence: f.jourdan@curtin.edu.au)
[2]Impacts and Astromaterials Research Centre (IARC), Imperial College London, SW7 2AZ, UK
[3]School of Earth and Space Exploration, Arizona State University, Tempe, AZ 85287, USA
[4]Meteoritics and Cosmic Mineralogy, Natural History Museum, Cromwell Road, London SW7 5BD

The Bunburra Rockhole (BR) meteorite is an anomalous basaltic achondrite recovered in Western Australia [1]. BR mineralogy, petrology [1] and mineral composition [2] resemble classical brecciated basaltic eucrites, generally associated with asteroid 4 Vesta. However, BR oxygen isotopic composition is distinct from the general HED fractionation line, suggesting that BR, along with 3 other anomalous eucrites, belongs to a distinct differentiated parent asteroid. Previous chronology studies indicate a reset of the ^{26}Al-^{26}Mg system and a ~4.1 Ga ^{207}Pb-^{206}Pb whole-rock reequilibration age for BR [2].

The ^{40}Ar/^{39}Ar chronometer has typical low closure temperature of few hundred °C and has the potential to record heating events such as large collisions between asteroids. We have analyzed 4 groundmass (fine-grained) and 5 breccia (medium- to coarse-grained) single-grain aliquots of BR using the ^{40}Ar/^{39}Ar laser step-heating technique. All samples yielded well-defined plateau ages. 7 grains yielded a weighted mean age of 3634±18 Ma (P=0.53) suggesting that BR recorded a major impact event on its parent body at this time. 2 breccia grains suggest a secondary minor heating event at 3538±24 Ma (P=0.54).

Generally, eucrites ^{40}Ar/^{39}Ar analyses yield complex age spectra with ambiguous apparent ages between 3.4 and 4.1 Ga [3]. Here, a unique well-defined age at 3.63±0.02 Ga based on several flat age spectra indicate that BR had a simpler history than eucrites from Vesta 4 and may suggest that BR belongs to a different parent asteroid.

[1] Bland *et al*. (2009) *Science* **325**, 1525-1527 [2] Spivak-Birndorf *et al*. (2010) 41th LPSC [3] Bogard & Garrison (2009) 40th LPSC.

https://doi.org/10.1180/S0026461X00006502 Published online by Cambridge University Press

Cu isotopes suggest Cu reduction during acquisition in higher plants

DELPHINE JOUVIN[1]*, DOMINIK WEISS[2], MATTHIEU N. BRAVIN[3], PASCALE LOUVAT[4], PHILIPPE HINSINGER[5] AND MARC F. BENEDETTI[6]

[1]IDES – Université Paris Sud, Orsay, France (*correspondence: delphine.jouvin@u-psud.fr)
[2]Department of Earth Science and Engineering – Imperial College, London, UK
[3]CIRAD, Saint-Denis, La Réunion, France
[4]Écologie fonctionnelle et Biogéochimie des Sols et Agrosystèmes – INRA, Montepllier, France
[5]Géochimie des Eaux, Université Paris Diderot – IPGP, Sorbone Paris Cité, UMR CNRS 7154, Paris, France
[6]Géochimie & Cosmochimie, IPGP - Université Paris Diderot, Sorbone Paris Cité, UMR 7154, Paris, France

Evidences from recent studies suggest that studying the natural isotope fractionation of metals in plants offers great potential to elucidate acquisition and translocation mechanisms. We conducted controlled hydroponic studies with lettuce, tomato, rice and durum wheat and tested the effect of copper (Cu) speciation and iron (Fe) supply in the nutrient solution. Next to Cu isotopes, we studied the zinc (Zn) isotopes since Zn is not sensitive to redox processes and a model of Zn isotopic fractionation in plants has been proposed [1].

Isotope fractionation patterns between nutrient solution, roots and shoots differ for Cu and Zn. Roots are enriched in ^{63}Cu (light isotope) but slightly enriched in Zn heavier isotopes compared to the nutrient solutions, suggesting that different processes occur for Cu and Zn at the root-solution interface. Different physical, chemical and biological processes can contribute to the isotopic fractionation during acquisition of Cu and Zn by plants. Abiotic processes, mainly complexation in the nutrient solution or adsorption onto root binding site, are expected to fractionate similarly for Cu and Zn. On the contrary, plant behaviour differs for Cu and Zn, as seen with the concentrations and isotopic ratios data.

The enrichment in light isotopes for Cu is associated with significant reduction of Cu at the root-solution interface, suggesting that this biogeochemical mechanism is predominant for the acquisition of this metal into plants. This is similar to mechanism of Fe uptake for strategy I plant species [2].

[1] Arnold T. *et al*. (2010) *Plant, Cell & Env*. **33**, 370–381. [2] Marschner H. Römheld V. (1994) *Plant & Soil* **165**, 261–274.

How are oceanic $\delta^{18}O$ changes imprinted in ice core records?

J. JOUZEL[1]*, G. HOFFMANN[1], A. LANDAIS[1], B. STENNI[2], V. MASSON-DELMOTTE[1] AND C. WAELBROECK[1]

[1]LSCE/IPSL CEA/CNRS/UVSQ, CEA saclay 91191, Gif/Yvette (*correspondence: jean.jouzel@lsce.ipsl.fr)
[2]Department of Geosciences, University of Trieste, 34127 Trieste, Italy

The deuterium and oxygen 18 composition of a precipitation and thus its deuterium-excess, $d = \delta D - 8\ \delta^{18}O$, depends, amongst other parameters, on the isotopic composition of surface waters in the oceanic source regions. As a result, the glacial-interglacial $\delta^{18}O$ change of surface oceanic waters is imprinted in the ice core d-excess record with, in Central Antarctica, a 3 to 4 ‰ d-excess increase directly attributable to the oceanic source. In the same line, changes in oceanic $\delta^{18}O$, globally averaged in this case, influence the $\delta^{18}O$ composition of atmospheric oxygen directly through oceanic productivity and indirectly over the continent. Obviously there are many other processes, most of them however relatively well identified, which govern the $\delta^{18}O$ oceanic record derived from foraminifera, on the one hand, and the d-excess and the air $\delta^{18}O$ measured respectively in polar ice and entrapped air bubbles, on the other. In this context, we will compare the amplitude and time sequence of these three isotopic signals from one deglaciation to the next, thanks to the d-excess and air $\delta^{18}O$ records now available on nine terminations from the EPICA Dome C ice core.

https://doi.org/10.1180/S0026461X00006502 Published online by Cambridge University Press

Nucleation and growth mechanisms and kinetics of environmentally important oxides and carbonates

YOUNG-SHIN JUN[1]*, BYEONGDU LEE[2], YANDI HU[1], JESSICA R. RAY[1], GLENN A. WAYCHUNAS[3] AND ALEJANDRO FERNANDEZ-MARTINEZ[3]

[1]Department of Energy, Environmental and Chemical Engineering, Washington University, St. Louis, MO 63130, USA (*correspondence: ysjun@seas.wustl.edu),
[2]Argonne National Laboratory
[3]Lawrence Berkeley National Laboratory

Nucleation and growth of hydrous oxide or carbonate nanoparticles can significantly influence the fate and transport of organic and heavy metal contaminants in the environment. Their particles' formation and tranport can alter the porosity and permeability of geo-media. Therefore, more accurate quantitative and qualitative information about mineral nucleation and growth is required.

In this work, we used a time-resolved simultaneous small angle x-ray scattering (SAXS)/grazing incidence (GISAXS) setup for real-time monitoring of water-mineral interfacial reactions. To observe the size, shape, distribution, and phase of hydrous iron oxide and calcium carbonate nanoparticles on quartz and mica surfaces as well as in solutions, we also used complemetary techniques, such as atomic force microscopy, high resolution transmission electron microscopy, high resolution X-ray diffraction, and grazing incidence wide angle x-ray scattering. The solutions included different ionic strengths of sodium nitrate, arsenate, aluminum, and polyaspartate. The mineral nucleation and growth modes were monitored as a function of exposure time. We delineated the quantitative contributions between homogenous and hetergeous mechanisms at varied environmental conditions. Hydrous iron oxide nanoparticles formed preferrentially along steps rather than terraces, while amorphous calcium carbonate did not show any clear preference. Under aqueous conditions, newly formed nanoparticles did not exhibit any facets. The presence of arsenate and aluminum ions significantly influenced the sizes and crystallinities of hydrous iron oxide nanoparticles and altered their nucleation and growth kinetics. This study provides more accurate depiction of nucleation and growth of environmentally important minerals in solution as well as at active interfaces. Our findings have implications not only for hydrous oxide- or carbonate-containing biogeochemical systems, but also for environmental remediation (heavy metal removal and nuclear waste deposition site remediation) and geoengineering applications (geologic CO_2 sequestration).

Effects of organic ligands on supercritical CO_2–induced phlogopite dissolution and secondary mineral formation

YOUNG-SHIN JUN* HONGBO SHAO, AND JESSICA R. RAY

Department of Energy, Environmental and Chemical Engineering, Washington University, St. Louis, MO 63130, USA (*correspondence: ysjun@seas.wustl.edu) (shaoh@seas.wustl.edu, jrr5@cec.wustl.edu)

To evaluate the long-term and short-term risks associated with geologic CO_2 sequestration (GCS), we need to understand both the reactions at supercritical CO_2 ($scCO_2$)-saline water-rock interfaces and the environmental factors affecting these interactions.[1, 2] This research investigated the effects of four organic ligands (oxalate, malonate, acetate, and propionate) on the dissolution and surface morphological changes of phlogopite [$KMg_{2.87}Si_{3.07}Al_{1.23}O_{10}$ (F, $OH)_2$] under GCS conditions (in particular, 95ºC and 102 atm). Phlogopite was chosen as a model clay mineral in potential GCS sites.

After CO_2 injection, the dissolution of CO_2 causes a pH decrease in saline water, which increases phlogopite dissolution, but this effect can be minimized by the buffering capacity of organic ligands. However, in this study, for ligands forming a strong complexation with surface metals, phlogopite dissolution rates (especially for Al) are increased by ligand-promoted dissolution, even though the pH increases. The experimentally observed dissolution rates of phlogopite were in the order: oxalate > malonate > acetate ≈ propionate. Based on results from ion-exchange chromatography, oxalate and malonate were stable in our reaction system; however, acetate and propionate concentrations continuously decreased due to the solvent exaction of acetic acid and propionic acid by $scCO_2$ at 95ºC and 102 atm. After 159 h, all of the acetate and propionate had disappeared from the aqueous solutions.

Interestingly, in the presence of oxalate, nanoscale precipitation of amorphous silica and fibrous illite was observed only three hours after CO_2 injection. At this early reaction time, illite fibers formed a honeycomb structure on phlogopite basal surfaces, but at a later reaction time these structures detached from the surface and triggered the formation of dissolution channels. In addition, kaolinite, boehmite, diaspore, and gibbsite were also identified. These results provide new information for understanding reactions at $scCO_2$–saline water–rock interfaces in deep saline aquifers.

[1] Shao, Ray & Jun (2010) *ES&T* **44**, 5999–6005. [2] Shao, Ray & Jun (2011) *ES&T* **45**, 1737–1743.

https://doi.org/10.1180/S0026461X00006502 Published online by Cambridge University Press

Laser-induced breakdown detection (LIBD) of uranium and silica colloids

E.C. JUNG*, H.-R. CHO AND M.R. PARK

Nuclear Chemistry Research Division, Korea Atomic Energy Research Institute, P.O. Box 105, Yuseong, Daejeon 305-600, Republic of Korea
(*correspondence: ecjung@kaeri.re.kr)

Introduction

Laser-induced breakdown detection (LIBD) is a well established technique using plasma formation in the high irradiance of a focused laser beam for measuring small size of colloidal particles in an aquatic environment. Over the last decades, several different LIBD systems which adopt different detection schemes by using a piezoelectric transducer, a charge-coupled device camera, and an optical probe beam were developed. These LIBD systems enable to detect extremely low concentration of nanoparticles. Thus, the LIBD technology can be applied in various fields such as, *in situ* observation of colloid mediated transport of polluants and measurement of solubility of radio-active elements.

Although LIBD methods allow one to determine a particle size in principle, until now, particle sizing capabilities in most LIBD experiments were inspected only for polystyrene particles of a well-defined size as a reference material. Therefore, it should be certified that these LIBD methods are whether suitable or not to determine the particle size for different materials.

Discussion of Results

In the present work, particle sizing capability using LIBD has been investigated for three different materials: uranium, polystyrene, and silica nanoparticles. It was observed that spatial distribution of breakdown events generated by laser pulse of 532 nm wavelength along the laser beam propagation axis was directly correlated with particle size for uranium and polystyrene, while there was no correlation between the spatial distribution of breakdown events and particle size for silica. The reason for these phenomena is understood based on the ionization potential (IP) of each material. IPs of these materials are about 6.17, 7.8, and 11.7 eV for UO_2, polystyrene, and SiO_2, respectively. When a focused laser pulse of 532 nm wavelength is used to generate laser-induced plasma, simultaneous three or four photon absorption is required to induce multiphoton ionization (MPI) of uranium and polystyrene. However, at least five photon absorption is required to induce MPI of silica. The result suggests that determination of particle size of silica particles with the aid of calibration curve obtained from the polystyrene reference particles may give incorrect values.

Seismic anisotropy produced by serpentine in the mantle wedge

H. JUNG*

School of Earth and Environmental Sciences, Seoul National University, Seoul 151-747, Korea
(*correspondence: hjung@snu.ac.kr)

Trench-parallel seismic anisotropy has been observed in many subduction zones in the upper mantle. In this study, crystal-preferred orientation (CPO) and seismic anisotropy of natural serpentine from Val Malenco in northern Italy and Punta Bettolina in western Italy were studied. It is found that [001] axes are aligned subnormal to the foliation but [010] axes of serpentine are aligned subparallel to the lineation which is significantly different from that produced in a recent high-pressure experiment. I show that the CPOs of serpentine found in this study can be used to explain trench-parallel seismic anisotropy in the mantle wedge, not only for serpentine deformed at high angles greater than 45° from the surface but also for serpentine deformed at low angles such as in horizontal shear, demonstrating that the CPO of serpentine has much broader implications for interpreting the seismic anisotropy than previously thought. It is also found that seismic anisotropy caused by the CPO of serpentine depends on the degree of serpentinization and flow geometry. Current data suggest that trench-parallel seismic anisotropy in the forearc mantle wedge in subduction zones can be attributed to the CPO of serpentine.

https://doi.org/10.1180/S0026461X00006502 Published online by Cambridge University Press

Wadi as collectors of drinking water in South Mongolia

DAVID JUŘIČKA[1], MAJIGSUREN YONDON[2], JITKA NOVOTNÁ[1] AND JINŘICH KYNICKÝ[1]

[1]Mendel University in Brno, 613 00 Brno, Czech Republic (25389@node.mendelu.cz)
[2]University of Science and Technology, Ulaanbaatal 46, Mongolia (majigsuren@yahoo.com)

Current drinking water resources of south Mongolia do not yield suitable quality and quantity to often. Solution of the drinking water deficit issue can partially solve the large wadi evaluation, such as drinking water collectors. We constructed the first evaluation of wadi water capacity for Khan Bogd complex, which is one of the largest known intrusions of peralkaline granite (*ca*. 1500 km^2). Watersheds and stream network and profiles carefully identified in the field were verified by comparison of supervised classifications of Landsat TM images. The possible sources yield almost 5.0×10^6 m^3 and average annual recharge rate for the Khan Bogd wadi aquifers is estimated at 1.892×10^6 m^3. The only risk of the aquifer contamination presents stock, but comparing the chemical composition of the water from wells used for animals feeding and samples of groundwater, we didn't observe any important contamination (ammonium up to 10 mg/l). Present study is the first attempt to describe and evaluate the potential wadi Khan Bogd as a source of drinking water in the Mongolia. Implication for use of this new water source accessible for drinking water in whole arid region of South Mongolia is clear.

Distinguishing mantle derived contributions at a continental arc volcano: Tatara-San Pedro

J. JWEDA[1], S.L. GOLDSTEIN[1], M.A. DUNGAN[2], C.H. LANGMUIR[3] AND J.P. DAVIDSON[4]

[1]Lamont-Doherty Earth Observatory, Columbia Univ., 61 Rt. 9W, Palisades, NY 10964, USA (*correspondence: jjweda@ldeo.columbia.edu)
[2]Université de Genéve, 13 rue des Maraîchers, CH-1205, Geneva, Switzerland
[3]Harvard University, 20 Oxford Street, Cambridge, MA 02138, USA
[4]University of Durham, South Road, Durham DH1 3LE, UK

Subduction recycling plays a key role in the distribution of elements between the mantle and crust. One of the important challenges in the study of arc magma genesis is identifing contributions from the subducted slab and mantle, and distinguishing them from crustal contamination at relatively thick crust continental arc volcanoes [1, 2]. The Quaternary Tatara-San Pedro complex (TSPC) of the Southern Volcanic Zone (SVZ) is a large, compositionally diverse frontal arc volcanic complex. High-density sampling has yielded one of the most complete eruptive chrono-stratigraphies (spanning over 930 kyr) of any arc volcano [3, 4, 5]. This provides us with a unique opportunity to elucidate magma source heterogeneity and the effects of recycled slab, mantle, and crustal input at a continental arc volcano.

This study augments an extensive XRF geochemical dataset with new isotope and ICP trace element analyses. Although most TSPC lavas appear impacted by crustal input, we distinguish three distinct mantle-derived magma types: (1) one derived from 'depleted mantle' fluxed by slab-derived hydrous fluids (high Sr/Nd, Zr/Nb and low $^{87}Sr/^{86}Sr$), (2) one from 'enriched mantle' (high incompatible elements, HFSE, and $^{87}Sr/^{86}Sr$), and (3) another that appears prevalent to the SVZ mantle wedge (subduction modified) with generally intermediate but still distinct chemistry (broadly similar to parental magmas at other SVZ volcanoes). Extensive MASH processing is precluded by the absence of significant garnet fractionation in the endmembers and by eruption of diverse parental magmas over short time intervals.

[1] Hilldreth & Moorbath (1988) *Contrib Mineral Petrol* **98**, 455–489. [2] Davidson *et al*. (1988) *Contrib Mineral Petrol* **100**, 429–445. [3] Fergueson *et al*. (1992) *J Petrol* **33**, 1–43. [4] Singer *et al*. (1997) *Geo Soc Am Bull* **109**, 127–142. [5] Dungan *et al*. (2001) *J Petrol* **42**, 555–626.

https://doi.org/10.1180/S0026461X00006502 Published online by Cambridge University Press

Role of Hydrogen and Oxygen fugacity in incorporation of Nitrogen in reduced magmas of the early Earth's mantle

A.A. KADIK[1]* AND Y.A. LITVIN[2]

[1]Vernadsky Institute of Geochemistry and Analytical Chemistry, Russian Academy of Sciences, 19, Kosygin str., Moscow, Russia (*correspondence: kadik@geokhi.ru)
[2]Institute of Experimental Mineralogy, Russian Academy of Sciences, Chernogolovka, Moscow district, 142432, Russia

In a series of experiments in the system Fe-bearing melt + molten Fe phase + N + H conducted at 4 GPa, 1550 °C, and fO_2 from 2 to 4 log units below IW buffer we have characterized the nature and quantified the abundance of N and H species dissolved in a model silicate melt (FeO + Na_2O + Al_2O_3 + SiO_2). To elucidate the mechanisms of nitrogen and hydrogen dissolution in magmas, we studied the glasses produced by quenching the melts using infrared and Raman spectroscopy's in a manner similar to that reported by [1]. Experiments indicate that under the reduced conditions corresponding to the fO_2 path during metal segregation and self-oxidized of mantle [2] and magma ocean [e.g. 3, 4] the silicate melt would contain species with N-H bonds (NH_3, NH^{4+}, NH^{2-}, NH^{2+}) as well as N_2 and oxidized H species (OH- and H_2O). Some hydrogen is present in the melt in molecular form. The formation of N–H bonds in the reduced silicate melts results in a significant increase in nitrogen solubility that can reach 1–2 wt. %. It is suggested that significant amounts of nitrogen, comparable to those estimated for the present-day mantle, could have been incorporated in the early Earth by dissolution in reduced magma ocean.

Support: Prog. No 24 RAS, RFBR grant No 11-05-00926, ESD RAS project No 8.

[1] Mysen *et al*. (2008*) AmMin* **93**, 1760–1770 [2] Galimov (2005) *EPSL* **233**, 263–276. [3] Wood *et al*. (2006) *Nature* **441**, 825–833. [4] Frost *et al*. (1008) *Phil Trans Royal Soc* **A 366**, 4315–437,

Differentiation of ophiolitic and nonophiolitic gabbros using confocal Raman spectroscopy: Central Anatolia Turkey

Y.K. KADIOĞLU, T. KORALAY, O. ZOROĞLU, B. GULLU, M.A. AKÇE, K. DENIZ AND B. YILDIRIM

Ankara Univ., Dept., of Geol., Eng., & YEBIM Ankara, Turkey (*correspondence: kadi@ankara.edu.tr)

Ophiolitic gabbros are mostly exposed at west of Tuz Lake and nonophiolitic gabbros are exposed at east of Tuz Lake in Central Anatolia. Ophiolitic and nonophiolitic gabbros have almost same mineral and geochemical compositions. Discrimination of the ophiolitic and nonophiolitic gabbros was carried out using the Raman spectra of the pyroxene minerals. Based on Raman peak positions, the major-element composition of the (Mg, Fe, Ca)-pyroxenes are determined and classified.

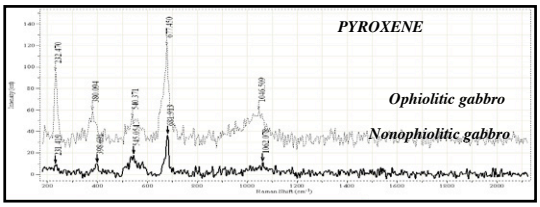

Results and Discussion

Raman vibrational modes were observed for the pyroxenes in the wave number range between 200 and 1200 cm^{-1} (Figure 1). The Raman modes showing the greatest variation in frequency with the $Fe^{2+}$and OH^{+}content are potentially capable of being used as an index for determining the ophiolite and nonophiolite pyroxenes of the gabbro series. The best Raman modes for this purpose in the ophiolite pyx series are ν_6 (232–540 cm^{-1}) and (677–1046 cm^{-1}) pairs that show about 60 cm^{-1}across the series. The ν_{15} (931–950 cm–1) mode can also serve as a supplementary mode for the determination of the composition. These modes are characteristic and fairly intense. However, in the nonophiolite pyx series, because only the ν_3 (231–545 cm^{-1}) and ν_3' (681–1046 cm^{-1}) pairs show a variation more than 20 cm^{-1}. These provide a weaker basis for the composition indices. The uncertainties in the determination of the Fe content with the Raman modes are of the order of 3 and 7%.

[1] Lin, I.H. (1995) *Raman Spectroscopy study of (Ca, Mg, Fe)-Pyroxene*. Master Thesis, National Taiwan University, **74** p.

https://doi.org/10.1180/S0026461X00006502 Published online by Cambridge University Press

Polyphase serpentinization history of Mariana forearc mantle: Observations on ultramafic clasts from ODP Leg 195, Site 1200

W.-A. KAHL[1]*, N. JÖNS[1], W. BACH[1] AND F. KLEIN[2]

[1]University of Bremen, 28359 Bremen, Germany (*correspondence: wakahl@uni-bremen.de)
[2]Woods Hole Oceanographic Institution, Woods Hole, USA

In the forearc of the Mariana subduction zone system, abundant seamounts form from extrusion of blueschist and serpentine mud. ODP Leg 195 drilled the South Chamorro seamount, where ultramafic clasts occur within the mud matrix. These clasts show a complex serpentinization history, which bears the potential for tracking the fluid history during uplift and cooling of mantle wedge rocks to the seafloor.

Highly serpentinized harzburgites, which are crosscut by different generations of late-stage veins, were examined. Preserved primary minerals include olivine (X_{Mg}= 0.91-0.92) and orthopyroxene ($X_{Mg}\approx$ 0.92). Magnesium-rich (X_{Mg}= 0.92-0.95) clinopyroxene is present as exsolution lamellae in orthopyroxene and in symplectitic intergrowths with spinel (X_{Cr}= 0.48-0.59).

Multiple serpentinization steps are documented: (I) Pervasive serpentinization led to ubiquitous breakdown of olivine and formation of serpentine (X_{Mg}= 0.92-0.94) and magnetite. Orthopyroxene was replaced to lesser extent by serpentine ($X_{Mg}\approx$ 0.90). Clinopyroxene remained stable during this stage. (II) The second hydration stage was bound to fractures crosscutting earlier serpentinization textures and is manifested as veins consisting of Mg-rich serpentine (X_{Mg}= 0.90-0.93). (III) Veins from stage II were re-activated and overprinted by serpentine + brucite assemblages. Replacement of magnetite is observed, leading to brucite with $X_{Mg}\approx$ 0.80 and serpentine with $X_{Mg}<$ 0.90. Furthermore, clinopyroxene breaks down and Fe-rich brucite ($X_{Mg}\approx$ 0.60) forms. (IV) Finally, late discontinuous serpentine veins formed perpendicular to the stage II and III veins.

Pervasive serpentinization (stage I) likely marks a comparatively high-T (i.e. T= 250-350°C) hydration that took place within the mantle wedge. The lower density of the hydrated rocks led to diapiric rise and associated fracture-bound serpentine formation (stage II). Formation of Fe-rich brucite as well as breakdown of magnetite and clinopyroxene (stage III) occurred after considerable cooling (T<< 200°C) during uplift. Petrography and mineral chemistry point to low-temperature demagnetization, which is in agreement with density-susceptibility relations and results of reaction-path modelling.

Incomplete recovery of mineral-bound lignin phenols

K. KAISER[1], P.J. HERNES[2], R.Y. DYDA[2], C. CERLI[3]

[1]Soil Sciences, Martin Luther University Halle-Wittenberg, 06120 Halle (Saale), Germany (*correspondence klaus.kaiser@landw.uni-halle.de)
[2]Department of Land, Air and Water Resources – Hydrology, University of California, Davis, CA 95616-8628, USA (pjhernes@ucdavis.edu, rydyda@ucdavis.edu)
[3]Institute of Biodiversity and Ecosystem Dynamics, Earth Surface Science, University of Amsterdam, 1098 XH Amsterdam, The Netherlands (c.cerli@uva.nl)

Intimate associations with minerals is one mechanism involved in the accumulation and stabilisation of organic matter (OM) in soils. Phenolic compounds derived from partial degradation of polyphenols such as lignin are among the most surface-reactive organic compounds. However, we still do not know to which extent lignin-derived phenols associated with soil minerals can be analytically assessed.

Here, we tested the extractability of mineral-bound lignin-derived phenols by alkaline CuO oxidation.

We used tree aqueous litter (blue oak, pine, annual grass) leachates and five minerals (ferrihydrite, goethite, kaolinite, illite, montmorillonite). In a first step, we determined the sorption capacity for dissolved organic carbon for each mineral, as well as the changes in specific UV absorption during the sorptive interaction between organic matter and minerals. Then, we produced organic–mineral associations under conditions well below the sorption maximum of the contained mineral. The mineral–organic associations, the dried out leachates and the equilibrium solutions were then subjcted to CuO oxidation. The amount of sorbed and not CuO-exctractable lignin-derived phenols were calculated by difference.

CuO-oxidation extracted lignin-derived phenols bound to ferrihydrite completely and without changes in composition, presumably due to complete dissolution of the mineral. For all other minerals, up to 44% of the bound phenols could not be extracted. The incomplete recovery of sorbed phenolic compounds was accompanied by different ratios of extracted individual phenols, suggesting different bonding strengths.

The results show that a substantial portion of lignin-derived phenols binds irreversibly to minerals, even escaping harsh extraction unless the mineral is completely dissolved. The difference in extractability of individual phenols suggests that abiotic processes, such as sorption/desorption, should be taken into account when using CuO oxidation data for assessing organic matter transformation in mineral matrixes.

https://doi.org/10.1180/S0026461X00006502 Published online by Cambridge University Press

Different paths of chemical alteration during grusification of granites from S Poland

B. KAJDAS* AND M. MICHALIK

Institute of Geological Sciences, Jagiellonian University, ul. Oleandry 2a, 30-063 Kraków, Poland (*correspondence: bartlomiej.kajdas@uj.edu.pl)

Four type of grusified granites were taken under consideration. Three of the investigated gruses were developed on the Variscan granites from Karkonosze Mts. (Kowary Średnie [KS] and Głębock [GL]) and Tatra Mts. (Skrajna Turnia Mt. [ST]), one on the Early Paleozoic (ca. 500 Ma) Izera Granite (Siedlęcin [SI]).

Each of studied gruses shows significant variation in the LOI (loss of ignition) value, what can be connected with degree of alteration of parent granite. Changes in contents of major elements differ for each grus localization. ST grus shows significant changes of amount of major elements in relation to degree of alteration of rock (decreasing trends in SiO_2, Na_2O, and CaO, and increasing trends in Al_2O_3, K_2O, MgO and Fe_2O_3 contents versus LOI); SI grus shows increasing trend for Fe_2O_3 and MgO and decreasing trend for SiO_2 (vs. LOI); in KS grus increasing trends occur for Fe_2O_3 and MgO, and decreasing trends for Na_2O and CaO, whereas SiO_2, Al_2O_3 and K_2O content variation is non-systematic in relation to LOI. In GL grus the only slightly increasing content of Fe_2O_3 is visible (vs. LOI).

Using several indices of alteration [1, 2] we were able to notice differences in the paths of chemical alteration during grusification. Because the main alteration process during grusification is connected with decomposition of plagioclase, chemical alterations can be observed on plots based on changes of alkali and Al_2O_3 content (e.g. CIA and PIA; [1, 2]). CIA and PIA plots for ST are steeper, for SI more flattened, and for KS and GL trends are less uniform (vs. LOI). The WPI [3], which use all major elements, shows most uniform plots for each of the investigated gruses, but PI [3] shows trends only for Tatra and Izera granites, what indicate, that silica was immobile during grusification of Karkonosze granite.

The Alteration Box Plot [4] used for hydrothermal and diagenetic alteration of rocks reveals sericitization and chloritization trends in ST, KS and GL and carbonatization trend in SI.

[1] Gupta & Rao (2001) *Bull Eng Geol Env* **60**, 201-221. [2] Price & Velbel (2001) *Chemgeo* **202**, 397-416. [3] Reiche (1943) *J Sediment Petrol* **13**, 58-68. [4] Large *et al*. (2001) *Econ. Geol* **96**, 957–972.

Fluid-fluid phase separation under metamorphic conditions: MD simulations of a generalized composition H_2O-CO_2-NaCl

ANDREY G. KALINICHEV

Laboratoire SUBATECH, UMR 6457 / Ecole des Mines de Nantes / IN2P3-CNRS / Université de Nantes, 4 rue Alfred Kastler, BP 20722, 44307 Nantes Cedex 03, France (kalinich@subatech.in2p3.fr)

Water and carbon dioxide are two most abundant volatile species in the Earth's crust and mantle. They represent the common solvents which, under high-temperature, high-pressure thermodynamic conditions, dissolve various amounts of other volatiles to form complex hydrothermal and metamorphic fluids. Thus, aqueous mixtures in the system H_2O-CO_2-NaCl can be considered a good approximation for most crustal and mantle fluids. Although there are many experimental thermodynamic data for this generalized system, the molecular-level understanding of their thermodynamic, transport, and phase equilibria properties is still inadequate in many respects. We performed molecular dynamics (MD) computer simulations of the H_2O-CO_2-NaCl fluids along three high-density isochores (1.0, 1.1, and 1.2 g/cm3) to systematically study their thermodynamic, structural, and transport properties in the range of temperatures from 400 to 1000ºC and pressures from 3 to 18 kbar.

The composition of H_2O/CO_2/NaCl = 60/28/12 mol%) was chosen to probe both homogeneous and heterogeneous regions of the phase diagram. It has been predicted from experimental data [1-3] and model calculations [4-5] that such fluid would undergo phase separation at approximately 700ºC by forming a CO_2-rich phase of low-salinity (H_2O/CO_2/NaCl ~ 50/48/2 mol%) and a concentrated brine (H_2O/CO_2/NaCl ~ 66/20/14 mol%). We try to uncover the molecular-level mechanisms driving this heterogenization process and to rationalize the properties of decompressing H_2O-CO_2-NaCl fluids under metamorphic conditions in terms of the effects of temperature and density on the molecular clusterization and ion pairing in the system controlled by the electrostatic and hydrogen-bonding interactions among the fluid species.

[1] Aranovich, L.Y. Newton, R.C. (1999) *Am. Mineral.* **84**, 1319–1332. [2] Shmulovich, K.I. Graham, C.M. (1999) *Contrib. Mineral. Petrol.* **136**, 247–257. [3] Shmulovich, K.I, Graham, C.M (2004) *Contrib. Mineral. Petrol.* **146**, 450–462. [4] Duan, Z.H. *et al*. (1995) *Geochim. Cosmochim. Acta*, **59**, 2869–2882. [5] Gerya, T.V. *et al*. (2000) *J. Geodynamics*, **29**, 17–35.

https://doi.org/10.1180/S0026461X00006502 Published online by Cambridge University Press

Hydrogen bonding and molecular ordering of water at mineral-solution interfaces

ANDREY G. KALINICHEV[1]*, JIANWEI WANG[2] AND R. JAMES KIRKPATRICK[3]

[1]Laboratoire SUBATECH, UMR 6457 / Ecole des Mines de Nantes / IN2P3-CNRS / Université de Nantes, 4 rue Alfred Kastler, BP 20722, 44307 Nantes Cedex 03, France (*correspondence: kalinich@subatech.in2p3.fr)
[2]Department of Geological Sciences, University of Michigan, Ann Arbor, MI 48109, USA
[3]College of Natural Science, Michigan State University, East Lansing, MI 48824, USA

Aqueous interfaces play crucial roles in many geochemical systems, and the atomic scale details of the mineral substrate structure and composition are essential to understanding and predicting their chemical and physical properties. Here we compare the results of molecular dynamics (MD) simulations for the atomic density profiles, atomic surface density distributions, hydrogen bonding configurations, and orientational ordering of H_2O molecules at interfaces with several minerals, which may be considered typical for many hydrophobic and hydrophilic inorganic oxide and hydroxide surfaces [1, 2]. The atomic density profiles of water show substantial layering at all surfaces, with the details significantly different and strongly dependent on the composition and crystal structure of the mineral substrate. Relative to bulk water, the average density of water at the hydrophobic talc (001) surface is reduced by about 9-15% within 6-10 Å from the interface, which is equivalent to a 0.8Å-thick depletion layer compared to the similar but hydrophilic (001) surface of muscovite.

At the hydroxide surfaces, both cations and anions are effectively stabilized in their adsorbed state via the development of an integrated hydrogen-bonding network among the ions, H_2O molecules, and surface OH-groups, even if the substrate does not charged. For organic anions, such as amino acids, the deprotonated carboxylate groups are the primary strong H-bond acceptors, whereas the deprotonated amine groups serve as only weak additional H-bond acceptors from the surface. The organic species preferably accept H-bonds from H_2O molecules rather than from surface OH-groups due to structural restrictions on the development of tetrahedrally coordinated H-bonding environments for the carboxylate groups at the surface.

[1] Wang, J. *et al*. (2009) *J. Phys. Chem. C*. **113**, 11077.
[2] Kalinichev, A.G. *et al*. (2010) *Phil. Mag*. **90**, 2475.

Paleoproductivity controls on microbical abundance in marine subsurface sediments

JENS KALLMEYER[1], DIEDERIK LIEBRAND[2], MITCH W. LYLE[3] AND THOMAS WESTERHOLD[4]

[1]University of Potsdam, Karl-Liebknecht Str. 24, 14476 Potsdam, Germany (kallm@geo.uni-potsdam.de)
[2]National Oceanography Centre, European Way, Southampton, UK, (Diederik.Liebrand@noc.soton.ac.uk)
[3]Texas A&M University, Oceanography and Meteorology, College Station, Texas 77843, USA, (mlyle@ocean.tamu.edu)
[4]MARUM, Leobener Str., 28359 Bremen, Germany (twesterhold@marum.de)

IODP Expeditions 320 and 321 (Paleocene-Eocene Age Transect, PEAT) recovered a continuous Cenozoic record of the equatorial Pacific by drilling at the paleopositions of the Equator at successive crustal ages on the Pacific plate. The drilled sites passed the high productivity area of the equatorial upwelling at different times.

Microbial cell abundance in several PEAT cores strongly deviates from the expected steady decrease with depth. We compared cell count profiles with several sedimentological, physical and geochemical parameters. Several of the observed excursions in cell abundance correlate with distinct sedimentological and geochemical horizons, which are ultimately caused by changes in paleoproductivity.

Colour changes in the sediment indicate changes in redox conditions from more oxidized to reducing, they also mark the time intervals during which the site was in the high productivity zone of the equatorial upwelling.
Also, distinct turning points in the cell count profiles correlate well with redox fronts, being indicated by peaks in dissolved porewater constituents like Fe^{2+} and Mn^{2+}.

The new PEAT data allow an insight into how past changes in productivity are influencing current patterns of microbial abundance and activity.

https://doi.org/10.1180/S0026461X00006502 Published online by Cambridge University Press

Revised ages of angrites

A. KALTENBACH[1]*, C.H. STIRLING[1] AND Y. AMELIN[2]

[1]Dept. of Chemistry, University of Otago, Dunedin, NZ (*correspondence: akaltenbach@chemistry.otago.ac.nz)
[2]RSES, The Australian National University, Canberra, Australia

Angrites are a small group of 18 differentiated achondrites and are among the oldest known rocks of our Solar System. These meteorites have low metamorphism and shock effects, are enriched in refractory elements and are well suited as anchors for short-lived nuclide chronology. Therefore it is crucial to accurately measure their ages according to the Pb-Pb chronometer, the only absolute geochronometer with sufficient precision to resolve age differences in the early Solar System processes.

To determine accurate ^{207}Pb-^{206}Pb ages, the isotopic ratio of ^{238}U/^{235}U must be known. This number was assumed to be invariant at 137.88 for several decades but recent studies [1, 2] have shown that variations occur not only in terrestrial rocks but also in meteorites. In this study, we analysed six bulk angrite samples: three quenched angrites and three plutonic angrites, for their uranium isotopic ratios using the double-spike MC-ICPMS procedure after [3]. The ratios are reported relative to the recently published value of 137.837 ± 0.015 (2σ) for the uranium isotopic standard CRM145 [4]. The ^{238}U/^{235}U ratios for the analysed angrites are uniform within error of each other, ranging from 137.763-137.802. Analytical errors are 0.018-0.049 (2σ), depending on the sample size. These data, combined with ^{206}Pb-^{207}Pb analysis by TIMS, are used to revise previously reported Pb-Pb ages to values with a higher accuracy, leading to a more reliable early Solar System chronometer.

The causes of variations in the ^{238}U/^{235}U ratios in meteorites are currently debated, including the possible decay of extant ^{247}Cm to ^{235}U. Th and Nd are used as present day proxies for the extinct Cm. Therefore, the correlation between Th/U or Nd/U and uranium isotopic ratios is used to find evidence for the decay of ^{247}Cm in the early stages of the Solar System [1, 2]. In addition to ^{238}U/^{235}U values, we analysed the rare earth element (REE) pattern and the U and Th concentrations of the samples to determine the environment in which the meteorites formed and the plausibility for Cm being present during angrite formation.

[1] Brennecka *et al*. (2010) *Science* **327**, 449–451. [2] Amelin *et al*. (2010) *EPSL* **300**, 343–350. [3] Stirling *et al*. (2006) *EPSL* **251**, 383–397. [4] Richter *et al*. (2010a) *International Journal of Mass Spectometry* 295(1-2) 94–97.

Mineralogy of atmospheric particles deposited on cypress leaves close to a nuclear plant

R. KALTENMEIER[1]*, R. GIERÉ[1] AND L. POURCELOT[2]

[1]Albert-Ludwigs-Universität, D-79104 Freiburg, Germany (*correspondence: giere@uni-freiburg.de)
[2]Institut de Radioprotection et de Sûreté Nucléaire, Cadarache, F-13115 St Paul lez Durance, France

Enhanced activity of actinides and some decay products has been reported for the leaves of cypress trees (*Chamaecyparis nootkatensis*) at the edge of the Malvési uranium-processing facility, SW France. The enhanced activity is due to the release of actinides via the smokestacks and artificial ponds inside the facility. This study was conducted to characterize the particulate matter deposited on the leaf surfaces from the atmosphere and to investigate whether or not radioactive particles may be identified.

Air-dried leaf samples were examined by scanning electron microscopy (SEM), in combination with energy-dispersive X-ray spectrometry (EDX). The samples were scanned systematically in both secondary and backscattered electron modes. EDX spectra were collected from particles and from areas devoid of particles (background spectra). These background spectra as well as the signals resulting from the C or Au coating were taken into account for the interpretation of the qualitative EDX spectra of the individual particles trapped on the leaf surface.

Particles ranging in size from <200 nm to ~40 μm were found on most portions of the adaxial leaf surface, but they are especially abundant at the boundary between facial and lateral leaves. We classified the particles chemically according to the most prominent peaks in the EDX spectra, yielding the following five principal classes: carbonates, silicates, sulfates, oxides/hydroxides, and halides. Approximately 80% of all analyzed particles could be attributed to these five classes. In addition, other types of particles were found, including Fe alloys; scheelite-group phases; phosphates; sulfides; and fly ash spheres.

Of special interest are U-rich particles, which were identified as U oxides, except for one particle, which was an U-oxide-fluoride. Clearly, these particles were released into the atmosphere by the nuclear facility prior to their deposition on the leaf surfaces. As most of the U-rich particles are ≤1 μm across, they are respirable.

Once inhaled, particles containing alpha-emitting isotopes represent a potentially long-term source of ionizing radiation inside the lungs and thus, pose a threat to the health of the people living nearby.

https://doi.org/10.1180/S0026461X00006502 Published online by Cambridge University Press

Petrogenetic implications of two contrasting granite types in the Çataldag Plutonic Complex, NW Turkey

O. KAMACI* AND S. ALTUNKAYNAK

Department of Geological Engineering, Istanbul Technical University, 34469, Maslak, Istanbul, Turkey (omer.kamaci@itu.edu.tr)

In late Oligocene and Early Miocene time, western Turkey was the site of extensive magmatic activity that produced voluminous plutonic associations. This magmatic activity was followed the continental collision between the Sakarya continent and Tauride-Anatolide carbonate platform along the Izmir-Ankara-Erzincan suture zone prior to middle Eocene. The Çataldag plutonic complex (CPC), one of the biggest plutonic associations, is a composite intrusive body consisting of both I- and S type granitic intrusions of similar age. $^{39}Ar/^{40}Ar$ dating obtained from CPC yields ages between 20 and 22 Ma as their cooling ages. These two intrusive groups display different textural, structural and also geochemical features. S-type, peraluminous granitic intrusion in CPC is represented by synkinematic, sheet like bodies situated in the eastern border of the plutonic complex. It includes leucocratic two-mica granites and milonitic granites which show petrographical features indicating ductile shear zone deformation. They are composed of quartz, feldspar with minor biotite, muscovite, epidote and garnet. Combined petrographical and geochemical features of this group reveal crustal origin for their genesis. I type granitic intrusion is made up of granite and granodiorite-quartz diorite showing gradational contact to each other. This group is late kinematic weakly deformed intrusion and displays hipidiomophic granular and porphyric textures. Geochemically, it has medium to high-K calc-alkaline and metaluminous compositions. Major and trace element compositions, and Sr-Nd-Pb isotope data indicate collectively that the I type granitic group of CPC has been originated from hybrid magma (s) including mantle and crustal components. Geochronological and petrological findings combined with bimodal character of CPC suggest that CPC is synextensional and therefore there was a close spatial and temporal relations between magmatism and extensional tectonics during the late Cenozoic geodynamic evolution of Turkey.

A combined U/Pb and Hf-isotope study of up to 4.0 Ga detrital zircon from the Wyoming Province

BALZ S. KAMBER, MARTIN J. WHITEHOUSE AND JON D. WOODHEAD[1,2,3]

[1]Laurentian University, Sudbury, Ontario, Canada
[2]Swedish Museum of Natural History, Stockholm, Sweden
[3]School of Earth Sciences, Melbourne, Australia

An extensive dataset (n=750) of new zircon U-Pb dates is presented for two quartz-rich metasediments from the eastern Beartooth Mountains, northern Wyoming craton, Montana. Both rocks yielded detrital zircon dates with comparable age populations, ranging from just under 4.0 Ga to the likely deposition age of ca. 3.0 Ga. Among the Meso-, Paleo-, and Eoarchean zircon there are age groupings. The most prominent population occurs between 3200 and 3325 Ma, followed by less abundant groupings at 3500, 3625, 3725, 3850 and 3950 Ma. A representative selection of grains (n=50) were subsequently analysed for Hf-isotopes by *in situ* MC-ICP-MS. Of these, 44 grains define a clear linear array in a Hf-isotope evolution diagram. The oldest zircon have chondritic initial Hf-isotope composition, with all younger grains defining a clear trend towards less radiogenic compositions. At 3.25 Ga, this trend averages -12 E_{Hf}.

Whereas no rocks of Eoarchean age have yet been found in the Wyoming craton, Pb-isotope signatures of 2.8 Ga ganodiorites have long been known to require involvement of an ancient high U/Pb silicate source. This could have been subduction zone modified mantle or a cratonic substrate. We discovered inherited Mesoarchean zircon in the 2.8 Ga granodiorites and heterogenous Hf-isotopes in zircon from one granodiorite, collectively favoring the *in situ* existence of a cratonic nucleus from the Hadean/Archean boundary but with no isotopic evidence for involvement of even older crust.

In agreement with most other Eoarchean and Hadean detrital zircon occurrences, it appears that the oldest zircon-bearing lithologies of the Wyoming craton became part of the erosional cycle only after a very extensive (ca. 1 Ga) period of residence in the crust. The internal structures of the oldest studied zircon grains reveal repeated reworking, testifying to a long and complex thermal history of the crust. This is consistent with a model of an originally quite zircon-poor mafic crust, whose internal heat, generated by radioactive decay, led to episodic remelting and reworking into a more evolved upper crust in which zircon became more abundant and a more refractory, depleted lower crust.

https://doi.org/10.1180/S0026461X00006502 Published online by Cambridge University Press

Volatiles in the kimberlite melt – What drives ascent and causes explosive eruption?

V.S. KAMENETSKY

School of Earth Sciences and CODES, University of Tasmania, Australia (Dima.Kamenetsky@utas.edu.au)

Existing reconstructions of the kimberlite melt emphasise carbonate-bearing ultramafic compositions with significant amounts of dissolved volatiles CO_2 and H_2O (10-20 wt%). These volatiles are considered to be a major factor in reducing viscosity of the kimberlite melt, governing fast ascent from mantle depths. The exsolution of these volatiles from the melt during ascent and emplacement is viewed as being responsible for violent eruption of the magma and related brecciation of country rocks and the kimberlite itself. Magmatic volatiles and groundwaters have an unequivocal role in present models of kimberlite emplacement (fluidisation and phreatomagmatism, respectively).

Studies of the diamondiferous Udachnaya-East pipe (Siberia) kimberlites [1-3] show that neither of major magmatic volatiles in the form of degassing fluids was responsible for well-known 'explosivity' of kimberlites. Exceptionally fresh kimberlites from the Udachnaya-East pipe have low H_2O (<0.5 wt%), but high CO_2 (up to 14 wt%), Cl and alkalis. The carbonatite-chloride composition of the Udachnaya-East kimberlite [1, 2] and similar compositions in olivine-hosted melt inclusions in other kimberlites worldwide [4] strongly support the previously assumed low viscosity and density of kimberlite magmas. Massive degassing of H_2O and CO_2 is unlikely in the case of the Udachnaya-East kimberlite, because the melt is poor in H_2O, whereas CO_2 is bonded in the carbonatitic melt. After crystallisation of olivine the kimberlite melt evolves towards essentially dry carbonate-chloride compositions [3]. The gravitational separation of silicate solids within the kimberlite pipes drives light, low viscosity carbonate-chloride melt to the top. The hydrogen species, such as H_2 and CH_4, some of magmatic origin, but mostly produced by post-magmatic serpentinisation of olivine in the kimberlite, are the main cause of explosions. Detonation of these gases at near-surface levels of the pipe can result in brecciation and even evacuation of already solid kimberlite and country rocks.

[1] Kamenetsky *et al*. (2004) *Geology* **32**, 845–848.
[2] Kamenetsky *et al*. (2007) *Chem. Geol*. **237**, 384–400.
[3] Kamenetsky *et al*. (2008) *J.Petrol*. **49**, 823–839.
[4] Kamenetsky *et al*. (2009) *Lithos* **112S**, 334–346.

Real composition of the Earth's lower mantle

FELIX V. KAMINSKY

KM Diamond Exploration Ltd., 2446 Shadbolt Lane, West Vancouver, BC, V7S 3J1 Canada (felixvkaminsky@cs.com)

Real composition of the Earth's lower mantle is based on a study of mineral inclusions in lower-mantle diamond from Brazil, Guinea, Canada and Australia. Three associations were established among them: juvenile ultramafic, analogues to eclogitic, and carbonatitic. The juvenile ultramafic association strongly predominates; it is composed of ferropericlase, MgSi-, CaSi- and CaTi-perovskites, stishovite, tetragonal almandine-pyrope phase (*TAPP*), and some others. The mineralogical composition of the lower mantle is now understood to be more complex than had been suggested in theoretic and experimental works. The frequencies of the lower mantle minerals for all areas are similar to each other, deviating from the average by only 10-15 %.

These figures differ drastically from the composition of the lower mantle as suggested from experimental data. In that the most common mineral is ferropericlase, which comprises 48.0-63.3 % (average 55.4 %) of all minerals in the lower mantle. This is in contrast to an abundance of ~ 18 % as suggested by experimental data, i.e. approximately three times higher. In contrast to ferropericlase, MgSi-perovskite comprises, in all studied regions, only 5.0-10.2 % (average 7.5 %), i.e. approximately ten times lower than has been suggested as an average composition in the lower mantle (~ 77 %); and its composition is more iron-rich (mg = 0.36-0.90) as compared to experimental and theoretical data. CaSi-perovskite, according to geological data, is more than twice as common compared to experimental data (10.0-14.3 % with an average of 12.0 % against ~ 5 %). The most important feature of the real composition of the lower mantle is a permanent presence, in all regions and areas, of free silica (as stishovite), in the lower mantle. Stishovite frequency, among the lower mantle minerals, is 2.1-15.0 % (average 8.4 %). The other minerals (CaTi-perovskite, *TAPP*, a phase with the composition of that of olivine, spinel, ilmenites, titanite, native nickel and iron, magnetite, and sulphides), have frequencies 0.1-4.3 % each. These discrepancies suggest that the composition of the lower mantle differs to that of the upper-mantle, and experiments based solely on 'pyrolitic' compositions are not, therefore, applicable to the lower mantle. These data indicate a probability of an alternative to the CI-chondrite model of the Earth's formation, for example, an enstatite-chondrite model.

https://doi.org/10.1180/S0026461X00006502 Published online by Cambridge University Press

Short-term CO_2-fluid-mineral interactions in a CO_2 injection experiment, Wyoming

N. KAMPMAN[1]*, M.J. BICKLE[1], A. GALY[1], H.J. CHAPMAN[1], Z. ZHOU[2], B. DUBACQ[1], M. WIGLEY[1], O. WARR[2], T. SIRIKITPUTTISAK[2] AND C.J. BALLENTINE[2]

[1]Dept. Earth Sciences, Downing Street, Cambridge CB2 3EQ, UK (*correspondence: nkam06@esc.cam.ac.uk)
[2]University of Manchester, M13 9PL, UK

During geological CO_2 storage short-term geochemical processes will be dominated by dissolution of CO_2 into the formation fluid and by the reaction of this acidic fluid with soluble minerals (e.g. carbonate, oxide, sulphide and organics) in the reservoir. Modelling the progress of the fluid-mineral reactions is frustrated by uncertainties in the absolute mineral surface reaction rates [1] and the significance, in natural systems, of CO_2 dissolution and transport in formation fluid as an overall rate limiting step.

We present preliminary results of water chemistry from an artificial noble gas tracer study in a commercial CO_2-EOR reservoir located in Wyoming, USA. In this study a noble gas spike (^{3}He & ^{129}X) was introduced to a single CO_2 injection well [2], and fluids and gases collected from the surrounding four-point production well pattern, from September 2010 to February 2011. Preliminary results from fluid chemistry measured over this period reflect: (1) mobilization and mixing of formation water, driven by the injection of CO_2; (2) the arrival of co-injected water and CO_2 at the production wells and; (3) dissolution of the CO_2 and subsequent reaction of this acidified fluid with soluble minerals in the reservoir. The spatial changes in fluid chemistry are consistent with the reservoir geology; the updip producers are dominated by processes related to the early arrival of the CO_2 front whereas changes in downdip fluid chemistry are dominated by the arrival of dense saline fluid from the injection well. Sigmoidal fronts in fluid chemistry are observed in the updip production wells, and correlate with changes in fluid temperature, a measure of CO_2 breakthrough. Elevated concentrations of divalent cations (Ca^{2+}, Mg^{2+}, Sr^{2+}, Fe^{2+} and Mn^{2+}), in excess of the original pore fluid and injected water, are thought to represent dissolution of carbonate minerals in the reservoir which drives neutralization of fluid acidity and progressively increasing fluid alkalinity.

[1] Kampman *et al*. (2009) *Earth Planet. Sci. Lett*. **284**, 473-488. [2] Zhou *et al*. (2011) This issue.

Multiple sulfur isotope fractionation during sulfur cycling in a warm, monomictic lake with sub-millimolar sulfate concentration

A. KAMYSHNY, JR.[1,2]*, W. ECKERT[3], J. GUN[4], O. LEV[4], A.L. ZERKLE[5], Z.F. MANSRAY AND J. FARQUHAR[2]

[1]Max Planck Institute for Marine Microbiology, Celsiusstrasse, 1, 28359, Bremen, Germany (*correspondence: alexey93@gmail.com)
[2]Department of Geology, University of Maryland, College Park, 20742, MD, USA
[3]Kinneret Limnological Laboratory, Israel Oceanographic and Limnological Research Ltd., P.O. Box 447, Migdal, 14950, Israel
[4]The Institute of Chemistry, The Hebrew University of Jerusalem, Jerusalem, 91904, Israel
[5]School of Civil Engineering and Geosciences, Newcastle University, Drummond Building, Newcastle upon Tyne, NE1 7RU, England, UK

Sub-millimolar concentrations of sulfate likely prevailed in the Archean Ocean. We studied the concentrations and quadruple isotope fractionation of sulfur species in the warm, monomictic Lake Kinneret (Tiberias), which has sulfate concentrations of <600 μM. The highest concentrations of zero-valent sulfur (ZVS), thiosulfate and sulfite occurred in the redox-transition zone (RTZ, c. a. 28 m depth), and were 5.0 μM, 1.35 μM and 0.76 μM, respectively.

In the vicinity of the RTZ, the δ^{34}S fractionations between sulfide and sulfate are small (-17 – -21‰), with large positive Δ^{33}S values (0.067 – 0.086 ‰), and can be attributed to sulfate reduction. ZVS is 0.1 – 4.7‰ more enriched in ^{34}S than sulfide, consistent with equilibrium isotope effects between sulfide – polysulfide – rhombic sulfur and fractionation via phototrophic sulfide oxidation.

In the deeper waters, δ^{34}S fractionations between sulfide and sulfate are larger (-37 – -44‰), with smaller differences in Δ^{33}S (0.009 – 0.073‰). Sulfur isotope values near the bottom of the lake can be explained by a combination of sulfate reduction and sulfur compounds disproportionation. High sulfur isotope fractionation is supported in this system even at very low sulfate concentrations by both the absence of sulfide scavenging by dissolved Fe (II) and the presence of the RTZ, where sulfide oxidation supplies zero-valent sulfur to deeper sulfidic waters.

https://doi.org/10.1180/S0026461X00006502 Published online by Cambridge University Press

Mineralogical and geochemical studies of the metasomatic rocks within Gachin, Kalat, Pohl and Hormuz Island salt plugs, Iran

A. KANANIAN[1], S. TAGHIPOUR[1], R. NEMATI[1] AND M.A. MACKIZADEH[2]

[1]School of Geology, College of science, University of Tehran, Tehran, Iran (kananian@khayam.ut.ac.ir)
[2]Mineralogy Department, College of Science, University of Isfahan, Isfahan, Iran (ma_mackizadeh@yahoo.com)

The Gachin, Kalat, Pohl and Hormuz Island salt domes are located in the Bandar Abbas province. They are a part of the Hormuz formation which situated in the Iran-Pakistan salt basin. The studied area centered at 25 ° 24´-27 ° 08´ N and 53 ° 55´-59 ° 15´ E at the geology map of the area [4]. The studied area is composed of some Infracambrian–Cambrian igneous and evaporites rocks. The igneous rocks composed of mafic to felsic composition and involve basalt, andesite, rhyolite, rhyolitic tuff and some hypabyssal bodies and occur in the within plate continental rift. On the basis of petrographic studies mineral assemblage has formed in magmatic (I) and metasomatic (II) stages. Clinopyroxene, amphibole, biotite, plagioclase, feldspar and quartz is the main magmatic minerals. Tremolite-actinolite, garnet, albite, epidote, sphen have occur in the metasomatic stage. According to the EPM analysis the chemical composition of the pyroxene is salite-frrosalite to augite. The composition of garnet is andradite-grossular ($An_{29.21}$ $Gros_{70.78}$), feldspar is albite ($An_{4.03}$-$Ab_{95.36}$-$Or_{0.60}$), epidote is pistachit. Clinopyroxene thermo-barometers range from 1060≤ T≤1290 °C and 1 ≤ P≤10 kbar [5], also chlorite [3] and plagioclase [2] geothermometer yielded a temperature of 330 °C and 500 °C for them respectively. Fluid inclusion studies have documented vapor bubbles, fluid and solid (cube halite) inclusions in the hydrothermal vein quarts. The salinity of the studied samples is 35-45 wt % NaCl and the homogenization temperature range 205 °C-320 °C. Fluid inclusion data on the salinity-temperature diagram [1] have plotted on the mixing magmatic-meteoric field. On the basis of field, petrography, mineral chemistry, thermo-barometery and fluid inclusion data we could proposed following conclusions:

At first stage, magmatic and evaporate rocks have formed in the within plate continental crust in the striking an aborted rift. At latter stage, meteoric water entering igneous-evaporite assemblage and a hydrothermal system has created so Na, Ca, Fe metasomatism occurred in the system and metasomatic minerals have formed.

[1] Beane (1983) *The magmatic-meteoric transition*. Geothermal Resources Council. Special Report. **13**, 245-253. [2] Benisek *et al*. (2010) *Contrib Mineral Petrol* **160**:327–337. [3] Cathelineu *et al*. (1985) *Contrib. Mineral. Petrol*., **91**, 235-244. [4] Kent (1970) *Journal of petroleum Geology*, **2**, 117-144. [5] Nimis (2000) *Contrb. Mineralo. Petrol*., **139**, 541-554.

Carbon cycling in the Pliocene Velenje Coal Basin, Slovenia, inferred from stable carbon isotopes

T. KANDUČ[1,], S. ŽIGON[1], M. MARKIČ[2], S. ZAVŠEK[3] AND J. MCINTOSH[4]

[1]Jožef Stefan Institute, Jamova 39, 1000 Ljubljana, Slovenia (*correspondence: tjasa.kanduc@ijs.si)
[2]Geological Survey of Slovenia, Dimičeva 14, SI-1000 Ljubljana, Slovenia
[3]Velenje Coal Mine, Partizanska 78, 3320 Velenje, Slovenia
[4]University of Arizona, Department of Hydrology and Water Resources, 1133 E. James E., Rogers Way, Tucson, Arizona

Introduction

In this study, stable isotopes of carbon were used to trace organic and inorganic carbon cycles and biogeochemical processes, especially methanogenesis within different geological media of the Pliocene lignite-bearing Velenje Basin in northern Slovenia. The study is based on investigations of carbon isotopic composition of the following geological media: 1) lithotypes of lignite, 2) coalbed gasses, 3) calcified woods and carbonate-rich sediments, and 4) groundwaters in various aquifers.

Discussion of Results

For different lignite lithotypes it was found that $\delta^{13}C$ values ranged from -28.1 to -23.0‰, the variability is being a consequence of original isotopic heterogeneity of the source plant ingredients and of biogeochemical processes (gelification, fusinitization, mineralization of organic matter). In the lignite seam the major gas components were found to be CO_2 and CH_4 with small amounts of N_2. The carbon isotope compositions of carbon in CO_2 ($\delta^{13}C_{CO2}$) and CH_4 ($\delta^{13}C_{CH4}$) were very variable and ranged from -9.7 to 0.6‰ and from -70.5 to -34.2‰, respectively. The presence of thermogenic gases is unlikely due to the low rank of the coal and lack of higher chain hydrocarbons. Calcified xylite enriched with ^{13}C ($\delta^{13}C$ values up to 17.1‰) indicated that CO_2 reduction process was present at the time of formation of the basin. The $\delta^{13}C_{DIC}$ values (from -17.4 to -3.2‰) of groundwaters recharging the basin from the Triassic aquifer were consistent with degradation of organic matter and dissolution of dolomite. Groundwaters from the Pliocene sandy and Lithotamnium carbonate aquifers had $\delta^{13}C_{DIC}$ values (from -9.1 to 0.2‰) suggestive of degradation of organic matter and biogenic CO_2 reduction.

https://doi.org/10.1180/S0026461X00006502 Published online by Cambridge University Press

Physical and chemical state of Fe-phases in Chinese aeolian dust

MAKOTO KANEKO[1], YUKI NAKAMATSU[1], ZHOUQING XIE[2] AND SATOSHI UTSUNOMIYA[1]*

[1]Department of Chemistry, Kyushu University, Fukuoka 812-8581, Japan (utu@chem.rc.kyushu-u.ac.jp)
[2]University of Science and Technology of China

Iron supplied by aeolian dust is a factor controlling the biomass of phytoplankton in high nutrient low chlorophyll (HNLC) regions, and dissolved Fe-stimulated biogeochemical activity can consume a large amount of CO_2 in atmosphere, which may have a significant impact on the global C-cycle. In order to understand the physical and chemical state of Fe in the asian dusts, aerosol samples collected in Fukuoka, Japan and Hefei, China in March 2010 have been investigated in detail from nano to bulk scale. The analytical techniques include an inductively coupled plasma mass spectrometry (ICP-MS), X-ray diffraction (XRD), scanning electron microscopy (SEM), and transmission electron microscopy (TEM). A sequential extraction of the Fe-phase was also perfomed based on the previous method [1].

The Fe concentrations in the Hefei and Fukuoka samples during the dust event are 11.8 and 4.31 times higher than that in the Fukuoka sample in the non-dust period. The fraction of Fe-phase (in wt.% = mass of Fe in each Fe-phase/total mass of Fe) in the Fukuoka dust samples determined by the sequential extraction is Fe-bearing sheet silicate (59-61 %), hematite and goethite (23-28 %), ferrihydirte (7.5-12 %), magnetite (3.0-4.3 %). The XRD pattern indicates that illite and chlorite are the major Fe-bearing minerals in all samples. TEM observation reveals that aggregates of nano-sized ferrihydrite are present on the surface of illite.

Based on the the solubilities of clays (4 %) and Fe oxides (<1 %) reported in the previous study [2] combined with our data, it is suggested that the clay minerals in the Chinese dust contribute predominantly to the Fe flux to the HNLC, which can potentially supply >6 times greater amount of Fe than that from Fe oxides [2]. It should be also noted that the ~10 % of Fe present as ferrihydrite may be an important contribution because it is readily consumed by some photosynthetic algae species [3]. Still, quantitative investigation of highly bioavailable and soluble minerals in dust materials such as demonstrated in the present study should be essential to the appropriate evaluation of the impact of atmospheric Fe input into HNLC region.

[1] Poulton & Canfield. (2005) *Chem. Geol.* **214**, 209–221. [2] Journet *et al.* (2008) *Geophys. Res. Lett.* **35**, L07805. [3] Wells *et al.* (1983) *J. Mar. Res.* **41**, 731-746.

Uniqueness of kimberlite magma: Its source characteristics and transportaion systems revealed by isotope signatures

ICHIRO KANEOKA

Earthquake Research Institute, University of Tokyo, Tokyo 113-0032, Japan (ikaneoka@aol.com)

Since kimberlite magma carries diamonds as xenoliths, it has been regarded to be formed at a depth of at least more than 150km and extruded to the surface within a few hours from the bottom of continental lithosphere. Based on Sr-Nd isotope systematics, kimberlites are classified into Group I and Group II [1]. Among them, Group I kimberlites show especially significant isotope signatures, which would reflect quite unique source characteristics and transportaion systems.

In the Sr-Nd and Nd-Hf isotope diagrams expressed as delta values, Group I kimberlites from different sites cluster close to the Bulk Earth values [2], while chondrite-normalized REE patterns show highly fractionated trend with L-REE enrichment. This implies that such high L-REE enrichment in a kimberlite magma should have occurred in the latest stage of magma transportaion system before eruption. To explain such high enrichment of L-REE, very small amount of partial melting of less than 1% is required. On the other hand, cluster of isotope signatures in Sr-Nd and Nd-Hf diagrams needs homogenization of magma source materials. Those isotope values mentioned above are often regarded to be a result of mixture between depleted (asthenosphere) and enriched (lithosphere) components. However, it seems quite difficult to attribute the cluster of isotope values of kimberlites with different sites and times to the process of small degree of partial melting. Our findings of high $^3He/^4He$ for Greenland kimberlites [3] and Ne isotope systematics for Russian kimberlites [4] definitely suggest that kimberlite (Group I) magma source materials have similar isotope sigantures with those of OIBs and would possibly be located in the lower mantle. Although He and Ne isotopes show a sign of interaction with lithospheric components before eruption, it would be only effective for He and Ne due to their higher diffusivity compared to that of solid elements. Hence, the cluster of Sr, Nd, Hf isotopes of kimberlites (Group I)would reflect the chratacteristics of source materials of magma in the less fractionated deep mantle.

[1] Smith, C.B. (1983) *Nature* **304**, 51–54. [2] Norwell, G.M. *et al.* (2004) *J. Petrology* **45**, 1–29. [3] Tachibana, Y. *et al.* (2006) *Geology* **34(4)** 273–276. [4] Sumino, K. *et al.* (2006) *Geophys. Res. Lett.* **33**, L16318.

https://doi.org/10.1180/S0026461X00006502 Published online by Cambridge University Press

Seasonal distribution and effects of herbicides on coral reefs around Okinawa, Japan

A. KANESHIRO[1], H. FUJIMURA[1]*, T. OOMORI[1], S. GIMA[1], T. HIGUCHI[2], B.E. CASARETO[2], Y. SUZUKI[2] AND T. SAGAWA[3]

[1]Univ. of the Ryukyus, 1 Senbaru, Nishihara, Okinawa 903-0213, Japan (*correspondence: fujimura@sci.u-ryukyu.ac.jp)
[2]Shizuoka Univ., 836 Ohya, Suruga-ku, Shizuoka-shi, Shizuoka 422-8529, Japan
[3]WWF Coral Reef Conservation and Research Centre, 118 Shiraho, Ishigaki, Okinawa 907-0242, Japan

Introduction

It is apprehensive about future degradation of coral reef caused by artificial chemicals such as herbicide and pesticides. Diuron [N'-(3, 4-dichlorophenyl)-N, N-dimethylurea] is one of the active substance contained in a herbicide. The used amount of diuron in Okinawa is the second highest in Japan [1]. Moreover, diuron has been using recently for antifoulant of ships as a replacement for organotin compounds. We investigated seasonal variation of herbicide contained in water and sediment around coral reef area in Ishigaki Island in Okinawa Japan, and carried out experiments to see the effect of the herbicide on coral metabolisms of photosynthesis and calcification.

Materials and Methods

Samples from twelve stations in the Shiraho lagoon and five in the Todoroki river were taken seasonally from August 2010 to May 2011. Diuron and other active substances were extracted using a solid-phase column and measured with a liquid chromatography with tandem mass spectrometry (LC–MS/MS).

Results and Discussion

Higher diuron of 222 ng/L was detected at the headwater of the Todoroki river in August. It decreased to 85 ng/L toward the river mouth. However, diuron in seawater and sediments at lagoon were significantly low level compared to the river. Because herbicide is mainly used in July to September in Okinawa and ground water from the catchment area flows geometrically to the headwater, the highest concentration was detected during summer season. The concentration in the lagoon has not reached to the level at which metabolic activity of coral colony is degraded.

[1] Sheikh *et al*. (2008) *Mar. Pollut. Bull*. **58**, 1922–1925.

Coral records of ocean acidification and physiological processes in the southern Great Barrier Reef

J.O. KANG[1,3]*, M.T. MCCULLOCH[2,3], S.M. EGGINS[1], M.K. GAGAN[1] AND G.E. MORTIMER[1]

[1]Research School of Earth Sciences, Australian National University, Canberra, ACT 0200, Australia (*correspondence: jung.kang@anu.edu.au)
[2]School of Earth and Environment, University of Western Australia, Crawley, WA 6009, Perth, Australia
[3]ARC Centre of Excellence in Coral Reef studies, Australia

Ocean acidification, the process of declining seawater pH due to increased uptake of CO_2 from anthropogenic emissions, is likely to have severe impacts on marine calcifiers and related ecosystems. However, long-term records of ocean acidification from marine biota have rarely been evaluated. Here, we present high-resolution records of boron isotopic compositions ($\delta^{11}B$) as a paleo-pH proxy and calcification rates from two *Porites* corals (over 150 year old) from the southern limits of the Great Barrier Reef, Australia.

Carbon isotopes ($\delta^{13}C$) and trace element ratios (Mg/Ca and Sr/Ca) were also determined. The results from coral boron isotopic systematics show the obvious impact of enhanced uptake of anthropogenic CO_2 on the ocean chemistry, resulting in a trend of decreasing seawater pH (-0.0016 ± 0.0002 pH unit yr^{-1}) and decreasing $\delta^{13}C$ compositions (-0.015 ± 0.002 ‰ yr^{-1} since 1960) due to fossil fuel burning (Suess effect). Ocean warming is also observed in the coral skeleton Sr/Ca record with slightly increased measured annual calcification from both corals during the observed period. This indicates that warming of the surface oceans may be countering the effect of decrease in carbonate ion concentration on coral calcification rates. Evidence of kinetic effects during coral calcification was also found in the long-term record; strong negative and positive correlation of coral growth with detrended $\delta^{13}C$ and Mg/Ca. This suggests that CO_2 hydroxylation is a dominant reaction in high calcifying conditions resulting in depleted $\delta^{13}C$. Also higher rate of coral growth could generate the kinetic effect on Mg partitioning and lead to greater incorporation into the aragonite skeleton of corals.

https://doi.org/10.1180/S0026461X00006502 Published online by Cambridge University Press

Validation of saltation flux parameterization with observation

J.-Y. KANG[1]*, M. MIKAMI[1], Y. SHAO[2], S.-C. YOON[3], T.Y. TANAKA[1] AND T.T. SEKIYAMA[1]

[1]Meteorological Research Institute, Tsukuba, Ibaraki, 305-0052, JAPAN (*correspondence: jykang@mri-jma.go.jp)
[2]University of Cologne, Cologne, D-50923, GERMANY (yshao@meteo.uni-koeln.de)
[3]Seoul National University, Seoul, 151-747, KOREA (yoon@snu.ac.kr)

Introduction

The estimation of natural dust emission amount is important to understand the effects of dust on climate. Many dust emission parameterizations have been developed and it is required to investigate emission parameterizations and validate them with observation data.

Results and Discussion

In this study, the saltation flux formulation given by White [1] is used and it is as follows:

$$Q=C\times\rho_a/g\times u_*^3\times(1-u_{*t}/u_*)\times(1+(u_{*t}/u_*)^2)$$

where C is coefficient, ρ_a and g are air density and gravity, respectively, and u_* is friction velocity, u_{*t} is threshold friction velocity. The White equation [1] is compared with observation data collected during the Japanese Australian Dust Experiment (JADE) [2]. The coefficient C is obtained by the iterative method to make the difference between observed and calculated fluxes minimize. Figure 1 shows the comparison of calculated flux using new linear coefficient with observation data. The result indicates that the saltation flux equation has a good ability to predict sand flux with tuning the linear coefficient only.

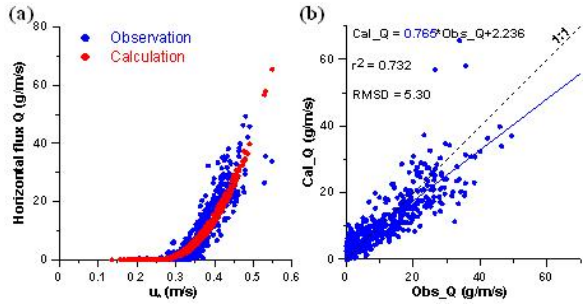

Figure 1: (a) Observed and calculated Q with friction velocity, (b)Scatter plot of observed Q versus calculated Q.

[1] White (1979) *J. Geophys. Res* **84**, 4643–4651. [2] Ishizuka *et al.* (2008) *J. Geophys. Res* **113**, D24212.

Geochronology and geochemistry of Hongqilapu granite in eastern Pamirs, China

LEI KANG, PEI-XI XIAO, XIAO-FENG GAO, REN-GANG XI, ZENG-CAN DONG AND LEI GUO

Xi'an Center of Geological Survey (Xi'an Institute of Geology and Mineral Resource), CGS, Xi'an, Shaanxi 710054, China (kang844@163.com)

Hongqilapu granite is distributed in the boundary of China and Pakistan, composed o f granodiorite and quartz dioite which developing dioritic enclave. The granite belongs to the sub-aluminum to peraluminous and calc-alkali series, and is characterized by rich in Al, Fe, Ca, and LILEs (Rb, Ba, Th), poor in Hf, Zr, Y, Yb. In particular, partial rock have the geochemistry character of adakite, such as SiO_2= $60.41\times10^2\sim72.02\times10^2$, $A1_2O_3$=$15.53\times10^2\sim16.13\times10^2$, MgO=0.66 $\times10^{-2}\sim2.56\times10^6$, Y=$9.61\times10^6\sim18\times10^6$, Yb=$0.8\times10^6\sim1.44\times10^6$, Sr=$393\times10^6\sim560\times10^-$, riching LREE, HFSEs' (Ti, Nb, Ta)content is as much as, Eu have negative anomaly faintly. In addition, these rocks' $K_2O/Na_2O>1$ and Sr-Y×10-Zr diagram show that them belong to C-form adakite with high kalium, proving that Hongqilapu granite is the production of thickened lower crust partial melting. LA-ICP-MS zircon U-Pb dating of the granite indicate that the weighted mean $^{206}Pb/^{238}U$ age are 107.20±0.76Ma (n=29, MSWD=1.09), which belongs to Early Cretaceous Epoch. In conclusion, these information show Bangonghu-Nujiang ocean basin of Neotethys had closed earlier than lower cretaceous, which provide a new valuable information on the time limit of colliding between Gangdise block and Qiangtang massif.

https://doi.org/10.1180/S0026461X00006502 Published online by Cambridge University Press

The Paleozoic minimum in $^{87}Sr/^{86}Sr$ ratio in the Capitanian (Middle Permian): Records from the mid-Panthalassa paleo-atoll limestones

T. KANI[1]*, D. KOFUKUDA[2] AND Y. ISOZAKI[2]

[1]Dept. of Earth Sci., Kumamoto Univ., Kumamoto, 860-8555, Japan (*correspondence: kani@sci.kumamoto-u.ac.jp)
[2]The University of Tokyo, Meguro, Tokyo 153-8902, Japan

We report a detailed secular change of the Middle-Late Permian seawater $^{87}Sr/^{86}Sr$ ratio with the unique 'Permian minimum' interval detected in mid-Panthalassa (superocean) paleo-atoll carbonates. The analyzed limestones at Kamura and Akasaka sections in Japan occur as exotic blocks within the Jurassic accretionary complex. On the basis of fusuline biostratigraphy, both sections span across the Middle-Upper Permian or the Guadalupian-Lopingian (G-L) boundary characterized by a major biotic crisis. Two sections are separated from each other for 500 km at present, thus were likely derived from different paleo-seamounts existed in mid-Panthalassa.

A 30 m-thick interval with low $^{87}Sr/^{86}Sr$ value (< 0.7070) was detected in the Capitanian (Upper Guadalupian) interval, i.e. the *Yabeina* (fusuline) Zone, *Lepidolina* Zone, and the barren interval in the Kamura section. Data from Akasaka section comfirm that extremely low $^{87}Sr/^{86}Sr$ values (0.70688) similarly characterize the *Yabeina* Zone and the barren interval. A remarkable rise in $^{87}Sr/^{86}Sr$ values for 0.00073 up to 0.70761 occurred in the barren interval after the 'Permian minimum' in both sections, suggesting a general isotopic trend in the superocean. This increase in Sr isotope after the 'Permian minimum' likely suggests that a huge amount of highly radiogenic terrigenous clastics have been shed into Panthalassa by connecting intra-Pangean drainage systems directly to the superocean. The development of the new drainage systems might be related to large-scale continental rifting, thus the initial breakup of Pangea. It is noteworthy that carbonate stable carbon isotope ratio ($\delta^{13}C_{carb}$) also shifted dramatically in the latest Capitanian barren interval immediately before the G-LB.

Fe(II) oxidation under very low O_2 conditions: New rate law and its implication

YOSHIKI KANZAKI* AND TAKASHI MURAKAMI

Department of Earth and Planetary Science, the University of Tokyo, Tokyo 113-0033, Japan
(*correspondence: kanzaki@eps.s.u-tokyo.ac.jp)

Many geological proxies point the great rise of atmospheric oxygen in the Paleoproterozoic (Great Oxidation Event). The proxies including mass independent fractionation in sulfur isotopes reveal that atmospheric oxygen increased from very low concentration (< ~10^{-6} atm of pO_2) to low concentration (> ~10^{-3} atm of pO_2) between 2.5 and 2.0 Ga. However, many of the proxies are useful for deciphering the timing of the transition in pO_2 levels rather than its quantitative pattern. On the other hand, paleosols formed during the Paleoproterozoic have recorded the ratios of Fe (III)/Fe (II) at the time of their formation and these kinetical data can give more quantitative estimates of pO_2. To quantitatively estimate pO_2 through the ratios of Fe (III)/Fe (II), the rate law of Fe (II) oxidation should be understood.

Experimental data of Fe (II) oxidation have been obtained under the conditions of $pO_2 = 10^{-3}$ - 10^{-5} atm and pH = 7.57 - 8.12. Combined with previous oxidation data at $pO_2 > 10^{-3}$ atm, newly discovered is that the rate law changes its form from $d[Fe(II)]/dt = -k[Fe(II)][OH^-]^2[O_2]$ at $pO_2 > \sim 5 \times 10^{-3}$ atm to $d[Fe(II)]/dt = -k'[Fe(II)][OH^-]^2[O_2]^{0.55}$ under the conditions of $pO_2 = 5 \times 10^{-3}$ - 10^{-5} atm.

In interpretation of this new rate law, especially the change in the power of $[O_2]$ from 1 to 0.55, we suggest that under the very low O_2 conditions intermediate oxygen species (superoxide, hydrogen peroxide and hydroxyl radical) attack Fe (II) more effectively, which results in faster Fe (II) oxidation rate than previously considered. Out of possible reactions that produce oxygen species from oxygen, the reaction,

$$O_2 + (18/11)H_2O = (16/11)H_2O_2 + (4/11)HO_2$$

gives the power of $[O_2]$ of 0.55. Combination of this reaction and those proposed by Haber and Weiss reproduces the experimental results well under the conditions of 10^{-5} - 0.2 atm of pO_2.

The new rate law was applied to the ratios of Fe (III)/Fe (II) of paleosols formed during the Paleoproterozoic, revealing that atmospheric oxygen increased gradually, linearly on the logarithmic scale, from < ~ 10^{-6} to > ~ 10^{-3} atm of pO_2 between 2.5 and 2.0 Ga.

https://doi.org/10.1180/S0026461X00006502 Published online by Cambridge University Press

Primary structures, petrography and geochemistry of Deccan flood basalts at Anantagiri Hills, Andhra Pradesh, India

ARCHANA B. KAOTEKWAR* AND S.N. CHARAN

National Geophysical Research Institute (CSIR) Hyderabad-500007, India
(*correspondence: archana.ngri@gmail.com)

The Cretaceous age Deccan flood basalts of Anantagiri Hills in south India represented by six lava flows show formation of columnar joints as the most conspicuous feature in each basalt flow unit. These flow units, exhibiting columnar structures, enable division into three well defined zones namely: Lower Colonnade Zone (LCZ); Middle Entablature Zone (MEZ) and Upper Colonnade Zone (UCZ). The columns in UCZ are five sided; MEZ separating the UCZ and the LCZ displays four sided intersecting, fanning and fragmented columns while the underlying LEZ has four to five sided vertical columns. These basalts show a mild affinity towards basaltic andesite on the TAS (Na_2O+K_2O vs. SiO_2) diagram, while in the Al-Fe+Ti-Mg ternary plot these basalts plot in the iron rich tholeiitic field. The major and trace element signatures of these tholeiitic basalts are similar to that of the Ambenali Formation basalts, suggesting possible extension of this Formation in SE Deccan Volcanic Province. REE plots define a nearly flat pattern with mild LREE enrichment and negative Eu anomaly. Primitive mantle normalized multielement patterns show mild LREE, LILE troughs positive Ba, Nb and Pb peaks and negative K, Sr and P anomalies in similarity with plume type CFB'S. The well developed sequence of colonnade structures in the different basalt flow units in Anantagiri Hills appear to have formed due to conductive cooling initiated both from the top and bottom portions of these flows. Geochemical signatures shown by these tholeiitic basalt flows suggest that the precursor was probably generated by low degree partial melting of an enriched mantle source.

Ectomycorrhizal fungi and silicate mineral weathering: Characterising nanoscale interactions using AFM

D. KAPITULČINOVÁ*, R.C.T. HOWE, S. JACKSON, S.A. GAZZE AND TERENCE J. MCMASTER

H.H. Wills Physics Laboratory, University of Bristol, Bristol, BS8 1TL (*correspondence: glxdk@bristol.ac.uk)

Ectomycorrhizal (ECM) fungi substantially affect mineral weathering [1, 2]. In order to understand the nanoscale processes occurring at the fungi-mineral interface, we have used Atomic Force Microscopy (AFM) to investigate the interactions of three *Suillus* ECM fungi, *S. bovinus*, *S. luteus* and *S. variegatus*, with sheet silicate minerals.

After 2-3 months of incubation under controlled laboratory conditions, the fungal hyphae and the mineral surface were imaged to nanometre resolution. To assess the effect of the fungi-mineral interaction on the mineral surface, a cleaning procedure was applied to biotite flakes colonised with *S. luteus*; this removed the organic material and exposed the 'reacted' mineral surface for further analysis. The cleaning protocol was also perfomed on a biotite control.

Our results show that all three *Suillus* species generate a large amount of organic material, forming typically a 1-5 nm thick coating on the mineral surface extending over many tens of microns. We have previously observed a similar 'biolayer' with *Paxillus involutus* [3]. AFM images of the cleaned biotite surface (Fig 1a), and the control biotite surface (Fig. 1b), show that both displayed a domain-like surface morphology. However, only on the fungi-colonised surface were round pits found, about 100 nm across and 5 nm in depth (Fig. 1a). These results indicate that the surface pitting is linked to the colonisation of the mineral with *S. luteus*.

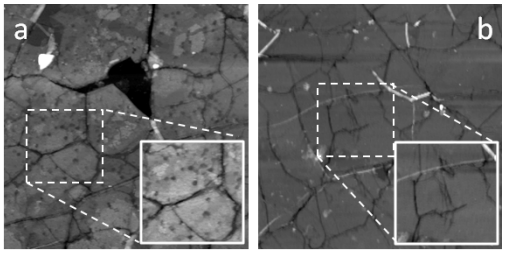

Figure 1: AFM images of a cleaned biotite surface: a) previously *Suillus luteus* colonised flake, note the pitting; b) control flake; field of view 8×8 μm, inserts 2.5×2.5 μm.

[1] Balogh-Brunstad *et al*. (2008) *GCA* **72**, 2601–2618.
[2] Landeweert *et al*. (2001) *TRENDS Ecol Evol* **16**, 248–254.
[3] Saccone *et al*. (2009) *GCA* **73**, A1140.

https://doi.org/10.1180/S0026461X00006502 Published online by Cambridge University Press

A ^{13}C DOC tracer approach to estimate the contribution of semi-labile dissolved organic carbon to stream ecosystem metabolism

LOUIS A. KAPLAN*, J. DENIS NEWBOLD AND ANTHONY K. AUFDENKAMPE

Stroud Water Research Center, 970 Spencer Rd, Avondale PA, 19390 (*correspondence: lakaplan@stroudcenter.org)

13C Tracer Method

In streams and rivers, dissolved organic carbon (DOC) supplies energy and carbon (C) to heterotrophic bacteria. The complexity of the DOC pool combined with simultaneous processes that continually produce, transform and consume DOC molecules in transport, makes *in situ* measurements of DOC uptake challenging. A tracer approach is a logical solution and we prepared a ^{13}C tracer of semi-labile DOC from soil-aged ^{13}C-labeled *Liriodendron tulipifera* tissues with a chemical composition reflective of the heterogeneity of terrestrially produced C that has been modified by sorptive fractionation onto mineral surfaces and oxidation by soil bacteria.

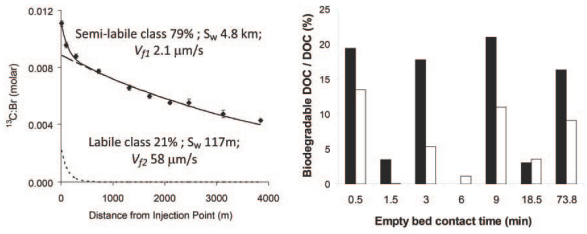

Figure 1: A. Whole-stream addition ^{13}C uptake; B. Lability profiles of stream water DOC (open) and ^{13}C tracer (solid).

Results

We used the tracer in a whole-stream injection coupled with bioreactor-based lability profiling to measure an uptake length of 4.5 km for semi-labile DOC constituents in a headwater piedmont stream and estimate support of ~10% of ecosystem metabolism.

Biogenic Fe(III) minerals lower the efficiency of iron-mineral-based commercial filter systems for arsenic removal

A. KAPPLER[1]*, S. KLEINERT[1], E..M. MUEHE[1], N.R. POSTH[1], U. DIPPON[1] AND BIRGIT DAUS[2]

[1]Geomicrobiology, University of Tuebingen, Germany (*correspondence: andreas.kappler@uni-tuebingen.de)
[2]Helmholtz-Zentrum für Umweltforschung GmbH – UFZ, Department Grundwassersanierung, Leipzig, Germany

Millions of people worldwide are affected by As-contaminated groundwater. Since abiogenic and biogenic Fe (III) (oxy)hydroxides sorb/co-precipitate As efficiently [1], filter systems containing Fe (III) minerals are applied to purify As-contaminated water. However, commercial filters containing abiogenic Fe (III) (oxy)hydroxides (granular ferric hydroxide, GFH) showed varying As removal efficiency depending on groundwater geochemistry and it was unclear whether Fe (II)-oxidizing bacteria influenced their efficiency. We found up to 10^7 Fe (II)-oxidizing bacteria/g dry weight in GFH-filters and determined the performance of the filters in the presence and absence of Fe (II)-oxidizing bacteria. GFH-material sorbed 1.7 mmol As (V)/g Fe. This was ~8 times more efficient than biogenic Fe (III) minerals alone that sorbed 208.3 μmol As (V)/g Fe. It was also ~5 times more efficient than a 10:1 mixture of GFH-material and biogenic Fe (III) minerals that bound 322.6 μmol As (V)/g Fe. Co-precipitation of As (V) with biogenic Fe (III) minerals in the absence of GFH-material removed 343.0 μmol As (V)/g Fe. As removal by co-precipitation with biogenic Fe (III) oxides in the presence of GFH-material bound 1.5 mmol As (V)/g Fe. This was slightly less efficient as by GFH-material alone. Since the formation of biogenic Fe (III) minerals lowers rather than increases the As removal efficiency of the filters, we recommend to exclude microorganisms from the filters (e.g. by activated carbon filters) to maintain their high As removal capacity.

[1] Hohmann *et al*. (2010) Anaerobic Fe(II)-oxidizing bacteria show As resistance & co-precipitate As during Fe(III) mineral precipitation. *Environmental Science & Technology*, **44**, 94–101.

https://doi.org/10.1180/S0026461X00006502 Published online by Cambridge University Press

Pressure-temperature diagenesis of Fe minerals and biomass produces hematite, siderite and magnetite as present in Banded Iron Formations

A. KAPPLER[1]*, N.R. POSTH[1], I. KOEHLER[1], C. SCHRÖDER[1], K.O. KONHAUSER[2], U. NEUMANN[1], C. BERTHOLD[1] AND M. NOWAK[1]

[1]University of Tuebingen, Germany (*correspondence: andreas.kappler@uni-tuebingen.de)
[2]Department of Earth and Atmospheric Sciences, University of Alberta, Edmonton, Alberta, Canada, T6G 2E3

The reconstruction of microbial life in ancient sedimentary deposits is complicated by the influence of temperature and pressure during diagenesis and metamorphism. While minerals and persistent organic molecules may be evident in ancient rock formations such as Banded Iron Formations (BIFs), the specific primary minerals, their (trans-)formation mechanisms and proposed microbial processes involved are not certain. Understanding the transformation of biogenic iron minerals is the key to constraining models of BIF deposition that occurred between 3.8-0.8 billion years ago [1]. Thermal and barometric transformations of Fe (III) minerals associated with organic carbon (biomass, e.g. microbial cells) have not yet been systematically tested in laboratory experiments. Here, we present experimental results of mineral transformations of Fe (III) hydroxide and organic matter (glucose as a proxy for biomass) in gold capsules at elevated pressures and temperatures. Iron speciation and mineralogical analysis show the conversion of ferrihydrite [Fe $(OH)_3$, ferric hydroxide] into hematite ($Fe_2^{III}O_3$), magnetite ($Fe^{II}Fe_2^{III}O_4$), and siderite ($Fe^{II}CO_3$). Our results suggest that the joint precipitation of biomass with primary Fe (III) hydroxides followed by pressure/temperature diagenesis produces minerals found in BIFs today. Moreover, this study shows that siderite and magnetite form, i.e. Fe (III) is partially reduced, under diagenetic conditions decoupled from conditions in the ocean/atmosphere. The experimental system presented herein offers a means to bridge the gap between geological evidence from the field and laboratory experiments with modern microbe analogues.

[1] Koehler *et al*. (2010) Role of microorganisms in Banded Iron Formations. *Geomicrobiology, Molecular & Environmental Perspective*. Larry Barton, Martin Mandl & Alexander Loy (Editors) 485p.

Source rock-oil correlation in the Sinop Basin (Northern Turkey)

REYHAN KARA-GÜLBAY* AND SADETTIN KORKMAZ

Karadeniz Technical University, Department of Geological Engineering 61080, Trabzon, Turkey (kara@ktu.edu.tr)

Lower Cretaceous aged Çağlayan Formation is exposed in the Sinop Basin consists of black coloured claystone, siltstone, shale and marl, and has source rock characteristics. An oil seep from Çağlayan Formation is located in the Ekinveren region of the Sinop Basin.

The average total organic carbon (TOC) values of the shale samples from the Çağlayan Formation in the Ekinveren and the Bürnük areas are 1.48, 1.26 % and HI values are 190, 244 mg HC/g TOC, respectively. The potential yield values of the sample from the Ekinveren and the Bürnük are >2 mg HC/g rock and these potential yield values indicate fair hydrocarbon potential for the Çağlayan Formation.

The unimodal n-alkane distribution with lower carbon number dominant is observed in the gas chromatograms of the shale samples from the Çağlayan Formation in the Ekinveren and the Bürnük locations. Low TAR, $(C_{19}+C_{20})/C_{23}$ tricyclic terpane ratios and type II kerogen content indicate that the shale samples from the Çağlayan Formation comprise dominantly marine organic matter. Pr/Ph ratios for the Ekinveren and the Bürnük shale samples are 1.39 and 0.89, respectively.

Average T_{max} values for the Ekinveren and the Bürnük locations are 429 and 433°C, respectively. According to T_{max} data, Çağlayan Formation has immature-early mature characteristics in the Ekinveren location and early mature-mature characteristics in the Bürnük location. CPI values, isoprenoid/n-alkane ratio, 20S/(20S+20R) and ββ/(ββ+αα) C_{29} sterane, 22S/(22S+22R) C_{32} homohopane ratios for the Ekinveren and Bürnük shale show that Bürnük shale are more mature than those of the Ekinveren shale.

A large UCM and n-alkanes, isoprenoids that were recorded in low amount in gas chromatogram for oil sample from the Ekinveren seep indicate that the Ekinveren oil seep were heavily biodegraded. Similar tricyclic terpane, C_{24} tetracyclic terpan, norhopane, hopane and homohopane distributions were recorded in m/z 191 and m/z 127 mass chromatograms of samples from the Çağlayan Formation and the Ekinveren oil seep. Higher diasterane and pregnane content is typical for oil and shale samples. C_{27}, C_{28}, C_{29} sterane distribution for oil and shale samples is similar. According to biomarker data, Çağlayan Formation and Ekinveren oil seep are well correlated to each other.

https://doi.org/10.1180/S0026461X00006502 Published online by Cambridge University Press

Mineralogical and chemical variations in kaolin and alunite deposits in vicinity of the Aksaray region (Central Anatolia, Turkey)

NECATI KARAKAYA AND MUAZZEZ ÇELIK KARAKAYA*

Selçuk Universitesi Muh.-Mim. Fakültesi Jeoloji Mühendisliği Bölümü, Konya, 42079, Türkiye
(*correspondence: mzzclk@hotmail.com)

The kaolin-alunite deposits were formed in Lower Miocene volcanic and volcanoclastic, mostly dacitic, rhyodacitic, and andesitic rocks. The deposits were derived from by supergene and hypogene alteration processes. Kaolinite/halloysite is clay minerals, sometimes pure and sometimes associated with α-quartz, K-feldspar, plagioclase, alunite, natroalunite and hematite, whereas other kaolinite accompanies smectite, which represents a moderate kaolinization. Massive zones of alunite deposits sometimes pure, and show gradational passing to kaolinite/halloysite, and they were cut by gypsum and native sulphur veins and contain partially cinnabar and realgar mottles and/or veinlet. Tridymite and rarely low-cristobalite are the dominant silica mineral in these kaolins. Barite, pyrophyllite, minamiite, hematite, and geotite/lepidocrosite are rarely observed. Bentonite deposits composed mainly of nearly pure Ca-montmorillonite, observed as gradually or sharply at the uppermost levels or lateral sides of the alunite and kaolinite deposits. The alunite and most of kaolinite are products of hypogene alteration. Alunite, kaolinite, and gypsum samples show very similar chondrite-normalized REE trends, suggesting that they may be linked to common source. The REE patterns of the alunite and kaolinite samples are characterized by strong LREE enrichment ((La/Lu)cn=54.7 and 170.5, whereas gypsum and bentonite samples show moderate enrichment (9.2 and 7.2), respectively. Most of the alunite and kaolinite samples have pronounced positive Eu anomalies (1.08) and gypsum and bentonite samples negative and/or weakly negative Eu anomalies ranging from 0.77 to 0.89. All of the samples have positive Ce anomalies. Alunite and native sulphur samples from the deposits have $\delta^{34}S$ values of 5.03-6.62%, and 5.97-7.49%, respectively, with values for gypsum of 4.5-5.24%. Therefore, the sulphur-rich minerals may have been formed by steam-heated hydrothermal environments. The isotopically slightly heavy sulphur in the minerals could be derived from H_2SO_4. Development of the hydrothermal alteration contemporaneous with extensional tectonic and strike-slip faulting movements have resulted in hypogene alunite and kaolinite deposits. Hydrothermal alteration strongly affected along fault zones but subsequent weathering (supergene) away from the fault zones, and much of the volcanoclastic rocks have been altered to a more smectite-rich and less kaolinite-bearing assemblage.

A new model of the asthenosphere

SHUN-ICHIRO KARATO

Yale University, Department of Geology & Geophysics, New Haven, USA, (shun-ichiro.karato@yale.edu)

Although the classic model of asthenosphere = a layer of partial melt has been questioned for more than two decades, such a model is revived recently based on seismological observations showing a sharp and large reduction in seismic wave velocity. In this presentation, I will argue that such a model is not consistent with physics of behavior of partailly molten materials nor with the seismological observations. First, in the gravity field, it is difficult to maintain a substantial amount of melt for a geologic time scale. Layering observed in some lab experiments is often invoked to explain the persistency of a mlet-rich layer, but the lab experiments show ~20° tilt and hence the melt-rich layer will be compacted. Second, if a large reduction of velocity (~5-10%) were to be due to the presence of sub-horizontal melt-rich layer, then the asthenosphere should show large anisotropy in SH/SV waves (5-10%), which is not observed.

I propose that the basic properties of the asthenosphere is best explained as a residue of partial melting near the 410-km discontinuity. Partial melting removes a large fraction of incompatible elements leading to the 'depleted' homogenous composition, and also leads to ~0.01 wt% of water in the asthenosphere. The lab data show that this much of water is consistent with the observed electrical conductivity of the asthenosphere including its regional variation. If water reduces the strength of grain-boundaries, it can easily exlpain the sharp drop in velocity as much as ~10%.

https://doi.org/10.1180/S0026461X00006502 Published online by Cambridge University Press

Sequential extraction of Pb, Zn, Cd, and Cu in contaminated soils due to mining operation in Isfahan-Iran

L. KARIMZADEH

(l_karimzad@yahoo.de)

Sequential extraction was applied on 6 soil samples collected from metal contaminated site due to Gooshfil mining operation (20 km south west of Isfahan) to evaluate the level of contamination and bioavailability of Pb, Zn, Cd, and Cu. The sequential extraction method which was used in this research has been introduced by Tesser *et al*. in 1979 and modified by Salbu *et al*. in 1998. This method separates metals in six operationally defined fractions: water soluble, exchangeable, carbonate bonds, oxides bonds, organic bonds and residual fractions.

From the results of this study it can be concluded that the study area is contaminated with led. Zn is lower but near the contamination level. Mining operation in the area is the major source of metal contamination. The results obtained from the sequential extraction indicate that up to 90 % of metals in soil samples were associated to low soluble and high stable fraction such as oxide, organic and residual fraction. Metal distribution in soil samples generally followed the order oxide fraction> residual fraction> organic fraction> carbonate fraction> exchangeable> water-soluble.

Metal mobility and bioavailability

Ratio of relatively metal bioavailable and mobile fractions to stable and less mobile fractions is defined as mobility factor.

Metal mobility factor (Mf) defined as the following equation:

MF = (water-soluble + exchangeable + carbonate fraction)/ total metal content *100

The high MF values have been interpreted of relatively high biological availability and bioaccessibility of metals in soils. Mobility factor for six soil samples was determined by using the result of sequential extraction. Results are presented in Table 1.

Table 1: Mobility factor for metals

Soil	Pb	Cd	Zn	Cu
S1	1.8	7.8	1.7	2.0
S2	0.7	6.9	0.6	0.7
S3	3.0	9.7	1.0	3.6
S4	3.9	10.2	1.4	8.1
S5	1.9	9.7	2.0	7.1
S6	3.1	10.2	1.0	4.1

Bioavailability for metals found to be very low. Metal mobility factor for four studied metals were lower than 12%. The highest mobility was measured for cadmium and the lowest obtained for Zn. The results of bioavailability and mobility factor for the studied metals in the soil samples generally show the following order: Cd>> Cu> Pb> Zn

Viscosity of MgO-SiO_2 melt system from first principles simulations

BIJAYA B KARKI

Department of Computer Science, Department of Geology and Geophysics, Center for Computation and Technology, Louisiana State University, Baton Rouge (karki@csc.lsu.edu)

Transport properties of silicate melts are crucial to our understanding of chemical and thermal evolution of Earth. In recent years, we have performed density functional theory-based molecular dynamics simulations to study from first principles several key properties including viscosity (η) of relevant melts in the MgO-SiO_2 system. Numerous simulations of durations from a couple of tens of picoseconds to a few nanoseconds were completed to sample the pressure-temperature-composition (P-T-X) space accurately. The calculated results show that the viscosity is strongly dependent on pressure and temperature showing large deviation from the normal Arrhenian behaviour. The melt viscosity varies by two to three orders of magnitude across the entire mantle pressure regime. The predicted anomaly (i.e. viscosity increasing on compression) becomes more pronounced in silica-richer melts. Such dynamical changes can be associated to the structural changes. The simulations results were used to derive a viscosity model, η (PTX), applicable for the parameter space considered. The predicted viscosities compare favourably with the available measured data.

https://doi.org/10.1180/S0026461X00006502 Published online by Cambridge University Press

Putting constraints on the life cycle of organic carbon based on ecosystem scale flux measurements

THOMAS KARL

National Center for Atmospheric Research, 3090 Center Green Drive, Boulder, CO, 80301, USA (tomkarl@ucar.edu)

Large quantities of volatile organic compounds (VOC) enter the atmosphere. The annual production of VOC (600 - 2000 TgC/a) likely exceeds that of methane and CO (~500 TgC/a each). Together these gases fuel tropospheric chemistry. Oxidation of VOC leads to the formation of aerosol [1] via complex organic chemistry [2, 3] in the gas and aerosol phase thereby modulating the oxidation capacity of the atmosphere [4]. It is currently believed that a large fraction of VOC originates from biogenic sources (e.g. >80%). The life cycle of organic carbon is ultimately controlled by emission and deposition processes at the surface. Uncertainties in budgets of VOC and potential ramifications for organic aerosol production in the atmosphere will be discussed based on a synthesis of direct VOC flux measurements performed in a range of different ecosystems. These direct flux measurements will be used to address some outstanding questions concerning (1) the amount of reactive biogenic organic aerosol precursors, (2) the magnitude of deposition processes and (3) the lifetime of reactive biogenic organic aerosol precursors in the atmosphere.

[1] Hallquist *et al*. (2009) Atmos. Chem. Phys. **9**, 5155–5235. [2] Atkinson & Arey (2003) *Chemical Reviews* **103**, 4605–4638. [3] Paulot *et al*. (2009) *Science* **325**, 730–733. [4] Lelieveld *et al*. (2008) *Nature* **452**, 737–740.

Molecular-level studies of Fe(III) in aquatic systems

T. KARLSSON[1]*, U. SKYLLBERG[2] AND P. PERSSON[1]

[1]Dept. of Chemistry, Umeå Univ., 901 87 Umeå, Sweden (*correspondence: torbjorn.karlsson@chem.umu.se)
[2]Dept. of Forest Ecology & Management, Swedish Univ. of Agri. Sci., 901 83 Umeå, Sweden

The fate and behavior of iron (Fe) in aquatic environments is highly dependent on chemical interactions with natural organic matter (NOM). There is however still limited knowledge about the molecular structure, strength and hydrolysis of the Fe species formed in association with aquatic NOM and few studies that present results obtained by molecular-level probes (e.g. [1, 2]). In this study we have used extended X-ray absorption fine structure (EXAFS) and Fourier transformed infrared (FTIR) spectroscopy in combination with chemical speciation modeling to characterize Fe (III) in different types of aquatic NOM and in dissolved and colloidal material in different size fractions from a boreal stream.

Our results show that Fe in association with NOM and fulvic acid from river water forms two predominant species; mononuclear Fe (III)-NOM complexes and polymeric Fe (III) (hydr)oxides. The distribution of the two species is largely dependent on pH and Fe concentration. The speciation in the boreal stream water is dominated by mononuclear organic Fe (III) complexes irrespective of pH and size fraction. In the organic complexes Fe is coordinated by carboxylic functional groups forming a structure consisting of five-membered chelate rings and these complexes are sufficiently strong to prevent hydrolytic polymerization of Fe even at pH 7.0.

Thus, in oxic aquatic environments, with organic matter present, the fate of Fe will to a large extent be controlled by the properties of the organic Fe (III) complexes. In addition, the stable Fe (III)-NOM complexes formed will have important implications for the biogeochemistry of other elements, such as phosphorus and arsenate, that are known to be strongly associated with Fe (III).

[1] Rose *et al*. (1998) *Colloids & Surf. A* **136**, 11–19. [2] Vilgé-Ritter *et al*. (1999) *Colloids & Surf. A* **147**, 297–308.

https://doi.org/10.1180/S0026461X00006502 Published online by Cambridge University Press

Temporal trend in anthropogenic sulfur aerosol transport from central and Eastern Europe to Israel

A. KARNIELI[1]*, D. YEVGENY[1,2], R. INDOITU[1], N. PANOV[1], R.C. LEVY[3], L.A. REMER[3] W. MAENHAUT[4] AND B.N. HOLBEN[3]

[1]Ben-Gurion University, Israel (*correspondence: karnieli@bgu.ac.il, panov@bgu.ac.il, indoitu@bgu.ac.il)
[2]Laboratoire d'Optique Atmospherique, France (derimian@loa.univ-lille1.fr)
[3]NASA/GFSC, Maryland, USA (robert.c.levy@nasa.gov, Lorraine.A.Remer@nasa.gov, Brent.N.Holben@nasa.gov)
[4]Ghent University, Gent, Belgium (Willy.Maenhaut@UGent.be)

Decrease of sulfur emissions in central and eastern Europe over the past 3 decades is well documented. These changes result in a decreasing trend of sulfate aerosol and aerosol forcing over the source region, but also at a receptor site located in southern Israel, thousands of kilometers downwind. A combination of several independent observations, namely, satellite and ground-based remote sensing, *in situ* aerosol sampling, and backward trajectory analysis, was implemented to show significant downward trends in fine particle aerosol optical thickness (AOT), in general, and sulfur aerosol, in particular. MODIS-Terra observations over central Europe show 38% reduction of fine AOT. At the reception site in southern Israel, 43% reduction of fine AOT was observed by a sunphotometer and 25% reduction of sampled fine aerosols was obtained. During the corresponding observation periods, the coarse mode AOT has remained constant. The majority of the backward trajectories, where meaningful sulfur events were observed at the receptor site, are originated from eastern and central Europe. The aerosol radiative effect at top of the atmosphere has become less negative during the past decade, decreasing by 30% in Europe and 67% in Israel.

Neoproterozoic ice ages, boron isotopes, and ocean acidification

S.A. KASEMANN[1]*, A.R. PRAVE[2], A.E. FALLICK[3], C.J. HAWKESWORTH[3] AND K.-H. HOFFMANN[4]

[1]Department of Geosciences, Univ. Bremen, 28334 Bremen, Germany (*correspondence: skasemann@marum.de)
[2]Earth Sciences, University of St Andrews, St Andrews KY16 9AL, UK (ap13@st-andrews.ac.uk, deputyprincipal@st-andrews.ac.uk)
[3]Scottish Universities Environmental Research Centre, East Kilbride G75 OQF, UK (T.Fallick@suerc.gla.ac.uk)
[4]Geological Survey of Namibia, P.O. Box 2168, Windhoek, Namibia (khhoffmann@mme.gov.na)

The Neoproterozoic Earth underwent at least two severe glaciations, each extending to low paleomagnetic latitudes and punctuating warmer climates. The two widespread older and younger Cryogenian glacial deposits in Namibia are directly overlain by cap carbonates deposited under inferred periods of high atmospheric carbon dioxide concentrations [1]. Oceanic uptake of carbon dioxide decreases ocean pH and here we present a record of Cryogenian inter-glacial ocean pH, based on boron isotopes in marine carbonates. Our data document characteristically different B isotope profiles of the two Cryogenian carbonate transects that are consistent with the presence of two 'pan-glacial' climate states, but indicate that each had its own distinct environmental conditions. The Marinoan interglacial $\delta^{11}B$ profiles are systematic and remarkably consistent, and they vary by up to 11‰. This yields a relative pH variation of up to 1.5 pH units, and implies a pH of 8.5 at the onset of cap carbonate deposition, followed by a decrease in pH to ~7 and then a return to pH ~8 for the upper part of the section. The transient ocean acidification excursion and the alkaline pH condition near the start and termination of the inferred greenhouse state suggests a rapid draw-down of CO_2 initiated at the start of the deglaciation and supports inferences of a thick, global sea-ice shield with minimal air-sea gas exchange during glaciation. In contrast, largely constant B isotope values for the Sturtian-aged glacial aftermath do not indicate extreme ocean pH (~8.3) conditions and do not support a contemporaneous major ocean acidification event and associated high pCO_2 at the time of the older Cryogenian glaciation and deglaciation. That leads us to speculate that the ocean during the older glaciation was not totally frozen and that the hydrological cycle was functioning [2].

[1] Hoffman *et al*. (1998) *Science* **281**, 1342–1346.
[2] Kasemann *et al*. (2010) *Geology* **38**, 775–778.

https://doi.org/10.1180/S0026461X00006502 Published online by Cambridge University Press

Molecular-scale mechanism of Mo isotopic fractionation during adsorption on ferromanganese oxides

TERUHIKO KASHIWABARA[1]*, YOSHIO TAKAHASHI[2] AND MASAHARU TANIMIZU[1]

[1]Japan Agency for Marine-Earth Science and Technology (JAMSTEC)
(*correspondence: teruhiko-kashiwa@jamstec.go.jp)
[2]Hiroshima University

Molybdenum (Mo) shows a large mass-dependent isotopic fractionation during adsorption on ferromanganese oxides, which is responsible for isotopic composition of Mo in modern oxic seawater [1]. The aim of this study is to reveal the fractionation mechanisms of Mo isotopes during adsorption on natural ferromanganese oxides. We investigated surface complex structures of Mo on various Fe/Mn (oxyhydr)oxides, key factors for the isotopic fractionation, and compared them with previously-reported isotopic fractionation.

Our XAFS analysis showed that symmetry of surface Mo species is different from MoO_4^{2-} (*Td*) in seawater in the case of its adsorption on some solids. This structural information showed the excellent correlation with the degree of isotopic fractionation of Mo reported in previous studies: the proportion of *Oh* species or their magnitude of distortion in surface Mo species becomes larger in the order of ferrihydrite < goethite < hematite < δ-MnO_2 [2], a trend identical to the degree of isotopic fractionation [3]. Based on the comparison with previous reports for surface Mo species on various oxides such as MgO, Al_2O_3, and TiO_2, the symmetric change from *Td* to *Oh* is suggested to be driven by the formation of inner-sphere complexes on specific sites of the oxide surfaces. In addition, the mode of attachment (inner- or outer-sphere) of surface Mo species is well correlated with the hydrolysis constant of the cation (e.g. Fe^{3+} and Mn^{4+}) in oxides.

[1] Barling *et al*. (2001) *Earth Planet. Sci. Lett*. **193**, 447. [2] Kashiwabara *et al*. (2009) *Geochem. J*. **43**, e31. [3] Goldberg *et al*. (2009) *Geochim. Cosmochim. Acta*, **73**, 6502.

EPMA study of sulfides in ultramafic suites of J.C.pura belt, Western Dharwar craton, India

NAMRATHA R. KASHYAP* AND B.C. PRABHAKAR

Department of geology, Bangalore University, Bangalore 560056, India
(*correspondence: namratharkashyap@gmail.com)

Significant ultramafic magmatism has been recorded in the western part of the Dharwar craton, southern India. J.C.Pura schist belt is one such ultramafic milieu with abundant dunite and peridotite which have been extensively serpentinised. Their komatiitic nature and extrusive mode of formation is evident from the field study. Some of the dunite bodies are chromitte in nature and contain veins and stringers of chromite. Highly altered bodies of chromitite show strong development of magnesite veins. They contain complex nickel sulfides which have been studied by ore microscopic method, besides analysing by EPMA. Camica (France Make) EPMA system was used for EPMA. Polished thin sections were prepared for this study and through a preliminary study the mineral-spots were marked for the EPMA studies. Selected representative samples from different rock types of dunite/peridotites, pyroxenites and cumulus schistose rocks were identified for this study. The chemical composition of different ore phases and the identified mineral phases are presented. From the analysis it is deciphered that cobalt–nickel-pyrite and pentlandite make the most abundant ore phase among the sulfides followed by pentlandite-pyrrohite-chalcopyrite assemblage. Occurrence of sulfides within the oxide phase (Chromite-Magnetite-ilmenite) is also noticed infrequently. This suggests to the possibility of sulfide evolution progressively with magma cooling. Strong immiscible and solid-solution relation are evident in the entire sulfide phase. The disseminated nature of them suggests to the possibility of poor sulfidation process during their formation i.e. either there was poor endowment of sulfur at the time of partial melting or during the ascent of magma through the crustal rocks. This is being reported for the first time for the J.C.Pura area. However detailed volcanic stratigraphy of the belt when studied, which is underway, and whole rock geochemistry including elemental ratios integrated, it will provide more insight in to the actual potential of the sulfides especially Ni sulfides in the said belt.

https://doi.org/10.1180/S0026461X00006502 Published online by Cambridge University Press

Microbial activity in gas field fluids and in laboratory experiments simulating geological CO_2 storage

ANDREA KASSAHUN[1]*, CLAUDIA GNIESE[2], MICHAELA HACHE[1], THOMAS MUSCHALLE[3] AND NILS HOTH[3]

[1]Dresdner Grundwasserforschungszentrum, 01217 Dresden, Germany (*correspondence: akassahun@dgfz.de)
[2]TU Bergakademie Freiberg, Inst. of Biosciences, 09599 Freiberg, Germany (claudia.gniese@ioez.tu-freiberg.de)
[3]TU Bergakademie Freiberg, Inst. of Drilling and Fluid Mining, 09596 Freiberg, Germany

Microbial activity in gas field fluids from two natural gas fields in Germany was assessed for evaluation of possible biochemical transformation of injected CO_2. 16S rDNA clone library construction revealed the presence of bacteria (*Thermoanaerobacterium* sp., *Petrotoga* sp. *Desulfotomaculum* sp.) in both gas fields and archaea (*Methanolobus, Methanoculleus*) in one gas field [1]. Gas field fluids of both fields contain free amino acids, polysaccharides, carbonic acids (formic acid, acetic acid) and alcohols (methanol, ethanol). Bio-molecules and metabolites form 25 to 50% of the total dissolved organic carbon of 2 to 10 μM. Moreover, both gas field fluids contain 0.1 to 250 μM dissolved H_2.

Laboratory experiments for simulation of geological CO_2 storage were conducted in high-pressure reactors (autoclaves) for 6 to 12 months. Gas field fluids and milled rock material from exploration drilling cores were reacted at p_{CO2}=6.5 bar, p_{H2}=3.5 bar, p_{N2}=4 bar and T=40°C. During the experiments, cell numbers of the reactor fluids rose and CO_2 and H_2 were consumed. DOC concentrations increased up to several hundred mM, while its composition remained comparable to the gas field fluid DOC. For one gas field, sulphate reduction was observed. Fatty acids, saturated hydrocarbons and elemental sulphur (in sulphate reducing systems) were detected in the sediments after the experiment. Fluorescence microscopy was used for visualisation of polysaccharides, proteins and calcium in the sediment samples. Both protein-calcium and polysaccharide-calcium associations were detected. REM-EDX analysis revealed biogenic sulphides and carbonates in sulphate reducing systems. Microbial activity at simulated CO_2 geological storage resulted in elevated concentrations of dissolved organic carbon, production of EPS and precipitation of biogenic minerals and thus might influence CO_2-storage capacities and rock physical properties of CO_2 storage units.

[1] Ehinger *et al*. (2009) *Geomicrobiology Journal* **26**, 326–338.

Analysis and application of water-rock-CO_2 reaction using basalt to underground CO_2 sequestration

T. KATAYAMA[1], N. SHIKAZONO[1], Y. TAKAYA[2] AND Y. KATO[2]

[1]Department of Science for Open and Environmental Systems, School of Science and Technology, Keio University, Kanagawa-ken, 223-8522, Japan (*correspondence: tomohirokatayama2487@yahoo.co.jp)
[2]Department of Systems Innovations, School of Engineering, the University of Tokyo, 113-8656, Tokyo, Japan

Water-rock-CO_2 reaction attract attention in many parts of science. It consists of three following reactions:

$CO_2 + H_2O = H_2CO_3 = H^+ + HCO_3^-$ (1)

$MSiO_3 + 2CO_2 + H_2O = M^{2+} + H_4SiO_4 + 2HCO_3^-$ (2)

$M^{2+} + 2HCO_3^- = MCO_3 + CO_2 + H_2O$ (3)

where M is bivalent metal ion.

There are two steps. First, CO_2 dissolves in the water by (1) or mineral and water react CO_2 by (2). Next, bivalent metal ion and hydrogen carbonate ion generate and carbonate minerals (MCO_3) precipitate by (3).

We are applying them to the CO_2 underground sequestration and the estimate of atmospheric CO_2 concentration of Archean and formation of mineral water, and global carbon cycle in earth system. In this paper we will focus on CO_2 underground sequestration based on experimental water-basalt-CO_2 reaction and computer simulation.

[1] Berger, G. (1994) *Geochimica et Cosmochimica Acta*, **58** (22), 4875-4886. [2] Gislason, S.R. and Oelkers, E.H. (2003) *Geochimca et Cosmochim Acta*, **67** (20), 3817-3832. [3] Holland, H.D. (2006) *Philosophical Transactions of the Royal Society Section B*, doi:10.10981 rstb. 1838. [4] Oelkers, E.H. and Gislason, S.R. (2001) *Geochimica et Cosmochimica Acta*, **65**(21), 3671-3681. [5] Shikazono, N. (2008) *Japanese Magazine of Mineralogical and Petlogical Sciences*, **37**(3), 69-77

https://doi.org/10.1180/S0026461X00006502 Published online by Cambridge University Press

Assessment of the nanoscopic dissolution rate of basic lead carbonate (hydrocerussite)

D. KATSIKOPOULOS[1]*, A. GODELITSAS[2] AND J.M. ASTILLEROS[3]

[1]University of Oviedo, Spain (*correspondence: dionisis@geol.uniovi.es)
[2]University of Athens, Greece
[3]Complutense University of Madrid, Spain

Hydrocerussite (Pb_3 $(CO_3)_2$ $(OH)_2$), related to shannonite and plumbonacrite phases, is reported to be a characteristic secondary mineral [e.g. 1] particularly associated with the weathering of industrial metallic Pb (e.g. bullets, shots, pipes) and the oxidation of Pb-Zn-Ag ore deposits. Such processes exhibit a straightforward connection between the dissolution-precipitation of hydrocerussite ($\log K_{sp}$=-43.7) and the mobility of Pb contaminants in the environment. Synthetic hydrocerussite (basic lead carbonate known as 'white lead' [e.g. 2]) has been broadly used in pigments and cosmetics. In this study, we present *in situ* AFM experiments that provide evidence of the nanoscopic reactivity behaviour of hydrocerussite {0001} surfaces in contact with deionized water. The AFM study shows that the edge pits, with initial depth ~1 nm, exhibit random shapes with flattened bottoms. However as the dissolution proceeds, terrace adatoms, corresponding approx. to the *c* unit cell parameter of hydrocerussite, appear near the edges of deeper etch pits (~3 nm, Fig. 1).

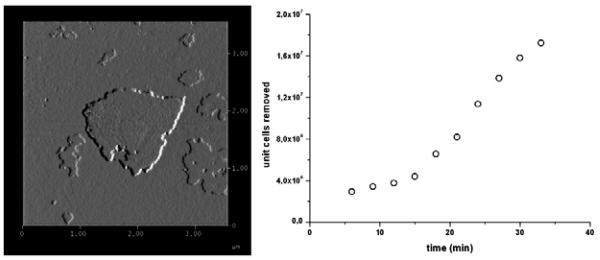

Figure 1: Nanoscopic dissolution rate of hydrocerussite

Following the methodology described by Rufe & Hochella [3], an assessment of the nanoscopic dissolution rate of hydrocerussite was obtained (**Fig. 1**) for the first time in the literature.

[1] Kokkoros P. & Vassiliadis K. (1953) *Tsch. Min. Petr. Mitt.* **3**, 298–304. [2] Martinetto P. *et al.* (2002) *Acta Cryst.* **C58**, i82-i84. [3] Rufe E. & Hochella F.Jr (1999) *Science*, **285**, 874–876.

The origin of Naxos migmatites: SIMS U-Pb and O isotope analysis of zircon

Y. KATZIR[1]*, Y. BE'ERI-SHLEVIN[2], J.WOODEN[3], J.W. VALLEY[4], K. KITAJIMA[4] AND C. GRIMES[5]

[1]Ben-Gurion University of the Negev, Be'er-Sheva 84105, Israel (*correspondence: ykatzir@bgu.ac.il)
[2]Heberew University of Jerusalem, Jeruslam 91904, Israel
[3]Stanford-USGS Micro Analysis Center, Stanford CA USA
[4]University of Wisconsin, Madison, WI 53706, USA
[5]Mississippy State University, Starkville, MS 39762, USA

The Naxos (Aegean Sea, Greece) structural and thermal dome is cored by migmatites that record the peak P-T conditions (6-8 kbar; ≤700°C) of a late Alpine (18 Ma) Barrovian type metamorphism [1]. The 'leucogneiss core' comprises various types of anatectic gneisses thought to derive from either 'pre-Alpine basement' or Mesozoic sedimentary protoliths or both. Early Miocene intense deformation and metamorphism has obliterated most prior evidence, leaving zircon as the major tool for unveiling the pre- and early-Alpine history of the Naxos core. SIMS U-Pb dating of zircons from the four major types of gneisses in the core shows that oscillatory zoned domains yield concordia ages of ca. 326, 315, 312 and 300 ± 5 Ma with inherited cores of ca. 500-2500 Ma. Clear overgrowths yield ages between 17 and 20 Ma. Intermediate ages between ca. 300 and 17 Ma are restricted to blurred or porous zircon domains and are aligned on discordia lines connecting these end points. The age data indicate that the protoliths of the migmatites were Variscan igneous intrusions with inheritance of Pan-African and older detritus. Zircons from a pelite raft within the core yield the same age pattern as the migmatites suggesting that these sediments were derived from a similar basement.

SIMS O isotope analysis of oscillatory zoned zircon domains of Variscan age yielded $\delta^{18}O$ (Zrn) of 6.5-8.5‰. However in each sample these values vary within a 1‰ range, further supporting the igneous origin of the Naxos migmatites.

[1] Buick & Holland (1989) *Geol Soc London Spec Publ* **43**, 365–369.

https://doi.org/10.1180/S0026461X00006502 Published online by Cambridge University Press

Noble gases used as an indicator of groundwater mixing in Azraq, Jordan

T. KAUDSE* AND W. AESCHBACH-HERTIG

Institute of Environmental Physics, Heidelberg University, 69120 Heidelberg, Germany (*correspondence: Tillmann.Kaudse@iup.uni-heidelberg.de)

Several sources contribute to the noble gas content in groundwater. One component arises from an equilibrium between soil air and percolating water. Excess air (EA) accounts for an additional noble gas contribution [1]. This applies to all noble gases. Helium has additional sources: ^{4}He is generated by radiogenic production within the aquifer matrix, while ^{3}He originates from tritium decay in young groundwater. A mantle helium component can shift the ^{3}He/^{4}He ratio to higher values. To determine the excess helium component all other noble gases need to be measured in order to separate the excess from the equilibrium and the EA component.

As part of an interdisciplinary research initiative to study water issues in Jordan, we use noble gases to investigate groundwater origin and recharge. In the region of Kerak in Western Jordan, a groundwater recharge estimation project is being conducted, based on tritium-^{3}He dating.

Here a study of groundwater origin in the Azraq Basin in Eastern Jordan, which is affected by groundwater depletion, is presented. The excess of ^{4}He as well as the ^{3}He/^{4}He ratio are used to identify groundwater mixing near the Azraq Oasis. In this area groundwater is used only from the upper aquifer, since the deeper one consists of highly saline water. However, a few production wells in the upper aquifer have shown a rising salt content over the past years. A correlation between the salinity and the ^{4}He excess is detected which argues for an inflow of water from the saline and old aquifer below. In the case of Azraq also the ^{3}He/^{4}He ratio seems to corroborate the above finding, as a ^{3}He/^{4}He vs. Ne/^{4}He isotope plot indicates mantle helium in the saline wells.

[1] Aeschbach-Hertig *et al*. (2000) *Nature* **405**, 1040–1044

Implications of U-Pb-Hf detrital zircon data on the Precambrian crustal evolution of NW India

PARAMPREET KAUR[1]*, ARMIN ZEH[2], NAVEEN CHAUDHRI[1], AXEL GERDES[2] AND MARTIN OKRUSCH[3]

[1]Centre of Advanced Study in Geology, Panjab University, Chandigarh-160 014, India (*correspondence: param.geol@gmail.com)
[2]Institut für Geowissenschaften, Goethe-Universität, Altenhöferallee 1, 60438 Frankfurt am Main, Germany
[3]Lehrstuhl für geodynamik und Geomaterialforschung, Universität Würzburg, 97074 Würzburg, Germany

We have integrated *in situ* U-Pb-Hf data for 217 zircon grains from two quartzite samples of NW Indian plate to understand the Precambrian crustal evolution of this region. The U-Pb data unravel prominent probability age peaks at ca. 1.77, 1.85, 2.2, 2.5, 2.7 and 2.9 Ga. Barring 1.77 and 2.2 Ga age peaks, others are correlatable with most of the magmatic events identified in the basement of NW India.

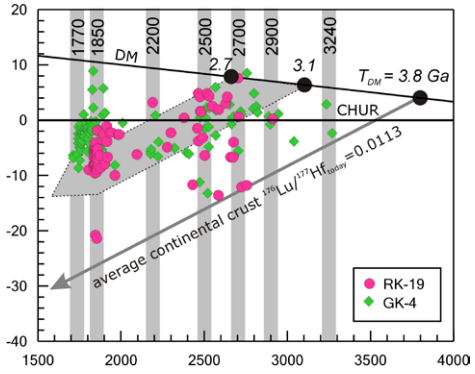

Figure 1: $\varepsilon Hf_{(t)}$ versus $^{207}Pb/^{206}Pb$ diagram showing results of detrital zircons from NW India.

The Lu-Hf isotope analyses indicate that at 1.77 and 1.85 Ga, reworking of Neoarchaean crust dominated over juvenile input as indicated by their largely subchondritic εHf values. At 2.5 Ga the zircons show a wide scatter in εHf values but the dominace of subchondritic values also indicate substantial reworking of older crust at this time. On the contrary, during 3.1–2.7 Ga, variable but mostly superchondritic to nearly chondritic εHf values suggest the dominant production of juvenile crust. The Hf model ages for Neoarchaean zircons also signify that the oldest crust in the NW Indian plate was formed from a depleted mantle source at around 3.8-3.7 Ga.

https://doi.org/10.1180/S0026461X00006502 Published online by Cambridge University Press

Impact of ferrihydrite coating and aeration conditions on microbial selenium (Se) reduction and retention in artificial soil aggregates

M.F. KAUSCH* AND C.E. PALLUD

ESPM, University of California at Berkeley, Berkeley, CA 94720, USA (*correspondence: mkausch@berkeley.edu)

Soils display large variations with respect to their physical, geochemical and biological characteristics at scales ranging from nanometers to kilometers. The impact of this heterogeneity on biogeochemical processes is as of yet poorly understood. In structured soils, the aggregate scale (mm-cm) is of particular interest due to the sharp transition in pore size at the surface of aggregates. Small intra-aggregate pores limit advective transport thus facilitating the formation of chemical concentration gradients that promote spatial variation in biogeochemical processes. One such process is the microbial reduction of selenium (Se), both an essential micronutrient and a toxicant. A mechanistic understanding of Se reduction within soil aggregates may lead to improved prediction of its transport and attenuation in soils of contaminated areas.

In order to investigate the coupling of physical and biogeochemical processes controlling Se reduction at the aggregate scale, we used artificial aggregates in flow-through reactor cells, mimicking the interface between soil micropores and macropores. Aggregates were constructed using either uncoated sand or ferrihydrite-coated sand homogenously inoculated with Se-reducing bacteria (*Thauera selenatis* and *Enterobacter cloacae* SLD1a-1 were compared). Saturated flow of aerobic or anaerobic artificial groundwater medium containing selenate and an electron donor, was initiated. Concentrations of selenite and total Se were measured in the outflow solution and in concentric sections of the aggregates' air dried solid phase.

Selenite export rates from aggregates increased by a factor of 600 between aerobic *T. selenatis* reactors with low selenate and acetate input and anaerobic *E. cloacae* reactors with high selenate and pyruvate input. Aerobic input solution significantly decreased Se reduction, however, the presence of a selenite signal indicates the occurrence of anaerobic/microaerobic microzones within aggregates. Solid phase selenite concentrations increased from the exterior to the core under aerobic as well as anaerobic conditions within both sand and ferrihydrite-coated sand aggregates. This is an indication that soil structure can impact Se retention in soils under a diverse set of conditions and that consideration of aggregate scale reactive transport may be essential for a complete understanding of field dynamics.

Metal mobility in clay formations – From batch experiments with mineral suspensions to column setup with compacted clay

R. KAUTENBURGER*, C. MOESER AND H.P. BECK

Institute of Inorganic and Analytical Chemistry and Radiochemistry, Saarland University, Saarbrücken, Germany
(*correspondence: r.kautenburger@mx.uni-saarland.de)

Nowadays, there is a broad consensus on the technical merits of the disposal of high-level nuclear waste (HLW) in deep and stable geological clay formations. For the long-term disposal of radioactive waste, detailed information about geochemical behaviour of radioactive and toxic metal ions under environmental conditions is necessary.

In our project europium, gadolinium (homologues of americium and curium) and uranium were used and their sorption and desorption behaviour onto Opalinus clay was studied [1]. Natural organic matter (NOM) can play an important role in the immobilisation or mobilisation of metal ions due to complexation and colloid formation. This complexation could interfere the sorption of metal ions onto clay. In addition to humic acid (HA) we used other natural appearing organics in Opalinus clay like lactate, formiate or propionate [2]. Therefore, we investigated the complexation behaviour of the metals with NOM as well as the influence of present NOM on the metal sorption onto clay [3].

Capillary electrophoresis hyphenated with inductively coupled plasma mass spectrometry (CE-ICP-MS) has been used to study the complexation behaviour of Eu (III), Gd (III) and U (VI) with HA. The influences of metal concentration as well as the presence of competing cations from clay dissolution as well as cations from clay porewater on the complexation behaviour was analysed [4]. For the sorption/desorption behaviour common batch experiments with mineral suspensions are performed, and in comparison a miniaturised column setup with compressed clay was used to study the influence of NOM on the metal mobility in compact Opalinus clay.

The authors thank the BMWi for financial support (grant no. 02E9683 and 02E10196).

[1] Kautenburger & Beck (2010) *J. Environ. Monit.* **12**, 1295–1301. [2] Courdouan *et al.* (2007) *Appl. Geochem.* **22**, 2926–2939. [3] Kautenburger & Beck (2008) *ChemSusChem* **1**, 295–297. [4] Kautenburger R. (2009) *J. Anal. At. Spectrom.* **24**, 934–938.

https://doi.org/10.1180/S0026461X00006502 Published online by Cambridge University Press

Boron isotope geochemistry of subseafloor hydrothermal ore deposits, Agrokipia B, in Troodos ophiolite, Cyprus

H. KAWAHATA[1]*, K. YAMAOKA[2], S. MATSUKURA[1] AND T. ISHIKAWA[3]

[1]Atmosphere and Ocean Research Institute, The University of Tokyo, 5-1-5 Kashiwanoha, Kashiwa, Chiba, 277-8564 Japan (*correspondence: kawahata@aori.u-tokyo.ac.jp)
[2]Geological Survey of Japan, National institute of Advanced Industrial Science and Technology, 1-1-1 Higashi, Tsukuba, Ibaraki 305-8567 Japan
[3]Kochi Institute for Core Sample Research, JAMSTEC, 200 Monobe Otsu, Nankoku, Kochi, 783-8502 Japan

Cyprus-type ore deposits in many ophiolites are regarded as fossil examples of ore forming processes occurring at modern hydrothermal vent area. Hole CY2A was drilled into stockwork zone of the subseafloor Agrokipia B deposit. Boron is a useful tracer for understanding geochemical mechanism of fluid-related processes because of its chemical properties of high incompatibility and fluid mobility.

Basalts altered at low temperature (Zone A) are relatively enriched in boron (6.2–31.7 ppm) and give the average value of 21.1 ppm. On the other hand, mineralized basalts and dolerites altered at high temperature (Zones B, C, and D) have lower boron contents (0.92–17.0 ppm) and show no trend with stratigraphic depth. The $\delta^{11}B$ values of basalts from upper 450 m slightly increase with depth from 2.4 to 4.8‰, whereas those of basalts and dolerites below 450 m show a significant decrease with increasing depth. The lowermost dolerite and sulfide-enriched part of dolerite have as low as –6‰ of $\delta^{11}B$. We conclude that the rocks around Agrokipia B experienced relatively low temperature in recharge zone when Agrokipia A deposits was formed and that high temperature alterations overprinted boron content and isotopic composition of altered rocks to form the subseafloor Agrokipia B deposit. This demonstrates that boron is a good new proxy to analyze and trace hydrothermal alteration and its stages.

Continental materials around the bottom of the mantle transition zone

K. KAWAI[1], S. YAMAMOTO[2], H. ICHIKAWA[3], T. TSUCHIYA[4] AND S. MARUYAMA[5]

[1]Department of Earth and Planetary Sciences, Tokyo Institute of Technology, Tokyo, Japan (kenji@geo.titech.ac.jp)
[2]Department of Earth Science & Astronomy, The University of Tokyo, Tokyo, Japan (syamamot@ea.c.u-tokyo.ac.jp)
[3]Geodyanmics Research Center, Ehime University, Ehime, Japan (h-ichikawa@sci.ehime-u.ac.jp)
[4]Geodyanmics Research Center, Ehime University, Ehime, Japan (takut@sci.ehime-u.ac.jp)
[5]Department of Earth and Planetary Sciences, Tokyo Institute of Technology, Tokyo Japan (smaruyam@geo.titech.ac.jp)

Recent progress in our understanding of the consuming plate boundary indicates the ubiquitous occurrence of tectonic erosion of the hanging wall of the continental margin, sediment-trapped subduction, and direct subduction of immature oceanic arcs into deep mantle. Geological studies have estimated the volume of subducted tonalite–trondhjemite–granodiorite (TTG) materials to about seven times the surface total volume of continental crust. To reveal the fate of subducted crusts and how they recycle within the Earth, we studied high-pressure densities and elastic properties of TTG by means of the first principles computation method and compared them to those of peridotite. We found that TTG is gravitationally stable and its seismic velocities are remarkably faster than peridotite in the depth range from 270 to 800 km, especially from 300 to 670 km. We, therefore, propose SiO_2-rich second continents around the bottom of the mantle transition zone, which used to form the TTG crust on the Earth's surface. Our proposed model may provide reasonable explanations of seismological observations such as the splitting of the 670 km discontinuity and seismic scatterers in the uppermost part of the lower mantle. The difference in seismic velocities between PREM model and experimental results in the lower part of the transition zone can be explained by 25 volumetric% of TTG, which would correspond to about several times the present volume of the continental crust. Formation and dynamics of those second continents would have controlled the Earth's thermal history over geologic time.

https://doi.org/10.1180/S0026461X00006502 Published online by Cambridge University Press

Zircon behavior in the upper amphibolite facies polymetamorphic terrane, Ryoke belt, Japan

T. KAWAKAMI*, I. YAMAGUCHI[1,2], T.D. YOKOYAMA[1], K. MAKI[1], T. HIRATA[1] AND T. SHIBATA[1]

[1]Dept. of Earth and Planetary Sciences, Kyoto Univ., Kyoto 606-8502, Japan (*correspondence: t-kawakami@kueps.kyoto-u.ac.jp)
[2]Dowa Holdings Co. Ltd., Tokyo 101-0021, Japan

In the Ryoke metamorphic belt at the Aoyama area, SW Japan, pelitic schists and migmatites are widely outcropped, and the *P-T* condition of the regional metamorphism by which they were formed is estimated to be 3.0–4.0kbar, 615–670ºC for the Sil-Kfs zone at the north, and 4.5–6.0kbar, 650–800ºC for the Grt-Crd zone at the south [1]. The U-Th-Pb dating of the monazite in migmatites yielded 96.5±1.9Ma mainly preserved in the monazite core, and domains and rims of 83.5±2.4Ma. Although the contact metamorphism by the Ao granite at the south (79.8±3.9Ma) was not detected from the major metamorphic minerals, the coincidence of the age suggests that the Younger Ryoke granite including the Ao granite caused the contact metamorphism to the regional metamorphic rocks [2].

In the Grt-Crd zone where metamorphic temperature increases toward the south, zircon grains larger than 20 μm in diameter were abundant in the north than in the south. The comparison between the modal amount of zircon larger than 20μm and the whole-rock Zr concentration suggests that most of the whole-rock Zr was resided in zircon larger than 20μm in the north, whereas zircon larger than 20μm can account for only 20-30% of the whole-rock Zr in the south. The U-Pb dating of zircon by LA-ICPMS showed that most of the zircon larger than 20μm from the northernmost part of the Grt-Crd zone are detrital in origin. On the other hand, in the pelitic migmatite from the area where metamorphic temperature of 720 °C is estimated, several grains of ~100Ma zircon larger than 20μm were found.

These observations suggest that upper amphibolite grade metamorphism that potentially lasted about 5Ma [3] is not sufficient enough to (re)crystallize new zircon larger than 20μm, although monazite is almost completely rejuvenated. It is necessary to date tiny-grained zircon less than 20μm, or instead, use monazite in order to date upper amphibolite facies metamorphism.

[1] Kawakami (2001) *JMG* **19**, 61–75. [2] Kawakami & Suzuki (2011) *JpGU meeting abst*. SCG008-01. [3] Suzuki *et al*. (1994) *EPSL* **128**, 391–405.

Increased stable carbon isotopic ratios of oxalic, malonic, and glyoxylic acids in the Arctic aerosols during polar sunrise and after

KIMITAKA KAWAMURA[1] AND LEONARD A. BARRIE[2]

[1]Institute of Low Temperature Science, Hokkaido University, Sapporo 060-0819, Japan (kawamura@lowtem.hokudai.ac.jp)
[2]The Cyprus Institute (CyI), P.O. Box 27456 CY-1645 Nicosia, Cyprus (barrie@cyi.ac.cy)

Low molecular weight dicarboxylic acids such as oxalic acid (C_2) are present abundantly in aerosols. Because they are water-soluble, dicarboxylic acids can enhance the hygroscopic properties of atmospheric particles. During the polar sunrise season at Alert, Canadian Arctic, we observed photochemical production and loss of small diacids [1]. Although C_2 is the dominant diacid species in winter to spring, it was replaced by succinic acid after polar sunrise in May. Oxalic acid was preferentially decomposed when a solar radiation was intensified and the atmospheric transport from mid latitudes was ended in May. In this study, we applied compound-specific stable isotope analysis for diacids and related compounds isolated from the Arctic aerosols collected from late winter to early summer including dark winter and polar sunrise seasons.

Stable carbon isotopic ratios ($\delta^{13}C$) of small dicarboxylic acids and ketoacids were measured in the Arctic aerosols after derivatization to butyl esters and/or dibutoxy acetals using a capillary gas chromatography combined to on-line combustion/isotope ratio mass spectrometer [2]. We found that $\delta^{13}C$ of C_2 increased from -23‰ in early March (before polar sunrise) to -5‰ in May (after polar sunrise). Malonic acid (C_3) also showed an increase of $\delta^{13}C$ from late February (-25‰) to early May (-17‰). Glyoxylic acid (HOC-COOH), a precursor of C_2, showed similar increase from -18‰ in late February to -10‰ in May. Glyoxal (HOC-CHO), another precursor of C_2, showed very high isotopic ratios up to +15‰. In contrast, isotopic composition of succinic acid (-32‰ to -24‰) did not show a systematic trend. An increase in $\delta^{13}C$ values is probably associated with photochemical ageing of aerosols. It is likely that ^{12}C-^{12}C bonds of oxalic and other species decompose preferentially over ^{12}C-^{13}C bonds during photochemical ageing. Isotopic fractionation of C_2 and its precursors may also be likely during the gas/particle portioning. Here, we propose that $\delta^{13}C$ of oxalic acid can be used as a photochemical tracer for the ageing of organic aerosols.

[1] Kawamura *et al*. (2010) *J. Geophys. Res*. **115**, D21306, doi, 10.1029/2010JD014299. [2] Kawamura & Watanabe (2004) *Anal. Chem*. **76**, 5762–5768.

https://doi.org/10.1180/S0026461X00006502 Published online by Cambridge University Press

Stable isotope approach for feeding structure of mudskipper *Periophthalmus argentilineatus* at different habitats in Okinawa Islands, Japan

R. KAWAMURA[1], H. FUJIMURA[1]*, R. UEMURA[1], T. HIGUCHI[2], B.E. CASARETO[2] AND Y. SUZUKI[2]

[1]Univ. of the Ryukyus, 1 Senbaru, Nishihara, Okinawa 903-0213, Japan (*correspondence: fujimura@sci.u-ryukyu.ac.jp)
[2]Shizuoka Univ., 836 Ohya, Suruga-ku, Shizuoka-shi, Shizuoka 422-8529, Japan

Introduction

Barred mudskipper *Periophthalmus argentilineatus* is an amphibious gobioid fish, inhabiting in mudflats, mangroves and port. Mudskippers are known as a carnivorous fish that feed insects as well as benthic animals such as small crustacea on intertidal area [1, 2]. While adult males of the mudskipper have territory around their nests, adult females move along with tidal migration front without their nests. Because the adult individuals have not been observed to move wide range habitats (e.g. between river systems), food differences of barred mudskippers are expected to reflect food availability of each habitat. Stable isotope is one of the powerful tools for studies of food chain in an ecosystem. This study is to reveal food differences attributed to differences of habitat environment and feeding behavior between males and females, using stable isotopic methods.

Materials and Methods

Mudskipper, other benthic animals, particulate matter and sediments were taken from intertidal area of mudflats and mangroves around tropical coral reefs of Okinawa, Japan. Mudskipper samples were separated into gut and muscular tissues. Then, all the organic tissue were freeze-dried and analyzed $\delta^{13}C$, $\delta^{15}N$, $\delta^{34}S$ using a continuous flow EA/IRMS (Delta V advantage, Thermo).

Results and Discussion

Muscular tissues of mudskipper showed $\delta^{13}C$ = -17.4‰ and $\delta^{15}N$ = 7.4‰ at Iriomote Island; $\delta^{13}C$ = -21.3‰ and $\delta^{15}N$ = 11.8‰ at Okinawa Island. These results suggested significantly different food sources and availabilities of the two islands.

[1] Kruitwagen *et al*. (2007) *J. Fish Biol*. **71**, 39–52. [2] Nanjo *et al*. (2008) *Fisheries Sci*. **74**, 1024–1033.

Assessment of cloud droplet growth based on the measurements of hygroscopicity and CCN activity of aerosol particles in Nagoya, Japan

K. KAWANA[1]*, M. MOCHIDA[1] AND N. KUBA[2]

[1]Graduate School of Environmental Studies, Nagoya, University, Nagoya, Japan (*correspondence: kawana.kaori@d.mbox.nagoya-u.ac.jp)
[2]Research Institute for Global Change, Japan Agency for Marine-Earth Science and Technology, Yokohama, Japan

To better understand the aerosol-cloud relationship in the atmosphere, we investigated hygroscopicity and CCN activity of aerosol particles by ground-based observation, and performed model calculations to predict the concentrations and the effective radii of cloud droplets (N_d and R_{eff}, respectively) formed from the observed particles. The field observation was conducted in the city of Nagoya, from 29 July to 3 August, 2010. The hygroscopic growth of aerosol particles were measured using a Hygroscopicity Tandem Differential Mobility Analyzer (HTDMA). The aerosol particles were classified by the dry mobility diameter in the first DMA, and were further classified by the diameter under the condition of 85% relative humidity in the second DMA. A CCN counter (CCNC) and a condensation particle counter to measure CCN and condensation nuclei were connected to the second DMA. The CCN were measured at supersaturations of 0.17%, 0.48%, and 0.93%. The hygroscopic growth factors (HGFs) of studied particles were 1.0, 1.1, 1.25, and 1.4.

The measured CCN activation diameters (d_{act}) were smaller than those predicted; i.e. the actual CCN activity was higher than that predicted. Whereas the differences between predicted and measured d_{act} were not very large for more hygroscopic particles, they were remarkable for particles with HGF of 1.0. Based on the HGF data, we performed model calculations to investigate how the differences of particle hygroscopicity and the differences between predicted and measured d_{act} for particles with HGF of ~1.0 affect the cloud droplet formation. If less hygroscopic aerosol particles in addition to more hygroscopic particles are considered in the cases of large updraft velocity conditions, N_d and R_{eff} are, respectively, substantially larger and smaller than those calculated with consideration of only more hygroscopic particles. Further, if we correct the model inputs based on the differences between predicted and measured d_{act}, N_d increase and R_{eff} decrease slightly. These results suggest that less hygroscopic aerosol particles in the urban area could contribute to the cloud droplet formation, and play an considerable role in the formation of clouds.

https://doi.org/10.1180/S0026461X00006502 Published online by Cambridge University Press

Högbomite from West Ongul Island, Lützow-Holm Complex, East Antarctica

TOSHISUKE KAWASAKI* AND SYOTA HAMADA

Ehime University, Matsuyama 790-8577, Japan
(*correspondence: toshkawa@sci.ehime-u.ac.jp)

Högbomite has been found within magnetite megacrysts (5 cm × 3 cm) from the upper amphibolite- to granulite-facies pegmatite cutting the medium-grained quartzo-feldspathic garnet-biotite gneiss at West Ongul Island, Lützow-Holm Complex, East Antarctica. Associated minerals included in magnetite are biotite, plagioclase, hercynite, sillimanite, corundum, quartz, rutile, ilmenite, hematite, and zircon. Högbomite occurs as very fine euhedral to subhedral crystal (5-20 μm) along grain boundaries between magnetite and ilmenite or less commonly enclosed in hercynite (Fig. 1) and in magnetite. Quartz is found in hercynite. Högbomite is in direct contact with hercynite. Ilmenite contains hematite exsolution lamellae. Hematite also forms exsolution lamellae in rutile, which is trapped in ilmenite. Corundum is in direct con-tact with magnetite, hercynite or sillimanite. Electron microprobe analyses of högbomite yield 2.6-7.9 wt% TiO_2, 60-64 wt% Al_2O_3, 0-0.1 wt% Cr_2O_3, 18-25 wt% Fe (as FeO), 0.3-0.6 wt% MnO, 2.9-4.4 wt% MgO, 4.8-10 wt% ZnO, 0.61-0.01 wt% SnO_2, and 0.20-0.36 X_{Mg}. Hercynite varies 4.9-14 wt% ZnO and 0.23-0.36 X_{Mg}. Sillimanite contains 0.6-3.6 wt% Fe_2O_3 from rim to core and < 0.1 wt% TiO_2. Textures and mineral chemistry suggest that the reaction, Mag + Ilm + H_2O + O_2 → Hög + Hc + Qtz, took place at retrograde stage (T < 600 °C) whereby magnetite and ilmenite contained impurities Si, Al, Zn and Mg. Hydrous and oxidized fluid, possibly supplied by crystallization process of pegmatite, were sufficiently enough to form högbomite and biotite. Subsequent cooling processes hematite crystallized as exsolution lamellae from ilmenite and rutile, and sillimanite and corundum became Fe_2O_3-poor at the rim.

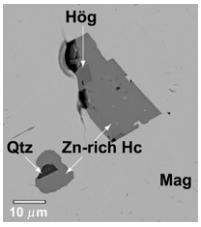

Figure 1: Backscattered image of högmatite + hercynite and her-cynite + quartz in magnetite.

Neogene Central Andean adakites, frontal arc migration and forearc subduction erosion at 27°-28.5°S

S. MAHLBURG KAY[1]*, A.R. GOSS[2] AND C. MPODOZIS[3]

[1]Dept. Earth Atm. Sci., Snee Hall, Cornell Univ., Ithaca, NY, 14853 USA (*correspondence: smk16@cornell.edu)
[2]Exxon Production Company, Houston, TX, U.S.A adam.r.goss@exxonmobil.com
[3]Antofagasta Minerals, Santiago, Chile

Glassy plagioclase phenocryst-free 8 to 2 Ma Andean andesitic lavas erupted at 27°-28.5°S can be argued to contain continental crust incorporated in the sub-arc mantle by forearc erosion as well as by melting in the overlaying ~65-70 km thick crust. These distinctive ~7.7 Ma pyx-bearing Dos Hermanos and 7-2 Ma amp-bearing Pircas Negras lavas (54-64% SiO_2) erupted as the frontal arc was being displaced ~50 km eastward over a developing bend in the Wadati-Benioff zone that now marks the Chilean flat-slab northern margin [1]. These lavas can show the most HFSE depletion (La/Ta=40-100) and adakitic-like character (Sm/Yb=4-9; Sr=600-1400 ppm) among Neogene lavas in the region and have higher $^{87}Sr/^{86}Sr$ (0.7055-0.7065) than 26-13 Ma lavas (<0.7055). Some 5-3 Ma lavas have high Mg# (to 61), Cr (to 250 ppm) and Ni (to 65 ppm). Their chemistry fits with trace element and isotopic models [2, 3] that begin with > 2 GPa partial melts of ~85:15 mixtures of mafic Jurassic and silicic Paleozoic Chilean forearc rocks reacting with sub-arc mantle peridotite. Mineral thermometry and MELTS program models for the Pircas Negras lavas indicate pre-eruption temperatures near 1050°C showing these magmas can then mix with and melt the overlying eclogitic crust. Given a constant arc-trench gap over the last 8 Ma, ~124 km^3/m. y./km of forearc crust needs to be removed to account for frontal arc migration at 8 to 2 Ma and is readily available to contaminate the mantle wedge.

[1] Mulcahy & 7 others (2010) *AGU* **91**, T11A-2050. [2] Goss & Kay (2009) *EPSL* **270**, 97–109. [3] Goss (2007) PhD thesis, Cornell Univ. Ithaca, NY, 351 pp.

https://doi.org/10.1180/S0026461X00006502 Published online by Cambridge University Press

Cathodoluminescence characterization of He^+ ion implanted plagioclase

M. KAYAMA[1]*, H. NISHIDO[1], S. TOYODA[2], K. KOMURO[3] AND K. NINAGAWA[22]

[1]Research Institute of Natural Sciences, Okayama University of Science, Japan
(*correspondence: kayama@rins.ous.ac.jp)
[2]Department of Applied Physics, Okayama University of Science, Japan
[3]Earth Evolution Sciences, University of Tsukuba, Japan

Cathodoluminescence (CL) techniques have been often used as an effective tool to visualize radiation halos in quartz. No investigation of radiation effects on CL of feldspar has been performed to date, although the visible halos can easily be found in the feldspar directly attached to radioactive minerals. In this study, CL of plagioclase implanted by He^+ ion has been conducted to clarify radiation effect on CL of plagioclase.

Single crystals of albite (Or_1Ab_{99}) from Minas Gerais, Brazil, oligoclase ($Or_2Ab_{82}An_{16}$) from Inabu, Japan, andesine ($Or_1Ab_{53}An_{46}$) from Bekily, Madagascar; and anorthite (Ab_5An_{95}) from Yoichi, Japan were selected for CL measurements. He^+ ion implantation with 4.0 MeV (dose density: 2.18×10^{-6} to 6.33×10^{-4} C/cm^2) on the samples was conducted using a 3M-tandem ion accelerator at at Takasaki Research Center of the Japan Atomic Energy Research Institute.

CL spectra of unimplanted and implanted plagioclase show emission bands at 350, 420, 580 and 740 nm. Implanted albite and oligoclase exhibit characteristic red emissions at 700–750 nm, where the intensities increase with an increase in radiation dose. Spectral deconvolution of albite and oligoclase samples can successfully separate the red emission into three Gaussian components at 1.861, 1.644, and 1.557 eV. Integral intensity of the component at 1.86 eV linearly correlates with radiation dose. The CL spectra of andesine and anorthite show no component at 1.861 eV. The component at 1.861 eV might be attributed to oxygen vacancy between Al and Si tetrahedra associated with two Na atoms ($O^{1-}/^{27}Al \times 2^{23}Na$ center). The component intensity clearly correlates with radiation dose as a function of $O^{1-}/^{27}Al \times 2^{23}Na$ center, but does not depend on the concentration and distribution of other emission centers, degree of Si-Al order and presence of microstructures or texture. CL spectral deconvolution, therefore, may be applied to evaluate radiation dose of alpha particles from natural radionuclides on Na-rich feldspar.

Semi detail orientation survey in semi arid conditions and mineral influenced basin, case study in Southestern Iran

A. KAZEMI MEHRNIA* AND I. RASA

University of Shahid Beheshti- Tehran, Iran
(*correspondence: akmehrnia@yahoo.com)
(I.Rasa@sbu.ac.ir)

Semi Detail orientation survey

The aim of this research is to find the optimum size fraction of stream sediment sampling in semi detail geochemical sampling and mineral influenced basin. In this study 21 stream sediment samples collected from of streams that draining Cu-Mo porphyry deposits in southeast of Iran.

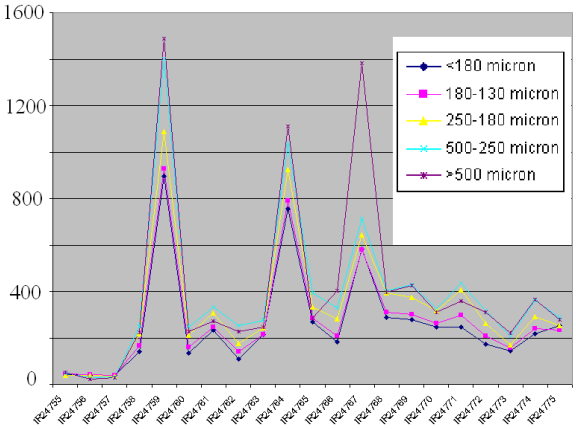

Figure 1: Sample Figure of Copper in stream sediments.

Discussion of Results

The charts (e.g. Fig. 1) suggest that >500 μm fractions give the strongest and most consistent anomalies for Cu, Mo and Au while 500-250 μm fractions give better Zn and Pb anomalies. The finer size fractions give a stronger anomaly response for gold [12]. By sampling the fine sediment fractions with high sampling density, uncertainty associated with the nuggety nature of gold can be reduced to a level [1]. In detail stream geochemistry the anomaly are not affected by Aeolian dust deposits respectively.

[1] Carlile, Digdowirogo, & Darius (1990) *Geochem. Explorer*. **35**, 105–140. [2] Melo & Fletcher (1999) *Journal of Geochemical Exploration*. **67**, 235–243.

https://doi.org/10.1180/S0026461X00006502 Published online by Cambridge University Press

Testing the 'post-glacial weathering peak' hypothesis – A lacustrine record of $^{87}Sr/^{86}Sr$

ANDREW R. KEECH[1]*, DEREK VANCE[1], COREY ARCHER[1] AND STEVE LUND[2]

[1]Bristol Isotope Group, School of Earth Sciences, University of Bristol, Queen's Road, Bristol, BS8 1RJ, UK
[3]Department of Earth Sciences, University of Southern California, Los Angeles, CA 90089-0740, USA
(*correspondence: andrew.keech@bristol.ac.uk)

Chemical weathering of the continents regulates levels of atmospheric CO_2, thereby acting as a primary control on Earth's climate [1]. The effect of continental ice sheets, as observed during the Pleistocene, on this regulation of global climate is not clear. It has been suggested that repeated transitions between glacial (high physical weathering) and interglacial (high chemical weathering) states may have enhanced CO_2 drawdown during the Quaternary [2].

[2] argue that present riverine inputs to the oceans are still distorted by the last glaciation and are above the long-term average. During the incipient stages of chemical weathering the Sr released is more radiogenic than the bulk rock [3, 4]. Therefore, associated with the landscape rejuvenation caused by each Pleistocene glaciation one might expect a peak in radiogenic Sr in continental runoff. Such a 'post-glacial weathering peak' is required to explain the modern marine Sr budget [2, 5].

We attempt to test the 'weathering peak' hypothesis by constructing a record of Sr isotope composition of waters draining the Sierra Nevada through the last glaciation using ostracods in previously studied sediment cores from Owens Lake, California (e.g. [6]). Preliminary data from ostracods in Holocene sediments show elevated $^{87}Sr/^{86}Sr$ relative to the modern flow-weighted mean $^{87}Sr/^{86}Sr$ of streams in the Owens Lake drainage (0.70911) [7]. Further analyses will complete a record of the Owens Lake Sr isotope composition from ~40ka to the present day and will allow for a comparision to the contemporaneous extent of glaciers in the Sierra Nevada [6] thus allowing us to test the 'post-glacial weathering peak' hypothesis.

[1] Walker, J.C.G. *et al*. (1981) *JGR* **86**, 9776–9782. [2] Vance *et al*. (2009) *Nature* **458**, 493–496. [3] Blum *et al*. (1997) *GCA* **61**, 3193–3204. [4] Keech *et al*. (2009) *GCA* **73**, 13 S1 A632. [5] Krabbenhoft *et al*. (2010) *GCA* **74**, 4097–4109. [6] Benson *et al*. (1996) *Science* **274**, 746–749. [7] Pretti & Stewart (2002) *Water Resour. Res*. **38**, 10.1029/2001 WR000370

As, Fe and S cycling during reductive biomineralisation of pedogenic jarosite

A.F. KEENE*, S.G. JOHNSTON, E.D. BURTON AND R.T. BUSH

Southern Cross GeoScience, Southern Cross University, Lismore NSW 2480, Australia
(*correspondence: annabelle.keene@scu.edu.au)

Jarosite (KFe_3 $(SO_4)^2$ $(OH)_6$) is an abundant Fe (III) mineral phase and important contaminant sorbent in coastal acid sulfate soils (ASS) [1]. Jarosite in these environments can be prone to reductive dissolution as a result of changes in local hydrology (e.g. sea-level rise and tidal seawater reflooding) [2]. However, very few studies have examined the reductive dissolution and transformation of K-jarosite, and the associated effects on contaminant mobility following seawater inundation of a jarosite-rich soil. Here we investigate the reductive biomineralisation of a natural As (V)-bearing pedogenic K-jarosite and explore the effects of a seawater gradient on the cycling of As, Fe and S. Solid and aqueous phase partitioning and speciation of As, Fe and S were determined using a wide variety of techniques including As- and S- K-edge XAS, TEM-SAED, SEM and XRD.

Whilst the rate and magnitude of fermentation processes were initially similar across the seawater gradient (100%, 10%, 1%), reductive dissolution of jarosite proceeded faster under 100% seawater conditions. Concentrations of $Fe^{2+}_{(aq)}$ were ~4-fold higher in 100% seawater and Fe^{2+}:K^+ ratios were initially congruent with respect to solid-phase jarosite. Evidence suggests both dissimiliatory reduction of jarosite-Fe (III) and abiotic reduction of Fe (III) by sulfide produced via sulfate-reducing bacteria. Residual jarosite became increasingly polycrystalline and developed hollow cores. Disordered nano-particulate mackinawite was a primary mineralisation product after 140 days in 100% seawater.

While As mobilisation was generally correlated with $Fe^{2+}_{(aq)}$ production, As displayed highly contrasting kinetics across the seawater gradient. Initial release of $As_{(aq)}$ was most rapid in low seawater treatments. Although As mobilisation in 100% seawater eventually exceeded the low seawater treatments, it was not substantially attentuated by the formation of mackinawite. The proportion of solid-phase As (III) increased over time and was greatest in 100% seawater. Findings provide important insights into the reductive dissolution of pedogenic jarosite following seawater inundation in coastal ASS environments.

[1] Keene *et al*. (2011) *Biogeochemistry* **103**, 263–279. [2] Johnston *et al*. (2011) *Chemical Geology* **2**, 257–280.

https://doi.org/10.1180/S0026461X00006502 Published online by Cambridge University Press

On the significance of ultra-magnesian olivines in basaltic rocks

J.K. KEIDING[1]*, R.B. TRUMBULL[1], I.V. VEKSLER[1,2] AND D AND A. JERRAM[3]

[1]GFZ German Research Centre for Geosciences Potsdam Germany (*correspondence: jakob@gfz-potsdam.de)
[2]Technical University of Berlin, Germany
[3]Dept. of Earth Sciences, Durham University, United Kingdom

The temperature regime in the Earth's mantle is of prime importance for models of mantle convection and a key test of the mantle plume hypothesis. Olivine thermometry is commonly used to constrain mantle potential temperatures in basaltic magmatic provinces. Ultra-magnesian olivines, here defined as Fo > 92, are common in Archean komatiites and occasionally observed in Phanerozoic LIPs. The presence of ultra-magnesian olivines is generally interpreted as evidence for melts with extremely high MgO concentration and high eruption temperatures. Such melts are considered to be a hallmark of a hotter mantle in the early Earth and of thermal anomalies related to Phanerozoic mantle plumes. Estimating primary melt compositions and temperature based on mineral and rock data is a common approach but subject to large uncertainties. A better alternative is direct study of melt inclusions trapped with early-formed crystals and isolated from the rest of the magma. Here we present data of olivine-hosted melt inclusions and their host crystals from the Henties Bay-Outjo (HOD) dyke swarm in NW Namibia. These dykes are interpreted to have been feeders to the Etendeka volcanics and are characterized by the local presence of high MgO (picritic) compositions. The composition of melt inclusions trapped in ultra-magnesian olivine ($Fo_{93.3}$) from the HOD contradict the predicted 24 wt. % MgO for parental melts and 1680 °C mantle potential temperature based on olivine whole-rock models [1]. Instead, the trapped melts do not exceed 17.5 wt. % MgO and the maximum potential temperature indicated by these compositions is 1520 °C. Most olivines in the HOD rocks with Fo > 85 are too Mg-rich to be in equilibrium with the whole-rock composition, indicating that the grains are entrained xenocrysts from earlier, more magnesian melts. We show that ultra-magnesian olivines can be produced by protracted melt extraction from the mantle source and that this process also leaves a distinctive depletion in the incompatible trace elements.

[1] Thompson, & Gibson (2000) *Nature* **407**, 502–506.

A poor man's enzyme? Effects of reactive Mn(III)-oxalate complexes on structurally intact plant cell walls

MARCO KEILUWEIT[1,2], JEREMY BOUGOURE[2], PETER S. NICO[3]*, JENNIFER A. SUMMERING[1], MARKUS KLEBER[1] AND JENNIFER PETT-RIDGE[2]

[1]Department of Crop and Soil Science, Soils Division, Oregon State University, Corvallis, OR-97331
[2]Lawrence Livermore National Laboratory, Physical and Life Sciences Directorate, Livermore, CA-94550
[3]Lawrence Berkeley National Laboratory, Earth Sciences Division, Berkeley, CA-94720 (*correspondence: PSNico@lbl.gov)

Manganese (III)-ligand complexes such as Mn (III)-oxalate are potent and highly diffusible oxidizers for lignin model compounds [1, 2]. Although there is clear indication for their potential role in lignin decomposition processes in soils [3, 4], few reports exist on mechanistic aspects such as substrate specificity, reaction kinetics and oxidizing power of Mn (III)-oxalate complexes reacting with structurally intact plant materials. This is of particular importance in the context of soil organic matter decomposition since lignin cannot be viewed as a single substance [5], but has to be seen as an integral component of ligno-carbohydrate complexes (LCC) in fresh plant cell walls (e.g. in litter, root and wood).

Here we tested the hypothesis that Mn (III)-oxalate complexes may act as a 'pretreatment' for structurally intact LCC components in plant cell walls. The diffusible oxidizers are thought to be small enough to penetrate and react with composite LCC in cell walls, thereby increasing porosity which permits access to more efficient lignin- and cellulose-decomposing ezymes. This was investigated by reacting cell walls of single *Zinnia elegans* tracheary elements with Mn (III)-oxalate complexes in a continuous flow-through micro-reactor. The uniformity of these individual plant cells allowed us to examine Mn (III)-induced changes in cell wall chemistry and ultrastructure on the micro-scale using fluorescence and electron microscopy as well as IR and X-ray spectromicroscopy. This presentation will discuss the specificity of Mn (III)-complexes for certain cell wall functionalities, the impact of such reactions on cell integrity, and potential implications for soil C cycling.

[1] Wariishi *et al*. (1992) *J. Biol. Chem*. **267**, 23688–23695. [2] Perez & Jeffries (1992) *Environ. Microbiol*. 58(8) 2402–2409. [3] Hofrichter (2002) *Enzyme Microb. Tech*. 30(4) 454–466. [4] Berg *et al*. (2010) *Biogeochemistry* **100**, 57–73. [5] Thevenot *et al*. (2010) *Soil Biol. Biochem*. **42**, 1200–1211.

https://doi.org/10.1180/S0026461X00006502 Published online by Cambridge University Press

The influence of co-contaminant complexing agents on radionuclide environmental behaviour

MIRANDA J. KEITH-ROACH[1,2]*, ESTELA REINOSO-MASET[1], COLIN C. MAY[1], LINDSAY YOUNG[1] AND PAUL J. WORSFOLD[1]

[1]Biogeochemistry Research Centre, University of Plymouth, Plymouth, PL4 8AA, UK
[2]Kemakta Konsult, S-11293 Stockholm, Sweden
(*correspondence: mkeith-roach@plymouth.ac.uk)

Organic complexing agents that are co-disposed in radioactive waste or formed *in situ* may enhance the migration of radionuclides at contaminated sites. However, the mechanisms of the interactions are poorly understood. We have therefore undertaken an extensive program of research to probe the speciation of radionuclide-organic co-contaminant complexes, competitive interactions with common metal ions and the mechanisms by which the complexing agents impact radionuclide sorption and transport. This work has utilised electrospray ionisation mass spectrometry for the characterisation of aqueous speciation, kinetic batch sorption experiments using a relevant, characterised terrestrial sand (Drigg sand) and dynamic column experiments coupled with the k1D transport code. Thorium (IV), U (VI), Sr (II) and Cs (I) were selected as model radionuclides of different oxidation states and EDTA, NTA, picolinic acid and isosaccharinic acid were included as key complexing agents.

The complexing agents generally influenced radionuclide behaviour in the expected order of Th>U (VI)>Sr, with no discernable effect on Cs, and EDTA generally exerted the greatest influence of the complexing agents. However, the results highlighted the complexity of these interactions. In several cases, the speciation of the complexes was more diverse than suggested by the existing speciation databases. Also, the kinetics of exchange between radionuclide complexes and common metal ions varied from occurring virtually instantaneously to over several months, and could involve precipitated metal phases.

Batch experiments demonstrated that the concentration of the radionuclide strongly influences the effect that a complexing agent can have, in terms of both the kinetics of sorption and the equilibrium position. Finally, transport experiments identified that the formation of ThEDTA complexes enhances Th transport, but that at higher Th concentrations, EDTA-mediated colloidal Th transport occurs. The key data from these studies will be presented and discussed in terms of the environmental importance of the complexing agents.

Geochemical study and U/Th dating of the Akköy fissure ridge travertine (SW-Turkey): Paleoclimatic and paleoseismic interpretations

S. KELE[1]*, M. ÖZKUL[2], A. GÖKGÖZ[2], C.-C. SHEN[3], I. FÓRIZS[1], M.O. BAYKARA[2] AND M.C. ALÇIÇEK[2]

[1]Hungarian Academy of Sci., Institute for Geochemical Research, Budaörsi út 45, H-1112 Budapest, Hungary (*correspondence: keles@geochem.hu)
[2]Pamukkale Univ., Dep. of Geol. Eng., TR-20070 Denizli, Turkey
[3]National Taiwan University, Taipei, Taiwan

Fissure ridge travertines are elongated, wedge-like nonmarine carbonate deposits formed due to CO_2 degassing from carbonate rich thermal spring waters. They are well-known indicators of past and present seismic activity, including Quaternary and prehistoric major earthquake events, as generally deposited from springs discharging in co-seismic extensional fissures along major active faults [1, 2]. The precipitation of travertines is strongly influenced by the water supply controlled mainly by climate, thus the question must be raised, whether the tectonic and/or climatic processes has the major role on their deposition.

To answer the question, we performed detailed U-series dating and stable isotope and trace elemental study of travertines collected along a vertical section, through the bedded layers of the Akköy, Karakaya Hill fissure ridge (Denizli Basin, SW-Turkey). The U-series age data range from 45±108 ka to 18±0.3 ka. The more or less continuous travertine deposition at the Akköy fissure ridge during cold-dry and warm-wet climatic events indicates that the travertine deposition was controlled strongly by tectonic processes, i.e. the area of the Denizli Basin was seismically active during the period mentioned above. The trace element concentrations of the bedded travertine deposits show temporal change in the geochemistry of the travertine depositing thermal water.

[1] Hancock *et al*. (1999) *J. Struct. Geol*. **21**, 903–916.
[2] Uysal *et al*. (2009) *Chem. Geol*. **265**, 442–454.

https://doi.org/10.1180/S0026461X00006502 Published online by Cambridge University Press

Mantle melting and melt transport beneath oceanic spreading ridges

PETER B. KELEMEN

LDEO, Columbia University (peterk@LDEO.columbia.edu)

Degree of melting & potential temperature

Reaction of cooling melt with shallow peridotite can reset indicators of degree of melting and potential temperature in both melt and residual peridotite. Yb concentration and spinel Cr# in peridotite are affected by (a) small scale variations in reactive melt transport, (b) variable extents of melt *extraction*, and (c) 'impregnation', i.e. partial crystallization of cooling melt in pore space. Also, many peridotites at ridges may have undergone several extensive partial melting events over Earth history, while others could be residues of extensive melt extraction from mafic heterogeneities in the mantle source.

Melt focusing to ridges

Modeled crystallization of cooling melt in the shallow mantle can create a permeability barrier guiding underlying melt diagonally toward the ridge, but field studies have not identified such barriers. Permeable 'shear bands' may guide melt to the ridge, but the nature of shear bands in open systems at natural grain size and strain rates is uncertain. 2D and 3D focused solid upwelling due to melt buoyancy and weakening as a function of permeability – especially increasing permeability with decreasing pyroxene content during melting – may warrant more attention.

Crustal thickness, spreading rate & melt productivity

The following three statements are inconsistent: (1) Modelled peridotite melt productivity beyond cpx exhaustion is ≥ 0.11%/GPa. (2) Crustal thickness is independent of spreading rate. (3) Thermal models predict, and observations confirm, thick thermal boundary layers beneath slow spreading ridges. Most sampled peridotites from ridges melted beyond cpx-out. Cpx in these rocks formed via impregnation and/or exsolution during cooling. The data can be understood if (a) melt productivity is << 0.1%/GPa beyond cpx-out, and (b) cpx-out occurs > 15 km below the seafloor beneath most ridges.

Conduit generation and geometry

Dunites, formed by pyroxene dissolution in olivine-saturated melt ascending by porous flow, are conduits for focused porous flow of melt, preserving disequilbrium between melt and pyroxene in surrounding peridotite at P < 1.5 GPa. Perturbations in permeability grow into dunite conduits because incongruent dissolution increases porosity and permeability. Perturbations may arise from 'shear bands' and/or heterogeneities in the mantle source. Conduits may also involve mechanical instabilities, if it is easier to open a pore than to close it. Most models and experiments do not produce the power law distribution of dunites at a given depth observed in peridotites, except for some shear band experiments.

Underplating of felsic rocks in arcs

PETER KELEMEN[1], BRADLEY HACKER[2] AND MARK BEHN[3]

[1]LDEO, Columbia University (peterk@LDEO.columbia.edu)
[2]UCSB (hacker@geol.ucsb.edu)
[3]WHOI (mbehn@whoi.edu)

Buoyant, felsic material may be subducted and then returned to the base of evolving crust via (a) relamination, (b) diapirs in the mantle wedge, and/or (c) imbrication (e.g. [1-5]). Subducting crust is carried to conditions (~700°C and P > 1 to 2 GPa) where garnet is stable, rendering some lithologies denser than mantle peridotite at the same PT, and where material is hot enough to flow viscously in response to buoyancy forces [6]. Whereas delamination and foundering can only remove dense lithologies from a narrow, high PT horizon at the base of typical crust, the *entire* subducting crustal section can undergo density sorting in subduction zones. Such efficient density sorting may explain why lower continental crustal compositions, including mafic estimates [7], are less dense than peridotite at the same PT [5, 6, 8].

Sediment subduction and 'subduction erosion' involve intermediate to felsic shale and greywacke. If they are in layers or blobs with dimensions > 100 m, they will rise buoyantly at > 700-800°C in times < 1 Myr [4]. Ascent in a 'subduction channel' involves isothermal decompression to a level of neutral buoyancy (a). Most UHP terrains record re-equilibration at 700°C and 0.5-1 GPa, in accord with this idea [5]. Diapric ascent through the hot mantle wedge (b) will induce extensive melting, producing the 'sediment component' in arc magmas [4]. Some trench sediments may be thrust directly into arc lower crust (c), producing andesitic paragneiss recording typical arc Moho PT (~ 800°C, 1 GPa [9]), as in the North Cascades. Indeed, the 35 km of crust beneath such exposures may itself have been added later, via continued underlplating of buoyant, felsic material. In general, arc magma flux estimates that assume subduction erosion always removes arc crust are overestimates.

Arc-arc or continental collision will also lead to efficient separation of dense, mafic rocks from bouyant, felsic metasediments and plutons that rise to neutral buoyancy [5].

As a result, much of the continental lower crust may be quite felsic, similar to typical granulite terrains. This is consistent with Vp and heat flow data provided that some U, Th and K are extracted via decompression melting [5].

[1] Kelemen *et al*. *Treatise on Geochem* 03 [2] Gerya & Yuen EPSL 03 [3] Currie *et al*. *Geol* 07 [4] Behn *et al*. *Nature Geosci* in revision [5] Hacker *et al*. *EPSL* in revision [6] Jull & Kelemen *JGR* 01 [7] Rudnick & Presper *in Granulites & Crustal Evolution*, D. Vielzeuf, & P. Vidal eds. 90 [8] Behn & Kelemen *JGR* 06 [9] Kelemen *et al*. *AGU Monograph* 03

https://doi.org/10.1180/S0026461X00006502 Published online by Cambridge University Press

Geochemical and ecological models of plant-driven chemical weathering: Insights into the sinks for atmospheric CO_2

C.K. KELLER[1]*, R. O'BRIEN[2], Z. BALOGH-BRUNSTAD[3] AND B.T. BORMANN[4]

[1]SEES, Washington State Univ., Pullman, WA 99164, USA (*correspondence: ckkeller@wsu.edu)
[2]Allegheny College, Meadville, PA 16335, USA
[3]Hartwick College, Oneonta, NY 13820, USA
[4]Forest Service PNW, Corvallis, OR 97331, USA

It is generally agreed that rhizospheric acidification of the shallow subsurface – the vascular-plant 'acid pump' – accelerates weathering and the loading of soil and drainage waters with base cations, thereby also promoting drainage losses of weathering products (chemical denudation) and lowering atmospheric CO_2 levels on geologic timescales [e.g. 1, 2]. Mass-balance tests of this model, in comparative studies of watersheds with different plant covers, report scattered results.

In our experimental mesocosm studies employing the same approach, a single ecosystem exhibits order-of-magnitude variations in chemical weathering and denudation rates over decadal timescales. Our results also show that the silicate-derived Ca+Mg denudation flux, i.e. the lithospheric CO_2 sink, is not equivalent to the alkalinity flux, i.e. the hydrospheric sink, because of disturbance-driven strong-acid generation. These results underline the idea that the efficacy of the plant-driven lithospheric CO_2 sink, and perhaps associated long-term climate control, may depend on the planet's geophysical, biological and ecological disturbance regime. It is true that the weathering power of vascular plant systems dwarfs that of nonvascular systems; but the vascular systems also have correspondingly great capacity to conserve the nutrients generated by weathering, by localizing water and nutrient cycles both during growth and following perturbations.

Our findings are consistent with an ecological model in which mechanisms of biologically mediated weathering are adaptive functions of ecosystem state. In this paradigm, which emphasizes the plant as chemical sink and builder of soil and ecosystem nutrient capital, vascular systems are likely to deploy varying portfolios of weathering and nutrient uptake strategies, involving a range of plant physiologies, rhizospheric symbioses, and mass transfer and transport mechanisms with a range of hydrochemical consequences.

[1] Keller & Wood (1993) *Nature* **364**, 223–225. [2] Berner (1997) *Science* **276**, 544–546.

Beyond the closure temperature concept: when does $^{40}Ar/^{39}Ar$ dating constrain exhumation?

S.P. KELLEY[1], C.J. WARREN[1] AND F. HANKE[2]

[1]CEPSAR, The Open University, Walton Hall, Milton Keynes, MK7 6AA, United Kingdom
[2]Surface Science Research Centre, Department of Chemistry, University of Liverpool, Liverpool, L69 3BX, United Kingdom

$^{40}Ar/^{39}Ar$ ages determined on metamorphic minerals are commonly assumed to reflect cooling and exhumation, but recently reported experimental results on muscovite suggest a significant pressure dependence of argon diffusion in muscovite, which acts to decrease argon diffusion rates at high pressure. Using numerical diffusion models, which include a pressure correction, we systematically interrogate the assumptions associated with $^{40}Ar/^{39}Ar$ dating of muscovite in such rocks. We show the pressure-temperature regions in which $^{40}Ar/^{39}Ar$ dating could constrain the timing of exhumation in an open system, and suggest a method for checking that the rock being dated has behaved as an open system during exhumation. The link between apparent $^{40}Ar/^{39}Ar$ age and traditional 'closure temperature' is shown to be valid only when muscovite crystallized under, or subsequently reached, high temperature and relatively low pressure conditions. Our modelling data suggest that HP and UHP rocks, particularly those that have experienced short orogenic cycles are unlikely to yield cooling and exhumation ages. The results and discussion presented here for muscovite are equally applicable to other metamorphic minerals commonly dated using the $^{40}Ar/^{39}Ar$ system.

https://doi.org/10.1180/S0026461X00006502 Published online by Cambridge University Press

Si isotope fractionation in high-temperature metal-silicate systems: Implications for core formation

J.KEMPL[1]*, P.Z. VROON[1], W.V. WESTRENEN[1], J.A. SMALL[2] AND H.G. JAK[3]

[1]FALW, VU University Amsterdam, The Netherlands (*correspondence: josepha.kempl@falw.vu.nl)
[2]CRC & [3]SPME, Tata Steel IJmuiden, The Netherlands

The observed difference in Si isotopic composition between CI chondrites and bulk silicate Earth has been explained by high P-T metal-silicate Si isotope fractionation accompanying Si incorporation into Earth's core [1, 2, 3].

We have measured Si isotopes in metal alloys and co-existing silicate slags that were produced at temperatures of ~1600°C in reducing atmospheric conditions in an industrial blast furnace at Tata Steel IJmuiden, the Netherlands.

Silicon isotopes were measured with a ThermoFinnigan Neptune MC-ICPMS [3] using a modified sample digestion procedure [3, 4]. Our results show an average mass difference of 0.75 ‰ for δ^{30}Si between metals and silicates (Fig.1).

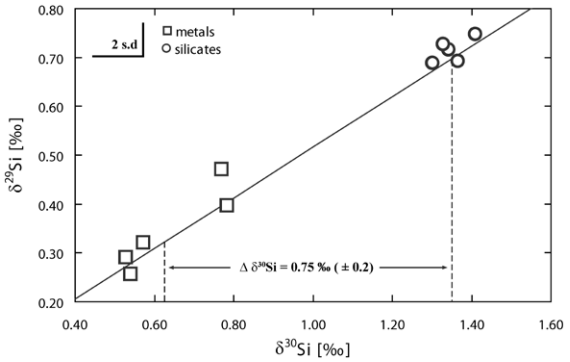

Figure 1: Three isotope plot showing Si isotope data of metals and silicates along the equilibrium fractionation line of Si.

Sign and magnitude of our results are in good agreement with results of high-pressure experiments [3] and theoretical predictions [1]. Si isotope fractionation clearly occurs in high-temperature metal-silicate systems under reducing atmospheric conditions, and high pressures are not required. Our data show that Si could have been incorporated into Earth's core during its early formation stages.

[1] Georg, R.B. *et al*. (2009) *Nature* **447**, 1102–1106. [2] Fitoussi, C. *et al*. (2009) *EPSL* **287**, 77–85. [3] Shahar, A. *et al*. (2009) *EPSL* **288**, 288–243. [4] Boorn, v.d. S. *et al*. (2006) *JAAS* **21**, 734–742.

First episode of widespread ocean oxygenation 551 Myr ago

B. KENDALL[1]*, T. KOMIYA[1,2,3], T.W. LYONS[4], S.M. BATES[4], G. JIANG[5], R.A. CREASER[6], S. XIAO[7], K. MCFADDEN[8], Y. SAWAKI[3,9], M. TAHATA[3,9], D. SHU[10], J. HAN[10], Y. LI[11], X. CHU[12] AND A.D. ANBAR[1]

[1]SESE, Arizona State Univ., Tempe, AZ 85287, USA (*correspondence: brian.kendall@asu.edu)
[2]Dept. Earth Science & Astronomy, Univ. Tokyo, Japan
[3]Research Ctr, Evolving Earth & Planets, Tokyo Tech., Japan
[4]Dept. Earth Sciences, Univ. California, Riverside, CA, USA
[5]Dept. Geoscience, Univ. Nevada, Las Vegas, NV, USA
[6]Dept. Earth & Atm. Sci., U. Alberta, Edmonton, AB, Canada
[7]Dept. Geosciences, Virginia Tech., Blacksburg, VA, USA
[8]ConocoPhillips, Houston, TX 77079 USA
[9]Dept. Earth & Planetary Sciences, Tokyo Tech., Japan
[10]Early Life Institute, Northwest Univ., Xi'an, China
[11]Earth Sciences & Resources, Chang'an Univ., China
[12]Inst. Geol. & Geophys., Chinese Acad. Sci., Beijing, China

Increasing ocean oxygenation may have spurred the evolution of large multicellular metazoans during the Ediacaran Period (635-542 Myr ago). Fe speciation and other geochemical data from sedimentary rocks indicate that regional ventilation of the deep oceans commenced no later than 580 Myr ago but parts of the Ediacaran deep ocean remained anoxic. Reconstructing the timeline of ocean oxygenation is critical to understanding metazoan evolution, but the spatiotemporal distribuition of dissolved O_2 remains poorly understood. In contrast, the Mo isotope composition of euxinic (anoxic/sulphidic) black shales represents a proxy for global seawater and constrains global ocean redox conditions.

Here, we present Mo isotope evidence for the first known episode of widespread ocean oxygenation 551 Myr ago. High-resolution profiles through black shales at the top of the Doushantuo Formation (South China) reveal a transient excursion to heavy $\delta^{98/95}$Mo (from ~0‰ to 2‰) that approaches modern global seawater (2.3‰). The latter has heavy $\delta^{98/95}$Mo largely because isotopically light Mo is preferentially removed into oxic Fe-Mn crusts. We infer a similar extent of Mo burial in oxic sediments 551 Myr ago.

Older euxinic shales deposited between 1840 and 551 Myr ago are enriched in isotopically light Mo and indicate expanded deep ocean anoxia, including a prevalence of euxinic conditions at mid-depths along ocean margins. Between 551 and 400 Myr ago, the Mo isotope database points to an intermediate extent of oxygenation relative to older and younger oceans. We propose that there was a major increase in ocean oxygenation 551 Myr ago which sparked a major diversification of complex macroscopic metazoans.

https://doi.org/10.1180/S0026461X00006502 Published online by Cambridge University Press

Halogens (Cl, Br, I) in basalt glasses

MARK A. KENDRICK[1], VADIM S. KAMENETSKY[2], JON D. WOODHEAD[1], DAVID PHILLIPS[1] AND MASAHIKO HONDA[3]

[1]School of Earth Sciences, University of Melbourne, Australia (mark.kendrick@unimelb.edu.au)
[2]ARC Centre of Excellence in Ore Deposits, University of Tasmania, Australia
[3]Research School of Earth Sciences, ANU, Australia

Halogens have highly variable concentrations in basalt glass with part of the variation related to mantle abundance. Serpentinites (hydrated mantle lithosphere) are major reservoirs for halogens in subducting slabs and previous work has shown Br/Cl and I/Cl are strongly fractionated during serpentine breakdown. As a result, fractionated and characteristic low Br/Cl and I/Cl ratios could be useful for tracing the presence of subducted halogens (and other volatiles) in basalts from different tectonic settings.

The halogen partition coefficients were investigated using a suite of Enriched Mid-Ocean Ridge Basalt glasses from Macquarie Island (70-1400 ppm Cl; MgO of 5.5-9 wt %; La/Sm of 1.4-7.9; typical MORB $^3He/^4He$ of ~8 Ra). Log-log covariation diagrams demonstrate Cl, Br, K and U have statistically indistinguishable partition coefficients similar to that of I. Therefore, Br/Cl, I/Cl, K/Cl and U/Cl are not easily fractionated during mantle processing, confirming variations potentially track subducted volatile components. The Macquarie MORB mantle has Br/Cl and I/Cl weight ratios of $(3.7 \pm 0.5)\times10^{-3}$ and $(130 \pm 100)\times10^{-6}$, respectively. Together with the Cl/K/U data, these ratios suggest 19 ± 6 ppm Cl, 67 ± 31 ppb Br and 7 ± 5 ppb I (2σ) in the bulk silicate Earth.

Preliminary data for Back-Arc Basin Basalt glasses from Lau and Manus have up to 3000 ppm Cl and variable Br/Cl and I/Cl signatures, including some of the lowest Br/Cl ratios obtained in this study. These data could be partly explained by a Cl contribution from serpentine breakdown fluids, but data are now required to determine the subduction potential of Br and I in organic-rich meta-sediments.

Oceanic Island Basalts from the Society and Pitcairn seamounts ($^3He/^4He$ of 1-10 Ra ± solar Ne indicate mixed recycled and primitive components) are characterised by MORB-like I/Cl and Br/Cl ratios. In contrast, low Br/Cl values are expected in dehydrated serpentinites and high I/Cl values are expected in subducted sediments. Therefore, halogens in basalts with 'EM-type' signatures do not carry an obvious recycled signature, but could be explained by mixing recycled, 'primitive (?)' and MORB mantle components.

Possible Platinum Group Element (PGE) clusters in magmatic systems; Using synthetic sulphide melts

B. KENNEDY[1]*, M. TREDOUX[1], C. BALLHAUS[2], H.M. HELMY[2], H.C. SWART[3] AND L. COETSEE[3]

[1]Department of Geology, University of the Free State, South Africa (*correspondence: kennedybia@gmail.com)
[2]Steinmann Institute, Universität Bonn, Bonn, Germany
[3]Department of Physics, NNSCF, University of the Free State, South Africa

The aim of the study is to verify whether or not the primary binding mechanism of PGE, in a magmatic environment, is a pure chemical or physical/- mechanical process. The monosulphide (mss) phases of temperature controlled synthetic melts were investigated for the existence of small Pt clusters or nano-structures (10-100 atoms). If such entitites are found, they would point towards an initial physical mechanism as the dominant process during early magma differentiation.

Exeriments were run with variable concnetrations of Pt, As, Cu, S and Fe, chosen to mimic a natural Cu-Ni-S ± PGE system. Samples were cooled down rapidly (from 1050-25°C in a few seconds) and slowly (1050-400 °C over 48 hours).

Pt forms large heterogeneously distributed Pt-As_x and Pt-Fe_x phases (0.2-50 μm i.e. approximately 700-166666 atoms) within the melt phase of both slow and fast cooled samples. Results indicate that Pt needs a suitable anion like As, Fe or Cu to form a stable phase in a magmatic system. Pt-Cu_x phases (200-1000nm i.e. approximately 700-3333 atoms) in the mss phase of faster cooled samples confirm that some kind of clustering process is at work in Cu-Ni-S systems. Faster cooled samples show exsolution textures of Pt out of the mss phases into the melt phase (Cu_x-Fe_x-S_x).

While chemical behaviour may govern the secondary distribution of Pt-phases, clustering is potentially the primary (physical) mechanism. The clusters can easily be taken up into a immiscible sulphide, oxide or silicate phase. Clustering behaviour may explain the high enrichment of PGE in early cumulus phases (olivine and chromite) of the Bushveld complex.

https://doi.org/10.1180/S0026461X00006502 Published online by Cambridge University Press

Terrestrialization of the Earth and its influence on the advent of complex life

MARTIN KENNEDY

School of Earth and Enironmental Science, University of Adelaide, Adelaide SA,5005, Australia (martin.kennedy@adelaide.edu.au)

For the first 3 billion years of life's history on Earth single celled organisms were Earth's sole residents. In the Late Precambrian this record changed dramatically with the appearance of complex multicellular life (metazoans) that rapidly diversified and radiated. This radiation was likely triggered by planetary changes, though what those changes were, how they interacted with intrinsic (genetic) influence and which changes were causes and which effects constitute principal questions in geobiology with important implications for the conditions on other planets necessary to support complex life. Much of what we know of this transformation comes from the marine record because of a strong preservational bias relative to terrestrial sediments. It is evident from studies of the modern biosphere, however, that the terrestrial realm has a critical influence on the sustainability of complex life. While it is widely accepted that the early terrestrial surface of the Earth was inhospitable to life, and the timing of the greening of the Earth's surface remains poorly constrained, the infleunce of vascular land plants beginning in the Silurian is commonly believed to have been an important step in establishing the present Earth system. However an earlier more cryptic and simple biomass likely colonized and expanded across the Precambrain landscape, modifying physical and chemical weathering patterns, soil clay mineral production, marine and terrrestrial carbon burial, nutrient flux to marine systems and the hydrological cycle. It is reasonable to hypothesize that biogeochemcial systems, like clay mineral associated organic carbon preservation and burial, that play an important role in CO_2 sequestration and atmospheric oxygen production today, were intitated during this earlier transition. Secular changes in clay mineral composition of sediments through late Precambrain continental margin sediments show a distinct rise in phyllosilicates in support of this hypothesis. Alteration of the carbon isotopic composition of coastal carbonates by dissolved organic mater in meteoric waters also becomes a pronounced influence during this period of time, and finally new fossil discoveries also point to the terrestrial surface as being an important component in planetary transformation.

A continental amplifier for marine carbon sequestration in a greenhouse ocean

MARTIN KENNEDY[1] AND THOMAS WAGNER[2]

[1]School of Earth and Environmental Science, University of Adelaide, Adelaide SA, 5005 Australia (martin.kennedy@adelaide.edu.au)

[2]School of Civil and Engineering and Geosciences, Newcastle University, Newcastle upon Tyne, NE1, &RU, UK

Recent evidence has increased concern that future climate will be influenced by natural processes and feedbacks more common to a warm climate mode. It is well known from past greenhouse periods that anomalous concentrations of organic carbon were associated with disruption of marine ecosystems, widespread anoxia, and climate perturbations. While most models of black shale formation focus on oceanographic controls, findings on modern continental margin sediments also identify a strong landward influence on marine carbon burial that is also consistent with current understanding of hypoxic zone expansion. Here we show evidence for a direct land-sea mechanism that translates the effects of changing continental climate to carbon burial in deep marine sediments via the preservative effects of detrital clay mineral surfaces. We show a correlation (r^2=0.75) at cm resolution between mineral surface area (MSA) and abrupt (centennial or less) high magnitude shifts in TOC from 1% to 15% in pelagic sediments from the tropical Cretaceous Atlantic (ODP 959). Carbon burial was maximized by an enhanced flux of high MSA clay minerals formed in response to increased seasonality in tropical Africa that were exported to hypoxic shelf waters with high dissolved organic carbon concentration. Not only do these data identify a dominating terrestrial influence for back shale formation during one of the 'Cretaceous Oceanic Anoxic Events' ~ 85 ma (OAE3), but show that climate under greenhouse conditions can cross a threshold into a highly sensitive mode in which organic carbon burial efficiency is amplified, providing a negative feedback to pCO_2,

https://doi.org/10.1180/S0026461X00006502 Published online by Cambridge University Press

Geochemistry of fluids from the Bruce nuclear site: Evidence for a geologically ancient Ordovician porewater system

LAURA KENNELL[1], TOM AL[2], IAN CLARK[3] AND MARK JENSEN[1]

[1]Nuclear Waste Management Organization, 3rd Floor 22 St. Clair Avenue East, Toronto ON, M4T 2S3
[2]Department of Earth Sciences, University of New Brunswick, P.O. Box 4400, Fredricton, NB, E3B 5A3
[3]Department of Earth Sciences, University of Ottawa, 140 Louis Pasteur, Ottawa, ON, K1N 6N5

Groundwater and porewater geochemistry data were collected at the Bruce nuclear site near Tiverton, ON, located on the northeastern margin of the Michigan Basin, as part of multi-disciplinary site characterization activities for the proposed development of a deep geologic repository (DGR) for low- and intermediate-level radioactive waste (L&ILW).

The site-specific geochemical data is consistent with regional data collected in various locations within the Michigan Basin, suggesting that the origin and evolution of the brines at the regional- and site-scales have been controlled by the same, or similar, processes. The natural tracer data ($\delta^{18}O$, $\delta^{2}H$, Cl, Br) collected at the Bruce nuclear site support the long-standing hypothesis that the sedimentary brines originated from seawater, or evaporated seawater (e.g. [1, 2]), and have been modified over hundreds of millions of years by various mixing and *in situ* water-rock interaction processes (e.g. dilution, halite dissolution, dolomitization). In addition, enriched $^{87}Sr/^{86}Sr$ isotopic signatures throughout the entire Ordovician sedimentary sequence suggest that solute residence times within the Ordovician brines are long and these values are consistent with regional observations (e.g. [3]).

Horizontal hydraulic conductivities (K_H) and matrix permeabilities were measured in the Ordovician formations and range between 10^{-15} and 10^{-12} m/s, and 10^{-20} to 10^{-15} m^2, respectively. Vertical hydraulic conductivities are estimated to be less than K_H by a factor of at least ten in the Ordovician formations, and the presence of high isotopic gradients in the methane and helium compositions ($\delta^{13}C_{CH4}$, $\delta^{2}H_{CH4}$, and $^{3}He/^{4}He$) indicate that a barrier to vertical solute transport may exist at the base of the Cobourg Formation at the Bruce nuclear site. The geochemistry, when partnered with the physical data, suggests that the Ordovician porewater system is geologically ancient.

[1] Wilson & Long (1993a) *Applied Geochemistry* **8**, 81–100. [2] Wilson & Long (1993b) *Applied Geochemistry* **8**, 507–524. [3] McNutt *et al*. (1987) *Applied Geochemistry* **2**, 495–505.

Characterising the Earth: Exploiting seismology and mineral physics

B.L.N. KENNETT

Research School of Earth Sciences, The Australian National University, Canberra ACT 0200, Australia (*correspondence: brian.kennett@anu.edu.au)

The dominant gradient in Earth properties is radial and this has enabled simple 1-D models to have considerable utility. Seismological reference models have been employed in ways that were not envisaged when they were created. In particular, the parameterizations were chosen for mathematical convenience rather than linked to any particular physical conditions. It should therefore come as no surprise that such seismological models do not conform to the properties expected for mineral physics predictions for reasonable mineral assemblage models and near adiabatic conditions. There will also be biases associated with lateral heterogeneity, e.g. the properties corresponding to the average temperature are not the same as the average of the same properties. Nevertheless seismology provides key tie points through well constrained discontinuities that can calibrate pressure scales, and mineral physics can investigate perfect aggregates and so explore a broad range of likely conditions. Rather than test a particular mineral physics configuration against a specific seismic reference model or a subset of seismological observations, we need to build new physical comparator models that recognise the limitations of both seismic and mineral physics models and provide explicit uncertainties on physical parameters. Such models should work with the standard seismological data sets and recognise the geodynamic state - non-adiabaticity is likely in a convecting system. We can examine the physical state implied by seismic tomography in terms of the predictions for different classes of parameter models and so gain insight into the controls we have on the Earth system.

https://doi.org/10.1180/S0026461X00006502 Published online by Cambridge University Press

Comparing the surface-promoted hydrolysis of phosphate mono- and diesters on goethite

JANICE P.L. KENNEY* AND PER PERSSON

Department of Chemistry, Umeå University, 901 87 Umeå Sweden (*correspondence: janice.kenney@chem.umu.se)

Phosphorus is an essential nutrient for both plants and microorganisms. However, in order for it to cross cell membranes, it must be in the form of orthophosphate or in some cases as small organophosphates. The majority of organic phosphates input into the biosphere are in the diester form, via pesticides, plasticizers, and hydraulic fluids. However, the P found in most soils is dominated by monoesters. Hydrolysis of phosphate esters in biological systems is important since it is a step that is required to make these large phosphate esters more bioavailable. While the hydrolysis of these phosphate esters is thermodynamically favourable, the reaction in water or a strong electrolyte solution is a slow process.

Phosphorus is a unique essential nutrient in its ability to strongly sorb to environmental particles. Therefore, reactions at the surfaces of these particles can control the fate and transport of phosphorus in the biosphere. Minerals, such as goethite, have been shown to increase the rate of hydrolysis of organophosphates by acting as a catalyst. In this study we have investigated the abiotic hydrolysis of a phosphate monoester and diester, p-nitrophenyl phosphate (pNPP) and Bis-[p-nitrophenyl] phosphate (BNPP), respectively. To determine the mechanisms and rate of the hydrolysis of pNPP and BNPP adsorbed on goethite surfaces we have used a combination of spectroscopic methods. The concentration of phosphate remaining in solution was determined by UV-vis spectroscopy, while the surface reactions were examined using infrared spectroscopy via the ATR sampling technique.

Spectroscopic results for the pNPP-goethite system show quick and complete adsorption of the ligand, followed by the subsequent hydrolysis, with the release of nitrophenol (NP) into solution. After 30 hours nearly 100% of the pNPP was hydrolyzed to NP and orthophosphate. Alternately, in the BNPP-goethite system, the ligand adsorbs much more slowly and to a lesser extent than the pNPP. Between pH 4 and 6, the maximum hydrolysis observed over 48 hours is less than 25%. Our results suggest that differences in surface affinity and surface-promoted hydrolysis between mono- and diesters are important factors to consider in order to explain differences in the overall biogeochmical behaviour of these two classes of phosphorus compounds.

Water in the mantle, melting, and the evolution of Earths atmosphere

HANS KEPPLER

(hans.keppler@uni-bayreuth.de)

Water and carbon are the most important volatiles in Earths´ interior, but they strongly differ in their behaviour. While carbon is mostly sequestered in accessory phases such as carbonates and elemental carbon, water mostly resides as OH point defects in the nominally anhydrous minerals of the mantle. In this presentation, I review (1) the observational constraints on water abundance in the mantle (2) the effect of water on mantle melting and the associated changes in electrical conductivity and (3) the coupling between the water abundance in Earth's mantle and the redox evolution of the atmosphere.

Water may be essential for inducing melting in the seismic low velocity zone of the upper mantle as well as above the 410 km discontinuity. Both effects are ultimately related to depth-dependent changes in the capability of mantle minerals to dissolve water as point defects. Major experimental advances in recent years have shown that both the solubility of water in olivine at the base of the upper mantle as well as the solubility of water in pyroxenes in the uppermost mantle are much higher than previously thought. Moreover, new *in situ* measurements show that water has a much stronger effect in enhancing the electrical conductivity of basaltic melts than anticipated and this effect increases with pressure. A consequence of these observations is that very likely, small fractions of hydrous melt can explain the electrical conductivity in the seismic low velocity zone of the upper mantle.

It has long been recognized that Earth's atmosphere became much more oxidized in the 'great oxidation event' 2.3 billion years ago. This event may be due to a change in oxidation state of volcanic gases or to photosynthesis by cyanobacteria. Changes in the oxidation state of volcanic gases 2.3 billion years ago have often been dismissed on the ground that there is no evidence for a corresponding change in mantle redox state at this time interval. However, the relevant gas equilibria between sulfur and nitrogen species do not only depend on oxygen fugacity, but also on water. I show that degassing of water from the mantle – at constant oxygen fugacity – may well induce the changes in the oxidation state of sulfur and nitrogen in volcanic gases required to oxidize the atmosphere.

https://doi.org/10.1180/S0026461X00006502 Published online by Cambridge University Press

Atomistic simulations of uranium in the environment: Diffusion, adsorption, and incorporation

S. KERISIT*, C. LIU, A.R. FELMY AND E.S. ILTON

Chemical and Materials Sciences Division, Pacific Northwest National Laboratory, Richland, WA 99352 USA (*correspondence: sebastien.kerisit@pnl.gov)

Uranium is the most common radionuclide contaminant in subsurface systems associated with the U.S. Department of Energy (DOE) sites where nuclear materials were processed and stored. We have used a suite of atomistic simulation techniques to provide an atomic-level characterization of U properties in model systems relevant to DOE sites.

U preferentially associates with intra-grain domains in U-contaminated sediments collected from the DOE Hanford site and diffusion is expected to control the future mobility of U in these sediments. Therefore, we present molecular dynamics simulations of the diffusion and adsorption of uranyl carbonate species in intra-grain micropores, using feldspar-water fractures as a model system. Uranyl carbonate species dominate U(VI) aqueous speciation in Hanford groundwater conditions. The simulations show the effects of confinment and of the presence of the mineral surface on the diffusion of water and several uranyl carbonate species [1-3].

Uranium sorption by Fe-(hydr)oxides, which are common minerals in soil systems, has been conceptualized as a surface process; however, sorption is not necessarily reversible. The potential for incorporation into the mineral structure is supported by EXAFS studies; however, the evidence for incorporation rests on distances that do not match distances claimed for simple adsorption. Therefore, independent data are needed to confirm the structural incorporation hypothesis.

In this paper, we present atomistic modeling performed to evaluate the coordination of U incorporation in three Fe-(hydr)oxides [4]. The simulations provided information on U-O and U-Fe distances, coordination numbers, and lattice distortion for U in different sites and oxidation states. Comparison of the simulations with available experimental data provides further evidence to support the structural incorporation hypothesis.

[1] Kerisit S. Ilton E.S. & Liu C. (2008) *Geochim. Cosmochim. Acta* **72**, 1481–1497. [2] Kerisit S. & Liu C. (2009) *Environ. Sci. Technol.* **43**, 777–782. [3] Kerisit S. & Liu C. (2010) *Geochim. Cosmochim. Acta* **74**, 4937–49521. [4] Kerisit S. Felmy A.R. & Ilton E.S. (2011) *Environ. Sci. Technol.* **45**, 2770–2776.

Probing mineral-water interfaces with computer simulation

S. KERISIT*, K.M. ROSSO AND A.R. FELMY

Chemical and Materials Sciences Division, Pacific Northwest National Laboratory, Richland, WA 99352 USA (*correspondence: sebastien.kerisit@pnl.gov)

The atomic-level structure of water at mineral sufaces is an important controlling factor in interfacial reactions. Therefore, differences in interfacial water structures could contribute to variations in surface reactivity between different surfaces of a single mineral. In this presentation, the water interfacial structure of three hematite surfaces, namely, the (012), (110), and (001) surfaces, will be contrasted [1]. An extensive comparison with X-ray scattering data provides further evidence that MD models can be used to reliably predict the structure of mineral-water interfaces. In addition, the MD trajectories were analyzed to gain insight into the surface structural controls on the interfacial water structure.

Mineral-water interactions also play an important role in carbonation reactions, which are one of the principal families of chemical interactions relevant to geological CO_2 capture and storage (CCS). Although carbonation of minerals in contact with a CO_2-containing aqueous phase has been extensively studied, carbonation reactions involving water-bearing supercritical CO_2 fluids (WBSF) have received comperatively little attention. However, the limited number of studies published to date all highlighted the dependence of the extent and rate of reaction on the water content of the WBSF. Therefore, a detailed understanding of the structure of the WBSF-mineral interface as a function of water content is critical to elucidating the mechanisms of carbonation reactions in conditions relevant to CCS.

MD simulations of a model forsterite surface in contact with WBSF of varying water content were performed to determine the partition of water between the WBSF and the mineral surface and the nature of CO_2 and H_2O bonding at the interface. The simulations show that water readily displaces CO_2 at the surface and that the formation of a water film at least three-monolayer thick can be exothermic even for water contents below saturation. The density, diffusion, and degree of hydration of CO_2 as well as the extent of CO_2/H_2O mixing at the interface were all predicted to depend strongly on the water content of the WBSF.

[1] Kerisit S. (2011) *Geochim. Cosmochim. Acta* **75**, 2043–2061.

https://doi.org/10.1180/S0026461X00006502 Published online by Cambridge University Press

Advancing studies of the origin and role of hydrocarbons in ore-forming systems

MITCHELL J. KERR* AND JACOB J. HANLEY

Saint Mary's University, Dept. Geology, Halifax, Canada (*correspondence: mitchell.kerr@utoronto.ca)

We have advanced an in-line rock crushing, gas chromatographic (GC) technique that can detect and quantify hydrocarbons present within fluid inclusions to a lower limit of 1 ppm. This technique has been adapted from developments by Bray *et al*. [2] and Salvi and Williams-Jones [1] in order to comprehensively analyze a much wider range of hydrocarbons (C1-C9 olefins and paraffins). The system is comprised of four stainless steel rock crushers that crush rock fragments in a sealed and sterile environment, passing the released volatiles into the GC to be separated and analyzed.

Rock types associated with various ore-forming systems, as well as a number of others are being investigated. These include: mantle-derived xenoliths, hydrothermal veins from major ore deposit types including MVT, VMS and magmatic sulfide deposits, porphyry systems, IOCG deposits, and epithermal/geothermal deposits. With this work, we are: (1) constraining the importance of hydrocarbons in transporting ore metals via olefins, alcohols and/or carboxylic acids that may facilitate metal complexation and transportation; (2) determining hydrocarbon origin (e.g. mantle-derived, remobilized from associated hydrocarbon deposits, *in situ* formation by metal catalyzed Fischer-Tropsch reactions [3]).

We suspect that the presence of particular metals (i.e. group VIII elements [3]) may effectively catalyze the respeciation/polymerization of light hydrocarbons into higher order compounds via the interaction between oxidized and/or reduced carbonic fluids within hydrothermal systems with various ore metal-bearing systems. Tentative results collected from analyzing hydrothermal quartz veins associated with base metal sulfide deposits in the Canadian Shield illustrate a high level of hydrocarbon speciation, including compounds such as butane, pentane, hexane and various saturated and unsaturated isomers thereof. Trace quantities of higher order compounds within the C6-C8 region were also found (possibly toluene, xylene, octane, etc.).

[1] Salvi & Williams-Jones (2003) *Min. Assoc. of Canada* **32**, 247–278. [2] Bray *et al*. (1991) *J. of Geochem. Exploration* **42**, 167–193. [3] Potter & Konnerup-Madsen (2003) *The Geol. Soc. of London, Spec. Pub.* **214**, 151–173.

Metallogenic provinces: Products of asthenosphere-thermal boundary layer-lithosphere interactions

R. KERRICH

Geological Sciences, University of Saskatchewan, Saskatoon, Canada S7N 5E2 (robert.kerrich@usask.ca)

Continental lithospheric mantle (CLM) was extensively modified by subduction-derived fluids especially at craton margins, and melts, from ~ 3 Ga as preserved in xenoliths of CLM. As well, melt-related metasomatism of CLM can be proxied by alkali basalts in ocean basins, by Dupal-type anomalies where a continental low-velocity zone is rafted into ocean basins as continents rift, and by continental alkali basalts all with high-LREE budgets.

Orogenic gold deposits, dominantly associated with accrertionary-type orogens, are generated at terrane boundaries where an accretionary wedge, and LVZ, are subcreted between the over-riding and subducting plates. Dehydration at low-water-rock ratios, during thermal rebound following cessation of subduction, generates low-salinity aqueous fluids enriched in Au, Ag, As, Sb, Hg and lithophile elements which advect along terrane boundaries where the deposits form. This element budget is a proxy for subduction-fluid induced metasomatism of the mantle wedge and sub-arc lithosphere during normall convergent margin magmatism.

During rifting of such metasomatised mantle in continental and oceanic settings, Au-rich fluids, and alkaline magmas, are generated as expressed in Au-porphyry deposits and epithermal systems. During plume impingement at craton margins ultramafic liquids interact with noritic melts generated from measomatised CLM raising Si- and H_2O-activities that trigger sulphide saturation for Ni-Cu-PGE deposits. At intracontinental rifts where plumes are focussed, the bimodal A-type granite and gabbro-anorthosite association is best expressed in the Proterozoic as controlled by the depth of the CLM. Fe-oxide, Cu, Au, REE deposits form by plume and decompressional melting and dehydration of metasomatised CLM with REE-contributed from entrained LVZ.

https://doi.org/10.1180/S0026461X00006502 Published online by Cambridge University Press

Glacial to Interglacial changes in the carbonate ion signature of deep and intermediate water masses in the Southern Ocean

F.KERSTEN* AND R. TIEDEMANN

Alfred Wegener Institute for Polar and Marine Research, 27570 Bremerhaven, Germany (*correspondence: Franziska.Kersten@awi.de)

The Southern Ocean (SO) currently acts as a sink for CO_2, which is transported to intermediate [1] and deep waters [2] and consequently alters the inorganic carbon chemistry there. With regard to the rise in atmospheric pCO_2 since the Last Glacial Maximum (LGM), we aim to reconstruct fluctuations in $[CO_3^{2-}]$ in the Circumpolar Deep Water (CPDW) and the Antarctic Intermediate Water (AAIW) in the Australian and Pacific Sector of the SO. For this purpose, B/Ca ratios in benthic foraminiferal shells (*C. wuellerstorfi, C. mundulus* and *Uvigerina spp.*) are obtained. Deep water samples from the South Tasman Rise show a clear decrease in average B/Ca ratios from the LGM (43 μmol/mol) towards the Holocene (29 μmol/mol), from which we reconstruct average LGM and Holocene carbonate ion contents of 130 μmol/kg and 81 μmol/kg, respectively. Holocene values are corroborated by data from nearby GLODAP sites and the observed drop in seawater- $[CO_3^{2-}]$ is consistent with an increase in atmospheric pCO_2 since the LGM. Reconstructed values from Challenger Plateau sediments (bathed by AAIW) follow the trend observed in deep water cores, showing a decrease in average $[CO_3^{2-}]$ from 93 μmol/kg (LGM) to 81 μmol/kg (Holocene). Results from the shallowest core (958 m water depth) however reveal rising $[CO_3^{2-}]$, which might reflect location- and depth-related differences in CO_2 uptake and release. To investigate this further, we are currently analysing sediments from the SE of New Zealand, which stem from AAIW and CPDW depths. Moreover, a continuous $[CO_3^{2-}]$- record for the last 20 ka will hopefully enable us to further constrain the temporal relationship between changes in SO carbonate chemistry and the step-wise release of CO_2 into the atmosphere.

[1] Sabine *et al*. (2004) *Science* **305**, 267–371. [2] Sandrini *et al*. (2007) *Antarctic Sci*. **19**, 395–407.

Plutonium transport: Identifying the biogeochemical mechanisms controlling its behavior

ANNIE B. KERSTING

Glenn T. Seaborg Institute, Physical & Life Sciences, Lawrence Livermore National Laboratory, L-231, PO Box 808, Livermore, CA 94550

A major challenge in predicting the mobility and transport of actinides is determining the dominant biogeochemical processes that control its behavior in the subsurface. Plutonium (Pu) is of particular concern do to its large worldwide production inventory, high toxicity to human health and long half-life. There is more than 2200 metric tons of Pu throughout the world (ISIS website). The long half-life of Pu (^{239}Pu ~ 2.4 x 10^4 years) together with existing inventories guarantees that significant quantities will remain in our environment for a very long time. Effectively managing, controlling, and disposing of these materials in order to stop inadvertent release and transport through the geosphere is a serious scientific challenge. Currently, scientists cannot reliable predict how or how much Pu will move once deposited in the subsurface preventing accurate assessment of risk to human health. The behavior of Pu is complex because the reaction chemistry of Pu (i.e. aqueous speciation, solubility, sorptivity, redox chemistry, and affinity for colloidal particles, both abiotic and microbially-mediated) is particularly complicated. Its migration is known to be oxidation-state dependent and facilitated by transport on particulate matter (i.e. colloidal particles). Yet very little is known about how and under what geochemical conditions colloids facilitate the transport of Pu.

Despite the gaps in our understanding, recent field and laboratory experiments are helping to shape our conceptual understanding. I will summarize our current understanding of the biogeochemical processes controlling Pu transport by discussing recent field and laboratory studies. Field studies include weapons facilities where contamination of large quantities of Pu have been deposited and migrated in the subsurface. These studies demonstrate that colloids can and do play an important role in the transport of low-solubility radionuclides; yet, colloids are not always responsible for transport. It is becoming clear that the depositional history of the contamination, as well as the site-specific hydrogeology is critical to assessing the dominant biogeochemical processes controlling the migration of Pu. In addition, the dominant biogeochemical processes controlling migration of Pu can change along the flow path from the sourse to the far-field environment.

https://doi.org/10.1180/S0026461X00006502 Published online by Cambridge University Press

Magmatic evolution of the Eastern Anatolian High Plateau, E. Turkey

M. KESKIN[1]*, V. OYAN[2], V.A. LEBEDEV[3], A. CHUGAEV[3], S.C. GENC[4], E.V. SHARKOV[3], E. UNAL[2] AND N. AYSAL[1]

[1]İstanbul University, Faculty of Engineering, Dept. of Geol. Engineering, 34320 Avcilar, Istanbul, Turkey (*correspondence: keskin@istanbul.edu.tr)
[2]Van YYU, Faculty of Engineering and Architecture, Dept. of Geol. Engineering, Zeve Campus, Van, Turkey
[3]RAS, IGEM, Staromonetny per., 35, Moscow 119017, Russia
[4]Istanbul Technical University, Faculty of Mines, Dept. of Geol. Engineering, 34469 Maslak, Istanbul, Turkey

The Eastern Anatolia High Plateau is an actively-deforming continental collision zone with a long-lasting volcanism from the end of Middle Miocene to historical times. It hosts some of the largest volcanic centers and plateaus of the circum Mediterranean region (e.g. Mt. Ararat, Nemrut, Tendurek and Suphan). Eastern Anatolia is a unique place in the world where the continental crust, most of which is represented by an accretionary complex, directly overlies the asthenospheric mantle [1]. So, the region is devoid of a lithospheric mantle. This unusual setting has been proposed to be linked to a major slab-steepening & breakoff event [1, 2].

To better understand the magma genesis and the geodynamic setting, we have been conducting a series of projects in E Anatolia since 2007, carefully studying the stratigraphy of the volcanoes and conducting radiometric datings and geochemical analyses. Results from our new and rather comprehensive database have revealed that the volcanism initiated around the N of Lake Van in the south at ~15 Ma with the eruption of calc-alkaline lavas containing a distinct subduction signature. The geochemical character of the volcanism changed from calc-alkaline to alkaline both in time (from Mid. Miocene to Quaternary) and space (from N to S), while the subduction signature temporally diminished. Our melting models suggest a region-wide temporal change from garnet- to spinel-dominated mantle mineralogy and an increase in the degree of melting. Our AFC and EC-AFC models indicate a significant crustal involvement increasing to the south. These findings may imply that the steepening of the slab has been a much faster event than we previously anticipated and the magma generation might have been influenced by the reformation of a new lithospheric mantle.

[1] Şengör *et al*. (2003) *GRL*, **30** (24) 8045. [2] Keskin (2003) *GRL*, **30** (24) 8046.

^{230}Th-^{234}U-^{238}U disequilibria along the river catchments from the Iberian Belt (Spain) affected by acid mine drainage (AMD)

M. KETTERER[1]*, A. HIERRO[2], L. BARBERO[3], M. OLÍAS[4], J.P. BOLIVAR[2], M. CASAS-RUIZ[5] AND M. BASKARAN[6].

[1]Chemistry and Biochemistry Department, Northern Arizona, University, Flagstaff, AZ 86011-5698, USA (*correspondence: Michael.Ketterer@nau.edu)
[2]Dpto. de Física Aplicada, Universidad de Huelva, Spain (almudena.hierro@dfa.uhu.es, bolivar@uhu.es)
[3]Dpto de Ciencias de la Tierra, Universidad de Cádiz, Spain (luis.barbero@uca.es)
[4]Dpto. Geología y Paleontología, Universidad de Huelv Spain (manuel.olias@dgyp.uhu.es)
[5]Dpto. de Física Aplicada, Universidad de Cádiz, Spain (melquiades.casas@uca.es)
[6]Department of Geology, Wayne State University, Detroit, MI, USA (baskaran@wayne.edu)

The Tinto and Odiel Rivers can be used as a natural laboratory to investigate how changes in the aqueous environment affect the mobility of U-series nuclides. These rivers have very low pH's of < 3 for most of their courses, as a result of acid mine drainage (AMD) processes. These AMD conditions generate preferential leaching of ^{234}U compared to ^{238}U from minerals in the background geological setting. Dissolved ^{238}U activities vary from 10 to 850 mBq/L, with the highest ^{238}U activities as well as the highest $^{234}U/^{238}U$ ratios (approaching 3.0) being present under the most acidic conditions. The acidic environment also promotes the dissolution of ^{230}Th, whose activities are up to several orders of magnitude higher than are commonplace in most natural waters. The mobilities of U and Th decrease as pH increases, resulting in precipitation of uranium-bearing minerals in the estuary. The high concentrations of sulfate appear to have an important role in complexation of dissolved Th. These results direct relevance to predicting the mobility behavior of other particle-reactive actinides under acidic conditions in the surface environment.

https://doi.org/10.1180/S0026461X00006502 Published online by Cambridge University Press

Liesegang banding and biochemically mediated geochemical self-organization

R.M. KETTLER[1]*, D.B. LOOPE[1] AND K.A. WEBER[1,2]

[1]Department of Earth and Atmospheric Sciences, University of Nebraska-Lincoln, Lincoln NE 68588-0340 USA(*correspondence: rkettler1@unl.edu, dloope1@unl.edu)

[2]School of Biological Sciences, University of Nebraska-Lincoln, Lincoln NE 68588-0118 USA (kweber2@unl.edu)

The Kanab Wonderstone is sandstone from the Shinarump member of the Chinle Formation that is variably cemented and stained with iron oxide. These sandstones contain approximately 5% Fe occurring as one to 5 mm thick, undulatory bands of iron oxide cement (IOC) that crosscut and obscure sedimentary structures. Between each pair of IOC bands are alternating bands of rock that are tinted with iron oxide stain (IOS) and unstained rock. The bands of IOS also crosscut and obscure sedimentary structures. The interior-most portion of the sandstone bed may contain a bleached sandstone core enclosed by a band of IOC. The IOC and IOS are related spatially to vertical joints that cut the sandstone at regular intervals. The IOC in the Shinarump comprises a mixture of acicular grains (goethite) and hexagonal plates with dendritic manganese oxide locally projecting from the cemented sandstone into more bleached rock. Although these features are unusual, they are not unique to the Shinarump member: similar features have been reported from other fluvial rocks worldwide. These features have been typically referred to as Liesegang bands, a type of geochemical self-organization.

The spacing of IOS is consistent with a Jablczynski coefficient [1] of 1.04 and the width of the IOS is a function of distance from the initial reaction front; characteristics that are typical of Liesegang bands [2]. Bands of IOC, on the other hand, exhibit more variable spacing and a relationship between IOC band thickness and distance between IOC. The Shinarump Wonderstone and similar rocks combine features of true Liesegang and biogenically mediated geochemical self-organization. Iron-oxidizing bacteria colonized the interface between siderite-cemented sand and porous sandstone, oxidizing iron and generating acid that caused dissolution of siderite. Aqueous ferrous iron diffused back to the biofilm where it was oxidized. Bands of IOS retain the morphology of reaction front fingers.

[1] Jablczynski (1923) *Bull. Chim. Soc. France* **33**, 1592–1597. [2] Chopard *et al.* (1994) *Phys. Rev. Letters* **72**, 1384–1387.

Origin and evolution of post-collisional volcanism: An example from Neoproterozoic Dokhan Volcanics at Gabal Nugara Area, Northeastern Desert, Egypt

EZZ EL DIN ABDEL HAKIM KHALAF

Geology Department, Faculty of Science, Cairo University (ezz_khalaf@hotmail.com)

Nugara volcanics are one of the northernmost outcrops of the Arabian-Nubian Shield (ANS). Two distinct volcanic successions are found in the Nugara basin: (1) old volcanic sequence composed of voluminous medium- to high-K calc-alkaline lavas, and minor alkali basalt; and (2) young volcanic sequence composed of subordinate tholeiitic mafic lavas. Their eruptions were punctuated by occasional volcaniclastic deposits that generated fall, flow or reworked suites compositionally identical to the lava flows. These volcanics are a part of a post-subduction and extensional-related magmatic event in Northeastern Desert of Egypt.

Volcanic rocks of the Nugara basin are characterized by strong enrichment in LILE relative to HESF, high LILE/HFSE ratios and depletions of Nb on MORB-normalized multi-element diagrams. Geochemical features of the volcanic rocks suggest that they experienced fractional crystallization, along with mixing processes. Crustal contributions to the magma sources may also have occurred during magmatic evolution. These processes have resulted in scattered major and trace element variations with respect to increasing silica contents. The model proposed for their origin involves contrasting ascent paths and differentiation histories through crustal columns with different thermal and density gradients.

Geochemical features of the most mafic samples suggest that the volcanic rocks in the region were derived from a mainly lithospheric mantle source that had been heterogeneously metasomatized by previous subduction events during convergence between the East and West Gondwanaland. The volcanic activity in the region is best explained by delamination of lithospheric mantle slices that were heterogeneously enriched by previous subduction-related processes.

https://doi.org/10.1180/S0026461X00006502 Published online by Cambridge University Press

Hydrogeochemistry and origin of cold high pCO_2 waters of Gonjinskoe spa (Priamurye, Russia)

N.A. KHARITONOVA, I.A. TARASENKO AND G.A. CHELNOKOV

690022, Russia, Primorsky region, Vladivostok, Prospect 100-letya 159, Far East Geological Institute Russian Academy of Science (tchenat@mail.ru)

Gonjinskoe is the most explored and popular spa with high pCO_2 groundwaters in the Priamurye. This spa is very actively used for treatments of gastrointestinal and heart diseases. In the last decade chemical composition of the spa was changed due to intensive exploitation so the main purpose of our study was to investigate the origin and evolution of the spa. Gonjinskoe spa is located in the Magdagachi area in the Valley of Bezimianniy River (Amur River basin) within the limits of the Mongolo-Okhotskaya geosynclinal area. Geologically, two rock formations were found of the study area. The oldest of these is Archeozoic metamorphic rocks of the Gonzhinsky horst. This formation essentially is composed of gneisses and marbles and often contents dykes of Early Cretaceous diorite and rhyolite. The tectonic structure of the spa is very complicated as two large regional faults northeast and sub-latitude directions are crossing here.

Groundwater mainly occurs in fractured Upper Cretaceous intrusive rocks of the area. Total area of the spa is 0, 9 Km^2 and three boreholes are actively utilized now. Water samples were collected over a ten-year period; additionally some published data were re-interpreted.

Two types of groundwater were distinguished here: fresh and high pCO_2 ones. Both types of water are very cold, the temperature is 0.5-1.0 ºC. Fresh water has very low TDS (up to 0.1 g/l) and belongs to Ca-Mg-Na-HCO_3 type. High pCO_2 groundwaters have TDS up to 3.5 g/l, CO_2dis. – 3.5 g/l and belongs to Ca-Mg-HCO_3 type. pH of waters very from 5.5 to 7.6.

Our bedrock and groundwater data indicates that both types of groundwater originate from meteoric water, and interactions between the water and these bedrocks have played a dominant role in the development of the chemical composition of the waters. Isotopic data indicates that CO_2 gas in the groundwater is mantle derived and its presence is critical for the development of the high pCO_2 groundwater. This type of groundwater evolves during gas-water-rock interactions only.

Flour content in the groundwater samples of Chahar-Farsakh area, South Khorasan, Iran

MARZIEH KHAZAII[1], AREZOO ABEDI[2] AND HANIYEH JALAYERY[3]

[1]Payamenour University, Nehbandan, Iran (mkhazaii@yahoo.com)

[2,3]Shahrood University of Technology,Shahrood,Iran (arezooabedi@shahroodut.ac.ir, hjalayeri@yahoo.com)

The study area is located about 24 km NW Nehbandan, South Khorasan province, Iran. Chahr -farsakh area was occurred at Iran's East Flysh belt junction with Lut block. This junction is a thin zone of crushed disruption, fault corrosion, extreme drift and metamorphism. Igneous, metamorphic and sedimentary rocks as granodiorite, quartz diorite, andesite, sandstone, shale, conglomerate, gneiss and schist with many other type of altered and crashed rocks from Jurassic to Neogen are the most rock formation in the area. In this study, the concentration of flour in 20 samples of groundwater sources as qanat and spring were determined. The results of analyses show that flour content were determined to range between 0.02-0.84 mg/l, lower than WHO 2008 limits. Temperature of waters distinguished between 19.4-30.6 C. The water PH were detected from 6.68 to 9.37. Flour show positive correlation with Na, Mg, Ca and HCO_3 in the water samples. Sandstone and shale seems to be the main aquifers in the study area. Mineralogical study by XRD shows that quartz is the main mineral in the aquifer and Illite, muscovite, shamosite, albite and calcite are subordinate minerals. Probably illite and muscovite are the main source of flour in the groundwater.

https://doi.org/10.1180/S0026461X00006502 Published online by Cambridge University Press

Boron contamination in the groundwater of Chahar-Farsakh area, South Khorasan, Iran

MARZIEH KHAZAII[1], AREZOO ABEDI[2] AND SOMAYEH TABASI[3]

[1]Payamenour University, Nehbandan, Iran (mkhazaii@yahoo.com)
[2,3]Shahrood University of Technology, Shahrood, Iran (arezooabedi@shahroodut.ac.ir, somayehtabasi@yahoo.com)

Groundwaters from 6 qanat and spring stations within the Chahar-Farsakh area, north-west of Nehbandan, South Khorasan province, Iran were sampled for metal contamination analysis. The data were used to calculate metal index (MI), all of the groundwater samples show metal index higher than 1. Among all analysis results, boron show high concentration in the groundwater samples. Concentrations of B in water samples from Chahar-Farsakh area were determined to range between 1.043-4.811 ppm, exceeding WHO (2009) limits (0.5 mg/L) for drinking waters. Naturally occurring boron is present in groundwater primarily as a result of leaching from rocks and soils containing borates and borosilicate. Geological surveying in the study area revealed some outcrops of pegmatite aplitic veins with tourmaline mineralization. Probably existence of tourmaline is the major natural source of boron in the water samples of Chahar-Farsakh area.

Petrography and mineralogy of Western Samen Metapelites

Z. KHODAIAN CHEGENI[1]*, A.A. BAHARIFA[2], M.H. EMAMI[3], M. MOHAJJEL[4] AND N. ASKARI[5]

[1]*Geological Survey of Iran, Research Institute for Earth Sciences, Tehran, Iran (khodaian@gsi.ir)
[2]Department of Earth Sciences, Abhar University, Abhar, Iran (baharifar@gmail.com)
[3]Geological Survey of Iran, Research Institute for Earth Sciences, Tehran, Iran (hashememami@yahoo.com)
[4]Department of Earth Sciences, Tarbiat Modares University, Tehran, Iran (mohajjel@modares.ac.ir)
[5]Geological Survey of Iran, Research Institute for Earth Sciences, Tehran, Iran (askari@gsi.ir)

The study area is located in southern of Hamadan, Sanandaj-Sirjan zone. Metamorphic rocks involve philite and Schist with green schist facies, advanced to amphibolite facies. These rocks composed of various metamorphic minerals. EPMA analysis is applied on some mineral to recognition of chemical composition of rock forming minerals. Mineral chemistry shows Muscovites that formed in rim of andalusite, have higher grade than those are in matrix and resulted of progressive metamorphism of andalusite to Muscovite, Staurolite and Fibrolite. Also Biotites are ferric and garnet is almandine and belongs to Piralespite groupe. Zoning pattern in garnet imply two progressive metamorphism and a retrogressive metamorphism that preserved in some garnets. Analytical data only show the composition of Staurolite.

https://doi.org/10.1180/S0026461X00006502 Published online by Cambridge University Press

Natural cementitious analogues of Jordan

HANI N. KHOURY

University of Jordan, Amman, Jordan (khouryhn@ju.edu.jo)

The pyrometamorphic rocks in Jordan (Daba-Siwaqa, Suweileh and Maqarin) are unique and represent *natural analogues* of Portland cement for sealing of nuclear waste. The Natural occurrences are of great aerial exposure and offer good example to study the interaction of cementitious hyperalkaline leachates on repository host rock. Similarity to cement processes and products is much more obvious than in any of the occurrences reported before. The similarity extends beyond strong mineralogical equivalence. The source of energy for this extremely energy intensive process was the same as cement kilns (fossil fuel from oil shale).

Maqarin area represents an early stage in the evolution of cementitious repository.

Suweileh and Daba-Siwaqa areas represent a later stage. Results on natural analogues in Jordan indicate that secondary minerals as smectites, sulphates, and hydrated aluminium silicates act as a sink for hazardous elements. Highly alkaline (pH = 12.7) ground water dissolves from the combusted bituminous marl the radionuclides and heavy metals (Cr, Zn, V) and reprecipitate it farther down when reducing conditions are encountered [1].

[1] Kamei *et al*. (2010) *ICEM2010*, 3–7 October, Tsukuba, Japan, ICEM10-40063.

Photochemical production of dissolved organic and inorganic nutrients from resuspended sediments

R.J. KIEBER*, M. SOUTHWELL, C.L. LAQUIRE, L. THOMPSON, S.A. SKRABAL, G.B. AVERY JR. AND R.N. MEAD

Department of Chemistry and Biochemistry, University of North carolina Wilmington, 601 South College Road, Wilmington, North Carolina 28403 (*correspondence: kieberr@uncw.edu)

A series of photolysis experiments were conducted in the presence and absence of tidal creek and continental shelf sediments to address the role of resuspension on nutrient fluxes in estuarine and coastal waters. There was a significant increase in TDN, phosphate and DOC when sediments were resuspended in overlying water and exposed to six hours of simulated sunlight. The majority of dissolved N was released as DON (87%) with relatively lesser amounts of ammonium (13%) and little or no nitrate. Results from autoclaved sediments suggest the mechanism of photolytic release was predominately abiotic. Results demonstrate that photoproduction from resuspended sediments is an episodically significant and previously unrecognized source of dissolved nutrients to coastal ecosystems receiving sediment plumes. This process may be especially important for continental margins where resuspension events occur as well as in regions experiencing high riverine sediment fluxes resulting from erosion associated with deforestation and desertification. The presentation also considers how photolytic fluxes of organics and nutrients may respond in the future during periods of salinity alteration as sea level rises.

https://doi.org/10.1180/S0026461X00006502 Published online by Cambridge University Press

Biogenic volatile emissions and their contribution to organic aerosol mass

A. KIENDLER-SCHARR[1], J. WILDT[2], TH.F. MENTEL[1], M. DAL MASO[3], E. KLEIST[2] AND R. TILLMANN[1]

[1]Institute of Energy and Climate Research, Troposphere (IEK-8), Forschungszentrum Jülich GmbH, Jülich, Germany
[2]Institute of Bio- and Geosciences, Plant Sciences (IBG-2), Forschungszentrum Jülich GmbH, Jülich, Germany
[3]Department of Physics, University of Helsinki, 00014 Helsinki, Finland

Land vegetation contributes 90% of the global volatile organic compound (VOC) emissions [1]. Atmospheric oxidation of these VOCs contributes to new particle formation and atmospheric organic aerosol mass [2]. The formation of aerosols from biogenic VOC emissions constitutes a possible feedback element in biosphere-atmosphere-climate interactions due to the overall cooling effect of aerosols [3]. This is based on increasing VOC emission strengths with increasing temperature and emission patterns being invariant to temperature changes. Recently evidence emerges that temperature induced changes in VOC emission patterns may alter the picture. It has been shown that increased isoprene emissions may suppress atmospheric new particle formation [4] thus dampening the cooling effect of aerosols formed from biogenic VOCs.

In addition the use of direct emissions of VOCs from plants in experiments studying secondary organic aerosol (SOA) formation shows that, beyond the so far considered main compound classes isoprene and its derivatives monoterpenes and sesquiterpenes, other VOC classes significantly impact SOA formation. Many of these VOCs are emitted under plant stress conditions.

An overview of the state of the art knowledge of SOA formation from biogenic VOCs with respect to different VOC classes will be given. In particular we will focus on the importance of non-classical VOC classes emitted under stress conditions.

[1] Guenther *et al*. (1995) *J. Geophys. Res.* **100**, 8873–8892
[2] Hallquist *et al*. (2010) *Atmos. Chem. Phys.* **9**, 5155–5236
[3] Kulmala *et al*. (2004) *Atmos. Chem. Phys.* **4**, 557–562
[4] Kiendler-Scharr *et al*. (2009) *Nature* **461**, 381–384

Factors affecting the stability of slags and metal release: The case study of historical Cu slags from Lower Silesia (SW Poland)

J. KIERCZAK*, A. PIETRANIK AND A. POTYSZ

University of Wroclaw, Cybulskiego 30, 50-205 Wroclaw, Poland
(*correspondence: jakub.kierczak@ing.uni.wroc.pl)

Historical slags originating from base metal smelting often contain considerable amounts of heavy metals and, when deposited, they may undergo potentially harmful interactions with surrounding soils, sediments and waters.

In this study we present mineralogical and chemical characteristics of historical slags from Rudawy Janowickie Mountains (Lower Silesia, SW Poland). We show that the studied slags are characterized by different cooling rates of the slag melt and we describe how these different rates affect slag properties (phase composition, metal distribution etc.). Furthermore, on the basis of leaching experiments, simulating various environmental conditions, we attempt to identify major factors controlling heavy metal release from slags.

Two types of slags produced during historical smelting of Cu ores occur in the studied area. The prevailing massive slag consists of silicate glass, olivine and hercynite. The second type is porous and comprises two types of silicate glass, olivine, ferrosilite, cristobalite and quartz. Both types contain important amounts of metals (up to 1.34 % of Cu).

The morphology of olivine crystals, phase assemblages, phase chemistry and distribution of trace elements in slag phases vary from sample to sample, which is consistent with different cooling rates. Careful investigation of cooling conditions is useful to predict susceptibility of slags to weathering. Leaching tests, performed on each type of slag show that the heavy metal release is more important for porous slags than for those having massive texture. Furthermore, larger proportions of heavy metals are released from slags formed under disequilibrium conditions than from those which cristallized under close to equilibrium conditions.

Mineralogical and geochemical analyses coupled with leaching experiments indicate that the most important factors controlling metal release from slags are: (1) textural characteristics and permeability of the material, (2) slag mineralogy and cooling rates, (3) environmental conditions (e.g. pH, organic matter content).

The work was financed by Polish Ministry of Science and Higher Education grant no. NN307051237.

Fluid microinclusions in octahedral diamonds

I. KIFLAWI[1], Y. WEISS[1]*, W.L. GRIFFIN[2] AND O. NAVON[1]

[1]The Institute of Earth Sciences, the Hebrew University of Jerusalem, Israel (*correspondence: yakov.weiss@mail.huji.ac.il)
[2]GEMOC, Macquarie University, NSW, Australia

Microinclusions carrying high-density fluids (HDFs) with silicic, carbonatitic and saline compositions are common in fibrous diamonds and represent the medium in which their host diamond grew. Such inclusions have not been documented previously in monocrystaline octahedral diamonds or in the octahedral cores of coated diamonds, allowing a debate on whether such fluids are responsible for the formation of octahedral diamonds as well. The other notable difference is that all nitrogen in microinclusion-bearing zones resides in A-centers, whereas most octahedral diamonds carry both A and B centers. We report the first finding of HDF microinclusion in an octahedral diamond from Finsch, South Africa and in the core of a coted diamond from Kankan, Guinea.

The microinclusions in the Finsch diamond are restricted to two thin layers (~10 μm), parallel to the (111) face, ~20 and 200 μm from the rim. Cathodoluminescence (CL) reveals concentric zoning and octahedral growth throughout the diamond. The inclusion-rich layers are easily recognized by their weak fluresence. The diamonds carry ~800-1200 ppm nitrogen. Absorbance of B centers is observed in the inner part (A/B=5) and between the inclusion rich layers and the rim (A/B=16). Forty-five inclusions of carbonatitic HDF were analyzed along the inner layer. Their major and trace element compositions and FTIR analyses are highly similar to the ones observed in HDFs from fibrous diamonds.

In the octahedral core of the Kankan diamond we found six microinclusions with saline composition. Unlike the case of the Finsch diamond, these inclusions are sporadically scattered, up to ~100 μm away from a sulfide mineral inclusion and were hard to find.

Supporting evidence for the involvement of HDF, similar to the ones capsulate in fibrous diamonds, in the formation of monocrystaline diamonds comes from LA-ICP-MS analyses of trace element patterns in monocrystalline diamonds (McNeill *et al*. 2009) and the sinosuidal REE patterns of garnet inclusions in diamonds (Stachel and Harris, 2008; Weiss *et al*. 2009).

Based on the above observation we have good reasons to believe that microinclusions and HDFs may be found in other octahedral diamonds, extending the role of HDFs to the formation of most natural diamonds.

Seasonal and temporal variations of uranium isotope ratio in atmospheric deposits in Japan

Y. KIKAWADA[1]*, R. YAMAUCHI[1], M. NOMURA[2], T. OI[1] AND K. HIROSE[1]

[1]Sophia University, Tokyo 102-8554, Japan (*correspondence: y-kikawa@sophia.ac.jp)
[2]Tokyo Institute of Technology, Tokyo 152-8550, Japan

The uranium isotope ratios, especially $^{235}U/^{238}U$, do not change substantially in the natural environment. The $^{235}U/^{238}U$ ratio in environmental samples differing from the natural ratio thus resulted from anthropogenic nuclear activities. The Japan Meteorological Agency (JMA) and the Meteorological Research Institute (MRI) have been monitoring the deposition amounts of anthropogenic radioisotopes, mainly ^{90}Sr and ^{137}Cs, using the atmospheric deposits collected with open surface samplers installed throughout the Japanese Islands since the 1950s. In our previous work, we had reported that the $^{235}U/^{238}U$ ratios in the deposits collected at Fukuoka, Kyushu, the most southwesterly one of the four Japanese main islands, were slightly but obviously higher than the natural ratio since the 1960s until today [1]. This time, we have measured the uranium isotope ratios in the atmospheric deposits collected at Akita, which is located at the northeastern region of Japan and faces to the Sea of Japan, in the months of March between 1964 and 2000 and every month in 1977 and 1978. The results revealed that the $^{235}U/^{238}U$ ratios in the atmospheric deposits had varied seasonally and temporally. The fluctuation pattern of the $^{235}U/^{238}U$ ratio in the Akita deposits through the 24 months in 1977 and 1978 is in good accordance with that of the deposition amounts of plutonium at Tokyo [2]. Contrary to this, the deposition amounts of ^{90}Sr and ^{137}Cs are not always connected with the uranium isotope ratio in the deposits. Our results suggest that a certain amount of depleted uranium (DU) had been transported to Japan in the 1970s with plutonium ejected into the atmosphere by the thermo nuclear tests then conducted in the test sites in the Central Asia. DU and plutonium had probably been transported by the mechanism different from that of radioactive strontium and cesium, although they all had come from the same source, neuclear test explosions.

[1] Kikawada *et al*. (2009) *J. Nucl. Sci. Technol*. **46**, 1094–1098. [2] Hirose *et al*. (2001) *Plutonium in the environment* A. Kudo (Ed.) Elsevier Science, 251–266.

https://doi.org/10.1180/S0026461X00006502 Published online by Cambridge University Press

Speciation of iron in natural and synthesized Bacteriogenic Iron Oxides (BIOS) using XAFS and μ-XRF-XAFS

S. KIKUCHI[1]*, H. MAKITA[2], S. MITSUNOBU[3], K. TAKAI[2] AND Y. TAKAHASHI[1]

[1]Hiroshima University, Hiroshima 739-8526 (*correspondence: m103384@hiroshima-u.ac.jp)
[2]Japan Agency for Marine-Earth Science and Technology (JAMSTEC), Kanagawa 237-0061, Japan
[3]University of Shizuoka, Shizuoka 422-8526, Japan

Speciation of Fe in natural and synthesized bacteriogenic iron oxides (BIOS) was studied using XAFS, μ-XRF-XAFS, SEM and EPMA. Natural BIOS were collected at 2 sampling sites: seafloor at Mariana trough and from groundwater stream discharged at Sambe Hot Spring in Shimane Prefecture. BIOS was synthesized using a diffusion cell which consists of two cells that are separated by a membrane. Anoxic and oxic conditions were created in each cell to simulate the appropriate condition to BIOS precipitation in natural environment. Chemoautotrophic iron-oxidizing bacterium (*Mariprofundus ferrooxydans* [1]) or heterotrophic iron-oxidizing bacterium (*Leptothrix discophora* [2]) were cultured in the oxic cell.

SEM and EPMA analysis suggested similar precipitation morphology to all samples where iron oxides precipitated around bacterial-induced organic materials. Although each natural BIOS were precipitated in different environment, the XAFS spectra exhibited similar structures. Synthesized BIOS also showed spectra similar to natural samples regardless of the species of iron oxidizing bacteria and the medium employed in culture. In addition, μ-XAFS spectra collected at several Fe-precipitated area within few micro scale in the stalk were approximately identical, which is consistent with our bulk XAFS results of natural and synthesized BIOS. These results suggest that minerals presented in BIOS were homogeniously distributed in micrometer scale. The liniar combination fitting suggested that ferrihydrite is one of the Fe species in BIOS. It is also implied that Fe-carboxylate complex or Fe (III)-phosphate is a second Fe species of BIOS. These results will provide better insights into understanding the role of BIOS in the migration of trace elements in natural waters.

[1] Emerson D. *et al*. (2007) *PLoS ONE* **2**,e667. [2] Plam C. *et al*. (1992) *Appl. Environ. Microbiol*. **58**, 450-454.

Origin of ultramafic rocks from Hero Fracture Zone, Antartic

Y. KIL[1] AND C.-S. PARK[2]

[1]Geological Musieum, Korea Institute of Geosciences and Mineral Resources, 92 Gwahang-no, Yuseong-gu, Daejeon 305-350, Korea (ykil@kigam.re.kr)
[2]Division of Earth and Environmental Sciences, Korea Basic Science Institute, 804-1 Yangcheong-ri, Ochang-eup, Cheongwon-gun, Chungcheongbuk-do 363-883, Korea (cspark@kbsir.re.kr)

Serpentinites are rocks composed predominantly of the serpentine minerals, lizardite, chrysotile, or antigorite that form through hydrothermal alteration of peridotite. Substantial exposures of serpentinized peridotites are commonly found in fracture zones and in slow spreading mid-ocean ridge settings. Serpentinites from the Hero Fracture Zone, Drake Passage, Antarctica, contain serpentine, amphibole, talc, chlorite, and magnetite as well as relict olivine, pyroxene, and spinel from a spinel peridotite precursor. Two episodes of serpentinization are recognized. The initial serpentinization event resulted in material that contains relatively abundant relict minerals and small amount of lizardite and antigorite. This event resulted from seawater infiltration at about 178 - 283 °C seawater and a water/rock ratio less than 5. The second serpentinization event resulted in a material highly enriched in serpentine. This second event was caused by seawater infiltration at 170 - 298 °C and a water/rock ratio in excess of 5. The buoyant serpentinite ridge model is invoked to explain the ascent of serpentinite from the upper mantle to the surface. Increasing fracturing and seawater infiltration during the process resulted in increasing degrees of serpentinization and decreasing rock density. Buoyant uplift of serpentinite resulted from the contrast in density between serpentinite and surrounding mafic rocks. Some serpentinite rock fragments were detached from the serpentinite during ascent and embedded in oceanic sediment after exposure to the surface.

https://doi.org/10.1180/S0026461X00006502 Published online by Cambridge University Press

CO_2, CH_4, N_2O flux measurements from a constructed wetland

DEUG-SOO KIM* AND UN-SUNG NA

Dept. of Environ. Engineering, Kunsan National Univ., Kunsan, Jeonbuk 573-701, Korea
(*correspondence: dskim@kunsan.ac.kr)
(raja85@nate.com)

Implication

It is recently reported that microbial activity in freshwater wetland soils transforms considerable amounts of CO_2 into CH_4, which is then released into the atmosphere [1]. Consequently, this is likely to enhance greenhouse effect as CH_4 has a global warming potential greater than CO_2. The current study was focused on quantifying the source strenths of these greenhouse gases (GHG) from a wetland water surface and elucidating relationship between GHG emissions and physicochemical parameters.

Sampling and Experimental Methods

A closed chamber system was utilized to measure GHG emissions from water surface in a constructed wetland at Kunsan, Korea for six-month period (August~December, 2010 and March 2011). The measurements were made on 20 days during a day time (1400~1600LST) for experimental period only when weather was clear, and 50 ml of three consecutive gas samples for one GHG flux calculation were taken at each 10 min interval from a half spherical plastic chamber floating on the wetland water surface with plastic syringes. GHG fluxes were calculated based on the rate of change of GHG concentration [2]. Chemical characteristics in water (NO_3^--N, NH_3^+-N and pH) and water temperature also were monitored on measurement days. Concentrations of CO_2, CH_4 and N_2O were analyzed by using a Gas Chromatography (equipped with ECD/FID) at laboratory.

Results and Discussion

In order to examine the role of temperature on the gas flux, the changes of GHGs' emissions were investigated in terms of water temperature measured during sampling period (warm season: 18~31 ºC, cool season: 8~12 ºC). Results from current wetland experiment shows that water surface of the wetland absorbs CO_2 (sink) and emits CH_4 and N_2O (source) in average over the experimental period. Those levels were greater in warm season than in cool season. Futher results in correlations between physicochemical controlling parameters and those GHG emissions will be discussed in the conference.

This work is supported by NRF Korea Grant (2009-0072936).

[1] Williams (2009) CCAR Tidal Wetland Issue Paper 02/04/09. [2] Kim *et al*. (2002) *J. Air & Waste Manage. Assoc*. **52**, 416–422.

The elemental and stable isotope geochemistry of Korean bottled waters: Characterization and identifying their origins

G. KIM[1], J.S. RYU[2], W.J. SHIN[2], M. CHOI[2] AND K.S. LEE*

[1]Graduate School of Analytical Science and Technology, Chungnam Nat'l Univ (goeun@kbsi.re.kr)
[2]Korea Basic Science Institute, Ochang Center, Chungbuk 363-883, Korea (*correspondence: kslee@kbsi.re.kr)

We investigated 54 Korean bottled waters to characterize their water types and to examine a good tool for identifying their origins using the elemental and isotopic geochemistry. The elemental and isotopic compositions of the bottled waters varied substantially in different types of bottled waters. Major ion chemistry and oxygen and hydrogen isotopes clearly discriminate marine waters from the other types of water. Fractionation of oxygen and hydrogen isotopes likely explains the altitude and latitude effects. Variations in dissolved inorganic carbon isotope values reflect artificial CO_2 addition in sparkling waters, and reveal fractionation during the desalination process of marine waters. Strontium isotope ratios ($^{87}Sr/^{86}Sr$) of bottled waters are clearly associated with those of basement rocks in which bottled waters were collected. The results suggest that combined elemental and stable isotope variations in bottled waters are useful for characterizing the bottled waters and identifying the origins. Furthermore, combined elemental and isotope geochemistry could be a powerful tool in the related research fields and forensic sciences.

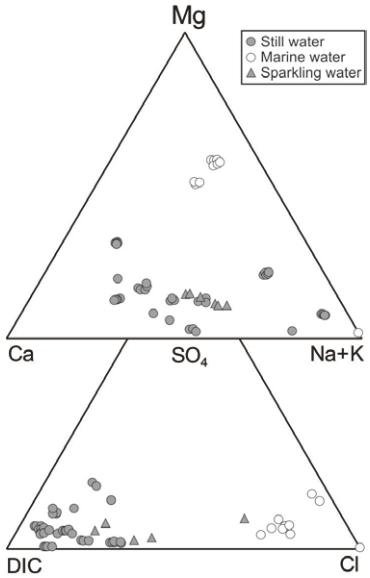

Figue 1: Ternary diagram showing chemical characteristics of bottled water.

https://doi.org/10.1180/S0026461X00006502 Published online by Cambridge University Press

Stabiliy of schwertmannite sorbed by oxyanions

JIYEON KIM, JONG-A CHOI, CHAN-YOUNG PARK, YEONGKYOO KIM* AND INCHANG RYU

Department of Geology, Kyungpook National University, Daegu, 702-701, Korea
(*correspondence: ygkim@knu.ac.kr)

Schwertmannite, commonly found iron-oxyhydroxysulfate in acid mine drainage has high sorption capacity and can play an important role in removing heavy metals in acid mine drainage. Heavy metals existing as oxyanions are known to have high affinity to schwertmannite compared with other heavy metals due to substitution for sulfate in the schwertmannite structure. However, schwertmannite is thermodynamically unstable and eventually transformed to goethite. The oxyanions such as AsO_4^{2-}, however, has been known to decrease the transformation rate. We made oxyanion-sorbed schwertmannite samples and studied their rates of transformation to geothite based on XRD patterns and pH values.

Schwertmannite was synthesized and oxyanion-sorbed schwertmannite was prepared by AsO_4^{2-}, SeO_3^{2-}, SeO_4^{2-}, MoO_4^{2-}, and CrO_4^{2-}. Because of the different sorption isotherms, the amount of sorbed oxyanions were fixed at 0.5 mmol/g for the samples. 0.1g of each samples were mixed with 40 ml distilled water and pH was adjusted at pH 9 at 30 ^oC to increase the transformation rate. The pH was measured every week pH values were adjusted to pH 9 again. The experiment was conducted for 3 months and during that period, 3 samples of each schwertmannite were analysed by XRD and compared.

Our results show that all the samples sorbed by oxyanions have slower transformation rate than pure schwertmannite, indicated by higher pH values. However, the transformation rates among oxyanions are different. Based on the pH value changes, the transformation rates to goethite are in the order of pure schwertmannite > SeO_4^{2-} > SeO_3^{2-} > CrO_4^{2-} > MO_4^{2-} > AsO_4^{2-}. XRD pattern of each sample shows that pure schwertmanite transformed to goethite after 1 month. After 3 months, the schwertmannite sorbed by SeO_4^{2-} almost transformed to goethite while other samples still have schwertmannite peaks. Therefore, the XRD patterns and pH values are quite closely matched. Our results show that sorption of oxyanions on schwertmannite decreases the transformation rate to goethite, and the rates of each samples are different.

Relations of arsenic concentrations among groundwater, soil, and bedrock in Geumsan, Korea: Implication for As mobilization according to changes in As-hosting minerals and land use

KANGJOO KIM[1]*, SEOK-HWI KIM[1], GI-YOUNG JEONG[2] AND PRAFULLA KUMAR SAHOO[1]

[1]Department of Environmental Engineering, Kunsan National University, Kunsan, Jeonbuk 573-701, Korea
(*correspondence: kangjoo@kunsan.ac.kr)
[2]Department of Earth and Environmental Sciences, Andong National University, Andong, Kyeongbuk 760-747, Korea

Arsenic concentrations and As-bearing minerals in bedrock, and soil, and their relations with groundwater concentrations were investigated in a small agricultural area of Korea to understand the changes in arsenic mobility by pedogenetic processes and changes in geochemical conditions. The arsenic concentration in bedrock shows a wide variation (<1 to 3990 mg/kg) and is well correlated with that in contacting groundwaters. Soils, the weathering product of bedrock, show much mitigated and dispersed, but still very high As concentrations (8.8 to 387 mg/kg). Furthermore, As concentrations in the shallow groundwaters were very low (<20 μg/L) and independent on the soil concentrations due to the differences in As hosts and geochemical conditions. Arsenopyrite is the major As-bearing mineral in bedrock and its oxidation controls the As levels in deep groundwater. In contrast, the As mostly resides in soil as Fe-(hydr)oxide bound forms. Due to low pH and oxidizing redox condition, the release of As from Fe (hydr)oxides are largely suppressed and the shallow groundwater show low As concentrations. However, it is suggested that the disturbance of geochemical conditions in soils by land use changes mobilize As and would cause serious As contamination in shallow groundwaters.

https://doi.org/10.1180/S0026461X00006502 Published online by Cambridge University Press

Hypoxia events in Cheonsu Bay, West coast of Korea, triggered by discharge of eutrophicated water from artificial lakes

KEE-HYUN KIM[1]* AND JAE-SUNG LEE[2]

[1]Chungnam National University, Daejeon 305-764, Korea (*correspondence: khkim@cnu.ac.kr)
[2]NFRDI, Busan 619-705, Korea, leejs728@nfrdi.go.kr

Frequent outbreaks of hypoxic water masses have been reported in Cheonsu Bay, west coast of Korea, due to the influx of eutrophicated waters heavily loaded with oxygen demanding material from artificial lakes formed by large-scale land reclamation and subsequent industrial development and rapid urbanization since early 1980s. The hypoxia events would give deteriorative impact on fisheries and aquaculture industry around the bay.

In summer 2010, we measured the concentration of dissolved oxygen (DO) and nutrients in bottom waters collected from 14 stations. We also measured the nutrient fluxes across the sediment-water interface in 3 stations by deploying a fully automated benthic lander, which collects time-series water samples inside a benthic chamber, on the seafloor for a couple of days.

We confirmed the on-going hypoxia in the northern parts of the bay into where the lakes discharged. DO content of the bottom water was below 2 mg/l, compared to that of 5 mg/l at the mouth of the bay. Organic carbon oxidation rate was estimated to be 55 mmol C m^{-2} d^{-1} and the oxygen consumption rates to be 50.4 mmol O_2 m^{-2} d^{-1}. These rates were about twice as fast as those at the bay mouth. Benthic fluxes of nutrients at the northern part of the bay were 4 to 6 times higher than those at the bay mouth.

Our results imply that it is necessary to keep keen eyes on hypoxia events since they would give severe damages to fisheries and aquaculture industry.

Oxygen isotope fractionation between calcium carbonate and water: Influence of ionic strength

SANG-TAE KIM

School of Geography and Earth Sciences, McMaster University, Hamilton, ON, L8S 4K1, Canada (sangtae@mcmaster.ca)

The conventional carbonate-water thermometer is one of the most successful paleotemperature proxies in the Earth sciences and it was developed on the theoretical basis of oxygen isotope fractionation between $CaCO_3$ and H_2O. As a result, numerous scientists have extensively studied the oxygen isotope systematics in the $CaCO_3$-H_2O system over the past several decades in order to establish a more reliable carbonate-water paleothermometer. Whereas the majority of natural calcium carbonate samples, such as corals and foraminifera, that are frequently used to reconstruct Earth's past climate changes on the basis of the conventional carbonate-water thermometer, are of oceanic origin, most of the experimental studies, that provide a baseline for the calibration of many of the species-specific carbonate-water paleotemperature proxies [1, 2], used calcium carbonates precipitated from parent solutions of low ionic strength (e.g. freshwater) rather than those precipitated from parent solutions of seawater salinity or ionic strength (e.g. ocean water).

In order to investigate the effect of a parent solution's ionic strength on the oxygen isotope fractionation between $CaCO_3$ and H_2O, calcium carbonates were synthesized in the laboratory from Na-Ca-(Mg)-Cl-HCO_3 solutions of seawater ionic strength (I = ~ 0.7). Subsequently, the oxygen isotope composition of the calcium carbonate precipitates and that of the parent solutions were determined. In particular, the passive CO_2 degassing and the constant addition methods, which are described in Kim *et al*. [3], were employed in this study. Our preliminary experimental results suggest that the oxygen isotope fractionation factors determined from calcium carbonates that were formed from high ionic strength solutions may not be always the same as those determined from low ionic strength solutions.

[1] Bemis *et al*. (1998) *Paleoceanography* **13**, 150–160. [2] Grossman & Ku (1986) *Chem. Geol*. **59**, 59–74. [3] Kim *et al*. (2007) *GCA* **71**, 4704–4715.

https://doi.org/10.1180/S0026461X00006502 Published online by Cambridge University Press

Extinction-to-backscatter ratio of Asian dust observed with a combined Raman elastic-backscatter lidar in Seoul, Korea

SANG-WOO KIM[1]*, MAN-HAE KIM[1], SOON-CHANG YOON[1] AND NOBUO SUGIMOTO[2]

[1]School of Earth and Environmental Sciences, Seoul National University, Seoul, Korea (*correspondence: kimsw@air.snu.ac.kr)

[2]Atmospheric Environment Division, National Institute for Environmental Studies, Tsukuba, Japan

The extinction-to-backscatter ratio (so called, lidar ratio), which is a key parameter in the issue of backscatter-lidar inversions, of Asian dust was observed with a combined Raman elastic-backscatter lidar in Seoul, Korea. The lidar ratio at 532 nm is calculated by the comparison of lidar-derived aerosol optical thickness (AOT) with sunphotometer-derived AOT for 4-year measurements (2006-2010). Here, the value of AOT 532 nm is calculated by the Ångström relationship using measurements at five wavelengths (400, 500, 675, 870, and 1020 nm). The annual mean lidar ratio (with standard deviation) is found to be 61.7±16.5 sr, and weak seasonal variations are noted with a maximum in summer (68.1±16.8 sr) and a minimum in winter (57.2±17.9 sr). The lidar ratios for clean, dust, and polluted conditions are estimated to be 45.0±9.5 sr, 51.7±13.7 sr, and 62.2±13.2 sr, respectively. While the lidar ratio for the polluted condition is appears to be consistent with previous studies (50-70 sr), clean and dust conditions tend to have larger values, compared to previous estimates (clean: 30-40 sr, dust: 40-50 sr). This discrepancy is thought to be mainly due to the anthropogenic aerosols existing in the atmospheric layer throughout the year around Seoul, which may cause increased S_a even for clean and dust conditions. For instance, the lower values of lidar ratio at 532 nm was directly estimated from Raman (inelastic) signals. The values of lidar ratio averaged for Asian dust layer was ranged from 25 and 40 sr on two Asian dust days (October 20, 2009 and March 15, 2010), with 10 ~ 20% of particle depolarization ratio.

Dependence of adiabaticity of stratiform clouds upon stability, and its relationship to aerosol-cloud interactions

Y.-J. KIM[1], B.-G. KIM[1]*, M. MILLER[2] AND C.-K. SONG[3]

[1]Department of Atmospheric Environmental Sciences, Gangneung-Wonju National Univ., Gangneung, 210-702, Korea (*correspondence: bgk@gwnu.ac.kr)

[2]Department of Environmental Sciences, Rutgers Univ., New Brunswick, NJ, 08901, United States

[3]Air Quality Research Department, National Institute of Environmental Research, Incheon, 404-708, Korea

The buffering mechanisms in the modifications of cloud microphysics and cloud albedo by cloud-active aerosol are only vaguely understood and are thought to include a myriad of processes that vary regionally and confound the application of simple physical models of cloud-aerosol sensitivity [1].

This study presents the relationship of aerosol-cloud interaction to cloud environment condition (adiabaticity and stability), using data from the Atmospheric Radiation Measurement (ARM) Southern Great Plain (SGP) site and the Pt. Reyes (PYE) deployment of the ARM Mobile Facility (AMF). Adiabaticity is defined as the ratio of the observed liquid water path (LWP) to corresponding adiabatic value in this study. The stability indicates the differences of potential temperature between 500 m above the mixed layer tops and the mixed layer tops. Strong inversions above the PYE cloud are shown to buffer marine stratocumulus from the effects of mixing with drier, warmer inversion air. This buffering reduces the variability of the cloud LWP and enables the clouds to remain nearly adiabatic. The critical comparison of cloud adiabaticity with static stability demonstrates the more adiabatic LWP in the condition of the stronger stability above the cloud. Weaker inversions above the SGP cloud promote variability in the LWP and sub-adiabatic LWPs. Aerosol-cloud interactions are probably more dominant in stratiform clouds that remain nearly addiabatic [2] and exhibit less variability in the LWP. This study implies static stability and adiabaticity are important controlling factors in the enhancement or attenuation of aerosol-cloud interactions.

This work was supported by the ‘National comprehensive measures against climate change’ by the ministry of environment, Korea (Grant no. 1600-1637-301-210-13).

[1] Stevens & Feingold (2009) *Nature* **461**, 607–613. [2] Kim *et al*. (2008) *J. Geophy. Res*. **113**, D05210.

https://doi.org/10.1180/S0026461X00006502 Published online by Cambridge University Press

Uranium minerals in black shale, South Korea

YOUNG JAE KIM[1], HYO EUN LEE[1], SUE-A KANG[1], JONG KI SHIN[2], SUNG YUN JUNG[2], YOUNG JAE LEE[1]*

[1]Department of Earth and Environmental Sciences, Korea University, Seoul 136-701, Korea (*correspondence: youngjlee@korea.ac.kr, jjbsnlove@korea.ac.kr, hyonim@korea.ac.kr, sue_a@korea.ac.kr)

[2]Coal & Uranium Exploration Team, Korea Resources Corporation, Seoul 156-406, Korea (jkshin1@kores.or.kr, jsy@kores.or.kr)

Uranium (U) in black shale, South Korea has been the subject of interest because of its potential roles in energy and mining industries. Previous reports found that balck shale in Korea is highly metalliferous with lead, uranium, and vanadium, but also that uranium content increases with increasing total carbon content in the black shale. Yet, identification and understanding of minerals for uranium and other elements in the black shale is still not clearly addressed. In the present study, U-containing minerals in the black shale is characterized by combination of geochemical compostion analysis and electron probe microanalyzer (EPMA) analysis.

Results show that uranium content is moderately proportional to the content of total organic carbon (TOC) in the black shale. XRF analysis shows that Al, Mg, Ba, and K are major elements with trace elements such as Zn, P, S, and Ti. Total uranium concentration is up to 0.13 wt. %, whereas total concentration of V and Ba are 0.17-1.6 wt. %, and 2.0-5.0 wt. %, respectively. Using EPMA, it is found that two different element series of U-P-Cu and U-V-Ba are found in U-containing minerals. Ratio of the series for U : V : Ba and U : P : Cu are 2 : 2 : 1 and 4 : 4 : 1, respectively. These results indicates that the U-containing minerals are francevillite ((Ba, Pb)$(UO_2)(V_2O_8)(H_2O)$) and torbernate (Cu $(UO_2)_2$ $(PO_4)_2$ $(H_2O)_8$) in the black shale. These findings are not consistent with previous reports showing that uraninite is a main mineral in U-containing minerals at a different area of the black shale, Korea. Upon our results, it is worthy to note that formation of uranium minerals are sensitively affected by geochemical environments and tectonic movements in the black shale, South Korea.

Uptake and retention of mercury by hydroxylapatite

YOUNG JAE KIM, HYO EUN LEE, SOO-OH PARK AND YOUNG JAE LEE*

Department of Earth and Environmental Sciences, Korea University, Seoul 136-701, Korea (*correspondence: youngjlee@korea.ac.kr, jjbsnlove@korea.ac.kr, hyonim@korea.ac.kr, orange261@korea.ac.kr)

Mercury (Hg) is well known as a toxic element for humans and ecosystems. Partitioning of the mercury to minerals and organics has been known to influence the fate and transport of mercury species in natural ecosystems. Despite the importance of mercury interaction with minerals, sorption mechanisms and modes are are not still clearly understood. Systematic characterization of mercury uptake by hydroxylapatite (HAP, $[Ca_5 (PO_4)_3OH]$) is little addressed over a wide range of physicochemical conditions.

Mercury sorption on HAP shows that the initial uptake of mercury by HAP sharply increases, levels off, and then followed by little changes as a function of concentration at pH 7.0 and 9.0, showing a typical pattern of Langmuir sorption. No obvious differences are found in the sorption pattern at the two pHs. Compared to that of the sorption at pH 7.0, however, the sorption of mercury on HAP decreases by a factor of 4 at pH 9.0. In addition, the mercury uptake by HAP decreases with increasing ionic strength of the solution. From $I = 0.01$ M to $I = 0.1$ M, total amount of the sorption decreases around by a factor of 2. During the duration of the kinetic experiments, the initial uptake and retension of mercury by HAP is rapid and ~85% of Hg is sorbed on the HAP within 30 mins, suggesting that adsorption plays an key role in the initial upatke of mercury at the HAP-water interface. Results reveals that different physicochemical conditions such as pH and I influence the mercury uptake by HAP sensitively.

https://doi.org/10.1180/S0026461X00006502 Published online by Cambridge University Press

Biogeochemical behaviour of Pu in a contaminated soil from Aldermaston, UK

R.L. KIMBER[1]*, P. PURDIE[2], C. BOOTHMAN[1], F.R. LIVENS[1] AND J.R. LLOYD[1]

[1]The University of Manchester, Oxford Road, Manchester, M13 9PL, United Kingdom (*correspondence: richard.kimber@postgrad.manchester.ac.uk)
[2]AWE Plc, Aldermaston, Reading, RG7 4PR, United Kingdom

Understanding the biogeochemical behaviour of actinides in the environment is essential for the long-term stewardship of radionuclide-contaminated land. Plutonium is of particular concern due its high radiotoxicity, long half-life and complex chemistry. Here, we investigate the biogeochemistry of Pu in a contaminated soil as microbial processes have the potential to mobilise Pu via the reduction of Pu (IV) to the potentially more mobile Pu (III). A series of microcosm experiments were designed to monitor changes in Pu solubility in an anaerobic environment stimulated via the addition of 10 mM glucose to Pu contaminated soils. A substantial shift in the 16S rRNA gene profile was observed between days 0 and 44 most notably with an increase in *Clostridia*, known glucose fermenters that have been reported to facilitate the reduction of Pu (IV) to Pu (III) [1]. A minor increase in Pu solubility was observed at day 44, decreasing to initial levels by day 118. The negligible change in Pu solubility, despite the onset of reducing conditions and formation of Fe (II), would suggest the Pu is highly refractory and unsusceptible to the influence of the surrounding geochemistry. To further examine the geochemistry of the Pu, a series of sequential extractions were performed. Around 75% of the Pu from the Aldermaston site was found to be associated with the highly refractory, residual fraction of the soils. This value greatly excedes the fraction of residual Pu at other nuclear sites reported in the literature after similar extraction protocols (34% at Sellafield and 8% at Dounreay [2]) and further suggests the Aldermaston Pu is highly resistant to changing geochemical conditions. Further work is currently being undertaken to investigate the impact of citric acid producing fungi on Pu solubility as citric acid has the potential to mobilize Pu. This information is important for understanding both the long-term mobility of Pu in the environment and for developing remediation options for Pu-contaminated soils.

[1] Francis *et al*. (2008) *Environ. Sci. Technol* **42**, 2355–2360.
[2] Kamosa (2002) *J. Radioanal. Nucl. Chem* **252**, 121–128.

What stays in the slab and what returns to the surface? A geochemical mass balance model perspective

J.-I. KIMURA, H. KAWABATA[1], B.R. HACKER[2], P.E. VAN KEKEN[3], J.B. GILL[4] AND R.J. STERN[5]

[1]Institute for Research on Earth Evolution (IFREE), Japan Agency for Marine-Earth Science and Technology (JAMSTEC) (jkimura@jamstec.go.jp, hiroshik@jamstec.go.jp)
[2]Department of Earth Science, University of California, Santa Barbara (hacker@geol.ucsb.edu)
[3]Department of Geological Sciences, University of Michigan (keken@umich.edu)
[4]Department of Geology, University of California Santa Cruz (jgill@pmc.ucsc.edu)
[5]Department of Geosciences, University of Texas at Dallas (rjstern@utdallas.edu)

We have developed the Arc Basalt Simulator (ABS), a quantitative forward model to calculate the mass balance of slab dehydration and melting, and slab fluid/melt-fluxed mantle melting, in order to quantitatively evaluate magma genesis beneath arcs. ABS models can reproduce magma compositions in many arcs.

The model suggests that the slab-derived component at volcanic fronts (VF) is mostly generated by dehydration, but successful models for most VF and all rear arc (RA) magmas also require the slab to melt. The compositions of slab fluids and melts are controlled primarily by the breakdown of amphibole and lawsonite beneath the VF and by the breakdown of phengite beneath the RA in addition to residual eclogite mineral phases including garnet, clinopyroxene, and quartz.

In the model, about 78-98% of relatively fluid-immobile elements including Nd and Hf in the arc lavas come from mantle peridotite. However, most liquid-mobile elements come from the slab. Modeled residual peridotite compositions are similar to those in some supra-subduction zone ophiolites and mantle xenoliths, providing constraints on reactions in the mantle wedge.

Altered oceanic crust (AOC) and sediment in the residual slab are modified by the subtraction of melt- and fluid-mobile elements. Unmodified AOC potentially becomes the EM I mantle component after 1 Ga, whereas melted AOC can have extremely fractionated U-Pb and become the HIMU source after 1-2 Ga. Element re-distribution beneath arcs can form the recycled materials that have been detected in ocean island basalts.

https://doi.org/10.1180/S0026461X00006502 Published online by Cambridge University Press

Interfacial reactions during olivine replacement

H.E. KING[1]*, H. SATOH[2], T. GEISLER[3] K. TSUKAMOTO[4] AND A. PUTNIS[1]

[1]Institut fuer Mineralogie, Westfaelische Wilhelms-Universitaet Muenster, Germany (*correspondence: hking_01@uni-muenster.de)
[2]Mitsubishi Materials Corporation, Japan
[3]Steinmann Institut, Universitaet Bonn, Germany
[4]Department of The Earth and Planetary Science, Tohoku University, Japan

Olivine-fluid interactions have a variety of applications in environmental remediation schemes, e.g. CO_2 sequestration and sulphate-rich acidic solution neutralization. We have conducted experiments to examine olivine reactivity within these systems, including mineral carbonation (200 °C, carbonated saline solution) and sulphuric acid neutralization (90 °C). Furthermore, we have used *in situ* phase-shift interferometry (PSI) to gain new insights into surface specific olivine dissolution.

The role of the interfacial solution composition was most pronounced in experiments with sulphuric acid, which produced an amorphous silica pseudomorph after olivine at high acid concentrations. Incorporation of ^{18}O into the silica layer in an isotope tracer experiment indicates that the replacement reaction occurred via an interface-coupled dissolution-reprecipitation mechanism. The formation of a pseudomorph in 3.6 M and 2 M solutions suggests that at these conditions olivine dissolution was the rate-limiting step. However, in 1 M solutions the formation of the amorphous silica layer controlled the rate, uncoupling the spatial relationship between dissolution and reprecipitation so that no pseudomorph was produced.

Dissolution of different olivine surfaces in saline solutions were studied with PSI, and showed that the fastest dissolving surface supersaturated the interfacial solution to precipitate a new phase at acidic conditions. This phase is predicted to be similar to the amorphous silica-enriched phase observed to form in the carbonation experiments indicating that the interfacial solution composition plays a critical role under a wide range of conditions.

Sulfur isotope studies in organic matter via SIMS using a statistical approach with heterogeneous standards

H.E. KING JR.[1], MINDY M. ZIMMER[1,2], WILLIAM C. HORN[1] AND WILLIAM A. LAMBERTI[1]

[1]ExxonMobil Research and Eng. Co., Annandale NJ (correspondence hubert.e.king@exxonmobil.com)
[2]current address Los Alamos National Lab, Los Alamos NM)

Solid bitumen, often found in rocks associated with a hydrocarbon phase, retains a paleo-signature reflecting the evolution of the hydrocarbon. For example, the $^{34}S/^{32}S$ ratio can provide information on the relative importance of thermal sulfate reduction over bacterial sulfate reduction during diagenesis. Such bitumen, distributed as small globules or grain coatings throughout the rock matrix, is a challenge to analyze. A technique with high-spatial resolution, Secondary Ion Mass Spectrometry (SIMS), is an excellent method, but there are challenges in applying this technique to such materials.

SIMS analysis of mineral phases is readily performed because standards allowing correction for instrument and matrix isotope fractionation have been developed. There are no comparable standards for sulfur isotopes in bitumen. Here we introduce the use of sulfur-bearing organic solids such as petroleum coke as such standards. They posses the required similarity in chemical bonding environment to that in bitumen. However to utilize these solids required that we develop a method to overcome their intrinsic chemical inhomogenity. For example, there are finely divided sulfate phases distributed in the organic matrix. Utilizing SIMS imaging to avoid secondary phases and a statistical analysis technique to mitigate the influence of unresolved secondary phases, we found that consistent correction factors for both instrument and matrix fractionation can be obtained. We have generated a Calibrated Matrix Correction that allows the systematic analysis of $\delta^{34}S$ values for bitumen, demonstrating those results by analyzing several bitumens from Brooks Range, Alaska and LaBarge, Wyoming.

https://doi.org/10.1180/S0026461X00006502 Published online by Cambridge University Press

Geocosmochronometer ^{146}Sm: A revised half-life value

N. KINOSHITA[1], M. PAUL[2]*, Y. KASHIV[3], M. ALCORTA[4], P. COLLON[3], C.M. DEIBEL[4,5], B. DIGIOVINE[4], J.P. GREENE[4], D.J. HENDERSON[4], C.L. JIANG[4], S.T. MARLEY[4], T. NAKANISHI[6], R.C. PARDO[4], K.E. REHM[4], D. ROBERTSON[3], R. SCOTT[3], C. SCHMITT[3], X.D. TANG[3], C. UGALDE[4], R. VONDRASEK[4] AND A. YOKOYAMA[6]

[1]Tandem Accelerator Complex, U. of Tsukuba, Japan
[2]Racah Institute of Physics, Hebrew U., Jerusalem, Israel 91904 (*correspondence: paul@vms.huji.ac.il)
[3]U. of Notre Dame, Notre Dame, IN 46556-5670
[4]Argonne National Laboratory, Argonne, IL 60439
[5]Joint Institute for Nuclear Astrophysics, Michigan State U., East Lansing, MI 48824
[6]Faculty of Chemistry, Kanazawa U., Japan

Alpha-decaying nuclide ^{146}Sm, now extinct, was extant in the Early Solar System (ESS) [1] and was proposed as a cosmochronometer measuring the time between *p*-process nucleosynthesis and ESS condensation. Positive isotopic anomalies in the ^{142}Nd daughter have been measured in Earth rocks [2] and in Moon [3] and Martian meteorite [4] samples, relative to chondritic meteorites. This indicates that geochemical fractionation between Sm and Nd occurred while ^{146}Sm was still live, possibly during mantle differentiation. These issues stress the importance of ^{146}Sm half-life, determined as $(1.03\pm0.05)\times10^8$ yr [5, 6]. We have performed a new determination of the ^{146}Sm half-life by measuring both alpha-activity ratio and atom ratio of ^{146}Sm to ^{147}Sm ($t_{1/2}$= $(1.07\pm0.09)\times10^{11}$ yr [7]) in artificially activated ^{147}Sm. The new value of ^{146}Sm half-life, $(0.68\pm0.07)\times10^8$ yr, is significantly shorter than previously measured and will have interesting implications for the chronology of *p*-process and planetary differentiation. The experimental determination of ^{146}Sm half-life will be described and discussed.

This work is supported in part by a Grant-in-Aid for Scientific Research Program of Japan Society for the Promotion of Science (20740161). This work is supported by the U.S. Department of Energy, Office of Nuclear Physics, under contract No. DE-AC02-06CH11357.

[1] Prinzhofer, Papanastassiou & Wasserburg (1992) *GCA* **56**, 797–815. [2] O'Neil *et al*. (2008) *Science* **321**, 1828–1831. [3] Boyet & Carlson (2007) *EPSL* **262**, 505–516. [4] Caro *et al*. (2008) *Nature* **452**, 336–339. [5] Friedman *et al*. (1966) *Radiochim. Acta* **5**, 192–194. [6] Meissner *et al*. (1987) *Z. Phys. A* **327**, 171–174. [7] Kossert *et al*. (2009) *Appl. Rad Iso*. **67**, 1702–1706.

Recycling of subducted sediments traced by HFSE and W systematics of K-rich mafic Aegean lavas

MARIA KIRCHENBAUR[1,2] AND CARSTEN MÜNKER[2]

[1]Steinmann-Institut, Universität Bonn, Germany (Kirchenbaur@uni-bonn.de)
[2]Institut für Geologie und Mineralogie, Universität zu Köln, Germany

Tungsten and other similar incompatible HFSE and LILE (Nb, Ta, Zr, Hf, Ba, Th, U) have been shown to be valuable monitors for assessing the flux of subducted sediments in arc systems [1]. In subduction-related tectonic settings, basalts of the K-rich series (medium-K, high-K and shoshonitic) are considered as the most incompatible element-rich endmembers, commonly being interpreted as tapping mantle sources that underwent a substantial flux of melts or fluids from subducted sediments. In order to constrain the behaviour of the extended HFSE group in the sources of K-rich lavas, we performed high-precision measurements of Nb- Ta-Zr-Hf and W concentrations by isotope dilution and MC-ICPMS on K-rich lavas from the Eo-Oligocene Eastern Rhodope province, Bulgaria and on mafic calc-alkaline lavas from the active Aegean Island arc (Santorini). Both suites share similar petrogenetic characteristics in that their sources were contaminated by subducted sediments from the African plate.

The concentrations of HFSE are enriched in all suites (e.g. 0.3 to 4.2 ppm W), similar to other incompatible elements such as K. The HFSE ratios of virtually all samples lie well within the MORB array (Nb/Ta = 12.8 – 15.1, Zr/Hf = 39.5 – 41.7). Only the absarokites exhibit elevated Nb/Ta (19.1 – 20.1) reflecting fractionation of phlogopite. The samples also exhibit lower Ta/W than MORB (0.19 to 0.68), similar as found for other arc suites [1].

The extended HFSE systematics for both Santorini and Bulgarian rocks can help to discriminate between different types of source overprint: lavas from Santorini, where source enrichment is controlled by melt-like components, exhibit consistently low W/Th (ca. 0.07), somewhat lower than MORB (ca. 0.15). In contrast, the HFSE and W budget in the Bulgarian K-rich rocks is dominated by both fluid- and melt-like components, and W/Th exhibit a large range from 0.07 to 0.3. Our data therefore confirm that W/Th in arc lavas can only be elevated in the presence of fluid-like subduction components. Conversely, in melt-controlled subduction regimes, W appears to behave slightly less mobile than Th.

[1] König *et al*. (2008) *EPSL* **274**, 82–92.

https://doi.org/10.1180/S0026461X00006502 Published online by Cambridge University Press

Towards a numerical model to constrain the time scales for vertically moving axial magma chambers beneath fast-spreading ocean ridges

C. KIRCHNER, J. KOEPKE AND H. BEHRENS

Institut für Mineralogie, Leibniz Universität Hannover, Callinstr. 3, 30167 Hannover, Germany (c.kirchner@mineralogie.uni-hannover.de)

It is well accepted that AMCs ('axial magma chamber') under fast spreading ocean ridges are dynamic systems with the potential to oscillate vertically. Unfortunately, the time scales of these movements are poorly contrained by several multidisciplinary studies, varying between 10 and 100.000 years.

The IODP multi-cruise mission „Superfast Spreading Crust' (Site 1256, equatorial East Pacific Rise), offers the possibility to study natural samples from the lower sheeted dikes from the 1256D drillcore. Detailed petrographic work led to the conclusion, that the ascent of the AMC led to the formation of 'granoblastic dikes' due to an intense metamorphic overprint under granulite facies conditions [1].

In this study, we apply tools of diffusion profile modeling to relictic plagioclase phenocrysts occuring in the granoblastic dikes located above the AMC. Since the plagioclases were affected by the thermal imprint of the AMC (~1200°C), the detailed analysis and modeling of the concentration profiles allows us a quantification of the residence time of the heat source (AMC) in a high position and hence, temporal information about the vertical fluctuations of the AMC can be assessed.

First estimations on the basis of CaAl-NaSi interdiffusion profiles yield average time scales of 19000 years for the development of the profiles. Calculations based on Mg concentration profiles revealed different results: The durations extracted from the profiles are much shorter in the range of ~150-400 years. This discrepancy presumably reflects different processes contributing to the development of the element distribution patterns in these plagioclase phenocrysts and its meaning has to be evaluated in the near future.

[1] Koepke *et al*. (2008) Petrography of the dike-gabbro transition at IODP Site 1256 (equatorial Pacific) The evolution of the granoblastic dikes, *Geochem. Geophys. Geosyst.* **9**, Q07O09, doi, 10.1029/2008GC001939.

Sub-micromolar oxygen dynamics at redox boundaries of lakes

M. KIRF[1,2], C.J. SCHUBERT[1] AND B. WEHRLI[1,2]

[1]Eawag, Seestr. 79, 6047 Kastanienbaum, Switzerland (mathias.kirf@eawag.ch, carsten.schubert@eawag.ch)
[2]Inst. Biogeochem. Pollutant Dynamics, ETH, 8092 Zurich, Switzerland (bernhard.wehrli@env.ethz.ch)

The oxic-anoxic interface in stratified lakes is a habitat of intense microbial activity where a cascade of redox processes occurs at low O_2 concentration levels. Here we report well resolved profiles based on a two-sensor technique: The stable but slower signal from low-level optodes was verified independently with profiles from highly amplified amperometric sensors. Pre-exposure to anoxic waters reduced the drift of electrochemical sensors.

The sub-micromolar oxygen zone

An field survey of the permanently anoxic basin of Lake Zug (Switzerland) [1] revealed the spatial structure and temporal variability of the oxic-anoxic interface in the water column. The depth interval from 1 μM O_2 down to the detection limit had an extension of 0.5 to 5 meters. While most profiles showed a steady decrease, several observations revealed sharp excursions due to the effect of turbulent mixing in the weakly stratified water column with a stability frequency of $N^2 < 10^{-6}$ s^{-2}.

Fast fluctuations were also confirmed when sensors were depoyed at constant depth. Concentrations changed by about 1 μM O_2 within ~ 10 seconds and then remained quasi constant on time-scales of minutes.

The chemical gradients right at the oxic-anoxic interface were on the order of 1 mmol O_2 m^{-4}. Temperature profiles showed local maxima of >0.01°C over the sub-micromolar zone. These temperature changes were not compatible with short-term oxygen fluctuations. Therefore, the position of the oxic-anoxic interface seemed to oscillate over a limited depth range of meters. Microbial communities such as methanotrophs need to cope with oscillating conditions on the time-scale of minutes but will face a rather stable diurnal O_2 supply.

The new setup will facilitate the high-resolution sampling at the redoxcline, the measurements of the *in situ* concentrations for important microbial reactions, and boundary conditions for more detailed reaction-transport models.

[1] Maerki *et al*. (2009) *Limnol. Oceanogr.* **54**, 428–438.

Age of the Pueblo Viejo epithermal deposit, Dominican Republic: Re-Os isotope data for sulfides from the Moore and Monte Negro deposits

J.D. KIRK[1]*, S.E. KESLER[2] AND J. RUIZ[1]

[1]University of Arizona, Tucson, Arizona 85721, USA (*correspondence: jdkirk@email.arizona.edu)
[2]University of Michigan, Ann Arbor, Michigan 48109, USA

Knowledge of the age of the giant Pueblo Viejo high-sulfidation epithermal deposit (23.7 M oz Au) in the Dominican Republic is critical to our understanding of the geologic environment in which these deposits form. Two possibilities have been suggested: 1) 118-111 Ma, coeval with formation of Los Ranchos Formation island-arc tholeiites that host the deposit and represent the earliest stage of magmatism in the Greater Antilles arc, or 2) 77-62 Ma, coeval with calc-alkaline intrusions that formed during later stages of arc magmatism typical of many other deposits of this type in Cordilleran settings.

Gold is hosted directly by pyrite and to a lesser extent other sulfides, and is found in both sulfide-rich veins and layers of sulfide along bedding planes in carbonaceous shale. Analyses of six heavy mineral concentrates (largely pyrite), five vein pyrite or sphalerite and one layer pyrite from the Moore and Monte Negro ore bodies, form an isochron yielding an age of 115.1 ± 5.4 Ma with an $^{187}Os/^{188}Os$ initial value of 0.30 ± 0.14 (MSWD = 0.38). Taken separately, the concentrate analyses yield an isochron with an age of 116.4 ± 7.5 Ma and the vein analyses give an age of 116.9 ± 9.9 Ma. The combined isochron age and $^{187}Os/^{188}Os$ initial are consistent with synvolcanic derivation of metals from juvenile arc tholeiites at ca. 115 Ma.

These results confirm that high-sulfidation epithermal mineralization can form during early stages of island arc volcanism and is not confined to calc-alkaline magmatic associations, thereby considerably expanding geologic terranes that are favorable for mineral exploration.

Sea water circulation in coastal aquifers as inferred from radium isotopes: The Dead Sea case

Y. KIRO[1,2]*, Y. WEINSTEIN[3], Y. YECHIELI[2] AND A. STARINSKY[1]

[1]Institute of Earth Sciences, The Hebrew University, Edmond J. Safra campus, Givat Ram, Jeruslaem, 91904
[2]Geological Survey of Israel, 30 Malkhe Israel St., Jerusalem, 95501, Israel
[3]Department of Geography and Environment, Bar-Ilan University, Ramat-Gan 52900

Saline water circulation in coastal aquifers may be a major process that controls trace element mass balances in coastal areas. This study uses radium isotopes in order to quantify lake water circulation in the Dead Sea aquifer.

The Dead Sea is extremely enriched in radium, where both ^{226}Ra and ^{228}Ra (140 and 1-2 dpm/L, respectively) are 3 orders of magnitude higher than in ocean water, whereas the salinity of the Dead Sea is only 10 times higher. The main sources of ^{226}Ra and ^{228}Ra to the lake are fresh springs and brines discharging along the lake shoreline.

Circulated Dead Sea water in the aquifer contains decreased activities of ^{226}Ra (60 dpm/L). This coincides with the lower Ba concentrations in this water compared with the lake (1.5 and 5 mg/l, respectively). We suggest that the low ^{226}Ra and Ba concentrations are due to precipitation of barite from the supersaturated Dead Sea water on entering the aquifer. ^{228}Ra and the shorter-lived ^{224}Ra and ^{223}Ra, which have much lower activities in the Dead Sea, are enriched in the circulated Dead Sea water (20, 45 and 35 dpm/L, respectively) due to recoil and desorption. This implies that the circulation of Dead Sea water in the aquifer removes ^{226}Ra and contributes ^{228}Ra, ^{223}Ra and ^{224}Ra to the lake. This adds a major source with relatively high $^{228}Ra/^{226}Ra$ ratios to the Dead Sea mass balance.

In order to study the processes affecting radium isotopes in the Dead Sea aquifer, considering the dynamic conditions of the Dead Sea, we used a multi-species density-dependent groundwater flow model (SUTRA-MS). The results show that the adsorption distribution coefficient is very low, indicating that the large decrease of ^{226}Ra in the groundwater cannot be due to adsorption, which supports the proposition that ^{226}Ra decrease is due to precipitation of barite.

Based on ^{226}Ra and ^{228}Ra mass balances in the Dead Sea, the calculated amount of Dead Sea water circulation in the aquifer is 200-300 million m^3/yr, which is of the same order of magnitude as all other known Dead Sea water sources at present.

https://doi.org/10.1180/S0026461X00006502 Published online by Cambridge University Press

Plutonium redox reactions with iron oxides under anoxic conditions

R. KIRSCH[1,2]*, D. FELLHAUER[3], M. ALTMAIER[4], A. ROSSBERG[1], TH. FANGHÄNEL[3], L. CHARLET[2] AND A.C. SCHEINOST[1]*

[1]Inst. of Radiochemisty, HZDR, 013 14 Dresden, Germany AND ROBL (BM20) at ESRF, BP220, 38043 Grenoble (*correspondence: kirsch@esrf.fr, scheinost@esrf.fr)
[2]ISTerre, UJF/CNRS, BP 53, 38041 Grenoble, France
[3]EC-JRC-ITU, P.O. Box 2340, 76125 Karlsruhe, Germany
[4]KIT-INE, P.O. Box 3640, 76021 Karlsruhe, Germany

The environmental fate of plutonium, the major transuranium actinide in nuclear waste, is largely impacted by its sorption onto and redox reactions with iron oxide minerals [1, 2] that form as corrosion products of steel in the 'near field' and occur widely in sediments. To obtain information on oxid-ation state and local structure, we reacted ^{242}Pu as electro-lytically prepared Pu (V) or Pu (III) (1×10^{-5} M) under anoxic conditions in carbonate free 0.1 M NaCl with hematite, goethite, maghemite and magnetite. Pu-L_{III}-edge XAFS spectra were collected after 40 d and 6 months of reaction.

Results and Discussion

After reaction of either Pu (III) or Pu (V) with hematite (> 99.9 % of added Pu is sorbed on α-Fe_2O_3), Pu is mainly present as Pu (IV), with up to 30 % Pu (V). Also after reaction with goethite (γ-FeOOH) both Pu (IV) (55 %) and Pu (V) (45 %) are present. For both minerals, EXAFS spectra show no strong Fe-backscattering from the substrate and also give no evidence for the formation of a solid PuO_2 phase. In contrast, EXAFS spectra of Pu reacted with maghemite (γ-Fe_2O_3) and magnetite (Fe_3O_4) are characterized by strong iron backscattering, indicating the formation of inner-sphere surface complexes. With maghemite, oxidation state mixtures of Pu (III) and Pu (IV) or Pu (IV) and Pu (V) were found while with magnetite, Pu (III) was the predominant oxidation state [3]. However, in one case and probably due to an increased Pu / magnetite surface area ratio, formation of PuO_2 after reaction of Pu (V) with magnetite was observed. These results highlight the importance of plutonium surface complexation, in addition to solid PuO_2 precipitation, in controlling envi-ronmental Pu concentrations. Further, under reducing con-ditions where Fe (II)-bearing oxides such as magnetite exist, it is necessary to consider trivalent in addition to tetravalent plutonium species and PuO_2 (am, hyd) for risk assessment.

[1] Novikov *et al*. (2006) *Science* **314**, 638–641. [2] Powell *et al*. (2005) *Environ. Sci. Technol*. **39**, 2107–2114. [3] Kirsch *et al*. (2011) submitted to *Environ. Sci. Technol*.

Monitoring CO_2-H_2O interactions using $\delta^{13}C$ & $\delta^{18}O$ at the CO2CRC Otway Project CO_2 storage pilot

D. KIRSTE[1,2], C. BOREHAM[1,3], L. STALKER[1,4] AND J. UNDERSCHULTZ[1,4]

[1]Cooperative Research Centre for Greenhouse Gas Technologies,
[2]Dept. of Earth Sciences, Simon Fraser University, Burnaby, BC V5A 1S6, Canada (dkirste@sfu.ca)
[3]Geoscience Australia, GPO Box 378, Canberra, ACT 2601, Australia (chris.boreham@ga.gov.au)
[4]Division of Petroleum Resources, CSIRO, Kensington, WA 6151, Australia (linda.stalker@csiro.au, james.underschultz@csiro.au)

The CO2CRC Otway Project is an extensively monitored demonstration site for the storage of CO_2 in a depleted gas field. Geochemical monitoring was carried out through the collection of high quality aqueous and supercritical fluid samples via a novel U-tube bottom hole sampling assembly. Several sampling zones within the depleted field were accessed using 3 separate U-tube lines, one completed in the methane-rich gas zone (U1) and two in the water leg at ~2 m (U2) and ~7 m (U3) below the initial gas-water contact. This configuration allowed for monitoring of the filling of the gas field by the injected CO_2. Injection of CO_2 began in late March, 2008 with breakthrough occurring between 101 and 121 days later and the transition to full self-lifting of U3 by day 303 Reservoir fluids were sampled for stable isotopic composition measurements of the $\delta^{13}C$ and $\delta^{18}O$ of the dissolved and immiscible phase CO_2 and the $\delta^{18}O$ and $\delta^{2}H$ of water. The U-tube assembly enabled sampling of fluids at reservoir pressure but cooling during sample lift meant that the subsurface temperatures were not maintained. The $\delta^{13}C$ of the pre-breakthough exsolved CO_2 and the gas phase CO_2 showed a fractionation consistent with that expected between $CO_{2\,(g)}$ and $CO_{2\,(aq)}$. As the injected CO_2 concentration increased the $\delta^{13}C$ shifted from that of the indigenous CO_2 to that of the injected. However, the $\delta^{13}C$ of the HCO_3^- showed a fractionation typical of a Rayleigh-type distillation and the fractionation factor reflected surface temperature conditions. The $\delta^{18}O$ of the water remained constant throughout the period for U2 and U3 until just prior to self-lift when there was an decrease. U3 showed considerable variability in the produced fluid immiscible/aqueous phase ratio near the transition and this is reflected in the oxygen isotopic of the aqueous and gas phase. Interestingly the $\delta^{18}O$ values showed no surface temperature fractionation like that seen for the $\delta^{13}C$.

https://doi.org/10.1180/S0026461X00006502 Published online by Cambridge University Press

Different coloured vitreous phases in obsidian

J. KIRSTE*, G. WAGNER, N. SCHULZE AND G. KLOESS

Institute for Mineralogy, Crystallography und Materials Science, Leipzig University, Scharnhorststrasse 20, 04275, Leipzig, Germany
(*correspondence: kirste@uni-leipzig.de)

Different coloured glass matrices obsidian are the object of the study. Their compositions and phase analyses of implemented nanocrystals were determined by Transmission Electron Microscopy (TEM). The analyses were carried out with an STEM Philips CM 200.

The Büyük Yayla obsidian (Eastern Pontides, Turkey) shows various bands, coloured black, red, and partially colourless. Moreover, a sharp black displacement (up to 1 cm) passes through the obsidian due to a still unknown shear process, displacing the several layers. Note, the different bands do not show a macroscopic 'schlieren-like' texture close to the displacement front.

The results of TEM-EDX analyses are given in the following table.

Oxide [wt-%]	red glass matrix	colour-less glass matrix	black glass matrix	glass close to the displacement trace
Na_2O	4.5	1.6	5.2	5.8
MgO	0.1	0.2	0.2	0
Al_2O_3	13.4	13.1	12.9	13.1
SiO_2	76.0	74.9	74.4	75.0
K_2O	4.7	8.4	5.3	4.6
CaO	1	0.9	1	1.1
TiO_2	0	0	0.2	0
MnO	0	0	0.1	0
Fe_2O_3 (Fe-tot)	0.4	0.9	0.6	0.5

Table 1: Chemical composition of different coloured glass matrices of the Büyük Yayla obsidian

Suprisingly the highest Fe-amount was detected in the colourless vitreous matrix. Hence, the iron soluted in the glass is not responsible for the different colours of the glass. The detected 0.3 – 0.5 wt-% of hematite- and magnetite-nanocrystals colour the vitreous matrices.

Calcium and magnesium isotopes in biogenic calcite

B. KISAKÜREK[1]*, A. EISENHAUER[1], M.N. MÜLLER[1,2], I. TAUBNER[1], J. FIETZKE[1], F. BÖHM[1], D. BUHL[3] AND J. EREZ[4]

[1]Leibniz Institute of Marine Sciences, IFM-GEOMAR, Kiel, Germany (*correspondence: bkisakurek@ifm-geomar.de)
[2]IMAS Institute for Marine and Antarctic Studies, Hobart, Australia
[3]Faculty of Geosciences, Ruhr-Universität Bochum, Germany
[4]Institute of Earth Sciences, The Hebrew Univ. of Jerusalem, Israel

As shown recently [1], the isotopic fractionation of calcium is strongly correlated with the partitioning of Sr in inorganically precipitated calcite, wherein the main control on both proxies is the precipitation rate. In a follow up study [2], the inorganic correlation between $\Delta^{44/40}$Ca and D_{Sr} has been verified for planktic foraminifera. We extend this approach to coccolithophores, including *Emiliania huxleyi* and *Coccolithus braarudii*, grown under controlled laboratory conditions. The slope of the regression between $\Delta^{44/40}$Ca (‰) and log D_{Sr} in coccolithophores (-1.8±0.9, [3]) is within error of that in inorganically precipitated calcite (-1.9±0.3, [1]), whereas there is a large offset between the inorganic and coccolithophorid regressions due to the higher Sr content in the latter.

Comparing the fractionation of magnesium isotopes versus the Mg content in the calcitic skeletons of the Alcyonarian soft coral *Rhythisma fulvum*, benthic foraminifer *Amphistegina* sp., coccolithophores *Emiliania huxleyi* and *Coccolithus braarudii*, echinoid *Echinocyamus pusillus*, red algea *Corallina officinalis*, brachiopod *Terebratula* sp. and sponge *Acanthochaetetes wellsi* [4, 5, 6] we find that species with high Mg content (>10 mol% $MgCO_3$) have a higher degree of fractionation ($\Delta^{26/24}$Mg<-2 ‰) compared to low Mg species (<5 mol% $MgCO_3$; $\Delta^{26/24}$Mg>-2 ‰). Planktic foraminifera and the blue mussel *Mytilus edulis* [5, 6] are exceptions with low Mg content but a high degree of fractionation ($\Delta^{26/24}$Mg<-3.5 ‰).

These results will be discussed in a comparative manner in terms of our understanding of the pathways of biomineralization in different calcifiers.

[1] Tang *et al*. (2008) *Geochim. Cosmochim. Acta* **72**, 3733–3745. [2] Kısakürek *et al*. (2011) *Geochim. Cosmochim. Acta* **75**, 427–443. [3] Müller *et al*. (2011) *Geochim. Cosmochim. Acta* **75**, 2088–2102. [4] Eisenhauer *et al*. (2009) *Elements* **5**, 365–368. [5] Hippler *et al*. (2009) *Geochim. Cosmochim. Acta* **73**, 6134–6146. [6] Wombacher *et al*. (2006) *Geophys. Res. Abstr*. **8**, 06353.

https://doi.org/10.1180/S0026461X00006502 Published online by Cambridge University Press

Post-deposition diffusion of ^{137}Cs in lake sediments

J. KLAMINDER[1], P. APPLEBY[2] AND I. RENBERG[1]

[1]Department of Ecology and Environmental Science, Umeå University, SE-901 87 Umeå, Sweden
[2]Department of Mathematical Sciences, University of Liverpool, P. O. Box 147, Liverpool, L69 3BX, UK

Large episodic emissions of radiocesium ^{137}Cs into the atmosphere, such as those generated by nuclear weapon testing programs in the 1960s and the Chernobyl accident in 1986, have been frequently utilized when dating lake sediments. The ongoing disaster at the reactors at Fukushima, Japan, is likely to generate a new chronological marker in sediments deposited over a large part of the region that can be recognized as subsurface peak in ^{137}Cs activities by future sedimentologists. However, the generation of a new ^{137}Cs dating horizon in lake sediment can eliminate the use of others due to significant post-depositional mobility and catchment processes as shown in this presentation. Here we show using archived sediment samples how the ^{137}Cs record within an annually varved sediment, from a lake situated about 1600 km from Chernobyl, is successively altered between 1985 to 2007 due to Chernobyl fallout and subsequent post-depositional diffusion and catchment inputs. The record reveals how Chernobyl ^{137}Cs becomes incorporated into the summer sediment in 1986 and diffuses downward in the core at a decreasing rate over time, making the marker of 1964 originally present in the core sampled three weeks before the Chernobyl accident unrecognizable two years after the accident. It is, therefore, questionable whether ^{137}Cs peaks in deep sediment can be used to recognize sediment deposited in the 1960s in regions that has received significant fallout from the accidents in Chernobyl or Fukushima.

Atomic force microscopy study of the dissolution of a calcite surface in the presence of phosphate ions

J. KLASA[1,2]*, E. RUIZ-AGUDO[3], C.V. PUTNIS[2], A. PUTNIS[2], P.F. SCHOFIELD[1], E. VALSAMI-JONES[1]

[1]Natural History Museum, Cromwell Road SW7 5BD, London, UK (*correspondence: j.klasa@nhm.ac.uk)
[2]Institute fuer Mineralogie, University of Muenster, Corrensstrasse 27, D-48149, Muenster
[3]Department of Mineralogy and Petrology, University of Granada, Fuentenueva, s/n, 18071, Granada, Spain

The dissolution of calcite in the presence of phosphate solutions has been studied using Atomic Force Microscopy (AFM). The presence of phosphate in aqueous solutions is known to inhibit calcite growth [1] and has been successfully used to reduce limescale formation. In this study, solutions containing phosphate salts such as ammonium and sodium phosphate were studied in order to compare their influence on the dissolution of a calcite surface {10-14} during continuous flow in the fluid cell of an AFM.

In the presence of phosphate solutions at pH ~ 8, a significant decrease in the dissolution rate was observed. However, the etch pit density, increased for both ammonium and sodium phosphate salts, suggesting a kosmotrope hydration character of phosphate ions and therefore similar behaviour to that of fluorine ions on calcite dissolution [2]. It was also observed that the dissolving calcite surface can act as a structurally suitable substrate for calcium phosphate growth, which may prove to be an environmentally important mineral replacement reaction for remediation of phosphate rich systems.

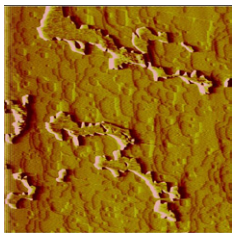

Figure 1: AFM image of calcium phosphate growth on a calcite cleavage surface. The process is limited by the release of Ca^{2+} from the dissolution of calcite.

[1] Lin & Singer (2005) *Water Research,* **39**, 4835-4843.
[2] Ruiz-Agudo *et al*. (2010) *GCA,* **74**, 1256-1267.

https://doi.org/10.1180/S0026461X00006502 Published online by Cambridge University Press

Origin of the nodules in the 18.6 ka Sarno plinian eruption of Mt. Somma-Vesuvius (Italy) and their significance

R. KLÉBESZ[1,2]*, R.J. BODNAR[1] AND B. DE VIVO[2]

[1]Dept. of Geosciences, Virginia Polytechnic Institute and State University, Blacksburg, VA 24061, USA (*correspondence: krita@vt.edu)

[2]Dept. of Earth Sciences, University of Naples "Federico II", Naples 80134, Italy (bdevivo@unina.it)

Nodules (coarse-grain 'plutonic' rocks) were collected from the phreato-magmatic phase of the Sarno eruption in C. Traianello quarry, located on the NE slope of Mt. Somma. Based on the mineral composition the rocks can be classified as monzonite-monzogabbro. They consist of An-rich plagioclase, K-feldspar, clinopyroxene (ferro-diopside), mica (phlogopite-biotite) ± olivine and amphibole. Unlike most of the nodules from the other eruptions, these samples do not have typical cumulative texture, but rather display a porphyrogranular texture. The phenocrysts are large (up to few mm) with variable compositional zoning. The phenocrysts are often partially to completely enclosed by later poikilitic feldspars. Sometimes irregular intergrowths of alkali feldspar and plagioclase and smaller unidentified crystals can be observed. These features are interpreted as crystallyzed melt pockets. Based on their textures, the nodules may represent the *in situ* crystallizing melt on the walls of the magma chamber. The lack of the interstitial glass, which is common in nodules from similar environments, can be explained by the time difference between the plinian and the phreatomagmatic phase. The time difference might have provided sufficient time for the interstitial melt in Sarno samples to crystallize.

Minerals, especially clinopyroxenes, are abundant in crystallized silicate melt inclusions. The inclusions consist of mica, oxide minerals, clinopyroxene and possibly apatite, feldspar, interstitial glass, bubble. Unlike nodules from other eruptions, all fluid inclusions in Sarno samples are single phase and secondary in origin, and not associated with melt inclusions. The different textures and inclusion populations may indicate different pre-eruptive conditions and processes, compared to other eruptions. Melt inclusions in clinopyroxenes have been analyzed by LA-ICP-MS. The major and trace element compositions of MI are similar to the products erupted during the plinian phase, indicating that they may be co-genetic. Melt inclusions have been rehomogenized for further analyzes to determine the volatile content, in order to estimate a minimum crystallization depth.

Monte Carlo study of aggregation of alkyltrimethylammonium ions at the montmorillonite-water interface

B. KLEBOW[1]* AND A. MELESHYN[1,2]

[1]Institute of Radioecology and Radiation Protection, Leibniz Universität Hannover, Germany (*correspondence: klebow@irs.uni-hannover.de)

[2]Present address: Gesellschaft für Anlagen- und Reaktorsicherheit (GRS) mbH, Brunswick, Germany

Unlike naturally occurring bentonites, organically modified ones exhibit adsorption capabilities not only for cationic but also for anionic contaminants. This property renders them valuable for various environmental and industrial processes like sewage treatment, groundwater remediation, production of nanocomposites, and waste disposal. An additional essential advantage regarding the application of organoclays to the remediation of contaminated groundwater is their effective adsorption of non-polar organic contaminants such as the highly persistent, toxic and carciogenic polycyclic aromatic hydrocarbons.

The precise molecular structures of organically modified clays as well as the mechanisms determining their observed adsorption properties are still not well understood. To establish a relation between experimental observations and underlying molecular structures, we performed classical molecular simulations of the external montmorillonite surface modified by alkyltrimethylammonium (C_nTMA^+, with n being the number of methyl (ene) groups in the alkyl chain).

The adsorption of alkyltrimethylammonium ions at the montmorillonite-water interface and the formation of interfacial C_nTMA^+ aggregates at higher concentrations of adsorbed C_nTMA^+ were studied. The simulations were performed in NVT-ensemble at a temperature of 298 K applying the Metropolis and the configurational-bias Monte Carlo algorithms for increasing surface concentrations of C_8TMA^+, $C_{12}TMA^+$, and $C_{16}TMA^+$ ions. The discussion will comprise the arrangement of adsorbed organic and inorganic ions, structure and type of adsorption complexes, conformation of alkyl chains, and the water structure at the organically modified montmorillonite-water interface taking into account findings of previous experimental and simulation studies.

https://doi.org/10.1180/S0026461X00006502 Published online by Cambridge University Press

Dolomitization of serpentinized harzburgite from the Atlantis Massif

FRIEDER KLEIN

Woods Hole Oceanographic Institution, (fklein@whoi.edu)

Ophicarbonate breccias consisting of fragments of serpentinized peridotite and carbonate cement have been reported from outcrops at the Atlantis Massif, MAR[1]. While the carbonate cement precipitates due to mixing of high-pH, Ca-rich serpentinization fluids with seawater, the direct replacement of serpentinite by dolomite is more difficult to explain. Here, I report on observations made in a dolomite-altered, strongly serpentinized, partly steatitized harzburgite, from the IODP Leg 304, Hole 1309B at the Atlantis Massif. Dolomite appears in mesh and hourglass texture of completely serpentinized olivine adjacent to a talc-tremolite altered shear zone. The dolomite in these samples is surrounded by a zone of serpentine (Mg# 98), and magnetite, which traces the former (sub-) grain boundaries of olivine. Orthopyroxene is partly serpentinized to bastite, which subsequently underwent partial steatitization but not dolomitization. Both clinopyroxene and Cr-spinel are unaltered.

Dolomite in serpentinite can form by conductive heating of seawater[2]; however, in samples from Hole 1309B petrographic observations and microprobe analyses suggest a direct replacement of brucite and serpentine by dolomite. Phase relations in the system MgO-CaO-SiO_2-H_2O-CO_2 indicate that brucite is the first mineral being replaced by dolomite at relatively low CO_2, aq actvities, while dolomitization of serpentine and talc requires higher CO_2, aq activities. However, it remains to be resolved whether the CO_2 is of magmatic or of seawater origin. The Mg needed for the formation of dolomite is likely contributed by brucite and/or serpentine themselves, whereas Ca may have been transported from the adjacent talc-tremolite shear zone. Alternatively, the Ca may have been contributed by the dissolution of the Ca-Tschermaks component of partly serpentinized orthopyroxene.

This pilot study indicates that serpentine and brucite can act as a sink for CO_2 in the oceanic lithosphere, in particular where seawater and/or magmatic fluids interact with hybrid mafic/ultramafic lithologies.

[1] Kelley, D.S. *et al*. (2005) *Science* **307**, 1428–1434.
[2] Eickmann, B. *et al*. (2009) *Chemical Geology* 268 (1-2) 97–106.

Chromium mobility in hydrous fluids at upper mantle conditions

O. KLEIN-BENDAVID[1], T. PETTKE[2] AND R. KESSEL[1]

[1]The Fredy & Nadine Herrmann Institute of Earth Sciences, the Hebrew University of Jerusalem, Jerusalem, Israel, 91904 (*correspondence: ofrak1@gmail.com)
[2]Institute of Geological Sciences, University of Bern, CH-3012 Bern, Switzerland

Chromium is a minor component in the earth's mantle and is considered to be immobile in aqueous fluid under crustal and most mantle conditions. Exceptions to this are for example K-rich diamond forming fluids, shown to contain up to 1 wt% Cr_2O_3 (on a volatile free basis). A series of high-P experiments on the solubility of Cr_2O_3 in KCl bearing water were done using rocking multi anvil diamond trap techniques (1000 and 1200 °C; 4 and 6 GPa) combined with cryogenic LA-ICP-MS in order to determine Cr mobility in saline fluids (e.g. diamond forming fluids) under mantle conditions and its possible involvement in deep metasomatism. Chromium solubility in KCl-bearing water increases with salinity (KCl). At 250 μg/g KCl, Cr solubility in water is between 100 and 200 μg/g, independent of pressure. At 4 GPa, an order of magnitude increase in Cr-solubility is observed only for the 3 wt% KCl solution, while at 6 GPa such increase is observed already at 1.3 wt% KCl. No significant effect of temperature is observed. Metasomatic Cr-rich mineral assemblages are encountered in both subduction zone and deep lithospheric mantle environments, where alkali-rich hydrous fluids, similar to those examined in this research, are regarded as major metasomatic agents. In some cases, unique minerals found as micro- and macro- inclusions within diamonds (e.g. chromite and phlogopite) have significantly different compositions than common mantle minerals and are much richer in Cr. Thus, saline hydrous fluids can be considered an important metasomatic agent at deep lithospheric mantle conditions and appear to be efficient in transporting elements such as Cr during rock water interaction.

https://doi.org/10.1180/S0026461X00006502 Published online by Cambridge University Press

Evidence of K-Fe metasomatism in the SW Scottish Highlands

B.I. KLEINE*, A.D.L. SKELTON AND I.K. PITCAIRN

Department of Geological Sciences, Stockholm University, 10691 Stockholm, Sweden
(*correspondence: barbara.kleine@geo.su.se)

Metamorphosed basaltic lava flows, tuffs, sills and dykes are emplaced within metasedimentary rocks which are part of the Dalradian Supergroup (Argyll Group) in the SW Scottish Highlands [1]. These metabasaltic sills were affected by at least three fluid-rock interaction events during greenschist facies regional metamorphism: pre-metamorphic spilitisation, syn-metamorphic carbonation of metabasaltic sills and post-metamorphic quartz-carbonate-sulphide veins [2]. The infiltration of H_2O-CO_2 fluids during carbonation led to a mineral assemblage zonation within the metabasalt with carbonate-free interiors and carbonate-rich margins [3].

These three fluid events and an additional K-Fe metasomatic event of uncertain timing could be identified in alterated metabasalt on the island of Islay in the SW Scottish Highlands. At this locality, the alterated metabasaltic sills display a distinct change in mineral assemblage which seems to be coupled to brittle to ductile faulting. Only the areas close to the fault seems to be affected by the K-Fe metasomatism. The mineral assemblage pl+zoi+chl+qtz+cc changes into ep+chl+qtz+cc+ht+bt towards the fault system which cuts through the outcrop. These results were achieved by petrographic analysis, point counting of 1000 evenly spaced points in selected thin sections, XRF and SEM analyses.

The fact, that hematization took place and zoisite changes into the more Fe-bearing epidote, suggests that iron was added during the fluid event. The formation of biotite leads to the assumption that K-metasomatism is also coupled by this fluid-rock interaction.

Is it possible to constrain a sequence of fluid events in this area? The hematite phenocrysts are only slightly affected by the foliation of the metabasalt which suggests that the K-Fe metasomatism occured after peak metamorphism (400-530°C, 10 kbar) [3]. Also its spatial association with faulting suggests that K-Fe metasomatism was occured late during the fluid-infiltration history.

[1] Roberts & Treagus (1977) *Scottish Journal of Geology* **13**, 87–99. [2] Skelton *et al*. (2010) *Journal of the Geological Society of London* **167**, 1049–1061. [3] Skelton *et al*. (1995) *Journal of Petrology* **36**, 563–586.

Hf-W chronometry of angrites: Implications for ^{26}Al heterogeneity and core formation in protoplanets

T. KLEINE[1]*, U. HANS[2], A.J. IRVING[3] AND B. BOURDON[2]

[1]Institute for Planetology, University of Muenster, Wilhelm-Klemm-Str. 10, 48149 Muenster, Germany (*correspondence: thorsten.kleine@uni-muenster.de)
[2]Institute for Geochemistry and Petrology, ETH Zurich, Clausiusstrasse 24, 8092 Zurich, Switzerland
[3]Department of Earth and Space Sciences, University of Washington, Seattle, WA 98195, USA

Angrites formed by some of the earliest igneous activity in the solar system and provide insights into the early stages of planetary melting and differentiation. Moreover, they are pivotal reference points for early solar system chronology [e.g. 1-3]. In order to study the processes and timescales of metal segregation in early protoplanets and to assess the distribution of short-lived radionuclides in the early solar system, the ^{182}Hf–^{182}W system was applied to a comprehensive suite of angrites. ^{182}Hf–^{182}W isochron ages for angrites are in excellent agreement with previously reported ^{207}Pb–^{206}Pb and ^{53}Mn–^{53}Cr results [e.g. 1] but are ~1 Myr older than ages obtained from ^{26}Al-^{26}Mg chronometry [e.g. 2]. These inconsistencies are best explained by a heterogeneous distribution of ^{26}Al in the early solar system, suggesting that at the time of CAI formation the angrite precursor material had an ^{26}Al/^{27}Al of ~1.8×10^{-5}, substantially lower than values commonly measured for CAI. Based on the Hf–W results four texturally and temporally resolved groups of angrites can be identified that were derived from at least two distinct mantle sources. These mantle sources are the result of separate events of core formation, both of which took place within ~2 Myr of CAI formation. Thus, core formation in the angrite parent body did not occur as a single event of metal segregation from a global magma ocean but rather took place under varying conditions by several more local events. Heterogeneities in the Hf-W systematics of the two distinct angrite source regions may result from inefficient core formation in some areas of the angrite parent body or may reflect variable redox conditions during metal segregation. The absence of global melting and homogenization in spite of an early accretion is consistent with a relatively low initial ^{26}Al/^{27}Al inferred here for the angrite precursor material.

[1] Nyquist *et al*. (2009) *Geochim. Cosmochim. Acta* **73**, 5115–5136. [2] Schiller *et al*. (2010) *Geochim. Cosmochim. Acta* **74**, 4844–4864. [3] Kleine *et al*. (2009) *Geochim. Cosmochim. Acta* **73**, 5150–5188.

https://doi.org/10.1180/S0026461X00006502 Published online by Cambridge University Press

Geodynamic implications of new U-Pb zircon ages for the Kamanjab Inlier (NW-Namibia)

I.C. KLEINHANNS[15], F. WILSKY[2], N. NOLTE[2], T. BECKER[3], B.T. HANSEN[2], R. KLEMD[4] AND D. FLIEGEL[5]

[1]Institute for Geoscience, University Tübingen, Germany, (kleinhanns@ifg.uni-tuebingen.de)
[2]GZG, University Göttingen, Germany
[3]BRGM, Orléans, France
[4]Geocentre Northern Bavaria, Erlangen, Germany
[5]Geoscience Institute, University Bergen, Norway

The Huab Metamorphic Complex (HMC) and Fransfontein Granitoid suite (FFG) are part of the Kamanjab Inlier (KI) in NW-Namibia. It is a poorly known pre-Pan African basement complex and, together with the Epupa complex (EC) further NW and the Grootfontein complex (GC) further E, marks the SW-margin of the Congo craton in N-Namibia. New LA-ICPMS U-Pb zircon ages frame FFG emplacement to 1.88-1.83Ga and protolith ages for HMC orthogneisses to 1.86-1.83Ga. These ages are roughly 100 m. y. older than protolith ages from the northern EC close to the Angolan border and roughly 100 m. y. younger than the GC. The southern EC in the Hoanib area is the only known Archean basement in Namibia, but shows eNd (1.83Ga) of -10.9 to -6.5 compared to those of the northern EC (-2 to 4.2), FFG (-5.9 to 1.2) and HMC (-2.3 to 2.3). Our study supports earlier speculations that the southern EC is an exotic terrane within the Namibian basement complexes. In contrast, the KI is comparable to the northern EC and GC and geochemical data indicate an active continental margin setting. This points to an event of Paleoproterozoic crustal growth at the SW border of the Congo Craton starting in the present E gradually moving towards the present NW.

The garnet-spinel transition in fertile and depleted mantle: Experimental data, thermodynamic calculations and implications for magmatic processes

S. KLEMME

Institut für Mineralogie, Universität Münster, Germany (stephan.klemme@uni-muenster.de)

With increasing depths in the Earth's mantle, the aluminous phase in the upper mantle changes from plagioclase to spinel to garnet. The transition from spinel lherzolite to garnet lherzolite could potentially influence the characteristics of some kinds of basalts, particularly mid-ocean ridge basalts (MORB), since this transition is thought to occur at about the same depths at which MORB may originate. Several studies have investigated the transition from garnet lherzolite to spinel lherzolite in simple systems (e.g. CaO-MgO-Al_2O_3-SiO_2) (e.g. [1-3]) but, due to experimental problems associated with slow reaction rates, few studies have tried to experimentally investigate the garnet-spinel transition in more complex and depleted composition (e.g. [4-5]). Here we set out to investigate phase relations from fertile to depleted mantle compositions using a new set of thermodynamic data and free energy minimization techniques [6]. We show that the stability fields of garnet and spinel in upper mantle lithosphere critically depend on the bulk composition of the peridotite. In fertile bulk compositions, the transition from spinel to garnet-bearing rocks is relatively sharp but in depleted bulk compositions there is a large pressure-temperature field where garnet and spinel coexist. We will show that the garnet-in reaction in depleted peridotite occurs in much greater depths than in fertile lherzolite. Furthermore, the results in depleted compositions may also be of relevance for the diamond exploration industry as the calculated Cr-rich spinel and garnet compositions may be used to quantitativly estimate pressures of origin and therefore evaluate the so-called diamond potential of mineral concentrates [7].

[1] O'Neill (1981) *Contrib Mineral Petrol* **77**, 185–194. [2] Walter *et al*. (2002) *Geochim. Cosmochim. Acta* **66**, 2109–2111. [3] Klemme & O'Neill (2000) *Contrib Mineral Petrol* **138**, 237–248. [4] Brey *et al*. (1999) *Eur J Mineral* **11**, 599–617. [5] Nickel (1986) *Neues Jahrb Mineral Abh* **155**, 259–287. [6] Klemme *et al*. (2009) *Lithos* **112**, 986–991 [7] Grütter *et al*. (2006) *J Petrol* **47**, 801–820.

https://doi.org/10.1180/S0026461X00006502 Published online by Cambridge University Press

Secondary minerals in mine wastes at Sb deposits in Slovakia

T. KLIMKO[1]*, J. MAJZLAN[2], B. LALINSKÁ[1], M. CHOVAN[1], J. GÖTTLICHER[3] AND R. STEININGER[3]

[1]Department of Mineralogy and Petrology, Comenius University, Bratislava, Slovakia (*correspondence: klimko@fns.uniba.sk)
[2]Institute of Geosciences, Friedrich-Schiller University, Jena, Germany
[3]Institute for Synchrotron Radiation, Karlsruhe Institute of Technology, Germany

In this work, we have summarized results from a detailed mineralogical study of the weathering products formed in the environment of tailing ponds and soils from five Sb deposits in Slovakia, based on 250 samples of flotation tailing materials and soils, 2500 electron microprobe analyses and 500 micro-X-ray diffraction (μ-XRD) analyses. All studied bulk samples are rich in Fe (24.2–181 g/kg), As (0.1–13.5 g/kg), and Sb (1.2–15.7 g/kg). The most frequent sulphides in the flotation wastes are pyrite (FeS_2) and arsenopyrite (FeAsS); stibnite (Sb_2S_3) is rare owing to its rapid oxidation.

The most common Sb-bearing secondary oxide is tripuhyite ($FeSbO_4$) with variable Sb (15.94-50.83 wt. %) and Fe content (4.13-41.52 wt. %). Unit cell volume is in the range from 64.70 Å^3 to 75.83 Å^3 and depends mostly on the Fe/(Fe+Sb) ratio of the tripuhyite grains. In the tailings and soils rich in Ca, secondary minerals with the pyrochlore structure have been identified. These phases are rich in Sb (up to 52.90 wt. %), Fe (up to 21.22 wt. %) and Ca (up to 7.40 wt. %) and the μ-XRD patterns fit well with the structural models of stibiconite ($Sb^{3+}Sb^{5+}{}_2O_6$ (OH)) and lewisite (Ca, Fe^{2+}, Na)$_2$ (Sb, Ti)$_2O_7$). The most frequent secondary mineral at all studied sites is goethite (α-FeOOH), with high content of Sb (up to 14.49 wt. %) and As (up to 6.49 wt. %). Cell parameters depend on incorporation of foreign elements, in agreement with earlier studies. Frequent are also X-ray amorphous Fe oxides with variable amounts of adsorbed elements (up to 6.66 wt. % of Mg, 13.91 wt. % of Sb and 10.64 wt. % of As). Simple secondary Sb oxides such as cervantite (α-Sb_2O_4) and senarmontite (Sb_2O_3) were observed each just in one soil sample. The most common product of arsenopyrite oxidation - scorodite ($FeAsO_4 \cdot 2H_2O$) occurs rarely. Beudantite ($PbFe_3$ (AsO_4)(SO_4)($OH)_6$) was identified in a few samples with increased content of Pb. In one sample, a porous secondary oxide rich in Pb and As was identified by μ-XRD as clinomimetite (Pb_5 ($AsO_4)_3Cl$).

This work was supported by Slovak Research and Development Agency under the contract No. VMSP-P-0115-09.

Experimental constraints on the composition of slab liquids below arc volcanoes

KEVIN KLIMM[1], FABIAN SCHRÖDER[1] AND JON D. BLUNDY[2]

[1]Institut für Geowissenschaften, Universität Frankfurt, D
[2]Department of Earth Sciences, University of Bristol, UK

The flux of elements from the slab into the mantle wedge is governed by the composition of the different subducted lithologies, the partitioning behaviour of trace elements and the subduction geotherm. Recently it has been shown that the concentration of key elements such as K, Zr, Ti, Nb and REE depends primarily on T and is controlled by the solubility of accessory phases, such as phengite, zircon, rutile and allanite, in the melt [1, 2]. This T-concentration relationship can be used as a geothermometer to determine the top slab T in subduction zones and suggests values that vary from 750 to 950 °C for different subduction zones [3]. Crucial questions that remain open are the effect of pressure and the presence of additional volatiles such as S, Cl and F on the stability of accessory phases and the composition of slab liquids.

Here we report preliminary results on crystallisation experiments on a H_2O-saturated and trace element-doped MORB composition at 5 GPa and 750-1000 °C. Together with previous results at 2.5 GPa and 750-900°C [2] the experimental dataset now covers the full range of P-T conditions predicted for the slab below volcanic arcs. The dataset will be augmented with a few runs containing additional S and F.

First results show that at 5 GPa the wet solidus of basalt is <900 °C. Experimental melts at 5 GPa are granitic compared to trondhjemitic melts at 2.5 GPa. With increasing P, D_{Na} in cpx increases and hence Na/K in the melt decreases. All runs contain gt, cpx and rutile. Allanite is present up to 950 °C. No effect of P on allanite composition has been recognised so far. Coesite is found to be stable at P >5 GPa. The trace element contents of the glasses are currently investigated by LA-ICPMS. One run at 950 °C and 5 GPa, containing small quantaties of F, crystallised REE-bearing CaF_2 and allanite. From these preliminary results we anticipate that a) increasing P (increasing depth of the slab) can explain the change from Na-rich to more K-rich signal in arc magmas and thus K is not only controlled by phengite stability and b) addition of F in the fluid stabilises REE-bearing CaF_2 in the solid residue.

[1] Hermann & Rubatto (2009) *Chem Geol* **265**, 512–526. [2] Klimm *et al*. (2008) *JPet* **49**, 523–553. [3] Plank *et al*. (2009) *Nature Geoscience* **2**, 611–615.

https://doi.org/10.1180/S0026461X00006502 Published online by Cambridge University Press

Translocation of synthetic inorganic nanoparticles in a water-saturated sediment column

SONDRA KLITZKE[1]*, SUSANN APELT[2] AND LARS DÜSTER[3]

[1,2]Federal Environment Agency, Schichauweg 58, 12307 Berlin, Germany (*corrspondence: sondra.klitzke@uba.de, susann.apelt@uba.de)

[3]Federal Institute of Hydrology, Am Mainzer Tor, 156068 Koblenz, Germany (duester@bafg.de)

Breakthrough of synthetic, inorganic nanoparticles (NP) in porous media observed in laboratory experiments [1] raises the assumption of NP posing a risk to drinking water treatment methods [2] such as riverbank filtration. Hence, the aim of this experiment was (i) to gain first hints on the fate of NP under near-natural conditions and (ii) to understand the processes of NP interactions taking place in the water phase and the sediment.

Four types of NP (TiO_2, Ag(0), CeO_2, Sb_2O_5) were suspended in the supernatant of a water-saturated sediment column (1 m length) implemented into a slow sand filtration pond. The column was filled with coarse-grained medium sand and was fed with surface water (pH 7, 8, I = 19 mM, turbidity = 3 FNU) from the surrounding pond. The column was sampled in various depths (20 cm, 40 cm, 60 cm, 80 cm) and at the outflow. The NP were fractionated by filtration (0.45 μm and 0.1 μm) and the respective analytes (Ti, Ag, Ce, Sb) were determined using ICP-MS.

In the water phase, NP concentrations were reduced by a factor of 1000 due to particle aggregation, which was predominantly caused by an increase in ionic strength in relation to the original NP suspension. This resulted in a shift of the particle size distribution towards larger sizes and NP were found to form hetero-aggregates with suspended particulate matter. Our observations demonstrate that hydrochemical conditions substantially affect size distribution and aggregation of the investigated NP.

In the sediment, Sb_2O_5, the NP with the most negative zeta potential, was the only NP showing breakthrough (up to a depth of 40 cm). This result confirms that the zeta potential is a key factor in NP suspension stability. The various conditions led to a change in particle size distribution during sediment passage, too. The processes which play a key role in NP translocation remain to be elucidated.

[1] Torkzaban, Kim, Mulvihill, Wan & Tokunaga (2010) *Journal of Contaminant Hydrology* **118**, 208–217. [2] Boxall, Tiede & Chaudhry (2007) *Nanomedicine* **2**, 919–927.

The role of mineral surface chemistry in the prebiotic selection of pentose sugars

K. KLOCHKO[1], D.A. SVERJENSKY[1,2], R.M. HAZEN[1] AND H.J. CLEAVES II[1]

[1]Geophysical Laboratory, Carnegie Institution of Washington, 5251 Broad Branch road, Washington DC 20015 (kklochko@ciw.edu)

[2]Department of Earth and Planetary Sciences, Johns Hopkins University, Baltimore, MD 21218.

Pentose sugars are major biochemical building blocks. Prebiotic syntheses have been proposed leading to complex mixtures including 4-, 5-, and 6-carbon sugars [1, 2]. However, the pentose sugar D-ribose has the greatest biological importance because it is the sugar found within modern nucleic acids. We are investigating whether this is due to some exceptional characteristic of ribose associated with its interaction with mineral surfaces.

Recent study of the adsorption of nucleosides and nucleotides on rutile [3] indicates that adjacent OH-groups on the ribose part of these molecules play a critical role in the attachment to mineral surfaces. The four pentose sugars ribose, xylose, lyxose and arabinose differ only in the arrangement of the OH-groups and their stereochemistry in solution. This suggests that the different structures of these sugars might lead to selective adsorption on mineral surfaces.

The present study is focused on interactions of D-ribose and D-xylose on rutile (α-TiO_2, pH_{PZC} = 5.4, BET = 18.1 m^2/g) in 10 and 100 mM NaCl solutions over a wide range of pH conditions (3-10). The rutile powder is the same as previously used for amino acid adsorption studies [4]. Batch adsorption experiments of the two sugars individually and in mixtures indicate that adsorption of both sugars increases with increasing pH of the solution. The pH dependancy of adsorption is more pronounced for ribose leading to a difference of ~20% adsorbed at pH > 8.5. Our preliminary results indicate a significant difference in the adsorption behavior of the two sugars.

[1] Springsteen & Joyce (2004) *J. Am. Chem. Soc.* **126**, 9578–9583. [2] Shapiro (1988) *Origin Life Evol. Biosphere* **18**, 71–85. [3] Cleaves *et al.* (2010) *Astrobiology* **10**, 311–323. [4] Jonsson *et al.* (2009) *Langmuir* **25**, 12127–12135.

https://doi.org/10.1180/S0026461X00006502 Published online by Cambridge University Press

Controls on lignin degradation in a temperate deciduous forest

THIMO KLOTZBÜCHER[1]* KLAUS KAISER[2] AND KARSTEN KALBITZ[1]

[1]Earth Surface Science, University of Amsterdam, Amsterdam, The Netherlands (*correspondence: thimo.klotzbuecher@gmail.com, k.kalbitz@uva.nl)

[2]Soil Sciences, Martin Luther University Halle-Wittenberg, Halle, Germany (klaus.kaiser@landw.uni-halle.de)

Degradation of lignin might play a critical role for carbon (C) storage in soils. Changes in climate or land-use affect inputs of nitrogen (N) and dissolved organic matter (DOM) to topsoils. We studied possible consequences for lignin degradation at a beech–oak site in Southern Germany. We hypothesized that degradation of lignin and other recalcitrant organic matter (OM) decreases with N inputs, but increases with input of easily degradable OM. The study also addressed effects of DOM composition on lignin degradation.

A column experiment using A horizon samples was conducted. Solutions differing in N and of different concentrations of DOM of various composition (i.e. glucose, DOM extracts of fresh or humified litter material) were added every 2-4 weeks for 11 months. Total N additions ranged from 0-32 mg N g^{-1} soil-N, organic C additons were 0 or 11 mg C g^{-1} soil-C (i.e. maximum C and N added equaled 2-3 times the annual input of dissolved organic C and total N from forest floors). Lignin degradation was assessed after 5 and 11 months using the CuO oxidation method.

In controls (no N or DOM added), the cummulated CO_2-C evolution (during 11 months of incubation) amounted to 13% of initial soil-C, while CO_2-evolution diminished during incubation indicating decreased C availability. Yields of lignin phenols decreased by 19% (0-11 months). Even in the later period (5-11 months), lignin degradation proeceeded, suggesting it was not limited by easily degradable OM. In line, glucose addition increased CO_2 evolution from soil-OM, but lignin degradation was not affected. However, addition of DOM led to enhanced lignin oxidation after 11 inubation months but the composition of DOM had no effect. This suggests that lignin degraders were stimulated by input of a complex mixture of organic compounds, but against expectations the share of easily degradable compounds played no role. Also N input did not affect CO_2 evolution or lignin degradation. To conclude, altered N inputs to topsoils due to land-use or climate change will not affect lignin degradation, whereas altered DOM inputs presumably has an effect. However, altered C availability seems not to be the reason. Other possible mechanisms will be discussed.

Basanite-phonolite mixing indicated by trace elements in green-core clinopyroxenes from La Palma

A. KLÜGEL

Geosciences Department, University of Bremen, Germany (akluegel@uni-bremen.de)

Green-core clinopyroxenes (Cpx) are ubiquitous in alkalic basalts worldwide. Commonly, anhedral and rounded green cores are enriched in Na, Fe and Mn compared to brownish rims and groundmass Cpx. Most are believed to have been formed by crystallization in evolved melts followed by magma mixing prior to eruption [1, 2].

This interpretation was tested by trace element analyses of Cpx phenocrysts in lavas from the active Cumbre Vieja volcano on La Palma (Canary Islands) where basanites and tephrites contain abundant green-core Cpx. Zoned and unzoned greenish Cpx in phonolites show a wide compositional range and characteristic S-shaped REE spectra with $(La/Nd)_N > 1$, $(La/Lu)_N > 1$ and $(Tm/Lu)_N \leq 1$. The spectra strongly differ from those of brownish Cpx rims and Cpx phenocrysts in basanites to tephrites, that have $(La/Nd)_N < 1$ and $(Tm/Lu)_N > 1$. The latter are also more restricted in composition and have higher compatible and lower incompatible trace element contents, and lower Zr/Hf and Nb/Ta, than phonolite-hosted Cpx. Calculated REE spectra of corresponding melts show strong enrichment of light relative to heavy REE, and are straight for basanites to tephrites but concave-upward for phonolites. All these differences are consistent with fractionation of observed phenocryst phases during the formation of phonolithic melts, with titanite being responsible for Nb/Ta fractionation.

Trace-element compositions of rounded cores from green-core Cpx overlap completely with green Cpx in phonolites, but differ systematically from brownish Cpx. This provides unequivocal evidence for formation of green-core Cpx in phonolitic melts, resorption after mixing with more primitive melt, and subsequent overgrowth by brownish Cpx. Mixing most likely occurs in the uppermost mantle at 430-780 MPa where La Palma magmes fractionate prior to eruption [3]. The commonness of green-core Cpx shows that mixing between basanitic and phonolitic melts periodically occurs beneath La Palma and is important to the evolution of magmas. The data also suggest that much more phonolite is produced at depth than inferred from erupted lavas.

[1] Brooks & Printzlau (1978) *JVGR* **4**, *315–331*. [2] Duda & Schmincke (1985) *CMP* **91**, *340–353*. [3] Klügel *et al*. (2005) *EPSL* **236**, *211–226*.

https://doi.org/10.1180/S0026461X00006502 Published online by Cambridge University Press

Fluid evolution in the Byngi gold deposit, central Urals, Russia

YU.I. KLYUKIN[1]*, V.V. MURZIN[1] AND R.J. BODNAR[2]

[1]Institute of Geology and Geochemistry of the UB, RAS, Yekaterinburg, Russia klukin@igg.uran (*correspondence: klukin@igg.uran.ru)
[2]Fluids Research Laboratory, Virginia Tech (VT), Blacksburg, VA 24061, USA

The Byngi gold deposit, located in the central Urals, consists of multiple quartz veins that occur in and above the apical part of a buried plagiogranite stock that is part of a gabbro-granitic complex. The volcanogenic country rocks that host the quartz veins have undergone metasomatic alteration that is associated with gold mineralization. Stock has been dated at 345-318 Ma.

The studied sample is vein quartz containing pyrite and chalcopyrite. Gold is closely associated with chalcopyrite. The ore minerals fill cracks in quartz, suggesting mineralization is later than at least some of the quartz. Pyrite shows two (or more) generations – the earliest is growth of idiomorphic crystals that trapped chalopyrite and grains of quartz inside. The second generation represents metasomatic growth of pyrite over the earlier pyrite. A later event produced fractures between the two generations of pyrite, and these were later filled by quartz and chalcopyrite. The final stage is represented by deformation of ore minerals. The sample thus contains three generations of quartz: early recrystallized quartz formed before ore minerals, quartz (± chalcopyrite) in cavities within pyrite, and finally quartz precipitated in later brecciated pyrite.

Fluid inclusion assemblages (FIAs) were measured from the earliest and latest stage quartz using a Linkam THMS-600 heating/cooling stage, Raman spectroscopy and cathodo-lumenecense. All FIA contain inclusions that contain an aqueous liquid phase and liquid±vapor CO_2 and contain about 10-20 mole% CO_2. CO_2 melts in the range -57.1 to -58.9°C, suggesting the presence of other volatiles, but no other gases were detected by Raman analysis. Salinity calculated from the melting temperature of clathrate [1] ranged from 1 to 9 wt% NaCl equivalent. Homogenization of the CO2 phase ranged from 10.5-30.1°C. FI in early quartz homognize at 110-145°C, those in intermediate quartz at 130-145°C, and the latest quartz at 200-240°C.

[1] Diamond L. W. (1992) *Geochimica et Cosmochimica Acta* **56**, 273–280.

Differences in coupling between AOM and SRR in marine sediments

NINA J. KNAB[1] AND BO B. JØRGENSEN[2]

[1]University of Southern California, 3616 Trousdale Parkway, AHF143, Los Angeles CA-90089, USA
[2]Max-Planck Institute for Marine Microbiology, Celsiusstr. 1, 28359 Bremen, Germany

Microbially mediated anaerobic oxidation of methane (AOM) is a major methane sink in the ocean, coupled to bacterial sulfate reduction (SRR) as electron accepting process. Yet, with increasing data of AOM and SRR measured in various sedimentary environments, ranging from cold seeps to diffusion dominated habitats, the regulation and linking of both processes remains controversial. In order to investigate if the regulation of AOM and the coupling between AOM and SRR is consistent in all environments, sediment from diffusion dominated sites on the continental shelf (Aarhus Bay and Kattegat/ Denmark) and a methane seep (Black Sea) were incubated under different combinations of methane and sulfate concentrations, and the response of both AOM and SRR evaluated. The experiments confirmed the strong dependence of AOM rates on methane concentrations at all sites but demonstrated differences in sulfate reduction rates with increasing concentrations of both, methane and sulfate. Whereas a close coupling of AOM and SRR, and respectively a strong dependence of rates on both substrates, was evident at the methane seep, the rate measurements from Aarhus Bay provide direct evidence for a decoupling of both processes. Furthermore, the ratio of both rates deviated from the even stoichiometry observed at the methane seep. The experiments demonstrate that there are significant differences in the regulation and coupling of AOM rates and SRR at different sites indicating that AOM might not be mediated in the same way at all sites.

https://doi.org/10.1180/S0026461X00006502 Published online by Cambridge University Press

Paleoenvironmental evolution of the Lower Miocene organic clays (the Sokolov Basin, Eger Graben, Czech Republic): Inorganic proxies

I. KNÉSL[1]*, B. KŘÍBEK[1], K. MARTÍNEK[2], P. ROJÍK[3] AND J. FRANCŮ[1]

[1]Czech Geological Survey, Klárov 3, 118 21 Prague 1, Czech Republic (*correspondence: ilja.knesl@geology.cz)
[2]Faculty of Science, Charles Univ. in Prague, Albertov 6, 128 43 Prague 2, Czech Republic
[3]Sokolovská uhelná JSC, Staré náměstí 69, 356 01 Sokolov, Czech Republic

Lacustrine sediments of the Cypris Formation cover in the Sokolov Basin approximately 20 km^2 of its area being represented chiefly by offshore organic matter and pyrite-rich clays of a thickness ranging from 130 m to 180 m, whereas near-shore facies are missing or preserved only rarely. Variations in Fe, Ca, K, Rb, S, Sr, Ti and Zr contents in lacustrine clays were studied in drill core (Dp 333-2009) using a portable XRF spectrometer Innov-X Alpha. The results of XRF measurements were verified by ICP-MS method after total digest of samples. The constant Ti/Zr ratio in the entire clay sequence indicates a uniform source of terrigeneous material brought into depositional area during the whole sedimentation period. Similarly, the Fe/Zr and Fe/Ti ratios are invariable thus indicating that most of the iron is confined to terrigenous material. Therefore, the correlation between Fe and S in clay is insignificant. The K/Zr and Rb/Zr ratios gradually increase from the bottom to the top of the studied sequence documenting an increase in the content of clay minerals in the sediments studied. Increase in Ca/Zr and Sr/Zr ratios upward in the section is attributed to the rising content of carbonates. The progressive increase in the content of clay minerals and carbonates towards the top of the sequence studied has been interpreted as indicating a gradual transition from the hydrologically open, relatively deep, freshwater lake environment, to the hydrologically closed, shallow water alkaline lake environment. This interpretation corresponds with the increasing content of anhydrite, montmorillonite and analcime upward in the clay sequence. Lacustrine clays of the Cypris Formation are usually laminated. The K/Zr and Rb/Zr ratios in organic matter-rich (10-18%TOC) and organic matter-poor (2-10% TOC) laminas are basically the same, but the Ca/Zr and Sr/Zr ratios are significantly higher in organic matter-poor laminas. Therefore, it is believed that the lamination reflects most likely seasonal variations in the organic matter and carbonate deposition.

This study was supported by the Grant Agency of the Czech Republic (GAČR 205/09/1162).

Modelling global trace gas emissions from biomass burning: Importance of emissions models vs. observed burned area

WOLFGAN KNORR, VEIKO LEHSTEN AND ALMUT ARNETH

Lund University, Sweden (almut.arneth@nateko.lu.se)

Biomass burning is one of the largest sources of atmospheric traces gases and aerosols globally. Emissions from biomass burning can be quantified by a combination of observed burned area, terrestrial ecosystem models to simulate fuel loads and the effect of fire on ecosystem dynamics, and emission factors that relate combusted biomass to the emission of various trace gases. However, different versions of global burned area data derived from satellite observations and emissions models still show major discrepancies. Studies on burned area products have so far focused on product inter-comparison, while the consequences of those discrepancies for fuel simulations and emissions modelling with ecosystem models are still unknown.

Here, we perform a sensitivity analysis of the influence of burned area products and emissions models using the ecosystem model LPJ-GUESS and modified version of the global fire model Spitfire. The emissions model follows two different strategies: a conventional one where fixed emission factors are multiplied by biomass combusted, and an alternative one where combustion efficiency depends on the ratio of grass to total combusted litter. Aerosol particle mass is also computed, following two different approaches derived.

https://doi.org/10.1180/S0026461X00006502 Published online by Cambridge University Press

Geochemical characterization of biosignatures in subseafloor basalts

E. KNOWLES[1]*, H. STAUDIGEL[2], N. MCLOUGHLIN[3] AND A. TEMPLETON[1]

[1]Deptartment of Geological Sciences, University of Colorado, Boulder, CO 80309 (*correspondence: knowlese@colorado.edu)

[2]Scripps Institution of Oceanography, University of California, La Jolla, CA 92093

[3]Centre for Geobiology & Department of Earth Science, University of Bergen, Bergen 5007, Norway

The discoveries of intriguing tubular and granular alteration features in subseafloor basalt glasses, ophiolites, and ancient greenstones [1, 2] has exciting implications for increasing our understanding of global geochemical cycling and the evolution of life on Earth, as well as for exploring other planets for signs of life. The suggestion that these features could represent some of the oldest signs of life on Earth [3] has sparked debate about their putative biogenicity. We have been working to constrain the physical and chemical conditions within the basalts at the time of alteration in order to put together a model of the mechanisms of alteration and preservation of the features.

Using a number of synchrotron-based X-ray microprobe and microspectroscopy techniques we have been able to geochemically characterize these alteration features at the sub-micron scale. We have mapped both major and trace element distributions in numerous tubular and granular alteration features, which shows intriguing patterns of mineral dissolution and authigenic precipitation. In addition, we have collected micro-diffraction patterns and analyzed the oxidation and coordination states of major and trace elements in potential biominerals, which may have formed as a result of microbial metabolic processes. We have been able to show that the mechanism of formation of the tubules clearly involves initial dissolution of the glass, followed by precipitation of authigenic minerals, with concomitant partial to complete oxidation of the reduced metals, such as Fe and sometimes Mn. XANES analyses have also revealed the coordination chemistries of these metals, leading to the identification of target phases that are potential biominerals.

[1] Furnes *et al*. (2004) *Science* **304**, 578–581. [2] Staudigel *et al*. (2008) *Earth Sci. Rev*. **89**, 156–176. [3] Banerjee *et al*. (2006) *EPSL* **241**, 707–722.

The study on arsenic stabilization using recycled mine sludge

M.S. KO[1], J.Y. KIM[1], J.S. LEE[2], J.I. KO[2] AND K.W. KIM[1]*

[1]School of Environmental Science and Engineering, Gwangju Institute of Science and Technology (GIST), Gwangju 500-712,Republic of Korea

[2]Technology Research Center, Mine Reclamation Corporation(MIRECO), Seoul, 110-727, Republic of Korea

Materials and methods

The stabilization efficiencies of arsenic (As) in contaminated soil were evaluated using mine sludge collected from an acid mine drainage (AMD) treatment system.. The soil samples were collected from the Chungyang area, where abandoned Au-Ag mines are located in South Korea. As (V) and As (III) sorption properties were investigate to eveluate the As sorption capacity of mine sludge. The stabilization experiments of As in soil carried out various ratio of mine sludge.

Results and discussion

The pH of the soil samples was 5.07, and the soil texture was silt loam (sand 33%, silt 63%, clay 4%). The CEC value and LOI were 19.8 meq/100 g and 25.6%, respectively. From the results of the SPLP and TCLP tests, the arsenic concentrations in the studied soil were 0.23 and 1.14 mg/kg, respectively. These results show a lower value for the TCLP than that proposed by the USEPA (5 mg/kg). The total arsenic concentration via aqua regia digestion of the soil was 145 mg/kg.

In the kinetic experiments, 99% of As (V) was removed within 3 min and 20% of As (III) was removed from the solution after 20 min and 98% within 12 hours. As (V) and As (III) adsorption process is not pH dependent, and the adsorption isotherm of As (V) and As (III) followed Langmuir isotherm model.

The pH variation depends on the mine sludge ratio (0, 0.5, 3 and 5 wt%) to total soil weight in As stabilization experiments. The extracted arsenic concentrations increased in the control experimental set. The average As concentration was 2.8 μg/L at the 0.5 wt% mine sludge mixed set, and 1.3 μg/L of As was extracted from both 3 and 5 wt% experimental sets. These results suggested that mine sludge influenced on As stabilization and 3 wt% of mine sludge suitable for stabilization of As in soil.

https://doi.org/10.1180/S0026461X00006502 Published online by Cambridge University Press

Predicting spatial and temporal concentrations of arsenic within the Mekong Delta

B.D. KOCAR[1], S.G. BENNER[2] AND S. FENDORF[1]

[1]Dept of EESS, Stanford University, Stanford CA, 94305 USA
[2]Department of Geosciences, Boise State University, Boise ID, 83725, USA

It is generally accepted that arsenic release from sediments within the vast deltaic plains of South and Southeast Asia transpires under reducing conditions, and microbially-mediated reductive dissolution of arsenic-bearing iron (hydr)oxides is the dominant reaction liberating arsenic to the aqueous phase. Further, strong links have been established between groundwater contamination and arsenic release within near and sub-surface environments, and it has become clear that hydrogeologic conditions impart a domineering effect on As distribution during and following liberation. The hydrologic systems of the deltaic aquifers throughout South and Southeast Asia, however, have drastically changed due to extensive groundwater extraction, and from massive anthropogenic alteration of the soil-sediment profile for numerous small and large-scale (excavation) projects. We here present a unifying biogeochemical-hydrogeologic analysis of processes governing arsenic using field-calibrated one- and two-dimensional reactive transport simulations, and utilize three-dimensional simulations to examine the possible effects of excavation and irrigation pumping—processes prevalent in other countries in South and Southeast Asia. The ability to project arsenic levels in space provides the critical capacity to assess optimal locations and depths for groundwater extraction—provided they exist—while projecting temporal changes allows us to determine long- and short-term threats to low-arsenic wells, particularly those arising from land use changes.

Arsenic mobility in a waste rock pile at Dlouhá Ves, Czech Republic

E. KOCOURKOVÁ[1]*, O. SRACEK[2,3], S. HOUZAR[1], J. CEMPÍREK[1], Z. LOSOS[4], J. FILIP[2] AND P. HRŠELOVÁ[2]

[1]Moravian Museum, Brno, Czech Republic
[2]Palacký University, Olomouc, Czech Republic
[3]OPV s.r.o., Praha, Czech Republic
[4]Masaryk University, Brno, Czech Republic
(*correspondence: ekocourkova@mzm.cz)

Products of fifty-years long alteration of a waste rock pile from a Pb, Zn-deposit at Dlouhá Ves, Vysočina region, Czech Republic, were studied in the pile centre (profile I) and on its slope (profile II). The pile material had initially high sulphide (10-20 wt. %) and very low carbonate content (1-2 wt. %); the only primary mineral of As was arsenopyrite.

Significant oxidation of sulphides (pyrite, pyrrhotite, arsenopyrite, sphalerite, galenite) took place in both profiles. The principal As-bearing phase at the top of the profile I is goethite, while down to its base most of As is present in the jarosite group minerals. Melanterite and anglesite were found in a sulfide-rich, lower part of the profile I. At the profile II, minerals of the jarosite-beudantite group, scorodite and kaňkite prevail and no Fe (II)-minerals were found. The paste pH was lower at the profile I (≥1.9) than at the profile II (≥2.8). Processes in the pile are affected by the ratio pyrite to arsenopyrite, where high pyrite content decreases the As/S ratio and results in the formation of jarosite group minerals and low pH conditions. Where arsenopyrite predominates, sulphides are coated by scorodite and other Fe-As phases like schwertmannite, which limit their further oxidation.

Arsenic concentrations released during the leaching experiments were generally low; maximum amounts (up to 0.56 ppm) were released from horizons with jarosite and arsenopyrite. In contrast, minimum amounts of arsenic were released from horizons with beudantite and scorodite. Differences between both profiles are caused mainly by limited water flow through the pile material and also limited penetration of oxygen into the deep parts of the excavation profile. It seems that beudantite and scorodite could represent a long-term option for immobilization of arsenic, but arsenic stored in jarosite can be mobilized relatively easily [1, 2]. However, potential mineralogical transformations and stability of arsenic in beudantite group minerals have yet to be evaluated, because the long-term stability of secondary arsenic minerals remains a serious problem [3].

[1] Kocourková *et al*. (2011) *J Geochem Expl*, in press. [2] Gieré *et al*. (2003) *Appl Geoch* **18**, 1347–1359. [3] Majzlan *et al*. (2007) *Geochim Cosmochim Acta* **71**, 4206–4220.

https://doi.org/10.1180/S0026461X00006502 Published online by Cambridge University Press

Analysis of nanoscale Zero Valent Iron particles upon arrival at a monitoring well

C.M. KOCUR[1]*, A.I. CHOWDHURY[1], H. BOPARAI[1], N. SAKULCHIACHAROEN[1], M. KROL[1], B.E. SLEEP[2], L. AUSTRINS[3] AND D.M. O'CARROLL[1],

[1]The University of Western Ontario, London, ON, Canada (*correspondence: ckocur@uwo.ca)
[2]University of Toronto, Toronto,ON, Canada
[3]CH2M HILL Canada Ltd. Kitchener, ON, Canada

Nanoscale Zero Valent Iron (nZVI) has received significant attention in recent years due to its ability to rapidly destroy numerous priority source zone contaminants in controlled laboratory studies. This has led to great optimism surrounding nZVI particle injection for insitu remediation. However, rapid nanometal settling and poor mobility has been encountered, reportedly due to the ferromagnetic attractive forces between particles leading to agglomeration [1]. Studies have proposed different methods to screen attractive forces between nZVI particles [2, 3, 4], thus protecting them from agglomeration and preventing rapid settling. Although analytical techniques used to characterize particles confirm that these methods yield high quality particles that are stable and readily reactive for extended periods of time in the lab, several important questions remain.

How well can nZVI particles travel through the subsurface?
What is their state when they reach target contamination?
Do current methods used to detect nZVI particles in the lab lend themselves to field application?

In this field study existing synthesis techniques [2] were scaled up and 800L of nZVI was injected into a contaminated utility corridor containing various chlorinated solvents. nZVI particles intercepted by monitoring wells were analyzed using transmission electron microscopy and dynamic light scattering that characterize their size. The zero valent iron content of the particles was also compared to nZVI immediately after synthesis to gain insight into the characteristics of nZVI being delivered to the contamination.

[1] Phenrat *et al*. (2007) *ES&T* **41** 284–290 [2] He *et al*. (2007) *ES&T* **41** 6216–6221 [3] Saleh *et al*. (2005) *Nanoletters* **5** 2489–2494 [4] Tiraferri *et al*. (2009) *J. Nanopart. Res*. **11** 635–645

Seismological constraints on an evolution of the Izu-Bonin intra-oceanic arc

SHUICHI KODAIRA, NARUMI TAKAHASHI AND TAKESHI SATO

IFREE JAMSTEC, Showa-machi 3175-25, Kanazawa-ku, Yokohama 236-0001 JAPAN (kodaira@jamstec.go.jp, narumi@jamstec.go.jp, tsato@jamstec.go.jp)

JAMSTEC has been conducting intensive active-source seismic surveys to cover the entire Izu-Bonin arc. New seismological constraints on formation and evolution processes of the arc crust are revealed from those data. For examples, a large volume of felsic-to-intermediate component crust having Vp of 6.0 - 6.8 km/s is predominantly observed beneath basaltic volcanic centers along the current volcanic front. We also discovered a similar along arc variation of the felsic-to-intermediate component crust in the rear-arc, which is proposed to be separated from the volcanic front after Oligocene. These findings suggest that the main part of the arc crust consisting of the felsic-to-intermediate component was created before the rear-arc has been separated from the volcanic front probably in Oligocene age. From recently obtained seismic data in the fore-arc, on the other hand, we found that the structure of the fore-arc region represents significantly different characters from that of the volcanic front. Petrological studies in the fore-arc region proposed a formation of oceanic crust associated with boninitic volcanism during an initial stage of subduction. The newly obtained seismic structures in the fore-arc strongly support this idea; i.e. the crust beneath the Bonin ridge in the fore-arc is remarkably thin (less than 10 km), and velocity-depth profiles in the fore-arc is almost identical to that of typical oceanic crust.

https://doi.org/10.1180/S0026461X00006502 Published online by Cambridge University Press

Magnesium isotope composition of presolar silicate grains

JÁNOS KODOLÁNYI* AND PETER HOPPE

Max Planck Institute for Chemistry, Mainz, 55128 Germany (*correspondence: j.kodolanyi@mpic.de)

We have measured the Mg isotope compositions of presolar silicate grains, to gain insights into the stellar nucleosynthesis and Galactic chemical evolution (GCE) of Mg isotopes.

More than half of the Mg in the interstellar medium (ISM) is hosted by oxide and silicate dust produced by evolved stars [1]. The Mg isotope composition of dust grains predating our Solar System could provide information about the Mg isotope 'inventory' of the local ISM at the time of Solar System formation. This is of particular interest, as the $^{25}Mg/^{24}Mg$ and $^{26}Mg/^{24}Mg$ ratios of the Sun (and the Solar System) appear to be substantially lower than that predicted by GCE models for stars of solar metallicity (Z_{solar};[2]). Presolar silicate grains represent the silicate fraction of the interstellar dust at the time of Solar System formation. They are 200-300 nm crystalline or amorphous grains, which escaped Solar System processing, thereby retaining their pristine isotope compositions [e.g. 3, 4].

Presolar silicate grains of the present study were found in the matrix of Acfer 094 (an ungrouped carbonaceous chondrite), based on their O isotope compositions and Si-Al-O systematics. These were determined by the NanoSIMS, as were the grains' Mg isotope compositions (for analytical conditions see [5]). Based on their O isotope composition, the identified 26 grains were produced in the stellar winds of AGB stars, with initial masses (M) of 1.15-2.2 × M_{solar} and Z ~ Z_{solar} [6], similar to the majority (~80 %) of presolar silicates reported in the literature previously [e.g. 4]. Two of the 3 grains analysed for Mg isotopes so far have solar $^{25}Mg/^{24}Mg$ ratios within analytical uncertainty (1 σ) whereas a third grain shows a slight enrichment in ^{25}Mg relative to solar ($\delta^{25}Mg$ = 32 ± 20 ‰). The ^{25}Mg-enriched grain also has elevated $^{26}Mg/^{24}Mg$ ($\delta^{26}Mg$ = 39 ± 20 ‰), as do one of the other two grains ($\delta^{26}Mg$ = 35 ± 16 ‰). Interestingly, in a $\delta^{25}Mg$ vs. $\delta^{26}Mg$ plot our silicate grains fall along a line with slope ~1 as predicted by the GCE model of [2] for stars with ~solar Z; however, at much lower $^{25}Mg/^{24}Mg$ and $^{26}Mg/^{24}Mg$ ratios than predicted, similar to presolar oxide grains from akin stellar sources [7].

[1] Fitzpatrick (1997) *Astrophys J* **482**, L199–L202. [2] Fenner *et al*. (2003) *Publ Astronom Soc Australia* **20**, 340–344. [3] Nguyen & Zinner (2004) *Science* **303**, 1496–1499. [4] Vollmer *et al*. (2009) *GCA* **73**, 7127–7149. [5] Kodolányi & Hoppe (2010) *Proc Sci (NIC XI)* 142 [6] Nittler (2009) *Publ Astronom Soc Australia* **26**, 271–277. [7] Zinner *et al*. (2005) *GCA* **69**, 4149–4165.

Fe acquisition from natural organic matter by an aerobic *Pseudomonad*: Siderophores and cellular Fe status

K. KOEHN[1], C. DEHNER[2], J. DUBOIS[2] AND P. MAURICE[1]*

[1]University of Notre Dame, 156 Fitzpatrick Hall, Notre Dame, IN 46556, USA (kkoehn@nd.edu, *correspondence: pmaurice@nd.edu)

[2]University of Notre Dame, 251 Nieuwland Hall, Notre Dame, IN 46556, USA (cdehner@nd.edu, jdubois@nd.edu)

Aerobic microorganisms have evolved various strategies to acquire nutrient Fe (often limiting in circumneutral environments), including the release of Fe-chelating siderophores. The potential importance of siderophores in Fe acquisition from natural organic matter (NOM) in the form of reverse osmosis (RO) and aquatic XAD-8-isolated humic samples (both with naturally associated Fe) was investigated using a wild type strain (WT) of aerobic *Pseudomonas mendocina* that produces siderophore (s) and an engineered mutant that cannot. Microbial growth under Fe-limited batch conditions was monitored via optical density, and a biosensor assay was used to report on transcriptional output as a measure of cellular Fe status. Both WT and mutant strains acquired Fe from NOM. Bacterially sensed Fe deficiency in the presence of the RO sample decreased with increasing [Fe] and was less for the WT than for the mutant. However, for both WT and mutant, maximum growth in the presence of the RO sample increased as: 1 mgC/L (0.2μM Fe) < 100 mgC/L (20μM Fe) < 10 mgC/L (2μM Fe); the highest concentration of NOM appeared to diminish numbers of free-swimming/planktonic bacteria, perhaps by inducing biofilm formation and/or as a result of associated Al. Growth was slightly more robust on the XAD-8 compared to the RO sample at 2 μM Fe, although there were no apparent differences in internal Fe status. Chelex® treatment to partially remove metals associated with the RO sample increased Fe stress but did not substantially affect growth. It was concluded that: (1) siderophores are useful but not necessary for Fe acquisition from NOM by *P. mendocina* and (2) NOM may have complex effects on microbial growth, related not just to Fe content but potentially to the presence of other (trace)metals such as Al and/or to effects on biofilm development.

https://doi.org/10.1180/S0026461X00006502 Published online by Cambridge University Press

No differences in Sr isotope ratios between ectomycorrhizal and arbuscular mycorrhizal ecosystems across a wide range of geological substrates

NINA KOELE[1]*, IAN DICKIE[1], JOEL BLUM[2], JAMES GLEASON[2], GARY LOVETT[3] AND MATT MCGLONE[1]

[1]Landcare Research - PO Box 40, 7640 Lincoln, New Zealand (*correspondence: koelen@landcareresearch.co.nz)
[2]University of Michigan, Dept. of Geological Sciences, Ann Arbor, MI 48109,USA
[3]Cary Institute of Ecosystem Studies, Box AB, Millbrook, New York 12545, USA

In highly weathered soils, where phosphorus (P) in particular may be a limiting nutrient, theory dictates that ectomycorrhizal (ECM) ecosystems are most efficient at uptake from mineral P through weathering of Ca-phosphate minerals and recycling of organic P. The ecological significance of mineral weathering by ECM fungi however remains unclear. We studied 10 pairs of pure arbuscular (AM) and pure ECM forests on different geological substrates on the South Island of New Zealand. Sr isotope ratios of dominant canopy tree foliage (AM *Dacrydium cupressinum* and ECM *Nothofagus menziesii*) were determined and in thin sections we analysed structural interactions between mycorrhizal hyphae and mineral and/or organic soil particles. Both AM and ECM forests had similar Sr isotope ratios that varied with geological substrates, indicating both forest types obtain Sr (and Ca-phosphate) from the same sources. Fungal weathering tunnels in feldspar grains were present in thin sections from both forest types. These preliminary data suggest there are no major differences in base cation nutrient uptake between AM and ECM ecosystems. This might challenge our understanding of the respective roles of ECM and AM fungi in ecosystem nutrient cycles.

Oceanic plagiogranites as products of hydrothermal activity at slow-spreading ridges

J. KOEPKE[1], P.E. WOLFF[1] AND S.T. FEIG[2]

[1]Institute for Mineralogy, Leibniz University of Hannover, Callinstr. 3, 30167 Hannover, Germany (Koepke@mineralogie.uni–hannover.de)
[2]CODES, University of Tasmania, Private Bag 126, Hobart, TAS 7001, Australia

We studied more than 100 oceanic gabbros from Mid-Atlantic Ridge and Southwest Indian Ridge by scanning electron microscopy and found in 90% of the samples microstructures suggesting that hydrous partial melting reactions proceeded. The best proxy for the underlying reaction is plagioclase strongly enriched in anorthite which is arranged in zones along grain boundaries implying that the partial melting process was triggered by fluids percolating on grain boundaries in a ductile regime. The composition of the new An-rich plagioclase is strongly impoverished in incompatible trace element excluding a model that these An-rich zones were precipitated by late, hydrous evolved melts. In some cases it is evidenced that the water-rich fluids are seawater-derived, suggesting a model that hydrothermal activity/circulation within the deep oceanic crust may trigger hydrous partial melting resulting in the production of oceanic plagiogranites, at temperatures exceeding 850° without any crack system, a prerequisite in current models for enabling hydrothermal circulation. This is in contrast with new findings of [1] stating that zircons of many plagiogranites from slow-spreading ridges show oxygen isotopes typically for equilibrium with mantle. However, new experimental work show that water activities prevailing during the melting reaction can be regarded as extremely low implying that a potential sea water source cannot be easily detected by stable isotopes.

[1] Grimes *et al*. (2011) *Contrib. Mineral. Petrol*. **161**, 13–33.

https://doi.org/10.1180/S0026461X00006502 Published online by Cambridge University Press

Lithium-boron isotope fractionation during degassing of rhyolitic magma

K.T. KOGA[1]*, E.F. ROSE-KOGA[1], D. LAPORTE[1], N. CLUZEL[1], N. SHIMIZU[2] AND E. DELOULE[3]

[1]Laboratoire Magmas et Volcans, Clermont Université, BP 10448, Université Blaise Pascal, CNRS UMR 6524, IRD M163, Clermont-Ferrand, France (*correspondence: k.koga@opgc.univ-bpclermont.fr)
[2]Woods Hole Oceanographic Institute, Woods Hole, MA 02543, USA
[3]Centre de Recherches Pétrographiques et Géochimiques, CNRS UPR 2300, Vandoeuvre-lés-Nancy, France

It has been considered that some volatile trace elements partition into a gas phase and leave the host magma during degassing events. For example, lithium and boron are light elements, which show strong affinity to fluid phase. Then, it is certainly possible to partition these elements into degassing fluid bubbles under pressure. Furthermore, during such element redistribution via diffusion transport, isotopes of lithium and boron may fractionate.

We have analyzed experimentally degassed natural rhyolitic obsidian, which was pre-saturated in H_2O at 210 MPa, 800 °C giving approximately 6 wt%. These samples were isothermally decompressed at the rate of 1000 and 27.8 kPa/s. The final pressure before quench was approximately 70 MPa. Here, a rhyolitic composition was chosen for their ability to retain bubbles within the melt matrix. A maximum element exchange is expected between gas phase and melt, while element diffusivities are slower in rhyolite than basalt. The result shows that significant lithium and boron depletion in the host lava can take place within 12 min of isothermal decompression at 800 °C. The duration of bubble growth was 20 sec and 12 min depending on the decompression rate.

The fast and slow decompression resulted in heterogeneous lithium and boron abundance in the charge. The areas further away from bubbles have lithium and boron abundance indistinguishable from the starting glass, and the areas close to bubbles show 43 and 18 % depletion of lithium and boron, respectively, while H_2O depletion is 50%. When significant abundance depletions were observed in the glass, in close vicinities, ^{7}Li is enriched by as much as 20.2 ± 1.5 permil, and ^{11}B is enriched by 8.8 ± 2.6 permil. The association of abundance depletion and heavy isotope enrichment strongly indicates isotope fractionation governed by diffusion transport.

Loparite composition in stratified Lovozero alkaline intrusion

L.N. KOGARKO[1], Y. LAHAYE[2] AND T.C. WILLIAMS[3]

[1]Vernadsky Institute, Moscow, Russia (kogarko@geokhi.ru)
[2]Institut für Geowissenschaften, University Frankfurt, Germany
[3]Natural History Museum, London, England

Lovozero massif, the largest of the Globe layered peralkaline intrusion, comprises super-large rare-metal (Nb, Ta, REE) deposit. The main ore mineral is loparite (Na, Ce, $Ca)_2$ (Ti, $Nb)_2O_6$ which was mined during many years. Compositional evolution of loparite has been investigated through a 2.35 km section of the Lovozero massif using LA-ICP-MS Institut für Geowissenschaften, University Frankfurt and CAMECA SX50 British Museum of Natural History (London) (Kogarko *et al*. 2002). The composition of cumulus loparite changed systematically upward through the intrusion with an increase in Na, Sr, Nb, Th, Nb/Ta, U/Th and decrease in REE, Zr, V, Zn, Ba and Ti. Our investigation indicates that the formation of loparite ore was the result of several factors including the chemical evolution of high alkaline magmatic system and mechanical accumulation of loparite at the base of convecting unit.

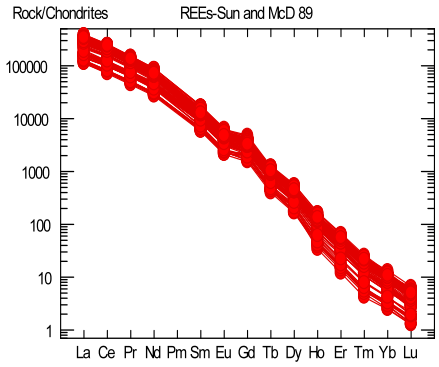

Figure 1: Range of REE contents in loparites.

https://doi.org/10.1180/S0026461X00006502 Published online by Cambridge University Press

Two- and three-dimensional imaging of platinum-group minerals at submicrometer scale with synchrotron X-ray

T. KOGISO[1]*, K. SUZUKI[2], T. SUZUKI[2] AND K. UESUGI[3]

[1]Graduate School of Human and Environmental Studies, Kyoto University, Kyoto 606-8501, Japan (*correspondence: kogiso@gaia.h.kyoto-u.ac.jp)
[2]IFREE, JAMSTEC, Yokosuka, Kanagawa 237-0061, Japan
[3]JASRI/SPring-8, Sayo, Hyogo 679-5198, Japan

Platinum-group elements (PGE) in the Earth's mantle are key tracers for understanding the differentiation history of the Earth. PGE in mantle peridotite are strongly concentrated in Fe-Ni-Cu sulfides [1], whereas platinum-group minerals (PGM) are also potential phases that host significant amounts of PGE in the mantle [2, 3]. PGM are too small to be detected with conventional analytical methods, and therefore it is difficult to know how abundantly and where PGM exist in the mantle. PGM ever found in peridotite samples are mostly associated with Fe-Ni-Cu sulfides [3, 4], implying that those PGM had exsolved from the Fe-Ni-Cu sulfides [1]. On the other hand, discrete PGM grains have been found from a sulfide-free harzburgite [5], but these PGM are interpreted to be residues formed in response to the complete consumption of Fe-Ni-Cu sulfides during partial melting of peridotite. Textural and morphological investigation of PGM in peridotites at submicrometer scale could be a powerful method to know whether PGM found in peridotites had originally existed as discrete grains in the mantle.

We did two- and three-dimensional imaging of PGM in peridotite samples using synchrotron X-ray at SPring-8 to reveal morphology of PGM and their textural relationship with surrounding minerals. Tho-dimensional mapping of PGM-bearing Fe-Ni-Cu sulfides with micro-XRF [4] demonstrated that PGM distributed near the rims of the slufide grains. Three-dimensional imaging of them with X-ray computed tomography and laminography revealed that some PGM grains are included within the sulfide grain. These observation suggests that not all of the PGM are exolusion products from the Fe-Ni-Cu slufides.

[1] Alard *et al*. (2000) *Nature* **407**, 891–894. [2] Keays *et al*. (1981) *Nature* **294**, 646–648. [3] Lorand *et al*. (2010) *EPSL* **289**, 298–310. [4] Kogiso *et al*. (2008) *G-cubed* **9**, 10.1029/2007GC001888. [5] Luguet *et al*. (2007) *GCA* **71**, 3082–3097.

Trends in buffer capacity, pH and Al at the Swedish integrated monitoring sites

S.J. KÖHLER[1]*, T. ZETTERBERG[2], M.N. FUTTER[1], J. FÖLSTER[1] AND S. LÖFGREN[1],

[1]Swedish University of Agricultural Sciences, SE750 07 Uppsala, SE (*correspondence: Stephan.Kohler@slu.se)
[2]IVL Svenska Miljöinstitutet AB, SE10031 Stockhom, SE

The lumped parameter model MAGIC [1] was applied to four Swedish long-term integrated monitoring sites. The largest part of the uncertainty in the model outcome was driven by the underlying deposition scenario, assumptions about sulphate (SO_4^{2-}) adsorption and soil mass. Estimated weathering rates varied in a relatively narrow range between 47-62 or (42-47) meq m^{-2} $year^{-1}$ depending on the choice of available soil cation exchange capacity (CEC). Varying Aluminium (Al) solubility or introducing a dynamic weathering feedback that allowed BC release to increase at more acidic pH had a systematic effect on predicted changes in acid neutralizing capacity (ANC; ca. 10-41 ueq L^{-1}) and pH (ca. 0.1 -0.6 pH units) at all sites. Uncertainties about weathering and modelled temporal changes in pools and respective fluxes of Al between compartments may lead to systematic differences for projected changes in pH and ANC and warrant further systematic study [2].

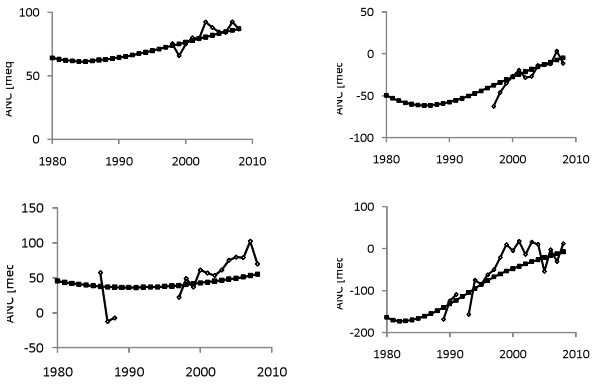

Figure 1: Time series of modelled and measured time series of ANC at each of the four sites.

[1] Cosby *et al*. (2001) *HESS* **5**, 499-517. [2] Köhler *et al*. (under review).

https://doi.org/10.1180/S0026461X00006502 Published online by Cambridge University Press

Low-temperature thermochronology of the Mesozoic uplift history in the Hardangerfjord area, SW Norway

F. KOHLMANN*, A.K. KSIENZYK, J. JACOBS AND H. FOSSEN

Department of Earth Science, University of Bergen, PB 7803, 5020, Bergen, Norway
(*correspondence: fabian.kohlmann@geo.uib.no)

The geology of the Hardangerfjord area is dominated by the Hardangerfjord Shear Zone (HSZ), a major crustal-scale structure that formed during Devonian extension shortly following the Caledonian orogeny. The HSZ might be part of an even larger zone of crustal deformation stretching across the North Sea into the Highland Boundary Fault in Scotland. The Hardangerfjord itself follows the trend of the shear zone and acted as one of the largest sediment pathways in the area. The amount of inland erosion and the corresponding depositional patterns are strongly affected by onshore tectonics.

The present project aims to constrain the amount and timing of post-Caledonian uplift in this area by fission track, (U-Th)/He and K/Ar dating. In particular the apparent absence of Mesozoic brittle reactivation of the HSZ in this area is targeted by sampling of detailed profiles parallel and across the HSZ. Furthermore, vertical profiles on steep flanks of the Hardangerfjord are analysed in order to obtain more precise uplift and erosion rates. This study will improve our understanding of onshore tectonic processes and their effect on offshore sedimentation cycles in the North Sea.

Subducted oceanic crust exhumed from the lower mantle

S.C. KOHN[1]*, M.J. WALTER[1], D. ARAUJO[2], G.P. BULANOVA[1] AND C.B. SMITH[1]

[1]School of Earth Sciences, University of Bristol, BS8 1RJ, UK (*correspondence: simon.kohn@bristol.ac.uk)
[2]Instituto de Geociências, Universidade de Brasília, Brasília-DF, 70910-900, Brazil

Over the last 25 years diamonds from several continents have yielded inclusions that have been interpreted as sub-lithospheric in origin. The mineralogy and compositions of the inclusions have been interpreted in terms of both peridotitic and basaltic protoliths and a range of pressures. There is now an abundance of samples of basaltic inclusions that record transition zone and lower asthenospheric pressures [1], but until now there has been no convincing evidence for diamonds that crystallised in the lower mantle from a basaltic protolith.

In this study we report on a suite of mineral inclusions in diamonds from Juina, Brazil, which have exactly the mineralogy and chemistry expected for a basaltic composition at depths of 700-1200 km. Syngenetic, composite mineral inclusions in diamonds from a single kimberlite pipe (Juina 5) are found to have the bulk chemistries of the 'calcium ferrite' phase (CF-phase), 'New Aluminium Silicate' phase (NAL-phase), Al- and Fe-rich Mg-perovskite, and Ti-rich Ca perovskite. CF- and NAL-phases have previously been observed only in high pressure and temperature experiments on basaltic bulk compositions. The inclusions therefore indicate an origin of the diamonds and inclusions in oceanic crust subducted into the lower mantle.

The relatively high density of subducted basalt, especially if it is cooler than the surrounding peridotitic mantle, means that the mechanism for exhumation of basaltic crust from the lower mantle is puzzling. Available time constraints from other sub-lithospheric diamonds from the Juina region [2] indicate uplift rates of buoyant plumes of subducted material of ~ 1 – 50 cm/yr. Various subduction-exhumation cycles that can explain all the data will be discussed.

[1] Harte (2010) *Min Mag*. **74** 189–215. [2] Bulanova *et al*. (2010) *Contrib. Min. Pet*. **160** 489–510.

https://doi.org/10.1180/S0026461X00006502 Published online by Cambridge University Press

Mineralogical residence of Platinum Group Elements (PGE) in the Fe-Ni-Cu sulfide deposits of the Ivrea Verbano Zone (Italy)

P. KOLLEGGER*, F. ZACCARINI, G. GARUTI AND O.A.R. THALHAMMER

University of Leoben, Dept. Appl. Geol. Sci. Geophysics, Leoben, Austria
(*correspondence: peter.kollegger@unileoben.ac.at)

We present a residence-study of platinum group elements (PGE) in base metals sulfides (BMS) as well as in specific platinum group minerals (PGM). The PGE, Te and Re contents were analyzed by electron microprobe. The investigated Fe-Ni-Cu deposits of the Ivrea Verbano zone occur: 1) within layers of the igneous complex, 2) within an ultramafic sill intruding metasediments and 3) within ultramafic pipes intruding gabbros and metasediments.

PGE hosted by base metals sulfides (BMS)

Pyrrhotite (Po), pentlandite (Pn) and chalcopyrite (Ccp) were analyzed. Nearly two thirds of the analysis (n=349) contain Ir, Rh, Pt and Pd above detection limits (d. l.) (100, 32, 93 and 30ppm). BMS from all the three types of deposits contain PGE. Generally Te is above d. l. (100ppm); enriched in Pn. Different analyses of one specific mineral showed that the PGE are distributed dishomogeneously and that the quantities do not correlate with Te. Pt and Ir are mainly hosted by Po and Pn but not by Ccp. Pd is carried by each of the mentioned minerals. Rh occurs mainly in Po and only rare in Ccp and Pn. Re is only hosted by Po. Ir is enriched in Po and Pn and Ccp contains no Ir above d. l. Re was only detected in Po. Os data was neglect due to an interference with Cu. Ru was always below the d. l. of 35ppm.

PGE hosted by platinum group minerals

We investigated several PGM included within the base metals sulfides (sizes <10μm). The following species were found: Pd-rich melonite, merenskyite, moncheite, sperrylite and irarsite in decreasing order of abundance. According to the mineral chemistry, Te was partly substituted by Bi.

Our mineralogical observations suggest that the PGE, together with other chalcogens, were initially dissolved and collected by an immiscible sulfide liquid probably as small clusters. Subsequently, they were exsolved together with Te, Bi and As and crystallized as discrete PGM which are described for our investigated samples.

REE patterns in the ore-bearing of the Chortovo Koryto gold deposit (Eastern Siberia)

YU.V. KOLMAKOV* AND P.A. TISHIN

Tomsk State University, Lenin avenu 36, 634050 Tomsk, Russia (*correspondence: kolmakovyv@tpu.ru)

REE are usually considered as inert components at the metamorphic and metasomatic processes. But in recent years more and more papers indicating their mobility in the hydrothermal systems are published. The REE distribution in the rock associations of the orogenic gold deposit Chortovo Koryto was studied by ICP-MS method.

This deposit is located on the boundary between Baical-Patom fold-thrust belt and Siberian Craton. The gold ore are represented by system of quartz vein in the metaterrigenous slice of the Early Paleozoic formation Mikhailovskaya. The rock metamorphism corresponds to the greenschist facies. The composition of ore beds includes metaaleurolite - Qtz + Ab + Mus + Chl ± Bt (SiO_2 60-80%; Al_2O_3 8-19%; CaO 0.1-0.6%; K_2O 1.7-3.5%), carbonaceous slates - Qtz + Ab + Mus + Chl + C (SiO_2 41-64%; Al_2O_3 13-29%; CaO 0.05-2.1%; K_2O 1.9-6.8%), and altered rocks - Anc + Cal + Mus + Ab + Chl (SiO_2 29-68%; Al_2O_3 9-16%; CaO 6-12%; K_2O 1.4-7.6%).

The morphology of Chondrite normalized REE patterns of metaaleurolite is similar to the main sedimentary standards (La/Yb 7.3-11.4; Eu/Eu* 0.62-0.81), but differs in lower accumulation level of lanthanides (37-88 ppm). In the carbonaceous slates Σ REE increases up to 186 ppm mostly due to light REE (La/Yb 18, 5-31, 2), at the same time an evident negative Eu anomaly is shown (Eu/Eu* 0.41-0.66). In the altered rocks a maximum enrichment (Σ TR 251-875 ppm), lanthanides differentiation (La/Yb 41, 3-50, 1) and absence of Eu anomaly (Eu/Eu* 0.89-1.02) are observed; from axil zone in direction of contacts Σ REE decreases from 413 to 251 ppm.

LILE and HFSE distribution in studied rocks indicates that the ore system was formed with presence of two source matters. Metaaleurolites and carbonaceous slates are compared with upper crust (Zr/Hf 31.4-39.1; Ta/Nb 12.02-17.01); altered rocks are similar to the rock basalt-andesite-rhyolite volcanic series of greenstone belts and they supplement with OIB.

The study was funded by Russian Ministry of Education and Science.

https://doi.org/10.1180/S0026461X00006502 Published online by Cambridge University Press

Phase relations of an Fe-Ni alloy determined in an internally-heated diamond anvil cell

TETSUYA KOMABAYASHI[1], KEI HIROSE[2] AND YASUO OHISHI[3]

[1]Tokyo Institute of Technology, 2-12-1 Ookayama, Meguro, Tokyo 152-8551, (komabayashi.t.aa@m.titech.ac.jp)
[2]Tokyo Institute of Technology, 2-12-1 Ookayama, Meguro, Tokyo 152-8551, (kei@geo.titech.ac.jp)
[3]Japan Synchrotron Radiation Research Institute, 1-1-1 Kouto, Sayo, Hyogo 679-5198, (ohishi@spring8.or.jp)

The Earth's core is believed to contain several amounts of nickel while its major component is iron. In order to understand the nature of the Earth's core, we conducted *in situ* X-ray diffraction study of an iron-nickel alloy in an internally-resistive heated diamond anvil cell (DAC) up to pressures (P) and temperatures (T) of 110 GPa and 2500 K. High-P-T experiments with the angle-dispersive X-ray diffraction system were conducted at the SPring-8. The improved internally heated DAC configuration provides stable heating with reliable temperature and pressure determination and phase identification [1]. Due to this configuration, we are able to put tight constraints on the P-T location and the width of the two phase loop of the γ (face-centered cubic structure) and ε (hexagonal close-packed structure) phase transition boundary.

Results show that γ and ε transition boundary in $Fe_{0.9}Ni_{0.1}$ is located at lower temperatures than that of pure iron, consistent with the previous works which used the laser-heated DAC [2, 3]. However, the width of the two-phase loop is narrower than those of previous works. We also evaluated the equation of state for the ε phase in $Fe_{0.9}Ni_{0.1}$ from the compression data to P =100 GPa.

We will present the P-T phase diagram and the density of ε phase in $Fe_{0.9}Ni_{0.1}$, and discuss possible roles of the addition of nickel to iron in the Earth's core.

[1] Komabayashi *et al*. (2009) *EPSL* **282**, 252–257. [2] Lin *et al*. (2002) GRL **29**, 10.1029/2002GL015089. [3] Mao *et al*. (2006) *PEPI* **155**, 146–151.

Environmental geochemistry of Cu in agricultural soils treated with Cu-based fungicides

M. KOMÁREK* AND E. ČADKOVÁ

Czech University of Life Sciences Prague, Czech Republic (*correspondence: komarek@af.czu.cz)

Introduction

Copper-based fungicides (such as the Bordeaux mixture - $CuSO_4$+Ca $(OH)_2$, Cu-oxychloride etc.) have been extensively used in Europe since the end of the 19th century to control fungal diseases on vine, such as downy mildew caused by *Plasmopara viticola*. Their long-term application and subsequent wash-off from the treated plants have resulted into extensive Cu accumulation in agricultural soils [1]. The aim of this paper is to provide information about the distribution, chemical fractionation and mobility of Cu in agricultural soils (vineyards, hop fields), including sorption processes and interactions with other commonly used organic fungicides (e.g. tebuconazole).

Results and Discussion

As in other contaminated soils, Cu in fungicide-impacted soils is mainly associated with the oxidizable and, to a lesser extent, with the reducible soil fraction, according to the soil organic matter and (hydr)oxide contents. The retention of Cu differs with the fungicide used (higher retention was observed for Cu originating from the Bordeaux mixture compared to Cu-oxychloride), which indicates that different retention processes occurs. The suggested mechanisms include: specific and non-specific adsorption (especially on soil organic matter) and precipitation of newly formed phases, such as CuO, Cu $(OH)_2$, various Cu-hydroxysulfates etc. The retention of fungicide-derived Cu in the studied soil types can be well described by the Freundlich isotherm and is directly controlled by its chemical form [2]. The presence of other organic-based fungicides, e.g. tebuconazole, can alter the adsorption behavior of Cu due to speciation changes (e.g. formation of Cu-tebuconazole complexes) [3].

[1] Komárek *et al*. (2010) *Environ. Inter*. **36**, 138–151. [2] Komárek *et al*. (2009) *J. Hazard. Mater*. **166**, 1395–1402. [3] Jaklová Dytrtová *et al*. (2011) *Rapid Commun. Mass Spectrom*. **25**, 1037–1042.

https://doi.org/10.1180/S0026461X00006502 Published online by Cambridge University Press

Observing the diurnal variability of Aerosol Optical Depth (AOD) from a geostationary satellite: Implications for air quality and climate monitoring

S. KONDRAGUNTA[1]*, P. CIREN[2], C. XU[2], I. LASLZO[1] AND H. ZHANG[3,4]

[1]NOAA/NESDIS, 5200 Auth Road, Camp Springs, MD 20746.
(*correspondence: Shobha.Kondragunta@noaa.gov)
[2]IMSG at NOAA/NESDIS, 5200 Auth Road, Camp Springs, MD 20746.
[3]University of Maryland, Baltimore County, 1000 Hilltop Circle, Baltimore, MD 21250.

NOAA has been providing AOD product from the GOES series of Imagers to users for a decade now. GOES AODs are derived from the single visible channel using a look-up-table approach; cloud screening is done using IR channels. GOES AODs, available at 30-minute temporal resolution and 4-km spatial resolution, have a root mean square error of 0.12; retrieval errors, however, are large when solar angles and/or view angles are large. Other sources of errors include cloud contamination, calibration errors, and errors in surface reflectance characterization. Analysis of GOES AODs over the United States indicates that spatial and temporal variability during pollution events is well captured; sub-urban/rural regions show good grid-to-grid correlation and the urban regions dominated by local pollution sources show less correlation with sub-urban regions. Analysis also shows that diurnal sampling improves the accuracy of monthly/seasonal mean AODs that has relevance to monitoring the impact of climate change. In addition to these results, we will show analysis of some case studies of pollution events that highlight the strengths of diurnal sampling with respect to policy implications as well as the capabilities of the future satellite instruments (e.g. GEO-CAPE) that will have better product accuracy and precision.

Gold-ore resources of Uzbekistan: Systematization and regularities of deposits' location

R.I. KONEEV

National University of Uzbekistan, VUZ-gorodok, Tashkent, 100174, Uzbekistan (rkoneev@yahoo.com)

The principles of the classification of gold-ore deposits

While classifying a geology-industrial approach with emphasis on main mineras of ores (quartz, sericite, adularia, alunite, pyrite, arsenopyrite), high-, lowsulphidized types is used. It was found [1] that on all hydrothermal gold ore deposits of the world, independently from host environment, a standard row of mineral, correspondingly, geochemical types is shown: scheelite-molybdenite (Au-W), pyrite-arsenopyrite (Au-As), telluride-polymetallic (Au-Te), sulphosalt-silver (Au-Ag), antimonite-sulphoantimonite (Au-Sb), realgar-cinnabar (Au-Hg). A porphiritic (Au-Cu, Mo) type is marked separately. An industrial resource of the deposit is determined by1-4 types.

Regularities of location and mineral-geochemical style

Uzbekistan is one of the leading countries in the world on reserves of gold. All deposits are located within the Kyzylkum-Kurama metallogenic belt and they form ore districts in the places of intersection of the Beltau-Kurama volcanino-plutonic belt (BKVB) with deep faults. Each ore district is characterized by its mineral-geochemical style that is explained by different depth of the formation, hypo-, meso-, epithermal conditions. From the West to the East of the BKVB the role of later types from Au-W to Au-Sb-Hg types increases. Elements' concentration coefficients in ores relatively to their clarks form following rows and mineral forms [2]: Muruntau – Bi-As-Te-Au-Se-Pd-W-Ag-Sb-Mo; tellurides of Bi, maldonite, arsenopyrite, scheelite, pyrite, Co-Ni minerals. Charmitan – As-Te-Bi-Au-Sb-Ag-Se-Pb-W-Mo; Bi tellurides, maldonite, aurostibite, Pb-Ag-Se sulphoantimonites, arsenopyrite, pyrite. Kochbulak – Te-Au-Bi-Sb-Ag-Se-As-Cu-Pb-Sn; tellurides of Au, Ag, Bi, Sb, Pb, Cu, Hg; pyrite, goldfieldite, tetrahedrite. Kalmakyr – Te-Re-Bi-Mo-Au-Se-Cu-Ag-As-Sb; tellurides of Bi, Au, Ag; Re-molybdenite, chalcopyrite, pyrite.

According to the statistics [3] 5-6 medium size deposits (15-20 tonnes) and 25-28 small deposits (<15 tonnes) usually form around one big deposit (>100 tonnes).

The resources of gold in Uzbekistan are highly evaluated.

[1] Rundkvist (1997) Geol.ore dep. **1**, 11–24. [2] Koneev *et al*. (2010) Geol.ore dep. **52**, **8**, 755–766. [3] Nekrasov (1999) Ores & metals, **3**, 48–62.

https://doi.org/10.1180/S0026461X00006502 Published online by Cambridge University Press

Chromium enrichment in iron formations record Earth's first acid rock drainage during the Great Oxidation Event

K. KONHAUSER[1], S. LALONDE, N. PLANAVSKY, E. PECOITS, T. LYONS, S. MOJZSIS, O. ROUXEL, M. BARLEY, C. ROSIERE, P. FRALICK, L. KUMP AND A. BEKKER[2]

[1](kurtk@ualberta.ca)
[2](bekker@cc.umanitoba.ca)

Iron formations (IF) are iron rich (~20-40% Fe) and siliceous (~40-50% SiO_2) sedimentary deposits that precipitated throughout much of the Precambrian. Their trace element composition have been used as a proxy for ancient seawater chemistry, with the view of better understanding nutrient availability for the ancient marine biosphere [1, 2]. Recently, their composition have also provided new insights into the chemical weathering processes on land and the transfer of solutes to the ocean. For instance, a recent compilation of Cr enrichment in IF shows a profound enrichment at 2.48 Gyr, coincident with the advent of the Great Oxidation Event. Given the insolubility of Cr minerals, its mobilization and incorporation into IF indicates enhanced chemical weathering at that time, most likely associated with continental pyrite oxidation. Today, aerobic chemo-lithoautotrophic bacteria are essential to this process, catalysing the continued oxidation of Fe (II) as pH values drop below the threshold for inorganic Fe (II) oxidation. We suggest that the Cr pulse beginning 2.48 Gyr ago indicates that such bacteria began utilising O_2 for the first time to oxidise a previously stable and abundant crustal pyrite reservoir. Sulphuric acid generated by this metabolism ultimately leached Cr from ultramafic source rocks and residual soils. This profound shift in weathering regimes constitutes Earth's first acid rock drainage and accounts for independent evidence for increased supply of sulphate and sulphide-hosted trace elements to the oceans at that time.

[1] Konhauser, K.O. Pecoits, E. Lalonde, S.V. Papineau, D. Nisbet, E.G. Barley, M.A. Arndt, N.T. Zahnle, K. & Kamber, B.S. (2009) Oceanic nickel depletion & a methanogen famine before the Great Oxidation Event. *Nature*, **458**, 750-753. [2] Planavsky, N.J. Rouxel, O. Bekker, A. Lalonde, S.V. Konhauser, K.O. Reinhard, C.T. & Lyons, T. (2010) The evolution of the marine phosphate reservoir. *Nature,* **467**, 1088-1090.

Deep versus shallow slab melt signatures recorded by Nb/Ta in modern island arc lavas

STEPHAN KÖNIG[1,2] AND STEPHAN SCHUTH[3]

[1]Universität Bonn, Germany (stephan.koenig@uni.bonn.de)
[2]Universität zu Köln, Germany
[3]Universität Hannover, Germany

The Solomon Islands cover over 1000 km of the SW Pacific plate border and constitute a modern intra-oceanic arc system devoid of subducted sediments and continental crust. Due to a change of subduction polarity, an Eocene deeply-subducted Pacific slab and a shallower, recently subducting Indian–Australian slab remain in the subarc mantle at depths of >100 km and 35-80 km, respectively [1]. Slab melt-related lavas from the Solomons therefore provide unique insights into the residual mineralogy of two slabs at different depths and their influence on the geochemical signatures of shallow and relatively deep slab melts.

Mafic to intermediate slab melt-related lavas from the southwestern volcanic chain of the Solomon Islands show the largest range of Nb/Ta ever reported in a single modern subduction environment. They range from low, subchondritic Nb/Ta (min. ~10) to superchondritic values (max. ~27) that correlate with slab melt signatures (e.g. Gd_N/Yb_N) [2]. Isotope dilution MC-ICP-MS data confirm this large range of Nb/Ta observed in Q-ICP-MS data. One minor slab melt component characterised by a low Nb/Ta is derived from the shallow and recently subducting Indian–Australian plate where amphibole is still a significant residual phase. In contrast, the high Nb/Ta signatures can only be explained by enrichment of the sub-arc mantle source by partial melts from subducted oceanic crust in the presence of residual rutile-bearing eclogite, where amphibole is either a minor phase or entirely absent. Only the old subducted Jurassic Pacific slab is located at depths required for such mineral assemblages. The slab melts that enriched the sub-arc mantle with an unusually high Nb/Ta signature are derived from an initially intact Pacific plate that was probably subject to a slab break-off event and subsequent melting at depths >100 km. Pb isotope data support a Pacific origin of these slab melts [3]. Altogether these geochemical constraints support recent geophysical studies in that partial slab melting may also affect initially intact oceanic plates older than 50 Ma [e.g. 4].

[1] Mann & Taira *Tectonophysics* (2004) **389**, 137–190. [2] König & Schuth *EPSL* (2011) **301**, 265–274. [3] Schuth *et al*. *J. Petrol*. (2009) **50**, 781–811. [4] Kelemen *et al*. *Geophys. Monogr*. (2003) **138**, 223–276.

https://doi.org/10.1180/S0026461X00006502 Published online by Cambridge University Press

Groundwater depletion: A U.S. national assessment and global perspective

LEONARD F. KONIKOW

U.S. Geological Survey, Reston, VA 20192 USA (lkonikow@usgs.gov)

Development of groundwater resources for agricultural, industrial, and municipal purposes greatly expanded during the 20th century, and economic gains from groundwater use have been dramatic. In many places, however, groundwater reserves have been depleted to the extent that well yields have decreased, pumping costs have increased, water quality has deteriorated, aquatic ecosystems have been damaged by reduced groundwater discharge, and land has subsided irreversibly. Some causes and effects of groundwater depletion are neither obvious nor easy to assess. If cumulative long-term global depletion is large, it will represent a substantial net transfer of mass from land to the oceans, thereby contributing to sea-level rise. Much groundwater pumped from confined aquifers is derived from storage losses in adjacent confining layers. Nevertheless, depletion in low-permeability layers is difficult to estimate, rarely monitored, and too often overlooked. A new simplified method for estimating depletion from confining layers was developed, tested, and applied. Results indicate that depletion in confining layers can greatly exceed the depletion from the confined aquifer itself. (For example, in the confined Dakota Aquifer, about 98 percent of the water removed from storage was derived from depletion in adjacent confining units.) A U.S. national groundwater depletion census indicates that about 800 km^3 of water was depleted from groundwater systems in the U.S. during the 20th century—equivalent to a sea-level rise of approximately 2.2 mm. Long-term global groundwater depletion since 1900 totalled about 3,400 km^3 through 2000 and 4,500 km^3 through 2008, equivalent to a sea-level rise of approximately 9.3 and 12.6 mm, respectively. The rate of annual depletion has increased markedly since about 1950, with maximum rates occurring during the most recent period (2000-2008), when it averaged about 145 km^3/yr (equivalent to 0.23 mm/yr of sea-level rise). This recent average rate would explain about 13 percent of the reported long-term rate of sea-level rise of 1.8 mm/yr. Worldwide, the magnitude of groundwater depletion is a small but nontrivial contribution to sea-level rise during the 20th century.

Discovery of new hydrothermal active fields in the South-West Pacific. Organic geochemistry of the fluids

C. KONN[1]*, J.L. CHARLOU[1], J.P. DONVAL[1], D. BIROT[1], V. GUYADER[1], F. PEREZ[2], P. JEAN-BAPTISTE[2], E. FOURRÉ[2], Y. FOUQUET[1] AND THE SCIENTIFIC PARTIES

[1]Ifremer c/Brest, Laboratoire de Géochimie et Métallogénie, BP70, 29280, Plouzané, France (*correspondence: cecile.konn@ifremer.fr)

[2]CEA-CNRS, LSCE, CEA-Saclay, 91191 Gif-sur-Yvette, France

Back-arc basins in the South-West Pacific have been investigated for hydrothermal activity in the last 20 years. Several hydrothermal fields have been discovered in the Lau basin, Manus basin and North Fiji basin. A new area off-shore the Futuna island was surveyed in fall 2010 during a French cruise conducted by Ifremer and two new hydrothermal active fields (Amanaki and Kulo Lasi) were discovered. The plumes were first evidenced by the use of physical and geochemical tracers. At Kulo Lasi, nephelometry, Mn, CH_4 He profiles strongly correlated and consistently showed a maximal anomaly in the water column at about 1200 m depth. Concentrations of CH_4 up to 1200 $nL.L^{-1}$ and up to 30 nM for Mn were detected. High-resolution bathymetry supported the tracers indications, showing a caldeira in the vicinity culminating at 1200 m. Numerous small black smokers were then discovered on the seafloor during our first submersible dive. CTD profiles were recorded around and on the field during 9 CTD operations and 6 Nautile dives. Alongside, water column samples and hydrothermal fluids samples were collected. On the one hand, physics and geochemistry of the Kulo Lasi plume will be discussed here. On the other hand, relatively elevated concentrations of H_2 and CO_2 have been measured in the fluids from Kulo Lasi (gas and inorganic geochemistry of the fluids will be the focus of another presentation by J.L. Charlou). In the presence of H_2 and CO_2, catalytic abiogenic reactions (e.g. Sabatier, Fischer Tropsch) may occur and generate hydrocarbons [1, 2]. Supercritical seawater (Pc = 298 bar, Tc = 407 °C) is a favourable media for cleavages, condensations, cyclisations, hydrolysis, oxydation, hydrogenation and hydroformylation. A great variety of organic compounds (heavier hydrocarbons, prebiotic molecules [3, 4]) may thus be produced at the Kulo Lasi hydrothermal field. The preliminary results on the organic geochemistry of the hot fluids will be presented here.

[1] Proskurowski *et al*. (2008) *Science*, **319**, 604–607. [2] Sherwood Lollar *et al.* (2006) *Chem. Geol.* **226**, 328–339. [3] Konn *et al*. (2009) *Chem. Geol*. **258**, 299–314. [4] Konn *et al.* (2011) *Geobiology,* **9**, 79–93.

https://doi.org/10.1180/S0026461X00006502 Published online by Cambridge University Press

Thermodynamic and trace element modeling to quantify fluid fluxes and fluid-rock interaction in high pressure rocks from the Sesia Zone (Western Alps)

MATTHIAS KONRAD-SCHMOLKE[1], THOMAS ZACK[2], PATRICK J. O'BRIEN[1] AND MATTHIAS BARTH[2]

[1]Institut für Erd- und Umweltwissenschaften, Universität Potsdam, Karl-Liebknecht-Straße 24-25, 14476 Potsdam, Germany

[2]Universität Mainz, Fachbereich Geowissenschaften, Becherweg 14, 55128 Mainz, Germany

The amount and composition of fluids percolating through high pressure rocks and the effect of resulting fluid-rock interaction on fluid and wall rock composition has been constrained by thermodynamic and trace element modeling of partially overprinted blueschist-facies rocks from the Sesia Zone (Western Alps). Deformation-induced differences in fluid flux led to a partial preservation of pristine mineral cores in weakly deformed phengite and sodic amphibole grains that were used to quantify Li, B, Sr and Pb distribution during mineral growth, -breakdown and -modification induced by fluid-rock interaction. Our results show that Li and B budgets are strongly fluid-controlled, thus acting as excellent tracers for fluid-rock interaction processes, whereas Sr and Pb budgets in our samples are mainly controlled by the fluid-induced formation of epidote. Our calculations show that fluid-rock interaction caused significant Li and B depletion in the affected rocks due to leaching effects, which in turn leads to an up to five-fold enrichment of these elements in the percolating fluid. Depending on available fluid-mineral trace element distribution coefficients modeled fluid rock ratios necessesary to produce the observed trace element patterns in the affected minerals were up to 1 in weakly deformed samples and at least 1 – 4 in shear zone mylonites. These values can be used to determine time integrated fluid fluxes that were up to 4. 10^2 m^3m^{-2} in the weakly deformed rocks and at least 2 – 8. 10^3 m^3m^{-2} in the mylonites. Combined thermodynamic and trace element models help to quantify metamorphic fluid fluxes and the associated element transfer in complex, reacting rock systems and to better understand commonly observed fluid-induced trace element trends in metamorphic and magmatic rocks and minerals from different geodynamic environments.

Evidence for a Hawaii-Emperor bend in the Rurutu hotspot track

J.G. KONTER[1]*, M.G. JACKSON[2] AND A.A.P. KOPPERS[3]

[1]Dept. Geological Sciences, University of Texas at El Paso, El Paso, TX 79968 (*correspondence: jgkonter@utep.edu)

[2]Dept. Earth Sciences, Boston University, Boston MA 02215

[3]Coll. Oceanic and Atmospheric Sciences, Oregon State University, Corvallis, OR 97331

Hotspots have long been used as an absolute and fixed reference frame for modeling plate motions. However, the paths of hotspot tracks may be complicated by factors related to mantle flow and/or plume motion. The two longest, continuous hotspot tracks recognized on the Pacific Plate, the Hawaiian-Emperor and Louisville chains, exhibit different behavior prior to ~50 Ma, where the Hawaiian-Emperor chain shows a pronounced 'kink', while the Louisville chain is gently curved [1]. Furthermore, the Hawaiian hotspot might have incurred a ~15° southern shift between 80 and 50 Ma, while the Louisville hotspot seems to have behaved more stationary (or moving west to east) over the same time period. The causes of these differences are not well understood, and they have some important ramifications for absolute plate motion models and our understanding of mantle dynamics. Despite suggestions to retire the plume hypothesis, a more conciliary view explains the variety of observations with three different types of hotspots. This would imply the major hotspots may still reflect plate motion with respect to the mantle, although a component of plume motion could also be recorded by the orientation of a volcanic chain.

Recent geochemical evidence and radiometric ages suggest that the Rurutu hotspot is long-lived (100 Ma) [2, 3] and follows a track midway between Hawaii and Louisville. Like Hawaii, the Rurutu hotspot exhibits a sharp bend in the Tuvalu region between Samoa and the Gilberts Ridge, around 35-55 Ma following the latest absolute plate motion models. The hotspot volcanoes are characterized by HIMU-type isotopic compositions [3], distinguishing them from other hotspots such as Samoa [4]. Therefore, the Rurutu hotspot may provide a third, long-lived Pacific hotspot track that can help to deconvolve the effects of plate motion from plume motion in determining the paths of hotspot tracks.

[1] Tarduno *et al*. (2009) *Science* **324**, 50–53. [2] Koppers *et al*. (2007) *Geochem. Geophys. Geosyst.* **8**, 10.1029/2006GC001489. [3] Konter *et al*. (2008) *EPSL* **275**, 285–295. [4] Jackson *et al*. (2011) *Geochem. Geophys. Geosyst.* **11**, 10.1029/2010GC003232.

https://doi.org/10.1180/S0026461X00006502 Published online by Cambridge University Press

Trace element systematics in HT metamorphic rutile: The robustness of the Zr geothermometer

E. KOOIJMAN[1]*, M.A. SMIT[1], K. MEZGER[2] AND J. BERNDT[1]

[1]Institut für Mineralogie, Westfälische Wilhelms-Universität, Corrensstraße 24, D-48149 Münster, Germany (*correspondence: e.kooijman@uni-muenster.de)
[2]Institut für Geologie, Universität Bern, Baltzerstraße 1-3, 3012 Bern, Switzerland

The Zr-in-rutile thermometer [1] has been successfully applied to a wide range of high-grade metamorphic rocks. However, experimental data indicate that rutile may be only moderately retentive to Zr [2]. Some field-based studies reported a large range of Zr concentrations from granulite facies metamorphic rocks suggesting post-peak diffusional resetting during slow cooling [3]. Further investigation into the Zr systematics in rutile is needed to improve the interpretation of Zr-in-rutile temperature estimates.

For this purpose, we analyzed rutile grains from zircon-bearing granulite-facies metapelites of the Archaean Pikwitonei granulite domain, Canada. The Zr concentrations were evaluated by acquiring compositional profiles and maps by electron probe micro-analysis. Profiles of Nb, Cr and V, which diffuse faster in rutile than Zr [4], were analyzed simultaneously. The variation in the concentrations of all elements is small within individual rutile grains (120-280 μm) from 3 different samples, but large differences are observed between grains only millimeters apart in the same sample.

The lack of diffusion profiles for all analyzed elements indicates that Zr concentrations are pristine. Zoning of high-Zr rutile (3000-4600 ppm) demonstrates Zr undersaturation during growth under dry UHT conditions in spite of the presence of zircon. Therefore, several rutile grains should be analyzed in a sample to obtain a useful minimum peak temperature estimate. The highest Zr-in-rutile temperatures for the samples from the Pikwitonei granulite domain are ca. 900 °C and thus exceed previous estimates of 820 °C based on two-feldspar thermometry [5], demonstrating the advantage of Zr-in-rutile thermometry for constraining peak temperatures of UHT rocks.

[1] Zack *et al*. (2004) *Contrib. Mineral. Petrol*. **148**, 471–488. [2] Cherniak *et al*. (2007) EPSL **261**, 267–279. [3] Luvizotto & Zack (2009) *Chem. Geol*. **261**, 303–317. [4] Dohmen *et al*. (2009) GCA **73**, A297. [5] Mezger *et al*. (1990) *J. Petrol*. **31**, 483–517.

In situ analysis of U-Th disequilibria in titanite by fs-LA-MC-ICPMS

J.M. KOORNNEEF[1,2]*, B. BOURDON[1,3], G. FONTAINE[4], L. DORTA[4], B. HATTENDORF[4], D. GÜNTHER[4], P. ULMER[1] AND A. STRACKE[5]

[1]Institute of Geochemistry and Petrology, ETH Zürich, Switzerland,
[2]Department of Petrology, VU Amsterdam, the Netherlands (*correspondence: janne.koornneef@falw.vu.nl)
[3]Ecole Normale Supérieure de Lyon, Lyon, France (CNRS)
[4]Laboratory of Inorganic chemistry, ETH Zürich, Switzerland
[5]Institut für Mineralogie, Westfälische Wilhelms Universität, Münster, Germany

A new technique for *in situ* analysis of U-Th disequilibria in titanite by fs-LA-MC-ICPMS is presented. An in-house titanite glass ([U] = 215 ppm), determined to be in secular equilibrium by solution mode MC-ICPMS, is used to correct for U-Th elemental fractionation by sample standard bracketing. SEM-Faraday gain and abundance sensitivity are determined on solution standards interspersed every 15 laser ablation analysis.

The effect of instrument settings to the accuracy and precision of (^{230}Th/^{238}U) ratios was investigated by multiple analyses of secondary titanite standards. The laser analysis mode (scanning or spot), laser energy and wavelength, and titanite material properties were all found to variably influence the U-Th elemental fractionation and compromise the accuracy of the data to different extents.

During spot analyses using near infra-red (NIR) wavelength and high laser energy, time-dependent elemental fractionation is observed, resulting in relatively large standard errors on the (^{230}Th/^{238}U). Decreasing the laser energy significantly reduces the time-dependent elemental fractionation but does not eliminate it completely, e.g. 2RSE on (^{230}Th/^{238}U) are 5.2% instead of 19%. NIR scanning mode analyses are not compromised by time-dependent elemental fractionation (2RSE on (^{230}Th/^{238}U) are 3.2%), but the absolute amount of fractionation between analyses of different materials (e.g. glass versus minerals) is variable.

Ultra violet (UV) mode LA analyses are significantly less affected by time-dependent elemental fractionation compared to NIR analyses, but are limited by counting statistics due to lower signal intensities. Furthermore, differences in fractionation behaviour between various titanite materials are still observed. The effect of adjusting plasma conditions, with the aim to reduce the elemental fractionation, is currently investigated.

https://doi.org/10.1180/S0026461X00006502 Published online by Cambridge University Press

Preliminary results from Integrated Ocean Drilling Program Expedition 330 to the Louisville Seamount Trail

A.A.P. KOPPERS[1]*, T. YAMAZAKI[2], J. GELDMACHER[3] AND IODP EXPEDITION 330 SCIENTIFIC PARTY

[1]College of Oceanic & Atmospheric Sciences, Oregon State University, Corvallis, OR, USA (*correspondence: akoppers@coas.oregonstate.edu)
[2]Geological Survey of Japan, AIST, 1-1-1 Higashi, Tsukuba 305-8567, Japan
[3]Integrated Ocean Drilling Program, Texas A/M University, 1000 Discovery Drive, College Station, TX 77845, USA

Integrated Ocean Drilling Program (IODP) Expedition 330 drilled five different guyots in the Louisville Seamount Trail ranging in age between 80 and 50 Ma. The primary goals of this expedition were to drill a sufficiently large number of *in situ* lava flows at each seamount for high-quality estimates of their paleolatitudes using paleomagnetic measurements, for improving the overall age progression using high-precision $^{40}Ar/^{39}Ar$ geochronology, and for detailed geochemical studies of the volcanic evolution of these seamounts. With these data we can provide the unique record of the paleolatitude shift (or lack thereof) of the Louisville mantle plume and compare it with the ~15° paleolatitude shift observed for seamounts in the Hawaiian-Emperor Seamount Trail over the same time period. It also allows us to directly compare the geochemical evolution of a typical Louisville seamount with seamounts in Hawaii and to test the apparent long-lived homogeneous geochemical character of the Louisville mantle source. These comparisons are of fundamental importance to determine whether these two primary hotspots have moved coherently or not, and to understand the nature of hotspots and convection in the Earth's mantle. Finally, the paleolatitude, age and geochemical data together will provide a more advanced test of whether the Louisville seamounts were formed from the same mantle source that also formed the Ontong Java Plateau. If this is found to be the case, it is possible that the plume head of the Louisville mantle upwelling caused the massive LIP volcanism that formed the Ontong Java Plateau around 120 Ma and at an average 24±2°S paleolatitude.

Diamondiferous conglomerate preserves evidence for kimberlite and the deep cratonic root of the Mesoarchean Southern Superior craton

M.G. KOPYLOVA[1], V.P. AFANASIEV[2], L. BRUCE[1] AND J. RYDER[3]

[1]University of British Columbia, Vancouver, Canada (mkopylov@eos.ubc.ca)
[2]Sobolev Institute of Geology and Mineralogy, Russian Academy of Sciences, Novosibirsk, Russia
[3]Dianor Resources, Inc, 649, 3rd avenue, 2nd floor Val-d'Or (Quebec) J9P 1S7, Canada

Current models of the Superior craton growth invoke formation of the cold diamondiferous root soon after the 2.7 Ga orogeny that consolidated the craton. We show that the Superior craton included an older cratonic nucleus that had developed the deep diamondiferous root prior to 2.7 Ga, and also provide evidence for a Mesoarchean Superoir kimberlite. This evidence contradicts current views that Archean diamondiferous volcanics differed from kimberlites, which became a major diamond–bearing primary rock only in the Proterozoic.

The evidence is found in 2.697-2.701 Ga diamondiferous conglomerates of the Michipicoten Greenstone Belt (MGB) of the Wawa subprovince. The conglomerate metamorphosed in the greenschist facies contains mainly lithic igneous mafic to felsic clasts of local provenance. The conglomerate matrix includes diamonds and paragenetic diamond indicator minerals with subtle signs of mechanical abrasion and varying degrees of chemical resorption. The diamonds are predominantly white single octahedral crystals. Comparison of the size distribution, resorbtion and N aggregation of diamonds in Wawa lamprophyres and the conglomerate diamonds confirms that the latter did not derive from the proximal lamprophyric source. Heavy minerals panned from the conglomerate and extracted in commercial labs include Cr-diopside, olivine, corundum, chromite, anorthite, magnetite, pyrope with kelyphitic rims and picroilmenite. Low abundances of heavy minerals (several grains per 4-70 tonnes of the conglomerate) are, in part, explained by their complete or partial replacement by the greenschist assemblage. Cr-diopside, olivine, chromite and anorthite were derived from mafic-ultramafic anorthosite- and chromitite-bearing layered complexes mapped in the MGB. Corundum may have come from kimberlites or other mafic rocks as the majority of corundum is the Cr-bearing ruby. The presence of pyrope with more than 6 wt% Cr_2O_3 suggests derivation from the cratonic root, as such high-Cr pyropes are never found in the off-cratonic continental or oceanic mantle. Picroilmenite has compositions typical of kimberlite and unlike that of ultramafic lamprophyres and other volcanics transitional to kimberlites. The Wawa conglomerate, therefore, should be considered analogous to the Witwatersrand conglomerate in recording indirect evidence for the Mesoarchean kimberlites.

https://doi.org/10.1180/S0026461X00006502 Published online by Cambridge University Press

Monitoring of plagiogranite of the Yeşilova Ophiolite: Geochemistry and confocal Raman spectroscopy, Southwest Anatolia, Turkey

TAMER KORALAY[1] AND YUSUF KAGAN KADIOGLU[2]

[1]Pamukkale Univ., Geol.Eng. Dept., 20017 Denizli Turkey
[2]Ankara Univ., Geol. Eng. Dept., 06100, Ankara-Turkey

In most ophiolitic suites observed around the world, there are small bodies of intrusive leucocratic rocks, usually called plagiogranites. It has clear differences from other subunits of the ophiolite in colour, texture and geochemical character. Yeşilova ophiolite exhibits an incomplete oceanic crust stratigraphy with missing sheeted dykes and epioceanic sediments. It is composed of tectonites, ultramafic-mafic cumulates, isotrope gabbros, plagiogranites and pillow basalts from the bottom to the top. Diabase and microgabbro usually cross-cut the peridotites. Plagiogranites crop out as veins, dikes and small intrusive bodies intruded into the isotrope gabbro having a sharp contact. They have light green, white in color and fine to medium-grain size, consisting predominantly of quartz, plagioclase, uralitized pyroxene, opaque minerals and supported by the Confocal Raman spectrometry. Plagiogranites have hypidiomorphic granular texture and mainly characterized by the micrographic and myrmekitic groundmass texture under the microscope.

Whole rock geochemical of plagiogranites are characterized by high SiO_2 (73.44±2.81) with remarkably low K_2O (0.62±0.48), and generally higher MgO (1.66±1.30), CaO (3.89±1.82) than the continental granite. Moreover; they have slightly high amount of Fe_2O_3/MgO ratio and similar Rb, Sr and Zr values to oceanic plagiogranite composition. On variation diagrams, CaO, Fe_2O_3, Sr, V, Co and Ta display clear negative correlations, whereas Na_2O, P_2O_5, Y, Zr, Hf, La, Ce show positive correlation with increasing of SiO_2 ratio. These can be explained by fractional crystallization processes in the late stage of magma generation. Plagiogranite samples display enrichment in LILE relative to HFSE in MORB and ORG normalized multi-element diagrams. In these diagrams, they exhibit depletions in Rb, Ba, Nb, P and Ti as characteristics of subduction-related magmas. Rare earth element (REE) patterns for plagiogranite show REE enrichment with respect to chondrite values. They exhibit slightly depletion in LREE ($(La/Sm)_N$ = 1.43-2.83) relative to HREE ($(Sm/Lu)_N$ = 0.43-0.92). Furthermore, all the samples of the plagiogranites have small positive Eu anomalies ($(Eu/Eu^*)_N$ = 1.14-1.35), indicating the significant role of plagioclase in the fractional crystallization.

As a result, despite the lack of isotopic data, the petrographic and geochemical results suggest that plagiogranites of the Yeşilova ophiolite are the most probably related to crystal-liquid differentiation process of the oceanic crust of the Alpine belt.

Urban dead seas: Natural and anthropogenic influences on redox-stratified lakes and wetlands

C. KORETSKY

Department of Geosciences, Western Michigan University, Kalamazoo, MI 49008, USA (carla.koretsky@wmich.edu)

Redox-stratification is a pervasive feature of dynamic near-surface earth systems, occurring on scales of micrometers to kilometers. Examples can be found in systems as diverse as microbial mats, soils and sediment pore waters, groundwaters, lakes and seas. Physical processes, such as advective flow through pores or wind mixing of surface waters, interact with chemical factors, for instance the availability of electron acceptors and donors, and biological processes, including organic matter fixation, macrophyte root exudation, bioirrigation, bioturbation and microbially-mediated reactions, to produce spatially and temporally heterogeneous systems.

Anthropogenic activities can also have an enormous influence on redox-stratified systems. For example, the addition of limiting nutrients and labile organic matter to surface and groundwaters leads to substantial, widespread problems such as eutrophication and the creation of dead zones. There is increasing recognition that the introduction of other contaminants, such as road salt deicers, may also have important biogeochemical consequences, albeit often through subtle or indirect effects. Deciers, typically NaCl or $CaCl_2$, are applied in enormous and growing quantities in urbanized settings throughout the world. In the U.S. alone, >15, 000, 000 tons of decier are applied to roads each year. It is well-known that application of these salts can have a profound impact on macro- and micro- biological communities, yet remarkably few studies have examined the effects on biogeochemical processes.

Recent work suggests that such effects could be quite significant. For example, mesocosm data show that addition of NaCl, and especially $CaCl_2$, can stimulate anaerobic respiration in wetland soils. Furthermore, an increasing body of literature demonstrates that road salt deicers may suppress physical mixing in lakes, potentially resulting in transition from dimictic to monomictic or even meromicitic conditions, and in pronounced redox-stratification of lake column waters. Particularly in eutrophic urban lakes, this is expected to have enormous consequences for biogeochemical cycling, and could lead to saline, persistently anoxic lake bottomwaters: ‘urban dead seas’. This emerging environmental problem deserves greater attention and further study.

https://doi.org/10.1180/S0026461X00006502 Published online by Cambridge University Press

Cr(VI) adsorption on γ-alumina

C.M. KORETSKY* AND T.J. REICH

Department of Geosciences, Western Michigan University, Kalamazoo, MI 49008, USA
(*correspondence: carla.koretsky@wmich.edu)

Cr (VI) is a toxic contaminant that has been introduced into numerous surface and subsurface systems through industrial activities such as electroplating, leather tanning and steel manufacturing. In solution, it forms anionic complexes (CrO_4^{-2}, $HCrO_4^-$), and as such, may bind to the surfaces of positively charged solids. High surface area, synthetic γ-alumina is often used as an analog for aluminum oxides found in soils and sediments. It has a high point of zero charge (~5.5-8.9), and thus may bind Cr (VI) even at relatively high pH. However, few studies have investigated Cr (VI) sorption on γ-alumina.

In this study, Cr (VI) sorption on γ-alumina (N_2 BET SA = 233 m^2/g) was measured as a function of pH (3-10), ionic strength (0.1 to 0.001 M $NaNO_3$), and pCO_2 (0, atmospheric, 2.5%). A large batch slurry of 2 g/L γ-alumina with 10^{-5} or 10^{-6} M Cr (VI) was titrated from pH 3 to 10, with aliquots removed at ~0.5 pH intervals. Individual aliquots were further equilibrated for 4 hrs, after which the supernantant was removed by centrifugation and syringe-filtration and analyzed for Cr (VI) by UV-vis spectrophotometry (diphenylcarbazide method) or for total Cr by ICP-OES using matrix-matched calibration standards.

Cr (VI) sorption is rapid, reaching equilibrium within 15 minutes, and is reversible, with 100% desorption occurring within 24 hrs. As expected, sorption decreases with increasing pH. For a given solution condition, more Cr (VI) uptake occurs in the 10^{-6} M compared to the 10^{-5} M Cr (VI) experiments. Adsorption edges show little dependence on ionic strength or pCO_2, except that Cr (VI) sorption is suppressed at low pH in experiments with high ionic strength and high pCO_2.

The measured adsorption edges were individually modeled using constant capacitance, diffuse double layer and triple layer surface complexation models. For each model, multiple site density, protonation/deprotonation stability constants, Cr (VI) reaction stoichiometries and capacitances were tested. In each case, good fits could be produced for individual edges. However, none of the models tested resulted in satisfactory fits over the complete range of measured pH, ionic strength, sorbate/sorbent, and pCO_2 conditions. The best fits were obtained using a constant capacitance model, because stability constants for this model are ionic-strength dependent.

Timing of denudation, erosion and surface uplift of the Hunza Karakoram – A case study of combined thermochronological and geomorphological approaches

D. KORINKOVA[1]*, M. SVOJTKA[1] AND J. KALVODA[2]

[1]Institute of Geology, Academy of Sciences CR v.v.i, Prague 6, 165 00, Czech Republic
(*correspondence: korinkova@gli.cas.cz)
[2]Charles University in Prague, Faculty of Science, Albertov 6, Prague 2, 128 43, Czech Republic
(kalvoda@natur.cuni.cz)

Geomorphological records of extreme surface uplifts of the Hunza Karakoram in the late Cenozoic are correlated with thermochronological history of relevant crystalline rocks during active collision orogeny. A set of studied samples dated by apatite fission-track (AFT) technique come from the SW-NE transect in the Hispar and Gharesa regions of the Hunza Karakoram. Variable lithological types of crystalline rocks were collected from 2 400 to 5 600 m a. s. l. and yielded ages between 3.9 ± 0.2 Ma to 9.7 ± 0.4 Ma. Our results confirmed effective denudation, erosion and transport of near-surface rock masses during the late Cenozoic.

Time-temperature modeling of AFT samples from the Hunza Karakoram shows a similar thermal history style, involving a period of total thermal annealing and a subsequent period of cooling corresponding to considerable denudation and erosion processes. Two dominant trends of cooling rate have been observed: (1) the Upper-Miocene to Pliocene period of a slow rate about 0.1 km/Ma followed by (2) the Quaternary period of a relatively rapid rate about 2.6 km/Ma. The later period of cooling can be associated with an approaching of (sampled) rock assemblages nearby late Cenozoic denudation and/or erosion surfaces.

Measured track-lengths vary from 10.3 ± 2.8 μm to 12.1 ± 2.2 μm with a negative skewness. The track-lengths-frequency histogram demonstrate a bimodal distribution with a short peak representing the higher temperature tracks and also with longer peaks derived from final cooling. These data give evidence of mixed ages as a result of (at least) two-stage cooling history of studied crystalline rocks.

Denudation and erosion of rock masses in the Hunza Karakoram estimated by a combination of current elevations of samples and depths of fossil apatite partial annealing zones reached up to 4 km from the Upper Miocene to the present.

https://doi.org/10.1180/S0026461X00006502 Published online by Cambridge University Press

Modern natural and technogenic iodine biogeochemical provinces: Spatial structure and health effects

E.M. KOROBOVA[1]*, S.L. ROMANOV[2], A.I. KUVYLIN[1], V.YU. BERIOZKIN[1] AND I.V. KURNOSOVA[3]

[1]Vernasky Institute of Geochemistry and Analytical Chemistry, Rus.Ac. of Sci., 119991 Moscow, Kosygin Str., 19, Russia (*correspondence: Korobova@geokhi.ru)
[2]Unitary Enterprise Geoinformation systems., Belarus National Ac. of Sciences, 220004 Minsk, Surganov Str., 6, Belarus (romanov_s_l@mail.ru)
[3]Bryansk Clinical and Diagnostic Center Bryansk, Bezhitskayay 2, Russia (irina_k@bkdc.ru)

The ubiquity of living matter proved its chemical coevolution with and adaptation to the Earth geochemical environment. However the existence of homeostatic concentration intervals providing normal functioning of biosystems has led to formation of endemic species and/or distribution of regional and local biogeochemical endemic diseases in cases of expansion of species to environments with concentrations outside thresholds or catastrophic releases of chemical elements and/or compounds. A failure of regulatory mechanisms in at least 20% of population may be a criterion for biogeochemical province with endemy [1].

The main goal of our study was to reveal and analyze the structures of natural and technogenic geofields of iodine in soil and food chain components and iodine-dependent medical effects.

The study of Bryansk oblast affected by the Cherbobyl fallout included: 1) estimation of the initial radioiodine contamination; 2) cartographic estimation of the soil iodine status; 3) determination of iodine in drinking water, milk, pasture plants, arable soil in private farms of 100 rural settlements provided with medical data on renal iodine excretion, endemic goiter and thyroid cancer.

Analysis of the obtained data organized as GIS data base allowed performing spatially adequate comparison of the geochemical and medical data and contouring of potential risk zones as a superposition of geofields of iodine.

The work has been supported by Russian foundation of basic research (grants #07-10-00912 [2] and 10-05-01148).

[1] Kovalsky (1983) Geochemical environment & life. Nauka, M. 77 p. [2] Korobova, Zvonova & Doroshchenko (2010) *RFBR report*, #07-10-00912, 34 p.

Raman spectroscopy of sodium silicates and germanates

O. KOROLEVA AND T. IVANOVA

Institute of mineralogy UrB RAS, Miass, Russia (koroleva@mineralogy.ru)

The approach to melt description we use here bases on idea of structural units make the basis of crystal chemistry of silicates and, when connected with one another via bridging bonds, form composite anions in melts or a disordered network in glass. The germanate system is of interest because of their analogy to silicates at high-pressure conditions. The local structure of silicate system can be presented as a set of silicon-oxygen tetrahedrons with various proportions of bridging and non-bridging oxigen atoms (Q^n-units, where n is the number of bridging oxygen atoms). The coordination number of germanium atoms in glasses has attracted much attention deu to a network forming cation can be in 4-coordinated and 6-coordinated states.

The concentrations of structural units Q^n can be determined experimentally by techniques of Raman spectroscopy, which has no principal limitations in terms of temperature, so that *in situ* structural studies can be carried on in melts. Sodium silicates and germanates of $x\%Na_2O\cdot(100-x)\%MO_2$ composition, where M - Si or Ge, x = 33, 40, 50, 55 и 60 were synthesized from sodium carbonate and SiO_2 (GeO_2). To study the quantity dependence of structural units presented in glass (melt) from modifier content and temperature spectra were deconvoluted on Gaussian components.

The work was supported by the Russian Foundation for Basic Research (grant № 10-05-96044) and grant of President of Russian Federation (MK-109.2011.5).

Early and Middle Jurassic $\delta^{13}C$ and $\delta^{18}O$ trends: A high resolution dataset from the UK

C. KORTE[1], S.P. HESSELBO[2] AND C.V. ULLMANN[1]

[1]Dept. of Geography and Geology & Nordic Center for Earth Evolution, University of Copenhagen, DK, (ck@geo.ku.dk)

[2]Dept. of Earth Sciences, University of Oxford, UK, (stephess@earth.ox.ac.uk)

Low-Mg-calcite fossils have been extensively utilized to obtain past seawater chemistry and to reveal major environmental changes in Earth history [1, 2]. The resolution of these first generation long-term studies is often at biozone levels only. Recent work on major Phanerozoic events showed that distinctly higher resolutions are possible, revealing short-term stable isotope fluctuations and helping to discover its causes. Here we present new carbon and oxygen isotope data from mollusks and brachiopods collected from marine Early to Middle Jurassic successions of the UK representing a new generation of data in terms of temporal resolution. Together with literature data for the T–J boundary [3] and the Toarcian OAE [4] a nearly complete high-resolution record is now available. The fossils have been screened by various techniques, such as scanning electron microscopy and chemical analysis, to check for post-depositional alteration. The carbon isotope fluctuations obtained from the analyzed samples are the following: (1) a positive excursion in the earliest Sinemurian *Conybeari* zone, (2) a negative shift in the Sinemurian *Bucklandi* zone, (3) a negative excursion at the Sinemurian–Pliensbachian boundary (upper *raricostatum* and lower *jamesoni* zones), and (4) a positive excursion in the Late Pliensbachian *margaritatus* zone. The new oxygen isotope fluctuations in general correspond to those of the carbon isotopes, but with the exception for the Sinemurian–Pliensbachian boundary event, which is characterized by a positive $\delta^{18}O$ trend during the negative $\delta^{13}C$ excursion. This positive trend represents most likely bottom water cooling as a result of the Early Pliensbachian transgression. In addition, an Aalenian–Bajocian positive $\delta^{18}O$ excursion is identified. The new high resolution dataset shows partly a strong similarity between the positions of the global warming and cooling events within transgressive and regressive phases of second-order depositional sequences though the Early Jurassic supporting the idea that second-order depositional sequences are a result of eustatic sea-level changes at that time.

[1] Veizer *et al*. (1999) *Chem. Geol*. **161**, 59–88. [2] Jenkyns *et al*. (2002) *J. Geol. Soc. London* **159**, 351–378. [3] Korte *et al*. (2009) *J. Geol. Soc. London* **166**, 431–445. [4] Bailey *et al*. (2003) *Earth Planet. Sci. Lett*. **212**, 307–320.

Geo-bio interactions in hydrothermal fluids and their potential role for hydrothermal metal fluxes

A. KOSCHINSKY[1]*, S. SANDER[2], V. KLEVENZ[1] AND M. PERNER[3]

[1]Jacobs University Bremen, D-28725 Bremen, Germany (*correspondence: a.koschinsky@jacobs-university.de)

[2]Dept. of Chemistry, University of Otago, Dunedin 9054, New Zealand

[3]Microbiology and Biotechnology, University of Hamburg, D-22609 Hamburg, Germany

Hydrothermal vents emit fluids with high concentrations of many metals at the seafloor. Until recently it was assumed that the precipitation of most metals (e.g. Cu and Fe) during mixing with seawater reduces their net fluxes from the hydrothermal systems into the open ocean to negligible values. However, the recent discovery of significant organic complexation of Cu and Fe in the hydrothermal fluids and rising plumes, has urged a revision of trace metal fluxes from deep-sea hydrothermal vents. We demonstrated using field data and geochemical modeling [1] that the presence of organic ligands stabilizing dissolved trace metals strongly competes with metal precipitation and significantly increases the dissolved metal concentrations in hydrothermal fluids and plumes. According to our calculations, hydrothermal metal fluxes may be significantly larger than previously assumed, i.e. up to 20% of the deep-ocean dissolved Fe and Cu budget can be assigned to hydrothermal sources.

While the importance of organic ligands for hydrothermal metal fluxes seems to be acknowledged by now, the nature and origin of these organic molecules is still unclear. Amino acids, probably of biogenic origin, which have been found in significant concentrations in hydrothermal fluids [2], and other organic molecules containing thiol groups would be potential candidates for stable metal complexation. In lab experiments with hydrothermal microbial cultures along Cu concentration gradients the production of organic Cu-binding ligands by the microbial communities due to increasing Cu stress was studied. Ligand production increased significantly with increasing Cu concentrations, implying microbial influence on dissolved metal concentrations, speciation and mineral precipitation in the hydrothermal vent environment. Our work suggests a significant modification of hydrothermal fluid chemistry and hydrothermal metal fluxes by biological processes.

[1] Sander & Koschinsky (2011) *Nature Geosc* **4**, 145–150. [2] Klevenz *et al*. (2010) *Geochem J* **44**, 387–397.

https://doi.org/10.1180/S0026461X00006502 Published online by Cambridge University Press

Fluid inclusion study of a sediment-hosted copper ore deposit in the Lubin area (Poland)

JOANNA KOSTYLEW[1,2]* AND CHRISTOPH A. HEINRICH[1]

[1]Institute of Geochemistry and Petrology, ETH Zürich, Clausiusstrasse 25, 8092 Zürich, Switzerland (*correspondence: joanna.kostylew@erdw.ethz.ch)
[2]Institute of Geological Sciences, University of Wrocław, ul. Cybulskiego 30, 50-205 Wrocław, Poland

The sediment-hosted copper ore deposit in the Fore-Sudetic Monocline (Lubin area, SW Poland) is one of the largest in the world. Copper mineralization (Cu and Cu-Fe sulphides) follows a redox front (*Rote Fäule*) and occurs close to the contact between the uppermost Lower Permian terrestrial sandstones (*Rotliegendes*), and Upper Permian (*Zechstein*) marine deposits (including siliciclastics, shales, dolomites, and evaporates). Mineralization is characteristically vertically zoned, and the sulphide type is unrelated to the host-rock lithology. This deposit is believed to be an equivalent to the German *Kupferschiefer* copper ore formation.

Processes leading to the ore formation in the Lubin region can be better understood with a modern fluid inclusion study, combining of classical microthermometry with LA-ICP-MS analysis. This provides valuable data on temperature, pressure and chemical composition (including concentrations of major and trace elements in individual fluid inclusions) of the hydrothermal fluids.

Samples collected from the three deep mines (Lubin, Rudna and Polkowice-Sieroszowiec) represent a variety of rock types (from both oxidized and reduced zones). Fluid inclusions were found in various rock types, but the most abundant are calcite veins and calcite infills of cavities in dolomites. Fluid inclusions are generally very small (<10μm), but diameters range up to 20-50 μm. Three main fluid inclusion types were identified: (1) aqueous two-phase primary fluid inclusions of irregular shapes, with small vapor bubble sizes (5-10 vol.%); (2) square single-phase aqueous fluid inclusions, distributed in the outer parts of the crystals; and, (3) very small secondary aqueous fluid inclusions with medium vapor bubble sizes (30 vol.%), present in late cracks.

Our combined microthermometry and LA-ICP-MS analysis provides the first data on the origin and geochemical evolution of low-temperature hydrothermal fluids in the Polish *Kupferschiefer* ore formation.

Extreme pressure dependence of sulphur solubility in silicate melts (experimental data)

A.V. KOSTYUK* AND N.S. GORBACHEV

Institute of Experimental Mineralogy, Academica Osipyana 4, Chernogolovka, Russia (*correspondence: nastya@iem.ac.ru, gor@iem.ac.ru)

Physicochemical conditions of sulphur concentration within fluid-bearing magmas in the upper mantle and the earth crust during sulphide-silicate immiscibility are very important for understanding of origin of magmatic sulphide deposits. Influence of pressure on solubility of sulphur is still controversial [1-3].

We studied influence of pressure on the SCSS (sulphur concentration at sulphide saturation) in H_2O and H_2O+CO_2-bearing silicate melts. We used Pt-peridotite ampoules filled with powder of olivine basalt and synthetic sulphide $Fe_{30}Ni_{30}Cu_{30}S_{10}$ as starting compositions. The highest concentrations of sulphur were 0.88-1.01 and 0.2 wt.% in H_2O-and H_2O+CO_2-bearing silicate melts respectively at 1.5-2.0 GPa (Fig. 1). The minimum concentrations were 0.1-0.2 wt.% both at low (0.1-0.8 GPa) and high (2.5-4.0 GPa) pressure.

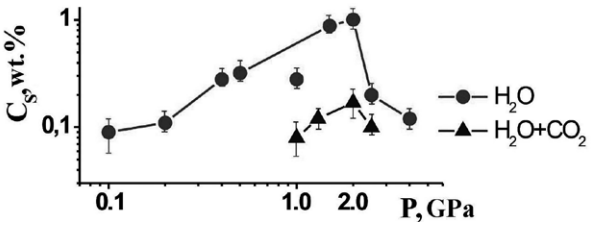

Figure 1: Relationships between pressure and SCSS in H_2O- and H_2O+CO_2-bearing silicate melts.

Inversion of relationships between pressure and SCSS in H_2O- and H_2O+CO_2-bearing silicate melts at P=1.5-2.0 GPa can be related to the inversion of volume effect of reactions and speciation of C, O, H and S in basalt melts at different pressure. Such inversion can play an important role in transport of sulphide sulphur and ore elements from the deep magmatic centres to the upper levels of the Earth crust where most of known sulphide ore deposits were discovered.

[1] Mavrogenes, O'Neill (1999) *Geochim. Cosmochim. Acta.* **63**, 1173–1180. [2] Mysen, Popp (1980) *Amer.J.Sci.* **280**, 78–92. [3] Wendlandt (1982) *Amer. Mineral.* **67**, 877–885.

https://doi.org/10.1180/S0026461X00006502 Published online by Cambridge University Press

New geochronological U–Pb isotopic data of granitoids from the Kuznetsk Alatau Ridge, SW Siberia

A.D. KOTELNIKOV AND V.V. VRUBLEVSKII

Tomsk State University

The Kuznetsk Alatau is a part of the Central-Asian mobile belt (CAMB) and represents the ensemble of the Caledonian fold-thrust structures. The Early Paleozoic large granitoid intrusives are extensively distributed on its south-east slope. The recent U-Pb isotope-geochronological data (SHRIMP-II) obtained by us from sparse grains of the accessory zircon enable three time borders to be established for the manifestation of the granitoid magmatism.

We have studied two massifs of the derivatives of the earliest Martaiga complex of the Middle Cambrian which are composed by quartz diorites, tonalites, granodiorites and plagiogranites. By the quartz diorites from these massifs, the concordant age of their intrusion has been established corresponding to the time interval T = 510 ± 7 and 506 ± 4 Ma. Subsequently, at the Cambrian-Ordovician transition, the formation of the Tigertysh granite complex has been in progress. The dating of granitoids in its three satellites has demonstrated the similar concordant age of their formation – T = 495 ± 8; 495 ± 5; 493 ± 8 Ma. In the closing stage of the development of the Early Paleozoic granitoid magmatism, the numerous small intrusions of the mixed composition has been going on in the region: from quartz-monzonites and diorite-porphyrites to granites and granite-porphyries. The isotopic dates T = 432 ± 4; 431 ± 6; 429 ± 6; 425 ± 4 Ma have been obtained from four rock varieties. This suggests the comparatively narrow time interval (Llandovery – Wenlock) for the final magmatic events in the Early Paleozoic. We assume that granitoids from the SE slope of the Kuznetsk Alatau aged 510–493 Ma, along with ultrabasite-basite massifs, granite batholites, alkali basaltoids, complexes of alkali rocks and carbonatites of the Caledonian stage of development CAMB (~ 510–470 Ma) seem to form the Early Paleozoic Large Igneous Province in its limits [1–3].

This study was funded by the Ministry of Education and Science of Russian Federation (project 2.1.1/208, Federal program of ‘Scientific and Scientific-Educational Personnel of Innovative Russia 2009-2013).

[1] Vladimirov *et al*. (1999) *Dokl. Earth Sci*. **369**, 795–798. [2] Izokh *et al*. (2007) In, *Abstr. Inter. Sympos. “LIPs of Asia, Mantle Plumes & Metallogeny”*, 30–32. [3] Vrublevskii *et al*. (2009) *Dokl. Earth Sci*. **427**, 846–850.

Fluid equilibria in water–salt (sodium fluoride, sulfate, carbonate) – silicate systems

Z.A. KOTELNIKOVA[1]* AND A.R. KOTELNIKOV[2]

[1]Institute of Geology of ore deposits of RAS. Staromonetny 35, Moscow, 119017, Russia (*correspondence: kotelnik@igem.ru)

[2]Institute of Experimental Mineralogy of RAS, Chernogolovka, Moscow district, 142432. Russia

Heterogeneous fluid equilibria in the P–Q_type H_2O–salt (Na_2CO_3, NaF, Na_2SO_4) systems in the presence of SiO_2 or SiO_2 + $NaAlSi_3O_8$ were studied experimentally at 700–800°C and P=1–3 kb. The method of synthetic fluid inclusions used. The microthermomemtric study of the synthesized inclusions showed that under experimental conditions the fluid did not remain inert with respect to quartz and albite and was heterogeneous. Some inclusions contained a glasslike phase, and liquid released from this phase by heating. Having been heated, some inclusions entrapped in the upper heterogeneous region, revealed liquid immiscibility in the presence of vapor within a temperature range of 200 to 400°C. The solutions of various concentrations, including oversaturated solutions in the presence of solid phase, underwent recurrent heterogenization. Near 400°C, vapor is either dissolved in one of immiscible liquids or absorbs this liquid.

Re-immiscibility of the liquid, entrapped in higher heterogeneous area is the significant peculiarity of studied system. Then heterogenization may take place in two (or more for multicomponent systems) stages at large scale of *TP*-parameters. The immiscibility is very sufficient mode of the matter re-distribution between immiscible phases. Owing to the multistage of that is important at the enrich or deplete of the fluid phase by specific components.

https://doi.org/10.1180/S0026461X00006502 Published online by Cambridge University Press

Discovery of diamond and coesite in Bohemian granulites

J. KOTKOVÁ[1,2]*, P.J.O'BRIEN[3] AND M.A.ZIEMANN[3]

[1]Czech Geological Survey, Klárov 3, 118 21 Prague 1, Czech Republic (*correspondence: jana.kotkova@geology.cz)
[2]Inst. of Geosciences, Masaryk University, Brno, CR
[3]Institute für Erd- und Umweltwissenschaften, Universität Potsdam, Germany

Microdiamond and coesite have been discovered in high-pressure granulites of North Bohemia. The newly found, 5-30 μm sized microdiamonds, documented by micro-Raman, occur as inclusions in garnet, kyanite and zircon. They range from well-formed octahedra in kyanite to ragged sub-rounded crystals in places forming clusters in garnet. Within garnet microdiamond commonly occurs with graphite, which forms also diamond-free aggregates of up to 0.1 mm in diameter with associated phases apatite, rutile, quartz and carbonate minerals whereas in kyanite associated graphite is minor. Diamond occurrence below the surface of the polished section, variable size and morphology and breakdown to graphite confirm the *in situ* origin. Coesite, with a thin rim of quartz, has been identified as an inclusion in kyanite which is itself completely enclosed in garnet, in one of the samples containing polycrystalline quartz aggregates. Thus the north Bohemian crystalline basement is an UHP terrane and it represents a fifth accepted location where diamond has been confirmed *in situ* in continental crust rather than mantle rocks (along with Kokchetav Massif, Kazakstan; Saidenbachtal, German Erzgebirge; Rhodope Massif, Greece and Qinling Mts., China).

The microdiamonds have been found in both felsic quartzofeldspathic and intermediate garnet-pyroxene granulites from exposures in the Eger Crystalline Complex as well as drill cores in the crystalline basement c. 50 km to the ENE. The Saidenbachtal in Central Erzgebirge, belonging to the same Variscan unit, is located c. 50 km to NNE. Whereas the Saidenbachtal diamond-bearing gneiss is an unusual, rare rock [1], our granulites are macroscopically indistinguishable from those covering thousands of square kilometers of the Variscan crystalline core. Garnet peridotites are commonly associated with these granulites. Our discovery indicates that the continental crust was subducted deep into the mantle and captured slices of mantle thus finally yielding an explanation for the long known but still disputed granulite - garnet-peridotite association. Further, it suggests that the Variscan belt may be one of the largest UHP terranes worldwide.

[1] Nasdala & Massonne (2000) *Eur. J. Mineral* **12**, 495–498.

The formation of organic molecules in solar system environments: The Miller-Urey Experiment in space preflight overview

J.M. KOTLER[1]*, P. EHRENFREUND[1], Z. MARTINS[2], A.J. RICCO[3], J. BLUM[4], R. SCHRAEPLER[4], J. VAN DONGEN[5], A. PALMANS[5], M.A. SEPHTON[2] AND H.J. CLEAVES[6]

[1]Leiden Institute of Chemistry, Leiden University, NL (*correspondence: J.M.Kotler@umail.leidenuniv.nl)
[2]Department of Earth Sciences and Engineering, Imperial College London, UK
[3]NASA Ames Research Center, Moffett Field, CA, USA
[4]Institute for Geophysics and extraterrestrial Physics, University of Braunschweig, D
[5]Department of Chemical Engineering, Technical University Eindhoven, NL
[6]Geophysical Laboratory, Carnegie Institute of Washington, Washington, DC, USA

The *Miller-Urey Experiment in space* (MUE) will investigate the formation of prebiotic organic compounds in the early solar system environment when it is sent to, and later retrieved from, the International Space Station in 2012. The dynamic environment of the solar nebula with the simultaneous presence of gas, particles, and energetic processes, including shock waves, electrical discharges, and radiation may trigger a rich organic chemistry leading to organic molecules. Two gas mixture compositions (CH_4, NH_3, H_2 and N_2, H_2, CO) will be tested and subjected to continuous spark discharges for 48, 96, and 192 hours. Silicate particles will serve as surfaces on which thin water ice mantles can accrete. The experiment will be performed at low temperatures (-5 °C), slowing hydrolysis and improving chances of detection of initial products, intermediates and their abundances. Conducting the Miller-Urey experiment in the space environment (microgravity) allows us to simulate conditions that could have prevailed in the low gravity, energetic early solar nebula and provides insights into the chemical pathways that may occur as planetary systems form.

https://doi.org/10.1180/S0026461X00006502 Published online by Cambridge University Press

Solute compositions and fluid residence times along an erosional gradient, Middle Fork of the Feather River, CA

C. KOUBA[1], K. MAHER[1], K. MAYER[1], K. YOO[2], B. WEINMAN[2], S. MUDD[3], M. HURST[3] AND M. ATTAL[3]

[1]Dept. of Geological & Environmental Sciences, Stanford, CA 94305 (*correspondence: kcouba@stanford.edu)

[2]Dept. of Soil, Water, and Climate, University of Minnesota, St. Paul, MN, 55108

[3]School of GeoSciences, University of Edinburgh, Edinburgh EH8 9XP, Scotland, UK

The residence time of water in the subsurface is known to be an important control on chemical weathering rates because longer contact times allow for waters to dissolve more minerals. A second control on weathering rates is erosion, which accelerates mineral dissolution by supplying fresh mineral to the soil environment from the bedrock below. However, on hillslopes erosion can also dramatically impact the hydrologic conditions. The rate of erosion may influence the slope of the terrain, the hydraulic gradient, and the amount of weathering products (e.g. clays and Fe-oxides). These effects result in shorter contact times and potentially decreased solute fluxes from rapidly eroding landscapes.

One conceptual model for assessing the relative importance of hydrologic and erosional processes is to consider the fluid residence time required to reach chemical equilibrium (which would determine the maximum solute flux) relative to the actual average fluid residence time of water in the hillslope. Weathering systems where these thermodynamic and physical time scales are closely matched should have the maximum rates of chemical denudation.

To test this model, we have studied the chemical and physical compositions solids and waters from three soil-covered hillslope transects within a tributary basin of the Middle Fork Feather River, CA. One of the hillslopes is located above the knickpoint, while the others are adjacent to and below the knickpoint. Water contents and solute chemistry are fairly constant across each hillslope but variable between hillslopes. In general, the solute concentrations are lowest in the soils of the steeper hillslopes suggesting that water residence time is an important factor.

A new methodology to experimentally determine water incorporation into upper mantle olivine and pyroxene

I. KOVÁCS[1,2], D.H. GREEN[2,3], A. ROSENTHAL[1], J. HERMANN[1], H.ST.C. O'NEILL[1], W.O. HIBBERSON[2] AND B. UDVARDI[1,4]

[1]Department of Data Management, Eötvös Loránd Geophysical Institute of Hungary, Colombus út 17-23, 1145, Budapest, Hungary (kovacsij@elgi.hu)

[2]Research School of Earth Sciences, The Australian National University, 0200, Canberra, ACT, Australia

[3]School of Earth Sciences and Centre for Ore Deposit Studies, University of Tasmania, Pte. Bag 79, Hobart, Tasmania, 7001, Australia (david.h.green@utas.edu.au)

[4]Lithosphere Fluid Research Lab, Eötvös University, Péter Pázmány sétány 1/C, 1117, Budapest, Hungray

This study explores experimentally the incorporation of water in olivine and pyroxene near the solidus of fertile lherzolite compositions at 2.5 and 4 GPa. A sensor-layer of olivine or pyroxenes was added to both sides of lherzolite material and their water contents were determined by Fourier-transform infrared spectroscopy. The IR absorption bands of the sensor crystals after the experiment are different from the bands present in the starting material, indicating that the sensor minerals equilibrated with the lherzolite material. The similarity of absorption characteristics in experimental runs to those from mantle derived rocks (summarised in the PULI spectral database) indicates that hydrogen defects in the sensor minerals can be successfully reproduced in chemically complex systems. Olivine, orthopyroxene and clinopyroxene contain 30-190, 290-320 and 910-980 ppm of water under the studied P-T conditions. The partition coefficients between orthopyroxene and clinopyroxene ($D^{cpx/opx}_{H_2O}$) are 2.7 and 3.5 at 2.5 and 4 GPa respectively, while values of $D^{opx/ol}_{H_2O}$ are ~7 and ~5, at 2.5 and 4 GPa respectively. Olivine and pyroxenes in our water-rich experiments display higher water concentrations than what is documented for most peridotites. They overlap only with the most water-rich natural samples from supra-subduction environments. Our experiments reproduce closely water-saturated conditions in the upper mantle in chemically analogue complex systems. Thus, our experimental strategy may be generally applied in the future for mapping out phase relations and maximum effective water storage capacity of the upper mantle.

https://doi.org/10.1180/S0026461X00006502 Published online by Cambridge University Press

Proxies for chemical weathering: Plio/Pleistocene red clay deposits from Hungary

J. KOVÁCS[1]*, B. RAUCSIK[1], G. ÚJVÁRI[2], A. VARGA[1] AND G. VARGA[3]

[1]Department of Geology, University of Pécs, H-7633 Pécs, Hungary (*correspondence: jones@gamma.ttk.pte.hu, raucsik.bela@gmail.com, andrea.varga.geol@gmail.com)
[2]Geodetic and Geophysical Research Institute, HAS, H-9400 Sopron, Hungary (ujvari@ggki.hu)
[3]Dept. Geomorphology & Quaternary Research, HAS, H-1112 Budapest, Hungary (eoliandust@gmail.com)

Introduction

Red clays in Hungary (Tengelic Red Clay Formation: TRCF; Kerecsend Red Clay Formation: KRCF) is overlain by loess paleosol sequences. The red clay sediments in the Carpathian Basin are known from both exposures and boreholes. The age of these formations is ~3.5–0.5 Ma.

Nature of clay mineral assemblages is primarily a function of climate, essentially affected by the length of time of weathering, slope, water-rock ratio, and water chemistry. Therefore, clay mineralogy, and geochemistry are considered to be a powerful tool for interpreting weathering conditions and paleoclimate.

Elemental oxide analyses of red clays were determined by x-ray florescence (XRF), and x-ray powder diffraction (XRD) was used for mineral identification. In this study, we aim to determine the changes of clay minerals due to chemical weathering and age.

Results

The older type (Beremend Mb, age: 3.3–2.4 Ma) of the TRCF is red kaolinitic clay containing typically disordered kaolinite, mixed-layer smectite/kaolinite, smectite and little gibbsite. It was formed in the local subaerial weathering crust in warm, humid, subtropical or monsoon climate. The younger member of the TRCF (age: 2.5–1.0 Ma) contains red (or 'reddish') clay beds. It contains relatively fresh material (illite, chlorite), the weathering products are predominantly smectite and goethite formed under warm and dry climate in environmental conditions of savannah and steppe or forest steppe. The basal red clay layers of the Paks Loess Fm. and KRCF (age: 1.7–0.5 Ma) contain similar material as the underlying red clays belonging to the younger member of the TRCF. The slightly but significantly lesser degree of weathering (more illite and chlorite, less smectite) indicates cooling of the climate.

The epithermal deposits as a potential source of Critical High-Tech Metals (Ga, Ge, In, Sb)

V.A. KOVALENKER

IGEM RAS, Russia, Moscow, 119017, Staromonetny per. 35 (kva@igem.ru)

In the recent evidences arise that some so-called 'Critical High-Tech Metals' of epithermal deposits are not only of academic interest. It is primarily concerns Sb and In which minerals in a number of deposits are appreciably accumulated. The IS-type epithermal deposits of Au-Ag-base metal usually accumulated in large of ore clusters (e.g. deposits Mexico, Peru, Romania, Serbia, Slovakia) can be considered as the potential source of Sb, produced by tetrahedrite - one of the main ore minerals. Some other deposits of this type (e.g. Tayoha, Goka in Japan, Prasolovskoe in Kunashir Island, Russia, etc) are enriched with In that is presented both, in the minerals (roquesite, sakuraiite, petrukite, and unnamed Zn-Fe-Ag-Cu-Sn-In-sulfides), and of high concentrations in sphalerite as well. In gold epithermal deposits of HS-type (e.g. Chelopech, Radka in Bulgaria) presence of Indium is provided mainly by high (to 4.7 wt. %) concentration in a sphalerite, unlike to rare roquesite. These and other similar deposits contain minerals of Ge (renierite, germanite, briartite, unnamed Cu-Fe-As-Ge-minerals) and Ga (gallite), as well. It is note, that considerable (to the first wt. %) concentrations of Ga are related to sphalerite too.

Thus contrary to existing conceptions that epithermal deposits mainly produce Au, Ag, as well as in some cases also Cu, Pb, Zn, some of these deposits already should be considered as byproducts sources of scarce rare, so-called Critical High-Tech Metals, such as Sb, In, Ge and, possibly Ga. While Sb, Ge, and Ga are more characteristic for IS-type deposits, In can accumulated in both types of epithermal mineralization.

This work was supported by ONZ RAS project 2-2 and RFBR project 10-05-00354.

Computation of Li equilibrium isotope fractionation between minerals and aqueous solution

PIOTR M. KOWALSKI AND SANDRO JAHN

GFZ German Research Centre for Geosciences, Telegrafenberg, 14473 Potsdam, Germany (kowalski@gfz-potsdam.de)

We present an efficient *ab initio* based computational method for prediction of the equilibrium isotope fractionation factors in the high pressure and temperature materials, including fluids. The method originates in the Bigeleisen and Mayer [1] approximation and requires only the knowledge of the force constants acting on the fractionating element. An important aspect of the proposed method is the explicit modelling of materials as continuous media. This allows for investigation of the expansion and compression effects, which influence the fractionation process in high -T and -P materials. We have tested our method by computing the Li isotope fractionation factors between complex Li-bearing crystalline solids (staurolite, spodumene and micas) and aqueous solution, and by comparison of the results with the existing experimental data [2]. We show that we are able to reproduce correctly the experimental isotope fractionation sequence: staurolite-fluid-mica-spodumene and reproduce the measured values within 1 ‰.

We also have investigated the predictive power of the widely used cluster approach, in which a fluid or solid is represented by a cluster of atoms and treated as a large molecule for derivation of the vibrational spectrum - the input for the computation of the equilibrium isotope fractionation factors. We show that representation of the aqueous solution by Li $(H_2O)_n$ cluster results in the correct estimation of the isotope fractionation at low pressure (P<1GPa) but dramatically fails even on the qualitative level for higher pressures. This is because when computing materials under extreme conditions one has to account for the volume effects, such as compression or expansion, and structural changes in the fluid. These effects cannot be modelled unambiguously using the cluster approach. The proposed method accounts for these effects and predicts increase of isotope fractionation with pressure, which is more realistic and in agreement with the recent high pressure (P=8GPa) measurements for spodumene [3].

[1] Bigeleisen J. & Mayer M.G. (1947) *J. Chem. Phys.* **15**, 262–267. [2] Wunder B. *et al.* (2006) *Contrib. Mineral. Petrol.* **151**, 112–120, Wunder B. *et al.* (2007) *Chem. Geol.* **238**, 277–290. [3] Wunder, B. Meixner, A. Romer, R. L. & Jahn, S. (2011) *Eur. Mineral.* in press. DOI, 10.1127/0935-1221/2011/022-2095

In situ $\delta^{18}O$ and Mg/Ca analyses of diagenetic and foraminiferal calcite: Implications for paleoceanographic proxy records

R. KOZDON*, D.C. KELLY, K. KITAJIMA, A. STRICKLAND AND J.W. VALLEY

WiscSIMS, Dept. of Geoscience, Univ. Wisconsin, Madison, WI 53706 USA (*correspondence: rkozdon@geology.wisc.edu)

The vast majority of planktic foraminiferal shells in deep-sea sediments are affected by various degrees of diagenesis; the effect on oxygen isotope ratios and minor/trace element abundances may be profound, but is debated. Previously, numerical models were applied to describe the oxygen isotope exchange during burial and recrystallization of deep-sea carbonate [1]. Furthermore, the partition coefficients for minor and trace element incorporation in diagenetic calcite are not clearly defined; in particular, the conversion of Mg/Ca ratios from diagenetically altered foraminiferal shells to water temperature is not straightforward.

We used an ion microprobe to analyze $\delta^{18}O$ and Mg/Ca in 200-500 μm sized diagenetic calcite crystallites cementing small aggregates of foraminiferal shells from the Early Paleogene section of ODP Site 865, Central Pacific. The $\delta^{18}O$ values of these diagenetic crystallites range from 0.1‰ to 2.2‰ [PDB] with an average of 1.2‰, and are in agreement with values predicted by numerical models [1]. The $\delta^{18}O$ of these diagenetic calcites are ~6‰ higher than that previously reported from *in situ* measurements of unaltered domains (basal areas of muricae) within planktic foraminiferal shells from the same core samples [2]. Thus, both the endmember biogenic and diagenetic $\delta^{18}O$ values are determined.

Mg/Ca of the diagenetic calcites range from ~25 to 100 mmol/mol with sharp gradients (variations of ~70 mmol/mol over 100 μm), implying complex, small-scale processes of dissolution and recrystallisation that are not reflected in the $\delta^{18}O$. The average Mg/Ca ratio of 60 mmol/mol confirms previous results from inorganic precipitation experiments [3] and is >10 times higher than the Mg/Ca of biogenic foraminiferal calcite. In contrast Mg/Ca ratios of diagenetically altered foraminiferal shells from the same core samples are not significantly elevated. Low Mg/Ca does not prove preservation of biogenetic values because the processes governing foraminiferal diagenesis differ from those that mediate the precipitation of interstitial cements.

[1] Schrag (1999) *Chem. Geol.* **161**, 215–224. [2] Kozdon *et al.* (2009) *Geochim. Cosmochim. Acta* **73**, A693. [3] Oomori *et al.* (1987) *Mar. Chem.* **20**, 327–336.

https://doi.org/10.1180/S0026461X00006502 Published online by Cambridge University Press

Mineral surface charge development in mixed electrolytes

PH.A. KOZIN AND J.-F. BOILY*

Department of Chemistry, Umeå University Umeå, Sweden
(*correspondence: jean-francois.boily@chem.umu.se)

Electrolyte ions play a central role in electric double layer formation at mineral/water interfaces. The presence of these ions in aqueous solutions is in fact essential for neutralizing charges of potential-determining ions (H^+, OH^-) coordinated to mineral surfaces. The charge-neutralizing capacity of electrolyte ions is notably controlled by their size-to-charge ratio as well as their ability at forming or breaking water structures. Although much has been learned through the study of Hofmeister-type series of ions, understanding effects of co-existing ions at mineral/water interfaces is central to the elucidation of multicomponent systems representative of geochemical settings.

This study was devised to follow charge development on surfaces of α- and γ-FeOOH submicron-sized particles in mixtures of NaCl and $NaClO_4$ electrolytes. Surface charge and zeta potential data notably show that end-member NaCl and $NaClO_4$ properties, such as capacitance and shear plane position, cannot be used to predict mixed systems (Fig. 1). Experiments on FeOOH particles of varied aspect ratios moreover point to important surface structural controls on these results as well. Mixed electrolyte systems are therefore likely to develop distinct interfacial water structures and ionic distributions.

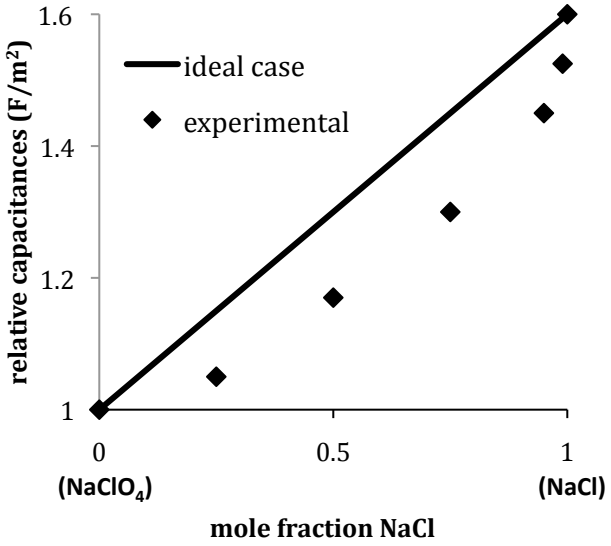

Figure 1: Relative capacitances of synthetic goethite (α-FeOOH) in mixed aqueous solutions of NaCl and $NaClO_4$. Total ionic strength 0.1M Na(Cl,ClO_4).

Comparative genome analysis of *Metallosphaera yellowstonensis* and a novel iron-oxidizing sulfolobales from Yellowstone National Park

M.A. KOZUBAL[1,*] AND W.P. INSKEEP[2]

[1]Department of Land Resources and Environmental Sciences and Thermal Biology Institute
(*correspondence: mark.kozubal@msu.montana.edu)
[2]Montana State University, Bozeman, MT 59717, USA
(binskeep@montana.edu)

Draft genomes have been completed for the iron and sulfur-oxidizing crenarchaea *Metallosphaera yellowstonensis* and Sulfolobales sp. strain MK5 (a novel member of the order Sulfolobales exhibiting only 89% 16S rRNA similarity to the closest *Sulfolobus* spp.). Both strains were obtained from a ferric iron mat within an acidic geothermal spring in YNP. This study compares the putative genes involved in iron and sulfur oxidation, heavy metal resistance, carbon fixation, and oxygen reduction between the two strains and with a diverse group of known iron-oxidizing acidophilic prokaryotes.

The draft genomes of each of these organisms contain sequences similar to putative iron-oxidizing open reading frames found in *M. sedula* and *S. tokodaii*, including a novel *fox* terminal oxidase gene cluster, a multicopper oxidase (*mco*), and the *cbs*AB-*sox*L2N operon. These genes differ considerably from the hypothesized cytochromes found in the genomes of *Acidithiobacillus ferrooxidans* and *Leptospirillum* sp. Group II. *M. yellowstonensis* and strain MK5 contain conserved heterodisulfide (*hdr*) gene clusters believed to be involved in the oxidation of elemental sulfur, as well as sequences that code for proteins involved in the oxidation of sulfide (*sqr*), sulfite (*som*), and thiosulfate oxidation (*tqo*). Multiple copies of the heme copper oxidase (HCO) subunit I were identified in both draft genomes. *M. yellowstonensis* also contains a *bd*-type terminal oxidase not found in other known members of the Sulfolobales.

M. yellowstonensis and strain MK5 are similar to other Sulfolobales in regards to genes involved in CO_2 fixation (i.e. 3-hydroxypropionate/ 4-hydroxybutyrate cycle) and heavy metal resistance; however, *M. yellowstonensis* is the only known archaeon to contain a methyl mercury lyase (*mer*B) gene. Analysis of gene sequence data suggest that, in addition to the diversity of HCO's, *M. yellowstonensis* and *Sulfolobales* strain MK5 exhibit novel mechanisms of iron oxidation, sulfur metabolism, autotrophy, and heavy metal resistance, all of which are consistent with the observed distribution of these organisms in high-temperature habitats of YNP.

https://doi.org/10.1180/S0026461X00006502 Published online by Cambridge University Press

Influence of different cleaning methods on seawater εNd extracted from planktonic foraminifera

STEFFANIE KRAFT[1]*, ED HATHORNE[1], MARTIN FRANK[1] AND SYEE WELDEAB[2]

[1]IFM-GEOMAR, Wischhofstr. 1-3, 24148 Kiel, Germany
[2]University of California, Santa Barbara, CA 93106-9630, USA

Seawater Nd isotope ratios extracted from foraminiferal calcite can be biased by contaminant phases, such as organic matter, ferromanganese coatings or secondary carbonates causing a shift towards bottom water signatures.

We compared two different cleaning methods to extract surface seawater neodymium isotope ratios from planktonic foraminiferal calcite. We used a modified version of the flow through method developed in [1] and a batch method following [2]. Single species samples (*G. menardii* and *G. ruber* pink) were obtained from core top sediments from the Gulf of Guinea to calibrate the method. Down core samples were investigated for paleoceanographic reconstruction of riverine input.

We tested the efficiency of two cleaning methods of the calcite by analysis of different element ratios (e.g. Al/Ca, Mn/Ca). The Al content was used as an indicator for successful clay removal whereas the Mn content reflects remaining early diagenetic coatings. Both elemental data and Nd isotope composition indicated indistinguishable levels of cleaning efficiency, whereby the batch method was less time consuming. For the different core top samples of our study clay particles had the strongest influence on the isotope and element ratios. To obtain a bottom water signature we analyzed mixed benthic foraminiferal carbonates from core top and down core samples. Additionally we compared these data with sediment leach data. The elemental ratios of the down core samples, both planktonic and benthic, showed elevated Mn/Ca ratios. To determine the origin of this contamination we analyzed the Fe/Ca and Mn/Fe ratios. The Mn/Fe ratios of planktonic and benthic samples presumably display different types of contamination.

In summary both planktonic and benthic foraminifera from the down core samples showed the same εNd values as the sediment leachates. Thus the Nd isotope compostition of the foraminiferal carbonate has most probably been overprinted by the bottom water isotope composition.

[1] B.A. Haley, G.P. Klinkhammer (2002) *Chemical Geology* **185**, 51–69. [2] D. Vance, K. Burton (1999) *Earth & Planetary Science Letters* **173**, 365–379.

Use of sequential extractions to evaluate the mobility of heavy metals in the Huanuni basin (Bolivia)

M. KRALJ[1]*, M. MARCHESI[2], E.DINELLI[1], A. SOLER[2], S.LAFUENTE[3] AND F.CORONADO[3]

[1]CIRSA, University of Bologna, 48100 Ravenna, Italy (*correspondence: martina.kralj2@unibo.it)
[2]MAIMA, Universitat de Barcelona, Barcelona, 080028, Spain (massimo.marchesi@ub.edu)
[3]PQII, Universidad Tecnica de Oruro, Bolivia

Water and sediment quality in the Huanuni river basin is affected by acid mine drainage (AMD) from three main mines (mainly on cassiterite deposits). The area, with a population over 50.000 inhabitants approx., is located in the Oruro department, Bolivia. Concentrations of trace metals and REE were determined in stream waters, groundwater wells, suspended materials and bedload sediments. Moreover, a BCR sequential extraction (four-stage) were applied in bedload and suspended sediment in order to better constrain mobility and relative sources of trace metals and REE.

The main stream and tributaries waters are characterized by strongly acidic conditions (pH 2.9-4.5), elevated SO_4^{2-} concentrations (up to 2400 mg/L), and high metal contents (especially Fe, Zn, Cd, Ni, Pb). Hydrochemistry coupled to sequential extraction allow the characterization of the contribution of the three considered main mines.

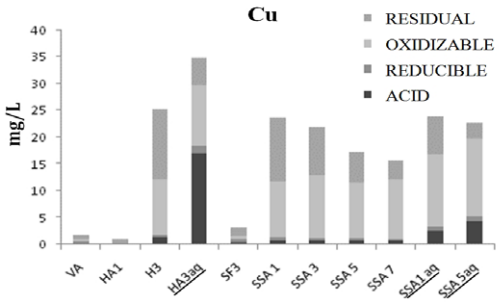

Figure 1: Cu concentration and fractionation pattern

The sequential extraction shows differences in partitioning and total concentration between suspended (in the figure indicated as codeaq, e. g HA3aq) and bedload sediment (e.g. HA3), with higher metal concentrations and exchangeable fraction in the suspended material. Cd, Zn and Cu (only Cu shown in Fig.1) seem related to the oxidizable fraction, whereas Cr and Ba with the reducible fraction.

Preliminary results suggest prioritizing remediation efforts on the suspended sediment.

https://doi.org/10.1180/S0026461X00006502 Published online by Cambridge University Press

Modeling of soil degradation in the Czech critical zone observatories

P. KRAM* AND J. HRUSKA

Czech Geological Survey, 11821 Prague 1, Czech Republic
(*correspondence: pavel.kram@geology.cz)

Three small catchments situated 5-7 km apart, with similar forest cover (Norway spruce), but underlain by contrasting bedrocks served as critical zone observatories (CZO). Sites are situated in the geochemically diverse Slavkov Forest [1] close to power plants with large S emissions in 1950s - mid 1990s. The MAGIC model [2] was used to simulate soil and water chemistry. Model parametrization at Lysina (LYS, area 27 ha, podzol on leucogranite) and Pluhuv Bor (PLB, 22 ha, stagnosol on serpentinite) was based on published data [3]. Parametrization at Na Zelenem (NAZ, 55 ha, cambisol on amphibolite) was based on recent sampling [4]. Simulated soil base saturation (BS) declined from 20% to 6% at LYS, from 56% to 31% at NAZ, and from 94% to 88% at PLB (Fig. 1). Contrasting soil and drainage water compositions were generated mainly by differences in chemical weathering rates of divalent base cations, Ca and Mg (0.4 keq/ha/a at LYS, 1.5 keq/ha/a at NAZ, and 2.4 keq/ha/a at PLB).

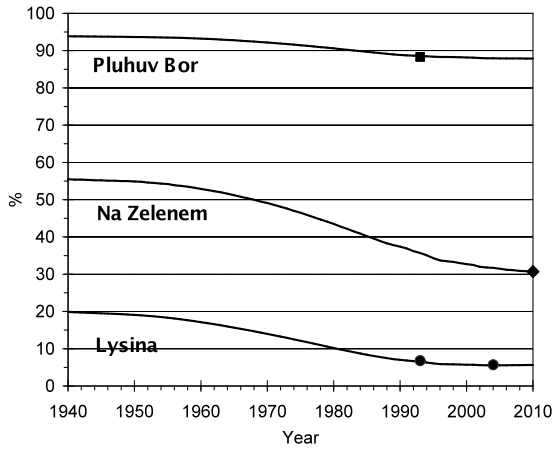

Figure 1: Simulated (lines) and measured (dots) soil base saturation at three Czech CZO in the Slavkov Forest.

[1] Kram (2010) *Geochim. Cosmochim. Acta*. **74**, A537. [2] Cosby *et al*. (2001) *Hydrol. Earth System Sci*. **5**, 499–517. [3] Hruska & Kram (2003) *Hydrol. Earth System Sci*. **7**, 525–539. [4] Rousseva *et al*. (2010) Datasets on soil physical, geochemical & biological properties. SoilTrEC Report.

Plant-microbe interactions in Cd-contaminated soils - Do Fe(III)-reducing bacteria influence the accumulation of Cd in the metal-hyperaccumulating plant *Arabidosis halleri*?

U. KRÄMER[1]*, E.M. MUEHE[2] AND A. KAPPLER[2]

[1]Plant Physiology, University of Bochum
(*correspondence: Ute.Kraemer@ruhr-uni-bochum.de)
[2]Geomicrobiology, University of Tuebingen

Soils worldwide have increasingly been contaminated with industrial waste metals, such as cadmium, which may subsequently enter the food chain through plants. These toxic metals can have dramatic effects on human and environmental health. Therefore, there is a need for the development and application of new techniques to efficiently remediate contaminated soils. In the present study, we combined phytoremediation and (microbially) enhanced natural attenuation to determine whether a more time- and cost-efficient removal of cadmium from contaminated sites can be achieved. In plant-microbe-soil microcosms, geochemical and microbial parameters are determined to trace the microbial release of cadmium from Cd-bearing Fe (III) minerals by the natural microbial community of the soil or by an isolated Cd-tolerant Fe (III)-reducing bacterium. Additionally, cadmium uptake and accumulation by the metallophyte Cd hyperaccumulator plant *Arabidopsis halleri* in the presence of these bacteria is quantified. Cadmium is made phytoavailable to the plant by the stimulation of naturally occurring Fe (III)-reducing bacteria which release cadmium from Fe (III) (hydr)oxides through reductive dissolution. Subsequently, the aqueous cadmium is actively taken up by the plant *A. halleri* and accumulated in the above ground tissue. By harvesting the plant regularly, an efficient removal of cadmium from contaminated sites may be achieved.

https://doi.org/10.1180/S0026461X00006502 Published online by Cambridge University Press

Calcium carbonate precipitation by the marine cyanobacterium *Trichodesmium*

SVEN A. KRANZ*, DIETER WOLF-GLADROW, GERNOT NEHRKE, GERALD LANGER AND BJÖRN ROST

Alfred Wegener Institute for Polar and Marine Research, Bremerhaven, Germany (*correspondence: Sven.kranz@awi.de, Dieter.Wolf-Gladrow@awi.de, Gernot.Nehrke@awi.de, Gerald.Langer@awi.de, Bjoern.Rost@awi.de)

Cyanobacteria are important primary producers of the contemporary oceans and have affected global biogeochemical cycles over geological timescales. The diazotrophic *Trichodesmium spp*. are known for their large-scale blooms and substantial input of 'reactive nitrogen' to the oligotrophic subtropical and tropical areas. In this laboratory study, we monitored the buildup of biomass and concomitant shift in seawater carbonate chemistry over the course of a *Trichodesmium* bloom under different phosphorus (P) availability. During exponential growth, dissolved inorganic carbon (DIC) decreased while pH increased until maximum cell densities were reached. Once P became depleted, DIC decreased even further and total alkalinity (TA) dropped, accompanied by precipitation of aragonite. Under P-replete conditions, DIC increased and TA remained constant in the post bloom phase while no aragonite was formed. A diffusion-reaction model was employed to estimate changes in carbonate chemistry of the diffusive boundary layer of an aggregate of *Trichodesmium*. This study demonstrates that *Trichodesmium* can induce precipitation of aragonite from seawater and further provides possible explanations about underlying mechanisms.

Parental melts of Avachinsky volcano (Kamchatka) recorded in melt inclusions

S. KRASHENINNIKOV[1]* AND M. PORTNYAGIN[1,2]

[1]V.I.Vernadsky Institute of Geochemistry and Analytical Chemistry, ul. Kosygina 19, Moscow 119991, Russia (*correspondence: spkrasheninnikov@mail.ru)

[2]Leibniz Institute of Marine Research, IFM-GEOMAR, Wischhofstrasse. 1-3, D-24148 Kiel, Germany

We studied ca. 700 melt inclusions (MIs) in 6 major minerals (Ol, Opx, Cpx, Pl, Amph and Mt) from 61 Holocene andesitic and basaltic andesites tephra of Avachinsky volcano erupted during the last 10 ^{14}C ky.

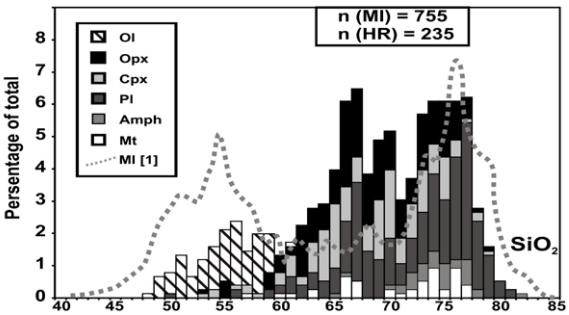

Figure 1: MIs compositions in Avachinsky tephra depending on host mineral phase. Dotted line – compilation of MIs from island-arc rocks after [1].

MIs have low-K to middle-K basaltic to rhyolitic compositions (fig. 1). The continuum of MIs can be well explained by fractional crystallization from parental basaltic melts. No apparent bimodality is observed in the dataset in comparison with [1, 2]. Melts of intermediate compositions are abundant and commonly found in minerals from basaltic andesites. In comparison with the host rocks, MIs have systematically more silicic compositions, and this difference increases with increasing SiO_2 content in the host rocks. Dacitic and rhyolitic MIs predominate in our dataset due to the prelevance of basaltic andesites and andesites on Avachinsky volcano.

These results show that the previously reported bimodality of MIs in island-arc rocks [1, 2] may result from unrepresentative sampling and does not reflect true volume proportions of melts with different SiO_2 content in island-arcs.

[1] Reubi & Blundy (2009) *Nature* **461**(7268) 1269–1273.
[2] Naumov *et al*. (1997) *Petrology* **5**, 586–596.

https://doi.org/10.1180/S0026461X00006502 Published online by Cambridge University Press

Mantle peridotites from the Stalemate F.Z. (NW Pacific)

E. KRASNOVA[1], M. PORTNYAGIN[1,2], S. SILANTYEV[1], R. WERNER[2] AND K. HOERNLE[2]

[1]V.I.Vernadsky Institute of Geochemistry and Analytical Chemistry, Kosygin St. 19, 119991 Moscow, Russia
[2]Leibniz Institute of Marine Sciences, IFM-GEOMAR, Wischhofstr. 1-3, 24114 Kiel, Germany

The Stalemate Fracture Zone (SFZ) is a 500 km long SE-NW trending transverse ridge between the northernmost Emperor Seamounts and the Aleutian Trench, which originated by flexural uplift of Cretaceous (?) oceanic lithosphere along a transform fault at the Kula-Pacific plate boundary [1].

The lithosphere cropping out along the NW flank of the SVZ was sampled by dredging during the R/V Sonne cruise SO201-KALMAR Leg 1b. Strongly altered mantle rocks ranging from pyroxene-rich lherzolites and pyroxene-poor dunites were obtained at the station DR37 at the northern SVZ bend. The compositions of primary minerals (*Cpx*, *Opx*, *Sp*) change systematically from lherzolites to dunites. *Sp* in lherzolites has higher Mg#, NiO, lower Cr#, Fe^{3+}# and TiO_2 (Mg#=0.65-0.68, NiO=0.26-0.34 wt%, Cr#=0.26-0.33, Fe^{3+}#=0.021-0.030, TiO_2=0.04-0.09 wt%) than spinel in dunites (Mg#=0.56-0.64, Cr#=0.38-0.43, TiO_2=0.19-0.28 wt%, NiO=0.19-0.26%, Fe^{3+}#=0.027-0.043). *Cpx* in lherzolites is moderately Mg- and Ni-rich, Ti- and Na-poor, has lower Cr# (Mg#=91.7-92.4, Cr#=0.12-0.16, TiO_2=0.06-0.15 wt%, Na_2O=0.19-0.41 wt%, NiO=0.06-0.09 wt%) and is extremely MREE- and Zr-depleted (C1-normalized Yb_n=4.0-5.6, Sm_n/Yb_n=0.05-0.14, Zr_n/Y_n=0.001-0.009) compared to clinopyroxenes analyzed in a sample of dunite DR37-3 (Mg#=93.7, Cr#=0.16, TiO_2=0.23wt%, Na_2O=0.85wt%, NiO=0.06wt%, Yb_n=5.7-7.4, Sm_n/Yb_n=0.22-0.27, Zr_n/Y_n=0.22). Some *Cpx* from lherzolites have flattened or strongly U-shaped patterns of REE (Sm_n/Yb_n=0.11-0.49, La_n/Sm_n=0.36-3.6) though their major element composition is indistinguishable from the more LREE depleted *Cpx*.

The variations of *Cpx* and *Sp* compositions can be explained by the two-stage process [2]: 1) near fractional melting of depleted mantle to 10-12%, 2) interaction of the residual lherzolite with N-MORB-like melts to form dunites. The protolith of lherzolites and dunites dredged from the SFZ can thus represent disintegrated parts of shallow oceanic mantle variably modified by melt percolation.

[1] Lonsdale (1988) *GSA Bulletin* **100**, 733–754. [2] Kelemen, Shimizu, Salters (1995) *Nature* **375**, 747-753

Unusual apatite crystals and pegmatites with Rare Earth Elements tetrad effect

STEPAN KREJSEK[1] AND JINRICH KYNICKY[2]

[1]Masaryk University, Faculty of science, 611 37 Brno (krejsek.stepan@seznam.cz)
[2]Mendel University in Brno, 613 00 Brno, Czech Republic (jindrich.kynicky@mendelu.cz)

Dolní Bory pegmatite deposit in the Czech Republic, display well developed zonality and different concentrations of rare earth elements with chondrite-normalized patterns that show a clear convex tetrad effect. Similar patterns and zonality exhibit also apatite crystals (Fig. 1). The Y/Ho and Sr/Eu ratios and very high Y and U content of the apatite samples correspond with evolved fractionation relative to the corresponding chondritic values. Based on the La/Lu, Sr/Eu and Y/Ho ratios of apatite, the apatite zones can be divided into two main groups which reflect two main stages of magma-fluid evolution, namely, a magmatic and a magmatic hydrothermal transition stage.

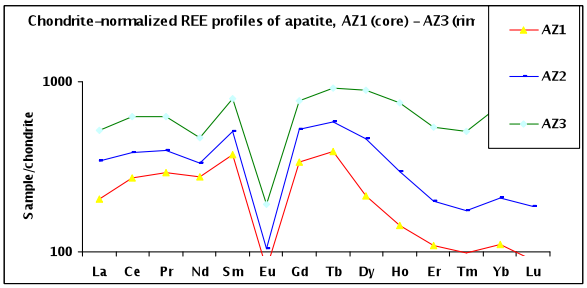

Figure 1: Chondrite-normalized REE profiles (apatite).

Interaction of a most evolved parental fluid with already formed pegmatite matrix and apatite probably produced the strongest REE tetrad effect in the youngest white zones of apatite rims (AZ3).

https://doi.org/10.1180/S0026461X00006502 Published online by Cambridge University Press

Deciphering the early fossil record of cyanobacterial mats based on their mode of mineralization

B. KREMER[1], J. KAZMIERCZAK[1] AND S. KEMPE[2]

[1]Institute of Paleobiology, Polish Academy of Sciences, Twarda 51/55, 00-818 Warsaw, Poland (kremer@twarda.pan.pl)
[2]Institut für Angewandte Geowissenschaften, Technische Universität Darmstadt, 64287 Darmstadt, Germany

Archean traces of life are vague and confusing due to poor preservation. Identifying traces of life in early geological record requires understanding the mode of fossil formation. Carbonaceous matter, although abundant in many Archean deposits, does not *per se* prove presence of life. Key to decipher earliest life forms could be their mode of mineralization. Etching of Neoarchean carbonates (Nauga Fm, South Africa) revealed coccoid cyanobacterial mats preserved as web-like structures composed of pits, mineralized with $CaCO_3$, and walls permineralized with Al-Fe-Mg-K silicates [1, 2].

Similarly permineralized web-like structures commonly occur in modern coccoid cyanobacterial mats. Studies on such mats from Lake Van (Turkey), Niuafo'ou Island (Tonga), and Satonda (Indonesia) showed that after death the mats undergo mineralization. The type of mineral phase(s) and the rate of mineralization depend chiefly on geochemical conditions within the degraded biomass. First to decompose is the cellular content and the thin mucilage sheaths surrounding individual cells and smaller groups of cells. Therefore cells are only exceptionally preserved. The most durable parts of the mat are the thicker outer web-like mucilagenous sheaths, which due to early permineralization with $CaCO_3$ and silicates, are fossilized.

Early diagenetic calcification and silicatization is associated with post mortem activity of heterotrophic bacteria. Bacteriolysis liberates cations complexed during cyanobacterial lifetime in their EPS. This process enhances mineral precipitation in the bacterially degraded mucilage sheaths and preserves their web-like texture. Morphology and mineral composition of Neoarchean web-like structures resemble those of modern mineralized cyanobacterial mats and can therefore be regarded as biosignatures of benthic coccoid cyanobacterial mats.

[1] Kazmierczak, J. Altermann, W. (2002) *Science* **298**, 2351.
[2] Kazmierczak, J. *et al*. (2009) *Precambrian Research* **173**, 79–92.

Density functional study of uranyl adsorption on solvated surfaces of clay minerals

ALENA KREMLEVA, SVEN KRÜGER AND NOTKER RÖSCH

Department Chemie & Catalysis Research Center, Technische Universität München, 85748 Garching, Germany (roesch@mytum.de)

Actinide adsorption on clay mineral surfaces represents an important retardation mechanism for these metal ions. With the topical issue of safe disposal of radioactive waste in mind, it is important to gain comprehensive knowledge of the environmental chemistry of radioactive elements and their compounds, where the interaction of actinides with mineral surfaces in general plays an important role. Various experimental techniques are being used to examine these issues, and these results are favorably complemented by computational chemistry studies.

We explored uranyl adsorption on solvated clay minerals with the plane-wave based projector augmented wave approach as implemented in the program VASP. Neutral 1:1 layered kaolinite was considered as a simple model clay mineral. We focused on (001) basal aluminol and (010) edge surfaces. Solvation plays a crucial role when modeling the latter type of surfaces. These effects were approximated by including a mono- or bi-layer of adsorbed water in the quantum mechanical models.

We mainly explored bidentate inner-sphere adsorption complexes on deprotonated sites representing neutral or slightly higher pH. Uranyl adsorption on kaolinite edge surfaces commonly leads to a deprotonation of aqua ligands of uranyl, resulting in monohydroxide as adsorbate. Aluminol adsorption sites are preferable for uranyl adsorption compared to mixed aluminol-silanol sites. The geometry of adsorption complexes is compared to available experimental results. Overall, complex formation energies suggest that several adsorbed species may simultaneously be present at kaolinite surfaces.

https://doi.org/10.1180/S0026461X00006502 Published online by Cambridge University Press

Speciation and micro-scale spatial distribution of As in a mining-affected river floodplain

R. KRETZSCHMAR[1]*, P. MANDALIEV[1], C. MIKUTTA[1], K. BARMETTLER[1] AND T. KOTSEV[2]

[1]Institute of Biogeochemistry and Pollutant Dynamics, ETH Zurich, Switzerland
(*correspondence: kretzschmar@env.ethz.ch)
[2]Institute of Geography, Bulgarian Academy of Sciences, Sofia, Bulgaria

Many rivers worldwide are polluted with trace elements originating from past or present mining. Even after closure and remediation of the mines, highly contaminated floodplains often remain as a source of contaminant release into river and ground water. Arsenic (As) has a high potential for mobilization unter reducing conditions, e.g. during soil flooding, but this strongly depends on the speciation of As among other factors.

We studied the speciation and micro-scale distribution of As in alluvial soils and sediments along the river Ogosta in NW-Bulgaria. Ogosta, an important tributary to the lower Danube river, was strongly affected by mining of Au, Fe, and Pb/Ag between 1951 and 1999.

Soil samples were collected along transects ranging from the river bed through the lower and upper floodplains, taking special precautions to minimize oxidation. All samples were analyzed for soil pH, mineralogy, elemental composition, and oxalate-extractable As and Fe. Arsenic speciation was investigated by As K-edge X-ray absorption spectroscopy (XAS). Thin sections of undisturbed soil were prepared and examined by micro-X-ray fluorescence (μ-XRF) spectrometry and μ-XAS. Additionally, selected soils were size-fractionated to explore the elemental composition, mineralogy, and As speciation as a function of particle size.

Soil As concentrations in the floodplain ranged between 40 and 37, 400 mg kg^{-1}. Highly As-contaminated soils were also enriched in Fe, Mn, S, Pb, Sb, and other trace elements. Bulk and micro-XAS, combined with oxalate-extractions, revealed that most As was present as As (V) sorbed to poorly-crystalline Fe (III)-oxyhydroxides, with smaller amounts of As bound in arsenopyrite. The fine particle size fractions <5 and 5-20 μm were strongly enriched in As (up to 93, 000 mg kg^{-1}) as compared to the corresponding bulk soils. These size separates contained only traces of arsenopyrite and exhibited very high oxalate-extractable As and Fe contents, reaching molar Fe/As ratios of <5. Our results suggest that As and Fe in these soils should be readily bioavailable for microbial reduction upon soil flooding.

Groundwater Recharge in the Santo Tomás Valley, Baja California, México

T. KRETZSCHMAR* AND W. THOMAS

CICESE, Ensenada, Mexico
(*correspondence: tkretzsc@cicese.mx)

Overview

The purpose of this study is to better understand Mountain Front Rrecharge (MFR) and Mountain Block Recharge (MBR) in a mountainous watershed in Baja California by creating a detailed fracture-trace map of the Santo Tomas basin along with stable isotope (O, H) and chemical analyses of spring water (thermal and cold), groundwater, and stream runoff throughout the study area.

This study focused on the topography, geology, vegetation and hydrologic characteristics of the eastern section of the Santo Tomas valley, located approximately 50 km southeast of Ensenada. Each method used in study was completed with the intention to integrate all data to better understand MBR in the study area.

Methods

Models of elevation, slope, lithology, vegetation, and fractures within the 300 km^2 watershed were created to help characterize the basin. Images were generated in ArcMap, using DEM data, field observations, and LandSat satellite imagery. Each visual was examined individually as well as in conjunction with other physical and chemical parameters to better understand the dynamic of the watershed.

Results

The stable isotope ($\delta^{18}O$ and $\delta^{2}H$) data show two distinct types of spring water within the watershed representing local and regional flow paths. Thermal springs, display a -1.9‰ $\delta^{18}O$ depletion compared to the other spring water, indicativing a higher elevations recharge or older waters. This distinct isotopic signal was found 15 km downstream in the alluvial aquifer, showing that a significant amount of water is recharging the basin aquifer via the mountain block along this flow regime. The thermal system and most cold-water springs surface along active faults, which appear to transmit more water than the undifferentiated fractures. An isotopic distinction can be seen between the hot and cold springs within the watershed despite that all the spring samples are taken between 400 - 550 m elevation.

https://doi.org/10.1180/S0026461X00006502 Published online by Cambridge University Press

Heavy minerals in the Kafue River sediments, Copperbelt Mining District, Zambia: Indicators of industrial contamination

B. KŘÍBEK[1]*, F. VESELOVSKÝ[1], I. KNÉSL[1] O. SRACEK[2], M. MIHALJEVIČ[3] AND V. ETTLER[3]

[1]Czech Geol. Survey, Geologická 6, 152 00 Prague 5, Czech Republic (*correspondence: bohdan.kribek@geology.cz)
[2]University Palacky, 17. listopadu 12, 771 46 Olomouc, Czech Republic
[3]Charles University, Faculty of Science, Albertov 6, 128 43 Prague 2, Czech Republic

Sediments of the Kafue River that drains the whole of the Copperbelt region were found to contain up to 1 wt% Cu, 0.1 wt% Co, 1.3 wt.% Mn and a number of other toxic elements like Pb, As and Hg. The study of heavy minerals in both types of sediments was intended to identify the sources of contamination. Heavy minerals found in uncontaminated sediments of this river comprise mostly of ilmenite, limonite, rutile, amphibole and tourmaline, while apatite, clinochlore epidote and zircon are minor. On the other hand, the contaminated sediments contain, besides rock-rorming minerals, chalcopyrite, pyrite, bornite, malachite and azurite the concentrations of which vary considerably. Chalcopyrite and pyrite evidently come from leaks of tailings still in operation in which the sulfides were not yet oxidized. Washing out and erosion of old flotation tailings ponds are responsible for enhanced contents of malachite, azurite, bornite, copper metal and chrysocolla together with limonite with high contents of copper and other elements in the contaminated Kafue River sediments. Particles of slag rich in magnetite and also particles of intermediate solid solution of Cu-Fe-S (ISS) affected by various degree of oxidation were found in sediments close to the smelters. The identification of heavy metals and their relative proportions enabled to assess the extent of contamination of stream sediments and also the character of individual sources of contamination. No extensive dissolution of copper and cobalt minerals in stream sediments takes place due to the neutral or slightly alcaline character of surface water in the area. However, occassional accidents in chemical plants processing copper and cobalt concentrate (acid spikes) result in short term but sharp increase in acidification of surface water (pH 3-4) which consequently leads to sharp increase in copper contents in these water. The study originated within the UNESCO/IGCP 594 Project 'The impact of ore mining and processing on the environment and human health in Africa'.

Combining phase petrology, reaction balancing and partial pseudosections – Theory and examples

L.M. KRIEGSMAN[1]* AND A.M. ÁLVAREZ-VALERO[1,2]

[1]NCB Naturalis, Leiden, The Netherlands (*correspondence: Leo.Kriegsman@ncbnaturalis.nl)
[2]Dept. of Earth, Atmospheric and Planetary Sciences, MIT

Both classical phase petrology and phase diagram modelling by pseudosections have their strengths and weaknesses. Phase petrology is well suited for generic P-T grids and phase diagrams in relatively simple chemical systems or subsystems (e.g. KFASH in metapelites), but is hard to use in more complex systems, unless pure phases exist from which to project. Pseudosections [1, 2] are complementary to grids in portraying all reactions that may potentially operate in a given bulk composition as a function of P and T. Both petrological tools assume equilibrium conditions that may not always be appropriate. Reaction overstepping, re-entering of inclusions into a reacting assemblage during host breakdown, kinetic barriers, etc., all highlight the local absence of equilibrium or the operation of patchy equilibrium [3]. In addition, pseudosections assume constant bulk chemistry, which may be invalid during melt loss [2] and when certain phases (e.g. inclusions) or cores of zoned minerals do not participate in a reaction [3].

Hence, deriving P-T-t paths is a subtle process that requires a multi-faceted approach combining textural analysis, mineral chemistry, reaction balancing [4], qualitative pseudosections using model reactions [5], quantitative P–T pseudosections for selected microdomains, and thermobarometry on selected textures apparently close to equilibrium. In addition, P-T vectors may be constrained by modelling of reaction line slopes [6], a technique that merits far more attention and use. Examples are given from migmatites (Finland), granulites (Sri Lanka) and xenoliths (Spain) to highlight this approach.

[1] Hensen (1971) *CMP* **33**, 191–214. [2] White *et al*. (2001) *JMG* **19**, 139-153. [3] Stüwe (1997) *CMP* **129**, 43–52. [4] Álvarez-Valero & Kriegsman (2010) *Lithos* **116**, 300–309. [5] Cenki *et al*. (2002) *JMG* **20**, 543–561. [6] Kriegsman (1996) *CMP* **126**, 38–50.

https://doi.org/10.1180/S0026461X00006502 Published online by Cambridge University Press

Trace and REE geochemistry of the Angola Basin sediments

E. KRIKUN, M. RIMSKAYA-KORSAKOVA AND A. DUBININ

P.P. Shirshov Institute of Oceanology RAS, Moscow, Russia (evgenia.krikun@gmail.com)

We studied chemical composition of sediment core samples collected from the Angola Basin (23°30´S, 4°17´W, 4990 m depth). Oxidized pelagic foraminifera oozes (60-98 wt% carbonate) represent the recovered core (length 210 cm). Mn and reactive Fe concentrations range from 0.1 to 0.3 % and decrease with $CaCO_3$ increase. The contents of Co, Ni, Mo and U along the core correlate with Mn concentrations due to scavenging on Mn-oxyhydroxides. Concentrations of REE decrease with $CaCO_3$ content increase. The values of Ce-anomaly range from negative in carbonate- rich sediments to positive in the carbonate-depleted layers. The concentrations of REE and Th correlate with reactive Fe content ($r > 0.9$). REE pattern indicates its hydrogenous origin.

Using negative correlation of each rare earth and carbonate concentration ($r>-0.9$), we calculated REE compositions in 100% $CaCO_3$. The latter is consistent with REEs in Atlantic ocean foraminifera from Palmer [1]. REE pattern of red clay component was obtained by extrapolation to 0% $CaCO_3$, and coincide with mean composition of pelagic red clays from Brazil Basin located symmetrically across the MAR. The REE are originated from the two main sources: biogenic carbonate and red clay component, and could be defined with variable content of these constituents. Biogenic carbonate is characterized with Ce depletion and low concentrations of REE, red clay component has positive Ce-anomaly and higher concentrations of trivalent REE.

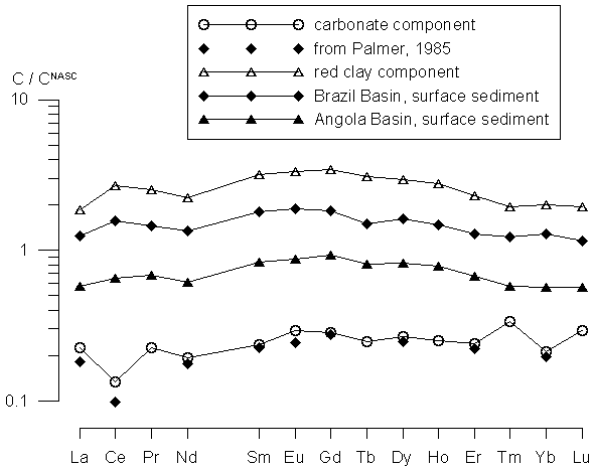

[1] Palmer (1985) *Earth & Planet. Sci. Lett.* **73**, 285–298.

Volatiles in Siberian flood basalts: Melt inclusions study

N.A. KRIVOLUTSKAYA[1]*, A.V. SOBOLEV[1,2,3], N.M. SVIRSKAYA[1], I.K. NIKOGOSIAN[1], S.G. SIMAKIN[1] AND D.V. KUZMIN[3]

[1]Vernadsky Institute of Geochemistry, RAS, 119991 Moscow, Russia (*correspondence: nakriv@mail.ru)

[2]ISTerre, University J. Fourier BP 53, 38041 Grenoble Cedex 9, France (alexander.sobolev@ujf-grenoble.fr)

[3]Max Planck Institute for Chemistry, Postfach 3060, 55020 Mainz, Germany

We report major, trace and volatile elements (Cl, F, B, S, H_2O) contents in melt inclusions in clinopyroxene phenocrysts from the Southern Maslovsky intrusion (Norilsk region) studied by EPMA, SIMS and LA-ICPMS technics. Modelling by PETROLOG software [1, 2] suggests that melts were saturated by both olivine (Fo 76-68) and CPX (Mg#78-69) and crystallized at shallow depth (below 100 MPa pressure) in the temperature range 1130-1080ºC. Incompatible elements patterns of melts are similar to typical Siberian flood basalt (La/Sm_n=1.4, Nb/La_n=0.6, Gd/Yb_n=1.1).

Melts are undersaturated by sulphur and have S/Dy=200, (150-300), markedly lower than for MORBs and OIBs (250-300, [3]). Water contents are variable (H_2O=0.08-0.45wt%) suggesting low pressure degasing of melt. The highest concentrations yields H_2O/Ce over 160, close to the typical range of OIB and MORB [3]. Chlorine and boron show significant excesses yielding Cl/K= 0.29, (0.24-0.40); B/K= $0.9*10^{-3}$, ($0.6\text{-}1.2*10^{-3}$), which are few times higher than those for typical MORB and OIB [3]. Contents of fluorine F/Ti= 0.045 (0.021-0.056) and F/Nd= 29 (18-38) are also higher than commonly found in MORB and OIB [3].

The recovered accesses of Cl and B of SFB melt are very uncommon for intraplate mantle derived magmas. But they are similar to those of Gudchikhinskaya suit (one of the lower units of Norilsk volcanic section) parental melt, which was proposed as a pyroxenite-derived end-member component of SFB originated from recycled oceanic crust [4]. This may suggest that the recycled oceanic crust was one of the sources of excessive Cl and B in SFB in general. The other source could be the actual continental crust. Anyway, data suggest significant emission of Cl to atmosphere at the time close to P-T environmental crisis.

[1] Danyushevsky, L.V. *et al.* (2000) *CMP* **138**, 68–83. [2] Danyushevsky, L.V. *et al.* (1996) *Mineral. Petrol.* **57**, 185–204. [3] Koleszar, A.M. *et al.* (2009) *EPSL* **287**, 442–452. [4] Sobolev, A.V. *et al.* (2009) *Petrology* **17**, 253–286.

https://doi.org/10.1180/S0026461X00006502 Published online by Cambridge University Press

Murataite-pyrochlore complex oxide series for actinide immobilization: Nanoscale structure and complexity

SERGEY V. KRIVOVICHEV[1]*, VADIM S. URUSOV[2], SERGEY V. YUDINTSEV[3], ANNA S. PAKHOMOVA[1] AND SERGEY V. STEFANOVSKY[4]

[1]Dept. Crystallography, St. Petersburg State Univ., University Emb. 7/9, 199034 St. Petersburg, Russia
[2]Dept. Crystallography and Crystal Chemistry, Moscow State Univ., 119992 Moscow Russia
[3]Institute of Geol. Ore Dep., Petrogr., Mineral. Geochem., Russ. Acad. Sci., 119017 Moscow Russia
[4]MosNPO Radon, 119121 Moscow Russia

Synthetic murataite, an analogue of a rare titanate mineral, was identified in Synroc ceramic designed for immobilization of high-level nuclear waste [1, 2]. Five volume percent of this phase accumulated about 40% of the total uranium present in the sample. Laverov *et al*. [3] discovered different murataite varieties, *Mu*-3, 5, 7, and 8, where numbers correspond to the multiplicity of murataite *a* cubic unit cell parameter with respect to the same parameter of the fluorite unit cell. Experimental studies demonstrated that the crystallization sequence of phases in the U (Pu)-Zr-Mn-Fe-Ti-Al-O complex system can be expressed as: Pyrochlore - *Mu*-7 - *Mu*-5 - *Mu*-8 - *Mu*-3. In murataite ceramic, typical grains contain pyrochlore and *Mu*-5 at the core surrounded by *Mu*-8 and *Mu*-3 phases. Since the most actinide-bearing phases are encapsulated by low-actinide varieties, this creates an additional barrier for actinide leaching and increases chemical durability of murataite ceramics. Recently, we have been able to structurally characterize *Mu*-3, 5 and 8 varieties of synthetic murataite and to demonstrate their polysomatic nature, in agreement with the earlier proposal by Urusov *et al*. [4]. It turns out that members of the murataite-pyrochlore series are the result of nanoscale mixing of murataite and pyrochlore structures. For instance, the structure of Mu-5 [5] is a complex framework consisting of pyrochlore unit cells uniformly distributed in murataite-type recombined structure. The structure of Mu-8 contains alternating murataite and pyrochlore unit cell modules separated by transitional structure.

[1] Morgan & Ryerson (1982) *J. Mater. Sci. Lett.* **1**, 351–352. [2] Laverov *et al*. (1998) *Dokl. Earth Sci.* **363**, 1104–1106. [3] Laverov *et al*. (1998) *Dokl. Earth Sci.* **363**, 1272–1274. [4] Urusovet al. (2005) *Dokl. Earth Sci.* **401**, 319–325. [5] Krivovichev *et al*. (2010) *Angew Chem. Int. Ed.* **49**, 9982–9984.

The lamprophyre problem: Return to the roots

LUKÁŠ KRMÍČEK

Institute of Geological Sciences, Masaryk University, Brno, CZ-61137, Czech Rep (l.krmicek@gmail.com)

The term ‘lamprophyre’ has been introduced in 1874 by Gümbel for Variscan mafic post-collisional dykes from the Bohemian Massif characterized by phenocrysts of mafic mica embedded in a feldspar groundmass (minette and kersantite type). In analogy to these, Rosenbusch in 1887 added the amphibole-bearing types such as vogesite and camptonite, from which spessartite was subsequently distinguished. Unfortunately, during the 20th century, petrologists enlarged this ill-understood group by incorporating different rocks containing mafic phenocrysts, such as kimberlites, lamproites, nepheline-, leucite- and melilite-bearing rocks. This resulted in a single large supergroup of polygenetic rocks termed the ‘lamprophyre clan’. In contrast, recent understanding of lamprophyres provides a sound basis for rejecting such a variable group of polygenetic origin [1, 2]. As true lamprophyres, we can now recognize five original types (end-members) among which there are continuous transitions: minette, kersantite, vogesite, spessartite and partly camptonite (in the original sense). It is important to note, that not every rock labelled as a true lamprophyre falls into this group. For example a ‘peralkaline minette’ is not a lamprophyre but very probably corresponds to a lamproite [c. f. 3, 4].

Since the term camptonite is usually used for an alkaline ‘lamprophyre’ variety (in fact volatile-rich basalt), I recommend not to use it in context with the true lamprophyres. Lamprophyre varieties containing kaersutitic amphibole can be easily described as titanospessartite or titanovogesite, respectively (Table 1). Moreover, the last proposed variety fills the gap in the current nomenclature.

	predominant mafic mineral with “OH” group		
predom. felsic mineral	**Al-undepleted phlogopite/ biotite**	**Mg-hastingsite + others Ca amphiboles**	**kaersutite**
Kfs	**minette**	**vogesite**	**titanovogesite**
Pl	**kersantite**	**spessartite**	**titanospessartite**

Table 1: Proposed principal subdivision for the true lamprophyres. (Kfs = K-feldspar, Pl = plagioclase)

[1] Le Bas (2007) *Geology Today* **23**, 167–168. [2] Krmíček (2010) *Acta Mus. Moraviae, Sci. geol.* **2**, 5–63. [3] Hall (1982) *Mineral. Mag.* **45**, 257–66. [4] Krmíček *et al*. (2011) *Lithos* **121**, 74–86.

https://doi.org/10.1180/S0026461X00006502 Published online by Cambridge University Press

Phlogopite/matrix, Cpx/matrix and Cpx/phlogopite trace element partitioning in true lamprophyres

M. KRMÍČKOVÁ[1]*, L. KRMÍČEK[2], V. KANICKÝ[3], T. VACULOVIČ[3] AND M. GALIOVÁ[3]

[1]Institute of Geotechnics, Brno University of Technology, Brno, CZ-602 00, Czech Rep (*correspondence: m.halavinova@gmail.com)
[2]Institute of Geological Sciences, Masaryk University, Brno, CZ-61137, Czech Rep
[3]Department of Chemistry, Masaryk University, Brno, CZ-61137, Czech Rep

Introduction

Partition coefficients for true lamprophyres (i.e. in their original sense [1]) are poorly known. Therefore, mineral/matrix and mineral/mineral partition coefficients were determined by LA-ICP-MS for clinopyroxene (Cpx) and phlogopite crystals from a Variscan calc-alkaline (agpaitic index = 0, 6) lamprophyre of minette-type from the Bohemian Massif (Křížanovice locality, Bohemicum). Quantification was performed using the glass reference material NIST SRM 612 as external standard, and microprobe analyses of Si as internal standard.

Results

Cpx/matrix partition coefficients (D) for 23 trace elements have values ~1 (0.9-1.1) for the HREE only. This suggest that HREE can be concentrated in clinopyroxene during crystallization from lamprophyre melts [2]. The coefficients differ significantly from published D-values for HREE (~0.3-0.4) in clinopyroxenes growing from 'lamprophyric' melt of alkaline composition [3].

In phlogopite, only 14 elements had concentrations above detection limit. Phlogopite/matrix partition coefficients have average values higher than 1 for Ba (D = 1.1), Rb (D = 1.7) and Ti (D = 1.5). On the other hand, D-values for LREE are extremely low (D < 0.02) and it was not possible to determine D-values for the majority of HREE.

During simultaneous crystallization of clinopyroxene and phlogopite phenocrysts, Th, Zr, Hf and REE are preferentially partitioned into clinopyroxene. The main reason for the behaviour of these elements may be found in the lack of a suitable crystallographic site in the phlogopite structure [5].

[1] Krmíček (2011) *MinMag*, this volume. [2] Plá Cid *et al*. (2005) *Contrib Mineral Petrol* **148**, 675–688. [3] Foley *et al*. (1996) *Geochim. Cosmochim. Acta* **60**, 529–538. [5] Schmidt *et al*. (1999) *Earth Planet. Sci. Lett*. **168**, 287–299.

Chronology of climate archives – A never-ending story

BERND KROMER

Curt-Engelhorn Centre for Archaeometry, C 4,8, D-68159 Mannheim, (bernd.kromer@cez-archeometrie.de)

Accurate dating of climate archives is essential for the reconstruction of past climate and to infer rates of climate change. Of special interest is the time range of the last Glacial and the transition into the Holocene, during which strong climate fluctuations are evident. Chronology of these archives is based on a number of dating systems, such as radiocarbon, U/Th and layer counting. Each clock has its strengths and limitations, and in the past decade important progress has been achieved to resolve inconsistencies within a dating method and between the methods. This keynote lecture will focus on this fascinating venture and the current status of establishing firm and consistent chronologies in the past 50.000 years.

https://doi.org/10.1180/S0026461X00006502 Published online by Cambridge University Press

O-isotope compositions of ferroan olivine in Ngawi (LL3–6) breccia

A.N. KROT[1]*, K. NAGASHIMA[1] AND M.I.PETAEV[2]

[1]University of Hawai'i, USA (sasha@higp.hawaii.edu)
[2]Harvard University, USA (mpetaev@fas.harvard.edu)

Ferroan olivine (*fa*, Fa_{50-100}) is one of the major minerals in matrices of unequilibrated ordinary (H, L, LL) and metamorphosed carbonaceous (CV, CK, CO) chondrites. The origin of matrix *fa* is not understood: high-T (>1000°C) gas-solid condensation under highly oxidizing conditions in the protoplanetary disk [1–3] and low-T (<300°C) formation during fluid-assisted thermal metamorphism on the chondrite parent bodies [4, 5] are being discussed. Here we report on the mineralogy and O-isotope compositions of secondary *fa* (Fa_{50-99}) in LL3 clasts of the Ngawi LL3–6 breccia. The *fa* coexists with phyllosilicates, replaces magnetite+sulfide nodules in chondrules and matrix and forms veins crosscutting fine-grained rims around chondrules. On a three-isotope diagram, oxygen compositions of *fa* measured *in situ* using the UH Cameca ims-1280 plot along mass-dependent fractionation line with $\Delta^{17}O$ value of 4.2±1.4‰ (2σ), well above the compositions of phenocrysts in LL3 chondrules [7]. The similar $\Delta^{17}O$ values, 4.9±1.9‰ (2σ), were reported for magnetite grains in Ngawi and Semarkona (LL3.0) [1]. We conclude that Ngawi *fa* formed *in situ* in the presence of aqueous solutions.

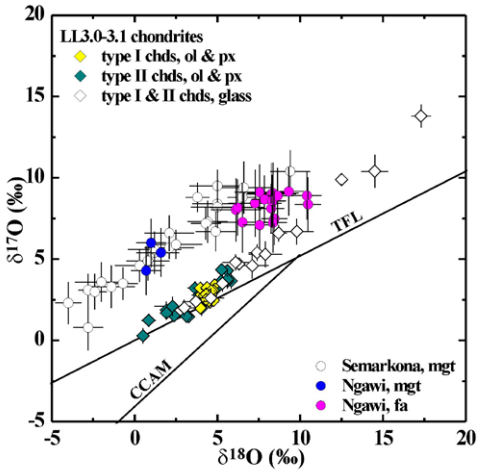

Figure 1: O-isotope compositions of the ferroan olivine [this study], magnetite [6], and phenocrysts and interstitial glass in chondrules [7] from LL3 chondrites.

[1] Palme & Fegley (1990) *EPSL* **101**, 180–195. [2] Weisberg *et al*. (1997) *MAPS* **32**, 791–801. [3] Lauretta *et al*. (2003) *GCA* **65**, 1337–1353. [4] Krot *et al*. (2004) *Proc. NIPR* **17**, 154–172. [5] Zolotov *et al*. (2006) *MAPS* **41**, 1775–1796. [6] Choi *et al*. (1998) *Nature* **35**, 1365–1387. [7] Kita *et al*. (2010) *GCA* **74**, 6610–6635.

Late Cretaceous alnöite from the Delitzsch (Germany) carbonatite – ultramafic complex

J.C. KRÜGER, R.L. ROMER AND H. KÄMPF

Deutsches GeoForschungsZentrum, 14473 Potsdam, Germany (jekruege@uni-potsdam.de, romer@gfz-potsdam.de kaempf@gfz-potsdam.de)

The Delitzsch complex consists of late Cretaceous ultramafic lamprophyres, alnöites and carbonatitic rocks, which are covered by up to 100 m thick sequences of Tertiary sedimentary rocks. Lamprophyre, alnöite and carbonatite dikes and diatrems are emplaced in Paleozoic to lower Permian volcanic and sedimentary rocks. The size and geometry of the Delitzsch complex is not well known, but exploration drilling has documented lamprophyres and carbonatites in an area of 150 km² [1]. The complex includes a diversity of magmatic and subvolcanic rocks, ranging from beforsites, rauhaugites, and alvikites for the carbonatitic rocks and aillikites, monchiquites, alkali picrites, and alnöites. Contact relations and distribution of xenolithic material indicates that phases of carbonatite and ultramafic lamprophyre magmatism overlapped.

The alnöite dike/diatrem at the northern flank of this complex is highly heterogenous with abundant wallrock xenoliths and reaction zones between alnöite and xenolithic material. The xenolithic material was incorperated during ascent and emplacement of the alnöite. Fresh alnöites have abundant melilithe, minor olivine, phlogopite, and pyroxene in a porphyritic texture. Acessory minerals are perovskite, apatite, chromian spinel, and magnetite. They are affected by post magmatic chloritization of olivine and especially pyroxene. The alnöites are relatively high in SiO_2 (~35%) and have high MgO, Cr, Ni, and Sr contents. The rocks have unradiogenic Sr and positive ε_{Nd} (T) values. Their Sr, Nd, and Pb isotopic compositions fall between HIMU and EM1 mantle components.

Xenolith-bearing alnöites show seperated areas with rounded quartz and K-feldspar. These texturally distinguished types are also geochemically and isotopically distinctive, with REE pattern similar to average crust and crustal Sr, Nd, and Pb isotope signatures. Xenolith-bearing alnöites show texturally and geochemically marked transition zones with selective enrichment of heavy REE, not attainable by simple assimilation of xenolithic material in the alnöite.

[1] Röllig *et al*. (1990) *Z. angew. Geol*. **36**, 49–54.

https://doi.org/10.1180/S0026461X00006502 Published online by Cambridge University Press

Microbial conversion of oil, coal and shales into methane – A future energy resource

M. KRÜGER[1]*, F. GRÜNDGER[1], M. SIEGERT[1], H.-M. SCHULZ[2] AND H.-H. RICHNOW[3]

[1]BGR, Hannover, Germany (*correspondence: Martin.Krueger@bgr.de)
[2]GFZ, Potsdam, Germany
[3]UFZ, Leipzig, Germany

Since decades it is known from stable isotope studies that large amounts of biogenic methane are formed in oil reservoirs. The investigation of this biodegradation process and of its biogeochemical controls are of great economical and social importance for: (1) The understanding of reservoir biodegradation may be of great use for the exploration industry, and (2) a biotechnological stimulation of methane formation in reservoirs could provide new economical perspectives for hydrocarbon recovery. Even under optimal conditions, today not more than 30-40 % of the total oil in a reservoir are actually recovered. The conversion of at least parts of the non-recoverable oil, coal or shales via an appropriate biotechnological treatment into easily recoverable methane would provide an extensive and ecologically sound energy resource. Laboratory mesocosms and high pressure autoclaves with samples from different geosystems showed high methane production rates after the addition of different oils, coals or shales. Stable isotope probing (SIP) combined with fingerprinting of the microbial enrichments showed a large bacterial but limited archaeal diversity involved in degradation. For the characterization of degradation pathways metabolite spectra will be analysed, combined with the use of SIP. The variability of carbon and hydrogen isotopes of produced methane falls in a relative narrow range. Further we have analysed the isotope composition of methane in reservoirs and oil-contaminated aquifer to test whether the isotope composition of methane can be used as an indicator for methanogenesis. The variability of carbon and hydrogen isotope composition *in situ* was almost identical with those obtained with the enrichment cultures. This implies a common methanogenic degradation mechanism resulting in consistent patterns of hydrocarbon alteration. This will provide an exploration tool to identify and assess these microbial processes in different reservoir geosystems. Mass balance calculations showed that significant fractions (2-10%) of added coals or oils were converted to methane. Current studies focus on the identification of stimulating or inhibiting factors for scale-up and field studies on MEOR.

Fluid inclusions in stalagmites used as a quantitative thermometer in paleoclimate research

Y. KRÜGER[1,3]*, D. MARTI[1], R. HIDALGO STAUB[1], D. FLEITMANN[2,3] AND M. FRENZ[1]

[1]Institute of Applied Physics, Univ. of Bern, Switzerland (*correspondence: yves.krueger@iap.unibe.ch)
[2]Institute of Geological Sciences, Univ. of Bern, Switzerland (fleitmann@geo.unibe.ch)
[3]Oeschger Centre for Climate Change Research, Univ. of Bern, Switzerland

We present a new approach to determine paleo-temperatures (mean annual surface temperatures) based on fluid inclusion liquid-vapour homogenisation temperatures (T_h) in stalagmites. A precondition for these measurements is to stimulate the nucleation of a vapour bubble in the initially monophase inclusions by means of single ultra-short laser pulses [1]. The aim of our study is to explore the potential and the limitations of this new paleothermometer and to develop a reliable methodology for routine applications in paleoclimate research. Therefore, we have investigated recent fluid inclusions from the top part of actively growing stalagmites from various caves to compare our results with the present-day cave air temperatures.

The method makes specific demands on the selection, handling and preparation of the stalagmites to avoid artificially induced modifications of the original fluid densities by leakage or stretching of the inclusions. Additionally, the measured homogenisation temperatures $T_{h\ (obs)}$ need to be corrected for the effect of surface tension to determine the nominal homogenisation temperature $T_{h\ (nom)}$ [2] that is expected to be equal to the stalagmite formation temperature and therefore closely corresponds to the mean annual surface temperature outside the cave. Based on our present results we may expect an accuracy in paleotemperature determinantions within ±0.3 °C. The application of this thermometer is, however, restricted to climate zones and periods with mean annual surface temperatures higher than 9–11 °C. Inclusions formed below this temperature limit do not feature a stable liquid-vapour state and thus T_h cannot be measured.

[1] Krüger *et al*. (2007) *Eur J Mineral* **19**, 693–706. [2] Marti *et al*. (submitted)

https://doi.org/10.1180/S0026461X00006502 Published online by Cambridge University Press

Hf-W evidence for rapid accretion and core formation in protoplanets

T. KRUIJER[1]*, P. SPRUNG[1], T. KLEINE[2], I. LEYA[3] AND R. WIELER[1]

[1]Inst. of Geochemistry and Petrology, ETH Zurich (*correspondence: thomas.kruijer@erdw.ethz.ch)
[2]Institute for Planetology, Universtity of Muenster
[3]Space Research and Planetary Sciences, University of Bern

Introduction

Several Hf-W studies [e.g. 1] showed that the parent bodies of magmatic iron meteorites formed very early, about contemporaneously to Ca-Al-rich inclusions (CAI). Cosmic-ray induced neutron capture reactions can, however, modify the W isotope budgets of iron meteorites [2] but no accurate method is yet available for correcting these effects [3, 4]. Consequently, the exact timing and duration of core formation in these bodies remain uncertain.

Approach

Cosmogenic noble gas abundances can help to select iron meteorite samples whose W isotope budgets likely remained unaffected by cosmic rays. Nevertheless, quantitative corrections of cosmic-ray induced shifts in W isotopes using a direct neutron dose monitor like ^{113}Cd [see e.g. 5] are desirable [2]. We here report results from a combined noble gas and W isotope study on different groups of magmatic irons. Complementing Cd isotope analyses on the same samples are currently on going.

Results

Cosmogenic noble gas concentrations in most of the analyzed samples are at the lowermost end of the range observed in iron meteorites [6]. Samples with the lowest cosmogenic noble gas abundances have ε^{182}W values (10^4 deviations from the terrestrial value) ranging from -3.3 to -3.2, indistinguishable from the CAI initial of -3.28±0.12 [7].

Implications

The (weighted) mean ε^{182}W of the weakly irradiated irons analyzed in this study is -3.25±0.05. Unlike in previous W isotope studies, this average value is higher than the CAI initial, not lower, demonstrating that ε^{182}W values lower than the CAI initial reflect cosmic-ray induced effects. Our W isotope data indicate that different iron meteorite parent bodies segregated their cores within a brief interval of less than 1 Myr. The average core formation age of the samples investigated here is $0.3^{+1.3}/_{-1.1}$ Myr after Solar System formation.

[1] Kleine *et al*. (2005) *Geochim. Cosmochim. Acta* **69**, 5805–5818. [2] Leya *et al*. (2003) *Geochim. Cosmochim. Acta* **67**, 529–541. [3] Markowski *et al*. (2006) *EPSL* **250**, 104–115. [4] Kleine *et al*. (2009) *Geochim. Cosmochim. Acta* **73**, 5150–5188. [5] Sands *et al*. (2001) *EPSL* **186**, 335–346. [6] Schultz & Franke (2004) MPI für Chemie, Mainz. [7] Burkhardt *et al*. (2008) *Geochim. Cosmochim. Acta* **72**, 6177–6197.

Sorption properties of supercritical carbon dioxide in nano-porous synthetic rocks

ELIZABETH G. KRUKOWSKI[1]*, GERNOT ROTHER[2†] AND ROBERT J.BODNAR[1]

[1]Department of Geosciences, Virginia Tech, 4044 Derring Hall, Blacksburg, VA 24061, USA (*correspondence: egk@vt.edu)
[2]Chemical Sciences Division, Oak Ridge National Laboratory, Oak Ridge, TN 37831-6110, USA ([†]rotherg@ornl.gov)

Carbon dioxide (CO_2) generated in fossil-fuel powered plants is a concern due to its potential contributions to global warming. Large-scale carbon capture and sequestration (CCS) can help to slow the rise of atmospheric CO_2 levels. In this process, CO_2 is stripped from the plant emissions, compressed and injected into subsurface reservoirs. Directly after injection, the dominant processes to contain the supercritical CO_2 in the reservoir are sorption and capillary trapping. Quantification and understanding of these processes is needed to estimate reservoir capacities and model long-term storage security. In this study, gravimetric sorption experiments were conducted from 0-200 bars and 35-50°C, using mesoporous silica, a synthetic proxy for quartz-rich rock. The CO_2 excess sorption isotherms were measured for samples with different pore sizes and morphologies. Strong adsorption of CO_2 to silica was found at low pressure, with the formation of a maximum in the excess sorption isotherm. The excess sorption is small or negative at high pressure. An inverse temperature dependence of the sorption strength was found in the adsorption region at low pressure, while the excess sorption showed little temperature dependence at high pressure. Our data suggest the existence of an optimum pressure, between 75–100 bars depending on temperature and pore size, for carbon storage in dry quartz-rich rocks.

We also studied the sorption of supercritical CO_2 to Na-montmorillonite clay, a proxy for cap rock materials. Limited amounts of CO_2 adsorbed to this clay mineral.

https://doi.org/10.1180/S0026461X00006502 Published online by Cambridge University Press

$\delta^{18}O$ and Cl/Nb evidence for fractional crystallization origin of silicic island arc magmas

S. KRUMM, K.M. HAASE, M. REGELOUS AND M.M. JOACHIMSKI

GeoZentrum Nordbayern, University of Erlangen-Nürnberg, Schlossgarten 5, D-91054 Erlangen, Germany (stefan.krumm@gzn.uni-erlangen.de)

Subduction-related silicic magmas may form either by extreme crystal fractionation or by partial melting of crustal rocks. Both mechanisms can be distinguished by their characteristic $\delta^{18}O$ and Cl signatures.

Laser-fluorination analysis of andesitic to rhyolitic volcanic glasses from the Kermadec island volcanoes and of basaltic to dacitic glasses from the Lau and Havre backarc rifts yielded very uniform $\delta^{18}O$ values of 5.4 to 6.5‰. This range is characteristic for mantle-derived magmas. The Cl concentrations show a positive correlation with the SiO_2 content while Cl/Nb ratios remain almost constant for the samples.

Magma generation by partial melting of sediments and/or low temperature hydrothermally altered oceanic crust, both typically having high $\delta^{18}O$, can be ruled out as these processes would cause much heavier isotopic values. A strong positive correlation between $\delta^{18}O$ and SiO_2 content would be expected but is not seen in our data.

Hydrothermal alteration of the oceanic crust leads to amphibolite with low $\delta^{18}O$, and melting of such rocks would lead to values much lower than observed. Assimilation of such materials also causes high and variable Cl concentrations and variable Cl/Nb ratios unlike the observed systematic trend.

The small variation of the $\delta^{18}O$ data as well as the very slight increase with SiO_2 content is best explained by fractional crystallization that modifies $\delta^{18}O$ values of the precursor mantle magma by 0.3 to 0.8‰ towards heavier values [1]. This is also consistent with a positive correlation between the incompatible Cl and SiO_2 content and with the constant Cl/Nb ratios in these samples. Both parameters prove monotonous enrichment of the magmas in Cl with increasing differentiation and indicate that degassing was insignificant at least for the submarine glasses.

[1] Bindeman *et al*. (2004) *GCA* **68**, 841–865.

Destruction of Paleoproterozoic crust: Deciphered from detrital zircon populations and geochemistry of quartzites (NE Poland)

E. KRZEMIŃSKA[1]*, L. KRZEMIŃSKI[1], I.S. WILLIAMS[2] AND J. WISZNIEWSKA[1]

[1]Polish Geological Institute-National Research Institute, Warsaw, Poland, (ewa.krzeminska@pgi.gov.pl)

[2]Research School of Earth Sciences, The Australian National University, Canberra, Australia

Among the many crystalline rocks sampled from the Precambrian basement of NE Poland, which is accessible only by drilling, there are local occurrences of quartzites and quartzitic schists. The quartzites were previously interpreted as Neoproterozoic quasi-platform cover which was formed during post-Gothian peneplanation after emplacement of Mezoproterozoic AMCG intrusions [1]. Correlation with Jotnian sediments exposed in Central Fennoscandia (Baltic Shield) was presumed. Here we present the first results of detrital zircon U-Pb and geochemical investigations of the provenance of quartzitic samples from two isolated drill holes (Mońki and Zabiele). Quartz meta-arenites and subarkoses in terms of Herron's chemical classification record a transition from an active continental margin towards a passive continental margin setting (Th–Sc–Zr/10, Th–La–Sc and Ti/Zr–La/Sc plots). A total of 70 detrital zircon grains from two drill core samples were analyzed by SHRIMP II. The U-Pb data demonstrate that the detritus was derived mainly from Paleoproterozoic crust (2.1–1.8 Ga). Archean grains are rare. No Mezoproterozoic component was detected. Three Paleoproterozic age populations were identified with a major peak at 1.95 Ga. The youngest concordant grains were dated at 1757 ± 24 Ma (Mońki depth 740 m) and 1745 ± 24 Ma (Zabiele depth 690 m) age. These data, however, do not support a Jotnian signature as deposition of Jotnian sediments in central Fennoscandia continued long after the 1.55 Ga anorogenic rapakivi magmatism up to 1.26 Ga A significant revision of the formerly assumed stratigraphic position of quartzitic rocks and correlation with uppermost mature Paleoproterozoic Västervik quartzites [2], S Sweden from the Fennoscandian continental margin, is proposed.

[1] Ryka W. (1998) *Prace Państ. Inst. Geol.* **161**, 19–26.
[2] Claesson S. & Sultan L. (2008) *33rd International Geological Congress, Oslo 6–14/8* ***2008***, session GDP-02

https://doi.org/10.1180/S0026461X00006502 Published online by Cambridge University Press

Geochemistry of tin in the southern part of the Silesian Upland

J. KUCHARZYK[1], W. BUREĆ-DREWNIAK[1], I. JAROŃ[1], W. NARKIEWICZ[1] AND A. PASIECZNA[2]

[1]Central Chemical Laboratory, Polish Geological Institute – National Research Institute, 4 Rakowiecka Street, 00-975 Warsaw, Poland (jkuc@pgi.gov.pl)

[2]Environmental Geology Department, Polish Geological Institute – National Research Institute, 4 Rakowiecka Street, 00-975 Warsaw, Poland

Introduction

Majority of soils from the southern part of the Silesian Upland are highly degraded and contain elevated levels of the toxic heavy metals [1]. Therefore, the purpose of presented studies was evaluation of tin pollution and determination of its mobility and bioavailability in soils from the investigated area.

In this work the soil samples were taken from industrial area. The soils samples were collected from two depths: topsoil (0, 0-0, 3 m) and subsoil (0, 8-1, 0 m). Comparison of elements concentration between topsoil and subsoil allows identification of the source of pollution (natural or anthropogenic).

Results

Considerably degree of chemical degradation was observed in both types of analyzed samples. The subsoil and topsoil samples were rich in tin (subsoil – 1265 mg/kg, topsoil – 37 mg/kg). Moreover, in both samples were noticed high concentration of copper, mercury, lead, arsenic and sulphur.

The sequential extraction experiments according to BCR method [2, 3] showed minimal tin mobility in the analyzed samples (almost 99% of tin was leached in the 4th step with aqua regia). The X-ray diffraction (XRD) analysis of selected samples showed the lack of tin minerals in the investigated soil. However, found the presence of quartz, clay minerals, calcite and gypsum.

[1] A. Pasieczna (2010) Detailed geochemical map of Upper Silesia 1:25000. [2] G. Rauret, J. F. López-Sánchez, A. Sahuquillo, R. Rubio, C. Davidson, A. Ure *et al*. (1999) *J. Environ. Monit*. **1**, 57–61. [3] J. M. Hernández-Moreno, J. I. Rodríguez-González, M. Espino-Mesa (2007) *Eur. J. Soil Sci*. **58**, 419–430.

Mesoarchean gabbroanorthosite magmatism of the Kola Region (Russia)

N.M. KUDRYASHOV AND A.V. MOKRUSHIN

Geological Institute of the Kola Science Centre of the Russian Academy of Sciences,14, Fersman str., Apatity, Russia (nik@geoksc.apatity.ru)

The Kola peninsula is the region marked with development of anorthosite magmatism in the NE Baltic Shield. The Archaean gabbroanorthosites intrusions - Tsaginsky, Achinsky and Medvezhe-Schucheozersky - have the age of 2.7-2.6 Ga. The Patchemvarek and Severny gabbroanorthosites intrusions are located in the junction zone of the Kolmozero-Voronja greenstone belt and the Murmansk domain. Age data for sedimentary-volcanogenic rocks of the Kolmozero-Voronja belt and Murmansk domain granitoids are 2.8-2.7 Ga.

The gabbroanorthosites intrusions have more calcic composition (70–85% An) of normative plagioclase, and low contents of TiO_2, FeO, and Fe_2O_3. U–Pb zircon dating established Mesoarchean ages of 2925±7 and 2935±8 Ma for the gabbroanorthosites of the Patchemvarek and Severny massifs, respectively. The gabbroanorthosites of the studied massifs have fairly low REE contents (Ce_n = 2.2–4.2, Yb_n = 1.6–2.6) and distinct positive Eu anomaly. Comagmatic ultrabasic differentiates have practically unfractionated REE pattern, low total REE contents (Ce_n = 1.2, Yb_n = 1.1, La/Yb_n = 1.32), and no Eu anomaly. The studied samples of the Archean gabbroanorthosites are characterized by positive εNd= +2.68 for the gabbroanorthosites of the Severny Massif and from +2.77 to +1.66 for the Patchemvarek Massif. The rocks of the Severny and Patchemvarek massifs has $^{87}Sr/^{86}Sr_i$ = 0.70204±8 and $^{87}Sr/^{86}Sr_i$ = 0.70258±8, respectively. The differences in the initial $^{143}Nd/^{144}Nd$ ratios between the Neoarchean and the Mesoarchean gabbroanorthosites suggest the existence of two mantle sources. One of them produced intrusions with an age of 2.67–2.66 Ga, while other was responsible for the formation of massifs with an age of 2.93-2.92 Ga.

The gabbroanorthosites of the Patchemvarek and Severny massifs were presumably derived from MORB-type basalts of oceanic settings, while the Tsaginsky, Achinsky, and other anorthosite massifs of the Neoarchean age were generated from subalkaline magma formed in within plate anorogenic setting. The Sm-Nd isotope data suggest the existence of several mantle sources in the Kola region, which produced melts for different-age gabbroanorthosite massifs since Mesoarchean to the middle Paleoproterozoic.

https://doi.org/10.1180/S0026461X00006502 Published online by Cambridge University Press

Chemical and mass changes of the vein type mineralizations in Çetilli area, (Ordu, Turkey)

KAMER KUDUN YOZGAT* AND NECATI TÜYSÜZ

Karadeniz Technical University, Department of Geological Engineering, 61080, Trabzon, Turkey (*correspondence: kameryozgat@gmail.com)

In this study, chemical and mass changes of Çetilli (Ordu) area vein type mineralization at the Eastern Black Sea region are investigated. The geology of the study area consists of volcanic, sedimentary and intrusive rock units. The study area is covered by Upper Cretaceous aged andesite, basalt and their pyroclastic equivalents, trachyandesite and its tuff, volcano-sedimentary sequence and limestone; Paleocene aged limestone, sandstone, claystone, marl, tuff and andesitic dyke; Eocene aged nummulites bearing limestone, andesite, basalt and their pyroclastics, monzonite; Upper Eocene aged basalt and Quvaterner aged travertine. Upper Cretaceous aged andesite, basalt and their pyroclastics are cut by E-W, NE-SW, NW-SE directed many fault systems. The Çetilli Orebody was formed by hydrothermal solutions arising throughout this fractured and cracked zones. Ore minerals are pyrite, sphalerite, chalcopyrite, galena and nabit gold.

Alteration of Çetilli Mineral Deposit display indistinct spatial zonation. Alteration zones are completely controlled by fault systems. Alteration types are observed silicification, calcification, zeolitization, clay, sericitization, limonization, hematization and pyritization. Chloritization and epidotization are observed cut distal part of veins. Alteration minerals are mainly quartz; lesser calcite, dickite, nacrite, ankerite, dolomite, kaolinite and a bit barite. The mass change calculations indicate a 19% volume increase in the ore zones, mainly due to addition of Si (24.45g/100g), Ca (1.06g/100g), K (0.61g/100g) and ore forming elements.

[1] Böhkle, J. K. (1989) Comparison of Metasomatic Reactions Between a Common CO_2-Rich Vein Fluid & Diverse Wall Rocks, Intensive variables, Mass Transfers, & Au Mineralization at Alleghany, California, *Econ. Geology* **84**, 2 91–327. [2] Huston, D. L. (1993) The Effect of Alteration & Metamorphism on Wall Rocks to the Balcooma & Dry River South Volcanics-Hosted Massive Sulphide Deposits, Queensland, Australia, *J. of Geoch. Expl.* **48**, 277–307

Iodide in kelp: An inorganic antioxidant in life impacting atmospheric chemistry

FRITHJOF C. KÜPPER

Scottish Association for Marine Science, Oban, Argyll PA37 1QA, Scotland, UK (*correspondence: fck@sams.ac.uk)

Brown algae of the Laminariales (kelps) are the strongest accumulators of iodine among living organisms. Not surprisingly, this element was discovered in kelp ashes 200 years ago. Kelps represent a major pump in the global biogeochemical cycle of iodine and in particular, the major source of iodocarbons in the coastal atmosphere. Nevertheless, the chemical state and biological significance of accumulated iodine have remained unknown to this date. Elucidation of these questions was the objective of this study. Using an interdisciplinary array of techniques, chiefly relying on synchrotron X-ray absorption spectroscopy, we show that the accumulated form is iodide, which readily scavenges a variety of reactive oxygen species (ROS). We propose here that its biological role is that of an inorganic antioxidant, the first ever to be described in a living system. Upon oxidative stress, a strong iodide efflux occurs. On the thallus surface and in the apoplast, iodide detoxifies both aqueous oxidants and ozone, the latter resulting in the release of high levels of molecular iodine and consequent formation of hygroscopic iodine oxides leading to particles, which are precursors to cloud condensation nuclei.

https://doi.org/10.1180/S0026461X00006502 Published online by Cambridge University Press

Comparison of internal and external metabolites produced by a diatom

ELIZABETH B. KUJAWINSKI*, MELISSA C. KIDO SOULE AND KRISTA LONGNECKER

Department of Marine Chemistry and Geochemistry, Woods Hole Oceanographic Institution, Woods Hole, MA 02543, USA (*correspondence: ekujawinski@whoi.edu) (msoule@whoi.edu, klongnecker@whoi.edu)

Introduction

Marine photosynthetic microorganisms play a key role in the global carbon cycle because they fix inorganic carbon into organic compounds. Many of these compounds are exuded into the environment during growth and collectively, they constitute a large fraction of dissolved organic matter in the surface ocean. Despite the significance of this carbon production mechanism, we know little about the molecular-level composition of photosynthetically-derived dissolved organic matter and the environmental factors that govern its production.

Methods

We sampled laboratory cultures of a marine phytoplankton (*Thalassiosira pseudonana*) at different stages of its growth. At each sampling point, we compared the molecular-level composition of dissolved organic matter released into the environment with the dissolved organic compounds retained within the phytoplankton cells. All measurements were made with an HPLC coupled to an ultrahigh resolution mass spectrometer (FT-ICR MS) in positive ion mode. Resulting mass and fragmentation data were compared to metabolite databases such as KEGG and MassBank.

Results

Our data reveal distinct differences between the dissolved organic compounds retained inside the phytoplankton compared to those compounds released into the surrounding media as well as some similarities in these two metabolite pools. Tentative identifications based on database comparisons and fragmentation data suggest a dynamic metabolome for *T. pseudonana*. From these identifications, we will present possible biomarkers for future quantitative metabolic studies of this diatom and related organisms.

Evolution of Variscan orogenic Popiel peridotite (SW Poland)

A. KUKUŁA[1], J. PUZIEWICZ[1]*, M. MATUSIAK-MAŁEK[1] AND T. NTAFLOS[2]

[1]Univ. Wrocław, Poland (*correspondence: jacek.puziewicz@ing.uni.wroc.pl)
[2]Univ. Wien, Austria (theodoros.ntaflos@univie.ac.at)

Small (few hundred metres in diameter) outcrop of peridotite occurs in the western part of the Sudetes (SW Poland) at the Intra-Sudetic Fault Zone, close to the NE margin of the Karkonosze granite, which is one of the main tectonic lines in NE Bohemian Massif.

The rock consists of olivine (Fo_{84-88}, NiO 0.17 – 0.36 wt %), orthopyroxene (mg# 0.84 - 0.88, Al_2O_3 0, 71- 4, 69 wt %) and spinel (typically $Mg_{0,68}Fe_{0,31}Ni_{0,01}Al_{1,79}Fe_{0,13}Cr_{0,08}O_4$) + chromiferous magnetite ($Fe_{0,99}Mg_{0,02}Mn_{0,01}Ni_{0,01}Fe_{1,68}Cr_{0,19}Al_{0,06}Ti_{0,03}O_4$ + very scarce ilmenite. The composition of minerals vary from sample to sample. The primary mineral assemblage is overprinted by tremolite (Si = 7.95 atoms pfu), overgrown by magnesiohornblende (Si = 6.78 a pfu). The serpentine is texturally later than the amphibole.

The rock composition: SiO_2 39 - 43, Al_2O_3 4 – 7, CaO 3- 6 wt %, MgO 24 – 32 wt % and Fe_2O_3 11 -13 wt % is Fe, Al and Ca enriched. Whole rock trace-element and REE patterns are slightly (1 – 10 times) enriched relative to primitive mantle, flat, with weak Zr and Eu negative anomalies. The rocks was altered by low-grade metamorphism producing tremolite, followed by contact metamorphism in the Karkonosze granite aureole (hornblende crystallization). The rock has been affected by metasomatism and later metamorphism under oxidizing conditions. It is the unique in Sudetes (NW margin of the Bohemian Massif) example of small orogenic peridotite body affected by metasomatic and metamorphic conditions.

https://doi.org/10.1180/S0026461X00006502 Published online by Cambridge University Press

On the application of jarosite and hematite thermochronology to assess aqueous environments on Mars

J. KULA* AND S.L. BALDWIN

Department of Earth Sciences, Syracuse University, Syracuse, NY 13244, USA (*correspondence: jkula@syr.edu)

Hematite and jarosite, identified in the Burns Formation by the Opportunity Mars Exploration Rover (MER), have been interpreted as *in situ* evidence for past aqueous conditions on the Martian surface. Hematite has been demonstrated as a useful (U-Th)/He chronometer, although it is not a commonly analyzed mineral. Likewise, jarosite has been used as a $^{40}Ar/^{39}Ar$ chronometer, although prior to this study, argon diffusion kinetics in jarosite were unknown. Using long-duration, low-temperature, furnace step heating, jarosite argon diffusion parameters (E, log D_o/a^2) have been determined. Incremental fractional loss measurements from three size fractions (75-125, 125-150, 150-200 μm) yield an average activation energy (E) of 38.80 ± 1.58 kcal/mol and a log D_o/a^2 of 6.09 ± 0.67 s^{-1} corresponding to a closure temperature (cooling rate 100°C/Ma) of 146 ± 30°C. Using published morphologic constraints and He diffusion kinetics on hematite spherules, and newly determined argon diffusion parameters for jarosite, we use the forward modeling program DECOMP to assess if these minerals will retain original (U-Th)/He and $^{40}Ar/^{39}Ar$ ages during long residence times (4.0 Ga) at Martian surface conditions (22°, 0°C). Model results indicate that for hematite spherules (≥1.0 mm in diameter), (U-Th)/He ages will record the timing of formation within analytical certainty. Jarosite (75-200 μm in diameter) is also expected to retain radiogenic ^{40}Ar, with predicted ages falling within 0.5% of the true age. We infer that in the absence of post-crystallization diffusive He or $^{40}Ar^*$ loss, (U-Th)/He and $^{40}Ar/^{39}Ar$ ages measured from Martian hematite spherules and jarosite respectively, can be used to constrain the time since water was present on Mars. Application of model results to the 'wetting-upwards' Burns Formation at Meridiani Planum, indicates that post depositional hematite from the lower eolian dune subunit would provide a minimum age of deposition, while possibly syndepositional hematite from the upper interdune/playa unit may yield the age of the unit. Jarosite ages throughout the section should record a downward migrating aridification front as the water table retreated. A vertical profile of hematite and jarosite ages may constrain the timing and rates of the transition from wet to dry conditions at Meridiani Planum. Application of hematite and jarosite thermochronology to samples returned from Mars may be key to determining if water was available for sufficient durations required for the development of life.

Rhine River: First case of anthropogenic lanthanum as a dissolved microcontaminant in the hydrosphere

SERKAN KULAKSIZ* AND MICHAEL BAU

Jacobs University Bremen, Earth and Space Sciences, Campus Ring 8, 28759, Bremen
(*correspondence: s.kulaksiz@jacobs-university.de)

The rare earth elements (REE) are a group of elements that behave coherently in natural systems, usually plotted with concentrations normalized to a known reference (e.g. shale). This style of representation makes the presence of anomalies easier to distinguish.

The first report of anthropogenic contamination of the natural REE distribution in river water appeared in the mid-1990s (Bau & Dulski, 1996). Gadolinium (Gd) concentrations in the Havel River downstream of the city of Berlin were up to 3 orders of magnitude higher than natural background concentrations. This study also reported on the Rhine River showing a similar excess of Gd concentration. Gadolinium is used in magnetic resonance imaging as a contrast agent, causing positive anthropogenic Gd anomalies in sewage effluent, rivers, estuaries and groundwater via several pathways in its highly-stable form (e.g. Gd-DTPA).

More recently, excess lanthanum (La) was also measured in the River Rhine, up to an order of magnitude higher than background values. The anomaly is introduced into the Rhine River north of the city of Worms at Rhine river-km 447.4. Samples taken a few hundred meters upstream/downstream of an effluent at this location show strong differences in La and light REE concentrations. The effluent itself shows 49 mg/kg La, well-above levels that are ecotoxicologically effective. Excess La is present 400 km downstream at the German-Dutch border where >93% of total La and Gd are of anthropogenic origin.

Since River Rhine water is used for artificial groundwater recharge and bank infiltration, anthropogenic La (and Gd) are both to be expected in tap water of those cities that rely on the Rhine River as a drinking water source. Indeed, several cities along the Rhine River carry positive anthropogenic Gd anomalies (e.g. Leverkusen, Koblenz, Düsseldorf, Duisburg, and Essen) and positive anthropogenic La anomalies (e.g. Leverkusen, Worms, and Kleve).

While several adverse health effects of Lanthanum are known, information on the potential health risks to the ecosystem inhabiting the river is lacking. Further research and monitoring is essential in order to avoid potential negative environmental consequences.

https://doi.org/10.1180/S0026461X00006502 Published online by Cambridge University Press

Risk assessment analysis of Kadji-Sai uranium tailings site, Kyrgyzstan

ZH. KULENBEKOV* AND BRODER J. MERKEL

TU Bergakademie Freiberg, Gustav Zeuner Str. 12, 09596, Germany (*correspondence: kulenbekov@gmail.com)

Sediment samples and coal ashes from Kadji-Sai uranium tailing site, Kyrgyzstan (a former coal and uranium mine) taken at depth of 0.1-0.2, 1, and 2 meters were investigated with gamma spectrometry and electron microscopy coupled with Energy-Dispersive X-ray Fluorescence Spectroscopy (SEM/EDX). Gamma spectroscopy showed significant elevated activities for uranium, radium, and lead-210 (Table 1).

Sampling points	Depths (m)	^{238}U kBq kg^{-1}	^{226}Ra kBq kg^{-1}	^{210}Pb kBq kg^{-1}
Catchment pool	0.1-0.2	0.43 to 1.2	0.10 to 0.07	0.11 to 0.07
Uranium tailing dump	1.0	6.8	31.2	23.9
Uranium tailing dump	2.0	7.2	26.6	24.2

Table 1: Gamma activity at shallow depths of the Kadji-Sai uranium tailing site

These results reveals that the uranium extraction technique was rather inefficient leaving about between 20 and 30% of the uranium in the tailings and that no sufficient cover of the tailings is in place. SEM/EDX was used to study the chemical forms and morphology of the coal ash and sediments particles. The precise knowledge of the elemental composition of radioactive wastes occurring in the tailings is important for future remediation and migration of radioactive elements and stability of secondary minerals being formed in the dump piles.

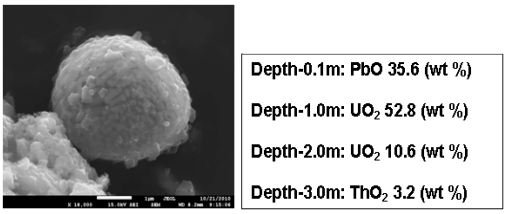

Figure 1: SEM image and EDX data of coal ash from different depths

Consistent treatment of entropy, enthalpy and volume effects of multi-dentate adsorption reactions

D.A. KULIK[1]* AND J. LÜTZENKIRCHEN[2]

[1]Paul Scherrer Institut, 5232 Villigen PSI, Switzerland (*correspondence: dmitrii.kulik@psi.ch)

[2]KIT INE, Postfach 3640, 76021 Karlsruhe, Germany (johannes.luetzenkirchen@kit.edu)

Evidence for aqueous ions binding to several oxygen atoms on mineral-water interfaces (MWI) has raised interest in multi-dentate surface complexation models [1, 2]. We investigated [3] how (fitted) intrinsic equilibrium constants [illegible] for a δ-dentate M adsorption reaction depend on the choice of concentration scale for ≡$_δ$M, e.g. molarity ($^{[]}$); relative surface fraction (^{o}); molecular surface density (^{r}, in mol·m^{-2}); or relative surface density Γ/Γ_o (^{o}, where $\Gamma_o = 2 \cdot 10^{-5}$ mol·m^{-2} [4]). We have shown that, for δ ≥ 2, only [illegible] and [illegible] are denticity-invariant, and only [illegible] is independent of the real site density Γ_C. This makes the (^{o}) scale the best choice for defining the standard state of a surface species.

In this contribution, our approach is extended to T and P corrections of [illegible] defined by the partial molal entropy $\Delta_r S$, enthalpy $\Delta_r H$, isobaric heat capacity ($\Delta_r Cp$), and volume $\Delta_r V$ effects (at T_r = 298 K) of the M adsorption reaction. These effects can be predicted, or fitted from [illegible] values known for several temperatures. For the same experimental data set, fitted $\Delta_r S$ values depend on the chosen concentration scale for [illegible]; the bias can reach 275 J·K^{-1}mol^{-1} for tetradentate cations on rutile surface. General conversions such as

$$\Delta_r^{[]} S^{\delta}_{M,298} - \Delta_r^{o} S_{M,298} = -R(\delta - 1)\ln[\equiv]_{TOT} \quad (1)$$

$$\Delta_r^{\Gamma} S^{\delta}_{M,298} - \Delta_r^{o} S_{M,298} = -R(\delta - 1)\ln \Gamma_o \quad (2)$$

($[\equiv]_{TOT}$ is the total molarity of sites ≡ at site density $\Gamma_{Co} = \Gamma_o$) depend on δ and on the chosen value of Γ_{Co} (1) or Γ_o (2).

Upon adsorption of aqueous M, several H_2O molecules must be liberated from its solvation shell and from the MWI. Thus, a standard-state density $\Gamma_◊$ should lead to 'standard' $\Delta_r^{o} S^{◊}_{M,298}$ and $\Delta_r^{o} V^{◊}_{M,298}$ effects consistent with known entropies and volumes of hydration of aqueous cations (cf. [5]). We find that $\Gamma_◊$ cannot be chosen arbitrarily; setting it close to the density of H_2O molecules in the surface monolayer ($2 \cdot 10^{-5} \pm 1 \cdot 10^{-5}$ mol·m^{-2} [6]) leads to entropy and volume effects related to $^{o}K^{◊}_{M}$ that are compatible with the available data on partial dehydration of aqueous ions and surfaces upon adsorption. In turn, this provides a constructive basis for future discussions aimed at reaching the ultimate thermodynamic convention on standard states of any-dentate surface complexes on MWIs.

[1] Zhang *et al*. (2004) *Langmuir* **20**, 4954–4969. [2] Ridley *et al*. (2009) *GCA* **73**, 1841–1856. [3] Kulik, Lützenkirchen, Payne (2010) *GCA* **74**(12S1) A544. [4] Kulik (2006) *Interf. Sci. Technol*. **11**, 171–250. [5] Marcus (1997) *Ion properties*. [6] Tamura *et al*. (1999) *JCIS* **209**, 225–231.

https://doi.org/10.1180/S0026461X00006502 Published online by Cambridge University Press

Mantle volatiles in groundwaters near the San Andreas Fault

JUSTIN T. KULONGOSKI[1], DAVID R. HILTON[2] AND KENNETH BELITZ[3]

[1]U.S. Geological Survey, California Water Science Center, San Diego, CA 92101 (kulongos@usgs.gov)
[2]Scripps Institution of Oceanography, UCSD, La Jolla, CA 92024-0244 (drhilton@ucsd.edu)
[3]U.S. Geological Survey, California Water Science Center, San Diego, CA 92101 (kbelitz@usgs.gov)

Groundwater samples were collected from 19 wells along the San Andreas Fault (SAF) in the Cuyama, Cuddy, and Mil Potrero Valleys in southern California, USA. Previous work has shown leakage of mantle He via the SAF indicative of a focused mantle contribution to the surface. In this study, we assess the relation between He, a major volatile phase, and CO_2, the hypothesized carrier of the helium from the mantle.

The isotopic composition and concentrations of dissolved gases were determined. Measured $^3He/^4He$ ratios were compared to the $^3He/^4He$ ratio of air = 1.4 x 10^{-6} = Ra, to determine whether groundwaters were enriched in crustal (0.02Ra) or mantle (8Ra) helium. Concentrations of ^4He, corrected for air-bubble entrainment, varied from 3.0 to 58.1 x 10^{-8} $cm^3STP\ g^{-1}H_2O$. $^3He/^4He$ ratios varied from 0.46 to 3.58 Ra, consistent with mantle He in all samples (up to ~50%). A subset of 10 samples were analyzed for CO_2 and $\delta^{13}C$; concentrations of CO_2 varied from 0.059 to 0.223 $cm^3STP\ g^{-1}H_2O$, and the $\delta^{13}C$ of the CO_2 varied from -21.50 to -11.87‰. In groundwater, $\delta^{13}C$ ratios of ~-6‰, and elevated CO_2 concentrations may indicate the presence of mantle volatiles, particularly when they co-occur with high $^3He/^4He$ ratios. Measured $CO_2/^3He$ ratios varied from 64.1 to 1632 x 10^9 (mantle $CO_2/^3He$ = ~1.5 x 10^9).

Samples were collected from Quaternary alluvium filled valleys formed by motion along the northwest-trending, right-lateral strike-slip SAF. The flux of deep mantle fluids to the seismogenic zone at high hydrostatic pressure may cause fault rupture, and transfer volatiles into the shallow crust. $^3He/^4He$ and $\delta^{13}C$ ratios, and ^4He and CO_2 concentrations are highest in the wells located in the Cuddy and Mil Potrero valleys, which are closest to the SAF. Samples with the highest $^3He/^4He$ ratios also had the lowest $CO_2/^3He$ ratios. However, the eight wells sampled in the Cuddy and Mil Potrero valleys were located <1km from the SAF, yet their $^3He/^4He$ and $CO_2/^3He$ ratios varied by up to an order of magnitude suggesting heterogeneous fluxes of mantle volatiles along this 40 km section of the SAF.

Biological precipitation of calcite in stalagmites

A. KUMAR[1], J. ROUTH[1] *, A. MANGINI[2], J. PATTANAIK[1] AND S. BASKAR[3]

[1]Dept of Earth Sciences, IISER-K, Kolkata741252, India (*correspondence: joyanto.routh@iiserkol.ac.in)
[2]Institut für Umweltphysik der Universität Heidelberg, Heidelberg, Germany
[3]Dept. of Environmental Science and Engineering, GJUST, Hisar, India

In recent years, spleothems have become an important archive for paleoclimate studies. To deduce paleoclimatic information from carbonate deposits, which is precipitated under non-equilibrium-conditions, it is important to improve the understanding of biological calcite precipitation.

In this study, laboratory experiments were conducted with calcium carbonate precipitating bacteria isolated from stalagmite deposits collected from Krem Syndai in Meghalaya, India. The medium used to culture these bacteria was designed in accordance to the drip water composition. We have isolated a new strain S4 that has been partially identified by 16S rDNA sequencing. The strain shows less than 95% similarity with any of the existing *Bacillus* stains involved in bio calcification. SEM and AFM studies are being carried out to understand the tomography of S4 strain.

Biocalcification rate of this strain was studied at regular intervals by studying the change in optical density, pH and calcite (wt%) precipitated in the medium. There is a positive correlation (r =0.925) between optical density and pH implying increased precipitation over the 40 day period. XRD was done to identify the minerals in the microbial precipitate. In addition the precipitate was analyzed for the isotopic composition of $\delta^{13}C$ and $\delta^{18}O$.

https://doi.org/10.1180/S0026461X00006502 Published online by Cambridge University Press

Dry deposition: A major pathway of atmospheric dust particle deposition

RANJIT KUMAR[1] AND K. MAHARAJ KUMARI[2]

[1]Department of Applied Chemistry, Technical College
[2]Department of Chemistry, Faculty of Science, Dayalbagh Educational Institute (Deemed University), Dayalbagh, Agra -282005. Ph: 0562-2801545, Fax: 0562-2801226 (rkschem@rediffmail.com)

Acidic deposition is of major concern due to their detrimental effects including wide spread acidification of soil, ponds, lakes, corrosion of building materials, injury to vegetation etc. The major mechanisms of removal of pollutants from the atmosphere to earth surface are dry deposition, wet deposition and occult deposition. Dry deposition is an important process for Indian climatic conditions as dry conditions prevail for most part of the year while rains are confined to short monsoon period. Direct measurements of dry deposition on natural surfaces are significant because measurements made so far are on surrogate surfaces that do not simulate the natural surfaces. Dry deposition flux was higher on rougher surface of Cassia leaf comparison to leaf of Ashok because it prevented the re-entrainment of deposited particles and therefore has higher deposition flux. Contribution of alkaline components is higher towards total dry deposition and hence dry deposition is basic in nature, which is dominated by the soil-derived elements Ca^{2+} and Mg^{2+}. NH_4^+ also plays important role in neutralization. Three major sources responsible for dry deposition of major ions are combustions for F^-, Cl^-, NO_3^-, SO_4^{2-} and K^+, road dust/soil for Ca^{2+}, Mg^{2+} and NH_4^+ and brick-kiln industries for Na^+ and F^+. The deposition velocities are relatively larger for cationic species than anionic species probably because the soil-derived aerosols (Na^+, K^+, Ca^{2+}, and Mg^{2+}) have higher MMDs.

Integrated GIS approach for characterisation of hydrogeochemical processes governing the groundwater quality in Sabarmati basin, Gujarat, India

RINA KUMARI, CHANDER KUMAR SINGH AND SAUMITRA MUKHERJEE

School of Environmental Sciences, Jawaharlal Nehru University, New Delhi-110067

Factors influencing the groundwater hydrochemistry in pre and post monsoon season were evaluated for a part of Sabarmati river basin of Gujarat, a hub of intense growth of agricultural and industrial activities. Samples were collected on the basis of spectral signature of vegetation and soil as observed on satellite image. 14 water quality parameters were analysed which formed the attribute database for spatial variation of respective parameter using GIS. Graphical plots were used to decipher the hydrogeochemical process occurring in the study area. Gibbs plot, USSL diagram, % sodium and SAR were used to verify the suitability of groundwater for irrigation. It was observed that leaching of wastes disposed from anthropogenic activities and agrichemicals is the major factor along with the natural processes such as weathering, dissolution and ion-exchange. Control of indiscriminate and unplanned exploitation of groundwater, application of fertilizers and disposal of industrial wastes in the affected areas can possibly ensure groundwater protection from further pollution and depletion.

https://doi.org/10.1180/S0026461X00006502 Published online by Cambridge University Press

Porewater composition of cores from Palinuro sea mountain, Italy

N. KUMMER[1]*, B. MERKEL[1], B. PLANER-FRIEDRICH[2] AND M. SCHIPEK[1]

[1]TU Bergakademie Freiberg, Freiberg, Germany (*correspondence: kummer1@geo.tu-freiberg.de)
[2]University of Bayreuth, Bayreuth, Germany

During RV Meteor cruise M73/2 (14-30 August 2007), cores were sampled from a submarine hydrothermal vent site at the Palinuro volcanic complex in the southeastern Tyrrhenian sea, Italy. Pore water samples were taken from the sediment cores using rhizon-samplers. Results from one of the cores are presented showing a distinct pattern for certain elements.

The redox potential changes from 100-200 mV in the upper one meter to strongly reducing conditions (-170 mV) at a depth of 280 cm. The pH has a minimum of 6.1 at a depth of 110 cm. While Fe and Mo show their highest concentrations in the upper parts of the profile, Mn increases with increasingly reducing conditions.

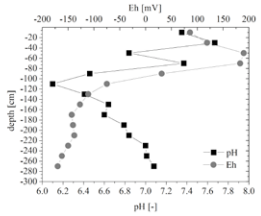

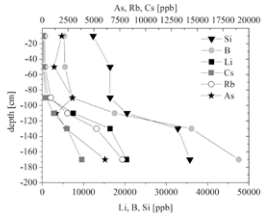

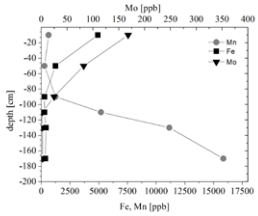

Si, B, Li, Cs, Rb, and As show the same behavior as Mn. While this is expected for As, it is quite surprising for all the other elements which are not redox-sensitive. Major cations and anions as well as electrical conductivity do not change significantly over depth. Arsenic speciation showed a predominance of arsenate and arsenite to a depth of 80 cm. At 90 and 110 cm, mono- (10%), di- (18%), and trithioarsenate (25%) were detected besides arsenate (34%) and arsenite (14%). At 110 cm, trithioarsenate was the predominant species with 64% of total As, followed by 28% dithioarsenate. The geochemical pattern is an indication for upwelling geothermal water and mixing with ocean water in the upper part where Fe and Mo is released from sediment under slightly oxidizing conditions.

Time-resolved emission of iodine from seaweed measured with a new on-line mass spectrometric technique

M. KUNDEL[1], U.R. THORENZ[1], J. BOSLE[1], R.J. HUANG[1,2] AND T. HOFFMANN[1]

[1]Johannes Gutenberg-University, Institute for Inorganic and Analytical Chemistry, Duesbergweg 10-14, 55128 Mainz
[2]School of Physics, Centre for Climate and Air Pollution Studies, National University of Ireland, Galway

Molecular iodine and iodocarbons are released by macroalgae and phytoplankton into the atmosphere. These volatile iodine-containing compounds are involved in the tropospheric ozone depletion and the marine new particle formation. Recent studies suggest that biogenic emissions of molecular iodine rather than iodocarbons are the dominant source of reactive iodine atoms in the marine boundaray layer [1]. Especially during low tide, when the seaweed is exposed to atmospheric air, increased levels of I_2 were detected at different measurement sites [2],[3]. In this work we present a new application of the time-of-flight aerosol mass spectrometer for the determination of I_2 in real-time. ToF-AMS were developed for the measurement of non-refractory atmospheric aerosols with high sensitivity [4]. In order to use the high sensitivity of the ToF-AMS for I_2 measurements, I_2 has to be converted from the gas phase into the particle phase by α-CD/NH_4Br particles inside a 0.5 L flow tube before entering the ToF-AMS. LOD of 300 ppt was achieved for 1 min time resolution and could be improved to 60 ppt for 30 min time resolution. Additionally this method was compared to a recent developed method that combines denuder sampling of I_2 and GC-MS analysis. The newly developed ToF-AMS method was used to explore the time-resolved emission of I_2 by various seaweed species from the eulittoral und sublittoral zone of Helgoland (North Sea, Germany). For our measurements entire seaweed species were removed from sea water, shaken free of excess water and introduced into a 4 L chamber made of glass to simulate low tide conditions. Additional stress was applied to the seaweed by flushing a continous flow of ozonated (20-150 ppb) synthetic air through the chamber to investigate the influence of ozone on the emission of I_2. Furthermore, volatile iodocarbons were quantified by TD-GC-MS and compared to I_2 measurements.

[1] McFiggans *et al*. (2004) *Atmos. Chem. Phys.* **4**, 701–713
[2] Mahajan *et al*. (2009) *Geophys. Res. Lett.* **36**, L16803.
[3] Huang *et al*. (2010) *Atmos. Chem. Phys.* **10**, 4823–4833.
[4] DeCarlo *et al*. (2006) *Anal. Chem.* **78**, 8281–8289.

https://doi.org/10.1180/S0026461X00006502 Published online by Cambridge University Press

Dynamical correlations in transition metal compounds

JAN KUNES

Institute of Physics, AS CR, Cukrovanicka 10, Praha 162 53, Czech Republic (kunes@fzu.cz)

The standard methods of density functional theory describe the eletronic structure of materials in terms of Slater determinants. While such description proved useful in many cases, in transition metal compounds it is often not sufficient. We use the dynamical mean-field theory (DMFT) [1] to study such systems and phenomena related to electronic correlations. The exmples include the spin state transitions in MnO [2] and Fe_2O_3 [3], driven by pressure, and in $LaCoO_3$ [4], driven by temperature. We discuss the relationship of the spin transition to the metal-insulator transition and tendencies towards long-range ordering.

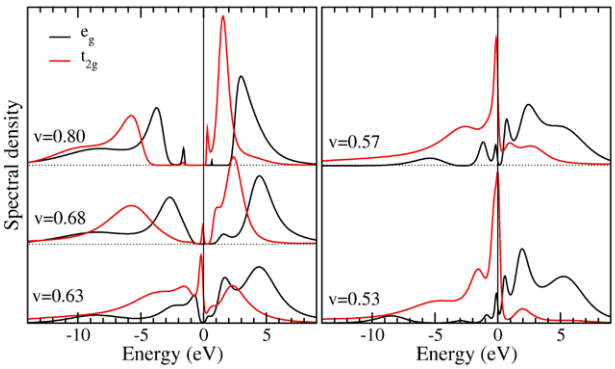

Figure 1: The orbital resolved Mn-*d* spectral density in MnO for various specific volumes. The results correspond to the temperature of 1160 K.

We will show how the local electronic correlation leads to emergence of non-fermionic degrees of freedom, such as the local magnetic moments, and how their fluctuations influence the material properties. The talk will focus on the qualitative differences between the DMFT description and static mean-field theories such as LDA or LDA+U.

[1] Georges *et al*. (1996) *Rev. Mod. Phys*. **68**, 13–125. [2] Kunes *et al*. (2008) *Nature Mater*. **7**, 198–202. [3] Kunes *et al*. (2009) *Phys. Rev. Lett*. **102**, 146402. [4] Kunes & Krapek (2011) arXiv, 1103.2249.

Phyllosilicate dissolution kinetics: experimental observations and Kinetic Monte Carlo modeling

INNA KURGANSKAYA*, ROLF. S. ARVIDSON AND ANDREAS LUTTGE

Dept. of Earth Science, Rice University, Houston 77005, USA (*correspondence: iak2@rice.edu)

We present our recent results in the study of phyllosilicate dissolution kinetics. The major problem in this field is the influence of the layered structure on dissolution mechanism and the difference in reactivity between edge and basal faces. We use an integrated approach including experiments and modelling to understand real crystallographic control of dissolution kinetics. Vertical Scanning Interferometry allows us to observe mineral surface topography during the dissolution process, measure dissolution rates and access their spatial and temporal variability. Detailed information about surface structure has also been obtained from AFM work. We simulate the dissolution of phyllosilicates using Kinetic Monte Carlo (KMC) approach. This stochastic method links elementary reactions taking place on the mineral surface with the topographic outcome of these processes. The KMC model has been parameterised using activation energies of elementary bond-hydrolysis reactions obtained from quantum mechanical calculations. As a result, we have reproduced experimentally-observed dissolution patterns in our KMC simulations (Fig.1). The combination of these techniques will help us to understand complex behaviour of crystalline systems in the dissolution process.

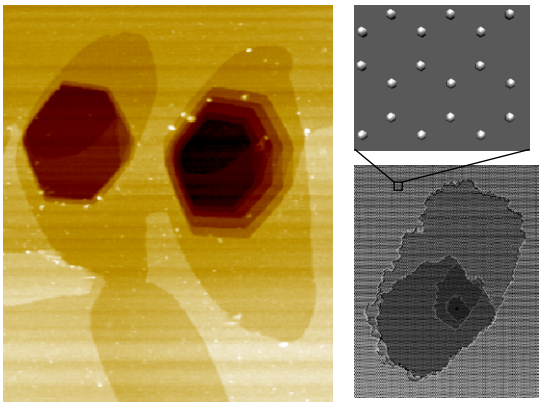

Figure 1: Left: AFM image of etch pit on muscovite {001} face 3x3 μm; Right: Etch pit (50 x 70 nm) obtained from KMC simulations with the enlarged area above showing arrangement of cations (Si/Al)

https://doi.org/10.1180/S0026461X00006502 Published online by Cambridge University Press

The influence of biofilms on fluid flow and contaminant transport in porous media

HANNA KURLANDA*, SUYIN YANG, BRYNE T. NGWENYA, IAN B. BULTER AND STEPHEN C. ELPHICK

School of GeoSciences, University of Edinburgh, Grant Institute, West Mains Rd, King's Buildings, EH9 3JW, Edinburgh, United Kingdom (*correspondence: hkurland@staffmail.ed.ac.uk)

Subsurface biofilm growth is a relatively novel and cost-effective method of bioremediation. Multiple injections of nutrients into the subsurface stimulate biofilm growth, forming a biobarrier. Biobarriers are known to reduce hydraulic conductivity, as well as immobilise metals in the matrix of the exopolymeric saccharides (EPS), produced by bacterial cells.

This research focuses on observing the influence of biofilm growth on transport in homogenous and heterogeneous column experiments under various nutrient conditions, as well as visualising and quantifying biomass of these biofilms *in situ* using x-ray micro computed tomography (μCT). This study will provide insight into materials and processes pertaining to groundwater vulnerability and assess the viability of biofilms to reduce the transport of aqueous metal contaminants. Biofilms were grown under continuous flow conditions in glass columns. A *Pseudomonas putida* culture was injected into the columns for biofilm growth. A decrease in hydraulic conductivity, column outflow and fluid velocity through the duration of the flow experiments was observed, which signifies bioclogging took place in the columns. Biomass distribution was examined using extraction methods and protein/ carbohydrate analysis. Additionally, syringe column experiments were carried out in order to observe and quantify microbially mediated mineral precipitation using μCT. In separate experiments *Sporosarcina pasteurii*, a ureolytic strain, was injected into the syringes to enable biofilm development and also $CaCO_3$ precipitation. The distribution of biomass, mineral precipitates and fluid flow paths in these experiments were visualised using x-ray μCT. Preliminary μCT imaging illustrates that for microbial processes in porous media, both biofilm growth and $CaCO_3$ precipitation as a result of ureolysis, can be visualised and quantified using CT techniques and software.

High-pressure single-crystal elasticity of $MgSiO_3$ and $(Mg,Fe)SiO_3$ perovskites at pressures of the Earth's lower mantle

A. KURNOSOV, D.M. TROTS, T. BOFFA BALLARAN, D. HARRIES[1] AND D.J. FROST

Bayerisches Geoinstitut, Universität Bayreuth, 95447 Bayreuth, Germany

Sound wave velocities obtained in seismology are at the moment the only direct measure of the properties of the Earth's lower mantle. In order to use such measurements to constrain the chemical and thermal state of the Earth's interior, however, knowledge of the pressure dependence of acoustic wave velocities of model minerals are essential. $MgSiO_3$ perovskite-type structures, with the end-member composition or containing some amount of Fe or Al, have been the subject of several studies, since are likely the primary lower mantle constituent. Experiments, however, are limited either to room pressure conditions [1, 2] or to aggregate materials [3, 4] due to the challenge of synthesizing and recovering high-quality single-crystals of this high-pressure mineral. Therefore the best knowledge so of the full elastic constant tensor of orthorhombic (Mg, Fe)SiO_3 perovskites results from first principle calculations [5, 6].

We succeeded to synthesize and select good quality single crystals of MgSiO3 perovskite (Mg - end member) and (Mg, Fe)SiO3 perovskite containing up to 4% of Fe. The crystals are prepared for high-pressure brillouin measurements using FIB (focused ion beam) technology providing double side parallel cutting of the surfaces with required dimensions and quality.

We present the data of simultaneous measurements of sound velocities (by brillouin spectroscopy) and density (by single crystal x-ray diffraction) vs. pressure of the perovskite single crystals loaded in diamond anvil cell with He pressure medium. Behavior of elastic constants calculated from these data and effect of Fe will be discussed in the presentation.

[1] Sinogeikin *et al*. (2004) *Geophys Res Lett* **31**, L06620. [2] Jackson *et al*. (2004) *Geophys Res Lett* **31**, L10614. [3] Murakami *et al*. (2007) *Earth Planet Sci Letters* **256**, 47–54. [4] Jackson *et al*. (2005) *Geophys Res Lett* **32**, L21305. [5] Karki *et al*. (1997) *Am Mineral* **82**, 635–638. [6] Kiefer *et al*. (2002) *Geophys Res Lett* **29**, 1539.

https://doi.org/10.1180/S0026461X00006502 Published online by Cambridge University Press

High magnitude MIF-S due to increased atmospheric $p(O_2)$

F. KURZWEIL[1]*, M. HANNINGTON[2] AND H. STRAUSS[1]

[1]Institut für Geologie und Paläontologie, WWU Münster, D-48149 Münster, Germany (*correspondence: f_kurz01@uni-muenster.de)
[2]University of Ottawa, Ottawa ON, Canada

Earth's atmosphere experienced several profound changes in the geological past. Among these was the Great Oxidation Event (GOE) at ~2.4 Ga as indicated by the subsequent absence of mass independently fractionated sulphur isotopes (MIF-S). The temporal evolution in MIF-S from low towards high magnitude was recently suggested to reflect changes in the total atmospheric composition and not exclusively resulting from variations in $p(O_2)$. [1] proposed that a rise in the atmospheric SO_2/H_2S ratio enlarged the magnitude of MIF-S.

Black shales from the Superior craton (2.71 Ga) record a high magnitude MIF-S signal ($\Delta^{33}S$ up to 4‰) following a period with greatly attenuated MIF-S between 3.2 and 2.7 Ga. Their $\Delta^{33}S$ vs. $\Delta^{36}S$ relationship shows a slope of -1, which appears to be a typical signature of rocks younger than 2.7 Ga. We interpret this shift towards high magnitude MIF-S and the concomitant change in the slope of $\Delta^{33}S$ vs. $\Delta^{36}S$ at 2.71 Ga as a consequence of a rise in atmospheric SO_2/H_2S. However, we suggest that a rise in atmospheric O_2 ultimately caused this increase, not variations in volcanic outgassing [1]. An increase in atmospheric $p(O_2)$ would have strengthened the conversion of H_2S to SO_2 resulting in a higher SO_2/H_2S ratio. Such a scenario would be consistent with a proposed onset of oxidative weathering already at 2.7 Ga [2]. Still, a generally reducing atmosphere kept oxygen levels below 10^{-5} PAL, low enough to allow for MIF-S until the GOE at ~2.4 Ga.

[1] Halevy *et al*. (2010) *Science* **329**, 204–207. [2] Frei *et al*. (2009) *Nature* **461**, 250–254.

Internal structure of icy satellites of Jupiter and Saturn and subsurface oceans

O.L. KUSKOV*, V.A. KRONROD AND A.P. ZHIDIKOVA

Vernadsky Institute of Geochemistry and Analytical Chemistry, Russian Academy of Sciences, 119991 Moscow, Russia (ol_kuskov@mail.ru)

Models of the internal structure of icy satellites have been constructed on the basis of the mass and moment of inertia constraints, geochemical constraints on composition of silicate fractions of ordinary and carbonaceous chondrites, and thermodynamic data on the equations of state of minerals and high-pressure ices [1, 2]. The mass and moment of inertia values are used as input data for determination of the thickness of an outer water-ice shell, the density distribution with depth, and the core sizes and masses. The equilibrium phase assemblages in the system Na_2O-TiO_2-CaO-FeO-MgO-Al_2O_3-SiO_2 were calculated using the technique of free energy minimization combined with the Mie-Grüneisen equation of state. The density variations in the mantle and Fe-S core radii are found by the Monte-Carlo method. The allowed thickness of Europa's H_2O layer (whether liquid or ice) ranges from 115 to 135 km (6-8% of total mass) for a L/LL-type chondritic mantle [2]. Two alternative models of Ganymede's outer shell composed of the high-pressure ice phases or of water and ice are considered. The thickness of the shell is in the range 800-900 km. The content of H_2O in Ganymede's outer shell is 46-48% [1]. We show that Callisto must only be partially differentiated into an outer ice-I layer, a water ocean, a rock-ice mantle, and a rock-iron core. The maximum thickness of the outer water-ice shell is up to ~300 km and that of the internal ocean is about 150 km. The total amount of H_2O in Callisto is found to be 48-55 wt%. The results of modelling support the hypothesis that Callisto may have an internal liquid-water ocean [2, 3]. The correspondence between the density and moment of inertia values for the Galilean satellites shows that their bulk compositions may be, in general, similar and may be described by the composition close to a material of the L/LL type chondrites [1-3]. Planetesimals composed of these types of ordinary chondrites could be considered as analogues of building material for the rock-iron cores of the Galilean satellites. A comparison of the internal structure of Ganymede and Callisto with that of Titan has been made.

[1] Kuskov O.L. & Kronrod V.A. (2001) *Icarus* **151**, 204–227. [2] Kuskov O.L. & Kronrod V.A. (2005) *Icarus* **177**, 550–569. [3] Kuskov O.L. & Kronrod V.A. (2005) *Solar Syst. Res*. **39**, 283–301.

https://doi.org/10.1180/S0026461X00006502 Published online by Cambridge University Press

Geochemical and isotopic analyses of non-volcanogenic hot springs in central Japan

C. KUSUDA[1]*, H. IWAMORI[2], K. KAZAHAYA[3], N. MORIKAWA[3], M. TAKAHASHI[3], H.A. TAKAHASHI[3], M. OHWADA[3], T. ISHIKAWA[4], M. TANIMIZU[4] AND K. NAGAISHI[4]

[1]Univ. Tokyo, Tokyo 113-0033, Japan (*correspondence: chiho-kusuda@eps.s.u-tokyo.ac.jp)
[2]TITECH, Tokyo 152-8550
[3]Geol. Surv. Japan, AIST
[4]Kochi Inst. Core Sample Res., JAMSTEC

The main aim of this study is to contribute to better understanding of fluid processes occurring in subduction zones with a comprehensive framework involving slab-derived fluids to near-surface fluids such as seawater, meteoric water and hot spring waters.

Our previous geochemical research on the Arima-type brine, anomalous non-volcanogenic hot springs with extreme high $^3He/^4He$ (e.g. [1, 2, 3]), identified and characterized the concentrated 'source' brine in a robust multi-elemental/isotopic space, and so far, supports the idea that NaCl-CO_2-rich aqueous fluids, which are possibly slab-derived fluids originated from subducting oceanic crusts, might have uprisen from a deep part of the forearc region and might supply solutes, gases and water itself to the brine.

While several other studies estimated the contribution of slab-derived fluids to island-arc magmatism (e.g. [4]), in non-volcanic or forearc regions, their involvements have been hardly found.

Therefore we extended our research area from the Kinki district in southwest Japan to forearc regions in central Japan, where two different slabs have been subducting, which might imply that one could expect involment of two different slab-derived fluids. Along the Median Tectonic Line, which divides the adjacent forearc region in two, there are several non-volcanogenic hot springs, some of which are thought to be classified as the Arima-type brine. Here we present the results of our geochemical and isotopic analyses of these hot springs in forearc regions in central Japan.

[1] Masuda *et al*. (1985) *Geochem. J.* **19**, 149–162. [2] Matsumoto *et al*. (2003) *Earth Planet. Sci. Lett.* **216**, 211–230. [3] Morikawa *et al*. (2008) *Geochem. J.* **42**, 61–74. [4] Nakamura *et al*. (2008) *Nature Geoscience* **6**, 380–384.

Structure and compositions of zircon grains from lower unites of Norilsk lava section

D.V. KUZMIN[1,2]*, A.V. SOBOLEV[1,3,4], O.B. KUZMINA[1] AND N.A. KRIVOLUTSKAYA[4]

[1]Max Planck Institute for Chemistry, Postfach 3060, 55020 Mainz, Germany (*correspondence: d.kuzmin@mpic.de)
[2]VS Sobolev Institute of Geology and Mineralogy, Novosibirsk, Russia
[3]ISTerre, University J. Fourier BP 53, 38041 Grenoble Cedex 9, France (alexander.sobolev@ugf-grenoble.fr)
[4]Vernadsky Institute of Geochemistry, RAS, 119991 Moscow, Russia

We intend to perform high precision absolute dating of lower unites of Norilsk volcanic section in order to understand evolution of Siberian flood basalts and their relation to P-T mass extinction [1]. For that purpose we picked up zircon grains from lower unites of Norilsk volcanic suit: Ivakinskaya (Iv), Severminskaya (Sv), Gudchikhinskaya (Gd) and Tuklonskaya (Tk) units. Here we report the first data on the structure and composition of 275 zircons grains obtained by CL, EPMA and LA ICP-MS techniques.

The studied zircons were subdivided into three groups. The group 1 (almost 70% of studied grains) includes euhedral grains with thin oscillatory zoning, group 2 (25% of population) consists of euhedral grains with low fluorescent cores surrounded by oscillatory zoned rims, and group 3 (5% of population) contains almost unzoned rounded low fluorescent grains. The groups 1 and 2 show week compositional zoning with slight decreasing of REE concentration towards the rim. They include the following minerals shown in the order of decreasing frequency: apatite, sphene, feldspars, crystalized melt, ilmenite and quartz. They possess relatively high Th/U ratios (0.3-2), are enriched in HREE and are similar to zircons of magmatic origin [2, 3]. Group 3 zircons have low Th/U ratios (0.05-0.25), are markedly depleted in HREE suggesting equilibrium with garnet and are likely of metamorphic origin.

We conclude that zircons of group 1 and 2 were likely crystallized *in situ* in basaltic flows and are good candidates for absolute dating.

[1] Sobolev, A.V. *et al*. (2009) *Petrology* **17**, 253–286. [2] Hoskin & Schaltegger (2003) *Am. Min. Soc.* **53**. [3] Belousova, E. *et al*. (2002) *CMP* **143**, 602–622.

https://doi.org/10.1180/S0026461X00006502 Published online by Cambridge University Press

Weathering and pore water evolution in the foreland of retreating glacier, SW Spitsbergen

M. KWAŚNIAK-KOMINEK, M. MANECKI, G. RZEPA AND J. CZERNY

AGH University of Science and Technology, al.Mickiewicza 30, 30-059 Cracow, Poland (*correspondence: monika.kwasniak@gmail.com)

Chemical weathering and soil forming processes which are associated with retreating glaciers contribute to high chemical denudation observed in polar regions. Retreating glaciers uncover fresh regolith, initial evolution of which may be dominated by few simple processes. The area of this study is the foreland of Werenskiold glacier near SW coast of Spitsbergen. This glacier has been countinuously retreating during the last century by several meters a year [1]. The objective of this study is correlation between the chemistry of pore waters and the mechanisms of alternation or dissolution of minerals present in regolith with respect to the distance from the glacier front (age of exposure). This is a part of large research effort on weathering, soil formation and initial microbiological activity on a foreland of Arctic glacier initiated with the International Polar Year in 2007.

Werenskiold glacier basin is eroded in metamorphic rocks which belong to Precambrian Hecla Hoek Succession. These are mostly carbonates, quartzites, phyllites, shists, greenshists and amphibolites [2]. In accordance with other studies, the carbonate dissolution dominates in the youngest glacial sediments while silicate weathering is relatively significant in the oldest sediments. The composition of water can be explained mostly by dissolution/crystallization accompanied with redox reactions. Alterations of minerals identified with optical microscopy, XRD and SEM-EDS include dissolution of carbonates and oxidation of pyrite accompanied with formation of clays. Systematic changes between water samples correlate with distance from the glacier front (with the age of soils): e.g. the pH decreases from 8, 6 to 7, 7 while TDS increases from 133 to 748 mg/L. Inverse modeling with PHREEQC was used to propose the mechanisms of mineral transformation. The waters evolve from carbonate-dominated to sulfate-dominated. This might indicate that with time, pore waters reach the equilibrium with carbonate minerals while being countinuously supplied with SO_4^{2-} from sulfides oxidation.

The research is supported by MNiSW grant N N307 473638.

[1] Bukowska-Jania (2007) *Pol. Polar Res.* **28**, 137–155. [2] Czerny J. Kieres A. Manecki M. & Rajchel J. 1993. Geological map of the SW part of Wedel Jarlsberg Land, Spitsbergen **1**, 25000. AGH-Kraków.

Roles of sulfate and Fe^{III} reduction on microbial community development

M.J. KWON[1,2], M.I. BOYANOV[1], D. ANTONOPOULOS[1], J. BRULC[1], K. KEMNER[1] AND E.J. O'LOUGHLIN[1]

[1]Biosciences Division, Argonne National Laboratory, Lemont, IL 60439 USA (mankwon73@gmail.com)

[2]Korea Institute of Science and Technology (KIST) – Gangneung Institute, Gangneung 210-340 S. Korea

To better understand the roles of sulfate- and/or iron-reduction on microbial community development, bicarbonate-buffered batch systems were created with acetate or lactate as the electron donor. Added electron acceptors included 2-line ferrihydrite, goethite, or lepidocrocite, in the presence or absence of sulfate. The batch systems were inoculated with the native microbial community present in a subsurface sediment. The rate of Fe^{III} reduction was low in the absence of sulfate. However, the rate and extent of Fe^{III} reduction increased more than 10 times with 10 mM sulfate. Sulfate reduction occurred concurrently with Fe^{III} reduction suggesting abiotic Fe^{III} reduction by sulfide. X-ray absorption fine-structure (XAFS) analysis confirmed the formation of ferrous sulfide as the major secondary mineral phase in these incubations. The rates of sulfate and Fe^{III} reduction were significantly faster with lactate than with acetate. Lactate promoted both sulfate and Fe^{III} reduction in all incubations, while acetate stimulated sulfate and Fe^{III} reduction only in ferrihydrite and goethite incubations. Acetate oxidation was coupled with sulfate and Fe^{III} reduction; however, lactate was rapidly fermented to acetate and propionate, followed by propionate oxidation coupled with sulfate reduction. Terminal Restriction Fragment Length Polymorphism (T-RFLP) yielded unique microbial community profiles. The presence of sulfate resulted in distinct community development likely due to the proliferation of acetate- or propionate-utilizing, sulfate-reducing bacteria. During the experiment, the community in lepidocrocite incubations evolved in a very different way compared to those in the other Fe^{III} (hydr)oxide incubations indicating that the nature of the Fe^{III} (hydr)oxide can affect microbial community development. However, after the complete consumption of sulfate the microbial community compositions in all incubations (except lepidocrocite plus acetate incubation) were similar to each other. These results show that the availability of sulfate, the type of Fe^{III} (hydr)oxide present, and the added electron donor can have a strong effect on the development of subsurface microbial communities.

https://doi.org/10.1180/S0026461X00006502 Published online by Cambridge University Press

Deciphering the evolution of continental crust: Insights through Laser Ablation Split-Stream (LASS) petrochronology

ANDREW R.C. KYLANDER-CLARK* AND BRADLEY R HACKER

University of California, Santa Barbara, 93106-9630 (*correspondence: kylander@geol.ucsb.edu)

One of the biggest challenges in the determination of the timing and rates of continental subduction is tying the age of a particular mineral to the conditions (i.e. pressure, temperature, fluid composition) at which that phase grew. Recent advances in microbeam techniques have greatly increased our understanding of crustal evolution by enabling this linkage. The most common target for U-Th-Pb petrochonology is zircon: its REE pattern reveals the coexistence of garnet (depleted HREE) and plagioclase (positive Eu/Eu*) and cathodoluminescence imaging can be used to link the ages and trace-element concentrations of spot analyses. The age of monazite can also be linked to certain conditions: most commonly, yttrium zoning is used a proxy for growth in the presence or absence of garnet.

Here we present a more accurate, comprehensive, and simplified procedure to obtain petrochronologic data and thus assess the P–T–t conditions of any individual spot analysis. The LASS—laser ablation split-stream—technique consists of concurrent analyses of single laser ablation spots on both a multi-collector (U-Th-Pb age) and single-collector (trace-element data) ICP-MS. LASS allows both rapid (<1 minute/spot analysis) and high-precision (<1%/age population) measurements and an unambiguous link between mineral age and (re)crystallization conditions.

The Western Gneiss Region of western Norway provides the perfect natural laboratory to exemplify the advantages of LASS petrochronology. Zircons from a garnet-bearing gneisses show >20 Myr of (re)crystallization, however, REE data show that these zircons grew under three distinct conditions: 1) garnet-poor prograde growth at 425.8 ± 4.6 Ma, 2) garnet-rich peak growth at 406.9 ± 5.7 Ma, and 3) garnet-breakdown retrograde growth at ~400 Ma. Without LASS, making this distinction would be nearly impossible. Monazite can also reveal complex age/element zoning; monazite analyzed from a meta-pelite yield high-Nd cores of 413.6 ± 3.9 Ma, Low-Nd mantles of 401.1 ± 4.4 Ma, and high-Y, low-Sr rims of 393.5 ± 3.4 Ma.

REE mineralization of high grade REE-Ba-Sr and REE-Mo deposits in Mongolia and China

J. KYNICKY[1]*, XU. CHENG[2], A.R. CHAKHMOURADIAN[3], E. REGUIR[3], H. CIHLÁŘOVÁ[1] AND M. BRTNICKÝ[1]

[1]Mendel University in Brno, 613 00 Brno, Czech Republic (*correspondence: jindrich.kynicky@mendelu.cz)
[2]Peking University, Beijing 100871, China (*correspondence: xucheng1999@hotmail.com)
[3]University of Manitoba, Winnipeg, Manitoba, Canada (*correspondence: chakhmou@cc.umanitoba.ca)

The exact causes and mechanisms responsible for the uniquely high levels of REE in carbonatites relative to any other igneous rock remain debated. To investigate these mechanisms, a large suite of REE-bearing carbonatites from Mongolia (Mushgai Khudag, Lugiin Gol, Omnot Olgii, Khurimt Khad Tolgod) and China (Daluxiang, Maoniuping, Huanglongpu, Huayangchuan, Bayan Obo) was examined.

All carbonatites are predominantly composed of medium- to coarse-grained calcite (60-90%). Accessory non-carbonate phases include mainly apatite, alkali feldspars, fluorite, phlogopite, sulphates and sulphides. The principal REE hosts are fluorocarbonates (<20 vol. %) and monazite (<5 vol. %).

Fluorocarbonates occur as complex intergrowths of bastnäsite with parasite or synchysite. Bastnäsite-(Ce), synchysite- (Ce) and monazite-(Ce) also rarely occur as discrete crystals. There is a structurally controlled compositional variation among the major REE minerals, but carbonatites from different deposits feature almost identical REE-HFSE mineralization patterns.

Chondrite-normalized whole-rock REE profiles exhibit a steep negative slope and lack detectable anomalies. The REE minerals show consistent enrichment in light REE [$(La/Nd)_n$=1.0–3.4]. In this respect, the carbonatite-hosted REE mineralization differs from that in the world's largest REE deposit at Bayan Obo, where the $(La/Nd)_n$ ratios are more variable and generally lower. The REE distribution patterns of individual REE minerals are similar, with the exception of Huanglongpu and Huayangchuan, where REE mineralization is associated with Mo and Mo-Th mineralization. At these two localities, whole-rock and mineral-specific REE patterns are broadly similar, but the latter show some enrichment in heavy REE.

We propose a similar mineralogical model for all investigated deposits with the exception of Bayan Obo. The high-grade carbonate-hosted REE deposits at Daluxiang and Maoniuping are nearly exhausted, but the little-explored Huanglongpu-Huayangchuan cluster has a definite potential as a viable REE resource of the future. Small- to medium-sized deposits in southern Mongolia may also have some economic value owing to their overall high grade (7-15 wt. % REE_2O_3) and a healthy global REE market.

https://doi.org/10.1180/S0026461X00006502 Published online by Cambridge University Press

Origin of the seamounts near Futuna Island, SW Pacific

S. LABANIEH[1], G. CHAZOT[1], J. ETOUBLEAU[2], Y. FOUQUET[2], L. DOSSO[1] AND C. HEMOND[1]

[1]IUEM, UBO, Brest, France
[2]IFREMER, Brest, France

Futuna Island, located in the SW pacific, is bordered by the North Fiji fracture zone, the active Tonga and Vanuatu subduction zones and associated Lau and North-Fiji back-arc basins, and the currently active Samoan hotspot. A cruise was conducted in August 2010 with the aim to map and sample the oceanic basement near Futuna Island. Bathymetric mapping reveals complex seafloor morphology with multiple areas of numerous seamounts and several very large and isolated caldeiras.

We measured major and trace elements and Pb isotopic ratios on samples collected from dredges or Nautile dives. Lavas collected on the seamount province range from sub-alkaline basalts to trachy-andesites, with SiO_2 content ranging from 45.6 to 60.1 wt%. Lavas exhibit variable La/Yb ratios that define a spatial gradient: north-western lavas are enriched in Light Rare Earth Elements (LREE) compared to Heavy Rare Earth Element (HREE) (La/Yb from 2.2 to 9.9) while south-eastern lavas are depleted in LREE (La/Yb from 0.74 to 1.1). In a Pb isotope diagram, lavas cover a fairly large array ($^{206}Pb/^{204}Pb$ from 18.0 to 19.0) and define a mixing trend. La/Yb and Pb isotopic ratios are positively correlated. We suggest that seamounts near Futuna Island are due to partial melting of an Indian-like mantle that has been variously metasomatised by an enriched end-member composed of Samoan plume material and a component similar to the subducting Louisville ridge basalts. The mixing proportions of end-members are geographically controlled by the infiltration in the mantle of the Samoan plume through the tearing of the Pacific plate at the junction between the Tonga arc and the North-Fiji fracture zone.

Multiple sulfur isotopes in basalts: Chemical geodynamics in the South Atlantic mantle

J. LABIDI*, P. CARTIGNY, J.J. BOURRAND AND N. ASSAYAG

Laboratoire de Géochimie des Isotopes stables, IPGP, 1 rue Jussieu, 75005 Paris (*correspondence: labidi@ipgp.fr)

Sulfur isotopes have placed significant constraints on past and present external cycle of sulfur. For example, the disappearance of non-zero $\Delta^{33}S$ values in archean sediments at 2.4 Ga show strong evidence for the atmosphere oxygenation [1].

Present day oceanic crust and sediments show a large range of $\delta^{34}S$: from -40‰ to +30‰, mostly between -7‰ and +5‰. The recycling of these crustal components in the mantle source of MORB may thus be identified with sulfur isotopes. Yet, the deep part of the sulfur cycle remains comparatively unconstrained: Only two studies have reported $\delta^{34}S$ of MORB (n=16; $\delta^{34}S_{MORB} = +0.8 \pm 1‰$)[2][3].

Using an improved method allowing quantitative recovery of sulfur from basaltic glasses, we report the first measurements of the four sulfur stable isotopes in 19 MORB from the South Atlantic ridge. The external precision and accuracy are ± 0.01‰, 0.25‰ and 0.20‰ in 2σ for $\Delta^{33}S$, $\delta^{34}S$, and $\Delta^{36}S$ respectively.

$\delta^{34}S$ values of our samples are all negative (mean $\delta^{34}S$ = -0.89 ± 0.6‰, 1σ) except for one sample at +1.1‰. The variability of $\delta^{34}S$ in our dataset is 3‰, which is significantly larger than the analytical precision. This enables us to discuss the $\delta^{34}S$ variability in MORB in terms of a meaningful geological tracer. We suggest than this variability rather reflect source heterogeneity rather than magmatic processes as it is correlated to radiogenic isotopes enrichments.

$\Delta^{33}S$ and $\Delta^{36}S$ of our samples are slightly but significantly non-equal to 0‰ and are of the same sign: -0.025‰ and -0.200‰ respectively (mean values). Both mixing with/within a subducting slab and/or revised terresrial original $\Delta^{33}S$ and $\Delta^{36}S$ could explain this feature. The respective contribution of these two extreme scenarios will be discussed at the conference.

[1] Farquhar *et al*. (2000) *Science* **289**, 256–258. [2] Sakai *et al*. (1983) *GCA* **48** 2433–2441. [3] Chaussidon *et al*. (1991) *Spec. Pub. J.Geochem. Soc*. **3**, 325–337.

https://doi.org/10.1180/S0026461X00006502 Published online by Cambridge University Press

Hydrothermal synthesis of lentil shaped $ThSiO_4$ nanoparticles

S. LABS, H. CURTIUS, D. BOSBACH

Institute of Energy and Climate Research, Forschungszentrum Jülich GmbH, 52425 Jülich, Germany (*correspondence: s.labs@fz-juelich.de)

We synthesized thorite ($ThSiO_4$) by a hydrothermal route for which we have adapted the protocol used by Fuchs and Hoekstra [1]. All samples were investigated by XRD and show the successful formation of $ThSiO_4$, molecular composition was confirmed by EDX. IR as well as DTA measurements suggest the well known phenomenon of the presence of H_2O in the crystal lattice in some samples. Complete new insight was obtained through SEM investigations, which reveal a rather unusual morphology of the synthesized $ThSiO_4$. Particles are uniform in size, lentil shaped and are 150 – 400 nm along the longest dimension. After heating up to 1000°C the shape and size of the particles remains merely unchanged.

The size of the nanoparticles, as well as their consistency can be influenced by synthesis temperature, concentration and pH-value. Therefore, particle growth most probably follows kinetically controlled mechanisms. However, further investigations and comparison to calculated data are essential. With the synthesis of $ThSiO_4$ being successfully accomplished, work on substituting Th for U is in progress, currently we are investigating the potential of UF_4 as a precursor for this matter.

[1] L.H. Fuchs, H.R. Hoekstra (1959) *Am. Min.* **44**, 1057-1063.

Recycling of juvenile supracrustal rocks in Mesozoic batholiths: Implications for crustal growth

JADE STAR LACKEY

Pomona College Geology Department, 185 E. Sixth Street, Claremont, CA, 91711, USA (*correspondence: jsl04747@pomona.edu)

The Mesozoic batholiths of the circum-Pacific region represent voluminous production of granitic crust; however, the proportion of these granitic batholiths that are re-worked, continental crust, versus young, recycled supracrustal rock (volcanogenic sedimentary rocks or ocean crust), remains uncertain.

Oxygen isotopes are particularly well suited to detect recycling of young rocks that have been hydrothermally altered at Earth's surface before being buried and re-melted. Moreover, because such rocks may be recycled before significant ingrowth occurs in radiogenic isotope systems, $\delta^{18}O$ and radiogenic systems can be decoupled.

Oxygen isotope studies of zircon in the Sierra Nevada batholith (SNB), California [1], show the highest $\delta^{18}O$ values (typically >7.0‰) in the Early Cretaceous western SNB, and the largest range of values, 5.3–8.7‰. $\delta^{18}O$ is commonly anti-correlated with radiogenic systems, indicating a significant (up to 20%) component of juvenile rocks in early arc magmas. In contrast, eastern SNB magmas, including the Late Cretaceous Sierra Crest magmatic centers, are typically lower $\delta^{18}O$ (<6.5‰) and vary by less than 1‰; radiogenic systems suggest greater input of age rock, likely lithospheric mantle [2], and not North American continental crust. The overall pattern of lower and more uniform $\delta^{18}O$ with time shows increasingly efficient magmatic recycling of pre-existing wallrock and hybridization with mantle derived magmas that averaged out $\delta^{18}O$ heterogeneity in the Sierran arc.

Thus, the contribution of juvenile supracrustal rocks to Mesozoic batholiths appears more significant that previously thought. Moreover, when accreted terranes are recycled in convergent margin arcs, an intermediate refinement step facilitates the conversion of juvenile arc terranes to granitoid crust. Recent work in other Mesozoic batholiths shows similar reworking of such rocks, suggesting the process is common operative, and an important step in the conversion oceanic arcs to continental crust.

[1] Lackey *et al.* (2008) *J. Petrol* **49**, 1397–1426. [2] Coleman *et al.* (1997) *I. Geol Rev.* **39**, 768–787.

https://doi.org/10.1180/S0026461X00006502 Published online by Cambridge University Press

Carbon storage technology potentials and difficulties

K. LACKNER

(kl2010@columbia.edu)

The challenges of capture and purification of carbon dioxide from flue gases or from the air is a subject that has received significant attention. Of equal impotance is addressing what to do with the carbon dioxide once it has been purified. Work on the subsequent safe and permanent disposal of carbon dioxide has focused on underground injection or the production of solid mineral carbonates. However, such permanent storage represents an enormous challenge mainly because of the sheer volume of emissions. This talk will also address storage technologies and put them in perspective with regard to technical difficulties, storage capacity, permanence of storage, storage safety and the ability to account for the stored carbon.

Sequestration of trace elements during nucleation and growth of serpentine minerals under hydrothermal conditions

ROMAIN LAFAY*, GERMAN MONTES-HERNANDEZ AND EMILIE JANOTS

Institut des Sciences de la Terre (ISTerre), UJF-CNRS, F-38041 Grenoble, Cedex 9, France (*correspondence: romain.lafay@ujf-grenoble.fr, german.montes-hernandez@obs.ujf-grenoble.fr)

Serpentinites observed in oceanic crust and exhumed mafic rocks contain high levels of trace elements or fluid mobile elements relative to primitive mantle. The concentrations in these elements are controlled by fluid-rock interactions and they represent excellent markers of mass transfert in complex geodynamics systems. Serpentinization processes have been experimentally investigated at different geological conditions, but, rare experimental studies have considered the presence of trace elements during nucleation and growth of serpentine minerals.

In the present study, serpentine nanofibers of chrysotile were nucleated-grown from H_2SiO_3-$MgCl_2$-NaOH hydrothermal system, referred as '*silica-gel system*' (300°C, Mg/Si=1.5, 76bar and pH>13). Liquid-solid distribution coefficients (K_D) for B, Cs, As, Sb and Li were estimated by fitting the experimental sequestration isotherms for each trace element (see for ex. [1]). Additionnnaly, small static-batch reactors were also used to simulate a more realistic serpentinization hydrothermal conditions in presence of the same trace elements. In this '*olivine system*', olivine (San Carlos) alteration was investigated at different physicochemical conditions of T (150-200°C), pH (0.5-13.5), particle size (1-150μm), liquid/solid weigh ratio (5-15), reaction duration (0.25-3 months). Trace element concentration in the fluid was fixed at 200mg/L.

Preliminary results by FESEM, XRDand BET reveal that the presence of trace elements has not significant effect on textural properties of chrysotile nanofibres grown from silica-gel system. Concerning the olivine system, three nanocrystal morphologies (conical, cylinder in cylinder and fibrous) of chrysotile and associated brucite nanoparticles were clearly observed at high pH (>13). Conversely, slight alteration of olivine was observed at low pH (<2) at the same T, particle size, reaction time and liquid/solid ratio conditions. More details for both experiment types (silica-gel and olivine systems) will be reported in [2].

[1] Montes-Hernandez *et al* (2009). *J. Hazard. Mater.* **166** 788–795. [2] Lafay *et al*. (in redaction)

https://doi.org/10.1180/S0026461X00006502 Published online by Cambridge University Press

Understanding O_2-deficient and CO_2-enriched gas production and migration in the subsurface above a coal post-mining area through *in situ* gas monitoring and modelling

S. LAFORTUNE, A. CHARMOILLE AND Z. POKRYSZKA

INERIS (French National Institute for Industrial Environment and Risks), Parc Technologique ALATA, BP 2, 60 550 Verneuil-en-Halatte, France (firstname.name@ineris.fr)

Context

INERIS works for 3 years on the characterization of O_2-deficient and CO_2-enriched gas production and migration processes above a former coal mining area where gas emissions occur at surface and which is close to a peat bog. The main objectives of this work were to determine the composition and origin of the emitted gas and the dynamics of its migration from the subsurface rock strata to the surface.

Study and results

In 2009, analyses (gas concentrations and $\delta^{13}C$ isotopic signatures) were performed during spells of low barometric pressure and gas flux was determined at surface of the studied area. Analyses were performed on field and in lab. Results have shown that emitted gas cannot be from mine or peat origin, respectively because it does not contain methane but CO_2 and because isotopic signatures do not match.

In 2010, a continuous gas monitoring was setup on field during a 6-month period. $\delta^{13}C$ isotopic signature of CO_2 was also monitored on field and gas/water samples have been collected for further analyses in lab. Results have shown that CO_2 emissions dynamics is linked to barometric pressure changes. We have also demonstrated that emitted gas cannot come from groundwater degassing, because dissolved gas quantity is not sufficient to explain gas concentrations measured at surface. That means that CO_2 is produced above the water table, in the saturated zone. A modelling study has shown that pyrite oxidation associated to carbonate dissolution is probably the reaction scheme that produces CO_2. Then main fractures lead CO_2 towards surface.

Scope of the presentation

The presentation will detail the methodological and metrological approaches that have been used in this study to characterize gas production and migration in the subsurface above a coal post-mining area. We will present our results, discuss the different gas origins that have been examined, describe migration processes and explain our conclusions.

Tracing crustal recycling in the mantle sources of the Cape Verde and Azores plumes using stable Mo isotope measurements

Y.J. LAI*, T. ELLIOTT AND M. WILLBOLD

Bristol Isotope Group, Dept. of Earth Sciences, Univ. of Bristol, Queens Road, Bristol, BS8 1RJ, UK (*correspondence: Y.J.Lai@bristol.ac.uk, tim.elliott@bristol.ac.uk, M.Willbold@bristol.ac.uk)

Constraining the role of crustal recycling is key to understanding the causes of mantle heterogeneity. In the past, radiogenic isotopes (Sr, Nd, Pb and Hf) and stable isotopes (Li) have been used as tracers to study this process, but none yield unequivocal signatures of recycling. In this study, we investigate the Mo stable isotope system as a new, potential tracer of recycled crust. Recent studies (see summary in [1] and unpublished data in [2-3]) have shown that the isotopic composition of Mo becomes fractionated in low temperature environments, with a notable offset of $\delta^{97}Mo$ between seawater (+1.6‰) and Mn-crust (-0.5‰). Mo isotopes could therefore be a potential tracer for deep mantle recycling of crustal components that have experienced low-temperature alteration on the Earth's surface. Literature $\delta^{97}Mo$ values of igneous rocks define a narrow range of $\delta^{97}Mo$ (-0.06 to +0.17 ‰) yet the uncertainties related to the analytical methods used so far (2S.D. < 0.1‰) do not allow much resolution of primary signature within this small range. Here we present Mo isotopes in oceanic island basalts from Cape Verde Islands and Azores archipelago that were determined using a newly-devised, higher-precision MC-ICPMS method (2S.D. is 0.03‰). Systematic variations of $\delta^{97}Mo$ values with key trace element ratios (i.e. Pr/Mo) indicate that the mantle sources of the Cape Verde and Azores contain various amounts of components that must have experienced alteration on the Earth surface in the past.

[1] Anbar (2004) *Rev. Min. Geochem.* **55**, *429–454*. [2] Vils *et al.* (2011) *this volumn*. [3] Freymuth *et al.* (2011) *this volume*.

https://doi.org/10.1180/S0026461X00006502 Published online by Cambridge University Press

Soil carbon build-up during soil formation, influenced by different forms of land use

G.J. LAIR AND W.E.H. BLUM

Institute of Soil Research, Dep. Forest and Soil Sciences, University of Natural Resources and Life Sciences Vienna (BOKU), Austria, (georg.lair@boku.ac.at, winfried.blum@boku.ac.at)

Soil carbon is the result of solar energy and one of the two important non-living components of soils, influencing physical, chemical and biological soil characteristics. Moreover, organic carbon is the driving force of mineral weathering and soil formation [1].

Based on a chronosequence of alluvial soils in the Danube River Basin near Vienna/Austria (covering an age range from approximately 50 – 6000 years of soil formation; [2]), carbon build-up under different forms of land use (forest, grassland and agricultural cropping) is shown, looking into the vertical C distribution as well as its influence on aggregate formation and distribution within different soil aggregates. The influence of N on C-build-up in the Chernozem-soils is discussed.

[1] Blum (2010) *Geochemica & Cosmochimica Acta*, Abstracts p99. [2] Lair *et al*. (2009) *QGC*, **4**, 260–266.

Imaging nanoparticle transport through porous media using magnetic resonance imaging

SUSITHRA LAKSHMANAN[1,*], W.M. HOMES[2], W.T. SLOAN[3] AND V.R. PHOENIX[1]

[1]Department of Geographical and Earth Sciences, University of Glasgow, G12 8QQ, UK (*correspondence: lakshmanan.susithra@ges.gla.ac.uk, Vernon.Phoenix@ges.gla.ac.uk)

[2]Wellcome Surgical Institute, University of Glasgow, UK (wmh5b@udcf.gla.ac.uk)

[3]Department of Civil Engineering, University of Glasgow, UK (w.sloan@civil.gla.ac.uk)

While most renowned for its use in the medical sciences, magnetic resonance imaging (MRI) has tremendous potential for revealing transport processes in engineered and geologic systems. Its ability to non-invasively image inside materials that are opaque to other imaging methods is a particular strength. Here, we report on the application of MRI to image nanoparticle transport through porous geologic media. Commercially available paramagnetically tagged (Gd) nanoparticles are used; the paramagnetic tag making the nanoparticle visible to MRI.

Nanoparticle transport was imaged as nanoparticles migrated through packed columns of quartz and dolomite sands and gravels. These images were calibrated using T_2 parameter maps to provide fully quantitative maps of nanoparticle concentration at regular time intervals throughout the column (T_2 being the spin-spin relaxation time of ^{1}H nuclei). Positively charged nanoparticle transport was significantly retarded in dolomite compared to quartz due to electrostatic attraction between nanoparticle and dolomite surfaces. Data was evaluated with CXTFIT to estimate solute transport parameters. MRI data fitted well to CXTFIT models of nanoparticle transport, indicating MRI was collecting usable and reliable datasets.

https://doi.org/10.1180/S0026461X00006502 Published online by Cambridge University Press

Alginate control on calcite precipitation rate

L.Z. LAKSHTANOV[1,2]*, N. BOVET[1] AND S.L.S. STIPP[1]

[1]Nano-Science Center, Deptartment of Chemistry, University of Copenhagen, Denmark (bovet@nano.ku.dk, stipp@nano.ku.dk)

[2]Inst of Experimental Mineralogy, 142432 Chernogolovka, Russia (*correspondence: leonid@iem.ac.ru)

The kinetics of calcite precipitation in the presence of alginate was investigated using the constant composition technique. In the concentration range investigated (0.0002 to 0.005 g L^{-1}), alginate inhibits calcite precipitation. The extent of inhibition increased with increased alginate concentration and decreased solution supersaturation.

Alginate adsorption, derived from normalized calcite precipitation rates, is described satisfactorily by the Langmuir adsorption model.

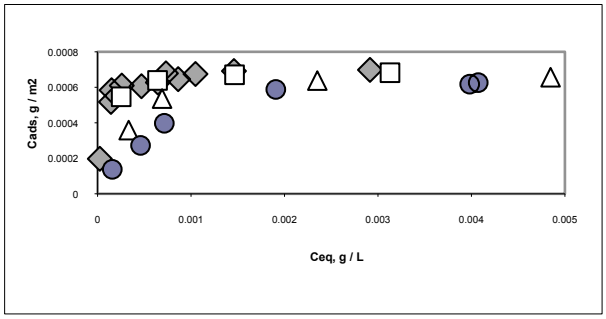

Figure 1: Alginate adsorption isotherms for four supersaturation values: Rhombs, σ = 1.40; squares, σ= 2.02; triangles, σ = 2.65; circles, σ = 3.55.

At lowest supersaturation, alginate adsorption onto calcite probably reaches its maximal uptake of 7.5E-4 g m^{-2}, corresponding to surface coverage of one molecule for each 200 to 300 nm^2, depending on the molecular mass of alginate. This means that one alginate molecule can be bound over 100 to 150 Ca surface sites. Initially, on the surface of the inhibited calcite.

XPS identified alginate but after further time in solution, when the system had recovered, XPS demonstrated that it disappeared from the surface, presumably buried under the newly formed calcite.

The alginate affinity constant decreases with increasing supersaturation, evidence for incomplete adsorption. A simple model based on competition between growth and desorption effectively describes the observed change in the adsorption constant.

Molybdenum and vanadium abundances in banded iron formation and the onset of oxidative continental weathering

STEFAN V. LALONDE[1]*, NOAH J. PLANAVSKY[2], OLIVIER J. ROUXEL[1,3], ERNESTO PECOITS[4] AND KURT O. KONHAUSER[4]

[1]Institut Universitaire Européen de la Mer (IUEM), Université Européene de Bretagne (UEB), Plouzané 29280, France (*correspondence: stefan.lalonde@univ-brest.fr)

[2]Department of Earth Sciences, University of California-Riverside, Riverside, CA 92521, USA

[3]IFREMER, Géoscience Marines, Plouzané 29280, France

[4]Department of Earth and Atmospheric Sciences, University of Alberta, Edmonton, AB T6G 2E3, Canada

The enrichment and isotopic composition of molybdenum in black shales provide insight into the history of atmospheric oxygenation via the coupling of molybdenum supply with the oxidative weathering of terrestrial sulfides [e.g. 1, 2]. However, the fidelity of preservation of Mo oxidative proxies in black shales may also be related to the degree to which euxinic conditions enable their capture [3, 4]. Similar to molybdenum, vanadium is also enriched in sediments deposited under euxinic conditions [4], but its marine supply should be independent of the oxidative weathering of terrestrial sulfides. Here we consider their combined history in order to better understand the black shale Mo record [2] in terms of changing oxidative sources and euxinic sinks in the geological past. We present a complimentary dataset for Mo and V abundances in banded iron formations (BIF), where the ferruginous conditions necessary for BIF deposition preclude euxinia, and sequestration of Mo and V likely occur by adsorption of their anions onto highly reactive ferric hydroxides. While V abundances remain relatively stable throughout the Precambrian, notable Mo enrichments are observed ca. 2.5-2.3 Ga; combined, these data point to the importance of changing sources, and reaffirm assertions that the Great Oxidation Event was marked by increased marine Mo supply driven by oxidative continental weathering. The BIF dataset is further evaluated in light of experimentally-determined Mo- and V- iron oxide partition coefficients that enable back-calculation to dissolved Mo and V concentrations in paleoseawater.

[1] Anbar *et al*. (2007) *Science* **317**, 1903–1906. [2] Scott *et al*. (2008) *Nature* **452**, 456–459. [3] Neubert *et al*. (2008) *Geology* **36**, 775–778. [4] Tribovillard *et al*. (2006) *Chem. Geol*. **232**, 12–32.

https://doi.org/10.1180/S0026461X00006502 Published online by Cambridge University Press

The speciation of marine particulate iron adjacent to active and passive continental margins

PHOEBE J. LAM[1], DANIEL C. OHNEMUS[2] AND MATTHEW A. MARCUS[3]

[1]Dept. of Marine Chemistry and Geochemistry, Woods Hole Oceanographic Institution, Woods Hole, MA 02543 (*correspondence: pjlam@whoi.edu)
[2]MIT-WHOI Joint Program in Oceanography, Woods Hole, MA (dan@whoi.edu)
[3]Advanced Light Source, Lawrence Berkeley National Laboratory, Berkeley, CA 94720 (mamarcus@lbl.gov)

We use synchrotron chemical-species mapping techniques to compare the speciation of marine particulate iron collected in two open ocean environments adjacent to active and passive continental margins. Chemical-species mapping combines the spatial information provided by microfocused X-ray fluorescence (XRF) mapping with chemical information gleaned from single particle X-ray absorption near-edge structure (XANES) spectroscopy to allow a rapid and statistically meaningful assessment of the speciation of a large number of heterogeneous micron-scale iron-rich particles. It is especially good for detecting spectroscopically distinct rare species that could not be detectable by other methods.

We find that the average oxidation state of marine particulate iron determined by chemical-species mapping is comparable to that determined by standard bulk X-ray Absorption Near Edge Structure spectroscopy. Fe (II)-containing minerals such as biotite, hornblende, and magnetite contribute up to 45% of total suspended marine particulate iron in the Northwest Pacific, with the balance comprised of Fe (III) compounds. Depth profiles of the mineralogy and oxidation state of marine particulate iron trace the source of iron to the volcanic Kuril-Kamchattka continental margin about 600km away. In contrast, particulate iron in the eastern tropical North Atlantic, which receives the highest dust deposition on Earth, is dominated by weathered and oxidized Fe compounds, with Fe (III) comprising 90% of total iron. The balance is composed primarily of Fe (II)-compounds, but we detected individual pyrite particles in some samples within an oxygen minimum zone in the upper thermocline. Several lines of evidence point to the adjacent Mauritanian continental shelf as the source of pyrite to the water column. We find that the speciation of suspended marine particulate iron reflects the mineralogy of iron from the adjacent continental margins.

Cd behaviour in arctic estuarine systems using Cd isotopes and concentrations analysis

M. LAMBELET[1], M. REHKÄMPER[1], T. VAN DE FLIERDT[1], Z. XUE[1], K. KREISSIG[1], B. COLES[1], P. ANDERSSON[2] AND D. PORCELLI[3]

[1]Department of Earth Science and Engineering, Imperial College London, UK (m.lambelet-salazar-serrudo09@imperial.ac.uk, markrehk@imperial.ac.uk)
[2]Swedish Museum of Natural History, Stockholm, Sweden
[3]Department of Earth Sciences, University of Oxford, UK

In the oceans, Cd exhibits a behaviour that is similar to the nutrient phosphate: the concentrations are low at the surface due to uptake by organisms, and higher in deep water where regeneration of biological debris occurs [1]. This behaviour is reflected in Cd isotope data, as surface waters commonly display large isotopic fractionations and heavy Cd isotope compositions [2].

Rivers are a significant source of marine Cd, but the behaviour of the element in estuaries is only poorly understood. Therefore, we have determined the Cd isotopic compositions and concentrations of 19 water samples collected along the Arctic Siberian Shelf during the ISSS-08 cruise.

The results for the majority of the samples are in accord with conservative mixing between river water and seawater. Six samples, however, deviate from the mixing trend. One displays a very light Cd isotope composition, which is in accord with release of anthropogenic Cd from particles. This interpretation is based on the light Cd isotope compositions reported for anthropogenic Cd in previous studies [3]. The remaining five samples also exhibit “excess” Cd and the isotope data indicate that this reflects release of natural Cd from particulates at intermediate salinities.

These observations emphasize the importance of trace metal stable isotope analyses for investigations of marine biogeochemical cycles. For Cd, the isotopic data (i) corroborate the reactive behaviour of Cd in estuaries, where Cd is released from particles and (ii) indicate that they may be a useful tool for tracing anthropogenic Cd in the environment.

[1] Boyle *et al*. (1976) *Nature* **263**, 42–44. [2] Ripperger *et al*. (2007) *EPSL* **261**, 670–684. [3] Cloquet *et al*. (2006) *ES&T* **40**, 2525–2530.

https://doi.org/10.1180/S0026461X00006502 Published online by Cambridge University Press

Zircon U-Pb and Hf isotopic data from granitic rocks of Taiwan

C.Y. LAN[1]*, T. USUKI[1], K.L. WANG[1], T.F. YUI[1], J.H. YANG[2], W. LIN[3] AND P.S. HSIEH[3]

[1]Institute of Earth Sciences, Academia Sinica, Nankang, Taipei, Taiwan, ROC (*correspondence: kyanite@earth.sinica.edu.tw)

[2]State Key Laboratory of Lithospheric Evolution, Institute of Geology and Geophysics, Chinese Academy of Sciences, Beijing,, PROC (jinhui@mail.igcas.ac.cn)

[3]Energy and Environment Research Laboratories, Industrial Technology Research Institute, Hsinchu, Taiwan, ROC (waynelin@itri.org.tw)

South China is famous for its widespread, voluminous Mesozoic Yanshanian igneous activity. Taiwan is situated at the eastern margin of South China. The timing and genesis of granitic rocks of Taiwan are curcial to understand the crustal evolution of Taiwan and thair relationship with South China.

In this study, six granitic rocks were collected from the Tailuko metamorphic basement of Taiwan for *in situ* zircon U-Pb dating and Hf isotopic measurement. They include four metagranites and one paragneiss from northern Taiwan and one metagranite from southern Taiwan. The metagranites present two magmatic age groups, 191±10 Ma [1]. and 84-90 Ma. Their relict zircon cores present Early Cretaceous to Early Permian ages with minor Paleoproterozic age. However, no unique magmatic age is found from the paragneiss. Its relict ages vary from Cretaceous to Late Carboniferous with minor Paleoproterozic ages and the youngest age being 88 Ma. The Early Jurassic metagranite outcropped in southern Taiwan gives positive zircon epsilon Hf (t) values, ranging from +8.6 to +11.8. Their T_{DM}^{C} Hf model ages of zircon range from 0.5 to 0.7 Ga. The Late Cretaceous metagranites outcropped in northern Taiwan yield positive to negative epsilon Hf (t) values, ranging from -3.8 to +6.5 and vary among different localities. Their T_{DM}^{C} Hf model ages of zircon range from 0.8 to 1.4 Ga and vary among different localities. Similar geochemical properties can be observed among the metagranites, such as initial Nd isotopic values, amount of normative corundum and peraluminosity [2]. Trace elements analyses on zircons are carried out for two Late Cretaceous metagranites. They exhibit REE patterns similar to magmatic zircons.

Our studies identified Middle Neoproterozoic and Middle Neoproterozic to Middle Mesoproterozoic Hf model age for the Early Jurassic metagranite from southern Taiwan and Late Cretaceous metagranites from northern Taiwan, respectively. These findings are consistent with the occurrences of Neo-proterozoic magmatism in the Yangtze and Cathaysia blocks.

Eoarchaean crustal evolution of the North Atlantic craton

PENELOPE J. LANCASTER*, CRAIG D. STOREY AND CHRIS J. HAWKESWORTH

University of Bristol, Dept. of Earth Sciences, Wills Memorial Building, Queen's Rd., Bristol BS8 1RJ, UK (*correspondence: penelope.lancaster@ucd.ie)

Recent studies suggest extraction of juvenile crust from the mantle has been globally continuous throughout Earth's history, but the crustal record is biased by preservation, particularly from supercontinents [e.g. 1, 2]. As a result, crust older than the first supercontinent at *c*. 2.7 Ga is now rare and frequently strongly reworked. However, younger sedimentary rocks may preserve fragments of Archaean basement by sampling wide areas, including those which have since been buried or destroyed, thereby providing a more complete record of the ancient crust. Of these sedimentary rocks, coarse basal units are most likely to preserve local basement, constraining the likely geographical distribution of those source areas and providing greater context for any detrital material.

Detrital zircons have been analyzed from basal units of the Meso/Neoproterozoic to Cambrian Stoer, Sleat, Ardvreck and Morar groups in NW Scotland to evaluate basement source ages and isotopic signatures. Widespread crustal extraction is recorded in Hf model ages between 4160–1410 Ma, peaking at c. 3350 Ma, with significant crystallisation and/or reworking between 3670–1070 Ma, peaking at c. 2700 Ma. Similar crystallisation and model ages have been identified around the North Atlantic Craton, suggesting a shared, but not consanguineous, origin. All four units contain Hf model ages that imply partial reworking of Eoarchaean crust, and model ages as old as 4200 Ma from the basal Ardvreck Gp. indicate the existence of much older crust in Scotland and the greater North Atlantic Craton. Such consistency around the craton reinforces the conclusion that crustal extraction and crystallisation are continuous, large-scale processes, and have been since the very earliest Earth.

[1] Lancaster *et al*. (2011) *Earth Planet. Sci. Lett*. In press.
[2] Hawkesworth *et al*. (2009) *Science* **323**, 49–50.

https://doi.org/10.1180/S0026461X00006502 Published online by Cambridge University Press

Microbial utilization of the products of serpentinization at the Lost City hydrothermal field

SUSAN Q. LANG[1]*, GRETCHEN L. FRÜH-GREEN[1], STEFANO M. BERNASCONI[1], DAVID A. BUTTERFIELD[2], MARVIN D. LILLEY[3], GIORA PROSKUROWSKI[3] AND SABINE MÉHAY[1]

[1]Department of Earth Sciences, ETH Zürich, 8092 Zürich, Switzerland
[2]JISAO, University of Washington, Seattle, WA 98195, USA
[3]School of Oceanography, University of Washington, Seattle, WA 98195, USA

The Lost City vent field (30°N, Mid-Atlantic Ridge) is characterized by extreme conditions: venting of pH 9-11, <90°C, metal-poor and hydrogren-rich fluids and formation of carbonate-brucite hydrothermal structures that reach up to 60 m high. Fluid-rock reactions in the underlying ultramafic rocks result in high concentrations of a number of chemical species proposed to be of abiological origin (hydrogen, methane, C_2^+ alkanes, formate) [1, 2]. Lost City is a possible analog to Early Earth or Martian environments and is potentially important to understanding the origin of life. For these reasons, a primary research focus has been to investigate the microbial communities that are sustained in this environment and examine their potential link with abiotically produced carbon species. We demonstrate here that in locations where microbial sulfate reduction is believed to be important, up to 50% of the microbial biomass in the carbonate chimneys is derived from mantle carbon. Conversely, mantle carbon contributes only ~10% of the biomass in locations that are minimally impacted by sulfate reduction. We argue that the difference can be attributed to the ability of sulfate reducing bacteria to convert formate to dissolved inorganic carbon which is then accessible by other microbial species such as the more abundant *Methanosarcinales* [3, 4].

[1] Proskurowski, G. *et al*. (2008) *Science* **319**, 604–607. [2] Lang, S. Q. *et al*. (2010) *Geochimica et Cosmochimica Acta* **74**, 941–952. [3] Schrenk *et al*. (2004) *Environmental Microbiology* **6**, 1086-1095 [4] Brazelton *et al*. (2006) *Applied & Environmental Microbiology* **72**, 6257–6270.

Natural organic matter as major sorbent for arsenic in a peatland

P. LANGNER, C. MIKUTTA* AND R. KRETZSCHMAR

Institute of Biogeochemistry and Pollutant Dynamics, ETH Zurich, Switzerland (*christian.mikutta@env.ethz.ch)

Arsenic (As) is a potentially toxic trace element, which is typically associated with metal-(hydr)oxides, silicates or sulfides in organic-rich soils and sediments. Natural organic matter (NOM) has also been suggested as important sorbent for As [1, 2] but the binding mechanisms are still elusive. In order to investigate the importance of NOM relative to reactive Fe species for As binding, we studied the solid-phase speciation of As and Fe in a minerotrophic peatland in Switzerland that contains high natural concentrations of As.

Anoxic peat samples were analyzed by bulk As and Fe K-edge X-ray absorption near edge structure (XANES) and extended X-ray absorption fine structure (EXAFS) spectroscopy at ~80 K. The EXAFS spectra were analyzed by means of principal component analysis and target testing followed by linear combination fitting. We focused our speciation analysis on shallow (<0.4 m) peat layers with 358-1810 mg As kg^{-1} and peat layers from greater depth (1.5-2.6 m) with 106-469 mg As kg^{-1}. Both depth intervals differed significantly in the molar S/Fe ratio of the peat: 0-1 at depths <0.4 m and 2-7 for 1.5-2.6 m depth.

Speciation analysis of As revealed that close to the peat surface As was mainly present as realgar (As_4S_4), As(III)-NOM complexes, and As(III)/As(V) sorbed to Fe(III)-(hydr)oxides. In the deep peat layers, however, As was entirely in its trivalent oxidation state and mostly coordinated to 2-3 S atoms of NOM ($R_{As\text{-}S}$ = 2.26 Å). The Fe speciation in the upper peat layers was dominated by Fe(III)-(hydr)oxides, chlorite, and Fe(III)-NOM complexes, indicating the presence of low-Fe/high-S microenvironments with high As activities. In the deep peat layers Fe(III)-NOM complexes and pyrite (FeS_2) were detected as main Fe species. Although these phases were shown or hypothesized to immobilize As(III), nearly all As was bound to sulfhydryl groups of NOM.

Our results suggest that As binding to sulfhydryl groups of NOM is the major As-NOM interaction scheme under sulfate-reducing conditions. This mechanism seems to impair As sequestration pathways involving Fe species such as the formation of As-bearing pyrite, the precipitation of arsenopyrite (FeAsS), or the formation of ternary As(III)-Fe(III)-NOM complexes.

[1] Buschmann *et al*. (2006) *Environ. Sci. Technol*. **40**, 6015. [2] Rothwell *et al*. (2010) *Environ. Sci. Technol*. **44**, 8497.

https://doi.org/10.1180/S0026461X00006502 Published online by Cambridge University Press

Exploring fracture dominated flow and spatially variable chemical weathering in the Boulder Creek Critical Zone Observatory, Colorado, USA

ABIGAIL L. LANGSTON[1,2]*, GREGORY E. TUCKER[1,2], ROBERT S. ANDERSON[1,3] AND SUZANNE P. ANDERSON[1,3]

[1]Department of Geological Sciences of Colorado
[2]CIRES
[3]INSTAAR

The spatial and temporal evolution of saprolite development on hillslopes controls soil production and sediment supply to rivers. We study the interaction between fluid flow and chemical weathering in the Boulder Creek watershed, a 1160 km^2 catchment that ranges in elevation from 4120 m at 1480 m. We developed our understanding of the formation of saprolite in a granitic mountain catchment by modelling the subsurface flow paths in an environment dominated by fracture flow. Two-dimensional hillslope hydrology models were constructed in a Richards equation-based model to visualize flow paths in the unsaturated zone. We expect fracture density and fracture size in the bedrock to exert the strongest control on both the depth of water penetration into the bedrock, and its residence time in the subsurface. The importance of fractures on the routing of water and development of saprolite in the unsaturated zone will be explored further through XRD and XRF analysis of selected samples of soil, saprolite, and bedrock collected along road cuts at specific points relative to the local fracture system

Geochemistry of tonalites formed by partial melting of eclogites: Experimental modelling

T. LARIKOVA[1]*, A. HOLZHEID[2] AND PH. KEGLER[2]

[1]Institute of Geology of Ore Deposits, Petrography, Mineralogy and Geochemistry IGEM RAS, Staromonetny 35, Moscow, Russia, (larik@igem.ru)
[2]Institute of Geosciences, University of Kiel, Germany

Processes of the partial melting of the metagabbroic rocks (eclogites) in subduction zones may lead to tonalites formation. Experiments aimed to study the formation mechanisms of the clinopyroxene-plagioclase symplectite textures that usually occur during decompression of eclogites. Piston cylinder experiments were performed at 700ºC and 9-11-13 kbar (corresponding to T-minima of wet basalt solidus) at the experimental petrology laboratory of the University Kiel. Run durations varied from 18 hours to 16 days. As fluid phase 0.1 M NaCl-H_2O was used. Starting material was unaltered bimineral (garnet+omphacite) eclogite from the Marun-Keu complex (Polar Urals), formed at 670-690ºC and 16-18 kbar.

During the experiments, the eclogitic garnet grains remained stable, but the composition of their rims changed. Primary omphacites were unstable and were partly or totally recrystallised. As a result, clinopyroxene and plagioclase intergrowth (often accompanied by hornblende) was formed. The compositions of newly formed minerals are in very good agreement with symplectites of the Marun-Keu eclogites. In the association with the symplectites, melt (quenched glass) was found. The melt formed domains, which are sometimes surrounded by a Cpx rim. Also the melt was found as a part of the newly formed symplectitic intergrowth and as a rim around primary eclogitic garnets. The melt (glass) corresponds to a tonalitic composition, with SiO_2 varying from 54 to 71 wt% and Al_2O_3 from 22 to 12 wt% accordingly. Furthermore, the melt contains up to 14 wt% of a fluid phase; the fluid amount increases with decreasing SiO_2 content. Trace elements compositions of the melt domains were obtained by ion microprobe. They show general depletion of the studied elements (exept for Sr) compared to the initial eclogites that correspond to MORB, while Sr is clearly enriched. Moreover a peak in Eu content is noticable.

In summary, our experimental results show formation of tonalitic melt with unusual low trace element content by partial melting of eclogite in equilibrium with garnet and newly formed clinopyroxene at 700°C.

The authors thank DFG (SFB 574), DAAD and RFBR for financial support.

https://doi.org/10.1180/S0026461X00006502 Published online by Cambridge University Press

A novel ion exchange separation for Cu prior to stable isotope analysis by MC-ICPMS

F. LARNER[1]*, M. REHKÄMPER[1,3], B. COLES[1,3], K. KREISSIG[1], D. WEISS[1,3], B. SAMPSON[2], C. UNSWORTH[3] AND S. STREKOPYTOV[3]

[1]Dept. of Earth Science & Engineering, Imperial College London, SW7 2AZ, UK (*correspondence: fiona.larner04@imperial.ac.uk)
[2]Dept. of Medicine, Imperial College London, W6 8RF, UK
[3]Natural History Museum, London, SW7 5BD, UK

The acquisition of stable isotope data with a precision of better than ±0.10‰ using multi-collector inductively coupled plasma mass spectrometry (MC-ICPMS) requires that target elements are separated from the sample matrix to enhance sensitivity, avoid spectral interferences and minimize matrix effects.

At present, the isolation of Cu is generally performed using anion exchange chromatography, with Cu in the +2 oxidation state. These methods suffer from the incomplete separation of Cu from matrix elements and multiple stages of column chemistry are therefore often required to produce a sufficiently purified Cu sample for isotopic analysis. Such problems appear to be particularly prominent for biological materials because (i) of the major interference of $^{40}Ar^{23}Na^{+}$ on $^{63}Cu^{+}$ and (ii) samples with high organic content appear to increase the overlap between the elution of Cu^{2+} and the bulk sample matrix.

To avoid these problems, we have developed a novel procedure that makes use of the different distribution coefficients of Cu (I) and Cu (II) to anion exchange resin, to significantly improve the separation of Cu from biological materials. The method was found to yield sufficiently pure Cu fractions for isotopic analyses after a single pass through the anion exchange columns and it routinely achieves recoveries of 100% ± 2%. Subsequent isotopic analyses of the Cu by MC-ICPMS, using admixed Ni for mass bias correction, yielded accurate Cu isotope data with a reproducibility of about ±0.05‰ (2s) for pure standard solutions and ±0.10‰ (2s) for samples.

Schwertmannite and Fe oxides formed by biological low-pH Fe(II) oxidation versus abiotic neutralization

L. LARSON[1], F. LUAN[1], L. TROYER[2], T. BORCH[2,3] AND W. BURGOS[1]*

[1]Dept. Civil Environ. Eng., Pennylvania State University, University Park, PA 16802, USA (*correspondence: wdb3@psu.edu, lnl5053@psu.edu, ful6@psu.edu)
[2]Dept. Chemistry, [3]Dept. Soil Crop Sci., Colorado State University, Fort Collins, CO 80523 (thomas.borch@colostate.edu, troyerld@lamar.colostate.edu)

We studied the mineralogy of three low-pH coal mine drainage (CMD) sites in central Pennsylvania. Water from one site was used in discontinuous titration/ neutralization experiments to produce Fe (III) minerals by abiotic precipitation for comparison with the field precipitates that were produced by biological low-pH Fe (II) oxidation. Sediments were characterized using X-ray diffraction, Fe K-edge extended X-ray absorption fine structure spectroscopy, and scanning electron microscopy with energy dispersive spectroscopy. Even though the hydrology and concentration of dissolved metals of the CMD varied considerably between the three field sites, the sediment mineralogy of the three iron terraces was found to be very similar. Schwertmannite was the predominant mineral phase precipitated at low-pH (2.5–4.0) along with lesser amounts of goethite. Schwertmannite particles occurred as micron sized spheroids with characteristic 'hedgehog' morphology at all sites. No trace metal incorporation was detected in sediments from the field sites, and no metals (other than Fe) were removed from the CMD at any of the field sites. Minerals formed by abiotic neutralization/precipitation (pH 4.4 – 8.4) were found to contain (in order of predominance) ferri-hydrite, schwertmannite and goethite. In contrast to low-pH precipitation, substantial trace metal removal occurred in the neutralized CMD. Biological low-pH Fe (II) oxidation can improve CMD treatment by reducing armouring and clogging of downstream limestone beds. A further benefit is that solids formed under these conditions may be of industrial value because they do not contain trace metals.

https://doi.org/10.1180/S0026461X00006502 Published online by Cambridge University Press

Towards the geochemical tricorder: Trends and needs in subsurface geochemical sensor systems for energy recovery and carbon management

STEVE LARTER AND LLOYD SNOWDON

PRG, University of Calgary, Calgary, Canada (slarter@ucalgary.ca Lloyd.Snowdon@ucalgary.ca)

Chemical and fluid property analysis of reservoir fluids extracted from reservoirs under *in situ* reservoir conditions (ISRC) is a holy grail of reservoir geochemistry. This is especially important in heavy oil fields where the petroleum often will not flow at native ISRC and is equally important in sampling fluids from CO_2 storage programs to provide monitoring capabilities. Great advances in our ability to sample and characterize reservoir fluids that flow under ISRC have been made in the last decade with dynamic well testing systems coupled to optical spectrometers leading the way currently. While developments have been dramatic and successful, current tools cannot provide the molecular information necessary for many organic or inorganic geochemical applications. Given our capabilities to send advanced analytical instrumentation across the solar system it is surprising that more sophisticated instrumentation is not used a mere few kilometers below our feet! We anticipate that reservoir geochemistry associated with carbon management and downhole sensors for CO_2 and storage reservoir water chemistry to be a large research and development area in the next decade as monitoring and verification of the quantities of large volume carbon dioxide storage programs becomes routine.

We summarize our own attempts to develop instrumentation for direct sampling and geochemical or fluid property analysis of reservoir fluids (oils, waters, gases) *in situ* and describe key technical boundaries to be crossed in terms of sensor technologies and proxy methods for determination of key flow and geochemical properties of hydrocarbon and aqueous fluids associated with energy recovery and CO_2 storage activities. We describe new approaches to sampling and assessing oil viscosity appropriate for *in situ* analysis in heavy oilfields and define *in situ* sensor specifications for performing reservoir geochemical applications such as permeability barrier detection and production allocation in petroleum reservoirs.

Chemistry of Li-Na-K-OH-H_2O brines up to high concentrations and temperatures

A. LASSIN[1]*, C. CHRISTOV[2], L. ANDRÉ[1] AND M. AZAROUAL[1]

[1]BRGM, 3 av. C. Guillemin, B.P. 36009, 45060 Orléans cedex 2, France (*correspondence: a.lassin@brgm.fr)

[2]GeoEco Consulting 2010, 514 E. Barham Drive, San Marcos, CA, USA, hristovi@sbcglobal.net

Lithium interest for industrial production has been increasing during the last few years. This alkali metal is of primary importance in the battery production for electricity storage, in vehicles and electronic devices. Because of very high solubility of lithium in water, the chemical behaviour of lithium minerals is mainly described in binary aqueous systems [1, 2] or at standard temperature [3-5]. Indeed, the chemistry of highly saline aqueous solutions is highly non-ideal and very complex. Its characterization requires specific approaches. The ion-specific interactions model developed by Pitzer [6] is particularly well suited for dealing with ionic strengths ranging from low up to very high salinities, *i.e.* above several tens of moles per kg of water.

In this work, we studied the Li-Na-K-OH-H_2O chemical system, and determined the relevant Pitzer interaction parameters using the procedure developed by André *et al.* [7]. In the binary LiOH-H_2O system, this set of parameters allows the description of the phase diagram for temperatures ranging from 0 to 240°C and for salinities up to saturation, *i.e.* up to 8 mol/kgw. In the ternary LiOH-KOH-H_2O and LiOH-NaOH-H_2O systems, phase diagrams can be satisfactorily described up to 30 mol/kgw, and 100°C, and up to 20 mol/kgw, and 150°C, respectively.

The set of parameters determined in this study should allow the description of the chemical behaviour of the quaternary LiOH-KOH-NaOH-H_2O system over a wide range of salinities and temperatures. The model presented here is a first step towards the possibility for optimizing the lithium extraction processes from natural hypersaline brines, geochemical resources, and industrial waste aqueous solutions.

[1] Monnin *et al.* (2002) *J. Chem. Eng. Data* **47**, 1331–1336 [2] Monnin & Dubois (2005) *J. Chem. Eng. Data* **50**, 1109–1113 [3] Christov *et al.* (1994) *J. Sol. Chem.* **23**, 595–604 [4] Christov *et al.* (2000) *J. Chem. Thermo.* **32**, 1505–1512 [5] El Guendouzi & Errougui (2009) *J. Chem. Eng. Data* **54**, 376–381 [6] Pitzer (1991) Activity coefficients in electrolyte solutions, 2nd ed. CRC Press [7] André *et al.* (2009) 19th Goldschmidt Conf.

https://doi.org/10.1180/S0026461X00006502 Published online by Cambridge University Press

Geochemical investigation of gabbroic xenoliths from Hualalai Volcano, Hawaii

J.C. LASSITER* AND R. GAO

Geological Sciences Dept., Jackson School of Geoscience, Univ. Texas, Austin, TX, USA (*correspondence: lassiter1@mail.utexas.edu)

The 1800-1801 Kaupulehu flow from Hualalai Volcano, Hawaii, contains abundant gabbroic and ultramafic xenoliths. These xenoliths provide insights into the plumbing systems of Hawaiian volcanes as well as constraints on the composition of the ~110 Ma Pacific crust and lithosphere upon which the Hawaiian Islands are constructed.

Clinopyroxenes from the majority of the Kaupulehu gabbros have convex-upward REE patterns consistent with derivation through fractional crystallization from LREE-enriched Hualalai magmas with little trapped interstital melt. Calculated parental melts have REE patterns spanning the entire range of Hualalai lava compositions. A small subset of xenoliths with LREE-enriched clinopyroxenes appear to be trapped Hualalai melts that crystallized as a closed system. The Hualalai-derived xenoliths have Sr-Nd-Pb isotopic compositions that span the full range reported for Hualalai lavas. These gabbros provide a nearly complete record (minus the stratigraphic context) of Hualalai magmatic history.

A small subset (~15%) of the Kaupulehu gabbros have LREE-depleted pyroxenes that crystallized from melts with MORB-like compositions. These xenoliths have unradiogenic $^{87}Sr/^{86}Sr$ (~0.7025-0.7028) and radiogenic $^{143}Nd/^{144}Nd$ (0.5130-0.5132) and overlap the field defined for Pacific MORB. Lead isotope compositions ($^{206}Pb/^{204}Pb \approx 18.0$-18.4) are generally less radiogenic than present-day Pb-isotope values reported for MORB from ODP Site 843 west of Hawaii, which suggests that the ODP 843 lavas may not be representative of the composition of the lower, less altered portions of the local Pacific crust beneath Hawaii. In particular, the MORB-related gabbros have lower $^{208}Pb/^{204}Pb$ for a given $^{206}Pb/^{204}Pb$ than the trend defined by Site 843 lavas [1], and overlap with post-erosional lavas from the Honolulu Volcanic Series. If the MORB-related gabbros are isotopically similar to the lithospheric mantle beneath Hawaii, then a role for lithospheric mantle in the generation of post-erosional lavas cannot be excluded based on the Pb-isotope compositions of Site 843 lavas, as some studies have previously concluded [2].

[1] Fekiacova *et al*. (2007) *EPSL* **261**, 65–83. [2] Garcia *et al*. (2010) *J. Petrol*. **51**, 1507–1540.

Sudbury asteroid impact triggered the emplacement of endogenous magma that produced a giant Ni-Cu-PGE deposit

RAIS LATYPOV

Department of Geosciences, University of Oulu, Oulu, FI-90014, Finland (*correspondence: rais.latypov@oulu.fi)

The Sudbury impact structure, Canada, comprises the up to 5 km thick Sudbury Igneous Complex (SIC) that is widely interpreted as an impact melt sheet produced by melting of target crustal rocks [1-6]. The Sudbury structure is renowned for showing clear evidence of asteroid impact and for hosting the largest known reserves of Ni, Cu and PGE sulfides that are closely associated with the SIC [6]. Two groups of igneous bodies closely associated with the SIC are thought to be representative of its initial magma composition. These are glassy dykes and sills that occur in the roof rocks (Onaping melt bodies) and dioritic dykes that cut the underlying basement rocks (Offset dyke). However, these two groups of igneous bodies have distinctly different major and trace element compositions, posing the question as to which magma produced the SIC. The quenched glassy texture of the Onaping bodies is indicative of their formation as superheated melts generated by asteroid impact [7]. Compositional changes of this initial impact melt by subsequent intra-chamber processes such as fractional differentiation [8], assimilation [9] or liquid immiscibility [4, 6, 10-11] do not lead to the magma compositions parental to the Offset dykes. The Offset dykes can therefore only represent an external, endogenous magma from below [12] that mixed with an impact melt to form the hybrid magma parental to the SIC. Identical ages for the SIC and Offset dykes indicate that emplacement of the endogenous magma was initiated by the Sudbury impact event. This suggests that Sudbury asteroid impact triggered endogenous magmatism that gave rise to formation of a giant Ni-Cu-PGE deposit.

[1] Faggart *et al*. (1985) *Science* **230**, 436–439. [2] Grieve *et al*. (1991) *J. Geophys. Res*. **96**, 22753–22764. [3] Grieve (1994) *Ont Geol Sur Sp Vol* **5**, 119–132. [4] Golightly (1994) *Ont Geol Sur Sp Vol* **5**, 105–117. [5] Mungall *et al*. (2004) *Nature* **429**, 546–548. [6] Naldrett (2004) Magmatic Sulfide Deposits. [7] Dressler & Reimold (2001) *Earth-Sci. Rev*. **56**, 205–284. [8] Therriault *et al*. (2002) *Econ Geol* **97**, 1521–1540. [9] Ames *et al*. (2002) *Econ Geol* **97**, 1541–1562. [10] Lightfoot *et al*. (2001) *Econ Geol* **96**, 1855–1875. [11] Zieg & Marsh (2005) *Geol. Soc. Am. Bul*. **117**, 1427–1450. [12] Norman (1994) *Geol. Soc. Am. Special Paper* **293**, 331–341.

https://doi.org/10.1180/S0026461X00006502 Published online by Cambridge University Press

Effects of absorbing aerosols on accelerated melting of snowpack in the Tibetan-Himalayas region

WILLIAM K.M. LAU

Laboratory for Atmospheres, NASA/GSFC, Greenbelt, MD 20771 (william.k.lau@nasa.gov)

The impacts of absorbing aerosol on melting of snowpack in the Hindu-Kush-Tibetan-Himalayas (HKTH) region are studied using NASA satellite and GEOS-5 GCM. Results from GCM experiments shows that a 8-10% in the rate of melting of snowpack over the western Himalayas and Tibetan Plateau can be attributed to the aerosol elevated-heat-pump (EHP) feedback effect (Lau *et al*. 2008), initiated by the absorption of solar radiation by absorbing aerosols accumulated over the Indo-Gangetic Plain and Himalayas foothills. On the other hand, deposition of black carbon on snow surface was estimated to give rise to a reduction in snow surface albedo of 2 - 5%, and an increased annual runoff of 9-24%. From case studies using satellite observations and re-analysis data, we find consistent signals of possible impacts of dust and black carbon aerosol in blackening snow surface, in accelerating spring melting of snowpack in the HKHT, and consequentially in influencing shifts in long-term Asian summer monsoon rainfall pattern.

Small-scale processes and mantle source heterogeneity recorded in melt inclusions from the Mid-Atlantic and Gakkel ridges

MURIEL LAUBIER* AND CHARLES H. LANGMUIR

Earth and Planetary Sciences, Harvard University, Cambridge, MA 02138, USA
(*correspondence: laubier@eps.harvard.edu)

Melt inclusions sample magmas that are less homogenized than lavas and provide new insights on magma generation, transport and mantle heterogeneity. Remarkably, at mid-ocean ridges few exhaustive studies of individual areas have taken place for olivine-hosted inclusions, to constrain to what extent major and trace elements provide coherent signal that reveals mantle composition and processes. We are carrying out such studies of ridges with very different spreading characteristics, from the FAMOUS segment (Mid-Atlantic Ridge) and the ultra-slow spreading Gakkel Ridge (Arctic Ocean). One aim is to test the hypothesis that melt inclusions record melts from various depths in the melting column, such that the most depleted melts are also high in Si and low in Fe.

188 new melt inclusions from 14 samples in the FAMOUS area display a large variability in major and trace elements that extends that of the lavas to more depleted compositions. Among them, high-Al, low-Si melts, found both as melt inclusions and lavas, are characterized by a strong depletion in the most incompatible elements and distinctively low MREE/HREE ratios. Although high-Al melts show evidence of assimilation of crustal plag-bearing cumulates, their trace element signature requires a distinct residual mantle formed by previous melt extraction in the garnet field. The low Si contents of the most depleted inclusions suggest that they reflect deep source processes, and not the 'top of the melting column'.

The Gakkel Ridge is the slowest spreading ridge on Earth, and should have a tens of km thick lithosphere that would be expected to influence melt inclusion compositions. The robust western volcanic zone has a continuous magmatic ridge, the sparsely magmatic zone consists largely of peridotite, and the eastern volcanic zone consists of isolated volcanoes. Large geochemical variations in the lavas along the ridge and within segments indicate small extents of melting (F), melt focusing and mantle source heterogeneity. Melt inclusion work will be reported on samples from all domains. The comparison between slow and ultraslow spreading ridges will constrain the changes in the melting dynamics, transport and sampling of mantle heterogeneity between the two environments.

https://doi.org/10.1180/S0026461X00006502 Published online by Cambridge University Press

Drillcore imaging spectroscopy for exploration and mining

C. LAUKAMP, I. SONNTAG, T. CUDAHY, M. HAEST AND A. RODGER

CSIRO, Kensington WA 6151, Australia
(*correspondence: Carsten.Laukamp@csiro.au)

Automated drill core logging techniques that measure the visible and infrared reflectance (e.g. line profiling systems such as HyLogging™) are increasingly used for mineral exploration and mining [1, 2]. Additionally, imaging spectrometers allow to capture mineralogical and textural information across the visible and infrared wavelength range (0.4 - 2.5µm). However, the automated extraction of mineral abundances and compositions from the resulting large spectral data sets is difficult and pure statistical methods can lead to questionable mineralogical conclusions.

This paper presents a case study using samples from orogenic gold deposits hosted by Archean greenstone belts of Western Australia, and iron-oxide copper gold deposits in the Mount Isa Inlier (Australia), to showcase the mineral feature extraction method [3, 4] for the interpretation of reflectance spectroscopic data and its application for drill core imaging spectroscopy. In this method mineral endmembers are not extracted from the analysed image, but are derived from physicochemical constraints characteristic for the minerals of interest. This enables the comparison of different samples and doesn't require spectral libraries for the interpretation of the reflectance spectra. Based on the image processing software ENVI™, routines were developed to create a suite of mineral maps, which show the spatial distribution and compositional changes of hydroxylated silicates and carbonates. The acquired mineral maps were compared with thin section petrography, SEM and electron microprobe work, and used to determine mineral phases that are visually difficult to identify in the greenschist to amphibolite facies host rocks. The results can be used to 1) better understand cross cutting and phase relationships of Au-related alteration assemblages (e.g. prehnite, white mica composition), and 2) improve the interpretation of automated drill core logging techniques, to deliver objective core logging results. The developed method is aimed to be globally applicable to a wide variety of mineral mixtures and geological settings.

[1] Cudahy *et al*. (2009) *Econ. Geol*. **16**, 223–235.
[2] Huntington *et al*. (2006) *MESA Journal*. **1**, 33–34.
[3] Cudahy *et al*. (2008) *CSIRO report*. **P2007/364**, 161pp.
[4] Laukamp *et al*. (2010) *AIG Bulletin*. **51**, 73–76.

The effect of sulfur on PGE solubility in silicate melts

V. LAURENZ[1]*, R.O.C. FONSECA[1], C. BALLHAUS[1], K.P. JOCHUM[2] AND P.J. SYLVESTER[3]

[1]Steinmann Institut, Rheinische Friedrich-Wilhelms Universität Bonn, Bonn, Germany (*correspondence: laurenz@uni-bonn.de)
[2]Max Planck Institut für Chemie, Abt. Biogeochemie, Mainz, Germany
[3]Department of Earth Sciences, Memorial University of Newfoundland, St. John's, Newfoundland, Canada

The solubility of platinum-group elements (PGE) in silicate melts depends on oxygen partial pressure, temperature, pressure and melt composition. In addition, sulfur plays an important role for PGE geochemistry in the Earth's mantle. Due to their chalcophile character, PGE are thought to be predominantly hosted by sulfides in the Earth's mantle. However, little is known about the the possible effect of sulfur partial pressure (pS_2) on the solubility of PGE in silicate melts. In addition to oxygen, dissolved S^{2-} may associate as a possible ligand with the PGE and enhance their solubility in a silicate melt relative to a S-free melt. A better understanding of the influence of sulfur on PGE solubility in silicate melts will provide deeper insights into the processes leading to the enrichment of PGE in sulfide in a sulfide-melt/silicate-melt system, as observed in sulfides of magmatic PGE ore deposits (e.g. Merensky Reef, Bushveld Complex).

In order to experimentally investigate the effect of S^{2-} on the solubility of PGE in silicate melts, a natural picrite was equilibrated with Ru or Pt metal at 1300°C in a 1 atm vertical gas mixing furnace under controlled pS_2 and pO_2. Sulfur fugacity was held below sulfide saturation. Run products were quenched to silicate glasses, which were subsequently analyzed for major elements and dissolveld S by EMP. Ru or Pt concentrations were determined by LA-ICP-MS to allow the detection of heterogeneities such as discrete metallic nanonuggets.

Experiments show that the solubility of Ru or Pt in the picritic melt is enhanced up to a factor of 20 in sulfur-bearing systems when compared to S-free melts at identical pO_2. Our results appear to indicate that Ru and Pt, and possibly other PGE as well, bond with S^{2-} anions dissolved in the silicate melt. This observation has important implications for ore-forming processes: The proportion of Ru or Pt associated with the S^{2-} ligand will be extracted straight into an exsolving sulfide melt, once sulfide saturation is reached. This leads to the observed enrichment of PGE in sulfide liquids forming magmatic sulfide ore deposits. Our results imply that our current understanding of PGE enrichment processes in sulfide melts have to be re-thought.

https://doi.org/10.1180/S0026461X00006502 Published online by Cambridge University Press

Himalayan erosion rates and ^{10}Be systematics in the Ganga basin

JÉRÔME LAVÉ[1], MAARTEN LUPKER[1], PIERRE-HENRI BLARD[1], CHRISTIAN FRANCE-LANORD[1], DIDIER BOURLÈS[2], JULIEN CHARREAU[1], LAETITIA LEANNI[2], RAPHAËL PIK[1] AND NICOLAS PUCHOL[1]

[1]CRPG-CNRS, Université de Lorraine, Vandoeuvre les Nancy, France
[2]CEREGE, UMR 6635 CNRS Aix-Marseille Université, BP80, Aix-en-Provence, France

A key parameter to understand the evolution of the Himalayan orogen and its impact on Earth surface processes is the mass of material removed from the system through physical erosion and sediment export. Himalayan erosion rates have been widely derived from thermochronological exhumation studies, river incision rates and sediment budgets covering both long-term exhumation rates and short-term events. Cosmogenic nucleids provide the opportunity to study large-scale basin average erosion rates at intermediate time scale [1, 2]. However, the use of ^{10}Be has yet remained limited for the major Himalayan basins [3].

Here we report ^{10}Be measurements from river sediments covering the Ganga basin that drains the central part of the Himalayan range. Sediments were collected between 2004 and 2010 at the Himalayan front in the main trans-Himalayan rivers, in the floodplain southern cratonic tributaries, and finally in the Ganga (Bangladesh) which integrates the whole basin. ^{10}Be concentrations measured at the Himalayan front range from (8 to 55)·10^3 at. g^{-1} and vary (up to a factor 2) interannually for most of the rivers. In Bangladesh, four different samples yield in contrast similar concentrations (~20·10^3 at. g^{-1}), close to the average of the upstream mountain-outlets values. Those results suggest several preliminary conclusions: (1) The sediment contribution of the southern tributaries of the Ganga is limited to <1%, consistently with their much higher ^{10}Be concentrations and erosion rates of ~0.008 mm. yr^{-1} for the Indian craton. (2) No systematic evolution of the average ^{10}Be concentrations is observed during floodplain transfer as it would be expected from long time transfer in the Ganga plain [4]. (3) Mixing and diffusion during transfer are, however, sufficiently efficient to smooth the lateral and temporal variations and to provide, in Bangladesh, a well constrained mean erosion rate of 1.3 ±0.3 mm. yr^{-1} for the central Himalayas.

[1] Granger *et al*. (1996) *J. Geology*, **104**, 249-257. [2] Wittmann *et al*. (2009) *EPSL*, **288**, 463-474. [3] Vance *et al*. (2003) *EPSL*, **206**, 273-288. [4] Granet *et al*. (2010) *GCA*, **74**, 2851-2865.

Potential rates of denitrification linked to iron and sulfur oxidation in aquatic sediments

ANNIET LAVERMAN[1], CHEN YAN[1], ERIC VIOLLIER[2], BRUNO DEFLANDRE[3], GEORGES ONA-NGUEMA[4] AND CÉLINE PALLUD[5]

[1]UMR 7619 Sisyphe, Université Pierre et Marie Curie, Campus Jussieu, Paris, France (Anniet.Laverman@upmc.fr)
[2]UMR 7154 Université Paris Diderot-Paris 7, 75205 Paris, France (viollier@ipgp.fr)
[3]UMR EPOC 5805, Université de Bordeaux 1, France. (b.deflandre@epoc.u-bordeaux1.fr)
[4]IMPMC UMR 7590 - Université Pierre et Marie Curie, Campus Jussieu, Paris, France (georges.ona-nguema@impmc.upmc.fr)
[5]ESPM Department, University of California, Berkeley, CA 94720, USA (cpallud@berkeley.edu)

Recent works have shown the existence and importance of chemoautotrophic denitrification via sulfur and iron. Relatively little is known, however regarding the environmental importance of these processes in anoxic sediments. Our goal was to investigate the potential of the two alternative nitrate-reducing processes and compare them to the classical, heterotrophic denitrification in freshwater (riverine) and coastal sediments.

Potential nitrate reduction rates in these sediments ranged from 200 to 700 nmol NO_3^- cm^{-3} h^{-1}. The addition of Fe (II) together with nitrate had little to no effect on total nitrate reduction rates. We observed however a significant effect on the rate of nitrite production in certain sediments; nitrite production was lower in the presence of Fe (II). We hypothesize that Fe (II) reacts, either biotically or abiotically, with nitrite that is produced during heterotrophic denitrification.

Sediments that were supplied under anoxic conditions with nitrate showed high nitrate reduction rates as well as sulfate release rates. No sulfate was supplied to these sediments and exceeded porewater flushing of sulfate indicating the coupling of nitrate reduction with sulfide oxidation resulting in the production of sulfate. The sulfate production rates reached values as high as 60 nmol SO_4^{2-} cm^{-3} h^{-1} and could make up for 15% of the nitrate reduction rates.

This study shows that nitrate reduction linked to iron oxidation in the investigated freshwater and coastal sediments, with ample carbon and high heterotrophic denitrification is of minor importance. The role of nitrite reduction by Fe (II) is under investigation. Sulfide oxidation by nitrate reduction appears to play a significant role in nitrogen cycling, potentially accounting for 1-15% of the nitrate reduction rates.

https://doi.org/10.1180/S0026461X00006502 Published online by Cambridge University Press

Anthropogenically induced changes in groundwater flow regimes in shallow high arsenic aquifers: Evidence from ^{3}H & ^{14}C data

M. LAWSON[1,2], C.J. BALLENTINE[1], D.A. POLYA[1]*, C.L. BRYANT[3] AND A. BOYCE[4]

[1]SEAES University of Manchester M13 9PL, UK (*correspondence: david.polya@manchester.ac.uk)
[2]ExxonMobil Upstream Research Company, Houston, USA
[3]Radiocarbon Facility, East Kilbride G75 0QF, UK
[4]SUERC, East Kilbride G75 0QF, UK

An estimated 100 million people in Asia are exposed to hazardously high concentrations of naturally occuring arsenic (As) in groundwater [1]. Although regional groundwater flow in high As aquifers is driven by topographically controlled hydraulic gradients, groundwater abstraction is thought to have altered the natural flow regime by developing transient flow paths, changing the location and mode of recharge, and the timescales over which these various processes operate [2]. The Nadia district of West Bengal is an example of such an area where there has been massive groundwater abstraction for 10s years. In contrast, the Kean Svay district of Cambodia has been relatively undeveloped, and as such provides a useful analogue for the assessment of conditions prior to massive groundwater abstraction [3]. We present here isotopic data collected from these two contrasting areas.

In Cambodia, ^{3}H data indicates that, even in the absence of extensive groundwater abstraction, there is considerable interaction between surface waters and the underlying shallow (< 20 m) groundwater operating over < 50 year timescales. Dissolved inorganic carbon (DIC) ^{14}C ages, however, indicate longer mean groundwater residence times of 100s to 1000s years at depths > 55 m. In West Bengal, groundwater contains a clear contribution of tritium active recharge to depths of as deep as 63 m in 90% of the samples. This is consistent with younger mean residence times of groundwater at depths of up to 100 m obtained from DIC ^{14}C ages. ^{14}C ages of dissolved organic carbon (DOC) are younger at greater depths in West Bengal compared to that present in Cambodian groundwaters. These data suggest that groundwater pumping practices may play a key role in the groundwater DOC composition which may ultimately influence the temporal evolution of groundwater arsenic.

[1] Ravenscroft *et al*. (2009) *Arsenic Pollution, A Global Synthesis*. Wiley-Blackwell. [2] Harvey *et al*. (2002) *Science* **298**, 1602–1606. [3] Polya *et al*. (2005) *MinMag* **69**, 807–823.

Halogen concentrations and $\delta^{37}Cl$ in apatite as a fluid probe to decipher fluid-rock interaction

G.D. LAYNE[1], T. JOHN[2], M.J. WHITEHOUSE[3], H. AUSTRHEIM[4] AND C. KUSEBAUCH[2]

[1]Department of Earth Sciences, Memorial University, St. John's, NL Canada (gdlayne@mun.ca)
[2]Institut für Mineralogie, WWU Münster, Germany
[3]Swedish Museum of Natural History, Stockholm, Sweden
[4]Physics of Geological Processes PGP, University of Oslo, Norway

Fundamental questions associated with fluid-rock interaction concern fluid flow in low-permeability crystalline rocks – How are fluids channelled? What is the geochemical signature of fluid flow on a regional scale? To better understand flow pattern formation and reaction front propagation, we need chemical tracers for the fluids involved (e.g. halogen ratios and $\delta^{37}Cl$) and fluid-composition indicative minerals that provide fluid probes. Apatite is a typical accessory vein-mineral in hydrothermal systems over a wide range of conditions. Apatite also reacts rather sensitively to changes in fluid composition by dissolution-reprecipitation, making it a reasonable candidate as a fluid probe. A primary advantage of apatite is that it routinely incorporates measurable concentrations of halogens.

We have performed ion microprobe (Cameca IMS1280, Nordsims facility) halogen isotope and elemental ratio measurements *in situ* on examples of 1) a hydrous shear zone cross cutting a dry gabbro (Kråkeneset, Norway) and, 2) the regional-scale scapolitization of gabbroic rocks (Bamble Sector, Norway). Within the shear zone sequence of study (1) we found a linear decrease in apatite F/Cl from 14, 000 $\times 10^{-3}$ in gabbro to ~2, 000 $\times 10^{-3}$ in sheared rock, while I/Cl decreased from ~30 $\times 10^{-6}$ to ~4 $\times 10^{-6}$. Conversely, apatite Br/Cl increased from ~0.2 $\times 10^{-3}$ to 1.1 $\times 10^{-3}$ from the most pristine gabbro to the centre of the shear zone. $\delta^{37}Cl$ in the gabbro apatites ranges from –1.0 to –0.5 ‰, and those of the shear zone cluster around +0.3 ‰. This implies a single fluid infiltration event that changed its composition during progressive fluid rock interaction.

In study (2), the least metasomatized gabbro has apatite F/Cl ~2, 000 $\times 10^{-3}$, I/Cl of ~5 $\times 10^{-6}$ and Br/Cl of ~0.9 $\times 10^{-3}$. Overprinting apatite (Cl-Ap) has F/Cl ~1.5 $\times 10^{-3}$, I/Cl of ~0.27 $\times 10^{-6}$ and Br/Cl of ~0.013 $\times 10^{-3}$, subsequently replaced by OH-Ap with F/Cl ~250 $\times 10^{-3}$, I/Cl of ~2-3 $\times 10^{-6}$ and Br/Cl of ~0.08 $\times 10^{-3}$. Apatite of the least metasomatized gabbro has $\delta^{37}Cl$ values of ~ –1 ‰, Cl-Ap of –0.2 ‰ and OH-Ap of +1.1 ‰. While the $\delta^{37}Cl$ values describe a continuous trend, the halogen ratios clearly require two distinct fluid events.

https://doi.org/10.1180/S0026461X00006502 Published online by Cambridge University Press

Open system U-Th ages of Red Sea corals indicate the activity of freshwater aquifers at the last interglacial

BOAZ LAZAR[1] AND MORDECHAI STEIN[2]

[1]Institute of Earth Sciences, The Hebrew University, Jerusalem 91904, Israel (boaz.lazar@huji.ac.il)
[2]Geological Survey of Israel, Malkhe Israel St., Jerusalem 95501, Israel (motistein@gsi.gov.il)

The Red Sea-Gulf of Aqaba is part of the 'Levantine corridor' where *H. sapiens* possibly migrated 'out of Africa' between 130, 000-100, 000 years BP. This 'corridor' however, lies currently in the heart of the most hyperarid desert belt on Earth, which imposes a formidable barrier to the supposed hominids migration. Yet, many fossil coral reefs scattered along the Red Sea show clear evidence for extensive interaction with fresh groundwater that resulted in recrystallization of the corals' primary aragonite skeleton to calcite. Thus, dating the age of recrystallization constrains the period when the Red Sea coastal aquifers were recharged with freshwater. However, traditional U-Th dating of corals requires close isotopic system. Therefore, we developed an open-system U-Th dating method and estimated the age of recrystallization of the tectonically uplifted fossil reef terraces along the shores of Aqaba. We found that ~140, 000 years ago, these reefs interacted with fresh groundwater and possibly also at ~118, 000 y. Apparently, the Red Sea region was wetter during the last interglacial than its current hyperarid conditions, thus facilitating the 'Levantine corridor' as the route of *H. sapience* 'out of Africa'.

Concentration of Ge in thermophilic cyano-bacterial community

E.V. LAZAREVA[1]*, A.V. BRYANSKAYA[2], O.P. TARAN[3], M.S. MELGUNOV[1], S.E. PELTEK[2] AND S.M. ZHMODIK[1]

[1]Institute of Geology and Mineralogy SB RAS, Pr. Koptug, 3, Novosibirsk, 630090, Russia (*correspondence: lazareva@igm.nsc.ru)
[2]Institute of Cytology and Genetics SB RAS, Pr. Lavrentyeva, 10, Novosibirsk, 630090, Russia
[3]Boreskov Institute of Catalysis SB RAS, Pr. Lavrentyeva, 5, Novosibirsk, 630090, Russia

It is known that Ge is a widely dispersed trace element. The crustal abundance of Ge ranges from 1 to 1.7 ppm. Higher concentrations are found in silicates, polymetallic sulfide ores, coal and petroleum [1].

This study consideres Ge accumulation in thermophilic cyano-bacterial communities. Numerous hot springs are localized in Barguzin Basin (Baikal Rift Zone). The presence of microbial communities is found in all the outlets of thermal waters. We studied 7 hot springs, which are alkaline hydrotherms with SO_4-HCO_3-Na and SO_4-Na water composition. Hot springs waters have a similar composition and different content of HS^- and Rn. The structure of dominant microorganisms in investigated communities is similar. It presented of filamentous forms: bacterium *Chloroflexus aurantiacus* and cyanobacterial genera *Phormidium*, *Leptolyngbya*, *Mastigocladus* and *Oscillatoria*.

Ge is concentrated in the cyano-bacterial communities, which grows in sulphide-less, Rn-bearing hot springs. Ge content in the microbial community of Garga and Uro hot springs is in average 270 and 350 ppm in dry weight (up to 1000 ppm), Rn content in waters is 110 and 60 Bk/L respectively. It is characteristic that the Ge is accumulating in parallel with radionuclides: ^{226}Ra, ^{228}Ra, ^{210}Pb in Garga cyano-bacterial mat (4000, 4000, 3000 Bk/kg in dry weight) and ^{210}Pb (700 Bk/kg) in the Uro microbial community. Previously was shown that organic compound of Ge exerted an antimutagenic effect on γ-ray-induced mutations in *Escherichia coli* [2]. Biological role of Ge currently not fully known, we proposed that Ge-accumulation in the thermophilic microbial communities in Barguzin Basin may be due to antimutagenic mechanism protected from high concentration of radionuclides.

This work was supported by the RFBR (11-05-00717); IP: 10.

[1] Bernstein L. R. (1985) *Geochimica et Cosmochimica Acta* **49**, 2409–2422. [2] Mochizuki, H. & Kada, T. (1982) *Int. J. Radiat. Biol.* **42**, 653–659.

https://doi.org/10.1180/S0026461X00006502 Published online by Cambridge University Press

Role of Fe- and Mn- redox coupling on the carbon cycle in a mixed land use watershed: Christina River Basin Critical Zone Observatory

O. LAZAREVA[1]*, D.L. SPARKS[1], A. AUFDENDAMPE[2], K.YOO[3], S. HICKS[2] AND J. KAN[2]

[1]University of Delaware Environmental Institute, Newark, DE, USA (olazarev@udel.edu, dlsparks@udel.edu)
[2]Stroud Water Research Center, Avondale, PA, USA (aufdenkampe@stroudcenter.org, shicks@stroudcenter.org, jkan@stroudcenter.org)
[3]University of Minnesota, St. Paul, MN, USA (kyoo@umn.edu)

A multitude of scientific publications have emphasized the importance of an organic carbon (C)-mineral complexation mechanism as a crucial factor in C stabilization and sequestration. Carbon-mineral complexation is strongly controlled by mineral surface area, mineralogy, pH, redox, polyvalent cations, ionic strength, and the chemical composition of organic matter. These factors vary spatially as a function of geomorphologic, hydrologic, and microbiological processes. Soil horizons and sediments with abundant Fe and Mn oxides/hydroxides have high mineral surface area and thus a high capacity to complex C, reducing its susceptibility to microbial degradation. Additionally, both sediment and hydrological fluxes transport mineral surface area in both solid and dissolved phases.

At the Christina River Basin-Critical Zone Observatory (CRB-CZO), one of six observatories funded by the National Science Foundation, we investigate how Fe- and Mn- redox coupling affects the C cycle under varying redox conditions across a wide range of landscape positions and uses, such as floodplain forest, upland forest, and agriculture.

This investigation will demonstrate preliminary data from a number of state-of-the-art *in situ* monitoring sensors, such as redox probes, soil moisture and temperature probes, gas probes (O_2, CO_2), pressure transducers and DO/temperature sensors, that have been installed within the White Clay Creek Watershed. In addition, we are conducting an extensive field sampling and analysis of soil cores, soil pore waters, stream water, and groundwater. The water samples are being analyzed for pH, temperature, DO, Fe^{2+}, conductivity, turbidity, TDS, DOC, TOC, NO_3, C, N, δD, $\delta^{18}O$ major anions, major cations, and metals. Soils samples will be examined for total chemical composition, C%, C isotopes, and mineral surface area. Selected samples will be analyzed by XRD, SEM, EPR, Mossbauer Spectroscopy, and molecular analysis on microbial communities.

Cu isotope fractionation in primary and secondary copper minerals from the Coka Marin and Bor mining areas (East Serbia)

M. LAZAROV[1]*, S. WEYER[1], A. PAČEVSKI[2] AND I. HORN[1]

[1]Institute für Mineralogie, Leibniz Universität Hannover, Callinstr. 13, 30167 Hannover, Germany (*correspondence: m.lazarov@mineralogie.uni-hannover.de)
[2]Faculty of Mining and Geology, University of Belgrade, Dusina 7, 11000 Belgrade, Serbia

The Coka Marin and Bor mines (east Serbia) belong to porphyry-copper deposits of the Carpathian-Balkan orogen belt connected with late Cretaceous calcalkaline magmatism. Hand specimens of massive sulphide and polymetallic ores were analysed for major and minor elements by EPMA. Several representative copper minerals were hand picked and their Cu isotope composition was measured using MC-ICP-MS.

Microscope and microprobe analyses showed complex copper mineral diversity. Copper minerals are generally homogeneous, but they display differences in their chemical compositions, like variable enrichment of Sb in enargite and the formation of tetrahedrite followed by variable enrichment of Fe and Zn.

Majority of primary copper sulphide minerals and native copper display a relatively narrow range of $\delta^{65}Cu$ around 0 ± 0.5‰. The Cu isotope compositions of secondary Cu sulphates and carbonates are systematically heavier by more than 2‰. These differences in $\delta^{65}Cu$ between primary and secondary copper minerals can be observed even within a single specimen. The best explanation implies that Cu isotope fractionation takes place during partial remobilisation of Cu under oxidising conditions.

Due to complex mineral composition and intimate intergrowth of copper minerals, it is not always possible to separate mineral phases even with careful hand picking. Therefore, *in situ* measurement by femtosecond LA-MC-ICP-MS will be performed in order to identify Cu flux on mineral scale.

https://doi.org/10.1180/S0026461X00006502 Published online by Cambridge University Press

Enzymatic extracellular superoxide in microbial Mn(II) oxidation

D.R. LEARMAN AND C.M. HANSEL*

School of Engineering and Applied Sciences, Harvard Univerisity, Cambridge, MA 02138 (*correspondence: hansel@seas.harvard.edu)

Manganese (Mn) oxide minerals are among the strongest sorbents and oxidants in the environment, controlling the fate of contaminants, degradation of recalcitrant carbon, and cycling of nutrients. We have recently shown that a common marine bacterium, *Roseobacter* sp. AzwK-3b, oxidizes Mn (II) through an indirect pathway, via enzymatic production of extracellular superoxide during exponential growth. Superoxide production and Mn (II) oxidation in cell-free filtrate was inhibited in the presence of proteases, suggesting that superoxide production is due to a soluble protein. NADH enhanced Mn (II) oxidation and inhibition by the oxidoreductase inhibitor DPI suggested that an NADH oxidase is involved in extracellular superoxide production, and subsequent Mn (II) oxidation, by this species.

Here we present new findings revealing the proteins and genes involved in extracellular superoxide production by *Roseobacter* AzwK-3b. A soluble fraction of proteins demonstrated the ability to oxidize Mn (II), which was also substantially enhanced by the presence of NADH and inhibited by superoxide dismutase (SOD). Global protein analysis using GeLC-MS/MS identified several soluble proteins related to oxidoreductases (e.g. ferredoxin-NADH reductase, NADH ubiquinone oxidoreductase). These types of proteins have previously been implicated in the production of extracellular superoxide by pathogenic bacteria. These proteins are currently being targeted by site-directed transposon mutagenesis. In-gel assays of this soluble protein fraction also showed a protein band active for Mn (II) oxidation. Surprisingly, we observe differences in Mn (II)-oxidizing proteins when *Roseobacter* is grown under different nutrient conditions. In the presence of a minimal medium, Mn (II)-oxidizing proteins are only detected when *Roseobacter* is grown in the presence of Mn (II). Using a comparative protein approach, we are identifying differences in the proteins produced under these two conditions, which will identify the protein involved in Mn (II) oxidation.

In combination, our past and current efforts have identified a new pathway for Mn (II) oxidation that is linked to a putative NADH oxidoreductase. Our current efforts will reveal the protein and genes involved in extracellular superoxide production by *Roseobacter*. Considering the abundance of *Roseobacter* in marine environments as well as the versatility of superoxide to act as both a metal oxidant and reductant, this research has large implications in the processes driving metal cycling within marine waters.

Measuring $\delta^{13}C$ in siderite and organic matter of lake sediments

O. LEBEAU, V. BUSIGNY, C. CHADUTEAU, D. JEZEQUEL AND M. ADER

IPGP-Sorbone Paris Cité, Univ. Paris Diderot, UMR7154 CNRS, Paris, France (olebeau@ipgp.fr)

The evolution of Earth surface biogeochemistry is still not completely understood. Among the various tracers available, the isotope compositions of C and N in Archean rocks are increasingly used but their interpretations remain ambiguous. The study of present stratified water body (oxic at the surface and anoxic in the deeper part) and of their sediments may help us to better interpret the isotopic signal from old sediments. Lake Pavin (French Massif Central) is permanently stratified with anoxic Fe-rich bottom water and can be regarded as an analogue of Archean oceans before the Great Oxidation Event (~2.5 Ga). We aim at analyzing C and N isotope of particulate matter sinking in the water column together with sediment cores from various water depths, in order to understand modifications related to early diagenesis within the water column and surface sediments. In this preliminary study, we develop protocols allowing the measurement of $\delta^{13}C$ values in both organic matter and siderite (Fe-carbonate) from sediment samples.

For organic matter analysis, the removal of siderite is necessary. Previous studies have shown that carbonate dissolution with HCl should not be used because immature organic matter can be partially attacked. Diluted HCl attacks (0.5, 1 and 2M) were tested on two siderite-free Pavin sediment samples. Despite a loss of carbon, no fractionation of C isotopes occurred. A siderite-rich sediment sample will be treated in the same way to check whether siderite is completely dissolved or not.

For C and O isotope analysis of siderite, the presence of organic matter might be problematic. Tests on mixtures of yeast with siderite show that organic matter reacts with phosphoric acid and modifies C and O isotopes signal of siderite. Organic matter removal with NaOCl 3.5% and H_2O_2 30% has been tested on the mixtures. While both reactants removed efficiently organic matter, siderite was also partially oxidized, but without $\delta^{13}C_{carb}$ and $\delta^{18}O_{carb}$ modifications. The chemical treatments thus improved greatly the siderite analysis. Vacuum pyrolysis and low temperature plasma ashing will also be tested to check if they can remove organic matter without destabilizing siderite.

https://doi.org/10.1180/S0026461X00006502 Published online by Cambridge University Press

Variability of the element content in clays of the Poznan series

D. LECH*, I. BOJAKOWSKA, P. BRAŃSKI AND I. JAROŃ

PGI-NRI, 00-975 Warsaw, Poland
(*correspondence: dariusz.lech@pgi.gov.pl)

Introduction

Miocene-Pliocene sediments of the Poznań series, occurring in central and northern Poland, were formed in a vast inland alluvial-lacustrine basin. In these series three lithostratigraphic horizons are distinguished: green clays, gray clay, and flamy clays.

Methods

129 samples were collected from 18 deposits of clays in order to characterize the variability of elements in clays of the Poznan series. In the samples after the full acid digesting, the contents of As, Ba, Cd, Co, Cr, Cu, Mn, Mo, Ni, Pb, Sn, Sr, Ti, V, Zn, Al, Ca, Fe, K, Mg, Na, P and S were determined using ICP-OES method, the Hg was determined by AAS.

Results

Differences were found in the element contents in Poznan clays depending on their lithotype. Green clays have higher average contents of Cr, Ni, Sr, Zn, Ca, Mg, Na, K, gray clays - higher content of Hg, Ba, Ti, and lower contents of Fe, Ca, Mg, Cr and V, and a flamy clay is marked by higher contents of As, Cu, Fe, Mn, P. Higher levels of the some elements in green clays are associated with the marine environment - Sr, Mg, Na and K. It was noted the variability of elements in clays depending on the region of their occurrence. Clays occurring in the northern part of the basin have higher contents of Na and Sr. In the western part of the basin clays contain less V, Cu, Fe and Mn than clays occurring in other parts of the reservoir. It was observed decline the content of Ba, Hg, K and P in clays in an easterly direction, while increasing Ca content. Clays occurring in northern coastal zone reservoir, fed from the East European Craton area, contain more Na, Sr and Ca as compared to clays located in the southern part, fed from an old Sudeten massif, characterized by a higher content of Ti and low contents of Fe and Ca. The clays formed in the reservoir, for which feeding area were mostly young Western Carpathian orogenic areas, contain more Cu, Zn, V and Mg.

Conclusions

It has been found differences in the contents of elements in the clays of Poznan series depending on their lithological variety and the region of deposition.

Rhodochrosite gemstones: Contrasting origin and evolution of related fluids

P. LECUMBERRI-SANCHEZ[1]*, R.L. ROMER[2], V. LÜDERS[2] AND R.J. BODNAR[1]

[1]4044 Derring Hall, VirginiaTech, Blacksburg, VA 24061 US
(pilar@vt.edu, rjb@vt.edu)
[2]GFZ, Telegrafenberg, D-14473, Potsdam, Germany
(romer@gfz-potsdam.de, volue@gfz-potsdam.de,)

The Wutong (Guanxi Province, China) and Sweet Home (Colorado, USA) are Pb-Zn-Ag deposits of similar mineralogy, originally exploited for Ag, and both are prolific producers of gem-quality rhodochrosite. The Sweet Home Mine is in the Colorado Mineral Belt (which includes several giant porphyry-Mo deposits), and the genesis of the Sweet Home deposit has been linked to the Mo deposits. Converesely, potential genetic relations of the Wutong Mine are unknown. The comparison between their fluid source and evolution provides a frame to understand which factors are critical in the formation of rhodochrosite gemstones.

At Wutong, narrow ranges in Sr and Pb isotopic compositions indicate that these elements were predominantly contributed by the same fluid source. Low variability in C and O isotopic compositions in rhodochrosite is additional evidence of a fairly simple fluid evolution, unaffected by strong mixing or partitioning events. Sweet Home Mine shows contrasting results: the wide Sr range suggests that several fluid sources contributed to the bulk Sr, and the distribution of C and O isotopic compositions may point to contributions from magmatic and meteoric derived fluids [1]. The Pb isotopic compositions in both deposits reflect as well the contrasting geologic history of the Pb source rocks.

Wutong fluid inclusions (FI) indicate that temperature and salinity decrease with time during the paragenesis, consistent with a magmatic fluid trend. The only observed exception to this trend is found in primary FI in fluorite where the temperature decreases but fluid salinities are higher than in previous or later generations. Pre-fluorite FI contain CO_2 while FI post-fluorite lack CO_2. The syn-fluorite peak in salinity and the disappearance of CO_2 in FI can be explained by several processes in the system including changes in pressure, boiling or mineral precipitation.

Magmatic fluids are responsible for the formation of Wutong. Despite the more complex history of Sweet Home, additional fluid sources do not seem to be a requirement for the formation of gem-quality rhodochrosite.

[1] Lüders *et al*. (2009) *Miner Deposita* **44**, 415–434.

https://doi.org/10.1180/S0026461X00006502 Published online by Cambridge University Press

Geochemical and synchrotron study of Barberton Greenstone Belt cherts (3.5-3.2 By), South Africa

M. LEDEVIN[1]*, A. SIMIONOVICI[1], N. ARNDT[1] AND F. WESTALL[2]

[1]ISTerre, BP53, 38041, Grenoble Cedex 9, France (*correspondence: morgane.ledevin@ujf-grenoble.fr)
[2]Centre de Biophysique Molléculaire, CNRS, rue Charles Sadron, 45071, Cedex 2, Orléans, France

To understand the formation of Archean cherts and the information they provide about conditions at the sea floor, we studied samples from four sites in the Barberton Greenstone Belt (3.5-3.2 By), South Africa. We identified cherts with three different origins: direct precipitation from seawater, precipitation in fractures from silica-rich hydrothermal fluids, and replacement of preexisting rocks at or near the surface.

Petrological criteria allow us to define specific chemical markers: rocks preserving sedimentary structures (e.g. laminations) have trace element patterns with high HREE and low LILE contents, and a strong negative Sr anomaly. In comparison, cherts precipitated in fractures have lower HREE and higher LILE contents, with a strong positive Ba anomaly. In one sample, the laminated portion has the chemical characteristics of the first type and a white fracture-filling chert has the features of the second type.

Another part of our study focused on petrology and rheology of Barberton cherts: both macro- and micro-structural observations are used to understand early physical behavior of chert, silica precipitation, and silicification processes. Field observations revealed complex rheological behavior, from ductile to brittle deformation, sometimes both in the same chert layer, with extremely fast diagenetic and induration processes, and some evidence of an early colloidal silica phase. Close correlation between micro-scale element repartition and microstructure by high-resolution analyses (RAMAN, X-Ray microfluorescence, cathodoluminescence, synchrotron) are currently underway.

In parallel, a petrological-geochemical study on siliceous chemical precipitates in modern volcanic lakes is being undertaken. The geochemical signatures of both Archean and modern cherts will then be used to infer physico-chemical conditions at the Archean sea floor and fractionation processes during silica transfer from fluids to rocks.

Determining the geographical origin of ginseng using strontium isotopes, multielements, and metabolite analysis

A.R. LEE[1], G. MUKESH[1], W.J. SHIN[1], M.S. CHOI[2], Y.S. BONG[1] AND K.S. LEE[1]*

[1]Korea Basic Science Institute, Ochang Center, Chungbuk 363-883, Korea (*correspondence: kslee@kbsi.re.kr)
[2]Chungnam National Univ. Daejeon 305-764, Korea (mschoi@cnu.ac.kr)

Asian ginseng (*Panax ginseng* C.A. Meyer) is widely used as an Oriental medicine in East Asian regions, particularly Korea and China. To develop a method to distinguish ginsengs cultivated in Korea with those cultivated in China, we analyzed multielements, strontium isotope ratios ($^{87}Sr/^{86}Sr$), and metabolite profiles in 35 ginseng samples collected from Korea and China. A multivariate statistical approach was performed to analyze the multiple elements and the ^{1}H nuclear magnetic resonance (NMR) data. Discriminating between the ginsengs from the two countries was generally successful when both the $^{87}Sr/^{86}Sr$ ratios and rare earth element contents were used together. Moreover, principal components analysis derived from the ^{1}H NMR data revealed a significant separation between the ginsengs originating from the two countries. The major metabolites responsible for differentiation were sugars such as glucose, xylose, and sucrose. The results suggest that this multi-platform approach offers a comprehensive method to distinguish the origin of ginsengs.

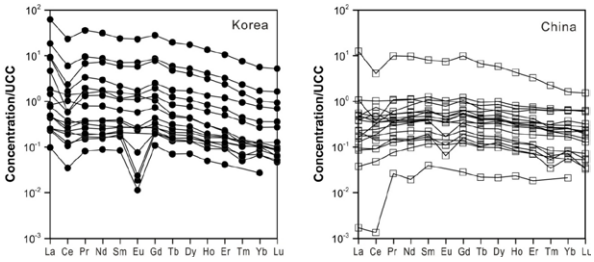

Figure 1: Upper continental crust (UCC)-normalized rare earth element (REE) patterns for the Korean (a) and Chinese (b) ginsengs.

https://doi.org/10.1180/S0026461X00006502 Published online by Cambridge University Press

Identification of the oldest carotenoid breakdown products in the geological record

C. LEE[1,2]* AND J.J. BROCKS[1]

[1]Research School of Earth Sciences, Australian National University, Canberra, Australia 0200
[2]Geological & Planetary Sciences, California Institute of Technology, Pasadena, CA 91125
(*correspondence: carinal@caltech.edu)

Carotenoids are often difficult to study in the geological record because of their low preservation potential. Preservation of the hydrocarbon equivalents of carotenoid molecules is rare due to their tendency to break into smaller units or undergo complex aromatisation and rearrangement reactions [1]. In rare instances where intact C_{40} carotenoid hydrocarbons are preserved by suitable diagenetic conditions, they are often subsequently cleaved into smaller fragments by increasing temperatures during burial of the host sediment (catagenesis).

Upper sections of the 1.64 billion year old (Ga) Barney Creek Formation (BCF) in the McArthur Basin of northern Australia preserves more than 22 different C_{40} carotenoid derivatives, including the hydrocarbons β-carotane, γ-carotane, and lycopane [2]. However, the C_{40} structures disappear in deeper strata, although reasons for this disappearance were unknown. It could either be a result of diagenesis, increasing thermal maturity, or change in the biological source organisms.

We simulated the natural degradation of the carotenoid hydrocarbon, β-carotane, by way of hydrous pyrolysis. Hydrous pyrolysis of β-carotane generated a mixture of systematic thermal cleavage products that were used as a new elution standard [3].

We were able to successfully identify β-/γ-carotane breakdown fragments even in deeper sections of the BCF. Given an intermittent disappearance and reappearance of these carotane fragments, as well as gradually declining concentrations with depth, we conclude that the combination of diagenesis and thermal maturity caused carotenoid decline. The fragments identified at 287 m depth in drill core GR-7 now represent the oldest evidence for non-aromatic carotenoids in the geological record.

[1] Koopmans *et al*. (1997) *Org. Geochem.* **26**(7-8) 451–466 [2] Brocks & Schaeffer, (2008) *Geochim. Cosmochim. Acta.* **72**, 1396–1414. [3] Lee & Brocks, (2011) *Org. Geochem. In Press*

Copper systematics in arc magmas and implications for the origin of continents, the Pb-paradox, and copper porphyry deposits

C.-T.A. LEE[1], E.J. CHIN[1], R. BOUCHET[1,2], P. LUFFI[1], R. DASGUPTA[1], D. MORTON[3], V. LE ROUX[4], Q.-Z. YIN[5], F. ALBAREDE[2] AND J. BLICHERT-TOFT[2]

[1]Rice University, TX, USA (ctlee@rice.edu)
[2]Ecole Normale Superieure, Lyon, France
[3]University of California, Riverside, CA, USA
[4]Woods Hole Oceanographic Institute, MA, USA
[5]University of California, Davis, CA, USA

Redox evolution during magma differentiation plays an important role in making continents, ore deposits, and the composition of the atmosphere. A powerful tracer of redox is S due to redox-sensitive speciation, but because S is easily disturbed by late-stage alteration, it is difficult to use as a robust tracer. However, Cu's unique affinity for sulfide makes it sensitive to S speciation and overall magma oxidation state. Here, we show that Cu in primitive arc and mid-ocean ridge basalts are similar and that the majority of arc magmas become depleted in Cu during differentiation. Thus, sulfide saturation and hence low oxygen fugacity generally characterize mantle melting and early magma differentiation in mid-ocean ridges and even most arcs. The fact that global continental crust is also depleted in Cu not only requires a missing Cu reservoir but also suggests that high oxygen fugacities are not critical in forming continental crust. We show that the missing Cu in arcs and continental crust is represented by sulfide-bearing pyroxenites formed as deep crustal cumulates that eventually founder into the mantle due to their high densities. Such foundering drives the residual crust towards felsic compositions and creates low U/Pb pyroxenite reservoirs in the deep mantle. Thus, the radiogenic Pb isotopic composition of the Earth's upper mantle is more likely attributed to continent formation than to protracted core formation. Instead of oxidized or metal-rich mantle sources, Cu-porphyries probably derive from Cu-rich pyroxenites. These pyroxenites are most prone to re-melting during arc thickening, but because the pyroxenites are given to foundering, the window for Cu-porphyry formation is narrow. An important implication of this work is that subduction does not lead to efficient oxidation of the mantle. Therefore, oxygenation of the Earth's atmosphere is not controlled by evolution of mantle redox.

https://doi.org/10.1180/S0026461X00006502 Published online by Cambridge University Press

The evolution of Zn and Cd isotopes in the South China Sea

DER-CHUEN LEE[1]*, SHUN-CHUN YANG[2,3] AND TUNG-YUAN HO[3]

[1]Institute of Earth Sciences, Academia Sinica, Taipei, Taiwan (*correspondence: dclee@earth.sinica.edu.tw)
[2]Dept of Geosciences, Nat. Taiwan Univ., Taipei, Taiwan
[3]Research Center for Environmental Changes, Academia Sinica, Taipei, Taiwan

Isotopic compositions of Zn and Cd for biogenetic particles and seawater samples from the South China Sea (SCS) have been determined in order to better constrain how do Zn and Cd isotopes evolve in the SCS. In general, the $\delta^{66/64}$Zn increases from -0.25‰ in the surface to 0.05‰ in the thermocline, and remains constant at 0.13‰ in the deep ocean. As for biogenic particles, they have the δZn of 0.04‰, suggesting that phytoplankton prefers heavy Zn isotopes. As a result, the vertical profile of Zn isotopes in the SCS appears to be governed by biological pump that transports heaver Zn into the deep ocean.

In contrast, the $\varepsilon^{114/110}$Cd in the seawater decreases from 9.6ε in the surface to 5.0ε in the thermocline, and remains constant at 3.5ε in the deep ocean. This seems to reflect the preferential uptake of light Cd isotope by phytoplankton in the surface water. However, the biogenic particles have the Cd isotopic signature of 9ε, comparable to that of the anthropogenic aeolian inputs, suggesting that the biological fractionation is perhaps insignificant in the SCS. Consequently, the vertical profile of Cd should reflect that of anthropogenic inputs to the surface ocean, and are subsequently transported into deeper ocean by vertical advection.

The diatom-dominated (during our sampling) SCS biogenic particles have similar Cd but heavier Zn relative to the surface water, consistent with previous findings that Cd is assimilated while Zn is mainly adsorbed in extracellular level by the phytoplankton.

Geochemical characteristics of the Nakdong River, Korea

GYEONGMIN LEE, JIYEON KIM AND YEONGKYOO KIM*

Department of Geology, Kyungpook National University, Daegu, 702-701, Korea (*correspondence: ygkim@knu.ac.kr)

The geochemical compositions of the river waters are influenced by many different factors including weathering and anthropogenic activity. Therefore, the informations on geochemical characteristics of river waters are required to get insight into the geological and hydrogeochemical processes of the river.

The Nakdong River is the second largest but the longest river in Korea. The length of the river is 506.17 km and the drainage area of the Nakdong basin is 23, 384.21 km^2. The water samples of river and tribuatry waters were collected three times in November, May, and July to see the effect of precipitation because July belongs to rainy season. The basin area of this river can be divided into two groups based on the geology: granitic and gneissic rocks in upstream region and sedimentary and granitic rocks in downstream one.

Piper diagram shows that the geochemical patterns changes from Ca-SO_4/Ca-HCO_3 type to Na-SO_4 one from upstream to downstream, showing the increase of the anthropogenic effects, and the influence of the different geology seems to be very small. The concentrations of the cations are in the order of Ca>Na>Mg>K, and those of anions are HCO_3>SO_4>Cl>NO_3, indicating that weathering is the main process controlling the geochemical compositions of the Nakdong River, especially in the upsteram region. The concentrations of Na abruptly increase at the sampling locations near Daegu, which is the third largest city in Korea, indicating a significant pollution by anthropogenic activity. The concentrations of cations in waters sampled in different months are in the order of November>July>May. However precipitation affects anion compositions differently. The concentrations of HCO_3 and Cl have the same trend as cations, but those of SO_4 and NO_3 are in the order of July>May>November, indicating possible influence of precipitation on the concentrations of these two anions.

https://doi.org/10.1180/S0026461X00006502 Published online by Cambridge University Press

Pilot scale feasibility test for *in situ* chemical oxidation and biodegradation process to remediate the diesel contaminated millitary site, Korea

HAJUNG LEE, INSU KIM, KYOUNGBAE BAEK AND MINHEE LEE

Department of Earth Environmnetal Sciences, Pukyong National University, Daeyon 3 dong, Namgu, Busan, 608-737, Republic of Korea (skyworld87@nate.com)

Pilot scale experiment was performed by using the *in situ* chemical oxidation and biodegradation process to remediate the diesel contaminated military site, Korea. The soil at this site was composed of sandy loam and silt loam and the initial average TPH concentration of soil was 5202.8 mg/kg.

The *in situ* chemical oxidation process was carried out on a pilot scale test site (2.5 m x 2.7 m x 1 m), by using 17.5 % hydrogen peroxide solution as an oxidizer. Five injection wells (IW-1, IW-2, IW-3, IW-4 and IW-5) and one extraction well (EW-1) were installed in the test site. The injection rate of hydrogen peroxide solution was 140 ml/min for 5 hours per day. The pumping from extraction well proceeded every 30 minutes. Total amount of H_2O_2 injected was 718 L and 400 L was extracted from the extraction well. After stabilizing the site for 7 days, indigenous microorganisms were cultivated from the contaminated soil and 86 L of solution having cultured microorganisms were added to the site, which was already treated by the chemical oxidation process, for 2 days (May 15th and 20th, 2010).

As a result of chemical oxidation process, TPH concentration of the treated soil decreased by 2138.1 mg/kg (59 % of removal efficiency). TPH concentration of site biodegraded by indigenous microorganisms for 17 days decreased by 729.6 mg/kg (92 % of removal efficiency), which was lower than Korean Soil Pollution Warning Limit (TPH : 2000 mg/kg).

From the results of the pilot scale test, it was investigated that the combination of chemical oxidation and the biodegradation process was complementary and it could effectively remediate diesel contaminated soil.

Arsenic uptake by natural sludge occurred at coal mine drainage

HYO EUN LEE[1], YOUNG JAE KIM[1], SOO-OH PARK[1], YOO HYUN SUNG[2], SAE GANG OH[3] AND YOUNG JAE LEE[1]*

[1]Department of Earth and Environmental Sciences, Korea University, Seoul 136-701, Korea (*correspondence: youngjlee@korea.ac.kr, hyonim@korea.ac.kr, jjbsnlove@korea.ac.kr, orange261@korea.ac.kr)

[2]Research and Development Team, Korea Resources Corporation, Seoul 156-406, Korea (yhsung@kores.or.kr)

[3]Office of Ecology Restoration, Mine Reclamation Corporation, Seoul 110-727, Korea (sgoh@mireco.or.kr)

Arsenic (As) is widely known as a toxic element for humans and ecosystems. Sorption of arsenic on minerals such as metal-(hydr)oxides has been known to play a key role in controlling the fate and transport of arsenic species in natural ecosystems. Despite the importance of arsenic interaction with natural minerals in ecosystems, uptake modes of arsenic by natural minerals under different physicochemical conditions are not clearly understood. Moreover, no systematic studies of arsenic uptake by naturally ocurring sludge at mine sites has been provided, especially by the combination of marcroscopic and microscopic observations.

Systematic studies, combined batch experiments with XRD, XRF, SEM, and X-ray absorption spectroscopy (XAS), have been used to investigate arsenic sorption on slugde occurred at Ham-Baek mine, South Korea. Results show that the sludeg is mainly composed of nano-sized schwertmannite (Fe_8O_8 $(OH)_6$ $(SO_4)\cdot nH_2O$). Compared to that of synthesized schwertmannite, however, XRD and SEM show that crystallinity of the sludge particles are very poor, suggesting that the surface reactivity of particles could be different. At pH 4.0 and 7.0, sorption of arsenite and arsenate on the sludge sharply increase at $[As]_{tot.} < 370$ μM, and then followed by gradually increase with increasing As concentration without reaching any plateau, indicative of Freundlich sorption behavior. At 7.0, however, the total amount of arsenate sorbed on the sludge decreases with increasing pH and ionic strength of the solution. It is found that both arsenite and arsenate uptake by the sludge is rapid and ~95% of As is sorbed on the sludge within 30 mins, suggesting that adsorption plays an important role in the initial upatke of arsenic at the sludge-water interface. XANES shows that arsenite species sorbed on the surface of the sludge particles is changed to arsenate during the duration of the experiment.

https://doi.org/10.1180/S0026461X00006502 Published online by Cambridge University Press

Hydrochemical and isotope study of groundwater contamination by fecal microbes

JEONG-HO LEE[1], SEONG-TAEK YUN[1]*, YONG SEOK JEONG[2], BERNHARD MAYER[3], WEON-WHA JHEONG[4] AND CHANG-HOON YOO[2]

[1]Department of Earth and Environmental Sciences, Korea University, Seoul 136-701, South Korea (*correspondence: styun@korea.ac.kr)
[2]Department of Biology, KyungHee University, Seoul, South Korea
[3]Department of Geoscience, University of Calgary, Calgary, Alberta, Canada T2N 1N4
[4]National Environmental Research Institute, Incheon, South Korea

In order to better understand the source (s) and behavior of the norovirus and other fecal microbes in groundwater systems we performed a hydrochemical and environmental isotope study in conjunction with a microbiological survey on total coliform, *E. coli*, fecal bacteria, coliphage and norovirus. In the study area with known norovirus contamination, groundwater samples were collected from 21 existing household wells and 3 multi-level monitoring wells (MLWs) installed around a latrine. The detection rate of the norovirus was high (10-19%) in household wells. Cl versus Cl/Br plots suggest that fecal microbes and potentially associated pollutants such as nitrate, chloride and sulfate are likely derived from septic effluents and animal wastes. Nitrogen and oxygen isotope ratios of nitrate in 21 groundwater samples [$\delta^{15}N_{nitrate}$ = 7.6 to 18.9‰ (avg. 13.5‰), $\delta^{18}O_{nitrate}$ = 3.6 to 13.4‰ (avg. 6.7‰)] also indicate the origin of nitrate from manure and/or sewage. Hydrochemistry data obtained from MLWs indicated the existence of one or two distinct reduction zones where denitrification occurred. In addition, groundwater from MLWs showed the frequent and considerable detection of total coliform and fecal bacteria. Detection rates of *E. coli*, coliphage and norovirus were negligible, possibly indicating that they are preferentially absorbed onto soil particles in unsaturated or saturated zones. Combined with local geologic features, we suggest that iron (hydro-)oxides in subsurface soils play a role as a sorbent of microbes. The results of this work will be helpful to evaluate the vulnerability of groundwater to fecal contamination, which can accompany norovirus and other fecal microbes.

Pb in a deep sea coral: Transfer of anthropogenic Pb to the deep North Atlantic Ocean over the last 500 years

JONG-MI LEE[1], SELENE F. ELTGROTH[2], EDWARD A. BOYLE[1] AND JESS F. ADKINS[2]

[1]Massachusetts Institute of Technology, 77 Massachusetts Ave, Cambridge, MA 02139, USA (jm_lee@mit.edu)
[2]California Institute of Technology, 1200 E. California Blvd. Pasadena, CA 91125, USA (jess@gps.caltech.edu)

Pb in the deep ocean depends on transit time distributions because its concentration and isotope composition in the surface ocean have varied significantly over time in response to anthropogenic Pb emissions. However, the use of Pb as a tracer has been limited by the lack of data in the ocean interior both in time and space. In this study, a ~500 year history of the evolution of Pb and Pb isotope ratios in the interior North Atlantic Ocean is established from a deep sea coral *E. rostrata* which was collected from ~1410m depth on the north Bermuda slope.

Coral Pb concentrations range between 1.1-4.5 nmol Pb/mol Ca from the early 16th century to the 17th century, and Pb isotope ratios ($^{206}Pb/^{207}Pb$ = 1.21, $^{208}Pb/^{207}Pb$ = 2.495) in this period agree with those found in pelagic sediments of the western North Atlantic Ocean. Slightly increased Pb/Ca ratios (~7 nmol Pb/mol Ca) are found between 1740s and 1860s, and the ratio increases rapidly from 1860s to 1997 by a factor of four. Both $^{206}Pb/^{207}Pb$ and $^{208}Pb/^{207}Pb$ ratios decrease from the mid-18th century as the Pb concentration increases, probably due to the penetration of anthropogenic Pb into the deep sea, which has lower $^{206}Pb/^{207}Pb$ and $^{208}Pb/^{207}Pb$ isotope compositions than natural Pb in this region. Comparison of this data to the 200-yr-record of surface Pb data from Bermuda corals shows that the transit time of Pb from the surface to the coral growth site is about 25 years. This estimate is consistent with that from radiocarbon measurements in the same coral. Reconstructed $\Delta^{14}C$ values also show that the bomb radiocarbon signal appears 20-25 years later than its first appearance in the surface ocean near Bermuda. However, the rise of $\Delta^{14}C$ is not as rapid in the deep as it is in the surface, potentially allowing us to reconstruct the relative effects of transport and diffusion on tracer movement from the surface to the intermediate North Atlantic Ocean.

https://doi.org/10.1180/S0026461X00006502 Published online by Cambridge University Press

Remediation of arsenic contaminated soil using soil washing with an acidic and reducing solution

J.H. LEE, J.G. KIM*, Y.C. CHO, C.H. LEE AND B.G. CHAE

Korea Institute of Geoscience and Mineral Resources, Daejeon 305-350, Korea (ljh@kigam.re.kr, *correspondence: jgkim@kigam.re.kr, choych@kigam.re.kr, chlee@kigam.re.kr, bgchae@kigam.re.kr)

Soil contamination with arsenic (As) is a serious environmental concern due to its highly toxicity and carcinogenic properity. Iron oxides are known a most important factor for the controlling As concentration in soil pore water. They absorb large amout of As and coprecipitate with As. We tried to develop a new washing method of As contaminated soil by the dissolution of iron oxide and desorption of As employing pH and redox potential adjustment. An As contaminated soil sample was collected at a rice paddy field near a copper smelter, Korea. The As concentration of the soil sample was determined with an aqua-regia extraction method. Washing solutions were prepared to be 0.001 – 0.1N HCl and 0 - 3 % Na-dithionite. The soil and washing solution were mixed at 1:4 ratio and the mixtures were reacted for 15, 30, 45 and 60 minutes. After the reaction, the soil and washing solution were separated with a centrifugation. The pH, Eh, and the concentrations of As, Fe and Mn of the washing solution were determined and the As concentration of the washed soil sample was also determined. The separated washing solution was treated with H_2O_2, $CaCl_2.2H_2O$ and cationic organic polymer to remove As.

The soil washing with the 0.01N HCl 3% Na-dithionite solution for 30 minutes was the most effective in the As removal from the soil reducing As concentration from 43 mg/kg to 18 mg/kg. The As concentration of the washing solution was reduce from 19.2 mg/L to 0.76 mg/L after the waste water treatment.

The stability of amino acids under redox-constrained hydrothermal conditions

NAMHEY LEE[1,2], D.I. FOUSTOUKOS[2], D.A. SVERJENSKY[1,2], H.J. CLEAVES II[2], K. KLOCHKO[2] AND R.M. HAZEN[2]

[1]Department of Earth and Planetary Sciences, Johns Hopkins University, Baltimore, MD, 21218 (namheyl@jhu.edu)
[2]Geophysical Laboratory, Carnegie Institution of Washington, 5251 Broad Branch Road, NW, Washington D.C., 20015

With the discovery of an extensive biosphere near deep-sea hydrothermal vents, the stability of amino acids at elevated temperatures and pressures is of great interest for the cycling of C and N within the crust and the overlying oceanic water column. Previous studies provide strong evidence that the decomposition properties of amino acids are very sensitive to parameters such as temperature, and catalytic reactor surfaces. However, despite the clear relevance, the redox state of the system has rarely been controlled in such studies. Here hydrothermal experiments were conducted to investigate the influence of redox conditions on the stability of glutamic acid at pressures and temperatures reflecting near-seafloor hydrothermal environments (100–250 °C, 136 bar). Reactions were conducted for 3 to 35 min. in a titanium flow-through cell. The oxidation state was controlled by equilibrating ~ 22 mmolal of H_2 (aq) with a glutamic acid solution with pH adjusted to ~10 at 25 °C. The products were identified and analyzed using gas chromatography and ionic chromatography with conductivity and electrochemical detectors. Results indicate that the reaction kinetics of glutamic acid under hydrothermal conditions is associated with conversion to the cyclic pyroglutamate via a dehydration reaction. Other products of glutamic acid included CO_2 (aq) and H_2 (aq). At temperatures above 200 °C formate was also observed, possibly produced via a decarboxylation and reduction. The conversion rate of glutamic acid to pyroglutamic acid, however, does not appear to be affected by the redox state of the system. The decomposition of glutamic acid is observed to obey first-order kinetics. From the temperature-dependent decay rate expressed by the Arrhenius equation, we obtained an activation energy of 39.6 kJ/mol with a pre-exponential factor as 74 sec^{-1}, whereas previous study estimated the activation energy of 152 kJ/mol with a pre-exponential factor as 10^{13} sec^{-1} using Pyrex glass and longer reaction times up to 15 hrs at 252 ºC [1].

[1] Povoledo & Vallentyne (1963) *Geochimica et Cosmochimica Acta* **28**, 731–734.

https://doi.org/10.1180/S0026461X00006502 Published online by Cambridge University Press

Geochemical significance of ^{14}C, ^{3}H, $\delta^{18}O$, $\delta^{2}H$ and $^{87}Sr/^{86}Sr$ isotopic data in the hot spring waters of South Korea

S-G. LEE[1]*, T. NAKAMURA[2], Y.Y. YOON[1], T-K. KIM[1], T. OHTA[2] AND T. LEE[1]

[1]Korea Institute of Geoscience and Mineral Resources, Daejeon 305-350, Korea (sgl@kigam.re.kr, yyyoon@kigam.re.kr, tkkim@kigam.re.kr, megi@kigam.re.kr)

[2]Center for Chronological Research, Nagoya University, Nagoya 464-8601, Japan (nakamura@nendai.nagoya-u.ac.jp)

Despite being a non-volcanic area, South Korea has a number of the hot springs with water temperatures of more than 40°C. The occurrence of these hot springs are related with Mesozoic granites in the Korean Prninsula. The hot springs are located at the fringes of the granite body rather than the center of the Mesozoic granites. Lee *et al.* [1] reported a geochemical characteristic of the $^{87}Sr/^{86}Sr$ in the hot spring waters, and suggested that the heat source of the hot spring water might be related with granite emplacement. Most hot springs are deep-drilled wells with depths of more than 100m, and motorized pumps are used. Here we report new data for $^{87}Sr/^{86}Sr$ ratio of the hot spring waters, and also report $\delta^{2}H$, $\delta^{18}O$, ^{14}C and ^{3}H isotopic data of hot spring waters in South Korea to discuss the origin of the hot spring waters.

Environmental isotope results such as $\delta^{2}H$ and $\delta^{18}O$ reveal that hot spring water and groundwater were originated from the meteoric water. However, there was no variation in chemical compostions and $^{87}Sr/^{86}Sr$ ratio of the hot spring waters during last eight years. ^{14}C activity of DIC in the hot spring waters in South Korea ranges from 1.7 pMC to 78 pMC. Such $^{87}Sr/^{86}Sr$ and ^{14}C isotope results show that the circulation between thermal water and current meteoric water including groundwater, surface water and rainwater at the southeastern part in the South Korea should be slow. Our data indicate that the high temperature hot spring water in South Korea might be derived from paleo-groundwater reservoir with high temperature rather than circulation of the modern meteoric water heated directly by a current heat souce. This also suggests that the hot spring water in the granite area might be one of limited groundwater resources.

[1] Lee, S.G. *et al*. (2007) *GCA* A558.

Zircon Hf isotopic study of the Mesozoic granitoids from Korea and Japan and tectonic implications

S.R. LEE[1]*, D.-L. CHO[1] AND F.-Y. WU[2]

[1]Geological Research Divison, Korea Institute of Geoscience and Mineral Resources, Daejeon 305-350, Korea (*correspondence: leesr@kigam.re.kr)

[2]Institute of Geology and Geophysics, Chinese Academy of Sciences, Beijing 100029, China

Before switching to the present-day island arc system during the Miocene, the Japanese Islands grew outboard of the older continental margin of East Asia, next to the Korean Peninsula [1]. The Hida belt, including the Precambrian rocks, represents the remant of the former Asian continental margin, but its tectonic correlation to the North China or South China cratons is uncertain. The Korean Peninsula consists of three Precambiran massifs: Nangrim, Gyeonggi and Yeongnam massifs. The first and last are considered as parts of the North China craton, while the middle as a part of the South China craton [2], though such correlations are still under debating [2, 3]. The correlative study among the Hida belt and Korean massifs thus provides some clues to the Mesozoic continental accretions of the eastern margin of the Asian continent.

In this study Hf isotopic compositions of the zircons are presented for the Late Paleozoic-Mesozoic granitoids from the Hida belt and Korean massifs. In the Hida belt, εHf (t) values range from +5 to -8 for the Triassic zircons, and from +12 to +6 for the Jurassic zircons, respectively. The εHf (t) values range from -10 to -26 for the Triassic zircons of the Gyeonggi massif, while they range from -4 to -12 for the Triassic zircons and -22 to -32 for the Jurassic zircons of the Yeongnam massif. Our data indicate that the source materials are similar to each other for the Triassic granitoids from the Hida belt and Yeongnam massif, and suggest that the Hida belt is more correlative to the Yeongnam massif (i.e. North China craton) rather than the Gyeonggi massif (i.e. South China craton). During the Jurassic, however, the source materials became more juvenile for the Hida granitoid, while they changed progressively to crustal-dominated ones for the granitoids from the Yeongnam massif. This feature suggests that the crustal thickness of the eastenmost part of the Asian continental margin (i.e. Hida belt) has extended enough to shift from continental arc setting to island arc setting during the Jurassic time.

[1] Taira (1997) *EPS* **325**, 467–478. [2] Chough *et al*. (2000) *ES Rev* **52**, 175–235. [3] Oh (2006) *Gond Res*. **9**, 47–61.

https://doi.org/10.1180/S0026461X00006502 Published online by Cambridge University Press

$Cr(OH)_3(s)$ oxidation by birnessite under common groundwater pH conditions

YEONJIN LEE AND GIEHYEON LEE*

Department of Earth System Sciences, Yonsei University, 50 Yonsei-ro, Seodaemun-gu, Seoul 120-749, Korea (*correspondence: ghlee@yonsei.ac.kr, ureca0125@yonsei.ac.kr)

Contamination of soil and groundwater by hexavalent chromium (Cr(VI)), which is the 2nd most common inorganic contaminant, was generally considered to be generated from anthropogenic sources. Recently, natural groundwater contamination by Cr(VI) without any anthropogenic sources have also been reported over the world. Previous studies showed that various Mn oxides effectively oxidized aqueous- or solid-phase Cr(III) under acidic pH conditions but not under neutral or higher pH conditions. Yet, the geochemical processes causing the natural contamination of Cr(VI) have not been clearly unravelled. This study examined the oxidation of $Cr(OH)_3(s)$ by birnessite, under common groundwater pH conditions. Both solids are ubiquitous in the environment. Practically, $Cr(OH)_3(s)$ has been thought to hinder the oxidation of dissolved Cr(III) by Mn oxides because the precipitation of this solid on Mn oxide would block the reactive surface sites.

Particle suspensions were prepared with synthetic $Cr(OH)_3(s)$ and/or birnessite in 50 mM $NaNO_3$ at pH 7, 8, or 9 open to the atmosphere. The individual solid concentration was 1 g/L in every case and the solution pH was maintained with a 10 mM buffer (Na-MOPS for pH 7 and 8, CHES for pH 9). In the presence of birnessite, Cr(VI) concentrations increased with increasing pH and reached up to 209, 613, 836 µM at pH 7, 8, and 9, respectively, within a month. These Cr(VI) concentrations were substantially higher than those in the absence of birnessite at all pHs. These results indicate that birnessite could effectivly oxidize $Cr(OH)_3(s)$, where the solubility of this solid is minimum. In addition, the apparent rate and extent of $Cr(OH)_3(s)$ oxidation appeared to be controlled by several accompanied reactions, the effects of which mainly depend on the pH of the system. It is noteworthy that the rate of $Cr(OH)_3(s)$ oxidation increased with time during the first 10 hr followed by a decrease in the rate with time for the rest of the reaction. These results suggest that the overall oxidation would likely be accelerated by a reaction intermediate in the early stage of the reaction. A potential reaction pathway of $Cr(OH)_3(s)$ oxidation will be briefly discussed.

Ternary surface complexes probed by attenuated total reflection-infrared spectroscopy

G. LEFÈVRE[1]*, F. MERCIER-BION[2], Y. ZHAO[2], V. SLADKOV[2], J. ROQUES[2] AND E. SIMONI[2]

[1]LECIME, UMR7575 CNRS-Chimie ParisTech, 75005 Paris, France (*correspondence: gregory-lefevre@enscp.fr)

[2]IPNO, UMR 8608 CNRS-Université Paris-Sud 11, 91406 Orsay, France

Attenuated Total Reflection-Infrared spectroscopy (ATR-IR) is amongst the most developped spectral techniques during the last decades to study the solid/solution interfaces. Its efficiency in determining the speciation of adsorbed ions has been proved in numerous works using different metallic oxides [1]. Its advantage is to probe the system in presence of solution, avoiding the modification of the structure consequently to the dehydration. Indeed, this phenomenon can occur for inner-sphere complexes, even though it is not systematic, while for outer-sphere complexes, the dehydration step has always a dramatic effect. Another field where the possibilities of ATR-IR are underexploited is the characterization of ternary surface complexes including the mineral surface / a bridging species / a second adsorbed species. The main question which can be adressed by ATR-IR is to determine which is the bridging species, and what type of chemical groups are bonded to the mineral surface or to the other adsorbed species. In literature, such studies have been performed on goethite/sulfate/Pb (II) [2] or hematite/carbonate/U (VI) [3], goethite/glyphosate/Cu (II) [4] for example. The purpose of our current works is to characterize the surface reactivity of silica towards uranyl ions in presence of small organic molecules to evaluate the role of organic matter on the transport of radionuclides in environment. We have first studied the system silica/uranyl/acetate, using ATR to show the presence of a ternary complex. The same work with more complex organic molecules is in progress.

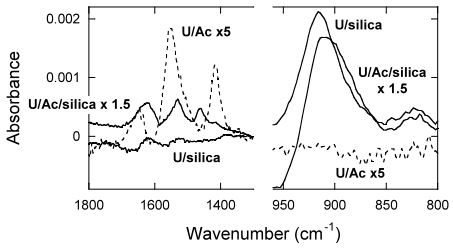

Figure 1: Spectra of U(VI) 0.05 mM in presence of acetic acid 10 mM (pH 5.5) and/or silica

[1] Lefèvre (2004) *Adv. Colloid Interface Sci.* **109**, 107–123. [2] Elzinga *et al.* (2011) *Geochim. Cosmochim. Acta* **14**, 2219–2230. [3] Bargar *et al.* (1999) *Environ. Sci. Technol.* **33**, 2481–2484. [4] Sheals (2002) *Environ. Sci. Technol.* **36**, 3090–3095.

https://doi.org/10.1180/S0026461X00006502 Published online by Cambridge University Press

Composition of the earliest hydrothermal fluids circulating along the South Range of the Sudbury Igneous Complex, Canada

DARREN LEFORT[1]*, JACOB HANLEY[1] AND JUNG HUN SEO[2]

[1]Dept. Geology, Saint Mary's University, Halifax, Canada (*correspondence: darrenlefort@gmail.com)
[2]ETH Zurich, Institute of Geochemistry and Petrology, CH-8092 Zürich, Switzerland

The Garson Ni-Cu-PGE deposit (Sudbury, Ontario, Canada) is hosted along the contact of the Sudbury Igneous Complex (SIC) and underlying Proterozoic-age metasediments and metavolcanic rocks. The deposit is strongly controlled by structural features and contains magmatic sulfides hosted in discrete shear zones. The main sulfides present are pyrrhotite, pentlandite and chalcopyrite with minor pyrite.

Massive sulfides overprint early quartz veins, forming sulfide-quartz stockworks. Fluid inclusions in the quartz are predominantly aqueous (30 vol% bubble) that contain a CO_2 vapor phase that homogenize upon heating between 2.8 and 29.0ºC, indicating a relatively low pressure of entrapment. A subordinate group of three phase (liquid-vapor-halite) inclusions are also present in the samples. Microthermometry showed the presence of clathrates in the primary inclusions. Clathrate destabilization temperatures yielded salinities between 12.1 to 14.4 wt% $NaCl_{equiv.}$. Some inclusions in which clathrates were not observed yielded a wide range salinities (from ice melting T) between 1 to 21 wt% $NaCl_{equiv.}$

LA-ICP-MS microanalysis of the primary aqueous inclusions show elevated concentrations of As, Pb, Zn and Sb, but very low concentrations of Cu, Fe and S, suggesting that these fluids did not equilibrate with typical magmatic sulfides or sulfide liquids, and were trapped prior to sulfide emplacement in the shear zones. Arsenic concentration in the fluids correlates to bulk salinity suggesting that the Cl complexation of As predominates at low T and low f_{O2}.

The circulation of early-stage CO_2-NaCl-H_2O fluids through metasedimentary wall rocks (and/or formation of these fluids from contact metamorphism of those wall rocks) may have been a factor in the local secondary enrichment of the Garson ores where As may be closely correlated to PGE distribution. Additionally, detection of As-rich fluid inclusions in quartz veins predating sulfide emplacement may serve as a discrimination tool for identifying areas along the South Range in which sulfide magmas may have been later contaminated through interaction with As-bearing country rocks.

Investigation of copper and zinc speciation in pig slurry by a multitechnique approach

S. LEGROS[1], E. DOELSCH[1,2], P. CHAURAND[2], J. ROSE[2], A. MASION[2], D. BORSCHNECK[2], O. PROUX[3], J.-L. HAZEMANN[4], V. BRIOIS[5], J.-H. FERRASSE[6], H. SAINT MACARY[1] AND J.-Y. BOTTERO[2]

[1]CIRAD, UPR Recyclage et risque, Montpellier, France
[2]CEREGE, Europôle Méditerranéen de l'Arbois, Aix-en-Provence, France
[3]CNRS, OSUG, St Martin d'Hères, France
[4]CNRS, Institut Néel, Grenoble, France
[5]Synchrotron SOLEIL, Gif-sur-Yvette, France
[6]MSNM-GP UMR 6181 CNRS Université Paul Cézanne, Aixen-Provence, France

The fate of pollutants associated with organic wastes is a key issue. For example, pig slurry presents high concentration of Copper (Cu) and Zinc (Zn) since they are used (at high concentration) as essential micronutrients in animal feeds. As a consequence, Cu and Zn accumulation was measured in soil surface layers that had been amended with pig slurry, inducing phytotoxicity as well as groundwater quality degradation. Better prediction of the mobility and bioavailability of Cu and Zn from pig slurry spreading can be achieved by determining the speciation of these elements.

The aim of this study is to investigate Cu and Zn speciation in pig slurry. A multitechnique approach was adopted including size fractionation, XRD, SEM-EDS, µXRF and XAS.

The present study demonstrated that only 0.2% of total Cu or Zn present in pig slurry was bound to particles smaller than 0.45 µm, while 75% of total Cu and Zn was bound to particles in the 0.45–20 µm size range. µXRF highlighted the colocalisation of Cu and sulfur. In addition, geochemical modelling demonstrated that physical chemical conditions within pig slurry lagoon are compatible with the precipitation of chalcocite (Cu_2S). Finally, XANES shows that Cu speciation in raw pig slurry and size fractions is described by Cu_2S and that its oxidation state is Cu (I). These Cu speciation in pig slurry may be the main reason for the observed Cu accumulation at the soil surface. Zn speciation revealed three patterns 49% Zn bound to organic matter, 37% amorphous Zn hydroxide, and 14% sphalerite (ZnS). The detected presence Zn sulphide, was unexpected and is reported for the first time. These three Zn forms seemed to be soluble in neutral or weakly acid soil systems, so the long-term impact of pig slurry spreading could lead to Zn leaching.

https://doi.org/10.1180/S0026461X00006502 Published online by Cambridge University Press

Aqueous alteration of organic matter and amorphous silicate in pristine chondrites: A multiscale study

C. LE GUILLOU[1], A. BREARLEY[1], L. REMUSAT[2] AND S. BERNARD[2]

[1]Dpt. of Earth and Planetary Sciences, University of New Mexico, Albuquerque, NM, USA (corentin.san@gmail.com)
[2]LMCM, MNHN, CNRS, Paris, France

Amorphous silicates have been observed in accretion disks of young stars[1]. On the other hand, amorphous silicates are also found in chondrites[2]. Therefore, the study of nanoparticles contained in the matrices of pristine chondrites may provide major insights into the nature of the nebular dust. We have explored the relationships between organics, water and silicates *in situ* by FIB-TEM, fluorescence microscopy, NanoSIMS and STXM (Scanning Transmission X-Ray Microscopy) in four carbonaceous chondrites with various alteration degree. Our goal is to assess the nature of the precursors (i.e. the dust) as well as the subsequent hydrothermal interactions which modified the accreted components.

We evidence the presence of hydrated amorphous silicate in MET00426 (CR3.0) and, for the first time, in Renazzo (CR2). Using ATEM, we estimate that this phase contains from 5 to 10 wt. % of water and has a very heterogeneous Fe/(Fe+Mg) ratio ranging from 30 to 75 at.%. Adjacent phyllosilicates which are probably genetically derived from the amorphous silicates have similar water contents and heterogeneous Fe/(Fe+Mg) ratios.

The spatial distribution of the organics shows a clear evolution with increasing aqueous alteration degree, detectable by TEM and fluorescence microscopy. In the least altered meteorites (CRs), mainly isolated grains are found (<500 nm) which sometimes share a preferential spatial relationship with phyllosilicates. In contrast, the more highly altered Murchison (CM2) and Orgueil (CI1) show a clear dichotomy between i) isolated grains and ii) a diffuse nanoscale mixture of organics and phyllosilicates. STXM results demonstrate the strong molecular heterogeneity of both types of grains at the sub-micrometer scale.

To explain these observations, we propose a scenario where organics trapped in water ice grains are mixed with amorphous silicates during accretion. Later, water melts, hydrates the amorphous silicate and redistributes the organic constituents which are entrapped within forming phyllosilicates during aqueous alteration.

[1] W. J. Forrest *et al*. (2004) *ApJS* **154**, 443. [2] N. Abreu & A. J. Brearley. (2010) *GCA* **74**, 1146–1171.

The assumption of a low pCO_2 during the Archean investigated with a 3D climate model

G. LE HIR[1]*, Y. TEITLER[1], F. FLUTEAU[1], Y. DONNADIEU[2] AND P. PHILIPPOT[1]

[1]IPGP, Université Paris 7-Denis Diderot, 1 rue Cuvier, Paris, France (*correspondence: lehir@ipgp.fr)
[2]LSCE, CNRS-CEA-UVSQ, 91191 Gif-sur-Yvette, France (Yannick.Donnadieu@lsce.ipsl.fr)

A new controversial assumption, based on banded iron formation mineralogy, supposes that the Archean atmosphere was potentially characterized by low concentrations of CO_2 [1]. To solve the young Sun problem, it hypothesized that a reduced albedo associated to less reflective clouds were able to prevent the early Earth to jump into a snowball state [1]. We have investigated the early Earth climate, using a general circulation model (GCM), to test this scenario including the ice albedo feedback [2]. Accounting for this feedback, we demonstrate that the faint young Sun problem is not solved. Hence we face again to the difficulty of maintaining a clement climate before 3Ga.

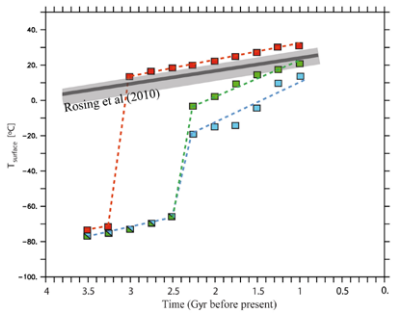

Figure 1: Surface temperature versus time assuming increasing irradiance**,** linear continental growth and a pCO_2 and pCH_4 of 900ppmv [1]. Blue, and red lines were obtained using liquid droplets size of 5 to 10μm (modern clouds), and 20μm (archean clouds), respectively [1]. The green line represents the no-clouds scenario.

[1] Rosing, M.T. *et al*. (2010) *Nature* **464**, 744-U117. [2] Kasting, J.F (2010) *Nature* **464**, 687-689.

https://doi.org/10.1180/S0026461X00006502 Published online by Cambridge University Press

Mantle source compositions of magmas from the North Atlantic Igneous Province

B. LEHMANN[1]*, A.V. SOBOLEV[1,2,3], N.T. ARNDT[1] AND C. CHAUVEL[1]

[1]ISTerre, University J. Fourier BP 53, 38041 Grenoble Cedex 9, France (*correspondence: benjamin-lehmann@hotmail.fr, alexander.sobolev@ujf-grenoble.fr)

[2]Max Planck Institute for Chemistry, Postfach 3060, 55020 Mainz, Germany

[3]Vernadsky Institute of Geochemistry, RAS, 119991 Moscow, Russia

It is widely accepted that the recycled oceanic crust plays an important role in the composition of mantle-derived magmas. In the case of North Atlantic Province, the amount of ancient oceanic crust is not well constrained. We used a new method of analysing the minor elements in olivine phenocrysts [1, 2] to determine the proportions of peridotite and eclogite in the source, and report new estimates for the lithology of mantle sources of Tertiary basalts in Northern Ireland and Scotland, which represent the oldest parts of the North Atlantic Province.

Preliminary results indicate significant and variable Ni excess and Mn deficiency in the compositions of magnesian olivine phenocrysts. This suggests a considerable but variable amount of non-peridotitic component (olivine-free pyroxenite) in the mantle sources of British Tertiary Province. Overall the estimated proportions of pyroxenite-derived melt are similar to that previously found for North Atlantic Province [1], and are markedly lower than in Hawaii.

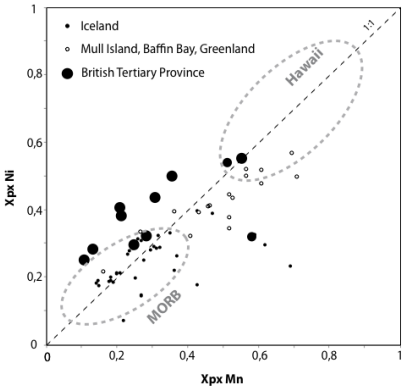

Figure 1: Proportion of pyroxenite derived melt from Ni excess and Mn deficiency in olivine composition (averaged per sample) [2]

[1] A. V. Sobolev *et al*. (2007) *Science* **316**, 412–417.
[2] A.V. Sobolev *et al*. (2008) *Science* **321**, 536.

Reconnaissance trace element and Os-Mo-Nd isotope geochemistry of Late Archean black shales in the Carajás iron ore district, Brazil

B. LEHMANN[1]*, R.A. CREASER[2], T. NÄGLER[3], A.R. VOEGELIN[3], B. BELYATSKY[4], A.R. CABRAL[1], H. GALBIATTI[5] AND A.A. SEABRA[5]

[1]Mineral Resources, Technical University of Clausthal, 38678 Clausthal-Zellerfeld, Germany (*correspondence: Lehmann@min.tu-clausthal.de)

[2]Earth and Atmospheric Sciences, University of Alberta, Edmonton, Alberta, Canada T6G 2E3

[3]Isotope Geology, Institute of Geological Sciences, University of Bern, CH-3012 Bern, Switzerland

[4]VNII Okeangeologia, Department of Antarctic Geology, 190121 St Petersburg, Russia

[4]Iron Ore Exploration, VALE, 34000-000 Nova Lima-MG, Brazil

The 250-300-m-thick Carajás Formation in the Carajás Mineral Province, northeastern Brazil, consists of banded iron formation (including giant iron ore deposits) and a lower shale-siltstone member, overlying several kms of 2.76-Ga-old meta-basalt. The shale-siltstone member hosts black shale units. The black shales (drillcore from the Serra Sul exploration project) have up to 29 ppm Mo, and trace element patterns reflect variable degree of clastic and hydrogenous input for a suite of redox-sensitive elements. We studied a 20-cm-drillcore interval in detail. The systematic $\delta^{98}/^{95}$Mo isotope pattern defines a clastic end-member with about 0.2 permil for continental input and 0.9 permil for seawater input. Five samples with the most euxinic signature give a Re-Os isochron of 2703 ± 64 Ma (2s) with an initial $^{187}/^{188}$Os of -0.26 ±0.55 (MSWD 0.57). Initial Os isotope ratios for the entire black shale population indicate mixing of continental material with a high $^{187}/^{188}$Os ratio up to 1.4 with a ~chondritic Os source (e.g. hydrothermal ridge input via seawater). Some black shale samples from deeper drillcore have astonishingly heavy Mo isotope compositions up to 1.8 permil $\delta^{98}/^{95}$Mo which suggests oxidative isotope fractionation similar to what has been described from the 2.5 Ga McRae Shale in Australia, but the Carajás samples are 200 Ma older. We interpret this finding as a very early 'whiff of oxygen'.

https://doi.org/10.1180/S0026461X00006502 Published online by Cambridge University Press

Functional group chemistry at the mineral-organic interface in soils

JOHANNES LEHMANN[1]*, DAWIT SOLOMON[1], DAVID MULLER[2], CHEE CHIA[3], HUOLIN XIN[2], STEPHEN JOSEPH[3] AND PAUL MUNROE[3]

[1]Department of Crop and Soil Sciences, Cornell University, Ithaca NY 14853, USA (*correspondence: CL273@cornell.edu)
[2]School of Applied and Engineering Physics, Cornell University, Ithaca, NY 14853, USA
[3]School of Materials Science and Engineering, University of New South Wales, Syndey, NSW 2052, Australia

We know that most organic matter enters the soil as readily recognizable plant and animal detritus, and is mineralized within short timescales of one or two years. The remaining organic C, however, is stabilized for longer timescales of up to thousands of years in the presence of Fe, Al, Mn oxide and hydroxides, phyllosilicates and other soil minerals. Changes in mineralogy can enhance the soil C storage potential several fold. It is, therefore, all the more astonishing that the precise mechanism for the interaction between minerals and C in soils is still largely unknown. One of the major limiting factors to past investigations of soil C sequestration is the fact that these processes operate well below the scale that most researchers have been able to observe. We have made significant progress over the past five years to examine C properties at sub-micrometer level using scanning transmission electron microscopy coupled with near edge x-ray absorption fine structure - STXM-NEXAFS spectroscopy, and clearly demonstrated, for the first time, the importance of the spatial distribution of organic C on a 25-100 nm scale. Here we show in addition aberration-corrected scanning transmission electron microscopy (STEM) combined with electron energy loss spectroscopy (EELS) enabling three-dimensional and high-resolution imaging, elemental identification and studies of nearest-neighbor bonding at the atomic scale of the organo-mineral interface in soils.

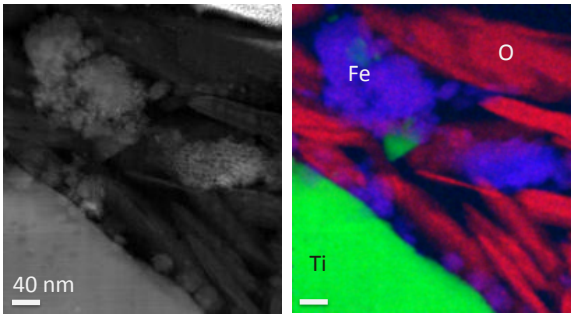

Uncoupled enrichment of ^{15}N and ^{18}O in nitrate – Constraints on nitrate regeneration in various aquatic environments

M.F. LEHMANN[1]*, C.B. WENK[1] AND A. BOURBONNAIS[2]

[1]University of Basel, Insitute of Environmental Geosciences, Bernoullistr. 30, CH-4056 Basel, Switzerland (*correspondence: moritz.lehmann@unibas.ch)
[2]School of Earth and Ocean Sciences, University of Victoria, Victoria, British Columbia, Canada, V8P 5C2

Measuring the nitrogen (N) and oxygen (O) isotope ratios in nitrate has been used to track N sources and transformations in freshwater and marine ecosystems. The deviation of nitrate N and O isotope values from parallel trends in $\delta^{15}N$ and $\delta^{18}O$ expected for nitrate uptake or denitrification has been taken as indication for nitrate production by nitrification. It still remains unclear, however, what controls O-isotope signatures of new nitrate in nature and, in turn, how sensitive the dual nitrate isotope signature is towards nitrate regeneration by nitrifying bacteria.

We will present nitrate isotope data from the open ocean, marine sediments, hydrothermal systems and a freshwater lake. Using a simple numerical model, nitrate isotope data are put into a quantitative framework for assessing nitrate production in net nitrate-consuming environments, and potential mechanisms involved in the generation of characteristic dual nitrate isotope signatures and anomalies in the various aquatic environments will be discussed.

https://doi.org/10.1180/S0026461X00006502 Published online by Cambridge University Press

Large ε_{Nd} change in South Indian seawater driven by Australian weathering at 15 Ma

S. LE HOUEDEC, L. MEYNADIER AND C.J. ALLEGRE

IPGP (Sorbonne Paris Cité, Université Paris Diderot, UMR7154 CNRS) 1 rue jussieu, 75005 Paris, France (lehouedec@ipgp.fr, meynadier@ipgp.fr, allegre@ipgp.fr)

We present Nd upper seawater data analysed on Indian Ocean carbonated oozes sediment from Site ODP 756 (located on the Ninety East Ridge, at 1518 m of water depth) and from Site ODP 762 (located on northwest Australian margin, at 1360 m of water depth). Our data cover the past 40 Ma at a resolution of two samples/Ma.

Amazingly, the records strongly mimic previous data from northern ODP Sites (ODP 757 and 707) (Gourlan *et al*. 2008; Martin and Scher, 2006).

We show that from 40 Ma to 10 Ma, the ε_{Nd} geographical distribution was homogenous over most of the Indian intermediate seawater, from a paleolatitute of 40°S up to the equator and over the entire Indian Ocean width. From 40 to 15 Ma, the ε_{Nd} value of Indian Ocean intermediate seawater recorded at all four ODP sites was almost constant, around -7 to -8 and increased by 3 ε_{Nd} units from 15 to 10 Ma. This sharp increase of ε_{Nd} is related to the enrichment by radiogenic Nd of the water mass originating from the Pacific as it flows through the Indonesian Passage. The numerous volcanic islands of this region corroborate the hypothesis of erosion and weathering of radiogenic Nd. By extending the studied area to the south, we demonstrated that this oceanic event is so strong that it can drive the ε_{Nd} of South Indian Ocean down to 40°S. With a two end-members model, we calculated that this event is characterized by an increase of ~1.7 time of the Nd transported through the Indonesian Pathway.

At 10 Ma, a large ε_{Nd} decrease (down to 6 ε_{Nd} units at Site ODP 762) is recorded. Such a large decrease was never observed in other northern Indian sites. Additional ε_{Nd} analyses on the detrital component of our two cores allow us to show that the seawater ε_{Nd} is then driven by detrital inputs linked to the weathering of Australia Continent. We estimate at about 20% the Nd contribution of this continental source to the oceanic Nd budget between 10 to 5 Ma. This could result of the beginning of the Australian drying (Bowler, 1976; Jonhson, 2009; Martin, 2006).

Long-term dynamics of differently stable soil organic matter fractions as function of soil management

PETER LEINWEBER[1]* AND SÖREN THIELE-BRUHN[2]

[1]Soil Science, University of Rostock, Justus-von-Liebig-Weg 6, 18051 Rostock, Germany

[2]Soil Science, University of Trier, Behringstraße 21, 54286 Trier, Germany

Rationale and experimental

Soil carbon is an integral part of soil organic matter (SOM), and modelling of its dynamics requires detailed information on the long-term fate of differently stable pools. Pyrolysis-field ionisation mass spectrometry (Py-FIMS) is the only method currently available that enables a rapid quantitation of ten different SOM compound classes and their thermal (biological) stability. We applied Py-FIMS to sample series from different treatments in one of the World´s oldest agricultural field experiments. First we determined temperature thresholds for 'labile' and 'stable' fractions of compound classes in laboratory incubation experiments. Next we applied these temperatures to quantitate differently stabile portions of compound classes, and test to what extent they have altered in various cropping systems from the early 1960ies until today.

Results and discussion

A kinetic model with coupled exponential functions was fitted to time series for relative abundances of compound classes. Cropping change from rye to maize led to (i) initial depletions in phenols & lignin monomers carbohydrates and N-compounds, the latter two being relatively enriched after 20 yrs, and (ii) initial enrichments in alkylaromatics, lipids and lignin dimers (for 15 yrs) followed by their net-decomposition over the next 30 yrs. This, however, was valid the labile proportions of compounds only (Fig. 1).

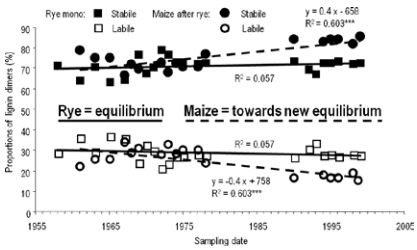

Figure 1: Proportions of labile and stabile lignin dimers in the "Eternal Rye Cultivation" as revealed by Py-FIMS.

Overall, we will demonstrate which SOM fractions were most susceptible to alterations according to cropping (rye, potato, maize) and fertilization (mineral vs. organic) practices.

https://doi.org/10.1180/S0026461X00006502 Published online by Cambridge University Press

Deciphering the offshore biogeochemical record of Holocene erosion in the Waipaoa watershed, New Zealand

E.L. LEITHOLD[1]*, N.E. BLAIR[2] AND L.B. CHILDRESS[2]

[1]Department of Marine, Earth, and Atmospheric Sciences, North Carolina State University, Raleigh, NC 27695, USA (*correspondence to leithold@ncsu.edu)

[2]Department of Civil and Environmental Engineering and Department of Earth and Planetary Sciences, Northwestern University, Evanston, IL 60208, USA (n_blair@northwestern.edu, lbchildr@northwestern.edu)

Continental margin sediments preserve a record of long-term changes in erosion in adjacent watersheds, and organic matter is one of the most useful components for decoding that record. ^{14}C in particular serves as an invaluable tool for resolving the relative contributions of sediment from shallow and deeper levels in the regolith, and therefore for reconstructing changes in the roles of various geomorphic processes over time. Here we report on a study of the sedimentary record preserved on the continental shelf offshore from the Waipaoa River, NZ. ^{14}C and $\delta^{13}C$analyses of bulk sediments as well as clay-sized, wood, and charcoal isolates provide evidence for a mid-Holocene episode of elevated bedrock OC input that is consistent with evidence for earthflow activity in the watershed and a stormy period in the region. Deforestation of the watershed by Polynesian settlers ca. 700 years ago is recorded by evidence for biomass burning as well as elevated levels of shallow landsliding and soil erosion. Finally, the development of deeply incised gullies following deforestation of the headwaters by European settlers is reflected by large contributions of bedrock OC to the riverine particulate carbon load during the past century. Our approach in the Waipaoa system offers promise for using biogeochemical stratigraphic records to reconstruct the influence of tectonics, climate, and human activities on geomorphic processes in watersheds around the world.

Arsenic mobilization in a high Andean watershed impacted by legacy mining

E.D. LEIVA, P.L. RÍOS, C.R. ESCAURIAZA, C.A. BONILLA, G.E. PIZARRO AND P.A. PASTEN*

Department of Hydraulic and Environmental Engineering Pontificia Universidad Catolica de Chile, Santiago, Chile (*correspondence: ppasten@ing.puc.cl)

Northern Chile is known by its water scarcity and rich mining activity. A complex mixture of contaminants from natural and anthropogenic sources limits the development of agricultural and industrial activities in the Lluta river watershed. A legacy sulfur mine site in the Altiplano is a key source of acid mine drainage on the upper section of the watershed. Tailings show high concentrations of arsenic (2-8 g/kg) (Fig 1) and sulfur (3-13 g/kg), with pH<1. The XRD analyses of tailings reveal a high proportion of elemental sulfur. Although this is a semi-arid environment (310 mm/year of precipitation), storms concentrate during the Bolivian winter. The RUSLE method estimates that ~14% of storms are erosive; thus sediments with acid formation potential are mobilized during the wet season. Downstream, mixing with neutral waters at varying proportions induce the occasional formation of Fe and Al oxides that become an arsenic repository. Fine colloids are mobilized by base flows, whereas coarse arsenic rich Fe-coated sediments are stored on the sediments. The sustainable development of water infrastructure (reservoir, irrigation works) needs to consider the interactions between hydrological, hydrodynamic and chemical processes.

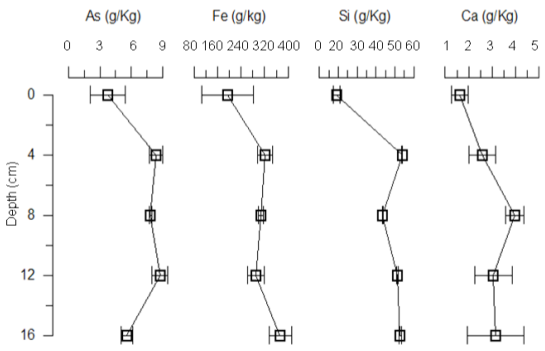

Figure 1: Geochemical analysis of tailings profile (As content and elemental associations [Fe, Si, Ca]). *Representative profile*.

Study supported by Fondecyt 1100943/2010

https://doi.org/10.1180/S0026461X00006502 Published online by Cambridge University Press

Water speciation in silicate melts investigated by Raman spectroscopy: Implication for volcanic process

CHARLES LE LOSQ[1], ROBERTO MORETTI[2,3] AND DANIEL R. NEUVILLE[1]

[1]CNRS-IPGP, Université Paris 7, Paris Sorbonne Cité, Laboratoire de Géochimie et Cosmochimie, 1 rue Jussieu, 75005 Paris, France (lelosq@ipgp.fr)
[2]Centro Interdipartimentale di Ricerca in Ingegneria Ambientale (CIRIAM) & Dipartimento di Ingegneria Civile, Seconda Università degli Studi di Napoli, Via Roma 29, Aversa (CE), Italy
[3]Istituto Nazionale di Geofisica e Vulcanologia, sezione di Napoli ‚Osservatorio Vesuviano', Italy

In addition to temperature, pressure and main chemical components, volatiles exert a strong influence on the physical properties of magmas. In particular, water plays a fundamental role in the dynamics and evolution of magmas in the deep interior and during volcano eruptions. However, water speciation in silicate melts is not fully understood. Infrared and NMR spectroscopy had provided some valuable informations about the H_2O/OH^- speciation. Nevertheless, some issues still remain unsolved about the OH^-/H_2O linkage to the silicate network.

Raman spectroscopy already allows quantifying the proportion of water dissolved in an aluminosilicate melt. Raman spectra are composed of i) a low wave number region that corresponds to vibrations of the silicate network (0-1500 cm^{-1}), and ii) a high wave-number region, which corresponds to the OH^- stretching vibrations and H_2O molecular vibrations (3100-3750 cm^{-1}). We have performed a first set of *in situ* experiments using a micro-furnace at ambient atmosphere. An evolution of the high wave-number region in function of the time and temperature is observed. New Raman peaks can be distinguished, particularly near 3650-3700 cm^{-1}. In this communication, we will present and discuss these observations between water and the silicate network in melts. Raman spectroscopy provides valuable informations to build a general model of water speciation, distinguishing the OH bonds between tetrahedral species and network modifiers for example. Results from this new model confirmed the amphoteric behavior of the water previously reported from polymeric modelling for instance, and opens new ways to study water in melts.

Near neutral seawater pH 3.45 billion years ago

D. LEMARCHAND[1]*, M. VAN BERGEN[2], M. JEAMBRUN[1], A-M. KARPOFF[3] AND P. VAN CAPPELLEN[4]

[1]LHYGES, CNRS-UDS, Strasbourg, France (*correspondence: lemarcha@unistra.Fr)
[2]DES, Utrecht University, the Netherland
[3]IPGS, CNRS-UDS, Strasbourg, France
[4]SEAS, Georgia Institute of Technology, Atlanta, USA

Many if not most known metabolic pathways had evolved by 3.5 Ga. The environmental conditions under which early evolution took place remain highly controversial and speculative, however. In particular, coeval ocean chemistry has been proposed to range anywhere from slightly acidic or modern like (NaCl type, pH<8.5) to strongly alkaline (Na_2CO_3 type, pH>10). Seawater pH is a key geochemical variable, which is tightly coupled to the composition of the atmosphere, and the nature and intensity of interactions between atmosphere, hydrosphere and lithosphere. Here, we extend the classical paleo-pH proxy method of boron isotopes in marine carbonates to a suite of well-preserved and extensively documented marine ferruginous cherts deposited 3.5 billion years ago. Like with carbonates, the approach is based on the large pH-dependent boron and boron isotope incorporation into solid phases, in particular Fe-(hydr)oxides. The samples are from the Pilbara craton (Western Ausltralia) that inlcude low metamorphic grade deposits showing alternation bands of pure and ferruginous silica, which are interpreted as resulting from chemical precipitation from silicon-rich seawater variably mixed with iron-rich hydrothermal fluids under quiet and probably deep water conditions.

We developed a mathematical model using Monte Carlo simulations coupled with a minimization routine to provide a set of self-consistent pH values of the hydrothermal-seawater mixture corresponding to each analyzed ferruginous band. Despite the large range of initial conditions tested and the methodological uncertainties involved, the simulations robustly converge to pH values ranging from 3.4 to 6.6. Mixing model combined with trace elements (REE) analyses imply circumneutral seawater (pH 7-9) and acidic hydrothermal fluids (pH ~3) discharging at the seafloor.

Altogether, the boron distribution and isotopic signatures of the Pilbara craton cherts are consistent with active buffering of the 3.5 Ga oceans by atmosphere-water-rock interactions not unlike those that have prevented dramatic shifts in seawater pH during the more recent geological past.

https://doi.org/10.1180/S0026461X00006502 Published online by Cambridge University Press

FT-ICR mass spectrometry of carbonate clusters: Magic clusters and pH effects

K.H. LEMKE[1]*, S.A. SADJADI[1] AND T.M. SEWARD[2]

[1]Department of Earth Sciences, University of Hong Kong, Pokfulam Road, Hong Kong, SAR (*correspondence: kono@hku.hk)

[2]SGEES, Victoria University of Wellington, Wellington, New Zealand

The only experimental data on solute clustering for aqueous carbonate systems stem from a recent electrochemcial study on $CaCO_3$ prenucleation-stage clusters, which suggested that nucleation of carbonates proceeds via cluster formation and aggregation [1]. However, there are no mass spectrometric studies that probe carbonate cluster distribution and composition in aqueous solutions as a function of pH or electrolyte concentration. Prompted by these recent experimental accounts of stable prenucleation carbonate clusters, we present results from Fourier transform ion cyclotron resonance (FT-ICR) mass spectrometric experiments pertaining to the stabililty, distribution and mass composition of a range of different carbonate clusters. We also report theoretical geometries and thermodynamic data of the above carbonate clusters using DFT calculations as well as the G4 and CBS-QB3 multi-step ab initio methods. All carbonate cluster experiments have been conducted on a Bruker 7T FT-ICR mass spectrometer equipped with electrospray ionization (ESI) source and a precision leak-valve system used for solvation studies. Stable carbonate species obtained from electrosprayed solutions (0.05mM/pH=11.20) containing Na_2CO_3 salts include the pure clusters $[Na\ (Na_2CO_3)_n]^+$ ($n \leq 12$), $[Na_2\ (Na_2CO_3)_n]^{+2}$ ($n \leq 19$), $[Na\ (NaHCO_3)_n]^+$ ($n \leq 9$) and $[Na\ (NaOH)_n]^+$ ($n \leq 11$) as well as the mixed clusters $[Na\ (NaHCO_3)(Na_2CO_3)_n]^+$ ($n \leq 8$), $[Na\ (NaHCO_3)_2\ (Na_2CO_3)_n]^+$ ($n \leq 6$) and $[Na\ (NaOH)\ (Na_2CO_3)_n]^+$ ($n \leq 10$). Moreover, upon acid titration with HFor to 3.50, we were able to observe a strong pH dependence of cluster composition and size distribution, especially in the pH vicinity of bulk carbonate solution pK values, e.g. at pH=10.32. In addition, ion mass spectra exhibit several marked discontinuities or „magic clusters' indicative of highly stable carbonate clusters. Solvation energies for the stepwise attachment of water onto individual cluster species will also be presented and compared with results from ab initio calculations.

[1] Gebauer *et al*. (2008) *Science* **322**, 1819.

OAE2 in marine sections at high Northern palaeolatitudes?

M. LENNIGER[1]*, G.K. PEDERSEN[2] AND C.J. BJERRUM[1]

[1]Department of Geography and Geology and Nordic Center for Earth Evolution (NordCEE), University of Copenhagen, 1350 Copenhagen, Denmark (*correspondence: mal@geo.ku.dk)

[2]Department of Geography and Geology, University of Copenhagen, 1350 Copenhagen, Denmark

The mid-Cretaceous world was characterised by unusually warm polar temperatures, extensive sea floor spreading and subsequent periods of major eustatic sea-level rise. At times volcanic outgassing increased the atmospheric pCO_2 and enhanced the terrestrial weathering. Weathering and rising sea level led to increased nutrient discharge and high organic productivity in the oceans. Associated increased decomposition of organic matter promoted the removal of oxygen, leading to anoxic conditions and elevated carbon burial in the sediments, a so called 'oceanic anoxic event'.

One of the global oceanic anoxic events is the Cenomanian–Turonian boundary event (OAE2). The event is characterised by a major positive $\delta^{13}C$ excursion (ca. 2-4 ‰) in marine carbonate and both marine and terrestrial organic matter, which indicates that a major disturbance of the global carbon cycle occurred in the ocean and atmosphere system. The OAE2 is thought to be a widespread event and evidence has been found all over the world, mostly at low and mid palaeolatitudes in the proto-Atlantic. However, records of the OAE2 from high palaeolatitudes are still scarce.

The ongoing work will establish the chemostratigraphy in different depositional environments in the Nuussuaq Basin in West Greenland and investigate the palaeoceanography that prevailed during the OAE2 in the basin. Three localities in a proximal–distal transect through the Nuussuaq Basin will be investigated for $\delta^{13}C$ bulk from organic material and redox sensitive trace metals. These investigations should help to understand, if black shale deposition in the Nuussuaq Basin is linked to the widespread occurring OAE2.

https://doi.org/10.1180/S0026461X00006502 Published online by Cambridge University Press

Is the oxygen isotope composition of zircon robust against aqueous alteration?

C. LENTING[1]*, T. GEISLER[2], J.B. CLIFF[3], M.R. KILBURN[3] AND A.A. NEMCHIN[4]

[1]Univ Münster, Institute for Mineralogy, Münster, Germany (*christoph.lenting@uni-muenster.de)
[2]Univ Bonn, Steinmann Institut, Bonn, Germany
[3]The University of Western Australia, Crawley, Australia
[4]Department of Applied Geology, Curtin Univ, Australia

The oxygen isotope composition of zircon is often used to unravel its (pre-)magmatic history, including the presence of liquid water on the surface of the Hadean Earth [1]. However, it has recently been questioned whether zircons retain their primary oxygen isotope signature during alteration and metamorphism [2], and experimental studies are likely to be most valuable in assesing this assumption. Here we report results from oxygen isotope hydrothermal tracer experiments with a heavily radiation-damaged zircon crystal from Sri Lanka. The experiments were conducted in ^{18}O-enriched water and in an enriched 0.1M HCl solution, as well as in milliQ water at temperatures between 100 and 700°C and pressures ranging from 1 to 1.6 kbar for 1 to 140 days. Preliminary SIMS analyses of altered zones formed at 400°C in milliQ water, known to have a negative $\delta^{18}O$, yielded a weighted average $\delta^{18}O$ of -6.46 ± 0.22 ‰ (2σ, n = 7) which is significantly different to the $\delta^{18}O$ of 6.68 ± 0.15 ‰ (n = 9) obtained from unaltered zircon areas. Furthermore, Raman spectroscopic measurements from altered zones formed in the ^{18}O-enriched solutions reveal a significant red-shift of the ν_3 (SiO_4) band when compared to altered zones that formed in milliQ water at the same temperature, indicating a mass-related frequency shift of the ν_3 (SiO_4) band due to the incorporation of significant amounts of ^{18}O from solution. The Raman measurements also indicate temperature-dependent structural recovery processes inside the altered areas which are accompanied by partial loss of radiogenic Pb, as revealed by SHRIMP analyses. Our preliminary data clearly show that, in contrast to the Hf isotope system [3], the oxygen isotope composition of radiation-damaged zircon can be altered signifcantly by the interaction with an external fluid, even during weathering. This has to be kept in mind when using the oxygen isotope composition of zircon to infer its (pre-) magmatic history.

[1] Wilde *et al*. (2001) *Nature* **409**, 175–178 [2] Nemchin *et al*. (2006) *Geochim Cosmochim Ac* **70**, 1864–1872 [3] Lenting *et al*. (2010) *Am Mineral* **95**, 1343–1348

The impact of Fe(III) oxide structure on shaping metal respiring microbial communities and carbon oxidation

CHRISTOPHER J. LENTINI* AND COLLEEN M. HANSEL

School of Engineering and Applied Sciences, Harvard University, Cambridge, MA USA
(*correspondence: lentini@fas.harvard.edu)

The importance of dissimilatory iron (III)-reducing microorganisms (DIRMs) in the iron (Fe) geochemical cycle has long been recognized. Their ability to reduce and thereby dissolve solid Fe (III) phases plays an important role in the cycling of trace nutrient and contaminants. In addition, metal oxide respiration plays a significant role in controlling organic matter mineralization in metal-rich environments. Despite this importance, our understnading of the role that Fe (III) (hydr)oxide mineralogy plays in controlling microbial Fe (III) respiration is poorly understood. For instance, while current model DIRMs in culture show the ability to greatly reduce ferrihydrite, these DIRMs show diminished abilities to reduce more crystalline phases (goethite and hematite), only reducing a small percent [1].

Through enrichment experiments, we found that both the Fe (III) mineral and carbon source provided specilized ecological niches for micrrooganisms. In fact, while acetate enrichments could support the reduction of ferrhydrite, the reduction of goehtite and hematite was not detected. However, with lactate and glucose as the carbon source, the reduction of these more crystalline phases was significant (30-70%). Clone library (16S rRNA) results indicated that a model Fe (III)-reducing microoganism, *Geobacter*, was prevalent on the ferrihydrite and acetate enrichments but did not occur on the hematite-acetate or goethite-acetate enrichments. Instead, in enrichments where goethite and hemtatie showed significant reduction, lactate and glucose supported the growth of less traditional Fe (III) reducers, *Desulfovibrio* and members of the family *Enterobacteriaceae*. Fe (III) reduction by these organisms is likely driven by indirect Fe (III) reduction coupled to sulfur cycling or fermentation.

Interstingly, our results also suggest that Fe (III) mineralogy will dictate competitive advantages between metal respiration and fermentation, possibly including acetategensis. These findings suggest that the oxidation of carbon and reduction of Fe (III) will be constrained by the host Fe (III) mineralogy of sediments/soils.

[1] C. M. Hansel, S. G. Benner, P. Nico *et al*. (2004) *Geochemica et Cosmochimica Acta* **68** (15), 3217

https://doi.org/10.1180/S0026461X00006502 Published online by Cambridge University Press

Land colonisation and Earth system change: A recurring pattern

TIMOTHY M. LENTON

College of Life and Environmental Sciences, University of Exeter, UK (t.m.lenton@exeter.ac.uk)

The colonisation of the land surface by complex life has occurred in several phases, each following a common pattern. All photosynthetic land colonisers must access mineral-bound essential elements, notably phosphorus. Fungi assist in this, being particularly effective at rock weathering, and forming symbiotic partnerships with algae in lichens, or with land plants as mycorrhizae. The resulting increase in the rate of silicate weathering lowers atmospheric CO_2 and global temperature. Meanwhile the selective enhancement of phosphorus weathering increases phosphorus supply to the ocean, organic carbon burial and hence atmospheric O_2.

It is widely accepted that the rise of rooted, vascular plants, including the first forests, through the Devonian-Carboniferous accelerated silicate weathering, causing a drawdown of atmospheric CO_2 and cooling the planet into glaciations. At the same time, acceleration of phosphorus weathering likely contributed to atmospheric O_2 rise.

Prior to this, the first pre-vascular plants colonised the land in the Mid-Late Ordovician. Existing models assume they had a negligible effect on weathering, but new experiments show that mosses amplify silicate weathering by factors of 1.5 to 6. We estimate that this roughly halved atmospheric CO_2, causing sustained global cooling of ~5 °C, and triggering the Late Ordovician glaciations. Mosses were also found to amplify phosphorus weathering by a factor of ~60. This could explain the extensive shallow water phosphate deposits, black shales, and two global positive excursions in marine carbonate $\delta^{13}C$ in the Late Ordovician.

Land colonisation is hypothesised to have begun much earlier still, in the Neoproterozoic, perhaps with lichen-like symbioses. This would neatly explain, with a single cause, both the extreme climate cooling and the 'lesser oxidation' (O_2 rise) that occured at that time. Whether the $\delta^{13}C$ record or other lines evidence support the hypothesis is hotly debated, but massive phosporite deposits support increased phosphorus weathering and input to the ocean.

An outstanding puzzle is why each phase of colonisation-driven cooling was not permanent? Perhaps the increasing ratio of O_2 to CO_2 in the atmosphere reduced the efficiency of photosynthesis, thus suppressing weathering. We also suggest that enhanced phosphorus weathering could not be sustained and ecosystems shifted to internal recycling of phosphorus, thus producing pulses of organic carbon burial and O_2 rise.

Tectonic evolution of a ~800-767 Ma continental arc back-arc system in South Brazil

C. LENZ[1], C. PORCHER[2], L.A. FERNANDES[2], R. CONCEIÇÃO[2], E. KOESTER[2] AND H. MASQUELIN[3]

[1]UFS-Brazil (crislenz@yahoo.com.br)
[2]UFRGS-Brazil (carla.porcher@ufrgs.br, ladfernandes@gmail.com, edineikoester@yahoo.com.br, rommulo.conceicao@ufrgs.br)
[3]Universidad de La Republica, Montevidéo (hmasquel@fcien.edu.uy)

In the southern region of Uruguay occur a sequence of Neoproterozoic para and orthogneisseic called Cerro Olivo Gneissic Complex. The orthogneissic unit yield crystallization ages (U-Pb SHRIMP) between 800-767 Ma. This unit is composed by a sequence of mafic gneisses, with gabbro to gabbro-diorite composition tectonically interleaved with a sequence of tonalitic and granodioritic gneisses. These rocks intrude the Chafalote paragneisses (pelite, quartzite and marbles) and were metamorphosed under high P-T conditions between ca. 676-654 Ma. Three different groups of rocks were distinguishing in the Cerro Bori Ortogneisses unit. Type I rocks are mafic gneisses with tholeiitic affinity and geochemical signatures characteristic of a back-arc setting. Type II rocks are mostly tonalitic gneisses with calc-alkaline affinity and geochemical signatures typical of a continental margin magmatic arc. Type III rocks are composed by biotite rich mafic gneisses with potassic to ultrapotassic affinity. These three rock types (I, II, III) show negative εNd values (between -2.12 and -6.67) and old TDM ages (between 1.2 and 2.0 Ga), indicating that assimilation of older crust and fractional crystallization were important during the evolution of these rocks. An Andean type magmatic arc setting with short distance between arc and back-arc is suggested for these rocks between 800-767 Ma. Thirty million years after the beginning of subduction the crystallization of a small volume of potassic and ultrapotassic rocks toke place. The nature, characteristics and ages of these rocks suggest the former existence of an ocean between Rio de La Plata and adjacent cratons (Brasilide Ocean) at a time that break up and dispersion of Rodinia supercontinent.

https://doi.org/10.1180/S0026461X00006502 Published online by Cambridge University Press

Characterization of biomineralized selenium solid phases by XAFS spectroscopy

M. LENZ[1,2], E.D. VAN HULLEBUSCH[3], F. FARGES[4] AND P.F.X. CORVINI[1,5]

[1]University of Applied Sciences Northwestern Switzerland (FHNW), School of Life Sciences, Institute for Ecopreneurship, Gründenstrasse 40, 4132 Muttenz, Switzerland
[2]Sub-Department of Environmental Technology, Wageningen University, 6700 EV Wageningen, The Netherlands
[3]Laboratoire Geomatériaux et Environnement (LGE), Université Paris-Est, EA 4508, 5 bd Descartes, 77454 Marne la Vallée Cedex 2, France
[4]Laboratoire de Minéralogie et de Cosmochimie du Muséum (LMCM), UMR CNRS 7202, Museum National Histoire Naturelle, 61 rue Buffon, 75005 Paris, France
[5]School of the Environment, Nanjing University, 22# Hankou Rd., Nanjing, 210093, P.R.China

The ability to reduce water soluble toxic selenium oxyanions is widespread in the microbial environment [1]. Firstly, specialized dissimilatory reducers can 'respire' selenium oxyanions to elemental selenium, producing energy for growth. Secondly, different microbial groups can catalyze selenium oxyanion reduction without gaining energy for growth (e.g. sulfate reducing bacteria) [2]. Since elemental selenium and most metal selenides are insoluble, microbially catalyzed reduction is thus thought to impact selenium environmental fate to large extents. However, little definitive information is available regarding the speciation of such (suppositional insoluble) phases, in particular in natural environments. We studied such phases formed by both mixed and pure cultures in metal poor and rich environments *in situ* by X-ray Absorption Fine Structure spectroscopy (XAFS). We demonstrated that in laboratory (i.e. metal depleted) incubations, amorphous elemental selenium is formed by most species, yet that natural (i.e. metal rich) environments are often rather dominated by complex mixtures of metal selenides.

[1] Lenz, M. & P. N. L. Lens (2009) *Science of the total Environment* **407**(12). [2] Stolz, J. E., P. Basu, J. M. Santini and R. S. Oremland (2006) *Annual Review of Microbiology* **60**.

Coupling $\delta^{34}S$ [SO_4^{2-}] and [^{206}Pb / ^{207}Pb]: Origin of trace metals in the urban Orge River, France

P. LE PAPE[1,2] *, S. AYRAULT[2], J-L. MICHELOT[1] AND C. QUANTIN[1]

[1]UMR 8148 IDES, UPS11 - CNRS, Orsay, 91405, France (*correspondence: pierre.le-pape@u-psud.fr)
[2]UMR 8212 LSCE, IPSL/CEA-CNRS-UVSQ, Gif-sur-Yvette, 91198, France

Several studies reported the close relationship existing between trace metal contamination in rivers and urbanization [1]. To reduce and constrain the emissions of urban trace metals and their transport due to runoff on urban surfaces, it is necessary to quantify the contribution of the different sources. It implies to study both the origins of water as a vector of transport (urban runoff, sewer network, groundwater...), the sources of metals and those of their bearing-phases. In that context, isotopic analyses are powerful tools to discriminate water and metal sources.

The study concerns the Orge-River urban catchment, part of the Seine-River watershed (Paris, France). Four sampling campaigns have been performed at a seasonal time scale from upstream (forestry and agricultural lands) to downstream (residential and urban areas). Sampled materials were water (filtrated at 0.45 μm), suspended particulate matter (SPM) and bed sediments.

Both dissolved (<0.45 μm) SO_4^{2-} and $\delta^{34}S$ [SO_4^{2-}] ratios increased from upstream to downstream, indicating sulfate inputs. Analysis of samples representing potential sources revealed that part of this additional sulfate was related to the leakages of sewer networks. In the particulate compartment, an anthropogenic Pb enrichment was clearly detected. Indeed, as Pb contents increased along the river, the [$^{206}Pb/^{207}Pb$] ratio evolved from a natural to an anthropogenic signature. Otherwise, anthropogenic contribution was especially noticed during low waterflow periods, when SPM load was low. [$^{206}Pb/^{207}Pb$] ratio also gave information about long term dynamics of particulate Pb in the watershed, indicating that the contribution of Pb from a Pb-gasoline endmember to SPM ended during the last decade.

Coupling of both $\delta^{34}S$ [SO_4^{2-}] and [$^{206}Pb/^{207}Pb$] ratios finally provided a good indicator of anthropogenic impact.

Furthermore, the isotopic approach described above was completed with studies at the particle scale (SEM or TEM-EDX), which revealed the presence of specific urban metal-bearing particles, such as barite or phosphate phases.

[1] Thévenot *et al*. (2007) *Sci.Tot Env*. **375**, 180–203.

https://doi.org/10.1180/S0026461X00006502 Published online by Cambridge University Press

Origin of isotopically heavy Fe in pyrite from 2.75 Ga Wilgie Mia BIF, Western Australia

AIVO LEPLAND[1]*, MARTIN J. VAN KRANENDONK[2] AND MARTIN J. WHITEHOUSE[3]

[1]Geological Survey of Norway, 7491 Trondheim, Norway (*correspondence: aivo.lepland@ngu.no)
[2]Geological Survey of Western Australia, 100 Plain St., East Perth WA, 6004 Australia
[3]Swedish Museum of Natural History, Box 50007, SE-104 05 Stockholm, Sweden

The 2.75 Ga Wilgie Mia Formation, Yilgarn Craton, Western Australia consists of a sequence of banded iron formation (jaspilitic chert, magnetite BIF), interlayered with minor black shales. Pyrite occurs abundantly in black shales and in trace amounts in BIFs, and has been studied for Fe and S isotopic composition using SIMS. Clustered framboidal diagenetic pyrite in shales is isotopically heterogeneous both in S ($\delta^{34}S$ from -6.9 to +4.7‰) and Fe ($\delta^{56}Fe$ from -3.3 to + 0.5‰). Analyzed BIF samples (c. 50 m stratigraphically above shale samples) exhibit a narrower range in $\delta^{34}S$ (-3 to +1‰) that overlap with $\delta^{34}S$ of secondary pyrite in veinlets in shale. Fe is considerably heavier in BIFs compared to shales with individual $\delta^{56}Fe$ measurements in three studied samples ranging from 0.6 to 1.3‰, 0.8 to 2.1‰ and 1.5 to 2.7‰. These $\delta^{56}Fe$ values from the Wilgie Mia BIF are among the heaviest so far reported from sedimentary rocks. Textural observations show that pyrite is the latest Fe phase in BIFs, post-dating both early hematite in jaspilitic chert and later hydrothermal magnetite. Pyrite formation in BIF appears to be related to hydrothermal S remobilization from shales and infiltration of framboidal pyrite derived sulfide bearing fluids into BIF. The S isotopic composition of dissolved hydrothermal sulfide was homogenized with respect to framboidal pyrite, and from this homogenized S source pyrite formed in veilets and BIFs. Previous Fe isotopic data using mineral separates [1] have indicated the presence of heavy pyrite with $\delta^{56}Fe$ values from 0.81 to 0.94‰ in the Wilgie Mia BIF. This was explained through the isotopic equilibrium of pyrite with magnetite ($\delta^{56}Fe$ from 0.37 to 0.60‰) and hematite-jaspilite ($\delta^{56}Fe$ from 0.54 to 0.72‰) [1]. As the $\delta^{56}Fe$ of many pyrite crystals studied here is heavier than predicted by equilibrium fractionation with Fe-oxides, and since pyrite is texturally late (clearly post-dating Fe-oxides) alternative fractionation mechanisms need to be considered. These may include the selective leaching of Fe-oxides by infiltrating sulfidic hydrothermal fluids, or equilibrium between magnetite/ hematite and Fe^{2+}_{aq}.

[1] Czaja *et al*. (2010) Abstract 5IAS

Nutrient content of mineral aeolian dust and its impacts on temperate forest nutrient cycles

E. LEQUY[1,2], S. CONIL[2], E. LECLERC[2] AND M-P. TURPAULT[1]*

[1]INRA 54280 Champenoux, France (*correspondence: turpault@nancy.inra.fr)
[2]ANDRA, 1-7 rue Jean Monnet, Châtenay-Malabry, France (sebastien.conil@andra.fr)

In Europe, mineral Aeolian dust is known to bring nutrients to Mediterranean forests [1] but its impact on acidic temperate forests has received little attention up to now. This study aims at quantifying the amount of nutrients released from Aeolian dust into the nutrient pool of two beech stands in the North of France. Mineral Aeolian dust was continuously collected in a clearing and below the canopy (throughfall and stemflow), showing deposition rates of 14±3 and 18±6 kg. ha^{-1} in 2010, respectively.

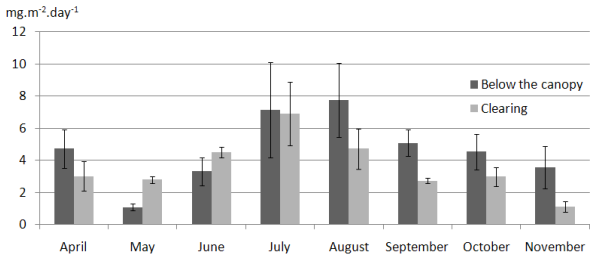

Figure 1: Aeolian dust deposition rates ($mg.m^{-2}.day^{-1}$) at the experimental site of Montiers-sur-Saulx

Particle size distribution, determined by a laser Coulter, was dominated by the fraction under 50 μm. Scanning electron microscopy and X-ray diffraction analyses of particles revealed the presence of quartz, phyllosilicates and feldspars. Our results suggest that Ca amounts released into forest nutrient pool by Aeolian dust and by soil weathering [2] are of the same order of magnitude.

[1] Avila *et al*. (1998) *Atmos Environ* **32**, 179–191. [2] Fichter *et al*. (1998) *Geoderma* **82**, 295–314

https://doi.org/10.1180/S0026461X00006502 Published online by Cambridge University Press

Preferential partitioning of copper into the vapor phase: An artifact?

LINDA LERCHBAUMER* AND ANDREAS AUDÉTAT

Bayerisches Geoinstitut, University of Bayreuth. 95447 Bayreuth, Germany
(*correspondence: linda.lerchbaumer@uni-bayreuth.de)

Studies on natural assemblages of coexisting vapor and brine inclusions revealed that Cu (± Au, As, Mo) commonly occurs at higher concentrations in the vapor phase, which has been interpreted to be due to the formation of stable hydrosulfide-bearing complexes. Although several experimental studies proved the existence of such complexes, none of them has succeeded in reproducing conditions under which Cu fractionates into the vapor phase (i.e. $D_{Cu}^{vap/brine} > 1$). An exception seemed to be the study of Nagaseki and Hayashi [1] who claimed to have obtained $D_{Cu}^{vap/brine}$ values up to 30. However, mass balance constraints and results of identical experiments performed in our laboratory suggest that these values are wrong and in fact are below unity.

In view of recent studies demonstrating that quartz-hosted fluid inclusions can diffusively loose or gain Cu after their formation we wanted to check whether the evidence from natural fluid inclusions could be compromised. For this purpose we synthesized vapor and brine inclusions from a Cu-H_2O-NaCl-S fluid at 800 °C/1.3 kbar and reequilibrated them in a second experiment with similar fluid at 800 °C/700 bar. After each step some of the inclusions were analyzed by LA-ICP-MS. Vapor inclusions indeed experienced a dramatic increase in their Cu content (from 0.3 ± 0.04 to 5.7 ± 3.3 wt% Cu) during this procedure, while brine inclusions remained unmodified, leading to a change in $D_{Cu}^{vap/brine}$ from a true value of 0.4 ± 0.05 to an apparent value of 8.3 ± 4.9. Subsequent experiments showed that the requirements for diffusional gain of Cu in fluid inclusions are a change in pH from ≤ 1 to a more basic value in the surrounding fluid, and the presence of S in the inclusions. These requirements are also fulfilled in nature: Cooling magmatic-hydrothermal fluids experience a change from acidic to more neutral pH due to buffering along the feldspar-mica join, and natural vapor inclusions typically contain significant amounts of S. $D_{Cu}^{vap/brine}$ values >1 observed on natural boiling assemblages could thus be a secondary feature, with original values being closer to 0.1. If true, then the role of vapor transport in the formation of magmatic-hydrothermal copper deposits has been severely overestimated.

[1] Nagaseki H. & Hayashi K. I. (2008) *Geology* **36**, 27–30.

Mineralogical heterogeneities in the Earth's mantle: Constraints from Mn, Co, Ni and Zn partitioning during partial melting

V. LE ROUX[1]*[,2], R. DASGUPTA[2] AND C.-T.A. LEE[2]

[1]Woods Hole Oceanographic Institution, 266 Woods Hole Road, Woods Hole, MA 02543, USA
(*correspondence: vleroux@whoi.edu)
[2]Department of Earth Science, Rice University, MS-126, 6100 Main Street, Houston, TX 77005, USA

The first-row transition elements (FRTE; Sc to Zn) are compatible to moderately incompatible during melting in mafic and ultramafic systems. Thus, because FRTE are sensitive to changes in mineralogy and major element composition, they are promising tracers of lithological heterogeneities in the mantle source regions of basalts. However, the partitioning behaviors of some FRTE at mantle conditions are still lacking despite growing interest in the application of these tracers to magmatic systems. Here we present mineral-melt partitioning experiments at 1.5-2.0 GPa and 1300-1500 °C for divalent FRTE – Zn, Fe, Mn, Co, and Ni. Our study, for the first time, provides Zn and Zn/Fe fractionation data between peridotitic olivine, orthopyroxene, clinopyroxene and basaltic melt. Using our new partition coefficients and combining multiple ratios (Zn/Fe, Ni/Co, Mn/Fe, Mn/Zn) we assess the role of FTRE as tracers of mineralogical composition of the mantle. We show that, during melting, olivine and orthopyroxene do not significantly fractionate Mn, Fe, and Zn from each other, and melts from peridotite would be expected to have similar Mn/Fe, Co/Fe and Zn/Fe as the source. In contrast, our results for clinopyroxene and published results for garnet show strong fractionations, such that melts of pyroxenites or eclogites would be expected to have low Mn/Fe, Co/Fe, Ni/Co, Mn/Zn and high Zn/Fe compared to peridotite partial melts. We compare Zn, Fe, Co, Mn and Ni contents of natural oceanic basalts to modeled compositions of peridotitic and pyroxenitic partial melts. Most MORB and near-ridge OIB can be explained by shallow melting of peridotite, but most OIB away from ridges deviate from predicted peridotite melt compositions. We use melting and mixing models of FRTE ratios in peridotite and in MORB-like eclogite to illustrate the potential contribution of eclogite- and peridotite derived melts in individual MORB and OIB lavas. We also present a melt-melt mixing model that estimates, under the assumptions of the present model, the amount of eclogite in the source of mantle end-members HIMU, EM1, and EM2.

https://doi.org/10.1180/S0026461X00006502 Published online by Cambridge University Press

Microbially enhanced ore weathering and surface anomaly development

K. LESLIE[1], C. IHLENFELD[2], C. OATES[2], J. BARR[2] AND D.A. FOWLE[1]

[1]Department of Geology, University of Kansas, Lawrence KS 66049, USA (kleslie@ku.edu)
[2]Geochemistry Division, Anglo American plc, 20 Carlton House Terrace, London, SW1Y5AN, United Kingdom

Biogeochemical processes in the subsurface have been found to affect the dispersion and accumulation of metals in soils overlying buried mineralized systems [1, 4]. Specific zones of metal accumulation, along with other secondary signals (such as isotopic anomalies, high pH and redox contrast, variations in microbial activity, gas flux and electrochemical anomalies) [1-5] have been used to successfully vector towards mineralization. Several models explaining the formation of these secondary features currently exist; electrochemical processes, expulsion of groundwater, dispersion of gas, and biogeochemical cycles [1, 4]. As microbiological processes play a significant role in many of these anomaly-developing processes, we hypothesize that the presence of microorganisms will enhance the mobility of metal ions in the subsurface.

Metal release from buried mineralization was examined in flow-through columns containing a variety of ore types (Cu porphyry, Magmatic Ni, Cu-Zn VMS) and a consortium of biogeochemically relevant microorganisms (Fe, S-oxidizers, Methanogens, Methanotrophs, Sulphate-reducers and Fe-reducers). Greater metal release was observed from all ore types, in comparison to un-inoculated controls. To examine the accumulation of metals in overlying soils we added soil and rock cover to the same ore types and microbial consortium used previously. Higher metal content was associated with the soil phase in the columns that had been inoculated. These results suggest that microbial processes may control metal dispersion and accumulation in the subsurface.

[1] Cameron *et al*. (2004) *Geochem-Explor Env A* **4**, 7–32. [2] Hamilton *et al*. (1998) *J Geochem Explor* **63**, 155–172. [3] Hamilton *et al*. (2004) *Geochem-Explor Env A* **4**, 33–44. [4] Kelly *et al*. (2006) *Econ Geol* **101**, 729–750. [5] Mann *et al*. (2005) *Geochem-Explor Env A* **5**, 201–210.

Time scales of magma differentiation and implications for the growth rate of the Torres del Paine laccolith

J. LEUTHOLD[1]*, O. MÜNTENER[1], L. BAUMGARTNER[1], B. PUTLITZ[1], M. OVTCHAROVA[2] AND U. SCHALTEGGER[2]

[1]Mineralogy and Geochemistry, University of Lausanne, Switzerland (*correspondence: julien.leuthold@unil.ch)
[2]Earth and Environmental Sciences, University of Geneva, Switzerland

The spectacularly exposed Torres del Paine laccolith (Southern Patagonia) has been constructed by successive injections of mafic and granitic melt batches. The sill complex is connected, at its western border, to a dike complex, interpreted as the laccolith feeder zone. A key unknown in sill complexes is the mechanism by which individual mafic and differentiated magma pulses are linked and assembled over time. We present high precision CA-ID-TIMS U-Pb data on mafic rocks zircons to constrain the time scales of differentiation. Feeder zone gabbronorite and Px-Hbl-gabbronorite with cumulate Px and Plg textures, display distinct positive Eu anomalies. Incompatible trace elements have been modelled to establish a fractionation relationship between mafic and granitic rocks. Zircon grains from the feeder zone gabbroic units have been dated at 12.59±0.01Ma, equivalent to the laccolith top granitic units, with a reported age of 12.59±0.02Ma [1]. Detailed field and petrographic studies evidence distinct Hbl-gabbro and diorite units within the laccolith, accreted sequentially. They display ages ranging from 12.47±0.01Ma for the lower Hbl-gabbro, 12.45±0.01Ma for diorite sills and 12.43±0.01Ma for upper Hbl-gabbro and diorite, all distinctly younger than the basal granite (12.51±0.03Ma [1]). These data show that, while the laccolith granitic complex is built up by under-accretion, the mafic complex itself grows by over-accretion, via amalgamation of successive sills. Emplacement dynamics involves a complex interplay between mafic and granitic magmas generating a volume of ~100km^3 over a time scale of ~160'000 years.

[1] Michel *et al*. (2008) *Geology* **36**, 459–462.

https://doi.org/10.1180/S0026461X00006502 Published online by Cambridge University Press

Imogolites as a tool for evaluating the hazard of HARN

C. LEVARD[1], W. LIU[2,3], A. MASION[2,3], A. THILL[3,4], J. ROSE[2,3], P. CHAURAND[2,3], M. AUFFAN[2,3], E. DOELSCH[3,5], O. PROUX[3,6], J.Y. BOTTERO[2,3]

[1]Stanford Univ. Dpt. GES
[2]CEREGE CNRS-Aix Marseille U.
[3]GDRI iCEINT
[4]CEA-IRAMIS-LIONS
[5]CIRAD
[6]ESRF

Since the discovery of carbon nanotubes (NTs), there has been great interest in the synthesis and characterization of similar shaped structures like inorganic nanotubes, nanorods, or nanowires. Imogolites (Al_2SiO_3 $(OH)_4$) are natural aluminosilicate single wall nanotubes. To date, only Ge-Al imogolite analogues have been successfully synthesized 100 times more concentrated than Si-Al imogolites.

The growth mechanisms of imogolite-like alumino-germanate nanotubes were examined using a combination of local- (XAS at the Ge-Kedge and 27Al NMR) and semilocal scale techniques (in situ SAXS). A model is proposed for the precursors of the nanotubular structure and consist in rooftile-shaped particles, up to 5 nm in size, with ca. 26% of Ge vacancies and varying curvatures. These precursors assemble to form short nanotubes/nanorings observed during the aging process. The final products are most likely obtained by an edge-edge assembly of these short nanotube segments.

Two structures are revealed by SAXS: at 0.25M of Al the Al-Ge imogolite are double-walled NTs whereas at 0.5 M single-walled NTs are obtained.

First tests to reveal cyto and genotoxicity on various vertebrates cells (human fibroblasts and CHO-K1) are interesting. They show a genotoxicity for concentrations from 8 10^{-5} g/L and effects decreasing from proto-imogolite to long tubes

Fossilization of microaerophilic iron oxidizing bacteria from marine hydrothermal vents

RICHARD J. LÉVEILLÉ[1]* AND KARINE LAPLANTE[1,2]

[1]Canadian Space Agency, 6767 route de l'Aéroport, Saint-Hubert, Québec, Canada, J3Y 8Y9 (*correspondence: richard.leveille@asc-csa.gc.ca)
[2]Institut de Biologie Intégrative et des Systèmes, Université Laval, 1030 rue de la Médecine, Québec, Québec, Canada, G1V 0A6 (karine.laplante.2@ulaval.ca)

Iron oxidizing bacteria are common in modern marine and terrestrial systems, where they often display distinctive cell morphologies and are commonly encrusted by minerals, especially bacteriogenic iron oxides and silica. Putative microfossils of iron oxidizing bacteria have also been found in ancient Si-Fe deposits and iron oxidation may be an ancient and widespread metabolic pathway. Microaerophilic iron oxidizing bacteria, in particular, could have thrived on the early Earth in circumneutral environments containing small amounts of oxygen (i.e. 'oxygen oases') produced either by locally concentrated photosynthetic microorganisms (e.g. cyanobacteria) or by chemical reactions. This work seeks to better understand the fossilization and biomineral formation processes associated with these organisms. Understanding the interplay between silica precipitation and biologically induced iron mineral precipitation is a key objective of this work and is essential for understanding preserved Fe-rich biominerals and silica microfossils in the rock record on Earth and possibly on Mars, where Fe-Si-rich hydrothermal systems likely existed.

We have studied samples of Fe-Si-rich deposits from extinct hydrothermal vents along the Explorer Ridge, NE Pacific Ocean. In addition, we have performed silicification experiments using the microaerophilic iron oxidizing bacterium Mariprofundus ferrooxidans, isolated from low-temperature diffuse marine hydrothermal vents, in a Fe-enriched seawater medium at constant pH (6.5) and oxygen concentration (5%) in a controlled bioreactor system. We present the results of characterization of the ultrastructure and composition of the natural samples and experimental reaction products using optical and flurorescent microsocopy, VP-SEM-EDS, FIB milling and FEG-SEM-EDS, and TEM-EDS.

https://doi.org/10.1180/S0026461X00006502 Published online by Cambridge University Press

Analogues between water in granite melts and petroleum formation

MICHAEL D. LEWAN

U. S. Geological Survey, Box 25046, MS 977 DFC, Denver, CO 80225, USA (mlewan@usgs.gov)

Water is ubiquitous within the Earth's crust and has long been recognized as a critical component in deep crustal areas undergoing metamorphism [1]. Similarly, water in granite melts has been shown to be critical to granite melting points, mineral phase relations, element partitioning between melt and mineral phases, and transport properties [2]. Although the specific role of water remains an issue in petroleum formation, experimental studies on petroleum source rocks pyrolysed with and without water clearly indicate that water is an important component [3]. Petroleum formation involves two overall reactions. The first of these reactions is the thermal decomposition of kerogen, which is the insoluble and dominant organic solid phase in thermally immature source rocks. With initial heating, kerogen partially breaks down to a soluble polar-rich high-molecular-weight tarry phase referred to as bitumen. A net volume increase associated with this reaction results in the bitumen expanding into the micro-porosity to form a continuous bitumen phase impregnating the groundmass of the source rock. Experiments have shown that water is not important in this step, but water in the original micro-pores and in surrounding fractures provides a source for dissolved water in the bitumen. Similar to water dissolved in granite melts, the solubility of water in bitumen plays a significant role. It is this dissolved water in the bitumen phase and not the surrounding bulk water in fractures or voids that becomes critical in the second overall reaction, which is the thermal decomposition of the polar-rich bitumen phase to a hydrocarbon-rich oil phase. During this overall reaction, the dissolved water provides a source of hydrogen that promotes thermal cracking and facilitates immiscibility between the bitumen and oil phases. These conditions result in a net volume increase and the expulsion of the oil from the water-laden bitumen in the source rock. The ability of water in pyrolysis experiments to simulate organic phases like those observed in nature helps petroleum-formation studies move away from sole emphasis on organic components (i.e. saturates/aromatic/resin/asphaltene) and, like granite-melt studies, allows examination of the collective behaviour of both components and phases.

[1] Winkler (1967) *Petrogenesis of Metamorphic Rocks*. Springer-Verlag, New York. [2] Mysen & Richet (2005) *Silicate Glasses and Melts*. Elsevier, New York. [3] Lewan (1997) *Geochim. Cosmochim. Acta* 61, 3691-3723.

Asphaltene content as a measure of oil losses related to the Deepwater Horizon oil spill

M.D. LEWAN, A. WARDEN, R.F. DIAS, Z.K. LOWRY, T.M. HANNAH, P.G. LILLIS, R. KOKALY, T.M. HOEFEN, G.A. SWAYZE, C. MILLS, S.H. HARRIS, G.S. PLUMLEE AND B.D. MARSHALL

U. S. Geological Survey, Box 25046, MS 977 DFC, Denver, CO 80225, USA (mlewan@usgs.gov)

The asphaltene content of spilled oil on open and coastal waters and coastal sediments was examined as a means of determining the fate of the estimated 4.9 million barrels of oil released from the damaged BP Macondo-1 wellhead of the Deepwater Horizon platform in the Gulf of Mexico (April 20 to July 15, 2010). A particularly salient issue is where has all of this spilled oil gone? Asphaltenes are the highest molecular-weight fraction in crude oils and are the most recalcitrant to water washing, volatilization, and biodegradation. Comparing the asphaltene content of spilled oils with those of the original oil released from the leaking wellhead allows one to determine the portion of oil lost. The lost portion of oil collectively includes that removed by volatilization, oxidation, water washing, dispersion, and microbial degradation. Critical to the application of this method is that a representative sample of the original oil is available and that degradation does not significantly affect the asphaltene content of the spilled oils. Two samples were collected from a riser insertion tube at the wellhead and are considered representative of the original oil. Although asphaltenes are the most recalcitrant fraction of crude oils, their composition can change with degradation. Possible alterations to the asphaltene fraction of the spilled oils were evaluated with stable carbon isotope and elemental analyses. Spilled-oil samples were collected between May 7 and July 10, 2010 and are divided into three groups; 1) open water, 2) coastal water, and 3) coastal sediment. The open-water group consists of spilled oils floating on the water at distances greater than 5 km from the coastline. Comparing the uncorrected asphaltene contents of these spilled oils with that of the original oils indicate spilled oil in open waters may represent less than 40 wt% of the original oil, and spilled oil in the coastal waters and sediments may represent less than 20 wt% of the original oil. These preliminary results suggest that significant quantities (more than 60 to 80 wt%) of the Deepwater Horizon spilled oil were lost within the first 81 days and provide input values for mass-balance calculations regarding the fate of the spilled oil.

https://doi.org/10.1180/S0026461X00006502 Published online by Cambridge University Press

Raman spectroscopy for geological applications

RENATA LEWANDOWSKA

HORIBA Scientific, 231 rue de Lille, 59650 Villeneuve d'Ascq, France, (renata.lewandowska@horiba.com)

Raman spectroscopy is a practical exploration tool to study geological materials. This technique is a rapid and reliable way to confirm a chemical composition of samples and the particle distribution. Chemical information can be obtained without any extraction procedure or sample preparation. Thus, the analysis can be achieved *in situ* and if necessary directly at the geological site. Raman imaging can be useful to study heterogeneous samples in various fields of application of Earth Science: mineralogy, gemmology, petrology, geoarcheology, paleontology, planetology or volcanology…

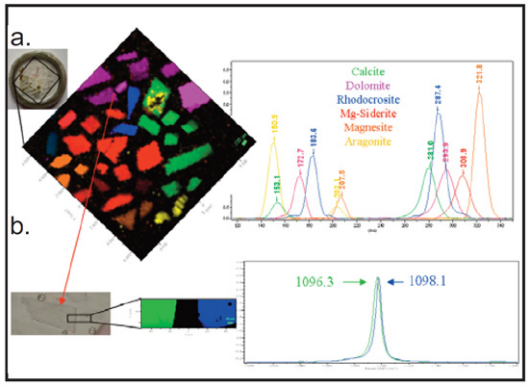

The latest developments in Raman instrumentation will be presented. A new Raman microscope will be introduced that combines high mobility, multi-laser excitation and ease-of-use. Its rugged design can withstand harsh environmental conditions for analysis in the field, and it is also equipped with a fiber port for probe measurements. We will also present a new imaging mode using scanning mirrors. This technique can be used in two modes: 'macro-mapping' mode to perform Raman imaging on large sample areas or for mapping small heterogeneities in large objects that cannot be moved easily with a motorized stage, such as big geological samples.

Structural incorporation of uranium during the Fe(II)-induced transformation of ferrihydrite

JUAN S LEZAMA PACHECO[1], MICHAEL S MASSEY[2], F. MARC MICHEL[1], JOHN R BARGAR[1] AND SCOTT FENDORF[3]

[1]SLAC National Accelerator Laboratory, 2575 Sand Hill Road, Menlo Park CA 94025 jlezama@slac.stanford.edu
[2]Department of Geological & Environmental Sciences, Stanford University, Stanford, CA 94305
[3]Department of Environmental Earth System Science, Stanford University, Stanford, CA 94305

Fe-(oxyhydr)oxides, among the most important metal-scavenging phases in soils and sediments, can undergo structural and compositional transformations during iron reducing conditions. Understanding the geochemical cycling and interaction of iron oxides with Uranium and other redox-active radionuclides, is of prime importance in the development of state-of-the art biogeochemical models to understand the fate and transport of these hazardous elements. In this work, X-ray diffraction and EXAFS analysis have been used to characterize the transformation products and local atomic structure around uranium in synthetic iron-oxide phases obtained by the Fe (II)-induced transformation of ferrihydrite. After transformation of ferrihydrite, U (IV)-bearing compounds and Fe-oxides are observed, with U (V/VI) being structurally incorporated into multiple sites in the goethite structure. We will discuss the incorporation mechanism, in which adsorption of uranium on the ferrihydrite starting material plays a key role in incorporation of this radionuclide into the resulting crystalline iron oxide phases. Our work also suggests that bioremediation strategies such as biostimulation can drive U sequestration not only through direct reduction of U, but also through Fe redox cycling.

https://doi.org/10.1180/S0026461X00006502 Published online by Cambridge University Press

The differences of fluid inclusions between ore minerals and gangue minerals of Huize lead-zinc deposit, Yunnan province, China

BO LI[1,2], RUNSHENG HAN[2], XIAOCHUN GU[1], SHUMING WEN[2] AND RUI SHENG[3]

[1]Yunnan Copper Industry (Group) Co.Ltd., Kunming Prospecting Design Institute of China Nonferrous Metals Industry, Kunming 650051, China (*correspondence: libo7_211@yahoo.com.cn)

[2]Kunming University of Science and Technology, Kunming 650093, China

[3]Huaneng Lancang River Hydropower Development Co.Ltd., Kunming 650051, China.

The Huize surperlarge lead-zinc deposit is a typical deposit in the Sichuan-Yunnan-Guizhou Zn-Pb polymetallic mineralization zone, the main ore minerals and gangue minerals are sphalerite and calcite respectively. Research of fluid inclusions in sphalerite and calcite indicate that there are differences in homogenization teperature, salinity, density and composition of fluid inclusion. *a. homogenization teperature*. The homogenization temperature of fluid inclusions in sphalerite range from 100.2°C to 344.5°C, for the average homogenization temperature of 179.5°C, which have two change temperature sectors obviously, 150°C~200°C and 250°C~350°C. Whereas, homogenization temperature of fluid inclusions in calcite range from 160°C to 220°C, and few can reach to 250°C. *b. salinity*. Salinity of fluid inclusions in sphalerite is similar to homogenization temperature, which range form 1.05wt% $NaCl_{eq}$ to 18.04 $wt\%NaCl_{eq}$, for the average salinity of 11.56 $wt\%NaCl_{eq}$, and have two change sectors, 1~13 $wt\%NaCl_{eq}$ and 13~20 $wt\%NaCl_{eq}$. Fluid inclusions in calcite are of low salinity, with a range from 0.18 $wt\%NaCl_{eq}$ to 10.8 $wt\%NaCl_{eq}$, and the average sallinity of calcite is 7.29 $wt\%NaCl_{eq}$. *c. density of fluid inclusion*. The densities of fluid inclusions in sphalerite range from 0.8884$g\cdot cm^{-3}$ to 1.0507 $g\cdot cm^{-3}$, and the average densities is 0.9735 $g\cdot cm^{-3}$, but densities of fluid inclusions in calcite range from 0.8811 $g\cdot cm^{-3}$ to 0.9556$g\cdot cm^{-3}$, with a change sectors of 0.900~0.930 $g\cdot cm^{-3}$. *d. composition of fluid inclusions*. The composition of fluid inclusions in sphalerite and calcite is similar, but composition content of fluid inclusions in calcite is higher than sphalerite. Liquid components of fluid inclusions are mainly Ca^{2+}, Mg^{2+}, Na^{+}, Cl^{-}, with minor amounts of F^{-}, K^{+}, Li^{+}. Gas components of fluid inclusions are mainly H_2O and CO_2, CO and CH_4 are less abundant.

Spatial and seasonal variations of iron species in the Changjiang (Yangtze River) sediment

CHAO LI AND SHOUYE YANG*

State Key Lab. of Marine Geology, Tongji Uni., Shanghai 200092, China (*correspondence: syyang@tongji.edu.cn)

The Changjiang River contributes huge amounts of dissolved and particulate matter to East Asian marginal seas. The complex provenance geology and source-to-sink pattern of terrigenous material into the sea complicate the fluvial flux and river chemistry. Geochemical cycle of key elements in the Changjiang, e.g. iron (Fe), has rarely been investigated. This study aims to investigate the spatial and seasonal variations of different chemical species of iron in the Changjiang sediment, and to reveal the low-temperature iron cycle in this large river.

The upper Changjiang sediment is higher in unreactive Fe (Fe_U) for its strong physical weathering and specific lithology, while the middle and lower reaches is relatively enriched highly reactive Fe (Fe_{HR}) because of hydrodynamic sorting and stronger chemical weathering. Seasonal variation of iron species in the lower mainstream is in consistent with variability of monsoon induced precipitation, with more significant supply from the upper reaches during flood season. Anthropogenic impact, such as the Three Gorge Dam, plays a key role in controlling sediment input, especially in dry season. Environmental magnetic study also suggests complicated and variable compositions of iron-bearing minerals within the river system. Thus, spatial and seasonal variations at different scales should be taken into account in the further study on elemental cycle and estimation of river flux.

This work was supported by NSFC research fund (Grant No: 41076018) and Scholarship Award for Excellent Doctoral Student granted by Ministry of Education.

https://doi.org/10.1180/S0026461X00006502 Published online by Cambridge University Press

Quantitative analysis of late Cenozoic tectonic deformation across the Northern foreland of the Chinese Tian Shan

CHUANXIN LI[1,2]* AND ZHAOJIE GUO[3]

[1]School of Energy Resources, China University of Geosciences, Beijing 100083, China (*correspondence: chuanxin_li@163.com)
[2]Research Institute of Petroleum Exploration & Development-Langfang, PetroChina, Langfang 065007, China
[3]Key Laboratory of Orogenic Belts and Crustal Evolution, Ministry of Education, School of Earth and Space Sciences, Peking University, Beijing 100871, China (zjguo@pku.edu.cn)

The East-West trending Tian Shan range has been reactivated and uplifted in the late Cenozoic in response to the northward propagation of deformation related to the India-Eurasia continental collision [1, 2]. Three paralleled rows of anticlinal belts have developed sequentially from south to north. Precise timing of and magnitude of the Tian Shan uplift are required to understand possible mechanisms of continental lithosphere deformation and interactions between climate, tectonism and erosion. Here, we provide structural analysis of seismic section and magnetostratigraphic and biostratigraphic age control on the stratigraphy of the northern Chinese Tian Shan foreland [3, 4]. In the southernmost row of the anticlinal belts, the magnitude of shortening is ~2.9km (15.1%), and the shortening rate is 0.41mm/yr based on the time of tectonic activity of ~6.0Ma. In the middle row, the magnitude of shortening is ~5.9km (23.7%), and the shortening rate is 2.9mm/yr based on the time of tectonic activity of ~2.0Ma. And the northernmost row, the magnitude of shortening is ~4.3km (15.7%), with a shortening rate of 4.3mm/yr. The results indicate that the intensity of the tectonic activity along the northern margin of the Tian Shan has been increasing since the late Cenozoic.

[1] Molnar *et al*. (1993) *Reviews of Geophysics* **31**, 357–396. [2] Tapponnier *et al* .(1979) *Journal of Geophysical Research* **84**, 3425–3459. [3] Li *et al*. (2010) *Basin Research* doi: 10.1111/j.1365-2117.2010.00475. x. [4] Li *et al*. (in press) *Journal of Asian Earth Sciences*, doi: 10.1016/j. jseaes. 2010.08.009.

Transient oxic conditions amid ferruginous deep waters after the Cryogenian Sturtian glaciation evidenced from Fe-C-S proxies

DA LI[1]*, HONGFEI LING[1], GRAHAM A. SHIELDS[2], LAWRENCE OCH[2] AND SIMON W. POULTON[3]

[1]School of Earth Sciences and Engineering, Nanjing University (*correspondence: maillida@gmail.com)
[2]Department of Earth Sciences, University College London
[3]School of Civil Engineering and Geosciences, Newcastle University

The Neoproterozoic ocean was characterized by profound perturbations which helped to trigger biological revolutions. While several lines of geochemical evidence indicate that the Ediacaran deep ocean was dominated by anoxic ferruginous conditions, much less is known about Cryogenian seawater. An iron-rich and sulfate-poor environment has been hypothesised for the post-'Sturtian' or late Cryogenian non-glacial interval, in accordance with the growth of a large organic carbon pool, as implied by decoupling between carbonate and organic carbon-isotopes [1].

Here we report iron speciation data from the basal Datangpo Formation which lies between the glacial deposits of the Tiesi'ao (Sturtian) and Nantuo (Marinoan) formations on the Yangtze Platform, South China. Our aim is to examine deep-water redox conditions after the Sturtian glaciation. Samples were collected from two underground rhodochrosite mines named Yuxin and Changxingpo, respectively.

Iron concentrations in different highly reactive species (Fe_{HR}), including $Fe_{carbonate}$, Fe_{oxide}, $Fe_{magnetite}$, were analyzed using the sequential leaching method outlined in reference [2] and performed at Newcastle University, UK.

Siltstone samples from the latest Tiesi'ao Fm. in the Yuxin section yielded Fe_{HR}/Fe_T above 0.38 and Fe_{py}/Fe_{HR} below 0.8, indicating ferruginous conditions. However, three samples from the uppermost Tiesi'ao Fm. at Changxingpo section have Fe_{HR}/Fe_T below 0.38, indicating oxic bottom waters during the melting of the Sturtian ice cover at c. 665 Ma. Organic- and manganese-rich carbonaceous siltstone samples from the lowermost Datangpo Fm. in both sections have Fe_{HR}/Fe_T above 0.38 and Fe_{py}/Fe_{HR} below 0.8, suggesting ferruginous deeper-waters during early interglacial time. This is consistent with a previous study of carbonate and organic matter C-isotope and pyrite S-isotope data from Yuxin section, which showed that the chemocline was initially close to the sediment-water interface and moved up into the water column during the early interglacial interval, as manganese was oxidized in the water column and then converted to manganese carbonates [3].

This study was co-funded by NSFC 40872025 and the DFG FOR736 program.

[1] Swanson-Hysell *et al*. (2010) *Science* **328**, 608–611. [2] Poulton & Canfield (2005) *Chem. Geol*. **214**, 209–221. [3] Chen, Li *et al*. (2008) *Prog. Nat. Sci*. **18**, 421–429.

Formation of summer hypoxia in the Yangtze River Estuary of China: 'Cold pool' and 'thermal barrier' effects

D.J. LI*, H.X. LIU, L. GAO AND P. WANG

State Key Laboratory of Estuarine and Coastal Research, East China Normal University, 3663 North Zhongshan Road, Shanghai 200062, China
(*correspondence: daojili@sklec.ecnu.edu.cn)

Hypoxia in the Yangtze River Estuary has received increasing attention. It occurs in summer and may last until early autumn, and it has recently become more serious. Based on survey data from October 1958 to September 1959, August 2009, and July 2005, we found that the hypoxia area is located in the trough off the Yangtze River Estuary and affected by many external forcing factors, including water temperature and salinity, runoff from the Yangtze River, the Taiwan Warm Current, upwelling, and the Yellow Sea Coastal Current. These factors promote the formation of hypoxia by influencing the dissolved oxygen saturation level, the strength of stratification, the distribution of temperature and salinity, and water movement. In addition to these factors, there was a cyclonic vortex in the hypoxia area, and the bottom water in the area was much more stable. The vortex was mainly made up of water from the Taiwan Warm Current, which is characterized by low temperature in summer. All these factors promote the formation of a cold pool (isolated, closed, and stable waters with lower temperature under a 15-meter layer of warmer water) in the hypoxia area, and a thermal barrier (water at the periphery of the cold pool with higher temperature that protects the stability of the cold pool and blocks the exchange of dissolved oxygen with surrounding waters) is formed. The existence of the cold pool and thermal barrier greatly increases the residence time of water in the hypoxia zones, restricts the supply of dissolved oxygen, and provides necessary preconditions for the formation of summer hypoxia.

This study was jointly funded by Ministry of Science and Technology of China (2010CR951203), Shanghai Municipality (10JC1404400), and State Key Laboratory of Estuarine and Coastal Research of China (2009KYYW03)

Balance of Cenozoic carbon cycle maintained by basalt weathering

GAOJUN LI

Department of Earth Sciences, Nanjing University, Nanjing 210093, China (ligaojun@nju.edu.cn)

The BLAG model proposed that the Cenozoic decline of atmospheric pCO_2 is primarily dirven by the decrease of CO_2 degassing through the pCO_2-weathering feedbacks [1]. However, the sea floor spreading rate, which is believed as the major control of CO_2 degassing, remained relatively constant [2]. Alternative explanation suggests that the drawdown of pCO_2 is forced by the enhanced silicate weathering in response to the widespread Cenozoic tectonic uplift [3], but the increasing CO_2 consumption would deplete the atmosphere of all its CO_2 within a million years [4].

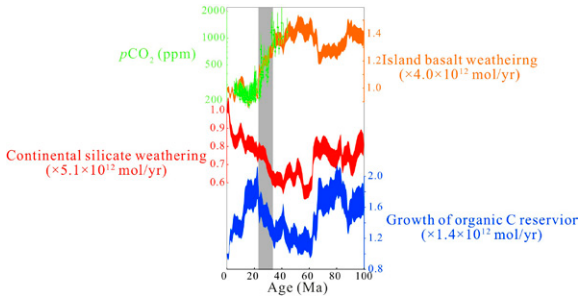

Figure 1: Atmospheric CO_2 sinks and pCO_2 [5] since 100 Ma

Here an reverse calculation coupling the marine isotopic records of C, Sr and Os suggest that the weathering of island basalt is largely controled by pCO_2 (Fig. 1), possibally through the CO_2 fertilization effect on plant weathering. The rate control of pCO_2 on basalt weathering imply that both the BLAG model and the 'uplift driven' hypothesis could stand for the Cenozoic pCO_2 evolution. Tectonic uplift enhanced the atmospheric CO_2 consumption by continental silicate weathering and accumulation of organic carbon during the Oligocene, left the unbalanced carbon cycle compensated by the decreasing island basalt weathering through the pCO_2 controlled basalt weathering rate. Since the Miocene, the increasing CO_2 sink of continental silicate weathering was roughly balanced by the decreasing accumulation rate of organic carbon reservoir, and thus the rate of basalt weathering and pCO_2 kept nearly constant.

[1] Berner *et al*. (1983) *Am. J. Sci*. **283**, 641. [2] Rowley (2002) *GSA Bulletin* **114**, 927. [3] Raymo *et al*. (1988) *Geology* **16**, 649. [4] Berner & Caldeira (1997) *Geology* **25**, 955.[5] Pagani *et al*. (2005) *Science* **309**, 600.

https://doi.org/10.1180/S0026461X00006502 Published online by Cambridge University Press

Trace elemental geochemistry of black shale from Chengkou district, Chongqing, southwest China and its genetic significances

H. LI, [1,2], Z. ZHU[1,2]*, C. ZHU[1] AND T. LUO[3]

[1]Chongqing Key Laboratory of Exogenic Minerallization and Mine Environment, Chongqing Institute of Geology and Mineral Resources, Chongqing 400042, China (*correspondence: zhuzhjie@163.com)

[2]Chongqing Research Center of State Key Laboratory of Coal Resources and Safe Mining 400042, China

[3]The State Key Laboratory of Ore Deposit Geochemistry, Institute of Geochemistry, Chinese Academy of Sciences, Guiyang 550002, China

The black rock series in Lower Cambrian are well developed in Chengkou district, Chongqing, representing a potentially large multi-metal deposit source in China. Previous study in Chengkou district showed that multi-metals including Ag, V, Se are enriched in black shale. In order to understand the genetic significances of black shale and multi-metal enrichment, ICP-MS techniques was used to analyze trace elemental contents in Lower Cambrian black rock series including cherts, black siltstones and multi-elements concentrated layers. The results indicated that REE is very low relative to other regions such as northern Guizhou, northwestern Hunan, and LREE is relative abundant. δCe shows almost negative anomaly, and δEu shows unconspicuous anomaly. The indicators of δCe, δU, V/Cr, Ni/Cr and V/(V+Ni) demonstrated that black rock series formed in the anoxic environment. REE geochemical characteristics and their diagrams, high enrichments of Cr, Sb, As, Bi and U/Th ratios indicated that black rock series mainly formed by hydrothermal deposition. Meanwhile, the petrogenesis of black rock series was associated with volcanism, and volcanism possibly provided the composition and dynamics to the hydrothermal activity.

This work is financially supported by Opening Fund of State Key Laboratory of Environmental Geochemistry (NO. HDH09001). and the Chongqing Administration of Land, Resources and Housing (NO. CIGMR0905)

[1] Blas *et al*. (1999) *Earth Planet. Sci. Lett*. **171**, 253-266.
[2] Teranes *et al*. (2005) *Limnol. Oceanogr*. **50**, 914-922.
[3] Hollander *et al*. (2001) *GCA* **65**, 4321-4337.

Metamorphic fluid activities and their effects on petrological and geochemical characteristics of UHP rocks, Southern Sulu UHP Terrane, China

HONGYAN LI*, DONG WANG AND XIANG CHENG

Institute of Mineral Resources, Chinese Academy of Geological Sciences, Beijing 100037, China (*correspondence: lihongyan@cags.ac.cn)

Since the 2000s, more and more research work disclosed metamorphic fluid activities during the deep subduction process of the continental materials in many UHP terranes. However, the property, scale and geological significance of the metamorphic fluid activities are still not clear.

Eclogites from the Qinglongshan area in the southern end of the Sulu UHP terrane have acquired celebrity in their unusual oxygen isotope compositions. We take two types of eclogites, an epidote-bearing and an epidote-free for this study in the Qinglongshan area. Four metamorphic stages are identified for the evolution of epidote-bearing eclogite. However, the epidote-free eclogite only records eclogite facies metamorphism. They have distinguished petrological, geochemical and Sr-Nd isotopic characteristics.

In the epidote-bearing eclogite, kyanite-zoisite-paragonite-quartz veins of several to decadal centimeters are developed. These veins were formed from the pre-existed hydrous UHP metamorphic mineral (lawsonite) and give a zircon U-Pb age of 219 ± 9 Ma, which indicate a metamorphic fluid activity in the early stage of the exhumation of the deep subducted continental materials.

U-Pb and Lu-Hf isotope studies of zircon are also carried out for the country gneiss of the epidote-bearing eclogite which develops kyanite-zoisite-paragonite-quartz veins. Zircons from the granitic gneiss have core-rim structure. Although the cores and rims have obviously different Hf isotopic characters, they show no difference in Th/U ratio, REE pattern and U-Pb age. Strongly in contrast with previously published zircon U-Pb ages of the Dabie-Sulu UHP metamorphic rocks where protolith ages of 700–800 Ma are commonly recorded, only metamorphic age of 218 ± 5 Ma, identified either in rim or core of the zircons, are recorded in this granitic gneiss. This result show that, in the locality with strong retrograde metamorphic fluid activities, the U-Pb isotope system of zircon could be reset completely from its magmatic precursor, while the Lu-Hf isotope system could remain relatively close.

https://doi.org/10.1180/S0026461X00006502 Published online by Cambridge University Press

Partitioning of chlorine and fluorine between apatite and felsic silicate melts at subduction zone conditions

H.J. LI* AND J. HERMANN

Research School of Earth Sciences, The Australian National University, Canberra, ACT 0200, Australia (*correspondence: huijuan.li@anu.edu.au)

The chemistry of subduction zone fluids has been a primary focus of geological studies in recent years. While the broader nature of the fluid phases remains a matter of debate, the specific role of ligands such as F and Cl are also pooly constrained, even though both elements can exert important controls on fluid chemistry due to their effects on H2O activity, mineral solubility and trace element partitioning, etc.

In this study, piston-cylinder experiments have been conducted to investigate chlorine and fluorine partitioning behaviour in felsic silicate systems at subduction zones conditions. A pelitic starting composition was synthesized with 6-7 wt% H_2O. Initial experiments were conducted over a pressure and temperature range of 25-45 kbar and 650-850°C, with 800 ppm Cl in the starting composition. Apatite was found to be the major mineral carrier of chlorine, with Cl concentrations ranging from ~0.1% at 750°C, 45kbar to 1.2% at 800°C, 25kbar. While an increasing Cl concentration in apatite correlates with increasing temperature, a decrease in Cl occurs with increasing pressure. Chlorine content in the coexisting melt was determined by both analysis and mass balance calculations. Partition coefficients between apatite and melt, $D^{Cl}_{ap\text{-}melt}$, vary from ~1 (e.g. at 750°C, 35kbar, and 800°C, 45kbar) to ~11 (at 800°C, 25kbar), with values rising with increasing temperature and falling with increasing pressure. The preliminary partition coefficient values for aqueous fluids, based on mass balance estimations, are found to be less than 1 at subsolidus conditions.

A further series of experiments was performed at 25 kbar and 800°C with various Cl (~0, 500, 1000, 2000, or 4000 ppm) and F (~0, 1000, or 2000 ppm) fractions in the starting compositions. $D^{Cl}_{ap\text{-}melt}$ values were found to remain relatively constant between experiments with identical F concentrations in the system. Linear regressions show the $D^{Cl}_{ap\text{-}melt}$, to be around 10.6 at 0 ppm F, ~3.5 at 1000 ppm F and ~1.9 at 2000 ppm F. The preliminary $D^{F}_{ap\text{-}melt}$ values range from 15 to 50, with the dominant influence being the F concentration in the system. The obtained results are the first ever reported in the literature, and will provide useful constraints on F and Cl contents in subduction zone fluids.

Geological evolution of Paleotethys: Constraints from Ar-Ar, U-Pb ages of gabbro in Jinshajiang Suture Zone

LI JIE[1,2]*, CHEN WEN[2], YONG YONG[2], SUN JINGBO[2] AND JI HONGWEI[1,2]

[1]China University of Geosciences(Beijing), Beijing, 100029 China (*correspondence: huaer3312@sina.com)

[2]Laboratory of Isotope Geology, Institute of Geology, CAGS, Beijing, 100037 China

Jinshajiang suture zone located in the northern and eastern of Qinghai-Tibet plateau, considered as the boundary of west-north Paleotethys. Therefore it is of significant in the research of the geological evolution of Paleotethys. We collected gabbro samples from ophiolitic melange in the area of Yushu, middle-west of the suture zone, and achieved a number of high-precision Ar-Ar and SHRIMP U-Pb age which with range of 295Ma-233Ma. According to these ages, the gabbro can be divided into three groups: (1) Late Carboniferous gabbro: Outcropped in the middle of Jinshajiang suture zone, with zircon SHRIMP U-Pb age of 295.3±5.2Ma. (2) Middle-late Permian gabbro: Distributing in central and north of the suture zone, with age ranges from 268 to 258Ma. (3) Mid-Triassic gabbro: Distributed in central and south parts of suture zone, the age is about 233Ma.

From above isotope ages of gabbro, we could extract some information for the geological evolution of Paleotethys: (1) The Jinshajiang ocean expansion lasted 60Ma. (2) Along Jinshajiang suture zone, the age of ophiolite from southeast to northwest reduce gradually, which indicate the Paleotethys Ocean opening is earlier in southern part than in northern part, from southeast to northwest, the Ocean basin opened in sharp of shear-like. (3) Considering the existence 362Ma of ophiolite in the south of Jinshajiang suture zone [1], Paleotethys existed more than 130Ma.

This work was supported by the Science and Technology Research Project of China (No.:2009CB421001; 201011027-1B; 1212011120293)

[1] Jian *et al*. (1998) *Acta Petrologica Sinica* **14**(2), 207-211.

https://doi.org/10.1180/S0026461X00006502 Published online by Cambridge University Press

Trace elements and REE geochemistry of copper-bearing sandstone in the middle submember of the Liuju Member of the Upper Cretaceous Matoushan Formation, Yunnan,China

JING LI[1], RUNSHENG HAN[2] AND PENG WU[2]*

[1]Kunming University of Science and Technology, Division of Laboratory Administration, Kunming 650093, China (*correspondence: lijing2409@yahoo.com.cn)
[2]Kunming University of Science and Technology, Southwes Institute of Geological Survey, Geological Survey Center for Non-ferrous Mineral Resources, Kunming 650093, China

Liuju sandstone-type copper deposit located in the North Centre of Chuxiong Basin in Yunnan province, China. The main ore-bearing strata is Liuju lower submember of the Upper Cretaceous Matoushan formation (K_2ml_1). The content of Cu is more than 2% recently discovered in Liuju middle submember (K_2ml_2) which has great prospecting futurities.

The metallogenic mechanism of K_2ml_2 is similar to that in the Liuju copper deposit (K_2ml_1). In K_2ml_2, Ta, Sc, Co, Ni, V are deficient, and chalcophile elements Mo, Cd, As, Cu enriched in grey sandstone, which has the feature of ore source rocks. It indicates that the enrichment of Cu is closely related to the water-rock interaction [1]. In terms of n (V)/n (V+Ni) >0.7, the copper ore formed in oxygen-poor environment.

The average contents of rocks $\sum$REE=123.04×10^{-6}, LREE/HREE=8.89, δEu=0.80, δCe=0.92. From the copper ore to gray bed, to purple bed, the average values of Mo、Cd、As and Hg reduced gradually, Nb、Zr、Hf、Th and $\sum$REE increased gradually.

Basis on geochemical research of copper-bearing sandstone in K_2ml_2, it indicates that the copper ore formed by water-rock interaction of ore-forming fluid and wall rocks, Cu is enriched in weak alkaline and reducing property environment.

Granted jointly by the Basic Applied Research Foundation of Yunnan Province (2010ZC013) and the Distinguishing Discipline of KUST (2008).

[1] Alex C. Brown (2006) *Journal of Geochemical Exploration* **89**, 23–26.

Diagenetic mobility of Mn and Fe crusts in organic-poor sediments of Lake Superior

J. LI[1]*, S.A. CROWE[2], E.T. BROWN[1], M. DITTRICH[3], D. MIKLESH[1] AND S. KATSEV[1]

[1]Large Lakes Observatory, University of Minnesota Duluth, Duluth, MN 55812 (*correspondence: lixx0590@d.umn.edu, skatsev@d.umn.edu)
[2]NordCEE, Univ. of S. Denmark (sacrowe1@gmail.com)
[3]University of Toronto Scarborough (dimaria@ethz.ch)

Sediment distributions of redox-sensitive metals, such as Fe and Mn, are often used as indicators of paleoceanographic redox conditions. Post-depositional changes in sediment redox conditions, however, may redistribute these metals within the sediment, complicating interpretations of sediment records. The rates and magnitudes of such redistributions in oceanic sediments, as well as their causes, are poorly known. We investigate the redistribution of diagenetically precipitated Fe and Mn phases in organic-poor modern sediments of Lake Superior. These sediments contain prominent (up to 10 wt%) multiple Fe and Mn-rich layers, often visible to a naked eye, and record vertical migrations of the sediment redox boundary in response to varying fluxes of organic carbon and actions of bottom currents. We use scanning XRF and chemical extractions to characterize these layers, and measure the concentrations of oxygen and dissolved metals in sediment porewaters to understand the *in situ* reaction rates and their links to past and present redox conditions. High levels of 0.5M HCl-extractable iron, as well as iron enrichment relative to Ti, within Fe-rich layers suggest that these layers formed diagnetically. Comparison of the porewater distributions of Fe (II), oxygen, and nitrate suggests a significant contribution of iron oxidation coupled to the reduction of nitrate, rather than oxygen. At one of our sampling sites, the depth of oxygen penetration has moved upwards by 4 cm and subsequently re-deepened over the course of ~40 years, as a result of sediment pollution by taconite tailings between 1950s and 1980s. The observed present-day distributions of sediment Fe and Mn and mass balance calculations show that these metals may become re-distributed over time scales as short as decades, even in a system where organic carbon is relatively unreactive (k=0.005 yr^{-1}) and in low quantity (2 wt%). Changes in organic carbon sedimentation within a factor of 2, or variations in the bottom-water oxygen concentrations by ~10% can alter the depth of oxygen penetration in these organic-poor sediments by several centimeters or more.

https://doi.org/10.1180/S0026461X00006502 Published online by Cambridge University Press

Magnesite dissolution rates at the column scale: The control of mineral spatial distribution

LI LI[1], FATEMEH SALEHIKHOO[1] AND SUSAN L. BRANTLEY[2]

[1]Department of Energy and Mineral Engineering, Penn State University, University Park, PA 16802

[2]Department of Geosciences, Earth and Environmental Systems Institute, Penn State University, University Park, PA 16802

Mineral dissolution plays a major role in various physical, chemical, and biological processes in nature. The rates of mineral dissolution in the field are often quantified by soil depth profiles and the sharpness of dissolution front within soil columns. Mineral dissolution rates can be affected not only by mineral reactivity, but also by other hydrogeochemical conditions, including flow velocity, inlet flow chemical composition, as well as the spatial distribution of minerals. Although potentially an important factor that determines the kinetics of mineral dissolution, the effects of mineral spatial distribution are often ignored. The objective of this work is to understand and quantify the effects of mineral spatial distribution on the overall dissolution rate at the column scale. Both column experiments and reactive transport modeling are used to investigate the dissolution of a reactive mineral (magnesite) imbedded in a sand column in different spatial patterns. The total mass ratios of the two minerals were kept constant. The variables include flow velocity, column length, and sub-column scale mineral spatial distribution. The results show that mineral spatial distribution is important under conditions where the flow velocities are relatively fast comparing to the reaction rates, and when the columns are relatively short. Under conditions where the small-scale heterogeneities are important, the column scale overall dissolution rates are larger when magnesite is spatially distributed evenly, compared to the case where all magnesite is clustered.

Distribution and release of strontium in rivers around mine: An indicator for the oxidation of sulfide minerals in carbonate area

LING LI[1], GUOPING ZHANG[1,*], HONG LIU[1], MENG XIANG[1,2] AND XIAOFEI WEI[1,2]

[1]State Key Laboratory of Environmental Geochemistry, Institute of Geochemistry, Chinese Academy of Sciences, Guiyang 550002, China (*correspondence: Guoping.zhang@tom.com) (lynnfirst@gmail.com)

[2]Graduate School, Chinese Academy of Sciences, Beijing 100049, China

Water samples from two mine areas were collected and analyzed for trace elements by ICP-MS. River water showed average Strontium concentration of 630 $\mu g \cdot L^{-1}$ in the Dachang multi-metalliferous mine area and of 790 $\mu g \cdot L^{-1}$ in the Yata gold mine area, were 4 and 5 times higher than the background values (Dachang mean: 155 $\mu g \cdot L^{-1}$; Yata mean: 160 $\mu g \cdot L^{-1}$), respectively. Especially, content of Sr was up to 1704 $\mu g \cdot L^{-1}$ in the adit water of the Dachang mine area.

Sr is abundant in carbonate rocks resulting from its similar ion radius with Ca. Actually, Dachang and Yata mine areas, as the carbonate rocks area, the former has one of the largest antimony deposit in China, and the latter has a significant gold deposit associated with As, Hg, Sb and Tl mineralisation in China. Although acid generated in the oxidation of sulfide minerals in mine tailings, the surface waters in the both of two mine areas are still circumneutral to slightly alkaline because of the neutralization of the carbonate rocks. However, when sulfide minerals such as antimony and arsenious sulphide are oxided, the sulfuric acid can react with carbonate rocks, and then can lead to the release of Sr from carbonate rocks. As a consequence, Sr shows a good correlation with Sb and As in the Pingcun river ($r = 0.99$ and 0.90, $n = 8$) and the downstream river ($r = 0.99$ and 0.94, $n = 6$) of Dachang mine area. Sr only shows a good correlation with As and but a poor correlation with Sb in the Yata mina area ($r = 0.94$ and 0.28, $n = 8$) [1]. Moreover, Sr in river water also shows a good correlation with SO_4^{2-} ($r = 0.96$, $n = 8$) in the Yata mine area. Therefore, it could be concluded that a strong release of Sr in water of mine area can be resulted from the neutralization of acid drainage. Furthermore, Sr can also be regarded as an indicator of the oxidation of sulfide minerals in the mining environment enriched in carbonates.

[1] Zhang *et al*. (2009) *J. Environ. Monit*. **11**, 1570–1578.

https://doi.org/10.1180/S0026461X00006502 Published online by Cambridge University Press

Archean sulfur may power modern microbial life in the deep subsurface in the Canadian Shield

LONG LI[1], BOSWELL WING[2], THI H. BUI[2], GREG F. SLATER[3], GEORGES LACRAMPE-COULOUME[1] AND BARBARA SHERWOOD LOLLAR[1]

[1]Department of Geology, University of Toronto, Toronto, ON, Cananda M5S 3B1

[2]Department of Earth and Planetary Sciences, McGill University, Montreal, QC, Canada H3A 2A7

[3]School of Geography and Earth Sciences, McMaster University, Hamilton, ON, Canada L8S 4K1

Saline fracture water in Archean rocks in the Canadian Shield and South Africa have been found to host microbes (mainly sulfate reducers) as deep as 3 km. This provides an important analog for the study of life on the early Earth and for search for life on other planets (e.g. Mars). In order to understand the source and sustainability of the sulfate that supports these deep microbial ecosystems, we carried out multiple sulfur (S) isotope analyses for dissolved sulfate and sulfide in the saline waters from up to 2.7 km depth in the Canadian Shield near Timmins, Ontario (ON) and Thompson, Manitoba (MN).

Prevalent S isotope mass independent fractionations (MIF) were observed: dissolved sulfate at the ON sites had $\delta^{34}S$ values from 3.3 to 8.4‰ and $\Delta^{33}S$ from -0.07 to -0.20‰. Dissolved sulfate at the MN sites had $\delta^{34}S$ values from 21.1 to 26.0‰ and $\Delta^{33}S$ from 0.13 to 0.19‰. One dissolved sulfide sample at the MN sites had $\delta^{34}S$ of 4.4‰ and $\Delta^{33}S$ of 0.13‰. The negative $\Delta^{33}S_{sulfate}$ values at ON are comparable to those of local 2.7Ga sulfide deposits. At MN, the S source of the hosting Proterozoic ore deposits has been inferred to be at least partially from recycling of sulfide in local Archean sedimentary rocks. The observed MIF of the saline waters suggests the possibility that the ultimate S sources of sulfate in these deep groundwater systems are the Archean sulfides. The large $\delta^{34}S$ and consistent $\Delta^{33}S$ between dissolved sulfate and sulfide, and the significantly elevated $\delta^{34}S_{sulfate}$ values in the MN samples relative to the reported values for the ore (2-6‰) suggest significant sulfate reduction (SR). The $\delta^{34}S_{sulfate}$ of the ON samples are also elevated by 1-6‰ compared to the published values of local ore deposits (0-2‰), implying SR may be also taking place at this site. Because all of these groundwaters have temperatures less than 30°C, the SR is most likely biological in origin. Our data raise the possibility that present-day elemental cycling by deep microbial communities can be supported by Archean S sources.

Measurement of intramolecular carbon isotopic distribution of acetaldehyde emitted from plant leaves

NA LI[1]*, KEITA YAMADA[1], RYOTA HATTORI[2], HIROKI SHIBATA[2], ALEXIS GILBERT[1], NAOHIRO YOSHIDA[1]

[1]Department of Environmental Science and Technology, Interdisciplinary Graduate School of Science and Engineering, Tokyo Institute of Technology, 4259 Nagatsuta, Yokohama 226-8502, Japan

[2]Central Laboratories for Frontier Technology, Center for Food Safety Science, Kirin Holdings Company Limited, 3 Miyahara, Takasaki Gunma 370-1295, Japan

Stable isotopic signatures within molecules record a wide range of phenomena in the chemical, biological, environmental, and earth sciences.

Here, we focus on acetaldehyde, which is an important metabolic intermediate in biological systems. Until now, there was only one study on intramolecular carbon isotopic composition ($\delta^{13}C$) of acetaldehyde, which derived from pyruvate decarboxylase during yeast incubation experiments [1]. However, in this study, the analytical protocol and the precision of the method, and the brief description made suggests that the technique was cumbersome, since it predated GC-IRMS techniques.

In this study, we examine the applicability of measurements of intramolecular $\delta^{13}C$ in acetaldehyde through GC-C-IRMS approaches. Using GC-C-IRMS combined with an off-line pyrolysis, we determined the certified values of the intramolecular $\delta^{13}C$ in acetaldehyde samples. Then, based on the certified value, we developed GC-Py-GC-C-IRMS combined with headspace solid-phase microextraction (time-saving and more sensitive than off-line pyrolysis) for the accurate determination of $\delta^{13}C$ of acetaldehyde. This method was applied to samples collected form chamber in which plants were grown. The results shown that the intrmolecular $\delta^{13}C$ of acetaldehyde emitted from plants was influenced by environmental factors, such as temperature, sunlight or humidity. These results suggest that environmental factors influence the fluxes related to acetaldehyde metabolism in plants, which gives us new insights into plant metabolic pathways and potentially plant-atmosphere interactions.

[1] DeNiro, M. & S. Epstein (1977) *Science* **197**, 261–263.

https://doi.org/10.1180/S0026461X00006502 Published online by Cambridge University Press

A study on volcanic minerals and hosted melt inclusions in newly-erupted Tengchong volcanic rocks, Yunnan Province

N. LI*, Q.C. FAN, L.Y. ZHANG

Institute of Geology, China Earthquake Administration, Chaoyang District, Beijing 100029 , China (*correspondence: nili@ies.ac.cn)

Tengchong volcanic clusters are located at the border area of western Yunnan Province and Myanmar. They consist of Heikong Mountain, Dakong Mountain, Xiaokong Mountain, Daying Mountain and Ma'an Mountain, etc., which are famous Quaternary volcanic clusters in our country and are divided by oldly- and newly-erupted volcanoes. Previous work testified Daying, Ma'an and Heikong Mountains are newly erupted ones, which had eruption activities in late Pleistocene and Holocene epochs [1].

The phenocrysts in these volcanic rocks are pyroxene, olivines and feldspars. The melt inclusions are found in hosted phenocrysts which have different shapes, randomly distributed and have some variations after entrapment. The compositional variation of melt inclusion in newly erupted volcanic rocks is larger than that of matrix glass. The chemical compositions of melt inclusion and matrix glass have covered basaltic trachyandesite, trachyandesite, trachyte and rhyolite etc., which are consistent with those of late Pleistocene and Holocene volcanic rocks in Tengchong. According to EMP analyses of melt inclusions in hosted phenocrysts, microcrystals and matrix glass, the content of volatile chlorine doesn't show large variations in melt inclusions and matrix glass, but those of volatile fluorine and SO_3 do have more variations in melt inclusions than in matrix glass.

In general, the degassing rate of newly-erupted Tengchong volcanic rocks was low and they didn't emitted more gas to the atmosphere, thus had small effect on the climate and environment by speculation. Nevertheless, future disaster shouldn't be ignored.

The work was supported by Special Project for Earthquake- 'Volcanic and Geologic Mapping of Tengchong'.

[1] Fan *et al*. (1999) *Geological Review* **45(supp.)**, 895–904.

A type of high Sr/Yb granite in North Qinling: The melting product of a pre-exiting source of arc environment

PING LI, JUN-LU CHEN, XUE-YI XU AND TING LI

Xi'an Center of Geological Survey (Xi'an Institute of Geology and Mineral Resource), CGS, Xi'an, Shaanxi 710054, China

Located in the North Qinling, the Wuguan intrusive rocks intruded into the Danfeng Group.It's rich in LILE and depleted in HFSE, with a high LILE/HFSE ratio. Moreover, the Wuguan intrusive rocks are rich in sodium and aluminum, having a high Sr/Yb and high CaO/Na_2O ratio, with no obvious negative Eu anomaly. Tthese geochemistry features suggest that there are formed by the remelting of the basaltic rocks with amphibole as a stable residual phase. The result of REE analogue calculation suggests that, plagioclase amphibolite which is formed in an island-arc environment in the Danfeng Group could form the Wuguan intrusive rock via partial melting. Besides, the residual mineral assemblage mainly is hornblende and also includes a small amount of plagioclase and clinopyroxene. The Zircon U-Pb isotopic age is later than the period of the subduction of Shangdan Ocean, but its chemical characters is closely related to the island-arc environments. The geochemical characters reflected in the Wuguan intrusive rocks may be some inherited chemical features of its sources in an arc-environment. However, the Wuguan intrusive rocks is formed in a collision orogenic process.

This work is supported by the National Science Foundation of China (Grant No. 40972150)

Precise age determination of the Paleozoic kimberlites in North China Craton and Hf isotopic constraint on the evolution of its subcontinental lithospheric mantle

QIU-LI LI*[,1], FU-YUAN WU[1], XIAN-HUA LI[1], ZHI-LI QIU[2], YU LIU[1], YUE-HENG YANG[1] AND GUO-QIANG TANG[1]

[1]State Key Laboratory of Lithospheric Evolution, Institute of Geology and Geophysics, Chinese Academy of Sciences, Beijing, 100029, China (*correspondence: liqiuli@mail.igcas.ac.cn)

[2]Department of Earth Sciences, Sun Yat-Sen University, Guangzhou 510275, China

Kimberlite, a kind of deep-sourced igneous rock, carries not only diamond, but also invaluable mantle xenolith and/or xenocryst, which are vital to track the evolution of subcontinental lithospheric mantle (SCLM). However, crustal and/or mantle contamination and post-emplacement alteration bring difficulties to determining the emplacement age of kimberlite and its compositions of primary magma. This paper finely constrains the emplacement age of diamondiferous kimberlites in Mengyin and Fuxian of the North China Craton (NCC) via three different dating methods. For Mengyin kimberlite, single grain phlogopite Rb–Sr dating yields an isochron age of 485 ± 4 Ma, U–Th–Pb analyses on perovskite give a U–Pb age of 480.6 ± 2.9 Ma and a Th–Pb age of 478.9 ±3.9 Ma, and baddeleyite yields a Pb–Pb age of 480.4 ± 3.9 Ma. For Fuxian kimberlite, baddeleyite gives a Pb–Pb age of 479.6 ± 3.9 Ma, indicating that the Paleozoic kimberlites in the NCC were emplaced at ~480 Ma. Numerous lines of evidence indicate that the studied baddeleyites are xenocrysts from the SCLM, and can be used to constrain Hf isotope compositions (~ –6) of the SCLM when kimberlite erupted. Combined with data from Mesozoic–Cenozoic mantle-derived rocks and xenoliths, the Hf isotope evolution trend of the SCLM beneath NCC before destruction was tentatively constructed, which suggested that the Archean SLCM was enriched by metasomatism at ~1.3 Ga. Further Hf isotope investigations on additional SCLM-derived materials could be compared with the constructed Hf isotope evolution trend before destruction to determine when the lithospheric thinning happened.

Late Mesozoic tectonic evolution of the Songliao basin, NE China: Evidence from detrital zircon ages and Sr-Nd isotopes

S.-Q. LI[1], F. CHEN[1]*, X.-Y. ZHU[1,2] AND W. SIEBEL[3]

[1]CAS Key Laboratory of Crust-Mantle Materials and Environments, University of Science and Technology of China, Hefei 230026, China (*correspondence: fkchen@ustc.edu.cn, lsq@mail.ustc.edu.cn)

[2]Institute of Geology and Geophysics, Chinese Academy of Sciences, Beijing 100029, China (zhuxiyan@mail.igcas.ac.cn)

[3]Institut für Geowissenschaften, Universität Tübingen, 72074 Tübingen, Germany (wolfgang.siebel@uni-tuebingen.de)

The Songliao basin, located in NE China, is one of the important oil and gas fields in China. The basin is tectonically bounded by the Jiamusi-Khanka, Erguna, Xing'an blocks between the North China and Siberian cratons. It is filled with thick Mesozoic sedimentary and volcanic rocks. This study presents detrital zircon ages and Sr-Nd isotopic compositions of two late Mesozoic sedimentary sequences, and discusses the tectonic evolution of the basin from the sedimentary record.

Dominant zircon populations of the underlying Denglouku Formation are Paleozoic (270-230 Ma) and Mesozoic (190-160 Ma) in age and are of magmatic origin. The overlying Quantou Formation contains older zircon populations of ~1800 Ma and ~2500-2900 Ma. The youngest detrital zircons place the deposition ages of both rock formations at about 110 Ma. The two sequences have distinguishable Sr-Nd isotopic features. The Denglouku Formation is characterized by higher initial ε_{Nd} values (-6.4 to -2.8) and lower initial $^{87}Sr/^{86}Sr$ ratios (0.707 to 0.709), compared to the Quantou Formation (-12.8 and 0.713).

Both rock formations appear to have been derived from different sedimentary sources. Most likely, Paleozoic and Mesozoic magmatic rocks were widespread in the northern periphery of the basin, and served as potential sources of the Denglouku Formation. In the south and in the east, old basement rocks of the North China craton provided major sedimentary material to the Quantou Formation. The south-eastward migration of erosion center(s) and the north-westward movement of the deposition center of the Songliao basin in late Mesozoic were probably related to the subduction of the western Pacific plate.

https://doi.org/10.1180/S0026461X00006502 Published online by Cambridge University Press

Oil-source correlation for severely biodegraded oils in Biyang Depression, China

S.F. LI*, S.Z. HU, S. HE AND D.M. ZHANG

Key Laboratory of Tectonics and Petroleum Resources (China University of Geosciences Wuhan), Ministry of Education, China (*correspondence: lishf@cug.edu.cn, hushzh@cug.edu.cn, shenghe@cug.edu.cn, zdm2007@cug.edu.cn)

There are multi-sources and kinds of crude oil types in Biyang Depression, which include normal oils and different-degree biodegraded oils [1]. Normal biomarker parameters, such as regular sterane and gammacerane index, are influenced by biodegradation [2], and the oil-source correlation for the whole area become very difficult. Some compounds with little or no influence should be chosen for oil-source correlation.

According to Peters [3], the 17α21β-norhopane is more resistant than 17α21β-hopane to biodegradation. Based on the analysis of more than three hundred samples which include source rock and crude oil distributed in six different basins, we proposed 2×αβ-norhopane in place of αβ-hopane and used this new gammacerane index (gammacerane/2×C_{29}hopane) to correlate those severely biodegraded oils and normal oils. Moreover, the different oils and source rocks in Biyang Depression can be distinguished clearly by the plate between gammacerane/2×C_{29}hopane and 2×C_{24} tetracyclic terpane/C_{26} tricyclic terpane (Fig. 1). Hence, the oil-source correlation for Biyang Depression has been made successfully.

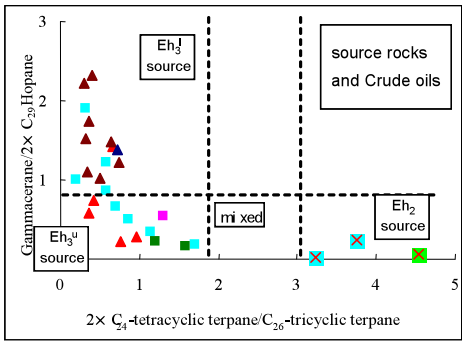

Figure 1: 2×C_{24} tetricyclic terpane / C_{26} tricyclic terpane versus gammacerane / 2×C_{29} hopane for oils and source rocks from Biyang Depression

[1] J.Q. Luo (2008) *Journal of Oil & Gas technology* **30**(2) 20–24. [2] Behar F (2006) *Organic Geochemistry* **37**(9) 1042–1051. [3] K.E.Peters (2005) *The Biomarker Guide* second editionII, 664–666.

Carbon isotope composition of DIC in the Yalong Jiang of Changjiang Basin, China

SI-LIANG LI, BENJAMIN CHETELAT, CONG-QIANG LIU, FUJUN YUE AND ZHIQI ZHAO

The State Key Laboratory of Environmental Geochemistry, Institute of Geochemistry, Chinese Academy of Sciences, Guiyang 550002, China (lisiliang@vip. skleg. cn)

Concentrations and isotopic compositions of carbon species in water samples are often used in studies of carbon biogeochemistry and rock weathering in rivers. Yalong Jiang is 2nd longest tributary of the Changjiang River in central and southern China. The Yalong rises in the Bayan Har Mountains in southern Qinghai Province at an elevation of nearly 5, 000 metres. The Yalong Jiang basin is covered by mesozoic sediments including low-grade metamorphic rocks and granitoid intrusive rocks. In this study, we surveyed carbon isotopic compositions of dissolved and suspended loads of Yalong Jiang and its main tributaries in August of 2009, with purposes of better understanding carbon sources and processes involved in the riverine carbon cycle.

The concentrations of HCO_3^- are in the range of 0.14 to 3.44 mmol L^{-1} for river waters. The $\delta^{13}C$ values of the dissolved inorganic carbon (DIC) in river waters range from -12.2‰ to -3.5‰ with a mean value of -7.1‰. The water collected from hot spring has high contents of HCO_3^- with 39.3 mmol L^{-1} and high carbon isotopic value of +0.9‰, suggesting dissolved inorganic carbon mainly derived from deep source CO_2. The $\delta^{13}C$ values of POC range from -25.4‰ to -21.9‰ for river waters with a mean value of -24.4‰, which suggests that they are mainly derived from C_3 plants. In the present study, the contents and isotopic composition of carbon species indicated that carbonate mineral and silicate weathering by CO_2 from C_3 plants and equilibration of DIC with atmospheric CO_2 involved riverine carbon cycle in Yalong Jiang of Changjiang Basin, China.

https://doi.org/10.1180/S0026461X00006502 Published online by Cambridge University Press

A LA-ICP-MS chronological and tectonic environment study of the ore-bearing volcanics in Baiyin orefield

XIANG-MIN LI, ZHONG-PING MA, JI-MIN SUN AND JI-YUAN YU

Xi'an Center of Geological Survey (Xi'an Institute of Geology and Mineral Resource), CGS, Xi'an, Shaanxi 710054, China

The Northern Qilian orogenic zone is one of the most important massive sulfide deposit provinces in our country and the world, especially, the Baiyin mine field which located at its east is a representative massive sulfide deposit. After the porphyroclastic lava extruding and the quartz albitophyre intruding which belong to the later acidic volcanic, The Baiyin mine field began mineralization, and ends at a relatively quiet period before a large-scale basic volcanism. Therefore, there is an important meaning to research the age and tectonic environment about the acid volcanic and the basic volcanic. In this paper, by using LA-ICP- MS zircon U-Pb isotope dating techniques we were determine the age of the basic volcanic in Baiyin orefield, the formation time of the basic volcanic in Baiyin orefield is 465.0±3.7Ma, this age should be belonging to Middle Ordovician ; Researched by predecessors and with the same method, the age of acid volcanic in Baiyin orefield is 467.3±2.9 Ma, So we think the age of the rocks and the mineralization of the Baiyin orefield shoud be appertaining the later Middle Ordovician. All the discovered industrial deposits were produced in marine bimodal volcanic rocks, the marine bimodal volcanic rocks are composition of quartz keratophyre、spilite and a small amount of keratophyre, Chondrite-normalized trace element distribution patterns display that there is a negative anomalies for the Nb, Ta and Ti, combined with tectonic evolution of the North Qilian Mountains, and the ore-bearing volcanic rocks of the Baiyin mine should be formed in the island arc--rift environment in the later Middle Ordovician. The results of the study has a very important significance for tectono-magmatic evolution of the Qilian orogenic belt and also for the guiding the regional geological prospecting.

This study is supported by National scientific and technological support projects (No. 2006BAB07B03-02) and China Geological Survey survey project (No. 1212010818090).

Sources and fate of nitrate in a dam-controlled subtropical river, Southwest China

X.D. LI[1]*, C.Q. LIU[1], Z.Y. YIN[1], X.Y. LIU[1] AND L.R. BAO[1,2]

[1]Institute of Geochemistry, Chinese Academy of Sciences, Guiyang, Guizhou, PR China (*correspondence: lixiaodong@mails.gyig.ac.cn)

[2]Graduate University of Chinese Academy of Sciences, Beijing, PR China

The concentrations and dual isotopic ($\delta^{15}N$ and $\delta^{18}O$) values in NO_3^- were analyzed from 23 samples collected along the Jialing River, a major tributary of upper Yangtze. Unlike other ions, the concentrations of NO_3^- were higher in rainy season than in dry season. Heavy use of nitrogen fertilizer with low use efficiency is responsible for nitrogen loss and high NO_3^- content in the river water during rainy season. The dammed river may provide preconditions for algal growth that would assimilate NO_3^-, which led to concentration of NO_3^- decreasing, $\delta^{15}N_{NO3}$ and $\delta^{18}O_{NO3}$ values increasing during rainy season. There was no obvious trend of $\delta^{15}N_{NO3}$ and $\delta^{18}O_{NO3}$ in dam area during dry season. To interpret the sources of nitrate, the co-variation of $\delta^{15}N_{NO3}$ and $\delta^{18}O_{NO3}$ was examined (Figure 1).

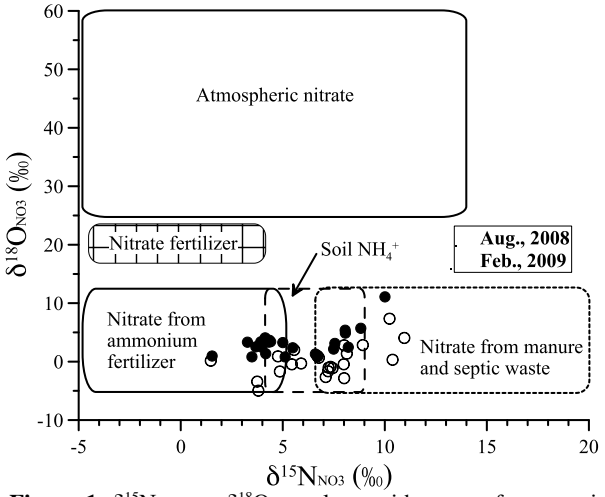

Figure 1: $\delta^{15}N_{NO3}$ *vs.* $\delta^{18}O_{NO3}$, along with ranges for potential sources. (Aug., 2008-rainy season; Feb., 2009-dry season)

The sources of NO_3^- are mainly resulted from the nitrification of ammonium fertilizer and demostic sewage during rainy season while the sewage is the major source during dry season in the Jialing River catchment.

This work was supported by the National Natural Science Foundation of China (Grant No. 40703004 and 40721002).

[1] Panno *et al*. (2008) *J Hydrol* **359**, 174–188. [2] Chen *et al*. (2009) *Biogeochemistry* **94**, 163–174.

Combining concentration-area method with indicator kriging analysis for geochemical anomaly identification of the typical deposit

X.H. LI, F. YUAN*, M.M. ZHANG AND T.F. ZHOU

School of Resources and Environmental Engineering, Hefei University of Technology, Hefei, China (*correspondence: yf_hfut@163.com)

Geochemical datasets always include outliers and potentially have skewed distributed data. Althought normal transformation can enhance the robustness of the kriging method, it can smooth the data more seriously. Indicator kriging method does not rely on the stationarity of the datasets, can make more robust and feasible against a series of outliers. The threshold is the most important factor of indicator kriging analysis. The concentration-area method [1] which baesd on the fractal and multifractal theory can provide great help for the threshold calculation.

When we carried out the anomaly identification analysis of Cu concentration in the typical deposit of China, we used the concentration-area method (ACAF) [2] to obtaine the threshold for the indicator kriging. The results of the indicator Kriging interpolation are shown in the figure below.

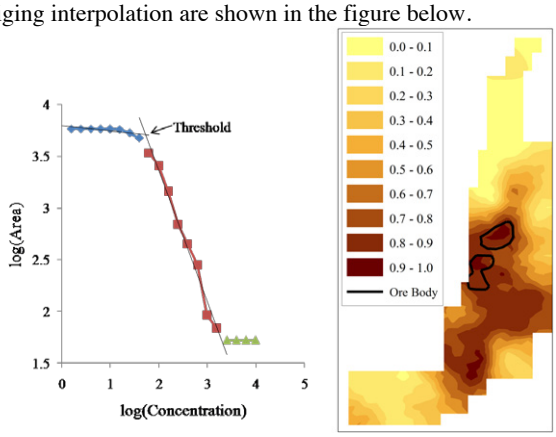

Figure 1: Indicator kriging interpolation results of Cu concentration

Discussion

Combining concentration-area method with indicator kriging analysis can highlight the known ore bodies and delineate mineralization centre more effectively, indicating that it is very suitable for the ore-hunting prognosis which is based on non-stationarity datasets and outliers.

This research was sponsored by the Key Technologies Research and Development Programme of Anhui Province, China(08010302200) and the Program for New Century Excellent Talents in University (NCET-10-0324).

[1] Cheng *et al*. (1994) *Journal of Geochemical Exploration* **43**, 91–109.[2] Xie *et al*. (2004) *Mathematical Geology* **36**, 847–864.

Equilibrium Se isotope fractionation parameters: A first-principles study

XUEFANG LI AND YUN LIU*

State Key Laboratory of Ore Deposit Geochemistry, Institute of Geochemistry, Chinese Academy of Sciences, Guiyang 550002, China (*correspondence: Liuyun@vip.gyig.ac.cn)

Introduction

Se belongs to one of the most redox-sensitive elements, so Se isotopes might be used to trace some redox and biointerference processes. But there are just a few pioneering studies [1, 2] that provided equilibrium Se isotope fractionation factors.

Based on the Urey model or the Bigeleisen–Mayer equation method, several important equilibrium Se isotope fractionation parameters are investigated by first-principles calculations. All the frequencies are obtained at B3LYP/6-311+G (d, p) level, with a frequency scaling factor of 1.05. Table 1 shows some of the calculated fractionation factors [3].

A-B	$10^3\ln(\alpha_{A\text{-}B})=a*10^6/T^2+b*10^3/T+c$
SeO_4^{2-}-SeO_3^{2-}	$10^3\ln(\alpha_{A\text{-}B})= 0.524637*10^6/T^2 + 2.94785*10^3/T-2.50587$
SeO_4^{2-}-$HSeO_3^-$	$10^3\ln(\alpha_{A\text{-}B})= 0.608479*10^6/T^2 + 2.77841*10^3/T-2.38642$
SeO_4^{2-}-HSe^-	$10^3\ln(\alpha_{A\text{-}B})= 1.709258*10^6/T^2 + 5.51101*10^3/T-5.02758$
SeO_3^{2-}-$HSeO_3^-$	$10^3\ln(\alpha_{A\text{-}B})= 0.083841*10^6/T^2 -0.16944*10^3/T+0.11944$
SeO_3^{2-}-HSe^-	$10^3\ln(\alpha_{A\text{-}B})= 1.184621*10^6/T^2 + 2.56316*10^3/T-2.52171$
SeO_4^{2-}-SeMet	$10^3\ln(\alpha_{A\text{-}B})= 1.236799*10^6/T^2 + 5.12772*10^3/T-4.42211$
SeO_4^{2-}-SeCyst	$10^3\ln(\alpha_{A\text{-}B})= 1.204255*10^6/T^2 +5.32442*10^3/T-4.59242$
SeO_4^{2-}-DMSe	$10^3\ln(\alpha_{A\text{-}B})=1.323029*10^6/T^2 +4.90539*10^3/T-4.22539$
SeO_4^{2-}-DMDSe	$10^3\ln(\alpha_{A\text{-}B})=1.306259*10^6/T^2 +5.48531*10^3/T-4.72162$
SeO_2-SeO	$10^3\ln(\alpha_{A\text{-}B})=0.438882*10^6/T^2 +2.57817*10^3/T-2.15291$
SeO_2-Se_2	$10^3\ln(\alpha_{A\text{-}B})=0.335359*10^6/T^2 +4.14586*10^3/T-3.45764$
SeO_2-H_2Se	$10^3\ln(\alpha_{A\text{-}B})=0.725619*10^6/T^2 +2.61754*10^3/T-2.71278$
SeO_2-Se(T)	$10^3\ln(\alpha_{A\text{-}B})=0.263308*10^6/T^2 +4.34169*10^3/T-3.63616$
SeO_2-Se(M)	$10^3\ln(\alpha_{A\text{-}B})=0.257529*10^6/T^2 +4.34519*10^3/T-3.63933$
SeO-Se(T)	$10^3\ln(\alpha_{A\text{-}B})=-0.175574*10^6/T^2 +1.76352*10^3/T-1.48325$
SeO_2-DMSe	$10^3\ln(\alpha_{A\text{-}B})=0.198796*10^6/T^2 +3.02243*10^3/T-2.49061$
SeMet-DMSe	$10^3\ln(\alpha_{A\text{-}B})=0.086231*10^6/T^2-0.22233*10^3/T+0.19672$

Table 1: The formula for Se isotope fractionations at different temperatures (see [3] for details).

Discussion of Results

Our results suggest that the magnitude of isotope fractionation is depended on Se valence states, and there is a trend of heavy Se isotopes enrichment as SeO_4^{2-} > SeO_3^{2-} > $HSeO_3^-$ > SeO_2 > selenoamino acids > alkylselenides > Se (0) or H_2Se > HSe^-. The equilibrium Se isotope fractionation factors provided here might be useful to explain Se isotope distributions in the biogeochemical cycle and also important to the study of Se global cycling.

[1] Krouse & Thode (1962) *Can. J. Chem.* **40**, 367–375. [2] Schauble (2004) *Rev. Mineral. Geochem.* **55**, 65–111. [3] Li & Liu (2011) *EPSL*. **304**, 113–120.

https://doi.org/10.1180/S0026461X00006502 Published online by Cambridge University Press

Geochemistry and metasomatic processes of spinel peridotite suite from mantle wedge of subduction zone, Western Tianshan

XU-PING LI[1]*, LI-FEI ZHANG[2] AND FAN-MEI KONG[1]

[1]College of Geological Science and Engineering, Shandong University of Science and Technology, Qingdao, 266510, China (*correspondence: lixuping@sdust.edu.cn)

[2]The Key Laboratory of Orogenic Belt and Crustal Evolution, MOE, School of Earth and Space Sciences, Peking University, Beijing 100871, China (lfzhang@pku.edu.cn)

Spinel peridotite and olivine amphibolite of the Western Tianshan orogenic belt are enclosed in micaschist and derive from an orogenic wedge environment, showing evidence of melt extraction and metasomatic enrichment and documenting a complex history of the shallow mantle. Al–spinel is closely intergrown with secondary hornblende, diopside and serpentine, indicating that it grows at the expense of former Cr-spinel. Compositions of orthopyroxene, olivine and spinel indicate equilibration within the spinel–peridotite facies of the upper mantle, at depths about 45–65 km and temperatures around 676–735 °C.

High Cr/Al ratio of relict primary spinel and no detected primary clinopyroxene indicate that the ultramafite of the Western Tianshan represents a high degree melting and highly depleted residual mantle. The spinel peridotites derive from a depleted mantle that became enriched in some large ion lithophile element (LILE) and light rare earth element (LREE). Whole-rock trace element patterns from the most spinel peridotite suite show distinct negative anomalies for Nd, Ti and positive anomalies for Pb and Sr. Early amphiboles generated in the mantle wedge above subduction zones are depleted in heavy rare earth element (HREE) with subchondritic Ti/Nb and Zr/Nb ratios, whiles late developed amphiboles are even more depleted in HREE, showing heavily effected by subduction-related fluid. The changing pattern of early edenite to late hornblende in peridotites and amphibolites indicate that the mantle rocks took place within the mantle wedge where a suprasubduction metasomatic event overprinted a probably early mantle metasomatic episode.

Geochemical characteristics of minerals and rocks indicate that the ultramafic rocks from subduction mantle wedge in the western Tianshan represent an island arc environment.

This study is supported by the National Natural Science Foundation of China (40973022), and the Chinese Ministry of Science and Technology (2009CB825007).

Atmospheric aerosol as the source of nitrate deposits in Turpan-Hami Basin, China: Evidence from oxygen and nitrogen isotopic compositions

LI YANHE *, QIN YAN, LIU FENG, HOU KEJUN AND WAN DEFANG

MLR Key Laboratory of Metallogeny and Mineral Assessment, Institute of Mineral Resource, Chinese Academy of Geological Sciences, Beijing, 100037, China (*correspondence: lyh@mx.cei.gov.cn)

The Turpan-Hami Basin, which located in eastern Xinjiang, China, is a closed inland basin and one of the driest regions on the Earth. Recently, a super-scale nitrate ore field was found in this basin. The total amount of nitrate resources in Turpan-Hami Basin is about 2.5 billion tons, as much as the amount in Atacama Desert of Chile. The Turpan-Hami nitrate deposits can be mainly divided into two types: (1) Quaternary alluvial-pluvial sediment fissures-filling sodium nitrate deposits, (2) Modern saline type niter deposit.

The N and O isotopic compositions are different in the two types of nitrate deposits. The $\delta^{15}N_{Air}$ values of sodium nitrate vary from 0.7‰ to 6.0‰, which are similar to atmospheric NO_3^-; The $\delta^{18}O_{V\text{-}SMOW}$ values are very high, range from 34.4‰ to 45.0‰, which are different from microbial nitrification nitrate, and similar to atmospheric NO_3^-; The $\Delta^{17}O$ values range from 12.20‰ to 20.70‰, mass-independent fractionation (MIF) of oxygen isotope is obviously. With these proofs of oxygen and nitrogen isotopic compositions of nitrate, we can conclude that sodium nitrate deposits in Turpan-Hami Basin were products of long term atmospheric deposition of nitrate aerosol particles, which produced by photochemical reactions. The niter deposits character with high $\delta^{15}N_{Air}$ (15.0‰ ~ 27.6‰), low $\delta^{18}O_{V\text{-}SMOW}$ (30.2‰ ~ 36.3‰) and $\Delta^{17}O$ (3.93‰ ~ 12.39‰) values.

The sodium nitrate and niter deposits in Turpan-Hami Basin are from the same source, and niter deposits experienced strong microbial denitrification during the formation.

https://doi.org/10.1180/S0026461X00006502 Published online by Cambridge University Press

Veterinary antibiotics in pig feces

Y.X. LI, W. LI, M. YANG AND C. LIN

School of Environment, Beijing Normal University, Beijing 100875, China (liyxbnu@bnu.edu.cn)

The intense livestock farming in China engenders a significant volume of manures with no other solution for farmers than land disposal. Continued land application of antibiotics-containing manure could detrimental to soil and water quality in the long term. 14 veterinary antibiotics (VAs) in pig feces were quantitatively determined using HPLC.

antibiotics	Appearance (%)	Mean value	Lowest value	Highest value	S.D.
TC	50.0	5.29	0.32	30.55	9.07
OTC	50.0	11.81	0.73	56.81	18.60
CTC	61.1	3.19	0.68	22.34	6.41
SG	22.2	0.63	0.15	1.90	0.85
SA	11.1	0.11	0.10	0.12	0.01
SMR	11.1	0.14	0.13	0.15	0.01
SMZ	27.8	1.07	0.21	2.16	0.85
SMM	27.8	1.14	0.12	4.84	2.07
SCP	16.7	0.85	0.13	2.13	1.11
NOR	27.8	1.10	0.41	3.18	1.18
CIP	27.8	0.49	0.31	0.96	0.27
ENR	44.4	0.87	0.36	2.22	0.75
DIF	5.6	0.14	0.14	0.14	0
TYL	22.2	0.69	0.23	1.88	0.80

Table 1: The residues of antibiotics in pig feces ($mg \cdot kg^{-1}$) (TC:tetracycline, OTC:oxytetracycline, CTC:chlortetracycline, SG:sulfaguanidine, SA:sulfanilamide, SMZ:sulfamethoxazole, SMM:sulfamonomethoxine, SMR:sulfamerazine, SCP:sulfachlorpyridazine, NOR:norfloxacin, CIP:ciprofloxacin, ENR: enrofloxacin, DIF:difloxacin, TYL: tylosin).

Result shows that 5.6-61.1% of four types of VAs could be detected in pig feces. The risk quotients (RQ) indicate a certain probability for adverse effects of VAs on soil microbial activity [1]. The largest RQ of OTC suggested that it should be the priority control of Vas in the study area.

Supported by EPPWP (200909042), NNSFC (20977010) and NBRPC (2007CB407302)

[1] Spaepen *et al*. (1997) *Environ. Toxicol. Chem*. **16**, 1977–1982.

Relationship between the longevous population and trace element in the soils of Xiayi County, China

Y.H. LI*, X.Y. ZOU AND W.Y. WANG

Institute of Geographical Sciences and Natural Resources Research, CAS, Beijing 100101, China (*correspondence: yhli@igsnrr.ac.cn)

Effects of environment on the longevous population

Health and longevity can be considered as the product of interactions between environment, heredity and lifestyle [1, 2]. A case study on Scandinavian twins concludes that the effect of heredity on life expectancy accounts for 20–30%, whereas that of environmental change accounts for at least 70% [3]. Most recently, soil, drinking water and climate were reported to be leading environmental factors influencing regional population longevity [4]. Based on field investigation and laboratory analysis, trace elements in the soils of Xiayi County, a Chinese longevous area, were investigated, and the key elements closely linked to health and longevity were evaluated.

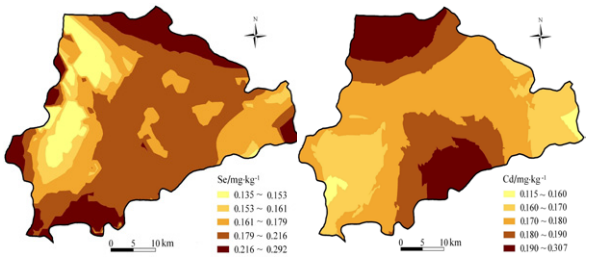

Figure 1: Spatial distribution of Se, Cd in the soil of Xiayi

Discussion of Results

The longevous population was distributed in a belt running across Xiayi County from northeast (NE) to southwest (SW). The longevity rate (number of population aged 95 or older per million) reached 83 in the NW region. Interestedly, it dramatically increased to 187 in the NE region, where the soils contained higher Se and Zn but lower Cd (Figure 1). The findings indicate that sufficient Zn and Se as well as low exposure to heavy metal pollution contribute to human longevity.

[1] Perls *et al*. (2002) *Mech. Ageing Dev*. **123**, 231–242. [2] Li *et al*. (2011) *Sci. Total Environ*. **409**, 1385–1390. [3] Ljungquist *et al*. (1998) *J. Gerontol. Ser. A , Biol. Sci. Med. Sci*. **53**, M441-M446. [4] Lv *et al*. (2011) *Arch. Gerontol Geriatr*. doi, 10.106/j.archger.2010.10.012.

https://doi.org/10.1180/S0026461X00006502 Published online by Cambridge University Press

Nitrogen speciation in mantle fluids

YUAN LI*, HANS KEPPLER AND ANDREAS AUDÉTAT

Bayerisches Geoinstitut, Universität Bayreuth, D-95440, Bayreuth, Germany
(*correspondence: Yuan.Li@uni-bayreuth.de)

Nitrogen speciation in N-H-O fluids at mantle conditions was studied by means of synthetic fluid inclusions trapped in HF etched quartz and pre-cracked San Carlos olivine. Experiments were performed at 600 - 1300 °C and 15 - 30 kbar using a piston cylinder apparatus, starting with a ~11 mol/L NH_3 solution. A modified double capsule technique was used to attain redox states of various oxygen buffers (Fe-FeO, Co-CoO, Ni-NiO). The recovered fluid inclusions were studied by Raman spectroscopy. The results show that NH_3 and N_2 are the two major nitrogen-bearing species, which stabilities strongly depend on the temperature, pressure, and oxygen fugacity. At conditions relevant to subduction zones, nitrogen occurs mainly as NH_3 and thus behaves similar to the lithophile element K; whereas in the overlying asthenospheric mantle it partially decomposes into N_2 and H_2. The ascent of the mantle fluids into the shallow crust results in complete transform of NH_3 into N_2. In the deep mantle along the geothermal profile, where oxygen fugacity is reduced and pressure is decreased, we expect nitrogen to be present significantly as NH_3 in the fluids, thus there could be much more nitrogen present in the bulk silicate Earth than the value estimated based on N/noble gas ratios in MORB [1].

[1] Marty, B. (1995) *Nature* **377**, 326–329.

Ecological stoichiometry of plant nutrients: A case study of degraded grassland in western Jilin Province, NE China

Y.F. LI, D.Y. WANG, C. SUN, D.Y. GUO, Y.Y. YANG AND X. SHI

College of Earth Sciences, Jilin University, Changchun 130061, China (yfli@jlu.edu.cn, wang_dy@jlu.edu.cn, scwutong@163.com, jluguodongyan@163.com, yyyang10@mails.jlu.edu.cn, awenxian@126.com)

Plant growth should be expected to be limited by nitrogen (N) and phosphorus (P) availability in most terrestrial ecosystems. The previous studies indicate that the N/P ratios be usually used to indicate N or P limitation on plant growth. However, how does N/P ratio influence vegetation composition and species richness? It has been one of the hotly discussed issues in the ecological stoichiometry. However, the N and P stoichiometry in the leaves of different plants from the Jiangjiadian grassland in Da'an city in western Jilin Province, NE China, provides insights for the above issue. The results indicate that N and P stoichiometry in the leaves of *Leymus chinensis, Phragmites australis, Chloris virgata, Puccinellia distans, Suaeda glauca* from the grassland are 1.09-3.4%, 0.68-2.94%, 1.69-2.76%, 1.47-2.35% and 1.88-8.7% for N and 0.056-0.254%, 0.082-0.184%, 0.105-0.122%, 0.057-0.107% and 0.067-0.072% for P, respectively. Their corresponding N/P ratios are 9.06-23.53, 8.31-18.12, 16.11-22.64, 22.02-25.88 and 28-28.06 respectively. The arithmetic means for the five species are 1.96%, 1.75%, 2.23%, 1.91% and 5.29 % for N, 0.119%, 0.120%, 0.113%, 0.082% and 0.069% for P, and 17.7, 13.83, 19.38, 23.95 and 28.03 for N/P ratios, respectively. The N and P contents as well as N/P ratios are high in the early stage of plant growth owing to small biomass, and then greatly decrease with leaf expansion during their fast growth period. With the increase of degree of grassland degradation, the *Leymus chinense, Phragmites australis, Chloris virgata, Puccinellia tenuiflora,* and *Suaeda glauca* subsequently appear. Taken together, it is suggested that the N and P contents as well as N/P ratios in plants differ greatly at different degredation stages because of the difference of components of the plant communities at the different degraded stages. Therefore, we conclude that stoichiometry ratios (N/P) in dominant plant species can serve as indicators of direction of plant succession in the degraded grassland.

https://doi.org/10.1180/S0026461X00006502 Published online by Cambridge University Press

The genetic feature and reservoir forming model of cracked gas in China

ZHENGWEN LI*, JUN LI AND SHIGUO LIN

Research Institute of Petroleum Exploration and Development-Langfang Branch, PetroChina Ltd, Langfang, Hebei, 065007, China (*correspondence: li-zhengwen@petrochina.com.cn)

Comprehensive research the domestic and foreign research fruit on cracked gas, further analyze the genetic features and reservoir forming differences of cracked gas among crude oil, marine facies source rock, lake facies sapropel type source rock and lake facies humic source rock.

Crude oil crack is the break of long chain fatty structure carbon. It begin to crack when the earth temperatures go beyond 180°C, the crack depth is deep, so its reservoir forming mainly controlled by palaeohigh. Source rock crack is the break of aromatics methyl and terminal methyl in kerogen structure. The gas generation potential of marine sapropel type would dry up when Ro near to 3%, but the gas generation potential of lake facies sapropel type source rock would generate about 201m^3/ton TOC when Ro near 3% to 5%. From simulate experiment, the gas-generating amount is about twenty percents of total [1]. Evolutionary trend of kerogen H/C atomic radtio may reflects that the coal still have large gas generation potential although it is in post-mature stage (Figure 1). The crack potential of lake faces sapropel type is between them and is controlled by the degree of sapropel type. as a whole, it is one of most important cracked gas source rock type. Source rock crack is controlled by the centre of generate hydrocarbon. transforming and reservoir condition are very important.

Divide cracked gas into four reservoir forming model, crude oil cracked gas palaeotectonic control reservoir, marine source rock cracked gas carbonate reef flat-unconformity control reservoir, lake facies source rock conventional and cracked mixed gas structure control reservoir and lake facies source rock cracked gas special lithology control reservoir.

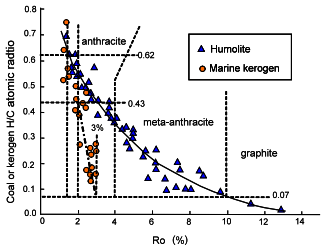

Figure 1: Relation of Coal or kerogen H/C atomic ratio with Ro

[1] Li Jian, Hu Guoyi, *et al*. (2001) *The Physical Chemistry Simulation Research of Gas Pool Forming in Large and Middle Scale Gasfileds in China*. Beijing: Petroleum Industry Press.

Carbon dioxide sequestration within Jinchuan copper-nickel mine tailing, China

ZIBO LI, LIANWEN LIU* AND JUNFENG JI

Institute of Surficial Geochemistry, School of Earth Sciences and Engineering, Nanjing University, Nanjing 210093 (*correspondence: Liulw@nju.eu.cn)

Anthropogenic greenhouse gas emissions may be offset by carbon dioxide mineral sequestration, which through the carbonation of magnesium silicate minerals to form magnesium carbonate minerals, and the ultramafic-hosted mine tailings are the ideal raw material for carbon dioxide mineral sequestration. Tailings that can be used to sequestrate carbon dioxide include copper-nickel mine tailings, chrysotile mine tailings, serpentine mine tailings, and V-Ti-magnetite mine tailings in China. We emphasis on particle size, mineral composition, major elements and trace elements, and the potential and capability of natural weathering for carbon dioxide sequestration in Jinchuan copper-nickel mine tailing. Jinchuan is located in central section of Gansu, China (38° 29' N, 102° 10' E) at elevation of 1563. To examine the capability of carbon dioxide fixed in Jinchuan copper-nickel mine tailing, a tailing profile was dug in NO. 1 tailing dam and 9 samples were collected at 10 cm intervals, and 5 other samples were collected from NO. 2 tailing dam. Analyses included particle size, XRF, FT-IR, XRD, and selective leaching, and we find that lansfordite content in NO. 1 and NO. 2 tailing dam is 4.19 wt% and 1.95wt% respectively. According to our preliminary estimate, 706.8 Kt CO_2 were sequestrated during the period of natural weathering in the Jinchuan copper-nickel mine tailing. Our study also indicate that the natural weathering of Jinchuan copper-nickel mine tailing are in abiotic environment, for lansfordite is formed in abiotic environment, and the main reasons may be drought condition, low temperature in Jinchuan, and the microenvironment of serpentine tailing have a high magnesium concentration, which will restrain the metastasis of bacteria. On the basis of tailing reserves and concentration of magnesium, it is about 40 Mt of carbon dioxide that could be fixed in Jinchuan copper-nickel mine tailing. Therefore, the potential of carbon dioxide that could be sequestrated in Jinchuan copper-nickel mine tailing is considerable. And the concentration of Ni, Cr and Cu are 2494 μg/g, 3094 μg/g and 1731 μg/g, hence comprehensive utilization of Ni, Cr and Cu would greatly cut down the investment of carbon dioxide sequestration.

This work was funded by the NSF of China through Grants 40773056.

https://doi.org/10.1180/S0026461X00006502 Published online by Cambridge University Press

Two types of gold mineralization from one ore district: Constraints on the genetic model of Yangshan gold deposit in western Qinling, China

J.L. LIANG[1]*AND W.D. SUN[2]

[1]Department of Geochemistry, Chengdu Univ. of Technology, No. 1, Roa. 3 of Eastern Erxianqiao, Chenghua District, Chengdu 610059, China (*correspondence: richardljl04@yahoo.com.cn)

[2]Guangzhou Institute of Geochemistry, the Chinese Academy of Sciences, 511 St. Kehua, Wushan, Tianhe District, Guangzhou 510640, China

Yangshan gold deposit, located in western Qinling orogenic belt, was classified by most previous researchers as Carlin-type mineralization, similar to those in Nevada [1, 2]. The host rocks are middle Devonian greenschist facies siliciclastic metasediments intercalated with carbonate. The distributions of orebodies are strictly controlled by a nearly west-east-striking fault system, Anchanghe Fault. Fine-grained (10s to 100s μm in size) arsenian pyrites and arsenopyrites are the major Au carriers, visible gold was not identified under scan electronic microscope.

Here we report coarse grained pyrite-bearing quartz ore veins through the tunnel of PD051 in Anba district, one of the major district in Yangshan. Significant amount of CO_2-rich fluid inclusions were found in quartz vein. Microthermometric analyses showed that the total homogenization temperature ranges from 221 °C to 310 °C, the salinity from 2.0 to 7.2 wt.% NaCl equivalent.

The new observations suggest that Yangshan gold deposit is actually an orogenic gold deposit in deep segments, and displayed as Carlin-type mineralization in shallow parts. This supports that those Carlin-type gold deposits in western Qinling displayed the charicteristics both epizonal orogenic and Carlin-type deposits [3].

[1] Mao *et al*. (2002) *Mineralium Deposita* **37**, 352–377. [2] Hu *et al*. (2002) *Mineralium Deposita* **37**, 378–392. [3] Cline *et al*. (2005) *Economic Geoogy* 100th Anniversary Volume 451–484.

Waves, channels, and diffusive porous flow: Geochemical implications for melt migration in an upwelling heterogeneous mantle

Y. LIANG[1] AND A. SCHIEMENZ[2]

[1]Department of Geological Sciences, Brown University, Providence, RI 02912, USA (yan_liang@brown.edu)

[2]Department of Earth and Environmental Sciences, Munich University, Theresienstr. 41, 80333 Munich, Germany

The style and mode of melt migration in the mantle are important to the interpretation of basalts erupted on the surface. Both grain-scale porous flow and channelized melt migration have been proposed to explain various geochemical observations of basalts. To better understand the mechanisms and consequences of melt migration in a heterogeneous mantle, we have undertaken a high-order numerical study of reactive dissolution in an upwelling mantle column where solubility of orthopyroxene increases upwards. Our setup is similar to that described in [1], except we use a larger domain size and longer simulation time. We show that strong nonlinear interactions among compaction, dissolution, and upwelling give rise to porosity waves and high-porosity melt channels, which may play an important role for melt migration in the upper part of the mantle directly beneath mid-ocean ridges. These compaction-dissolution waves have well organized but time-dependent structures in the lower part of the simulation domain. High-porosity melt channels nucleate along nodal lines of the porosity waves, growing downwards. The upper part of the melt channel is pyroxene-free dunite, whereas the lower part is harzburgite.

Transient melt flow in the wave regime results in significant lateral mixing and chromatographic fractionation of elements of different incompatibility during melt migration in the mantle even when mantle source compositions are independent of time. In one simulation with time-independent sources, we observe strong time-dependent variations in isotopic ratios in melts both within and at top of the domain: Fields of isotopically labelled melts are quickly distorted by differential flows upon entering the column from below, resulting in expansion, contraction, stretching, folding, and mixing in the mid to upper part of the column. Caution therefore must be exercised when inferring the geometry and spatial distribution of mantle heterogeneity based on spatial and temporal variations in isotopic ratios recorded in basalts.

[1] Liang *et al*. (2010) *GRL* **37**, L15306, doi, 10.1029/2010GL044162.

https://doi.org/10.1180/S0026461X00006502 Published online by Cambridge University Press

Molybdenum isotopic studies of mantle reservoirs

Y.-H. LIANG*, C. SIEBERT, J. YANG AND A.N. HALLIDAY

Department of Earth Sciences, University of Oxford, South Parks Road, Oxford, OX1 3AN, UK (*correspondence: Yu-Hsuan.Liang@earth.ox.ac.uk)

Mass dependent isotope fractionation of (for example) silicon isotopes between meteorites and planetary materials has been used to assess processes that occurred during formation of Earth and its core (e.g. [1, 2]).

Thus far little is known about the mass dependent isotope fractionation of Mo in the solar system. Molybdenum is a refractory and moderately siderophile element. The processes that might have fractionated Mo in the early solar system include condensation and evaporation of dust grains, metal-silicate segregation, core crystallization, and aqueous alteration. To make comparisons with the silicate Earth it is first necessary to assess how much fractionation takes place during mantle melting.

Although we know much about the behavior of Mo in low temperature environments, little is known of Mo isotope behavior during high temperature processes. In this study we analyzed mafic and ultramafic rocks from a variety of settings. The $\delta^{95/98}$Mo values of mid-ocean ridge basalts (MORB) range from -0.18 to +0.10, and the $\delta^{95/98}$Mo values of oceanic island basalts (OIB) vary from -0.04 to +0.25 (+-<0.1permil (2s. d.) on $^{98/95}$Mo by double spike and MC-ICP-MS, this study; [3]). There is no significant variation in Mo isotope composition in a differentiation sequence from Ketla on Iceland over a range of Si contents. The mean isotope composition of OIB is slightly higher than MORB, but withinuncertainty the same. According to these preliminary results, it seems unlikely that there could exist any significant isotopic variability between these mantle Mo reservoirs. Our results also make Mo isotope fractionation during fractional crystallization unlikely.

[1] Georg *et al*. (2007) *Nature* **447**, 1102-1106. [2] Ziegler *et al*. (2010) *Earth & Planetary Science Letters* **295**, 487-496. [3] Siebert *et al*. (2001) *Geochemistry, Geophysics, Geosystems* **2**, 2000GC000124.

Geochemical characteristics and genetic types of natural gas in the Yinggehai Basin, China

FENGRONG LIAO

PetroChina Research Institute of Petroleum Exploration and Development, Beijing 100083, China (liao_xiaoke@163.com)

The genetic types of natural gas in the Yinggehai Basin are complex and dominated by thermogenic gas, with a small quantity of microbial gas and microbial-thermogenic mixed gas. The $\delta^{13}C_1$ values of natural gas in this area range from -28.6‰ to -74.7‰, and the $\delta^{13}C_2$ values range from -21.8‰ to -27‰, showing humic characteristics. In the C_1/C_{2+3}-$\delta^{13}C_1$ diagram (Fig.1), proportion of samples locate in the range of kerogen type III, and the others out of the range for mixing or migration. This phenomenon may be induced by episodic fluid flow in the Yinggehai Basin. The $\delta^{13}C_1$ values of microbial gas range from -74.4‰ to -62.5‰ and the δD values are heavy, ranging from -172.1‰ to -108.5‰. The previous studies suggested that the δD values were influenced by the sedimentary environment and the δD values of microbial gas in this area indicated that the microbial gas was generated in marine environment. Compared to the microbial-thermogenic mixed gas, the thermogenic gas and microbial gas are mixed in proportion and the results indicate that in the microbial-thermogenic mixed gas, the contents of the microbial gas range from 10% to 30%, and those of the thermogenic gas range from 70% to 90%.

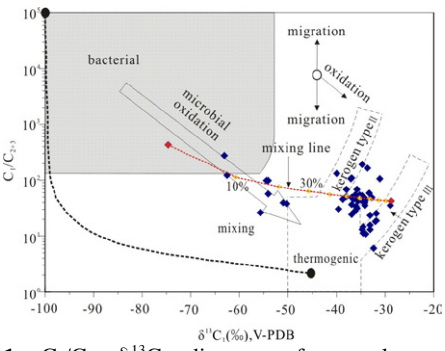

Figure 1: C_1/C_{2+3}-$\delta^{13}C_1$ diagram of natural gas in the Yinggehai Basin(the base map is according to Whiticar [1], the data are according to previous authors [2-6]).

[1] Whiticar *et al*. (1999) *Chem Geol* **161**, 291–314. [2] Dai *et al*. (2003) *China Offshore Oil & Gas(Geol)* **63**, 149-150. [3] Zhao *et al*. (2005) *Acta Sediment Sin* **23**, 156–161. [5] Hao *et al*. (2000) *AAPG Bull* **84**, 607–626. [6] Shen *et al*. (1996) *Nal Gas Geosci* **7**, 7–16.

https://doi.org/10.1180/S0026461X00006502 Published online by Cambridge University Press

Indoor seismology

ROBERT C. LIEBERMANN, BAOSHENG LI, JENNIFER KUNG, IAN JACKSON, GABRIEL GWANMESIA, SYTLE ANTAO AND JOHN B. PARISE

Mineral Physics Institute, Stony Brook University, Stony Brook, NY USA Robert.Liebermann@stonybrook.edu

In the last decade, considerable progress has been made in our laboratory in conducting acoustic velocity measurements of the elasticity of materials at high pressures and temperatures using ultrasonic interferometric techniques in multi-anvil, high-pressure apparatus. By combining these ultrasonic measurements with synchrotron X-radiation, we have extended the experimental capabilities in multi-dimensions, thereby enabling more complete characterization of solid and liquid materials to pressures of P>25 GPa and temperatures T>1600K. These expanded facilities now allow us to conduct simultaneous measurements of sound velocities using ultrasonic interferometry, crystal structure and unit cell parameters using X-ray diffraction, and sample length using X-radiographic imaging, all *in situ* at high P & T.

Experiments using these new techniques have been conducted on many minerals of the Earth's mantle in the form of polycrystalline and single crystal specimens, including San Carlos olivine [$(Mg, Fe)_2SiO_4$], ortho- and high-pressure clino-pyroxene [$MgSiO_3$], pyrope [$Mg_3Al_2Si_3O_{12}$]-garnet, wadsleyite and ringwoodite [Mg_2SiO_4], magnesium silicate perovskite [$MgSiO_3$] and ferropericlase [(Mg, Fe)O]. We report here new data from our laboratory for pyrope-majorite garnets and high-temperature elasticity of orthoenstatite ($MgSiO_3$) and magnesioferrite spinel ($MgFe_2O_4$).

Paired Sr isotope ($^{87}Sr/^{86}Sr$, $\delta^{88/86}Sr$) systematic of pore water profiles: A new perspective in marine weathering and seepage studies

V. LIEBETRAU*, M. HAECKEL, A. EISENHAUER, F. SCHOLZ, C. HENSEN AND A. REITZ

Leibniz Institute of Marine Sciences, IFM-GEOMAR, Kiel, 24148, Germany
(*correspondence: vliebetrau@ifm-geomar.de)

The simultaneous and independent determination of the radiogenic ($^{87}Sr/^{86}Sr$) and the fractionation reflecting stable ($\delta^{88/86}Sr$) Sr isotope ratio on pore waters, sediments and precipitates (e.g. carbonates and sulfates) opens a new perspective in the field of submarine weathering and Sr contribution to the ocean chemistry.

Four initial case studies covering (1.) CO_2 seeps of the Okinawa Trough (OT), (2.) mud volcanoes (MV) and mounds in the Gulf of Cadiz (GoC) and the (3.) Central American Fore Arc as well as first results from the (4.) Black Sea are conducted and reflect a stable Sr perspective on seeps from a broad range of geological settings.

Referred to NIST-SRM-987, in this study the IAPSO seawater (SW) standard has a $\delta^{88/86}Sr$ of 0.39 ‰ (±0.03, 2SD). As a prominent systematic deviation the OT pore water (PW) data from a site with CO_2 hydrate and liquid CO_2 occurence show values ranging from 0.27 to 0.59 ‰ (286 to 64 cm sediment depth), accompanied by a weak inversely correlated trend from 0.2 to 0.15 ‰ for the corresponding bulk sediment (286 to 36 cm).

In contradiction to a simple fluid/SW-mixing approach as driving mechanism for the PW stable Sr trend the $^{87}Sr/^{86}Sr$ signature stays within analytical uncertainty constant with depth (0.70980 (1)) and differs significantly from SW (0.70917 (1)) and the more radiogenic, slightly heterogeneous sediment (0.71892-0.71731).

Potential explanation for the observed $\delta^{88/86}Sr$ trend and PW signatures heavier than SW are (a) strong fractionation processes enriching light isotopes in secondary precipitates and remineralisation products and heavier signatures in the remaining fluid and/or (b) preferential dissolution of heavier mineral phases.

Examples for the latter kind of sediment component are determined in a detailed study of the Mercator MV (GoC) by high $\delta^{88/86}Sr$ ratios of 0.72 for authigenic and 0.92 ‰ for potentially extruded gypsum crystals.

Combined with PW data from the other seep settings (0.2 to 0.52 ‰) a broad range of Sr contribution and fractionation processes becomes evident.

https://doi.org/10.1180/S0026461X00006502 Published online by Cambridge University Press

Precambrian P-T-t history of the Yenisey Ridge as a consequence of contrasting tectonic settings in the western margin of the Siberian craton

I.I. LIKHANOV* AND V.V. REVERDATTO

Sobolev Institute of Geology and Mineralogy, Novosibirsk, Russia (*correspondence: likh@uiggm.nsc.ru)

The Riphean evolution of the Yenisey Ridge was not marked by the prominent tectonic events except for the rift-related bimodal magmatism at ~1380 Ma. The closure of this basin was accompanied by the orogeny with deformation and metamorphism. The early stage is marked by the formation of low-pressure (LP) metamorphic complexes of the And-Sil type (T=400-650°C at P=3.3-5.2 kbar), indicating a normal metamorphic field gradient with dT/dH of about 25-35 °C/km. The relationship between this process and the Grenville-age orogeny was supported by the U-Pb and ^{40}Ar-^{39}Ar dating of metapelites from the Teya complex (~970 Ma). These LP/HT assemblages structurally overlie mid-crustal rocks of the Garevka complex that underwent medium-pressure (MP) metamorphism in the range from amphibolite- to granulite facies conditions of T=582-631ºC at P=7.72-8.64 kbar at depths of ca. 27-28 km.

Rocks closest to the thrusts underwent the MP metamorphism of the Ky-Sil type. A number of specific features and low metamorphic field gradient with dT/dH from 5-7 to 14°C/km are typical of collisional metamorphism during overthrusting of continental blocks, and are evidence of near-isothermal loading in accordance with the transient emplacement of thrust sheets and subsequent rapid exhumation. The proposed model suggests that, given an estimated exhumation rate of 0.368 mm/yr, the peak of collision-related metamorphic conditions occurred at 849-862 and 798-802 Ma.

The 849-862 Ma collisional evens are contemporaneous with the emplacement of low-alkali granite plutons responsible for the heating of rocks at a P=2.5-3.5 kbar, indicating a high gradient with dT/dH >100°C/km. Approximately at the same time (900-880 Ma) the mid-crustal amphibolite-facies rocks have experienced exhumation to a 14-16 km depth of upper-crustal structural levels. D_2-blastomylonites, which localized in narrow strike-slip fault zones, were re-equilibrated under LP conditions at 3.9-4.9 kbar associated with a low metamorphic field gradient with dT/dH ≤10°C/km.

The first occurrence of Siberian equivalents of the mid-Mesoproterozoic event, coupled with evidence of the Grenville-age orogenic events in the Yenisey Ridge, provide the basis for any paleoreconstructions showing a tight connection between Laurentia and Siberia in Rodinia configuration.

Developing models to assess fine scale energy change in soil organic matter under different forest managements

GARRETT C. LILES* AND WILLIAM R. HORWATH

Univ. of California, Davis – Dept of Land, Air and Water Resources (gcliles@ucdavis.edu, wrhorwath@ucdavis.edu)

The energy captured by primary productivity drives the biosphere but we do not view soil and SOM from an energetic perspective. SOM represents a complex thermochemical continuum from ordered energy rich macromolecules and assemblages through less ordered energy 'poor' aromatics and microbial byproducts. This complexity has been reduced conceptually and analytically into a 'black box' where biophysical parameters are summed into pools describing biological function and stability or turnover dynamics.

Simple conceptual models are useful for characterizing gross processes and rates such as ecosystem scale N cycling but fail to provide insight into long-term stability of C and energy dynamics. There is a dearth of information on the effect of simple or mixed litter inputs on SOM stability. Development of quantitative relationships between energy rich inputs and their transformation into a continuum of meta-stable SOM constituents is needed to support mechanistic understanding of ecosystem resilience related to disturbance, management and climate change. Differential Scanning Calorimetry- Thermogravimetry (DSC-TG) provides the flexibility, resolution and reproducibility to quantify distributions of thermochemical stability in soils and SOM across biophysical and management gradients to construct a mechanistic biophysical basis of SOM dynamics and stability.

We present results and models from long-term forestry experiments that manipulated N availability and litter inputs across varying soil mineralogy sequences. Our dataset (field replicated sample) supports robust DSC and TG models for statistical analyses on fine scale temperature subdivision bins (5-20°C). Thermal regions of significant energetic enrichment (associated with fertilization) or reduced litter diversity were detected. In both cases, the differences are apparent at the fine scale temperature subdivision but loose their clarity at coarse scales (150°C exothermic approach) or changes in soil C mass alone. In addition, we developed ratios and relationships between DSC-TG quantities and rates to detangle exotherm SOM signals from varying mineral constituents. These results illustrate the varying capacity of short-range order minerals to support the stability of new inputs or the release of existing SOM related to treatment. Our results illustrate the potential of numerical and modelling approaches to move from coarse aggregated metrics to process based relationships. This is a logical step towards developing a continuous and mechanistic understanding of the complex thermochemical nature of SOM.

https://doi.org/10.1180/S0026461X00006502 Published online by Cambridge University Press

Microbial controls on CH_4 cycling in water-saturated mineral soils

K.L.H. LIM[1], P.J. MAXFIELD[1], E.R.C. HORNIBROOK[2], R.D. PANCOST[1], R.P. EVERSHED[1]*

[1]Organic Geochemistry Unit, School of Chemistry, University of Bristol, Cantock's Close, Bristol BS8 1TS, UK (*correspondence: R.P.Eversheed@bristol.ac.uk)
[2]School of Earth Sciences, University of Bristol, Wills Memorial Building, Queen's Road, Bristol, BS8 1RJ, UK

Mineral soils are generally regarded as methane (CH_4) sinks however those which experience regular water saturation, although not always fully anoxic, may host significant methanogenic communities and even act as CH_4 sources [1]. It is evident that the balance between methanogenesis and methanotrophy in such soils, termed 'transitional soils', may be disrupted by marginal increases in water-content. Hence, internal CH_4 production may be underestimated, potentially causing a 'tipping-point' to occur which may increase the capacity of the soil to act as a net CH_4 source.

CH_4 cycling in soils susceptible to frequent seasonal water-logging was investigated using a combination of CH_4 flux measurements, ^{13}C-stable isotope probing and biomarker analyses [2]. In particular the use of archaeol as a potential proxy to assess methanogenic archaeal communities, determined using gas chromatography/mass spectrometry (GC/MS), was explored. The results indicate for the first time in UK mineral soils an increased population of methanogenic archaea at depth due to the anoxic conditions induced by increased water content. Significantly, >90% of the total archaeol was present in 'bound' glycolipid and phospholipid forms, indicating an origin from living archaeal biomass. We are now using these techniques to assess the true 'sink'/'source' capacity of mineral soils subjected to frequent water saturation.

[1] Teh *et al*. (2005) *Glob. Change Biol*. **11**, 1283–1297. [2] Maxfield *et al*. (2006) *Appl. Environ. Microb*. **72**, 3901–3907.

Multipurpose geochemistry project of CPRM in the Pernambuco State, Brazil – Current stage of work

E.A. M. LIMA*, M. FRANZEN, R. CAVALCANTE AND F.G. CUNHA

CPRM – Geological Survey of Brazil (*correspondence: enjolras.lima@cprm.gov.br, melissa.franzen@cprm.gov.br, rogerio.cavalcante@cprm.gov.br, fernanda.cunha@cprm.gov.br)

The work of environmental geochemical mapping and prospective low density are being developed in Pernambuco State, includes Fernando de Noronha Archipelago. We completed work to collect samples of soil, drainage and public water supply as well as stream sediment, with the aim of generating data that can configure the geochemistry of the physical landscape and explain the areas of chemical species impoverished or enriched relative to normal background values of global and regional. Aimed at diagnosing the quality of soils, sediments and water and identify metallogenetic areas looking targets that will be consequential studies involving greater detail.

Results

The phase of interpretation and evaluation of analytical data was started, having achieved the following results of colected samples: 1178 stream sediment samples, 212 soil samples, 338 samples of drinking water, 209 samples of drainage water. Through this regional geochemical mapping of low density at the drainage of the Pernambuco State, is being demonstrated knowledge of the distribution of trace elements. It is being made a database from the results of chemical analysis of collected samples and analytical information. Will also be provided some additional information such as the extent of the contamination plume in surface waters, and indications of anomalous concentrations of metals, indicative of possible mineral deposits.

Thus, the Project was set up not only by geochemical evidence, which could target prospective metallogenic investigations of greater accuracy, but mainly to be used as an efficient tool to diagnose the quality of the environment sampled, and their relationship to public health and the surrounding biota.

https://doi.org/10.1180/S0026461X00006502 Published online by Cambridge University Press

Environmental geochemistry and magnetic susceptibility in the estuarine clastics sediments of Jaboatao River, Pernambuco, Brazil

M.R.B.F. LIMA[1]*, E.A.M. LIMA[2], A.S. MORAES[1], M.T.T. CASTRO[3], V.H.M. NEUMANN[1], E.S. LIMA AND P.B. CORREIA[1]

[1]Universidade Federal de Pernambuco, Brazil (*correspondence: martamfg@yahoo.com.br)
[2]Geological Survey of Brazil (enjolras.lima@cprm.gov.br)
[3]Universidade de A Coruña, España (teresat@udc.es)

The Jaboatão river estuary is located in the southern coastal area of the Pernambuco state (Northeastern Brazil). A continuous sediment record measuring 50cm in length was collected 4 km from the river mouth. Sediments were sampled at 5cm intervals and the geochemical sub recent evolution registered from this estuary was investigated by chemical analysis and Magnetic Susceptibility.

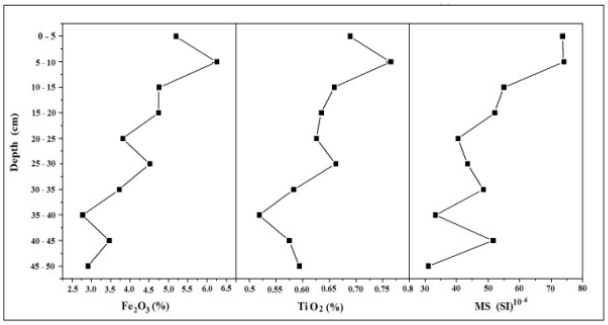

Figure 1: Evolution contents of Fe_2O_3, TiO_2 and MS in core profile.

Discussion of Results

Magnetic susceptibility measured in these samples showed relation to the Fe and Ti content and a sympathetic increase to the top of the core. Similar results have also been found in other parts of the world in industrialized areas [1].

The Enrichment Factor (EF), based in local and global reference values, showed the possible impacts in the considered ecosystem. Presented values below the USEPA´s (ERL, ERM) [2], except for As and Cr. Based on the EF found for the studied sediment core samples the estuarine sediment environment can be classified as below the geochemical contamination level.

[1] Lu *et al*. (2008) *Pedosphere* **18**, 479–485. [2] USEPA (1998) *USEPA*, EPA-**823**, 98-001.

Arsenic partition in the native and As-sorbed sediment

C. LIN, M.C. HE, Y.X. LI AND X.T. LIU

School of Environment, Beijing Normal University, Beijing 100875, China (c.lin@bnu.edu.cn)

Arsenic in the native and As-sorbed sediment samples was fractionized to understand how sorbed As partioned into various solid mineral phases with a selective dissolution method [1] (Fig. 1).

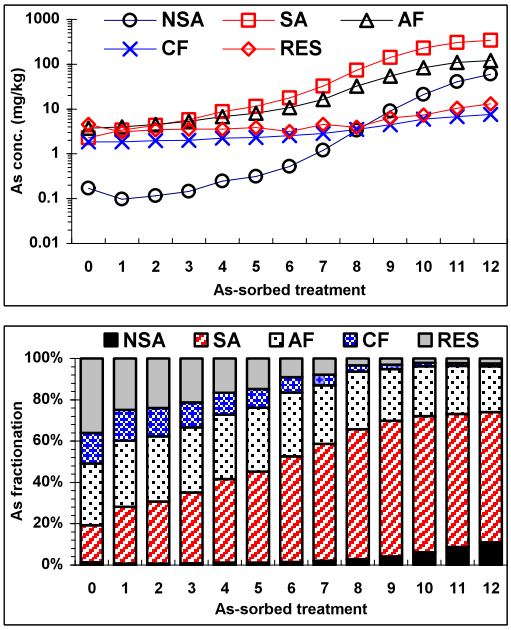

Figure 1: Contents and proportions of As in the native and As-sorbed sediment (0: native sediment, NSA: non-specific adsorption, SA: specific adsorption, AF: amorphos iron oxides, CF: crystalline iron oxides, RES: residual) .

Results showed As in the NSA, SA, AF greatly increased with gradual increasment of sorbed As, while As in CF and RES only slightly increased. On other hand, sorbed As was mostly bound to SA. Whereas Han and Banin observed that metal-added soils tend to return to the fractional quasi-equilibrium state of the non-amended soil [2], this process may take long time scale.

Supported by NNSFC (40971058, 40873077) and PCSIRT (No.IRT0809)

[1] Wenzel *et al*. (2001) *Anal Chim Acta* **436**, 309–323. [2] Han & Banin (1999) *Water Soil Water Poll* **114**, 221–250.

https://doi.org/10.1180/S0026461X00006502 Published online by Cambridge University Press

Microbial communities in shallow-sea hydrothermal environment of the Kueishantao Island, Taiwan

LI-HUNG LIN[1], WEN-YU TSAI[1], GUNG-HSIN LU[1], PEI-LING WANG[2], TING-WEN CHENG[1] AND ROY E. PRICE[3]

[1]Department of Geosciences, National Taiwan University
[2]Institute of Oceanography, National Taiwan University
[3]Earth and Planetary Sciences, Washington University in St. Louis

Shallow-sea hydrothermal systems provide easy access to investigating the extent of microbial communities residing in oceanic crustal environments, and the biotic and abiotic interactions along steep physiochemical gradients. This study analyzed venting fluids, pore fluids, surface biofilms and sediments collected from the yellow and white vent areas of the Kueishantao hydrothermal field offshore northeastern Taiwan. Molecular screening of 16S rRNA genes revealed that bacteria and archaea existed ubiquitously in nearly all samples (except for the absence of archaea in biofilms). Of all sequences detected, the bacterial members were affiliated with *Proteobacteria, Bacteroidetes, Cyanobacteria, Chloroflexi, Verrucomicrobia,* and *Firmicutes,* whereas the archaeal members were related to *Thermococci, Thermoplasmata*, and *Thermoprotei*. Communities in the yellow vent area were composed of all phyla and classes described above. In contrast, only ε-*Proteobacteria, Firmicutes, Thermococci,* and *Thermo-plasmata* were detected in the white vent area. The ε-*Proteobacteria* related sequences generally constituted a significant proportion of bacterial libraries, and were more abundant in the white vent area. Thirty strains were isolated from enrichments incubated at 40 ºC. Theses strains were phylogenetically affiliated with α- and γ-*Proteobacteria*, and grew autotrophically or organotrophically by using H_2/O_2, S^o/O_2, As^{3+}/O_2, or complex organic carbon for energy acquisition at acidic or neutral pH. Sequences related to these strains only constituted a small proportion of bacterial libraries in some samples. Overall, the prevalence of potential sulfur-respiring microorganisms, such as ε-*Proteobacteria* and *Thermococci* suggests elemental sulfur as an important energy source, and is consistent with the enriched content of elemental sulfur observed during sampling. The contrasting diversities in different areas and highly similar structures within individual areas further indicate that hydrothermal fluids might entrain variable fractions of seawater along different circulation pathways, enabling the proliferation of microbial communities sustained by distinct energy sources and geochemical characteristics.

'Biogenic natural gas' formation in a pressurized lab scale reactor

R.E.F. LINDEBOOM[1]*, J. WEIJMA[1], K. ZAGT[2] AND J.B. VAN LIER[3]

[1]Environmental Technology, Wageningen University, 6700 EV The Netherlands (*correspondence: ralph.lindeboom@wur.nl)
[2]Bareau Sustainable Technology BV, Heerenveen, The Netherlands (www.bareau.nl; kirsten.zagt@bareau.nl)
[3]Section Sanitary Engineering, Dep. of Water Management, CITG, Delft University of Technology, The Netherlands

It is known that methanogenic micro-organisms produce biogenic natural gas by degrading organic matter in natural gas fields. Methanogens also produce biogas in anaerobic digestion technology [1]. However, biogas generally consists of 55-65% CH_4, ~35% CO_2, and some H_2O, H_2S and NH_3. Our aim was to simulate biogenic natural gas formation in a lab scale pressurized reactor vessel, to see whether natural gas quality could be obtained in a single step reactor system. To do so, pressure reactors were used to simulate CH_4 and CO_2 production from organic matter by mixed culture methanogenic biomass under varying reactor conditions. Temperature, pressure and pH were monitored online with pressure resistant sensors. The lab-scale setup allowed sampling at short time intervals under varying environmental conditions. To determine microbiological organic intermediates, CH_4 and CO_2 production, HPLC and GC were used. Cryo-SEM EDX, FT-IR and TGA-MS were used to acquire information on carbonate precipitates.

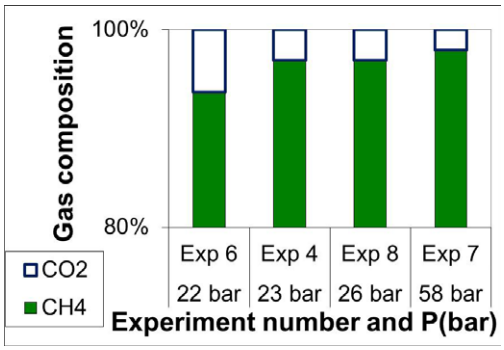

Figure 1: Overview of some experimental gas compositions

Discussion of results

The combination of analytical results highlighted the influence of microbe-mineral interactions on lab-scale biogenic natural gas formation. As a consequence, we found a way to biologically generate pressures up to 90 bar, with 80-97% CH_4-content within a week [2], only limited by the reactor safety limitations.

[1] Stams & Plugge (2009) *Nature Review Microbiology* **7**, 568–577. [2] Lindeboom *et al*. (accepted for publication) *Water Science & Technology*.

https://doi.org/10.1180/S0026461X00006502 Published online by Cambridge University Press

Phase transformation in simulated acid mine drainage precipitates

MALIN LINDEGREN* AND LARS LÖVGREN

Department of Chemistry, Umeå University, SE-901 87 Umeå, Sweden (*correspondence: malin.lindegren@chem.umu.se)

Metal ions released by oxidation of sulfide minerals in mine tailings may be immobilized from mine drainage by natural attenuation processes involving association to mineral phases. Secondary iron precipitates formed when the discharging drainage is exposed to the atmosphere have the potential to play a particularly important role in this context. However, the mineralogy of these precipitates changes over time, possibly affecting the attenuation.

The phase transformation of a mixture of schwertmannite and goethite, likely to be found in precipitates from acid mine drainage, was monitored over time. In order to investigate the possible influence of metal adsorbed to the mineral surfaces on this process, the precipitates were partially coated with copper or lead ions and compared to un-coated blanks run in parallel. As the formation of goethite from schwertmannite produces sulfuric acid, the amount of OH^- required to maintain suspension pH at 6 and the release of sulfate ions into solution can be used to quantify the phase transformation. To further verify the phase transformation over time, we used the relative intensities of the peaks originating from goethite and schwertmannite in FT-IR spectra of the dried solids. X-ray powder diffractograms of the solids were used to confirm the mineralogy of the original material and reacted samples.

No copper or lead could be detected in the aqueous phase of the samples, suggesting fully adsorbed metal ions. However, in terms of rate of phase transformation, no significant distinction could be made between the coated and un-coated samples, which suggests that the transformation of schwertmannite into goethite is unaffected by adsorbed metal ions.

Origin of hydrothermal fluids of uranium deposits hosted in granite: Constraints from redox conditions

HONG-FEI LING*

State Key Lab for Mineral Deposits Research, School of Earth Sciences and Engineering, Nanjing University, Nanjing 210093, China (*correspondence: hfling@nju.edu.cn)

Based on experimental data and theoretic calculation results from the literatures, this paper has summarized the valences and geochemical behaviors of uranium in melts and redox and other conditions of uranium being dissolved into fluids. Then the cause for the large difference in ages of uranium deposits and host granites, the source of uranium and the origin of hydrothermal fluids have been elucidated in this paper.

The oxygen fugacity of either mantle-derived melts or granitic magma is below that of the magnetite-hematite (MH) buffer, while the oxygen fugacity for uranyl ion (U (VI)) stable in fluids is much higher than MH. This implies that neither mantle-derived melts nor granitic magma could reach the oxygen fugacity for U (VI). Uranium in magmas occurs predominately as uranous ion (U (IV)) which enters crystals of uraninite and/or other accessory minerals in late stage of magma evolution and hardly enters magma-derived fluids unless under F-rich alkaline magma condition. This is why there is almost no uranium deposit formed by granitic magma-derived fluids. As uranium in fluids occurs as uranyl complexes, it is the key process for forming granite-hosted hydrothermal uranium deposits that high oxygen fugacity fluids ultimately originated from meteoric water leach uranium from uranium-rich granitic rocks. As for the granite-hosted uranium deposits in South China, Indosinian uranium -rich prealuminous leucogranites were the uranium source rocks, and late Yanshanian tectonic extension and dike magmatism provided the heat and the fissure system in granites for meteoric water infiltrating and cycling to leach uranium from the granites. Such fluids became uranium -rich hydrothermal fluids and finally formed the uranium deposits hosted in granties, South China.

https://doi.org/10.1180/S0026461X00006502 Published online by Cambridge University Press

Recognition of the Archean high-grade terrain in the South Qinglin orogen and its conection with the South China Block tectonics

W.L. LING[1,2], S.S. LU[1], Z.W. CHEN[1], X.M. LIU[2] AND R.C. DUAN[1]

[1]State Key Laboratory of Geological Processes and Mineral Resources, China Univ. of Geosciences, Wuhan 430074, China (wlling@cug.edu.cn, xiaomingliu@263.com)
[2]State Key Laboratory of Continental Dynamics, Department of Geology, Northwest University, Xi'an 710069, China

The South- and North China blocks were welded by the late Paleozoic to early Mesozoic Qinling-Dabie-Sulu orogen. However, timing of some isolated Precambrian terrains within the South Qinling unit and their correlation with the South China Block (SCB) are still poorly understood. The Yudongzi terrain in western South Qinling comprises crystalline basement gneisses and cover layers of banded iron formations (BIF). The basement rocks are dominated by trondhjemite with subordinate tonalite and granodiorite and show upper amphibolite- to granulite facies metamorphism. High precision zircon dating by the present work reveals that the gneisses were formed at 2650-2680Ma, whereas the BIF inherited zircons give an age cluster at 2.1-2.0 Ga with scattered Neoarchean grains, suggesting an early-mid Paleoproterozoic dominated provenance.

In the SCB, the Kongling area is the only terrain where the 2.9-2.7 Ga Archean high grade basement is well proved, whereas the unique early-mid Paleoproterozoic arc-related igneous suites (2150-2120 Ma), the Houhe intrusive rocks, occur at the northwestern SCB. Integrating with our documented works, we suggest that Yudongzi and Kongling terrains were two independent subordinate continents, which likely were welded during 2.0-1.9 Ga along the northwestern Yangtze margin, and were re-separated at ~755 Ma during the break-up of Rodinia.

This work was supported by the NSFC (Grant Nos. 40873017, 40673025).

Plant uptake of metals of economic importance: Laboratory studies

M.J. LINTERN[1]*, R.M. HOUGH[1], R.R. ANAND[1] AND C.G. RYAN[2]

[1]CSIRO Minerals Downunder Flagship, Kensington, WA 6152, Australia (*correspondence: lin082@csiro.au)
[2]CSIRO School of Geosciences, Monash University, Clayton, Vic. 3168, Australia

Biogeochemistry for mineral exploration has been undergoing a renaissance in recent years particularly in Australia. However, fundamental research into uptake of metals of economic importance by plants that are sampled for mineral exploration purposes has been lacking. Previous studies have taken place on crops of agricultural interest or for those pertaining to animal health or environmental monitoring. In this study we examine the uptake of several metals (Au, Cu, Ni, Pb and Zn) at variable concentrations in a series of trials using a sand-based, ebb and flow hydroponic system. Metal concentrations are analysed and the siting of these metals is investigated to understand if, how and where metals are located in biogeochemical sampling media..

Several trays containing several hundred plants were tested during each trial to quantify natural variability. Initially a large selection of Australian native plants were used but this was later reduced to two principal species, both of which are frequently used in mineral exploration, namely Mulga *Acacia aneura* (F.Muell. ex Benth.) and River Red Gum *Eucalyptus camuldulensis* (Dehnh.). In our experiments plant uptake of metal concentrations over three orders of magnitude were examined to test whether there were any barrier mechanisms to uptake at or near concentrations commonly observed in natural ecosystems. Competitive and enhanced interactions between metal uptake were also investigated to see whether certain metals were restricted or enhanced by the presence of others. The effect of pH and salinity variability was examined to emulate the range of natural groundwater conditions on which these plants grow. We used SEM, PIXE and SXRF to determine the location of metals in plant tissues (collected during sampling and from the hydroponic experiments) and establish if dust or anthropogenic contamination had occurred or whether the metals are truly absorbed in the plants. This is important when mineral exploration sampling is done in polluted mining environments.

We will discuss our results and show that they are encouraging for those using biogeochemistry for mineral exploration purposes as well as phytoremediation and phytomining.

https://doi.org/10.1180/S0026461X00006502 Published online by Cambridge University Press

Neon identifies two billion year old fluid component in Kaapvaal Craton

J. LIPPMANN-PIPKE[1]*, B. SHERWOOD LOLLAR[2], S. NIEDERMANN[3], N.A. STRONCIK[3], R. NAUMANN[3], E. VAN HEERDEN[4] AND T.C. ONSTOTT[5]

[1]Helmholtz-Zentrum Dresden-Rossendorf, Research Site Leipzig, Permoserstr. 15, 04318 Leipzig, Germany (*correspondence: j.lippmann-pipke@hzdr.de)
[2]University of Toronto, 22 Russell Street, Toronto, M5S 3B1, Canada (bslollar@chem.utoronto.ca)
[3]Helmholtz-Zentrum Potsdam – Deutsches GeoForschungsZentrum, Telegrafenberg, 14473 Potsdam, Germany (nied@gfz-potsdam.de)
[4]University of the Free State, P.O. Box 339, Bloemfontein 9300, South Africa (vheerde@ufs.ac.za)
[5]Princeton University, Guyot Hall, Princeton, NJ 08544, USA (tullis@princeton.edu)

We analysed shallow (to ~1 km) and deep fracture waters (to > 3 km) from the Witwatersrand Basin, South Africa for their noble gas isotopic composition. Their neon signature clearly differentiates a group of typical crustal fluids from another one with a significantly enriched nucleogenic neon signal with the highest $^{21}Ne/^{22}Ne$ ratios (0.160 ± 0.003) ever reported in groundwater [1]. Fluid inclusions in adjacent rocks yield even higher $^{21}Ne/^{22}Ne$ ratios between 0.219 and 0.515, consistent with an extrapolated $^{21}Ne/^{22}Ne$ value of 3.3 ± 0.2 at $^{20}Ne/^{22}Ne = 0$. We show that this enriched nucleogenic neon end-member represents a fluid component that was produced in the fluorine-depleted Archaean formations and trapped in fluid inclusions > 2 Ga ago [1]. The observation of enriched nucleogenic neon signatures in deep fracture water implies the release of this billion-year-old neon component from the fluid inclusions and its accumulation in exceptionally isolated fracture water systems. The observed association of this Archaean neon signature with H_2-hydrocarbon-rich geogases of proposed abiogenic origin [2] dissolved in the same deep groundwater suggests that the fracture systems have also allowed for the accumulation of various products of water-rock reactions throughout geologic times. One of these fracture systems contained a chemolithotrophic, single species ecosystem surviving on radiolytically produced H_2 and sulfate completely independent of the surface photosphere [3, 4].

[1] Lippmann-Pipke *et al*. (2011) *Chem. Geol*. **283**, 287–296. [2] Sherwood Lollar *et al*. (2002) *Nature* **416** (6880) 522-524. [3] Lin L.-H. *et al*. (2006) *Science* **314**(5798) 479–482. [4] Chivian D. *et al*. (2008) *Science* **322** (5899) 275–278.

An Atlantic Ocean $^{231}Pa/^{230}Th$ survey

JÖRG LIPPOLD[1], SYLVAIN PICHAT[2], YIMING LUO[3], JEANNE-MARIE GHERARDI[4] AND ROGER FRANCOIS[3]

[1]Heidelberg Academy of Sciences, Institute of Environmental Physics, University of Heidelberg, Germany
[2]Laboratoire de Géologie de Lyon, Ecole normale supérieure de Lyon et Université Claude Bernard Lyon, France
[3]Department of Earth and Ocean Sciences, University of British Columbia, Canada
[4]LSCE/IPSL Laboratoire CNRS/CEA/UVSQ, domaine du CNRS, 91198 Gif sur Yvette, France

The Atlantic Ocean circulation is an important contributor to Earth's meridional heat flux and much effort has been devoted to reconstructing its past variability. In particular, downcore records of the ratio of ^{231}Pa and ^{230}Th from marine sediments are increasingly used to infer past changes in the strength and structure of the Atlantic meridional overturning circulation (AMOC) [1, 2]. Modelling studies support the use of this tracer [3, 4], but they also indicate that an extensive database is required to apply the method to its full potential [5, 6]. A given strength and geometry of AMOC generates a unique distribution pattern of $^{231}Pa/^{230}Th$ in the water column and sediments. Documenting past changes in this pattern requires systematic sampling on bathymetric profiles at different latitudes to fully capture the vertical and horizontal gradients in sediment $^{231}Pa/^{230}Th$ generated by the AMOC. At any single location, the same $^{231}Pa/^{230}Th$ ratio can be generated by various combinations of AMOC strength and geometry and cannot be uniquely interpreted. Likewise, the pattern generated by an overturning circulation, particularly the vertical gradient, is quite distinct from that generated by changes in opal flux. Here we present a compilation of Atlantic Ocean $^{231}Pa/^{230}Th$ from the literature and new measurements for the Holocene and the Last Glacial Maximum (LGM). Comparing the data to the outputs of a 2D scavenging model [6] indicates that the Holocene $^{231}Pa/^{230}Th$ pattern is consistent with the strength and geometry of the modern AMOC, while the LGM $^{231}Pa/^{230}Th$ distribution pattern points to a different mode of AMOC with a stronger but shallower North Atlantic overturning cell, consistent with paleonutrient proxies [7].

[1] McManus *et al*. (2004) *Nature*, **428**, 834–837. [2] Gherardi *et al*. (2009) *Paleoceanography,* **24**, PA2204. [3] Marchal *et al*. (2000) *J. Phy. Oceanogr*. **38**, 2014–2037. [4] Siddall *et al*. (2007) *Paleoceanography,* **22** PA2214. [5] Luo *et al*. (2010) *Ocean Science*, **6**, 381–400. [6] Burke *et al*. (2011) *Paleoceanography,* **26**, PA1212. [7] Lynch-Stieglitz *et al*. (2007) *Science* **316**, 66.

https://doi.org/10.1180/S0026461X00006502 Published online by Cambridge University Press

Paleoredox changes of the Yangtze Sea during the Ordovician-Silurian transition and its deposition of black shales, south China

ZHANG LIQIN

Key Laboratory of Geospace Environment and Geodesy of Ministry of Education, Wuhan University, Wuhan 430079, China (lqzhang@sgg.whu.edu.cn)

The redox chemistry of Paleozoic oceans has important implications for understanding the processes of deposition and organic matter preservation of black shale, but empirical constraints on competing environmental models are scarce [1, 2]. To investigate the redox condition changes in the Ordovician-Silurian transition series of the Yangtze Sea, we examine the organic carbon content (TOC), pyrite sulphur content, pyrite sulphur isotope, and Fe species–including dithionite-extractable Fe (FeD), pyrite Fe (FeP), HCL-extractable Fe (FeH), and total Fe (FeT)–in black shale. Fe-TOC-S relationship and several ratios, that C/S ratio, the ratio between highly reactive Fe (FeHR=FeD+FeP) and FeT, and the ratio FeP/(Fep+FeH), known as the degree of pyritization (DOP), are used to evaluate the redox state of Yangtze Sea and the processes that led to the accumulation of organic matter-rich black shale deposits. These redox indices through three intervals, the mid Ashgill, Hirnantian, and early Rhuddanian, indicate that the anoxic–sulfidic marine water occupy most of the Yangtze Sea during the mid Ashgill and early Rhuddanian, while the Hirnantian possesses oxic marine water [3, 4]. Sulfate reduction occurs in euxinic water column and results in characteristic C/S ratio, FeHR/ FeT ratio, DOP, and Fe–TOC–S relationships. Elevated productivity, anoxia and high sedimentation rates support the formation of black shale deposits. For Hirnantian interval, organic matter sedimentation takes place through an oxygenated water column. We suggest that the Hirnantian oxic marine water is the integrative result of glacioeustatic sea-level fall and the influx of cold and oxygen-laden Boreal waters, however, the abrupt transition from oxic to anoxic marine water occurs in the early Rhuddanian resulting from the post-glacial rise in sea level and corresponding increase in surface-water nutrient availability [5].

[1] Calvert *et al*. (1992) *Geology* **20**, 757–760. [2] Pedersen & Calvert (l990) *Bul1. Am. Assoc. Petrol. Geol.* **74**, 454–466. [3] Yan *et al*. (2010) *Geology* **37**, 599–603. [4] Zhang *et al*. (2000) *Global & Planetary Change*. **24**, 133–152. [5] Yan *et al*. (2009) *Palaeogeogr. Palaeoclimat. Palaeoecol*. **274**, 32–39.

Pervasive reactive melt migration though the lower oceanic crust: Implications for the evolution of mid-ocean ridge basalt

C. JOHAN LISSENBERG[1]*, CHRISTOPHER J MACLEOD[1], KERRY A HOWARD[1] AND MARGUERITE GODARD[2]

[1]School of Earth and Ocean Sciences, Cardiff University, Park Place, Cardiff CF10 3AT, United Kingdom (*correspondence: lissenbergcj@cardiff.ac.uk)

[2]Géosciences Montpellier, UMR CNRS-UM2 5243, Universite Montpellier 2 - cc60 Place Eugène Bataillon, 34095 Montpellier cedex 5, France

Mid-ocean ridge basalt (MORB) is the most abundant magma on Earth. It is generated beneath mid-ocean ridges by decompression melting of upwelling mantle, and, following processing in lower crustal magma chambers, erupted onto the seafloor. For more then four decades igneous petrologists and geochemists have relied upon MORB as their major window into the mantle, deriving its composition, melting processes and melt migration mechanisms from the erupted lavas. However, this approach assumes that modification of melts in crustal magma chambers occurs exclusively by fractional crystallisation, and can thus be easily corrected for.

Data from an extensive suite of lower crustal rocks from Hess Deep (equatorial Pacific Ocean) demonstrate that melts do not simply evolve by fractional crystallisation. The gabbros crystallised from melts that underwent extensive reactive porous flow, which modified both their major- and trace element composition. The degree to which this reactive signature is present increases up section throughout the lower crust, suggesting that it occurs on a crustal scale. Thus, magma in the lower oceanic crust evolves by a combination of fractional crystallisation and melt-rock reaction. If a reactive signature is present in MORB, this requires a reassessment of its use as a messenger from the mantle.

https://doi.org/10.1180/S0026461X00006502 Published online by Cambridge University Press

High degradation efficiency of deicing chemicals affects the natural redox system in airfield soils

H. LISSNER*, M. WEHRER AND K.U. TOTSCHE

University of Jena, Institute of Geosciences, Burgweg 11, 07749 Jena (*correspondence: heidi.lissner@uni-jena.de)

Large amounts of the deicing chemicals (DIC) propylene glycol (PG) and formate are spread for removal of snow and ice on the aircrafts and airfields every winter. A considerable amount of these chemicals are carried into surrounding areas, where they mix with snow and infiltrate in the soil during snowmelt. Even though DIC are easily degradable, the high mobility and the high biological oxygen demand of PG in particular can influence the hydrogeochemistry of the unsaturated and saturated zone. The aims of the study were to evaluate and quantify transport of deicing chemicals during snowmelt under field conditions, and to study effects of DIC degradation on the hydrogeochemistry of the unsaturated zone. Eight undisturbed soil cores (0.3 m x 1 m, 0.071 m^3) were retrieved at the Gardermoen Airport, Norway, and installed as non-weighable small scale lysimeters at a nearby field site. Before snowmelt in March 2010, a mix of snow containing 350 g/m^2 PG, 71 g/m^2 formate, and 17 g/m^2 of bromide were added to the lysimeters. To determine the fate and transport of PG we monitored PG and its metabolites, bromide, manganese, and iron in the seepage water.

High cumulative infiltration and marginal degradation of PG during the snowmelt period allowed up to 50 % of the PG to leave the upper, microbially most active, region of the soil. Only marginal concentrations of formate were analysed in all lysimeters, indicating fast degradation and favoured metabolism by soil bacteria compared to PG. Low contents of metabolites and the concurrent breakthrough of PG and Br in the seepage water even imply that PG was not significantly degraded before June. Redox values down to 200 mV in April, the detection of propionate and manganese, as well as a rise in pH, suggest partially anearobic localities in the soil, not only during high soil water saturation in April and May but also during summer when PG degradation was very efficient. In the longterm, the intense depletion of secondary electron acceptors such as Mn (hydr)oxides lowers the potential of the unsaturated zone to buffer high loads of DIC. Therefore, it is necessary to carefully assess the buffering capacity of the soil and to develop suitable remediation techniques to sustain the natural redox buffer system.

Melting in the peridotite and eclogite, coexisting with reduced C-O-H fluid at 3-16 GPa

K.D. LITASOV[1,2]*, A. SHATSKIY[1,2] AND E. OHTANI[1]

[1]Tohoku University, Sendai, 9808578, Japan (*correspondence: klitasov@m.tohoku.ac.jp)

[2]Institute of Geology and Mineralogy SB RAS, Novosibirsk, 630090, Russia

Melting phase relations of peridotite and eclogite systems coexisting with reduced C-O-H fluid has been studied at 3-16 GPa and 1200-1600ºC. In order to perform these experiments the double-capsule technique with fO_2 control by outer Mo- or Fe-buffer capsule was designed and developed for multianvil experiments at pressures above 3 GPa. The inner capsule contained silicate starting material with an addition of 8-10 wt% stearic acid, which served as a fluid source, whereas outer capsule contained talc, which served as a hydrogen transmitting medium to maximize fH_2 in the inner capsule.

Silicate phase assemblages resemble those in volatile-free lithologies. Melting was detected by appearance of quenched crystals of pyroxene, feldspar and glassy silica. Abundant voids indicate presence of fluid in all runs. The fluid composition was not measured, but should correspond to CH_4-H_2O-bearing one, according to estimations from equations of state. The compositions of partial melt were estimated from mass-balances. The partial melt from peridotite runs has CaO-poor (6-9 wt%) basaltic composition with 44-47 wt% SiO_2 and 1.1-1.6 wt% Na_2O (recalculated to 100% of dry residue). Eclogitic melts contain more SiO_2 (47-49 wt%) and are enriched in CaO (9-15 wt%), Na_2O (9-14 wt%), and K_2O (1.3-2.2 wt%). All runs contained graphite or diamond crystals along with porous carbon aggregate with microinclusions of silicate phases.

The solidi have relatively steep slope in the pressure range between 3 and 16 GPa. Estimated solidus temperatures for peridotite+C-O-H-fluid with fO_2 control by Fe-FeO buffer are 1200ºC at 3 GPa and 1700ºC at 16 GPa. The solidus of the system with fO_2 control by Mo-MoO_2 buffer was about 100ºC lower. Solidi in the eclogite systems are located at another 100ºC lower than peridotitic ones for both buffers. The obtained solidi are much higher (300-500ºC) then those for peridotite/eclogite systems with H_2O and CO_2. However, they are still about 300ºC lower than solidi of volatile-free peridotite and eclogite at 12-16 GPa. Thus, we provide new direct evidences for redox melting by change of oxidation state across a mantle section.

https://doi.org/10.1180/S0026461X00006502 Published online by Cambridge University Press

Abiotic and biotic control of the $\delta^{65}Cu$ and $\delta^{66}Zn$ composition of seawater

S.H. LITTLE*, D. VANCE AND D.M. SHERMAN

Bristol Isotope Group, School of Earth Sciences, University of Bristol, Bristol BS8 1RJ UK
(*correspondence: s.little@bristol.ac.uk)

Dissolved copper in seawater is isotopically heavy (1.1‰) relative to both rocks (0‰) and the riverine input (0.7‰). Particulate Cu in the oceans is adsorbed to ferromanganese crusts and is isotopically lighter than seawater, at 0.1-0.4‰. EXAFS and μ-XRF indicate that Cu in the crusts is predominantly associated with the Mn-oxide, δ-MnO_2. Consistent with these observations, the experimental $\Delta^{65}Cu_{solid\text{-}soln}$ on inorganic sorption of Cu to δ-MnO_2 is -0.5‰. Thus, abiotic fractionation of Cu in large part explains the heavy isotopic composition of seawater.

The additional control can be sought in the dissolved Cu fraction, the speciation of which is dominated by complexation to siderophore-like ligands, likely exuded by phytoplankton. We have cultured cyanobacteria, and show that there is indeed a small positive $\Delta^{65}Cu_{ligand\text{-}soln}$ associated with this complexation. Similarly, Cu sorbs to deprotonated surfaces of dissolved organic matter with an isotopic fractionation of +0.27‰ [1], and several species of bacteria preferentially take up ^{63}Cu [2]. All of the above provide mechanisms to enrich the dissolved fraction in heavy ^{65}Cu.

$\delta^{65}Cu$ in the oceans is hence a balance of both inorganic and organic complexation, and our observations contribute to an internally consistent picture. This is not yet the case for zinc, however. Lab experiments [3] and our synchrotron-based study indicate that Zn behaves similarly to Cu in terms of its crystal chemistry and abiotic fractionation. Unlike Cu, however, Zn in ferromanganese crusts is isotopically heavier than the $\delta^{66}Zn$ of seawater. Further work is required to understand this discrepancy.

[1] Bigalke *et al*. (2010) *Env. Sci. Tech* **44**, 5496–5502 [2] Navarrete *et al*. (2011) *GCA* **75**, 784–799 [3] Pokrovsky *et al*. (2005) *J. Colloid Interf. Sci*. **291**, 192–200.

Origin and evolution of carbonatite magma parental for diamond and syngenetic inclusions

YU.A. LITVIN

Institute of Experimental Mineralogy, Russian Acad. Sci., Chernogolovka, Moscow Dstr. 142432, Russia
(litvin@iem.ac.ru)

Introductory remarks

Mantle-carbonatite model of diamond genesis [1], genetic classification of primary inclusions in mantle-derived diamond [2] and generalized composition diagram for multi-component heterogeneous parental medium for diamond and syngenetic inclusions [3] are the key findings based on integration of mineralogical and experimental data.

Origin of diamond-parent carbonatite magma

In the making stationary chamber of diamond-parent carbonatite magma, two episodes are of a significant part: (1) Mg-Ca-carbonatite primary melts can result from mantle peridotite in response to chemical attack of high-temperature "metasomatic agents" rich in CO_2, K-Na-alkaline carbonates and silicates, minor incompatible and REE elements;

(2) primary carbonatite melts dissolve peridotite minerals, solid and dispersed carbon, minor soluble phases and involve xenogenetic ones. Diamond-forming activity of mantle carbonatite chamber begins when diamond solubility concentration in the magma is attained. During cooling, carbon oversaturation in respect to diamond is reached producing nucleation and growth of diamond.

Evolution of diamond-parent carbonatite magma

In compositional evolution of the fractionated parental magma during cooling, two physicochemical mechanisms which control magmatic ultrabasic-to-basic and peridotite-to-eclogite paragenetic transitions have a dominant role: (1) carbonatization of olivine and orthopyroxene; (2) garnetization of olivine due to reaction between olivine and jadeite components [4]. The both reaction mechanisms control continuous transition from formation of peridotite mineral paragenesis to the eclogite one in diamond-parent carbonatite magma.

Syngenesis diagrams for diamond, paragenetic and xenogenetic inclusions

Syngenesis melting relations of the eclogite-carbonatite-sulfide-diamond system are studied at 7 GPa. Syngenesis diagrams offer a clearer view of how diamond and paragenetic phases have formed. These reveal physicochemical mechanism of origin of natural diamond, PT-conditions of formation of paragenetic silicate and carbonate minerals and their coexistence with xenogenetic minerals and melts. Thus physicochemical conditions of primary caption of paragenetic and xenogenetic phases by growing diamond are revealed. Support: RFBR 1105/00401.

[1] Litvin (2007) *Geol Soc Amer Spec Pap* **421**, 83-103 [2] Litvin (2009) *Rus Geol Geoph* **50**, 1188-1200 [3] Litvin (2010) *Proceed XI Rus Min Soc General Meeting*, 77-78 [4] Gasparik, Litvin (1997) *Eur J Mineral* **9**, 311-326.

https://doi.org/10.1180/S0026461X00006502 Published online by Cambridge University Press

Cr^{6+} reduction by sulfate-reducing bacteria in salt marsh sediments

C.H. LIU*, C. TANG, S.P. YAO AND Y.R. XUE

Nanjing University, 22 Hankou Road, Nanjing 210093 (*correspondence: chliu@nju.edu.cn)

Chromium is one of the most toxic and carcinogenic heavy metals. Cr^{2+} and Cr^{3+} species are the most stable and least toxic species, while Cr^{6+} is highly toxic to eukaryote and prokaryote. Recently, many bacteria have been proved to be an efficient Cr^{6+} removal in the chromium-contaminated sediment. In this study, 34 culturable sulfate-reducing bacteria (SRB) isolated from salt marsh along Yellow Sea of China were evaluated for their potential in Cr^{6+} removal. All procedures regarding bacterial manipulations were performed under aerobic condition with addition of 5mM of ethanol as carbon source and 100mg/L of Cr^{6+} in the medium (pH 7.3). Cells were grown in an shaker at 37 °C, 110 rpm for 6d. Cr^{6+} was quantified by the colorimetric diphenylcarbazide method at 540 nm, while the cell growth was measured at 600nm. Ten of the test SRB showed tolerant to high concentration of Cr^{6+} and 6 were able to reduce Cr^{6+} to Cr^{3+}, which were identified to be *Pseudomonas* sp.(3 isolates), *Bacillus sphaericus*, *Rhiodococcus erythropolis* and *Oceanimonas* sp.. The highest reduction of Cr^{6+} (82.6%) was by *Oceanimonas* sp., while 66.4%-79.7% were reduced by the others. However, the highest reduction rate per cell was by one of the *Pseudomonas* species. Except for *Pseudomonas* and *R. erythropolis* that were confirmed to be able to reduce Cr^{6+} to Cr^{3+}, *Bacillus sphaericus* and *Oceanimonas* were demonstrated at the first time to have a potential ecological role in soil or water bioremediation due to their tolerance or reduction of Cr^{6+} the removal of Cr^{6+}.

[1] Lee S.E. Lee J.U. Lee J.S. & Chon H.T. (2006) *Geophysical Research Abstracts* **8**, 03237. [2] Badar U. Ahmed N. Beswick A.J. Pattanapipitpaisa P. & Macaskie L.E. (2000) *Biotechnol. Lett.* **22**, 829–836.

Geothermal gradient and heat flow distributions of Northeastern Taiwan and its implication

CHIA-MEI LIU[1]*, SHENG-RONG SONG[1], FU-SHU JENG[2], EN-CHAO YEH[3], TAI-TIEN WANG[4] AND YI-CHIA LU[1]

[1]Institute of Geosciences, National Taiwan University, Taiwan (*correspondence: pollynismo@gmail.com, srsong@ntu.edu.tw, yichialu@ntu.edu.tw)

[2]Depart/ment of Civil Engineer, National Taiwan University, Taiwan (fsjeng@ntu.edu.tw)

[3]Department of Earth Sciences, National Taiwan Normal University, Taiwan (ecyeh@ntnu.edu.tw)

[4]Institute of Mineral Resources Engineering, National Taipei University of Technology, Taiwan (ttwang@ntut.edu.tw)

The continental heat flow map shows the characteristics of regional thermal structures and displays the phenomena of geology and geophysics. Taiwan Island is located in the boundary of Philippine Sea plate obliquely colliding with the Eurasia plate to form an orogenic belt. Meantime, the Philippine Sea plate also subducts northwardly under the Eurasian plate to produce the Ryukyu Trench-Okinawa Trough system in northern Taiwan. Based on the collision maturity in terms of geological and geophysical data, the tectonic of northeastern Taiwan belongs to the arc collapse/subduction zone. In this study, we apply the hydro-geochemical data to gain geothermal gradient and heat flow distributions of northeastern Taiwan, and discuss the possible mechanism inducing the thermal anomaly in this region.

The thermal profile across northeastern Taiwan indicates that the peak with a silica heat flow value about 150 mW/m^2 is located at the Chingshui area, and decreases northeastwardly to Ilan Plain and southwestwardly to Lushan area. According to the results of geodetic monitoring and micro-earthquakes, it has shown the extending southwestwardly from the southwest of the Okinawa Trough into the Ilan Plain, which induced widely the normal faulting and magmatic intrusion. Thus, the origin of the abnormally high silica heat flow in the Chingshui area is likely due to the southwestward propagation of hot fluids from the Okinawa Trough into the Ilan Plain.

https://doi.org/10.1180/S0026461X00006502 Published online by Cambridge University Press

Pore-scale process coupling and its effect on the apparent rates of uranyl surface complexation

CHONGXUAN LIU[1]*, SEBASTIEN KERISIT[1], ROBERT EWING[2], JIANYING SHANG[1] AND JOHN ZACHARA[1]

[1]Pacific Northwest National Laboratory, Richland, WA 99354 (*correspondence: Chongxuan.liu@pnl.gov)
[2]Iowa State University, Ames, IA 50011 (ewing@iastate.edu)

Surface complexation is a major process that affects uranyl [U (VI)] fate and reactive transport in subsurface sediments. Surface complexation reactions occur at the pore-scale in coupling with other processes including aqueous speciation reactions, diffusion, and advection. Extensive characterization of U (VI)-contaminated sediments collected from US DOE Hanford site has revealed that U (VI) preferentially associates with certain types of porous domains including intragranular fractures, grain-coating regions, and grain-aggregates. This presentation discusses the nature and complexity of process coupling at the scales of single pore, intragranular domain, and pore-network in flow media that fundamentally control the apparent rates of U (VI) surface complexation reactions and reactive transport in subsurface porous media. Experiments and modeling studies at various scales revealed that the molecular rate of U (VI) surface complexation reactions in a single pore domain was fast with a first-order rate constant of 10^2 - 10^4 s^{-1}. The apparent rate of U (VI) surface complexation, however, decreased to 10^{-3} s^{-1} at the grain scale as a result of coupling of intragranular diffusion and reactions, and further decreased to 10^{-5} - 10^{-6} s^{-1} in flow domains where complex pore-scale coupling of flow, diffusion and reactions occurred in both inter-granular and intragranular domains in field-textured sediments. The scale-dependent reaction rates present a significant challenge to apply laboratory-determined reactions and parameters to predict field-scale reactive transport, and indicate that conceptual and numerical upscaling approaches to scale reaction rates are critically needed. This presentation will also discuss pore-network-based upscaling concepts and theories to scale reactions from the intragranular pore-network to the grain-scale, and from the grain-scale to the flow media. These upscaling approaches explicitly considered pore size and connectivity variability in porous media that affect pore-scale flow and diffusion, and their coupling with intrinsic reactions.

Fragments of hot and metasomatized mantle lithosphere sampled by mid-Miocene ultrapotassic lavas, Southern Tibet

CHUAN-ZHOU LIU[1], FU-YUAN WU[1], SUN-LIN CHUNG[2] AND ZHI-DAN ZHAO[3]

[1]Institute of Geology and Geophysics, Chinese Academy of Sciences, Beijing, 100029
[2]Department of Geosciences National Taiwan University, Taipei, 10699
[3]China University of Geosciences, Beijing, 100083

The first suite of mantle peridotite xenoliths have been discovered in mid-Miocene (~ 17 Ma) ultrapotassic lavas from Salipu, southern Tibet [1]. The Sailipu mantle xenoliths are very tiny with diameters of less than 1 cm, and characterized by presence of abundant phlogopite. Olivines of Salipu xenoliths have Fo [100×Mg/ (Mg+Fe)] content of 83~89, lower than typical upper mantle olivines. Both orthopyroxene and clinopyroxene in Salipu xenoliths also became iron-rich with Mg# [Mg/(Mg+Fe)] values of 0.83~0.91 and 0.84~0.89, respectively. Equilibrium temperatures of 1050~1250 ºC have been obtained for the Salipu mantle xenoliths by two-pyroxene geothermometer gives. Spinels reacted with phlogopites became Al-rich with a Cr# [Al/(Cr+Al)] of 0.1~0.2, whereas spinels that are not surrounded by phlogopites have higher Cr# values (0.32 vs. 0.36, respectively). Phlogopites in Salipu xenoliths with Mg# values of 0.82~0.94 are F-rich (2.64~8.1 %), Ti-rich (0.92~4.48 %) and contain variable contents of H_2O (0.5-5 %). Clinopyroxenes in Salipu xenoliths display convex upward rare earth element (REE) patterns, with enrichment of light rare earth elements (LREE) over heavy rare earth elements (HREE). They also mimic some trace element characteristics shown by ultrapotassic lavas in southern Tibet, especially the negative Sr, Nb, Ta, Zr, Hf and Ti anomalies. These features suggest that the metasomatic melts should be subduction-related rather than asthenosphere-derived.

Results of the Sailipu mantle xenoliths indicate the existence of hot, highly metasomatized lithospheric mantle beneath southern Tibet during the mid-Miocene, and thus support the idea that convective thinning of the lithosphere was responsible for the uplift of the plateau. The relict mantle was later removed or squeezed northward by the underthrusting Indian continental lithosphere, which terminated magmatism in southern Tibet and played a role in creating the entire plateau.

[1] Zhao, ZD. *et al*. (2008) *Acta Petrologica Sinica* **24**, 193–202.

https://doi.org/10.1180/S0026461X00006502 Published online by Cambridge University Press

Erosion rate estimated from surface and profile of cosmogenic ^{36}Cl in carbonates in China

C.Q. LIU[1], S. XU[2]*, S.P.H.T. FREEMAN[2], Y.C. LANG[1], R. PHILLIPS[3], C.L. TU[1] AND K. WILCKEN[2]

[1]Institute of Geochemistry, Chinese Academy of Sciences, Guiyang, Guizhou 550002, China
[2]Scottish Universities Environmental Research Centre, East Kilbride, G75 0QF, UK
(*correspondence: s.xu@suerc.gla.ac.uk)
[3]University of Leeds, Leeds, LS2 9LT, UK

This study attempted to quantify long-term subaerial erosion of bare carbonate rock surfaces by using in situ-produced cosmogenic ^{36}Cl in carbonates. Carbonate samples were collected from the topmost 5 cm of exposed pinnacles at several non-glaciated karst or carbonate areas in modern monsoon (Guizhou), arid (Gansu) and transition (Beijing) regions in China. Samples from a 30m-depth profile were also collected in Guizhou karst area. Concentrations of natural Cl and ^{36}Cl in carbonates were determined by accelerator mass spectrometry with isotope dilution with ^{35}Cl-enriched carrier spike. Local ^{36}Cl production rates are calculated on the basis of geomorphological locations and chemical compositions of carbonates. The total Cl concentrations in carbonates were in range of 10-200 ppm. The ^{36}Cl nuclide concentrations were of the order of 10^5–10^7 atom g^{-1}, and converted to total erosion rates averaged over a 10^5 yr-timescale of chemical and physical processes acting on the karst surfaces. The erosion rates were 20–50 mm kyr^{-1} in Guizhou. Variations and mechanisms of the local erosion rates are discussed and the results are compared with the existing observations obtained by other measurement techniques.

U-Pb dating, and Lu-Hf property of zircon from granitic leucosome within orthogneiss from Sulu UHP terrane, Eastern China

F.L. LIU[1]* AND A. GERDES[2]

[1]Institute of Geology, Chinese Academy of Geological Sciences, Beijing, 100037, China
[2]Institute of Geosciences, Mineralogy, J.W. Goethe University, Frankfurt, 60054, Germany

Granitic leucosomes as thin veins are widely distributed within orthogneiss in the Sulu UHP terrane, eastern China. A combined study of mineral inclusions, cathodoluminescence (CL) images, U-Pb SHRIMP dates, and *in situ* trace element and Lu-Hf isotope analyses of zircons provided insight into the nature and timing of partial melting in these rocks. Zircons from orthogneisses have three distinct domains: (1) inherited magmatic cores with Coe + Phe + Ap inclusions, which record a Neoproterozoic protolith age of 790-750 Ma, (2) mantles with Coe + Phe + Ap inclusions that record Triassic UHP age of 230-225 Ma, and (3) rims with Qtz inclusions that record retrograde metamorphism at 215-210 Ma. In contrast, zircons from granitic leucosomes have only two distinct domains: (1) the central UHP domains with Coe + Phe + Ap iclusions record Triassic UHP age of 230-225 Ma, and outmost rims with Qtz + Kfs + Ab + Ap inclusions record partial melting time of 214-210 Ma. Theses data indicate that partial melting in the Sulu UHP orthogneisses took place during late retrograde amphibolite-facies metamorphism. Inherited magmatic zircon cores from orthogneisses give uniform $^{176}Hf/^{177}Hf$ of 0.28187 ± 0.00003 corresponding to εHf (t) and Hf model ages of about -16.3 and 2.41 Ga, respectively. This is consistent with the generation of its protolith by reworking of Paleoproterozoic to late Archean crust. In contrast, UHP zircon domains from orthogneisses and granitic leucosomes are characterized by low Lu/Hf (<0.006), low Th/U (<0.1) and significantly higher $^{176}Hf/^{177}Hf$ (0.28233 ± 0.00002) than the inherited magmatic cores. The uniform but significantly different Hf isotope composition between the UHP and inherited zircon domains indicates equilibrium of the Lu-Hf isotope system only within the UHP metamorphic mineral assemblage. Zircon domains crystallized during partial melting at 214-210 Ma in granitic leucosomes have a Hf isotope composition indistinguishable from that of the UHP zircon domains. This suggests that only Hf (and Zr) equilibrated during UHP metamorphism was remobiliazed during partial melting while inherited magmatic zircons remained stable or was not accessible.

https://doi.org/10.1180/S0026461X00006502 Published online by Cambridge University Press

High pressure diffraction tomography technique for mineral physics reseraches

HAOZHE LIU, LUHONG WANG, ZHENHAI YU, LINGPING KONG, JINGGENG ZHAO, DAWEI DONG AND CHUNYU LI

Natural Science Research Center, Harbin Institute of Technology, Harbin 150080, China

The high-pressure behaviors for Olivine and selenium will be presented using synchrotron x-ray diffraction and micro-tomography techniques. The novel development for the combination of synchrotron x-ray microtomography and diffraction techniques in diamond anvil cell high-pressure conditions, which provides new insight for many mineral physics research, will be introduced. The phase transition procedure of iron was studied, and the 3-D distribution of low pressure and high-pressure phases at about 11 GPa was obtain. The deviatoric stress between the parent and new phases in the iron sample, as well as the phase transition mechanism will be discussed based on the 3 dimensional data. The potential application for the diffraction tomography development in diamond anvil cell to the mineral materials will be emphasized.

Comparative Sr-Nd-Pb-Hf-Os isotopic systematics of xenolithic peridotites from Yangyuan, North China Craton

JINGAO LIU[1]*, RICHARD W. CARLSON[2], ROBERTA L. RUDNICK[1], RICHARD J. WALKER[1], FU-YUAN WU[3] AND SHAN GAO[4]

[1]Department of Geology, University of Maryland, College Park, MD20742 USA (*correspondence: gobyliu@umd.edu)
[2]DTM, Carnegie Institution, Washington, DC 20015 USA
[3]IGG/CAS, P.O. Box 9825, Beijing 100029 China
[4]China University of Geosciences, Wuhan 430074 China

Trace element concentrations and Sr, Nd, Pb and Hf isotopic compositions were determined for clinopyroxenes separated from 11 well-characterized spinel peridotites, carried in the ~30 Ma Yangyuan alkali basalts from the central region of the North China Craton. Our objective was to use these isotope tracers to determine the history of initial melt depletion and later metasomatic enrichment of incompatible trace elements in the mantle. Clinopyroxenes were selected from samples for which whole-rock Re-Os isotopic compositions were previously determined, and to span a wide range of rare earth element (REE) patterns (chondrite-normalized $(La/Yb)_N$ = 0.13 to 13.5). Present-day isotopic ratios are $^{87}Sr/^{86}Sr$ = 0.70229-0.70443, ε_{Nd} = -0.6 to +24, $^{206}Pb/^{204}Pb$ = 15.74-19.08, and ε_{Hf} = +13.5 to +167). Some peridotites retain original ancient melt depletion signatures characterized by prominent depletions of light REE (LREE) relative to heavy REE and highly radiogenic Nd (ε_{Nd} up to +24) and Hf (ε_{Hf} up to +167) isotopic compositions, and very non-radiogenic Pb isotopic compositions ($^{206}Pb/^{204}Pb$ as low as 15.74). Ancient metasomatism may have occurred in a few samples, given their elevated LREE, Paleoproterozoic Nd model ages and non-radiogenic Pb isotopic compositions that, on a $^{206}Pb/^{204}Pb$ vs. $^{207}Pb/^{204}Pb$ diagram, plot just to the right of the 1.8 Ga geochron. The remaining samples with LREE-enriched patterns were likely affected by incompatible element re-enrichment more recently, as evidenced by a limited range of $^{143}Nd/^{144}Nd$ (0.5128 to 0.5132), but a large range of $^{147}Sm/^{144}Nd$ (0.13 to 0.28), as well as Pb isotopic compositions that plot along a mixing line between the host basalt and the least radiogenic samples in a plot of $^{206}Pb/^{204}Pb$ vs. 1/Pb. In spite of these re-enrichment events, both the clinopyroxene Lu-Hf isotope and whole-rock Re-Os isotope systems appear to provide robust chronologic information regarding melt depletion in these peridotites. A Lu-Hf 'errorchron' (1.66 ± 0.10 Ga) and Os model ages (1.8 ± 0.2 Ga) are both consistent with Paleoproterozoic (~1.8 Ga) melt depletion in the Yangyuan peridotites. This age is consistent with the oldest (Paleoproterozoic) Nd model ages and non-radiogenic Pb isotopic compositions observed in some samples. The younger age of the lithospheric mantle compared to the overlying Archean crust suggests the removal and replacement of original underlying lithospheric mantle during a ~1.8 Ga collision in this region of the North China Craton.

https://doi.org/10.1180/S0026461X00006502 Published online by Cambridge University Press

Apatite from eclogite and veins from Sulu-Dabie eclogite-bearing belt

JINGBO LIU*, LINGMIN ZHANG, KAI YE, YI CHEN AND SHUN GUO

Institute of Geology and Geophysics, Chinese Academy of Sciences, Beijing 100029, China (*correspondence: jingboliu@mail.igcas.ac.cn)

We analysed apatites of eclogites and veins hosted in eclogite bodies in Chizhuang, Qinlongshan, Maobei from the Sulu ultrahigh-pressure (UHP) belt, and Bixiling, Maowu, Hualiangtin, Zhujiachong from the Dabie Mountains in order to unravel whether or not saline as a predominant fluid type was involved in high-pressure (HP) or UHP metamorphic process.

The apatites in eclogites have the Cl contents of 0.01-2.0 wt % from Chizhuang, 0.04-0.36 wt % from Qinlongshan, 0.04-0.6 wt % from Maobei, 0.2-1.5 wt % from Bixiling, 0.01-7.0 wt % from Maowu, and 0-0.05 wt % from Hualiangtin and Zhujiachong. The results suggest that the fluids equilibrated with apatites were from very low salinity (Hualiangtin and Zhujiachong) to very high salinity (Chizhuang, Bixiling and Maowu). At the same time, for one sample or outcrop of eclogite, large variability of Cl content in apatites also indicates that the salinity of fluids was greatly changed during HP or UHP metamorphic process.

The apatites in veins from Chizhuang, Maobei, Bixiling, Hualiangtin and Zhujiachong were also analysed. The apatites of kyanite (Ky)-zoisite (Zo)-quartz (Qtz) vein from Chizhuang have Cl content of 0-1.7 wt %, whereas the apatites from other three types of vein (Qtz vein, omphacite (Omp)-rich-Qtz vein and phengite (Phn)-rich-Qtz vein) show less 0.20 wt % Cl content. The apatites of three types of veins from Maobei (Omp, Ky-Qtz and Zo-Qtz) display 0-0.36 wt % Cl contnets. Two types of veins from Bixiling (Omp and Ky-Phn-Qtz) have the apatites with 0.2-1.0 wt % Cl contents. The apatites of epidote-talc-Ky-Qtz vein from Hualiangtin show 0.02-0.30 wt % Cl content, and of Phn-Qtz and Zo-Ky-Qtz veins from Zhujiachong have less 0.05 wt % Cl content. These analytical data indicate that the fluids equilibrated with apatites were also from very low salinity (Zhujiachong) to very high salinity (Chizhuang, Bixiling). Meanwhile, for one vein, significant variability of Cl content in apatites also indicates that the salinity of fluids was greatly variable during the formation process of vein.

Adsorption of thallium(I) onto geological materials: Effect of pH and humic matter

J. LIU[1,2]*, H. LIPPOLD[2], J. WANG[1], J. LIPPMANN-PIPKE[2] AND Y.H. CHEN[1]

[1]School of Environmental Science and Engineering, Guangzhou University, Guangzhou 510006, China (*correspondence: liujuan858585@163.com)

[2]Institute of Radiochemistry, Helmholtz-Zentrum Dresden-Rossendorf, Research Site Leipzigmailto:, 04318 Leipzig, Germany

Thallium (Tl) is a typical toxic heavy metal, with higher toxicity than Hg, Cd, Pb. Anthropogenic sources such as coal combustion or mining/smelting activities generated high enrichments of Tl in some areas. For long-term risk assessments, the mobility in geochemical systems is a topic of major interest. Adsorption onto mineral surfaces can be considerably affected by dissolved humic acids (HAs), which are ubiquitous in natural waters. By using radioactive tracers, we were able to investigate co-adsorption of Tl and HAs at low concentration levels to be considered in real scenarios [1].

Two natural HAs were extracted from river sediments collected in a contaminated mining area in South China (regions of Guangzhou and Yunfu City). They were radiolabeled by an azo-coupling reaction with ^{14}C-aniline. ^{204}Tl (I) was employed as a radiotracer for Tl (I). The geological materials used in this study were goethite, pyrolusite and a natural sediment sample taken from Yunfu City.

For all these substrates, metal adsorption was found to be promoted with increasing pH since more binding sites are provided by deprotonation of surface hydroxyl groups. In contrast, adsorption of HAs was counteracted with increasing pH, which is explained by increasing electrostatic repulsion as a consequence of deprotonation. As expected, the extent of Tl (I)-HA complexation turned out to be very low, with a slight increase at higher pH.

Based on these data, a combined distribution model (Linear Additive Model) was tested for suitability in predicting the pH-dependent influence of HAs on Tl (I) adsorption. Our experimental results could not be reproduced in this way. In view of the fact that the approach worked well in other studies, criteria for its applicability need to be identified. Selectivities within the multicomponent system of humic material, regarding adsorption as well as complexation, are one possible reason for a failure of the model.

[1] Liu J. Lippold H. Wang J. Lippmann-Pipke J. & Chen Y.H. (2011) *Chemosphere* **82** 866–871.

https://doi.org/10.1180/S0026461X00006502 Published online by Cambridge University Press

^{40}Ar-^{39}Ar isotopic dating of muscovite from the Hukeng tungsten deposit, Jiangxi Province, South China

JUN LIU, MAOYAN MA, GUODONG SHI, HAIJIAO YOU, YONG ZHAN AND YOUFEI GUAN

The Civil Engineering School, Anhui University of Architecture, P.R. China (fzel@tom.com)

Hukeng tungsten deposit, located in central part of Jiangxi Province, South China, is one large-scale quartz vein type wolframite deposit, which is in the south margin of Hukeng granite intrusion, covering the area of 6 km^2. The deposit can be divided into quartz-wolframite, quartz-fluorite-wolframite and quartz-pyrite-sphalerite-wolframite three metallogenic stages [1].

The muscovite for ^{40}Ar-^{39}Ar dating has eminent cleavage, weak pleochroism and high interference color, coexisted with wolframite in ore veins at depth of -60m of the Hukeng tungsten deposit. The variation of apparent age in low temperature (600-800℃) released stage of muscovite is large, varying between 92.0±15.0Ma and 132.7±1.4Ma, and ^{39}Ar only accounts for about 5.4% of the total ^{39}Ar released, which may be caused by lattice defect of mineral of minor argon loss in the periphery of mineral. Five high temperature released stages (1100-1400℃, ^{39}Ar occupies 94.6% of the total ^{39}Ar released) form a plateau age of 147.2 ± 1.4 Ma and an isochron age of 148.0± 2.8 Ma with MSWD of 0.51. The intercept of isochron ((^{40}Ar/^{36}Ar)$_0$) is 280, suggesting certain argon loss may exist in the lattice of muscovite. However, in the fitting process of plateau age, 94.6% ^{39}Ar conforms to plateau-forming conditions, and isoshron is adapted to compare and just the age, which can correct the influence of argon loss efficiently. Therefore, the plateau age of muscovite has geological significance and can represent the cooling age for the formation of muscovite.

In the deposit, homogenization temperatures for quartz from three mineralization stages range from 200 to 300°C [1], obviously lower than the closure temperatures of the ^{40}Ar-^{39}Ar mica chronometers. The closure temperature for the K-Ar isotope system in muscovite is 350–640°C [2]. Therefore, we can assume that the K-Ar system for muscovite remained closed after mineral precipitation, and thus, the ^{40}Ar-^{39}Ar date reported in this study is taken as the age of ore formation in the Hukeng tungsten deposit. Therefore, the absolute timing of tungsten mineralization in Hukeng is about 150 Ma.

This research was financially supported by the Doctoral Fund of Anhui University of Architecture of China (No.K02415).

[1] Liu. (2008) doctoral dissertation, 76–78. [2] Hames & Bowing. (1994) *EPSL* **124**, 161-167.

The inclusions of carbonates in UHP eclogite from the South Altyn Tagh, Northwest China: A new constraint for its peak metamorphic pressure

L. LIU*, Y.T. CAO, C. WANG, D.L. CHEN, L. KANG AND W.Q. YANG

State Key Laboratory of Continental Dynamics, Department of Geology, Northwest University, Xi'an 710069, P R China (*correspondence: liuliang@nwu.edu.cn)

Previous studies have revealed that eclogites from the South Altyn Tagh have been underwent UHPM according to coesite pseudomorphs in garnet and omphacite [1, 2], and the P-T conditions of the eclogites were estimated to be about 3GPa and 800°C. But the peak metamorphic pressure of the eclogite remains uncertain due to the absence of confident mineralogical constraints.

Recently, abundant inclusions of carbonations are recognized in garnet and omphacite in the eclogite by detailed petrography observations, Raman spectrum and eclectron probe analyses. Two most remarkable textures of the inclusions are as follow: 1) magnesite was found as relict, rounded inclusions with reaction rims of dolomite within garnet and omphacite. The transition from magnisite to dolomite is by means of the reaction of magnesite + aragonite = dolomite [3]; 2) inclusions of calcite aggregates have well developed radial fractures in garnet and omphacite, and have very similar textures to quartz pseudomorphs after coesite inclusions in garnet and omphacite in other UHP eclogites, which are interpreted as the aragonite pseudomorph. These textures reflect that the peak mineral assemblage of the eclogite is Grt+Omp+Mgs+Arg±Coe.

The reaction of dolomite = magnesite + aragonite has been experimentally and extensively investigated to be stable at mantle conditions (>5-20GPa) [4], and identified in many mantle xenoliths and UHP metamorphic rocks [3, 5]. The assemblage of Grt + Omp + Mgs + Arg ± Coe is observed at >6 GPa in recent experiment of cabonated eclogite [6]. According to the experimental data above, we estimate the peak metamorphic pressure of the eclogite is to be >6GPa, and the subducted depth should be at least 180 km.

[1] Zhang *et al*. (2002) *CSB* **47**, 751–755. [2] Liu *et al*. (2009) *JAES* **263**, 180–191. [3] Dobrzhinetskaya *et al*. (2006) *EPSL* **243**, 85–93. [4] Liu *et al*. (1995) *EPSL* **134**, 297–305. [5] Zhang *et al*. (2003) *JMG* **21** , 523-529. [6] Hammouda (2003) *EPSL* **214**, 232–244.

https://doi.org/10.1180/S0026461X00006502 Published online by Cambridge University Press

Catalytic spectrophotometric determination of iodine in vegetable matter digested by pyrohydrolysis

L. LIU, D. WU*AND P. LI

College of Environmental and Chemical Engineering, Nanchang University, Nanchang 330031, PR China (*correspondence: dswu@ncu.edu.cn)

Revolutionary New Method

The low I contents, complexity of the matrix, chemical interferences, possibility of contamination, and loss during sample dissolution are some of the potential limiting factors for the determination of I in vegetable matter [1]. The reported analytical methods (except RNAA) have the lower detection limit ranging from 5μg/kg to 3 mg/kg [2-6]. Thus few methods can be adapted to determine I in the inland vegetable matter, which usually has I content of a few μg/kg. We have developed a method that combines pyrohydrolysis digestion with catalytic spectrophotometry (CS) to determine I in vegetable matter. The pretreatment program of pyrohydrolysis was designed to decompose the vegetable matter steadily and completely. The conditions of CS were optimized to enhance the sensitivity of iodine determination. Excellent limit of detection has been achieved and meet the analytical requirements.

Discussion of Results

The conditions of pyrohydrolysis optimized through orthogonal experiment are as follows: 0.5 g vegetable matter sample, a temperature of 1100 °C, 20 minutes for pyrohydrolysis, 100 mL/min of oxygen flux and 15 mL 0.2 M NaOH of absorption solution. The conditions of CS are optimized as follows: reaction temperature of 45 °C and reaction time of 35 minutes. The limit of detection and quantification are 0.3 ng/g and 0.9 ng/g, respectively. Hence it can be applied to determine trace I in vegetable matter. Precision and accuracy were evaluated by the analysis of Chinese vegetable matter reference materials.

Owing to the low cost of instruments and analysis, low limit of detection, high accuracy and precision, pyrohydrolysis-CS method is very suitable for the daily analysis of the iodine contents in vegetable matter.

[1] Rao & Chatt (1991) *Anal. Chem* **83**, 1298–1303. [2] Schnetger & Muramatsu (1996) *Analyst* **121**, 1627-1631. [3] Niedobova *et al.* (2005) *Microchim. Acta* **150**, 103–107. [4] Tagami *et al.* (2006) *Anal. Chim. Acta* **570**, 88–92. [5] Varga (2007) *Microchem. J* **85**, 127–131. [6] Bhagat *et al.* (2009) *Food Chem* **115**, 706–710.

Accumulation of organic carbon in typical hillslope soils in karst area, Southwest China

T.Z. LIU*, C.Q. LIU, X.D. LI AND C.L. TU

State Key Laboratory of Environmental Geochemistry, Institute of Geochemistry, Chinese Academy of Sciences, Guiyang 550002, China (*correspondence: liutaoze@mails.gyig.ac.cn)

The content of soil organic carbon (SOC) has long been recognized as a key characteristic of soil quality. During an earlier survey, we observed that a lot of SOC stocked in a hillslope under natural conditions for 10 years of revegetation in karst area, Southwest China. Here, we analyzed the content and ^{13}C isotope of SOC in size-fractionated particles (mainly as sand 53μm~2000μm, silt 2μm~53μm, clay <2μm) of soils in this hillslope, to elucidate the generation and stability of organic carbon.

The results showed that the content of SOC in the upper hillslope was higher than that in down hillslope area. Though the larger SOC accumulation was found in the sand fraction in the upper hillslope, the organic carbon pool was unstable. Oppositely, in down hillslope area, the organic carbon was mainly stored in the slit and clay fraction and has been in relatively stable state (Fig.1). Comparing the $\delta^{13}C$ values of SOC in soil and its three fractions (sand, silt, clay) with $\delta^{13}C$ values of litters, we found that $\delta^{13}C$ values of SOC in sand fraction were strongly correlated with the values of litters, which implying sand fraction was more sensitive to the change of vegetation types in the hillslope.

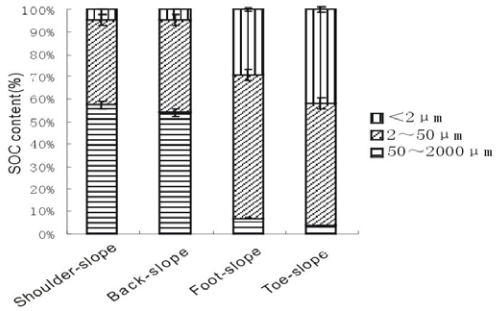

Figure 1: Proportion of organic carbon of different fraction in soil profiles

Our findings indicate that revegetation on hillslope can increase SOC stocks, but distribution has significant difference. And $\delta^{13}C$ value of SOC should be a good tracer for assessing the formation and stability of organic carbon.

This work was supported by the National Natural Science Foundation of China (Grant No. 41003008 and 40721002).

https://doi.org/10.1180/S0026461X00006502 Published online by Cambridge University Press

A synthetic silica glass reference material for determination of Ti in zircon by LA-ICP-MS

XIAOMING LIU[1], SHAN GAO[2] AND JOHN.C. AYERS[3]

[1]State Key Laboratory of Continental Dynamics, Department of Geology, Northwest University, Xi'an 710069, China
[2]Faculty of Earth Sciences, China University of Geosciences, Wuhan 430074, China
[3]Department of Earth and Environmental Science, College of Arts and Science, Vanderbilt University, Nashville TN, USA

The proper use of Ti-in-zircon thermometer mostly depends on the accurate determination of Ti content in zircon. Because of lacking homogeneous matrix-matched mineral standards available, a silica glass (LCD-1) was fused at 1680°C. The major element contents of the glass, SiO_2 (73.89±0.29)%, Al_2O_3 (8.22±0.14)%, ZrO_2 (5.96±0.09)%, K_2O (5.53±0.04)% and Na_2O (7.35±0.11)% (all in1σ), were determined by electron microprobe. The Ti content in the glass is 998±23μg/g (1σ) measured by using solution-ICP-MS method and 1009±22μg/g (1σ) using LA-ICP-MS method calibrated by taking ^{29}Si as an internal standard and NIST SRM 610 as the reference material.

The fractionation index of Ti/Zr is less than Ti/Si in zircon. So, LCD-1 as reference material, Ti contents in zircon 91500, GJ-1 and M257 are determined by LA-ICP-MS. The result for one analysis calibrated using ^{29}Si as an internal standard is lower 16-20% than that using ^{96}Zr. The results calibrated using NIST 610 and LCD-1 as reference material and ^{29}Si as an internal standard are nearly same, their differences are less than 2.3%. All these facts suggested that LCD-1 glass is a better reference material than NIST 610 in determination of Ti in zircon.

Scanning transmission X-ray and atomic force microscopy mapping of exopolymer fractionation in *Bacillus subtilis* biofilms on goethite

X. LIU[1]*, K. EUSTERHUES[1], J. THIEME[2], K. KÜSEL[3] AND K.U. TOTSCHE[1]

[1]Institut für Geowissenschaften, Friedrich–Schiller-Universität Jena, Germany (*correspondence: xinran.liu@uni-jena.com)
[2]NSLS-II, Brookhaven National Laboratory, Upton, NY, USA (jthieme@bnl.gov)
[3]Institut für Ökologie, Friedrich-Schiller-Universität Jena, Germany (kirsten.kuesel@uni-jena.de)

The surface properties of goethite are vital for many environmental processes, such as adsorption and transport of contaminants and nutrients. This study aims at understanding of how biofilm formation changes the mineral surface. Adhesion and mechanical properties (e.g. elastic modulus) were investigated by atomic force microscopy (AFM), while the chemical composition of the biofilm was mapped by scanning transmission X-ray microscopy (STXM).

We investigated single-layered biofilms formed by *Bacillus subtilis* on Lysogeny broth-agar plates in the presence or absence of goethite. Synchrotron-based STXM C K-edge image sequences, recorded at a spatial resolution of ≤ 25 nm, were converted to component maps of proteins, polysaccharides, nucleic acids and lipids by linear combination fitting. STXM revealed that proteins, nucleic acids and lipids were mainly located inside the cells, while polysaccharides dominate in the extracellular polymeric substances (EPS). In the presence of goethite, we found a higher concentration of nucleic acids in the EPS and the goethite needles were covered by nucleic acids. This supports the view that nucleic acids mediate EPS binding to mineral surfaces and are required for establishing biofilms [1].

Quantitative nanomechanical properties measurement by AFM indicated that the DMT modulus (elastic modulus) of the goethite surface decreased from ~40 GPa to ~84 MPa after biofilm formation. The adhesion between the AFM tip and the goethite surface in air increased from ~2 nN to ~12 nN after biofilm formation.

We hypothesize that nucleic acids are intentionally excreted by *B. subtilis* when e.g. goethite surfaces are present. This preferentially adsorbed nucleic acid-rich material is responsible for the observed changes in the mechanical surface properties of goethite.

[1] Whitchurch (2002) *Science* **295**, 1487.

https://doi.org/10.1180/S0026461X00006502 Published online by Cambridge University Press

A novel mutant strain of *Acidithiobacillus ferrooxidans* adapted to extremely low pH

LIU YAJIE[1,2] LI JIANG[2] XU LINGLING[2] CHEN GONGXIN[2] AND LIU JIANSHE[1]*

[1]School of Envrionmental Science and Engineering, Donghua University, No.2999 Renmin North Rd.China. 201620 (*correspondence: liujianshe@dhu.edu.cn)

[2] School of Civil and Environmental Engineering, East China Institute of Technology, Fuzhou, Jiangxi Province, China. 344000 (yjliu@ecit.cn, lij@ecit.cn, llxu@ecit.cn, gxchen@ecit.cn)

Introduction

Although *Acidithiobacillus ferrooxidans* (*At. f*) is widely used in mining and metallurgy technologies nearly over thirty countries at present, its application still stay in laboratory and pilot experiments for uranium recovery in China [1]. One of the key problem inhibited its industrialization application is lack of better adaptative strains with strong ferrous-oxidizing activity and stability at very low pH and high conductivity.

Results

A mutant strain of *At. f* was obtained by ultraviolet mutagenesis and directional screening with optimum pH between 1.2-1.8 and iron oxidized rate of 0.2g/L. h^{-1} (Fig.1). Physiological and 16SrDNA

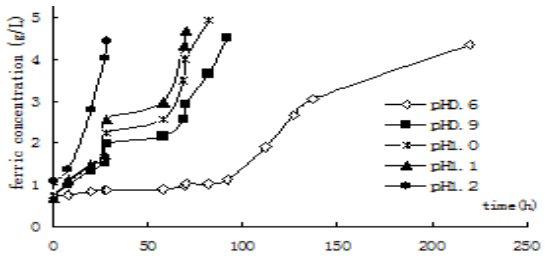

Figure 1: Iron oxidizing capacity with time at extremely low pH sequencing indicated it was *Acidithiobacillus ferrooxidans*.

Compared with the original strain, the characteristics of this mutant strain are as the following: (1) Relatively strong oxidized activity at pH1.2; (2) Relatively Stable in mineral medium after 8 times inoculations; (3) Growing at extremely low pH, even at pH=0.6. It is a promising strain likely being applied in comercial bioleaching.

Thanks for the supports of Jiangxi Provincial Department of Education Project (GJJ08309) and National Natrual Science Foudation (50974043).

[1] L.Zhong-er, H.Yun-hong & C.Zhao-ling (2002) *Chinese Journal of Process Engineering* **2**(5), 415–419.

Estimating ground level $PM_{2.5}$ concentrations in Atlanta Metro Area using spatial statistical models

Y. LIU[1]*, X. HU[1], L. WALLER[1], M. AL-HAMDAN[2], W. CROSSON[2], M. ESTES[2], S. ESTES[2] AND D. QUATTROCHI[2]

[1]Emory University, Rollins School of Public Health, Atlanta, GA 30322, USA (*correspondence: yang.liu@emory.edu, xuefei.hu@emory.edu, lwaller@emory.edu)

[2]NASA Marshall Space Flight Center, Huntsville, AL 35805, USA (mohammad.alhamdan@nasa.gov, bill.crosson@nasa.gov, Maury.G.Estes@nasa.gov, sue.m.estes@nasa.gov, Dale.Quattrochi@nasa.gov)

Studies have shown that exposure to $PM_{2.5}$ (airborne particles less than 2.5 μm in size) may increase the risk of cardiovascular and respiratory diseases. Current $PM_{2.5}$ health effects studies rely on the often sparse ground monitoring networks to provide exposure estimates. We developed a geographically weighted regression (GWR) model to examine the relationship among $PM_{2.5}$, MODIS AOD, meteorological parameters, and land use information. Additionally, Two meteorological datasets: North American Regional Reanalysis (NARR) and North America Land Data Assimilation System (NLDAS), were fitted into the model separately to compare their performances. The root mean squared prediction error (RMSPE) showed that the prediction accuracy was 83.6% and 83.9% for NARR and NLDAS in model fitting, and 69.9% and 72.5% in cross validation. The results indicated that GWR combined with AOD, meteorological parameters, and land use information as the predictor variables could generate a better fit and achieve high accuracy in PM2.5 exposure estimation, and NLDAS could be used as an alternative of the NARR to provide some of the meteorological fields.

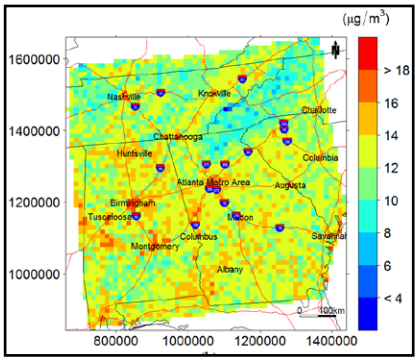

Figure 1: Predicted annual mean PM2.5 concentrations in 2003 using NLDAS meteorological fields.

https://doi.org/10.1180/S0026461X00006502 Published online by Cambridge University Press

Constraints of the concentration of the platinum-group elements in Pobei Ni-Cu Sulfide Deposit, Xinjiang Province

YANRONG LIU[1,2], XINBIAO LÜ[1]*, WEI MEI[1] AND YUCHAI DAI[3]

[1]Faculty of Earth Resources, China University of Geosciences, Wuhan 430074, China (*correspondence: lvxb_01@163.com, fwjlyr@ 163.com)
[2]Key Laboratory of Western Mineral Resources and Geological Engineering of Ministry of Education, Chang'an University, Xi'an 710054, China
[3]No.6 Geological Party, Xinjiang Bureau of Geology and Mineral Exploration and Development, Hami 839000, China

Pobei Cu-Ni sulfide deposit hosted in mafic-ultramafic intrusion is located in the Beishan rift valley belts, Northern Talimu plate, Xinjiang Province, NW China. The sulfide ores are mainly disseminated. The disseminated sulfide ores are characterized by variable but generally high Cu, Ni and PGE concentrations:70225-102951ppm Cu, 108691-307454ppm Ni, 175-1637ppb Pt, 214-593ppb Pd, 23.2-80.6ppb Ir, 59-216 ppb Ru, and12-52ppb Rh in 100% sulfides.

All of rocks and ores Pd/Ir ratios (4.34 to 27.75) in Pobei Cu-Ni deposit are less than 100 [1], indicating that the effects of late hydrothermal fluids are weak. The positive correlations between Ir and Pd indicate that sulfide didn't experience fractionation. Pobei deposit has very higher Cu/Pd ratios (90-1626×10^3) than primitive mantle (Cu/Pd=7.5×10^3), which suggest that the sulfide ores formed from the silicate magmas had already experienced prior-sulfide [2].

Assuming a partition coefficient between sulfide liquid and silicate melt for Pd, Pt and Ir of 20000 and for Cu of 1000, for Ni of 500 [3, 4], the primary magma of the Pobei intrusion comes from the primitive mantle.Our calculations indicate that the basaltic magma of melting degree 25% had contained 120ppm Cu, 490ppmNi, 9.4ppb Pt, 16ppb Pd, and 0.48ppb Ir, then 0.02% sulfide removal would result in PGE-depletion in the residual magma with 98ppm Cu, 443ppm Ni, 0.172ppb Pt, 0.293ppb Pd, and 0.009ppb Ir, then sulfer come to saturation again and sulfide segregate from the PGE-depleted magma under silicate/sulfide liquid ratios (R-factor) ranging from 500 to 5000.

[1] Keays (1995) *Lithos* **34**, 1–18. [2] Maier *et al*. (1998) *South African Geol* **3**, 237–253. [3] Fleet *et al*. (1993) *Contrib Mineral Petrol* **115**, 36–44. [4] Francis (1990) *Chem Geol* **85**, 199–213.

Spectral and electrochemical evidence for kinetically separate cytochrome compartments in *Geobacter* biofilms

YING LIU[1], RHONDA R. FRANKLIN[2] AND DANIEL R. BOND[1]*

[1]BioTechnology Institute and Department of Microbiology, University of Minnesota, St. Paul MN 55108 (*correspondence: dbond@umn.edu) (liux0820@umn.edu)
[2]Department of Electrical Engineering and Computer Science University of Minnesota, (drayton@umn.edu)

This work seeks to unite recent reports of the redox potential and putative locations of multiheme c-type cytochromes expressed by *Geobacter* with new electrochemical and spectral data collected during transfer of electrons to electrodes. Spectral monitoring of biofilms revealed that early 40% of *G. sulfurreducens* cytochromes were oxidized at lower potentials (-0.4 V to -0.2 V, the range of extracellular cytochromes OmcS and OmcZ) [1-4], yet sustained electron transfer does not occur at these potentials [5,6]. A second oxidation event was centered at the midpoint potential of the periplasmic cytochrome PpcA (-0.15 V [7]).

The fact that extracellular cytochromes have lower potentials than periplasmic cytochromes is the opposite of how electron transfer chains are typically designed. A hypothesis is that this guarantees the outer surface is in equilibrium with insoluble acceptors, to serve as a sink for the periplasm. If self-exchange and cytochrome-metal transfer rates are rapid, such schemes are possible.

A prediction from this hypothesis is that the periplasmic pool would be slower to respond to changes in electrode potential, as electrons must first travel through extracellular cytochromes. This behavior was observed in scan rate analysis: spectral changes at low potential (-0.4 to -0.2 V) responded immediately to potential steps, while the –0.15 V pool lagged behind. A second prediction is that the redox status of periplasmic cytochromes would kinetically 'gate' electron flow to the exterior, consistent with the -0.15 V midpoint potential observed during catalytic cyclic voltammetry [8]. Further work using mutants lacking key cytochromes are being used to test this model.

[1] Qian, X., *et al*. (2011) *BBA* **1807**, 404-412. [2] Leang, C., *et al*. (2010) *Appl. Environ. Microbiol*. **76**, 4080-4084. [3] Inoue, K., *et al*. (2010) *Appl. Environ. Microbiol*. **76**, 3999-4007. [4] Inoue, K. *et al*. (2010) *Env. Microbiol. Reports*. [5] Richter, H. *et al*. (2009) *Energy Environ. Sci*. **2**, 506-516. [6] Marsili, E. *et al*. (2010) *Electroanalysis* **22**, 865-874. [7] Pessanha, M., *et al*. (2006) *Biochemistry* **45**, 13910-13917. [8] Strycharz, S. M., *et al*. (2011) *Energy Environ. Sci*. **4**, 896-913.

https://doi.org/10.1180/S0026461X00006502 Published online by Cambridge University Press

Geology and fluid origin of Mohailaheng Pb-Zn deposit in Tibet

YINGCHAO LIU[1], ZENGQIAN HOU[1], ZHUSEN YANG[2] AND SHIHONG TIAN[2]

[1]Institute of Geology, CAGS, Beijing 100037, China (lychappy@126.com)
[2]Institute of Mineral Resources,CAGS,Beijing 100037, China

The Mohailaheng Pb-Zn deposit in south Qinghai, China, is a stratabound epigenetic deposit hosted by Early Carboniferous limestone in the hanging wall of a Cenozoic thrust fault system. Four mineralization stages are recognized in the deposit. During Stage I, xenomorphic grass-green sphalerite, galena, and pyrite precipitated as dissemination with dolomite and calcite. In Stage II, xenomorphic and less colloform brown sphalerite, galena and pyrite precipitated with barite, quartz, fluorite and calcite as cements of limestone breccias. It is followed by calcite-pyrite vein in Stage III and pure calcite vein in Stage IV. Most sulfides in the deposit were produced during Stage II.

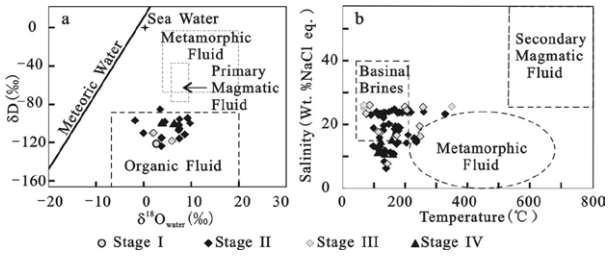

Figure 1: a-Diagram of $\delta D_{v\text{-}snow}$-$\delta^{18}O_{fluid}$ (base diagram after [1]) and b-Diagram of salinity-temperature of fluid inclusions (base diagram after [2])

Raman microprobe analyses indicate that CO_2, CH_4, H_2S and H_2O are common in vapor phases of fluid inclusions in Stage II. The H-O isotopic data of fluid show the character of organic matter or gas (Fig.1a). Most salinity-temperature data of primary fluid inclusions fall into the basinal brine field and some fall near or into the metamorphic fluid field (Fig.1b). The results above give two possible fluid origins which are basinal brine possibly providing CH_4 and metamorphic fluid possibly providing CO_2.

The geology and fluid orogin of this deposit indicate the characters including MVT and fracture controlled Pb-Zn deposit, so it is just considerded as a carbonate hosted Pb-Zn deposit controlled by thrust systerms in the orogenic belt.

This work was supported by grants (Contract No. 2006BAB01A08, 2011CB403106 and U0933605).

[1] Lu H Z *et al*. (2004) Beijing, Science Press, 19–20. [2] Beane (1983) *Geothermal resources council Special Report*, 245–253.

Autotrophic denitrification potential: An experimental study on nitrate-N removal from groundwater by pyrite in mining wastes as electron donor

Y. LIU[1]* AND Y.X. LI[2]

[1]School of Biotechnology and Food Engineering, Hefei University of Technology, Hefei 230009, China (liuy99999@163.com)
[2]Hefei University of Technology, Hefei 230009, China

New Method

Groundwater nitrate pollution is a common problem in the world, especially in North China [1-2]. It becomes a serious threat to source of drinking water in fractured media where how to control and remedy it is an open question [3-8]. In addition, there are lots of mining waste including pyrite often causing acid mine drainage. The new method is to use the pyrite as electron donor combining with the *thiobacillus* to remedy nitrate pollution by the experimental study [2].

Discussion of Results

The mixed *denitrogenation thiobacillus* (T.D) is concentrated and separated from the charcoal factory's soil. Then a strain with strong denitrification ability is isolated, which is self-supportive and facultative anaerobic. Based on the analysis of physiological and biochemical measurements, this stain is preliminary judged to Thiobacillus. The mixed T.D is employed to reduce Nitrate nitrogen from the groundwater using pyrite as electron donor. The effect of the ratio by Sulfur and Nitrogen (S/N), iron disulfide quantity and vaccination quantity is investigated experimentally. Results show that: the most suitable S/N is 5/2, the quantity of Sulfur in iron disulfide reach to 250 mg/L is the most suitable iron disulfide quantity, and the best vaccination quantity is 9%. At the condition mentioned above, the nitrate removal rate is 62.17%. The effect of nitrogen removal on chemical synthesis culture medium of pure T.D is better than that using mixed T.D. Conclusions show that the strain isolated can be used to remove the nitrate-N (high concentration) from groundwater using pyrite as electron donor with potential value. (Grant no: 2009HGCX0233)

[1] Liu *et al.*(2009) *Geochim.Cosmochim. Acta* **73**, 783–783. [2] Qian *et al*. (2011, in press) *Environ. Technol*. [3] Qian *et al*. (2005) *J. Hydrol.* **311**, 134–142. [4] Zhou *et al*. (2004) *Int. J. Rock Mech. Min. Sci*. **41**, 402. [5] Qian *et al*. (2006) *Hydrogeol. J*. **14**, 1192–1205. [6] Chen *et al*. (2009) *Journal of Hydrodynamics* **21**(6) 820–825. [7] Qian *et al*. (2009) *Hydrogeol. J*. **17**, 1749–1760. [8] Qian *et al*. (2011) *Hydrol. Process*. **25**, 614–622.

https://doi.org/10.1180/S0026461X00006502 Published online by Cambridge University Press

Crust recycling-induced melt-peridotite interactions in the northern margin of the North China Craton

YONGSHENG LIU, SHAN GAO AND ZHAOCHU HU

State Key Laboratory of Geological Processes and Mineral Resources, Faculty of Earth Sciences, China University of Geosciences, Wuhan 430074, China

Recycling and subsequent melting of crustal rocks (via delamination or subduction) in the upper mantle is thought to be partially responsible for generating mantle heterogeneity and drive evolution of the continental crust to a bulk andesitic composition. It could have induced widely silicate melt-peridotite interaction, and a network of pyroxenite veins in the lithospheric mantle of different ages is then expected. Such pyroxenites have been sampled as garnet/spinel pyroxenite veins hosted in the spinel lherzolite xenoliths carried by the basalts in the northern margin of the North China Craton (NCC). Zircon U-Pb age, single melt inclusions and profile analyses of minerals of peridotite and pyroxenite xenoliths carried by the Neogene basalts are combined to investigate the mantle peridotite-melt interactions in the northern margin of the North China Craton.

Continental crust-derived Precambrian zircon xenocrysts and igneous zircons of 315 ± 3 Ma (2σ), 80 - 170 Ma and 48 - 64 Ma were separated from the pyroxenite veins, which provide evidence for the lower continental crust and oceanic crust recycling-induced multi-episodic melt-peridotite interactions in the central zone of the NCC. The combination of the positive εHf (t) values (2.91-24.6) of the 315 Ma zircons with the rare occurrence of subduction-related diorite-granite plutons of 302 - 324 Ma in the northern margin of the NCC implies that the igneous zircons of 315 Ma could record the melt-peridotite interactions in the lithospheric mantle induced by the Palaeo-Asian oceanic crust subduction. Igneous zircons of 80 - 170 Ma generally co-exist with the Precambrian metamorphic zircons. The 170-110 Ma zircons are generally characterized by negative εHf (t) values, while the 110-100 Ma zircons are featured by positive εHf (t) values. These observations suggest that the melt-peridotite interactions at 80-170 Ma were induced by partial melting of a recycled continental crust. The igneous zircons of 48 - 64 Ma are characterized by negligible Ce anomaly, unusually high REE, U and Th contents and positive εHf (t) values. These features imply that the melt-peridotite interactions at 48 - 64 Ma could be associated with a depleted mantle-derived carbonate melt/fluid.

The 4.2ka BP climate event and its influence on Neolithic Cultures around the middle reaches of Yangtze River, China

YUHUI LIU*, XIA SUN, CHAOYONG HU, JIAOYANG RUAN AND SHUCHENG XIE

China University of Geosciences, Wuhan, 430074, China (*correspondence: yhliu@cug.edu.cn)

A sudden collapse of Neolithic Cultures in China around 4ka BP presents a problem for archaeologists. Recently reported records of the 4.2ka BP event in China [1], raises the possibility of Chinese cultural collapse corresponding to this climate anomaly [2]. However, climate change in China around 4ka BP is not well studied as sites, materials and proxies differ in their sensitivity, response time, duration and temporal resolution. To address this question, information on the 4.2ka BP event at high temporal resolution is required.

A precisely dated stalagmite, HS4, covering the last 9000 years, with clear annual growth banding [3], collected from Heshang Cave in the middle reaches of Yangtze River (30.44°N, 110.42°E), provides an apparent record of 4.2ka BP event. Oxygen isotope data from HS4 with an average resolution of ~16a suggests there is a weak monsoon event between 4.4 ka and 4.1 ka. Following this event, the subsequent 2000 year oxygen isotope average value shows an increase of ~1‰, compared with the previous 3000 year, suggesting the 4.2ka BP event is a marker of the end of the Holocene Climate Optimum. Growth rates of HS4 around 4.2ka BP also show a decrease from 300 μm/yr to 200 μm/yr, extending for 240 years, suggesting less water supply to the cave. Furthermore, Mg/Ca ratios from HS4 at seasonal resolution during this event show a prominent increase by ~40% with large variations, indicating an unstable and severe drought condition.

Consistent climate information from all three proxies from HS4 appears to support the thesis of a severe drought during 4.2ka BP around the middle reaches of Yangtze River. An extensive drought covering a period of over 200 years would devastate rain based agricultural and be a prime cause of the collapse of the flourishing Shijiahe Culture, marking the disappearance of local Neolithic Cultures in the middle reaches of Yangtze River.

[1] Xu *et al*. (2006) *PALAEO* **230**, 155–164. [2] Wu & Liu (2004) *INQUA* **117**, 153–166. [3] Hu *et al*. (2008) *EPSL* **266**, 221–232.

https://doi.org/10.1180/S0026461X00006502 Published online by Cambridge University Press

Application of remote sensing method for detecting and monitoring water contamination

YUMING LIU[1], JING ZHANG[1]*, XIAOJUAN LI[2] AND HUILI GONG[2]

[1]The Key Laboratory of Resource Environment and GIS of Beijing, Capital Normal University, Beijing 100048, P.R. China (*correspondence: maggie2008zj@yahoo.com)
[2]College of Resource Environment and Tourism, Capital Normal University, Beijing 100048, P.R. China

With the global shortage of fresh water resources and freshwater ecosystems continue to be disrupted, the traditional research based on the objectives and methodology of single-disciplinary, has difficulties to face the complexity of the new challenges of global environmental changes. Beijing as the capital of China, due to continuous years of drought, the amount of available water resources has been greatly attenuated. Two drinking water reservoirs for residents, the Miyun reservoir and Guanting reservoir are only 7.2 billion and 2 billion m3 respectively. In recent years, additionally with water pollution and water quality issues, making available drinking water situation is quite serious. Remote sensing techniques play an important role recently in frequent deterioration of the status of aquatic ecology for drinking water. In this study, landsat imagery was used to detect and monitor water quality in Guanting Reservoir, Beijing, China. This talk will focus on the use of remote sensing technique to determine the nature and extent of water pollution from nitrogen materials which have much more effects on the quality of drinking water in Guanting Reservoir .

Under the auspices of National Natural Science Foundation of China (No.40901026) & Supported by Beijing Municipal Science & Technology New Star Project Funds (No.2010B046)

Equilibrium isotope fractionation calculation beyond harmonic level

YUN LIU[1]*, QI LIU[1] AND JOHN A. TOSSELL[2,3]

[1]State Key Laboratory of Ore Deposit Geochemistry, Institute of Geochemistry, Chinese Academy of Sciences, Guiyang 550002, China (Liuyun@vip.gyig.ac.cn)
[2]Dept. of Chemistry and Institute for Basic Energy Science and Technology, George Washington University, Washington, DC 20052
[3]Dept. of Chemistry and Biochemistry, University of Maryland, College Park, MD 20742

The Bigeleisen-Mayer equation has been the theoretical corner-stone of stable isotope geochemistry for decades. The advantage of using this method is that it largely simplified the calculation procedure by cancelling out as many identical energy terms as possible before the final numerical calculation, concentrating on the vibrational frequency shifts of the different isotopologues. However, Bigeleisen-Mayer equation is purely based on harmonic vibration and rigid rotator approximations. In this study, corrections beyond the harmonic level to the Bigeleisen-Mayer equation have been discussed and compared. The hindered internal rotation correction on isotope effects is found to be significant for H/D exchanges of some organic molecules. Anharmonic correction for ZPE, including the G_0 term, has been found to be very important for all kinds of isotope exchange reactions. For the H/D exchange reactions, almost all the high order corrections discussed in this study are important. The temperature dependences of six higher-order corrections are checked. These higher-order corrections are strongly suggested to be included not only for H/D exchanges but also for several other non-H/D exchange reactions, such as those in B isotope and clumped isotope systems.

[1] Qi Liu, John A. Tossell & Yun Liu*(2010) On the proper use of the Bigeleisen-Mayer equation & corrections to it in the calculation of isotopic fractionation equilibrium constants. *Geochimica et Cosmochimica Acta* **74**, 6965–6983.

https://doi.org/10.1180/S0026461X00006502 Published online by Cambridge University Press

Complex tectonic-thermal history of the Red River Shear Zone: Evidence on Zircon SHRIMP and LA-ICP-MS dating of the Yaoshan Group, SE Yunnan, China

LIU Y-P[1], LI Z-X[2], LIAO Z[1], YE L[1], PI D-H[1] AND LI C-Y[1,3]

[1]State Key Laboratory of Ore Deposit Geochemistry, Institute of Geochemistry, Chinese Academy of Sciences, Guiyang 550002, China (liuyuping@vip.gyig.ac.cn)

[2]Department of Applied Geology, Curtin University of Sciences and Technology, Bentley, WA6102, Australia (Z.Li@curtin.edu.au)

[3]Guangzhou Institute of Geochemistry, Chinese Academy of Sciences, Guangzhou 510640, China (lcy5736@gig.ac.cn)

The Yaoshan Group is located on the southeastern part of the Ailao Shan-Red River strike-slip fault zone. It has experienced the high-amphibolite facie metamorphism and chorismitization, thus it was thought as one part of the Precambrian basement of the South China Block in the traditional Chinese literatures. According to CL images and optical microscope analysis, the zircons derivered from the Yaoshan Group, which are very complicated with the metamorphosed recrystal and overgrowth, could be divided into inherited, metamorphic, anatectic or magamatic types. In order to probe the history of the Red River Shear Zone, zircons derived from the Yaoshan Group have been dating through SHRIMP and LA-ICP-MS. The inherited zircon yielded the $^{206}Pb/^{238}U$ ages in the range of 235±1.7 Ma and 261±3.6Ma with the weighted mean value of 250.8±9.8Ma (N=4, MSWD=4.1) , suggested that the protoliths of the Yaoshan Group should be a sedimenrary series youger than the Permain period. The $^{206}Pb/^{238}U$ ages of metamorphic, anatectic/magmatic zircons could be divided into five groups, which are ~85 Ma, ~75 Ma, ~43 Ma, ~37 Ma and ~32 Ma, respectively. The five zircon age groups mention above could be taken as important episodes of five intensive activities in Red River fault. The first and second age groups, which related to two magmatic and high-temperature metamorphic episodes, indicated that the Red River Fault acted since the later Cretaceous. The other three age groups, which corresponded with the dating of the Ailaoshan region and North Vietnam, might indicated the three main left-direction activities in the Red River Shear Zone.

Supported by NBRSPC (2007BC04008) and NSFC (40972129)

Surface structures on rutile guide organic molecule attachment

K.J.T. LIVI[1]*, B. SCHAFFER[2,3], D. AZZOLINI[1], T. HARDCASTLE[4], C.R. SEABOURNE[4], A.J. SCOTT[4], D. SVERJENSKY[1,5], R. HAZEN[5] AND R. BRYDSON[4]

[1]Johns Hopkins Univ., Baltimore, MD 21218 USA (*correspondence: klivi@jhu.edu)

[2]SuperSTEM Laboratory, Warrington WA4 4AD, UK

[3]University of Glasgow, Glasgow G12 8QQ, UK

[4]SPEME, University of Leeds, Leeds LS2 9JT, UK

[5]Geophysical Laboratory, Washington, DC 20015 USA

Interactions of aqueous organic molecules with the surfaces of metal oxides, such as rutile, are of fundamental interest in a wide range of topics from human implants to the origin of life on Earth. Previous adsorption studies of metals and organic molecules have focused on the {110} form that often dominates macroscopic crystals. However, recent experimental and theoretical studies of glutamate and aspartate adsorption on a synthetic rutile are consistent with attachment to functional groups such as >Ti (OH)2 or >Ti (OH)O which are not present on ideal {110} surfaces but are instead present on the pyramidal {111} or {101} surfaces [1, 2]. The pyramidal forms would have to be sufficiently abundant as steps on {110} to account for the measured adsorption of amino acids. We have used aberration-corrected atomic-resolution scanning transmission electron microscopy high-angle annular dark-field (HAADF) imaging to locate surface Ti atoms and determine the structures present on {110} and {111} faces. HAADF images of {110} prism edges show three structures: Ti-Ti pairs parallel to {110}, {111}, and {11-1} edges. The proportion of these are 4:1:1, respectively, regardless of the roughness of the edges on the μm-scale. This also matches the proportion of crystal prism to pyramidal face lengths. The majority of surface structures consist of only half unit-cell steps. These half steps comprise about 33% of the {110} prism edges. If these extend across the {110} faces, they could account for the sites necessary for amino acid adsorption. Interestingly, odd numbers of Ti pairs between steps requires that bounding steps have different structures not related by symmetry. The calculated energies of the (110) (0.40 J/m2) and (111) (1.41 J/m2) surfaces are also nearly 4:1, suggesting a relationship between growth rate and surface energy. We conclude that: (1) the presence of {111}-type steps on {110} confirms inferences from theoretical and experimental adsorption studies, (2) adsorption models and experiments can be integrated with sub-unit cell surface structures, the detailed nature of which should be characterized with electron microscopy.

[1] Jonsson *et al*. (2009) *Langmuir* **25**, 12127–12135. [2] Park *et al*. (2011) *Langmuir* **27**, 1778–1787.

https://doi.org/10.1180/S0026461X00006502 Published online by Cambridge University Press

Impact of microbial metabolism on radionuclide solubility in natural and engineered environments

J.R. LLOYD[1]*, A. GEISSLER[2], G.T.W. LAW[1], C.L. THORPE[1], V.E. EVANS[1], A.R. BROWN[1], R. KIMBER[1], D.R. BROOKSHAW[1], C. BOOTHMAN[1], F.R. LIVENS[1] AND K. MORRIS[1]

[1]SEAES, WRC and RCRD, University of Manchester, M13 9PL, UK (*correspondence: jon.lloyd@manchester.ac.uk)
[2]Forschungszentrum Dresden Rossendorf, Inst Radiochem, Dresden, Germany

Microbial metabolism can have a controlling influence on the solubility of actinides and fission products in engineered and natural environments. In the 'far field' surrounding a nuclear repository, microbial processes can immobilise redox active radionuclides via respiratory processes that either change directly the oxidation state of the element, or produce new biogenic phases for enhanced sorption. In the 'near field' of the repository, the direct and indirect impacts of microbial metabolism are less well characterised but have the potential to have a significant impact on wasteform evolution and radionuclide mobility, and must be incorporated into the safety case of the repository.

Recent work on the redox cycling of U, Np, Pu and Tc will be discussed, including both reduction and oxidation reactions and their impact on soluble and insoluble radionuclide inventories. The roles of proteins, secreted electron shuttles and other microbial products will be discussed alongside additional controls coupled to bulk element cycles e.g. the production of new mineral phases or significant changes in the geochemical environment such as pH. Studies from a range of contrasting natural and engineered systems will highlight how microbial communities can respond to the radioactive inventory and the extreme (radio)chemistry of some disposed wasteforms, and ultimately control the biogeochemical fate of key radioactive elements.

Laser ablation with the NEPTUNE *Plus* MC-ICP-MS

N.S. LLOYD[1]*, S. SHUTTLEWORTH[2], J.B. SCHWIETERS[1] AND C. BOUMAN[1]

[1]Thermo Fisher Scientific, Hanna-Kunath-Str. 11, 28199 Bremen, Germany (*correspondence: nicholas.lloyd@thermofisher.com)
[2]Photon Machines, 15030 N.E. 95th St., Redmond, WA 98052, USA (shutts@photon-machines.com)

The Thermo Scientific NEPTUNE *Plus* with Jet Interface offers unparalleled MC-ICP-MS sensitivity for all elements across the mass range. An ion yield of > 3 % has previously been reported for uranium solutions [1]. Sensitivity enhancements have been achieved through a combination of a dry high-capacity (up to 130 m^3/h) interface pump, X-cone, Jet cone, and desolvating nebuliser system.

The Thermo Scientific NEPTUNE *Plus* with Jet Interface was coupled with a Photon Machines excimer laser ablation system. This system features a short pulse width (4ns) 193 nm excimer laser and the HELEX 2 volume sample cell. The 193nm wavelength has been shown to reduce the particle size distribution of the aerosol produced by the laser ablation process [2] and this in turn has been shown to help minimize the effects of fractionation by ensuring that particles are in a size range so as to avoid incomplete vaporization and ionization in the plasma [3].

The sensitivity of the Jet Interface for small spot size (< 10 μm diameter) LA-MC-ICP-MS was trialled for natural uraninite and for NBS U-030 certified reference material. The minor uranium isotopes, ^{234}U and ^{236}U, were measured simultaneously on discrete dynode SEMs, with RPQ abundance sensitivity filters, whilst ^{238}U and ^{235}U were measured on Faraday cups with 10^{11} Ω amplifiers. This 'nuclear forensic' application was previously demonstrated with an older generation of MC-ICP-MS instrument, which required larger ablation volumes due to lower analyte sensitivity [4].

Hafnium isotope ratios were measured from zircon reference material 91500 using Faraday cups with 10^{11} Ω amplifiers. Figures of merit are given for precision from decreasing ablation spot sizes (i.e. improved spatial resolution).

[1] Bouman, C. *et al*. (2009) *Geochim. Cosmochim. Acta*. **73**(13, Supplement 1) [2] Guillong *et al*. (2003) *J. Anal. At. Spectrom*. **18** 1224–1230. [3] Kuhn *et al*. (2004) *Anal. Bioanal. Chem*. **378** 1069–1074. [4] Lloyd, N.S. *et al*. (2009) *J. Anal. At. Spectrom*. **24** 752–758.

https://doi.org/10.1180/S0026461X00006502 Published online by Cambridge University Press

Invasion of warm, saline, and well ventilated intermediate water in the cold stadials during the last 30,000 years? Evidence from the middle Okinawa Trough site MD01-2404

LI LO[1], YUAN-PIN CHANG[2]*, CHUAN-CHOU SHEN[1], MIN-TE CHEN[3] AND KUO-YEN WEI[1]

[1]Dept. of Geosciences, Natioal Taiwan Univ., Taipei 106, Taiwan (lo.rogerloli@gmail.com)
[2]Institute of Marine of Geology and Chemistry, National Sun-Yet Sen Univ., Kaohsiung, Taiwan (*correspondence: yuanpin.chang@mail.nsysu.edu.tw)
[3]Institute of Applied Geosciences, National Taiwan Ocean Univ., Keelung 20224, Taiwan (mtchen@ntou.edu.tw)

It has been proposed that the North Pacific may play an important role on the glacial deep water formation during the cold stadials in the last glacial[1]. This deep water formation hypothesis would impact the understanding of deep ocean circulation model and the interpretation of various geochemical proxies. Less evidence, however, could be found in the intermediate water (IW) in the western North Pacific Ocean (NPO). Here we present: 1) benthic foraminiferal (*Uvigerina peregrina*, >250 μm) $\delta^{18}O$[2], Mg/Ca ratios, and calculated $\delta^{18}O_w$ from Site MD01-2404 (24°48'N, 122°30'E, water depth 1397 m) in the middle Okinawa Trough (mid-OT), and 2) composite western NPO IW ventilation ages during the last 30, 000 years.

First, IW temperatures in the mid-OT showed rapid millennial timescale oscillation from 0 to 4 °C, and $\delta^{18}O_w$ were flucutated from -0.8 to 0.3 ‰. Druing the cold stadial periods, e.g. Younger Dryas (YD), Older Dryas, Heinrich events 1 (H1) and 2, and the stadial between Dansgaard-Oeschger interstadials 4 to 5, warm and saline IW could be recognized in the mid-OT region. Second, the ventilation age from the intermediate depth (978-1397 m) in the mid-OT and the western NPO were composited to further identify this warm-saline water mass origin. The age differences could as low as 800-1000 yrs in H1 and YD periods, and as high as ~2000 yrs druing Bølling-Allerød period.

In short, this study proposed a warm, saline and relatively well ventilated IW mass intrusion to the mid-OT during the cold stadial periods through the last 30, 000 years.

[1] Okazaki *et al*. (2010) *Science* **329**, 200–204. [2] Chang *et al*. (2009) *Paleoceanography*, doi, 10.1029/2007PA001577.

Geochemical study of the stone deterioration in a granitic monument of Oporto, Northern Portugal

J. LOBO[1] AND A. ALMEIDA[2]*

[1]ES/3 Daniel Faria – Baltar, Portugal
[2]CGUP, Universidade do Porto, 4169-007 Porto, Portugal (*correspondence: aalmeida@fc.up.pt)

The lighthouse of St Michael the Angel in the mouth of the Douro river, Porto, Portugal, has been selected for a geochemical study of the deterioration of the granite stone. The lighthouse-chapel was built in 1527, under a design by the Italian Francesco de Carmona. It has three entries, contemporary of its foundation. The dome exhibits a purity of Renaissance architecture. It constitutes a single copy in Portugal and the oldest in Europe. It is an emblematic building due to the historical features and also to the stone diseases associated to it.

The recognition of the main deterioration processes was based on the study of the representative granite facies of the Lighthouse of St. Michael the Angel. For this purpose a mineralogical and geochemical study of the granite stone deterioration and of the joint mortars, using various experimental techniques that include stereoscopic binocular microscopy, X-ray diffraction, scanning electron microscopy (SEM- EDS) and the Raman spectroscopy, was carried out. The diagnosis of the deterioration types show granular disintegration, plates, flakes, black crusts, thin black layers, biological colonization and fissuration. The geochemical study of the pathologies puts into evidence the formation of soluble salts and minerals, namely halite, gypsum, barite and calcite. The close proximity to the Atlantic Ocean in the river mouth is an important factor in the composition of rain water and in the formation of marine aerosols, with sodium chloride and sulphate ions.

The stones applied in the lighthouse were extracted from a local quarry of peraluminous two-mica granite, affected by late- to post-magmatic alteration processes well illustrated by the muscovitization of biotite and plagioclase. The potassic feldspar was strongly kaolinized. Hence, during the construction of the building, the stones already exhibited some chemical alteration inherited from the quarry, a fact that is confirmed by the presence of gibbsite and kaolinite that indicate a high degree of mineralogical evolution. The natural deterioration factors, mainly the long exposure to climate conditions and the rock susceptibility to weathering, are aggravated by the reaction of mortars with the rock minerals and by industrial and traffic pollution.

https://doi.org/10.1180/S0026461X00006502 Published online by Cambridge University Press

Fluoride complexation of yttrium under hydrothermal conditions

A. LOGES[1]*, A.A. MIGDISOV[2], T. WAGNER[3], A.E. WILLIAMS-JONES[2] AND G. MARKL[1]

[1]Institut für Geowissenschaften, University Tübingen, D-72070 Tübingen, Germany (*correspondence: anselm.loges@uni-tuebingen.de)
[2]Dept. of Earth and Planetary Sciences, McGill University, Montreal, Que., Canada H3A 2A7
[3]Institute of Geochemistry and Petrology, ETH Zurich CH-8902 Zurich, Switzerland

As a result of the recent upsurge in demand for new resources of the REE, there is an urgent need to better understand their behavior in hydrothermal systems. Here we report results of a study designed to determine formation constants for yttrium fluoride species by measuring the solubility of YF_3 in fluoride-bearing solutions. The experiments were performed at 150, 200, and 250°C and saturated water pressure, using the method of Migdisov *et al*. [1]. The pH and fluorine concentration were 0.85 to 3.05 and 3e-4 to 1e-1 mol/kg, respectively. Based on these experiments, Y speciation is dominated by mono-fluoride and di-fluoride complexes.

The elements Y and Ho are geochemical twins, with nearly identical ionic radii (900 pm and 901 pm) and the same oxidation state (3+) in nature. Consequently, they do not fractionate strongly in most geological systems. Important exceptions are fluorine-rich hydrothermal systems, in which their fractionation is pronounced. Our results allow us to assess fluoride-induced fractionation as a function of temperature and fluoride concentration and can be used to quantitatively model Y/Ho ratios in hydrothermal systems. This important geochemical indicator can extend our understanding of the transport processes of the economically important and geochemically interesting Rare Earth Elements.

[1] Migdisov, A.A. Williams-Jones, A.E. & Wagner, T. (2009) *Geochim. Cosmochim. Acta* **73**, 7087–7109.

Geochemical modeling of reactive minerals associated with *in situ* recovery of uranium

P. LONGMIRE, V. LAGNEAU AND M. BOUZID

MINES ParisTech, Centre de Géosciences, 35 rue Saint Honoré, 77305 Fontainebleau, France (patrick.longmire@mines-paristech.fr, vincent.lagneau@mines-paristech.fr)

Dissolution of uraninite and pyrite in the presence of oxidants and SO_4^{2-} derived from H_2SO_4 are important geochemical processes taking place during *in situ* recovery (ISR) of uranium worldwide. During ISR of uranium using H_2SO_4, pH values of 3 or less are typically achieved depending on the buffering capacity of reactive (intermediate kinetic) minerals. Reactions involve significant dissolution of uraninite and primary silicate minerals. Possible precipitation of secondary minerals (gypsum, alunite, and jurbanite) can also occur under localized acidic conditions. Geochemical modeling using PHREEQC and HYTEC was conducted to quantify dissolution and redox reactions. The pre-extraction geochemistry is built, in agreement with observations, by equilibrating groundwater with primary phases (uraninite, pyrite, K-feldspar, hematite, calcite, kaolinite, Mg-montmorillonite, and Ca-nontronite). Acidification results in early-stage dissolution of Fe (III) minerals, which initiates oxidative and irreversible dissolution of uraninite and pyrite. Surface-controlled dissolution of K-feldspar, kaolinite, and Mg-montmorillonite with intermediate kinetics produces an acidic, mixed solute [Al-Ca-Fe (II)-SO_4] composition, enhancing precipitation of alunite and jurbanite. 2D simulations were then performed to study mixing effects, particularly near the production wells. Flow velocities can be much smaller for longer stream-tubes allowing for slower kinetic reactions to be effective. The amount of buffering by calcite increases along these flow paths characterized by increasing pH- buffering capacity.

https://doi.org/10.1180/S0026461X00006502 Published online by Cambridge University Press

Modeling local and remote impacts of Amazonian biomass burning aerosols

K.M. LONGO[1]*, S.R. FREITAS[2], N.E. ROSÁRIO[3,2], R. SIQUEIRA[1], J. HOELZEMMAN[1], M.S. GÁCITA[2] AND E. IGNOTTI[4]

[1]Center for Earth Science System, Brazilian Nacional Institute for Space Research, São José dos Campos, SP, Brazil (*correspondence: karla.longo@inpe.br) (ricardo.siqueira@inpe.br) (judith.hoelzemman@inpe.br)

[2]Center for Weather Forecast and Climate Studies, Brazilian Nacional Institute for Space Research, São José dos Campos, SP, Brazil (saulo.freitas@cptec.inpe.br) (madeleine.sanchez@cptec.inpe.br)

[3]Atmospheric Science Department, University of São Paulo, São Paulo, SP, Brazil (nrosario@model.iag.usp.br)

[4]University of Mato Grosso State, Alta Floresta, MT, Brazil (eignotti@ensp.fiocruz.br)

Every year, biomass burning in Amazonia releases large amounts of aerosols into the atmosphere. The consequent change from low to very high atmospheric concentration of aerosols therefore affects the radiative, cloud physical and chemical properties of the atmosphere over Amazonia. This represents a dramatic perturbation to the local and regional climate, ecology, water and nutrients cycles, and human life. Given the magnitude of biomass burning in Amazonia and the efficiency of the process of atmospheric transport of fire emissions, there perturbations are very likely to affect the climate system even on a global scale. Here, we examine the smoke aerosols simulated by CCATT-BRAMS model (an aerosol and chemistry transport model coupled on-line to a non-hydrostatic and compressible mesoscale model) over South America, aiming to use the model results to assess the local and remote impacts. We will present the current model status, summarizing the efforts made in terms of numerical model development, in order to better represent within the model the atmospheric processes that are the main drivers of the fate of fire emissions and that lead to smoke impacts. Based on a 13-year numerical simulation, we will draw the general pattern of smoke long-range transport over the South American continent and explore local and remote impacts. We will discuss the smoke radiative impacts on the hydrological cycle, surface processes as well as on the troposheric chemistry over the affected areas. Finally, the human dimension of the problem will be visualized throughout correlations between the hospitalization rate of children and elderly people and the level of smoke exposition.

Geochemistry of xenoliths from the Gibeon Kimberlite Province, Namibia

M. LONGO[1], P. NIMIS[1], L. ZIBERNA[1], A. MARZOLI[1], A. ZANETTI[2] AND L. FRANZ[3]

[1]University of Padua, Department of Geosciences, Italy (micaela.longo@unipd.it, paolo.nimis@unipd.it, luca.ziberna@studenti-unipd.it, andrea.marzoli@unipd.it)

[2]IGG-CNR, Italy (zanetti@crystal.unipv.it)

[3]University of Basel, Switzerland (leander.franz@unibas.ch)

Mantle xenoliths from the off-craton Gibeon Kimberlite Province (southern Namibia) include garnet peridotites with coarse equant (CE) to mosaic porphyroclastic (MP) textures. The Gibeon mantle is characterized by a perturbed geotherm, with displacement of the most deformed MP-samples to ca. 200°C higher T [1, 2]. We have analysed by LA-ICP-MS the trace element compositions of garnets (Grt) and clinopyroxenes (Cpx) in ten Grt-peridotites from the Gibeon Townsland 1 pipe. The samples included Cpx-bearing and Cpx-free xenoliths showing CE to MP textures and varying estimated equilibrium T. One Grt shows a sinusoidal REE_{CI} profile, with peak at Eu and HREE between 2 and 5xCI, typical of depleted peridotites affected by fluid-metasomatism [3]. The other Grts are richer in HREE (≈10xCI) and show normal or sloped REE_{CI} profiles. The coexisting Cpxs show LREE-enriched profiles with variable La_{CI}/Sm_{CI} ratios (0.6-5.1). Zr vs. HREE (Y) relations are typical of more fertile peridotites affected by variable degrees of melt-metasomatism, possibly involving both PIC- and MARID-type agents [4]. No relationship has been observed between geochemical compositions and xenolith texture or PT conditions. This suggests that the recorded thermal perturbation postdated the above peridotite metasomatism and refertilisation.

[1] Franz *et al*. (1996) *Contrib Min Petr* **126**, 181–198. [2] Franz *et al*. (1996) *J Geol* **104**, 599–615. [3] Creighton *et al*. (2009) *Contrib Min Petr* **157**, 491–504. [4] Grégoire *et al*. (2003) *J Petrol* **44**, 629–657.

https://doi.org/10.1180/S0026461X00006502 Published online by Cambridge University Press

Preliminary account of the Silurian carbon isotope record ($\delta^{13}C_{org}$) from the Barrancos region, Ossa Morena Zone, Portugal

G. LOPES[1,3]*, P. FERNANDES[1], R. GOODHUE[2], Z. PEREIRA[3] AND J.M. PIÇARRA[4]

[1]CIMA, University of the Algarve, Campus de Gambelas, 8005-139 Faro, Portugal (*correspondence: gilda.lopes@lneg.pt)
[2]Department of Geology, Trinity College Dublin, Ireland
[3]LNEG, Ap.1089, 4466-956 S. M. Infesta, Portugal
[4]LNEG, Ap. 104, 7801-902 Beja, Portugal

The Barrancos region provides one of the reference sections for the Silurian of the Ossa Morena Zone in Portugal. In this area the Silurian succession is condensed, with a maximum thickness of 50 m and the ages provided by graptolite faunas indicates that all the Silurian system is represented here. The lithologies are fairly homogenous throughout the succession consisting of black carbonaceous shales interbedded with black cherts, that were deposited in marine basins that developed at the northen margins of the Gondwana continent. This study is the first attempt to characterize the variation of $\delta^{13}C_{org}$ in this region, in order to assess well-documented Silurian climatic events.

The studied section is located at Monte do Carreba, near Barrancos village, and consists of a 45 m thick succession of black shales and cherts with graptolite faunas that indicates a Llandovery to lower Ludlow age. The base of the section is faulted against Upper Ordovician greywackes and quartzites. In this section $\delta^{13}C_{org}$ shows a baseline of consistent low values ranging from -25.88 to -25.10‰. This is interrupted by three positive excursions with maximum values of: -22.73‰ at the transition between the Llandovery (Telychian) and Wenlock (Sheinwoodian), -23.33‰ at the Homerian and -23.09‰ at the transition between the Wenlock and Ludlow (Gorstian). The excursions have positive shifts between +2.55 and +3.15‰ and are tentatively related to the three first global climatic events recognized for the Silurian (Ireviken, Mulde and Linde). Although this study is a preliminary account of $\delta^{13}C_{org}$ in this region, it could provide usefull data for the recognition and discussion of climatic global events in high latitude regions as was the OMZ located during Silurian times and for sections with high level of thermal maturation.

This study was sponsored by FCT (PhD grant SFRH/BD/48534/2008).

Isotope geochemistry of São Tomé Island (Cameroon Volcanic Line): Implications for mantle source components

J.M.R. LOPES[1], R. CALDEIRA[2,3]*, U.G. CORDANI[1] AND J.M. MUNHÁ[3]

[1]IGC-USP – Instituto de Geociências - Univ. São Paulo, BR
[2]LNEG – Laboratório Nacional de Energia e Geologia, PT (*correspondence: rita.caldeira@lneg.pt)
[3]CeGUL – Centro de Geologia da Univ. Lisboa, PT

An asthenospheric origin for the Cameroon Volcanic Line (CVL) is today an accepted fact. Its mantle source has been ascribed to a mixture of HIMU with DMM enriched with EM I components. However, in view of the redefined FOZO (Focal Zone) it has been suggested that CVL basalts are generally outside the typical HIMU field and instead encompass de FOZO domain, a component suggested to be common to all OIBs. Here we present new Sr and Nd isotopic data for the previously defined São Tomé Island main volcanic units (CMZ: 6 -8 Ma; CRA: 2.5 - 5 Ma; CST: < 1.5 Ma). São Tomé basalts ($^{87}Sr/^{86}Sr)_i$ = 0.703046 to 0.703530 and εNd = 3.15 to 5.56 isotopic data are similar to values found for other CVL basalts and fit within the projection plane defined by isotopic compositions of the HIMU, DMM and EMI mantle components, displaying a trend between these two. However they also fit, almost perfectly, within the FOZO domain. In addition, already published $^{206}Pb/^{204}Pb$ (19.4 to 20.1) data on São Tomé is consistent with a FOZO contribution, pointing out to FOZO prevalence as the main source component over HIMU. The new data also show an increase in $^{143}Nd/^{144}Nd$ towards the younger volcanic unit, which can be interpreted as a waning of the EMI component with a resulting increase of DMM. Accordingly we propose that the São Tomé magmatism was derived from a deep-seated (FOZO) signature, mixed with DMM and EMI components.

https://doi.org/10.1180/S0026461X00006502 Published online by Cambridge University Press

Microbial populations of clay formations and their interactions with uranium

M. López Fernández, O. Fernández Sanfrancisco, M. Martinéz García, P. Ranea Robles, T. Galera Monge, A. Moreno García and M.L. Merroun

Department of Microbiology, University of Granada, Spain (merroun@ugr.es)

Clay formations are considered a very important part of many deep geological repository designs for the final geological disposal of radioactive wastes. The present work describes the culture-dependent bacterial diversity of two different bentonite samples (BI and BII) recovered from clay deposits of 'Cortijo de Archidona' (Almeria, Spain), chosen as potential host rock model for the deep geological disposal of radioactive wastes. The mineralogy of these two samples dominated by smectite phases, slightly differs by the presence of the iron sulphate mineral phase, jarosite (KFe^{3+}_3 $(SO_4)_2$ $(OH)_6$), for the sample BII. The culture dependent microbial diversity studies were performed using media based on clay porewater supplemented with different organic carbon sources, oligotrophic media, etc. The evaluation of aerobic bacterial populations clearly indicated the presence of high numbers of cultivable bacteria in both samples. Bacteria belonging to *Actinobacteria* (*Arthrobacter*, *Micrococcus*, *Amycolotapsis, Kocuria, Isoptericola*), *Gammaproteobacteria* (*Pseudomonas*, *Stenotrophomonas*), *Bacilli* (*Bacillus*), etc. were identified. The interactions of selected isolated bacteria with uranium were studied using a combination of spectroscopic, microscopic and microbiological techniques. A high fraction of the bacterial population (e.g. *Stenotrophomonas* sp.) was able to tolerate high concentrations of uranium up to 10 mM, etc. U precipitation as uranium phosphate mineral phases (e.g. meta-autunite) was involved in the bacterial tolerance to this radionuclide and in the immobilization of this element in the environment.

Geochemical evidence of mud volcano activity in the West Alboran Sea

C. Lopez-Rodriguez[1]*, F. Martinez-Ruiz[1], M.C. Comas[1], C. Hensen[2], E. Piñero[2], M.E. Böttcher[3], O. Dellwig[3] and C. Lenz[3]

[1]Instituto Andaluz de Ciencias de la Tierra (CSIC-University of Granada), 18100 Granada, Spain (*correspondence: carmina@ugr.es)

[2]Leibniz Institute of Marine Sciences, IFM-GEOMAR, Wischhofstr.1-3, D-24148 Kiel, Germany

[3]Leibniz Institute for Baltic Sea Research (IOW), Seestr. 15, D-18119 Warnemünde, Germany

A broad field of mud volcanoes ('MVs') and pockmarks occur in the West Alboran Sea behind of the Gibraltar Arc. These sea-floor structures appear upon a major sedimentary depocenter encompassing Miocene to Holocene sedimentary sequences more than 7 km thick. The MVs are rooted at diapirs formed by undercompacted units from the older sediments, as demonstrated by geophysical data. Here we provide geochemical results of pore waters obtained with rhizons from two gravity cores drilled in the Southern Mud-volcano Field: the Carmen MV ('CMV') and the Unnamed Pockmark ('UPM'), which locates SW near CMV. In order to estimate their actual activity and determine if fluid composition is influenced by the presence of hydrocarbons, dissolved anions (SO_4^{2-}, Cl^-, I^-, and Br^-) and major and trace cations (Li^+, Na^+, K^+, Mg^{2+}, Ca^{2+}, Sr^{2+}, Ba^{2+}, Mn^{2+}, Fe^{2+}), besides boric acid and silica, were analysed using IC and ICP-OES. CMV fluids are depleted with depth in SO_4^{2-}, Mg^{2+}, K^+ and Br^- and enriched in Li^+ and B. Such dissimilarities evidence that CMV is active. Furthermore, CMV fluids show freshening at depth, similar to results found at active MVs from the Gulf of Cadiz, which suggests that the decrease in chlorinity is related with gas hydrate dissociation. By contrast, the UPM fluids show constant vertical trends for dissolved concentrations of non-metabolites. The profiles of salinity and conservative ions (Na^+ and Cl^-) indicate Mediterranean seawater as the major source at the UPM and therefore no clear evidence for seepage activity at present. Our results point to the close coexistence of active -methane emission- and inactive seepages structures in the Southern Mud-volcano Field of the Alboran Sea.

Supported by projects CTM2009-07715, TOPOMED-CGL2008-03474 and CONSOLIDER-INGENIO2010-CSD2006- 00041 (MICINN and FEDER funds, Spain), RNM3713, RNM5212 & RNM215 (PAI-JA, Spain)

https://doi.org/10.1180/S0026461X00006502 Published online by Cambridge University Press

Tungstate polymerization and its role in sorption on iron and aluminum oxyhydroxides

E.A. LORENZ[1], H. HUR[2] AND R.J. REEDER[1]*

[1]Dept. of Geosciences, Stony Brook Univ., Stony Brook, NY 11794 USA (*correspondence: rjreeder@stonybrook.edu)
[2]Dept. of Chemistry, Stony Brook Univ., Stony Brook, NY 11794 USA

Tungsten, although largely unregulated as an environmental pollutant, is now identified as an emerging contaminant, partly as a consequence of its widespread use in commercial, industrial, and military applications. Interaction with mineral substrates is considered an important process governing the mobility of dissolved tungsten species in aquatic and soil systems. We examined the uptake of tungstate species by iron and aluminum oxyhdroxide phases in model systems. Results indicate that W(VI) uptake is strongly dependent on pH and W concentration. The pH dependence determined from batch studies (pH 4-8) shows sorption behavior typical of anions, with only minor dependence on ionic strength. Sorption isotherms of tungstate on iron and aluminum oxyhydroxide phases show Langmuir-like uptake at low W(VI) concentrations, but increasing uptake at higher concentrations. Solution speciation calculations suggest that a monomeric tungstate species dominates at pH > 7, with formation of polymeric tungstate species favored at lower pH and with increasing W concentration. W L_3-edge EXAFS and W L_1-edge XANES of tungstate solutions are consistent with a monomeric tungstate species at pH 8 and at least one polymeric tungstate species present in solution at pH 4, which is consistent with speciation calculations. EXAFS and XANES of tungstate sorbed on goethite over the pH range 4-8 and at W concentrations 25-1000 uM show spectra that are similar and suggest that tungstate polymerization occurs at the surface, either forming a polytungstate sorption complex or a surface precipitate. This conclusion is supported by differential pair distribution function data, which show correlations extending to 11 Å that are likely attributable to the W-W pair correlations present in polytungstates. EXAFS and XANES spectra of tungstate sorbed onto bohemite over similar pH and W concentrations show differences in uptake mechanism not observed for goethite. Desorption experiments reveal limited reversibility of uptake, consistent with formation of a surface precipitate. These initial findings emphasize the need for additional research to assess the importance of sorption in limiting the mobility of dissolved tungstate in the environment.

Talvivaara Ni deposit and ore potential of Palaeoproterozoic black shale formations in Finland

K. LOUKOLA-RUSKEENIEMI[1]*, E. HYVÖNEN[2], H. ARKIMAA[1], M.-L. AIRO[1], J. VANNE[3], J. LERSSI[3] AND S. VUORIAINEN[1]

[1]Geological Survey of Finland, P.O. Box 96, FI-02151 Espoo, Finland (*correspondence: kirsti.loukola-ruskeeniemi@gtk.fi)
[2]Geological Survey of Finland, P.O. Box 77, FI-96101 Rovaniemi, Finland
[3]Geological Survey of Finland, P.O. Box 1237, FI-70211 Kuopio, Finland

The black-shale-hosted Talvivaara deposit contains more than 1 000 Mt of low-grade Ni-Cu-Co-Zn-Mn ore. The two ore bodies are from 20 m to > 450 m thick, less than 2 km long and almost 0.5 km wide. The textures, mineralogy and geochemistry of the black shales have been studied earlier [e.g. 1, 2].

Talvivaara black shales are characterized by high organic C and S concentrations with median values of 7.6% and 9%, respectively, and the occurrence of horizons with Mn≥0.8%. Nickel precipitated in organic-rich mud from Ni-rich bottom waters in an epicontinental stratified marine basin. The Mn-rich horizons were probably deposited on the margins of the euxinic basin or, alternatively, Mn was derived via upwelling from oxygen-minimum zones.

The ore potential of black shale formations in Finland was first evaluated by nation-wide airborne geophysical surveys, because the geophysical properties of black shales can be used for preliminary classification [3, 4]. Textures, mineralogy, geochemistry and petrophysical properties were studied from altogether 800 black shale samples. Concentrations of organic C and S were as high as at Talvivaara in many localities in eastern and northern Finland, but Ni-Cu-Co-Zn and/or Mn concentrations were lower. High Pd and Pt concentrations were found in some prospects.

A mass extinction for 2 Ga ago has been suggested for the origin of the high C in certain thick (> 50 m) black shale formations in eastern and northern Finland [5].

[1] Loukola-Ruskeeniemi & Heino (1996) *Econ. Geol.* **91**, 80–110. [2] Loukola-Ruskeeniemi (2011) *Geological Survey of Finland, Special Paper* **51**. [3] Arkimaa *et al.* (2000) Black Shale Map 1 , 1 000 000. Geological Survey of Finland. [4] Airo & Loukola-Ruskeeniemi (2004) *Ore Geology Reviews* **24**, 67–84. [5] Loukola-Ruskeeniemi (2000) *Geol. Soc. of America*. Abstracts with Programs **32**(7) A-5.

https://doi.org/10.1180/S0026461X00006502 Published online by Cambridge University Press

Magnetic parameters of soils developed on different geologic backgrounds, Central Portugal

A. LOURENÇO[1], H. SANT'OVAIA[2] AND C. GOMES[3]

[1]CGUC, DCT, Universidade de Coimbra, Universidade de Coimbra, Largo Marquês de Pombal, 3000 - 272 Coimbra (*correspondence: ana.lourenco@dct.uc.pt)
[2]Centro de Geologia da U. Porto, DGAOT, FCUP, R Campo Alegre, 4169-007 Porto, Portugal
[3]CGUC, DCT, Universidade de Coimbra, Largo Marquês de Pombal, 3000 - 272 Coimbra, Portugal

Three different types of soils were studied using the environmental magnetism method in the Coimbra region, Central Portugal. Mass specific magnetic susceptibility and isothermal remanent magnetization imparted at 1 tesla (IRM_{1T}) were determined in order to characterize and map the topsoils in an area of 200 km^2. The soils studied are Fluvisols, Cambisols and Leptosols, according to FAO classification. Fluvisols are formed on the alluvial plain of Mondego River (Holocene age). Leptosols and Cambisols are formed on metamorphic rocks of Proterozoic age and red sandstones of Upper Triassic age. Magnetic susceptibility was measured on 48 surface soil samples. This parameter ranges between 0.10 and 1.04 (10^{-6} m^3kg^{-1}) in Fluvisols, between 0.09 and 4.06 (10^{-6} m^3kg^{-1}) in Cambisols and between 0.35 and 6.20 (10^{-6} m^3kg^{-1}) in Leptosols. The IRM_{1T} measured on 32 samples of Cambisols and Leptosols. IRM_{1T} values ranges between 0.60 and 107.40 (10^{-3} Am^2kg^{-1}) in Cambisols and between 4.10 and 49.04 (10^{-3} Am^2kg^{-1}) in Leptosols. The results revealed that the magnetic parameters are higher in soils formed on metamorphic rocks than on sandstones. In this case study the differences obtained are mainly due to the lithological and pedological influences and the role of the geological background is clear. The anthropogenic Fe-particles contribution is only obvious near roads and rivers. Topsoil magnetic parameters can be useful as a proxy to anthropogenic pollution particles and an auxiliary tool for geologic and soil mapping.

Assessing cementation in the El Capitan Reef Complex and Lincolnshire Limestone using ^{13}C-^{18}O bond abundances in carbonates

SEAN J. LOYD[1]*, TONY DICKSON[2], JOHN D. HUDSON[3], JOHN M. EILER[4] AND ARADHNA K. TRIPATI[1]

[1]University of California, Los Angeles, Los Angeles CA USA (*correspondence: seanloyd@ucla.edu)
[2]Univ. of Cambridge, Cambridge, UK
[3]Univ. of Leicester, Leicester, UK
[3]Calif. Inst. Of Tech., Pasadena CA, USA

The Permian El Capitan and Jurassic Lincolnshire limestones have been intensely studied for their stratigraphy, depositional setting and paleoecology. Nevertheless, the diagenetic development of these two units remains controversial, particularly with regard to diagenetic carbonate formation. Calcite cement phases have previously been characterized via $\delta^{18}O$ and $\delta^{13}C$ in order to determine precipitation temperatures and carbon sources, however, these results have lead to conflicting hypotheses.

Here, we present clumped isotope data (values corresponding to of the relative abundance of the ^{13}C-^{18}O bond in carbonates) from cements of the El Capitan and Lincolnshire limestones in an attempt to more robustly characterize precipitation temperatures and directly calculate fluid $\delta^{18}O$ values, a previously elusive measurement. Intriguingly, the resultant data display a fairly tight positive correlation between these two parameters ($R^2 \sim 0.7$ for both units). In El Capitan calcites, cements with elevated fluid $\delta^{18}O$ closer to seawater values (from ~ –2‰ VSMOW) exhibit higher precipitation temperatures (up to 70°C) than those with isotopic compositions more like meteoric fluids (down to ~ –10‰ and 28°C). The Lincolnshire Limestone calcites formed in fluids with $\delta^{18}O$ values and temperatures ranging from ~ –3‰ and 50°C to ~ –6.5‰ and 32°C, respectively.

These results suggest a tight coupling between pore water evolution and cement precipitation temperature, a somewhat intuitive finding. However, the trajectory of the combined fluid $\delta^{18}O$ and temperature trend is intriguing and potentially transformative in our understanding of the cementation of carbonate rock units. In both units, progressive cementation follows a trend toward increasingly meteoric-like fluids potentially suggesting precipitation in mixed-zone settings rather that a strictly marine environment. The nature of cementation, its bearing on the reported geochemical signatures and the implications for standing hypotheses will be discussed further.

https://doi.org/10.1180/S0026461X00006502 Published online by Cambridge University Press

Synergistic effects of biocatalysis and mineral photocatalysis

ANHUAI LU AND YAN LI

School of Earth and Space Sciences, Peking University, Beijing 100871, P.R. China (ahlu@pku.edu.cn)

Geophotocatalysis of natural semiconducting minerals play key roles in driving redox reactions on earth surface. Whether it is related to microbial metabolism remains unknown. This study focused on revealing the potential interactions among light, microbes and minerals by studying the relationship between bacterial metabolism and semiconducting mineral photocatalysis. To achieve this goal, a photoelectrochemical approach was employed by using a microbial fuel cell (MFC)-based equipment. To distinguish from traditional MFC, the novel system is named as light fuel cell (LFC), which is specifically used for investigating the biophotochemical reactions participated by microorganisms and semiconducting minerals. When using O_2 as the cathodic electron acceptor, the volumetric power density of a LFC with a microbial anode and a visible light-irradiated rutile-cathode was 12.1 W/m^3, 1.6 times higher than that obtained in the dark (7.5 W/m^3). Electrochemical impedance spectroscopy (EIS) data indicated that the cathodic polarization resistance of the LFC in light was 196 Ω, while that operated in the dark was 2820 Ω. These results manifested the synergistic effect of biocatalysis and semiconductor photocatalysis significantly improved the electron transfer efficiency. Further experiments showed a broad range of pollutants (e.g. hexavalent chromium, azo dyes, landfill leachate) were effectively treated in this system. The finding that microorganisms can donate electrons to photoexcited semiconducting minerals not only indicated a new aspect of microbe-mineral interactive pathway, but also predicted a new environmental remediation strategy. Based on our study, we believe the exploration of LFC will help in discovery of natural solar-driven biogeochemical process and development of interdisciplinary techniques in environmental remediation.

Two contrasting ore-bearing granites: Sn-bearing Qitianling granite and W-bearing Xintianling granite, Hunan province, China

JIANJUN LU, RONGQING ZHANG AND RUCHEN WANG

State Key Laboratory for Mineral Deposits Research, School of Earth Sciences and Engineering, Nanjing University, Nanjing, 210093, China (lujj@nju.edu.cn)

The Xintianling skarn type scheelite deposit is located to the northern of the Qitianling composite pluton associated with Furong tin deposit and was considered genetically to be relative to the Qitianling granite pluton. The authors had carried out in detail investigations to the age, Hf isotope and geochemical features of the Qitianling granite and the granite spatially associated with the Xintianling tungsten deposit.

The Qitianling composite pluton is mainly composed of hornblende biotite monzogranite with an age of 160~163 Ma, biotite monzogranite with an age of 153~157 Ma and fine-grained granite with an age of 146~150 Ma. These granitic rocks have higher contents of TiO_2, MgO, FeOt, HFSE (Zr+Nb+Y+Ce), total REE and LREE and higher ratio values of 10000×(Ga/Al), Th/U and LREE/HREE. They have an average values of 0.53 wt%, 0.62 wt%, 3.31 wt%, 491.48 ppm, 335.92 ppm, 305.59 ppm, 3.13, 3.51 and 10.87, respectively. The average values of A/CNK and zircon saturation temperature are 0.96 and 818 °C respectively. The ε_{Hf} (t) values of the zircons in the Qitianling granite vary from -8.1 to -3.7. These geochemical features indicate that the Qitianling granite belongs to A_2-type granite.

The granite relating to Xintianling skarn type scheelite deposit (named as Xintianling granite) consists mainly of fine to medium grained biotite granite with an age of 165 Ma and fine-grained biotite granite with an age of 154.5 Ma. The Xintianling granite has lower contents of TiO_2, MgO, FeOt, HFSE (Zr+Nb+Y+Ce), total REE and LREE and lower ratio values of 10000×(Ga/Al), Th/U and LREE/HREE. They have an average values of 0.18 wt%, 0.21 wt%, 1.15 wt%, 164.25 ppm, 87.65 ppm, 75.40 ppm, 2.43, 1.57 and 5.90, respectively. The average values of A/CNK and zircon saturation temperature are 1.03 and 734 °C respectively. The ε_{Hf} (t) values of the zircons vary from -12.7 to -6.1. The Xintianling granite belongs to S-type granite.

The geochemical characters discussed above demonstrate that the W-bearing Xintianling granite is genetically entirely different from the Sn-bearing Qitianling granite.

This work was financially supported by the NSFC (40873029) and China Geological Survey (1212010632100).

https://doi.org/10.1180/S0026461X00006502 Published online by Cambridge University Press

Environmental protection design of Chinese highway tunnel

LU JUN-FU[1]* AND CUI GUANG-YAO[2]

[1]State Key Laboratory of Geohazard Prevention and Geoenvironment Protection, Chengdu University of Technology, Chengdu, 610059, China (*correspondence: jyyuan521@126.com)
[2]School of Civil Engineering, Southwest Jiaotong University, Chengdu, 610031, China

The environmental protection design of highway tunnel mainly includes 3 aspects: environmental protection design for tunnel portal, water-proof and drainage environment protection design, environmental protection landscape and illumination design in tunnel.

The principle of environmental protection design for tunnel portal is 'natural, concise, harmonious with environment, not exaggerating deliberately and protecting original natural landscape of tunnel'. The content of environmental protection design for tunnel portal is the selection of tunnel portal placement and type. The selection of tunnel portal placement should be a placement that protects the natural status of mountain massif to a largest degree. The selection of tunnel portal placement should avoid high side slope and is good for being compatible with environment. Bamboo-truncating and end wall portal types are recommended because of convenient in construction, handsome appearance, reasonable strength distribution and good seismic behavior.

The principle of water-proof and drainage environment protection design is 'prevention first, blocking and intercepting coordination, and supported by clearing'. The main method to deal with this problem of adopting combined lining to prevent water, improving the anti-permeability of concrete, dealing with the deformation joint and construction joint and so on.

The purpose of environmental protection landscape and illumination design in tunnel is to improve the driving environment and the comfort index. The main methods are: to increase light illumination in tunnel, to arrange artificial green landscape in tunnel, to plant green plants at the tunnel portal and so on.

[1] CUI GUANG-YAO (2010) *Geochimica et Cosmochimica Acta,* **74**(12) Supplement **1**, A199. [2] Xu WL, Zhang JQ(2010) *Geochimica et Cosmochimica Acta,* **74**(12) Supplement **1**, A1162.

Elucidating the functions of the active microbial community of Iron Snow in an acidic lake

S. LU[1]*, K. CHOUREY[2], M. REICHE[1], V. CIOBOTĂ[1], S. NIETZSCHE[1], R.L. HETTICH[2] AND K. KÜSEL[1]

[1]Friedrich Schiller University Jena, 07743 Jena, Germany (*correspondence: shipeng.lu@uni-jena.de)
[2]Oak Ridge National Laboratory, Oak Ridge, TN, USA

Lignite mine lakes are characterized by low pH, low nutrient status, and high concentrations of Fe (II) and sulfate. In lignite mine lake 77, located in Brandenburg, Germany, microbial oxidation of Fe (II) at redoxclines with opposing Fe (II) and oxygen gradients leads to the formation of iron-rich macroscopic aggregates (Iron Snow, IS). The IS provides an important input for the reduction of Fe (III) in the anoxic hypolimnion which shows different pH values ranging from 3.3 - 4 to 3.4 - 5.9 in the center basin (CB) or north basin (NB), respectively. Thus, the diversity and function of the IS microbial communities responsible for Fe-cycling may be dissimilar. This study aimed to i) characterize microbial communities from CB and NB and ii) explore active Fe-cycling microorganisms through RNA- and proteomic-based methods. Fe (III) mineral schwertmannite was the dominating iron oxide in CB and NB samples using SEM, EDX and Raman spectroscopy. Metaproteomics analyses was performed using detergent-based cellular lysis for total protein extraction followed by LC-MS/MS interrogation. Spectral matches were accomplished using an artificial metagenome, (assembled using 175 genomes of sequenced reference isolates) and yielded a total of 390 different proteins representing 43 microorganisms in NB samples, and 105 proteins tracing back to 27 genus from CB samples. Proteins of *Chlorobium*, *Acidiphilium*, *Acidovarax*, *Azoarcus*, *Burkhoderia* and *Geobacter* species were detected in both NB and CB samples. *Acidothiobacillus* related proteins were only determined in NB while those related to *Ferroplasma* and *Sulfolobus* were discovered in CB primarily. Detections of cytochrome c class I of *Acidiphilium* JF5 in both NB and CB indicated its active role in Fe (III) reduction among the lake. Carboxysome proteins were found in *Acidimicrobium ferrooxidans* and *Acidithiobacillus* species, suggesting their capacity of CO_2-fixation coupled to Fe (II) oxidation in the upper oxic water epilimnion in Lake 77. 16S rRNA gene libraries and q-PCR for functional proteins will further provide insights into the ecophysiology of the Fe-cycling microorganisms in acidic environments.

https://doi.org/10.1180/S0026461X00006502 Published online by Cambridge University Press

The crystal morphology of aragonite and its implications in pumping pipe of hot spring, Taiwan

YI-CHIA LU*, SHENG-RONG SONG, CHIA-MEI LIU AND LIN HUANG

Department of Geosciences, National Taiwan University (*correspondence: yichialu@ntu.edu.tw, srsong@ntu.edu.tw, d91224006@ntu.edu.tw, linhuang@ntu.edu.tw)

This study investigates crystal morphology of sinter and discusses what kinds of factors controlling crystal morphology of aragonite to reconstruct the pumping history of hot spring.

The pipe sinter of this study is collected from Ho-Ya SPA hotel, located in Rui-Shui, Hualien County of Taiwan. Precipitated minerals of it are predominantly composed of aragonite (>99.4%) with preferred orientation by Electron Backscatter Diffraction (EBSD). The sinter displays the rings of gray, white and gray from outside to inside. The white ring of sinter is composed of many strips, but the gray one is not by naked-eyes. Under optical microscope, there are two particle morphologies of aragonite in Ho-Ya SPA white sinter. One is small and rounded crystal gathered to strips, while the other is needle. However, the gray ring almost consists of needle shape of aragonite.

Holcomb *et al*. (2009) [1] simulated the coral's growth and concluded that the small and rounded crystal is owing to high pH and saturation state in the solution. In coral, the gathered small and round crystals are called centres of calcification (COC).

In this case, we propose that the higher pumping rate causes the rapid depressurization to over-saturate quickly, and then crystals nucleate and grow. This process may generate higher porosity and rounded shape of aragonite.

In low season with low pumping rate, the aragonite grows the fine and elongate crystal due to slow supply of hot spring. However, in peak season with high pumping rate causes the quick degassing of CO_2 to occur over-saturated in solutions, then precipitate aragonite rapidly and generate rounded crystals with larger porosity. The crystal morphology, therefore, of the colorful rings implies that the sinter of Ho-Ya hot spring grows at the summer-winter-summer during one and a halfyears.

[1] Holcomb *et al*. (2009) *Geochimica et Cosochimica Acta* **73**, 4166–4179.

Reaching part-per-quadrillion: detection of ^{39}Ar in environmental samples using ATTA

Z.-T. LU[1,2]*, K. BAILEY[1], A.M. DAVIS[3], S.-M. HU[4], W. JIANG[1], P. MUELLER[1], T.P. O'CONNOR[1], R. PURTSCHERT[5], N.C. STURCHIO[6], Y.R. SUN[4] AND W. WILLIAMS[1]

[1]Physics Division, Argonne National Lab (*correspondence: LU@ANL.GOV)
[2]Department of Physics, University of Chicago
[3]Dept. of Geophysical Sciences, University of Chicago
[4]Hefei National Laboratory, USTC, China
[5]Climate and Environmental Physics, University of Bern
[6]Earth & Environmental Science, Univ of Illinois at Chicago

The Atom Trap Trace Analysis (ATTA) method has been used to analyze the cosmogenic isotope ^{39}Ar (half-life = 269 yr, isotopic abundance ~ 8×10^{-16}) in the atmosphere [1, 2]. With this demonstration, ATTA has reached a new milestone of detecting isotopes at the abundance level of less than one part per quadrillion. Along with the previously demonstrated analyses of ^{81}Kr (229, 000 yr, ~10^{-12}) and ^{85}Kr (10.8 yr, ~10^{-11}), ATTA can now analyze all three long-lived noble gas radioisotopes covering a wide range of ages and applications in the earth sciences. The detection of ^{39}Ar was made possible by a large improvement (x 100) in both the counting rate and counting efficiency of the ATTA method. We have developed a new apparatus (ATTA-3) to perform ^{81}Kr dating with a required sample size of 10-100 liters of water or ice. This work is supported by DOE, Office of Nuclear Physics, and by NSF, Division of Earth Sciences.

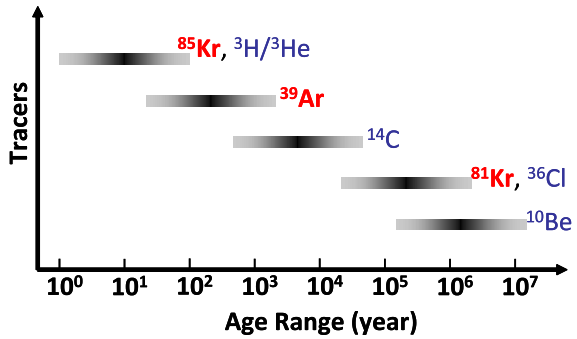

[1] Jiang W. *et al*. (2011) *Phys. Rev. Lett.* **106**, 103001.
[2] Chen C. Y. *et al*. (1999) *Science* **286**, 1139.

https://doi.org/10.1180/S0026461X00006502 Published online by Cambridge University Press

Preliminary high-resolution Ge/Si data in early Archaean BIFs

BEATRICE LUAIS[1]*, PHILIPPE LACH[2], EMILIE THOMASSOT[1], MARC CHAUSSIDON[1] AND MARIE-CHRISTINE BOIRON[2]

[1]CRPG-CNRS, Nancy Université, BP 20, 54501 Vandoeuvre-lès-Nancy, France (*correspondence: luais@crpg.cnrs-nancy.fr)
[2]G2R-CNRS, Nancy Université, Boulevard des Aiguillettes, B.P. 70239, 54506 Vandoeuvre-lès-Nancy, France

Banded iron formations are laminated sediments consisting of alternate banding of Fe-oxides layers and quartz layers which predominate in the Precambrian. Many aspects of their genesis are still controversial, but some observations such as the disappearance of BIFs at the time of atmospheric oxygenation (~2.3Ga), in spite of some recurrences between 0.8-0.6 Ga, indicate that the oceanic and atmospheric conditions have played an important role for their deposition. The Ge/Si ratios have been long used in studies concerning paleochemistry of oceans as a proxy for understanding the geochemical cycle of Si and Si sources in surface environments. It has been shown that Ge/Si ratio is higher in hydrothermal environments than that from continental weathering, and that the solubility of Ge in aqueous fluids varies with temperature [1]. This can suggest that Ge/Si ratios could be a potential tracer of Archaean environmental conditions and sources for BIFs deposition.

BIF samples from Isua-Greenland (≈ 3.7-3.8 Ga) and Nuvvuagittuq-Canada (likely as old as 4.28 Ga [2]) have been studied in order to decipher the chronological evolution of their trace elements, Ge/Si and O, Si isotopic compositions. The main focus is the identification of compositional variations within bands and between bands of quartz and Fe-oxides. High-resolution *in situ* measurements of trace element concentrations have been performed using laser ablation ICP-MS. First results for Isua BIFs indicate that Ge concentrations range from ≈ 7 to ≈ 12 ppm in quartz, with variations of few ppm between large quartz and small quartz bands. The calculated Ge/Si ratios range from ≈ 0.6 to 1* 10^{-5}mole/mole, which is significantly smaller than previously determined data (Ge/Si ≥ 2*10^{-5}mole/mole [2]) on bulk individual mesobands. This discrepancy can be explained by the presence of scarse amphiboles with measured Ge contents of ≈ 100ppm, which bias the Ge budget of individual bands. *In situ* Ge/Si, together with O and Si isotopes will provide insights on BIFs depositional environments.

[1] Pokrovski G. *et al*. (1998) *Geochim. Cosmochim. Acta* **62**, 1631–1642. [2] O'Neil *et al*. (2008) *Science* **321**, 1828–1831. [3] Frei R. & Polat A. (2007) *Earth Planet. Sci. Lett.* **253**, 266–281.

Alkaline particle size and delivery for settling and dissolution: Optimising ocean-based enhanced weathering geoengineering

A.S. LUBANSKY[1]*, M. TANNENBERGER[2], T. KRUGER[3] AND R.C. DARTON[1]

[1]Department of Engineering Science, University of Oxford, Oxford UK OX1 3PJ (*correspondence: alex.lubansky@eng.ox.ac.uk)
[2]BASF SE, GTE/AB - Q920, 67056 Ludwigshafen, Germany
[3]Oxford Geoengineering Programme, Oxford Martin School, University of Oxford, Oxford UK OX1 3BD

Among the many geoengineering techniques proposed for climate remediation by removing carbon dioxide from the atmosphere, a major benefit of ocean-based enhanced weathering is that it also holds the promise of being able to directly counteract ocean acidification. Operating such a geoengineering scheme successfully involves optimising many fine details. Arguably the most crucial detail is the size and delivery of the alkaline particles into the ocean: if the particle dissolution depth is too high, the particles will leave the mixed layer, underutilising the mineral, while if the particle dissolution depth is too low, there will be high localised concentrations of the alkaline mineral, risking undesirable side-reactions.

In this presentation, we present an analytical model for calculating the settling and dissolution rates for a suspension of multiple particles into ocean water in order to determine the optimum rates for dispersing alkalinity into the ocean. We develop a theoretical framework that can be used to determine the most efficient method for adding multiple alkaline particles, taking into account particle size and concentration as they are being dispersed.

Through our model, extending simple single-particle Stokesian analysis by taking into account average particle spacing as well as flows between and around the particles, the model enables the prediction of local conditions throughout the system to be determined in a straightforward manner. By predicting local conditions, the deleterious effects of side reactions, particularly those on the surface of the particles, can be minimised. By predicting the details of dissolution, such as concentration vs depth and time, our model predicts the efficacy of a given delivery system for adding alkalinity to the ocean.

In this presentation, a discussion will also be provided highlighting some of the applications of the model to geoengineering for removing atmospheric carbon dioxide and for moderating ocean acidification.

https://doi.org/10.1180/S0026461X00006502 Published online by Cambridge University Press

Modifying the diffusive gradients in thin films technique for the geochemical exploration of gold

ANDREW LUCAS[1], ANDREW RATE[1], HAO ZHANG[2] AND URSULA SALMON[1]

[1]School of Earth and Environment, University of Western Australia, 35 Stirling Highway, Crawley, WA 6009, Australia

[2]Lancaster Environmental Centre, Lancaster University, Lancaster LA1 4YQ, UK

Using DGT for Gold

Gold is a precious metal that exists in the environment in extremely low concentrations (>1ppb). Any technique which is sensitive enough to usefully determine ultra-low quantities of metals such as gold is of interest to exploration geochemists and mining companies alike. As such, the diffusive gradients in thin films (DGT) technique, which has been used extensively to monitor ultra-low concentrations of metals in soils, sediments and freshwater [1], is likely to be ideally suited for geochemical exploration of gold in the environment.

Methodology and Discussion

This research details the development of a DGT method for the geochemical exploration of gold, and introduces a new binding-layer based on activated carbon. The performance of this new technique was assessed by: 1) determining the diffusion coefficient of gold (as soluble gold (III) chloride); 2) assessing the new binding layer's capacity to uptake gold; 3) determining the elution methodology from the binding layer; 4) assessing possible interference from other environmentally labile metals, and; 5) the effect of ionic strength and pH on performance.

The results of this study show that the technique has significant potential to be used for the geochemical exploration of gold in aqueous environments. Further method development will include assessing the technique's potential with gold species other than the gold (III) chloride used in this study, and further modification to measure gold concentrations in soils and sediments.

[1] Zhang & Davison (1999) *Anal. Chim. Act.* **398**, 329–340.

Element redistribution during rutile dissolution and titanite precipitation

F. LUCASSEN[1,2], G. FRANZ[1] AND D. RHEDE[2]

[1]Technische Universität Berlin, FG Petrologie, Berlin, Germany (lucassen@gfz-potsdam.de)

[2]Deutsches Geoforschungszentrum, Potsdam, Germany

We investigated the dissolution-precipitation reaction rutile + Ca, Si, Al in fluid = titanite at 400 MPa and 600°C. Solid sources of Ti, rutile (Nb, W bearing natural or Cr doped synthetic rutile) and Ca, Si, Al (wollastonite and Al_2O_3 or grossular) are separated by using a double capsule technique. All element exchange is via an aqueous NaCl fluid. The purpose of the study is to find out what are the rate controlling steps and how are major (Al-Ti) and trace elements distributed.

Titanite growth is very rapid; overgrowth is complete after 1 day. With longer run-time, substantial increase of crystal size and changing crystal habits of the titanite imprint spatially related dissolution patterns on the rutile surface. The reaction progress is controlled by the low solubility of Ti and element transport from and to the dissolution front on rutile along titanite–titanite grain boundaries. Titanium is not transported away from the reaction site, but Al, which is always present in the quench, is perfectly mobile. This contrasting behaviour leads to an irregular 'patchy' Al-Ti distribution in titanite [1]. The Ti/Al is likely dominated by the availability of Ti rather than of Al. We assume quantitative incorporation of dissolved Ti in titanite.

Trace element (Nb, W) contents in titanite around rutile is variable and shows no clear spatial relation to the variable trace element contents of the zoned natural rutile. It is also neither related to core-rim relations in titanite corresponding to the time of the experiment, nor controlled crystallographically. Chromium (source: homogeneous synthetic rutile with 2000 ppm Cr) shows a similar behaviour. It is between ~400 to ~1400 ppm with a few higher values up to ~5000 ppm. From mass balance calculation, ~800 ppm Cr are expected if Cr is quantitatively incorporated and homogeneously distributed in the titanite. Chromium and Ti/Al are not correlated. Decoupling of Cr and Ti, which are released together by rutile dissolution, must origin from randomly different transport of both elements.

[1] Lucassen *et al.* (2010) *American Mineralogist* **95**, 1365–1378.

https://doi.org/10.1180/S0026461X00006502 Published online by Cambridge University Press

Chronological and thermal history of the lithospheric mantle underneath the Gibeon kimberlite field, Namibia

TIMO LUCHS*, GERHARD BREY AND AXEL GERDES

Institut für Geowissenschaften, Goethe Universitaet, Frankfurt am Main (*correspondence: luchs@em.uni-frankfurt.de)

The 70 Ma kimberlite volcanism in the Gibeon Province in Namibia was triggered by the drift of the African continent over the Discovery plume [1]. It brought garnet peridotites, megacrysts and few crustal xenoliths to the surface. The volcanic field is situated in the Rehoboth province which gives crustal basement ages between 1.7 – 2.3 Ga [e.g. 2-3]. The neighbouring Namaqua-Natal belt is charactarised by ages of 0.9 to 1.3 Ga. Rhenium depletion ages of the peridotites range from less than 1 to 2.2 Ga and point towards an early proterozoic depletion event [4].

Major and trace elements of garnets and clinopyroxenes of 19 more or less altered peridotites from Hanaus and Gibeon were analysed by EPMA and LA-SF-ICPMS; the Lu/Hf and Sm/Nd isotope ratios were measured in cpx and grt mineral separates from 12 of these samples by ID-MC-ICPMS.

Garnets from 14 samples have LREE depleted patterns (with corresponding equilibrium patterns in the coexisting clinopyroxenes), five garnets show sigmoidal patterns of the type commonly observed in Archean garnets. The latter show a tendency to higher temperatures (~ 1250 °C) compared to samples with LREE depleted garnet patterns (~ 1100 °C) at same pressures (~ 40 Kbar).

Bulk rock isotopic compositions were calculated from the modal abundances and isotopic composition of the minerals. Three sigmoidal and five LREE depleted peridotites yield two separate Lu-Hf isochrones of 1.88 Ga and 933 Ma respectively. Both isochrones are interpreted as reflecting enrichment events of previously depleted mantle. Timing and extent of depletion must have been very different because the former yield $\varepsilon H = +29$, the latter +5. The younger enrichment age points to an event connected with the Namaqua orogeny, the older to processes connected with the manifestation of the Rehoboth province.

Sm-Nd whole rock isotope systematics indicate a late metasomatic overprint at around 500 Ma during the Damara orogeny.

[1] Davies, G. R. *et al*.. (2001) *J.Pet*. [2] Becker, T. *et al*. (2004) *Comm.Geol.Surv.Nam*. [3] Ziegler, U. R. F. *et al*. (1991) *Com. Geol. Surv. Nam*. [4] Hoal *et al*. (1995) *S. A. J. Geol*.

The significance of Rotliegend brines in mineralizing processes and hydrocarbon systems in the Southern Permian Basin

V. LÜDERS[1]*, B. PLESSEN[1], H.B. VONHOF[2] AND J. SCHNEIDER[3]

[1]Helmholtz Centre Potsdam GFZ, Telegrafenberg, D-14473, Potsdam, Germany (*correspondence: volue@gfz-potsdam.de, birgit.plessen@gfz-potsdam.de)

[2]Vrije Universiteit Amsterdam, De Boelelaan 1085 1081 HV Amsterdam, The Netherlands (vonh@falw.vu.nl)

[3]Badstr. 5-9, D-35792 Löhnberg, Germany (j.schneider@mineral.tu-freiberg.de)

Studies of sedimentary brines from the central part of the Southern Permian Basin (SPB) show that formation water stored in Rotliegend sandstones differs clearly in elemental abundances and isotopic composition from formation waters from the overlying Zechstein and Mesozoic units [1, 2]. The Permian depositional conditions in the central part of the SPB (Rotliegend salt lake) and subsequent Zechstein transgression which caused to the formation of huge evaporite caps led to the preservation of original Rotliegend formation waters that changed their pristine chemical character by water-rock interaction (WRI) during basin subsidence. These 'altered' Rotliegend formation waters are characterized by positive δD and $\delta^{18}O$ values due to evaporation of meteoric water of the Rotliegend salt lake and high radiogenic $^{87}Sr/^{86}Sr$ isotopic ratios due to WRI with surrounding host rocks [1]. Fluid flow of Rotliegend brines is recorded by abundant fracture-fill and vein mineralization within Rotliegend sediments and even in deeper-lying Paleozoic units. Fracture-fill anhydrite shows unusual $\delta^{34}S$ isotopic composition of about +5‰ suggesting that sulphur was derived by WRI between Rotliegend formation waters and Rotliegend sediments of magmatic origin rather than being derived from the overlying Zechstein. Furthermore, Rotliegend brines played a significant role in the formation of nitrogen-rich gas reservoirs in the central and eastern part of the SPB.

[1] Lüders *et al*. (2010) *Chem. Geol*. **276**, 198–208. [2] Möller *et al*. (2007) *Int. J. Earth Sci*. **97**, 1057–1073.

https://doi.org/10.1180/S0026461X00006502 Published online by Cambridge University Press

Reactive melt transport in the oceanic lithosphere: Implications to MORB thermobarometry

PETER LUFFI* AND CIN-TY A. LEE

Rice University, Houston, TX 77005, USA
(*correspondence: pluffi@rice.edu)

Basalt compositions reflect physico-chemical factors controlling magma generation, transport, and emplacement, and it is widely thought that, if chemical variables are known (e.g. Mg# and fO_2 in source peridotites) or properly corrected for (e.g. olivine fractionation), then the P-T conditions of mantle melting can be reasonably constrained. In this respect, mid-ocean ridge basalts (MORB) are of major interest: they encapsulate information regarding the present thermal state of Earth's mantle. Thermobarometry based on Si and Mg in basalts indicates that fractionation-corrected 'primary' MORB form a narrow P-T array between 1300-1400 °C and 0.7-1.7 GPa, overlapping the 10-15% melting isopleths of dry lherzolite [1]. This P-T array is evident even at short lengthscales, making it difficult to explain the spread by variations in mantle potential temperatures (T_p). More likely, short-lengthscale MORB temperature variability is the result of melt-rock reactions in the oceanic lithosphere, and reflects differences in axial lithosphere thickness [2].

Here we assess to what extent the 'primary' MORB P-T array can be caused by reactive melt transport in oceanic lithosphere. Using Adiabat_1ph [3] with pMELTS [4], we calibrate a synthetic Mg-Si thermobarometer for basalts equilibrated with peridotite at P < 3 GPa, analogous to experiment-based calibrations [1]. We apply this thermobarometer to aggregated melts obtained by simulating polybaric fractional melting of peridotite along relevant T_p and show that, in the absence of low-P melt-rock reaction, MORB P-T values reflect the conditions of mean extent of melting. However, our simulations of percolation of aggregate melts through residual harzburgites at low-P show that reactive melt transport in the oceanic lithosphere decreases Mg and increases Si in melt such that thermobarometry will produce P-T arrays overlapping those observed in MORB. These results render T_p variability unnecessary for explaining most of the global MORB P-T, corroborate the view that short-scale MORB P-T variability is a measure of reactive melt transport, and help constrain geotherms beneath mid-ocean ridge axes.

[1] Lee *et al*. (2009) *EPSL* **279**, 20–33. [2] Collier & Kelemen (2010) *J. Pet*. **51**, 1913-1940. [3] Smith & Asimow (2005) *G-cubed* 6/Q02004. [4] Ghiorso *et al*. (2002) *G-cubed* 3/1030.

Re-Os and Lu-Hf dating in Letlhakane peridotite xenoliths (Botswana)

AMBRE LUGUET[1], MELANIE BEHRENS[1], DANIEL HERWARTZ[1] AND D. GRAHAM PEARSON[2]

[1]Steinmann Institute, Poppelsdorfer Schloss, Universitaet Bonn, Germany (Ambre.luguet@uni-bonn.de)
[2]Department of Earth and Atmospheric Sciences, University of Alberta, Edmonton, Canada

In order to better understand the lithosphere structure and evolution under the Paleoproterozoic Magondi Belt (NW margin of Zimbabwe craton), 11 peridotites from the Letlhakane diamondiferous kimberlite were studied for HSE, Lu-Hf and Re-Os isotope systematics. These peridotites experienced both high degrees of partial melting and metasomatism as evidenced by the presence of phlogopite and significant enrichments in incompatible trace elements. Their HSE systematics show progressive metasomatic Pt and Pd enrichments, with CI-normalised patterns ranging from those typical of residues of high partial melting degree (PdN/IrN<0.03, PtN/IrN<0.1) to patterns having chondritic to suprachondritic PtN/IrN and PdN/IrN (0.9-1 and 1.06-1.4, respectively). All but 1 sample show Re enrichments (ReN/PdN=0.3-7.6). Re depletion ages range from 2.2 to 2.8 Ga, clearly indicating the presence of Archean mantle beneath this area [1]. Whole-rock Lu-Hf isotope systematics show significant scatter in 176Hf/177Hf vs. 176Lu/177Hf space, but 3 samples yield a ca. 2.1 Ga errorchron age (MSWD = 4.8) with a radiogenic initial 176Hf/177Hf ratio. Apart from 1 peridotite yielding a Lu-Hf model age of 2.5 Ga, the Lu-model ages of Letlhakane peridotites cluster at 0.7-1.1 Ga. Moreover, a clinopyroxene-garnet pair from a single sample defines a 2-point isochron age of 132±38 Ma, within error of the eruption age of the Orapa kimberlite (93 Ma, [2]), which is assumed to be erupted in the same phase of magmatic activity as Letlhakane kimberlite [3].

None of the Lu-Hf isotope systematics is consistent with the Archean depletion event indicated by the Re-Os isotope system. The Lu-Hf isotopic systematics have been highly disturbed by the petrological modifications experienced by the lithospheric mantle under Letlhakane and thus indicate the vulnerability of the Lu-Hf isotopic system in metasomatised peridotites for dating depletion age and formation of the mantle root.

[1] Carlson *et al*. (1999) *Proceedings 7th IKC*, 99–108. [2] Davies (1977) *2nd IKC*, unpaginated. [3] Stiefenhofer *et al*. (1997) *CMP* **127**, 147–158.

https://doi.org/10.1180/S0026461X00006502 Published online by Cambridge University Press

Solubility and species of Zn and Pb in water-chloride fluids at T-P conditions of granite magmas degassing

O.A. LUKANIN, N.A. KUROVSKAYA AND B.N. RYZHENKO

Vernadsky Institute of Geochemistry and Analytical Chemistry, Moscow, Russia (lukanin@geokhi.ru)

Results of thermodynamic modeling of equilibrium relationship of complexes of Zn and Pb in water-chloride solutions as a function of T (600 - 900ºC), P (0.7-5 kbar), the composition and acidity of the fluid (NaCl, KCl, NaCl+HCl), as well as the initial concentration of Zn and Pb in the system in the form of $ZnO_{(c)}$, $PbO_{(c)}$ or $ZnCl_2$, $PbCl_2$ are presented. At 'magmatic' T-P parameters Cl-complexes fraction and total solubility of ore metals in solutions equilibrated with their solid oxides essentially increase with the increase of chloride ion concentration (C_{Cl}) and decrease of pH. The form of prevailing Cl-complexes varies with growth of C_{Cl} towards the increase of quantity of their Cl atoms as follows: $ZnCl^+$, $ZnCl_2^o$ - $ZnCl_4^{2-}$; $PbCl_2^o$ - $PbCl^{3-}$ - $PbCl_4^{2-}$. The increase of pressure and temperature decrease contributes to stability of Zn and Pb Cl-complexes. Zn/Pb (at.) > 1 in solutions equilibrated with $ZnO_{(c)}$ and $PbO_{(c)}$ within wide range of T-P-X parameters. It increases with the increase of C_{Cl} and acidity of the solution.

Results of thermodynamic simulation confirm the assumption about the leading role of Cl-complexes in the distribution of Zn and Pb between water-chloride fluids and granite melts during their degassing and agree with experimental data obtained at 800ºC and 1-5 kbar (Urabe, 1987; etc.) that show: (1) the increase of Zn and Pb distribution coefficients between fluid and granite melt ($D(Zn)^{f/m}$, $D(Pb)^{f/m}$) with the increase of Na and K chloride concentration in a water fluid, (2) the particularly sharp increase of $D(Zn)^{f/m}$ and $D(Pb)^{f/m}$ with addition of HCl to fluid phase (at T, P, C_{Cl} = const), (3) the higher values of $D(Zn)^{f/m}$ in comparison with that of $D(Pb)^{f/m}$ at given T-P-X conditions.

The work was supported by RFBR (grant 08-05-00022) and Branch of Earth Sciences of the RAS (the program 2, 2011).

Production of the Cordillera del Paine igneous complex by thermal migration zone refinining

C.C. LUNDSTROM[1], N. GAJOS[1] AND P.J. MICHAEL[2]

[1]Dept of Geology, Univ of Illinois, Urbana IL 61801 (lundstro@uiuc.edu)

[2]Dept. Geosciences, Univ of. Tulsa, Tulsa, OK 74104 (pjm@utulsa.edu)

The Torres del Paine igneous complex consists of a silicic granitoid pluton overlying a contemporaneous mafic gabbro complex that are possibly cogenetic; recent dating studies indicate progressively decreasing age with stratigraphic depth [1, 2]. Descending through the ~1.5 km vertical stratigraphy, the upper 1 km consists of 70-72% SiO2 granite with abundant silicic aplites along the margins including the top. Beneath the granite is a zone of mixed diorite, which is underlain by a few hundred meters of hornblende gabbros. A recent model for graniotid formation by top down sill injection and reaction [3] predicts a similar overall vertical stratigraphy; isotopic measurements of a vertical Torres del Paine transect provides a first order test of this hypothesis.

We have undertaken Fe isotope analyses of previously characterized samples from the studies of Michael (1984, 1991)[4, 5]. We used high resolution MCICPMS techniques and a ^{57}Fe-^{58}Fe double spike method. Analytical precision is ~0.08 permil. Results indicate that 4 granite and evolved granite samples (SiO_2 >71%) have consistently heavy isotopic compositions relative to the IRMM standard (0.23 ± 0.08). Six monzogabbro/diorite samples average 0.09 ± 0.07. Notably, a mafic monzodiorite and two gabbros at the bottom of the Paine mafic complex average -0.80 ± 0.48, representing the lightest Fe isotopic compositions yet observed in igneous rocks. Finally, a dike porphyry sample also has a light isotopic composition of -0.39.

While further analyses are in progress, results thus far are consistent with the prediction that the isotopic variations reflect the role of thermal gradients and thermal diffusion in fractionating Fe isotopes. Specifically, heavier isotopic ratios for granites compared to diorites follows previoius observations of isotopic variations with silica content [6]. However, significantly light isotopic compositions in the bottom of the system provides evidence for a complimentary signature at the hotter part of an igneous body. Trace element modeling using IRIDIUM of top down differentiation will further assess the plausibility of this model.

[1] Michel *et al*. (2008) *Geology*. [2] Leuthold *et al*. (2009) *AGU*. [3] Lundstrom (2009) *GCA*. [4] Michael (1984) *Cont. Min Petrol*. [5] Michael (1991) *Cont. Min. Petrol*. [6] Poitrasson (2006) *Chem Geol*.

https://doi.org/10.1180/S0026461X00006502 Published online by Cambridge University Press

Impact of parent rocks and diagenetic evolution on sandstone reservoir quality with low to very low permeability

JING-LAN LUO

State Key Laboratory of Continental Dynamics, Northwest University, Xi'an, 710069, China (jlluo@nwu.edu.cn)

Sandstone types, characteristics of fragments and cements, pore types and reservoir quality, and their horizontal distribution of the He 8 and Shan 1 Group, Permian of the Upper Paleozoic from the northern Ordos Basin, China is studied, based upon observation of bore cores, use of multiple analytic measurements. The major factors impacting the reservoir quality is discussed. Results show that feature of parent rocks and diagenetic evolution is the major element which affects the reservoir quality. Parent rocks determined sandstone types and primary pore skeleton, resulting in three types of quartzarenite, lithic quartzarenite and lithicarenite with average primary porosity of 35.1%, 34.2% and 33.6%, respectively. Parent rocks also influenced diagenetic paths and types of cements, which led to diversity pores and pore throats, thus varied reservoir qualities. The sandstones experienced the early (P-T) and late (T_3-K_1) diagentic evolution phases, and three hydrocarbon charging stages during T_3, J_2-J_3 and K_1 as well. Compaction occurred in the early diagenetic phase caused average porosity for quartzarenite, lithic quartzarenite and lithicarenite is 17.4%, 18.3% and 18.5%, respectively. Cementation mainly occurred in the late diagenetic phase resulted in average porosity for quartzarenite, lithic quartzarenite and lithicarenite is 15.0%, 15.8% and 14.8%, respectively. The quartzarenite, with average macro-pores of 3.8%, is the excellent natural-bearing reservoir sandstone type in the studied area.

This study is supported by the National Natural Science Foundation of China (Grant No. 40872083) and the Natural Key Project of Science and Technology (Grant No. 2008ZX05008-004-076).

Migration of toxic elements in biogeochemistry chains in residents and farmlands near a Pb-Zn Mine

L. LUO[1]*, B. CHU[1], T. XU[1], X. WANG[1], Y. LIU[1], Y. BO[2] AND J. SUN[1]

[1]National Research Center of Geoanalysis, Beijing, 100037
[2]Institute of Mineral Resources, CAGS, Beijing, 100037

Biogeochemistry investigation has been conducted in the last five years in the human residents and farmlands near a lead-zinc mine in the suburb of Nanjing city, southeast China. People have lived very close to the mine. Water, soils, plants and animal tissues, as well as human blood, were sampled, and Pb, As, Cd and other minor and trace elements in them were determined by X-ray fluorescence spectrometry, inductively couple plasma atomic emission spectrometry and mass spectrometry.

Pb, As and Cd in the samples of water, soil and dust particles taken from the investigation areas were partly or generally higher than the critical level ruled by Chinese environmental standards. For example, the maximum of Pb concentrations in irrigation water was about four times higher than the standards. The concentrations of Pb, As and Cd in farmland soils were beyond the national quality standards for the edible vegetable soils. Parts of data were shown in Table 1.

Pb and As in leaf vegetable samples were beyond the national quality standards. Parts of Pb, As and Cd in animal tissues displayed the same trends. High concentrations of Pb in human blood and bone were observed.

	Max. in Irrigation Water	Means in Vegetable soils
Pb	13.2	296
As	0.17	59
Cd	0.16	1.4

Table 1: Concentrations of toxic elements

https://doi.org/10.1180/S0026461X00006502 Published online by Cambridge University Press

Soil leaf-wax n-alkane δD along altitudinal and latitudinal transects: Implications for paleoelevation and paleohydrology reconstructions

P. LUO[1]*, P.A. PENG[2] AND G. GLEIXNER[3]

[1]Research Institute of Petroleum Exploration & Development, PetroChina, Beijing 100083, China (*correspondence: ipanluo@gmail.com)
[2]Guangzhou Institute of Geochemistry, CAS, Guangzhou 510640, China (pinganp@gig.ac.cn)
[3]Max Planck Institute for Biogeochemistry, 07745 Jena,Germany (ggleix@bgc-jena.mpg.de)

δD values of leaf wax-derived *n*-alkane (δD_{wax}) preserved in soils or sediments could reflect spatial and temporal variations of precipitation δD (δD_p), which develops a way to paleohydrology reconstruction and a proxy for paleoaltimetry.

We find that soil δD_{wax} values track altitudinal variations of δD_p along four altitudinal transects in China that span variable environment conditions and vertical vegetation spectra [1]. An empirical δD_{wax}-altitude relationship, that is the average δD_{wax} lapse rate of -2.27±0.38‰/100m, would be used to estimate paleoelevation change. Additionally, a reversal of altitude effect in the vertical variation of δD_{wax} exists in the alpine zone of the Tianshan Mountains, which might be caused by atmospheric circulation change with altitude. This implies that the paleo-circulation pattern and its changes should be evaluated firstly when stable isotope-based paleoaltimetry is applied.

The apparent fractionation between leaf wax and precipitation ($\varepsilon_{wax\text{-}p}$) in the extreme humid Wuyi Mountains is quite negative (-154‰), compared to the humid Shennongjia (-129‰) and the arid (but with abundant summer precipitation) Tianshan Mountains (-130‰), which suggests aridity or water availability in the growing season is the primary factor controlling soil/sediment $\varepsilon_{wax\text{-}p}$. Moreover, this climatic dependency of soil $\varepsilon_{wax\text{-}p}$ also is present along the N-S latitudinal soil transect. From the wet southeast to the arid northwest of China, values of $\varepsilon_{wax\text{-}p}$ become more positive increasingly. This variation of soil $\varepsilon_{wax\text{-}p}$ might be independent on temperature or elevation change, and could not be interpreted by the vegetation shift. Therefore, we suggest climate-specific $\varepsilon_{wax\text{-}p}$ for δD_p reconstruction: -150‰ for extremely humid climate, -130‰ for moderately wet climate (or no water stress in growing season) and -100‰ for typical arid climate. Also, paleoelevation would be estimated using empirical (observation) or theoretical (Rayleigh model) δD_p-altitude relationship.

[1] Luo *et al*. (2011) *EPSL* **301**, 285–296.

Insight and analysis on the interior surface characteristic of a single fracture in granite sample

S.H. LUO[1]*, T. GOTO[2] AND J. KODAMA[2]

[1]School of Resources and Environment, Henan Polytechnic University, Jiaozuo 454010, China (luosh@hpu.edu.cn)
[2]Muroran Institute of Technology, Muroran 050-8585 Japan

New Measuring Method for Fracture

Fluid flow in a single fracture is an important research subject in CO_2 sequestration, hydrogeology, engineering geology and petroleum engineering [1, 2]. Recent years, some authors study mechanism on flow and transport in laboratory [1-5] and situ [6-8]. However, the main question that has still not been answered satisfactorily is: How to correlate fluid flow with fracture geometry and roughness. Therefore, we study a new method to measure and characterize the surface of fractures.

Results and Discussion

As shown in the research, fracture state *in situ* measurement applied in the experimental method is feasible.The fracture was visualized based on coordinate values of fracture Surface by the cross-sectional photographs of samples without separating the fracture surfaces (Fig.1). And New methods can show the view of fracture surface (Fig.2).

Fracture aperture is large around the borehole wall where fracture is thought to occur, and the farther away from the borehole wall, the narrower the fraction opening is.

There are more high opening angles (> 10 degree) around the borehole wall, and more low opening angles far away from the borehole wall. The fractal dimension of profiles of fracture surface is between 1.17 and 1.68.

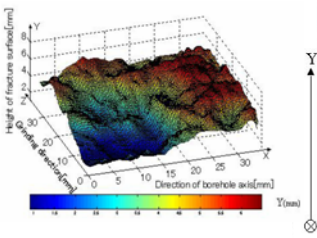

Fig. 1: Image of a single fracture.

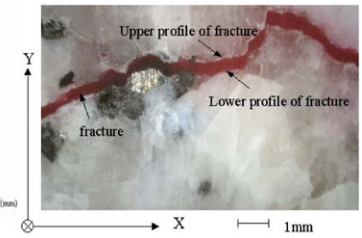

Fig. 2: Lower surface of fracture

[1] Luo *et al*.(2009) *Geochim.Cosmochim. Acta* **73**: A802. [2] Qian *et al*. (2011) *J. Hydrol.* **399**: 246-254. [3] Qian *et al*. (2005) *J. Hydrol.* **311**: 134-142. [4] Qian *et al*.(2007) *J. Hydrol.* **339**: 206-219. [5] Qian *et al*. (2011) *Hydrol. Process.* **25**: 614-622. [6] Zhou *et al*. (2004) *Int. J. Rock Mech. Min. Sci*. **41**:402. [7] Qian *et al*. (2006) *Hydrogeol. J*. **14**: 1192-1205. [8] Qian *et al*. (2009) *Hydrogeol. J*. **17**: 1749-1760.

https://doi.org/10.1180/S0026461X00006502 Published online by Cambridge University Press

Biogas generating simulation from source rock and oil in Jiyang Depression, Bohai bay Basin, China

X. LUO, L.H HOU, C.YANG AND J.H WANG

Research Institute of Petroleum Exploration and Development, Beijing, China (luoxia69@petrochina.com.cn, lhhou@petrochina.com.cn, yangchunzs@petrochina.com.cn, 284174762@qq.com)

Bacterium detection is carried out in rocks, which are different types of formation, lithology and depth in Jiyang depression, Bohai bay Basin in this paper. The results are that *methanococcales* are widely existed in different rocks such as mudstone and sandstone and in different formations such as Es_3, Es_1 and Ed formation and in wide depth from 1297 to 2522 meters (the formation temperatures are about 45°C and 80°C). The above results indicate that the living of *methanococcales* only depends on its survival environment and is independent of formation and lithology of rocks. Similar results were got from the characteristics of biogas generating simulation from source rocks and oils. The results are as follows: all kinds of rocks and oils can and only generate CH_4 and CO_2 during simulation. 45°C and 65°C are biogas generating peaks and the productivities are 20-160m^3/t TOC and 10-15m^3/t oil respectively. Carbon isotope compositions of methane ranging between -80.2‰ and -41.5‰ change lighter with simulation temperature rising while carbon isotope compositions of carbon dioxide change heavier. The hydrogen isotope compositions of methane ranging between -300‰ and -350‰ change little but deviation with biogas ranging between -240‰ and -270‰ from gas filed such as Luliang basin in Yunnan province as affected by the geological environment.

Himalayan weathering evolution from LGM to present

MAARTEN LUPKER[1], CHRISTIAN FRANCE-LANORD[1], VALIER GALY[2], JEROME LAVE[1] AND HERMANN KUDRASS[3]

[1]CRPG - 15 rue Notre Dame des Pauvres, 54501 Vandoeuvre, France

[2]WHOI-Department of Marine Chemistry, Woods Hole, MA, USA

[3]Federal Institute for Geosciences and Natural Resources (BGR), Hannover, Germany

We use the sedimentary record from the Bay of Bengal (BoB) spanning from the Last Glacial Maximum (LGM) to document the weathering intensity in the Himalayan system. These cores record the Himalayan erosion products transported by the Ganga and Brahmaputra (G&B) through their floodplains. The physical setting of the G&B basin remained essentially unchanged over the Quaternary. Therefore, climate change marked by reduced river runoff and lower snowline during the LGM are the main forcing variables in the basin.

We use the classical mobile elements geochemistry but also introduce the less conventional sediment hydration [H_2O^+] and detrital carbonate concentration as weathering tracers. These tracers were first applied to the modern Ganga basin, showing the predominant role of the floodplain in weathering Himalayan sediments. These tracers also highlight that mineral sorting has to be accounted for, to derive a weathering signal from detrital sediments. The BoB sediment record is then compared to the modern system. Source proxies such as Sr and Nd isotopic composition suggest that the G&B balance between both rivers has remained constant since LGM [2]. The evolution of [H_2O^+], [K] and [Carbonates] of the cores, corrected for mineral sorting, shows that the sediments exported by the system during the LGM were significantly less weathered than modern sediments. Reduced monsoon intensity [1, 3] during glacial periods yields lower precipitation, which reduces the overall weathering intensity. Lower discharge and base level likely inhibits river avulsion and limit the reworking of mature, weathered, floodplain sediments. We thus hypothesize that during LGM, river-floodplain interactions were more limited reducing the weathering of Himalayan sediments.

[1] Duplessy (1982) *Nature* **295**, 494–498. [2] Galy *et al*. (2008) *QSR* **27**, 1396–1409. [3] Kudrass *et al*. (2001) *Geology* **29**, 63–66.

https://doi.org/10.1180/S0026461X00006502 Published online by Cambridge University Press

Distinguishing arc, backarc, and hotspot affinities using helium isotope and C/^{3}He ratios

J. LUPTON[1], J. RESING[2], M. LILLEY[3], D. BUTTERFIELD[2], N. KELLER[4], R. ARCULUS[5], E. BAKER[2] AND R. EMBLEY[1]

[1]NOAA/PMEL, Newport, OR, USA
[2]NOAA/PMEL, Seattle, WA, USA
[3]School of Oceanography, Univ. of Washington, Seattle, WA, USA
[4]IES, Univ. of Iceland, Reykjavik, Iceland
[5]RSES, Australian National University, Canberra, ACT, Australia

The northern Lau Basin is host to a complicated pattern of volcanic activity, including the volcanoes of the Tofua Arc and several back-arc spreading centers. Farther west along the NW Lau Spreading Center, elevated ^{3}He/^{4}He ratios in the seafloor lavas suggest that an OIB or mantle plume signature, possibly from Samoa, has influenced this extensional zone. Helium isotope and C/^{3}He ratios have proved useful for differentiating between arc vs. back-arc influences. True back-arc systems are similar to mid-ocean ridge (MOR) systems with ^{3}He/^{4}He of ~ 8 Ra (R = ^{3}He/^{4}He and Ra = Rair) and C/^{3}He of ~10^9. In contrast, arc volcanoes typically have lower ^{3}He/^{4}He ratios and higher C/^{3}He ratios ($\geq 10^{10}$), presumably due to downgoing slab components. For example, the recently erupting West Mata submarine volcano in the NE Lau Basin has 7.3 Ra and C/^{3}He of ~10^{10}, indicating strong arc affinities. In contrast, lavas and hydrothermal fluids from the NELSC have 8.0 – 8.6 Ra and C/^{3}He of 1 – 3 x 10^9, typical MOR or back-arc signatures. Other volcanic centers in the region show varying degrees of arc or downgoing slab influence based on their ^{3}He/^{4}He - C/^{3}He fingerprint. A broader view of the entire northern Lau Basin indicates that elevated ^{3}He/^{4}He ratios indicative of an OIB signature are confined to the Northwest Lau Spreading Center, and that the NE Lau Basin is characterized by both arc and back-arc signatures.

Thermodynamics of one and two electron transfer steps: Implications for iodide oxidation and iodine environmental cycling

GEORGE W. LUTHER, III

School of Marine Science and Policy, College of Earth, Ocean and Environment, University of Delaware, Lewes, DE 19958, USA (luther@udel.edu)

In oxygenated waters, chloride and bromide are the thermodynamically stable halogen species that exist whereas iodate, the thermodynamically stable form of iodine, and iodide can co-exist. The stability and oxidation of halides in the environment is related to the unfavorable thermodynamics for the first electron transfer with oxygen to form X· atoms. However, reactive oxygen species (ROS) such as $^1O_2$, H_2O_2 and O_3 can oxidize the halides to X_2 and HOX in two electron transfer processes; these reactions become less favorable with increasing pH. Fe (III) and Mn (III, IV) solid phases can oxidize halides with similar patterns as ROS.

The best oxidants in aqueous solution appear to be the one electron oxidant, ·OH, and the two electron oxidants, $^1O_2$, H_2O_2 or O_3. However, thermodynamic favorability depends on the halide with iodide being the easiest to oxidize as well as on pH with thermodynamic favorability decreasing with increasing pH. In sediments, Mn (III) (oxy)hydroxides are possible oxidants at near neutral pH for iodide; however, chloride and bromide reactions can only occur at pH values ≤ 2-3. I_2 and HOI form on iodide oxidation and can react with natural organic matter with formation of organo-iodine (R-I) compounds. During the treatment of drinking water, unwanted R-I disinfectant byproducts can form when the oxidant is not capable of quantitatively converting iodide to iodate.

In the atmosphere, halogen oxidation reactions are more likely due to photodecomposition of C-X bonds to X atoms, which react with O_3, NO, XO and other species by O atom transfer, a two electron transfer process. In the case of iodine, iodine oxide species form aerosol nanoparticles leading to cloud condensation nuclei.

https://doi.org/10.1180/S0026461X00006502 Published online by Cambridge University Press

How crystalline matter dissolves: Contours of a comprehensive stochastic model

ANDREAS LUTTGE[1]*,[2], ROLF S. ARVIDSON[1], INNA KURGANSKAYA[1] AND CORNELIUS FISCHER[3]

[1]Department of Earth Science MS-126, Rice University, Houston TX 77005, USA (*correspondence: aluttge@rice.edu)
[2]Department of Chemistry MS-60, Rice University, Houston TX 77005, USA
[3]Georg-August-Universität, D-37077 Göttingen, Germany

In the 1950's Burton, Cabrera and Frank developed BCF theory for crystal growth and some specific cases of crystal dissolution, e.g. the formation of etch pits along screw dislocations. Subsequently, we have struggled with attempts to develop a comprehensive theory and model that will describe and correctly predict how crystalline matter dissolves.

Today, we can point to a large pool of experimental and field data and a correspondingly large number of so-called rate laws that mainly attempt to fit these data. At the same time, we have identified a number of obstacles that potentially prevent us from understanding fundamental problems, including the measured discrepancies between field and laboratory data, 'reactive' surface area, and related issues. This situation cripples our ability to quantitatively predict how crystalline matter dissolves, and thus has significant consequences for important decisions involving, e.g. the licensing of repositories for nuclear waste, the treatment of hazardous waste, and regulations to ensure groundwater and aquifer quality during the 'fracing' process used by the energy industry to generate shale gas.

As an alternative we have developed a new approach that treats the dissolution and growth of crystalline matter stochastically as a many-body problem. Laboratory studies using vertical scanning interferometry and atomic force microscopy demonstrate that computer simulations of reaction kinetics based on parameterized Monte Carlo simulations are increasingly capable of correctly predicting how a specific surface or an entire crystal dissolves.

Our study shows that variations of up to 2.5 orders of magnitude in dissolution rates are likely real and not an experimental artifact. Thus, the concept of an intrinsic dissolution rate, i.e. the 'rate constant' as a material constant, is indeed fiction. Even if we postulate that the development of a steady-state surface is possible for dissolving crystals, this scenario would not be realistic for most natural processes under ambient conditions.

^{17}O anomaly of dissolved O_2 in the deep Atlantic Ocean

BOAZ LUZ[1]*, EUGENI BARKAN[1], GIDEON HENDERSON[2], WILLIAM SMETHIE[3]

[1]The Institute of Earth Sciences, The Hebrew University of Jerusalem, Jerusalem 91904, Israel (*correspondence: boaz.luz@huji.ac.il)
[2]Department of Earth Sciences, Oxford University, Oxford OX1 3AN, UK (gideonh@earth.ox.ac.uk)
[3]Lamont-Doherty Earth Observatory, Palisades NY 10964-8000, USA (bsmeth@ldeo.columbia.edu)

It is well established that oceanic dissolved O_2 contains an excess of ^{17}O ($^{17}\Delta$) with respect to atmospheric oxygen [1, 2]. This excess originates from newly produced O_2 by marine photosynthesis. $^{17}\Delta$ is unaffected by respiration and therefore behaves conservatively in the deep sea. In contrast, air-sea gas exchange drives $^{17}\Delta$ towards zero in surface water. As a result, $^{17}\Delta$ is low (20-40 per meg) in the oceanic mixed layer, but high values (up to ~200 per meg) are typical in the seasonal thermocline, where exchange with air is slow and new production of O_2 by photosynthesis is the main factor affecting $^{17}\Delta$. Below the seasonal thermocline, in layers that originate in winter at high latitudes, $^{17}\Delta$ tends again toward low values indicating the dominance of gas exchange over photosynthesis in the source areas. Yet, there is no information on $^{17}\Delta$ below 300 m.

Here we report results of the first measurements in the deep sea. In the Sargasso Sea, $^{17}\Delta$ is ~50 per meg at 500 m and gradually declines to ~30 per meg at 4700 m. These values are expected according to the explanation above and the high latitude origin of the water in this depth range. In contrast, high $^{17}\Delta$ values (79 to 97 per meg) were measured over the depth range of 1250 to 5000 m in two stations in the S. Atlantic (~35º and ~39ºS). Such high values in both NADW and AABW are unexpected and we will discuss possible explanations for their origin.

[1] Luz&Barkan (2000) *Science* **288**, 2028–2031. [2] Luz & Barkan (2009) *AME* **56**, 133–145.

https://doi.org/10.1180/S0026461X00006502 Published online by Cambridge University Press

Research on hyperspectral remote sensing estimation model of heavy metal pollution in vegetation

LV KAIYUN[1,2] AND ZHANG MING[1,2]

[1]Key Laboratory of Nuclear Resources and Environment (East China Institute of Technology), Ministry of Education,Nanchang 330013, P.R. China
[2]East China Institute of Technology, Fuzhou in Jiangxi, 344000, P.R. China

Hyperspectral remote sensing, which can provide higher spectrum resolution and super multi-band image spectrum data, and can well reflect the inherent spectral characteristics and differences of various vegetation in nature, has a wide range of applications in the vegetation monitoring. After the heavy metals getting into the interior of vegetation, they will cause changes in various physical and chemical parameters of vegetation, so that they will lead to the changes of spectral characteristics. This paper will take the corn in heavy metal copper pollution as an example, through analyzing the main spectrum features under hyperspectral remote sensing, and extracting the feature parameters of the red edge from the spectral, analyze the movement rules of the red edge of the corn in different pollution degrees and the relationships between the physiological index of the corn under the heavy metal pollution and them. According to multiple statistical analysis technique, regarded the red edge feature parameters as independent variable, establish the multiple regression estimation model of physiological index, and invert various physical and chemical parameters of vegetation polluted by heavy metals, which is helpful for the pollution degrees of vegetation to diagnose and evaluate. By analyzing the test data, based on the regression model of the red edge feature parameters with the character of simple and practical and high accuracy, it will be able to well reflect the pollution degrees of vegetation polluted by heavy metals, so it is worth doing and applying in practice.

This work was supported by the Jiangxi Province Natural Science Foundation of China (Grant No: 2009GQS0001) and Key Laboratory of Geospace Environment & Geodesy ministry of Education. China (Grant No:08-01-04).

Photochemistry and the observed enrichment of O, C, N, and H isotopes in meteorite IOM

J.R. LYONS

Institute of Geophysics & Planetary Physics, UCLA, Los Angeles, CA 90095-1567 USA (jimlyons@ucla.edu)

Recently measured large isotope excursions in IOM

The remarkable O MIF signatures seen in acid-insoluble organic matter (IOM) from a CR2 meteorite [1] show some correlation with enhanced $\delta^{13}C$ values, suggesting that both enrichments may be a result of CO photochemistry. ^{2}H and ^{15}N enrichments in the same IOM do not correlate with $^{17,18}O$ and/or ^{13}C enrichments, but do show some correlation with each other [1]. Both N and H isotopes have been shown to be strongly fractionated by ion-molecule reactions in molecular clouds [2, 3]. The question I address here is are these results, particularly those for meteorite IOM [1], consistent with expected photochemical and ion-molecule processes.

Photochemical models of clouds and the solar nebula

It is well established that CO self-shielding produces large enrichment in product ^{17}O and ^{18}O, which are then stored in H_2O. Product C is similarly enriched in ^{13}C, although by a factor of ~2 less than the enrichment in ^{17}O and ^{18}O [4]. Self-shielding enrichment of ^{13}C is predicted by photochemical models of disks [5], but CO exchange with C^+ and CO condensation [6, 7], are also important. Disk model calculations, including ^{13}C at temperatures well above CO condensation, are in progress. As with CO, N_2 also undergoes self-shielding, producing enriched N and N (^2D), with the N stored in HCN. The N (^2D) rapidly forms NH, leading to reformation of N_2 by reaction of N and NH. Large ^{15}N enrichments are possible by N_2 self-shielding, but the total amount of enriched material produced is small [8]. Finally, H_2 also has a line-type absorption spectrum, and so also undergoes self-shielding at the edges of clouds and high surface of disks. At greater depths into these objects, where CO and N_2 self-shielding become important, H_2 lines are very broadened and will shield HD lines, thus reducing D enrichment. These results are consistent with a photochemical origin for O and (possibly) C isotopes signatures in IOM, and ion-molecule origin for H and N isotopes signatures in IOM.

[1] Hashizume *et al*. (2011*) Nature Geo*. **4**, 165. [2] Rogers & Charnley (2008) *MNRAS* **385**, L48. [3] Aleon & Robert (2004) *Icarus* **167**, 424. [4] Visser *et al*. (2009) *A&A* **503**, 323. [5] Woods & Willacy (2009) *ApJ* **693**, 1360. [6] Smith *et al*. (2011) *42nd LPSC* abs. 1281. [7] Young & Schauble (2011) *42nd LPSC* abs. 1323. [8] Lyons (2010) *73rd MetSoc* abs. 5424.

https://doi.org/10.1180/S0026461X00006502 Published online by Cambridge University Press

Molybdenum as a paleoredox proxy: An update

T.W. LYONS[1]*, G.L. ARNOLD[2], A. CHAPPAZ[1], B.C. GILL[3], N.J. PLANAVSKY[1], C.T. REINHARD[1], N. RIEDINGER[1], C.T. SCOTT[4] AND A.D. ANBAR[5]

[1]Dept. of Earth Sciences, Univ. of California, Riverside, CA 92521 USA (*correspondence: timothy.lyons@ucr.edu)
[2]Max Planck Instit. for Marine Microbiology, 28359 Bremen, Germany
[3]Dept. of Earth and Planetary Sciences, Harvard Univ., Cambridge, MA 02138 USA
[4]Dept. of Earth and Planetary Sciences, McGill Univ., Montreal, Quebec H3A 2A7 Canada
[5]School of Earth and Space Exploration and Dept. of Chemistry & Biochemistry, Arizona State Univ. Tempe, AZ 85287 USA

Concentrations and isotope trends of molybdenum in organic-rich shales are among the favored tracers for euxinia in the ancient ocean on local and global scales. With the successes, however, has also come increasing awareness of the complexity.

The purpose of this talk is to synthesize the broad range of refining and defining proxy developments and applications over the past several years, as a progress report and roadmap for future applications. Among the key topics are (1) our new and refined models for Mo uptake and burial under euxinic conditions, including a rigorous mechanistic understanding of the apparent coupling between Mo and organic matter sinks; (2) our comprehensive view of how Mo is taken up, fractionated isotopically, and buried [or recycled] beneath oxic bottom waters, particularly as coupled to Mn and Fe cycles; (3) our improved perspective on how and when Mo isotopes can be fractionated under permanent or transient euxinia, leading to a more effective use of the global redox proxy and to novel estimates of dissolved sulfide concentrations and their variability within ancient euxinic settings; and (4) our new, all-inclusive understanding of the cycling and mass balance of Mo in the ocean. We are encouraged by emerging consistency with the very latest models for the redox structure of the Proterozoic ocean; inferrences about Mo-limited early eukaryotic and prokaryotic life; and our ability to use Mo isotopes, with caution, to estimate global redox conditions.

https://doi.org/10.1180/S0026461X00006502 Published online by Cambridge University Press

Structural phase transition of ammonia hydrate under high pressure

CHUNLI MA, QIANG ZHOU, FANGFEI LI, JIAN HAO, JINGSHU WANG, FENGXIAN HUANG AND QILIANG CUI*

State key Laboratory of Superhard Materials, Jilin University, Changchun, 130012, P.R.China
(*correspondence: cql@jlu.edu.cn)

High pressure Raman scattering studies and angle-dispersive synchrotron x-ray diffraction measurements have performed on water-ammonia binary system up to 29.92GPa and 45.11GPa, respectively. Moreover, with pressure increased slowly, it was found from microscope that the appearance of lozenge blocked solid in the sample chamber at 3.48GPa. Compared with the Raman spectrum of ice and solid ammonia, we observed that the new appeared solid was ammonia hydrate. Hence, Raman spectrum of water-ammonia binary system and ammonia hydrate would be obtained at same pressure, respectively. Therefore, it was observed that the water-ammonia binary system transformed from liquid to solid phase at 3.8GPa but the ammonia hydrate had no phase transition up to 20.34GPa because of the disappearance of Raman spectrum. However, high pressure angle-dispersive synchrotron x-ray diffraction measurements showed that there was a solid to solid phase transition of ammonia hydrate at about 20GPa. And the mechanism of this phase transition is in processing.

This work was financial supported by the National Natural Science Foundation of China (No.10574054, No.10976011 and No.11004074); the National Basic Research Program of China (2011CB808200).

Characteristic of mineral component in carlin-type gold deposit in Qinling area

MA GUANG[1], GONG LI[1]*, DONG YUN FENG[2], CHEN KUIKUI[1] AND ZHANG GUIPING[3]

[1]Henan Polytechnic University, Heana 454001, China (*correspondence: gongli5678@163.com)
[2]Liaoning Geological environment monitor station, Liaoning 100032, China
[3]China Geological Library, Beijing, 100083

Introduction

The intergrowth combination of ore mineral in different Carlin-type gold deposits in the Qinling area are roughly consistent, and, the gold mainly forms in the first stage of the hydrothermal period—arsenic-rich sulfide phase, Gold existed mainly in the form of native gold with irregular granular shape, secondly, it assumes the sub-microscopic gold existing in the arsenic sulfide.

Experiment and Results

Gold minerals output mainly in the form of native gold and have irregular granular primarily, also show the shape of flake, clavate, arborization and so on. Particle size are generally small and mostly exists as the form of microscopic gold - sub-microscopic gold, a few may be visible to the naked eye. Most of the sub-micro golden are located within the arsenic-sulfide mineral (80.4%~85.2%). The major minerals are the arsenical pyrites and arsenopyrite, in the next place are the tennantite, the realgar, the orpiment, the stibnite and so on, sometimes associated with the few chalcopyrite, the galena and the sphalerite. It has the characteristic of proliferation annulus in crystal grain interior of the arsenical pyrites, according this, may determine the ore deposit type and the provide effective prospecting method.

In the metallogenesis hydrothermal stage of ore deposit, arsenic pyrite and arsenopyrite is the gold-bearing mineral crystallized earliest and distributed widely in most deposits, however, the arsenopyrite content change large in the different ore deposit. Minerals above constituent uppermost stage of gold mineralization—rich-arsenic sulfide stage, this stage has formed the stable Au-As element combination and the mineral association, the stibnite, the cinnabar, the realgar and the orpiment forms late and fill in opening space with vein shape. After rich-arsenic sulfide hydrothermal stage, appear the vein with intense silicification, calcilized and the barite arteries, the veins forms in the late stages of metallogenesis under oxidation.In this stage, gold-bearing arsenic sulfide has suffered intense oxidation and hydrolysis, submicroscopic gold dissociating has obvious enrichment in the surface.

https://doi.org/10.1180/S0026461X00006502 Published online by Cambridge University Press

Mine hydrochemistry evolution and water-inrush discrimination based on GIS: A case in Panyi

L. MA[1]*, X.M. WANG[2] AND X.P. ZHOU[1]

[1]School of Resources and Environmental Engineering, Hefei University of Technology, Hefei 230009, China (Lei8505@gmail.com)
[2]Public Geological Survey Management Center of Anhui Province 230001, China

New Method

With the increase of the coal exploitation depth, intensity, rate and scale, coal mining has been under the serious threat of fracture-karst groundwater [1-2]. Many studies show that groundwater flows in fractures are nonlinear and difficult to identify [3-8]. An alternative mothod is to make use of groundwater hydrochemical characteristics and groundwater temperature for discriminating the source of water-inrush. Based on ArcSDE and Microsoft SQL Server, the spatial database for discrimination of water-inrush source of Panyi Coal mine was designed and established. Spatial data mining technology was introduced and applied to the analysis of mine groundwater. Based on Voronoi diagram and DEM methods, the distribution rules of the hydrochemical types and the spatial association rules of groundwater chemistry and structure were mined from the above spatial database. The models for water-inrush source discrimination were studied and coupled with GIS.

Results and Discussion

Spatial data mining technology was applied to analyze the groundwater of mine, and based on Voronoi diagram and DEM methods the distribution rules of the chemical types of groundwater were mined.

A GIS-based identification method of mine water-inrush source with comprehensive information which integrated water level, water chemical and water temperature was proposed, and the application in Panyi Mine showed that the method can improve the precision of discrimination.

A simple, rapid and practical GIS-based system for mine water-inrush source rapid discrimination with comprehensive information was developed. (Grant no: 2009HGCX0233)

[1] Qian *et al*. (2006) *Hydrogeol. J*. **14**, 1192–1205. [2] Qian *et al*. (2009) *Hydrogeol. J*. **17**, 1749–1760. [3] Zhou *et al*. (2004) *Int. J. Rock Mech. Min. Sci*. **41**, 402. [4] Qian *et al*. (2005) *J. Hydrol.* **311**, 134–142. [5] Qian *et al.*(2007) *J. Hydrol.* **339**, 206–219. [6] Qian *et al*. (2011) *Hydrol. Process*. **25**, 614–622. [7] Qian *et al*. (2011) *J. Hydrol.* **399**, 246–254. [8] Chen *et al.*(2009) *Journal of Hydrodynamics* **21**, 820–825.

Olympic Dam U-Cu-Au deposit, Australia: New age constraints

R. MAAS[1], V. KAMENETSKY[2], K. EHRIG[3], S. MEFFRE[2], J. MCPHIE[2] AND G. DIEMAR[3]

[1]University of Melbourne, Australia, maasr@unimelb.edu.au
[2]CODES, University of Tasmania, Hobart, Australia
[3]BHP-Billiton, Adelaide, Australia

The Olympic Dam supergiant U-Cu-Au-REE deposit is located in the Olympic Dam IOCG province of the mid-Archean-Proterozoic Gawler Craton, South Australia. Mineralization is hosted in hematite-rich breccia within the 1590 Ma Roxby Downs Granite, part of the strongly mineralized Gawler Range Volcanic LIP. Initially linked to the GRV event, recent work supports a post-GRV, late-Mesoproteroic age of mineralization. Our Sm-Nd data for step-leached ores are similar to published whole rock data and define an (imprecise) ~1300 Ma apparent age. This is broadly supported by Rb-Sr isochrons for the same step-leach fractions. ε_{Nd} and $^{87}Sr/^{86}Sr$ (at 1300 Ma) are ~-7.5 and ~0.708. Pb isotopes in isotopically zoned pyrite from mineralized clastic sediments and galena in the ore have common Pb model ages which suggest sediment deposition/diagenesis and U introduction no earlier than 1.3-1.1 Ga. These age constraints are consistent with earlier work (ionprobe U-Pb ages in uraninite no older than 1.4 Ga, ReOs dating of chalcopyrite ~1.26 Ga). Evidence for post-ore disturbance is preserved in the form of 450-550 Ma apparent ages for a step-leached sericite-rich ore (Rb-Sr) and a texturally late fluorite-rich vein (Sm-Nd); the ~500 Ma apparent ages are associated with $^{87}Sr/^{86}Sr = 0.715$-0.722.

Extraction of unequivocal age evidence for this very complex deposit is difficult, and all ages – previously published and new – need to be treated with caution. For example, Sm-Nd isotope systematics are easily modified by local REE redistribution involving Nd-rich 'nuggets' of bastnaesite and florencite. Nevertheless, the balance of evidence now indicates a post-1590 Ma age for much of the mineralization in the period 1.4-1.1 Ga. Metal deposition in several stages, from the magmatic GRV event to renewed crustal-scale fluid flow during amalgamation of Rodinia at 1.2-1.1 Ga may explain the enormous size of the deposit.

https://doi.org/10.1180/S0026461X00006502 Published online by Cambridge University Press

Variations in atmospheric helium isotopes

J.C. MABRY*, B. MARTY, P. BURNARD

CRPG-CNRS, 54501 Nancy, France
(*correspondence: jmabry@crpg.cnrs-nancy.fr)

The purpose of this work is to look for variations in the isotopic helium composition in the atmosphere. Anthropogenic activities such as oil and gas exploitation release crustal helium, which has excess ^{4}He compared to atmospheric helium. This may give rise to detectable spatial and temporal variations in the atmospheric ^{3}He/^{4}He [1].

These differences, if they exist, would be very small [2], and thus require very high precision measurements. However, high precision measurements of atmospheric helium presents a significant analytical challenge because helium is only present in trace quantities in the air (5.24 ppm) and there are are many of orders of magnitude difference in the abundance of the two isotopes (^{3}He/^{4}He$_{air}$ = 1.38 x10^{-6}). We are designing a method to reliably measure ^{3}He/^{4}He with 2‰ or better precision.

Air samples are collected in copper tubes which are then sealed manually at the sample site with steel clamps. Each tube holds a volume of approximately 20 cm^3. Samples collected cover a wide range of longitudes and latitudes, with a particular emphasis on sampling across many latitudes since the largest spatial variation is expected to be seen in latitude.

For each measurement we purify a relatively large amount of gas (~5-15 cm^3) so that we can make many repeat analyses of the same sample gas. We have constructed an automated extraction line which can rapidly switch between measuring aliquots of sample with standards. A major component of our method features an adjustable bellows on the sample aliquot volume that enables us to adjust the size of a sample aliquot to precisely match the standard, eliminating biases arising from nonlinear pressure effects in the mass spectrometer. The measurements are made using a Helix split flight tube multi-collector mass spectrometer.

At present, the measured ratios of a sample have a 1σ reproducibility of 2-3‰, which is still too large to detect variations. We have planned several changes to further improve the next round of measurements including installing a quadrupole mass spectrometer to monitor the gas purification process and the addition of a cold trap to the mass spectrometer volume.

[1] Oliver *et al*. (1984) *GCA* **48**, 1759–1767. [2] Sano *et al*. (2010) *GCA* **74**, 4893–4901.

On the origins of dissolved natural organic matter (DNOM) in rivers and lakes

DONALD L. MACALADY[1]
AND KATHERINE WALTON-DAY[2]

[1]Colorado School of Mines, Golden, CO, USA
(dmacalad@mines.edu)
[2]U.S. Geological Survey, Denver, CO USA
(kwaltond@usgs.gov)

One of the most important characteristics of DNOM, at least with respect to reversible chemical reactivity, is its aromatic carbon content. The DNOM (measured as dissolved organic carbon, DOC) that dominates most rivers and lakes is derived primarily from land plants, including various species of woody trees and shrubs, grasses, fungi and mosses. The specific ultraviolet absorbance (SUVA, absorbance at 254 nm in a 1.0 cm cell divided by DOC in mgL^{-1}) of DNOM provides a simple, widely applicable indication of a sample's aromatic content. Examination of SUVA values of water samples from rivers and lakes, then comparison of these to SUVA values for DNOM samples derived from precursor materials, shows little apparent commonality. These precursor materials consist of senescent materials from plant species common to the catchment basins of the rivers and lakes. This paper examines the effects of geochemical processes on the SUVA values of natural waters and associated precursor materials in order to develop an understanding of the primary factors affecting the origins and aromatic content of DNOM in natural waters.

https://doi.org/10.1180/S0026461X00006502 Published online by Cambridge University Press

Proterozoic analog ecosystem and organic biomarkers in a Florida sinkhole

J.L. MACALADY[1]*, H.L. ALBRECHT[1], P.V. WELANDER[2], J.M. FULTON[1], I. SCHAPERDOTH[1], T.S. WHITE[1], K.H. FREEMAN[1], D.K. NEWMAN[3] AND R.E. SUMMONS[2]

[1]Geosciences Dept., Penn State Univ., University Park, PA 16802 USA (*correspondence: jlm80@psu.edu)
[2]Dept. EAPS, MIT, Cambridge, MA 02139 USA
[3]California Inst. Technology, Pasadena, CA 91125 USA

Competition between oxygenic and anoxygenic phototrophs has been proposed as a mechanism that delayed the oxygenation of the Earth's oceans and atmosphere in the Proterozoic [1]. Factors affecting competition among modern phototrophs are not well understood, especially under low oxygen conditions thought to have been prevalent in Precambrian oceans. Little Salt Spring (Sarasota County, FL, USA) is a brackish, sulfidic sinkhole hosting a mixed community of oxygenic and anoxygenic phototrophs. Groundwater vents discharge into the bottom water at 73 m depth, and thick, purple microbial mats cover sediment surfaces in the sunlit upper basin. 16S rRNA clones from the mat were affiliated with *Cyanobacteria* and *Chlorobi*, with smaller numbers of *Deltaproteobacteria* in sulfate-reducing clades. Six bacteriochlorophyll e homologues and isorenieratene reflect contributions from *Chlorobi,* and abundant chlorophyll a and pheophytin a likely derive from *Cyanobacteria*. Hopanoid content of the mat is high (29% of total membrane lipids). The relative abundances of polar hopanoids in the mat are preserved in organic-rich surface sediments accumulating in the deep portion of the sink. Remarkably, more than half of the hopanoids in the mat and surface sediments have 2-methyl structures, which are preserved in the geologic record as 2-methyl hopanes and have been interpreted as biomarkers for *Cyanobacteria*. PCR amplification of the hopanol 2-methylase (*hpnP*) from mat DNA retrieved a sequence affiliated with other cyanobacterial HpnP homologs. Ongoing work at the site is aimed at: (1) a quantitative model of anoxygenic and oxygenic contributions to net primary productivity and biomarker production; (2) understanding the ecological factors that promote the co-existence of oxygenic and anoxygenic phototrophs in the mat; and (3) describing the timescale and chemical changes associated with diagenesis of organic biomarkers.

[1] Johnston (2009) *Proc. Nat. Acad. Sci.* **106**, 16925–16929.

Combined SIMS U-Pb ages and Ti-in-zircon geothermometry fingerprints long deep crustal residence in the Archaean

JOHN MACDONALD[1], JOHN WHEELER[1], KATHRYN GOODENOUGH[2], SIMON HARLEY[3], QUENTIN CROWLEY[4] AND ELISABETTA MARIANI[1]

[1]School of Environmental Sciences, University of Liverpool, Liverpool, L69 3GP jmacd@liv.ac.uk
[2]British Geological Survey, Edinburgh EH9 3LA
[3]School of GeoSciences, University of Edinburgh, Edinburgh EH9 3JW
[4]School of Natural Sciences, Trinity College, Dublin

Combined SIMS U-Pb ages and Ti-in-zircon geothermometer temperatures for a population of zircons from Archaean gneisses indicate long deep crustal residence at >780°C for >350Ma. This technique of having both an age and minimum temperature for each analytical spot is a new and direct way of showing that heat flux from the mantle to the base of the crust was higher in the Archaean than the present day.

The rocks are TTG gneisses from the polymetamorphic Archaean-Palaeoproterozoic Lewisian Gneiss Complex of NW Scotland. The analysed zircon population comprises a small number of primary magmatic cores and a range of metamorphic domains; CL imaging showed that the metamorphic domains were either rims or whole crystals of uniform CL. The metamorphic domains comprised a mix of anatectic growth and recrystallisation textures. U-Pb data produced a spread of ages from 2.5-2.8Ga with some ages older than this. Tight discordance limits (+5/-2%) were applied so only the best, most concordant age data were used. Ti analyses were filtered to exclude those from plastically-deformed (EBSD data) and contaminated (Ba >1ppm) zircons.

We interpret the data as TTG protolith formation around 2.8-3.0Ga followed by granulite-facies metamorphism at 2.8Ga. The studied part of the Lewisian Complex remained at >780°C up until 2.5Ga when it was cooled, possibly by uplift and erosion. This 300 My period of elevated temperature contrasts with Phanerozoic crustal behaviour, in which such high grade rocks are cooled over much shorter timescales.

https://doi.org/10.1180/S0026461X00006502 Published online by Cambridge University Press

Assessment of heavy metal contamination in soils around Chinnaeru river sub-basin, Nalgonda District, India

G. MACHENDER[2], S. YASHODA[1], M.N. REDDY[2] AND P.K. GOVIL[1]

[1]National Geophysical Research Institute (Council of Scientific and Industrial Research) Uppal Road, Hyderabad-500007, A.P., India
[2]Dept. of Geology, Osmania University, Hyderabad-500007, A.P., India

The concentration of heavy metals such as As, Ba, Co, Cr, Cu, Ni, Pb, Rb, Sr, V, Y, Zn and Zr were studied in soils to understand metal contamination due to agriculture and geogenic activities in Chinnaeru river basin, Nalgonda district, India. This area is affected by the geogenic fluoride contamination. The contamination of the soils was assessed on the basis of geoaccumulation index, enrichment factor (EF), contamination factor and degree of contamination. Forty four soil samples were collected from the agricultural field from the study area from top 10-50 cm layer of soil. Soil samples were analyzed for heavy metals by using X-ray fluorescence spectrometer. Data revealed that, soils in the study area are significantly contaminated, showing high level of toxic elements than normal distribution. The ranges of concentration of Ba (370-1710 mg/kg), Cr (8.7-543 mg/kg), Cu (7.7-96.6 mg/kg), Ni (5.4-168 mg/kg), Rb (29.6-223 mg/kg), Sr (134-438 mg/kg), Zr (141.2-8232 mg/kg) and Zn (29-478 mg/kg). The concentration of other elements was similar to the levels in the earth's crust or pointed to metal depletion in the soil (EF<1). The high EFs for some heavy metals obtained in soil samples show that there is a considerable heavy metal pollution, which could be due to excessive use of fertilizers and pesticides used for agricultural or may be due to geogenic activities in the area. A contamination site poses significant environmental hazards for terrestrial and aquatic ecosystems. They are important sources of pollution and may results in ecotoxicological effects on terrestrial, groundwater and aquatic ecosystems.

Influence of interfacial water structure on surface protonation and ion adsorption at metal oxide surfaces

M.L. MACHESKY[1]*, D.J. WESOLOWSKI[2], L. VLCEK[2], E. MAMONTOV[2], P.R.C. KENT[2], M. PŘEDOTA[3], J. ROSENQVIST[4], M.K. RIDLEY[5], P.T. CUMMINGS[6], J.D. KUBICKI[7], J.O. SOFO[7], N.KUMAR[7], S.N. LVOV[7], A.V. BANDURA[8], P. FENTER[9] AND Z. ZHANG[9]

[1]Univ. of Illinois, Champaign, IL 61820, USA (*correspondence: machesky@illinois.edu)
[2]Oak Ridge National Laboratory, Oak Ridge, TN 37831, USA (dqw@ornl.gov, vlcekl1@ornl.gov, mamontove@ornl.gov, kentpr@ornl.gov)
[3]Univ. South Bohemia, České Budějovice, Czech Republic, 370 04 (predota@prf.jcu.cz)
[4]University of Leeds, Leeds LS2 9JT, UK (J.Rosenqvist@leeds.ac.uk)
[5]Texas Tech University, Lubbock, TX 79409, USA (moira.ridley@ttu.edu)
[6]Vanderbilt Univ., Nashville, TN 37235, USA (peter.cummings@vanderbilt.edu)
[7]The Pennsylvania State Univ., University Park, PA 16802, USA (jdk7@psu.edu, sofo@psu.edu, nkz116@psu.edu, lvov@psu.edu)
[8]St. Petersburg State Univ., St. Petersburg, Russia (andrei@ab1955.spb.edu)
[9]Argonne National Laboratory, Argonne, IL 60439, USA (Fenter@anl.gov, zhanzhang@anl.gov)

The overall goal of our research is to quantitatively link experimental and computational results to elucidate the atomic scale structure and dynamics of aqueous solutions at metal oxide surfaces and to link these atomistic interfacial properties with their macroscopic manifestations. Most of our efforts have been directed toward the isostructural oxides rutile (TiO_2) and cassitertite (SnO_2). The surfaces of these oxides (primarily the 110 face) have been probed by X-ray and neutron scattering, second harmonic generation, pH and zeta potential titrations, and ab initio and classical MD. In total, these techniques reveal a fairly consistent picture of interfacial water structure and cation binding. Directly bound water molecules are more tightly held at the cassiterite 110 surface than rutile 110 surface, and this difference helps account for the observed differences in surface protonation and ion binding exhibited by these oxides.

This research has been largely supported by the Division of Chemical Sciences, Geosciences and Biosciences, Office of Basic Energy Sciences, U.S. Deparment of Energy.

https://doi.org/10.1180/S0026461X00006502 Published online by Cambridge University Press

Sr, Nd, and Pb isotopes of basalts along hotspot-influenced Central Indian Ridge

S. MACHIDA[1], Y. ORIHASHI[2], N. NEO[3], M. TANIMIZU[4], S.C. UNSWORTH[5] AND K. TAMAKI[6]

[1]School of Creative Science and Engineering, Waseda University, 3-4-1 Okubo, Shinjuku, Tokyo 169-8555, Japan (m-shikit@aoni.waseda.jp)
[2]Earthquake Research Institute, the University of Tokyo
[3]Faculty of Sciences, Niigata University
[4]Kochi Core Center, JAMSTEC
[5]National Oceanography Centre, University of Southampton
[6]Graduate School of Engineering, the University of Tokyo

A type of distal ridge-hotspot interaction is observed between the Central Indian Ridge (CIR) and the Réunion hotspot. The Rodrigues, Three Magi, and Gasitao Ridges clearly indicate topographic connection of CIR at 20°S and the Réunion hotspot track. However, northward geochemical enrichment of MORB along a segment of CIR at 18-20°S still remains a contentious issue, and is explained by an inflow of plume materials from the Réunion hotspot [1, 2] or ancient recycling process [3]. In order to define what factor regulates melt production along hotspot-influenced CIR, it is important to clarify extensive distribution of the plume-related or -unrelated MORB. We thus report Sr, Nd, and Pb isotopic compositions, with geochemical data set [4] and H_2O content, of fresh quenched glasses and basalts along CIR at 15-20°S.

Variation of isotopic compositions, Ba/Nb (Ba/La, Nb/Zr), and H_2O content are interpreted by mixing of three mantle endmembers: depleted MORB mantle (DMM); enriched source mantle for the Rodrigues Ridge [5] and intermediate series of the Mauritius Island [e.g. 6]; and enriched source mantle for the Gasitao Ridge [3]. These two enriched components are geochemically distinct from the Réunion plume. In fact, geochemical variation of MORB doesn't relate to the pollution of the upper mantle by the Réunion plume. Melting of the ancient recycled plate materials with a low melting point by the heat brought from the Réunion hotspot regulates voluminous magma production along CIR around 19°S. These results strongly support that small-scale plume-unrelated heterogeneity widespread in upper mantle [7].

[1] J.J. Mahoney *et al*. (1989) *JGR*, **94**, 4033–4052. [2] B.J. Murton *et al*. (2005) *G3,* **6**, 2004GC000798. [3] F. Nauret *et al*. (2006) *EPSL*, **245**, 137–152. [4] Y. Orihashi *et al*. (2009) *GCA*, **73** (13) Sup. **1**, A975. [5] A.N. Baxter *et al*. (1985) *CMP*, **89**, 90–101. [6] S. Nohda *et al*. (2005) *J. Petrol*. **46** (3) 505–522. [7] S. Machida *et al*. (2009) *GCA*, **73**, 3028–3037.

A field method for the *in situ* determination of excess air and oxygen consumption in groundwater

L. MÄCHLER[1]*,[2], M.S. BRENNWALD[1] AND R. KIPFER[1,3]

[1]Eawag, Swiss Federal Institute of Aquatic Science and Technology, Duebendorf, Switzerland. (*correspondence lars.maechler@eawag.ch)
[2]Institute of Geochemistry and Petrology, ETH Zürich, Switzerland
[3]Institute of Biogeochemistry and Pollutant Dynamics, ETH Zürich, Switzerland

Measurements of dissolved gases play a crucial role in studying aquatic systems in the environment. An important example is the study of oxygen consumption in groundwater. For its determination, the input of oxygen into the water body must be estimated. This input not only depends on the temperature at recharge, but also on a common phenomenon called "excess air", i.e. the entrapment and dissolution of air bubbles into the water, caused by water-table fluctuations, that lead to an excess of dissolved gases in water relative to solubility equilibration.

Noble gases are chemically inert and therefore ideal tracers to study gas transport in groundwater and gas-exchange mechanism at the air-water boundary. The light noble gases (He, Ne) are sensitive indicators for excess air formation, while the heavy noble gases (Kr, Xe) are good proxies to reconstruct the physical conditions (i.e. temperature and salinity) of the water body during the last gas exchange with atmosphere. Furthermore, Ar has similar physical properties as O_2 and can be used to estimate the O_2-input into groundwater.

Common methods to measure noble-gas concentrations are all based on sampling the water in the field and transporting the sample to the laboratory, where the analysis is performed. However, changes in dissolved-gas concentration, in river-groundwater interactions, can occur within minutes/hours and cannot be studied using the conventional approaches for noble-gas analysis.

Therefore, we developed a membrane-inlet mass-spectrometric system to analyse *in situ* O_2, He, Ar, Kr, and CO_2 concentrations in groundwater in the field. The system is based on a commercially available quadrupole mass-spectrometer connected to a membrane-contactor module. We optimized the system to a measurement cycle of about 15 minutes in order to measure gas-concentration changes in groundwater occurring in response to river table fluctuations.

https://doi.org/10.1180/S0026461X00006502 Published online by Cambridge University Press

Natural Fe-Oxidizing Lagoon as a pretreatment in AMD remediation

FRANCISCO MACÍAS[1], CARLOS AYORA[2], MANUEL A. CARABALLO[1], JOSÉ MIGUEL NIETO[1] AND TOBIAS S. RÖTTING[3]

[1]Department of Geology, University of Huelva. Avda Fuerzas Armadas s/n 21071 Huelva, Spain
[2]Institute of Environmental Assessment and Water Research, CSIC, Jordi Girona 18, E-08034 Barcelona, Spain
[3]Department of Geotechnical Engineering and Geosciences, Technical University of Catalonia UPC-Barcelona Tech, Jordi Girona 1-3, D2-005b, E-08034 Barcelona, Spain

A concept called Natural Fe-Oxidizing Lagoon (NFOL) has been developed as an AMD pretreatment to enhance the iron oxidation and remotion processes involved in the natural attenuation of the AMD pollution, by the recreation, at a larger scale, of the iron terraces and pools observed in the Fe-rich AMD systems tipically found in the Iberian Pyrite Belt, SW Spain.

The NFOL comprises a first section formed by several preexisting iron terraces followed by a lagoon with a capacity of 100 m^3. The AMD pretreated in the NFOL, mean flow of 1.5 L/s, displayed a pH near 3 and contains 275 mg/L Fe (99% Fe (II)), 440 mg/L Zn, 3, 400 mg/L SO_4, 250 mg/L Ca, 100 mg/L Al, 18 mg/L Mn, 5 mg/L Cu and 0.1-1 mg/L As, Pb, Cr, Cd, Co and Ni. The NFOL was built following the recommendations offered by Piramid Consortium (2003) [1] according to surface area (m^2) and inflow (L/s) for lagoons and aerobic wetlands, but facing an inflow Fe concentration 5 times higher.

During the 6 months period of study, the NFOL pretreatment oxidized an average of 65% of the inflowing Fe (II) and precipitated a mean of 38% of total inflowing Fe. Additionally, over 80% of As in the inflow water was retained. Schwertmannite, subsequently aged to goethite, are the minerals responsible for the Fe (III) and As removal. The NFOL showed a mean Fe removal rate as high as 100 $g/m^2/day$, this value is one order of magnitude higher than the common standards for the efficient operation of a lagoon or an aerobic wetland in AMD environments.

NFOL pretreatment can be considered an efficient option to oxide and remove Fe and As prior to the treatment in the alkaline-based passive remediation system dispersed alkaline substrate (DAS) [2].

[1] PIRAMID-Consortium (2003) University of Newcastle Upon Tyne, Newcastle Upon Tyne UK. [2] Rötting *et al*. (2008) Appl Geochem (2008) **23**, 1660–1674.

Skarn bearing clintonite from Kuhe-Dor, Shirkuh, Yazd Province, Iran

MOHAMMAD ALI MACKIZADEH[1] AND BATOUL TAGHIPOUR[2]

[1]Department of geology, faculty of sciences, Isfahan University, Isfahan, Iran (ma_mackizadeh@yahoo.com)
[2]Department of earth sciences, faculty of sciences, Shiraz University, Shiraz, Iran (taghipour@shirazu.ac.ir)

Shirkuh skarns (Kuhe Dor) are located in Cenozoic magmatic belt of Central Iran. There is a diorite intrusion in lower Cretaceous limestone's are detected:

Pyroxene – spinel – clintonite – phligopite – garnet – vesuvianite – calcite

Kuhe Dor skarn, is characteristic with rare mineral clintonite. Clintonite shows the transition processes from mg – skarn to ca – skarn and is formed in geologic environment with high X H_2O, low X CO_2 and depletion in SiO_2. Content mineral texture evidences show unstable boundaries when clintonite is in contact with spinel. Such petrographic evidence suggests the formation of clintonites at the expense of aluminum rich phase (spinel) is taken place. Skarn formation is started in peak temperature about 800°C.

Due to post Cretaceous intrusions, various marble-skarn mineralization are formed in eastern Shirkuh fault zone. Marbles are made the last zone in contact metamorphic aureole. Marbles are characterized by following mineral assemblages:

brucite+serpentine+forstrite+hydromagnesite+calcite+dolomite.

The marbles are undergone to pyroxene hornfels facies with temperature between 450°C to 600°C (p<2kb). There is three different stages in the formation of marbles; decarbonation, hydration and carbonation which revealed by mineral paragenes is and textures.

https://doi.org/10.1180/S0026461X00006502 Published online by Cambridge University Press

Adsorption of Cr(VI) on hydrous manganese oxide

A. MACLEOD* AND C.M. KORETSKY

Department of Geosciences, Western Michigan University, Kalamazoo, MI 49008, USA
(*correspondence: andrew.k.macleod@wmich.edu)

Hexavalent chromium is used in a variety of industrial processes. When released into the environment, it can be quite mobile and is highly toxic. Understanding and accurately predicting Cr(VI) speciation and transport is key to remediating contaminated sites. Cr(VI) forms chromate (CrO_4^{-2}) and bichromate ($HCrO_4^-$) anions in natural systems, which adsorb to various substrates at low pH and desorb at high pH. The goal of this study is to investigate sorption of Cr(VI) on hydrous manganese oxide (HMO) as a function of ionic strength, pH and pCO_2.

Hydrous manganese oxide was synthesized by alkametric titation and subsequently stored under 0 pCO_2 conditions. HMO was confirmed by XRD, and N_2-BET indicated a surface area of ~230 m^2/g. Experiments were conducted by adding 20 g/L HMO to a solution of $NaNO_3$ (0.001, 0.01 or 0.1 M) containing 10^{-5} M Cr(VI). The batch solution was titrated to an initial pH of 3, and by small additions of NaOH was titrated upwards to pH 10 with ~10 mL aliquots drawn off at ~0.8 pH intervals. These aliquots were further equilibrated for 24 hrs under varying pCO_2 (0, atmospheric or 2.5%), then centrifuged and the supernatant filtered and tested for Cr(VI) concentrations using UV-vis spectrophotometry or total Cr by ICP-OES.

Cr(VI) sorption decreases as pH increases, from nearly 95% (0.1 M $NaNO_3$) or 75% (0.001 M $NaNO_3$) sorbed at pH 3 to 0% sorbed at pH > 7. Cr(VI) sorption depends strongly on ionic strength, with ~50% of the Cr(VI) sorbed at pH~6 in 0.1 M $NaNO_3$, compared to ~4 in 0.001 M $NaNO_3$ experiments. In contrast, Cr(VI) sorption on HMO was nearly identical for a given ionic strength under atmospheric compared to elevated (2.5%) pCO_2 conditions.

Future work will focus on investigating possible competitive sorption interactions between carbonate and chromate at pCO_2 levels $\geq$5%, and on Cr(VI) adsorption under other Cr(VI) loadings and ionic strength conditions. The data will be used to parameterize a surface complexation model, so that results can be readily incorporated into reactive transport models. This will further advance our predictive understanding of Cr(VI) mobility and speciation in natural environments.

Fractionation of HSE in the Tonga arc: Flux melting of a depleted source

C.G. MACPHERSON[1]*, C.W. DALE[1], D.G. PEARSON[1,2], S.J. HAMMOND[3] AND R.J. ARCULUS[4]

[1]Dept. of Earth Sciences, Durham University, DH1 3LE, UK (*correspondence: colin.macpherson@durham.ac.uk)
[2]Dept. for Earth & Atmos Sci, University of Alberta, Edmonton, Canada
[3]Dept. of Earth & Environ. Sciences, Open University, UK
[4]Dept. of Earth & Marine Sciences, ANU, Australia

Highly siderophile element concentrations (Os, Ir, Ru, Pt, Pd, Re) have been determined for a suite of fresh, submarine mafic lavas from the Tonga arc front and the nascent Fonualei backarc spreading centre (FSC). The highly depleted Tongan mantle wedge combined with a high fluid flux is thought to have produced boninitic magmas at several arc and FSC locations. As such, this arc system provides an opportunity to assess the fluid mobility of PGE and to investigate the effects of fluid-induced melting and prior melt depletion on PGE behaviour during both mantle melting and magma evolution.

Tongan lavas display extreme fractionation of the platinum-group PGE (P-PGE) from the iridium-group PGE (I-PGE) which is inherited at source and is significantly greater than MORB. All of the PGE display low bulk compatibility during magma evolution, reflecting sulphide undersaturation. Rather than source PPGE enrichment by slab fluids, the fractionation of the PPGE from the IPGE can be explained by relatively low-temperature yet high-degree melting of fluid-fluxed depleted mantle. Prior melt depletion increases the likelihood of complete consumption of sulphide in the source during melting, which typically produces melts with high concentrations of all the PGE. In the Tonga arc, however, the high PPGE contents can be explained by the exhaustion of sulphide liquid in the source [e.g. 1], while the retention of the IPGE requires residual monosulphide solid solution (mss) or platinum-group minerals. Complete sulphide exhaustion is likely given high aggregate degrees of partial melting (≥25%) of a DMM source which is sufficiently hot to melt mss. If so, the presence of laurite (Ru-Os-(Ir) sulphide) or IPGE alloys may explain the retention of IPGE in the source residue.

Flux-melting investigated here and a previously proposed PGE flux from the slab indicate that subduction zones are undoubtedly an environment where significant fractionation of Re and Pt from Os occurs, further indicating that the core contribution hypothesis to explain the coupled enrichments of ^{186}Os and ^{187}Os may be non-unique.

[1] Mungall *et al*. (2005) *GCA* **69**(17), 4349–4360.

https://doi.org/10.1180/S0026461X00006502 Published online by Cambridge University Press

New insights into San Carlos mantle xenoliths using iron isotopes

C.A. MACRIS[1]*, E.D.YOUNG[1,2], C.E. MANNING[1] AND E.A. SCHAUBLE[1]

[1]Department of Earth and Space Sciences, UCLA, CA (*correspondence: cmacris@ucla.edu)
[2]Institute of Geophysics and Planetary Physics, UCLA, CA

Iron isotopic compositions of mantle minerals can provide powerful tracers for geochemical processes in the mantle, such as partial melting, metasomatism, and oxidation. Predictions of equilibrium fractionation from theory and Mössbauer data conflict, making the meaning of Fe isotope fractionation in the mantle uncertain. To address this, we studied inter-mineral iron isotopic fractionation of minerals from five distinct mantle-xenolith lithologies from San Carlos, Arizona. The samples represent a broad range of mineral modes and include a clinopyroxenite, a websterite, a lherzolite, a harzburgite, and a dunite. All samples except for the websterite are Group I inclusions, which are typically rich in Mg and Cr, and consist of mainly olivine-rich rocks. Group II inclusions, represented here by the websterite, are enriched in Al and Ti, and commonly contain more clinopyroxene than orthopyroxene [1]. Each xenolith exhibits Fe-isotopic variation between minerals in a single sample, and between samples. In all cases where spinel and olivine coexist in a sample, the $^{57}Fe/^{54}Fe$ of spinel is greater than that of the corresponding olivine, agreeing with predictions of equilibrium fractionation from theory. $^{57}Fe/^{54}Fe$ values of clinopyroxenes and orthopyroxenes from the xenoliths show no clear systematic differences. Plots of $\delta^{57}Fe$ of the pyroxenes versus $\delta^{57}Fe$ of the other minerals show that the pyroxenes underwent some open-system processes and are not in equilibrium with the coexisting olivine and spinel. We interpret this as a result of varying degrees of disequilibration in the samples due to late stage open-system processes, such as metasomatism or partial melting, affecting the pyroxenes only. A strongly linear reverse correlation between olivine content and bulk rock $^{57}Fe/^{54}Fe$ was found for all samples except the websterite (the only type II xenolith measured). The strong linear relationship among Group I samples, and deviation from the trend in websterite, suggests Fe isotope systematics can be added to the list of differences used to distinguish between Group I and Group II xenoliths.

[1] Frey & Prinz 1978 *EPSL* **38**, 129–176.

Soluble Mn(III), Mn(II) and total Mn in sediment porewaters: Soluble Mn(III) is ubiquitous

ANDREW S. MADISON[1], ALFONSO MUCCI[2], BJØRN SUNDBY[2], BRADLEY M. TEBO[3] AND GEORGE W. LUTHER, III[1]*

[1]School of Marine Science and Policy, College of Earth, Ocean and Environment, University of Delaware, Lewes, DE 19958, USA (*correspondence: luther@udel.edu) (amadison@udel.edu)
[2]Department of Earth and Planetary Sciences, McGill University, Montreal, QC., Canada H3A 2A7 (alfonso.mucci@mcgill.ca, bjorn_sundby@uqar.ca)
[3]Division of Environmental and Biomolecular Systems, Oregon Health and Science University, Beaverton, OR 97006, USA (tebo@ebs.ogi.edu)

Recent research shows that soluble manganese(III) or $[Mn(III)]_{aq}$, that material which passes through a 0.2 μm filter, exists in natural waters such as the Black Sea, the Baltic Sea and Chesapeake Bay and can constitute a large fraction of the dissolved Mn pool at the oxic/anoxic interface. Recently Madison *et al*. [1] have reported a direct and accurate spectrophotometric method to measure $[Mn(III)]_{aq}$ in sediment porewaters. The method is capable of rapid and simultaneous determination of $[Mn(III)]_{aq}$, $[Mn(II)]_{aq}$, and total soluble Mn. This method was successfully applied to the determination of all soluble Mn species in sediment porewaters of the Lower St. Lawrence Estuary collected during cruises in 2009 and 2010 and in Delaware salt marsh sediments. In all samples, $[Mn(III)]_{aq}$ accounts for up to 80% of the total dissolved Mn pool in the upper oxic and suboxic sediments with concentrations ranging from the detection limit of 50 nM to 80 μM. Data will be presented that highlight the role $[Mn(III)]_{aq}$ plays in Mn cycling and how it can impact several important geochemical cycles.

[1] A.S. Madison, B. M. Tebo, G. W. Luther, III. (2011) *Talanta* **84**, 374–381.

https://doi.org/10.1180/S0026461X00006502 Published online by Cambridge University Press

He and Ne isotopic ratios from the Terceira Rift (Azores): Constraints on the boundary between Eurasia and Nubia mantle sources

PEDRO MADUREIRA[1,4], MANUEL MOREIRA[2], JOÃO CARLOS NUNES[3], NUNO LOURENÇO[4], CÉCILE GAUTHERON[5], ROSÁRIO CARVALHO[6], JOÃO MATA[6] AND MANUEL PINTO DE ABREU[4]

[1]Univ. Évora, CGE, Dep. Geociências, Rua Romão Ramalho, 59, 7000-671 Évora, Portugal (pedro@uevora.pt)
[2]Equipe de Géochimie et Cosmochimie, IPGP, Sorbonne Paris Cité, CNRS (UMR 7154), 1 rue Jussieu, 75238 Paris Cedex, France (moreira@ipgp.fr)
[3]Univ. dos Açores, Dep. Geociências, R. Mãe de Deus, Apartado 1422, 9501-801 Ponta Delgada, Açores, Portugal (jcnunes@uac.pt)
[4]EMAM, Rua Costa Pinto, 165, 2770-047 Paço d'Arcos, Portugal (nlourenco@am-em.org, mapabreu@am-em.org)
[5]UMR Interactions et Dynamique des Environnements de Surface-CNRS 8148, Université Paris Sud, 91405 Orsay, France (cecile.gautheron@u-psud.fr)
[6]Univ. Lisboa, Faculdade de Ciências, Dep. Geologia (GeoFCUL), CeGUL, Edifício C6, Campo Grande, 1749-016, Lisboa, Portugal (mdrcarvalho@fc.ul.pt, jmata@fc.ul.pt)

We present He and Ne isotopic data from subaerial and submarine samples collected along the Terceira Rift. Graciosa Island as well as the western end of S. Miguel Island and D. João de Castro Bank display $^4He/^3He$ ratios similar to those observed along the MAR segments located to the north of the Azores Triple Junction area. Conversely, samples from the south Hirondelle Basin display a $^4He/^3He$ ratio similar to that of the MAR segments located to the south of the Azores Plateau. The Terceira Rift is thus characterized by the mingling of two different mantle domains referred as 'Eurasia' and 'Nubia' type. He and Ne systematics shows that the influence of the relatively primitive source sampled by the Azores plume can be followed along the Terceira Rift from the Graciosa Island towards the south Hirondelle Basin. Moreover, samples from the south Hirondelle Basin, D. João de Castro Bank and Graciosa Island cannot be explained by the same hyperbolic mixing model that encloses Terceira data.

SHRIMP studies of the uranium oxide-based U/Pb SIMS calibration

C.W. MAGEE

Australian Scientific Instruments 111/113 Gladstone St. Fyshwick ACT 2609 Australia (cwmagee@gmail.com)

Since the earliest days of SIMS U/Pb geochronology, it has been necessary to correct for variations in the relative ionization efficiency of Pb and U. Extensive research during the twentieth century has resulted in the empirical derivation of calibration cures based on observed relationships between Pb/U and UO_x/U, where x is equal to 1 or 2. This calibration is the precision-limiting step in SIMS U-Pb data reduction.

Both oxygen activity and secondary ion energy have been proposed asmachanisms for measured Pb/U variation. For example, the extreme sensitivity of Pb ionization to oxygen flooding in some SIMS instruments suggests that oxygen activity at the sample surface may important to relative Pb and U ionization. As is shown in figure 1, this is consistent with the ability to use a variety of Zr, Hf, Th, or U oxide pairs as a rough calibration, with about ~3% accuracy and precision.

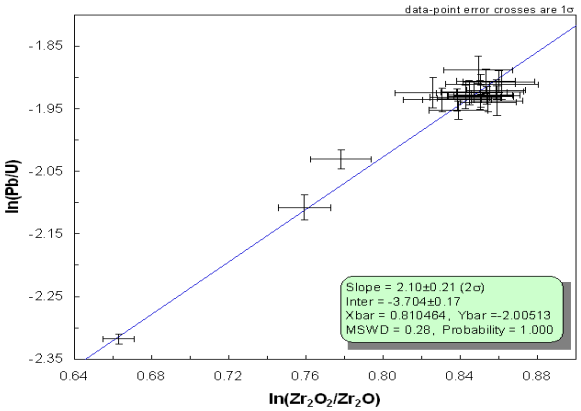

Figure 1: Arbitrary oxide calibration of SHRIMP U/Pb data. This and similar Hf and Th-based calibrations yield less scatter than raw Pb/U or Pb/UO_2.

Additional effects beyond fO_2 must be responsible for the superior performance of UO_x based calibrations compared to randomly selected metal oxide pairs. While the effect of secondary ion energy has been discussed previously, the effect of primary ion energy is less well studied. Primary energies as low is 2.5kV have been investigated to determine the change in calibration due to changes in Pb ionization efficiency, secondary ion energy dispersion, and uranium oxide speciation.

https://doi.org/10.1180/S0026461X00006502 Published online by Cambridge University Press

Reconstructing ancient landscapes: Molecular insights to spatial patterns in ecosystems and water

CLAYTON R. MAGILL[1]*, GAIL M ASHLEY[2] AND KATHERINE H. FREEMAN[1]

[1]Pennsylvania State University, University Park PA 16802 (*correspondence: clayton.magill@psu.edu)
[2]Rutgers University, Piscataway NJ 08854

Water shapes vegetation and natural landscapes at different spatial and temporal scales – defining habitats, selective pressures and the evolution of fauna. Hydroclimate may have catalyzed morphologic and behavioural adaptations in early humans through changing spatial patterns in ecosystem structure. These can be evaluated using molecular and isotopic 'landscape biomarkers' lending insights to ancient habitats and providing means to test links between evolution and environment. We apply these to landscapes at spatial scales of human habitation (~1 km^2) from paleosol and lake deposits at Olduvai Gorge (*ca*. 1.845 million years ago).

Biomarker signatures reveal heterogeneity in sources and composition of sedimentary organic matter. Near to a freshwater spring (tufa) deposit, algae (heptadecane [nC_{17}]) and sedge (*n*-alkylresorcinol [*n*AR]) biomarkers are associated with positive ratios between the lignin monomers syringic acid/vanillic acid (S/V) and *p*-coumaric acid/vanillic acid (C/V). In contrast, sediments associated with early human remains contain nominal nC_{17}, *n*AR and C/V, instead showing high plant-wax (hentriacontane [nC_{31}]) abundances. Plant-wax biomarkers $\delta^{13}C$ values range nearly 14‰ across the 1 km paleosol transect, between sediments associated with early human remains (-33.0‰) and grass phytoliths (-19.3‰).

Our data indicate pronounced heterogeneity in this early human habitat, consistent with geochemical and faunal data.[1] Near the spring deposit, biomarkers suggest a shallow wetland environment with emergent vegetation. Nearby, depleted $\delta^{13}C_{31}$ values and nominal C/V indicate a shrubby or wooded environment. This area is proximal to sites with $\delta^{13}C_{31}$ and C/V ratios that indicate grassland. This study focuses on a time slice with dominant grassland (C_4) signals captured in lake sediments. In this dry time, woody and wetland vegetation drew early humans[2] to their resources.

[1] Dominguez-Rodrigo *et al*. (2010) *Quat. Res*. **74**, 315–332.
[2] Blumenschine *et al*. (2002) *Science* **299**, 1217–1220.

Lithium – Light metallic traveller through crusts of the Earth and beyond

TOMÁŠ MAGNA[1,2]

[1]Universität Münster, Germany (tomas.magna@uni-muenster.de)
[2]Czech Geological Survey, Prague, Czech Republic (tomas.magna@geology.cz)

Lithium isotopes have become an increasingly used tool for unraveling metasomatic processes in the mantle, extent and duration of fluid transfer in subduction settings or alteration of oceanic crust, for example. Only recently have Li isotopes been employed to study the magmatic evolution, metamorphism, alteration and weathering of continental crust. This is rather surprising considering the large economic potential of Li deposited in the crust and its utility in modern technologies. Available data suggest a dominant control of protolith heterogeneities and modal mineralogy for bulk terrestrial crust, superimposed on long-term secular evolution of Li in the continental crust as a response to weathering and recycling through subduction zones.

For the Moon, the limited dataset for highland crust shows a dramatic difference between mafic lower crust and calcic plagioclase-dominated rocks of the upper anorthositic layer, with the latter showing extreme net Li depletions coupled with high δ^7Li that extends far beyond the range of mare basalts. Whether plagioclase segregation from lunar magma ocean exerts a major control on crust–mantle Li isotope fractionation remains to be investigated.

That as yet unsampled evolved (crustal?) reservoirs may exist on Mars can be deduced from the nakhlite lava sequence as well as from two distinctive lithologies found in Zagami and having different Li (and also Ca) systematics. Yet, this finding is still consistent with linear Li-δ^7Li relationship recorded for the enriched shergotittes, thought to contain larger proportion of evolved crustal material among shergottites. These data point toward a low-Li high-δ^7Li reservoir that may have once existed early in Martian history. On the contrary, bulk Martian crust appears basalt-andesitic in composition, leaving granitic rocks subordinate although, on Earth, granitic rocks develop distinctive Li fingerprints as a consequence of complete geological cycles. This applies perhaps to 4 Vesta too despite local exposures of highly evolved terrains.

It may well be that juvenile crust in general develops a uniform Li isotope signature as observed in Iceland, for example, with invariant δ^7Li over a large range of chemical compositions. Only with ample time would Li become enriched and fractionated in the crust relative to the mantle on a planetary scale.

https://doi.org/10.1180/S0026461X00006502 Published online by Cambridge University Press

Lithium isotope composition of lunar crust – Rapid crystallization and post-solidification quiescence?

TOMÁŠ MAGNA[1,2] AND CLIVE R. NEAL[3]

[1]Universität Münster, Germany (tomas.magna@uni-muenster.de)
[2]Czech Geological Survey, Prague, Czech Republic
[3]University of Notre Dame, USA

Lunar crust consists of ferroan anorthosites (~80%) and Mg-rich suite lithologies (~20%). It represents products from the most ancient lunar magmatic events (>4.1 Gyr [1]) and is accepted to have formed through plagioclase flotation on the lunar magma ocean (LMO) [2], from which significant amounts of incompatible elements (e.g. K, Th and U) were concentrated in the residual LMO melt (KREEP). Lithium has received little attention [3–6] despite its utility in tracking the history of the terrestrial crust [7–9].

New Li data show that anorthosites are the most Li-depleted lunar material known to date with <1 ppm in pristine samples. This is consistent with [6] and opposite to Earth's continental crust [7, 8] and may in part be explained by limited Li partitioning into plagioclase ($K_d^{plg\text{-}melt}$ ~0.2, [10]) from progressively crystallizing LMO for which ~3–4 ppm Li would thus be estimated. This appears higher than Li content of the Earth's mantle [3, 4]; the nature of such a difference is currently unclear but it could perhaps reflect a lack of net Li depletion before the accretion of the Moon [11]. Anorthosites show uniformly high δ^7Li>5.7‰ (up to 9.4‰), distinct from mare basalts [3–5] as well as the Earth's continental crust [7, 8]. δ^7Li of norite 77215 with a KREEP affinity is resolved from other KREEP-rich lithologies [5]. The tight positive correlation of δ^7Li with Na across the whole suite may reflect fractional crystallization of clinopyroxene appearing on the liquidus shortly after plagioclase during LMO crystallization. Overall, the Li data suggest (i) rapid plagioclase segregation without further re-equilibration with remaining LMO (through equilibrium Li isotope fractionation) and (ii) little subsequent modification of the lunar crust without an influence from younger magmatic events.

[1] Wieczorek *et al*. (2006) *RiMG* **60**, 221–364. [2] Taylor & Jakeš (1974) *LPSC* **V**, 1287–1305. [3] Magna *et al*. (2006) *EPSL* **243**, 336–353. [4] Seitz *et al*. (2006) *EPSL* **245**, 6–18. [5] Magna *et al*. (2009) *GCA* **73**, A816. [6] Steele *et al*. (1980) *LPSC* **XI**, 571–590. [7] Teng *et al*. (2004) *GCA* **68**, 4167–4178. [8] Magna *et al*. (2010) *ChG* **274**, 94–107. [9] Ushikubo *et al*. (2008) *EPSL* **272**, 666–676. [10] Bindeman *et al*. (1998) *GCA* **62**, 1175–1193. [11] Magna *et al*. (2011) *GCA* **75**, 2137–2158

Surface and subsurface geochemical monitoring of an EOR-CO_2 field: Buracica, Brazil

C. MAGNIER[1], V. ROUCHON[1], C. BANDEIRA[2], R. GONÇALVES[2], D. MILLER[2] AND R. DINO[2]

[1]IFP Énergies nouvelles,1-4 avenue du bois Préau, 92852 Rueil Malmaison, France (caroline.magnier@ifpen.fr)
[2]PETROBRAS-CENPES/PDEXP Rua Horácio Macedo n.950, Cidade Universitária, Ilha do Fundão, Rio de Janeiro, Brasil, 21941-915

We present a surface and subsurface geochemical survey of the Buracica EOR-CO_2 field on-shore Brazil. A methodology coupling the stable isotopes of carbon with the noble gases was adopted to investigate the adequacy of a geochemical monitoring to track deep fluid leakage at the surface, with a scope of future application in the developping CCS industry. Three campaigns of CO_2 flux and concentration in soils were performed to understand the CO_2 variability across the field. The distribution of the CO_2 soil contents between 0.8 to 14 % is correlated with the proprieties of the soil, with a first order topographic control. These results, together with a $\delta^{13}C_{CO2}$ between -15 and -23 ‰, suggest that the bulk of the soil CO_2 flux at Buracica is biological.

The gas injected and produced at numerous wells across the field showed a great spatial and somewhat temporal heterogeneity with respect to molecular, $\delta^{13}C_{CO2}$ and noble gas compositions. The injected CO_2 is characterized by $\delta^{13}C_{CO2}$ near -31 ‰ and a peculiar noble gas composition enriched in Kr with respect to atmospheric values, while being depleted in the lighter noble gases. The heterogeneity of the gas produced from the reservoir is a consequence of the EOR-induced sweeping of the indigenous fluids by the injected CO_2, producing a heterogeneous mixing controlled by 1) the production scheme and 2) the distribution in reservoir permeability. In the light of the $\delta^{13}C_{CO2}$ found in the reservoir (from -36 to +6 ‰), the stable isotopic composition of carbon revealed insufficient to track CO_2 leaks at the surface. We demonstrate how noble gases may be powerful leak discriminators, even for CO_2 abundances in soils in the bottom range of the biological baseline (~1 %). The results presented in this study show the potentiality of geochemical monitoring techniques, involving stable isotopes and noble gases at the reservoir and soil levels, for tracing CO_2 in CCS and EOR projects.

https://doi.org/10.1180/S0026461X00006502 Published online by Cambridge University Press

Geology and mineralogy of Bidakhavid indusrial soil

A. MAHDAVI AND B. TAGHIPOUR

Department of earth sciences, student of sciences, shiraz university, shiraz, Iran (amirmahdavi1984@yahoo.com, taghipour@shirazu.ac.ir)

Bidakhavid industrial soil is located 70 km southwester of ayzd city, central Iran. this area is a part of Cenozoeic magmatic belt. According the geological map of geology survey of Iran (1:250000 map of Yazd, Iran).

Bidakhavide feldspar mine is near the Shir-Kuh massive intrusion and Jamal limestone formation with Jurassic age, Darreh-Zereshk is the main fault in this area.

Petrologicaly, predominant rock is sandstone in this area. with attention the Folk classification this sandstones are including: litarenite, arkosic arenite, arenite and sublitarenite. Quartz, alkali-feldspar and jarosite are the main minerals and biotite, muscovite and hematite are minor minerals.

X-ray diffractometery results show, quartz, albite, orthoclase, jarosite and clay minerals are the main minerals in the Biakhavid sandstones (Fig. 1).

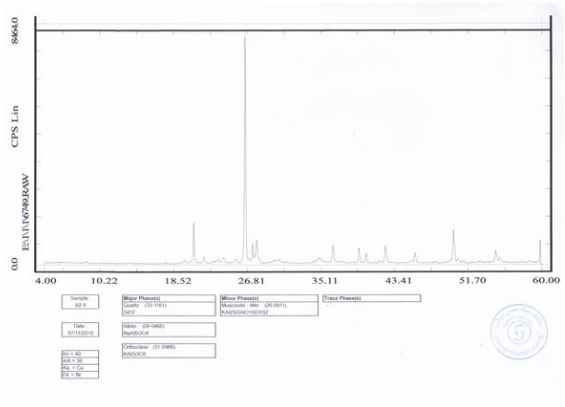

Figure 1: sample figures of XRD diagram

Because of weak roundness structure and poorly sorted of sandstones grain it is obvious that, parent rock is near the Biakhavid mine. According to fild evidence, petrography and mineralogy studies sandstones composition is similar to the Shir-Kuh granite. So we can conclude that Shi-kuh intrusion has an important role for the providing of primary material for the industrial soil in the Biakhavid area. Also it must be noted that Darreh-Zereshk fault movements may have supported fluids for alteration of Shir-Kuh granite.

[1] 1:250000 map of Yazd, Iran. [2] Folk R.L. (1965) *Petrology of Sedimentary Rocks*, Hemphill.

The role of fluid residence times in controlling the chemical fluxes and isotopic compositions of rivers

K. MAHER*, A. SCHNEIDER-MOR AND J.L. OSTER

Dept. of Geological and Environmental Sciences, Stanford University, Stanford, CA, 94305, USA (*correspondence: kmaher@stanford.edu)

The role of fluid residence times and catchment length scales in controlling the chemical composition of rivers is evaluated by comparing numerical simulations and scaling arguments to concentration-discharge data from small catchments and global rivers. The analysis suggests that the actual residence time of fluid relative to the residence time required to approach chemical equilibrium is likely a dominant control on solute fluxes. Catchments that show little variability in concentration with discharge (or 'chemostatic behavior') likely have average fluid residence times that exceed the time required to reach chemical equilibrium. Conversely, decreases in concentration with increasing discharge are explained by average residence times shorter than required to approach equilibrium, resulting in dilution. Increases in runoff associated with climate change can result in either a proportional increase in weathering fluxes, or a plateau in weathering fluxes if the fluid residence times become shorter than the time required for equilibrium. The same theoretical considerations can be applied to interpret the behavior of Sr and U isotopes in rivers. The extent of isotopic equilibrium and the final isotopic composition reflected by river waters will also depend on the ratio of the fluid residence time to the time required to reach isotopic equilibrium, where the later varies widely across isotopic systems and weathering environments.

This framework also has implications for weathering rates in the past. As a consequence of the thermodynamic and hydrologic restrictions on the amount of weathering outlined above, global solute fluxes may depend more strongly on the geometry, relief, runoff and permeability of basins then on temperature and rates of erosion. If fluid residence times and catchment length scales are a dominant control on weathering fluxes, the chemistry and isotopic composition of different rivers could vary entirely as a function of the nature subsurface flow paths and the composition of the system at chemical equilibrium, which is complex to predict and strongly coupled to biological processes.

https://doi.org/10.1180/S0026461X00006502 Published online by Cambridge University Press

Latitudinal changes in sea surface temperature and salinity over the Eastern Arabian Sea during the Last Glacial Maximum through Holocene

B.S. MAHESH* AND V.K. BANAKAR

National Institute of Oceanography (CSIR), Goa, India.
(*correspondence: maheshsbadanal@gmail.com)

Three sediment cores dated by radiocarbon spanning the last ~35 kyr have been utilized to reconstruct the past hydrography in the Eastern Arabian Sea (EAS). These three sediment cores were collected in a North-South transect where significant hydrographic differences occur between their locations. The EAS receives significant amount of overhead precipitation as it borders the orographic barrier all along the western margin of peninsular India due to Deccan Mountains. As a result the sea surface temperature (SST) and surface salinity (salinity) in the EAS respond to subtle changes in the intensity of the monsoons. Here we reconstruct the SST and salinity from by the paired measurement of $\delta^{18}O$ and SST utilizing *Globigerinoides sacculifer*, an upper mixed layer dwelling foraminifera. The last glacial maximum (LGM) could be defined as the heaviest $\delta^{18}O_{G.sacculifer}$ (-0.07±0.08‰) and is evident between 23 – 15 ka BP. The $\delta^{18}O_{G.sacculifer}$ shift between the LGM and Holocene in all the three sediment cores is ~ 2‰. The SSTs show an overall warming of 2°C from the LGM to Holocene (28°C to 30°C). However, coldest SSTs are observed prior to LGM (~27 ka BP) in all the three records. The salinity is higher (~ 38 psu) throughout most of the last glacial period (32.5 – 15 ka BP) compared to the salinity during the Holocene (~36 psu). During the LGM, the North-South salinity gradient was higher than that of modern gradient. The increased North-South salinity gradient during LGM may suggest not only reduced summer monsoons but also relatively intensified winter monsoons. The higher salinity together with generally lower SSTs indicates sustained weaker summer or stronger winter monsoons. The deglacial warming is associated with rapid reorganization of monsoons and is reflected in decreased salinity to a modern level of ~ 36.5 psu within a period of ~ 5 kyr, which indicates process of intensification of summer monsoons during cold to warm climate transition.

Adsorption behaviour of copper in natural composite sedimentary materials

FLÁVIA MAIA* AND MÁRIO A. GONÇALVES

Dep. Geologia and CREMINER/LA-ISR, Fac. Ciências da Universidade de Lisboa, Campo Grande, 1749-016, Lisboa, Portugal,
(*correspondence: flavia.maia@amphos21.com)

The understanding of adsorption processes is important both to evaluate the potential hazard related to contaminants as well as to minimize their impact on the environment. The aim of this work is to carry out comprehensive adsorption experiments using composite natural materials corresponding to matrices of continental alluvial deposits (so called raña deposits) from Macedo de Cavaleiros in the NE of Portugal. These materials were considered to evaluate their capacity for the attenuation of metal dispersion, as well as for the retention of low to intermediate level radioactive waste. The main minerals present in the matrices include quartz, montmorillonite, illite and kaolinite, with abundant poorly crystallized iron oxyhydroxides. The matrices also contain substantial amounts of organic matter.

A protocol was developed to characterise the adsorption behaviour of copper onto the main constituents of the natural matrices (clay minerals, organic matter, and iron oxyhydroxides). They were designed as to reflect the removal efficiency of copper by the various constituents while maintaining the structural integrity of the clay minerals.

The adsorption behaviour of copper has been evaluated by carrying out batch experiments with Cu^{2+} on a series of samples without previous treatment, removal of organic matter, removal of Fe oxyhydroxides, and removal of both organic matter and Fe oxyhydroxides in a range of pH between 4 and 6.

The results show that the adsorption capacity of these materials is rather limitted but slightly enhanced as the pH gets higher. However, the pre-treatments had some influence on the enhancement of the adsorption results, especially Fe oxyhydroxides and organic matter. The low equilibrium pH of these samples was shown to be derived from the presence of organic matter which on itself is also likely to alter the adsorption capacity of these matrices.

Contribution of Project KADRWaste PTDC/CTE-GEX/82678/2006 funded by FCT (Portugal)

https://doi.org/10.1180/S0026461X00006502 Published online by Cambridge University Press

Ptychography: A powerful X-ray imaging tool

A.M. MAIDEN[1]*, G.R. MORRISON[2], B. KAULICH[3], A. GIANONCELLI[3], G. KAKONYI[1] AND J.M. RODENBURG[1]

[1]Kroto Research Institute, University of Sheffield, Broad Lane, Sheffield, S3 7HQ, UK (*correspondence: a.maiden@sheffield.ac.uk)
[2]King's College London, Dept. of Physics, Strand, London, WC2R 2LS, UK (graeme.morrison@kcl.ac.uk)
[3]ELETTRA, S.S. 14, km 163.5 in Area Science Park, I-34012 Trieste, Italy (burkhard.kaulich / alessandra.gianoncelli@elettra.trieste.it)

Ptychography is a form of diffractive imaging in which overlapping regions of a specimen are illuminated by coherent radiation, the resulting scatter patterns recorded, and an image formed using iterative algorithms [1, 2]. The method is currently undergoing a renaissance as a tool for X-ray imaging [3, 4], since its genesis as an electron microscopy technique in the late 1960s.

The principal benefit of ptychography is its experimental simplicity: no focussing optics are required in a ptychographic experiment, with resolution being limited only by the angular width of the recorded scatter patterns. Despite being successfully demonstrated only recently in the X-ray regime, ptychographic imaging has advanced to a stage where sub 50nm resolution is obtainable using hard X-rays [5]. Ptychography also produces quantitative phase images that in the x-ray regime can be used to measure electron densities accurately. By varying the beam energy ptychography can provide chemical contrast and it can be combined very effectively with tomography to produce three-dimensional images [6].

Here we will introduce the ptychographic method and describe how it works. We will discuss the merits and drawbacks of the technique relative to more established methods such as Scanning Transmission X-ray Microscopy (STXM), and we will present results from recent soft X-ray experiments at the ELETTRA synchrotron in Trieste, where ptychography was used to image iron nanoparticles within cells.

[1] Rodenburg (2008) *Advances in Imaging & Electron Physics* **150**, 87–182. [2] Maiden (2009) *Ultramicroscopy* **109**, 1256–1262. [3] Thibault (2008) *Science* **321** 378–382. [4] Giewekemeyer (2011) *Optics Express* **19**, 1037–1050. [5] Schropp (2011) *J. of Microsc.* **241**, 9-12. [6] Dierolf (2010) *Nature* **467**, 436-439.

Detailed field relations of pre-3.85 Ga zircon bearing metasediments from southern Montana (USA)

A.C. MAIER*, N.L. CATES AND S.J. MOJZSIS

University of Colorado, Department of Geological Sciences, 2200 Colorado Avenue, Boulder, CO 80309-0399 USA (*correspondence: analisa.maier@colorado.edu)

Paleoarchean fuchsitic detrital quartzites in the Bearthtooth Mountains (Wyoming craton, southern Montana, USA) are one of the few documented localities that host Hadean (>3.85 Ga) detrital zircons [1]. Our high-resolution mapping (1:250) revealed several other rock-types in the area that include intrusive granitoids and mafic dikes, banded iron-formation (BIF), paragneisses, and a possible meta-conglomerate. Zircon geochronology from quartzites and paragneisses [1; this study] reveals several age populations: >3.6-4.0 Ga; 3.4-3.6 Ga; 3.2-3.3 Ga; 3.0-3.1 Ga; and 2.7-2.8 Ga. Some of these are coincident with known metamorphic events [2] responsible for discordant ages seen in much of the data. We find that there is no obvious correlation between degree of discordance and zircon-bearing lithology.

Zirconiferous quartzites are Cr- (40-360 ppm) and SiO_2-(93-95 wt.%) rich with low Zr (37-81 ppm). Paragneisses resemble the quartzites (Cr: 230 ppm), but with less SiO_2 (75 wt.%) and more Al_2O_3 (14 wt.%) and high Zr (348 ppm); paragneisses and quartzites follow expected weathering trends for a mixed granitoid + mafic source [3]. A candidate conglomerate (SiO_2 77 wt.%; Al_2O_3 14 wt.%) and (intrusive) granitoids (SiO_2 73 wt.%; Al_2O_3 15 wt.%) resemble the paragneisses, but the conglomerate has 70 ppm Cr and 49 ppm Zr, whereas the intrusive felsite body is Cr-poor (<D.L.), with typical orthogneissic Zr (167 ppm). The BIF is Fe_2O_3-rich (51 wt.%) with low SiO_2 (44 wt.%) and minor Al_2O_3 (3 wt.%), Cr (50 ppm) and Zr (26 ppm) pointing to a detrital component; multi-element plots compared to other BIFs and normalized to NASC shows a similar positive slope, but with no Eu anomaly and low (but still superchondritic) Y/Ho (28.7). In PM-normalized spider diagrams, detrital and igneous 'felsic' lithologies show enriched LILE, negative Nb anomalies, with depletions in Sr and Ti.

Ancient detrital/xenocrystic zircons confirm that older crustal components existed in the area, suggestive of a genetic link between the Beartooth quartzites and the geology of the Western Slave Province [1] and perhaps the Thelon Basin in Nunavut [3] and the Assean Lake Complex (Manitoba; [4]).

[1] Mueller *et al.* (1992) *Geology* **20**, 327–330. [2] Mueller *et al.* (1998) *Precamb. Res.* **91**, 295–307 [3] Palmer *et al.* (2004) *Precamb. Res.* **129**, 115–140. [4] Böhm *et al.* (2000) *Geology* **28**, 75–78.

https://doi.org/10.1180/S0026461X00006502 Published online by Cambridge University Press

Gold contents of the cratonic sub-continental lithospheric mantle: Implications for orogenic gold deposits

W.D. MAIER[1]*, A KONTINEN[2] AND I. MCDONALD[3]

[1]University of Oulu, Oulu, 90014, Finland (*correspondence: wolfgang.maier@oulu.fi)
[2]Geological Survey of Finland, Kuopio, 70211, Finland
[3]Cardiff University, Cardiff, CF10 3YE, Uk

The occurence of many orogenic gold deposits within Archaean cratons suggests that the gold could be sourced from the sub-cratonic lithospheric mantle. The model has been difficult to test because the available cratonic mantle samples consist almost entirely of kimberlite-borne xenoliths, few of which have been analysed for Au. Furthermore, Au levels in mantle rocks tend to be close to the detection limit of current analytical methods. In the present study we have determined Au contents in 81 kimberlite borne peridotite and MARID mantle samples from the southern Africa, using ICP-MS after Ni-sulfide fire assay and Te co-precipitation at Cardiff University. The blank contained 0.11±0.03Au, resulting in a procedural detection limit of 0.1 ppb Au and a quantification limit of 0.33 ppb Au. On average, the Kaapvaal xenoliths contain 1.09 ppb Au, broadly in the range of primitive upper mantle estimates. In order to exclude the possibility that the xenoliths could be non-representative of the SCLM we have also analysed Au in 24 samples of the Jormua massif in Finland, interpreted to represent Archean cratonic SCLM that was obducted onto the Karelian craton margin at ca 1.95 Ga. The average Au content of 23 Jormua samples is 1.01 ppb, with one additional highly talc-carbonate replaced sample containing more than 100 ppb Au.

Our samples, as well as many other samples from non-cratonic lithospheric mantle, show high primitive-mantle normalized Au/Pd ratios, due to pervasive Pd depletion.

We infer that introduction of Au during contamination with host kimberlite is unlikely to account for the observed positive anomalies. One could alternatively suggest that Au is stabilized in refractory alloys during mantle melting, based on the observation that Au does not enter into mantle sulfides. However, the Au enrichment in magmatic sulfide ores clearly indicates that Au behaves incompatible during mantle melting, consistent with the high D values of Au with regard to sulphide liquid (D ~ 1000, Barnes and Lightfoot, 2005). The formation of distinct Au-rich phases associated with sulfides can be explained by the fact that the ionic radius of Au is too large to fit into the structure of mss or iss. As the solubility of Au in basaltic magmas is >10 ppm, Au will be released to the magma during partial melting of the mantle. In conclusion, our preferred model is that the relative Au enrichment in the cratonic SCLM formed through metasomatic introduction of Au, implying mobility of Au in the mantle. This is consistent with derivation of at least some orogenic gold from the SCLM.

Local structure of poorly ordered nanosized iron oxides. Implications for contaminants scavenging

F. MAILLOT[1], G. MORIN[1], C. CASIOT[2], Y. WANG[1], D. BONNIN[3], C. CHANEAC[4] AND G. CALAS[1]

[1]IMPMC, CNRS – UPMC, Paris, France
[2]Hydrosciences, CNRS-Universités Montpellier I and II-IRD, Montpellier, France
[3]Laboratoire de Physique et d'Etude des Matériaux, ESPCI ParisTech, Paris, France
[4]CMCP, CNRS – UPMC, Paris, France

Iron (oxyhydr)oxides nanoparticles are ubiquitous in natural environments (soils, rivers, sediments…), as well as in impacted systems such as acid mine drainage, where they strongly impact the mobility of most trace elements. Among these (oxyhydr)oxides, the poorly crystalline minerals ferrihydrite and schwertmannite are the most efficient in the scavenging of toxic solutes such as arsenic, either via sorption or coprecipitation mechanisms. The knowledge of the structure of these compounds is a prerequisite to the understanding of their surface reactivity. However, due to their nanoparticulate nature and to the lack of well-crystallized isomorph compounds, their structure remains poorly constrained. Recent X-ray scattering studies [1, 2] have yield unique information on the medium-range order in these materials. However, for such disordered nanomaterials, scattering techniques that yield average periodic structural models may fail at accurately describing the local coordination sphere of cations. To overcome this difficulty, we have used Extended X-ray absorption fine structure (EXAFS) spectroscopy to determine the local coordination and arrangement of cations in these poorly ordered solids. Using EXAFS data recorded at liquid helium temperature over a wide energy range, we will particularly discuss the presence of tetrahedral iron in ferrihydrite [3], and the structural specificities of natural and synthetic schwertmannites coprecipitated in the presence of arsenic. The structural information derived from these data will be compared with existing structural models, and yield clues for better understanding the reactivity of these materials.

[1] F.M. Michel *et al*. (2007) *Science* **316**, 1726–172. [2] A. Fernandez-Martinez *et al*. (2010) *Am. Mineral*. **95**, 1312–1322. [3] F. Maillot *et al*. (2011) *Geochim. Cosmochim. Acta* **75** 2708- 2720

https://doi.org/10.1180/S0026461X00006502 Published online by Cambridge University Press

Inverse estimates of the air-sea flux of carbon using surface pCO_2 measurements

JOSEPH MAJKUT AND JORGE L. SARMIENTO

Princeton University, Princeton, NJ, USA 08544
(*correspondence: jmajkut@princeton.edu)

A new method of estimating the historical pCO_2 at the sea-surface is used to estimate the air-sea CO_2 flux and the time rate of change of ΔpCO_2 from 1980 through 2010. Using a large surface pCO_2 measurement database [1], which despite its size sparsely represents much of the ocean over the past 40 years, we find optimal estimates of the pCO_2 using information from global circulation models and a simplified model of pCO_2 in the surface water. The simplified model describes the time evolution of surface pCO_2 on a 5x4 ° grid according to

$$pCO_2(t) = At + B + C \cdot pCO_2'(t).$$

The third term, pCO_2' (t), represents the interannually-varying seasonal cycle and other interannual variations in pCO_2 diagnosed from a series of simulations using the GFDL MOM4.1 ocean general circulation model and the BLING biogeochemistry model (OGCM). For each grid box, we estimate the model parameters A, B and C by evaluating likelihood against the data using a bayesian markov chain monte carlo technique (MCMC) [2].

The resulting pCO_2 trends and diagnosed fluxes are provocative. The method indicates an ocean sink for anthropogenic carbon of 2.7 $\pm$.15 Pg C for the year 2000. The estimated annual rate of change of the ΔpCO_2, used as an indicator of flux trends, shows where the ocean is changing at a rate significantly different than the atmosphere. The implied air-sea carbon flux is increasing over much of the ocean, with exceptions in the Northern Atlantic and Pacific basins.

Projections and hindcasts of the ocean carbon sink that are based on OGCM simulations rely on the response of the OGCM to climate change. The framework proposed here allows us to evaluate that modeled response, of the carbon cycle to climate change, against the observations. We present regional analysis indicating whether or not modeled trends and feedbacks are occuring in the real earth system.

[1] Takahashi *et al*. (2010) ORNL/CDIAC-152, NDP 088
[2] Hastings, W. K. (1970) *Biometrika* **57**(1), 97–109.

Using discrimination analysis for anomaly separation and distinguish the mineralized factors

M.J. MAJLESI[1]*, M. MEMARZADEH[1],
R. GHAVAMI- RIABI[1] AND H. ASADI-HARONI[2]

[1]Mining, Petrolum and Geophysics Faculty, Shahrood Univ. of Tech, 7 Tir square, Danshgh Bolv
(*correspondence: mj.majlesi@gmail.com)
[2]Mining Engineering Dept., Isfahan Univ. of Tech., Khomani shahr Bolv

Distinguish the mineralized factors in anomaly data

In the current research, the abilities of the discriminant analysis in distinguishing anomaly from background [1, 2, 3] for soil lithogeochemical samples in porphyry Cu-Au- Dalli area (Iran) was shown. A group of 163 samples with sample space of 50*50 m^2 were used. According to the results (Fig. 1), three populations were separated in data set (Fig. 1a). The second group (code 2) is related to the anomalous sub-population, the first group (code 1) is considered as mixture of background and anomalous sub-population and the zero group (code 0) is shown the background sub-population. In the anomalous sub-population, the elements of Au and Cu (Fig. 1b) are introduced as mineralized factors, the elements of V, Fe, P, Y, Ba, and Sc are important in the mixed sub-population.

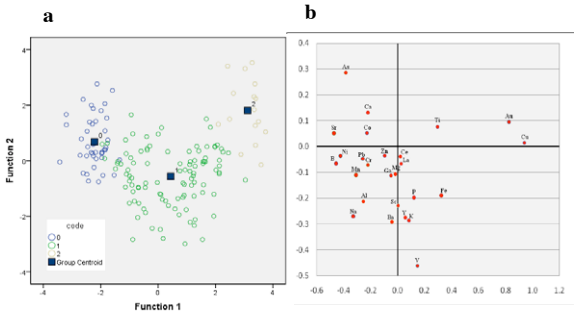

Figure 1: Discrimination analysis, anomly separation (a) and mineralized factor (b).

Conclusion

One of the charactristic of the discrimination analysis as anomaly separation method in compare with the other methods is the identification of the mineralized factors or elements.

[1] Davis, J.C. (2002) John Wiley & Sons, 646 pp. [2] Peh, Z. & Halamić, J (2010) *J. Geo. Expl.* **107**, 30–38.
[3] www.statsoft.com/textbook/stathome.html.

https://doi.org/10.1180/S0026461X00006502 Published online by Cambridge University Press

Thermodynamics of crystalline iron(III) arsenates scorodite, kaňkite, and bukovskýite

J. MAJZLAN[1], P. DRAHOTA[2], M. FILIPPI[3], M. NOVÁK[4], J. LOUN[4] AND K.-D. GREVEL[1]

[1]Institute of Geosciences, Friedrich-Schiller University, Jena, Germany (*correspondence: Juraj.Majzlan@uni-jena.de)
[2]Institute of Geochemistry, Mineralogy and Mineral Resources, Charles University, Prague, Czech Republic
[3]Institute of Geology AS CR, Prague, Czech Republic
[4]Department of Geological Sciences, Masaryk University, Brno, Czech Republic

The crystalline ferric arsenates are candidates for arsenic storage at sites contaminated by this metalloid. The remediation technologies today usually involve precipitation of poorly crystalline hydrous ferric oxide which is capable of adsorbing As(V) or crystalline scorodite ($FeAsO_4 \cdot 2H_2O$). We seek alternatives which could be used for such processes, if found to be advantageous. To this end, we study the mineralogy and geochemistry of various sites polluted with arsenic and measure the solubility of the arsenate minerals by calorimetric techniques.

In this work, we present the formation enthalpies ($\Delta_f H^o$) of three arsenates, scorodite, kaňkite ($FeAsO_4 \cdot 3.5H_2O$), and bukovskýite ($Fe_2(AsO_4)(SO_4)(OH) \cdot 9H_2O$). The $\Delta_f H^o$ values were determined by acid-solution calorimetry at T = 298 K in 5 N HCl as the solvent, using $HCl \cdot 9.96H_2O$, γ-FeOOH, α-$MgSO_4$, MgO, KCl, and KH_2AsO_4 as the reference compounds. The resulting values for scorodite, kaňkite, and bukovskýite are –1508.9±2.9, –1940.2±2.8, and –4742.2±3.8 kJ/mol, respectively. We have also determined the $\Delta_f H^o$ value for anhydrous $FeAsO_4$ (not known as a mineral) as –899.0 ±3.0 kJ/mol.

Scorodite served as a test of our approach as many studies have been conducted on this phase (e.g. [1]). Using our $\Delta_f H^o$ value and a Kopp rule estimate of entropy of 180.3 J/mol·K, we arrive at a solubility product of –25.4, in good agreement with –25.8 in [1] or –25.4 in [2]. Our data also predict kaňkite to be unstable with respect to scorodite, in line with the rare occurrence of kaňkite in nature.

The results presented here will be soon complemented by heat capacity measurements and entropy calculations. Once these data are secured, calculations of phase diagrams for the title and related phases will be done and presented.

[1] Langmuir, D. Mahoney, J. Rowson, J. (2006) *Geochim. Cosmochim. Acta* **70**, 2942–2956. [2] Bluteau, M.-C. Demopoulos, G.P. (2007) *Hydrometallurgy* **87**, 163–177.

Sr and Nd isotope disequilibrium in migmatites and leucogranites, the Higo metamorphic terrane, Japan

K. MAKI[1,2]*, J.G. SHELLNUTT[2], T.W. WU[3], Y. MORI[4], K. MIYAZAKI[5], T.F. YUI[2] AND B.M. JAHN[2,6]

[1]Kyoto University, Kyoto 606-8502, Japan (*correspondence: k-maki@kueps.kyoto-u.ac.jp)
[2]Academia Sinica, Taipei 11529, Taiwan
[3]University of Western Ontario, Ontario N6A 5B7, Canada
[4]Kitakyushu Museum of Natural History and Human History, Kitakyushu 805-0071, Japan
[5]Geological Survey of Japan, AIST, Tsukuba 305-8567, Japan
[6]National Taiwan University, Taipei 106, Taiwan

Sr and Nd isotope compositions of migmatites and leucogranites in the highest grade zone of the Higo low-*P*/high-*T* (andalusite-sillimanite type) metamorphic terrane, central Kyushu, Japan, suggest that the nebulitic migmatites (diatexite) formed due to melt infiltration into the pelitic gneisses, and the stromatic migmatites (metatexite) due to *in situ* partial melting of the pelitic gneisses. The nebulitic migmatites occur as a 3 m-thick layer and is sandwiched between 2 m-thick layers of storomatic migmatites within pelitic gneisses. Both types of migmatites are parallel to the foliation of the gneisses. The leucogranites occur as a few to ten cm-thick layer or lens within the gneisses. The nebulitic migmatites preserve a record of large magnitude Sr and Nd isotope disequilibrium with the pelitic gneisses, which show the isotope equilibrium with the stromatic migmatites. The nebulitic migmatites have higher epsilon Nd (T) values of -0.6 and P_2O_5 contents of 0.42 wt.% than those of the pelitic gneisses (-2.1 and 0.18 wt.%) and stromatic migmatites (-3.1 and 0.10 wt.%). The initial $^{87}Sr/^{86}Sr$ ratio, I_{Sr}, of the nubulitic migmatite, 0.70572, is lower than that of the pelitic gneisses and stromatic migmatites ranging from 0.70792 to 0.70857. Some leucogranites with high P_2O_5 contens of 0.91 wt.% have the higher epsilon Nd (T) values of +3.4 than, and similar I_{Sr} value of 0.70800 to that of the pelitic gneiss and stromatic migmatites. Based on the Sr and Nd isotope characteristics and P_2O_5 contents, *in situ* partial melting of the pelitic gneisses could form the stromatic migmatites, but could not produce the nebulitic migmatites with the higher epsilon Nd (T) value and P_2O_5 contents. The higher epsilon Nd (T) value and P_2O_5 contents may imply the participation of externally derived melt during the formation of nebulitic migmatites. Dissolution of apatite into the melt under dry and high-temperature conditions might produce such a high degree of Nd isotope disequilibrium and high P_2O_5 contents.

https://doi.org/10.1180/S0026461X00006502 Published online by Cambridge University Press

Adsorption of organophosphorous compounds on well-characterized iron mineral nanoparticles

PETER MÄKIE[1], PER PERSSON[1] AND LARS ÖSTERLUND[2,3]

[1]Dep. of Chemistry, Umeå Univ., SE-901 87 Umeå, Sweden (peter.makie@chem.umu.se, per.persson@chem.umu.se)
[2]FOI CBRN Defence and Security, SE-901 82 Umeå, Sweden (lars.osterlund@foi.se)
[3]Dep. of Engineering Sciences, The Ångström Laboratory, Uppsala Univ. SE-751 21 Uppsala, Sweden (laost@angstrom.uu.se)

Particles of iron (hydr)oxides in the eartht's crust are highly reactive towards phosphates, and sorption of organophosphorous (OP) compounds constitutes an important part of the anthropogenic phosphor cycle [1]. In this study, three different polymorphs of well-characterized nanoparticles were chosen as model systems for iron minerals, i.e. hematite (α-Fe_2O_3), maghemite (γ-Fe_2O_3) and and goethite (α-FeOOH). Comparative studies of structure-specific sorption processes were performed using three OP compounds, namely trimethyl phosphate (TMP), triethyl phosphate (TEP) and dimethyl-methyl phosphonate (DMMP). Using *in situ* infrared vibrational spectroscopy, calibrated OP adsorption measurements were performed in a temperature controlled system under different conditions: Dry sorption with and without irradiation by simulated sunlight, and sorption under controlled humidity with and without sunlight.

The surface reactivity was shown to be strongly dependent on detailed bonding coordination of the central P atom, the structre of iron mineral surface, and environmental parameters (humidity and sunlight). All OPs were found to adsorb through the phosphoryl O atom on unsaturated iron cation surface sites (Lewis acids) on hematite and maghemite. In contrast, on goethite hydrogen bonding to surface OH (Brønstedt acid sites) dominates. On the iron oxides dissociative adsorption is facile yielding predominantly methoxy and formate reaction intermediates (oxidative pathway), and predominantly methoxy and phosphoric acid on the hydroxide (hydrolysis). The reactivity increases in the order goethite < maghemite < hematite. Addition of water blocks reactive adsorption sites, whereas sunlight strongly promotes OP dissociation on all minerals. Absence of water favours oxidation on hematite and maghemite, whereas presence of water during sunlight irradiation yields a combined oxidation/hydrolysis pathway.

[1] Schnurer, Y. *et al*. (2006) *Env. Sci. & Technol*. **40**, 4145–4150.

Microbiological investigation of the Iron-containing floculent mats in various deep sea environments

H. MAKITA[1]*, S. KIKUCHI[2], S. MITSUNOBU[3], K. NAKAMURA[1], T. TOKI[4], S. KAWAGUCCI[1], T. NOGUCHI[5], M. ABE[1], J. MIYAZAKI[1], T. YAMANAKA[6], S. TSUCHIDA[1], H. NOMAKI[1], Y. TAKAHASHI[2] AND K. TAKAI[1]

[1]Japan Agency for Marine-Earth Science and Technology (JAMSTEC), Kanagawa 237-0061, Japan (*corrspondence: makita@jamstec.go.jp)
[2]Hiroshima University, Hiroshima 739-8526, Japan
[3]University of Shizuoka, Shizuoka 422-8526, Japan
[4]University of the Ryukyus, Okinawa 903-0213, Japan
[5]Kochi University, Kochi, 783-8502, Japan
[6]Okayama University, Okayama, 700-8530, Japan

It is believed that most important energy source in ocean crust or subseafloor is vastly abundant iron. Therefore, it is suggested that the iron-oxidizing chemolithoautotrophic microbe is a key player for the microbial ecosystem. However, there were no direct evidences because cultivation of iron oxidizer was difficult.

Recently, '*Mariprofundus ferrooxidans*' belong to the ζ (zeta)-proteobacteria [1] was isolated. This microbe can oxidize ferrous iron as the elctron donor and can be widely observed in various deep-sea low-temperature hydrothermal fields [2].

However, the diversity, distribution and role of these iron-oxidizing ζ-proteobacteria are still unknown. In addition, it is still unclear how these microbes cope with iron predominantly from oceanic basalts.

Therefore, to clarify these questions, we have investigated several iron-containing flocculent mats from deep-sea hydrothermal fields in the Mariana Vocanic Arc and the Okinawa Trough. Culture independent analysis of these mats demostrated that ζ-proteobacteria was the most dominant phylotypes. The X-ray analysis (XANES and EXAFS) revealed that the abundance of potentially biogenic Fe-oxides-species would be relevant with the abundance of ζ-proteobacteria population in the iron-containing flocculent mats. These results strongly supported that iron-oxidizing chemolithoautotrophs have significant ecological roles for iron and carbon cycles in deep-sea low-temperature hydrothermal systems.

[1] Emerson D. *et al*. (2007) *PLoS ONE* **2**, e667. [2] Emerson D. & C. L. Moyer (2010) *Oceanography* **23**, 148-163.

https://doi.org/10.1180/S0026461X00006502 Published online by Cambridge University Press

Recycled crust in the source of Deccan flood basalts

K. MALAMOUD[1]*, A.V. SOBOLEV[1,2], D.V.KUZMIN[2], S. VILADKAR[3] AND A.W. HOFMANN[2]

[1]ISTerre, University J. Fourier BP 53, 38041 Grenoble Cedex 9, France (*correspondence: karim.malamoud@gmail.com)
[2]Max Planck Institute for Chemistry, Postfach 3060, 55020 Mainz, Germany
[3]Carbonatite Research Centre, Amba Dongar, Kadipani, District Vadodara 390117, India

The Deccan Flood Basalts (DFB), Seychelles plateau and Mascarene Islands (e.g. Réunion) are thought to trace the evolution of a single mantle plume from its initial stage under thick continental lithosphere to a hot-spot stage under thinner oceanic lithosphere. DFB may also have contributed to the Cretaceous-Tertiary-boundary mass extinction [1].

We intend to reconstruct the source compositions of lavas from the DFB and the Mascarene Islands using the compositions of melt inclusions and host olivine phenocrysts following [2]. Preliminary results on samples from the Kutch district (Gujarat state, India) indicate significant Ni excess and Mn deficiency in the composition of olivine phenocrysts similar to Hawaiian magmas (see Fig). This suggests a large contribution of pyroxenite-derived melt (recycled oceanic crust). Furthermore, this component appears compatible with that of lavas from the Réunion Island.

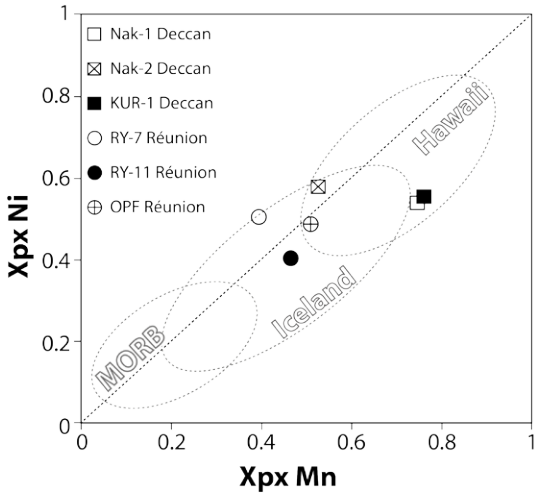

Figure 1: Proportion of pyroxenite derived melt from Ni excess and Mn deficiency in averaged (per sample) olivine compositions [2].

[1] Courtillot, V. *et al*. (1988) *Nature* **333**, 843–846.
[2] Sobolev, A.V. *et al*. (2008) *Science* **321**, 536.

Serpentinite channel and the role of serpentinite buoyancy for exhumation of HP rocks (Voltri Massif, Western Alps)

C. MALATESTA[1], T. GERYA[2], M. SCAMBELLURI[1], L. FEDERICO[1], L. CRISPINI[1], G. CAPPONI[1]

[1]Dipartimento per lo studio del territorio e delle sue Risorse, Università di Genova, Corso Europa 26, Genova - Italy
[2]Institute of Geophysics, ETH Zentrum, Sonneggstrasse 5, 8092 Zürich (Switzerland)

The high-pressure (HP) Voltri Massif (at the eastern end of the Western Alps) consists of meta-ophiolites and metasediments recording peak blueschist (Palmaro-Caffarella Unit) to eclogite (Voltri Unit) facies. Eclogite and blueschist metagabbro lenses within highly sheared serpentinite or metasediments reveal strain heterogeneity within the lenses and between lenses and host-rocks. P-T pseudosections of these rocks indicate clockwise P-T paths for subduction and exhumation. Peak conditions range from 10-15 kbar and 450-500°C (Palmaro-Caffarella), to 21 kbar and 450-490°C, and to 22-28 kbar, 460-500°C (Voltri). To constrain exhumation of these rocks, we performed 2D numerical models simulating intraoceanic subduction in a basin surrounded by continental margins, same as the Mesozoic Ligurian Tethys. We reproduced a non-layered lithosphere typical of slow and ultra-slow spreading ridges, where serpentinized lithospheric mantle hosts discrete gabbro intrusions and is discontinuously covered by basalts. As the result of slab dehydration, a viscous serpentinite channel forms in the mantle wedge, whose evolution is strongly controlled by rheology of serpentine. Ductile deformation of serpentine within the channel enhances mixing of parts of the overriding plate with slab-derived sediments, oceanic crust and mantle. The simulations show that serpentinites decreased the bulk density of HP terrains below the mantle value, causing exhumation of part of the serpentinite channel. They also provide P-T paths of selected rock volumes with close correspondence with the P-T paths of the Voltri gabbroic lenses. The dominance of highly sheared serpentinite, the strong strain-partitioning, the metamorphic peaks attained by the various rock volumes within the Massif, and the similarity of natural and simulated P-T paths, suggest that the Voltri Massif may represent a ‘fossil’ serpentinite channel.

https://doi.org/10.1180/S0026461X00006502 Published online by Cambridge University Press

Sr and Nd isotope studies on sediment core samples from Cauvery delta, South India: Evidence for monsoon induced changes in provenance

MALIK ZUBAIR AHMAD, S. BALAKRISHNAN AND P. SINGH*

Department of Earth Sciences, Pondicherry University, Pondicherry 605014, India
(*correspondence: pramods@yahoo.com)

Sr and Nd isotope composition of sediments are useful to trace their provenance and past changes in climate [1]. Here, we present $^{87}Sr/^{86}Sr$ ratios of four different leachate fractions and Sr and Nd isotopic composition of the residual detrital phase of the sediments from a 25 m core obtained from the distal part of the Cauvery River delta. The $^{87}Sr/^{86}Sr$ ratios of exchangeable, carbonate, Fe-Mn and organic phases of the sediments exhibit similar trends falling between seawater and river water values (Fig.1). All these phases exhibit a sharp positive excursion at 3.8 m depth. This could be due to stabilization of vadoze zone for a long period, permitting greater microbial assisted weathering of minerals to release more radiogenic Sr.

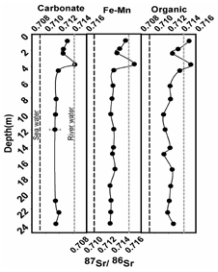

Figure 1.

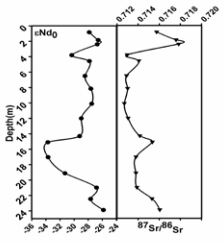

Figure 2.

Comparison of trends of εNd_o and $^{87}Sr/^{86}Sr$ ratios in the detrital phase of the sediments shows five excursions (Fig. 2). Comparing the isotope ratios of rocks exposed from the catchment of Cauvery river suggest that the dominant source of sediments varied from (1) granitic gneisses and basalts of Dharwar craton exposed along northern westcoast, receiving rains during southwest monsoon (2) enderbites and granulites of Nilgiri mountains that receive rainfall during both southwest and northeast monsoon and (3) gneisses and granulites found along Moyar, Bhavani and Cauvery shear zones and Southern Granulite Terrain receiving rains during NE monsoon. Evidence for intensification of SW monsoon is observed at a depth of 4 m upward (~7800 years B.P.) to 1.85m (upto ~5990 years B.P.).

[1] Goodbred (2003) *Sedimentary Geology* **162**, 83–104.

Redox conditions of formation of osmium-rich alloys from dunite and chromitite of the Guli massif (Maimecha-Kotui Province, Russia)

K.N. MALITCH[1]*, A.A. KADIK[2], BADANINA I.YU.[1] AND E.V. ZHARKOVA[2]

[1]Russian Geological Research Institute, St. Petersburg, 199106, Russia (*correspondence: dunite@yandex.ru)
[2]Institute of Geochemistry and Analytical Chemistry, Russian Academy of Sciences, Moscow, 119991, Russia (kadik@geokhi.ru)

This study presents the new data on mineral composition and physico-chemical conditions of formation of Os-rich alloy grains derived from dunite and chromitite of the Guli clinopyroxenite-dunite massif (Maimecha-Kotui Province, Russia). The study employed a multitechnique approach that utilized electron microprobe analysis and experimental determination of the intrinsic oxygen fugacity (fO_2) of Os-rich alloys using solid electromechanical cells.

Measured fO_2 values of native osmium ($Os_{84}Ir_{11}Ru_5$) and iridian osmium ($Os_{66}Ir_{28}Ru_5$) are plotted (Fig. 1) between standard equilibrium buffers of wustite – magnetite (WM) and quartz – fayalite – iron (QFI). The similarity of fO2 for Os-rich alloys from dunite and chromitite indicates that formation of these minerals occurred in compatible redox conditions, characteristic of the region of generation of mantle peridotites.

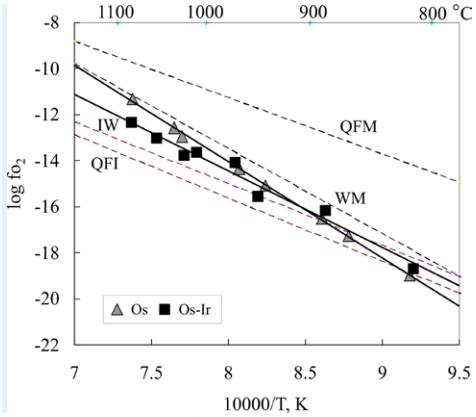

Figure 1: Plot log fO_2 - 10^4/T (K) for the measured samples of native osmium from dunite and iridium osmium from chromitite.

The study was supported by Russian Foundation for Basic Research (grant № 09-05-01242).

https://doi.org/10.1180/S0026461X00006502 Published online by Cambridge University Press

Late metasomatic addition of garnet to the SCLM: Os-isotope evidence

V.G. MALKOVETS[1]*, W.L. GRIFFIN[2], N.J. PEARSON[2], D.I. REZVUKHIN[1], S.Y. O'REILLY[2], N.P. POKHILENKO[1], V.K. GARANIN[3], Z.V. SPETSIUS[4] AND K.D. LITASOV[1]

[1]V.S. Sobolev Institute of Geology and Mineralogy, Novosibirsk, 630090, Russia (*correspondence: vladimir.malkovets@gmail.com)
[2]GEMOC National Key Centre, Macquarie University, Sydney, 2109, Australia (wgriffin@els.mq.edu.au)
[3]Moscow State University, Moscow, Russia
[4]ALROSA Ltd., Mirny, Russia

Archean cratons are underlain by highly depleted subcontinental lithospheric mantle (SCLM). However, xenolith and xenocryst data [1; references therein] suggest that Archean SCLM has been extensively refertilized by metasomatic processes, with the addition of Fe, Ca, and Al to depleted protoliths. The distribution of sub-calcic garnets in the SCLM beneath the Siberian craton suggests (1) sub-calcic garnets and diamonds are metasomatic phases in the cratonic SCLM; (2) the distribution of both phases is laterally heterogeneous on relatively small scales and related to ancient structural controls [2].

Re-Os isotopic compositions of sulfide inclusions in lherzolitic Cr-pyropes from four Siberian middle Paleozoic diamond mines have been determined by laser ablation MC-ICP-MS: Mir (n=17) and Internationalnaya (n=109), Malobotuobiya field, Udachnaya (n=17), Daldyn field, and Nyurbinskaya (n=12), Nakyn field.

Most analysed sulfides (~84%) have very low Re/Os ratios (<0.07), and their Re-depletion ages (T_{RD}) fall between 2.2 and 3.0 Ga (±0.03 Ga, mean 2s analytical uncertainty). 10 to 15% of the sulfides give younger T_{RD} down to 600 Ma.

Our previous study [3] of sulfide inclusions in megacrystic olivines from the Udachnaya pipe suggests that most of the SCLM beneath the Daldyn kimberlite field formed at 3-3.5 Ga, and that lithosphere formation culminated at ca 2.9 Ga. Our new data suggest that refertilization of the highly depleted SCLM and the introduction of Cr-pyrope garnet occurred between 2.2 and 3.0 Ga; little garnet was present before 3 Ga. Pyropes with young sulfides (between ~1.9 and ~2.2 Ga) may have crystallised during the amalgamation of the Siberian craton in Paleoproterozoic time.

[1] Griffin *et al*. (2009) *Jour. of Petrol*. **50**, 1185–1204. [2] Malkovets *et al*. (2007) *Geology* **35**, 339–342. [3] Griffin *et al*. (2002) *Geochem. Geophys. Geosyst*. **3**, 1069.

On dating of groundwater with a high $^{234}U/^{238}U$ and Eh> 100mV

A.I. MALOV

Institute of the Ecologic Problems of the Northern Region, Naberezhnaya Severnoi Dviny, Arkhangelsk, 163061, Russia (malovai@yandex.ru)

In this report, on the basis of geological dating and developed PI Chalov method for determining the age of surface water for non-equilibrium uranium, attempted to assess the possibility of using isotopes U to determine the age of groundwater. In alpha-decay of ^{238}U atoms in an unbroken part of the mineral species appears disorders (disordered) region (*d. r.*) formed by atom recoil ^{234}Th. Among disordered may be the atom itself and the impact that formed this region. The probability of this event, p: $0 < p < 1$. If the groundwater is constantly supplied nonequilibrium uranium $^{234}U/^{238}U > 1$ ($\gamma_{d.\,r.}$) within a certain time t, then the following expression:

$$\gamma_{d.r.} = \left(\gamma_{t.water} - 1\right)\frac{\lambda_2 t}{1 - ?^{-\lambda_2 t}} + 1.$$

Therefore, asking a few randomly chosen values of t, we can define the corresponding values $\gamma_{d.\,r.}$. Then get some corresponding values N_{1rocks} / p:

$$\frac{N_{1rocks}}{?} = \frac{\lambda_2}{\lambda_1\left(\gamma_{dr} - \gamma_{rocks}\right)}.,$$

where N_{1rocks} - the number of atoms of ^{238}U, $\lambda_1 = 1.55 \cdot 10^{-10}$ years^{-1} and $\lambda_2 = 2.75 \cdot 10^{-6}$ years^{-1} - decay constant of ^{238}U and ^{234}U. Knowing the number of atoms of ^{238}U, located in the water contained in a unit volume of rock V_{unit} is currently $N_{1unit..\,water}$, and the activity of ^{238}U of the mineral species in the same volume $A_{1unit.\,rocks}$, you can roughly estimate the average number of atoms N_{1rocks} goes into the water from a disordered region:

$$N_{1rocks} \approx \frac{N_{1unit.water}}{?_{1unit.rocks} \cdot t}.$$

Having obtained the values N_{1rocks}/p and N_{1rocks}, we define p. As a result, for each of several arbitrarily chosen values of t we obtain the corresponding value of probability p. The values of t and p are related by a power dependence. Therefore, defining p, for several values of t, we can derive an equation of type $t = ap^{-0.971}$, where a - the age of groundwater at p=1%, and construct the corresponding diagram. The key point of the proposed method is the choice for charting the calculated value of p, on which is t, age-appropriate groundwater. On the example of North Dvina basin (northwest Russia) have shown that for aquifers with a high $^{234}U/^{238}U$ and Eh> 100 mV in increments homogeneous sandy rocks, p value is 0.35%. It is important to note that the chemical dissolution of equilibrium uranium contained in areas of undisturbed radioactive decay of rocks, as well as sorption to the results of calculations by the proposed method is not influenced.

https://doi.org/10.1180/S0026461X00006502 Published online by Cambridge University Press

Progress in understanding of sulfur in subduction zone magmas

C. MANDEVILLE[1]*, N. SHIMIZU[2], K. KELLEY[3], N. METRICH[4], A. FIEGE[5] AND H. BEHRENS[5]

[1]US Geological Survey (cmandeville@usgs.gov)
[2]Woods Hole Oceanographic Institution (nshimizu@whoi.edu)
[3]University of Rhode Island (kelley@gso.uri.edu)
[4]Institut de Physique du Globe de Paris (metrich@ipgp.fr)
[5]Univ. of Hannover (a.fiege@mineralogie.uni-hannover.de)

Progress in developing a better understanding of sulfur's behavior and origin in subduction zone magmas has now been facilitated through new *in situ* analytical techniques and recent conduction of high pressure and temperature (P-T) partitioning and isotopic fractionation experiments. Development of an *in situ* secondary ionization mass spectrometry (SIMS) technique for measurement of $^{34}S/^{32}S$ ratios in silicate glasses now allows for direct measurements of experimental glasses and melt inclusions from mafic arc magmas. Complementary SIMS calibrations for sulfur isotope ratio measurements of pyrrhotite and anhydrite now allow for investigation of S isotopic fractionation between sulfur-bearing melt and condensed sulfur phases at magmatic temperatures. Conventional and SIMS analysis of run products from high (P-T) decompression experiments investigating S partitioning between vapor and melt (Fiege *et al*. [1]) provide direct measurement of isotopic fractionations that can now be compared to estimates derived from previous extrapolations of data from lower temperature experiments, analogue materials and/or theoretical models [2]. Advances in S and Fe micro-X-ray Absorption Near Edge Structure Spectroscopy (XANES) has allowed for determination of the oxidation state of S and Fe in both natural and experimental samples.

Measured $^{34}S/^{32}S$ ratios via SIMS in olivine-hosted basaltic melt inclusions (MI's) from Krakatau and Galunggung volcanoes in Indonesia and Augustine volcano, Alaska yield $\delta^{34}S$ values from -2.8‰ to 17.2‰. Highest $\delta^{34}S$ values of 9.6‰ to 17.2‰ were measured in MI's from a Pleistocene basalt from Augustine volcano that have high disolved volatiles of 8.0 wt.% H_2O, 2624 to 5100 ppm S, 3900 ppm Cl, and sulfur XANES spectra with prominent peaks at 2482 eV indicating 100% SO_4^{2-} species in melt. Melt inclusions from the 1982 eruption of Galunggung yield $\delta^{34}S$ of -2.8‰ to 9.6‰. Melt inclusions from Krakatau pre-1883 basaltic scoria yield $\delta^{34}S$ values of 1.6‰ to 8.7‰. $A^{34}S$-enriched material is present in these magma source regions.

[1] Fiege *et al*. (2011) *MinMag*, this volume. [2] Mandeville *et al*. (2009) *GCA* **73**, 2978–3012.

Mn-crusts record deep ocean ventilation changes

AUGUSTO MANGINI

Heidelberger Akademie der Wissenschaften, INF 229, D-69120 Heidelberg (amangini@iup.uni-heidelberg.de)

The end of glacial stages is accompanied by an increase of atmospheric CO_2. During the last Termination this increase goes along with a drastic drop of atmospheric ^{14}C by about 190‰. The probable explanation assumes the release of old carbon stored from a poorly ventilated glacial Ocean. This period was addressed by Broecker as the 'Mystery Interval' due to lacking higher glacial Benthic-Planktic foraminifera ages. However, the mystery could be an artefact of the tool applied, as benthic foraminifera cannot survive in an anoxic ocean.

More than 20 years ago we had measured profiles of ^{230}Th in the top mm of two Mn-crusts from the Central Pacific, from 4, 400 m and 1, 500 m water depth at a resolution of 20μm. In both samples growth rates during the past 300, 000 years were faster in Interglacials than in Glacials. We attributed the extremely slow growth rate during stage 2, and, especially, stops of growth during glacial stages 6 and 8 to periods of anoxia of the deep ocean, impeding formation of Mn-oxides. However, these conclusions were ignored, arguing that the occurrence of benthic forams and the lack of peaks of uranium in sediments contradicted periods of anoxia. In the meantime, however, there are a number of indications that the deep glacial Pacific Ocean was less ventilated than at present and that the shut down of N. Atlantic deep water formation during Heinrich 1 could have led to a short anoxic period in the deep Pacific. Reconsidering the data from the Mn crusts may help to solve the mystery.

https://doi.org/10.1180/S0026461X00006502 Published online by Cambridge University Press

Geochemical implications of iodine distribution in Indian soils

DEVLEENA MANI*, D.J. PATIL AND A.M. DAYAL

Petroleum Geochemistry Group, National Geophysical Research Institute(CSIR), Hyderabad-500007 (*correspondence: devleenatiwari@ngri.res.in)

Iodine plays a pivotal role in many of the geological, chemical and biological processes because of its litho-, bio-, atmo-, hydro- and chalco-philic nature. Speciation of iodine as inorganic iodine (iodides and iodates), molecular iodine and organically bound iodine provides its chemical signature in diverse forms in the earth crust. Contrasting distributions of iodine are observed in the Indian soils; wherein iodine lows below the permissible limits of WHO are observed in several parts of India, especially in the northern region [1], and on the other side, elevated iodine concentrations in hydrocarbon prospective/petroliferous sedimentary basins of India have been documented [2].

Soil iodine studies have been carried out in Saurashtra and Deccan Syneclise basins, which are potentially prospective hydrocarbon realms in the western and west central India, respectively. Results show the concentration (in mg/kg) of iodine to be in the range of 1.5-68.5 and 1.1-19.3 in the surficial soils of Saurashtra and Deccan Syneclise, respectively. The values are quite high compared to average distribution of iodine in soils (0.01-6mg/kg) [3]. The iodine highs in these regions appear to be associated with the hydrocarbon prone organic matter of the sedimentary basins.

The geological and geophysical variations occurring in different regions and sedimentary basins of India corroborate the concentration distribution pattern of iodine in the soils and the related geochemical anomalies.

[1] Ghose, *et al*. (2003) *Journal of Geol. Soc. of India* **62**, 91–98. [2] Mani *et al*. (2011) *Natural Resources Research* **20**, **1**, 75–88. [3] Kebata-Pendias & Pendias, (1984) *Trace elements in soils & plants*, CRC Press.

HIMU-EMI type OIBs from the Neoarchean Penakacherla greenstone belt, Dharwar craton, India: Implications on Recycling of Mesoarchean crust

C. MANIKYAMBA[1] AND R. KERRICH[2]

[1]National Geophysical Research Institute (CSIR), Hyderabad-606, India; (cmaningri@yahoo.com)

[2]Univeristy of Saskatchewan, Skatoon, Canada S7N 5E2, (rbkerrich@shaw.ca)

Alkaline basalts, having relict aegirine, leucite and nepheline mineralogy, are associated with high-Mg and island arc basalts in the Neoarchean Penakacherla greenstone belt, eastern Dharwar craton, India. These are compositionally uniform, where SiO_2 = 43 to 46 wt%, Mg# = 0.70 to 0.58, and Ni = 183-85 ppm, enriched in alkalies (K_2O+Na_2O ~7 wt.%), TiO_2 (2.3-2.1 wt.%), and exhibit fractionated REE patterns with $(La/Yb)_N$ ranging from 23 to 29. On the Ni-Zr diagram, alkaline basalts plot with counterparts from the ocean island of Tubuai, Cook-Austral volcanic chain. On paired REE and primitive mantle normalized multi-element diagrams these basalts are characterized by coherent patterns: (1) smoothly fractionated REE [(La/Sm)N 4.08-5.00, (Gd/Yb)N 3.09-4.27]; (2) uniform Th/U ratios (4.1-5.4); (3) no Ce or Eu anomalies; (4) depletions of Th relative to Nb and La, yielding small negative anomalies of Nb relative to La (Nb/La = 0.78-1.01 vs.1.04 the primitive mantle ratio, in common with compositional characteristics of Phanerozoic alkaline ocean island basalts (OIB). These basalts plot with Recent counterparts from Aitutaki and Heard OIB on SiO_2 vs Nb/Y plot. High-μ, EM1 and EM2 OIB have distinct to overlapping trace element characteristics, of which HIMU OIB alone are characterized by positive Nb-anomalies. Comparison of PT-alkaline basalts with average trace elements ratios of OIB end members of Greenough *et al*. (2005) exhibit resemblance with some features of HIMU and EM1. Ratios of Zr/Nb (2.7-3.61), and La/Yb (32 - 41) compared to respective values in HIMU (3.4, 30), EM1 (5.4, 36), and EM2 (6.3, 21). Ti/Y (559) and Y/Yb (14) compare to respective values in HIMU (598, 13), EM1 (680, 15) and EM2 (638, 16). Consequently, PT alkaline basalts have trace element ratios intermediate between HIMU and EM endmembers. This occurrence of alkaline basalts indicates subduction, recycling, and incubation of Mesoarchaean oceanic and continental crust in the mantle, and generation of a mantle plume at 2.7 Ga.

https://doi.org/10.1180/S0026461X00006502 Published online by Cambridge University Press

Nutrient uptake at the fungi-mineral interface

UTRA MANKASINGH[1]*, SALVATORE A. GAZZE[2], LOREDANA SACCONE[2], ADELE L. DURAN[3], JONATHAN R. LEAKE[3] AND KRISTIN VALA RAGNARSDOTTIR[1]

[1]Faculty of Earth Sciences, School of Engineering and Natural Sciences, University of Iceland, Askja, Sturlugata 7, Reykjavik 107, Iceland (*correspondence: utra@hi.is)
[2]H.H. Wills Physics Laboratory, University of Bristol, Tyndall Avenue., Bristol, BS8 1TL, UK
[3]Department of Animal and Plant Sciences, University of Sheffield, Western Bank, Sheffield, S10 2TN, UK

This study focuses on the central role of soil fungi to acquire mineral nutrients from rocks and minerals, and thus participate in the weathering of bedrock to soil. We investigate fungal uptake of nutrient elements from minerals via direct contact and transport across the organism membrane.

Plant seedlings (*Pinus sylvestris*) in symbiosis with ectomycorhyzal fungi were grown directly on mineral surfaces in a controlled microcosm environment with regulated light, nutrients, moisture and carbon dioxide. The seedlings were grown in mixed mineral microcosms that were starved of a single essential nutrient. Initial chemical analysis of foliage and roots from microcosms starved of the major nutrients K and Mg showed lower concentrations of these elements in plant tissue compared to plants from microcosms that were not starved of these elements. However, despite systems being starved of K, an appreciably greater K concentration was observed in the shoots vs roots, suggestive of K storage in the foliage. Ca was also higher in shoots than roots. This trend is perhaps indicative of water efflux in the plants. Similarly, the essential nutrients P, Mg, Mn and Zn were higher in the foliage than in the roots,

Conversely, Fe and Al concentrations are higher in the roots than the shoots. Similar trends have been observed in the literature, suggesting low mobility of Al and Fe in plants [1]. Al, which is a non-essential element to plants, is toxic to fungi and they excrete it. The ready supply of Al to the roots system and the selective uptake to the shoots could imply that fungi may act as a filter for Al uptake by the seedlings. Fe uptake needs to be further investigated through comparison of systems with varying Fe nutrient supply.

[1] Hobbie *et al*. (2009) *Comm Soil Sci Plan* **40**, 3503–3523.

The role of North Atlantic asthenosphere in the genesis of Icelandic lavas: Evidence from Heimaey

C.J. MANNING* AND M.F. THIRLWALL

Royal Holloway University of London, Egham Hill, Egham Surrey TW20 0EX
(*correspondence: c.manning@es.rhul.ac.uk)

Recent work on Iceland has indicated minimal involvement of North Atlantic asthenosphere (NAA) in the genesis of Icelandic lavas [1, 2]. Whilst the variation in isotopic and trace element compositions of Icelandic lavas requires several distinct mantle sources, these are all suggested to be derived from the Iceland plume rather than the surrounding asthenosphere [2, 3, 4]. It follows that areas remote from the current plume position are more likely to exhibit evidence for interation with NAA. We present new high-precision isotopic and elemental data for samples from the island of Heimaey which is proposed to be the tip of the propagating Eastern Rift Zone in South East Iceland.

In contrast to the incompatible element enrichment expected in the small degree melts produced at off-rift zones, the Heimaey samples exhibit lower concentrations (up to 21%) at a given MgO% than the South Iceland central volcanoes. Despite this the Heimaey lavas still plot in the alkali field on a TAS diagram which is a consequence of enrichment in Na that is not coupled with enrichment in other incompatible elements.

Relationships between K/Nb, Na_2O/TiO_2, and radiogenic isotopes indicate mixing between an enriched component with an 'Icelandic' signature and a depleted component similar to NAA. Na_2O/TiO_2 has been shown to vary as a function of melting depth [5] and polybaric melting models for Na_2O/TiO_2 indicate that the high values seen within the Heimaey samples can be generated by mixing between <40% of an 'Icelandic' source melting in the garnet facies (~45kbar) and <72% of a North Atlantic MORB source melting in the spinel facies (~10kbar).

[1] Fitton *et al*. (1997) *EPSL* ***153***, 197–208. [2] Thirlwall *et al*. (2004) *GCA* ***68***, 361–386. [3] Chauvel & Hemond (2000) *G*^{3} **1**. [4] Kokfelt *et al*. (2006) *J.Pet*. **47**, 1705–1749. [5] Putirka (1999) *JGR* ***104****(B2)* 2817–2829

https://doi.org/10.1180/S0026461X00006502 Published online by Cambridge University Press

New roles for rutile in tracing petrogenetic processes

C.E. MANNING

Department of Earth and Space Sciences, University of California Los Angeles, Los Angeles, CA 90095-1567 (manning@ess.ucla.edu)

Rutile is common in a wide range of igneous and metamorphic systems. Its wide stability and mechanical durability make it an important addition to the petrologist's accessory-phase toolkit. And, for at least two jobs, it may be a better tool than its more commonly deployed partner, zircon. First, rutile is nominally anhydrous but can contain up to 3000 ppm H_2O, significantly more than zircon [1]. Thus, OH in rutile can help evaluate the role of hydrous components during petrogenesis. Colasanti *et al*. [2] determined OH solubility in pure synthetic rutile at 0.5-2.0 GPa, 500-900 °C and four fO_2 buffers using FTIR spectroscopy. OH solubility increases with decreasing fO_2 at fixed *P*-*T*, and with *T* or *P* at isobarically or isothermally buffered fO_2. Data support OH substitution via $Ti^{4+}O_2 + {}^1/_2H_2O = Ti^{3+}O(OH) + {}^1/_4O_2$, and yield nearly ideal, multi-site mixing of the TiO_2-TiOOH solid solution along with $\Delta V_r°$, $\Delta H_r°$ and $\Delta S_r°$ of 1.90±0.48 cm^3/mol, 219.3±1.3 kJ/mol, and 19.9±1.4 J/molK (1σ). OH in rutile can be deployed as a thermobarometer and/or oxybarometer. Elevated OH in rutile may imply unexpectedly high Ti^{3+} in some terrestrial settings.

A second role for rutile arises from its participation in net-transfer reactions, which is rare for zircon [3]. This makes it especially useful in thermobarometry [4]. Kapp *et al*. [5] showed that solid solution in titanite leads to titanite-rutile coexistence over a range of *P* and *T*, in turn permitting titanite-rutile barometry. Evaluation of 2 zoisite/clinozoisite + rutile + quartz = 3 anorthite + titanite + water (TZARS) and anorthite + 2 titanite = grossular + 2 rutile + quartz (GRATiS) reveals that using appropriate solution models both return *P* within 0.5 kbar of independent constraints for a range of lithologies and cotexts. Moreover, crustal rocks possess nearly constant titanite activity, so accurate *P* is recorded even if only one Ti-phase is present, greatly expanding the range of assemblages on which TZARS and GRATiS can be deployed. These two examples show that rutile may provide key insights into conditions attending igneous and metamorphic processes.

[1] Johnson (2006) *Rev. Mineral. Geochem.* **62**, 117–154. [2] Colasanti *et al*. (2011) *Am. Min.* in press. [3] Ferry *et al*. (2002) *Am. Mineral.* **87**, 1342–1350. [4] Manning & Bohlen (1991) *Contrib. Mineral. Petrol.* **109**, 1–9. [5] Kapp *et al*. (2009) *J. Metamorphic Geol.* **27**, 509–521.

Aqueous complexing and element recycling by subduction-zone fluids

C.E. MANNING

Department of Earth and Space Sciences, University of California Los Angeles, Los Angeles, CA 90095-1567 (manning@ess.ucla.edu)

Mineral solubility in pure H_2O is a poor guide to assessing minor-element transfer by subduction-zone fluids. This is because all such fluids exist in a soluble rock matrix, and it is the interactions with the major solutes derived from host lithologies that exert the dominant controls on element mobility. This can be seen with three examples. First, low rutile solubility in pure H_2O at subduction zone conditions [1] fails to explain occurrence of this phase in veins in high *P* rocks. However, TiO_2 solubility is greatly enhanced dissolved Na-Al silicates, via incorporation in Na-Ti complexes or Na-Al-Si oligomers [1, 2]. Experimentally constrained solubility data indicate that at 600 °C along model slab geotherms, rutile solubility in H_2O is 2 ppm Ti, whereas in H_2O equilibrated with cpx+mica+quartz the high dissolved Na-Al-Si [3] yield 88 ppm Ti. If albite-H_2O fluids are supercritical, even greater Ti transport is possible [4]. Alkali halides are also important complexing agents. Tropper *et al*. [5] showed that at 800°C, 1 GPa, $CePO_4$ monazite and YPO_4 xenotime solubilities are very low in pure H_2O but are significantly enhanced by NaCl via REE/Y-chloride and Na-phosphate complexing. This may promote REE mobility; for example, H_2O/Ce inferred for subduction-zone melts and silicate-rich fluids [6] can also be produced by a $CePO_4$-saturated fluid with $X_{NaCl} = 0.1$. Finally, mineral-solute interactions fix pH in a given lithology and set of conditions. The pH controls the solubility of amphoteric metal oxides. It also governs volatile transfers, e.g. carbon. Molecular CO_2 from carbonate minerals is low along slab geotherms. Most carbon is dissolved instead as carbonate. The strong dependence of aragonite solubility on pH translates to important controls by buffering mineral assemblages. Changes in pH with *P*, *T* and bulk composition must be the primary factors governing loss of carbon from slabs before they reach sub-arc depths. In general, the strong influence of aqueous complexing on element solubility highlights that the role of fluids in element recycling can vary widely.

[1] Antignano & Manning (2008) *Chem. Geol.* **255**, 283–293. [2] Manning *et al*. (2008) *Earth Planet. Sci. Lett.* **272**, 730–737. [3] Wohlers *et al*. (2011) *Geochim. Cosmochim. Acta* in press. [4] Hayden & Manning (2011) *Chem. Geol.* **284**, 74–81. [5] Tropper *et al*. (2011) *Chem. Geol.* **282**, 58–66. [6] Plank *et al*. (2009) *Nature Geosci.* **2**, 611–615.

https://doi.org/10.1180/S0026461X00006502 Published online by Cambridge University Press

Chemical fractionation of Pb and Zn and determination of Pb isotopes in deposited blast-furnace sludge

TIM MANSFELDT, HENNING SCHIEDUNG AND STEPHAN SCHUTH

Department of Geosciences, Soil Geography/Soil Science, University of Köln, Germany (tim.mansfeldt@uni-koeln.de)

Blast-furnace sludge is a waste of pig iron production and was deposited in large surface landfills. Since it contains high amounts of Zn and Pb it is of environmental concern. The first aim of this study was to investigate the solubility and binding forms of Zn and Pb in this industrial waste.

We performed a five step sequential chemical fractionation on 32 samples: (A) 1 M NH_4NO_3; (B) 1 M NH_4OAc, buffered at pH 5.4; (C) 0.2 M NH_4-oxalate-buffer, pH 3.25; (D) 0.1 M ascorbic acid + 0.2 M NH_4-oxalate-buffer, pH 3.25; (E) aqua regia.

The second aim was to determine the Pb isotope ratios of representative bulk samples (n = 10) and related fractions (n = 3) with MC-ICP-MS.

Total contents of Zn ranged from 15, 720 to 86, 400 mg kg^{-1} (median 30, 360 mg kg^{-1}) and from 1, 420 to 19, 510 mg kg^{-1} (median 9, 835 mg kg^{-1}) for Pb. The proportion of the mobile fraction (A) ranged from 0.09 to 2.11% (median 0.26%) for Zn and from 0 to 0.3% (median 0.04%) for Pb. For the easily mobilized fraction (B) we obtained a range from 2 to 23% (median 7%) for Zn and from 5 to 68% (median 19%) for Pb. In contrast to Zn, which is largely associated (63 to 96%, median 85%) to fraction C, i.e. poorly crystalline iron oxides, Pb is much more distributed over the fractions D (4 to 26%, median 18%), i.e. crystalline iron oxides, and E (9 to 64%, median 39%). Sequential fractionation indicates that Zn and Pb are bonded differently in blast-furnace sludge, resulting in a contrasting mobility of these two elements.

The Pb isotope ratios of the bulk samples are clearly distinguishable and ranged from 18.088 to 18.634 ($^{206}Pb/^{204}Pb$), 15.595 to 15.670 ($Pb^{207}/^{204}Pb$) and 37.709 to 38.402 ($^{208}Pb/^{204}Pb$). In contrast, the isotope ratios of the different fractions show little variation, especially the ^{207}Pb-^{204}Pb ratios overlap within analytical uncertainty. No mass-dependent fractionation was observed between the different fractions, because variation is higher for $^{207}Pb/^{204}Pb$ and $^{206}Pb/^{204}Pb$ than for $^{208}Pb/^{204}Pb$.

Seasonal variation in the clay mineral and Sr-Nd isotopic compositions of the suspended sediments of the lower Changjiang River at Nanjing, China

CHANGPING MAO[1,2]*, JUN CHEN[1] AND JUNFENG JI[1]

[1]Institute of Surficial Geochemistry, School of Earth Sciences and Engineering, Nanjing University

[2]State Key Laboratory of Pollution Control and Resource Reuse, School of Environment, Nanjing University, Nanjing 210093, China (*correspondence: chpmao@nju.edu.cn)

The clay minerals and Sr-Nd isotope signatures have been extensively used to characterise the provenance of detrital sediments and wheathering processes. The Changjiang (CR) River is one of the largest rivers in the world. The CR originates on the Tibetan Plateau and enters the East China Sea. A large part of the CR Basin has a subtropical monsoon climate. To examine seasonal changes in clay minerals and Sr-Nd isotopic compositions of the CR, suspended sediment (SS) samples were collected monthly for two hydrological cycles in Nanjing city.

The results indicate that the concentration of CR SS ranges from 11.3 to 152 mg/L and is highly correlated to the rate of water discharge with a higher concentration in flood season. Illite dominates the clay minerals of the CR SS, followed by chlorite, kaolinite and smectite. Illite and kaolinite show distinctly seasonal variations; SS has more illite and less kaolinite contents during flood season than the dry seasons. The illite chemistry index and crystallinity as well as kaolinite/illite ratio all indicate intense physical erosion in the upper CR basin during the flood season.

The Sr-Nd isotopic compositions (silicate fraction) also show distinctly seasonal variations. The results indicate that the $^{87}Sr/^{86}Sr$ ratios of CR SS ranges from 0.725352 to 0.738128, and the εNd (0) values ranges from −10.55 to −12.29. The relative decrease in $^{87}Sr/^{86}Sr$ ratios and increase in εNd (0) values during the flood season can be interpreted to reflect an increasing in the mechanical erosion rate in the upper basin and contribution of more radiogenic Nd and non-radiogenic Sr to the suspended load in flood season.

The Sr-Nd isotopic compositions correlate well with the clay mineral associations, indicating that the seasonal variations primarily reflect the controls of provenance rocks and erosion between different sub-catchments. Furthermore, these signatures can be now used to decipher past discharge and flow regimes of the rivers from sediment cores offshore.

https://doi.org/10.1180/S0026461X00006502 Published online by Cambridge University Press

^{230}Th inventories in new sediment cores from the eastern equatorial Pacific: Constraints on the ^{230}Th constant-flux proxy

FRANCO MARCANTONIO[1], RAMI IBRAHIM[1], AJAY K. SINGH[1] AND MITCHELL LYLE[2]

[1]Department of Geology & Geophysics, Texas A&M University, College Station, TX 77843, USA (*correspondence: marcantonio@tamu.edu)
[2]Department of Oceanography, Texas A&M University, College Station, TX 77843, USA

We have conducted an oceanographic survey in the eastern equatorial Pacific Ocean to assess the water and sedimentary budget of ^{230}Th along water flow paths into the Panama Basin. Our survey, along ~85°W, included bathymetric mapping, sub-bottom profiling, seismic reflection data acquisition, and collection of water and new sediment cores. Our goal is to address the controversy concerning the use of ^{230}Th activities as a constant-flux proxy in the Pacific Ocean. Proponents of the ^{230}Th technique maintain that sediment redistribution is widespread in the eastern equatorial Pacific and that the flux of laterally advected sediment can surpass the vertically rained flux by up to 2-4 times. Others suggest that there may be a discrepancy between the ^{230}Th flux and its rate of production which, in turn, causes accumulation rates to be underestimated due to potential lateral transport of ^{230}Th in the water column. The crux of the disagreement amounts to how one explains the larger-than-expected inventories of sedimentary ^{230}Th along the equator in the Pacific, inventories above those expected from a constant water column production rate.

The Carnegie gap region, bounding the southern border of the Panama Basin, is the main deep water flow path into the basin, and provides an ideal testing ground for investigating sediment advection. Our seismic and sub-bottom profiling surveys determined 'end-member' areas within this region with both thick and thin sediment cover, and several of these sites were multi- and piston-cored. The cores have been dated via radiocarbon and XRF-major-element correlation, which has enabled us to construct common stratigraphies in each survey region. A high-resolution assessment of a ^{230}Th deficit or excess from each end-member region (bathymetric highs versus lows; thin versus thick sediment piles) will be presented. The processes that control this distribution will be assessed in relation to the present-day ^{230}Th water column systematics, which we present elsewhere at this conference (Singh *et al*.).

Geochemistry of antigorite serpentinite and chlorite harzburgite from the Cerro del Almirez (S. Spain): Compositional constraints on fluids released by dehydration of mantle serpentinites

C. MARCHESI[1]*, C.J. GARRIDO[1], J.A. PADRÓN-NAVARTA[2], M.T. GÓMEZ-PUGNAIRE[2] AND V. LÓPEZ SÁNCHEZ-VIZCAÍNO[3]

[1]Instituto Andaluz de Ciencias de la Tierra, Granada, Spain (*correspondence: claudio@iact.ugr-csic.es) (garrido@iact.ugr-csic.es)
[2]Dpt. of Mineralogy and Petrology, UGR, Granada, Spain (padron@ugr.es, teresa@ugr.es)
[3]Dpt. of Geology, University of Jaén, Jaén, Spain (vlopez@ujaen.es)

In the Cerro del Almirez massif (Betic cordillera, S. Spain) hydrous antigorite (Atg)- serpentinite exceptionally records prograde dehydration to chlorite (Chl)- harzburgite under eclogite facies conditions (680-710°C and 1.6-1.9 GPa). Al_2O_3 contents of Atg-serpentinites and Chl-harzburgites match those of variable fertile mantle peridotites. SiO_2 is rather higher in some Atg-serpentinites than the values usually reported for oceanic peridotites, probably owing to normalization of the whole rock compositions after partial MgO loss during seafloor weathering.

The REE patterns of Atg-serpentinites are flat or LREE-depleted and show a negative anomaly in Eu. On the other hand, Chl-harzburgites have 'U-shaped' patterns enriched in LREE and HREE relative to MREE, or are depleted in LREE. Chl-harzburgites also show negative anomalies in Eu and their REE concentrations generally coincide with those of Atg-serpentinites except for lower abundances in MREE. The concentrations of lithophile trace elements are usually above 0.1 the values of the primitive mantle and well overlap those of abyssal peridotites from ocean ridges.

Chl-harzburgites have significantly higher Nb/La, Ta/La, Zr/Sm and Hf/Sm than precursor Atg-serpentinites. This indicates that fluids released during the formation of prograde Chl-harzburgites had complementary low Nb-Ta/LREE and Zr-Hf/MREE ratios. Zr and HREE concentrations of most Chl-harzburgites are similar to those of Atg-serpentinites, and these elements were hence effectively immobile during deserpentinization. The high Zr/Sm and Hf/Sm ratios of Chl-harzburgites are therefore due primarily to the preferential mobility of MREE into fluids. Additionally, Chl-harzburgites have also lower Ba/Th than Atg-serpentinites, consistently with the higher solubility of Ba in fluids compared to Th.

https://doi.org/10.1180/S0026461X00006502 Published online by Cambridge University Press

Low latitude surface ocean contribution to the deglacial atmospheric radiocarbon decline

T.M. MARCHITTO[1]*, S.J. LEHMAN[1], C. LINDSAY[1], S.P. BRYAN[2], J.D. ORTIZ[3] AND A. VAN GEEN[4]

[1]University of Colorado, Boulder, CO 80309, USA (*correspondence: tom.marchitto@colorado.edu) (scott.lehman@colorado.edu, colin.lindsay@colorado.edu)
[2]Woods Hole Oceanographic Institution, Woods Hole, MA 02543, USA (sbryan@whoi.edu)
[3]Kent State University, Kent, OH 44242, USA (jortiz@kent.edu)
[4]Lamont-Doherty Earth Observatory of Columbia University, Palisades, NY 10964, USA (avangeen@ldeo.columbia.edu)

The bulk of the atmospheric radiocarbon decline across the last deglaciation was likely driven by a release of ^{14}C-depleted CO_2 from the deep ocean. Renewed deep mixing in the Southern Ocean is most often cited as the main mechanism of that release. However, observations from the intermediate-depth Indo-Pacific suggest that ^{14}C-depleted waters were also present at low latitudes during deglaciation. If those waters impacted the sea surface via upwelling, then part of the atmospheric Δ^{14}C drop might be attributable to radiocarbon isofluxes across the air-sea interface in the tropics and subtropics.

Here we present new radiocarbon results from two species of shallow-dwelling planktonic foraminifera in Baja California core MV99-PC08 (23.5°N, 111.6°W, 705 m water depth). Calendar ages are estimated by stratigraphic correlation to the GISP2 ice core in Greenland, allowing us to calculate seawater Δ^{14}C through time. We find that the two deglacial Δ^{14}C minima previously seen in intermediate waters at this site are also reflected in the planktonic foraminifera, but in attenuated form. The rate of decline in *Globigerinoides ruber* Δ^{14}C across Heinrich Stadial 1 was slower than in intermediate waters, but faster than in the atmosphere. These observations are consistent with partial upwelling of the Δ^{14}C minima to the sea surface. Additional constraint on the vertical transfer is provided by new benthic Δ^{14}C data from nearby Soledad Basin (290 m sill depth). We diagnose the potential impact of low latitude ^{14}C exchange on the atmosphere using a simple numerical model of the atmospheric radiocarbon balance.

Phases and phase transitions of tropospheric aerosols

C. MARCOLLI[1]*, M. SONG[1], V.G. CIOBANU[1], A. ZUEND[2], G. GANBAVALE[1], B. ZOBRIST[1], B.P. LUO[1], V. SOONSIN[1], U.K. KRIEGER[1] AND T. PETER[1]

[1]ETH Zurich, Institute for Atmospheric and Climate Science, Switzerland (*correspondence: claudia.marcolli@env.ethz.ch)
[2]Department of Chemical Engineering, California Institute of Technology, Pasadena, California, United States

Submicron aerosol particles exert a potentially large but not well constrained effect on the radiative balance of Earth's atmosphere by direct interaction with solar radiation and indirectly by modifying cloud properties. They typically consist of a high variety of organic substances, sulfate and other inorganic ions such as ammonium and nitrate. Knowledge of the physical state and morphology of these particles is needed to predict hygroscopicity and gas/particle partitioning of semivolatile species, to improve knowledge of heterogeneous and multiphase chemistry, and to quantify light scattering and absorption.

However, it is difficult to infer the physical state of atmospheric aerosol particles directly from field measurements. Laboratory experiments on model mixtures and thermodynamic models are thus required to gain insight into the phases and phase transitions of aerosols. The high variety of organic substances impedes crystallization and the organic fraction remains as a liquid or glass even at low relative humidty (RH) and cold temperatures. The way this organic phase interacts with inorganic salts depends on its hydrophilicity. We use Raman microscopy to investigate the phase transitions of micrometer-sized particles during humidity cycles and a high-speed video camera to observe the efflorescence process. For particles consisting of dicarboxylic acids and ammonium sulfate, liquid-liquid phase separation into an organic-rich and an aqueous electrolyte phase occurs for O:C ratios of 0.7 or lower. Using the thermodynamic model AIOMFAC (Aerosol Inorganic-Organic Mixtures Functional groups Activity Coefficients) we can also model liquid-liquid equilibria and gas/particle partitioning of such particles. While crystal growth occurs within milliseconds in the aqueous electrolyte phase, it is drastically slowed in the highly viscous organic-rich phase. Slow diffusion in glassy aerosol particles indeed keeps particles off thermodynamic equilibrium during humidity cycles, as we have shown for sucrose particles levitated in an electrodynamic balance. This highlights the need to also consider deviations from thermodynamic equilibria caused by diffusion limitations especially at cold and dry conditions.

https://doi.org/10.1180/S0026461X00006502 Published online by Cambridge University Press

Geoneutrino observations and the Earth energy budget

JEAN-CLAUDE MARESCHAL[1], CATHERINE PHANEUF[1], CLAIRE PERRY[1] AND CLAUDE JAUPART[2]

[1]GEOTOP, Université du Québec à Montréal, PO8888, Station Downtown, Montréal, H3C 3P8, Canada
[2]Institut de Physique du Globe de Paris, 1, rue Jussieu, 75238, Paris Cedex 5, France

The total energy loss of the Earth has been calculated to be 46+/-2TW. The heat loss is balanced by the radio-activity of the Earth's crust and mantle, the core heat flow and the mantle secular cooling. The crustal radioactivity is relatively well constrained (6.5+/1TW), but the uncertainty on all the other components is very large. Estimates of core heat flow vary between 5 and 14TW. Mantle cooling could provide between 6 and 18TW. Bulk silicate earth models predict about 13TW for the heat generation in the mantle, but proposed values of mantle heat production vary between 9 and 20TW.

Underground neutrino observatories now have the capability of detecting geo-neutrinos, anti-neutrinos produced by β decay in radio-elements U and Th series.

It is thus hoped that geoneutrino observations will put constraints on the abundance and distribution of U and Th in the mantle and their contribution to the earth's energy budget.

A small error on the crustal heat generation has a large impact on the estimates of the abundance of U and Th in the mantle, because the contribution of the crust to the geoneutrino flux is 4 to 5 times larger than that of the mantle,. Combining heat flux and heat production data is the most robust method to determine with high precision the crustal radio-activity and to predict the crustal geo-neutrino's contribition.

Rare earth element (REE) quantification in geochemical samples: Can we trust commercially available ICP-MS calibration solutions?

E. MARILLO SIALER AND T. MEISEL*

General and Analytical Chemistry, Montanuniversitaet, 8700 Leoben, Austria
(*correspondence: thomas.meisel@unileoben.ac.at)

The ICP-MS technique allows the analyses of individual REE concentrations in a wide range of matrices relevant for geochemists. However, the quantification of concentrations via in the mass spectrum still faces complications due to the vast potential chemical and spectral interferences, arising from complex sample matrices, when quantification is needed. To overcome these interferences, a number of measures including internal standardization, matrix separation, isotope-dilution, the standard addition method, algebraic correction, among others, are employed.

In this work we report the results from the isotopic analysis of fourteen REE in geological materials by ICP-MS. Three different analytical approaches were studied: 1) ICP-MS using matrix matched reference materials (RM) for calibration and 2) HPLC-ICP-MS after Tm addition 3) Isotope Dilution ICP-MS with and without chemical separation. All approaches involve sample dissolution by sodium peroxide sintering to assure complete dissolutions of refractory minerals. The first analytical procedure for determination by ICP-MS uses external calibration curves generated from certified and well characterized, matrix matched geological RM (CRM, provided and certified by the International Association of Geoanalysts, IAG) which were prepared in the same way as the studied samples. The determination by HPLC-ICP-MS comprises spiking with Tm before sample dissolution and a straightforward chromatographic matrix separation procedure. Oxalic and diglycolic acid were used as complexing agents on a Dionex Ionpac CS5A analytical column. Synthetic standard solutions obtained from Inorganic ventures, High Purity Standards and Spex were used for calibration of the HPLC-ICP-MS.

The findings of this study, and the advantages and disadvantages of all methodologies used are discussed. Significant differences between the three calibration strategies were observed for some of the ICP-MS solutions. Thus the traceability of the so called certified ICP-MS standard solutions is questioned and the reliability of the new CRM is highlighted.

https://doi.org/10.1180/S0026461X00006502 Published online by Cambridge University Press

The diagenesis effect on paleo-temperature reconstruction from Precambrian cherts

JOHANNA MARIN-CARBONNE[1,2]*, MARC CHAUSSIDON[1] AND FRANCOIS ROBERT[3]

[1]Universite de Lorraine, CRPG-CNRS 54500 Vandoeuvre les Nancy, France (chocho@crpg.cnrs-nancy.fr)
[2]Department of Earth and Space Sciences, UCLA, CA 90095 USA (*correspondence: jmarin@ess.ucla.edu)
[3]Laboratoire de Mineralogie et Cosmochimie du Museum, Museum d'Histoire Naturelle Paris, France (robert@mnhn.fr)

Cherts are considered as possible proxies of paleo-environmental conditions of the Early Earth. Variations in $\delta^{18}O$ and $\delta^{30}Si$ in Precambrian cherts have been used to reconstruct oceanic temperature [1, 2], and to try to address the Faint Young Sun Paradox. However, these reconstructions did not calculate the diagenesis effect, assumed small, on the isotopic compositions. The *in situ* ion microprobe study $\delta^{18}O$ and $\delta^{30}Si$ of microquartz in cherts of different ages, from 3.50 Ga to 1.88 Ga, allowed better understanding of the origin and the formation of these rocks. These results impact the paleo-temperatures reconstruction for Precambrian seawater [3].

The correlation between Al_2O_3 content and $\delta^{30}Si$ can discriminate diagenetic cherts from hydrothermal or silicified cherts. The diagenetic cherts are from the Gunflint Iron formation (1.88 Ga). These cherts show a typical 2-14 ‰ range for $\delta^{18}O$ and 2-5 ‰ range for $\delta^{30}Si$ at the scale of microquartz grains (~ 2 μm). We interpret this heterogeneity as inherited from the diagenesis. Hence, these variations could be explained by a simple model of dissolution-precipitation of an amorphous silica precursor.

The calculated temperatures from this model ranges from +37° to +52 °C, suggesting an hot ocean during the Precambrian Era if Gunflint cherts are representative of global environment conditions [3]. Taking the diagenesis account decrease the seawater temperatures found by bulk analysis previously.

[1] Knauth L.P. Lowe R.D. (1978) *Earth & Planetary Science Letters*. **41**, 209–222. [2] Robert F. Chaussidon M. (2006) *Nature* **443**, 969–971. [3] Marin-Carbonne *et al*. (2010) *GCA* **74**, 116–130.

The Manicouagan impact crater: A site for testing the accuracy of revisions to the K-Ar system

DARREN F. MARK[1] AND LEAH E. MORGAN[2]

[1]Scottish Universities Environmental Research Centre, East Kilbride, Scotland, G75 0QF, UK
[2]Dept. of Petrology, Vrije Universitiet, De Bolelaan 1085, 1081HV Amsterdam, Netherlands

Compared with the U-Pb geochronometer the K-Ar system still retains relatively large systematic uncertainties. Recent studies have attempted to improve the accuracy of the Ar/Ar method by determination of an accurate age for Fish Canyon sanidine (FCs) [2, 4] and the K-Ar decay constants [3]. The results vary by 1%, beyond what is expected from analytical precision. Although the magnitude of this uncertainty is difficult to assess in single experiments, one can examine whether the amount of dispersion in the three latest revisions represent true external reproducibility and thus reflect geological uncertainties?

Inter-comparison of one Ar/Ar (sanidine) age with one U-Pb (zircon) age is problematic (e.g. zircon magma residence time). Sanidine and zircon have markedly different closure temperatures for the retention of daughter products so we are commonly faced with the question: what are these minerals dating and at what level can we assume equivalence?

Melt rocks from large terrestrial impact events are an ideal target for an Ar/Ar – U-Pb inter-comparison study as they have a somewhat simple crystallization and cooling history and do not suffer the protracted crystallization histories that typify magma-chamber process. Ramezani *et al*. [1] determined a high-precision ID-TIMS ^{206}U-^{238}Pb age for zircon from the Manicouagan impact crater. Here we present a high-precision Ar/Ar age for the coeval sanidine. We will discuss revisions to the age of FCs and the K-Ar decay constants, and show that the latest proposed age for FCs (Channell *et al*. 2010) is not consistent with our data. The approach allows us to get beyond the question of 'what are we dating?' and assess the inter-calibration of the Ar/Ar and U-Pb chronometers at a level approaching analytical precision.

[1] Ramezani *et al*. (2005) 19th Goldschmidt Conference abstract, 321. [2] Kuiper *et al*. (2008) *Science* **320**, 500–504. [3] Renne *et al*. (2010) *GCA* **74**, 5349–5367. [4] Channell *et al*. 2010, *G-Cubed* **11**, 1–21.

https://doi.org/10.1180/S0026461X00006502 Published online by Cambridge University Press

Mineralizations monitor depth and composition variations of paleohydrothermal fluid systems

G. MARKL* AND S. STAUDE

Eberhard Karls Universität Tübingen, Wilhelmstrasse 56, 72072 Tübingen, Germany
(*correspondence: markl@uni-tuebingen.de)

More than 1000 hydrothermal mineralizations in the Schwarzwald ore district of SW Germany formed discontinuously over the last 300 Ma [1]. Fluid inclusions, structural and mineralogical specifics allow to distinguish six different mineralizing fluid systems [2]. Most mineralizations formed by mixing of a deep-seated and a near-surface fluid. Interestingly, ore mineral compositions (especially fahlore [3]) and fluid inclusion systematics appear to reflect the relative importance of the deep and the shallow fluid systems, while e.g. Sr or Pb isotope systematics allow to quantify their contributions more precisely in some cases. Stable sulfur, oxygen and carbon isotope systematics allow to draw conclusions regarding the source of these (and geochemically similar) elements.

Combination of these various methods allows to characterize paleofluid systems with respect to their composition, their timing and their ore-forming potential in great detail on a district-wide scale and thereby help to understand the communication of deep and shallow aquifers over time in a typical crustal block of 100x50 km size.

[1] Pfaff *et al*. (2009) *Eur. J. Min.* **21**, 817. [2] Staude *et al*. (2009) *EPSL* **286**, 387. [2] Staude *et al*. (2010) *Min. Mag.* **74**, 309.

Volatile elements in apatite: An integrated analytical approach with special focus on bromine

M.A.W. MARKS[1]*, M. WHITEHOUSE[2], T. WENZEL[1], H. STOSNACH[3] AND G. MARKL[1]

[1]Universität Tübingen, 72074 Tübingen, Germany (*correspondence: michael.marks@uni-tuebingen.de)
[2]Swedish Museum of Natural History, Stockholm, Sweden
[3]Bruker Nano GmbH, Schwarzschildstrasse 12, D-12489 Berlin, Germany

We analyzed a Durango apatite crystal and apatites from five plutonic samples from the alkaline Mt. Saint Hilaire Complex (Canada) by means of Electron Microprobe Analysis (EPMA), Laser Ablation ICP-MS (LA-ICP-MS), Secondary Ion Mass Spectrometry (SIMS), pyrohydrolysis combined with ion chromatography, Fourier Transformed Infrared Spectroscopy (FTIR), Instrumental Neutron Activation Analysis (INAA) and Total Reflection X-ray Fluorescence Analysis (TXRF).

The focus of our study are volatile elements (F, Cl, Br, S, C) with a special emphasis on Br, since the analytical possibilities for this element are especially in the low- to sub-μg/g range restricted and thus, reliable concentration data for Br in rock-forming minerals are scarce. We demonstrate here that TXRF, which is barely used in geosciences so far, is suitable for analyzing the bulk content of Br and Cl as well as of a range of important minor and trace elements (e.g. Sr, Ce, Fe, Mn, As) in apatite simultaneously. The TXRF method combines the advantages of low to very low detection limits (μg/g- to sub-μg/g range), small sample amounts needed (mg range) and a relatively fast and inexpensive analytical procedure. In the case of apatite, reliable concentration data for Br can be produced with detection limits in the sub-μg/g range. The analysis of Cl is also possible, if a suitable correction method, which accounts for the observed systematic underestimation, is applied. For investigations, where space-resolved data are needed, a large geometry SIMS machine offers the possibility to analyze F, Cl, Br and S if reliable data for suitable reference materials exist.

Based on our data, we propose an average Br concentration of around 0.1 μg/g as a preliminary reference value for the Durango apatite. However, more data on the Br content of the Durango apatite are needed in order to validate this value.

https://doi.org/10.1180/S0026461X00006502 Published online by Cambridge University Press

Endolithic anaerobic methane oxidation at cold seeps

JEFFREY J. MARLOW*, JOSHUA STEELE AND VICTORIA J. ORPHAN

California Institute of Technology, MC 100-23, 1200 E. California Blvd., Pasadena, CA 91125 (*correspondence: jjmarlow@caltech.edu)

The anaerobic oxidation of methane (AOM) at deep sea cold seeps has been the target of much work over the last decade, as researchers have sought to characterize complicated syntrophic relationships [1], identify metabolically relevant chemical species [2], and understand the role of AOM in the broader carbon cycle [3]. However, much of this work has focused on cold seep sediments, and comparatively little is known about the associated authigenic carbonates that are formed as a product of AOM. If biologically active, these rocks would contribute significantly to AOM processes in the global deep ocean environment.

Here we describe a unique microscopy and molecular study of cold seep endolithic environments that compares sediments, protolithic carbonate nodules, carbonate rocks associated with active methane seepage ('active'), and carbonate rocks from dormant seep areas ('inactive'). Image analysis and cell staining with DAPI and domain-specific CARD-FISH probes showed abundant cell aggregates in all environments including the interiors of the 'inactive' carbonates. Carbonate rocks from active seep habitats contained the largest and most abundant cell aggregates, with average diameters around 10 um. 16s rRNA gene sequences and T-RFLP analyses revealed syntrophic methane oxidizing archaea and sulfate reducing bacteria, in keeping with previous studies. X-ray diffraction exposed mineralogical differences between samples; a relative abundance of metal-based minerals in rock interiors could expose cells to additional electron acceptors and accommodate larger, more abundant aggregates.

A quantitative model of methane uptake based on aggregate density, theoretical enzyme kinetics, measured methane concentrations, and carbonate rock porosity will be presented to demonstrate the role of carbonate pavements in overall methane consumption. The finding of active endolithic AOM consortia expands our understanding of where and how AOM occurs, suggesting that a significant – possibly dominant – component of AOM activity in cold seep habitats may occur within lithified carbonates at and within the seabed.

[1] Orphan *et al*. (2002) *PNAS* **99**, 7663–7668. [2] Beal, E.J. *et al*. (2009) *Science* **325**, 184–187. [3] Reeburgh, W.S. (2007) *Chemical Reviews* **107**, 486–513.

Elastic properties of nano-crystalline MgO to high pressures by Brillouin scattering

HAUKE MARQUARDT[1], ARIANNA GLEASON[2], KATHARINA MARQUARDT[1], SERGIO SPEZIALE[1], LOWELL MIYAGI[3], GREGOR NEUSSER[4], HANS-RUDOLF WENK[2] AND RAYMOND JEANLOZ[2]

[1]German Research Center for Geosciences (GFZ), Telegrafenberg, 14473 Potsdam, (hama@gfz-potsdam.de)
[2]Department of Earth and Planetary Science, University of California, Berkeley, CA 94720
[3]Geology and Geophysics Department, Yale University, P.O. Box 208109, New Haven, CT 06520
[4]Institute for Geological Sciences, Freie Universität Berlin, 12249 Berlin, Germany

Recent Brillouin scattering results on the sound wave velocities of MgO powder compressed under non-hydrostatic conditions show velocities that are around 20% lower than expected from single-crystal data [1]. These results question the reliability of Brillouin scattering of polycrystalline materials and they illustrate that several poorly understood processes might affect the derived sound wave velocities, including a preferred orientation of the crystallites (texturing), non-hydrostatic conditions in the diamond-anvil cell, and grain size effects.

Here, we report the elastic properties of nano-crystalline MgO powder determined by Brillouin scattering to pressures above 30 GPa. We find the acoustic velocities to be significantly lower than reported data on single-crystal MgO. A careful characterization of the crystallite sizes in our sample material by synchrotron x-ray diffraction and high-resolution scanning and transmission electron microscopy shows that the average crystallite size stabilizes at about 7 nm at high pressures. The small crystallite size has a profound effect on the elastic properties and is responsible for the observed low velocities in MgO. We show that this effect prevails at high pressures.

Based on our first data analysis, zero-pressure bulk and shear moduli of the intercrystalline material (mostly grain boundaries) are reduced by about 70 % and 80 %, respectively, as compared to the crystalline material. The effect of grain size on the measured velocities is by far exceeding any effects of non-hydrostaticity and texturing. Our findings imply that a thorough characterisation of the crystallite size distribution is crucial for the interpretation of Brillouin scattering results from polycrystalline materials.

[1] Gleason *et al*. (2011) *GRL* **38**, L03304.

https://doi.org/10.1180/S0026461X00006502 Published online by Cambridge University Press

Synchrotron X-ray diffraction of nano-crystalline MgO Powder to 65 GPa

HAUKE MARQUARDT[1], SERGIO SPEZIALE[1], HANS JOSEF REICHMANN[1] AND HANNS-PETER LIERMANN[2]

[1]German Research Center for Geosciences (GFZ), Telegrafenberg, 14473 Potsdam (hama@gfz-potsdam.de)
[2]DESY, PETRA III, Notkestr. 85, 22607 Hamburg

The compression behavior of nano-crystalline materials (crystallite sizes smaller than 100 nm) might significantly differ from the behavior of larger grained materials.

We compressed MgO powder with an average crystallite size of about 20 nm in a diamond-anvil cell. The sample material was loaded either with or without a pressure-transmitting medium. Our results indicate that the crystallite size is preserved in the quasi-hydrostatic experimental run, whereas it reduced to below 10 nm in the non-hydrostatic experiment.

High-pressure synchrotron x-ray diffraction was performed at DESY/PETRA III beamline P02.2 using an energy of about 42.8 keV, a focusing spot of ~2 x 2 μm^2, and a collection time of 30-60 seconds. Up to nine diffraction lines could be detected at high-pressures.

Our results that were collected in hydrostatic conditions indicate that the zero-pressure bulk modulus is slightly decreased as compared to large-grained MgO [1], but both zero-pressure volume and zero-pressure derivative of the bulk modulus are unaffected within the experimental uncertainties. The material that was non-hydrostatically compressed appears to be less compressible compared to the same (starting) material that was quasi-hydrostatically pressurized. The compression behaviour in this run is, however, likely also influenced by a continuous crystallite size reduction and the consequent increase of the volume fraction of intercrystalline material in the sample, that occurs upon compression in non-hydrostatic conditions.

[1] Speziale *et al*. (2001) *JGR* **106**, 515–528.

Focused ion beam cutting of large samples for Brillouin spectroscopy

KATHARINA MARQUARDT AND HAUKE MARQUARDT

German Research Center for Geosciences (GFZ), Telegrafenberg, 14473 Potsdam (hama@gfz-potsdam.de)

Brillouin spectroscopy is a major technique for the determination of elastic properties of single-crystals at high-pressures and high-temperatures. Brillouin scattering at extreme conditions is usually carried out in symmetric platelet forward scattering geometry, which allows for a straightforward evaluation of shear and compressional velocities. However, well-polished platelet samples with parallel faces are required. Mechanical polishing is restricted to materials of sufficient size and mechanical stability. This precludes the preparation of a number of compounds with significant geophysical relevance, including both natural samples and candidate Earth materials that are synthesised at high-pressure/high-temperature conditions (for instance ferropericlase, perovskite).

Here, we show that ion cutting and polishing is a very elegant approach to prepare μm-sized samples of well-defined thickness with high surface quality. It does not expose the samples to mechanical forces, thus allows for preparing materials that are brittle, meta-stable, or show a strong cleavage. In addition, it offers the chance to cut more than one sample from a piece of material, for instance two platelets with different orientation from one single-crystal (fig. 1). A transmission electron microscopy (TEM) foil can be produced simultaneously. This allows for a detailed characterization, including chemical composition, crystallographic orientation, defect structure and secondary phases, of the same sample material, i.e. the same single-crystal, that is later used for optical spectroscopy.

We successfully tested this method on different geomaterials, including perovskite, ferropericlase, spinel, and antigorite.

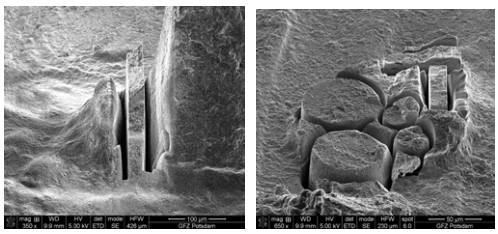

Figure 1: Secondary electron images of a perovskite single-crystal platelet that was cut from an aggregate made up of several single-crystals. The platelet, with approximate dimensions of 180 x 180 x 30 μm^3, was double-side polished (left). The platelet was manually flipped by 90° and again inserted into the dual beam machine (right). Several samples were cut for Brillouin spectroscopy, single-crystal x-ray diffraction and TEM analysis.

https://doi.org/10.1180/S0026461X00006502 Published online by Cambridge University Press

Geochemistry and mineralogy of volcanic ash red paleosol from Fogo island (Cape Verde)

R. MARQUES[1,3], M.I. PRUDÊNCIO[1,3], J.C. WAERENBORGH[1], F. ROCHA[2,3], M.I. DIAS[1,3] AND E. FERREIRA DA SILVA[2]

[1]Instituto Tecnológico e Nuclear, EN 10, Sacavém, Portugal
[2]Dep. Geociências, Univ. Aveiro, Aveiro, Portugal
[3]GeoBioTec, Univ. Aveiro, Aveiro, Portugal

Introduction

Red paleosols developed on volcanic ashes occur in Fogo island (Cape Verde, semi-arid climate). Four samples were collected in a vertical profile (70 cm depth) of paleoweathered volcanic ashes (Monte Almada, western Fogo) with decreasing grain size upwards and varying in colour: P1-1- dark gray + dark reddish brown; P1-2 – dark yellowish brown + yellowish brown; P1-3 – red; and P-4 – weak red at the top. The paleosol is underlayed by carbonatite and covered by nephelinite lavas. Chemical and mineralogical analyses were done by INAA, Mössbauer spectroscopy and XRD.

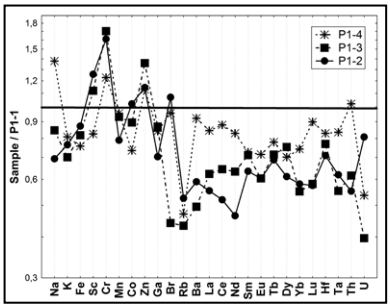

Figure 1: Chemical variations with depth.

Discussion of Results

A general decrease of the analysed chemical elements (rare earth elements included) occur in the upper levels (Fig.1, where sample P1-1, collected at the bottom, was used as reference). Exceptions were found for Cr and Zn. Na is enriched at the top level. Quartz, augite and phyllosilicates are ubiquitous. Magnetite is present in the lower P1-1 and P1-2 levels and gradually oxidizes towards maghemite in P1-3 and P1-4. Hematite is observed in all samples, its content increasing upwards. Fe^{2+} is incorporated in phyllosilicates and augite throughout the profile. The Fe^{2+}/Fe^{3+} ratio is slightly lower in the surface level.

Horozontial and vertical water mass tracing of the SW Pacific Ocean during the last deglaciation

J.P. MARR[1], J.A. BAKER[1], L. CARTER[1], A. ALLAN[1], K. CHRISTENSEN[1] AND H.C. BOSTOCK[2]

[1]Victoria University of Wellington, Wellington, New Zealand (*correspondence: julene.marr@vuw.ac.nz)
[2]National Institute of Water and Atmospheric Research, Wellington, New Zealand

We have measured Mg, Al, Mn, Zn, Sr and Ba/Ca ratios for *Globigerina bulloides* by LA-ICPMS, in a high-resolution marine sediment core (MD97-2121, 40°22.935′S; 177°59.68′E; 25 ka to present) from the SW Pacific Ocean at centennial scale resolution. The core site resides beneath two major, interacting surface water masses (Subtropical Water [STW], Sub-Antarctic Water [SAW]). Mg/Ca ratios record a change in mean ocean temperature of 6°C from the last glacial period to the Holocene, with a maximum regional temperature difference of 11°C. Alkenone paleo-ocean temperatures from the same core record significant differences with an earlier (2 kyr) onset of deglaciation, subdued short-term temperature variability and do not define the Antarctic Cold Reversal, which is clearly visible in the Mg/Ca record. Mg/Ca ratios in the final (*f*) and antepenultimate (*f-2*) chamber of *G. bulloides* appear to reflect its migration through the water column at differing stages of its life cycle. Holocene Mg/Ca values have a 20% difference between chambers f and f-2 compared to 10% during the last glacial period, suggesting a reduction in the glacial surface ocean thermal stratification. Measurement of Mn, Ba and Zn in *G. bulloides* from a regional suite of core-tops potentially discriminates STW and SAW. The down-core results demonstrate a dominance of SAW during the last glaciation when enhanced winds forced northward transport of surface waters, accompanied by increased upwelling, and a prominence of STW during the Holocene.

https://doi.org/10.1180/S0026461X00006502 Published online by Cambridge University Press

Controls on modern and paleo-shell weights of *G. bulloides* in the SW Pacific Ocean

JULENE MARR, ANNETTE BOLTON, KYLIE CHRISTIANSEN, JOEL BAKER* AND LIONEL CARTER

Victoria University of Wellington, P.O. Box 600, Wellington, New Zealand (*correspondence: joel.baker@vuw.ac.nz)

Shell weights of the planktic foraminfera *G. bulloides* have been used to track changes in near-surface ocean carbonate ion concentrations over the past 50 kyr in the Atlantic Ocean [1], and to hypothesize that anthropogenic atmospheric CO_2 increases and ocean acidification resulted in decreases in modern *G. bulloides* shell weights as compared to mean Holocene weights in the Southern Ocean [2]. We have carried out a study of the test sizes and weights, and trace element chemistry of 'modern' *G. bulloides* in sediment core-tops from the SW Pacific Ocean (latitudes 33-53°S; T=7-19°C). Mean size-normalized shell weights (SNW) correlate negatively with near-surface ocean temperature in the SW Pacific Ocean ($T = 31.8 \times e^{-30.5 \times SNW}$) and, unlike the study of [1], shell weights are heaviest in southernmost sites of *lowest* temperatures and *lowest* carbonate ion concentrations. Similar suites of data have been obtained for *G. bulloides* from sites offshore of eastern New Zealand for the past 25 kyr covering the last deglaciaton, and MIS-33 to MIS-29 encompassing the warm MIS-31 interglacial when collapse of the Ross Ice Shelf and substantive ice loss from West Antarctica may have occurred [3]. Hypothetical *G. bulloides* SNW can be calculated for these paleo-records using the modern relationship between ocean temperature and SNW, Mg/Ca paleo-ocean temperatures, and then compared with measured SNW. In the current interglacial (<10 kyr) and the MIS-29 interglacial, measured SNW are in good agreement (within 10%) of predicted values. However, during the last and MIS-30 glacial periods, measured SNW are often more different (up to 30%) than predicted SNW, although the modern ocean temperature-SNW relationship is still the prominent control on SNW. During and prior to MIS-31, measured SNW deviate significantly (up to 100%) from predicted vaues and, in fact, correlate positively with Mg/Ca paleo-ocean temperatures and, presumably, are largely controlled by carbonate ion concentrations. These results demonstrate the complexity in attributing changes in *G. bulloides* SNW to one process both in different ocean settings and also back in time at a single site in the SW Pacific Ocean.

[1] Barker & Elderfield (2002) *Science* **297**, 833–836. [2] Moy *et al*. (2009) *Nature Geoscience* **2**, 276–280. [3] Pollard & deConto (2009) *Nature* **458**, 329–332.

Water dynamics in clay as a function of temperature: Coupling Neutron Spin Echo and molecular dynamics

V. MARRY[1]*, E. DUBOIS[1], N. MALIKOVA[2], M. SALANNE[1], S. LONGEVILLE[2], W. HAUSSLER[3] AND J. BREU[4]

[1]Univ Pierre et Marie Curie – Paris 6, UMR-UPMC-CNRS-ESPCI 7195, Case 51, 4 Place Jussieu, 75252 Paris, France (*correspondence: virginie.marry@upmc.fr)
[2]Laboratoire Léon Brillouin, UMR CEA-CNRS 12, CEA Saclay, 91191 Gif-sur-Yvette, France
[3]FRM-II & E21, Technishe Universität München, Lichtenbergstrasse 1, 85747 Garching, Germany
[3]Institut für Anorganische Chemie, Universität Regensburg, 93040 Regensburg, Germany

In the context of underground storage of radioactive waste, investigating water molecules dynamics in swelling clays considered in engineered barriers is of prime importance. In the vicinity of the canisters containing the nuclear waste, the temperature can reach more than 350K. Swelling clay minerals are lamellar alumino-silicates with permanent negative charge compensated by exchangeable cations situated between clay layers. In contact with water, the cations hydrate, leading to the formation of one, two or more layers of water confined between clay surfaces.

We study the translational dynamics of water in clays in low hydrated states by coupling quasi-elastic neutron scattering experiments (Neutron Spin Echo or NSE) and molecular dynamics (MD) on a large scale of temperature range where water remains liquid. As the natural montmorillonite clay of interest is complex to analyze because of interstratification, we chose to model it by a synthetic clay with well-defined states of hydration [1]. The activation energies of the diffusion processes determined by NSE are around 6 kJ/mol higher than for bulk water, for both the hydration states studied. The simulations are found to be in good agreement with experiments for relevant set of conditions [2] and they allow more insight into the origin of the observed dynamics, like the influence of hydrogen bonding and specific interactions with the surfaces.

[1] Malikova,N. *et al*. (2007) *J. Phys. Chem. C* **111**, 17603–17611. [2] Marry,V. *et al*. (2011) *Environ. Sci. Technol*. **45**, 2850–2855.

https://doi.org/10.1180/S0026461X00006502 Published online by Cambridge University Press

Competition between lanthanides and Al for humic acid binding

R. MARSAC*, M. DAVRANCHE, G. GRUAU AND A. DIA

Geosciences Rennes, Rennes 1 Univ., UMR 6118 CNRS, France (*correspondence: remi.marsac@univ-rennes1.fr)

Lanthanides or rare earth elements (REE) are commonly studied as analogues of actinides. This group of 14 elements present a unique feature related to their similar and coherent chemical properties. In natural waters, REE aqueous concentrations and transport is strongly affected by dissolved organic matter such as humic acids (HA). However, in organic-rich waters, different REE concentration patterns are observed. A first explanation is the heterogeneity of HA binding sites: REE-HA pattern is the fingerprint of the dominant REE binding HA sites. Previous study showed that light REE (LREE) are more bound to HA carboxylic sites whereas heavy REE (HREE) are more bound to HA phenolic sites. Secondly, in natural waters, various cations are also bound to HA and might therefore affect REE-HA binding and subsequent pattern. Al is one of the major competitor cation for REE regards to its high affinity for HA and it strong concentration in natural waters.

Al-REE competition experiments for HA binding were performed between pH 3 and 6. Results were modelled with Model VI, a specific humic-ion binding model. It appeared that Al^{3+} and $Al(OH)^{2+}$ present the same affinity for HA sites as already assumed in Model VI. However, Al^{3+} and $Al(OH)^{2+}$ are stronger competitors for HREE than LREE, which is not expected in the model and was attributed to Al strong affinity for HA phenolic groups. From pH 5 to 6, Al competitive effect decreases because of $Al(OH)_3$ precipitation. However, Al becomes more competitive for LREE than HREE regards to the $Al(OH)_2^+$ binding to HA carboxylic groups. Model VI parameters were re-evaluated and, for the first time, $Al(OH)_2^+$ was also considered to bind to HA. The new set of Al parameters improved model accuracy for both our REE-Al competitive experiments and Al-HA data from literature.

REE-Al competitive study for HA shows a new Al-HA binding mechanisms which was not observed before. These results highlight the strong impact of competitor cations on the REE-HA binding behaviour in natural organic-rich waters. This study provides a more accurate description of Al-HA binding and, therefore, will indirectly improve REE and actinides speciation modelling in environmental systems.

Recycling agents in subduction zones: Fluids, melts and solids!

HORST R. MARSCHALL[1] AND JOHN C. SCHUMACHER[2]

[1]Dep. of Geology & Geophysics, WHOI, Woods Hole, MA 02543, USA, (hmarschall@whoi.edu)

[2]Dep. of Earth Sciences, University of Bristol, Bristol BS8 1RJ, UK, (j.c.schumacher@bristol.ac.uk)

Sediment melts and hydrous fluids loaded with solutes generated in the subducting slab at elevated *P-T* conditions are thought to transport differing amounts of trace elements and variable isotopic signatures from the subducting slab into the overlying mantle, where they ultimately contribute to the source region of magmas produced at convergent plate margins. Conventional geochemical models of subduction zones consider trace elements to be derived from two distinct sources: hydrous fluids derived from altered oceanic crust during subduction and partial melts derived from the thin sedimentary veneer. However, the physical processes of transport and mixing of these contributors within the subduction factory are largely enigmatic.

Studies on exhumed subduction mélanges suggest that hybrid rocks with newly grown minerals concentrate, sequester and redistribute water and key trace elements [1, 2]. The strong petrologic and chemical contrast at the slab-mantle interface, produces these hybrid rock compositions by metasomatic reactions, diffusion and mechanical mixing: the Al-, Si- and alkali-rich slab that carries crustal isotopic signatures and trace-element abundances is juxtaposed with the Mg-rich ultramafic rocks of the harzburgitic mantle. Mechanical mixing of crustal and mantle rocks will propagate the formation of hybrid rocks, and fluxing by hydrous fluids derived from the dehydrating slab will enhance reactivity and lead to fluid saturation of the newly formed rocks.

The identification of cold plumes in high-resolution numerical experiments [3] provides a mechanism to transport buoyant hybrid rocks from the slab-mantle interface towards the source region of arc magmas. Mélange rocks travelling into the mantle wedge in ‘wet’ diapirs would be subjected to *P-T* conditions dramatically different from those at the slab surface. Partial melting of hybrid rocks may produce the large range of major and trace-element compositions found in modern island arc volcanic rocks.

[1] Bebout & Barton (2002) *Chem. Geol.* **187**, 79–106. [2] Miller *et al.* (2009) *Lithos* **107**, 53–67. [3] Zhu *et al.* (2009) *G-cubed* **10**, Q11006.

https://doi.org/10.1180/S0026461X00006502 Published online by Cambridge University Press

Erosion monitored by riverine sediment Ti-in-quartz, Southern Alps, New Zealand

C.E. MARTIN*, K.B. MCKERCHER AND J.M. PALIN

Dept. of Geology, Univ. of Otago, P.O. Box 56, Dunedin 9054 NZ (*correspondence: candace.martin@otago.ac.nz)

Quartz is an abundant mineral in the surface environment, and can have as its source a variety of primary and recycled sources. Recent developments have shown that Ti incorporation into quartz is proportional to crystallization temperature, pressure, and *a* (TiO_2) [1, 2]. We have explored the use of Ti and other trace elements as a fingerprint of the source of quartz sediment in rivers draining the actively uplifting and eroding Southern Alps of New Zealand.

The Haast River drains the western side of the Southern Alps and experiences very high rainfall and erosion rates. The bedrock schist within the catchment exhibits a metamorphic field gradient from chlorite through garnet-oligoclase zone. Quartz in these rocks have Ti concentrations that reflect prograde re-equilibration of detrital grains and crystallization of new quartz in the presence of ilmenite or titanite at appropriate pressures [3].

Sediment was collected along the length of the river system and sieved to obtain grain size fractions. Quartz grains from each size fraction were mounted in epoxy, polished and analyzed by LA-ICP-MS. Raw intensity data were normalized via analyses of the NIST 610 standard to obtain trace element concentrations. Ti-in-quartz temperatures [1, 2] were calculated using estimated pressure and *a* (TiO_2) for the schist bedrock.

Quartz sediment shows changes in trace element concentrations and Ti-temperature with location that reflect the metamorphic grade of the upstream bedrock. Several samples exhibit smooth variations with grain size. Bulk chemistry and mineralogy of bedload sediment have previously shown that physical erosion dominates over chemical weathering processes in the Haast River catchment but were unable to discriminate the bedrock sources [4]. Our results for the Haast River indicate that Ti-in-quartz can be a sensitive provenance tracer for sand; we are currently analyzing quartz sediment from other active river systems and sedimentary basins on the South Island in order to assess the robustness of the method.

[1] Wark & Watson (2006) *Contrib. Min. Petrol.* **152**, 743–754. [2] Thomas *et al.* (2010) *Contrib. Min. Petrol.* **160**, 743–759. [3] Palin *et al.* (2011) *MinMag,* this volume. [4] Kautz & Martin (2007) *Appl. Geochem.* **22**, 1715–1735.

Contribution of groundwater to chemical weathering fluxes in the Pingtung Plain, Taiwan

CAROLINE MARTIN[1]*, ALBERT GALY[1], NIELS HOVIUS[1], MIKE BICKLE[1], IN-TIAN LIN[2], MING-JAME HORNG[3], DAMIEN CALMELS[4], HAZEL CHAPMAN[1] AND HONGEY CHEN[5]

[1]Dept. Earth Sciences, University of Cambridge (*correspondence: ceam4@cam.ac.uk)
[2]Institute of Earth Sciences, Academia Sinica, Taipei, Taiwan
[3]Water Resources Agency, Ministry of Economic Affairs, Hsin-Yi Road, Taipei, Taiwan
[4]Institute de Physique du Globe, Paris, France
[5]Dept. of Geosciences, National Taiwan University

The concentration of dissolved cations in flowing groundwaters of the Pingtung Plain gravel, sand and clay aquifer systems in southwest Taiwan demonstrates that underground circulation is a significant source of major and trace ions to the ocean for Taiwan, comparable in magnitude to the weathering flux measured in the surface runoff of the Pingtung Plain in the Kaoping River. The waters from 33 wells at varying depths through a 280 m window in the plain were analysed for cations: Ca^{2+}, Mg^{2+}, Na^{+}, K^{+}, Sr^{2+}, Fe^{2+} and Ba^{2+}, and anions: Cl^{-}, SO_4^{2-} and NO_3^{-}, and compared with a 5-year bi-weekly time series from the Kaoping River. Multi-year hydrological head data gives the direction of groundwater flow through the drilled depth of the basin, and indicates that pumping of the aquifer for irrigation and fish farming has had a limited effect on the hydrological stability of the system. Hydraulic conductivities for each well location show that hydrological connectivity exists throughout the drilled depth of the basin whereas chemical gradients suggest that stratified flow is in operation. At the proximal position of the groundwater flow paths, the concentration of dissolved species in the groundwater ranges from 1.1 to 3.3 times that of the Kaoping River; increasing to 2.3 to 8.5 times the Kaoping River values at the coastal region of the aquifer, indicating that net chemical weathering occurs along subsurface flow pathways. When compared to the 5-year time series for the Kaoping River, the relative contribution of subsurface fluxes is between 40 to 50% for Na, K, Sr, Ca and around 30% for Mg and SO_4. The results suggest submarine groundwater discharges in the Taiwan strait and that the impacts of groundwater from active margins on global ocean geochemcial budgets need to be much better constrained.

https://doi.org/10.1180/S0026461X00006502 Published online by Cambridge University Press

Nd and Hf model ages in the Western Gneiss Region, Norway: A new way to better understand mantle-crust evolution

CÉLINE MARTIN[1,2], STÉPHANIE DUCHÊNE[1,3], BÉATRICE LUAIS[1] AND ETIENNE DELOULE[1]

[1]CRPG, Nancy-Université, CNRS, 15 rue Notre Dame des Pauvres 54501 Vandoeuvre les Nancy cedex
[2]present adress: DGLG – WE - Vrije Universiteit Brussel, Pleinlaan, 2 B-1050 Brussels
[3]present adress: LMTG, UMR 5563, CNRS - UPS Toulouse III - IRD, 14 rue Edouard Belin, 31400 Toulouse

The signification of Hf model ages is revisited through the study of metabasites and their gneissic host-rock of Vårdalsneset (Western Gneiss Region, Norway), with the comparison of Nd and Hf model ages, that are assumed to be similar for a given sample.

Three different mantle-crust differentiation models currently exist on the basis of Nd and Hf isotope systematics: (i) the canonical model with chondritic Earth and an unique early step of differentiation, (ii) a model with chondritic Earth and a continual growing crust since 3 Ga and (iii) a model with sub-chondritic Earth and a continual growing crust since 4.56 Ga, and they remain to debate. It is therefore expected that Nd and Hf model ages calculations could allow the validation of one of these models.

Rock protoliths as well as trace-element mobility are characterized by a petrological and geochemical study. Metabasic samples likely came from cumulates and MORB-type basalt whereas gneiss could represent paragneiss and not orthogneiss as usually accepted in the WGR of Norway.

As the trace elements appear slightly mobile, the Nd and Hf isotopic data enable to calculate model ages.

Interestingly, whatever the crust-mantle differentiation model used, Nd model ages are equal within error contrarily to Hf model ages (Table 1).

	Nd (i)	Hf (i)	Nd (ii)	Hf (ii)	Nd (iii)	Hf (iii)
min	1.44±0.35	2.18±0.39	1.16±0.30	1.44±0.38	1.09±0.34	1.22±0.39
max	1.87±0.02	3.21±0.52	1.44±0.06	1.97±0.78	1.31±0.04	1.56±0.38

Table 1: Nd and Hf model ages in Ga calculated on metabasites for the three mantle-crust differentiation model.

We assume that both Nd and Hf model ages should be in agreement with metabasites zircon U-Pb age (1.15 ± 0.20 Ga). Thus, we show that only the third model with sub-chondritic Earth and a continual growing crust since 4.56 Ga allows to obtain significant model ages with both Nd and Hf isotopic systems ranging from 1.09 ± 0.34 to 1.56 ± 0.38 Ga.

Pb isotopic history of weathering on Antarctica during the Eocene-Oligocene transition

ELLEN E. MARTIN[1] AND CHANDRANATH BASAK

Dept. of Geological Sciences, Univ. of Florida, Gainesville, Fl 32611, USA (eemartin@ufl.edu, basakc1@ufl.edu)

The initiation of Antarctic continental glaciation at the end of the Eocene is one of the most dramatic climate events in the Cenozoic. Drawdown of atmospheric CO_2 below a threshold value is considered one of the prerequisites for this glacial transition, suggesting a possible role for silicate weathering. In this study we compare Pb isotopes recorded in Hydroxylamine Hydrochloride extractions (seawater) and residual terrigenous material from two intermediate water, circum-Antarctic sites (ODP Sites 689 and 738) to evaluate the extent of chemical weathering and the composition of weathered material during the Eocene/Oligocene transition (EOT). Prior to the EOT, seawater and residues record similar $^{206}Pb/^{204}Pb$, $^{207}Pb/^{204}Pb$ and $^{208}Pb/^{204}Pb$ values. At the EOT, both sites record increasing seawater and residue $^{207}Pb/^{204}Pb$ and $^{208}Pb/^{204}Pb$ values, with some structure apparent in the higher resolution record of Site 738 that matches the two-step glacial transition defined by $\delta^{18}O$. In contrast, $^{206}Pb/^{204}Pb$ values for seawater become more radiogenic at both sites, while values for residues become less radiogenic.

The similarity between seawater and residue values for all three Pb isotopic systems suggest extensive, congruent chemical weathering that may have started during the warm Eocene, an interpretation supported by other proxies. Variations in residue Pb isotopes starting at the EOT imply intensified mechanical weathering that incorporated multiple silicate source rocks with different chemical compositions. This interpretation is consistent with the idea that the glaciers weathered rocks from a broader region as they grew. The fact that seawater Pb isotopic values track residue values argues that the silicate mechanical weathering products from the glaciers were exposed to active chemical weathering and controlled the local seawater Pb isotopic signal. This silicate weathering could have contributed to the drawdown of atmospheric CO_2. The correlation with the $\delta^{18}O$ two-step also implies that intervals of cooling and ice growth were associated with weathering pulses. The pattern for $^{206}Pb/^{204}Pb$ values is distinct from the other two isotopic systems after the EOT and is interpreted to represent weathering of Phanerozoic carbonates that contribute uranogenic, but not thorogenic, Pb. Weathering inputs from these carbonate source rocks may have contributed to deepening of the carbonate compensation depth.

https://doi.org/10.1180/S0026461X00006502 Published online by Cambridge University Press

Experimental determination of CO_2/H_2O in subduction zone fluids by GC-TCD analysis

LAURE A.J. MARTIN[1] AND JOERG HERMANN[2]

[1]Research School of Earth Sciences, The Australian National University, 0200 Canberra (laure.martin@anu.edu.au)
[2]Research School of Earth Sciences, The Australian National University, 0200 Canberra (joerg.hermann@anu.edu.au)

Carbon recycling in subduction zones plays an important role in the evolution of climate through geological time and in the formation of diamonds in the deep mantle. Carbonates formed during seafloor alteration of the oceanic crust are buried into the deep Earth along subduction zones. Experimental studies on the phase stability in H_2O-CO_2-bearing basaltic compositions indicate that the fluid at sub-arc depth is dominated by H_2O [1]. However, experimental studies are hampered by the difficulty to estimate accurately the H_2O/CO_2 of the fluid in the experimental products.

We conducted experiments with a starting material made of a synthetic K_2O, CO_2 and H_2O-bearing basaltic composition between 3.0 and 3.5 GPa, 700 - 775°C in a piston-cylinder apparatus. The experimental results indicate that the solidus occurs between 700 and 750°C at both 3.0 and 3.5 GPa. At T≤750°C, dolomite and magnesite coexist with garnet, omphacite, phengite, epidote, coesite, rutile ± kyanite. At T≥750°C, Mg-calcite±dolomite coexist with melt, garnet, omphacite, epidote, rutile ± coesite and phengite.

The experimental capsules have been pierced under vacuum and the experimental gas, mixed with pure He, has then been directly analysed with an Agilent Technologies 6850 gas chromatograph equipped with a thermal conductivity detector (GC-TCD). The accurate determination (±5%) of small quantities of CO_2 and H_2O in a He mixture by GC-TCD method has been validated in using pure standards of these gas and the elaboration of the calibration lines between their partial pressures in a He mixture versus the peak area read in the chromatograms. P_{CO2}/P_{H2O} of the gas mixture in equilibrium with the sub-solidus assemblages decreases with pressure from 6.3 to 4.0, confirming the previous estimations of low CO_2 contents in such aqueous fluids [1]. The gas mixture released from experiments above the solidus is characterised by P_{CO2}/P_{H2O} ranging from 6.1 to 3.6. This indicates that some H_2O and CO_2 are released from the glass during quenching. Therefore, analyses of the glass and the quench fluid are needed in order to quantify the CO_2 release during partial melting of altered oceanic crust.

[1] Poli *et al*. (2009) *EPSL* **278**, 350–360.

Influence of different sources on cloud condensation nuclei numbers in the high Arctic

M. MARTIN[1]*, B. SIERAU[1], C. LECK[2] AND U. LOHMANN[1]

[1]ETH Zurich, Institute for Atmospheric and Climate Science, Universitätsstr. 16, 8092 Zurich, Switzerland (*correspondence: maria.martin@env.ethz.ch)
[2]Department of Meteorology, Stockholm University, Stockholm, Sweden

Introduction

A thin cloud layer is often observed in the high Arctic in summer. The sources of particles in this region that act as cloud condensation nuclei (CCN) can be long-range transport from continental sources, but also primary particles emitted from the Central Arctic Ocean including the pack ice area, and secondary formed from local sources or transported precursors might contribute.

The ASCOS (Arctic Summer Cloud Ocean Study) campaign on board an icebreaker was undertaken into the high Arctic in summer 2008 to investigate aerosol properties. Measurements from two CCN counters are presented.

Results and Discussion

CCN properties were analysed and classified based on different meteorological conditions, and CCN number concentrations were correlated with different air mass source regions. The CCN concentration and the activated fraction was very variable throughout the campaign.

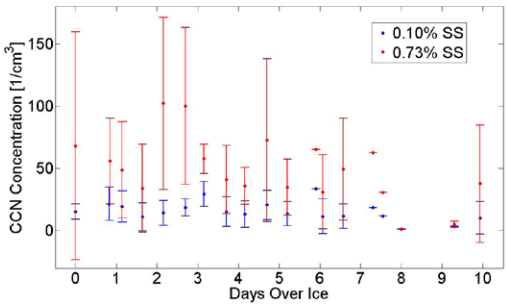

Figure 1. Measured CCN concentration at 0.10 and 0.73% supersaturation as a function of the number of days the air spent over the ice.

The data was also investigated using the time, which the air masses spent over the pack ice before reaching the ship (see Fig. 1). High concentrations after a few days over the ice can be taken as a hint for local particle sources.

https://doi.org/10.1180/S0026461X00006502 Published online by Cambridge University Press

Which is more ionic? UO_2 or PuO_2

RICHARD L. MARTIN

Theoretical Division, Los Alamos National Labnoratory, Los Alamos, NM (rlmartin@lanl.gov)

The electronic structure of many of the oxides containing *d*- and *f*-elements has long been a challenge for theory. For example, the traditional workhorses of density functional theory, the local density approximation (LDA) and the generalized gradient approximations (GGA), predict most of these systems to be metallic, when in fact they are insulators with band gaps of several eV. These problems reflect the localization/delocalization dilemma faced in systems with weak overlap and seem to be largely overcome by the new generation of hybrid density functionals developed for molecular studies. Only fairly recently has it been possible to apply these functionals to solids but in the cases studied thus far we find a distinct improvement when comparing with experiment. Hybrid functionals have also made a counterintuitive prediction: that of significant covalency in PuO_2, as opposed to UO_2; a prediction that has now been addressed by experiment. I will review predictions of the theory and recent experimental work on the first single-crystal quality samples of PuO_2.

Covalency in the actinides probed with ligand K-edge X-ray absorption spectroscopy

RICHARD L. MARTIN AND ENRIQUE R. BATISTA

Theoretical Division, Los Alamos National Laboratory, Los Alamos, NM 87544 (rlmartin@lanl.gov, erb@lanl.gov)

I will discuss experimental and theoretical investigations of ligand K-edge X-ray absorption spectroscopy for a number of actinide complexes and solids. Evidence for *f*-orbital – ligand bonding interactions will be presented, and the ramifications of this for actinide electronic structure discussed.

https://doi.org/10.1180/S0026461X00006502 Published online by Cambridge University Press

Corals constrain $CaCO_3$ chemistry at the Triassic–Jurassic boundary, a potential ocean acidification event

ROWAN C. MARTINDALE, WILLIAM M. BERELSON, FRANK A. CORSETTI, DAVID J. BOTTJER AND A. JOSHUA WEST

University of Southern California, Los Angeles, USA (rmartind@usc.edu, berelson@usc.edu, fcorsett@usc.edu, dbottjer@usc.edu, joshwest@usc.edu)

Ocean acidification associated with emplacement of the Central Atlantic Magmatic Province (CAMP) has been suggested as a kill mechanism for the Triassic–Jurassic (T–J) mass extinction (~200Ma), but few direct proxies for ocean acidity are available in the Mesozoic. In this work, we show that the presence of corals and reefs in the fossil record can provide a proxy for saturation state, and we use this proxy to determine the plausibility of an acidification event at the T-J.

The new proxy for surface aragonite saturation (Ω_{Arag}) proposed here uses the physiological constraints of modern corals to determine minimum Ω_{Arag} during the intervals when coral are preserved in the fossil record. Corals lose the ability to biomineralise below aragonite saturation (Ω_{Arag}) of 2 and coral reefs are restricted to $\Omega_{Arag} > 3$, so when scleractinians are preserved in the rock record, surface ocean Ω_{Arag} was > 2, and when coral reefs are preserved, $\Omega_{Arag} > 3$. Coral reefs are preserved throughout the latest Triassic but disappear from the fossil record at the T–J boundary, reappearing in the mid Hettangian (~370 kyr coral gap).

We use atmospheric pCO_2 reconstructions from the literature in conjunction with these Ω_{Arag} limitations to calculate the total dissolved inorganic carbon (TCO_2) in the T-J ocean. Our results suggest that the T-J pCO_2 increases recorded by stomatal and pedogenic carbonate proxies would depress saturation state to the point where it would be extremely difficult for corals to biomineralise ($\Omega_{Arag} < 2$), resulting in a coral and reef gap in the fossil record. However, the Jurassic elevation of pCO_2 observed in the proxies does not produce complete carbonate undersaturation in the surface ocean. Models suggest that higher pCO_2 values (between 3000 ppm and 7000 ppm) could be possible, and at these levels, the saturation state would have been low enough for aragonite undersaturation in the surface ocean. This short but extreme acidification in an ocean with low TCO_2 would explain the significant extinction of calcareous organisms and the Early Hettangian coral gap.

Surface $\delta^{11}B$-pH reconstructions and insights into the dynamics of the oceanic carbonate system during the last deglaciation

M.A. MARTÍNEZ-BOTÍ[1]*, G.L. FOSTER[1] AND D. VANCE[2]

[1]School of Ocean and Earth Science, National Oceanography Centre Southampton, University of Southampton, Southampton SO14 3ZH, UK (*correspondence: M.A.Martinez-Boti@noc.soton.ac.uk)

[2]Bristol Isotope Group, Department of Earth Sciences, University of Bristol, Bristol SO8 1RJ, UK

There is a long-standing debate about the role of an isolated deep-ocean carbon-rich reservoir in the rise of atmospheric CO_2 during the last deglaciation. One of the most commonly invoked hypotheses implies that CO_2 is 'stored' in the deep ocean during glacial periods, and that re-communication of this reservoir with the surface ocean and atmosphere at deglaciations (mainly via upwelling in the Southern Ocean) increases atmospheric pCO_2. While several studies in the Southern Ocean, Eastern Equatorial Pacific and Indian Ocean have confirmed the validity of this hypothesis, others have cast doubt on the existence and even the feasibility of such ^{14}C-depleted reservoir [1-5].

Boron isotopes in planktic foraminifera are a proven proxy for surface oceanic pH [6, 7], which has been shown to provide valuable insights into past changes in the ocean carbonate system and ultimately into past atmospheric pCO_2. Here we will present novel results from sediment cores retrieved from the equatorial regions of several ocean basins that provide valuable insights into the causes and mechanisms of deglacial pCO_2 rise.

[1] Marchitto, Lehman, Ortiz, Fluckiger & van Geen (2007) *Science* **316**, 1456–1459. [2] Anderson, Ali, Bradtmiller, Nielsen, Fleisher, Anderson & Burckle (2009) *Science* **323**, 1443–1448. [3] Bryan, Marchitto & Lehman (2010) *Earth Planet. Sci. Lett.* **298**, 244–254. [4] Rose, Sikes, Guilderson, Shane, Hill, Zahn & Spero (2010) *Nature* **466**, 1093–1097. [5] Hain, Sigman & Haug (2011) *Geophys. Res. Lett.* **38**, L04604. [6] Sanyal, Bijma, Spero & Lea (2001) Paleoceanography **16**, 515–519. [7] Foster (2008) *Earth Planet. Sci. Lett.* **271**, 254–266.

https://doi.org/10.1180/S0026461X00006502 Published online by Cambridge University Press

Preliminary estimation of scavenging rates in the Guadalete estuary (Bay of Cádiz, Spain) based on U-Th disequilibrium series

C. MARTÍNEZ-RAMOS[1], E. CUESTA[2], M. CASAS-RUIZ[1], J.P. BOLÍVAR[2], E.G. SAN MIGUEL[2], L. BARBERO[3], AND M. BASKARAN[4]

[1]Departamento de Física Aplicada, Universidad de Cádiz (celia.martiramos@uca.es)
[2]Departamento de Física Aplicada, Universidad de Huelva, Spain (estefania.cuesta@dfa.uhu.es)
[3]Departamento de Ciencias de la Tierra, Universidad de Cádiz, Spain
[4]Department of Geology, Wayne State University, Detroit, USA

Several samples were taken along salinity gradient in the Guadalete River estuary (SW Spain), with the aim of estimating the scavenging rates and residence times of U and Th. Scavenging processes can be quantified from the measurements of members of the U-Th series, such as ^{234}Th and ^{238}U, based on the differences in the geochemical behaviour with respect to sorption on to particulate matter. We analyzed the dissolved and particulate ^{234}Th in a suite of water samples. Our results show that the dissolved U is conserved in the estuarine mixing zone. Using a simple box model for the particulate and dissolved ^{234}Th, the calculated scavenging rate constant k and the residence time τ in the lower salinity samples are 0.96±0.28 d^{-1} and 1.01±0.28 d, respectively. At intermediate salinity, these values are 0.74±0.11 d^{-1} and 1.30±0.11 d, respectively. Scavenging rates and residence times from samples in the surrounding Bay of Cádiz, are 0.56±0.08 d^{-1} and 1.69±0.08 d, respectively. A comparison of these values indicate that there is active scavenging (lower residence time) at low salinity region compared to high salinity region towards the sea. Furthermore, these results imply high scavenging rates in the Guadalete River estuary as well as short residence times, as is normally the case in estuarine areas.

Biogeochemistry of Devonian shale gas resources of the Midwest USA: Antrim and New Albany Shales

A.M. MARTINI[1], S.T. PETSCH[2]*, J.C. MCINTOSH[3], M. SCHLEGEL[3], J. DAMASHEK[4], S.E. MILLER[5] AND M. KIRK[6]

[1]Dept. of Geology, Amherst College, Amherst, MA 01002 (ammartini@amherst.edu)
[2]Dept. of Geosciences, University of Massachusetts Amherst, Amherst, MA 01003 (*correspondence: spetsch@geo.umass.edu)
[3]Dept. of Hydrology and Water Resources, University of Arizona, Tucson, AZ 85721
[4]Dept. of Environmental Earth System Science, Stanford University, Stanford, CA 94305
[5]Dept. of Geophysical Sciences, University of Chicago, Chicago, IL 60637
[6]Sandia National Laboratory, Albuquerque, NM 87185

To better understand the role of subsurface microbial communities in natural gas generation in shales, we have pursued comparison of the aqueous geochemistry, gas isotope geochemistry, organic geochemistry, and microbial ecology in two US gas shale formations. Both formations exhibit key geochemical/isotopic indicators of methanogenesis, including high concentrations of HCO_3^-; $\delta^{13}C$ values of HCO_3^- between 10-33 ‰; low concentrations of SO_4^{2-} and CH_3COO^-; and a strong co-variance of H_2O and CH_4 δD values. These indicators reach more extreme values in the Antrim compared to the New Albany, suggesting greater overall microbial gas generation and/or a more active microbial community in the Antrim. Analysis of extractable hydrocarbons from shale core samples also reveal that biodegradation is much less severe in the New Albany compared to the Antrim. 16S rRNA partial gene sequences from production waters of both formations include both Archaea and Bacteria. Phylogenetic analyses suggest different microbial communities occur both between and within the two formations, yet all exhibit broadly similar functions of bacterial fermentation of hydrocarbons accompanied by predominantly hydrogenotrophic methanogenesis.

https://doi.org/10.1180/S0026461X00006502 Published online by Cambridge University Press

Assessment of trace element concentration related to the K-Pg event by the use of PXRF

FRANCISCO J. MARTÍN-PEINADO[1]*
AND FRANCISCO J. RODRÍGUEZ-TOVAR[2]

[1]Department of Soil Science, University of Granada, Spain (*correspondence: fjmartin@ugr.es)
[2]Department of Stratigraphy and Paleontology, University of Granada, Spain

The field portable X-ray fluorescence (PXRF) analyser is a useful tool for screening and assessing contaminated areas. This equipment allows *in situ* trace-element concentrations to be determined both rapidly and easily. According to its advantages, the method reveals especially appropriate when sampling is difficult or even forbidden (e.g. scarce sample, difficult access to sampling or protected areas), as is the case of the K-Pg boundary layer in some sections. To check its potential applicability, the K-Pg boundary layer at the Caravaca section (Murcia province, SE Spain), has been analyzed. In this section, the 2-3 mm thick K-Pg rust-red boundary layer has been previously characterized by the presence of Ir and other geochemical anomalies that, together with other evidences, where related to a extraterrestrial origin. Samples were taken to analyse *in situ* the element concentrations in the sediments of the K-Pg boundary interval, from the uppermost Maastrichtian to the lowermost Danian, including the boundary layer, as well as in the infilling material of trace fossils registered at the K-Pg boundary interval. The results indicated statistical significant differences between the different samples analysed for the following elements: Zn, As, Ti, Fe, Sr, Ca and K. Maximum values of these elements (up to 1480 ppm of As, 1272 ppm of Zn and 166 g/kg of Fe) were detected in the K-Pg boundary layer. Cretaceous sediments were characterized by the lowest concentration of these elements but the maximum values of calcium. Tertiary materials statistically differ from the Cretaceous sediments, with significant increase in Sr, Fe, and Ti and strong decrease in Ca content. Finally, trace fossils registered at the K-Pg boundary interval show variable concentrations according to the type of infilling material.

In this study, PXRF has proved to be a useful tool for screening and assessing particular fossil examples as that from the K-Pg boundary for quick and easy *in situ* determination of trace-element concentrations related to this type of events.

Zircon typologies and internal structures as petrogenetic indicators in contrasting Variscan biotite-rich granite plutons from Northern Portugal

H.C.B. MARTINS[1] AND P.P. SIMÕES[2]

[1]Centro de Geologia, Faculdade de Ciências, Universidade do Porto, Rua do Campo Alegre, 4169-007 (hbrites@fc.up.pt)
[2]Centro de Geologia da Universidade do Porto/ Universidade do Minho, Campus de Gualtar (pimenta@dct.uminho.pt)

The aim of the present morphological zircon study is to characterize the sources reservoirs involved in the generation of the different type of granites, testing the classic 'Pupin method' and zircon geochemistry against the petrogenetic indications given by geochemical and isotopic data. In northern Portugal large volumes of granitoids were emplaced during the last stage (D3) of the Variscan orogeny and display a wide range of petrological signatures. We studied the morphologies, internal structures and geochemistry of zircons from (1) Syn-D_3 biotite granitoids: Ucanha–Vilar, Lamego, Felgueiras, Sameiro and Refoios do Lima plutons (2) Late- D_3 biotite-dominant granitoids: Vieira do Minho pluton and (3) post- D_3 biotite granitoids: Vila Pouca de Aguiar pluton. The typological evolutionary trends suggest a crustal or dominantly crustal origin for the syn-D_3 Refois do Lima granite and for the late- D_3 pluton whereas an hibridisation process is proposed for the Ucanha-Vilar, Lamego and Sameiro granites. The zircon population from the post- D_3 granites define a typological evolutionary trend betweeen calc-alkaline and subalkaline granites suggesting a under crustal or mantle source. The petrogenetic model proposed by zircon typological and geochemical study in all plutons is in accordance with geochemical and isotopic data. In fact the Syn-D_3 biotite granitoids display Sr_i ratios and εNd values varying in the range 0.7072-0.7116 and - 4.4 to - 6.3, respectively; the late- D_3 pluton present Sr_i= 0.7089-0.7090 and εNd = - 5.6 to - 5.7 and finally post- D_3 biotite granitoids present weakly evolved isotopic compositions, Sri=0.7044–0.7077 and εNd=–2.0 to –2.6.

https://doi.org/10.1180/S0026461X00006502 Published online by Cambridge University Press

Radon risk and their geological controle in the region of Amarante (Northern Portugal)

L. MARTINS[1], M.E.P. GOMES[1], L. NEVES[2] AND A. PEREIRA[2]

[1]Dep. of Geology, UTAD, 5001-801 Vila Real, Centro de Geociências, Portugal
[2]IMAR, Dep. of Earth Sciences, 3000-272 Coimbra, Portugal

Amarante is located in the border of an extensive tardi-tectonic massif, formed by Hercynian granites. Around Amarante city, two types of the granitic rocks occur: AT1 is a coarse-grained, porphyritic, bi>mu (biotite>muscovite) and AT2 is granite with medium-grained, bi>mu, porphyritic. Other units are metamorphic rocks of Silurian and Devonian in Aboim village. Representative samples of granitic rocks unaltered and with different degrees of alteration were studied. The variations of SiO_2, TiO_2, Fe_2O_3t, MgO, V, Zr, Sr, Ba, U, Fe/(Fe+Mg), their subparallel REE of two unaltered granites suggest a relation by crystal fractionation; and AT2 is the most differentiated granite. The average uranium content of the AT2 granite was found to be 18 ppm, higher than the crustal average, subsequently showing a high radon potential. Accessory minerals from granites were studied through SEM suggesting that, U and Th are mainly concentrated in zircon, monazite, uraninite, thorite and thorianite. In three geological units was evaluated a radioactive background with gamma-ray portable spectrometers and in the granitic rock a gamma ray flux of 289 ηGy/h measured in direct contact with the rock was observed; a lower flux of 155 ηGy/h was observed for metamorphic rocks that also outcrop in the area. An important measured system of fractures with tardi-hercynian directions affects the studied area. Some fractures that crosscut the Amarante granite show a moderate degree of uranium enrichment (26 ppm), with gamma ray fluxes up to 420 ηGy/h.

The indoor radon concentrations, during the winter, were measured in 73 dwellings with CR39 passive detectors. The highest radon levels occur in 35 dwellings and built over the granite AT2 (geometric mean of 430 Bq/m^3), which also shows the highest uranium. Buildings from Aboim village show the lowest U contents and consequent lowest radon levels. Fourteen representative samples of groundwater were analysed for Rn, gross α and β. Groundwater related with AT2 has the highest radon (up to 2295 Bq/l) and the highest gross α (up to 0, 83 Bq/l) allowed by Portuguese legislation. Overall, we can conclude that the area of Amarante city presents a moderate to high radon risk and the area of Aboim presents low to moderate radon risk.

Nitrogen fixation through early Earth history

F. JAVIER MARTIN-TORRES* AND ALFONSO DELGADO-BONAL

Centro de Astrobiologia (CSIC-INTA), Carretera de Ajalvir, km.4, 28850, Torrejón de Ardoz, Madrid, Spain (*correspondence: javiermt@cab.inta-csic.es)

Nitrogen is an essential part of many of the chemical compounds, such as proteins and nucleic acids, which are the basis of all life forms. However, N_2 cannot be used directly by biological systems to build the chemicals required for growth and reproduction. Before its incorporation into a living system, N_2 must first be combined with hydrogen. This process of reduction of N_2, commonly referred to as *nitrogen fixation* may be accomplished chemically or biologically. In this paper we present a study of the evolution of nitrogen fixation through Earth history between 3.4 and 0.5 Gyr ago and its effects on the geophysical Earth system.

https://doi.org/10.1180/S0026461X00006502 Published online by Cambridge University Press

Metal-rich brown layers in Arctic Ocean sediments: Climate versus diagenesis

C. MÄRZ[1]*,[2], A. STRATMANN[2], S. ECKERT[2], B. SCHNETGER[2], S.W. POULTON[1] AND H.-J. BRUMSACK[2]

[1]CEGS, Newcastle University, NE1 7RU Newcastle upon Tyne, UK (*correspondence: christian.maerz@ncl.ac.uk)
[2]ICBM, Universität Oldenburg, 26111 Oldenburg, Germany

The sediments of the central Arctic Ocean are a unique archive for past climate and environmental changes in this highly sensitive ocean region. Amongst the most prominent and widespread features of Arctic Quaternary deposits are marked cm- to dm-thick brown layers. Their origin is unclear, and might either be related to specific environmental conditions during either deposition, or to diagenesis. To understand the genesis and composition of these layers, we studied sediments cores from the southern Mendeleev Ridge (RV *Polarstern* Expedition ARK-XXIII/3) by inorganic-geochemical methods (XRF, ICP-MS, Fe extraction) at high resolution.

The brown layers are consistently enriched in Mn and Fe (oxyhydr)oxides, but also in various trace metals (As, Co, Cu, Mo, Ni) that most probably adsorbed to Mn and Fe phases and were scavenged from the water column. These metal enrichments are likely related to enhanced riverine input to the Arctic Ocean, as Arctic river waters are known to be metal-rich. Increased fluvial runoff should be related to a more intense hydrological cycle under warmer (interglacial-type) climate conditions.

However, pore water data indicate ongoing Mn (but not Fe) diagenesis in the recovered sediments, questioning the primary nature of the observed metal enrichments. We suggest that relative changes in the enrichment patterns of specific trace metals (especially of Co and Mo) in individual brown layers might be used to determine if the composition of the respective layers was overprinted by diagenetic processes.

In detail, we observe that brown layers currently serving as pore water Mn sources have Co/Mo ratios above 5, while those layers acting as pore water Mn sinks have Co/Mo ratios below 5. This trace metal pattern may be explained by preferential retention of Co in dissolving Mn (oxyhydr)oxide layers. In contrast, Mo is preferentially desorbed, diffuses through the pore space in conjunction with Mn, and re-adsorbs onto freshly precipitating, authigenic Mn (oxyhydr)oxides. However, the wider application of trace metal ratios as 'diagenetic markers' in Arctic sediments requires further investigation.

Nitrate reduction drives distant sulfide oxidation

U. MARZOCCHI[1]*, N. RISGAARD-PETERSEN[2], N.P. REVSBECH[1] AND L.P. NIELSEN[1]

[1]Section for Microbiology, Department of Biological Sciences, Aarhus University, 8000 Aarhus C, Denmark (*correspondence: ugo.marzocchi@biology.au.dk) (revsbech@biology.au.dk) (biolpn@biology.au.dk)
[2]Center for Geomicrobiology, Aarhus University, 8000 Aarhus C, Denmark (nils.risgaard-petersen@biology.au.dk)

Recent observations in marine sediments show that electric currents may couple oxygen reduction at the sediments surface to sulfide oxidation deep within the sediment [1]. In this study we tested if electric currents can couple also nitrate reduction to sulfide oxidation

Sediment collected from Aarhus bay (Denmark) was pre-incubated for 2 months in two different aquaria: one with oxic seawater and another where oxygen was replaced with nitrate. After the pre-incubation, sulfide, oxygen and pH distribution in the sediment were determined with microsensors whilst a biomicrosensor was used to measure nitrate & nitrite.

Our concentration profiles showed a 4 mm separation between nitrate and sulfide in sediments incubated with nitrate in the water column. In sediments incubated with oxygen in the water column, oxygen and sulfide were separated by 25 mm. In both types of incubation, the pH signature indicated the presence of electric currents coupling spatially segregated biogeochemical processes.

These results provide an important indication of the capacity of nitrate to sustain sulfide depletion over distances not coverable by diffusion only. Moreover demonstrating that oxygen is not the only electron acceptor able to sustain such a system, implies that this distant coupling can be more spread in nature than previously expected.

[1] Nielsen *et al*. (2010) *Nature* **463**, 1071-1074.

https://doi.org/10.1180/S0026461X00006502 Published online by Cambridge University Press

Origin of Cameroon Line basanites from metasomatized lithosphere

A. MARZOLI[1]*, F.T AKA[2], M. CHIARADIA[3], L. REISBERG[4] AND R. MERLE[1]

[1]University of Padua, Italy (renaud.merle@unipd.it) (*correspondence: andrea.marzoli@unipd.it)
[2]IRGM-ARGV, Ekona, Cameroon (akatongwa@yahoo.com)
[3]Université de Genève, Switzerland (Massimo.Chiaradia@unige.ch)
[4]CRPG (CNRS UPR2300), Université de Lorraine, France (reisberg@crpg.cnrs-nancy.fr)

The Cameroon Line is located above a zone where a sharp gradient in lithospheric thickness occurs north of the Congo Craton keel [1]. This zone was the site of magmatic activity since (at least) the beginning of the Cenozoic until the Present. Here we investigate the Miocene basic-ultrabasic magmatism of Mt. Bambouto volcano (Western Cameroon). Its 20 to 15 Ma old basanitic flows and alkali-basaltic dykes are characterized by extreme enrichments in Sr (up to 2200 ppm), Ba, and P and by generally high TiO_2 (up to 4.6 wt%). The other alkali basaltic flows from Mt. Bambouto lack such extreme compositions and resemble other typical continetal and oceanic Cameroon Line basalts. Compared to the alkali basaltic flows, the Mt. Bambouto basanites yield also slightly higher initial $^{87}Sr/^{86}Sr$ (0.7034-0.7036 vs 0.7030-0.7033) and $^{143}Nd/^{144}Nd$ (0.51290-0.51285 vs 0.51285-0.51283) and lower $^{206}Pb/^{204}Pb$ (19.4-19.6 vs 19.6-19.9). Moreover, basanites are characterized by higher initial $^{187}Os/^{188}Os$ (0.191-0.220) than the only analyzed alkali basalt ($^{187}Os/^{188}Os$ = 0.127). The high Os isotopic compositions of basanites would seem to suggest a significant amount of crustal assimilation (ca. 25 or 35% of silicic upper or mafic lower crust, respectively). However such an interpretation is not easy to reconcile with their OIB-like Sr-Nd-Pb isotopic compositions, their little evolved whole-rock compositions (e.g. MgO 9-11 wt%, Cr 350-550 ppm) and their mineralogy (high-Mg olivines: Fo_{80-88}, high pressure clinopyroxenes: crystallized at ca. 10 kbar [2]). Alternatvely, we suggest that basanites derived from mafic material entrapped within the mantle, which would also be compatible with their major and trace element compositions. In particular, we propose that these mafic veins may have metasomatically pervaded the continental lithosphere during the early stages of Cameroon Line magmatism and developed relatively high $^{187}Os/^{188}Os$ prior to the Mt. Bambouto volcanism.

[1] Reusch *et al*. (2010) *G-3* **11**, Q10W07. [2] Putirka (2008) *Rev. Mineral. Geochem.* **69**, 61–120.

Magnetic anisotropy of artificial deposits

A.V. MASHUKOV*, A.E. MASHUKOVA AND S.A. SIMINCHUK

Siberian Federal Univ., Krashoyarskiy Rabochiy, 95, Krasnoyarsk, 660025, Russia (*correspondence: avmashukov@sfu-kras.ru)

There was studied the influence of the sizes of grains of Fe_3O_4 in the artificial deposits, precipitating in the Earth magnetic field, on magnetic characteristics of the samples. To obtain most of the information, for the same samples, there was used a complex of investigations of research of same samples was used for obtaining more information.

The dependences of uniaxial anisotropy constant (K), maximum losses from the rotator hysteresis (W_m), the value of the alternating magnetic field, half reducing residual magnetization ($\tilde{H}_{1/2}$) on grain size, are shown in table 1.

Grain size Fe_3O_4, mcm	K, Joule /m^3	W_m, Joule /m^3	$\tilde{H}_{1/2}$, Oe	Intensity
0 < d ≤ 8	410,0	1020,0	320,0	1,9
8 < d ≤ 16	305,0	820,0	280,0	1,8
16 < d ≤ 32	180,0	500,0	200,0	1,5
32 < d ≤ 44	130,0	410,0	120,0	1,3
44 < d ≤ 64	115,0	225,0	110,0	1,2
64 < d ≤ 100	105,0	160,0	105,0	1,1
100 < d ≤ 150	105,0	160,0	100,0	1,1

Table 1: Dependences of magnetic characteristics on grain size

The X-ray technique of straight pole figures (intensity in table 1) shows anisotropic distribution of axes for particles d > 40 mcm.

Thus, the magnetic characteristics of rocks are controlled by ferrimagnetic particle size as well as its crystallographic ordering.

https://doi.org/10.1180/S0026461X00006502 Published online by Cambridge University Press

Geochemical variation of fracture carbonates in crystalline bedrock

O. MASKENSKAYA*, H. DRAKE, P. PELTOLA AND M. ÅSTRÖM

Geochemistry research group, School of Natural Science, Linnaeus University, SE Sweden (*correspondence: olga.maskenskaya@lnu.se)

The current study is focused on trace and rare earth elements (REE) in carbonates from two fracture mineral generations formed at separate events at very different conditions, but in the same granitoid fracture system. Both generations are well-characterized and separation is based on paragenesis, $\delta^{13}C$, $\delta^{18}O$, $^{87}Sr/^{86}Sr$ and crystal habit [1]. The oldest generation was formed in the Proterozoic era (~1.4 Ga) [2] and the youngest in the Paleozoic era (~440-400 Ma) [2, 3].

In total, 41 calcite samples and 1 dolomite sample from 17 drill cores (up to 1 km depth), originating from the Swedish Nuclear Fuel and Waste Management Co's investigations in the Laxemar-Simpevarp area, SE Sweden, were analysed (with ICP-MS of calcite leachates).

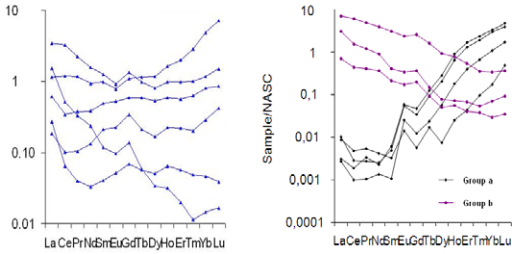

Figure 1: NASC-normalized REE patterns (REE_n) of Proterozoic carbonates (left) and Paleozoic carbonates (right), NASC according to [4].

Proterozoic carbonate shows two groups (a and b) which differ both in REE_n patterns and trace element compositions, accordingly: a) positive Eu_n- and La_n-anomalies, very low light REE concentrations, gradually enriched in REE_n from Gd_n to Lu_n, relatively high amounts of Sr, Mg and Fe; b) no Eu_n- or La_n-anomalies, gradual decrease in REE_n from La_n to Lu_n, depleted in other trace elements.

Paleozoic calcite shows larger REE_n variation including e.g. both slightly enriched heavy or middle REE_n, as well as gradual depletion from La_n to Lu_n. All Paleozoic calcite samples show low trace element concentrations and large Mn and Y variations. Observed trace element variations in different generations are predominantly caused by factors that influenced composition of parental solutions. Intense hydrothermal wall rock alteration in the Proterozoic, and microbial activity and descending organic-rich fluids in the Paleozoic might be these factors.

[1] Drake & Tullborg (2009) *Appl. Geochemistry* **23**, 715-732. [2] Drake *et al.* (2009) *Lithos* **110,** 37-49. [3] Alm *et al.* (2005) *Report* **SKB-R-05-66**. www.skb.se. [4] Haskin *et al.* (1968) *Pergamon* **vol.1**, 889-911.

Microbial sulfur isotope fractionation in littoral sediments: Interpreting $\delta^{34}S$ variability in Archean rocks

PAUL R.D. MASON[1], MARJOLIJN C. STAM[1], ANNIET M. LAVERMAN[2], CELINE PALLUD[3] AND PHILIPPE VAN CAPPELLEN[1,4]

[1]Utrecht University, The Netherlands (mason@geo.uu.nl)
[2]Universite Pierre et Marie Curie, Paris, France
[3]UC Berkeley, Ca, USA
[4]Georgia Institute of Technology, Atlanta, Ga, USA

Sulfur isotope variations in Archean rocks have been used to argue for the presence of sulfate reducing mircoorganisms as one of the earliest forms of life in the early Archean, back to 3.49 Ga [1-3]. Extensive laboratory pure culture and incubation studies with modern sediments have been used to support these interpretations with measured and predicted $\delta^{34}S$ values up to 49 ‰ for a single reduction step of sulfate to sulfide (e.g. [4, 5]). Here we expand the available data for isotope fractionation by natural communities of microorganisms, with an extensive laboratory flow through reactor study, that enables sulfate reduction under close to *in situ* conditions. Sediments were collected from a brackish marine estuary (Sheldt estuary, The Netherlands), a hypersaline soda lake (Mono Lake, California), a freshwater river (Scheldt, Belgium) and a shallow marine hydrothermal system (Vulcano, Italy).

Sulfate reduction rates (SRR) varied between 5 and 180 nmol cm^{-3} h^{-1} with corresponding isotope fractionations (ε), calculated as the difference between inflow sulfate and product sulfide, of 5 to 43 ‰. No overall relationship was found between SRR and ε , but weak correlations were found within the individual sites. Isotope fractionation data fall within the range predicted by standard models with lowest values at highest rates, but do not fall towards the smallest values predicted by the Rees model [5]. Our data indicate that relatively small isotope fractionations (<20 ‰) would be typical for sulfate reducing communities, under optimum growth conditions, and in the absence of competition from other metabolisms. Without an oxidative component in the sulfur cycle, widespread microbial sulfate reduction would result in minor $\delta^{34}S$ variations and may be more widespread in the Archean than previously envisaged.

[1] Shen *et al.* (2001) *Nature* **410**, 77–81. [2] Ueno *et al.* (2008) *GCA* **72**, 5675–5691. [3] Shen *et al.* (2009) *EPSL* **279**, 383–391. [4] Detmers *et al.* (2001) *Appl. Env. Microbiol* **67**, 888–894. [5] Rees (1973) *GCA* **37**, 1141–1162.

https://doi.org/10.1180/S0026461X00006502 Published online by Cambridge University Press

Catching a collapsing solidification front through thermal gradient experiments

M. MASOTTA[1]*, C. FREDA[2] AND M. GAETA[1,2]

[1]Sapienza - Università di Roma, Italy
(*correspondence: matteo.masotta@uniroma1.it)
[2]Istituto Nazionale di Geofisica e Vulcanologia, Rome, Italy

Large explosive eruptions commonly emplace differentiated (i.e. rhyolite, phonolite), crystal-poor juveniles. This is a well-known paradox in volcanology, considering that magmatic differentiation implies crystallization and that crystal-melt separation processes (e.g. crystal settling) are more efficient in high-temperature, primitive magmas. Conversely, differentiated, crystal-poor juveniles are usually associated to shallow, thermally-zoned feeding systems. Here, the generation of differentiated, crystal-poor magmas may be explained throughout the development of a 'solidification front' [1] at the roof of the chamber. Although natural evidences and theoretical models support the solidification front concept, its capability to originate differentiated, crystal-poor magmas remains unconstrained.

By experimentally investigating the formation of a solidification front in a thermally zoned environment we demonstrate its capability to originate glassy belts and pockets phonolitic in composition (figure 1). We recognize in the instability and collapse of rigid crystal frame the driving mechanism producing segregation and upward accumulation of crystal-poor melts and suggest this model may apply to thermally zoned magma chambers.

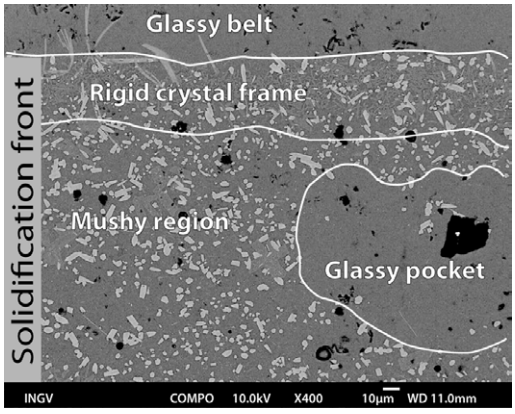

Figure 1: Solidification front obtained in a thermal gradient experiment performed at 300 MPa and T ranging 1000-850°C. The glassy belt (top, cooler zone of the capsule) is phonolitic in composition.

[1] Marsh (2002) *Geochim. Cosmochim. Acta* **66**, 2211–2229.

Promoting As release by aerobic water infiltration into Holocene aquifer, Bangladesh

H. MASUDA[1]*, S. MAEDA[1], K. OKABAYASHI[1], A.A. SEDDIQUE[2], M. MITAMURA[1], N. MORIKAWA[3] AND S. NAKAYA[4]

[1]Dep. Geosciences, Osaka City Univ., Osaka 558-8585, Japan
(*correspondence: harue@sci.osaka-cu.ac.jp)
(shunsuke@sci.osaka-cu.ac.jp, okarin@sci.osaka-cu.ac.jp, mitamura@sci.osaka-cu.ac.jp)
[2]Jessore Sci. Tech. Univ., Jessore-7407, Bangladesh
(aseddique@yahoo.com)
[3]GSJ, AIST, Tsukuba, 305-8563, Japan
(n.morikawa@aist.go.jp)
[4]Dep. Eng., Shinshu Univ., Nagano 380-8553, Japan
(nakayas@shinshu-u.ac.jp)

In order to investigate the timing of As release in the Holocene groundwater aquifer, Sonargaon, Bangradesh, age of groundwaters were determined using $^3He/^4He$ ratio. Among the ten well waters collected from the active recharging zone of the Holocene aquifer within 300 m diameters, the lowest $^3He/^4He$ ratio was found in the groundwater containing highest concentration of As >1000 µg/L. Groundwater giving the highest $^3He/^4He$ ratio contained <1µg/L As. Compared with the histrical tritium unit in the air of New Delhi, the former groundwater was recharged after 1980, while, the latter was before 1970. As concentration of the groundwater increases decreasing $^3He/^4He$ ratio, indicating that the As release started after 1980.

In this area, the As conmtaninated Holocene aquifer directly contacts to As-free Pleistocene aquifer due to lack of the Pleistocene impermeable clay layer. Presumably, the As release is triggered by increasing infiltration of groundwater into the Holocene aquifer in association with the increasing withdrawel of groundwaters from the Pleistocene aquifer to cause drastic change of the Holocene aquifer condition.

Fe rich chlorite was found to be a primary source of As, and this mineral was oxidized to precipitate goethite in the aquifer. Thus, the rapid infiltration of aerobic water into the Holocene reducing aquifer is the trigger to cause oxidation-decomposition of the As-bearing chlorite.

https://doi.org/10.1180/S0026461X00006502 Published online by Cambridge University Press

Experimental study on As and Cd releases from anoxic sedimentary rock under anoxic and aerobic conditions

S. MASUDA, Y. OGAWA*, K. SUTO AND C. INOUE

Graduate School of Environmental Studies, Tohoku University, Miyagi 980-8579, Japan (*correspondence: ogawa@geo.kankyo.tohoku.ac.jp)

The dissolution behaviors of As and Cd from the anoxic sedimentary rock and subsequent immobilization mechanism were investigated under anoxic and aerobic conditions.

Under aerobic condition, the decrease in pH and concomitant Cd release were attributable to oxidative dissolution of sulfide minerals, and 22 % of Cd in rock sample was dissolved out for 2 months. On the contrary, Cd concentration in the solution reacted under anoxic condition was maintained low level, and the contribution of dissolved Cd was only 0.14 %.

Arsenic was released as arsenite under both conditions. The As concentrations in extracts under both conditions was small, and the maximum contributions of As dissolution were about 1 %. The XANES spectra reveal that samples before the extraction contained the sulfide form As and As(V). Under aerobic condition, the As sulfide completely decomposed within a month and only As(V) existed in the samples after extraction.

The chemical state of As in samples oxidized under 100% humidity was changed to sulphide form to oxide and/or strongly sorbed ones. This experiment shows the change in chemical states of As within rock sample before the contact with water, and the result reveals that the oxidation of As sulfide did not lead to large amounts of As release. On the contrary, under anoxic condition, As and Cd concentrations were maintained low and the sulfate-rich acidic solution was not produced. Furthermore, the sulfide As were still remained in samples extracted for 2 months. These results indicate that the sulfide minerals containing As and Cd in anoxic sedimentary rock almost remained during extraction experiment for 2 months.

The Mesozoic evolution of the West Iberian Margin as witnessed by magma geochemistry

J. MATA[1], C.F. ALVES[1], R. MIRANDA[1,2], L. MARTINS[1], J. MADEIRA[2], P. TERRINHA[2], N. YOUBI[1,3], M.K. BENSALAH[1,3] AND M.R. AZEVEDO[4]

[1]Centro de Geologia da Univ.Lisboa (jmata@fc.ul.pt)
[2]Lattex/IDL
[3]Université Cadi Ayyad Marrakech, Morocco
[4]GeoBioTec, University of Aveiro

The main phases of the onshore West Iberian Margin (WIM) Mesozoic evolution were marked by the occurrence of 3 magmatic cycles separated by time lags of ≈50 Ma. The first cycle (202 - 198Ma) is linked to the initial stages of the Central Atlantic opening, being considered part of an important LIP: the Central Atlantic Magmatic Province. Magmatism produced low-Ti tholeiites characterized by $(La/Yb)n < 4$, $(^{87}Sr/^{86}Sr)_0 > 0.7050$ and $(^{143}Nd/1^{44}Nd)_0$ down to 0.512268 which post-date the beginning of syn-rift sedimentation by ≈ 20-30 Ma. The second cycle (147 - 141Ma) was coeval of the westward rift axis migration from the Lusitanian Basin to the location where oceanization was successfully reached. Preserved rocks are hypabyssal with transitional affinities (moderately alkaline to subalkaline), $6 < (La/Yb)n < 12$, $(^{87}Sr/^{86}Sr)_0 = 0.70403$ to 0.70456 and $(^{143}Nd/^{144}Nd)_0 = 0.512531$ to 0.512664. The third cycle (94 to 72 Ma) was synchronous with the opening of the Bay of Biscay and of the rotation of the Iberia. It was characterized by the formation of abundant alkaline magmatism presenting $(La/Yb)n$ up to 21, $(^{87}Sr/^{86}Sr)_0$ down to 0.702870 and $(^{143}Nd/1^{44}Nd)_0$ up to 0.512897. The geochemical evolution depicted by WIM magmas expresses the diminishing role of lithospheric sources. They prevailed during the first cycle, when magmas present fingerprints of supra-subduction processes probably developed in the lithosphere during the Upper Paleozoic Variscan orogeny.

https://doi.org/10.1180/S0026461X00006502 Published online by Cambridge University Press

Molybdate sorption from steel slag eluates by soils

K. MATERN[1]*, T. MANSFELDT.[1] AND T. RENNERT[2]

[1]Department of Geosciences, Soil Geography/Soil Science, University of Cologne, Albertus-Magnus-Platz, 50923 Cologne, Germany (*correspondence: katrin.matern@uni-koeln.de)
[2]Institute of Earth Sciences, Friedrich Schiller University of Jena, Burgweg 11, 07749 Jena, Germany (thilo.rennert@uni-jena.de)

Steel slags are an industrial by-product. The latest statistic of 2009 show a use which amounted to 4.62 mio. t slag in Germany [1]. Over 60 % have been used as construction material (ways, roads, earthworks). Molybdenum is added during steel processing in order to harden the steel. The objective of this study was to evaluate the sorption behavior of molybdate from slag eluates towards different soils to assess the risk that may arise from contamination of ground water by leaching of molybdate.

Molybdate sorption batch experiments were carried out with eluates obtained from (i) steel slag (Linz-Donawitz operation, LD) and (ii) electric furnace slag (EF).

Six different soils and sediments were chosen to provide a wide range of chemical properties (pH 4.0 to 7.6; dithionit-extractable Fe 0.73 to 14.69 mg kg^{-1}). Molybdate sorption experiments were carried out at pH of the steel slag eluates (pH 11 to 12) as well as at pH adjusted to soil pH. The data were evaluated with the Freundlich equation.

Molybdate sorption exhibited a maximum near pH 4 for steel slag eluates which were adjusted to soil pH and decreased rapidly with increasing pH until sorption was virtually zero at pH > 11. Sorption was greater for soils with high amounts of dithionite-extractable iron oxides. Molybdate sorption behavior of both eluates was similar. After reaching equilibrium, the pH of the EF steel slag eluate was lower than the pH of the LD steel slag eluate that was caused by different buffer capacities. Some soils were able to decrease the pH of the EF steel slag eluates by about four pH units enhancing the sorption of molybdate.

The Mo-sorption behavior from steel slag eluates is similar to sorption experiments with commercial Mo standard solutions. The same factors affect Mo-sorption, but Mo-sorption from steel slag eluates is more complex as a result of eluate chemistry.

[1] Merkel (2010) *Report des FEhS-Institutes* **1**, 14.

Brackish marine water intrusion in deep fractured granitic bedrock

F.A. MATHURIN[1]*, B.E. KALINOWSKI[2], M. ÅSTRÖM[1] AND M. LAAKSOHARJU[3]

[1]Department of Natural Sciences, Linnaeus Univ., Kalmar, Sweden (*correspondence: frederic.mathurin@lnu.se)
[2]Swedish Nuclear Fuel and Waste Management Co, Stockholm, Sweden
[3]Geopoint AB, Stockholm, Sweden

Groundwater residing in the fractures of granitic bedrock in a costal environment can be related to the climate changes and seawater stages. The purpose of this study is to hydrogeochemically characterise the different brackish marine water types present at the Äspö Hard Rock Laboratory, an underground bedrock laboratory situated at the Baltic Sea shore, in south-east Sweden [1].

Groundwater samples collected from the different boreholes along the tunnel at 50-560m depth were classified according to their Cl content and $\delta^{18}O$ signature. Groundwater classified as brackish marine component was used to study the Mg/Cl and Mg/K ratios in detail.

For samples with Mg/Cl ratio higher than 0.03, two different trends can be observed both with respect to the Mg and the Cl concentrations. One group of samples is distributed along an evolution line from the present Baltic Sea water (Cl = 3380 mg.L^{-1}). The other group, consisting of fewer samples and higher Cl concentration, appears to gather along an evolution line from the ancient Baltic Sea, also called the Littorina Sea (Cl = 6500mg.L^{-1}; [2]). However, the samples of the second group have lower Mg and Cl concentration than the original Littorina Sea composition. The brackish marine water considered to be influenced by Littorina Sea water is located in relatively shallow fracture sections at 30-180m depth. This suggests storage of Littorina Sea water as pockets in some fractures. Nevertheless the high Mg/K ratio, which is more than four times the ratio of the Littorina Sea water, indicates that a strong water-rock interaction occurred since the Littorina sea water intrusion. The alignment of the samples along different evolution lines of the two different brackish Sea water types shows that mixing processes with other water types [3] take place in the fracture network.

[1] Laaksoharju *et al*. (1999) *Appl. Geoch* **14**, 835–859. [2] Sjöberg *et al*. (1984) *Chem. Geol*. **42**, 147–158. [3] Smellie *et al*. (1995) *Jour Hydro* **172**, 147–169.

https://doi.org/10.1180/S0026461X00006502 Published online by Cambridge University Press

Depth profile of $^{129}I/^{127}I$ ratio in Andisol collected in preserved field of NIAES, Tsukuba, Japan

H. MATSUZAKI[1]*, Y. MAEJIMA[2], T. OHKURA[2], Y.S. TSUCHIYA[1], K. ABE[1], Y. MIYAIRI[3] AND Y. MURAMATSU[4]

[1]The University of Tokyo, Tokyo 113-8656, Japan (*correspondence: hmatsu@n.t.u-tokyo.ac.jp)
[2]NIAES, Tsukuba 305-8604, Japan
[3]AORI, The University of Tokyo, Chiba 277-8564, Japan
[4]Gakushuin University, Tokyo 171-8588, Japan

Depth profile of $^{129}I/^{127}I$ ratio were measured as well as iodine concentration, carbon concentration and $^{14}C/^{12}C$ in Japanese Andisol collected in the well preserved field of National Institute for Agro-Environmental Sciences, Tsukuba, Japan. Today, most of ^{129}I in the surface environment involving soils is originated in the human nuclear activities: atmospheric nuclear bomb testing, spent nuclear fuel reprocessing, and nuclear acceident. To estimate total deposition of ^{129}I in soil precisely and to investigate iodine transfer process correctly, the depth profile information is essential. From the gradient of the profile iodine transfer model can be constructed. If $^{14}C/^{12}C$ profile shows the signal from the bomb testing (110 pMC just below the surface), the sampling field has been undisturbed at least several decades [1]. This study was the case.

Resulting $^{129}I/^{127}I$ depth profile shows steep decreasing trend above 20cm depth. This part can be fitted simple diffusion curve (error function). Below this depth $^{129}I/^{127}I$ come to be rather constant. This observation suggests that there are at least two component of iodine: quick diffusion component (with which most of recent ^{129}I is carried) and rather static component (maybe as old as the mother material of the soil).

The maximum $^{129}I/^{127}I$ ratio in Tsukuba (this study) is 1.67 x 10^{-8} at 1.5cm deep which is as twice as higher than the Shimokita soil (7.29 x 10^{-9}) [1]. This should be due to the influence of a nuclear fuel reprocessing plant at Tokai area located about 60km northern east of Tsukuba. Total deposition density of ^{129}I was calculated using $^{129}I/^{127}I$ ratio profile and iodine concentration of each depth and soil density. That was 0.036 Bq/m^2 corresponding to 2.6 x 10^{13} atoms/m^2. These data should be a reference for the evaluation of the influence of the nuclear power plant acceident like the Fukushima dai-ichi power plant.

[1] H. Matsuzaki *et al*. (2010) *Radiocarbon* **52**(2–3), 1487–1497.

Tracking permanent CO_2 storage in basaltic rocks using conservative and reactive tracers at the CarbFix injection site, Iceland

J.M. MATTER, M. STUTE AND W. BROECKER

LDEO, Palisades, NY 10964 (jmatter@ldeo.columbia.edu)

Injection of CO_2 modifies ambient formation waters, inducing fluid-rock reactions that may lead to mineral carbonation of the CO_2. In the CarbFix pilot CO_2 injection project in Iceland, we are investigating *in situ* mineral carbonation of CO_2 in a basaltic aquifer. At the moment, the pilot test involves the injection of 2, 200 tons of CO_2. The CO_2 is injected dissolved in water at a rate of 0.07 kg/s of CO_2 in 2 kg/s of water at 19°C [1].

The success of mineral carbonation in basaltic rocks depends on the ability to monitor and understand the behavior of the injected CO_2. The currently existing monitoring techniques in CO_2 capture and storage are insufficient to characterize mineral carbonation in any storage reservoir. Most geophysical detection methods require that CO_2 is present as a supercritical phase. Dissolved CO_2 and chemically transformed carbon thus avoid detection.

We are using a multi tracer approach, including conservative and reactive tracers to track CO_2 storage in basaltic rocks. Trifluormethylsulphur pentafluoride (SF_5CF_3), a conservative tracer, is injected in pulses into the CO_2 gas stream at a concentration of 2700 pptv. It is used to characterize the physical transport processes of advection and dispersion of the CO_2 solution. Furthermore, the injected CO_2 is tagged with radiocarbon (^{14}C). Radiocarbon is injected as dissolved bicarbonate at a concentration of 1.20x10^1 Bq/kg of injected water. This results in 5x enrichment compared to the 1850 background. The total ^{14}C activity needed for the 2, 200-ton injection is 7.44x10^8 Bq or 20 mCi. We use ^{14}C as a tracer to monitor the CO_2 reactivity in the storage reservoir. Its ratio to carbon in the groundwater of the basaltic aquifer will change as a result of dissolution and precipitation of carbonate minerals. Thus, by measuring the carbon isotopic ratio in water samples collected in monitoring wells, we are able to quantify and verify *in situ* mineral carbonation and therefore long term storage.

[1] Gislason *et al*. (2010) *Int. J. Greenh. Gas Con*. **4**.

https://doi.org/10.1180/S0026461X00006502 Published online by Cambridge University Press

Fluid-flow controls of low δ^{57}Fe hydrothermal iron mineralization

A. MATTHEWS[1]*, Y. EREL[1], D. STERN[1], U.RYB[1] AND Y. AVNI[2]

[1]Institute of Earth Sciences, Hebrew University of Jerusalem, Israel (*correspondence: alan@vms.huji.ac.il)
[2]Geological Survey of Israel, Jerusalem 95501, Israel

Low δ^{57}Fe values are characteristic of iron isotope fractionation during bacterial and abiogenic reduction. However, experiments on the Fe isotopic fractionation during sorption-desorption of aqueous Fe on quartz [1, 2] indicate alternative mechanisms for generating isotopically light iron.

We investigate the controls of Fe-isotopic fractionation during low temperature hydrothermal iron mineralization along a 70 km section of a fault (Paran Fault) adjacent to the Dead Sea Transform (DST), which separates the Arabian plate from the Sinai Sub-plate. The MVT type mineralization comprises iron oxide lenses in the fault zone and iron oxide-bearing dolomites in the adjacent Cretaceous host rock limestone. The Mg-Fe rich brines were sourced in evaporite-bearing sandstones (Nubian) underlying the limestone.

Fe isotopic compositions from two 10 km long segments in the west (Haspas) and East (Menuha) parts of the fault show uniformly negative values: Menuha: δ^{57}Fe (Fe-ox) = -1.08±0.4‰ (n=23); (Fe-dol) = -0.87±0.26‰ (n=15); Haspas δ^{57}Fe (Fe-ox) = -0.86±0.26‰ (n=17); (Fe-dol) = -0.61±0.21‰ (n=13). These values represent isotopically light source solutions formed by the dissolution of clastic iron minerals in the sandstone with δ^{57}Fe = 0.34±0.19‰. (n=8).

Both bacterial and abiotic reduction of the clastic iron oxides could have provided isotopically light Fe (II) solutions. However, the highly saline conditions of the sandstone fluids do not necesssarily favour bacterial intervention. An alternative fluid flow model is examined whereby the isotopically light Fe compositions are generated by sorption on sandstone grain surfaces. The uniformity of the Fe isotope composition suggests that fluid flow was generally orthogonal to the E-W trending fault. Northward fluid flow is consistent with the topographic recharge being to the south (present-day Suez Rift) at the Oligocene time of the major pulse of mineralization. Slightly lighter δ^{57}Fe values (≤ -1.0 ‰) in dolomites closer to the DST possibly represent Miocene reactivation related to creation of the transform [3].

[1] Matthews *et al*. (2008) *GCA* **72**, 5908–5919. [2] Mikutta *et al*. (2009) *GCA* **73**, 1795–1812. [3] Erel *et al*. (2006) *GCA* **70**, 5552–5570.

Using atomic force microscopy to probe pore surfaces of oil-bearing sandstone

J. MATTHIESEN*, T. HASSENKAM, N. BOVET AND S.L.S. STIPP

Nano-Science Center, Department of Chemistry, University of Copenhagen, Denmark
(*correspondence: jmatth@nano.ku.dk, tue@nano.ku.dk)

Pore surface properties of oil-bearing sandstone control the oil recovery from sandstone reservoirs. The wettabillity of the pore surface, i.e. the tendency of the surface to cover itself with a fluid, plays a key role in recovery. Pore surface wetting behavior for chalk reservoirs has previously been shown to be inhomogeneous over scales of 10's of nanometers [1]. Here we investigate whether the same applies for sandstone.

Using atomic force microscopy/spectroscopy (AFM/AFS), we have probed the surface wetting properties at the nanoscale of natural oil-bearing sandstones. A self-assembled monolayer of alkane-thiols is formed on the AFM tip surface, creating a hydrophobic layer. Force curves measuring the adhesion between the hydrophobic tip and the sandstone surface were acquired in a 50x50 grid over a 5x5 μm area thereby forming a map of adhesion. Properties such as topography and elasticity were also extracted from these measurements.

We observe that sandstone wettability varies on a sub-micrometer scale. In some areas, the degree of adhesion of the hydrophobic tip decreases with number of scans over the area and the force curves indicate that material is pulled off the surface. Using X-ray photoelectron spectroscopy (XPS) measurements, we saw that the initial surfaces were covered with several layers of carbon containing material. The wetting behavior of the pore surface is thus controlled by adsorbed organic material and not by the actual surface of the mineral. This improved understanding about the wetting behavior of reservoir minerals will hopefully provide clues for increasing oil recovery.

[1] Hassenkam *et al*. (2009) *PNAS* **106**, 6071–6076.

https://doi.org/10.1180/S0026461X00006502 Published online by Cambridge University Press

George R. Tilton and the development of U-Pb geochronology

J.M. MATTINSON

Department of Earth Science, Univ. of California, Santa Barbara, CA 93106-9630 USA (mattinson@geol.ucsb.edu)

In the early decades of U-Pb geochronology, following the discovery of radioactivity and the recognition of the decay products of U decay, ages based on U/Pb ratios were determined using classical chemical methods. As a result, age determinations were limited to U ore minerals containing large amounts of U and Pb. The application of mass spectrometry to U-Pb studies, e.g. Nier [1, 2], was a major advance, but did not change the sample requirements -- the early mass spectrometric methods required several milligrams of Pb per determination.

From the late 1940's to the mid-1950's, George Tilton and his fellow graduate student at the University of Chicago, Clair 'Pat' Patterson completely revolutionized U-Pb geochronology. They developed the clean chemistry, isotope dilution, and thermal ionization mass spectrometry techniques to accurately measure the low concentrations and isotopic compositions of U, Th, and Pb in meteorites [3] and in virtually every mineral in a sample of ca. 1 Ga granite [4]. The new techniques reduced the amounts of Pb required for accurate measurements of concentration and isotopic composition by ca. three orders of magnitude, allowing application of $^{207}Pb/^{206}Pb$ dating to meteorites and the Earth [3], and of U-Pb dating to small amounts of zircon, sphene (titanite), apatite [4] and monazite [5], thus setting the stage for the modern era of U-Pb geochronology.

[1] Nier (1939) *Phys. Rev.* **55**, 150–153. [2] Nier (1939) *Phys. Rev.* **55**, 153–163. [3] Patterson *et al.* (1955) *Science* **121**, 69–75. [4] Tilton *et al.* (1955) *Bull. Geol. Soc. Amer.* **66**, 1131–1148. [5] Tilton & Nicolayson (1956) *Geochim. Cosmochim. Acta* **11**, 28–40.

Fe –metasomatism in upper mantle beneath SW Poland

M. MATUSIAK-MAŁEK[1]*, J. PUZIEWICZ[1], M. GREGOIRE[2] AND T. NTAFLOS[3]

[1]Univ. Wroclaw, Poland (*correspondence: magdalena.matusiak@ing.uni.wroc.pl)
[2]CNRS-UMR 5562, Univ. Toulouse, France (michel.gregoire@get.obs-mip.fr)
[3]Univ. Wien, Austria (theodoros.ntaflos@univie.ac.at)

Cenozoic alkaline volcanic rocks from SW Poland make the NE termination of Cenozoic Central European Volcanic Province. The volcanics occur on both sides of the NW-SE trending Intrasudetic Fault Zone (IFZ), a major Variscan dislocation feature separating crustal blocks of different geological record. Two peaks of volcanic activity (30-26 and 23-15 Ma) are recorded in volcanics occurring to the north of IFZ, whereas Cenozoic eruptive rocks located south from the fault zone (Lądek Zdrój volcanic field, Kozákov volcano) are much younger (5 – 3 Ma). All of the mantle xenoliths occurring in alkaline rocks are from the mantle spinel peridotite facies.

The xenoliths occurring in volcanic rocks located N of the IFZ record significant depletion, especially in basaltic components followed by various style of melt-related metasomatism. Significant part of peridotites are enriched in Fe, which is evidenced by low (83-89 %) forsterite content in olivine, and low #mg in orthopyroxene (0.85-0.86) and locally cpx (0.87-0.88). Textures of these peridotites exludes cumulative origin linked to crystal sellting. Some of mineral chemical features (e.g. NiO in Ol 0.30 – 0.44 wt.%) indicate upper mantle origin. We suggest that the Fe – enriched peridotites represent parts of mantle affected by Fe (and Mn) – rich metasomatic agent, which appearts to be alkaline silicate melt in the Księginki locality [1]. Lack of bulk rock Ca enrichment, typical for other Fe – peridotites [2] suggests low fraction of carbonated-eclogite-derived melts [3, 4] to be a metasomatic agent in Krzeniów locality.

The Fe-enriched peridotites among mantle xenoliths have not been found to the south of IFZ (Lądek Zdrój [3], Kozákov [5]). Moreover, xenoliths from the southern and northern domains differ in respect to texture, modal composition and style of metasomatic processes. Hence, we suggest that IFZ constitutes also a boundary between two litospheric mantle domains.

[1] Puziewicz *et al.* (submitted) *J Petrol.* [2] Ionov (2005) *Contr Miner Petr* **150**, 335–353. [3] Dasgupta *et al.* (2006) *J Petrol* **47**, 647–671. [4] Matusiak-Małek *et al.* (2010) *Lithos* **117**, 49–60. [4] Ackerman *et al.* (2008) *J Petrol* **48**, 2235–2260.

https://doi.org/10.1180/S0026461X00006502 Published online by Cambridge University Press

Analysis of heavy metals in floodplains of the Morava and Jizera rivers

TOMAS MATYS GRYGAR[2], TEREZA NOVAKOVA[1,2]*, VERONIKA LUKESOVA[2,3] AND MARTIN MIHALJEVIC[1]

[1]Charles University, Faculty of Science, Albertov 6, 128 43, Prague (Mihal@natur.cuni.cz) (*correspondence: Tereza.Novakova@natur.cuni.cz)
[2]Institute of Inorganic Chemistry AS CR (grygar@iic.cas.cz)
[3]Department of Soil Science and Soil Protection, Faculty of Agrobiology, Food and Natural Resources, Czech University of Life Sciences in Prague (lukesovav@af.czu.cz)

Regional pollution by Cu, Pb and Zn during the 20th century was studied in floodplains of two rivers in Czech Republic, usually considered less contaminated - the Morava and the Jizera; the latter is one of three water sources for Prague. Sediments were obtained by hand-drilled cores (2-4 m long) and in the case of the Morava River from outcrops in erosion banks. To describe realistically the pollution of floodplain sediments, facial analysis and outline of floodplain architecture are essential for two main reasons: to distinguish anthropogenic impact from natural background and evaluate possible post-depositional migration of pollutants. Geochemical analysis by laboratory ED XRF spectrometer offers handy tools for both these subtasks, which we have learnt in the Morava River floodplain and now apply to Jizera River floodplain. Additional subtask is sediment dating, which can be achieved by careful examination of depth dependences of activities of ^{137}Cs and unsupported ^{210}Pb; the use of ^{14}C of plant debris is, unfortunately, limited. For reliable reconstruction of the past pollution, fine sediments (silty clay with small sand content) should be used, which slow down the vertical migration of both pollutants and ^{137}Cs. Cu, Pb and Zn start to migrate substantially in floodplain sediments of both studied rivers at depths larger than 1.5 m, where they follow lithofacial boundaries and redox accumulations of Fe and Mn oxides. Extensive correlations of densely and continuously sampled cores must be performed to avoid lithofacial biases and migration - and only that can allow sound interpretations. Approximate dating of sediments from the Morava River area can be based on the onset of Pb and Zn contamination at about 1900, Pb fastest enhancement at moderate Zn in the 1950's, stagnating Pb 1960's – 1980's), and stagnating Zn and declining Pb since 1990's.

Acquisition of Fe by aerobic microorganisms: Effects of Fe oxide nanoparticle size

P.A. MAURICE[1], C. DEHNER[2], J. DUBOIS[2] AND L.E. BARTON[1]

[1]Dept. of Civil Engineering & Geological Sciences, and
[2]Dept. of Chemistry and Biochemistry, University of Notre Dame, Notre Dame, IN, 46556, USA (pmaurice@nd.edu, cdehner@nd.edu, jdubois@nd.edu, lbarton@nd.edu)

Most organisms require Fe as a fundamental nutrient; yet, Fe-bearing minerals tend to be highly insoluble in circum-neutral aerobic environments. Many aerobic microorganisms overcome Fe limitation by releasing low molecular weight organic ligands known as siderophores into the environment. Siderophore-Fe(III) 1:1 complex stability constants range from 10^{23}-10^{52}.

Using an obligate aerobic bacterium *Pseudomonas mendocina* ymp wild type (WT) and a siderphore (-) mutant of the species (MT; i.e. a mutant that can not produce siderophore), along with a reporter strain that signals Fe deficiency, our group investigated Fe acquisition from hematite (nano)particles of different average particle sizes. Fe associated with < 10 nm hematite was considerably more bioavailable than Fe associated with larger particles. Hematite nanoparticles < 10 nm have more transient or labile Fe, dissolve at about an order of magnitude faster rate in siderophore at circumneutral pH, and support enhanced growth (relative to growth on 72 nm hematite) by *P. mendocina* WT under Fe-limited conditions. The greater bioavailability is also related in part to mechanism (s) that depend on cell/nanomineral proximity, but not on siderophores. MT bacteria readily acquire Fe from particles < 10 nm but must be in direct physical proximity to the nanomineral. Addition of the reducing ligand ascorbate is particularly effective at supplying nano-hematite Fe to the bacteria under siderophore-free conditions. Even a small amount of cell-surface associated reducing activity, as further suggested by results of ferrozine assay, therefore would be likely to enhance cell growth considerably.

https://doi.org/10.1180/S0026461X00006502 Published online by Cambridge University Press

P-T-t evolution of metapelitic rocks from the Bushveld contact aureole: Using garnet isopleths thermobarometry and Lu-Hf garnet dating

P.K. MAVIMBELA*, M.J. RIGBY, P.G. ERIKSSON AND P. GRÄSER

University of Pretoria, Pretoria 0002, South Africa (*correspondence philani.mavimbela@up.ac.za, matin.rigby@up.ac.za, pat.eriksson@up.ac.za, peter.graser@up.ac.za)

We employ garnet isopleth thermobarometry and Lu-Hf garnet isotopic system in order to investigate the P-T-t evolution of two garnet bearing metapelitic samples (DY954 and DY918) from the Bushveld contact aureole. Two types of garnets porphyroblast were identified in sample DY954, garnet included in biotite which records peak metamorphic condition of 551 $\pm 15^0$C at 3.1±0.2kb and a non reactive garnet which records 527±8^0C at 3±0.35kb. The slightly higher temperature of the former may be interpreted to have resulted from garnet reaction overstepping. The DY918 amalgamated garnet porphyroblast does records different P-T conditions (~601^0C at 1.3kb) as compared to the DY954 sample and the fusion of the garnets which will require significant re-crystallization [1] can be attributed to these higher temperatures. The weighted average Lu-Hf garnets isochron ages obtain for the two samples (DY954 and DY918) are 2061.5±5.1Ma and, 2061.4±3.5Ma respectively. The nearly identical garnet isochron ages marks the first robust age of the BIC contact aureole which can be indirectly interpreted as constraints to the emplacement age of the RLS.

[1]Taylor, J. & Stevens, G. (2010) *Lithos* **120**, 277–292.

Heavy metal fractionation in high temperature fumaroles

JOHN A. MAVROGENES* AND RICHARD W. HENLEY

Research School of Earth Sciences, Australian National University, ACT Australia 0200 (*correspondence: john.mavrogenes@anu.edu.au)

Some volcanoes discharge high temperature gases from which unique metal suites are formed as sublimates. Examples include Vulcano, Italy, where sublimates contain a wide range of rare bismuth-lead sulfosalt minerals. Paradoxically, arsenic minerals do not occur in fumarole discharges but are common in crater lakes. In paleo-fumarole environments such as Chinkuashih, Taiwan, enargite and related sulfosalts occur as almost mono-mineralic assemblages over a depth range of more than 1000 meters. Modelling of vapor-phase stabilities shows that decompressing volcanic gases deposit pyrite below 700°C followed by rapid precipitation of enargite as depressurization proceeds. In consequence, surface discharges are strongly depleted in arsenic, iron, copper and a range of heavy metals.

Based on high resolution microanalysis of As-rich sulfosalt assemblages in paleo-fumaroles, we suggest that fractionation occurs between arsenic-rich sulfosalt melt and vapor within the upper few hundred meters of the surface, leading to heavy metal (Sb, Bi, Te, etc) enrichment of the vapor phase and consequent formation of lead-bismuth sulfosalt minerals and tellurides in surface discharges, such as the metallic snow of the Venus Highlands region. Similar sub-surface fractionation processes result in molybdenum-rhenium enrichment in volcanic systems such as Kudryavy (Kurile Arc, Russia), and gold and silver in others (e.g.Kudryavy and Colima, Mexico). Similar sulfosalt –sulfide melt segregation occurs in the magmatic environment resulting in metal fractionation during the formation of the so-called 'high sulfidation' and porphyry copper-gold deposits.

https://doi.org/10.1180/S0026461X00006502 Published online by Cambridge University Press

Effect of aqueous organic ligands on Mg-isotope fractionation during magnesite precipitation

V. MAVROMATIS*, Q. GAUTIER, J. SCHOTT AND E.H. OELKERS

Geoscience and Environment Toulouse (GET), CNRS, UMR 5563, OMP, 14 Avenue Edouard Belin, 31400 Toulouse, France (*correspondence: mavromat@get.obs-mip.fr)

Organic ligands are present in most Earth's surface environments and play a significant role on mineral formation and transformation. This study aims to illuminate the effect of the presence of these organic ligands on isotopic fractionation during mineral dissolution and growth.

Magnesite precipitation experiments were conducted in mixed flow reactors at 120 and 150 ºC following the methods described by Saldi *et al*. [1], in the reactive fluids containing various concentrations of aqueous oxalate and citrate. Supersaturation of the reactive fluid in the reactor was facilitated by the retrograde solubility of magnesite. Magnesite precipitation favored incorporation of isotopically lighter Mg into solid phase, as shown by enrichment of ^{26}Mg in the outlet solutions. Experiments conducted at 120 ºC show larger isotopic fractionation factors $\Delta^{26}Mg_{solid\text{-}solution}$ compared to those performed at 150 ºC indicating a temperature effect on isotopic fractionation. Furthermore, experiments performed in the presence of oxalate and citrate, exhibit lower $\Delta^{26}Mg_{solid\text{-}solution}$ values at similar precipitation rates compared to corresponding experiments performed in the absence of aqueous organic ligands. These observations suggest the preferential complexation of the heavier Mg isotopes by the organic ligands in aqueous solution.

Overall the observations obtained in this study demonstrate that $\Delta^{26}Mg_{solid\text{-}solution}$ during magnesite precipitation depends not only on precipitation rates, but also on the concentration of aqueous organic ligands. This result suggests that the presence of organic ligands may also effect the isotopic fractionation of a large number of other elements, and may be responsible, at least in part for the degree of isotopic fractionation observed in natural systems.

[1] Saldi *et al*. (2009) *Geochim. Cosmochim. Acta* **73**, 5646–5657.

$^{146,147}Sm$-$^{142,143}Nd$ studies of komatiites from western Dharwar Craton, India: Implications for depleted mantle evolution in Early Archean

J.M. MAYA, RAJNEESH BHUTANI* AND S. BALAKRISHNAN

Department of Earth Sciences Pondicherry University, Puducherry 605014 (*correspondence: rbhutani@gmail.com)

Early Earth Differentiation

Variation of $^{142}Nd/^{144}Nd$ ratio in terrestrial samples compared to chondrites has now been demonstrated by several studies indicating an early global chemical differentiation of Bulk Silicate Earth (BSE). (see [1] for a recent review).

These studies, however, raised several outstanding questions related to nature of Early Enriched Reservoir (EER) and Early Depleted Mantle (EDM) and their subsequent evolution.

Results

We have carried out measurements of $^{142}Nd/^{144}Nd$ ratios, along with conventional ^{147}Sm-^{143}Nd studies, on well preserved komatiites with spinifex texture characterized by MgO > 20% that occur at Banasandra, in the western limb of Chitradurga greenstone belt of Dharwar craton in India.

$^{142}Nd/^{144}Nd$ ratios of these komatiites are same as La Jolla and AMES standards within 10 ppm (2 σ) uncertainity. The ^{147}Sm-^{143}Nd whole rock isochron age as yielded by 9 samples is 3136 ± 200 Ma (MSWD =74) with initial $^{143}Nd/^{144}Nd$ =0.50872 ± 0.00033 corresponding to $\varepsilon_{Nd\ (t=3.15)}$=+ 3.5.

Discussion

We calculated time-integrated $^{147}Sm/^{144}Nd$ ratio of source of 3.15 Ga old komatiites of Dharwar craton with the constraints that it got differentiated at 4.2 Ga (No radiogenic $^{142}Nd/^{144}Nd$ anomaly) and that by 3.15 Ga ago it evolved to $\varepsilon_{Nd\ (t=3.15)}$=+ 3.5. The time-integrated $^{147}Sm/^{144}Nd$ ratio of the source, thus obtained, is significantly higher than what has been predicted by Blichert-toft and Puchtel [2] for the source of this age. These results can be explained if source of these komatiites is originated from a second differentiation of the EDM at 4.2 Ga. Further, these results also indicate that Archean depleted mantle has not been homogenous in time and space.

[1] Caro G (2011) *Annu. Rev. Earth Planet. Sci.* **39**, 31–58.
[2] Blichert-Toft & Puchtel (2010) *Earth & Planetary Science Letters* **297**, 598–606.

https://doi.org/10.1180/S0026461X00006502 Published online by Cambridge University Press

Variability of nitrogen stable isotope in suspended organic matter in waters of the western continental shelf of India and the Mandovi estuary

M.V. MAYA[1]*, S.G. KARAPURKAR[1], M.A. SOARES[1], R. AGNIHOTRI[2], R. ROY[1], H. NAIK[1] AND S.W. A. NAQVI[1]

[1]National Institute of Oceanography (Council for Scientific and Industrial Research), Dona Paula, Goa - 403004, India (*correspondence: mmayae11@gmail.com)

[2]National Physical Laboratory, New Delhi, India (rajagni9@gmail.com)

First direct evidence for the addition of substantial amount of isotopically light nitrogen by *Trichodesmium* in the western continental shelf of India (WCSI), a region of global significance on account of being the largest natural seasonally-occurring coastal oxygen-deficient zone in the world with large efflux of N_2O to the atmosphere. The results for the WCSI and the Mandovi estuary are summarized in Fig. 1, which reveal significant shifts in $\delta^{15}N$ of suspended particulate organic matter (SPOM) before and after the onset of the south-west (SW) monsoon.

Discussion of results

The development of *Trichodesmium* blooms significantly lowers the $\delta^{15}N$ of SPOM during the pre-monsoon season, whereas water-column denitrification makes SPOM enriched in $\delta^{15}N$ during late SW monsoon. Another important result of this study states that the $\delta^{15}N$ of SPOM is generally lower than the mean value (7.38‰) for surficial sediments. The $\delta^{15}N$ of SPOM in the Mandovi estuary also shows significant variation during and after the cessation of SW monsoon. Depletion of $\delta^{15}N$ in SPOM during the SW monsoon could be preferential utilization of $^{14}NO_3^-$ by phytoplankton, as has been observed in other NO_3^- replete areas, whereas post-monsoon season are characterized by relatively high $\delta^{15}N$ of SPOM.

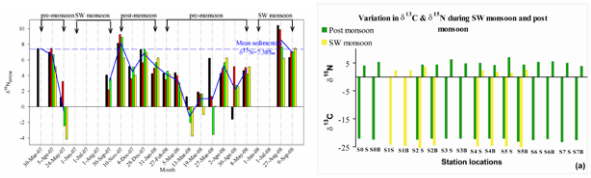

Figure 1: A) Intra-annual variations in $\delta^{15}N$ of SPOM along the WCSI. B) SW monsoon and post-monsoon changes in the Mandovi estuary.

Isotopic analysis of microarrays to link microbial identity and function

X. MAYALI[1]*, P.K. WEBER[1], E.L. BRODIE[2], S. MABERY[1], P.D. HOEPRICH[1] AND J. PETT-RIDGE[1]

[1]Lawrence Livermore National Laboratory, Livermore CA 94550, USA (*correspondence: mayali1@llnl.gov)

[2]Lawrence Berkeley National Laboratory, Berkeley CA 94720 USA

Most microorganisms remain uncultivated, and typically their ecological roles are inferred from diversity and genomic studies. To directly measure functional roles of uncultivated microbes, we developed Chip-SIP, a high-sensitivity, high-throughput stable isotope probing (SIP [1]) method performed on a phylogenetic microarray. For this approach, we incubate microbial communities with isotopically labeled substrates, hybridize community rRNA to a microarray, and measure isotope incorporation—and therefore substrate use—by secondary ion mass spectrometer imaging (NanoSIMS).

Chip-SIP analysis of an estuarine community quantified amino acid, nucleic acid or fatty acid incorporation by 81 taxa. The resulting resource use profile (Figure 1) demonstrates that some generalist bacteria can incorporate multiple organic substrates while others specialize in 1 or 2 out of 3. We also found that bacterial functional capacity can be decoupled from phylogeny. This approach provides a means to test genomics-generated hypotheses about biogeochemical function in natural environments.

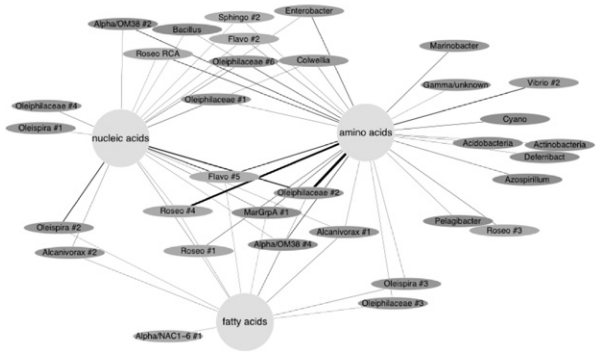

Figure 1: summary network diagram of Chip-SIP analysis of San Francisco Bay, linking substrates (circles) to microbial taxa (ovals). The thickness of the lines is proportional to the amount of substrate incorporated.

[1] Radajewski *et al*. (2000) *Nature* **403**, 646–649.

https://doi.org/10.1180/S0026461X00006502 Published online by Cambridge University Press

Absolute isotopic composition of molybdenum reference materials using double spike MC-ICP-MS

A.J. MAYER[1]*, B. PROEMSE[2] AND M.E. WIESER[1]

[1]Department of Physics and Astronomy, 2500 University Drive NW, University of Calgary, Calgary, AB, T2N 1N4, Canada (*correspondence: ajmayer@ucalgary.ca)
[2]Department of Geoscience, 2500 University Drive NW, University of Calgary, Calgary, AB T2N 1N4, Canada

Molybdenum isotope abundance measurements have enabled unique insights into the study of oxic conditions in the oceans [1], high-temperature hydrothermal ore deposits [2], and the heterogeneity of molybdenum in the early solar system [3]. Useful interpretations are only possible when isotopic compositions are reported relative to commonly available reference materials. Chemical processing of samples can alter isotopic composition, so it is important to test methods on matrices of known molybdenum isotopic composition and concentration.

At present, researchers are using a variety of commercially available and in-house standards. Recently, Wen *et al*. measured the relative isotopic composition of five reference solutions and proposed using NIST SRM 3134 as the delta zero reference for molybdenum [4]. However, the absolute isotopic compositions of these standards were not reported and none of the chosen materials were in a natural matrix.

In this study, we have determined the absolute isotopic composition of molybdenum in a variety of reference materials including NIST SRM 3134, BCR-1, BCR-2 (basalt), USGS SCo-1 (shale), SRM 1547 (peach leaves), Johnson-Matthey pure Mo metal rod, and SCP Science Mo PlasmaCal. Measurements were made using a Thermo Scientific Neptune MC-ICP-MS. Instrumental fractionation was corrected by measuring a mixture of the sample with a fully calibrated double spike. The fractionation correction assumed an exponential fractionation law and used computational root finding methods to solve for the fractionation due to chemical processing and instrumental mass bias.

[1] Barling *et al*. (2001) *EPSL* **193**, 447–457. [2] Mathur *et al*. (2010) *Miner Deposita* **45**, 43–50. [3] Dauphas *et al*. (2002) *ApJ*. **565**, 640–644. [4] Wen *et al*. (2010) *J. Anal. At. Spectrom*. **25**, 716–721.

Chemical and isotopic composition of Cenozoic hornblende-bearing basalts from the Rhön area (Germany)

B. MAYER[1]*, S. JUNG[1] AND A. STRACKE[2]

[1]Mineralogisch-Petrographisches Institut, Universität Hamburg, Grindelallee 48, 20146 Hamburg, Germany (*correspondence: Bernhard.Mayer@uni-hamburg.de)
[2]Westfälische Wilhelms Universität, Institut für Mineralogie, Corrensstraße 24, 48149 Münster, Germany

Primitive, alkaline mafic volcanic rocks provide important information about the chemical composition of the Earth's mantle. The source of intra-continental volcanic rocks are either the subcontinental lithospheric mantle, the asthenospheric upper mantle or upwelling mantle material (mantle plumes). In contrast to the asthenosphere, the lithospheric part of the mantle has been isolated from the convecting part and may have had a complex geological history of ancient depletion and enrichment events.

Unusual hornblende-bearing basanites from the Rhön area (Central European Volcanic Province; CEVP) are mostly primitive to differentiated volcanic rocks (Mg#: 65-45, Ni: 190-60 ppm, Cr: 400-100 ppm) with higher TiO_2, lower MgO contents and slightly lower Ce/Pb ratios (15-20) at a given SiO_2 content relative to other alkaline rocks from the CEVP. Rare Earth element patterns show LREE enrichment but only moderate depletion in HREE relative to primitive mantle. Rare earth element patterns can be reproduced by about 4 to 8 % partial melting of a spinel peridotite containing 10 % of modal amphibole. In multi-element diagrams, the basanites are enriched in Nb, but depleted in Rb and K relative to the neighboring elements, compatible with partial melting with residual amphibole.

Incompatible trace element abundances and ratios and Nd and Sr isotopes overlap those of other volcanic rocks from the CEVP. Initial $^{87}Sr/^{86}Sr$ ratios range from 0.7034 to 0.7040 at almost constant initial $^{143}Nd/^{144}Nd$ of ca. 0.51279-0.51285 (εNd of +3.3 to +4.6). The Sr and Nd isotope data suggest that contamination of the lavas with the ambient lower crustal rocks is relatively minor (< 5%). The variable Sr at constant Nd isotope compositions could also result from melting heterogeneous sources with variable Rb/Sr ratios as a result of mantle metasomatism. Based on their high TiO_2 but low MgO, elevated $^{87}Sr/^{86}Sr$ ratios and low Ce/Pb ratios relative to other basanites from the CEVP, the hornblende-bearing basanites appear to contain a signifcant proportion of the lithospheric upper mantle.

https://doi.org/10.1180/S0026461X00006502 Published online by Cambridge University Press

Modeling the relationship between sorption and residence times

M.A. MAYES*, S. JAGADAMMA, W.M. POST, J. FRERICHS AND G. WANG

P.O. Box 2008, Oak Ridge, TN 37831
(*correspondence: mayesma@ornl.gov)

We seek to improve representations of stabilization and degradation of organic carbon in soils in terrestrial C cycling models. Major processes considered in the model include sorption of dissolved compounds onto mineral and particulate soil fractions, incorporation into microbial biomass, enzyme-facilitated degradation, and mineralization of dissolved and native carbon. Soils from temperate, tropical, and arctic climates will be used. The sorptive capacity of three orders of magnitudes of dissolved compounds common to soil solutions (sugars, starch, lipids, etc.) will be measured using ^{14}C labelling. Subsequently, the soils containing adsorbed compounds will be subjected to short-term incubation experiments to determine rates of mineralization from each soil fraction. Chloroform fumigation will be used to measure ^{14}C allocated to microbial biomass. Enzyme assays will be used to determine the potential for enzyme activities in response to various treatments. This presentation will consist of initial experimental findings and presentation of the model framework. The initial findings will be evaluated in terms of project goals produce a testbed for modelling microbially-faciliated sorptive and degradative processes at the soil mineral interface.

The effect of *M. thermoflexus* on the Fe-bearing mineral assemblage associated with low temperature basalt-water reactions

L. MAYHEW[1]*, G. LAU[1], T. MCCOLLOM[2] AND A. TEMPLETON[1]

[1]Dept. Geological Sciences, University of Colorado–Boulder (*correspondence: mayhewl@colorado.edu)

[2]Laboratory for Atmospheric and Space Physics, University of Colorado–Boulder

Water-rock reactions, such as serpentinization of ultramafic rocks in the ocean crust, alter Fe(II)-bearing silicate minerals producing secondary minerals and H_2 gas and are therefore thought to support chemolithotrophic life in extreme environments (e.g. the deep subsurface). However, the alteration of Fe-bearing silicate minerals present in these rocks has not been extensively studied under low temperature, anoxic conditions. We inoculated a low temperature (55°C), anoxic water-Fe^0-basalt system with a methanogenic Archaeon, to determine if 1) microbial growth could be supported by *in situ* production of H_2 gas and 2) the presence of the microorganisms influenced the production of H_2 gas and the Fe-bearing secondary mineral assemblage.

Growth of *M. thermoflexus* is evidenced by time series measurements of H_2 and CH_4 showing the continuous production of H_2 in the abiotic control while in cultures microbial methanogenesis draws down H_2 and produces CH_4. Upon saturation, purging the headspace gases destabilizes Fe-bearing minerals and releases Fe and Si to solution. $[Si_{(aq)}]$, while buffered to relatively constant values, was lower in the abiotic control than cultures. $[H_2]$ appears to affect the speciation of Fe in the solid phase products. Collection of synchrotron-based μXRF maps at multiple energies within the Fe K-edge and μXANES analyses integrated with principal components analyses and XANES fitting enables visualization and quantification of the distribution of the Fe-species. After ~1 year of reaction, Fe-bearing secondary mineral assemblages associated with high $[H_2]$ (abiotic control) are different than those associated with low $[H_2]$ (culture experiments). For example, minnesotaite, an Fe-phyllosilicate, is ubiquitous in the abiotic control but much less abundant in the culture experiments. We will discuss how the geochemical reaction paths and Fe-speciation differ between the abiotic control and the culture experiments. This work suggests that at low temperatures microorganisms may have a profound effect on what has long been thought to be solely an abiotic reaction and may produce diagnostic mineral assemblages that may be preserved in the geological record.

https://doi.org/10.1180/S0026461X00006502 Published online by Cambridge University Press

The petrological, geochemical and tectonic setting of metabasites from Mashhad, North East of Iran

S.A. MAZAHERI[1], R. BIERESDORFER[2] AND F. ARMSTRONG[2]

[1]Geology Department, Faculty of Sciences, Ferdowsi University of Mashhad, Mashhad, 91775-1436, Iran
[2]Department of geological and Environmental Studies, Youngstown State University, Ohio 44555, USA (mazaheri@ferdowsi.um.ac.ir)

Metabasites of Mashhad area are part of Virani (Nourabad) Ophiolite in the Binaloud region. The ophiolite extends to Aghdarband area, north east of Fariman. Ultramafic rocks are predominantly peridotite (lherzolite, wherlite and hursburgite). Mafic rocks are mainly metabasalt, metagabbro and metadolerite. Large pillow lavas (>45 Cm in diameter) crops out in Zakaria and Nowdarreh areas.

Metabasites subjected to a low to medium grade metamorphism (greenschist to amphibolites facies), characterized by Ab + Act + Epid + Chlo; Na-Plag + Hbld + Epid and Ca – Na Plag + Hbld assemblages. Plagioclase (Ab to Ande), Amphiboles (Actinolite and Hornblende), Epidote, Chlorite, Quartz, Sphene, Apatite and Iron – Oxides are the most common minerals of metabasites.

Selected samples have analysed by XRD, XRF and ICP methods. Major and trace elements data indicates that metabasites are tholeiitic in nature and characterized by low potassium (0.25 wt%), and high magnesium (maximum 23.23 wt%), high chromium (maximum 2110 ppm), and high nickel (maximum 2970 ppm) contents. The metabasite samples have low Zr/TiO2 (0.0011 – 0.0092) and Nb/Y (0.06 – 0.15) ratios, similar to those of tholeiitic basalts.

The Metabasites of Mashhad area are believed to be remnant of the Paleo – Tethys oceanic plate that were subducted beneath the Turan plate. Later on the Turan plate have obducted over the Iranian Micrcontinent, and formed the northeasten Iran.

Importance of syntrophic acetate oxidation during thermophilic municipal solid wastes anerobic digestion

L. MAZEAS[1]*, J. GROSSIN-DEBATTISTA[1], X. QU[1,2], A. GUENNE[1], P.J. HE[2], H. BUDZINSKI[3], M. LE MUNIER[4] AND T. BOUCHEZ[1]

[1]Cemagref-HBAN, parc de Tourvoie, BP 44, 92163 Antony cedex, France (*correspondence: laurent.mazeas@cemagref.fr)
[2]State Key Laboratory of Pollution Control and Resources Reuse, Tongji University, Shanghai 200092, China
[3]Institut des Sciences Moléculaires (ISM) – UMR 5255 CNRS - Université Bordeaux 1, 33405 Talence, France
[4]Suez Environnement, CIRSEE, 38 rue du Président Wilson, 78230 Le Pecq, France

During anaerobic digestion of organic matter, acetate and H_2/CO_2 are expected to be responsible of around 67% and 33% of the methane production respectively [1]. Our results show that temperature has a significant influence on methanogenic pathways as indicated by the different CH_4 isotopic composition ($\delta^{13}CH_4$) evolutions observed under mesophilic and thermophilic conditions. The contribution of the hydrogenotrophic pathway appears to be much more important in thermophilic condition due to the occurrence of the syntrophic acetate oxidation (SAO) reaction.

Using different molecular microbiological tools (Fluorescent *in situ* hybridization and cloning sequencing) microbial communities involved during those MSW incubations have been identified. It appears that strict hydrogenotrophic archaea from the Methanomicrobiales order are highly dominant in thermophilic condition which is in accordance with a SAO reaction implication.

[1] Conrad (1999) *FEMS Microbiol Ecol* **28**, 193–202.

https://doi.org/10.1180/S0026461X00006502 Published online by Cambridge University Press

Petrogenesis of Zoozan pluton, NE of Lut, Eastern Iran

S.A. MAZHARI[1]* AND M. SAFARI[2]

[1]Department of Geology, Payame Noor University, 19395-4697 Tehran, I.R. of Iran (*correspodence: ali54894@yahoo.com)

[2]Geological Survey of Iran, North-East Territory, Mashhad, Iran (petrolsaf@yahoo.com)

The Zoozan pluton is one of the Tertiary plutonic bodies in the northeastern of the micro-continental Lut block in Eastern Iran. This pluton is composed of two geochemically unrelated mafic and granitoid units. All rocks are calc-alkaline, with LILE/REE and HFSE/REE compatible with arc magmas. Mafic phase consists of gabbro to quartz diorite and emplaced as small stocks and dykes. These rocks exhibit relatively high contents of incompatible elements, low Na_2O and Mg#>44.0. These features suggest their origin from enriched lithospheric mantle above subducted slab.

Granitoid phase includes granite-granodiorites which show high-K calc-alkaline metaluminous to slightly peraluminous I-type granitoid characteristics. Their Chondrite-normalized REE patterns mark enrichment of LREE (La_N/Lu_N= 7.6-12.5) and small negative anomaly (Eu/Eu^*= 0.63-0.74). They have geochemical composition typical of volcanic arc granitoids and have been originated from metabasaltic to tonalitic sources. Furthermore, fractional crystallization may have played significant role during the formation of Zoozan granitoids.

Variation in carbon stable isotope ratios of organic matter in Bay of Bengal during the last glacial episode

A.MAZUMDAR*, R.K. JOSHI, A. PEKETI AND B.G. NAIK

Geological Oceanography, National Institute of Oceanography, Donapaula, Goa, 403004, India (*correspondence: correspondence: maninda@nio.org)

We report here a high resolution total organic carbon content (TOC) and $\delta^{13}C_{TOC}$ variations from a 30m long core from Bay of Bengal. The core (MD161-8, water depth: 1033 m) was collected on board *Marion Dufresne* as part of our on going gas hydrate exploration program in the Krishna-Godavari basin. TOC content is constrained within 1-2 wt%. Our studies show dependence of TOC content on grain size distribution. During the last glacial episode, the $\delta^{13}C_{TOC}$ varied between 14 and 17‰ VPDB indicating a significant contribution of C4 vegetation. Within 16-18 mbsf we have observed presence of pentamethyl icosane with carbon isotope ratios <-100‰. Presence of PMI has resulted in the isotope excursion. Post LGM rise in pCO_2 resulted in the diminished C4 contribution. Most depleted C isotope ratio is noted at ~7-8 ky BP suggesting enhanced contribution of terrestrial organic matter. For rest of the Holocene contribution from marine productivity dominates.

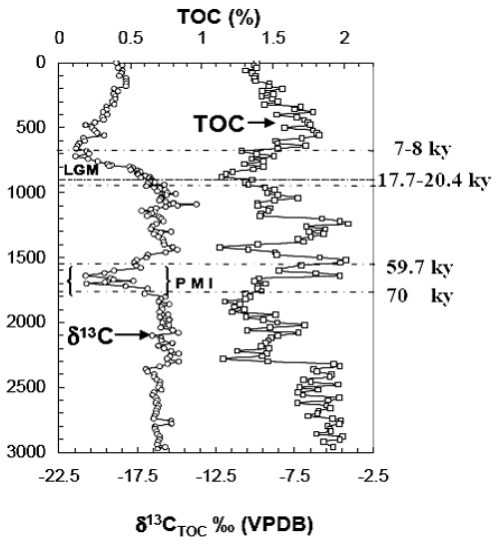

Figure 1: TOC and $\delta^{13}C_{TOC}$ profile of MD161-8

https://doi.org/10.1180/S0026461X00006502 Published online by Cambridge University Press

Pristine mantle xenoliths from the active Bismarck Arc

SARLAE R.B. MCALPINE* AND RICHARD J. ARCULUS

Research School of Earth Sciences, Australian National University, ACT Australia 0200
(*correspondence: sarlae.mcalpine@anu.edu.au)

Peridotites samples were recovered during the Marine National Facility Voyage (SS06-2007; WeBiVE) from three volcanic cones northwest of Ritter Volcano, New Britain-West Bismarck Arc system of Papua New Guinea. Wedge-derived peridotites are extremely rare even in well-explored subaerial arcs; the Ritter suite is the first global occurrence of peridotites recovered from an active submarine volcanic arc front edifice.

The peridotites occur as rounded (≤15cm diameter) and angular blocks and fragments. The host basalt is a Cr spinel-olivine-diopsidic augite-bearing, medium-K tholeiite. It is the most MgO-rich basalt (~15wt%) reported in the West-Bismarck-New Britain Arc system; the high-MgO might derive in part from the cumulative and/or xenocrystic nature of some olivine.

The xenoliths are pristine (serpentine-free), predominantly harzburgitic but also include lherzolite, orthopyroxenite, and a single gabbro. Preliminary petrological analysis shows complex textural relationships between the constituent minerals olivine ($Fo_{94.4-86.3}$), orthopyroxene, clinopyroxene, and spinel. The spinel is highly refractory with Cr/(Cr+Al) > 0.9 accompanied by high Mg/(Mg+Fe^{2+}) consistent with quenching from high-temperature. Deformation textures include olivine kink-banding and wavy exsolution lamellae in the pyroxene. Secondary clinopyroxene reflects some metasomatism. Bulk trace element charateristics include relatively unfractionated rare earth element abundances (0.6 to 1*chondritic), elevated Pb/Ce (>1), and negative Nb, Ta, Zr, Hf, and Ti anomalies.

Temperatures range from ~900 to 1100 °C; fO_2 ranges from ΔFMQ -2 to +0.5. These samples show extremely refractory, relatively reduced harzburgites are present in the mantle section beneath a modern subduction system. Ongoing detailed mineralogical and petrological studies will provide important insight into the mantle below the New Britain-West Bismarck Island Arc.

Arsenic in Ground Water

J.M. MCARTHUR

Earth Sciences, UCL, London WC1E 6BT, UK.
(j.mcarthur@ucl.ac.uk)

Arsenic in groundwater presents a hazard to health globally [1]. In the Bengal Basin, one of the regions worst affected by such pollution [2, 3], the distribution of pollution reflects the geological evolution of the basin during the past 125,000 years [3], and the same explanation, with local modifications, must apply to As-polluted deltaic aquifers worldwide. The As-pollution is confined largely to sediments laid down after the last glacial maximum, a fact that explains the vertical inhomogeneity in As-pollution. The lateral inhomogeneity in As-pollution reflects, in part, the distribution of As-polluted palaeo-channel aquifers and As-free palaeo-interfluvial aquifers [4].

Flow of As-polluted palaeo-channel water into As-free palaeo-interfluvial aquifers has been ongoing since sea-level stabilized around 6 ka. The flow has been accelerated by abstraction of water for irrigation since the 1970s. Natural and enhanced flows explain the development of a strong redox gradient at the palaeo-interfluvial margins. Flows enhanced by abstraction for irrigation explain rising concentrations of As in marginal palaeo-interfluvial wells, especially where the flow is counter to the natural hydraulic gradient. In this talk, some of these aspects will be explored.

[1] Ravenscroft, P. *et al*. (2009) *.Arsenic pollution: a global synthesis*. Wiley-Blackwell [2] Frisbie SH, *et al*. (1999) The nature and extent of arsenic-affected drinking water in Bangladesh. *In*: *Metals and Genetics* (Sarkar B, ed). New York: Plenum Publishing Co,; 67–85. [3] DPHE; (1999) *Groundwater Studies for Arsenic Contamination in Bangladesh*. *Final Report, Rapid Investigation Phase*. Department of Public Health Engineering, Government of Bangladesh. Mott MacDonald and British Geological Survey (6 vols), Dhaka [4] McArthur J.M. *et al*. (2011). Palaeosol control on groundwater flow and pollutant distribution: the example of arsenic. *Environ. Sci. Technol*., **45**, 1376–1383. dx.doi.org/10.1021/es1032376.

https://doi.org/10.1180/S0026461X00006502 Published online by Cambridge University Press

Reaction rind formation in Mèlange in the Catalina Schist, California

C.A. McCallum[1]*,
S.C. Penniston-Dorland[1] and G.E. Bebout[2]

[1]Department of Geology, University of Maryland, College Park, MD 20742, USA
(*correspondence: mccallum@umd.edu)
[2]Department of Earth and Environmental Sciences, Lehigh University, Bethlehem, PA 18015, USA

Reaction rinds between differing lithologies are commonly thought to have formed due to fluid-assisted metasomatic alteration, however, enrichment in relatively fluid-immobile elements such as Cr and Ni suggests an additional process may be responsible for their formation. Eleven samples along a 17cm transect through one amphibolite grade block and a reaction rind with an ultramafic-rich matrix from the Catalina Schist, CA show distinct changes across the block-rind contact in mineral abundance and whole rock major and trace element and Li isotope composition. Whole rock rind concentrations of SiO_2, K_2O, Rb, Ba, MgO, Cr and Ni are enriched in the rind relative to the core and FeO is depleted. Lithium concentrations are enriched in the rind (10-16ppm) relative to the core (8-11ppm) with δ^7Li ranging from -3 to +1‰. The distribution of Li concentrations and isotope compositions is consistent with diffusion on the scale of almost the entire 17-cm profile. Garnets in the core and rind are similar in FeO content, however whole-rock FeO of the core and rind differs significantly, suggesting garnet growth before the depletion in whole-rock FeO. Rind garnets are pseudomorphed extensively by decussate chlorite, suggesting that infiltration by H_2O-rich fluid occurred after garnet growth. Rind concentrations of Cr, Ni Al_2O_3 and CaO can be most simply explained by mechanical mixing of mafic block (50-70%) with melange matrix (30-50%). Mixing cannot explain the increases in SiO_2, K_2O, Li, Rb and Ba or the depletions in FeO, and we propose that the concentrations of these elements in the rind are due to relatively late-stage fluid infiltration. We propose an early episode of mechanical mixing where mixing of mafic block and melange matrix produced rind-like material which was then accreted onto the outside of basaltic blocks. Garnets likely grew in both block core and rind after mechanical mixing. Fluid infiltration in the rind occurred after peak metamorphism of the block. The source of this fluid was likely metasedimentary rocks within the subduction zone, as has been proposed based on O isotope compositions of this amphibolite-facies mélange unit.

Serpentinization and hydrogen generation

T.M. McCollom[1], F. Klein[2], W. Bach[3],
N. Jöns[3] and A. Templeton[4]

[1]Laboratory for Atmospheric and Space Physics, University of Colorado, Boulder, 80309, USA
(mccollom@lasp.colorado.edu)
[2]Woods Hole Oceanographic Institution, MA, USA
[3]University of Bremen, Germany
[4]University of Colorado, Boulder, CO, USA

Much of the current scientific interest in serpentinites revolves around the production of molecular hydrogen (H_2) during serpentinization, which can serve as a source of metabolic energy for autotrophic microbial communities, or as the reductant for abiotic formation of organic compounds. While it has been known for some time that fluids generated during serpentinization can be highly reducing and enriched in H_2, the processes responsible for producing these conditions remain poorly understood. Serpentinization of ultramafic rocks is commonly portrayed by the simple generalized reaction: olivine + water → serpentine + brucite + magnetite + H_2, where production of H_2 occurs as a result of oxidation of ferrous Fe [FeO] from the mineral comp-onents of the original rock (olivine and pyroxene) to ferric Fe [$FeO_{1.5}$] in the reaction products, especially magnetite. However, petrologic studies and laboratory experiments make it increasingly evident that the process is much more complex than this simple expression would indicate. For instance, rather than going directly into magnetite, Fe from the reactant minerals is partitioned among all solid products including serpentine and brucite, so that the relative distribution and oxidation state of Fe among these minerals determines the amount of H_2 generated. Petrologic, lab-oratory, and theoretical studies indicate that the proportions and oxidation state of Fe in the product minerals is highly variable, and appears to be dependent on a number of factors including temperature, bulk rock composition, extent of reaction, and 'openess' of the system. To complicate matters further, the Fe components of serpentine and brucite may become unstable as the reaction progresses, so that Fe-rich minerals formed during the initial stages of serpentinization may decompose over time in favor of more Fe-poor compositions and magnetite. We will present results from ongoing laboratory experiments and modeling studies that are an attempt to unravel the sequence of reactions controlling Fe distribution and H_2 formation during serpentinization, and their dependence on reaction conditions.

https://doi.org/10.1180/S0026461X00006502 Published online by Cambridge University Press

The future of marine calcifiers in a high CO_2 world: Boron isotope systematics of pH up-regulation

M.T. McCulloch[1,2], J.A. Trotter[1], J. Falter[1,2] and P. Montagna[3]

[1]The University of Western Australia Oceans Institute and School of Earth and Environment, Western Australia
[2]ARC Centre of Excellence in Coral Reef Studies, UWA
[3]Laboratoire des Sciences du Climat et de l'Environnement, Av. de la Terrasse, 91198, Gif-sur-Yvette, France

Rising atmospheric CO_2 is not only causing global warming, but also lowering the oceans pH and hence carbonate ion concentration upon which many marine organisms depend to calcify their skeletons. Declining calcification rates combined with an increased frequency of coral bleaching from unusually high seawater temperatures has the potential to cause major disruption to marine ecosystems. Which marine calcifiers can sustain skeletal development as pCO_2 increases is however highly uncertain. Here we present new boron isotopic constraints on the degree of physiological control of the pH of the calcifying medium. Biological up-regulation of pH is linked to abiotic calcification rates using the inorganic kinetics of carbonate precipitation.

Boron isotope systematics of aragonitic corals show a species dependent ability to up-regulate the pH at their site of calcification, with changes in internal pH being approximately one-half of those in ambient seawater [1]. This pH buffering capacity is present in both non-symbiont and symbiont bearing aragonitic corals and serves to raise the saturation state of the calcifying fluid, thereby increasing their potential rate of calcification. The ability of biogenic calcifiers to raise the internal saturation state via pH up-regulation is not however ubiquitous, being absent for example in many key species of calcitic foraminifera. Ocean acidification and global warming are thus likely to cause a major bi-polar shift in the abundance and distribution of marine calcifiers. Those that lack internal pH regulation will continue to undergo rapid declines, while in cold-water corals enhanced rates of aragonite precipitation from pH elevation and rising temperatures has the potential to counter the effects of decreasing seawater pH. However the ability of tropical corals to maintain calcification rates by pH up-regulation will mainly depend on their capacity to adapt to thermal stress caused by rapid increases in ocean temperatures.

[1] Trotter *et al*. (2011) *Earth Planet Sci Lett*. **303**, 163-173.

Interfaces and exchange coupling

S.A. McEnroe[1], P. Robinson[1], K. Fabian[1], R.J. Harrison[2], N. Miyajima[3] and F. Langenhorst[3]

[1]Geological Survey of Norway, Trondheim 7041 Norway (*correspondence, suzanne.mcenroe@ngu.no)
[2]Cambridge University, Cambridge, UK
[3]BGI, Universitaet Bayreuth Bayreuth Germany

Natural oxides in the ilmenite-hematite system are now known to have contact layers [1] at the interface between the two phases. Contact layers, reduce charge imbalance at interfaces [2] and result in magnetic properties that are different from the bulk host or lamellae. Magnetic coupling across interfaces provide a mechanism for the stability of extremely small lamellae. These samples with lamellae < 1nm thick show exchange bias with shifted hysteresis loops more than 13, 000 Oe. This shift is the largest that has ever been measured in any material, natural or synthetic.

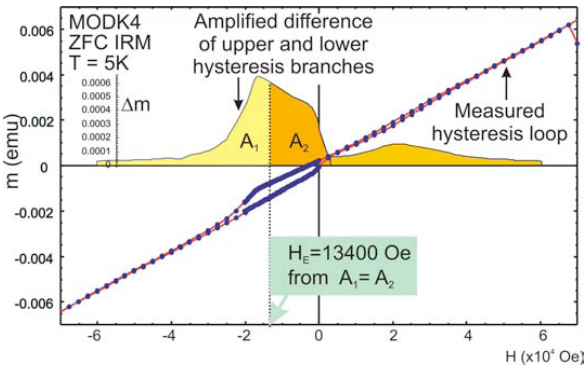

Figure 1: Shifted hystereis loop measured at 5 K. [3]

Combined TEM analyses and images with low-temperature magnetic studies are powerful tools to describe the chemical, structural and electronic nature of the interfaces. To date these are the smallest stable magnets ever known. There is wide interest in under-standing these natural samples and their interfaces, which may well provide blueprints for future technological designs.

[1] Robinson *et al*.(2002) *Nature* **418**, 517–520. [2] Robinson *et al*.(2006) *Am Min*. **91**, 67–72. [3] McEnroe *et al*.(2007) *Nature Nanotechnology* **2**, 631–634.

https://doi.org/10.1180/S0026461X00006502 Published online by Cambridge University Press

Simulations of multicomponent aerosol processes on the regional scale

G. McFiggans*, S.R. Utembe, D. Lowe, S. Archer-Nicholls and D.O. Topping

Centre for Atmospheric Science, SEAES, The University of Manchester, Oxford Road, Manchester, M13 9PL, UK (*corresponence: g.mcfiggans@manchester.ac.uk)

Organic material is a significant and variable component of tropospheric aerosol, accounting for between 10 and 90 % of fine particle mass. Owing to its complexity, large-scale models must represent the organic fraction and its interactions with inorganic aerosol components using highly simplified methods. Bottom-up representations usually underestimate organic particulate mass and more simplified bottom-up treatments may be expected to perform even more poorly. It is difficult to evaluate the reasons for such behaviour, in part because of the lack of traceability of the representation to more complex and realistic mechanistic approaches.

In this work, we present the coupling of the reduced Common Representative Intermediates (CRIv2-R5) scheme [1] describing tropospheric degradation of methane and 22 emitted non-methane hydrocarbons and oxygenated volatile organic compounds (comprising 220 species and 609 reactions), and traceable to the Master Chemical Mechanism (v3.1), to a sectional aerosol microphysics representation within the WRF-Chem model to enable prediction of the regional transformation of multicomponent aerosol in the oxidising atmosphere. The aerosol treatment uses the hyprid Partial Derivative Fitted Taylor Expansion (PD-FiTE) [2] coupled to the MTEM inorganic reprentation in WRF-Chem to provide computationally efficient calculation of the multicomponent gas / liquid equilibria in the particles. The model can be used to investigate the regional evolution of aerosol in the moist atmosphere and the organic contribution to aerosol mass predicted by a mechanism traceable to a more realistic representation of tropospheric VOC oxidation.

We will present results of the first simulations investigating the formation and transformation of tropospheric aerosols in the UK under a range of changing emission profiles and oxidant conditions.

[1] Watson, L. Shallcross, D. E. Utembe, S. R. & Jenkin, M. E. (2008) *Atmos. Environ.* **42**, 7196–7204. [2] Topping, D. Lowe, D. & McFiggans, G. (2009) *J. Geophys. Res.* **114**, doi: 10.1029/2008JD010099.

Monogenetic, but not monotonous: Basaltic eruptions in the Auckland Volcanic Field, New Zealand

L.E. McGee[1]*, I.E.M. Smith[1], M.-A. Millet[2], C. Beier[3,4], J.M. Lindsay[1] and H. Handley[3]

[1]School of Environment, Auckland University, Private Bag 92019, Auckland 1142, NZ (*correspondence: l.mcgee@auckland.ac.nz)
[2]SGEES, Victoria University, PO Box 600, Wellington, NZ
[3]GEMOC, Maquarie University, Sydney, Australia
[4]Now at Universität Erlangen-Nürnberg, Germany

How melts are extracted from their mantle sources and what happens to them *en route* to the surface are fundamental questions in the workings of basaltic volcanic fields. The well-sampled Auckland Volcanic Field (AVF) – an intraplate volcanic system in northern New Zealand – offers excellent opportunities to build up a more detailed picture of the plumbing systems feeding such fields. Here we present major and trace element data along with new Sr-Nd-Pb and U-series isotopic data, in order to investigate the processes involved in the large chemical heterogeneity seen in the AVF.

Detailed sampling has shown that individual trends for each centre can be explained by either high-pressure clinopyroxene or shallow olivine fractionation. Near-primary magmas show a range in degrees of partial melting from ~5% down to <0.5% in the smallest centres. Trace element ratios and high (^{230}Th/^{232}Th) ratios (1.16-1.33) show melts are primarily formed within the garnet stability zone and involve two mantle sources: a FOZO-like source and a source displaying more radiogenic Pb isotope ratios. Mixing between these 2 end-members is seen at both the single volcano and the field-wide scale.

U-series isotopic data for the two most chemically extreme centres, both of which erupted twice, are used to model subtle changes in magma dynamics. Both volcanoes follow the same trend of eruption of an early, less primitive, smaller-volume magma with a higher ^{230}Th-excess, then a more voluminous, more primitive magma with a lower ^{230}Th-excess. Parameters including melting and upwelling rates, conduit lengths and porosities are modelled and found to be within the range of other intraplate volcanic fields, yet show considerable variation between AVF eruptions. Together with the lack of any spatial or temporal trend in the chemistry of the field, these results suggest that melt batches evolve in isolation, being subject to differing processes and are able to move at variable speeds and through variable porosities in the mantle, resulting in dispersed plumbing systems for such fields and an erratic pattern of eruptions.

https://doi.org/10.1180/S0026461X00006502 Published online by Cambridge University Press

Unusual U-REE deposits at Mt Isa, Australia and potential links to mid-crustal anorogenic granites

M. McGloin[1]*, A.G. Tomkins[1] and C.M. MacRae[2]

[1]School of Geosciences, Monash Univ, VIC, 3800, Australia (*correspondence: matthew.mcgloin@monash.edu)
[2]Microbeam Laboratory, Minerals Down Under Flagship, CSIRO, Clayton, VIC, 3168, Australia

The unusual Uranium-Rare Earth Element (U-REE) deposits of Mount Isa, Queensland, associated with immobile element enrichment (Y, Zr, Nb, LREE, locally Ti) show a significant spatial relationship to radiometrically anomalous intrusive phases of the mid-crustal Sybella Granite Batholith. The high K and U radiometric anomalies in recent phases of the Sybella Batholith suggest a possible link with the U-REE deposits. Geochemical results for the most anomalous Sybella microgranite phase, indicates enrichment in several incompatible and high field strength elements, including elevated mean LREE content (189ppm Zr, 26ppm Y, 44ppm La and 90ppm Ce).

In the largest U-REE deposit, Valhalla, LREE enrichment (≥500ppm) is well correlated with the highest U (≥3.2wt% U_3O_8), associated with brannerite and uraniferous zircon [1]. The textural association of fluoroapatite surrounding brannerite [2, 1] suggests involvement of F in controlling U, REE and Zr mobility. The Sybella microgranite phase has geochemical characteristics typical of anorogenic granites [3], which are associated with U-REE mineralisation at other localities worldwide. Previous geochronological work on the Sybella microgranite gives ambiguous emplacement age constraints, allowing the possibility of a syn-Isan intrusion significantly later than the main intrusive Sybella phase (ca. 1670Ma [4]), possibly around 1555-1510Ma [1].

Our geochemical results, combined with a younger microgranite age, would support a genetic association with the ~1530Ma U-REE deposits, and more geochronological work is in progress to further test this possibility. Given that magmatic fractionation promotes enrichment of the incompatible elements seen at Valhalla, and that these elements are generally immobile in typical metamorphic fluids, we suggest that this unusual style of mineralisation most likely has a magmatic-hydrothermal origin.

[1] Polito *et al*. (2009) *Min Dep* **44**, 11–40. [2] Gregory *et al*. (2005) *Econ Geol* **100**, 537–546. [3] Eby (1990) *Lithos* **26**, 115–134. [4] Page & Bell (1986) *Journal Geol* **94**, 365–379.

Impact of biotic and abiotic factors on the mobilization of heavy metals in Al-Ghadir river sediments (Lebanon)

Amale Mcheik[1], Mohamad Fakih[2], Noureddine Bousserrhine[1], Joumana Toufaily[2], Vanessa Alphonse[1], Hiba Noureddine[2] and Evelyne Garnier-Zarli[1]

[1]IBIOS – BIOEMCO, Faculty of sciences and technology, University Paris-Est, 61 avenue de general chales de gaulles, 94010 Creteil Cedex, France
[2]Laboratory MCEMA, Faculty of Sciences (I), Lebanese University, Hadath Beirut, Lebanon

Although there is no doubt about the importance of bacterial activity on solubilisation and distribution of metal in aquatic sediments, hydromorphic soils and ground waters very little is known about the involvement of bacterial dissolution in periodically anaerobic environments like that found in dredged sediments and little is known about the processes and environmental factor controlling this process.

Our study aims at underlining the role of autochthonous bacteria in the biodegradation of organic matters and the mobilization of metals (Zn, Pb, Co, Cr, Cd, Al, Mn and Fe) contained in sediments in Al-Ghadir river. In order to do so, we have follow over time the evolution of carbon metabolism (Organic matter evolved, carbon consumption, organic acids production) and metals release in batch reactor where the sediments were mixed with a culture medium. The experiments were monitored under standard anaerobic conditions.

Under the adopted conditions, the incubated sediments showed a significant release of organic carbon corresponding to bacterial development.

Mineral analysis showed an important solubilisation of iron and manganese (in reduced form) indicating the presence of Fe and Mn-reducing bacteria in sediments. Co and Cr solubilisation were also observed and appeared concomitant to Fe and Mn indicating that Co and Cr are associated to Fe and Mn in sediment. Al and Zn were associated to organic matter while Cd and Cu were associated to organic matter and to Fe and Mn oxides.

At the end of the incubation, the molecular techniques showed (i) the disappearance of some bacterial strains due to the toxicity of the released heavy metals and (ii) the growth of new population of microorganisms tolerant to the same heavy metals.

https://doi.org/10.1180/S0026461X00006502 Published online by Cambridge University Press

Silicic acid: An experimental and *ab initio* study of explicit solvation and reaction kinetics

G.J. McIntosh*, P.J. Swedlund and T. Söhnel

Department of Chemistry, University of Auckland, Private Bag 92019, Auckland, New Zealand (*correspondence: g.mcintosh@auckland.ac.nz)

Ab initio quantum chemistry has become a powerful supplement to experimental studies of gas-phase systems in particular. However, while the application to species of geochemical interest such as silicic acid, H_4SiO_4, is achievable, it is dramatically complicated by the presence of water. As both computer speed and the efficiency of quantum chemical algorithms progress, it is becoming increasingly feasible to go beyond simple continuum descriptions of the solvent to the inclusion of explicit solute-solvent interactions.

We have recently benchmarked the effects of explicit solvation in a theoretical study of a counter-intuitive reverse isotope shift observed in the vibrational spectra of aqueous H_4SiO_4 and D_4SiO_4 [1]. Upon deuteration, the antisymmetric ν (Si-O) stretching modes shifts to higher frequencies, in opposition to what is anticipated from reduced mass arguments. DFT/B3LYP/6-31+G (d)-based models are unable to describe this shift without the inclusion of explicit water molecules. Specific hydrogen bonding interactions, present only within an explicit solvation framework, are found to significantly stiffen and blueshift the δ (Si-O-H/D) bending modes. In D_4SiO_4, these bends subsequently couple with the ν (Si-O) modes; resonance effects blueshift the stretching modes by a greater extent than the increased mass-induced red shift, leading to a net reverse-isotope shift. Similarly, the positions of δ (Si-O-H/D) modes in the IR and symmetric ν (Si-O) modes in the Raman, and peak widths and heights are also only reproduced with the inclusion of explicit solvation effects.

On the strength of these results, we have begun exploring the feasibility of deriving a kinetic model of silicate polymerization and hydrolysis almost entirely from first principles. We present preliminary results benchmarking transition state theory approximations and the roles of implicit and explicit solvation in modelling the kinetics of H_4SiO_4 dimerization. Early results suggest that this approach may provide a surprisingly good model of reaction kinetics and thermodynamics in pH- and temperature-dependent systems.

[1] McIntosh *et al*. (2011) *Phys. Chem. Chem. Phys.* **13**, 2314–2322.

How and where redox-sensitive trace metals can answer the question productivity or ventilation

J.L. McKay[1]*, T. Ivanochko[2] and T.F. Pedersen[3]

[1]COAS, Oregon State University, Corvallis, OR 97330, USA (*correspondence: mckay@coas.oregonstate.edu)

[2]EOS, University of British Columbia, Vancouver, BC, V6T 1Z4, Canada (tivanoch@eos.ubc.ca)

[3]SEOS, University of Victoria, Victoria, BC, V8W 2Y2, Canada (tfp@uvic.ca)

The enrichment of redox-sensitive trace metals such as Re and Mo is commonly used to infer changes in paleo redox conditions of marine sediments. Determining why redox conditions changed is trickier because both organic carbon flux (e.g. export productivity) and changes in bottom water oxygen (e.g. ventilation) can influence sedimentary redox. Which of these factors is the dominant control can be sorted out by analyzing Ag along with the redox-sensitive metals noted above. Unlike these other metals, Ag does not accumulate after sediment deposition. Rather it is scavenged from the water column by organic particles and transported to the sediment as part of the biogenic particle flux. Its accumulation in sediments is therefore related to productivity. Thus, high Ag in combination with high Re and/or Mo suggests that high productivity is controlling sedimentary redox while a combination of low Ag and high Re and/or Mo suggests a lack of ventilation. Some environments, however, don't lend themselves well to the use of redox-sensitive trace metals. Surface sediments from the OMZ on the Pakistan Margin, for example, are characterized by relatively low Re and Mo concentrations in comparison to oceanographically similar regions off Mexico and Peru. Silver concentrations are also anomalously low except near the base of the OMZ indicating post-depositional oxidation and loss of Ag. Together these trace metal data suggest that OMZ sediments on the Pakistan Margin are at best weakly suboxic despite their high organic carbon content and the low bottom water oxygen values.

https://doi.org/10.1180/S0026461X00006502 Published online by Cambridge University Press

Integration of the intrusive and extrusive cycles of Palaeogene igneous activity in N.E. Ireland

C. McKenna[1]*, J.A. Gamble[1], P.R. Renne[2], R.M. Ellam[3], J.G. Fitton[4] and P. Lyle[1]

[1]School of BEES, National University of Ireland, Cork, Rep. of Ireland (*correspondence: mckennca@gmail.com)
[2]Berkeley Geochronology Centre, 2455 Ridge Road, Berkeley, CA 94709, USA (prenne@bgc.org)
[3]Scottish Universitites Environmental ResearchCentre, East Kilbride G75 0QF, UK (r.ellam@suerc.gla.ac.uk)
[4]School of GeoSciences, , University of Edinburgh, Edinburgh EH9 3JW, UK (Godfrey.Fitton@ed.ac.uk)

We compare trace element and isotopic (Sr, Nd, and Pb) geochemical data from the mafic intrusive complex of Slieve Gullion with new data from the thick sills (up to 100 m) at Portrush, Carrickarede and Fair Head in N Antrim and make comparisons to the Antrim Lava Group (ALG) flood basalts.

Slieve Gullion rocks (56.5±1.3 Ma) are characterised by flat ~10x chondritic HREE with slight +ve Eu-anomalies and LREE enrichment ($(La/Pr)_{CN}$ = ~2.5). Portrush sill rocks (54.9±0.6 Ma) show similar flat HREE patterns, +ve Eu anomalies and faint LREE enrichment ($(La/Pr)_{CN}$ >1). By way of contrast Carrickarede and Fair Head (60.2±0.3 Ma) rocks show convex upward REE patterns, with maximum REE enrichment at Nd ($(La/Pr)_{CN}$ < 1, $(Nd/Lu)_{CN}$ ~ 4). Multielement plots of incompatible elements for Slieve Gullion and Portrush rocks display similar flat patterns for HREE and HFSE, with distinctive +ve spikes at Pb, Sr and Rb and –ve Nb anomalies, that strongly resemble subduction modified melts or continental crust. The Fair Head rocks show distinctive, smooth upwardly convex patterns.

The Lower Basalts (~60-62 Ma) of the ALG show similar convex upwards REE patterns as the Fair Head and Carrickarede rocks, whereas many of the younger Upper Basalts (~59-57 Ma) resemble the younger intrusions at Portrush and Slieve Gullion, but with flat or LREE depleted REE patterns.

A key to understanding the evolution of the N.E. Irish sector of the North Atlantic Igneous Province is explaining such differences in temporally related rocks, which cannot be rationalised solely by partial melting of a similar source. We suggest that the LREE enrichment and Pb, Sr, Rb spikes so distinctive of the Slieve Gullion magmas, and also hinted at in Portrush, might derive from a lithospheric mantle component, as the melting regime penetrates into lithospheric mantle as extension developed across the Province.

Complex Al and P zoning in pallasite olivine: Constraints on high-T history

Seann J. McKibbin[1]*, Hugh St.C. O'Neill[1], Guilherme Mallmann[1,2] and Angela Halfpenny[1,3]

[1]Research School of Earth Sciences, Australian National University, Canberra ACT, Australia (*correspondence: seann.mckibbin@anu.edu.au) (hugh.oneill@anu.edu.au)
[2]Institute of Geosciences, University of São Paulo, São Paulo SP 05508-080, Brazil (guil.mallmann@gmail.com)
[3]Earth Science and Resource Engineering, CSIRO, Kensington WA, Australia (angela.halfpenny@csiro.com)

Pallasites are mixtures of olivine and Fe-Ni metal, possibly formed near the core-mantle boundary of a differentiated asteroid [1]. The distribution of trace elements in pallasite olivine appears to reflect diffusion profiles [2] although complex structure has also been reported [3]. It has recently been shown experimentally [4] and in various natural samples [5] that Al and P diffuse very slowly in olivine and these elements can preserve early distributions which are resistant to later thermal modification.

To search for evidence of the early history of pallasite olivine, we have used Laser-Ablation Inductively-Coupled-Plasma Mass-Spectrometry (LA-ICP-MS) to produce trace-element maps of olivine from two pallasites: Brahin (with fragmental olivine) and Brenham (rounded olivine). Heterogeneous distributions are found over scales of ~100 microns for Al and elements likely to associate with it in coupled substitutions. P is also heterogeneously distributed but is negatively correlated with or unrelated to Al. In Brahin, these distributions bear no relationship to the olivine morphology; for Brenham, Al concentrations decrease at grain margins but the interiors have complex distributions.

Heterogeneous distributions of Al and P in pallasite olivine provides some constraints on its residence time in a high-T environment. Taking the diffusion parameters for Si [6] as a proxy for the diffusion behaviour of these elements (since they reside in the same crystallographic site), at 1650 K (~OPX out for a fertile peridotite composition; [7]) the characteristic timescale for diffusion over 100 microns is ~1 Ma. This represents an upper limit on the time between the establishment of trace element systematics in olivine and formation of pallasites by mixing with metal.

[1] Scott, E.R.D. (1977) *GCA* **41**, 693. [2] Miyamoto, M. (1997) *JGR* **102**, 21613. [3] Tomiyama T. & Huss G.R. (2006) *LPSC* **37**, 2132. [4] Spandler C. & O'Neill H.St.C. (2010) *CM&P* **159**, 791. [5] Milman-Barris M. *et al*. (2008) *CM&P* **155**, 739. [6] Dohmen R. *et al*. (2002) *GRL* **29**, 2030. [7] Walter M. J. (2003) in *Treatise on Geochemistry* 2.08, 363–394.

https://doi.org/10.1180/S0026461X00006502 Published online by Cambridge University Press

Relationships between the composition of planetary crusts and their sedimentary records

SCOTT M. MCLENNAN

Dept. of Geosciences, SUNY at Stony Brook, Stony Brook, NY, 11794-2100, USA (Scott.McLennan@sunysb.edu)

Planetary crusts possess variable sedimentary records in terms of origin, size, lithology, age and composition. At one extreme, Earth has a complex sedimentary record formed in response to weathering, erosion, transport, deposition and recycling. The highly dynamic terrestrial rock cycle precludes preservation of any significant planetary regolith (eolian deposits being the closest analog). At the other extreme, airless bodies like the Moon, and probably Mercury, possess classic impact-derived planetary regoliths as their only sedimentary deposit. Mars provides the intermediate case where a long-lived sedimentary rock record exists but the surface is also covered widely by regolith. Controls on planetary sedimentary records are related to (1) impact and volcanic history, (2) presence and nature of atmospheres (i.e. climate), (3) occurrence, composition and physical state of near-surface volatiles, and (4) presence and nature of crustal tectonics, crustal evolution, and so forth. In turn, the composition of planetary sediments reflects their crustal sources in complex, but generally understandable ways. The terrestrial sedimentary record is lithologically differentiated (shales, sands, carbonates, evaporites) due mainly to large bodies of water. Nevertheless, terrestrial sediments reflect widespread sources and accordingly have long been used to estimate upper crustal composition and to trace crustal evolution. For impact-derived lunar regolith, absence of water and air restricts reworking or transport on any significant scale after initial deposition. Disruption and mixing take place but by impact gardening that operates on local scales and largely in a vertical sense. The result is that lunar regoliths do not sample widespread regions and so are compositionally variable, matching the crust in the vicinity of where they form. Martian sedimentary rocks and regolith formed by a wider array of processes than did lunar regolith, including impact, volcanic, glacial, eolian and subaqueous processes, and are far more complex mineralogically. On the other hand, much less lithological differentiation takes place than is seen on Earth. Sedimentary mixing processes at the surface (e.g. eolian, glacial, impact gardening) were of sufficient scale to minimize variations in regolith composition. Although local geological influences are observed, Martian regolith is of broadly uniform composition, reflecting the average upper crust even for the major elements.

A 4-dimemsional landscape geochemical framework for the remote arid landscapes of Australia's Musgrave Province

S.M. MCLENNAN[1]* AND S.M. HILL[2]

[1]The University of Adelaide, Adelaide, 5005, Australia (*correspondence: stephanie.mclennan@adelaide.edu.au)
[2]The University of Adelaide, Adelaide, 5005, Australia (steven.hill@adelaide.edu.au)

This study integrates geochemical and biogeochemical datasets generated from the remote arid landscape of the Musgrave Province in Central Australia. It demonstrates the inter-relationships between the chemistry of the region and its landscape evolution. Many previous geochemical studies of the arid landscapes of Australia have tended to focus on a single system or sampling medium. Where datasets for several media are combined and compared they have tended to be considered within the context of a featureless ‘space’ rather than their landscape setting. In this study bedrock geochemical, regolith geochemical, groundwater hydrogeochemical and plant biogeochemical systems are sampled, chemically characterised and compared based on their landscape setting. This study utilises the importance of the evolution of regolith materials that have evolved within the landscape's history as the context.

An initial focus has centred on the Mt Caroline ultra-mafic intrusion, which is considered prospective for Ni-Cu sulphide deposits. Variably think sedimentary cover (10s to 100s m), Aboriginal land access restrictions, and a lack of tracks and roads through the region have limited the development of previous landscape geochemical models. Access to some exploration tenements, however, has allowed the development of a geochemical sampling program incorporating regolith materials, biota (especially Triodia basedowii), and groundwater. Given the extent and variation in thickness of sedimentary cover in the area, however, plotting and comparing these datasets in two dimensions is an over-simplification of the dispersion processes at play in this system. This project optimises the presentation of these datasets to show differences between the results and similarities between anomalies to assist in further developing future exploration programs. The study proposes an effective means of presenting data that incorporates the geochemistry across the landscape in two dimensions but also the role of landforms and varying lithologies in surface expression of concealed mineral deposits.

https://doi.org/10.1180/S0026461X00006502 Published online by Cambridge University Press

The origin of carbonate globules in silicate melts: Solids or liquids?

S.C. McMahon*, D.K. Bailey, M.J. Walter and L. Caricchi

Department of Earth Sciences, University of Bristol, BS8 1RJ (*correspondence: Sorcha.McMahon@bristol.ac.uk)

Carbonate globules found in mantle xenoliths, as inclusions in mantle minerals and in juvenile silicate melt lapilli are possible examples of primitive carbonatitic melts from the mantle [1]. Here we present findings from carbonate globules from Finca La Nava, a matrix-supported carbonatite tuff in the Calatrava Volcanic Province in central Spain; an alkaline mafic-ultramafic province comprising over 250 monogenetic cones and vents [1]. Carbonate globules are prolific within silicate melt lapilli. Silicate melts of at least two different compositions, melilitite and kamafugite, have been discovered within this one outcrop.

The origin of the carbonate globules within melt lapilli is debatable. Globule textures including curved menisci against silicate melt, budding, and coalescing of the globules, are compelling evidence for liquid immiscibility. However, recent experimental results suggest that similarly-shaped globules formed as solid calcite crystals in equilibrium with silicate melt [2]. Many, but not all, globule interiors in the Calatrava lapilli are apparently nearly phase-pure calcium carbonate with minor Mg, but Si, Al, and Na are virtually absent. Yet experiments show that carbonatitic melts equilibrated with mantle silicates or silicate melts can dissolve significant amounts of these elements, suggesting that the globules may have originated as solid calcite, as in the experiments. So did these carbonate globules originate as solids or liquids?

The 'pure' globules are in fact both compositionally and texturally heterogeneous on a micron scale. Initial findings made on the basis of sub-micron elemental mapping using a FEG-SEM demonstrate that considerable quantities of additional components of Si and Al, amongst other major elements, appear to have been exsolved and segregated to the globule rims during crystallisation. Such a mechanism may explain the observed 'pure' calcium carbonate composition of many globule interiors, and supports an immiscible liquid model for carbonatite tuff genesis in Calatrava.

[1] Bailey *et al*. (2005). *Mineral Mag* **69**, 907-915. [2] Brooker & Kjarsgaard (2010) *Journal of Petrology* doi: 10.1093/petrology/egq081

Timing and duration of Heinrich events in the North Atlantic

Jerry F. McManus

Lamont-Doherty Earth Observatory of Columbia University, Palisades, NY 10964, USA (*correspondence: jmcmanus@ldeo.columbia.edu)

The repeated iceberg discharges into the North Atlantic during the Pleistocene, known as Heinrich events, are widely believed to have influenced the global climate. Their millennial pacing, abrupt occurrence, and widespread impact make them important targets for understanding the rates of climate change. Efforts to date the sedimentary layers associated with these events have achieved some success, particularly for the few events within the range of ^{14}C methods. Similarly, the duration of the youngest events has been estimated by foraminifera ^{14}C and sedimentary ^{230}Thxs. Beyond these most recent events, the Heinrich layers of ice-rafted sediments have typically been dated by correlation to other sedimentary archives with independent chronologies, such as ice cores and speleothems. In this study, two different approaches to ^{230}Thxs profiling have been utilized to explore directly the absolute timing and duration of each of the Heinrich events that occurred during the last large climate cycle of the Pleistocene. Both approaches incorporate new sedimentary data generated by ICP-MS at locations where initial results were produced by alpha counting. Heinrich event H11 is shown to occur within the penultimate deglaciation identified in foraminifera $\delta^{18}O$. Using Thxs profiling in a core from the Caribbean sea with an approximately constant accumulation rate, an age estimate of 133 ky is derived for the timing of H11, following Broecker and van Donk [1]. In core V28-82 from the subpolar North Atlantic, with a variable accumulation rate, the inventory of sedimentary ^{230}Th is shown to be in balance with the overlying seawater production of ^{230}Th, and Sackett's method [2] to quantifying the passage of time can be applied to estimate both the absolute age and duration of each of the Heinrich events. The results support previous estimates that the sedimentary layers associated with the events were deposited rapidly over the course of centuries, not millennia.

[1] Broecker, W. S. & van Donk, J. (1970) Insolation changes, ice volumes & the O18 record in deep-sea cores. *Reviews of Geophysics & Space Physics* **8**, 169–198. [2] Sackett, W. M. (1965) *Deposition rates by the protactinium method. In* "Symposium Volume." (D. R. Schink, & J. T. Corless, Eds.) pp. 29–40. URI.

https://doi.org/10.1180/S0026461X00006502 Published online by Cambridge University Press

Maximising precision and accuracy in laser quadrupole ICPMS U-Pb geochronology

SEBASTIEN MEFFRE, LEONID DANYUSHEVSKY, MARCEL GUILLONG AND SARAH GILBERT

School of Earth Sciences & Australian Research Council Centre for Excellence in Ore Deposit Studies, University of Tasmania, Australia, (smeffre@utas.edu.au)

Laser mass spectrometry is widely used to determine the age of rocks throughout the earth science. However, analytical problems related to ablation cells, standards, mass spectrometers and calculations have meant that it is difficult to fully characterise precision and accuracy of the technique.

Experiments performed at the University of Tasmania over the last 10 years have shown that the following parameters affect the precision and accuracy of measurements: 1) homogeneity of the signal in the ablation cell, 2) type, number and position of standards analysed within the analytical sequence 3) accuracy dead time corrections 4) amount of instrumental drift, 5) contamination during cleaning and polishing 6) calculation method used 7) tuning parameters and signal intensity 8) harmonic interference between the laser and the mass spectrometer (spectral skew).

The contribution of each of these parameters to the uncertainty of the final measurements is complex and changes with age and uranium concentration of the crystals. For example young and low U zircons (those which have accumulated <0.2 ppm radiogenic Pb) must be carefully cleaned and calculated using the 'ratio of the mean' rather than the 'mean of the ratio' method but are relatively insensitive to the position and homogeneity of the standards, dead time corrections, harmonic interferences and instrumental drift compared to older high U zircons.

Mechanical instabilities induced by sulfate adsorption

M. MEGAWATI[1]*, A. HIORTH[2] AND M.V. MADLAND[3]

[1]University of Stavanger, 4036 Norway (*correspondence: megawati.megawati@uis.no)

[2]International Research Institute Stavanger, 4068 Norway (ah@iris.no)

[3]University of Stavanger, 4036 Norway (merete.v.madland@uis.no)

We present experimental data and analytical calculations which demonstrate the effect of negative surface charge caused by sulfate adsorption in high porosity chalks. Rock mechanical tests on three high-porosity outcrop chalks flooded with Na_2SO_4 at 130 ^{0}C show a significant decrease in the yield strength and in the bulk modulus compared to that of NaCl flooding. At 50 ^{0}C, however, no significant difference in the mechanical strength between cores exposed to Na_2SO_4 and NaCl is observed. Relative to that of the distilled water flooding (i.e. no sulfate present) a decreasing strength of 20-40% in the yield and 10-70% in the bulk modulus are correlated well with the increasing sulfate concentration in the pore water at higher temperature (130 °C). In addition standard creep tests at constant stress level of 10.7 and 18.9 MPa show similarly high creep rate along the creep stages. We measured sulfate adsorption of 0.2 μmol/m^2 and 0.5-1 μmol/m^2 at 50 °C and 130 °C, respectively, while dissolution was found to be low (below 0.4 mM Ca^{2+} produced after 14 PV's flooded). The sulfate adsorption process is interpreted by using surface complexation model together with Gouy-Chapman theory to describe the electrical double layer. The analytical calculations give fairly good agreement with the measured sulfate adsorption and comparable with ζ -potential measurement data respectively. The reduced mechanical strength is related to the sulfate adsorption which leads to a negative (pH dependent) surface charge. We suggest that the interaction between charged surfaces specifically in the weak overlaps of electrical double layer gives rise to the total disjoining pressure, which acts as normal forces in the grains vicinity, and it counteracts the shear forces during the failure mechanism. Increasing magnitude of the disjoining pressure when chalk cores are exposed to different Na_2SO_4 concentration at 130 °C correlate well with the reduced strength from the mechanical test results. The correlation remarkably reproduces the same trend as observed in the yield strength and bulk modulus as a function of Na_2SO_4 concentrations.

https://doi.org/10.1180/S0026461X00006502 Published online by Cambridge University Press

The effect of sulfate adsorption on the cation exchange capacity of high porosity chalks

M. MEGAWATI[1], A. HIORTH[2]* AND M.V. MADLAND[3]

[1]University of Stavanger, 4036 Norway (megawati.megawati@uis.no)
[2]International Research Institute Stavanger, 4068 Norway (*correspondence: ah@iris.no)
[3]University of Stavanger, 4036 Norway (merete.v.madland@uis.no)

Understanding the process of sulfate adsorption onto the chalk surfaces is important as it has been associated with wettability change [1, 3] and it was also shown to impact the mechanical stability of high porosity chalks [2]. In this paper we determine the cation exchange capacity (CEC) from core floods with and without sulfate present in the pore fluids. We model the sulphate adsorption in terms of interaction with positive Ca sites at the calcite mineral surface [1]; resulting in a net negative surface charge. The cation exchange is believed to take place in the diffusive counter ion layer. Our experimental results remarkably show that CEC increases with almost a factor of 2 upon adsorption of sulfate and the retardation of Na+/K+ front as well increases significantly (see Table 1). The enhanced CEC due to sulfate adsorption could thus contribute to an improved understanding of the enhanced compaction as observed during rock mechanical tests.

Chalk	T	Sulfate ads.	With adsorbed SO4		Without adsorbed SO4	
			CEC	Retard. of Na^+/K^+	CEC (Exp.)	Retard. of Na^+
	^{0}C	μmol/m^2	mEq/L	PV	mEq/L	PV
Liege	50	0.36	0.10	2.18	0.06	1.35
	90	0.80	0.11	2.05	0.05	1.28
	130	1.04	0.10	1.94	0.06	1.28
S.Klint	50	0.49	0.02	1.14	0.01	1.03
	90	0.81	0.02	1.12	0.01	1.04
	130	1.16	0.02	1.12	0.01	1.05

Table 1: Increasing trend in the CEC upon adsorption of sulfate.

[1] Hiorth *et al*. (2010) *TIPM* 10.1007/s11242-010-9543-6. [2] Korsnes *et al*. (2008) *Journal Pet.Sci.Eng* **60**, 183–193. [3] Strand *et al*. (2001) *Journal Pet. Sci.Eng* **52**, 187–197.

The structural determinants of silicon fractionation properties of silicate minerals: A first-principles density functional study

M. MÉHEUT[1]* AND E.A. SCHAUBLE[2]

[1]GET, Université Paul Sabatier, Toulouse, France (*correspondence: meheut@lmtg.obs-mip.fr)
[2]ESS Dept., UCLA, Los Angeles, USA

Ab initio methods based on density functional theory have proven to be successful in reproducing the physical and chemical properties of complex systems. Within this framework, we have recently developed a methodology to predict equilibrium fractionation factors as a function of temperature (1). We use PBE functionals, combined with the use of pseudopotentials and planewave basis sets. Our previous work focused on the effect of the polymerization of the silicate network on Si-isotope fractionation (2), which had previously been predicted to be a determining factor. Our work does not confirm this assumption. To investigate the origin of this fractionation, we studied minerals with identical polymerization structures such as talc, pyrophyllite, muscovite, phlogopite or clinochlore. In the case of muscovite and phlogopite, the calculated quartz-mineral fractionations are in qualitative agreement with natural estimates. In this family of silicates, a strong correlation can be shown between the mineral-quartz fractionation of silicon and cationic content. Together with the simple shape of the fractionation laws, this permits to propose the following approximate law, valid for any temperature T (in K):
$\ln\alpha(\text{phyllo.,qtz,Si,T}) = a(T)*[Mg(o)] + b(T)*([Al(o)]+2*[Al(t)])$, where [Mg(o)], [Al(o)] and [Al(t)] represent the content of octahedric magnesium, aluminium and tetrahedric aluminium relative to 4 tetrahedral units, and $a(T) = -12.834x^2 + 14.39x^3$; $b(T) = -5.040x^2 + 4.20x^3$, with $x = 10^2/T$

This relationship can apparently be extrapolated to fractionation properties of tectosilicates (quartz and albite) and inosilicates (enstatite) but fails to reproduce the properties of forsterite. To better understand the limits of this apparently general correlation, we plan to present calculations for several chain silicates (diopside, wollastonite, jadeite), and potentially nesosilicates (fayalite, zircon, garnet). We will also focus on the interpretation of this relationship in terms of cationic force field effects.

[1] Meheut *et al*. (2007) *GCA* **71**, 3170–3181. [2] Meheut *et al*. (2009) *Chem. Geol*. **258**, 28.

https://doi.org/10.1180/S0026461X00006502 Published online by Cambridge University Press

Petrogenesis and geochemistry of the Dajing Cu-Sn-Pb-Zn-Ag Ore Deposit in Chifeng, Inner Mongolia

WEI MEI[1], XINBIAO LÜ[1,2]*, ZHILONG AI[1], RANKUN TANG[1] AND ZHI LIU[1]

[1]Faculty of Earth Resources, China University of Geosciences, Wuhan 430074, China (meiwei09@qq.com) (*correspondence: lvxb_01@163.com)

[2]State Key Laboratory of Geological Processes and Mineral Resources, China University of Geosciences, Wuhan 430074, China

The Dajing deposit is the largest tin deposit at the north of North China, which is a fissure-filling hydrothermal ore deposit located at the south of Daxinggan Mountain with Sn, Cu, Pb, Zn, Ag mineralisation. The deposit is controlled by multistage of fracture systems, mainly including NE striking sinistral compresso-shear fractures, a suite of SN striking compresso-shear fractures, and NW striking tenso-shear fractures (with ore veins mainly filling in this group of fractures). The widely outcropped magmatic rocks in the ore district are sub-volcanic rocks. They intruded into the Upper Permian Linxi Group that was formed in the inshore lake basins environment. The sub-volcanic dykes are divided into four main types: aphanophyre, acidic to intermediate rocks (dacite porphyry, rhyolite porphyry and granite porphyry), intermediate to basic rocks (andesitic porphyrite, diabasic porphyrite and basaltic prophyrite) and lamprohpyre, which scattered in the ore district. However, the subvolcanic rocks are dominated by acidic rocks in the central part, and intermdiate to basic rocks in the eastern part. K-Ar bulk isotopic age of the dykes ranges from 155.3 to 177.2 Ma. Wall rock alterations are weak silicification, carbonatization, chloritization and sericitization. They occur on both sides of ore veins.

The acidic rocks in the central are a suit of high-K calc-alkaline dacite with high content of Cu and Sn, while the basic rocks in the eastern are a suit of shoshonitic basalt to basaltic-andesite rocks with high content of Pb and Zn. All the rocks are characterized by enriched LILE and LREE, but acidic rocks have lower REE content with intermediate negative Eu anomaly (δEu=0.56-0.58). All the rocks originated from the same mantle source. They underwent high degree of differentiation and evolution when entered into the secondary magma chamber.

This work is founded by 305 Project of State Science and Technology Support Program (Grant No. 2007BAB25B04).

Ab initio molecular dynamics simulation of copper(I) complexation in chloride/sulfide fluids

YUAN MEI[1,2,3], DAVID M SHERMAN[2], JOËL BRUGGER[1] AND WEIHUA LIU[3]

[1]School of Earth and Environmental Sciences, The University of Adelaide, Adelaide, SA 5000, Australia

[2]Department of Earth Sciences, University of Bristol, Bristol, BS8 1RJ, UK

[3]CSIRO Earth Science and Resource Engineering, Clayton, VIC 3168, Australia

Chloride and hydrosulfide are the primary ligands believed to control the transport of copper in hydrothermal fluids. Recent studies of Cu complexation in hydrothermal Cl^-, HS^- solutions have been done using X-ray Absorption Spectroscopy (XAS). However, coordination numbers have a large uncertainty and are strongly correlated with Debye-Waller factors; moreover, it is very difficult to distinguish between chloride and sulfur ligands. *Ab initio* molecular dynamics simulations based on density functional theory enable us to interpret EXAFS results and, potentially, predict stability constants of metal complexes.

In this study, we investigated the species of copper(I) complexes via *ab initio* Car-Parrinello Molecular Dynamics simulations for copper(I) solutions with different hydrosulfide/chloride ratios at 500bar and 600K. Calculations were done using Vanderbilt ultrasoft pseudopotentials and the PBE exchange-correlation functional.

In the absence of Cl-ligands, copper forms a $Cu(HS)_2^-$ complex with a Cu-S bond length of 2.17 Å (vs. an expt. value of 2.15 Å); moreover, the S-Cu-S bond angle is ~162°, in excellent agreement with experiment (150-160°). In the presence of excess chloride, however, we find that Cu forms previously unknown $Cu(HS)Cl^-$ and (minor) $CuCl_2(HS)^{-2}$ complexes. Such complexes would be difficult to resolve from $CuCl_2^-$ or $Cu(HS)_2^-$ using EXAFS. We also explored the complexation of Cu in a low density (0.29 g/cm^3), high T (1273K) fluid (vapour). Here, we find that Cu forms $Cu(HS)_2^-$ (not the neutral CuHS, as expected). We tentatively suggest that charged complexes may be significant in high temperature, low density fluids.

Ultimately, we hope to predict stability constants of metal complexes. To this end, we are testing metadynamics and thermodynamic integration with respect to metal-ligand distances or coordination numbers. Using these techniques, we estimate the free energy difference between $CuCl_2^- + HS^-$ and $CuCl(HS)^- + Cl^-$ to be ~40 KJ/mol.

https://doi.org/10.1180/S0026461X00006502 Published online by Cambridge University Press

NanoSIMS: New results of relevance to biomineralization and biology

ANDERS MEIBOM

Muséum d'Histoire Naturelle, Paris, France

The NanoSIMS is a relatively new type of ion microprobe that can deliver a primary beam of Cs^+ or O^- to a sample surface, focused to a minimum spot size of ~50 nanometers and ~150 nanometers, respectively. (On non-conducting materials, bombardment with Cs+ causes strong charging effects. Such positive charge build-ups are compensated by electrons, which can be delivered to the sample surface by an electron gun.) Secondary ions sputtered from the sample surface and charged opposite to the primary beam are transferred with high transmission to a high mass-resolution, multi-collection mass-spectrometer that allows simultaneous collection of five or seven (depending on the model) different isotopes in electron multipliers and/or Faraday cups. This means that five (or seven) different images can be simultaneously recorded from the same sputtered volume. This capability can be used to create images or maps of elemental and isotopic variation within a sample. Such images can be generated from the lightest elements, such as H (D/H ratios), C ($^{13}C/^{12}C$ ratios), N ($^{15}N/^{14}N$ ratios), O ($^{17}O/^{16}O$ and $^{18}O/^{16}O$ ratios) and S (e.g. $^{34}S/^{32}S$ ratios) to the heaviest elements in the periodic table, including uranium.

Ion images of the sample surface are created by a precisely controlled raster of the primary beam across the sample surface. The NanoSIMS is therefore a powerful analytical instrument in conjunction with biological labeling experiments, where high spatial resolution is required and high analytical precision is not a requirement. Importantly, it is possible to do high quality NanoSIMS imaging even on very thin sections prepared for TEM analysis.

This presentation will include examples of the combination between dynamic isotopic labeling experiments, SEM, TEM, STXM, and NanoSIMS imaging to study skeletal formation dynamics and single-cell-level ammonium assimilation in reef-building corals.

Quantification of environmental proxy precision

ANDERS MEIBOM AND CHRISTOPHE KOPP

Muséum d'Histoire Naturelle, Paris, France

The extent and causes of recent environmental variations represent a vitally important problem for scientists, lawmakers and society in general. Essential to the ongoing scientific debate is the development of proxies that can reconstruct environmental change on both short (10-1000 years) and long (i.e. geologic) timescales. However, for every such proxy, a fundamental question exists that is rarely addressed: To what *precision* can the proxy reconstruct environmental variation? Only by answering this question quantitatively is it possible to decide if a given proxy is precise enough to be applicable and useful.

Here, we illustrate and discuss the vital effects that plague the major proxies for e.g. ocean sea-surface temperature. This will be based on recently acquired micro-analytical data, in particular with the NanoSIMS ion microprobe. Subsequently, the precision of linear environmental proxies is quantified with a general and easily applicable method. The precision of a selection of existing proxies is evaluated against the requirements of e.g. anthropogenic global warming.

https://doi.org/10.1180/S0026461X00006502 Published online by Cambridge University Press

Automated characterization of Eyjafjallajökull ash cloud particles

M.F. MEIER[1]*, K. WEBER[2], A. VOGEL[2], C. FISCHER[2] AND B. GROBÉTY[1,3]

[1]Univ. of Fribourg, Dept. of Geosciences, 1700 Fribourg, Switzerland (*correspondence: mario.meier@unifr.ch)
[2]Univ. of Applied Science, 40474 Düsseldorf, Germany
[3]Univ. of Fribourg, FRIMAT, 1700 Fribourg, Switzerland

The Eyjafjallajökull (EFJ) ash cloud crisis caused an airspace closure over Europe in April 2010 and had an important impact on economy. During this crisis the Dusseldorf University of Applied Sciences performed several measurment flights over north-western Germany with a light aircraft equipped among other with an optical particle counter (OPC) [1]. The primary goal of the airborne campaign (two flights F1 and F2, 18th May, different routes) was to compare the model calculation of the Volcanic Ash Advisory Center (VAAC) with *in situ* observation. The aim of this work is to present results of computer controlled scanning electron microscopy (CCSEM) coupled with engergy dispersive X-ray spectroscopy (EDX) applied on particles sampled on PTFE filters obtained from the OPC outlet. CCSEM/EDX generates morpho-chemical data of over 1000 particles in a few hours.

Many of the particles sampled during F1 were silicate dominated particles with compositions similar to the ones obtained from ash particles sampled on Iceland during and after the eruption of EFJ. Augitic clinopyroxenes could be identified morphologically. X-ray diffraction analyses of the eruption products confirm the presence of augite phenocryst. This points to the conclusion that the aerosol sampled during F1 was indeed volcanic ash from EFJ. Volcanic particles up to 6.5 µm were present, much larger than the conventional dispersion model would predict. The maximum mass concentration recorded inside the ash cloud by OPC was 330 µg/m^3. On the filter, sampled during F2, clays, carbonates, sulfates and quartz were present. Volcanic ash particles, however, were almost absent.

Chemical fingerprints of *in situ* collected samples are one way to ascertain the volcanic nature of an aerosol cloud. CCSEM can deliver such fingerprints. We were able to confirm the presence of the volcanic cloud over some parts of north-western Germany the 18th May 2010, but also to show that not all higher aerosol concentrations in the free troposphere could be attributed to the presence of volcanic ash. The obtained results from the measurement flights agree with the model of VAAC at its scale.

[1] Weber *et al*. (2011) *Atm. Env*. S-11-00415, submitted.

A record of Paleoproterozoic sulfur cycling from ~2 Ga Zaonega Formation, NW Russia

D. MEISTER[1]*, V.A. MELEZHIK[2,3], A. LEPLAND[2] AND H. STRAUSS[1]

[1]Institut für Geologie und Paläontologie, WWU Münster, 48149 Münster, Germany (*correspondence: dmeis_01@uni-muenster.de)
[2]Geological Survey of Norway (NGU), Trondheim, Norway
[3]University of Bergen, Centre of Geobiology, Bergen, Norway

Major environmental upheavals of global nature characterize the early Paleoproterozoic including the deposition of unprecedented amounts of organic matter during the Shunga Event ~2 billion years ago. Within the depositional environment, this organic matter fueled respiratory processes, among them the microbial reduction of an oceanic sulfate pool that developed in the aftermath of the Great Oxidation Event (GOE ~2.4 Ga). Ample evidence for microbially driven turnover of sulfate is provided by sedimentary pyrite in the organic-rich deposits of the Zaonega Formation, Onega Paleobasin, NW Russia.

Three drillcores were obtained from the Zaonega Formation in the course of the Fennoscandian Arctic Russia – Drilling Early Earth Project (FAR-DEEP) under the auspices of the International Continental Drilling Program (ICDP). Organic carbon rich samples from the Zaonega Formation contain abundant sedimentary Fe-sulfides exhibiting different morphologies suggestive of multiple stages of sulfide generations. In terms of diagenetic timing, these range from early diagenetic sedimentary pyrite to late generation pyrite and pyrrhotite occurring in cross cutting veins together with migrated bitumen.

Different forms of sulfur (AVS: acid volatile sulfide; CRS: chromium reducible sulfur) extracted from bulk rock samples throughout the succession yielded highly variable $\delta^{34}S$ values ranging between -8.1 and +25.6‰. Stratigraphic variations are discernible. The observed range in $\delta^{34}S$ values is consistent with a microbial origin via sulfate reduction and confirms previously published sulfur isotope data [1]. Guided by petrographic observations using transmitted and reflected light microscopy, a detailed sampling of different pyrite generations for subsequent sulfur isotopic work has been performed.

[1] Melezhik *et al*. (1999) *Earth-Science Reviews* **47**, 1–40.

https://doi.org/10.1180/S0026461X00006502 Published online by Cambridge University Press

Dynamic subsurface biosphere fuelled by organic matter from the past

P. MEISTER[1]*, S. CONTRERAS QUINTANA[1,2], B. LIU[1], A. KHALILI[1,3], T.G. FERDELMAN[1], M. KUYPERS[1] AND B.B. JØRGENSEN[1,4]

[1]Max Planck Institute for Marine Microbiology, 28359 Bremen, Germany (*correspondence: pmeister@mpi-bremen.de)
[2]Large Lakes Observatory (LLO), University of Minnesota, Duluth, MN 55812, USA
[3]Earth & Space Sciences Program, School of Engineering and Science, Jacobs University, 28725 Bremen, Germany
[4]Center for Geomicrobiology, Århus University, 8000 Århus, Denmark

Microbial degradation of organic matter deposited on the seafloor and buried over geological time within marine sediments leads to the onset of a redox zonation. This zonation may strongly shift over geological timescales due to variations of organic matter composition and burial rate. However, such dynamics in subsurface redox zonation is generally not obvious from measured porewater profiles.

Redox zonations may leave characteristic imprints in the geological record and therefore document the diagenetic history of a particular biogeochemical setting. We report the finding of diagenetic barite and dolomite layers that document past positions of the sulphate/methane transition zone (SMTZ) at ODP Site 1229 drilled on the Peruvian continental shelf. The layers co-occur with a focussed enrichment in isotopically light archeol, a lipid biomarker indicative of anaerobic methane oxidation.

Using a time-transient reactive transport model for sulphate and methane allowed to reproduce a SMTZ migrating upward and downward over a depth range of 30 m (below seafloor) over a time period of 100 ka. These variations were caused by variation in the organic matter content, the initial age of organic matter, and burial rate. Organic matter was assumed to decay according the reactive continuum model [1] whereby the different parameters were constrained by bulk TOC and ^{35}S radiotracer rate data.

The diagenetic imprints and modelling results are evidence of a sub-surface redox zonation more dynamic than we would expect from measured porewater profiles. Therefore, the diagenetic record in combination with non-steady state geochemical modelling must be taken into account for an assessment of diffusive fluxes between marine sediments and the water column and their contribution to global biogeochemical cycling.

[1] Boudreau and Ruddick, (1991) *Am. J. Sci.* **291**, 507-538.

Development of methodologies based on Field-Flow Fractionation for the characterization of engineered nanoparticles in complex samples

B. MEISTERJAHN, S. LEGROS, F. VON DER KAMMER* AND T. HOFMANN

Univ. of Vienna, Dept. of Env. Geosciences, Vienna, Austria (*correspondence: frank.kammer@univie.ac.at)

Engineered nanoparticles (ENPs) are more and more introduced into consumer products, leading to environmental and health concern. This development has been so rapid that methods to detect, quantify and characterize ENPs in environmental and biological media are still widely lacking. Field Flow Fractionation (FFF) is one of the most promising techniques currently developed for these tasks.

The strategy adopted for the analysis of ENPs in complex matrices depend strongly on the type of the ENPs and the nature of the matrix. Therefore, different methodologies have to be specifically developed for the e.g. analysis of nanoparticles of silver (AgNP) in an environmental matrix and nanoparticles of silica (SiO_2NP) in a biological matrix. These new developments have been performed on reference samples and are presented here.

Standard AgNP (i.e. 15-20 nm NM300 from OECD repository) were spiked to a standard soil (i.e. IME RefeSol from the German Federal Environment Agency) while Standard SiO_2NP (here 40 and 100 nm) were spiked to tomato soup (preparation from JRC in the course of FP7 Nanolyse project). The sample preparation can be done by density separation (AgNP) and by acid digestion (SiO_2NP). Flow-FFF coupled to UV-DAD spectrometry, online static and dynamic light scattering and ICP-MS were used to characterize compositions and properties of nanoparticles as a function of size.

Conventional ICP-MS coupled to FFF seems to be suitable for complex samples containing AgNP, because Ag has a low background in the environment.

These optimized methods helped in the investigation of complex mixtures of ENPs and matrix which finally led to the conclusion that ENPs do not always intensively interact with natural nanoparticles coming from the matrices and can occur as stable single particles in the environment. This results mitigate the current assumption that hetero-aggregation will be the most probable mechanism occurring in the environment. This is important in order to predict the impact of ENPs on the environment and human health.

https://doi.org/10.1180/S0026461X00006502 Published online by Cambridge University Press

Melts migrating through the mantle wedge: evidences from Patagonian and Western Pacific mantle xenoliths

M. MELCHIORRE[1], B. FACCINI[1], M. COLTORTI[1], M. GREGOIRE[2], C. BONADIMAN[1] AND M. BENOIT[2]

[1]Department Earth Sciences, University of Ferrara, Italy (massimiliano.melchiorre@unife.it)
[2]Observatoire Midi Pyrénéese, Université de Toulouse, France (gregoire@dtp.obs-mip.fr)

A suite of anhydrous spinel-bearing mantle xenoliths from Estancia Sol de Mayo (ESM, Patagonia) has been studied and compared with a large number of mantle xenoliths from other Patagonian localities. ESM xenoliths are devoid of modal metasomatic features as well as of amphibole. ESM cpx and opx plot on the high mg# side of three different trends, depicted by peridotites and pyroxenites of the other Patagonia localities. On the whole the three trends point towards refertilization/metasomatic events caused by saturated and undersaturated melts which largely affected the Patagonian sublithospheric mantle. These melts are similar to those responsible for the formation of various plateaux located behind the Austral Volcanic Zone. Cpx and opx of mantle xenoliths found in calc-alkaline lavas from the western part of the Pacific plate are also included in the comparison. They appear to be substantially depleted in Al_2O_3 and depict the fourth distinct trend. Investigation is currently undertaken to evaluate if this difference can be 'simply' related to different partial melting degree or to compositionally distinct metasomatic agents.

Diverse mantle sources for Ninetyeast Ridge volcanoes

P. MELENEY[1]*, F.A. FREY[1], M. PRINGLE[1], E. O'BRIEN[1], S. HUANG[2], I. NOBRE SILVA[3] AND D. WEIS[3]

[1]EAPS, MIT, Cambridge, MA 02139, USA (*pmeleney@mit.edu)
[2]EPS, Harvard University, Cambridge, MA 02138, USA
[3]EOS, UBC, Vancouver, B.C., Canada V6T 1Z4

The Ninetyeast Ridge (NER) is a 5, 000 km long N-S oriented submarine volcanic ridge in the eastern Indian Ocean. The N to S linear decrease in age, 77 to 43 Ma, is consistent with the NER forming as a hotspot track as the Indian Plate migrated northward over the Kerguelen hotspot. In 2007 the R/V Revelle recovered over 2, 000 kg of dominantly tholeiitic basalt from 22 dredge sites along 3, 200 km of the NER. The basalts have been variably altered in the submarine environment and 7 whole rock-glass pairs show that Rb and U are enriched and Ba is depleted in the altered whole rocks. Based on abundance ratios of REE and HFSE, and their correlations with Nd and Hf isotopic ratios, we identify several mantle sources that contributed to formation of the NER (see Fig. 1). We infer that two are related to the hotspot: one enriched in incompatible trace elements similar to the source of flood basalt in the Kerguelen Archipelago and the other is depleted in incompatible elements, but some trace element ratios (like Y/Nb) differ from the source of recently erupted SEIR MORB [1] (see Fig. 2). A third source is incompatible element-depleted similar to the source of SEIR MORB; this source is consistent with the inferred proximity of the hotspot to a spreading ridge during NER construction. However, Sr and Pb isotopic ratios of acid-leached whole rocks are not consistent with this inference [2, 3].

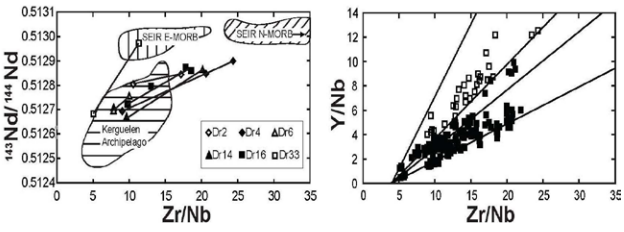

Figure 1: Dredges show trends between KA and SEIR E-MORB and N-MORB
Figure 2: Y/Nb anomalies in NER basalts.

[1] Frey *et al*. (2011) *EPSL* **303** 315–224. [2] Nobre Silva *et al*. (2007) *GCA* **71**, 15S A721. [3] Nobre Silva *et al*. (2011) *PhD Thesis* UBC.

https://doi.org/10.1180/S0026461X00006502 Published online by Cambridge University Press

Abundant marine sulphate in the Palaeoproterozoic: Models come and go, but the rock record endures

V.A. MELEZHIK[1,2]*, A.E. FALLICK[3], D.V. RYCHANCHIK[4] AND FAR-DEEP DRILLING TEAM

[1]NGU, Postboks 6315, N-7491 Trondheim, Norway (*correspondence: victor.melezhik@ngu.no)
[2]University of Bergen, Postboks 7803, N-5020 Bergen, Norway
[3]SUERC, East Kilbride, Glasgow G75 0QF Scotland
[4]Geological Institute, 185610 Ptrozavodsk, Russia

An important consequence of progressive oxygenation of the Earth's biosphere through the Proterozoic was an increased rate of sulphide oxidation during continental weathering, with concomitant increase in marine sulphate concentration. Hence, accurate assessment of the marine sulphate reservoir is crucial for correct interpretation and reconstruction of the oxygenation history of Earth's early emvironments. The currently accepted view is that the Proterozoic biosphere shows protracted oxidation, but marine sulphate remains low until c. 800 Ma [1]. This view and the estimated size of the marine sulphate reservoir through the Proterozoic, was essentially based on (*i*) a model that involves S isotope variability, and (*ii*) the absence of massive Ca-sulphates in the geological record until the late Mesoproterozoic. A contrasting, and less popular view, based on geological evidence, suggests otherwise [2]. Recently, the controversy has been resolved by discovery of massive anhydrites [3]. At a depth of 2115 m in a c. 3500-m-deep drillhole in the Onega Basin in eastern Fennoscandian Shield ^{13}C-rich dolostones of Lomagundi-Jatuli age (335 m) were intersected followed by massive anhydrite and anhydrite-magnesite rocks (c. 100 m), nodular shale interbedded with massive anhydrite (190 m) and a c. 194-m-thick halite formation (70-75% halite, 12-20% anhydrite, 10-15% magnesite) containing large blocks (up to 1 m) of bedded, coarse-grained anhydrite and magnesite. The c. 500-m-thick sulphate-halite interval survived orogenic deformation and associated greenschist metamorphism. Thick dissolution-collapse breccias occurring basin-wide at more shallow depths suggest that the preserved section represents only a small fraction from that what was originally precipitated. Hence, the geological record in the Onega basin endured and revision of current models is essential.

[1] Kah *et al*. (2004) *Nature* **431**, 834–838. [2] Melezhik *et al*. (2005) *Terra Nova* **17**, 141–148. [3] Morozov *et al*. (2010) *Doklady Earth Science, Geochemistry* **435**, 230–233.

U-Pb dating of columbite-tantalite from Variscan rare-elements granites and pegmatites

J. MELLETON[1], E. GLOAGUEN[1], D. FREI[2] AND A. LIMA[3]

[1]BRGM, Mineral Resources Division, Orléans, France (j.melleton@bgrm.fr, e.gloaguen@brgm.fr)
[2]Stellenbosch University, Central Analytical Facility & Department of Earth Sciences, Stellenbosch, South Africa (dirkfrei@sun.ac.za)
[3]Porto University, Center of Geology, Porto, Portugal (allima@fc.up.pt)

Rare-elements (Li, Cs, Ta, Be, Sn…) magmatism is well expressed in the European Variscan belt with mainly pegmatites and granites. These bodies are known in most of the different realms of the belt, but they are particularly abundants in localized parts of the Iberian massif, the French Massif Central and the Bohemian Massif.

U-Pb dating of columbite-tantalite from selected Variscan rare-elements granites and pegmatites of these three massifs has been performed using laser ablation system connected to a single collector magnetic SectorField - Inductively Coupled Plasma - Mass Spectrometer (LA-SF-ICP-MS). The main aims of this study are to investigate the timing of this magmatism in the Variscan belt and the chronological relationship with the surrounding granitoid suites. Our results highlighted the existence of several emplacement episods :

- in the Moldanubian domain of the Bohemian Massif, rare-elements pegmatites emplaced at around 340-330 Ma.
- in the North of French Massif Central, the Montebras and Beauvoir granites and the Chèdeville pegmatite lead to emplacement age at 315-310 Ma.
- in the North of Iberian massif, three different events have been recognized, with the emplacement of the Argemela granite at 326 ± 3 Ma, a first group of pegmatites emplaced at 310 ± 5 Ma, a second at 301 ± 3 Ma.

In this context, rare-elements magmatism do not look to be related to lower crust processes (i.e. granulitic metamorphism) and rare metal magmatism event appears diachroneous and polyphased.

https://doi.org/10.1180/S0026461X00006502 Published online by Cambridge University Press

Microbial iron(II) oxidation in littoral freshwater lake sediments; Competition between phototrophic versus nitrate-reducing iron(II)-oxidizers

E.D. MELTON*, C. SCHMIDT AND A. KAPPLER

Geomicrobiology, University of Tuebingen (*correspondence: emily-denise.melton@uni-tuebingen.de)

The temporal and spatial distribution of microbial iron redox transformations are determined by local geochemical conditions and the resident microbial diversity. In the anoxic part of the top layer of littoral freshwater lake sediments, nitrate-reducing and photoferrotrophic microorganisms compete for the same electron-donor, i.e. reduced iron. Though a conceptual framework for biogeochemical iron cycling has been proposed [1], it is not yet empirically understood how these microbes co-exist in the sediment, what their spatial distribution is relative to one another and what role they play in the overall iron cycle. In this study, freshwater littoral lake sediment from Lake Constance was incubated in microcosm experiments with various additives to stimulate microbial photoferrotrophic and nitrate-reducing iron (II) oxidation in order to distinguish between the two processes and assess their individual contributions to the sedimentary iron cycle. One set was incubated under constant light, whilst a parallel set was incubated in the dark at 23°C. Additionally, a high-resolution MPN depth profile was performed for iron (II)-oxidizing organisms utilizing light or nitrate to reveal their spatial distribution in the natural sediment. These experiments combine microbial and geochemical techniques to provide key information needed not only to determine the contribution of microbial activity to the overall iron oxidation budget and their spatial distribution, but also to define the role of geo (photo)chemical iron conversion rates and its general importance in littoral freshwater lake sediments.

[1] Schmidt *et al*. (2010) *Environmental Chemistry* **7**, 399–405.

Unraveling microbes-minerals interactions in the deep biosphere

B. MENEZ[1,2]*, E. GERARD[1,2], D. BRUNELLI[3], V. PASINI[31], P. LE CAMPION[1,2], S. DUPRAZ[1,2], M.C. MARINOZZI[1,2], M. AMOR[1] AND F. GUYOT[1,24]

[1]IPGP, UMR CNRS 7154, 1 rue Jussieu, 75005 Paris, France (*correspondence: menez@ipgp.fr)

[2]Centre de Recherches sur le Stockage Géologique du CO_2 (IPGP/TOTAL/SCHLUMBERGER/ADEME)

[3]Dipartimento di Scienze della Terra, Università di Modena, L.go St. Eufemia 19, 41100 Modena, Italy

[4]IMPMC, UMR CNRS 7590, 4 place Jussieu, 75005 Paris, France

Subsurface environments harbor diverse and active microbial populations that influenced the Earth's chemistry throughout geological times by mediating elemental fluxes from the lithosphere to the oceans and atmosphere. However, the exploration of their metabolic diversity, energy sources, and biogeochemical transformations at the appropriate scale remains highly challenging, especially within hard rocks. We present here dedicated cutting-edge approaches combining molecular labelling (as fluorescence *in situ* hybridization and immunodetection) with an array of high-resolution techniques (coupled confocal laser scanning microscopy and Raman spectroscopy, transmission and scanning electron microscopies, synchrotron-based X-ray microimaging). Altogether they allow localizing specifically individual prokaryotic cells, investigating their phylogenetic affiliation at the micrometric scale while characterizing concomitantly the nature and the stucture of their microhabitats and past interactions (i.e. mineral dissolution and metabolic byproducts such as biomineralizations). Our ability to reveal chemical, mineralogical, genetic and metabolic diversity in subsurface environments will be illustrated by integrated field and laboratory investigations. Special attention will be dedicated to hydrogen-driven chemolithoautotrophic ecosystems associated with ultramafic rocks from the oceanic lithosphere, in the double fundamental perspective: to explore analogs for early biological systems on the primitive Earth or other planetary bodies, and for industrial purposes being a major target for CO_2 geological storage where microbial activity allow enhancing carbonation processes and reducing the energetic balance.

https://doi.org/10.1180/S0026461X00006502 Published online by Cambridge University Press

Late Paleozoic tectonic evolution in eastern Heillongjiang Province, NE China: Constraints from detrital zircons and volcanisms

E. MENG, W.L. XU*, F.P. PEI AND F. WANG

College of Earth Sciences, Jilin University, Changchun 130061, China (mengen08@mails.jlu.edu.cn) (*correspondence: xuwl@jlu.edu.cn, mengen08@mails.jlu.edu.cn)

Geochronology of detrital and magmatic zircons and geochemistry of the volcanic rocks from the late Paleozoic strata in eastern Heilongjiang province of NE China, provide constraints on the Late Paleozoic tectonic evolution of the eastern segment of the Central Asian Orogenic Belt between the Siberian and the North China cratons [1].

LA-ICP-MS U-Pb dating results for detrital zircons from the Early Devonian sandstones show that the detrital zircons from the rocks in the Songnen-Zhangguangcai Range Massif (SZM) have age populations of 2503, 1833, 903~802, and 551~403 Ma, different from those from the coeval rocks in the Jiamusi Massif (JM) with ages of 569, 542, 509, and 484 Ma [2]. This finding indicates that (1) they deposited after 403 and 484 Ma, respectively; (2) ancient crustal remnants existed in the SZM in the Late Paleozoic; (3) the amalgamation of the SZM and JM could happen before 403 Ma.

Zircon U-Pb dating results for the magmatic zircons from the Late Paleozoic volcanic rocks in the region indicate that three volcanical events exist in the Late Paleozoic, i.e. the Middle Devonian (386 Ma), Early Permian (291 Ma), and Middle Permian (268 Ma). Their geochemical data and Sr-Nd-Hf isotopes reveal that: (1) the Middle Devonian volcanic rocks in eastern margin of the JM consist of basalt and rhyolite, a bimodal volcanism, suggesting an extensional environment, which is consistent with the existence of coeval A-type rhyolites in the SZM; (2) the Early Permian volcanic rcoks in the eastern margin of the JM are composed mainly of a calc-alkaline volcanic rocks such as basalt, basalt-andesite, and minor dacite, indicating an active continental margin setting, whereas the coeval bimodal volcanical rocks in the SZ suggests an extensional environment similar to a back-arc basin setting [3];. and (3) the Middle Permian syn-collisional rhyolites in the southeastern margin of the JM imply the amalgamation of the JM and the Khanka Massif.

[1] Sengör A.M.C. *et al*. (1993) *Nature* **364**, 299–307. [2] Meng *et al*. (2010) *Tectonophysics*. **485**, 42–51. [3] Meng *et al*. (2011) *J. Asian Earth Sci*. **41,** 119-132.

Hf-Nd isotope decoupling during partial melting of thickened eclogitic lower continental crust

F.X. MENG[1]*, S. GAO[1,2], W.L. XU[3], J.L. GUO[1] AND C.L. ZONG[2]

[1]State Key Laboratory of Geological Processes and Mineral Resources, China University of Geosciences, Wuhan 430074, China (*correspondence: mfx1117@163.com) (sgao@263.net)

[2]State Key Laboratory of Continental Dynamics, Northwest University, Xi'an 710069, China

[3]School of Earth Sciences, Jilin University, Changchun 130061, China (xuwl@jlu.edu.cn)

Worldwide granulites usually do not exhibit decoupled Hf-Nd systems expected for crustal melting at the presence of garnet. Here we present whole-rock Nd–Hf isotopic data for a rare suite of lower crustal eclogitic xenoliths and their host early Cretaceous high-Mg adakitic porphyries from the Xuhuai area from the eastern North China craton. The xenoliths and their host intrusions are considered to represent residues and melt formed by melting of eclogitic lower crust that foundered into the convecting mantle based on their complementary major and trace element compositions and similar zircon age patterns. Nine of the eleven analyzed xenoliths plot significantly above the terrestrial Hf-Nd array with ε_{Hf} up to +60, while the porphyries fall essentially along the array. Hf-Nd isotopic modelling shows that the eclogitic xenoliths can be interpreted by 30-50% extraction of melt, which after reaction with 10-30% depleted mantle can produce the observed porphyry. The retarded time-integrated Hf isotope ingrowth of the porphyries is due to its very low Lu/Hf ratio and a relatively short time span after its formation. Our results also indicate that garnet is the major factor controlling Lu/Hf ratio of the residue with accessory minerals rutile and titanite also playing a role. Granulite with <10% garnet will not evolve to show significant decoupled Hf-Nd isotopic signatures even after 500 Ma of melt extraction. The generally terrestrial Hf-Nd compositions of worldwide granulites may be because they have never experienced partial melting at presence of abundant garnet. Instead, the lower crustal granulite may transform into eclogite during crustal thickening. Such an eclogitic lower crust is short-lived, and will be recycled into the mantle. Decoupled Hf-Nd isotopic signatures are expected to be more pronounced in eclogite foundering-related basaltic magma than eclogite-derived TTG melt, as observed in some of Cenozoic basalts from the eastern North China craton.

https://doi.org/10.1180/S0026461X00006502 Published online by Cambridge University Press

Thermometry of quartz from the metaconglomerate of Jack Hills, Western Australia

M. MENNEKEN[1]*, A.A. NEMCHIN[2] AND T. GEISLER[3]

[1]Institut für Mineralogie, Westf. Wilhelms Univ. Münster Correnstr. 24, 48149 Münster , Germany (*correspondence: m.menneken@uni-muenster.de)
[2]Department of Applied Geology, Curtin Univ. of Technlogy, Kent Str. Bentley, 6102 WA, Australia
[3]Steinmann Institut, Rheinische-Friedrich-Wilhems Univ. Bonn, Poppelsdorfer Schloss, 53115 Bonn, Germany

The original sample site W74 in the Jack Hills meta-sedimetary belt, Western Australia [1], is well known for containing detrital zircon grains as old as 4.4 Ga [2]. Various geochemical investigations on these detrital zircons and their inclusions have been utilized in trying to establish conditions that existed on the early Earth [3 and ref. therein]. We extended the focus of this research to quartz, the main component of the conglomerate containing old zircons. In a comparative study we determined Ti temperatures of quartz [4] in both the quartzite pebbles and the matrix of the conglomerate, as well as of quartz from inclusions in zircons. The quartz grains of the conglomerate pebble record an average temperature of 437 ± 22°C (2σ, n=21), which is significantly lower than the temperature of 509 ± 80°C (n=15) obtained from the matrix quartz. The temperatures obtained from quartz inclusions in separated zircon grains, on the other hand, are all around 700°C, and are in agreement with Ti-in-zircon temperatures obtained from the host zircons, proving previous assumption that the quartz inclusions were incorporated during zircon growth. We interpret the matrix quartz temperature as recording the late metamorphism of the Jack Hills sedimentary belt at upper greenschist lower amphibolite conditions [5]. The pebble quartz, however, might inherit the temperature of an earlier metamorphic event in the source region. This, in combination with the restriction of the mineral paragenesis to nearly purely quartz, suggests that grains, deposited in the Jack Hill sedimentary belt, are derived from a meta-sedimentary host rock. Zircons, found in the conglomerate, would thus have experienced at least one metamorphic event before being re-deposited in the Jack Hill sedimentary belt.

[1] Compston & Pidgeon (1986) *Nature* **321** 766–769. [2] Wilde *et al*. (2001) *Nature* **409** 175–178. [3] Kemp *et al*. (2010) *EPSL* **296** 45–56. [4] Wark & Watson (2006) Contrib Mineral Petrol **152** 743–754 [5] Rasmussen *et al*. (2010) *Precambrian Research* **180** 26–46.

SoilTrEC: An international consortium to assess soil processes and functions using a global network of Critical Zone Observatories

M. MENON AND SOILTREC RESEARCH TEAM

Kroto Research Institute, University of Sheffield, Broad Lane, Sheffield, S3 7HQ, United Kingdom (m.menon@sheffield.ac.uk)

Soil Transformation in **E**uropean **C**atchments (SoilTrEC) is an international consortium that aims to develop a comprehensive understanding of soil processes and functions. The project will combine experiments and modelling to describe soil formation and functions using a global network of Critical Zone Observatories (CZOs) that focus multidisciplinary expertise onto the study of soil processes. The specific objectives of the project are the following: (1) describe from 1st principles how soil structure impacts processes and function at soil profile scale, (2) establish 4 EU Critical Zone Observatories to study soil processes at field scale (3) develop a Critical Zone Integrated Model of soil processes and function (4) create a GIS-based modelling framework to delineate soil threats and assess mitigation at EU scale (5) quantify impacts of changing land use, climate and biodiversity on soil function and economic value (6) form with international partners a global network of CZOs for soils research, and (7) deliver a programme of public outreach and research transfer on soil sustainability [1].

Four experimental CZOs are chosen for this study [1]; the Damma Glacier CZO (Switzerland) allows the study of incipient soil formation in the glacial forefield as the glacier retreats, to study earliest stages of soil formation. Lysina CZO (Czech Republic) and Fuchsenbigl CZO (Austria) are included to study soil processes under well managed forest and arable landscapes, respectively. The Koiliaris CZO (Greece) represents highly degraded soils after millennia of intensive agricultural land use, including grazing, and is under additional threat from desertification due to modern climate change. These CZOs provide field data and new measurements which will be used for the modelling of water flow, reactive transport, biogeochemical processes and nutrient cycles. Finally, an intergrated regional scale model will be developed for soil ecosystem services and threats in Europe, which will be further validated with other CZOs in Europe, USA and China. Soil profile sampling from the CZOs was completed in 2010 and preliminary data will be presented.

[1] Banwart *et al*. *Vadose Zone Journal* (in review).

https://doi.org/10.1180/S0026461X00006502 Published online by Cambridge University Press

Quantitative reconstruction of millennial-scale temperature variations in Central Europe

G. MENOT* AND E. BARD

CEREGE, Univ. Aix-Marseille, CNRS, IRD & College de France, Technopole de l'Arbois BP 80, 13545 Aix-en-Provence Cedex 04, France
(*correspondence: menot@cerege.fr, bard@cerege.fr)

The amplitude of the environmental changes associated with the Last Deglaciation provides a useful test bench for the climatic and oceanic responses and their attendant feedbacks to major reorganizations of the atmospheric circulation and the surface hydrology. We present the first quantitative reconstruction of millennial-scale temperature variations in Central Europe during the last 40, 000 years based on newly developed temperature proxies measured in a sediment core from the Black Sea (MD04-2790). Despite the shift from lacustrine to marine conditions (and therefore associated salinity changes) that affected the basin, the tetraether-based paleothermometer (TEX_{86}) properly records the increase in surface water temperatures during the Last Deglaciation. To our knowledge, no quantitative temperature reconstruction has been published for the Black Sea area so far, a comparison of the amplitude of temperature changes reconstructed for the Last Glacial Maximum and the actual in the Mediterranean basin shows that the Black Sea values are consistent with that of the western basin and colder than the eastern basin [1]. Interestingly and in contrary to what is seen in nearby archives (pollen assemblages [2], [3] and speleothems [4]) Heinrich events deeply imprint our glacial temperature record, whereas the signature of Dansgaard-Oeschger interstadials are comparatively attenuated. The high-resolution record also provides snapshots of the basin responses to specific abrupt climatic events such as the Younger Dryas and the Bølling-Allerød.

[1] Hayes *et al*. (2005) *Quaternary Science Reviews* **24**, 999–1016. [2] Naughton *et al*. (2007) *Marine Micropaleontology*, **62**, 91–114. [3] Fletcher *et al*. (2010) *Quaternary Science Reviews*, **29 (21-22)** 2839–2864. [4] Fleitmann *et al*. (2009) *Geophys. Res. Let*. **36**.

Application of thermal analysis and NMR to study soil organic matter biodiversity and biodegradability in afforested lands

AGUSTÍN MERINO*, CÉSAR PÉREZ-CRUZADO, JOSEFA SALGADO AND NIEVES BARROS.

Escuela Politécnica Superior, University of Santiago de Compostela, Lugo, Spain

Calorimetry and thermal analysis can be applied to studies of the stabilization of soil organic matter (SOM) under different environment situations and types of management. In this study, differential scanning calorimetry (DSC) and isothermal calorimetry were applied, along with ^{13}C CPMAS NMR, to assess the changes in SOM quality in afforested lands under pine and eucalypt in a humid temperate region.

Samples with the highest carbon percentages contained highly diverse mixture of aliphatic fractions, carbohydrates, cellulose, aromatic C and carboxyl groups. The heat of combustion was also highest in these samples. The loss of SOM and the C decay affected the aliphatic fraction and carbonyl groups, which could not be identified in the NMR spectrum or in the DSC curves of those samples. Carbohydrates and aromatic C persisted in the samples with the lowest C percentages. C gain after afforestation predominantly affected the aliphatic and aromatic fractions in the pine stands and the aliphatic and carbohydrate fractions in the eucalypt stands. The method was sensitive to detect differences in the OM nature attributable to the tree species.

https://doi.org/10.1180/S0026461X00006502 Published online by Cambridge University Press

Sr-Nd-Pb-Os isotopes of CAMP tholeiites from northeast America

R. MERLE[1]*, A. MARZOLI[1], H. BERTRAND[2], L. REISBERG[3], M. CHIARADIA[4] AND G. BELLIENI[1]

[1]Università di Padova, via Gradenigo 6, 35100 Padova, Italia (*correspondence: renaud.merle@unipd.it) (andrea.marzol@unipd.it, giuliano.bellieni@nipd.it)
[2]UMR-CNRS 5570, 46 Allée d'Italie, 69364 Lyon, France (herve.bertrand@ens-lyon.fr)
[3]CRPG (CNRS UPR2300), BP 20, 54501 Vandoeuvre-lès-Nancy, France (reisberg@crpg.cnrs-nancy.fr)
[4]Université de Genève, 13 rue des Maraîchers, 1205 Genève, Switzerland (Massimo.Chiaradia@unige.ch)

The Central Atlantic Magmatic Province (CAMP) is one of the largest CFB provinces on Earth, extending over a surface in excess of 10^7 km^2 in circum-Atlantic regions. Here we document the geochemical characteristics of CAMP lavas flows, sills and dikes from NE U.S.A. and Nova Scotia (Canada).

All the samples are low-Ti basalts and compared to N-MORBs they display LILE and LREE enriched patterns with negative Nb anomalies. Based on major and trace element characteristics (REE patterns, TiO_2 vs La/Yb diagrams), three groups can be defined: (1) the Talcott-Orange-Mt Zion Church flow units, all the Nova Scotia samples (North Mountain basalts and Shelbourne dike) and the lower part of the Palisades sill (TiO_2 ≈ 0.5-1.3 wt%, La/Yb ≈ 4-6), (2) the Holyoke-Preakness-Sander-Hickory flow units (TiO_2 ≈ 0.7-1.1 Wt%, La/Yb ≈ 2.5-3.5) and (3) the Hampden-Hook flow units (TiO_2 ~ 1.3-1.5 wt%, La/Yb ~ 2).

All the samples plot in the field of CAMP low-Ti basalts in Pb-Pb and Sr-Nd isotope plots ($^{206}Pb/^{204}Pb$ = 18.16-18.69, $^{207}Pb/^{204}Pb$ = 15.57-15.67, εNd from -4.1 to 2.3). Most of the samples display initial $^{187}Os/^{188}Os$ ratios in the range of typical upper mantle magmas. Nevertheless, some samples have quite radiogenic initial ratios (up to 0.479) suggestive of crustal contamination.

The Talcott-Mt Zion Church-Orange-North Mountain-Shelbourne group shows continental-like Sr-Nd-Pb isotopic ratios, which coupled with their mostly non-radiogenic Os compositions, may argue for a dominant source contribution from subduction-metasomatised sub-continental lithospheric mantle (SCLM). The Hook-Hampden and the Holyoke-Sander-Preakness-Hickory units as well as the Rapidan sill are slightly distinct from the other samples since they yield $^{206}Pb/^{204}Pb$ >18.5 and are closer to the NHRL. These characteristics may suggest a contribution from an asthenospheric component.

Evaluating the impact of marine organic aerosols on climate

NICHOLAS MESKHIDZE, JUN XU AND BRETT GANTT

Department of Marine, Earth, and Atmsospheric Sciences, North Carolina State University, Raleigh, NC, USA (nmeskhisze@ncsu.edu, jxu5@ncsu.edu, bdgantt@gmail.com)

A large fraction of the uncertainty in predicting future climate may be related to the number concentration of marine aerosol that are prescribed or diagnosed in global climate models. Therefore, correct assessments of aerosol number concentration, size distribution and chemical composition over pristine marine regions may have profound effect on model predicted extent of human-induced climate change.

The effects of marine organic aerosols on microphysical properties of shallow clouds and the Earth's radiative budget are explored by the NCAR Community Atmosphere Model (CAM5.0), coupled with the PNNL Modal Aerosol Model. Sea spray enrichment by organics is estimated using wind speed dependent size-resolved parameterization, while marine-source secondary organic aerosol is inferred from the ocean emissions of biogenic trace gases. The ability of sea spray to act as cloud condensation nuclei (CCN) are not fully understood; therefore CAM5 simulations cover the range of possible scenarios in aerosol mixing sate and hyroscopicity parameter based on our recent lab experiments. The size, number, and CCN distributions of aerosols generated by a bubble-bursting process were determined using a differential mobility analyzer (DMA)-condensation particle counter (CPC)-CCN counter (CCNc) system. Predicted concentration of organic aerosol and CCN in remote marine atmosphere was compared to *in situ* data. Simulations show that over the oceans marine organics can yield up to 10% increase in surface CCN (0.2%) (see Fig. 1). Changes associated with liquid water path and droplet number can increase short-wave forcing by -0.2Wm^{-2}. The disproportional effects of marine aerosols between pre-industrial and current climate and land vs. ocean have also been observed.

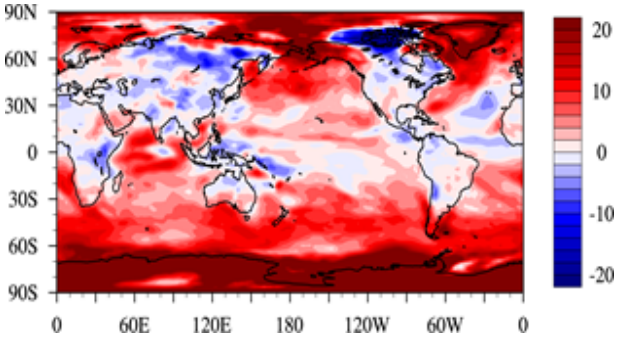

Figure 1: Annual average percentage change in surface CCN (0.2%) concentration due to marine emissions.

https://doi.org/10.1180/S0026461X00006502 Published online by Cambridge University Press

Evolution of the δD value in water-rich basaltic melt inclusions during volcanic processes

N. METRICH[1]*, E. DELOULE[2] AND A. DI MURO[1]

[1]Institut de Physique du Globe, Sorbonne Paris Cité, UMR CNRS 7154, Univ. Paris Diderot, Paris, France (*correspondence: metrich@ipgp.fr, dimuro@ipgp.fr)
[2]CRPG-CNRS, Vandoeuvre Les Nancy, France (deloule@crpg.cnrs-nancy.fr)

Melt inclusions (MI*s*) hosted in Mg-rich olivines are powerful tools to record magma evolution and degassing during their decompression and ascent toward the surface. However their ability to loose H_2O during magma ascent and degassing through proton diffusion is widely debated [e.g. 1].

H_2O contents and δD values were measured in two series of melt inclusions representative of Ca-rich basalts to arc basalts, rich in H_2O, in using the Cameca IMS 1270 ion microprobe (CRPG-CNRS, Nancy, France) and Raman spectroscopy (Saclay, France, [2]), respectively. In lapilli samples from Vulcano island (Aeolian arc), MIs are hosted in olivine Fo_{89-90}, they contain on average 4.4 wt% of H_2O (±0.2 wt%; 18 measurements) and the post-entrapment olivine crystallizaton is negligible. In Aoba samples (Vanuatu arc), MIs are entrapped in olivine Fo_{86-90}, with 2 to 5 % of post-entrapment crystallization; their H_2O is more variable (1.7-2.3 wt%). In both cases their low CO_2 concentrations indicate shallow olivine crystallization.

As a whole the δD values (42 measurements) vary from -96‰ to +38‰ (with two values even higher). Isotopic analyses have been duplicated in single inclusions of Vulcano samples to verify the data reproducibility.

Hydrogen diffusion out of Mi*s* is required to explain negative trends between the H_2O concentrations and δD, in particular in one series of Aoba samples showing δD values ≥0‰. Leaving apart these latter values, most of the measured δD are comprise between -19‰ and -40‰. They plot in the field of Mariana arc Mi*s* (from -55‰ to -12‰; [3]). The question that arises is to what extent our δD values are representative of the last stage of melt equilibration with their surroundings at time of their entrapment and olivine crystallization or bring constraints on the magma source. The different processes able to reproduce the trends registered by Aoba and Vulcano MI*s* will be discussed.

[1] Gaetani *et al*. (2009) *Eos Trans AGU* 90(52) Fall Meeting supp. Abst. V51E-1770. [2] Mercier *et al*. (2010) *Geochim Cosmochim Acta* **74**, 5641–5656. [3] Shaw *et al*. (2008) *Earth Planet. Sci. Lett*. **275**, 138–145.

Am(III) retention by cement corrosion products under highly saline conditions

V. METZ, C. BUBE, E. BOHNERT, M. SCHLIEKER AND B. KIENZLER

Institute for Nuclear Waste Disposal (INE), Karlsruhe Institute of Technology, Herrmann-von-Helmholtz-Platz, 76344 Eggenstein-Leopoldshafen (volker.metz@kit.edu, bube@kit.edu, elke.bohnert@kit.edu, schlieker@kit.edu, bernhard.kienzler@kit.edu)

Cementition is a common method to fix and solidify low and intermediate radioactive waste (LLW/ILW). Alteration of radionuclide bearing cement products in diluted aqueous solutions has been studied quite extensively. Yet, in chloride-rich solutions, which are relevant for final LLW/ILW disposal in rock salt, there is still a lack of thermodynamic data and understanding with respect to both cement corrosion and radionuclide behaviour. In the present work, cement interaction with $MgCl_2$-rich brines have been studied experimentally on laboratory-scale and with full-scale waste simulates. In addition, Am (III) retention by cement corrosion products was quantified from the laboratory experiments.

Due to dissolution of portlandite, ettringite and other solid cement phases, the initially $MgCl_2$-rich solutions alter to alkaline $CaCl_2$-rich solutions. Besides reprecipitation of gypsum, formation of hydrotalcite phases, Mg-Ca-Al hydroxochloride and brucite is observed. Compositions of the altered solution and solid phases depend strongly on the cement / brine ratio. Measured solution compositions agree well with results of thermodynamic calculations for the studied cement / brine systems. After equilibration of the systems, they are doped with small quantities of acidic ^{241}Am (III) and ^{243}Am (III) solutions (10^{-9}, 10^{-8} and 10^{-7} mol Am (kg H_2O)$^{-1}$). Am concentrations and solution composition have been monitored for 1000 days in the non-agitated batch experiments. Within six months a sorption equilibrium is achieved, demonstrating strong retention of Am (III) by the corroded cement products. Data of equlibrated systems are characterized by linear sorption isotherms, which allow determining apparent sorption coefficients, R_s. In $MgCl_2$-$CaCl_2$ and weakly alkaline $CaCl_2$ systems ($7.3 < -\log(m_{H+}) < 9.0$), R_s is measured in the range of 3000 to 6000 ml g^{-1}, whereas in highly alkaline $CaCl_2$ systems ($-\log(m_{H+}) \sim 11.5$) R_s = 10000 ml g^{-1} is observed. The retention of radionuclides on corroded cement products has often been claimed not only for dilute solutions, but also for saline brines. This work enables to quantify the retention of Am and thus corroborates previous estimations with experimental data.

https://doi.org/10.1180/S0026461X00006502 Published online by Cambridge University Press

Coupled high-resolution $\delta^{13}C_{carb}$ and $^{87}Sr/^{86}Sr$ chemostratigraphy on the North American craton: Identifying the source of the Late Ordovician Guttenberg Isotopic Carbon Excursion

J.G. METZGER AND D.A. FIKE

Dept. of Earth and Plentary Sciences, Washington Univ., St. Louis, MO 63130, USA. (gmetzger@levee.wustl.edu, dfike@levee.wustl.edu)

The Guttenberg isotopic carbon excursion (GICE) is a ~2‰ positive excursion in $\delta^{13}C_{carb}$ found in Late Ordovician (Early Katian) strata on three different continents and represents a major perturbation of the global biogeochemical carbon cycle. We applied $\delta^{13}C_{carb}$ chemostratigraphy to two Missouri (MO) sections containing the GICE in the Decorah Formation. Our data show the Kings Lake Member of southern MO and the Guttenberg Member of northern MO are coeval rather than successive, thereby revising the erosional and depositional history of Late Ordovician sediments in MO.

The cause of the GICE remains uncertain. Although enhanced burial of organic carbon is often invoked, definitive evidence for this has yet to arise. We couple $\delta^{13}C_{carb}$ and $^{87}Sr/^{86}Sr$ chemostratigraphy with biogeochemical cycling models of C and Sr to constrain possible causes for the GICE. Parallel variation in $\delta^{13}C_{carb}$ and $^{87}Sr/^{86}Sr$ suggest a change in oceanic weathering inputs as the most likely explanation for the GICE. Modelling results indicate that a single mechanism, a drop in the total weathering flux (F_w) and/or proportion of silicates being weathered, can explain the apparent inverse relationship between $\delta^{13}C_{carb}$ and $^{87}Sr/^{86}Sr$ in our two sections from MO. The drop in F_w could have resulted from flooding of the North American craton, which thereby lowered the amount of exposed land. Significant stratigraphic evidence of sea level rise is found across the North America craton and is coincident with the onset of the excursions in both isotopic systems. However, a widespread drowning surface at the end-GICE across the Upper Mississippi Valley suggests a decoupling between $\delta^{13}C_{carb}$ and sea level or the presence of more than one mechanism. Despite the challenges of non-uniqueness in reconciling chemostratigraphy and model results, we are able to show that coupling multi isotopic systems and elemental cycling models can constrain the range of possible source mechanisms, while precluding others. Furthermore, our results suggest that small excursions in $^{87}Sr/^{86}Sr$ may exist over relatively short periods of time (<1 Myr) in Paleozoic deposits.

Characteristics and origin of the Lala iron oxide Cu-Co-(U, REE) deposit: Sichuan, Southern China

F.M. MEYER[1]*, C. SCHARDT[1], S. SINDERN[1], M. GEHLEN[1], P.E. HALBACH[2], J. LAHR[2] AND J. LI[3]

[1]Institute of Mineralogy and Economic Geology, RWTH Aachen University, Wüllnerstr. 2, 52062 Aachen, Germany (*correspondence: m.meyer@rwth-aachen.de)

[2]Institute of Geological Sciences, Free University Berlin, Malteserstr. 74-100, 12249 Berlin, Germany

[3]Qingdao Institute of Marine Geology, 62 Fuzhou Nan Road, Qingdao, 266071, People's Republic of China

Cu-Co-REE-U mineralization at the Lala mine is multistage, controlled by the geologic-tectonic evolution of the region. The deposit has been interpreted as volcanic-hosted massive sulfide [1], metavolcanic-sedimentary with hydrothermal remobilization [2], or IOCG-type mineralization [3, 4]. The ore deposit is hosted by a Middle Proterozoic volcano-sedimentary succession, metamorphosed at upper-greenschist to amphibolite-facies conditions, early during the Sibao Orogeny (~1 Ga). Mineralization occurred during the Neoproterozoic at ca. 830 Ma [5].

The host rocks are metamorphosed and hydrothermally altered intermediate to mafic volcanics and mica schist. The main alteration styles include albitization and sericitization. Textural evidence allows recognition of 3 modes of sulphide mineralization with a distinct sequence of formation, indicating a complex and multiphase genetic evolution. There are strong indications that the mineralization is essentially epigenetic-hydrothermal in origin and the formation of hydrothermal breccias may be attributed to fluid release from an underlying magma. While there is no strict statistical correlation between La and Cu, Cu-rich samples are always enriched in REE elements. Other characteristic features include the abundance of iron-oxides and Cu-sulfides, a low-Ti magnetite chemistry, REE-mineralogy, and the presence of uraninite.

These new data lend evidence to the conclusion that, in contrast to previously proposed ore genesis models, the mineralization at Lala possesses many features that warrant its inclusion within the global IOCG deposit class.

[1] Zaw *et al*. (2007) *Ore Geol. Rev*. **31**, 3–47. [2] Baoyong & Zhengnan (1986) *J. Min. Pet*. **6**, 111–121. [3] Wang *et al*. (2005) *GCA* **69**, 573. [4] Li *et al*. (2002) *Bull. Chin. Soc. Min Petr. Geochem*. **21**, 258–260. [5] Sun *et al*. (2006) *Geochim*. **35**, 553–559.

https://doi.org/10.1180/S0026461X00006502 Published online by Cambridge University Press

Biogeochemical cycling in shallow-sea and terrestrial hydrothermal systems

D'ARCY R. MEYER-DOMBARD[1]*, DAWN CARDACE[2], SARA T. LOIACONO[1], YASEMIN GÜLEÇAL[1,3], KRISTIN WOYCHEESE[1] AND JAN P. AMEND[4]

[1]University of Illinois at Chicago (*correspondance: drmd@uic.edu, slafre2@uic.edu, kwoych2@uic.edu)
[2]University of Rhode Island (dawn.cardace@gmail.com)
[3]Istanbul University (yasegulecal@gmail.com)
[4]Washington University in St. Louis (amend@wustl.edu)

Mounting evidence indicates that microbial diversity varies substantially between hydrothermal systems of differing provenances. For example, among terrestrial hydrothermal systems, it has been shown that diversity and distribution of microorganisms may be related to geographical location or physical separation [1, 2]. There is, however, minimal evidence concerning differences in the diversity and distribution of genes associated with biogeochemical functions. Of particular interest is the nature of biogeochemical cycles such as nitrogen or carbon cycling in hydrothermal systems. Recent work has revealed snapshots of genetic potential for nitrogen cycling processes in hydrothermal systems such as nitrogen fixation and nitrification, and potential correlation with geography and other physicochemical parameters [for example, 3-6]. As of yet, no comparison of these processes between terrestrial and shallow-sea hydrothermal systems has been made.

We surveyed over 100 locations, representing terrestrial hydrothermal systems in Yellowstone National Park [USA] and Turkey, and shallow-sea hydrothermal systems in Sicily [Italy] and Papua New Guinea. In each area, we have characterized the geochemical environment, energetic potential, and functional genes diagnostic for stages of the nitrogen cycle. Our results show that the distribution of nifH [nitrogen fixation], amoA [nitrification], and narG/nirKS/nosZ [denitrification] genes differs between samples in sediments and biofilms. In addition, the genetic potential for nitrogen cycling is dependent on metabolic zonation within the hydrothermal system; for example, chemosynthetic vs. photosynthetic zones. The diversity of nitrogen cycling genes also varies with the provenace of the sample location, showing evidence for adaptation.

[1] Takacs-Vesbach *et al*. (2008) *Env. Micro.* **10**. [2] Whittaker *et al*. (2003) *Science* **301**. [3] Mehta *et al*. (2005) *Env. Micro.* **7**. [4] Zhang *et al*. (2008) *AEM* **74**. [5] Hamilton *et al*. (2011). [6] Hall *et al*. (2008) *AEM* **74**.

Multi-proxy ($\delta^{18}O$, χ_m , Nd and Pb isotopes) study for paleoclimate and paleoweathering in the Maldives area

L. MEYNADIER[1], C.J. ALLEGRE[1], A.T. GOURLAN[1] AND F.M. BASSINOT[2]

[1]IPGP (Sorbonne Paris Cité, Université Paris Diderot, UMR7154 CNRS), 1 rue Jussieu, 75238 Paris Cedex 05, France
[2]LSCE (CNRS/CEA/UVSQ), Domaine du CNRS, 91190 Gif-sur-Yvette, France (allegre@ipgp.fr, meynadier@ipgp.fr, gourlan@ujf-grenoble.fr, franck.bassinot@lsce.ipsl.fr)

On the MD900963 sediment archive cored on the edge of the Maldives Plateau (Equatorial Indian Ocean), we measured $\delta^{18}O$, $CaCO_3$, Magnetic susceptibility (χ_m), Neodymium and Lead isotopic compositions of both the ancient seawater and the detrital fraction. Our analyses cover the last 250 Ka.

The observed variations show fluctuations, which mimics the glacial-interglacial variations shown by $\partial^{18}O$. The two dominant frequencies are 100 Ka and 23 Ka.

The coherent results of Nd (ε_{Nd}) and Pb isotopes on the detrital fraction and carbonated corrected χ_m on one hand and Nd and Pb isotopes of the ancient seawater on the other hand show without doubt that these variations reflect the regional weathering and regional sedimentation. These data will also be in perspective with ODP Site 758 [1] and additional lead isotopes data from this eastern site.

All together, these results confirm that rain, physical & chemical erosion were larger during warm periods than during cold periods. These variations reflect the fluctuations of the summer monsoon rain intensity. Therefore the study gives strong limitations for the processes driving the relationship between climate, rain and weathering in the equatorial Indian Ocean region over the Glacial/Interglacial alternate.

[1] Gourlan, A. T. L. Meynadier, C. J. Allègre, P. Tapponnier, J.-L. Birck, & J.-L. Joron (2010) *Quaternary Science Reviews,* **29**(19-20) DOI: 10.1016/j.quascirev.2010.05.003.

Origin of Earth's volatile elements: Constraints from Rb isotopes

K. MEZGER[1], O. NEBEL[2] AND W. VAN WESTRENEN[3]

[1]Universität Bern, Switzerland (klaus.mezger@geo.unibe.ch)
[2]The Australian National University, Canberra, Australia
[3]Free University Amsterdam, Amsterdam, The Netherlands

Compared to the composition of C1-meteorites the Earth is strongly depleted in volatile elements. This depletions may be due to incomplete condensation or volatile loss caused by impact heating during the early stages of the planet formation. The elemental depletion correlates roughly with the half-condensation temperatures of the elements. This general depletion trend for the volatile element abundances in bulk silicate Earth (BSE) is modified due to core formation which further fractioned elements based on their siderophile and/or chalcophile behavior. The combined cosmochemical and geochemical effects result in the irregular trends observed in the abundances of the volatile elements in BSE. In order to separate the different depletion processes that affected the final composition of BSE we compare the abundances of Rb and Pb and their isotope compositions in terrestrial samples and meteorites In order to evaluate the variability of Rb isotopes in different solar system materials the Rb-isotope compositions of 17 primitive meteorites and terrestrial samples was analysed by MC-ICP-MS with Zr as an internal standard. This technique results in a reproducibility of ± 0.2 ‰ for $^{87}Rb/^{85}Rb$. The observed variation of the Rb-isotopes in all materials studied is less than 2 ‰. The variation does not correlate with the Rb elemental abundances. The unfractionated Rb-isotopes of the Earth imply that the volatile element depletion is not due to evaporation or incomplete condensation alone but requires at least a two step process. A more realistic model is that the Earth consists primarily of a large component of essentially volatile free material that was later mixed with a component that was not depleted in volatile elements. In this model the Rb-isotope composition of the mixture is dominated by the isotope composition of the undepleted component. Mass balancing with a 90% depleted Proto-Earth and gain of 10% C1 material can account for the Rb isotope distribution and abundance in the present day BSE. If Pb behaved approximately like Rb, as is suggested by its similar half condensation temperature, BSE requires an additional Pb depletion event to account for its observed U/Pb and Pb-isotope systematics. Comparison of Rb abundances and isotopes with Pb abundances and isotopes implies that the Pb-depletion in the BSE was not solely due to core formation but most of the Pb was already missing from the Earth prior to final core mantle equilibration.

Simulating experiments on gas generation of coal under different fluid pressure

MI JINGKUI, ZHANG SHUICHANG AND HE KUN

Key Laboratory for Petroleum Geochemistry, China National Petroleum Corporation.

It is still a controversy whether fluid pressure has a retardation for the hydrocarbon generation of source rock or not [1-2]. 4 groups experiments of gas generation of coal were conducted under different fluid pressure (25Mpa, 50Mpa, 75Mpa and 100Mpa) and temperature (300°C-650°C) in gold tube closed system. The maximum amount of total hydrocarbon gas are 102.32ml/g. coal, 95.63ml/g. coal, 122.26ml/g. coal and 124.56 ml/g. coal under 25Mpa, 50Mpa, 75Mpa and 100Mpa, respectively. So, fluid pressure action on gas generation of coal is not acceleration or retardation simply, but retardation in a relatively low scope of fluid pressure, and acceleration for gas generation of coal with fluid pressure increasing. The amount variation of methane generated by coal with fluid pressure increasing is consistent with that of total gases, but the volume variations of other gas components (such as H_2, H_2S, CO_2) have great difference, this indicate the influences of fluid pressure on these gases formation are different.

There is no explicit correlation between the value of $\delta^{13}C_1$ and the fluid pressure below 430°C, the value of $\delta^{13}C_1$ becomes from light to heavy first, then to light with the fluid pressure increasing in main period of gas generation (above 470°C) in all 4 groups experiments. The more of gas generating from coal is, the lower of H/C value of coal residue is. The R_O value of pyrolysis residue under 50MPa is lower than that under others fluid pressure in 470°C-575°C, in a point of other range temperature, there is no measurable difference of residue R_O in 4 group experiments

[1] Dalla Torre M. *et al*. (1997) *Org Geochem* **61**, 2921–2928.
[2] Wei Tao *et al*. (2010) *Fuel* **89**, 3590–3597.

https://doi.org/10.1180/S0026461X00006502 Published online by Cambridge University Press

Transport of solutes through hydraulically and chemically heterogeneous sediments of the Bengal Basin

H.A. MICHAEL

University of Delaware, Newark, DE 19716, USA (hmichael@udel.edu)

The sedimentary history of the Bengal Basin has determined the structure and pattern of an aquifer system more than 250, 000 km^2 in area and up to 16 km deep. Rivers carrying huge sediment loads from the Himalayas have deposited and eroded floodplain sediments through avulsion cycles; this combined with transgressions and regressions of sea level have produced complex stratigraphic sequences that make up a highly heterogeneous hydrogeologic system.

The sedimentary architecture plays a major role in determining groundwater flowpaths and subsurface transport of solutes. The depositional history also contributes to sediment chemistry, which can affect sorptive properties and other biogeochemical reactions. The effects of hydraulic and chemical heterogeneity in the Bengal Basin are considered generally and in two specific contexts: sustainability of arsenic-safe groundwater resources and groundwater salinization in the coastal zone.

Widespread contamination of shallow groundwater with As concentrations above world health standards occurs throughout much of the lower Bengal Basin, in Bangladesh and West Bengal, India. High concentrations are limited to the upper 100m in many areas; thus deep groundwater has been targeted as a mitigation option. The sustainability of deep resources depends on hydraulics and chemistry: both flowpaths and sorption may reduce vulnerability. Simulation of these protection mechanisms on a regional scale assuming basin-wide effective properties suggests a sustainable resource if properly managed. However, small-scale simulations that incorporate explicit heterogeneity in physical and chemical properties suggest that As migration may be highly variable, with short breakthrough times in some areas.

In the coastal zone, groundwater resources are threatened by salinization, which may become worse as sea level rises in the future. Currently, fresh groundwater exists at depth (>~200m) beneath a brackish zone. Mechanisms and timescales of salinization, both lateral and vertical, were investigated with variable-density numerical models. Subsurface salinity distributions, particularly in transient states, are highly dependent on heterogeneity in hydrogeologic properties as well as the history of sea level and storm surge inundations.

Geologic and hydrologic control of porewater chemistry and submarine groundwater discharge into Indian River Bay, Delaware

H.A. MICHAEL[1]*, C. FERNANDEZ[1], C.J. RUSSONIELLO[1], A.S. ANDRES[2], K.D. KROEGER[3], D.E. KRANTZ[4], J.F. BANASZAK[4], A. MUSETTO[1], K. MYERS[1], L.F. KONIKOW[5] AND J.F. BRATTON[6]

[1]University of Delaware, Newark, DE 19716, USA (*correspondence: hmichael@udel.edu)
[2]Delaware Geological Survey, Newark, DE 19716, USA
[3]U.S. Geological Survey, Woods Hole, MA 02543, USA
[4]University of Toledo, Toledo, OH 43606, USA
[5]U.S. Geological Survey, Reston, VA 12201, USA
[6]NOAA Great Lakes Environmental Research Laboratory, Ann Arbor, MI 48108, USA

Fluxes of nutrients transported by groundwater contribute to eutrophication in Indian River Bay, Delaware. Fresh and saline groundwater discharge rates and porewater salinity depend on system hydrology, mechanisms of groundwater-baywater exchange, and geologic heterogeneity. The interactions between these factors produce complex flowpaths and mixing that may affect nutrient bioavailability by causing biogeochemical transformations prior to discharge.

The hydrology, stratigraphy, subsurface salinity and N-species distributions, and submarine groundwater discharge (SGD) rates and patterns were characterized at Holts Landing State Park. A buried paleochannel and near-bottom confining beds, expected to control both flow and mixing in the subsurface, were located with offshore chirp seismic profiling and coring. Electrical resistivity surveys and vertical porewater salinity profiles to depths of up to 17m indicate that a zone of freshened groundwater extends hundreds of meters offshore. Onshore and offshore multi-level wells were sampled to obtain a 3D distribution of N species in the subsurface. SGD measurements from Lee-type seepage meters were collected to better understand discharge salinity, rates, and spatial and temporal SGD patterns. Measurements indicate that SGD is primarily saline, and that the lowest salinity groundwater discharges near the shoreline in the area away from the paleochannel feature and along the submerged paleochannel/interfluve boundary. Hydraulic head and permeability measurements in onshore and offshore wells provide information on site hydrology and temporal change. Data were incorporated into a groundwater flow model of the Indian River Bay watershed, which provides a larger-scale estimate of groundwater flowpaths and SGD fluxes and patterns along the entire bay shoreline.

https://doi.org/10.1180/S0026461X00006502 Published online by Cambridge University Press

Chemical composition of low-temperature biomass ash

M. MICHALIK[1]*, R. GASEK[2], W. WILCZYŃSKA-MICHALIK[2]

[1]Institute of Geological Sciences, Jagiellonian University, ul. Oleandry 2a, 30-063 Kraków, Poland (*correspondence: marek.michalik@uj.edu.pl)
[2]Institute of Geography, Pedagogical University, ul. Podchorążych 2, 30-085 Kraków, Poland (wmichali@up.krakow.pl)

The aim of the study of chemical composition of biomass ash is to evaluate its possible influence on composition of ash obtained during co-combustion of biomass and coal. Modification of composition of fly ash by biomass co-combustion with coal often reduce possibility of its utilization. Environmental impact of biomass combustion is poorly studied. There is a common opinion that biomass ash does not contain toxic metals like in the case of coal ash. The study is based on eight samples of biomass used in power plants in southern Poland.

Biomass was ashed at 475ºC and the yield of ash was from 0.5wt% (sawdust) to 10.8 wt% (olive kernel). Ash is usually rich in Ca (highest content ca. 16wt% in sawdust ash; content above 10wt% in three other samples; and the lowest ca. 1.9wt% in bran biomass ash), K (six samples with content above 10wt%, the lowest value for beechwood biomass), and P (two samples with content above 5wt% and the lowest content ca 0.5wt%).

Content of trace elements in studied samples of ash in often higher comparing with typical coal ash, e.g. Mn from 321 to >10 000 ppm; Ag from 0.02 to 5.3 ppm; Cd from 0.13 to 71.3 ppm; Cr from 3.8 to 988 ppm; Cu from 18 to 588 ppm; Mo from 2 to 14.7 ppm; Zn 106 to 1923 ppm and Hg from <5 to 35 ppb.

Ash is usually enriched in metals comparing with biomass samples. Highest enrichment (measured as ratio of content of element in ash/content of element in biomass) is observed for sawdust ash (e.g. Mo – 150; Cu - 193; Zn – 196; Ag – 143; Ni – 91; Co – 287; Mn – 156, Fe - 270; Cd – 230; Bi – 250; Cr – 177; Ba – 198; B – 464).

Obtained results indicate that both the composition of low temperature biomass ash and degree of enrichment in selected elements during ashing varies within broad range. Systematic study is necessary to predict the influence of biomass co-combustion on properties of ash and possible environmental impact.

Evidence for habitable environments deep in the Martian crust

J.R. MICHALSKI[1,2] P.B. NILES[3] AND J. CUADROS[1]

[1]Natural History Museum, South Kensington, London, UK
[2]Planetary Science Institute, Tucson, AZ, USA (*correspondence: michalski@psi.edu)
[3]NASA Johnson Space Center, Houston, TX, USA

Observations

Using infrared reflectance spectroscopy and high-resolution imaging, we have detected the presence of Fe/Ca-carbonates and Fe/Mg-rich phyllosilicates on Mars within rocks exhumed from deep in the subsurface by meteor impact [1]. The carbonates occur within layers or bands that are interbedded with or injected into layered and foliated chlorite, chlorite-smectite-, pumpellyite-, and possibly serpentine-bearing bedrock (Figure 1). This category of deposit is fundamentally different from previous detections of clay minerals [2-3] and carbonates [4-5] on Mars because in this case: a) carbonates and putative hydrothermal phyllosilicates occur together, b) the materials reflect a subsurface environment, rather than surface materials, and c) the minerals occur within rocks that have metamorphic and hydrothermal textures.

Implications

The carbonate- and clay-bearing rocks observed within Leighton Crater were excavated from ~6 km depth. These rocks may represent some of the most ancient sedimentary rocks on Mars (also in the Solar System) that were subsequently buried and metamorphosed. Alternatively, they may be evidence for deep-seated hydrothermal activity in a habitable subsurface environment.

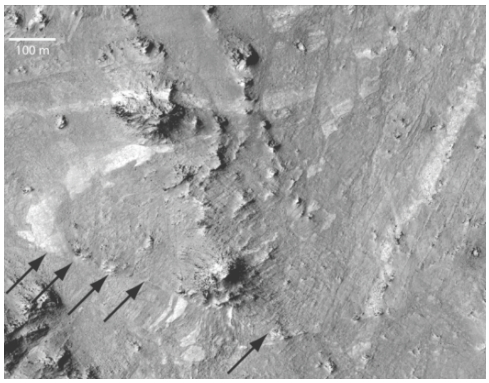

Figure 1: A HiRISE image of the central peak of Leighton Crater, Mars, where carbonates are detected within light-toned rocks that occur within exhumed, phyllosilicate-rich bedrock. Arrows point to a fault that offsets carbonates.

[1] Michalski & Niles (2010) *Nature Geo.* **3**, 751–755. [2] Bibring *et al.* (2006) *Science* **312**, 400–404. [3] Murchie *et al.* (2009) *J. Geophys. Res.* **114**, 1–30. [4] Ehlmann *et al.* (2008) *Science* **322**, 1828–1832. [5] Morris *et al.* (2010) *Science* **329**, 421–424.

https://doi.org/10.1180/S0026461X00006502 Published online by Cambridge University Press

Geochemical and geophysical coupling study of the karstic aquifer between Saïs Basin and the Causses of the Middle Atlas (Morocco). Fez-Meknès area

HÉLÈNE MICHE[1], ADRIANO MAYER[1], GINETTE SARACCO[1], MOHAMED ROUAI[2], ABDELILAH DEKAYIR[2], KONSTANTINOS CHALIKAKIS[3] AND CHRISTOPHE EMBLANCH[3]

[1]CNRS-UMR6635, CEREGE, UPCAM, Europole de l'Arbois, BP 80, F-13545 Aix en Provence, France (*correspondence: saracco@cerege.fr)
[2]Université M. Ismail, Département de Géologie, Quartier Zitoune, Meknès, Marocco
[3]EMMAH (UAPV, INRA) CNRS-UMR_A 1114, 33 rue pasteur, 84000, Avignon, France

The population growth in the region of Fez-Meknès (1.6 Million), accentuated by the increasing number of wells for agriculture, and by the increasing aridity in recent years, poses the problem of controlling water of sufficient quality and quantity over time.

This fractured karstic Basin mainly composed of Liassic dolomitic limestones overlying Triassic basalts, shales and evaporites, is the main drinking water supply in the region. The karstic reservoir presents a decline in its chemical quality and ponctually some turbidity problems.

To better understand this system and the interactions between different aquifers and aquitards, we conducted coupling study on:

i) geochemistry (major and minor elements, $\delta^{18}O$, δD and ^{222}Rn) of the main springs of Liassic and Triassic origin that could be connected each other and with the major spring of Bittit;

ii) electromagnetic multi-scale tomography for separating draining faults from not draining faults (geological structure).

The geochemistry of water during the three surveys in 2009 and 2010 shows a major Liassic origin for Bittit, Ribaa, Aguemguam, Amansayarmine, Bou Youssef and El Hajeb springs, and a major Triassic origin for El Mir, Sbaa 2, Maarouf1 and Maarouf2 springs. Radon 222 (T=3.85days) has highlighted the existence of areas of rapid exchange between waters of Liassic aquifers characterized by low Radon activity (3500 Bq/m^3) and waters of Triassic aquitards characterized by a high Radon activity (> 12000 Bq/m^3). The transit time from the Triassic aquifer is less than two weeks. Analyses of $\delta^{18}O$ versus δD show only a slight excess of Deuterium, this characterizes a local recharge of the groundwater.

Geophysical measurements of resistivity and conductivity show anomalies in the direction of Bittit and perpendicularly to the Causses, confirming the presence of a preferential drainage where Liassic waters of high quality mix with those in contact with the Triassic aquitard.

Acknowledgment: These studies are funded by the CNRS, Program of the Fédération de Recherche ECCOREV, and the Conseil Régional PACA, BREMEX Program.

Natural ferrihydrite: Impact of structure and composition on redox cycling

F.M. MICHEL[1,2], A.C. CISMASU[1], J.S. LEZAMA[2], M. MASSEY[1], S. FENDORF[3], G.E. BROWN, JR.[1,2] AND J.R. BARGAR[2]

[1]Geological & Environmental Sciences, Stanford University, Stanford, CA 94305, USA
[2]SLAC National Accelerator Laboratory, Menlo Park, CA 94025, USA
[3]Department of Environmental Earth System Science, Stanford University, Stanford, CA 94305, USA

Synthetic ferrihydrite (Fh) is typically used in laboratory studies and in the field, to a lesser extent, as a model compound for natural Fh in terms of understanding its sorption capacity, reactivity, stability, and dissolution and transformation behavior. All are properties that make naturally occuring Fh one of the most important natural Fe (III) oxyhydroxides in geochemical systems undergoing biogeochemical cycling of iron and redox-active contaminant metals such as U.Although much is known about synthetic Fh, recent research by our group calls into questions its relevance to natural systems. Many past studies have suggested that natural Fh often contains a suite of impurities (e.g. Zn^{2+}, Cr^{3+}, Al^{3+}, silicate, phosphate, organic carbon complexes) that can range widely depending on the conditions of Fh formation. It is less clear, however, how impurities impact the bulk and surface structure of Fh and its reactivity and stability. Our recent work [1] on natural Fh formed in an acid mine drainage system demonstrated that impurities, mainly Al, Si, and natural organic matter, increased structural disorder and decreased average particle size. Such details are important as they are likely to have significant impact on the biogeochemical reactivity of Fh.

While our picture of synthetic Fh structure continues to improve, little is known about the individual and cumulative effects of structural disorder (e.g. lattice strain and cationic vacancies), size, and composition on electron transfer processes occurring in Fh under reducing conditions. Processes related to the Fe (II)-induced reductive transformation are important, for example, because of the potential for environmental contaminants such as uranium to be directly incorporated in Fh transformation products. Our current work aims to better understand the links between the structure/composition and biogeochemical reactivity for both natural Fh and synthetic analogues to natural samples.

[1] Cismasu *et al*. (2011) *Comptes Rendus Geosci*. In press.

https://doi.org/10.1180/S0026461X00006502 Published online by Cambridge University Press

Oxygen and hydrogen stable isotope composition of precipitation in Friuli-Venezia Giulia (Northeastern Italy)

M. MICHELINI*, F. CUCCHI, O. FLORA, B. STENNI, F. TREU AND L. ZINI

Department of Geosciences, University of Trieste, Italy (*correspondence: marzia.michelini@phd.units.it)

Introduction

Oxygen and hydrogen stable isotopes, being natural tracers of the hydrological cycle, have been extensively used as tools to characterize regional aquifers. In particular, the knowledge of the mean annual-weighted isotopic composition of precipitation is a very important tool to determine the origin of the waters that feed aquifers and rivers, their recharge area and its mean altitude, thanks to the definition of the vertical isotope gradient. The knowledge of the relationship between isotopic composition of local precipitation and local environmental conditions is also essential for hydrological studies. In order to provide an overview of the isotopic composition of the precipitation in Friuli-Venezia Giulia region a monitoring of the regional rain gauge network has been carried out at the University of Trieste from 2004 to 2010.

Results and Discussion

Here we present $\delta^{18}O$ data obtained from monthly precipitation collected by rain gauges; where possible the $\delta^{18}O$ data were compared with temperature data weighted for precipitation (fig. 1) showing generally a good correlation. Vertical $\delta^{18}O$ gradients for homogenuos areas and an average gradient for the region as a whole were also calculated.
Finally the local meteoric water line was calculated using $\delta^{18}O$ and δD long-term weighted values for all the sampling sites.

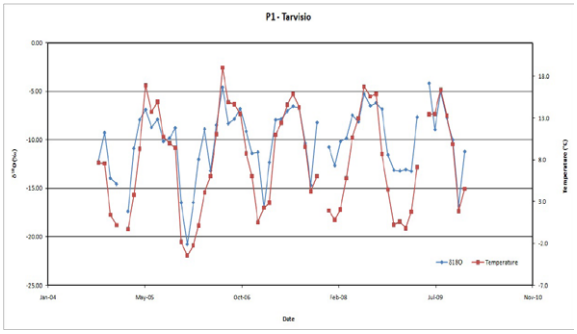

Figure 1: Monthly trends of $\delta^{18}O$ and temperature for the Tarvisio sampling site.

Metastable accessory phases in high heat-producing felsic igneous rocks

A.W. MIDDLETON*, S.D. GOLDING AND I.T. UYSAL

University of Queensland, St. Lucia, QLD 4066, Australia (*correspondence: alexander.middleton@uqconnect.edu.au)

High heat-producing felsic igneous rocks are characterised by enriched values of U, Th and K relative to upper continental crust, and are of specific interest when seeking to exploit geothermal energy through enhanced geothermal systems. The elevated values reflect the evolved nature of the felsic rock; common examples include granites and rhyolites. The current study focuses on famous HHP systems of Soultz-sous-Forêts, France, Cornwall, UK, and the novel HHP rhyolite of central Queensland, Australia.

Samples from Soultz and central Queensland show evidence that metasomatised titanite can form rutile + calcite + quartz with accessory hydrothermal zircon and Ca (REE, Y)CO_3 (OH, F)$_?$ or cheralite, respectively. The accessory phases reflect how Zr, Th, Y and REE can substitute into titanite's structure in an evolved system. EPMA of the anhedral hydroxyl-, fluoro-carbonate phase found elevated values of both Ca and Ce with variable LREE, Y and Th. The occurrence of Ca (REE, Y)CO_3 (OH, F)$_?$ in place of cheralite may result from elevated [CO_2] and [F-] as opposed to [PO_4^{3-}] and [CO_2]; as indicated by cogenetic chloritisation of F-bearing biotite and intercleavage-grown ankerite. Mobilisation of incompatible elements as fluoro-carbonate ligand complexes was minimised by the presence of Ca^{2+}, resulting in precipitation within or proximal to the titanite void. By contrast, SEM analyses of the F^--dominated Cornish metasomatic system shows monazite solid-solution phases along cleavage planes of chloritised biotite, implicating the uncommon mobilisation of Th^{4+}. Further EMPA will better define these phases and constrain their palaeometasomatic conditions.

Analysed primary accessory phases such as titanite were relatively enriched in incompatible elements that formed polymineralic assemblages following metasomatism. The volatile content of metasomatising fluids played a significant role in the production of these metastable phases. Titanite specifically, destabilised in the presence of CO_2 or F- [1, 2]. Volatiles not only helped destabilise the primary phases but also mobilised constituent elements; as seen when halide ligands drastically increase the mobility of incompatible elements such as REE and HFSE [3]. By analysing metastable accessory phases, this study will further constrain under which conditions HHP systems undergo metasomatism as well as better understand the extent of metasomatic incompatible element immobility.

[1] Markl & Piazolo (1991) *Am. Min.* **84**, 37–47. [2] Hunt & Kerrick (1977) *G&C Acta* **41**, 279–288. [3] Wood (1990) *Chem. Geo.* **88**, 99–125.

https://doi.org/10.1180/S0026461X00006502 Published online by Cambridge University Press

An experimental study of the stability of hydrosulfide species of Fe(II) at hydrothermal conditions

ART. MIGDISOV[1]*, D. ZEZIN[2] AND A.E. WILLIAMS-JONES[1]

[1]Earth & Planet. Sci., McGill Univ., Montreal, H3A 2A7 Canada (*correspondence: artas65@gmail.com)
[2]Institute of Geochemistry and Petrology, ETH Zurich, CH-8902 Zurich, Switzerland

Iron is one of the most abundant elements in the Earth's crust, and is actively involved in the processes of hydrothermal alteration and ore mineralisation. Iron-bearing sulphides dominate most hydrothermal sulphide ore bodies and form in a wide variety of geological environments at conditions ranging from those of magmatic intrusions to those of sediments undergoing diagenesis. However, our knowledge of the speciation of this metal in sulphide-bearing fluids is surprisingly limited. Despite the participation of iron in processes involving reduced sulphur-bearing fluids, the behaviour of the hydrosulphide species of this metal is effectively unknown at elevated temperature. Partly because of this, the hydrothermal transport and deposition of iron is commonly modelled exclusively using chloride species. The goal of our study was therefore to determine stability constants for hydrosulfide complexes of Fe (II) experimentally at temperatures up to 350-400 °C, and to evaluate the contribution of these complexes to the mobilisation of iron in nature.

Our experiments were performed in light-weight titanium autoclaves and involved measurement of the solubility of pyrite (FeS_2) in acidic solutions (pH<3) saturated with respect to H_2S at partial pressures of this gas varying from 15 to 120 bars. The acidity of the solutions was controlled using $HClO_4$ for experiments at T≤250 °C, and HCl at higher temperature. After equilibrium was attained, the autoclaves were quenched, pyrite was removed, and samples of the quenched solutions were analysed for Fe and Cl. Precipitates that formed during quenching were dissolved by washing the autoclaves with HCl; the washing solutions were also analysed for Fe. All analyses were performed using NAA.

The data obtained in our study suggest that, at temperatures up to 300 °C, the dominant hydrosulphide species of iron are $FeHS^+$ and $Fe(HS)_2°$. They also suggest that the concentration of these species is sufficient for them to play an important role in the transport and deposition of Fe (II) in H_2S-rich hydrothermal systems.

Isotope-geochemical features of enriched mantle source of rift tholeiites from Bouvet Triple Junction (South Atlantic)

NATALIA A. MIGDISOVA[1]*, NADEZHDA M. SUSHCHEVSKAYA[1] AND BORIS V. BELYATSKY[2]

[1]Vernasky Institute of Geochemistry RAS, Moscow, Russian Federation (*correspondence: nat-mig@yandex.ru)
[2]VNIIOkeanologia, Antarctic Geology, St.Petersburg, Russian Federation (bbelytsky@hotmail.ru)

Bouvet triple junction (BTJ) is formed by three spreading ridges: Mid-Atlantic (MAR), American-Antarctic (AAR), South-West Indian (SWIR) and is marked by especially complicated construction and evolution. The isotopic analysis of glasses from the Spiess Ridge and Bouvet segment of SWIR revealed the relatively high $^{206}Pb/^{204}Pb$ (18.4 to 19.2) and low $^{143}Nd/^{144}Nd$ values (0.512603-0.513103) indicating the source enrichment compared to the depleted oceanic mantle [1]. Differences in $^{207}Pb/^{204}Pb$ vs $^{206}Pb/^{204}Pb$ contents in tholeiites from BTJ region and adjacent structures imply diverse magmatic sources. We assume that type of enrichment of BTJ mantle source is like HIMU and is close to those of lamprophyres from Antarctic Ferrar province formed during the Karroo - Ferrar plume influence about 180 m. y. ago [2]. Pyroxenite component in parental source was established by olivine composition [3] and generally constituted about 30-40 % of parental melts [3, 4].

One of the plausible explanations of so considerable amount of the ancient substance is the formation of the west end of SWIR over some crustal blocks which were separated during/ after Gondwana breakup. These microplates could comprise parts of a pre-existing retro-arc fold thrust belt [5].

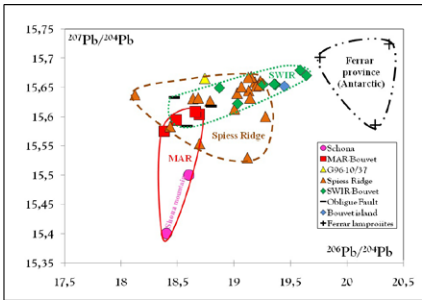

[1] Hauri & Hart (1994) *J. Geophys. Res.* **99**, 24301–24321. [2] Riley *et al.* (2003) *Lithos* **66**, 63–76. [3] Sobolev *et al.* (2007) Science **316**, 412–417. **112.** [4] Migdisova *et al.* (2009) *Alpine Ophiolites & Modern Analogues, Continental rifting to oceanic lithosphere, insights from the Alpine ophiolites & modern oceans. Abstract volume,* ***47***. [5] Martin (2009) *USGS OF-2007-1047, Extended Abstract* ***112***.

https://doi.org/10.1180/S0026461X00006502 Published online by Cambridge University Press

Cu isotope geochemistry in the unusual Las Cruces supergene copper deposit

N.G. MIGUELEZ[1]*, R. MATHUR[2], F. TORNOS[1], F. VELASCO[3] AND J.C. VIDEIRA[4]

[1]IGME, Rios Rosas, 23. 28003, Madrid, Spain & UNIA, 21819 La Rábida, Huelva, Spain (f.tornos@igme.es) (*correspondence: n.miguelez@igme.es)

[2]Juniata College, Department of Geology, Huntingdon, PA 16652, USA (mathur@juniata.edu)

[3]Universidad del País Vasco, Apdo. 644, 48080 Bilbao, Spain (francisco.velasco@ehu.es)

[4]Cobre Las Cruces, S.A., 41860, Gerena,, Sevilla, Spain (juancarlos.videira@cobrelascruces.com)

The Las Cruces deposit (17 Mt @ 6.7% Cu) is the last on-going mine of the Iberian Pyrite Belt (IPB). The ore deposit consists of an unusual supergene copper enrichment zone of a common late Devonian VMS. This is located below the Guadalquivir river Basin, which hosts an aquifer on its base that is still interacting with the deposit nowadays. Late Alpine faults crosscut the deposit and act as fluid pathways related to the latest enrichment process; thus, three Cu-sulphides generations are identified: granular non-cemented Cu-sulphides formed during the weathering process, chalcocite related to late calcite-quartz veins, and euhedral chalcocite crystals grown over calcite veins. Textures and isotope geochemistry suggest a critical influence of microbial activity during the enrichment processes.

The primary sulphides show enrichment on δ^{65}Cu (1.96±0.70‰) in comparison to other primary sulphides worldwide [1]. The secondary Cu-sulphides are largely depleted on δ^{65}Cu and they show consecutively steeply enrichment on δ^{65}Cu in the three Cu-sulphides mineralization generations: δ^{65}Cu=-6.39±0.10‰ in granular non-cemented Cu-sulphides, δ^{65}Cu= -5.36±0.19‰, in chalcocite related to late calcite-quartz veins and δ^{65}Cu= -3.77±0.17‰ in euhedral chalcocite crystals. These would show the three steps of the evolution of a mineralizing fluid, which is also enhanced by biogenic activity [2]. Finally, the gossan samples show a very large variation in δ^{65}Cu, including both positive and negative values (δ^{65}Cu= -7.79‰ & 3.84‰).

The δ65Cu composition of the Las Cruces ore deposit present unusual values in comparison with studies developed on other VMS and gossan related.

[1] Larson *et al*. (2003) *Chem. Geol*. **201**, 337–350.
[2] Mathur *et al*. (2005) *Geochim. Cosmochim. Acta* **69**, 5233–5246.

The nanoscale structure of complex perovskite-type oxides with superb dielectric properties

BORIANA MIHAILOVA

Mineralogisch-Petrogrpahisches Institut, Universität Hamburg, Grindelallee 48, 20146 Hamburg, Germany, email: boriana.mihailova@uni-hamburg.de

The perovksite (ABO_3) structure type is an outstanding example of how chemical variations can tune the nanoscale atomic arrangements and thus influence the properties of complex oxide materials. Thanks to V. M. Goldschmidt who formulated the relation between the chemical composition and the structural stability, the perovksite-type crystals are nowadays key functional materials used in a number of technological applications. Pb-based relaxors are advanced ferroelectrics with remarkable dielectric, electromechanical and electrooptic responses. The exceptional properties of relaxors are due to their structural inhomogeneities. At ambient conditions, the average structure is pseudocubic but rich in ferroic nanoregions too small to be directly studied by conventional diffraction analysis. However, combining *in situ* temperature and pressure diffraction and Raman scattering allows us to resolve the structural complexity of relaxors. Due to the different length and time scales of sensitivity, diffraction probes the long-range order, i.e. the structure averaged over time and space, while Raman spectroscopy can detect local structural deviations from the average structure via the anomalous Raman activity of the phonon modes that, when the symmetry of the average structure is considered, should not generate Raman peaks. Hence, the combined analysis of the long-range order induced at low temperatures or high pressures and of the phonon anomalies enhanced on temperature decrease or pressure increase can reveal the energetically preferred structural nanoclusters existing at ambient conditions. The structural analysis of series of model compounds, namely stoichiometric and A-site doped (Ba^{2+}, Bi^{3+}, La^{3+}, Sr^{2+}) $PbSc_{0.5}Ta_{0.5}O_3$ and $PbSc_{0.5}Na_{0.5}O_3$ as well as solid solutions with three cationic types on the B-site showed that at ambient conditions, on the mesoscopic scale, polar order coexists with antiferrodistortive order, which may be the key reason for the relaxor behaviour. Chemically-induced local elastic fields influence the nanoscale atomic clustering more strongly than chemically-induced local electric fields do.

https://doi.org/10.1180/S0026461X00006502 Published online by Cambridge University Press

Dissolution kinetics of Pd and Pt from automobile catalysts by naturally occurring complexing agents

MARTIN MIHALJEVIČ[1], ONDŘEJ ŠEBEK[2], LADISLAV STRNAD[2], VOJTĚCH ETTLER[1], JOSEF JEŽEK[3], ROBIN ŠTEDRÝ[1] AND PETR DRAHOTA[1]

[1]Institute of Geochemistry, Mineralogy and Mineral Resources, Charles University in Prague, Albertov 6, CZ-128 43 Prague 2, Czech Republic

[2]Laboratories of the Geological Institutes, Charles University in Prague, Albertov 6, CZ-128 43 Prague 2, Czech Republic

[3]Institute of Applications of Mathematics and Information Technologies, Charles University in Prague, Faculty of Science, Albertov 6, CZ-128 43 Praha 2, Czech Republic

Powder samples prepared from gasoline (Pt, Pd, Rh, new GN/old GO) and diesel (Pt, new DN/old DO) catalysts and recycled catalyst NIST 2556 were tested by kinetic leaching experiments following 1, 12, 24, 48, 168, 360, 720 and 1440-hour interaction with solutions of 20 mM citric acid (CA), 20 mM $Na_2P_4O_7$ (NaPyr), 1 g L^{-1} NaCl (NaCl) and a fulvic acid solution (FA- DOC 50 mg L^{-1}). The mobilization of Pt metals into solution was fastest through the effect of CA and NaPyr. In the other interactions (NaCl, FA), the release of PGE is probably followed by immobilization processes and the interactions cannot be considered to correspond to simple release of Pt metals into solution. Because of their low concentrations, the individual complexing agents did not have any effect on the speciation of Pd and Pt in the extracts; both metals are present in solution as complexes ($Me(OH)_2$, $Me(OH)^+$). Immobilization can take place through the adsorption of the positively charged hydroxyl complexes or flocculation of fulvic acid complexing the Pt metals on the surface of the extracted catalysts. The calculated normalized bulk released NRi values are similar to the reaction rate, highest in solutions of CA and NaPyr.

$^{87}Sr/^{86}Sr$ isotope ratios in single benthic foraminifera by LA-MC-ICPMS

TAMÁS MIKES[1,2]*, AXEL GERDES[2], NATÁLIA HUDÁČKOVÁ[3] AND ANDREAS MULCH[1,2]

[1]Biodiversity and Climate Research Centre (BiK-F), Frankfurt am Main, Germany

[2]Institute of Geosciences, Goethe University, Frankfurt am Main, Germany
(*correspondence: mikes@em.uni-frankfurt.de)

[3]Department of Geology and Palaeontology, Comenius University, Bratislava, Slovakia.

$^{87}Sr/^{86}Sr$ analysis of foraminifera is usually performed from solution samples using either TIMS or MC-ICPMS techniques. With increasing precision offered by recent advances of laser ablation instrumentation, the LA-MC-ICPMS approach rivals solution work in terms of precision, and outperforms conventional solution techniques in terms of sample throughput and time needed per analysis.

Within an ongoing paleoclimatic study, we have determined $^{87}Sr/^{86}Sr$ isotope ratios from single tests of the benthic foraminifera *Quinqueloculina* sp. from a Neogene hyperhaline paralic sequence in Central Anatolia, Turkey. The analytical setup used consists of a RESOlution M-50 excimer LA instrument (λ=193 nm) including a factory-built Laurin two-volume sample cell, coupled to a Thermo Neptune MC-ICPMS. During 60 seconds of data acquisition a 200-300 μm long line was ablated (8 Hz, 3.5 J/cm^2) with pit diameter varying between 53 to 140 μm. After correction for interferences from Rb, Kr, Ca-dimers and doubly-charged REE, all Sr isotope data were corrected for mass fractionation ($^{86}Sr/^{88}Sr$ = 0.1194) and normalized to NIST SRM987 using $^{87}Sr/^{86}Sr$ of 0.71025. Repeated measurements on a recent coral from the Red Sea (~3000 ppm Sr) yielded $^{87}Sr/^{86}Sr$ ratios of 0.709235 ± 0.000023 (2σ s. d.).

For the *Quinqueloculina* sp. tests, pit diameter were adjusted to 80 or 120 µm and the ablation path was located at the topmost part of the curved, quasi-globular test surface. $^{87}Sr/^{86}Sr$ ratios cover a range from 0.707174 ± 0.000032 to 0.707255 ± 0.000027, with calculated net reproducibilities being in the range of as low as ±0.00004 (2σ s. d.).

Overall, the LA-based analysis of $^{87}Sr/^{86}Sr$ in foraminifera is likely most suitable in cases where low sample amounts (e.g. high-resolution stratigraphic work on drillcores) and/or high sample numbers are dealt with; i.e. for material otherwise not providing the necessary Sr concentration in the final solution, or requiring time-consuming Sr separation and solution work.

https://doi.org/10.1180/S0026461X00006502 Published online by Cambridge University Press

The abiogenic generation of low $\delta^{13}C$ reservoirs in the deep Earth

S. MIKHAIL[1,2]*, A. SHAHAR[3], S.A. HUNT[1], A.B. VERCHOVSKY[2], I.A. FRANCHI[2], S, BASU[1] AND A.P. JONES[1]

[1]Department of Earth Sciences, UCL, Gower Street, London, WC1E 6BT, UK (*correspondence: s.mikhil@ucl.ac.uk)
[2]PSSRI, The Open University, Walton Hall, Milton Keynes, UK
[3]Geophysical Laboratory, Carnegie Institution of Washington, Broad Branch road, Washington, DC 20015, USA

The stable isotopes of carbon from mantle diamonds (expressed as $\delta^{13}C$) provide a direct proxy used to understand the Earth's deep carbon cycle (carbon speciation, reservoir identification and exchanges between such reservoirs). Carbon speciation is highly dependent upon the local fO_2 and variations of this parameter in an open system can result in isotopic fractionation of carbon where two species are stable and one is mobilised and removed [1]. The largest measured fractionation factor in nature for ^{13}C under mantle conditions is between graphite and Fe-carbide (circa +12 ‰) [2] and at a higher temperature between diamond and Fe-carbide (circa +7 ‰) [3]. This system may have a large impact on the BSE deep carbon cycle and if not considered, and well quantified, may cause significant errors in the interpretation of low $\delta^{13}C$ values determined from terrestrial and extra-terrestrial mantle samples. This system requires fO_2 conditions to be lower than the IW buffer and also requires the presence of Fe^0. Frost *et al*. [4] provided experimental evidence for the stability and predicted existence of Fe^0 with magnesium silicate perovskite and ferropericlase in the lower mantle. More recently Rohrbach *et al*. [5] demonstrated that from depths < 250 km, the upper mantle can also host stable Fe^0 with subcalcic pyroxene and majoritic garnet buffering the fO_2 to IW -2. Therefore it is plausible that two solid phases of carbon could be stable; diamond and Fe-carbide. We present new data for a measured fractionation factor between natural and synthetic diamond and Fe-carbide samples and place constraints upon the P-T effects of ^{13}C fractionation from 2-25 GPa and 14-2000 K in the system Fe-C. This data probes conventional ideas surrounding the modelling of ^{13}C fractionation during mantle-core differentiation, geodynamic cycling of carbon as inferred using empirical data from mantle xenoliths and xenocrysts and the nature and source (abiogenic vs. biogenic) of low $\delta^{13}C$ values determined from terrestrial and extra-terrestrial mantle samples.

[1] Cartigny *et al*. (1998) *Science* **280**, 1421. [2] Deines & Wickman (1975) *GCA* **39**, 547. [3] Mikhail *et al*. (2010) AGU Abstract [4] Frost *et al*. (2004) *Nature* **428**, 6981. [5] Rohrbach *et al*. (2010) *J. Petrol* **52**, 717-731.

Kirschsteinite exsolution lamellae in olivine from young angrites: Implications for their thermal history

T. MIKOUCHI[1]*, M. MIYAMOTO[1] AND G.A. MCKAY[2]

[1]Dept. Earth & Planet. Sci., Univ. of Tokyo, Tokyo 113-0033, Japan (*correspondence: mikouchi@eps.s.u-tokyo.ac.jp)
[2]NASA-JSC, Houston, TX 77058, USA (deceased)

Angrites are among the oldest known basaltic rocks in the solar system characterized by unique mineralogy and chemistry. They can be mainly divided into two subgroups by difference in texture and crystallization ages (~4564 Ma 'quenched' angrites and ~4558 Ma 'plutonic' angrites) [e.g. 1]. Among them, young plutonic angrites are important to understand prolonged igneous activity in the angrite parent body (APB), and understanding of their geological settings can offer good information about the crustal evolution of APB. Kirschsteinite exsolution lamellae present in olivine from LEW86010 (LEW) plutonic angrite could be used to estimate its cooling rate and burial depth by calculating Ca diffusion profiles [2]. Similar exsolution was found in recently discovered plutonic angrite NWA4590 (NWA) [3], and we performed the same calculation. The obtained cooling rate of NWA olivine is 0.15 ºC/year, corresponding to the burial depth of 240 m. This cooling rate is ~1 order of magnitude slower than that of LEW (1.7 ºC/year: 75 m depth [2]). The lamella growth in NWA was from 975 to 700 ºC, and the LEW lamellae grew in a similar temperature range (1000-700 ºC) [2, 4]. Amelin *et al*. [5] obtained a cooling rate of 540±290 ºC/Ma for NWA by using the Pb-Pb age difference of pyroxene and silico-apatite. This cooling rate is too slow and will homogenize pyroxene zoning observed in NWA, and thus the age difference is unrelated to cooling as also suggested by [5]. A geological setting for the 75~240 m depth might be in a lava lake or hypabyssal intrusion. Although LEW and NWA share similar mineralogy and crystallization ages [1, 2, 5], their cosmic-ray exposure ages are different [6], suggesting sampling from different regions of APB. If this is the case, a rock unit with the lithology similar to LEW and NWA may show wide and deep spatial distribution in the crust of APB.

[1] Amelin (2008) *GCA* **72**, 221–232. [2] McKay *et al*. (1998) *MAPS* **33**, 977–983. [3] Kuehner & Irving (2007) *LPSC* **XXXVIII**, #1522. [4] Davidson & Mukhopadhyay (1984) *Contrib. Mineral. Petrol.* **86**, 256–263. [5] Amelin *et al*. (2011) *LPSC* **XLII**, #1682. [6] Nakashima D. *et al*. (2008) *MAPS* **43**, Suppl. A112.

https://doi.org/10.1180/S0026461X00006502 Published online by Cambridge University Press

Evaluation of matrix effects during laser ablation MC ICP-MS analysis of boron isotopes in tourmaline

JITKA MÍKOVÁ[1,2]*, JAN KOŠLER[2] AND MICHAEL WIEDENBECK[3]

[1]Czech Geological Survey, Klárov 3, Prague 1, CZ-118 21, Czech Republic (*correspondence: jitka.mikova@geology.cz)
[2]Centre for Geobiology and Department of Earth Science, University of Bergen, Allegaten 41, Bergen, N-5007, Norway
[3]Helmholtz Centre Potsdam, GFZm German Research Centre for Geosciences, Telegrafenberg, 14473 Potsdam, Germany

This study evaluates the effects of laser ablation ICP-MS instrument parameters and sample matrix composition on data accuracy and precision. Laser ablation MC ICP-MS was used to determine boron isotopic compositions of several natural tourmaline group minerals with variable chemical composition. Some of the studied samples have been previously used as reference materials for *in situ* isotopic analysis (98144 elbaite [1, 2], 108796 dravite [1, 2], 112566 schorl [1, 2] and B4 [3]). The choice of laser and ICP-MS instrument parameters has a significant effect on the measured $^{11}B/^{10}B$ ratios, namely as a result of different signal intensities and $^{40}Ar^{4+}$ spectral interferes on the ^{10}B mass peak. This interference can be suppressed by optimizing mass resolution of the instrument. Laser induced isotopic fractionation of B was negligible for single laser spot and laser raster sampling strategies, allowing for a choice of an optimal sampling mode depending on the size, shape and homogeneity of the sample. It can be demonstrated that the tourmaline matrix affects significantly the obtained $\delta^{11}B$ values and impacts on data accuracy, especially if a non matrix-matched reference material is used for calibration. In case of matrix-matched calibration, the accuracy of LA MC ICP-MS boron isotopic data is comparable to the previously published values obtained by TIMS technique. The measurement precisions associated with the average $\delta^{11}B$ values achieved by LA MC ICP-MS are between 0.2 and 0.5‰ (1 s).

[1] M.D. Dyar *et al*. (2001) *Geostand. Newsl*. **25**(2-3), 441–463. [2] W.P. Leeman, S. Tonarini (2001) *Geostand. Newsl*. **25**(2-3), 399–403. [3] Tonarini *et al*. (2003) *Geostand. Newsl*. **27**, 21–39.

Re-Os age of molybdenite from the Tatra Mountains, Poland

S.Z. MIKULSKI[1], A. GAWĘDA[2] AND H.J. STEIN[3,4]

[1]Dept. of Mineral Deposits Geology, Polish Geological Institute - National Research Institute, Warsaw, Poland (stanislaw.mikulski @pgi.gov.pl)
[2]Faculty of Earth Sciences, University of Silesia, 41-200 Sosnowiec, Poland (gaweda@us.edu.pl
[3]AIRIE Program, Colorado State University, USA (hstein@cnr.colostate.edu)
[4]Norges Geologiske Undersøkelse, 7491 Trondheim, Norway

The Tatra Mountains are a tectonically uplifted piece of Variscan crust emplaced during the Alpine orogeny and forming part of the Central Western Carpathians. Mesozoic sedimentary formations overlie a pre-Alpine core composed of a polygenetic granitoid intrusion and its metamorphic envelope, extensively migmatized [1]. The contact zone of metamorphic rocks and hybrid granite [2] is well exposed in the western part, called Western Tatra Mts.Textural, geochemical, and isotopic studies point to a mixed I- and S-type character for the Tatra granitoid intrusion, formed by multiple magma batches in the age interval 370–345 Ma [2, 3, 5]. The polygenetic granitoid intrusion, defined as a tongue-shaped, tabular body [4], is concordant with regional metamorphic foliation.

Molybdenite was collected from the northern debris slope (*ca*. 1580 m a. s. l.) below the Wołowiec peak. Molybdenite is observed as single isolated blades (<3 mm) or small aggregates of crystals (<5 mm in diameter) in pegmatite, within a coarse-grained leucocratic porphyritic granite. Molybdenite is associated with K-feldspar, albite, quartz and coarse-grained muscovite. In this area the local brecciation of the granite and its envelope by boron-rich fluid is observed.

The analyzed molybdenite sample has a Re concentration of 16.58 ± 0.01 ppm, and an ^{187}Os concentration of 61.04 ± 5 ppb, providing a ^{187}Re-^{187}Os model age of 350 ± 1 Ma indicating a period of molybdenite crystallization in Carboniferous Lower Missisippian (Tournaisian) and is in accordance (within brackets) with WR Rb-Sr isotopic age of pegmatites and U-Pb dating of magmatic zircons [6]. We suggest molybdenite crystallized from fluids locally derived from the hosting coarse-grained leucocratic granite. This is the first report on the presence of molybdenite in the Tatra Mts. and its age can be interpreted as the timing of fluid exsolution from the cooling granite.

This work was financially supported by Polish Ministry of Science and Higher Education, Grant N N 525 393739.

[1] Burda & Gawęda (2009) *Lithos* **110**, 373–385. [2] Burda *et al*. (2011) *Mineralogy & Petrology (in print). [*3] Gawęda (2008) *Geol. Carpathica* **59**, **4**, 295–306. [4] Kohut & Janak (1994) *Geol. Carpathica* **45**, **5**, 301–311. [5] Poller *et al*. (2000) *Inter. Jour. Earth Sci*. **89**, 336–349. [6] Gawęda (1995) *Geol. Carpathica* **46**, **2**, 95–99.

https://doi.org/10.1180/S0026461X00006502 Published online by Cambridge University Press

Linking structural isomerism of organic ligands to the precipitation and structure of ferrihydrite

C. MIKUTTA

Institute of Biogeochemistry and Pollutant Dynamics , ETH Zurich, Switzerland (christian.mikutta@env.ethz.ch)

The extent of interference of organic ligands with the polymerization of Fe(III) has not been systematically studied as a function of structural ligand properties. Here I tested how the number and relative phenol group positions in hydroxybenzoic acids affect both ferrihydrite formation and its local (<5 Å) Fe coordination. To this end, acid Fe(III) nitrate solutions were neutralized up to pH 6.0 in the presence of increasing concentrations of 4-hydroxybenzoic acid (4HB), and the two constitutional isomers 2,4-dihydroxybenzoic acid (2,4DHB) and 3,4-dihydroxybenzoic acid (3,4DHB). The precipitates formed were dialyzed, lyophilized, and subsequently studied by means of X-ray absorption spectroscopy and synchrotron X-ray diffraction.

The solids contained up to 32 wt% organic C. Only precipitates formed in 3,4DHB solutions comprised significant Fe(II) ($Fe(II)/Fe_{tot}$ ≤6 mol%), implying the abiotic mineralization of the catechol-group bearing ligand during Fe (III) hydrolysis under oxic conditions. Ferrihydrite formation was significantly impaired by the ligands (4HB ~ 2,4DHB << 3,4DHB). Coordination numbers of edge- and corner-sharing Fe in the precipitates decreased with increasing initial ligand concentration by up to 100%. Linear combination fitting (LCF) of Fe K-edge X-ray absorption near edge structure (XANES) and extended X-ray absorption fine structure (EXAFS) spectra, however, revealed that these decreases were due to increasing proportions of organic Fe(III) complexes. All ligands reduced the coherently scattering domain (CSD) size of ferrihydrite as indicated by synchrotron X-ray diffraction analysis (4HB < 2,4DHB << 3,4DHB). With decreasing particle size of ferrihydrite its $Fe(O,OH)_6$ octahedra became progressively distorted as evidenced by an increasing loss of centrosymmetry of the Fe sites. Pre-edge peak analysis of the Fe K-edge XANES spectra in conjunction with LCF results implied that ferrihydrite contains 11 ± 2% tetrahedral Fe(III).

The results suggest that especially hydroquinone moieties of NOM effectively suppress Fe(III) polymerization and ferrihydrite formation. Organic chelates seem to control ferrihydrite formation mainly by kinetically modulating the availability of Fe(III) for nucleation and/or polymerization reactions. As a consequence, NOM may trigger the formation of smaller ferrihydrite nanoparticles possessing increased structural strain.

Helium rain and core erosion in gas giant planets

BURKHARD MILITZER*

University of California, Berkeley, CA 94720, USA (*correspondence: militzer@berkeley.edu)

Starting with a brief overview over the search for extrasolar planets, this talk will discuss the state of matter at high temperature and pressure conditions that prevail in the interiors of giant planets. We describe how data from the Galileo mission to Jupiter has been combined with *ab initio* simulations to demonstrate that there exists helium rain on this planet [1]. Furthermore we use such simulations to predict two new phases of water ice (figure) at megabar pressures and characterize the associated structural and electronic transitions [2]. Since water ice is assumed to be one of the primary components of the cores of gas giants, we analyzed its stability when it is exposed to metallic hydrogen. We show that the cores of Jupiter and Saturn have been eroded [3]. We conclude with discussing the erosion of heavier materials.

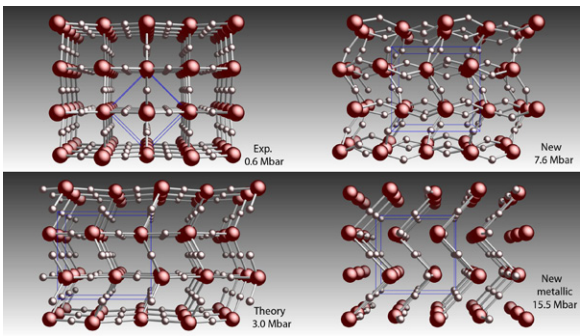

Figure 1: High pressure phases of water ice. The large and small spheres denote the oxygen hydrogen atoms, respectively.

The top left panel shows ice X, the highest pressure phase seen in experiments. On the lower left, the Pbcm phase is shown that was predicted theoretically in 1996. Recently we used *ab initio* simulations to predict the existence of the two new phases shown on the right [2]. The lower one is metallic.

[1] H. F. Wilson & B. Militzer (2010) *Phys. Rev. Lett.* **104**, 121101. [2] B. Militzer, H. F. Wilson (2010) *Phys. Rev. Lett.* **105**, 195701.[3] H. F. Wilson, B. Militzer, '*Erosion of Icy Cores in Giant Gas Planets*', http://arxiv.org/abs/1009.4722

https://doi.org/10.1180/S0026461X00006502 Published online by Cambridge University Press

Isotope distribution of dissolved carbonate species in Serbian thermal waters

N. MILJEVIC[1]*, D. GOLOBOCANIN[2], J. COLIC[1] AND M. MARTINOVIC[3]

[1]Jaroslav Cerni Institute for Development of Water Resources, Jaroslava Cernog 80, 11226 Belgrade, Serbia (*correspondence: emiljevi@vinca.rs)
[2]Vinca Institute for Nuclear Sciences, POB 522, 11001 Belgrade, Serbia
[3]University of Belgrade, Faculty of Mining and Geology, Belgrade, Serbia (martinovic@rgf.bg.ac.rs)

In this paper we will discuss the results relative to the major ion composition of the thermal waters, along with the $\delta^{13}C$ composition of the dissolved inorganic carbon, and to evaluate the interaction processes occurring between gas and thermal reservoirs in different geodynamic environments as well as the origin of dissolved CO_2. The $\delta^{13}C$ of CO_2 leaving thermal springs ranges from -8.2 to 5.6 ‰ (vs. PDB, n=9), while the $\delta^{13}C$ of dissolved inorganic carbon (DIC) in water ranges from -18.4 to +1.8 ‰ (n=53) [1] (Fig. 1).

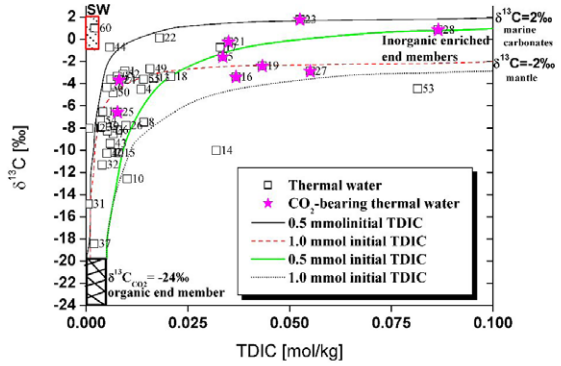

Figure 1: TDIC (Total Dissolved Inorganic Carbon) contents vs. $\delta^{13}C_{DIC}$ togather with $\delta^{13}C_{CO2gas}$ (theoretical) for thermal waters [2].

Water isotope compositions indicate that most waters are meteoric in origin or resulting from mixing between meteoric water and heavy isotope end members.

[1] Miljevic *et al.*(1996) *J. Serb. Chem. Soc.* **61**, 831–840.
[2] Grassa *et al.* (2006) *Pure Appl. Geophys.* **163**, 781–807.

Effect of ocean acidification on processes in the ocean

FRANK J. MILLERO

Rosenstiel School of Marine and Atmospheric Science, University of Miami, Miami, FL USA 33149

The burning of fossil fuels has increased the pCO_2 in the atmosphere from 280 ppmv to 385 ppmv over the last 200 years. This increase is larger than has occurred over the past 800 ky. Equilibration of this CO_2 with surface waters will decrease the pH (called Ocean Acidification) from current values of 8.1 to values as low as 7.4 over the next 200 years. The decrease in the pH of ocean waters can affect chemical and biological processes that occur in the oceans. Many recent studies have shown that ocean acidification can affect the production and dissolution of $CaCO_3$ (s) microorganisms in surface waters. Ocean acidification can also affect ionic equilibria such as acid-base and the formation of metal complexes. Many oxidation-reduction reactions of metals are also affected by changes in the pH.

In this paper, I will examine how ocean acidification of seawater can affect the state of metal ions. The decrease in pH can cause a decrease in the concentration of inorganic (OH^-, CO_3^{2+} ions) and organic ligands that complex many metals in natural waters. This will change the speciation of many metals in seawater. Uncomplexed Cu^{2+} is toxic to bacteria and phytoplankton while uncomplexed Fe^{2+} is more available for the growth of phytoplankton Since organic ligands in natural waters can form strong complexes with metals, more studies are needed on the effect of metal organic complexes.

https://doi.org/10.1180/S0026461X00006502 Published online by Cambridge University Press

Redox- and diffusion-controlled fractionation of Fe stable isotopes in silicate minerals of igneous rocks

MARC-ALBAN MILLET, JOEL BAKER, MONICA HANDLER, CONSTANCE PAYNE AND JESSICA DALLAS

School of Geography, Environment and Earth Sciences, Victoria University of Wellington, New Zealand

Amongst the non-traditional stable isotopic systems available for study in high temperature geochemistry, Fe isotopes have received particular attention. However, the controls of Fe stable isotope fractionation in high temperature magmatic systems are not fully understood, mainly due to poorly constrained isotopic fractionation factors between silicate minerals and melts.

We present new Fe stable isotope data obtained using a high precision double-spike technique ($\delta^{56}Fe \pm 0.02‰$, 2 sd) for minerals from terrestrial (basalt-rhyolite, gabbro-granite, boninite) and extraterrestrial igneous rocks (angrites, eucrites, mesosiderites). Results show that significant mineral isotopic fractionations exist in terrestrial samples that appear to be controlled by Fe redox state ($\delta^{56}Fe_{IRMM-14}$ = -1.0 to +0.85‰). Fe^{2+}-rich minerals like olivine display enrichments in light Fe ($\delta^{56}Fe_{IRMM-14}$ = -0.35 to -0.25‰) compared to host melt ($\delta^{56}Fe_{IRMM-14}$ = +0.05 to +0.22‰). Conversely, Fe^{3+}-rich minerals like plagioclase have heavy Fe ($\delta^{56}Fe_{IRMM-14}$ = +0.25 to +0.42‰), and alkali feldspar exhibits markedly heavy Fe ($\delta^{56}Fe_{IRMM-14}$ = +0.85‰). Clinopyroxene typically has a Fe stable isotopic composition the same or only slightly lower than host melt. In contrast to the terrestrial samples, olivine, pyroxene and plagioclase from basaltic meteorites formed on planetesimals that differentiated in the early Solar System under reducing magmatic conditions do not show measurable Fe stable isotope fractionations. This demonstrates isotopic fractionation between Fe^{2+} and Fe^{3+} in high temperature magmatic systems, which is then captured in terrestrial igneous rocks when minerals incorporate various proportions of these two Fe pools according to their mineral chemistry.

Analyses of single olivine crystals from a basaltic andesite erupted in a subduction zone setting display an extreme isotopic range ($\delta^{56}Fe_{IRMM-14}$ = -0.96 to +0.19‰). Evidence for chemical zonation in the olivine related to Fe-Mg interdiffusion between olivine and melt suggests that significant stable Fe isotopic fractionation in the olivines may be due to diffusion-driven processes. This dataset will be complemented by Mg stable isotopes of the same grains in order to assess the relative importance of redox- and diffusion-controlled processes on Fe stable isotopic fractionation in high temperature magmatic systems.

Carbon isotope fractionation associated with $CaCO_3$ precipitation induced by ureolysis

S.C. MILLO*, M. DUPRAZ, F. ADER, C. GUYOT, R. THALER AND B. MENEZ

IPGP-Sorbone Paris Cité, Univ. Paris Diderot, UMR7154 CNRS, Paris, France (*correspondence: millo@ipgp.fr)

It is increasingly recognized that carbonate precipitation by microorganisms presents some similarities with the carbonate biomineralization of skeleton-forming organisms. For example, in both processes crystallization often starts with the formation of amorphous carbonate, and the polymorphism and habit of carbonate crystals are influenced by interactions with the cell membrane or with extracellular organic products. However, if the occurrence of vital isotopic effects has been extensively documented for skeleton-forming organisms, so far the potential vital effects associated with microbial carbonate precipitation have remained unexplored. Paleoenvironmental reconstructions based on microbial carbonates therefore rely on the assumption that the carbon isotope fractionation expressed during microbial carbonate precipitation is equal to that expressed during inorganic precipitation at isotopic equilibrium.

We performed an experimental study of the carbon isotope fractionation expressed during $CaCO_3$ precipitation associated with ureolysis induced by *Sporosarcina pasteurii* used as a model organism for carbonate precipitation by heterotrophic bacteria. The crystallization sequence initiates with the formation of amorphous calcium phosphate followed by vaterite and then calcite, which dominates the $CaCO_3$ products at the end of precipitation. The carbon isotope composition of $CaCO_3$ evolves following a typical Rayleigh distillation pattern, which can be modeled assuming precipitation with no isotopic re–equilibration between $CaCO_3$ crystals and dissolved inorganic carbon (DIC). According to this model, the first stage of precipitation, possibly of vaterite, is characterized by an increasing ^{13}C–depletion of $CaCO_3$ relative to DIC of up to 2‰. The second stage, probably of calcite, proceeds very close to calcite precipitation isotope equilibrium. These results suggest that vital isotopic effects are probably not limited to skeleton-forming organisms but may also occur during microbial biomineralization, where they might be related to the initial precipitation of metastable mineral phases.

https://doi.org/10.1180/S0026461X00006502 Published online by Cambridge University Press

U-Pb geochronology and Lu-Hf isotope data from meta-carbonatites in the southern Canadian Cordillera

LEO J. MILLONIG[1]*, AXEL GERDES[2] AND LEE A. GROAT[1]

[1]Department of Earth and Ocean Sciences, University of British Columbia, 6339 Stores Road, Vancouver, BC, Canada, V6T 1Z4 (*correspondence: lmilloni@eos.ubc.ca) (lgroat@eos.ubc.ca)

[2]Institut fuer Geowissenschaften, Goethe University Frankfurt, Altenhoeferallee 1, Germany (gerdes@em.uni-frankfurt.de)

Of the 14 carbonatites in British Columbia [1] only 7 have been dated yielding a wide range of dates interpreted as intrusion ages, which cannot be explained within a coherent tectonic setting. The scope of this study is to provide reliable age data for several undated and/or previously unknown carbonatites.

U-Pb and Th-Pb ages of zircons and accessory phases from meta-carbonatites, obtained by LA-SF-ICP-MS techniques, of the southern Canadian Cordillera provide evidence for two episodes of carbonatitic magmatism during the Cambrian at around 500 Ma and the Late Devonian to Early Carboniferous at ~360-340 Ma. Furthermore, episodes of regional metamorphism are recorded by Pb-loss of the zircons and/or new zircon growth at ~170 Ma, 70-65 Ma and ~50 Ma. Lu-Hf isotope data from these zircons show a complex pattern of homogenous to strongly varying values between and within samples, indicating isotopic differences in the magmatic sources or different degrees of isotopic disturbance during metamorphism. In addition, U-Pb age dating of the accessory phases allanite, apatite, baddeleyite, monazite, pyrochlore, titanite and zirconolite will be conducted in order to determine the intrusion ages and the timing of high-grade metamorphism as well as its effect on the different minerals.

In this study 10 carbonatite, 2 mafic and 4 syenite samples are currently being processed and the results will provide new constraints on the geodynamic evolution of the Canadian Cordillera with regard to carbonatitic-alkaline magmatism. This in turn will help to elucidate why some of the investigated carbonatite-alkaline complexes are of economic interest with regard to the Rare Earth Elements (REE) and Ta and Nb.

[1] Woolley & Kjarsgaard (2008) *Carbonatite occurences of the world, Map & Database*. Geological Survey of Canada, Open File 5796.

Long period oscillations in the Neoproterozoic carbon cycle

BENJAMIN MILLS[1]*, ANDREW J. WATSON[1], COLIN GOLDBLATT[2], RICHARD BOYLE[1] AND TIMOTHY M. LENTON[1]

[1]School of Environmental Sciences, University of East Anglia, Norwich, NR4 7TJ, U.K (*correspondence: b.mills@uea.ac.uk)

[2]Astronomy department and Virtual Planetary Laboratory, University of Washington, Box351580, Seattle, WA 98195, USA

The proposed Neoproterozoic snowball Earth events imply a super-greenhouse period following deglaciation, in which the high CO_2 concentration required to initiate glacial retreat coupled with the decrease in planetary albedo causes greatly elevated surface temperature [1]. In this situation, increased reaction kinetics would drive greater silicate weathering fluxes, which draw down CO_2 until a steady state is achieved [2].

However, the speed at which the system returns to steady state is highly dependent on the global erosion rate. When temperature and runoff are very high, the supply of cations to the weathering zone becomes a limiting factor for silicate weathering [3]. Using estimates for post-snowball CO_2 concentration [1, 4] and the Phanerozoic average erosion rate [5] yields a stabilisation time of $>10^7$ years in the COPSE biogeochemical model [6], comparable with the timing of Neoproterozoic glaciations.

Extended periods of high temperature and nuteirnt abundance following a snowball glaciation may help to explain the biological advances made over the Neoproterozoic, as well as the geochemical features such as long positive excursions in $\delta^{13}C$ and massive deposition of phosphorus. Conversely, evidence that CO_2 concentration quickly returned to low levels might help constrain our views on snowball Earth.

[1] Hoffman *et al*. (1998) *Science* **281**, p. 1342–1346. [2] Walker *et al*. (1981) *JGR* **86**, p. 9776–9782. [3] West *et al*. (2005) *EPSL* **235**, p. 211–228. [4] Pierrehumbert (2005) *JGR* **110**. [5] Wilkinson & McElroy (2007) *GSA Bulletin* **119**, p. 140–156. [6] Bergman *et al*. (2004) *Am.J.Sci*. **304**, p. 397–437.

https://doi.org/10.1180/S0026461X00006502 Published online by Cambridge University Press

Experimental evidence for coarsening of crystals and bubbles during thermal cycling of mafic and silicic magmas

R.D. MILLS* AND A.F. GLAZNER

Dept. of Geological Sciences, Univ. of North Carolina, Chapel Hill, NC 27599, USA
(*correspondence: rdmills@email.unc.edu)

Porphyritic textures in igneous rocks are commonly interpreted as evidence for low nucleation rates and/or high growth rates, but experiments in both magma analog systems and ice cream show that temperature oscillations can promote crystal cannibalism and coarsening, and thus porphyritic texture. Here we show that thermal cycling significantly increases crystal and bubble size during experiments on a basalt at 1-atm in a gas-mixing furnace and on a water-saturated rhyolite at 100 MPa in a cold-seal furnace.

The basalt experiments clearly show that temperature cycling dramatically increases crystal sizes. Experiments were performed on an alkali basalt at 1160°C, Ni-NiO buffer, for durations of 20 to 120 hours. After thermal cycling with amplitudes of 5 to 20°C and periods of 20 to 40 minutes, the larger plagioclase crystals were ~20 times more massive, and the larger olivine crystals ~5 times more massive, than in comparable static experiments. Cycle amplitude and period interact in complex ways with crystal structure to produce coarsening, but all cycled experiments show increased coarsening compared to the experiments at constant temperature.

Initial results from experiments in a water-saturated rhyolitic system at 100 MPa and 810°C indicate that cycling of 10°C at a period of 40 minutes greatly increases the size of plagioclase (mass ratio ~12) and hornblende (~4). These results indicate that temperature cycling may offer a way to attack the kinetic problems inherent in experimental work in high-silica systems.

In both sets of experiments, thermal cycling caused marked coarsening of bubbles. Although the processes by which bubbles coarsen are probably different from those that govern crystal coarsening, the results are very similar. Thermal cycling greatly increases the size of bubbles and decreases their number, suggesting that thermal cycling could play an important role in degassing of magmas and ultimately in determining the explosivity of eruptions.

Jiaodong gold district, Northeast China: Discrepancies with orogenic gold mineralisation

S.E. MILLS* AND A.G. TOMKINS

School of Geosciences, Monash Uni, Melbourne, Australia
(*correspondence: stephanie.mills@monash.edu)

The world-class gold deposits of the Jiaodong Peninsula represent the most important gold-producing area in the world's leading gold-producing country. They are considered by some researchers to be orogenic gold deposits; however this study shows this classification ignores fundamental differences in mineralisation character.

Typical orogenic gold mineralisation is associated with compressional or transpressional tectonics in a collisional/accretionary setting and is commonly hosted in metamorphosed terranes. In Jiaodong, it is well accepted that mineralisation occured in extensional tectonics that included lithospheric thinning and large-scale granitic emplacement [1]; fieldwork from this study also shows evidence for mineralisation during normal faulting. Likewise, at the time of mineralisation Jiaodong was far inboard of the active subduction front (Paleo-Pacific Plate subducting benath the East Asian margin), and although metamorphosed Precambrian basement is present, mineralisation is almost exculsively hosted in Mesozoic granitic intrusions. Also, the Precambrian basement reached upper-amphibolite to granulite facies metamorphism at ~2.5Ga, resulting in devolitalization and making it unlikely that mineralisation is related to basement metamorphism [2].

Results from this study also illustrate that deposit scale characteristics are contrary to orogenic deposits, including high base-metal enrichment (600, 150, 35 times background for Cu, Pb, and Zn respectively) in the form of polymetallic mineralisation (chalcopyrite and galena) proximal to controlling faults in high-grade Au zones. Gold-associated enrichments include Ag, Bi, As ± Sb, Mo, W with low Au:Ag (0.005 to 1.66, average 0.4). Sulfur isotope analyses on pyrite show $\delta^{34}S$ values ranging from +6‰ to +13‰ with an average of +9‰.

These regional to deposit scale characteristics show that although Jiaodong deposits have some similarities to orogenic systems, major discrepancies exist. It is likely that dynamic processes in the lithosphere and asthenosphere (i.e. mantle lithosphere destruction, asthenospheric upwelling) were instead the regional drivers behind mineralisation.

[1] Mao, J. *et al*. (2008) *Ore Geology Reviews* **33**, 361–381.
[2] Zhao, G. *et al*. (2001) *Precambrian Research* **107**, 45–73.

https://doi.org/10.1180/S0026461X00006502 Published online by Cambridge University Press

The fate of organic pollutants in soil – Emerging views on the relevance of non-extractable residues

ANJA MILTNER[1]*, KAROLINA NOWAK[1], CRISTOBAL GIRARDI[1], ANDREAS SCHÄFFER[2] AND MATTHIAS KÄSTNER[1]

[1]UFZ - Centre for Environmental Research, Department of Environmental Biotechnology, Leipzig, Germany (*correspondence: anja.miltner@ufz.de)

[2]RWTH Aachen, Department of Environmental Biology and Chemodynamics, Aachen, Germany

C from soil pollutants partitions into parent compound, metabolites, non-extractable residues (NER), CO_2 and microbial biomass. This distribution must be known to assess the fate of a compound in soil, but simulation tests in soils are rarely performed because they are expensive and complex. Data from aqueous systems are much more abundant, and using them for fate assessment in soils would increase the database enormously. The main obstacle for this is that NER formation cannot be simulated in aqueous systems. In the past, NER were considered to mainly consist of adsorbed and sequestered parent compound or metabolites and thus hazardous. However, they may partly derive from bacterial biomass, resulting in harmless biogenic residues. We compared the biodegradation of isotope labeled 2, 4-D, ibuprofen and ciprofloxacin in aqueous systems and soil and quantified the contribution of microbial residues to NER in soil. Both 2, 4-D and ibuprofen were mineralized fast in aqueous systems. In soil, mineralization was lower, and significant amounts of NER were formed. The amount of label found in biomolecules indicated that virtually all of the NER derived from microbial biomass. We found no mineralization of ciprofloxacin in aqueous systems, but a low mineralization in soil. NER formation from ciprofloxacin was fast and independent of microbial activity. Ciprofloxacin reduced microbial activity more in aqueous systems than in soil, because sorption and spatial inaccessibility reduced the toxicity in soil. In conclusion, for readily degradable compounds, mineralization is lower in soil than in water, and a significant part of the carbon is channeled to microbial biomass, which later is stabilized in soil organic matter, resulting in biogenic residues. Toxic compounds are mineralized more easily in soil than in water, because NER formation, spatial heterogeneity, and microbial biodiversity in soil reduce the toxicity of the compounds. NER formation without corresponding mineralization indicates formation of potentially hazardous NER derived from the parent compounds or (toxic) metabolites. In contrast, NER formed along with significant mineralization are biogenic and thus non-hazardous.

Boron isotopes by laser ablation MC-ICPMS

J. ANDY MILTON*, FRANCES DEMUTH, GAVIN L. FOSTER AND MARTIN R. PALMER

School of Ocean and Earth Science, National Oceanography Centre, Southampton, Southampton, UK (*correspondence: jam2@soton.ac.uk)

The invention of multicollector inductively coupled plasma mass spectrometers (MC-ICPMS) has revolutionised the way in which a number of isotope systems are measured. Not least the light dual-isotope systems such as boron where the large, but stable, mass fractionation of the plasma ion source allows accurate correction using bracketing standards of known isotope composition [1]. An additional advantage of these instruments is the ability use a laser ablation introduction system that allows relatively precise isotopic analysis, without prior chemical purification, on the scale of 10-100's of microns (e.g. [2]). The few studies that report boron isotopes by LA-MCICPMS [3, 4] are very encouraging, especially given the obvious advantages offered by rapid sample throughput and high spatial precision by LA and the difficulties associated with boron isotope analysis by solution MC-ICPMS (e.g. poor washout, low sensitivity, and the difficulties associated with silicate dissolution).

Here we present our recent efforts investigating the accuracy and precision of boron isotope analysis by LA-MCICPMS of a variety of samples and reference materials (glass, tourmaline, carbonates). Our initial results suggest accurate and precise data, rivalling the most precise solution analyses [1], can be generated *in situ* on samples amounting to <0.5 ng of boron.

[1] Foster (2008) *EPSL,* **271**, 254–266. [2] Foster & Vance (2006) *Nature*, **444**, 918–921. [3] le Roux *et al*. (2004) *Chem. Geol*. **203**, 123–138. [4] Fietzke *et al*. (2010) *JAAS* doi, 10.1039/c0ja00036a.

https://doi.org/10.1180/S0026461X00006502 Published online by Cambridge University Press

Assessing the role of microorganisms in biogeochemical processes by protein immunodetection using nanoSIMS

J. MILUCKA[1]*, L. POLERECKY[1], I. LIEBERWIRTH[2], M. SCHÜLER[3], T. KEIL[3], T. VAGNER[1], F. WIDDEL[1] AND M.M. M. KUYPERS[1]

[1]Max Planck Institute for Marine Microbiology, 28359 Bremen, Germany (*correspondence: jmilucka@mpi-bremen.de)
[2]Max Planck Institute for Polymer Research, 55128 Mainz, Germany
[3]Max Planck Institute of Biochemistry, 82152 Martinsried, Germany

Anaerobic oxidation of methane (AOM) coupled to sulfate reduction, performed by consortia of methanotrophic archaea (ANME) and sulfate-reducing *Deltaproteobacteria*, plays a crucial role in biogeochemical carbon and sulfur cycling in marine sediments. We developed a method that allowed us to visualize single cells in AOM consortia, identify these cells based on the presence of key enzymes and determine their elemental and isotopic composition.

First, thin sections of AOM aggregates were prepared and examined by fluorescence microscopy. The discrimination between ANME and *Deltaproteobacteria* was achieved by using fluorescent antibodies targeting specific enzymes of each of the two organisms. Next, the sample preparation and immunolabeling protocol was successfully adapted for nanometer-scale secondary ion mass spectrometry (nanoSIMS). We selectively targeted the ANME with primary antibodies against methyl-CoM reductase – the key enzyme of AOM – and NanoGold-coupled secondary antibodies. The obtained nanoSIMS images revealed an unusually high phosphorus and iron content of the ANME-associated bacteria. The transmission electron microscopy coupled to energy-dispersive X-ray spectroscopy (TEM/EDX) showed that these bacterial cells contained peculiar amorphous iron- and phosphorus-rich particles in their cytoplasm.

Based on these results we speculate that AOM might also play a – yet unrecognized – role in iron and/or phosphorus cycling in marine sediments. This demonstrates that imunodetection of key enzymes in combination with nanoSIMS can be used to assess the involvement of functional groups of organisms in biogeochemical processes.

Reaction of silicate with released CO_2 by inorganic precipitations of marine carbonate in sandstone: Evidence from $^{87}Sr/^{86}Sr$, $\delta^{18}O$ and $\delta^{13}C$ isotopes in calcareous sandstone

MASAYO MINAMI[1], TSUYOSHI TANAKA[2]*, MAKOTO TAKEUCHI[3] AND SAEKO MITO[4]

[1]Center for Chronological Res., Nagoya Univ., Nagoya 464-8602 Japan (minami@nendai.nagoya-u.ac.jp)
[2]Center for Chronological Res., Nagoya Univ., Nagoya 464-8602 Japan and RITE, Kyoto 619-0292 Japan (*correspondence: tanakat@nagoya-u.jp)
[3]Earth and Environmental Sci., Nagoya Univ., Nagoya 464-8602 Japan (takeuchi@eps.nagoya-u.ac.jp)
[4]Res. Inst. of Innovative Technology for the Earth, Kizugawa, Kyoto 619-0292 Japan (mito@rite.or.jp)

$^{87}Sr/^{86}Sr$, $\delta^{18}O$ and $\delta^{13}C$ isotopes of carbonate in calcareous sandstone show intermediate values between marine carbonate and silicate phase of the sandstone.

Triassic Hiraiso Formation of the South Kitakami Terrane in Japan contains calcareous sandstone. The carbonate distributed homogeneously in lithic fragments and partly replaced plagioclase of the sandstone. It is considered that the early Triassic period was a dried climate and the Hiraiso Formation was deposited at near shore marine. The carbonate phase and silicate phase were separately examined. $^{87}Sr/^{86}Sr$ and $\delta^{18}O$ isotopes of the carbonate phase are lower than the values of limestone at that Triassic period. The values show the intermediate between silicate minerals and marine carbonate, while $\delta^{13}C$ shows the value of marine carbonate. The $^{87}Sr/^{86}Sr$ and $\delta^{18}O$ isotopes indicate that these are the mixed ones of marine Sr and oxygen with those in silicate phase. Very few carbon is contained in the silicate phase and the $\delta^{13}C$ value shows always that of marine. It shows *simultaneous* formations of the 1st: Carbonate precipitation from seawater in the sandstone with 2nd: Precipitation of carbonate by the quick reaction of silicates and the nascent carbon dioxide released at that time.

https://doi.org/10.1180/S0026461X00006502 Published online by Cambridge University Press

Anthropogenic aerosols and the weakening of the South Asian summer monsoon

YI MING[1], MASSIMO BOLLASINA[2] AND V. RAMASWAMY[3]

[1]Geophysical Fluid Dynamics Laboratory/NOAA, 201 Forrestal Road, Princeton, NJ 08540 (Yi.Ming@noaa.gov)
[2]Program in Atmospheric and Oceanic Sciences, Princeton University, Princeton, NJ 08540 (Massimo.Bollasina@noaa.gov)
[3]Geophysical Fluid Dynamics Laboratory/NOAA, 201 Forrestal Road, Princeton, NJ 08540 (V.Ramaswamy@noaa.gov)

an integral component of the Earth's hydrological cycle, the South Asian summer monsoon is critical for the well-being of over one-fifth of the world's population. Observations show that South Asia underwent a widespread drying during the second half of the twentieth century, but it is still largely unclear whether this prolonged shift was due to natural variations or human activities. Here we use a series of perturbation experiments with a state-of-the-art climate model, which realistically simulates the observed historical trend when driven with all known climate forcings, to investigate the South Asian monsoon response to natural and anthropogenic factors, with particular focus on aerosols and greenhouse gases. We find that the observed precipitation decrease is very likely to be of anthropogenic origin, and can be attributed almost entirely to aerosols. The drying is a robust outcome of a slowdown of the tropical meridional overturning circulation, which is fundamentally driven by the need to counteract the aerosol-induced energy imbalance between the northern and southern hemispheres. In contrast, greenhouse gases give rise primarily to a weakening of the equatorial zonal overturning circulation. These results provide compelling evidence of the prominent role of aerosols in shaping regional climate change over South Asia.

Volatiles (H_2O, CO_2, S, Cl, F) in primary magmas of Kliuchevskoy volcano (Kamchatka)

N. MIRONOV[1]* AND M. PORTNYAGIN[1,2]

[1]V.I. Vernadsky Institute of Geochemistry and Analytical Chemistry (GEOKHI RAS), Kosygin str. 19, 119991 Moscow, Russian (*correspondence: nmironov@geokhi.ru)
[2]Leibniz Institute of Marine Sciences (IFM-GEOMAR), Wischhofstr. 1-3, 24148 Kiel, Germany

We carried out a melt and fluid inclusion study to estimate the amount of volatiles (H_2O, CO_2, S, Cl, F) in primary magmas of Kliuchevskoy volcano in Kamchatka. Volatiles in melt inclusions were analyzed by EMP (S, Cl), SIMS (H_2O, F) and FTIR (CO_2, H_2O). Fluid inclusions were studied criometrically. More than 400 melt and fluid inclusions in olivine (Fo_{92-67}) were studied. We found that diffusive H_2O loss from inclusions, redistribution of CO_2 between melt and fluid and sulfide immiscibility inside inclusions preclude straightforward interpretation of volatile concentration in glasses of primitive MIs (Ol-host Fo>85) as representative for primary melts. Careful selection of the least modified after entrapment melt inclusions allowed us to define the most plausible range of volatile concentrations in primitive Klyuchevskoy magmas (minimum-maximum, average, wt. %): H_2O=2.8-3.6, 3.2; S=0.13-0.23, 0.16; Cl=0.02-0.13, 0.08; F=0.022-0.051, 0.032. A minimum CO_2 content in primitive melts is estimated from density of CO_2 fluid inclusions in primitive olivines to be 3500 ppm. Inclusions in more evolved olivines (Fo<80), which were trapped shortly before eruption, reflect variable extent of magma degassing and were nearly undisturbed by the later processes of melt modification after entrapment.

The concentration of volatiles in Kliuchevskoy melts are similar to those estimated in other, much less productive Kamchatkan volcanoes [3]. Given the large productivity of this volcano (on average 60 Mt /year), the flux of volatiles from Kliuchevskoy volcano is however very high during the Holocene (e.g. H_2O flux amounts at 3.27 Mt/year). The high volatile flux may indicate a large part of subducting plate delivered fluids focused to the source of Kliuchevskoy and/or perhaps additional contribution of volatiles from serpentinites in the subducted plate.

[1] Minerals, inclusions & volcanic processes (2008) *Reviews in mineralogy & geochemistry*, **69**. [2] Mironov, Portnyagin (2011) *Russian Geology & Geophysics*, in press. [3] Portnyagin *et al*. (2007) *Earth & Planetary Science Letters* **255**, 53–69.

https://doi.org/10.1180/S0026461X00006502 Published online by Cambridge University Press

Chronology of early solar system inferred from precise Al-Mg isotope systematics of Vigarano CAIs

R.K. MISHRA AND M. CHAUSSIDON

Centre de Recherches Petrographiques et Géochimiques, CRPG - CNRS, UPR 2300, 15 rue Notre Dame des Pauvres, BP 20, 54501Vandoeuvre les Nancy, France (ritesh@crpg.cnrs-nancy.fr, chocho@crpg.cnrs-nancy.fr)

Calcium, Aluminium-rich Inclusions (CAIs) are the oldest solar system solids that have been absolutely dated to have an age of ~4.57 Ga [1-2]. High precision *in situ* Al-Mg isotope systematics studies of CAIs, and other early formed solar system objects, using secondary ion mass spectrometer (SIMS) provides an opportunity to obtain very precisely time of last melting event (from $^{26}Al/^{27}Al$ ratio) and Mg isotope composition at this time (from $\delta^{26}Mg_0$) [3-6]. This allows better understanding of high temperature events in the solar accretion disk by constraining their durations with greater precision (~10^5 years), the components involved (gas or solids) and the history of these components. Eight CAIs of different types from one of the least altered meteorite Vigarano ($CV_{reduced}$ 3.1-3.4) were analysed for Al-Mg isotopic composition in order to answer several first order questions: (i) did condensation/melting of CAI precursors happen only during a unique single event in the accretion disk, (ii) how many high temperature events did CAI undergo, (iii) whether some of these events were related with chondrule formation? In addition, it provides arguments for quantifying the level of homogeneity of Al, and Mg isotopes in the inner solar system [3, 7]. Results obtained so far suggest melting of CAIs at different periods of time from precursors extracted earlier, in a short time interval, from the solar gas. No indication of ^{26}Al heterogeneity has been found.

[1] Bouvier & Wadhwa (2010) *Nature geo*. **3**, 637–641. [2] Amelin *et al*. (2010) *EPSL* **300**, 343–350. [3] Villeneuve *et al*. (2009) *Science* **325**, 985–8. [4] Kita *et al*. (2010) *LPSC 41* 2154. [5] Davis *et al*. (2010) *LPSC 41* 2496. [6] MacPherson *et al*. (2010) *ApJ* **711**, L117-121. [7] Jacobsen *et al*. (2008) *EPSL* **272**, 353–364.

Formation of the nitrogen B-aggregates in type Ib diamond

Y. MITA[1]*, Y. NISIDA[1] AND M. OKADA[2]

[1]Graduate School of Engineering Science, Osaka University, Toyonaka, Osaka 560-8531, Japan (*correspondence: mita@mp.es.osaka-u.ac.jp)

[2]Research Reactor Institute, Kyoto University, Sennan, Osaka 590-0451, Japan

Most of natural diamonds contain nitrogen atoms more or less and they form many types of aggregates by annealing. When the diamonds contain nitrogen atoms in single substitutional form, in substitutional nitrogen pairs (named A-centers) or in B-aggregate form, they called type Ib, type IaA or type IaB, respectively. As many natural diamonds are their mixed types and contain impurity atoms in reality, all types of diamonds must be obtained artificially for investigation. However to form the nitrogen B-aggregates consist of four substitutional nitrogen atoms surrounding a vacancy from isolated nitrogen atoms of type Ib diamond the samples must be annealed for an extraordinary long time under high temperature and high pressure conditions. Therefore it was thought till recently that to form the B-aggregates artificially is preposterously difficult and a diamond which contains the B-aggregates is natural. Collins [1] observed formation of the A-centers in the electron irradiated and annealed type Ib diamond and thought that the aggregation of nitrogen is enhanced by vacancies introduced due to the electron irradiation. However this treatment was not enough powerful for generating big nitrogen aggregates like the B-aggregate.

We studied the neutron irradiation effects on the nitrogen aggregation in type Ib diamonds. The nitrogen concenteration of samples were ranged from 50 to 340 ppm and the neutron irradiation was carried out with doses of 1.1×10^{16} n/cm^2 to 2.8×10^{18} n/cm^2. The samples were annealed at various temperatures between 1000 to 1700 centigrade degrees for several annealing times under a pressure of 6 GPa. It was observed that the aggregation due to the high temperature and high pressure annealing is highly accelarated by vacancies introduced through the neutron irradiation and a large amount of B-aggregate was generated from single nitrogen. The best record of generation time of B-aggregates at present is shorter than 30 minutes.

[1] Collins (1980) *J. Phys. C, Solid St. Phys*. **13** 2641–2650.

https://doi.org/10.1180/S0026461X00006502 Published online by Cambridge University Press

River red gum biogeochemical expression of buried Broken Hill type mineralisation

C. MITCHELL[1]* AND S.M. HILL[2]

[1]The University of Adelaide, Adelaide, 5005, Australia (*correspondence: charlotte.mitchell@adelaide.edu.au)
[2]The University of Adelaide, Adelaide, 5005, Australia (steven.hill@adelaide.edu.au)

River red gums (*Eucalyptus camaldulensis*) are a tree native to Australia but now widely grown in warm and semi-arid parts of the world. In Australia, they are one of the most widely distributed tree species, especially in riparian zones of arid regions. Their distribution closely corresponds to areas where sediments and and alluvial aquifers are well developed. As such, they tend to colonise settings where the underlying bedrock geochemistry is poorly defined. These long-lived and deep-rooted trees therefore have potential to provide important biogeochemical expressions of the geochemistry of buried bedrock. This study provides an overview of multi-element (ICP-MS and XRF) analysis of leaf samples from about 500 river red gum trees from the Broken Hill region in semi-arid central Australia. Particular attention is given to the biogeochemical expression of sites of known Broken Hill type (Ag-Pb-Zn) mineralisation. It shows that biogeochemistry can provide an effective recognition of buried mineralisation, even when the overlying sediments do not contain a geochemical expression that distinctly highlights mineralisation. It also provides an indication of some of the highly elevated metal and trace element contents that can be hosted in native vegetation near the natural occurrences of ore bodies.

Samples from trees overlying mineralisation near the Pinnacles Mine and along the Broken Hill Line of Lode show highly elevated contents of Ag (max. 1.36 ppm), Pb (max. 411 ppm) and Zn (max. 338 ppm), where regional 'background' values are typically low or approaching analytical detection limits (e.g. Ag 0.01 ppm; Pb 1 ppm; and, Zn 17 ppm). Some samples from near mineralisation also contain elevated Cd, Au, In and Tl contents, however, values are variable, and these elements are best considered within the context of the major ore forming elements (e.g. In/Zn). The spatial extent of the elevated biogeochemical response depends on the size and grade of mineralisation but also the characteristics of the physical and chemical dispersion that vary in different parts of riparian zones.

Selenium adsorption and associated selenium isotope fractionation

K. MITCHELL[1]*, R.-M. COUTURE[1], T.M. JOHNSON[2], P.R.D. MASON[3] AND P. VAN CAPPELLEN[1]

[1]Georgia Institute of Technology, Atlanta, USA (*correspondence: kristen.mitchell@eas.gatech.edu)
[2]University of Illinois at Urbana-Champaign, Urbana, IL, USA
[3]Utrecht University, Utrecht, The Netherlands

Riverine input is a source of selenium to the coastal oceans: between 5 and 12% of Se input consists of particulate selenium. Depending on the site, particulate organic Se is estimated to account for 40 to 100% of the particulate Se pool, suggesting that up to 60% of particulate selenium is in another form, possibly as selenium oxyanions adsorbed onto either organic matter or iron (Fe) oxides

Among the Fe oxides, goethite has been put forth as the dominant authigenic Fe(III) phase in freshwater and marine sediments. Hematite is found in association with goethite, though generally it is not as widespread. Ferryhydrite, while short lived, is a precursor to the latter phases. Thus, these ubiquitous phases are important carrier of adsorbed Se species to oceans.

Nevertheless, sorption behavior of selenate and selenite as well as the isotope fractionations associated with these reactions has not been systematically investigated. Here, we measured total Se concentrations as a function of time during the equilibration of selenate and selenite with suspensions of 2-line ferryhydrite, hematite, goethite (Table 1).

	2-line ferryhydrite	Hematite	Goethite
Selenite	50	0.5	275
Selenate	~0	~0	1

Table 1: Calculated partition coefficient (Kd; L g^{-1}) for Se sorption onto selected Fe(III) oxyhydroxide minerals.

We show that selenate does sorb onto goethite (Table 1), contrary to expectation, albeit to a much lower extent than selenite. We conclude by discussing the isotope shifts associated with these sorption reactions and the potential use of Se isotopes to fingerprint the sorption mechanism of Se removal by Fe oxides in the aquatic environment.

https://doi.org/10.1180/S0026461X00006502 Published online by Cambridge University Press

Adsorption and sorption of Zn^{2+} on the surface of aluminum hydroxide

A. MIYAZAKI[1]*, M. NUMATA[1], M. ETOU[2], K. YONEZU[3], I. BALINT[4] AND T. YOKOYAMA[2]

[1]Japan Women's University, Tokyo 112-8681, Japan (*correspondence: miyazakia@fc.jwu.ac.jp)
[2]Faculty of Science, Kyusyu University, Fukuoka 810-8560, Japan
[3]Faculty of Engineering, Kyusyu University, Fukuoka 819-0395, Japan
[4]Institute of Physical Chemistry, 77208 Bucharest, Romania

Adsorption/sorption of heavy metal ions on clay minerals

Clay minerals are expected as one of the most effective adsorbent/sorbent for heavy metal ions in soil. Miyazaki *et al*. [1] reported that solid-liquid interfacial reaction of Zn^{2+} ions on alumina can be divided into three processes: adsorption due to formation of inner-spehre complex, desorption of Zn^{2+} accompanied with dissolution of Al^{3+} and then co-precipitation of Zn^{2+} with Al $(OH)_3$. Shlegel and Manceau [2] reported that after adsorption of Zn^{2+} onto montmorillonite, which was exchanged with Al^{3+} or Keggin Al_{13}, the Zn^{2+} located in vacant octahedra of gibbsite-like layers. These reactions for Zn^{2+} may correspond to transfer from adsorption to sorption. In order to access and control the mobility of heavy metals in soil systems, it is essential to understand the relationship between their sorption and adsorption onto clay minerals. One of the crucial problems is the role of Al^{3+} in the process of adsorption/sorption. In this study, Zn^{2+} was adsorbed onto Al $(OH)_3$ and change in the chemical state of Al^{3+} in Al $(OH)_3$ after the adorption was analyzed using ^{27}Al MAS NMR.

Results and discussion

Al $(OH)_3$ was prepared by hydrolisis of Al^{3+} in $KAl(SO_4)_2{\cdot}12H_2O$ solution. In the ^{27}Al MAS NMR spectra for Al $(OH)_3$, a peak was observed around 5 ppm. In case of Al $(OH)_3$ after adsorption of Zn^{2+}, the NMR peaks were observed around 15 and 60 ppm depending on the experimental condition such as pH, concentration etc. These peaks may be AlO_6 octahedral species adsorbing Zn^{2+} and AlO_4 tetrahedral species, respectively. Interestingly, the peak at 60 ppm was also found in the co-precipitates of Zn^{2+} with Al $(OH)_3$. From these results, it can be assumed that adsorption of Zn^{2+} onto Al $(OH)_3$ induces Al^{3+} dissolution and the Al^{3+} precipitates on the solid forming Keggin-like structure which correspond to the sorption.

[1] Miyazaki *et al*, (2003) *Geochim. Cosmoschim. Acta* **67**, 3833–3844. [2] Shlegel & Manceau (2007) *Environ. Sci. Technol*. **41**, 1942–1948.

The composition of Earth's oldest iron formations: The Nuvvuagittuq Supracrustal Belt (Québec, Canada)

A.M. MLOSZEWSKA*, E. PECOITS[1], N.L CATES[2], S.J. MOJZSIS[2], J. O'NEIL[3] AND K.O. KONHAUSER[1]

[1]Earth and Atmopsheric Sciences, University of Alberta, Edmonton, Alberta, T6E 1Y1 (*correspondence: mloszews@ualberta.ca)
[2]Geological Sciences, University of Colorado at Boulder, 90309-0399, USA
[3]Terrestrial Magnetism, Carnegie Institution of Washington, Washington DC, 20015-1305, USA

The composition of iron formations in the >3.8 Ga year old [1, 2] Nuvvuagittuq Supracrustal Belt in northern Québec provide a proxy for seawater composition of the Eoarchean, and perhaps Hadean oceans, as well as constraints on the types of nutrients available to Earth's earliest life forms. Having precipitated directly out of seawater, it is thought that the primary iron minerals that comprised the initial BIF sediments (e.g. ferric oxyhydroxides) retained the chemical signature of this seawater in the process. Integrated petrologic and geochemical relationships mapped between mineral phases in thin section and whole-rock chemistry provides a framework for interpreting bulk and micro-scale variations in these chemical sedimentary precipitates. Results show that there are two distinct chemical sedimentary units in the Nuvvuagittuq belt: i) a BIF unit, consisting of alternating micro-bands of magnetite, Fe-Mg-Ca-silicates and quartz, and ii) a more silicate-rich (Fe-poor) banded silicate-formation (BSF) unit of alternating micro-bands of quartz and Fe-Ca-silicates. Precursor BIF and BSF deposits were layered amorphous silica and ferric oxyhydroxides, fine-grained carbonate oozes and/or Ca-Mg-Fe rich silicate gels deposited in a marine setting. Low Al_2O_3, TiO_2 and HFSE concentrations show that they are relatively detritus-free, with distinctively seawater-like REE+Y profiles and consistently positive Eu anomalies. These features suggest that the rocks preserved their seawater-like compositions despite metamorphic overprinting. The most significant trace elements in the sediments are Ni and Zn. Experimentally-derived partitioning coefficients show that Earth's earliest oceans had relatively high dissolved Ni concentrations (up to ~300 ppm) while those for Zn were relative low (up to ~20 ppm) compared to modern seawater. Compositional resemblances between the Nuvvuagittuq sediments and those documented in the ca. 3.8 Ga Isua supracrustals (west Greenland) provide a plausible case that global ocean processes had reached steady-state by the Eoarchean.

[1] Cates & Mojzsis (2007) *EPSL*. **255**, 9–21. [2] O'Neil *et al*. (2008) *Science* **132**, 1828–1831.

https://doi.org/10.1180/S0026461X00006502 Published online by Cambridge University Press

Petrogenesis and tectonic significance of Shuangjianshan highly evolved I-type granite, Beishan orogen, NW China

YALONG MO[1,3], XINBIAO LÜ[1,2]*, ZHUJIANG[1], DENGJIE[1], XIAOFENG CAO[1] AND YUCAI DAI[4]

[1]Faculty of Earth Resources, China University of Geosciences, Wuhan 430074, China (*correspondence: lvxb_01@163.com, myl7004@126.com)

[2]State Key Laboratory of Geological Processes and Mineral Resources, China University of Geosciences, Wuhan 430074, China

[3]Yunnan provincial tourism school, Kunming 650221, China

[4]No. 6 Geological Party, Xinjiang Bureau of Geology and Mineral Exploration, Hami 839000, China

We have studied the petrology, major and trace element geochemistry, isotope geochemistry of the Shuangjianshan intrusion and discussed its petrogenesis and tectonic significance. The Shuangjianshan intrusion is located in south of Hongshishan ophiolitic mélange in Beishan orogeny belt, Gansu, north of Tarim. It is a monzogranite. The content of SiO_2 is 73.04-74.39 %, A/CNK ranges from 0.996 to 1.065, total alkalis ranges from 8.29 to 8.44 % with Na_2O over 3%, calculated corundum is less than 1 % and DI ranges from 91.29 to 93.26. Thus, it is a highly evolved I-type granite with total REE (146.79-157.5 ppm), $(La/Yb)_N$ (8.08-8.80) and δEu (0.64-0.73). It is enriched in Rb, Ba, Th, U and depleted in Ta, Nb, Sr, Ti. Its geochemistry characters show the affinity of island arc magmatic rock. LA-ICP-MS zircon U-Pb dating gave the intrusive age of 322.3±1.7Ma (weighted $^{206}Pb/^{238}U$ age). Its has high εNd (t) (+1.9 to +2.7), low $(^{87}Sr/^{86}Sr)_i$ (0.70312 ~ 0.70343) and the samples from the intrusion plots in the orogeny evolution trend on the $^{206}Pb/^{204}Pb$ vs. $^{207}Pb/^{204}Pb$ diagram. It falls in the area of syn-collisional granite area on R1-R2 diagram, however in the volcanic arc granite area on the Y vs. Y+Nb and Y vs. Nb diagrams. The characteristics described above indicate that the Shuangjianshan intrusion is a highly evolved I-type granite originating from the mantle wedge. Trace elements exibit the characteristics of subduction zone. The granite also contaminated by crust and underwent highly fractional crystallization. Combining with the 334 Ma adakite, we believe that the intrusion is a later product of the subducted North Tianshan ocean crust, which closed before 322 Ma and then came to the syn-collisional stage.

This work is founded by 305 Project of State Science and Technology Support Program (Grant No. 2007BAB25B04).

Quaternary soil and climate change inferred from TL Dating of Quaternary terraces in Taleghan basin, Iran

A. MOEINI[1] AND E. ALIZADE PAEEN AFRAKATY[2]

[1]Department of Agriculture and Natural Resources, Science & Research Branch, Islamic Azad University (IAU), Iran (abmoeini@yahoo.com)

[2]Faculty of Environment, University of Tehran, Iran.

Introduction and methods

We report the first thermoluminescence ages for the quaternary sediments of the Taleghan Drainage Basin, Tehran, Iran.

Results

Teracces	Terrace Name	Age (y)
Q4	Toria War	4650+ 520
Q3	Wurm	9100 ± 800
Q2	Wurm	15600 ± 2000
Q1	Riss	54900± 8700

Table1. Result of TL dating [1, 2]

The carbonates appeared in the field as nodules in the wurm terrace and laminar or conglomeratic massive cemented accumulation (Petrocalcic horizons) in the Riss terrace and the Toria war (youngest terraces), rejuvenates by flooding, and has not secondary carbonate within the profile.

Discussion

Based upon the above observations, we theorize that, at the ~100 ky ago climate was cold and arid, at the ~15 ky ago climate was tardi glacial, at the ~9 ky ago climate was pluvial and temperate with arid transitions and at the ~4 ky ago climate was flooding [3].

[1] Aitken, M.J. (1998) Oxford University Press, Oxford. [2] Shannon, M. (2000) (USGS) October 13, 2000. [3] Thomas, M.F. (2004) *Catena* **55** (2),107–124.

https://doi.org/10.1180/S0026461X00006502 Published online by Cambridge University Press

Cu, Zn and Fe isotope systematics of low-T hydrothermal Fe-Si deposits

K. MOELLER[1]*, R. SCHOENBERG[2], I.H. THORSETH[1] AND R.B. PEDERSEN[1]

[1]Centre for Geobiology and Department of Earth Science, University of Bergen, Allegaten 41, 5007 Bergen, Norway (*correspondence: Kirsten.Moller@geo.uib.no)
[2]Institute for Geoscience, University of Tuebingen, Wilhelmstrasse 56, 72076 Tuebingen, Germany

The formation of Si-rich ferric oxyhydroxide deposits is observed distal to the white smoker-type Jan Mayen hydrothermal vent fields at the Mohns Ridge, North Atlantic, in an area of diffuse low-temperature venting. Individual stratified laminated layers within these deposits are largely composed of branching, twisted filaments resembling encrusted stalks of Fe-oxidising bacteria, indicating biologically influenced precipitation of ferric iron.

In this study, we used stable isotope systematics of transition metals from different layers of the Fe-Si deposits in order to trace the evolution of hydrothermal fluids within the oceanic crust, from which these deposits ultimately formed. Isotope measurements show fractionation of the redox-sensitive elements Fe and Cu, whereas Zn with its singular oxidation state behaves more conservatively. Isotopically light Fe (δ^{56}Fe = -2.09 to -0.66 ‰) points to abiogenic partial, subsurface Fe oxidation [1] and/or dissimilatory iron reduction in combination with re-oxidation by Fe-oxidising bacteria. The reactive surface of the ferric oxyhydroxides of the Fe-Si deposits may absorb Cu and Zn from the venting fluid, thereby preferentially incorporating the heavy isotopes of these elements [2]. However, measured Zn isotope data do not show a significant enrichment relative to hydrothermal fluids [3] and Cu is isotopically lighter than primary hydrothermal Cu sulphides [4]. We hypothesize that precipitation and/or adsorption processes below the seafloor lead to the depletion of heavy isotopes in the evolved hydrothermal fluids from which the Fe-Si deposits formed.

[1] Rouxel *et al*. (2003) *Chem. Geol*. **202**, 155–182. [2] Balistrieri *et al*. (2009) *GCA* **72**, 311–328. [3] John *et al*. (2008) *EPSL* **269**, 17–28. [4] Rouxel *et al*. (2004) *Econ. Geol*. **99**, 585–600.

Geochemistry of Cheshmeh Sefid manganese deposit, Sabzevar, Khorasan province, Iran

S.J. MOGHADDASI* AND M. GANBARI

Payame Noor University, Department of Geology, 19395-4697, Tehran, Iran (*correspondence: sjmoghad@pnu.ac.ir)

Cheshmeh Sefid manganese deposit is located in 60 km south of Sabzevar, a major city in Khorasan province, northeast of Iran. The study area is situated in central Iran structural zone. Manganese mineralization is occurred in a volcano-sedimentary succession consisted of grey limestone, submarine volcanic, Neogene sediments and flysch-like deposits. Manganese mineralization is mainly hosted by green colored rhyolitic tuffs of Eocene age. Manganese rich stratiform bodies are enclosed in jasper and overlain by grey colored dacite and rhyodacite. They are often syngenetic, based upon the stratigraphic persistence of the manganese horizon and the observed interstratification of manganese ore and hosting volcanics. Manganese deposits occur as lenses and stratiform bodies of different sizes. Upper and lower contacts of the ore bodies are characteristically sharp. Ore mineralography and XRD examinations were indicated that pyrolusite, psilomelane and cryptomelane were major manganese ore minerals in the studied deposit.

Geochemically, iron and manganese were characteristically fractionated, producing low Fe/Mn ratios. Si-Mn-Fe and Al-Si discrimination diagrams were also used to recognize between hydrothermal and hydrogenous manganese deposits. The collected geochemical data from the study area plot in the characteristic field of hydrothermal deposits. The manganese ores were indicated relatively low concentrations of Ni, Co, and Cu compared with those concentrations in hydrogenous manganese deposits. Diagnostic plot to Mn-Fe-10 (Ni+Co+Cu) discrimination diagram was indicated a characteristic depletion in Ni, Co, and Cu, suggesting a hydrothermal origin for the studied manganese deposit. Geochemical composition of manganese deposits of the studied area and their host rocks indicates that manganese oxides of the study area are the result of rapid deposition from Mn-rich fluids. These fluids have a hydrothermal exhalative nature and were probably associated with volcanic activities in Eocene period.

https://doi.org/10.1180/S0026461X00006502 Published online by Cambridge University Press

Removal of seawater ^{234}U incorporated in Holocene basaltic sediments from the Reykjanes ridge

K.J. MOHAMED[1,2]*, L.F. ROBINSON[2,3] AND J.F. MCMANUS[2,4]

[1]University of Vigo, Vigo, Spain (*correspondence: kmohamed@uvigo.es)
[2]Woods Hole Oceanographic Instit., Woods Hole, MA, USA
[3]University of Bristol, Bristol, UK
[4]Columbia University, Lamont-Doherty Earth Observatory, Palisades, NY, USA

The ratio ($^{234}U/^{238}U$) of detrital sediments is a potential tool for direct determinations of sediment transport time and provenance. Changes in grain size, shape and mineralogy after deposition can obscure the ($^{234}U/^{238}U$) variation with time, providing erroneous estimates of transport time. Addition of Uranium from external sources can also change this ratio, even to values higher than secular equilibrium.

Icelandic sediments recovered from the eastern flank of the Reykjanes ridge, in the Björn drift, showed ($^{234}U/^{238}U$) values higher than 1. Basalts, the main rock in the area, are known to incorporate Uranium from seawater with a ($^{234}U/^{238}U$) of 1.14, which may explain the anomalously high ($^{234}U/^{238}U$) measured in our samples. To identify the source of this ^{234}U addition, we performed a leaching of Holocene and deglacial sediments from the same site with increasing concentrations of HCl.

Older sediments with initially low ($^{234}U/^{238}U$) showed little variation with increasing acid concentration. On the contrary, younger samples with high ($^{234}U/^{238}U$) show steep decreases at concentrations lower than ~2.5 N HCl, and little changes from 3 to 9 N.

Leachates exhibit higher ($^{234}U/^{238}U$) than residues in all cases. In low ($^{234}U/^{238}U$) samples, leachates decrease initially and reverse the trend at HCL concentrations higher than 2.5 N HCl reaching values close to secular equilibrium. Leachates from samples with high ($^{234}U/^{238}U$) show similar behavior as the residues.

The incorporation of seawater uranium in Holocene samples suggests that these sediments have a higher contribution from Icelandic basalts. This ^{234}U contamination from seawater can be removed by leaching with 2.5 N HCl, which increases the reliability of transport time estimates based on the ($^{234}U/^{238}U$) ratio. Higher HCl concentrations may dissolve the sediment grains, which releases detrital ^{234}U and would explain the reversed trend observed in the leachates above 2.5 N HCl.

Helium in Michigan Basin sediments: A tracer for pore fluid migration and age

R.K. MOHAPATRA[1]*, I.D. CLARK[1], R.E. JACKSON[2], K. RAVEN[2] AND M. JENSEN[3]

[1]Dept. of Earth Sciences, University of Ottawa, Ottawa, ON Canada, K1N 6N5 (*correspondence: ratan.mohapatra@uottawa.ca)
[2]Geofirma Engineering, Ottawa
[3]Nuclear Waste Management Organization, Toronto

As a central component of hydrogeological investigations at a proposed site for low and intermediate level nuclear waste disposal, we have measured He in Ordovician strata from the Deep Geological Repository site in the Michigan Basin near Tiverton, Southern Ontario. Samples were micro-cored (6mm dia., 20mm length) from full 76 mm core samples of shales and argillaceous limestones shortly after recovery from depths between 450 and 850 m, for measurement of He on a MAP 215-50 mass spectrometer (MAPL). Supplemented by stable isotope measurements and major and trace element geochemistry, the labile helium fraction is used to estimate pore fluid age and source location. The xRa profile shows a consistent value near 0.0200 ± 0.0015 in the very low permeability Upper Ordovician shales, with a shift to 0.0360 ±0.0020 in the underlying Middle Ordovician limestones. *In situ* production rates for ^{3}He from ^{6}Li fission and ^{4}He from U and Th decay in the shales provide a calculated xRa that, within the margin of uncertainty, is the same as the measured ratio, suggesting an autochthonous source for He in that section. Pore fluid age, based on the calculated ^{4}He production rate and measured He concentrations in the shales, indicates accumulation over ~ 200 Ma. In the very low permeability limestones the calculated *in situ* xRa of 0.001 to 0.004 suggests an allochthonous He source. The xRa value of 0.036 measured in the limestones was indistinguishable from that measured in the thin basal Cambrian sandstone aquifer groundwater collected during the study. This value may be explained by a mixture of a mantle ^{3}He-enriched end member derived from the rifted base of the Michigan Basin and He from the Canadian Shield.

https://doi.org/10.1180/S0026461X00006502 Published online by Cambridge University Press

Isotopic data from the Pomarinho enclave swarm (SW Iberian Chain)

P. MOITA[1], J.F. SANTOS[2] AND P. SILVA[3]

[1]HERCULES, CGE, Univ. Évora (pmoita@uevora.pt)
[2]GeoBiotec, Univ. de Aveiro (jfsantos@ua.pt)
[3]IDL, ISEL, Lisboa (pmsilva@fc.ul.pt)

Mafic microgranular enclaves are a common feature of calc-alkaline granitoids (e.g. tonalites and granodiorites) in active continental margins and collisional orogens. They correspond to dark-coloured globules that, although widespread throughout the host rock, usually constitute only a small proportion of the whole volume of the intrusion. When the enclaves occur strongly concentrated in a restricted area, they form an enclave swarm (e.g. [3]). At Pomarinho, the Granialpa quarry is a privileged exposure of a cluster of dark igneous enclaves that has been targeted for geochemical and geophysical studies (GeoRadar and AMS).

The Pomarinho swarm is located in the SW edge of Évora granitoid (Carvalhosa, 1983), in the Portuguese sector of the Ossa-Morena Zone (Iberian Variscides). The enclaves have tonalitic and granodioritic compositions, whereas the host correspond to a very homogeneous light-coloured granodiorite. Preliminary geochemical information, based on major and trace elements [2], suggests that the enclaves and the host rock are probably derived from co-genetic magmas.

Rb-Sr isotope data now obtained in four enclaves and three host-rock samples yield an isochron corresponding to 335±14Ma (MSWD=0.96), which fits into the spectrum of ages of the Variscan granitoids in the region. Additionally, the homogeneity of both $^{87}Sr/^{86}Sr_{335}$ (0.704758 to 0.705133) and εNd_{335} (-0.10 to 1.13) values corroborates the hypothesis of derivation of the enclaves and the host granodiorite from a common primitive melt through magmatic differentiation. Low $^{87}Sr/^{86}Sr_{335}$ and high εNd_{335} values suggest that ultimately the parental melt is related to a mantle source, with no or only small contribution of metasedimentary crustal materials.

Funding: Petrochron project (PTDC/CTE-GIX/112561/2009)

[1] Carvalhosa, A. 1983. Esquema geológico do Maciço de Évora. *Comun. Serv. Geol. Portugal* **69** (2), 201–208. [2] Moita, P. Santos, J.F. Silva, P. & Pardal, E. (2011) Geochemical signature of the Pomarinho enclave swarm (Ossa-Morena Zone, Portugal) Abstract, Hutton Symposium. [3] Tobish, O.T. McNulty, B.A. & Vernon, R.H. (1997) Microgranitoid enclave swarms in granitic plutons, central Sierra Nevada, California. *Lithos* **40**, 321–339.

The ca. 4.2-3.7 Ga history of the Acasta Gneiss Complex (Northwest Territories, Canada)

S. MOJZSIS[1]*, N. CATES[1], A. MAIER[1], M. HOPKINS[1], D. TRAIL[2], M. GUITREAU[3], O. ABRAMOV[1,4] AND W. BLEEKER[5]

[1]CU, Geol. Sci., Boulder, CO 80309-0399 USA (*correspondence: mojzsis@colorado.edu)
[2]RPI, Earth & Environ. Sci., Troy, NY 12180 USA
[3]ENS, LGLTPE, 69007 Lyon, France
[4]LPI, Houston, TX 77058 USA
[5]GSC, Ottawa, ON K1A 0E4 Canada

Compiled U-Pb zircon ages of the oldest components of the Acasta Gneiss Complex (AGC) on the western margin of the Archean Slave Province [1] span 4.05-3.90 Ga [2-5]; even older (4.2 Ga) ages [2, 3] have also been noted. AGC outcrops cover a large (>50 km) area across several domal basement antiforms, but only a small subset of these is documented. We report ion microprobe conventional 2-D spot and 3-D depth-profile geochronology coupled with whole-rock (WR) and zircon REE and Ti thermometry, in petrographic thin sections and from mineral separates, of a diverse suite of AGC lithologies including orthogneisses and gabbroic hornblende schist enclaves. Samples were collected from photo-mapped outcrops (1:25) to guide sampling. Discrete cm-scale gneissic domains show distinctive $[Th/U]_{zirc}$ vs. $[Ti]_{zirc}$ temperatures correlative with zircon U-Pb ages and rock compositions. We used lattice-strain theory to model zircon/WR REE of zircon domains (cores/rims) in different generations of gneisses and relate these to ages of original igneous emplacement and subsequent polyphase metamorphic histories. We confirm that the earliest geological history of the AGC is at 4.2 Ga, followed by magmatic incursions at mid-crustal depths (4.05-4.02 Ga) and thermal modifications at 3.96-3.85 Ga concurrent with some lunar basin formation ages. Eoarchean AGC ages (3.74-3.72) are also preserved, contemporaneous with documented emplacement times for the 3.85-3.71 Ga Itsaq Gneiss Complex in West Greenland [6] and 3.78-3.75 Ga Nuvvuagittuq belt in northern Québec [7].

[1] St-Onge *et al.* (1988) *Geol. Surv. Canada, Open Files Report* **1923**. [2] Iizuka *et al.* (2006) *Geology* **34**, 245–248. [3] Bowring & Housh (1995) *Science* **269**, 1535–1540. [4] Iizuka *et al.* (2007) *Precamb. Res.* **153**, 179–208. [5] Stern & Bleeker (1998) *Geosci. Canada* **25**, 27–31. [6] Nutman *et al.* (1996) *Precamb. Res.* **78**, 1–39. [7] Cates & Mojzsis (2009) *Chem. Geol.* **261** 98–113.

https://doi.org/10.1180/S0026461X00006502 Published online by Cambridge University Press

REE geochemistry of iron-apatite deposits in Central Iran

M.A.A. MOKHTARI[1], M.H. EMAMI[1], N. ABEDIAN[1], M. KHEZRI[1] AND J. BABUREK[2]

[1]Geological survey of Iran, Exploration, Regional exploration group (Mokhtari1031@gmail.com)
[2]Czech geological Survey (Jiri.baburek@geology.cz)

REEs in different ore types display characteristic patterns, related to different modes of formation of the ore. The apatites of iron- apatite ores of Bafq region (Central Iran) show a strong LREE/HREE ratio and a pronounced negative Eu anomaly. This pattern is a distinct characteristic of igneous apatites. Mentioned REE pattern is similar to that of apatites from Kiruna iron ore and the other Kiruna- type iron ores in elsewhere of the world.

In the all Iron-Apatite deposits of Central Iran, the REE patterns of apatites, phosphate- bearing iron ores and iron ores with no or very little phosphate, are similar and have a different REE contents. This similarity indicates a common source for these rocks and deposits. On the other hand, the REE patterns of granitic intrusions which are located adjacent to the iron-apatite ores have a similar REE patterns to that of iron- apatite ores. This similarity, in turn, also indicates a genetic relation for these rocks.

In general, it can be consider a basic alkaline magma rich in iron and some incompatible elements such as P, REE, Th-U, Cl and F, have been parent magma for Iron-Apatite ores and granitic intrusions. This parent magma had been differentiated into immiscible silicate- oxide- phosphate units in route of ascend to the earth's surface.

Modelling of nanoparticles: Aggregation of oxides and hydroxides

M. MOLINARI[1]* D.C. SAYLE[2] AND S.C. PARKER[1]

[1]Dept. of Chemistry, University of Bath, Bath, BA2 7AY, UK (*correspondence: m.molinari@bath.ac.uk)
[2]Dept. of Engineering and Applied Science, Cranfield University, Shrivenham, SN6 8LA, UK

We use molecular dynamics simulations to study the aggregation of CeO_2 (ceria) and $Mg(OH)_2$ (brucite) nanoparticles (NPs). Calculations are running in vacuum and in water in order to include the effect the solvent during aggregation. We employ the DL_POLY code [1] and a potential model fitted in the METADISE [2] and the GULP [3] codes against *ab initio* data derived using the VASP code [4]. We use ceria, an extended solid oxide, and brucite, a layered material, as models. Forcing oriented aggregation during the crystal growth of such important materials for catalysis and sorption processes can facilitate the production of tailor-made structures with enhanced properties.

The free energy change due to aggregation NPs can be evaluated considering different interparticle orientations. Results for 1ns run for ceria NPs in vacuum are shown in Figure 1. The calculations predict no free energy barrier to aggregation when the NPs approach along crystallographic orientations as previously reported by Spagnoli *et al*. [5]. Finally, a comparison between aggregation in dry and wet conditions is considered.

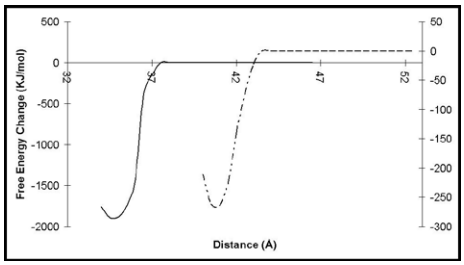

Figure 1: Free energy change of aggregation as a function of distance for a 5nm diameter octahedral CeO_2 NPs with a fixed orientations: dashed line, approaching edges; solid line, approaching faces.

[1] W. Smith, T.R. Forester, J. (1996) *Mol. Graph.* **14**, 136. [2] G. Watson *et al*. (1996) *J. Chem. Soc. Faraday Trans.* **92**, 433. [3] J. Gale (1997) *J. Chem. Soc. Faraday Trans.* **93**, 629. [4] G. Kresse, J. Furthmuller (1996*) Phys. ReV. B* **54**, 11169. [5] D. Spagnoli *et al*. (2008) *J. Phys. Chem. C*. **112**, 14731.

https://doi.org/10.1180/S0026461X00006502 Published online by Cambridge University Press

Direct pore-scale numerical simulation of precipitation and dissolution

S. MOLINS*, D.B. SILIN, D. TREBOTICH AND C.I .STEEFEL

Lawrence Berkeley National Laboratory 1 Cyclotron Road, Berkeley, CA 94720 USA (*correspondence: SMolins@lbl.gov, MS 90R1116) (DSilin@lbl.gov, DPTrebotich@lbl.gov, CISteefel@lbl.gov)

Mineral precipitation and dissolution driven by field applications such as carbon sequestration or remediation strategies can modify the geometry and structure of porous media in relatively short time scales. In this context, feedback processes between geochemical reactions and flow that take place at the pore scale affect continuum scale parameters such as permeability or reaction rates. Beyond the insights gained by innovative experimental and imaging techniques such as x-ray computed micro-tomography, modeling provides a unique tool to mechanistically understand and quantify these feedback processes at the pore scale and inform continuum scale models. In this work, we develop strategies to perform efficient direct numerical simulation of flow and reactive transport on idealized and complex pore scale geometries building on existing platforms. We apply these approaches to a range of pore geometries from single pores to 1-cm-long columns to calculate average reactions rates and porosity-permeability evolution and illustrate model capabilities and limitations.

Simulations show that dissolution and precipitation reactions affect the pore space nonuniformly. As a result, a simple porosity-permeability correlation may be insufficient to describe the complexity of the reaction-induced pore space evolution. The relative magnitude of the reaction rate constants affects the evolution of the permeability-porosity relationship. In dissolution simulations, fast reactions result in localized effects and further evolution of permeability is relatively unaffected by subsequent porosity increase. In contrast, slow reactions cause a less localized dissolution, with the result that the permeability increase is consistent with the porosity increment. Simulations show that in columns with the same average parameters, including column porosity, reactive surface area, and flow rate, different pore structures with different flow patterns can result in different average reactions rates.

Sequential coupling between transport and geochemical reactions allowed us to use an efficient and flexible computational fluid dynamics platform that implements higher-order algorithms, while implicit coupling shows promising results for efficient simulation of pore geometry evolution. We discuss further model development for interpretation of experimental results.

Genetic relation between Skarn ore deposits and magmatic activity in the Ahar region, Western Albuorz, northwest of Iran: Evidence for metasomatism and copper mineralization

HABIB MOLLAEI AND RAHIM DABIRI

Department of Geology, Mashhad Branch. Islamic Azad University, Mashhad -Iran. Office Phone No.: 0098 5118446361 (mollai@mshdiau.ac.ir)

Numerous skarn deposits formed in the contact between the Upper Cretaceous impure carbonate rocks and Oligocene–Miocene Magmatic rocks in the Ahar region. The aim of this study is to understand how magmatic activity led to the copper skarn mineralization in this region. The history of skarn formation starts with the emplacement and upwelling pluton body, followed by the assimilation of limestone by the magma. The skarnification process occurred mainly in two stages: the first stage is starting with prograde metasomatism and anhydrous minerals, this stage followed by four stages of retrograde skarn deposit. In addition to Fe, Si and Mg, substantial amounts of Cu, along with volatile components such as H_2S and CO_2 were added to the skarn system. Consequently considerable amounts of hydrous calc-silicates, sulfides, oxides and carbonates replaced the anhydrous calc-silicates and the chemistry of the host granodiorites, Mineralogical and chemical characteristic indicate that an island arc or Subduction-related origin of Fe-Cu skarn deposit.

https://doi.org/10.1180/S0026461X00006502 Published online by Cambridge University Press

Thermodynamic models of aqueous systems to high temperature and concentration

N. MOLLER* AND J.H. WEARE

Chemistry and Biochemistry, UCSD, San Diego, CA, 92093 (*correspondence: nweare@ucsd.edu)

We have developed thermodynamic models, using the Pitzer specific interaction equations, that describe interactions as well as solid-liquid-gas equilibria to high temperature and concentration within the H^+, Na^+, K^+, Ca^{2+}, Mg^{2+}, Al^{3+}, Al $(OH)^{2+}$, Al $(OH)_2^+$, Al $(OH)_3^0$, Al $(OH)_4^-$ Cl^-, OH^-, HSO_4^-, SO_4^{2-}, HCO_3^-, CO_3^{2-}, Si $(OH)_4$, SiO $(OH)_3^-$, SiO_2 (aq), CO_2 (aq/g), H_2S (aq/g), CH_3 (aq/g), H_2O system. In this presentation, the construction of two models that produce predictions with accuracy near the uncertainty of the experiments is discussed. One, correctly calculates solute/solvent activities and solid-liquid equilibria in the H-Na-K-OH-Cl-HSO_4-SO_4-H_2O system from dilute to high solution concentration and from low to high pH within the 0° to 250°C temperature range. The other correctly predicts solvent/solute activities and monomeric aluminum hydrolysis speciation as well as solid-liquid equilibria in the H^+, Na^+, Al^{3+}, Cl^-, Si $(OH)_4$, SiO $(OH)_3^-$, OH^-, Al $(OH)^{2+}$, Al $(OH)_2^+$, Al $(OH)_3^0$, Al $(OH)_4^-$ system as a function of pH to high salt concentrations ($I \leq 5$ m NaCl), for temperatures up to 300°C and for saturation pressures. The latter model accurately predicts the fluid compositions for the low Al ($\leq 10^{-5}$ m) and Si $(OH)_4$ ($\leq 10^{-4}$ m) concentrations commonly encountered in the intermediate pH ranges typical of most natural fluids. For high and low pH regions where the formation of polymeric Al hydrolysis species is low, the model will apply to higher total aluminum concentrations. The successful prediction of the solubility of aluminiosilicate solid phases falling within this system is also described.

REE in groundwater as indicators of catchment lithology in semi-arid regions

P. MÖLLER[1], C. SIEBERT[2] AND S. GEYER[2]

[1]Helmholtz Zentrum Potsdam, Deutsches GeoForschungsZentrum, D-14473 Potsdam

[2]Helmholtz Center for Environmental Research-UFZ, Halle/Saale 06120, Germany

REE in groundwater (GW) in regions with little soil coverage characterize the lithology of its recharge area because interaction of precipitation with soil coverage is short to absent. Under such conditions the dissolution of minerals in the catchment area becomes an important tool in particular in regions with dominant transboundary GW flow in politically unstable regions.

REE patterns in GW recharged over limestones resemble those of the limestones. GW recharged over olivine bearing basalts yield REE patterns that are controlled by dissolution of the least stable minerals such as olivine and by scavenging during weathering by ferric hydroxides and calcite. Bowl-shaped REE patterns are typical. REE in GW from sandstones are controlled by leachable minerals of their cements. In the presences of gypsum and phosphates the intermediate REE are enriched in GW.

REE in GW from aquifers of the same lithology of fthe recharge area are controlled by strong sorption of REE onto mineral surfaces. In case of limestones overlaying basalts the GW from basalts shows nearly the same pattern as in GW from the limestone above because the high REE abundance in GW is adsorbed by minerals of the basalt and thus with time GW passes the basalt without significant changes. In case of basalts overlaying limestones the REE abundance in the final GW is lower than expected from interaction with limestones. Due to high Ca and Mg concentration from weathering of plagioclase and olivine in basalts dissolution of calcite from limestones is limited and thus the REE patterns achieved from the basalt is not significantly altered during the passage of limestone.

https://doi.org/10.1180/S0026461X00006502 Published online by Cambridge University Press

Mineral textures and fluid inclusion characteristics of ore samples from the Guanajuato district, Mexico

D. MONCADA* AND R.J. BODNAR

Dept. of Geosciences, Virginia Tech, Blacksburg, VA 24061 USA (*correspondence: moncada@vt.edu, rjb@vt.edu)

Successful exploration for mineral deposits requires tools that the explorationist can use to distinguish between targets with high potential for mineralization and those with lower economic potential. In this study, we describe a technique based on petrographic and fluid inclusion characteristics that may be applied in exploration for precious metal deposits to identify areas of high-grade mineralization.

The Guanajuato mining district in Mexico is one of the largest silver producing districts in the world with continuous mining activity for nearly 500 years. Ore shoots in the district are localized along three major northwest trending vein systems, the La Luz, the Veta Madre and the Vetas de la Sierra. Mineralization in the district shows much variability between and within individual deposits, from precious metal-rich to more base-metal-rich zones, and from gold-rich to silver-rich zones. Ore textures also vary and include void space that formed during multiple fissuring events, banded quartz veins, massive quartz veins and stockworks. More than 1, 200 samples representing all the different mineralization styles were collected from all three vein systems in the Guanajuato mining district, and the mineral textures and fluid inclusion characteristics of each sample have been defined. In addition, each sample was assayed for Au, Ag, Cu, Pb, Zn, As and Sb.

Samples from the Guanajuato district show a wide range in silica textures. Some of these textures, including colloform texture, plumose texture and jigsaw texture, are indicative of rapid precipitation, such as occurs when fluids boil. Other mineral phases, including illite, rhombic adularia and bladed calcite are also indicative of rapid growth in a hydrothermal system and are characteristic of boiling systems. Because boiling is an effective mechanism for precipitating gold and silver from hydrothermal fluids, the presence of mineral textures indicative of boiling is a desirable feature in exploration. In many samples, textural evidence for boiling is supported by coexisting liquid-rich and vapor-rich fluid inclusions, or Fluid Inclusion Assemblages consisting of only vapor-rich inclusions, suggesting 'flashing' of the hydrothermal fluids. Textural and fluid inclusion evidence for boiling has been observed in the deepest levels of the Guanajuato mining district, suggesting that additional precious metal resources may occur beneath these levels.

Sulfide mineralogy of West Greenland kimberlitic mantle xenoliths

SISIR K. MONDAL[1]*, STEFAN BERNSTEIN[2] AND MINIK T. ROSING[2]

[1]Department of Geological Sciences, Jadavpur University, Kolkata-700032, India (*correspondence: sisir.mondal@gmail.com)

[2]Natural History Museum of Denmark, University of Copenhagen, 1350 Copenhagen, Denmark (sb@avannaa.com, Minik@snm.ku.dk)

Sulfide minerals control the platinum group element (PGE) budget of mantle rocks along with PGE behaviour during melting and thus trace the Earth's differentiation processes. We have conducted mineralogical study of the sulfide assemblages of mantle xenoliths sampled from two West Greenland kimberlites dykes of presumed Neoproterozoic age. One dyke from the Sarfartoq area, is situated in 2.8 Ga continental crust, and part of the ca. 1.8 Ga Nagsoqtoqidian mobile belt. The second kimberlite dyke comes from the Aasivik terrain which represent early Archaean, 3.5 to 3.7 Ga crust. The Sarfartoq- and Aasivik-dykes can therefore be classified as Proton and Archon, respectively. The xenoliths from the Sarfartoq kimberlite dyke are relatively fresh but commonly contain pockets of fine-grained magnetite, mica and hydrothermally altered silicates interpreted to represent melts invaded from the kimberlitic host. The Sarfartoq-dyke xenoliths are garnet-lherzolite (olivine Fo 86.8-91.1), garnet-dunite (olivine Fo 90.1-91.2), spinel-dunite (olivine Fo 91.4-93.0) and dunite (olivine Fo 89.2-92.5). Sulfide minerals are present as rounded blobs mostly within olivine and rarely within garnet and clinopyroxene. Minor amount of interstitial sulfide is also present. Both types commonly occur in a single sample. Blobs are dominated by pentlandite with minor chalcopyrite and pyrrhotite and veined by late generated magnetite. The xenoliths from the Aasivik kimberlite dyke are nearly all extensively altered and appear to be mostly dunite (olivine Fo 87.8-92.5). Only relicts of olivine grains are present, and these contain blobs of sulfides as inclusions. Our study suggests that the sulfide was initially monosulfide solid solution, re-equilibrated at low temperature.

https://doi.org/10.1180/S0026461X00006502 Published online by Cambridge University Press

The Pan-African reconstruction of NW Angola: Petro-structural and temporal constraints

P. MONIÉ[1], D. BOSCH[1], O. BRUGUIER[1], A. VAUCHEZ[1], P. NSUNGANI[1,2] AND Y. ROLLAND[3]

[1]Géosciences Montpellier, UMR-CNRS-5243, Univ. Montpellier 2, Place E. Bataillon, 34095 Montpellier, Cedex 05, France (bosch@gm.univ-montp2.fr)
[2]Agostinho Neto University, Avenida 4 de Fevereiro 7, Luanda, Angola
[3]Géosciences Azur, UMR 6526 CNRS, Université de Nice Sophia Antipolis, Parc Valrose, 06108 Nice cedex 2 – France

At the end of Neoproterozoic times, assembly of the Gondwana supercontinent resulted in the closure of several oceanic domains and accretion of large cratons. Various tectono-metamorphic belts developed et the margins of these cratons during the Panafrican orogeny. During this work, we developed a study combining petro-structural and geochronological investigations on the West Congolian belt (NW Angola) resulting from the collision between the Congo and Sao Francisco cratons. Two main tectono-metamorphic units have been recognized in the studied area, namely eastern and western internal units, and show a westward increase of deformation and metamorphic grade. The WIU consists of high-grade gneisses and migmatites with intercalation of amphibolites, quartzites and pegmatites. This sub-unit experienced metamorphic conditions that increase upward and westward. Maximum P-T conditions for high-grade gneisses have been estimated at 10-12 Kbar and 600-650°C. One garnet amphibolite intercalated with gneisses has been dated and yields ages of 539±7Ma and 498±5Ma for U-Pb and Ar-Ar methods, respectively. A pegmatitic dyke concordant to the regional foliation provides a concordant U-Pb age of 544±13Ma taken as our best estimate for pegmatite emplacement. Two paragneisses have been also dated with ages ranging from 589±12Ma to 678±48Ma suggesting a detrital origine and indicating that detritus was derived from Neoproterozoic source material. At least monazites from one of this gneiss show a complex U-Pb age distribution (three batches between 560-490Ma) and Ar-Ar biotite age of 487±5Ma. All this age underlines the predominance of the Pan-African deformation and metamorphism in the construction of this belt.

Characterization of hyperalkaline fluids produced by serpentinization of mantle peridotites in Oman and in Liguria (Northern Italy)

C. MONNIN*, V. CHAVAGNAC, G. CEULENEER, C. BOULART AND G. HOAREAU

Geosciences Environement Toulouse, 14 Avenue Edouard Belin, 31400 Toulouse, France (*correspondence: monnin@get.obs-mip.fr)

High pH waters and gases produced by serpentinization of mantle peridotites as well as precipitates forming at the springs have been sampled between 2008 and 2011 in the Semail nappe of the Oman Mountains and the Voltri group of the Ligurian Alps (Northern Italy).

Factors influencing the composition of the hyperalkaline waters are: 1) alteration of the ultramafic basement, 2) formation of precipitates at the water discharge, 3) interaction of the waters with the atmosphere, 4) mixing with surface (runoff) waters, 5) concentration by evaporation.

In Oman the springs are located along major geological discontinuities (Moho, basal contact between the ophiolite and the underlying Cretaceous sedimentary formations).
The increase in the Na, K and Ca contents of the Oman waters with chlorinity cannot be explained by evaporation, pointing to the reactivity of these elements (formation of clays and Ca-carbonates).

In Liguria, the alkaline springs are located above the river beds and their waters do not mix with the river waters. In Oman this mixing leads to a continuous range of pH from the normal runoff (6 to 8) and the extreme values (12.1). In this case, the pH change can be very rapid (dropping by two pH units in half a meter at the site 'Grande Ligurie'). Conversely the pH drop of the alkaline waters collected in the irrigation channels (falaj) is very slow, being due to the sole uptake of atmospheric CO_2.

Minerals forming at the springs are mainly calcite, aragonite and brucite.

Larger values of the H_2 content of the gas phase bubbling at the springs are found in Oman while CH_4 is more important in Liguria.

The reaction of the infiltrating surface waters with the ultramafic formation almost entirely removes the Dissolved Inorganic Carbon indicating that the alteration of ophiolites is indeed an efficient sink for carbon.

Our observations ask the question of the hydrologic pathways of the water in ophiolites: percolation through the ultramafic formation or circulation along major geological discontinuities?

https://doi.org/10.1180/S0026461X00006502 Published online by Cambridge University Press

Towards modelling biogenic magnetite, Fe_3O_4

AMY MONNINGTON[1], DAVID J COOKE[1] AND COLIN L FREEMAN[2]

[1]Department of Chemical and Biological Sciences, University of Huddersfield, UK (Amy.Monnington@hud.ac.uk)
[2]Department of Engineering Materials, University of Sheffield, UK (c.l.freeman@sheffield.ac.uk)

There is an increasing number of new, exciting and dynamic uses for magnetic nanoparticles (MNPs), including many in the field of medicine (site-specific chemotherapy), technology (spintronics) and industry (ferrofluids). Magnetotactic bacteria produce chains of nanosized magnetite, Fe_3O_4, particles that operate as internal magnets. This biosynthesis of magnetite is the earliest known example of biomineralisation, having first occured some two billion years ago. Despite this, much of the detailed atomistic mechanism by which the process occurs is unknown. Therefore, we have begun to develop an atomistic model for the system, in an attempt to understand the processes involved, particularly the role of the 1-5% Co that is present in the biomineral.

In this work we report initial results for modelling the different surfaces of magnetite, using differing methods. Comparison of the related surface energies produced for these methods, using energy minimisation (METADISE [1]) and molecular dynamics (DL_POLY [2]), identified the {100} surface as the most stable. For all methods, elasticity constants were compared to the data produced from previous studies [3]. Subsequent to this, attachments of simple organic molecules to the magnetite were analysed and modelling of interactions between these molecules and the {100} surface were performed.

Future work will validate the potentials for the interactions between the simple organic molecules and the magnetite surface, enabling us to fit the required organic/ inorganic cross parameters to a system where the stable surfaces are well defined, allowing us to better access the validity of each of the components of the model. This is in the aim of progressing to more complex protein attachments.

[1] Watson, G. W. *et al*. (1996) *J. Chem. Soc. Faraday Trans.* **92**(3), 433. [2] Smith, W. & Forester, T. R. (1996) *J. Mol. Graphics* **14**(3), 136. [3] Doraiswami, M. S. (1947) *Proc. Math. Sci*. **25**(5), 413.

Neodymium isotopic composition of gorgonian corals as reliable tool to reconstruct water mass circulation

P. MONTAGNA[1,2,3]*, M. LOPEZ CORREA[4], S. GOLDSTEIN[2], M.T. MCCULLOCH[5], A. FREIWALD[6], M. TAVIANI[3], J.A. TROTTER[5] AND J. RADDATZ[7]

[1]LSCE-CEA, 91198, Gif-sur-Yvette, France (*correspondence: paolo.montagna@lsce.ipsl.fr)
[2]LDEO, Palisades, NY 10964, USA
[3]ISMAR-CNR, Via Gobetti 101, 40129 Bologna, Italy
[4]GeoZentrum Nordbayern, 91054 Erlangen, Germany
[5]University of Western Australia, 6009 Crawley, Australia
[6]Senckenberg am Meer, Abteilung für Meeresforschung, D-26384, Wilhelmshaven, Germany
[7]IFM-GEOMAR, D-24148 Kiel, Germany

It has recently been shown that intermediate and deep ocean circulation can be reliably reconstructed using the neodymium (Nd) isotopic composition of the aragonitic skeleton of scleractinian deep-water corals [1,2,3,4]. Motivated by these findings, we have investigated the Nd systematics of the high-magnesium calcite skeleton of deep-water gorgonian octocorals. These corals have centennial-scale lifespans and are distributed worldwide, representing potential archives of past oceanic circulation at sub-decadal resolution. Live-collected corals, belonging to the families *Isididae* (genus *Keratoisis*) and *Coralliidae* (genus *Corallium)*, were retrieved from the Atlantic, Pacific, and Southern Oceans as well as from the Mediterranean Sea at water depths between ~500 to ~1300m. Seawater samples from two profiles in the Mediterranean Sea were collected at the same locations and depths as the coral samples in order to compare seawater Nd isotopic compositions with the coral skeletons. The isotopic ratio ($^{143}Nd/^{144}Nd$) was obtained using a VG Sector 54-30 thermal ionization mass spectrometer by dynamic multicollection. The neodymium concentration was analysed along different tracks parallel to the growth bands using a 193nm laser ablation microsampling system connected to a Varian 820 inductively coupled plasma mass spectrometer.

The gorgonian calcite skeletons and the surrounding seawater share equivalent Nd isotopic compositions, which clearly show that these calcite corals are reliable archives of water mass circulation.

[1] van de Flierdt *et al*. (2010) *GCA* 74, 6014-6032. [2] Copart *et al*. (2010) *QSR* **29**, 2499-2508. [3] Colin *et al*. (2010) *QSR* **29**, 2509-2517. [4] Montagna *et al*. (2010) AGU meeting, San Francisco.

https://doi.org/10.1180/S0026461X00006502 Published online by Cambridge University Press

OIB's from South Eastern Pacific: Notes from key geochemical features

P. MONTECINOS MUÑOZ* AND K. PINTO LOGUERCIO

Emilio Vaisse 332c, Santiago, Chile
(*correspondence: pmonteci@gmail.com)

We summarize some geochemical features of basalts from Easter, Juan Fernandez and Galapagos. Data were obtained from GEOROC on March 2011. Elemental concentration were normalized to primitive mantle displaying strong enrichment for Juan Fernandez ($[U]_N$~98, $[Pb]_N$~49, $[Th]_N$~40, $[Nb]_N$~70, $[Ta]_N$~78) similar to EM2 source [1]. Easter and Galapagos exhibit a moderately enrichment for Nb and Ta ($[Nb]_N$~35,$[Ta]_N$~50), and small enrichment for U, Pb, Th ($[U]_N$~22,$[Pb]_N$~9,$[Th]_N$~17). These enrichment factors are less than those for samples from EM and HIMU sources, and the $[U/Pb]_N$ and $[Th/Pb]_N$ ratios of Easter and Galapagos are different from EM and HIMU sources, suggesting that the sources of the two islands contain Pb whose origins were not explained by subduction-related process invoked for EM2 [1] and HIMU [2].

That statement is supported by Pb isotopes plotted on a ^{206}Pb-normalized space (Fig. 1). In this plot a linear trend composed by ~90% of Easter (**Line e**) is noticeable. Principal component analysis calculation shows that Line e is an eigenvector explaining a 94% of variability of Easter. Some Easter samples are outside FOZO field [3] suggesting influence from DM source and possibly other extreme component located at left beyond FOZO. Azores samples composing Az3 line (Fig.1) seems to confirm such extreme component. Az1-Az2 lines go beyond Fozo field suggesting another possible component different to HIMU and FOZO.

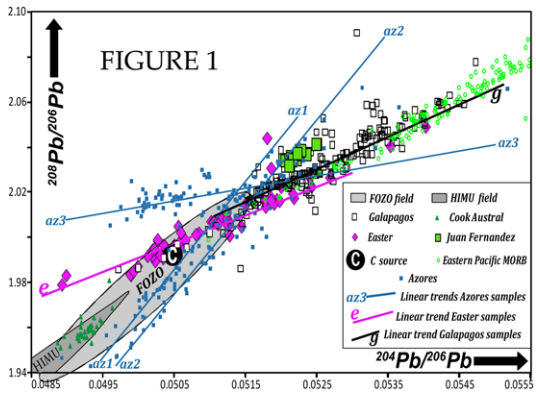

We thank to Professor Shun'ichi Nakai (University of Tokyo) by his suggestions.

[1] Jackson *et al*. (2008) *Gcubed* **9**. [2] Hanyu *et al*. (2011) *Gcubed* **12** . [3] Stracke *et al*. (2005) *Gcubed* **6**.

Style and chronology of growth by oblique accretion and oroclinal bending: The Panama Isthmus

C. MONTES*[1,2], A. CARDONA[1,2], G.A. BAYONA[2], R. MCFADDEN[1], S.E. MORON[1], C.A. SILVA[1], S.RESTEPO-MORENO[1] AND D.A. RAMIREZ[1]

[1]Smithsonian Tropical Research Institute, Box 0843-03092, Balboa, Ancon Republic of Panama, (montesc@si.edu)
[2]Corporación Geológica Ares, Calle 44a # 53-96, Bogotá, Colombia

The Panama Isthums displays, in approximatley 500 km (or ~15 Ma), the transition from: 1) ongoing subduction and magmatism in a normal intra-oceanic arc setting; 2) a deformed, exhumed and extinct magmatic arc, still in an intraoceanic setting, and 3) an extinct arc accreted to a continental margin. This west to east geographic progression from active arc to accreted is also a proxy for the chronology of this arc-continent collisions. The oblique accretion of the Panama arc to northwestern South America is documented with geologic mapping and multidisciplinary analytical studies. A new geologic map with >2000 field stations, 40 petrographic analyses, 24 paleomagnetic sites, and over 30 new geochronological and thermochronological analyses, supports the middle Miocene accretion of the Panama arc to northwestern South America and a late Eocene initiation of tectonic interaction. The extinct arc segment in central Panama arc is composed of a folded-faulted, ~ 3 km-thick basaltic sequence, intruded by granitoid bodies and onlapped by mostly undeformed shallow marine and continental strata. Existing geochronological data, and new whole-rock Ar/Ar (2), and U/Pb zircon ages (6), reveal intense late Paleocene to middle Eocene magmatism, a temporary cessation of magmatic activity between 38 and 28 Ma, and renewed magmatism after 28 Ma in a position approximately 75 km south of the former magmatic axis in central Panama. The geographic patterns of these magmatic pulses is interpreted as a collison that left-laterally offset, and oroclinally bent the axis of the arc, and terminated magmatic activity in the 28 to 38 Ma interval. Magmatic activity restarted after 28 Ma but lasted only until ~15 Ma east of the Canal Basin and west of the Uramita suture, defining an arc segment approximately 400 km in length that shows no sign of magmatic activity younger than 15 Ma, probably the result of this part of the arc getting detached and overthrusted the Caribbean Plate to the north. The sigmoidal part of the Panama arc is therefore the result of an extinct arc that has been obliquely accreting to the northwestern margin of South America for the last 15 Ma.

https://doi.org/10.1180/S0026461X00006502 Published online by Cambridge University Press

Nucleation and growth of acicular goethite from ferric hydroxide gel under moderate temperature (30 and 70°C)

G. MONTES-HERNANDEZ[1]*, P. BECK[2], F. RENARD[1], E. QUIRICO[2], B. LANSON[1], R. CHIRIAC[3] AND N. FINDLING[2]

[1]CNRS-UJF, Institute of Earth Sciences (ISTerre), OSUG/INSU, BP 53, 38041 Grenoble Cedex 9, France (*german.montes-hernandez@obs.ujf-grenoble.fr)

[2]CNRS-UJF, IPAG, OSUG/INSU, BP 53, 38041 Grenoble Cedex 9, France

[3]Laboratoire des Multimatériaux et Interfaces UMR CNRS 5615, 43 bd du 11 novembre 1918, 69622 Villeurbanne Cedex, France

The present study describes a simple and novel synthesis route for sub-micrometric acicular goethite (α-FeOOH) using high OH/Fe molar ratio (=5) and moderate temperature (30 and 70°C). Two different alkaline sources (NaOH and Ca $(OH)_2$) and two iron (III) sources ($FeCl_3.6H_2O$ and Fe $(NO_3)_3.9H_2O$) were investigated. FESEM, XRD, FTIR, N_2 sorption isotherms, colour evolution and pH monitoring have been used to determine the formation mechanism, the particle size, specific surface area, and morphology of goethite. Three pH regions were determined during goethite formation and each region was qualitatively associated to (I) the formation of ferric hydroxide gel, leading to acid conditions (pH<2.5); (II) spontaneous nucleation of goethite, leading to alkaline conditions (pH>11) and fine sedimentable particles; (III) growth of goethite in alkaline conditions (11<pH<13.5). The kinetic behaviour depends clearly on the reaction temperature; globally the nucleation-growth of goethite at 70 °C was about three times faster than at 30 °C. For example, well-crystallized goethite particles (high acicular goethite < 1μm in length with moderate specific surface area, S_{BET}=31.2m^2/g) were produced after 7h of reaction at 70 °C while about 24h of reaction are required to produce well-crystallized goethite particles (low acicular goethite < 0.5μm in length with high specific surface area, S_{BET}=133.8m^2/g) at 30 °C using in both cases iron chloride. In summary, the temperature and iron (III) source have a significant effect on the particle size, specific surface area and morphology of goethite. Herein, single-phase goethite particles were formed. When Ca $(OH)_2$ particles are used as alkaline source, a complex mineral composite with high specific surface area (87.3 m^2/g) was synthesized; this powdered material was mainly composed of unreacted Ca $(OH)_2$ coated by nanosized particles (possibly amorphous iron hydroxide), calcium iron oxide chloride hydrate and calcite. The best conditions to prepare uniform goethite particles, possibly with high potential as adsorbents or pigments, have been established.

Uncertainty assessment in quantification of silicate weathering rates in global rivers

SEULGI MOON[1]*, C. PAGE CHAMBERLAIN[2] AND GEORGE E. HILLEY[1]

[1]Department of Geological and Environmental Sciences, Stanford University, Stanford, CA 94305, USA (*correspondence: sgmoon@stanford.edu, hilley@stanford.edu)

[2]Department of Environmental Earth System Science, Stanford University, Stanford, CA 94305, USA Department of Geology, University of California, Davis, CA 95616 (chamb@stanford.edu)

Chemical weathering is important for understanding landscape evolution, nutrient supply to ecosystems, and global geochemical cycles. Total silicate weathering fluxes to oceans have been quantified using compilations of catchment-wide measurements of concentration and water discharge [1-3]. Sources of chemical elements were differentiated using geochemical mass balance models (forward and inverse models) to partition the fluxes of each of the measured elements into carbonate, silicate, evaporite, and rain-water pools.

In this research, we analyze time-series of elemental concentrations and discharge from 52 global rivers provided by the GEMS/Water compilation, which together constitute a database of ~9000 data points. With these comprehensive datasets, we estimate uncertainties within silicate weathering rates in global rivers that consider the effects of infrequent sampling, covariation between river discharge and concentration, and uniqueness of attribution of weathering fluxes to the different pools. This is accomplished using a Bayesian Metrolpolis-Hastings algorithm to estimate the overall uncertainties within, and covaration between weathering fluxes that are attributed to the different pools based on the GEMS/Water database. Knowing the overall uncertainties in global estimates will provide information about required sampling frequencies, number of sites, and chemical elements that will help to design future catchment-scale studies.

[1] Gaillardet *et al*. (1999) *Chem. Geol*. **159**, 3–30. [2] Meybeck (2003) in *Treatise on Geochemistry, Surface & Ground Water, Weathering, & Soils,* vol. **5**, 207–223. [3] Meybeck & Ragu (1997) UNEP Publication.

https://doi.org/10.1180/S0026461X00006502 Published online by Cambridge University Press

The origin of Darreh-Zanjir lead-zinc Deposit, 'Central Iran'

F. MOORE, E. SAJEDIAN, B. TAGHIPOUR

Department of Earth Science, College of Science, Shiraz University, Shiraz, Iran

The Darreh-Zanjir Zn-Pb deposit is located 25 km south-west of Yazd province within Cenozoic magmatic belt of central Iran. It occurs in the Lower Cretaceous dolomitized limestones of Taft Formation and is underlained by Albian shales of Biabanak Formation. A major fault known as Darreh-Zanjir thrust fault is associated with minor faults and trending east, north-east seems to control the mineralization. This fault is also responsible for pushing Lower Cretaceous carbonate strata over the older Albian shales. Cretaceous dolomite formed by metasomatism of Lower Cretaceous orbitolinous limestone, hosts the Pb-Zn mineralization.

The carbonated-hosted epigenetic mineralization consists of primary galena and sphalerite and secondary carbonates such as cerussite and smithsonite. The principal type of mineralization is irregular, open space filling, forming vein and stockworks. Two stages of mineralization are indicated. The first being the dolomitization of limestone followed by invasion of metal-bearing hydrothermal solutions. Mineralization is confined to fault planes, fractures and their margins. Several factors including geologic setting, lithology, and hydrothermal solutions have played a role in the mineralization. Minor faults and fractures have also provided suitable conditions for secondary dolomitization and mineralization. Field observations, mineralogy and geochemical investigations show that Darreh-Zanjir Pb-Zn deposit is a Mississippi Valley Type deposit.

[1] Report of GSI (1996) **96**, 13-28.

Natural attenuation of metal contaminants in a large mine-impacted river: A long-term case study of temporal and spatial trends

J.N. MOORE AND H.W. LANGNER*

University of Montana, Missoula, MT 59812-1296, USA (*correspondence: heiko.langner@umontana.edu)

We conducted a 20-yr study to determine environmental trends in a mine-impacted watershed in Northwestern Montana, USA. About 100 million tons of waste from copper and precious metals mining were disposed of in the headwaters of the Clark Fork River (CFR) between 1880 and 1982. Large amounts of contaminated material were transported downstream and deposited on the floodplain, where it acts as a secondary source of contamination to the river. Our study focuses on spatial and temporal trends of As, Cu, Cd, Pb and Zn in fine-grained bed sediments along a 200-km river section below a set of tailings ponds that were constructed to cut off the source of contaminants upstream. Remediation in this section has been minimal, providing an excellent area to study natural attenuation of contamination. We collected monthly sediment samples from three locations for most months between 1991 and 2010. In addition, four sets of about 40 sediment samples were collected longitudinally in 1991, 1998, 2001 and 2009. The longitudinal concentration profiles showed decreasing contaminant concentrations, with temporal trends being less obvious than for monthly samples at the three sites. Initial concentrations for As, Cd, Cu, Pb and Zn at the most upstream monthly sampling site were 140, 8.3, 1400, 220, 1500 mg/kg, respectively, in 1991. Monthly samples for all elements and sites trended down over time following a first-order exponential decay model. However, half-lives of sediment concentrations differed considerably between elements, suggesting element-specific processes affecting their transport and retention in the system. Half-lives for Cd were 10 ± 0.5 yr for the three locations in the watershed. Half-lives for Cu, Pb and Zn were 22 ± 5 yr, and for As 35 ± 10 yr. Our monthly sampling also revealed high variability without obvious relationships to seasonal or annual variations of the hydrograph, showing that sediment sampling in long intervals (e.g. annually) is insufficient to accurately estimate trends. Our exponential 'decay' model predicts when acceptable contaminant levels will occur without human intervention. Thus, these results may assist with the selection of cleanup strategies, for example where natural mixing and transport processes may be preferable over engineering approaches to remediation.

https://doi.org/10.1180/S0026461X00006502 Published online by Cambridge University Press

The lower regolith boundary revisited in unmatched detail with a new global lithological map

NILS MOOSDORF, JENS HARTMANN AND RONNY LAUERWALD

Institute for Biogeochemistry and Marine Chemistry, KlimaCampus, University of Hamburg, Bundesstrasse 55, 20146 Hamburg, Germany (nils@moosdorf.de)

Bedrock is the lower boundary of the regolith column. It represents one control on regolith formation. For this bedrock types and properties are more relevant than its age, which most geological maps focus on. A new high-resolution global lithological map (GLiM) could provide a valuable tool for global analyses of the regolith zone.

GLiM consists now of more than one million polygons that were assembled from more than 65 geological maps; some natively in digital format, some digitized by hand. Most of the maps are at a scale of 1: 2, 500, 000 or finer. The lithology information was gathered from metadata of the maps or from additional literature, totalling more than 220 different sources. The classification was expanded from the system introduced by Dürr *et al*. [1, 2]. The map distinguishes six classes of sediments, six classes of igneous rocks, as well as metamorphic rocks. Additional information levels add further detail (e.g. sediment grain size).

A presented comparison between maps of the uppermost regolith layer (soil) and GLiM shows expected significant spatial correlations between the lithological classes and soil types. This highlights the impact of lithology on regolith generation, which is one possible explaination of the impact of lithology on chemical erosion[3]. Due to its high resolution, the new global lithological map can be applied to numerous global problems that require high levels of detail.

[1] Dürr, H. H. Meybeck, M. & Dürr, S. H. (2005) *Global Biogeochemical Cycles* **19**, GB4S10. [2] Moosdorf, N. Hartmann, J. & Dürr, H. H. (2010) *Geochem. Geophys. Geosyst*. **11**, Q11003. [3] Hartmann, J. Dürr, H. H. Moosdorf, N. Meybeck, M. & Kempe, S. (in press) *International Journal of Earth Science*.

Organic nitrogen cycling during organic matter decomposition

M. MOOSHAMMER[1]*, W. WANEK[1], A.H. FRANK[1], F. HOFHANSL[1], K.M. KEIBLINGER[2], S. ZECHMEISTER-BOLTENSTERN[2] AND A. RICHTER[1]

[1]Dept. of Chemical Ecology and Ecosystem Research, University of Vienna, 1090 Vienna, Austria (*correspondence: maria.mooshammer@univie.ac.at)

[2]Federal Research and Training Centre for Forests, Natural Hazards and Landscape, BFW, 1131 Vienna, Austria

Proteins represent the dominant input of organic N into soil ecosystems. The breakdown of proteins to amino acids is anticipated to be the critical process determining the underlying mechanisms in litter and soil N dynamics. This includes initiating the N mineralization sequence by providing substrates for ammonification and microbial uptake. However, the release and fate of organic N-containing compounds during decomposition of organic matter is largely unknown.

We developed a new ^{15}N pool dilution assay to quantify gross rates of protein depolymerization (i.e. amino acid production) and amino acid immobilization [1]. The assay is based on the concurrent labeling of the pool of 18 proteinogenic amino acids, which are present in a free form in soil and litter, and the measurement of ^{15}N:^{14}N ratios in the individual amino acids by GC-MS over time.

The results from a litter decomposition experiment showed that gross protein depolymerization exceeded gross N mineralization by >8 fold indicating that only a small fraction of amino acids released by extracellular enzymes was actually mineralized to ammonium. These results point to an important direct role of dissolved organic N (i.e. amino acids) for microbial N nutrition and a negligible contribution of MIT ('mineralization-immobilization turnover'; extracellular deamination of amino acids) to N mineralization in decomposing litter. Furthermore, controls such as litter quality and microbial community structure and the effect of stress (i.e. temperature) on organic and inorganic N cycling processes will be discussed in more detail.

[1] Wanek *et al*. (2011) *Soil Biology & Biochemistry* **43**, 221–221.

https://doi.org/10.1180/S0026461X00006502 Published online by Cambridge University Press

Synthesis of magnetite nanoparticles and using them for separating toxic elements from the wastewater of sulphuric gold mines

M.A. MORADIAN[1], M.O. MORADIAN[2], AND Z. BOROUMAND[3]

[1]NanoBioEarth Group, Applied Research Center of Geological Survey of Iran (marzi.moradian@gmail.com)
[2]Chemistry faculty of Kashan University (mohsen.moradian158@gmail.com)
[3]NanoBioEarth Group, Applied Research Center of Geological Survey of Iran (zohre.boromand@gmail.com)

Arsenic is a toxic element that the maximum allowable concentration for it in drinking water is about 0.5 mg/lit. Arsenic Inorganic compounds include As_2O_3, FeAsS, AsS and As_2S_3. Although arsenic has a multi allotrope element with yellow, gray and black colors, but only the gray ones that are solid metalloid, crystalline and fragile, are persistent in the nature. Approximately 100, 000 tones arsenic are produced per year in the world because of excavating metals such as copper, lead, cobalt and gold. It causes cancer because of impairing synthesis of DNA and RNA.

One of the most essential problems in Zarshouran gold mine, in northwest of Iran, is existence of too much arsenic in wastewater of mining. Different methods are presented to remove arsenic from the wastewaters such as: Arsenic can be removed by composite of graphene oxide and ion exchange method, but these methods are so high expense that has limited using them. We prepared magnetic nanoparticles with different methods in laboratory. These nanoparticles were less than 50 nanometers in diameter that we used it for removing arsenic as a very light expense method from Zarshouran wastewaters. A natural bond creates between arsenic and magnetic nanoparticles. After separating of arsenic, nanoparticles can be separate from the solution with a simple magnet. We succeed to remove arsenic with over 99 percent in volume by this method.

Mobility of nitrogen and heavy metals in biosolid amended soil

D. MORAETIS*, S. VOUTSADAKI, M. KOTRONAKIS, G. KONTOLAIMAKIS[1], F.E. STAMATI, N.P. NIKOLAIDIS AND N. KALOGERAKIS

Technical University of Crete, Chania 73100 Greece (*correspondence: moraetis@mred.tuc.gr)

The potential leaching and availability of nitrogen and heavy metals in biosolid-amended soil were investigated using batch and column studies. The mobility of heavy metals were assessed with SPLP and TCLP tests while the availability of nitrogen with a KCl extraction test. In addition semi-continuous column studies were conducted to assess the leachability of nitrogen and heavy metals from biosolid-amended soil under simulated-unsaturated soil conditions. One type of biosolids, a compost derived from municipal solid waste recycling of the organic fraction together with a clayey soil typical of Crete were used in this study. Two application rates of 100 and 200 t/ha were tested. The results were compared with soil lysimeter measurements of a parallel experiment in an olive grove.

Results

The total input of N was 1160 and 2320kg/ha for the two amendments. KCl extraction showed that 15 and 96 kg/ha of N ($N\text{-}NO_3$+$N\text{-}NH_4$) was bio-available which correspond to 1.3% and 4.2% of the total N input for the 100 and 200t/ha application rates respectively. Columns packed with soil amended with 200t/ha compost and receiving synthetic rain released 34 kg/ha of N ($N\text{-}NO_3$+$N\text{-}NH_4$). Using lysimeter measurements the average release of N in olive grove compost amended soil was estimated to be 16kg/ha N. The results from all measurements were consistent.

Heavy metal mobility from compost-amended soil was assessed with the SPLP and TCLP batch tests, semi-continuous column studies and field measurements with lysimeters. All results were consistent and orders of magnitude lower than EPA standards [1]. Zn was shown to be the most mobile metal in all measurements. Results suggest that one-time application of biosolids at agronomic rates will not impact the groundwater.

[1] EPA (1996) *Soil Screening Guidance,* Document 540/R-96/018.

https://doi.org/10.1180/S0026461X00006502 Published online by Cambridge University Press

Long-distance transport of North Gondwana Cambro-Ordovician sandstones: Evidence from detrital zircon Hf isotopic composition

NAVOT MORAG[1]*, DOV AVIGAD[1], AXEL GERDES[2], ELENA BELOUSOVA[3] AND YEHUDIT HARLAVAN[4]

[1]Institute of Earth Sciences, The Hebrew University of Jerusalem, Jerusalem 91904, Israel (*correspondence: navot.morag@mail.huji.ac.il)
[2]Institut für Geowissenschaften, Johann Wolfgang Goethe Universität, D-60438 Frankfurt am Main, Germany
[3]GEMOC, Department of Earth and Planetary Sciences, Macquarie University, NSW 2109, Australia
[4]The Geological Survey of Israel, Jerusalem 95501, Israel

A voluminous Early Paleozoic sequence of quartz-rich sandstones was deposited in northern Gondwana following its assembly during the Neoproterozoic-Cambrian Pan-African Orogeny. Field evidence for the sense of transport indicate that sediments were carried from Gondwana hinterland towards the supercontinent margins in the North (present coordinates). Derivation from Pan-African terranes is evident from the ubiquity of detrital zircons with Neoproterozoic U-Pb ages, but the exact provenance of these siliciclastic deposits remains unclear. Herein we present new Hf isotopic data from U-Pb dated detrital zircons of the Cambro-Ordovician sandstone that top the juvenile Neoproterozoic basement of the Arabian-Nubian Shield in Israel and Jordan. Remarkably, the detrital zircon Hf isotopic signal stands in marked contrast with Nd and Hf isotopic signature of the underlying basement. A preponderance (61%) of the Neoproterozoic-aged detrital zircons from the Cambro-Ordovician sandstones in Israel and Jordan yielded negative $\varepsilon_{Hf(t)}$ values incompatible with a juvenile source. Therefore, rather than from the adjacent Arabian-Nubian Shield, most of the detrital zircons were derived from distant terrane(s), comprising pre-Neoproterozoic crust reworked during Pan-African orogeny. Because our sampling sites are situated at the northern tip of the Arabian-Nubian Shield, sand must have been transported several thousand kilometers before deposition. This finding also implies that the Arabian-Nubian Shield and other Pan-African orogens of NE Africa were completely warned down by the onset of Cambro-Ordovician deposition and that vast areas in the northern part of Gondwana were then low-lying such as to allow transfer of sand across the continent.

Macroscopic anhydrite interacted with Pb-doped solutions

JUAN MORALES[1], J.M. ASTILLEROS[1,2], AMALIA JIMÉNEZ[3] AND L. FERNÁNDEZ-DÍAZ[1,2]

[1]Dpto. Cristalografía y Mineralogía. Universidad Complutense de Madrid. 28040 Madrid. Spain
[2]Instituto de Geociencias (UCM-CSIC). 28040 Madrid, Spain
[3]Facultad de Geología de la Universidad de Oviedo, 33005, Oviedo, Spain

Pb is a toxic metal that affects the vital functions of living organisms. A previous study showed that Pb sorption by gypsum is an effective uptake mechanism [1]. Here the ability of anhydrite to uptake Pb from aqueous solutions is evaluated and its effectiveness as Pb-remover compared with that of gypsum. Experiments were performed by placing 2g of crushed pure anhydrite in 100 mL of Pb-bearing aqueous solutions (ranged from 10 to 1000 mg/L) and, after specific reaction periods (1 minute to 5 weeks), analyzing the aqueous solution and examining the solids formed on the surface of the anhydrite crystals. DRX data revealed that anglesite formed on anhydrite after short interaction periods (Figure 1). ICP-OES analyses showed that when the initial Pb concentration, [Pb]ini, was ≥ 50 ppm, it decreased very rapidly to reach a constant value (≈ 5 ppm) after about six hours. The evolution of the solution composition is consistent with a coupling between anhydrite dissolution and anglesite precipitation. Our results indicate that anhydrite and gypsum surfaces have similar ability to remove Pb from aqueous solutions.

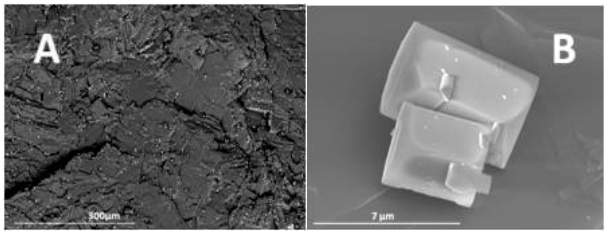

Figure 1: SEM images of anhydrite surface after interaction with a Pb-bearing aqueous solution ($[Pb]_{ini}$ =100ppm). (A) BSE image showing the distribution of anglesite crystals (bright spots) formed on anhydrite surface after 5 minutes interaction. (B) After a 24 hours interaction period of anglesite reach sizes in the range 3 to 10 microns.

[1] J.M. Astilleros *et al*. (2010) *Applied Geochemistry* **25**(7), pp. 1008–1016.

https://doi.org/10.1180/S0026461X00006502 Published online by Cambridge University Press

Partitionning of Pt-Re-Os between solid and liquid metal in the Fe-Ni-Si system

G. MORARD[1,2], J. SIEBERT[1,2], D. ANTONANGELI[1,2] AND J. BADRO[1]

[1]Institut de Physique du Globe de Paris, France
[2]Institut de Minéralogie et de Physique des Milieux Condensés, Paris, France

The Earth evolved into a layered body early in its history with silicates and oxides forming the mantle while molten metal was gravitationally segregated to form the core. Cooling of the Earth causes the liquid core to crystallize. In the meantime, small amount of liquid outer core material could be remixed by dynamical entrainment in the deep mantle. This mechanism was proposed as responsible for the Os isotopic anomalies observed in some mantle-plume derived lavas (OIBs). In that model, a radiogenic Os signature would be produced in the outer core as a result of inner core crystallization, and would then be remixed with the mantle and imprint the isotopic composition of some OIBs.

Here we investigate the solid-liquid fractionation of Os, Re and Pt in the metal at high pressure. As these partition coefficients depend on metal composition, we choose to study the most realistic candidate for core composition, the Fe-Ni-Si system, for which no data exist so far.

He-Pb lead evidence for marble cake under the Pacific-Antarctic ridge

M. MOREIRA[1]*, C. HAMELIN[1] AND L. DOSSO[2]

[1]Institut de Physique du Globe de Paris, Sorbonne Paris Cité, CNRS (UMR 7154), 1 rue Jussieu, 75238, Paris Cedex, France (*correspondence: moreira@ipgp.fr)
[2]CNRS, UMR6538, Domaines Océaniques, IFREMER, B.P.70, 29280 Plouzané, France

Lead isotopes and Helium isotopes were analyzed in glass samples from 10 seamounts located off-axis of the Pacific-Antarctic Ridge between 50.5°S and 41.5°S. Samples were dredged during the Pacantarctic 2 cruise of the R/V L'Atalante in Dec. 2004-Jan. 2005. Helium isotopic ratios vary between the local mean MORB value ($^4He/^3He$=95, 300; R/Ra=7.58) and more radiogenic values ($^4He/^3He$=182, 460; R/Ra=3.96) associated with high He abundances (~10μccSTP/g). The $^{206}Pb/^{204}Pb$ ratio goes up to 20.2. $^4He/^3He$ ratio and $^{206}Pb/^{204}Pb$ ratios are correlated in samples from the pacific ridges [1] and off-axis seamounts (figure). Clearly, this correlation between helium and lead isotopes reflects the marble-cake structure of the mantle where the fertile component carries the radiogenic signatures. Because of a thicker off-axis lithosphere, this fertile component is more likely to be sampled off-axis as it melts preferentially to the peridotitic mantle.

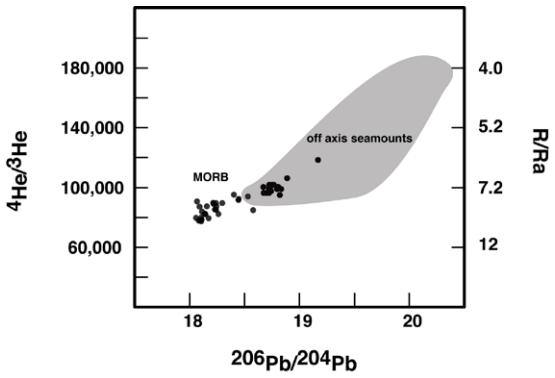

[1] Hamelin *et al*. (2011) *Earth & Planetary Science Letters* **302**, 154–162.

https://doi.org/10.1180/S0026461X00006502 Published online by Cambridge University Press

A geochemical approach to the Sado saltmarshes (Portugal)

S. MOREIRA[1]*, M.C. FREITAS[1], C. ANDRADE[1] AND M.F. ARAÚJO[2]

[1]Universidade de Lisboa, Faculdade Ciências, Departamento de Geologia & Centro de Geologia, 1749-016 Lisboa, Portugal (*correspondence: scmoreira@fc.ul.pt)
[2]Instituto Tecnológico e Nuclear, EN 10, 2686-953 Sacavém, Portugal

The Sado estuary develops ca. 20 km south of Lisbon and studies of its subtidal and intertidal sediments, (namely of marginal marshes - Malha da Costa, Faralhão, Carrasqueira, Alcácer) showed that upper estuarine (Alcácer) sediments yield a Zn/Al-normalized ratio up to 14x (channel) and 7x (marsh) higher than in all remaining areas [1, 2]. Zn is sourced in the Iberian Pyrite Belt terranes - exploited for ore since the Calcolithic - which are intersected by the Sado's watershed; weathering and lixiviation of waste-piles input inorganic carriers of Zn into the drainage system, the metal progressing downstream until reaching the high-salinity upper estuarine domain.

This motivated the sedimentological and geochemical study of a 2.7 m-long core taken from the Alcácer saltmarsh, to investigate the variatons in Zn and other heavy metals along time. The core consists of a monotonous accumulation of muddy sediment (coarse fraction <8%), with compatible values of Si (26-28%) and Al (~9%), high in organic matter (~7-10%) and $CaCO_3$-free, thus low (<0.5%) in Ca.

The vertical profiles of terrigenous elements are fairly invariant. K (1.7-1, 9%) and Ti (0.5-0.6%) usually associate with Al-silicates, and may be replaced by Rb (145-157 mg/kg) and Zr (129-161mg/kg), respectively, in those minerals; these elements and Al present identical vertical variation profiles. The elemental content in Zn decreases upcore (3200 to 443mg/kg) and the Al-normalized values range between 50×10^{-4} and 365×10^{-4}. The lowermost 6 cm of the core yielded Zn/Al $>100\times10^{-4}$. The contents of Cr, Ni, Cu and Pb are 95-153, 41-59, 91-228 and 44-73mg/kg, respectively. The vertical variation of the Al-normalized values of these metals show a slight increase of Cr and Pb upward and a clear decrease in Ni and Cu in the top meter.

The closure of several mines and rehabilitation of tailing areas should have decreased the supply of Zn to River Sado tributaries, and consequently in the lower reaches of the river. At this point it is not possible to indicate the factor responsible for the increment of Cr and Pb to the surface.

[1] Cortesão & Vale (1995) *Mar Pollut Bull* **30**, 34–37.
[2] Moreira *et al*. (2009) *J Coastal Res* **SI 56**, 1380–1384.

The plumbing system of the Ischia island: A physico-chemical window on the fluid-saturated and CO_2-sustained Neapolitan volcanism (Southern Italy)

R. MORETTI[1,2], I. ARIENZO[2], G. ORSI[2], L. CIVETTA[2,3] AND M. D'ANTONIO[4]

[1]Dipartimento di Ingegneria Civile, Seconda Università di Napoli, Aversa (CE), Italy
[2]INGV-Osservatorio Vesuviano, Via Diocleziano 328, Napoli, Italy
[3]Dipartimento di Scienze Fisiche, Università di Napoli "Federico II", Napoli, Italy
[4]Dipartimento di Scienze della Terra, Università di Napoli "Federico II", Napoli, Italy

Ischia, a small island located 18 miles NW offshore Naples (Southern Italy), is a densely populated active caldera (last eruption 1302 A.D.). Melt inclusions in phenocrysts of poorly differentiated eruptive products constrain structure and nature of the Ischia deep magmatic feeding system. Volcanic products bear clear evidence for CO_2-dominated gas fluxing, under very oxidized conditions, and CO_2 enrichment in magma portions stagnating at major crustal discontinuities. Volatile concentrations require gas-melt equilibria between 3 and 18 km depth. At Ischia there is much less magma than that needed to directly supply the amount of released magmatic fluid. Comparison with data from the other nearby Neapolitan volcanoes (Procida, Campi Flegrei –CF-, and Somma-Vesuvius –SV-) highlights the pivotal role of deep fluids in originating the volcanism. Despite the compositional and eruptive style differences observed within the small extension of the Neapolitan Volcanic District, and the variable occurrence of mixing, crustal assimilation and fractional crystallization, the different kinds of volcanism are mostly linked by supercritical CO_2 fluids produced by the devolatilization of subducted terrigenous-carbonatic metasediments. Geochemical and isotopic differences among Ischia, CF and SV from one side, and Procida from the other one, reflect the tectonically controlled slab-derived fluids release and upraise trough the mantle wedge, that, in turns, control magma generation.

https://doi.org/10.1180/S0026461X00006502 Published online by Cambridge University Press

Climatic conditions during the Holocene based on Levantine continental shelf sediment cores

T. MOR-FEDERMAN[1], R. BOOKMAN[1]*, A. ALMOGI-LABIN[2] AND B. HERUT[1,3]

[1]Dept. of Marine Geosciences, Charney School of Marine Sciences, University of Haifa, Mt. Carmel, Haifa 31905, Israel (*correspondence: rbookman@sci.haifa.ac.il)

[2]Geological Survey of Israel, 30 Malkhe Israel, Jerusalem 95501, Israel

[3]Israel Oceanographic & Limnolological Research, Tel Shikmona, Haifa 31080, Israel

Sediments deposited on the southeastern continental shelf of the Levantine Basin are sensitive recorders of climatic and oceanographic variability affected by the north Atlantic and indirectly by monsoonal systems. In order to reconstruct the influence of these climatic systems on Holocene sediments two cores were taken off shore the southern (V115) and central (V101) Israeli coast at water depths of ~35 m. The cores, dated to 7, 630 and 8, 440 ^{14}C years BP, show two distinct sedimentation regimes. High rates, of 190-140 cm/ka, in the lower Holocene, and significantly lower rates of 50-60 cm/ka during the last 5, 500 years. The cores were analyzed for grain size, TOC, $\delta^{13}C$, major and trace elements, and Sr isotopes. Selected results are shown in the figures below. The full data set indicates clearly that two distinct climatic periods governed the eastern Mediterranean and its surroundings during the Holocene.

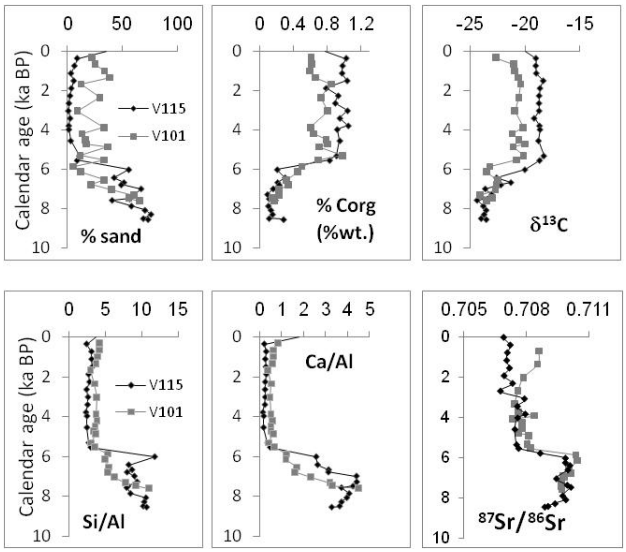

Timescales of eruption triggering and magma transport from element diffusion in minerals

DAN MORGAN*

School of Earth & Environment, University of Leeds, LS2 9JT UK (*correspondence: d.j.morgan@leeds.ac.uk)

Mixing of magmas of contrasting temperatures and compositions can act as a trigger of a subsequent volcanic eruption. Heating of a magmatic system by basaltic injection can remobilise magma that is close to its solidus, and mixing can further change the character of the magma, lowering viscosity and promoting eruption.

Upon mixing, if the magma system remains saturated in mineral phases inherited from one or both parental melts, strongly-zoned mineral grains will form, as a product of changes in mineral-melt equilibria and melt composition. Subsequent residence at magmatic temperatures will allow such abrupt chemical zoning profiles to relax by diffusion. If magma temperatures are known, we can place constraints on diffusion time and thereby investigate the amount of time that passes between a magma injection – ultimately our eruption trigger – and the ensuing eruption.

Study of large silicic systems implies crystal residence times at magmatic temperatures of the order of tens of years (e.g. Whakamaru Ignimbrite, NZ, [1]) to thousands of years (e.g. Fish Canyon Tuff, USA, [2]), which is still relatively rapid given the large volumes concerned. Looking at smaller systems, the Nea Kameni Dacite of Santorini suggests a remobilisation time of the order of a month between basaltic injection and dacite eruption [3], whilst study of the recent Eyjafjallajokull eruption of 2010 resolves multiple mixing events occurring in the months prior to, and during, the eruption. In contrast, work on Piton de la Fournaise volcano is less clear-cut, and perhaps sounds a cautionary note for determining magmatic timescales from diffusion profiles.

Developments of new software tools and methodologies, and the utilisation of new mineral-element systems promise an expansion of these techniques. However, the petrological context has to be a major concern in these studies as it entirely determines the significance of the results.

[1] Saunders, Morgan, Baker & Wysoczanski (2010) *Journal of Petrology* **51**, 2465–2488. [2] Charlier, Bachmann, Davidson, Dungan & Morgan (2007) *Journal of Petrology* **48**, 1875–1894. [3] Martin, Morgan, Jerram, Caddick, Prior & Davidson (2008) *Science* **321**, 1178.

https://doi.org/10.1180/S0026461X00006502 Published online by Cambridge University Press

Rapidly assessing changes in bone mineral balance using natural stable calcium isotopes

J.L.L. MORGAN[1]*, G.W. GORDON[1], S.J. ROMANIELLO[1], J.L. SKULAN[2], S.M. SMITH[3] AND A.D. ANBAR[1]

[1]Arizona State Univ., Tempe, AZ 85287 (*correspondence: jlmorga3@asu.edu, gwyneth.gordon@asu.edu, sromanie@asu.edu, anbar@asu.edu)

[2]Geology Museum, Univ. of Wisconsin, Madison, WI 53706 (jlskulan@geology.wisc.edu)

[3]HACD, NASA Johnson Space Center, Houston, TX 77058 (scott.m.smith@nasa.gov)

We demonstrate that variations in the Ca isotope ratios in urine rapidly and quantitatively reflect changes in bone mineral balance. This variation occurs because bone formation depletes soft tissue of light Ca isotopes, while bone resorption releases that isotopically light Ca back into soft tissue.

In a study of 12 individuals confined to bed rest, a condition known to induce bone resorption, we show that Ca isotope ratios shift in a direction consistent with net bone loss after just 7 days, long before detectible changes in bone density occur. Consistent with this interpretation, the Ca isotope variations track changes observed in N-teleopeptide, a bone resorption biomarker, while bone-specific alkaline phosphatase, a bone formation biomarker, is unchanged. Ca isotopes can in principle be used to quantify net changes in bone mass. Ca isotopes indicate an average loss of 0.62 ± 0.16 % in bone mass over the course of this 30-day study. The Ca isotope technique should accelerate the pace of discovery of new treatments for bone disease and provide novel insights into the dynamics of bone metabolism.

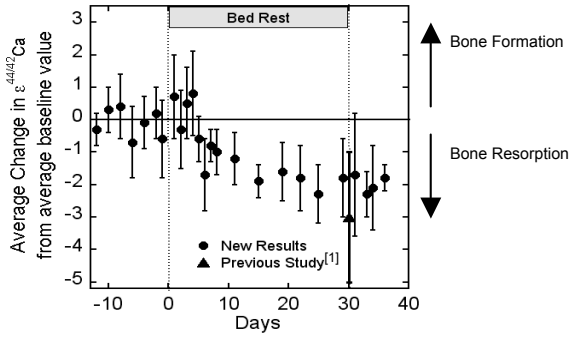

Figure 1: Change in Ca isotope ratios of urine as a result of bed rest.

[1] Skulan *et al*. (2007) *Clinical Chem*. **53**, 1155–1158.

Improving the accuracy of the $^{40}Ar/^{39}Ar$ geochronometer

L.E. MORGAN[1]*, D.F. MARK[2], K.F. KUIPER[1], O. POSTMA[1], I.M. VILLA[3] AND J.R. WIJBRANS[1]

[1]Faculty of Earth & Life Science, Vrije Universiteit, De Boelelaan 1085, 1081HV, Amsterdam, The Netherlands (*correspondence: leah.morgan@falw.vu.nl)

[2]NERC Argon Isotope Facility, Scottish Univ. Environmental Research Centre, East Kilbride, G75 0QF, UK

[3]Universität Bern, Institut für Geologie, Baltzerstrasse 3, CH-3012 Bern, Switzerland

The accuracy of the $^{40}Ar/^{39}Ar$ system relies on a number of parameters, most notably decay constants for the branched decay of ^{40}K to ^{40}Ar and ^{40}Ca, and the $^{40}Ar/^{40}K$ ratios (or ages) of mineral standards used as neutron flux monitors.

Although these parameters can be assessed to an extent through intercalibration efforts (e.g. [1]), a serious effort to better constrain these parameters based on metrologically traceable measurements, modern technologies, and rigorous uncertainty analyses is overdue [2, 3, 4].

Here we present steps towards a 'first principles' calibration of the $^{40}Ar/^{39}Ar$ system by measurement of ^{40}Ar and ^{40}K concentrations. These measurements will be used both to determine the $^{40}Ar/^{40}K$ ratios of mineral standards (thus allowing for calculations of their K-Ar ages) and also the ^{40}Ar branch of the ^{40}K decay constant via ingrowth experiments in material enriched in ^{40}K.

^{40}Ar concentration measurements are based on sensitivity corrections via a calibrated pipette system working under the principles of the ideal gas law. This system relies on components with calibrations traceable to international standards and will be both renewable, with a lifetime of ca. 1 month for gas in the reservoir, and portable, to permit interlaboratory calibrations.

^{40}K concentration measurements are based on TIMS measurements and NIST standard reference materials for elemental (SRM999b) and isotopic (SRM985) potassium.

This series of measurements aims to directly calibrate the $^{40}Ar/^{39}Ar$ system using measurements traceable to international standards, similar to recent steps taken by the U-Pb community [6].

The research leading to these results has received funding from the European Community's Seventh Framework Programme (FP7/2007-2013) under grant agreement n° 215458.

[1] Kuiper *et al*. (2008) *Science* **320**, 500–504. [2] Min *et al*. (2000) *GCA* **64**, 73–98. [3] Begemann *et al*. (2001) *GCA* **65**, 111–121. [4] McDougall & Wellman (2010) *Chem.Geol*. **280**, 19–25. [6] Condon *et al*. (2010) *GCA* **74**, 7127–7143.

https://doi.org/10.1180/S0026461X00006502 Published online by Cambridge University Press

Two pyroxene-garnet rock of the Gridino area of Belomorian mobile belt (Northern Karelia), Karelia, Russia: Record of the prograde and retrograde metamorphic events

A.A. MORGUNOVA[1]* AND A.L. PERCHUK[1,2]

[1]Institute of Experimental Mineralogy, Academica Osipyana Street 4, Moscow distr. 142432, Chernogolovka, Russia (*correspondence: almor@iem.ac.ru)

[2]Lomonosov Moscow State University, Geological Faculty, GSP-1, Leninskie Gory, Moscow, Russia (alp@geol.msu.ru)

Archean felsic gneisses in the high pressure Gridino complex host lenses boudins and dikes of eclogitized mafic (gabbro, gabbro-norite) and ultramafic (garnet-pyroxene rock, orthopyroxenite) rocks. The paper is aimed to reconstruct metamorphic evolution of the two pyroxene-garnet rock forms a boudin of size 4*5 m in the amphibole-biotite gneisses on the Visokii Island of the White Sea.

The early episode of the rock evolution is characterized by inclusions of calcite and diabantite (rare Fe-Si chlorite). The diabantite is well-known as product of metasomatic alteration of peridotites. Inclusions of this mineral were found in all rock-forming minerals (garnet, clino- and orthopyroxene). They often associate with REE and U, Th-rich minerals, which tend to crystallize at the walls of the vacuoles. The inclusions are very unusual in term of the surrounding cracks. The inclusions hosted by pyroxenes are surrounded by the both concentric and radial cracks, whereas inclusions in garnets are surrounded by the only radial cracks. Theses features indicate that the inclusions have been recrystallized after their trapping. Thermobarometric study of the rock indicates that unhydrous mineral assemble garnet+clinopyroxene+orthopyroxene that replaced diabantite-bearing metasomatic rock was formed under T-P conditions (690ºC/1.7 GPa) of eclogite facies similar to those determinated for the Archean mafic eclogites within the complex. Rim zones of the rock-forming minerals indicate isothermal decompression down to $P \sim 1.2$ GPa, followed by the episode of cooling to $T \sim 650$ºC and decompression to $P \sim 0.9$ GPa recorded by development of the retrograde amphibole-garnet-orthopyroxene association [1].

[1] Morgunova & Perchuk (2011) *Russian Geology & Geophysics*, in press.

Dispersal of tritium and ^{3}He along the outer rim of the Weddell gyre

R. MORIARTY*, Z. ZHOU AND C.J. BALLENTINE

SEAES, University of Manchester, M13 9PL, UK (*correspondence: roisin.moriarty@manchester.ac.uk)

Weddell gyre plays an important role in the southern closure of the Meridional Overturning Circulation (MOC) and in the ventilation of the deep ocean through the formation of Antarctic Bottom Water (AABW). Estimates of AABW production in the region are not very well constrained and range between 3 and 11Sv ($1Sv=10^6$ m^3 s^{-1})[1]. Recent observations [2, 3] suggest that the Weddell gyre may not be the primary region of AABW formation as previously thought. Exchange between the Weddell gyre and the world oceans occurs at the outer rim of the gyre. Determination of the transport of water masses across this boundary is needed to quantify the production and export of AABW in and from the gyre and to determine its contribution to global ocean circulation.

Seawater samples (~500) for tritium and helium-3 analysis were collected along the outer rim of the gyre as part of ANtarctic Deep Rates of EXport (ANDREX) project between (Dec. 2008 and April 2010). These samples covered 48 stations and ranged from suface to a depth of 6000m. Helium-3 values in conjunction with another steady state tracer, PO_4*, will allow the calculation of dilution times using optimum multiparameter techniques. Tritium in conjunction with CFCs and SF_6 will allow the quantification of ventilation ages and the trasist times since a water parcel was last in contact with the atmosphere. They will also give a second estimation of dilution times. Preliminary results for tritium indicate values ~0.15 TU in surface waters, a tritium dead layer at intermediate depths and an increase in tritium concentration at depths ≥4000m. These data provide the basis for modelling mechanisms that control the dispersal and calculation of the AABW production rates.

[1] Naveira Garabato, *et al*. (2002) *Deep-Sea Res. II* **49**, 3735-3769. [2] Meredith, *et al*. (2000) *J. Geophys. Res*. **105**, 1093-1104. [3] Hoppema, *et al*. (2001) *J. Mar. Res*. **59**, 257-279.

https://doi.org/10.1180/S0026461X00006502 Published online by Cambridge University Press

How biogenic nano-iron oxides can control the fate of pollutants

G. MORIN[1], G. ONA-NGUEMA[1], F. JUILLOT[1], F. MAILLOT, Y. WANG[1], M. EGAL[2], O. BRUNEEL[2], C. CASIOT[2], F. ELBAZ-POULICHET[2], G. CALAS[1] AND G.E. BROWN, JR.[3]

[1]Institut de Minéralogie et de Physique des Milieux Condensés (IMPMC), CNRS, UPMC, Univ Paris 7, 4, Place Jussieu, 75252 Paris Cedex 05, France (guillaume.morin@impmc.upmc.fr)

[2]Hydrosciences UMR 5569, CNRS, Universités Montpellier I and II, IRD, Place Eugène Bataillon, CC MSE, 34095 Montpellier cedex 5, France (egal@msem.univ-montp2.fr)

[3]Surface & Aqueous Geochemistry Group, Department of Geological & Environmental Sciences, Stanford University, Stanford, CA 94305-2115, USA (gordon.brown@stanford.edu)

Nanominerals have been the subject of extensive research for the last decade, especially because of their exceptional surface properties. These properties indeed confer to these nanoparticles an important role in pollutant dynamics via sorption and precipitation reactions, colloidal transport, and redox surface reactions (e.g. [1]).

In this communication we will present recent advances in the identification of such processes in impacted natural systems as contaminated soils and mining environments as well as in laboratory systems relevant of water treatment processes. Microscopic and spectroscopic investigations of these systems emphasize the role of nano – iron oxides [2, 3], oxyhydroxides [1], hydroxides [4, 5] and hydroxysulfates [6, 7] from abiotic or microbial origin. Particular attention will be paid to better understanding the respective roles of physico-chemical factors and microbial metabolisms in controlling the kinetics of nano-mineral nucleation and evolution, and the ability of these solids to scavenge inorganic pollutants, especially arsenic. Finally, recent evidence for surface redox reactions involving reactive oxygen species [8] will be discussed as a promising process for remediation of contaminated surface waters.

[1] Charlet *et al*. (2011) *CR Geoscience* **343**, 123–139. [2] Morin *et al*. (2009) *Langmuir* ***25***, 9119–9128. [3] Wang *et al*. (2008) *GCA* ***72***, 2573–2586. [4] Ona-Nguema *et al*. (2009) *GCA* ***73***, 1359–1381. [5] Wang *et al*. (2010) *ES&T* ***44***, 109–115. [6] Egal *et al*. (2009) *Chemical Geol*. **265**, 432–441. [7] Egal *et al*. (2010) *Appl*. *Geochem*. **25**, 1949–1957. [8] Ona-Nguema *et al*. (2010) *ES&T* **44**, 5416–5422.

Removal of fluoride on Mg–Al mixed oxides prepared at different temperatures

S. MORIYAMA*, K. SASAKI AND T. HIRAJIMA

Department of Earth Resource Engineering, Kyushu University, Motooka 744 Fukuoka, Japan (*correspondence: s-moriyama09@mine.kyushu-u.ac.jp)

Hydrotalcite is in layered double hydroxides (LDHs) structures, the general chemical formula is represented $[M_1 (II)_{1-x}M_2 (III)_x (OH_2)]A_{n-x/n}\cdot mH_2O$, where M_1 (II) = divalent cation (Mg^{2+}, Zn^{2+}, Ni^{2+}, Co^{2+}, Mn^{2+}, Cd^{2+}), M_2 (III) = trivalent cation (Al^{3+}, Fe^{3+}, Cr^{3+}), An^- = interlayer anion with valence n, x is M_2 (III/M_1 (II) + M_2 (III). In the present study Mg–Al mixed oxides, which were obtained by thermal decomposition of precipitated hydrotalcite-like compounds, were used as sorbents to remove fluoride in aqueous systems. Calcination temperatures were 873 K, 1073 K, and 1273 K.

The XRD peaks for co-precipitation products were assigned to hydrotalcite, but this pattern completely disappeared and assigned to MgO after calcination at each temperature, spinel phase was also observed at 1273 K. Higher calcination temperature provided higher crystallinities and larger crystal size of mixed oxide which was confirmed by TEM images. Fluoride sorption on mixed oxides can be mainly explained by ionic exchange of OH^- to F^-. Mg and Al ions were released during the sorption of fluoride; the behaviors of released Mg and Al during the sorption of fluoride have been affected by the elemental distributions of the surface on mixed oxides. The molar ratio of Al/Mg in hydrotalcite-like compounds before calcinations was determined to 0.33 after acid decomposition; however XPS results indicate that the molarl ratio of Al/Mg on the surface of mixed oxide increased by the calcination temperatures. After sorption of fluoride, hydrotalcite have been reconstructed again with mixed oxide calcined at 873 K and 1073 K, however, less crystalline hydrotalcite, Mg $(OH)_2$, and spinel were observed on mixed oxides calcined at 1273 K. The lowest sorption efficiency of mixed oxide calcined at 1273 K probably due to the small amount of MgO by the phase transition to spinel because the spinel was stable in water and doesn't react with fluoride. On the other hand, removal of fluoride was more easily achieved in mixed oxides calcined at 1073 K than another mixed oxides; this may be caused by good correlation with lattice parameter of MgO. Mg–Al mixed oxides is one of promising products to remove anion including fluoride, but the sorption efficiency are affected by properties of the surface molar ratio and structures, therefore calcination temperatures must to be considered.

https://doi.org/10.1180/S0026461X00006502 Published online by Cambridge University Press

H_2O-CO_2 solubility in mafic melts

Y. MORIZET[1], G. IACONO-MARZIANO[2]* AND F. GAILLARD[2]

[1]Université de Nantes, UMR 6112, France
[2]ISTO, UMR 6113 CNRS-Université d'Orléans, France
(*correspondence: giada.iacono@cnrs-orleans.fr)

Water and carbon dioxide are the two most abundant volatile species in volcanic gases. Accurate laws describing their solubilities in silicate melts are therefore crucial to understand volcanic degassing and interpret melt inclusion entrapment depths. We present here new experimental data on H_2O-CO_2 solubility in mafic melts with variable chemical compositions (alkali basalt, lamproite and kamafugite) that extend the existing database. We show that potassium and calcium-rich melts can dissolve ~ 1 wt% CO_2 at 3500 bar and 1200°C, whereas conventional models predicts solubilities of 0.2-0.5 wt%, under similar P-T conditions. These new data, together with those already existing in the literature, stress the fundamental control of melt chemical composition on CO_2 solubility. We present a H_2O-CO_2 solubility model for mafic melts, which employs simplified concepts of gas-melt thermodynamics and accounts for the combined effects of melt chemical composition and structure. The model is calibrated on a selected database consisting of 270 experiments with 43 different mafic compositions. The statistic analyses of the experimental data indicate that the structure and the chemical composition of the melt play a fundamental role in CO_2 solubility in mafic melts, whereas H_2O solubility is negligibly affected by melt composition and structure. CO_2 solubility mainly depends on the amount of non-bridging oxygen per oxygen (NBO/O) in the melt, but the nature of the cation bounded to NBO is also critical. Alkalis (Na+K) bounded to NBO result in a strong enhancement of CO_2 solubility, whereas Ca has a more moderate effect. Mg and Fe bounded to NBO have the weakest effect on CO_2 solubility. Other structural parameters, such as the agpaitic index (Al_2O_3/ [CaO + K_2O + Na_2O]), are shown significant, though not as critical as NBO/O. Finally, we modelled the effect of water on CO_2 solubility and suggest that molecular H_2O enhances its solubility, whereas hydroxyls appear to have the opposite effect. In contrast with CO_2, H_2O solubility in mafic melts shows a weak correlation with NBO/O, and is statistically independent on melt composition.

Migration of europium and uranium in opalinus clay influenced by pH and temperature

C. MÖSER*, R. KAUTENBURGER AND H.P. BECK

Institute of Inorganic and Analytical Chemistry and Radiochemistry, Saarland University, Saarbrücken, Germany
(*correspondence: c.moeser@mx.uni-saarland.de)

Introduction

The development of a disposal in deep geological formations for high-level radioactive waste is a very important task for the future. The migration of radionuclides through soil is one of the critical paths from leaked stored container to the environment [1]. As metals of interest, europium as homologue of americium and uranium as principal component of nuclear fuel elements were used.

Spotlight of our investigations is the sorption of europium and uranium onto Opalinus clay. To get a first understanding for the different sorption processes we used batch experiments. During this experiments we varied the conditions like pH and temperature.

Results

The sorption of the metal ions is strongly pH-dependent. At pH<7 the Eu sorption decreases strongly. The uranium sorption decreases strongly between pH 6 and 9. An explanation afford the formation of the neutral $Ca_2UO_2(CO_3)_3$ species, which doesn´t sorbed onto the clay [2, 3]. The necessary carbonate and calcium was dissolved out of the Opalinus clay. For the investigations synthetic porewater was used. It has an ionic strength of 0.4 M and the concentration of cations is more than $7 g \cdot L^{-1}$. These porewater cations influence the sorption of europium in a pH range <7 significantly. Due to the presence of competing cations the sorption of Eu is inhibited. The uranium sorption is nearly independent from the competing cations. The influence of pH and temperature is significant higher. With an increasing temperature from 298 to 333 K the sorption of the metals increases, too. Investigations at different temperatures allow it to calculate the entropies and enthalpies for the reactions with uranium and europium derived from Van´t Hoff plots.

[1] Wang *et al*. (2011) *J. Radioanal. Nucl. Chem.* **287**, 231–237. [2] Liu *et al*. (2005) *Environ. Sci. Technol.* **39**, 4125–4133. [3] Meleshyn *et al*. (2009) *Environ. Sci. Technol.* **43**, 4896–4901.

https://doi.org/10.1180/S0026461X00006502 Published online by Cambridge University Press

Monitoring emissions from the Athabasca Oil Sands using stable isotopes from black spruce (*Picea mariana*)

HEATHER MOSHER* AND ALEXANDER P. WOLFE

University of Alberta, Edmonton T6G 2E3, AB, Canada
(*correspondence: hmosher@ualberta.ca)

Atmospheric deposition in boreal forest ecosystems

The Athabasca Oil Sands industrial complex in northeastern Alberta, Canada, emits tons of CO_2, NO_x and SO_x daily, as well as various trace metals and aromatic hydrocarbons. The effects of these emissions on the surrounding, nutrient-limited, boreal forest ecosystem is not yet fully understood, especially with regards to deposition of bio-available reactive nitrogen (Nr). The possibility exists that industrial nitrogen subsidies may increase forest production, although this has not yet been assessed.

Nitrogen and carbon stable isotope data from year-old black spruce needles (*Picea mariana*) collected around the Athabasca Oil Sands suggest a possible fertilization effect promoting tree growth. Observed depleted nitrogen values correspond well with depleted carbon values regionally. However, the most proximal sites show clear signals that increased deposition may result in tree physiological stress, most likely related to the deposition of trace metals, and thus locally annulling any positive effects of Nr deposition on tree growth. Paired C and N sotopes from wood cellulose generally support needle measurements, together providing a detailed overview of the interactions between atmospheric deposition, nutrient cycling and tree ecophysiological stress.

Initial results from a new time resolved microfocus XEOL facility at the Diamond Light Source

J.F.W. MOSSELMANS[1], R.P TAYLOR[1,2], A.A. FINCH[2] AND P.D. QUINN[1]

[1]Diamond Light Source, Didcot, OX11 0DE, UK
(*correspondence fred.mosselmans@diamond.ac.uk)
[2]Dept. of Earth Sciences, St Andrews, KY16 9AL, UK
(aaf1@st-andrews.ac.uk)

Time Resolved spectrometer

We have constructed a Time-Resolved X-ray Excited Optical Luminescence (TR-XEOL) detection system at the Micofocus Spectroscopy beamline I18 at the Diamond Light Source. TR-XEOL allows the study of short lived states in isolation from long-lived cascade generated signals and thus potentially identify and study transient luminescent centres.

The system uses a Horiba-Jobin Triax Spectrometer and Hamamatsu R3809U-50 microchannel-plate photo multiplier tube. Triggering on the RF clock, we are able to record data in time bins of 6.2 ps in the 230 ns gap between the hybrid bunch photons and those from the main group of electron bunches orbiting the ring. We can detect light over the range 180-850 nm using a bespoke optical fibre, with X-ray excitation energies between 2 and 20 keV.

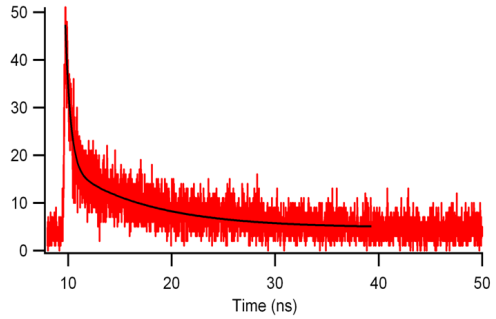

Figure 1: TR_XEOL spectrum from Labradorite Feldspar at 400 nm fitted with 2 exponentials of 1.6 and 29.7 ns.

Initial results

We have examined several different feldspars looking at the short-lived emissions in the UV region. We have observed two exponential decay lifetimes at 400 nm one with a lifetime of 1.6 ns and a second of 29.7 ns from a single crystal labradorite plagioclase feldspar (RT50c, Smithsonian Institute), an untreated single crystal collected from Clear lake Utah USA. In contrast, R1-11a, a microcline cryptoperthite from the Prins Christians Sund granite suite South Greenland [1], showed variable lifetimes at 400 nm, a short lifetime whose mean value was 0.20±0.13 ns and a longer life component of 13.5 ns. The potential of TR-optically detected XAS will be discussed.

[1] Finch & Klein (1999) *Contr. Mineral. Petrol.* **135**, 234–243.

https://doi.org/10.1180/S0026461X00006502 Published online by Cambridge University Press

Serpentine and brucite intergrowths: effects on $\delta^{11}B$

F.E. MOTHERSOLE[1]*, K.A. EVANS[1] AND J. CLIFF[2]

[1]Curtin University of Technology, Bentley, WA 6845, Australia (*correspondence: f.mothersole@postgrad.curtin.edu.au)
[2]Centre for Microscopy, Characterisation and Analysis, University of Western Australia, Australia

A quantitative understanding of fluid:rock interaction is important for understanding the transfer of elements and fluid circulation within the crust. Serpentinites can provide a sensitive record of fluid-rock interaction, particularly via analysis of isotopes of fluid mobile elements, such as boron.

Previous studies of boron in serpentinised rocks have provided a wide range of values. ^{11}B partitions into seawater, so heavy $\delta^{11}B$ values indicate a sewater influence, while lighter $\delta^{11}B$ reflects mantle influences. Strong fractionation between the two isotopes at temperatures of serpentinisation enables elucidation of the evolving fluid:rock system with progressive serpentinisation.

However, boron isotopic fractionation is influenced by temperature and pH because ^{11}B is preferentially incorporated into trigonal environments, such as those found in the $B(OH)_3$ aqueous species, while ^{10}B is preferentially hosted by the $B(OH)_4^-$ tetragonal species, which dominates in solution at high pH [1]. Additionally serpentine minerals, particularly early grown serpentine, can be intimately intergrown with brucite. Brucite cations are held in a trigonal site, so the presence of brucite is expected to increase $\delta^{11}B$. If this is not recognised, $\delta^{11}B$ values heavier than the true serpentine $\delta^{11}B$ values will be inferred, and erroneous interpretations may be made.

In this study, brucite, serpentine and brucite-serpentine intergrowths of partially serpentinised peridotites from ODP Leg 209 and New Caledonia were identified using micro-raman spectroscopy. Secondary Ion Mass Spectrometry (SIMS) was used to assess the extent to which the presence of brucite affects $\delta^{11}B$. The results enable a quantitative assessment of the magnitude of the effect of brucite on $\delta^{11}B$ and the implications of this for interpretation of fluid:rock interaction during serpentinisation.

[1] Foustoukos *et al*. (2008) *Geochimica et Cosmochimica Acta* **72**(22) 5457–5474.

Direct molecular simulation of aqueous electrolyte solubility

F. MOUCKA[1,2] AND W.R. SMITH[1]*

[1]Un. of Ontario Institute of Technology, Oshawa, ON Canada L1H 7K4 (*correspondence: william.smith@uoit.ca)
[2]J. E. Purkinje University, 40096 Usti n. Labem, Czech Republic

Introduction

We describe a new and computationally efficient methodology using Osmotic Ensemble Monte Carlo (OEMC) simulation to calculate the solubility of aqueous electrolytes [1]. We apply it to directly determine solubility without the need for calculating chemical potentials. The method avoids calculations for the solid phase, directly incorporating readily available data from thermochemical tables based on well-defined reference states [2].

Methodology

The method performs simulations of the aqueous solution at a fixed number of water molecules, pressure, temperature and specified overall electrolyte chemical potential. Insertion/deletion of ions to/from the system is implemented using fractional ion states, and transitions between the states incorporates Wang-Landau sampling.

Results and Discussion

We have applied the approach to calculate the solubilities of a range of alkali halides, using several water and ionic force-field models from the literature. We consider both individual alkali halides and their mixtures, dissolved in both H_2O and HCl-H_2O solutions. The solubility predictions are generally good. The solubility is very sensitive to the force field employed.

[1] F. Moucka, M. Lisal, J.Skvor, J. Jirsak, I. Nezbeda & W.R. Smith (2011) *J. Phys. Chem. B*, submitted.[2] M. Chase, Jr. (1998) NIST-JANAF Thermochemical Tables, *J. Phys. & Chem. Reference Data Monograph No.* ***9***, Am. Chem. Society, Am. Inst. Physics.

https://doi.org/10.1180/S0026461X00006502 Published online by Cambridge University Press

An unusual Hf-Pb signature below the East Pacific Rise – Mathematician Hotspot system

BÉRENGÈRE MOUGEL, ARNAUD AGRANIER, CHRISTOPHE HÉMOND AND PASCAL GENTE

UMR 6538 Domaines Océaniques, IUEM, Université de Brestagne Occidentale, 26980 Plouzané, France

The Northern part of the East Pacific Rise (EPR), between the Riviera and Orozco Fracture zones shows an atypical morphology. It is 300m shallower than the rest of the ridge and is unusually wide. On its western side, a strong alignment of seamounts intersects perpendicularly the ridge in its most inflated part, suggesting a hotspot-ridge interaction.

This study reports new Hf and Pb isotopes and trace element concentrations for 57 MORB samples, collected by submersible 'Nautile' during cruise PARISUB (2010). It covers a 15 km transect along the ridge axis from 15°37'N to 15°47°N with an average sampling of space ~300m.

REE patterns shows typical intermediate E-MORB compositions with relatively flat LREE profiles and significant depletions in HREE.

$^{206}Pb/^{204}Pb$ range from 17.5 to 18.2; $^{208}Pb/^{204}Pb$=36.8-37.6; $^{207}Pb/^{204}Pb$= 15.46-15.51; ε_{Hf}= 8.7-11.5. All the Pb ratios over ^{204}Pb are correlated with each other, as well as with $^{176}Hf/^{177}Hf$. These clean correlations most likely reflect binary mixings occurring in the mantle source between the local DMM and enriched material (EM). $^{206}Pb/^{204}Pb$ and $^{208}Pb/^{204}Pb$ ratios are also unusually low even for MORB. They are actually the lowest values ever reported for the EPR, which is unexpected for a plume-ridge interaction. Moreover, alignments in $^{207}Pb/^{204}Pb$ vs $^{206}Pb/^{204}Pb$ or $^{208}Pb/^{204}Pb$ diagrams are distinct from any geochemical trend known for this ridge ($^{207}Pb/^{204}Pb$, too high for given $^{206}Pb/^{204}Pb$ and $^{208}Pb/^{204}Pb$).

The positive correlation between Hf and Pb isotopes is even more remarkable, that geochemical enrichments typically lead to radiogenic Pb and un-radiogenic Hf signatures and, therefore, that DMM-EM mixtures usually appear as negative correlations in the Hf-Pb isotope spaces.

The least radiogenic Hf and Pb correspond to the samples the closest to the Seamounts-ridge intersection (15°43'N) suggesting that these unusual compositions reflect the Mathematician EM material.

Interperetaion of microtexture and microstructure in the dynamic metamorphic rocks in Mouteh Mine area, Iran

SEYED ZAHED MOUSAVI[1]* AND KHATEREH PANAHI[2]

[1]Basic Science Department, Islamic Azad University(I.A.U), Meshkinshahr Branch,Meshkinshahr, Iran (*correspondence: z.mousavi@meshkin-iau.ac.ir) (khaterehpanahi@gmail.com)

Introduction

The studied area is located in the central part of Sanadaj-Sirjan belt, 60 km south part of Delijan city, the Muteh mine area. The formations at this area are Devonian silicic volcanic and volcano clastic rocks that have been metmorphed at green schist –amphiboloit facies.This rocks have altered by some Basic intrusive.

Methods and Results

Above 60 thin section have taken from drilling core samples. The aim of this studding is a interpretation of micro texture & microstructure by microscope. The result of studding show some micro texture like CS, C/ fabric, Mineral Fish, Bookshelf Structure, Boudinage, Strain Shadow, σ, δ, Φ pyroclast. In addition we can find three metamorphism setting (D_1, D_2, D_3) at this area. Every one this micro texture & microstructure have made in various metamorphism and deformation setting.

[1] Cees W. Passchier & Rudolph A.J. Trouw (2005) *Microtectonics* 2th edition.springer, 140–143, 152–153.
[2] David A.Ferrill, Alan P Morris, Mark A. Evance, Martin Burkhard, Richard H. Groshong Jr. (2004) *Journal of Structural Geology* **26**, 1521-1529.

https://doi.org/10.1180/S0026461X00006502 Published online by Cambridge University Press

Sulfur and strontium isotope study of hydrothermal mineralization from the SE Afar Rift

N. MOUSSA[1,2,3]*, O. ROUXEL[1,2], P. NONNOTTE[2], Y. FOUQUET[1], E. PONZEVERA[1] AND J. ETOUBLEAU[1]

[1]IFREMER, Centre de Brest, BP 70- 29280 Plouzané, France
[2]UMR 6538 Domaines Océaniques, UBO-IUEM, Place Copernic, 29280, Plouzané, France
[3]IST, Centre d'Etude et de Recherche de Djibouti, BP 486, Djibouti
(*correspondence: nima.moussa.egueh@ifremer.fr)

Epithermal mineralization was recently described in the SE Afar Rift (Republic of Djibouti). To infer fluid sources in hydrothermal veins, sulfur and strontium isotopic analyses were performed on thirty mineralized samples of chalcedony, and/or quartz, ± carbonate containing gold and sulfides. Gypsum occurs as individual mounds and shallow stockwork zones. Isotopic composition of sulfides and sulfates were determined using Multicollector-Inductively Coupled Plasma Mass Spectrometer (MC ICPMS) and Thermal Ionisation Mass Spectrometer (TIMS) methods [1]. Sulfur isotopic composition of sulfides (mainly pyrite) vary from –0.2 to +6.8‰. These values are classically reported for volcanic rocks and hydrothermal sources. Strontium isotopic ratios ($^{87}Sr/^{86}Sr$) of mineralized veins range from 0.70391 to 0.70799. The lowest values of $^{87}Sr/^{86}Sr$ ratios indicate volcanic source of fluid while the highest isotopic composition indicate significant seawater contribution (defined at 0.70903, [2]). Coupled sulfur and strontium isotope compositions of eight sulfate samples hosted in (i) gypsum mound; (ii) evaporites (iii) stockwork veins in sediment or in volcanic rocks were also investigated to characterize the sources of Sr and S. The $\delta^{34}S$ values of the sulfate range from –1 to +14.3‰ while the $^{87}Sr/^{86}Sr$ compositions fall in the range 0.70389-0.70639. The highest values of $^{87}Sr/^{86}Sr$ ratios (0.70639) in gypsum correspond to the lighter values of $\delta^{34}S$ (+14.3‰.). These relatively light $\delta^{34}S$ values can be explained by the disproportionation of magmatic SO_2. This implies that both acidic fluid of magmatic origin and saline fluids contribute to the hydrothermal system in the Afar Rift.

[1] Craddock *et al*. (2008) *Chem. Geol* **253**, 102–113. [2] Barrat *et al*. (1993) *GCA* **57**, 2291–2302.

Isotopic fractionation of zinc in planetary basalts

F. MOYNIER[1], R. PANIELLO[1] AND J.M.D. DAY[2]

[1]Dept. Earth Planet. Sci, Washington Univ. St Louis, MO 63130 (moynier@wustl.edu, PanielloR@ent.wustl.edu)
[2]Geosci. Res. Div., Scripps Institution of Oceanography, La Jolla, CA 92093-0244 (jmdday@ucsd.edu)

Zinc is a moderately volatile chalcophile trace element and so preserves evidence for volatility-driven processes during planetary accretion. For this reason, Zn can be used to understand the origin and evolution of planetary bodies, including Earth-Moon system formation. Terrestrial igneous rocks exhibit a limited range in zinc isotopic composition ($\delta^{66}Zn$ = +0.3±0.1‰, 2SE), whereas large variations have been found in lunar soils ($\delta^{66}Zn$ up to +6.4‰ [1]) and tektites (up to +2.04‰ [2]) associated with volatilization processes.

Here we report new Zn isotopic data for low- and high-Ti mare basalts to directly address the origin of the Earth and Moon. We also present new Zn isotopic data for martian meteorites, which have identical Zn isotopic compositions, within uncertainties ($\delta^{66}Zn$ = +0.25±0.03‰, 2SE, n=10), to terrestrial lavas. Absolute Zn concentrations in mare basalts (0.6-12ppm) are generally significantly lower than for terrestrial lavas (typically >75ppm), silicate Earth estimates (~55ppm), CI chondrites (>300ppm), or lunar pyroclastic beads (>90ppm) [1]. With the exception of two outliers, low-Ti and the high-Ti lunar basalts have similar mean $\delta^{66}Zn$ values of +1.31±0.13‰ (n=11) and +1.39±0.31‰ (n=8), respectively, and similar ranges (+0.8 to +1.6‰ and +0.5 to +1.9‰, respectively). By comparison, lunar regolith materials have higher $\delta^{66}Zn$ values due to micrometeorite impacts and/or cosmic ray sputtering, and lunar pyroclastic beads are enriched in light isotopes (-3.7±0.3‰ [1,3]).

Zinc isotopic homogeneity in terrestrial and martian igneous rocks and lack of obvious isotopic fractionation of Zn in low- and high-Ti mare basalts (versus O or Fe [4]) suggest that igneous processes do not fractionated Zn isotopes significantly. Values of $\delta^{66}Zn$ were probably not inherited from the proto-Earth (for Earth) or Theia (for the Moon) because chondrite meteorites have lower $\delta^{66}Zn$ (<0.8‰) than mare basalts [5]. Instead, enrichments in heavy Zn isotopes for mare basalts are likely a consequence of degassing either following giant impact, or during basaltic eruption. Alternatively, Zn isotopic fractionation during giant impact, followed by stochastic late accretion [6,7] led to the Zn isotopic compositions seen in terrestrial, martian and lunar igneous rocks.

[1] Herzog (2009) *GCA* **73**, 5884. [2] Moynier (2009) *EPSL* **277**, 482. [3] Moynier (2006) *GCA* **70**, 6103. [4] Liu (2010) *GCA* **74**, 6249, [5] Luck (2005) *GCA* **69**, 535. [6] Bottke (2010) *Science* **330**, 1527. [7] Albarede (2009) Nature **461**, 1227.

https://doi.org/10.1180/S0026461X00006502 Published online by Cambridge University Press

Sediment response to persistently low oxygen levels in bottom waters: The Lower St. Lawrence Estuary

A. MUCCI,[1]* S. LEFORT[1] AND B. SUNDBY[1,2]

[1]Dept. of Earth and Planetary Sciences, McGill University, Montreal, Quebec Canada H3A 2A7 (*correspondence: alfonso.mucci@mcgill.ca)

[2]Institut des sciences de la mer de Rimouski, Rimouski, Quebec, Canada

Reports of hypoxia (O_2 concentrations < 62.5 μmol L^{-1}) in the bottom waters of the coastal ocean, and the extent of the areas that are affected by hypoxia, have increased at an alarming rate. Most studies of hypoxic environments focused on the impacts on pelagic and benthic populations, but the impact of hypoxia on sediment chemistry is poorly documented. We compared the chemical composition of sediment and porewater in cores recovered between 1982 and 2007 at two sites in the Lower St. Lawrence Estuary (LSLE), where the bottom water has been persistently hypoxic for more than 25 years. The concentrations and the vertical distributions of total Fe and As in the cores have not changed since the 1980s, but the speciation of solid phase Fe and As have changed significantly. The proportions of reactive Fe and As components have increased while the degree of pyritization of Fe and As has decreased by 50% and 75%, respectively. In addition, the concentrations of porewater Fe and As have increased since 1982. We propose that in marine, iron-rich environments, such as the LSLE, the hypoxia interferes with pyritization, which normally would immobilize elements such as As by incorporating them into stable authigenic pyrite phases.

Fate of As upon microbial Fe(III) reduction of As-bearing biogenic Fe minerals

E.M. MUEHE*, L. SCHEER AND A. KAPPLER

Geomicrobiology, University of Tuebingen (*correspondence: eva-marie.muehe@uni-tuebingen.de)

In arsenic-contaminated groundwater and soil, aqueous arsenic enters the human food chain directly via drinking water or indirectly via plants and animals, potentially leading to devastating health effects on people. Hence, research has focused on the geochemical and biogeochemical processes leading to the mobilization (release) and immobilization (removal) of arsenic from aquifers and soil. Former studies by Hohmann *et al*. [1] demonstrated that Fe(II)-oxidizing bacteria can efficiently immobilize arsenic by forming biogenic Fe(III) hydroxides. In the presence of arsenic these microorganisms form co-precipitates of Fe(III) (hydr)oxides and arsenic and additionally arsenic is sorbed to the mineral surfaces.

However, the co-existence of Fe(II)-oxidizing with Fe(III)-reducing bacteria in the environment could result in Fe cycling by the reduction of biogenic Fe(III) (hydr)oxides. This could lead either to a dissolution of the Fe(III) minerals causing a release of the bound arsenic or alternatively to the formation of secondary Fe(II/III) mineral phases [2] and an immobilization of arsenic.

In this study, we followed the reduction of biogenic arsenic-bearing Fe(III) minerals by the Fe(III)-reducer *Shewanella oneidensis* MR-1. We then compared the As (im-)mobilization during the reduction of these biogenic Fe(III) hydroxides to the As (im-)mobilization from chemically-synthesized Fe(III) minerals including the poorly-crystalline mineral ferrihydrite and the highly crystalline mineral goethite.

The resulting iron minerals were identified and characterized by X-ray diffraction, Mössbauer spectroscopy and electron microscopy. First results show that arsenic is only partially remobilized during microbial reduction of biogenic Fe-As-co-precipitates and that the remaining arsenic is bound either to the non-reduced goethite or to the newly formed Fe (II) carbonate and phosphate mineral phases.

[1] Hohmann *et al*. (2010) *ES&T* **44**, 94-101. [2] Tufano and Fendorf (2008) *ES&T* **42**, 4777-4783.

https://doi.org/10.1180/S0026461X00006502 Published online by Cambridge University Press

Measuring the elastic properties under simulated Earth's mantle conditions

H.J. MUELLER[1]*, J. LAUTERJUNG[1], F.R. SCHILLING[2], C. LATHE[1] AND M. WEHBER[2]

[1]GFZ German Research Centre for Geosciences, Telegraphenbergm D-14473, Potsdam, Germany (*correspondence: hjmuel@gfz-potsdam.de)
[2]KIT Karlsruher Institute of Technology – Universität Karlsruhe, Engler-Bunte-Ring 14, D-76131, Karlsruhe, Germany (frank.schilling@kit.edu)

The Earth's mantle is only accessible by indirect methods, above all seismological studies. The interpretation of seismic data from the Earth's deep interior requires measurements of the physical properties of Earth materials under experimental simulated mantle conditions. In principle there are 2 common ways of simulating these *in situ* conditions by high pressure techniques - diamond anvil cells (DAC), large volume presses (LVP). The latters are more limited in pressure, but provide sample volumes 3 to 7 orders of magnitude bigger. They also offer small and even adjustable temperature gradients over the whole sample. Ultrasonic interferometry allows the highly precise travel time measurement at a sample enclosed in a LVP under *in situ* conditions. The data transfer function technique (DTF) even makes transient measurements possible. From geophysical point of view the up to 6 orders of magnitude lower frequency range as used for optical techniques in DAC and the option of using complex samples, i.e. polycrystalline, polyphase mineral assemblages, make the results much more representative for comparison with field data. Simultaneous structural and deformation measurements require the installation at a 3rd generation synchrotron light source. We present recent techniques and results of elastic properties measurements performed at different large volume presses.

Using Ambient Pressure X-ray Photoelectron Spectroscopy to investigate the reduction of c(2x2)-O/Ni(100) by hydrogen

KATHRIN MÜLLER[1], ANDERY SHAVORSKIY[2], HENDRIK BLUHM[2] AND DAVID STARR[1]*

[1]Center for Functional Nanomaterials, Brookhaven National Laboratory, Upton, NY 11973, USA (*correspondence: dstarr@bnl.gov)
[2]Chemical Sciences Division, Lawrence Berkeley National Laboratory, Berkeley, CA 94720, USA

X-ray Photoelectron Spectroscopy (XPS) is a powerful tool for the chemical analysis of surfaces. Typically XPS measurments are performed under ultra-high vacuum conditions, which are far removed from many environmental or technologically relevant conditions. The development of synchrotron based Ambient Pressure XPS (AP-XPS) that incorporates a differentially pumped electrostatic lens system into the electron energy analyzer has made possible XPS measurments at pressure up to about 5 Torr. In this presentation, after a brief introduction to the AP-XPS technique, results using AP-XPS to investigate the reduction of a chemisorbed oxygen layer on Ni (100) by hydrogen will be discussed.

Among transition metal oxides, NiO has been the focus of extensive fundamental studies due to its applications in catalysis and potential magnetic devices. The reduction of NiO has been studied at elevated pressure conditions using a broad range of techniques including X-ray Diffraction [1], and Near Edge X-ray Absorbtion Spectroscopy [2] among others. Relatively unexplored is the reduction of chemisorbed oxygen on the surfaces of Ni single crystals at elevated pressures.

We have investigated the reduction of the c (2x2)-O chemisorbed layer on Ni (100) using AP-XPS at temperatures from 100 °C to 150 °C and pressures up to 0.5 Torr. The presence of small NiO clusters, located at step edges as shown by scanning tunneling microscopy, have a significant impact on the reduction kinetics of the c (2x2)-O layer. These clusters are preferntially reduced compared to the c (2x2)-O layer and increase the reduction rate of the c (2x2)-O layer, quite likely from spill-over of dissociated hydrogen from the NiO islands.

[1] J. A. Rodriguez, J. C. Hanson, A. I. Frenkel, J. Y. Kim, M. Perez (2002) *JACS* **124**, 346–354. [2] J. G. Chen, D. A. Fischer, J. H. Hardenbergh, R. B. Hall (1992) *Surf. Sci.* **279**, 13–22.

https://doi.org/10.1180/S0026461X00006502 Published online by Cambridge University Press

Monazite dating of base-metal mineralization, Earaheedy Basin, Western Australia

J.R. MUHLING[1]*, I.R. FLETCHER[2] AND B. RASMUSSEN[2]

[1]CMCA, Univ. Western Australia, Crawley, 6009, Australia (*correspondence: janet.muhling@uwa.edu.au)
[2]Dept Applied Geology, Curtin Univ., Bentley, 6102, Australia (I.Fletcher@curtin.edu.au, B.Rasmussen@curtin.edu.au)

The Paleoproterozoic Earaheedy Basin occupies the eastern end of the Capricorn Orogen that separates the Archean Pilbara and Yilgarn Cratons. The maximum depositional age of the Yelma Formation at the base of the Earaheedy Group is less than ~2.0 Ga from detrital zircon dating [1], while the minimum age is very poorly constrained. Sandstones of the Yelma Formation overlie granitic rocks of the Yilgarn Craton in the Earaheedy Basin, and outliers that extend up to 100 km south of the basin overlie Yilgarn Craton rocks or metasedimentary rocks of the Yerrida Group. The Yelma Formation was deposited on a broad shallow shelf over an extensive area of the northern margin of the Yilgarn Craton. Within the basin, carbonates of the Sweetwaters Well Member of the Yelma Formation host minor Pb-Zn sulphide mineralization of Mississippi Valley type [2]. Secondary Pb mineralization, interpreted to have resulted from weathering and remobilization of sulphide mineralization [3, 4], is being mined in ouliers of Yelma Formation at Magellan and Cano.

$^{207}Pb/^{206}Pb$ dating of authigenic monazite in sandstones of the Yelma Formation within the Earaheedy Basin gave an age of 1.81 Ga, which is interpreted to be the age of metamorphic or hydrothermal fluid flow, and may be related to the MVT mineralization. This age provides a firm minimum for deposition of the formation. At Cano, monazite is intergrown with iron oxides, interpreted to have replaced pyrite, in Pb-bearing greywacke. $^{207}Pb/^{206}Pb$ dating gave a similar, though imprecise, age, with many analyses recording high levels of common Pb. A Pb/Pb isochron age derived from outgrowths of xenotime on detrital zircon gave the same age, within error, and Pb isotope compositions support consanguinity with the MVT mineralization.

REE phosphates are very sensitive to the passage of metamorphic and hydrothermal fluids, often recording multiple fluid events. In the Earaheedy Basin, they constrain the depositional age of the Yelma Formation to ~2.0-1.81 Ga, and the timing of base metal mineralization to ~1.81 Ga.

[1] Halilovic *et al*. (2004) *Precambr. Res*. **128**, 343–366. [2] Teen (1996) BSc (Hons) thesis, U. Tas, 128 pp. [3] McQuitty & Pascoe (1998) *Aust. Inst. Min. Metall. Mon*. **22**, 293–296. [4] Pirajno (2004) *Precambr. Res*. **128**, 411–439.

Volatiles in the mantle: Impact on intraplate magmatism

SAMUEL B. MUKASA[1]*, CHRIS STEFANO[2], MARIA MARCANO[2], THOMAS HUDGINS[2], MARY PETERSON[3] AND NOBU SHIMIZU[4]

[1]Department of Earth Sciences, University of New Hampshire, Durham, NH 03824 (*correspondence: sam.mukasa@unh.edu)
[2]Department of Geological Sciences, University of Michigan, Ann Arbor, MI 48109
[3]Department of Geological Sciences, Brown University, Providence, RI 02912
[4]Woods Hole Oceanographic Institution, Woods Hole, MA 02543

Concentrations of the volatiles H_2O, CO_2, S, Cl, and F and elemental compositions of primary magmas and their sources can be estimated through the study of olivine-hosted melt inclusions in volcanic rocks, thereby providing insights about melting processes in the mantle. These volatiles play a major role in both the formation and evolution of mantle melts, and yet their impact on intraplate volcanism on the continents and in the ocean basins may be grossly underestimated. We have determined the major-oxide, trace-element and volatile (H_2O, CO_2, S, Cl, and F) concentrations of olivine-hosted melt inclusions from the Columbia River Plateau (CRP)-Snake River Plain (SRP) large igneous province, West Antarctic Rift System, and Iceland, all three areas with intraplate volcanism hypothesized to be related to plume activity.

Most of the samples we have analyzed record minimum H_2O concentrations of 1 wt% or higher, exceeding the largest values obtained for subaerial eruptions in Hawaii of 0.8 wt%. The most H_2O-rich lava in the SRP has 3.3 wt%, and in the Columbia River Basalts (CRB) values reach 4.2 wt% H_2O. Concentrations in Icelandic and West Antarctic Rift melt inclusions reach values of 3.0 and 2.2 wt% H_2O, respectively. Water and CO_2 are correlated and follow magmatic degassing curves. Furthermore, the highest volatile concentrations are always found in the more primitive melt inclusions, based on major oxide and trace element abundances, indicating that the volatiles are of mantle origin, not artefacts of differentiation in the crust. The trace element and volatile variability, high concentrations of water, and recent studies of Os isotopes in these tectonic settings provide compelling evidence that the volatiles and chemical heterogeneity of the magma sources may be caused by the recycling of ancient oceanic crust.

https://doi.org/10.1180/S0026461X00006502 Published online by Cambridge University Press

I-Pu-Xe in OIBs and the early separation of the plume source from the MORB source mantle

SUJOY MUKHOPADHYAY

Dept. of Earth and Planetary Sciences, Harvard University, Cambridge, MA 02138, USA (sujoy@eps.harvard.edu)

The noble gases provide unique insights into mantle structure and the origin of the different mantle reservoirs. In particular, the noble gases are thought to provide one of the strongest evidence for regions of the deep mantle to have largely escaped melt extraction. However, the interpretation of the noble gas data remains a matter of active debate. For example, OIBs have lower $^{40}Ar/^{36}Ar$ and $^{129}Xe/^{130}Xe$ ratios than MORBs. This observation has been variously interpreted to reflect the sampling of a relatively undegassed mantle reservoir or preferential sampling of recycled plates with seawater derived atmospheric Ar and Xe. These two interpretations have very different implications for mantle differentiation, and the creation and destruction of mantle heterogeneities. Here I will present new He, Ne, Ar, and Xe data from Iceland that will allow the above interpretations to be critically evaluated.

The relative abundances of ^{4}He, ^{21}Ne, and Ar in the Iceland sample are in the same proportion as the mantle production rates for these isotopes. As a result, the sample preserves an elementally unfractionated pattern that allows the abundance pattern of the priomordial noble gases in the plume source to be reconstructed. Strong linear relationships are observed between isotope ratios and elemental ratios (e.g. $^{40}Ar/^{36}Ar$-$^{3}He/^{36}Ar$, $^{129}Xe/^{130}Xe$-$^{3}He/^{130}Xe$) that reflect mixing between mantle-derived noble gases and shallow-level atmospheric contamination. Importantly, while the gas-rich 'popping rock' from the N. Atlantic ridge and the Iceland sample share a common shallow-level atmospheric contaminant, they trend towards very different mantle $^{40}Ar/^{36}Ar$ and $^{129}Xe/^{130}Xe$ ratios. Additionally, the Iceland sample has a large proportion of Pu-derived to U-derived fission xenon. Hence, for the first time, the Iceland data provides unequivocal evidence that the differences in Ar and Xe isotopic compositions between MORBs and OIBs cannot be generated solely through preferential re-circulation of atmospheric noble gases into the OIB source. The differences reflect a lower degree of outgassing of the plume source. Further, because ^{129}Xe is produced from extinct ^{129}I, the result demonstrates that chemical differences between OIBs and MORBs must have been established within the first 100 Myrs of Earth history and subsequent mantle convection has not wiped out the differences established in the early Earth.

Architecture of submicron organo-mineral domains in soil aggregates – Evaluation by NanoSIMS

C.W. MÜLLER, C. HÖSCHEN AND I. KÖGEL-KNABNER

Lehrstuhl für Bodenkunde, Technische Universität München, 85350 Freising-Weihenstephan, Germany (*correspondence: carsten.mueller@wzw.tum.de)

During soil aggregation primary soil particles such as clay and silt, iron and aluminium (hydro)oxides and particulate organic matter are bound together to complex aggregates. The spatial mixture of mineral and organic components results in diverse interfaces controlling soil organic matter stabilization but also sorption processes. Until nowadays it was hard to analyse the spatial distribution of mineral and organic domains within intact soil aggregates together with its turnover.

The nano-scale secondary ion mass spectrometry (NanoSIMS) enables us to analyse biogeochemical processes and properties of inner aggregate spheres at a submicron scale. NanoSIMS allows the simultaneous analysis of up to seven ion species with high sensitivity and lateral resolution. With Cs^{+} as primary ions, negatively charged ions, like e.g. $^{12}C^{-}$, $^{13}C^{-}$, $^{12}C^{14}N^{-}$, $^{12}C^{15}N^{-}$, $^{27}Al^{16}O^{-}$ and $^{28}Si^{-}$, are collected with a lateral resolution down to 50 nm. Using O^{-} as primary ion, positively charged ions like e.g. $^{24}Mg^{+}$, $^{40}Ca^{+}$ and $^{56}Fe^{+}$, are collected with a lateral resolution down to 150 nm.

For the present study we used soil material of topsoils from an agricultural cropland and a forest. Both soils were derived from labelling experiments using litter enriched in ^{15}N (mustard litter on cropland soil, beech litter on forest soil). The air dried soil aggregates were embedded in an epoxy-resin, cut and polished in order to obtain a smooth inner aggregate surface. A cascade from reflectance light microscopy, scanning electron microscopy to NanoSIMS was used to evaluate architecture, elemental composition and ^{15}N location within intact soil aggregates.

A spatial mixing of mineral compounds into plant residues with still visible cell structures was shown within aggregates. We can demonstrate that the incorporated ^{15}N-labelled organic matter is not distributed homogeneously, but resides at specific micron-scale spots within soil aggregates. The packing of mineral and organic domains in soil aggregates showed distinctively alternating spatial patterns. The NanoSIMS technique therefore allows the combined *in situ* evaluation of specific aggregate structures and their possible functions in terms of organic matter sorption and turnover.

https://doi.org/10.1180/S0026461X00006502 Published online by Cambridge University Press

Comparative study of the U(VI) complexation onto γ-Al_2O_3 by ATR FT-IR and EXAFS spectroscopy

KATHARINA MÜLLER*, HARALD FOERSTENDORF, ANDRÉ ROSSBERG, KAROLINE STOLZE AND KATHARINA GÜCKEL

Helmholtz-Zentrum Dresden-Rossendorf, Institute of Radiochemistry, Dresden, Germany (*correspondence: k.mueller@hzdr.de)

Aluminates, representing an essential component of clay minerals, play a decisive role in regulating the mobility of contaminants in rock and soil formations, in particular due to their tendency to form coatings on mineral surfaces [1].

In this work, U(VI) sorption on γ-Al_2O_3 is comparatively investigated using *in situ* vibrational and X-ray absorption spectroscopy. The focus was set to micromolar U(VI) concentrations and a variety of environmentally relevant sorption parameters in order to resolve discrepancies reported earlier [2-4].

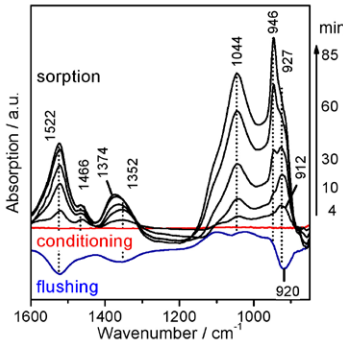

Figure 1: TR ATR FT-IR spectra of U(VI) soprtion on γ-Al_2O_3.

Time-resolved (TR)IR spectroscopic sorption experiments at the alumina-water interface evidence the formation of three different species as a function of surface loading (c. f. Figure 1): a monomeric carbonate complex, an oligomeric surface complex and a surface precipitate. These results are confirmed by IR experiments performed at different flow rates, pH values, ionic strengths, U(VI) concentrations, and in inert gas atmosphere. Results of EXAFS experiments of batch samples are consistent to these findings.

[1] Guillaumont, R. (1994) *Radiochimica Acta* 66–7, 231–242. [2] Catalano, J. G. *et al*. (2005) *Geochim. Cosmochim. Acta* **69**, 3555–3572. [3] Moskaleva, L.V. *et al*. (2006) *Langmuir* **22**, 2141–2145. [4] Sylwester, E. R. *et al*. (2000) *Geochim. Cosmochim. Acta* **64**, 2431–2438.

The role of comets as possible contributors of water and prebiotic organics to terrestrial planets

M.J. MUMMA* AND S.B. CHARNLEY

NASA-Goddard Space Flight Center, Solar System Exploration Division, Greenbelt, MD, 20771, USA (*correspondence: michael.j.mumma@nasa.gov)

The question of exogenous delivery of organics and water to Earth and other young planets is of critical importance for understanding the origin of Earth's water, and for assessing the prospects for existence of Earth-like exo-planets. Viewed from a cosmic perspective, Earth is a dry planet yet its oceans are enriched in deuterium by a large factor relative to nebular hydrogen. Can comets have delivered Earth's water? The deuterium content of comets is key to assessing their role as contributors of water to Earth.

Icy bodies today reside in two distinct reservoirs, the Oort Cloud and the Kuiper Disk (divided into the classical disk, the scattered disk, and the detached or extended disk populations). Orbital parameters can indicate the cosmic storage reservoir for a given comet. Knowledge of the diversity of comets within a reservoir assists in assessing their possible contribution to early Earth, but requires quantitative knowledge of their components – dust and ice. Strong gradients in temperature and chemistry in the proto-planetary disk, coupled with dynamical dispersion of an outer disk of icy planetesimals, imply that comets from KD and OC reservoirs should have diverse composition.

The primary volatiles (native to the nucleus) provide the preferred metric for building a taxonomy for comets, and the number of comets so quantified is growing rapidly. Taxonomies based on native species (primary volatiles) are now beginning to emerge [1, 2, 3]. The measurement of cosmic parameters such as the nuclear spin temperatures for H_2O, NH_3, and CH_4, and of enrichment factors for isotopologues (D/H in water and hydrogen cyanide, $^{14}N/^{15}N$ in CN and hydrogen cyanide) provide additional tests of the origin of cometary material. I will provide an overview of these aspects, and implications for the origin of Earth's water and prebiotic organics

[1] Mumma & Charnley (2011) *Ann. Rev. Astron. Astrophys.* in press. [2] DiSanti & Mumma (2008) *Sp. Sci. Rev.* **138**, 127. [3] Crovisier *et al*. (2009) *Earth, Moon, Planets* **105**, 267.

https://doi.org/10.1180/S0026461X00006502 Published online by Cambridge University Press

Change in lead sorption during transformation of monohydrocalcite to aragonite

T. MUNEMOTO AND T. MURAKAMI

Department of Earth and Planetary Science, the University of Tokyo, Tokyo 113-0033, Japan
(*correspondence: munemoto@eps.s.u-tokyo.ac.jp)

Monohydrocalcite ($CaCO_3 \cdot H_2O$) (MHC) is a metastable calcium carbonate found in the sediments of mordern saline and alkaline lakes. MHC transforms to anhydrous calcium carbonates such as calcite and aragonite [1]. The sorption behavior of aqueous metal ions to calcite, the most stable calcium carbonate, is well known [2], but little to metastable calcium carbonates. We conducted uptake experiments of lead ion on monohydrocalcite to examine change in sorption behavior of lead ion during transformation of monohydrocalcite to aragonite.

Solutions of Na_2CO_3, $NaHCO_3$, $NaNO_3$, NaOH, HNO_3, and 1μM of Pb^{2+} (I = 0.13) were adjusted to pH 8.50, 9.00, and 9.50 by changing the concentrations; the concentration of CO_3^{2-} was kept constant for any solutions. Then, 2g/L of synthesized monohydrocalcite was added to the solutions at 25 °C, and the concentrations of lead and some other cations were measured at the end of each batch experiment. The run duration was up to 15 hours.

Aragonite increased in amount gradually with time while monohydrocalcite decreased with time; the growth rates of aragonite were almost the same between the three different pH conditions. Monohydrocalcite was almost completely replaced by aragonite for 15 hours. The distribution coefficient, $k_d=(Pb)_{sold}/(Pb)_{solution}$ (L/g), generally decreased with time; the difference in pH did not show a significant difference in k_d. The k_d values were almost the same between the three different pH conditions after the 15 hour experiments. And the final uptake of Pb^{2+} was nearly 90% for all the three different-pH experiments. The k_d values during the transformation were higher than those of calcite and aragonite [2]. Our results suggest that the k_d value decreases with increase in aragonite, i.e. during the transformation of monohydrocalcite to aragonite.

[1] Munemoto & Fukushi (2008) *JMPS* **103**, 345–349. [2] Rouff, *et al*. (2005) *J. Colloid Interface Sci*. **286**, 61–67.

Indistinguishable Hf/W in the silicate Earth and the silicate Moon

CARSTEN MÜNKER[1,2], STEPHAN KÖNIG[1,2] AND TONI SCHULZ[1,2,3]

[1]Institut für Geologie und Mineralogie, Universität zu Köln
[2]Steinmann Institut, Universität Bonn
[3]Institut für Geologie, Universität Wien

The W isotope composition and the Hf/W ratio of the silicate Earth and the silicate Moon can help to unravel the relative chronology of the Moon-forming giant impact event and core formation on Earth. It has been established by now that the silicate Earth and the Moon are indistinguishable in terms of their W isotope signature [1]. Yet, it has long been assumed that the Hf/W ratio of the silicate Moon (26.5 [1])is higher than that estimated for the silicate Earth (18.7) [2]. Based on these two values and the similar W isotope composition, a maximum age of the Moon-forming giant impact has been estimated to ca. 60 Ma after solar system formation [1]. Here we evaluate new Hf/W estimates of the silicate Earth and the silicate Moon.

The Hf/W ratio of the silicate Earth has traditionally been estimated assuming near constant W/Th or W/U and chondritic Hf/U or Hf/Th ratios [2, 3]. Our recently published mass balance estimate for W in the silicate Earth challenges this view, as W has been shown to be highly mobile in subduction systems. This leads to substantial W/Th and W/U fractionations in arc lavas/OIBs. An improved mass balance estimate for the silicate Earth, based on Ta/W systematics in major silicate reservoirs has yielded a Hf/W of 25.8 [4].

For the Moon, a re-evaluation of existing W-Th-U-Ta data together with new high precision data yields a Hf/W of 24.9 for the silicate Moon [5], similar within error to previous estimates. Notably, the lunar value is indistinguishable from the revised Hf/W for the silicate Earth.

Together with the identical ^{182}W compositions of the silicate Earth and the silicate Moon [1], the similar Hf/W ratios now strongly imply that the Moon forming giant impact might have triggered an efficient metal-silicate re-equilibration on Earth. It is therefore likely, that radiogenic ingrowth of excess ^{182}W in the Earth's mantle relative to chondrites largely occurred after the giant impact and is to a lesser extent an inherited feature from early formed planetesimals. Morover, the model age for single stage core formation on Earth may in fact be close in time to the age of the Moon forming giant impact.

[1] Touboul M. *et al*. 2007 *Nature* **450**. [2] Newsom H.E. *et al*. 1996 *GCA* **60**. [3] Arevalo R. & McDonough W.F. 2008 *EPSL* **272**. [4] König *et al*. 2011 *GCA* **75**. [5] Münker 2010 *GCA* **74**.

https://doi.org/10.1180/S0026461X00006502 Published online by Cambridge University Press

Dynamical properties of $CaIrO_3$ under high pressure from *ab initio* calculations

A. MUÑOZ AND P. RODRÍGUEZ-HERNÁNDEZ

MALTA Consolider Team, Departamento de Física Fundamental II, and Instituto Universitario de Materiales y Nanotecnologia, Universidad de La Laguna, 38205La Laguna, Tenerife, Spain (amunoz@marengo.dfis.ull.es)

$CaIrO_3$ crystallizes in the orthorhombic Cmcm at normal conditions. This compound is attracting important interest as a low-pressure isostructural analog of the predicted postperovskite high pressure phase of $MgSiO_3$. Here we perform an ab initio density functional calculations of the structural and dynamical properties under hydrostatic pressure for the Cmcm and the Pbnm phase of of $CaIrO_3$.

Our studies have been performed in the framework of DFT with echange correlation taken in generalized gradient approximation (GGA) with the PBEsol prescription. We use the pseudopotential method with ultrasoft PAW pseudopotentials with an energy cutoff of 520 eV. Such a large cutoff was required to achieve highly converged results within the projector augmented wave (PAW) scheme. The PAW method takes into account the full nodal character of all the electron charge density distribution in the core region. We use a dense grid of k-special points for integrations along the Brillouin zone (BZ) in order to assure highly converged results.

Lattice dynamics calculations of phonon modes were performed at the zone centre (Γ point) of the BZ. The calculations provided information about the frequency, symmetry and polarization vector of the vibrational modes in each structure. We use direct force-constant approach (or supercell method). Diagonalization of the dynamical matrix provides both the frequencies of the normal modes and their polarization vectors. It allows us to identify the irreducible representations and the character of phonon modes at the Γ point. We will report the Raman and IR actives modes, the pressure derivarives, the phonon dispersion, the phonon density of states and the projected DOS.

Vertical distribution of iodine in pore water collected from Japan Sea sediments: Origin of iodine-rich fluid associated with methane hydrate

Y. MURAMATSU[1], H. ANZAI[1], H. TOMARU[2], R. MATSUMOTO[2] AND H. MATSUZAKI[3]

[1]Dept. of Chemistry, Gakushuin University, Toshima, Tokyo, 171-8588, Japan: (yasuyuki.muramatsu@gakushuin.ac.jp)
[2]Dept. of Earth and Planetary Sciences, University of Tokyo, Bunkyo, Tokyo, 113-0032, Japan
[3]Dept. of Nuclear Engineering and Management, University of Tokyo, Bunkyo, Tokyo, 113-0032, Japan

In our previous studies, we have analyzed iodine in many geochemical samples systematically and found that nearly 70% of iodine in the Earth's crust is estimated to exist in marine sediments (Muramatsu and Wedepohl 1998). We also studied occurrences of iodine rich brine associated with methane seepage in different areas surrounding Japan (Muramatsu *et al*. 2001, 2007).

In this study we have analyzed halogens and some other elements in pore water samples collected from Japan Sea sediments of methane hydrate areas. Sediment cores were recovered from the Umitaka Spur and the Joetsu Knoll region, eastern margin of the Japan Sea, during the cruises of Umitaka-Maru in 2009 and R/V Marion Dufresne in 2010 (MD179). The depth of the sediments collected were down to about 40m below sea floor. Concentrations of iodine, bromine and some other elements were analyzed by ICP-MS and those of chloride and sulfate were by ion-chromatography.

Analytical results showed that iodine concentration in pore water increased markedly with depth. The slope of the increase was rather constant. The highest concentration found in the Umitaka Spur was 0.4 mM (about 50ppm) which is nearly 1000 times higher than the seawater concentration. No marked increases of iodine were found in the samples collected from control areas without methane seepage.

We also determined $^{129}I/^{127}I$ ratios by AMS in pore water samples at defferent depth. As a result, the $^{129}I/^{127}I$ ratios tended to be lower in the deeper layers. The lowest ratio was about 0.13×10^{-12}, which was older than 50 Ma. This age is before the opening event of Japan Sea. Considering the age of iodine obtained and the depth profile of the iodine concentrations, iodine and possibly methane are originated from deeper layers and transported with aqueous fluids into the surface layers.

This study was supported by MH21 Research Consortium Japan

https://doi.org/10.1180/S0026461X00006502 Published online by Cambridge University Press

Sr, Nd, Hf and Pb isotope characterisation of basalts from IODP Site U1346, Shirshov Massif the youngest edifice of the Shatsky Rise, northwest Pacific

DAVID MURPHY[1]*, JÖRG GELDMACHER[2] AND IRINA ROMANOVA[3]

[1]Discipline of Biogeosciences, Queensland University of Technology, Brisbane, Qld. 4001, Australia (*correspondence: david.murphy@qut.edu.au)
[2]USIO- IODP, Texas A&M University, College Station, TX 77845-9547, USA
[3]Discipline of Biogeosciences, Queensland University of Technology, Brisbane, Qld. 4001, Australia

The Shatsky Rise is a large volcanic plateau in the northwest Pacific that formed between 140–150 Ma on the Pacific oceanic crust [1, 2]. Magnetic lineations indicate that the plateau formed along the trace of a triple junction of oceanic spreading ridges [1]. Shirshov Massif is the northern most of the large seamounts within Shatsky Rise. It is a subcircular edifice, ~100 km in diameter. The Shirshov Massif represents a waning phase in the evolution of the Shatsky Rise, intermediate between the main phase of plateau formation at the Tamu Massif to the southeast and the much lower levels of magmatism represented by the younger Papanin Ridge to the northeast. In the parlance of the plume head hypothesis, Shirshov Massif is in the transition between plume head and tail.

During IODP Expedition 324 Hole U1346A, situated on the northern flank of the Shirshov massif, was drilled, penetrating thin sediment cover and into igneous basement. Two volcanic units were recognised, a 1.6m volcanic debris flow and a 50.1m thick succession of pillow lavas (and/or inflation units) that represent a single volcanic event [3].

Here we present Sr, Nd, Hf and Pb isotope data from the basaltic basement samples. We compare the isotope data to previous analyses from the Shatsky Rise [2], to other oceanic plateaus and to estimated mantle end member compositions in order to assess the nature of the mantle material that melted to form the final stage of plateau volcanism at Shatsky Rise.

[1] Nakanishi, *et al*. (1999) *Journal of Geophysical Research Solid Earth* **104**, 7539–7556. [2] Mahoney, *et al*. (2005) *Geology* **33**, 185–188. [3] Expedition 324 Scientists (2010) Site U1346. *In* Sager, W.W. Sano, T. Geldmacher, J. & the Expedition 324 Scientists, *Proc. IODP,* **324**, Tokyo (IODP-MI) doi, 10.2204/iodp.proc.324.103.2010

U-Series disequilibrium in groundwater as a vector for U mineralisation

MELISSA J. MURPHY[1]*, ANTHONY DOSSETO[2], SIMON P. TURNER[1] AND BRUCE F. SCHAEFER[1]

[1]GEMOC, Department of Earth and Planetary Sciences, Macquarie University, Australia (*correspondence: melissa.murphy@mq.edu.au)
[2]GeoQuEST Research Centre, School of Earth and Environmental Sciences, University of Wollongong, Australia

Groundwaters often exhibit ($^{234}U/^{238}U$) activity ratios greater than one as a result of fractionation between ^{234}U and ^{238}U nuclides during rock/water interactions. However, when groundwaters pass through high-grade uranium mineralisation, congruent dissolution of uranium minerals should impart a ($^{234}U/^{238}U$) activity ratio which is at or very close to secular equilibrium.

This research characterises the uranium-series (U-series) disequilibria in groundwater surrounding a high-grade uranium deposit, and investigates the use of disequilibria in groundwater as a proxy for uranium exploration. U-Series isotopes have been analysed by isotope dilution MC-ICP-MS in groundwater samples along the groundwater flow path, within and surrounding the South Australian Four Mile and Pepegoona sediment-hosted uranium mineralised systems.

Samples collected down-gradient of the Four Mile mineralisation have ($^{234}U/^{238}U$) activity ratios ranging from 1.12 proximal to mineralisation, up to 2.08 approximately 10 kms down-gradient from mineralisation. U concentrations range from 0.5 – 200 ppb, with highest concentrations found in samples collected in mineralisation. Groundwaters sampled within the high-grade mineralisation show ($^{234}U/^{238}U$) activity ratios close to unity (1.05), which is consistent with the congruent dissolution of uranium minerals.

The observation of increasing disequilibrium with distance from mineralisation highlights the potential application of U-series isotopes as an indicator of high-grade uranium deposits.

However, the extent and distribution of disequilibrium at the Pepegoona deposit is not entirely consistant with proximity to the mineralisation. Groundwaters samples within mineralisation exhibit much higher ($^{234}U/^{238}U$) activity ratios than at Four Mile, averaging 1.41. Samples collected down-gradient have typically lower U concentrations and ($^{234}U/^{238}U$) activity ratios approaching unity. This signature reflects the highly variable local geology of the Pepegoona deposit.

https://doi.org/10.1180/S0026461X00006502 Published online by Cambridge University Press

Global warming and climate change: Impact on India

K.S. MURTY

101/28 Hindustan colony, Amaravati Rd., Nagpur 440033, India (murtysk1931@yahoo. co. in)

Global warming is here to stay and climate change will be intense. The warming could range from 1.8 dgrees to 4 degrees C. , which could lead to water scarcity and droughts as well as higher rainfall and floods. The impact will also affect biodiversity, forests and agriculture. India has seen stupendous growth in the agricultural sector and has become from once-food-importing to food-exportring country, after adopting new technologies and agriculture and its allied industries contribute to nearly 19 per cent of the total Gross Domestic Product (GDP). More than 60 per cent of the work force is dependent on this sector. Nearly two-thirds of the cropped areas in the region is rain-fed. Apart from this, the northern rivers derive much of their waters from the Himalayan glaciers. It has been reported that there has been accelerated rate of melting of these glaciers. Still higher rate of melting could affect fresh water supply sources in the Ganga-Brahnmaputra basin which could directly affect the biodiversity, livelihood of people in that region and lead to dramatc consequences of the country's economy. Hydropower generation could be drastically reduced, leading to an energy crisis. The country has a coastline of 6,000 km around which about 400 million people live. Any rise in the sea level, say by a meter, can lead to welfare loss of $1.859 million in India. As it is, tropical cyclones in the Bay of Bengal cause havoc in the coastal areas and any rise in sea level could mean a loss of 15 per cent of land area by 2020. Biospheres like the Sunderbans can be lost for ever and other mangrove forests may meet the same fate. Forests play a crucial role in the social, economic and cultural spheres of India. Many river systems originate in the forests and anchor rich biodiversity. Some 200,000 villages are located inside or on the fringes of forests and some 200 million people depend on forests for their livelihood. The Indian subcontinent is projected to experience a warming of 2 to 6 degrees by the end of the current century with consequences of reduced or increased rainfall, threat to biodiversity and in general to the rate of growth of its economy. Urgent steps are needed to face these threats and the Government of India is grappling with this problem.

Direct aerosol effect from multimodel simulations in AeroCom

G. MYHRE

Center for International Climate and Environmental Research – Oslo (CICERO), Norway, (gunnar.myhre@cicero.uio.no)

There has been a substantially development of the global aerosol models over the last decade. Despite this development and advanced aerosol observations uncertainties in the direct aerosol effect is substantial. AeroCom is a global aerosol model intercomparison exercise [1, 2] and Phase II simulations have recently been performed. Here we present results from several global aerosol models with simulations of the direct aerosol effect based on aerosol emissions for present and pre-industrial conditions. The solar radiative forcing (RF) of the total direct aerosol effect range between -0.6 and -0.05 Wm^{-2}. All models in the study include anthropogenic changes in sulphate, black carbon (BC) from fossil fuel, organic carbon (OC) from fossil fuel, and biomass burning aerosols (BC and OC). Some of the models also include anthropogenic changes in secondary organic aerosols and nitrate in the model simulations. The spread in the RF is large for the carbonaceous aerosols, with RF for BC from fossil fuel ranging from 0.14 to 0.37 Wm^{-2}. The few models performing RF of secondary organic carbon and nitrate shows even larger relative range in the RF.

We analyze the results with respect to burden, aerosol optical depth, and extinction coefficients to explore the causes for the differences. Further, vertical profile differences which are particularly important for BC is quantified in terms of RF.

[1] Schulz, M. Textor, C. Kinne, S. Balkanski, Y. Bauer, S. *et al*. (2006) *Atmos. Chem. Phys*. 5225–5246. [2] Textor, C. Schulz, M. Guibert, S. Kinne, S. Balkanski, Y. *et al*. (2006) *Atmos. Chem. Phys*. **6**, 1777–1813.

https://doi.org/10.1180/S0026461X00006502 Published online by Cambridge University Press

X-ray analysis of reactive C-, N-, P-, and S-functional groups in NOM

S.C.B. MYNENI

Department of Geosciences, Princeton University, Princeton, NJ 08544, USA

NOM plays an important role in many biogeochemical processes, and the conentration and chemistry of functional groups of NOM dictate their role in different processes. Traditional laboratory techniques, such as NMR and IR, have been used for decades to examine the functional group composition of isolated NOM. In the last decade, synchrotron based X-ray absorption spectroscopy (XAS) and spectromicroscopy methods allowed the examination of functional groups of NOM in their pristine state in soils and sediments at nanometer resolution. A discussion of XAS of reactive functional groups in NOM and their cycling in terrestrial systems will be presented.

Using XAS, we examined isolated NOM from different environments, and NOM in selected soils without any isolation. The XAS of several simple molecules containing different C-, N-, P-, and S-groups were also examined, and their spectra helped in interpreting the electronic states of different functional groups of NOM. X-ray spectra were also collected in different ways (using electron and fluorescence yield, and transmission) to identify the best detection schemes.

While several functional groups are identified using XAS, the ability to detect different C-moieties with X-rays is not as good as NMR. However, XAS contributes new information on the aromatic-N, amides, and nitrosyls. The detection of P groups using XAS is at par with that of NMR. However, small variations in the XAS of P can be used to detect the bonding environments of phosphate or phosphonate groups. The S-XAS spectra of NOM provide unique information on both the reduced and oxidized functional groups of S.

The electronic transitions, probed using XAS, are highly sensitive to small changes in the local coordination environments of functional groups, and the X-ray spectra change with changes in the protonation state, metal complexation (type of metal, and the number of metals), and symmetry of functional groups. The X-ray spectra are also sensitive to sample thickness and the concentration of the reactive groups, which can influence the relative concentration estimates. Ignoring these variations can result in the incorrect identification of the functional groups.

Geochemical monitoring of reactive percolation experiments using carbon stable isotopes

A. MYRTTINEN[1]*, E. JEANDEL[2], O. UKELIS[2], ALAIN DIMIER[2], V. BECKER[1], R. VAN GELDERN[1] AND J.A.C. BARTH[1]

[1]GeoZentrum Nordbayern, Friedrich-Alexander Universität Erlangen-Nürnberg, 91056 Erlangen, Germany (*correspondence: myrttinen@geol.uni-erlangen.de)

[2]European Institute for Energy Research, D-76131 Karlsruhe, Germany

Reservoir petrophysical property changes (permeability/porosity) are crucial issues, which need to be considered in carbon capture and storage (CCS) and enhanced oil and gas recovery (EOR and EGR). The potential hydrodynamic and geochemical reactions during such initiatives need to be well understood for planning, as well as for monitoring purposes. CO_2-rock-brine interactions are often analysed using geochemical parameters such as ion concentration changes. Stable isotope measurements of carbon ($\delta^{13}C$)are currently used as a method to montor and quantify geochemical changes during CO_2-injection. The applicability of using these isotopes as an additional and new monitoring tool to verify permeabiliy changes in the host rock has been tested in a series of laboratory experiments with a new reactive percolation bench, ICARE 4. Reservoirs, considered suitable for CO_2 injection, often host carbonate phases in contact with brine. Carbonate dissolution, plays a major role in host rock permeability changes during CO_2 injection. In order to test the geochemical effects of such a scenario, supercritical CO_2 was injected into brine in contact with quarzitic limestone. Results indicate good correlations between permeability, $\delta^{13}C$, DIC and calcium concentration data. Once CO_2-breakthrough occurred, permeability increased from a minimum of 0.1 millidarcy (mD) to a maximum of ~ 1.4 mD. This was accompanied by a $\delta^{13}C_{DIC}$ increase from ~ -5 ‰ to 0 ‰; DIC concentration increase from 0 mg L^{-1} to 3000 mg L^{-1} and a calcium concentration increase from below 100 mg L^{-1} to ~ 1400 mg L^{-}. These first data imply that $\delta^{13}C$ is a valid monitoring parameter for observing critical geochemical changes indicating CO_2 rock-brine interaction, which may be used to verify permeability development during CO_2 injection.

https://doi.org/10.1180/S0026461X00006502 Published online by Cambridge University Press

P^{5+} and Ti^{4+} solution mechanisms of and partitioning between fluids and melts at crustal and upper mantle pressure and temperature

BJORN O. MYSEN

Geohysical Laboratory, Carnegie Instn. Washington, 5251 Broad Branch Rd., NW, USA (bmysen@ciw.edu)

Solution mechanisms of P- and Ti-bearing, H_2O-saturated silicate melts, silicate-saturated aqueous fluids, and silicate-rich single phase (supercritical) liquids have been characterized *in situ* to 900°C/2.2 GPa with vibrational spectroscopy as structural tool. Partitioning of P- and Ti species between fluid and melt was also determined. Starting materials were aluminum-free $Na_2O•4SiO_2$ (NS4) and with 10 mol % Al_2O_3 (NA10) substituting for SiO_2, with 10 mol % TiO_2 or 5 mol % P_2O_5. The structure of Ti-bearing aqueous fluids in equilibrium with rutile was also characterized.

Aluminosilicate species of Q^o, Q^1, Q^2, and Q^3 type exist in coexisting fluid and melt in both Ti- and P-bearing systems. In melts, the abundance of the most depolymerized silicate species, Q^o, is positively correlated with temperature and pressure, whereas that of the most polymerized species, Q^3, decreases with temperature and pressure. In the silicate solute in aqueous fluids, Q^3 (and Q^1 and Q^2) abundance increases with temperature and pressure. The phosphate species in melts and fluids are of PO_4, P_2O_7, and Q^nP type. In the Ti-bearing silicate systems, isolated TiO_4 tetrahedra in melts and fluids probably share oxygen with neighboring silicate tetrahedra. The Ti in aqueous fluids in TiO_2 (rutile)-H_2O comprises polyhedra with greater oxygen coordination numbers.

The fluid/melt partition coefficients for P_2O_7 and Q^nP species are in the 0.15-0.7 range. The PO_4 fluid/melt partition coefficients are <0.2. These partition coefficients increase with increasing temperature and pressure. There is no clear influence of Al_2O_3. The fluid/melt partition coefficient of Ti in the equivalent Ti-bearing systems increases from ~0.1 to ~0.5 in the 200°-500°C and 0.4-1 GPa temperature and pressure range with greater values in Al-bearing systems. The Ti concentration in aqueous fluids coexisting with rutile in the same pressure and temperature range is ≤10% of that in the silicate systems.

The P-bearing complexes in fluids and melts are associated with Na^+ in the silicate systems, whereas Ti^{4+} in silicate systems may form more complex complexes that involve both Na^+ and Al^{3+}. Formation of such complexes can enhance Ti and P solubility in aqueous fluids can enhance their solubility by at least and order of magnitude compared with silicate-saturated systems.

In situ, high-pressure/-temperature experimental determination of structure-property relations in silicate melt-COHN systems

BJORN O. MYSEN

Geohysical Laboratory, Carnegie Instn. Washington, 5251 Broad Branch Rd., NW, USA (bmysen@ciw.edu)

Voletiles in the COHN system, when dissolved in silicate melts, affect their transport and thermodynamic properties. Quantitative characterization of solution mechanisms, central to characterization of melt properties, has been carried out while melts and coexisting COHN fluids were at the desired pressure and temperature.

In aluminosilicate melt-H_2O, the ΔH of the water speciation equilibrium, $H_2O°(melt) + O(melt) \leftrightharpoons 2OH(melt)$, is ~30 kJ/mol with ΔH positively correlated with Al/(Al+Si) of the melt. This speciation equilibrium coupled with an appropriate silicate speciation equilibrium becomes, Q^n (M) + $H_2O \leftrightharpoons Q^{n-1}$ (H), where (M) and (H) denotes metal cation and protons associated with nonbridging oxygen. The ΔH for the reaction is ~6±2 kJ/mol with a slight positive correlation with Al/(Al+Si).

In melt-COH and melt-NOH systems, f_{O2} is an additional variable affecting solubility and solution mechanisms. From haplobasalt to haploandesite melt-COH, the carbon solubility at upper mantle pressures and temperatures decreases from ~2 wt% to ~1 wt% in equilibrium with CO_2 gas, whereas under reducing conditions, decrease is from about 0.3 to about 0.15 wt% in equilibrium with NH_4+H_2 gas. Oxidized carbon is dissolved dominantly as CO_3 groups, whereas reduced carbon in the COH system is dissolved as a mixture of CH_3 groups and CH_4 molecules. In compositionally analogous NOH-saturated melts, under oxidizing conditions, nitrogen solubity is insensitive to melt composition, whereas in reduced melts, the solubility decreases from ~1 wt% to ~0.3 wt% in equilibrium with NH_3 gas in the composition range from haploandesite to haplobasalt. The solubility increases rapidly with decreasing f_{O2}. Oxidized N is dossolved as N_2 molecules, whereas reduced nitrogen is dissolved as NH_2 groups and NH_3.

By changing f_{O2} from oxidized to reduced, resultant changes of C and N solution mechanisms in melt-COHN systems cause NBO/T changes, which affect transport properties. For example, melt viscosity under oxidizing and conditions is, $\eta=4.4+0.75[0.35-(X_{CO2}/50)]^{-4.1}$, whereas under reducing conditions it is, $\eta=4.4+0.75[0.35+(X_{CH4}/30.3)]^{-4.1}$. This illustrates how redox conditions alone can change melt properties relevant to magmatic processes in the Earth's interior.

https://doi.org/10.1180/S0026461X00006502 Published online by Cambridge University Press

Lithium isotope fractionation at the soil–plant interface

O. MYŠKA[1], T. MAGNA[1,2], M. NOVÁK[1], J. ŠIKL[1], V.ZOULKOVÁ[1] AND F. OULEHLE[1]

[1]Czech Geological Survey, Prague, Czech Republic
[2]Universität Münster, Germany

Lithium abundances and isotope compositions were determined for an extensively studied site in the Krušné hory Mts. in order to search for previously unknown stable isotope fractionations of non-nutrient trace elements between soils and vegetation cover (Picea *sp*., Fagus *sp*.). In the soil profile, Li contents decrease from ~60 ppm at 40–80 cm depth to 20 ppm at 0–10 cm depth und to 6 ppm in the uppermost organic layer (Oi+Oe) whereas sup-ppm Li levels were consistently found in roots, stem and needles. Stems have the lowest Li contents of all analyzed tree compartments. The Li contents show tight positive linear correlation with Mg both in soils and trees but less defined correlation with other alkali elements (Na, K). Soil, developed on granitoid bedrock, appears to reflect its magmatic precursor with only limited modification through weathering or fluid circulation. Roots of both Picea *sp*. and Fagus *sp*. show no significant difference relative to δ^7Li of underlying soils despite different rooting depth (shallow for Picea, deep for Fagus). In contrast, stem wood of both species consistently shows significant enrichments in ^{7}Li relative to roots and soils (cf. [1]); in particular, δ^7Li difference of >16‰ has been found for Picea stem and roots. It thus appears that stem may fractionate Li isotopes significantly, irrespective of botanic classification or taxonomy of the corresponding species (gymnospermous, angiospermous) but the extent of this fractionation may depend on qualitative characteristics of the wood, such as proportion of xylem and phloem, structural bonding of celulose etc. In either case, the data require more complex examination of interaction between plants and substrate with respect to different rooting depths, chemistry, bottom water flow, nutrient availability etc.

Overall, the results are best explained by low utilization of Li in biological matter despite modest bioavailability of Li from grown substrate. Whether or not net ^{7}Li enrichments in plants are a general feature remains unconstrained but it could be consistent with positive Li–Mg correlation in plants and high δ^{26}Mg in wheat that has been found to result from preferential uptake of heavy Mg from the nutrient supply into plants [2].

[1] Lemarchand *et al*. (2010) *GCA* **74**, 4612–4628. [2] Black *et al*. (2008) *Env. Sci. Tech*. **42**, 7831–7836.

https://doi.org/10.1180/S0026461X00006502 Published online by Cambridge University Press

Tracing the source of IRD in the Heinrich Layers of the North Atlantic

B. DAVID A. NAAFS[1,2]*, JENS HEFTER[1], SHUNXIN ZHANG[3] AND RUEDIGER STEIN[1]

[1]Alfred Wegener Institute for Polar and Marine Research, (*correspondence: david.naafs@awi.de) D-27568 Bremerhaven, Germany
[2]Leibniz Center for Earth Surface and Climate Studies, Potsdam University, D-14476 Potsdam, Germany
[3]Nunavut Geosciences Office, NU X0A 0H0 Iqaluit, Canada

Heinrich Events (HEs) are among the most dramatic examples of millennial-scale climate variability. During HEs large amounts of ice-rafted debris (IRD) derived from glacial erosion of continental bedrock accumulated in the sediment of the North Atlantic, forming Heinrich Layers (HLs) [1]. One of the key issues in understanding the still poorly understood mechanisms behind HEs is the development of specific provenance indicators that provide information about the source areas of the IRD [2]. Here we present an organic geochemical study on the type, distribution and relative abundance of biomarker compounds of extractable organic matter from the different HLs of the last glacial at multiple locations in the North Atlantic.

The results demonstrate that an unique assemblage of organic 'petrogenic' compounds such as (benzo)hopanes, mono- and triaromatic steroids, and palaerenieratene and isorenieratene-derivatives characterize the HLs in the North Atlantic. The presence of aromatic counterparts and dominance of mature isomers in the hopanoids and steroids indicates that the biomarker distribution within HLs is incompatible with recent sediments [3]. Rather, these compounds derive from the transportation of ancient organic matter by icebergs because of glacial erosion of bedrock in the Hudson Bay Area. Comparison of the biomarker assemblage of HLs with available geologic and organic-geochemical data allowed narrowing down the assumed source of IRD to a sequence of Upper Ordovician oil shales and limestones outcropping in and close to the Hudson Strait, which have a strikingly similar biomarker signature to that of HLs. Monitoring the presence of these petrogenic compounds in marine sediments thus allows to distinguish organic matter in HLs from adjacent samples and can be used as specific organic-geochemical tracers for the input of continental material from the Hudson Bay Area in northern Canada.

[1] Heinrich (1988). *Quaternary Research* **29**, 142.
[2] Hemming (2004). *Review of Geophysics* **42**, RG1005.
[3] Rashid & Grosjean (2006) *Paleoceanography* **21**, PA3014

The nature of fluid flow through vertical formations in the aureole of the EJB pluton, White Mountains, California

P.I. NABELEK[1]* AND S.S. MORGAN[2]

[1]Dept. of Geological Sciences, Univ. of Missouri, Columbia, MO 65211, USA (nabelekp@missouri.edu)
[2]Dept. of Geology and Meteorology, Central Michigan University, Mt. Pleasant, MI 48859, USA (morga1ss@cmich.edu)

Petrology and stable isotope compositions of metamorphic rocks in the aureole of the Eureka Valley-Joshua Flat-Beer Creek (EJB) composite pluton, White Mountains, eastern California, were examined to determine nature of fluid flow in the aureole. The White Mountains were an arc terrain in the Jurassic and Cretaceous periods. The metamorphosed sedimentary rocks in the aureole are distinguished by having vertical orientations due to rotation and stretching resulting from forceful emplacement of magma. The sedimentary formations include Cambrian marbles, calc-silicates, schists, and quartzites. Each lithology behaved differently during contact metamorphism. Clean dolomite and calcite marbles did not equilibrate with an external fluid as revealed by unshifted $\delta^{18}O$ and $\delta^{13}C$ values of 20 to 25‰ and –1 to +2‰, respectively. Largest isotopic shifts occurred in calc-silicates where $\delta^{18}O$ decreased to ~15‰. The moderate $\delta^{18}O$ shift suggests that the calc-silicates equilibrated with an aqueous fluid whose oxygen isotope ratio was buffered by surrounding silicate metamorphic rocks. Infiltration of calc-silicates in the inner aureole by an aqueous fluid is also demonstrated by the presence of grossular garnet and vesuvianite.

Variation in mineralogy of schists reflects the variation in the Al/K ratio. Schists with higher ratios have andalusite whereas schists with lower ratios have K-feldspar. On the western side of the pluton, partial melting of inner aureole schists was driven by focused flow of aqueous fluids between the pluton and marbles. *P-T* pseudosections for the schists suggest that partial melting has occurred between 2.5 and 3 kbar and >660°C, and they predict a narrow subsolidus cordierite field. However, cordierite, feldspars, and other silicate minerals were altered by late pervasive fluid flow through the schists below 500°C. This fluid flow was probably driven by slow cooling of the large EJB pluton and/or continued magmatism in the arc terrain.

Overall, the data from the EJB aureole point to highly localized heterogenous flow in vertical calc-silicates and marbles, and pervasive and protracted flow through schists.

https://doi.org/10.1180/S0026461X00006502 Published online by Cambridge University Press

Kinetics of condensastion and cosmochemical fractionation of the planet forming materials in the early solar nebula

H. NAGAHARA* AND K. OZAWA

Dept. Earth Planet. Sci., The Univ. Tokyo, Hongo, Tokyo 113-0033, Japan
(*correspondence: hiroko@eps.s.u-tokyo.ac.jp)

Chemical Fractionation

Condensation is the first step of planet formation. The isotopic homogeneity except for oxygen of the planetary and meteoritic materials indicates that the early solar nebula was once totally evaporated and the precursor materials of the planets were subsequently condensed. Homogeneity of heterogeneity of the precursor materials of the planets is controlled by the competition between cooling time scale of the nebula, time scale of condensation, and time scale of transportation of the condensed phases.

Kinetic Condensation Experiments

We have carried out condensation experiments for Mg-silicates and metallic iron, which are the two most important solids for terrestrial planets, and obtained condensation coefficients (probability of condensation against number of collided molecules). The experimental results also showed unexpectedly wetted relationship between silicates and metallic iron, which further indicates heterogeneous condensation of planet forming materials.

Model and Results

We have developed kinetic condensation model and calculated the development of condensed phases as a function of gas cooling time scale, which includes physical separation of the dusts. The model contains two free parameters, the critical size for gas/dust separation and gas cooling time scale. The results show the relationship between the gas cooling time scale and the critical size for dust separation in order to generate chemical (Mg/Si/Fe) condensation. If the dust separation size was 1micron, the cooling time scale of the gas was 1-10^2 years, whereas the separation size was 1mm, the gas cooling time scale was 10^3-10^6 years. Thus, the precursor of the planets could have been fractionated depending on the viscosity of the disc, which predicts planets with diverse compositions in exoplanetary systems.

Molybdenum isotope fractionation in pelagic euxinia: Evidence from the modern Black and Baltic Seas

T.F. NÄGLER[1]*, N. NEUBERT[2], M.E. BÖTTCHER[3], O. DELLWIG[3] AND B. SCHNETGER[4]

[1]Institute für Geologie, Universität Bern, Switzerland (*correspondence: naegler@geo.unibe.ch)
[2]Institut für Mineralogie, Leibniz Universität Hannover, Germany
[3]Marine Geology Section, Leibniz Institute for Baltic Sea Research, Warnemünde, Germany
[4]Institute for Chemistry and Biology of the Marine Environment, University of Oldenburg, Germany

We present a model to explain isotope data of vertical profiles of dissolved molybdenum (Mo) of the Black Sea and the Baltic Sea. The entire water column of the Black Sea, as well as the anoxic waters of the euxinic deeps of the Baltic Sea show δ^{98}Mo values (up to 2.9 ‰) significantly above the homogeneous, open ocean waters (2.3 ‰). Further all water samples are enriched in the heavy isotope compared to published data of sedimentary Mo from the same range of water depths. The observed isotope fractionation between sediments and the anoxic water column of the Black Sea can be reconciled by a model involving published ab initio calculations of Mo isotope fractionation and thermodynamic thiomolybdate distributions parameters in dependence of H_2S_{aq}. The observed pattern can readily be explained as decreasing importance of mono-, di-, or tri- thiomolybdate scavenging with increasing H_2S_{aq}. The model results further imply that Mo isotopic composition of the water column is in equilibrium with that of the sediments. The effective equilibrium fractionation factor at any given depth depends on the relative abundances of the different thiomolybdates, and thus H_2S_{aq} abundance. An extrapolation to a theoretical pure MoS_4^{2-} solution indicates a fractionation constant between MoS_4^{2-} and authigenic solid Mo of 0.5 ± 0.3‰. Results from the Baltic Sea are in principle agreement with themodel, but are slightly offset. The latter is probably related to the occasional large scale inflow events which lead to temporary disequilibrium distribution of thiomolybdate species, due to the slow reaction kinetics of the $MoOS_3^{2-}$ to MoS_4^{2-} transition. δ^{98}Mo values of the upper oxic waters of both basins are higher than predicted by mixing models based on salinity. The results can be explained by non-conservative behaviour of Mo under suboxic to anoxic conditions in the shallow bottom parts of the basin, most pronounced on the NW shelf of the Black Sea.

https://doi.org/10.1180/S0026461X00006502 Published online by Cambridge University Press

Isotope study of Neoproterozoic to Lower Palaeozoic successions of the southern Kalahari craton

THANUSHA NAIDOO[1]*, UDO ZIMMERMANN[1], J.T. MIYAZAKI[2] AND J. VERVOORT[3]

[1]Institutt for petroleumsteknologi, Universitetet i Stavanger, Norway (*correspondence: thanusha.naidoo@uis.no)
[2]Institute For Research on Earth Evolution, JAMSTEC Natsushimacho, Yokosuka, Japan (tmiyazaki@jamstec.go.jp)
[3]School of Earth and Environmental Sciences, Washington State University, Pullman, USA (vervoort@wsu.edu)

The southern area of the Kalahari Craton is characterized by isolated Neoproterozoic to Lower Palaeozoic basins containing mostly immature psammites and pelites, and few carbonates. Outcropping conglomerates were falsely interpreted as glacial deposits in the wake of the snowball earth hypothesis, as none of the sedimentary rocks of the basins contain any characteristics of a glacial event or associated cap carbonates. Age constraints for the rocks are weak. Pb-Pb isotopes on carbonates point to an Ediacaran age but might reflect a metamorphic age. Sr and C isotope values do not always reflect primary seawater composition since clastic input and other environmental factors have hampered the results. Microfossil analyses show a low-species assemblage typical for the Early Ediacaran and alternatively the Uppermost Ediacaran, and global biostratigraphic markers are absent. Trace element geochemistry proposes, for some of the rocks, the influence of a mafic source mixed with felsic sediments, but high Ti, Nb and Ta concentration exclude a direct arc source. Detrital zircon analysis revealed the occurrence of Ediacaran zircons, in addition to Mesoproterozoic zircons as major source rock ages. Pb and Nd isotopes are comparable to those from the basement of Patagonia and the Arequipa-West Pampeanas Terrane. Nd model ages vary between 1.3 and 1.8 Ga, which is unexpected for the Kalahari Craton. This similarity to Patagonia suggests that, during the formation of Rodinia, the southern margin of the Kalahari Craton faced Patagonia or even shared the same basement. If so, then Patagonia possibly drifted slightly off the Kalahari craton during the Lower Palaeozoic and finally, into its modern position during the Late Palaeozoic.

Sorption of uranyl and arsenate on SiO_2, Al_2O_3, TiO_2 and FeOOH

SREEJESH NAIR* AND BRODER J MERKEL

Department of Hydrogeology, Technische Universität Bergakademie Freiberg,Gustav-Zeuner Str.12, 09599 Freiberg, Germany (*correspondence: sreejeshmc@gmail.com)

Migration of uranium or arsenic in aquatic environments is often controlled by sorption on minerals present along the water flow path. One of the major controlling factors of sorption is the aqueous speciation of these elements. Hence it is important to know the major species in order to predict the sorption behaviour in the environment. The formation of uranium-phosphate complexes was investigated rather well, but thermodynamic data are still contradictory. On contrary, less information is available about the formation of uranium-arsenate complexes. To investigate the sorption behaviour, batch experiments were conducted for uranium (0.5 μM/l), arsenic (0.5 μM/l) and uranium-arsenic (0.5:0.5 μM/l) together with SiO_2, Al_2O_3, TiO_2 and FeOOH at a pH ranging from 3 to 9. Sorption of U (VI) and As (V) on SiO_2 is almost similar in solutions containing either U (VI) or As (V) separately, or both together. Similar sorption behavior was observed for FeOOH too. In the presence of equimolar U (VI) and As (V) together, a considerable retardation of U (VI) sorption and an enhancement of As (V) sorption on Al_2O_3 was observed for a wide range of pH (Fig. 1). While Al_2O_3 was replaced with TiO_2, an increase in sorption was observed for both uranium and arsenic. This change in sorption retardation/enhancement can be explained by the formation of uranylarsenate complexes or competitive sorption between uranyl and arsenate species.

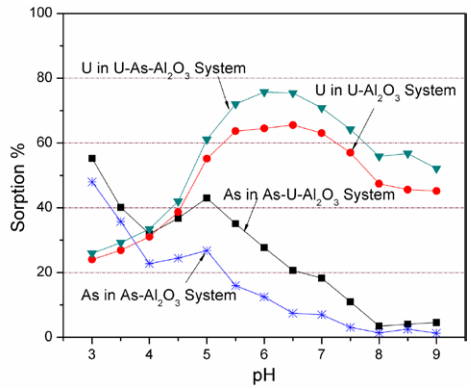

Figure 1: Sorption of U(VI) and As(V) on Al_2O_3 as a function of pH. Either U(VI) or As(V) separately, or both together. (0.5 μM/l U & As, 23ºC, pCO_2 10-3.5 hPa).

https://doi.org/10.1180/S0026461X00006502 Published online by Cambridge University Press

Rare Earth Elements in crude oil

R. NAKADA[1]*, Y. TAKAHASHI[1], G. ZHENG[2], S. KATO[3] AND A. WASEDA[4]

[1]Dept. of Earth and Planetary Systems Science, Hiroshima Univ., Hiroshima 739-8626, Japan (*correspondence: ryo-nakada@hiroshima-u.ac.jp)
[2]Institute of Geology and Geophysics, CAS, 382 West Donggang Road, Lanzhou 730000, China
[3]JGI, Inc., Tokyo 112-0012, Japan
[4]Japan Petroleum Exploration Co., Ltd (JAPEX) Research Center

Patterns of the entire range of rare earth element (REE) in crude oils and coexisting water, collected from mud volcanoes in Xinjiang Province of China, are recently reported [1]. Crude oils show light REE enriched patterns with flat or depleted patterns in heavy REE, when normalized to chondrite. Surprisingly, the REE concentrations in crude oils are larger than those in coexisting water by a factor of more than one hundred. Considering the hydrophobicity of oil and the high ionic characteristics of REE, it is strongly suggested that REE forms complexes with ligands present in the crude oils. Based on the ^{13}C NMR spectroscopy, it was found that small amounts of phenol and carboxyl groups are contained in the crude oil samples, which could possibly provide complexing sites for REE.

On the other hand, the REE concentrations in crude oils collected from Sagara and Nagaoka-Higashiyama oil fields, Japan which have much lesser amounts of carboxyl and phenol groups compared with those in Xinjiang. This fact suggests that REE is released from carboxyl and phenol groups during maturation of crude oil. The important key reaction can be the kerogen decarboxylation. By this reaction, carboxyl groups are decomposed into carbon dioxide gas. Since REE cannot form complexes with gas, it can be released from organic phase during maturation from kerogen to crude oil.

[1] Nakada *et al*. (2010) *Geochem. J*. **44**, 411–418.

Electron transport across a black smoker chimney

R. NAKAMURA[1]*, T. TAKASHIMA[1], S. KATO[1], K. TAKAI[2], M. YAMAMOTO[2] ANDK. HASHIMOTO[1]

[1]Dep. Applied Chemistry, The University of Tokyo, Tokyo, 113-8656, Japan (*correspondence: nakamura@light.t.u-tokyo.ac.jp)
[2]SUGAR Project, Japan Agency for Marine-earth Science and Technology, Yokosuka, 273-0061, Japan

At deep-sea hydrothermal vent systems, sulfide-rich emissions generate a columnar black-smoker chimney structure, which serves as an ideal habitat for physiologically and phylogenetically diverse extremophiles in the present and ancient deep ocean. Here we report the data that suggest a new form of efficient and robust energy transfer from such hot, sulfur-rich hydrothermal fluids to cold, oxygenated seawater via electrical current generation. Black smoker sulfide chimney was found to display a significant electrical conduction potential owing to the densely interconnected structure of micron and submicron crystalline particles of chalcopyrite and pyrite. The current–voltage characteristics, combined with electrocatalysis measurements, clarified that their metal-like conduction generates an electron transport conduit longer than 10 cm across the chimney wall and converts the spatially discrete redox potential to electrical current. These findings suggest that not only the emitted reductive compounds, but also the high-energy electrons delivered from the inner hydrothermal fluid conduit via conductive sulfide networks, supports primary production at the deep-sea hydrothermal vent systems (Figure 1).

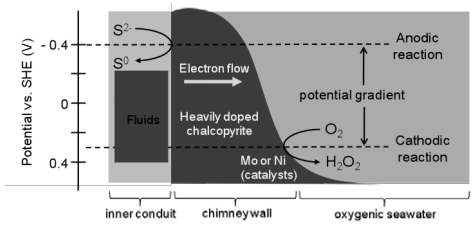

Figure 1: An energy diagram for the anodic and cathodic reactions occurring at the inner and outer surfaces, respectively, of the chimney.

[1] Nakamura et al. (2010) *Angew. Chem. Int. Ed*. **49**, 7692-7694.

https://doi.org/10.1180/S0026461X00006502 Published online by Cambridge University Press

$Cr(OH)_3(s)$ oxidation coupled with heterogeneous Mn(II) oxidation

SEONYI NAMGUNG AND GIEHYEON LEE*

Department of Earth System Sciences, Yonsei University, Seoul, Korea (hysy0514@yonsei.ac.kr)
(*correspondence: ghlee@yonsei.ac.kr)

Soil and groundwater contamination by Cr(VI) of natural origin has been reported over the world. Cr is 21st most abundant element in the earth's crust and commonly exists in the oxidation state of +III as a trace constituent of various aluminosilicate minerals. Under natural conditions, Cr(III) oxidaiton by dissolved oxygen or Mn oxides is thermodynamically feasible. Previous studies showed that Cr(VI) could be effectively oxidized by various Mn oxides under acidic conditions, but the oxidation became ineffective under neutral or higher pH conditions. This inhibition of Cr(III) oxidation was attributed to the precipitation of $Cr(OH)_3(s)$ on the surface of Mn oxides, which blocks the reactive surface sites. Moreover, the oxidation of Cr(III) by dissolved oxygen is known to be kinetically sluggish and favorable only at high pH conditions. The geochemical processes causing the natural contamination of Cr(VI) have not been unveiled yet. This study examined whether $Cr(OH)_3(s)$, which is the most common and stable solid phase of Cr(III) in the environment, could be oxidized indirectly by the product of Mn (II) oxidation. Although dissolved oxygen does not readily oxidize Cr(III), it effectively oxidizes Mn(II) heterogeneously under moderately alkaline pH conditions.

The suspensions were prepared with 1 g/L $Cr(OH)_3(s)$ and/or 50 μM Mn (II) in 50 mM $NaNO_3$ at pH 7 – 9 in the presence or absence of dissolved oxygen. The solution pH was maintained with 10 or 50 mM buffers (MOPS for pH 7 and 8; CHES for pH 9). Under anaerobic conditions, Cr(VI) was not detected at all pHs regardless of the presence of Mn(II). Under aerobic conditions, Cr(VI) was released from $Cr(OH)_3(s)$ oxidation both in the presence and absence of Mn (II) at pH ≥ 8. The amounts of Cr(VI), however, were substantially higher in the presence than absence of Mn(II) and increased with increasing pH. These results indicate that the rate and extent of $Cr(OH)_3(s)$ oxidation would likely be controlled by those of heterogneous Mn(II) oxidation.

Interaction between metamorphism and deformation in eclogite facies shear zones, Lofoten, Norway

P. NASIPURI*, H. STUNITZ, E.J. K. RAVNA, L. MENEGON AND K. KULLERUD

Department of Geology, University of Tromso, Norway
(*correspondence: pritam.nasipuri@uit.no)

Eclogite facies shear zones in lower crustal rocks are argued to have formed by infiltrating fluids during eclogitization [1]. Weakening of the rocks is pronounced during shear zone formation [1]. Our study on eclogites from Lofoten [2], Norway deals with shear zones developed due to near isothermal decompression and subsequent symplectite formation. Mineral abbreviations are after Kretz [3]. Metamorphic Opx and Grt_I corona (M_1) at Ol – Pl interface characterize the undeformed eclogite. Alternate bands of mixture of Pl–amphibole (Amph) and Grt_I (M_1) – Opx – Omp (M_{2A}) characterize the shear zone (D_1). Recrystallized Opx grains and Cpx - Pl symplectite (M_{2B}) mantle Opx (D_{1A}) and Omp porphyroblasts respectively. Grt_{II} (M_3) occurs along the contact of deformed Opx and Pl. Amph (M_4) overgrows the finer grained pyroxene.

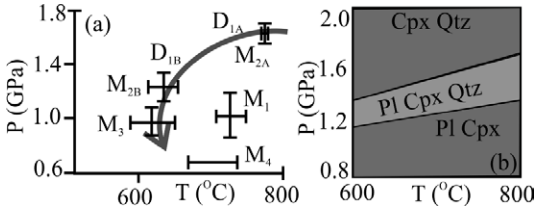

Figure 1: (a) PT estimate [GTB, 4] of different metamorphic stages. $Fe^{total} = Fe^{2+}$ is assumed for Omp. Shear zone PT path is also shown. (b) PT pseudosection [5] of reintegrated composition of Omp shows that exhumation is essential to generate fine-grained reaction products.

We suggest near isothermal decompression for the shear zone development in eclogite. The deformation of Opx and Omp commenced in the Omp stability field. Oriented inclusions of feldspar in Grt_{II} (M_3) indicate that shear zone developed before the Grt_{II} growth. This study reveals that fine-grained anhydrous reaction products can accommodate large amount of strains due to a decrease in grain size and a switch to diffusion creep deformation.

[1] Austrheim (1987) *EPSL* **81**, 221–232. [2] Krogh (1977) *Nature* **267**, 17–19. [3] Kretz (1983) *Am. Min.* **68**, 277–279. [4] http://ees2.geo.rpi.edu/spear/spear.html [5] Connolly (2005) *EPSL* **236**, 524–541.

https://doi.org/10.1180/S0026461X00006502 Published online by Cambridge University Press

Petrogenesis of Oligo-Miocene granitoid intrusive in west Natanz, central part of Uroma-Dokhtar magmatic belt, NE Isfahan, Iran

ALI KHAN NASR ESFAHANI [1]* AND BEHAFARIN SHOJAEI[2]

[1]Islamic Azad University, Khorasgan Branch, Geology department, Isfahan, Iran.
(*correspondence: nasr@khuisf.ac.ir)
[2]Islamic Azad University, Khorasgan Branch, Petrology department, Isfahan, Iran.

Oigo-Miocene granitoid intrusive is located in west Natanz city, NE Isfahan and is a central part of Uromia-Dokhtar magmatic assemblage in Iran. This plutonic rock is the result of extensive magmatism which occurred during and after the Alpine Orogeny. The Plutonic composition is Granodiorite to Tonalite. The main minerals consist of quartz, plagioclase, alkali-feldspar. It contains a number of dioritic enclaves of different sizes. This granitiod is similar to those of the subalkaline, calc-alkaline series, metaluminous, and displays typical features of magnesian I-type granites. The chondrite normalized REE patterns are characterized by moderate to high LREE enrichment and unfractionated HREE. This granitoid magma involves partial melting of crustal protoliths and mantle-derived basaltic magmas emplaced into the lower crust. The Natanz granitoid stock has mineralogical field and geochemical characteristics typical of volcanic arc granites related to an active continental margin. Probably, Oigo-Miocene granitoid is the result of the subduction of Neo-Tethyan oceanic plate below the Lut microcontinent and this oceanic residual plate during Mesozoic to Cenozoeic time.

The isotopic composition of carbon and oxygen in calcite of veinlets and host rocks within the limits of the Kokhanivka oil field (Carpathian Foredeep, Ukraine)

I. NAUMKO[1]*, V. ZAGNITKO[2] AND YU. BELETS'KA[1]

[1]Institute of Geology and Geochemistry of the Combustible Minerals of NAS of Ukraine, 3a, Naukova St., Lviv, 79060, Ukraine (igggk@mail.lviv.ua)
[2]Taras Shevchenko Kyiv National University of MESYoS of Ukraine, 90, Vasylkivska St., Kyiv, 03022, Ukraine (zagnitko@igmr.relc.com)

Conditions of postsedimentogenous mineralogenesis in sedimentary strata within the limits of the Kokhanivka oil field in Jurassic limestones (Carpathian Foredeep) [1] were specified according to data of isotopic composition of carbon and oxygen research in calcite of veinlets and host rocks.

The isotopic analysis has revealed sufficiently homogenous values both of $\delta^{13}C$, correspondingly, -3.13÷+2.16 and -0.46÷+2.56 ‰ (standard PDB), and $\delta^{18}O$ – 24.25÷25.75 and 25.11÷29.21 ‰ (standard SMOW) that are not correlated with a depth of occurrence and a spatial distribution of a veinlet etc. It is established too that carbon and oxygen from veinlet's calcite is almost always somewhat lighter (enriched by isotope ^{12}C and ^{16}O) compared with carbon and oxygen in calcite of host rocks.

The predominance of CH_4 (56.3–62.8 vol. per cent) and steam among volatile as well as high relative water-saturation (93.9–98.9 vol. per cent) of fluid inclusions and closed cavities in rosks (by data of chemical mass-spectrometry [2]) indicates the important role of carbon-water fluids relicts of which were captured by defects in minerals into processes of postsedimentary transformations of oil-saturated strata.

Migrative processes were reduced to the formation, on the one hand, of oil deposit of the Kokhanivka field, but on the other hand, veinlet-impregnated mineralization at host rocks. Healing of fractures by the mineral substance of deep-seated high-temperature fluid [3, 4] with the formation of the calcite veinlets probably occurred from the single homogenized source similarity to the Lopushna oil field (Ukrainian Carpathians) [5].

[1] *Atlas of oil & gas fields of Ukraine* (1998). [2] Naumko *et al*. (2008) Moscow, IGEM RAS, 218–220 (http://www.minsoc.ru/2008-1-113-0). [3] Naumko (2006) *Thesis for a doctor's degree*, 52 p. [4] Naumko, Svoren' (2008) *Rep. of the NAS of Ukraine* **9**, 112–114. [5] Naumko *et al*. (2011) *Rep. of the NAS of Ukraine* **2**, 100–115.

https://doi.org/10.1180/S0026461X00006502 Published online by Cambridge University Press

Changes to porosity and pore structure of mudstones resulting from reaction with CO_2 and brine

ALEXIS NAVARRE-SITCHLER[1], KATHERINE MOUZAKIS[1], JASON HEATH[2], TOM DEWERS[2], GERNOT ROTHER[3], XIUYU WANG[4], JOHN KASZUBA[4] AND JOHN MCCRAY[1]

[1]Environemntal Science and Engineering Division, Colorado School of Mines, Golden CO (asitchle@mines.edu)
[2]Sandia National Laboratory, Albuquerque NM
[3]Oak Ridge National Laboratory, Oak Ridge TN
[4]Department of Geology and Geophysics, University of Wyoming, Laramie WY

Modeling transport and reactivity of CO_2 at multiple scales is important for evaluating CO_2 sequestration or containment in geological formations. One limitation of modeling complex coupled reaction and flow processes at the pore scale is the challenge of describing the dynamic complex 3D pore structures of real rocks in a reactive environment. Stacked scanning electron microscopy (SEM) images, 3D pore reconstructions and small angle neutron scattering (SANS) provide quantitative information on pore networks at length scales inaccessible by other techniques such as x-ray computed tomography. Data from five CCS carock samples demonstrate the complex nature of the pore network.

Fractal dimensions (determined from SANS data) describing the pore network are similar for four of the five mudstones. These samples are described by a combination of mass and surface fractal dimensions. In contrast, a single mass fractal dimension describes the fifth sample. Differences in pore network geometry appear to be related to lithologic variations. Calculated volume, surface area and pore size distributions from SANS, image analysis and mercury intrusion porosimetry are in agreement.

Two of the caprock samples were reacted with CO_2 and brine at 160C and 150 bars for ~50 days to evaluate pore network changes in a reactive environment. Field-emission SEM images show a marked increase in pores at length scales ranging from 10s of nm to >1 μm. In some cases new precipitates have grown into this porespace. Dissolution features such as pitting and etching is observed on mineral grain faces. Changes in porosity and surface area are quantified with SANS, image analysis and gas adsorption techniques. SANS also provides a measure of changes to the fractal structure of the pore network at nm to 100's of nm length scales.

Sandia is a multiprogram laboratory operated by Sandia Corporation, a Lockheed Martin Company, for the U.S. DOE under contract DE-ACOC4-94AL85000.

Field scale organic management of vineyard soils controls copper distribution and bioavailability at the micro-aggregate scale

ALINE NAVEL AND JEAN M.F. MARTINS

LTHE-CNRS-Univ. Grenoble I (UMR 5564), Domaine Universitaire BP 53, 38041 Grenoble Cedex 9, France (jean.martins@hmg.inpg.fr)

In this study we evaluated the effect of organic management of a vineyard soil on the distribution of copper at the micro-aggregate scale. The model vineyard soil used in this study (Macon, Burgundy, France) experienced a field experiment over twenty years that consisted in amendments and vegetations with various materials and plants. We studied specifically the effect of straw (S) and conifer compost (CC) organic amendments and clover (Cl) and fescue (F) vegetation on the fate of copper, used as fungicide, in the surface layer of this loamy soil (non amended, NA, control soil). These five soils were collected in June 2009 and immediately physically fractionated in order to obtain 5 granulometric subfractions, supposed to represent specific habitats for soil microorganisms as well as variable copper-reactive compartments. All soil fractions were quantitatively characterized in terms of contents of solid mass, total nitrogen and organic carbon, major inorganic elements and of copper (total, Ca-exchangeable, free and bioavailable to bacteria or plants). The results showed that each soil fraction presents a specific inorganic and organic composition. Indeed, whatever the treatment, amendment or vegetation, major elements and TOC distribution are highly variable in the soil sub-fractions and between soils. All soil treatments induced TOC increases, especially in Cl and CC soils (x1.8 and x2.8, respectively). Organic carbon accumulated preferentially in the 20-2μm fraction of the 5 soils (ranging from 6.3 to 10.3 mgC g^{-1}) and also in the coarser fraction (>250μm) where freshly added carbon first accumulates. Copper microscale distribution was shown to be different among the five soils. The amended soils accumulated more Cu in the coarser fractions, especially the CC soil, probably in relation with the reactivity increase of added recalcitrant carbon. The vegetated soils, and especially the Cl soil, accumulated much more Cu in the finest and micro-aggregated (20-2μm) subfractions, probably due to the increased rhizospheric development well known to increase soil micro-aggregation. This differential Cu accumulation was also shown to modify copper bioavailability to plants and soil bacteria. Altogether our results show that the field scale organic management clearly modifies the micro-scale Cu distribution and its bioavailability to living soil organisms.

https://doi.org/10.1180/S0026461X00006502 Published online by Cambridge University Press

'Table' *vs* 'Bench': Trace elements in fibrous diamonds

O. NAVON[1]*, W.L. GRIFFIN[2] AND Y. WEISS[1]

[1]The Institute of Earth Sciences, the Hebrew University of Jerusalem, Israel
(*correspondence: oded.navon@huji.ac.il)
[2]GEMOC, Macquarie University, NSW, Australia

Fibrous diamonds encapsulate pristine metasomatic high-density fluids (HDFs) of silicic, carbonatitic and saline compositions. In general, the trace element patterns are similar in all HDFs. The REEs are fractionated and most samples show variable negative anomalies of Sr, Ti, Zr, Hf and Y relative to the corresponding REE. Larger diversity exists in the highly incompatible elements (Cs-La), where two patterns are distinguished: one is mostly flat with no significant anomalies and shows a moderate decrease of concentrations with decreasing ionic radius ('Bench'); the other ('Table') has elevated Ba, U, Th and LREE and depleted Nb, Ta, K, Rb and Cs. The two can be best distinguished by the ratios (Nb, Rb)/(La, Pr, U, Th).

The similar signature of incompatible elements in diamonds-forming fluids from various mantle localities, well separated in space and time, the persistence of 'Table' and 'Bench' patterns in HDFs of such diverse major-element compositions and the uniform carbon isotopic composition of fibrous diamonds is fascinating. We seek to explain these features, which require collection from a large source region and/or interaction of the HDFs with a relatively large volume of mantle rocks.

The Nb/(Th, U, La) ratios in HDFs with 'Bench' patterns fall within a narrow range and are similar to MORB/OIB/PM values. This smooth pattern can be approximated by very small degree of melting of a source with PM trace element concentrations. In HDFs with the more fractionated 'Table' patterns the above ratios deviate from the strict MORB/OIB/PM range and decrease by ~2 orders of magnitude with decreasing Nb content. The patterns can be closely produced by low-degree partial melting of a metasomatised continental lithosphere with carbonate, phlogopite and rutile as accessory phases.

Searching for a possible relation between the two patterns, we examined fractional crystallization and percolation. Major elements allow only <20% phlogopite removal from HDFs with 'Bench' patterns, not enough to produce the high depletion in alkalis of the 'Table' patterns. Percolation of a melt with a 'Bench' pattern through SCLM rocks with the above accessory phases does lead to evolution of a 'Table' pattern, with minimal changes to the major elements.

Contrasting sediment and water geochemistry between low and very high arsenic affected areas in Murshidabad, West Bengal, India

A. NEAL[1], K, TELFEYAN[2], J. HAUG[2], R. TAPPERO[3], T. OCHELTREE[4], K. JOHANNESSON[2] AND S. DATTA[1]

[1]Dept of Geology, Kansas State Univ, Manhattan, KS 66506
[2]Dept of Earth and Environmental Sciences, Tulane Univ, New Orleans, LA 70118
[3]NSLS, Brookhaven National Laboratory, Upton, NY 11973
[4]Dept of Biology, Kansas State Univ, Manhattan, KS 66506

Arsenic contamination of shallow groundwater is among the most severe environmental and health threats in SE Asia. Murshidabad, an eastern district in West Bengal, India, where groundwaters are highly As-affected (up to ~4000 µg/l), was chosen as our study area. Objectives were: (1) characterize sediment cores and groundwaters in areas with contrasting As concentrations; (2) describe the extent of spatial variability of dissolved As concentrations in shallow (< 60m) aquifers; (3) identify source (s) of aquifer recharge to understand the bioavailability and mobilization of As from sediments to groundwaters. Surface (0-2m) and core (2-40m) sediments and water from shallow and deep tubewells, irrigation, ponds, and major rivers were collected during two field seasons.

The low-As Pleistocene terrace sediments are orange-brown, whereas the high-As Holocene floodplain sediments are grey. Mineralogical examination reveals the Pleistocene sediments as mainly quartz and feldspars coated with Fe (III) oxides/hydroxides, whereas the Holocene sediments also contain clay minerals, micas, amphiboles, carbonates, and accessories. Sequential extractions show As present chiefly in specifically-sorbed phases and associated with amorphous and poorly-crystalline hydrous oxides of Fe (Al and Mn). Hydrochemistry shows reducing conditions in high-As waters (high Fe, HCO_3^-, PO_4^{3-}, NH_4^+, As (III):As_T; low NO_3^-, NO_2^-, Cl^-, SO_4^{2-}); low-As areas showed converse relationships with these values. The complex spatial variability of dissolved As levels may result from variable flow paths induced by well-pumping and seasonal flooding, buried As-rich lenses, distribution of microbial communities, etc. Stable isotope values for δ^2H and $\delta^{18}O$ in water samples plot on the local meteoric water line between summer monsoon and dry season precipitation, indicating the high As groundwater originates as local precipitation that has not experienced any appreciable evaporation. Furthermore, the stable isotopes demonstrate that the high As groundwaters are not recharged by local pond waters, which have undergone substantial evaporation.

https://doi.org/10.1180/S0026461X00006502 Published online by Cambridge University Press

A new Moon

CLIVE R. NEAL

Dept. of Civil Eng. & Geological Sci., University of Notre Dame, Notre Dame, IN 46556, USA (neal.1@nd.edu)

International and commercial interest in exploring the Moon has exploded over the last 5 years. Missions from China, India, Japan, and the USA have explored and are exploring our closest celestial neighbour from lunar orbit. The Google Lunar X-Prize has stimulated commercial teams to compete in landing on the Moon, demonstrating mobility and transmitting data back to Earth. Recent and current lunar missions have revolutionized our view of the Moon through high-resolution photography [1], confirmation of polar volatile deposits [2, 3], as well as diurnal cycling of OH/H_2O [4], and identification of lithologies that are not represented in the return sample collections [5, 6]. New global datasets have been/are being collected (e.g. microwave emissions, gravity, temperature, rock abundance, etc.) that still need to be fully interpreted. Interpretation of 30+ years of laser ranging data indicates the presence of a fuid core [7]. Re-examination of the Apollo seismic data with modern computing techniques suggests that the Moon contains a solid inner and liquid outer core [8]. Continued examination of returned samples have shown that the interior of the Moon may be more volatile rich than previously thought [9-12], although interpretation of Cl isotope data [13] suggests otherwise Finally, quantitative petrography presents a promising method for distinguishing impact melts from pristine basalts [14] and crystal stratigraphy studies allow insights into basalt petrogenesis heretofore unattainable [15, 16]. These new advances demonstrate that old data are still relevant, that lunar samples are 'the gift that keeps on giving, and that new lunar missions always yield exciting results. With lunar missions being launched by NASA in 2011 (GRAIL) and 2013 (LADEE), others being planned (US, Russia, India, Japan), and continued sample and data analysis, lunar research will inevitably produce new and exciting insights into solar system processes.

[1] Watters *et al*. (2010) *Science* **329**, 936–940. [2] Colaprete *et al*. (2010) *Science* **330**, 463–468. [3] Mitrofanov *et al*. (2010) *Science* **330**, 483–486. [4] Pieters *et al*. (2009) *Science* **326**, 568–572. [5] Ohtake *et al*. (2009) *Nature* **461**, 236–240. [6] Pieters *et al*. (2011) *LPSC* **42**, #2173.[7] Williams *et al*. (2006) *Adv*. *Space Res*. **37**, 67–71. [8] Weber *et al*. (2011) *Science* **331**, 309–312. [9] Saal *et al*. (2008) *Nature* **454**, 192–195. [10] McCubbin *et al*. (2010) *PNAS* **107**, 11223–11228. [11] Boyce *et al*. (2010) *Nature* **466**, 466–469. [12] Greenwood *et al*. (2011) *Nat*. *Geosci*. **4**, 79–82. [13] Sharp *et al*. (2010) *LPSC* **41**, #2424. [14] Neal *et al*. (2011) *LPSC* **42**, #2668. [15] Fagan & Neal (2011) *LPSC* **42**, #2137. [16] Hiu *et al*. (2011) *LPSC* **42**, #1461.

Hafnium isotope constraints on the origin of layered intrusions and the stabilisation of the Yilgarn cratonic lithosphere

O. NEBEL[1], R.J. ARCULUS[1], J.A. MAVROGENES[1], Y.J. NEBEL-JACOBSEN[2] AND T. IVANIC[3]

[1]Research School of Earth Sciences, ANU, Australia
[2]Centre for Sustainable Energy Systems, School of Engineering, ANU, Australia
[3]Department of Mines and Petroleum, Geological Survey of Western Australia, Australia

Primitive mantle-derived magmas forming the Archaean (~3 Ga) Windimurra layered mafic intrusion (LMI) in the Yilgarn Craton yield radiogenic $^{176}Hf/^{177}Hf$ considerably exceeding that of the age-corrected depleted MORB mantle source. This isotopic character is consistent with derivation from ultra-depleted mantle established as a primitive mantle reservoir in Hadaean/Early Archaean time. Ancient refractory mantle is believed to reside either in deep mantle or buoyantly underpin cratonic sub-continental lithospheric mantle (SCLM). We suggest either an ultra-depleted deep mantle reservoir was tapped by upwelling mantle or the SCLM of the Yilgarn Craton was partly re-melted; both scenarios require the involvement of a hot mantle plume. The refractory Hf isotope signal is complementary to the Hadaean zircon record from the North-Western Yilgarn, suggesting a co-genetic relationship. Unlike the ~2 Ga old Bushveld LMI that partly samples the Kaapvaal SCLM, Windimurra lacks continental isotope signatures or primary hydrous minerals. If LMI share common processes of mantle melting, we conclude: (1) LMI are sourced from deep mantle plumes; (2) the Yilgarn SCLM was not hydrated or metasomatised until ~3 Ga; (3) establishment of the Yilgarn SCLM may be related to melt events complementary to the formation of the Narryer Terrane zircon record.

https://doi.org/10.1180/S0026461X00006502 Published online by Cambridge University Press

Characterization of the microbe-biotite interface on field samples from a mine site, Derome, Sweden

K. NEGRICH[1]*, Z. BALOGH-BRUNSTAD[1,2]*, T. HASSENKAM[2] AND S.L.S. STIPP[2]

[1]Hartwick College, Oneonta, NY 13820, USA (*correspondence: negrichk@hartwick.edu, balogh_brunz@hartwick.edu)

[2]NanoGeoScience, Nano-Science Center, Dept. of Chemistry, University of Copenhagen, Denmark

Biological processes, specifically mediated by fungal hyphae and biofilms, play a major role in mineral weathering and facilitating nutrient uptake. This study examines field samples of biotite from an abandoned mine site that was naturally re-vegetated by a mixed conifer and hardwood forest. We hypothesized that hyphal-sized etched channels formed on biotite surfaces by the weathering action of fungal hyphae under protective biofilm cover. Biotite surfaces were examined with atomic force microscopy (AFM) and environmental scanning electron microscopy (ESEM) in their natural state and after removing the biological material from the mineral surfaces [1, 2].

The AFM and ESEM images show extensive hyphal colonization and biofilm cover of the entire biotite surface. Fungal hyphae also grew between layers of the biotite sheets exhibiting an intensive exploration of the available weatherable surfaces. The biofilm that also covers the hyphae shows unique globular features of diameter 10-100 nm on all surfaces (Figure 1).

Force spectroscopy mode of AFM showed that both biofilm and hyphal surfaces are hydrophobic with hyphal surfaces providing higher adhesive forces. However, removal of the biological material resulted in smooth and non-etched surfaces indicating that regardless of the strong surface attachment, etching of the basal surface is not the main mechanism for base-cation nutrient acquisition in these natural biotite samples.

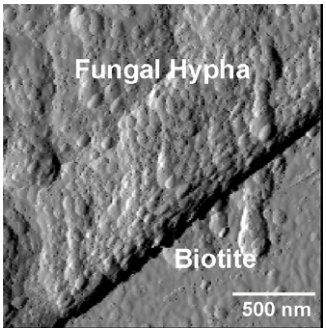

Figure 1: An AFM contact mode deflection image of the globular features of the biofilm layer covering the fungal hypha on a sample of biotite.

[1] Balogh-Brunstad *et al*. (2008) *GCA* **72**, 2601–2618.
[2] Buss *et al*. (2003) *Geomicrobiol J* **20**, 25–42.

Precipitation and surface complexation in systems containing Cu(II), As(V) and goethite

H. NELSON, S. SJÖBERG AND L. LÖVGREN

Department of Chemistry, Umeå University, SE-901 87 Umeå, Sweden (hanna.nelson@chem.umu.se)

The main objective of the present study has been to establish a model for equilibria in the four component system H^+-$HAsO_4^{2-}$-Cu^{2+}-goethite (α-FeOOH). Before the complete four component system can be tackled, equilibria in the different subsystems must be known. Due to the scarce information available in the literature on interactions between Cu (II) and As (V), the possible formation of complexes involving Cu (II) and As (V) in aqueous solution, as well as formation of solid phases were studied. All experiments were performed in 0.1 M NaCl ionic medium. Potentiometric titrations at different Cu to As ratios gave no evidence for the existence of Cu (II)-As (V) complexes in solution below pH of the precipitation boundaries (pH ≈ 4). Mixing of solutions of Cu (II) and As (V) at different proportions and adjusting pH to values ranging from 4 to 9 resulted in precipitation of five different solid phases. The elemental composition of the solids was analysed using XPS and SEM. The average Cu/As ratio was determined by dissolving the solids and analyzing of aqueous solutions. Two of the solids contained significant fractions of Na^+. Stability constants for the five solid phases have been calculated.

The co-adsorption of copper (II) and arsenate onto the surface of goethite were studied by potentimetric titrations and batch uptake experiments. A surface complexation model was developed to describe the experimental results. Models for the binary systems Cu (II) -goethite and As (V)-goethite were acquired separately and the parameters were included together with the stabilities of copper-arsenate solid phases. The adsorption of copper (II) could best be described with four different surface complexes. The surface complexes of As (V) on goethite were best modelled invoking a monodentate coordination of arsenate ions to singly coordinated surface hydroxyls and the arsenate ions are hydrogen-bonded to neighboring triply coordinated surface sites. In the case of co-adsorption of copper (II) and arsenate, the adsorption could not be described by applying the combined model from the two binary systems only. Two ternary copper- arsenate-goethite surface complexes were required.

https://doi.org/10.1180/S0026461X00006502 Published online by Cambridge University Press

An isotopic glimpse of the lithospheric mantle beneath the East African Rift System

WENDY R. NELSON[1]*, STEVEN B. SHIREY[1] AND TANYA FURMAN[2]

[1]DTM, Carnegie Institution of Washington, Washington, DC USA (*correspondence: wnelson@dtm.ciw.edu)
[2]Dept. of Gesciences, Pennsylvania State University, University Park, PA 16802, USA

Discerning the influence of various source components (mantle plumes, mantle lithosphere, crust) contributing to >30 Myrs of volcanism in the East African Rift System is difficult because the composition, age, and extent of the lithospheric mantle beneath Ethiopia have remained enigmatic. To better understand the potential role of the lithosphere, we analyzed Re-Os and PGE's of whole rock powders and Sr-Nd-Pb-Hf on clinopyroxene separates of peridotites from NW and S Ethiopia. The peridotites range from lherzolites to harzburgites and websterites. Compared to fertile mantle, all samples have low Os (0.73-2.55 ppb) and Re (0.004-0.075 ppb) concentrations, excepting one websterite (0.56 ppb Os, 0.37 ppb Re). Lherzolites are mildly unradiogenic ($^{187}Os/^{188}Os$ = 0.1236-0.1286) and overlap compositionally with 30 Ma high-Ti flood basalts in NW Ethiopia (0.1247-0.1329 [1, 2]). However, the peridotites have high ε_{Nd} (12.6-18.5), high ε_{Hf} (13.8-27.6), low $^{87}Sr/^{86}Sr$ (0.7019-0.7029) and variable $^{206}Pb/^{204}Pb$ (17.1-17.9 and 18.7-19.3) which, except for Pb, contrasts sharply with flood basalt compositions (ε_{Nd} = 4.7-6.7 [3]; ε_{Hf} = 12.1-13.5 [2]; $^{87}Sr/^{86}Sr$ = 0.7037-0.7043 [2, 3]. This difference demonstrates the lithospheric mantle did not contribute significantly to the production of Ethiopian high-Ti flood basalts. Instead, these flood basalts are derived from the upwelling Afar plume.

Lherzolite model ages calculated for the Re-Os and Sm-Nd isotopic systems vary widely: Re-Os T_{MA} = 0.2-0.6 Ga with one outlier at 1.35 Ga; Sm-Nd T_{DM} = 0.3-0.5 Ga and 1.2-2.6 Ga. Both the model ages and isotopic composition of the peridotites are consistent with mantle xenoliths from Eritrea [4] and Jordan [5]. Not only do the xenolith suites in Afro-Arabia all record the 500-900 Ma Pan-African orogeny, the range in model ages preserve evidence for an earlier, widespread Proterozoic metasomatic event that previously introduced heterogeneities in the lithospheric mantle [5].

[1] Rogers *et al*. (2010) *EPSL* **296**, 413–422. [2] Nelson *et al*. (in review) *Chem Geol*. [3] Pik *et al*. (1999) *GCA* **63**, 2263–2279. [4] Teklay *et al*. (2010) *Contrib Min Pet* **159**, 731–751. [5] Shaw *et al*. (2007) *J Pet* **48**, 1494–1512.

Did the AD 1452 Kuwae eruption have global climatic impact?

K. NÉMETH[1]*, S.J. CRONIN[1] AND I.E.M. SMITH[2]

[1]Massey University, Palmerston North, New Zealand (*correspondence: k.nemeth@massey.ac.nz)
[2]The University of Auckland, Auckland, New Zealand

The eruption and formation of Kuwae caldera, Vanuatu, was inferred to have induced a major atmospheric impact and climate cooling event in the mid-15th century [1]. C^{14} dating of charcoal from non-welded ignimbrite deposits on the adjacent Tongoa Island, provided an age of AD 1425 [2], later recalculated to AD 1452 and linked to sulphur spikes of ice cores from Greenland and Antarctica [3]. Oral traditions [4] were linked to this catastrophic event, and more-recently tsunami deposits locally as well as on Futuna, Wallis and Efate Islands [5]. Volatile, halogen and sulphur analyses, along with assumptions of the eruption volume based on the caldera dimensions indicate that the Kuwae magma could have been strongly climate-forcing [1]. However, the interpretation of this caldera was formed in a single huge volcanic event may be too simple, based on its complex double-shape and deposit geometry and sedimentology [4]. New stratigraphy, along with whole rock, major element composition of juvenile pyroclasts from the eruptives of Kuwae caldera show evidence for multiple explosive events with very similar compositions, separated by soil-forming breaks. This implies that the caldera was formed in a series of eruptions of the same type of magma, some potentially submarine. The most recent of these events (the AD1452 event) produced a basal basaltic andesitic and capping dacitic ignimbrite in localised areas from multiple apparent vent locations at the edges of a complex caldera. Its volume was probably half to a quarter of whole-caldera estimates (c. f., 1), but its impact was clearly globally relevant in terms of atmospheric chemistry. Earlier explosive eruptions at this centre may also have been violent enough to also generate high eruption columns and a series of earlier atmospheric cooling events. Further dating and geochemical study of this volcano is required to evaluate its past climatic influences and evaluate its potential for future large-scale events of a similar nature.

[1] Witter & Self (2007) *Bull. Volc* **69**, 301–318. [2] Monzier *et al*. (1994) *J. Volc. Geotherm. Res* **59**, 207–218. [3] Gao *et al*. (2006) *J. Geophys. Res* **111**, D12107. [4] Németh *et al*. (2007) The Open Geol. J. **1**, 7–11. [5] Goff *et al*. (2011) *Earth-Scie Rev*. doi, 10.1016/j.earsirev.2010.11.003

https://doi.org/10.1180/S0026461X00006502 Published online by Cambridge University Press

Marine productivity: Impacts on aerosols and clouds

ATHANASIOS NENES[1,2]

[1]School of Earth and Atmospheric Sciences, Georgia Institute of Technology, Atlanta, GA
[2]School of Chemical and Biomolecular Engineering, Georgia Institute of Technology, Atlanta, GA

Aerosols influence the planetary radiation balance directly by scattering and absorbing sunlight, and indirectly by modifying cloud microphysical properties. Marine aerosols are a particularly important class of particles, as they contribute considerably to the global aerosol load, are emitted from a large surface area, and are emitted in areas where cloud properties are especially sensitive to changes in aerosol concentration.

Aerosols over the remote oceans consist of a mixture of sea salt particles, organics, and sulfates from the oxidation of biogenic dimethyl sulfide, with additional contributions from mineral dust, biomass burning and anthropogenic sources. The biological sulfur cycle has long been thought a major source of oceanic cloud condensation nuclei. In recent years, significant abundances of organic carbon (OC) aerosols have been identified in marine environments and attributed to biological activity. The concentrations of marine-source OC aerosols are particularly high over regions of enhanced oceanic biological activity. Despite recognizing their crucial role, the source strength and chemical composition of biogenic marine aerosols remain highly uncertain.

This talk will give an overview of the state of knowledge of the links between marine productivity, aerosols and clouds.

Atmospheric acidification of mineral aerosols: A source of bioavailable phosphorus for the oceans

ATHANASIOS NENES[1,2,3], MICHAEL D. KROM[4], NIKOLAOS MIHALOPOULOS[5,3], PHILIPPE VAN CAPPELLEN[1], ZONBGO SHI[4], AIKATERINI BOUGIATIOTI[5], PAVLOS ZARMPAS[5] AND BARAK HERUT[6]

[1]School of Earth and Atmospheric Sciences, Georgia Institute of Technology, Atlanta, GA
[2]School of Chemical and Biomolecular Engineering, Georgia Institute of Technology, Atlanta, GA
[3]Institute of Chemical Engineering and High Temperature Chemical Processes, Foundation for Research and Technology Hellas, Patras, Greece
[4]School of Earth and Environment, University of Leeds, Leeds, United Kingdom
[5]Department of Chemistry, University of Crete, Heraklion, Crete, Greece
[6]Israel Oceanographic Limnological Research, Tel Shikmona, Haifa, Israel

Primary productivity of continental and marine ecosystems is often limited or co-limited by phosphorus. Deposition of atmospheric aerosols provides the major external source of phosphorus to surface waters. However, only a fraction of deposited aerosol phosphorus is water soluble and available for uptake by phytoplankton. We propose that atmospheric acidification of aerosols is a prime mechanism producing soluble phosphorus from soil-derived minerals. Acid mobilization is expected to be pronounced where polluted and dust-laden air masses mix. Our hypothesis is supported by the soluble compositions and reconstructed pH values for atmospheric particulate matter samples collected over a 5-year period at Finokalia, Crete. At least tenfold increase in soluble phosphorus is observed when Saharan soil and dust were acidified in laboratory experiments which simulate atmospheric conditions. Aerosol acidification links bioavailable phosphorus supply to anthropogenic and natural acidic gas emissions, and may be a key regulator of ocean biogeochemistry.

https://doi.org/10.1180/S0026461X00006502 Published online by Cambridge University Press

Crystallographic relationships between diamond and its olivine inclusions

F. NESTOLA[1], P. NIMIS[1] AND J.W. HARRIS[2]

[1]Dipartimento di Geoscienze, Università di Padova
[2]School of Geographical and Earth Sciences, University of Glasgow

Modern single-crystal X-ray analysis of minerals still encapsulated in diamond not only permits the determination of both the chemical composition of inclusions and of the residual internal pressures [1], but also provides a three dimensional analysis of the crystallographic relationships between inclusions and diamond hosts. Although the syngenicity of inclusions in diamonds is generally assumed on the basis of strong morphological criteria, the crystallographic relationships between inclusions and their host are rarely determined and a systematic survey of them for the different mineral species is lacking. We will present results of an on-going single-crystal X-ray diffraction study of olivines included in diamonds from the Udachnaya kimberlite (Russia). Implications on the syngenetic or protogenetic nature of the inclusions will be discussed.

[1] Nestola, Nimis, Ziberna, Longo, Marzoli, Manghnani, Fedortchouk (2011) *Earth & Planetary Science Letters* **305**, 249–255.

Size dependent element interaction and speciation in environmental nanoparticles

E. NEUBAUER, F. VON DER KAMMER, S.M. KRAEMER AND T. HOFMANN*

Univ. of Vienna, Dept of Env. Geosciences, A-1090-Vienna, Austria (*correspondence: thilo.hofmann@univie.ac.at)

Environmental nanoparticles play an important role e.g. in the binding of trace metals [1]. Increasing evidence is found that material <20 nm, such as natural organic matter (NOM) and Fe-rich mineral-like nanophases, play a key role in the fixation of trace elements in many natural systems, including soil and peat bog systems.

Size Exclusion Chromatography (SEC) and Flow Field-Flow Fractionation (FlowFFF), both coupled to ICP-MS, are used as complementary high-resolution size separation techniques, providing size dependent element information. In the < 30 nm fraction of natural waters we observe NOM and Fe-rich mineral-like particles with significantly different affinities to trace elements. The presence of Fe-rich nanoparticles governs the binding of e.g. Pb, Ti, and Mn. Cu is predominantly associated with NOM.

While the complexation of inorganic As with NOM and Fe-minerals has been investigated previously, a particular focus of this work is their interaction with organic As species. We observe that substantial fractions of As are associated with low molecular weight NOM (Figure 1) despite the reported high affinity of Fe minerals for As binding [2].

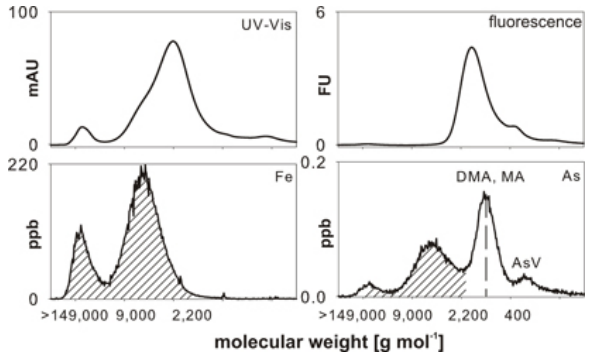

Figure 1: Size exclusion chromatogram of a peat bog drainage.

Combined FlowFFF/SEC size fractionation and IC speciation analysis can show, however, that some of the fractions are not colloid-bound but present as organic As species such as DMA and MA, as well as inorganic As (V).

[1] Hassellöv & von der Kammer (2008) *Elements* **4**, 401–406. [2] Sharma et al. (2010) *ES&T*. **44**, 4479–4485.

https://doi.org/10.1180/S0026461X00006502 Published online by Cambridge University Press

Arsenic removal with composite iron matrix filters from Bangladesh

A. NEUMANN[1]*, R. KAEGI[1], A. VOEGELIN[1], A. HUSSAM[2], A.K.M. MUNIR[3] AND S.J. HUG[1]

[1]Eawag, Swiss Federal Institute of Aquatic Science and Technology, Ueberlandstrasse 133, CH 8600 Duebendorf, Switzerland (*correspondence: anke.neumann@eawag.ch)
[2]Center for Clean Water and Sustainable Technologies, George Mason University, Fairfax, Virginia 22030, USA
[3]Sono Technology and Research Inc, Courtpara, Kushtia, Bangladesh

In Bangladesh, 30–50 million people are exposed to toxic levels of arsenic (As) in drinking water from shallow tube wells. With more than 50% of the affected population still exposed, inexpensive, reliable, and low-maintenance filters to remove As from well water could lead to a significant reduction of As exposure. The SONO water filter, which was developed in Bangladesh and is produced there from local materials, fulfills these criteria as well as the requirements for potable water. It has been used in large numbers in Bangladesh for years and was recently approved by the Bangladesh government.

The removal of As with SONO filters is based on the transformation of zero-valent iron (ZVI) to a porous solid matrix known as composite iron matrix (CIM) and subsequent reactions. Although some of the general pathways for the removal of As with ZVI are known, the complex chemistry within the CIM is not yet fully understood. In particular, a more detailed identification of formed solids and proper mass balances could improve the assessment of the filters' sustainability and environmental impact and would help in the development of a consistent model for As removal with ZVI-based filter systems.

In a combined long-term field and laboratory study, we investigated the chemical reactions involved in As removal with SONO filters. The effect of the water components Ca, P, Fe, and dissolved oxygen (DO) on the As removal efficiency has been investigated for 13 months in the field and was complemented with experiments with small-scale columns in the laboratory. The sampling of the percolating solution and of filter material at different depths enabled the detailed analysis of the chemical gradients within the filter. We identified the main components in the solid samples with X-ray based methods (XRF, XRD) and microscopy (Raman, ESEM) and investigated whether the mode of filtration and the influent DO content had an effect on the solids formed in these filters over time.

The hydrogeochemistry of pond and rice field recharge: Implications for the arsenic contaminated aquifers in Bangladesh

REBECCA B. NEUMANN[1]*, KHANDAKER N. ASHFAQUE[2], MATTHEW L. POLIZZOTTO[3], A. BORHAN M. BADRUZZAMAN[4], M. ASHRAF ALI[4] AND CHARLES F. HARVEY[5]

[1]Department of Civil and Environmental Engineering, University of Washington, Seattle, WA, USA (*correspondence: rbneum@u.washington.edu)
[2]Arcadis Environmental Consultants, Baltimore, MD, USA
[3]Department of Soil Science, North Carolina State University, Raleigh, NC, USA
[4]Department of Civil Engineering, Bangladesh University of Engineering and Technology, Dhaka, Bangladesh
[5]Department of Civil and Environmental Engineering, Massachusetts Institute of Technology, Cambridge, MA, USA

Researchers have puzzled over the origin of dissolved arsenic in the aquifers of the Ganges Delta since widespread arsenic poisoning from groundwater was publicized two decades ago. Previous work has concluded that biological oxidation of organic carbon drives geochemical transformations that mobilize arsenic from sediments; however, the source of the organic carbon that fuels these processes remains controversial. A combined hydrologic and biogeochemical analysis of a typical site in Bangladesh, where constructed ponds and groundwater-irrigated rice fields are the main sources of recharge, shows that only recharge through pond sediments provides the biologically degradable organic carbon that can drive arsenic mobilization. Chemical and isotopic indicators suggest that contaminated groundwater originates from excavated ponds and that water originating from rice fields is low in arsenic. In fact, rice fields act as an arsenic sink. Irrigation moves arsenic-rich groundwater from the aquifers and deposits it on the rice fields. Most of the deposited arsenic does not return to the aquifers; it is sorbed by the field's surface soil and bunds, and is swept away in the monsoon floods. The findings indicate that patterns of arsenic contamination in the shallow aquifer are due to recharge-source variation and complex three-dimensional flow.

https://doi.org/10.1180/S0026461X00006502 Published online by Cambridge University Press

'Ordering' in glasses and melts: Structural observations and their properties implications

DANIEL R. NEUVILLE[1]*, CHARLES LE LOSQ[1], FLORIAN PIERRE[2], ALAIN BARONNET[3] AND DOMINIQUE MASSIOT[2]

[1]CNRS-IPGP, 1 rue Jussieu, 75005 Paris
[2]CEHMTI-CNRS, 1d rue de la recherche scientifique, 45000 Orléans
[3]CINaM, Université de Marseille, Marseille

As the chemical and physical behavior of magmas dominates many geological processes, and as most technological glasses and glass ceramics start off in the molten state, understanding of the physical chemistry of silicate glasses and melts is important in both the earth and material sciences. Our present knowledge of these systems is limited, however, by the technical difficulties of working at high temperatures, and the theoretical complexities of materials whose structure and dynamics lie somewhere between the relatively well-understood field of organic polymers and that of molten salts. One of the most important questions concerns the link between macroscopic properties and structure at the nano-scales of the glassy state but also of the liquid and in the melts with changing intensive properties.

One of the more challenging and controversial idea is about middle and long range order in glass. Greaves *et al*. [1981] and Greaves [1985] proposed the *Modified Random Network* (MRN) model, where a glass can be a mixing of between rich domain in network former and rich domain with cation modifier that create some channels. This assumption can be used to explain alkali diffusion in glass [Roling *et al*. 2001; Sunyer *et al*. 2002; Meyer *et al*. 2004], and even if EXAFS experiments were over interpreted to build this original structural view, the channel idea works well to explain glass structure.

Following this idea, a glass is a non-random structure composed of two interpenetrated sub-networks: one rich in network former, surrounded by the other rich in network modifier or charge compensator, concentrated in channels already observed by Frischat *et al*. [2004] using high resolution AFM on Duran® borosilicate glass surface. These two different domains can be also interpret in term of low and high density region following Tanaka works to explain fracture, unmixing, polyamorphism and crystallization in glass [Kurita and Tanaka, 2004; Shintani and Tanaka, 2006; Patrick Royall *et al*. 2008; Furukawa and Tanaka, 2009].

We plan to discuss and complete this idea using some new rheological and structural investigation on alkali aluminosilicate glasses and melts. These considerations are of prime importance for glasses industry, earth sciences and more particular for explosive volcanos activity.

Volatile and major element zonation within melt inclusions: A natural diffusion experiment

M. NEWCOMBE[1]*, A. FABBRIZIO[2], YOUXUE ZHANG[3], Y. GUAN[1], C. MA[1], M. LE VOYER[1], J. EILER[1], A. SAAL[4] AND E. STOLPER[1]

[1]California Institute of Technology, Pasadena, CA 91125, USA (*correspondence: megan@gps.caltech.edu)
[2]Institut für Mineralogie und Petrographie, Universität Innsbruck, Innrain 52f, 6020 Innsbruck, Austria
[3]University of Michigan, Ann Arbor, MI 48109-1005, USA
[4]Brown University, Providence, RI 02912, USA

The diffusivities of volatile elements in silicate melts significantly impact petrological processes [e.g. 1, 2]. Although many studies of volatile diffusion in silicic melts have been undertaken, there have been few studies in basaltic melts [e.g. 3], and most of these have concentrated on the diffusion of only one or two elements in each experiment.

Significant zonation in volatile and major elements has been discovered in olivine-hosted melt inclusions from the Siqueiros Fracture Zone [samples previously studied in 4]. Elements that are compatible in olivine, such as Mg and Fe, are depleted at the edges of the zoned melt inclusions relative to their centers, whereas elements that are incompatible in olivine, such as Al, Ca, Si, Na and S, are enriched. Preservation of this zonation suggests that it formed during crystallization of olivine on the walls of the inclusions in response to cooling during or just prior to eruption. Although all melt inclusions from this sample suite exhibit zoning profiles, there are few previous reports [e.g. 5] of comparable concentration profiles in melt inclusions, so it is not known if this feature is widespread.

The MgO concentration profiles in two melt inclusions have been used to constrain the cooling history of the inclusions using the results of [6]. The profiles are consistent with an initial slow cooling rate followed by a period of more rapid cooling. For other components, their zoning profiles can be used to estimate their diffusivities relative to that of MgO. Of the volatile elements, we have demonstrated such profiles in S, and have preliminary results on Cl and F that allow constraints to be placed on their relative diffusivities in basaltic melt.

[1] Saal *et al*. (2008) *Nature*, **454**, 192–195. [2] Sparks *et al*. (1994) *Rev. Mineral*. **30**, 413–445. [3] Zhang *et al*. (2010) *Rev. Mineral*. **72**, 311–408. [4] Saal *et al*. (2002) *Nature*, **419**, 451–455. [5] Mercier (2009) *PhD thesis*, Université Paris - Sud 11 [6] Chen & Zhang (2008) *GCA*, **72**, 4756–4777.

https://doi.org/10.1180/S0026461X00006502 Published online by Cambridge University Press

Theories of fluids at extreme conditions

I. NEZBEDA[1,2]

[1]Faculty of Science, J. E. Purkinje University, 40096 Usti n. L., Czech Republic
(*correspondence: IvoNez@icpf.cas.cz)
[2]E. Hala Lab. of Thermodyn., Acad. Sci., 16502 Prague, Czech Republic

Introduction

In this contribution two completely different methods to estimate by means of theory properties of fluids at conditions encountered in geochemical applications will be presented and discussed.

It is been well known that at these conditions most of compounds can be treated fairly well by a softly repulsive EXP6 potential. Consequently, common theories of fluids making use, either directly or indirectly, of the properties of the fluid of hard spheres (HS) are inapplicable in this case. Following the recently established idea of a uniform view of fluids [1] we have developed a theory, called augmented van der Waals theory [2], based on a Yukawa reference. Within this theory the EXP6 fluid may be described either directly by means of a 2-Yukawa model or by a simple Yukawa-based van der Waals equation, vdW (Y), with a simple mean field term. Both methods make use of the knowledge of theory-based analytic expressions for the thermodynamic properties of the Yukawa fluids.

The other method follows the common experimental setup, namely, to operate at fixed temperature, T, and pressure, P, and is based on P-explicit analytic equations of state for both pure HS fluids [3] and general hard-body fluid mixtures [4]. It is shown that the volume, as a function of T and P, estimated by means of the hard body equations captures extremely well the behavior of real fluids and that the additional mean field term is sufficient to bring theoretical results to agreement with experiment.

[1] Nezbeda (2005) Mol. Phys. **103**, 59–76. [2] Nezbeda *et al*. (2010) J. supercrit. Fluids **55**, 448–454. [3] Nezbeda *et al*. (1989) *Z. phys. Chem. (Leipzig)* **270**, 533–539. [4] Voertler & Nezbeda (1990) *Ber. Bunsenges. Phys. Chem.* **94**, 559–563.

First-principles simulations of alkali aluminosilicate liquids

HUAIWEI NI* AND NICO DE KOKER

Bayerisches Geoinstitut, Universität Bayreuth, 95440 Bayreuth, Germany
(*correspndence: huaiwei.ni@uni-bayreuth.de)

We have investigated the thermodynamics, diffusion, and structure of alkali aluminosilicate liquids at mantle conditions using first-principles molecular dynamics. Results for $NaAlSi_2O_6$ and $NaAlSi_3O_8$ liquid have been obtained at temperatures of 3000-6000 K and pressures up to 150 GPa. We find that fourth order finite strain expansions are required to account for the pressure-volume equations of state. Thermodynamic properties derived from simulation results agree well with experimental measurements. Isochoric heat capacity decreases with pressure, but the Grüneisen parameter increases with pressure. Liquid structure changes continuously with pressure, showing trends in mean coordination numbers and relative abundances of distinct coordination species consistent with previous studies of other silicate liquids. Self-diffusivities for Si and O increase with pressure below 16 GPa at 3000 K, while low-pressure diffusivities of Na are 3–6 times higher than values for other components. Activation volume for Na diffusion is much larger than that for Al, Si, and O diffusion, so that Na diffusivities become comparable to those of the other components at lower mantle pressures. This disappearance of mobility contrast implies that alkali-rich silicate liquids associated with low degree melting in Earth's interior are unlikely to have high electrical conductivity and will be more difficult than previously expected to detect by magnetotelluric sounding.

https://doi.org/10.1180/S0026461X00006502 Published online by Cambridge University Press

Mineral sources of arsenic from glacial aquifer sediments to well water in Minnesota, USA

SARAH L. NICHOLAS[1], BRANDY M. TONER[1]*, MELINDA L. ERICKSON[2], LAUREL G. WOODRUFF[2], ALAN R. KNAEBLE[3] AND GARY N. MEYER[3]

[1]Department of Soil, Water and Climate, University of Minnesota, USA (nich0160@umn.edu) (*corespondence: toner@umn.edu)

[2]United States Geological Survey, Mounds View, Minnesota, USA (merickso@usgs.gov, woodruff@usgs.gov)

[3]Minnesota Geological Survey, St. Paul, Minnesota, USA (knaeb001@umn.edu)

In Minnesota, USA, domestic wells with arsenic concentrations exceeding 10μgL^{-1} are predominantly found within the footprint of the Des Moines Lobe glacial advance (12-14 kya). The arsenic concentrations in groundwater are variable over short distances. Although the exact mineral source of arsenic remains unknown, a frequent hypothesis is that arsenic-bearing pyrites in Cretaceous shale fragments common to these glacial sediments release arsenic to groundwater. The abundance of arsenic in reduced well-water and groundwaters suggests that the solid source of some of the arsenic may be oxidized, sorbed species.

The goals of this study are to identify the mineral and chemical species of the arsenic in the solid phase, and better understand the mechanisms liberating arsenic to well-water. This information may provide guidelines to well-drillers for future well construction.

In our analysis, we use sequential extractions to identify arsenic species operationally, and whole-rock chemistry to describe total elemental abundances of the strata. Bulk and microprobe X-ray absorption spectroscopy (XAS) is used to identify and quantify arsenic and iron species. Powder and microprobe X-ray diffraction (XRD) are used to describe the bulk and arsenic-bearing mineralogy of the glacial deposits. Nested analysis of resulting datasets across the landscape and as a function of depth is accomplished in a geographic information systems (GIS) and geostatistical framework.

Glacial sediments sampled from ten rotary-sonic drill cores (20-70m depth) were examined. Arsenic speciation in strata above, at, and below transitions between fine-grained glacial tills (confining layers) and sand-gravel deposits (aquifers) was measured. Arsenic is present in three distinct oxidation states: As^{5+}, As^{3+}, and As^{1-}. The presence of three arsenic species, with varying proportions in the solids, may explain some of the observed spatial heterogeneity in well-water arsenic concentrations These forms of arsenic will be labile under different redox conditions in waters.

Approaching a consistent set of cosmogenic ^{3}He, ^{21}Ne and ^{10}Be production rates

S. NIEDERMANN* AND C.R. FENTON

Helmholtz-Zentrum Potsdam – Deutsches GeoForschungs-Zentrum, Telegrafenberg, D-14473 Potsdam, Germany (*correspondence: nied@gfz-potsdam.de)

Cross-calibrations of production rates for cosmogenic ^{3}He, ^{21}Ne and ^{10}Be in olivine, pyroxene and quartz have revealed an inconsistency between earlier production rate calibrations, mainly because the ^{3}He (ol, px)/^{21}Ne (qz) ratio of 8.19 ± 0.19 was found to be considerably higher than the predicted ratio of ~6.1 [1]. Recently however, several new ^{3}He and ^{10}Be production rate determinations have indicated that the discrepancy may be less severe than anticipated. In particular, three regional studies in northeastern North America, New Zealand and Norway [2, 3, 4] have yielded ^{10}Be production rates that are consistently ~15% smaller than the earlier 'global mean' of Balco *et al*. [5]. It seems unlikely that all calibration sites, which are at latitudes from 42° to 70°N and ~44°S, are characterized by a uniform reduction in production rates due to untypical conditions of the atmosphere or the geomagnetic field. Rather, we believe that earlier work included in the 'global mean' [5] may have overestimated the ^{10}Be production rate. Similarly, a recent compilation [6] as well as an additional calibration study [7] indicate ~10% higher ^{3}He production rates in olivine and pyroxene than reported earlier [5]. Using these new production rate values, the discrepancy between direct production rate determinations and cross-calibrations is substantially reduced. In this respect, ^{3}He and ^{10}Be production rate values that have been scaled by the De, Du and Li methods [cf. 5 and references therein] perform distinctly better than those scaled by the St or Lm methods (11-12% vs. 19% remaining discrepancy). Indeed, the directly determined and cross-calibrated production rates overlap within error limits for the former three scaling methods. Therefore, the apparent inconsistency is largely resolved when the new set of production rates is used. ^{10}Be and ^{21}Ne exposure ages will however increase by ~15%.

[1] Niedermann *et al*. (2009) *Geochim. Cosmochim. Acta* **73**, A940. [2] Balco *et al*. (2009) *Quat. Geochron*. **4**, 93-107. [3] Putnam *et al*. (2010) *Quat. Geochron*. **5**, 392-409. [4] Fenton *et al*. (2011) *Quat. Geochron*., in press. [5] Balco *et al*. (2008) *Quat. Geochron*. **3**, 174-195. [6] Goehring *et al*. (2010) *Quat. Geochron*. **5**, 410-418. [7] Amidon & Farley (2011) *Quat. Geochron*. **6**, 10-21.

https://doi.org/10.1180/S0026461X00006502 Published online by Cambridge University Press

Formation and inhibition of calcite, aragonite and vaterite

A. NIEDERMAYR[1,2], M. DIETZEL[2] AND S.J. KÖHLER[3]

[1]Institute of Geology, Mineralogy and Geophysics, Ruhr-University Bochum, Germany (andrea.niedermayr@rub.de)
[2]Institute of Applied Geosciences, TU Graz, Austria
[3]Swedish University of Agricultural Sciences, Uppsala, SE

Calcium carbonates ($CaCO_3$) are widespread in sediments and organisms and highly relevant materials for industrial applications. The formation of calcium carbonate is strongly affected by dissolved magnesium ions (Mg) and polyaspartic acid (Pasp). In the present study the formation of the anhydrous $CaCO_3$ polymorphs calcite, aragonite and vaterite were investigated at various temperatures ($6 < T < 40°C$), carbonate accumulation rates ($0.15 < R_{CO3} < 320$ μmol h^{-1}), concentrations of Mg (≤ 55 mmol l^{-1}) and Pasp (≤ 3.4 mg l^{-1}) by using the CO_2 diffusion technique at constant pH. Nucleation of $CaCO_3$ was retarded from few minutes up to several hours at $T \leq 10°C$, and up to several hundreds of hours at elevated [Mg] and [Pasp]. Distinct $CaCO_3$ polymorph formation is mainly controlled by [Mg], [Pasp], T and R_{CO3}. [Mg]/[Ca] > 0.2 (40°C) to [Mg]/[Ca] > 2 (6°C) promote the formation of aragonite and suppress the formation of vaterite. Pasp inhibits aragonite formation and favours vaterite formation, whereas combining both Pasp and Mg causes calcite formation. In the presence of Pasp, $CaCO_3$ nucleates only in case of supersaturation with respect to monohydrocalcite. The present study provides conditions to synthesize tailored $CaCO_3$ polymorphs. Moreover, the results can be used to obtain an advanced understanding for the mechanisms of $CaCO_3$ biomineralization and to evaluate $CaCO_3$ scaling mechanisms with special regard on inhibition of $CaCO_3$ polymorphs and nucleation times.

Conductive filaments and electric fields associated with electric currents in marine sediment

L.P. NIELSEN[1]*, N. RISGAARD-PETERSEN[1], Y. GORBY[2], A. REVIL[3], G. WANGER[4], M. EL-NAGGAR[5] AND T. YUZVINSKY[5]

[1]Dep. of Biological Sciences, Aarhus Univ., Denmark (*correspondence: biolpn@biology.au.dk) (nils.risgaard-petersen@biology.au.dk)
[2]Geobiology, Univ. S. California, USA (ygorby@usc.edu)
[3]Dep. of Geophysics, Colorado School of Mines, Golden, Colorado, USA (arevil@mines.edu)
[4]The J. Craig Venter Institute, San Diego, California, USA (gwanger@jcvi.org)
[5]Dep. of Physics and Astronomy, Univ. of S. California, USA (mnaggar@usc.edu) (yuzvinsky@gmail.com)

Electric currents have been found to explain tightly coupled but spatially separated sulphide oxidation and oxygen reduction in marine sediment [1]. In the present study we searched for electron conductors and additional measures of electric activity in the sediment. Networks of filaments resembling bacterial conductive pili ('nanowires') were observed in the sediments and electron conductivity was documented with nanofabrication approaches [2]. Down-core measurements of self-potentials revealed an electric field that matched the geochemical evidence of electric circuits extending from the sediment surface to a depth of 2 cm. The upwards charge transfer by electrons was thus balanced by ion drift in the pore water.

The results suggest that sediment electric networks are engineered by microorganisms using nanowires as electron conductors.

[1] Nielsen *et al*. (2010) *Nature* **463**, 1071–1074. [2] El-Naggar *et al*. (2010) *PNAS* **107**, 18127–18131.

https://doi.org/10.1180/S0026461X00006502 Published online by Cambridge University Press

Molecular model of kinetic isotope fractionation during surface-controlled growth of $CaCO_3$ from aqueous solution

LAURA C. NIELSEN*, DONALD J. DEPAOLO AND JAMES J. DE YOREO

Lawrence Berkeley National Laboratory, Berkeley, CA 94720, USA (*correspondence: lnielsen@berkeley.edu)

The attachment and detachment of cations and anions at the mineral-aqueous solution interface control rates of crystal growth and dissolution, and also affect isotope fractionation and trace element partitioning. Recent experimental work has begun to characterize kinetic isotope fractionation during precipitation of $CaCO_3$ and other di-ionic solids. Proposed models for isotopic and trace element effects deal only with macroscopic properties such as solution saturation state and solid state diffusivity. In this study, we apply molecular models of di-ionic crystal growth to deduce the dependence of kinetic isotope fractionation on growth mechanism, and both solution saturation state and stoichiometry. Recent theoretical advances have underscored the significance of solution stoichiometry—e.g. the ratio of Ca to CO_3 ion activities in solution—for controlling mineral surface kink density and composition and thus growth rate and growth mechanism. Our approach incorporates the effect of solution composition on microscopic mineral surface structure and composition, providing testable hypotheses for growth of sparingly soluble AB crystals such as calcite, namely:

1) Oversaturation and solution stoichiometry control growth rate and partitioning of A and B isotopes during precipitation;
2) For step growth, distinct rate laws describe dislocation- and 2D nucleation-driven growth, while the expression describing isotope fractionation requires no change;
3) Formation of amorphous precursors will generate isotope effects incompatible with ion-by-ion growth theory.

As observed during calcite growth, increasing oversaturation increases growth rate and drives isotope partitioning towards the kinetic limit. Also, increasing concentration of Ca^{2+} relative to CO_3^{2-} should drive new growth towards isotopic equilibrium. These competing effects, as well as the formation of an amorphous precursor, determine the observed magnitude of isotope fractionation. This model provides a clear mechanistic description of processes controlling the cross-over from the near-equilibrium to the kinetic limit of isotope fractionation, allowing us to relate trends in experimental data to environmental conditions of growth.

Large vanadium isotope difference between silicate Earth and meteorites

S.G. NIELSEN[1,2], J. PRYTULAK[1], B.J. WOOD[1] AND A.N. HALLIDAY[1]

[1]University of Oxford, Dept. of Earth Science, South Parks Rd, OX1 3AN, Oxford, UK
[2]WHOI, Dept. of Geology and Geophysics, 266 Woods Hole Rd, 02543 Woods Hole, MA, USA

We have recently developed a technique to measure precise and accurate vanadium (V) isotope ratios [1, 2]. All data are reported in parts per thousand as $\delta^{51}V$ relative to an Alfa Aesar (AA) standard. Processing multiple aliquots of the same sample, including dissolution and column chemistry, yields a long-term external reproducibility of about 0.15‰ (2sd) [2].

Here, we present the first high precision $^{51}V/^{50}V$ isotope composition data for a range of extraterrestrial materials. The sample set comprises CI, CO, CM, CV and CK carbonaceous chondrites, one ordinary chondrite, one ureilite, three HED parent body achondrites and the martian meteorite Nakhla. The data fall in a relatively narrow range about 1.5 to 2‰ lighter than AA.

If the meteorites are considered as one sample group then they are 0.5-0.8‰ lighter than our current best estimate for bulk silicate Earth [3]. The isotopic offset between Earth and meteorites may be explained by partitioning of isotopically light V into the Earth's core. This conclusion, however, is at odds with the insignificant V isotopic fractionation observed for three metal-silicate equilibration experiments.

Alternatively, the Earth does not have a V isotope composition identical to chondrites. The abundance of ^{50}V is sensitive to irradiation [4] and it is therefore conceivable that early solar system processes may have generated a V isotope gradient that could be preserved today in meteorites.

[1] Nielsen, S.G. J. Prytulak, & A.N. Halliday (2011) *Geostand. Geoanal. Res.* in press. [2] Prytulak, J. S.G. Nielsen, & A.N. Halliday (2011, in press) *Geostand. Geoanal. Res.* [3] Prytulak, J. S.G. Nielsen, & A.N. Halliday (2011, in press) *Geochim. Cosmochim. Acta.* [4] Gounelle, M. *et al.* (2001) *Astrophys. J.* **548**(2): 1051–1070.

https://doi.org/10.1180/S0026461X00006502 Published online by Cambridge University Press

Validation and application of a novel, terrestrial biomarker-based paleo thermometer to Holocene sediments of Lake Cadagno, Switzerland

H. NIEMANN[1], S.B. WIRTH[2], A. STADNITSKAIA[3], A. GILLI[2], F.S. ANSELMETTI[4], J.S. SINNINGHE DAMSTÉ[3], S. SCHOUTEN[3], E.C. HOPPMANS[3], M.F. LEHMANN[1]

[1]Institute for Environmental Geosciences, University of Basel (helge.niemann@unibas.ch)
[2]Geological Institute, ETH Zurich
[3]Royal Netherland Institute for Sea Research (NIOZ), Texel
[4]Swiss Federal Institute of Aquatic Science and Technology (EAWAG), Dübendorf

Lake Cadagno is a relatively small glacial lake in southern Switzerland (1921 m altitude). We recovered a 10.5 m long composite core from the lake covering the sedimentary sequence of the last 11000 yrs. Our aim was to reconstruct past mean annual air temperature (MAAT) using a novel, lipid-based proxy, the MBT/CBT paleothermometer. The MBT/CBT ratios comprise fossilised methyl-branched and cyclic Glycerol Dialkyl Glycerol Tetraethers (GDGTs) of presumably soil bacterial origin that are preserved in the sediments. Our results stand in good agreement with instrumental MAAT values for Lake Cadagno (ca. 0°C, Swiss Meteo). Furthermore, temperature variations recorded by the MBT/CBT paleothermometer match published temperature reconstructions for the last two millennia at nearby locations in timing and magnitude. Major climate anomalies recorded by the independent proxies and by the MBT/CBT paleothermometer are, for instance, the Little Ice Age and the Medieval Warm Period. Furthermore, we detected a cold period lasting from about 2400 - 2000 yrs BP (-0.7°C), which correlates with the disappearance of the last lake dwellings in the European Alps. We also found a cold period during the Bronze Age (3500 - 4500 yrs BP; -0.5°C). In alpine regions, strong rain falls typically lead to increased erosion and flood activities, which are recorded in the sedimentary sequence (frequency and layer thickness of flood deposits). Similarly, pronounced precipitation can induce leaching of basic elements and thus acidification of soils, which has an impact on the CBT ratios. We found strongly enhanced flood activities concomitant with a decrease in soil pH during time periods of major cold spells, which also agrees with earlier reports on alpine lake level stands. Our results strongly emphasise the usefulness of the MBT/CBT paleothermometer for terrestrial climate reconstructions.

Soil carbon sequestration in olive grove with different soil management

O. NIETO[1], J. CASTRO[2] AND E. FERNÁNDEZ-ONDOÑO[1]*

[1]Dpto. Edafología y Química Agrícola. Facultad de Ciencias University of Granada (*correspondence: efernand@ugr.es)
[2]IFAPA Camino de Purchil. Junta de Andalucía

Introduction

We have simulated the dynamics of carbon (OC) under two soil management systems (tillage soil and cover plant soil) in a Mediterranean olive grove with the RothC model. We choose two soil management (tillage and cover crop) in three locations (L). The soil OC storage was calculate as difference between the content in both management. Carbon sequestration was calculated as difference between simulated RothC input and soil respiration.

Discussion of Results

	Clay	OC input	Carbon storage	Carbon sequestration
	%	Mg C ha^{-1} yr^{-1}		
L1	45	9.39	4.53	6.48
L2	50	5.51	2.18	3.63
L3	25	8.88	5.35	7.63

Table 1: clay content and carbon fluxes in the three locations for the first year after soil management change.

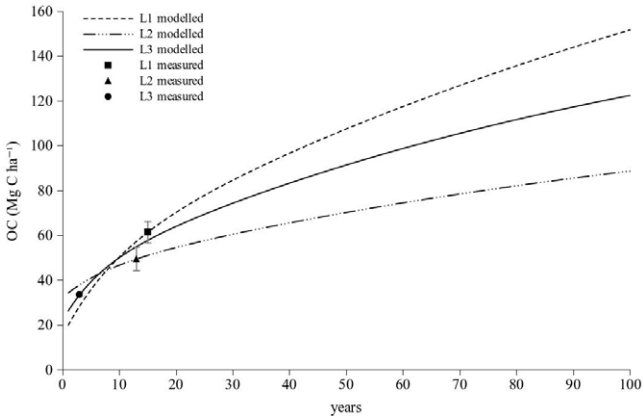

Figure 1: OC modelled for the three locations under cover crop.

Differences between the three locations were due to the amount of biomass generated by the cover crop and the clay content. L1 and L2, with high clay content but different carbon input, resulted in high OC for L1 after 100 years (Figure 1). The lower clay content whit high input (L3) was an intermediate position.

https://doi.org/10.1180/S0026461X00006502 Published online by Cambridge University Press

'Geo-metabolomics' — A key for understanding function and reactivity of dissolved organic matter

JUTTA NIGGEMANN[1]*, GUNNAR GERDTS[2] AND THORSTEN DITTMAR[1]

[1]Max Planck Research Group for Marine Geochemistry, ICBM, University of Oldenburg, Germany (*correspondence: jniggema@mpi-bremen.de) (tdittmar@mpi-bremen.de)

[2]Alfred Wegener Institute, Helgoland, Germany (Gunnar.Gerdts@awi.de)

Dissolved organic matter (DOM) in the ocean contains as much carbon as the earth atmosphere. This huge pool of energy- and nutrient-rich compounds provides an important base for microbial life in the water column. We hypothesize that the microbial community shapes DOM composition (and vice versa), thereby determining the dynamics of individual molecules and the entity of DOM. The entity of DOM is considered as a population of compounds, each characterized by a specific function and reactivity in the cycling of energy and elements. We propose 'geo-metabolomics' as the principle that a most comprehensive characterization of molecular DOM composition and its abiotic and biotic sources and sinks reveals a correlation of properties and behavior, ultimately allowing for the prediction of function and reactivity.

We present results from a long-term study of molecular DOM composition in the open North Sea. Ten-thousands of molecular formulae were identified in DOM by ultrahigh resolution mass spectrometry analysis (FT-ICR-MS, Fourier-Transform Ion Cyclotron Resonance Mass Spectrometry). For the 'geo-metabolomics' approach we include abiotic environmental factors and information on abundance and composition of phytoplankton and microbial communities.

The DOM pool in the North Sea is highly dynamic and influenced by a complex interplay of processes that produce, transform and degrade dissolved molecules. Phytoplankton blooms significantly change the molecular composition of DOM, strongly increasing the inherent molecular diversity. The temporal variability of individual molecular formulae in the 'geo-metabolome' provides novel information on their function and reactivity. This is a crucial step towards assigning structures to molecular formulae and finally the key for understanding DOM dynamics and interactions.

Near-source compositions of Italian kamafugite melt

I.K. NIKOGOSIAN* AND M.J. VAN BERGEN

Department of Earth Sciences, Utrecht University, The Netherlands (*correspondence: iniki@geo.uu.nl)

Within the wide compositional spectrum of K-rich magmatism in Central Italy, kamafugitic rocks in the Intra-Apennine Volcanic Province constitute the most alkalic, Si-undersaturated end-member, showing the highest enrichment in many incompatible trace elements. Longstanding debate concerning magmagenesis and geodynamic controls has been fuelled by questions concerning the extent to which crustal-interaction processes modified primary melt compositions. Here we present the results of a detailed study of melt-inclusions (MI) and host olivines from a representative kamafugite specimen from San Venanzo, that enabled us to constrain the primary composition (s) of mantle-derived melt.

Olivine phenocrysts show complex textures indicative of drastic late-stage changes in the crystallization regime. Pristine core parts, characterized by Fo_{93-90}, low CaO (0.2-0.3 wt.%) and Cr-spinel inclusions (Cr# ~ 0.7) are considered to to have crystallized from primary mantle-derived melt. Modified rim zones, showing a strong compositional gradient of decreasing forsterite (down to Fo_{70}) and increasing CaO (up to 1.8 wt.%), and hosting compositionally deviating MI, point to re-equilibration in response to drastic compositional changes induced by interaction with carbonate-rich rock types at shallow crustal levels.

Melt inclusions in the unmodified central parts of the olivines have compositional characteristics consistent with mantle derivation (8-12 wt.% MgO) but span a continuous range between 3 and 9 wt.% K_2O. The K-richest MI have compositions are relatively enriched in Na_2O, P_2O_5 and TiO_2. The K-poor end-member is characterized by very high CaO contents (up to 22 wt.%). From an average of the entire group of MI (n=25) the approximate volatile-free composition of the kamafugite parental magma is 43.0% SiO_2, 12.1% Al_2O_3, 2.15% TiO_2, 6.5% FeO, 0.11% MnO, 8.9% MgO, 17.6% CaO, 6.8% K_2O, 1.9% Na_2O, 0.95% P_2O_5.

We propose that this kamafugite composition represents an assembly of primary melts with differentiated compositions controlled by small-scale variations in the source. These would fit with different imprints by siliceous potassium-rich and carbonate-rich metasomatic agents derived from subducted carbonate-bearing metapelitic sediments.

https://doi.org/10.1180/S0026461X00006502 Published online by Cambridge University Press

Native iron in association with forsterite, experimental research

E.I. NIKOLENKO* AND E.I. ZHIMULEV

V.S. Sobolev Institute of Geology and Mineralogy SB RAS, Novosibirsk 630090, Russia
(*correspondence: nevgeny@gmail.com)

Experimental research of zonal ilmenite formation in low oxygen fugacity conditions was spent on a high-pressure pressless 'split sphere' (BARS type). The investigated sample consisting of a haemoilmenite (Geik 10 mol. %, Ilm 44 mol. %, Hem 46 mol. %), powdered kimberlite and metal titanium was located in a platinum capsule which was placed in a high pressure cell. The longest experiment proceeded 5520 minutes at pressure 2.0±0.25 GPa and temperature 1100 ±20 °C. Highly reducing conditions in a capsule were supported at the expense of the metal titanium, which bonds oxidizing components. As a result of experiments a rim of Mg-rich ilmenite on a grain of haemoilmenite was obtained. It was formed by interaction of haemoilmenite with melt. Thus, the iron reduced from a haemoilmenite was accumulated in a native form in interstitial area, near to a titanium tablet. Native iron composition was estimated by EDS spectrometer (Oxford instruments): Fe 92.4-97.5, P up to 5.9, S up to 3.2, Ni up to 4.5, Ti up to 0.5 (wt.%). Olivine have the following composition near the titanium tablet (wt.%): SiO_2 - 41.06; Cr_2O_3 - 0.04; FeO - 7.67; MnO – 0.06; MgO - 50.27; CaO - 0.18; NiO - 0.41. With increasing distance from a titanium tablet iron content in olivine rises from 7.67 to 14.76 wt.% (Fo 92.1 - 84.5 mol. %).

In this case the dependence of olivine composition from redox conditions is clearly shown. At low values of oxygen fugacity native iron coexists with forsteritic olivine (Fo 92.1). Obtained data indicate the possibility of highly reducing conditions in a mantle at which some silicate phases could lose iron. These results are confirmed by finds of native iron together with Fe-poor silicate inclusions in natural diamonds [1, 2].

Work is executed under the Russian Federation President's grant MK-908.2011.5.

[1] Fedorov *et al.* (1999) *Geochemistry International* **37**, 860–865. [2] Sobolev *et al.* (1981) *Geologiya i Geofizika* **22**, 25–29 (in Russian).

Fluid inclusion and stable isotope studies of the Kharape Epizonal Orogenic Gold Deposit, West Azerbaijan Province, Iran

S. NIROOMAND, R.J. GOLDFARB AND F. MOORE

(sh.niroomand@gmail.com, goldfarb@ usgs.gov, moore@geology.shirazu.ac.ir)

The Kharapeh epizonal orogenic gold deposit is located the Sanandaj-Sirjan Zone (SSZ) in the West Azerbaijan province, Iran. The deposit area is underlain by folded Cretaceous metamorphic rocks. The gold-bearing quartz veins are >1 km in length and average about 6 m in width; breccia zones are 10-50 m in length and ≤1 m in width. Four fluid inclusion types were recognized in cogenetic quartz: monophase aqueous inclusions, monophase carbonic inclusions, two-phase aqueous inclusions and three-phase carbonic-aqueous inclusions. Fluid inclusion data suggest mineral deposition at temperatures of at least 220 to 255°C, and depths of at least 1.4-1.8 km, from a H_2O-CO_2±CH_4 fluid of relatively high salinity (12-14 equiv. wt% NaCl). Ore fluid $\delta^{18}O$ values between about 7 and 9 per mil suggest no significant meteoric water input, despite gold deposition in a relatively shallow epizonal environment.

https://doi.org/10.1180/S0026461X00006502 Published online by Cambridge University Press

Cathodoluminescence of high-pressure feldspar minerals

H. NISHIDO[1]*, M. KAYAMA[1], T. SEKINE[2] AND K. NINAGAWA[3]

[1]Research Institute of Natural Sciences, Okayama University of Science, Japan (*correspondence: nishido@rins.ous.ac.jp)
[2]Department of Earth and Planetary Systems Science, Graduate School of Science, Hiroshima University
[3]Department of Applied Physics, Okayama University of Science, Japan

Cathodoluminescence (CL) of high-pressure silica minerals have been investigated, although high-pressure feldspar minerals such as $KAlSi_3O_8$-hollandite has not been studied from the perspective of CL spectroscopy. In this study, high-pressure feldspar minerals have been characterized by CL spectral analysis to clarify their emission mechanisms.

$KAlSi_3O_8$-hollandite ($Or_{97}Ab_3$) synthesized from adularia at a static condition of ~15 GPa and ~1200°C for 1 hour and experimentally shock-induced sanidine ($Or_{87}Ab_{13}$) from Eifel, Germany at pressure of 10 to 40 GPa by a propellant gun were selected for CL measurements. A scanning electron microscopy-cathodoluminescence (SEM-CL) was used to obtain CL spectra of these minerals.

CL spectrum of $KAlSi_3O_8$-hollandite consists of emission bands at 330 and 380 nm in UV-blue region. Similar UV-blue emission bands were detected in experimentally shocked sanidine above 20 GPa (diaplectic glass), but not observed in the samples below 20 GPa (diaplectic feldspar), where these emission intensities increase with increasing shock pressure. Diaplectic glasses in shergottites also exhibit UV-blue emissions at 330 and 380 nm. $KAlSi_3O_8$-hollandite has higher intensities of the UV-blue emissions than shocked samples at 40 GPa as well as diaplectic glasses in shergottite which might be responsible for completely octahedral coordination of Si (Al) in $KAlSi_3O_8$-hollandite and partially one in diaplectic glass. The UV emissions at 330 and 380 nm might be assigned to defect centers in Al and Si octahedral coordination produced by static and shock metamorphism. Furthermore, CL spectrum of $KAlSi_3O_8$-hollandite shows emissions at 550, 580, 660, 710 and 730 nm, which were undetectable in experimentally shocked sanidine above 20 GPa and diaplectic glasses in shergottite. These emission bands are characteristics of CL signals derived from $KAlSi_3O_8$-hollandite. Therefore, the CL signals can be used to identify high-pressure feldspar minerals and to observe its distribution in meteorite with high spatial resolution (~1 μm).

Long-term production rates of cosmogenic nuclides: Millions of years of rock exposure in Antarctica and the Atacama Desert

K. NISHIIZUMI[1]*, M.W. CAFFEE[2], S.A. BINNIE[1], R.C. FINKEL[3], J.J. OWEN[4], R. AMUNDSON[4], W.E. DIETRICH[5] AND G. FAURE[6]

[1]Space Sciences Lab., Univ. of California, Berkeley, CA 94720, USA (*correspondence: kuni@ssl.berkeley.edu)
[2]Dept of Physics, Purdue Univ, W. Lafayette, IN 47906, USA
[3]CAMS, LLNL, Livermore, CA 94550, USA
[4]Dept of ESPM, Univ. of Calif., Berkeley, CA 94720, USA
[5]Dept of EPS, Univ. of Calif., Berkeley, CA 94720, USA
[6]SES, Ohio State Univ., Columbus, OH 43210, USA

Introduction

Production rates (PR) for terrestrial cosmogenic nuclides are typically estimated by measurements of independently dated samples, by exposure of artificial targets for a known duration or by coupling cross-sections with model-generated particle fluxes. The determination of PRs for extraterrestrial samples, on the other hand, utlizes samples that have achieved secular equilibrium during long exposure in a low erosion environment. Here we adopt this approach to derive terrestrial cosmogenic ^{10}Be and ^{26}Al production rates.

Results and Discussion

Sets of paired ^{10}Be-^{26}Al results were selected from our published and unpublished data (28 Antarctica, 45 Atacama Desert). All samples contain more than $4x10^6$ atoms ^{10}Be/g quartz, sea level at high latitude. The ^{10}Be concentrations were plotted against corresponding $^{26}Al/^{10}Be$ values, and a range of possible 'saturated' ^{10}Be production rates.

A ^{10}Be production rate (P_{10}) of 5.1-5.3 atom/yr g-quartz is the best fit to the measurements. This P_{10} is much higher than the recently proposed P_{10} of ~4.5. Known geologic processes cannot reconcile these two production rates. In fact, the P_{10} based on Atacama and Antarctic samples is a minimum production rate since: (1) samples must have experienced some erosion and even 5 cm/Myr erosion yields a 16 % P_{10} increase; (2) any soil, ash or snow cover would artificially depress our PR estimate; (3) saturation may not have been achieved, since for many samples ^{26}Al-^{21}Ne exposure ages do not show more than 8 Myr exposure age (98 % saturation for ^{10}Be); (4) uplift of the Transantarctic Mountains and Atacama Desert moves the samples into higher PR. The high P_{10} indicates that the long-term cosmic ray flux is higher than that of the last few tens of thousands of years, probably due to a higher GCR flux and lower geomagnetic field in the past.

https://doi.org/10.1180/S0026461X00006502 Published online by Cambridge University Press

Relationship between water saturation and mineral-water contact area of a sandstone

N. NISHIYAMA* AND T. YOKOYAMA

Department of Earth and Space Science, Osaka University, 1-1 Machikaneyama-cho, Toyonaka, Osaka, Japan (*correspondence: nnishiyama@ess.sci.osaka-u.ac.jp)

Mineral-water contact area (reactive surface area) of a rock is an essential parameter for quantitative treatment of water-rock interaction. Although mineral-water contact areas have been often estimated by the gas adsorption method and image analysis, pore spaces in rocks near the Earth's surface are not always filled only with water but also with air. In such unsaturated condition, only a portion of mineral surfaces may contact water. However, knowledge of the dependence of mineral-water contact area on water saturation (the proportion of pore water volume to total pore volume) has been very limited. In the present study, we performed the dissolution experiments using a sandstone under various water saturations. Fontainebleau sandstone from France, having a porosity of 7% and being composed of ~100% quartz, was used. In the experiments (Fig. 1), a constant water pressure was applied to the rock core whose water saturation was adjusted in advance, and volumetric flow rate Q [m^3 s^{-1}] and concentration of dissolved Si [mol m^{-3}] were measured. Mineral-water contact ratio α, the proportion of mineral-water contact area at the given water saturation to that at the saturated condition, can be calculated by the following relationship: $Q \times [Si] = k_{diss} \times A \times \alpha$, where k_{diss} [mol m^{-2} s^{-1}] is the dissoluton rate of quartz and A [m^2] mineral-water contact area at the saturated condition. It was found that the mineral-water contact ratio is almost unchanged even if water saturation decreases. We attribute this result to the existence of water films wetting mineral surfaces.

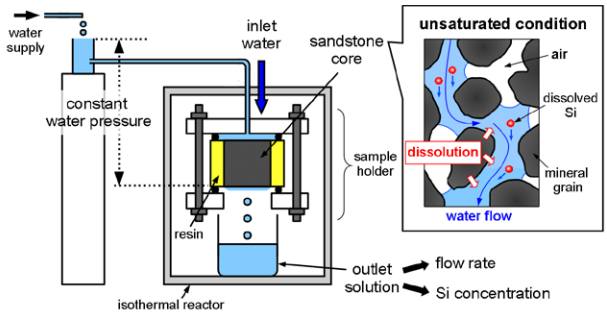

Figure 1: Experimental setup for measuring mineral-water contact area at various water saturations.

Linking nitrogen isotope systematics and microbiology in a subsurface geothermal water stream, Hishikari Gold mine, Japan

MANABU NISHIZAWA[1]*, KEISUKE KOBA[2], AKIKO MAKABE[2], NAOHIRO YOSHIDA[3], MIHO HIRAI[4], JUNICHI MIYAZAKI[1,4], TAKURO NUNOURA[4] AND KEN TAKAI[1,4]

[1]Precambrian Ecosystem Laboratory, JAMSTEC, 237-0061, Japan (*correspondence: m_nishizawa@jamstec.go.jp)
[2]Tokyo University of Agriculture and Technology, Japan
[3]Tokyo Institute of Technology, Japan
[4]Subsurface Geobiology Advanced Research Program, JAMSTEC, 237-0061, Japan

We report biogeochemistry of a subsurface geothermal water stream in the Hishikari gold mine, Japan. The stream, which is derived from a subsurface anaerobic aquifer containing plentiful CO_2, CH_4, H_2, and NH_4^+, emerges in a mine tunnel 320 m below the surface, providing nutrients for a lush microbial community that extends to a distance of approximately 10 m in the absence of sunlight-irradiation. 16S rRNA gene analyses showed a change of microbial community structure along the stream. In the upstream site (72°C), dominant phylotypes were methane-oxidizing bacteria, and hydrogen- and sulfur-oxidizing bacteria. In contrast, dominant phylotypes were closely related to ammonia-oxidizing archaea (AOA) and nitrite oxidizing bacteria (NOB) in the midstream and downstream sites (65 and 57°C). Abundance of archaeal *amoA* gene (10^9 copies/g mat) is much higher than that of bacterial *amoA* gene ($10^{5\sim6}$ copies/g mat). Water chemistry systematically changes along the stream. From the upstream to downstream sites, CH_4, H_2 and NH_4^+ contents decrease, while NO_2^- and NO_3^- contents increase, respectively. These results indicate a tight coupling of microbial community structure and chemical dynamics of C, H, and N in the subsurface hydrothermal ecosystem.

We extensively studied the nitrogen dynamics driven by thermophilic AOA and NOB. Contents and $\delta^{15}N$ values of inorganic N species in the geothermal water are as follows: NH_4^+: 166 to 255 μM, 0 to 7‰; NO_2^-: 0 to 27 μM, -25 to -27‰; NO_3^-: 0 to 67μM, -1.8 to -2.3‰. Importantly, content and $\delta^{15}N$ value of total fixed-N little change along the stream. By using two-step reactions model in a closed system, we have estimated apparent isotopic fractionations and relative ratio of reaction rate coefficients of ammonia oxidation and nitrite oxidation in the subsurface hydrothermal ecosystem.

https://doi.org/10.1180/S0026461X00006502 Published online by Cambridge University Press

Plutonium interactions with pure and substituted iron and manganese oxyhydroxide minerals

H. NITSCHE[1,2]*, Y.-J. HU[1,2], D.L. WANG[1,2] AND L.K. SCHWAIGER[1,2]

[1]Department of Chemistry, University of California, Berkeley, CA 94720-1460, USA (*correspondence: hnitsche@berkeley.edu)

[2]Nuclear Science Division, Lawrence Berkeley National Laboratory, Berkeley, CA, 94720-816, USA

Due to its long half live 239-Pu is a major concern for radioactive contaminated sites and risk assessment of high-level geologic nuclear waste repositories. Plutonium can co-exist in four stable oxidation states [Pu^{3+}, Pu^{4+}, $Pu(V)O_2^+$, and $Pu(VI)O_2^{2+}$] under environmental conditions. Solubility and speciation can vary widely depending on oxidation state and ultimately affect the transport properties. Oxidized plutonium is orders of magnitude more soluble than the reduced forms, Pu(III) and Pu(IV), and thus Pu(V) and Pu(VI) are more mobile in the environment. Plutonium is highly redox active; contact with the surrounding environment could potentially reduce the more soluble forms of plutonium, causing them to become more insoluble.

We studied the interaction iron oxyhydroxide minerals (ferrihydrite and goethite), as environmentally prevalent mineral phases with hexavalent plutonium. XAS analysis for the sorption of Pu(VI) to pure goethite, showed that Pu(VI) was reduced to Pu(V).

We also investigated the interaction of Pu(VI) with pure manganese oxyhydroxide minerals manganite (MnOOH) and hausmannite (Mn_3O_4). These are minor minerals that have been shown to be present at many current and potential geologic nuclear storage sites as coatings on iron minerals. XANES measurements showed that upon contact with the minerals, all the plutonium sorbed to the minerals was reduced to either Pu(V) or Pu(IV). Fits to the EXAFS imply that the Pu is sorbed to the manganite and hausmannite surfaces in an inner-sphere coordination.

We also studied the influence of manganese as a minor component with synthetic manganese-substituted goethite. Pu(VI) was reduced to Pu(V) or Pu(IV) upon contact with the mineral. The results suggest that manganese is the species responsible for the reduction of Pu(VI) to the more insoluble Pu(IV) oxidation state, and indicate the possibility of limited plutonium migration in the environment through interaction with Mn-containing minerals

Influence of oil price fluctuation to Chinese Economy

NIU JIANYING[1]*, ZHAO LIANRONG[1] AND ZHOU JINSHENG[2]

[1]School of Humanities and Economic Management, China University of Geosciences (Beijing), Xue Yuan Road 29#, Hai Dian District, Beijing, China (*correspondence: niujy@cugb.edu.cn)

[2]China University of Geosciences (Beijing)

Research aiming at relation between oil price and economic activities dated back to 1970's when economic depression happened in main oil consuming countries because of twice oil crisis. However, initial research took energy economy as one part of resources & environmental economics, afterwards research emphasis gradually turned to aspects such as how government policies affect energy consumption and improve efficiency of energy utilization. In recent years, by establishing models, each research conducted analysis, measurement and predict of affection to economic activity index by oil price fluctuation [1]. Research results indicate that large fluctuation of crude oil price caused a certain affects to OECD countries [2].

From the turn of this century up to the present, dramatic rise of oil price has caused a certain affect to Chinese economic operation. By following oil consumption material flow and value chain analysis principle, we have established oil price fluctuation and micro-economic growth related analysis model. We also calculated relative industrial departments oil consumption coefficient. We formed a model of affect by international oil price fluctuation to Chinese economy, overcoming shortage of previous research. We conducted sensitivity analysis and projection about oil price fluctuation affecting Chinese economy, providing scientific evidence to the nation for formulating early warming mechanism on guarding against oil price risk.

[1] George Filis (2010) *Energy Economics* (2010) **32**, 877–886. [2] Fabio Milani (2009) *Energy Economics* (2009) **31**, 827–837.

https://doi.org/10.1180/S0026461X00006502 Published online by Cambridge University Press

Intra-plate magmatism of the Al Haruj Volcanic Field, Libya

SARAH NIXON*, JOHN MACLENNAN AND NICKY WHITE

Department of Earth Sciences, University of Cambridge, Cambridge, CB2 3EQ, UK
(*correspondence: sn340@cam.ac.uk)

The Al Haruj volcanic field covers a 45,000 km^2 area in central Libya. The volcanic field is comprised of a sequence of 6 volcanic phases and a series of lava shields and scoria cones. The volcanic phases were distinguished using ASTER images and field observations. The age of the Al Haruj has been estimated to range from 5.27-0.1 Ma. New ^{3}He exposure dates on the youngest lava flow extend this age range, revealing recent activity with an age of 2.31±0.81 ka (1σ, n=5). Initial phases of volcanism 1-3, consist of both alkali and tholeiitic basalts which were erupted in close spatial proximity. The younger phases 4-6 can be attributed to better preserved continuous lava flows and show a more consistent geochemical signature evolving from transitional to sub-alkaline lavas.

The alkali basalts are incompatible trace element enriched and isotopically depleted relative to the tholeiitic samples. Fractional crystallisation occurred at depths of 25-39 km and temperatures between 1215-1360°C. 0-4% combined assimilation and fractional crystallisation introduced a heterogeneous crustal component to the mantle melts. Differentiation processes cannot account for all compositional variability. REE inversion modelling predicts generation of alkali and tholeiitic basalts can be accounted for by melting of a predominately anhydrous mixed mantle source in an upper mantle plume with a mantle Tp of ~1460-1480°C. The maximum melt fractions are 18.9 and 13.5%, extracted at depths of 70 and 74 km for tholeiitic and alkali basalts, respectively.

Across North Africa volcanism is predominately of alkaline affinity. The lithospheric thickness influences the melt fraction; small degree (0.5-2.2%), incompatible element enriched melts, are found beneath regions of thicker lithosphere at Hoggar and Air Massifs. These melts are also isotopically depleted. At the Jebel Marra and Tibesti volcanic provinces, values of Vs are lower and predicted melts fractions are larger (4.4-8.2%) and melts are enriched isotopically. The larger melt fractions estimated for the Al Haruj lavas and the abundance of tholeiitic basalts in comparison to other North African volcanic fields is attributed to a higher Tp in addition to the occurrence of thinner lithosphere (<80 km). North African Cenozoic volcanic provinces can be explained by diapiric upwellings or hot fingers originating in the upper mantle. Isotopic enrichment of larger melt fractions may represent a greater proportion of a lithospheric or plume component in the source.

Pb-Sr-Nd systematics of the early Mauna Kea Shield Phase and insight into the Pacific deep mantle

INÊS GARCIA NOBRE SILVA*, DOMINIQUE WEIS AND JAMES S. SCOATES

PCIGR, EOS, University of British Columbia, Canada
(*correspondence: inobre@eos.ubc.ca)

High-precision Pb, Sr and Nd isotopic compositions of 40 basalts from the bottom 408 metres of core recovered during the final phase of the Hawai'i Scientific Drilling Project (HSDP2-B and -C) reveal compositional continuity of the >650 ka stratigraphic record of Mauna Kea volcano, with the majority of the basalts plotting along the 'Kea-mid8' array [1]. Compared to the previous ~3099 m of drill core, the upper 210 m (3098.2 to 3308.2 m) of samples from this drilling phase show very restricted isotopic variations (e.g. 5x and 3x smaller variation for ^{206}Pb/^{204}Pb and ^{86}Sr/^{87}Sr, respectively). This indicates sampling of a more homogeneous source domain during the time interval represented by the eruption of these basalts. In contrast, samples from the deeper 170 metres show the largest range of ^{206}Pb/^{204}Pb (18.304–18.693) and ^{208}Pb/^{204}Pb (37.923–38.270). These older lavas extend the isotopic record of Mauna Kea both to significantly more radiogenic values, similar to the isotopic compositions shown by 'ancestral' Kilauea lavas [2], and to significantly less radiogenic values, similar to those observed in Mauna Kea and Kohala post-shield lavas [3]. Based on their older ages (> 650 kyr) and compositional characteristics, these basalts likely erupted in the very early shield phase of Mauna Kea, rather than representing part of the output of Kohala or another unknown volcano [4]. Similar to Mauna Loa [5], the earlier stages (older lavas) of Mauna Kea volcanism are isotopically more variable than subsequent stages. Overall, the isotopic heterogeneity in Mauna Kea shield lavas can be explained by mixing variable proportions of four isotopically distinct components intrinsic to the Hawaiian mantle plume: the more radiogenic 'Kea' component, a high ^{208}Pb*/^{206}Pb* (producing low-SiO_2 basalts) component similar to Loihi, and two components with less radiogenic Pb isotopic compositions. Besides being a common, long-lived component in the Hawaiian plume, 'Kea' has isotopic similarities to the common mantle component 'C'. The fact that it is positioned at the convergence between other Pacific Ocean island basalt groups suggests that 'Kea' is a common composition in the deep mantle beneath the Pacific Ocean basin.

[1] Eisele *et al*. (2003) *G*^{3} **4**, 1–32. [2] Kimura *et al*. (2006) *JVGR* **151**, 51–72. [3] Holcomb *et al*. (2000) *Geology*, **28**, 547–550. [4] Blichert-Toft & Albarède (2009) *EPSL* **282**, 190–200. [5] D. Weis (in preparation)

https://doi.org/10.1180/S0026461X00006502 Published online by Cambridge University Press

Nucleation and growth of calcite particles: Comparing modelling and experimental approaches

C. NOGUERA[1]*, B. FRITZ[2] AND A. CLÉMENT[2] AND G. MONTES-HERNANDEZ[3]

[1]INSP, CNRS-UPMC, Paris, France (*correspondence: noguera@insp.jussieu.fr)
[2]LHYGES, Université de Strasbourg/EOST, CNRS, France
[3]ISTerre, Université J. Fourier, CNRS, Grenoble, France

The development of CO_2 storage projects stimulates an extensive use of geochemical models for the precipitation of mineral phases and particularly carbonate phases. A thorough modelling of the formation of secondary minerals in geochemical processes requires an account of nucleation and growth mechanisms in a generalized kinetic approach. We have developed the Nanokin code [1-3] which models kinetic dissolution of primary minerals and precipitation of secondary minerals, relating the nucleation and growth of precipitated particles to the saturation state of the aqueous solution. This model predicts the size evolution of created particles and the feedback effect on the aqueous composition.

We present an application of the Nanokin code to the formation of calcite from a supersaturated solution produced by the dissolution of portlandite at 30°C with a high pH value around 12. These conditions correspond to those selected by Montes *et al*. [4] in their recent experimental approach. The simulated calcite particles are produced by heterogeneous nucleation and tri-dimensional growth.

The results show that the nucleation of calcite occurs rapidly from the initial dissolution stages of portlandite as obtained experimentally during the first 5 hours of reaction. The nucleated particles grow over 24 hours, reaching sizes of about 70-75 nm which compare well to the sizes obtained experimentally (64 nm).

This modelling approach validated at 30°C may be extended to higher temperatures up to 90°C as in the experimental approach.

[1] B. Fritz, A. Clément, Y. Amal, & C. Noguera (2009) *GCA* **73**, 1340–1358. [2] Noguera C. Fritz B. Clément A. & Amal Y. (2010) *Chem Geol*. **269**, 89–99. [3] Noguera C. Fritz B. & Clément A. (2011) *GCA* (in press) DOI: 10.1016/j.gca.2011.03.016. [4] F. Montes-Hernandez, A. Fernandez-Martinez & F. Renard (2009) *Crystal Growth & Design* **9**(10), 4567–4573.

Spin crossover and iron-rich silicate melt in the Earth's deep mantle

R. NOMURA[1]*, H. OZAWA[1,2], S. TATENO[1], K. HIROSE[1,2], J. HERNLUND[3], S. MUTO[4], H. ISHII[5] AND N. HIRAOKA[5]

[1]Tokyo Institute of Technology, Tokyo 152-8551, Japan (*correspondence: nomura.r.ab@m.titech.ac.jp)
[2]Japan Agency for Marine-Earth Science and Technology, Kanagawa 237-0061, Japan
[3]University of California, Berkeley, California 94720, USA
[4]Nagoya University, Nagoya 464-8603, Japan
[5]National Synchrotron Radiation Research Center, Hsinchu 30076, Taiwan

The density crossover between melt and solid in the deep mantle has long been speculated with profound implications for chemical evolution of our planet[1]. Recent *ab-initio* calculations[2] suggested that melt-solid iron partitioning is the key to cause density crossover, which has been examined only at low pressures (25 GPa)[3].

In this study, we performed melting experiments on $(Mg_{0.89}Fe_{0.11})_2SiO_4$ olivine using laser-heated diamond anvil cell (LHDAC) and extended measurements of iron partitioning over the entire mantle pressure range.

The calculated Mg-Fe distribution coefficient K_D between melt and liquidus phase (Fig. 1) showed the sudden drop of K_D value at about 76 GPa, which could be explained by a Fe^{2+} spin crossover (from high-spin to low-spin) in melt suggested by additional X-ray emission spectroscopy (XES) measurements in $(Mg_{0.95}Fe_{0.05})SiO_3$ glass which observed the change of spin state at about 70 GPa and room temperature.

The culculated density of (Mg, Fe)SiO_3 liquid coexisting with $(Mg_{0.92}Fe_{0.08})SiO_3$ perovskite shows that melt is denser than solid below 1800 km depth in the Earth. These results suggest that dense basal magma ocean in the early Earth whose subsequent crystallization may have formed large low shear velocity provinces (LLSVPs) and ultra low velocity zone (ULVZ).

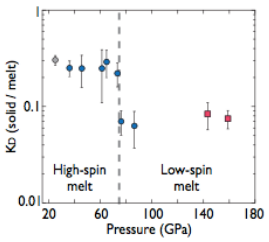

Figure 1: Change in Fe-Mg distribution coefficient K_D between perovskite (blue circle) or post-perovskite (red square) and melt. The datum of previous experiment is shown in grey circle [3].

[1] Labrosse *et al*. (2007) *Nature* **450**, 866–869. [2] Stixrude *et al*. (2009) *EPSL* **278**, 226–232. [3] Corgne *et al*. (2005) *GCA* **69**, 485–496

https://doi.org/10.1180/S0026461X00006502 Published online by Cambridge University Press

Fractionation of $^{238}U/^{235}U$ during weathering and hydrothermal alteration

J. NOORDMANN[1]*, S. WEYER[1], M. SHARMA[2], R.B. GEORG[3], S. RAUSCH[4] AND W. BACH[4]

[1]Institute of Mineralogy, University of Hanover, Germany (*correspondence: j.noordmann@mineralogie.uni-hannover.de)
[2]Department of Earth Sciences, Dartmouth Collage, New Hampshire, USA
[3]Worsfold Water Quality Centre, Trent University, Canada
[4]Geosciences Department, University of Bremen, Germany

Recently, fractionation of $^{238}U/^{235}U$ has been observed between oxic and anoxic oceanic environments [1]. To use U isotopes as a proxy to constrain mass fluxes or the redox evolution of the oceans [2], we need detailed information on the U isotope mass balance. However, U isotope fractionation during continental weathering and transport to the oceans, as well as during hydrothermal alteration (the second most important sink for U) is yet unknown.

Here, we analysed $\delta^{238}U$ of water samples from rivers of different climatic conditions, granites of different localities, five different hydrothermal fluids from the Juan de Fuca Ridge and altered oceanic crust from the Bermuda Rise, Reykjanes Ridge and Pigafetta Basin

Large rivers display an average $\delta^{238}U$ of -0.24 ‰ (relative to CRM-112A) which is very similar to the average value of granites ($\delta^{238}U$ = -0.30 ‰) and basalts ($\delta^{238}U$ = -0.28 ‰), indicating that in average only minor U isotope fractionation occurs during weathering and transport. Only smaller rivers display larger U isotope variations (between 0.01 and -0.28 ‰) likely monitoring U isotope variations of their bed rocks. The hydrothermal waters display a tight range of $\delta^{238}U$ (-0.28 and -0.50 ‰) around the seawater value of $\delta^{238}U$= -0.37 ‰ (modified after [1]), however, at much lower U concentration levels (0.08 to 0.24 ppb) compared to that of seawater (3.3 ppb, [1]). Also, most of the analyzed altered basalts have $\delta^{238}U$ similar to that of fresh basalts ($\delta^{238}U$= -0.42 to -0.23 ‰), with two notable exceptions (0.18 and 0.31 ‰). Accordingly, removal of U from the ocean water during hydrothermal alteration of the oceanic crust appears not to result in significant U isotope fractionation in most cases.

[1] Weyer *et al*. (2008) *GCA* **72**, 345–359. [2] Montoya-Pino *et al*. (2010) *Geology* **38**, 315–318.

Geochemistry in a boreal stream after a major forest fire — Implications for a changing climate

FREDRIK NORDBLAD[1], FRAUKE ECKE[1,2] AND JOHAN INGRI[1]

[1]Division of Geosciences, Luleå University of Technology, S-97187 Luleå, Sweden (*correspondence: fredrik.nordblad@ltu.se)
[2]Department of Aquatic Sciences and Assessment, Swedish University of Agricultural Sciences, Box 7050, S-750 07 Uppsala, Sweden

In August 2006, a major wildfire burned 15 km^2 of boreal forest land near Harads, a town in the north of Sweden. The purpose of this work was to examine wildfire effects on surface water geochemistry in a boreal catchment.

In 2007, increased dissolved output of major elements Ca, K, Mg, Na and elevated conductivity was measured in a stream draining the burnt area. Repeated measurements in 2009 showed a considerable decrease in conductivity and post-fire release of major elements from the burned catchment, which was interpreted as regression towards pre-fire conditions.

A nearby stream not draining the burned area was used as a reference. Conductivity and concentrations of Ca, K, Mg & Na were 1.5 – 7 times lower compared to the burnt creek in 2007. The 2009 re-measurements showed equivalent levels of Ca & Na concentrations and conductivity in both creeks but K & Mg concentrations were still higher in the burnt creek.

The elevated concentrations in the burnt creek in 2007 were interpreted to originate from leaching ash and remainders of burnt organic material on the forest floor. The maintained elevation of K & Mg concentrations in 2009 is likely to be caused by inhibited plant uptake as the biomass was severely reduced by the fire.

Diurnal specific transport rates ($\mu mol/m^2$) in the burnt creek were 1.8 – 2.6 times higher in 2007 compared to 2009. This implies there is a potential for increased transport of major elements from boreal areas since it is likely that wildfire frequency and the extent of burned area will increase according to current climate change scenarios [1].

[1] Soja *et al*. (2007) *Global and Planetary Change* **56**, 274-296.

https://doi.org/10.1180/S0026461X00006502 Published online by Cambridge University Press

Acid mine drainage and responsible mining

D.K. NORDSTROM

U.S. Geological Survey, Boulder, Colorado, 80303, USA (dkn@usgs.gov)

One of the most challenging environmental problems to mitigate or remediate is acid mine drainage (AMD) from metal and coal mining. Until relatively recently, planning for a new mine did not consider the production of AMD or even an accounting of the water cycle (recharge, flowpaths, and discharge). Environmental managers were not considered part of the mining work force and hydrogeologists, geochemists, land use planners, and socio-economic planners were mocked for being irrelevant. Fortunately, this situation has been reversed for many companies and today there are several industry consortiums whose goal is to prevent or mitigate AMD**.** Professionals in the hydrologic, geochemical, geological, and microbiological sciences are being asked more frequently to investigate and advise on water-quality issues and remediation scenarios related to mining and mineral processing. Unfortunately we still have a long ways to go. I suggest that even more fundamental changes are needed: (a) support environmental scientists in hydrology, environmental geology, and geochemistry and involve them in the initial planning stages, in background studies, and in testing of waste materials and modeling their environmental effects. (b) The word mine 'wastes' should be dropped from common usage. An attitude needs to be developed that every bit of earth removed but not economic for ore processing is economic and utilizable for something. (c) Contaminant water pathways can be anticipated beforehand with hydrogeochemical expertise and after waterways have been polluted, careful investigations through synoptic sampling and tracer-injection test can establish sources and sinks of AMD, simulate potential remediation scenarios, and determine the reasons for successes and failures of remediation from properly monitored sites.

Geochemical and physical characteriation of palaeo and contemporary redox interfaces within Late Palaeozoic sediment sequences in South Australia

VERITY NORMINGTON*, S.M. HILL AND ROBERT C. DART

Deep Exploration Technologies Cooperative Research Centre. School of Earth and Environmental Sciences. University of Adelaide. SA 5005 (*correspondence: verity.normington@adelaide.edu.au)

The record of Late Carboniferous to Permian glacial erosion and deposition in South Australia is part of the Late Palaeozoic Gondwanan glaciation. Although there have been many different sedimentological and palaeogeographical studies of these sediments, they have not been mutli-element, geochemically characterised. This study identifies and briefly characterises some of the redox interfaces within these sediments that have important attributes in accounting for the multi-element characteristics of these sediments from ICP-MS and XRF.

Lodgement tills, fluvial-glacial, lacustine-glacial and glacial-marine sediments are abundant within these sequences, with some of the larger and deeper depositional areas (e.g. Arckaringa Basin) also containing fluvial and coal swamp deposits. Some of the most extensive redox interfaces are associated with the interfaces between geochemically reduced lignite beds and geochemically oxidised sandstone beds. These interfaces are major repositories for a range of redox-sensitive elements, in particular U. Another important setting for redox interfaces is within the predominantly geochemically reduced clays and interbedded oxidised fine sands within the glacial marine sediments. These interfaces typically feature tabular sheets of calcareous and silicified sandstones, as well as silica-indurated, discoidal reduction spots and in some sites irregular masses of alunite concretions. The third major type of redox interface identified contains variably ferruginised and minor manganiferrous induration. This may be constrained by the hydromorphic attrubites of particular sediment lithologies (e.g. preferentially confined to sandstone or clay beds) or fractures sets within the sequence. Alternatively ferruginisation is associated with redox and weathering profiles associated with palaeosurfaces, with oxidation typically extending vertically downwards into otherwise geochemically reduced sediment.

https://doi.org/10.1180/S0026461X00006502 Published online by Cambridge University Press

Enhancing heavy metal immobilization in SuDS

M. NORRIS[1]*, V. PHOENIX[1], I. PULFORD[1], H. HAYNES[1] AND C. DOREA[2]

[1]University of Glasgow College of Science and Engineering, Glasgow, Scotland G12 8QQ (*correspondence: norris@civil.gla.ac.uk)
[2]Université Laval Département de génie civil et génie des eaux, Québec, QC, Canada G1V 0A6

Introduction

Diffuse water pollution from urban runoff has the potential to carry a variety of heavy metals and other pollutants throughout the environment. Sustainable urban drainage systems (SuDS) are increasingly being used as a first defence for stormwater-borne pollutant removal. One example of a SuDS system is a filter drain; a trench filled with gravel filter material intended to filter pollutants from road runoff and act as storage during high rainfall events.

Since a major component of stormwater runoff can include heavy metals such as Cd, Cu, Pb and Zn, the aim of this study is to increase the heavy metal immobilization of gravel filter media within filter drains. Chemical amendments (iron-oxide coatings) were made to typical filter drain gravel with the aim of increasing affinity for metals. These amendments have already been shown to enhance metal immobilization by finer media such as sand [1, 2] and polyethelyne beads [3].

Experimentation and Results

A process adapted from Liu *et al*. [3] was used to coat 10mm gravel with iron oxide. Initial batch experiments showed that heavy metal removal was pH dependent due to the coating method altering the pH buffering capacity of the gravel. Different coating proceedures generated gravels which buffered batch reaction solutions between pH 3 and 10, (despite repeated washing). Perfecting of the coating method is ongoing, as well as further amendments to gravel which include manganese oxide and clay.

In order to verify geochemical processes, the PHREEQC modelling program was used to determine metal speciation and saturation indices of the solutions. When increased metal removal is observed at higher pH, the solutions are shown to be supersaturated. This is corroborated in batch experiments which show that the immobilization process is non-reversible, and thus likely precipitation dominated.

[1] Edwards *et al*. (1989) *Res J Water Pollut C* **61**, 1523–1533. [2] Lo *et al*. (1997) *Water Sci Technol* **35**, 63–70. [3] Liu *et al*. (2001) *J Environ Eng-Asce* **127**, 868–878.

Usefulness of stable isotopes in small catchment studies: Overview of results from the stressed ecosystems of Central Europe

M. NOVAK*, F. BUZEK, I. JACKOVA, V. CHRASTNY, J. FARKAS, D. FOTTOVA, P. VOLDRICHOVA, M. STEPANOVA AND E. PRECHOVA

Czech Geological Survey, Geologická 6, Prague 5, Czech Republic (*correspondence: martin.novak@geology.cz)

Over the past 20 years, a number of stable isotopes (C, N, S, O, Pb and Zn) have been used in Central European catchments as diagnostic tools in biogeochemical studies or tracers of dispersion pathways of pollutants. Here we summarize the main isotope success stories in a hydrochemical monitoring network of 13 headwater catchments in the Czech Republic. The network, known as GEOMON, has been supplying monthly hydrochemical input-output data since 1994. The monitoring has coincided with a major decrease in industrial emissions, that had peaked in the 1980s, and are now lower. We have documented linkages between the behaviour of C, N and S in ecosystems. Assimilation of all three elements by plants is associated with an isotope fractionation. Plant tissues tend to accumulate lighter isotopes. In soils, both in upland and wetland locations, degradation of organic molecules is associated with preferential release of the lighter isotopes of C, N and S. The residual vertical soil profiles exhibit isotopically heavier C, N and S with an increasing depth. In retrospective studies, comparing isotope data from emanating greenhouse gases and from organic soils can provide an insight into terminal C, N and S mineralization. Vertical stratification of S isotopes in soils has been used to calculate the proportion of organically cycled anthropogenic S in stream discharge. It appears that most acidifying S was stored in the topmost organic soil horizon and is now flushed out of the ecosystem. Soil solutions, taken by lysimeters, contain newly formed nitrate and sulfate, isotopically different from that in rainfall/canopy throughfall. Sulfate oxygen isotopes systematically show that throughfall sulfate was mainly formed by heterogeneous oxidation of SO_2, wherese sulfate deposited in open areas was mainly formed by homogeneous oxidation of SO_2. Lead isotopes in tree rings and peat profiles are useful as archives of past pollution rates and for apportionment of pollution sources (coal burning, traffic, ore smelting). Zinc isotope ratios, recently determined in ice accretions and snow, fingerprint pollution sources that are rarely situated upwind from the receptor sites.

https://doi.org/10.1180/S0026461X00006502 Published online by Cambridge University Press

Lithium isotope fractionation in pegmatites — Function of bond length

M. NOVÁK[1], T. MAGNA[2,3], J. CEMPÍREK[4], V. JANOUŠEK[3], C.V. ULLMANN[5] AND U. WIECHERT[5]

[1]Masaryk University Brno, Czech Republic
[2]Universität Münster, Germany (tomas.magna@geology.cz)
[3]Czech Geological Survey, Prague, Czech Republic
[4]Moravian Museum, Brno, Czech Republic
[5]Freie Universität Berlin, Germany

Large ranges in Li isotope compositions of pegmatites have recently been reported and δ^7Li variations variously ascribed to melt–exsolving fluid fractionation [1], source variations [2], the ^{7}Li affinity to occupy stronger (i.e. shorter) Li–O bonds [3] or extensive crystal–melt fractionation [4].

Petalite, spodumene, amblygonite, lepidolite, tourmaline, beryl, muscovite and secondary lithiophosphate and cookeite from two pegmatites with similar mineral assemblages but distinct ages (Nová Ves, Czech Republic, ~335 Ma; Tanco, Canada, ~2640 Ma), show large range in Li (770–154, 000 ppm) and δ^7Li (from -2 to +32‰). The Nová Ves pegmatite has δ^7Li comparable with crustal rocks from wider area [5, 6] while the Tanco pegmatite has uniformly high δ^7Li >9‰, indicative of distinct sources (melting of upper continental crust vs. ^{7}Li-rich brines) for the two localities. δ^7Li tends to increase with decreasing coordination number of Li in the crystal lattice (see also [3, 4]). More notably, tight negative δ^7Li correlation with the Li–O bond length is observed with nearly identical slopes for both localities, perhaps suggestive of general rule driving the Li isotope fractionation at moderate temperatures (500–250°C), overall confirming experimental results [3]. These observations are further tied by broadly similar order of crystallizing mineral phases but the crystallization sequence does not result in uni-directional evolution of δ^7Li. Thus, the Li–O bond length appears to be the key factor in fractionating Li isotopes, irrespective of genetic context (parental melt, sub-solidus or hydrothermal origin). Also, pegmatite zones crystallized from Na–Li-rich melts during the final phase of solidification are the most important carriers of Li, implying (i) behavior of the whole system as a near-infinite Li reservoir and (ii) high Li mobility in Na–Li–F-rich melts and hydrothermal fluids that impedes development of Li isotope heterogeneity.

[1] Maloney *et al*. (2008) *Eur J Min* **20**, 905–916. [2] Shabaga *et al*. (2010) *Min Mag* **74**, 241–255. [3] Wunder *et al*. (2011) *Eur J Min* **23**, doi, 10.1127/0935-1221/2011/0022-2095. [4] Teng *et al*. (2006) *Am Min* **91**, 1488–1498. [5] Janoušek *et al*. (2009) *GCA* **73**, A586. [6] Magna *et al*. (2010) *Chem Geol* **274**, 94–107.

Water contents of incipient partial melts in equilibrium with peridotite at upper mantle conditions

D. NOVELLA* AND D.J. FROST

Bayerisches Geoinstitut, Universität Bayreuth, D-95440 Bayreuth, Germany
(*correspondence: davide.novella@uni-bayreuth.de)

Beneath mid ocean ridges the onset of adiabatic melting in the mantle is thought to first occur through the formation of small degree melts likely rich in H_2O. Small degree melts produced from a mantle with a relatively low bulk H_2O content still have the potential to strip trace elements from larger regions of the mantle compared to dry melting processes. Also, the presence of such melts may be responsible for the low viscosity of the asthenospheric mantle and for the regular metasomatism of the lithospheric mantle. Therefore, the compositions of incipient melts in particular the H_2O content and H_2O partitioning between the melts and peridotite minerals are very important and need to be constrained.

The aim of this study is to determine the chemical composition and H_2O content of small degree partial melts that form by melting a hydrous peridotite at pressures and temperatures compatible to the upper mantle and to determine the H_2O mineral-melt partitioning.

Sandwich experiments have been performed at 6 GPa and 1400°C, the adiabatic temperature at this depth. In our experiments, an initial guess melt composition containing H_2O is sandwiched between layers of peridotite and equilibrated at high P and T. Changes in the melt composition during the equilibration result in a new melt composition, which is then used as a starting material in a second experiment. After several iterations a melt composition is found saturated in the same peridotite assemblage as found under anhydrous conditions at the same P and T. The water content of each experiment has to be assessed through mass balance. We then measure the mineral/melt partition coefficients. Our results have implications in terms of melt production in the Earth's upper mantle and observed anomalies in the propagation of seismic waves.

https://doi.org/10.1180/S0026461X00006502 Published online by Cambridge University Press

Cenozoic volcanic activity in North Sudetic Basin (Lower Silesia, SW Poland) —Possible evolution model based on combineded petrological, geochemical and isotopic investigation of litospheric xenoliths and volcanic host-rocks

M. NOWAK[1]*, A. MUSZYŃSKI[1] AND P. MICHALAK[1,2]

[1]Institute of Geology, Adam Mickiewicz University in Poznań (*correspondence:mnap@amu.edu.pl)
[2]Institut für Mineralogie, TU Bergakademie Freiberg

The Cenozoic volcanism in the North-Sudetic Basin (CEVP) took place ca. 30 to 18 Ma [1]. Throughout the basin (Złotoryja and Jawor area) there are about 26 outcrops on the surface, mostly in the form of necks, lava flows and veins [1, 2].

The model was based on considerate microscopic observations of all xenoliths (after excluding such effects as decompression melting, interaction with a host rock etc.), analysis of petrological, chemical and isotopic variation of the host-rocks and literature data [1, 2, 3].

As the orogenic movements and asthenospheric activity intensified, the lithospheric mantle was penetrated by melts that caused crystallization of pyroxenites and early cumulates. Subsequent uplift of the asthenospheric mantle resulted in partial melting of the lithospheric mantle and first significant peak of volcanic activity in the area (Oligocene). The material supplied form deeper parts of the lithosphere/asthenosphere caused an increase in metasomatism of the lithospheric mantle, mainly cryptic metasomatism and locally modal metasomatism [4, 5].

The supply of deeper melts (garnet stability field) in the last phase of the volcanic activity (Miocene) along with partial melting of the metasomatized lithospheric mantle resulted in changes in chemical and isotopic composition of the studied rocks.

The work was support by MNiSW grant No. NN307040736.

[1] Birkanmajer *et al*. (2007) *Ann. Soc. Geol. Pol*. **77**, 1–16. [2] Ladenberger (2006) *Min. Pol. Spec. Pap*. **29**, 40–48. [3] Majdański *et al*. (2006) *Tectonophysics* **413**, 249–269. [4] Matusiak-Małek *et al*. (2010) *Lithos*, **117**, 49–60. [5] Nowak *et al*. (2010) *EGU* 2010-9299.

Crust-mantle links and a major Mesoproterozoic melting event

G.M. NOWELL[1]*, C.W. DALE[1], D.G. PEARSON[1,2], T. OBERTHÜR[3], A.H. DIJKSTRA[4] AND S.W. PARMAN[5]

[1]Dept. of Earth Sciences, Durham University, DH1 3LE, UK (*correspondence: g.m.nowell@durham.ac.uk)
[2]Dept. for Earth & Atmos Sci, University of Alberta, Canada
[3]Bundesanstalt für Geowissenschaften und Rohstoffe, Hannover, Germany
[4]Centre for Research in Earth Sciences, Plymouth Univ., UK
[5]Dept. of Geological Sciences, Brown University, USA

The evolution of $^{187}Os/^{188}Os$ in residual mantle effectively ceases after large-degree mantle melting events, due to almost complete depletion of Re in the residue. Thus, Os isotopes in mantle rocks can be used to constrain the timing of major melting episodes, by comparison with a chondritic evolution curve, and to investigate the scale of such events through time (e.g. [1]). Platinum-group minerals (PGM) are formed in the mantle and in mantle-derived ultramafic rocks rich in platinum-group elements (PGE). Although difficult to locate and extract directly, PGM are sampled and preconcentrated by fluvial systems. The Os isotope compositions of detrital PGM retain a record of mantle depletion events, owing to their high Os and low Re contents and their resistance to alteration [2]. Laser ablation MC-ICPMS provides a rapid, accurate and precise method for the analysis of large suites of PGM.

Osmium isotope analyses of over 300 PGM from the Witwatersrand Supergroup, the largest recognised Archaean sedimentary basin, indicate major mantle melting in the region at around 3.0 Ga to 3.2 Ga, with the oldest ages (~3.5 Ga). The range of Os isotope values in Wits detrital PGM may reflect multiple ultramafic sources. Unlike Phanerozoic ophiolite-derived suites [2], the Wits PGM do not have a pronounced skew towards older ages, confirming that Archean mantle is less heterogeneous than modern day mantle.

Suites of PGM from a Philippine ophiolite and the Rhine river system, the latter sampling various ultramafic bodies of the Alps, have major modes in $^{187}Os/^{188}Os$ corresponding to a depletion age of ~0.5 Ga, but also display subsidiary peaks at ~1.2 Ga and possibly around ~2 Ga, similar to ages found in other global ophiolites [2]. This confirms the global nature of the 1.2 Ga event and indicates a significant mantle to crust mass flux at that time, as documented in the zircon record.

[1] Shirey & Walker (1998) *Annu. Rev. Earth Planet. Sci*. **26**, 423–500. [2] Pearson *et al*. (2007) *Nature* **449** (7159) 202–205.

Re-Os ages of Besshi-type massive sulfide deposits associated with *in situ* basalt as a new age constraint for ridge subduction

T. NOZAKI[1,2], Y. KATO[2], K. SUZUKI[1], Y. TAKAYA[2] AND K. NAKAYAMA[3]

[1]IFREE/JAMSTEC, 2-15 Natsushima-cho, Yokosuka, Kanagawa 237-0061, Japan (nozaki@jamstec.go.jp)
[2]Univ. of Tokyo, 7-3-1 Hongo, Bunkyo-ku, Tokyo 113-8656, Japan (ykato@sys.t.u-tokyo.ac.jp)
[3]Nittetsu Mining Consultants Co. Ltd., 4-2-3 Shiba, Minato-ku, Tokyo 108-0014, Japan (nakayama@nmconsults.co.jp)

Introduction

We report two Re-Os ages for the Makimine and Shimokawa (Kyusyu and Hokkaido area, southwestern and northeastern parts of Japan, respectively) Besshi-type massive sulfide deposits in the Northern Shimanto Belt. These Besshi-type deposits are characterized by close association with an *in situ* basalt whose geochemical composition is similar to those of mid-ocean ridge basalts. Terrigenous clastic materials such as sandstone and mudstone directly overlie massive sulfide layers, indicating that the Makimine and Shimokawa deposits were formed in the marginal sea.

Results and Discussions

The Re-Os ages obtained for the Makimine and Shimokawa deposits are ca. 89 Ma and 48 Ma, respectively. Based on the stratigraphic and geochemical features of two Besshi-type deposits, we interpret these Re-Os ages as a timing of sulfide deposition on a paleo-seafloor when the Kula-Ridge subducted to the paleo Japanese island arc in the Late Cretaceous. The Re-Os age of the Makimine deposit (89 Ma) is generally consistent with the timing of the ridge subduction determined by microfossils in the sedimentary rocks. The plate motion model has documented the the northeastward migration of ridge subduction occurred at the Late Cretaceous Japanese island arc. Considering that the distance between two Besshi-type deposits is about 1, 600 km, this migration speed is estimated to be 4 cm/yr, which is very consistent with the model estimation.

Asthenospheric signature in mantle xenoliths from Enmelen, NE-Russia?

TH. NTAFLOS[1]*, C. TSCHEGG[1], M. BIZIMIS[2] AND V.V. AKININ[3]

[1]Dept. of Lithospheric Research, Univ. Vienna, Austria (*correspondence: theodoros.ntaflos@univie.ac.at)
[2]Dept. Earth and Ocean Sciences, Univ. S. Carolina, USA
[3]NE Interdisciplinary Science Research Institute, Russia

The late Cenozoic intra-plate Bering Sea Basalt Province (BSBP) comprise 17 volcanic fields that occur on islands in the Bering Sea, on the west coast of Alaska and on the northeast cost of Russia. The lavas are mainly tholeiitic and alkaline olivine basalts with subordinate basanites and nephelinites. The Enmelen volcanic field in east Chukotka, NE Russia, differs from the other volcanic fields in that the majority of the lavas are strongly undersaturated (nephelinites, olivine melanephelinites and basanites) and carry abundant mantle xenoliths. The sampled xenoliths hosted by the lavas are mainly fertile spinel lherzolites but few depleted spinel lherzolites occur as well.

Based on the bulk rock and clinopyroxene trace element analyses the Enmelen spinel lherzolites can be divided into three groups. Group A represents non-metasomatized xenoliths that have experienced 3-4% fractional melting. Group B is represented by spinel lherzolites that have whole-rock chondrite-normalized REE patterns with strongly enriched LREE relative to HREE (La_N/Yb_N=9). Their clinopyroxenes are also enriched in LREE and plot sub-parallel to the whole-rock REE patterns (La_N/Yb_N=7). The lack of hydrous phases suggests that group B has experienced cryptic metasomatism. Group C is characterized by the presence of amphibole. Chondrite-normalized REE from the core of clinopyroxenes have patterns with depleted LREE similar to those of group A. However, their rims show, relative to the core, an increase of the LREE (La_N/Sm_N = 0.21 and 2.44 for core and rim respectively). The introduction of fluids, rich in H_2O, LREE, Sr and Ti and the formation of amphibole must have taken place shortly prior to the incorporation of the rocks into the host lavas and before re-equilibration could be achieved.

The clinopyroxene Sr, Nd, and Hf isotope systematics generally overalap the range of MORBs $^{86}Sr/^{87}Sr$= 0.70222-0.7310, $^{143}Nd/^{144}Nd$=0.51303-0.51333 $^{176}Hf/^{177}Hf$=0.28303-0.28363). These depleted isotopic compositions coupled with the trace element enrichements suggests that any metasomatc overprint must have been relatively recent. These data colectively suggest that the Enmelen peridotite xenoliths most likely originate from the convective asthenosphere.

https://doi.org/10.1180/S0026461X00006502 Published online by Cambridge University Press

Basaltic volcanism in NE-Russia; Evidence for metasomatized depleted mantle underneath Bering Sea Basalt Province

TH. NTAFLOS[1]*, C. TSCHEGG[1], M. BIZIMIS[2] AND V.V. AKININ[3]

[1]Dept. of Lithospheric Research, Univ. Vienna, AUSTRIA (*correspondence: theodoros.ntaflos@univie.ac.at)
[2]Dept. Earth and Ocean Sciences, Univ. S. Carolina, USA
[3]NE Interdisciplinary Science Research Institute, RUSSIA

Small volcanic fields, which are diffuse and widespread in the Bering Sea and in NE-Russia and Alaska define the Bering Sea Basalt Province (BSBP). The Late Neogene Enmelen volcanoes on Chukotka Peninsula, NE-Russia, belong to the BSBP and consist of nephelinites, olivine-melanephelintes and basanites that are relatively MgO-rich with average 1ooxMg# 58, 65 and 64, respectively. The nephelinites have the highest total alkalis (7.5 wt.%) and basanites the lowest (5 wt.%). The high concentrations of REE in the lavas indicate that they have been formed after low degrees of partial melting, whereas the high $(Dy/Yb)_N$ ratios (1.9-2.6) suggest melting in the garnet peridotite field, leaving garnet in the residue.

While the nephelinites have Ba/Ce ratio that vary around the Primitive Mantle value of 4.5, the olivine melanephelinites and basanites have considerably higher ratios ranging from 9 and 10 that point to LILE enrichments in their source.

Radiogenic Sr, Nd, Hf and Pb isotopic ratios aproach MORB-values, with $^{87}Sr/^{86}Sr$ ranging from 0.703094 to 0.703225, $^{143}Nd/^{144}Nd$ from 0.512990 to 0.513031, $^{176}Hf/^{177}Hf$ from 0.283069 to 0.2830907 and $^{208}Pb/^{204}Pb$ vs. $^{206}Pb/^{204}Pb$ values that lie on the NHRL line within the MORB field. Calculated melt segregation T and P vary around 1400 °C and 3.5 GPa respectivevely. For the estimated 0.15 % melt fraction, a Tp of 1450 °C can be inferred precluding any plume activity beneath BSBP. Similar geochemical characteristics have been described for the Pribilof Island, Alaska [1] suggesting that lavas along the BSBP reflect common petrogenetic conditions. Lithospheric extention with addition of LILE-rich fluids to the source could account for the magma generation.

The elevated LILE and high LREE/HREE all support an enriched source, while the radiogenic isotope ratios suggest recent enrichment of a long lived depleted source by fluids from the depleted upper mantle.

[1] Chang *et al*. (2009) *J. Petrol* **50**, 2249–2286.

The Barbados Cloud Observatory: Controls on precipitating shallow cumulus convection

L. NUIJENS*, I. SERIKOV, L.HIRSCH AND K. LONITZ

Max-Planck Institute for Meteorology, Bundesstrasse 53, 20146 Hamburg, Germany (*correspondence: louise.nuijens@zmaw.de)

Shallow cumulus clouds are ubiquitous over the subtropical oceans in regions called the “trades”, after the steady surface winds that once made foreign commerce flourish. These clouds help regulate the transport of moisture and heat between the ocean and the free troposphere and are therefore crucial to the climate system. Their small footprint and limited vertical extent, however, make it challenging to observe them from space or to simulate them accurately in coarse resolution models. Important questions regarding the statistical properties of trade-wind cumuli and what controls their aggregate behavior are therefore still left unanswered.

The cloud observatory on Barbados, an island exposed to the relatively undisturbed trade winds, is a collaborative initiative of the Max-Planck Institute for Meteorology and the Caribbean Institute for Meteorology and Hydrology, and strives to improve our understanding of the interplay between clouds, precipitation, the aerosol and large-scale meteorology. The instrument platform includes a scanning cloud radar and microwave radiometer, as well as a vertically-pointing Raman lidar, water vapor lidar, micro-rain radar and ceilometer, and is operational since April 2010 for a duration of at least three years.

We shall present one year of data from the observatory to indicate the large variability present in cloudiness, even within this meteorological regime (the undisturbed trades). Relationships between cloudiness and rainfall are explored in comparison with the humidity structure derived from Raman lidar water vapor profiles. The presence of features such as a well-defined inversion height and a transition layer near cloud base, and the extent to which they regulate convection, is discussed.

https://doi.org/10.1180/S0026461X00006502 Published online by Cambridge University Press

Unravelling P-T-t paths: Pseudo-sections versus classical phase petrology

P.J. O'BRIEN

Institute für Erd- und Umweltwissenschaften, Universität Potsdam, Germany (obrien@geo.uni-potsdam.de)

Crystalline rocks record critical information about the magnitude and rates of geodynamic processes. Important factors such as: how deep; how hot; how fast; and for how long are all in some way encoded in the mineral assemblages, mineral compositions and microstructures. Our ability to estimate metamorphic pressure–temperature (*P-T*) conditions has improved markedly with the increased availability of thermodynamic data for both simple and complex solid-solution phases, internally-consistent thermodynamic datasets and powerful computer programs to manipulate this data for a variety of equilibrium calculations. An increasingly popular tool is the single composition *P-T* section (commonly termed pseudosection) which allows rapid determination of mineral assemblages, compositions and their modal amounts for a given bulk composition within a specified *P-T* window. Unfortunately, with the increasing popularity has come an increasing disregard for the fact that a rock in equilibrium can only define a single point on such a diagram and that *P-T* paths, interpreted due to compositional zoning, inclusion suites and reaction textures, cannot be reliably indicated on the same, single pseudosection. Fortunately, the solution to this dilemma already exists. It is possible to model the consequences of bulk compositional fractionation along a P-T-path and even to define local bulk chemical sub-domains (e.g. for a single inclusion or between two specific grains). Conventional geothermobarometry, typically utilising standardised formulations of exchange, net transfer or solvus reactions, is only of limited, indicative use. However, if one is confident of having identified a preserved equilibrium assemblage, and assuming that the compositions of the phases have not been subsequently modified, the same conventional thermobarometric reactions can be determined with thorough consideration of the *P*- and *T*- dependence of thermodynamic parameters, including activities, with the internally consistent data. Rocks in perfect (metastable) equilibrium are ideal for studying by a single pseudosection but of zero use for determining *P-T*-time paths. It is only by the combination of petrography, careful microanalysis and thoughtful application of various equilibrium thermodynamic tools, including pseudosections, that we will advance to a better quantification of, and thus also ability to model and predict, geodynamic processes.

Mercury distribution and speciation in a seasonal wetland impacted by mine waste

P.A. O'DAY[1]*, S. SERRANO[1], T. STILSON[1] AND D. VLASSOPOULOUS[2]

[1]University of California, Merced, CA 95343 USA (*correspondence: poday@ucmerced.edu)
[2]Anchor QEA, LLC, Portland OR 97224 USA (dvlassopoulos@anchorqea.com)

Ephemeral pond waters and surface sediments were studied in a seasonal wetland adjacent to the former Sulphur Bank Mercury Mine and Clear Lake (CA, USA) in order to evaluate *in situ* stabilization treatments as a remedial option for Hg-contaminated sediments. Surface ponds fed during winter by acidic groundwater seepage from a pit lake on the adjacent mine site have high and variable total dissolved Hg concentrations ($[Hg]_{tot}$ = 70-2300 ng l^{-1}), but low methyl-mercury (Me-Hg) (<0.1% of $[Hg]_{tot}$). Higher dissolved Me-Hg concentrations, comprising 22-41% of total Hg, are correlated with pond waters influenced by groundwater flux from Clear Lake with circum-neutral pH (~6.6-8.6) and relatively high dissolved organic carbon (~30 mg l^{-1}). Characterization by X-ray diffraction and X-ray absorption spectroscopy (XAS) showed sulfate-rich (gypsum, jarosite) and clay alteration phases in surface sediments influenced by acidic groundwater, and less altered primary minerals and the presence of calcite in neutral pH sediments. Results from bulk and micro-focused Hg XAS of sediments indicated the presence of metacinnabar (HgS (s)), most likely as residual mine waste particles, nearest the former mine with high sediment $[Hg]_{tot}$ concentrations (100-500 mg kg^{-1}). Sediments from weakly acidic and neutral pH ponds had lower $[Hg]_{tot}$ (3-15 mg kg^{-1}), but a higher fraction of Hg associated with extractable organic matter. There was no evidence in sediment Fe or S XANES spectra for the presence of reduced Fe-sulfide minerals, and all surface pond waters were oxidized, with measureable dissolved oxygen and low dissolved Fe. The lack of evidence for active sulfate or Fe reduction in neutral pH ponds with high dissolved Me-Hg suggests that Hg methylation is occurring in the subsurface, with possible transport of Me-Hg by organic matter complexation. Thus, remediation strategies must consider both (1) stabilization of residual HgS (s) particles, but limiting bacterial sulfate reduction and Hg methylation as pond water pH increases with remediation of the pit lake, and (2) transport of Me-Hg in groundwater to surface biological receptors where Hg bioaccumulation may occur.

https://doi.org/10.1180/S0026461X00006502 Published online by Cambridge University Press

Effects of microbial activity and electron shuttles on the reduction of U(VI) under sulfidogenic conditions

E.J. O'Loughlin[1]*, M.I. Boyanov[1] M.J. Kwon[1], P.E. Long[2], K.H. Williams[3] and K.M. Kemner[1]

[1]Argonne National Laboratory, Argonne, IL, 60439, USA (*correspondence: oloughlin@anl.gov)
[2]Pacific Northwest National Laboratory, Richland, WA, 99352, USA
[3]Lawrence Berkeley National Laboratory, Berkeley, CA, 94720, USA

Introduction

Recent studies suggest that electron shuttles such as low molecular mass quinones and humic substances may play a role in many redox reactions involved in contaminant transformations and the biogeochemical cycling of redox active elements. This study investigates the effects of 9, 10-anthraquinone-2, 6-disulfonate (AQDS), a synthetic electron shuttle often used as a surrogate for quinone moieties in humic substances, on transformations of Fe, S, and U under reducing conditions.

Experimental Methodology

Experiments were conducted in defined mineral medium containing 30 mM Fe (III), 5 mM sulfate, and 10 mM acetate, with and without 100 μM AQDS and inoculated with sediment from the Rifle, CO, USA, Integrated Field Research Challenge (IFRC) Site. After the system reached steady state with respect to Fe (III) and sulfate reduction, aliquots of suspension were collected from each system and one set was pasteurized at 70 °C for 1 hr. The suspensions were then spiked with 500 µM U (VI).

Discussion of Results

After 48 h, 100% of the added U was removed from solution in the non-pasteurized AQDS system. However, only 58%, 25%, and 11% of added U was removed in the no AQDS non-pasteurized, AQDS pasteurized, and no AQDS pasteurized systems, respectively. U XANES analysis of the hydrated solids indicated that, with the exception of the pasteurized system without AQDS, the majority (85-95%) of the U associated with the solids was reduced to U (IV). The results of the EXAFS analysis of U (IV) in the systems with and without AQDS (not pasteurized) are consistent with the formation of nanoparticulate uraninite. The results of this study suggest that microbial reduction was the dominant process contributing to the reduction of U (VI) over the timescale of this experiment and that the presence of AQDS enhanced both biotic and abtiotic/microbially mediated U (VI) reduction.

Age and origin of the Nuvvuagittuq Greenstone Belt

J. O'Neil[1], R.W. Carlson[1], D.E. Moser[2], L.M. Heaman[3]and D. Francis[4]

[1]Carnegie Institution of Washington, DC, USA, 20015
[2]University of Western Ontario, London, Canada, N6A 3K7
[3]University of Alberta, Edmonton, Canada, T6G 2E3
[4]McGill University, Montreal, Qc, Canada, H3A 2A7

The Nuvvuagittuq belt is dominated by mafic and ultramafic rocks metamorphosed to at least upper amphibolite facies. Primary U-rich minerals that might provide reliable dates for rock formation have yet to be found in the dominant lithology called the Ujaraaluk unit. Metamorphic zircons, rutiles and monazites are, however, present in the unit locally and give variably discordant results with $^{207}Pb/^{206}Pb$ ages ranging from 2.8 Ga to 2.5 Ga. The younger ages overlap 2686±4 Ma zircon ages for intruding pegmatites and Sm-Nd ages for garnet formation in the Ujaraaluk rocks suggesting this era as the time of peak metamorphism and metasomatism in the Nuvvuagittuq belt, coeval with regional metamorphism of the Superior craton. ^{147}Sm-^{143}Nd data for Ujaraaluk whole rocks provide a statistically poor isochron of 3814±300 Ma, but when separated by compositional groups, this 'isochron' is seen to consist of a series of ~2.7 Ga slopes emanating from a baseline distribution older than 4 Ga. Metamorphism at 2.7 Ga will have less effect on the ^{146}Sm-^{142}Nd chronometer because of ^{146}Sm extinction prior to ~4 Ga. Expansion of the ^{142}Nd dataset for the Ujaraaluk rocks and associated ultramafic cumulates continues to show a good correlation between Sm/Nd and $^{142}Nd/^{144}Nd$ that corresponds to an age of 4.359^{+45}_{-67} Ga. The dataset now includes samples with superchondritic Sm/Nd ratios that extend the correlation to values of $^{142}Nd/^{144}Nd$ slightly higher than the terrestrial standard with a total range in $\varepsilon^{142}Nd$ of more than 24 ppm. The upper Sm/Nd end of this correlation is defined by rocks that are interpreted as cumulates to compositionally related extrusive rocks indicating that this crystal fractionation had to occur while ^{146}Sm decay was active, i.e. well before 4 Ga. Intruding gabbros give ^{143}Nd and ^{142}Nd isochron ages overlapping within error at 4.16 Ga also supporting an Hadean age for the belt. Eoarchean tonalites surrounding the Nuvvuagittuq belt show a deficit in ^{142}Nd compared to the terrestrial standard, but plot to the low Sm/Nd side of the Ujaraaluk isochron suggesting that they are remelts of this type of mafic basement. The Nuvvuagittuq belt thus preserves over 1.6 billion years of early Earth history including an expanse of mafic crust formed only ~200Ma after Earth formation.

https://doi.org/10.1180/S0026461X00006502 Published online by Cambridge University Press

The punctuated evolution of the Earth: Geodynamic constraints and model predictions

CRAIG O'NEILL[1],
ADRIAN LENARDIC[2] AND KENT CONDIE[3]

[1]CCFS Centre of Excellence, Macquarie University, Sydney, NSW, Australia
[2]Rice University, USA
[3]New Mexico Tech, USA

The preserved Precambrian crustal record is strongly episodic, and observation that has been attributed to preservational effects or episodic crustal production. These age peaks are associated with juvenile crustal production, voluminous high-temperature volcanism, massive mantle depletion, widespread orogeny and mineralisation, large apparent polar wander velocity spikes, and subsequent paleointensity increases. The impact of these events impinged on the glaciation record, atmospheric and ocean chemistry, and on the rise of oxygen. Here we assess a variety of geodynamic models for Precambrian dynamics against the swath of observational constraints available. We find that episodic behaviour from non-linear slab-driven models - such as mantle avalanches or episodic subduction events - are best able to simultaneously satisfy the majority of geological constraints. In such models, rapid descent of subducted material into the mantle drives fast plate motions and convergence at the surface. This is accompanied by large-scale upwellings of deep hot mantle which contribute to voluminous volcanism. Currently, it is not possible to differentiate the ultimate cause of non-linear plate behaviour solely from the geological record, however, dynamic simulations under Earth-like conditions may be able to secern.

Redox variable trace elements

HUGH ST.C. O'NEILL[1],
ANDREW J. BERRY[2] AND GUILHERME MALLMANN[3]

[1]Research School of Earth Sciences, ANU, Canberra, Australia (hugh.oneill@anu.edu.au)
[2] Department of Earth Science and Engineering, Imperial College London, London SW7 2AZ, UK
[3] Institute of Geosciences, University of São Paulo, São Paulo SP, 05508-080, Brazil

As a change in the oxidation state of an element is usually accompanied by a profound change in its geochemical properties, redox variable elements are potentially sensitive indicators of mantle differentiation processes. Prominent redox variable elements include V, Cr, Mo, the PGEs, Re and U, as well as the volatiles C, H, and S. While Fe is the most abundant redox variable element, likely amounts of Cr, C and S are enough to affect the complex interactions between oxygen content and oxygen chemical potential (or oxygen fugacity, fO_2) that must be understood to quantify the redox state of a system. The presence of abundant Fe^{3+} and Fe^{2+} may obscure the redox state of a trace element in glasses quenched from natural silicate melts because electron exchange reactions (e.g. $Cr^{2+} + Fe^{3+} = Cr^{3+} + Fe^{2+}$) can be too fast for the high temperature speciation to be preserved. Hence spectroscopic measurements on natural materials at room temperature may be misleading.

V occurs in three oxidation states under terrestrial mantle conditions, V^{3+}, V^{4+} and V^{5+}, with a huge variation in incompatibility, making this element a good monitor of mantle redox processes. Its properties may be utilized either through whole-rock abundances to deduce redox conditions during partial melting, or from phenocryst/matrix partitioning, to study magma crystallization. When applied to arc basalts, the two methods show disconcertingly disparate results, crystallization mostly being under oxidized conditions (long known from Fe^{3+}/Fe^{2+} ratios), but from a source of similar redox character to MORB source. Mo systematics show promise for further investigation of this conundrum. U is of particular interest because of the importance of U-Th-Pb systematics in evaluating mantle evolution, and of U series disequilibria in understanding rate processes. While U^{4+} is slightly less incompatible than Th, U^{5+} and U^{6+} are much more incompatible. Significant fractions of U^{6+} are expected at natural fO_2s, with U^{5+} making an unexpected but intriguing appearance at low pressures.

https://doi.org/10.1180/S0026461X00006502 Published online by Cambridge University Press

Petrogenesis of the oceanic crust from trace elements in basalt glasses

HUGH ST.C. O'NEILL* AND FRANCES E. JENNER

Research School of Earth Sciences, ANU,Australia
(*correspondence: hugh.oneill@anu.edu.au)

Laser-ablation ICP-MS gives precise trace-element analyses on small areas of basaltic glasses, not only for the traditionally analysed trace elements (REE, HFSE, LILE and first-row transition elements), but also elements such as Be, Ga, Ge, As, Se, Ag, Cd, In, Sn, Sb, W, Tl and Bi. We have analysed >350 Ocean Floor Basaltic (OFB) glass samples from the Smithsonian collection [1] covering a global range in OFB from the Atlantic, Pacific and Indian oceans, for 53 trace elements, plus sulfur by electron microprobe. EMP analyses of the major elements are given in [1]. Principal Component Analysis of a set of 29 precisely determined (±2%) highly incompatible trace elements (HICE: here, all 26 Refractory Lithophile trace elements plus P, K and Pb) shows that 96% of their variance is contained in the first two PCs (93% with PCA on the correlation matrix). The further statistical treatment of this large data set uncovers a highly systematic variation of HICE with degree of low pressure evolution from beneath the variability due to source heterogeneity and melting processes. This cannot be explained by simple fractional crystallization but reflects magma eruption/discharge processes [2, 3], not evident from major elements, which are buffered along the olivine-plagioclase-clinopyroxene cotectic. This evolution systematically fractionates the HICE among themselves in a way that is not consistent with simple fractional crystallization, e.g. mean Th/U increses from 2.3 at 9.5% MgO to 3.3 at 5.5% MgO. Inverting the parental OFB composition allows average mantle source composition and degree of melting to be calculated independently of assumptions about ocean crust recycling. The result shows that OFBs are a product of a high degree of melting (20 to 25 %), from a source that is too depleted to be balanced by estimates of the composition of the continental crust. This seems to require a non-chondritic Earth [4].

[1] Melson WG, O'Hearn TJ & Jarosewich E (2002) *Geochem Geophys Geosyst* **3**, #1023. [2] Albarede F (1985) *Nature* **318**, 256–258. [3] O'Hara MJ & Herzberg C (2002) *Geochim Cosmochim Acta* **66**, 2167–2191. [4] O'Neill HStC & Palme H (2008) *Phil Trans Royal Soc A* **366**, 4205–4238.

Coupling, decoupling and metasomatism: A saga of crust-mantle relationships beneath NW Spitsbergen (Arctic Norway)

SUZANNE Y. O'REILLY*, N. NICOLIC, W.L. GRIFFIN AND N.J. PEARSON

GEMOC/CCFS, Earth and Planetary Sciences, Macquarie University, NSW 2109 Australia
(*correspondence: sue.oreilly@mq.edu.au)

Recent studies integrating mantle and lower crustal geochronology on xenolith samples, isotopic information from crustal zircons worldwide, and seismic tomographic imaging of deep lithosphere domains, suggest that over 70% of the present deep lithosphere formed by about 3 Ga. Subsequent tectonism has modified the lithospheric mantle and caused crustal reworking. The Bockfjord area of NW Spitsbergen (Norwegian Arctic) provides an ideal natural laboratory to track crust/mantle evolution and tectonism over >3.2Ga. Quaternary alkali-basalt volcanism provides abundant xenoliths of mantle and crustal rocks from both sides of a major translithospheric N-S fault. Zircons from lower-crustal xenoliths (from both sides of the fault) have mainly Neoarchean/ Paleoproterozoic or Paleozoic U-Pb ages; several show ages and/or Hf model ages >3.2 Ga. Mantle-derived peridotite xenoliths east of the fault contain common metasomatic minerals rare in those west of the fault. Re-Os analysis of sulfides in xenoliths west of the fault show T_{RD} model ages to 3.3 Ga; major populations are 2.4-2.6 Ga, 1.6-1.8 Ga and 1.2-1.3 Ga, with rare Caledonian ages. However, sulfides in xenoliths east of the fault show maximum T_{RD} of 2.3 Ga with major peaks at 900-1100 and 400-500 Ma, identical to the spectrum of zircon ages of protoliths for exposed gneisses and schists east of the fault

These data demonstrate a major disjunct, on both sides of the B-B fault, between the Archean lower crust and a Proterozoic-Paleozoic upper crust; this suggests that the original Archean upper (and middle?) crust was detached from the lower crust and replaced by thrust sheets of younger material, probably during the major overthrusting of the Caledonian orogeny. The striking differences in the SCLM on either side of the B-B fault suggest major transcurrent movement, juxtaposing lithospheric sections that evolved discretely at some distance from one another. West of the B-B fault, the presence of Archean lower crust overlying Archean SCLM suggests coupling of the crust and mantle for ≥3 Ga

https://doi.org/10.1180/S0026461X00006502 Published online by Cambridge University Press

In situ U-Pb dating of rutile in UHT granulites from the Gruf Complex, European Central Alps

JEFFREY OALMANN[1]*, ANDREAS MÖLLER[1] AND ROMAIN BOUSQUET[2]

[1]Department of Geology, Univ. of Kansas, 1475 Jayhawk Blvd, Rm. 120, Lawrence, KS 66045, USA (*correspondence: joalmann@ku.edu)

[2]Géosciences Rennes, Université de Rennes 1, Campus Beaulieu, 35042 Rennes Cedex, France (romain.bousquet@univ-rennes1.fr)

In situ U-Pb dating of rutile directly in thin sections preserves textural information including inclusion relationships. Grains included in some minerals such as garnet may preserve older U-Pb ages than matrix grains due to sluggish Pb diffusion through the host mineral and can provide additional constraints on P-T-t evolution.

The Gruf Complex of the Central Alps consists of amphibolite migmatitic gneisses and relict ultra high temperature (UHT) charnockite and sapphirine-bearing granulites. Whether the UHT event occurred during the Permian Variscan orogeny or the Tertiary Alpine orogeny is a matter of debate [e.g. 1, 2, 3]. Amphibolite facies metamorphism and migmatization began at ~32 Ma in the Central Alps, and temperature may have remained >640°C until 22 Ma [4, 5]. The Gruf Complex lies structurally below the Bergell pluton, which crystallized between 32 and 30 Ma [6], and was intruded by the Novate granite at 24 Ma [7].

Rutile in the Gruf granulites was analyzed using laser ablation inductively coupled mass spectrometry. Inclusions in garnet, orthopyroxene, biotite, and sapphirine as well as grains in the matrix and leucosomes were dated to determine if included grains preserve older ages than matrix grains. Average $^{206}Pb/^{238}U$ ages uncorrected for common Pb range from 21-25 Ma for different samples. There is no clear correlation between age and textural setting; however, the oldest concordant date of ~30 Ma is from a grain included in garnet. These ages suggest that cooling from 640°C to below the closure temperature of Pb diffusion in rutile was rapid and possibly occurred as early as 25 Ma in the Gruf Complex.

[1] Liati & Gebauer (2003) *Schweiz Miner Petrog* **83**, 159–172. [2] Schmitz *et al*. (2009) *Eur J Mineral* **21**, 927–945. [3] Galli *et al*. (2011) *Contrib Mineral Petr,* in revision. [4] Rubatto *et al*. (2009) *Contrib Mineral Petr* **158**, 703–722. [5] Berger *et al*. (2011) *Tectonics* **30**, TC1007. [6] Von Blanckenburg (1992) *Chem Geol* **100**, 19–40. [7] Liati *et al*. (2000) *Schweiz Miner Petrog* **80**, 305–316.

Is mineral precipitation the reverse of dissolution?

E.H. OELKERS[1]* G.D. SALDI[2] AND J. SCHOTT[1]

[1]Geoscience and Environment Toulouse (GET), CNRS, UMR 5563, OMP, 14 Avenue Edouard Belin, 31400 Toulouse, France (*correspondence: oelkers@get.obs-mip.fr)

[2]Earth Science Division, Lawrence Berkeley Laboratory, 1 Cyclotron Rd. Berkeley CA 94720, United States

Mineral precipitation and dissolution are fundamental processes governing fluid-solid reactions in nature and chemical mass transfer in the crust; the accurate description of the rates of these reactions within geochemical modelling codes holds the promise to quantify in real time the fate and consequences of processes ranging from radioactive waste disposal and carbon storage to the formation of hydrothermal ore deposits. Based, on the principle of detailed balancing, it has been commonly been assumed that mineral precipitation can be described as the reverse of dissolution; transition state theory rate expressions that successfully describe mineral dissolution as a function of degree of fluid saturation state have been adopted to predict corresponding precipitation rates.

Surface sensitive microscopy suggests similar mechanisms at near to equilibrium; both dissolution and precipitation adds or removes material to existing active sites resulting in a linear dependence of rates on chemical affinity. At far from equilibrium etch pits form on dissolving surfaces, and analogous nuclei form on precipitating surfaces. The differences between dissolution and precipitation, however, stem from the existence of grain edges, which are active sites for dissolution but not precipitation. Moreover, the removal of material from edge sites creates additional active sites for dissolution, but precipitation fills active sites. As a consequence, steady state precipitation is dominated by nucleation in contrast to dissolution which removes material from continuously renewed active sites. This conclusion is supported by our recent measurement of quartz and magnesite dissolution and precipitation rates [1, 2]. Precipitation on grains having pre-existing active sites is consistent with the reversibility of dissolution whereas precipitation on pristine crystals is inconsistent and following independent rate equations.

[1] Saldi *et al*. (2009) *Geochim. Cosmochim. Acta,* **73**, 5646–5657. [2] Saldi *et al*. (2010) *Geochim. Cosmochim. Acta,* **74**, 6344–6356.

https://doi.org/10.1180/S0026461X00006502 Published online by Cambridge University Press

Si isotope fractionation during precipitation of silica by cyclic freezing and adsorption of monosilicic acid on gibbsite

M. OELZE[1], F. VON BLANCKENBURG[1], D. HÖLLEN[2] AND M. DIETZEL[2]

[1]Earth Surface Geochemistry at GFZ German Centre for Geosciences, Potsdam, Germany (Oelze@gfz-potsdam.de)
[2]Institute of Applied Geosciences, Graz University of Technology, Austria

Cyclic freezing of aqueous solutions containing silicic acid can be used to precipitate amorphous silica through complex precipitation-dissolution reactions. In such a dynamic system kinetic isotope effects during an unidirectional transfer from silicic acid to a solid may be equalized by cyclic dissolution of the previous precipitated silica and slow isotopic equilibrium between solutions and solids is potentially attained.

We performed several sets of freeze-thawing experiments to decipher the silicon isotope fractionation during precipitation of amorphous silica at pH 4.5 and 7. The initial solutions contain 1.6 mmol L^{-1} of Si and 0.1 or 1 mmol L^{-1} of Al (TEOS and $AlNO_3 \cdot 9H_2O$). The solutions were frozen and thawed within 24 hours by up to 130 cycles and sampled at regular intervals.

Experiments with high initial Al concentration ([Al] = 1mmolL^{-1}) show changing $\delta^{30}Si$ values with time. The $\delta^{30}Si$ solution values increased during the first 20 freeze-thaw cycles to up to 2.4‰ and then showed a decline to almost starting values of 0‰ after 130 days. Experiments with low Al concentrations ([Al] = 0.1mmolL^{-1}) remained at the value of the initial solution throughout.

Supplementary adsorption experiments, with monosilicic acid (0.36 mmol L^{-1} Si) and gibbsite (55 m^2 L^{-1}) were carried out at pH 7. Adsorption of silicic acid results in an increase of $\delta^{30}Si$ values and a quasi isotopic/chemical steady state is reached at ~ 300 h.

We developed a mass balance approach and applied time-dependent fractionation factors consisting of $\alpha 1_{precipitate\text{-}solution}$ and $\alpha 2_{precipitate\text{-}solution}$ to the freeze-thaw system. Model results predict that during the first 20 freeze-thaw cycles presumably kinetic fractionation was dominant with a 1000ln (α1) = -4.5‰. This value is close to what is observed by adsorption of silicic acid onto gibbsite. Once the system reaches a steady-state the modeled fractionation factor changes to 1000ln (α2) = 0‰. α2 = 1 possibly represents the equilibrium isotope fractionation factor and indicates no discrimination of silicon isotopes between dissolved silicic acid and newly formed amorphous silica or hydroxyalumosilicate.

A profile of multiple Sulfur isotopes for the Oman ophiolite

M. OESER[1,2,*], H. STRAUSS[1], M. PETERS[1], P.E. WOLFF[2], J. KOEPKE[2], D. GARBE-SCHÖNBERG[3] AND M. DIETRICH[2]

[1]Westfälische Wilhelms-Universität, Institut für Geologie und Paläontologie, 48149 Münster, Germany (*correspondence: m.oeser@mineralogie.uni-hannover.de)
[2]Leibniz Universität Hannover, Institut für Mineralogie, 30167 Hannover, Germany
[3]Christian-Albrechts-Universität zu Kiel, Institut für Geowissenschaften, 24118 Kiel, Germany

The Oman ophiolite is regarded to represent the best example of fast-spreading oceanic lithosphere on land. Here, we present the first multiple sulfur isotope profile through all components of the (ancient) oceanic lithosphere (Fig. 1), together with sulfur abundances and a petrographic study.

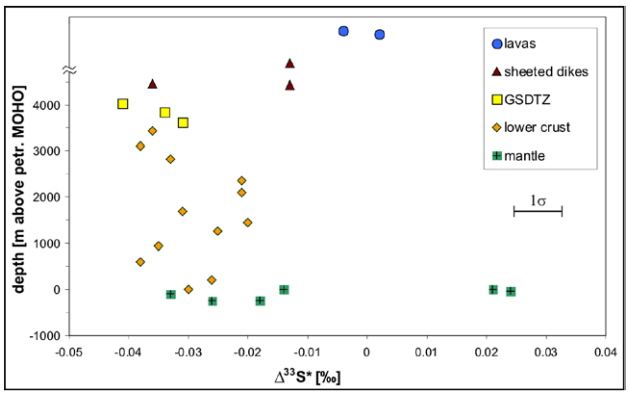

Figure 1: $\Delta^{33}S^*$ values of Cr-reducible sulfur versus depth for a composite section through the Oman ophiolite; $\Delta^{33}S^* = \delta^{33}S - 1000 \times ((1 + \delta^{34}S / 1000)^{0.515} - 1)$ [1]; GSDTZ represents the gabbro/sheeted dike transition zone.

Our results indicate that upper crustal rocks of the Oman ophiolite (lavas and sheeted dikes) exhibit: (i) pervasive alteration due to intense circulation of seawater; and (ii) microbial reduction of seawater sulfate occurring within the lavas during low-temperature alteration. Samples from the gabbro/sheeted dike transition zone and lower crustal rocks are affected by a high-temperature alteration resulting in leaching and redistribution of sulfide-S. $\Delta^{33}S^*$ values of Cr-reducible sulfur (CRS) between -0.020‰ and -0.038‰ clearly differ from those of upper crustal rocks (Fig. 1). This could either suggest that intense sulfur leaching processes operate in those units, or that oceanic lower crust has a primary multiple sulfur isotopic composition that deviates from the postulated mantle value ($\Delta^{33}S^* = 0.0$‰; [1]). Samples from the mantle portion of the Oman ophiolite display the widest ranges in $\delta^{34}S$ and $\Delta^{33}S^*$ reflecting multi-stage serpentinization processes.

[1] Farquhar *et al*. (2002) *Science* **298**, 2369–2372.

https://doi.org/10.1180/S0026461X00006502 Published online by Cambridge University Press

Geochemical behavior of As originated from acidic thermal water during river transport and sedimentation mechanism

Y. OGAWA[1]*, N. SHIKAZONO[2], K. IWANE[2], Y. TAKAHASHI[3], K. SUTO[1] AND C. INOUE[1]

[1]Graduate School of Environmental Stidies, Tohoku University, Miyagi 980-8579, Japan (*correspondence: ogawa@geo.kankyo.tohoku.ac.jp)
[2]Department of Applied Chemistry, Faculty of Science and Technology, Keio University, Kanagawa 223-8522, Japan
[3]Marine Microbiology, Atomosphere and Ocean Research Institute, University of Tokyo, Chiba 277-8564, Japan

We investigated change in the physico-chemical and redox status of As originated from the acidic Tamagawa thermal waters during transport in Shibukuro and Tama Rivers and sedimentation mechanism in the watershed.

The predominant dissolved As species in the thermal water was arsenite. However, this specie was rapidly oxidized. Thus, the geochemical mobility of arsenate was mainly controlled by the sorption onto hydrous ferric oxides (HFO). Most HFO sorbing As was transported and effectively settled onto the downstream man-made lake.

Most of As in riverbed and shallow part of lake sediments were extracted as reducible phase, indicating that they are originated from the Tamagawa hot spring area transported as HFO sorbates. Furthermore, XANES spectra reveal that As existed as As (V). On the other hand, As in deep part of lake sediments could not be extracted by reducing agent and XANES spectra reveal the conversion to As (III). The arsenite and ferrous ion was also detected in the interstitial water. These results indicate that HFO sorbing As was reduced during the sedimentation process.

The iron-oxidizing bacteria inhabited in acidic river water. The inhabitations of several microorganism including sulfate-reducing bacteria in deep part of lake sediment were also confirmed. Taking these facts into consideration, the As mobility in this river system would be possibly controlled by the bacterial activities.

Development of the modern-style geochemical cycle of uranium by 3.5 Ga: A solution to the 'lead paradox'

H. OHMOTO[1], Y. WATANABE[1], K.E. YAMAGUCHI[2], D.C. BEVACQUA[1], I. JOHNSON[1] AND T. RUSHTON[1]

[1]NASA Astrobiology Institute and Dept. of Geosience, Penn State University, University Park, PA 16802, USA and hqo@psu.edu
[2]Department of Chemistry, Toho University, Funabashi, Chiba, 274-8510, Japan

From analyses of redox-sensitive elements in many paleosol-, shale-, and submarine basalt- sections 3.5-2.5 Ga in age, we have recognized: (1) depletions of S and C, and depletions/enrichments of U, Mo, Fe, Mn, Cr and Cu in the paleosols; (2) enrichments of U and Mo in many of the black shales; (3) enrichments of U, Fe^{III} and Mo in the basalts that were affected by submarine alteration; and (4) Ce anomalies in many of the paleosols and submarine basalts. Therefore, the behaviours of redox-sensitive elements in these Archean rocks are essentially the same as those in Phanerozoic rocks. This suggests that the Archean oceans were poor in Fe, but rich in U and Mo, and that the modern-style geochemical cycles of redox-sensitive elements through the continental crust, oceans, oceanic crust, and mantle reservoirs have operated since at least ~3.5 Ga. The presence of highly radiogenic Pb in many Archean-age submarine basalts also supports this suggestion. The atmospheric pO_2 >0.5 PAL is necessary to operate the modern-style geochemical cycle of U. Subduction of Fe^{III}- and U-enriched oceanic crust may have created a large-scale heterogeneity of the mantle since ~3.5 Ga, including: (a) the Fe^{III}/Fe^{II} ratio, and (b) the 'lead paradox' where the Pb in the mantle, especially in the source regions of OIBs and MORBs, is more radiogenic than in the chondrite-modeled bulk Earth. Therefore, through the creation of the oxygenated oceans and atmosphere, microbes have influenced the geochemistry of the deep Earth and the nature of volcanism since ~3.5 Ga.

https://doi.org/10.1180/S0026461X00006502 Published online by Cambridge University Press

Trace element composition of size-fractionated particulates in the Mauritanian upwelling zone of the Eastern North Atlantic U.S. GEOTRACES section

DANIEL C. OHNEMUS[1,2] AND PHOEBE J. LAM[2]*

[1]MIT/WHOI Joint Program in Chemical Oceanography, Woods Hole, MA (*correspondence: dan@whoi.edu)
[2]Department of Marine Chemistry and Geochemistry, Woods Hole Oceanographic Inst., Woods Hole MA (pjlam@whoi.edu)

Sinking (>51μm) and suspended (<51μm) particulates were collected via *in situ* filtration during the first US GEOTRACES North Atlantic Zonal Transect on the *R/V Knorr* in October-November, 2010. Total and acetic-acid leachable compositional profiles for key trace elements and isotopes (TEIs—Fe, Al, Zn, Mn, Cd, Cu) and other TEIs of interest (Co, Ti, Ba, V, Ni, Mo) are presented from four stations along the eastern tropical North Atlantic oxygen minimum zone (OMZ) extending from the coast of Mauritania to the Cape Verde Islands.

This dataset provides the first look at full (16-point) ocean-depth profiles of size-fractionated particulate trace elements in this productive and biogeochemically complex region. Particulate inputs, including mineral dust deposition from the Sahara, resuspended particles from the African margin, and in bottom nepheloid layers, are examined via bulk compositional data. Acetic acid-leachable phases are used to examine scavenging and remineralization processes of redox-sensitive and surface-active TEIs, especially within the Mauritanian OMZ and along upwelling-driven transport pathways away from the African continent.

Information from these particulate analyses, and soon the full particulate section of the US GEOTRACES North Atlantic zonal transect, will provide critical insights into TEI remineralization length and depth scales, elemental scavenging behavior in the OMZ and benthic nepheloid zones, and trace nutrient recycling rates within and below the euphotic zone.

Isotopic fractionation of Mg, Ca and Sr in calcite and aragonite

TAKESHI OHNO[1], TAKAHIRO WAKABAYASHI[2], TAKAFUMI HIRATA[3], EDWARD TIPPER[4] AND ALBERT GALY[4]

[1]Department of Chemistry, Gakushuin University, Mejiro 1-5-1, Toshima-ku, Tokyo, Japan (takeshi.ohno@gakushuin.ac.jp)
[2]Department of Earth and Planetary Sciences, Tokyo Institute of Technology, Japan
[3]Department of Earth and Planetary Sciences, University of Kyoto, Japan
[4]Department of Earth Sciences, The University of Cambridge, UK

The alkaline earth metals such as magnesium, calcium and strontium play an important role in a variety of geochemical and biological processes. The element ratios (Mg/Ca and Sr/Ca) in marine carbonates have been used as proxies for reconstruction of the past environment. Recently several studies suggested that the study for the isotopic fractionation of the alkaline earth metals in marine carbonates has a potentially significant influence in geochemical research fields (e.g. Eisenhauer *et al*. 2009). However there are few studies for possible correlations between the level of isotopic fractionation of Ca and that of other alkaline earth metals during carbonate precipitation.

The purpose of this study is to see if there are any correlations between the isotope fractionation factor of Ca during carbonate precipitation and that of Mg and Sr. Moreover, we investigated whether fractionations of Mg, Ca and Sr isotopes could differ between calcium carbonate polymorphs (Calcite and Aragonite). In order to examine the isotope fractionation factor of Mg, Ca and Sr during carbonate precipitation, calcite and aragonite were synthesized from calcium bicarbonate solution in which the amount of magnesium was controlled based on Kitano method (Kitano, 1962). Calcium carbonates were also prepared from the mixture of calcium chlorite and sodium hydrogen carbonate solutions for the purpose of comparison among the methods. The isotope fractionation factors were measured by MC-ICPMS (Nu plasma).

Results suggested that the level of isotopic fractionation of Mg during carbonate precipitation was correlated with that of Sr and that the change of the carbonate crystal structure could make differences of isotopic fractionations of Mg and Ca, however no difference was found in the case of Sr. In this presentation, the possible mechanism will be discussed.

https://doi.org/10.1180/S0026461X00006502 Published online by Cambridge University Press

Biotransformation Rare Earth Elements

T. OHNUKI

Advanced Science Research Center, Japan Atomic Energy Agency (JAEA), Tokai, Ibaraki, 319-1195 Japan (ohnuki.toshihiko@jaea.go.jp)

Geochemical behaviors of rare earth elements (REEs of La, Ce, Pr, Nd, Sm, Eu, Gd, Tb, Dy, Ho, Er, Tm, Yb, Lu) are important to understand the migration of trivalent actinides fission genic REEs from nuclear power plants and high level radioactive waste. When REEs migrates in environemnts, their chemical states may change by the interaction with inorganic and organic materials. Many researchers have studied the interaction of REEs with inorganic materials. However, the biotransformation of REEs have not fully understood. We have conducted the research on the effects of microorganisms on chemical states change of REEs.

The REEs patterns of the distribution coefficients (K_d) for hyphae of *Acremonium* sp. showed no Ce anomaly. On the contrary, the REEs pattern of K_d for biogenic Mn oxides with *Acremonium* sp. showed positive Ce anomaly at pH 3.7 by oxidization of Ce (III) to Ce (IV) by Mn oxides. With increase of pH in solution positive Ce anomaly became smaller, and the polarity of Ce anomaly shifted from positive to negative around pH 6.5. This anomaly shift is probably caused by organic molecules released from the hyphae.

Presence of desferrioxamine B (DFO) showed negative anomaly of Ce in the REEs patterns of K_d for *Pseudomonas fluorescens*. Negative Ce anomaly came smaller with increasing contact time, caused by oxidaton states change of Ce (IV) in the Ce-DFO complex to Ce (III).

We found that Ce (III) phosphate nano minerals were formed on the cells surface of yeast *Saccharomyces serevisiae* after exposure of Ce (III) solution with the resting cells, even though no phosphate is added. Ce (III) ions were first adsorbed by the functional groups of cells surface, followed by the chemical states change by the reaction with phosphate ions released from inside the yeast cells.

These findings indicate that microorganisms affect geochemical behavior of REEs.

Carbonate dissolution at oceanic atolls: A CO_2 sequestration option

T. OHSUMI

CRIEPI, Abiko, Chiba 270-1194, Japan (*correspondence: ohsumitk@ohsumi-jp.com)

Carbon dioxide storage in the ocean will eventually bring about the dissolution of carbonate in the ocean floor. Ohsumi [1] suggested the purposeful *in situ* reaction of CO_2 with the ocean-floor carbonate as a storage option of captured CO_2. However, the carbonate dissolution method [2, 3] proposed and discussed technically and geochemically so far has put the focus on siting the reactor vessel on land near emission sources of CO_2. The ocean bottom covered with carbonate sediments may not be suitable in applying the carbonate-dissolution method, because of high implementation cost as revealed by the research and development effort of the deep-sea Mn nodule mining and also of the associated environmental impacts on the open ocean. If the partial pressure of CO_2 is raised up more above one atmosphere by selecting the site of the dissolution underground, the volume of water required for the reaction to proceed could be saved, the reaction being:

$$CO_2\,(g) + CaCO_3\,(s) + H_2O\,(l) \Rightarrow Ca^{2+}(aq) + 2HCO_3^-(aq).$$

Large scale coral atolls found typically in the Pacific ocean give an appropriate example of the installation site of the reaction system. When several hundreds tonnes H_2O coexisting with one tonne CO_2 are to be reacted with the ambient carbonate rocks at depths of a few hundred meters inside the atoll, *ca*. 20% of the injected CO_2 would be transformed into bicarbonate, reaching to the equilibrium where the pH value is above 6 and the CO_2 partial pressure is below one atmosphere. The drainage waste water containing the residual CO_2 (aq) and the reaction products, *i.e*. calcium bicarbonate solution would be discharged directly to the deep ocean for further dilution of CO_2 (aq). The discharge operation offers an opportunity for the measurement of CO_2 inventory, and more importantly contributes avoidance of the long term possible erosion of the atoll and its consequent impacts to the island surface.

The presented storage concept of captured CO_2 is essentially the ocean storage by dissolution of carbonate minerals, but eliminates the large-scale surface reaction plant.

[1] Ohsumi (1993) *Energy Convers. Mgmt.* **34**, 1059–1064. [2] Rau & Caldeira (1999) *Energy Convers. Mgmt.* **40**, 1803–1813. [3] Caldeira & Rau (2000) *Geophys. Res. Lett.* **27**, 225–228.

https://doi.org/10.1180/S0026461X00006502 Published online by Cambridge University Press

Natural analogue study on long-term reaction of bentonite and highly alkaline groundwater

MASAYA OI[1], NAOTATSU SHIKAZONO, MINORU YAMAKAWA[2] AND NAOKI FUJII[3]

[1]3-14-1, Hiyoshi, Kouhokuku,Yokohamashi, Kanagawa, Japan (ooimasaya@gmail.com, sikazono@applc.keio.ac.jp)
[2]1-15-7, Tsukishima, tyuoku,Tokyo, Japan (amakawa_ytmy@ybb.ne.jp, fujii@rwmc.or.jp)

Geological disposal of high-level nuclear waste has been planned and developed in many countries worldwide. In Japan, it is to be vitrified and an overpack enclosing metallic containers that contain the vitrified waste is to be placed in a deep geological repository with the multibarrier system consisting of an engineered barrier and a natural barrier by geological formations. One of the possible buffer materials for the engineered barrier is bentonite, which should possess the property of long-term stability, although the functions required for it depend on the method of disposal of the waste. When used with cement materials as reinforcing agents, however, the functions required for the bentonite-based barrier material may deteriorate due to such phenomena as dissolution and change of properties by highly alkaline groundwater formed by reactions of the cement materials with groundwater. Since it takes hundreds of thousands of years for the radioactivity of high-level nuclear waste to decrease to the natural background level, it is impossible to clarify the reaction mechanism of bentonite and highly alkaline groundwater in the laboratory for such a long time. An appropriate method to examine such a long-term system is natural analogue study that is an investigation of a natural system that has some similarities with a radioactive waste repository and its surrounding environment.

The Mangatarem district, in the Philippines, was chosen as a study area in this natural analogue study. Through the investigation of the Mangatarem district, we tried to elucidate the long-term interaction of bentonite with highly alkaline groundwater

Analytical results reveal some differences between the trench and outcrop samples. Assuming that the source rock of bentonite and zeolite is common for the rock samples of the two sampling points, those differences are probably attributable to the difference in the reaction of the source rock with the highly alkaline groundwater that had come up along faults.

Iron isotopic signature for weathered ordinary chondrites: Application of the LAL sampling-ICP-MS technique for cosmochemical sample

S. OKABAYASHI[1]*, T.D. YOKOYAMA[1], T. YOKOYAMA[2] AND T. HIRATA[1]

[1]Laboratory for Planetary Sciences, Kyoto University, Kitashirakawa Oiwakecho, Kyoto, 606-0582, Japan (*correspondence: okabayashi-s-aa@kueps.kyoto-u.ac.jp)
[2]Department of Earth and Planetary Sciences, Tokyo Institute of Technology, O-okayama 2-12-1, Meguro, Tokyo, 152-8551, Japan

The laser ablation in liquid (LAL) is one of the most versatile techniques to produce the nanoparticles of the solid materials. Our recent research revealed the LAL can be also applied for the sampling technique of the solid samples to measure the elemental and isotopic composition using the mass spectrometer [1, 2]. The LAL sampling technique provides the micro scale sampling, sample integration, and the elimination of the coexistent elements through the ion exchange chromatography. These advantages enable the high-precision measurement of the micro region on the solid samples.

In this study, we have measured the δ^{56}Fe and δ^{57}Fe values of the Fe-Ni grains and the related weathering products in the ordinary chondrites. The cut pipette tip filled with deionized water was placed on the polished meteorite surface and the laser ablation was performed through the water layer. After the LAL procedure, the sample suspension was collected using the micropipette. The resulting sample suspension was decomposed and dissolved in conc. HCl, then the resulting solution was used for the ^{56}Fe/^{54}Fe and ^{57}Fe/^{54}Fe ratio measurements using the multiple collector-ICP-MS technique. The measured $\delta^{56, 57}$Fe values of metal grains showed good agreement with the previously reported values [3]. In contrast, the iron isotopic signature for weathering products found in the identical meteorite samples revealed that the measured $\delta^{56, 57}$Fe values were significantly higher than those for the inherent metal grains. It should be noted that the inherent part of the metallic grains were commonly surrounded by the weathered parts. Possible cause of the present large difference in the measured iron isotope ratios between the fresh and weathered metal grains will be discussed in this presentation.

[1] Okabayashi *et al*. (2011) *J. Anal. At. Spectrom*. DOI, 10.1039/c0ja00200c. [2] Douglas *et al*. (2011) *J. Anal. At. Spectrom*. DOI, 10.1039/c0ja00144a. [3] Theis *et al*. (2008) *Geochim. Cosmochim. Acta* **72**, 4440–4456.

https://doi.org/10.1180/S0026461X00006502 Published online by Cambridge University Press

Water and ethanol reactivity on chalk from water- and gas-saturated zones

D. OKHRIMENKO*, K.N. DALBY, N. BOVET AND S.L.S. STIPP

Nano-Science Center, Department of Chemistry, University of Copenhagen, Denmark (*correspondence: denisokr@nano.ku.dk)

Adsorption and wettability properties of chalk in oil-reservoirs are highly affected by many factors. These factors include: the presence of inorganic, polymeric, and especially, organic additives on the surface.

To compare the behavior of samples with different levels of surface coatings, we analyzed the solid surfaces of chalk sampled from a water and a gas zone. We also examined how the adsorbed organic material affects the ability of chalk to interact with polar molecules such as water and ethanol. The changes in adsorption energy of water can be used to predict the changes in surface wettability, while ethanol adsorption studies can help in understanding adsorption mechanisms for polar organic compounds. For investigating porous solids such as chalk, vapour adsorption isotherm determination is an appropriate alternative technique to the methods usually used for adsorption studies.

Isosteric enthalpies of water and ethanol adsorption were examined on chalk samples before and after liquid (chloroform) – solid extraction of the organic matter and compared with the results for synthetic calcite. The chemical composition of the extracted organic fraction was established by chromato-mass-spectrometry and qualitative changes on chalk before and after the extraction procedure were monitored with X-ray photoelectron spectroscopy (XPS).

The XPS spectra show that extraction with chloroform leads to a relative increase in concentration of polar groups on the chalk surface. This is consistent with the extraction experiments, which show that the liquid extract from both chalk samples contains mainly nonpolar long-chain alkanes.

We observed a difference in water and ethanol adsorption behaviour caused by the nature of the solid and the adsorbate. Water adsorption depends on the presence of adsorbed polar groups and enthalpy of asorption increases with decrease in amount of preadsorbed nonpolar organic matter, while ethanol adsorption is not influenced by amount of polar groups on the chalk surface. At the same time, ethanol bonds specifically to synthetic calcite with an energy of ~200 kJ/mol, which is 3-4 times higher than on chalk. The results can be used in interpretating the adsorption mechanisms for organic matter on natural oil reservoir materials and for modifying surface properties.

Low temperature alteration of serpentinized dunite; A case study from the Leka ophiolite complex

INGEBORG ØKLAND, INGUNN THORSETH, SHANSHAN HUANG AND ROLF B. PEDERSEN

Centre for Geobiology and Department of Earth Science, University of Bergen, Allegaten 41, 5007 Bergen, Norway (Ingeborg.Okland@geo.uib.no)

Ecosystems based on water-rock interactions independent of photosynthesis have been known for the last decades. Systems where processes like serpentinization produce H_2 and simple hydrocarbons supports the hypothesis of a H_2 based subsurface biosphere. Such environments could be important analogues to systems where life originated. The low temperature water-rock interactions in ultramafic rock is poorly constrained. In this study we try to understand ongoing low-temperature reactions through textural, mineralogical and geochemical characterisation of a 50 m long rock core from the dunitic part of the Leka ophiolite complex, mid-Norway, in combination with geochemical analyses of groundwater emanating from this drill hole, and rainwater. Geochemical modelling has been used to describe ongoing processes in this system.

The core show different degrees of alteration from olivine-dominated, near unaltered dunite to nearly completely altered dunite consisting mainly of blocky serpentine with partly open veins lined with fibrous serpentine and brucite. Groundwater infiltration is thought to take mainly place in three major fracture zones in the most altered parts. Analysis of the groundwater show that the pH increases and the Mg and Si decrease as the groundwater evolves. The most evolved groundwater also has elevated levels of H_2 and traces of CH_4.

Since the main part of the water-rock reactions take place in the serpentine dominated part of the rock it is suggested that the H_2 is a result of the reduction? of water due to oxidation of ferrous iron from dissolving serpentine and brucite.

https://doi.org/10.1180/S0026461X00006502 Published online by Cambridge University Press

Experimental study of partition of rare elements between minerals and melts of diamond forming eclogite-carbonatite and peridotite-carbonatite systems

V.YU. OKOEMOVA[1], P.G. VASILIEV[1], A.V. KUZYURA[2]*, YU.A. LITVIN[2], F. WALL[3] AND T. JEFFRIES[4]

[1]Geological Dept. of Moscow State Univ., Russia, 119991, Vorobievy Gory, GSP-1 (arowanaok@gmail.com, prokvasiliev@gmail.com)
[2]Institute of Experimental Mineralogy RAS, Russia, 142432, Moscow dstr., Chernogolovka, ulica Akademika Osip'yana, 4, IEM RAS (*correspondence: shushkanova@iem.ac.ru)
[3]Camborne School of Mines, University of Exeter, Cornwall Campus, Truro, TR10 9EZ, UK
[4]Dept. of Mineralogy, Natural History Museum, Cromwell Road, London, SW7 5BD, UK

The goal was to study interphase partitioning of trace elements in high-pressure melted eclogite-carbonatite $[[CPx_{40-64}Grt_{16-40}(SiO_2)_{20}]_{59.3}Carb_{39.3}]_{98.6}RE_{1.4}$ and peridotite-carbonatite $[[Ol_{36-60}OPx_{16}CPx_{12-24}Grt_{12-24}]_{30}Carb_{70}]_{99}RE_1$ systems doped with a set of trace elements: Li, Rb, Cs, Ba, Th, U, Ta, Nb, La, Ce, Pb, Pr, Sr, Nd, Zr, Hf, Sm, Eu, Gd, Tb, Dy, Y, Ho, Er, Tm, Yb, Lu, Sc, and Zn. Concentrations of trace elements in coexisting phases were determined using LAICPMS and the mineral-melt partitioning coefficients were calculated. The main feature of the trace element partitioning in high-pressure experiments is the different behaviour of light REE (La, Ce, Pr) in relation to medium and heavy REE (Nd, Zr, Hf, Sm, Eu, Gd, Tb, Dy, Y, Ho, Er, Tm, Yb, Lu). Light REE are partitioned favourably into the melt phase, and the rest REE go into garnet, when the last is presenting. Comparison of the new experimental and published data for partitioning between garnet, clinopyroxene and carbonatite melt, as well as for garnet, clinopyroxene and silicate melt [1-4] shows a similarity in respect of trace element distribution of diamond-forming homogeneous carbonate-silicate melts studied and carbonatite or silicate melts equilibrated with the mantle silicate minerals.

Supported by the President of Russian Federation № MK-913.2011.5, RFBR №№ 10-05-00654 and 11-05-00401.

[1] Sweeney *et al*. (1992) *Earth & Planetary Science Letters* **114**, № 1–2, 1–14. [2] Sweeney *et al*. (1995) *Geochimica et Cosmochimica Acta,* **59**, 3671–3683. [3] Van Westrenen *et al*. (1999) *American Mineralogist*, **84**, 838–847. [4] Walter *et al*. (2008) *Nature*, **454**, 622–626.

REE geochemistry, mineralogy and origin of manganese mineralization in the Derbent (Mahkeme Hill), Yozgat (Turkey)

N. OKSUZ[1]*, A. KARAKUŞ[2] AND C. YURTERI[3]

[1]Bozok University, Department of Geology, Yozgat, Turkey (*correspondence: nursel.oksuz@gmail.com)
[2]Ankara University, Department of Geology, Ankara, Turkey(karakusalpay@hotmail.com)
[3]Hacettepe University, Department of Geology, Ankara, Turkey (cansu.yurteri@hotmail.com)

Artova ophiolite complex is located along the North western and east margin in Yozgat (Turkey). The Mn-deposits in the Derbent area is part of this ophiolite complex. This deposit banded and lenticular forms, is hosted by radiolarite and is generally overlying volcanics. Manyetite, manganite, pyrolusite and goethite are main constituents of the manganese ores in Mahkeme Hill (Derbent-Yozgat) area. The gang minerals in Derbent are quartz and calcite.

In chondrite normalized REE graphics samples are characterized by highly negative and positive Ce anomalies in area. Europium shows negative anomaly in all samples. The negative Ce anomaly is typical to submarine hydrothermal deposits and positive Ce anomaly is indicative of hydrogenous deposits [1]. The negative Eu anomaly shows contamination from the continental crust and/or sediment contribution via dehydration [2].

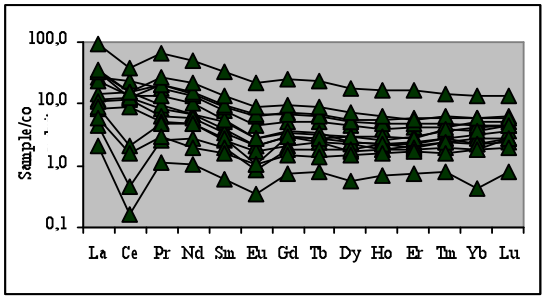

Figure 1: Chondrite normalized REE diagram for ore samples

Ce values in the Mahkeme Hill mineralization were computed and the anomalies were found as $Ce_{anom} < -0.1$ in 9 samples and $Ce_{anom} > -0.1$ in 5 samples. These values are indicative of both oxic and anoxic sedimentation conditions. Chemically, the studied manganese deposit and associated radiolarite are very similar to these formed by hydrothermal – hydrogenous processes.

[1] Hein et al., (1997) *Geological Society, Spec. Publ.* London. **119**, 123–138. [2] Sun and Mc Donough (1989) *Geol. Soc. Spec. Publ.*, London. **42**, 313-345

https://doi.org/10.1180/S0026461X00006502 Published online by Cambridge University Press

Beyond petroleomics – Petroleum geochemistry for the 21st Century

THOMAS B.P. OLDENBURG*, NORKA MARCANO, HAIPING HUANG, BEN HSIEH AND STEVE R. LARTER

Petroleum Reservoir Group (prg), Department of Geoscience, University of Calgary, Calgary, AB, Canada (*correspondence: toldenbu@ucalgary.ca)

Petroleum geochemistry has been driven by analytical developments since the development of gas chromatography in the 1950's and practical computerized GCMS technologies in the 1970's heralding, in the 70's and 80's, the development of practical biomarker technologies and most of the source rock facies and maturity molecular concepts that we still use today. Recent advances in Fourier Transform Ion Cyclotron Resonance Mass Spectrometry (FT-ICR-MS) technology now allow a more comprehensive analysis of polar constituents of fossil fuels. This new technology allows for the first time routine analysis of the broad range of complex polar compound mixtures that dominate source rock extracts and heavy oils.

In this study we will show the use of FTMS derived high molecular weight multi hetero component (HMWMH) complex compound class distributions to discriminate biodegraded oils from different source rocks from marine versus lacustrine systems and also differentiate oil charges from mixed facies marine source rocks. These new proxies are independent of microbial biodegradation alteration levels from Peters & Moldowan levels 0 to 8 (Peters and Moldowan, 1994) and show that it is likely that FTMS techniques and parameters may offer substantial advances over conventional GCMS based approaches to petroleum system characterisation. In addition, new insights into the compositional changes during *in situ* thermal recovery processes simulated in the lab under aquathermolysis and hydrotreating conditions will be shown.

The environmental impact of sewage effluent discharges in the Pracana River - Portugal

N. OLIVEIRA, P. ALMEIDA, N. CARVALHO, A. SILVA, I.M.H.R. ANTUNES, A. FERREIRA AND T. ALBUQUERQUE

Polytechnic Institute of Castelo Branco, 6000-243 Castelo Branco, Portugal (teresal@ipcb.pt)

The Pracana River is an important tributary of the Ocreza River. The Ocreza River is located in Central Portugal and has it source in an important Alpine chain called Gardunha. It starts at 1160 m altitude and stretches for 80 km until draining into the Tagus River. It has several creeks and tributaries along which there are several rural villages. The Pracana's waters has an important role by being abundantly used in agriculture, the main economic activity of these communities, and for human consumption. Characterization, monitorization and control of the impact due to several wastewaters treatment plants discharges on water quality is of crucial importance.

This paper focuses on the Proença-a-Nova wastewaters treatment plant, which discharges directly into the Freixada River, a Pracana's tributary. Twelve georeferenced water samples were collected between the sewage effluent discharge and the Pracana river confluence. Secondary inflows were identified and water samples collected downstream at approximately equal distances. The core of our study is the hydrological year of 2010. Sampling campaigns were conducted during three different periods: rainy winter (January), intermediate conditions (March) and dry season (June). The following chemical parameters were analyzed: biochemical oxygen demand (BOD), dissolved oxygen concentration (DO), dry residue, P_{total}, N_{total}; pH, temperature and microbiological parameters. The dissolved oxygen concentration (DO), biochemical oxygen demand (BOD) and the microbiological parameters were used as indicators for the presence of organic matter in the body of water, and as parameters for evaluating the environmental pollution.

The pollution simulation in the Pracana river was performed by a coupled hydrodynamic and water dispersion model. A water quality model was constructed applying to QUAL2kw software. The simulation results are consistent with field observations and demonstrate that the model has been correctly calibrated. The model is suitable for evaluating the environmental impact of wastewaters plant discharges on the Pracana River, allowing feasibility studies of different treatment schemes and the development of specific monitoring activities.

https://doi.org/10.1180/S0026461X00006502 Published online by Cambridge University Press

U-Pb dating of very low-grade metamorphic titanite

V. Oliveros[1]*, A. Simonetti[2] and D. Morata[3]

[1]Departamento Ciencias de la Tierra, Universidad de Concepción, Casilla 160-C, Concepción, Chile (*correspondence: voliveros@udec.cl)
[2]Civil Engineering and Geological Sciences, University of Notre Dame, Notre Dame, IN 46556, USA
[3]Departamento de Geología, Universidad de Chile, Plaza Ercilla 803, Santiago, Chile

Titanite is a common secondary mineral present in metabasites in the Chilean Andes. Its rather high closure temperature (<550°C) renders it very suitable for dating sub-to-low-grade metamorphism or hydrothermal alteration. In this study we tested the feasibility of dating very small grains of secondary titanite. Thirteen standard petrographic thin sections of Mesozoic volcanic rocks outcropping in the Main and Coastal cordilleras of central Chile (33-35°S) were selected for U-Pb dating by LA-MC-ICP-MS. The analyzed titanites occur as four different varieties: infilling amygdales or veins, within the groundmass, and replacing both former pyroxene and magnetite phenocrysts. The radiogenic Pb content is generally low and correlates with the type of titanite, i.e. the large titanites within amygdales (~200 μm) contain the most radiogenic Pb. The mean ages range from 48.5±6.5 to 147±22 Ma, with three distinct groups at 102-108 Ma, 80-85 Ma, and 49-62 Ma. One sample from the Coastal Cordillera yielded an age of 119.8±3.6 Ma (Fig. 1). The U-Pb ages do not correlate with either the amount of common Pb, or with the varietal type of titanite (Fig. 1). The U-Pb ages overlap with those previously obtained by K-Ar and Ar-Ar methods, which have been attributed to either very low-grade metamorphism, or approach the age of volcanism; however, several samples yield Cenozoic ages, which may represent a geologic event or related to secondary Pb loss.

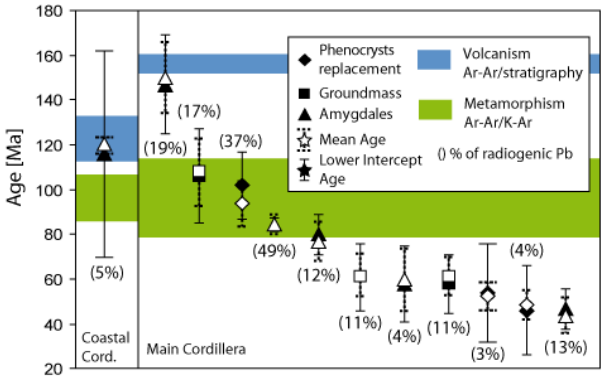

Figure 1: Titanite U-Pb ages.

Low biodiversity tropics in a high CO_2 median Mesozoic world

Paul E. Olsen[1], Jessica H. Whiteside[2] and Morgan F. Schaller[3]

[1]Lamont-Doherty Earth Observatory, Palisades, NY 10968, USA (*correspondence: polsen@ldeo.columbia.edu)
[2]Dept. of Geological Sciences, Brown Univ., Providence, RI 02912, USA (jessica_whiteside@brown.edu)
[3]Dept. of Earth and Planetary Sciences, Rutgers Univ., Piscataway, NJ 08854, USA (schaller@rci.rutgers.edu)

A strong latitudinal gradient in biodiversity, increasing to the tropics, is one of the most striking of modern ecological patterns. Late Triassic to Early Cretaceous tropical assemblages do not show this pattern, however. Most tropical and subtropical floral records from this time are characterized by low diversity and are overwhelmingly dominated by cheirolepidaceous conifers and their pollen, *Classopollis*. These conifers have been traditionally described as arid-adapted with features such as microphyllus leaves and thickened cuticle with sunken or papillate stomata. While some subtropical occurrences of cheirolepidaceous conifers are indeed associated with sedimentological evidence for aridity such as evaporites, many from the tropics are not and instead are found in settings incompatible with aridity. In contrast, the temporal distribution of these low-diversity assemblages tracks Mesozoic CO_2, rising through the Triassic and falling through the Cretaceous as angiosperms become more prevalent. We suggest that these conifers were not so much arid-adapted, but rather specialized in extraordinarily hot, high-CO_2 environments, regardless of precipitation.

The same pattern maintains at finer time scales. The end-Triassic extinction (ETE) exhibits a dramatic drop in biodiversity at pulsed 2-3X increases in CO_2 associated with Central Atlantic Magmatic Province (CAMP) basaltic eruptions. *Classopollis* massively increased in the tropics and subtropics as generic diversity of other pollen and spores dropped in direct association with the eruptions. However, perennial lake sediments and other indications of an enhanced hydrological cycle increased dramatically at the same time consistent with high CO_2 and extremely hot temperatures, being the main drivers of cheirolepidaceous dominance and low biodiversity, not the lack of water.

High latitudes had dramatically higher diversity. At the ETE, these assemblages also suffered a huge drop in diversity among broader leaf forms consistent with thermal damage, but they never became as skewed as the tropics. Thus, relative to now, latitudinal diversity gradients were reversed at all temporal scales during times of very high CO_2, plausibly because of near lethal temperatures.

https://doi.org/10.1180/S0026461X00006502 Published online by Cambridge University Press

Incorporation of heavy metals into recent travertine formations at the Eyjafjallajökull volcano

J. OLSSON[1,2]*, S.L. S. STIPP[2], K.N. DALBY[2] AND S.R. GISLASON[1]

[1]Nordic Volcanological Institute, Institute of Earth Sciences, University of Iceland, Iceland (*correspondence: jolsson@hi.is) (sigrg@raunvis.hi.is)

[2]Nano-Science Center, Chemistry Department, University of Copenhagen, Denmark (stipp@nano.ku.dk, kdalby@nano.ku.dk)

The release of heavy metals from water-volcanic rock-gas interaction and pristine volcanic ash-water interactions pose a serious environmental problem for water supplies. Thus it is interesting that the concentrations of waterborne pollutants monitored in the vicinity of active volcanoes are often much lower than predicted. Released heavy metals from the iniaial water-rock interactions are probably scavanged by and/or reincorporated into secondary precipitates including aluminium silicates, iron (hydr)oxides and carbonates. The purpose of this study was to investigate the capacity of naturally formed travertine to immobilise heavy metals.

Following the eruption of the Eyjafalljökull Iceland volcano in the spring 2010, a new strong outlet of riverine CO_2 was observed via the river Hvanná, which indicates deep degassing into the water. A white mineral layer; at some places several cm thick, for hundreds of meters downstream was observed. The precipitation was identified solely as calcite with X-ray diffraction. Low concentrations of riverine Al and Fe provide a unique opportunity to examine the scavenging role of the precipitating carbonates exclusively. A gradual decrease of: conductivity from 1.8 to 1.1 mS/cm, alkalinity from 20.8 to 8.8 meq/kg, concentration of Ca, Mg, Cd, Cu, Mn, Sr, Ba and CO_2, and increase in the pH from 6.5 to 8.5, strongly correlated with the amount of precipitated travertine. Dissolution experiments show that bulk travertine incorporates the same metals. The water temperature was below 5 °C and an elevated atmospheric CO_2 partial pressure was detected near the river. The river water degassed downstream and pH increased, resulting in calcite supersaturation and precipitation. Our thermodynamic models suggest that, in addition to $CaCO_3$, Mg-, Sr- and Ba-carbonates and two phyllosilicate phases were supersaturated.

Our study provides valuable information for assessing environmental impacts for, e.g. volcanic eruptions or carbon capture and storage (CCS) projects in basaltic rock, such as the Icelandic multi-collaborator project 'Carbfix'.

Enzymatic and abiotic hydrolysis of glucose phosphate adsorbed on goethite

R. OLSSON[1]*, R. GIESLER[2], J.S. LORING[3] AND P. PERSSON[1]

[1]Department of Chemistry, Umeå University, 901 87 Umeå, Sweden (*correspondence: rickard.olsson@chem.umu.se) (per.persson@chem.umu.se)

[2]Climate Impacts Research Centre, Department of Ecology and Environmental Science, Umeå University, 901 87 Umeå, Sweden (reiner.giesler@emg.umu.se)

[3]Pacific Northwest National Laboratory, Richland,Washington 99352, USA

Organophosphates constitute a substantial part of the total phosphorus in soil. However, hydrolysis of the phosphate ester bond may be required in order to produce bioavailable phosphate. Adsorption on mineral surfaces can facilitate abiotic hydrolysis, but has also been suggested to block enzymatic hydrolysis. In this study we have investigated the enzymatic and abiotic hydrolysis of glucose-1-phosphate and glucose-6-phosphate adsorbed at the water-goethite interface. Sugar monoesters such as these have been indicated to occur at significant concentrations in soils.

To study the kinetics and molecular mechanisms of the abiotic and enzymatic hydrolysis we have used wet-chemical and spectroscopic techniques. Ion chromatography was used to obtain quantitative data, while a setup for simultaneous infrared and potentiometric titrations was used to investigate *in situ* the goethite-water interface reactions. We found that glucose phosphate forms three surface complexes on goethite in the pH range 3 – 10 differing in protonation states and hydrogen bonding interactions with neighboring surface groups. Below pH 7 the glucose-1-phosphate complexes are stable with respect to hydrolysis whereas at higher pH values a small extent of hydrolysis is detected. With glucose-6-phosphate the trend is reversed, i.e. hydrolysis occurs at low pH values. When an enzyme (acid phosphatase) is added the hydrolysis increases considerably. This increase coincides with adsorption of enzyme, and all experimental data indicate that the enzymatic hydrolysis is a strictly interfacial process. Furthermore, the enzymatic hydrolysis is strongly dependent on the amount of glucose phosphate adsorbed since the properties of the surface affect the enzyme's mode of adsorption and hence it's activity.

https://doi.org/10.1180/S0026461X00006502 Published online by Cambridge University Press

A study on the beach sediments of The Gulf of Fethiye (SW Turkey), focus on geochemical data

Z. ONAL, B. ESER-DOGDU*, M. ERGIN, Z.S. KARAKAS, K. SOZER AND E.S. DURMUS

Ankara University, Department of Geological Engineering, 06100, Tandoğan, Ankara (*correspondence: edogdu@eng.ankara.edu.tr)

This study is carried out to investigate sedimentary transport and depositional processes, heavy mineral distribution and possible economically important placer potentials of coastal beaches of the Fethiye Gulf. Investigation also forms part of a Project supported by the Ankara University Scientific Research Projects Office. To perform this, in September 2009, a large number of sediment samples were collected along the shoreline (A) and backshore (B) parts of coastal beaches of Fethiye and subjected to well-known sedimentary petrographic methods.

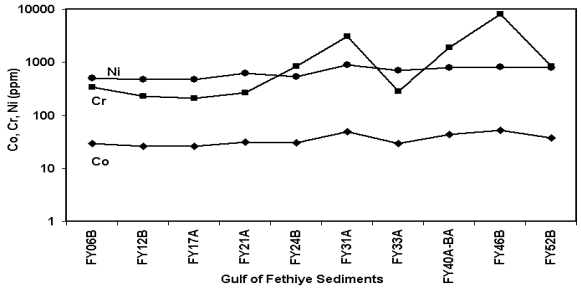

Figure 1: The distribution of Co, Cr and Ni concentrations in the beach sediments of Fethiye.

According to multielement analysis of sediments, Ni (657 ppm), Co (35, 5 ppm) and Cr (1605 ppm) contents are found to be higher than average values of Earth's crust and sandstones values. Earth' s crust averages (ppm) for Co 25, Cr 100 and Ni are also given for comparison [1]. High concentrations of the elements can be related to the occurrences of ophiolites and bearing chromites on the coastal hinterland of the Fethiye Gulf. The total heavy mineral contents of the sediments showed parallel trend with an some element contents.

[1] Mason & Moore (1982) *Principles of Geochemistry*.

Experimental tests for the origin of Archean sulfur mass-independent fractionation during SO_2 photolysis

SHUHEI ONO* AND ANDREW WHITEHILL

Earth, Atmospheric, and Planetary Sciences, Massachusetts Institute of Technology, 77 Massachusetts Avenue, Cambridge, MA 02139 (*correspondence: sono@mit.edu)

The signatures of Archean sulfur isotope mass-independent fractionation (S-MIF) provide critical constraints on the redox evolution of the early Earth's atmosphere. Although S-MIF is likely to be sourced from SO_2 photolysis, the physical origin of this unique isotope effect is yet to be identified. Recent studies suggest 1) selfshielding [1] or 2) isotopologue specific photoexcitation [2, 3] as the origin of observed S-MIF signatures. These two models imply the pattern of S-MIF is sensitive to the UV spectrum, and thus, the atmospheric components that absorb UV region between 190 to 220 nm, potentially providing significant new constraints on the chemical compositions of early atmosphere.

A series of laboratory experiments are in progress to test above two hypotheses during UV photolysis of SO_2 ($3SO_2 + h\nu \rightarrow 2SO_3 + S$). A flow-though photochemical reactor is used to examine S-MIF as a function of SO_2 mixing ratio. Two broad band light souces (D and Xe arc lamp), with or without 200 nm bandpass filter, are used to test the effect of light spectrum. Detailed photohemial model using available rate constants suggests that S is formed by SO bimolecular collision ($SO+SO \rightarrow SO_2 + S$), and the photolysis of SO ($SO + h\nu \rightarrow S + O$) is a minor channel.

Experiments with D and Xe lamp produced similar MIF patterns ($\delta^{33}S/\delta^{34}S$ and $\Delta^{36}S/\Delta^{33}S$ ratios), suggesting S-MIF is not sensitive to the detailed shape of the UV spectrum. Although large $\delta^{34}S$ isotope effect is consistent with [2], their cross section predicts the opposite signs of $\Delta^{33}S$ for D and Xe lamp experiments. This suggests that the photoexcitation step itself may contribute relatively little to S-MIF. Instead, S-MIF may be originating from the isotope-sensitive quantum yield, such as curve crossing among various excited states SO_2. We will also report the results from a newly constructed dual-flow cell system designed to test the SO_2 selfshielding model at optically thin condisions.

[1] Lyons (2007) *Geophy. Res. Lett.* **34**, L22811
[2] Danielache *et al.* (2008) *J. Geophy. Res.* **113**, D17314
[3] Ueno *et al.* (2009) *Proc. Nat. Aca. Sci.* **106**, 14784

https://doi.org/10.1180/S0026461X00006502 Published online by Cambridge University Press

The role of hydroxyl group (OH) in forming minerals

V.V. ONUFRIENOK*, A.M. SAZONOV, A.V. TEREHOVA AND A.G. NIKIFOROV

Siberian Federal University, Krasnoyarsk, Russia (*correspondence: VOnufriynok@sfu-kras.ru)

There was studied the changes of the pyrrhotites structure when hydroxyl group (OH) is introduced into it. After synthesis (1273 K) the samples were maintained at the room temperature (~ 25°C) for 29 years in atmospheric conditions.

The X-ray and chemical analysis analysis of the samples, which were maintained, showed that there are compounds containing hydroxyl group (OH) in the crystal structure. The samples contained parabutlerite, goethite, szomolnokite, rozenite, rhomboclase, pyrite and pyrrhotite.

For example the influence of hydroxyl group (OH) on the content of the formed szomolnokite was considered on the basis of calculating the thermodynamic potentials using the Bose-Einstein statistics. The theoretical calculations were compared with X-ray phase analysis data (table 1).

S/Fe ratio	Percentage hydroxyl group (OH)	Szomolnokite percentage	
		X-ray	As calculated
1.710	4.25	21.21	16.779
1.684	2.72	12.92	18.533
1.670	4.42	23.70	19.553
1.660	2.38	11.65	20.315
1.580	5.11	25.61	27.586
1.571	5.27	17.36	28.552
1.497	7.99	41.55	41.127
1.382	4.25	26.60	21.780
1.380	9.35	21.04	21.540
1.250	0.85	5.07	10.499
1.158	2.03	6.19	6.314
1.157	1.70	3.29	6.279
1.052	0.34	2.07	3.514

Table 1. The szomolnokite percentage in the samples

As it is shown in the table, tendency to decreasing both with increasing of szomolnokite content with decreasing S/Fe ratio is observed both X-ray data and the theoretical calculation results.

Seasonal magnesium isotope variations in soil solutions reflecting physico-chemical processes controlling soil weathering fluxes

S. OPFERGELT[1,2], R.B. GEORG[3], K.W. BURTON[1], R. GUICHARNAUD[4], C. SIEBERT[1], S.R. GISLASON[5] AND A.N. HALLIDAY[1]

[1]Department of Earth Sciences, University of Oxford, Oxford, United Kingdom

[2]Earth and Life Institute, Université catholique de Louvain, Louvain-la-Neuve, Belgium (sophie.opfergelt@uclouvain.be)

[3]Trent University, Water Quality Centre, Peterborough, Ontario, Canada

[4]Agricultural University of Iceland, Reykjavik, Iceland

[5]Institute of Earth Sciences, University of Iceland, Reykjavík, Iceland

Chemical weathering supplies base cations controlling the long-term availability of nutrients. Base cations, including magnesium, lost by plant uptake or leaching, are replaced by mineral weathering and partly retained on the soil exchange complex. Despite Mg isotopes being used as a weathering proxy, the fractionation mechanisms in the critical zone are still unclear. Here we report the first look into the seasonal variability of Mg isotope compositions in soil solutions derived from a well-defined protolith, Icelandic basalt, which was exposed to seasonal freeze-thaw cycles. Less weathered freely drained Brown and Gleyic Andosol (BA-GA) are compared with more weathered poorly drained Histosol and Histic Andosol (H-HA). The difference in clay content (35 and 48%) and proportions of exchangeable Mg (2 and 7%) in BA-GA and H-HA, respectively, allow for a direct assessment of the processes controlling Mg isotope ratios (δ^{26}Mg relative to DSM-3). Vegetation (-0.30 to -0.18‰) is heavier than parental basalt (-0.31‰) and bulk soils (-0.79 to -0.25‰). Soil solutions (-1.16 to -0.53‰) are relatively lighter than the basalt. Magnesium retention on the soil exchange complex is larger in neutral than in acid soils and discriminates against light Mg isotopes (-0.88 to -0.51‰) contributing towards isotopically lighter soil solutions in BA-GA. Seasonal variations (from June to September) of Mg isotope ratios in soil solutions from organic-rich H-HA are likely to reflect the release of heavier Mg isotopes from the decomposition of plant material during thaw. Our results show that Mg isotopes have a great potential as a proxy for seasonal soil processes, especially in sub-arctic soils where environmental changes would potentially affect vegetation decomposition, CO_2 release, and associated nutrient delivery to the hydrosphere.

https://doi.org/10.1180/S0026461X00006502 Published online by Cambridge University Press

Erebus: A laboratory volcano in Antarctica

CLIVE OPPENHEIMER[1,2], PHILIP KYLE[3], LAURA JONES[3], WILLIAM MCINTOSH[3], NELIA DUNBAR[3], TEHNUKA ILANKO[2], NIAL PETERS[2], YVES MOUSSALLAM[2], KAYLA IACOVINO[2], MARIE BOICHU[4], GEORGINA SAWYER[2], VITCHKO TSANEV[2], BRUNO SCAILLET[1], MICHEL PICHAVANT[1], ALAIN BURGISSER[1], MARINA ALLETTI[1] AND INDIRA MOLINA[1]

[1]ISTO-CNRS, 1A rue de la Férolerie, 45071 Orléans, France (co200@cam.ac.uk, bruno.scaillet@cnrs-orleans.fr, pichavan@cnrs-orleans.fr, burgisse@cnrs-orleans.fr, marina.alletti@cnrs-orleans.fr, imolina@cnrs-orleans.fr)

[2]Department of Geography, Downing Place, Cambridge CB2 3EN, UK (ti235@cam.ac.uk, njp39@cam.ac.uk, ym286@cam.ac.uk, ki247@cam.ac.uk, gms26@cam.ac.uk, vip20@cam.ac.uk)

[3]Department of Earth and Environmental Science, Department of Earth & Environmental Science, New Mexico Institute of Mining and Technology, 801 Leroy Place, Socorro, N.M. 87801-4796, USA (kyle@nmt.edu, ljon01@nmt.edu, mcintosh@nmt.edu, nelia@nmt.edu)

[4]Institut Pierre Simon Laplace, Laboratoire de Météorologie Dynamique, Ecole Polytechnique, 91128 Palaiseau cedex (mboichu@lmd.polytechnique.fr)

Erebus, the only presently erupting phonolite volcano, offers an exceptional opportunity to examine the complexities that accompany degassing and the evolution of magmas from deep to shallow levels. These include aspects of magmatic differentiation, redox chemistry and eruptive transitions widely relevant to understanding other volcanoes. Its long-lived anorthoclase phonolite lava lake, sustained degassing and hyperarid environment provide uncommonly favourable circumstances for direct measurement of the lava lake – the uppermost portion of the magmatic system.

Several features distinguish Erebus: the decadal persistence of the lava lake; evidence for continuous fractionation (the Erebus Lineage) from basanite to phonolite; episodic Strombolian activity at the lava lake (which provides samples for analysis); and the abundance of megacrysts (up to 10-cm-long) of anorthoclase feldspar in the lava lake. The longevity of the lava lake implies counterflow of vesicular and degassed magma within the (<10 m) feeder conduit. Flow instabilities and diffusional processes allow complex transfers of gas, melt and crystals up and down the conduit.

This contribution focuses on integration of field measurements of volcanic gas emissions (composition and flux) and the vigour of lava lake motion, and how the observations map to characteristics of magma flow and degassing. It aims to showcase key findings of recent annual field seasons on Erebus, to review some of the challenges of volcano surveillance in the extreme Antarctic environment, and to stimulate comparative studies of Erebus and volcanoes such as Vesuvio, Stromboli, Nyiragongo, and others, with shared characteristics.

Halophilic microorganisms: Modern and ancient, on Earth and in Space

AHARON OREN

Department of Plant and Environmental Sciences, The Alexander Silberman Institute of Life Sciences, The Hebrew University of Jerusalem, 91904 Jerusalem, Israel

Salt-saturated environments on Earth are inhabited by a great diversity of halophilic microorganisms. They are found in all three domains of life: Bacteria, Archaea, and Eucarya. Many can thrive not only at low water activities, but are also adapted to high divalent cations concentrations (the Dead Sea) and to extremes of pH and temperature. Different groups of halophiles can be detected using biomarkers such as the archaeal isoprenoid ether lipids, pigments (the archaeal C-50 bacterioruberins, β-carotene from the alga *Dunaliella salina*), and osmotic solutes such as glycine betaine and ectoine in Bacteria, glycerol in *Dunaliella*.

When halite crystallizes from salt-saturated brines, microorganisms are often trapped within fluid inclusions in the crystals, where they can survive for prolonged periods. Live microorganisms have been recovered from ancient halite, e.g. *Virgibacillus marismortui* from Permian salts of New Mexico, Archaea (*Halobacterium*, *Natronobacterium*) from Cretaceous halite crystals from Brazil. DNA encoding bacterial and archaeal rRNA genes was recovered from Cretaceous (Brazil) and Silurian (Michigan) salt. Salt crystals deposited 35,000 years ago in Death Valley, CA, contained microscopically recognizable prokaryotes, as well as *Dunaliella*, which may have provided the prokaryotes with glycerol and other organic compounds as a source of energy for survival. In spite of the earlier scepticism, compelling evidence for long-term survival of halophilic microorganisms within salt crystals has accumulated in the past decade.

Some species of halophilic Archaea can survive large doses of UV radiation, desiccation and exposure to low temperatures, but not all halophiles are equally adapted. Some strains of halophiles have survived flights on the Biopan facility of the space shuttle, including a species named *Halorubrum chaoviator*, 'the traveller of the void'.

Halite has been detected on Mars and in meteorites. In view of the ability of some halophiles to survive in salt at low water activity, high radiation levels, and in a broad range of pH, salt crystals are promising material to search for life elsewhere in the universe, using a combination of techniques: microscopy, gene-based approaches, and detection of specific biomarkers. Model systems on Earth – recent and ancient – provide plentiful material to evaluate the different methods.

https://doi.org/10.1180/S0026461X00006502 Published online by Cambridge University Press

Numerical study of weathering fluxes at the catchment scale in a boreal watershed: A coupled thermo-hydro-geochemical mechanistic approach

L. ORGOGOZO[1]*, Y. GODDÉRIS[1], O.S. POKROVSKI[1], J. VIERS[1], D. LABAT[1], A.S. PROKUSHKIN[2] AND B. DUPRÉ[1]

[1]GET, 31400, Toulouse, France (*correspondence: laurent.orgogozo@get.obs-mip.fr) (yves.godderis@get.obs-mip.fr, oleg.pokrovsky@get.obs-mip.fr, jerome.viers@get.obs-mip.fr, david.labat@get.obs-mip.fr, bernard.dupre@get.obs-mip.fr)

[2]V.N. Sukachev Institute of Forest, SB RAS, Akademgorodok, Russia (prokushkin@ksc.krasn.ru)

This work deals with the assessment of the impact of the climatic changes on weathering processes in boreal catchments which are characterized by the occurrence of a continuous permafrost. The two main goals of this study are : (i) to quantify the influence of seasonal cycles of freezing and thawing of the active layer on the fluxes of chemical elements generated by the weathering processes and (ii) to estimate the effect on the weathering fluxes of possible interannual variations of these cycles caused by climatic changes. Our approach is based on the development and the validation of a coupled thermo-hydrological mechanistic modelling at the catchment scale for current climatic conditions. This thermo-hydrological model is designed to give the entrance data (the seasonal evolutions of the average thickness and of the average water content of the active layer) for the computation of weathering fluxes with the WHITCH geochemical model (e.g. [1]). This modelling approach at the catchment scale is established on the basis of the data available in the International Research Group CAR WET SIB ([2], [3]). In further studies, the model developed here will allow to forecast the impact of various scenarios of climatic changes on the weathering fluxes.

[1] Goddéris *et al*. (2006) *Geochim. Cosmochim. Acta* **70**, 1128–1147. [2] Bagard *et al*. (in press) *Geochim. Cosmochim. Acta*. [3] Pokrovsky *et al*. (2005) *Geochim. Cosmochim. Acta* **69**, 5659–5680.

Geochronological fingerprint revealed the evolution of the crust underlying Cerro Pampa adakite, Argentine Patagonia

Y. ORIHASHI[1], R. ANMA[2], A. MOTOKI[3], M.J. HALLER[4], V.A. RAMOS[5] AND D. HIRATA[6]

[1]ERI, University of Tokyo, Tokyo 113-0032, Japan (*correspondence: oripachi@eri.u-tokyo.ac.jp)

[2]Tukuba University, Ibaragi 305-8572, Japan

[3]Rio de Janeiro State University, Rio de Janeiro, Brazil

[4]Centro Patagonico Nacional, Chubut, Argentina

[5]Universidad de Buenos Aires, Buenos Aires, Argentina

[6]Kanagawa Prefecture Museum of Natural History, Kanagawa 250-0031, Japan

We reports the results of U-Pb dating for 282 zircon crystals separated from a Middle Miocene adakite in Cerro Pampa, southern Argentine Patagonia, using LA-ICP-MS. With the exception of 3 spot ages, 140 of the concordia ages are significantly older (> 94 Ma) than the cooling ages of the adakite magma (~ 12 Ma). Kay *et al*. [1] attributed the origin of adakite magmas to partial melting of subducted slab of the Nasca plate. Presence of exotic zircon crystals clearly indicates crustal contaminations to produce the adakitic magma in Cerro Pampa. The obtained concordia ages of exotic zircons range from 94 Ma to 1441 Ma and could be divided into five groups having distinctive peaks on a population diagram. The first (100-125 Ma) and second age groups (125 to 145 Ma) correspond to the age of plutonic activities that formed main body of the South Patagonian Batholith [2]. The third to fifth groups correspond to activities of El Qumado-Ibañez volcanic complex (145-170 Ma) [2], gabbroic rocks scarcely distributed in Central Patagonia (170-200 Ma), and the Eastern Andean metamorphic complex of Late Paleozoic to Early Mesozoic ages (200-380 Ma) [3], respectively.

Our data suggests that the crust underneath Cerro Pampa were mostly formed after 380 Ma and majority of the upper crust was formed during early Cretaceous to middle Jurassic. The processes of crustal development ceased ~ 94 Ma until the activity of the Cerro Pampa adakite in ~ 12 Ma. There was no evidence for Archean-Paleoproterozoic crust.

[1] Kay *et al*. (1993) *J. Geol*. **101**, 703–714. [2] Herve *et al*. (2007) *Lithos*, **97**, 373–394. [3] Bahlburg *et al*. (2009) *Earth-Sci. Rev*. **97**, 215–241.

https://doi.org/10.1180/S0026461X00006502 Published online by Cambridge University Press

Microbial partnerships and methane-oxidation in the deep sea

V.J. ORPHAN[1], A. DEKAS[1], A. GREEN[1], C. HOUSE[2], J. MARLOW[1], J. STEELE[1], S. MCGLYNN[1] AND L. LEVIN[3]

[1]California Institute of Technology, Pasadena, CA 91125 vorphan@gps.caltech.edu
[2]Pennsylvania State University, University Park, PA 16802
[3]Scripps Institute of Oceanography, La Jolla, CA 92093

The ability to decipher the metabolic roles of microorganisms within living microbial ecosystems and to connect microbial metabolism with biosignatures preserved in the rock record represents some of the grand challenges in the field of Microbial Geobiology. The combination of molecular methods with stable isotope analysis (both natural abundance and as tracers) in modern environments represents a multidisciplinary approach that has been used successfully to characterize links between specific microorganisms and their ecophysiology in situ. In particular, the introduction of micron-scale isotopic analyses by secondary ion mass spectrometry (SIMS and nanoSIMS) [1] to the study of microorganisms has enabled an unprecedented level of inquiry into the inner workings of microbial ecosystems. Integrating SIMS-based stable isotope analysis with microscopy and culture-independent metagenomics techniques, we have been investigating carbon and nutrient utilization by deep-sea microorganisms and symbiotic microbial consortia fuelled by methane in sediments and associated authigenic carbonates. Single cell characterization of methane-cycling archaea and sulphate-reducing bacteria have revealed significant inter and intra-group heterogeneity in both stable carbon isotopic signatures and nitrogen utilization, including differences in nitrogen fixation [2] and assimilatory nitrate reduction. These cell-specific analyses have yielded new information regarding the isotopic variability, metabolic potential and interactions between individual microorganisms and the greater biological community in methane-based ecosystems.

[1] Orphan. V.J. and House. C.H. (2009) Geobiological investigations using secondary ion mass spectrometry (SIMS): microanalysis of extant and paleo-microbial processes. *Geobiology*. **7**, 360-372 [2] Dekas. A.D. *et al*. (2009) Deep-sea archea fix and share nitrogen in methane-consuming microbial consortia. *Science*. **326**. 422-426

Combining electrochemical and spectroscopic methods to obtain speciation of quinones

S. ORSETTI*, S. SPAHR, C. LASKOV AND S. HADERLEIN

Center for Applied Geosciences, University of Tübingen, Sigwartstrasse 10, D-72076 Tübingen, Germany (*correspondence: silvia.orsetti@uni-tuebingen.de)

In anoxic aquifers, the presence of goethite-Fe(II) systems plays a major role in electron transfer processes, such as degradation of organic pollutants [1]. To investigate the role of organic matter as potential electron shuttles commonly model quinones such as AQDS, juglone and lawsone were used [2, 3]. To address this question we studied interactions with iron minerals and the speciation of model quinones.

Defined redox and acid-base species of the model quinones were obtained by electrochemical methods, varying systematically the reduction potential, pH and ionic strength. The UV-visible spectra of these species were used as reference to obtain the redox speciation of quinones in goethite-Fe(II) systems. From these data information on electron transfer processes, redox potential and equilibrium states of the redox sensitive quinone and iron species can be derived.

[1] Tratnyek *et al*. (2001) *Water Res*. **35**, 4435–4443. [2] Aeschbacher *et al*. (2010) *Environ. Sci. Technol*. **44**, 87–93. [3] Doong *et al*. (2005) *Environ. Sci. Technol*. **39**, 7460–7468.

https://doi.org/10.1180/S0026461X00006502 Published online by Cambridge University Press

PGE distribution in base-metal sulfides from the Merensky Reef of the Bushveld Complex, South Africa

I. OSBAHR[1]*, T. OBERTHÜR[2] AND R. KLEMD[1]

[1]GeoZentrum Nordbayern, University of Erlangen, Schlossgarten 5a, 91054 Erlangen, Germany (*correspondence: osbahr@geol.uni-erlangen.de)
[2]Federal Institute for Geoscience and Natural Resources (BGR), Stilleweg 2, 30655 Hannover, Germany

Introduction

Several studies were undertaken to elucidate the distribution of PGE between various sulfides such as pentlandite, pyrrhotite or chalcopyrite [1, 2]. This present study concentrates on the PGE distribution in BMS in profiles of the Merensky Reef of the Bushveld Complex using whloe-rock, electron microprobe and LA-ICP-MS analysis.

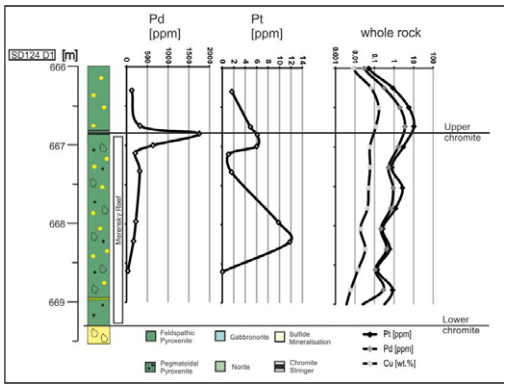

Figure 1: Pd and Pt distribution in pentlandite and whole-rock.

Results

Pentlandite is a principal host of Pd (and Rh) whereas Pt is mainly hosted by PGM. The distribution of Pt and Pd in two profiles from the western Bushveld reveals a top-loaded mineralization – max. concentrations of Pd and Pt occur in the area of the upper chromite stringer in the whole-rock, coinciding with max. concentrations of Pd in pentlandite (Fig. 1). Two profiles from the eastern Bushveld reveal 'offset patterns' – max. concentration of Pd in pentlandite is displaced ny 0.5 – 1 m below the max. concentration of whole-rock Pd and Pt. Downward percolation of sulfides or post-magmatic processes such as selective diffusion may be responsible for the observed offset feature.

[1] Godel *et al*. (2007) *J. Petrol* **248**, 272–294. [2] Barnes *et al*. (2006) *Contrib Mineral Petrol* **152**, 187–200.

The evolution of surface, intermediate and deep water connections during the closure of the Central American Seaway

A. OSBORNE[1]* M. FRANK[1] AND R. TIEDEMANN[2]

[1]IFM-GEOMAR, Leibniz Institute of Marine Sciences at the University of Kiel, Wischhofstrasse 1-3, 24148 Kiel, Germany (*correspondence: aosborne@ifm-geomar.de)
[2]AWI, Alfred Wegener Institute for Polar and Marine Research, Am Alten Hafen 26, 27568 Bremerhaven, Germany

The progressive closure of the Central American Seaway and the associated reorganisation of deep-ocean circulation have been controversially reported as contributing to a warming and a cooling of global climate, as well as increasing moisture supply to the northern hemisphere and hence preconditioning the inception of Northern Hemisphere Glaciation. Here we use radiogenic isotopes of Nd and Pb to reconstruct the history of shallow, intermediate and deep water connections between the Caribbean Sea and the eastern Equatorial Pacific Ocean from 5.0 to 2.0 million years ago. Surface water exchange and mixing is characterised using the Nd isotope composition of planktonic foraminiferal calcite. The Nd and Pb isotope compositions of early diagenetic ferromanganese coatings of the same sediment samples are employed to determine intermediate and deep water exchange.

A core-top survey compares ε_{Nd} in surface sediments, with the expected water mass signature. Leaches of core-top sediments taken from intermediate water depths (~1000m) in the central Caribbean Sea give values between ε_{Nd} = -7.5 and -10.2. Planktic foraminifera from the same samples have ε_{Nd} between -8 and -10.8. Around a deeper central Caribbean site (~3000m), leaches give between -5.9 and -8.2 in ε_{Nd}, which is 2 to 6 ε_{Nd} units more radiogenic than published data from ferromanganese crusts in the Lesser Antilles[1, 2], but still significantly less radiogenic than core-top leaches from the Eastern Equatorial Pacific (EEP), which have ε_{Nd} between 2 and 0. These latter measurements are broadly consistent with data from an EEP ferromanganese crust [3]. These findings form the basis for the down-core survey and the reconstruction of the exact timing of the closure of the seaway and corresponding water mass exchange at different water depths.

[1] Reynolds *et al*. (1999) *EPSL* **173**, 381–396. [2] Frank *et al*. (2006) *G*^{3} **7**, doi, 10.1029/2005GC001140. [3] Frank *et al*. (1999) *Geology* **27**, 1147–1150.

https://doi.org/10.1180/S0026461X00006502 Published online by Cambridge University Press

3 stages of Earth evolution — Core formation, ocean emergence and the 2.3 Ga rise of atmospheric oxygen: How are they linked?

MILES F. OSMASTON

The White Cottage, Sendmarsh, Ripley, Woking, Surrey GU23 6JT, UK (miles@osmaston.demon.co.uk)

Recognized nearly a century ago [1], the mean specific angular momentum (a. m.) of SS planetary materials is $>10^5$ times the Sun's, so it is an important constraint upon how the planets were built. Nebula is the only conceivable agent for this partition. And it must do this for both the protoplanet and all of its feedstock, so planetary growth must be essentially complete before it departs (<5 Ma?). This rules out the post-nebula growth in cores-by-Fe-percolation models, for which isotopic (Hf-W, etc) data have been interpreted as needing upwards of 30 Ma for completion, though this interval may actually relate to post-core-completion exchange at the CMB.

Those models also do nothing for the origin of SS water. Ringwood's model (1960-1978) invokes a cool nebula, achievable with other advantages [2-4], to give high-*f*O2 accretion. It then uses the nebula to reduce hot erupted FeO at the protoplanet's surface; the Fe then being 'subducted' to form the core. Nebular departure halted this, leaving some FeO in the mantle. Incorporation into its mineral structure of a few of the >400 Earth-ocean volumes of reaction water thus generated greatly water-weakened it, facilitating convective loss of early heating.

But at ~2.49Ga, ocean production caused parts of the upper mantle to reach a critical loss of water-weakening in the presence of interstitial melt [5], halting convective motion for ~270Ma [6, 7]. MOR collapse lowered sea-level by >3km, exposing cratons to erosion, unroofing TTG, lowering atmospheric CO2 and causing Huronian glaciation (2.4 Ga). During this hiatus, oxygenic life, previously confined to the top 200m of oceans, won its battle against MOR effusions, depositing BIF and oxygenating the atmosphere, which is why we are here [5, 7]. The restart after 2.22Ga left cratons with the deep-keeled tectospheres of stiffened mantle, manifest in plate dynamics behaviour for at least the past 90Ma [8].

[1] Jeans (1919) Problems of cosmogony & stellar dynamics. Adams Prize Essay, Clarendon Press. [2] Osmaston (2006) *GCA* **70** (18S) A465. [3] Osmaston (2009) *Geophys. Res. Abstr.* **11**, EGU2009-12204. [4] Osmaston (2009) *EPSC Abstr.* **4** EPSC2009-264. [5] Hirth & Kohlstedt (1996) *EPSL* **144**, 93–108. [6] Osmaston (2001) *J.Conf Abstr* **6** (1) 417. [7] Condie, O'Neill & Aster (2008) *GCA* **72** (12S) A175. [8] Osmaston (2009) *Geophys.Res.Abstr.* **11**, EGU2009-6359.

Experimental study of nucleation and phase stability of calcium sulfate

M. OSSORIO[1]*, A.E.S. VAN DRIESSCHE AND J.M. GARCÍA-RUIZ

LEC, IACT, CSIC - U.Granada, 18100 Granada, Spain (*correspondence: mercedes@lec.csic.es)

Calcium sulfate presents three common phases when precipitated from aqueous solution in nature or in the laboratory: gypsum ($CaSO_4{\cdot}2H_2O$), bassanite ($CaSO_4{\cdot}0.5H_2O$) and anhydrite ($CaSO_4$) [1]. The conversion of these phases into each other takes place in nature but also represents the basis of gypsum-based building materials. Therefore many studies have been performed on the phase stability of calcium sulfate in solution, as a function of temperature but, at present, the mechanisms by which precipitation, phase transition and phase stability occur in solution are not well defined [2].

We performed an experimental study in order to identify the factors that influence the nucleation, growth and phase stability of calcium sulfate at laboratory scale. The crystallization was carried out by chemical reaction by varying temperature (40°C-120ºC), salinity (0.8, 2.8, 4.3 M NaCl) and duration of the experiments (2 min – 3 months). The reaction products were characterized by Powder X-Ray Diffraction, SEM and TEM.

Our results show a clear dependence on temperature and salinity of the precipitated phase of calcium sulfate; at low temperatures, gypsum is the most stable phase (<60°C). As temperature increases, direct precipitation of bassanite (80-110°C) and anhydrite (120°C) occurs. The temperature at which primary bassanite appears decreases with increasing salinity (110-80°C) while anhydrite shows a more complex dependence. Besides primary precipitation phase transition of calcium sulfate in contact with the mother solution occurs over time (>days). With time the temperature at which bassanite and anhydrite appear decreases. This behavior is generalized for the three salinities studied but at the highest salinity this phase transition occurs faster.

A plausible explanation for the mechanism of phase transition is the dissolution of the phase that precipitates first (less stable) and subsequent 'recrystallization' of the more stable phases with passing time. The kinetics of dissolution/precipitation of these compounds plays a decisive role in the transition rates of calcium sulfate phases and are mainly controlled by temperature and solution salinity.

[1] Christensen *et al.* (2008) *Chem. Mater.* **20,** 2124-2132 [2] Freyer & Voigt (2003) *Monatshefte für Chemie* **134**, 693-719.

https://doi.org/10.1180/S0026461X00006502 Published online by Cambridge University Press

Petrogenesis of syn-orogenic leucogranites (Damara orogen, Namibia)

J. OSTENDORF[1] AND S. JUNG[2]

[1]Institut für Mineralogie, TU Bergakademie Freiberg, 09596 Freiberg, Germany (joerg.ostendorf@mineral.tu-freiberg.de)
[2]Mineralogisch-Petrographisches Institut, Universität Hamburg, 20146 Hamburg, Germany

The granite-dominated part of the Central Damara Orogen (Namibia) consists of basement gneisses, high-grade metamorphic metasedimentary rocks, and crust-derived granites. Granites that crop out in the Kubas area fall into two groups; 553±8 Ma-old grey granites and 513±6 Ma-old red leucogranites. The grey granites have a common granitic composition but the red leucogranites are highly fractionated melts shown by extremely high Rb/Sr ratios, fractionated REE patterns and the presence of euhedral Mn-rich garnet. Digested remnants of upper crustal pelites are clusters of biotite, sillimanite and cordierite indicating some crustal contamination. The grey granites have less evolved isotopic compositions (init. $^{87}Sr/^{86}Sr$: 0.720; init. ε Nd: -16; large variation in $^{207}Pb/^{204}Pb$ (15.55-15.61) at $^{206}Pb/^{204}Pb$ ratios lower than the red leucogranites). The red leucogranites have more evolved isotopic compositions (init. $^{87}Sr/^{86}Sr$: 0.725-0.750; init. ε Nd: -16; large variation in $^{206}Pb/^{204}Pb$ trending towards the composition of common pelitic metasediments from the Damara orogen). These isotopic features indicate that both granite types represent melts from a similar source (Proterozoic/Archaean basement?) but have undergone different processes. The grey granites appear to be uncontaminated and hence, their composition mirror their sources. The red leucogranites have apparently interacted with upper crustal rocks via AFC processes (digested xenoliths, fractionated REE patterns, large variation in Sr and Pb isotopes), probably during stagnation within the crust. Such lower crustal melts are apparently confined to the pre-to syn-collisional phase of the orogeny and it is therefore likely that they have also contributed to the heat budget that controlled high-temperature metamorphism. Even in complex terranes granites can preserve a record of their sources and can be used to place limits on possible compositions of the unexposed sources of the granites and thus on the nature of the terranes through which the melts ascended.

Level of ^{129}I and ^{127}I in terrestrial environment of Slovenia: A two-year study of background areas

A. OSTERC AND V. STIBILJ*

Institute Jožef Stefan, Jamova 39, 1000, Ljubljana, Slovenia (*correspondence: vekoslava.stibilj@ijs.si)

Introduction

Iodine has two natural isotopes – ^{127}I is a stable isotope, while ^{129}I is a radioactive isotope formed naturally by spallation of cosmic rays on atmospheric Xe and spontaneous fission of ^{238}U. However, the main sources of ^{129}I in the environment are anthropogenic from nuclear fuel reprocessing plants (NFRP). Current levels of ^{129}I do not represent any radiological hazard to humans, but the discharges of ^{129}I from NFRP can be used as an environmental tracer [1]. Our aim was to investigate levels of ^{129}I in environment of Slovenia, because no data exist.

Experimental

Samples of precipitation, soil from opened field and forest, and pine needles were collected three times at four various locations in period 2009–2010. Total concentrations of ^{127}I and ^{129}I were determined with radiochemical neutron activation analysis [2].

Results

Sample	**^{127}I** ($\mu g\ g^{-1}$)	**$^{129}I/^{127}I$** (10^{-8})
precipitation (n = 10)	0.0017–0.0065	<2.3–91.0
soil		
opened field (n = 12)	2.4–22.2	0.7–7.1
forest (n = 12)	3.9–35.2	0.7–7.4
pine needles (n = 12)	0.058–0.413	15–189

Table 1: Range of concentration levels and $^{129}I/^{127}I$ ratios

Discussion

The highest concentrations of ^{127}I and ^{129}I were found in soil samples. Soil samples collected in forest, where more organic matter is present; contained more ^{129}I and ^{127}I than soil from opened field, although the $^{129}I/^{127}I$ isotopic ratio is the same. The highest $^{129}I/^{127}I$ isotopic ratio was found for pine needles. Obtained results are the first for terrestrial environment of South Europe and are comparable to values found in literature for background areas.

[1] Hou (2004) *J. Radioanal. Nucl. Chem* **262**, 67–75.
[2] Osterc *et al*. (2007) *Acta Chim. Slov* **54**, 273–283.

https://doi.org/10.1180/S0026461X00006502 Published online by Cambridge University Press

Transformation of nitrogen during sediment burial history

CHRISTIAN OSTERTAG-HENNING[1] AND CHRISTIAN ILLING[2]

[1]Bundesanstalt für Geowissenschaften und Rohstoffe, Stilleweg 2, D-30655 Hannover, Germany (*correspondence: Christian.Ostertag-Henning@bgr.de)
[2]Westfälische Wilhelms-Universität, Institut für Geologie, Corrensstr. 24, D-48149 Münster, Germany

Many gas reservoirs contain appreciable percentages of gaseous dinitrogen besides the commercial valuable hydrocarbon gases. The source of this nitrogen and its transformation path to gaseous dinitrogen is still a matter of ongoing research (cf. [1], [2]).

To follow the transformation of nitrogen in organic rich sediments and sedimentary rocks during burial history with increasing pressure and temperature different approaches have been followed in this study: (1) Two sets of natural maturity series of type II or type III kerogen containing sediments and sedimentary rocks have been analysed with respect to several forms of nitrogen: exchangeable NH_4^+, N in the bitumen, HCl-hydrolysable N (amino-N in kerogen and N in clay minerals), kerogen bound N and N fixed in feldspars and other acid-stable minerals. In addition to the concentrations of the different nitrogen forms the nitrogen isotopic composition was investigated. (2) For the low maturity sediment and sedimentary rock samples artificial heating experiments in closed gold capsules as well as in flexible gold-titanium cells at high pressures and temperatures have been conducted to simulate the natural maturation process.

The results clearly document the release of organically bound nitrogen during early maturation – and a concomittant increase in dissolved inorganic nitrogen concentrations. With elevated ammonium concentrations in the pore water the incorporation of ammonium into authigenic minerals increases. This mineral-bound nitrogen is fixed until the mineral phase is destabilised by higher p-T-conditions or changing aqueous fluid compositions. The final transformation of ammonium released from minerals to gaseous dinitrogen might be a consequence of redox reactions involving mineral surfaces. At very high temperatures dinitrogen might be formed from organically bound nitrogen in type III kerogen.

[1] Jurisch & Krooss (2008) *Org. Geochem.* **39**, 924–928. [2] Mingram *et al.* (2005) *Int. J Earth Sci.* **94**, 1010–22.

U-Pb and Pb-Pb dating of phosphates in Martian meteorites

YOSHI. OTA[1]*, N. TAKAHATA[2], Y. SANO[3] AND N. SUGIURA[4]

[1]School of Sci., Univ. of Tokyo, Tokyo 113-0033 Japan (*correspondence: y_ohta@aori.u-tokyo.ac.jp)
[2]AORI. Univ. of Tokyo, Kashiwa 277-8564 Japan (ntaka@aori.u-tokyo.ac.jp)
[3]AORI. Univ. of Tokyo (ysano@aori.u-tokyo.ac.jp)
[4]Sch.of Sci., Univ. of Tokyo (sugiura@eps.s.u-tokyo.ac.jp)

There are many studies that measured U-Pb and Pb-Pb ages in phosphates of Martian meteorites. The ages of Shergottites are controversial, ranging from 4 billion years [1] to 200 million years [2] and are not well constrained. The ages are very important for understanding Martian evolution.

Here we show the U-Pb and Pb-Pb ages in several Martian meteorites. ALH84001, Zagami, DaG476 and some other Martian meteorites were investigated. For U-Pb and Pb-Pb dating by NanoSIMS, primary O- ions with a beam intensity of 10nA were used in a spot diameter of about 10-20 micrometer. An apatite from Prairie Lake called PRAP with a known age [3] was used as a standard for Pb/UO-UO/UO_2 calibration. The age of ALH84001 is about 4 billion years and it is consistent with those of the previous studies [4] within the experimental error. Our U-Pb age of phosphate minerals in Zagami are very young, suggesting that it was reset by some recent metamorphism. However the Pb-Pb isochron age at the same spots of U-Pb dating is about 4 billion years. This age is derived from two grains. Our data suggest that Zagami crystallized at 4 billion years ago, and it experienced some recent metamorphism to reset the U-Pb age. At the poster session I will discuss the implication of the U-Pb and Pb-Pb ages of ALH84001, Zagami and other Martian meteorites.

[1] A. Bouvier. *et al.*(2009) *Earth & Planetary Sci. Lett.* **280** 285–295. [2] Nyquist *et al.* (1998) *Journal of Geophysical Res.* **103**, E13, **31**, 445-31, **455**. [3] Sano Y. *et al.*(1999) *Chem. Geol.* **153**, 171–179. [4] Terada K. *et al.*(2003) *Meteoritics&Planet.Sci.* **38** 1697–1703.

https://doi.org/10.1180/S0026461X00006502 Published online by Cambridge University Press

Origins of chromite found in chemical and clastic sedimentary rocks of the 3.2 Ga Moodies Group, South Afirica

T. OTAKE[1]*, Y. SAKAMOTO AND T. KAKEGAWA

Department of Earth Science, Tohoku University, Aoba 6-3, Aramaki, Aoba-ku, Sendai, 980-8578, Japan (*correspondance : totake@m.tohoku.ac.jp) (y-sakamoto@m.tains.tohoku.ac.jp, kakegawa@m.tohoku.ac.jp

The timing of the emergence of oxygenic photoautotrophs (e.g. cyanobacteria) is critical for understanding the evolution of life and the earth's surface environments. Yet, no palaeontological or geochemical signature in sedimentary rocks has provided unequivocal evidence for the emergence of cyanobacteria in the Archean era. The objective of this study was to find mineralogical and geochemical signatures that mark the emergence of cyanobacteria in a shallow ocean environment from the the Moodies Group, South Africa (~3.2 Gyr), in which Javaux *et al*. (2010) [1] discovered large, well-preserved microfossils, possibly the remnants of eukaryotes. We were particularly focused on the origins of chromite ($FeCr_2O_4$) and magnetite (Fe_3O_4), which contain the redox-sensitive elements, iron (Fe) and chromium (Cr), found in the chemical and clastic sedimentary rocks.

Our samples collected from underground mines (e.g. Sheba gold mine) were divided into 3 groups, based on the dominant iron-bearing mineral: the Siderite ($FeCO_3$), Mgnetite, and Hematite (Fe_2O_3) groups. While fine-grained (<5 μm in diameter) hematite, or ferric hydroxide ($Fe(OH)_3$) as its precuror, was interpreted to have been directly precipitated from seawater, large-grained (>50 μm in diameter) magnetite and siderite were interpreted to have formed during early diagenesis. We identified two types of chromite: eudheral and unhedral chromite. All eudheral chromite, which was observed in the Magnetite group, was overgrown by magnetite. This suggests that both euhderal chromite and magnetite in the Magnetite group were formed during diagenesis. On the other hand, unhedral chromite in the Siderite group was often included in silicate minerals (e.g. chlorite and biotite), indicating that it is detrital in origin. A positive correaltion between the Cr/Ti ratio and the U/Th ratio in the bulk chemical composition of the Magnetite group may suggest that both Cr and U were transported to the ocean through oxidative chemical weathering, and therefore that cyanobacteria was emerged before 3.2Ga.

[1] Javaux *et al*. (2010) *Nature* **463**, 934–938.

Uranium speciation in opals from the Nopal I deposit (Mexico)

G. OTHMANE[1]*, T. ALLARD[1], N. MENGUY[1], T. VERCOUTER[2], G. MORIN[1], G. CALAS[1] AND M. FAYEK[3]

[1]IMPMC, CNRS UMR 7590, UPMC, Paris, France (*correspondence: guillaume.othmane@impmc.upmc.fr)
[2]LSRM, CEA Saclay, Gif-sur-Yvette, France
[3]University of Manitoba, Canada

The study of uranium migration and trapping in the environment is relevant to assess the safety of potential high-level nuclear waste repositories (HLNWR). The Nopal I uranium deposit (Sierra Peña Blanca, Mexico) is a natural analogue of HLNWR located in volcanic tuff. Secondary uranyl minerals such as uranophane and weeksite occur in the deposit and are coated by opal [1], [2].

The aim of this study is to determine the uranium speciation in these opals to reveal the low temperature conditions of trapping of this element, from the micrometer scale of electron microscopy to the molecular scale provided by fluorescence spectroscopy.

Uranium speciation was found to be various and complex. We evidenced by scanning electron microscopy (SEM) microparticles of ß-uranophane Ca $[(UO_2)(SiO_3OH)]_2$ $(H_2O)_5$ and apatite Ca_5 $(PO_4)_3$ (OH, Cl, F) containing small amounts of uranium. However the major part of uranium is concentrated in Ca-U-enriched zones with a Ca:U ratio of 1:1 and displaying spherical features (Fig. 1).

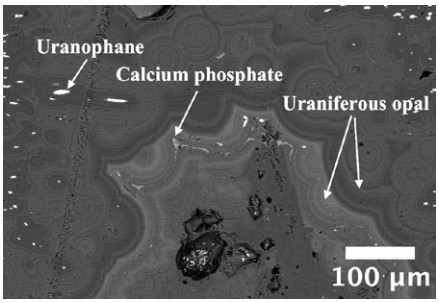

Figure 1: SEM back-scattered electron picture of a yellow opal cross-section from the Nopal I uranium deposit, Mexico.

The exact nature of Ca-U species in these zones was not determined but transmission electron microscopy (TEM), cathodoluminescence and time-resolved laser fluorescence spectrocopy (TRLFS) analyses suggest the presence of Ca_m-$(UO_2)_m$-$(O/OH/H_2O)_n$ complexes adsorbed or incorporated in opal. These results will be discussed in terms of chemical conditions that prevailed during U incorporation.

[1] Calas *et al*. (2008) *Terra Nova* **20**, 206–212. [2] Schindler & Fayek (2010) *Geochim. Cosmochim. Ac*, **74**, 187–202.

https://doi.org/10.1180/S0026461X00006502 Published online by Cambridge University Press

Density functional theory study of the interaction of arsenic complexes with FeOOH surfaces

KATRIN OTTE*, WOLFGANG W. SCHMAHL AND ROSSITZA PENTCHEVA

Department of Earth and Environmental Sciences, University of Munich, Theresienstr. 41, 80333 Munich, Germany (*correspondence: Katrin.Otte@lrz.uni-muenchen.de, Pentcheva@lrz.uni-muenchen.de)

Iron oxyhydroxides (FeOOH) possess high surface areas which are relevant for cycling and retention in a series of environmental and technological processes [1]. Using density functional theory (DFT), we explore the stability and electronic properties of the goethite (101), akaganeite (100), and lepidocrocite (010) surfaces under different environmental conditions. The GGA+*U* calculations reveal that the termination impacts the oxidation state of the surface iron ions, providing a possibility to tune the catalytic activity. The energetics and bonding mechanisms of arsenic complexes in different adsorption geometries (e.g. mono- and bidentate) on the surfaces are investigated.

Funding by the BMBF programme Geotechnologies: Mineral Surfaces (Project SURFTRAP) and Elitenetzwerk Bayern is acknowledged.

[1] R. M. Cornell & U. Schwertmann, *The Iron Oxides* (Wiley, Weinheim, 2001).

Quantification of primary marine organic aerosol properties using aerosol mass spectrometry

J. OVADNEVAITE[1]*, D. CEBURNIS[1], H. BERRESHEIM[1], M. DALL'OSTO[1,2], J. BIALEK[1], C. MONAHAN[1], D.R. WORSNOP[3,4] AND C.D. O'DOWD[1]

[1]School of Physics and Center for Climate and Air Pollution Studies, Ryan Institute, National University of Ireland Galway, Galway, Ireland (*correspondence: jurgita.ovadnevaite@nuigalway.ie)

[2]Institute of Environmental Assessment and Water Research, Consejo Superior de Investigaciones Científicas, Barcelona, Spain

[3]Aerodyne Research, Inc., Billerica, Massachusetts, USA

[4]Physics Department, University of Helsinki, Helsinki, Finland

Marine aerosol has a strong impact on both the Earth's albedo and climate; however, its inherently complex composition ranging from inorganic components (sea salt, nss sulfate) to complex organic carbon mixtures of water soluble and insoluble components [1, 2] and bio - aerosol components [3] complicates the quantification of those impacts. In recent years, the dominant organic matter (OM) contribution (in particular, the primary organic matter) to submicron marine aerosol during periods of high biological activity over N.E. Atlantic has been quantified on a seasonal basis [1] as well as in real-time [4]. However, the character of its influence on cloud formation is still undergoing an intense discussion. Here, we present the comprehensive long term real time ambient aersol measurements which reveal the important role of marine organics to cloud formation: the recurrent enhancement of cloud formation activity (cloud condensation nuclei) under aerosol enrichment by primary organics with low hygroscopic growth factor is reported for the first time. Moreover, the complexity of organic matter identified by high resolution time of flight aerosol mass spectrometry (HR-ToF-AMS) and its interpretation from HR-PMF (Positive matrix factorization) revealed a dominant contribution of primary sources to marine organic aerosol, with unique marine organic aerosol fingerprint, when compared to anthropogenic organic aerosol.

[1] O'Dowd, C.D. *et al*. (2004) *Nature* **431**, 676-680. [2] Russell, L.M. *et al*. (2010) *P. Natl. Acad. Sci. USA* **107**(15) 6652–6657. [3] Leck, C. & E.K. Bigg (2005) *Geophys. Res. Lett*. **32**(19) L19803. [4] Ovadnevaite, J. *et al*. (2011) *Geophys. Res. Lett*. **38**(2) L02807.

https://doi.org/10.1180/S0026461X00006502 Published online by Cambridge University Press

First principles investigation of manganese oxide surface chemistry

GLORIA A.E. OXFORD* AND ANNE M. CHAKA

National Institute of Standards and Technology, Gaithersburg, MD 20899, USA
(*correspondence: gloria.oxford@nist.gov)

Manganese oxides, which are ubiquitous in geological settings, play an important role in heavy metal adsorption and oxidation in the environment. In particular, the ability of manganese oxides to oxidize trivalent chromium to hexavalent chromium has garnered considerable attention, but questions remain concerning the mechanim of oxidation. To accurately model hexavalent chromium transport and its fate in the environment, the specific interactions between chromium ions and manganese oxide surfaces must be ascertained. Because structure, composition, and chemical properties of surfaces are intimately related to reactivity, a fundamental understanding of manganese oxide surface reconstructions and redox behavior lays the foundation for investigating oxidation mechanisms involving manganese oxides. However, detailed structural analyses of manganese oxide surfaces under environmentally relevant conditions are scarce.

We have combined periodic density functional theory calculations and *ab initio* thermodynamics to identify stable surface terminations of the β-MnO_2 (110) and γ-MnOOH (010) surfaces and to determine their redox behavior in response to varying oxygen and water chemical potentials. Reduction of the surfaces produces interesting surface reconstructions driven by the competition between lattice constraints and optimal *d*-orbital occupation and manganese coordination geometry. Multiple oxidation states are found at the surfaces due to Jahn-Teller effects. Under ambient conditions, oxidation of the γ-MnOOH (010) surfaces is predicted to be favorable, while the reduced β-MnO_2 (110) and γ-MnOOH (010) surfaces are not stable but may become relevant during heavy metal oxidation processes at the surface. Molecular and dissociative adsorption of water on the clean surfaces significantly lower the surface free energies. Binding sites for trivalent chromium on the hydrated surfaces will be presented with a focus on the effect of manganese oxidation state on adsorption geometry.

Modeling oceanic anoxia/euxinia induced by massive CO_2 injection

K. OZAKI[1]* AND E. TAJIKA[2]

[1]University of Tokyo, Tokyo, 113-0033, Japan
(*correspondence: ozaki@eps.s.u-tokyo.ac.jp)
[2]University of Tokyo, Chiba-ken, 277-8561, Japan

Atmosphere-ocean biogeochemical cycle model

Rapid global warming caused by large igneous provinces (LIPs) has been suggested as the cause of ocean anoxia. To constrain the required conditions for the occurrence of oceanic anoxic event (OAE) and investigate the climate change during OAE, we constructed the atmosphere-ocean biogeochemical cycle model. The ocean model [1] can reproduce the vertical distribution of several dissolved components (e.g. PO_4, O_2, H_2S, DIC, Alk) in the water column. We also consider the kinetic treatment of carbonate dissolution in the ocean. Hence, carbonate compensation depth (CCD) can also be calculated. The simplified chemical (carbonate and silicate) weatheriing on land and air-sea exchange of CO_2 were also included.

Results and discussions

We conducted the sensitivity analyses of CO_2 injection event systematically with several initial conditions (we especially focused on pCO_2, pO_2, SST, and shelf area) because climate and geographical setting would affect the required amount of CO_2 and behaviour of climate change. Simulations indicate that (1) enhanced nutrient (phosphorus) input to ocean effectively promote the oceanic productivity, resulting in an expantion of oxygen minimum zone and nutrient efflux from the surface sediments to the bottom waters, (2) global eutrophication (and anoxia) can be induced by a positive feedback loop among anoxia, phosphorus regeneration, and surface productivity, (3) once global anoxia achieve, enhanced accumulation of organic carbon in marine sediments acts as a buffer against global warming, resulting in climate cooling during OAE in some cases.

In this presentation, we will also discuss the effect of initial conditions on the required amount of CO_2 for the occurrence of global anoxia. We conclude that historical background has an important role in the required conditions for OAEs.

[1] Ozaki, Tajima & Tajika (2011) *EPSL* **304**, 270–279.

https://doi.org/10.1180/S0026461X00006502 Published online by Cambridge University Press

Petrographic and geochemicial characteristics of dolomites in the Golbogazı Formation (Upper Devonian) at SW of Hadim, (Konya - Turkey)

ALI MUJDAT OZKAN AND EMRE BICER

Selcuk University, Engineering Faculty, Department of Geological Engineering, Konya – Turkey (mujdatozkan@selcuk.edu.tr)

Upper Devonian units, locating Central Taurus composed of thick dolomite with massive limestones layers and thinner dolomite layers with intercalated limestone are described. Various dolomite types include: Type I) dolomite formed as dolomicrite as mimic replacement, Type II) the planar-e texture dolomites are scattered in a micritic matrix, Type III) fracture and void filling dolomite (zoned dolomite, overgrowth and saddle), Type IV) brecciated dolomite, and V) polymodal dolomite.

The Sr content in the Golbogazı Formation (184 to 74 ppm in the early dolomites, and 105 to 78 ppm in the late dolomites, respectively) is compatible with the Sr concentration mixing-zone dolomites. The Na content in the Golbogazı Formation (593 to 148 ppm in the early dolomites, and 519 to 297 ppm in the late dolomites, respectively) is compatible with the Na concentration mixing-zone dolomites. The investigated dolomites exhibit -1.95 to -3.46 PDB in $\delta^{18}O$ values relative to their $\delta^{13}C$ values (1.33 to -1.33 PDB) in the early diagenetic dolomites. The late diagenetic dolomites display -3.96 to -9.44 PDB in $\delta^{18}O$ values relative to their $\delta^{13}C$ values (2.52 to -1.58 PDB).

REE	Samples		Normalized values			
	Rocks	Str. Sed.	Chondrite	Peridotite	MORB	NASC
La	22,1	24,1	67,0	22,3	6,0	0,7
Ce	44,8	49,2	52,1	17,0	3,9	0,6
Pr	5,4	5,3	44,8	15,8	3,0	0,6
Nd	20,7	20,3	33,3	11,5	2,1	0,7
Sm	4,1	4,1	20,3	7,5	1,2	0,7
$\sum_{LREE}$	97,1	103				
Eu	0,8	0,9	11,4	3,8	0,6	0,6
Gd	3,7	3,8	13,8	5,0	0,8	0,7
Tb	0,7	0,7	13,7	4,9	0,8	0,7
Dy	3,8	4	11,6	4,0	0,7	0,7
Ho	0,7	0,8	10,3	3,4	0,6	0,6
Er	2,4	2,5	11,0	4,0	0,7	0,7
Tm	0,4	0,4	12,0	4,0	1,1	0,7
Yb	2,4	2,5	10,8	4,0	1,1	0,8
Lu	0,3	0,4	12,3	3,7	1,0	0,8
$\sum_{HREE}$	15,2	16				
$\sum_{REE}$	112,3	119				

As a result, the Golbogazı Formation dolomites have been formed as early diagenetic at the shallow marine environment and as the late diagenetic at the shallow-deep burial depths.

Comparison of REE concentrations between the Bozkir ophiolitic rocks and stream sediments derived from these rocks in the Bozkır Region (Konya – Turkey)

A. ÖZTÜRK*, F. ARIK AND M. KARADAG

Selcuk University, Geological Engineering Department, Konya, Turkey (*correspondence: acan@selcuk.edu.tr)

The study area located in south and east of Bozkır (Konya-TURKEY), covers approximately 250 km^2. The units cropped out in the study area are Geyikdağı (slightly metamorphic detricious and carbonaceous rock), Bozkır (ophiolitic rocks such as serpentinite, pyroxenite, gabbro, radiolarite, chert, limestone) and Bolkardağ (generally limestones) tectonic units from bottom to top. This study aims investigation of REE concentration of the rocks and stream sediment samples derived from Bozkir Ophiolitic Melange and comparison between the two mentioned groups [1, 2].

REE contents of the rock samples higher than those of the chondrite and peridotite while lower than that of NASC. $\sum$REE, HREE $_{(La-Sm)}$ and LREE $_{(Gd-Lu)}$ of the rocks are 112.2, 97 and 15.2 ppm respectively. REE contents of stream sediments higher than that of the rock samples (Table 1).

Table 1. REE contents of the rock and stream sediment and normalized values to the some reference rocks.

Some normalized values of the rock samples to the chondrite such as La/Lu, Gd/Yb, Eu/Eu* and Ce/Ce* are 5.44, 1.27, 0.68 and 0.93.

[1] Öztürk (2008) PhD Thesis *Selcuk Univ. N.A.S.I 222p.* [2] Öztürk (2010) *Geology of Nat. Sys._ Geo* 209–210p.

https://doi.org/10.1180/S0026461X00006502 Published online by Cambridge University Press

Mineralogy and geochemistry of the Yellice magnetite occurrences of Sivas-Central Anatolia, Turkey

C. OZTURK*, T. UNLU AND İ.S. SAYILI

Ankara University, Department of Geological Engineering, 06100, Tandoğan, Ankara
(*correspondence: cozturk@eng.ankara.edu.tr)

Ophiolitic rocks, trusted tectonically over Munzur limestones of Taurus platform and emplaced during Maastrichtian form the basement of the study area.

The primary ore mineral at Yellice is magnetite in serpentinized ultramaphic rocks of ophiolites. Other ore minerals are chromite, machinavite inclusions bearing pentlandite, pyrrhotite, cubanite lamellae bearing chalcopyrite and pyrite characterizing a liquid magmatic phase. Secondary magnetites of a subsequent phase are formed from ferromagnesian minerals during serpentinization processes.

XRD studies carried on post-tectonic basin deposits (e.g. basalts) indicate albite, calcite, augite, chlorite, olivine and lizardite minerals which point out to minerals occurred by ocean floor metamorphism [1]. Two different mineral assemblages occur in serpentinites. The first paragenesis is antigorite, talc, magnetite, magnezite and chlorite which indicate nearly 400-500 °C temperature conditions [2]. The second paragenesis represented by chrysotile, lizardite, diopside, augite, tremolite, actinolite, calcite, quartz, chromite, magnetite, olivine and talc characterize approximately 350-400°C temperatures and suggests an ocean floor (or hydrothermal) metamorphism [3].

Raman studies revealed that the plagioclases of basaltic rocks are albitized by the affects of sea water. Some pyroxenes are replaced by actinolites due to uralitization.

Consequently, lens shaped magnetite ores with an average grade of 18-20 % Fe_3O_4 and 125 millions tons of tonnages in serpentinites suggest an assemblage of primary minerals formed in upper mantle conditions and a further element association by serpentinization processes.

[1] Stern *et al*. (1979) *Tectonophysics* **55**, 179–213. [2] Iyer *et al*. (2008) *Chem. Geol*. **249**, 66–90. [3] Coleman (1977) *Ophiolites*, **229**.

https://doi.org/10.1180/S0026461X00006502 Published online by Cambridge University Press

Arsenic and its compounds in plants growing in soils contaminated by mining activities

I. PACÁKOVÁ[1], J. SZÁKOVÁ[1]*, W. GOESSLER[2] AND P. TLUSTOŠ[1]

[1]Czech University of Life Sciences, CZ-165 21 Prague 6, Czech Republic (*correspondence: szakova@af.czu.cz)
[2]Karl-Franzens-University Graz, Universitaetsplatz 1, A-8010 Graz, Austria (walter.goessler@uni-graz.at)

Areas of silver and gold ore deposits associated with elevated concentrations of arsenic-bearing elements of the Bohemian Massif were investigated to assess uptake of arsenic species by individual plant species growing at these sites. The areas of the interest were: i) Kaňk near Kutná Hora, Central Bohemia, where the plant species were collected at dump remaining after medieval silver mining. The total arsenic contents in the soil ranged from 100 to 450 mg kg^{-1}. ii) Spoil close to former gold mine in Roudný, Central Bohemia, where the mining activities were stopped in 1930's. The total arsenic contents in the soil ranged from 50 to 1100 mg kg^{-1}. iii) Former mining area Nalžovské Hory, Western Bohemia, where silver was mined till the beginning of 17th century with total As concentrationsin the soil between 70 and 75 mg kg^{-1}.

Results and Discussion

Arsenite, arsenate, dimethylarsinic acid (DMA), methylarsonic acid (MA), trimethylarsine oxide (TMAO), the tetramethylarsonium ion (TETRA), arsenocholine (AC), and arsenobetaine (AB) were commonly found in the plant species. Among the species determined, high arsenobetaine concentrations represent the most interesting finding. Among the plant families, AB was identified in the species representing *Poaceae, Cyperaceae*, and *Plantaginaceae families*. *Similar findings were already published by* Geiszinger *et al*. [1] where arsenocholine and arsenobetaine were detected in *Trifolium pratense*, *Dactylis glomerata*, and *Plantago lanceolata* collected at an arsenic containing ore vein. The results showed the ability of higher plants to produce and/or accumulate a wide spectrum of arsenic species. Their fate and transformations in plant tissues needs intensive research especially when elevated total As concentrations are in the plant biomass.

[1] Geiszinger *et al*. (2002) *Appl. Organomet. Chem*. **16**, 245–249. Financial support for these investigations was provided by Aktion 061002 project.

The $\delta^{18}O$ fingerprint of spring water pathways with evaporating recharge areas

F.A.L. PACHECO [1] AND C.H. VAN DER WEIJDEN[2]

[1]Department of Geology and Centre for Chemistry, UTAD, Vila Real, Portugal (fpacheco@utad.pt)
[2]Utrecht University, The Netherlands (chvdw@geo.uu.nl)

Evaluation of the mean recharge elevation of a spring in a mountainous area by extrapolation using the vertical isotopic gradient of local precipitation assumes that evaporation is limited during the period of recharge. Usually, this assumption fails when recharge takes place in low permeability rocks (e.g. granites). In these cases, water remains variable periods of time in the recharge cells to ensure replenishment of local, intermediate and regional flow circuits. Preservation in the recharge area potentiates evaporation and therefore the enrichment of recharge water in ^{18}O. Resulting from evaporation, an isotopic gradient develops for spring waters, represented by a negative correlation between $\delta^{18}O$ in spring water and elevation. The lines representing the isotopic gradients of precipitation and spring water are expected to converge towards the recharge area and diverge in the opposite direction. The recharge area will be defined by the sectors of the catchment where $\delta^{18}O$ (precipitation) - $\delta^{18}O$ (spring) = 0. A result corroborating this approach is illustrated in Fig. 1 for the Sordo River basin (North of Portugal).

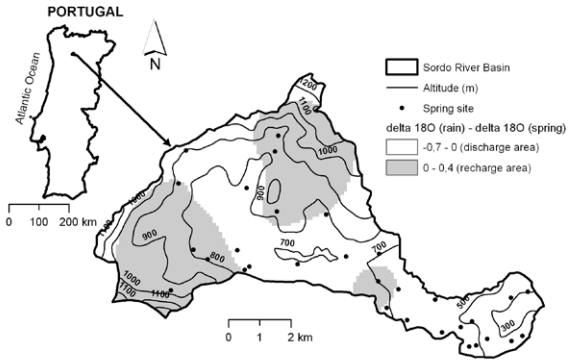

Figure 1: Recharge areas of Sordo River basin

https://doi.org/10.1180/S0026461X00006502 Published online by Cambridge University Press

Holographic interferometry study of the inhibition of gypsum dissolution

E.A. PACHON-RODRIGUEZ AND J. COLOMBANI

Laboratoire de Physique de la Matière Condensée et Nanostructures, Université de Lyon, Université Claude Bernard Lyon 1 and CNRS, 69622 Villerbanne, France (Jean.Colombani@univ-lyon1.fr)

The knowledge of the dissolution properties of gypsum in aqueous solutions is of primary importance in many situations, among which the weathering of rocks, the gypsum karst formation, the quality of drinking water, the scale formation in the oil and gas industry, and the liberation of calcium ions, useful for the geological storage of CO_2.

In standard dissolution experiments, the mineral is dissolving in stirred water. So the dissolution kinetics is blurred by diffusive and convective contributions. For hard minerals, dissolution is so slow that it drives the whole kinetics and the convection contribution can be neglected. But for softer minerals like gypsum, dissolution, diffusion and convection timescales are of the same order of magnitude and their respective contribution can be difficult to distinguish.

We have collected dissolution rates of gypsum in water measured by various methods found in the literature. The deduced dissolution rate constants span over several decades. Therefore we have analysed the hydrodynamics of the experimental setups, eliminated the convective contribution and deduced from them the pure surface reaction rate constant of gypsum in water. It appears to be much smaller than expected from the literature results. An holographic interferometry experiment, performed in still water, is carried out and enables to measure directly this rate constant. Both values agree within experimental uncertainty.

We have made use of this methodology to investigate the influence of various salts, known for their calcium-complexing influence, on the dissolution rate of gypsum. These agents provoke a decrease of the surface reaction rate constant of gypsum of up to more than one order of magnitude (cf. Fig. 1).

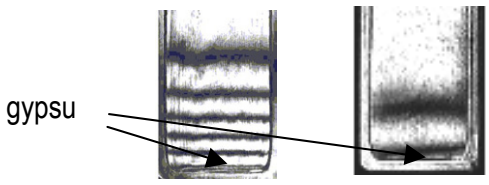

Figure 1: Holointerferograms of the dissolution of a gypsum sample in pure water (left) and in a phosphate salt aqueous solution (right) at rest.

Viruses: A key role in microbial mat mineralization

MURIEL PACTON[1]*, DAVID WACEY[2,3], MATT R. KILBURN[2], GEORGES E. GORIN[4] AND CRISOGONO VASCONCELOS[1]

[1]ETH Zurich, Geological Institute, Zurich, Switzerland (*correspondence: muriel.pacton@erdw.ethz.ch)

[2]Centre for Microscopy, Characterisation and Analysis, The University of Western Australia, Crawley, WA, Australia

[3]School of Earth and Environment, The University of Western Australia, Crawley, WA, Australia

[4]Earth Science Section, University of Geneva, Geneva, Switzerland

In microbial mats, microbes mediate the formation of mineral layers, most commonly carbonates, through the process of organomineralisation, and in doing so enhance their preservation potential in the geological record; Cell walls, sheaths and extracellular polymeric substances (EPS) matrix are currently thought to be the main templates for such mineral precipitation. Nanometer-scale spheroids (20-200 nm) have been widely found in the geological record and are thought to initiate precipitation. Previously, these nano-spheres have been interpreted as fossilised bacterial remains [1] such as nannobacteria, proteins and, more recently, EPS [2].

This study focuses on organomineralisation in a living, hypersaline, non-lithifying microbial mat from Lagoa Vermelha, Brazil, where mineralized nano-scale spheroids have been found. Correlative NanoSIMS and TEM analyses of the same sample area show a one-to-one correlation of nano-scale spheroid morphology, organic material and mineralogy. These results indicate that viruses, which cause the death of the bacteria and then become mineralized upon release, are the most likely origin of these spheroids. The infection of microbial mats by viruses appears to be significant in preserving one of Earth's most primitive and enduring ecosystems in the fossil record.

[1] Kirkland, B.L. Lynch, F.L. Folk, R.L. Lawrence, A.M. & Corley, M.E. (2008) Nanobacteria, organic matter, & precipitation in hot springs, Viterbo, Italy, distinctions & relevance. *Microscopy Today* **16**, 58–60. [2] Benzerara, K. Menguy, N. Lopez-Garcia, P. Yoon, T-H. Kazmierczak, J. Tyliszczak, T. Guyot, F. Brown & G.E. Jr. (2006) Nanoscale detection of organic signatures in carbonate microbialites. *Proc. Natl. Acad. Sci.* **103**, 9440–9445.

https://doi.org/10.1180/S0026461X00006502 Published online by Cambridge University Press

The arrested HP antigorite dehydration front from Cerro del Almirez (SE Spain)

J.A. PADRÓN-NAVARTA[1]*, V. LÓPEZ SÁNCHEZ-VIZCAÍNO[2], C.J. GARRIDO[3], M.T. GÓMEZ-PUGNAIRE[1,3] AND C. MARCHESI[3]

[1]Departamento de Mineralogía y Petrología, Universidad de Granada, 18002 Spain (*correspondence: padron@ugr.es)
[2]Departamento de Geología, Universidad de Jaén, Escuela Politécnica Superior, 23700 Linares, Spain
[3]Instituto Andaluz de Ciencias de la Tierra (IACT), CSIC & UGR, Facultad de Ciencias. 18002 Granada, Spain

Dehydration fronts in metamorphic terrains are mechanically distinct zones where fluids and grain-scale porosity are generatated. Their temporal evolution is a complex interelationship between metamorphic and compactation timescales leading to several mechanisms of fluid expulsion and kinetic fluctuations [1]. An exceptionally well preserved dehydration front, corresponding to the high-pressure (680-710°C and 1.6-1.9 GPa) antigorite breakdown reaction (Atg-out), crops out in Cerro del Almirez (Betic Cordillera, Spain), which displays a complete sequence of metamorphic reactions and allied textures [2, 3]. Detailed mapping of the Atg-out front shows that, between Atg-serpentinite and prograde Chl-harzburgite, a narrow band (up to 8 m thick) occurs of transitional lithologies consisting of chlorite-antigorite-olivine-serpentinite (Chl-serpentinite), grading through antigorite-chlorite-orthopyroxene-olivine (Atg-Chl-Opx-Ol) rocks to Chl-harzburgite (Ol-Opx-Chl). Mass balance calculations and phase diagram considerations indicate that HP Atg breakdown occurred by the sequential formation of: Chl-serpentinite through the reaction,

$$\text{Atg (Al-rich)} + \text{Ol} = \text{Atg (Al-poor)} + \text{Chl} + \text{fluid} \quad (1)$$

and Atg-Chl-Opx-Ol assemblage through the reaction,

$$\text{Atg} = \text{Ol} + \text{Opx} + \text{Chl} + \text{fluid} \quad (2)$$

Observed continuous chemical changes and progresive grain coarsening suggest that these reactions took place at near equilibrium conditions. These observations are important to unravel the kinetics and fluid expulsion mechanisms of this natural dehydrating system.

[1] Connolly (2010) *Elements* **6**, 165–172. [2] Padrón-Navarta *et al*. (2008) *Contrib Mineral Petr* **156**, 679–688. [3] Padrón-Navarta *et al*. (2010) *Contrib Mineral Petr* **159**, 25–42.

Methane and the PETM: All good things must come to an end?

M. PAGANI[1], R. DECONTO[2], S. GALEOTTI[3] AND D. BEERLING[4]

[1]Yale University, Deptartment of Geology and Geophysics, New Haven, CT, 06520 USA (mark.pagani@yale.edu)
[2]Univ. of Massachusetts, Department of Geosciences, Amherst, MA, 01002 USA (deconto@geo.umass.edu)
[3]Università degli Studi di Urbino, Dipartimento GeoTeCA, Urbino, Italy 61029, Italy (simone.galeotti@uniurb.it)
[4]Department of Animal and Plant Sciences, University of Sheffield, Sheffield S10 2TN, UK (d.j.beerling@sheffield.ac.uk)

Global warming during the Paleocene Eocene Thermal Maximum is often explained by a massive release of methane hydrates. However, modeled methane hydrate abundances during warm climates are lower than required to explain the carbon isotope shift that characterizes the PETM. Even if ancient hydrate abundances were greater than model predictions, a very high climate sensitivity to CO_2 would be required to explain the magnitude of warming during the event. While some portion of this high apparent climate sensitivity could be related to an assumed pre-warming that triggered hydrate instability, evidence for that warming is weak at best, and why this warming occurred repeatedly to trigger successive hyperthermals has never been adequately addressed.

In contrast to the methane paradigm, an emerging supposition involving the storage and orbitally controlled release of terrestrial carbon from the arguably vast permafrost reservoirs of Antarctica and the high Arctic region readily explains the warming characteristics of the early Cenozoic hyperthermals. Modeled permafrost carbon estimates and simulations accounting for rising background greenhouse gas concentrations and orbital variability demonstrate terrestrial permafrost thawed during high eccentricity and obliquity orbital nodes once a long-term warming threshold was reached. This new supposition allows for the massive amount of carbon necessary to explain the magnitude of carbon isotope shifts, a reasonable climate sensitivity to CO_2, and the mechanistic basis for repeated warming events during an ever-warming planet.

https://doi.org/10.1180/S0026461X00006502 Published online by Cambridge University Press

Oxidized organic aerosol components in Cabauw, Netherlands, during the May 2008 EUCAARI IOP: NMR spectroscopic characterization and factor analysis

M. PAGLIONE[1], E. FINESSI[1], S. DECESARI[1], A. KIENDLER-SCHARR[2], A. MENSAH[2], M. STOCCHERO[3] AND M.C. FACCHINI[1]

[1]National Research Council (CNR), Institute of Atmospheric Sciences and Climate (ISAC), Bologna, Italy, +39-051-6399578 (m.paglione@isac.cnr.it)
[2]Forschungzentrum Jülich (ICG), Germany
[3]S-IN Soluzioni Informatiche, Vicenza, Italy

Outside urban areas, oxidized organic aerosols (OOA) dominate the composition of the organic atmospheric particulate matter. In the frame of the EUCAARI (European integrated project on Aerosol Cloud Climate Air Quality Interactions) project, the submicron aerosol chemical composition in Cabauw, Netherlands, was characterized by means of proton-Nuclear Magnetic Resonance (^{1}H-NMR) spectroscopy with aim of organic aerosol characterization and source apportionment. The analysis was applied to water-soluble organic aerosols (WSOA), which is a proxy for OOA.

A set of 25 PM1 filter samples, collected in a period of prolonged stable anticyclonic conditions and of accumulation of pollutants, were analysed by ^{1}H-NMR spectroscopy and the resulting collection of spectra was processed using a suite of chemometric techniques, including PCA, cluster analysis and factor analysis (PMF, NMF, MCR) aiming to identify recurrent spectral profiles, to quantify their relative contributions and so to identify different prevalent sources.

Factor analysis identified three factors with characteristic spectral profile: (a) OOA associated to metanesulphonic acid (MSA), (b) humic-like substances (HULIS) and (c) other complex OOA enriched in aliphatic acids. The analysis of metadata (meteorological variables, concentrations of nitrate, sulfate, ammonium, potassium, black carbon, and air masses origin), shows that the MSA-containing OOA factor is associated to northerly marine air masses, the HULIS are carried by polluted continental air masses, whereas the aliphatic-rich OOA have no clear dependence on wind direction.

The comparison of these results with those of Positive Matrix Factorization (PMF) applied to a parallel AMS dataset showed a good agreement between NMR 'HULIS'-factor and one type of AMS 'LV-OOA' (a-type).

Volatile loss via outgassing of the lunar magma ocean

KAVEH PAHLEVAN* AND SHUN-ICHIRO KARATO

Department of Geology and Geophysics, Yale University, New Haven, CT 06520
(*correspondence: kaveh.pahlevan@yale.edu)

Among the most striking observations made of the Apollo samples is the depletion of trace elements in lunar materials [1] including moderately volatile elements (i.e. potassium) that condense from the solar nebula at relatively high temperature (T > 1000 K). While initially thought to be a feature of the degassing of lunar magmas into vacuum, the depletion of volatile elements in lunar samples has since been established as a feature of interior reservoirs [2] and therefore potentially diagnostic of the processes of lunar formation. While this observation is generally thought to be consistent with the high energy events associated with a giant impact, no quantitative scenario has been put forward to explain it. In particular, the settings and processes relevant to the volatile loss episode(s) have not been identified, and the isotopic signatures expected for the various scenarios have not been developed.

The energy released in the Moon-forming giant impact is sufficient to melt and partially vaporize both the Earth and the impactor. The timescale to eliminate this heat by radiation is ~10^3 years [3]. Hence, the Earth-Moon system is expected to be in a melt-vapor state for the first thousand years after the giant impact. Moreover, the Moon-forming material may revaporize during the process of lunar accretion from a disk if the process is sufficiently rapid [4]. Previous work has shown that silicate vapors are gravitationally bound to the gravity field of the Earth, even at the high temperatures encountered after a giant impact [5]. We have investigated the conditions necessary for the efficient outgassing of the lunar magma ocean and hydrodynamic escape of the resulting transient atmosphere from the weak lunar gravity field. We will present predictions for isotopic signatures that can test and constrain such a scenairo experimentally.

[1] Wolf, R. Anders, E. (1980) *Geochem. Cosmochem. Acta* **44** 2111–2124. [2] Ringwood, A.E. (1979) *Origin of the Earth & Moon*. Springer-Verlag, New York. [3] Pahlevan, K. Stevenson, D.J. (2007) *Earth & Planet. Sci. Letters* **262** 438–449. [4] Zahnle, K. Abe, Y. Hashimoto, A. (2000) *Bull. Am. Astron. Soc.* **32** 857. [5] Stevenson, D.J. (1987) *Annu. Rev. Earth Planet. Sci.* **15** 271–315.

https://doi.org/10.1180/S0026461X00006502 Published online by Cambridge University Press

Benthic fluxes of iron and manganese under various redox conditions

S. PAKHOMOVA

P.P.Shirshov Institute of Oceanology RAS, Moscow, Russia (s-pakhomova@yandex.ru)

Fluxes of dissolved forms of iron and manganese across the sediment-water interface were studied *in situ* in the Gulf of Finland and the Vistula Lagoon (Baltic Sea), and in the Golubaya Bay (Black Sea) from 2001 to 2005. Fluxes were measured using chamber incubations (Jch), and sediment cores were collected to assess the porewater and solid phase metal distribution at different depths to calculate diffusive flux (Jpw). Measured and calculated benthic fluxes of manganese and iron were directed out of sediment for all sites and were found to vary between 70–4450 and 5–1000 μmole m^{-2} day^{-1} for manganese and iron, respectively. Benthic fluxes of manganese were found to correlate with manganese concentration in the porewater of the top sediment layer positively. The manganese fluxes were not influenced by redox conditions in the near-bottom water. On a large timescale manganese fluxes depend on redox conditions in bottom water, because a change of redox conditions would lead to a change of dissolved manganese content of the porewater. However, on a timescale of a single chamber incubation manganese fluxes did not depend on oxygen concentration (redox conditions), because for dissolved manganese the rate of oxidation is much lower than the rate of release from sediment. Diffusive flux of manganese constitutes 25–70% of the measured flux determined with the chamber incubation (on average Jch/Jpw=3). This indicates that another processes such as bacterial dissolution or bio-irrigation also play an important role in manganese benthic flux formation. Our results showed the importance of bottom water redox conditions for benthic iron fluxes. We measured no fluxes at oxic conditions, intermediate fluxes at anoxic conditions and high fluxes at suboxic conditions. Oxidation of released dissolved iron occurred very rapidly under oxic conditions right after its release from the sediment. Under suboxic and anoxic conditions in the bottom water, the iron flux was dependent both on its concentration in porewater of the surface sediment and on the content of iron in the solid phase of sediment. The chamber measured and diffusive fluxes of total iron differed much more than for manganese, 0.01<Jch/Jpw<50. Thus, bio-irrigation, sediment resuspension and chemical processes at the interface are much more important for iron fluxes than for manganese fluxes.

Peformance characteristics of an enhanced Daly ion counting system for TIMS

ZENON PALACZ*, TONY JONES, DAMIAN TOOTELL, ROBERT GUEST AND STEVE LOCKE

Isotopx Ltd, Middlewich, Cheshire CW10 0GE,UK (*correspondence: Zenon.Palacz@isotopx.com)

We have developed matched and close-coupled pulse amplification electronics for the ion-counting Daly detector used on Phoenix and IsoProbe-T thermal ionization mass spectrometers. These developments have largely eliminated post pulse ringing and permit the use of very low discrimination thresholds resulting in a new ion-counting Daly detector system which is linear (within ~0.05%) from zero to 3.5e6cps (~50-60mV) using a single deadtime correction.

The large dynamic range of the new Daly provides a significant overlap with the range of the Faraday detectors. This provides an exciting opportunity to obtain high precision measurements of minor isotopes such as ^{234}U and ^{230}Th using a combination of Faraday and ion-counting Daly. It also extends the range of large ratios that can be measured by peak jumping on the Daly alone, eliminating the requirement for a Daly/Faraday gain calibration. The large dynamic range also provides the ability to resolve small differences in deadtime (<0.1ns) to allow accurate and precise measurements of Pb isotopes by peak jumping i.e. for high resolution geochronological applications.

A further benefit of the large dynamic range is the ability to measure 20-30mV ion signals with zero noise. This will be of real benefit for the measurement of sub-ng levels of e.g. Nd by peak jumping. It could also offer an alternative to the use of $1e^{12}\Omega$ gain resistors on Faraday detectors since noise, linearity and signal decay times are significantly better than can be attained using these resistors.

Examples of different applications will be presented with indications of the level of precision that can be attained using different analytical combinations.

https://doi.org/10.1180/S0026461X00006502 Published online by Cambridge University Press

Red Sea detritus provenance during MIS 6/5 and MIS 2/1 transitions

D. PALCHAN[1,2], M. STEIN[2], A. ALMOGI-LABIN[2], Y. EREL[1] AND S.L. GOLDSTEIN[3]

[1]Institute of Earth Science, The Hebrew University, Jerusalem, Israel (Pdanielos@gmail.com, yerel@vms.huji.ac.il)
[2]The Geological survey of Israel, 30 Malkhe Israel St, Jerusalem, Israel (motistein@gsi.gov.il, almogi@gsi.gov.il)
[3]Lamont-Doherty Earth Observatory and Columbia University, 10964 Palisade, NY, USA (steveg@ldeo.columbia.edu)

The Red Sea (RS), located in the midst of the Arabian-Sahara desert belt, comprises a sedimentray trap for fine-grain detritus that is transported from its neigbouring continental terrains. Interpreting the fine detritus as desert dust we explored the mineralogy, grain-size, major and trace elements chemistry and Sr-Nd-Hf isotope composition of silicate material (insolbule in acetic acid) recovered from the sedimentary core KL-23, which was drilled in the northern RS (25°44' 88N 35°03' 28E). Core chronology is based on the SPECMAP $\delta^{18}O$ age model indicating that the core spans over 370 ka. We focused on two glacial interglacial transitions: MIS 6 to 5 and MIS 2 to 1 (~160-110 kyr BP and ~20-8 kyr BP, respectively) and analyzed the <63μm fraction of the insoluble material. The Nd-Sr-Hf isotopic ratios indicate contribution from two main lithological sources: 'granitic' material, which is common over the Arabian and Sahara crustal terrains and a 'basaltic' material, which possibly originated from the Cenozoic basaltic terrains at the southern margins of the RS. The 'granitic' source was more dominant during glacials while the 'basaltic' source contributes fine detritus immediately after glacial terminations and transitions to interglacials. Major elements reveal different effects of diagenetic–alteration processes reflecting possibly enhanced alteration during wetter periods in the basaltic source regions during interglacials.

Ti-in-quartz thermometry of siliciclastic metasedimentary rocks of the Otago Schist, New Zealand

J.M. PALIN*, C.L. KING, A. WILSON AND C.E. MARTIN

Department of Geology, University of Otago, P.O. Box 56, Dunedin 9054 New Zealand (*correspondence: michael.palin@otago.ac.nz)

We have used exposures of silicilcastic metasedimentary rocks of increasing grade from the margins to the core of the Otago Schist belt of New Zealand to examine changes in quartz Ti concentration due to re-equilibration and new crystallization at increasing P-T [1, 2]. Samples were taken across three well-documented metamorphic field gradients: Dansey Pass [3], Lindis Pass [4], and Lake Hawea/Haast River [5]. Quartz in thin sections and mineral separates was analyzed using LA-ICP-MS. Raw intensity data were normalized via the NIST 610 standard to obtain trace element concentrations.

There are systematic changes in the concentrations of Ti in quartz: (a) variability is greatest at low grade where re-equilibration of primary igneous signatures of detrital quartz is incomplete; and (b) quartz Ti concentrations increase systematically from moderate to high metamorphic grade. The latter provide metamorphic P-T constraints that agree with previous geothermometry for the rocks [6] for a reduced a (TiO_2) appropriate for textural equilibrium of quartz with titanite at low metamorphic grade and ilmenite at higher grades (Fig. 1).

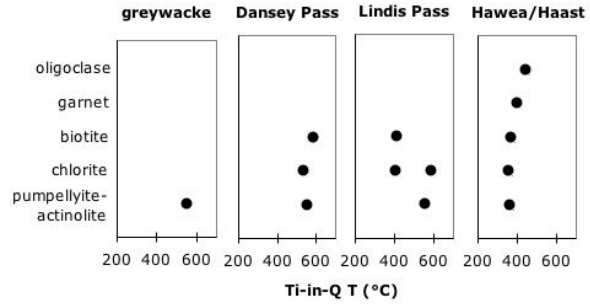

Figure 1: Ti-in-quartz temperatures calculated for P = 5 kb and $a(TiO_2)$ of 0.8 ± 0.2.

[1] Wark & Watson (2006) *Contrib. Min. Petrol.* **152**, 743–754. [2] Thomas *et al.* (2010) *Contrib. Min. Petrol.* **160**, 743–759. [3] Bishop (1972) *Bull. GSA* **83**, 3177–3198. [4] Stallard *et al.* (2005) *J. Meta. Geol.* **23**, 443-459 [5] Cox (1993) unpubl. PhD thesis. [6] Mortimer (2001) *Int. J. Earth Sci.* **89**, 295-306.

https://doi.org/10.1180/S0026461X00006502 Published online by Cambridge University Press

Al and Fe substitution in $MgSiO_3$ perovskite: An ^{27}Al and ^{29}Si NMR study

A.C. PALKE[1]*, J.F. STEBBINS[1], D.J. FROST[2] AND C.A. MCCAMMON[2]

[1]Department of Geological and Environmental Sciences, Stanford University, Stanford, CA 94305, USA (*correspondence: apalke@stanford.edu)
[2]Bayerisches Geoinstitut, Universität Bayreuth, D-95440 Bayreuth, Germany

This study involves ^{27}Al and ^{29}Si NMR spectroscopy on ^{29}Si- and ^{57}Fe-enriched, Al- and Fe-bearing $MgSiO_3$ perovskite of nominal composition $(Mg_{1-x}Fe_x)(Si_{1-x}Al_x)O_3$ ($x < 0.05$) in order to elucidate the substitutional mechanisms of Al and Fe. Previous ^{27}Al NMR studies have focused on Fe-free, Al-bearing $MgSiO_3$ perovskite; however, it is known that Fe has a dramatic impact on the incorporation of Al due to a coupled substitution of Al^{3+} and Fe^{3+} [1]. Nonetheless, the exact nature of Al substitution in the presence of iron (i.e. site occupancy of Al^{3+} and Fe^{3+}, order/disorder and distribution of the substituting cations, etc…) is incompletely understood. Mössbauer spectroscopy of our samples found bulk sample Fe^{3+}/Fe_{total} = 40-60%, indicating that coupled substitution of Fe^{3+} and Al^{3+} occurs to a significant extent. An analysis of ^{27}Al and ^{29}Si signal losses and peak widths with increasing Al and Fe content suggests a strong ordering of Fe^{3+} occurring in Mg^{2+} sites with Al^{3+} occupying adjacent Si^{4+} sites. However, particularly at higher concentrations of Al and Fe, it is clear that this coupled substitution is not the only mechanism operating in these samples. This study is an extension of previous work involving natural Fe-bearing pyrope garnet [2] and rare earth orthophosphates and builds on the insights obtained therein.

[1] Frost & Langenhorst (2002) *Earth Planet. Sci. Lett.* **199**, 227–241. [2] Palke & Stebbins (2011) *Am. Min.* in press.

Environmental controls on potential nitrate and sulfate reduction rates in a range of aquatic sediments

CELINE PALLUD[1], ANNIET LAVERMAN[2], CHUANHUI GU[3] AND PHILIPPE VAN CAPPELLEN[4]

[1]ESPM Department, University of California, Berkeley, CA 94720, USA (cpallud@berkeley.edu)
[2]UMR 7619 Sisyphe, Université Pierre et Marie Curie, 75005 Paris Cedex 05, France (Anniet.Laverman@upmc.fr)
[3]Department of Geology, Appalachian State University, Boone, NC 28608, USA (guc@appstate.edu)
[4]School of Earth and Atmospheric Sciences, Georgia Institute of Technology, Atlanta, GA 30332, USA (pvc@eas.gatech.edu)

Nitrate and sulfate are two important terminal electron acceptors for anaerobic respiration in littoral sediments. We investigated the environmental factors controlling potential rates of nitrate reduction and sulfate reduction (NRR and SRR) in a range of aquatic sediments. Reaction rates were determined on intact surface sediment slices sampled at 14 sites using flow-through reactors. Nitrate and sulfate were added separately or simultaneously. We used redundancy analysis to assess how environmental factors might control the variability of these rates.

On average, NRR exceeded SRR by one order of magnitude and 9% of the NRR can be accounted for by nitrate-mediated sulfide oxidation to sulfate in the studied sediments. When nitrate and sulfate were supplied simultaneously, the effect of nitrate on SRR was variable, ranging from near complete inhibition to 25% enhancement. Redundancy analysis showed that overlying water pH and salinity were the two most important predictors of variability of sediment potential NRR and SRR under all conditions. However, when nitrate and sulfate were added separately, sulfate concentration in the overlying water and sediment N content were additional factors explaining the variations of potential NRR and SRR. Furthermore, when the two electron acceptors were both present, the potential NRR and SRR were also controlled by sediment arsenic content besides pH and salinity. It suggests that different biogeochemical processes are involved in the N and S cycles in response to separate and simultaneous addition of nitrate and sulfate. These results indicate that controls on elemental cycling in systems subject to S and N pollution are more complex than formerly thought and point to the need to critically reassess the representation of anaerobic respiration kinetics and their interactions in diagenetic models.

https://doi.org/10.1180/S0026461X00006502 Published online by Cambridge University Press

Combining spot samples and continuous sampling to study small catchment storm runoff

M.R. PALMER[1]*, A. GKRITZALIS-PAPADOPOULOS[2] AND M.C. MOWLEM[2]

[1]School of Ocean & Earth Science, University of Southampton, Southampton SO14 3ZH, UK (*correspondence: pmrp@noc.soton.ac.uk)
[2]National Oceanography Centre, Southampton SO14 3ZH, UK

We have used two different sampling techniques to study the geochemical response of a small lowland rural catchment to episodic storm run off. The first method involves traditional daily spot sampling and has been used to develop a standard end member mixing analysis (EMMA) of the relative contributions of ground water flow and surface run off to the total stream flow. The second method utilises a continuous sampling device, powered by an osmotic pump, to produce an integrated 24-hour sample of the stream flow.

There is generally very good agreement between the patterns of solute chemistry measured from both sampling methods. The spot sample data can be used to construct a hydrograph separation model for the river chemistry that indicates the export chemistry is dominated by groundwater flow during low flow conditions and surface runoff during high flow conditions, but that the groundwater flux also increased during periods of high flow. Comparison between the chemistry predicted from the hydrograph separation model and the concentrations recorded by the continuous sampler are generally very good for most solutes. For NO_3, however, data from the continuous sampler indicates that there is a stored soil water reservoir that contains high NO_3 concentrations and is flushed during the rising hydrograph limb of a storm event. The continuous sampler data also indicates that the NO_3 concentration of this reservoir takes >7 days before it is replenished to pre-flushing event levels. Combined use of spot sample and continuous sample data can yield insights into the behaviour of nitrate during storm events, that are not apparent from spot sample data alone.

The elasticity of hydrous minerals in the lower mantle

M.G. PAMATO*, T. BOFFA BALLARAN, D.J. FROST, A. KURNOSOV AND D.M. TROTS

Bayerisches Geoinstitut, Universität Bayreuth, D-95440 Bayreuth, Germany (*correspondence: martha.pamato@uni-bayreuth.de)

Water is recycled into the Earth's interior by hydrous minerals in descending slabs and the amount of water that is transported into the deep mantle depends on the stability of high-pressure hydrous phases. As water plays an important role in mantle dynamics and planetary evolution, the study of the structure, elastic properties and stability of possible hydrous high-pressure phases in subducting slabs is of crucial importance.

A number of hydrous phases have been experimentally synthesized at pressures and temperatures compatible with subduction zone conditions. Very recently, a super aluminous version of the dense hydrous magnesium phase D (Al-phase D), was synthesized in a simplified basaltic bulk composition at lower mantle conditions [1]. The high temperature stability of this new form of phase D, which is stable up to 1600°C at 26 GPa, suggests that this phase may be an important host for water within portions of subducted oceanic crust in the Earth's lower mantle. Given the importance of such a hydrous aluminous phase and the fact that no similar phases have been previously reported, we investigated its elasticity.

High-pressure single crystal X-ray diffraction measurements were performed using a diamond anvil cell. Simultaneously S and P elastic wave velocities were measured using Brillouin spectroscopy. Preliminary results indicate that although Al-phase D can contain up to 16 wt% H_2O, the measured Vs and Vp are similar to that expected for an anhydrous lower mantle assemblage. Consequently if larger amounts of H_2O were present in this phase within the lower mantle it would have an undetectable seismic signature.

[1] Boffa Ballaran *et al*. (2010) *Am. Mineral*. **95**, 1113–1116.

https://doi.org/10.1180/S0026461X00006502 Published online by Cambridge University Press

Interfacial thermodynamics: Inherent limitations of classical adsorption theories

G. PAN

Research Center for Eco-environmental Sciences, Chinese Academy of Sciences, Beijing, China (gpan@rcees.ac.cn)

Equilibrium adsorption properties defined by macroscopic parameters of adsorption densities (mol/m^2) are inherently ambiguous and do not obey conventional thermodynamic adsorption theories, because the energy states for different microscopic metastable-equilibrium adsorption (MEA) modes that construct real equilibrium state cannot be described by the macroscopic methodology such as adsorption density [1-2]. An initial concentration (C_0) effect, i.e. the dependence of equilibrium adsorption isotherms on the initial adsorbate concentration, was first found to be a fundamental macroscopic adsorption phenomenon [3-5]. A multi-batch adsorption experiment was designed to test this phenomenon in arsenate-TiO_2 system. Under the same thermodynamic conditions, when the initial adsorbate was added by multiple batches, adsorption isotherms declined as the multi-batch increased. Microscopic EXAFS analysis showed that at least two MEA states co-existed in the equilibrium samples: monodentate mononuclear (MM) and bidentate binuclear (BB) modes. The ratio of BB:MM increased as the multi-batch increased or as the C_0 decreased. Experimentally measured equilibrium isotherms/constants therefore fundamentally depend on the initial reactant concentrations (e.g. initial absorbate concentration and/or adsorbent concentration) and kinetic pathways since the surface molecular structures of different MEA states are generally affected by the kinetic/danamic processes [6-10]. Failure in recognizing this principle has greatly hindered our understanding and interpretation on many interfacial processes in earth, environmental, and engineering sciences.

[1] Pan & Liss (1998) *J. Colloid Interface Sci.* **201**, 71–76. [2] Pan *et al.* (2011) *Interfacial Thermodynamics* ISBN 978–953-307-318-7. [3] He *et al.* (2009) *J. Phys. Chem. C* **113**, 21679–21686. [4] He *et al.* (2009) *J. Phys. Chem. C* **113**, 17076–17081. [5] Zhang *et al.* (2009) *J. Colloid Interface Sci.* **338**, 284–286. [6] Pan & Liss (1998) *J. Colloid Interface Sci.* **201**, 77–85. [7] Pan *et al.* (2004) *J. Colloid Interface Sci.* **271**, 28–34. [8] Li *et al.* (2004) *J. Colloid Interface Sci.* **271**, 35–40. [8] Li *et al.* (2008) *J. Colloid Interface Sci.* **319**, 385–391. [9] Pan *et al.* (1999) *Colloids Surf. A* **151**, 127–133. [10] He *et al.* (2011) *Environ. Sci. Technol.* **45**, 1873–1879.

Studying on tectono-geochemistry and rock ore specimens appraisal of Bangwei copper mine

PAN PING[1,2]*, HAN RUNSHENG[1] AND CHANG HE[1]

[1]Kunming University of Science and Technology, Southwest Institute of Geological Survey, Geological Survey Center for Non-ferrous Mineral Resources, Kunming, China (*correspondence: panping0815@vip.qq.com)

[2]Scientific Research Department, Kunming Metallurgy college, Kunming 650033,China

Bangwei copper mine is located in the east of Wendong-Fubang folded bundle, the copper-bearing limonite-quartz vein penetrate north-south fracture and 50 meters width fractured zone which along the Huimin group of Lancang of Proterozoic. The Occurrence is 300∠600, The thickness of single vein is about 1meter, mineralized zone extend 3 kilometers spasmodically. Mineral is mainly copper-bearing limonite. The gangue is composed of quartz and sericite, with a Honeycomb structure.The spectrum of ore contains: Cu-7000ppm, As-600ppm, Y-100ppm. It can be determined that the background value of ore-forming element by the statistical analysis of obtained data. It shows that the content changes of element of Sn, W, Cu, Pb, Zn focus on the rock mass of Indosinian and fracture of metamorphic rock nearby. There is significantly positive correlation between the content of element.

This paper studies on tectono-geochemistry of Bangwei copper and rock ore specimens appraisal, the results of ICP-AES is that the higher copper content reach 350ppm, 198ppm, and doesn't discover copper metallic minerals in rock ore appraisal. Based on previous work this paper considers that the metallogenic province is Cu, Fe abnormal of mineralization.

Granted by the project of the Distinguishing Discipline of KUST (2008)

https://doi.org/10.1180/S0026461X00006502 Published online by Cambridge University Press

Response of continental biogeochemical processes to short- and long-term global warming

R.D. PANCOST[1]*, K. TAYLOR[1], C. HOLLIS[2], L. HANDLEY[1], R. REES-OWEN[1], E.M. CROUCH[2] AND S. SCHOUTEN[3]

[1]Organic Geochemistry Unit, School of Chemistry, University of Bristol, UK (*correspondence: r.d.pancost@bris.ac.uk, kyle.taylor@bris.ac.uk, luke.handley@gmail.com)
[2]Geological and Nuclear Sciences, P.O Box30-368, Lower Hutt, NZ (c.hollis@gns.cri.nz, e.crouch@gns.cri.nz)
[3]Royal Netherlands Institute for Sea Research, Texel, The Netherlands (schouten@nioz.nl)

Much work on past hyperthermals, and especially the Paleocene-EoceneThermal Maximum (PETM), illustrates that rapid global warming caused dramatic changes in the continental hydrological, erosional and weathering regime. Evidence for such changes include higher plant δD records indicative of increased moisture transport to the poles, lithlogical and organic geochemical evidence for increased erosion and transport of sediments to marginal marine settings, and osmium isotopic evidence for increased chemical weathering. Here we compare the impact of these transient events to that of the longer term global warming that occurred from the mid-Paleocene to mid-Eocene.

New short-term records from Tanzania and NZ provide further evidence for a reorganisation of the global hydrological cycle coinciding with the onset of the PETM. They also document increased inputs of terrigenous biomarkers into marginal sediments, complementing previous work from, for example, the North American margin, the Arctic Ocean and the Tethyan realm.

In contrast, longer term terrigenous biomarker records document no difference between relatively cooler (Late Paleocene, Middle Eocene) and warmer (Early Eocene) intervals. Where the records do exhibit variability, they do not inidcate elevated terrigenous inputs during warm intervals. This is expected as the long-term control on erosion will be dictated by the temperature-mediated balance between uplift and denudation. By comparison, the dramatic perturbations at the PETM must reflect the consequence of temporary but dramatic deviations from this steady state due either directly to elevated temperatures or consequential changes in hydrology. This highlights the importance of examining the rapid climate change events of the past if we wish to understand the consequences of comparably rapid Anthropocene climate change.

Chlorine and CO_2 rich Fluids in 2.5 Ga amphibolite-granulite facies basement below the Killari earthquake region, India and seismogenesis

O.P. PANDEY[1], G. PARTHASARATHY[1], PRIYANKA TRIPATHI[1], V. RAJAGOPALAN[2] AND B. SREEDHAR[3]

[1]National Geophysical Research Institute (CSIR),Hyderabad-500606, India (om_pandey@rediffmail.com)
[2]Atomic Minerals Directorate for Expl.Res (DAE), Hyderabad, 500 016, India
[3]Indian Institute of Chemical Technology (CSIR), Hyderabad,500007 India

Halogens form an important component in the upper mantle fluids and play a significant role in understanding the evolutionary processes of the earth's crust and upper mantle. Killari-Latur earthquake (M 6.2) region of Maharashtra (central India), concealed below a thick suite of Deccan volcanics, is one such region where massive exhumation of mafic crust has taken place [1]. In order to understand the role of mantle fluids in the seismogenesis, we have carried out a detailed mineralogical investigation on the 2.5 Ga Archean basement core samples from a 617m deep Killari borehole, drilled in the epicentral region for seismotectonic studies. Our study indicates that the crystalline basement, covered by a 338m thick Deccan volcanics, is made up of CO_2, Cl, FeO and CaO-rich, high density (2.82 g/cm^3) - high velocity (avg. Vp: 6.20 km/s) amphibolite-granulite facies rocks, which underwent pervasive Ca-metasomatism due to infiltration of mantle fluids. Primary source of such fluids apparently existed in the upper mantle, from where it moved to lower crust due to thermal remobilization. Input of mantle heat flow in this region is estimated to be quite high at about 32 mW/m^2. Present study reveals an interesting possibility that nucleation of large intraplate earthquakes may be related to the regional metasomatism, which is also fluid controlled and alters the basic fabric and composition of the rocks considerably due to recrystallisation.

[1] Pandey O.P. *et al*. (2009) *J.Asian Earth Science* **34**, 781–795.

https://doi.org/10.1180/S0026461X00006502 Published online by Cambridge University Press

A $\delta^{30}Si_{diatom}$ reconstruction of Holocene productivity of the Southern Ocean, east Antarctica

VIRGINIA PANIZZO[1]*, DAMIEN CARDINAL[2,3], XAVIER CROSTA[4] AND NADINE MATTIELLI[1]

[1]Department of Earth and Environmental Sciences, Université Libre de Bruxelles, CP160/02 Avenue F.D. Roosevelt 50, 1050 Brussels, Belgium (*correspondence: virginia.panizzo@ulb.ac.be)

[2]LOCEAN – IPSL, Université Pierre et Marie Curie, 4 Place Jussieu, Boite 100, F-75252 PARIS Cedex 05

[3]Section of Mineralogy and Geochemistry, Royal Museum for Central Africa, Leuvensesteenweg, 13, B-3080 Tervuren - Belgium

[4]UMR-CNRS 5805 EPOC, Avenue des Facultés, Université Bordeaux I, 33405 Talence Cedex, France

Coastal and continental shelf zones are among the most productive ecological provinces of the Southern Ocean and account for c.76% and 3.5% of the total primary productivity of the marginal ice zone and southern ocean respectively [1]. Diatoms account for a large proportion of primary productivity in these regions. Piston core MD03-2601 was recovered in 2003 off the coast of Adélie Land, east Antarctica (66°03.07′S, 138°33.43′E, 746 m water depth) and $\delta^{30}Si_{diatom}$ as analysed by MC-ICP-MS were conducted on a total of 29 samples at regular intervals across a total 2700 cm (c.1000-8000 years BP) of the core to reconstruct productivity changes. $\delta^{30}Si_{diatom}$ is reported as delta values relative to the NBS28 standard. $\delta^{30}Si_{diatom}$ values fluctuate between -0.01 and +0.82‰, with analytical standard errors less than ±0.08, over the duration of the record, with higher values indicating increased utilisation. Increasing $\delta^{30}Si_{diatom}$ values are concomitant with increases in *Chaetoceros* resting spores, reflecting periods of higher diatom productivity associated with longer periods of surface water stratification. These correspond with millennial periodicities of increased productivity [1]. Main trends in the percentage abundance of summer diatom species (predominantly *Fragilariopsis kerguelensis*) show a decline after c.3500 years BP and a change to the dominance of spring diatom assemblages (e.g. *Fragilariopsis curta*), reflecting prolonged sea ice cover [2]. Overall results show that after the Hypsithermal period (c.3500 years BP), during the late Holocene Neoglacial, productivity is reduced.

[1] Denis *et al*. (2009) *Paleoceanography* **24**, PA3207. [2] Crosta *et al*. (2008) *Marine Micropaleontology* **66**, 222–232.

Isotopically heavy sulfur in banded iron formations from the Eoarchean Nuvvuagittuq Supracrustal Belt

DOMINIC PAPINEAU[1,2] AND ERIK HAURI[3]

[1]Department of Earth and Environmental Sciences, Boston College, United States (dominic.papineau@bc.edu)

[2]Geophysical Laboratory, Carnegie Institution of Washington, United States

[3]Department of Terrestrial Magnetism, Carnegie Institution of Washington, United States

All known Eoarchean (*c*. 3.85–3.60 Ga) volcano-sedimentary successions (i.e. supracrustal rocks) are restricted to high-grade gneissic terranes where biological signatures are challenging to recognize. Although they can be complicated by metamorphic overprinting, sulfur isotopes from Archean supracrustal rocks have the potential to preserve signatures of atmospheric redox chemistry and metabolic fractionation from the original depositional environment. Such sulfur isotope signatures have pushed the record of microbial sulfur metabolism back to 3.49 Ga (Shen *et al*. 2001; Philippot *et al*. 2007) and that of the anoxic atmosphere to 3.8 Ga (e.g. Papineau and Mojzsis, 2006). In order to further extend the Eoarchean sulfur isotope record, we undertook a study of multiple sulfur isotopes from various types of banded iron formations (BIFs) and associated rocks in the 3.77 to 4.28 Ga Nuvvuagittuq Supracrustal Belt (NSB). NanoSIMS was used to analyze sulfides with spot sizes of 15x15 μm for ^{32}S, ^{33}S, and ^{34}S. Analytical conditions yield a 2σ reproducibility for $\delta^{34}S$ and $\delta^{33}S$ better than 0.6 and 0.4‰, respectively, for a combined $\Delta^{33}S$ reproducibility better than 0.3‰. In sulfides from NSB BIFs, we measured the largest range of $\delta^{34}S$ values between -5.7 and +14.6‰ so far reported in Eoarchean rocks, along with a range of $\Delta^{33}S$ values between -0.9 to +3.3‰, that point to an anoxic sulfur cycle. The heaviest $\delta^{34}S$ values were of chalcopyrite grains, up to 2 mm in size, randomly distributed in jaspilitic BIFs in the southwestern part of the NSB. Associated metavolcanic rocks had a comparatively small range of $\delta^{34}S$ values between -2.8 to +1.1‰ along with a range of MIF $\Delta^{33}S$ values between -2.6 to +1.7‰, that suggest that some sedimentary sulfur was remobilized in volcanic rocks. The heavy $\delta^{34}S$ values in NSB BIFs may be an indication of biological metabolic fractionation, but alteration of isotope compositions by post-depositional isotope diffusion cannot be excluded. To independently verify the ranges measured by NanoSIMS, we are currently performing continuous flow isotope ratio mass spectrometric analyses of multiple sulfur isotopes in microdrilled sulfides from polished slabs from these rocks.

https://doi.org/10.1180/S0026461X00006502 Published online by Cambridge University Press

Geology and geochemistry of carbonate-hosted nonsulphide Zn-Pb mineralization in Southern and Central British Columbia, Canada

S. PARADIS[1], G.J. SIMANDL[2], H. KEEVIL[3] AND M. RAUDSEPP[3]

[1]Geological Survey of Canada, Box 6000, Sidney, BC, V8L 4B2, Canana (*correspondence: suparadi@NRCan.gc.ca)
[2]British Columbia Ministry of Energy, Mines and Petroleum Resources, British Columbia, Canada
[3]Earth and Ocean Sciences, University of British Columbia, Vancouver, British Columbia, Canada

Carbonate-hosted, nonsulphide base metal deposits are derived from sulphide mineralization (i.e. MVT, SEDEX, Irish-type, vein-type deposits and skarns) by supergene processes. Several carbonate-hosted sulphide deposits in BC have near-surface Zn- and Pb-bearing iron oxide-rich gossans. Such gossans form when carbonate-hosted, base-metal sulphide mineralization is subject to intense weathering and metals are liberated by the oxidation of sulphide minerals. The metals can be trapped locally, forming direct replacement, nonsulphide ore deposits (‘red ores’) or they can be transported by percolating waters down and away from the sulphide protore, forming wallrock replacement nonsulphide deposits (‘white ores’). The direct replacement nonsulphide deposits consist predominantly of Fe-oxyhydroxides, goethite, hematite, hemimorphite, and minor smithsonite, hydrozincite, cerussite, and anglesite; they contain 0.8-23 wt.% Zn, 0.7-5 wt.% Pb, and >20 wt.% Fe. Zinc content of sphalerite ranges from 56.6 to 67.3 wt.%, and iron content of sphalerite ranges from 0.03 to 9.4 wt.%; both show a negative correlation with a general increase in Fe from the southern to the northern deposits. The wallrock replacement deposits consist mainly of hemimorphite, smithsonite and hydrozincite, and minor Fe-oxyhydroxides and carbonates. No remnants of sulphides were observed. They contain 31.5-49.8% Zn, 0.13-0.19% Pb and <3% Fe.

Effects of municipal solid waste compost amendments on carbon and nitrogen cycling in a clayey soil

N.V. PARANYCHIANAKIS*, G. GIANNAKIS, N.P. NIKOLAIDIS AND N. KALOGERAKIS

Dept of Environmental Engineering, Technical University of Crete, 73100

The decline of organic matter is currently recognized as an important threat to soil quality. Land application of biosolids has been employed as a common management practice worldwide to restore soil C content. In this work, we provide findings from a six-month study investigating the effects of various compost amendments (0, 50, 100 t/ha) on the kinetics of carbon (C) and nitrogen (N) mineralization in soil microcosms either spiked or not with inorganic N. N application at rates of 50 kg/ha further stimulated CO_2 evolution at compost application rates of 50 t/ha, but it did not at the higher application dose (100 t/ha). N addition in compost-treated microcosms also increased potential nitrification rates compared to the treatments not spiked with N. In addition, the application of compost up-regulated enzyme activities involved in C and N cycling, including proteases, β-glucosaminidase, arginase and glutamine. Finally, data regarding genes copy number variation, involved in the N cycling (bacterial-*amoA*, archaeal-*amoA* and *nir*S), throughout the study are discussed and interpreted with enzyme activities and N-forms availability.

https://doi.org/10.1180/S0026461X00006502 Published online by Cambridge University Press

Crystal-rich basaltic andesites of the current Arenal eruption in light of experiments with crystal-poor basalt

F. PARAT[1,2]*, M.J. STRECK[3], F. HOLTZ[4] AND R. ALMEEV[4]

[1]Géosciences Montpellier, Univ. Montpellier, France (*correspondence: Fleurice.Parat@gm.univ-montp2.fr)
[2]Mineralogie-Geochemie, Univ. Freiburg, Germany
[3]Department of Geology, Portland State Univ., Portland, OR 97207, USA (streckm@pdx.edu)
[4]Institute of Mineralogy, Univ Hannover, Germany (f.holtz@mineralogie.uni-hannover.de)

Arenal volcano is nearly unique with its 43 year long continuous activity erupting remarkably monotonous basaltic andesites but mineral zoning records indicate complex open-system processes including the episodic injections of basalt. The condition of the mafic input as well as the evolution to the currently erupting basaltic andesite were addressed by an experimental study on a phenocryst-poor (~3%) Arenal-type basalt (50.5 wt% SiO_2) from a nearby scoria cone containing olivine (ol, Fo_{92}), plagioclase (pl, An_{86}), clinopyroxene (cpx, mg#=82) and magnetite (mag, X_{ulvo}=0.13).

Our experiments (200 MPa, 900-1050°C, oxidizing and fluid-saturated conditions with various water activities, XH_2O_{fluid}=0.3 to 1) produced at 1050°C and water-saturated conditions (H_2O_{melt}=5 wt%), only magnetite, whereas mag+cpx+ol crystallized at low water activity. Plagioclase and cpx crystallized at water-saturated conditions with olivine at 1000°C and with amphibole at 950-900°C, whereas they crystallized with opx at low water activity (for T=1000-900°C). The mineral assemblage as well as the mineral compositions of the natural basalt were reproduced at 1000°C with basaltic andesitic melt (55 wt% SiO_2) with 5 wt% H_2O.

Our results can be used to substantiate previously envisioned crystallization environments beneath Arenal. Basaltic magma inputs are water-rich at relatively high pressure and high temperature. Evolution to more evolved magmas would have happened under fluid-saturated conditions but variably water activities. A decrease of water activity (degassing?) induces the change of the mineral assemblage pl+ol+cpx to pl+cpx+opx observed in basalt (e.g. ET3-1) to andesitic tephras (e.g. Ar7/68). On the other hand, the lack of opx and the presence of amphibole also in basaltic andesitic tephra units of earlier eruptive phases (e.g. ET3-2) indicate water-saturated conditions at temperature lower than 950°C. Continuous degassing may contribute to persistent small-scale explosive activity - so characteristic for the current eruption-, likely prevailed during crystallization of the water-rich magmas at Arenal. Mixing of magma batches (with subtle but distinct compositional and mineralogical differences) plus the occasional process of concentrating mineral contents by melt expulsion will do the rest to make crystal-rich basaltic andesites of the current eruption.

Iron reduction by a *Clostridia* consortium

MADHAVI PARIKH, CHU-CHING LIN, TAMAR BARKAY AND NATHAN YEE*

School of Environmental and Biological Sciences, Rutgers University, New Brunswick, NJ, USA (*correspondence: nyee@envsci.rutgers.edu)

Background

One of the major pathways of inorganic contaminant (e.g. Cr, Hg, Pu and U) transformation in Earth's critical zone is through redox reactions with Fe (II). Reactive Fe (II)-bearing minerals are known to form during microbial respiration of ferrihydrite. However, the common crystalline iron oxide phases in the critical zone are notoriously recalcitrant towards microbial reduction. Here we report the cultivation of a microbial consortium, enriched from subsurface sediments, that rapidly reduces crystalline goethite (α-FeOOH) and hematite (Fe_3O_2), and produces highly reactive Fe (II)-bearing particles.

Materials and Methods

A sediment core collected from the United States Department of Energy Field Research Center (FRC) in Oak Ridge Tennessee was used as inoculum for anaerobic enrichment cultures. The media were initially amended with acetate and citrate as the electron donors, and active cultures were eventually tranferred to media containing fumarate as the carbon source. After a purified consortium was obtained, the genomic DNA was extracted and DGGE analysis was performed to determine the microbial community composition. Iron reduction experiments were conducted to evaluate the ability of this consortium to reduce goethite and hematite when provided with alternate electron donors. Periodically, samples were collected and the mineral transformation products were analyzed using powder X-ray diffraction (XRD).

Results and Discussion

Enrichment cultures Oak Ridge FRC resulted in the cultivation of a microbial consortium that exhibited robust iron reducing activity. This consortium consisted of two strictly anaeorbic spore-forming microorganisms. 16S rRNA gene sequences indicated that both organisms belong to the class *Clostridia* in the *Firmicutes* phylum. When given peptone, the consortium was able to reduce goethite and hematite at rates an order of magnitude faster than any pure culture reported to date. The biogenic ferrous iron produced by this consortium was largely retained in the solid phase. The Fe (II) precipitates exhibited distinct coloration and were highly reactive towards oxygen. Notably, these secondary ferrous iron phases were not detectable by XRD, suggesting that the Fe (II)-bearing solids were amorphous.

https://doi.org/10.1180/S0026461X00006502 Published online by Cambridge University Press

In-diffusion of some chemical species in a weathered granite

C.K. PARK*, M.H. BAEK AND JT. JEONG

Atomic Energy Research Institute, Yousung-gu Daedukdaero 1045, Daejin, Korea
(*correspondence: ckpark@kaeri.re.kr)

An in-diffusion experiment for some chemical species onto a weathered granite core of Φ5x 20 (cm) was carried out in a glove box under a reducing condition. After nine months, the rock samples was recovered, cut into two parts along its axis. The one part was scanned with a cyclone, a kind of autoradiographe, to identy the distrubution of radionuclide on the rock surface with the diffusional direction. The other part cut into several slices of 1cm thickness. In order to identify sorption types of the species, a sequential chemical extraction was carried out on the slices. The considered sorption types are physiosorption, ion exchange, association with ferro-manganese oxides, and incorporation into mineral structure.

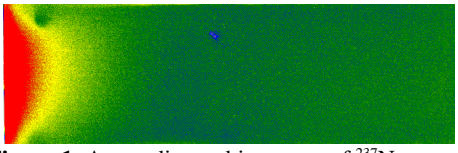

Figure 1: Autoradiographic amage of ^{237}Np

Fig.1. shows the concentration distribution of ^{237}Np on the rock surface. Np sorbed mainly within 2`3 cm and penetrated about 6 cm. Sr and Co penetrated more deeply than the other species. And some species such as Th, Cs and Eu were sorbed mainly on the contacting surface and their diffusion depth were within 3 cm.

The most interesting finding in this experiment is that the sorption mechanisms of some species were changed along their penetration depth. For examples, at the contacting surface U and Co sorbed mainly by ion exchange but association with ferro-manganese oxides became important with going into the inside of the rock. On the other hand, Np mainly associated with ferro-manganes oxides on the contacting surface and ion exchange becomes main sorption type in the deeper region.

[1] J.Berry *et al*. (1994) *Radiochimica Acta* **66/67**, 447.
[2] Vilks *et al*.(2003) *J.of Cont. Hydrol*. **61**, 191.
[3] Braitwaite *et al*.(2000) *Czechoslovak J.of Physics* **50**, 265.

Study for the geochemical reaction of Bukpyong CO_2 sequestration site, Korea

JINYOUNG PARK*, HYUNMIN KANG, MINHO PARK AND MINHEE LEE

Deprtment of Environmental Geosciences, Pukyong National University, 599-1 Daeyon 3 Dong, Namgu, Busan, 608-737, Republic of Korea (pjy9614@naver.com)

The objective of this study is to investigate the geochemical reaction of rock in Bukpyong CO_2 sequestration site, Korea. Target formations were mostly composed of porous sandstone and conglomerate beds. For the experiment, the high pressurized cell system (100 bar and 50 ºC) was designed to create supercritical CO_2 in the cell. The dissolution and precipitation of sandstone and mudstone were observed while the rock reacted with supercritical CO_2 and saline water in the cell for 30 days. Ten g of rock powder type and 50 ml of saline water were contacted with supercritical CO_2 in the cell. For the experiment, saline water was sampled from a hot-spring well (800 m in depth) in Busan. SEM-EDS analysis was conducted to measure the precipitated minerals and ICP/OES was used to quantify main compounds dissoved in solution of the high pressure cell. The mineral surface was observed by using a reflection microscope. Three locations were randomly selected on the surface and the average roughness value of those locations was measured by SPM (Scanning Probe Microscope) to investigate the change of mineral surface.

For the mudstone, concentrations of Ca^{2+}, Fe^{2+}, Mg^{2+}, Na^{2+} and K^{+} in solution increased to 348.9 mg/L, 185.2 mg/L, 134.1 mg/L, 66.9 mg/L and 7.5 mg/L, respectively, after 30 days. For the sandstone, concetrations of Ca^{2+}, Fe^{2+}, Mg^{2+}, Na^{2+} and K^{+} in solution increased to 3895.9 mg/L, 378 mg/L, 23.8 mg/L, 63.1 mg/L and 9.9 mg/L, respectively. These results suggested that ions such as Ca^{2+}, Fe^{2+}, Mg^{2+} and Na^{2+} would be significantly dissolved when it contact with the supercritical CO_2 and saline water in Bukpyong CO_2 sequestration site. The average roughness value of the plagioclase surface was 1.04 nm before the reaction, but it considerably increased to 11.26 nm after 30 days. For the orthoclase, the average roughness increased from 2.74 nm to 18.56 nm, suggesting that the dissolution of plagioclase and orthoclase occurs in active when the feldspars contact with supercritical CO_2 and saline water at Bukpyong CO_2 sequestration site.

https://doi.org/10.1180/S0026461X00006502 Published online by Cambridge University Press

Study for TPH removal efficiency of landfarming process using indigenous microorganisms to diesel contaminated site

MINHO PARK* AND MINHEE LEE

Department of Earth Environmental Sciences, Pukyong National University, Daeyon 3 Dong, Namgu, Busan, 608-737, Republic of Korea
(*correspondence: minhop1008@gmail.com)

Landfarming is the representative process to use the biodegradation by using microorganisms and it is considered to be more economical and pre-environmental than other process to remediate fuel-contaminated sites. The feasibility of landfarming process using indigenous microorganisms, living in diesel contaminated soils of a military camp was investigated by batch experiment. Initial TPH concentration of soil sample in the study was 3, 819 mg/kg and the soil was classified to 'Sand' for USDA soil texture group. The average water content was 1.19 % and soil pH was 8.29. For the experiment using indigenous microorganisms, total four microorganisms (*Arthrobacter* sp., *Burkhoderia* sp., *Cupriavidus* sp. and *Bacillus* sp.) were isolated from two diesel contaminated soils from a military camp, Korea. Batch experiments were performed to investigate the TPH removal efficiency with different conditions for 1 month. In the petri dish (15 cm in diameter x 2 cm in depth), 300 g of soil were mixed with each isolated microorganism solutions (0.3 ml and 0.6 ml) and nutrient (0.3 ml). The ratio of C:N:P in the nutrient was 100:10:1. Various water contents (10 % and 20 %) and temperature (20 ℃, 30 ℃ and 40 ℃) were applied to the experiments. The humidity of batch soil decreased due to the vaporization and the distilled water was added into the batch soil every 48 hours to maintain a constant humidity.

After 31 days of experiment, the greatest TPH removal efficiency was 95 % by using *bacillus* sp.. The average TPH removal efficiency of four microorganisms was 76.5 %, suggesting that the landfarming process using indigenous microorganisms is successful to remove TPH from diesel contaminated soils.

Microstructure of Yuka eclogite, North Qaidam HP/UHP terrane, Northwestern China

M. PARK AND H. JUNG*

School of Earth and Environmental Sciences, Seoul National University, Seoul, Republic of Korea
(*correspondence: hjung@snu.ac.kr)

This study aims at further understanding of the mechanisms how lattice-preferred orientation (LPO) developed during the HP-UHP metamorphism in the eclogites. Microstructures of Yuka eclogites from North Qaidam HP/UHP terrane, northwestern China were analyzed using optical microscopy and electron backscattered diffraction (EBSD) in order to determine the LPOs of minerals and deformation mechanisms. The LPOs of omphacite showed that [001] axes are alligned parallel to lineation and [010] axes distributed within a girdle normal to lineation which is known as the L-type fabric, while the garnets showed a week LPO. The fabrics of quartz showed a weak rhomb <a> slip system which the C{0001} axis pole figures present patterns which form a girdle in the plane normal to the lineation. To determine water content of minerals we used the Nicolete 6700 FTIR with a Continuum IR microcroscope in the Tectonophysics Laboratory in SEES in Seoul National University. Unpolarized FTIR analysis of samples showed that two hydroxyl absorption bands at 3430 – 3530 cm^{-1} and 3600 – 3620 cm^{-1} exist in the omphacite grains indicating the deforrmation of omphacite in a wet condition, while there was no O-H peak observed in garnet and quartz minerals indicating deformation of the minerals in a dry condition. The presence of strong LPOs in omphacite suggests that dislocation creep was a dominant deformation mechanism of omphacite, but the garnet grains appear to be deformed by other mechanisms (e.g. grain boundary sliding). Quartz grains appear to be deformed by the dislocation creep mechanism in a dry condition, and the weak LPOs of quartz may have been caused by the later stage deformation and metamorphisms.

https://doi.org/10.1180/S0026461X00006502 Published online by Cambridge University Press

Effects of future climate change on air quality over East Asia

ROKJIN J. PARK[1]*, MINJOONG KIM[1], JAEIN JEONG[1] AND CHANG-KEUN SONG[2]

[1]School of Earth and Environmental Sciences, Seoul National University, Seoul, Korea (*correspondence: rjpark@snu.ac.kr)

[2]Global Environment Research Center, National Institute of Environmental Research, Incheon, Korea

Air pollutant concentrations such as troposheric ozone and aerosols are affected by meteorological variables including temperature, mixing depth, precipitation, and so on. Future climate is expected to be different from the present and so are those meteorological variables due to human perturbation to the atmospheric levels of the long-lived greenhouse gases and aerosols. East Asia is one of important source regions of both anthropogenic and natural greenhouse gases and air pollutant precursors. Therefore, significant environmental changes are expected in the future. We here use an offline coupling of a 3-D chemical transport model (GEOS-Chem) and a climate model (CAM3) to examine the effects of future climate change on air pollutatnt concentrations over East Asia. We conduct several model simulations with the IPCC SRES emission scenarions. Simulated air pollutant concentrations over East Asia in the future are found to be sensitively perturbed relative to the present depending on the different emission scenarios. Important meteorological factors affecting air pollutant concentrations include temperature, cloud covers, and precipitation over the continent. Changes in synoptic meteorological patterns induce different transport pathways of air pollutatns. Future climate changes may in general exacerbate air quality degradation that requires more stringent emission reductions over East Asia.

Column experiments for biosorption by immobilized carrier beads using *Bacillus* sp. and polysulfone to remove Pb from aqueous solution

SANGHEE PARK, INSU KIM, HAJUNG LEE AND MINHEE LEE

Department of Earth Environmnetal Sciences, Pukyong National University, Daeyon 3 dong, Namgu, Busan, 608-737, Republic of Korea (sthico0911@gmail.com)

Biosorption of Pb from aqueous solution has been investigated in column experiments. Sorption column experiments were used the immobilized carrier beads with dead biomass and polysulfone. *Bacillus* sp. was isolated from soil contaminated with oil and heavy metals at a military site in Repubilic of Korea. Dead biomass prepared by freeze-drying and autoclaving at 121 ℃ was mixed with 10 % polysulfone in DMF (*N, N*-dimethyl formamide) solution to produce the immobilized carrier beads which were spherical and porous beads (1 mm in diameter).

The column was designed with an internal diameter 2.5 cm and 100 cm height. Experiments were carried out in glass column filled with 5 % of dead biomass in carrier beads which were investigated to Pb removal efficiency in batch experiments. The initial concentration of Pb in the synthetic aqueous solution was titrated as 10 mg/L. Pb solution was pumped through peristaltic pump connected to the bottom of the column at a flow rate of 2.2 ml/min. From the top of the column, water samples were collected at regular time intavals (1, 2, 3, 4, 5, 6, 7, 8, 12, 15, 18, 24, 30, 36, 42, 48, 54, 60, 66, 78 pore volume). Samples were analyzed on ICP-OES for residual Pb concentrations in solution.

From the results of the column experiments, the Pb removal efficiency of immobilized carrier beads was kept over 98 % until the Pb solution was injected quantity of 30 pore volume. The amount of Pb adsorbed per unit weight of beads was 12.78 mg/g. A small quantity of immobilized beads could remove a lot of Pb in aqueous solution, therefore immobilized beads have a great passibility to clean up the heavy metal contaminated groundwater at the field.

https://doi.org/10.1180/S0026461X00006502 Published online by Cambridge University Press

Evaluation of anthropogenic contamination of bedrock groundwater using hydrochemical data: An example from suburban areas in Korea

SEONG-SOOK PARK[1,2], SEONG-TAEK YUN[1]*, KYOUNG-HO KIM[1], HYANG MI KIM[3] AND EUN-SEON JANG[1]

[1]Department of Earth and Environmental Sciences, Korea University, Seoul 136-701, South Korea (*correspondence: styun@korea.ac.kr)
[2]Department of Natural Resources and Environmental Engineering, Hanyang University, Seoul, South Korea
[3]Department of Mathmatics and Statistics, University of Calgary, Calgary, Alberta, Canada T2N1N4

A better evaluation of the relative contribution from natural versus anthropogenic sources to the observed groundwater quality is highly needed for better groundwater management. In this work, we evaluated hydrochemical data of 102 bedrock groundwater samples from two suburban areas using multivariate statistical techniques, in order to distinguish between anthropogenic contamination and natural process. The hydrochemistry of groundwater changed gradually from Ca-Na-HCO_3 to Ca-HCO_3-Cl type, concomitantly with the general increase of nitrate. The estimation of the distribution using the non-parametric kernel algorithm showed the bimodality for F and NO_3. The collected samples could be divided into natural versus anthropogenic groups via multivariate hierarchical, k-means, and fuzzy c-means clustering methods. The results from those multivariate clustering showed a drawback in terms of definite classification. On the other hand, the model-based clustering with a mixture model was a preferred method for identifying the two groups. Careful examination of hydrochemistry data for the two clustered groups suggests that the formation of Ca-Na-HCO_3 type groundwater is mainly controlled by plagioclase hydrolysis accompanying subordinate cation exchange (between Ca and Na) and calcite precipitation, while Ca-HCO_3-Cl type groundwater with noticeable NO_3 reflects varying degrees of anthropogenic contamination by agrochemicals and sewage/manure. This study provides an example of the successful application of the model-based clustering with mixture model to the regional groundwater quality evaluation.

Preliminary results of a recent expedition to the Australian-Antartic Ridge

S.H. PARK[1]*, C.H. LANGMUIR[2], J. LIN[3], D. HAHM[1], S.S. KIM[4], S.G. HONG[1], Y.M. LEE[1] AND P. MICHAEL[5]

[1]Korea Polar Research Institute, Incheon, Korea (*correspondence: shpark314@kopri.re.kr)
[2]Harvard University, Cambridge, MA, USA
[3]Woods Hole Oceanographic Institution, MA, USA
[4]Seoul National University, Seoul, Korea
[5]University of Tulsa, Tulsa, OK, USA

The Australian-Antarctic Ridge (AAR) is the largest unexplored expanse of the global mid-ocean ridge system. In early 2011, the Korea Polar Research Institute conducted a short survey of two segments at 160°E (K1) and 152.5°E (K2) using the icebreaker Araon. As a result, we have a multi-beam map and 16 rock core samples from the two segments. Also, we found strong signals of hydrothermal venting using MAPR (Miniature Autonomous Plume Recorder) profiles from the ridge. The AAR is intermediate spreading ridge and its axial depth is relatively shallow (~2100m). The axial morphology varies from an axial high to well-developed rift valley in the K1 segment, suggesting magma supply has varied on short spatial scales. The K1 western end abuts a transform with a strike towards the Balleny Islands, providing a possible source of excess magma supply and the shallow axial depth. MgO varies from 1.72 to 7.63 wt.%, mostly between 6~7wt.%. Fe-Ti basalt and dacite are at the western end of the K1 segment where magma supply appears most robust. The K2 segment samples are more primitive, and include E-MORB with 0.65% K_2O. Na_8 (2.5) is lower than the EPR but slightly high in the context of the global correlation with axial depth. It falls on trend with the slightly higher Na of Indian Ocean ridges. Trace elements and isotopes will be analyzed to characterize the mantle source. It appears that hydrothermal vents are distributed in the central part of the K1 segment. In the K2 segment, hydrothermal vent signals were mainly found in the western part of the segment.

https://doi.org/10.1180/S0026461X00006502 Published online by Cambridge University Press

Structure and stability of mineral interfaces

S.C. PARKER[1]*, M. MOLINARI[1], R ZHU[1], W SMITH[2] AND C. NOGUERA[3]

[1]Department of Chemistry, University of Bath, Bath BA2 7AY, United Kingdom (*correspondence: s.c.parker@bath.ac.uk)
[2]STFC Daresbury Laboratory, Warrington WA4 4AD, United Kingdom
[3]INSP, Université Pierre et Marie Curie, Paris, France

The aim of this presentation is to describe some recent applications of atomistic simulation studies for extending the range of applications to mineral interfaces. Two main themes will be addressed. The first is to describe our recent work on using Path Integral Molecular Dynamics. The approach is to provide quantum treatment of nuclear motion and particularly improve the description of proton motion. As a way of disentangling the electronic from nuclear motions we begin by presenting preliminary results for a number of mineral water interfaces using PIMD in the DL_POLY [1] code and employing interatomic potentials.

The second area is the application of both potential-based and DFT simulations towards modelling increasingly complex mineral interfaces. Two areas where we have investigating ways of improving the mineral surface description are (i) the simulation of polar surfaces and (ii) the interaction of nanoparticles with mineral surfaces.

A number of strategies in which the mineral can remove a surface dipole will be discussed and illustrated with several examples including the layered mineral: lizardite, where each layer is comprised of a silica sheet linked to brucite.

Finally, modelling the nanoparticle-surface interaction will be discussed. The release of nanoparticles into the environment could cause adverse ecological problems, and thus the transport of nanoparticles in the environment and the interaction of nanoparticles with the geosorbents are of concern. There are currently few studies that have addressed the interactions of nanoparticles with soil minerals, although numerous reports already showed that soil minerals such as clays can have strong interactions with organic contaminants. Here we will report our current work on these interactions. One example where all techniques can be applied is the interaction and transport of fullerene and its interaction with clay surfaces. Our results indicate that adsorption of fullerene on soil clay minerals could significantly influence its transport in the environment.

[1] Smith & Forester (1996) *J. Mol Graph* **14**, 136–141.

Mine water geochemistry and biogeochemical modeling

MARC PARMENTIER, NOLWENN CROISET, FABIENNE BATTAGLIA-BRUNET AND MOHAMED AZAROUAL

BRGM – Water Division, Hydrogeological and Hydrogeochemical Modelling, 3 av. C. Guillemin, BP 36009, 45060 France (m.parmentier@brgm.fr)

In mine tailings sites, where sulfide minerals are in contact with atmospheric humidity and meteoritic water, oxidation of sulfides generate acidity leading to mobilization of metals and metalloids through the soil to surface and underground waters. The resulting acid mine drainage can impair dramatic environmental problems (i.e. toxicity of arsenic III, etc.). In the old gold mine of Chéni (France), large physical, chemical and microbiological datasets are available: mineralogical compositions of the tailings [1], long-term survey of drainage waters chemistry [2] and microbiological characterizations [3]. The pH/Eh of sampled waters through the tailing column (unsaturated and saturated zones) is in the range of 2.9–7.6 and 0-700mV respectively. Analysis of these data permitted to identify the key processes of mine water behavior. Numerical simulations, using the geochemical software PHREEQC [4], were performed aiming to identify the key mechanisms and understand those coupling processes.

First analysis of geochemistry show different redox potentials for each element (Fe, As, O_2, N, S). Such redox disequilibrium, known in natural waters [5] is rarely take into account in modeling. In our work, redox decoupling of the thermodynamical database is used to model redox behavior of mine water.

Biological oxidation of arsenic was identified as an active and sustained process in such systems. Experimental results of biological As oxidation was used to develop a thermokinetic model coupling geochemistry and biologic activity [6] and reproducing the pH-dependant activity of bacterial population.

Finally, we elaborate a mixed biogeochemical model to reproduce the behavior of an acid mine drainage, which takes into account major processes including bacterial activities, precipitation of Fe-containing minerals (Schwertmannite, ferrihydrite, jarosite) and surface complexation.

[1] Roussel (1998) *PhD thesis*, Univ. Limoges. [2] Bodénan *et al*. (2004) *Appl. Geochem*. **19**, 1785–1800. [3] Battgalia (2002) *J. Appl. Micr*. **93**, 656–667. [4] Parkhurst et Appelo (1999) USGS Rep. **99**, 4529. [5] Lindberg & Runnels (1984) *Science* **225**, 925–927. [6] Jin & Bethke (2005) *Geoch. Cosm. Acta* **69**, 1133–1143.

https://doi.org/10.1180/S0026461X00006502 Published online by Cambridge University Press

Modelling methyl halide emissions from plants: From cytosol to the atmosphere

L. PARSHOTAM[1], D. CHRISTOPOULOU[2] AND K.R. REDEKER[1]*

[1]University of York, Department of Mathematics (lep506@york.ac.uk)
[2]University of York, Department of Mathematics (dc685@york.ac.uk)
[3]University of York, Department of Biology, *correspondance:(kelly.redeker@york.ac.uk)

Methyl halides affect climate through a number of important atmsopheric chemical processes, from ozone depletion to reduction of the cleansing capacity of the lower atmosphere to enhancing regional aerosol formation potentials. Despite these recognized concerns global budgets for methyl halides, including methyl chloride, methyl bromide and methyl iodide, remain poorly quantified. One major source of uncertainty within methyl halide budgets is the terrestrial biosphere. Only a few ecosystems have been quantitatively measured over full season life-cycles and our understanding of environmental parameter effects on plant emissions remains limited.

Here we present a 'from the ground up' model which predicts methyl halide emissions from plant tissues based upon estimated production rates within leaf mesophyll cell cytosol and diffusional transport through stomata, cuticle, leaf boundary layer and into the free atmosphere. This is the first model that the authors are aware of that follows trace gas transport from within plant cell tissues through diffusion to the free atmosphere.

Modelled results are compared to observational data from several plant systems to establish critical knowledge gaps within the methyl halide plant-atmosphere system. An inverse approach has also been performed to answer one of the persistent questions regarding the terrestrial biosphere and methyl halides: 'Do plants produce methyl halides as a defense mechanism'?

The effect of flood-induced redox oscillations on arsenic mobility in a calcareous fluvisol

C. PARSONS[1]*, R.-M. COUTURE[2], E. OMEREGIE[3], F. BARDELLI[1], G.ROMAN-ROSS[4] AND L. CHARLET[1]

[1]Environmental Geochemistry Group, ISTerre, University of Grenoble I, B. P. 53, 38041 Grenoble, France. (*correspondence: Chris.Parsons@aquatrain.eu)
[2]Georgia Institute of Technology, Atlanta, USA
[3]Williamson Research Centre for Molecular Environmental Science, University of Manchester, M13 9PL, UK
[4]Department of Chemistry, Faculty of Sciences, University of Girona, Campus de Montilivi, 17071 Girona, Spain

Contamination of floodplain soils with metals and metalloids is widespread, particularly in areas with a legacy of intense industrial activities [1], as is the case for much of Western Europe. It is well established that arsenic associated with metal oxides in soils and sediments can be released under reducing conditions experienced during flooding [2], due to desorption processes, speciation changes or mineral dissolution [3].

We show, through a combination of batch experiments, spectroscopy and thermodynamic and kinetic modelling, that the cumulative effects of redox cycling, often neglected in floodplain studies, also control arsenic mobility and that repetitive cycling in a closed system can help to attenuate arsenic mobilized during reducing conditions after a severe contamination event.

We demonstrate that this attenuation is due to a combination of fast reversible surface complexation of As to iron oxide minerals and slow irreversible adsorption/co-precipitation. This has implications for management of contaminated floodplains and suggests that controlled flooding and draining may help reduce the risk posed by arsenic in soils.

[1] Du Laing *et al*. (2009) *Sci Total Environ* **407**, 3972–3985. [2] McGeehan & Naylor (1994) *Soil Sci Soc Am J* **58**, **2**, 337–342. [3] Masscheleyn *et al*. (1991) *Environ Sci Technol* **25**, **8**, 1414–1419.

https://doi.org/10.1180/S0026461X00006502 Published online by Cambridge University Press

Establishing baseline geochemical conditions at historic gold mines for risk assessment and remediation

M.B. PARSONS[1]*, T.A. GOODWIN[2] AND M.E. LITTLE[1]

[1]Natural Resources Canada, Geological Survey of Canada (Atlantic), Dartmouth, Nova Scotia, Canada (*correspondence: Michael.Parsons@NRCan.gc.ca)
[2]Nova Scotia Department of Natural Resources, Mineral Resources Branch, Halifax, Nova Scotia, Canada

The mining and milling of Au from orogenic lode Au deposits can result in risks to the environment and human health without appropriate mine planning, environmental management, and monitoring programs. These deposits are the main source of Au in Canada, and are presently the focus of considerable exploration and development. Arsenopyrite occurs naturally in the ore and surrounding bedrock in these deposits, and As is generally present at high concentrations in mine wastes and drainage waters. Historically, Hg amalgamation was often used to extract Au from the ore, and high Hg concentrations are common in mine tailings and near abandoned mill sites. The recent surge in global Au prices has generated renewed interest in many former mining districts, and in the possibility of reprocessing historic Au mine wastes. To develop appropriate environmental management plans for these sites, it is essential to characterize both the pre-mining concentrations of metal (oid)s in waters, sediments and soils, as well as the impact from previous mining operations.

This presentation will summarize recent studies of geochemical baselines at lode gold deposits in Nova Scotia and British Columbia, Canada. In Nova Scotia, we determined the vertical distribution of As and Hg in forest soils surrounding two abandoned gold mines to evaluate pre-mining baseline conditions, and the extent of historical mine wastes. In general, the concentrations of As are highest in B and C horizon soils, whereas Hg concentrations are highest in the organic-rich humus (H) layer. Arsenic concentrations in naturally mineralized soils range from 2-270 mg/kg, and are generally greater than the 12 mg/kg Canadian Soil Quality Guideline for As. In British Columbia, samples of stream water and sediment were collected around the past-producing Bralorne, King, and Pioneer Au mines. Background concentrations of As, Hg, and Sb commonly exceed environmental guidelines in sediments, but impacts on water quality were restricted to the immediate vicinity of former mine sites. The results of these studies are being used to inform environmental site assessments and to develop suitable monitoring and remediation strategies for orogenic lode gold deposits across Canada.

Major ion chemistry of subsurface water samples around waste disposal sites of Hyderabad city, India

VANDANA PARTH[1] *, N.N. MURTHY[1] AND PRAVEEN RAJ SAXENA[2]

[1]National Geophysical Research Institute, Council of Scientific and Industrial Research, Hyderabad, India (*correspondence: vandana.parth@gmail.com)
[2]Department of Applied Geochemistry, Osmania University, Hyderabad, India

The present study deals with hydrogeochemistry of groundwater around dumpsites, Hyderabad city, India. The city witness ~4000 tons of solid waste per day dumped in low-lying areas as landfills, affecting groundwater quality. Three waste dumpsites namely; Jawaharnagar, Autonagar and Dundigal were chosen for major ions study in the groundwater. The samples were collected from sixty location points around dumpsites covering entire area and were precisely analysed for physicochemical characters using the standard procedures recommended by APHA [1]. F^- and NO_3^- were determined by double junction electrode at 25°C. The type of water that predominated in the study area was assessed based on hydro-chemical facies. Suitability of groundwater for irrigation was evaluated based on sodium adsorption ratio, per cent sodium, residual sodium carbonate and the US salinity diagram. High concentrations of major ions (Ca^{++}, Mg^{++}, Na^+, F^-) observed in bore wells can be attributed to differential weathering of minerals such as pyroxenes, plagioclase feldspars, and apatite together with dissolution/precipitation reactions along fractures and joints in the granites. The high NO_3^- level >50 mg/l is ascribed to consequence of the oxidation of ammonia and similar sources from leachate emanating from waste. Although the water in the study area is not potable, it is found to be suitable for irrigation purposes with little risk in the development of detrimental level of exchangeable sodium. Based on piper diagram, the groundwater is being classified into Ca-HCO_3^- type, Ca-Cl^- type, Mg-HCO_3^- type and Mg-Cl^- type. The carbonate hardness exceeds 50% of the total ionic composition, which signifies that the chemical properties are dominated by alkaline earth (Ca^{2+}+Mg^{2+}) and week acids (CO_3^{2-}+HCO_3^-). Though the suitability of water for irrigation in the present study is determined based on SAR, RSC, %Na and USSL diagram, it is only an experimental conclusion. In addition to water quality, other factors like soil type, crop pattern, frequency and recharge (precipitation), climatic conditions, etc. have a vital role in determining the suitability of water.

[1] APHA (1998) *Standard methods for the examination of water & wastewater*. American Public Health Association, Washington DC, 20th edn.

https://doi.org/10.1180/S0026461X00006502 Published online by Cambridge University Press

Pressure dependence of electrical resistivity of cummingtonite from the world's deepest Kola super deep-borehole (KSDB-3), Russia

G. PARTHASARATHY[1] AND F.F. GORBATSEVICH[2]

[1]National Geophysical Research Institute (CSIR), Hyderabad-7, India (gpngri@rediffmail.com)
[2]Geological Institute Russian Academy of Sciences, Apatity, Murmansk 184209, Russia

We present here for first time the temperature and pressure dependence of the electrical resistivity of cummingtonite from the Kola super-deep borehole (KSDB-3) up to 700 K and 4 GPa. The Kola super-deep borehole near Zapolyarny, Kola Peninsula, Russia is the deepest borehole in the world (12261 m deep) that has penetrated Proterozoic complex from the surface to 6840 meters, with mafic meta-volcanic on the top 1000m, metasedimentary rocks from 2800m to 4500 m, and intermediate metavolcanics dominating from down to 6800 m depth, further in the depth region 6800 m to 12261 meters the KSDB-3 intersects an Archaean gneiss-migmatite complex with ubiquitous amphibolites bodies up to 30 meters thickness. About 1/3 of the total cross section of the borehole consists of amphibolites [1]. High-pressure electrical resistivity measurements were carried out in a Bridgman opposed anvil system, up to 9 GPa [2]. We have observed a distinct slope change in the Arrhenius plot of the electrical conductivity of cummingtonite at 455 K, which can be explained as a $Mg^{2+} \rightarrow Fe^{2+}$ cation order-disorder phase transition, which is due to the migration of Fe^{2+} from M4 to M1, M2, M3 sites at 683 K [3]. The conductivity activation energy has been measured at different pressures, and found to be decreasing from 065 eV at room pressure to 0.35 eV at 6GPa.

[1] Mitrofanov FP & Gorbatsevich FF (2000) *IGCP project* **408**, Apatitty, Russian Academy of Sciences. 153pp. [2] Parthasarathy, G (2006) *J. Applied Geophys.* **58**, 321. [3] Ghose, S & Weidner JR (1972) *Earth. Planet. Sci. Lett* **16**, 346.

Spectroscopic investigations on natural stichtite and synthetic hydrotalcites

G. PARTHASARATHY[1] AND CH.VENKAT REDDY[2]

[1]National Geophysical Research Institute(CSIR) Hyderabad-500606, India (gpsarathy@ngri.res.in)
[2]Indian Institute of Chemical Technology (CSIR), Hyderabad-500607, India Presently Dept of Chemsitry, Iowa state university, Ames, IA-50011,USA
E-mail: chvekatreddy@gmail.com

We present here structural and thermal properties of synthetic hydrotalcites and natural stichtite. Stichtite, a rare hydrated carbonate-hydroxide of Mg and Cr with ideal formula $Mg_6Cr_2(OH)_{16}CO_3 \cdot 4H_2O$, occurs in chromite bearing serpentenites of Nuggihalli Archaean greenstone belt, India.[1]. The efficiency of CO_2 adsorption based separation is based on the structural and thermal characteristics of the adsorbent. There are several naturally occurring minerals like zeolites, in the Deccan Trap area with high CO_2 adsorption capacity. However, most of these adsorbents suffer from low capacity at high temperature (seen in the combustion processes). Hydrotalcite is one of the few minerals with significant anion exchange capacity, and stands in contrasts to the more common mesoporous clay minerals, which have cation exchange properties. Carbon-dioxide adsorbing capacity has been investigated by using hydrotalcites as high temperature adsorbents. We present here the compositional and structural characteristics of the naturally occurring stichtite and synthetic hydrotalcites by using spectroscopic methods, and the potential applications of synthetic hydrotalcites and naturally occurring stichtite in the study of the adsorption of carbon dioxide are discussed. Infrared spectroscopic studies on the stichtite shown several absorbtion bands at 1460, 1380, 745 and 685 cm-1, all of them are assigned as per the standard vibrational modes described by Frost and Erickson [2]. High temperature DTA/TG studies showed a thermal dehydration reaction at about 530 K and decarbonation reaction at 825 K, similar to Al based synthetic hydrotalcites.

We thank PLANEX, ISRO Govt. of India, for funding.

[1] Nijagunappa R & Naganna C (1983) *Econ. Geol.* **79**, 507-513. [2] Frost.R.L.Erickson K (2004) *Spectrochim. Acta. A* **60**, 3001. [3] Parthasarathy G *et al.* (2002) *Microporous Mesoporous Materials* **56**, 147–152.

https://doi.org/10.1180/S0026461X00006502 Published online by Cambridge University Press

Re-Os geochemistry and geochronology of the Ransko gabbro-peridotite massif, Czech Republic

JAN PAŠAVA[1], LUKÁŠ ACKERMAN[1,2]* AND VOJTĚCH ERBAN[1]

[1]Czech Geological Survey, Geologická 6, 152 00 Praha 5, Czech Republic

[2]Institute of Geology v.v.i., Academy of Sciences of the Czech Republic, Rozvojová 269, 165 00 Praha 6, Czech Republic (*correspondence: ackerman@gli.cas.cz)

The Ransko gabbro-peridotite massif is located in a transition zone between Moldabian and Kutná Hora crystalline unit of Bohemian Massif, Czech Republic. It represents a strongly differentiated intrusive complex with zoned structure which hosts low grade Ni-Cu-(PGE) ores. This mineralization is mainly developed close to the contact of olivine-rich rocks with gabbros, in troctolites, and to a much lesser extent in both pyroxene and olivine gabbros and plagioclase-rich peridotites [1].

We analyzed eleven samples of gabbro, troctolite, peridotite and Ni-Cu ore for Re-Os concentrations and Os isotopic ratios. Barren gabbro and troctolite have very low Os concentrations (0.02 to 0.1 ppb), high Re contents (0.6 to 2.4 ppb) and corresponding high Re/Os ratios. Their $^{187}Os/^{188}Os$ ratios display very variable strongly radiogenic values ranging from 0.4358 to 2.1372. This heterogeneity in Os isotopic ratios is most likely connected with different degrees of crustal contamination involved in the parent basaltic melt. The Ni-Cu low mineralized rock (peridotite, troctolite) and massive Ni-Cu-(PGE) ores have high Re (from 1.67 to 121.2 ppb) and Os (0.81 to 206.8 ppb) contents and consequently low Re/Os ratios (0.5 až 5.1). The subchondtritic to superchondritic $^{187}Os/^{188}Os$ ratios (from 0.1264 to 2.1372) show variable contribution of mantle- and crustal-derived ^{187}Os in Ni-Cu-(PGE) mineralization.

Four selected samples with suggested closure of the Re-Os system after emplacement of Ni-Cu mineralization have similar Os model ages and yield the Re-Os isochron age of 550 ± 49 Ma. This is in agreement with the results of [2] who suggested Lower Cambrian age of the Ransko massif based on geological and paleomagnetic studies.

[1] Mísař, Z (1979) *Canadian Mineralogist* **17**, 299–307.
[2] Marek, F (1970) *Věstník Ústředního Ústavu Geologického* **45**, 99–102 (in Czech with English abstract)

Cryptoendolithic colonization in the hydrating mantle along mid ocean ridges

V. PASINI[1,2]*, B. MÉNEZ[1] AND D. BRUNELLI[13]

[1]Dipartimento di Scienze della Terra, Università di Modena e Reggio Emilia, L.go St. Eufemia 19, 41100 Modena, Italy (*correspondence: valerio.pasini@unimore.it)

[2]IPGP, UMR CNRS 7154, 1 rue Jussieu, 75005 Paris, France

[3]Istituto di Scienze del Mare – CNR, Via Gobetti 101, 49100 Bologna, Italy

The basaltic oceanic crust and associated sediments are recognized to harbor an active microbial life involved in the geochemical fluxes between geosphere and hydrosphere while the underlying mantle-derived peridotitic lithosphere remains until now underexplored. Nonetheless, the progressive hydration of peridotite-forming minerals (i.e. serpentinization) releases great amount of molecular hydrogen, that constitutes a valuable source of metabolic energy for chemiolithoautotrophic microorganisms. Although recent studies have demonstrated the presence of extremophile microbial life at hydrothermal vents related to oceanic serpentinization, as illustrated at Lost City (Mid Atlantic Ridge, 13° N), the presence and the level of activity of hydrogen-driven subseafloor communities inside the hydrating mantle rocks are still under debate.

By implementing a suite of microspectroscopic and microimaging techniques (i.e. coupled confocal laser scanning microscopy and Raman spectroscopy, transmission and scanning electron microscopies on focused-ion-beam ultrathin sections) we evidenced the presence of deep endogenic organic-carbon accumulations that sign a past mineralizing bioactivity in deeply serpentinized mantle rocks collected along the Mid-Atlantic Ridge (6°03.3'N-33°25.4'W). These niches are constituted by chains of porous hydroandraditic garnets harboring polyhedral/polygonal serpentines and iron oxides. Their strict association with remnants of multiple organic polymers carrying biological functionalities and thermally-evolved carbonaceous matter, proves that cryptoendolithic life drives hydrogarnet dissolution and concomitantly serpentine ± iron oxides formation while sequestrating carbon through primary production. Mass balance shows these activities to be local source for Ca and a sink for Mg. Our results support the existence of deep ecosystems within the low-temperature hydrating mantle sustained by the process of serpentinization that mediate chemical fluxes from the Earth's lithosphere to oceans and potentially impact the overall chemical transfer between the Earth's mantle and the exosphere.

https://doi.org/10.1180/S0026461X00006502 Published online by Cambridge University Press

Mesoarchaean tectono-metamorphic event from Bundelkhand craton, central India

J.K. PATI[1]* AND L. SAHA[2]

[1]Department of Earth and Planetary Sciences, UA, Allahabad, India (*correspondence: jkpati@yahoo.co.in)
[2]School of Geological Sciences, UKZN, Durban, SA

Bundelkhand craton is exposed over ~29, 000km^2 area in north-central India. The craton consists of slivers of Archaean greenstone successions within granitoids and gneisses, latter containing components with ages: 3.5 Ga [1], 3.3 Ga, 2.7 Ga and 2.56-2.49 Ga [2]. The amphibolites from the greenstone slivers yield depleted mantle ages clustering around 4.9-4.2 Ga and 3.4-3.3 Ga [3]. While the older age range may correspond to protolith formation, the younger cluster may indicate age of metamorphism.

Our study concentrates on a greenstone sequence SW of Mauranipur. The sequence consists of interlayered amphibolite-calc silicate-biotite schist-quartzite and have steeply dipping foliation. Amphibolites are of two types: Type-1, retrogressed amphibolites with garnet porphyroblasts in a matrix of chlorite-quartz, Type-2 amphibolites with hornblende-defined foliation and cross-cutting quartzo-feldspathic veins. Garnet porphyroblasts are extensively replaced by chlorite in Type-1 amphibolite. The Type-1 amphibolite is interbanded with a calc-silicate, latter consisting of alternate bands of garnet-amphibole-calcite-quartz and clinopyroxene-epidote-calcite-quartz. Garnets in the Type-1 amphibolite and in calc-silicate have compositions: $Prp_{11-14}Grs_{13-15}Alm_{65-69}Sps_{5-9}$ and $Grs_{30-50}Alm_{15-32}Sps_{34-37,}$ respectively. The P-T condition of metamorphism is ~5.7 kbar, 425-450°C and this has been obtained from the garnet-bearing layer of calc-silicate by determining the intersection of stable reactions by using THERMOCALC.

We conclude that the age of this metamorphic event from Bundelkhand craton was probably ~3.3 Ga, as obtained from the Nd isotope systematics of the amphibolites. The P-T conditions of metamorphism indicates a high geothermal gradient of ~30°C/km in contrast to ~ 12°C/km recorded during Neoarchean [5] from the craton.

[1] Sarkar *et al*. (1996) *Rec. Res. in Geology* **16**, 76–92. [2] Mondal *et al*. (2002) *Pre. Res*. **117**, 85–100. [3] Malviya *et al*. (2005) Joint Meeting Earth & Planetary Sciences, Japan. [5] Saha *et al*. (2010) *Contrib. Mineral. Petrol*. **161**, 511–530.

C, O, Sr isotope compositions of sediments of the Mesozoic Kutch basin, NW India

D.J. PATIL[1], B. SREENIVAS[1], C. SRIKARNI[2], P.B. RAMAMURTHY[1], E.V.S.S.K. BABU[1], B. VIJAYA GOPAL[1] AND A.M. DAYAL[1]

[1]National Geophysical Research Institute (CSIR), Hyderabad 500007, India (djpatil@ngri.res.in)
[2]Geological Survey of India, Itanagar, Arunachal Pradesh, India

The Mesozoic period of earth history is known for the preservation of bulk of global hydrocarbon reservoirs. It is also known that this period is marked by global scale anoxic events reflecting in the C, O and Sr isotope records of marine carbonates [1]. In this work we report C, O and Sr isotope compositions of marine carbonate rocks belonging to the Mesozoic Kutch sedimentary basin of NW India. The sediments of the Kutch basin range in age from Bathonian stage (169.2 Ma) of Middle Jurasssic to the Albian (98.9 Ma) of the Cretaceous. Carbonate sediments belonging to the lower Jhurio (Bathonian to Callovian) and Jumara (Callovian to Oxfordian) Formations have been analyzed for their $\delta^{13}C$, $\delta^{18}O$ and $^{87}Sr/^{86}Sr$ values showing wide ranges mainly due to the effect of later diagenesis. Using the proxies such as Mn/Sr, $\delta^{18}O$ and $^{87}Sr/^{86}Sr$ the best-preserved C, O and Sr isotope compositons of ambient seawater compositions has been estimated (Table 1).

Formation	$\delta^{13}C_{Carb}$	$\delta^{18}O$	$\delta^{13}C_{Org}$	$^{87}Sr/^{86}Sr$
Jumara	-1.5 to 1.6 (n = 15)	-10.7 to -5.8 (n = 15)	-29.4 to -24.6 (n = 12)	0.707080 to 0.707441 (n = 15)
Jhurio	-1.0 to -1.6 (n = 2)	-6.4 to -9.4 (n = 2)	-30.9 to -26.9 (n = 2)	

Table 1: Best-preserved C, O and Sr isotope compositions of Mesozoic Kutch carbonates

While the best-preserved $\delta^{13}C$ and $^{87}Sr/^{86}Sr$ values of Kutch carbonates are well in agreement with the global curves, the $\delta^{18}O$ values show large depletion up to 5‰ when compared to the ambient global mean. The observed diagenetic trends indicate possible thermal maturity of organic matter and hence generation of hydrocarbon reservoirs as also corroborated by surface geochemical prospecting methods.

[1] Jones, C.E. & Jenkyns, H.C. (2001) *Am. J. Sci*. **301**, 112–149.

https://doi.org/10.1180/S0026461X00006502 Published online by Cambridge University Press

Improved $^{27}Al/^{24}Mg$ ratio measurement using a modified isotope-dilution approach

C. PATON*, M. SCHILLER, D. ULFBECK AND M. BIZZARRO

Center for Star and Planet Formation, Natural History Museum, University of Copenhagen, Øster Voldgade 5–7, 1350, Copenhagen, Denmark (*correspondence: cpaton@snm.ku.dk)

With its half-life of ~0.73 Myr, the decay of (now extinct) ^{26}Al to ^{26}Mg is capable of providing extremely precise relative ages, and as a result the ^{26}Al–^{26}Mg system is widely employed in constraining the timing of events in the early solar system. The popularity of ^{26}Al as a chronometer has stimulated a continual refinement in the analytical methods of Mg-isotope determination, resulting in a present day reproducibility for $^{26}Mg^*$ values of better than 3 ppm [1]. However, methods for the measurement of $^{27}Al/^{24}Mg$ ratios (as a proxy for parent/daughter ratios) have seen little improvement, and the present accuracy of ±2% [2] is no better than it was a decade ago [3]. As a result, the uncertainties in Al/Mg isochrons are now dominated by uncertainties in the measured $^{27}Al/^{24}Mg$ ratio.

By modifying conventional mixed-spike isotope-dilution methods we have developed a technique using a spike consisting of isotopically enriched ^{25}Mg and isotopically normal Al, which incorporates an approach analogous to standard-sample bracketing. The method employs isotope dilution to determine the spike to sample ratio for magnesium, but utilises bracketing of spiked and unspiked sample solutions to obtain the spike to sample ratio for aluminium. A typical run consists of four spiked measurements, bracketed by five unspiked measurements, and consumes < 2 μg of Mg.

This technique overcomes the problem of aluminium being monoisotopic, and measurements of international rock standards, as well as a gravimetric calibrant solution, indicate a reproducibility approaching conventional mixed-spike isotope dilution (i.e. 2 s. d. of <0.5%). Measurements are made on a single unpurified aliquot of the sample, so no chromatographic separation is required, and the method is less susceptible to biases generated by differences in sample matrix composition.

[1] Bizzarro *et al*. (2011) *Journal of Analytical Atomic Spectrometry* **26**, 565–577. [2] Schiller *et al*. (2010) *Geochimica et Cosmochimica Acta* **74**, 4844–4864. [3] Galy *et al*. (2000) *Science* **290**, 1751–1753.

Concentration of chalcophile and siderophile elements in MORB sulphide droplets: New sulphide melt-silicate melt partition coefficients

C. PATTEN[1], S.-J. BARNES[2] AND E.A. MATHEZ[3]

[1]Sciences de la Terre, Université du Québec à Chicoutimi (clifford.patten@uqac.ca)

[2]Sciences de la Terre, Université du Québec à Chicoutimi (Sarah-Jane_Barnes@uqac.ca)

[3]Department of Earth and Planetary Sciences, American Museum of Natural History, New York (mathez@amnh.org)

We have determined the concentrations of chalcophile and siderophile elements by LA-ICP-MS from sulphide droplets and fresh glass in contact with them from MORB pillow rims. MORBs play an important role in the understanding of mantle petrogenesis, providing information on chemical fractionation of elements in the mantle. However, chalcophile element behaviour is not completely understood, partly due to the lack of data for partition coefficients between sulphide and silicate melts.

Some droplets present homogenous textures and others portions rich in monosulphide solid solution (Mss) and intermediate solid solution (Iss) indicating that they have undergone crystal fractionation. For homogenous droplets, concentrations of Ni and Cu are 10 to 1%; Co and Zn 1000 to 100 ppm; Se, Te, Ag and Pb 100 to 10 ppm; Cd, Sn, Pd, Bi and Pt 10 to 1 ppm; Au, Ru and Re 1 to 0.1 ppm. For some of these elements it was also possible to obtain data in fresh glass allowing the calculation of partition coefficients. These were calculated for Ni (745± 252), Cu (1219 ± 381), Co (42 ± 5.5), Zn (3.4 ± 0.9), Sn (10.4 ± 1.8) and Pb (55.6 ± 9.3). Values for Ni, Cu and Co are in agreement with literature [1], suggesting that values for Zn, Sn and Pb are realistic.

[1] Peach *et al*. (1990) Sulfide melt-silicate melt distribution coefficients for noble metals & other chalcophile elements as deduced from MORB, Implications for partial melting, *Geochimica et Cosmochimica Acta* **54**, 3379–3389.

https://doi.org/10.1180/S0026461X00006502 Published online by Cambridge University Press

Radiation damage in biotite: Defined by Micro XAS and XRD

RICHARD PATTRICK[1], TINA GERAKI[2], JOHN CHARNOCK[1], CAROLYN PEARCE[3], SIMON PIMBLOTT[1] AND GILES DROOP[1]

[1]RCRD, University of Manchester, Manchester, UK, M13 9PL
[2]Diamond Light Source, Harwell, Oxfordshire, OX11 0DE
[3]PNNL, Richland, WA 99352, USA

Radiation damage in mineral structures is of interest because of their consideration as radioactive waste forms. Examples of damage occuring on geological timescales are available in nature. Alpha particle damage around actinide-bearing inclusions in silicates is best observed in the mineral biotite where a *ca* 35 micron damage halo is seen. By using combined synchrotron XAS and XRD at the Diamond Light Source, UK, the changes across the damaged zone around a U/Th-bearing monazite inclusion was investigated. Fe K-edge XANES from a traverse shows that within the damaged zone the biotite Fe^{3+} is reduced, perhaps as a consequence of radiolysis of the OH groups in the octahedral layers. The Fe K-edge EXAFS show an increase in disorder in the damaged zone. The micro XRD showed major changes in the biotite lattice as the U/Th containing inclusion was approached. The use of a single crystal positioned perpendicular to (001) enhanced the a, b plane reflections. The diffraction spots representing 110 and other sub-parallel planes show evidence of amorphisation of the biotite lattice. Also new reflections appear at d-spacings close to the main reflections, indicating local changes to the structure as a result of atomic displacements during the development of Frenkel pairs.

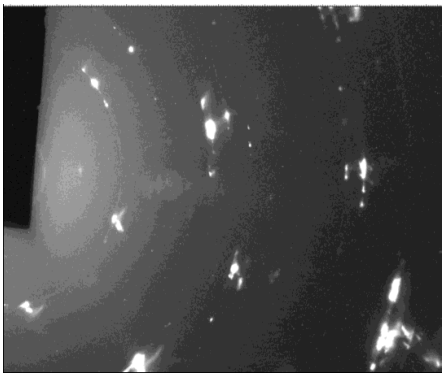

Figure. 1. Synchrotron diffraction image of biotite adjacent to an alpha particle emitting inclusion.

Melt inclusion Pb-isotope analysis by LA-MC-ICPMS: Assessment of analytical performance and application to OIB genesis

BENCE PAUL[1,2]*, JON D WOODHEAD[1], JANET HERGT[1] AND LEONID DANYUSHEVSKY[2]

[1]School of Earth Sciences, The University of Melbourne, Victoria, Australia (*correspondence: bpaul@unimelb.edu.au)
[2]CODES ARC Centre of Excellence in Ore Deposits, University of Tasmania, Tasmania, Australia (L.Dan@utas.edu.au)

We present laser ablation MC-ICPMS lead isotope measurements of olivine-hosted melt inclusions, analyses that include the low abundance Pb-isotope, ^{204}Pb, measured on an ion counter. These data were collected using a unique parallel ion counter-faraday cup method, developed for melt inclusion isotope analysis [1]. We tested this technique on an isotopically homogeneous sample from Tonga to provide constraints on both precision and accuracy. Using the variability of these data we then re-investigate two OIB inclusion suites. These new data demonstrate that greater variability than would be expected from analytical errors alone can be discerned in the two OIB suites.

Our data suggest that melt inclusions are not biased towards grain-scale phenomena and thus may indeed be representative of geologically significant processes in magma chambers. In the case of the Pitcairn Seamounts, we find that each sample contains melt inclusion compositions with the same variablity as the entire whole-rock sample population for these seamounts. Similarly, melt inclusion data from the island Mangaia show the same degree of compositional variability as defined by all lavas on the island.

In addition, our Pb isotope measurements of individual samples suggest that discrete batches of isotopically distinct melt exist to high levels in magmatic plumbing systems.

We also present two preliminary combined trace element/Pb isotope measurements for two inclusions, which we believe demonstrate the potential of such an approach for future studies. Results from the Pitcairn Seamounts suggest that isotopic variability is inherited from the mantle source and not necessarily from late stage crustal contamination.

[1] Paul *et al*. (2005) *J.A.A.S*. **20**, 1350–1357.

https://doi.org/10.1180/S0026461X00006502 Published online by Cambridge University Press

Fe(II) exchange at titanomagnetite-water interfaces

C.I. PEARCE[1]*, J. LIU[1], O. QAFOKU[1], E. ARENHOLZ[2], S.M. HEALD[3] AND K.M. ROSSO[1]

[1]Pacific Northwest National Laboratory, Richland WA, USA (*correspondence: carolyn.pearce@pnl.gov)
[2]Advanced Light Source, Lawrence Berkeley National Laboratory, Berkeley, CA 94720, USA
[3]Argonne National Laboratory, Argonne, IL 60439, USA

Spinel-type iron oxides such as magnetite are an important source of solid-state Fe (II) that can affect the transport of redox-active contaminants, such as ^{99}Tc (VII), in the subsurface. Natural magnetites present in sediments are typically highly impure with titanium, and structural Fe (III) replacement by Ti (IV) yields a proportional increase in the relative Fe (II) content in the metal sublattice to maintain bulk charge neutrality. Titanomagnetite ($Fe_{3-x}Ti_xO_4$) nanoparticles provide a high surface area pristine material for batch studies to evaluate the availability and reactivity of Fe (II) at the mineral surface. $Fe_{3-x}Ti_xO_4$ nanoparticles accept structural Ti (IV) into the octahedral metal sublattice up to $x = 0.4$; higher values up to $x = 0.6$ yield discrete amorphous Fe (II)/Ti (IV) phases on particle exteriors. In aqueous suspension, there is a net driving force for the movement of Fe (II) from the bulk $Fe_{3-x}Ti_xO_4$ structure to the nanoparticle surface with subsequent release of Fe (II) into solution to reach an equilibrium distribution between interior structural Fe (II)/Fe (III), near-surface Fe (II)/Fe (III), and aqueous Fe (II). Consumption of structural Fe (II) through both dissolution and redox reactions results in the replacement of octahedral cations with vacancies to form an Fe (II)-deficient titanomaghemitized surface. Spontaneous Fe (II) release from the solid into solution increases in extent systematically with both Ti-content and decreasing pH. The presence of Tc (VII) in solution, as an electron accepting probe molecule, also increases this driving force as Fe (II) at the surface reacts with the Tc (VII) to form of a mixed Fe (III)-Tc (IV) co-precipitate. In principle, this titanomaghemitization process is reversible and, under reducing conditions, structural reducing equivalents can be restored by an external Fe (II) source. Pre-oxidized $Fe_{3-x}Ti_xO_4$ nanoparticles were found to be systematically restorable to Tc (VII) reduction rate behavior of pristine titanomagnetites by exposure to various concentrations of aqueous Fe (II). The findings demonstrate that the reactive structural Fe (II) pool can be resupplied in these $Fe_{3-x}Ti_xO_4$ phases and suggest that the mechanism involves facile coupled electron/ion transport across the mineral-water interface.

Stable strontium (δ^{88}Sr) isotopic fractionation during hydrological cycling

CHRISTOPHER R. PEARCE[1]*, IAN J. PARKINSON[1], KEVIN W. BURTON[2] AND JEROME GAILLARDET[3]

[1]Department of Earth and Environmental Sciences, CEPSAR, The Open Universtiy, Walton Hall, Milton Keynes, MK7 6AA, UK (*correspondence: c.pearce@open.ac.uk)
[2]Department of Earth Sciences, Oxford University, Parks Road, Oxford, OX1 3PR, UK
[3]Laboratoire de Geochimie-Cosmochimie, Institute de Physique du Globe de Paris, 7 Place Jussieu 75252, Paris, Cedex 05, France

The stable strontium (δ^{88}Sr) isotope system has considerable promise for resolving source and flux variations during elemental transfer to the oceans by continental weathering. In combination with radiogenic Sr isotope ratios (^{87}Sr/^{86}Sr), δ^{88}Sr provides an additional compositional space in which the riverine source and weathering flux effects can be distinguished.

Analysis of >40 % of the global Sr flux to the oceans has revealed an average riverine δ^{88}Sr composition of 0.34 ‰ [1], similar to the mean seawater value of 0.36 ‰ [2]. Most continental rivers vary about this mean (between 0.2 ‰ and 0.5 ‰), although a broader range of values (0.1–0.9 ‰) is observed in rivers draining basaltic and carbonate terrains where fractionation processes relating to carbonate precipitation and dissolution are thought to occur [1].

The largest δ^{88}Sr offset in the modern hydrological cycle is observed in continental ice, with Langjökull glacier in west Iceland having a value of -0.24 ‰. The δ^{88}Sr composition of Parisian rainwater, 0.26 ‰, is also significantly lighter than seawater, and similar offsets have been previously reported in glacial meltwaters from Switzerland [3]. This evidence for the compositional differentiation of stable Sr isotopes between seawater and precipitation contrasts with results from other isotope systems (such as Li, Mg, Mo and Si), and implies that Sr-specific fractionation may be occurring during the evaporation-precipitation and/or freeze-thaw processes. This study explores the potential mechanisms responsible for this isotopic fractionation and the possibilities for using δ^{88}Sr as a monitor of the hydrological cycle.

[1] Pearce *et al*. (2010) *AGU*, *Fall Meet*. *Abstract*. **B21D-0342**. [2] Stevenson *et al*. (2010) *AGU*, *Fall Meet*. *Abstract*. **B21D-0343**. [3] de Souza *et al*. (2010) *GCA*, **74**, 2596–2614.

https://doi.org/10.1180/S0026461X00006502 Published online by Cambridge University Press

Newly-discovered abyssal peridotite mantle xenoliths constrain mid-ocean ridge melting models

JULIAN A. PEARCE[1], PHILIP T. LEAT[2], TIFFANY L. BARRY[3] AND ANDREW G. TINDLE[4]

[1]School of Earth and Ocean Sciences, Cardiff University, Cardiff CF10 3YE, UK (PearceJA@cf.ac.uk)
[2]British Antarctic Survey, Cambridge CB3 0ET, UK (ptle@bas.ac.uk)
[3]Dept. of Geology, University of Leicester, Leicester LE1 7RH, UK (tbl2@leicester.ac.uk)
[4]Dept. of Earth Sciences, The Open University, Milton Keynes MK7 6AA, UK (a.g.tindle@open.ac.uk)

Much of our knowledge of mantle melting beneath mid-ocean ridges comes from modelling based on the composition of MORB and of variably-serpentinized abyssal peridotites tectonically exposed on the ocean floor. Here, we report a unique occurrence of fresh nodules of young, deep, sub-ridge oceanic lithosphere with the potential to test these melting models. The setting is the West Scotia Ridge spreading centre which actively spread at intermediate-slow rates for c.25Ma. Following the cessation of spreading at c.5.5Ma (Ar-Ar and magnetic anomaly dating), a final pulse of alkali basalt erupted at c.0.3Ma carrying the peridotite nodules to the sea-floor. Thermobarometry places these nodules at an original depth of c.1±0.3 GPa (Ca-in-olivine) and a temperature of c.1050°±35C (olivine-spinel and Ca-in-orthopyroxene), the latter consistent with c.6Ma of cooling of oceanic lithosphere at c.25-30km depth. Geochemical interpretation of the nodules (spinel Cr# and clinopyroxene REE) indicates that they have experienced c.12% of fractional melting, c.5% in garnet facies and c.7% in spinel facies, so supporting models for initiation of ridge melting in garnet facies and supporting some estimates for melt production rates (dF/dP). The host alkali basalt has REE concentrations and MREE-HREE gradients consistent with formation by a small degree of mainly garnet facies melting and so supports models requiring a contribution to MORB of a deep, small-volume melt with high incompatible element concentrations. The Nd isotope ratio of the alkali basalt is less than that of the MORB/nodule (0.513015 cf. 0.513095), which may result from sources of different compositions but could also be explained by fractional melting of a heterogeneous mantle. Thus the dying ridge setting provides a useful opportunity to sample the small melt fractions and deep near-ridge lithosphere normally unavailable during active spreading and facilitates the ground-truthing of ridge melting models.

Crust-mantle links in cratons

D.G. PEARSON[1]*, S. TAPPE[1], K.A. SMART[1], K.A. MATHER[2], C.W. DALE[2] AND B.A. KJARSGAARD[3]

[1]University of Alberta, Edmonton AB, T6G 2E3, Canada (*correspondence: gdpearso@ualberta.ca)
[2]Durham University, Durham, DH1 3LE, UK
[3]Geological Survey of Canada, Ottawa, Canada

Cratonic crust and its underlying mantle root are both bouyant survivors of the Archean tectonic regime. A central issue in constraining the formation of continents in this Eon is the genetic relationship between these two 'stable' units. Peridotite and eclogite xenoliths erupted by kimberlites provide vital clues that can be matched to a growing database of crustal geochemistry and geochronology. We illustrate the diverse relations between crust and mantle in three different cratons over Gyr periods.

(i) *Crust mantle coupling:-* In the North Atlantic Craton, West Greenland, newly discovered eclogite xenoliths are of similar age to the main peridotitic lithosphere. Their elemental geochemistry shows a clear genetic relationship to the TTG crust in that region [1], providing compelling support for craton root construction via tectonic stacking.

(ii) *Crust-mantle decoupling:-* Detrital Pt-alloy grains from late Archean sedimentary basins provide robust age data to compare with depletion ages from the underlying peridotitic root. These ages are generally distinct from the main craton-building events and appear to document earlier differentiation of oceanic mantle prior to craton formation.

(iii) *Major magmatic modification of lithosphere:-*

The Slave and Kaapvaal cratons both show evidence of major magmatic crustal addition and lithospheric mantle modification/growth due to the impact of some of the planet's largest igneous events. The entire lithosphere beneath the N. Slave craton is modified by the 1.3 Ga McKenzie LIP, with significant mass addition into the deeper cratonic crust that may go undetected in zircon studies of crustal evolution.

The Kaapvaal craton has been extensively modified by the 2.0 Ga Bushveld/Malopo Farms event that left a clear compositional imprint in the Kaapvaal lithospheric mantle. In contrast, the major 1.1-1.3 Ga Namaqua-Natal crustal event left a more subtle record on the root of the central craton but more strongly affected peri-cratonic lithospheric mantle to the SW of the craton margin. In detail, multiple linked crust-mantle events are evident over the 3.5 Gyr history of this and other cratons indicating that cratonic roots are more dynamic than usually assumed.

[1] Tappe *et al*. (2011 - submitted) *Geology*.

https://doi.org/10.1180/S0026461X00006502 Published online by Cambridge University Press

Matrix effects and Hf isotope analysis of zircon by laser ablation MC-ICP-MS

NORMAN J. PEARSON[1], JUSTIN L. PAYNE[2] AND KEVIN J. GRANT[1]

[1]GEMOC/CCFS, Earth and Planetary Sciences, Macquarie University, NSW 2109 Australia (norman.pearson@mq.edu.au, kevin.grant@mq.edu.au)
[2]Centre for Tectonics, Resources and Exploration, University of Adelaide, SA Australia 5005 (justin.payne@adelaide.edu.au)

In the last decade there have been significant advances made in the *in situ* measurement of Hf isotopes in zircon and the application of the Lu-Hf isotopic system to help constrain the sources that contributed to zircon formation. The information obtained from the *in situ* Hf analysis of zircon has been used to monitor magmatic processes, to identify inherited and juvenile components in magmatic sources, and to evaluate models of crustal evolution. Despite the success of the technique, its application is still limited by the contribution to the total uncertainty by corrections for isobaric interferences, especially for zircons with high REE/Hf ratios. A significant effort has been devoted to demonstrating the robustness of correction methods for isobaric interferences of ^{176}Yb and ^{176}Lu on ^{176}Hf but little attention has been paid to the contribution of molecular interferences.

In this study the accuracy and precision of isobaric corrections and the contribution of REE-oxides on Hf isotopes are evaluated using a suite of synthetic glass beads doped with the JMC475 Hf standard and varying concentrations of Yb, Gd and Dy. The results demonstrate the robustness of the isobaric interference correction procedures for ^{176}Yb/^{177}Hf ratios greater than 0.8 (i.e. approx. three times that of ^{176}Hf/^{177}Hf ratio).

Theoretical calculations and measurement of Gd- and Dy-doped glass beads demonstrate that REE-oxides are also able to bias Hf-isotope data. Gd oxides can produce interferences on a number of Yb isotopes and Dy oxides overlap several Hf isotopes. The significance of these interferences depends on the oxide production of the mass spectrometer as well as the slope of the REE patterns (Gd/Yb) and REE/Hf ratios (Dy/Hf). The results can potentially explain a number of observed correlations between REE content of zircon and measured Hf isotope ratios. These 'matrix-effects' are most apparent in high REE zircons and in zircons with high Gd/Yb ratios and leads us to recommend monitoring of REE levels and oxide interference corrections.

Assimilation of lithospheric mantle melts by West Greenland tholeiitic magmas recorded by melt inclusions

D.W. PEATE[1]*, I. UKSTINS PEATE[1], A.J.R. KENT[2] AND M.C. ROWE[1,3]

[1]University of Iowa, Iowa City, IA 52242, USA (*correspondence: david-peate@uiowa.edu)
[2]Oregon State University, Corvallis, OR 97331, USA
[3]Washington State University, Pullman, WA 99164, USA

An issue in many flood basalt provinces is how to distinguish crustal assimilation from lithospheric mantle inputs. We have studied olivine-hosted melt inclusions in five high MgO samples (olivine separates from [1]) from the Paleocene picrite-dominated Vaigat Formation in West Greenland [2]. Melt inclusions can preserve a diversity of compositions that record petrogenetic processes taking place within the magmatic plumbing system. Inclusions were rehomogenized to glass in a 1-atm gas-mixing furnace prior to EPMA and LA-ICP-MS analysis. One sample (332788) has lower ^{143}Nd/^{144}Nd and higher ^{206}Pb/^{204}Pb than the other samples. Inclusions from the other four samples show limited compositional variability, limiting any role for crustal assimilation, and inclusions in rare high Fo% (~92) olivines are similar to inclusions in less forsteritic olivines in terms of incompatible element ratios, indicating that the high Fo% olivines are not xenocrystic. Whole rock data on more evolved flows [1] show isotopic evidence for assimilation by crust with low ^{143}Nd/^{144}Nd and low ^{206}Pb/^{204}Pb, different to the displacement trend of sample 332788. Inclusions in sample 332788 show significant compositional variability, with K/Ti varying from 0.14 to 0.33 (compared to 0.12 to 0.19 in inclusions from the other samples). Trace element data show that K/Ti in inclusions from sample 332788 correlates with incompatible element ratios such as Zr/Y and Zr/Nb but not with La/Nb and Ba/Nb that might have been expected for crustal assimilation. Small-volume, incompatible-element-enriched, alkali picrite flows, interpreted as melts of old metasomatized lithospheric mantle, are found at a similar stratigraphic level elsewhere in the province [3]. Their isotopic composition is consistent with the displacement of sample 332788 from the other samples, and their trace element composition can explain the variations in the inclusions. The presence of these melts near the surface suggests a shallow-level magma mixing model rather than assimilation during ascent through the lithosphere.

[1] Larsen *et al*. (2009) *JPet* **50**, 1667–1711. [2] Graham *et al*. (1998) *EPSL* **160**, 241–255. [3] Larsen *et al*. (2003) *JPet* **44**, 3–28.

https://doi.org/10.1180/S0026461X00006502 Published online by Cambridge University Press

D/H composition of leaf waxes from C_3 plants along a transect from the UK to central Siberia, Russia

N. PEDENTCHOUK[1]* AND K. FISHER[2]

[1]School of Environmental Sciences, the University of East Anglia, Norwich, NR4 7TJ, UK (*correspondence: n.pedentchouk@uea.ac.uk)
[2]Department of Georgraphy, the University of Leicester, UK

The δD values of individual organic compounds from leaf waxes are being increasingly used in environmental sciences. Extracting palaeoecological and palaeoclimatological information from the organic D/H signal requires a clear understanding of hydrogen isotope fractionation between the source water and biosynthates. The purpose of this work is to investigate differences in hydrogen apparent fractionation factor (ε) among several common deciduous and conifer plant species in northern Eurasia.

We determined the D/H composition of *n*-alkanes derived from leaf waxes extracted from several extant plants representing conifer (*Pinus*) and deciduous angiosperm (*Betula* and *Salix*) genera along a longitudinal transect from the UK to central Siberia in 11 locations. We also measured the δD values of tap waters collected at the same locations. The *n*-alkane and leaf water data were then used to calculate ε values. Our initial results show the following.

The δD values of *n*-C_{27} alkane from individual genera correlate with the δD values of tap water along the transect. The R^2 values for *Betula* (9 locations), *Salix* (5 locations) and *Pinus* (6 locations) are 0.95, 0.97, and 0.82, respectively. However, the ε values calculated between *n*-C_{27} alkane and tap water differ significantly among the genera: *Betula* -84‰, *Salix* -142‰, and *Pinus* -119‰. We suggest that there are at least two possible explanation that could account for such large difference in the ε values. Because of the differences in tree morphology and habitat, the plants could be using isotopically different soil water, so that *Betula* consumed soil water that underwent a larger D-enrichement than *Pinus* and *Salix*. Additionally, or alternatively, plants could vary in terms of their leaf morphology and biochemistry of photosynthesis so that the differences in biosynthate D/H composition – and thus in the ε values – arise during the processes that take place at the leaf level.

Further research involving analysis of the δD values of soil and leaf water as well as plant physiological variables at individual locations will help clarify which factors and to what extent control D/H fractionation between the individual compounds in leaf waxes and the source water.

Desorption of quinoline from clay: An investigation of the LoSal™ mechanism

C.S. PEDERSEN*, C.P. HEM AND S.L.S. STIPP

Nano-Science Center, Department of Chemistry, University of Copenhagen, Denmark (*correspondence: cspe@nano.ku.dk)

Oil recovery from reservoirs is often less than 30%; increasing this would be an efficient way of increasing the available global oil resources. In traditional water flooding, recycled reservoir brine or sea water is injected to flush out interstitial oil. When this high salinity water is substituted with low salinity water (LoSal™), oil recovery from sandstone reservoirs has been shown to increase by 5 to 15% [1]. We have investigated the interaction between aromatic base compounds, as models for crude oil, and clay to gain understanding about the mechanism behind the LoSal™ effect.

Quinoline, a model for aromatic bases in oil, was adsorbed from aqueous solution onto kaolinite and Ca-montmorillonite. The clay samples were subsequently rinsed with high (36000 ppm) or low salinity water (1400 ppm). We found that high salinity water was more than 50% more effective in removing quinoline from both kaolinite and Ca-montmorillonite. Quinoline is adsorbed as a cation and therefore increased desorption can be explained by cation exchange. These results contrast with the LoSal™ effect, suggesting that the LoSal™ effect is not associated with the adsorption of aromatic bases on clays. We are currently investigating the interaction of other functional groups and minerals in an attempt to mimic the LoSal™ effect. This is the first step toward improving understanding of oil-water-mineral interactions in reservoirs at the molecular level.

[1] Lager, Webb & Collins (2008) *SPE/DOE Symposium on Improved Oil Recovery* 113976-MS

https://doi.org/10.1180/S0026461X00006502 Published online by Cambridge University Press

A study on the effect of pore geometry on mineral changes

J. PEDERSEN[1], E. JETTESTUEN[1]*, J.L. VINNINGLAND[1], M. MADLAND[2], L.M. CATHLES III[3] AND A. HIORTH[1,2]

[1]International Research Institute of Stavanger (IRIS), P. O. Box 8046, 4068 Stavanger, Norway (*correspondence: eje@iris.no)
[2]The University of Stavanger, 4036 Stavanger, Norway
[3]Cornell University, Ithaca, New York, USA

Injection of seawater in 130°C offshore chalk oil fields will induce chemical alterations as the seawater is not in equilibrium with the formation. This has been confirmed by core experiments. Furthermore, the core experiments reveal that the chemical alteration induces enhanced compaction and enhanced oil production. Many conceptual models have been suggested for this phenomenon, but quantitative geochemical simulations on the pore scale is missing. We investigate the spatial distribution of the chemical alterations induced by seawater and $MgCl_2$ flooding at 130°C; the net chemical change in the pore space is compared with the net chemical change observed in the core experiments.

A full geochemical solver integrated with a lattice Boltzmann (LB) model is used to model the pore scale reactive flow. The LB model solves the fluid flow and the advection-diffusion of the chemical species, while the geochemical model gives the interaction between the aqua chemical species and the pore mineral-surfaces. The geochemical solver has been compared successfully with PHREEQC and effluent from core experiments. A simulation on a carbonate sample is shown in Fig.1.

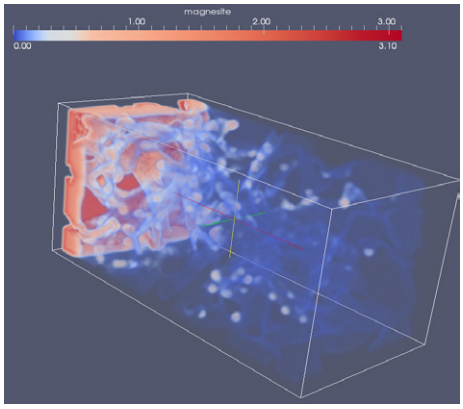

Figure 1: 0.219M $MgCl_2$ is flooded from the left at 130°C, the pore space is initial in equilibrium with distilled water. After 2 pore volumes of flooding magnesite is precipitated non-uniformly in the pore space (blue (opaque) to red (solid) colours). Only calcite is present initially.

Key impact of soil (Fe/organic C) ratio on REE shallow groundwater patterns

M. PÉDROT*, A. DIA, M. DAVRANCHE AND G. GRUAU

CNRS - UMR 6118 Géosciences Rennes, 35042 Rennes cedex, France (*correspondence: mathieu.pedrot@univ-rennes1.fr)

A number of studies have been carried out over the last two decades on the chemistry of rare earth elements (REE) in stream waters and groundwaters. They occur usually as simple REE (III) species, with the exception of Ce. Indeed, among the REE, Ce is the only element that can be oxidized to the (+IV) state, modifying its behaviour. REE are potentially used as tracers of rock/water interaction processes, groundwater flow and mixing, soil genesis, and notably, as proxies for evaluating paleoceanographic and paleoclimatic change by using Ce anomaly development.

Previous investigations of the REE geochemistry in groundwaters of the Kervidy/Coët-Dan catchment (Brittany, France) showed a systematic, topography related variation of REE signatures, notably a large negative Ce anomaly in the upper part which decreases from top to bottom of the transect. These studies also showed that REE are carried by organic colloids in these waters. A recent study showed that the strong spatial variation of negative Ce anomaly would be due to the input into the aquifer of REE-rich, Ce anomaly-free, organic colloids located in the uppermost, organic-rich soil horizons. Consequently, one major question arises: why organic colloids show a large negative Ce anomaly at the top and Ce anomaly-free at the bottom?

In this context, soil/water interactions performed through soil column experiments, were carried out with several soil samples recovered from top to bottom of two toposequences to understand the origin of the variability of REE patterns in the Kervidy/Coët-Dan catchment. The major carriers phases of the REE pools were determined. Moreover, batch experiments were carried out to investigate the role of organic molecules in the development of Ce anomaly in solution.

The results showed: (i) a strong Ce sequestration in oxidized phases such as secondary minerals formed at the frond of altered shale, (ii) a close relationship between soil Fe/Organic C ratio and Ce anomaly in soil solution. Moreover, this study showed (iii) the strong influence of organic molecules in the lack of Ce anomaly in waters by Fe oxyhydroxide dissolution. Furthermore, the REE signature in the Kervidy/Coët-Dan groundwaters appears to be provided in major part by the upper horizon of soil.

https://doi.org/10.1180/S0026461X00006502 Published online by Cambridge University Press

Oxygen isotope analysis of experimental glasses by SIMS: A calibration attempt

K. PEDROZA[1], E.M. JOLIS[1], V.R. TROLL[1,2], C. FREDA[2], C. HARRIS[3], F.M. DEEGAN[1], M.J. WHITEHOUSE[4], I. BINDEMAN[5], H. ANNERSTEN[1] AND B. ELLIS[6]

[1]Dept. of Earth Sci (CEMPEG), Uppsala University, Sweden (kirsten.pedroza@geo.uu.se)
[2]Istituto Nazionale di Geofisica e Vulcanologia, Rome, Italy
[3]Dept. Geol. Sci, University of Cape Town, South Africa
[4]Swedish Museum of Natural History, Stockholm, Sweden
[5]Dept. Geol. Sci, University of Oregon, USA
[6]School Earth & Enviro. Sci., Washington State University, USA

Analysis of oxygen isotopes in minerals is increasingly performed by Secondary Ionisation Mass Spectrometry (SIMS) [1, 2, 3, 4]. However, the application of SIMS to analyse $\delta^{18}O$ values in silicate glasses has been limited due to calibration difficulties related to the highly variable chemical composition of different glasses. In response to this problem, we have initiated the synthesis of a set of glass standards, selected natural samples and other existing experimental glasses [5] for a large-scale calibration program. To date we have fused a series of natural rhyolitic and phonolitic rock powders to produce the first experimental glasses, which have been tested for homogeneity by Electron Microprobe (EMP). We subsequently determined their $\delta^{18}O$ values using: a) a conventional silicate oxygen extraction line, b) laser fluorination and c) SIMS. The data we present here complements other recent SIMS studies of silicate glasses [6] and represent the first stage in our long-term efforts to develop a new SIMS analytical protocol. We plan to expand our glass standards to encompass intermediate to mafic glass compositions. Ultimately this work will significantly contribute to the fields of oxygen isotope geochemistry by SIMS, which can be used not only to study glasses in natural and synthetic systems [e.g. 7, 8], but will have a wide utility for geochemistry and geology in general.

[1] Valby & Kita (2009) *SIMS in the Earth Science* **41**, 19–63. [2] Valby (2003) *Rev. Mineral. Geochem.* **53**, 343–385. [3] Whitehouse & Nemchin (2009) *Chem. Geol.* **261**, 32–42.[4] Bindemann *et al.* (2008) *Geochim. Cosmochim. Acta*, **71**, 4397-4420. [5] Jochum *et al.* (2006) *Geochem. Geophys. Geosyst.* **7**, Q02008. [6] Ickert *et al.* (2008) *Chem. Geol.* **257**, 114–128. [7] Deegan *et al.* (2010) *J. Petrol.* **51**, 1027–1057. [8] Jolis *et al.* (2011) *Geochim. Cosmochim. Acta*, this issue.

Early Cretaceous bimodal magmatism in Tonghua area, Jilin province, China: Implications for the destruction of the North China Craton

F.P. PEI, W.L. XU, F. WANG, H.H. CAO AND S.M. LU

College of Earth Sciences, Jilin University, Changchun 130061, China (peifp@jlu.edu.cn,xuwl@jlu.edu.cn)

Chronological, geochemical and zircon Hf isotopic data of the Early Cretaceous granitoids, diabases, and gabbros in the Tonghua area, Jilin province, China, provide insights into the spatial extent of the destruction of the North China Craton (NCC). LA-ICP-MS zircon U-Pb dating results indicate that the granitoids, disbases, and gabbros emplaced in the Early Cretaceous (115-134 Ma), consistent with the timing of the intensive magmatism in eastern China in the Mesozoic [1].

The Early Cretaceous granitoids consist chiefly of granite-porphyry. Chemically, they display high SiO_2, and rich in alkali and are characterized by enrichment in LREEs and LILEs, and depletion in HREE, and Ba, P, Ti and Eu, smilar to A-type granite. ε_{Hf} (t) values and Hf model ages of zircons from the granitoids range from -10.8 to -20.8 and from 1.9Ga to 2.5Ga, respectively, indicating that they were mainly derived from the partial melting of the Neoarchean-Paleoproterozoic basement rocks within the NCC.

In contrast, the Early Cretaceous diabases and gabbros exhibit low SiO_2 and high Mg#, and high Cr, Ni and Sc contents, and are characterized by enrichment in LILEs, depletion in HFSEs and P, and no Eu anomaly. They belong chemically to tholeiitic series. The above-mentioned geochemical data indicate that these mafic igneous rocks could be derived from partial melting of the metasomatized lithospheric mantle.

The Early Cretaceous granitoids, diabase, and gabbro in the Tonghua area consititute a bimodal igneous rock association, implying an extensional setting. Combined with the researches on the coeval granitoids and mafic-ultramafic rocks in eastern Liaoning Peninsula [1, 2], we propose that the spatial extent of the NCC destruction should include the northeastern segment of the NCC.

This research was financially supported by the Natural Science Foundation of China (Grant 40872049 and 90814003) and the Chinese Ministry of Education (200801831102).

[1] Wu *et al.* (2005) *Earth Planet. Sci. Lett.* **233**, 103–119. [2] Pei *et al.* (2011) *J.Asian Earth Sci.* **40**, 636–650.

https://doi.org/10.1180/S0026461X00006502 Published online by Cambridge University Press

Hydrological constraints for biogeochemical processes in acidic mining lakes

STEFAN PEIFFER

Department of Hydrology, University of Bayreuth, Germany (s.peiffer@uni-bayreuth.de)

Recovery or remediation of acidic mining lakes (AML) is severly impeded through the occurrence of schwertmannite, its transformation and an associated acidity-driven iron cycle that prevents generation of alkalinity [1]

This concept was derived based on evaluuation of sediment pore water data using a diffusion-controlled reactive-transport approach. It has, however, been demonstrated that ground water dynamics may have severe effects on the biogeochemical processes in sediments [2]. In this presentation I will therefore discuss some general aspects as to how hydrological processes interfere with biogeochemical process. Examples that will be discussed are

- The inflow of sulfate load on acidity formation from percolated sedimentary schwertmannite.

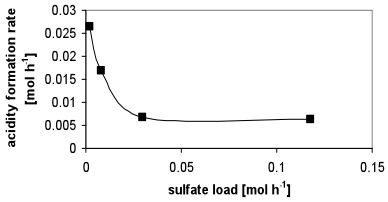

Figure 1: Acidity formation rate as a function of sulfate load measured in column experiments with schwertmannite (data from [3].

- The effect of flow rate on competition between chemical (through sulfide leading to fixation of iron sulfides) and microbial (amplifying the acidity driven iron cycle) reductive dissolution of iron oxides.

- The spatial decoupling between oxidaton of ground-water borne Fe(II) in lake water and and the precipitation of schwertmannite through lake-water travel-path controlled reaction kinetics.

Implications of ground-water flow on biogeochemical processes in an AML will be discussed in a companion paper [4].

[1] Peine, Küsel, Tritschler, Peiffer (2000) *Limnol Oceanogr* **45**, 1077–1087. [2] Blodau (2005) *Acta Hydrochim. Hydrobiol.* **33**, 104–117. [3] Blodau & Knorr (2006) *J. Geophysic. Res.* **111**, G0202610.1029/2006JG000165. [4] Beer *et al. this session*.

High resolution sulfur isotope analyses across sulphate-methane transition zone

A. PEKETI AND A. MAZUMDAR*

Geological Oceanography, National Institute of Oceanography, Donapaula, Goa, 403004, India (*correspondence: maninda@nio.org)

We report here for the first time high resolution pyrite sulfur isotope ratios from Bay of Bengal. Pyrite from the sediment samples was extracted following chromium reduction method. Prior to CRS extraction, elemental sulfur and acid volatile sulphide were extracted using acetone and 6N HCl respectively. Two 30m long sediment cores, MD161-13 and MD161-8 were recovered at water depths of 647m and 1033 m respectively on-board *Marion Dufresne*. The cores were collected as part of our on going methane hydrate exploration program in the Krishna-Godavari basin. The CRS content at MD161-13 increases from 0.005 to 0.26 wt% down depth. CRS content varies from 0.04 to 0.41 wt% in the top 7.3 m at MD161-8. Below this depth CRS content shows marked fluctuations. Figure-1 shows the sulfur isotope ratios observed at the two locations. In both the cores $\delta^{34}S_{CRS}$ values increases with depth below seafloor. Highly depleted sulfur isotope ratios (-36 to -44‰ VCDT) at MD161-8 are attributed to sulfide oxidation and disproportionation of intermediate sulfur compounds. Sulfate limitation due to burial diagenesis resulted in enrichment in sulfur isotope ratios above SMTZ. Across SMTZ, $\delta^{34}S_{CRS}$ increases sharply due to sulfate reduction by anaerobic methane oxidation. AMO cause rapid sulfate limitation.

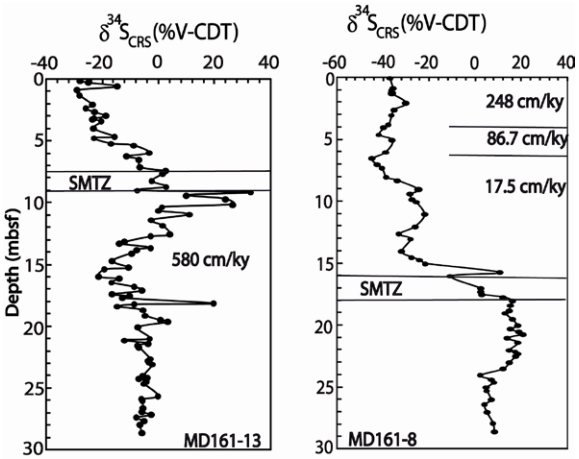

Figure 1: $\delta^{34}S$ of CRS in MD161-8 and MD161-13.

https://doi.org/10.1180/S0026461X00006502 Published online by Cambridge University Press

Insights on ocean acidification from instrumental monitoring and experiments in aquaria

C. PELEJERO[1], J. MOVILLA[2], E. CALVO[2], R. COMA[3], E. SERRANO[3], M. RIBES[2] AND E. FERNÁNDEZ-GUALLART[2]

[1]ICREA and Institut de Ciències del Mar, CSIC, Pg. Marítim de la Barceloneta 37-49, Barcelona, Catalonia, Spain (*correspondence: carles.pelejero@icrea.cat)
[2]Institut de Ciències del Mar, CSIC, Pg. Marítim de la Barceloneta 37-49, Barcelona, Catalonia, Spain
[3]Centre d'Estudis Avançats de Blanes, Accés Cala Sant Francesc 14, Blanes, Girona, Catalonia, Spain

The anthropogenic rise in atmospheric CO_2 is driving fundamental and unprecedented changes in the chemistry of the world's oceans, with detrimental consequences for a wide variety of marine organisms. In this presentation I will review recent advances in our understanding of ocean acidification, with a focus on the Mediterranean Sea, from an integration of new data on high frequency variability of seawater chemistry and on the outputs from a suite of pH manipulative experiments in aquaria. Over the last centuries, paleoreconstructions of seawater pH in coral reefs have shown a certain degree of interdecadal variability. In coastal sites of the Mediterranean, from data measured using autonomous systems, we have also detected significant changes in seawater pH on the order of hours to days, possibly linked to vertical mixing and movement of water masses. To complement this information on natural variability, we have undertaken several experiments of pH manipulation, some of which are currently underway. I will show results from a first experiment of several months of duration on two species of Mediterranean corals, *Cladocora caespitosa* and *Oculina patagonica*, which have confirmed the expected decrease in skeletal growth with decreasing pH. In addition, a second experiment with the Mediterranean sponges *Chondrosia reniformis*, *Agelas oroides* and *Dysidea avara* has shown a varying species response. In this last experiment, changes in the abundance and diversity of sponge associated bacteria are being assessed, to seek for clues on possible groups that may be benefitted from ocean acidification.

Fe-poor and sulfide-rich: Mangrove Lake as a Precambrian analogue?

ANDRÉ PELLERIN[1]*, BOSWELL WING[1], THI HAO BUI[1], ALFONSO MUCCI[1], MIKAELLA ROUGH[1] AND DONALD E. CANFIELD[2]

[1]Departement of Earth and Planetary Sciences, McGill University, Montreal, Quebec, H3A 2A7, Canada (*correspondence: andrepellerin@gmail.com)
[2]Institute of Biological Sciences, Odense University, Campusvej 55, 5230 Odense M, Denmark

Minor sulfur (S) isotopes produce an integrated picture of biogeochemical S cycling through metabolism-specific deviations from reference isotope fractionations, and have become a recent tool in investigating the biogeochemical state of Precambrian oceans. We used this tool to investigate the S cycle of Mangrove Lake, Bermuda: a permanently stratified lake characterized by high levels of algal-derived organic matter (up to 32mM) and high sulfide concentrations (>15mM) below a wind-mixed layer. The sulfate concentration in the mixed layer is controlled by infiltration of seawater from the nearby ocean (~400 m), and is characterized by a $\delta^{34}S$ ~22‰, and $\Delta^{33}S$ ~0.04‰. Sulfate is nearly depleted 30 cm below the mixed layer, with $\delta^{34}S$ values approaching 80‰ and $\Delta^{33}S$ values of ~0.11‰. Proxies for sulfate in the Precambrian oceans that exhibit similar isotopic characteristics have been taken as evidence for a microbially complex marine S cycle, with active S re-oxidation and disproportionation. Nevertheless, we can nearly reproduce our $\Delta^{33}S$- $\delta^{34}S$ trajectories with a simple 1-D diffusion-reaction model that only considers microbial sulfate reduction. We will explore whether this apparent discrepancy represents the peculiar mechanisms of sulfide removal in Mangrove Lake, the inappropriate application of model parsimony, or limitations of retrodicting Precambrian oceanic conditions from modern analogue environments.

https://doi.org/10.1180/S0026461X00006502 Published online by Cambridge University Press

Influence of dust deposits to the budget of U-series nuclides in mount Cameroon basaltic soils

E. PELT[1], F. CHABAUX[1], C. INNOCENT[2], B. GHALEB[3] AND P. STILLE[1]

[1]LHYGES Strasbourg, UDS/CNRS, France
[2]BRGM Orléans, France
[3]GEOTOP Montréal, Canada

The timescale of soil formation can be inferred from U-series disequilibria. This requires a complete comprehension of sources and fractionation of U-series nuclides during soil formation processes [1]. Usually, aeolian inputs are not considered to be an important source of U-series nuclides in soils. We therefore propose to evaluate the impact of dust deposition on U-series nuclides in soils, by working on present and paleo-soils from the mount Cameroon volcano. Sr-Nd-Pb isotopic data for these samples have documented significant inputs of Saharan dusts in these soils [2]. Comparison of ^{238}U-^{234}U-^{230}Th isotopic data with Sr-Nd-Pb isotopic ratios indicates a significant impact of the dust inputs onto U-Th budget of the soils, with a mean value of 15% dust contribution for both U and Th. The dust pool estimate for both U-Th concentrations and U-Th isotope ratios is compatible with data obtained on Saharan dusts collected in Barbados [3]. However, according to U/Th elemental ratios, a secondary uranium migration associated with chemical weathering has affected both soils and paleo-soils. The quantification of this small U mobile pool (~10%) highlights that in this context the effect of dust accretion onto U-Th budget in soils can be as important as chemical weathering effect. This conclusion means that atmospheric dust cannot be systematically neglected in chemical weathering studies using U-series nuclides. Nevertheless, in basaltic terrains of mount Cameroon large dust inputs from continental crust of Sahara with high U-Th content contaminate soils with low U-Th contents. In other contexts where dust inputs are lower, or the soils more concentrated in U and Th, the dust contribution might not significantly influence U-series chronometry.

[1] Chabaux *et al*. (2011) *Applied Geochemistry*, In press. [2] Dia *et al*. (2006) *Chem. Geol*. **226**, 232–252. [3] Rydell H.S. & Prospero J.M. (1972) *EPSL* **14**, 397–402.

Organic geochemistry of mudstones in the Upper Permian Linxi Formation, NE China: Implications for hydrocarbon-forming potential in the Late Paleozoic strata

X.L. PENG*, L. LIU, N. LIU AND X.P. ZENG

College of Earth Sciences, Jilin University, Changchun, 130061, China (*correspondence: Pengxl@jlu.edu.cn)

It has been a hotly discussed issue whether the Late Paleozoic strata in the Xing-Meng orogenic belt (NE China) have hydrocarbon-forming potential or not. However, organic geochemical data of the mudstones from the Upper Permian Linxi Formation in northeastern Inner Mongolia provide insights for that. The Upper Permian Linxi Formation consists mainly of dark mudstone, shale, siltstone, fine sandstone. The thickness of the mudstones in the Formation is about 276 m in Solon. Organic geochemical analytical results for 30 mudstone samples indicate that their residual organic carbon contents range from 0.45~3.55% (average 1.09%). TOC values for about 87% samples are over threshold of the organic matter abundance (0.5%), and TOC values for about 73% samples are more than 0.6%, suggesting that the source rocks are of the midium-good hydrocarbon-forming potential. The organic matter includes sapropelinite and vitrinite, with a typical kerogen type of II_1-II_2. The Ro values range from 1.57% to 2.71%, and the maximum pyrolysis temperature is 475~507°C (average 488°C). Taken together, it is suggested that the source rocks are high maturity. Combined with the high-evolutionary hydrocarbon source rocks from the Tarim and Sichuan basins, we consider that the Upper Permian Linxi Formation could have the gas-forming potential, and that the marine source rocks from the Late Paleozoic strata in NE China could be of a good hydrocarbon -forming prospects.

This research was financially supported by the Natural Science Foundation of China (40972075) and the Strategic Research Center of Oil & Gas Resources (14B09XQ1201).

https://doi.org/10.1180/S0026461X00006502 Published online by Cambridge University Press

The fluid inclusion characteristics and metallogenic mechanism of Dashui Gold Deposit in Gansu Province, China

XIUHONG PENG[1,2], JIANGSU ZHANG[3], HUI DENG[4]*, YUAN HU[1], CHENGSHI QING[1] AND LIUYI ZHANG[5]

[1]Geochemistry Dep., Chengdu University of Technology China
[2]Key Laboratory of Nuclear Techniques in Geosciences, China
[3]Third Geology and Mineral Resources Exploration Academy of Gansu Province, Lanzhou, China (*correspondence: dh@cdut.edu.cn)
[4]State Key Laboratory of Geohazard Prevention and Geoenvironment Protection, Chengdu University of Technology
[5]Institute of Geology, China Earthquake Administration

Dashui Gold Deposit in Maqu, Gansu found in west Qinling mountain area is a gold deposit with extra unique mineralization characteristics. Ore bodies mainly outcrop in the hematitization silicified limestone, hematitization silicified granodiorite and their contact zone. The ores are red, brown and very poor in sulfides.

Hydrothermal calcite veins within the mining area are well developed. They are closely associated with gold mineralization temporally and spatially, and often constituting the roof and floor of ore bodies. According to the calcite veins' spatial output form, crystal habits and the relationship with gold mineralization, the process can be divided into three stages, and the calcite from second stage is closely related to mineralization. In this research there were total 12 inclusion samples collected, two calcite samples from first stage, seven from second stage and three from the third stage.

The inclusion characteristics of Dashui Gold Deposit indicate that ore-forming temperature is bounded up with metallogenic depth. The maximum metallogenic depth in 3490m middle section is 0.59km with a maximum ore-forming temperature 370.1°C. The metallogenic depth of 3530m middle section is low. There are two samples collected from 0.29km and 0.30km separately with low ore-forming temperatures 168.2°C and 168.3°C of each other. This indicates that the the ore-forming fluid was upward migrating from the depth.

Regnonally the ore-forming temperature of fluid is decreasing from east to west. The average homogeneous temperature of east zone is 240.66°C, the general temperature are 217.4°C, 243.7°C and 276.3°C. The west zone's is decreasing to 174°C, showing that the migration of ore-forming fluid was from east to west. The ore-forming temperature can be divided into three intervals: 370.1°C, 217.4°C-276.3°C and 168.2°C-174°C, which can also stand for three metallogenic stages

The solubilities and phase diagram of the aqueous system containing with vanadate at 298 K

Y. PENG[1,2] AND Y. ZENG[1,2]*

[1]College of Materials and Chemistry & Chemical Engineering, Chengdu University of Technology, Chengdu, Sichuan, P. R. China.
[2]Mineral Resources Chemistry Key Laboratory of Sichuan Higher Education Institutions, P. R. China (*correspondence: zengyster@gmail.com)

The solubility of vanadium in soil solution is effected by coexisting ions in soil, such as potassium, sodium, phosphorus and so on. In this article, the solubility of the metavanadate coexists with them has been determined. The phase equilibria of the quaternary system Na^+, K^+// VO_3^-, $H_2PO_4^-$ - H_2O were studied at 298 K using an isothermal dissolution equilibrium method.

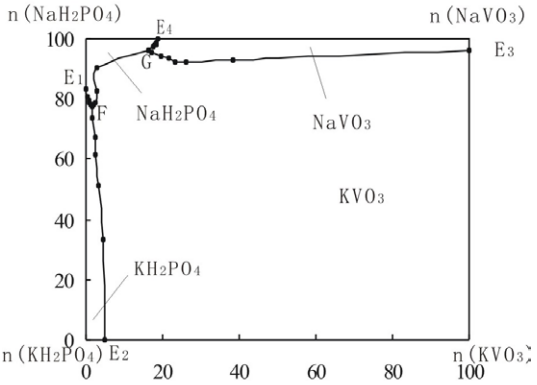

Figure 1: The solubility isotherms of the quaternary system Na^+, K^+// VO_3^-, $H_2PO_4^-$ - H_2O at 298 K

The phase diagram, as shown in Figure 1, is consists of four crystallization fields, five univariant curves, and two invariant points. No double salt or solid solution was formed at research temperature. The crystallizing field of KVO_3 is larger than that of $NaVO_3$, which indicates the solubility of KVO_3 is smaller than that of $NaVO_3$. In this weakly acid system, the crystallization form of metavanadate is polyoxovanadate. The dissolution and migration of vanadium in aqueous solution has negative correlation with dihydrogen phosphate ion.

The authors acknowledge the support of the Program for New Century Excellent Talents in University (NCET-08-0900) and the National Nature Science Foundation of China (No. 40673050).

https://doi.org/10.1180/S0026461X00006502 Published online by Cambridge University Press

Boron proxy evidence for surface ocean acidification & elevated pCO_2 during the PETM

DONALD E. PENMAN[1], JAMES C. ZACHOS[1], BÄRBEL HÖNISCH[2], STEPHEN EGGINS[3] AND RICHARD E. ZEEBE[4]

[1]Earth & Planetary Sciences, University of California, Santa Cruz, CA 95064 USA (dpenman@ucsc.edu)
[2]LDEO of Columbia University, 61 Route 9W Palisades, NY 10964 USA
[3]Research School of Earth Sciences, ANU, Canberra 0200, ACT, Australia
[4]Dept. of Oceanography, University of Hawaii at Manoa, Honolulu, HI 96822 USA

The Paleocene-Eocene Thermal Maximum (~55Ma) is recognized as a rapid (<10ka) input of a large mass (~4500-6000 GtC) of ^{12}C-enriched carbon into the ocean-atmosphere system. Patterns of $CaCO_3$ dissolution at the suggest that this was accompanied by a rapid decrease in ocean pH, followed by a gradual recovery phase. A further result of such modeling studies is the suggestion of an 'overshoot' or supersaturated ocean phase after the recovery, when the carbonate lysocline deepened to below its Paleocene depth and surface water carbonate saturation states rose to above pre-excursion levels. In an effort to quantify changes in the carbonate chemistry of surface waters and infer potential effects on calcifying organisms and Mg/Ca and $\delta^{18}O$-based temperature estimates, we have measured B/Ca and Mg/Ca in mixed-layer planktic foraminifers from IODP site 1209 in the Pacific and sites 1262 and 1263 in the Atlantic. Previous work at these sites has documented large increases (~50%) in Mg/Ca ratios in the mixed-layer planktic foraminifer species *M. velascoensis* and *A. soldadoensis* consistent with 5 to 6°C of sea surface warming. Our B/Ca measurements in both species suggest a large drop in surface water pH and $[CO_3^=]$ coincident with the rise in temperature at the onset of the carbon isotope excursion, followed by a gradual recovery to pre-excursion levels. The latter feature, coupled with the rise in total alkalinity caused by the dissolution of $CaCO_3$ is taken as evidence of an overshoot phase starting ~100ka after the onset of the event. We are currently measuring boron isotopes in the same taxa in order to quantify the pH changes suggested by the B/Ca data. Additionally, we plan to measure B/Ca and $\delta^{11}B$ in thermocline-dwelling planktic species in order to examine the depth-dependence of the pH changes. Estimating the magnitude of the pH drop at the onset of the event will facilitate calculations of the mass and rate of carbon input that triggered the PETM, as well as the magnitude of change in atmospheric pCO_2 levels and Paleogene climate sensitivity.

Can multiple sulfur isotopes be used as a tracer of sub-continental lithospheric mantle in the Bushveld?

S.C. PENNISTON-DORLAND[1]*, J. FARQUHAR[2], G.J. POLLEY[1], E.A. MATHEZ[3] AND J.A. KINNAIRD[4]

[1]Department of Geology, University of Maryland, College Park, MD 20742, USA (*correspondence: sarahpd@umd.edu)
[2]Department of Geology and ESSIC, University of Maryland, College Park, MD 20742, USA
[3]Department of Earth and Planetary Sciences, American Museum of Natural History, New York, NY, 10024, USA
[4]Department of Geological Sciences, University of the Witwatersrand, Private Bag 3, Johannesburg, Wits, 2050, South Africa

The Bushveld Complex (BC) is the world's largest layered intrusion and contains most of its reserves of platinum group elements. The ultimate source of BC magma is thought to have been the mantle. Strontium, Nd and Os isotopic compositions of BC rocks are heterogeneous, however, and along with O isotopes indicate a source contaminated by sedimentary-derived material. Sub-continental lithospheric mantle (SCLM) has been proposed as a source of some of these anomalies. The multiple S isotopic composition of primitive mantle is thought to be $\Delta^{33}S = 0 \pm 0.01‰$ (1σ). Thirty whole-rock and sulfide separate analyses from a variety of locations within the BC have positive $\Delta^{33}S$ values, with an average $\Delta^{33}S = 0.13 \pm 0.05‰$(1σ). Since high-temperature processes are not thought to produce significant change in $\Delta^{33}S$, this high $\Delta^{33}S$ indicates that the BC sulfur contains a sedimentary or surface-derived component. There are geographic and stratigraphic variations in $\delta^{34}S$ and $\Delta^{33}S$ possibly reflecting hydrothermal alteration and/or localized wall rock interaction. Platreef $\delta^{34}S$=+2.7 to +9.2‰, $\Delta^{33}S$=0.03 to 0.26‰; Main Zone $\delta^{34}S$=-3.5 to -1.6‰, $\Delta^{33}S$=0.1 to 0.2‰; UG2 and Merensky Reef $\delta^{34}S$=-6.2 to +3.2‰, $\Delta^{33}S$=0.05 to 0.15‰. We are measuring the $\Delta^{33}S$ of Premier kimberlite mantle xenoliths to evaluate the hypothesis that SCLM has a non-zero $\Delta^{33}S$.

https://doi.org/10.1180/S0026461X00006502 Published online by Cambridge University Press

Control of charge and orbital order at the Fe_3O_4(001)-surface via adsorbates: Insights from density functional theory calculations

R. PENTCHEVA[1]*, N. MULAKALURI[1,2] AND M. SCHEFFLER[3]

[1]Dept. of Earth and Environmental Sciences, University of Munich, Theresienstr. 41, 80333 Munich, Germany (*correspondence: Rossitza.Pentcheva@lrz.uni-muenchen.de)
[2]Insitute of Solid State Research, Research Center Jülich, Leo-Brandt-Straße, D-52428 Jülich, Germany
[3]Fritz-Haber-Institut der Max-Planck-Gesellschaft Faradayweg 4-6, D-14195 Berlin, Germany

Besides being a potential spintronics material magnetite plays an important role in a number of environmental processes. As the surface reactivity depends critically on the electronic state of the mineral surface, we explore the interaction of water and hydrogen with the Fe_3O_4 (001)-surface using density functional theory (DFT) calculations with an on-site Coulomb repulsion term (GGA+*U*). The surface phase diagram compiled in the framework of *ab -initio* thermodynamics shows dissociation of isolated water molecules especially at oxygen vacancies and a crossover to a partial dissociation with chains of alternating H_2O and OH groups stabilised by hydrogen bonding with increasing oxygen and water pressures [1]. The DFT results reveal that defects and adsorbates induce a unique charge and orbital order at the Fe_3O_4 (001) surface: While the clean, water and OH-covered surfaces exhibit an exclusively Fe^{3+} surface layer with Fe^{2+}, Fe^{3+} ordering in the deeper layers [1], hydrogen adsorption can be used to reduce the surface layer to Fe^{2+} [2] with implications for the catalytic activity of the mineral surface, as well as the spin-polarization of carriers.

[1] N. Mulakaluri, R. Pentcheva, M.Wieland, W. Moritz & M. Scheffler (2009) *Phys. Rev. Lett* **103**, 176102. [2] G. S. Parkinson, N. Mulakaluri, Y. Losovyj, P. Jacobson, R. Pentcheva, & U. Diebold (2010) *Phys. Rev. B* **82**, 125413.

Decarbonation of subducting slab at subarc depth: Experimental modeling

A.L. PERCHUK[1,2]*, O.S. KOREPANOVA[2] AND V.O. YAPASKURT[1]

[1]Lomonosov Moscow State University, Geological Faculty, Moscow, Russia (*correspondence: alp@geol.msu.ru)
[2]Institute of Experimental Mineralogy, RAS, Chernogolovka, Moscow DC, Russia

We present UHP experimental results that model H_2O-CO_2 fluid release from the natural analogues of the oceanic crust and the mantle wedge. The experiments were conducted with two layer 'sandwich' materials consisting of calcite-bearing blueschist (BS) and olivine (OL) and three layer 'sandwich' with siliceous marble layer in between BS and OL. The experiments were carried out at 2.7 GPa under the conditions of imposed temperature gradient of ac. 40-50 ºC/mm so that to keep GS at the lower temperatures conditions than the OL [1]. The maximum temperature at the top of the capsules was 1000 °C. P-T conditions at the bottom of the capsules were corresponded to so-called 'hot' subduction zones.

The experiments reveal crucial role of hyrous fluid on decarbonation of calcite (the only carbonate in the starting materials) and contrasting behaviour of CO_2 in different types of sandwich materials. Aqueous fluid was produced mainly by the reaction of glaucophane breakdown: glaucophane => omphacite+quartz±Ca-Na amphibole+H_2O operated in the both types of sandwiches. Flux of H_2O (and solutes like Si, Al etc) in the OL zone of the two layer sandwich was resulted in the development of the Al-bearing orthopyroxene layer at contact with the glaucophane zone. Some of the released CO_2 was stored within abundant vermicular magnesite randomly distributed among olivine crystals above the orthopyroxene layer. Such magnesite occurrences are rare in the olivine from the three layer sandwich. However, upward migration of the H_2O-bearing fluid through the marble in this sandwich was resulted in the formation of ultrahigh pressure metasomatic column which consists of 4 zones: Fe-Mg-Ca carbonate| dolomite | diopside | magnesite in between the marble and OL, respectively. Multiple clinochlore flakes in lower part of the OL zone also witnesses migration of the hydrous fluid.

Storage of CO_2 in the mantle wedge minerals at the subarc depth may have valuable effect on an imbalance in the carbon budget in subduction zones. Further investigation of the slab-mantle interaction is necessary to explain existing discrepancies.

[1] Perchuk & Korepanova (2011) *Doklady Earth Sciences* **437**, 393–395.

https://doi.org/10.1180/S0026461X00006502 Published online by Cambridge University Press

Impact of water sources and flow paths on carbon in streams of seasonally snow-covered catchments

JULIA PERDRIAL[1]*, PAUL BROOKS[2], JON CHOROVER[1], ADRIAN HARPOLD[2], INGO HEIDBUECHEL[2], JENNIFER MCINTOSH[2], JAMES RAY[3] AND XAVIER ZAPATA-RIOS[2]

[1]University of Arizona, SWES, Tucson, AZ, USA (*correspondence: jnperdri@email.arizona.edu)
[2]University of Arizona, HWR, Tucson, AZ, USA
[3]University of Puget Sound, Tacoma, WA, USA

Stream waters from seasonally snow-covered catchments of the Jemez River Basin Critical Zone Observatory in northern New Mexico are characterized by two distinct main water sources. While groundwater from deeper flow paths dominates the streams throughout the year, snowmelt and monsoon inputs additionally enter the streams through shallow soil flow paths. To investigate how changes in water sources influences dissolved carbon characteristics, 5 flumed streams at catchment outlets located around Redondo peak were sampled 10 times between March and October 2010 to analyze for total dissolved organic and inorganic carbon (DOC and DIC), DOC quality and stable isotopes of DIC. Stream water DOC showed a flushing pattern in all catchments, with highest concentrations during peak snowmelt and low concentrations during the dry season. $SUVA_{254}$ confirms presence of organic soil constituents of lignin based precursors during snow melt and monsoon season. Preliminary results of organic matter (OM) PARAFAC quantification identified a component with fluorescence in region II that dominates when shallow flow paths are activated. DIC concentrations show a dilution pattern with low concentrations during snowmelt. $\delta^{13}C$ values of DIC progressively increase with time since snowmelt, suggesting increasing inputs of groundwater enriched in ^{13}C, possibly from microbial cycling of carbon in long transit time reservoirs. In waters from deeper flow paths, low $SUVA_{254}$ values and a PARAFAC component with fluorescence in region I dominate. Those results indicate that differences in source waters, flow paths and residence times have important impacts on stream water carbon characteristics.

Predicting the fate of radionuclides at the Hanford tank farm using analog sediments

N. PERDRIAL[1]*, A. THOMPSON[2], N.A. RIVERA[3], Y.-T. DENG[2], P.A. O'DAY[3] AND J. CHOROVER[1]

[1]SWES, University of Arizona, Tucson, AZ 85721, USA (*correspondence: perdrial@email.arizona.edu)
[2]Crop and Soil Science, University of Georgia, Athens, GA 30602, USA
[3]School of Natural Sciences, University of California, Merced, CA 95343, USA

Due to challenges in studying *in situ* samples induced by the extreme conditions encountered at the USDOE facility at Hanford (WA, USA) and in order to predict the impact of the cleanup strategy on contaminant transfer, we investigated the geochemical behavior of Hanford sediments impacted by a synthetic tank waste (i.e. 'analog contaminated sediments') before and after removal of the waste source.

The reaction of pristine Hanford sediments with synthetic waste containing Sr, Cs and I led to the producion of 8 analog sediments reflecting different contamination scenarios. Amongst the variables tested (contaminant concentrations, pCO_2, reaction time), the level of trace contaminant had the greatest effect on the mineral transformation reactions that gave rise to sequestration of Sr and Cs. Reaction product formation was correlated with trace contaminant (mM vs. μM) concentration. Sodalite/cancrinite formation at μM levels and chabazite formation at mM levels affected the binding environment of incorporated Sr and Cs.

The effect of source removal was investigated by infiltrating the sediments with a synthetic porewater solution that reflected aquifer recharge, and monitoring elemental release in dissolved and colloidal pools, as well as solid phase transformation, over time. The observed release mechanisms helped constrain a contaminant transport model used as a predictive tool for contaminant release at Hanford. Contaminant stability differed according to the reaction time and contaminant levels, consistent with neophase ripening and structural modifications occuring during desorption. Cs and Sr release depended on neophase stability, whereas I was rapidly desorbed Elemental release monitored during wet-dry cycling did not significantly modify desorption rates. Sr particulate ($Ø < 20\mu m$) transport was observed in some cases.

The observation of contaminant dynamics in analog Hanford sediments helps predict the fate of contaminants, and highlights the strong potential for long-term natural sequestration of Sr and Cs (not I) after retrieval of the sources.

https://doi.org/10.1180/S0026461X00006502 Published online by Cambridge University Press

Uranium mobility in the Beiras granite (Central Portugal): Implications for radon exhalation

A.J.S.C. PEREIRA AND L.J.P.F. NEVES

IMAR-CMA, Department of Earth Sciences, University of Coimbra (apereira@dct.uc.pt, luisneves@dct.uc.pt)

The medium to coarse grained porphyritc biotite granite of the Beiras region is the dominant facies of a late Hercynian batholith outcroping in Central Portugal, associated with a large number of secondary uranium mineralizations exploited in the past (*ca*. 60). Geochemical and isotopic data indicates that it is a moderately evolved rock, slightly peraluminous, and likely originated from a heterogeneous portion of the lower crust. It's accessory mineralogy includes uraninite, which is a likely primary source for the thousands of local uranium anomalies detected in the region, usually associated with fault filling materials and metasedimentary rocks of the contact aureole and enclaves.

A total of 18 representative samples from the batholith were collected, 16 of granite and 2 of hornfelses. Granitic samples include fresh rock, some stages of slight and moderate weathering and also specimens showing hydrothermal alteration, characterized by the development of pink/red feldspars and strong chloritization; some of these last samples were colected in the vicinity of the Cunha Baixa old uranium mine. Thin sections coupled with mica detectors were prepared and irradiated with fast neutrons in a nuclear reactor. The study of fission tracks produced by ^{235}U decay and recorded in the mica detectors allowed to study the mineralogical distribution of U. In parallel, ^{226}Ra activity and total U concentration was estimated for all samples using a 3x3" Ortec NaI(Tl) gamma ray spectrometer; radon exhalation rate was determined placing the same samples inside sealed containers of known volume and measuring the radon activity in the air of the container after equilibrium being achieved (*ca*. 4 weeks) with an Alphaguard monitor.

Uranium concentration in the samples shows a wide range of variation, from 6 to 29 ppm, with a median of 13 ppm. Accordingly, exhalation rates are in the range 0.7 up to 7.3 $Bq.kg^{-1}.h^{-1}$, with a median of 1.4 $Bq.kg^{-1}.h^{-1}$. Fission-track observations indicate a generalized secondary uranium mobilization, even in fresh samples, with a large proportion of this element related with mineral borders, alteration surfaces and oxi-hydroxide fillings of microfractures; this is in good agreement with the very high exhalation rates measured.

IMS 1280-HR: A versatile SIMS instrument for Geosciences

P. PERES, F. FERNANDES, M. SCHUHMACHER AND P. SALIOT

CAMECA, 29 quai des Grésillons, 92622 Gennevilliers Cedex, France (peres@cameca.com)

SIMS (Secondary Ion Mass Spectrometry) is applied to a variety of applications in Geosciences, because it provides *in situ* measurement of elemental and isotopic composition in selected µm-size areas of the sample.

The CAMECA IMS 1280-HR large geometry SIMS offers outstanding capabilities for a wide range of geological applications, thanks to its very high transmission mass spectrometer combined to a versatile multicollection system. The IMS 1280-HR is also able to map the lateral distribution of major, minor, and trace elements, both in microscope and microprobe mode.

Hundreds of scientific papers have been published covering major application fields in geo- and cosmochemistry, geochronology, environmental studies,...:

- stable isotope ratio measurements on different systems: Hydrogen [1], Lithium [2], Carbon [3-5], Oxygen [6-10], Magnesium [11], Silicon [12], Sulfur [13-14],...
- U-Pb dating in Zircon [10, 15-18],
- trace element analyses [10, 19-20],

A review of recent analytical data obtained with the IMS 1280-HR on different domains will be presented.

[1] J.P. Greenwood *et al*. (2011) *Nature Geoscience* (in press). [2] T. Ushikubo *et al*. (2008) *EPSL* **272**, 666. [3] J.A. Craven *et al*. (2009) *Mineral Mag*. **73**, 193. [4] J.M. Ferry *et al*. (2010) *GCA* **74**, 6517. [5] A.A. Nemchin *et al*. (2008) *Nature* **454**, 92. [6] N.N. Hanson *et al*. (2010) *Rapid Commun. Mass Spectr*. **24**, 2491. [7] A.I.S. Kemp *et al*. (2007) *Science* **315**, 980. [8] R. Kozdon *et al*. (2009) *Chem. Geology* **258**, 327. [9] T. Nakamura *et al*. (2008) *Science* **321**, 1664. [10] F. Z. Page *et al*. (2007) *GCA* **71**, 3887. [11] J. Villeneuve *et al*. (2009) *Science*, **325**, 985. [12] F. Robert, M. Chaussidon (2007) *Nature* **447**, E1-E2 [13] A. El Albani *et al*. (2010) *Nature* **466**, 100. [14] P. Philippot *et al*. (2007) *Science* **317**, 1534. [15] X.-H. Li *et al*. (2009) *Geochemistry, Geophysics, Geosystems* **10**, N. 4. [16] G. Srinivasan *et al*. (2007) *Science* **317**, 345. [17] A.A. Nemchin *et al*. (2008) *GCA*, **72**, 668. [18] D. Trail *et al*. (2007) *GCA* **71**, 4044. [19] T. M. Harrison *et al*. (2007) *EPSL* **261**, 9 [20] M. J. Whitehouse *et al*. (2003) *Contrib. Mineral. Petrology* **145**, 61.

https://doi.org/10.1180/S0026461X00006502 Published online by Cambridge University Press

Modeling of ultramafic-hosted hydrothermal systems using CAST3M

F. PEREZ[1]*, C. MUGLER[1], P. JEAN-BAPTISTE[1] AND J.L. CHARLOU[2]

[1]LSCE, CEA-CNRS-UVSQ, Gif-Sur-Yvette, France (*correspondence: florian.perez@lsce.ipsl.fr)
[2]Géosciences Marines, IFREMER, Brest, France

Along the Mid-Atlantic Ridge, ultramafic-hosted active hydrothermal sites such as Rainbow and Ashaze release unusual high fluxes of methane and hydrogen relatively to the hydrothermal sites in basaltic environments [1, 2]. This has been interpretated as the result of serpentinization processes. The purpose of this ongoing work is to simulate the hydrothermal circulation and fluid-rock interactions in such ultramafic environments with a thermo-hydraulic model in order to investigate hydrogen fluxes. We thus developed a two-dimensional numerical model of the ridge using a Finite Volume method to simulate heat driven fluid flows in the framework of the CAST3M code [3]. This thermo-hydrogeological model was then coupled with a geochemistry module to simulate the serpentinization reaction. The latter was built thanks to laboratory experiments [4, 5] and speciation calculations performed with the EQ3/6 code.

Preliminary results for the Rainbow site show that the model produces realistic temperatures for the exiting fluids (Fig. 1).

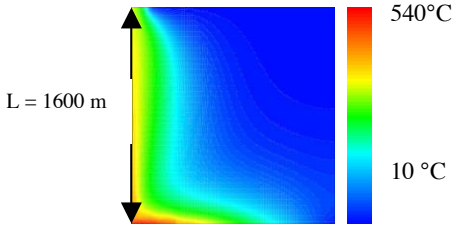

Figure 1: Simulated temperature field.

The next step will be to simulate hydrogen production and to compare it to available field data [1, 2] to gain further insight into the ongoing serpentinization process at Rainbow.

[1] Charlou *et al*. 2010 AGU Monograph series. [2] Seyfried *et al*. (2011) *Geochim. Cosmochim. Acta* **75**, 1574–1593. [3] http,//www-cast3m.cea.fr. [4] Martin & Fyfe(1970) *Chem. Geol*. **6**, 185-202. [5] Marcaillou *et al*. (2011) *Earth & Planet. Sci. Lett*. **303**, 281-290.

Controls on microbes in an actively venting chimney and in low-temperature hydrothermal fluids

M. PERNER[1]* AND J. LAROCHE[2]

[1]Microbiology and Biotechnology, University of Hamburg, D-22609 Hamburg, Germany
[2]Marine Biogeochemistry, Leibniz Institute of Marine Science, IFM-GEOMAR, Düsternbrooker Weg 20, 24105 Kiel, Germany

Two types of venting are recognised in hydrothermal habitats: hot and low-temperature emissions. Hot venting is commonly accompanied by formation of chimneys, which precipitate when ascending hot, reduced liquids come into contact with cold, oxygenated, ambient seawater. Alternatively, low-temperature emissions exist. These areas are often covered by microbial mats or symbiotic mussels. Besides the possibility of the type of host rock contributing to the chemical signature, the degree of seawater admixed to endmembers defines temperature and fluid chemistry in these liquids/habitats.

To understand the feedbacks of temperature and chemistry on the indigenous microbial community of hydrothermal biotopes, we collected a flank from an actively venting chimney and low-temperature hydrothermal emissions from two basalt-hosted sites on the southern Mid-Atlantic Ridge. As anticipated, measured sulfide (~6 mM), and hydrogen (~50 μM) is considerably higher in the hot chimney fluids (375°C) than in the low-temperature (9°C) emissions (47 μM, and 0, 9 μM, respectively). Oxygen was below detection limit in the former and around 71 μM in the latter fluids. The metagenomes of the chimney and the diffuse fluids clearly reflect the thermal and anoxic/oxic conditions of the two environments. From the metagenomic data, the importance of different pathways and enzymes for sulfur, nitrogen and carbon cycling can be deduced for the two biotopes. However, while microbial hydrogen and sulfide consumption rates were similar for both sites, hydrogen and sulfide only stimulated microbial CO_2 fixation considerably in the low-temperature fluids. Besides chemical controls, alternative factors may govern the microbial community structure. For example, more divergent transposases were in the chimney, but a higher divergence and abundance of phages, plasmid-related-functions as well as virulence, defense and disease strategies were found in the low-temperature liquids. Since conditions in the hot chimney are already highly selective for specific lifestyles, these type of defense/transfer strategies may be of profound importance for survival in low-temeprature venting habitats.

https://doi.org/10.1180/S0026461X00006502 Published online by Cambridge University Press

Magmatic plumbing dynamics along the Northern Rift Zone, NE Iceland

J.F. PERNET-FISHER* AND M.F. THIRLWALL

Department of Earth Sciences, Royal Holloway, University of London, Egham, Surrey, TW20 0EX, UK (*correspondence: j.pernet-fisher@es.rhul.ac.uk)

Previous pressure studies of Icelandic magmas have shown that most basalts crystallise at a wide range of depths within the crust (e.g. [1]). In addition [2] have shown that most central volcanoes have discreet multiple stacked chambers of crystallisation. The majority of these studies, however, either have very small data sets or focus on specific locations.

In this study crystallisation pressures have been calculated using the method of [3] from an extensive collection of 121 post, inter- and intra- glacial basalts from the Krafla, Fremri-Namur, Askja and Kverkfjöll central volcanoes as well as a section of Plio-Tertiary lavas from the surrounding area. This has enabled the location and depth of significant bodies of crystallisation under the length of the Northern Rift Zone (NRZ) to be resolved.

The identification of these bodies as well as comparisons between volcanic centres over time can provide clues into the structure of the Icelandic crust. It is clear that minimal change has occurred within the last 0.7 Ma with lavas crystallising at similar pressures over this time period. Furthermore it is apparent that the shield central volcanoes of Fremri-Namur and Theistareykir have much more complicated plumbing, lacking the presence of stacked bodies that is seen under all other volcanic centres in the NRZ.

The detailed understanding of crustal structure is critical when assessing the role of processes such as magma mixing or assimilation that are occurring within the crust. Many authors have noted that individual lava flows can have complex crystal cargos (e.g. [2]; [4]); in addition to the plumbing dynamics along the NRZ we present olivine data from selected flows that will allow the assessment of the crustal processes that contribute to these complex cargos over time.

[1] Maclennan *et al*. (2001) *Earth & Planetary Science Letters*, **191**, 295–310. [2] Kelly & Barton (2008) *Journal of Petrology* **49**, 465-492. [3] Yang *et al*. (1996) *Contributions to Mineral Petrology* **124**, 1–18. [4] Maclennan (2008) *Journal of Petrology* **49**, 1931-1953.

Discovery and description with scintillometric and geochemistry of gossans above amethyst deposits in altered volcanic rocks of the Paraná province, South America

JULIANA PERTILLE AND LÉO A. HARTMANN

Instituto de Geociências, Universidade Federal do Rio Grande do Sul, Avenida Bento Gonçalves, 9500, 91501-970 Porto Alegre, Rio Grande do Sul Brazil

We discovered a large number (probably thousands) of gossans in the intraplate volcanic rocks of the Paraná volcanic province, South America, based on observations of satellite images and field work associated with geochemistry and geophysics. We thus define a straitforward propecting guide for agate and amethyst deposits. The study area is located on the border between Brazil and Uruguay, covering the Los Catalanes gemological district and the Quaraí mining district. Anomalies in Google Earth satellite images were identified above six underground mines in the Los Catalanes gemological district, characterized in the pampas of the region as irregular structures of intense green color and sometimes with brownish, rough texture. The vegetation, scintillometric and geochemical anomalies occur at several stratigraphic levels in the volcanic group. Three scintillometric profiles performed on the Maurício Mine in the Los Catalanes gemological disctric indicate low emission rates near 55 cps (sd = 4.7) in the gossan compared with the regional average of colada Cordillera (63 cps). Whole rock geochemical analyses of three samples collected within the underground mine indicate high loss on ignition (4.5, 3.4, 4.5 wt.%). LOI higher than 2% is considered a strong indicator of intense hydrothermal alteration in the gossan. In the Quaraí mining district, gossans were studied in five areas, two in colada Catalán, two in colada Muralha, and one in colada Cordillera. The world-class deposits of amethyst and agate geodes are in coladas Catalán and Cordillera. Negative radiometric anomalies (higher than one standard deviation) occur in these gossans. The detailed study of one gossan included a geophysical grid spacing of 50 x 50 m (K, U, Th and total emission rate) and whole rock geochemical analyses (ACME, Canadá). The whole rock geochemical analyses of 17 samples collected within and outside the gossan classify the rocks as basaltic andesites, low–Ti, Gramado chemical type. The samples inside the gossan display high values of loss on ignition (2.3, 2.8, 2.9, 2.8, 2.9, 2.4, 2.6, 2.6, 2.3 and 2.3 wt.%), while outside the gossan the values are lower (0.8, 2.3, 0.5, 0.5, 1.6, 0.5, 0.6, 0.7, 1.1, 1.3 and 1.9 wt.%). SiO_2, K_2O and Rb show strong negative correlation with loss on ignition, while MgO has a slight enrichment. Were identified by electron microprobe analysis clinoptilolite associated with smectite, as products of hydrothermal alteration in the samples of Gossan.

https://doi.org/10.1180/S0026461X00006502 Published online by Cambridge University Press

Magma mixing as a petrological clock to measure the timescale of volcanic eruptions: Experiments and numerical models

D. PERUGINI

University of Perugia, Italy (diegop@unipg.it)

Magma mixing processes generate different fluid dynamic domains in which chemical exchanges between magmas can be strongly modulated, depending on the ability of the two melts to spread across the magmatic system. These structural domains, tightly linked to the chaotic nature of the mixing, are preserved in volcanic glasses as fractal structures.

Detailed petrological studies of lava microstructures generated by magma mixing reveal the presence, in the same system, of highly heterogeneous volumes of melts in which both depletion and enrichment of trace elements occurs, depending on the values of their diffusivity, triggering a 'diffusive fractionation' process.

Numerical simulations in which the mixing process is induced by applying a chaotic advection numerical scheme and a chemical diffusion model, reveal that the 'diffusive fractionation' of trace elements, analogous to that observed in lava flows, can be readily achieved and that the extent of this process depends upon the mixing time.

Chaotic magma mixing experiments were performed by mixing natural magmatic compositions from Phlegrean Fields. Experiments were carried out at different mixing times. Micro-analysis of experimental runs confirms a very variable mobility for the different trace elements, depending on their diffusivity. Equations relating the degree of 'diffusive fractionation' of trace elements to the time-scales of mixing are derived from experimental data.

Application of the 'diffusive fractionation' conceptual model to several pyroclastic sequences from Phlegrean Fields (Italy) allows us to apply the relationships derived from numerical models and experiments to estimate mixing time-scales. Results indicate that mixing processes lasted for a few days prior to eruption. These short time-scales for the mixing process argue in favor of the hypothesis that refilling of magma chambers and magma mixing processes likely was the key processes triggering eruptions.

We show that the combination of chaos theory, classic petrology, microtextural evidence, numerical simulations and experimental petrology is a highly effective and much needed approach to increase our knowledge on the behavior of volcanic systems, especially for the key issue of constraining time-scales of volcanic eruptions and hazard assessment at active volcanic centres.

Competitive ligand exchange between Cu-humate complexes and methanobactin

M.-L. PESCH[1]*, I. CHRISTL[1], S.M. KRAEMER[2] AND R. KRETZSCHMAR[1]

[1]Institute of Biogeochemistry and Pollutant Dynamics, ETH Zurich, Switzerland (*correspondence: laurie.pesch@env.ethz.ch)

[2]Department of Environmental Geosciences, University of Vienna, Austria

Methane oxidation by methanotrophs depends on the availability of copper and the efficiency of copper acquisition by methanotrophic bacteria. In natural environments such as soils, peat bogs, and surface waters, the presence of natural organic matter, having a high affinity for copper, can potentially control the bioavailability of copper. To mobilize copper, methanotrophs have developed a unique copper uptake system, similar to the siderophore-based iron uptake systems, involving the synthesis of a copper-binding ligand (so-called methanobactin). The aim of the current study is to investigate the competition between methanobactin and natural organic matter for copper binding.

Methanobactin used in the experiments has been isolated and purified from *Methylosinus trichosporium* OB3b cultures [1]. A well characterized humic acid extracted from a humified organic horizon of a Humic Gleysol was used as a model for natural organic matter. Kinetics of ligand exchange between Cu-humate complexes and methanobactin have been studied by means of UV–vis absorption spectroscopy. Concurrent competition of humic substances and methanobactin for copper binding were investigated in batch experiments and analyzed by size exclusion chromatography (SEC) coupled to an ICP-MS. Online monitoring of SEC eluates allowed the direct determination of the amount of copper bound to methanobactin and humic acid, respectively.

UV–vis absorption spectra indicated a fast uptake of Cu from humic acid. A substantial partitioning of methanobactin into humic acid was not observed. The observed equilibrium Cu speciation was quantitatively compared to model calculations using the previously derived conditional stability constants for proton and copper binding by methanobactin and the NICA-Donnan parameters determined for the humic acid used in this study [2].

[1] Pesch, M.-L. *et al*. (2011) *Geochemical Transactions* **12**: 2. [2] Christl, I. *et al*. (2001) *Environ. Sci. Technol*. **35**, 2512-2517.

https://doi.org/10.1180/S0026461X00006502 Published online by Cambridge University Press

Sulfate reduction in peatlands – Ecophysiology of a rare microorganism that contributes to a process with increasing importance for the global climate

MICHAEL PESTER, BELA HAUSMANN, PINSURANG DEEVONG, MICHAEL WAGNER AND ALEXANDER LOY

Department of Microbial Ecology, University of Vienna, Austria (loy@microbial-ecology.net)

Methane emission from peatlands contributes substantially to global warming but is significantly reduced by sulfate reduction, which is fuelled by globally increasing aerial sulfur pollution. However, the biology behind sulfate reduction in terrestrial ecosystems is not well understood and the key players for this process as well as their abundance remained unidentified. Linking (phylo)genetic information, obtained through gene-specific or metagenomic/-transcriptomic surveys, to the ecosystem process sulfate reduction is notoriously difficult because (i) known sulfate reducers are phylogenetically intermingled with non sulfate reducers and (ii) marker genes for sulfate reduction [such as *dsrAB*, encoding subunits of dissimilatory (bi)sulfite reductase] are also present and transcribed in some bacteria that lack the capability for sulfate reduction. Here we demonstrate, by comparative 16S rRNA gene stable isotope probing in the presence and absence of sulfate, that a *Desulfosporosinus* species, which constitutes only 0.006% of the total microbial community, is a main sulfate reducer at a long-term study peatland. Parallel stable isotope probing of *dsrAB*, confirmed that no other microorganisms contributed substantially to sulfate reduction in the incubations supplied with *in situ* concentrations of short-chained fatty acids and lactate. Subsequent single substrate incubations revealed that sulfate reduction was stimulated best with lactate, propionate, and butyrate, but not with acetate or formate. For the identified *Desulfosporosinus* species a high cell-specific sulfate reduction rate of 341 fmol SO_4^{2-} $cell^{-1}$ day^{-1} was determined. Thus, the small *Desulfosporosinus* population has the potential to reduce sulfate *in situ* at a rate of 4.0-36.8 nmol (g soil w. wt.)$^{-1}$ day^{-1}, sufficient to account for a considerable part of sulfate reduction in the peat soil. These data show that the identified *Desulfosporosinus* species, despite being a member of the 'rare biosphere', contributes to an important biogeochemical process that diverts the carbon flow in peatlands from methane to CO_2 and, thus, alters their contribution to global warming.

Abiogenic formation of carbon species at hydrothermal conditions using a novel flow apparatus

NICHOLAS J. PESTER* AND WILLIAM E. SEYFRIED, JR

Dept. of Earth Sciences, University of Minnesota, Minneapolis, MN 55455, USA (*correspondence: peste005@umn.edu)

We present an experimental configuration that permits constant high-pressure flow through hydrothermal cells while at the same time maintaining uniform concentrations of multiple dissolved gases. This system provides an additional benefit for kinetic studies as it allows precise redox control without the presence of mineral buffers or the need to rely on the hydothermal breakdown of unstable intermediates in the source fluid. Steady-state equilibrium can be determined when a target species concentration no longer changes with increasing residence time at equivalent temperature, pressure and source fluid composition. For example, we have calibrated the equilibrium constant for the water-gas shift (WGS) reaction ($CO_2 + H_2 = CO + H_2O$) in pure water between 225-374°C and 220-325 bars, including the critical point. In this region the log K_{WGS} is linear with respect to water density. These equilibrium constants, as well as those for formic acid (thought to be the WGS reaction intermediate) are in good agreement with those derived from the HKF equation of state if recent updates for the involved species are incorporated. This is especially noteworthy due to the uncertainty of thermodynamic calculations near the critical point of water with implications for modeling natural hydrothermal systems.

While the low concentrations of CO appear in equilbrium with the WGS reaction, controls on the appreciably higher concentrations of methane in deep-sea hydrothermal fluids are still unclear. However, this methane is often thought abiogenic and CO_2 is the dominant source of carbon. This is an important consideration when studying the kinetically prohibitive synthesis of reduced hydrocarbon species (e.g. $CO_2 + 4H_2 = CH_4 + 2H_2O$). Using a source fluid containing geologically relevant concentrations of H_2 and CO_2, we have observed the formation of C1-C3 hydrocarbons in reaction cells constructed of both titanium and gold, with and without the presence of magnetite, between 200-400°C. Methane generation is linear with respect to residence time in the cells and synthesis is maximized at temperatures near 300°C. Our results demonstrate that hydrocarbon formation is enhanced as much as 200X in the gold cell relative to the titanium cell, while magnetite appears relatively ineffectual as a catalyst for hydrocarbon formation.

https://doi.org/10.1180/S0026461X00006502 Published online by Cambridge University Press

Ship emissions and their influence on large scale cloud fields

K. PETERS[1,2]*, J. QUAAS[1], H. GRASSL[1] AND P. STIER[3]

[1]Max-Planck-Institut für Meteorologie, Hamburg, Germany (*correspondence: karsten.peters@zmaw.de)
[2]International Max Planck Research School on Earth System Modelling, Hamburg, Germany
[3]Department of Physics, University of Oxford, UK.

Our study assesses the possibility of detecting an influence of global shipping emissions on the micro- and macrophysical properties of large-scale cloud fields in remote regions of the tropical oceans. We utilise cloud- and aerosol properties as retrieved from satellite measurements as well as results from global aerosol modelling for this purpose.

Our satellite data-based approach differs from many previous studies on ships' influence on clouds because we do not specifically attempt to detect and characterise linear features in stratocumulus cloud-decks known as 'ship tracks'. Ships emit large amounts of aerosols and aerosol precursor gases in remote oceanic areas thereby modifying the composition of marine boundary layer (MBL) aerosol composition and –concentration. It is this modification of MBL characteristics which may alter the properties of liquid water clouds on large scales; a factor which remains to be investigated by use of satellite- and model data.

For the satellite-data based part of our study, we combine cloud- and aerosol properties as derived from satellite measurements (MODIS) and ERA-Interim reanalysis data. We identify regions of large spatial contrast in shipping emissions from an up-to-date shipping emissions inventory. With this data, we separate 'clean' from 'polluted' oceanic regions by using the wind direction as provided by the reanalysis data. The reanalysis data also enable us to characterize the ambient meteorological conditions for the observed scenes.

For the modelling-based part of our study, we use the ECHAM5-HAM aerosol-climate model to assess the climate impact of shipping emissions provided by the shipping emissions inventory. We also sample the model data according to the sampling strategy of the satellite data.

The analysis of the satellite data reveals a potential Twomey-effect on the properties of large-scale cloud fields with regard to shipping emissions. Nevertheless, the results suggest that the observed effects could also be due to a change in dynamical drivers, such as a change in sea surface temperatures. This highlights the difficulty to separate aerosol effects from ambient conditions in satellite based studies. The modelling results generally confirm the findings from the satellite data analysis and enable us to pinpoint the effect of shipping emissions more precisely.

Amphibole antecrysts in deposits of Merapi volcano, Indonesia: A plutonic phase in extrusive magmas

S.T.M. PETERS[1,2]*, J.P. CHADWICK[2] AND V.R. TROLL[3]

[1]Institut für Geologie und Mineralogie, Universität zu Köln, Germany (*correspondence: peterss1@uni-koeln.de)
[2]VU University, Amsterdam, The Netherlands
[3]Dept. of Earth Science, Uppsala University, Uppsala Sweden

Amphibole crystals are present in, but typically in disequilibrium with, the high-K basaltic andesite deposits of Mount Merapi, an active stratovolcano of the Sunda volcanic arc at central Java, Indonesia [1-2]. These *antecrysts* form a potential tool for tracing the physical interaction between the deep and shallow parts of the magmatic system. Moreover, they provide a window into the plutonic REE (rare earth element) evolution of arc magmas, for which amphibole fractionation has been inferred to be a controlling process [3]. We studied amphibole antecrysts from block and ash flow deposits of the 1998 eruption by petrographic and EMP analysis of ten thin sections. Six samples with limited to no visible alteration were selected for REE (Quadrupole ICPMS) and radiogenic Sr and Nd isotope analyses (TIMS).

Major element trends combined with the Al based geobarometer that was developed by [4] indicate that amphibole crystallized from a basic magma at the base of the crust (20-31 km) and re-equilibrated with a more silicic magma at a shallower level (13-18 km). The crystals have similar Nd isotope compositions to the bulk rock whereas their Sr compositions are less radiogenic, most likely reflecting a lesser degree of crustal contamination with respect to later grown phases such as feldspar [5]. Both findings are consistent with a model in which magma ponds at the base of the crust, partially crystallizes and subsequently feeds a shallower, more silicic plumbing system that is increasingly affected by crustal contamination. REE ratios show high Dy/Yb and low La/Yb, but concentrations are typically too low to counterbalance the respectively low and high ratios of the hostrock. Fractionation of an additional phase with similar REE partitioning behaviour but with higher partition coefficients, possibly clinopyroxene, is therefore implied in the deeper parts of the Merapi system.

[1] van Bemmelen (1949) **1A** 732p. [2] Camus (2000) *J Volc Geoth Res* **100**, 139–163. [3] Davidson *et al*. (2007) *Geology* **35**, 787–790. [4] Ridolfi *et al*. (2010) *Contrib to miner petr* **160**, 45–66. [5] Chadwick *et al*. (2007) *J of Pet*. **48**, 1793–1812.

https://doi.org/10.1180/S0026461X00006502 Published online by Cambridge University Press

Investigation of ^{36}Cl distribution in the North-Western Sahara aquifer system

J.O. PETERSEN[1], F. HADJ AMMAR[1,2], P. DESCHAMPS[1]*, B. HAMELIN[1], J. GONCALVES[1], K. ZOUARI[2], A. GUENDOUZ[3], J.-L. MICHELOT[4] AND ASTER TEAM[1]

[1]CEREGE, B.P. 80, 13545 Aix-en-Provence cedex 4, France (*correspondence: deschamps@cerege.fr)
[2]LRAE (ENIS) B.P. 1173-3038 Sfax,Tunisia
[3]University of Blida, BP. 270, Soummaa Blida, Algeria
[4]IDES, Bat. 504, Université Paris-Sud, 91405 Orsay, France

In spite of its pivotal significance for resource management, the concept of 'groundwater age' remains in many cases elusive. Among various methods proposed for dating groundwater, naturally occurring radioactive isotopes such as ^{36}Cl or ^{81}K and ^{4}He appear as more promising to characterize groundwater transport in the large aquifer bodies where residence times are on the order of 100 kyr to 1 Myr [1-3]. Here, we present new ^{36}Cl analyses obtained on groundwater samples collected in the Tunisian part of the Continental Intercalaire (CI) and Complex Terminal (CT) aquifers that form the North-Western Sahara Aquifer System. These analyses were performed at CEREGE, on the French 5 MV AMS National Facility 'ASTER'. Procedural blanks are routinely measured as less than 1×10^{-16} $^{36}Cl/Cl$ ratio.

In the Tunisian CT, ^{36}Cl contents up to 12×10^{8} at. l^{-1} are observed while $^{36}Cl/Cl$ ratios vary from 13 to 75×10^{-15} at at^{-1}. Lower values are generally obtained in the samples collected in the Tunisian part of the CI ([^{36}Cl]< 2.5×10^{8} at. l^{-1}), as expected from their deeper setting. By comparison, the data obtained by Gendouz and Michelot in the Algerian region of the CI show lower ^{36}Cl contents (<3.7×10^{8} at. l^{-1}) but comparable $^{36}Cl/Cl$ due to lower salinities of the groundwater. The data also show a high heterogeneity in the area of the Tunisian Chotts, probably related to the complex inter-connexions of the aquifer layers in this tectonically fractured basement and/or the complex flowpaths in this area.

The data will be compared to direct predictions obtained from hydrodynamic modelling using MODFLOW implemented with an age-mass calculation subroutine [5], and hydrodynamic parameters and aquifer geometry published previously by Baba Sy [6].

[1] Lehmann, B.E. *et al*. (2003) *EPSL*. [2] Sturchio, N.C. *et al*. (2004) *GRL*. [3] Mahara, Y. *et al*. (2009) *EPSL*. [4] Guendouz, A. & J.L. Michelot (2006) *J. of Hydrology*. [5] Goode, D. J. (1996) *WRR*. [6] Baba Sy, O. (2005) *PhD Thesis*, Université Tunis El Manar.

Pb isotopes and the origin of the 'ghost plagioclase' signature in melt inclusions from the Galapagos Archipelago

M. PETERSON[1]*, A. SAAL[1], E. NAKAMURA[2], K. BURGESS[1] AND H. KITAGAWA[2]

[1]Brown University, Providence, RI, 029012, USA (*correspondence: mary_peterson@brown.edu, alberto_saal@brown.edu, katherine_burgess@brown.edu)
[2]ISEI, Okayama University, Misasa, Tottori 682-0193, Japan (eizonak@misasa.okayama-u.ac.jp, kitagawa@pheasant.misasa.okayama-u.ac.jp)

This study looks at olivine-hosted melt inclusions from Santiago and Fernandina islands, Galapagos Archipelago. Although both suites of melt inclusions show plagioclase signature in primitive mantle normalized diagrams, melt inclusions from Santiago show major element composition indicative of plagioclase assimilation. In contrast, the Fernandina inclusions that have the trace-element signature of plagioclase do not show the major element compositions expected during plagioclase assimilation. Thus, the trace-element signature of the original plagioclase is present only as a 'ghost' [1]. Two main hypotheses have been proposed to explain the ghost plagioclase signature, either an ancient recycled plagioclase-rich cumulate intrinsic to the plume [1], or the interaction of melts with plagioclase cumulates within the present day oceanic lithosphere [2, 3]. *In situ* measurement of Pb isotopes in melt inclusions can be used to distinguish between the proposed origins of the ghost plagioclase. We expect that an ancient recycled plagioclase-rich cumulate will have a very different Pb isotopic composition from the present day MORB and FOZO components typical of Santiago and Fernandina lavas [4, 5].

Pb isotopes were measured using the Cameca 1270 SIMS of the Institute for the Study of the Earth's Interior, Okayama University, Misasa, Japan. The 2s errors in our measurements ranged from 0.4 to 2% for $^{207}Pb/^{206}Pb$ and from 0.3 to 1.6% for $^{208}Pb/^{206}Pb$ at a range in ^{208}Pb of 219 to 10 cps. The results show that melt inclusions with plagioclase signature have Pb isotopes that are indistinguishable from the present day MORB and FOZO components typical of Santiago and Fernandina lavas. Therefore, the ghost plagioclase signature in Fernandina melt inclusions is produced by melt-plagioclase cumulate interaction within the crystal mush zone beneath Fernandina Island.

[1] Sobolev *et al*. (2000) *Nature* **404**, 986–990. [2] Saal, *et al*. (2007) *EPSL* **257**, 391–406. [3] Danyushevsky *et al*. (2004) *J. Petrology* **45**, 2531–2553. [4] White *et al*. (1993) *JGR* ***98***, 19533–19563. [5] Kurz & Geist (1999) *GCA* ***63***, 4139–4156

https://doi.org/10.1180/S0026461X00006502 Published online by Cambridge University Press

Zircon U-Pb, Hf and O isotope constraints on growth versus recycling of continental crust in the Grenville orogen, Ohio, USA

ANDREAS PETERSSON[1], ANDERS SCHERSTÉN[1], JENNY ANDERSSON[2], MARTIN WHITEHOUSE[3], JOHN M. HANCHAR[4] AND CHRIS FISHER[4]

[1]Department of Earth and Ecosystem Sciences, Lund University, Sölvegatan 12, SE-223 62 Lund, Sweden (andreas.zircon@gmail.com)
[2]Geological Survey of Sweden, Box 670, SE-751 28 Uppsala, Sweden
[3]Laboratory for Isotope Geology, Swedish Museum of Natural History, Box 50 007, SE-104 05 Stockholm, Sweden
[4]Department of Earth Sciences, Memorial University of Newfoundland, St. John's, NL A1B 3X5 Canada

The Grenville orogen extends along the present day North American continent, from Labrador in the north to Mexico in the south. It is, however, largely covered by thick piles of Phanerozoic rocks, and the geological evolution of the extensive covered parts of the orogen is poorly known. We present zircon U-Pb, Hf- and O-isotope analyses for six drill-cores in Ohio (USA). U–Pb data dates magmatic and metamorphic zircon crystallization that span from 1643 ±54 Ma to 1025 ±8 Ma. Zircon $\varepsilon Hf_{(t: 1650\text{-}1025\ Ma)}$ values at 1.9 ±1.2 to 9.0 ±0.6 is explained by reworking of a single crustal reservoir derived from the mantle at 1640 ±40 Ma, that evolved with a $^{176}Lu/^{177}Hf$ value of 0.014. One sample, deviates from this trend and its spread in εHf t=1230 Ma indicates a 0-33 wt% contribution of a depleted mantle component to the t_{DM}=1650 Ma reservoir. Zircon (SIMS) $\delta^{18}O$ weighted mean values range from 5.36 ±0.65‰ to 10.88 ±0.21‰, which corresponds to juvenile mantle and recycled crustal oxygen signatures respectively. There is a broad negative correlation between zircon Th/U and $\delta^{18}O$ and age respectively. The general increase in $\delta^{18}O$ with time and progressive metamorphic recrystallization is best explained by the increasing effect of heavy $\delta^{18}O$ metamorphic fluids during Grenvillian continent-continent collision. Together, the new data presented here suggests that the crustal evolution of this part of the North American continent is significantly older, and that the influence of metamorphic fluids on the O-isotope system in zircon is stronger than previously reported.

Glacial interglacial aerosol input over Antarctica and the global hydrological cycle

J.R. PETIT[1]* AND B. DELMONTE[2]

[1]LGGE, CNRS UJF, BP 96 38402 St Martin d'Hères cedex, France (*correspondence: petit@lgge.obs.ujf-grenoble.fr)
[2]DSAT, Università degli Studi di Milano-Bicocca, Piazza della Scienza, 1, 20126 – Milano, Italy (barbara.delmonte@unimib.it)

Questions rise for simulating and interpreting the 5 fold marine and the 50-to-70 fold dust enhancement observed from Antarctic ice core records during the past glacial interglacial cycles. Amongst uncertainties the repective contribution from source, from transport which would be consistent for aerosols of different origin are challenging.

A semi-empirical model has been developed to reproduce the large glacial-interglacial changes of Antarctic dust and sodium concentrations [1]. Tthe model uses a life-time parameter that depends on atmospheric temperature (stable isotope content of ice) which drives the global hydrological cycle and the atmospheric cleansing and which was applied to conceptual pathways for aerosols.

The model reproduces most of the increase in dust concentrations during cold periods with respect to Holocene climate, as observed in Epica Dome C (EDC) and Vostok ice records, on the basis of synergetic changes of three factors associated with temperature (source, transport efficiency, accumulation rate over Antarctica). As supportive results, our model provide source amplitude (up to X 4) and mimics the pattern of a south Atlantic marine record covering the last 300, 000 yr (Martinez Garcia, 2009) along with consistent 3-5°C atmospheric temperature change over the Southern Ocean [2]. The calculated source changes (mostly Patagonia) share the pattern of the sea ice extends over the south Atlantic.

When applied to the sodium, the concentration changes could be reproduced by our model by using two main factors (accumulation rate and transport efficiency) while the source effect is not discernable from an atmopheric temperature effect.

[1] Petit, J.R. and B. Delmonte (2009) *Tellus* **61B**, 768–790. [2] Martinez Garcia *et al*. (2009) *Paleoceanograpghy*, **24** PA 1207.

https://doi.org/10.1180/S0026461X00006502 Published online by Cambridge University Press

In situ insights to partitioning of highly siderophile elements between silicate and iron rich liquids at extreme conditions

S. PETITGIRARD[1], M. BORCHERT[2], D. ANDRAULT[3], K. APPEL[2] AND H.-P. LIERMANN[2]

[1]European Synchrotron Radiation Facility (ESRF), Grenoble, France
[2]Deutsches Elektronen-Synchrotron (DESY), Hamburg, Germany (manuela.borchert@desy.de)
[3]Universite Blaise Pascal, Laboratoire des Magmas & Volcans, Clermont-Ferrand, France

Experimental data indicate that highly siderophile elements (HSE) sunk down with the iron in the Earth's core at the early stage of the Earth's formation [1]. Consequently, the Earth´s mantle and crust should be depleted in HSE. Thus, the apparent excess of these elements in the Earth´s upper mantle and crust has been a long-lasting enigma in the interpretation of geochemical signatures of the Earth's mantle and the geochemistry of core-mantle differentiation.

So far, all metal-silicate partitioning studies make use of 'classical' HP-HT techniques and therefore are limited to PT conditions of the Earth's upper mantle. There is urgent need for experiments at much higher pressures and temperatures to simulate conditions of core-mantle boundary because it remains unclear if determined metal-silicate partition coefficients of HSE can simply be extrapolated to lower mantle conditions. Here, we present first preliminary data on metal-silicate trace element partitioning from a new experimental approach to obtain *in-situ* information at simultaneous high pressures and high temperatures using synchrotron radiation (SR). First experiments were performed at beamline ID27 (ESRF, France) using laser-heated diamond-anvil cells up to ~50 GPa and 4200 K. Samples are analysed before, during and after laser heating by SR-μXRF/XRD. The sample chamber is loaded with a HSE- doped chondrite glass chip placed next to a HSE-free metal foil ($Fe_{90}Ni_{10}$). MgO is used as pressure media and insulator. Laser heating was performed at the interface between the chondrite glass and metal foil. During stepwise heating, *in-situ* μXRF spectra and μXRD pattern of the metal foil were synchronously collected. Fluorescence analysis is used to quantify trace element concentration whereas diffraction patterns give information on melting stage and appearance of high pressure phases in the laser spot. First qualitative analysis verify existing data and show a strong partitioning of HSE into the metal liquid with increasing temperature. Quantitative data analysis is currently in progress.

[1] Ertel et al. (1999). GCA, 63, 2439-2449

Heavy noble gases from the Northern Lau Basin: The Xenon perspective on mantle heterogeneity

MARIA PETŐ[1], SUJOY MUKHOPADHYAY[1] AND KATHERINE A. KELLEY[2]

[1]Deptartment of Earth and Planetary Sciences, Harvard University, Cambridge, MA02138, USA (mpeto@fas.harvard.edu, sujoy@eps.harvard.edu)
[2]Graduate School of Oceanography, University of Rhode Island, RI 02282, USA (kelley@gso.uri.edu)

Constraining the Xenon isotopic composition of the MORB and plume sources is critical to understand Earth structure, mixing between different reservoirs in the mantle, and early degassing. Recent high-precision Xe measurements from Iceland by our group indicate that the $^{129}Xe/^{130}Xe$ ratio in the Iceland plume is low compared to MORBs because of a lower I/Xe ratio. Since ^{129}Xe is produced from now extinct ^{129}I, the Xe data limits the degree of mixing between the Iceland plume source and the MORB source over Earth history.

We will also present CO_2, and noble gas data (He, Ne, Ar and Xe) from gas-rich basalt glasses along the Rochambeau Rift (RR) in the Northern Lau Basin. Our goal is to investigate whether the Xe composition of the Iceland plume is representative of other mantle plumes.

The samples selected for the study have $^3He/^4He$ ratios between 15.8 to 28.2 R_A. Recent work suggests that the high $^3He/^4He$ ratios reflect the presence of a 'Samoan-like' OIB source in the northern Lau Basin [1]. The measured $^{129}Xe/^{130}Xe$ ratios in the 28.2 R_A sample reaches 7.01. Mixing systematics between Xenon and the other noble gases in the samples demonstrate that the maximum $^{129}Xe/^{130}Xe$ ratios in the mantle source is ~7.1**,** much lower than measured values in MORBs. Additionally, the $^4He/^{40}Ar$ ratio of one of the samples is ~3, indicating it to be largely undegassed. Data obtained by multiple step crushes of this sample display a linear trend in $^{129}Xe/^{130}Xe$ vs $^3He/^{130}Xe$ space that overlaps with the Iceland data, but is quite distinct from MORBs. Our new data corroborates observations from Iceland and suggests that OIBs and MORBs evolved with different I/Xe ratios. Further, Xe in the MORB source cannot be derived from the plume source, refuting predictions for the steady-state upper mantle model. Additional work is ongoing to characterize the Pu- to U-derived fission xenon in the RR samples.

[1] Lupton (2009) *GRL* **36**.

https://doi.org/10.1180/S0026461X00006502 Published online by Cambridge University Press

Mn(IV) reduction: A driving mechanism for Mg^{2+}-enrichment in shallow marine carbonates?

D.A. PETRASH[1]*, S.V. LALONDE[2], M.K. GINGRAS[1] AND K.O. KONHAUSER[1]

[1]University of Alberta, Edmonton, AB T6G 2E3, Canada (*correspondence: petrash@ualberta.ca)
[2]IUEM Technopôle Brest-Iroise, France

A wide variety of bacterial metabolisms have been suggested to facilitate the precipitation of penecontemporaneous dolomite (e.g. aerobic respiration, sulfide oxidation, sulfate reduction, and methanogenesis), highlighting a strong need for additional insights from modern near-surface dolomite-forming locales. In the transition from intertidal to supratidal settings in a Ca-dolomite-forming lagoon, Archipelago Los Roques, Venezuela, early diagenesis is strongly influenced by a complex microbial mat system. The overlying evaporated seawater is characterized by temperatures in excess of 30°C; elevated alkalinity, ~245 meq/L (as total $CaCO_3$) and pH, ~9.3. Sedimentation in the lagoonal system is dominated by allochemical aragonite, authigenic calcite and gypsum. In the sediment, there is a slightly cemented zone, 8-12 cm below the surface, consisting of aragonite, calcite and Ca-dolomite. EPMA show that within this layer, gypsum is actually being calcified. Such evidence would suggest that the enrichment of Mg in carbonate cements might have been mediated by the terminal stages of degradation of organic matter [1], however, the Mg-enriched zone also corresponds with a local increase in the total organic carbon. Sediment major and trace element data yield a more complex picture of diagenetic processes leading to dolomitization. The trends in sediment trace element concentrations reveal marked changes in redox conditions with increasing depth. Carbonates in the cemented zone have maximum [Mn^{2+}] and minimum [Fe^{2+}], and as compared with underlying sediments, they also record highest Ni and Co concentrations. The incorporation of these elements in authigenic carbonates is though dependent on their solubilisation by Mn (IV) reduction [2], and the trends described here strongly suggest that at this depth, manganese reduction outcompetes sulfate reduction for labile organic carbon. Our results suggest that the trace element composition of carbonate minerals may track the biogeochemical processes that take place during low-temperature diagenesis, and importantly, offers new insight into the formation of penecontemporaneous dolomite.

[1] Fernández-Díaz L. *et al*. (2009) *Am. Mineral*. **94**, 1223-34.
[2] Ehrlich H.L. Dianne K. (2009) Taylor Francis, pp. 400.

LP-HT signature from the Adria-Europe plate boundary realm: The role of mantle/crust interaction in granite generation

Z. PETRINEC* AND D. BALEN

University of Zagreb, Faculty of Science, Croatia (*correspondence: zoricap@geol.pmf.hr)

The final geodynamic position of the Moslavačka Gora (MG) on the SW margin of the Pannonian Basin (PB) is related to Mesozoic and Cenozoic evolution of the Dinaric segment of the Alpine-Himalayan orogenic belt formed along the Adria-Europe active continental margin. Overall lithology of the MG crystalline can be broadly divided into three main groups: S-type granites which make the core of the MG complex and high- to medium-grade metamorphic rocks (migmatites, gneisses, amphibolites, metapelites) which are present in form of foreign enclaves i.e. xenoliths inside the MG granite pluton.

Dm- to m-sized xenoliths bear signature of the polyphase metamorphic evolution of the MG complex with at least two phases being identifiable through specific mineral assemblages. First phase (recorded in amphibolites), which preceded granite intrusion, reached maximum conditions of amphibolite facies metamorphism. The second, Late Cretaceous LP-HT phase, can be separated into two closely related metamorphic events (recorded in the metapelite xenoliths) that took place under low-P amphibolite facies conditions. Pseudosection modelling gave temperature range 585-600 °C and pressure range 390-460 MPa for assemblage Bt + Cd + Pl + Grt + Sil + Qtz while younger assemblage Bt + Chl + Pl + And + Qtz gave temperature 540°C and pressure <250 MPa).

Major and trace element chemical data (including REE) favor anatexis of a crustal (meta)pelitic source as a dominant process in the genesis of two dominant types of the Late Cretaceous MG peraluminous granites: two-mica granite (Tmg), and leucogranites (Lg). Occurrence of different types of cognate enclaves, e.g. tourmaline nodules, together with presence of miaroles and magmatic andalusite in the assemblage points to upper crust emplacement level of the intrusion (avg. 5-6 km). Rare MME field occurrences imply genetic link of the MG granite intrusion with Late Cretacoeus LP-HT event and the upper mantle/lower crust mafic intrusion that might be the same that was responsible for Cretaceous gabbro occurences of the MG crystalline complex.

https://doi.org/10.1180/S0026461X00006502 Published online by Cambridge University Press

Sorption of Np on magnetite in solutions of different ionic strengths

V.G. PETROV*, A.A. ZADORIN AND S.N. KALMYKOV

119991, Leninskie gory, 1/3, Chemistry Department, MSU, Moscow, Russia
(*correspondence: vladimir.g.petrov@gmail.com)

Neptunium is an element of interest due its high content in spent nuclear fuel and its physico-chemical properties, such as long half-life ($T_{1/2}$ (^{237}Np) = $2.14 \cdot 10^6$ years) and high potential mobility of Np (V) which is the most stable valent state under the environment conditions. Among numerous geochemical reactions controlling the migration behavior of actinides, sorption processes are of main importance. Magnetite is one of the possible iron oxide phases forming as a result of steel containers corrosion. There are number of research works dealing with sorption of neptunium onto different iron oxides in solutions with low ionic strengths in literature. However in near-field conditions due to dissolving of cementitious materials and host rocks formation of brine solutions is possible.

The objective of this work is to investigate sorption of pentavalent neptunium on magnetite in sodium chloride solutions of different concentrations both in aerobic and anaerobic conditions.

Experiments in aerobic conditions were done in contact with atmospheric air in the pHc (pHc = -log [H^+]) range 2.0 – 8.0. Experiments in anaerobic conditions were done in N_2 glove box in the pHc range 2.0 – 10.0. All solutions were prepared using deionized water and NaOH/NaCl, HCl/NaCl for adjusting pHc. The initial neptunium concentration was $1 \cdot 10^{-9}$ M. For activity measurements short-lived gamma-emitting isotope ^{239}Np ($T_{1/2}$ = 2.36 days) was used. Solid/solution ratio was 1 g/L.

The shift of the sorption edge to higher values of pHc (6.5 – 7.5) and decreasing of maximum sorption with increasing ionic strength was observed in both aerobic and anaerobic conditions (from 98% in 0.1 M NaCl solution to 67% in 5 M NaCl solution). In the 0.1 M NaCl solutions typical for cation sorption curve was observed with pHc_{50} (50 % sorption) 6.5. Unusual sorption behavior was observed for 1-5 M NaCl solutions in aerobic conditions with additional maximum in the pHc range 4.5-5.5, that could be explained by reduction of pentavalent neptunium in the presence of iron (II). This maximum has the highest value of 70% for 1 M NaCl and decreases to 20% with increasing of the ionic strength to 5 M NaCl. Further thermodynamic calculations are required for accurate description of obtained results.

Modeling reconciles observations for Traps in East and West Siberia

A.G. PETRUNIN AND S.V. SOBOLEV

GFZ, German Research Centre for Geosciences, 14473 Potsdam, Germany
(*correspondence: stephan@gfz-potsdam.de)

The Permo-Triassic Siberian Traps – the type example and the largest continental Large Igneous Province, is located on both thick cratonic lithosphere of Precambrian Siberian Craton in the East Siberia and on much thinner lithosphere of the Mesozoic West Siberian Basin. Based on largest volumes of the exposed basalts and on highest source temperatures of basalts in the East Siberia, it is believed that the head of a hot mantle plume, which was probably the source of basalts, arrived in the East Siberia. However, there is no evidence of the expected pre-magmatic uplift nor of a large lithospheric stretching of the basaltic sequence in the East Siberia, while these features are reported for the West Siberian Basin [1]. Based on these observations it was suggested [1] that mantle plume head arrived to the base of the lithosphere of the West Siberian Basin and only later leaked below the East Siberian Craton.

Here we test scenarios with different locations of the mantle plume, using thermomechanical modeling technique. The model employs petrological constraints for the source composition and temperature [2, 3], non-linear temperature- and stress-dependent elasto-visco-plastic rheology [4] and pressure- and temperature-dependent melting of a heterogeneous mantle. We show that observations for the West and East Siberian Traps can be reconciled for the large (more than 400 km in radius) and hot (potential temperature up to 1600°C) plume head containing large amount (up to 15 Wt%) of the recycled oceanic crust, that arrived to the thick lithosphere of the East Siberia and was then deflected towards the thin lithosphere of the West Siberia. In this case no uplift and stretching is generated in the East Siberia and major basaltic eruptions may occur first in the West Siberia.

[1] Saunders, A.D. *et al*. (2005) *Earth Planet. Sci. Lett*. **79**, 407–424. [2] Sobolev, A.V. *et al*. (2009) *Petrology* **17**, 253–286. [3] Sobolev, A.V. *et al*. (2009) *Russian Geology & Geophysics* (2009) **50**, 999–1033. [4] Sobolev, S.V. & Babeyko, A.Y. (2005) *Geology* **33**, 617–620.

https://doi.org/10.1180/S0026461X00006502 Published online by Cambridge University Press

VisualAge: A novel approach to U-Pb LA-ICP-MS geochronology

JOSEPH A. PETRUS* AND BALZ S. KAMBER

Laurentian University, Sudbury, ON, Canada
(*correspondence: japetrus@gmail.com)

This contribution presents VisualAge, a new tool for reducing and visualizing U-Pb geochronology data obtained by LA-ICP-MS. VisualAge was developed as an add-on for Iolite (the freely available ICP-MS data analysis tool [1]) and consists of two main components: an Iolite data reduction scheme (DRS) and Igor Pro visualization routines. The VisualAge DRS improves upon the existing Iolite U-Pb geochronology DRS by calculating the $^{207}Pb/^{206}Pb$ age as well as the common lead corrected ratios and ages (either via the measured ^{204}Pb signal or where ^{204}Pb is unavailable, with Andersen's approach [2]) for each point of the raw ICP-MS data. By far the most important feature of VisualAge is its ability to display a 'live' concordia diagram. This feature allows one to visualize the data of an Iolite integration on a concordia diagram as it is being selected and adjusted, thus providing immediate visual feedback regarding data discordance, uncertainty, and common lead contamination for different regions of the ICP-MS signal. The 'live' concordia diagram is particularly useful for LA-ICP-MS zircon data, where the signal from a single grain can consist of zones of concordance, disturbed or metamict areas, as well as inherited cores or younger overgrowths. Once integrations have been selected in Iolite, VisualAge can also be used to quickly construct age histograms and probability distributions, standard and Tera-Wasserburg style concordia diagrams (including the computation of a concordia age [3]), as well as 3D U-Th-Pb and total U-Pb concordia diagrams.

[1] Hellstrom *et al*. (2008) *Mineral. Assoc. Can. Short Course Ser*. **40**, 135–145. [2] Andersen (2002) *Chem. Geol*. **192**, 59–79. [3] Ludwig (1998) *Geochim. Cosmochim. Acta* **62**, 665–676.

Cloud droplet activation of organic aerosols: The role of molecule size, polarity, and functional group composition

M.D. PETTERS[1], P.J. ZIEMANN[2], S.M. KREIDENWEIS[3], S.R. SUDA[1], C.M. CARRICO[3], A. FAULHABER[2], A. MATSUNAGA[2], R.C. SULLIVAN[3], L. MINAMBRES[4] AND A.J. PRENNI[3]

[1]Department of Marine Earth and Atmospheric Sciences, North Carolina State University, Raleigh, NC, USA
[2]Air Pollution Research Center, University of California, Riverside, CA, USA
[3]Department of Atmospheric Science, Colorado State University, Fort Collins, CO, USA
[4]Department of Physical Chemistry, University of País Vasco, Spain

Secondary organic aerosols (SOA) comprise a significant fraction of the atmospheric aerosol burden and play an important role in direct and indirect aerosol effects on climate. To model SOA-cloud interactions we ultimately seek relationships that can predict a compound's contribution to a particle's ability to serve as a cloud condensation nucleus (CCN) based on its chemical composition. The relative CCN efficiency of a compound is described by the hygroscopicity parameter κ. We find that for sufficiently functionalized molecules, κ can be modeled within a factor two using predictions based on molar volume. Compounds with fewer functional groups strongly deviate from this model, resulting in a continuum of reduced κ values between the molar volume model and zero. We use experimentally determined derivatives of d (κ)/d (number of functional groups of type i) to quantify this effect and to develop a framework that can be used to compute κ based on the molar volume, number of carbon atoms, and the number and type of functional groups present in the molecule.

Ambient organic aerosols consist of a large number of different compounds. We developed a new technique to characterize this distribution by collecting aerosol on filters, extracting the compounds into solvent, separating the extract using high pressure liquid chromatography, and measuring the κ value of each seperated component as a function of column retention time using scanning flow CCN analysis. Kappa generally decreased with retention time, suggesting a relationship between a compound's polarity and its κ value. The frequency distributions of component κ's that make up the mixture provide detailed information linking chemical mechanisms of SOA formation and organic aerosol CCN activity.

https://doi.org/10.1180/S0026461X00006502 Published online by Cambridge University Press

LA-ICP-MS Sr isotope ratio analysis of individual fluid inclusions

THOMAS PETTKE[1], FELIX OBERLI[2] AND JACOB J. HANLEY[3]

[1]University of Bern, Institute of Geological Sciences, CH-3012 Bern, Switzerland. (Pettke@geo.unibe.ch)
[2]ETH Zurich, Institute of Geochemistry and Petrology, CH-8092 Zurich, Switzerland

This pilot study addresses the feasibility of precise and accurate Sr isotope ratio analysis by laser-ablation multiple collector ICP-MS of fast transient signals as obtained from the ablation of individual fluid inclusions. We used synthetic (Na±Ca)Cl inclusions containing variable amounts of SRM 987 Sr and Rb.

The principal analytical and data reduction procedures follow those reported in Pettke *et al*. [1] and Burla *et al*. [2]. Masses 83, 84, 85, 86, 87, 88 were recorded on Faraday detectors at 0.2s integration intervals. Raw readings were first corrected for incongruent amplifier response using the quadratic tau correction scheme [1]. Background correction is followed by interference correction, altogether removing overlap by Kr, Ca-argides and Ca-dimers. ^{87}Rb overlap is then corrected by peak stripping using fractionated Rb based on mass bias values obtained for Sr, and the resulting ^{87}Sr/^{86}Sr ratio is then mass bias corrected.

Evaluation of results based on individual readings reveals incongruent signal intensity evolution for ^{85}Rb and ^{86}Sr across the fluid inclusion signal. Tau- and interference-corrected ^{87}Sr/^{86}Sr data are constant (at given analytical precision) across the transient fluid inclusion signal, however.

^{87}Sr/^{86}Sr ratios of synthetic fluid inclusions with variable Rb/Sr abundance ratios were obtained by bulk signal integration. As for synthetic fluid inclusions Sr isotope equilibrium between phases prevails, uncertainties of ^{87}Sr/^{86}Sr ratios could be minimized by cutting off low-intensity and thus imprecise transient signal tails.

Final ^{87}Sr/^{86}Sr ratios correlate with ^{85}Rb/^{86}Sr ratios. The least squares linear fit intercept is at ^{87}Sr/^{86}Sr = 0.71028 ±0.00019, identical to the nominal value of SRM 987 = 0.710245. The correlation could be eliminated by adjustment of ^{85}Rb/^{87}Rb to 2.58676, a value very close to that reported earlier [3], suggesting that an offset in mass bias between Sr and Rb by 5.3% in β values can account for the observed trend.

[1] Pettke, T. *et al*. (2011) *J. Anal. Atom. Spectrom*. **26**, 475. [2] Burla, S. *et al*. (2009) *Terra Nova* **21**, 401. [3] Jackson, M.G. Hart, S.R. (2006) *EPSL* **245**, 260.

Association of amino sugars (chitin) with Fe oxyhydroxides in mycorrhizal mat soils – A STXM/NanoSIMS investigation

JENNIFER PETT-RIDGE[1]*, MARCO KEILUWEIT[1,2], JEREMY BOUGOURE[1], PETER S. NICO[3], PETER K. WEBER[1], LYDIA ZEGLIN[2], DAVID D. MYROLD[2] AND MARKUS KLEBER[2]

[1]Lawrence Livermore National Laboratory, Physical and Life Sciences Directorate, Livermore, CA (*correspondence: pettridge2@llnl.gov)
[2]Department of Crop and Soil Science, Soils Division, Oregon State University, Corvallis, OR
[3]Lawrence Berkeley National Laboratory, Earth Sciences Division, Berkeley, CA

Amino sugars and polymers such as chitin represent a major constituent of fungal cell walls and hydrolyzed soil organic matter. Despite their potential importance in soil nitrogen and carbon cycling, comparatively little is known about their dynamics in soils. Here we present the results of an investigation into the mineral interactions and micro-scale behavior of chitin in ectomycorrhizal mats – a system adapted to rapid cycling of amino sugars. The aim of this study was to follow the micro-scale dynamics of ^{13}C- and ^{15}N-labeled chitin during a 3-week incubation in mycorrhizal mat soil collected from a Oregon andic soil under Douglas-fir forest. Based upon previous findings, we hypothesized that the isotopic label would accumulate in bacterial cells associated with fungal hyphae due to their ability to rapidly process amino sugars. In contrast, nano-scale secondary ion mass-spectrometry (NanoSIMS) imaging of hyphae-associated soil organic matter, minerals, and bacteria revealed a preferential association of ^{15}N with Fe-rich particles at the end of the experiment. Synchrotron-based Scanning Transmission X-ray spectromicroscopy (STXM/NEXAFS) at the C, N and Fe K-edge suggests that these hyphae-associated microstructures consist of thin coatings of amine N on Fe (oxyhydr)oxides. Our results are consistent with recent observations of preferential binding of amine N to Fe-rich minerals and suggest a role of Fe (oxyhydr)oxide surfaces in N cycling of organic layers soils. No enrichment of ^{13}C was found at these locations, possibly due to the lower levels of overall ^{13}C abundance. We further discuss advantages and challenges (e.g. data representation, replication, appropriate controls) of the combined application of isotopic and spectroscopic imaging techniques for the investigation of soil C and N cycling.

https://doi.org/10.1180/S0026461X00006502 Published online by Cambridge University Press

CO_2 sequestration in olivine rich basaltic aquifers: A reactive percolation experimental study

S. PEUBLE, M. GODARD, P. GOUZE AND L. LUQUOT

Géosciences, CNRS-Université Montpellier 2, France

Injection of CO_2-rich fluids into basaltic aquifers is one of the methods envisaged for mitigation of increasing atmospheric CO_2. Basalts are rich in Mg, Fe and Ca and have a high potential to trap CO_2 as carbonate minerals. However, the role of reaction-transport processes has yet to be investigated in order to predict the capacity and sustainability for CO_2 storage of these highly reactive systems.

We present the results of three percolation experiments performed on the ICARE-2 experimental bench at 180°C and total pressure of 12 MPa. $NaHCO_3$ rich water (0.5 mol/L) mixed with CO_2 (Pco_2 = 10 MPa) was injected through sintered analogues of olivine-accumulation zones in basaltic flows (~95% olivine Fo_{87}, MORB glass, minor chromite). The injection rate was 1 mL/h for exp. 1 and 2, and 0.1 mL/h for exp. 3. The initial porosity and permeability of samples ranges from 4 to 7% and $30x10^{-18}$ to $400x10^{-18}$ m^2 respectively.

All experiments show a strong permeability decrease (down to 10^{-18} m^2) after 90 hours for exp. 1 and 2, earlier for exp 3. Yet dissolution occurs: high concentrations of Zr and Al and of Co in the outlet fluids indicates dissolution of basaltic glass and olivine respectively. Si concentration changes reveal a more complex system with olivine dissolution and the precipitation of Si rich phases. We observed the growth of relatively large (up to 5 microns) Mg-Fe rich phyllosilicates perpendicular to (at the expense of ?) olivine surface. This reaction is typically associated to hydration of (ultra-)mafic rocks and may explain the decrease in permeability during experiments. Finally, the low Ca and Mg fluid concentrations suggests trapping by Ca-Mg rich phases. Ankerite and dolomite were identified by Raman spectrometry in the samples of exp. 1 and 2, while exp. 3 was characterised by precipitation of well developped and abundant magnesite ($Mg_{0.88}Fe_{0.11}Ca_{0.01}CO_3$) replacing dissolved olivine. Carbonation appears to be an efficient process: ~ 0.015g of CO_2 per gram of sample is stored as carbonates during exp. 1, that is, if these results were directly upscaled to the size of an injection site, an average yield of ~45 kg/m^3/day. Our results indicate a strong control of flow rates on carbonation, but also on hydration reactions. This implies not only variations of the CO_2 storage capacity of the basaltic aquifer with distance to the injection well, but also that controlling the injection rate could allow to enhance the efficiency of *in situ* carbonation.

Diffusion of nanoparticles in waters and biofilms-implications for bioavailability

T.-O. PEULEN[1], R.F. DOMINGOS[2], D.F. SIMON[3] AND K.J. WILKINSON[3]

[1]Institute of Molecular Physical Chemistry, Heinrich-Heine-University Düsseldorf, Building 26.32.02, Universitätsstraße 1, 40225 Düsseldorf, Germany

[2]Centro de Química Estrutural, Instituto Superior Técnico/Universidade Técnica de Lisboa, Torre Sul lab 11-6.3, Av. Rovisco Pais # 1, 1049-001 Lisbon, Portugal

[3]Département de Chimie, Université de Montréal, C.P. 6128, succursale Centre-ville, Montréal QC, H3C 3J7, Canada

In order to properly assess the environmental risk of engineered nanoparticles (ENP), it is necessary to determine their fate (including dissolution, aggregation and bioaccumulation) and mobility under representative environmental conditions. While the mass transport of nanoparticles in the environment is necessarily lower than that of ions, it is not clear that reduced mobility will result in reduced bioavailability. In this study, two lines of study were examined to determine the effect of increased particle size on the mobility and bioavailability of nanoparticles. The bioaccumulation (and biological effects) of CdTe/CdS quantum dots (QD) was compared with that of free Cd^{2+}. While the bioaccumulation of the QD was largely accounted for by dissolved Cd, whole transcriptome screening using RNA-Seq analysis showed that the free Cd and the QD had distinctly different biological effects. In a second line of experiments, the diffusion of several model nanoparticles (dextrans, fluorescent microspheres, Ag nanoparticles) were studied *in situ* using confocal microscopy and fluorescence correlation spectroscopy in a biofilm. For the most part, relative self-diffusion coefficients decreased exponentially with the square of the radius of the nanoparticle. The nature of the biofilm was also shown to be an important parameter controlling the diffusion of the nanoparticles. Finally, the charge of the nanoparticles also appeared to be important – a greater than predicted decrease in the self-diffusion coefficient was observed for the negatively charged nano Ag, especially in dense biofilms. In order to understand the role of nanoparticles in the environment, it is necessary to understand the important factors affecting their mobility.

https://doi.org/10.1180/S0026461X00006502 Published online by Cambridge University Press

Removal Pb^{2+} from water sample, by using Natural Zeolites of Aftar mine (Semnan, Iran)

S. PEYRAVI[1], R. ZAHIRI[2] AND K. MORADI HERSINI[3]

[1]M.Sc in Economic Geology, School of Earth Sciences, Damghan University, Damghan, Iran
[2]Assistant Professor, School of Earth Sciences, Damghan University, Damghan, Iran (zahiri@du.ac.ir)
[3]Assistant Professor, School of Earth Sciences, Damghan University, Damghan, Iran

Zeolites are naturally occurring hydrated Aluminosilicate minerals [1]. The isomorphous replacement of Si^{4+} by Al^{3+} produces a negative charge in the lattice. The net negative charge is balanced by the exchangeable cations (sodium, potassium, or calcium). These cations are exchangeable with certain cations in solutions such as lead [2, 3].

This study represents usage zeolite Aftar mine in ability the zeolites in the removal of lead from water sample. For this purpose, the first crushed zeolites and using the mesh sieve ASTM.E-11 standard classification in size by 1 mm, 0.71 mm and 0.25 mm for use in testing were falling head.

According to falling head test, and calculated parameter such as K (Permeability) water samples (with concentrations of certain lead) the cross of the zeolite and ICP-OES analysis on them. The results show that zeolite of Aftar mine be able removal lead. XRF analysis on the zeolite shows that After passing the water sample in the composition of zeolites lead sensible.

PbO	K_2O	Na_2O	CaO	Fe_2O_3	Al_2O_3	SiO_2	Components
0	1.93	1.46	2.78	1.19	10.96	70.85	Before
0.38	1.89	1.64	1.83	1.18	10.94	71.75	After

Table 1: XRF analysis of the zeolite samples before and after removal lead

[1] Badillo-Almaraz *et al*. (2003) *Instrum. Methods Phys. Res.* **B 210**, 424. [2] Barer. (1987) Academic Press, New York. [3] Breck (1964) *Chem. Edu.* **41**, 678.

Biogeoelectric networks in marine sediments – A 'first cut' study

C. PFEFFER[1]*, N. RISGAARD-PETERSEN[1] AND L.P. NIELSEN[2]

[1]Center for Geomicrobiology, Department of Biological Sciences, Aarhus University, 8000 Aarhus C, Denmark (*correspondence: christian.pfeffer@biology.au.dk) (nils.risgaard-petersen@biology.au.dk)
[2]Section for Microbiology, Department of Biological Sciences, Aarhus University, 8000 Aarhus C, Denmark (biolpn@biology.au.dk)

Electric Currents in Marine Sediments

A recent study showed that electric currents can run through marine sediments coupling hydrogen sulphide oxidation at depth and oxygen reduction at the sediment surface [1]. A microbially assisted composition of bacterial nanowires and possibly semiconductive minerals was suggested to play a role in the electron transfer. However, this concept remained hypothetical.

Evaluating the Type of Electron Transmission

We hypothesised that an electric network is entirely composed of solid conduits, performing true electronic conductance (in contrast to electron shuttling).

To test this hypothesis, we first cut horizontally through electrically active sediment systems using a very thin platinum filament. Monitoring proton and oxygen consumptions revealed that the electrochemical reduction of oxygen was instantaneously interrupted by the cut. Moreover, the electric field was equally affected upon cutting.

In a second approach, polycarbonate filters embedded in the sediment were found to obstruct the development of an electric connection, although diffusion of electron shuttles were not impeded by the filters.

Conclusion

The results provide strong evidence that the conductive elements in marine sediments comprise a solid matrix of electronic conduits. Thus, our findings support the proposed involvement of microbial nanowires and semiconductive minerals, i.e. the occurrence of biogeoelectric networks in marine sediments.

[1] Nielsen *et al*. (2010) *Nature* **463**, 1071–1074.

https://doi.org/10.1180/S0026461X00006502 Published online by Cambridge University Press

Arsenic uptake and speciation in the green marine alga *Ulva lactuca*: Development of a coastal aquatic bioindicator

CATHERINE PHAM[1,2]*, LAURENT CHARLET[2] AND GARRISON SPOSITO[1]

[1]Division of Ecosystem Sciences, University of California, Berkeley, CA 94720-3114, USA (*correspondence: pham@cal.berkeley.edu, gsposito@berkeley.edu)

[2]ISTerre, University of Grenoble, BP 53, 38041, Grenoble, France (charlet38@gmail.com)

Algae are ubiquitous in surface waters and are known to influence the biodynamics of the priority toxic metalloid arsenic (As) in polluted marine environments. In the present study, we investigated the bioavailability and chemical forms of As in algae sampled from contaminated coastal waters in France and California in order to understand As cycling in the marine environment using synchrotron-based spectroscopic techniques.

Given the alga's unique morphology and cell size (15-50 µm cell diameter; 50-100 µm thallus thickness), STXM and µXRF were used for the first time to date to analyze *Ulva lactuca* to distinguish the different target organelles and map As speciation *in situ*. We observed shifts at the carbon 1s edge in response to As and phosphate gradients and are exploring the importance of arsenosugars.

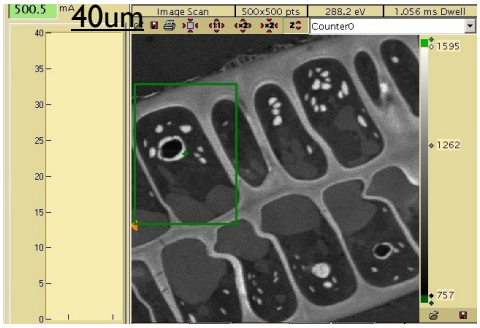

Figure 1: Cross-section of *Ulva lactuca* perpendicular to the axis of the thallus using STXM at 288.2 eV.

We are characterizing the potential risks As may pose to both ecological and human health as it is transformed into various chemical forms and moves from algae up trophic levels, potentially to fish and humans. Our research may serve as a basis for the future use of algae in biomonitoring and phytoremediation scenarios related to metalloid contamination in aquatic ecosystems.

Evidence from zircon ages and Hf isotopic composition for Paleoproterozoic crustal evolution in Northwestern Vietnam

PHAM TRUNG HIEU[1,2]* AND F. CHEN[3]

[1]Institute of Geology and Geophysics, Chinese Academy of Sciences, Beijing, 100029, China (*correspondence: fanzhongxiao@126.com)

[2]Hanoi University of Mining and Geology, Vietnam

[3]School of Earth and Space Sciences, University of Science and Technology of China, Hefei, China (fkchen@ustc.edu.cn)

The Phan Si Pan area of NW Vietnam is one of the oldest basements in SE Asia. Paleoproterozoic is worldwide an important era in crustal evolution with occurrence of megascale tectonothermal activities, but the record is not much clear in NW Vietnam. In order to reveal the nature of Paleoproterozoic events in NW Vietnam, a combined study of zircon U-Pb ages and Hf isotopic composition was done on metamorphosed sedimentary rock and migmatite in the Phan Si Pan area, being an Archean basement exposed in NW Vietnam. Zircons yield U-Pb ages of 1.83 ±0.08 Ga. These Paleoproterozoic zircons have Th/U ratios of 0.02-0.25, indicating both magmatic and metamorphic origins. They are characterized by old Hf model ages of ~3.1 Ga and negative ε_{Hf} (t) values of about -10, implying Archean source (s). From these results, it is proposed that the Paleoproterozoic global thermal event (s) must have been taken place in NW Vietnam at least with reworking of Archean continental nucleus.

Based on a survey of the Paleoproterozoic events throughout the Phan Si Pan area, it can be observed that metamorphic and simultaneous magmatic event (s) have occurred in the northern part connected with the South China craton, but only magmatic activity have been distinguished in the southern part (the Bao Ha complex) so far. These metamorphic and magmatic activities were probably associated with the formation of a unified basement in NW Vietnam and likely imply continental accretion during the assembly of the Columbia supercontinent in Paleoproterozoic.

https://doi.org/10.1180/S0026461X00006502 Published online by Cambridge University Press

On the potential for CO_2 mineral storage in continental flood basalts

VAN T.H. PHAM *, HELGE HELLEVANG AND PER AAGAARD

Department of Geosciences, Univ. Oslo, Norway (*correspondence: per.aagaard@geo.uio.no)

Continental flood basalts (cfb) are considered as potential objectives for CO_2 storage because they contain abundant divalent cations and therefore have a potential for mineral trapping of CO_2 [1]. Lateral extensive cfb are found in many place in the world within distance from major CO_2 point emission sources.

The potential of cfb to store CO_2 in secondary carbonates was evaluated. Based on mineral assemblage, formation water composition of Colombia River Basalt [2], we estimated the reactive surface of the basalt to be approximately 1/1000 of the total pore space surface. Kinetic dissolution of primary basalt-minerals (pyroxene, feldspar and glass) and local equilibrium assumption for secondary phases (weathering products) were applied for the simulations.

According to the simulations result, formation of carbonates in basalt rock at 40 ºC and CO_2 100 bar is limited, and only small amount of siderite and ankerite formed. Calcium was largely consumed by zeolite instead of forming Ca-carbonates (Figure 1). Potential of carbonate formation is sensitive to reservoir temperature and CO_2 pressure, with intermediate pressures giving more secondary carbonates than the highest pressures. The amount of carbon stored in solid phases after 10.000 years is small relative to solution trapping (approximately 0.23 %).

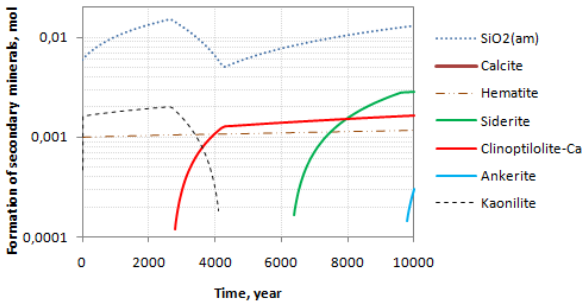

Figure 1: Secondary minerals formed in the batch simulation with the present of injection CO_2 at 40 °C, 100 bar. Only amounts of siderite and ankerite formed in thousand years.

[1] Oelkers *et al*. 2008. *Elements* **4**, 305–310. [2] Reidel *et al*. 2002. *Report Pacific Northwest National Laboratory*, PNNL-13962.

Crustal contribution to the geo-neutrino flux at the Sudbury Neutrino Observatory (SNOLAB)

CATHERINE PHANEUF[1], JEAN-CLAUDE MARESCHAL[1], CLAIRE PERRY[1] AND CLAUDE JAUPART[2]

[1]GEOTOP , Université du Québec à Montréal, PO8888, Station Downtown, Montréal, H3C 3P8, Canada

[2]Institut de Physique du Globe de Paris, 1, rue Jussieu, 75238, Paris Cedex 5, France

Recent improvement in the observation of geo-neutrinos, i.e. low energy anti-neutrinos produced by β decays in the series of radioactive elements U and Th, will permit a direct determination of the abundance of these radio-elements in the mantle and their contribution to the earth's energy budget.

The major fraction, about 80%, of the geo-neutrinos, that will be detected in continental observatories come from the continental crust nearby. In order to estimate the flux from the mantle, we need to precisely account for the crustal contribution.

Crustal radio-activity can be best determined from surface heat flux data which integrate the entire crustal column and are unaffected by small scale heterogeneities.

We analyze heat flux and heat production data to calculate the crustal contribution to the total geo-neutrino flux that will be observed at the Sudbury Neutrino Observatory (SNOLAB).

With all the available data, we show that the heat production is very heterogeneous but that the Sudbury region has significantly higher heat flux than the average Canadian shield (53 mWm^{-2} vs 42 mWm^{-2}). This elevated heat flux is due to the high heat production (>1.5 μWm^{-3}) in the upper part of the crust which is usually enriched in radio-elements.

This high crustal radio-activity leads to as much as 50% increase of the local crustal component of the geo-neutrino flux that will be observed at SNOLAB.

https://doi.org/10.1180/S0026461X00006502 Published online by Cambridge University Press

Reconciling the sulfur atmospheric cycle of early Earth with the geological record

PASCAL PHILIPPOT AND MARK VAN ZUILEN

Geobiosphere, Institut de Physique du Globe, Sorbonne Paris Cité, Université Paris Diderot, CNRS, 1 rue Jussieu, 75238 Paris, France

The reports of mass-independent sulfur isotope anomalies (MIF-S) in sediments older than 2.45 Ga have been attributed to photolytic reactions involving volcanic SO_2 in an oxygen-poor atmosphere. Photolysis experiments of SO_2 coupled with various UV shielding scenarios provided additional links to the early atmosphere. However, no simple model can reproduce the mismatch in the $\Delta^{33}S$-$\delta^{34}S$ relationship between the reference Archaean sulfide array (positive $\Delta^{33}S$-$\delta^{34}S$ correlation) and product sulfate (negative $\Delta^{33}S$ but positive $\delta^{34}S$). The discrepancy in the temporal and spatial record of sulfur isotope anomalies, with three main sulfate horizons deposited within less than 300 Ma compare to a global distribution of sulfide over more than 1, 500 Ma, is also unexplained. Here we report a new $\Delta^{33}S$-$\delta^{34}S$ linear trends recovered in two felsic volcanic ash layers of the 3.2 Ga Mapepe Formation in South Africa. This « felsic volcanic array » forms a tight $\Delta^{33}S$-$\delta^{34}S$ linear correlation that is best approximated by SO_2 photolysis experiments at deep UV wavelength. The perfect match to the $\Delta^{33}S$-$\delta^{34}S$ values of associated sulfate and equivalent felsic volcanoclastic and sulfate horizons of the 3.5 Ga old Dresser Formation, Western Australia, indicates that the exogenic sulfur cycle that produced this array was linked to felsic volcanism and sulfate precipitation. An emerging scenario for the early Earth atmosphere is a continuous photochemical haze that is perturbed between 3.5 and 3.2 Gyr by massive and optically thick volcanic plumes. This volcanic activity coincides in time with a period of rapid crust formation (Valbaara supercontinent).

Microbial iron reduction under deep subsurface pressure conditions

AUDE PICARD[1,2,3]*, DENIS TESTEMALE[4], JEAN-LOUIS HAZEMANN[4] AND ISABELLE DANIEL[3]

[1]Max Planck Institute for Marine Microbiology, Biogeochemistry Department, Celsiusstraße 1, 28359 Bremen, Germany (*correspondence: apicard@mpi-bremen.de)

[2]MARUM, Center for Marine Environmental Sciences, Bremen, Germany

[3]Université de Lyon, F-69622, Lyon, France, Université Lyon 1, ENS Lyon, CNRS, UMR 5570, Laboratoire de Géologie de Lyon, 46 allée d'Italie, 69364 Lyon Cedex 07, France

[4]Institut Néel, CNRS, Université Joseph Fourier, BP166, F-38042 Grenoble Cedex 9, France

Pressure is a key parameter in the deep subsurface which has been estimated to contain a large microbial population [1]. However the effects of pressure on microbial processes involved in important biogeochemical cycles are not constrained yet. At present, iron oxides are recognized as the most abundant terminal acceptors for the oxidation of organic matter in anoxic environments imposing dissimilatory iron reduction (DIR) as a biogeochemically important process in aquatic sediments, soils and aquifers [2]. Many factors are known to influence iron reduction rate and extent, however to our knowledge pressure effects on microbial iron reduction have not been investigated. We investigated the pressure dependence on Fe (III) reduction by the bacterium *Shewanella oneidensis* MR-1 up to 100 MPa using *in situ* X-ray Absorption Spectroscopy (XAS). At pressures up to 70 MPa, MR-1 was able to reduce all 5 mM Fe (III) citrate provided. Above 70 MPa, the final amount of Fe (III) that MR-1 could reduce decreased linearly and DIR was estimated to stop at 109 ±7 MPa. The initial reduction rate was enhanced by pressure up to 40 MPa then decreased to reach 0 at ca 110 MPa. MR-1 is a piezosensitive bacterium with growth rate maximum at atmospheric pressure. However, it can still grow at relatively high rates up to 40 MPa. MR-1 could thus be a potential significant player of the iron cycle in most of the metal-rich freshwater and marine sediments where moderate pressures occur.

[1] Whitman W.B. Coleman D.C. Wiebe W.J. (1998) *Proc. Natl. Acad. Sci. USA* **95**, 6578-6583. [2] Nealson K.H. & Saffarini D. (1994) *Annu. Rev. Microbiol.* **48**, 311–343.

https://doi.org/10.1180/S0026461X00006502 Published online by Cambridge University Press

Diatom-bound trace metals: A tracer for past changes in micronutrients availability?

LAETITIA E. PICHEVIN*, WALTER GEIBERT AND RAJA S. GANESHRAM

School of Geosciences, Grant Institute, West Mains Road, Edinburgh EH9 3JW, UK
(*correspondence: laetitia.pichevin@ed.ac.uk)

Micronutrient input to the ocean is considered to have played a modulating role on the marine carbon pump and global climate throughout the past. An appropriate proxy for micronutrient bioavailability in the surface ocean and uptake by the phytoplankton was hitherto lacking. Culture experiments have shown that diatoms incorporate elements such as Zn and (potentially) Fe into their frustules in proportion with their availability in the medium [1, 2]. Hence, diatom-bound metals concentrations could be used to track past changes in marine micronutrients availability. However, whether the signal recorded by the living diatoms is fully transferred to the sediment has never been tested. In order to measure the impact of diagenetic processes during settling and burial on the trace metals signal biologically incorporated into the frustules, we compared diatom-bound trace metals content in surface sediments, traps and in suspended particles collected in the overlying surface water. Both ICP-OES and the ion microprobe techniques were used. Our results suggest that for most of the metals considered in this study, diagenetic processes alter the recording of the signal with the notable exception of Zn and, potentially, Mg.

[1] Ellwood, M. J. & Hunter, K. A. Limnology & (2000) *Oceanography* **45**, 1517–1524. [2] Jaccard, T. Ariztegui, D. & Wilkinson, K. J. (2009) *Chemical Geology* **265**, 381–386.

Experimental investigation of garnet-cpx geobarometers in eclogites

J. PICKLES*, J.D. BLUNDY, R. SWEENEY AND C.B. SMITH

University of Bristol, Bristol. UK
(*correspondence: Joe.Pickles@bristol.ac.uk)

The development of accurate geothermometers has greatly helped in the understanding of metamorphic petrology and magmatic processes. The development of geobarometers applicable to eclogitic assemblages has previously not received the same attention. Here we present both empirical and thermodynamic models based on the partitioning of major and minor elements between garnet and cpx as determined experimentally in the P-T range 1-11 GPa and 800-1700 °C.

The cpx-garnet partitioning of Na, Ca and Ti are found to be strongly sensitive to pressure, with Dgt/cpx increasing with increasing pressure. The sensitivity of D_{Ca} to pressure increases with decreasing garnet mg#. An empirical model of D_{Ca} was derived from over 150 mineral pairs from experiments. For garnets with an mg#< 0.7 the following calibration is valid for pressures between 1 and 11 GPa and temperatures between 800 and 1300 °C.

The barometer is:

$$P = (\ln D_{Ca} - 4.48 + 1.26 Si^{gnt} + 0.19 Fe^{gnt} + 1.46 Mn^{gnt} + 0.87 Mg^{gnt}) * 4.17$$

Where D_{Ca} is the concentration of Ca in garnet divided by Ca in cpx and Si^{gnt} is Si in garnet, all in atoms pfu. This model is insensitive to temperature, thus avoiding errors associated with geothermometers. Based on the regression of the data we estimate that the model has a standard error of 0.5 GPa.

We also investigated a number of exchange reactions as potential barometers, including reactions involving silica and rutile. These exchange reactions show considerable compositional sensitivity at fixed P and T, testifying to non-ideality in garnet and cpx. Using a ternary asymmetric model we derive non-ideal interaction parameters for each mineral. We find that barometers based on the exchange of Ca between garnet and cpx provide the most robust barometers.

https://doi.org/10.1180/S0026461X00006502 Published online by Cambridge University Press

The structure and lability of Re(VII)-sodalite

ERIC M. PIERCE[1]*, JAMES B. HARSH AND[2] AND JOHNBULL O. DICKSON[2]

[1]Oak Ridge National Laboratory, Oak Ridge, TN 37831 USA (*correspondence: pierceem@ornl.gov)
[2]Washington State University, Pullman, WA 99164 USA (harsh@wsu.edu, j.dickson@ wsu.edu)

^{99}Tc (Tc), a long-lived radionuclide, is one of the most widespread contaminants within the Hanford subsurface with an estimated inventory of 5.31×10^3 curies. For example, Tc contamination has been found in the sediments beneath the C, S, SX, T, and TX Tank Farms as a result of high-level waste (HLW) solutions that have leaked or spilled from Hanford Tanks. The HLW solutions are characterized as highly alkaline (hydroxide ion concentration > 8.5 M) and high ionic strength solutions (up to saturation with respect to $NaNO_3$). Previous research focused on ^{90}Sr and ^{137}Cs has demonstrated that these elements are incorporated into feldspathoid minerals, such as sodalite [Na_8 ($Al_6Si_6O_{24}$)Cl_2], that formed as a result of the contact between Hanford sediments and the HLW solutions [1, 2]. The desire to immobilize Tc in aluminosilicate minerals through the application of subsurface amendments for contaminated sediments as well as the production of mineralized wasteforms further emphasizes the need to understand the long-term stability and release of Tc from aluminosilicate minerals, specifically the feldspathoid mineral sodalite.

In an attempt to determine the structure and reactivity of Re-sodalite (as a chemical analogue for Tc-sodalite), a combination of spectroscopy analyses along with single-pass flow-through experiments were performed under dilute and near saturated conditions at pH (23°C) = 9.0 and 40°C. These initial experimental results suggest the release of elements from Re-sodalite is complex; the saturation state of the solution changes and this behavior may be associated with the formation of other mineral phases.

[1] Chorover, J. Choi, S. Rotenberg, P. Serne, R.J. Rivera, N. Strepka, C. Thompson, A. Mueller, K.T. O'Day, P.A. (2008) Silicon control of strontium & cesium partitioning in hydroxide-weathered sediments. *Geochimica Et Cosmochimica Acta* **72**, 2024–2047. [2] Deng, Y. Harsh, J.B. Flury, M. Young, J.S. & Boyle, J.S. (2006) Mineral formation during simulated leaks of Hanford waste tanks. *Applied Geochemistry* **21**, 1392–1409.

Long term chemical variations in stream waters draining a granitic catchment (1986-2010). Link between hydrology and weathering (Strengbach catchment, France)

MARIE-CLAIRE PIERRET[1], DANIEL VIVILLE[1], FRANÇOIS CHABAUX[1], PETER STILLE[1] AND ANNE PROBST[2]

[1]LHYGES EOST Université de Strasbourg, 1 rue Blessig 67000 Strasbourg, France (marie-claire.pierret@unistra.fr)
[2]ECOLAB ENSAT, Avenue de l'Agrobiopole 31326 Castanet Tolosan, France (anne.probst@ensat.fr)

The forested Strengbach catchment is an experimental site for which hydrological, geochemical and meteorological data have been collected since 1986. It is located in the Vosges massif on a granitic bedrock with temperate oceanic mountainous climate. The site suffered from acid rains and tree decline was acknowledged in the 1980s.

At the end of the 1980s, in parallel with the decrease of the acid atmospheric depositions, the pH of surface waters increased. At the same time, the chemical composition of the stream water evolved to significant lower cation (Ca, Mg) and anion (SO_4, NO_3) concentrations. Similarly, soil solutions show a decrease in Ca and Mg concentrations since 1986.

The decreasing sulfate concentrations are related to the reduction of anthropogenic acidic rain depositions as well as combination of sorption/desorption in soils**.** The variations of nitrate concentrations, which are not continuous over time, might be related to extremely dry periods causing modification of the N biogeochemical cycle at the catchment scale.

The decreasing cation concentrations cannot be explained by diminishing atmospheric wet and dry depositions. Similarly, hydrological processes do not explain these compositional changes. But the annual chemical fluxes out of the catchment are strongly correlated to the annual water fluxes, which were highly variable during the past 25 years.

Only changes in water-rock interaction and in the nature of the weathered sources might explain the Ca, Mg and K concentration variations at the catchment scale. The mechanisms involved include the formation of secondary soil minerals (mainly clays), cation exchange processes as well as weathering of primary, granite-derived and secondary minerals with resulting cation depletion in soil and saprolite.

Therefore, the long term monitoring of rain, throughfalls, spring and stream waters allows to follow the geochemical evolution of the ecosystem over time in response to changes in atmospheric pollution and forest management.

https://doi.org/10.1180/S0026461X00006502 Published online by Cambridge University Press

Chemical and mineralogical profile of the local wind-blown surface soil contribution to respirable airborne PM in Rome (Italy)

A. PIETRODANGELO*, R. SALZANO, S. PARETI, E. RANTICA AND C. PERRINO

Institute for Atmospheric Pollution Research, C.N.R., Italy, 00016 Monterotondo St (Rome)
(*correspondence: Pietrodangelo@iia.cnr.it)

We present the chemical and mineralogical profile of the respirable fraction of resuspended surface soil contributing to airborne particulate matter (PM) in the southern area of Rome. Mineral dust either from rocks and soil or from human activities share an exchangeable fate in the PBL [1] and result often not separable by receptor modelling. Nevertheless, discriminating among dust contributions is critical both for legislative purposes and for modelling improvement. In this work 12 bulk samples of surface rocks were collected at locations where the various geological lithosomes of the southern area of Rome emerge from soil [2]. From these samples the PM10 fraction was extracted. The PM_{10} soil fraction was analysed by ED-XRF and for single–particle microanalysis by SEM–EDX. The mineralogical content of samples was obtained by XRD. Analytical performances of single-particle microanalysis were evaluated against ED-XRF and XRD results. Single particles were classified for mineralogy, by matching the EDS spectra with the database of the RRUFF and/or of the GEOROC projects [3, 4]. Estimated aerodynamic diameter and size-segregation of the mineralogical classes identified in the PM_{10} soil fraction are discussed.

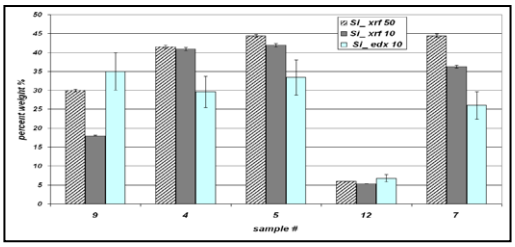

Figure 1: Performance evaluation for the Si determination by field and single-particle SEM-EDX microanalysis.

[1] Korcz *et al*. (2009) *Atm Env* **43**, 1410-. [2] Giordano *et al*. (2006) *J. Volcanol Geotherm Res* **155**, 49–80. [3] Downs (2006) http://rruff.info. [4] Sarbas & Nohl (2006) http://georoc.mpch-mainz.gwdg.de/georoc/Entry.html

Slow mantle upwelling on the margin of the Hawaiian plume based on ^{230}Th-^{238}U disequilibria at Lōih‘i Seamount

AARON J. PIETRUSZKA[1], ERIK H. HAURI[2], RICHARD W. CARLSON[2] AND MICHAEL O. GARCIA[3]

[1]Department of Geological Sciences, San Diego State University, San Diego, CA 92182-1020, USA
[2]Department of Terrestrial Magnetism, Carnegie Institution of Washington, Washington DC 20015, USA
[3]Department of Geology and Geophysics, University of Hawaii, Honolulu, HI 96822, USA

The shield stage of a Hawaiian volcano is dominated by the eruption of tholeiitic basalts, whereas alkalic lavas are commonly erupted during the submarine pre-shield stage. Geochemical studies (e.g. [1]) relate this difference in lava chemistry to an increase in the degree of partial melting as the volcano drifts onto the Hawaiian mantle plume. We present high-precision U-series isotopic measurements for sixteen volcanic glasses from Lōih‘i Seamount to examine the time scale of the melt generation process during the pre-shield stage of a Hawaiian volcano. All of the samples have small amounts of excess ^{234}U (~0.2-1.0%) due to contamination with seawater-derived U (with ~14.6% excess ^{234}U). These signatures cannot be explained by syn- or post-eruptive interaction between lava and seawater. Instead, mantle-derived magmas at Lōih‘i are probably contaminated by hydrothermally altered rocks within the volcanic edifice. These altered rocks were likely enriched in U that was precipitated from seawater-derived hydrothermal fluids in the region above the volcano’s magmatic plumbing system. The Lōih‘i glasses display a wide measured range in the amount of excess ^{230}Th from ~1-7% (due to the addition of seawater-derived U) that overlaps with lavas from the nearby shield-stage volcano, Kīlauea (~2% excess ^{230}Th [2]). We correct the ^{230}Th-^{238}U disequilibria of the Lōih‘i glasses back to their pre-contamination values using their ^{234}U-^{238}U disequilibria and a simple mass-balance calculation. This correction suggests that mantle-derived magmas at Lōih‘i have a narrow range of ~6-9% excess ^{230}Th, which is significantly larger than observed at Kīlauea. This difference is consistent with the idea that Lōih‘i is tapping mantle that is upwelling slowly (~5-6 cm/yr) on the margin of the Hawaiian plume. This rate is at least an order of magnitude slower than the 50-1000 cm/yr range inferred for the mantle beneath Kīlauea [2].

[1] Garcia *et al*. (1995) *J. Petrol*. **36**, 1647–1674. [2] Pietruszka *et al*. (2001) *EPSL* **186**, 15–31.

https://doi.org/10.1180/S0026461X00006502 Published online by Cambridge University Press

Melt compositions and processes in the kimberlite provience of southern West Greenland

L. PILBEAM[1,2]*, T.F.D. NIELSEN[1] AND T.WAIGHT[2]

[1]Geological Survey of Denmark and Greenland, Øster Voldgade 10, 1350 KBH K, Denmark (*corresponence: lpi@geus.dk)
[2]Institute of Geography and Geology, Univ. of Copenhagen, Øster Voldgade 10, 1350 KBH K, Denmark

The kimberlite province of southern West Greenland (600-560Ma) comprises kimberlite *sensu stricto* on the Archean craton and aillikites on the paleoproterzoic sheild to the North. Carbonatite melt and xenocrystic olivine dominate the kimberlite *sensu stricto* occurrences of the Manitsoq region [1] whilst the silica content and H_2O/CO_2 ratio of the bulk rocks increases towards Sisimuit [2, 3]. A common carbonatite rich end-member is implicated [2]. This is in contrast to the prevailing dogma of a continuum from carbonatite though aillikite to kimberlite with increasing melting degree [4].

The authors have demonstrated that a process of DFC (digestion fractional crystallisation) whereby the cognate olivine crystallisation is coupled to entrained xenocrystic orthopyroxene assimilation is a key process during the formation of the Majugaa occurrence of the Manitsoq region [5]. Mass balance considerations are here applied to the Majuagaa bulk rock in term of the DFC mechanism obtaining an estimate of parental melt and magma composition for the Majuagaa kimberlite.

We use bulk rock major and trace element geochemistry together with mineral chemistry to investigate the range of melt compositions involved in the region. Melting models involving introduction of a carbonatite melt are applied to inferred lithospheric mantle compositions based upon nodule assemblages. Compositional variations across the southern West Greenland province are explained by interaction of an aesthenospheric carbonatite melt with lithospheric mantle. The major and trace element budgets are understood as a combination of melting regime together with mixing and reaction between the primary melts and the dispersed xenocryst assemblages. Variations of the mineral assemblages of the cognate groundmass are similarly explained.

[1] Nielsen & Sand (2008) *Can. Min.* **46**, 1043–1061. [2] Nielsen *et al.* (2009) *Lithos* **112S**, 358–371. [3] Tappe *et al.* (2011) *EPSL* doi: 10.1016/j.epsl.2011.03.005. [4] Dalton & Presnall (1998) *J.Pet.* **39**, 1953–1964. [5] Pilbeam *et al.* In prep.

Evidence for metasomatic enrichment in the oceanic lithosphere and implication for the generation of enriched reservoirs

S. PILET[1]*, D. BUCHS[2], M. COSCA[3], K. FLORES[4], A. BANDINI[5] AND P. BAUMGARTNER[1]

[1]University of Lausanne, Switzerland (*correspondence: Sebastien.Pilet@unil.ch)
[2]IFM-Geomar, Kiel, Germany.
[3]US Geological Survey, Denver, USA
[4]American Museum of Natural History
[5]UWA, Perth, Australia

Recycled metasomatized deep portions of oceanic lithosphere are potential candidates for enriched fertile mantle sources accounting for the overall enriched geochemistry of OIBs. However, the mechanisms of metasomatic enrichment in the oceanic lithosphere are poorly constrained. Here we report new petrological data that support the existence of metasomatic veins in the oceanic lithosphere, and explore the isotopic evolution of metasomatized lithosphere after its recycling and storage in the convecting mantle.

Metasomatic veins in the oceanic lithosphere are documented by cpx xenocrysts in accreted basaltic sills from northern Costa Rica. New field observations, ^{40}Ar-^{39}Ar radiometric dating, biostratigraphic ages and geochemical analyses indicate that the sills represent a possible, ancient analogue of petit-spot volcanoes formed by oceanic plate flexure offshore Japan [1]. The cpx xenocrysts are interpreted as relic of metasomatic veins based on their compositions which are similar to cpx from metasomatic veins observed in mantle outcrops and xenoliths. We interpret the formation of these veins as an early stage of the process that led to formation of the basaltic sills; some low degree melts do not reach the surface but differentiate within the lithosphere and form metasomatic cumulates (i.e. veins).

The generation of low degree melts at the base of the lithosphere by plate flexure is likely to represent a common mechanism in the oceanic lithosphere. Our data suggest that oceanic lithosphere is metasomatized before subduction. Monte Carlo simulations of this enrichment process [2] show that such metasomatized oceanic lithosphere is highly enriched in incompatible trace elements and its recycling and storage for 1 to 1.5 Ga could produce an enriched mantle reservoir with trace element and isotope compositions similar to HIMU mantle ‘end-member’.

[1] Hirano *et al.* (2007) *Science* **313**, 1426. [2] Pilet *et al.* (2011) *J.Pet* doi: 10.1093/petrology/egr007.

https://doi.org/10.1180/S0026461X00006502 Published online by Cambridge University Press

A close look at the carbon cycle from the Roselend Natural Laboratory using laser-based isotope ratio spectrometry

E. PILI[1,2]*, S. GUILLON[1,2], P. AGRINIER[2] AND M. DELLINGER[2]

[1]CEA,DAM,DIF, F-91297 Arpajon
[2]Institut de Physique du Globe de Paris, 1 rue Jussieu, F 75005 Paris

We study the carbon cycle (fluxes and isotope ratios) in a section of a crystalline mountain belt. At the Roselend Natural Laboratory (French Alps), a tunnel provides access to the heart of the fractured-rock unsaturated zone, at 55m depth below ground surface. From dedicated sampling of matrix flow, fracture flow and runoff, we compute the contributions to Dissolved Inorganic Carbon due to carbonic acid weathering of carbonates and silicates as well as sulfuric acid weathering of carbonates. This reveals that this system is a net source of CO_2.

A recent laser-based CO_2 Carbon Isotope Analyzer (CCIA DLT-100, Los Gatos Research Inc.) allows *in situ* continuous monitoring of CO_2 concentration and carbon isotope composition. We thoroughly assess the performance of this instrument in the view of using it in harsh geological conditions (high water content, large concentration range).

CO_2 degassing can be characterized by flux measurements in closed chambers. In our setting, this requires a preliminary purge with CO_2-free air. Isoflux measurements are performed in small (7 L) horizontal boreholes drilled from the tunnel wall and in an isolated chamber (60 m^3) at the end of the tunnel. We also apply a Keeling plot approach that is well-suited for open systems, such as the entire tunnel ventilated by the atmosphere.

These CCIA measurements confirm that CO_2 is contributed from the rock, and indicate multiple sources (soil respiration, DIC degassing, carbonate precipitation). CO_2 fluxes are highly dynamic in response to meteorological, hydrogeological and mechanical forcing.

The understanding of the natural carbon cycle in the Roselend Natural Laboratory is a preliminary basis for a forthcoming tracing experiment between the isolated chamber of the tunnel and the atmosphere above through 55 m of fractured rocks.

Atomic force microscopy observations of nanostructures and crystal growth in bivalves

C.M. PINA[1], A.G. CHECA[2], C.I. SAINZ-DÍAZ[3] AND J.H.E. CARTWRIGHT[3]

[1]Dept. de Cristalografía y Mineralogía, Universidad Complutense de Madrid, E-28040 Madrid, Spain (cmpina@geo.ucm.es)
[2]Dept. de Estratigrafía y Paleontología, Universidad de Granada, E-18071 Granada, Spain (acheca@ugr.es)
[3]Instituto Andaluz de Ciencias de la Tierra, CSIC-Universidad de Granada, E-18071 Granada, Spain (cisainz@ugr.es, julyan.cartwright@csic.es)

The shells of bivalves are complex nanostructured materials formed by calcium carbonate and organic membranes. Both the variety of hierarchical structures and the selective usage of calcite and aragonite in their shells, reveal the extraordinary ability of bivalves to control crystal growth processes at various length scales. The result of such a multiple scale control is the generation of composite materials with outstanding mechanical properties.

Here we present atomic force microscopy (AFM) observations of calcitic and aragonitic internal structures in shells of a number of bivalves. These structures are constructed by micrometric tablets, whose shape, size and coalescence schemes vary from one species to another. However, in all the species, the surfaces of the tablets are built up by granules and subgranules down to the nanometric scale. These highly hierarchical structures of the tablets provide them with a multiple scale roughness which differs from that commonly observed on inorganic mineral surfaces. To further study the nature of the tablets, we also conducted a series of crystal growth experiments using the inner part of bivalves' shells as a substrate. Crystal growth was promoted by passing supersaturated aqueous solutions with respect to calcite and aragonite over the arrangements of micrometric tablets. The growth on the bivalve's shells was observed in real time by AFM. The analysis of the morphology and orientation of the overgrown crystals provided information about the crystallographic features of the tablets that form the interior of bivalves' shells.

https://doi.org/10.1180/S0026461X00006502 Published online by Cambridge University Press

Graphite-bearing norites (Cortegana Igneous Complex, SW Spain): Mantle-derived carbon or crustal contamination?

R. PIÑA[1], E. CRESPO-FEO[1], L. ORTEGA[1], J.F. BARRENECHEA[1,2] AND F.J. LUQUE[1,2]

[1]Faculty of Geology, Univ. Complutense of Madrid, Spain
[2]Institute of Geosciences (UCM-CSIC), Madrid, Spain

The Cortegana Igneous Complex comprises a number of small lens-like intrusive mafic bodies (Tejadillas, Sojalva, El Merendero, La Caballona and Tabarca) located in the southern part of the Aracena Metamorphic Belt (Ossa-Morena Zone of the Iberian Massif). Among these bodies, the Sojalva stock is especially interesting due to the presence of abundant graphite in the igneous rocks (up to 26 wt.% C). Norite is the predominant lithology and consists of plagioclase (An_{80-46}), orthopyroxene (Mg#, 0.53-0.71) and minor biotite, along with cordierite, quartz, hercynite, graphite and Fe-Ni-Cu sulfides, mainly pyrrhotite and minor pentlandite and chalcopyrite. Partially-digested metamorphic xenoliths commonly occur in the igneous rock. The mineral assemblage (qtz+pl+bt+crd+grt+sil+sp) of these metamorphic xenoliths resembles that found in the high-grade gneisses and graphite-rich quartzites from the 'aluminous series' of the Aracena Metamorphic Belt.

Graphite occurs as flakes and aggregates of flakes both in the igneous rock and within the xenoliths. Graphite flakes in the igneous rock may reach up to 200x20 μm and they are usually associated with the sulfides which, in turn, are intersticial with respect to the silicate phases. Locally, small graphite flakes (less than 80 μm) are included within silicates (mostly cordierite, plagioclase and pyroxene).

The study of graphite by XRD reveals that it corresponds to the hexagonal politype and has a high degree of structural order along the stacking direction (c-axis).

The stable carbon isotope ratios of bulk graphite samples are light, with $\delta^{13}C$ values ranging from -19.5 to -23.6 ‰. These values are compatible with biogenic carbon and point to derivation from the assimilation of metasedimentary rocks. This hypothesis is also in agreement with the mineralogical and textural features of the igneous rocks.

The results of this study reveal therefore that mantle-derived rocks may acquire their carbon content also by assimilation during their emplacement rather than from the mantle itself and that petrographic and isotopic studies are crucial to establish the ultimate origin of carbon in these rocks.

$(Ba, Cu)(UO_2)_2(PO_4)_2.nH_2O$ solid solution occurences from an uranyl-phosphate deposit in Portugal

A.J. PINTO[1]*, M. GONÇALVES[1], C. PRAZERES[2] AND M.J. BATISTA[2]

[1]CREMINER, Dep. of Geology, Fac. of Sciences. Univ. of Lisbon, Ed. C6, Campo Grande 1749-016 Portugal (*correspondence: afipinto@fc.ul.pt)
[2]LNEG, Laboratório Nacional de Energia e Geologia, Estrada da Portela, Alfragide, Ap. 7586 2611-901 Amadora

The occurrence of solid solution systems of both anionic and cationic substitution in secondary uranyl phosphate deposits is acknowledged in the scientific literature (e.g. [1] and [2]). Our work focuses on the Ba^{2+}/Cu^{2+} substitution found in uranyl phosphates from Tarabau deposit, Nisa, Portugal, as depicted in the image below.

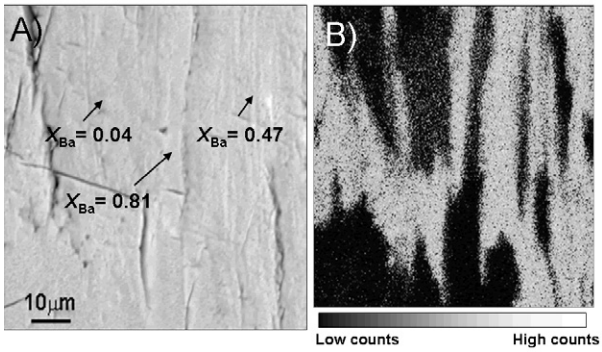

Figure 1: a) Backscattered electron micrograph of a (001) cleavage surface of a Ba-bearing uranyl-phosphate grain. Quantitative point analyses expressed in Ba mole fraction (X_{Ba} = 1-X_{Cu}) are also included, **b)** Electron microprobe X-ray map relative to Ba on the surface shown in a).

A close inspection of the obtained results reveals that the studied materials are not chemically homogeneous, yielding intermediate compositions between pure Cu and Ba-endmember compositions. Moreover, an inverse relationship is found between surface composition in Ba and U, suggesting the occurrence of surface dissolution of a meta-torbernite substrate coupled with co-precipitation of an uranyl defficient (Ba, Cu) solid solution. Powder X-ray diffraction results point towards meta-torbernite-type structures, which implies that such phases are members of the meta-torbernite – meta-uranocircite solid solution system.

[1] Jerden *et al*. (2003) *Chem. Geol.* **199**, 129–157.
[2] Yakubovich *et al*. (2008) *Cryst. Rep.* **53**(5), 764–770.

https://doi.org/10.1180/S0026461X00006502 Published online by Cambridge University Press

Reconstructing Southern and Pacific Ocean deep circulation using Nd isotopes

A.M. PIOTROWSKI*, T.L. NOBLE AND I.N. MCCAVE

Department of Earth Sciences, University of Cambridge, Cambridge, CB2 3EQ, United Kingdom (*correspondence: amp58@cam.ac.uk)

The southwestern Pacific is an important region to reconstruct past ocean circulation since it is the entry point for Southern Ocean waters into the Deep Western Boundary Current of the Pacific. The relationship between deep water neodymium and carbon isotopes in the southwestern Pacific, and their comparison to records from the South Atlantic [1] and Indian Ocean [2], have the potential to provide new information about changes in water mass sourcing and nutrient generation along different deep water flow paths in the Southern Hemisphere [3].

Here we present a new Nd isotope record from ODP Site 1123 on the Chatham Rise (42 S, 172 W, 3.3 km-bsl), and glacial-interglacial Nd isotope changes from Chatham Rise transect of four cores, ranging from 1.4 to 4.8 km-bsl. Nd isotopes were measured by three methods, acid-reductive leaching of bulk detritus, mixed planktonic foraminifera which have authigenic coatings, and those which have been reductively cleaned. The foraminifera with authigenic coatings yeild the expected deep seawater Nd isotopic composition, matching nearby water and Fe-Mn nodules measurements, while bulk detrital leachates do not. Reductively cleaned and uncleaned planktonic foraminifera have Nd isotopic compositions within error of each other, suggesting that the host phase of Nd is difficult to remove.

The Nd isotopic composition of ODP Site 1123 changes on glacial-interglacial timescales, recording a deglacial Nd isotopic shift from -5 ε_{Nd} during the Last Glacial Maximum (LGM) to -7 ε_{Nd} during the Holocene. The 'Pacific-like' Nd isotopic compositions during the LGM suggests reduced Atlantic-sourced water, and is also replicated at the deeper CHAT transect cores. The intermediate depth (1 to 2 km-bsl) cores have a more constant Pacific-like sourcing of waters of -4 ε_{Nd} during the deglaciation. The ODP Site 1123 Nd isotope record appears to track, but is offset from, the South Atlantic [1] and Equatorial Indian Ocean [2] Nd isotope records, suggesting that Atlantic-sector deep water changes are propigated through the Southern Ocean.

[1] Piotrowski *et al*. (2005) *Science* **307**, 1933–1938. [2] Piotrowski *et al*. (2009) *EPSL* **285**, 179–189. [3] McCave *et al*. (2008) *QSR* **27**, 19–20, 1886–1908.

Evidence of slab melt transfer in the New Caledonian fore-arc ophiolite

CASSIAN PIRARD[1], JÖRG HERMANN[2] AND HUGH O'NEILL[2]

[1]Department of Petrology, Vrije Universiteit Amsterdam, 1081HV Amsterdam (cassian.pirard@falw.vu.nl)

[2]Research School of Earth Sciences, The Australian National University, 0200 Canberra (joerg.hermann@anu.edu.au, hugh.oneill@anu.edu.au)

The highly depleted harzburgite of the Massif du Sud ophiolite of New Caledonia hosts several late intrusive bodies (hornblendites, granitoids, gabbros) in an area expanding from the crust-mantle transition zone to a couple of kilometers under the palaeo-Moho. The absence of relationship with the basement and lateral variations related to the paleo-depth of the mantle suggest an emplacement in an oceanic environment, several millions years prior to the obductive event. The granitoid intrusions of the Massif du Sud ophiolite are the first known reported case of large amount of felsic magma hosted in a sub-arc mantle.

U-Pb dating of the magmatic bodies provides a similar age than igneous zircon cores occuring in the eclogite terrane in the northern part of the island. This overlap of ages suggests that the magmatic activity witnessed in the felsic intrusions within the ophiolite corresponds to arc volcanic events that produced volcanoclastic sediments representing the protolith of New Caledonia eclogite facies rocks.

Magmatic intrusions are all alkali-rich and cover intermediate to felsic compositions. Mg-numbers range from 0.45 to 0.92 and are positively correlated with sodium and silica contents, ruling out that diorites and trondhjemites are related by differentiation processes. Instead we suggest that the high Mg# trondhjemites represent slab melts that interacted with the mantle wedge.

Pyroxenite reaction zones rimming these intrusions show a direct chemical relationship with pyroxenite dykes occuring deeper in the mantle. These dykes are interpreted as feeder conduits for slab melts which accumulate in large pods at the crust-mantle transition.

A study of amphibole trace element composition in the granitoid intrusions also show a link with amphibole-bearing peridotite and mafic rocks which are located in an area of the ophiolite inferred as a near-trench environment. This lateral variation is interpreted as the result of a thermal gradient in the sub-arc mantle. Slab melt metasomatism affects peridotites at subsolidus conditions in colder part of the fore-arc whereas large pockets of melt accumulate under the oceanic crust in hotter parts of the sub-arc mantle.

https://doi.org/10.1180/S0026461X00006502 Published online by Cambridge University Press

U/Pb dating of geodic calcites: A tool for paleohydrological reconstructions

C. PISAPIA[1,2]*, P. DESCHAMPS[1], B. HAMELIN[1], A. BATTANI[2,3], S. BUSCHAERT[2] AND J. DAVID[4]

[1]CEREGE, Univ. Aix-Marseille, France (*correspondence: pisapia@cerege.fr)
[2]ANDRA, Chatenay-Malabry, France
[3]IFP-EN, Paris, France
[4]GEOTOP, Univ. du Québec, Montréal, Canada

This study presents U/Pb dating of secondary geodic calcites carried out to provide chronological constraints on diagenetic processes and past fluid circulations that affected the deep sedimentary formations of the East of the Paris Basin. It is part of projects developed by the French Agency for Nuclear Waste Management (ANDRA) in order to test the feasibility for nuclear waste storage in the Callovo-Oxfordian argillite. This layer is embedded between two carbonated shelf formations, Dogger and Oxfordian in age, characterized by very low porosity due to secondary sparite precipitation. These calcites are thougth to reflect main diagenetic events and phases of fluid circulation within the sedimentary basin since the early Cretaceous period. But the absolute ages of these events are uncertain and still subjet to debate. The aim of this project was thus to date secondary geodic calcites related to these fluid circulations in order to reconstruct the diagenetic and palaeohydrological history of the site.

The U/Pb dating method was optimized to large secondary calcites samples with very low concentrations of lead (from 3 to 26 ppb) and uranium (from 22 ppb to 1ppm). Geodic calcites from Oxfordian and Dogger formations were sampled from drilling cores and were analyzed by TIMS (VG 54 Sector at CEREGE) using a ^{205}Pb-^{236}U-^{233}U-^{229}Th spike.

Results depict clear isochrons and several phases of secondary calcite precipitation were identified. Two ages were obtained on 4 geodes from the Dogger formations at -149.2±5.8Ma and -99.1±1.9Ma. They strongly suggest two phases of sparite precipitation: (1) during early diagenetic processes and (2) during a later recristallization process. On the contrary, 6 geodes from the Oxfordian formations gave a unique age at -33.2±5.5Ma indicating a more recent and unique phase of porosity infilling. This precipitation phase is very likely related to a major fluid circulation event synchronous with the Late Eocene/Oligocene tectonic extension responsible for the formation of major rifts in northern Europe (e.g. Rhine graben). This event affected the whole Oxfordian formations in the eastern part of the basin but did not affect the Dogger formations.

U/Pb dating of geodic calcites thus offers a new powerful way for reconstructing the coupled palaeohydrological and tectonic history of sedimentary basins.

Iron and other metals in the Proterozoic oceans

NOAH PLANAVSKY[1], CLINT SCOTT[1], PETER MCGOLDRICK[2], CHAO LI[1], CHRIS REINHARD[1], ANDREY BEKKER[3], GORDON LOVE[1] AND TIMOTHY LYONS[1]

[1]Department of Earth Sciences, University of California, Riverside, CA 92521, USA
[2]CODES ARC Centre of Excellence in Ore Deposits, University of Tasmania, Private Bag 126, Hobart, TAS 7001, Australia
[3]Department of Geological Sciences, University of Manitoba, Winnipeg, MB, R3T 2N2 Canada

The chemical composition of the ocean changed dramatically with the oxidation of the Earth's surface, and this process has profoundly influenced the evolutionary and ecological history of life. The early Earth was characterized by a reducing ocean-atmosphere system, while the Phanerozoic Eon (<542 million years ago) is known for a stable and oxygenated biosphere conducive to the radiation of animals. The redox characteristics of surface environments during the Earth's middle age (1.8 to 1 billion years ago) are less well known, but over the past decade it has been commonly assumed that the mid-Proterozoic was home to a globally sulfidic (euxinic) deep ocean. Here, we present iron data from a suite of mid-Proterozoic marine shales. Contrary to the popular model, our results indicate that ferruginous (anoxic and Fe^{2+}-rich) conditions were both spatially and temporally extensive across diverse paleogeographic settings in the mid-Proterozoic ocean, inviting new models for the temporal distribution of iron formations and the availability of bioessential trace elements during a critical window for eukaryotic evolution. We suggest that ferruginous shales are not large sinks for bioessential chalcophile elements. In this light, the presence of widespread Fe^{2+}-rich conditions may allow for substantial redox-sensitive trace metal reservoirs in a largely reducing ocean.

https://doi.org/10.1180/S0026461X00006502 Published online by Cambridge University Press

Does monsoon rainfall drive arsenic mobilization and organic carbon release in Bangladesh aquifers?

B. PLANER-FRIEDRICH[1]*, C. HÄRTIG[1,4], H. LISSNER[2,4], J. STEINBORN[3,4], E. SÜSS[1,4], M.Q. HASSAN[5], A. ZAHID[5,6], M. ALAM[5] AND B. MERKEL[4]

[1]University of Bayreuth, Bayreuth, Germany (*correspondence: b.planer-friedrich@uni-bayreuth.de)
[2]Friedrich-Schiller University Jena, Jena, Germany
[3]Landesamt für Geologie und Bergwesen, Halle, Germany
[4]TU Bergakademie Freiberg, Freiberg, Germany
[5]University of Dhaka, Department of Geology, Bangladesh
[6]Bangladesh Water Development Board, Dhaka, Bangladesh

Organic carbon (DOC) is believed to be the main driver for arsenic (As) release during reductive dissolution of iron hydroxides from sediments in the Bengal Delta. However, the source of the organic carbon remains controversial. Recharge from man-made ponds has recently been claimed as the main source and installation of 'As-safe' wells away from ponds beneath rice fields has been suggested. Our study questions the validity of this approach throughout Bangladesh. Based on a one-year weekly sampling of wells at different depths in the Titas district, 60 km SE' of Dhaka, we propose a model of natural organic carbon and As mobilization from clay and peat layers following monsoonal changes in specific storativity. During the dry season a natural decline in hydraulic heads boosted by intensive pumping for irrigation causes release of porewaters with high DOC concentrations from clay and peat layers. Flushing, diffusion, and water re-storage decrease initially released DOC concentrations in the rainy season. Maximum As concentrations and an increase in the share of arsenite follow DOC peak concentrations with a time lag which we interpret as delayed response in microbially catalyzed arsenate reduction and release of arsenite previously sorbed to sediment. Over time, aqueous As concentrations will decrease in most parts of the Holocene unconfined aquifer as organic matter is consumed. Based on our model, organic carbon and As from clay and peat layers will continue to pose a problem for underlying aquifers as they are seasonally released by changes in specific storativity. Though sorption capacities are higher in the Pleistocene sediments, long-term continuous As input from overlying clay and peat layers as in our study area eventually also leads to increased aqueous As concentrations. Before exploiting deeper aquifers the overlying clay and peat layers should thus be studied for their history of fresh-water flushing, their current pore water biogeochemistry and hydraulic properties.

Why do mafic arc magmas contain 4 wt% water on average?

TERRY PLANK[1]*, KATHERINE A. KELLEY[2], MINDY ZIMMER[3], ERIK HAURI[4] AND PAUL WALLACE[5]

[1]LDEO, Palisades, NY 10960, USA (*correspondence: tplank@ldeo.columbia.edu)
[2]URI/GSO, Narragansett, RI 02882, USA
[3]Los Alamos National Lab, Los Alamos, NM 87544, USA
[4]DTM/CIW, Washington, DC 20015, USA
[5]Univ. of Oregon, Eugene, OR 97403, USA

Over the last fifteen years there has been an explosion in data on the volatile contents of magmas parental to arc volcanoes. This has occurred due to the intense study of melt inclusions, trapped primarily within olivine, as aliquots of magma that have escaped degassing during eruption. The surprising first-order result is the narrow range in H_2O concentrations of the least degassed melt inclusions when averaged by volcano (based on 7 arcs for which such data exist for > 5 volcanoes: Central America, Mexico, Kamchatka, Marianas, Cascades, Tonga and the Aleutians). Nearly all arc volcanoes are sourced with mafic magmas that contain 2-6 wt% H_2O. Moreover, the average for each arc varies even less, from 3.2 (for the Cascades) to 4.5 (for the Marianas), with an average for all seven arcs of 3.8 ± 0.5 wt% H_2O. The narrow range and common average value for H_2O is in stark contrast to that for most other subduction tracers, such as Nb or Ba, which vary by orders of magnitude.

A modulating process, either in the crust or mantle, is likely responsible for the restricted range in the H_2O contents of melt inclusions. One possibility is that melt inclusions reflects vapor saturation at the last storage depth prior to eruption. Magmas rise from the mantle with variable H_2O contents (> 4 wt%), start degassing at the depth of H_2O-saturation, and continue to degas up until the depth at which they stall. If the stalling depths were ~6 km, not atypical for storage depths beneath volcanoes, magmas would be saturated at ~4 wt% H_2O, and melt inclusions, which become sealed during ascent, would thus record ≤ 4 wt% H_2O. Another possibility is that the melting process modulates water content in the melt such that magmas rise out of the mantle with ~4 wt% H_2O. A strong relationship between the water content of the source (H_2O_o) and the degree of melting (F) maintains nearly constant water contents in the melt for a restricted range in mantle temperature. Magmas with 3-4 wt% H_2O can be generated at 1230-1280°C and 1.5 GPa for a wide range in F and H_2O_o. Crust and mantle controls may dominate in different regions and may be distinguished from coupled trace element or CO_2 variations.

https://doi.org/10.1180/S0026461X00006502 Published online by Cambridge University Press

Fate of U(IV) during microbially-driven Mn(II) oxidation in sediments

K.L. PLATHE[1]*, S-W. LEE[2], J.S. LEZAMA-PACHECO[3], B.M. TEBO[2], J.R. BARGAR[3] AND R. BERNIER-LATMANI[1]

[1]École Polytechnique Fédérale de Lausanne, Lausanne, Switzerland (*correspondence: kelly.plathe@epfl.ch)
[2]Oregon Health & Science Univ., Portland, OR 97239, USA
[3]Stanford Synchotron Radiation Lightsource, Menlo Park, CA 94025, USA

Uranium is a toxic radionuclide and its contamination of soil and groundwater is a worldwide problem. The oxidized form of U, hexavalent uranium (U (VI)), is the most soluble and mobile form of uranium and therefore, an understanding of its behavior in contaminated environments is of utmost importance. It is known that U (VI) can be biologically reduced to less soluble U (IV) species such as the mineral uraninite (UO_2) or monomeric U (IV) and the stimulation of biological activity to this end is a salient remediation strategy; however, it is as yet unknown if these materials remain stable in their subsurface formation environments. Manganese oxides, also formed biogenically in the subsurface, are capable of rapidly oxidizing U (IV) to U (VI) [1].

Here, we evaluate the effect of Mn redox cycling on the mobility and stability of U in contaminated subsurface environments on various scales. Batch experiments were conducted in which agarose gels, containing Mn-oxidizing spores and biogenic UO_2, were exposed to Mn (II). After optimization of experimental variables using these batch reactors, the redox reactions were analyzed in sediment from a U-contaminated site in Rifle, Colorado USA. Results to date indicate biogenic UO_2 oxidation to U (VI) by nano-scale bio Mn oxides. The U (VI) product is retained within the agarose gel or the sediment matrix suggesting the formation of U (VI) precipitates or strong surface complexes. Various methods, including inductively coupled plasma mass spectroscopy (ICPMS), transmission electron microscopy (TEM) and X-ray absorption spectroscopy (XAS), are used to pinpoint the speciation and spatial distribution of U (VI) relative to Mn. The feasibility of bioreduction as a strategy to immobilize uranium in the contaminated subsurface is contingent on the long-term stability of immobilized U. Hence it is critical that the role of Mn–present at sufficiently high concentrations at Rifle–in this stability be assessed. This study furthers our knowledge of the coupled U/Mn system and therefore is expected to inform future remediation efforts.

[1] Chini (2008) *Environ. Sci. Technol.* **42**, 8709–8714.

Thermal state of subducting plate beneath Kamchatka inferred from H_2O/Ce in melt inclusions

A.A. PLECHOVA[1]* AND M.V. PORTNYAGIN[1,2]

[1]V.I. Vernadsky Institute of Geochemistry and Analytical Chemistry, ul. Kosygina 19, Moscow 119991, Russia (*correspondence: aplech@geokhi.ru)
[2]IFM-GEOMAR, Kiel, Germany

We measured water and trace element contents in a new large set of naturally quenched and reheated melt inclusions in olivine from volcanoes along the Eastern Volcanic Front of Kamchatka (Zhupanosky, Karymsky, Vysokiy, Zavaritsky, Zheltovsky, Ksudach and others), which are located 100-190 km above the subducting plate. H_2O/Ce ratios in the least degassed inclusions correlate inversely with the distance from volcano to slab surface (fig. 1b) and suggest a systematic a change in the composition of slab component with increasing slab depth [1]. This data is used to estimate the temperature of equilibrium of water-bearing components with subducting sediments at the slab top [2].

The data indicate sharp temperature increase (740-800º) at relatively shallow depths (100-110 km) and less efficient slab heating at greater depths (800-950 ºC, 110-190 km). These results are in qualitative agreement with modern numeric SZ models (e.g. [3]) though our petrologic data predict ~50ºC hotter slab for 110-190 km depths beneath Kamchatka.

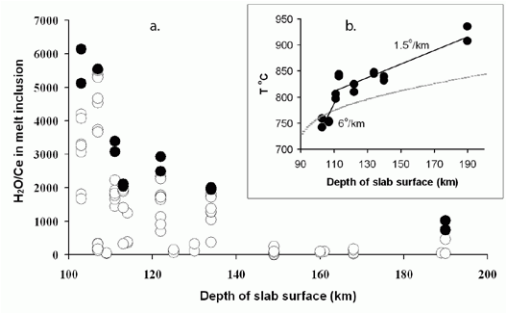

Figure 1: (a) H_2O/Ce ratios in melt inclusions from Kamchatkan volcanoes and (b) calculated temperature of slab fluids [2] versus slab depth beneath volcanoes. Filled circles denote the least degassed inclusions. Gray line in (b) shows a model depth-temperature path of the Pacific plate surface beneath Kamchatka [3].

[1] Portnyagin *et al.* (2007) *EPSL* **255**, 53–69. [2] Plank *et al.* (2009) *Nature Geoscience* **2**, 611–615. [3] Van Keken *et al.* (2011) *JGR* **116**, B01401.

https://doi.org/10.1180/S0026461X00006502 Published online by Cambridge University Press

Geochemical characterization of the hydrocarbons in Domanik Rocks, Tatarstan Republic

IRINA N. PLOTNIKOVA, FIDANIA F. NOSOVA, AND NIKITA V. PRONIN

Kazan Federal University (irena-2005@rambler.ru)

On the basis of combined geological-geochemical analysis of the conditions of hydrocarbon generation and formation of basins, the total petroleum-generating potencial of domanic formation (DF) is estimated at 126 billion tons of liquid hydrocarbons. High-bituminous argillo-siliceous carbonate deposits of DF occurring within pale depressions and down warps in the east of the Russian platform are treated by many investigators as a main source of oil and gas in the Volga-Ural province.

In this study a special attention was turned to organic-rich rocks DF witch outcrop in the central part (Uratminskaya area 792, 806 boreholes) and in the west part (Sviyagskaya, 423) of the Tatarstan Republic.

The aim of the present paper is to characterize the organic matter: origin, depositional environments, thermal maturity and biodegradation-weathering effects.

Nowadays the most informative geochemical parameters are some biomarkers which qualitatively and are quantitatively defined from distributions of n-alkanes and branched alkanes.

Methodology used in this study included sampling, bitumen extraction, liquid-column chromatography and gas chromatography/mass spectrometry analyses. The bitumen was fractionated by column chromatography on silica gel. Non-aromatic or alifatics, aromatics and polar compounds were obtained.

Alifatic were analysed by gas chromatography/mass spectrometry Perkin Elmer. The hydrocarbons present in the sediments of DF and have a carbon numbers ranging from 12 through 38. The samples contain variably inputs from both terrigenous and non-terrigenous (probably marine algal) organic matter as evident in bimodal GC fingerprints of some samples. Pristane and phytane, also, occur in very high concentration in sample extracts. The relatively low Pr/Ph ratios, CPI and OEP<1 imply that the domanik organic matter was deposited in reducing environments.

Mass chromatograms show the distribution of regular steranes, iso-steranes, lower molecular weight C_{21} and C_{22} steranes (pregnanes) (m/z 217) and triterpanes (m/z 191). The biomarkers distribution of the domanic samples generally suggests a major marine phytoplankton contribution relative to terrigenous land plant source input. The marine affinity is evident from the relatively abundant C_{27} steranes, which are biomarkers for marine algal contribution to organic matter and low C_{29} sterane contens.

In this present study, samples are dominated by 5α, 14α, 17α (H)-20R and 5β, 14α, 17α (H)-20R steranes (biological configuration). The ratios of 20S/(20S+20R) for αααC_{29}

The legacy of plastic deformation and pre-existing microstructures during olivine serpentinization

O. PLÜMPER[1], H. AUSTRHEIM[1], S. PIAZOLO[2] AND H. JUNG[3]

[1]Physics of Geological Processes (PGP), University of Oslo, Oslo 0316, Norway (*correspondence: oliver.pluemper@fys.uio.no)

[2]Department of Earth and Planetary Sciences, Macquarie University, NSW 2109, Australia

[3]School of Earth and Environmental Science, Seoul National University, Seoul 151-747, Republic of Korea

High-temperature crystal-plastic deformation of olivine is an inevitable consequence of asthenospheric mantle flow. In this environment olivine commonly yields by dislocation creep to form dislocation walls. Solid-state diffusion along these imperfections is faster than through the bulk crystal. At low temperatures, olivine serpentinization modifies the petrophysical and geochemical properties of the oceanic lithosphere. Under these conditions olivine generally fails to compositionally readjust via diffusion and re-equilibrates via dissolution-reprecipitation. Although plastic deformation and serpentinization are decoupled, we identified compositional readjustments expressed as striped zonings in partially serpentinized and deformed olivine grains from the Leka Ophiolite Complex (LOC), Norway. Combining focused ion beam sample preparation and (scanning) transmission electron microscopy reveals that every zone is immediately related to a subgrain boundary composed of edge dislocations. The zonings are a result of the Fe-Mg exchange potential between olivine and antigorite, where Fe enrichment or depletion is controlled by the silica activity imposed on the system by orthopyroxene and magnetite stability. Nanometer-sized serpentine precipitates along olivine dislocation walls and crystallographic relationships gained by electron backscatter diffraction (EBSD) suggest that hydration was also initiated along these intracrystalline imperfections. The legacy of pre-existing microstructures in the LOC is exhibited by localized occurances of parallel but highly misorientated olivine grains seperated by plastically deformed diopside lamellae. Microtomography combined with EBSD suggest that these areas are a consequence of a hydration-dehydration sequence to result in a complex pseudomorphism of primary mantle orthopyroxene to olivine and the cryptic survival of the primary microstructure.

Our observations provide new insights into the role of primary microstructures and crystal-plastic deformation on subsequent fluid-mediated reactions.

https://doi.org/10.1180/S0026461X00006502 Published online by Cambridge University Press

The evolution of a serpentinizing environment inferred from andradite vein networks

O. PLÜMPER[1], A. BEINLICH[1,2], E. JANOTS[3] AND H. AUSTRHEIM[1,2]

[1]Physics of Geological Processes (PGP), University of Oslo, Oslo 0316, Norway (*correspondence: oliver.pluemper@fys.uio.no)
[2]Department of Geosciences, University of Oslo, Norway
[3]ISTerre, F-38000 Grenoble

Serpentinization of the oceanic lithosphere produces a unique geochemical environment. Vein networks from the Feragen Ultramafic Body (Norway) provide new insight into the evolution of a serpentinizing system and the critical role of ortho- and clinopyroxene. The veins are composed of polyhedral serpentine spheres, botryoidal andradite spheres, ferroan brucite, and awaruite. By combining X-ray fluorescence mapping and reactive transport modeling we illustrate how Ca from the dissolving clinopyroxene serves as a proxy for the determination of the system's geochemical evolution. Crystal morphology analysis allows us to infer that stagnant fluid domains were present during vein formation. Microtomography reveals that isolated andradite spheres float in a serpentine matrix within the vein. Calculated particle settling velocity in the vein indicates that rapid crystallization or a gel-type framework prevented the andradite spheres from descending to the vein walls. We infer that the required geochemical conditions, in terms of silica activity and redox conditions were short-lived and vein minerals precipitated rapidly once critical supersaturation was reached. Our observations have implication for the lifetime of the distinct geochemical conditions within a serpentinizing environment.

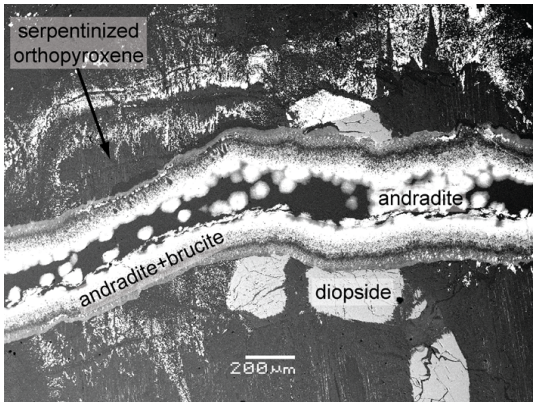

Figure 1: Andradite vein within a meta-harzburgite interlayering meta-dunite.

Se isotope evidence for atmospheric oxidation at ~0.6 Ga

P.A.E. POGGE VON STRANDMANN[1]*, T. ELLIOTT[1], D. CATLING[2] AND S.W. POULTON[3]

[1]BIG, School of Earth Sciences, Bristol University, Bristol, UK (*correspondence: P.PoggevonStrandmann@bristol.ac.uk)
[2]Department of Earth and Space Sciences, Univeristy of Washington, Seattle, USA
[3]School of Civil Engineering and Geosciences, Newcastle University, Newcastle, UK

It is generally thought that atmospheric O_2 levels rose irreversibly twice during Earth history, with the 2nd rise at ~0.8-0.6 Ga [1]. However, the magnitude of the O_2 increase is unclear (estimates range between ~10–100% of the present level), and the specific causes and consequences are uncertain. Knowledge of redox change is fundamental for our understanding of biological evolution and climate systems, because redox constrains the development of a modern biogeochemical cycle. Here we explore the 2nd O_2 rise, using the novel tracer of selenium (Se) isotopes.

Se is a micronutrient. It is strongly redox-dependent and chemically similar to sulphur (S). However, its redox reactions occur at different Eh-pH from S, and therefore Se can provide additional constraints on global redox transitions [2]. Se isotopes are significantly fractionated by microbial reduction, and the degree of fractionation likely depends on atmospheric O_2 in a way similar to S isotopes. This is because when little O_2 is present, microbes will utilise all isotopes, whereas as O_2 increases, more fractionation will occur.

We have analysed Se isotopes in black shales spanning the time of the 2nd O_2 rise, from the Yangtze Platform and the Mackenzie Mountains. Se concentrations in the shales range from the lowest levels so far recorded in shales [3], and show an increase of ~2 orders of magnitude (from 0.02-0.1 to ~10 µg/g), with the highest concentrations in the most recent shales. An overall increase in oceanic Se is consistent with greater supply via oxidative weathering and less hydrothermal scavenging into seafloor selenides once the deep ocean becomes fully oxic. Se isotope ratios in the same samples ($\delta^{82/76}$Se) show a negative excursion of >6‰ across the same period, with a correlated trend of Se and δ^{82}Se. These characteristics suggest that the O_2 content of the atmosphere rapidly increased, providing more selenate and nutrients to the oceans via chemical weathering, allowing microbial reduction to fractionate Se isotopes to a greater degree.

[1] Catling & Claire (2005) *EPSL*, **237**, 1–20. [2] Johnson & Bullen (2004) *Reviews Min. Geochem.* **55**, 289–317. [3] Wen & Carignan (2011) *GCA* **75**, 1411–1427.

https://doi.org/10.1180/S0026461X00006502 Published online by Cambridge University Press

Rare earth elements: Indicators of redox conditions and surface water-groundwater mixing in an estuarine wetland

S.C. POH[1,2,3]* AND M.GASPARON[1,2]

[1]School of Earth Sciences, The University of Queensland, Brisbane, Queensland, Australia (*correspondence: s.poh@uq.edu.au)
[2]National Centre for Groundwater Research and Training, Australia
[3]Department of Chemical Sciences, University Malaysia Terengganu, Kuala Terengganu, Malaysia.

This study was conducted on the Tinchi Tamba Wetlands (TTW) of Moreton Bay, southeast Queensland, as part of a project aimed at characterizing the wetlands' water fluxes. The TTW aquifer is a bowl-shaped aquifer of a semi-confined type, sitting on top of an impermeable clayey layer, with a maximum depth no greater than 20m. The aquifer material comprises high percentage of clay and some medium to coarse sand and gravel. In most cases, coarse grains usually occur as lenses and interbeds. Groundwater flow paths and the extent of mixing of surface and groundwater in the wetlands are difficult to quantify because of the complexity of the geological substrate. In this study we combined field hydrogeological and geochemical data to trace the spatial and temporal evolution of rare earth elements (REEs) distribution in TTW and the adjacent watershed.

Groundwater, ponds, and estuarine waters were sampled monthly over a ten-month period, with additional samples collected during a major storm event that caused significant flooding. Results indicate that a) meteoric water infiltration and evaporation heavily influence the aquifer's geochemistry (electrical conductivity ranging from 3 to 48 ms/cm), b) different sources contribute to the surface water budget, c) REE patterns respond rapidly to changes in redox conditions in the aquifer (redox ranging from -80 to 450mV), d) in areas dominated by low-permeability units, REE patterns are fractionated and exhibited Ce, Pr, Nd, Sm, and Eu depletions, e) the spatio-temporal pattern of REEs indicates mixing of different water sources. In conclusion, the results show that REEs can be used to accurately characterize the surface water and groundwater sources from different reservoirs, as well as the extent of mixing between recharged surface water and groundwater in an estuarine environment.

2-D thermodynamic and trace element models of subduction zones

MICHAEL PÖHLE[1], MATTHIAS KONRAD-SCHMOLKE[1] AND SANDRO JAHN[2]

[1]Institut für Erd- und Umweltwissenschaften, Universität Potsdam, Karl-Liebknecht-Straße 24-25, 14476 Potsdam, Germany
[2]GeoForschungsZentrum Potsdam, Telegrafenberg, 14473 Potsdam, Germany

Fluids derived from dehydration reactions in subducting slabs display major carriers of trace elements tranferred into the mantle wedge. During ascent the fluids interact with the wall rock within the subducted plate, thus it is necessary to quantify element distribution during this fluid-rock interaction in order to get information about the amount and composition of fluids entering the mantle wedge. Complexities in modeling trace element compositions of subduction zone fluids arise from the fact that migrating fluids interact with rocks of different major and trace element compositions undergoing continuous metamorpic transformation within a complex pressure-temperature framework. Based on modeled isotherm patterns of different subduction zone settings we calculate phase relations in the entire subducted slab, considering upward migration of liberated fluids during subduction utilising incremental Gibbs energy minimisation models. The modeled phase relations and fluid amounts are then used to calculate mass balanced trace element distribution among the stable phases at every increment within the slab. Trace element transport occurs within the migrating fluid that equilibrates with the wall rock during ascent, which controls trace element depletion and/or enrichment of fluid and wall rock. With these models we can constrain the absolute amount and the resulting trace element composition of the fluid at the slab surface after fluid-rock interaction within the subducted plate. Preliminary results show that the fluid flux on top of the slab is strongly dicontinuous and shows distinct maxima between 35 and 60 as well as 70 and 80 km slab depth, depending on slab temperature. Potentially fluid-mobile trace elements, such as Li, Be and B show a significant intra-slab fluid rock interaction. Trace element concentration trends of these elements are similar to those observed in arc volcanics, such that Li, Be and B are continuously depleted during subduction and B/Be is significantly decreasing with increasing slab depth. However, in our models the transfer of fluid mobile elements into the mantle wedge already occurs at fore-arc depths, which indicates that mantle dynamics play an important role for element transfer to the sites of melt production beneath the volcanic arc.

https://doi.org/10.1180/S0026461X00006502 Published online by Cambridge University Press

Osmium isotopes in manganese nodules from the Labrador Sea

A. POIRIER[1], C. HILLAIRE-MARCEL[1], S. MEREDYK[2] AND E. EDINGER[2]

[1]GEOTOP-UQAM, CP. 8888, Succ. Centre-ville, Montréal, H3C 3P8, Canada (poirier.andre@uqam.ca, chm@uqam.ca)

[2]Memorial University, St. John's, NL, A1B 3X9, Canada (smeredyk@mun.ca , eedinger@mun.ca)

Using a remotely operated vehicle, manganese nodules were retrieved in 2010, at the base (2870 m depth) of a small bedrock-cored mound, south-east of Orphan Knoll (southern Labrador Sea), in a field of rounded polymetallic balls found at the base of a small cliff of weakly consolidated calcareous ooze.

Using a Thermo Triton™ (NTIMS), we measured the osmium $^{187}Os/^{188}Os$ isotopic ratio in the outer <1mm-thick layer of three nodules. These outer layers were expected to yield the Os isotopic composition of modern seawater (ca. 1.06), in relation with recent co-precipitation of hydrogenous osmium and Fe/Mn oxyhydroxides.

We obtained Os-isotopic values (<0.92) much lower than expected, both for the bulk analysis of the Fe/Mn material, and for mild cold HBr-leachates. We are currently investigating possible reasons for such low values, notably a lower than average growth rate (less than few mm/Ma), or a recent gap in precipitation, or some on-site contamination by the calcareous ooze found within the nodules field area. These contain nanofossils of Eocene age and yielded a low Os-composition (0.59) reflecting typical marine-Os values of this interval.

Isotope composition of iron delivered to the oceans by intertropical rivers: The Amazon River case

F. POITRASSON[1,2]*, L.C. VIEIRA[1], P. SEYLER[2], G.M. DOS SANTOS PINHEIRO[1,2], D. MULHOLLAND[1,2], B.A. FERREIRA LIMA[1], M.P. BONNET[1,2], J.M. MARTINEZ[1,2] AND J. PRUNIER[2]

[1]Instituto de Geociências, Universidade de Brasilia, Campus Darcy Ribeiro, 70904-970 Brasilia-DF, Brazil

[2]Laboratoire Géosciences Environnement Toulouse, IRD-CNRS, 14-16, av. E. Belin, 31400 Toulouse, France (*correspondence: Franck.Poitrasson@get.obs-mip.fr)

Riverborne iron is a notable source for this biogeochemically key element to the oceans. A proper understanding of the Fe cycle at the surface of the Earth require a good characterization of the isotopic composition of the various reservoirs of this element.

However, as the database growths, it appears that the isotope composition of the riverborne Fe delivered to the oceans may be more varied than initially thought, in agreement with inferences from soil studies from different climatic contexts. It is therefore important to compare major rivers from different latitudes. We focused our attention on the Amazon River and its tributaries that represent ca. 20% of the freshwater delivered to the oceans by world rivers.

Preliminary experiment suggests that water filtration may induce biases in stable Fe isotope composition. Therefore, we worked first on bulk waters, sampled through multidisciplinary field campaigns on the Amazon River and its tributaries, including the Solimoes, Negro, Madeira and Tapajos Rivers. Besides a complete sample physical-chemical characterization, Fe isotope determinations were conduced after water sample mineralization, iron purification and MC-ICP-MS analysis.

Our first results reveal that most bulk water samples cluster close to the continental crust value (0.1‰ $\delta^{57}Fe_{IRMM-14}$) with an overall range of 0.2‰. This is consistent with the restricted range found in lateritic soils elsewhere that represent 80% of the Amazon basin surface. This result holds whatever the relative proportion of dissolved Fe in the bulk waters budget, that ranges from 5 to 50% in these waters, whatever the sample depth and whenever the samples were taken in the river cycle. Hence, the bulk waters from the Amazon River delivered to the ocean have an isotopic composition that is close to that of the continental crust.

https://doi.org/10.1180/S0026461X00006502 Published online by Cambridge University Press

A new view on sulfur speciation in geological fluids at elevated temperatures and pressures

G.S. POKROVSKI[1]*, L.S. DUBROVINSKY[2] AND J. DUBESSY[3]

[1]GET, Géosciences Environnement Toulouse, 31400, Toulouse, France (*correspondence: gleb.pokrovski@get.obs-mip.fr)
[2]Bayerisches Geoinstitut, Bayreuth, Germany (leonid.dubrovinsky@uni-bayreuth.de)
[3]G2R, Géologie et Gestion des Ressources Minérales et Energétiques, Vandoeuvre-lès-Nancy, 54506, France (jean.dubessy@g2r.uhp-nancy.fr)

The amount and chemical speciation of sulfur in geological fluids are controlling factors in the formation of magmatic-hydrothermal deposits of many economically critical metals [1]. The two major forms of sulfur in crustal fluids over a wide range of temperature and pressure are believed to be sulfate (HSO_4^- and SO_4^{2-}) and sulfide (H_2S, HS^- and S^{2-}). They are regarded as the key agents controlling the transport and precipitation of metals by deep and hot fluids. However, this belief is based almost exclusively on observations of sulfate and sulfide in minerals, silicate glasses, and fluid inclusions brought to the Earth's surface and/or extrapolations of thermodynamic data for most aqueous sulfur species obtained at near-ambient conditions. It thus suffers from the lack of *in situ* approaches for analyzing sulfur in geological fluids and melts at elevated temperatures and pressures.

In this keynote contribution, we present *in situ* measurements using Raman spectroscopy [2] in model sulfur and thiosulfate aqueous solutions and vapors across a wide range of acidity (pH~2–8), sulfur concentration (0.3–6 wt%), temperature (150–500°C), and pressure (5–50000 bars). Results show that sulfur in the low-density vapor phase is represented by $H_2S \pm SO_2$. In contrast, the dominant stable sulfur species is the dense liquid and supercritical fluid phase is the trisulfur ion S_3^- that forms rapidly and reversibly at the expense of sulfide and sulfate above ~250°C in a wide pressure and acidity range. The large stability of S_3^- may favor the mobility of sulfur and chalcophile metals such as Au, Cu and Pt in hydrothermal fluids over a range of depth, and thus provide the source of these elements for the important types of gold deposits in Achaean greenstone belts and porphyry-epithermal systems.

[1] Pokrovski *et al*. (2008) *Earth Planet. Sci. Lett.* **266**, 345–362. [2] Pokrovski & Dubrovinsky (2011) *Science* **331**, 1052–1054.

Stuctural study of copper chemical status adsorbed onto and incorporated by benthic algae and periphytic biofilm

O.S. POKROVSKY[1]*, A.COUTAUD[1,2], G.S. POKROVSKI[1] AND J.L. ROLS[2]

[1]GET,CNRS/UPS, 14 av Edouard Belin, 31400 Toulouse, France (*correspondence: oleg@get.obs-mip.fr)
[2]EcoLab, CNRS/UPS, 118 rte de Narbonne, 31062 Toulouse cedex 9, France (aude .coutaud@get.obs-mip.fr)

While the major macroscopic parameters of metals interactions with inorganic constituents of continental aquatic systems are well known, the role of biota remains poorly understood. Here we studied the interaction of one of the most phyto-toxic metals, copper, with different phototrophic microorganisms as a function of exposure time via physico-chemical characterization of metal adsorption on and incorporation into cells under controlled laboratory conditions. For this purpose, we have combined two different approaches, the 'macroscopic' stable-isotope techniques with the 'microscopic' molecular-level observations using XAS spectroscopy of the complexes formed.

Results show that drastic changes in local chemical environment of copper occur upon its adsorption onto or incorporation in the cells, similarly to Zn and Cd [1-3]. To investigate the local atomic environment of Cu in peryphytic biofilms, freeze-dried samples with 1 to 5000 ppm Cu were examined by XAS at ID26 beamline (ESRF). The high-resolution mode, for the first time used for copper in biological matrices, allowed establishing specific features of the Cu pre-edge and quantifying the oxidation state and nature and number of neighbours around Cu. Low-concentrated samples (1-20 ppm), demonstrate the presence of sulfur in the nearest atomic shell of Cu, whereas in concentrated samples, carboxylic complexes of Cu predominate. These findings help establish the interaction mechanism of autotrophic photosynthetic microorganims with copper at trace and toxic level. The results of this integrated study can be useful for tracing the environmental effects of metal-biota interactions, and may provide new insights on the mechanisms of Cu stable isotope fractionation in biological systems.

[1] Guiné *et al*. (2006) *Environ. Sci. Technol.* **40**, 1806–1813. [2] Pokrovsky *et al*. (2005) *Environ. Sci. Technol.* **39**, 4490–4498. [3] Pokrovsky *et al*. (2008) *Geochim. Cosmochim. Acta.* **72**, 1742–1757.

https://doi.org/10.1180/S0026461X00006502 Published online by Cambridge University Press

Influence of conditions past and present on bacterial mineral precipitation

T.K. POLACSEK *, C.S. COCKELL AND T.L. GLADDING

The Open University, Walton Hall, Milton Keynes, Buckinghamshire, MK7 6AA, United Kingdom (*correspondence: t.k.polacsek@open.ac.uk) (c.s.cockell@open.ac.uk, t.l.gladding@open.ac.uk)

Bacterial mineral precipitation is thought to be a complex process, being influenced by biological, chemical and geological factors throughout time [1, 2]. This study focused on calcium mineral precipitation in the Cretaceous (~120Ma ago) and the present day, using marine bacteria. We investigated parameters such as (i) the Magnesium: Calcium ratio of seawater [3] and (ii) the atmospheric partial pressure of carbon dioxide [4], both of which showed great variations over time. We further investigated (iii) possible inhibitors of precipitation, (iv) availability of nutrients and (v) the necessity of metabolic active cells.

Electron-microscopy (EM) techniques, powder X-Ray diffraction and elemental spectra were used to screen the cultures for precipitates and to analyse polymorph mineralogy. For some bacterial strains, calcium mineral spheres were observed in the Cretaceous-like medium only, with a nutrient concentration of > 0.25% yeast promoting their formation. EM analysis not only revealed micropores and bacterial matter on the surface of the spheres but also demonstrated such pores in the interior of the spheres, containing cells being entombed in precipitate. For the first time these data elucidate the interplay of different parameters and their influence on the formation of bacterially induced calcium minerals in the Cretaceous.

[1] Ehrlich (1996) *Chem. Geol.* **132**, 5–9. [2] Bosak (2005) *JSR* **75**, 190–199. [3] Stanley (2008) *Chem. Rev.* **144**, 3–19. [4] Berner (1994) *Am. J. Sci.* **294**, 56–91.

Microbial communities as palaeoenvironmental indicators during black shale-hosted manganese ore formation

M. POLGÁRI[1]*, J.R. HEIN[2], T. NÉMETH[1], J. GUTZMER[3], T. HAHN[3]; A. MÜLLER[4], T. VIGH[5] AND L. BÍRÓ[4]

[1]Institute for Geochemical Research, Hungarian Academy of Sciences, 1112 Budapest, Budaörsi út. 45 (rodokrozit@gmail.com)

[2]USGS, MS 999, 345 Middlefield Rd. Menlo Park, CA 94025, USA

[3]TU Bergakademie Freiberg Institute of Mineralogy, Brennhausgasse 14. D-09596 Freiberg, Germany

[4]Szeged University, Dept. of Mineralogy, Geochemistry and Petrology, 6702 Szeged, Egyetem str. 2-6, Hungary

[5]Mangán Ltd, Úrkút, Külterület 1. 8409 Hungary

The Jurassic (Lias) black shale-hosted Mn-carbonate ore deposit was studied by XRD mineralogy (260) and rock microscopy (80) to determine mineral components and microstructure to better understand the sequence of microbial communities that existed during ore accumulation. Formation of the main Mn ore bed in the Úrkút deposit occurred via a two-cycle bacterial sequence: (1) an aerobic, chemolithoautotrophic microbial cycle, followed by (2) an anaerobic bacterial cycle. During cycle 1, microbial Mn (II) enzymatic oxidation resulted in the fine-grained accumulation of biooxides (with reactive organic matter), which later transformed during diagenesis into Ca-rhodochrosite via bacterially mediated processes during early suboxic diagenesis [1, 2]. These redox conditions supported celadonite formation from the mixing of warm geofluids with seawater. This clay formation occurred at the sediment/seawater interface or near it during synsedimentation or very early diagenesis under neutrophylic pH. The near seabed environment was continuously dysoxic-suboxic and was colonized by Fe (II) oxidizing microbes. Those microbs were interlaced with the host sediment and probably initially concentrated ferrihydrite, which was later transformed to goethite. Conditions became more reducing with a higher rock/water ratio during burial. This resulted in smectite formation and pyritization of goethite in the zone of bacterially mediated sulphate reduction.

The study was supported by Hungarian Science Foundation (OTKA-NKTH No. K 68992).

[1] Polgári *et al.* (1991) *JSP* **61**, **3**, 384–393. [2] Polgári *et al.* (2011) *OGR* submitted.

https://doi.org/10.1180/S0026461X00006502 Published online by Cambridge University Press

In situ O & Si isotopic microanalysis of diagenetic cements: Basin brines vs. weathering, low vs. high T

ANTHONY D. POLLINGTON*, REINHARD KOZDON, KOUKI KITAJIMA, ARIEL STRICKLAND AND J.W. VALLEY

WiscSIMS, Dept. Geoscience, Univ. Wisconsin, Madison, WI 53706, USA
(*correspondence: apolling@geology.wisc.edu)

Secondary minerals, such as diagenetic overgrowths, are potential recorders of processes in surface and shallow sub-surface environments. Quartz overgrowths incorporate chemical and isotopic signatures of the fluids from which they grow; the composition of these fluids in turn being influenced by factors such as chemical weathering of the source region and interactions with rocks along a flow path.

In situ microanalyses of $\delta^{18}O$ in isotopically-zoned quartz overgrowths from the Cambrian Mt. Simon Sandstone in central North America reveal growth from a compositionally ($\delta^{18}O$) constant fluid during an evolving temperature history of burial and heating [1]. The temperatures calculated from $\delta^{18}O$ values indicate that drill core samples from the Illinois Basin grew in response to burial/heating and are consistent with geotherm temperature-depth estimates (50 to 110°C). However, overgrowths from most outcrop samples on the Wisconsin Dome, which have never been deeply buried, indicate growth at low temperatures (~35°C).

We have also measured Si isotope ratios and trace element concentrations in the same overgrowths. The $\delta^{30}Si$ values for most samples indicate growth from a source dominated by primary igneous Si (such as detrital sand grains). However, samples from one outcrop, ~5m above the Precambrian unconformity, have $\delta^{30}Si$ values that are among the lowest terrestrial values reported (-5.44‰ to -0.40‰) as well as unusually low $\delta^{18}O$ values suggesting hydrothermal precipitation. Chemical weathering has been proposed as a mechanism to explain low $\delta^{30}Si$ values in overgrowths [2].

Trace element concentrations are relatively low in detrital quartz, and overgrowths from the basin samples. In quartz overgrowths from outcrop samples though, concentrations of some elements (in particular Li and Al) are at least 1-2 orders of magnitude higher than the detrital material. Trace element concentrations, $\delta^{18}O$ and $\delta^{30}Si$ values are distinctly different for outcrop samples versus basin samples. This possibly reflects interaction of fluids with a weathered protolith, such as the nearby paleosol that underlies the formation on the Cambrian-Precambrian unconformity.

[1] Pollington *et al*. (2010) *Geochimica et Cosmochimica Acta Suppl*. **74**, A823. [2] Basile-Doelsch *et al*. (2005) *Nature* **433**, 399–402.

Reaction paths and volume changes of solid solutions in coupled dissolution-precipitation reactions: The role of endmember solubility

K. POLLOK[1]*, C.V. PUTNIS[2] AND A. PUTNIS[2]

[1]Bayerisches Geoinstitut, Universität Bayreuth, D-95440 Bayreuth, Germany
(*correspondence: kilian.pollok@uni-bayreuth.de)
[2]Institut für Mineralogie, Universität Münster, Corrensstr. 24, D-48149 Münster, Germany

Mineral-fluid reactions towards equilibration involve readjustment of the phase assemblage and its composition. Such reequilibration is commonly accomplished by dissolution and precipitation reactions at Earth's surface and at crustal conditions when fluid flow is pervasive. As most rock-forming mineral systems are, to various extents, solid solutions, they respond to the fluid chemistry by readjusting their composition. This can be often observed as a pseudomorphic replacement. In this context, the concept of solubility becomes complicated once solid solution-aqueous solution (SS-AS) relationships are taken into account [1].

Based on the internally consistent description of solubility and SS-AS equilibrium states in the model KBr-KCl-H_2O system [2] a quantitative treatment of various reaction paths and their associated volume changes is presented. It allows to derive various scenarios for dissolution-precipitation reactions based on solid-fluid ratio, local equilibrium or limited transport at the reacting interface which in turn can provide qualitative predictions on the kinetics of the replacement reaction.

In many cases, volume changes are preserved in replaced minerals as intracrystalline porosity which can facilitate transport from and to the reaction front [3]. Data on the solubility of solid solutions in complex aqueous fluids at higher temperature and pressure is still limited. However, the determined porosity in partly replaced minerals (either natural or experimental) can be used to roughly estimate the solubility difference of the parent and product phases. This concept as well as its limitations will be demonstrated for various rock-forming minerals and is intended to facilitate more experimental work to ascertain the role of porosity generation in interface-coupled dissolution-precipitation reactions.

[1] Prieto, M. (2009) *Rev Min Geochem* **70**, 47–85. [2] Pollok, K. *et al*. (2011) *Am J Sci* **311**, DOI: 10.2475/03.2011.02. [3] Putnis, A. (2009) *Rev Min Geochem* **70**, 87–124.

https://doi.org/10.1180/S0026461X00006502 Published online by Cambridge University Press

Adsorption and oxidative transformation of aromatic acids by Fe(III)-montmorillonite

T. POLUBESOVA*, S. ELDAD AND B. CHEFETZ

Department of Soil and Water Sciences, the Robert H. Smith Faculty of Agriculture, Food and Environment, The Hebrew University of Jerusalem, P. O. Box 12, Rehovot 76100, Israel
(*correspondence: polubeso@agri.huji.ac.il)

Aromatic acids are involved in important soil processes, such as mobilization of microelements by plants and formation of humic components. The interactions of aromatic acids (ferulic, p-coumaric, syringic, vanillic and benzoic) with montmorillonite enriched with Fe (III) was investigated. Adsorption of the phenolic acids on Fe (III)-montmorillonite was accompanied by their oxidative transformation and formation of Fe (II). Oxidative transformation of phenolic acids was affected by their molecular structure. The order of maximal transformation at the initial acid concentration of 20 mg/L on the surface of Fe (III)-montmorillonite was: ferulic (94%), syringic (60%), p-coumaric (35%) and vanillic (25%). Benzoic acid which was used as a reference aromatic compound exhibited only 5% transformation [1]. Adsorption of benzoic acid by Fe (III)-montmorillonite increased in the presence of 5 mM $CaCl_2$. Desorption of benzoic acid from Fe (III)-Ca^{2+}-montmorillonite was greater than that from Fe (III)-montmorillonite [2]. Removal of aromatic acids from solution by Fe (III)-montmorillnite increased with decreasing pH. LC-MS analysis demonstrated the presence of dimers, trimers, and tetramers of ferulic acid on the surface of Fe (III)-montmorillonite [1]. Oxidation and transformation of ferulic acid were more intense on the surface of Fe (III)-montmorillonite as compared to Fe (III) in solution due to stronger complexation on the clay surface: 90% of the ferulic acid was transformed following by interaction with Fe (III)-montmorillonite at an initial concentration of 0.1 mM, whereas only 20% was transformed in $FeCl_3$ solution. The concentrations of Fe (II) formed in Fe (III)-montmorillonite-ferulic acid suspensions at equilibrium was 0.46 mM. In the corresponding $FeCl_3$-ferulic acid system, the concentrations of Fe (II) was 0.06 mM [1]. The results of the current study demonstrate the importance of Fe (III)-clay surfaces for the abiotic formation of humic materials and for the transformation of aromatic (phenolic) pollutants.

[1] Polubesova, Eldad & Chefetz (2010) *Environ. Sci. Technol.* **44**, 4203–4209. [2] Chefetz, Eldad & Polubesova (2011) *Geoderma* **160**, 608–613.

Isotope fractionation between metallic Fe and Fe^{3+}- and Fe^{4+}-bearing compounds

V.B.POLYAKOV* AND D.M.SOULTANOV

Institute of experimental mineralogy, RAS, Chernogolovka, Moscow region, 142432, Russia
(*correspondence: polyakov@iem.ac.ru, dll@iem.ac.ru)

We determined β-factors for Fe^{3+} and Fe^{4+} ($CaFeO_3$ and $SrFeO_3$) compounds at ambient pressure from Mössbauer and inelastic nuclear resonant x-ray scattering (INRXS) spectra [1-6] using techniques developed previously [7-10]. The pressure effect on Fe β-factors were estimated from a relation between pressure and temperature derivatives of β-factors [11]. For metallic Fe, we used the pressure dependence of β-factors [12] calculated from INRXS spectra [13].

Compound	Equilibrium fractionation factor (‰)			
	2000 K		3000 K	
	ambient	24 GPa	ambient	32 GPa
Fe_2O_3	0.05 - 0.07	0.07 - 0.09	0.03 - 0.04	0.05 - 0.06
$ReFeO_3$-Pv*	0.03 - 0.09	0.05 - 0.12	0.02 - 0.06	0.03 - 0.10
$CaFeO_3$-Pv	0.12 - 0.17	0.15 - 0.21	0.06 - 0.09	0.07 - 0.12
$SrFeO_3$-Pv	0.15 - 0.25	0.19 - 0.30	0.08 - 0.13	0.10 - 0.17
(Mg, Fe)SiO_3-Pv ferric	0.04 - 0.09	0.06 - 0.11	0.02 - 0.04	0.03 - 0.05

Table 1: Equilibrium isotope fractionation factor between Fe^{3+}- and Fe^{4+}-bearing compounds and metallic Fe.
* Re is the rare earth element, except Yb.

The isotope fractionation between Fe^{3+} compounds and Fe-metal is smaller than observed isotopic shifts (~0.1‰ [14]) between Earth's basalts and those from Mars and Vesta. The putative disproportionation via Fe^{4+} species might allow one to agree estimations and observations. Addition of S, H, and C to the Fe metallic phase is also a favorable factor for the enrichment of Earth's core in light Fe isotope [15].

[1] Eibschütz *et al.* (1967) *Phys Rev.* **156**, 562–568. [2] McCammon (1996) *Phase Transition* **58**, 1–26. [3] Seto *et. al.* (2004) *J. Phys. Soc. Jpn.* **73**, 1669–1672. [4] Rykov *et. al.* (2004) *Physica B.* **350**, 287–304. [5] McCammon (1998) *Phys. Chem. Minerals* **25**, 292–300. [6] Sturhahn (2000) *Hyp. Interact.* **125**, 149–172 [7] Polyakov (1997) *GCA,* **61**, 4213–4217. [8] Polyakov & Mineev (2000) *GCA* **64**, 849 865. [9] Polyakov *et. al.* (2005) *GCA* **69**, 5531–5536. [10] Polyakov *et. al.* (2007) *GCA* **71**, 3833–3846. [11] Polyakov & Kharlashina (1994) *GCA* **58**, 4739–4750. [12] Polyakov (2009) *Science* **323**, 912–914. [13] Mao *et. al.* (2001) *Science* **292**, 914–917. [14] Poitrasson *et. al.* (2004) **223**, 253–266. [15] Polyakov (2009) *Eos Trans.AGU,* **90** Suppl. V148-01.

https://doi.org/10.1180/S0026461X00006502 Published online by Cambridge University Press

Arsenic concentration influences secondary mineral formation during simultaneous As(V) and Fe(III) reduction by *Shewanella* sp.

S.A. POMBO[1]*, J.-H. HUANG[1], C. MIKUTTA[1], U. DIPPON[2], A. KAPPLER[2] AND R. KRETZSCHMAR[1]

[1]Institute of Biogeochemistry and Pollutant Dynamics, ETH Zurich, Switzerland (*correspondence: silvina.pombo@env.ethz.ch)

[2]Geomicrobiology, Center for Applied Geosciences, University of Tuebingen, 72076 Tuebingen, Germany

Microbial reduction of As (V) and Fe (III)-oxyhydroxides largely controls the solubility and mobility of As in soils and natural waters. Under most conditions, As (III) is sorbed less strongly to oxide mineral surfaces than is As (V), and changes in specific surface area and reactivity resulting from reductive Fe-mineral transformations also influence the sorption of As.

The extent of simultaneous microbial reduction of Fe (III) in ferrihydrite and sorbed As (V), as well as secondary Fe-mineral formation, were studied in batch cultures (serum bottles). Ferrihydrite suspensions (2 g L^{-1}) containing 20, 200 or 2000 μM As (V) and 20 mM lactate in mineral medium were incubated for 38 days in the presence of *Shewanella* sp. ANA-3 under anoxic conditions at 25°C. Iron mineral transformations were monitored by Fe K-edge EXAFS (extended X-ray absorption fine structure) and ^{57}Fe Mössbauer spectroscopies.

Increasing As concentrations resulted in an increase in the percentage of As (V) reduced during 38 days (from 40 to 90%). The average As (V) reduction rate increased from 0.24 to 86 μmol As L^{-1} d^{-1}. The concentrations of dissolved As, mainly As (III), also increased with time up to 80 μM at the higher As concentration, whereas no dissolved As was detected in suspensions containing 20 μM As. The average Fe reduction rate decreased from 32 to 26 mmol Fe L^{-1} d^{-1} with increasing total As concentration, while the dissolved Fe (II) concentration decreased by 50%. EXAFS and Mössbauer spectra revealed that mainly magnetite was formed in the presence of 20 μM As, while chloride green rust was identified as the dominating secondary mineral in the presence of 2000 μM As.

In conclusion, the presence of a high As concentration (molar ratio As/Fe~0.1) resulted in an increased As (V) reduction rate, a decreased Fe reduction rate, and inhibited magnetite formation in favor of formation of chloride green rust.

Reactivity of chemically modified nanodisperse anatase

A.V. PONARYADOV AND O.B. KOTOVA

Institute of Geology of Komi SC UB RAS, Russia, 167982, Syktyvkar (alex401@rambler.ru)

Titanium minerals are the most important source of titanium, a strategic metal of modern industry. They act in natural and technological processes as interacting substances, homogeneous and heterogeneous catalysts coated on surface of support and consisting of relatively small particles of metal or metal oxides (1–2 nm). Mechanism of nucleation and growth of minerals on nanoscale as well as nonautonomous phases on mineral surfaces could be studied using synthetic analogues of titanium minerals as research model.

Three different TiO_2 have been used as support of Au-systems: commercial Aldrich Titanium (IV) oxide, nanopowder, 99.7 %, anatase and two nanotube-structured TiO_2 with different pH and geometrical parameters. Nonautonomous phases were deposited on the surface of supports by means of a liquid dispensing robot. Chemical reactivity of prepared samples were tested in reaction of preferential oxidation of carbon monoxide. In temperature programmed reactions (TPR) conversion of CO and O_2 as well as selectivity of O_2 towards CO has been determined as a function of temperature.

As CO conversion over the Au-only sample is very low, the selectivity of this system is much smaller, than that obtained over the modified multicomponent systems. Hence, the main role of the modifiers in case of catalysts supported on commercial TiO_2 and titaniun dioxide nanotubes is the enhancement of the selectivity. On the bases of previous studies it is very probable that Pb is alloyed with Au, which is main reason for the selectivity enhancement [1]. The bimetallic Au-Pb particle suppresses adsorption of hydrogen; therefore oxidation of CO obtains higher probability.

Addition of Sm can change the nanoenvironment of Au in such a way that it stabilizes dispersion of gold during the reaction, as well as the interfaces between the Au nanoparticles and Sm_2O_3 can facilitate oxygen adsorption. Moreover, due to the atomic contact between oxide modifiers and gold the formation of metal ion – gold nanocluster ensemble sites can activate CO oxidation over the multicomponent catalysts. All these effects contribute to the enhancement of CO oxidation rate.

[1] Tompos *et al*. (2009) *J. Catal*. **266**, 207–217.

https://doi.org/10.1180/S0026461X00006502 Published online by Cambridge University Press

250-Ma old nature carbon nanostructuring materials and nanotubes in inrusive rocks

V.A. PONOMARCHUK*, D.V.SEMENOVA, T.N. MOROZ, A.T. TITOV AND V.V. RYABOV

Sobolev Institute of Geology and Mineralogy SB RAS, 630090 Novosibirsk, Acad. Koptyug av., 3, Russia (*correspondence: ponomar@igm.nsc.ru)

Numerous studies of the synthesis of carbon nanostructuring materials were conducted after publication [1] (1952 year), and [2] (1991 year), and it was thought after that the nanotubes can be obtained only by artificial means in the laboratory. However, studies of graphite-like globules (size - 2 ÷ 10 mm) from leykogabbro with age of 250 million years have shown the possibility of formation of carbon nanotubes in magmatic processes.

Analytical procedures include following steps: 1) acid decomposition of silicate rocks, 2) selection of graphite particles under a microscope, 3) study of morphology and composition using a scanning microscope, and 4) identification of the C-C bond (Raman microscopy) and carbon isotopic composition.

'Anatomy' of globule (from the edge to the center) is as follows: 1) the thin layer of carbon film (graphene?), 2) outer shell, made of a porous carbon material with thickness of ~ 20μm (turbostatic graphite), 3) the inside of the shell is covered by 'forest' of carbon microtubes; 4) the length of the microtubes – 0.2-0.3 mm, diameter - 1-5μm (Fig. 1, left part); 5) multi-walled carbon nanotubes 'growing' from the microtubes (Fig.1, right part). Temperature of the carbon nanostructuring material formation (Raman spectroscopy) ranges from 650 to 470°C. $\delta^{13}C$ values of different forms vary from -16 to -12‰. In general, the data, obtained in this study, have shown that nano- and microtubes were formed in gaseous environment (from CO^2) through the molecular dynamic mechanism.

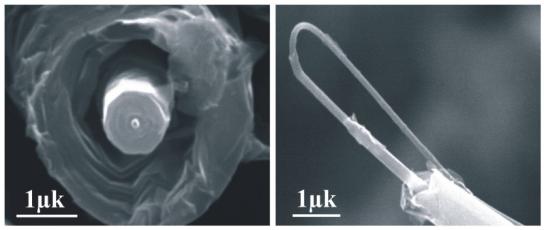

Figure 1: left - section of the carbon microtube, right – nanotube growing from microtube.

[1] Radushkevich *et al*. (1952) *J. of Phys. Chem*. **26**, 88–95. [2] Lijima (1991) *Nature* **354**, 56–58.

Stable isotope composition and volume of Early Archaean oceans

E.C. POPE[1]*, M.T. ROSING[2] AND D.K. BIRD[3]

[1]Geological Museum, University of Copenhagen, 1350 Copenhagen K., Denmark (*correspondence: ecpope@stanford.edu)
[2]Geological Museum, University of Copenhagen, Denmark (minik@snm.ku.dk)
[3]Dept. of Geological and Environmental Sciences, Stanford University, Stanford, CA, 94305, USA (dbird@stanford.edu)

Oxygen and hydrogen isotope compositions of seawater are controlled by volatile fluxes between mantle, lithospheric (oceanic and continental crust) and atmospheric reservoirs. Throughout geologic time oxygen was likely conserved within these Earth system reservoirs, but hydrogen was not, as it can escape to space [1]. Hydrogen isotope ratios of serpentinites from the ~3.8Ga Isua Supracrustal Belt in West Greenland are between -53 and -99‰; the highest values are in antigorite ± lizardite serpentinites from a low-strain lithologic domain where hydrothermal reaction of Archaean seawater with oceanic crust at elevated temperatures was geochemically preserved, indicating that the $\delta D_{SEAWATER}$ was at most 25 ± 5‰ lower than modern VSMOW. We propose that the progressive increase in $\delta D_{SEAWATER}$ since this time is due to preferential uptake of hydrogen in continent-forming minerals and to hydrogen escape via biogenic methanogenesis [2]. Mass balance considerations within the Earth system places a cumulative upper limit on elemental hydrogen loss to space of ~$1.8x10^{22}$mol elemental hydrogen H, constraining maximum Archaean atmospheric methane levels at ~3.8Ga to <500ppmv (depending on the volume of continents present at that time), and the mass of Early Archaean oceans to ~109 to 126% of present day oceans. Oxygen isotope analyses from these Isua serpentinites ($\delta^{18}O$ = +0.1 to 5.6‰ relative to VSMOW) indicate that early Archaean $\delta^{18}O_{SEAWATER}$ similar to modern oceans. Our observations suggest that the low-$\delta^{18}O$ values of Precambrian sedimentary cherts and carbonates are not a consequence of isotope variability of seawater or extreme ocean temperatures [3, 4], but rather are due to isotopic exchange with shallow hydrothermal fluids on the ocean floor or during diagenesis [5].

[1] Lécuyer *et al*. (1998) *Chem. Geol*. **145**, 249–261. [2] Catling *et al*. (2001) *Science* **293**, 839–843. [3] Hren *et al*. (2009) *Nature* **462**, 205–208. [4] Jaffrés *et al*. (2007) *Earth-Science Reviews* **83**, 83–122. [5] Blake *et al*. (2010) *Nature* **464**, 1029–1032.

https://doi.org/10.1180/S0026461X00006502 Published online by Cambridge University Press

REE behavior during the formation of Sn-W deposits

J.A. POPOVA[1]*, A.YU. BYCHKOV[1], S.YU. NEKRASOV[1] AND T. SUSCHEVSKAJA[2]

[1]Moscow State Universiy, Moscow,Russia (*correspondence: julka_p@rambler.ru)
[2]GEOKHI RAS, Moscow, Russia

REE behaviour was considered for two Sn-W deposits, Svetloe and Iul'tin (Chukotka, Russia). Both deposits take place within the Iul'tin ore district. The isotopic composition of oxygen and hydrogen allowed to conclude that meteoric waters were probable source of hydrothermal fluids in these deposits [1]. REE content in fluorites may be used as an indicator to determine the nature and the evolution of fluids [2]. Regularities of REE spectra changes indicate the presence of two generations of fluorite. REE concentations in thehydrothermal solutions in equilibrium with fluorites were obtained by conversion of two generations of fluorite into fluids using the distribution coefficients of mineral / fluid [2]. For the first fluorite generation the fluid is magmatic one, for the second fluorite generation the fluid is exogenous. Mixing these two fluids leads to the deposition of ore. The deposition of cassiterite and arsenopyrite occurs when acidic magmatic fluid carrying the ore elements mixed with alkaline meteoric water. As a result pH increases and the following association is formed:

$3Sn^{II}Cl_2^{\circ}+2As^{III}(OH)_3^{\circ}+2FeCl_2^{\circ}+2H_2S^{\circ}=$
$=3Sn^{IV}O_2+2FeAs^{\circ}S+10HCl^{\circ}.$

The wolframite deposition occurs under the following reaction:

$NaHWO_4^{\circ}+FeCl_2^{\circ}=FeWO_4+Na^{+}+2Cl^{-}+H^{+}.$

The compositon of wolframite changes in the vertical section of Iul'tin deposite from 47% to 64% mol% FeWO4. For Svetloe deposite it is shown that wolframite is depleted of iron (from 39 to 5 mol% FeWO4) under the joint deposition of wolframite and arsenopyrite.

[1] Sushchevskaya T. *et al*. (2000) *Geochem. Int*. **38**. Suppl. 2 . P. 123. [2] Raimbault L. (1985) *Bull. Mineral* **108.** P.737.

Methylotrophy in Yellowstone National Park hot springs

A.T. PORET-PETERSON[1]*, S.J. ROMANIELLO[1], N. ZOLOTOVA[1], Z. MARTINEZ[1], J.J. ELSER[2] AND A.D. ANBAR[1,3]

[1]School of Earth and Space Exploration, Arizona State University, PO Box 871404, Tempe, AZ 85287, USA (*correspondence: aporetpe@asu.edu)
[2]School of Life Sciences, Arizona State University, PO Box 874501, Tempe, AZ 85287, USA
[3]Department of Chemistry and Biochemistry, Arizona State University, PO Box 871604, Tempe, AZ 85287, USA

Autotrophic microorganisms in hot springs, like their mesophilic counterparts in other aquatic ecosystesm, likely play a major role in supplying reduced organic C to these systems [1]. However, hot springs are surface expressions of geologic activity that releases compounds that may serve equally well as sources of C, such methane (CH_4). Indeed, CH_4 assimilation pathways may be less energetically expensive in terms of ATP and reductant than the Calvin Cycle or alternative pathways for CO_2 fixation [2]. Thermodynamic calculations also show that microbes capable of aerobic CH_4 oxidation can thrive in hydrothermal ecosystems due to the amount of energy released from its catabolism [3]. Several recent studies have isolated CH_4-oxidizers from geothermal environemnts [4].

The goal of this study was to investigate whether methylotrophs (utilizers of reduced C_1 compounds) were present and active in various thermal features in Yellowstone National Park. To accomplish this objective, we incubated hot spring sediments and microbial mats in microcosms amended with stable-isotope labeled and unlabeled methanol (CH_3OH) overnight at *in situ* temperatures. We found evidence for methylotrophy in the sediments of slightly acidic hot springs (pH 6.0) based on ^{13}C enrichment of CO_2 and bulk sediment. To complement our isotopic data, we extracted DNA from hot spring sediments and retrieved functional genes encoding key enzymes in aerobic CH_4 and CH_3OH oxidation. Sequencing of these genes suggests that a complex methylotrophic community may be present in the hot spring, as clones grouped with gammaproteobacterial obli-gate methanotrophs and betaproteobacterial obligate methylo-trophs.

[1] Azam & Malfatti (2007) *Nature* **5**, 782–791. [2] Berg (2011) *Appl. Environ. Microbiol*. **77**, 1925–1936. [3] Shock *et al*. (2010) *Geochim. Cosmochim. Ac*. **17**, 4005–4043. [4] Trotsenko *et al*. (2009) *Microbiol*. **78**, 387–401.

https://doi.org/10.1180/S0026461X00006502 Published online by Cambridge University Press

Understanding Early Jurassic ocean connectivity using Os isotopes

SARAH J. PORTER[1], DAVID SELBY[1], KATSUHIKO SUZUKI[2] AND DARREN R. GRÖCKE[1]

[1]Department of Earth Sciences, Durham University, Durham, DH1 3LE, UK
[2]Japan Agency for Marine-Earth Science and Technology, Yokosuka, 237-006, Japan

Marine organic-rich sedimentary rocks (ORS) hold the key to understanding past chemical changes to the oceans. The osmium isotope system ($^{187}Os/^{188}Os$) is a particularly powerful tool for tracing these changes, and as such makes it possible to determine the effects of continental weathering, meteorite impact and mantle-derived fluxes [1].

Although the present-day seawater Os isotope composition is relatively uniform ($^{187}Os/^{188}Os$ ratio of ~ 1.06), it has varied significantly throughout geological time [2, 3]. The Jurassic was a particularly dynamic period that witnessed full-scale plate reorganisation associated with the supercontinental break-up of Pangea. The Triassic-Jurassic boundary saw the onset of Central Atlantic Magmatic Province (CAMP) volcanism as the Central Atlantic lineament began to rift. Ocean chemistry at this time was therefore subject to significant fluctuations.

The marine ORS sequence of the Sinemurian-Pliensbachian GSSP, Robin Hood's Bay, UK, was located on the margins of the shallow European epicontinental sea in relative proximity to the rifting Central Atlantic, making it an ideal candidate for studying the affect of the CAMP on seawater chemistry.

Our results indicate that there was a significant contribution of unradiogenic Os to the oceans across the Sinemurian-Pliensbachian boundary, that can only be resolved by a mantle-derived, hydrothermal Os input. Evidence for sudden increased faunal exchange between the western Tethyan and eastern Pacific Oceans at this time, suggests that initiation of flooding of the Hispanic Corridor occurred close to this boundary. Our Os data provides evidence for opening of this seaway and better constrains the timing of flooding, therefore improving our understanding of palaeogeography and ocean connectivity during the Early Jurassic.

[1] Cohen, A.S. Coe, A. L. Bartlett, J. M. & Hawkesworth, C. J. (1999) *EPSL*, **167**, 159–173.[2] Levasseur, S. Birck, J.-L. & Allegre, C. J. (1998) *Science*, **282**, 272–274.[3] Peucker-Ehrenbrink, B. & Ravizza, G. (2000) *Terra Nova*, **12**, 205–219.

Arc magmas from slab to eruption: The case of Kliuchevskoy volcano

M. PORTNYAGIN[1,2]*, N. MIRONOV[2], V. PONOMAREVA[3], I. BINDEMAN[4], F. HAUFF[1], A. SOBOLEV[2,5], T. KAYZAR[6]D. GARBE-SCHÖNBERG[7] AND K. HOERNLE[1]

[1]Leibniz Institute of Marine Sciences (IFM-GEOMAR), Wischhofstr. 1-3, 24148 Kiel, Germany (*correspondence: mportnyagin@ifm-geomar.de)
[2]V.I. Vernadsky Inst. of Geochemistry and Analytical Chemistry, Moscow, Russia
[3]Inst. Volcanology and Seismology, Petropavlovsk-Kamchatsky, Russia
[4]Geological Sciences, Univ. Oregon, Eugene, USA
[5]Laboratoire de Géodynamique des Chaînes Alpines (LGCA), Univ. Joseph Fourier, Grenoble, France
[6]Univ. Washington, Earth and Space Sciences, Seattle, USA
[7]Inst. Geosciences, Christian-Albrechts-Univ., Kiel, Germany

Arc magmas are generated by a number of mantle and crustal processes. Our multidisciplinary, long-term research is aimed at deciphering these processes for a single arc volcano, Kliuchevskoy volcano in Kamchatka. Some key results of the study follow:

1) Modeling of trace element and H_2O contents in melt inclusions suggests that the primary magmas originate via hydrous flux-melting of the mantle wedge at temperatures close to the dry peridotite solidus. The role of decompression melting is minor or absent at Kliuchevskoy and other arc volcanoes built on relatively thick crust.

2) Geochemistry of high-Mg olivine suggests that primary Kliuchevskoy magmas have substantial contribution from olivine-free pyroxenite (up to 30 %), which could be formed by reaction of slab melts (or supercritical fluids) with mantle wedge peridotite.

3) Parental Kliuchevskoy melts start to crystallize as deep as the Moho boundary, and the erupted magmas reflect multi-stage and complex processes of crystallization, magma mixing and crustal assimilation. None of the Kliuchevskoy rocks analyzed thus far represent true primary melt compositions.

4) The Kliuchevskoy Holocene eruptive history is not steady-state in terms of eruption rate and geochemistry. There are two millenial cycles with major and trace element and O-Sr-Nd-Pb and U-series isotope compositions of the magmas changing gradually from more to less affected by crustal (?) assimilation. The onset of the cycles correlates with periods of enhanced volcanic activity in Kamchatka, suggesting that the extent of magma-crust interaction is inversely related to magma production rate and thus magma flux from the mantle.

https://doi.org/10.1180/S0026461X00006502 Published online by Cambridge University Press

The formation of micro-diamonds in cracks caused by a C-O-H rich fluid under medium to low pressure conditions

J. POTGIETER[1], H. SOMMER[2]*, K. REGENAUER-LIEB[3,4], H. JUNG[2] AND B. GASHAROVA[5]

[1]Department of Geology, University of the Free State, PO Box 339, Bloemfontein 9301, South Africa
[2]School of Earth and Environmental Sciences, Seoul National University, Seoul 151-747, Korea (*correspondence: info@holgersommer.de)
[3]School of Earth & Geographical Sciences, The University of Western Australia, Perth, Western Australia 6009, Australia
[4]CSIRO Exploration & Mining, PO Box 1130, Bentley, WA 6102, Australia
[5]ANKA/Inst.Synchotron Radiation, Forschungszentrum Karlsruhe GmbH, Hermann-von-Helmholtz-Platz 1, Eggenstein-Leopoldshafen, D-76344 Germany

There is new evidence that micro-diamonds not only formed at high pressure and high temperature conditions in the diamond window. We found that, under favorable thermodynamic, stoichiometric and kinetic circumstances, micro diamonds can be synthesized by polycondensation of light carbon bearing molecules at medium to low pressure conditions, even close to the Earth's surface in the studied eclogites from the Victor Diamond Mine, South Africa. The studied eclogites contain OH, CO_2, CO, CH_4, CH_2O and CH_3OH around totally embedded micro-cracks in nominally anhydrous minerals (NAMS). Micro cracks act like monomineralic and interphase grain boundaries, and can also interpreted as two dimensional defect structures. We used high-resolution synchrotron based FT-IR to detect C-O-H bearing volatiles around two-dimensional defect structures in NAMS as garnet. At micro diamond bearing defect structures, a correlation between the different C-O-H bearing volatiles is visible, whereas in inclusion free defect structures no correlation of the different C:O:H containing volatiles can be recognized. The findings from our study show that the C:O:H bearing volatiles, and their distribution pattern around the studied micro cracks, are indicative for the formation of micro diamonds in natural eclogites. Our outcomes confirm the results from experimental studies on the growth and synthesis of diamond crystals as a consequence of polycondensation of light carbon molecules.

This research was supported by the Mid-career Researcher Program through an NRF grant funded by the MEST (No. 3345-20100013) and is a contribution to UNESCO IGCP 557.

Iron mineralization in anoxic, non-sulphidic systems

SIMON W. POULTON

School of Civil Engineering and Geosciences, Newcastle University, Newcastle upon Tyne, NE1 7RU, UK (s.w.poulton@ncl.ac.uk)

It has long been considered that Earth's early oceans were anoxic and rich in dissolved Fe (ferruginous). The evidence for this comes from the widespread preservation of banded iron formations (BIF) in the geologic record. Although BIF deposition occurred in pulses, recent reconstructions of oceanic redox conditions during deposition of marine shales have increasingly provided evidence for persistent deep water ferruginous conditions throughout the Archean. It has been proposed that following the termination of global BIF deposition ~1.8 billion years ago, the oceans underwent a fundamental change in response to rising Earth surface oxygenation. The most recent reconstructions suggest that this may have led to widespread euxinia along continental margins and in epicontinental seas, with the deep ocean remaining ferruginous. Deep ocean ferruginous conditions have also been advocated for much of the Neoproterozoic, while recent high resolution reconstructions of ocean redox conditions during Phanerozoic oceanic anoxic events have also shown distinct orbital timescale cycling between deep water euxinic and ferruginous conditions.

Yet, despite the significance of ferruginous conditions during past periods of ocean anoxia, very little is known about biogeochemical cycling of elements and nutrients under such conditions. To address this we have recently focussed on assessing Fe mineralization in anoxic, non-sulphidic settings, in particular Lake Matano, Indonesia, and Golfo Dulce, Costa Rica. At Lake Matano, we find clear evidence for water column precipitation of the mixed ferrous-ferric mineral, green rust, at the oxycline. This is the first identification of green rust in a natural water body and we propose that this mineral would have played a major role in elemental cycling during precipitation (through adsorption/co-precipitation) and during subsequent transformation processes. At both Lake Matano and Golfo Dulce, we also find evidence for authigenic magnetite formation on an unprecedented scale, both in the water column and during diagenesis. This new insight ultimately provides process understanding of mineralization pathways and associated elemental cycling under anoxic, ferruginous conditions, and provides insight into the genesis of BIFs, while also aiding the reconstruction of environment conditions based on BIF geochemistry.

https://doi.org/10.1180/S0026461X00006502 Published online by Cambridge University Press

The anatomy of the Great Oxidation Event

SIMON W. POULTON[1], ANDREY BEKKER[2], JAMES FARQUHAR[3], AUBREY L. ZERKLE[1], DAVID T. JOHNSTON[4] AND DONALD E. CANFIELD[5]

[1]School of Civil Engineering and Geosciences, Newcastle University, UK (s.w.poulton@ncl.ac.uk)
[2]Department of Geological Sciences, University of Manitoba, Canada
[3]Department of Geology, University of Maryland, USA
[4]Department of Earth and Planetary Sciences, Harvard University, USA
[5]Nordic Center for Earth Evolution, University of Southern Denmark

The Palaeoproterozoic was characterised by three major glaciations that coincided with the transition from a dominantly anoxic to a well-oxygenated atmosphere (the Great Oxidation Event; GOE). This transition has been dated at 2.32 Gyr ago, based on a loss of S isotope mass-independent fractionations (MIF) in sediments from the Transvaal Supergroup, South Africa [1]. These South African sediments are considered to correlate with the second of three widescale glaciations recorded in the Huronian Supergroup, Canada [2].

To provide more insight into links between the detailed dynamics of the GOE and Paleoproterozoic glaciations and ocean chemistry, we have performed a multi-proxy reconstruction of Earth surface oxygenation across the second Huronian glaciation. We combine a variety of sensitive indicators of oxygenation, including the role that sulphate exerts on ocean redox state, Mo concentrations, and multiple S isotopes. We find clear evidence for euxinic depositional conditions during deposition of the Bruce glacial diamictite. Coupled with enrichments in Mo, this implies significant pervasive atmospheric oxygenation that was glacially-driven. However, persistence of mass-independent S isotope fractionations suggests that this was at a low level. The MIF signal is possibly transiently lost in the lower part of the overlying Espanola Formation, implying that oxygenation may have been close to the upper threshold for MIF generation. However, a clear S isotope MIF signal is present throughout the upper succession, despite enrichments in Mo, suggesting that atmospheric oxygen levels fluctuated around a low level between the second and third glaciations.

[1] Guo, Q. *et al*. (2009) *Geology* **37**, 399–402. [2] Bekker, A. *et al*. (2005) *Precamb. Res* **137**, 167–206.

High precision analysis of all REEs in chondrites and Earth

A. POURMAND[1,2]*, N. DAUPHAS[1] AND T.J. IRELAND[1]

[1]Origins Lab., Dept. of Geophys. Sci., Univ. of Chicago, Chicago, IL 60637, USA
[2]RSMAS - Division of Marine Geology and Geophys., Univ. of Miami, Miami, FL 33149, USA (*correspondence: apourmand@rsmas.miami.edu)

Advances in rare earth element (REE) analyses have succeeded in increasing the precision of measurements, while concurrently decreasing preparation time (e.g. [1, 2]). Here, we present high precision data for the REEs, Sc and Y that were collected following an innovative technique that we developed for the separation and purification of these elements. This technique applies a low-blank flux fusion procedure to ensure the complete digestion of a sample, followed by column chromatography to separate the REEs, Sc and Y from matrix elements, prior to analysis on a Neptune multi-collector ICP-MS [1, 3]. The REE patterns in all geostandards are in excellent agreement with compilations of literature values, albeit at a higher precision.

Rare-earth element, Sc and Y data were obtained for 10 carbonaceous chondrites, 16 enstatite chondrites and 15 ordinary chondrites. Previously, U, Th and Hf concentration, as well as Hf isotopic data were gathered for these meteorites [4]. In general, REE patterns for carbonaceous chondrites are relatively flat, although some CV3 samples (e.g. Allende) show a group-2 CAI pattern. Other chondrite groups show evidence for REE re-distribution during metamorphism, consistent with Dauphas and Pourmand [4].

A critical goal of this study was to re-evaluate CI-chondrite abundances, and if necessary, suggest a revised composition for normalizing purposes. We analyzed three CI-chondrites (Orguiel, n=5; Ivuna, n=2; Alais, n=1) and based on these 8 measurements, we propose a revised CI-composition for the REEs [3].

In addition to chondrites, we analyzed several terrestrial samples. When normalized to our revised CI composition, terrestrial rocks show smooth REE patterns except possibly for a small anomaly at Tm (also reported by [5]). This REE is seldom reported in literature, as it is mono-isotopic and often used as an internal standard. Further work is currently in progress to assess whether this effect is real.

[1] Pourmand & Dauphas (2010) *Talanta* **81**, 741–753. [2] Baker *et al*. (2002) *GCA* **66**, 3635–3646. [3] Pourmand *et al*. (2011) submitted. [4] Dauphas & Pourmand (2011) *Nature*, in press. [5] Bendel *et al*. (2011) *Lunar & Planetary Science Conference* ***2011***, abstract #1711.

https://doi.org/10.1180/S0026461X00006502 Published online by Cambridge University Press

Importance of correlation effects in first-principles simulations of iron at high-pressure

L.V. POUROVSKII[1,2], K. GLAZYRIN[3], L. DUBROVINKY[3], F. TASNADI[1], M. EKHOLM[1], M.I. KATSNELSON[4], A.V. RUBAN[5] AND I.A. ABRIKOSOV[1]*

[1]Department of Physics, Chemistry and Biology (IFM), Linköping University, Linköping, Sweden (leopo@ifm.liu.se, tasnadi@ifm.liu.se, marek@ifm.liu.se, *correspondence: igor.abrikosov@ifm.liu.se)

[2]Center de Physique Theorique, Ecole Polytechnique, 91128 Palaiseau Cedex, France (Leonid.Pourovskii@cpht.polytechnique.fr)

[3]Bayerisches Geoinstitut, Universität Bayreuth, Bayreuth, Germany (konstantin.glazyrin@uni-bayreuth.de, Leonid.Dubrovinsky@uni-bayreuth.de)

[4]Radboud University Nijmegen, Institute for Molecules and Materials, 6525 AJ, Nijmegen, Netherlands (m.katsnelson@science.ru.nl)

[5]Department of Materials Science and Engineering, Royal Institute of Technology, SE-10044, Stockholm, Sweden (a.v.ruban@gmail.com)

The importance of magnetic and correlation effects in high-pressure research is often overlooked. The usual motivation here is that under compression the overlap between localized states increases and so does the bandwidth W, while the local Coulomb repulsion U between those states is screened more efficiently. The reduction of U/W ratio is used to rationalize the neglect of electronic correlations beyond state-of-the art local density approximation (LDA) or semi-local generalized gradient approximation (GGA) at high-pressure conditions. Concerning magnetism, the Stoner theory becomes more realistic at very high temperature $T >> T_c$ (T_c is the Curie temperature) where the disappearance of local magnetic moments can be expected.

In particular, based on these arguments iron at the inner Earth's core conditions is modeled as non-magnetic within LDA-based approaches. To challenge this point of view, we have performed calculations with a new implementation of the dynamical mean-field theory (DMFT). It is based on a highly precise full-potential linear augmented plane wave (FLAPW) method for the band structure calculation combined with DMFT in conjunction with a continuous-time quantum Monte Carlo (CTQMC) impurity solver for treating the strong correlations [1]. The application of the methodology has shown anumbigously that inclusion of correlation effects beyond LDA/GGA has led to qualitatively new physical effects predicted in Fe at moderate, as well as at ultra-high pressure and temperature.

[1] Aichhorn *et al.* (2009) *Phys. Rev. B* **80**, 085101.

Cadmium isotopes in the western North Atlantic — GEOTRACES cruise PE319

C. POWELL[1]*, W. ABOUCHAMI[1], S.J.G GALER[1], M.O. ANDREAE[1], J. DE JONG[2], L. GERRINGA[2] AND H. DE BAAR[2]

[1]Max Planck Institute for Chemistry, PO Box 3060, 55020 Mainz, Germany (*correspondence: Claire.Powell@mpic.de)

[2]Royal Netherlands Institute for Sea Research, PO Box 59, 1790 AB Den Burg, The Netherlands

We present cadmium concentration and isotopic composition data for four depth profiles from GEOTRACES cruise PE319, which sailed from Scrabster, UK to Bermuda during April and May 2010, following the eruption of the Eyjafjallajoekull volcano in Iceland.

Recent Cd isotope data have shown that the cadmium biogeochemical cycle in the high nutrient, low chlorophyll (HNLC) regions of the Southern Ocean is controlled by both ocean circulation and primary production [1]. In contrast, the surface waters of North Atlantic subtropical gyre are considered oligotrophic for much of the year, and the high latitude (>55°N) North West Atlantic is seasonally HNLC [2].

Seawater samples, collected using a titanium frame and ultra clean sampling techniques [3], were analysed for cadmium isotopic composition and concentration using a double-spike technique using Thermal Ionization Mass Spectrometry (DS-TIMS) at MPI. One litre seawater samples were processed as described by Abouchami *et al.*[1]. Data are reported relative to our NIST SRM 3108 standard ($^{110}Cd/^{112}Cd$=0.520121±4 (2SD, n=14)).

Preliminary results from the Irminger Basin (at 64.0°N, 34.25°W) show relatively constant cadmium concentrations, with a mean concentration of 0.25 ± 0.02 nmol kg^{-1} in the upper water column. The $\varepsilon^{112/110}Cd$ show little variation, with a mean value of +2.9 ± 0.26, and are similar to those reported in surface waters from the Arctic and North Atlantic [4]. Additionally, the ratio of phosphate to cadmium concentration appears to be coherent with models and observations of this ratio at low phosphate concentrations [5]. These results are consistent with seasonal observations of hydrographic mixing and stratification in the region [6].

[1] Abouchami *et al.* (2011) *EPSL* **305**, 83–91. [2] Nielsdóttir *et al.* (2009) *GBC* **23**, GB3001. [3] De Baar *et al.* (2008) *Mar.Chem.* **111**, 4–21. [4] Ripperger *et al.* (2007) *EPSL* **261**, 670–684. [5] Boyle (1988) *Paleoceanography*, **3**, 471–489. [6] Holliday *et al.* (2006) *J. Marine Systems* **59**, 201–208.

https://doi.org/10.1180/S0026461X00006502 Published online by Cambridge University Press

Studies of metalotolerant vegetable species and their potential for biogeochemical prospecting and environmental restoration (Cavalo old mining area, Central Portugal)

JOÃO PRATAS[1,3], PAULO FAVAS[2,3] AND LUIS CONDE[1]

[1]Dep. of Earth Sciences, University of Coimbra, Largo Marquês de Pombal, 3001-401 Coimbra, Portugal
[2]Dep. of Geology, UTAD, Ap.1013, 5000-801 Vila Real, Portugal (pjcf@utad.pt)
[3]Geosciences Center, University of Coimbra

Biogeochemical prospecting and the environmental control in highly polluted areas presume the correct selection of the biogeochemical material for sampling and the interpretation of the analytical results that takes into account the physiological mechanisms of plant adaptation and, in particular, the pedogeochemical phenomena.

In this work, have been characterised the species present in the old mining area of Cavalo (Oleiros, Castelo Branco, Central Portugal); environment with important W, As and some Cu contamination.

The species were selected envisaging their use as bioindicators, meaning that they are able to detect the pollution present in soils for use in mineral exploration; and seeking their potential use in the restoration with metalotolerant species able to tolerate the geochemical stress imposed by these conditions. The analyzed species included: *Erica australis, Erica umbellata, Pterospartum tridentatum, Halimium ocymoides, Arbutus unedo, Cistus salvifolius, Hypochaeris radicata, Pinus pinaster, Anarrhinum bellidifolium, Conyza canadensis, Andryala integrifolia, Agrostis delicatula* and *Agrostis curtisii*.

The results of analysis show that the species best suited for biogeochemical indicating are by order of importance: *Erica australis, Arbutus unedo* (leaves), *Halimium ocymoides, Erica umbellata, Cistus salvifolius* and *Pterospartum tridentatum* for As; *Halimium ocymoides* for Cu; *Erica umbellata, Arbutus unedo* (leaves and stems), *Erica australis, Pterospartum tridentatum, Halimium ocymoides* e *Cistus salvifolius* for W.

On the possibility of using these species in revegetation of areas with this type of contamination, it appears that all species accumulate in their tissues the main elements causing contamination (As and W). On the other hand, these species only have medium physiological barriers, not implying a high intake of these elements in the ecosystem.

Uranium in aquatic plants from uranium contaminated water in Central Portugal

JOÃO PRATAS[1,4], PAULO FAVAS[2,4] AND M.N.V. PRASAD[3]

[1]Dep. of Earth Sciences, University of Coimbra, Largo Marquês de Pombal, 3001-401 Coimbra, Portugal (jpratas@dct.uc.pt)
[2]Dep. of Geology, UTAD, Ap.1013, 5000-801 Vila Real, Portugal (pjcf@utad.pt)
[3]Department of Plant Sciences, University of Hyderabad, India
[4]Geosciences Center, University of Coimbra

The work presented here is a part of an on-going study on the uraniferous geochemical province of Central Portugal in which, the use of aquatic plants as indicators of uranium (U) contamination is being probed using aquatic plants emphasizing their potential use in the emerging phytotechnologies.

Several of the uraniferous deposits were exploited either by underground or surface mining methods. Many of the places were left in different stages of degradation.

The samples were collected in running and in standing waters (lentic and lotic) in the places where it was possible to observe aquatic species. In these sites, samples of the waters and of the vegetable species were taken. The plants collected represented the free floating and the rooted emergent plants. In the ponds, only free floating plants were found growing. The methodology adopted for the determination of the U content in the water and plants was fluorometry.

Even though we have observed very low concentration of U in the fresh waters of the studied sites we found a set of vegetable species with the ability to accumulate U in concentrations which are orders of magnitude higher than the surrounding environment. We have observed that *Callitriche stagnalis* (1948.41 mg/kg DW), *Lemna minor* (52.98 mg/kg DW) and *Fontinalis antipyretica* (234.79 mg/kg DW) accumulated significant amounts of uranium, whereas *Oenanthe crocata* excluded U. These results indicate substantial scope for proper radiophytoremediation and phytosociological investigation exploiting the native flora. These species show great potential for phytoremediation because they are endemic and easy to grow in their native conditions. *C. stagnalis* have high bioproductivity and yield good biomass.

https://doi.org/10.1180/S0026461X00006502 Published online by Cambridge University Press

Electrokinetic properties of the rutile/water interface: Zeta-potential prediction from computer simulations

MILAN PŘEDOTA[1], MICHAEL L. MACHESKY[2], D.J. WESOLOWSKI[3] AND P.T. CUMMINGS[4]

[1]Faculty of Science, University of South Bohemia, Ceske Budejovice, Czech Republic (predota@prf.jcu.cz)
[2]Illinois State Water Survey, Champaign, Illinois 61820-7495, USA
[3]Chemical Sciences Division, Oak Ridge National Laboratory, Oak Ridge, TN 37831-6110, USA
[4]Department of Chemical Engineering, Vanderbilt University, Nashville, Tennessee 37235, USA

In the last 10 years we have been studying by molecular dynamics (MD) the structural and dynamic properties of aqueous solutions in contact with metal-oxide surfaces, mainly rutile [1-3]. We will present the results of our non-equilibrium MD simulations focusing on the molecular level origin of electrokinetic phenomena - electroosmosis and electrophoresis. We will comment on the asymmetry of the density profiles of cations and anions at positive and negative surfaces, discuss the properties of the diffuse and shear layers, if definable at all on the molecular scale, and present our zeta potential predictions from molecular simulations. Our results of zeta potential are in qualitative agreement with experimental data [5]. However, our molecular explanation is rather contradictory to at least some of the commonly used theories of the solid-liquid interface including the common double- or triple- layer models. We observe that the composition and structure at the interface, influenced by the surface charge, are the key factors, while the electrostatics of the aqueous solution is rather independent of the surface charge.

[1] M. Předota, A. V. Bandura, P. T. Cummings, J. D. Kubicki, D. J. Wesolowski, A. A. Chialvo, & M. L. Machesky (2004) *J. Phys. Chem. B* **108**, 12049–12060. [2] M. Předota, Z. Zhang, P. Fenter, D. J. Wesolowski, & P. T. Cummings (2004) *J. Phys. Chem. B* **108**, 12061–12072. [3] M. Předota, P. T. Cummings, & D. J. Wesolowski (2007) *J. Phys. Chem. C* **111**, 3071–3079. [4] M. L. Machesky *et al.* (2008) *Langmuir* **24**, 12331–12339. [5] M. V. Fedkin, X. Y. Zhou, J. D. Kubicki, A. V. Bandura, S. N. Lvov (2003) *Langmuir* **19**, 3797–3804.

Recycling plus: A new recipe for making orogenic mantle

D. PRELEVIC

University of Mainz, Germany, (prelevic@uni-mainz.de)

Fluids and melts liberated from the subducting oceanic crust ± sediments recycle a number of chemical elements back into the mantle wedge. The recycling rate of key chemical elements is controled by the dichotomy of subsolidus dehydration vs. melting. Thermal models based on active subduction zones suggest that the majority of arcs are able to activate fluid-related transport dominantly, while the melt-related material recycling is only possible in unusually hot arcs. Paleo-subduction zones within orogenic belts, such as these within the Cenozoic Alpine-Himalayan belt, may serve as an advanced source of information regarding recycling styles during subduction. The composition of their mantle section is poorly constrained, but may be studied using postcollisional mantle-derived ultrapotassic lavas as a proxy.

The whole rock and mineral chemistry of postcollisional lavas suggests that the orogenic mantle underwent much more intense and complex material recycling than anticipated only by fluid- or melt-dominated transport. This is based on several fundamental constraints: i) Extremely enriched Sr, Nd, Hf, Pb and Os isotopic signature, which complement exceptionally low Ce/Pb and Nb/U ratios, are recognized in all mantle-derived postcollisional lavas along the Alpine-Himalayan belt; ii) Mixed ultra-depleted+ultra-enriched character of olivine phenocrysts and xenocrysts, with high Mg and Ni contents coupled with extremely high Li concentrations. Phenocrystal olivines have more than 40 ppm Li, and xenocrystal ones up to 10 ppm Li. iii) Extremely high Th/La coupled with high Sm/La of ultrapotassic mantle-derived lavas.

The above observations suggest that neither fluids nor melts alone are able to precondition orogenic mantle using known mechanisms, thus a new model is required. In my contribution, I will use the peculiar compositions of ultrapotassic mantle-derived lavas from across the Mediterranean for fingerprinting processes within the continental lithosphere. I will present a hypothesis that orogenic mantle is produced by accretion of suprasubduction fore-arc oceanic lithosphere plus trench sediments beneath older lithosphere during collisional tectonic events. The model demands conversion of principally oceanic lithosphere into the phlogopite-bearing continental lithospheric mantle and production of ultrapotassic lavas, which is a multi-episodic process.

https://doi.org/10.1180/S0026461X00006502 Published online by Cambridge University Press

Marine and terrestrial palaeoclimate proxies from the stable isotope analysis of North African molluscs

AMY L. PRENDERGAST[1], RHIANNON E. STEVENS[2], TAMSIN C. O'CONNELL[2], CHRISTOPHER HUNT[3] AND GRAEME BARKER[2]

[1]Department of Archaeology, University of Cambridge, Downing Street, Cambridge
[2]McDonald Institute for Archaeological Research, University of Cambridge, Downing Street, CB2 3ER
[3]Queens University Belfast, School of Geography, Archaeology and Palaeoecology, 42 Fitzwilliam Street, Belfast

Stable isotope analyses from the topshell *Osilinus turbinatus* and the pulmonate snail *Helix melanostoma* from the Haua Fteah, an archaeological site in North Africa have allowed the construction of paired marine and terrestrial climate curves that extend from c.20, 000 years ago to c. 7000 years ago. These analyses have been interpreted with reference to analogue studies on modern marine and terrestrial molluscs from Libya. In marine molluscs, $\delta^{18}O$ records fluctuations in sea surface temperature. In terrestrial molluscs, $\delta^{18}O$ varies according to the water ingested by the animal as the shell grows, which in turn is linked to water and air temperature at the moment of precipitation whilst $\delta^{13}C$ provides a proxy for palaeovegetation patterns and water stress. Intrashell stable isotope series from the Haua Fteah record snapshots of sub-seasonal climatic variations covering rapid and profound climatic fluctuations from MIS 2 to MIS 1. This high-resolution climatic framework coupled with the well-dated record of cultural change in the archaeological record, allows an examination of human-environment interactions during critical periods of late Pleistocene to early Holocene climate change.

Effects of ocean acidification in a supersaturated ocean (Carnian, Late Triassic)

N. PRETO[1], J. DAL CORSO[1] AND G. ROGHI[2]

[1]Dipartimento di Geoscienze, Iniversità degli Studi di Padova, via Gradenigo 6, 35131, Padova, Italy (*correspondence: nereo.preto@unipd.it)
[2]Istituto di Geoscienze e Georisorse, CNR, via Gradenigo 6, 35131, Padova, Italy

Ocean acidification triggered by recent anthropogenic emission of CO_2 is predicted to impact negatively on calcifying organisms. Here we present the response of lower Carnian shallow-water microbial carbonate platforms to an early-Late Triassic (~230 Myrs) episode of increased pCO_2. A negative carbon isotope excursion (CIE) of 2-4‰ was discovered in the lower Carnian (Upper Triassic) of the Dolomites (Southern Alps, Italy) which testifies for a rapid injection of light carbon in the atmosphere-ocean system linked to the eruption of Wrangellia large igneous province. The observed rise of the Carbonate Compensation Depth (CCD) in the deep-water succession and the crisis of shallow water carbonate systems [1] is best explained by an episode of ocean acidification triggered by increasing pCO_2.

Point-counting of calciturbidites and carbonate storm layers interbedded with the shales of the Carnian San Cassiano and Heiligkreuz formations show that carbonate grains with microbial origin are dominant below the CIE, but fall to less than 10% above, where skeletal grains and ooids become dominant. The turnover point coincides exactly with the CIE. It seems that ocean acidification favored metazoans and higher carbonate-secreting organisms over calcifying microbes. Thus, the Carnian case study seems a counter-example of today ocean acidification. However, Carnian seawater where microbes flourished was extremely supersaturated ('Neritan ocean' state [2]), and the effect of CO_2 injection in the system was probably just to drive supersaturation closer to present-day values. The Carnian case study demonstrates, at least at the short time-scale of the Carnian CIE, that the effects of ocean acidification can be strongly non-linear, and dependent on boundary conditions as the local saturation state of seawater with respect to carbonate.

[1] Rigo *et al*. (2007) *Palaeogeogr. Palaeocl. Palaeoecol.* **246**, 188–205. [2] Zeebe & Westbroeck (2003) **4**, *Geochem. Geophys. Geosyst.* **4**, doi: 10.1029/2003GC000538.

https://doi.org/10.1180/S0026461X00006502 Published online by Cambridge University Press

Zinc sulfide in suspended matter from an oxic river (Seine, France)

C. PRIADI[1]*, G. MORIN[2], S. AYRAULT[1], F. MAILLOT[2], F. JUILLOT[2], I. LLORENS[3], D. TESTEMALE[4], O. PROUX[5] AND GORDON E. BROWN JR.[6,7]

[1]LSCE, IPSL/CEA/CNRS-UVSQ, Gif-sur-Yvette, 91198, France (*correspondence: crpriadi@gmail.com, sophie.ayrault@lsce.ipsl.fr)
[2]IMPMC UMR7590 CNRS - UPMC – UP7, Paris 75252 cedex 05, France (guillaume.morin@impmc.upmc.fr)
[3]CEA INAC/SP2M/NRS, Grenoble, 38054 Cedex 9, France
[4]Institut Néel MCMF, CNRS, Grenoble, 38042, France
[5]OSUG, Grenoble, 38041 Cedex 9, France
[6]Surface & Aqueous Geochemistry Group, Dept. Geological and Environmental Sciences, Stanford University, Palo-Alto, CA, USA
[7]SSRL, SLAC National Accelerator Laboratory, Menlo Park, CA, USA

Several studies have underlined the importance of sulfide phases as trace element carrier in anoxic river and estuarine bottom sediments. Moreover, thermodynamic and kinetic studies in oxic waters have shown that the oxidation process of this reduced phase process may be relatively slow [1].

In the present study, Zn speciation was investigated in suspended particulate matter (SPM) in an oxic water column of the Seine River downstream of Paris, an urbanized watershed significantly impacted by Zn contamination [2].

First coordination shell around Zn was determined using Synchrotron-based Extended X-ray Absorption Fine Structure (EXAFS) spectroscopy at the Zn K-edge. Analysis of samples dried under pure nitrogen atmosphere indicated a dominant sulfur first coordination environment around Zn in the form of amorphous/poorly crystalline. In contrast, an oxygen first coordination environment around Zn was observed in the samples dried under ambient oxygenated atmosphere. The presence of ZnS solid phases in nitrogen-dried samples was confirmed by scanning electron microscopic observations coupled with energy dispersive x-ray spectroscopy analyses.

This study highlights the importance of preserving oxidation state for metal speciation studies, even in an oxic water column.

[1] Luther *et al*. (2005) *J. Nanopart. Res*. **7**, 389–407. [2] Priadi *et al*. *Environmental Science & Technology*, submitted.

The Longwood Igneous Complex of southern New Zealand: An intra-oceanic, subduction-related batholith

R.C. PRICE[1]*, C. SPANDLER[2] AND R.J. ARCULUS[3]

[1]Science and Engineering, University of Waikato, Hamilton, New Zealand (*correspondence: r.price@waikato.ac.nz)
[2]Earth and Environmental Sciences, James Cook University, Townsville, Queensland 4811, Australia (carl.spandler@jcu.edu.au)
[3]Research School of Earth Sciences, Australian National University, Canberra, ACT 0200, Australia (Richard.arculus@anu.edu.au)

The Longwood Igneous Complex (LIC), which is located in Southland, New Zealand, is a batholith-scale plutonic complex made up of troctolite, gabbro, gabbroic diorite, granite and basaltic dyke rocks ranging in age from Permian to Jurassic. Whole rock samples of the LIC have the trace element patterns of intra-ocaeanic, subduction-related magmas. Mineral chemistry and mineral phase relationships indicate emplacement depths of 15 to 25 km.

Ultramafic rocks and most of the gabbros of the LIC have petrographic and geochemical features indicating that they formed as cumulates. Few have direct compositional analogues among modern intra-oceanic volcanic rocks (e.g. [1, 2]). LIC intrusions represent crystal cumulates and mushes left over from the processes that generated the magmas that would have been erupted at the contemporaneous volcanic arc (c.f. [3]).

Across the LIC, there is a systematic change in the age of the intrusives from 254 Ma in the east to 142 Ma in the west. There is also a correlation between age of emplacement and Sr and Nd isotopic compositions, which together with inheritance in zircons dated by ion probe, suggests that crustal recycling became significant as the LIC subduction system evolved and matured. The LIC can therefore be used to estimate the composition of lower – middle crust assembled beneath an intra-oceanic arc over a 100 Ma time scale. LIC crust is on average andesitic and compositionally similar to bulk continental crust.

[1] Glazner *et al*. (2008) *Geology* **36**, 183–186. [2] Kent *et al*. (2010) *Nature Geoscience* **3**, doi: 10.038/NGEO924. [3] Bachmann & Bergantz (2008) *J. Petrology* **49**, 2277–2285.

https://doi.org/10.1180/S0026461X00006502 Published online by Cambridge University Press

Subcritical phase separation, extreme arsenic enrichment, and the search for arsenotrophs in the marine shallow-water hydrothermal vents off Milos Island, Greece

ROY E. PRICE[1]*, KATJA NITZSCHE[2], ANKE MEYERDIERKS[2] AND JAN P. AMEND[1]

[1]Earth and Planetary Sciences, Washington University, St. Louis (*correspondence: royprice@wustl.edu)
[2]Max Planck Institute for Marine Microbiology, Bremen, Germany

Recent investigations [1] revealed the highest arsenic concentrations measured to date for any submarine hydrothermal vent fluid, occurring in the shallow waters (<20 m) of Paleochori and Spathi Bay, off the southeast coast of Milos Island, Greece. Concentrations reached as high as 79 μM, which equals nearly 3000 times the concentration of seawater As and far exceeds the concentrations typically found in mid-ocean ridge (MOR) and back-arc basin (BAB) fluids (typically >10 μM). Orange hydrotheral precipitates at the site were characterized as non-crystalline orpiment. Both a high Cl (enriched in Cl by up to 47% compared to seawater) and a low Cl fluid (depleted by up to 66%) were encountered, and geochemical data indicate that the hydrothermal fluids underwent subcritical phase separation (boiling) and vapor/brine segregation prior to discharge.

We utilized both culture-dependent and molecular microbiological approaches to search for arsenotrophs in white and orange mats found on the seafloor in the area of venting. Field inoculations were performed using hydrothermal fluids and sediment slurries on designer growth media, including autotrophic and heterotrophic arsenate (AsV) reduction, as well as aerobic and anarobic arsenite (AsIII) oxidation, and incubated at 50 and 80 °C. Thusfar, enrichments in autotrophic AsV reduction with H_2S as the electron donor were successful, and efforts to characterize this community continue.

16S rRNA analysis showed a high diversity in the bacterial community, while archaea constituted only a minor fraction of the microbial community, with low diversity. The presence of diverse genes for the large subunit of arsenic oxidase (*aro*A) in the white and orange mats at Milos indicates the capability of the microbial community to metabolise arsenic.

[1] Price, R.E. Pichler, T. Planer-Friedrich, B. Bühring, S.I. Savov, I. (2011) The behavior of arsenic in subcritically phase-separated hydrothermal fluids from the marine shallow-water hydrothermal vents off Milos Island, Aegean arc, Greece. Submitted.

Interfacial tension, metastability, and solubility of solid solutions

M. PRIETO*, D. KATSIKOPOULOS AND A. FERNÁNDEZ GONZÁLEZ

Dept. Geology, University of Oviedo, Oviedo, Spain (*correspondence: mprieto@geol.uniovi.es)

The existence of a relationship between metastability and solubility is widely recognized in the crystal growth literature [1]. In general, the lower the solubility of a substance the higher is its 'ability' to form supersaturated solutions. The metastability limit of a supersaturated solution can be defined by the threshold below which the solution can remain supersaturated longer than an arbitrarily chosen waiting time. This definition is in the framework of the classical nucleation theory (CNT), which connects metastability, interfacial tension (σ) and solubility. The nucleation rate depends strongly on σ, which is in turn related to the solubility by the rule that the higher the solubility, the lower σ. In CNT, the interfacial tension is actually an 'artificial' parameter, but empirical estimations [2] of σ are typically used to account for precipitation in natural systems [3] and to model the precipitation in sequential order of lesser and lesser soluble minerals constituted of the same elements, according the Ostwald step rule. In a similar way, when solid-solutions crystallize from supersaturated solutions, the partitioning of the substituting ions usually differs from the equilibrium values [4]. 'More soluble' solid solution compositions are kinetically favored and tend to nucleate even though the aqueous solution is less supersaturated for these compositions than for less soluble members. This effect has been modeled by considering the differences between the interfacial tensions of the end-members [5], but empirical estimations of σ for intermediate members of solid solutions are rare.

The aim of this work was to determine interfacial tensions of intermediate members of a number of binary (ideal and non-ideal) solid solutions and to correlate them with the corresponding solubilities (Lippmann's solidus relationships). The interfacial tensions were determined from nucleation experiments carried out at 25 °C in a solution calorimeter. As a final outcome, for each solid solution system an empirical $\sigma(x)$ function of composition is proposed.

[1] Sangwal (1989) *J. Cryst. Growth* **97**, 393–405. [2] Söhnel (1982) *J. Cryst. Growth* **57**, 101–108. [3] Fritz & Noguera (2009) *Rev. Min. Geochem.* **70**, 371–410. [4] Prieto (2009) *Rev. Min. Geochem.* **70**, 47–85. [5] Pina & Putnis (2002) *Geochim. Cosmochim. Acta* **66**, 185–192.

https://doi.org/10.1180/S0026461X00006502 Published online by Cambridge University Press

Tracing anthropogenic nitrogen in the vicinity of industrial emitters in the Athabasca oilsands region, Alberta, Canada

B. PROEMSE[1]*, B. MAYER[1] AND M. FENN[2]

[1]Department of Geoscience, University of Calgary, 2500 University Drive NW, Calgary, Alberta, T2N 1N4 (*correspondence: bcpromse@ucalgary.ca)
[2]USDA, Forest Fire Laboratory, 4955 Canyon Crest Dr., Riverside, CA 92507, USA

The Athabasca oilsands deposit in northeastern Alberta, Canada, constitutes an unconventional energy source that is becoming increasingly important as the supply of conventional oil decreases. However, the rapid expansion in the exploitation of this oil resource over the last few years has caused increasing concerns regarding potential effects of elevated nitrogen (N) deposition. Hence, monitoring of N deposition and a better understanding of the N cycle in the Athabasca oilsands region are crucial for a thorough assessment of the impacts of elevated N emissions and depositions on surrounding terrestrial and aquatic ecosystems. Stable isotope techniques were used to trace the sources and fate of anthropogenic N emitted from the oilsands development. We determined $\delta^{18}O$ and $\Delta^{17}O$ values of atmospheric nitrate and $\delta^{15}N$ values of nitrate and ammonium collected in bulk deposition at various distances from the industrial emission sources to gain a better understanding of atmospheric N cycling in the vicinity of the industrial emitters. $\delta^{15}N$ values of total N in bitumen and oil sand samples were ~2‰. $\delta^{15}N$ values of atmospheric nitrate and ammonium varied with season and distance from the industrial emission source. Biogenic nitrogen emissions appeared to affect the isotopic composition of atmospheric nitrate in the summer ($\delta^{15}N$ -4.9 to +1.9‰), while vehicle exhaust appeared to be a major NO_x contributor influencing $\delta^{15}N$ values of atmospheric nitrate in the winter (-2.0 to +6.3‰). $\delta^{15}N$ values of ammonium as high as +10‰ close to the emission stack are believed to be associated with NH_3 released by the bitumen desulfurization process. $\Delta^{17}O$ analyses on atmospheric nitrate (n=22) showed non-zero values (+15.3 to +32.0‰) and hence mass-independent isotope fractionation. There was a trend towards higher $\Delta^{17}O$ values of atmospheric nitrate with increasing distance from the emission source, confirming the anthropogenic origin of nitrate in the vicinity of Athabasca oilsands development. We conclude that isotope analyses on atmospheric N compounds can reveal important information about sources and fate of natural and anthropogenic N compounds.

High-temperature gold deposits of Transbaykalia (Russia): Ore fluids compositions and its connection with magmatic process

V.Y. PROKOFIEV[1], N.N. AKINFIEV[1] AND L.D. ZORINA[2]

[1]IGEM RAS, Russia, Moscow, Staromonetny st., 35 (vpr@igem.ru)
[2]Vinogradov Imstitute of geochemistry, 664033, Russia, Irkutsk, Favorsky st., 1a (irazor@rambler.ru)

There are some atypical gold deposits with high-temperature veinlets-dissiminated ore at the territory of East Zabaykaliya (Talatuy, Kariyskoe, Pilinenskoe and others). Except Au, from the ore of these deposits can be extracted Ag, Cu, W, Mo, Bi. The Main mineral ore assotiation – tourmaline-pyrite-magnetite. The early native gold has high fineness (up to 996‰), silver deposits in late associations under low temperatures. Alteration of host rocks are presented by prophilites and orthoklasites. Three types of fluid inclusions are recognized: (1) inclusions of chloride brine that contain a gas bubble, water solution, one or several isotropic crystals, and occasionally an opaque ore mineral; (2) substantially gas inclusions that contain gas with a thin rim of aqueous solution and an occasional cubic isotropic crystal; and (3) two-phase gas–liquid inclusions of diluted solutions. The results of thermo- and cryometric studies, which involved 440 individual fluid inclusions in quartz and calcite, indicate that Mg, Na, and occasionally Ca chlorides participated in the ore formation. The complete homogenization of brine inclusions is achieved at a temperature of 610–270°C, and the salt concentration amounts to 56.3–29.9 wt % NaCl equiv. The gas fluid inclusions are homogenized into gas at 590–290°C and contain a fluid with salt concentrations ranging from 33.8 to 0.9 wt % NaCl equiv. Some inclusions contain carbon dioxide. The pressure estimates based on the inclusions of this type are 1170–110 bar. The two-phase gas–liquid inclusions of diluted solutions are homogenized into liquid at 495–145°C. The salt concentration in solutions that fill inclusions varies from 23.2 to 0.4 wt % NaCl equiv. The chemical composition of fluid inclusion was studied. Fe, Cu, Mo, Zn, Pb, Au, Ag, Bi and the other elements were determined into fluid composition. The ore formation at the deposits of this type took place against the background of boil-off (heterogenization) of chloride fluid near the cooling magma pocket. The particularities of the chemical fluid composition witness about the occurrence of magmatic fluid. The thermodynamic model of gold and silver separation in such fluid-magmatic system was built.

https://doi.org/10.1180/S0026461X00006502 Published online by Cambridge University Press

Organic matter alteration due to high heat flow in the northern Gulf of California

ROSA M. PROL-LEDESMA[1], CATALINA ANGELES[2], RUTH VILLANUEVA-ESTRADA[1] AND CARLES CANET[1]

[1]Departamento de Recursos Naturales, Instituto de Geofísica, Universidad Nacional Autónoma de México, Ciudad Universitaria, Delegación Coyoacán, 04510 México D.F., México

[2]Posgrado en Ciencias del Mar, Instituto de Ciencias del Mar y Limnología, Universidad Nacional Autónoma de México, Ciudad Universitaria, Delegación Coyoacán, 04510 México D.F., México

Studies in the northern Gulf of California have discovered high heat flow anomalies related to intensive gas discharge in the Wagner and Consag basins. The basins present a thick sediment cover of at least 5 km and bathymetry data show a maximum depth of 200m. Both basins have intense seismic activity and they are similar to other tectonically active basins in the Gulf of California plate border system. Intense gas discharge has been reported along the Wagner Fault, which is a continuation of the San Andreas transform fault. Chemical studies of the sediments from the Wagner Basin show that they have been subject to alteration of the sediment organic matter due to hydrothermal activity, similarly to what has been reported in the Central Gulf of California (Guaymas Basin), where high heat flow has been related to hydrocarbon generation and thermogenic methane abundance. Identification of the isoprenoid (PM1) related to the phylum Crenarchaeota is evidence of high temperature (75 to 105 °C) as this is the optimal temperatura for those organisms. High variability was observed in the maturity of organic matter in the sediments of the basins in correlation with the presence of hydrothermal activity.

Microbial community development and mineral-organic matter interactions in an artificial soil incubation experiment

GEERTJE J. PRONK[1], KATJA HEISTER[1], GUO-CHUN DING[2], KORNELIA SMALLA[2] AND INGRID KÖGEL-KNABNER[1]

[1]Lehrstuhl für Bodenkunde, Technische Universität München, Freising-Weihenstephan, Germany

[2]Julius Kühn-Institut (JKI), Institute for Epidemiology and Pathogen Diagnostics, Braunschweig, Germany

Artificial soils with 8 different mixtures of illite, montmorillonite, ferrihydrite, boehmite, charcoal and quartz sand, and manure as organic matter (OM) source were inoculated with the same microbial extract and incubated up to 18 months. The artificial soils were incubated under constant environmental conditions so that the effect of microbial activity on OM-mineral interactions alone could be studied.

The amount of organic carbon (OC) associated with minerals and microaggregates was determined by density fractionation. Solid state ^{13}C nuclear magnetic resonance (NMR) spectroscopy was used to characterize OC composition. Development of the microbial community in the first 90 days was followed by denaturing gradient gel electrophoresis (DGGE) analysis of 16S rRNA gene fragments amplified from total community DNA.

Density fractionation showed that significant microaggregation took place within 3 months of incubation and up to 24% of the OC present was associated with microaggregates and minerals in all mixtures at the end of incubation. This indicates that a fast development of OM-mineral interactions took place, providing microbial habitats. This is supported by the development of the bacterial community structure in the artificial soils, which depended on the mineral composition. Charcoal was shown to strongly influence the reassembly of bacterial communities. Effects of montmorillonite, illite and iron oxide on microbial communities were observed at day 90.

The results clearly show that mineral composition shaped the microbial community structure. This experiment therefore allows for the study of the development of organic matter-mineral associations, facilitated by micro-organisms, from clean model materials to soil-like systems.

https://doi.org/10.1180/S0026461X00006502 Published online by Cambridge University Press

Funginite and secretinite in coals Southern Pechora basin

O.S. PROTSKO

Institute of Geology of Komi Science Center Ural Branch of Russian Academy of Sciences, Syktyvkar (procko@geo.komisc.ru)

Funginite and Secretinite are one of not enough studied components inertinite maceral group. Earlier these components were called Sclerotinite. These components are rare in the Permian coals and sedimentary rocks (1-3 %). Content funginite and secretinite a increased to 10 % in Permian coals of their Nechensky layer. Nechensky low-rank coal deposits located in southern Pechora basin. The well section consists from is thin-is rhythmical alternating layers of different types coals, coals argillites and clays.

Secretinite occur in 15 samples, contents <1 - 9.5 %, on the average 3-5 %. The maximum content is revealed in the high part of a layer coals argillite, in other samples don't observed defined dependence to concrete types of rocks, it meets both in argillite, and in semibrilliant coals. The small part of inclusions secretinite it is concentrated in gelification layers and it is possibly characterized by the transferred forms. Funginite is found out in 29 samples, its content changes <1 – 10 %, on the average 5 %. Variation of funginite also non-uniformly on a section also meets in all rocks types. Its maximum content of 10 % mets in a layer coals argillite, height 100 mm. Often secretinite occurs together with funginite, e.g. in a layer of semimatte coal (обр 408-42) occur inclusions funginite (to 8 %) and secretinite (to 2 %). High contents the inertinite maceral group and minerals matter occurs together with for samples with inclusions funginite. Probably, these components indicate to oxidizing conditions sedimentation and swamp conditions with active hydrodynamics.

Classical geothermobarometry versus pseudosections: Practical experiences and strange encounters

A. PROYER[1]* AND E. BRUAND[2]

[1]Institute of Earth Sciences, University of Graz, 8010 Graz, Austria (*correspondence: alexander.proyer@uni-graz.at) p.a.: Inst. of Geological Sciences, FU Berlin, 12249, Berlin

[2]SEES, University of Portsmouth, Portsmouth PO1 3QL, UK

Practical experiences with geothermobarometry of the classical type and with pseudosections have revealed a number of particularities that might be of interest to both petrologists and geodynamicists trying to transform *P-T* data into geodynamic models. As an example, Fe-Mg geothermometry with grt-cpx in an eclogite can err considerably when ferric iron is not measured but calculated from stoichiometry. Such a deviation by >200°C could only be detected after Moessbauer microspectroscopy on garnet and clinopyroxene. The average*PT*-method (av*PT*) of THERMOCALC however, as a multi-equilibrium technique, is not as sensitive to these Fe-Mg exchange reactions and produced the correct result in the first place. Av*PT* has the potential to highlight a wrong choice of 'phases in equilibrium' but can also give (apparently correct) results on disequilibrium assemblages if its statistical elimination procedure is not used with proper diligence. Pseudosection modelling of eclogites with PERPLEX revealed two weaknesses. One is intrinsic to PERPLEX: significant changes in the shape and topology of some assemblage fields when the grid refinement parameters are changed. The second is due to the activity-composition models, mainly of amphibole, which results in more or less unrealistic assemblages and or mineral compositions, no matter what amphibole model is used. Two examples of THERMOCALC pseudosection modelling also produced significant inconsistencies with observation, i.e. 'unpublishable' diagrams. In a metapelite, the rather open secret of poor thermodynamic data for Mn-phases resulted in the fact that the calculated garnet composition isopleth just would not match those observed in the rock. In a metabasite, quartz predicted as stable in a large *P-T* range around peak conditions is not found in the rock – reason hitherto unknown. As 'failed results' usually (not always) escape publication, such weak points of methods are probably discussed less than they ought to be. The main problem is still the lack or scarcity of good thermodynamic data for many substances. Whereas pseudosection and geothermobarometry calculations are popular tools, we find that segment of experimental petrology which generates the fundamental data largely abandoned today.

https://doi.org/10.1180/S0026461X00006502 Published online by Cambridge University Press

The stable vanadium isotope composition of the bulk silicate Earth

J. PRYTULAK[1]*, S.G. NIELSEN[1,2] AND A.N. HALLIDAY[1]

[1]University of Oxford, Dept. of Earth Sciences, South Parks Road, Oxford, OX1 3AN, UK (*correspondence: Julie.Prytulak@earth.ox.ac.uk, alex.halliday@earth.ox.ac.uk)

[2]WHOI, Department of Geology and Geophysics, 266 Woods Hole Road, 02543, Woods Hole, MA, USA (snielsen@whoi.edu)

We have developed the first analytical method capable of producing accurate stable vanadium isotope ($^{51}V/^{50}V$) compositions to a precision useful for geologic problems [1, 2]. Vanadium exists in multiple valence states (V^{2+}, V^{3+}, V^{4+}, V^{5+}) and its partitioning is directly related to changing oxidation states. Stable vanadium isotopes are expected to respond to oxidation-reduction processes, although this has yet to be demonstrated. USGS reference materials display significant, resolvable isotope variation [2] and the system appears to have great potential for a variety of geologic applications including studies of oceanography, igneous petrology, oxygen fugacity, cosmochemistry, and hydrocarbon genesis. The first step to enable the application of new 'non-traditional' stable isotope systems is to estimate and define the bulk silicate earth (BSE). Here we present measurements of peridotites, suites of Mid-Ocean ridge basalts, picrites and other primitive mantle-derived magmas to permit an initial estimate of BSE. Our results support an analytically significant difference between terrestrial and extraterrestrial material [2, 3].

[1] Nielsen, S.G. Prytulak, J. Halliday, A.N. (2011) *Geostand. Geoanal. Res.* in press. [2] Prytulak, J. Nielsen, S.G. Halliday, A.N. (2011) *Geostand. Geoanal. Res.* in press. [3] Nielsen, S.G. Prytulak, J. Wood, B.J. Halliday, A.N. (2011) *MinMag*, this volume.

Mechanisms controlling the release, transport and attenuation of mercury in riverine sediments

C.J. PTACEK*, K.A.N. DESROCHERS, B.D. GIBSON, P. LIU, O. WANG, J.A. TORDIFF, S.D. DAUGHERTY, K.E. BLOWES, J. VAN DE VALK, M.B.J. LINDSAY, AND D.W. BLOWES

Department of Earth and Environmental Sciences, University of Waterloo, Waterloo, ON, Canada (*correspondence: ptacek@uwaterloo.ca)

The release and transport of Hg at industrial sites are controlled by a complex series of interrelated physical and biogeochemical processes. This study evaluated mechanisms controlling the release and transport of soluble and particulate forms of Hg from contaminated river sediments and the effectiveness of amending the sediments with reactive media to stabilize Hg. The sediment was characterized using sequential extractions and synchrotron radiation based techniques. Long-term column experiments, 6-8 months in duration, were conducted under variable flow conditions. During the early stages of the experiments, concentrations of Hg in the column effluent increased sharply after periods of flow stagnation, whereas, during later stages, the releases were lower and spikes were not observed after stagnations. The observed releases were not correlated to the masses of Hg released in the sequential extraction analyses. Reactive media, including clay, C, S and Fe bearing media, were added in batch style experiments as single-media additions or in combinations. Amendment of the sediments reduced the aqueous Hg concentrations by 50 to >99%. Under continuous saturated flow conditions, concentrations of Hg in the column effluent were maintained in the low ng L^{-1} range for the amended sediment. Following periods of stagnation, concentrations of Hg increased in the column containing the unamended sediment and the sediment amended with clay, whereas sediment amended with C, S, and Fe bearing media showed no increases. These results indicate that large decreases in Hg concentrations can be achieved under varying flow conditions through the addition of reactive media.

https://doi.org/10.1180/S0026461X00006502 Published online by Cambridge University Press

Evolution of deep mantle sources as inferred from Os-Nd isotope systematics of Archean komatiites

IGOR S. PUCHTEL AND RICHARD J. WALKER

Dept. of Geology, University of MD, College Park, MD 20742, USA (ipuchtel@umd.edu, rjwalker@umd.edu)

We present ^{190}Pt-^{186}Os and ^{187}Re-^{187}Os isotopic and highly siderophile element (HSE) abundance data for eight well preserved komatiite systems from around the globe, including 3.6 Ga Schapenburg, 3.5 Ga Komati, 3.3 Ga Weltevreden, 2.9 Ga Kamennoozero, 2.8 Ga Kostomuksha, 2.7 Ga Belingwe, 2.7 Ga Abitibi, and 2.5 Ga Vetreny. These data provide important insights to the evolution of absolute and relative HSE abundances in the deep mantle throughout the Archean. Based on precise initial $^{186}Os/^{188}Os$ and $^{187}Os/^{188}Os$, models for the komatiite sources suggest long-term evolution to the times of melting with $^{190}Pt/^{188}Os$ and $^{187}Re/^{188}Os$ of 0.00183±15 and 0.412±8, respectively ($2\sigma_{mean}$). These source parameters are remarkably uniform and fall well within the range of those measured in chondritic meteorites. The evolution of the komatiite sources over >1 Ga generally shows no shifts in trajectory that would reflect major changes in Pt/Os or Re/Os, as might occur due to progressive melt extraction or crustal recycling. Over the same time interval, absolute HSE abundances in the komatiite sources increase. The trend, however, is far from linear; e.g. Pt abundances in the sources increase from 2 ppb to 6 ppb between 3.6 and 3.3 Ga and then level at 6 ppb through the rest of the Archean. In contrast, the komatiite sources were characterized by strong depletions in highly incompatible lithophile trace elements, as compared with chondrites. Sm-Nd isotopic data indicate evolution with time-integrated $^{147}Sm/^{144}Nd$ averaged at 0.214±3 and 0.209±1 for the early and late Archean systems, respectively. The collective Os-Nd results indicate that during the period of time examined, processes acting on the mantle sources affected Sm/Nd, yet did not substantially modify Re/Os or Pt/Os. These characteristics are consistent with mixing between two mantle reservoirs. The Sm-Nd constraints on the earliest reservoir are similar to the hypothesized Early Depleted Reservoir of Boyet and Carlson (2006). This could represent either a primitive early crust, or a reservoir created during magma ocean crystallization. The lower HSE, yet chondritic Re/Os and Pt/Os, would be consistent with the establishment of this reservoir by late accretion, but prior to accumulating a full complement of HSE. The second reservoir would potentially be representative of the upper mantle.

Chondritic-like xenon in the Archean atmosphere

MAGALI PUJOL[1] AND BERNARD MARTY[2]

[1]ETH - Zürich, Switzerland (magali.pujol@erdw.ethz.ch)
[2]CRPG-CNRS, Nancy Université, Vandoeuvre les Nancy France (bmarty@crpg.cnrs-nancy.fr)

Xenon in the present-day atmospheric is depleted compared to lighter atmospheric noble gases and isotopically fractionated (i.e. enriched in heavy isotopes) by 3-4 % par amu related to condritic or solar Xe. Because it is the heaviest noble gas, any mass dependent process such as atmospheric escape would have resulted in the reverse situation, that is, bettter retention of Xe and lower isotopic fractionation of Xe compared to e.g. Kr. This observation, known as the xenon paradox is one of the most intersting problems in geochemistry. It has resisted decades of modeling efforts.

We have reported in [1] the analyses of xenon and other noble gases in meso-Archean sedimentary rocks (baryte and fluid inclusions in hydrothermal quartz) from North Pole (Pilbara, Australia), which show that Xe alone is isotopically fractionated and intermediate between chondritic and modern atmospheric compositions. This observation suggests that Xe isotopic fractionation, and, by inference, Xe depletion in the atmosphere was still ongoing 1 Ga after Earth's formation and was not limited to the Earth's building period as previously thought. In laboratory experiments, the only processes able to fractionate Xe isotopes at the percent level require ionization (e.g. [2]), suggesting that the fractionation of atmospheric Xe was related to the solar UV light during the first half of Earth's history. Independent evidence for deep UV penetration in the atmosphere stems from mass independent fractionation of sulfur isotopes trapped in Archean sedimentary rocks [3]. A delayed loss of atmospheric xenon has implications for the early evolution of Earth. The age of the Earth computed from retention of ^{129}Xe produced by the decay of ^{129}I ($T_{1/2}$ = 16 Ma) becomes ~50 Ma instead of ~110 Ma computed previously with the present-day inventory of atmospheric Xe. The depletion in the mantle and atmosphere of Xe isotopes produced by extinct ^{244}Pu ($T_{1/2}$ = 82 Ma) is more understandable if Xe loss continued well after the decay of plutonium-244.

[1] Pujol *et al*. (in press) *Earth Planet. Sci. Lett*. [2] Frick *et al*. (1979) *Proc. Lunar Planet. Sci. Conf. 10th,* 1961. [3] Farquhar *et al*. (2000) *Science* **289**, 756.

https://doi.org/10.1180/S0026461X00006502 Published online by Cambridge University Press

Noble Gas in Basin Centred Gas: Sampling techniques and preliminary results

MAGALI PUJOL[1]*, SANDER VAN DEN BOORN[2], BERNARD BOURDON[3], ROLF KIPFER[4], RAINER WIELER[1] AND MATTHIAS BRENNWALD[4]

[1]ETH Zürich, 8092 Zürich, Switzerland (*correspondence: pujol@erdw.ethz.ch)
[2]Shell P. and T., 2288GS Rijswijk, the Netherlands
[3]ENS Lyon, 69364 Lyon, France
[4]EAWAG, 8600 Dübendorf, Switzerland

Noble gas have become a powerful tool to constrain the origin of fluids as well as the rates of fluid migration in sedimentary basins and have found applications in environmental and petroleum research [1]. The aim of this study is to apply some of these concepts to understand the genesis and evolution of Basin Centred (Hydrocarbon, HC) Gas (BCG) systems, which are abnormally pressured pervasive accumulations of gas in tight reservoirs. Poor understanding of HC gas-water interaction in the subsurface and the mechanism of gas transport make the inert noble gasses ideally suited for the geochemical investigation of these systems' dynamics. Natural lab for this study is the Deep Basin of the Western Canadian Sedimentary Basin (WCSB) in Alberta (Canada) where HC gas is being produced from tight Cretaceous sandstones [2].

Twenty wells were selected in the Deep Basin including a transect from the deep southwestern part of the basin to shallower regions in the northeast. Samples were collected in 500cc stainless steel cylinders using two different sampling techniques: (1) collection in pre-evacuated cylinders without purging ('vacuum technique'), and (2) collection in cylinders that were purged for 15 seconds ('purged technique'). All samples were analyzed for He, Ne, Ar, Kr and Xe concentrations and selected isotopes.

Noble gas concentrations in HC gas from the Deep Basin are extremely low and large differences were observed between 'purged' and 'vacuum' samples from individual wells. These inconsistencies are believed to be largely the result of contamination of the vacuum samples by dead volumes in the sampling line. Lab experiments demonstrate that purging cylinders for 15 seconds is sufficient to eliminate potential mass fractionation artefacts. Despite some remaining uncertainties related to the sampling protocol, the preliminary noble gas data of Deep Basin natural gas show some interesting trends which may provide new insights into gas-water interactions in the subsurface.

[1] Gilfillan *et al*. (2008) *GCA* **72**, 1174–1198. [2] Hiyagon & Kennedy (1992) *GCA* **56**, 1569–1589.

Coexistent aqueous fluid phase and melt in lherzolites from Bultfontein, South Africa

M. PURCHASE[1], H. SOMMER[2]*, K. REGENAUER-LIEB[3,4], H. JUNG[2] AND B. GASHAROVA[5]

[1]Department of Geology, University of the Free State, PO Box 339, Bloemfontein 9301, South Africa
[2]School of Earth and Environmental Sciences, Seoul National University, Seoul 151-747, Korea (*correspondence: info@holgersommer.de)
[3]School of Earth & Geographical Sciences, The University of Western Australia, Perth, Western Australia 6009, Australia
[4]CSIRO Exploration & Mining, PO Box 1130, Bentley, WA 6102, Australia
[5]ANKA/Inst.Synchotron Radiation, Forschungszentrum Karlsruhe GmbH, Hermann-von-Helmholtz-Platz 1, Eggenstein-Leopoldshafen, D-76344 Germany

The transfer of aqueous fluid and melt at high pressures is an essential mechanism in the creation, evolution and dynamics of terrestrial planets like Earth's. Volatiles control the density and viscosity of magmas generated in the Earth's interior and have an important effect of melt segregation processes. The densification of melt under high pressure conditions and the general density between the melt and solid components are very important to understand the heterogeneities of the Earth's mantle. Experimental studies show coexisting aqueous fluid and melt phases at high pressure and temperature conditions. Therefore, the current paradigm in geosciences is if aqueous fluid and melt can be coexist in natural peridotites formed at P-T conditions of 5GPa and 1300°C. Aqueous fluid and initially formed melt moves preferably along grain boundaries. The problem to detect aqueous fluid along grain boundaries is that H_2O has a higher solubility in the melt as in anhydrous nominally minerals. Thus, the aqueous fluid will partitioning in the melt during the uplift of the peridotite xenoliths to the Earth's surface. We have overcome this problem by using high-resolution synchrotron based FTIR images of higher dimensional defect structures within garnet revealing a strong variation of aqueous fluid and melt concentration at all length scales. Our analysis has three major ramifications: *i)* it shows aqueous fluid around monomineralic grain boundaries in the lithospheric mantle; *ii)* it shows coexisting aqueous fluid and melt under P-T conditions of 5GPa and 1300°C; *iii)* it shows fundamental reassessment of the dynamics of aqueous fluid transfer within the lithospheric mantle. This research was supported by the Mid-career Researcher Program through an NRF grant funded by the MEST (No. 3345-20100013) and is a contribution to UNESCO IGCP 557.

https://doi.org/10.1180/S0026461X00006502 Published online by Cambridge University Press

Mantle-protocore system evolution in the case of heterogenic accretion: Paleomagnetic and isotopic evidences

Y.D. PUSHKAREV[1]* AND S.V. STARCHENKO[2]

[1]Institute of Precambrian Geology and Geochronology, St.-Petersburg, Russia
(*correspondence: ydcanon@rambler.ru)
[2]Institute of Terrestrial Magnetism, Troitsk, Moscow, Russia

The Earth evolution model for the case of heterogeneous accretion is developed as alternative to traditional hypotheses. According to this model the considerable part of the Fe and Ni should initially concentrate in the protocore in which content of the metal component was decreasing to the periphery, but content of chondrite silicates was increasing. The evolution of such 'mantle-protocore' system begins with fast formation of the liquid core geosphere in outer part of the planet. This geosphere expands while moving down, but due to growth of pressure the melting of metal is replaced by its slow erosion on the protocore surfaces. It occurs owing to interaction of metal and such component of the liquid core as S or FeO which lowers temperature of melting. During the protocore erosion its silicate component is liberated and than floats-up through liquid core, producing composite convection which is the main drive of geodynamo. The model calculations show that this process could culminate in early Precambrian, and so the evolution of paleomagnetc records should be observed. At the same time the emerging of the protocore silicate component to the lower mantle should be accompanied by appearance of elements having isotope characteristics of the chondritic material (the high contents of ^{3}He, ^{20}Ne, ^{129}Xe, ^{204}Pb). All these effects most likely confirm the reality of the described scenario of the 'mantle-protocore' system evolution. It is noteworthy that the energy released due to the protocore density differentiation (up to 20 TWT during 4 Ga) could be enough for a long overheat of the core-mantle boundary and for the plum-formation. The analysis of evolution of the geodynamic activity demonstrates that maximum of such endogenous energy generation also corresponds to the early Precambrian.

The interplay between chemical and textural evolution across a shear zone

ANDREW PUTNIS[1]*, HÅKON AUSTRHEIM[2] AND CHRISTINE V. PUTNIS[1]

[1]Institut für Mineralogie, University of Münster, Germany
(*correspondence: putnis@uni-muenster.de)
[2]Physics of Geological Processes, University of Oslo, Norway

The extent to which chemical reactions and mineral replacement reactions due to fluid infiltration influence textural evolution during the formation of shear zones is described from anorthositic granulites in the Lindås Nappe, Bergen Arcs, Norway, where the Grenvillian age granulites (~930 My) are transected by Caledonian age (~420My) eclogite and amphibolite facies shear zones [1, 2]. We focus on the evidence for fluid-induced reactions in the plagioclases which form coarse, clear crystals with composition ~An_{50} in the most pristine anorthositic granulites and become milky as the shear zone is approached, reacting with fluid to form more albitic plagioclase (~An_{25}) with numerous inclusions of clinozoisite, and finally developing an intracrystalline domain structure defined by planar zones of composition ~An_{64} within the plagioclase (~An_{25}) crystals. This apparent 'chemical fragmentation' of the plagioclase single crystals is a precursor to the formation of the much smaller grain size plagioclase crystals within the shear zone. A combination of electron microscopic and analytical techniques is used to describe the interplay between the chemical reactions, the recrystallisation of the plagioclase and the physical deformation forming the shear zone.

[1] Bingen *et al*. (2001) *J. Petrol*. **42**, 355–357. [2] Bingen *et al*. (2004) *Contribs. Min. Pet*. **147**, 671–638.

https://doi.org/10.1180/S0026461X00006502 Published online by Cambridge University Press

The importance of the fluid-mineral interface in the control of crystal growth

CHRISTINE V. PUTNIS[1]*, ENCARNACIÓN RUIZ-AGUDO[2], LIJUN WANG[3], JOLANTA KLASA[1,4] AND ANDREW PUTNIS[1]

[1]Institut für Mineralogie, University of Münster, D-48149 Germany (*correspondence: putnisc@uni-muenster.de)
[2]Department of Mineralogy and Petrology, University of Granada, 18071 Granada, Spain (encaruiz@egr.es)
[3]Huazhong Agricultural University, Hubei 430070, Wuhan, China (ljwang@mail.hzau.edu.cn)
[4]Mineralogy Department, Natural History Museum, SW7 5BD London, UK (j_klas03@uni-muenster.de)

Atomic force microscopy (AFM) experiments have shown that growth on mineral surfaces can occur from solutions when the bulk fluid composition is undersaturated with respect to the precipitating phase. The implication is that the composition of the solution in the fluid boundary layer in contact with the mineral surface must become supersaturated with respect to the new phase growing at the mineral surface. This has been reported in a number of systems, including the growth of new phases on calcite cleavage surfaces, such as Ca phosphonates [1], and on gypsum surfaces, such as Ca phosphates [2], where the dissolution of the substrate provides ions included in the new phase. The thickness of the boundary layer can be estimated by considering the following: the solubility of the solid in the fluid phase; the diffusion rate of the dissolved ions in the fluid phase; the composition of the fluid; the saturation state of the fluid with respect to all possible phases; possible epitaxial relationships between the mineral surface and the new phase.

The concept of a boundary layer becoming supersaturated with respect to another phase, which then precipitates, is essential for the understanding of coupled dissolution-precipitation as a mechanism of mineral replacement [3]. Real-time phase-shift interferometry has been used to show the steep compositional gradient at the surface of a crystal of KBr being pseudomorphically replaced by KCl [4] and this has been used as a model system for more complex Earth systems involving mineral-fluid reactions during such processes as metasomatism, metamorphism and weathering. This concept is also relevant to many industrial processes and nuclear waste management.

[1] Ruiz-Agudo E. *et al*. (2010) *Crystal Growth & Design*. [2] Pinto A. *et al*. (2010) *American Mineralogist*. [3] Putnis A. & Putnis C.V. (2007) *Journal of Solid State Chemistry*. [4] Putnis C.V. *et al*. (2005) *American Mineralogist*.

Mantle metasomatic events related to alkaline volcanism during incipient rifting: NE Eger Rift (Central Europe) example

J. PUZIEWICZ[1]*, M. MATUSIAK-MAŁEK[1], T. NTAFLOS[2] AND M. GREGOIRE[3]

[1]Univ. Wroclaw, Poland (*correspondence: jacek.puziewicz@ing.uni.wroc.pl)
[2]Univ. Wien, Austria (theodoros.ntaflos@univie.ac.at)
[3]CNRS-UMR 5562, Univ. Toulouse, France (michel.gregoire@get.obs-mip.fr)

Mantle metasomatism is preceding alkaline volcanism at initial stages of continental rifting. The complete example of its various effects is offered by xenolith suite occurring in the Miocene Księginki nephelinite (SW Poland). The latter occurs at the NE termination of the Eger Rift, the easternmost of the rifts forming the European Cenozoic Rift System.

The lithospheric mantle was infiltrated by alkaline silica-undersaturated magma resembling the Księginki nephelinite. Olivine clinopyroxenites originated by crystal accumulation in channelized magma flow. The 'Fe-metasomatism' operated in mantle harzburgites subjected to pervasive magma flow. It lowered olivine Fo (down to 86 %) and resulted in REE patterns of clinopyroxene identical to those ocurring in olivine clinopyroxenites. The clinopyroxene megacrysts occurring in the Księginki nephelinite are the remnants of very coarse-grained clinopyroxene cumulates, uncompletely solidified and disaggregated during eruption. The fine-grained glass-bearing aggregates of olivine + clinopyroxene ± plagioclase or titanian phlogopite offer the snap-shot picture of the various stages of metasomatism and show that part of the xenoliths resided shortly in transient magma chambers located near the Moho, under pressures enabling plagioclase crystallization. Alternatively plagioclase crystallization in melt pockets could take place en route to the surface at low pressures. All the lithospheric mantle section sampled by the Księginki nephelinite was thermally rejuvenated during volcanism and shows the temperatures of 1060 - 1120 °C.

https://doi.org/10.1180/S0026461X00006502 Published online by Cambridge University Press

The Lower Pre-Cambrian, the Urals

A.M. PYSTIN AND YU.I. PYSTINA

Institute of Geology, Komi Science Centre, Uralian Branch of RAS, Syktyvkar

The presence of Early Pre-Cambrian complexes is mostly proved in the western paleocontinental part of the Urals (to the west from the Main Uralian Deep Fault). Polymetamorphic complexes, different in material composition, structure, and metamorphic peculiarities of rocks, are related to them. The main types can be established among them: gneiss-granulite, gneiss-migmatite, crystallo-schist, granulite-metabasite, eclogite-gneiss, and eclogite-schist one [1].

The metamorphic evolution of rocks constituting the polymetamorphic complexes in the western part of the Urals (the western slope of the Urals) falls down within the interval 2.7–0.35 Ga.

Distinctions in material composition, as well as facial conditions, and especially the type of rock metamorphism allow for distinguishing two groups of the polymetamorphic complexes. One of them is characterized by moderate-pressure metamorphism and prevalence of acidic rocks in a section, mainly of initially-sedimentary origin. In the other group, the essential role belongs to initially-magmatic formations, mainly of the basic series, which underwent high-pressure metamorphism. It is possible to allocate vertical (age) series of the polymetamorphic complexes in each of the named two groups. The first vertical (age) series is composed of (from below-upwards): gneiss-granulite →gneiss-migmatite →crystallo-schist complexes. The second vertical series is made of (from below-upwards): granulite-metabasite → eclogite-gneiss→ eglogite-schist complexes.

Along with the vertical series, certain lateral relations between the various complexes, indicating their formation in different geodynamic settings, are outlined.

Available geochronological data allow one to conclude that distinctions in geodynamic settings during formation of the considered structural-material complexes existed, beginning at least with the Late Archaean and then lasting throughout the Early Proterozoic. The established regularities in composition and structure of the polymetamorphic complexes of the Western Uralian slope, as well as ages of initial high-temperature metamorphic manifestations (the granulitic and eclogitic facies) give reason to think that they are fragments of the crystalline basement of Volgo-Uralian part of Baltica.

[1] Pystin A. M. *et al*. (2009) *Typification of the Lower Pre-Cambrian, Timan–Northern Urals region*. Syktyvkar, Geoprint. 36 p.

https://doi.org/10.1180/S0026461X00006502 Published online by Cambridge University Press

Modern sedimentation rate and heavy metal accumulation in Jiaozhou Bay sediments

J. QI

Guangdong Food and Drug Vocational College, Guangzhou 510520, PR China (jungzh@163.com)

Introduction

The sediments that accumulate in Jiaozhou Bay of the Shandong Peninsula recorded the information about the history of changes in the source of the material, the rate of deposition and the influence of human activies [1, 2]. Six cores were collected from the Jiaozhou Bay by the Cruise work on Gold Star boat on Sep. 6th, 2003. The ^{210}Pb radioactivities of the sediments were determined by ^{210}Pb geochronology method and ICP-MS was employed for the determination of Zn, Cu, Cr, Ni, Pb, Cd and Co concentrations.

Discussion of Results

The sedimentation rates were found to be higher in margin areas of the bay, especially in the dumping areas, where the rates were about 0.77cm/a ~ 3.96cm/a. While in the central region of the bay, there was a patch of fine-grained mud, with the sedimentation rates being lower. The profiles ^{210}Pb radioactivity at sample cores mostly appeared in two-segment model, which indicate that the modern sedimentary environment of this region was very stable. Differences in the profiles reflect spatial and temporal variations in hydrodynamic conditions and the grain size of sediments in the Jiaozhou Bay.

The main heavy metals in the sediments of Jiaozhou Bay were Zn, Cu, Cr, Ni and Pb, while the concentrations of the elements Cd and Co were much lower. The concentrations of the main heavy metals of the sediments in Jiaozhou Bay were higher than that in the China Shelf Sea, which showed that the area had been contaminated to a certain extent. But these concentrations were low in comparison with the highest background level in former global modern industrialization times and that in other industrialized areas. The heavy metal profiles Zn, Cr, Ni, Co and Pb from the six cores showed a high variability, but also a decreasing trend since 1980s, while the element Cu presented an increasing trend and the element Cd presented a more chaotic profile than the other elements.

[1] Stanley *et al*. (2000) *Geology* **28**, 259–298. [2] Ruiz-Fermandez *et al*. (2004) *J Environ Radioactiv* **76**, 161–175.

The bioavailability of selenium and risk assessment for human selenium poisoning in Se-high areas, China

H-B. QIN[1,2], J-M. ZHU[1]* AND H. SU[3]

[1]State Key Laboratory of Environmental Geochemistry, Institute of Geochemistry, Chinese Academy of Sciences, Guiyang 550002, China (*correspondence: zhujianming@vip.gyig.ac.cn)

[2]Graduate University of Chinese Academy of Sciences, Beijing 100049, China

[3]Center for Disease Control and Prevention of Enshi Prefecture, Enshi 445000, China

Enshi, China, is one of the selenosis areas in the world, where sporadic cases of selenium (Se) poisoning in livestock and human were still being found at present. However, selenium bioavailibility in soils and current situation on intake of Se by human have not been reported in detail. In this study, selenium levels and its speciation in water and cropland soils, Se content in crops from Enshi were investigated, as well as estimating the daily intake of Se by local residents. Results showed that the geometric mean of Se concentration was 54.2 μg/L (2.0-519.3 μg/L, *n*=62) and 6.2 mg/kg (2.67-87.3 mg/kg, *n*=37) in water and soils, respectively. Selenium content ranged from 0.18 mg/kg to 37.1 mg/kg in crops, which was dependent on crop species and Se bioavailability in soils. On the basis of consumption and Se contents of foods, cereal consumption is the major pathway of Se intake by local residents, followed by vegetables, meats, and drinking water. The total daily intake of Se was approximately 3000 μg/day for human in Se-high areas in Enshi, which was considerably higher than the upper tolerable nutrient levels (UL, 400 μg/day) referred by WHO and US EPA, suggesting that a high risk for human chronic Se poisoning still exists in this areas. Furthermore, the daily Se intake through drinking water (108.4 μg/day) was up to 27.1% of referred Se UL. Thus, unlike previous studies, it is should not ignore the contribution of Se in drinking water when assessing the health risk for human daily intake of Se in Se-high areas. Local residents should be advised to avoid planting crops in areas with Se-high soils or irrigated by Se-high water, and to consume foods mixed with the exotic.

The study was supported by the Knowledge Innovation Program of the Chinese Academy of Sciences (KZCX2-YW-JC101), and the National Natural Science Foundation of China (40973085, 40721002, 40573050).

https://doi.org/10.1180/S0026461X00006502 Published online by Cambridge University Press

Cr isotope fractionation during biogeochemical reduction of Cr(VI) by Hanford native aquifer microbial communities

L. QIN*, J.N. CHRISTENSEN, S.T. BROWN, L. YANG, M.E. CONRAD, E. SONNENTHAL AND H.R. BELLER

Lawrence Berkeley National Laboratory, 1 Cyclotron Rd., Berkeley, CA 94720 (*correspondence: lqin@lbl.gov)

Hexavalent Cr contamination in groundwater within the DOE complex has been a long-standing issue. Injection of electron donors, such as lactate, to Cr contaminated aquifers to stimulate the growth of native microbial communities, and thus promote reduction of Cr (VI) to Cr (III), has become a widely utilized remediation practice. However, whether these conditions are optimal for Cr reduction is to a large extent unknown. It has been demontrated that reduction of Cr (VI) can cause Cr isotope fractionation [1, 2]. The Cr fractionation factor changes under varying experimental conditions even with the same bacterial strain [2]. Cr isotopic measurements are more direct and effective than concentration analyses to distinguish between different reduction pathways, and also between reduction and simple dilution.

To evaluate the effects of differing electron acceptors on Cr (VI) reduction by native microbes, small-scale column experiments with homogenized material from the Hanford 100H aquifer were conducted. All columns had a continuous inflow of solutions with constant concentrations of Cr (VI), lactate, and the targeted electron acceptor (nitrate, sulfate, no electron acceptor added). Different Cr fractionation behaviors were observed under different conditions. The least extensive Cr reduction occurred in no-electron-acceptor-added columns and had the largest Cr isotope fractionation (α~0.997). The greatest Cr reduction occurred in two sulfate-containing columns that were fermenting the lactate. Samples from one such column had the smallest Cr fractionation (α~0.999). Denitrifying columns had intermediate α values. One sulfate-added (not fermentative) column showed two distinctive stages of fractionation, suggesting a change in reduction processes. Our α values mostly fall in the range 0.997-0.999, which are smaller than those observed in cell suspension experiments with *Shewanella oneidensis* and much lower lactate concentrations [2]. Reactive tranport modeling will be conducted to further evaluate the effects of various experimental parameters on Cr isotope fractionation.

[1] Ellis, Johnson & Bullen (2002) *Science* **295**, 260–262.
[2] Sikora, Johnson & Bullen (2008) *Geochim. Cosmochim. Acta* **72**, 3631–3641.

Precise $^{40}Ar/^{39}Ar$ geochronology of gas migration and accumulation

H.N. QIU[1], J.B. YUN[1,2], H.Y. WU[2] AND Z.H. FENG[2]

[1]State Key Laboratory of Isotope Geochemistry, Guangzhou Institute of Geochemistry, CAS, Guangzhou 510640
[2]Exploration and Development Research Institute, Daqing Oilfield Company Ltd., Daqing 163712, China

It is very difficult to determine the exact age of natural gas emplacement because no suitable mineral for dating with common isotope geochronometers was formed during gas migration and accumulation, although illite K-Ar dating has been widely used to constrain the maximum ages of petroleum accumulation since Lee *et al*.'s [1] report. Selby *et al*. [4] demonstrated a possibility to date hydrocarbon deposits by Re-Os isotopes. Mark *et al*. [2] obtained oil migration age by UV laser microprobe $^{40}Ar/^{39}Ar$ dating of authigenic K-feldspar bearing oil fluid inclusions.

In this study, we show a novel promising approach to obtain high precision ages of gas emplacement into the Songliao Basin, NE China, by $^{40}Ar/^{39}Ar$ progressive crushing technique. The igneous quartz from the Cretaceous volcanic rocks in Yingcheng Formation (117–111 Ma) hosting the gas reservoir contains abundant K-rich secondary fluid inclusions (8.3–0.4 wt% in salinity) with high partial pressures of methane (66–9 MPa) trapped during gas emplacement. Based on our previous studies, quartz with abundant K-rich fluid inclusions provides an excellent closed system well suited for $^{40}Ar/^{39}Ar$ progressive crushing technique. Three irradiated igneous quartz samples were measured by stepwise crushing to release these secondary fluid inclusions. All three samples yielded well-defined $^{40}Ar/^{39}Ar$ isochrons with ages in close agreement, precisely constraining that the gas emplacement occurred at 42.4 ± 0.5 Ma (2SD) below the famous Daqing Oil Field in the Songliao Basin, extending possible gas reservoirs from the upper Cretaceous to the middle Eocene.

This study provides a new effective solution to gain the ages of gas emplacement. See [3] for detail.

[1] Lee M, Aronson JL, Savin SM. (1985) *AAPG Bull*. **69**(9), 1381–1385. [2] Mark DF, Parnell J, Kelley SP, Lee MR, Sherlock SC. (2010) *Geology* **38**(1), 75–78. doi: 10.1130/g30237.1. [3] Qiu HN, Wu HY, Yun JB, Feng ZH, Xu YG, Mei LF, Wijbrans JR. (2011) *Geology* **39**(5) 451–454. doi: 10.1130/G31885.1. [4] Selby D, Creaser RA. (2005) *Science* **308**(5726), 1293–1295 doi: 10.1126/science.1111081.

The relationship between gabbros and I-type granites in the southeast coast of Fujian, South China: Evidence from *in situ* zircon U-Pb dating, Hf isotopes and whole-rock geochemistry

JIAN-SHENG QIU* AND ZHEN LI

State Key Lab for Mineral Deposits Research, School of Earth Sciences and Engineering, Nanjing University, Nanjing 210093, China (*correspondence: jsqiu@nju.edu.cn)

Two representative gabbro–granite complexes from Quanzhou (QZ) and Huacuo (HC) in the southeast coast of Fujian, South China have been selected for a detailed geochronological and geochemical study, aiming to probe the genetic relations between the acid and basic magmas.

These complexes are composed predominantly of I-type granitoids, with lesser amounts of hornblende gabbro (<5% of the total igneous rocks). Zircon U-Pb dating yields consistent crystallisation ages of 109 ± 1 and 108 ± 1 Ma for the QZ gabbros and granites, and an age of 111 ± 1 Ma for the HC gabbros, which is contemporaneous with the spatially coexisted HC granites. Both the gabbros and granitoids are enriched in light rare earth elements and large ion lithophile elements (e.g. Rb, Ba, Th and U), and depleted in high field strength elements (e.g. Nb and Ta). Moreover, they show similarly homogeneous Sr–Nd isotopic compositions. All these factors indicate that they are genetically related.

Although the Sr–Nd isotopic signatures of the QZ and HC gabbros seemingly point to an enriched mantle source (EM-1), they have highly variable zircon Hf isotopic compositions, with ε_{Hf} (t) values ranging from negative to positive (specifically –4.6 to +6.1 for the QZ gabbros and –4.8 to +11.6 for the HC gabbros). On the other hand, their associated granitoids show relatively high whole-rock $\varepsilon_{Nd}(t)$ values (–2.5 and –4.1 for the QZ and HC granites, respectively), and homogeneous and neutral zircon $\varepsilon_{Hf}(t)$ values (–1.9 to +1.8 for the QZ granite). Based on an integration of petrography, geochronology and geochemistry, we interpret the parental basic magmas of these gabbros have originated from a depleted mantle source, but experienced a significant crustal contamination by the felsic melts that gave rise to the associated granitoids. Contributions from such a depleted mantle source resulted in the growth of juvenile basaltic lower crust, the partial melting of which generated the parental felsic magmas of the QZ and HC complexes.

A new recognition of Grenvillian volcanic suite in the South China Block and its connection with Rodinia assembly

X.F. QIU[1], W.L. LING[1]* AND X.M. LIU[2]

[1]State Key Laboratory of Geological Processes and Mineral Resources, China Univ. of Geosciences, Wuhan 430074, China (qxf_424@yahoo.com.cn,) (*correspondence: wlling@cug.edu.cn)

[2]State Key Laboratory of Continental Dynamics, Department of Geology, Northwest University, Xi'an 710069, China (xiaomingliu@263.com)

Contrasting proposals have been suggested for the position of the South China Block (SCB) in the Rodinia reconstruction, which is partly due to a poor understanding of the SCB history during the late Mesoproterozoic to early Neoproterozoic. Here we report a newly recognized Grenvillian arc-volcanic sequence in the Shennongjia area, western SCB. It comprises alkali-, calc-alkaline basalts and tholeiitic andesitic rocks, and is dated at 1152±24 Ma. The alkali basalts have high TiO2, low Mg# (42-55) and positive εNd, and display OIB-like elemental patterns. By contrast, the calc-alkaline basalts have higher Mg# (57-68), Cr and Ni contents and large negative εNd, and exhibit pronounced depletion in HFSE. The andesites show Eu deficiency, HFSE depletion and small negative εNd.

The alkali-, calc-alkaline basalts are suggested to have been derived from depleted asthenospheric- and metasomatised lithospheric mantle sources, respectively, whereas the andesites from mafic lower crustal anatexis; the volcanic sequence was developed within an island-arc setting. Integrating with previously documented works, the western Yangtze craton is suggested to have comprised a collage of microcontinents during the Grenvillian period and underwent a westward lateral continental growth by subduction accretion and subduction-related collision. Increasing lines of evidence infer a western Yangtze-South Australia connection during Rodinia assembly, which provides a new insight into the SCB position in the supercontinent.

This work is financially supported by the National Natural Science Foundation of China (Grant No. 40673025)

https://doi.org/10.1180/S0026461X00006502 Published online by Cambridge University Press

Raman spectroscopic analysis of heterogeneous carbonaceous matter in the 2.0 Ga Zaonega Fm, Karelia, Russia

Y. QU[1]*, M.A. VAN ZUILEN[1,2] AND A. LEPLAND[3]

[1]Centre for Geobiology, University of Bergen, Allegaten 41, 5007, Bergen, Norway (*correspondence: Yuangao.Qu@geo.uib.no)

[2]Equipe Geobiosphere, Institut de Physique du Globe - Sorbonne Paris Cité, Université Paris Diderot, CNRS, 1 rue Jussieu, 75238 Paris cedex 5, France (vanzuilen@ipgp.fr)

[3]Geological Survey of Norway, Leiv Eirikssons vei 39, 7491 Trondheim, Norway (Aivo.Lepland@NGU.NO)

Carbonaceous matter in sediments is gradually matured during metamorphism, as increased temperature causes structurally disordered organic molecules to rearrange themselves progressively into crystalline graphite. Raman spectroscopy is commonly used to describe the degree of this transformation, since the relative band intensities at 1350 cm-1 (D1) and at 1580 cm-1 (G) can be directly related to the defect-bound crystal domain size of graphitic crystallites. Intensity-based (R1) and especially area-based (R2) band ratios of carbonaceous matter have therefore been used as reliable indicators for the metamorphic grade that a rock has experienced.

The 2.0 Ga old Zaonega Formation in Karelia, Russia, contains sediments that are highly enriched in organic carbon. They represent the first known record of oil generation and migration on Earth, and form a key target for drill-core-based studies on the evolution of life during the Archean-Paleoproterozoic transition period. Carbonaceous matter consisting of residual kerogen and pyrobitumen throughout the succession has experienced local contact-metamorphism caused by gabbroic sills and lava flows, regional greenschist-facies metamorphism, and migration in silicate saturated fluid systems. This complex geologic history prevents simple straightforward interpretation of original isotopic ($\delta^{13}C$) and chemical characteristics of carbonaceous matter, and requires an *in situ* tool such as Raman spectroscopy to distinguish between variously altered carbonaceous fractions and small scale heterogeneities.

Here we report the variation in Raman spectral indicators R1 and R2 of carbonaceous matter throughout a 7 m long drill-core section that represents the upper contact zone of a gabbroic sill. Considerable heterogeneity in both R1 and R2 on a small spatial scale, indicates that factors other than temperature - such as organic precursor material, mineral matrix, and local variation in stress and strain - have influenced the overall process of graphitization. The implications for Raman-based geothermometry on complex metamorphic terrains will be discussed.

Estimating aerosol forcings using the MACC aerosol reanalysis

JOHANNES QUAAS[1]* AND NICOLAS BELLOUIN[2]

[1]Institute for Meteorology, University of Leipzig, Stephanstr. 3, D-04103 Leipzig, Germany (*correspondence: johannes.quaas@uni-leipzig.de)

[2]Hadley Centre, Met Office, FitzRoy Road, Exeter EX1 3PB, United Kingdom (nicolas.bellouin@metoffice.gov.uk)

In the EU-funded project 'Monitoring Atmospheric Composition and Climate' (MACC), MODIS satellite retrievals of aerosol optical depth (AOD) are assimilated into the IFS global atmospheric model enhanced by an aerosol module, and used for quasi-operational numerical weather forecasts. This MACC aerosol reanalysis yields a 3D field of concentrations of different aerosol components consistent with the MODIS AOD retrievals, along with the reanalysis of meteorological fields, and cloud and radiation distributions as computed by the model. This new dataset provides a unique opportunity to estimate aerosol climate forcings. On the basis of the method by Bellouin *et al*. [1] and Quaas *et al*. [2], where the aerosol radiative forcings have been derived from satellite data, we develop an improved method using this new dataset. Preliminary results show a global annual (year 2003) mean radiative forcing by the aerosol direct effect of -0.5 Wm^{-2}, and an indirect effect (first indirect effect or Twomey effect) of -0.3 Wm^{-2}. The product now also allows for a detailed analysis of the spatial and temporal variability of aerosol forcings.

[1] Bellouin *et al*. (2005) *Nature* **438**, 1138–1141. [2] Quaas *et al*. (2008) *J. Geophys. Res*. **113**, D05204.

https://doi.org/10.1180/S0026461X00006502 Published online by Cambridge University Press

Diamond-facies fluid flow during subduction: Evidence & consequence

ALEX QUAS-COHEN[1]*, SIMON CUTHBERT[2], GILES DROOP[1], CHRIS J. BALLENTINE[1] AND RAY BURGESS[1]

[1]School of Earth, Atmospheric and Environmental Sciences, University of Manchester, Manchester, UK (*correspondence: alexandra.quas-cohen@postgrad.manchester.ac.uk)
[2]School of Sciences, University of the West of Scotland, Paisley, UK (Simon.Cuthbert@uws.ac.uk)

Exhumed, subducted crustal terranes record the most extreme metamorphic conditions that continental rocks are known to experience and enable us to gain insight into the more elusive systems and processes of the Earth. Abundant fluid flow and fluid-rock interaction is evident during subduction even at the highest-grade conditions: numerous veins within a Fe-Ti, crustal garnet peridotite body in the Western Gneiss Region (WGR) of Norway contain microdiamonds [1]. Many questions remain unanswered regarding fluids and interactions at these depths. Our study focuses on the metasomatism of ultra-high pressure (UHP) rocks in the WGR; in particular, on determining the signature, source and recycling of noble gases and halogens. I present field maps and sketches of various UHP WGR localities to demonstrate the petrophysical relationships between various rock-types and features which demonstrate the nature and composition of intruding fluids; particularly, the associations of pegmatitic garnet websterites, carbonaceous and hydrous phases and different vein-types with Fe-Ti garnet peridotite and bimineralic eclogite bodies. I also present preliminary geochemical data demonstrating phase compositions, P-T conditions, chemical change due to fluid-rock interaction and noble gas compositions. Data gathered so far indicates that garnet websterites represent metasomatised domains of the peridotite and eclogite bodies within the WGR.

[1] Vrijmoed *et al*. (2006) *Mineral. Petrol*. **88**, 381–405.

The impact of transported pollution on Arctic climate

P.K. QUINN[1] *, A.S. STOHL[2], A. ARNETH[3], T. BERNTSEN[4], J. BURKHART[2], M. FLANNER[5], K. KUPIAINEN[6], M. SHEPHERD[7], V. SHEVCHENKO[8], H. SKOV[9] AND V. VESTRENG[10]

[1]NOAA PMEL, Seattle, WA, USA (*correspondence: patrcia.k.quinn@noaa.gov)
[2]Norwegian Institute for Air Research, Kjeller, Norway (ast@nilu.no, jfb@nilu.no)
[3]Lund University, Lund, Sweden (Almut.Arneth@nateko.lu.se)
[4]University of Oslo, Oslo, Norway (t.k.berntsen@geo.uio.no)
[5]University of Michigan, Ann Arbor, MI , USA (flanner@umich.edu)
[6]Finnish Environment Institute, Helsinki, Finland (Kaarle.Kupiainen@ymparisto.fi)
[7]Environment Canada, Toronto, Canada (marjorie.Shepherd@ec.gc.ca)
[8]P.P. Shirshov Institute of Oceanology of the Russian Academy of Sciences, Moscow, Russia (vshevch@ocean.ru)
[9]Aarhus University, Roskilde, Denmark (hsk@dmu.dk)
[10]Norwegian Pollution Control Authorities, Oslo, Norway (Vigdis.Vestreng@klif.no)

Arctic temperatures have increased at almost twice the global average rate over the past 100 years [1]. Warming in the Arctic has been accompanied by an earlier onset of spring melt, a lengthening of the melt season, changes in the mass balance of the Greenland ice sheet, and a decrease in sea ice extent. Short-lived, climate warming pollutants such as black carbon (BC) have recently gained attention as a target for immediate mitigation of Arctic warming in addition to reductions in long lived greenhouse gases. Model calculations indicate that BC increases surface temperatures within the Arctic primarily through deposition on snow and ice surfaces with a resulting decrease in surface albedo and increase in absorbed solar radiation. In 2009, the Arctic Monitoring and Assessment Program (AMAP) established an Expert Group on BC with the goal of identifying source regions and energy sectors that have the largest impact on Arctic climate. Here we present the results of this work and investigate links between mid-latitude pollutants and Arctic climate.

[1] IPCC (Intergovernmental Panel on Climate Change) (2007) *Summary for Policymakers, Contribution of Working Group 1 to the 4th Assessment Report*.

https://doi.org/10.1180/S0026461X00006502 Published online by Cambridge University Press

Pressure induced phase transitions in $MnTiO_3$: Insights from first principles

CARMEN QUIROGA* AND ROSSITZA PENTCHEVA

Section Crystallography, Department of Earth and Environmental Sciences, Ludwig-Maximilians Universität München
(*correspondence:
Carmen.Quiroga@lrz.uni-muenchen.de,
Pentcheva@lrz.uni-muenchen.de)

$MnTiO_3$ is an example of an ABO_3 compound which at ambient conditions crystallizes in the ilmenite structure and remains stable at least up to 26 GPa [1]. A denser $LiNbO_3$ phase can be quenched from high pressure and high temperature experiments to ambient conditions [2].

Using density functional theory calculations we determine the ground state properties and magnetic coupling of $MnTiO_3$ in the ilmenite, perovskite, $LiNbO_3$ and postperovskite phases. As $MnTiO_3$ is a strongly correlated material, we explore the influence of the exchange correlation functional beyond the local density and the generalized gradient approximations within LDA/GGA+*U* method and hybrid functionals. Our calculations show that ilmenite is the most stable phase at ambient conditions. The $LiNbO_3$ transforms into the perovskite phase at ~2.5 GPa in agreement with experiments [3]. A transition from perovskite to the post-perovskite phase ($CaIrO_3$-type) is predicted at pressures above 50 GPa.

Funding by DFG SPP1236 (PE883/8-1) and computational time at the Leibniz Rechenzentrum is acknowledged.

[1] Wu, Qin & Dubrovinsky (2010) *Geoscience Frontiers* **2**, 107–114. [2] Ko & Prewitt. (1988*) Phys. Chem. Minerals* **15**, 355–362. [3] Ross, Ko & Prewitt (1989) *Phys. Chem. Minerals* **16**, 621–629.

https://doi.org/10.1180/S0026461X00006502 Published online by Cambridge University Press

Tourmaline from porphyry copper belts as a proxy to assess boron budget in arc magmas

O.M. RABBIA AND L.B. HERNÁNDEZ

Instituto de Geología Económica Aplicada, Universidad de Concepción, Casilla 160c, Concepción, Chile (rabbia@udec.cl, lahernan@udec.cl)

In the Andes, world-class porphyry Cu deposits are intimately associated to major changes in the subduction geometry (progressive flattening) resulting in episodes of intense deformation, crustal thickening, rapid uplift and erosion (major orogenic phases), accompanied by migration of the volcanic front and changes in the geochemistry of magmas (appearance of the adakitic signature). As consequence of these highly compressive events, volcanism tends to vanish leaving mostly plutonic rocks in the geologic record. Whole-rock analysis of these intrusive rocks offers no quantitative appraisal of the B content in their magmas if volatile exsolution has taken place. On the other hand, during these particular periods of the Andean orogen evolution, volatiles exsolved from magmas are the main source of B-bearing hydrothermal fluids from which tourmaline may precipitate in porphyry Cu deposits. Therefore, the assessment of the relative abundance of this borosilicate in copper deposit belts could cast some light on B abundance in the associated arc magmas during metallogenic periods.

Tourmaline breccia complexes, with up to ~20 vol% of tourmaline, are a characteristic feature of world-class porphyry Cu deposits from the ~370 km long, Late Miocene-Early Pliocene Cu belt from Central Chile, as well as, of prospects and deposits from the ~1500 km long, Paleocene-Early Eocene Cu belt from Northern Chile and Southern Peru. In contrast, tourmaline is rarely developed or relatively uncommon in most porphyry Cu deposits from the ~2000 km long, Late Eocene-Early Oligocene belt from Southern Peru and Northern Chile.

Considering that the amount of fluid involved in giant porphyry Cu deposits formation requires huge volumes of magma (up to ~2000 km^3), the tourmaline-poor nature of the Late Eocene-Early Oligocene Cu belt, hosting giant Cu deposits (e.g.: Chuquicamata, La Escondida), suggests that the associated magmatism, and by extension its source, was fluid-bearing but B-poor. A possible explanation for the low B budget in these arc magmas could be related to a particular thermal configuration of the downgoing oceanic plate.

A high-resolution paleohydrological record of the Younger Dryas episode from Western Europe – Using lipid biomarker D/H ratios

OLIVER RACH[1]*, ACHIM BRAUER[2], HEINZ WILKES[2] AND DIRK SACHSE[1]

[1]University of Potsdam, Institute of Earth andEnvironmental Science, Karl-Liebknecht-Str. 24-25 14476 Potsdam-Golm (Germany) (*correspondence: rach@geo.uni-potsdam.de)
[2]GeoForschungsZentrum Potsdam, 14473 Potdsdam

Despite the recognized importance of the hydrological cycle within the climate system it is difficult to predict hydrological consequences of current and future climatic changes on regional scales. However, regional climatic variations on the continents are often most dramatically expressed through hydrological changes. A key tool to better understand the underlying mechanisms is the reconstruction of the past climate changes from high-resolution lacustrine proxy data. We investigated how fast hydrological changes have taken place during abrupt climatic shifts, such as the Younger Dryas cold episode (YD) ca. 12 ky BP. We assessed this question with a novel proxy, the stable hydrogen isotope composition of higher-plant derived lipid biomarkers.

We analyzed sediments from Lake Meerfelder Maar (Germany), with a continuous annual varving during the YD, which provide an excellent archive to resolve this issue. We measured the hydrogen isotope ratios of higher plant lipid biomarkers (long-chain *n*-alkanes) and conducted X-Ray fluorescence analyses (XRF), with focus on catchment-typical allochthonous elements (K, Al, Ti) in high-resolution (8-33 years per sample). The average chain length of the *n*-alkanes shows short-term variabilities, suggesting changes in lake catchment ecology. While *n*-alkanes with the highest concentration are long-chain homologues (nC_{25}, nC_{27}, nC_{29}, nC_{31}) of terrestrial origin, an increase in nC_{23} produced mainly by aquatic macrophytes suggests changes in the aquatic ecology during the early YD. XRF data show pronounced changes in sedimentary conditions with more allochthonous sediments in the later YD, probably related to hydrological variations. Indeed, the results from hydrogen isotope analysis, with a significant isotopic depletion in leaf-wax *n*-alkanes of about 20 ‰ during the initial part of the YD relative to Allerød, suggest colder conditions and/or enhanced precipitation. Furthermore, our data provide additional evidence for two hydrologically distinct periods within the YD interval. Through a combination of biomarker D/H ratios with XRF data our results deliver new insights into the timing and magnitude of regional hydrological changes as a consequence of abrupt global climatic variations.

https://doi.org/10.1180/S0026461X00006502 Published online by Cambridge University Press

Chemical weathering and erosion rates in Lesser Antilles: An overview in Guadeloupe, Martinique and Dominica

SÉTAREH RAD[1], KARINE RIVE[2], OLIVIER CERDAN[1], VITTECOQ BENOIT[1] AND CLAUDE ALLÈGRE[3]

[1]BRGM, 3, avenue Claude-Guillemin, Orléans, France
[2]CEGEO, 159 allee chardin, Villeneuve d'ascq, France
[3]IPGP, PRES Paris Cite´ , 75238 Paris Cedex 05, France

Guadeloupe, Martinique and Dominica Islands alike numerous tropical environment present extreme weathering regimes.

Physical denudation is mainly controlled by landside, This reflects the torrential dynamics of the rivers. For Guadeloupe, the mechanical weathering rates are 800-4000 t/km^2/yr.

The lithology is very porous with high infiltration rates, which induces that most of the elements fluxes are produced on subsurface as the chemical erosion rates are 2 to 5 time higher than the rates from surface water. We show how kinetic of chemical weathering rates depends on the age of the lava and subsurface circulation.

In addition, timescale of erosion have been calculated from U-series analyses sediments from rivers. Our results show a large range: from 0 to 150 ka in Martinique and from 0 to 60 ka Guadeloupe. From analyses from the dissolved loads, we propose to evaluate residence times in the river water. It would appear that waters circulation is globally 3 times longer for subsurface water than for surficial water (Rad *et al*. 2011).

Moreover these islands are highly impacted by agriculture. It is therefore interesting to assess the impact of such influence on the weathering rates. Our result show that human activity brings no disturbance on Critical zone processes contrary to what one might think. Indeed, we show that among the combined impact of all parameters (climate, runoff, slopes, vegetation…), the basins age seems to be the control parameter on chemical weathering and land use: the younger the basin, the higher the weathering rate.

We could observe a combined effect between the higher erodibility and a higher climate erosivity of the younger reliefs.

Impact of a small downstream reservoir on metal cycling in acid mine drainage impacted waters

L.K. RADEMACHER[1]*, K.L. FAUL[2] AND G. MCDANIEL[1]

[1]University of the Pacific, Stockton, CA 95211, USA (*correspondence: lrademacher@pacific.edu)
[2]Mills College, Oakland, CA 94613, USA (kfaul@mills.edu)

The results of ongoing work in an acid mine drainage impacted watershed suggests downstream reservoirs play an important role in the cycling of metals and trace elements under variable flow conditions. The former Leona Heights Sulfur mine in Oakland, California produces acid mine drainage (AMD) that enters the Lion Creek watershed. These waters flow into the Lake Aliso reservoir, which is kept full during the dry summer months, thus contributing to the development of chemical gradients. Lake Aliso is drained during the wet winter months, allowing Lion Creek to flow freely across the lake bottom. The different flow regimes in Lake Aliso provide a wide range of geochemical conditions under which to study metal cycling in a single system.

Beginning in July 2009, monthly water samples were collected from Lion Creek and its two tributaries, Leona and Horseshoe Creeks, as well as from the inlet and outlet of Lake Aliso. Leona Creek is the source of AMD impacts within the watershed and Horseshoe Creek represents background watershed conditions. Lion Creek intergrates these two tributaries and discharges into Lake Aliso. Sediment cores collected from Lake Aliso provide a history of lake conditions and metals cycling.

Metals concentrations, including Pb, Cd, Fe, Ni, Cu, and Zn, in the AMD impacted Leona Creek tributary are significantly elevated above levels in the Horseshoe Creek tributary. After these tributaries mix in Lion Creek, measured concentrations of metals at the Lake Aliso inlet are lower than those measured in Leona Creek, due part to dilution by Horseshoe Creek waters. However, dilution alone cannot explain the reduction in metals concentration. Although all metal conentrations are lowered, only Cu (on most sampling dates), Fe, and Pb approach background levels. In addition, whether concentrations of metals at the Lake Aliso outlet are greater than or less than the lake inlet depends on whether the lake is full or empty, as well as the recent precipitation history. Depth profiles of lake temperature, pH, and dissolved oxygen suggest the chemical gradients that develop when the lake is full likely control the mobility of metals. Additionally, sediment cores from the lake exhibit fine scale (sub cm) oscillations in redox conditions.

https://doi.org/10.1180/S0026461X00006502 Published online by Cambridge University Press

Polar twins? Deglacial carbon and circulation records from the deep North Pacific and Southern oceans

J.W.B. RAE[1]*, G.L. FOSTER[2], M. GUTJAHR[1], M. SARNTHEIN[3], L.C. SKINNER[4], D.N. SCHMIDT[1] AND T. ELLIOTT[1]

[1]Bristol Isotope Group, Department of Earth Sciences, University of Bristol, UK (*correspondence: james.rae@bristol.ac.uk)
[2]School of Ocean and Earth Science, National Oceanography Centre, University of Southampton, Southampton, UK
[3]Institut für Geowissenschaften, U. of Kiel, Kiel, Germany
[4]Godwin Laboratory, Department of Earth Sciences, University of Cambridge, Downing St, Cambridge, UK

The cause of glacial – interglacial CO_2 transfer between the deep ocean and the atmosphere is one of the oldest puzzles in palaeoclimatology. The regularity of these cycles, and their strong coupling to a range of climate proxies, suggests a well-ordered set of controlling mechanisms [1]. The Southern Ocean is thought to play a key role by providing a (stemable) link for carbon and nutrients between the deep ocean and the atmosphere [2]. The North Pacific shares some of these nutrient and mixing characteristics; records from both locations may thus help us understand the fundamental processes driving glacial deep ocean CO_2 storage and release [3].

We present novel proxy data from the deep North Pacific and Southern oceans that provide new constraints on deep ocean chemistry and circulation changes during deglacial pCO_2 rise. Boron isotopes ($\delta^{11}B$) from benthic foraminifera are used to record the state of the deep ocean carbonate system, and are coupled with neodymium isotopes (ε_{Nd}) and benthic-planktic radiocarbon ($\Delta^{14}C$; [4]) to explore the influences of water mass mixing and ventilation age changes. Our $\delta^{11}B$ data show a pronounced pattern of millennial carbonate system variations that is consistent between two cores in the Southern Ocean and one in the North Pacific. In contrast, Southern Ocean ε_{Nd} shows a relatively smooth deglacial transition, suggesting that mixing of differently sourced water masses has minimal control on our millennial carbonate system variations. Rather, the $\delta^{11}B$ and $\Delta^{14}C$ data are best explained by increases in vertical mixing, consistent with the breakdown of glacial stratification in these high latitude oceans during the Heinrich Stadial 1 and Younger Dryas intervals of atmospheric CO_2 rise.

[1] Broecker & Henderson (1998) *Paleoceanogr*. **13**, 352–364. [2] Sigman *et al*. (2010) *Nature* **466**, 47–55. [3] Haug & Sigman. (2009) *Nature Geoscience* **2**, 91–92. [4] Gebhardt *et al*. (2008) Paleoceanogr. **23**, PA4212, 1–21.

Response of coralline alga *Lithothamnion glaciale* Kjellman to ocean acidification

F. RAGAZZOLA[1]*, A. FORM[1], L. FOSTER[2], J. BÜSCHER[1], T. HANSTEEN[1] AND J. FIETZKE[1]

[1]IFM-GEOMAR, Leibniz Institut für Meereswissenschaften Wischhofstraße 1-3 , 24148 Kiel, Germany (*correspondence: fragazzola@ifm-geomar.de)
[2]Dept. of Earth Sciences, University of Bristol, Wills Memorial Building, Queen's Road, BS8 1RJ, UK

Since the industrial revolution, the partial pressure of carbon dioxide in the atmosphere has been rising. The increase of carbon dioxide in the atmosphere and the related uptake by the oceans [1] will result in a decrease in ocean pH by 0.2-0.4 units over the next century [2] and in a decline of calcium carbonate saturation states in the seawater surface. The potential for marine life to adapt to increasing CO_2 concentration are not well known, especially for the organisms living at high latitudes in waters which have naturally low saturation levels.

The effects of elevated pCO_2 were investigated in the high latitude coralline alga *L. glaciale*, an high Mg-Calcite calcifier. The algae were kept in the aquaria for 3 months at 8 ± 0.5 °C with 20 µmol photons m^{-2} sec^{-1} in 12 hours light/ dark cycle at four different CO_2 concentrations: 410 ppm (control), 563 ppm, 838 ppm and 1120 ppm according to the IPCC prediction.

During this incubation period, *L. glaciale* showed a significant linear trend towards lower 'apical tip' growth rates (from 1.0 mm $year^{-1}$ to 0.8 mm $year^{-1}$) with increasing pCO_2 in the water. In water undersaturated with respect to aragonite (pCO_2 1120 ppm- ΩAr = 0.9), the cell density of the newly grown thallus was 68 % less compared to the control together with a 56 % decrease in the cell walls thickness. Reduced growth rates and the weakening of the coralline thallus could have severe consequences for the biodiversity, growth and stabilization of carbonate reefs.

[1] Sabine *et al*. (2004) *Science* **305**, 367–371. [2] Caldeira & Wickett (2003) *Nature* **425**, 365.

https://doi.org/10.1180/S0026461X00006502 Published online by Cambridge University Press

Ba, Sr and $^{87}Sr/^{86}Sr$ in Indian estuaries: Impact of submarine groundwater discharge

WALIUR RAHAMAN AND SUNIL K. SINGH

Physical Research Laboratory, Ahmedabad-380009, India (waliur@prl.res.in, sunil@prl.res.in)

Dissolved Sr, Ba and $^{87}Sr/^{86}Sr$ were studied in three Indian estuaries linked to the Arabian Sea i.e. the Narmada, Tapi and the Mandovi. The concentration of dissolved Sr and Ba in the rivers show significant variations; ranges from 0.7-2.5 μmol/kg, 27-207 nmol/kg respectively whereas $^{87}Sr/^{86}Sr$ vary between 0.70875 and 0.71062 reflecting the lithologies they drain. The Sr/salinity profile in all these estuaries shows conservative mixing between river water and seawater end members whereas Ba shows nonconservative mixing with its gain in mid salinity region (10-15‰). The $^{87}Sr/^{86}Sr$ shows non-conservative behaviour; its distribution exhibits significant departures from the expected conservative mixing lines in all these estuaries. This difference in the behaviour between dissolved Sr and its $^{87}Sr/^{86}Sr$ is intriguing and suggests that there is supply of Sr from additional sources to these estuaries. Similarly, Ba gain could not be explained by Ba release from particles in the estuaries and river-seawater mixing and requires its additional source. The additional source seems to be submarine groundwater discharge (SGD). The non-conservative behaviour of $^{87}Sr/^{86}Sr$ provides a handle to estimate the quantum of SGD to these estuaries. Inverse model calculations have been used to characterize the Sr concentration, $^{87}Sr/^{86}Sr$ and salinity of the SGD and estimate its water fluxes to the Narmada estuary. The model derived SGD flow rates to the Narmada estuary are ~7 and 275 cm/day during nonmonsoon and monsoon respectively indicating large seasonal variability of SGD. This estimate is consistent with those reported from the south-west coast of India using dissolved ^{222}Rn [1] and other coastal regions of the world [2].

[1] Jacob *et al*. (2009) *Curr. Sci*. **97**, 1313–1320. [2] Burnett *et al*. (2003) *Spec Issue, Biogeochemistry* **66**, 202.

Constraints on the formation of a lunar core from metal-silicate partitioning of siderophile elements

NACHIKETA RAI AND WIM VAN WESTRENEN

Faculty of Earth and Life Sciences, VU University Amsterdam, The Netherlands (nachiketa.rai@falw.vu.nl)

Most models for the interior of the Moon include a small iron–rich core with a maximum diameter of several 100 km [1], but the composition and formation conditions of the lunar core are poorly constrained. One major consequence of core-mantle differentiation in planetary bodies is that the majority of the siderophile elements are strongly partitioned into the iron-rich core. Since the degree of extraction of these elements into the metallic phases is governed according to their metal/silicate partition coefficients (D) and the pressure-temperature-composition conditions during core formation, abundances of these elements in the silicate Moon can in principle be used to constrain lunar core formation and chemistry.

Estimates of siderophile element abundances in the lunar mantle have previously been used to argue for the presence of a small metallic core (0.1-5.5 wt%) [2-4], but recent improved approaches to terrestrial core formation models (including better thermodynamic models and the ability to model changing conditions through time) have not yet been applied to the Moon.

Here we re-examine whether a consistent set of conditions can be obtained to match observed siderophile element depletions in the silicate Moon. We combine new metal-silicate partitioning data for Ni, Co, Cr, Mn, Ga, P, Pb, W and V with literature data and characterize the dependence of the partition coefficients on temperature, pressure, oxygen fugacity and silicate melt structure and composition to derive equations of the following form: $\log D = \alpha + \beta (\Delta IW) + \delta (1/T) + \varepsilon (P/T) + \chi (nbo/t)$.

Initial results suggest that when using the proposed bulk Moon composition of [5] and siderophile element abundances from [6], data are consistent with the Moon possessing a small metallic core, with metal-silicate equilibration pressures close to the current core-mantle boundary, consistent with whole-Moon melting at the time of core formation.

[1] Weber *et al*. (2011) *Science* **331**, 309–312. [2] Righter & Drake (1996) *Icarus* **124**, 513–529. [3] O'Neill (1991) *GCA* **55**, 1135–1157. [4] Walter *et al*. (2000) In *Origin of the Earth & Moon*, U of A Press, Tucson, pp.265–289.

https://doi.org/10.1180/S0026461X00006502 Published online by Cambridge University Press

Geochemical and isotopic composition of quartzites near the MCT zone (Garhwal Himalaya, India): Implications to their provenance & deposition

SANTOSH K. RAI[1], SUNIL K. SINGH[2] AND H .K. SACHAN[1]

[1]Wadia Institute of Himalayan Geology, Dehradun (India) (rksant@wihg.res.in, hksachan@wihg.res.in)
[2]Physical Research Laboratory, Navrangpura, Ahmedabad (sunil@prl.res.in)

Quartzites are one of the major clastic sedimentary rocks in the Himalaya that had deposited in the Tethys Ocean basin and exhibit varying chemical composition, protoliths, age (pre-Himalaya) and depositional settings [1, 2, 3]. In this study, geochemical and isotopic composition were determined in the quartzite samples collected form the either side of MCT zone of the Garhwal Himalaya to determine their provenances and nature of the protoliths.

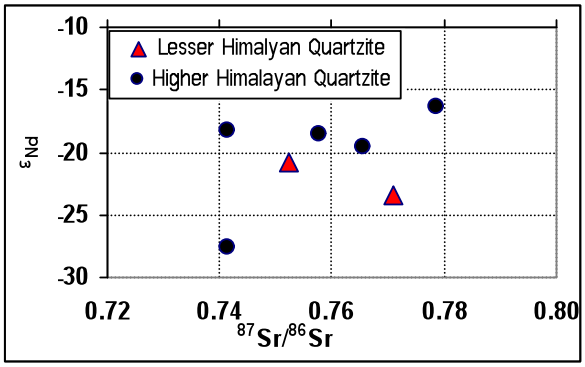

Figure 1: $^{87}Sr/^{86}Sr$ & ε_{Nd} of the Himalayan Quartzites near the MCT zone of the Garhwal Himalaya (India).

Major elements data of the Lesser Himalayan quartzites (Kaliasaud-Alaknanda region) demonstrate significant difference from those of the Higher Himalaya. For example, TiO_2/SiO_2, Al_2O_3/SiO_2, Fe_2O_3/SiO_2 are one to two order of magnitude higher for Higher Himalayan quartzites compared to those from the Lesser Himalaya. These differences could be related either to source variability or to mineralogical sorting during their weathering, transport and deposition. The limited samples measured in this study indicate overlapping Sr and Nd isotope composition between Higher (ε_{Nd} -16.5 to -27.7; $^{87}Sr/^{86}Sr$ 0.7414-0.7788) and the Lesser (ε_{Nd} -20.8 to -23.5; $^{87}Sr/^{86}Sr$ 0.7524-0.7714) Himalayan quartzites making it difficult to differentiate their sources. More work is underway to generate larger data set to study their protoliths.

[1] Ahmad, *et al*. (2000) *Geol. Soc. Am. Bull*. **112**, 467–477. [2] Spencer, *et al*. (2011) *JAES* (in press). [3] Jain A.K. (1972) *Journ. Sed. Ptrol*. **42**(4), 941–960.

Heat flow in the laser-heated diamond anvil cell and the thermal conductivity of the lower mantle

E.S. G. RAINEY[1]*, A. KAVNER[1] AND J. HERNLUND[2]

[1]Department of Earth and Space Sciences, University of California Los Angeles, Los Angeles, CA 90095 (*correspondence: erainey@ucla.edu)
[2]Department of Earth and Planetary Science, University of California Berkeley, Berkeley, CA 94720

The thermal conductivity of the lower mantle is a critical parameter for understanding the current heat budget and thermal evolution of the Earth. However, thermal conductivity measurements at high pressure and temperature are difficult due to the small sample volumes and large temperature gradients characteristic of the laser-heated diamond anvil cell (LHDAC) [1]. Temperature distributions in the LHDAC are determined by laser and sample geometry as well as physical properties such as sample absorbance and thermal conductivity [2]. During heating experiments, precise measurements of peak sample temperatures and 2-D hotspot intensity gradients can be made [3]. In order to infer physical properties of a sample using measured temperature distributions in the LHDAC, a quantitative understanding of heat flow in the LHDAC is needed.

We have developed a 3-D numerical model of steady-state heat conduction for continuous heating experiments in the LHDAC. The numerical model has been benchmarked against an existing 2-D analytic solution [2], yielding agreement in predictions of temperature distributions as a function of input laser power, sample geometry, and sample thermal conductivity. Model calculations show that peak temperature and hotspot width are strongly correlated and dependent on laser power, laser and sample geometry, and sample thermal conductivity. The rate of change of the peak temperature and hotspot width as a function of input laser power is especially dependent on sample thermal conductivity, all other variables being equal.

[1] Benedetti & Loubeyre (2004) *High Pressure Res*. **24**, 423–445. [2] Panero & Jeanloz (2001) *J. Geophys. Res*. **106**, 6493–6498. [3] Kavner & Nugent (2008) *Rev. Sci. Inst*. **79**, 024902.

https://doi.org/10.1180/S0026461X00006502 Published online by Cambridge University Press

In situ U-Pb dating of scheelite: Constraints on the age and genesis of the Felbertal tungsten deposit

J.G. RAITH[1]*, A. GERDES[2] AND D.H. CORNELL[3]

[1]Chair of Resource Mineralogy, Montanuniversitaet Leoben, 8700 Leoben, Austria (*correspondence: johann.raith@unileoben.ac.at)
[2]Institut für Geowissenschaften, Goethe Universität Frankfurt (gerdes@em.uni-frankfurt.de)
[3]Geovetarcentrum, Gothenburg Sweden (cornell@gvc.gu.se)

The Felbertal scheelite deposit, Salzburg province, Austria, is one of the biggest tungsten producers in the world. It has long been regarded as the type locality of stratiform-stratabound scheelite deposits. The deposit is situated in the Habach Complex, an Early Cambrian to Ordovician metavolcano-sedimentary ophiolitic to arc sequence. A chemically unusual W-bearing granite, the K1 orthogneiss, was emplaced in the Early Carboniferous into the western ore zone of the deposit. Several economic scheelite ore bodies are spatially associated with this orthogneiss. The ore deposit was overprinted during the Variscan (~330 Ma) and Alpine (~30 Ma) orogenies. Economic scheelite mineralisation is associated with SiO_2-rich lithologies including foliated fine-grained scheelite-quartz ores ('Scheelite-rich quartzite'), deformed quartz veins and stockwork like mineralisation. Trace element analyses using LA-ICP-MS techniques, controlled by cathodoluminescence (CL) images, confirmed the previously established classification of scheelite stages. Scheelite 1 is preserved as relict cores in fine-grained scheelite in the mylonitic scheelite-quartz ores. It preserves delicate oscillatory growth zoning, is characterised by flat wing-shaped REE patterns, and contains between 50 to 1120 ppm U. *In situ* U-Pb dating by LA-SF-ICP-MS of Scheelite 1 yielded a concordia age of 335.5 ± 4.6 (2 sigma). This new age constrains the timing of scheelite formation of this ore type for which a Cambrian age was previously assumed [1]. Within the uncertainty this new age is indistinguishable from the published 336 ± 19 Ma emplacement age of the K1 orthogneiss. The new scheelite age is inconsistent with previous genetic models, which proposed either syngenetic ore formation in the Cambrian or two stages of epigenetic ore formation, the first in the Cambrian and the second in the Early Carboniferous [1]. The Felbertal scheelite deposit is best interpreted as a metamorphosed granite-related magmatic-hydrothermal ore deposit of exclusively Early Carboniferous age.

[1] Eichhorn *et al*. (1999) *Int. J. Earth Sci*. **88**, 496–512.

Geochemical and mineralogical features of coal combustion wastes (CCW) of Angren Thermal Power Station (TPS) and possible ways of their recycling, Uzbekistan

SH.SH. RAKHMONKULOV A.* AND N.E. SHUKUROV

Institute of Geology and Geophysics Academy of Science of Uzbekistan, 49, Khodjibaeva Str. Tashkent, 100041, Republic of Uzbekistan (*correspondence: rshakhnoza@yahoo.com)

The Angren TPS working on the basis of Angren lignite was found in 1958, during this 53 years functioning were generated 13 million tons of CCW and disposed in 3 coal ash dumps (203 acre). The physical and chemical characteristics of CCW have bearing on both its potential for use and its potential to present some level of risk to human health and the environment. Elemental and mineralogical content of samples from Angren CCW were checked by XRF and JEOL Superprobe microzond. The results of chemical and mineralogical analyses showed high content of metals and minerals with magnetic features (magnetite, haematite, titan-magnetite etc.), concentration of trace elements, as well as rare- earth elements etc. were elevated also. Subsamples were subjected to magnetic separation, results show that content of minerals with ferromagnetic feature is 65% of total mass. Investigations under the JEOL microanalizer show that in spherical magnetic aggregates are containing Fe, Ti, Mn and W in high value.

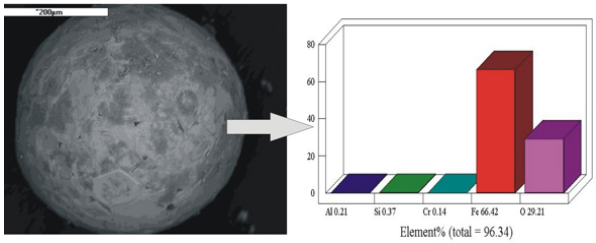

Figure 1: SEM image of magnetic particle and distribution ratio some magnetic elements.

High concentration of Fe and Mn in studied CCW samples showing their effective utilization and bright perspective for using as a raw material for producing several kinds of Ferroalloy for metallurgical industry.

https://doi.org/10.1180/S0026461X00006502 Published online by Cambridge University Press

Magnetic resonance imaging of pollutant mass transport in biofilms

B. RAMANAN[1,2,3], W.M. HOLMES[2], W.T. SLOAN[3] AND V.R. PHOENIX[1]*

[1]School of Geographical and Earth Sciences, University of Glasgow, G12 8QQ, UK (*correspondence: vernon.phoenix@glasgow.ac.uk)
[2]GEMRIC, Wellcome Surgical Institute, University of Glasgow (william.holmes@glasgow.ac.uk)
[3]School of Engineering, University of Glasgow (william.sloan@glasgow.ac.uk)

Introduction

Biofilms play a key role in immobilizing and degrading pollutants in both natural and engineered systems. Quantifying the mass transport of these pollutants in biofilms is critical for effective modelling of biofilm performance. Thus methods are needed which spatially image pollutant transport in a non-invasive manner. However, imaging inside biofilms thicker than several hundreds of microns becomes challenging for photon based methods such as CLSM due to attenuation of photon penetration and the fluorescent signal. These thicker biofilms, however, are by no means rare. For these, such as phototrophic biofilms in natural systems and those in granular waste-water treatment systems, alternative imaging methods must be sought.

Results and Discussion.

Here we report the use of Magnetic Resonance Imaging (MRI) for structural and mass transport imaging in a 2.5 mm thick phototrophic biofilm using a small (5 mm diameter), simple-to-construct RF coil. Notably, the RF coil is also far less expensive than similar commercially available coils.

Gd [DTPA] (molecular mass 547 g/mol) was chosen as a surrogate for an organic contaminant; the parmagnetic Gd making the molecule visible to MRI. The transport of Gd [DTPA] through the biofilm was imaged by aquiring a series of T_2 weighted images (T_2 being the spin-spin relaxation rate of ^{1}H nuclei in the water surrounding the Gd [DTPA]). Because T_2 is inversely proportional to the concentration of Gd [DTPA], fully quantitative maps of Gd [DTPA] transport inside the biofilm were constructed. MRI was also used to image structural heterogeneity and water diffusion within the biofilm. Biofilm structure, water diffusivity and Gd [DTPA] transport were clearly correlated. MRI is a valuable tool for imaging pollutant transport and fate in biofilms too thick for photon based imaging methods.

$Au_3(Pb,Sb)_4$ mineral phase from Tetrem gold deposits, Ghana, West Africa

R.P. RAMDOHR[1] AND T.L. EVSTIGNEEVA[2]

[1]High River Gold Exploration Burkina SARL 01 BP 4418 Ouagadougou Burkina Faso (reinramdohr@yahoo.com)
[2]IGEM RAS, 35, Satromonetny, 119017, Moscou, RF (evst@igem.ru)

The new Au-mineral phase with the composition ~$Au_6Pb_5Sb_3$ [Au_3 (Pb, Sb)$_4$] and parameters (Å) of tetragonal cell a=8.401 (2), c=8.239 (1) is found in the gold deposit Tetrem, SW Ghana, Tarkwa area. The orebodies consist of a series of sedimentary Banket quartz reef conglomerates similar to those in the Witwatersrand Basin. Gold mineralization in Tetrem deposits is located in quartz veins, and appears to have formed during Eburnean II (2, 116-2, 080 Ma) within shear and fault networks developed during contraction deformation.

Gold minerals occur as free particles with an average size of 50-150 μm. The main gold mineral is native gold. There are only minor electrum and Au with 3-7% Ag. Gold is associated with sulphides: pyrite, sphalerite, galena, chalcopyrite, arsenopyrite, pyrrhotite, and molybdenite. Accessory oxides in the ore are magnetite, goethite, ilmenite, and rutile. The mineral proportions vary in gold occurrences of the area. Ore minerals occur in silicified and albitized (?) granite cut by numerous quartz veins and stringers.

The mineral $Au_6Pb_5Sb_3$ was found in quartz veins in association with: free gold containing up to 7.2 Wt% Ag, and up to 5.7 Wt% Hg, and hunchunite, Au_2Pb. Native Au in the sample contain also tiny, <5-10 μm grains of aurostibite, and altaite.

Data of study obtained using MRSA, SEM+EDD, and XRDA. show that by composition, physical properties, and crystallochemical characteristics $Au_6Pb_5Sb_3$ differs from other natural compounds of gold with metals and 'semi-metals': Au and Au-Ag tellurides; aurostibite, $AuSb_2$; maldonite, Au_2Bi; hunchunite, Au_2Pb; anyuiite, $AuPb_2$; and yuanjiangite, AuSn.

$Au_6Pb_5Sb_3$ analogue has been synthesized from the melt in multi-component Ag-Pb-Bi-Sb system for detail study of mineral properties and associations.

Financial support of Fundamental Researches Program n.5 of Dept.Earth.Sci. of Russian Academie of Sciences.

[1] Evstigneeva *et al*. http://geo.web.ru/conf/khitariada/1-2003/informbul-1_2003/mineral-14e.pdf

https://doi.org/10.1180/S0026461X00006502 Published online by Cambridge University Press

Petrography and chemistry of zircons from the Chaltén Plutonic Complex and implication on the interpretation of U-Pb zircon ages

CRISTÓBAL RAMÍREZ DE ARELLANO[1], BENITA PUTLITZ[1], OTHMAR MÜNTENER[1] AND MARÍA OVTCHAROVA[2]

[1]Institute of Mineralogy and Geochemistry, University of Lausanne, Switzerland. (ramirez.andes@gmail.com)
[2]Department of Mineralogy, University of Geneva, Switzerland

The absolute geochronology of the Chaltén Plutonic Complex (CHPC), located in the Southernmost Andes, has a strong influence on the geodynamic interpretation of Patagonia. In addition, the textural and chemical features of zircons from the different plutonic units of this composite intrusion provide important constraints for understanding the growth of zircons in magmas with variable degree of differentiation. These features should be taken into account for the interpretation of zircon ages, since increasing precision of ages is obtained thanks to the development of the U-Pb CA-TIMS dating techniques during the last decades.

The CHPC is a calc-alkaline (arc related) intrusion, which was emplaced at upper crustal levels (3.5 to 2 kbar). The zircon ages (16.90 ± 0.05 to 16.37 ± 0.02 Ma) are consistent with the relative geochronology inferred from field relationships. Where undulated ductile contacts are observed, the age difference cannot be resolved. In the case of brecciated contacts a minimum age difference of 80ky was obtained, which is at the limit of the obtained precission (±40ky).

The petrographic textures of zircons from mafic rocks indicate crystallization in isolated pockets, i.e. interstitial. The application of the Ti-in-zircon thermometer yield constistently low temperatures (~760°C). This indicates that most zircons from these samples might have crystallize near solidus temperatures and consequently post-date the emplacement. In contrast, the textures of zircons from granitic rocks indicate a more protracted crystallization. The chemistry (LA-ICP-MS analysis) of zircons from granitic rocks displays systematic variation of U/Th and U/Ta ratios between core and rim. This pattern can be correlated with the observed variations of calculated temperatures and Ce^{III}/Ce^{IV} ratios. These features suggest that in granitic melts there could be several episodes of zircon crystallization at different temperatures. These temperatures are 100° to 200° higher than the solidus, which implies that many zircons might have crystallize prior to the emplacement (antecryst).

Predicting the character of future eruptions: Insights from single crystal analyses

F.C. RAMOS[1]*, J.B. GILL[2], J.A. WOLFF[3], C.A. DIMOND[1] AND D.L. TOLLSTRUP[4]

[1]Dept. of Geological Sciences, New Mexico State University, Las Cruces, NM, 88003, USA (*correspondence: framos@nmsu.edu)
[2]Dept. of Earth and Marines Sciences, UC Santa Cruz, Santa Cruz, CA, 95064, USA
[3]School of Earth and Environmental Sciences, Washington State University, Pullman, WA, 99164, USA
[4]Thermo Fisher Scientific, 1400 N. Pointe PWKY, West Palm Beach, FL, 33407, USA

While the science of predicting volcanic eruptions is becoming a viable practice, few constraints exist as to the chemical nature of future eruptions, especially regarding the composition and character of the magma or magmas to be erupted. Usually compositional assessments can only be undertaken post-eruption. However, volcanoes characterized by a variety of volcanic products (i.e. a variety of erupted rock compositions) that erupt in short geological time periods (e.g. <10ky), may allow for assessing magma composition/ character prior to when an eruption actually occurs. Baitoushan volcano, located along the China/North Korean border, is known for the largest rhyolitic, caldera forming eruption in the last 2000 years and has shown signs of recent seismic activity. Baitoushan is characterized by at least three recent eruptions (<5000 ka) involving at least four distinctive highly evolved magma compositions. Following a detailed approach involving Sr and Pb isotopes of single mineral crystals, we have identified specific mineral populations that cannot have originated from host magmas, but rather, must have originated from magmas seen only in later eruptions. These populations become more common in subsequent eruptions until they become the dominant mineral population in the latest-erupted magmas. Results suggest the presence of crystals in older erupted materials up to 5000 years prior to eruptions where these crystals are the dominant population. Results are consistent with a magma residence age of ~10 ky and document the first time in which crystals associated with future magmatic activity are observed in materials from earlier eruptions. In addition, isotope variations in selected crystals suggest open system processes occurring ~3000 years prior to eruption in highly viscous, high-silica rhyolites. Ultimately, detailed crystal evaluations offer compositional constraints of magmas resident under volcanoes 1000s of years prior to their eventual eruption.

https://doi.org/10.1180/S0026461X00006502 Published online by Cambridge University Press

Li-O-Pb-Nd-Hf isotope and trace element systematics and S in residual peridotites: Evidences for ancient hydrothermal fluid-rock interactions at mid-ocean ridges

L.V. RANAWEERA, T. MORIGUTI, R. TANAKA, A. MAKISHIMA AND E. NAKAMURA*

The Pheasant Memorial Laboratory (PML), Institute for Study of the Earth's Interior, Okayama University at Misasa, Tottori-Ken, 682-0193, Japan
(*correspondence: eizonak@misasa.okayama-u.ac.jp)

Massive plagioclase lherzolite (MSPL) from the Horoman orogenic massif, Japan, which formed at ~ 1 Ga at a mid-ocean ridge (MOR), represents the most unradiogenic Pb reservoir ever found in the mantle [1]. New data for O and Li isotopes of these MSPL combined with previously published trace element, S contents, and Pb, Nd and Hf isotope data reveal evidences for ancient hydrothermal fluid-rock interaction (HFRI) at mid-ocean ridges.

The trace element patterns of MSPL show element enrichment and depletion in variably melt extracted residues. They show 2-43 times lower U/Pb and 3-11 times lower Ce/Pb than those of the depleted MORB mantle or DMM indicating Pb enrichment. Several MSPLs show bulk rock S elemental abundance (146-273 ppm) higher than those of the DMM (116 ppm) and primitive mantle (250 ppm) also suggesting S enrichment. In addition, S positively correlates with Pb. $\delta^{18}O$ (5.11-5.49 ‰) and $\delta^{7}Li$ (-0.83-3.96 ‰) compositions of MSPL suggest a mixing between DMM and a light Li and O isotope source. These oxygen isotope values negatively and positively correlate with age corrected Pb and Nd and Hf, respectively at ~ 1 Ga.

The correlation in O-Li isotope system indicates hydrothermal fluid and MSPL interaction. Hydrothermal fluids can react with residual peridotites at MORs giving rise to sulfide which can sequester Pb and increase S. The correlation of O with Pb, Nd and Hf indicates that HFRI of MSPLs occurring around 1 Ga. Thus, our data reveal evidences for hydrothermal fluid alteration of peridotites occurred at ancient time at MORs and account for origin of highly unradiogenic Pb reservoirs in the mantle.

[1] Malaviarachchi *et al*. (2008) *Nature Geosci*. **1**, 859–863.

Variation in contribution of Bay of Bengal moisture source derived from stable isotopic composition of cave carbonates in Meghalaya, India

R. RANGARAJAN[1], J. ROUTH[2], P. GHOSH[1], A. MANGINI[3], J. FOHLMEISTER[3] S. BASKAR[4], R. BASKAR[4] AND S. HOLZKÄMPER[5]

[1]Center for Earth Sciences, IISc, India (ravi@ceas.iisc.ernet.in. pghosh@ceas.iisc.ernet.in)
[2]Department of Earth Sciences, IISER, India
[3]HeidelbergerAkademie der Wissenschaften, Germany
[4]Guru Jambheshwar University, India
[5]Johannes Gutenberg University Mainz, Germany

Stable isotope (SI) ratio of calcites in stalagmite samples collected from 3 different caves in the Jaintia (Krem Syndai and Rupasor; N25°09′ and E92°00′) and Khasi Hills (Krem Mawmluh; N25°20′ and E42°45′) of Meghalaya in northeast Himalayas reveals change in rainfall intensity during the last 21 ka BP. Analysis of stalagmite collected from Mawmluh Cave (6.95 – 21.6 ± 0.5 ka) revealed signature of the glacial maxima registered as an abrupt drop in $\delta^{18}O$ values by ~7‰. This is the first observation documenting large variability in isotopic ratio. The Syndai stalagmite (1.8 ± 0.05 ka – 4.69 ± 0.15 ka) captures climatic amelioration across 2.5 to 5 ka. The actively growing Rupasor stalagmite covers the period 0.42 ± 0.14 ka – 2.5 ± 0.03 ka. The late Holocene events, like the Medieval Warm Period (MWP) and Little Ice Age (LIA) have also been captured. Comparing the seasonal variability of present day average rainwater SI record from the Shillong region and wind speed observation from the nearest meteorological observatory allows defining an empirical relationship for predicting the contribution of BoB moisture. The estimates suggests more than 60% drop in the Wind speed (WS) vector corresponding to the ~7‰ difference observed between glacial and non-glacial times.

https://doi.org/10.1180/S0026461X00006502 Published online by Cambridge University Press

Geospeedometry applied to El'gygytgyn impact glass

U. RANTZSCH[1]*, T. HABER[1], D. KLIMM[2] AND G. KLOESS[1]

[1]Institute for Mineralogy, Crystallography and Materials Science, University of Leipzig, Germany (*correspondence: rantzsch@uni-leipzig.de)
[2]Leibniz Institute for Crystal Growth, Berlin, Germany

The El'gygytgyn impact glass has been investigated with the method of relaxation geospeedometry. The sibirian impactite was found in the 3.6 Myr old El'gygytgyn impact structure in lacustrine terraces.

The aim of this research was to determine the natural cooling rate of the El'gygytgyn rhyolitic glass (71.3 % SiO_2, 14.9 % Al_2O_3, 4.1 % K_2O, 2.8 % CaO, 2.8 % Na_2O_3, 2.7 % FeO, 1.1 % MgO, 0.3 % TiO_2, in wt-% by 20 EMPA analysis).

The method of geospeedometry based on the structural relaxation in silicate melts was first applied to natural glasses by [1]. The procedure is referred to the Tool-Narayanaswamy approach [2]. The cooling history of the impactite is frozen in its structure. The temperature-dependent reheating across the glass transformation was used to obtain the original cooling history. The relaxation of the enthalpy was achieved by measurements of the heat capacity.

Therefore, differential scanning calorimetry (DSC) measurements with certain heating and cooling rates were performed. The impact glass was heated above the glass transition (T_g) to ensure the complete relaxation of the glass structure. Thereupon, the kinetic parameters were adjusted for each thermal cycle.

We can deduce that the cooling rate for the impact glass is between 0.15-0.85 K/min. The cooling rate is comparable to the data determined for phonolite obsidian flows on Tenerife [3] but significantly slower than for tektites reported in literature. Hence, we present that the final cooling of the El'gygytgyn impact glass originated witin the hot impact structure.

[1] Wilding, M.C. Webb, S.L. Dingwell, D.B. (1995) *Chem. Geol.* **125**, 137–148. [2] Narayanaswamy, O.S. (1971) *J. Am. Ceram. Soc.* **54**, 491–498. [3] Gottsmann, J. Dingwell, D. B. (2001) *J. Volcanol. Geotherm. Res.* **105**, 323–342.

The influence of physically-induced porewater advection, benthic photosynthesis and respiration on $CaCO_3$ dynamics in reef sands

ALEXANDRA RAO[1,2,3]*, LUBOS POLERECKY[3], DANNY IONESCU[3], FILIP MEYSMAN[1,2] AND DIRK DE BEER[3]

[1]Laboratory of Analytical and Environmental Chemistry, Earth System Science Research Unit, Vrije Universiteit Brussel, Pleinlaan 2, 1050 Brussels, Belgium
[2]Centre for Estuarine and Marine Ecology, Netherlands Institute of Ecology, PO Box 140, 4400 AC Yerseke, The Netherlands (*correspondence: a.rao@nioo.knaw.nl)
[3]Microsensor Group, Max Planck Institute for Marine Microbiology, Celsiusstr. 1, 28359 Bremen, Germany

Reduced net calcification owing to increasing pCO_2 from the burning of fossil fuels suggests a potential reduction in carbonate accumulation in continental margins, where a large fraction of global carbonate accumulation occurs. This feedback in the ocean carbonate cycle lends particular importance to understanding the factors controlling carbonate accumulation and dissolution in coastal and shelf deposits. Permeable biogenic carbonate sediments in reef environments are poised to play a crucial role in the response of ocean margin environments to ocean acidification, because of the interplay between porewater exchange, benthic community metabolism and $CaCO_3$ dynamics in these deposits.

Sediment oxygen consumption rates, porewater profiles and benthic fluxes of oxygen, pH, calcium, alkalinity, and dissolved inorganic carbon were determined in reef sands (Heron Island, Australia) of different permeability across a range of hydrodynamic conditions. In these biogenic deposits, porewater advection and light stimulate rates of benthic photosynthesis, which, in turn, fuels calcification in surface sediments. Furthermore, our results indicate an important damping effect of porewater advection on the efficiency of respiration-driven carbonate dissolution in sediments. Therefore, we argue that the synergistic effects of porewater advection, benthic respiration, photosynthesis, calcification and carbonate dissolution promote carbonate preservation in permeable ocean margin deposits, and have a direct bearing on past, present and future changes in the ocean carbonate cycle.

https://doi.org/10.1180/S0026461X00006502 Published online by Cambridge University Press

The impact of sea level rise on salt water intrusion into coastal aquifers

JOHN RAPAGLIA[1], HENRY BOKUNIEWICZ[2], ATHANASIOS VAFEIDIS[3] AND TSVI PICK[4]

[1]The Future Ocean Excellence Cluster, Institute of Geography, Christian Albrechts University, Kiel,Germany 24098 (rapaglia@geographie.uni-kiel.de)
[2]School of Marine and Atmospheric Science, Stony Brook University, Stony Brook, NY 11794 (hbokuniewicz@notes.cc.sunysb.edu)
[3]The Future Ocean Excellence Cluster, Institute of Geography, Christian Albrechts University, Kiel,Germany 24098 (vafeidis@geographie.uni-kiel.de)
[4]School of Marine and Atmospheric Science, Stony Brook University, Stony Brook, NY 11794 (tpick@ic.sunysb.edu)

According to the IPCC (2007) sea level rise is one of the more certain consequences of climate change. Salt water intrusion into coastal aquifers is an important impact of sea level rise, which has received some attention among the coastal scientific community in recent years (e.g. [1]).

Several studies have produced global scale salt water intrusion maps, buth these maps are at a coarse spatial resolution, which limits their use. We contend that there remains a need to investigate how future changes in climate will affect freshwater-seawater interactions in coastal aquifers both in terms of seawater intrusion as well as groundwater discharge.

We present a first order, global model intended to predict change in the salt water intrusion length into coastal aquifers under different sea level rise scenarios. Forecasts are made up to a pixel resolution of 30 arc-seconds. This model is based on existing sea level rise scenarios, the Bruun Rule and assumptions concerning the relation between surface topology and the hydraulic head which is expected to be a function of aquifer recharge and public consumption. Saltwater intrusion lengths in water stressed areas are likely to increase with sea level rise but that the effect of changing consumption rates due to population change is often greater than the effect of sea level rise alone.

Several limitations remain regarding the utility of the analysis based on data quality; however the model remains a useful first step towards understading future salt water intrusion at a global level.

[1] Döll, P. (2009) Vulnerability to the impact of climate change on renewable groundwater resources: a global-scale assessment. *Environmental Research Letters* **4**(3), 12pp.

Exploring geoengineering using climate and detailed modelling strategies

PHILIP J. RASCH*, HAILONG WANG, JIN-HO YOON, DILIP GANGULY, PO-LUN MA AND VINOJ VELU

Pacific Northwest National Laboratory (PNNL) (*correspondence: philip.rasch@pnl.gov)

Geoengineering (the deliberate perturbation of the planet to counteract some of the effects of increasing CO_2 concentrations) has received increasing attention in scientific and policy communities due to concern about the difficulty of transforming the planet's energy infrastructure and the scientific consensus that reductions in emissions must take place soon to avoid the risk of undesirable impacts and dangerous climate change. Due to the difficulty of energy transformation, societies have been slow to respond, in spite of the risks.

As a stopgap measure, a number of geoengineering strategies have been suggested that introduce aerosols into the atmosphere to increase the planetary albedo, or to reduce the opacity of the atmosphere to longwave energy to cool the planet. The conflation of aerosols, energy, and climate make these strategies a natural topic for this Goldschmidt session. I will describe some modeling studies that explore three geoengineering strategies: 1) introducing sources of stratospheric aerosols; 2) introducing sea salt aerosols to brighten marine stratocumulus clouds; 3) introducing aerosols that act as ice nuclei to reduce the opacity of cirrus clouds.

Geoengineering is complex, and it is important to consider a variety of issues in considering this topic:

1. What are the consequences of particular geoengineering strategies to climate, ecosystems, and society?
2. How do these geoengineering strategies compare to each other?
3. How well do we understand the fundamental physics and chemistry of the processes employed by each strategy? Are climate models providing an adequate representation of these processes so that they may be used for studying geoengineering consequences?

Climate models can be used to explore the planetary response to geoengineering. Process models can be used to better understand the fundamental physics and chemistry that the strategies depend upon. I will describe a number of studies performed by our group using both types of models and identify some of the remaining challenges.

https://doi.org/10.1180/S0026461X00006502 Published online by Cambridge University Press

Secondary origin for 'primary' mineral inclusions in detrital zircons from Jack Hills, Western Australia

B. RASMUSSEN[1]*, I.R. FLETCHER[1], J.R. MUHLING[2], C.J. GREGORY[1] AND S.A.W. WILDE[1]

[1]Dept Applied Geology, Curtin Univ., Bentley, 6102, Australia (*correspondence: B.Rasmussen@curtin.edu.au, I.Fletcher@curtin.edu.au, C.Gregory@curtin.edu.au, S.Wilde@curtin.edu.au)

[2]CMCA, Univ. Western Australia, Crawley, 6009, Australia (janet.muhling@uwa.edu.au)

The Hadean crust has long been regarded to comprise mainly primitive mafic and ultramafic rocks. However, detrital zircons up to 4.4 Ga from Jack Hills, Australia, have been used to infer the existence of extensive granitic crust during the Hadean. Mineral inclusions in these zircons have been interpreted to be primary and magmatic, and therefore to provide important clues about the chemistry of the early crust.

In situ U-Pb dating of monazite and xenotime inclusions in detrital zircon grains from Jack Hills, shows that the inclusions are much younger than their zircon host, and formed during episodes of regional metamorphism at 2.68 Ga or 0.8 Ga. Monazite-xenotime thermometry of intergrowths in the inclusions and the quartz-muscovite rock matrix constrain temperatures to ~450°C, corresponding with conditions during peak metamorphism. Evidence from inclusions in zircon from other localities indicates that the replacement of primary inclusions may commence in the granite host-rock and continue after deposition through to high-grade metamorphism. In metasedimentary rocks, the inclusion assemblage in detrital zircon may increasingly resemble the composition of the rock matrix. In Jack Hills, the most abundant minerals filling inclusions are also the main matrix minerals (quartz and muscovite), consistent with their formation during metamorphism.

Our results show that detrital zircon is not impermeable to post-depositional fluids. We suggest that many of the primary inclusions were replaced by secondary minerals during metamorphism, raising doubts about the use of mineral inclusions in zircon to infer magma chemistry.

Integrating climate and landscape controls on regolith depth, chemistry and mineral assemblage

CRAIG RASMUSSEN[1]*, REBECCA LYBRAND[1], ANGIE JARDINE[2], JON PELLETIER[3], PETER TROCH[2] AND JON CHOROVER[1]

[1]Dept. of Soil, Water, and Environmental Science, Univ. of Arizona, AZ-85721, USA (*correspondence: crasmuss@cals.arizona.edu)

[2]Dept. of Hydrology and Water Resources, Univ. of Arizona, AZ-85721, USA

[3]Dept. of Geosciences, Univ. of Arizona, AZ-85721, USA.

Linkages among climate, erosion and mineral weathering are central to pedogenesis and critical zone evolution. We approach these linkages through synthesis of climate, erosion and regolith geochemical data for upland terrain, coupled with detailed studies on climate and landscape position controls on pedon-scale regolith weathering patterns across the steep semiarid climate gradient encompassed by the Santa Catalina Mountain (SCM) Critical Zone Observatory in southern Arizona, USA. Climate forcing was quantified in terms of effective energy and mass transfer (*EEMT*), that includes energy flux to the subsurface critical zone in the form of primary production and effective precipitation, whereas chemical depeletion and mineral transformation were quantifed using a combination of geochemical, isotopic and mineralgocial analyses. The regional synthesis indicated regolith chemical depletion increased exponentially with water availability and *EEMT* for sites with annual temperature greater than 5°C and erosion rates greater than 10 $g/m^2/yr$, suggesting first order control of climate on chemical depletion, and second order control of temperature and erosion. SCM geochemical and mineralogical data indicated strong linkages among *EEMT*, phyiscal erosion, regolith depth, chemical depletion and mineral assemblage. Specifically, divergent landscape positions demonstrated a pattern similar to that in the regional synthesis of increasing chemical depletion with increasing *EEMT*. In contrast, convergent landscape positions demonstrated minimal mineral mass loss and relatively greater content of neogenic secondary mineral phases. Solution chemistry data suggest the convergent positions concentrate soluble weathering products from adjacent divergent positions, thus resulting in locally reduced mineral-solution weathering gradients and promotion of neogenic mineral precipitation. The coupled datasets indicate that timing and amount of available water is a central control on regolith weathering with strong local-scale modification related to landscape position.

https://doi.org/10.1180/S0026461X00006502 Published online by Cambridge University Press

Behaviour of Zr/Hf and Y/Ho ratios during transition between seawater column and deep-sea brines

M. RASO[1], F. SAIANO[2], E. OLIVERI[3], M. YAKIMOV[4] AND P. CENSI[1,3]

[1]Dipartimento DiSTeM, Università di Palermo, Via Archirafi, 36 90123 - Palermo (Italy)
[2]Dipartimento S.A.G.A., Università di Palermo, Viale delle Scienze, ed.4, 90128 Palermo, Italy
[3]I.A.M.C.-CNR –UOS di Capo Granitola, Via del mare, 3 - 91026 Torretta Granitola, C.bello di Mazara (Italy)
[4]I.A.M.C.-CNR –UOS di Messina, Spianata S. Raineri, 86 - 98122 Messina (Italy)

During the oceanic cruise Mamba 2011 in the Eastern Mediterranean Sea seawater, biogeochemistry of the oxic layers and of the underlying anoxic deep-sea brines was studied. In order to extend the knowledge of processes occurring at oxic-anoxic interface in seawater, Zr/Hf ratio, coupled for the first time with Y/Ho and lanthanide behaviour, was investigated. Lanthanides and especially Y/Ho ratio are considered powerful probes of geochemical processes and a coherent behaviour with respect to Y/Ho was shown by the Zr/Hf ratio in several geochemical systems [1]. Observed covariance of Zr/Hf ratio with respect to dissolved Mn and Fe in anoxic brine, suggest that Zr was preferentially scavenged on MnO_2 surfaces under oxic conditions and the same process occurred for Hf onto FeOOH. These data confirm the observed behaviour in pore water studies [2] and extend the knowledge of Zr and Hf reactivity also onto Mn-oxides.

Different is the Y/Ho behaviour that correlates with dissolved Fe content, especially in brine from Tyro basin but not with Mn content, neither in brines, nor in oxic seawater. The observed lack of correlation observed among Y/Ho and Zr/Hf with respect Fe and Mn contents in seawater is probably due to the delivery of detrital materials in shallowest water layers.

[1] Bau (1996) *Contrib. Miner. Petrol* **123**, 323–333.
[2] McKelvey (1994) *PhD Thesis*, Univ. British Columbia.

The role of multicomponent diffusion and electromigration for reactive transport in porous media

PEJMAN RASOULI[1]*, K. ULRICH MAYER[1] AND SERGIO A. BEA[1,2]

[1]Department of Earth and Ocean Scinces, University of British Columbia, Vancouver, BC, Canada (umayer@eos.ubc.ca) (*correspondence: prasouli@eos.ubc.ca)
[2]now at: Earth Sciences Division, Lawrence Berkeley National Laboratory, Berkeley, CA, USA (sabea@lbl.gov)

Aqueous diffusion is the dominant mass transport process in low permeability formations or in the absence of significant advection. There are systems in which electrostatic interactions between diffusing molecules strongly affect the apparent diffusion coefficients. Neglecting electromigration may lead to the inability of reactive transport models to adequately simulate diffusion dominated transport and to properly reproduce key phenomena such as mineral dissolution and precipitation [1]. An application for which electrochemical migration plays a significant role is the electrokinetic remediation of contaminated groundwater. Electrokinetic remediation is based on controlled application of low intensity direct current through the soil between electrodes. The change of redox condition induced near the electrodes shifts the thermodynamic conditions and ionic mobility with the goal to decontaminate the soil.

The formulation for numerical modeling of reactive transport including multicomponent diffusion and electromigration will be presented and preliminary results from simulations of electrokinetic remediation of metal contaminated soils will be discussed.

This modelling effort evaluates the importance of feedback mechanisms between electromigration, applied electric current, and homogenous and heterogeneous reactions in the aqueous phase and attempts to integrate the simulated response with observed geochemical data.

[1] Galíndez, J. M. & Molinero, J. (2010) On the relevance of electrochemical diffusion for the modeling of degradation of cementitious materials. *Cement & Concrete Composites* **32**, 351–359.

https://doi.org/10.1180/S0026461X00006502 Published online by Cambridge University Press

Mineral compositions indicate magma recharge processes in the Ilímaussaq Complex, Greenland

B. RATSCHBACHER*, M. MARKS, K. PFAFF AND G. MARKL

Eberhard Karls Universität Tübingen, 72072 Tübingen, Germany
(*correspondence: barbara.ratschbacher@yahoo.de)

The peralkaline Ilímaussaq intrusion, South Greenland, exhibits various types of syenites and nepheline syenites. The latest magma pulse represents the most evolved rocks (lujavrites), which mainly consist of eudialyte group minerals (EGM), feldspar, Na-pyroxene (aegirine) and sodic amphibole (arfvedsonite). Based on varying proportions of aegirine or arfvedsonite the lujavrites are subdivided into several units (Fig. 1). Our investigated samples cover the whole sequence of these rocks, including the upper part of the underlying cumulates (kakortokites). We analyzed early magmatic EGM to track the geochemical evolution of their parental melt. Textures (change from poikilitic to dispersed amphibole) and compositional variations (Fe/Mn and Ca/REE ratio systematics) imply that aegirine lujavrites I & IIA continuously evolved from the underlying kakortokites (Fig. 1). Data for arfvedsonite lujavrite A shift back to similar element ratios as aegirine lujavrite I and evolve further on a comparable trend. In contrast, aegirine lujavrite IIB and arfvedsonite lujavrite B data seem to evolve differently. We take these data as indication for the presence of three melts batches responsible for the formation of the lujavrite sequence, which is in contrast to earlier interpretations, who suggested that the kakortokite-lujavrite sequence formed from one single magma batch [1].

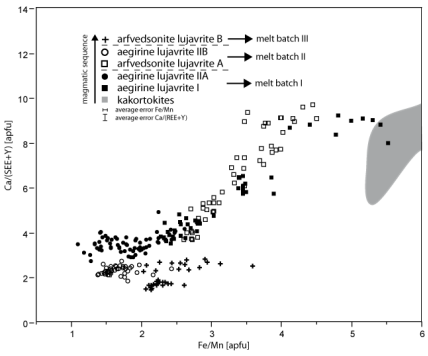

Figure 1: Element ratios in eudialyte; combined with data from [2].

[1] Sørensen *et al*. (2006) *Lithos* **91**, 286. [2] Pfaff *et al*. (2008) *Lithos* **106**, 280.

Electrochemical enhancement of carbonate and silicate weathering for CO_2 mitigation

GREG H. RAU[1,2]* AND SUSAN A. CARROLL[2]

[1]Inst. Marine Sciences, Univ. Calif., Santa Cruz, CA 95064
[2]Carbon Management Program, Lawrence Livermore Nat. Lab., Livermore, CA 94550, USA
(*correspondence: rau4@llnl.gov)

Given the urgent need to stabilize if not reduce atmospheric CO_2 levels, might it be possible to safely and cost-effectively accelerate the consumption and storage of CO_2 via mineral weathering? Exposure of silicate and especially carbonate minerals to elevated CO_2 (e.g. flue gas) can effectively increase the reaction rates leading to CO_2 capture and storage via bicarbonate and/or carbonate formation (1). However, the slow kinetics of the silicate/CO_2 reactions appear to require additional chemical and/or physical treatment, especially in consuming more dilute CO_2 such as found in air. Because of the sensitivity of carbonate and silicate mineral dissolution to acids, and given the ability of saline water electrolysis to generate strong acids, it has been previously shown that electrochemistry can be used to accelerate mineral weathering for purposes of air CO_2 mitigation (2, 3). To explore this further, powdered wollastonite or ultramafic rock standard (UM-4) was encased around the acidic anode of a saline water electrolysis cell composed of graphite electrodes and a 0.25M Na_2SO_4 electrolyte solution. After 0.5 to 1.5 hrs of electricity application (3.5V_{dc}, 5-10mA), the electrolyte pH rose to as much as 11.1 (initial and blank pH's <6.6). Subequent bubbling of these basic solutions with air lowered pH by at least 2 units and increased dissolve carbon content (primarily bicarbonate) by as much as 50X that of the blanks. While Ca^{2+} and Mg^{2+} concentrations were elevated, these were insufficient to balance the majority of the bicarbonate anions in solution. We suggest that in these experiments the silicate minerals acted as acid absorbers, forming mostly insoluble $CaSO_4$ and $MgSO_4$ at the anode, thus allowing NaOH formation at the cathode to accumulate in solution, in turn reacting with air CO_2 to form $NaHCO_3$. Longer electrolysis times and/or alternative electrolyte solutions might allow formation and precipitation of Ca or Mg carbonates. Such electrochemistry might ultimately provide a safe, efficient way to harness the planet's: i) large, off-peak or off-grid renewable electricity potential, ii) abundant basic minerals, and iii) vast natural brine electrolytes for air CO_2 mitigation and carbon-negative H_2 production.

[1] Rau, G.H. (2011) *Environ Sci. Techol.* **45**, 1088–. [2] House, K.Z. *et al*. (2007) *Environ Sci. Techol.* **41**, 8464–. [3] Rau, G.H. (2008) *Environ Sci. Techol.* **42**, 8935–.

https://doi.org/10.1180/S0026461X00006502 Published online by Cambridge University Press

Calcium carbonate veins in ocean crust record a threefold increase of seawater Mg/Ca and Sr/Ca in the past 30 Million years

SVENJA RAUSCH[1], FLORIAN BÖHM[2], ANTON EISENHAUER[2], ANDREAS KLÜGEL[1] AND WOLFGANG BACH[1]

[1]Geoscience Department, University of Bremen, Germany (srausch@uni-bremen.de)
[2]IfM-GEOMAR, 24148 Kiel, Germany

Carbonates in the basaltic ocean crust form during low-temperature alteration and provide a significant sink of CO_2 in the global carbon cycle. Coggon *et al*. [1] calculated ancient seawater Mg/Ca and Sr/Ca ratios based on the record of calcium carbonate veins in the ocean crust and proposed that these ratios were quite uniform throughout the period between 170 and 24 Ma, but then suddenly increased by a factor of 4 to present-day seawater composition. This increase, although delayed by tens of millions of years, is interpreted as an effect of decreasing ridge flank hydrothermal activity, which may be related to a decrease in ocean crust production rate in the late Cretaceous. The goal of this study was to use calcium carbonate veins in reconstructing seawater Mg/Ca and Sr/Ca ratios with a specific emphasis on young sites (≤ 57 Ma) in cold ridge flanks. While our data fill gaps in the critical interval of compositional change in the past 30 Ma, they strongly corroborate the results of Coggon *et al*. [1] in showing simultaneous increases in Mg/Ca and Sr/Ca. Our data also indicate that the Mg/Sr ratio of seawater did not change in the Neogene. We find this to be at odds with a hydrothermal driver of seawater compositional change which should not leave Mg/Sr unchanged. We suggest that a scenario first proposed by Wallmann [2], can explain both the observed trends and the time lag between the late-Cretaceous and the Neogene compositional canges of seawater. The late Cenozoic decrease in ocean crust production rate led to an increase in the average age of the crust und thus to a sea level drop. Lower sea level caused a shift of carbonate deposition from the shelves to the pelagic ocean. Finally, subduction-recycle delayed transfer of CO_2 from deep-sea carbonates to volcanic arcs in combination with accelerated erosion increased the carbonate alkalinity input to the oceans and boosted the Ca sink flux by carbonate formation.

[1] Coggon *et al*. (2010) *Science* **327**, 1114–1117. [2] Wallmann (2001) *Geochim. Cosmochim. Acta* **65**, 3005–3025.

How Jupiter's two-phase gas-driven migration shaped the inner Solar System

SEAN N. RAYMOND[1], KEVIN J. WALSH[2], ALESSANDRO MORBIDELLI[2], DAVID P. O'BRIEN[3] AND AVI M. MANDELL[4]

[1]Laboratoire d'Astrophysique de Bordeaux, BP 89, 33271 Floirac, France (rayray.sean@gmail.com)
[2]Observatoire de la Cote d'Azur, Nice (kwalsh@boulder.swri.edu, morby@oca.eu)
[3]Planetary Science Institute, Tucson, AZ , USA
[4]NASA Goddard Space Flight Center, MD, USA

Accretion simulations cannot adequately reproduce the terrestrial planets, in particular Mars' small mass [1]. Currently, the best solution to this problem assumes that the terrestrial building blocks were initially concentrated in a narrow annulus from 0.7-1 AU [2]. These initial conditions could have been sculpted by Jupiter's two-phase migration in the gaseous Solar Nebula: Jupiter first migrated inward due to standard type 2 torques, then back outward once Saturn grew and was trapped in 2:3 resonance [3]. If the turnaround point or "tack" occurred when Jupiter was at 1.5 AU then the inner disk of material would be truncated at 1 AU, forming a small Mars (Figure 1). In this scenario, the asteroid belt was first emptied and then re-filled by Jupiter: S-type asteroids (red in Figure 1) originated between 1-3 AU and C-types (blue) originated between the giant planets and beyond Neptune [4].

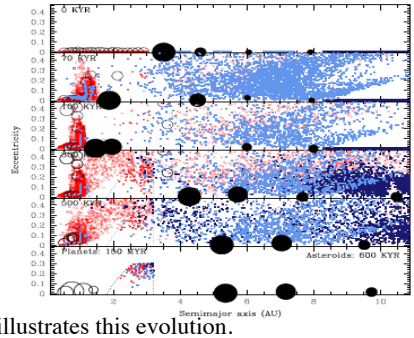

Figure 1: illustrates this evolution.

In the absence of migration, primitive C-type asteroids represent a plausible source for Earth's water [5]. In the context of the 'grand tack' model [4], this same population may still deliver water to the growing Earth: for every C-type planetesimal injected into the asteroid belt, ~10 were scattered onto eccentric orbits that intersect the terrestrial planet-forming region. These scattered C-types can deliver several oceans of water to the growing Earth.

[1] Raymond *et al*. (2009) *Icarus* **203**, 644–662. [2] Hansen (2009) *ApJ* **703**, 1131–1140. [3] Masset & Snellgrove (2001) *MNRAS* **320**, L55-L59. [4] Walsh *et al*. (2011, in press) *Nature*. [5] Morbidelli *et al*. (2000) *M&PS* **35**, 1309–1320.

https://doi.org/10.1180/S0026461X00006502 Published online by Cambridge University Press

Juvenile glass fragments in phreatic explosion debris from Turrialba Volcano, Costa Rica

MARK K. REAGAN[1], MICHAEL C. ROWE[2], ELIECER DUARTE[3] AND ERICK FERNANDEZ[3]

[1]U. Iowa, Iowa City IA, 52242 USA, (mark-reagan@uiowa.edu)
[2]Washington State U., Pullman WA, 99164 USA
[3]OVSICORI, UNA, Costa Rica

After several years of increasing fumarolic activity, Turrialba volcano experienced small phreatic explosions on January 5-6, 2010, leaving a 55x20 m crater with an incandescent floor. Ash and lapilli from the explosions consists mostly of crystal-rich and altered material originally erupted in 1864-1866 and earlier. Nevertheless, careful examination of the tephra revealed that ~1% of the medium to coarse ash-sized particles consists of fresh glass. The freshness of the glass and its unusual chemical traits suggest that this glass is juvenile. EMP analysis of the glass fragments showed them to be calcalkaline andesites, whose major element compositions were largely consistent with derevation by low-P crystal fractionation of basaltic parental magmas. Na_2O, however, is depleted in most glass fragments (1.1-2.8 wt. %) compared to Turrialba's basaltic lavas (2.8-3.8). Incompatible trace element compositions determined by LA-ICPMS are broadly similar to those of the 1864-1866 basalts. REE element patterns are strongly light enriched and most fragments have the elevated Ba/Ce and La/Nb ratios (8-16 and 1.8-2.2 respectively, which is commonplace for calcalkaline lavas. However, one fragment had Ba/Ce and La/Nb ratios (5 and 1.1) more typical of an ocean island basalt, but was otherwise similar in composition to the other fragments.

The concentrations of S in all fragments were near the EMP detection limit, and Cl in most samples were also unusually low for a Turrialba basalt. The concentrations of F, however, were highly variable, ranging from 0.03 to 0.6 wt. %. High F was associated lower concentrations of Na, REE and HFS elements. We speculate the F was enriched by interaction with high-T fumarolic gasses which also leached highly-charged cations and Na.

Important findings are: (1) phreatic explosion debris can contain juvenile glass fragments that provide compositional information about the magma triggering the unrest; (2) magmas intruding into Turrialba's upper edifice at present are basalts or basaltic andesites with varying La/Nb; and (3) gas streaming can affect compositions of apparently fresh glass, particularly Na concentrations.

Glass composition impact on water reactivity at the glass surface

D. REBISCOUL[1]*, F. BRUGUIER[1], V. MAGNIN[2] AND S. GIN[1]

[1]CEA Marcoule,CEA/LCLT, BP 17171, 30207 Bagnols-sur-Ceze BP 17171, 30207 Bagnols sur FRANCE (*correspondence: diane.rebiscoul@cea.fr, florence.bruguier@cea.fr, stephane.gin@cea.fr)
[2]ICSM,/LDD, BP 17171, 30207 Bagnols-sur-Ceze, FRANCE (valerie.magnin@cea.fr)

Understanding the interactions of water with glass surface is of great interest to improve glass alteration models. In this study, the impacts of soda-lime borosilicate glass composition [1] and particularly the effect of network formers such Si and Zr, and of charge compensators such Ca and Na, on water penetration and water structure at the first time of alteration were investigated. Two surface characterizations were used: X-ray reflectometry to determine the thickness and density of the modified glass zone and attenuated total reflection infrared spectroscopy to precise the predominant alteration mechanisms (water diffusion through glass network or hydrolisis) resolving the O-H streching band into four components corresponding to different types of water in glass (hydroxilic group, free, newtwork and ion bounded water). The results of glass alteration at pH=3 and 30°C have shown that hydrolisis was the predominant mechanism after few seconds for glass having a low ZrO_2/SiO_2 ratio. This phenomenon can be explained by the high amount of NBO content. For the other glasses, the diffusion was the limiting reaction characterized by a modified zone having a density close to the hydrated glass and a high amount of free water. The calculated water diffusion coefficients hilighted a decrease of the water diffusion with an increase of Ca content in glass probably due to the compaction of the network by incorporation of divalent cations [2].

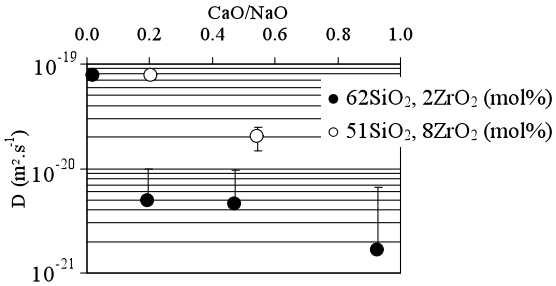

Figure 1: Diffusion coefficients of water through the glasses at pH=3 and 30°C calculated from the first Fick law.

[1] Angéli *et al*. (2010) *J. Am. Ceram. Soc*. **93**, 2693–2704.
[2] Indris *et al*. (2005) *Phys. Rev. B* **71**, 064205.

https://doi.org/10.1180/S0026461X00006502 Published online by Cambridge University Press

The combined use of CALIOP, MODIS and OMI aerosol and cloud products for calculating direct aerosol radiative effects

JENS REDEMANN[1], M. VAUGHAN[2], Y. SHINOZUKA[1], P. RUSSELL[3], J. LIVINGSTON[4] AND L. REMER[5]

[1]BAER Institute/NASA Ames, 290 Maple Ct. Ste. 268, Ventura, CA 93003, USA (*correspondence: Jens.Redemann-1@nasa.gov)
[2]NASA Langley Research Center, Hampton, VA 23681, USA
[3]NASA Ames Research Center, MS 245-5, Bldg. 245, P.O. Box 1, Moffett Field, CA 94035, USA
[4]SRI, International, G-179, 333 Ravenswood Ave., Menlo Park, CA 94025, USA
[5]NASA Goddard Space Flight Center, code 613.2, Bldg. 33, Greenbelt, MD 20771, USA

We describe a technique for combining CALIOP aerosol backscatter, MODIS spectral AOD (aerosol optical depth), and OMI AAOD (absorption aerosol optical depth) measurements for the purpose of estimating full spectral sets of aerosol radiative properties, and ultimately for calculating direct aerosol radiative effects. We will present first results using 1-month of collocated CALIOP V3, MODIS and OMI data collected in October 2007, as well as a test of our methodology using airborne observations in the ARCTAS field experiment. As a prerequisite for the application of our methodology to the actual satellite observations, we assessed the consistency between comparable measurement quantities from the different A-Train sensors. For eight months in 2007 and 2009, comparisons of the standard MODIS-Aqua AOD data to AOD calculated from CALIOP aerosol extinction profile data show differences in global, monthly mean, over-ocean AOD (532nm) between CALIOP and MODIS ranging between between 0.025 and 0.04 for CALIOP V3, with CALIOP generally biased low. Differences for CALIOP V2 are often smaller, but correlation with MODIS AOD is significantly lower.

Anelastic processes in minerals at high temperature: Examples of quartz and spinel

S. REDFERN*, Z. PENG, J. WALSH AND M. DARAKTCHIEV

Department of Earth Sciences, University of Cambridge, Downing Street, Cambridge, CB4 2BD, UK (*correspondence: satr@cam.ac.uk)

Features of recent mechanical spectroscopic studies in Cambridge will be reviewed. The first measurements of higher-order harmonic responses of coelastic materials at displacive phase transitions are reported: Second and third harmonics of strain have been measured by forced torsion pendulum for quartz at the high-low transition. The incommensurate phase and the highly non-linear thermal expansion of quartz at this transition may play a role in controlling higher order elastic moduli. Jerky elastic and strain responses to applied stress also reveal themselves in such experimental arrangements, and we have seen the development of power law distributions of such elastic noise in a number of systems. Self-induced defects appear to lead to such crackling microstructures.

As a contrasting example, the high temperature behaviour of $MgAl_2O_4$ spinel is known to be dominated by kinetic rearrangements of Mg and Al cations as the system undergoes non-convergent order-disorder. We have measured the anelastic loss associated with such order-disorder processes in crystals and ceramics of spinel at ambient and high pressure. The loss is revealed as a strong anelastic relaxation, with well-defined activation energy and relaxation time, in the seismic frequency range. Finally, the implications for seismic damping in ringwoodite spinel are considered.

https://doi.org/10.1180/S0026461X00006502 Published online by Cambridge University Press

Methane geochemistry's 'stealth' process: Microbial oxidation

WILLIAM S. REEBURGH

Earth System Science, University of California Irvine, Irvine, CA, 92697, USA (reeburgh@uci.edu)

For the purposes of this presentation, I consider a 'stealth' process as one that cannot be directly measured. Microbial methane oxidation, aerobic and anaerobic, are examples. Most of the fluxes used to assemble the global methane budget are net fluxes, the difference between production and consumption, so direct measurements of production and consumption require tracer measurements. Several recent high-profile climate modeling papers have fallen into the 'stealth process' trap by failing to explicitly consider microbial oxidation.

This talk reviews recent developments in quantifying methane oxidation in the oxic ocean and estimates the global importance of both aerobic and anaerobic oxidation in a range of environments as controls on global change induced production. New methods sre discussed and remaining challenges are enumerated.

Phase separation, degassing and anomalous methane at the Menez Gwen hydrothermal field

EOGHAN P. REEVES[1], X. PRIETO[1], M. HENTSCHER[1], M. ROSNER[2], J. SEEWALD[3], K.-U. HINRICHS[1] AND W. BACH[1]

[1]MARUM Center for Marine Environmental Sciences, Universität Bremen, Bremen 28359, Germany (*correspondence: reeves@uni-bremen.de)

[2]Fachbereich Geowissenschaften, Freie Universität Berlin, Berlin 12249, Germany

[3]Woods Hole Oceanographic Institution, Woods Hole MA 02543, USA

The Menez Gwen neovolcanic dome, lying at ~800m depth, hosts one of the shallowest basalt-hosted hydrothermal systems on the Mid-Atlantic Ridge and vent fluids there have unusually high CH_4/H_2 ratios relative to ultramafic- and other basalt-hosted systems [1]. To further constrain the origin of this CH_4, fluids were sampled in 2010 from vents on the dome's eastern flank, and from a newly discovered vent field, Bubbylon, 5km to the south of the Menez Gwen dome.

Maximum vent temperatures (270–298°C) in the eastern Hot Sands and AzorAna areas are near the 2-phase boundary and near-seafloor subcritical phase seperation (boiling) is pervasive. Endmember CH_4 (0.37–3.6mmol/kg) and CO_2 (11–78mmol/kg) concentrations are high, but H_2 (0.06–0.57mmol/kg) is low, and only a narrow Cl range (202–368mmol/kg) is evident. Two volatile-rich diffuse fluids (91–117°C) sampled appear to have formed by subsurface mixing of near zero salinity vapor phases with entrained seawater, with apparent CH_4 and CO_2 end-member concentrations of ~30 and ~600mmol/kg, respectively. Such extreme volatile enrichments due to boiling are likely responsible for the ubiquitous gas bubble exsolution evident at the seafloor, releasing substantial CO_2 and CH_4 to the water column. Despite boiling-related variability, endmember CH_4/H_2 ratios (2.5–18) remain anomalously high in 2010. Trace NH_4^+ concentrations (<5µmol/kg) and $\delta^{13}C_{CH4}$ values (-16.6‰ to -19.9‰) within the typical range of unsedimented systems preclude any subsurface sedimentary source of thermogenic CH_4 [2]. Thermodynamic considerations also exclude abiotic CO_2 reduction to CH_4 at the conditions encountered by fluids. This suggests a deeper source of CH_4, such as the volatile-rich fluid inclusions found in oceanic crust Layer 3 [3]. CH_4 radiocarbon and C_{2+} hydrocarbon analyses are ongoing.

[1] Charlou *et al*. (2000) *Chem. Geol*. **171**, 49–75. [2] Lilley *et al*. (1993) *Nature* **364**, 45–47. [3] Kelley & Früh-Green (1999) *J. Geophys. Res*. **104**, 10439–10460.

https://doi.org/10.1180/S0026461X00006502 Published online by Cambridge University Press

Oceanic basalts provide a biased view of mantle composition

MARCEL REGELOUS, KARSTEN M. HAASE AND PHILIPP A. BRANDL

GeoZentrum Nordbayern, Universität Erlangen-Nürnberg, Erlangen, Germany (regelous@geol.uni-erlangen.de)

Chemical and isotopic variations in oceanic basalts are commonly used to infer the chemical structure and evolution of the Earth's mantle. The mantle source of intraplate oceanic basalts is thought to be more 'enriched' than that which melts beneath spreading ridges, due to a greater contribution from recycled oceanic crust or sediment, which can be identified using incompatible trace element and isotope ratios. This approach assumes that mantle melts inherit the incompatible trace element and isotope ratios of their mantle source, an assumption which is also inherent in many geochemical models for melting at spreading ridges and ocean islands.

We will present geochemical data for lavas erupted during slowdown and after the end of active spreading on the fossil Galapagos Rise spreading centre, which show that many oceanic basalts probably do not faithfully record the average composition of the volume of mantle that is melted. Galapagos Rise lavas were generated by variable degrees of melting from 'normal' depleted upper mantle, yet display an enormous range of compositions. At 9.2 Ma, before spreading ceased, incompatible element depleted NMORB (0.75 ppm Nb, Nb/Zr 0.011, $^{87}Sr/^{86}Sr$ 0.70251) were erupted. Younger post spreading lavas, dated at between 7.5 and 5.7 Ma, were produced by smaller degrees of melting and are increasingly enriched. The youngest basalts are trace element enriched EMORB with 77.9 ppm Nb, Nb/Zr 0.256, $^{87}Sr/^{86}Sr$ 0.70311.

The correlated trace element and isotope variations in Galapagos Rise lavas are inconsistent with simple mixing of endmember melt compositions, and also cannot be explained by melting of variably heterogeneous mantle in which enriched and depleted materials contribute equally to melting. Instead, our data can be explained by variable degrees of melting of heterogeneous mantle, within which incompatible element enriched lithologies melt to a greater extent than the more depleted 'matrix'. Our results have implications for the way in which oceanic basalts can be used to infer mantle melting processes and source compositions. For example, the 'garnet signatures' inferred from rare earth element and Nd isotope compositions in MORB may be more sensitive to variations in mantle composition, than to the average depth of melting. Melts of heterogeneous mantle will be biased towards the compositions of more fertile, enriched lithologies, so that the mantle may be significantly more depleted than is often assumed.

Monitoring fluid properties in a geothermal plant

SIMONA REGENSPURG*, HARALD MILSCH, RONNY GIESE AND MATHIAS POSER

Helmholtz-Centre Potsdam, German Research Centre for Geosciences (GFZ) Potsdam, Germany (*correspondence: regens@gfz-potsdam.de)

Measuring chemical properties of geothermal fluids, processed in a geothermal plant is challenging due to high temperatures, salinities and change of conditions resulting in chemical reactions such as corrosion or scaling (=mineral precipitation). At the geothermal *in situ* research laboratory Groß Schönebeck (Germany) chemical reactions of a fluid produced from a Permian sandstone at ~ 4300 m depth, are investigated by a newly developed, fluid-chemical monitoring unit. The apparatus can be connected to different locations at the above ground installations. At these adapters, part of the fluid from the main pipe, would flow through a bypass containing a small heat exchanger. On both sites of the heat exchanger a sampling unit as well as probes to measure pH value and redox potential are installed which can be operated at 150 and 70°C, respectively. Besides high temperatures, the sensors need to be corrosion resistent due to the high chloride concentration typically found in geothermal brines (up to 5 M).

The device simulates processes occuring at heat exchangers which are typically installed in geothermal plants to transfer the heat of the fluid for electric energy production. The chemical informations obtained from this monitoring unit describe not only the compositional variability of the produced fluid over time, but also chemical processes and their kinetics potentially occurring within the plant due to temperature decrease, which could result in corrosion or clogging of the pipes and components. In Groß Schönebeck, chemical equilibrium caculations indicated oversaturation of sulfate-, silicate-, iron- and lead minerals due to temperature drop. The monitoring validates modeled reactions and thus gives evidence on these reactions and might finally predict plant failures.

https://doi.org/10.1180/S0026461X00006502 Published online by Cambridge University Press

The ^{129}I isotopic composition of supergene iodine minerals in Chile and Australia

MARTIN REICH[1,2], FERNANDA ALVAREZ[1], ALIDA PÉREZ[1], GLEN T. SNYDER[3], C. PALACIOS[1], G. VARGAS[1], Y. MURAMATSU[4], EION M. CAMERON[5] AND UDO FEHN[6]

[1]Department of Geology, Universidad de Chile, Santiago Chile (mreich@ing.uchile.cl)
[2]Andean Geothermal Center of Excellence, Universidad de Chile, Santiago, Chile
[3]Department of Earth Sciences, Rice University, Houston, TX
[4]Department of Chemistry, Gakushuin University, Tokyo, Japan
[5]Eion Cameron Geochemical Inc., Carp, ON, Canada
[6]Department of Earth and Environmental Sciences, University of Rochester, Rochester, NY

Because of its large ionic radius, iodine (I) is rarely incorporated into minerals and remains in the aqueous phase much longer than other halogens. Naturally-formed I minerals are very rare, but are found in the nitrate ore fields of the Atacama Desert in Chile and the supergene zones of base and precious ore deposits in extremely arid environments (Chile, Australia). The presence of I in Cu deposits in northern Chile has not been investigated previously, but provides the opportunity to apply the ^{129}I system for the study of the tectonic history of the area and of climatic changes, particularly the desiccation of the Atacama region.

Here, we report the first ^{129}I data of iodide minerals from supergene zones of Cu and Ag deposits from the hyperarid Atacama Desert. Two marshite (CuI) samples from the supergene zone of the Chuquicamata Cu deposit show ^{129}I/I ratios of 218 ± 72 and 562 ± 77 ($\times 10^{-15}$ at·at^{-1}), similar to the ^{129}I isotopic signature of a geochemically anomalous, iodine-rich soil sampled above the Spence porphyry Cu deposit (473 ± 75). Therefore, mineral and soil samples range between typical volcanic arc fluids (^{129}I/I~700-1000) and forearc fluids (^{129}I/I~100-250). In contrast, marshites and iodargyrites (AgI) from the Broken Hill Pb-Zn-Ag deposit in Australia and the Chañarcillo Ag deposit in Chile show a wider dispersion of ^{129}I/I ratios, ranging from ~100 to 2000, indicating a significant meteoric influence.

We suggest that I-rich fluids were involved in supergene enrichment and recycling of Cu in the Atacama region, revealing a complex link between mutliple sources of fluids, active tectonics and climate change.

Melting conditions associated with the Colorado Plateau, USA

M.R. REID[1]*, ROMAIN A. BOUCHET[2] AND J. BLICHERT-TOFT[2]

[1]School of Earth Sciences and Environmental Sustainabiliy, Northern Arizona University, Flagstaff, AZ 86011-4099 USA (mary.reid@nau.edu)
[2]Ecole Normale Supérieure de Lyon, 69007 Lyon, France

Continental foundering occurs by lithospheric detachments associated with gravitational instabilities as well as by shear-related thinning. Volcanic activity is progressively encroaching on the otherwise tectonically stable Colorado Plateau in the southwestern U.S. We show that decompression melting of local ambient enriched mantle lithosphere - rather than compression melting of lithospheric mantle drips or delaminations, or decompression melting of the asthenospheric mantle return flow - is likely responsible for this volcanism. New Hf and Nd isotope data (>120 analyses) significantly expand evidence for heterogeneous enriched mantle sources beneath the Colorado Plateau. ^{206}Pb/^{204}Pb values <18.5 and as low as 17, characterize those samples with Hf-Nd isotope signatures that are evocative of mantle enrichment by mixing with pelagic ± terrigenous sediments: values >18.5 would be expected if Cordilleran and other sediments had been incorporated into their sources during Laramide-aged (80–40 Ma) shallow subduction. Relative abundances of minor and trace elements further show that the more volumetrically significant melts are sourced dominantly in peridotite rather than in pyroxenite or eclogite. Silica- and MgO-based thermobarometry supports evidence from trace element fractionation that melting locally transcends the garnet-spinel transition (~75 km), with shallower melts characterized by higher degrees of partial melting. Low P- and S-wave velocity domains, pronounced thinning of the lithosphere beneath the margins of the Colorado Plateau, and possible evidence for lithospheric delamination [1] may be further evidence that localized mantle upwelling is responsible for Colorado Plateau volcanism.

[1] Levander *et al*. (in press) *Nature*.

https://doi.org/10.1180/S0026461X00006502 Published online by Cambridge University Press

Biogeochemistry as a regional mineral exploration tool: Northeast Yilgarn Craton, Western Australia

N. REID[1]*, M.J. LINTERN[1], R.R.P. NOBLE[1], R.R. ANAND[1], D.J. GRAY[1], G. SUTTON[2] AND R. JARRETT[2]

[1]CSIRO Earth Science and Resource Engineering, Kensington WA 6151, Australia (*correspondence: nathan.reid@csiro.au)

[2]CSIRO Mathematics, Informatics and Statistics, Urrbrae SA 5064, Australia

Regional biogeochemical surveys can potentially be of great use for mineral exploration where access problems and the hindrance of transported overburden make other techniques problematic. A large area of the north Yilgarn Craton hosting numerous Ni, Au, U and VMS deposits was selected for this proof of concept study. *Acacia aneura* (mulga) was sampled approximately every 8 km in this region as it is one of the most widespread plant species across Australia. Mulga samples were collected at water wells and bores corresponding to a regional hydrogeochemistry sampling program. Vegetation samples were dried, split, milled, digested in aqua regia then analysed using ICP-MS/OES. A large, robust, statistically verified geochemical data set was generated which provides the ability to detect lithological signatures using geochemical indices and multivariate statistics (with around 20% error of prediction). Uranium in mulga was the only distinct target element for secondary U deposits, and was successful for most known prospects. Gold exploration potential was improved by the use of multi-element indices. Nickel prospects were identified where the samples were close to the prospects (<2 km) or where supergene mineralisation was dispersed. The Leinster and Murrin Murrin areas were highlighted by elevated Ni, Co, Cr and Fe concentrations compared to background with haloes up to 20 km wide. Detection of VMS style deposits is hampered by Zn and Cu being essential plant nutrients however, high Zn values seen on the regional scale may warrant further investigation. Little correlation exists between hydrogeochemistry and biogeochemistry, meaning one cannot be used as a surrogate for the other; however, both are useful tools in detecting mineralisation and lithological signatures using different chemical properties for a regional setting. Also, mulga can be sampled without the need for drilling to access groundwater.

Sensitivity and feedback in the oceanic molybdenum cycle

C.T. REINHARD[1]*, C.T. SCOTT[2] AND T.W. LYONS[1]

[1]Dept. of Earth Sciences, Univ. of California, Riverside, Riverside, CA 92521 (timothyl@ucr.edu) (*correspondence: christopher.reinhard@ucr.edu)

[2]Dept. of Earth and Planetary Sciences, McGill Univ., Montreal, QC H3A 2A7 (clinton.scott@mcgill.ca)

The oceanic inventories of trace elements have fluctuated markedly during Earth's history as a function of prevailing Earth surface redox conditions. Given the importance of many trace elements in a wide variety of enzymatic processes, such changes may have had significant downstream effects on the global biogeochemical cycling of carbon, nitrogen, and oxygen [1]. Molybdenum (Mo) is particularly important in this regard, being a crucial catalytic component of enzymes involved in biological N_2 fixation, assimilation of NO_3^-, and oxygen atom transfer reactions.

Here, we explore the response of the oceanic Mo reservoir to perturbations in marine redox in a one-box ocean model in which Mo enrichment and burial are first-order with respect to the ambient Mo reservoir. Despite imposing this negative feedback, we find that relatively small changes in ocean redox can have significant effects on the concentration of Mo in seawater ($[Mo]_{sw}$) at steady state, and that relaxation to steady state following perturbation occurs relatively quickly. In addition, although it is possible to draw down $[Mo]_{sw}$ to levels that would have been likely to exert negative effects on some biological processes, the muted enrichments seen in many Proterozoic black shales [2] are likely not compatible with global-scale sulfidic conditions.

In order to further explore the feasibility of attaining varying degress of expanded anoxia we employ a simple oxygen budget for the modern North Atlantic. This exercise corroborates that of [3], and suggests that the redox state of the deep ocean could have been severely impacted purely by air-sea gas exchange limitations at presumed Proterozoic atmospheric oxygen levels. Further, a simple regional budget of sulfide and highly reactive iron (Fe_{HR}) fluxes to marine sediments suggests that were the ocean to become anoxic due to limited O_2 supply (as in the Proterozoic) the deep ocean would most likely have become ferruginous (anoxic and Fe-rich) [4] while marginal environments would likely have been prone to sulfidic conditions.

[1] Anbar & Knoll (2002) *Science* **297**, 1137–1142. [2] Scott *et al*. (2008) *Nature* **452**, 456–459. [3] Canfield (1998) *Nature* **396**, 450–453. [4] Poulton & Canfield (2011) *Elements* **7**, 107–112.

https://doi.org/10.1180/S0026461X00006502 Published online by Cambridge University Press

Transformations of silver nanoparticles in environmental systems

B.C. REINSCH[1,2], R MA[1,2], C. LEVARD[2,3], N. KABENGI[2,4], G.E. BROWN JR.[2,3], C.S. KIM[5] AND G.V. LOWRY[1,2]*

[1]Carnegie Mellon University, Pittsburgh, PA 15213, USA (*correspondence: glowry@cmu.edu)
[2]Center for the Environmental Implications of Nanotechnology (CEINT)
[3]Stanford University, Stanford, CA 94305, USA
[4]University of Kentucky, KY 40546, USA
[5]Chapman University, Orange, CA 92866, USA

The persistence, toxicity, and effects of silver nanoparticles (AgNPs) released to the environment depends on their eventual speciation. Reduced sulfur-silver species are predicted to dominate the eventual species that form. However, in the environment, especially in aerobic conditions, other ligands are more abundant, such as Cl^-, organic thiols, SO_4^{2-}, Br, and I^-. To idenity important transformations from 'weathering' and predict the speciation of silver naoparticles weathered in environmental samples, engineered AgNPs were weathered in various environmental conditions including: wastewater treatment byproducts, aerobic and anaerobic soils, and in simulated wetland mesocosms. Synchrotron-based X-ray absorption spectroscopy was used to speciate AgNPs aged under simulated weathering conditions in the laboratory. Comparisons between the speciation of AgNPs that had been weathered for up to 18 months in a simulated wetland and laboratory weathering can be used to create particles that mimic the observed changes in environmental samples. Protocols to rapidly weather engineered nanomaterails will allow researchers to use NPs with properties representative of the materials that will be in the environment rather than those of the pristine materials. This will enable better predictions of the environmental fate, transport, and effects of engineered nanoparticles.

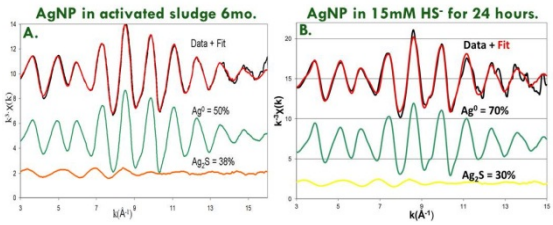

Figure 1: The original AgNPs containing ~90% Ag^0 have been transformed to approximately 50% Ag^0 and 30%Ag_2S after 6 months of ageing in activated sludge, shown in A. B shows the resulting particles from a laboratory ageing process that has produced a particle of somewhat similar composition after only 24 hours of ageing in Na_2S.

The Os isotopic record of organic rich sediments from the Benguela Upwelling System, Namibia

L. REISBERG[1]*, D. BLAMART[2] AND C. ZIMMERMANN[1]

[1]CRPG (CNRS UPR2300), Université de Lorraine, BP 20, 54501 Vandoeuvre-les-Nancy, France (*correspondence: reisberg@crpg.cnrs-nancy.fr)
[2]LSCE (CEA-CNRS-UVSQ), Avenue de la Terrasse, 91198 Gif-sur-Yvette Cedex, France

Several recent studies [1-5] have shown a correlation between osmium isotopic variations in marine sediments and glacial-interglacial cycling. These correlated variations have been used to argue for direct climatic control on weathering intensity and/or on the composition of erosional products. However these rapid fluctuations in the marine Os isotopic records suggest a residence time for Os in seawater (3 to 10 ka) that is much shorter than that inferred from mass balance (~ 25 to 40 ka, [6-8]). Furthermore, potential problems linked to sampling site or sediment type, such as basin isolation, detrital contributions, and low sedimentation rate, could bias many of the existing Os records.

To obtain a reliable, high resolution record of marine Os isotopic variations in Quaternary times, we are analyzing sediments from ODP Leg 175, Site 1084, drilled off the coast of Namibia beneath the Benguela Upwelling System. This is an open ocean site containing rapidly deposited (~ 18 cm/kyr) organic rich sediments, which should be unaffected by the possible problems that may have plagued earlier studies. We currently have results for 9 samples spanning the most recent 35 ka of this record. These samples have extremely high Re and Os concentrations (58-157 ppb and 0.19-0.34 ppb, respectively). Their $^{187}Os/^{188}Os$ ratios are quite constant (1.044 ±0.013, 2σ), and show only a tiny hint of the nearly 7% decrease in $^{187}Os/^{188}Os$ during the last glacial maximum observed in several previous studies. Instead, the uniformity of the Benguela Os record is similar to that reported for an early Pleistocene record from the equatorial Pacific Ocean [9]. The discrepancies between the Os records from different sediment types and localities must be better understood before these records can be used to constrain relationships between climate and weathering.

[1] Oxburgh (1998) *EPSL* **159**, 181–191. [2] Dalai *et al.* (2005) *Chem. Geol.* **220**, 303–314. [3] Williams & Turekian (2004) *EPSL* **228**, 379–389. [4] Oxburgh *et al.* (2007) *EPSL* **263**, 246–258. [5] Burton *et al.* (2010) *EPSL* **295**, 58–68. [6] Oxburgh (2001) *G-cubed* 2000GC000104. [7] Levasseur *et al.* (1998) *EPSL* **174**, 7–23. [8] Paul *et al.* (2010) *GCA* **74**, 3432–3448. [9] Dalai & Ravizza (2010) *GCA* **74**, 4332–4345.

https://doi.org/10.1180/S0026461X00006502 Published online by Cambridge University Press

The geomicrobiology of gold: Fundamental processes to industrial applications

FRANK REITH[1], GREGOR GRASS[2], CARLA ZAMMIT[1], GORDON SOUTHAM[3] AND JOËL BRUGGER[1]

[1]The University of Adelaide, Geol. & Geophys., Adelaide SA5005, Australia (Frank.Reith@csiro.au)
[2]University of Nebraska-Lincoln, Lincoln NE 68588-0666, USA
[3]University of Western Ontario, London, ON, Canada N6A 5B7

The biosphere catalyzes a variety of biogeochemical reactions that transform gold (Au) [1, 2]. Microbial weathering contributes to the mobilization of Au by releasing Au trapped in minerals and by solubilizing it via complexation. Subsequent microbial destabilization of Au (I/III)-complexes coupled to bio-precipitation and biomineralization leads to secondary Au formation, completing the cycle. Secondary Au occurs as nano-particles as well as micro-crystalline and 'bacteriomorphic' Au, the latter being a controversial form of 'biogenic' Au. Recent research provides an understanding of genetic and biochemical mechanisms that microorganisms utilize to drive this biogeochemical cycle. These studies show that: (1) microorganisms mediate Au solubilization via excretion of metabolites, e.g. cyanide, amino acids and thiosulfate; (2) precipitate Au intra- and extracellularly, and in products of their metabolism leading to the formation of Au biominerals; and to achieve this (3) have developed biochemical responses to deal with toxic Au (I/III)-complexes.

Using genomic, proteomic and synchrotron spectroscopic techniques genes and proteins involved in Au detoxification have been characterized. For example, a transcriptional regulator (GolS) in the bacterium *Salmonella enterica* is activated specifically by Au-complexes. Activated GolS then activates the expression of a metallochaperone gene (*golB*) and of a transmembrane efflux ATPase (*golT*), which promote Au resistance [3]. Using these results a biosensor for Au is in development allowing the quantification of Au from environmental samples. This will provide a cost-efficient and environmentally sustainable technique for the improvement of Au exploration and ore processing.

[1] Reith *et al*. (2007) *ISME Journal* **1**, 567–584. [2] Southam *et al*. (2009) *Elements* **5**, 303–307. [3] Checa *et al*. (2007) *Mol.. Microbiol*. **63**, 1307–1318.

Mobility of platinum and gold in the Australian regolith – Spectroscopic and electron microscopic analyses

FRANK REITH[1], CHRISTINE TA[2], BARBARA ETSCHMANN[1], CLAIRE LENEHAN[2] AND JOËL BRUGGER[1]

[1]The University of Adelaide, Geol. & Geophys., Adelaide SA5005, Australia (Frank.Reith@csiro.au)
[2]Flinders University, Adelaide SA5001, Australia

Biogeochemical cycling of gold (Au) and platinum (Pt) appears to play a fundamental role in the formation of secondary Pt and Au in placer deposits, and secondary 'biogenic' Pt and Au has been reported from Brazil and Australia [1, 2]. To compare Pt and Au mobility, Pt/Au nuggets, soils and groundwaters were collected from a platinoferous and auriferous site near Fifield, New South Wales, Australia. Collected materials were analyzed using (FIB)-SEM-(EDXA/EBSD), ICP-MS, EPMA, ICP-MS/OES, X-ray tomography, synchrotron-μXRF, and thermodynamic modeling.

Secondary morphologies, presence of nano-particle and formation of micro-crystalline enrichment zones of Pt/Au on surfaces of Pt/Au grains suggest (bio)geochemical dissolution and re-precipitation that promote the mobility of Pt and Au in surface environment. This is supported by X-ray tomography of a rare specimen of deep lead material (Fe-oxides, silicates and clays) with embedded Pt- and Au grains. Grain surfaces display filigree and perforated structures, strong rounding of grains and the formation of nano- and micro-particles. Synchrotron μXRF-mapping and FIB-SEM of polished sections uncovers differences in Au and Pt mobility. This is supported by groundwater data and geochemical modeling, suggesting lower Pt compared Au reactivity, and hence mobility, in surface environments.

[1] Cabral *et al*. (2011) *Chem. Geol*. **281**, 125–132. [2] Reith *et al*. (2010) *Geology* **38**, 843–846.

https://doi.org/10.1180/S0026461X00006502 Published online by Cambridge University Press

Distinguishing periods of crustal growth and recycling by U-Pb dating, Sr, Pb and Hf isotopes among the Eastern Cordilleran granitoids of South Peru

MARIËL REITSMA[1]*, U. SCHALTEGGER[1], R. SPIKINGS[1], M. CHIARADIA[1], A. ULIANOV[2] AND A. GERDES[3]

[1]Université de Genève, Rue des Maraîchers 13, 1205 Geneva, Switzerland (*correspondence: martje.reitsma@unige.ch)
[2]Université de Lausanne, Switzerland
[3]Goethe University, Frankfurt am Main, Germany

The backbone of the Eastern Cordillera of south Peru is built of plutons that have previously been mapped as Permo-Triassic. They were related to an extensional event that generated continental basins at the surface, filled with the sediments of the Mitu Group.

The aim of this study is to decipher age trends among the granitoids and asses their contribution to crustal growth. U-Pb laser ablation ICPMS dating of zircons shows that the plutons of the north-west trending Cordillera de Carabaya are middle to upper Triassic in age, while the plutons in the Abancay deflection are older: Ordovician, Carboniferous and Permian. Triassic plutons continue in north-western direction to the south of the Abancay deflection.

Hf-isotope data show positive εHf (~+2 to +4) for the Paleozoic plutons indicating a mantle dominated source while the Triassic plutons have εHf around 0 to -4 indicating mixing of mantle and crustal sources.

The Triassic plutons match exactly the age of the sediments of the Mitu group. Therefore, we conclude that these granitoids formed via partial crustal anatexis associated with extension. The offset of the plutons around the Abancay deflection could be interpreted as a step over in the Mitu rift. The Ordovician, Carboniferous and Permian plutons coincide with times of known continental arc magmatism along the western Gondwana margin and were emplaced in a back-arc setting.

Hf-isotope results for both tectonic settings indicate variable amounts of juvenile input from the mantle and/or from a lower crustal source, reflecting an increasing importance of a crustal component in the Triassic. However, with the present data we cannot quantify crustal growth versus crustal recycling yet.

Historical perspective of passive aerosol remote sensing: Bridging the years

LORRAINE A. REMER AND OMAR TORRES

NASA Goddard Space Flight Center, Greenbelt MD 20771 USA (Lorraine.A.Remer@nasa.gov, Omar.O.Torres@nasa.gov)

For nearly three decades space sensors designed for other purposes were used to observe, quantify and characterize atmospheric aerosols. During this ‘heritage period’, algorithm development focused on three primary methods. (1) Occultation methods that measure the extinction of solar radiation and provide vertical profiles of aerosol extinction through the stratosphere. (2) Dark target methods that use the brightening of the scene to infer aerosol loading. (3) UV methods that use the deviation of the observed signal from expected Rayleigh scattering values. Besides these three main methods applied to the SAM/SAGE, AVHRR and TOMS measurements, respectively, to produce long aerosol time series, other methods have been developed to make use of multiangle, polarization and geosynchronous capabilities. These satellite aerosol products applied to data collected in the 1980s and 1990s made way for the era of the modern sensors that began with the launch of Terra in late 1999. The modern sensors: MODIS, MISR, OMI etc., were designed with aerosol in mind, but specifically with the goal of providing information that would help reduce uncertainties in estimates of climate forcing. The quantitative information they provided was unexpectedly also used in other applications including air quality forecasting, public health studies, and long-range transport of dust and pollutants. Thus, the modern satellite data helps to bridge the scales, as well as the years.

https://doi.org/10.1180/S0026461X00006502 Published online by Cambridge University Press

An experimental study of brine-CO_2 metal fractionation: Applications to the geological storage of CO_2

KIRSTEN U. REMPEL*, AXEL LIEBSCHER, WILHELM HEINRICH AND GEORG SCHETTLER

GFZ German Research Centre for Geosciences, Telegrafenberg, 14473 Potsdam, Germany (*correspondence: rempel@gfz-potsdam.de)

In this study, we have measured the fractionation of Fe, Cu, Zn and Na between brine and carbon dioxide at pressure-temperature conditions applicable to the saline aquifers used for the geological storage of CO_2, in order to evaluate the potential for trace element remobilization within the injected CO_2 plume. The experiments were carried out at 6.5-16 MPa and 60°C in a Ti autoclave loaded with a 20 wt% NaCl solution containing a known concentration of Fe, Cu or Zn, in addition to pressurized CO_2. Paired samples of brine and CO_2 were extracted from separate capillary lines and analyzed for metal concentrations.

The vapour-brine partition coefficients $(D_i^{V/L} = C_i^V/C_i^L)$ ranged from $4x10^{-4}$ - $2x10^{-3}$ for Fe, $8x10^{-5}$ - $4x10^{-4}$ for Cu, $4x10^{-6}$ - $2x10^{-4}$ for Zn, and $1x10^{-6}$ - $1x10^{-3}$ for Na. The fractionation of these elements into the CO_2 did not cause a measureable decrease of their concentrations in the brine. The total element concentrations in the CO_2 samples ranged from 0.2 to 1.4 mg/kg (ppm) Fe, 0.1 to 0.6 mg/kg Cu, 0.004 to 0.4 mg/kg Zn and 0.6 to 92 mg/kg Na, and generally displayed a small positive correlation with CO_2 density. The values of $D_i^{V/L}$ in a CO_2 storage reservoir at 7-28.5 MPa and 35-98°C, in which the density of CO_2 is ~0.3-0.7 g/cm^3 (as compared to 0.1-0.6 g/cm^3 in this study), could be expected to be approximately equivalent to those determined from these experiments.

Considering the metal concentrations typical of brines in CO_2 storage aquifers that have reacted with CO_2 and sandstone (20-200 mg/kg Fe, 0.3-1 mg/kg of Cu, 3-5 mg/kg Zn), and neglecting the increased solvent capability of higher-density CO_2, these results suggest that a plume of injected CO_2 could contain up to 0.1 mg/kg Fe, 0.3 µg/kg Cu and 1 µg/kg (ppb) Zn, in addition to 16 mg/kg Na. At a Sleipner (North Sea)-sized reservoir used to store 14 Mt of CO_2, this would lead to the mobilization of about 1 t Fe, 5-10 kg Cu and Zn, and 200 t Na. In terms of long-term CO_2 storage, the potential consequences of these results include the precipitation of carbonate minerals in shallower, more distal regions of the aquifer and the transferral of metals to adjacent aquifer systems.

Combining NanoSIMS with STXM/TEM imaging to shed new light on organic matter contained in micron-sized particles

L. REMUSAT[1]*, D. DERRIEN[2], P.J. HATTON[2], P. NICO[3] AND J.-N. ROUZAUD[4]

[1]CNRS/Muséum National d'Histoire Naturelle, Paris, France (*correspondence : remusat@mnhn.fr)
[2]INRA Nancy, Champenoux, France
[3]Earth Science Division, LBNL, Berkeley, USA
[4]CNRS / ENS Paris, Paris, France

During the past 10 years, NanoSIMS has opened a new window on the study of the spatial distribution of light elements and their isotopic composition in natural samples. This instrument, with its high sensitivity, high precision and high spatial resolution, is suitable to study organic matter (OM) in meteorites and soil aggregates. Nevertheless, this technique suffers from the influence of the nature and the topography of the sample surface on the ion yield (the so called matrix effect) making the unambiguous characterization of the carbonaceous phases sometimes problematic. Moreover, the intrument cannot deliver molecular information, often required for the study of OM.

We illustrate here, through several examples, the benefits to combine NanoSIMS imaging with TEM and STXM, in order to improve the characterization of the carbonaceous materials and to strengthen the conclusions arisen from NanoSIMS images. This is a challenging task because these cutting edge techniques, while sharing high spatial resolution capabilities, have very different intrumental constrains.

The combination TEM+NanoSIMS was used to characterize the carbonaceous phases isolated from an Enstatite chondrite by HF/HCl dissolution. Graphite and poorly organised OM were identified by TEM (and Raman spectroscopy). With NanoSIMS, we measured the D/H and $^{13}C/^{12}C$ isotopic ratios along with the H/C and N/C elemental ratios of each phase, without ambiguity. Hence, we entirely characterized the carbonaceous phases separately to understand their relationship and origin.

We could also assess the fate of labelled OM after a 10 years *in situ* incubation experiment in a natural forest by combining NanoSIMS and STXM. While NanoSIMS was able to map ^{15}N-labelled OM in soil microaggregates recovered from this forest, it has to be combined with STXM imaging (of the same aggregates) to reveal the molecular structure of the organic constituents. The combination of these instruments allows us to follow, at the submicron scale, the processes leading to the soil OM recycling.

https://doi.org/10.1180/S0026461X00006502 Published online by Cambridge University Press

Trace and rare earth elements characteristics of scheelite from the Sanjiazi tungsten deposit in Siping area, Northeastern China

Y.S. REN[1]*, H. WANG[1], N. JU[1] AND C.Z. WU[2]

[1]College of Earth Sciences, Jilin University, Changchun 130061, China (*correspondence: renys@jlu.edu.cn)
[2]State Key Laboratory for Mineral Deposits Research (Nanjing University), Nanjing 210093, China

The Sanjiazi skarn scheelite deposit is lately discovered in northeast China and there are many key questions on its genesis still unresolved. Scheelite is a widespread mineral in many hydrothermal deposits, its trace and rare earth elements can be used to constrain the derivation of the metal and mineralising fluids [1, 2]. Trace elements and rare earth elements (REE) compositions of the scheelite from Sanjiazi deposit were analyzed by ICP-AES.

Scheelite in Sanjiazi deposit is depleted in Sr, Be, Co, Ni, Ta and with enrichment of such metallogenic elements as Pb, Zn, Mo, Bi and Ag. Generally, these enriched trace elements, together with W, are prone to accumulate in magmatic hydrothermal fluids and precipitate in mesothermal condition. Moreover, scheelite shows accordant primitive mantle-normalized trace element spidergram with the Mesozoic granite and pre-mineralizing diorite porphyry dikes, indicating that they have the common material source.

The total content of REE in scheelite is 134.59ppm. The content of the LREE is nearly equal to that of the HREE. Chondrite-normalized REE patterns of the scheelite are overall flat curves with obvious Eu peak, which indicates a strong LREE/HREE fractionation. Scheelite has strong positive Eu anomalies (δEu=2.05), weak negative Ce anomalies (δCe=0.77), low LREE/HREE (1.09) and $(La/Yb)_N$ (0.54). The REE characteristics of scheelite in Sanjiazi deposit is similar to those in some skarn tungstern deposits in south China associated with magmatic hydrothermal fluid [4].

A conclusion can be safely drawn that the Sanjiazi tungsten deposit belongs to skarn ones, its ore source was derived from the granitic magmatic fluid instead of ore-hosting skarn. The Mesozoic granitic magmatism played an important role in scheelite mineralization in this area.

This research was supported by basic research grants from Jilin University (Grants 200903025 and 201004001).

[1] Brugger *et al*. (2000) *Contrib Mineral Petrol*. **139**, 251–264. [2] Xiong *et al*. (2006) *Acta Petrologica Sinica*. **22**(3), 733-741. [3] Zeng *et al*. (1998) *Geology-Geochemistry*. **26**(2), 34–38.

REE fractionation during crustal anatexis: Constraints from the South Bohemian batholith (Bohemian Massif)

M. RENÉ

Institute of Rock Structure and Mechanics, Academy of Sciences, Prague 8, Czech Republic (rene@irsm.cas.cz)

The processes controlling rare earth element (REE) behaviour during origin of S-type granite melts have profound implications for REE abundances in these granites. For typical protoliths of S-type two-mica granites, such as are metapelites of the Moldanubian Zone from the Bohemian Massif (Central European Variscides), a high amount of bulk rock LREE are sited in monazite and of HREE in garnet, apatite and zircon. The LREE and Th concentrations of a metapelite-derived melt are buffered by monazite stability. During anatexis, dissolution of monazite, apatite and zircon in the melt results in increasing bulk REE abundances and LREE/HREE ratios with increasing temperature of melting and a negative Eu anomaly in the melt. Both these features are displayed in the REE geochemistry of two-mica granites from the South Bohemian batholith (SBB) in the Bohemian Massif.

Three main geochemical two-mica granite types can be distinguished in the SBB: the low-Th Deštná granite, the intermediate-Th Eisgarn granite and the high-Th Lipnice and Steinberg granites. Th concentrations and REE element patterns are quite distinct class marks for the above mentioned three geochemical types of two-mica granites. The highest bulk content of REE is significant for the Lipnice and Steinberg granites (207–242 ppm), whereas the lowest bulk of REE was observed in the Deštná granites (33–69 ppm). The content of REE is controlled by variable amount of apatite, monazite and zircon enclosed usually in biotite and/or in apatite. The accessory minerals assemblage in the Deštná granite consists of monazite, zircon, apatite and xenotime usually enclosed in K-feldspar. The Eisgarn granitic melt was generated from dehydration melting of biotite at temperatures in the range 830–850 °C, whereas the Deštná granitic melt was generated by dehydration melting of muscovite at temperatures in range 670–750 °C, in agreement with REE concentrations. The highest Th contents in monazite and high Th/U ratios are significant for monazites from the Lipnice and Steinberg granites. On the other hand, monazites from the Deštná granites show higher values of U and Y.

This study was supported by the Ministry of Education, Youth and Sports of the Czech Republic (project No. ME10083).

Quantification of waste silicates for mineral carbonation

P. RENFORTH[1]*,
C-L. WASHBOURNE[2] AND D.A.C MANNING[2]

[1]Department of Earth Sciences, University of Oxford, Oxford, OX1 3AN, United Kingdom (*correspondence: Phil.Renforth@earth.ox.ac.uk)
[2]School of Civil Engineering and Geosciences, Newcastle University, NE1 7RU, United Kingdom

Historic Production

Silicate minerals are an ubiquitous component of some anthropogenic material streams (cement, construction waste, slag, fuel ash etc.). Generally, they are produced by calcining carbonate minerals in the presence of silica (mine/aggregate waste is composed of naturally occuring silicates). We estimate that humans have produced approximately 89-103 billion tonnes (Gt) of silicate material since the early 1800's (Table 1; [1]). The fate of this material is likely one of several namely, disposal in the ocean or in lanfill, spread onto land, or material in engineering. While some of this material has carbonated in the environment [e.g. 2], it is possible that a substantial quantity remains available for carbon capture (with a total potential in the order of 10^3 MtC).

Material	Current (Mt a^{-1})	Historic (Mt)
Aggregate fines	3, 300	unknown
Mine waste	2, 000-6, 500	unknown
Cement kiln dust	420-568	9, 000-12, 000
C & D waste	1, 400-5, 900	*
Slag	380-500	12, 100-15, 900
Fuel Ash	198-383	76, 000-14, 600

Table 1: Global production estimates for anthropogenic silicates since the early 19th century. *historic production of C&D waste is unknown, but the upper limit is based on the historic production of cement (60 Gt). See [1] for more details.

Current production

Current annual production of silicate material is estimated to be approximately 7.6-17.2 Gt. With an estimated carbon capture potential of around 190-332 Mt of carbon. Production of silicates is increasing by approximately 2 % a^{-1}, largely in China, carbonation of which is likely to an increasly important role for mitigating some of the associated carbon emissions.

[1] Renforth, *et al*. (2011) *Environ Sci Technol* ***45****(6), 2035-41*. [2] Manning (2001) *Min Mag* **65**(5), 603-10.

Further progress towards synchronizing geochronometers

PAUL R. RENNE[1,2]

[1]Berkeley Geochronology Center, 2455 Ridge Rd., Berkeley, CA, USA 94709 (prenne@bgc.org)
[2]Dept. of Earth and Planetary Science, Univ. California, Berkeley, CA, USA 94709

A recent calibration of the $^{40}Ar/^{39}Ar$ system [1] has largely reconciled the $^{40}Ar/^{39}Ar$ and $^{238}U/^{206}Pb$ geochron-ometers, but reveals several apparent inconsistencies with previous results. For example, recalculating a previous result [2] for the Cretaceous/Paleogene boundary (KPB) produces an age of 66.236 ±0.060 Ma (1σ here and throughout), slightly older beyond stated errors than an astronomically tuned age of 65.957 ±0.040 Ma [3] for the KPB at Zumaia (Spain). To investigate this disparity, renewed analysis of circum-KPB events has been initiated. Arguably the most definitive age for the KPB would be that for the Beloc (Haiti) tektites. Previous results for these tektites are consistent with a KPB age though not with sufficient precision to advance the present discussion. With rigorous attention to neutron fluence monitoring via the Fish Canyon sanidine (FCs) standard, a suite of Beloc tektites was irradiated along with sanidine from a Z-coal tonstein (stratigraphically ~60 cm above the KPB) from the Hell Creek area of Montana (USA). Three positions of the standard closely bracketing the samples yielded an average *J*-value with 0.02% precision. Seven tektites with Ca/K between 2.8 and 4.8 heated incrementally in 14-18 steps with a CO_2 laser and analyzed with a single collector MAP 215 mass spectrometer all yielded 100% concordant age spectra. The weighted mean of the seven plateau ages, calibrated per [1], is 65.946 ±0.067 Ma, indistinguishable from the astronomical age [3]. Combined with previous results [4, 5] a weighted mean age of 66.043 ±0.049 Ma is obtained for the Beloc tektites. Additional work in progress will further refine the age of the tektites and enhance their importance to a precise age for the KPB. Calibrated per [1], 71 single crystals of sanidine from the Z-coal yielded an age of 65.926 ±0.066 Ma. No xenocrysts are evident in the data, justifying step-heating analysis of multigrained aliquots currently in progress. These results disfavor the possibility raised by [1] that the astronomical age [3] of the KPB is miscalibrated by a 405 ka eccentricity cycle and serve to validate intercalibration between the Ar/Ar, U/Pb and robust astronomical chronometers.

[1] Renne *et al*. (2010) *GCA* **74**, 5349–5367. [2] Swisher *et al*. (1993) *CJES* **30**, 1981–1996. [3] Kuiper *et al*. (2008) *Science* **320**, 500–504. [4] Izett *et al*. (1991) *Science* **252**, 1539–1542. [5] Swisher *et al*. (1992) *Science* **257**, 954–958.

https://doi.org/10.1180/S0026461X00006502 Published online by Cambridge University Press

Continental flood basalts and biotic crises: Does the Paraná-Etendeka exception prove the rule?

PAUL R. RENNE[1,2]

[1]Berkeley Geochronology Center, 2455 Ridge Rd., Berkeley, CA, 94709, USA (prenne@bgc.org)
[2]Dept. Earth & Planetary Science, Univ. California, Berkeley, CA, 94720

The temporal correlation between continental flood volcanism and severe paleoenvironmental effects including mass extinctions are well known although the causal mechanism (s) remain unclear. Various metrics of the magnitude of either phenomenon (e.g. % taxa extinct or volume of magma erupted) define positive correlations but the extent of scatter in such relationships implies that other variables are important. Some of the larger CFB's that fail to coincide with profound extinction events (e.g. Ferrar-Karoo) turn out to be temporally distributed over several million years and their anomalously feeble impact may be due to lower effusion rates reducing atmosheric loading rates for volcanogenic volatiles. Among the largest CFB's clearly erupted mainly over a short time interval (< 3 Ma; e.g. Siberian, CAMP and Deccan), the Paraná-Etendeka province (PEP) stands out distinctly as an outlier in the correlation with biotic crises. Extensive incremental-heating Ar/Ar data demonstrate unequivocally that the PEP was brief (>90% erupted 135-132 Ma; calibration per [1]), and previous studies suggesting a protracted event spanning ~10 Ma were flawed. The resolution of this apparent conundrum may lie in the importance of thermogenic volatiles (mainly CO_2, methane and sulfates) released from country rocks during CFB events, as has been proposed in many recent studies. Virtually throughout the PEP, volcanic effusions were emplaced atop up to 450 m of eolian sands of the Botucatu and Etjo Fms., and the nearest-surface carbonaceous strata (< 80 m thick Iratí Fm.) at the time of the PEP event were >2 km beneath the surface. We suggest that thermogenic CO_2 was minimal in the PEP event due to a combination of (1) relatively sparse carbonaceous sediments in the thermal aurole; (2) depth (lithstatic pressure) of these sediments being sufficiently high to retain CO_2 in metamorphic assemblages and inhibit brittle fracturing, limiting transmissivity for thermogenic volatiles. Moreover, PEP magmas are exceptional among the largest brief CFB's in the dominance of lithospheric melt sources, suggesting minimal magmatic contributions to volatile loading of sulfates and CO_2.

[1] Renne *et al*. (2010) *GCA* **74**, 5349–5367.

Iron species in soils on a mofette site studied by Fe *K*-edge XANES

T. RENNERT[1]*, K. EUSTERHUES[1], V. DE ANDRADE[2], J. PRIETZEL[3] AND K.U. TOTSCHE[1]

[1]Institut für Geowissenschaften, FSU Jena, Germany (*correspondence: thilo.rennert@uni-jena.de)
[2]NSLS-II, Brookhaven, USA
[3]Lehrstuhl für Bodenkunde, TU München, Germany

Ascending geogenic CO_2 is a soil-forming factor on mofette sites: With increasing soil CO_2, the amounts of pedogenic Fe decrease, and Fe oxides are poorly crystalline according to extraction with oxalate and dithionite [1]. To further study the Fe speciation (especially that of Fe (II)), we applied spatially resolved X-ray absorption near-edge spectroscopy (XANES) to soil samples from a mofette site in the NW Czech Republic. The samples originated from spots with 4 and 100% CO_2 in the soil atmosphere. Point XANES spectra (1 μm^2) at the Fe *K*-edge (7112 eV) were collected at beamline ID 21 of the ESRF, Grenoble, in fluorescence mode. Altogether, we recorded 73 spectra on regions of interest identified from 5 fluorescence maps of 3 thin sections prepared from undisturbed soil samples. Linear combination fitting of reference spectra from a whole of 51 references including various Fe (II)- and Fe (III)-bearing minerals and organic species was used for Fe-species identification. In almost all cases, two references were sufficient as checked by the sum of squared differences.

The Fe-fluorescence maps explicitely showed a heterogeneous spatial distribution of Fe with accumulation in larger pores (e.g. former root channels) and depletion in the soil matrix. We conclude small particles (< 1 μm), because point spectra could not be explained by a single reference spectrum. We identified smectites, illite and ferrihydrite in the Fe-accumulation zones. Iron in the Fe-depletion zones was mostly present in clay minerals such as different smectites, illites and chlorites in 68 spectra. Especially at 100% CO_2, we identified Fe (II)-containing minerals such as green rust, vivianite, siderite and magnetite in the soil matrix. According to XANES, Fe sulphates and Fe sulphides were not present. We detected only slightly more Fe (II) complexed by organic species at 4% CO_2 than at 100% CO_2 indicating that CO_2 impedes the association of organic matter with Fe-containing minerals. This is in line with the observation of mainly non-decomposed, probably particulate organic matter in soils on mofette sites and only a small fraction of organo–mineral associations [1].

[1] Rennert *et al*. (2011) *Eur. J. Soil Sci*. in press

https://doi.org/10.1180/S0026461X00006502 Published online by Cambridge University Press

Constraining the fidelity of sulfate-oxygen in the geological record

VICTORIA RENNIE* AND ALEXANDRA V. TURCHYN

Dept. Earth Sciences, University of Cambridge (*correspondence: vcr22@cam.ac.uk)

The oxygen isotope composition of aqueous sulfate ($\delta^{18}O_{SO4}$) in natural environments reflects microbially-mediated oxygen isotope exchange with water during bacterial sulfate reduction, as well as oxygen isotope fractionation during sulfide oxidation. When the $\delta^{18}O_{SO4}$ is preserved in the geological record, it is a potentially powerful tool for reconstructing these key microbial metabolisms (sulfate reduction and sulfide reoxidation) over time. This may be of critical importance in the NeoProterozoic, when the existence and evolution of these metabolisms is intimately related to the redox evolution of the Earth's surface environment.

The viability of using the $\delta^{18}O_{SO4}$ to elucidate these processes in both modern and ancient environments rests on the assumption that there is minimal abiotic exchange between sulfate-oxygen and water-oxygen during the variety of conditions imposed by sample storage, mineral extraction, and laboratory processing. Previous work has shown that oxygen isotope exchange between sulfate and water occurs readily at very low pH (<1) and/or at high temperatures (>100°C). Aqueous samples are routinely acidifed prior to analysis, but current estimates for timescales of exchange under these conditions rely on extrapolation from highly dissimilar solutions.

We present results from exchange experiments mimicking pore fluids under a variety of conditions. These rule out short and medium-term exchange of sulfate-oxygen with water during sample treatment over a range of acidic conditions. Additionally, the presence of aqueous sulfide in sedimentary pore fluids may facilitate sulfate-oxygen exchange with water-oxygen via the transient formation of thiosulfite complexes. Our experiments constrain the range of pore fluid (and natural) conditions over which $\delta^{18}O_{SO4}$ will remain stable. Finally, in contrast with aqueous sulfate, results from extracted carbonate-associated-sulfate (CAS) show that mineral bound $\delta^{18}O_{SO4}$ is not solely a function of the oxygen isotope composition of the aqueous sulfate during carbonate crystallization. This points towards further controls on $\delta^{18}O_{SO4}$ in CAS possibly imposed by the presence of the carbonate lattice.

Investigating the transport of strontium through biogenic hydroxyapatite Barriers

J.C. RENSHAW*, S. HANDLEY-SIDHU, F. SINCLAIR SMITH, Q. GRAIL, M. CUTHBERT, M RILEY AND L.E. MACASKIE

University of Birmingham, Edgbaston, Birmingham B15 2TT, UK (*correspondence: j.c.renshaw@bham.ac.uk)

Hydroxyapatite (HAp) has potential as a material for the remediation of metal contaminated waters [1] and in reactive barriers [2]. *Serratia* sp. cells bio-manufacture nanophase hydroxyapatite (Bio-HAp) from the substrates glycerol 2-phosphate and Ca^{2+} [3]. This Bio-HAp has properties that increase metal uptake (e.g. decreasing crystallite size, increasing specific surface area and organic content).

Column experiments were conducted to investigate the transport of Sr^{2+} (0.5 mg) through Drigg sand (sampled near low level waste repository) and Drigg sand containing either 0.25% commercial (Com-HAp) or Bio-HAp. Figure 1 shows the elution of Sr^{2+} through columns containing groundwaters (GW) with high levels of competing ions (100 and 50 mg L^{-1} of Ca^{2+} and Mg^{2+}, respectively). The Com-HAp and Bio-HAp retained 2.5 and 3.7 mg of Sr^{2+} per 1 g of HAp, respectively. Work is now been undertaken with GW containing lower cation concentrations. Numerical modelling is also being carried out to test various hypotheses regarding Sr^{2+} transport processes.

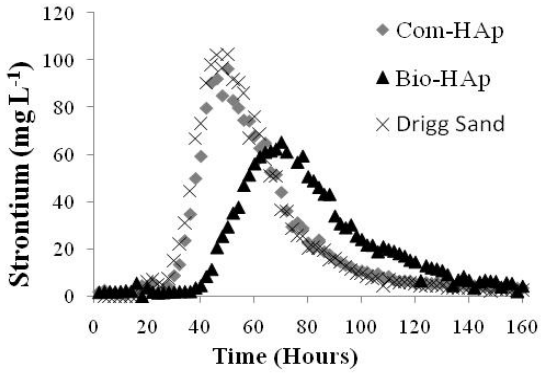

Figure 1: The Transport of Sr^{2+} through Drigg Sand (x), with Com-HAP (♦) and Bio-HAp (▲)

[1] Handley-Sidhu (2011) *Biotechnol. Lett.* **33**, 79–87. [2] Simon (2004) *Sci. Total Environ.*. **326**, 249–256. [3] Thackray (2004) *J. Mater. Sci. Mater. Med.* **15**, 403–406.

https://doi.org/10.1180/S0026461X00006502 Published online by Cambridge University Press

Time scales of metasomatism, differentiation and degassing at Volcán de Colima

O. REUBI[1], K.W.W. SIMS[2], J. EIKENBERG[3], M.K. REAGAN[4], N.R. VARLEY[5] AND B. BOURDON[1,6]

[1]ETH Zurich, Switzerland (olivier.reubi@erdw.ethz.ch)
[2]University of Wyoming, USA
[3]Paul Scherrer Institute, Switzerland
[4]University of Iowa, USA
[5]Universidad de Colima, Mexico,
[6]Ecole Normale Supérieure de Lyon and CNRS, France

Volcán de Colima, Mexico (VDC) nearly continuous activity since 1998 provides a unique opportunity to asses the times scales characteristic of intermediate arc volcanoes. VDC andesites have ($^{238}U/^{230}Th$) = 1, but have significant excesses of ^{231}Pa and ^{226}Ra. These excesses, and relatively low Th contents, indicate that addition of Th-rich sediments in secular equilibrium to the mantle source cannot account for ^{238}U-^{230}Th equilibrium, as generally advocated. In the VDC case, the U-series suggest that slab fluids carrying U were not added to the mantle wedge in the last 350 kyr and ^{226}Ra excesses are most likely mantle melting signals. ^{226}Ra and ^{231}Pa excesses indicate that the time scales of differentiation from primary mafic to dacitic melt (composition of the crystallizing melt) are short and < 1.6 kyr.

Most 1998-2010 magmas have ($^{210}Pb/^{226}Ra$) = 1, however small ^{210}Pb deficits are measured in few samples. This indicates that the magmas erupted at the onset of the eruptive phase (1998) degassed either more than 100 yr ago or within few months of eruption. Observed changes in petrology and the SO_2 flux measured prior to 1998 concur to suggest that significant degassing occurred within few months of eruption. Increasing maximum ^{210}Pb deficits with time are consistent with progressive degassing of a magma batch since 1998, but require several influxes of undegassed magmas and incomplete mixing between the magma batches. Influxes of undegassed magmas may cause the observed shifts in activity from Vulcanian to effusive.

Long residence (> 6 Ma) time of Paleoproterozoic seawater sulfate revealed by *in situ* and *ex situ* sulfur isotope measurements

MARLENE REUSCHEL[1]*, M. WHITEHOUSE[2],, V.A. MELEZHIK[3], A. LEPLAND[3], A.E. FALLICK[4] AND H. STRAUSS[1]

[1]Corrensstrasse 24, D-48149 Münster, Germany (*correspondence: marlene.reuschel@uni-muenster.de)
[2]Swedish Museum of National History, Box 50007, SE-10405 Stockholm, Sweden
[3]Geological Survey of Norway, Leiv Erikssons vei 39, N-7491 Trondheim, Norway
[4]Scottish Universities Environmental Research Centre, Rankine Avenue, East Kilbride, G75 0QF, Scotland, UK

The 2.0 Ga Tulomozero Formation, Fennoscandian Shield, NW Russia, consists of shallow marine carbonates and silicilastics, dissolution breccias and widespread syndepositional marine evaporites, now mostly present as pseudomorphs after Ca-sulfates.

Ex situ measured carbonate-associated sulfate (CAS) and breccia-associated sulfate (BAS) throughout the entire formation ($\delta^{34}S_{CAS}$= 10.9±2.7 ‰, $\delta^{34}S_{BAS}$=9.0± 1.1 ‰) resemble the *in situ* SIMS sulfur isotope data from relics of sulfate evaporites in ubiquitous pseudomorphs after Ca-sulfates ($\delta^{34}S_{anhydrite}$= 9.6 ±1.0 ‰; $\delta^{34}S_{barite}$= 11.0±3.1 ‰).

The $\delta^{34}S$ record of the Tulomozero sulfates matches the sulfur isotopic composition of other broadly time equivalent evaporite successions [1, 2]. Furthermore, the homogeneity of the sulfate sulfur isotope record within the Tulomozero Formation together with an estimated minimum depositional time of the formation (based on average carbonate precipitation rates) suggests a residence time of seawater sulfate in the Mid-Proterozoic of at least 6.5 Ma.

Consequently, the apparent presence of Ca-sulfate evaporites and the homogeneity of sulfate sulfur isotope data from various lithologies support the existence of a sizeable seawater sulfate reservoir already in the Mid-Paleoproterozoic ocean.

[1] Schröder *et al*. (2008) *Terra Nova* **20**, 108–117. [2] Guo *et al*. (2009) *Geology* **37**, 399–402.

https://doi.org/10.1180/S0026461X00006502 Published online by Cambridge University Press

Electrical conductivity of the serpentinised mantle and fluid flow in subduction zones

BRUNO REYNARD[1,2], KENJI MIBE[2] AND BERTRAND VAN DE MOORTELE[1]

[1]Université de Lyon, CNRS, ENS de Lyon, Parvis Descartes, 69007, Lyon, France (bruno.reynard@ens-lyon.fr)

[2]Earthquake Research Institute, University of Tokyo, 1-1-1 Yayoi, Bunkyo-ku, Tokyo 113-0032 Japan (mibe@eri.u-tokyo.ac.jp)

In the mantle wedge of subduction zones, electromagnetic profiles reveal high electrical-conductivity bodies. In hot areas (> 700°C), water released by dehydration of the slab induces melting of the mantle under volcanic arcs that can explain the observed high conductivities. In the cold (<700°C) melt-free fore-arc mantle wedge, fluid water migrates and causes serpentinisation detected as low seismic wave velocities in the mantle wedge. High conductivities in the serpentinized wedge may picture serpentinisation or instantaneous fluid flow depending on serpentine electrical conductivity. We measured the electrical conductivities of three natural serpentine samples from subduction zone context using complex impedance measurements, and find they have low electrical conductivities ($< 10^{-4}$ S. m^{-1}) similar to those of dry mantle minerals below 700°C. Because of the negligible conductivity of serpentine, electrical conductivity in the hydrated mantle wedge is only sensitive to the fluid content and salinity, not to serpentinisation. A small fraction (*ca*. 1% in volume) of connective high-salinity fluids accounts for the highest observed conductivities. The low-salinity fluids (≤ 0.1 *m*) released by slab dehydration evolve towards high-salinity (≥ 1 *m*) fluids during progressive serpentinisation of the mantle wedge. These fluids can mix with arc magmas at depths and account for high chlorine/water ratios in arc lavas.

Modelling vertical stable isotope and elemental distributions in the upper ocean

BEN C. REYNOLDS AND GREGORY F. DE SOUZA

ETH Zurich, Institute of Geochemistry and Petrology, Zurich, Switzerland (*correspondence: reynolds@erdw.ethz.ch)

The stable isotope compositions of elements dissolved in seawater are a valuable source of information on ocean biogeochemistry. Depth profiles of elemental ratios and isotope compositions often show large vertical gradients near the surface due to the uptake and fractionation by biota in the surface ocean. However, interpretations of observed distributions are often based on overly simplistic models of the fractionation behaviour, such as the Rayleigh equation [1], which ignore dynamic mixing in the oceans. The processes governing the spatial and chemical gradients do not fit the fundamental assumptions underlying Rayleigh-type behaviour. In order to more effectively describe the processes governing the depth profiles we argue that simple one-dimensional advection-diffusion-reaction (1-D ADR) models should be applied. These models incorporate the interaction between biogeochemical cycling and physical redistribution, and thus help to realise the true potential of stable isotopic tracers to quantify biogeochemical cycling.

Applications of our models to stable isotope variations in the upper ocean demonstrate that, within the thermocline, elemental concentration gradients and isotope distributions are strongly affected by physical mixing processes. The biological cycling, however, controls the composition of the surface mixed layer. Our models provide a combined physical-biological framework for the interpretation of novel metal stable isotope variations currently being determined. It is apparent from the models that estimations of the fractionation factors derived using the Rayleigh equation will systematically underestimate the true values; the degree of underestimation depending upon the relative importance of mixing. We show how our models can be applied to published datasets.

[1] Rayleigh (1902) On the distillation of binary mixtures. *Phil. Mag.* **4**, 521.

https://doi.org/10.1180/S0026461X00006502 Published online by Cambridge University Press

Assessment of water/rock interaction to safeguarding drinking water quality

M. REZVANIKHALILABAD

Mahabghodss, Integrated studies on water,soil and environment Division, Affilated to Ministry of Power, Tehran, IRAN, P.O. Box: 19395-6875 (mahnazrezvany@yahoo.com)

Water storage, transfer and deliver to end users for drinking and sanitary purposes have been a challenge over the years in IRAN. IWRM strategies were focused to ease the Scio-economical aspects of the water shortage that vulnerability of the resources and the Environmental flow simply was ignored. Geological characteristics of artificial lakes and their natural or manmade transfer routs, exclusively studied from geotechnical prospects. Water/Rock interaction of bed rocks or reservoir body was neglected.

Chamgardalan dam located in IYLAM province, which water/rock interaction made an odor and taste problem in reservoir water is the best example [1]. Reservoir rocks consist of interbeded coal layers highly rich in sulfur and iron changed the quality of the dam lake water over years. The costly remediation study is ongoing (2009 till now). Contamination changes the quality of the water as effective as intensive interaction of water with bed rocks. In small projects in local or regional scale considering such studies will be costly and developers may not include it in their action plans. National or international fundamental research should provide such information.

In the new approach a methodology established to consider the effect of geological formation on the quality of surface water in the basin scale. Faults, intrusives, salt domes & massive evaporation sediments, closed & operating mines, progressive alteration, and etc. were assessed. Defined guideline played a major role in IWRM study of Caspian and Uromieh lake basins in north of Iran which has been carried out in 2010 [2]. The result concluded in generating a 1:250000 scale geological map on potential effect of geological formations on surface water quality regarding the heavy metals & trace elements, salinity and sediment production. The integrated map will give a glimpse of possible potential which has to be assessed meticultly.

[1] Khajehzadeh (2011) '*Clean Water*' Work shop, Iran
[2] Chehrehnegar (2010) Iran water Resource management Conf. Proc.

The variation of magnetic susceptibility with grain size: Its implication on forensic studies

C. RIBEIRO, A. GUEDES*, B. VALENTIM, H. SANT'OVAIA, H. RIBEIRO AND F. NORONHA

Centro de Geologia da Universidade do Porto e Departamento de Geociências, Ambiente e Ordenamento do Território, Faculdade de Ciências, Universidade do Porto, Rua do Campo Alegre 687, Porto, Portugal (*correspondence: aguedes@fc.up.pt)

Detectable quantities of magnetic and paramagnetic minerals are almost always found in soils, being the magnetic susceptibility the sum of all contributions from the forming minerals, and varying due to concentration and composition those minerals. The magnetic susceptibility (MS) measurements of soils at room temperature are non-destructive. Additionally, does not require sample preparation, and can be used as a simple and fast method which may be operable in small samples. So, MS is an excellent tool for studies of soils being used as trace evidence in forensic investigations.

During this study, twenty four soil samples were collected on two different coastal sites from North Portugal, Mindelo and Cabedelo. At each site twelve samples were collected with a plastic spade from the surface soil. The samples were subjected to dry sieving using a column of sieves, resulting in different size classes: >2mm; [2mm-1mm]; [1mm-0.5mm]; [0.5mm-0.25mm]; [0.25mm-0.125mm]; [0.125mm-0.063mm] and <0.063mm. The MS analyses were performed directly on 1g of each size fraction after homogenisation, applying an external magnetic field of 300 A/m to the sample, and a Kappabridge, model KLY-4S of Agico balance equipped with the Sumean software used. The MS was calculated in m^3/kg. It was observed that in all samples the MS increases from coarse to fine grain size. The coarser fractions >2mm and [2mm-1mm] generally show negative values of MS and this is generally followed by low positive values of MS that increase ten times on the next fine fraction. These data show that fine fractions are the mostly enhanced in terms of MS. Finally, higher reproducibility was observed on the lower size fractions.

We conclude that although the magnetic susceptibility analysis is suitable to be used in a forensic soil investigation, it is important to adopt the same protocol during the analysis.

This research was supported by Project PTDC/CTE-GEX/67442/2006 of FCT (Portugal).

https://doi.org/10.1180/S0026461X00006502 Published online by Cambridge University Press

Phosphorus mobility in lake sediments

D.C. RIBEIRO, G. MARTINS, A.G. BRITO, AND R. NOGUEIRA

University of Minho, Campus de Gualtar, 4710-057 Braga, Portugal (dcribeiro@deb.uminho.pt)

For several decades, the paradigm that phosphorus release in sediments is the consequence of the absence of oxygen in the hypolimnium is recurrent among limnologists. At that time, the relation between the reduction of Fe (III) complexes and phosphorus (P) release in anoxic sediments was stated as hypothesis and later demonstrated. Although the theoretical statements matched the practical findings, these could not be generalized since several field observations and laboratory experiments lead to other conclusions. This has lead to a need of deeper understanding of factors that influence the phosphorus mobility besides oxygen concentration.

P mobility in lake sediments was assess through a microcosm experiment. Sediments from Lake Furnas (Portugal) were examined through a P sequential extraction procedure before and after a shift in redox potential achieved by means of O_2 concentration variation. Microsensors were used to measure pH and O_2 concentration in the sediments, during oxic and anoxic periods. The sediments that were under anoxic conditions released P from Fe minerals (BD fraction) compared with the initial conditions. The P bounded to Al minerals remained approximately the same comparing with the initial conditions (NaOH fraction), indicating the this fraction remains stable with redox potential changes. When the reactor was exposed to O_2, Fe minerals re-adsorbed P which is consistent with the classical paradigm. However, we found that Al minerals released P in the oxic phase of the experiment leading to a P concentration raise in water column. The reason was not due directly to O_2 concentration but to a raise in pH. A possible explanation is related with the recent findings that oxygen in the oxic layers could oxidize H_2S in deeper sediment layers trough a microbial network connected with nano-wires from H_2S in the deep anoxic sediment layer to oxygen in the upper layers, with concomitant pH raise.

Calcium minerals bounded to P remained stable between anoxic and oxic conditions (HCl fraction), as well as the refractory pool (NaOH 85 °C). P bounded to Al and Fe represent the most mobile fraction and is an indicator of exhaustion of sediments' retention capacity.

Zoned calc-silicated boudins in quartz-pelitic metatexitic rocks, NW Portugal

M.A. RIBEIRO*, M. AREIAS, A. DÓRIA AND P. FERREIRA

Centro Geologia, Faculdade de Ciências, Univ. Porto R. Campo Alegre, 4169-007 Porto, Portugal (*correspondence: maribeir@fc.up.pt)

In the coastal zone of NW Portugal, at north of Porto, a banded and sheared migmatitic structure outcrops, with a general NNW-SSE to NW-SE trend. This structure shows strong asymmetric interlayer folds with generally subvertical axes, plunging to SE. Metatexites are widely prevalent, over diatexite lithologies. These are leucocratic to mesocratic with no foliation or locally with an incipient one, with a very irregular orientation. The metatexite lithologies present a well defined foliation in the metapelitic or quartz-pelitic melanosome, trending N160°-N175°, 75°-90° NE, or N15°, 90°, but with considerable dispersion. The neosome occurs as irregular lenticules, elongated parallel to this foliation.

Calc-silicated rocks occur in small ovoid or ellipsoid bodies, always with internal zoning, more or less concentric: in the core, a zone of granoblastic texture with quartz +clinopyroxene+wollastonite+garnet+sphene+ plagioclase +/- biotite, surrounded by a zone of granoblastic texture of lower granularity with quartz+biotite+plagioclase+sphene+ garnet+/- clinopyroxene+amphibole. The outer zone (metatexites) is more irregular and presents heterogranular texture with variation in the % of biotite associated with quartz, muscovite and feldspar +/-sillimanite. The core zone of the ellipsoid bodies is relatively richer in CaO and Al_2O_3 while the intermediate zone is enriched in SiO_2 and Na_2O. The surrounding metatexites present higher content of K_2O and similar content of Na_2O, regarding the buffer zone.

The foliation of the metataxites is deflected around the calc-silicated ellipsoidal bodies of variable size (5 cm to 1 m), and its major axis elongation has general direction NNW-SSE, parallel to the foliation of the surrounding migmatites. These bodies represent 'resister' of palaeosome in the migmatites that have undergone metasomatism during the migmatisation and boudinage during the coeval shear deformation of the surrounding metaxites, trending NNW-SSE. The protolith of these calc-silicated rocks may be a Ca-rich quartz-pelitic metasedimentary rock. It is thought to correspond to a Ca-plagioclase-rich greywacke.

This work has been financially supported by POCI 2010 (FCT-Portugal, COMPETE/FEDER).

https://doi.org/10.1180/S0026461X00006502 Published online by Cambridge University Press

Conditions for uranium transport in unconformity-related U deposits

A. RICHARD[1]*, C. ROZSYPAL[1], J. MERCADIER[1], D.A. BANKS[2], M. CUNEY[1], M.C. BOIRON[1] AND M. CATHELINEAU[1]

[1]G2R, Nancy-Université, CNRS, BP 239, 54506 Vandoeuvre-lès-Nancy Cedex, France (*correspondence: antonin.richard@g2r.uhp-nancy.fr)
[2]School of Earth and Environment, University of Leeds, Woodhouse Lane, Leeds LS2 9JT, UK

Our knowledge of massive metal transfer within the Earth's crust is limited by the lack of direct analysis of deep fluids and experimental work. During the Mesoproterozoic Era (1.6-1.0 Gyr ago), giant uranium deposits were formed from large-scale circulation of uranium-bearing brines at the interface between sedimentary basins and their crystalline basements (unconformity-related uranium deposits) [1, 2].

However, the key processes leading the exceptionally high ore grades and tonnages of these deposits, especially the transport of uranium in the brines, remained poorly understood.

Here, we show that the uranium was transported under unexpectedly low pH conditions and at the highest concentrations recorded for crustal fluids so far.

By using laser ablation inductively coupled plasma mass spectrometry analysis of natural fluid inclusions we found that the uranium concentration varies over four orders of magnitudes in the ore-forming brines (from 10^{-6} up to 2.8×10^{-3} mol. l^{-1} U).

We combined these results with the first experimental determination of the solubility of U (VI) in H_2O-NaCl mixtures analogous to the ore-forming brines (up to 6 mol. l^{-1} NaCl) and we found that the pH (between 3 and 4 at 155°C) is the major control on U (VI) solubility in these conditions.

More generally, models for the formation of 'world-class' hydrothermal ore deposits imply either protracted fluid flow with relatively low metal concentration, or more discrete events characterised by exceptionally metal-rich fluids. Our results strongly suggest that the second hypothesis can be applied to the world's richest uranium deposits.

[1] Richard *et al*. (2010) *Terra Nova* **22**, 303–308. [2] Boiron *et al*. (2010) *Geofluids* **10**, 270–292.

Taking advantage of both U-Th and U-Pb disequilibrium methods for speleothem geochronology

D.A. RICHARDS[1]*, C.J.M. SMITH[1], P.L. SMART[1], A.R. FARRANT[2], R.R. PARRISH[3] AND D.C. FORD[3]

[1]Geographical Sciences & Bristol Isotope Group, Univ. Bristol, UK (*correspondence: david.richards@bristol.ac.uk)
[2]British Geological Survey, UK
[3]NERC Isotope Geosciences Laboratory, UK
[4]Geography and Earth Sciences, McMaster Univ. Canada

The success of speleothems as accurate chronological markers of landscape evolution and climate change is well acknowledged, but accuracy and precision become particularly limiting beyond 350 ka for a number of reasons beyond the theoretical, including interlaboratory comparison and common standard/half-life usage. We illustrate here plans to take advantage of high-precision U-Th methods in concert with U-Pb techniques [1-3], which have the added advantage of community-supported accuracy (via EARTHTIME), to date important material in the range 0.35 to 1 Ma.

We are currently optimising a combination of U-Th-Pb techniques that utilise solution and *in situ* methods with MC-ICP-MS at the BIG and NIGL to analyse a variety of secondary calcite deposits previously demonstrated to be beyond the age range of traditional methods. We focus on an unusually U-rich flowstone sample (>60 μg g^{-1} ^{238}U) from the Grotte Valerie system in the Mackenzie Mountains, NWT, Canada [4]. Ten high-resolution sub-samples were cut as wafers from the growth layers identified in original publication. Several sub-samples have a extremely high ^{230}Th/^{232}Th atomic ratio (> 3), which demonstrates that the Th isotope signal is dominated by the radiogenic component. We obtained an age and 2σ uncertainty of 120 ± 1.2 ka from the youngest phase of growth. U-Th ages for older sub-samples, between 8.5 and 30 mm above base are not finite, and are therefore > 500 ka. We present preliminary U-Pb ages and *in situ* LA U-Th-Pb and gamma mapping for this older material. The latter are also used to screen future sub-samples useful for a host of applications.

[1] Cliff *et al*. (2010) *Quat. Geochron* **5**, 452–258. [2] Polyak *et al*. (2008) *Science*, **319**, 1377–1380. [3] Woodhead *et al*. (2006) *Quat. Geochron*, **1**, 208–221. [4] Harmon *et al*. (1977) *Canadian J. Earth Sci* **14**, 2543–2552.

https://doi.org/10.1180/S0026461X00006502 Published online by Cambridge University Press

From the Lower Amazon to the Mekong: How floodplains modulate fluxes of carbon from land to the sea

JEFFREY E. RICHEY*, JOHN M. MELACK AND KIMBERLEY N. IRVINE

(*correspondence: jrichey@uw.edu)

The large rivers of the tropics account for a significant fraction of the flux of carbon to the oceans and of fluvial and lacustrine CO2 and CH4 to the atmosphere. Through dynamic hydrologic, geomorphological, and biogeochemical processes, their floodplains and deltas provide a significant modulation to the materials transported by the river. In the process, the template set by these surface processes produces strong chemical disequilibria at the interface between water and sediments, impacting reactions down through the sediment column. But the magnitude, and even the specific dynamics, of these processes is poorly known. The last sampling stations on major rivers are typically above the delta and channel regions of tidally-impacted lower rivers, precisely to avoid dealing with the complexities. Which means that not only are time-series of the fluxes and controls from upriver not well-known, what happens in the lower river is even more poorly characterized. Here we examine recent results from the lower Amazon River and its floodplain, in comparison to the lower Mekong and the Tonle Sap Great Lake. About 20% of the Amazon basin is seasonally inundated, with extensive floodplains along several thousand kilometers of the main channel. These aquatic environments are sites of high evasion rates of methane and carbon dioxide, up to ten times the riverine flux to the ocean, and equivalent to sequestration by the forest. Considerable spatial and seasonal differences in carbon dioxide concentrations and evasion occur in the large shallow lakes common in the lower floodplains, with floodplain and geomorphological processes attenuating the chemical signal at the 'traditional' measuring station of Obidos. In contrast, floodplains of the Mekong are constrained to the lower reaches, with fluxes impacted by the Tonle Sap great lake. Higher pH than the Amazon results in greater export of respired carbon as bicarbonate relative to pCO_2. Implications for boundary conditions for deltaic sediment chemistry will be discussed.

High-temperature kinetic isotope fractionation in silicate systems: Laboratory and natural examples

F.M. RICHTER

Geophysical Sciences, The University of Chicago, Chicago, IL 60637, USA (richter@geosci.uchicago.edu)

The talk will focus on kinetic processes (see Table below) in silicate systems that result in easily measured stable isotope fractionations. The table below provides selected references that will provide the interested reader with a good introduction to the present state of affairs.

Process	Isotopic systems	laboratory examples	natural examples
Evaporation	Mg,Fe,Si, O	[1], [2], [3], [4]	CAIs [5] spherules [6]
Chemical diffusion	Li,Ca,Mg, K	[7],[8], [9]	Vinal Cove, Maine [10]
Grain-boundary diffusion	Li		Tin Mtn.[11] Pegmatite
Thermal diffusion	Mg,Ca, Fe, Si, O	[12],[13]	

In those cases where there is both laboratory and natural examples, I will focus on the commonality of what has been found. Recent developments in better understanding kinetic isotope fractionations by molecular dynamics simulations [8] and transition state theory [14] will also be discussed.

[1] Davis *et al*. (1990) *Nature* **347**, 655–658. [4] Dauphas *et al*. (2004) *Anal. Chem*. **76**, 5855–5863. [3] Richter *et al*. (2007) *GCA* **71**, 5544–5564. [4] Knight *et al*. (2009) *GCA* **73**, 6390–6401. [5] Clayton *et al*. (1988) *Phil. Trans. Roy. Soc. London A* **325**, 483–501. [6] Taylor *et al*. (2005) *GCA* **69**, 2647–2662. [7] Richter *et al*. (2003) *GCA* **67**, 3905–3923. [8] Bourg *et al*. (2010) *GCA* **74** 2249–2256. [9] Watkins *et al*. (2011) *GCA in press*. [10] Chopra (2010) *PhD dissertation*, Univ. Chicago. [11] Teng *et al*. (2006) *EPSL* **243**, 701–710. [12] Richter *et al*. (2009) *GCA* **73**, 4250–4263. [13] Huang *et al*. (2010) *Nature* **464**, 396–400. [14] Dominguez *et al*. (2011) *Nature in press*.

https://doi.org/10.1180/S0026461X00006502 Published online by Cambridge University Press

Cytochromes and iron reduction

K. RICHTER AND J. GESCHER*

Department for Microbiology, University of Freiburg, Germany (*correspondence: johannes.gescher@biologie.uni-freiburg.de)

The key innovation that enables cells to respire on metals like ferric iron or manganese is the development of a respiratory chain to the cell surface. Most of the known bacterial ferric iron reducers are proteobacteria. These cells all have in common the canonical blueprint of a Gram-negative cell with cytoplasm, cytoplasmic membrane, periplasm and outer membrane as separated reaction compartments. We study the electron transport chain to the cell surface using *Shewanella oneidensis* MR-1 as a model organism. *C*-type cytochromes are the dominant electron transferring proteins in *Shewanella*. They establish a conductive connection to the cell surface and catalyze the final reduction step onto a metallic electron acceptor. Interestingly, *S. oneidensis* as well as other dissimilatory iron reducers produces a multitude of different cytochromes while growing under dissimilatory ferric iron reducing conditions. Our work aims at elucidating as to why expression of this high number of cytochromes might result in a selective advantage. We can show that periplasmic cytochromes build a dynamic electron-transferring network. We can furthermore show that these cytochromes can catalyze ferric iron reduction. Hence, so called outer membrane cytochromes that are localized to the cell surface simply allow for contact between respiratory electrons and the electron acceptor. Although these surface localized cytochromes are crucial for wild type cells to respire on ferric iron or manganese, we could surprisingly establish that they are not necessary. Two simple point mutations can enable a *Shewanella* mutant to find a way around this necessity for outer membrane cytochromes. We currently complete our studies concerning these point mutations but will already provide evidence for the possible functions of the genetic exchanges.

The relase of Hf isotopes during weathering

J. RICKLI, A.R. KEECH, C. ARCHER AND D. VANCE

Bristol Isotope Group, School of Earth Sciences, University of Bristol, Wills Memorial Building, Queen′s Road, Bristol, BS8 1RJ, UK (*correspondence: J.Rickli@bristol.ac.uk)

Studies of river and ocean waters suggest that Hf isotopes are released incongruently during weathering of the continental crust. The governing processes in soils are poorly understood because the release of Hf isotopes from soils during weathering has thus far hardly been explored. Such an understanding is crucial to the eventual use of Hf isotopes for the reconstruction of past weathering conditions. Here we explore Hf isotope behaviour in a soil chronosequence from Scotland, spanning an age-range of 0.1-13ka.

Bulk soil Hf isotopes digested in a pressure bomb span a relativley small range between εHf = -22.1 and -19.7. Hot plate digests, which exclude most Hf from zircons, are more radiogenic and also show a larger isotopic range (εHf = -20.1 to -16.0). The isotopic compositions of both digestion procedures are well correlated, which indicates that zircons attenuate the variabilty that is imparted by weathering of the zircon-free portion and seem largely inert on the time scales of the chronosequence. Although all soil profiles consistently show a depletion of radiogenic Hf in their upper horizons, documenting the removal of radiogenic Hf, the evolution of the soils with time is not very systematic. In particular the 10 ka profile is less radiogenic throughout, which is likely to indicate heterogenity in the parent material of the chronosequence.

Currently, it is diffult to asses the proportion of removed Hf from the soils and derive an estimate of the corresponding Hf isotopic composition released to the hydrosphere. Hf/Zr ratios in the bulk soils (bomb digestions) are relatively homogenous and a calculation of the depletion of Hf from these geochemical twins seems inappropriate. A correlation of Hf/Zr with Hf isotopes which would support such an approach is not observed.

In summary the data shows that Hf isotopes removed from soils is more radiogenic than the bulk. This preferential removal of radiogenic Hf mainly relates to the zircon free portion of the soil, in which weathering imparts a variablity of 4 εHf. These findings will be consolidated by establishing the Hf budget of the rocks (zircon free crustal Hf vs bulk Hf) and the measurement of Hf isotopes in the draining rivers.

https://doi.org/10.1180/S0026461X00006502 Published online by Cambridge University Press

Oxygen and silicon partitioning between molten iron and silicate melts up to 70 GPa and 4000 K

A. RICOLLEAU[1]*, J. BADRO[1], J. SIEBERT[1,2], D. ANTONANGELI[1,2], M. CANTONI[3], C. HEBERT[3], D.T.L. ALEXANDER[3] AND P. GILLET[3]

[1]Institut de Physique du Globe de Paris, France (*correspondence: ricolleau@ipgp.fr)
[2]Institut de Minéralogie et de Physique des Milieux Condensés, Paris, France
[3]École Polytechnique Fédérale de Lausanne, Switzerland

The Earth's core is mainly composed of a Fe-Ni alloy. The core density compared to that of pure iron highlights a deficit that calls for the presence of light elements in addition to Fe and Ni to be explained. Si and O are among the likely candidates. Core formation is speculated to occur in a deep magma ocean in which the molten metal equilibrates with the silicate melt. The depth of this magma ocean, constrained by siderophile element partitioning, appears larger than previously thought. Thus, the experimental studies carried so far that have focused on Si and O partitioning between molten metal and silicates only up to 25 GPa, or at higher pressure, between metal and (Mg, Fe)O to interpret the behavior of oxygen in iron melts, have to be extrapolate to be relevant for the conditions of Earth's core formation.

In this study, we investigated directly the partitioning of oxygen and silicon between molten iron and silicate melts from 40 to 70 GPa using the laser-heated diamond anvil cell. We loaded the DAC with samples of olivine surrounding pure iron metal. Three olivine compositions, from 0 to 8 wt% FeO, were loaded with iron at 50 GPa to study the effect of oxygen fugacity on partitioning. Recovered samples were milled with the Focused Ion Beam technique and analyzed with electron microprobe and Transmission Electron Microscopes to obtain compositions of quench metal and silicate. The partition coefficients of oxygen and silicon between metal and silicate were determined as a function of pressure and oxygen fugacity. Quenched analyzed samples clearly show an oxidation of the silicate during the experiments. We report large amounts of oxygen (6-12 wt%) and silicon (2-10 wt%) in the metal at fO_2 around IW-1. The obtained results are used with literature lower-pressure data to thermodynamically parameterize the partitioning of oxygen and silicon. Oxygen and silicon solubility trends at high pressure are different than what expected on the basis of the extrapolation of lower pressure data.

A comparison of the reactivity at the solid-solution interface of nano- and micro-crystalline TiO_2 phases

MOIRA K. RIDLEY[1]*, MICHAEL L. MACHESKY[2] AND JAMES D. KUBICKI[3]

[1]Texas Tech University, Lubbock, TX 79409, USA (*correspondence: moira.ridley@ttu.edu)
[2]Illinois State Water Survey, Champaign, IL 61821, USA (machesky@illinois.edu)
[3]The Pennsylvania State University, University Park, PA 16802, USA (jdk7@psu.edu)

The acid–base surface reactivity of rutile (α-TiO_2), with the (110) crystal face predominant, has been studied extensively. Specifically, theoretical simulations, X-ray techniques and potentiometric titration studies have provided molecular-scale and macroscopic details on the ion adsorption behaviour of rutile. Results of the collective studies have been integrated into the multisite complexation (MUSIC) model. Similar detailed studies examining the surface charging properties of nano-crystalline anatase samples are now being conducted.

Primary surface charging curves of rutile in LiCl, NaCl, KCl, and RbCl electrolyte media are compared with similar titration data for nanoparticle anatase samples. The effect of electrolyte media and ionic strength on the primary charging behaviour of anatase was studied as a function of nanoparticle size (3–40 nm diameter). The primary charging curves of rutile and all nano-anatase samples are generally analogous, when normalized to their respective pH_{znpc} values. At low ionic strength (0.03 m) the development of negative surface charge was similar for all electrolyte cations. However, with increasing ionic strength negative surface charge development was enhanced as the bare crystallographic radii of the cations decreased. Subtle differences in the macroscopic charging behaviour of the 3 nm diameter anatase sample were noted, particularly below the pH_{znpc} value were Cl^- counterions screen the surface from bulk solution.

For rutile, X-ray data and MD simulations show that electrolyte cations are adsorbed as inner-sphere complexes, principally in tetradentate geometry. Similarly, DFT-MD simulations show inner-sphere sorption of monovalent cations onto anatase; however, bidentate sorption predominates. For both anatase and rutile, a CD-MUSIC model, coupled with a Basic Stern layer description of the electric double (EDL), successfully integrates all microscopic information with the macroscopic experimental results. Though for the smallest anatase particles, it is necessary to account for some curvature of the EDL.

https://doi.org/10.1180/S0026461X00006502 Published online by Cambridge University Press

Supply-limited and kinetic-limited chemical erosion

CLIFFORD S. RIEBE[1]*, KEN L. FERRIER[2], W. JESSE HAHM[1] AND JAMES W. KIRCHNER[3,4]

[1]Dept. Geology & Geophysics, U. Wyoming, WY, USA (*correspondence: criebe@uwyo.edu)
[2]Dept. Earth Atmospheric & Planetary Sciences, MIT, USA
[3]Dept. Earth & Planetary Science, U. Calif., Berkeley, USA
[4]Swiss Federal Institute for Forest, Snow, & Landscape Research (WSL), CH

Downslope transport of hillslope sediment is often usefully cast in terms of two end-members of a spectrum of erosional regimes. At one end of the spectrum, 'transport-limited' physical erosion develops when downward propagation of weathering outpaces erosional losses from a slope, such that the removal of material is limited only by the sediment transport rate [1]. At the other end of the spectrum, 'weathering-limited' erosion develops when sediment transport matches the rate at which physically competent material loses its structural integrity, such that erosional removal of material is limited by how fast it breaks down by weathering [1]. As originally defined, the concepts of transport-limited and weathering-limited erosion only strictly apply to physical fluxes, yet they are commonly misappropriated in discussions of chemical fluxes. We suggest the interpretive framework for hillslope processes needs to be clarified and expanded for studies of chemical fluxes. Here we define and discuss two end-members in a spectrum of possible chemical erosion regimes. On one end, 'supply-limited' chemical erosion develops when physical erosion rates are slow enough (or regolith residence times are long enough) that further chemical erosion of regolith is not possible due to exhaustive depletion of reactive phases [2, 3]. On the other end, 'kinetic-limited' chemical erosion develops when physical erosion is so fast that chemical erosion can only partially deplete regolith of its weatherable phases before they are removed from slopes [3]. Using published data from field and modeling studies, we show how supply-limited and kinetic-limited chemical erosion can be distinguished from one another based on differences in relationships between chemical erosion rates and mineral supply rates—two variables that can be measured in mountainous landscapes using cosmogenic nuclides.

[1] Carson & Kirkby (1972) *Hillslope Form & Process*. [2] Riebe *et al*. (2004) *Earth Planet. Sci. Lett*. **224**, 547–562. [3] West *et al*. (2005) *Earth Planet. Sci. Lett*. **235**, 211–228.

Inferring process from provenance using apatite (U-Th)/He ages of coarse sediment in mountain streams

CLIFFORD S. RIEBE[1]*, CLAIRE E. LUKENS[1], LEONARD S. SKLAR[2], JONATHAN D. BEYELER[2] AND DAVID L. SHUSTER[3]

[1]Dept. Geology & Geophysics, U. Wyoming, WY, USA (*correspondence: criebe@uwyo.edu)
[2]Dept. Geosciences, San Francisco State Univ., CA, USA
[3]Berkeley Geochronology Center, CA, USA

The lithology and size distribution of sediment in a streambed reflects a jumble of integrated processes, from the breakdown of bedrock on slopes to selective transport and comminution as particles bash together in transit downstream. If this jumble could somehow be disentangled, it would reveal much about how physical and chemical processes shape landscapes. Here we show how processes of sediment production, transport, and breakdown can be resolved in new quantitiative light using a novel methodological adaptation of existing sediment tracing techniques. If apatite-helium (AHe) cooling ages in bedrock increase with elevation, the distribution of AHe ages in stream sediment reveals the distribution of elevations of sediment source areas [e.g. 1]. To the extent that differences in source elevations reflect differences in geomorphic processes [1, 2], AHe ages in sediment can provide a powerful indicator of the dominant modes of landscape change in a watershed [1, 3]. However, previous AHe tracer studies have focused solely on sand, which represents a small fraction of bed sediment in steep mountain streams where the technique has been applied. Hence, insight on the production and delivery of sediment from hillslopes remains incomplete. Moreover, source elevations of sand reveal little about the movement and downstream fining of coarse sediment in channel networks. Here we show how a much fuller understanding of weathering, erosion, and sediment transport can be obtained by quantifying AHe ages in all grain size classes, including sand, gravel, cobbles, and boulders. What controls the grain size distribution of sediment supplied to channels? Where do boulders come from? How long do they persist in mountain streams? How important is particle comminution in the downstream evolution of grain size distributions? We show that answers to such fundamental questions about surface processes are within closer reach through AHe tracing of coarse sediment.

[1] Stock *et al*. (2006) *Geology* **34**, 725–728. [2] Tranel *et al*. (2011) *Bas. Res*. **23**. [3] McPhillips & Brandon (2010) *Earth Planet. Sci. Lett*. **296**, 373–383.

https://doi.org/10.1180/S0026461X00006502 Published online by Cambridge University Press

A HPSEC-ICP-MS study on the affinity of trace elements (Fe, Cu, I) to dissolved organic matter in natural water samples

T. RIEDEL AND H. BIESTER

Institut für Umweltgeologie, Technische Universität Braunschweig, Germany (thomas.riedel@tu-bs.de)

The speciation of trace elements in natural waters strongly influences their mobility and geochemical behavior in the environment. Especially, the presence of dissolved organic matter (DOM) in soil and peat runoff may favor complexation of certain metals, thereby increasing the solubility. Earlier studies were focused on the concept of metal binding to organic molecules which were thought to be of considerable size (some ten to hundred thousand Da in molecular weight). The existence of large organic substances, however, has recently been challenged. It was proposed, on the basis of several different studies, that DOM may consist of much smaller molecules, probably in the size fraction of only a few hundred to thousand Da. This raises the question if these smaller fractions can be separated by analytical techniques thereby enabling a study of the metal-binding capacity of 'small' DOM.

To resolve this question we used inductively coupled plasma mass spectrometry hyphenated with gel filtration liquid chromatography. The size exclusion column used was selected to efficiently separate substances with relatively low ionic radii thus resolving predominantly smaller fractions of DOM. Samples were river waters taken from remotes sites in Patagonia, Chile as well as from the Harz mountain region, Northern Germany. All samples were filtered with 0.45 μm. Samples were initially measured in their original composition. The influence of pH was studied via the addition of nitric acid.

We found remarkable differences between the investigated metals with up to four different peaks in the chromatograms suggesting that a number of colloids/complexes of different size exist which can be separated. While some elements occurred exclusively in one or two fractions (Fe) others occur in all fractions (I, Cu) suggesting a rather non-specific binding. The addition of protons yielded the expected shift from larger to smaller fractions, possibly because metals desorb from the binding sites on the DOM or colloids/particles dissolve.

Further investigations aim to exploit the characteristic size distributions observed to create fingerprints of natural waters that help to understand the environmental distribution and cycling of these trace metals.

Microbially mediated iron reduction in the methanic zone of sediments from the Western Argentine Basin

N. RIEDINGER[1]*, M.J. FORMOLO[2], S. HENKEL[3], B.K. REESE[4], H.J. MILLS[4], A. VOSSMEYER[5], G.L. ARNOLD[6], J. SAWICKA[6], J. TOMASINI[7], G.D. LOVE[1], T.W. LYONS[1] AND S. KASTEN[3]

[1]Dept. of Earth Sciences, Univ. of California, Riverside, CA 92521 USA (*correspondence: natascha.riedinger@ucr.edu)
[2]Dept. of Geosciences, The Univ. of Tulsa, OK 74104 USA
[3]Alfred Wegener Instit. for Polar and Marine Research, 27570 Bremerhaven, Germany
[4]Dept. of Oceanography, Texas A&M Univ., College Station TX 77843 USA
[5]Dept. of Marine Sciences, Univ. of Georgia GA 30602 USA
[6]Max Planck Instit. for Marine Microbiology, 28359 Bremen, Germany
[7]ANCAP, Montevideo, 11100, Uruguay

Variable depositional conditions in marine sediments can have a strong impact on the associated biogeochemical cycles. In areas with high sedimentation rates, including mass transport-related deposition, (highly-) reactive mineral phases can be buried rapidly. This situation leads to the availability of reactive compounds for microorganisms in deep-subsurface anoxic environments. To unravel the influence of dynamic depositional conditions on biogeochemical processes in rapidly deposited sediments we applied inorganic and organic geochemical analyses and microbiological methods on marine sediments from the western Argentine Basin collected during the RV Meteor Expedition M78/3 (May-July) 2009. Our results show that the sediments are characterized by high concentrations of highly reactive iron phases accompanied by low amounts of organic carbon throughout the sediment column. Pore water accumulations of hydrogen sulfide are restricted to a small interval at the sulfate-methane transition zone. Below this zone, methane concentrations increase strongly with depth in association with appreciable availability of highly reactive Fe (III) phases. Elevated iron concentrations in the pore water in the same depth interval indicate ongoing iron reduction. Based on preliminary results we suggest that contributions from organo-clastic Fe reduction in these sulfide-depleted sediments can be neglected. Instead, because of the abundance of methane and reactive ferric Fe in the absence of sulfide, we propose that reduction of biologically available Fe phases in the methanic zone is coupled to methanogens via hydrogen or to anaerobic oxidation of methane.

https://doi.org/10.1180/S0026461X00006502 Published online by Cambridge University Press

Short-lived nuclides of the U and Th-series probing recent pedogenic processes in soils

S. RIHS[1]*, J. PRUNIER[1,2], B. THIEN[1,3], D. LEMARCHAND[1], M.C. PIERRET[1] AND F. CHABAUX[1]

[1]LHyGeS/UdS, 1 rue Blessig, 67084 Strasbourg cedex, France (*correspondence: rihs@unistra.fr)

[2]Present address: LMTG/ Université Paul Sabatier, 14 avenue Edouard Belin 31400 Toulouse, France

[3]Present address: Paul Scherrer Institut, CH-5232 Villigen PSI, Switzerland

The recent chemical dynamic occurring in a podzolic forest soil section (from the Strengbach watershed, France) was investigated using U and Th-series nuclides, including short-lived nuclides. Analyses of (^{230}Th), (^{226}Ra), (^{232}Th), (^{228}Ra) and (^{228}Th) activities in the soil particles, the seepage waters, the roots and the mature leaves of the beeches growing on this soil were performed by mass spectrometry (TIMS) or gamma spectrometry. Moreover, the exchangeable fraction was extracted from the soil particle and analysed. The simultaneous analysis of the different soil (*sl*) compartments allows to demonstrate that the overall Ra and Th transfer scheme is fully consistent with the acido-complexolysis weathering mechanism prevailing in podzols. Using a continuous open-system leaching model, the coupled (^{226}Ra/^{230}Th) and (^{228}Ra/^{232}Th) disequilibria measured in the different soil layers permit to date the contemporary processes such as recent (< 18 years) change in organic-colloids migration occurring in the shallow soil horizons. The Monte Carlo simulation approach used to resolve this system shows that a semi-infinite range of Th-isotopes leaching rates can explain the observed data, but minimum values can be inferred, leading to an upper limit age for the beginning of the perturbation. The model predicts distinct leaching rates of Th isotopes, in excellent agreement with the apparent preferential ^{230}Th over ^{232}Th leaching recorded in seepage water. The lower soil horizons are also affected by such Th mobilization, though lasting over several centuries at least, with a much smaller leaching rate.

Ra and Th isotopic ratios also appear to be valuable tracers of some mineral-water-plant interactions occurring in a soil. The (^{228}Ra/^{226}Ra) ratio discriminate the Ra flux originating from leaves degradation and from mineral weathering in the shallow -10cm seepage soil waters. This ratio, combined to the ^{232}Th-^{228}Ra-^{228}Th radioactive disequilibria measured in the different soil compartments allows to constaint the shallow bio-geochemical cycle of Ra, including residence time in vegetation cycling and scavenging in the soil exchangeable fraction.

Intrabasaltic paleosols from the North Atlantic Igneous Province record late Paleocene global climate trends and hyperthermals

M.S. RIISHUUS[1]* AND D.K. BIRD[2]

[1]Nordic Volcanological Center, Institute of Earth Sciences, University of Iceland, IS-101 Reykjavik, Iceland (*correspondence: riishuus@hi.is)

[2]Department of Geological and Environmental Sciences, Stanford University, Stanford, California 94305, USA (dbird@stanford.edu)

Weathering of basaltic tephra and lava produces clays preserved in intrabasaltic paleosols. We propose that hydrogen isotopes of smectite clays formed by weathering of intraflow tephras (redbeds) of the North Atlantic Igneous Province preserve isotopic records of past global climate. In support we present smectite δD compositions of 70 tephras from West (~61.5-60.0 Ma) and East (~56.5-55.0 Ma) Greenland (64-66°N paleolatitude) for comparative analysis with global paleoclimate trends and aberrations recorded in higher-resolution marine records.

The observed smectite δD compositions range from -145 to -104 ‰. In the East Greenland section smectite δD varies around -130 to -120 ‰ at ~56 Ma prior to an abrupt increase to a maximum of -104 ‰ before returning gradually to -117 ‰ at ~55 Ma. This trend corresponds inversely to the δ^{18}O deep-sea foraminifera record depicting a warming trend from mid-Paleocene (~59 Ma) towards the Early Eocene Climatic Optimum (~52 Ma) superimposed with the Paleocene-Eocene Thermal Maximum (~55.5 Ma). The ~5 m. y. older West Greenland tephras display an initial abrupt increase in smectite δD from around -135 to -130 ‰ up to ~-120 ‰, followed by a more gradual decrease to ~-140 ‰. The more depleted δD compositions reported from West Greenland relative to East Greenland are in agreement with the cooler global conditions that prevailed in the earliest Paleocene (65-58 Ma). While the general decrease to ~-140 ‰ correlates with global cooling towards 59 Ma, we suggest that the initial increase in smectite δD from West Greenland could be recording a similar, but weaker, hyperthermal as the PETM.

We speculate that both the East and West Greenland continental flood basalt volcanism had an indirect short-lived warming effect through release of methane from organic-rich sediments by contact metamorphism from overflowing lavas and sill intrusions, as well as a direct longer-lasting cooling effect through degassing of SO_2.

https://doi.org/10.1180/S0026461X00006502 Published online by Cambridge University Press

Dissolved Fe in the Western Atlantic Ocean: Distribution, sources, sinks and cycling

M.J.A. RIJKENBERG [1]*, L.J.A. GERRINGA, [1], P. LAAN [1], V. SCHOEMANN [1], R. MIDDAG [1], S.M.A.C. VAN HEUVEN [2], L. SALT [1], H.M. VAN AKEN [1], J.T.M. DE JONG [1] AND H.J.W. DE BAAR [1,2]

[1]Royal Netherlands Institute for Sea Research, PO Box 59, 1790 AB Den Burg, The Netherlands (*correspondence: Micha.Rijkenberg@nioz.nl)
[2]University of Groningen, PO Box 11103, 9700 CC Groningen, The Netherlands

Iron (Fe) plays a key role in the regulation of primary production and dinitrogen fixation in large parts of the world oceans. Because there is an increasing urgency to understand the role of the oceans in global climate, it is paramount that we understand the biogeochemical cycle of bio-essential elements such as Fe. Despite this recognized importance there is still limited knowledge of the sources, sinks, chemistry and internal cycling of Fe. To fill this gap in our knowledge, the distribution and organic speciation of dissolved Fe (DFe) have been measured during three Dutch GEOTRACES cruises. Together, these cruises form a comprehensive, high resolution, full-depth section through the western Atlantic Ocean from Iceland to 58°S. In this presentation we will evaluate the distribution of DFe and its speciation using many other parameters such as dissolved inorganic carbon, total alkalinity, pH, dissolved oxygen, fluorescence, the macronutrients phosphate, nitrate and silicate and trace elements like dissolved aluminum (DAl) and dissolved manganese (DMn), to understand the processes that determine the distribution of DFe.

The influence of CO_2 on phase relations at Mount St. Helens

J.M. RIKER[1], J. BLUNDY[1], C.J.G. VAN HOEK[2] AND S.R. VAN DER LAAN[2]

[1]School of Earth Sciences, University of Bristol, Bristol, BS8 1RJ, UK (*correspondence: jenny.riker@bristol.ac.uk)
[2]Ceramics Research Centre, TATA Steel RD&T, P.O. Box 10000, 1970 CA, Ijmuiden, The Netherlands

Volatile components play a fundamental role in the ascent and eruption of silicic arc magmas. Although the effect of water on phase relations in these systems is well-studied, CO_2 is also present and may at times be abundant, for example, during instances of gas fluxing. Recent work on melt inclusions from Mount St. Helens suggests CO_2 may exert a strong influence on both depths of vapor saturation and shallow crystallization [1].

To this end, we have performed a series of experiments at shallow crustal pressures in rapid-quench cold seal pressure vessels. Experiments were designed to simulate equilibrium crystallization at depths between the magma chamber and the surface. Run temperatures (880 °C), pressures (<3 kbars), and fugacties (NNO+1) are constrained by natural erupted products, while fluid compositions vary from pure H_2O to XCO_2 = 0.5. This work builds on previous experimental studies of phase equilibria at Mount St. Helens [e.g. 2, 3].

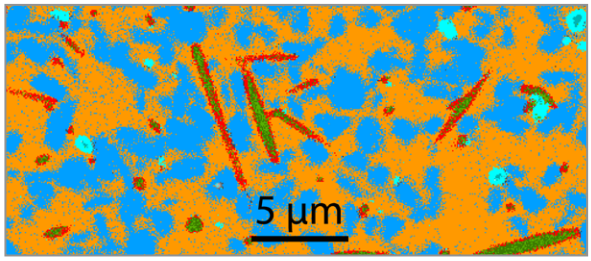

Figure 1: Phase map produced by PARC (880 °C, 500 bars).

High-resolution spectral maps allowed for detailed characterization of run products. Maps were acquired on a Field Emission Gun SEM and processed using a novel software program for automated **Ph**ase **R**ecognition and **C**haracterization (PARC) [Fig. 1]. PARC enabled rapid identification of sub-micron crystals and compositional analysis of all phases by quantitative EDS. Our results shed light on the conditions of crystallization and melt inclusion formation at Mount St. Helens, with implications for the volatile budgets of arc magmas.

[1] Blundy *et al*. (2010) *EPSL* **290**, 289–301. [2] Rutherford *et al*. (1985) *JGR* **90**, 2929–2947. [3] Gardner *et al*. (1995) *BV* **57**, 1–17.

https://doi.org/10.1180/S0026461X00006502 Published online by Cambridge University Press

Contribution of the reactive mineral surface area on CO_2 mineralization under natural conditions

JEAN RILLARD[1,2] AND PIERPAOLO ZUDDAS[1]

[1]Earth Sciences Department, University of Lyon1 (jean.rillard@etu.univ-lyon1.fr)
[2]INERIS, French National Institute for industrial Environment and RISk- FRANCE

A natural hydrothermal field is considered to be a useful analogue of carbon dioxide mineralization because it integrates the long-term interaction signal. The hydrothermal field of Galicia is characterized fluids resulting from a granit reservoir with pCO_2 from 103 to 105 Pa and pH from 10 to 6. Fluids are characterized by an increase of major elements correlated to pCO_2. We evaluated the effect of deep CO_2 perturbation We evaluated the effects of deep CO_2 perturbation on the fluid-rock interaction system. Mineral reactivity which produces changes in the fluid mineral composition is mainly dependent on the 'real' reactive surface area.

The mineral surface area participating in reactions resulting from this pCO_2 gradient was estimated by an inverse model approach. Input data was based on the chemical composition of the fluids we sampled. The rate of mineral dissolution was estimated by the observed pH and equilibrium conditions.

Moreover, the major elemental concentrations allowed us to quantify the variation of the reactive surface area of minerals involved with the overall water-rock interaction.

The irreversible mass transfer process, ruled by the continuum equilibrium condition, was defined by the overall degree of reaction advancement, using a set of polynomial equations solved independently of time scale.We found that reactive surface area of calcite, albite and K-feldspar increases by 2 orders of magnitude over the entire CO_2 fluid-rock interaction process, while the reactive surface area of biotite increases by 4 orders of magnitude. This shows that fluid neutralisation and consequent CO_2 mineralization under the form of carbonate species is greatly dependent on the behaviour of the reactive surface area of the mineral association in this geological context. We propose that biotite plays a basic role on the pH stabilisation and redox control of environmental perturbation and CO_2 mineralization.

Origin and evolution of ferromanganese crusts from South Altantic

M. RIMSKAYA-KORSAKOVA, I. VVEDENSKAYA AND A. DUBININ

P.P. Shirshov Institute of Oceanology RAS, Moscow, Russia (korsakova@ocean.ru)

Ferromanganese crusts are important tools in palaeooceanography for seawater microelement composition reconstruction and palaeocurrents identification. In this study the trace element content of crusts collected in South Atlantic at Mid Atlantic Ridge (st.2176), Angola Basin (st.2179) and Cape Basin (st.2188 and seamount st.2193) was determined.

We perform the layer-specific chemical analysis to estimate hydrogenous and hydrothermal contribution into crust formation. All crusts surfaces are dominantly hydrogenous that is proved with their chemical composition, namely trace elements enrichment and high positive Ce anomaly. Sample 2176 enriched with iron (up to 27%) and Mn/Fe ratio across the whole crust is about 0.4. We found high Co (up to 0.24%), Cu (0.1%) and As (0.04%) concentrations. Content of typical hydrogenous elements decreases from surface into deep crust layers reflecting changes in origin of matter.

The surface of sample 2179 (Angola Basin) abnormally enriched with Co (0.92%), Th (89 ppm) and Ce (0.29%). The REE composition of the crust upper layers exhibit high Ce anomaly (3.8-5.4) manifesting their hydrogenous signature, in contrast to lower layers with Ce anomaly value about 1.3. The lower layers are also depleted with other trivalent REEs and Y, and enriched with chalcophile elements like Zn and Cu, that indicates the hydrothermal origin of Fe oxyhydroxides.

The crust sample 2193 comes up to 20 kg in weight and characterized with dense texture without visible layers. Preliminary results show the sample enrichment with trace elements (Co – 0.82%, Ni – 0.33%, Pb – 0.22%, Ce – 0.20%, W – up to 170 ppm, Bi – 52 ppm, Th – 47 ppm) and Mn in contrast to other samples. The surface of crust probably undergo the dissolution due to strong near bottom currents flow.

The obtained data reveal a complex history of crusts formation, which origin often associated with submarine weathering (halmyrolysis), hydrothermal transportation reflected in chalcophile elements Cu and Zn concentrations. Subsequent crusts growth supplied with hydrogenous accumulation of matter from seawater.

https://doi.org/10.1180/S0026461X00006502 Published online by Cambridge University Press

Marine aerosol oxalic acid from in-cloud oxidation of glyoxal

MATTEO RINALDI[1]*, STEFANO DECESARI[1], SANDRO FUZZI[1], DARIUS CEBURNIS[2], COLIN D. O'DOWD[2], JEAN SCIARE[3], JOHN P. BURROWS[4], BARBARA ERVENS[5,6] AND MARIA CRISTINA FACCHINI[1]

[1]Institute of Atmospheric Sciences and Climate, National Research Council, Bologna, Italy (*correspondence: m.rinaldi@isac.cnr.it)
[2]School of Experimental Physics & Environmental Change Institute, National University of Ireland Galway, Ireland
[3]Laboratoire des Sciences du Climat et de l'Environnement, CNRS-CEA-IPSL, Gif-sur-Yvette, France
[4]Institute of Environmental Physics and Remote Sensing, University of Bremen, Germany
[5]Cooperative Institute for Research in Environmental Sciences, University of Colorado, Boulder, CO, USA
[6]Chemical Sciences Division, Earth System Research Laboratory, NOAA, Boulder, CO, USA

Oxalate was detected in 'clean sector' marine aerosol samples at Mace Head (53°20′N, 9°54′W) and Amsterdam Island (37°48′S, 77°34′E) in concentrations ranging from few ng m^{-3} to tens of ng m^{-3}. Measurements went on in 2006 at Mace Head and from 2003 to 2007 at Amsterdam Island. The oxalate concentration in marine aerosol showed a clear seasonal trend at both sites, with maxima in spring-summer and minima in fall-winter, as other marine biogenic aerosol components (e.g. methanesulfonic acid, non-sea-salt-sulfate and aliphatic amines). These results suggest the existence of a natural source of oxalic acid over the oceans.

Observed oxalate was distributed along the whole aerosol size spectrum, with both a sub and a supermicrometer mode, suggesting the co-exhistence of different formation routes over remote oceanic regions.

Several formation processes can explain the presence of oxalate in marine aerosol. Here, it is proposed that the cloud mediated oxidation of gaseous glyoxal, recently detected over remote oceanic regions in concentrations of the order of 100 ppt, may be an important source of submicrometer oxalate in the marine boundary layer. Supporting this hypothesis, satellite retrieved glyoxal column concentrations over the two sampling sites exhibited the same seasonal concentration trend of marine aerosol oxalate. Furthermore, chemical box model simulations showed that the observed submicrometer oxalate concentrations were consistent with the in-cloud oxidation of typical marine air glyoxal mixing ratios, as retrieved by satellite measurements, at both sites.

Monoterpene emission dynamics from Arctic to Tropics

JANNE RINNE[1], ALMUT ARNETH[2], JÖRG-PETER SCHNITZLER[3] AND ALEX GUENTHER[4]

[1]University of Helsinki, POB 48, 00014 U. Helsinki, Finland (*correspondence: janne.rinne@helsinki.fi)
[2]Lund University, Soelvegatan 12, 22362 Lund, Sweden (almut.arneth@nateko.lu.se)
[3]Helmholz Zentrum Münich, Ingolstädter Landstr. 1, 85764 Neuherberg, Germany (jp.schnitzler@helmholtz-muenchen.de)
[4]National Center for Atmospheric Research, POB 3000, Boulder CO 80307, USA (guenther@ucar.edu)

Monoterpene emissions, while globally much smaller than isoprene emissions, can dominate emissions from certain regions and ecosystems [1]. As larger molecules, they are also much more likely to take part in secondary aerosol formation than isoprene.

The traditional monoterpene emission algorithm by Guenther *et al*. [2] was based on an assumption that the monoterpene emission can be described as evaporation from large storage pools. This leads to temperature dependent emission algorithm. However, quite soon it became obvious that monoterpene emission from certain plants and ecosystems showed more or less light dependent behavior [3, 4]. This was taken as indication that a part of the emission originates directly from synthesis. The ^{13}C labeling experiments, in which rapid labeling of a part of monoterpenes is observed, further confirm the linkages between photosynthesis and part of the monoterpene emission [4, 5]. The importance of large storage reservoirs as important source of emission from many coniferous species is indicated by large unlabeled fraction of monoterpene emission from these plants [5]. Thus one can describe the emission using a scheme of parallel emission pathways.

By combining data on monoterpene emissions, content in plant tissue, and labeling patterns reported in literature we can generalize the emission dynamics within plant functional types. This will yield a more comprehensive picture on monoterpene emission dynamics from ecosystems ranging from Arctic to Tropics.

[1] Guenther *et al*. (1995) *J. Geophys. Res.* **100**, 8873–8892.
[2] Guenther *et al*. (1991) *J. Geophys. Res.* **96**, 10799–10808.
[3] Staudt & Seufert (1995) *Naturwissenschafen* **82**, 89–92.
[4] Shao *et al*. (2001) *J. Geophys. Res.* **106**, 20483–20491.
[5] Ghirardo *et al*. (2010) *Plant Cell Environ*. **33**, 781–792.

https://doi.org/10.1180/S0026461X00006502 Published online by Cambridge University Press

Characterization and identification of minerals in rocks by ToF-SIMS and principal component analysis

S. RINNEN[1]*, C. STROTH[1], A. RISSE[2], C. OSTERTAG-HENNING[2] AND H.F. ARLINGHAUS[1]

[1]Physikalisches Institut, University of Muenster, 48149 Muenster, Germany (*correspondence: stefan.rinnen@wwu.de)

[2]Bundesanstalt fuer Geowissenschaften und Rohstoffe, 30655 Hannover, German (Christian.Ostertag-Henning@bgr.de)

For a variety of geoscientific topics a technique which unambiguously identifies minerals in rock samples would be very advantegous. In addition to optical methods, chemical mapping on the element level with different techniques has gained importance during recent years. For investigating gas-fluid-rock reactions it is important to be able to detect small secondary minerals and mineral alterations formed during the reactions – in combination with a high spatial resolution this could be achieved by mapping the incorporation of isotope labels. Therefore, a method using time-of-flight-secondary mass spectrometry (ToF-SIMS) is being developed that aims at identifying minerals and mineral alterations.

ToF-SIMS has the advantage that the entire mass spectrum is recorded quasi-simultaneously, so that a great number of elemental and molecular ion signals can be used to characterize the minerals. Here, the statistical method of principal component analysis (PCA) is a powerful tool for identifying the ion signals with great differentiation potential between individual minerals. We have used ToF-SIMS and PCA to analyze various rock-forming minerals. A spectral library was produced for all minerals investigated. For this, positive and negative ToF-SIMS spectra were taken from polished grains of rock-forming minerals (silicates, carbonates, sulfates, oxides, etc.). Signals from elemental and molecular ions that allocate to at least one of the minerals were used for the PCA analysis.

Afterwards, we used ToF-SIMS to image areas of rock samples containing unknown minerals. Spectra from individual zones were extracted and used to identify these minerals either by comparing them with the spectral library or by PCA analysis. The data clearly show that the high lateral resolution achievable with ToF-SIMS is very advantageous for the detection and identification of e.g. small newly formed phases of minerals at the edges of other components. Additionally, PCA was successfully used to classify silicates according to their crystal structures by comparing SixOy signal ratios and chemical compositions.

Assessing the factors controlling the temporal variations of weathering fluxes in a tropical watershed: Mule-Hole (South India)

J. RIOTTE[1], J.J. BRAUN[1,2], J.C. MARECHAL, A. VIOLETTE[1], P. DESCHAMPS[1,3], L. RUIZ[4], C. LAGANE[1], M. SEKHAR[2], S. SUBRAMANIAN[2], C. KUMAR[2] AND S. AUDRY[1]

[1]GET, UMR 5563, UPS-IRD-CNRS 14 av. E. Belin 31400 Toulouse, France

[2]IFCWS, Indian Institute of Science, Bangalore 560012 India

[3]CEREGE, CNRS-Aix-Marseille University, BP80 13545 Aix-en-Provence, France

[4]INRA, UMR1069, SAS, 35000 Rennes, France

We investigated the present-day and long term weathering and erosion fluxes in tropical forested watershed (Mule Hole, South India). The watershed, monitored since 2003, is located in the sub-humid zone (MAR = 1100mm/yr) of a sharp climatic gradient induced by the Western Ghats and mostly fed by the South West monsoon.

The present-day evapotranspiration from the forest accounts for 85% of the annual rainfall, with two major consequences: (1) limitation of groundwater recharge and disconnexion with the stream, and (2) limitation of the stream flow, which is highly ephemeral [1]. However, the stream deconvolution indicates that almost 80% of dissolved species but Na transited through the vegetation as a result of leaf recretion and litter decay. These results emphasis the ambigous role of the vegetation that limits the runoff but enhances dissolved fluxes in the stream.

The present-day denudation rate is 28mm/kyr. It is dominated by erosion, ~25mm/ky, and by groundwater flux, 3mm/kyr, whereas the dissolved flux in the stream is very low, 0.3mm/kyr. The long term -100kyr- denudation rate was measured by ^{10}Be on the stream bedload. It accounts for only one third of the present-day value which means that the watershed experienced much lower erosion fluxes during the last climatic cycle, likeky under drier climate. This is confirmed by the occurrences of pedogenic carbonates in the basin soils. Their U-Th datings reveal the coexistence of several generations, essentially during the Last Glacial Maximum and to a lesser extent during the Holocene [2]. Rainfall conditions during the carbonate formation were semi-arid (MAR= 400 to 700mm/yr), i.e. enough for deepening the weathering front, but not for maintaining erosion fluxes.

[1] Maréchal *et al*. (2009) *J. Hydrol*. **364**, 272–284. [2] Violette *et al*. (2010) *Geochim. Cosmochim. Acta* **74**, 7059–7085.

https://doi.org/10.1180/S0026461X00006502 Published online by Cambridge University Press

Mechanisms for the attainment of sulfide saturation in magmas derived from subcontinental lithospheric mantle

EDWARD M. RIPLEY

Department of Geological Sciences, Indiana University, Bloomington, Indiana, USA 47405 (ripley@indiana.edu)

Magmatic, sulfide-rich, Ni-Cu-(PGE) deposits occur in settings where potential interaction between mantle-derived magma and country is enhanced (and hence a particular significance to subcontinental lithospheric mantle). Although the presence of S-bearing country rocks should not be dismissed when exploring for Ni-Cu-(PGE) deposits, it is clear that immediate country rocks often may have very little to do with the process of ore genesis. For this reason local country rocks may be poor choices for end-members in various types of geochemical mixing calculations, and data collected from the igneous rocks and associated sulfide mineralization must be carefully evaluated to assess the extent of magma interaction with country rocks. In the case of komatiites the introduction of sulfur from relatively local country rocks has been well-documented. For deeper-seated systems the involvement of immediate country rocks as magma contaminants has been more difficult to prove.

Troctolitic intrusions of the Duluth Complex (Midcontinent Rift System) are hosted by sulfide-bearing pelitic rocks which provide a viable source of sulfur in a contamination process. Sulfur isotope values of the mineralized rocks show a strong crustal signature, but their variability also signifies the involvement of multiple sulfide-saturated pulses. In a system of multiple intrusions various pulses may interact with different country rocks in the conduit system, and as a result be characterized by distinct chemical and isotpic signatures. Situations such as these lead to a conclusion that assimilation of crustal S occurred in deeper chambers within the magmatic system.

When the incorporation of S from country rocks is not indicated, the size of the magma system becomes particularly important. Contamination of mafic magmas by silicic country rocks may lead to sulfide saturation and if orthopyroxene crystallizion results rather than olivine, an added benefit is the availability of Ni (D-Ni (pyr) < D-Ni (ol)). However, in cases where S addition has not occurred extremely efficient collection of sulfide, from large masses of magma, is required for the formation of economically viable mineralization.

Long distance electron transmission couples sulphur, iron, calcium and oxygen cycling in marine sediment

N. RISGAARD-PETERSEN[1]* AND L.P. NIELSEN[2]

[1]Center for Geomicrobiology, Department of Biological Sciences, Aarhus University, 8000 Aarhus C, Denmark (*correspondence: nils.risgaard-petersen@biology.au.dk)

[2]Section for Microbiology, Department of Biological Sciences, Aarhus University, 8000 Aarhus C, Denmark (biolpn@biology.au.dk)

Geochemical observations in marine sediment have recently documented that electric currents may intimately couple spatially separated biogeochemical processes (1). When marine sediment rich in iron sulphide was exposed to oxygen we observed how the electric currents resulted in significant geochemical alterations in the upper centimetres of the anoxic sediment:

Sulphides were oxidized to sulphate in anoxic sediment layers. Electrons from this half-reaction were passed to the oxic layers cm above. In this way the domain of oxygen was extended far beyond it's physically presence. Bioelectrical sulfide oxidation leads to electric field formation, sulfide depletion and acidification of the upper centimeters of the sediment. This promoted ion migration and dissolution of carbonates and iron sulfides. Sulfide released from iron sulfides was the major e-donor in the system. Ferrous iron released from iron sulfides was to a large extend deposited in the oxic zone as iron oxides and Ca^{2+} eventually precipitates at the surface as due to high pH caused by cathodic oxygen reduction.

The result show how long distance electron transmission allows oxygen to drive the allocation of important minerals and possibly many trace elements deep in marine sediment.

[1] Nielsen *et al*. (2010) *Nature* **463**, 1071-1074.

https://doi.org/10.1180/S0026461X00006502 Published online by Cambridge University Press

Alteration of carbonates in saline aquifers due to CO_2 and accessory gases at geological storage conditions

A. RISSE*, K. HEESCHEN, S. STADLER AND C. OSTERTAG-HENNING

Federal Institute for Geosciences and Natural Resources (BGR), Stilleweg 2, D-30655 Hannover, Germany (*correspondence: Andreas.Risse@bgr.de)

The estimation of an environmentally and economically feasible purity of carbon dioxide for geological storage presumes a comprehensive understanding of the geochemical interactions of CO_2, accessory gas components in the separated gas stream, e.g. H_2O, O_2, N_2, SO_x, NO_x, CO, H_2, H_2S, aqueous highly saline fluids and natural minerals.

The main focus of this geochemical subtask within the project COORAL (= CO_2 - Purity for Capture and Storage) is on experimental work with mineral-H_2O-CO_2-electrolyte-(accessory gas, e.g. SO_2, O_2, NO_x)-systems at *in situ* pressure (p) and temperature (T) conditions and the combination with geochemical modeling applying the numerical code PHREEQC.

A literature survey and systematic parameter evaluation demonstrated that some mineral-fluid-gas systems (shown for calcite-H_2O-CO_2-electrolyte) cannot be adequately described as to a partially simplified incorporation into the model, a lack of data at relevant pT conditions, and/or extrapolation-induced errors of the underlying thermodynamic data sets, confirming the need for additional experimental work at elevated pT conditions.

We show natural mineral and fluid alteration data of dissolution experiments of up to 700 h duration in the system calcite-H_2O-CO_2-(SO_2)-NaCl. Results were obtained with a static batch reactor system equipped with chemically inert and flexible gold-titanium-cells at operating conditions of 200 bars and 120 °C. Dissolution data indicate a stronger release of Ca from calcite in the presence of NaCl or/and CO_2 (and acid generating SO_2) in agreement with published findings. Net dissolution rates of calcite at various calcite-H_2O-CO_2-(SO_2)-NaCl systems will be presented and discussed.

While experimental data without CO_2 are well represented by thermodynamic calculations, rather strong discrepancies from measured data are e.g. observed for simulations of experiments in the presence of CO_2. We discuss reasons for deviations and limitations induced by the databases used.

STXM and XAS study of kaolinite conversion into berthierine-like mineral

C. RIVARD[1]*, E. MONTARGES-PELLETIER[1], M. PELLETIER[1], L.J. MICHOT[1], D. VANTELON[2], C. KARUNAKARAN[3], F. VILLIERAS[1] AND N. MICHAU[4]

[1]LEM, Université de Lorraine-CNRS, BP40, 54501 Vandoeuvre-lès-Nancy, France (*camille.rivard@ensg.inpl-nancy.fr)
[2]Synchrotron Soleil, Gif-sur-Yvette, 91192, France
[3]Canadian Light Source, University of Saskatchewan, Saskatoon, SK S7N 5C9, Canada
[4]ANDRA, 1/7 rue Jean Monnet, Parc de la Croix Blanche, 92298 Châtenay-Malabry Cedex, France

Experiments

In the context of radioactive waste repository in geological formation, kaolinite-Fe^0 interactions were investigated at the cristallochemical level. Batch experiments were carried out in anoxic conditions at 90°C, for durations of one, three and nine months, by mixing Georgia Kaolinite (KGa2), powder Fe^0 and aqueous solution (NaCl, $CaCl_2$). Such parameters were chosen to mimic repository conditions.

Results

First results indicated very fast iron metal consumption, morphological changes and iron-enrichment of clay particles.

X-ray diffraction, Fe K- and L-edges microspectroscopy (µ-XAS, STXM) evidence the rapid formation of an iron-rich 7 Å clay phase, with a structure close to that of berthierine or chamosite. At micrometric and nanometric scales, most iron is ferrous and octahedrally coordinated. However, some of the newly formed iron-rich clay particles display significant amounts of Fe^{3+} with variable Fe^{2+}/Fe^{3+} ratio (Figure 1). In order to get further crystallochemical information, iron data were complemented by experiments at both the Si and Al-K edges. Si K-edge spectra display variations mainly due to particles orientation. Al K-edge spectra reveal no change in aluminium status of pristine clay. Although berthierine and chamosite bear both Al^{IV} and Al^{VI}, only Al^{VI} seems to be present in the neoformed iron rich-clays.

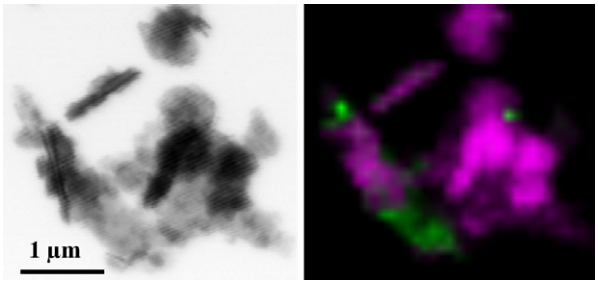

Figure 1: STXM image at 715 eV (Fe L3-edge) and corresponding two components fit (pink Fe^{2+}, green Fe^{3+}).

https://doi.org/10.1180/S0026461X00006502 Published online by Cambridge University Press

Li isotopes a powerful tool to trace hydrothermal impact during chemical weathering processes

KARINE RIVÉ[1], SÉTAREH RAD[2], MANUEL GARCIN[2] AND ROMAIN MILLOT[2]

[1]CEGEO, 159 allee chardin, Villeneuve d'ascq, France
[2]BRGM, 3, avenue Claude-Guillemin, Orléans, France

Li isotopes has been recently used to study water-rock interactions at Earth surface. Li is a fluid-mobile element that tends to preferentially partition into the fluid phase during water-rock interaction. The relative mass difference between the two isotopes is considerable, generating large mass dependent fractionation during chemical weathering processes, even at high temperature.

In the present work, the $^{7}Li/^{6}Li$ (expressed as $\delta^{7}Li$) was analyzed in Allier River, one of the major river basins of France. We have undertaken a systematic study of weathering products of the river. The lithology is dominant by granite rocks with current upstream, while it is mainly basaltic and Oligocene sediments in the downstream with hydrothermal manifestation.

Water samples were collected during several field trips. Our results show a large variation in Li isotopes within the catchment from 4.44 ‰ to 23.52 ‰. Li signature show a geographical distribution as it decreases from upstream to downstream over 400km. It appears that the upstream portion of the river present Li signature with higher fractionation with a mean value of 18 ‰ whereas it is only 6 ‰ in the downstream. This last portion of the river is impacted by hydrothermal activity, indeed these values reflect low temperature water-rock interaction in upstream and high water-rock interactions in the downstream, which the lowest values correspond to thermal mineral water plant. Li isotopes can be used here as a tracer of hydrothermalism. Moreover it seems that Li isotopes present a negative correlation with metal elements concentrations, which means that in a natural system hydrothermal activity induce liberation of those elements in the dissolved phase of the river during chemical alteration.

Those promising applications from Li isotopes to better understand chemical weathering processes will be discussed.

Identification of transboundary geothermal aquifers by hydrogeochemistry

N. RMAN[1]*, T. SZŐCS[2] AND A. LAPANJE[1]

[1]Geological Survey of Slovenia, Dimičeva ul. 14, 1000 Ljubljana, Slovenia
(*correspondence: nina.rman@geo-zs.si
[2]Geological Institute of Hungary, Stefánia út 14., 1143 Budapest, Hungary

Problem identification and applied methodology

The transboundary character of the Mesozoic, Miocene and Pliocene geothermal aquifers in the Mura-Zala basin in the SW Hungary and NE Slovenia was investigated by various hydrogeochemical techniques. Chemical analyses of 24 cold- and thermal groundwater samples were performed in 2010 for the T-JAM project, followed by additional sampling in 2011 for the TRANSENERGY project.

Results and discussion

Main components and trace elements analyses confirm the vertical stratification of geothermal aquifers as already suggested by many [1, 2, 3], but also indicate transboundary flow systems. Hydrogeological connections and groundwater age are interpreted from the stable ($\delta^{18}O$, δD, $\delta^{13}C$) and radioactive groundwater isotope (tritium, ^{14}C) analyses.

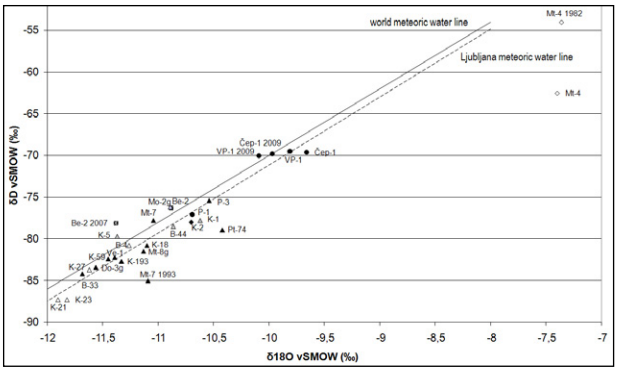

Figure 1: Distribution of $\delta^{18}O$ and δD in the samples.

Organic compounds, dissolved and separated gas, and noble gas analyses indicate differences in evolution and prevalent geochemical processes in the aquifers. Distinction between active and stagnant flow systems is also evident from our results.

[1] Kralj & Kralj (2000) *Env. Geol* **39/5**, 488–500. [2] Lapanje (2006) *Geol* **49/2**, 347–370. [3] Tóth *et al.* (2006) MÁFI Report

https://doi.org/10.1180/S0026461X00006502 Published online by Cambridge University Press

Proteogenomics of a marine sediment community dominated by ANME-1

I. ROALKVAM[1], R. STOKKE[1], H. HAFLIDASON[2] AND I.H. STEEN[1]*

[1]Department of Biology, Centre for Geobiology, University of Bergen, 5020 Bergen, Norway (*correspondence: ida.steen@bio.uib.no)

[2]Department of Earth Science, University of Bergen, 5020 Bergen, Norway

Sulfate-reducing methanotrophy by anaerobic methanotrophic archaea (ANME) and sulfate-reducing bacteria (SRB) is a major biological sink of the green house gas methane in anoxic methane-enriched marine sediments. The physiology of a microbial community in the G11 pockmark at Nyegga dominated by free-living ANME-1 was investigated by a proteogenomic approach. Total DNA was subjected to 454-pyrosequencing (829, 527 reads) and 16.6 Mbp sequence information was assembled into contigs Taxonomic analysis supported a high abundance of Euryarchaea (70%) with 66% of the assembled metagenome belonging to ANME-1. Extracted proteins were separated on 1D-SDS-PAGE, and gel slices were in-gel tryptic digested and subjected to liquid chromatography and mass spectrometry (LTQ-Orbitrap XL). Of 356 identified proteins, 245 were expressed by ANME-1. Expression of cold-adaptations and gas vesicle proteins reflects adaptation of the ANME-1 community to a permanently cold environment and possibly to positioning in specific sediment depths, respectively. Furthermore, except N_5N_{10}-methylene-tetrahydro-methanopterin reductase all enzymes in the reverse metanogenesis pathway as well as red-ox protein components homologous to SRB, were expressed by ANME-1. Sulfite reductase and adenosine-5'-phosphosulfate (APS) -reductase in the dissimilatory sulfate reduction pathway were expressed by sulfate reducing δ-proteobacteria. In addition, an APS-reductase affiliated with cluster IV comprising Gram-positive SRB and related sequences [1], was present in the proteome.

[1] Meyer and Kuever (2007), Microbiology **153**, 2026-2044

Deep-sea coral records of surface water properties in Gulf of Mexico and the South Eastern United States over the last millennium

E.B. ROARK[1]*, N.G. PROUTY[2], A.E. KOENING[3] AND S.W. ROSS[4]

[1]Department of Geography, Texas A&M University, College Station, TX 77843 (*correspondence: broark@geos.tamu.edu)

[2]US Geological Survey, 400 Natural Bridges Drive Santa Cruz, CA 95060

[3]US Geological Survey, MS 973 Denver Federal Center Denver, CO 80225

[4]Center for Marine Science, University of North Carolina at Wilmington, Wilmington, NC 28409

In this study we report on the use of radiocarbon measurements to investigate growth rates and age distributions of deep-water black corals (*Leiopathes* sp.) in the Gulf of Mexico and the southeastern Unites States. Results from five specimens show that these animals have been growing continuously for at least the last two millennia, with growth rates ranging from 8 to 22 μm yr^{-1}. These results are compared to SEM work to image growth rings and measure relative trace elements concentrations. The counting growth rings counts by two different methods on the SEM images and peaks in iodine concentration are in good agreement (typically within the ^{14}C uncertainty and a 10% counting uncertainty) with the radiocarbon results allowing for the development of independent age models

In this study we also use a multi-proxy approach in order to better understand the combination of biological and physical factors controlling the isotopic and trace element content of deep-sea corals. Both $\delta^{15}N$ and $\delta^{13}C$ signatures along with trace element paleoindicators of eutrophication and oxygen levels (V, Mo, U, Re, Cu and I) can be used to infer changes in surface water conditions related to nutrient loading, eutrophication, and hypoxia in the Gulf of Mexico over the last millennium. Important changes are noted over the last 900 years and over the last century.

https://doi.org/10.1180/S0026461X00006502 Published online by Cambridge University Press

The evolution of the marine Zn reservoir: Comparing the proteomic and sedimentary records

L.J. ROBBINS[1]*, S.V. LALONDE[2] AND K.O. KONHAUSER[1]

[1]1-26 Earth Science Bldg., Univeristy of Alberta, Edmonton, Ab. T6G 2E3, Canada (*correspondence: lrobbins@ualberta.ca)

[2]European Institute for Marine Studies, Technopôle Brest-Iroise, Place Nicholas Copernic [2]9280 Plouzané, France (stefan.lalonde@univ-brest.fr)

Banded iron formations as proxies for Zn

In the transition-metal complement of living cells, zinc plays a central role. It is the most common inorganic co-factor employed by eukaryotic metalloenzymes, and second or equal to iron in prokaryotic metalloenzymes [1]. In Eukarya, many Zn-binding proteins appear to have evolved relatively recently, leading to the proposal that limited marine Zn availability prior to the Neoproterozoic may have impacted the course of eukaryotic evolution [1]. We seek to evaluate this hypothesis by examining sedimentary proxies for the evolution of the marine Zn reservoir over geological time, specifically Precambrian banded iron formations (BIF), younger ironstones and exhalites. By combining the BIF record with experimental results for Fe-Zn-Si co-precipitation we are able account for the competitive effects of silica during absorption. We present estimates of seawater Zn concentrations from the Archean through to the modern; while there appears to be mild enrichment in the Phanerozoic, we extrapolate Archean Zn concentrations that are roughly comparable to modern. These findings have strong bearing on potential consistency between genetic and geological records for the evolution of Earth's surface environment.

[1] Dupont *et al*. (2010) *PNAS* **107**, 10567–10572.

Rheological constraints on the deformation of Snake River-type ignimbrites: An experimental study

GENEVIEVE ROBERT[1]*, GRAHAM D. ANDREWS[2], JIYANG YE[1] AND ALAN G. WHITTINGTON[1]

[1]Department of Geological Sciences, University of Missouri – Columbia , Columbia, MO, USA (*correspondence: genevieve.robert@mail.mizzou.edu)

[2]Department of Earth and Environment, Franklin and Marshall College, Lancaster, PA, USA

We have studied the rheology of two ashfall units associated with the eruption of the pervasively rheomorphic Grey's Landing (GL) ignimbrite (a Snake River-type ignimbrite) from the Miocene Rogerson formation, Snake River Plain volcanic province, USA. Lava-like lithofacies of the GL ignimbrite are either crystallized, devitrified, or perlitized, and do not necessarily represent the original material that came out of the vent to be subsequently deposited, welded and deformed by flow (rheomorphism). We therefore chose to use the fused basal co-ignimbrite ashfall tuff (GLB) and the upper co-ignimbrite tuff (GLU) as potential 'starting material' for the GL ignimbrite. The basal ash is laminated, moderately porous (~15%), and contains 10–20% crystals; in contrast the upper ash is massive, nearly aphyric, glassy and contains ~5% porosity.

We measured the apparent viscosity of each unit over ~835-1005°C, a range of temperatures relevant to eruption and deposition of these ignimbrites. The viscosities of the upper and lower units converge in the low-temperature range (~835°C) and diverge at higher temperatures (at 900°C, the viscosity of GLU is $10^{10.3}$ Pa s whereas that of GLB is $10^{10.8}$ Pa s).

Strains ranging from 10 up to 1000 are recorded in the Grey's Landing ignimbrite. However, our viscometry results suggest that dry melts making up the deposit either require unreasonably high stresses (>1MPa) or long deformation timescales (days to weeks) inconsistent with field observations to produce the observed strain in the deposit. It follows that dissolved water reducing the viscosity of the pyroclasts at the deposition temperature and/or strain heating keeping temperatures high or even increasing temperatures during deposition and deformation are necessary to explain the field observations. Models investigating the relative contributions of dissolved water and strain heating in facilitating rheomorphism will be presented.

https://doi.org/10.1180/S0026461X00006502 Published online by Cambridge University Press

Potential REE deposits along the Red Sea coast of Egypt

JAMES ROBERTS[1]* AND TAREK IBRAHIM[2]

[1]University of Pretoria, Pretoria, South Africa (*correspondence: james.roberts@up.ac.za)
[2]El Mansoura University, Cairo, Egypt, (elsahabi@yahoo.com)

In Egypt, exploration for heavy mineral deposits with their associated REE minerals has traditionally concentrated on the Mediterranean coast, and large garnetiferous heavy mineral sands have been identified at localities near Alexandria. However, the Red Sea coast is also an ideal environment for the formation of such deposits [1].The Red Sea Coast in the southernmost portion of Egypt has a long geological history of erosion and sediment transportation, and several alluvial deposits rich in economic heavy minerals have been identified in the coastal strip between Ras Banas and the border with Sudan. Accumulations of heavy minerals have been observed along Red Sea beaches at Ras Manazel, Khudaa, Shalateen, Wadi Diit, and along the coastal stretches between these locations. These deposits have formed not only by transport processes related to offshore currents in the Red Sea, but also by drainage networks operating in the Eastern Desert of Egypt. Satellite imagery of the drainage networks indicates that the granites of the Sudanese highlands are the source of the heavy minerals, with minor input from granites in the southern Egyptian highlands. Deposits inland from the current Red Sea coastline may have been formed before the opening of the Red Sea, and subsequent erosion and reworking through flash flooding and other catastrophic transport mechanisms has created more recent deposits along the current coastline. The deposits contain not only illmenite, rutile, magnetite, and garnet, but also large concentrations of radioactive minerals such as thorite, zircon and monazite. Preliminary studies have shown that some of the deposits are extremely rich in REE minerals (1-2% zircon by weight, 0.5% monazite by weight). The mineralogical composition of the deposits matches those of the granites in Sudan and southern Egypt, which have been explored extensively for uranium for the last 10 years. These deposits are thus a viable target for further exploration, with the intent to extract the REE minerals as well as the titaniferous ilmenite.

[1] Dawood, El-Naby (2007) *Mineralogical Magazine* **71**, 389–406. [2] Balestrieri, Abbate, Bigazzi , Ali (2009) *Earth Surf. Process. Landforms* **34**, 1279–1290.

Rare earth element association with foraminifera

N.L. ROBERTS[1]*, A.M. PIOTROWSKI[1], T.I. EGLINTON[2] AND M.L. LOMAS[3]

[1]Department of Earth Sciences, Downing Street, Cambridge, UK (*correspondence: nr297@cam.ac.uk)
[2]Geological Institute, Sonneggstasse 5, Zürich, Switzerland
[3]Bermuda Institute of Ocean Sciences, St George's, Bermuda

Nd isotopes are becoming widely used as a paleoceanographic tool for reconstructing past changes in water mass source [1]. Recent analysis of Nd isotopes on sedimentary planktonic foraminifera at the Bermuda Rise has proven to be a robust alternative to bulk sediment leachates, for reconstructing bottom water circulation [2]. However, in order to use foraminiferal Nd isotopes as a proxy for bottom water composition, we need to establish how, where and when rare earth elements (REEs) become associated with foraminifera.

We have measured REE concentrations and Nd isotopes on plankton tow and sediment trap foraminifera from the NW Atlantic, and compared with sedimentary foraminifera from marine cores in the same region. This allowed an evaluation of REE association with planktonic foraminifera at various stages of settling through the water column, and diagenesis near the sediment-water interface.

We find approximately 80% of plankton tow and sediment trap Nd is scavenged by particulate organic carbon and metal oxides. These phases are remineralised as particles fall through the water column allowing partial equilibration of foraminiferal Nd isotopes with ambient dissolved sea water. Once at the sediment-water interface, respiration of organic matter between foraminiferal primary calcite layers provides a reducing micro-environment within which diagenetic phases precipitate. These phases increase foraminiferal REE concentrations by ~10 fold through inorganic partitioning from bottom and pore waters.

Calculated partition coefficients suggest manganese carbonate is the predominant diagenetic host for REEs in planktonic foraminifera at the Bermuda Rise. This carbonate phase is difficult to remove during reductive cleaning, and is also resistant to down core REDOX changes, allowing reconstruction of robust bottom water Nd isotope records by measuring mixed planktonic foraminfera. Our findings have important implications for the use of planktonic foraminifera, both for surface and bottom water Nd isotope reconstruction.

[1] Piotrowski *et al*. (2005) *Science* **307**, 1933–1938. [2] Roberts *et al*. (2009) *Science* **327**, 75–78.

https://doi.org/10.1180/S0026461X00006502 Published online by Cambridge University Press

Continental growth spurts during supercontinent break-up

NICK M.W. ROBERTS

NERC Isotope Geosciences Laboratory, Kingsley Dunham Centre, Keyworth, Nottingham, NG12 5GG, UK (nickmwroberts@gmail.com)

Accretionary orogens are the primary host of both growth and loss of continental crust, at least since the Archaean. At present-day, growth and loss are balanced globally, leading to a constant continental volume [1]. Retreating accretionary orogens will feature greater continental growth than those in advancing mode (e.g. [2, 3]). Continental growth largely occurs via subdcuction-driven magmatism, whereas continental loss largely occurs via subduction erosion and sediment subduction. Since the latter typically involves partial recycling into magmas, both growth and loss of continental crust are represented in the magmatic record.

Using a global zircon-Hf datset [4], the magmatic record preserved in zircons is examined to determine the relative amount of global continental growth versus recycling. Excursions into positive and negative εHf-time space relative to a global mean, represent increased continental growth and recycling respectively. The data show strong negative excursions at ~2.0-1.7 Ga, ~1.0 Ga, and ~550 Ma, reflecting increased continental recycling during periods of supercontinent amalgamation. Well-defined positive excursions are seen at ~1.7-1.3 Ga and ~0.8-0.6 Ga, interpreted as increased continental growth-rate during periods of supercontinent break-up, and likely reflecting an increased degree of retreating accretionary orogens. The Archaean lacks strong positive or negative excursions, reflecting either a lack of supercontinent formation, or a differing role of accretionary orogenesis during this period.

Preservational bias during the supercontinent cycle may lead to an increased zircon record during supercontinent formation [5]; however, the degree of mantle input recorded by Hf-in-zircon indicates that continental growth-rate is actually increased during supercontinent break-up. Elucidating the exact degree of continental loss through Earth history remains a challenge, but is vital for determining the true nature of continental growth.

[1] Hawkesworth *et al*. (2010) *Jour. Geol. Soc. London* **167**, 229–248. [2] Kay *et al*. (2005) *Geol. Soc. Am. Bull*. **117**, 67–88. [3] Kemp *et al*. (2009) *EPSL* **284**, 455–466. [4] Belousova *et al*. (2010) *Lithos* **119**, 457–466. [5] Hawkesworth *et al*. (2005*) Science* **323**, 49–50.

Marine controls on atmospheric radiocarbon: The glacial and deglaciation

LAURA F. ROBINSON[1], ANDREA BURKE[2] AND JESS F. ADKINS[3]

[1]Dept. Marine Chemistry & Geochemistry, Woods Hole Oceanographic Institution, 266 Woods Hole Rd. 02543 Woods Hole, MA. USA (lrobinson@whoi.edu)

[2]Dept. Geology & Geophysics, Woods Hole Oceanographic Institution, 266 Woods Hole Rd. 02543 Woods Hole, MA. USA (aburke@whoi.edu)

[3]MC 100-23, 1200 E. California Blvd. Pasadena, CA 91125 (jess@gps.caltech.edu)

Radiocarbon is an important isotope because its radioactive decay provides constraints on the rates and timing of processes today and in the past. It is well mixed in the atmosphere, where its history is reasonably well constrained back through the last 50,000 years. By contrast the radiocarbon content of the ocean varies by about 150 per mil depending on equilibration with the atmosphere and subsequent isolation that allows decay to proceed.

There is evidence for an even greater dynamic range in the marine realm during the last glacial and deglaciation. For example, published records from intermediate waters in the northern hemisphere are up to 500 per mil depleted relative to the contemporaneous atmosphere, and have been used as evidence for a isolated, carbon-rich reservoir in the deep ocean. There is little doubt that interaction with the ocean is a major driver of atmospheric CO_2 and radiocarbon on these timescales, but the mechanisms continue to be debated in the literature. In this abstract we focus on building a coherent compilation of the state-of the-art of marine radiocarbon records, and then use these records to discuss potential mechanisms for abrupt changes in atmospheric carbon and radiocarbon.

https://doi.org/10.1180/S0026461X00006502 Published online by Cambridge University Press

Transfer of nutrients and carbon from the Southern Ocean to the Atlantic during the last deglaciation

LAURA F. ROBINSON, ANDREA BURKE AND KATHARINE R.HENDRY

Woods Hole Oceanographic Institution, 360 Woods Hole Rd. 02543 Woods Hole, MA. USA

The interconnection of ocean circulation and nutrient cycling appears to be closely linked to atmospheric carbon dioxide and global temperature. In this abstract we make use of a novel proxy for silicic acid concentration, $d^{30}Si$ in deep-sea sponge spicules, together with new and published ^{14}C records to examine carbon and nutrient cycling in the deep Southern Ocean. We then link this cycling to intermediate and deep locations in the western basin of the Atlantic during the abrupt climate events of the last deglaciation to investigate how circulation, nutrients and CO_2 are coupled.

We have documented little difference between the silicic acid concentration of the deep Southern Ocean at the last glacial maximum compared to the modern. By contrast, it appears that circumpolar deep waters were significantly depleted in radiocarbon during the glacial period, indicative of a build up of carbon. Within the Southern Ocean itself we observe a break down of deep-water stratification during the deglaciation, at around the time of the Bolling Allerod.

Ocean circulation and nutrient cycling in the Atlantic during the three most recent Heinrich events, H2, H1 and the Younger Dryas appear to share certain characteristics, but the CO_2 response is not the same in each case. For example meridional circulation from sedimentary Pa/Th ratios appears to have been somewhat similar during H2 and H1. At the same time there is evidence for northward export of Si and low $^{14}C/^{12}C$ waters into the Atlantic. However in one case atmospheric CO_2 increased markedly, and in the other it did not. During the Younger Dryas when CO_2 was increasing, Pa/Th indicates only a partial reduction in advection but silicic acid and Cd/Ca indicate export of virtually unadulterated circumpolar deep waters throughout the intermediate depths of the Atlantic. Concurrently $^{14}C/^{12}C$ ratios at deep and intermediate depths in the North Atlantic were somewhat depleted, consistent with carbon-rich southern-source waters escaping from the Southern Ocean. We will use these similarities and differences to link our knowledge of the circulation of the ocean to atmospheric carbon records.

Deep subduction of crustal minerals in the mantle: Evidence from ophiolites

P. ROBINSON[1], R. TRUMBULL[2], J.-S. YANG[3] AND A. SCHMITT[4]

[1]Department of Earth Sciences, Dalhousie University, Halifax, Nova Scotia, Canada

[2] Helmholtz Centre Potsdam , GFZ German Research Centre for Geosciences , D14473, Potsdam, Germany

[3] Key Laboratory for Continental Dynamics, Institute of Geology, Chinese Academy of Sciences , Beijing, 100037 China

[4] Department of Earth and Space Sciences, University of California, Los Angeles, Los Angeles, California 90095-1567, USA

Crustal minerals, including zircon, corundum, feldspar, almandine garnet, kyanite, sillimanite and rutile, associated with ultrahigh pressure minerals, such as coesite, diamond, kyanite, and moissanite have been recovered in varying proportions from podiform chromitites of the Luobusa and Donqiao ophiolites of Tibet and the Semail ophiolite of Oman. The UHP minerals, and some of the crustal minerals, have been found in situ; the other grains have been recovered from mineral separates. Zircon is common in all three ophiolites and occurs as rounded to subangular grains, about 50-300 microns across, typically with very complex internal textures. A few euhedral prisms have regular oscillatory zoning indicative of a magmatic origin. $^{206}Pb/^{208}U$ SIMS dates for the Luobusa zircons range from 549±19 to 1657±48 Ma, whereas those from Donqiao have ages of 484±49 to 2515± Ma, all much older than the ophiolites. Sixteen dates on zircons from the Semail ophiolite range in age from 84±4 to 1386±48 Ma. Most zircons from Oman are older than the ophiolite but 3 grains are essentially the same age as the ophiolite (92±4 to 99±5 Ma. These are euhedral prisms with oscillatory zoning. The zircons typically contain a variety of low-pressure inclusions, including quartz, rutile, orthoclase, mica, ilmenite and apatite. In addition, all of the zircons from the three ophiolites have REE and trace element compositions compatible with a crustal origin. The assemblage of crustal minerals, combined with the morphology and age of the zircon, strongly suggest derivation from crustal sediments subducted into the mantle, where they were mixed with UHP and highly reduced phases. The preservation of these minerals can be explained by their occurrence as inclusions in chromite grains.

https://doi.org/10.1180/S0026461X00006502 Published online by Cambridge University Press

Southern Ocean nitrogen and silicon dynamics during the last deglaciation

REBECCA S. ROBINSON[1], MATTHEW G. HORN[1], CHARLOTTE P. BEUCHER[2] AND MARK A. BRZEZINSKI[2]

[1]Graduate School of Oceanography, University of Rhode Island, Narragansett, Rhode Island, USA
[2]The Marine Science Institute, University of California Santa Barbara, Santa Barbara, California, USA

The reinvigoration of overturning in the Southern Ocean is hypothesized to have returned CO_2 from the deep ocean to the atmosphere at the end of the last ice age. Large peaks in opal accumulation have been put forward as evidence for an increase in wind driven upwelling between 10 and 15 kyr BP [1]. Here, we use coupled nitrogen and silicon isotope records alongside opal accumulation rates to provide quasi-quantitative estimates of Southern Ocean nutrient supply, by upwelling, and nutrient utilization across this interval. Significant changes in the consumption of N and Si across the two opal accumulation peaks indicate major changes in both upwelling and nutrient demand. We find N and Si consumption to be relatively incomplete during peak opal accumulation. Nutrient supply must have been significantly enhanced. Differences between the Si and N responses during opal peaks may stem from decreasing iron availability across the glacial termination. The reinvigoration of overturning circulation during the deglaciation is hypothesized to cause a transient peak in nutrient supply to the low latitudes [2]. This is supported by our data, which indicate that relatively high macronutrient concentrations were maintained in the Southern Ocean surface waters despite high demand.

[1] Anderson *et al*. (2009) *Science* **323**, 1443–1448. [2] Spero & Lea (2002) *Science* **296**, 522–525.

A re-compiling of Cretaceous SST proxy data

STUART A. ROBINSON, KATE LITTLER, PAUL BOWN AND JACKIE LEES

Department of Earth Sciences, University College London, Gower Street, London, WC1E 6BT, UK (stuart.robinson@ucl.ac.uk)

The Cretaceous was generally a period of extreme global warmth, most likely caused by elevated atmospheric pCO_2 levels, during which geologically brief (<1 Myr duration) carbon-cycle perturbations were common. Thus, the geological recod of this time period may hold clues as to the mechanics of the Earth system under different conditions to those experienced at the present-day and, also, to the long-term response of the planet to severe environmental perturbation. However, extraction of meaningful inferences about the Earth system from the Cretaceous geological record requires confidence in the proxies used to reconstruct environmental variables, such as temperature and pCO_2.

The last decade has seen significant shifts in the understanding and number of geochemical proxies used to reconstruct sea-surface temperatures (SSTs) in the Cretaceous. The recognition of early bottom-water recrystallization of planktic foraminifera has resulted in the re-appraisal of what is considered ‘excellent’ calcite preservation suitable for oxygen-isotope and Mg/Ca analysis. Organic geochemistry has provided a new proxy, TEX_{86}, that has permitted the generation of SST records in time periods and environments that were previously unobtainable by calcite $\delta^{18}O$. Additional insights have been provided by $\delta^{18}O$ of phoshate from biogenic apatites and new water-phosphate fractionation equations have been defined. These new insights and developments provide the justification for a re-appraisal of the temporal and spatial variability in Cretaceous SSTs. We attempt here to provide an up-to-date synthesis of Cretaceous proxy SST data that is mindful of the lessons and developments of the last decade. Using this new compilation allows us to build a more comprehensive view of Cretaceous palaeoclimates and to explore a number of questions that are pertinent both to Cretaceous palaeoclimatology and wider inferences about the mechanics of the Earth system.

https://doi.org/10.1180/S0026461X00006502 Published online by Cambridge University Press

Rapid weathering of arsenopyrite in agricultural soils

T.C. ROBSON*, C.B. BRAUNGARDT AND M.J. KEITH-ROACH

University of Plymouth, Plymouth, PL4 8AA, UK (*correspondence: thomas.robson@plymouth.ac.uk)

Aerially distributed fine mineral waste particles (< 250 μm), the product of mining processes, are an important source of potentially toxic elements (PTEs) in the surface environment. However, there is a paucity of data on the short-term stability of PTE-rich particles in agricultural soils and the associated risk of producing contaminated crops when PTEs are released from mineral matrices.

This study aimed to determine whether sulphide ore minerals undergo geochemical alterations (i.e. oxidation-dissolution) at a rate that is relevant to crop growth (in the order of months – years). Arsenopyrite (FeAsS) was selected for this proof-of-concept experiment due to the toxicity of arsenic at low concentrations [1].

Two soils, contrasting in organic matter content and pH, were spiked with ground FeAsS (1, 600 μmol/kg As), sown with spring wheat (*Triticum aestivum)* and incubated under controlled conditions until the wheat ripened (90 days).

Following the incubation period, soluble (soil water extract) and exchangeable (0.1 mol/L phosphate buffer extract, pH 7.2) arsenic concentrations were significantly ($p<0.05$) higher in spiked soils, compared with controls. Low soluble arsenic concentrations suggested that less than 0.1% m/m of the mineral-bound arsenic had been released and remained present as soluble species. On the other hand, exchangeable As concentrations indicated that up to 9 % m/m (in acid soil, pH 4.5) of the mineral-bound arsenic had been released and loosely bound within the spiked acid soil matrix. The lower exchangeable concentrations extracted from the organic, neutral pH soil (0.5% m/m) were consistent with the reported FeAsS dissolution rate minima at pH 7-8 [2].

Short-term weathering of FeAsS did not yield dangerous arsenic concentrations (4.2-5.3 nmol/g) in edible plant tissues under the test conditions, based on cereal consumption rates [3]. However, this study provides evidence for significant arsenic release from arsenopyrite within an agriculturally relevant, short exposure period. Further experiments are underway, with the aim of determing the alteration rate of FeAsS and other related minerals in agricultural systems.

[1] World Health Organisation (1983) WHO Food Additive Report Series, Geneva. [2] Yu *et al*. (2007) ES&T **41**, 6460-6464. [3] European Food Standards Agency (2010) Concise European Food Consumption Database.

Ecosystem-level impact signals of groundwater borne continental nitrate transfer to the Ria Formosa lagoon by Submarine Groundwater Discharge (SGD) traced along the mixing gradient by a multi-indicator approach

C. ROCHA[1]*, C. VEIGA-PIRES[2], J. WILSON[1], J. ANIBAL[2], J-P. MONTEIRO[3] AND J. SCHOLTEN[4]

[1]Biogeochemistry Research Group, School of Natural Sciences, Trinity College Dublin, Dublin 2, Ireland (*correspondence: rochac@tcd.ie, jewilson@tcd.ie)

[2]Faculdade de Ciencias e Tecnologia, CIMA – Ed. 7. Universidade do Algarve, Campus de Gambelas, 8000 Faro, Portugal (cvpires@ualg.pt, janibal@ualg.pt)

[3]Faculdade de Ciencias e Tecnologia, Universidade do Algarve, Campus de Gambelas, 8005-139 Faro, Portugal (jpmontei@ualg.pt)

[4]IAEA, Marine Environment Laboratories, 4 Quai Antoine 1[er], MC-98000 Monaco (J.Scholten@iaea.org)

Recognition of the role played by SGD in the transfer of contaminants to near shore marine environments underscores the need for tools and approaches that will facilitate regional assessments of its environmental impact, including localization, spatial extent and magnitude as well as the provision of uninterrupted chains of evidence that effectively demonstrate links between polluted groundwater sources on land and ecosystem level effects in the coastal zone.

We present an uninterrupted chain of evidence linking groundwater pollution to coastal ecosystem function for a leaky coastal lagoon system. Here, for the first time, this causal link is demonstrated in its entirety for a single ecosystem. The approach used combines Earth observation techniques, hydrological mass balance approaches, conservative, radiogenic and stable isotope tracers, nutrient dynamics along the mixing line and finally, direct physiological indicators of primary producer assimilation of groundwater borne nutrients at the marine end member.

https://doi.org/10.1180/S0026461X00006502 Published online by Cambridge University Press

Petroleomics: Past, present and future

RYAN P RODGERS[1], AMY M. MCKENNA[1], CHRISOPHER L. HENDRICKSON[1] AND ALAN G. MARSHALL[2]

[1]National High Magnetic Field Laboratory, 1800 E. Paul Dirac Drive, Tallahassee, FL 32310 USA (rodgers@magnet.fsu.edu, mckenna@magnet.fsu.edu, hendrick@magnet.fsu.edu)

[2]Department of Chemistry and Biochemistry, Florida State Univ., 95 Chieftan Way, Tallahassee, FL 32306 USA (marshall@magnet.fsu.edu)

Advances in mass spectrometry enable identification of tens of thousands of species in petroleum and environmental samples at the molecular level (elemental composition assignment). Current ionization methods amplify the utility of such detailed compositional information through the selective ionization of basic, acidic and aromatic species (± ESI and APPI). The ability to fingerprint, identify and track compositional changes in complex natural mixtures spawned the field of 'Petroleomics'. Although the past and current applications are largely limited to high resolution Fourier transform ion cyclotron resonance mass spectrometry, the future of 'Petroleomics' lies in the expansion and method development on the latest instruments in all areas of analytical chemistry.

Here we present an overview of the birth and development of Petroleomics and highlight the latest developments in our 'petroleomic' research efforts with an emphasis on the diversification of analytical workflows to maximize attainable compositional information. Specifically, microdistillation, 2-D HPLC, GC x GC, LC-TOF, preparative scale LC and FT-ICR MS will be discussed. Geochemical, oil production and refinery applications that include down-hole, deposits, offshore platform, terrestrial production and distillate samples reveal the need for a diversified analytical approach combined with high field FT-ICR mass spectrometry for problem solving and advances in the fundamental knowledge of the composition and behavior of petroleum derived materials.

Work supported by Shell Global Solutions (Houston, TX), NSF CHE-10-49753, DMR-06-54118, and the State of Florida.

High-frequency climate cycles in the Westernmost Mediterranean during the last 20,000 yrs

M. RODRIGO-GÁMIZ[1]*, F. MARTÍNEZ-RUIZ[1], F.J. RODRÍGUEZ-TOVAR[2], F.J. JIMÉNEZ-ESPEJO[1] AND E. PARDO-IGÚZQUIZA[3]

[1]Instituto Andaluz de Ciencias de la Tierra (IACT-CSIC-UGR), Granada, Spain (*correspondence: martarodrigo@ugr.es, fmruiz@ugr.es, fjjspejo@ugr.es)

[2]Departamento de Estratigrafía y Paleontología, Universidad de Granada, Granada, Spain (fjrtovar@ugr.es)

[3]Instituto Geológico y Minero de España, Madrid, Spain (e.pardo@igme.es)

High-sedimentation rates in the westernmost Mediterranean (Alboran Sea basin) allow excellent resolution for paleoclimate reconstructions at millennial- to centennial-scales. Here, a novel cyclostratigraphic analysis has been conducted on a marine record, revealing major and secondary peaks related to climate cycles during the last 20,000 yrs. Spectral analysis on time-series corresponds to several multi-proxy groups, including detrital, redox, paleoproductivity, and paleotemperature-paleosalinity, which reveals cycles of different confidence level at particular periodicities. Main periodicities at 1,300, 1,515, 2,000, and 5,000 yrs plus secondary harmonics at 650, 1,087, and 3,000 yrs derive from diverse climate forcing mechanisms. Thus, the 1,300 yr cycle appear to be principally influenced by North Atlantic freshwater inflow. The 1,515 yr cycle, equivalence to the Bond cycle in the North Atlantic, is linked to the North Atlantic thermohaline circulation and changes in the intensity and position of the North Atlantic Oscillation (NAO) and the Inter-Tropical Convergence Zone migrations (ITCZ). Although the 2,000 yr cycle is only punctually registered, it supports a global connection with records distributed at high-, mid-, and low-latitudes, pointing to variations in solar activity as main climate forcing mechanism. In contrast, the cycle at 5,000 yrs is well-registered and presents a direct relationship with orbital forcing responses, also accompanied by monsoonal variations and NAO oscillations. Thus, the obtained spectral periodicities reinforce the evidence on the strong connection between Mediterranean and North Atlantic climates, being climate oscillations mainly forced by solar variations, the NAO and the ITCZ migrations.

Acknowledgements: Projects CGL2009-07603, CGL2008-03007, CTM2009-07715, CSD2006-00041, MARM 200800050084447, RNM-5212, RNM-3715, RNM-179, RNM-178.

https://doi.org/10.1180/S0026461X00006502 Published online by Cambridge University Press

Discrimination of sediment samples for forensic application using REE

A. RODRIGUES, A. GUEDES*, H. RIBEIRO, B. VALENTIM AND F. NORONHA

Centro de Geologia da Universidade do Porto e Departamento de Geociências, Ambiente e Ordenamento do Território, Faculdade de Ciências, Universidade do Porto, Rua do Campo Alegre 687, Porto, Portugal (*correspondence: aguedes@fc.up.pt)

The geochemical signature of sediments is currently used as trace evidence in forensic investigations. In this research, geochemical studies have been carried out on Portuguese coastal sands aiming to ascertain its use for forensic purposes.

Rare Earth Elements (REE) concentrations were determined on samples collected on three coastal areas surrounded by different geological contexts, namely limestone, granite and metasediment. Eight sand samples were collected along transects perpendicular to the coastline, in beach and dune from each site. Each sample was manually collected with a plastic spade from the surface sediment, at a depth of approximately 0-5cm. From the sediment samples a standardized particle size fraction of <150 μm was obtained by dry sieving method and subsequently grinded to minimise the variation in the geochemical properties due to particle size.

The REE composition fraction was determined using four acid digestions ultratrace ICP-MS analysis at ACME labs (Canada), and concentrations calculated. Although the measured REEs concentrations can be compared directly for forensic purposes a normalisation reported to condrite meteorites was performed [1].

A REEs normalised concentration and a hierarchical cluster analyses were performed to obtain discrimination between samples. They reveal differences between samples associated with different geological context, and permitted the discrimination between samples surrounded by granite from samples surrounded by limestone and metasediments. It was also possible to discriminate some of the samples based on their REE concentration and profile.

This research was supported by Project PTDC/CTE-GEX/67442/2006 of FCT (Portugal).

[1] Taylor & McLennan (1985) Blackwell Scientific Publications, 312p.

Geochemical signatures in detrital tourmalines as indicators for sediment provenance: The Baixo Alentejo Flysch Group, South Portuguese Zone

B. RODRIGUES[1]*, P. DIAS[2], R.C.G.S. JORGE[3] AND P. FERNANDES[1]

[1]CIMA, University of the Algarve, Campus de Gambelas, 8005-139 Faro, Portugal (*correspondence: bmgrodrigues@sapo.pt, pfernandes@ualg.pt)
[2]CIG-R, University of Minho (patriciasdias@gmail.com)
[3]CREMINER LA/ISR, Dep. Geologia, Fac. Ciências da Universidade de Lisboa (rjorge@fc.ul.pt)

Microprobe analyses were made to infer the source of detrital tourmalines from the Mid to Late Carboniferous turbiditic deposits of the Baixo Alentejo Flysch Group (BAFG) of the South Portuguese Zone. A representative group of greywacke samples covering the whole range of the BAFG ages was collected for this study. Tourmalines have brown to brownish gray colors and do not show any optical zonation. In the Fe-Mg-Al diagram, the tourmalines fall into the fields of Ca-poor metapelites, metapsammites and quartz-tourmaline rocks. Microprobe analyses revealed a range of values between schorl and dravite end members, being closer to the latter, with variable contents of X-site vacancies (0.05-0.255 apfu), Ca (0.078-0.2 apfu), Na (0.627-0.924 and Al (5.746-6.622 apfu). The Fe/(Fe+Mg) and Na/(Na+Ca) ratios range from 0.32-0.45 and 0.79-0.91, respectively.

The presence of well-rounded tourmaline grains suggests that they could have derived from a source located at a great distance from the sedimentary basin, or from reworked sedimentary rocks. The occurrence of few euhedral grains indicates minor contribution from first cycle sediments. Together, these data suggest that the detrital BAFG tourmalines derived from multiple sources with the predominance of rocks with a felsic composition.

Bruno Rodrigues holds a PhD grant from the Portuguese Foundation for Science and Technology (n.° SFRH/BD/62213/2009).

https://doi.org/10.1180/S0026461X00006502 Published online by Cambridge University Press

The role of Mg in the formation of monohydrocalcite

J.D. RODRIGUEZ-BLANCO, P. BOTS, T. RONCAL-HERRERO, S. SHAW AND L.G. BENNING

School of Earth and Environment. University of Leeds. Leeds, LS29JT. UK (earjdrb@see.leeds.ac.uk)

Monohydrocalcite (MHC, $CaCO_3{\cdot}H_2O$) is a calcium carbonate mineral which forms by biological and abiotic processes in a number of environments including caves or lake-bed sediments. MHC often forms in Mg-rich aqueous environments, but is metastable with respect to aragonite and calcite [1]. However, the mechanisms of its formation and the role or effect of Mg on its nucleation and growth are not understood. Hence, using a combination of *in situ* and real-time synchrotron-based scattering and off-line micro-spectroscopic characterization, we followed and quantitatively assessed the formation mechanism of MHC.

Experiments were carried out by mixing equimolar Ca, Mg and CO_3 solutions (0.7:0.3:1) and reacting them at 21°C for 12 hours. The MHC crystallisation reaction was followed *in situ* (1 min/frame) using Small and Wide Angle Scattering (SAXS/WAXS, Diamond Light Source, UK), and equivalent off-line experiments were quenched at various times for solids and solution analysis.

The WAXS profile (Fig. 1 main plot) revealed after ~ 50 minutes MHC crystals grew via a two-step reaction. Step 1 is the transformation of a poorly-ordered amorphous calcium carbonate precursor (inset 1) into MHC nanocrystals (inset 2). This stage is followed by a second growth step after ~8.5 hr of reaction (inset 3) which occurs concomitantly with the formation of minor hydromagnesite (HMg). The combined on- and off-line data have allowed us to elucidate the key role of Mg^{2+} in both the precursor stabilization as well as in the structure, crystallinity and growth mechanisms of MHC.

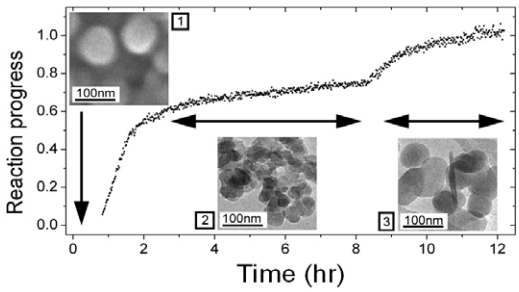

Figure 1: Reaction progress profile (***1***) precursor (***2***) MHC spheres at 3 h (***3***) MHC and HMg (plates) at 11 hr.

[1] Munemoto and Fukushi (2008) *Journal of Mineralogical and Petrological Sciences* **103**, 345-349.

High-pressure phases and dynamical properties of $ZnAl_2O_4$ and $ZnGa_2O_4$

P. RODRÍGUEZ-HERNANDEZ[1], A. MUÑOZ[1], S. LÓPEZ´-MORENO[1,2] AND A. ROMERO[2]

[1]MALTA Consolider Team, Departamento de Física Fundamental II and Instituto Univ. de Materiales y Nanotecnología, Universidad de La Laguna, 38205 La Laguna, Tenerife Spain (placida@marengo.dfis.ull.es)

[2]CINVESTAV-Querétaro, Libramiento Norponiente No 2000, Real de Juriquilla, Querétaro, Qro. Mexico

The structural dependence of oxide spinel AB_2O_4 compounds (A: divalent cation and B: trivalent cation) under pressure has received a lot of attention, mainly due to their occurrence in many geological settings of the Earth's crust and mantle, as well as in lunar rocks and meteorites. Many AB_2O_4 compounds crystallize in the cubic spinel structure (*Fd*3*m*), exemplified by $MgAl_2O_4$. In this work, we report first-principles calculations of the structural, electronic, and vibrational properties of the cubic spinels $ZnAl_2O_4$ and $ZnGa_2O_4$ compounds under hydrostatic pressure. Besides, we report the variation in the structural parameters under pressure and compare directly with recent experimental

results. Finally, we study the possible pressure induced structural phase transitions for both compounds that have been confirmed from X-Ray diffraction experiments [1] and from *ab initio* studies [2]. Total energy calculations were done within the framework of the density functional theory (DFT) and the projector-augmented wave (PAW) method. The exchange and correlation energy was described within the local density approximation (LDA). We use a plane-wave energy cutoff of 500 eV to ensure a high precision in the calculations. Monkhorst-Pack scheme was employed for the Brillouin-zone (BZ) integrations with dense meshes to ensure convergence. We will report the Raman and IR phonon modes as well as the pressure coefficients and Grüneisen parameters of the spinel structure and the pressure dependence of the Raman and IR active modes in other high-pressure structures.

[1] Errandonea, D. Kumar, R.S. Manjon, F.J. Ursaki, V.V. & Rusu, E.V. (2009) *Phys. Rev. B* **79**, 024103. [2] López, S. Romero, A.H. Rodríguez-Hernández. P. & Muñoz, A. (2009) *Phys. Rev. B* **79**, 214103.

https://doi.org/10.1180/S0026461X00006502 Published online by Cambridge University Press

Colonization of contaminated sediments: Implications in recovery of mass extinctions events

FRANCISCO J. RODRÍGUEZ-TOVAR[1]* AND FRANCISCO J. MARTÍN-PEINADO[2]

[1]Department of Stratigraphy and Paleontology, University of Granada, Spain (*correspondence: fjrtovar@ugr.es)
[2]Department of Soil Science, University of Granada, Spain

Biotic recovery after past bio-events is one of the difficult questions to interpret from mass extinction events. One of the recently proved useful approaches is the comparison with similar unfavourable environmental conditions in recent examples. To interpret the biotic recovery after the K-Pg impact event, characterized by an ejecta layer with high values in Ir as well as by positive anomalies of platinum-group elements and other elements (Zn, As, Cu, Ni, Co, Cr, Fe, etc.), the study of a contaminated area at the Tinto river has been conducted.

The marsh area of the Tinto river, next to the estuary of Huelva (SW Spain), is characterized by high concentrations of heavy metals accumulated in soils and sediments. These elements come from the draining and lixiviation of the river in relation to the Iberian Pyrite Belt, one of the most important polymetallic sulphide formation in Europe that has been exploited by human mining since ancient times. High concentrations of Zn, As, Cu and Tl, were found in the sediments of the marsh areas of two close locations (Palos de la Frontera, and Moguer). Values up to 1688 ppm of Zn, and 125 ppm of As were registered in the surface layer of the sediments; these levels are 2.2 and 2.5-fold, respectively, above the ecotoxicological levels reported in the bibliography. These concentrations should convert the substrate as inhabitable by organisms, but evidences of trace makers were found in this adverse media. Presence of biota colonizing into this high-polluted substrate prevents on a direct interpretation of the dramatic effect of some past bio-events based exclusively in the presence of high levels of toxic components.

The results agree with the recent ichnological evidence of a rapid colonization of the K-Pg boundary ejecta layer, classically interpreted as an inhabitable substrate, by organisms with a high independence with respect to substrate composition.

Paleoarchean barites record microbial reduction of a well-mixed marine sulfate reservoir

DESIREE L. ROERDINK[1], PAUL R.D. MASON, JAMES FARQUHAR[2] AND THOMAS REIMER[3]

[1]Department of Earth Sciences, Utrecht University, The Netherlands (roerdink@geo.uu.nl, mason@geo.uu.nl)
[2]Department of Geology and ESSIC, University of Maryland, College Park, USA (jfarquha@glue.umd.edu)
[3]Bernard-May-Str. 43, Wiesbaden, Germany (tobareim@alice.de)

Bedded barites from the Barberton greenstone belt (South-Africa) preserve a unique record of atmospheric, oceanic and microbial processes involved in the formation and evolution of the Paleoarchean (3.6-3.2 Ga) marine sulfate reservoir [1, 2]. Here, we present multiple sulfur isotope data from the ca. 3.5 Ga Londozi barite deposit in Swaziland, and the ca. 3.4 Ga Vergelegen, 3.26 Ga Stentor and 3.26-3.23 Ga Barite Valley deposits in South Africa. Individual deposits show relatively homogeneous mass-independent signatures ($\Delta^{33}S$, $\Delta^{36}S$) that support a significant contribution of sulfate from photochemical reactions in a low-oxygen atmosphere. Barites are enriched in ^{34}S (average $\delta^{34}S$ = 4.9‰) relative to the inferred composition of atmospheric sulfate ($\delta^{34}S \approx$ -0.5‰), suggesting an important role for global-scale microbial sulfate reduction as a ^{34}S-depleted sink. Modeling shows that variations in $\delta^{34}S$ per deposit can also be linked to active basin-scale biological reduction processes. Observation of relatively constant $\Delta^{33}S$ and $\Delta^{36}S$ in individual deposits and in barites of similar age from other cratons suggests that sulfate accumulated in a well-mixed oceanic sulfate pool, with a residence time similar to or slightly longer than the millenial timescale of barite formation. This global sulfate reservoir fed basins where barite precipitated and sulfate was microbially reduced, with minimal contributions from re-oxidation of sulfide and other sources of juvenile sulfur. Our results demonstrate that sulfate reducing micro-organisms played an important role in the early sulfate cycle similar to modern times, but with considerably less sulfide oxidation than seen in for example the Neoarchean [3].

[1] Huston, D.L. & Logan, G.A. (2004) *EPSL* **220**, 41–55.
[2] Reimer, T.O. (1980) *Precambrian Research* **12**, 393–410.
[3] Ono, S. *et al*. (2003) *EPSL* **213**, 15–30.

https://doi.org/10.1180/S0026461X00006502 Published online by Cambridge University Press

ID-TIMS as a tool for terrane provenance studies in polyorogenic complexes: A case from the SW-Norwegian Caledonides

CORNELIA ROFFEIS, FERNADO CORFU, ROY H. GABRIELSEN

Department of Geosciences, University of Oslo, Norway (cornelia.roffeis@geo.uio.no, fernando.corfu@geo.uio.no, r.h.gabrielsen@geo.uio.no)

The Caledonian mountain range along the western coast of Norway formed by the collision between Baltica and Laurentia in Silurian times. Several nappe sheets were thrust onto the Baltic basement and built up a mountain range which collapsed during following extensional tectonics and suffered severe erosion. Today the SW-Norwegian Caledonian nappe pile is fragmented into different tectonic units, overlying Baltic basement, without lateral connections.

In this work we look at the provenance of the Hardangervidda-Ryfylke Nappe Complex and its relations to the other nappes in the Caledonides. This nappe complex has been subdivided into three distinct nappe sheets, from bottom to top: the Dyrskard, Kvitenut and the Revsegg nappes. Previous dating with the Rb-Sr method had shown that the rocks formed in the Meso- to Neoproterozoic, but there was considerable uncertainty on the timing of metamorphic overprints and deformation. One specific question is whether the nappes have been emplaced together as one block, or as separate units, during the Caledonian orogeny.

We use ID-TIMS analyses, mainly on single grains of zircon, titanite and rutile from orthogneisses, metavolcanics, neosomes and pegmatites. Some of the main differences emerging at this stage concern the oldest units in the different nappes, which in the Kvitenut nappe point towards 1600 Ma whereas both the Revsegg and the Dyrskard nappes are around 1500 Ma. All three nappes have been affected by the Sveconorwegian orogeny. A most prominent effect is the emplacement of a large granitic body in the Kvitenut nappe at around 990 Ma, coeval with formation of local neosomes and the metamorphism of amphibolite and orthogneiss. The Caledonian overprint was also quite strong in all three nappe segments, disturbing the U-Pb systematics of zircon, forming new rutile, some titanite and local pegmatites. The latter have been affected by regional deformation and hence their age can be used to constrain the dynamics of the Caledonian processes in the region.

Redox-freezing and -melting of carbonates in the deep mantle and the role of transient carbides

A. ROHRBACH[1,2] AND M.W. SCHMIDT[1]

[1]Inst. f. Geochemistry and Petrology, ETH Zürich, Switzerland

[2]Inst. f. Mineralogy, University of Münster, Germany (arno.rohrbach@uni–muenster.de)

The onset of deep melting in the Earth's mantle is likely to be related to small amounts of CO_2/carbonate [1] buried to depths below the 660 km discontinuity as a component in subducted oceanic lithosphere. Thus, we investigate redox processes between oxidized carbonates and the reduced ambient mantle that potentially hosts an Fe, Ni metal phase [2–4]. We locate the carbon/carbonate redox equilibrium in terms of f_{O2} and the solidus temperature of carbonated peridotite at P and T relevant for the transition zone and lower mantle. Experiments were performed on a fertile peridotite composition containing 5 wt.% CO_2 at ETH. At 10–23 GPa, solidi temperatures are in the range of a mantle geotherm implying that small degree carbonatite melting is generally possible through thermal relaxation of subducted lithosphere. f_{O2} controlled experiments indicate that the carbon/carbonate equilibrium is situated ≥2 log units above IW at 10–23 GPa, i.e. ≥2 log units higher than likely f_{O2} conditions of ambient mantle. Consequently, carbonatite melts infiltrating the mantle are unstable and will suffer redox freezing through reduction of CO_2 to diamond causing their immobilization. On a local scale, carbonatite melts will consume Fe, Ni metal to leave a mantle domain that contains all iron as Fe^{2+} and Fe^{3+} in silicates and ferropericlase and all carbon as diamond [5]. The inverse process, carbonatitic redox melting, consuming Fe^{3+} and diamond would occur when such heterogeneities are entrained by upwelling mantle. Such melts cannot travel far within the metal bearing mantle matrix (as they would again reduce at depths > 250 km) and will only escape at less than ~120 km because the ambient f_{O2} remains too low also in metal free mantle to about this depth [6]. We expect a zone of Fe, Ni carbides to form at the boundaries of such domains where the mass of carbonatite is insufficient to oxidize all metal present. Preliminary data indicate that such carbides melt surprisingly at a few 100 degrees below the mantle geotherm.

[1] Dasgupta & Hirschmann (2006) *Nature* **440**, 659–662. [2] Frost *et al*. (2004) *Nature* **428**, 409–412. [3] Rohrbach *et al*. (2007) *Nature* **449**, 456–458. [4] Rohrbach *et al*. (2011) *J. Petrol*. **52**, 717–731. [5] Rohrbach & Schmidt (2011) *Nature* **472**, 209–212. [6] Stagno & Frost (2010) *EPSL* **300**, 72–84.

https://doi.org/10.1180/S0026461X00006502 Published online by Cambridge University Press

Compound-specific transverse dispersion in porous media: Darcy-scale experiments and pore-scale modeling interpretation

M. ROLLE[1]*, D. HOCHSTETLER[2], G. CHIOGNA[1], P.K. KITANIDIS[2] AND P. GRATHWOHL[1]

[1]Center for Applied Geosciences, University of Tübingen, 72076 Tübingen, Germany (*correspondence: massimo.rolle@uni-tuebingen.de)
[2]Department of Civil and Environmental Engineering, Stanford University, CA 94305, Stanford, USA

Multitracer laboratory bench-scale experiments and pore-scale simulations in different homogeneous saturated porous media were performed to (i) gain an improved understanding of the role of basic transport processes (i.e. advection and molecular diffusion) at the sub-continuum scale and their effect on the macroscopic description of transverse mixing in porous media; (ii) quantify the importance of compound-specific properties such as aqueous diffusivities for transport of different solutes.

A non-linear compound-dependent parameterization of transverse hydrodynamic dispersion is required to capture the lateral displacement observed in the experiments over a wide range of seepage velocities (0.1-35 m/day). With pore-scale simulations we can prove the hypothesis that the interplay between advective and diffusive mass transfer results in vertical concentration gradients leading to incomplete mixing in the pore channels. We quantify mixing in the pore channels using the concept of flux-related dilution index and show that different solutes undergoing transport in a flow-through system with a given average velocity can show a different degree of incomplete mixing. We conclude that physical processes at the microscopic level significantly determine the observed macroscopic behavior and, therefore, should be properly reflected in up-scaled parameterizations of transport processes such as local hydrodynamic dispersion coefficients. These findings are relevant also for the interpretation of isotopic signatures in groundwater [1] and for mixing-controlled reactive transport. In the latter case, a correct quantification of transverse mixing is of utmost importance to assess the length of contaminant plumes [2].

[1] Rolle *et al*. (2010) *Environ. Sci. Technol*. **44**, 6167–6173.
[2] Chiogna *et al*. (2011) *Water Resour. Res*. **47**, W02505, doi: 10.1029/2010WR009608.

Boron isotopes as pH proxy: Combination of boron speciation and isotope composition data

C. ROLLION-BARD[1]*, D. BLAMART[2], J. TREBOSC[3], G. TRICOT[3], A. MUSSI[4] AND J.-P. CUIF[5]

[1]CRPG-CNRS, BP20, 54501, Nancy, France (*correspondence: rollion@crpg.cnrs-nancy.fr)
[2]LSCE, 91198 Gif-sur-Yvette, France
[3]UCCS, 59652 Villeneuve d'Ascq, France
[4]UMET, Univ. Lille 1, 59655 Villeneuve d'Ascq, France
[5]IDES, Univ. Paris XI, 91405 Orsay, France

Reconstructing past atmospheric CO_2 level and elucidating its link with climate evolution is one of the most fundamental questions in Earth sciences. Boron isotopic composition ($\delta^{11}B$) of marine biocarbonates is considered to be a proxy for ocean pH. This technique has mainly been used in foraminifera and in tropical corals during previous climatic cycles and on longer geological time scales.

Dissolved boron in modern seawater occurs in the form of two species, trigonal boric acid $B(OH)_3$ and tetrahedral borate ion $B(OH)_4^-$, the proportion of which is dependent on pH of the solution. One of the key assumption in the use of $\delta^{11}B$ of carbonates as pH proxy is that only borate ions are incorporated into the carbonate. Here, we investigate the speciation of boron in deep-sea coral microstructures (*Lophelia pertusa* specimen) by using high field magic angle spinning nuclear magnetic resonance (^{11}B MAS NMR) and electron energy-loss spectroscopy (EELS). We observe both boron coordination species, but in different proportions depending on the coral microstructure, i.e. centres of calcification versus fibres. These results suggest that careful sampling is necessary before performing boron isotopic measurements in deep-sea corals. By combining the proportions of $B(OH)_3$ and $B(OH)_4^-$ determined by NMR and our previous ion microprobe boron isotope measurements, we propose a new equation for the relation between seawater pH and boron isotopic composition in deep-sea corals.

https://doi.org/10.1180/S0026461X00006502 Published online by Cambridge University Press

The interaction of Pd- and Pt-bearing chloride solutions with sulfide minerals: XPS, SPM and electrochemical study

A.S. ROMANCHENKO[1], O.F. GAYNULLOVA[2] AND YU.L. MIKHLIN[1]

[1]Institute of Chemistry and Chemical Technology SB RAS, K. Marx Str., 42, Krasnoyarsk 660049, Russia (alexrom@icct.ru)

[2]Siberian Federal University, Svobodny Av., 79 Krasnoyarsk 660062, Russia

The majority of platinum group element (PGE) deposits are of magmatic origin, and it has generally been assumed that PGEs are unreactive in aqueous media. However, Pt, Pd, and other metals may be mobile in surface environments, so adsorption and precipitation of PGE at sulfide minerals are of particular interest for the mineral processing, PGE analysis, etc. There are only few studies on this matter in the literature, for example, [1].

In the present work, we examined precipitation of Pd and Pt from aqueous PdCl42- and PtCl62- solutions onto pyrite, pyrrhotite and galena, including those previously reacted under different conditions, applying XPS, AFM, STM/STS, SEM, and cyclic voltammetry. It was found, in particular, that the deposition of Pt is slower than Pd; the quantities of the metals precipitated on pyrrhotite and pyrite are close. Preliminary oxidation of pyrrhotite surface results in an increase in the deposition of Pt, whereas the opposite trend was observed for pyrite. The results were interpreted in terms of the formation of Cl-, O- or S-bearing nanoscale species of Pd and Pt, with their proportion being a function of the reaction time and mineral pre-treatment (Fig. 1). The behaviour of the precipitated Pt and Pd entities was also studied.

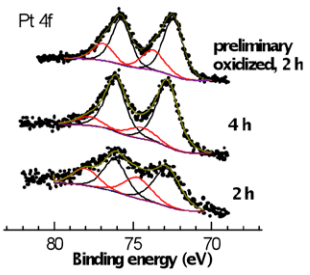

Figure 1: XP spectra from Pt deposited at pyrrhotite under various conditions (room temperature, 1 mM PtCl62-).

This work was supported by Grants from the Ministry of Education and Science of RF 02.740.11.0269, RFBR 09-05-98019, Grant of President of RF MK-5193.2011.5.

[1] Hyland *et al*. (1989) *Geochim. Cosmochim. Acta* **54**, 117-130.

$PuO_{2+x}{\cdot}nH_2O$ nanoparticles formation upon Pu(V,VI) sorption onto hematite

A.YU. ROMANCHUK[1]*, A.V. EGOROV[1], Y.V. ZUBAVICHUS[2], A.A. SHIRYAEV[3] AND S.N. KALMYKOV[1]

[1]Lomonosov Moscow State University, Moscow, Russia (*correspondence: romanchuk.anna@gmail.com)

[2]Kurchatov Institute, Moscow, Russia

[3]Frumkin Institute of Physical and Electrochemistry of RAS, Moscow, Russia

Plutonium (IV) as well as most of highly hydrolyzable cations forms intrinsic colloids that is demonstrated in many laboratory experiments mostly at relatively low pH values and high Pu concentrations. The gap of knowledge exists on the possibility and mechanisms of intrinsic colloids formation under conditions more relevant to the environment. The purpose of this study was to define the mechanisms of Pu (V, VI) interaction with hematite colloids including redox reactions and formation of intrinsic colloids.

It was previosly shown [1] that Pu in high valence states is reduced to Pu (IV) upon sorption onto hematite. In case of Pu (IV) at very low total concentrations, e.g. ~10^{-14} M, the fast sorption of monomeric species on hematite occur, while in case of Pu (VI), the sorption is kinetically controlled by slow reduction on the surface. For total concentrations of Pu around 10^{-6} the reduction of Pu (V, VI) upon sorption onto hematite is confirmed by Pu L_{III} XANES. The reduction is accompanied by the formation of PuO_{2+x} crystalline nanoparticles with average size of 1-2 nm that was independently demonstrated by HR-TEM and Pu L_{III} EXAFS measurements.

The most challenging question is concerning Pu behavior at lower concentrations, i.e. around 10^{-9} M and less. Due to the increase of concentration near the surface, Pu (IV) could polymerize even at this relatively concentration that strongly effect both kinetics of sorption and leaching behavior. For the first time it was demonstrated by HRTEM that Pu (V, VI) reduction upon sorption result in the formation of low-crystallinity PuO_{2+x} nanoparticles.

[1] Romanchuk *et al*. (2011) *Radiochim.Acta* **99**, 137–144.

https://doi.org/10.1180/S0026461X00006502 Published online by Cambridge University Press

Nitrogen limitation in extremophilic hydrothermal ecosystems of Yellowstone National Park

S.J. ROMANIELLO[1]*, H.E. HARTNETT[1,2], A.D. ANBAR[1,2], J.J. ELSER[3] AND E.L. SHOCK[1,2]

[1]School of Earth and Space Exploration, Arizona State University, Tempe, AZ 85287-1404 (*correspondence: sromanie@asu.edu)

[2]Department of Chemistry and Biochemistry, Arizona State University, Tempe, AZ 85287-1406

[3]School of Life Sciences, Arizona State University, Tempe, AZ

We present the results of ^{15}N assimilation experiments conducted with hydrothermal chemotrophic and phototrophic microbial mats in Yellowstone National Park (YNP), USA. *In situ* ^{15}N incubations were carried out with $^{15}NO_3^-$, $^{15}NH_4^+$, and $^{15}N_2$ during the summer 2009 and 2010 field seasons over a wide range of temperature and pH (50-92°C, pH = 2.1-9.3).

Measured rates of NO_3^-, NH_4^+, and N_2 assimilation vary widely between sites. The highest assimilation rates were generally found in photosynthetic mats. NO_3^--assimilation was detected at some high temperature sites but was conspicuously absent at others, even when these sites exhibited remarkable geochemical simularity. Measurable rates of N_2-fixation were measured in the phototrophic cyanobacterial mats. However attempts to detect N_2 assimilation in high temperature, alkaline, chemotrophic communities were unsuccessful.

NO_3^- assimilation rates determined in 2009 using 1-4 μM initial NO_3^- were generally <10% of 2010 rates using 100 μM initial NO_3^- at reoccupied sites (e.g. Figure 1). These results imply that nitrate assimilation may be strongly understaturated at *in situ* NO_3^- concentrations (<1.5 μM). This suggests that nitrogen limitation may be an underappreciated aspect of hydrothermal ecosystem biogeochemistry.

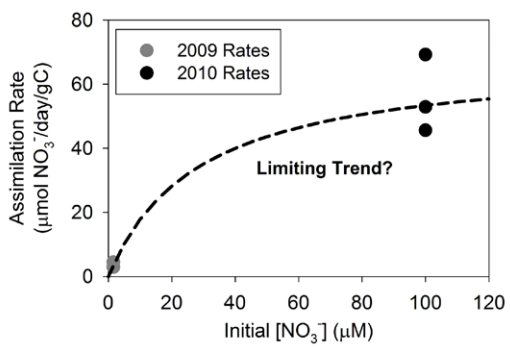

Figure 1: Nitrate assimilation rate as a function of initial NO_3^- concentration at a hot spring near Obsidian Pool, YNP.

Concerning organization of geochemical environment as a study object for geochemistry

S.L. ROMANOV[1]* AND E.M. KOROBOVA[2]

[1]Unitary Enterprise .Geoinformation systems., Belarus National Ac. of Sciences, 220004 Minsk, Surganov Str., 6, Belarus (*correspondence: romanov_s_l@mail.ru)

[2]Vernasky Institute of Geochemistry and Analytical Chemistry, Rus.Ac. of Sci., 119991 Moscow, Kosygin Str., 19, Russia, Korobova@geokhi.ru)

In the light of concepts of theoretical geochemistry the environment is presented by a set of hierarchically ordered and geochemically discontinuous objects such as biosphere or lithosphere which in their part consist of a quantity of the smaller structural units – rocks, gases, proteins. On the molecular level the latter present sets of typical components made of a relatively limited number of chemical elements. In general the environment is treated as the present result of the continuous chemical reactions. However the paradox is that the observed environment can not be interpreted as a result of all the possible chemical reactions. To produce such an object as the World Ocean, or an ore deposit the necessary chemical elements should occur in the corresponding volume, the corresponding form and sufficient quantity. In the other words the physically significant result of interaction of all the substances is characterized by significant masses presented in the particular volume. Therefore the quantity of all the chemical elements present on the Earth may be treated as material bodies of the particular elements such as iron, oxygen or actinium.

Such an approach is logically unrepugnant and permit to formulate an important corollary. All chemical elements and compounds that are in the environment regardless of form, quantity and aggregate state are organized as material bodies which have general and specific properties such as weight, dynamics and space configuration. Furthermore, theirs bodies exhibit characteristics of a three-dimensional fractal.

This assertion does not contradict any of the basic tenets of science and allows us make a more general conclusion. Parameters of the existing geochemical environment at all levels of organization are naturally predetermined by specific interaction of a small number of material bodies, that are stable in time and space and are the basic components of the universe.

If these statements are true (they are at least logically consistent) then the environment can be considered as constantly evolving, naturally organized and well-balanced superposition of special geochemical bodies, which in framework of notions of theoretical geochemistry may become the main object of this science. Such object is in full measure able to provide formal interpretation and comparison of all the existing geochemical data using the means of modern physics and mathematics.

https://doi.org/10.1180/S0026461X00006502 Published online by Cambridge University Press

Assessment of arsenic toxicity using bioassays. Application in contaminated soils

A. ROMERO-FREIRE[1], G.N. ANTÚNEZ, F. MARTÍN-PEINADO[1]*, M.O. ESCOTO[2] AND A. ROCA[1]

[1]Soil Science Department. Faculty of Sciences. University of Granada. 18002 Granada, Spain (*correspondence: fjmartin@ugr.es)

[2]Natural Resource Management and Environment. National University of Agriculture. P.C. 9. Catacamas. Honduras

In last decades, arsenic has become a serious environmental problem due to the extensive use and to its potential high toxicity [1]. Arsenic trends to accumulate in soils because its low mobility in this media, although water-soluble fractions are highly bioavailable [2]. Soil toxicity bioassays are based on the evaluation of the toxic effect of the solid phase or the soil solution over a living organism [3].

Potential As toxicity from bioassays with *Vibrio fischeri* and *Lactuca sativa* germination test was estimated. These assays were done in artificially contaminated solutions (ranging from 0.1 to 100 ppm As), and in water extracts from soils spiked with 100 ppm As. Both bioassays had a different response in the artificially contaminated solutions. According to the EC50 values (Table 1), the *Lactuca sativa* test showed higher sensitivity to the toxicity than *Vibrio fischeri* bioassay.

	EC50 (mg/kg)	
	Value	95% CI
Lactuca sativa	2.46	1.36 - 4.48
Vibrio fischeri	12.33	7.83 - 19.42

Table 1: EC50 values in the contaminated solutions. CI: Confidence interval at 95%.

Four soils with different properties were contaminated with 100 mg As kg^{-1} soil. Soil organic matter ranged from 1.2 to 6.8%, calcium carbonate from 0 to 39%, and clay content from 9 to 33%. In all cases the As concentration in soil solutions was below 0.03 mg kg^{-1}. The results of toxicity bioassay with the solutions coming from the contaminated soils indicated no toxic response in the case of lettuce germination test or *Vibrio fischeri* bioassay. Further studies are needed to check the main parameters controlling the reduction of toxicity in relation to soil properties.

Acknowledgement: Research project CGL2010-19902.

[1] Adriano (1986) Springer-Valag. 533 p. [2] Beesley *et al*. (2010) *Env*. *Poll*. **158**, 2282–2287. [3] Martín *et al*. (2010) *Int*. *J*. *Chem*. *Eng*. *Art* ID 101390.

Imaging the removal of radionuclides from solution by NZVI using HRTEM

M.E. ROMERO-GONZALEZ[1]*, GABRIELLA KAKONYI[1] AND IAN M ROSS[2]

[1]Cell-Mineral Research Centre, The University of Sheffield, Kroto Research Institute, Sheffield, UK (*correspondence: m.e.romero-gonzalez@sheffield.ac.uk)

[2]Kroto Centre for High Resolution Imaging and Analysis, The University of Sheffield, Kroto Research Institute, Sheffield S3 7HQ, UK

Nano zero valent iron (NZVI) has been promoted as a remedial strategy for a range of contaminants present in the environment. Its applications range from the remediation of chlorinated compounds in sediments to arsenic in groundwater and aquifer material. Its properties such as size, mobility through porous media and reactivity offer advantages for remediation of contaminants under a variety of remedial strategies: used as complement material on iron barriers, direct injection to aquifers and targeted emplacement in subsurface zones.

We explore here the use of NZVI as an external barrier to radionuclide deep nuclear repository waste containment. Rates of removal of U (VI) removal in suspensions of NZVI (nanoFer 25 and 25S) were performed in batch systems in presence of ordinary portland cement (OPC) at pH 9 and 12. All experiments were conducted in an anoxic glovebox free of CO_2. Samples were taken for the quantification of U (VI), Ca and total Fe by ICP-MS. Samples were also analysed using a HRTEM JEOL 2200FSC. The HRTEM provides a maximum 0.05 nm spatial resolution, this allowed the imaging of the reaction products at atomic scale.

The results showed that NZVI can effectively remove uranium (VI) from solution under a range of conditions. The presence of high Ca concentrations reduce the efficiency of NZVI to remove U (VI) when compared to systems without Ca. However, the overall efficiency of the NZVI-cement system was little compromised since U (VI) was effectively removed from solution under all studied conditions.

The HRTEM results indicated mainly a coprecipitation mechanism for the removal of U (VI) from solution at highly alkaline pH. Therefore the potential to use NZVI technology to increase the efficiency of barriers around a deep nuclear waste repository is very promising. Additionally, HRTEM has proven to be a very valuable tool on the investigation of nanoparticle interactions with porous media.

https://doi.org/10.1180/S0026461X00006502 Published online by Cambridge University Press

Hydrogen isotopic signatures of algal biomarkers as a proxy of hydroclimatic variability in Lake Isabel, Mexico

L. ROMERO[1]*, H.G. HAUG[1,2], U. KIENEL[1,3] AND D. SACHSE[1].

[1]Institut für Erd- und Umweltwissenschaften, Karl-Liebknecht-Strasse 24, 14476 Potsdam, Germany (*correspondence: romero@geo.uni-potsdam.de)
[2]Geologisches Institut, Department Erdwissenchaften, ETH Zürich, Sonneggstrasse 5, 8092 Zürich, Switzerland
[3]German Research Centre for Geosciences-Helmholtz-Centre Potsdam. Telegrafenberg. 14473 Potsdam, Germany

Based on the observed linear relationships between the isotopic composition of the source water and the δD values of aquatic and terrestrial lipid biomarkers, the analysis of the isotopic signature in these organic molecules preserved in sediments has become a new tool for paleohydrological reconstruction. However the influence of additional factors (i.e. growth rate, salinity, and temperature) on the δD values of algal lipids remains poorly understood. Therefore, sediments from a short core corresponding to the time period 1943-2003 A.D from a hypersaline crater lake located on Isla Isabel, 30km off the Pacific Coast of Mexico, were analysed for lipid biomarker δD values and compared to instrumental climate data. δD values of the 1,15C_{32} diol, a specific biomarker for algal populations, showed a significant relationship with the instrumental record of rainfall amount confirming its potential as a proxy of past hydroclimatic conditions. Unexpectedly, deuterium-enrichment in diols was observed during wetter conditions while these were significantly depleted during drier periods. We hypothesize that under this strongly seasonal climate regime algal growth conditions play an important role in determining algal lipid δD values. This calibration study between the isotopic signatures and the climatic record shows the complexity but also the potential of hydrogen isotope analyses of lipids as proxy to reconstruct the past climatic variability.

The role of inorganic additives in evaporitic carbonate precipitation

T. RONCAL-HERRERO[1,2]*, P. BOTS[2], J.D. RODRIGUEZ-BLANCO[2], S. SHAW[2] AND L.G. BENNING[2]

[1]Department of Geosciences, University of Oslo, PB 1047, Blindern, Oslo, Norway
[2]School of Earth and Environment, University of Leeds, Leeds, LS2 9JT, United Kingdom (*correspondence: eartr@leeds.ac.uk)

Interactions between carbonate-bearing groundwaters and sulphate minerals in evaporitic settings lead to the formation of carbonate deposits [1]. However, our understanding of the reaction kinetics in these processes is still fragmented.

An experimental study following the formation of $CaCO_3$ phases from gypsum (GYP, $CaSO_4.2H_2O$) in the presence of 1 to 100 mM of Mg, Zn, Sr, or PO_4 was carried out at 25°C. GYP (Ø < 420 μm) was reacted with 50 mM Na_2CO_3 at a GYP/liquid ratio of ~ 0.007 in stirred closed reactors. The experiments were run at two different initial pH settings (***a***) pH ≈ 11.4, due to the Na_2CO_3 or (***b***) pH ≈ 6.8, where the solutions was also supersaturated with $CO_{2\ (g)}$. Solids were characterized over time by X-ray diffraction and high-resolution microcopy imaging while changes in aqueous contentrations were determined by ion chromatography.

The results of both sets showed that the dissolution of GYP (release of Ca^{2+}) lead to a relatively fast nucleation and growth of $CaCO_3$ polymorphs. As long as the solution had excess carbonate, the continuous dissolution of gypsum was mirrored by a simultaneous precipitation of $CaCO_3$. In all cases, the first phase nucleating on the gypsum surface was amorphous $CaCO_3$ (ACC). Depending on experimental approach or the presence of additives, ACC transformed gradually to various $CaCO_3$ polymorphs. At condition (***a***) the GYP completely dissolved in ~ 24 h and the initial ACC transformed into calcite within 2 days, while in approach (***b***) GYP took only ~ 5 h to fully dissolve and the carbonate that formed after 30 h was 'stable' vaterite [2]. The presence of additive ions strongly influenced both the reaction kinetics and the nature of the crystalline end products. For example, using approach (***b***) but adding 1 mM Zn produced calcite (instead of vaterite) with Zn becoming incorporated into the calcite structure; conversely, with 100 mM Mg present in the initial solution, ACC transformed to aragonite after 12 h and calcite was not observed. These results revealed that aqueous additives play a fundamental role in controlling the nature and formation pathway of the end product and this has major implications for biomineralization, industrial applications, and CO_2 sequestration.

[1] Sanz-Rubio *et al*. (2001) *Sedim. Geology* **140**, 123–142.
[2] Bots *et al*. (2011) *Geology* **39**, 331–334.

https://doi.org/10.1180/S0026461X00006502 Published online by Cambridge University Press

Re-Os geochronology of the Neoproterozoic Coppercap and Twitya Formations: Implications for the Rapitan-Sturtian glaciation

A.D. ROONEY[1]*, F.A. MACDONALD[2] AND D. SELBY[1]

[1]Earth Sciences Department, Durham University, DH1 3LE, UK (*correspondence: alan.rooney@durham.ac.uk)
[2]Department of Earth & Planetary Sciences, Harvard University, Cambridge MA, 02138

The late Neoproterozoic Windermere Supergroup of NW Canada is a ~7 km thick mixed carbonate-siliciclastic succession deposited on the margin of Laurentia. The Coppercap Formation of the Coates Lake Group consists of ~300 m of TOC-rich limestone that unconformably underlie glaciogenic deposits of the Rapitan Group. U-Pb zircon ages below and within the Rapitan Group in the Yukon constrain the onset of the Rapitan glaciation to ca. 717 Ma. The Rapitan Group is conformably overlain by the Twitya Formation, which is ~900 m thick and consists predominantly of carbonate and siliciclastic turbidites.

A 21 m interval of organic-rich carbonate of the Coppercap Formation yields a Model 1 depositional isochron age of 733 ± 4 Ma. Further Re-Os geochronology of a ~2 m interval of organic-rich carbonate of the Twitya Formation yield a Model 1 depositional isochron age of 655 ± 26 Ma. Combined with U-Pb zircon data, these ages constrain the minimum duration of the Rapitan glaciation to 36 Myrs.

Initial Os isotope composition (Os_i) derived from the Re-Os isotope data of the Coppercap Formation reveals an unradiogenic Os_i (0.14) for seawater prior to the Rapitan glaciation. This unradiogenic Os seawater signal may be derived from the erosion of basalts of the underlying Little Dal Group as well as the Gunbarrel magmatic events, and hydrothermal vents associated with rifting during the break-up of Rodinia. The Os_i data from the Twitya Formation yields a radiogenic composition (~0.83) suggesting that post-glaciation; the crustal Os flux from rivers exerted a strong influence on ocean Os composition. These data are consistent with Sr isotope data, which show a large increase to more radiogenic values across the Rapitan-Sturtian glaciation.

Both the Re-Os isochron age and the Os_i data for the Twitya are identical, within uncertainty, to that of the Aralka Formation, which overlies the glaciogenic Areyonga Formation of Central Australia suggesting that de-glaciation was broadly penecontemporaneous, and that the Sturtian and Rapitan glaciations are correlative. The Re-Os geochronology and Os_i data presented here has profound implications for our understanding of Late Proterozoic ocean chemistry and the Snowball Earth hypothesis.

Synchrotron XAS and XRF study of microbially reduced arsenic and iron in iron-based remediation media

ROBERT A. ROOT[1]*, FERNANDO J. ALDAY[2], SAHAR FATHORDOOBADI[2], WENDELL P. ELA[2] AND JON CHOROVER[1]

[1]Department of Soil, Water and Environmental Science, University of Arizona, Tucson AZ, USA (*correspondence: rroot@email.arizona.edu)
[2]Department of Chemical and Environmental Engineering, University of Arizona, Tucson AZ, USA

Arsenic remediation technologies exploiting the high affinity of ferric (oxy)hydroxides for oxyanion sorption has resulted in a significant increase in the volume of arsenic-bearing solid residuals generated by drinking water utilities. These iron sorbents widely utilized for water treatment may be legally disposed in municipal solid-waste landfills if they pass the USEPA toxicity characteristic leaching procedure (TCLP). However, conditions in a mature landfill are biotic and generally suboxic where iron and arsenic may be reduced and released to the leachate; a consequence not simulated with the TCLP test. To examine the effect of biotically induced reducing conditions, controlled flow through column experiments were used to simulate conditions similar to those found in a landfill. Upflow 30 cm x 2.5 cm reactors were packed with 15 g (dry wt.) ferric arsenate sludge (Fe:As = 20:1; pH 7-8) and 73 g of 0.8 mm glass beads then reacted for 432 days (864 pore volumes) with a synthetic landfill leachate containing nutrients (e.g. components: $[SO_4]$ = 64μM, [Na] = 12 μM, [CO3]= 24 μM etc.) and a consortium of microorganisms from an anaerobic digester sludge collected from a water treatment plant.

Columns were sub-sectioned and investigated with Synchrotron X-ray absorption spectroscopy and fluorescence microprobe (μXRF) to determine the bulk As, Fe, and S speciation and to spatially resolve As and Fe species with energy difference μXRF mapping. Reducing conditions prevail at the inlet of the column and the primary iron phase there is siderite, whereas vivianite, green rust and ferric (oxy)hydroxide form as the conditions become more oxic. Arsenic is present as As (III) and As (V) sorbed to ferric (oxy)hydroxide in suboxic and oxic environments respectively. When the columns are run at sulfate influent concentrations increased from 64 μM to 2.1 mM, the primary iron and arsenic phases are amorphous iron sulfide (FeS) and realgar (AsS), indicating sulfate and iron concentrations are important for As sequestration in landfills.

https://doi.org/10.1180/S0026461X00006502 Published online by Cambridge University Press

Contaminated soil diagnosis by electrical resistivity tomography in underground storage tanks of different petrol stations in SE Spain

R.M. ROSALES*, P. MARTÍNEZ AND A. FAZ

Technical University of Cartagena, Cartagena 30203, Spain (*correspondence: rosamaria.rosales@upct.es, p.martinez@upct.es, angel.fazcano@upct.es)

Introduction

Soil contamination could be produced by petroleum products spill and leaks related to activities of refinement and fuel dispensing in Service Stations. Although pipelines and Underground Storage Tanks (UST) are designed to avoid this kind of accidents, the large amount of fuel dispensed at petrol stations during years may cause a very important damage in the surrounding uncontaminated area.Through this research it has been made an environmental diagnosis to identify possible leaks in UST as plumes in the subsoil by applying Electrical Resistivity Tomography 2D (ERT 2D), a non destructive geophysical technique in three petrol stations located in Murcia Region, Spain. Three ERT profiles were carried out in each petrol station per campaign (wet and dry seasons).

Results and discussion

Figure1 shows electrical pseudosections obtained by processing ERT data with PROSYS II and RES2DINV softwares corresponding to one petrol station in wet season.These results may define different confined zones in the subsoil with electrical resistivity values up to 2000 Ω·m, very high values for a natural soil. Hydrocarbons are excellent insulators and exhibit very high values of electrical resistivity [1] around 2500 Ω·m, values assigned to a possible fuel leak [2].

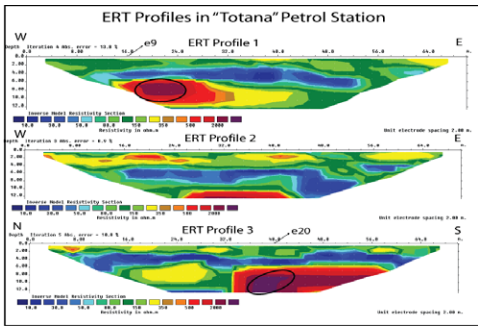

Figure 1: Processed pseudosection from ERT 2D profiles in "Totana" petrol station corresponding to wet season.

[1] Delaney *et al*. (2001) *Cold Reg. Sci. Techn.* **32**, 107–119.
[2] Znamensky (1980) *Field Geophysics. Nedra* **351**, 279–284.

On the variability of aerosol intensive optical properties over South America

N.E. ROSARIO[1,2]*, M.A. YAMASOE[1] AND K.M. LONGO[2]

[1]University of São Paulo, São Paulo, Brazil (*correspondence: nrosario@model.iag.usp.br) (akemi@model.iag.usp.br)
[2]National Institute for Space Research, São José dos Campos, Brazil (karla.longo@inpe.br)

The variability of aerosol intensive optical properties, specifically single scattering albedo ($\omega_{o\lambda}$) and asymmetry parameter (g_λ), over South America have been analyzed using data from Aerosol RObotic NETwork [1]. The stations considered in the study are installed in distinct environment: Alta Floresta and Belterra are in the biomass burning regions of the southern and northeast of the Amazon basin, respectively, Cuiaba is in the *Cerrado* area, São Paulo is an urban center in the southeast of Brazil, and Arica and Surinam are coastal sites on the west and north coast of South America, respectively. The variability of aerosol optical properties inter and intra stations is significant, in particular for those located downwind of the biomass burning regions. Further differences emerge when the signal of smoke aerosols from the southern of Amazon basin are excluded from the mean calculation. For instance, São Paulo and Cuiaba locally produced aerosol is more absorbing than the indiscriminate average of optical properties suggests. The smoke transport from the southern Amazonia tends to reduce the heterogeneity that characterizes optical properties elsewhere. A clustering analysis based on the magnitude and spectral dependence of $\omega_{o\lambda}$ and g_λ was performed for each station. The factors associated with the occurrence of the identified clusters vary among the stations. For São Paulo and Cuiaba, as expected, the clusters occurrence are indeed correlated to the smoke transport. In Alta Floresta less absorbing clusters are in general associated with wetter and/or highly polluted conditions. Arica presents the lowest variability in optical properties, although a dependence on the wind diurnal cycle was observed. These results have been analyzed from the perspective of the representation of aerosol intensive optical properties in regional circulation models. Ongoing analysis evaluating the impact of the variability in optical properties on radiative balance using the Coupled Aerosol and Tracer Transport model to the Brazilian developments on the Regional Atmospheric Modelling System [2] are discussed.

[1] Holben *et al*.(1994) *Rem. Sens. Environ*, **66**, 1–16.
[2] Freitas *et al*.(2010) *Chem. Phys. Discuss*. **7**. 8525–8569.

https://doi.org/10.1180/S0026461X00006502 Published online by Cambridge University Press

Exploring the first steps of iron(III) oxyhydroxide nucleation using a competitive ligand kinetic approach

ANDREW L. ROSE

Southern Cross GeoScience, Southern Cross University, Lismore 2480, Australia
(*correspondence: andrew.rose@scu.edu.au)

Under favourable conditions, nucleation of iron (III) oxyhydroxides (FeOx) is typically rapid compared to subsequent processes. To date, little work has been done to examine the first steps of FeOx nucleation, namely the initial polymerisation of dissolved monomeric iron (III) complexes, which may be rate-limiting in the nucleation process.

I have investigated the kinetics of iron (III) polymerisation over a wide range of pH values using a competitive ligand approach in which the complexation of monomeric iron (III) by desferrioxamine B (DFB) competes with iron (III) polymerisation when conditions conducive to nucleation are induced. Polymerisation was induced by the rapid (< 5 ms) mixing of acidified solutions of dissolved iron (III) with a pH-buffered DFB solution using a micromixer chip. Formation of the orange coloured iron (III)-DFB complex was quantified over time from 100 ms after mixing onwards at concentrations down to ~10 nM with a stopped-flow long (1 m) optical pathlength spectrophotometry system (Figure 1).

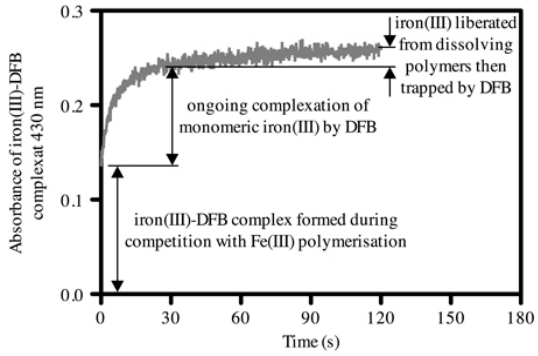

Figure 1: Kinetic traces reveal initial rapid partitioning of iron(III) between the iron(III)-DFB complex and iron(III) polymers, followed by the slow redissolution of polymers.

Kinetic parameters for FeOx polymerisation (obtained by simultaneously fitting data from multiple iron (III) and DFB concentrations at each pH) varied with pH in a manner consistent with control of the initial polymerisation step by the exchange of water bound to monomeric iron (III). The initial steps in FeOx nucleation can thus be interpreted in a similar context to other aquatic chemical processes.

Environmental impact of engineered nanoparticles and nanomaterials through their life cycle

JÉRÔME ROSE[1,2], MÉLANIE AUFFAN[1,2], PERRINE CHAURAND[1,2], JÉRÔME LABILLE[1,2], DANIEL BORSCHNECK[1,2], ARMAND MASION[1,2], HELENE MICHE[1,2], CÉLINE BOTTA[1], CHRISTOPHE GEANTET[3], ERIC PUZENAT[3], PAVEL AFANASIEV[3], EMMANUEL LECELRC[3], JEANNE GARRIC[4], FOUQUERAY MANUELA[4], BERNARD VOLLAT[4]; PATRICE NOURY[4]; KHEDIDJA ABBA CI[4], KRZYSZTOF PIELICHOWSKIAZE[5], AGNIESZKA LESZCZYNSKA[5], SLAWOMIR MICHALOWSKI[5], JAMES NJUGUNA[6], SOPHIA SACHSE[6] AND JEAN-YVES BOTTERO[1,2]

[1]CEREGE UMR 6635- CNRS, Aix-Marseille Université, 13545 Aix-en-Provence France
[2]ICEINT: international Center for the Environmental Implications of Nanotechnology, CNRS-CEA, www.i-ceint.org
[3]IRCELYON, UMR 5256 CNRS/Université LYON 1, F-69626 Villeurbanne France
[4]CEMAGREF Lyon UR MALY, Ecotoxicologie, F-69336 Lyon France
[5]Cracow University of Technology, Krakow, Poland
[6]Cranfield University , Bedfordshire MK43 0AL ,United Kingdom

Even though preliminary risk assessments of manufactured nanoparticles (NPs) are emerging, information on NPs bioavailability to aquatic biota and trophic transfer are largely lacking, and early studies have yielded incomplete and contradictory results. Moreover, a considerable confusion exists concerning the distinction between 'nanotechnology' and 'nanomaterial' which are most often considered to be synonymous of nanoparticles. But for most applications nanoparticles can be surface modified and generally are embedded in the final product and therefore do not come into direct contact with consumers or the environment. So what about their toxic effects when surface modified?

The aim of our stufy is to better constrain the transfer, transformation and ecotoxicity of by-products released from nanomaterials during their life cycle. Two examples will be detailed 1) nano-TiO_2 incorporated as UV filter in sunscreens ii) nano-SiO_2 based composite (polymeric matrixes including polyamides, polypropylenes and polyurethanes as bulk materials) to compare impact between by-products and bare nanoparticles. Methodology and experimental issues concerning durability characterisation using accelerated aging protocols, characterisation will be adressed.

The project is supported by the French national programs NANOALTER (INSU/EC2CO/CYTRIX), AGING NANO & TROPH (ANR-08-CESA-001) and the FP7 NEPHH project (CP-FP 228536-2).

https://doi.org/10.1180/S0026461X00006502 Published online by Cambridge University Press

Medically-derived ^{131}I as a tracer in aquatic environments

P.S. ROSE[1,2]*, J.P. SMITH[2], J.K. COCHRAN[1], R.C. ALLER[1], R.L. SWANSON[1] AND R.B. COFFIN[2]

[1]SoMAS, Stony Brook University, Stony Brook, NY 11794-5000, USA

[2]Marine Biogeochemistry, Code 6114, US Naval Research Laboratory, Washington, DC 20375, USA (paula.rose.ctr@nrl.navy.mil)

Iodine-131 ($t_{½}$ = 8.04 d) has been measured in Potomac River water and sediments in the vicinity of Blue Plains, the world's largest advanced wastewater treatment plant. It serves all of Washington, DC, treats an average of 1.4 x 10^9 L d^{-1} and has a maximum capacity of >4 x 10^9 L d^{-1}. Concentrations of ^{131}I detected in sewage effluent and in the river suggest a continuous dischage of the isotope from Blue Plains. Surface water ^{131}I ranged from 0.076 ± 0.006 to 6.07 ± 0.07 Bq L^{-1}. Partitioning in sewage effluent and river water suggests that ^{131}I is associated with colloidal and particulate organic material. Iodine-131 was detected in sediments to depths of 5 cm with specific activites between 1.3 ± 0.8 and 117 ± 2 Bq kg^{-1} dry weight. The behavior of ^{131}I in the Potomac River is consistent with the cycling of natural iodine in aquatic environments. It is discharged to the river via sewage effluent, incorporated into particulate matter and deposited in sediments where it is subject to diagenetic remineralization.

Additionally, dissolved ^{131}I showed a strong, postive correlation with $\delta^{15}N$ values of nitrate in the river. Surface water $\delta^{15}NO_3$ values ranged from 8.7 ± 0.3 to 33.4 ± 7.3‰ with dissolved inorganic nitrogen (NO_3+NO_2) concentrations between 0.38 ± 0.02 and 2.79 ± 0.13 mgN L^{-1}. $\delta^{15}N$ in sediments ranged from 4.7 ± 0.1 to 9.3 ± 0.1‰. Sediment profiles of particulate ^{131}I and $\delta^{15}N$ indicate rapid mixing or sedimentation and in many cases remineralization of a heavy nitrogen source consistent with wastewater nitrogen.

Sewage effluent discharges of ^{131}I to surface water can be used to study the rates and mechanisms controlling natural iodine cycling. Iodine-131 coupled with $\delta^{15}N$ can be an excellent tracer for the short-term fate of wastewater nitrogen. The utility of ^{131}I is not limited to the Potomac River. The presence of medically-derived ^{131}I has been documented in several aquatic environments and is readily measureable in sewage effluent. Continuous discharges of this radioisotope in sewage effluent are likely to be widespread. Further study of ^{131}I in receiving waters can provide valuable insight into the fate and transport of this radioisotope in the context of large scale accidental releases.

Volatile abundances and Pb isotopes in melt inclusions from Iwate volcano, Japan

E.F. ROSE-KOGA[1]*, K.T. KOGA[1], M. HAMADA[2], T. HELOUIS[1], M.J. WHITEHOUSE[3] AND N. SHIMIZU[4]

[1]Laboratoire Magmas et Volcans, Universite Blaise Pascal, CNRS, UMR 6524, IRD, R 163, Clermont-Ferrand, France (*correspondence: ekoga@opgc.univ-bpclermont.fr)

[2]Department of Earth and Planetary Sciences, Tokyo Institute of Technology, Japan

[3]Swedish Museum of Natural History & Nordic Center for Earth Evolution, Stockholm, Sweden

[4]Woods Hole Oceanographic Institution, Woods Hole, MA 02543, USA

The pre-eruptive volatile content of magma is of fundamental importance for understanding melting processes, as well as eruption dynamics. However, since volatiles in magma are largely degassed during subaerial eruptions, it is difficult to estimate their pre-eruptive concentrations based on the measurements of volcanic whole rocks. Melt inclusions trapped in early crystallizing olivine retain dissolved volatiles of magmas at depth (e.g. [1]).

Iwate volcano is located on the volcanic front of the North-east Japan arc on the Honshu Island. The Iwate samples are one of the most undifferentiated rocks on the volcanic front of Japanese island arcs. The olivine hosted melt inclusions of the 1686 eruption of Iwate volcano are basaltic to basaltic-andesitic in composition.

The melt inclusions have Pb isotope compositions $^{207}Pb/^{206}Pb$ (0.836 to 0.850) and $^{208}Pb/^{206}Pb$ (2.079 to 2.094). These compositions are homogeneous and close to MORB values. The volatile contents (H_2O, S) are highly variable and reaches values comparable to that of Izu Oshima melt inclusions (up to 3.57 wt% and 1798 ppm, respectively; [2]). F and Cl concentrations are highly clustered between 113 and 183 ppm and 285 and 408 ppm, respectively. This low F and Cl magma, yet with arc H_2O content, may represent partial melting of a highly depleted mantle wedge with no or little metasomatism.

[1] Sobolev (1996) *Petrol.* 209–220. [2] Ikehata, Yasuda & Notsu (2010) *Miner. Petrol.* 143–152.

https://doi.org/10.1180/S0026461X00006502 Published online by Cambridge University Press

U/Pb age spectra of detrital rutile as a powerful tool for provenance analysis

DELIA RÖSEL[1], THOMAS ZACK[1], MATTHIAS BARTH[1], ANDREAS MÖLLER[2] AND JEFFREY OALMANN[2]

[1]Institut für Geowissenschaften, Universität Mainz, Becher Weg 21, 55128 Mainz (*correspondence: roeseld@uni-mainz.de)

[2]University of Kansas, Dept. of Geology, Lawrence, KS, 66045, USA

Compared with zircon, rutile is assumed to be unstable during low-grade metamorphic conditions, so that rutile grown under prograde metamorphic conditions should not contain inherited cores of older metamorphic events. Therefore rutile predominantly reflects the age of the latest metamorphic overprint. In general, metamorphic overprint is orogen-wide with similar ages in large areas. We therefore propose that detrital rutile age spectra can be utilized to distinguish between local sources (unimodal age distribution) and continent-wide catchment areas (several age peaks).

As part of a larger project aiming at detrital rutile of sub-greenschist facies meta-psammitic rocks, several samples from the Saxo-Thuringian Zone of the Variscan Orogen have been dated. All detrital rutiles from the Neoproterozoic to Lower Silurian depositional ages show pre-depositional ages indicating that the rutiles are detrital and that the Variscan overprint has not reset the ages. Most samples show an unimodal age distribution, with Pan African ages between 600 and 800 Ma. However, rutiles out of one meta-sandstone with Late Ordovician / Early Silurian depositional age show a multimodal age spectrum. 30 % of the ages are > 1000 Ma and reaching a maximal age of 2200 Ma. This age distribution suggests erosion of other metamorphic domains and transport of the eroded material at the same time and to the same sedimentary environment as those from the Pan African Orogen. The Late Ordovician of the Saxo-Thuringian strata characterizes the transition from rift basin to a passive margin setting on the northern periphery from Gondwana [1]. The age spectrum indicates a direct sedimentary connection between Saxo-Thuringia and Gondwana during that period, perhaps by a continent-wide river system.

Alternatively, another source of multimodal detrital rutiles can be deposits of the Late Ordovician Hirnantian glaciation of Gondwana, which are found stratigraphically below the meta-sandstones [1]. However, this possibility would still imply a sedimentary connection between Gondwana and Saxothuringia.

[1] Linnemann *et al*. (2004) *Int J Earth Sci* **93**, 683–705.

Reactivity of mafic and ultramafic rocks with CO_2-charged fluids and the autocatalytic reduction of CO_2 to form CH_4

R.J. ROSENBAUER[1]*, C. OZE[2], L.C. JONES[1], B. THOMAS[1], G.I. GOLDSMITH[3] AND J.L. BISCHOFF[1]

[1]US Geological Survey, 345 Middlefield Rd., Menlo Park, CA 94025 (*correspondence: brosenbauer@usgs.gov)

[2]Department of Geological Sciences, University of Canterbury, Christchurch, New Zealand

[3]Department of Chemistry, Bryn Mawr College, 101 N. Merion Ave., Bryn Mawr, PA 19010

Mafic and ultramafic rocks are highly reactive to carbon dioxide (CO_2). They may be potential repositories for sequestering CO_2 because of their capacity for trapping CO_2 in carbonate minerals. They are also capable of reducing CO_2 to form CH_4 via molecular hydrogen (H_2) from serpentinization reactions. Geochemical laboratory experiments, reacting tholeite, picrite, and olivine with CO_2-charged fluids over a range of temperature (50 - 200°C) and pressure (100 - 300 bar) conditions, resulted in a high degree of rock alteration, secondary mineral formation and gas synthesis. In tholeite and picrite experiments, CO_2 is taken up from solution at all temperatures but the maximum extent and rate of reaction occurs at 100°C and 300 bar. The amount of CO_2 uptake at 100°C, 300 bar ranged from 8 wt% for a typical tholeite to 26 wt% for a picrite, where the amount of uptake coincides with the Mg content of the rock as a reaction limiting factor. Although geochemical modeling predicts an equilibrium carbonate alteration assemblage of calcite, magnesite, and siderite, only secondary ferroan magnesite was identified in the residual solids.

An alternate fate for CO_2 when reacted with ultramafic rocks is conversion to CH_4. In olivine hydrolysis experiments (200°C, 300 bar), Fe^{2+} from olivine is incorporated into carbonates more rapidly than Fe^{2+} oxidation (and concomitant H_2 formation) leading to diminished yields of H_2 and H_2-dependent CH_4 production. At carbonate equilibrium or under-saturated conditions, the experimental data suggest that produced magnetite catalyzes the reduction of CO_2 to form CH_4. Rate calculations suggest that the kinetic balance between the production of H_2 and CH_4 in natural systems undergoing serpentinization may serve to discriminate between abiotic and biotic processes.

https://doi.org/10.1180/S0026461X00006502 Published online by Cambridge University Press

The Co-precipitation of Ra in a large scale evaporitic system

Y.O. ROSENBERG*[,1], V. METZ[2] AND J. GANOR[1]

[1]Dept. of Geological and Environmental Sciences, Ben-Gurion Univ., P.O.B. 653, Beer Sheva 84105, Israel (*correspondence: yoavoved@gmail.com)

[2]Institute for Nuclear Waste Disposal, Karlsruhe Institute of Technology, P.O.B. 3640, 76021 Karlsruhe, Germany

High concentrations of radium pose environmental and health concerns in natural and industrial aqueous systems. Co-precipitation of Ra^{2+} with barite is an effective process in decreasing its concentration, and was extensively addressed in laboratory experiments. The outcome of such small scale experiments often serves in theoretical risk assessments simulation, but was hardly validated over large field systems.

The co-precipitation of Ra^{2+} with barite was studied in a large scale field system, comprising 6 sequential evaporation ponds, having a total volume of $3.25 \cdot 10^5$ m^3, in which a rejected brine of a desalination plant is evaporated. The non evaporated brine has an ionic strength of 0.7 m, ^{226}Ra concentration of 12 Bq kg^{-1}, and it is oversaturated with respect to gypsum, celestite and barite. Upon its evaporation the ionic strength increases up to 8.4 m, and a total amount of $\sim 4 \cdot 10^6$ kg $year^{-1}$ of sulphate minerals precipitates.

Brine and salt samples were collected and analyzed for their chemical composition and radium isotopes. Precipitation rate of the different ions was calculated by assuming a steady state at each pond. The *apparent* partition coefficient of Ra in barite for pond n was calculated as: $K'_{d,\,n}=ln\{[Ra_n]/([Ra_{n-1}]\cdot EF)\}/ln\{[Ba_n]/([Ba_{n-1}]\cdot EF)\}$, where $[i]$ is the concentration of component i (mol kg^{-1}), and EF is the evaporation factor which corrects for concentration changes due to evaporation. Assuming that Mg is conservative, $EF=[Mg]_n/[Mg]_{n-1}$.

Preliminary results demonstrate that the increase in the amount of ^{226}Ra and Ba in the solid is concurrent and is not correlated with the increase of neither Ca or Sr. This indicates that barite precipitates as a separate phase and that Ra co-precipitates with barite. On the average, K'_d among all the ponds was calculated to be 1.1±0.1 in agreement with laboratory experiments carried out with the same brine (1.04±0.01). However, close examination reveals that K'_d increases by a factor of ~2 from 0.7±0.3 to 1.5±0.1 as barite precipitation rate decreases ~20 fold. This trend suggests that similarly to laboratory observations, kinetic effect lowers Ra co-precipitation.

Constrains given by the above field observations support experimental data, and thus strengthen the validity of the parameters needed for risk assessments.

Solubility of carbon dioxide in aqueous fluids at subcritical pressure: Testing the models

JÖRGEN ROSENQVIST*, ANDREW D. KILPATRICK AND BRUCE W.D. YARDLEY

School of Earth and Environment, University of Leeds, Leeds LS2 9JT, United Kingdom (*correspondence: j.rosenqvist@leeds.ac.uk)

Modelling of CO_2 storage in geological reservoirs indicates that solution trapping will become significant with time. However, there is little direct experimental data for CO_2 solubility in aqueous fluids at subcritical and near-critical pressures. We have therefore performed CO_2 solubility experiments in an intermediate pressure range, and made comparisons with model predictions.

Experiments are conducted at temperatures from RT to 70°C, with absolute pressures ranging from 4 bar to tens of bars. Our experimental setup allows pH-measurements to be conducted at pressure, for pressures ≤ 10 bar. The solution phase can be sampled at any pressure and the CO_2 solubility is determined to within 1% using alkalinity titrations.

Figure 1 shows coupled pH – solubility data at a total pressure of 4 bar. At this pressure the agreement between experiment and PHREEQC modelling is generally good, but anomalously high solubilities are predicted for calcite-bearing assemblages giving relatively high pH fluids. If confirmed at higher pressures, this discrepancy will have important implications for modelling CO_2 storage.

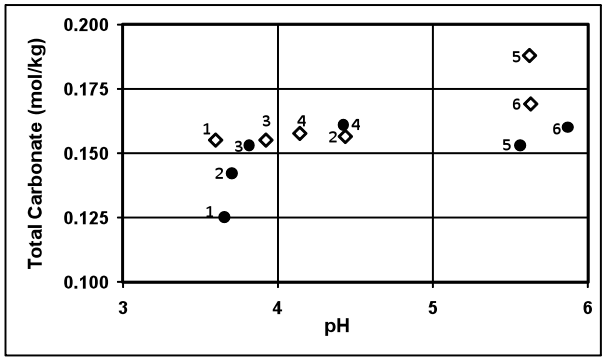

Figure 1: Solid symbols show experimental CO_2 solubility and pH, open symbols show results from PHREEQC calculations. Symbols numbered 1 are for pure H_2O - CO_2, while the others are for H_2O - CO_2 – mineral systems as follows: 2: K-feldspar 3: kaolinite 4: Na-montmorillonite 5: calcite 6: Na-montmorillonite + calcite.

https://doi.org/10.1180/S0026461X00006502 Published online by Cambridge University Press

New offset $\delta^{11}B$ isotope reference materials for geochemical and environmental boron isotope studies

M. ROSNER[1,2]* AND J. VOGL[2]

[1]IsoAnalysis UG, 10829 Berlin, Germany
(*correspondence: martin.rosner@bam.de)
[2]BAM Federal Institute for Materials Research and Testing, 12205 Berlin, Germany

The isotopic composition of boron is a well established tool in various areas of science and industries. Boron isotope compositions are typically reported as $\delta^{11}B$ values which indicate the isotopic difference of a sample relative to the internationally accepted isotope reference material NIST SRM 951. A significant drawback of all of the available boron isotope reference materials is that non covers a natural boron isotope composition apart from NIST SRM 951.

To fill this gap of required offset $\delta^{11}B$ reference materials we produced three new solution boric acid reference materials that cover two-thirds of the natural boron isotope variation (-20 to 40 ‰ $\delta^{11}B$) of about 100 ‰. The new reference materials are certified for their $\delta^{11}B$ values. The certified $\delta^{11}B$ values of -20.2 ‰ for ERM-AE120, +19.9 ‰ for ERM-AE121 and 39.7 ‰ for ERM-AE122 have been established by three independent analytical methods (gravimetric, TIMS $Na_2BO_2^+$ and $Cs_2BO_2^+$). The $\delta^{11}B$ reference materials are commercially available through European Reference Materials (http://www. erm-crm. org) or the webshop of the BAM Federal Institute of Materials Research and Testing (http://www. webshop. bam. de).

The newly produced and certified boron isotope reference materials will allow straight forward method validation and quality control of boron isotope data.

Micro-XRD and ICP-MS analysis of sub-milligram sized mineral samples

KIRK C. ROSS AND BALZ S. KAMBER

Laurentian University, Sudbury On Ca (kross@laurentian.ca)

We present a study that combined micro-analytical X-ray diffraction (XRD), emplying the image plate - diffraction image integration software (IP-DIIS) method, with trace element analysis on the very same grain fragment via ultra-low blank solution inductively coupled plasma – mass spectrometry (ICP-MS). The experimental procedure involves three steps. First, trace element homogeneity in the mineral is studied via laser ablation ICP-MS by analysis of multiple spots. Subsequently, a very small fragment of material (typical edge length ~15-25μm) is removed adjacent to the laser ablation pit. This is then mounted in a 114.6 mm Gandolfi camera. An IP is used to quantitatively record the diffraction inter-planar spacing (d-spacing) and intersity (I). The latent image on the IP is digitized through a propietary IP scanner, after which the image plate can be erased and reused. The scanned image is then converted to a digital diffractogram using appropriate not-for-profit software. We demonstrate that simple XRD technique yields a fully quantitative digital diffractogram amenable to Rietveld structural refinement. The accurate and percise crystallo-graphic parameters are thus known for the mineral fragment from the structural refinement. The final analytical step involves ultra-low blank miniaturized mineral acid digestion of the mineral fragments that typically weigh between 0.1 and 1 milligrams. The digests are subsequently analyzed for the trace element suite of interest by solution ICP-MS.

When crystallographic parameters and chemical information are combined in this fashion, it is possible to empirically test the control excerted by the crystal lattice on apparent trace element partition coefficients. In particular, this method allows a test of the theoretically derived and experimentally confirmed crystal lattice strain model (CLSM) [1, 2]) for naturally occuring mineral phases. Namely, the fundamental premise of the CLSM is that isovalent trace element distribution (D) in a mineral is controlled by the size (Ro) and elastic modulus (E) of the substituent crystallographic site. The XRD data can be used to compute Ro while the trace element data can be used to calculate an independent value for Ro from the strain-free admittance of a fictitious atom of radius Ro.

[1] Brice J.C. (1975) *J Cryst. Growth* **28**, 249–253. [2] Blundy JD, Wood BJ (1994) *Nature* **372**, 452–454.

https://doi.org/10.1180/S0026461X00006502 Published online by Cambridge University Press

Thermodynamic properties of hydration layers on surfaces of metal oxide nanoparticles

N.L. ROSS[1]*, E.C. SPENCER[1], B.F. WOODFIELD[2], A. NAVRTOSKY[3], S.F. PARKER[4] AND A.I. KOLESNIKOV[5]

[1]VirginiaTech, Blacksburg, VA 24061, USA (*correspondence: nross@vt.edu)
[2]Brigham Young University, Provo, UT 84602, USA
[3]NEAT, UC Davis, Davis, CA 95616, USA
[4]ISIS, RAL, Didcot, OX11 0QX, UK
[5]ORNL, Oak Ridge, TN 37831, USA

Water is ubiquitous on the surface of oxide nanoparticles and can exert a profound influence on the thermodynamic properties of the oxide [1]. We have measured inelastic neutron scattering (INS) spectra for several hydrated metal oxide nanoparticles systems, including 6nm SnO_2, 7nm rutile-TiO_2, 16nm Co_3O_4, and 10nm CoO, and determined the isochoric heat capacity and vibrational entropy of the water confined to their surfaces [2-4]. The results from these studies have been combined with complementary calorimetric data and show that the surface energy of the underlying metal oxide particles exerts a strong influence on the heat capacity of the hydration layers. The surface water adsorbed on metal oxide nanoparticles with higher surface energies have lower heat capacities and vibrational entropies. For example, isostructural SnO_2 and rutile-TiO_2 have surface energies of 1.72±0.01 and 2.22±0.07 Jm^{-2}, respectively, with S_{298} values of their hydration layers equal to 37.17 and 32.34 $JK^{-1}mol^{-1}$, respectively [3, 5]. In addition, Co_3O_4 spinel and CoO rocksalt nanoparticles, although chemically similar, have surface energies of 1.96±0.05 and 3.57±0.20 Jm^{-2}, respectively, with S_{298} values of their hydration layers equal to 38.13 and 37.03 $JK^{-1}mol^{-1}$, respectively [4, 5].

[1] Boerio-Goates *et al*. (2006) *Nano Lett*. **6**, 750.
[2] E.C. Spencer *et al*. (2009) *J. Phys. Chem. A*, **113**, 2796.
[3] E.C. Spencer *et al*. (2011) *J. Phys. Chem. A*, submitted.
[4] E.C. Spencer *et al*. (2011) *J. Phys. Condens. Matt,* in press.
[5] A. Navrotsky *et al*. (2010) *Science* **330**, 199.

The Late Jurassic Andean back-arc volcanism, Northern Chile (26-31°S)

P. ROSSEL[1], V. OLIVEROS[1]*, M.N. DUCEA[2], M. LABBE[1] AND R. CHARRIER[3]

[1]Departamento Ciencias de la Tierra, Universidad de Concepción, Casilla 160-C, Concepción, Chile (*correspondence: voliveros@udec.cl)
[2]Univ. of Arizona, Dept. of Geociences, Tucson, AZ, 85721, USA
[3]Departamento de Geología, Universidad de Chile, Casilla 13518, Correo 21, Santiago, Chile

The configuration of the Andes in southwestern Gondwana during the Jurassic and Early Cretaceous was characterized by abundant primitive arc magmatism, and marine to continental extensional back-arc basins controlled by hemigraben fault systems. Occasional effusion of volcanic material occurred along the eastern flanks of these basins. Between 26°and 31°, two parallel belts of volcanic rocks crop out to the east of the contemporary Upper Jurassic arc. The volcanic rocks located closer to the arc (G1), have a maximum age of 163.2 Ma, range from basaltic-andesite to andesite, with minor rhyolites, and have calc-alcaline affinities but with higher alkali content than the arc rocks. The more distant volcanics (G2) have a maximum age of ca. 153 Ma and are mostly alkaline basalts.

Spider diagrams show enrichment in LILE, usually not higher than 100, relative to the primordial mantle, and concentrations of HREE below 10. The rocks of G1 are characterized by Nb-Ta troughs and La_n/Nb_n ratios between 2.2 and 8.1, while G2 trace elements patterns have a concave-down shape, similar to that of the OIB, and La_n/Nb_n ratios between 1.8 and 2.5 or Nb-Ta anomalies commonly absent. Rocks from both groups have flat REE patterns, with minor negative Eu anomalies for G1, and positive Eu anomalies for some G2 lavas. The Ni concentrations (44-223 vs 20-130 ppm), Dy/Yb (1.8-2.8 vs 1.9-2.1) and La/Yb (7-23 vs 8-17) are higher for the G2 lavas, which is consistent with the greatest distance of this group from the trench, and lower degrees of partial melting of their mantle source. The lower Nb/Yb for the G1 lavas (2-37 vs 3-8) suggests a more depleted source than that of the G2 lavas, but more enriched relative to the source of the arc rocks (0.1-3). Isotopic ratios ($^{87}Sr/^{86}Sr$=0.7035-0.70501, $^{143}Nd/^{144}Nd$=0.512455-0.512742, $^{206}Pb/^{204}Pb$=18.4-19.34, $^{207}Pb/^{204}Pb$=15.6-15.67, $^{208}Pb/^{204}Pb$= 38.43-39.0) are indicative of an enrichment in the magma source from the arc eastwards; the spatial and temporal geochemical variations suggest progressive increase of lithospheric contributions to the back-arc magmatism.

https://doi.org/10.1180/S0026461X00006502 Published online by Cambridge University Press

Large-scale simulation of molecular structure and electron transfer in microbial cytochromes

KEVIN M. ROSSO[1]*, PIOTR ZARZYCKI[1], MARIAN BREUER[2], JOCHEN BLUMBERGER[2], LIANG SHI[1], DAVID J. RICHARDSON[3], THOMAS A. CLARKE[3], MARCUS EDWARDS[3], JULEA BUTT[3], JOHN M. ZACHARA[1] AND JIM K. FREDRICKSON[1]

[1]Pacific Northwest National Laboratory, Richland Washington, USA (*correspondence: kevin.rosso@pnl.gov)
[2]University College London, London, UK
[3]University of East Anglia, Norwich, UK

This research seeks to understand rates and molecular mechanisms used by microbial multiheme c-type cytochromes (c-Cyts) for mediating extracellular Fe valence transformation, an important biogeochemical process affecting the availability and supply of reactive Fe (II) in subsurface environments. The structure of MtrF, an outer-membrane decaheme c-type cytochrome from an iron-reducing bacterium, has been determined by synchrotron diffraction measurements. Results show that the ten hemes of MtrF are organized into a unique 'wire cross', in which a staggered 65 Å octa-heme chain transects the length of the protein and is crossed at the middle by a 45 Å tetra-heme chain. Each heme is within 7 Å of its nearest neighbors, in principle permitting rapid interheme electron transfer.

Large-scale molecular dynamics simulations are being carried out to understand the free energy landscape for electron hopping along various trajectories of the wire cross. Using the technique of thermodynamic integration, relative redox potentials of all possible intraprotein electron transfer steps have been computed, which shows that upon possible electron entry into heme 5, only a 0.84 kcal/mol (1.4 kT) activation free energy barrier for electron transfer to heme 4 opposes otherwise net thermodynamically downhill heme-to-heme conductance to hemes 2, 7, and 10 at the protein-environment interface. It is therefore proposed that heme 5 is the input site of electrons from partner proteins MtrDE up the electron transport chain, and that MtrF transfers electrons down the chain directly to Fe (III)-oxides via highly solvent-exposed heme 10. The combined experimental and computational simulation activity is collectively providing a comprehensive understanding of bacterial outer-membrane c-Cyt functioning at the level of individual heme redox potentials, heme-to-heme electron transfer rates across the protein, and insights into dynamical effects of protein fluctuation and solvent reorganization on overall electron transfer conductance.

Reactive Fe(II) and electron exchange dynamics in iron oxides

K.M. ROSSO[1]*, P. ZARZYCKI[1], C.I. PEARCE[1], J. KATZ[2], B. GILBERT[2], R.M. HANDLER[3], M.M. SCHERER[3] AND P. MEAKIN[4]

[1]Pacific Northwest National Laboratory, Richland WA, USA (*correspondence: kevin.rosso@pnl.gov)
[2]Lawrence Berkeley National Laboratory, Berkeley, CA, USA
[3]University of Iowa, Iowa City, IA, USA
[4]Idaho National Laboratory, Idaho Falls, ID, USA

Ferrous-ferric electron exchange is central to the biogeochemical cycle of iron and determines iron forms and availability in the subsurface. For most environmentally relevant conditions this exchange involves interaction between soluble ferrous iron and solid-phase iron oxides and oxyhydroxides, with complex involvement of solid-state charge migration. Examples include Fe (II)-catalyzed transformation of Fe (III)-oxides and oxyhydroxides, and spinel ferrite nanoparticles acting as a mineralogic source and sink for reactive Fe (II) due to their topotactic solid-solution property and stable multi-valent nature. This presentation focuses on the interdependence of Fe (II) fluxes at these mineral-water interfaces with structural and electronic properties of mineralogic iron oxide forms. Using combined experiment and computational molecular simulation, we examine the underlying mechanisms of observed complete iron atom exchange without change in mineralogy, crystallinity, crystal size or shape between an aqueous Fe (II) pool and well-defined goethite (FeOOH) crystallites, the accessibility of solid-state Fe (II) in titanomagnetite ($Fe_{3-x}Ti_xO_4$) nanoparticles in which the structural Fe (II)/Fe (III) ratio is intentionally tuned by the Ti (IV) content, and the highly time-resolved dynamics and fate of Fe (II) electrons photoinjected into maghemite ($Fe_{8/3}O_4$) nanoparticles. Aspects covered will include thermodynamic energy requirements for bulk crystal conduction and possible free energy sources sustaining bulk currents, ferrous iron adsorption energies at iron oxide surfaces and the kinetics of interfacial electron exchange, the structural dependence of ferrous-ferric electron exchange in the solid, and internal charge compensation mechanisms. These lines of research are collectively converging on a picture of rapid electron exchange dynamics between aqueous ferrous iron and iron oxides, with broad-reaching implications for the biogeochemistry iron in the subsurface.

https://doi.org/10.1180/S0026461X00006502 Published online by Cambridge University Press

New approaches to assess the responses of phytoplankton to ocean acidification

BJÖRN ROST

Alfred Wegener Institute for Polar and Marine Research, Bremerhaven, Germany (Bjoern.Rost@awi.de)

Global Change will affect phytoplankton in many ways, altering the complex balance of biogeochemical cycles and climate feedback mechanisms. Hence, predictions of how phytoplankton may respond to these perturbations at the cellular and ecosystem levels are a major challenge in global change research. In this presentation, I will outline the expected physico-chemical changes in the marine environment (e.g. ocean acidification, light regime, nutrients supply) and describe how these may affect different phytoplankton groups. Focusing on coccolithophores, diatoms, dinoflagellates and cyanobacteria, results from laboratory and field studies will be analyzed in view of the overall sensitivity (e.g. elemental composition, growth rate, productivity) to ocean acidification. To go beyond this descriptive level, methods on cellular processes are increasingly applied in the context of global change research. They yield information about underlying mechanisms causing processes like photosynthesis, calcification or N_2 fixation to be responsive to ocean acidification.

Overall results indicate major species- and taxa-specific differences in the sensitivity towards ocean acidification. While some species are not responsive at all, others will clearly benefit or have to face detrimental effects. The presented data will stress, however, that responses to ocean acidification are strongly modulated by other environmental conditions, such as light or nutrient levels. As these factors are also influenced in the framework of global change, the combined effects have to be considered. Some of the observed responses can meanwhile be related to species- or taxa-specific physiological traits. Next to *direct* CO_2 effects (e.g. on processes like the CO_2 concentrating mechanism), the aspect of energy allocation between physiological processes seems to play an crucial role in causing *indirect* CO_2 effects (e.g. on processes like N_2 fixation). As the cellular changes imposed by ocean acidification likely influence the competitive abilities of species, implications for the natural phytoplankton communities and biogeochemical cycling may be even be larger than indicated from results obtained in mono-specific incubations.

Wetland extension on the Russian Plain over the past 40 kyr: A biomarker approach from the Black Sea

F. ROSTEK* AND E. BARD

CEREGE, Univ. Aix-Marseille, CNRS, IRD & College de France, Technopole de l'Arbois BP 80 13545 Aix-en-Provence Cedex 04, France
(*correspondence: rostek@cerege.fr, bard@cerege.fr)

The Black Sea is a catchment basin for large areas of the European Russian Plain, the Alps and southeastern Europe. In order to study the hydrological changes in this basin over the last 40 kyr, we measured a continous series of terrestrial long-chain *n*-alkan-2-ones and *n*-alkanes as paleoclimate proxies in well dated glacial lacustrine to Holocene marine sediments from the NW Black Sea.

Two specific molecules of these homologuous series are normalized to total organic carbon (TOC), respectively Ket27/TOC for *n*-alkan-2-ones and C23/TOC for n-alkanes and interpreted as characteristic biomarkers for *Sphagnum* mosses, a dominant vegetation component in wetlands. Decreased concentrations of *Sphagnum* biomarkers are found for the North Atlantic icebergs surges and cooling events known as Heinrich Events, the Last Glacial Maximum and the Younger Dryas. These drops are pointing to low erosional input to the Black Sea with cold and dry climate conditions. Increased biomarker inputs characterize the mild climate phases known as Dansgaard/Oeschger Interstadials, pointing to increased erosion due to permafrost degradation and/or wetland extension on the Russian Plain.

The final retreat of the Fennoscandian ice sheet is concomitant with Heinrich Event 1 and expressed by increased biomarker concentrations in the so-called Red Layers, a typical series of deglacial clay layers. The two biomarker signals are decoupled at the start of the Bølling/Allerød: C23/TOC is decreasing whereas Ket27/TOC variations are in phase with the major climate events like the Bølling/Allerød, the Younger Dryas event and the early Holocene. The paleoclimatic record is interrupted by the final reconnection of the Black Sea with the Mediterranean Sea which led to marine conditions.

https://doi.org/10.1180/S0026461X00006502 Published online by Cambridge University Press

Halogen composition of the early Solar System inferred from meteoritic apatites

J. ROSZJAR[1]*, T. JOHN[2], M. WHITEHOUSE[3], G. LAYNE[4] AND A. BISCHOFF[1]

[1]Institut für Planetologie, WWU Münster, Germany (*correspondence: j_rosz01@uni-muenster.de)
[2]Institut für Mineralogie, WWU Münster, Germany
[3]Laboratory for Isotope Geology, Naturhistoriska Riksmuseet Stockholm, Sweden
[4]Department of Earth Sciences, Memorial University, St. John's, NL Canada

The volatile halogens are important tracers in constraining Solar System processes, such as degassing, and as abundant anionic components in fluids they are also useful in deciphering fluid-rock interactions. So far, there is limited information about halogen ratios and the $\delta^{37}Cl$ isotope composition of planetary reservoirs, such as the chondritic reservoir, depleted Earth mantle or bulk silica Earth.

The halogen budget of individual meteorite samples appears dominantly controlled by apatites that preferentially incorporate halogens. To constrain the halogen budget of the early Solar System planetesimals we determined F, Cl, Br, and I concentrations, and the $\delta^{37}Cl$ of individual apatite grains in meteoritic materials - including ordinary and Rumuruti chondrites, primitive achondrites, eucrites, and iron meteorites. Phosphate grains were documented by SEM and their mineral chemistry was determined by EPMA. Halogen concentrations and $\delta^{37}Cl$ were determined using a Cameca IMS 1280 (NORDSIMS). Mass balance calculations were carried out to evaluate the potential of apatite to act as a probe for the halogen chemistry.

$\delta^{37}Cl$ values of different meteorite groups span a range from about -1 ‰ to +1 ‰ [1; this study]. We found an evolutionary trend in $\delta^{37}Cl$ from chondritic through differentiated material, with the latter probably being balanced by silicate-bearing iron meteorites, such as Campo del Cielo. This trend is also seen for F/Cl of apatites from different meteorite groups, which ranges from ~100×10^{-3} in chondritic material to ~32, 500×10^{-3} in differentiated meteorites. I/Cl range from ~0.6×10^{-6} to 6×10^{-6}, - except for eucrites, which have I/Cl two orders of magnitude higher. Br/Cl vary from ~0.02×10^{-3} in ordinary chondrites to ~1.7×10^{-3} in iron meteorites. This implies discernible variation of halogens among different meteorite groups but, compared to Earth's halogen reservoirs, a relatively homogeneous halogen composition for the early Solar System.

(1) Sharp *et al*. (2007) *Nature* **446**, 1062-1065.

Inherited ^{142}Nd anomalies in the Nuvvuagittuq supracrustal belt

A.S.G. ROTH[1], B. BOURDON[2], T. KLEINE[3], S.J. MOJZSIS[4] AND M. TOUBOUL[5]

[1]Institute of Geochemistry and Petrology, ETH Zurich, 8092 Zurich, Switzerland (antoine.roth@erdw.ethz.ch)
[2]ENS Lyon, UMR 5276, CNRS, France
[3]Institut für Planetologie, Universität Münster, 48149 Münster, Germany
[4]Department of Geological Sciences, University of Colorado, Boulder, CO 80309-0399, USA
[5]Department of Geology, University of Maryland, College Park, MD 20742, USA

The short-lived ^{146}Sm-^{142}Nd chronometer is a sensitive tool to trace early silicate Earth differentiation. Mantle depletions prior to ~4.2 Ga are documented as positive ^{142}Nd anomalies in Eoarchean rocks [e.g. 1]. O'Neil *et al*. [2] reported evidence for an early enriched reservoir from negative ^{142}Nd anomalies in pre-3750 Ma rocks of the Nuvvuagittuq supracrustal belt (NSB) in Québec. These authors derived a ^{146}Sm-^{142}Nd isochron with a 4.28 Ga age and concluded that the NSB may be the oldest crust.

We present new coupled $^{147, 146}Sm$-$^{143, 142}Nd$ systematics for six different NSB lithotypes. Samples yield a range of $^{147}Sm/^{144}Nd$ ratios from about 0.07 to 0.17. Nd data were collected on a Triton (TIMS) at ETH; repeat measurements of the JNdi-1 standard yield an external precision of ±4 ppm (2 SD) for the $^{142}Nd/^{144}Nd$ ratio (n=39). We reproduced negative ^{142}Nd anomalies for sample powders reported in [2], and for a cummingtonite amphibolite from the mapped area in [3]. A mafic (tonalitic) gneiss and a quartz-biotite schist from an Inukjuak supracrustal enclave NE of the NSB show $^{142}Nd/^{144}Nd$ ratios lower than the terrestrial standard ($\varepsilon^{142}Nd$ = -0.08 to -0.13). Taken together, these negative ^{142}Nd anomalies are uncorrelatable with $^{147}Sm/^{144}Nd$ for mafic or felsic lithologies and do not produce a ~4.28 Ga isochron as in [2]. In ^{147}Sm-^{143}Nd isochron diagrams our NSB whole rock samples define an array with an imprecise age of ~3.75 Ga similar to ages from U-Pb ion microprobe zircon geochronology [3]. Data indicate that the NSB rocks suffered a complex protracted history and that the Sm-Nd system is disturbed. We conclude that the absence of concordant ages in the ^{143}Nd-^{142}Nd system suggests that the negative ^{142}Nd anomalies were inherited from an early enriched reservoir and do not represent the age of the formation of the NSB rocks.

[1] Caro *et al*. (2006) *GCA* **70**, 164-191. [2] O'Neil *et al*. (2008) *Science* **321**, 1828-1831. [3] Cates and Mojzsis (2007) *EPSL* **255**, 9-21.

https://doi.org/10.1180/S0026461X00006502 Published online by Cambridge University Press

Use of TGA/DSC-IR to assess the effect of Cr on struvite stability

ASHAKI A. ROUFF

School of Earth and Environmental Sciences, Queens College, CUNY, Flushing NY 11367, USA (Ashaki.Rouff@qc.cuny.edu)

A TGA/DSC-IR hyphenated technique was used to evaluate the effect of sorbed Cr on the thermal properties of struvite ($NH_4MgPO_4 \cdot 6H_2O$, MAP). MAP occurs in guano deposits, peat, and lake sediments [1, 2]. It is also found in agroecosystems as a fertilizer decomposition product, and as a component of animal manure and poultry litter [3]. These systems can have high metal content, including Cr, which may substitute for P in MAP. Simultaneous thermal analysis has been used to determine the effect of Cr on the thermodynamic properties and stability of phosphate minerals [3, 4]. Addition of IR spectroscopy allows direct identification and quantification of decomposition products. Cr-MAP solids were generated from solutions with 0-100 μM Cr (III) and Cr (VI). DSC indicated an endothermic peak for all solids at 127 ± 0.5 °C, accompanied by >50% sample weight loss based on TGA, due to evolution of H_2O (g) and NH_3 (g) as identified by IR. The enthalpy, weight loss, and moles of evolved gases varied with initial Cr oxidation state and concentration. This was suggestive of diverse sorption complexes and mechanisms, further investigated using FT-IR and XAFS. The overall effect of sorbed Cr was to increase the structural H_2O content of MAP and to reduce the enthalpy of the endothermic transition. This indicates that Cr reduces the stability of MAP, increasing susceptibility to decomposition and thus release of the metalloid. This has implications for cycling of Cr, P and N in MAP-bearing natural and agricultural systems.

[1] Abdelrazig & Sharp (1988) *Thermochim. Acta* **129**, 197–215. [2] Donovan *et al.* (2007) *The Holocene* **17**, 1155–1169. [3] Hunger *et al.* (2008) *J. Environ. Qual.* **37**, 1617–1625. [3] Wakamura *et al.* (1997) *Polyhedron* **16**, 2047–2053. [4] Yasuda & Hishinuma (1995) *Solid State Ionics* **78**, 109–114.

Identification of geochemical processes in groundwater at the Chernobyl Pilot Site and preliminary contamination characterization with $^{36}Cl/Cl$ ratios

C. ROUX[1,2]*, C. LE GAL LA SALLE[1], C. SIMONUCCI[2], S. BASSOT[2], J.-L. MICHELOT[3], K. FIFIELD[4], N. VAN MEIR[2], D. BUGAI[5] AND J. LANCELOT

[1]GIS/CEREGE, UMR 6635, CNRS/University of Nîmes and Aix-Marseille, F-30035, Nîmes cedex 1, France (*correspondence: celine.roux.1@etu.univ-cezanne.fr, corinne.legallasalle@unimes.fr)

[2]IRSN, POB 17, F-92262 Fontenay-aux-Roses, France (caroline.simonucci@irsn.fr)

[3]IDES, UMR 8148, CNRS/University of Paris 11, F-91405, Orsay, France

[4]Department of Nuclear Physics, Australian National University, Canberra ACT 0200, Australia

[5]IGS, National Ukrainian Sciences Academia, U-01054 Kiev, Ukraine

After the accident at the Chernobyl Nuclear Power Plant in april 1986, 12.10^{18} Bq of radionuclides (RN) were released in the atmosphere and most of them were redeposited around the facility. To prevent atmospheric resuspension, about 800 trenches were dug on site to dispose contaminated material (debris, organic matter, topsoil containing reactor fuel particles). Since 1999, the EPIC (Experimental Platform In Chernobyl) project has been set to study migration of radionuclides from one of these trenches, the trench T22, through the unsaturated and saturated zone. A plume of ^{90}Sr was identified downstream from the trench. The aim of this study is to contribute to the understanding of the migration of ^{90}Sr and other RN in groundwater. Water stable isotopes indicate winter recharge and groundwater stratification. Major elements show an increase in concentration with depth, linked to mixing and/or water-rock interaction processes. Preliminary results in $^{36}Cl/Cl$ show ratios in the order of those observed in concrete of proton-accelerator facilities [1] and 2 to 3 orders of magnitude higher than the theoretical ratio in precipitation. The source of this contamination may be contaminated particles released during the explosion and/or background activity and/or waste buried in the trench. Characterization of transport processes will be further investigated based on $^{235}U/^{238}U$, $^{86}Sr/^{88}Sr$ and $^{87}Sr/^{86}Sr$ ratios and additional $^{36}Cl/Cl$ measurments.

[1] Bessho (2007) *Nucl. Instr. & Meth. in Phys Research B* **259**, 702–707.

https://doi.org/10.1180/S0026461X00006502 Published online by Cambridge University Press

Energy content of soil organic matter as studied by bomb calorimetry

PERE ROVIRA* AND RITA HENRIQUES

Forest Sciences Center of Catalonia (CTFC), Solsona, Spain (*correspondence: pere.rovira@ctfc.cat)

Calorimetry has been applied to the study of soil organic matter for decades. Differential scanning calorimetry (DSC) has been the most widely used technique: this method submits the soil sample to a controlled temperature increase (often, 10°C per minute), and records the energy released by the combustion of organic matter. The components of organic matter (cellulose, lignin, polyphenolics, etc) have contrasting ignition temperatures; thus the graph of energy released *versus* temperature characterizes a given substrate [1]. In spite of the obvious attractive of this technique, it has the problem that during the temperature increase (and as a consequence of it) some components of the sample may volatilize before being affected by combustion, a fact that may result in underestimations of the amount of energy stored within the structure of the organic matter under study.

Bomb calorimetry is an alternative procedure. This technique does not allow a detailed study of the release of energy along a range of temperatures, because it gives just a single value, the total energy released by the combustion of the sample. Nevertheless, since the combustion occurs within a closed vessel, no losses of material occur. Therefore, the recorded release of energy reflects the amount of energy stored in the sample probably better than DSC techniques.

We applied bomb calorimetry to quantify the energy stored in soil organic matter in a set of mediterranean forest soils, under *Pinus halepensis* and over calcareous substrates (limestones, marls, etc). Methodological problems were observed; for instance, for soil samples below 7% of OC it was not possible to start a combustion by the standard method (electrical flash in the O_2-saturated vessel), and a comburent was needed.

The amount of energy released was linearly related to the organic carbon content. The relationship was very close, with r^2 values higher than 0.9. Translated to stored energy per unit of organic matter, the obtained values were around 34 Joules per mg C. This ratio, however, was not constant, for it increased with the total organic matter of the sample. In soil horizons very rich in organic matter (some OH horizons) it can reach almost 40 Joules per mg C, whereas it may drop down to less than 30 in mineral soil horizons. The relationships between energy stored and characteristics of the soil organic matter are under study.

[1] Rovira *et al*. (2008) *Soil Biol. Biochem*. **40**, 172–185.

Basaltic magmatism and mantle metasomatism in the Rio Grande Rift

M.C. ROWE[1]*, J.C. LASSITER[2] AND B.M. SCHMANDT[3]

[1]Washington State University, School of Earth and Environmental Sciences, Pullman, WA 99164, USA (*correspondence: mcrowe@wsu.edu)
[2]University of Texas at Austin, Jackson School of Geosciences, Austin, TX 78712, USA
[3]University of Oregon, Department of Geological Sciences, Eugene, OR 97403, USA

The Rio Grande Rift in the southwest United States provides an excellent opportunity to investigate temporal and spatial variations in mantle sources and basaltic magmatism in an active continental rift setting. The Rio Grande Rift, extending from northern Mexico to northwest Colorado, has undergone varying amounts of extension, with extension decreasing to the north. Prior rheological studies have indicated that metasomatism and hydration may have a significant effect on the strength of the lithospheric mantle. Here we combine primitive melt inclusion geochemistry (major-, trace-, and volatile elements), whole rock Sr-Nd-Pb isotopic analysis, and tomographic imaging to examine potential mantle metasomatism and its effects on basaltic magma compositions in the Rio Grande Rift.

Melt incusions and whole rock compositions are screened for potential crustal contamination based on negative correlations between Cl/K and Ba/Nb as described by Rowe & Lassiter [1]. Here we focus on Cl variations in melt inclusions, specifically variations in Cl/Nb, to identify mantle metasomatism. The only significant temporal variation along the rift in Cl/Nb is in the southernmost region where the highest Cl/Nb ratios are observed in olivine-hosted melt inclusiosn from a ~37Ma basalt (~150 Cl/Nb) compared to melt inclusions from a young (<50ka) basalt (~10 Cl/Nb). Correlations between age of magmatism, Cl/Nb, and whole rock $^{143}Nd/^{144}Nd$, particularly in the southern rift segment, indicates changes in Cl/Nb are likely related a transition from lithospheric to asthenospheric melting over time.

For basaltic volcanism younger than 5 m. y. the highest Cl/Nb ratios are in the central Rio Grande Rift, suggesting little systematic Cl/Nb fluctuations along the rift (N to S). However, for young volcanics, tenative correlations between whole rock Pb isotopes and mantle seismic velocity models (Vs/Vp at 60-100km depth) may further support diverse mantle sources for basaltic magmatism.

[1] Rowe & Lassiter (2009) *Geology* **37**, 439–442.

https://doi.org/10.1180/S0026461X00006502 Published online by Cambridge University Press

The Fe L_3-edge as a probe for Fe oxide speciation

A.N. ROYCHOUDHURY[1]*, B.P. VON DER HEYDEN[1], M. FRITH[2] AND S.C.B MYNENI[2]

[1]Dept. of Earth Sciences, Stellenbosch University, Stellenbosch 7602, South Africa (*correspondence: roy@sun.ac.za)

[2]Dept. of Geosciences, Princeton University, Princeton, NJ 08544, USA

L-edge XANES spectroscopy has been used to identify the speciation of Fe in natural samples. The majority of previous analyses are limited to the identification of Fe (II) versus Fe (III) speciation in complex natural samples however, these spectra are rarely used to identify different mineral phases in soils and sediments. Using the fine spectral variations between different crystalline and amorphous Fe phases, we developed a technique to evaluate the local co-ordination environment of Fe in natural samples. The technique makes use of splitting of the main electronic transitions in the L_3 edge (ΔeV) region, and the ratio of their peak intensities. These spectral parameters are sensitive to the valence state, electronegativity of the coordinated ligands and the degree of distortion of the polyhedra of Fe. We collected L-edge XANES spectra of several synthetic Fe-oxides and oxyhydroxides, and also compiled the spectra of several published spectra in the literature.

When compared for the characteristic ΔeV values and intensity ratio values; the common Fe (III) minerals, goethite, akaganeite, lepidocrocite, amorphous Fe, hematite, and maghemite fall within their own discreet oblong fields, with minor overlap between some of the phases. Similarly, the Fe (II) rich phases occupy their own positions on the plot characterized by greater intensity ratios. The differences in the characteristic intensity ratio values of the fields for the ferric standards is defined predominantly by the number of hydroxyls co-ordinating, and the characteristic ΔeV values are governed predominantly by the magnitude of the ligand field splitting. The arrangement of the fields is also a function of the polyhedral linkages and this is reflected in the average metal-metal distances. However, this analysis is limited by the saturation effects, an artifact of the XANES analysis of thicker and Fe-rich particles.

Details of these spectral analyses, the effects of cation substitution in Fe-oxides that influence these spectral parameters, and an application of this technique to study the natural samples will be presented.

Redox stratification of the White Sea sediments

ALEXANDER ROZANOV

P.P. Shirshov Institute of Oceanology, Russian Academy of Sciences, Moscow (rozanov@ocean.ru)

Redox stratification is formed by the consequence of biogeochemical reactions of oxidation and reduction of organic and inorganic components of the sediments. Organic matter on the surface of the White Sea sediments is oxidized by oxygen dissolved in bottom water. However, in the subsurface horizons the oxygen is rapidly disappearing and other carriers of oxygen, namely, oxygen compounds of nitrogen, manganese, iron and sulfur serve as oxidants. The most striking manifestation of diagenesis is an extremely high content of Mn^{2+} in the pore water (sometimes more than 500 μM), which determines its flux from the sediments to the bottom water and oxidation at the contact with oxygen to form oxyhydroxides MnO_2, enriching the surface layers of the sediments. In lesser extent, migration and oxidation are characteristic of iron. After exhaustion of oxygen in the surface layer at the stage of anaerobic diagenesis newly formed oxyhydroxides (MnO_2 and FeOOH) themselves become oxidants of organic matter. Estimation of the diffusion flux of manganese from the sediments (280 μM/(m2day) and the corresponding amount of MnO_2 formed, compared with the opposite flux of oxygen to the sediments (1-10 mM/(m2 day), shows that over 10% of the organic matter of the surface layer of the sediments can be oxidized with MnO2. The role of other oxidants of organic matter (FeOOH and SO_4^{2-}) is prominent in the deeper horizons. In the upper package of sediments (0 - 100 cm) 61% of the anaerobic oxidation of Corg accounted for MnO2, the proportions of FeOOH and SO_4^{2-} are 14 and 25% respectively. At the same time in the topmost surface layer (0-5 cm) MnO_2 is practically 100 per cent oxidant agent, and at 100 cm the 100-percent oxidizer is SO_4^{2-}. A detailed calculation of the balance of reduction process shows the higher consumption of organic matter in diagenesis of surface sediments than gives a direct determination of Corg. The most active processes of redox diagenesis end at 25-50cm. Layers of manganese enrichment in the deeper horizons are in the nature of metastable relics of the surface accumulation (pobably, manganese nodules), subject to gradual dissipation withtin the sediment column.

https://doi.org/10.1180/S0026461X00006502 Published online by Cambridge University Press

Core formation in the Earth and the terrestrial planets

D.C. RUBIE[1]*, D.J. FROST[1], D.P. O'BRIEN[2], F. NIMMO[3], A. MORBIDELLI[4] AND H. PALME[5]

[1]Bayerisches Geoinstitut, Univ. Bayreuth, D-95440 Bayreuth, Germany (*correspondence: dave.rubie@uni-bayreuth.de)
[2]Planetary Science Institute, Tucson, AZ 85719, USA
[3]Dept. of Earth and Planetary Sciences, University of California, Santa Cruz, CA 95064, USA
[4]Observatoire de Nice, F-06304 Nice Cedex 4, France
[5]Forschungsinstitut und Naturmuseum Senckenberg, D-60325 Frankfurt am Main, Germany

Accretion of the terrestrial planets occurred through a series of impacts/mergers with smaller differentiated embryos and planetesimals (e.g. [1]). In addition to adding Fe metal to proto-planets, impacting bodies provide sufficient energy to cause large scale melting, the establishment of deep magma oceans and therefore episodes of metal-silicate segregation. In our recent model of multistage core formation [2], collisions result in an impactor's core partially or fully equilibrating in a magma ocean before merging with the planet's proto-core. Compositions of metal and silicate that result from the equilibration process are determined from the bulk composition by a novel approach involving mass balance combined with element partitioning. In the case of the Earth, model parameters (e.g. metal-silicate equilibration pressures) are determined by a least squares regression based on constraints provided by the concentrations of major and trace elements in the Earth's mantle. Results show that accretion of the Earth was heterogeneous: early accreting material was highly-reduced and volatile-poor and later accreted material was more oxidized and volatile-rich. This is consistent with dynamical simulations which suggest that late-accreting material originates from greater heliocentric distances and should thus be more volatile rich [1]. Oxygen fugacity and the FeO content of the mantle both increase during accretion due to (a) the dissolution of Si into the core by a reaction that releases oxygen and (b) the late addition of oxidized material. In contrast to early models of heterogeneous accretion, equilibration at pressures up to 60-80 GPa and a significant degree of disequilibrium both play a critical role.

The model is currently being integrated with N-body accretion simulations [1] in order to investigate the chemical evolution of all the terrestrial planets simultaneously. Some simulations suggest an increase in mantle FeO contents (e.g. from 4 to 14 wt%) and a decrease in mantle Mg/Si ratios and core mass fractions as heliocentric distance increases from 0.5 to 2 AU [3]. Finally, the model is used to investigate the causes of ^{182}W anomalies in planetary mantles.

[1] O'Brien *et al*. (2006) *) Icarus* **184**, 39–58. [2] Rubie *et al*. (2011) *EPSL* **301**, 31–42. [3] Rubie *et al*. (2011) *42nd LPSC*, Abstract #1061.

Do erupted mafic lavas accurately reflect mantle magmatic timescales?

K.H. RUBIN

Dept. of Geology & Geophysics, Univ. of Hawaii, Honolulu, HI 96822 USA (krubin@hawaii.edu)

Mantle melting and melt transport encompass a range of processes that vary in duration, magnitude and length scale, and depend upon variables such as tectonic setting, volcano maturity, volcano spacing, and mantle physical characteristics (e.g. thermal state, composition, lithology, upwelling rate). Multiple compositional attributes of mantle derived magmas provide information on melting processes and conditions. The U-series nuclides are nearly unique in their ability to provide information about rates of such processes because chemical fractionation creates radioactive disequilibria between decay chain nuclides, which then decay away on characteristic timescales once fractionation ceases. Some surprising results from this literature suggest that the duration of melting is highly variable over short temporal and spatial scales in the mantle, and that melt transport is generally quite fast. But how trustworthy are these interpretations? Early studies were content to use the presence or absence of radioactive disequilibria in magmas to crudely estimate the duration of magma generation and transport in the mantle. Yet since the 1970s, development of much more sophisticated melting models and of analytical methods for nuclide activity measurements with 100-fold precision improvements have led to more specified time scale assessments in the U-series literature. Despite these refinements, the geological errors introduced by the melting and melt transport processes in the mantle place severe and often underestimated limits on our ability to tell time with these tracers in erupted magmas. Situations such as multiple melting lithologies, magma mixing, fluid-addition (at convergent margins) and reactive transport create a large amount of non-uniqueness to the way U-series data sets can be interpreted. Add crustal/magma chamber processes to this list and the challenge of deriving a unique temporal solution to the duration of magmagenesis and transport using a combined U-series, major/trace element and radiogenic isotope data set is nearly insurmountable. Nevertheless, results from U-series studies have much to tell us about magmatic timescales so long as data are not over-interpreted or modeled with a false sense of precision to the parameterization. This presentation will discuss the current state of the art and successful strategies for limiting the uncertainty of timescale assessments from magma chemistry, and present examples where results are generally consistent with independent geological and geophysical observations.

https://doi.org/10.1180/S0026461X00006502 Published online by Cambridge University Press

Local and regional magmatic modulators to mantle signatures in erupted mid-ocean ridge lavas

K.H. RUBIN[1]*, JOHN MACLENNAN[2], JOHN SINTON[1] AND ERIC HELLEBRAND[1]

[1]Dept. of Geology & Geophysics, Univ. of Hawaii, Honolulu, HI 96822 USA (*correspondence: krubin@hawaii.edu)
[2]Department of Earth Sciences, University of Cambridge, CB2 3EQ, UK

Although nearly all mid-ocean ridge magmas are formed in the mantle and inherit local compositional characteristics of the mantle source, a range of processes that occur between melt generation at depth and eruption on the sea-floor modulate the chemical signals of mantle heterogeneity that is sampled by ridge volcanoes. Increased time-integrated magma supply from mantle to crust is one characteristic that dramatically impacts (reduces) true mantle compositional variance in MORB by promoting coupled magma mixing and differentiation in the crust (e.g. [1]) Studies at local and regional spatial scales underscore the importance of geological conditions for interpreting mantle signatures in erupted lavas and provide a means for studying non-steady-state aspects of magma transport and crustal construction on decadal to millennial timescales. The inherent complexity in MORB compositions reflects the processes and rates of magma delivery to and accumulation in the crust, as well as the extent of mixing and heat loss prior to eruption, with implications for the spatial scales of mantle compositional variation thereby recorded in MORB. This talk will discuss global variations in MORB compositions and new results of recently conducted local/regional studies at a range of spreading rates where there are melt supply 'anomalies' along axis (e.g. from hot spots) and clear short-term differences in magma supply and eruptive activity at neighboring ridge segments. In general, these studies demonstrate that short term fluctuations in magma supply are driven by mantle heterogeneity, and that globally inferred linkages between magma supply, mantle compositional variance, and differentiation degree hold at these shorter spatial and temporal scales as well. They also demonstrate the importance of understanding geological context of lava samples, the need to have a sufficiently well sampled eruptive unit, and the preference for less differentiated (generally, high MgO) lavas in order to begin to decipher mantle compositional variation patterns in MORB.

[1] Rubin & Sinton (2007) *EPSL* **260**, 257–276.

Intermediate water $\Delta^{14}C$ off Brazil between 3-40 ka BP

M. RUCKELSHAUSEN[1]*, R. KOWSMANN[2], J.M. GODOY[4], G.M. SANTOS[3] AND A. MANGINI[1]

[1]Heidelberger Akademie der Wissenschaften, Im Neuenheimer Feld 229, 69120 Heidelberg, Germany (*correspondence: mario.ruckelshausen@iup.uni-heidelberg.de)
[2]Petrobras-CENPES, Cidade Universitaria, Quadra 7, Ilha do Fundao, CEP 21949-900, Rio de Janeiro, RJ, Brazil
[3]Keck-CCAMS Facility, Earth Systems Science, B321 Croul Hall, Univ. of California, Irvine, CA 92697-3100, USA
[4]Instituto de Radioprotecao e Dosimetria, Barra da Tijuca, CEP 22643-970, Rio de Janeiro, RJ, Brazil

The Southern Ocean is thought to play a key role in understanding the atmospheric rise of CO_2 at the end of the last glacial period accompanied by a decline of atmospheric $\Delta^{14}C$. Here we present reconstructed marine $\Delta^{14}C$ activities from corals of intermediate depth off Brazil. The corals stem from two new sediment cores in the direct vicinity to our cores already reported in [1]. This new dataset expands the older one and encompasses now the ages from 3-40 ka BP. First measurements validated our $\Delta^{14}C$ findings already published in [1]. The new data show that the continuous $\Delta^{14}C$ decline starting in our previous study with the Younger Dryas (YD) extends to 5 ka BP reaching an absolute minimum with an apparent ventilation age of over 6200 ^{14}C years. These observations are compatible with the scenario suggesting the existence of an abyssal reservoir in the Pacific Ocean that was isolated for several thousand years from the atmosphere before deglaciation. The observed continuous $\Delta^{14}C$ decline during Heinrich Stadial 1 (HS1) and the YD would then suggest a further weakening of ventilation of the deep water and the injection of this old carbon dioxide signature from the deep Pacific reservoir into the Circumpolar Water around Antarctica that is the source of Atlantic Intermediate Water. This follow-up study also attempts to trace back the history of the $\Delta^{14}C$ activity beyond HS1 (HS2, HS3 and HS4). First results lead to the conclusion that even during HS4 (38-35 ka), the water on the continental shelf off Brazil was highly depleted in ^{14}C with apparent ventilation ages of 4.84±1.35 ka (2σ). Recurring events of old water masses advance at intermediate depth off Brazil indicate a coupling between the intensity of deep water formation in the North Atlantic and the ventilation of the deep Pacific Ocean.

[1] Mangini *et al*. (2010) *EPSL* **293**, 269–276

https://doi.org/10.1180/S0026461X00006502 Published online by Cambridge University Press

Statistical sampling of mantle heterogeneity

JOHN F. RUDGE[1]*, JOHN MACLENNAN[2] AND ANDREAS STRACKE[3]

[1]Bullard Laboratories, Department of Earth Sciences, University of Cambridge, Madingley Road, Cambridge, CB3 0EZ, UK (*correspondence: rudge@esc.cam.ac.uk)
[2]Department of Earth Sciences, University of Cambridge, Downing Street, Cambridge, CB2 3EQ, UK (jcm1004@cam.ac.uk)
[3]Institut für Mineralogie, Westfälische Wilhelms-Universität Münster, Corrensstraße 24, 48149 Münster, Germany (stracke.andreas@uni-muenster.de)

The Earth's mantle is chemically, isotopically, and perhaps even lithologically, heterogeneous. This heterogeneity provides key information on Earth's evolution through time. Unfortunately much of this information is destroyed and overprinted by the melting and melt mixing processes that occur during the formation of basalt, which is then sampled at the Earth's surface.

The aim of this study is to better understand how mantle heterogeneity is filtered to produce the heterogeneity we observe in basalts. Since the physical processes of melting, melt mixing, and melt extraction are complex and still poorly understood, we focus here on developing simple statistical models of the sampling process. In these models we consider the melting of a two lithology source consisting of an enriched, more fusible, lithology (e.g. pyroxenite), and a more depleted, less fusible, lithology (e.g. peridotite). We fractionally melt these two lithologies, and then mix the resultant fractional melts together to form a sample, i.e. an erupted basalt.

There are many different ways in which the fractional melts can be mixed together to produce a sample, and we compare a number of different models for this mixing process. We focus in particular on the effects of biasing the mixing according to the different depths at which the fractional melts are generated. To constrain our models we compare the results with isotopic, major, and trace element observations of both whole rocks and melt inclusions from tightly constrained regions (e.g. Theistareykir, NE Iceland [1, 2]). Models in which deep melts mix more thoroughly than shallow melts can account for several key characteristics of these geochemical observations. We suggest that mixing of deep melts occurs during melt generation and migration in the mantle, prior to extensive mixing in lower crustal magma chambers.

[1] Stracke *et al*. (2003) *Geochem. Geophys. Geosyst.* **4**, 8507.
[2] Maclennan *et al*. (2003) *Geochem. Geophys. Geosyst.* **4**, 8624.

A novel proxy links CAMP volcanism with end-Triassic mass extinction *and* early Jurassic evolution

M. RUHL*, C.J. BJERRUM, R. FREI AND C. KORTE

Nordic Centre for Earth Evolution, University of Copenhagen, Oester Voldgade 10, DK-1350 Copenhagen K, Denmark (*correspondence: micharuhl@gmail.com)

Phanerozoic mass extinctions are marked by global marine and terrestrial biodiversity loss and often linked to the formation of large igneous provinces (LIPs). Large-scale greenhouse gas release during these major volcanic events had a profound impact on the global exogenic carbon cycle, initiating strong perturbations in $\delta^{13}C$ records. Hence, they can be regarded as natural deep-time analogues of global environmental change. However, high resolution stratigraphic correlation between LIP formation, biotic crises and isotopic perturbations are poorly constraint. Here we present a novel proxy for volcanic activity, based on relative abundance changes of Lu, Hf, Y and Nb trace elements (ratio: $^{(Lu/\ Hf)}/_{(Y/\ Nb)}$), in a marine sedimentary record across the Triassic-Jurassic boundary. We show that peak ($^{(Lu/\ Hf)}/_{(Y/\ Nb)}$) values exactly match up with consecutive continental flood basalt emplacements in the Central Atlantic Magmatic Province (CAMP). The observed ($^{(Lu/\ Hf)}/_{(Y/\ Nb)}$)-peaks also coincide with the end-Triassic mass extinction, one of the largest Phanerozoic extinctions (at ~201.38 Ma), *and* with early Jurassic recovery patterns, suggesting that volcanism also governs (the speed of) early Jurassic evolution. Hence, this proxy for the first time allows very detailed causality studies on increased volcanic activity, disruption of global geochemical cycles and global biodiversity/ ecosystem turnovers, in unprecedented stratigraphic resolution. We furthermore test this method on the end-Permian mass extinction, the largest extinction event in earth history. Furthermore, the abundance of these trace elements in different CAMP basalt units, suggests a transition in magmatic source for the flood basalts. Lu/Hf and Y/Nb values in the oldest CAMP units are similar to the upper crust and gradually change (within ~600 kyr) to MORB values in the youngest CAMP units. In addition, highly reactive iron and trace element (Mo, U etc.) data allow interpretation of water column conditions in terms of oxic vs. anoxic and ferruginous vs. euxinic conditions. Periods of ocean anoxia/ euxinia (based on increased Fe-HR/Fe-T, Fe (Py)/Fe-HR, Mo values) coincides with the CAMP volcanic phase, but a direct link to individual CAMP pulses is yet less clear.

https://doi.org/10.1180/S0026461X00006502 Published online by Cambridge University Press

Reduction of biogenic uranyl phosphate nanoparticles by three metal-reducing bacteria

X. RUI[1], M.I. BOYANOV[2], M.J.KWON[2], E.J.O'LOUGHLIN[2], S. DUNHAM-CHEATHAM[3], J.B. FEIN[3], B.A. BUNKER[1] AND K.M. KEMNER[2]

[1]Department of Physics, University of Notre Dame, Notre Dame, IN 46556 (xrui@nd.edu)
[2]Bioscience Division, Argonne National Laboratory, Argonne, IL 60439
[3]Department of Civil Engineering and Geological Sciences, Univserity of Notre Dame, Notre Dame, IN 46556

The transformations of U in subsurface environments are controlled by a number of bacterially-driven precipitation and redox reactions. We examined the ability of three dissimilatory metal-reducing bacteria (*Anaeromyxobacter dehalogenans* strain K, *Geobacter sulfurreducens* PCA, and *Shewanella putrefaciens* CN32) to reduce U (VI) in three forms: hydrogen uranyl phosphate (HUP) nanoparticles on the cell wall of *Bacillus subtilis* bacteria precipitated by passive cell wall biomineralization; abiotically precipitated HUP; and aqueous uranyl ion. The reduction experiments were conducted at pH=6.8 with presence and absence of bicarbonate and phosphate. X-ray Absorption Fine Structure spectroscopy (XANES and EXAFS) showed varied reduction extent of U (VI) by the three bacteria. The biogenic HUP mineral was consistently more easily reduced than the abiotic HUP under the same experimental conditions. Higher extent of reduction was observed in the presence of bicarbonate. Reduction experiments under conditions that inhibited the HUP dissolution (i.e. high phosphate concentrations) showed smaller extents of U (VI) reduction. These results indicate reduction of the dissolved U (VI) species in the system, as opposed to direct electron transfer to the HUP mineral. EXAFS analysis shows that the reduced U (IV) species are consistent with mono-and bi-dentate phosphate complexation of the U (IV) atoms, as found in the $U^{IV}Ca(PO_4)_2$ mineral ningyoite.

Radioactive element abundances, paleo-heat flows, and the internal evolution of Mars

JAVIER RUIZ[1]*, ALBERTO JIMÉNEZ-DÍAZ[1], VALLE LÓPEZ[2,3], PATRICK J. MCGOVERN[4], JEAN-PIERRE WILLIAMS[5], BRIAN C. HAHN[6] AND ROSA TEJERO[1,3]

[1]Departamento de Geodinámica, Universidad Complutense de Madrid, Madrid, Spain (*correspondence: jaruiz@geo.ucm.es)
[2]Instituto de Geología Económica, CSIC-UCM, Madrid, Spain
[3]Instituto de Geociencias, CSIC-UCM, Madrid, Spain
[4]Lunar and Planetary Institute, Houston, USA
[5]Department of Earth and Space Sciences, University of California, Los Angeles, USA
[6]Department of Earth and Planetary Sciences, University of Tennessee, Knoxville, USA

Lithospheric strength, crustal and mantle lithosphere composition and orbital measurements of radioactive element abundances can be used together to estimate paleo-heat flows for Mars (e.g. [1]), which help us to constrain the thermal evolution of this planet. In this work we present estimates of paleo-heat flow for several martian regions of different periods and geological context, derived from lithospheric strength and regional radioactive element abundances obtained with the *Mars Odyssey* Gamma Ray Spectrometer. The obtained surface heat flows are in general lower than the equivalent radioactive heat production of Mars in each time, suggesting a limited contribution from secular cooling to the heat flow during the majority of the history of Mars. This is contrary to the predictions from the majority of thermal history models [2], but it would be consistent with an inefficient cycling of volatiles to and from the mantle [3], as might be expected for Mars, which has lacked a plate tectonic cycle.

[1] Ruiz *et al*. (2008) *EPSL* **270**, 1–12. [2] Hauck & Phillips (2002) *JGR* **107**, 5052. [3] Sandu *et al*. (2011) *JGR*, submitted.

https://doi.org/10.1180/S0026461X00006502 Published online by Cambridge University Press

Dissolution/precipitation processes during low-temperature mineral weathering

E. RUIZ-AGUDO[1]*, M. UROSEVIC[1], C.V. PUTNIS[2], C. CARDELL[1], C. RODRIGUEZ-NAVARRO[1] AND A. PUTNIS[2]

[1]Dept. Mineralogy and Petrology, University of Granada, Spain (*correspondence: encaruiz@ugr.es)
[2]Institut für Mineralogie, Universität Münster, Germany

Low-temperature weathering of rock-forming minerals is critical for understanding earth-surface geochemical processes. Many of these minerals are reported to dissolve non-stoichiometrically, i.e. the elemental ratios in the solid are different to those in the fluid. This phenomenon is commonly called *incongruent dissolution*, and it is attributed to the preferential release of certain cations to the solution (due to differences in the bonding strength of the mineral components), leading to the formation of the so-called *leached layers* [1]. In this study, chemical analysis of the output solutions during mineral dissolution (dolomite, as an example of a mineral that reportedly dissolves 'incongruently' [2]) and in situ, nanoscale observations of the reacting surfaces using AFM are combined with the aim of establishing a realistic mechanism for the reaction. From our observations of the reacting surface we found no experimental evidence that supports the hypothesis of a preferential release of any of the cations. Moreover, our AFM results clearly indicate that the 'incongruent' behavior is the result of a dissolution-precipitation process, with the formation of a Mg-rich precipitate on dolomite dissolving surfaces. This process seems to be controlled by the composition of a boundary layer at the carbonate-fluid interface. Dissolution of the carbonate causes this fluid boundary layer to become supersaturated with respect to the secondary phase, which then precipitates.

[1] Busenberg E. & Plummer L.N. (1982) *Am. J. Sci.* **282**(1), 45–78. [2] Casey *et al.* (1993) *Nature* **366**, 253–256.

Optimized hydrofluoric acid demineralization for quantitative isolation of soil organic matter

M. RUPPENTHAL[1]*, Y. OELMANN[1] AND W. WILCKE[2]

[1]Institute of Integrated Natural Sciences, Department of Geography, University of Koblenz, Germany (*correspondence: ruppenthal@uni-koblenz.de)
[2]Soil Science Group, Geographic Institute, University of Berne, Switzerland

Many analytical methods for chemical characterization of soil organic matter (SOM) require a precedent separation of SOM and soil mineral matrix [1]. For example, δ^2H measurements of SOM are hampered by the interference of constitutional water of clay minerals [2]. During demineralization of soil samples with hydrofluoric acid (HF), the hydrolyzed fraction of SOM is frequently discarded. Moreover, neoformed fluorides after HF treatment are often removed with highly concentrated acids resulting in additional SOM hydrolysis. Particularly from subsoil horizons considerable amounts of SOM are lost because of demineralization (losses of organic carbon [C_{org}] up to 70%).

In order to increase the C_{org}-recovery after HF treatment of soil samples and to minimize chemical alterations of SOM induced by the acid attack, we demineralized soil samples from three depth profiles. We used a new method involving density fractionation or dilute acid washings to reduce the amount of neoformed fluorides in SOM concentrates. Furthermore, we recovered the SOM dissolved in HF via precipitation of dissolved metals as hydroxides in the presence of sodium pyrophosphate to avoid coprecipitation of dissolved organic matter, followed by desalting the supernatant by means of dialysis.

Our results show that the new method allows for a better demineralization compared to established procedures, especially for subsoil horizons. We were able to minimize hydrolysis of SOM, double the C enrichment factors (ratio of C_{org} concentration after to that before treatment) and reduce C_{org}-losses to below 15%. We will discuss potential effects of the demineralization method on δ^2H values of SOM.

[1] Gélinas *et al.* 2001 *Organic Geochemistry* **32**, 677–693. [2] Ruppenthal *et al.* 2010 *Geoderma* **155**, 231–241.

https://doi.org/10.1180/S0026461X00006502 Published online by Cambridge University Press

Magma mixing and the assembly of complex eruption sequences

PHILIPP RUPRECHT AND TERRY PLANK

Lamont-Doherty Earth Observatory, Columbia University, 61 Route 9W, Palisades, NY 10964, USA (*correspondence: ruprecht@ldeo.columbia.edu, tplank@ldeo.columbia.edu)

Elemental diffusion in plagioclase and olivine [1, 2] can provide an integrated timescale of the sequence of magma mixing until eruption. For example, at Quizapu volcano (Chile) textural observations and Mg diffusion in plagioclase constrain a succession of magma recharge, mixing and eruption to a few days to three weeks [3]. One major caveat in using elemental diffusion, however, is the potential competing effect of crystal growth, which may lead to similar normal zoning patterns when magma mixes, cools and crystallizes with more evolved compositions.

In order to deconvolve crystal growth from diffusion, we have obtained by LA-ICPMS multi-element zoning patterns for olivines from the 1963-5 eruption of Irazu volcano (Costa Rica) for elements that span a wide range of diffusivities (Fe-Mg, Mn, Li, Ca, P, Sc, Ti V, Cr, Mn, Fe-Mg, Co, Ni, Zn). The 1963-65 eruption is characterized by phreatomagmatic deposits of basaltic andesites (54-57 wt% SiO_2, [4]). In three samples spanning a large sequence of the eruption we identify olivines of different origin (Fo70-91, crustal olivine cumulates and mantle-derived recharge olivines). Some olivines are dominated by growth signatures (primarily based on P profiles) and others record the timing of magma mixing through their diffusion profiles (Fe-Mg, Ni). The initial phase is dominated by mantle-melt derived olivines with a thin low Fo growth rim consistent with decompression growth over a few weeks in a mixed magma and a slightly normal zoned interior (Fo84-90) resulting from an extended time of diffusive exchange (months to years) at evolving but still mafic compositions. The later eruptive sequence shows much larger variety of olivines that records the syn-eruptive addition of distinct magmas that wax and wane through the eruption, though olivines still present from the early stage have much thicker growth rims indicating longer residence prior to eruption. Thus, multi-element zonation profiles record crystal growth during magma ascent and diffusive exchange during crystal storage, as an eruptive system evolves.

[1] Costa F *et al*. (2003) *GCA* **67**, 2189–2200. [2] Martin VM *et al*. (2008) *Science* **321**, 1178. [3] Ruprecht P (2009) PhD thesis, Univ. of Washington. [4] Alvarado GE *et al*. (2006) *GSA Spec*. *Paper* **412**, 259–276.

A complex network analysis of growth and mixing dynamics in natural metal-silicate systems

TRACY RUSHMER[1]*, ANTOINETTE TORDESILLAS[2] AND DAVID M. WALKER[2]

[1]GEMOC/Department of Earth and Planetary Sciences, Macquarie University, NSW 2109 Australia (*correspondence: Tracy.Rushmer@mq.edu.au)

[2] Department of Mathematics and Statistics, University of Melbourne, Victoria 3052 Australia

Core Formation in Partially Molten Planetesimals

The segregation of metallic cores from silicate mantles is one of the earliest, and most important, differentiation process involved in the evolution of terrestrial planetary bodies and reconciling our estimates of primary bulk silicate mantle with candidate planetary bulk compositions requires an understanding of the different regimes in which core forming material may have been mobile. This includes regimes that are dynamic and may result in transient states of high stress due to impact. Recent scenarios of core formation in planetesimals using calculations from extinct radionuclides (e.g. ^{26}Al, ^{60}Fe) call for segregation of a metal liquid (core) from partially molten silicate – a silicate mush matrix. This segregation scenario requires growth of molten core material into blebs large enough to overcome the strength of the mush matrix so that separation can occur. However, currently there is no satisfactory explanation as to how or why metallic liquid blebs in the presence of silicate melt actually grow. Experimental work has suggested deformation and shear can help coalesce metallic blebs. Here, we have developed an innovative approach that combines textures in experimental deformation experiments on a partially molten natural meteorite with complex network analyses. This approach can elucidate and quantify the growth of metallic blebs in regions where a silicate mush matrix is present and help predict separation.

https://doi.org/10.1180/S0026461X00006502 Published online by Cambridge University Press

Fate of nutrients in the fresh-saline water interface in coastal aquifers

A. RUSSAK[1,2]*, O. SIVAN[1], Y. YECHIELI[2], B. LAZAR[3] AND B. HERUT[4]

[1]Department of Geological and Environmental Sciences, Ben Gurion University of the Negev, Beer Sheva, Israel (*correspondence: russak@bgu.ac.il, oritsi@bgu.ac.il)
[2]Geological Survey of Israel, Jerusalem, Israel (yechieli@gsi.gov.il)
[3]Institute of Earth Sciences, Hebrew University, Jerusalem, Israel (boaz.lazar@huji.ac.il)
[4]Isreal Oceanographic and Limnological Research, National Institute of Oceanography, Haifa, Israel (barak@ocean.org.il)

The fresh-saline water interface (FSI) is the transition zone between fresh and saline groundwater in coastal aquifers. Major ions composition indicate if the FSI deviates from conservative mixing between fresh and saline end-members, mainly attributed to cation exchange.

This study aims to quantify the changes in nutrient concentrations (NH_4^+, NO_3^-, NO_2^-, PO_4^{3-} and $Si(OH)_4$) across the FSI at the Israeli coastal aquifer due to freshening and salinization processes. In addition to field sampling in boreholes at the coastal aquifer, experimental studies were conducted to simulate salinization and freshening events using sediment columns and a flow-through system.

The field results show that the FSI acts as a redoxcline. The oxidized fresh groundwater zone is charecterized by relatively high NO_3^- and low NH_4^+ and NO_2^- concentrations, while the saline groundwater is almost anoxic with high NH_4^+ and low NO_3^- and NO_2^-. Within the FSI NO_2^- was enriched.

During the experiments the nutrients behavior was not conservative as well. This was attributed to denitrification, adsorption/desorption and dissolution processes, similar to the field observations.

$\delta^{18}O$ zoning in eclogite garnet

A.K. RUSSELL*, K. KITAJIMA, A. STRICKLAND, L.G. MEDARIS JR., M.J. SPICUZZA AND J.W. VALLEY

Department of Geoscience, Univ. of Wisconsin, Madison, WI 53703, USA (*correspondence: akrussell@wisc.edu)

Metamorphic garnets record history and can preserve evidence, through chemical zoning, of chemical changes and fluid interactions. O isotope ratios in minerals are valuable as monitors of fluid interactions. Secondary Ion Mass Spectrometry (SIMS) allows the measurement of $\delta^{18}O$ at 10 μm scale in garnet with a precision of ±0.3‰ (2sd) [1].

Nine garnets from eight different eclogite localites across Europe were analyzed for $\delta^{18}O$ zoning. Samples are from the Saxothuringian and Moldanubian Zones of the Variscan Bohemian Massif; Trescolmen, Alps, and the Scandian-age Nordfjord region, Norway. Analyzed by laser fluoination, eight garnets had bulk $\delta^{18}O$ values between -0.41 and 3.75‰, and the ninth, 8.18‰ [2].

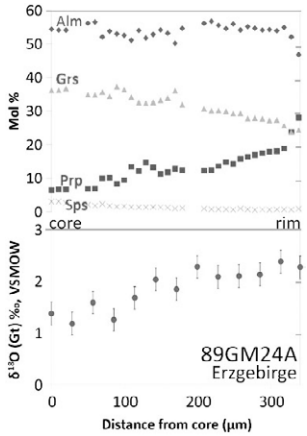

Figure: $\delta^{18}O$ and major element zoning from core to rim in garnet from the Erzgebirge[4].

This first detailed study of $\delta^{18}O$ zoning in eclogite garnet reveals a common pattern: low $\delta^{18}O$ in the core with higher $\delta^{18}O$ rims (Figure). Seven out of nine garnets analyzed have this type of zoning, independent of garnet size, geological setting, peak metamorphic conditions, age, and garnet composition.

Our results are consistent with an inherited low $\delta^{18}O$ core derived from hydrothermally altered mafic protoliths formed at an oceanic spreading center. Due to small oxygen fractionations at high T between garnet and other minerals [3], and the refractory nature of garnet, we conclude that the increase of $\delta^{18}O$ toward the rims represents interaction with a high $\delta^{18}O$ reservoir at high pressures.

[1] Page *et al*. (2010) *Chem. Geol*. **270**, 9–19. [2] Wiesli (2002) Geochem. ecl. & metapel. Adula Nappe, Central Alps, Switzerland. *PhD thesis*, University of Tennessee at Knoxville. [3] Eiler (2001) *Rev. Min & Geochem* **43**, 319–359. [4] Klápová *et al*. (1998) *J. Geol Soc*. **155**, 567–583.

https://doi.org/10.1180/S0026461X00006502 Published online by Cambridge University Press

Comparing ambient and generated marine particle composition, size, and production

L.M. RUSSELL[1]*, A.A. FROSSARD[1], R. MODINI[1], G.B. DEANE[1], M.D. STOKES[1], W.C. KEENE[2], P.K. QUINN[3] AND T.S. BATES[3]

[1]Scripps Institution of Oceanography, University of California, San Diego, La Jolla, CA 92093-0221, USA (*correspondence: lmrussell@ucsd.edu)

[2]Department of Environmental Science, University of Virginia, Charlottesville, VA 22904, USA

[3]Pacific Marine Environmental Laboratory, NOAA, Seattle, WA 98115, USA

Oceans cover two-thirds of the Earth's surface, and the particles emitted by waves breaking on the ocean surface provide an important contribution to the planetary albedo. The contribution of sea salt particles to atmospheric aerosol has been recognized and qualitatively understood for almost a century. The quantity, size distribution, and composition of submicron particles released into the atmosphere from bubble bursting remains unknown because measurements of particle production in controlled conditions have never fully explained open ocean observations. This presentation compares ambient-observed and artificially-generated composition, size, and production of marine particles.

In addition to physical measurements of particle number distributions, chemical analyses are used to illustrate the important role of surface seawater composition in forming particles. Filter samples were analyzed using Fourier transform infrared (FTIR) spectroscopy to determine the functional group composition and total organic mass (OM) of the ambient and generated marine particles. Positive matrix factorization (PMF) of the ambient particle FTIR spectra was used to separate the marine and anthropogenically-influenced sources of OM in ambient observations. Samples from marine aerosol bubbling generation showed similar organic compositions to those determined from ambient marine factors, all showing high fractions of hydroxyl functional groups. Number concentrations of artificially-generated particles were also related to the properties of the seawater from which they were generated.

To evaluate the role of organic and inorganic components of seawater in forming particles, we also investigated particle production from laboratory bubbling in controlled conditions with simple seawater model solutions. These experiments serve to illustrate the important role of sea surface components in the film bursting process that leads to particle production.

Magma degassing processes during Plinian eruptions of La Montagne Pelée (Martinique, F.W.I.)

LORRAINE RUZIÉ* AND MANUEL MOREIRA

Équipe de Géochimie et Cosmochimie, Institut de Physique du Globe de Paris, Sorbonne Paris Cité, Univ. Paris Diderot, UMR 7154 CNRS, F-75005 Paris, France (*correspondence: ruzie@ipgp.jussieu.fr)

Magma degassing process is the driving force behind explosive eruptions. To assess our knowledge on this phenomena, we have measured noble gas abundances and isotopic ratios in pumices produced by fragmentation of volatile-enriched magma.

Ruzié et Moreira (2009) [1] conducted analyses on pumice samples coming from worldwide Plinian eruptions. All samples are characterized by a systematic enrichment in neon over argon, a depletion of krypton relative to argon and an isotopically fractioned $^{38}Ar/^{36}Ar$ ratio. These features do not depend on geological setting, or on pumice age, or eruption intensity. However, they are similar for pumices from the same eruption. A correlation is observed between $^{84}Kr/^{36}Ar$ and $^{38}Ar/^{36}Ar$ ratio. This illustrates that only one physical process is at the origin of the fractionation. We therefore proposed a model of kinetic magma degassing before fragmentation to explain the elemental and isotopic fractionation. Noble gases diffuse in a magma shell surrounding a preexisting bubble with constant radius. The model explains measurements and shows the rapidity of the magma degassing process in the conduit (few hundreds of seconds).

We apply a more elaborate model taking into account bubble growth in pumices coming from La Montagne Pelée volcano (Martinique), which produced Plinian eruptions with various intensities. A detailed stratigraphic study for the last three Plinian eruptions is still in progress.

[1] Ruzié et Moreira (2009) *JVGR* **192**, 142–150.

https://doi.org/10.1180/S0026461X00006502 Published online by Cambridge University Press

Regime of volatile components in magmatism of LIP (Siberian traps)

I.D. RYABCHIKOV

Institute for Geology of Ore Deposits, Russian Academy of Sciences, 119017, Moscow, Russia (iryab@igem.ru)

To assess the formation conditions of Siberian traps we investigated melt and fluid inclusions in the phenocrysts of these rocks, which were analyzed for major and trace elements (EMPA and SIMS methods).

Ion microprobe data for reheated melt inclusions show relatively low concentrations of water by comparison with non-volatile components of comparable incompatibility (H_2O/Ce=4.5 vs 170 for MORB). Similar decoupling of H_2O and light REE was found for OIBs which belong to EM2 mantle reservoir. This has been interpreted as diffusive dehydration of the EM2 source during its storage in a drier ambient mantle (Workman *et al*. 2006). Similar mechanism of diffusive loss of water to the surrounding mantle may be proposed for magmas in Siberian Trap Province. Fluorine whose partition coefficients for major minerals of mantle rocks are similar to those of water is characterized in the investigated melts by close correlation with its non-volatile analogue (F/Nd=17 vs 21 for MORB+OIB). Concentrations of volatiles other than water in the mantle source of Siberian magmas are similar to the estimates for the sources of OIB magmas.

Low concentration of H_2O and moderate contents of other volatiles imply that the estimates of near-solidus temperature based on comparison with volatile free systems would not be changed significantly. Comparison of the estimated from melt inclusion data pressures with experimental data shows that the temperature of rising plume material was ca 400°C higher by comparison with the convecting upper mantle at the same depth. This proves that plume material arrived from deep levels in the mantle below certain thermal boundary layer.

Predicting the properties and behavior of multiphase materials in disposal environments

J.V. RYAN*, C-W. CHUNG, R.E. WILLIFORD, L.A. TURO, N.M. WASHTON AND A.L. WARD

Pacific Northwest National Laboratory (*correspondence: joe.ryan@pnl.gov)

Multiphase materials such as cement, ceramics, metals, glasses, and glass-ceramics, are being considered for stabilization of primary and secondary radioactive wastes. These materials are hydrophysically, chemically, and structurally complex with properties varying across multiple length scales. Hydrophysical properties exert control over percolation processes that help to define the relationship between microstructure and transport properties. Chemically, each form contains several components and phases, some of which can be amorphous or poorly crystalline with metastable solid-solution compositions varying over a fairly wide range. Transport properties are generally not well understood; their dependences on microstructure are non-unique such that empirical relations cannot be universally applied with confidence and modeling of interactions is under-constrained. In addition, the characteristics, and thus performance, of multiphase materials will change as the system evolves and degrades. Prediction of these changes is necessary for an improved understanding of service life in the disposal environment. A direct consequence of this complexity is that the evolution and degradation of waste form systems (comprised of the waste form and the near-field environment) are difficult to measure and, consequently, long-term performance is difficult to predict.

This research uses an integration of computational materials science, multiphase hydraulics, and geophysical techniques with careful experimentation to develop the tools necessary for analyzing and predicting the changes accompanying the evolution and degradation of multiphase waste form systems. Two waste form systems have been chosen for analysis: corroded HLW glass and cementitious cast stone. Both subject materials are multi-scale in their heterogeneity, with variations in microstructure from nanometers to millimeters. Inverse modeling techniques are coupled with physically-realistic composite physico-chemical models to determine critical parameters. These are then investigated with targeted experiments utilizing a suite of experimental techniques covering the range of scales of interest to these particular problems, including nuclear magnetic resonance, electron microscopy, x-ray tomography, and impedance spectroscopy.

https://doi.org/10.1180/S0026461X00006502 Published online by Cambridge University Press

Intra-transform magmatism; Melt migration and two-component mantle

A.E. SAAL, A.N. NAGLE, R.C. PICKLE AND D.W. FORSYTH

Brown University Department of Geological Sciences, Providence, RI (asaal@brown.edu)

Oceanic intra-transform magmatism is not supported by long-lived magma chambers or along-axis transport of melt from other parts of the spreading system, thus providing well-defined locations of melt delivery and crustal formation. Intra-transform basalts therefore represent pre-aggregated melts and their compositions provide insight into models of melt generation and transport processes beneath mid-ocean ridges. The Quebrada/Discovery/Gofar (QDG) transform fault system offsets the fast-slipping East Pacific Rise (3°-5°S) by approximately 400km and is composed of 8 active intra-transform spreading centers ranging in length from 5 to 70 km. Forty-seven dredges of young intra-transform basalts were collected and geochemically characterized from this area.

QDG basalts exhibit varying degrees of differentiation, which correlate with the estimates of crustal thickness of each ridge segment derived from gravity models. The incompatible trace element ratios (e.g. Th/La) of these lavas range significantly from depleted to enriched compositions at similar MgO content, and the level of enrichment correlates well with indicators of depth of melt segregation (e.g. Sm/Yb). Overall, the chemical variation of these basalts is greater than that previously found in fracture zones (such as Siqueiros and Garrett FZ) and is similar to the compositional range defined by northern EPR seamounts.

A simple geochemical model reproducing the trace and isotopic data of QDG basalts suggest that melting of a two-mantle component and the effect of melt migration can easily explain the compositional range observed at mid-ocean ridges.

Arsenic in siliceous deposits formed from geothermal water

A. SABITA[1], K. YONEZU[2], Y. OKAUE[1] AND T. YOKOYAMA[1]*

[1]Faculty of Science, Kyushu University, Fukuoka 812-8581, Japan (*correspondence: yokoyamatakushi@chem.kyushu-univ.jp)

[2]Faculty of Engineering, Kyushu University, Fukuoka 819-0395, Japan

Arsenic in geothermal power plants

Geothermal water, which discharges from deep underground, contains various harmful elements since it is volcanic origin. Especially, arsenic (As) concentration of geothermal water is outstanding and is generally several ppm. Therefore, the geothermal water after water/vapor separation for electric generation has been returned into deep underground again through re-injection wells at geothermal power plants. On the other hand, siliceous deposits, which are formed from geothermal waters, have been discharged into environment as industrial wastes. However, they are possible to take up As from geothermal water during the formation. Whereas, the uptake mechanism of As by siliceous deposits formed from geothermal water and its chemical state have never been investigated. In this study, the uptake mechanism of As by siliceous deposits in geothermal water at a geothermal power plant and change in the chemical state of As during the formation of siliceous deposits was investigated.

Results and Discussion

From the correlation analysis between elements in siliceous deposits formed from geothermal water at the Hatchobaru geothermal power plant, Japan and rare earth element pattern of the geothermal water, As can be concluded to be taken up by coprecipitation with hydrous iron (III) oxide. Although the siliceous deposits were formed from oxidizing geothermal water, the inside of the deposits was considered to be in reducing environment because of the conversion of hydrous iron (III) oxide to pyrite. No As was contained in the pyrite. Due to the conversion, the As may immigrate from Fe phase to silicate phase based on the result of chemical leaching treatment.

https://doi.org/10.1180/S0026461X00006502 Published online by Cambridge University Press

Mineralogy of speleothems in the Khas-e-Tarash Cave, northeast Isfahan, Iran

F. SABOKKHIZ[1], S.H. HEJAZI[2]*, A.R. NADIMI[3] AND A. ABED ESFAHANY[4]

[1]Department of Geology, Islamic Azad University, Isfahan Branch (Khurasgan), P.O. Box 81595-158, Isfahan, Iran (f.sabokkhiz@ yahoo.com)

[2]Department of Geology, Islamic Azad University, Isfahan Branch (Khurasgan), P.O. Box 81595- 158, Isfahan, Iran (*correspondence: hhejazi@khuisf.ac.ir)

[3]Department of Geology, Payeme Noor University of Isfahan, Isfahan, Iran

[4]Department of Basic Sciences, Islamic Azad University, Khurasgan Branch, P.O. Box 81595-158, Isfahan, Iran

New Method and Discussion

Speleothems are a kind of secondary minerals that form in caves. These deposits have different landscapes and mineralogy properties. In this research, the Khas-e-Tarash Cave, which is in the northeast of Isfahan, centeral Iran, is studied and introduced for the first time. We considered 59 stations in the cave and all of 19 speleothem samples are studied. Results of the scanning electron microscope (SEM) and X-ray powder diffraction (XRD) analyses indicate that calcite ($CaCO_3$), aragonite ($CaCO_3$) and the other minerals are gypsum ($CaSo_4.2H_2O$), thenardite, halite and in some cases quartz minerals are formed by groundwater along joints, fractures and main cave saloons (A sample of XRD figure 1).

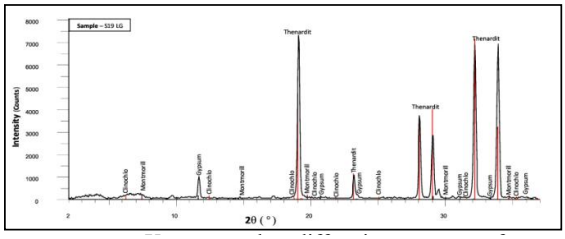

Figure 1: X-ray powder diffraction pattern of one sample, it shows that minerals are sulfates with clay minerals.

A new method, in AAS analyses, stransium Measured and the results show some samples only consist of carbonate. This survey shows that carbonate speleothems have calcite and aragonite. The evaporite minerals consist of different shapes in gypsum minerals (very fine to coarse), halite and thnardite. Silicon observed is in some cave deposits that indicate a change in groundwater composition. Later erosion and solution by groundwater have deformed old speleothems.

These minerals contain from four different chemicals classes; carbonates, sulfates, halides and silicates that sometimes stained by clay minerals and Iron oxide.

The tectonic setting where faults allowed the ascension of hydrothermal solutions and the deposition of the quartz minerals.

These minerals precipitated in low-temperature vadose solutions (calcite, aragonite, hydromagnesite, etc.).

Preliminary results of magnetic fabric of the Gole-zard pluton, Aligoodars, Iran

M. SADEGHIAN, S. BADALLOI* AND M. SHEIBI

Faculty of earth Science, Shahrood University of Technology, Shahrood, Iran (*correspondence: simin_badallo@yahoo.com, Sadeghianm1386@yahoo.com, Sheibi58@gmail.com)

A magnetic fabric study was performed on the Gole-zard pluton in an attempt to understand its emplacement history. Gole-zard granitoidic body (~20 km^2) is located in the north of Aligoodarz cities (SW of Iran), Sanandaj-Sirjan structural zone and ranges compositionally from granodiorite-granite to leucogranite. The pluton intruded in middle Jurassic metapelitic rocks and base on age determinations on the Sanandaj-Sirjan magmatic and metamorphic belt, it belongs to middle Jurassic (155-175 Ma). The presence of metaplitic and metasandstone enclaves, silica veins xenoliths with metamorphic origin, xenocrysts of andalusite and garnet confirm its S-type character. According to the geochemistry data, the rocks are peraluminous and calc-alkaline.

The mean magnetic susceptibility obtained from different rock groups are as follows: granodiorites (225 μSI), leucogranites (56 μSI), and chloritized granodiorites (510 μSI). Obtained results characterize that granodiorites (the main part of this pluton) associated with leucogranites are belong to paramagnetic granitoids (0<Km<500) which is accommodates with S-type granite. Km values increase in proportion to abundance of biotite and ilmenite. Km values reduce from granodiorites to leucogranites and finally tourmaline bearing leucogranites. In spite of distribution of magmatic microstructures in all parts of pluton, the eastern part show some evidences of solid state deformation microstructures including alteration of biotite to muscovite, chlorite and hematite; kinked biotite; mechanical twining in plagioclase and chessboard pattern in quartz.

Anisotropy percentage (P %) and shape parameter of magnetic ellipsoid (T) values vary from 1 to 3, and -0.43 to, in respectively. With respect to variation of (P) and (T) values and microstructural evidences, eastern parts of Gole -Zard g pluton have undergone more intensive deformation.

https://doi.org/10.1180/S0026461X00006502 Published online by Cambridge University Press

Magmatic evolution of Azna-Aligoudarz granitoidic plutons, SW of Iran: A typical example of S type granitization

M. SADEGHIAN, S. BAGHBANI* AND M. SHEIBI

Faculty of earth Science, Shahrood University of Technology, Shahrood, Iran
(*correspondence: Shiva.baghbani@gmail.com, Sadeghianm1386@yahoo.com, Sheibi58@gmail.com)

Darreh Bagh, Gol-e Zard and Azna plutons located in the Sanandaj- Sirjan zone, SW Iran. Based on mineralogy and geochemistry, these plutons are S -type granites with compositional range from granodiorite to leucogranite. Special characteristics of them are: presence of andalusitic xenocrysts, andalusite bearing metapelitic enclaves, xenolithic silica (quartz fragments), metasandstone and micaschistic enclaves, microgabbroic (or basaltic) dikes cutting Gol- e- Zard granitoid pluton. Field relationships show evidences for intrusion of basic – intermediats magmas (with gabbro to diorite compositions) into metapletic rocks (slate, phyllite, micashiste and garnet micashist) and resulted in contact metamorphism and converting the metapletic rocks to cordierite hornfels, andalusite hornfels and silimanite hornfels. With increasing temperature, migmatites appeared and produced granitoidic melt. Then, they ascended to higher levels in the upper crust. More differentiated members including pegmatite and leucogranites dikes, tourmaline veins and veinlets, and tourmalinites cut granitic- granodioritic rocks. Since these plutons are believed that belong to the tectonomagmatic events in Sanandaj-Sirjan zone and subuction of neothethys, basic – inter mediate magmas derived from melting oceanic slab undergoing or mantle source. In conclusion, it seems interval time between emplacement of basic – intermediate and felsic magmas is not so long.

Microstructural and AMS investigation of Darre Bagh granitoidic pluton (SW Iran)

M. SADEGHIAN, S. SHEKARI* AND M. SHEIBI

Faculty of earth Science, Shahrood University of Technology, Shahrood, Iran
(*correspondence: Shekari_2002@yahoo.com, Sadeghianm1386@yahoo.com, Sheibi58@gmail.com)

Darre Bagh granitoidic pluton (60 km^2) is located in the north of Azna-Aligoodarz cities (SW Iran) and in Sanandaj-Sirjan structural zone. The pluton intruded in middle Jurassic metapelitic rocks and base on age determinations on the Sanandaj-Sirjan magmatic and metamorphic belt, its age is obtained 169-170 Ma. This pluton compositionally ranges from granodiorite, granite to leucogranite. Small tourmaline bearing pegmatites are also observed in some parts of the studied pluton. The presence of metaplitic and metasandstone enclaves, xenolithes of silica veins with metamorphic origin, xenocrysts of andalusite and garnet, ubiquitous presence of biotite association with metapelitic host rocks confirm peraluminous and S-type granite nature of the studied rocks.

This pluton has been examined by anisotropy of magnetic susceptibility method (AMS) for the first time. Based on our investigations in 86 stations (249 cores and 854 fragments), average of measured mean magnetic susceptibility (Km) for different rock groups are as follows: granodiorites (Km=248.5 μSI), leucogranites (Km=52.6 μSI), migmatites (Km=415.1 μSI) and enclaves (Km=391.3 μSI). Obtained Km values (in Geomagnetic Lab of Shahrood University of Technology) indicate that main part of this granitoidic pluton (biotite bearing granodiorites) belong to paramagnetic granitoids (0<Km<500 μSI). Mean magnetic susceptibility is decreased from granodiorites to leucogranites which accommodates with decrease of ferromagnesian minerals (in particular biotite). The other magnetic behavior carriers are sphene, ilmenite and tourmaline. Therefore, there is a direct and logical relationship between lithological and mineralogical compositions and Km values. Hence, we can use Km values with reliable, for interpretations of compositional evolutions of granitoidic rocks.

Submagmatic and high to medium temperature subsolidus microstructures are visible in most of the thin sections prepared from core samples. The most interesting features of deformation in Darreh Bagh pluton are as follow: subgraining of quartz, plagioclase, orthoclase and biotite; mechanical twining in plagioclase; producing kinked biotite, chessboard pattern and undulose extinction in quartz, plagioclase and orthoclase; myrmekite rim along the margin of plagioclase; alteration of biotite to muscovite and chlorite and neoformation of secondary sphene and finally sericitization of orthoclase and plagioclase. The percentage of anisotropy (P%) values vary from 2 to 10 and show positive correlation with degree of deformation. Shape parameter of magnetic ellipsoid (T) values varies from 0.78 to -0.58 and most of magnetic ellipsoids are oblate.

https://doi.org/10.1180/S0026461X00006502 Published online by Cambridge University Press

Deciphering the significance of hopanoids in the marine geologic record

JAMES P. SÁENZ[1,2,3], STUART G. WAKEHAM[4], TIMOTHY I. EGLINTON[3,5] AND ROGER E. SUMMONS[2]

[1]MPI-CBG, 01307 Dresden, Germany (saenz@mpi-cbg.de)
[2]MIT EAPS, Cambridge, MA 02139, USA
[3]WHOI MCG, Woods Hole, MA 02543, USA
[4]UW School of Oceanography Seattle, WA 98195, USA
[5]ETH, Geologic Institute, 8092 Zurich, Switzerland

Hopanoids are pentacyclic triterpenoids produced by some bacteria that have been dubbed bacterial 'sterol surrogates.' Hopanoids have been broadly applied in the marine sedimentary record as taxonomic markers for certain groups of bacteria and their associated biogeochemical processes. However, our ability to rigorously interpret the significance of hopanoids in the geologic record has been greatly limited by a dearth of knowledge surrounding the sources of hopanoids in marine environments. Despite the ubiquity of hopanoids in modern and ancient marine sediments, their precise provenance in the modern oceans is largely unknown. In this study, we present a survey of bacteriohopanepolyols (BHPs) in a diverse selection of marine and proximal marine environments. Our work establishes the presence and ubiquity of hopanoids in the oceans, and provides fresh insight on the environmental sources and biogeochemical significance of hopanoids in marine sediments. We observe pronounced heterogeneity in the spatial and temporal distribution of BHPs, indicating the potential for the application of hopanoids as biomarkers for biological processes in the upper ocean and as tracers for organic matter input to sediments. In particular, BHPs appear to be relatively abundant and structurally diverse in low oxygen and oligotrophic environments and in particulate organic matter (OM) transported by rivers from terrestrial environments. Given the rich structural diversity of BHPs in terrigenous OM, interpretations of the sedimentary record of hopanoids in coastal marine settings must resolve inputs from marine pelagic and terrestrial sources. Furthermore, BHPs produced in suboxic and anoxic pelagic environments likely represent an important input to the sedimentary hopanoid inventory in upwelling environments and anoxic marine basins.

The Shatsky Rise supervolcano

WILLIAM W. SAGER[1], TAKASHI SANO[2] AND JUN KORENAGA[3]

[1]Texas A&M University, College Station, TX 77843, USA (*correspondence: wsager@tamu.edu)
[2]National Museum of Nature and Science, Tokyo 169-0073, Japan
[3]Yale University, New Haven, CT, 06520, USA

Oceanic plateaus are igneous mountains constructed by massive eruptions of basalt and related igneous rocks. Because they are hidden beneath remote parts of the oceans, the structure and evolution of these mountains are poorly known. Shatsky Rise, in the northwest Pacific, is an oceanic plateau that formed during the Late Jurassic and Early Cretacous (~145-125 Ma) near a triple junction of spreading ridges. It consists of three large volcanic massifs and a narrow volcanic ridge. It is inferred that eruptions began with the largest massif (Tamu Massif) and waned through time through the formation of the other massifs. Tamu Massif is a supervolcano, i.e. a single volcanic edifice, like a seamount, but much bigger. It has an area similar to Olympus Mons on Mars, the largest volcano in the solar system. Geophysical data show that Tamu Massif has a central summit, and a shape that is symmetric across its axis. Volcanic slopes are low, implying long, low viscosity lava flows. A seismic profile across the volcano axis shows lava flows flowed outward from the axis. Seismic profiles in some spots over these axes show normal faulting that imply volcanic rift zones. Coring on Integrated Ocean Drilling Program (IODP) Expedition 324 recovered basalt flows of two types: pillows and massive flows. Pillows are indicative of normal seamount volcanism at low effusion rates whereas the massive flows imply high volume lava flows with high effusion rates. Massive flows are typical of continental flood basalts and are also found on other large plateaus. On Shatsky Rise, thick massive flows are found on Tamu Massif, whereas pillows and thin massive flows characterize the other massifs. This trend supports the idea that Tamu Massif was formed by an initial massive eruptive event and afterwards volcanism waned as other massifs were erupted. Shallow water fossils and depth-diagnostic rocks and sediments indicate that the summits of Shatsky Rise massifs were near sea level at the time of formation. Expedition 324 cores recovered hyalo-clastites and volcanic sedimentary rocks implying that explosive volcanism was significant near the volcano summit. Heavy alteration of rocks from the shallower parts of the volcanoes suggests that warm fluids flowed through the volcano summit rocks. In sum, the structure and evolution of Tamu Massif appears much like that of a typical seamount, except that it is much bigger and was built by correspondingly larger and widespread eruptions.

https://doi.org/10.1180/S0026461X00006502 Published online by Cambridge University Press

Environmental impacts of abandoned VMS deposits: An example case from NE Turkey

E.S. SAĞLAM[1]*, M. AKÇAY[1] AND D.N. ÇOLAK[2]

[1]Dept. of Geology, Karadeniz Technical University, 61080, Trabzon, Turkey (*correspondence: ssaglam@ktu.edu.tr, akcay@ktu.edu.tr)

[2]Dept. of Biology, Karadeniz Technical University, 61080, Trabzon, Turkey (dilsatcolak@hotmail.com)

The eastern Black Sea Region (NE Turkey) is well known for massive sulphide deposits. The abandoned mines near Espiye (Giresun, NE Turkey) are characterised by widespread slag disposed of along valleys into streams and tributaries causing serious environmental pollution. This study presents physical and chemical features of stream and spring waters and their degrees of pollution based on a sampling programme in August, 2010.

In the Ficklin diagram [1], three groups of samples collected from highly polluted mine effluent (along Acısu tributary), areas of slag disposal sites and upstream from the mine effects plot in high acid-extreme metal and high acid-high metal fields, acid-high metal field and near neutral-low metal field, respectively. The water samples from the zones near the effluent are highly polluted and contain extremely anomalous values of S, Fe, Cu, Zn, As, Cd, Pb with values as high as 1375, 1130.12, 71.37, 53.08, 2.15, 0.21, 0.1 mg/L, respectively. After about a km downstream from the effluent, these values are diluted to a great extent, especially for Pb, Fe and As. Elevated levels of other elements continue further. In contrast, the waters of tributaries draining slag piles have much lower levels of heavy metals, with some elements such as As and Fe having undetectable concentrations.

In the Acısu tributary, SO_4 is highly enriched (up to 5410 mg/L) due to microbial oxidation of sulfides. 16S rRNA analyses on water samples from this area indicates presence of *Acidithiobacillus ferrooxidans* at 98% precision.

The sediments are in compliance with this, and are enriched in As, Mo, Pb, Cu, Cd, Zn, Hg and Fe based on geoaccumulation (I geo) values [2]. These values are significantly high and denote heavy contamination in stream sediments along the Acısu tributary. The sediments with the surface waters are potentially hazardous to the environment adjacent to the abandoned Karaerik mine and thus are in need of remediation.

[1] Plumlee *et al*. (1999) *Economic Geology* **6 (B) 70**, 373–407. [2] Muller (1969) *Geo. Journal* **2**, 109–118.

Prograde P-T path of a ~3.2 Ga tectonometamorphic event from Assegaai greenstone belt, SE Kaapvaal Craton

L. SAHA[1]*, A. HOFMANN[2] AND H. XIE[3]

[1]School of Geological Sciences, UKZN, Durban, SA (*correspondence: saha.lopamudra@gmail.com)

[2]Department of Geology, UJ, Johannesburg, SA

[3]Beijing SHRIMP Center, Beijing, China

P-T pseudosections are being used extensively in modern petrological studies not only to determine the P-T conditions of peak metamorphism but to establish how these conditions have been achieved, i.e. the tectonic scenario related to such processes [1]. In the present study we have used P-T pseudosection to determine the prograde P-T path from amphibolite facies garnet-staurolite-chlorite-albite-quartz-ilmenite-bearing pelitic schist from the Archaean Assegaai greenstone belt, SE Kaapvaal craton.

The pelitic schist forms part of a supracrustal sequence consisting of amphibolite, BIF, talc-tremolite schist, quartzite and calc-silicate. Within the metapelite, garnet and staurolite form the peak metamorphic assemblage and are replaced by chlorite. Absence of inclusions of any prograde mineral within garnet and staurolite porphyroblasts hinders application of any conventional thermobarometry to determine the prograde and peak metamorphic conditions.

Pesudosection analysis reveals that the garnet and staurolite assemblage was formed along a clockwise P-T path by breakdown of chloritoid: Fe-Chloritoid = almandine + Fe-Staurolite, a common reaction in pelitic rocks under amphibolite-facies conditions. Peak P-T conditions are estimated at~ 8 kbar, 600-625°C. Chlorite and albite were formed during post-peak decompression and cooling by breakdown of garnet-staurolite and paragonite, respectively.

Zircon crystallisation ages ($^{207}Pb/^{206}Pb$, SHRIMP) obtained from syntectonic quartzofeldspathic veins derived from partial melting reveal that peak metamorphism occurred ~3.18 Ga. The clockwise P-T path from the metapelite indicates a collisional tectonic event similar to that reported from other greenstone belts of SE Kaapvaal craton [2, 3], that marked stabilisation of the craton at ~3.2 Ga.

[1] O' Brien, P. (2011) *GRA* **13**, 11043. [2] Saha *et al*. (2010) *Am. J. Sci*. DOI 10.2475/04.2010.00. [3] Moyen *et al*. (2006) *Nature* **443**, 559–562.

https://doi.org/10.1180/S0026461X00006502 Published online by Cambridge University Press

Geochemical and age of collision-related volcanism following the closure of the Neotethys Ocean (Lesser Caucasus, Armenia)

L. SAHAKYAN[1]*, D. BOSCH[2], M. SOSSON[3], O. BRUGUIER[2], Y. ROLLAND[3], GH. GALOYAN[1] AND A. AVAGYAN[1]

[1]Institute of Geological Sciences, National Academy of Sciences, 24[a] Baghramyan avenue, Yerevan, 0019, Armenia (*correspondence: lilitsahakyan@yahoo.com)
[2]University Montpellier 2, Place Eugene Bataillon 34095, Cedex 05, France (bosch@)gm.univ-montp2.fr)
[3]University of Nice-Sophia Antipolis, UMR Geoazur, OCA, 250 rue A Einstein 06560 Valbonne 2, France

In the Lesser Caucasus in Armenia, collision of the South-Armenian Block (SAB) and Eurasia started during the Paleocene and was forming the Amasia-Sevan-Akera Suture zone (ASASZ). Magmatism covering the suture zone occurred during this collision and is particularly widespread since Middle Eocene. Moreover magmatism occurred after the Arabian plate collision with Eurasia since Miocene. In order to add constraints to the geodynamic context of these magmatisms, an extensive geochemical study (major & trace elements, isotopes) and geochronological study has been developped on 19 magmatic rocks. Only scarce geochemical and geochronological data are available on the Middle to Late Eocene volcanism which is associated to calc-alkaline to alkaline mildly alkaline compositions.

12 zircon grains extracted from a rhyodacite sample from SAB have been dated by U-Pb laser ICP-MS ablation which gives a well-concordant middle Miocene age of 14.6±0.2 My.

The rocks are overall characterized by enrichment in large ion lithophile elements (LILE) and show significant enrichment in light rare earth elements (LREE) compared to heavy rare earth elements (HREE) with $(La/Sm)_N$ evolving from 2.2-7.3 and $(La/Yb)_N$ ratios ranging between 2.5 and 16 and up to 47 for the rhyodacite. Extended rock-patterns of the ASASZ samples show positive anomalies in Pb, Sr, Ba associated to negative Nb and Ta spikes typical of subduction or back-arc environments. A more continental character is evidenced for trachyandesites of late Eocene and rhyodacite of middle Miocene ages due to possible slab retreat, a break off and continental crust heating by rising of the astenospheric mantle (Sosson *et al*. 2010).

[1] Sosson *et al*. (2010) *Geological Society of London, Special publication* **340**, 328–350.

Geochemical reactivity of submarine tailings from the Batu Hijau Mine

ALI SAHAMI[1], JORINA WAWORUNTU[2] AND SKYA FAWCETT[1]

[1]Lorax Environmental Services Ltd, 2289 Burard Street, Vancouver, British Columbia, Canada (alis@lorax.ca, Skya.Fawcett@lorax.ca)
[2]PT Newmont Nusa Tenggara, Jl Sriwijaya 258, Mataram, NTB, Indonesia (Jorina.Waworuntu@nnt.co.id)

Batu Hijau is an open pit mine, located in south-western Sumbawa, Indonesia, with economic mineral recovery achieved through sulphide flotation and copper-gold concentrate production. Mine tailings are discharged to Senunu Submarine Canyon via an engineered deep sea tailings placement (DSTP) system. The tailings pipeline terminus is at a water depth of 125 meters from which solid tailings flow down the canyon slope to settle at depths approximately 2,000-4,000 meters. The ore processed at Batu Hijau is categorized as fresh ore from the pit, medium and low grade, with the majority of the latter two reporting to the ore stockpile where they may be stored for several years prior to processing. The fresh ore tailings contain primarily unreactive gangue material and residual sulphides. Extensive global scientific research as well as site-specific data has conclusively demonstrated that fresh sulphidic tailings are geochemically stable when permanently stored under a water cover due to greatly reduced sulphide oxidation rates arising from the limited availability and diffusibility of oxygen in water as compared to air. Conversely, the stockpiled ore is exposed to oxygen and rain prior to processing resulting in the partial oxidation of precursor sulphides and formation of secondary weathering and oxidation products. Disposal of oxidized minerals within the tailings to the marine environment may result in the reductive dissolution of oxide and oxyhydroxide phases potentially resulting in an increase in mobility of metals to overlying seawater. Field experiments were conducted in 2010 to assess the geochemical reactivity of tailings derived from processing of fresh and partially oxidized ore in the marine environment. Redox sensitive parameters and trace metals in tailings porewater and the overlying seawater were measured at high spatial resolution through the use of dialysis arrays (peepers). Mobility of contaminants of concern and the geochemical reactions governing the reactivity of submarine tailings were assessed from the porewater geochemical data. Copper efflux rates of less than 0.7 $\mu g/cm^2$/year were calculated for both types of tailings from the porewater chemical profiles.

https://doi.org/10.1180/S0026461X00006502 Published online by Cambridge University Press

Studying soft X-ray absorption edges under extreme conditions

CHRISTOPH J. SAHLE[1], CHRISTIAN STERNEMANN[1], ALEXANDER NYROW[1], KOLJA MENDE[1], MAX WILKE[2], CHRISTIAN SCHMIDT[2], JULIEN DUBRAIL[2], METIN TOLAN[1], LAURA SIMONELLI[3], VALENTINA GIORDANO[4] AND JOHN S. TSE[5]

[1]Fakultät Physik/DELTA, 44227 Dortmund, Germany
[2]Deutsches GeoForschungsZentrum GFZ, Telegraphenberg, 14773 Potsdam, Germany
[3]ESRF, rue Jules Horowitz, 38043 Grenoble Cedex, France
[4]CNRS, LPMCN, Lyon, France.
[5]Department of Physics, University of Saskatchewan, Saskatoon S7N0W0, Canada

The study of absorption edges has proven a powerful tool to investigate the local and electronic structure of materials. [1] Absorption edges of medium or high Z elements can be accessed using X-ray absorption spectroscopy even under extreme conditions. However, the *in situ* study of low Z elements absorption edges under extreme conditions, i.e. high temperature and high pressure, is not feasible using soft X-rays or electrons as probe. Here, non-resonant X-ray Raman scattering (XRS) as an energy loss technique enables one to choose the energy of the primary X-ray beam freely and thus gives access to shallow absorption edges even in highly absorbing sample environments such as diamond anvil cells. [2]

In this contribution we enlighten the approach of XRS as a tool to access shallow absorption edges under extreme conditions and present first results of *in situ* studies of solids and liquids under high temperature and high-pressure conditions. In particular, the Ba N_{45}- and Si L_{23}-edges of the silicon clathrate Ba_8Si_{46} was studied at pressures up to 19.4 GPa. Data of the Si and Al L_{23}-edges of hydrous sodium silicate and alumosilicate glasses are presented and compared to the first *in situ* high pressure - high temperature data on hydrous silicate melts. In addition, the O K-edge of supercritical water was studied to acquire insights into its local structure. Finally, the potential of XRS for determining the Fe oxidation state from the Fe L and/or M-edge is explored.

[1] D.C. Koningsberger, & R. Prins (1988) *X-Ray Absorption, Principles, Applications, Techniques of Exafs, Sexafs & Xanes*, Wiley & Sons. [2] W. Schülke (2007) *Electron Dynamics by Inelastic X-Ray Scattering*, Oxford University Press.

An oxygen window for early Ediacaran animal life

S.K. SAHOO[1]*, G. JIANG[1], B. KENDALL[2], N.J. PLANAVSKY[3], X. WANG[4], X. SHI[4], A.D. ANBAR[2,5] AND T.W. LYONS[3]

[1]Dept. Geoscience, Univ. Nevada, Las Vegas, NV, USA (*correspondence: sahoos@unlv.nevada.edu)
[2]SESE, Arizona State Univ. Tempe, AZ, USA
[3]Dept. Earth Science, Univ. California, Riverside, CA, USA
[4]Sch. Earth Sc. & Res., Univ. Geosciences, Beijing, China
[5]Dept. Chem/Biochem, Arizona State Univ. Tempe, AZ, USA

Complex multicellular organisms including early metazoans appeared in the Ediacaran Period shortly after the termination of the late Cryogenian (Marinoan) glaciation about 635 million years (Myr) ago. Given that metazoans have high respiratory demands, it has been speculated that the termination of the Marinoan glaciation, the rise of oxygen, and evolution of complex life forms were casually linked. Previously published geochemical data, however, suggest that a major increase in the extent of ocean oxygenation did not happen until the middle Ediacaran Period, 50 Myr after the first appearance of animal fossils. This later oxygenation is arguably linked to the termination of a much less severe Gaskiers glaciation around 580 Myr ago. Here we report new geochemical data from early Ediacaran (ca. 632 Myr ago) organic-rich black shales of the basal Doushantuo Formation in South China. Iron speciation and sulfur isotope data indicate pervasive deep-water euxinia (anoxic and sulphidic) and an increase in the marine sulphate reservoir from the oxidative weathering of crustal sulphides. High molybdenum (Mo) and vanadium (V) enrichments (Mo: 120 parts per million [ppm] and V: 6000 ppm) in these shales record an increase in the oceanic Mo and V reservoirs and hence point toward a significant post-glacial oxygenation event. Our data provide evidence for co-evolution of marine redox conditions and early animals in the immediate aftermath of the Marinoan glaciation.

https://doi.org/10.1180/S0026461X00006502 Published online by Cambridge University Press

Inventory of particulate matter from all possible major sources for air quality forecasting during Commonwealth Games 2010 in Mega City Delhi

S.K. SAHU* AND G. BEIG

Indian Institute of Tropical Meteorology, Pune-411008 India (*corresponding author: saroj@tropmet.res.in)

Mega city Delhi, is facing large urban agglomerations which is one of the largest urban concentrations in South Asia and a fast growing economic center. Adverse impact of air pollution on human health, welfare and ecosystem is a key environmental problem in Indian mega cities as well as worldwide. High resolution emission inventory (EI) is one of the important and essential critical input to air quality modeling and should be as latest as possible. As part of the System of Air quality Forecasting and Research (SAFAR) project developed for air quality forecasting during the Commonwealth Games (CWG) – 2010, a high resolution emission inventory of PM_{10} and $PM_{2.5}$ have been developed for the mega city Delhi for the year 2010. The comprehensive inventory involves detailed activity data and developed for a domain of 70km×65km with a 1.67km×1.67km resolution covering Delhi and surrounding region using Geographical Information System (GIS) based statistical modeling. Developed high resolution EIs of PM_{10} and $PM_{2.5\ for}$ the air quality forecasting includes the technological specific activity data for different sectors were collected from primary source through one year field campaign as well as from secondary source which is first of its kind of attempt have been made in this work not only to fill the gap but also improve the understanding, uncertainty and accuracy of inventory.. It has been found that total emission of PM_{10} and $PM_{2.5}$ over the study area is found to be 236 Gg/yr (as shown in Fig.1) and 94 Gg/yr respectively. The contribution of windblown road dust is found to be as high as 131 Gg/yr for PM_{10} which is unusual. The relative contributions of different sectors are discussed with possible target for mitigation.

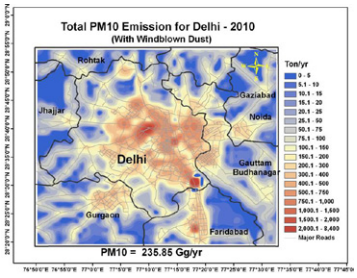

Figure 1: PM_{10} emission from different sources over Mega city Delhi.

Positive Ce anomalies and U-enrichment in Archean volcanics: Implications for oxygenated oceans

N. SAID[1]*, R. KERRICH[2] AND C. MANIKYAMBA[3]

[1]School of Earth Sciences, University of Western Australia, Western Australia 6011 (*correspondence: nsaid@cyllene.uwa.edu.au)

[2]Geological Sciences, University of Saskatchewan, Canada S7N 5E2 (robert.kerrich@usask.ca)

[3]NGRI, Hyderabad 500 007, India (cmaningri@yahoo.com)

Inference of reducing conditions in the Archean are mostly based on local evidence such as paleosols. Accordingly, new data from the scale of ocean basins is presented. Boninites in unweathered volcanic sequences of the 2.7 Ga Gadwal greenstone terrane, Dharwar craton, India, record systematic positive anomalies of U relative to Th on primitive mantle normalised diagrams, where Th/U spans 0.9-2.1 versus ~ 4 in tholeiitic basalts [1]. Such patterns are present in Phanerozoic forearc boninites where oxygenated fluids are released from the subducting slab into forearc mantle wedge. Adakites, interbedded with pillow basalts, of the ~ 2.6 Ga Hutti greenstone terrane, Dharwar craton, record Ce/Ce* ~ 1.2-1.3 with Th/U ratios <4 consistent with additions of Ce and Th from oxygenated ocean waters. Systematic positive anomalies of Ce, where Ce/Ce* spans 2.1 to 11.4, are present in basalts and rhyolites of a 2.9 Ga submarine volcanic sequence, Murchison Province, Western Australia; these are true Ce anomalies as Pr/Pr*<1. These extreme anomalies are attributed to a stratified ocean, with oxygenated surface waters but reduced bottom waters, in which Ce^{4+} was sequestered, then co-precipitated with Fe-, Mn-oxides and hydroxides distal to a submarine hydrothermal system that generated the Golden Grove Zn-Cu VMS deposit. Archean BIF of the Dharwar craton preserve negative Ce anomalies, complementary to the positive anomalies in volcanic sequences. Collectively, these observations, at the scale of ocean basins, preserve the record of an oxygenated marine environment ~ 400 Ma before the so-called great oxidation event (GOE) at ~ 2.4 Ga.

[1] Manikyamba *et al.*(2005) *EPSL* **230**, 65–83.

https://doi.org/10.1180/S0026461X00006502 Published online by Cambridge University Press

Spectroscopic estimation of SiO_2 for characterizing clays in the Brahmaputra river sediment

BHASKAR J SAIKIA

Department of Physics, ADP College, Nagaon -782 002, India (vaskar_r@rediffmail.com)

We report here the characterization of sediments from the Brahmaputra river. The samples were collected along the stretch of the Brahmaputra river channel. Analysis of the sediment is presented with the help of FTIR and XRF spectroscopic methods. Clay mineral analyses provide evidence for diagenesis. The maturity index of sediment and extinction coefficient of SiO_2 inclusion reflects the nature of erosion quality of the river.The major constituents of the samples are silica, alumina, which confirms the chemical analysis of clay. The LOI was determined at 800°C. The relatively large difference in the LOI values between 9.87 wt % and 22.21 wt % indicates that greater loss on ignition took place during the calcination step. This is largely due to the giving off of structural hydroxyl water and volatile organic components. The samples showed SiO_2 contents between 34.77 and 56.41 wt%. The grain size of the sediment samples are measured from the SiO_2/Al_2O_3 (wt %) ratio. The maturity index is invalidating with gain size of the samples, which indicate that the maturity increases with the decrease of quartz content and grain size. The correlation of the K_2O, TiO_2, Na_2O and MgO with Al_2O_3 indicate that these compounds of the sediment samples are completely associated with detrital phases of erosion process of the river. The region 400-800 cm^{-1} represents generally the bands assigned to the O-Si-O and O-Al-O bending region. The region 800-2000 cm^{-1} contains the Si-O and Al-O stretching modes and the region 2600-4000 cm^{-1} represents the OH stretching modes. In the O-Si-O and O-Al-O bending region of the infrared spectra of the studied samples are complex and there is a significant overlap between the quartz and kaolinite bands. The deposition of kaolinite in the sediment samples of the different stages of the river track can be differentiated on the basis of its quartz content. Comparison between the maturity index and extinction coefficient of the sediment samples shows a marked increase of SiO_2 content.

Spectroscopic characterization of olivine due to Fe/Mg in Dergaon H5 chondrite

BHASKAR J. SAIKIA[1], G. PARTHASARATHY[2] AND R.R. BORAH[3]

[1]Department of Physics, ADP College, Nagaon -782 002, India (vaskar_r@rediffmail.com)

[2]National Geophysical Research Institute (CSIR), Hyderabad-500 007, India (gpsarathy@ngri.res.in)

[3]Department of Physics, Nowgong College, Nagaon -782 001, India (rashmirekha_b@rediffmail.com)

The effect of the Fe and Mg ratio of olivine group $[(Mg_nFe_{2-n})SiO_4]$ in the Dergaon H5 chondrite has been investigated by Fourier Transform infrared (FTIR) and X-ray florescence (XRF) analysis. The change of peak positions of the SiO_4 tetrahedra in the stretching region have been observed with the Fe, Mg contents. The special interest is given in systematic band shifts in forsterite- fayalite series. The SiO44– tetrahedra are isolated in the structure and linked by cations Fe^{2+} or Mg^{2+} in octahedral positions. The cation positions in the structure can be filled with iron and magnesium in all possible ratios and sometimes it is occupied by Ca^{2+} or Mn^{2+}. The iron and magnesium (Fe/Mg) ratio in olivine is expressed as the forsterite content, and is calculated from the atomic percentage of Fe and Mg in the measurements. The variation of fosterite and fayalite compositions are Fo 66-89 and Fa 10-33 mol % respectively. The plot of Fo and Fa against the corresponds wavenumbers for the bands 1to5 of olivine group of the meteorite sample shows a linear variation for Fo and Fa in a different direction. The factors responsible for the frequency decrease of the absorption bands with an increase in iron may be the effects of replacing an ion of smaller radius (Mg^{2+} of radius 0.66Å) with a larger one (Fe^{2+} of radius 0.74 Å). The infrared bands in the 10mm region of the meteorite sample exhibits good agreement with the XRF results. In the 600 - 400 cm^{-1} region, the pyroxene shows a ‘V’ shape in the infrared spectra. This band shape depends upon the Mg/Fe ratio in the sample.

https://doi.org/10.1180/S0026461X00006502 Published online by Cambridge University Press

Spectroscopic studies of silicate minerals from North-Eastern India

BHASKAR J SAIKIA[1] AND N C SARMAH[2]

[1]Department of Physics, ADP College, Nagaon -782 002, India (vaskar_r@rediffmail.com)
[2]Department of Physics, Dibrugarh University, Dibrugarh-786 004, India (ncsdu@yahoo.com)

The samples we reported here are collected from North-Eastern region of India in their almost pure form of quartz crystal and silicates. Here an overview of the basic morphological, physico-chemical and crystallographic characteristics of the silicates is given. Particular emphasis is given to make a catalogue of silicates on the basis of structural classifications. The colour of the quartz crystal of these locations indicates the inclusion of the trace elements present in the host rocks. The compositional and structural studies were carried out at room temperature by using X-ray fluorescence (XRF), electron microprobe (EPMA) analyses and Fourier transform infrared (FTIR) spectroscopic techniques. Differential thermal analysis (DTA) and thermo gravimetric studies were also performed. The results of the compositional analysis of the samples are comparable to the standard literature. The compositional analysis of the samples exhibits that the major trace elements are Fe, Al, Ca and Mg. The optical properties are compared with the standard literature and the results are found to be satisfactory. An attempt to identify the minerals using the FTIR spectroscopy and to classify them according to their structural characteristics is performed. The crystallinity investigation throws light on the dependency on temperature and pressure during formation. The purity and distributions of the samples can also helps on the economic and industrial values of the silicates of the study region.

A rough idea about the silicate minerals of the study area can be lead from this investigation. Since silicates are known as rock forming mineral, one can have a fairly good idea about the rocks found in these areas.

Complexation of Eu^{3+} with humic substances studied by time-resolved laser fluorescence spectroscopy and parallel factor analysis

TAKUMI SAITO[1]*, STEVEN LUKMAN[1], NOBORU AOYAGI[2], TAKAUMI KIMURA[2] AND SHINYA NAGASAKI[1]

[1]The University of Tokyo, 7-3-1 Hongo, Bunkyo-ku, Tokyo, 113-8656, Japan (*correspondence: takumi@flanker.n.t.u-tokyo.ac.jp, stevenlukman@flanker.n.t.u-tokyo.ac.jp, nagasaki@nucler.jp)
[2]Japana Atomic Energy Agency, 2-4 Shirakatashirane, Tokai-mura, Ibaraki 319-1195, Japan (aoyagi.noboru@jaea.go.jp, kimura.takaumi@jaea.go.jp)

Humic substances (HS) are heterogeneous and ill-defined organic nanoparticles widely found in soil and aqueous environments. HS are known as effective complexants for inorganic and organic contaminants, mediating their migration through geosphere. Although many researches have been devoted to study binding of metal ions to HS mostly in terms of macroscopic binding amounts, detailed information on the binding processes are still limited, because of the heterogeneity and variety of HS from different origins. In this research, we investigated the binding of Eu^{3+} to various HS by time-resolved laser fluorescence spectroscopy (TRLFS) hyphnated with parallel factor analysis (PARAFAC). TRLFS is an analytical technique sensitive to physico-chemical forms of a target fluorescent metal ion, which can be further reinforced by combining with a powerful multivariate data analysis, PARARAC [1].

Binding of Eu^{3+} to HS purchased from the International and Japanese Humic Substances Societies was examined by TRLFS as a function of pH. A series of TRLFS data obtained for a certain HS were processed by PARAFAC to determine the number, spectra, decays and relative concentrations of factors. Except for one HS, three factors were necessary and enough to describe the variations in the data sets. These factors were distinctive with each other and could correspond to different Eu^{3+} species bound to HS. Each of the factors has some similarity among different HS, suggesting the presence of similar binding environments in different HS. It was further revealed that there were systematic trends between the spectra, decays and concentrations of the factors and the physical and chemical properties of HS. The observed trends will be used to deduce the characteristics of the different binding environments for Eu^{3+} in HS.

[1] Saito *et al*. (2010) *Environ. Sci. Technol*. **44**, 5055-5060.

https://doi.org/10.1180/S0026461X00006502 Published online by Cambridge University Press

Viscosity measurements of FeO-rich silicate melts and its implication for the lunar crust formation

R. SAKAI*, I. KUSHIRO, H. NAGAHARA, K. OZAWA AND S. TACHIBANA

Department of Earth and Planetary Science, The University of Tokyo, 7-3-1 Hongo, Tokyo 113-0033, Japan (*correspondence: rsakai@eps.s.u-tokyo.ac.jp)

The anorthite crust of the Moon has been thought to be the product of large-scale differentiation in the cooling lunar magma ocean, and the bulk composition of the Moon has been estimated to be richer in FeO than the bulk silicate Earth (e.g. [1]). The FeO content is a critical parameter for density and viscosity of silicate melt, and precise determination of those parameters is important for quantitative evaluation of the lunar curst. Contrary to the density, viscosity of silicate melts show complicated dependence on pressure and composition. Hence, experimental determination of viscosity of FeO-rich silicate melts is important. We have carried out viscosity measurements with the falling sphere method for silicate melts suitable for the lunar magma ocean.

The starting materials are glasses with three different compositions, which are fractionated in terms of mantle minerals to the first appearance of anorthite from the bulk silicate Earth with FeO-enrichment with various degrees.

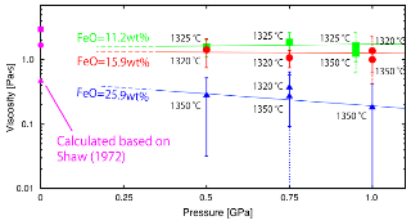

Figure 1: Viscosity of silicate melts responsible for differentiation of the Moon.

The results are shown in Figure 1, which shows weak (or slightly negative) dependence of viscosity on pressure and clear negative dependence on the FeO contents.

Figure 1 suggests little pressure dependence of viscosity for the lunar magma ocean melt at least to P>1GPa (~ 100km). The little or weak negative pressure dependence of the melt of the magma ocean in addition to high density due to high FeO contents result in effective flotation of anorthite, that is, effective formation of the anorthite crust. Our quantitative model predicts that the initial FeO content of the Moon that finally generated the anorthosite crust with the thickness of 45km was 10 - 13 wt%, which is more than the bulk silicate Earth.

[1] Khan *et al*. (2006) *Jour. Geophys. Res.* **111**, E05005, doi: 10.1029/2005/JE002608. [2] Sakai *et al*. (2011) *Lunar Planet. Sci*. **XXXXII**, abstract #1636.

Behavior of biological and terrigenous elements during the late Cenozoic in the Bering Sea: Paleoceanographic constraints of the IODP Exp. 323 sediments by high resolution non-destructive TATSCAN scanning

T. SAKAMOTO[1]*, S. SAKAI[1], A.C. MIX[2], K. TAKAHASHI[3], H. ASAHI[4], M. IKEHARA[4], M. OKADA[5], A. IJIRI[6], J. ONODERA[7], Y. OKAZAKI[7], K. HORIKAWA[8], O. SEKI[9], K. AOKI[10] AND IODP EXPEDITION 323 SCIENTIFIC PARTY[11]

[1]Institute of Biogeosciences, JAMSTEC, Natsushima-cho 2015, Yokosuka, 237-0061Japan (*correspondence: tats-ron@jamstec.go.jp)
[2]Oregon State University, Corvallis, OR, United States.
[3]Kyushu University, Fukuoka, Japan.
[4]Kochi Universaity, Kochi, Japan.
[5]Ibaraki University Ibraki, Japan
[6]The University of Tokyo, Tokyo, Japan.
[7]JAMSTEC, Yokosuka, Japan.
[8]Toyama University, Toyama, Japan.
[9]Hokkaido University, Sapporo, Japan
[10]Rissho Universtity, Saitama, Japan
[11]Integrated Ocean Drilling Program (IODP)

Continuous marine sediment cores during 5 myrs in the Bowers Ridge (Sites U1340 and U1341) and continental slope of the Aleutian Basin (Sites U1341, U1343, and U1344) of the Bering sea obtained by the IODP expedition 323 in 2009. Age models of the drilled cores are constructed using oxygen isotope stratigraphy, bio- and magneto-stratigraphy with astronomical calibration of non-destructive XRF core measurements (TATSCAN-F2). Estimated sedimentation rates during interglacials are two to three times higher than that of glacials.

Marine primary productivity, Si/Al ratio measured using TATSCAN-F2 representing biogenic silica content, exhibits large glacial-interglacial cycles during the Plio-Pleistocene. and. The productivity is relatively high, similar to that of today's 'green-belt', during the interglacial periods with increasing glacial-interglacial variability after NHG, and even larger amplitude variations during last 500 kyrs. Changes of biological productivily were closely related to terrigenosu inputs representing by K/Al and Fe/Al ratio that those elements derived from the Alaskan large rivers during the past 5 myrs.

https://doi.org/10.1180/S0026461X00006502 Published online by Cambridge University Press

Geochemical studies in Piraeus port sediments, Greece

F. SAKELLARIADOU

Dept of Maritime Studies, University of Piraeus, 18532 Piraeus, Gr (fsakelar@unipi.gr)

Introduction and methodology

Piraeus port surface sediments were geochemically studied. Total metal content and metal partitioning [1] were determined by Atomic Absorption Spectrophotometry. Metal partitioning is presented as percentages in pie diagrams. The DOM aqueous extracts were characterized by fluorescence spectroscopy for distinguishing different classes of organic components. Mono dimensional spectra [2] and contour plots (EEMS) are given.

Discussion of Results

Sediments show a high metal enrichment, especially in the outer part of the central port for Fe, Pb, Zn, Cu, Cd and Sn while seawards the outer cargo terminal for Mn, Ni, Cr and Zn. In all samples there are significant easily hydrolyzed Zn, Cu and Cd components, easily available to the biota. A carbonate related contribution of Mn and Ni was found. More than half of Cu is either bound to various forms of organic matter and/or present in sulphide minerals.

DOM consists of either simple aromatic units [2, 3] (phenolic- like, hydroxyl substituted benzoic and cinnamic acid derivatives, coumarins and alkaloid-like hydroxyquinolines) or compounds such as humic- and fulvic-like moieties and protein derived materials [4].

[1] Tessier *et al*. (1979) *Analytical Chemistry* **51**, 844–851. [2] Senesi *et al*. (1991) *Soil Science* **152**, 259–271. [3] Wolfbeis (1985) *Molecular Luminescence Spectroscopy*, 167–370. [4] Baker & Genty (1999) *Journal of Hydrology*, **217**, 19–34.

Iron isotope composition of the Middle Eocene ooidal-oncoidal ironstones and the associated lateritic paleosols from the Bahariya Depression, Western Desert, Egypt

W. SALAMA[1]*, S. WEYER[2], R. GAUPP[3] AND M.M. EL AREF[1]

[1]Department of Geology, Faculty of Science, Cairo University, Giza 12613, Egypt (*correspondence: walidsamir@daad-alumni.de)

[2]Institute of Mineralogy, Leibniz University Hannover, Callinstr. 3, 30167 Hannover

[3]Institute of Earth Sciences, Friedrich Schiller University, 07749 Jena, Germany

The Middle Eocene ironstones of the Bahariya depression, Western Desert, Egypt are subdivided into two marine sequences. The lower ironstone sequence consists mainly of peritidal stromatolitic and ooidal-oncoidal ironstone facies that were later subjected to subsurface alteration by acidic hot groundwater. The upper ironstone sequence consists mainly of mud-ironstones. The upper surfaces of these ironstone sequences were exposed to subaerial weathering processes, along which lateritic iron ores and paleosols were formed.

Iron isotope measurements were used to differentiate between the subaerial and subsurface alteration processes affecting the original marine ironstones. The iron isotope composition of the lateritic paleosols displays low δ^{56}Fe values of -0.15‰ to -0.85‰, while the stromatolitic and ooidal-oncoidal ironstones have high δ^{56}Fe values of +1.14 ‰ to +2.28 ‰. The negative δ^{56}Fe values of the paleosol are compatible with the simple internal redistribution of originally light (i.e. organically- bound) iron by dissolution-reprecipitation processes in a closed system. Multiphase iron recycling through multiple oxidation and reduction steps may have resulted in lower δ^{56}Fe [1, 2]. The negative δ^{56}Fe may have been preserved by complete or near-complete oxidation of low δ^{56}Fe aqueous Fe^{2+}. The positive δ^{56}Fe values of the marine ironstones are most probably related to a secondary subsurface alteration by ascending acidic groundwater. The acidity and the redox gradient of the groundwater resulted in the oxidation of pyrite pockets of the Cenomanian glauconitic clastics. This process involved transport of aqueous Fe^{2+} through the marine ironstone sequences. The production of high δ^{56}Fe values can be attributed to partial oxidation of low δ^{56}Fe Fe^{2+}_{aq} in a close proximity to an aqueous anoxic-oxic boundary. The high δ^{56}Fe values for oxides indicate an open system with respect to Fe [3]. Our findings indicate that the application of iron isotopes may provide important information about environmental conditions dominated during the Middle-Eocene ironstone formation and helps to determine precisely the paleoweathering surfaces within the marine ironstone sequences.

[1] Fantle & DePaolo (2004) *EPSL* **228**, 547-562. [2] Emmanuel *et al.* 2005) *Chem. Geol.* **222**, 23-34. [3] Yamagushi *et al* (2007) *EPSL* **256**, 577-587.

https://doi.org/10.1180/S0026461X00006502 Published online by Cambridge University Press

Development of steady-state surface topography and the determination of dolomite dissolution rates

G.D. SALDI[1]*, D. DAVAL[1], M. XU[2], S.R. HIGGINS[2] AND K.G. KNAUSS[1]

[1]ESD, LBNL, Berkeley CA 94720, USA (*correspondence: gdsaldi@lbl.gov)
[2]Department of Chemistry, WSU, Dayton, OH 45435, USA

The knowledge of the elementary mechanisms controlling the reactivity of mineral surfaces which undergo dissolution is critical to the development of rate-models that can accurately describe the processes occurring at the mineral/water interface. The correct interpretation of experimentally measured steady-state dissolution rates is affected by the duration of the experiments and by the development of a steady-state surface morphology, particularly at conditions close to equilibrium [1, 2].

Dolomite dissolution has been studied by hydrothermal atomic force microscopy (HAFM) on fresh-cleaved crystal surfaces as a function of the chemical affinity from 60 to 100 C, while a parallel series of experiments has been performed on a mineral powder of the same origin, under the same conditions, using a mixed-flow reactor.

The microscopic observations show the development of rectangular-shaped etch pits at mildly acidic pH's and a progressive decrease of the step velocities accompanied by a concurrent rounding of the acute step morphology when a carbonate-rich solution is introduced in the AFM cell. This change required several hours to be clearly manifested and effectively slow the rates of dissolution. Depending on the previous history of the sample, the same morphological steady-state may even require a few days to be attained. The results obtained from bulk experiments confirm the inhibiting effect of both carbonate species and aqueous Ca on dissolution and indicate that this drastic decrease of the rates is the consequence of a lower etch pit density.

[1] Bose S. *et al*. (2008) *Geochim. Cosmochim. Acta* **72**, 759–770. [2] Arvidson R.S. & Luttge A. (2010) *Chem. Geo*. **269**, 79–88.

Biologically enhanced silicate mineral dissolution for CO_2 sequestration

S.S.S. SALEK[1], R. KLEEREBEZEM[1], H.M. JONKERS[2] AND M.C.M. VAN LOOSDRECHT[1]

[1]Delft University of Technology, 2628BC Delft, The Netherlands
[2]Delft University of Technology, 2628CN Delft, The Netherlands

During the past two centuries release rate of CO_2 to atmospheric reservoir has been increased by combustion of fossil fuels [1]. The consequence of CO2 accumulation in the atmosphere is reflected as global climate change which is one of the main challenges facing humanity today [2]. CO_2 fixation as carbonates has been introduced as one the most sustainable and promising mitigation methods [3]. The efficiency of this method however is mainly limited by the raw material availability (Ca or similar divalent cations) [4]. Naturally occurring alkaline silicates are rich in divalent cations and have large reservoirs on earth; however with low dissolution rate. In the present study we describe dissolution enhancement of an alkaline silicate (wollastonite) during microbial anaerobic fermentation producing organic acids. Fermentation is an intermediate step in the anaerobic digestion process, a common process used for industrial or domestic purposes to manage waste and/or to release energy. Integration of wollastonite in an anaerobic fermentation process can result in release of Ca to the solution and neutralization of the process. ICP-OES and HPLC measurements showed an increase of dissolution rate by both proton release resulted from dissociated organic acids and complexation of Ca with these organic-products. Upon subsequent degradation of the organic acids to biogas, inorganic CO2 will be sequestered as carbonate mineral. This work could provide an alternative route to reduce climate impacts from waste treatment plants.

[1] Falkowski, P. *et al*. (2000) *Science* **290**(5490), 291–296. [2] Rockstrom, J. *et al*. (2009) *Nature* **461**(7263), 472–475. [3] Lackner, K. S. *et al*. (1995) *Energy* **20**(11), 1153–1170. [4] Renforth, P. *et al*. (2011) *Environmental Science & Technology* **45**(6), 2035–2041.

https://doi.org/10.1180/S0026461X00006502 Published online by Cambridge University Press

TIMS U-Pb dating of bastnäsite, calzirtite and tantalite as a powerful tool for timing of rare-metal granites and carbonatites (Eastern Siberia)

E.B. SALNIKOVA*, S.Z. YAKOVLEVA, A.B. KOTOV AND YU.V. PLOTKINA

IPGG RAS, St.Petersburg, Russia
(*correspondence: katesalnikova@yandex.ru)

Complex Ti, Nb-Ta and Zr oxides, primary HFSE hosts like baddeleyite, zirconolite, perovskite, pyrochlore are well known minerals appropriated for U-Pb dating of carbonatites, phoscorites as well as granitic pegmatites of the rare-element class. We propose to extend this list with calzirtite, tazheranite and bastnäsite.

Bastnäsite ((LREE)(CO_3)F) is a typomorphic mineral of siderite carbonatites from the Karasug (REE, Ba, Sr, F, Fe) deposit (Tuva Republic) Concordant U-Pb age at 118±1 Ma was obtained for bastnäsite which is in good agreement with Sm–Nd and Rb–Sr ages [1]. The minerals of this group are widespread and, in particular, represent the major economic LREE minerals in the deposits related to nontraditional carbonatite complexes, as well as occur in highly alkaline pegmatites, alkaline granites and scarns.

Tazheranite ($CaTiZr_2O_8$) and calzirtite ($Ca_2Zr_5Ti_2O_{16}$) are the characteristic accessory minerals in alkalic and ultramafic complexes associated with carbonatites. A Tazheran (SW Lake Baykal) calzirtite and tazheranite yielded a Concordia U-Pb ages at 466±2 Ma and 464±2 Ma respectively which are consistent with zircon U-Pb age at 471±5 Ma [2] as well as perovskite U-Pb age at 462.8±2.5 Ma [3].

For the first time U-Pb isotopic analyses were carried out on tantalites from three suites of pegmatites in East Sayan large-scale rare-metal province. The ages of 1838±3 Ma 1824±7 Ma and 1738±5 Ma have been obtained. These data demonstrate that mineralization is just for 30-100 Ma younger than country post-collisional Sayan granites (1858±20 Ma) [4].

Our study advertises bastnäsite, calzirtite, tazheranite as well as tantalite as promising tool for U-Pb timing of mineralization related to plumasitic type rare-metal granites and some of carbonatites.

[1] Salnikova *et al*. (2010) *Doklady Earth Sciences* **430**, 134–136. [2] Sklyarov *et al*. (2009) *Russian Geology & Geophysicse* **50**, 1091–1106. [3] Qiu-Li Li *et al*. (2010) *Chem Geol* **269**, 396–405. [4] Levitsky *et al*. (2002) *Russian Geology & Geophysics* **8**, 717–731.

A new debate on the origin of granitoid rocks from Dehnow area (NE Iran), based on isotopic data

R. SAMADI[1]* AND N. SHIRDASHTZADEH[2]

[1]Science and Research Branch, Islamic Azad University, Tehran, Iran
(*correspondence: ramin_samadi@hotmail.com)
[2]Department of Geology, University of Isfahan, Isfahan, Iran

Introduction

Magma origin of Dehnow tonalite was always under debate. [1] revealed valuable isotopic data for these rocks and suggested that they are S-type. [2] introduced them I-type based on whole rock geochemistry (e.g. Zr & Zn vs. SiO_2 plots, etc) and mineralogy. In this work, we try to illuminate the fact by putting isotopic values from [1] on figure below.

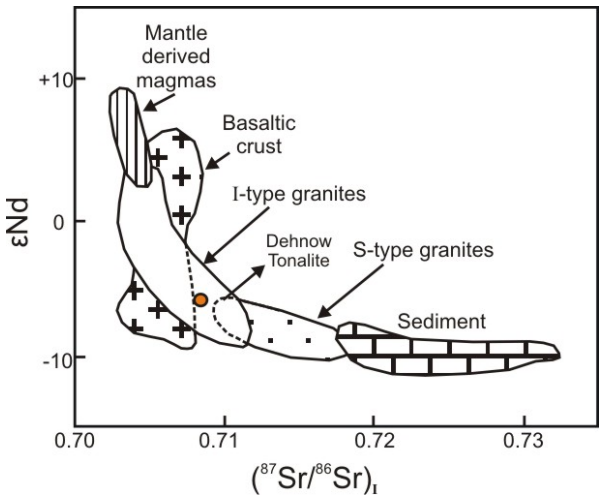

Figure 1: εNd vs. Sr isotope ratio [3, 4].

Discussion

In fact, according to figure 1, isotopic data of [1] ($^{87}Sr/^{86}Sr$=0.7079-0.7085 and εNd=-6.63 to -5.90) completely confirm the results by [2] and simply underline I-type granitoids nature of these rocks.

[1] Karimpour *et al*. (2010) *J Asian Earth Sci* **37**, 384–393. [2] Samadi *et al*. (2010) *1st IAGC* 1265. [3] Dickin (2005) *Radio Iso Geol* 492. [4] Keay *et al*. (1997) *Geol* **25**, 307–310.

https://doi.org/10.1180/S0026461X00006502 Published online by Cambridge University Press

XPS analysis of corrosion products formed on mild steel surface

A. SAMIDE[1], B. TUTUNARU[1]* AND C. NEGRILA[2]

[1]University of Craiova, Calea Bucuresti 107i, Craiova, Romania (*correspondence: tutunaruchim@yahoo.com)
[2]National Institute of Materials Physics, Bucharest, Romania

Methods of investigation

Effect of an antibacterial drug, sulfacetamide (SA), on the composition of corrosion products formed on mild steel surface in 1.0 M HCl solution has been investigated using potentiodynamic polarization, electrochemical impedance spectroscopy and XPS analysis. Fig.1 shows XPS spectra.

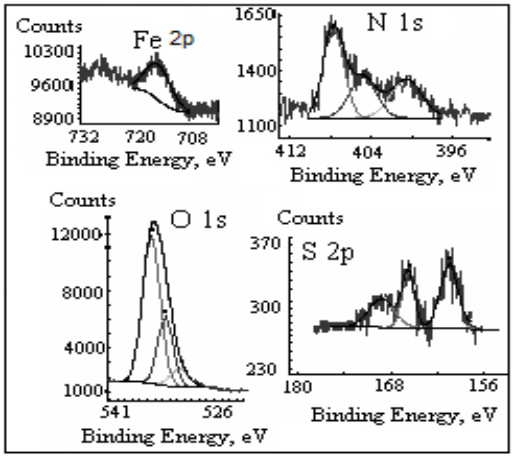

Figure 1: XPS spectra of mild steel surface corroded in 1.0 M HCl solution containing 4 mM sulfacetamide

Discussion of Results

In presence of SA, the surface layer consists of FeO (OH) rather than pure oxide [1, 2], adsorbed molecules of SA [2] and inorganic compounds (sulfides, carbonates, sulphates, nitrates) which were obtained by electrochemical decomposition of sulfacetamide [2]. More or less hypothetical compound such as schwertmannite, an iron-oxyhydroxysulfate mineral with an ideal chemical formula of Fe_8O_8 $(OH)_6$ $(SO_4)\cdot nH_2O$ or $Fe^{3+}{}_{16}O_{16}$ $(OH, SO_4)_{12\text{-}13}\cdot$10-12 H_2O may be formed. It can be considered that the SA acts as an incipient 'rust transformer' and favors the formation of a 'superficial closed layer'.

The authors thank for the financial support to the IDEI/Grant-Program, 422/2008 competition.

[1] Grosvenor *et al*. (2004) *Surf. Interf. Anal*. **36**, 1564–1574.
[2] Samide *et al*. (2011) *Digest J. Nanomat.Biost*. **6**, 663–673.

Stable isotope constraints on fluid flow in the Cascadia accretionary prism: Evidence for large flow transients during recent deformation

J.C. SAMPLE[1]* AND A. TRIPATI[2]

[1]SESES, Northern Arizona Univ., Flagstaff, AZ 86011, USA (*correspondence: james.sample@nau.edu)
[2]Earth and Space Sciences, UCLA, Los Angeles, CA 90095 (ripple@ess.ucla.edu)

The Cascadia subduction zone is a site of significant earthquakes with a recurrence interval of 240 to 530 years [1]. ODP drilling near the deformation front and on Hydrate Ridge has revealed pervasive deformation, and the formation of abundant gas hydrate, and in addition carbonate cements and veins [2]. The carbonates are proxies for fluid characteristics during he most recent active deformation and perhaps extending back to 2 Ma bp. Conventional and ion microprobe isotopic studies have shown that several fault horizons preserve carbonates with δ^{18}OVPDB values as low as -22‰, substantially out of equilibrium with modern pore water isotopic compositions and temperature. The values can be explained by transient flow events bringing in fluids from several kilometers remote from the drill sites, with substantially different isotopic compositions and temperatures. At one of the drill sites, δ18O values are consistent with precipitation temperatures of >100°C at a depth of only 67 meters below seafloor (mbsf). Conventional and ion microprobe analyses cannot distinguish between fluid isotopic and temperature causation of the carbonate isotopic anomalies. We are planning to measure samples using the technique of clumped isotope analysis, which relies on the correlation between the prevalence of ^{13}C-^{18}O-^{16}O isotopologues (Δ47 measurements) in carbonate with temperature during carbonate formation, to determine temperature and oxygen isotopic composition of fluids. The new data presented here will bear on our model of periodic, nonsteady-state fluid migration in the Cascadia accretionary prism. These transient flow events likely occur at time scales of less than a year, and may be related to periodic large-magnitude earthquakes. Widespread pulses of warm fluids could potentially destabilize clathrates at Hydrate Ridge and result in release of large quantities of methane into the overlying water column and atmosphere.

[1] Goldfinger *et al*. (in press) *USGS Prof. Paper* **1661-F**.
[2] Sample (2010) *EPSL* **293**, 300–312.

https://doi.org/10.1180/S0026461X00006502 Published online by Cambridge University Press

Study of Naryn river (Central Asia) runoff formation by stable isotope

A.A. SAMSONOVA[1]* AND I.V. TOKAREV[2]

[1]IWPH NAS KR, Bishkek, 720033 Kyrgyz Republic (aasamson@yandex.ru)
[2]SPbSU, Sredniy 41, of. 519, Saint-Petersburg, 199004 (*correspondence: tokarevigor@gmail.com)

Monitoring of the isotope composition ($\delta^{18}O$, $\delta^{2}H$) of precipitations, Naryn river and its tributaries, groundwater, and Toktogul reservoir was carried out in 2007-2009. Isotope composition of precipitations vary from $\delta^{18}O$ = -1.2 and $\delta^{2}H$ = -17 ‰ to $\delta^{18}O$ = -26.5 and $\delta^{2}H$ = -206 ‰ and fits the global meteoric water line. Mean seasonal composition of precipitation in summer (Jun.-Jul.-Aug.) is $\delta^{18}O$ = -9.5 and $\delta^{2}H$ = -70 ‰; in spring (Mar.-Apr.-May) is $\delta^{18}O$ = -11.6 and $\delta^{2}H$ = -83 ‰, in autumn (Sep.-Oct.-Nov.) is $\delta^{18}O$ = -11.0 and $\delta^{2}H$ = -79 ‰, in winter (Dec.-Jan.-Feb.) is $\delta^{18}O$ = -17.3 and $\delta^{2}H$ = -130 ‰.

End-member isotopic compositions varies: a) Naryn river head $\delta^{18}O$ = -15.2 and $\delta^{2}H$ = -134 ‰ to $\delta^{18}O$ = -10 and $\delta^{2}H$ = -82 ‰; b) middle reach of Naryn river and its tributaries $\delta^{18}O$ = -10.9 and $\delta^{2}H$ = -79 ‰ to $\delta^{18}O$ = -14.5 and $\delta^{2}H$ = -104 ‰; c) Toktogul reservoir $\delta^{18}O$ = -14.1 and $\delta^{2}H$ = -103 ‰ to $\delta^{18}O$ = -11.8 and $\delta^{2}H$ = -84 ‰; d) groundwater $\delta^{18}O$ = -17 and $\delta^{2}H$ = -126 ‰ to $\delta^{18}O$ = -13 and $\delta^{2}H$ = -94 ‰. The average isotopic composition of Naryn river just before flowing into the Toktogul reservoir is $\delta^{18}O$ = -13.0 and $\delta^{2}H$ = -93.2 ‰, and in the reservoir itself – $\delta^{18}O$ = -13.0 and $\delta^{2}H$ = -94.4 ‰; both are close to the mean annual precipitation $\delta^{18}O$ = -12.8 and $\delta^{2}H$ = -92.5 ‰. Consequently, there is strong averaging of precipitations in the some reservoirs, and averaging increases with runoff.

Naryn river runoff practically has no the glacier water, because of a) isotopic composition of water in rivers is weighted in summer and lighted in winter; b) water isotopic composition in the middle reaches is heavier, than in river head, where water has moreover fingerprint of cryogenic metamorphism in isotope composition; c) river water significantly differs from the isotopic composition of ice cores on the Inylchek glacier $\delta^{18}O$ = -16.5 and $\delta^{2}H$ = -105 ‰.

In conclusion, Naryn river runoff is formed at the expense of winter and spring precipitations. Summer precipitations can be neglected, as their volume is insignificant, and at altitudes to 1600 m precipitations are completely absorbed by evaporation. Disappearance of glaciers won't render essential influence on a river Naryn runoff.

The breakup and chemical equilibration of metal diapirs in terrestrial magma oceans

HENRI SAMUEL

Bayerisches Geoinsitut, Universitaet Bayreuth (henri.samuel@uni-bayreuth.de)

The early history of the Earth is most likely marked by at least one global magma ocean stage. During this time window, iron diapirs of various sizes delivered by differentiated impactors may have plunged through a few hundred kilometer thick silicate magma ocean. Understanding the breakup of metallic cores in such context is key to constrain the degree of metal-silicate equilibration processes.

To address this problem, I have conducted a series of numerical experiments where I follow the sinking of iron diapirs until breakup. These models include an accurate treatment of surface tension, inertial effects, stress and composition dependent viscosity. The influence of rheological properties and diapir sizes was systematically investigated. Scaling laws for the conditions of diapir breakup have been derived and are used to determine the stable size of sinking iron bodies in a silicate magma ocean.

Using these relationships I investigate the conditions and timing for metal-silicate chemical equilibration in terrestrial magma oceans.

https://doi.org/10.1180/S0026461X00006502 Published online by Cambridge University Press

Determination of U-Th and Pb isotope ratios in crude oil, kerogen and asphaltenes: Potential application for dating age of expulsion of crude oil from the rock source

GEORGIA SANABRIA[1], CHRISTOPHE PECHEYRAN[1]*, SYLVAIN BERAIL[1], ALAIN PRIZHOFER[2] AND OLIVIER F.X. DONARD[1]

[1]LCABIE, IPREM UMR 5254, CNRS – Université de Pau es des Pays de l'Adour, 64053, Pau cedex 9, France
[2]IFP, Direction Géologie-Geochimie, 1 et 4, Av. de Bois Préau, 92852 Rueil Malmaison Cedex, France

The Pb-Pb, U-Pb and Th-Pb methods of dating have become in geochromometers widely used to determine ages of minerals and rocks. However, there is scarce information about their application for dating hydrocarbon samples.

A simplified concept for U-Th-Pb geochronometers is proposed to estimate the expulsion age of crude oil from the source rock. Elemental isotopic ratio U/Pb and Th/Pb were determined by Q-ICPMS after sample acid digestion. Due to the matrix composition, classical anion exchange procedures used for lead isolation in inorganic samples (like sediments, minerals or rocks) can not be applied directly in crude oil, kerogenes and asphaltenes samples. Therefore purification procedures were evaluated in-depth for experimental optimal conditions and the optimized method was compared with a new developed method which consists in a two purification steps: first Pb ethylation with $NaBEt_4$ and solvent extraction followed by second separation stage in a gas chromatograph coupled to the MC-ICPMS. This new approach providing limited sample preparation is an efficient alternative to conventional geochimical procedures, with a great potential for micro geochemical samples.

Isotopic ratios results were used for dating hydrocarbon accumulation of two petroleum basin. These results were in good agreement with the theoretical model, hence, representing a new potential tool in petroleum prospection.

Root litter decomposition and stabilisation in three different soil depths related to microbial community dynamics and enzyme activity

M. SANAULLAH[1], A. CHABBI[1,2], P.A. MARON[3], A. SARR[3], E. BLADOTSKAYA[4] AND C. RUMPEL[1]

[1]CNRS, BIOEMCO, Thiverval-Grignon, France (cornelia.rumpel@grignon.inra.fr)
[2]UEFE, INRA, Lusignan, France
[3]INRA, Dijon, France
[4]Uni Bayreuth, Bayreuth, Germany

Subsoil horizons located below the A horizon are known to store important amounts of organic carbon characterised by high mean residence times. Microbial biomass and activity in these horizons are most probably contrasting to those of topsoil horizons and thus influence root litter degradation in different soil depths [1]. The aim of this study was to follow ^{13}C labelled root litter degradation in three different soil depths during a three year field incubation experiment and to establish a relation to the dynamics of microbial communities analysed by DNA fingerprinting and enzyme activities.

Our results showed contrasting decomposition dynamics in top- and subsoil horizons despite similar stabilisation processes [2]. Subsoil horizons showed a lag phase during the first months of incubation, but this retard in decomposition was compensated at the end of incubation probably by slightly better abiotic conditions at depth [2].

Enzyme activities showed distinct dynamics in different soil depths. Chitinase was the only enzyme that showed similar activity in top-and subsoil horizons; all other enzyme activities were much higher in topsoil. Activity of the enzyme involved in the N-cycle was evident in subsoil only within a short period after plant litter addition.

Dynamics of microbial populations evolved with time especially in the first year of the experiment. Thereafter changes in community composition were less pronounced. Stucture of microbial communities showed a depth gradient with the lowest soil layer being most different from the other two. This was mainly related to the first six months, where fresh root litter input obviously caused drastic changes.

We conclude, that microbial biomass and activity at soil depth are more limited by lack of fresh plant litter than by physical conditions. Both parameters can rapidely be stimulated and reach topsoil level in the first few months after root litter addition. However, these changes were only transient at 90 cm depth.

Funding was provided by the french science foundation ANR (project DIMMIMOS) and EGIDE (program PROCOPE).

[1] Rumpel *et al*. (2011) *Plant & Soil*, **338**, 143–158.
[2] Sanaullah *et al*. (2011) *Plant & Soil,* **338**, 127–141.

https://doi.org/10.1180/S0026461X00006502 Published online by Cambridge University Press

Microbial Fe(III)-reduction in highly calcareous agricultural soils

I. SÁNCHEZ-ALCALA[1], K.L. STRAUB[2]*, M.C. DEL CAMPILLO[1], S.M. KRAEMER[2] AND J. TORRENT[1]

[1]Departamento de Ciencias y Recursos Agrícolas y Forestales, Universidad de Córdoba, Edificio C4, Campus de Rabanales, 14071 Córdoba, Spain
[2]Department of Environmental Geosciences, University of Vienna, Althanstraße 14, 1090 Vienna, Austria (*correspondence: kristina.straub@univie.ac.at)

Although iron is the fourth most abundant element in the Earth's crust, plants may develop iron deficiency symptoms (iron chlorosis) due to low iron bioavailability. Iron chlorosis symptoms include insufficient leave chlorophyll content, poor growth and low crop yield. In particular, plants grown on calcareous soils of arid and semi-arid regions are prone to iron chlorosis because calcium carbonate buffers pH at high pH values where iron solubility is low and soil acidification strategies of diverse plant families – which would otherwise increase iron solubility and hence availability – are compromised. Agronomic practices to alleviate iron chlorosis include the application of inorganic iron fertilizers or synthetic iron chelators. Occasionally, temporary flooding of soils was shown to increase iron phytoavailability; it was speculated that microbial iron reducing activities mobilized iron during such flooding events. However, information on microorganisms with Fe(III)-reducing capabilities inhabiting calcareous soils is scant. To study flooding effects in relation to microbial activity in greater detail, we incubated soil slurries prepared from twenty-four different calcareous soils from southern Spain in the laboratory and monitored changes in iron mineralogy. The concentration of ferrous iron remained constant in control experiments with sterilized soils. In contrast, native soils produced significant amounts of ferrous iron from soil ferric minerals and the extent of ferrous iron production correlated well with native contents of dissolved organic carbon. The addition of organic acids that are typically found in root exudates further increased the production of ferrous iron. Comparative examination of soil samples suggests significant microbial mobilization of both poorly crystalline and crystalline soil iron oxides. Threshold values required for adequate iron nutrition of tolerant plants were reached in 18 slurries of native soils and 22 of the native soils that had been amended with organic acids. Microbial mechanisms that probably contributed to the mobilization of iron include respiration, fermentation and sulfur-cycle mediated reduction of soil iron minerals.

Distribution of branched tetraether lipids in a Black Sea sediment core: Insights into continental temperature evolution in Central Europe over the past 40000 years

L. SANCHI*, G. MENOTAND E. BARD

CEREGE, Univ. Aix-Marseille, CNRS, IRD & College de France, Technopole de l'Arbois BP 80, 13545 Aix-en-Provence Cedex 04, France (*correspondence: sanchi@cerege.fr, menot@cerege.fr, bard@cerege.fr)

The MBT/CBT proxy based on the relative distribution of branched tetraether membrane lipids found in peat bogs, soils and ancient sediments is a promising tool for past annual air temperature and soil pH estimations. The first studies support its application in marine sediments (e.g. [1, 2]). Nevertheless the uncertainties on the source of the biomarkers (producing organisms and/or possible aquatic production) and the need of new calibration datasets clearly speak for more studies.

We present the first paleo-record of branched tetraether lipids in Central Europe from a sediment core retrieved in the Black Sea, over the past 40000 yrs BP. As the Black Sea encountered a transition from a lacustrine to a marine stage at the beginning of the Holocene period, we could explore the MBT/CBT proxy in the two realms. During the marine stage and especially during the reconnection of the Black Sea to the Mediterranean Sea, MBT/CBT-derived temperature profile seems to be biased possibly due to the major reorganization in the water column and/or the salinity shifts. However, using the MBT/CBT global lake calibration [3], the core-top yields reconstructed temperatures similar to the instrumental spring temperature in the Black Sea basin and to the present mean annual atmosphere temperature registered above the core.

Whatever calibration datasets, the Holocene/LGM reconstructed temperature drop is consistent with existing paleo datasets from the area. Furthermore, the temperature profile of the last glacial period shows synchronous variations with major climatic events recorded elsewhere in the Northern Hemisphere.

[1] Weijers *et al*. (2007) *Science* **315**, 1701–1704. [2] Rueda *et al*. (2009) *Org. Geochem*. **40**, 287–291. [3] Sun *et al*. (2011) *J Geophy Res-Biogeo* **116.**

https://doi.org/10.1180/S0026461X00006502 Published online by Cambridge University Press

$CaCO_3$ polymorph growth and stabilization in water-ethanol mixtures

K.K. SAND[1]*, J.D. RODRIGUEZ-BLANCO[2], E. MAKOVICKY[3], L.G. BENNING[2] AND S.L.S. STIPP[1]

[1]Nano-Science Center, Dept. of Chemistry, University of Copenhagen, Denmark (kks@nano.ku.dk)
[2]School of Earth and Environment, University of Leeds, UK
[3]Dept. for Geography and Geology, University of Copenhagen, Denmark

Alcohol-water mixtures can control the mode of precipitation and morphology of crystalline $CaCO_3$. However, these two characteristics are sensitive to experimental parameters such as concentration, calcium source, temperature, precipitation method and mixing speed. An understanding of the growth of $CaCO_3$ in alcohol-water mixtures is important because control of the precipitating polymorph and its morphology are two central parameters for successful biomineralization of $CaCO_3$.

We used a simple, homogeneous precipitation method, where we fixed temperature (24 °C) and total concentration of $CaCl_2$ and Na_2CO_3 (25 mM) and varied the proportion (10 and 50%) of alcohol, shaking speed, type of alcohol (ethanol, 1-propanol and 2-propanol) and reaction time (1 h to 4 m). Diffraction and imaging results show that shaking speed and alcohol concentration are the determining parameters for vaterite and aragonite stabilization. They also control vaterite morphology, which varies from cauliflower shaped aggregates to dendrites (Figure 1). We also present an equation for controlling the synthesis of aragonite:vaterite and aragonite:calcite ratios.

The evolution of the precipitates over time lead us to conclude that this system is described by classical growth with twinned aragonite and spherulitic vaterite and aragonite. Solutions with a low water activity can be used as a switch for control of polymorph and morphology and thus define new possible pathways for biomineralization processes.

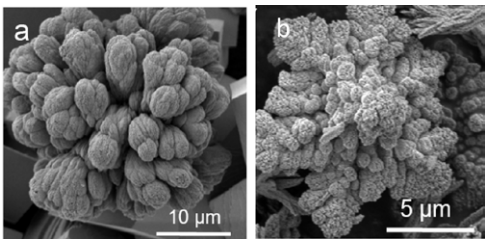

Figure 1: Vaterite precipitated in (a) 10% and (b) 50% alcohol under vigorous shaking. With gentle shaking, vaterite did not form in experiments with 50% alcohol.

Electron donating properties of humic substances and implications for pollutant phototransformation

MICHAEL SANDER[1]*, MICHAEL AESCHBACHER[1], JANNIS WENK[1,2], SILVIO CANONICA[2], URS VON GUNTEN[1,2,3], ELISABETH SALHI[2] AND RENÉ P. SCHWARZENBACH[1]

[1]Institute of Biogeochemistry and Pollutant Dynamics, Swiss Federal Institute of Technology, ETH Zurich (*correspondence: michael.sander@env.ethz.ch)
[2]Water Resources and Drinking Water, Swiss Federal Institute of Aquatic Science and Technology, eawag
[3]Civil and Environmental Engineering, Ecole Polytechnique Fédérale de Lausanne (EPFL)

Humic substances (HS) play a key role in many biogeochemical and pollutant electron transfer reactions. Past research primarily focused on HS redox properties under anoxic conditions. This contribution will present the results of a systematic characterization of the electron donating properties of a diverse set of HS under oxic conditions and, for selected HS, relate their antioxidant properties to inhibitory effects on the indirect phototransformation of organic pollutants.

Electron donating capacities (EDCs) were measured by electrochemical oxidation using 2, 2'-azino-bis (3-ethylbenz-thiazoline-6-sulphonic acid) radicals to mediate electron transfer from HS to the working electrode [1]. The number of oxidizable moieties at constant pH and applied reduction potential, E_h, increased from microbial to terrestrial HS and was highest for mixed aquatic-terrestrial HS. For a given HS, EDC values increased with increasing pH and E_h. Strong positive correlations of EDC with HS titrated phenol contents and, for mixed terrestrial-aquatic HS with aromaticities indicates that phenols and hydroquinones are the major electron donating moieties in HS.

HS may decrease indirect phototransformation rates of organic pollutants by donating electrons to oxidized reaction intermediates [2]. Combined electro- and photo-chemical experiments with anilines as model pollutants showed that the inhibition efficiencies of HS on pollutant phototransformation increased with their EDCs. Furthermore, the inhibition efficiency for a given HS increased with increasing pH, in parallel with increasing EDC. Pre-treatment of HS with chemical oxidants, including ozone and chlorine dioxide, reduced the number of electron donating moieties, reflected by significant reduction in both inhibition efficiency and EDC values. These results suggest that EDC and inhibition efficiency on organic pollutant phototransformation are determined by the number and potential distribution of hydroxybenzene moieties present in HS.

[1] Aeschbacher, A. M. Sander, & R.P. Schwarzenbach (2010) *Environmental Science & Technology,* **44**, 87–93. [2] Wenk, J. U. von Gunten, & S. Canonica (2011) *Environmental Science & Technology*, **45**, 1334–1340.

https://doi.org/10.1180/S0026461X00006502 Published online by Cambridge University Press

Sulfur isotope data from Beaver Brook Antimony deposit, Central Newfoundland, Canada: A hint for the source of mineralization?

DIRK SANDMANN*, THOMAS SEIFERT AND JENS GUTZMER

Department of Mineralogy, TU Bergakademie Freiberg, Brennhausgasse 14, D-09596 Freiberg, Germany (*correspondence: dirk.sandmann@mineral.tu-freiberg.de, thomas.seifert@mineral.tu-freiberg.de, jens.gutzmer@mineral.tu-freiberg.de)

The Beaver Brook Mine exploits one of the largest antimony deposits in the Americas. It has a current production level of 12,000 metric tons antimony concentrate (grading around 65% Sb) per year with current reserves sufficient for an estimated ten-year operating life. The mineralization (dominantly stibnite with traces of pyrite as well as quartz and carbonate gangue) is hosted by meta-sedimentary rocks of Ordovician to Silurian age and structurally controlled by faults and breccia zones. The conditions of formation of the deposit remain unknown, but it has characteristics similar to other Sb-dominated hydrothermal deposits that form at variable temperatures (100-400°C).

Stable sulfur isotope data of ten monomineralic stibnite samples were analyzed at the Department of Mineralogy, TU Bergakademie Freiberg. $\delta^{34}S_{VCDT}$ values for the stibnite samples occupy a very narrow range from -6.6 to -6.0‰ with an total analytical error of ≤ ±0.3‰. The narrow range of $\delta^{34}S$ values of stibnites from Beaver Brook suggests stable physico-chemical conditions as well as a large well-mixed sulfur reservoir. Obolensky *et al*. [1] suggest that mixing of neutral or alkaline metal-containing solutions with H_2S-bearing fluids sourced from sulfide-rich host rocks are well-suited for stibnite ore deposition. Accordingly, we suggest that the sulfur contained in the Beaver Brook deposit was provided by meta-sedimentary host rocks. The metal source, on the other hand, remains unconstrained [2, 3].

[1] Obolensky *et al*. (2007) Russ Geol Geophys **48**, 992–1001. [2] Evans (1992) *Curr. Res. Nfld. Dep. Mines Energy, Geol. Surv. Branch,* Report **92–1**, 231–243. [3] Evans & Wilson (1994) *Curr. Res. Nfld. Dep. of Mines Energy, Geol. Surv. Branch,* Report **94–1**, 211–223.

Sediment-water nutrient and Oxygen fluxes in two Antarctic continental shelf areas differently affected by climate change

E. SAÑÉ[1]*, E. ISLA[1] AND A. GRÉMARE[2]

[1]Instituto de Ciencias del Mar (ICM-CSIC), 08003 Barcelona, Spain (*correspondence: sane@icm.csic.es)

[2]UMR EPOC, Université Bordeaux 1- CNRS, Station Marine d'Arcachon, 33120 Arcachon, France

Larsen A and B ice shelves, in the Eastern Antarctic Peninsula (EAP), collapsed in 1995 and 2002, respectively. In 2006, during Antarctic expedition ANTXXIII/8, respiration experiments were carried out onboard R/V Polarstern to measure nutrient and oxygen water-sediment fluxes beneath the extinct Larsen ice shelves and off of the Northern Antarctic Peninsula (NAP), a region which has been free of ice shelves in the last 1000 years [1, 2]. Nutrient and oxygen water-sediment fluxes in EAP were studied to investigate how Larsen ecosystems evolved from a situation of negligible primary production and negligible vertical flux of organic matter to the sea floor under ice shelves [3] to a situation of ongoing primary production after Larsen ice shelves collapse [4]. We found higher nutrient and oxygen fluxes in NAP than in EAP probably related to the higher concentration of particulate organic matter found in NAP sediments [5]. Studies on benthic recolonization after iceberg scouring events suggested that the recovery time for an Antarctic mature benthic community is comprised between 230 and 500 yr [6, 7], with early recovery stages that may take up to 10 yr long, presumably like those found in the EAP benthic ecosystem [8].

[1] Ingólfsson *et al*. (1998) *Ant. Sci*. **10**, 326–344. [2] Anderson *et al*. (2002) *Quat. Sci. Rev*. **21**, 49–70. [3] Littlepage & Pearse (1962) *Science* **137**, 679–681. [4] Bertolin & Schloss (2009) *Polar Biol*. **32**, 1435–1446. [5] Sañé *et al*. (2011) *J. Sea Res*. **65**, 94–102. [6] Gutt *et al*. (1996) *Mar. Ecol. Progr. Ser*. **137**, 311–316. [7] Gutt & Starmans (2001) *Polar Biol*. **24**, 615–619. [8] Gutt *et al*. (2010) *Deep-Sea Research II*, doi: 10.1016/ j.physletb.2003.10.071.

https://doi.org/10.1180/S0026461X00006502 Published online by Cambridge University Press

Equation of state of water and melting curve of Ice VII based on simultaneous measurements of sound velocity and X-ray diffraction of Ice VII to 19 GPa and 873 K

L. SANG[1]*, D.L. FARBER[2,3], C.R. ARACNE[2], J. ZHANG[1], V. PRAKAPENKA[4], I. KANTOR[4], S. TKACHEV[4], K. ZHURAVLEV[4] AND J.D. BASS[1]

[1]Department of Geology, University of Illinois at Urbana-Champaign, Urbana, Illinois 61801, USA (*correspondence: sang1@illinois.edu)
[2]University of California, Lawrence Livermore National Laboratory, Livermore, California 94550, USA
[3]University of California, Santa Cruz, Santa Cruz, California 95064, USA
[4]GSECARS, Advanced Photon Source, Argonne National Laboratory, Argonne, Illinois 60439, USA

We have measured the sound velocity of H_2O by Brillouin spectroscopy using membrane-style diamond anvil cell with resistance heating at elevated temperatures and pressures up to 873 K and 19 GPa. The unit cells of Ice VII and Au were determined by synchrotron X-ray diffraction, using Au as an *in situ* pressure gauge. All our samples were contained within and chemically insulated from the Re-gasket hole by a gold liner. Measurements of the sound velocity in liquid water have been extended to 8.0 GPa and 873K. We observed, generally, lower velocities (up to 10% at 723 K) than those given by previous studies [1, 2]. The melting of Ice VII was determined by monitoring the sound velocity drop and the disappearance of diffraction pattern of Ice VII upon melting. Our determination of the melting temperatures differ significantly from those given by previous studies [3, 4], with an observed discrepancy of 130 K at 8 GPa. Given the care taken in the present experiments to avoid potential contamination of the water sample due to reactions at high temperatures between the sample and the gaskets and/or pressure gauges, our new measurements likely provide the first measurements on pure water which displays an extended stability field of the solid phase. Thus, our new measurements suggest that the melting curve of H_2O at high pressure needs to be reevaluated.

[1] Abramson & Brown (2003) *GCA* **68**, 1827–1835. [2] Decremps *et al*. (2006) *Ultrasonics* **44**, 1495–1498. [3] Datchi *et al*. (2000) *Phys. Rev. B* **61**, 6535–6546. [4] Lin *et al*. (2004) *J. Chem. Phys*. **121**, 8423–8427.

Solid - liquid Equilibria in the quaternary $K_2B_4O_7$-K_2SO_4-KCl-H_2O system at 323 K

SHI-HUA SANG*, XIAO ZHANG AND DAN WANG

College of Materials and Chemistry & Chemical Engineering, Chengdu University of Technology, ChengDu 610059, P.R. China (*correspondence: sangsh@cdut.edu.cn)
Mineral Resources Chemistry Key Laboratory of Sichuan Higher Education Institutions, ChengDu 610059, P.R. China

Introduction

A huge store of underground brine was discovered in Sichuan western basin of China. Sodium chloride, potassium and boron are the major chemical compositions of the underground brines. For exploiting brine resources of the underground brines, the measurement of mineral solubilities at different temperatures is used widely.

Discussion of Results

The solid - liquid equilibria in the quaternary system $K_2B_4O_7$-K_2SO_4-KCl-H_2O at 323 K were studied experimentally using the method of isothermal solution saturation. Solubilities and densities of the solution of the quaternary system were measured experimentally. In the phase diagram of the quaternary system $K_2B_4O_7$ -K_2SO_4-KCl-H_2O at 323 K, there are one invariant point E and three univariant curves E1E, E2E and E3E, and three crystallization fields corresponding to KCl, $K_2B_4O_7{\cdot}4H_2O$ and K_2SO_4 in the studied quaternary system. The experimental results show that K_2SO_4 has the biggest crystallization field (E2EE1 field) in the phase diagram (Figure 1).

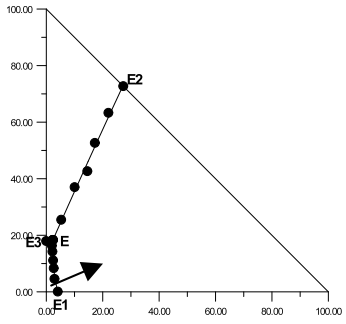

Figure 1: Phase diagram of the quaternary system $K_2B_4O_7$ - K_2SO_4-KCl-H_2O at 323 K(KB: $K_2B_4O_7{\cdot}4H_2O$)

This project was supported by the National Natural Science Foundation of China (No. 40973047), the Young Science Foundation of Sichuan Province in China (08ZQ026-017), and the New Century Excellent Talents in Universities of China (NCET-07-0125).

https://doi.org/10.1180/S0026461X00006502 Published online by Cambridge University Press

Compressibility change in Fe-rich melt and implications for core formation models

C. SANLOUP[1,2], W. VAN WESTRENEN[3], R. DASGUPTA[4], H. MAYNARD-CASELY[2] AND J.-P. PERRILLAT[5]

[1]UPMC Univ Paris 06, UMR 7193, ISTEP, F-75005, Paris, France
[2]Center for Science at Extreme Conditions and School of Physics, University of Edinburgh, EH9 3JZ Edinburgh, UK
[3]Faculty of Earth and Life Sciences, VU University Amsterdam, The Netherlands
[4]Department of Earth Science, Rice University, Houston, TX 77005, USA
[5]European Synchrotron Radiation Facility, Grenoble, France

Density measurements

The physical and chemical properties of molten iron play a key role in core formation, the largest chemical differentiation event in the early evolution of the Earth [1]. We have performed density measurements of molten iron containing an appropriate amount of light elements (5.7 wt.% carbon) up to 8 GPa using the *in situ* X-ray absorption technique [2, 3].

Discussion of the results

A liquid–liquid transition is identified by a significant compressibility increase in the vicinity of the δ-γ-liquid triple point at 5.2 GPa [4]. The observed increased compressibility of the melt is consistent with the reported molar volume difference between δ and γ phases that increases by a factor of 2 along the Fe melting curve between 0 and 5 GPa [5].

This transition pressure coincides with a marked change in the pressure evolution of the distributions of nickel, cobalt and tungsten between liquid metal and silicate melt that form a cornerstone of geochemical models of core formation. The identification of a clear link between molten metal polymorphism and metal-silicate element partitioning implies that reliable geochemical core formation models will need to incorporate the effects of these additional liquid metal transitions.

[1] Stevenson (2008) *Nature* **451**, 261–265. [2] Katayama (1996) *High Pressure Res.* **14**, 383–391. [3] Sanloup *et al.* (2000) *Geophys. Res. Lett.* **27**, 811–814. [4] Sanloup *et al.* (2011) *Earth Planet. Sci. Lett.* accepted. [5] Besson & Nicol (1990) *J. Geophys. Res.* **95**, 21717–21720.

Diurnal cycle of Strontium/Calcium ratio in a giant clam shell: A super-fine pyrheliometer

YUJI SANO[1]*, S. KOBAYASHI[2], K. SHIRAI[3], N. TAKAHATA[4], T. WATANABE[5], K. SOWA[6] AND K. IWAI[7]

[1]Atmo. Ocean Res. Inst., Univ. of Tokyo (*correspondence: ysano@aori.u-tokyo.ac.jp)
[2]AORI, Univ. Tokyo (gioiellocrlespacio@yahoo.co.jp)
[3]AORI, Univ. Tokyo (kshirai@aori.u-tokyo.ac.jp)
[4]AORI, Univ. Tokyo (ntaka@aori.u-tokyo.ac.jp)
[5]DEPS, Hokkaido Univ (nabe@mail.sci.hokudai.ac.jp)
[6]DEPS, Hokkaido Univ (sowa@mail.sci.hokudai.ac.jp)
[7]RCFO at Okinawa Pref (iwaikenj@pref.okinawa.lg.jp)

Insolation is an important meteorological parameter and a primary determinant of the Earth's climate system. The historical record of insolation in tropical and sub-tropical regions is short. Moreover, it remains difficult to extract solar radiation from a past marine environmental proxy, even though past seawater temperature [1], salinity [2], pH [3], and nutrients [4] were successfully estimated from geochemical data of biogenic marine carbonates such as coral skeletons, foraminifera tests, and mollusk shells. Herein, we describe the precise analysis of Sr/Ca ratio by using a NanoSIMS [5] with 2 micro-meter resolution in a cultivated giant clam shell exhibiting striking diurnal variations, elevated as high as 25% relative to the mean, associated with regional hourly solar radiation. This is the finest proxy among all data ever published. Annual variation of the Sr/Ca ratio is also observed in the sample by a 10 micro-meter spot with 50 micro-meter interval, again correlated with daily insolation record with similar amplitude. Light enhanced calcification and elemental transportation processes in giant clam and symbiotic algae may explain these diurnal and annual variations. Therefore, the Sr/Ca ratio of a giant clam shell might be a useful paleo-chemical-pyrheliometer.

[1] T. Felis *et al.* (2004) *Nature* **429**, 164–168. [2] N.J. Abram *et al.* (2007) *Nature* **445**, 299–302. [3] A.K. Tripati *et al.* (2009) *Science* **326**, 1394–1397. [4] H. Ren *et al.* (2009) *Science* **323**, 244–248. [5] Y. Sano *et al.* (2005) *Anal. Sci.* **21**, 1091–1097.

https://doi.org/10.1180/S0026461X00006502 Published online by Cambridge University Press

An attempt to trace the redox state of the post Marinoan glaciation (≈635Ma) ocean at the Araras platform (Brazil)

P. SANSJOFRE[1,2]*, M. ADER[1], R.I.F. TRINDADE[2], M. REUSCHEL[3] AND A.C.R. NOGUEIRA[4]

[1]Institut de Physique du Globe de Paris, Univ Paris Diderot, UMR 7154 CNRS, F-75005 Paris, France (*correspondence: sansjofre@ipgp.fr)
[2]Universidade de São Paulo, Rua do Matão 1226, 05508-900 São Paulo, Brazil
[3]Institut für Geologie und Paläontologie, Corrensstrasse 24, D-48149 Münster, Germany
[4]Universidade Federal do Pará, CEP 66.075-110, Belém, Brazil

Oceans and atmosphere oxidation in the Ediacaran paved the way for one of the biggest evolutionary leaps in Earth's history – the dawn of animals. In an attempt to trace such a major oxidation event, we investigated carbonate layers deposited at the base of the Ediacaran period which cap Marinoan glacial deposits in central Brazil. The stratigraphic section in the Araras Group comprises 13 meters of pink dolostone overlain by 25 meters of gray limestone, separated by a transition zone of gray dolostone with higher organic carbon content. Well-preserved sedimentary structures along the section indicate a transgressive tract from shallow marine to deep water deposition environments. Applied redox proxies show two different oxidation states along the sedimentary column: oxic in the dolomitic part and dysoxic-anoxic in the limestone, suggesting that respective carbonates have formed in a redox stratified water column. In the transition zone between oxic and dysoxic-anoxic environments, nitrogen, vanadium, manganese, iron and sulfur show successive variations in their concentrations or isotopic compositions. These variations likely record the succession of nitrogenous, manganeous, ferruginous and sulfidic zones, thus indicating a progressive upward transition from oxic to anoxic conditions. However, some geochemical proxies (e.g. Ce anomaly, Ni/Co) as well as the classical iron speciation redox indicator FeHR/FeT show contradictory results, providing thus conflicting interpretations for our dataset. We explain the different interpretations of the data in terms of either a paleo-redox state for the post Marinoan Ocean, or a diagenetic overprint.

Metamorphic evolution recorded by amphiboles in the metadolerites from the Frido Unit ophiolites (Southern Apennine-Italy)

MARIA T. CRISTI SANSONE[1], GIACOMO PROSSER[1], GIOVANNA RIZZO[2], PAOLA TARTAROTTI[3]

[1]Dipartimento di Scienze Geologiche-Università degli Studi Della Basilicata
[2]Dipartimento di Chimica-Università degli Studi Della Basilicata
[3]Dipartimento di Scienze della Terra- Università degli Studi di Milano

Metadolerites of the Frido Unit Ophiolites have different kinds of texture reflecting various degree of *crystallinity*. Primary clinopyroxene is replaced by brown and green amphiboles interpreted as being of oceanic origin; brown amphiboles show Mg-hastingsite, edenite, pargasite, Fe-hastingsite, Mg-horneblende and tschermakite compositions, whereas green amphiboles show Mg-hastingsite, hastingsite, edenite, Mg-horneblende, tschermakite and Fe-tschermakite compositions. The blue amphibole rims of the brown amphibole has a winchite and barrowisite compositions; we infer that it crystallized during the early stages of the orogenic metamorphism, likely under static conditions. The different composition of amphiboles occurring in the metadolerites suggest that the ophiolitic rocks from the Frido Unit has been affected by both ocean-floor metamorphism in the amphibolite to greenschist facies conditions and subsequent orogenic metamorphism under HP/LT conditions.

https://doi.org/10.1180/S0026461X00006502 Published online by Cambridge University Press

Multidisciplinary study of Santa Eulalia Plutonic Complex (Central Portugal): Preliminary insight

H. SANT'OVAIA[1]*, J. CARRILHO LOPES[2] AND P. NOGUEIRA[2]

[1]DGAOT, Centro de Geologia, FCUP, Portugal (*correspondence: hsantov@fc.up.pt)
[2]Dep. Geo., Univ. Évora, Centro de Geologia UL, Portugal

The Santa Eulália Plutonic Complex (SEPC) is a late-Variscan calcalkaline granitic body that occupies an area of 400 km^2 and is located in the Variscan Iberian sector. The host rocks of the complex are composed by metamorphic formations from Proterozoic to Lower Paleozoic. The SEPC has two main facies which present different compositions and textures. From the rim to the core, there is a medium- to coarse-grained pinkish granite (G0) involving large masses of mafic to intermediate rocks and a central gray monzonitic granite (G1). The central facies can be divided into a porphyritic facies (G1A) and a central medium-grained facies (G1B). Multidisciplinary studies that include petrography, mineral and whole-rock chemistry, Anisotropy of Magnetic Susceptibility (AMS) and microstructural analyses were carried out. Besides petrographic and mineral chemistry data, whole-rock analytical results reveal clear differences between these two main granitic facies. G0 granites represent more evolved liquids (>SiO_2 wt.% and <MgO wt.%), plot closer to metaluminous and A-type fields, and present negative Eu anomalies, while G1 facies are typically monzonitic granites with a strong peraluminous character. The AMS study was based on 50 sampling sites. The magnetic susceptibility ranges between 55.09 and 7343.67 x 10^{-6} SI. Two major groups can be established: facies G0, with Km > 10^{-3} SI which supports the presence of magnetite, and the central facies (G1A, G1B) with Km< 10^{-4} SI. In the central facies the paramagnetic behaviour is due to ferromagnesian minerals, such as biotite, and ilmenite. Magnetic anisotropy ranges between 2.2 and 18.2% being in mean >5% in facies G0 and <4% in the central facies. The high P% in G0 facies may be caused by the magnetic bearer, magnetite. Nevertheless, microscope observations show signs of a post-magmatic deformation in G0. These preliminary data support that the facies G0 and the central facies (G1) have a distinct magnetic behaviour which may suggest different redox conditions in magma genesis.

This work has been financially supported by PTDC/CTE-GIX/099447/2008 (FCT-Portugal, COMPETE/FEDER).

Fe(II) and organic exudates interaction in seawater

J. MAGDALENA SANTANA-CASIANO*, ARIDANE G. GONZÁLEZ, NORMA PÉREZ AND MELCHOR GONZÁLEZ-DÁVILA

Departamento de Química, Facultad de Ciencias del Mar, Universidad de Las Palmas de Gran Canaria, Campus de Tafira, 35017 Las Palmas, Spain

Fe(II) oxidation kinetic was studied in seawater and in seawater enriched with exudates excreted by *Phaeodactylum tricornutum*. The exudates produced after 2, 4 and 8 days of culture at $6.21 \cdot 10^7$ cell/L, $2.29 \cdot 10^8$ cell/L and $4.98 \cdot 10^8$ cell/L were selected. The effects of the pH (7.2-8.2), temperature (5-35°C) and salinity (10-36.72) on the Fe(II) oxidation rate were studied. All the data was compared with the results for seawater without exudates (seawater control). The Fe(II) rate constants decreased as a function of culture time and cell concentration at different pH, temperature and salinity. The experimental data was fitted to a polynomial function in order to quantify the fractional contribution of the organic exudates from the diatoms to the Fe(II) oxidation rate in natural seawater. Experimental results showed that the organic exudates excreted by *Phaeodactylum tricornutum* affect the Fe(II) oxidation, increasing the life time of the Fe(II) in seawater. A kinetic model approach was carried out in order to account for the speciation of each Fe(II) species together with its contribution to the overall oxidation rate.

https://doi.org/10.1180/S0026461X00006502 Published online by Cambridge University Press

Biomineralization of Mn oxides by Mn(II)-oxidizing fungi

C.M. SANTELLI[1,2]*, S.M. WEBB[3], A.C. DOHNALKOVA[4] AND C.M. HANSEL[2]

[1]Smithsonian Institution, Washington, DC 20560, USA (*correspondence: santellic@si.edu)
[2]Harvard University, Cambridge, MA 02138, USA (hansel@seas.harvard.edu)
[3]Stanford Synchrotron Radiation Lightsource, Menlo Park, CA 94025, USA (samwebb@slac.stanford.edu)
[4]Environmental Molecular Sciences Laborary, PNNL, Richland, WA 99352, USA (Alice.Dohnalkova@pnl.gov)

Manganese (Mn) oxides are environmentally abundant, highly reactive mineral phases that play important roles in the biogeochemical cycling of nutrients, contaminants, carbon, and numerous other elements. The oxidation of Mn(II) to these sparingly soluble, nanocrystalline Mn(III/IV) oxide phases is believed to be largely driven by microbiological activity. The majority of studies thus far have focused on the contributions of bacteria to the biogeochemical cycling of Mn, however recent studies have suggested that fungi may substanially contribute to the biomineralization of Mn oxide minerals in some environments. Understanding the environmental impact of these fungally precipitated mineral phases requires detailed analysis of their size, composition, and structure.

Several species of Mn(II)-oxidizing Ascomycete fungi were isolated from metal-contaminated and freshwater environments. A microscopic examination of these fungi revealed that the patterns of Mn oxide deposition varied amongst the different species. In this study, representative Mn(II)-oxidizing fungi were grown under the same chemical and physical conditions to determine if the species of fungus impacts the size, morphology, or structure of Mn biooxides. A combination of electron microscopy annd synchrotron radiation X-ray absorption spectroscopy (SR-XAS) were utilized to characterize the Mn oxide phases produced by these representative fungal species.

Our study reveals that the initial phase produced by different species of Mn(II)-oxidizing fungi grown under the same conditions is a highly disordered, nanocrystalline phyllomanganate similar to δ-MnO_2. Amongst the different species, however, differences in mineral size, morphology, and secondary products are observed. Changes in solution chemistry (e.g. Mn concentration) further impacts the structure of these biominerals, which could translate to large influences on biogeochemical processes in the environment.

Changes in the Fe(II)/Fe(III) ratio by bacterial activity according to dynamics of an acid pit lake

E. SANTOFIMIA[1], E. LÓPEZ-PAMO[1], E. GONZÁLEZ-TORIL[2] AND A. AGUILERA[2]

[1]Instituto Geológico y Minero de España, Ríos Rosas 23, Madrid, España
[2]Centro de Astrobiología, Torrejón-Ajalvir road km 4, Torrejón de Ardoz, Madrid, España

Nuestra Señora del Carmen acidic pit lake (Iberian Pyrite Belt) generally presents a chemical stratification, differentiating two layers: 1) a thin upper layer of ~2 m depth, pH between 2.5-2.7, EC from 2 to 8 mS/cm and Eh 820 mV, which corresponds to oxic conditions where iron is predominantly Fe(III), and 2) a thick bottom layer from 2 m to 35 m depth, homogeneous in depth, with pH ~2.5, EC 9 mS/cm, anoxic (<0.2 mg/L) and Eh between 640-680 mV, where Fe is both Fe(II) and Fe(III). Microbial community composition was analyzed by 16S and 18S rRNA gene cloning and sequencing in this layer, detecting oxidising bacteria (*Leptospirillum*) and the facultative iron-reducing bacteria such as *At. ferrooxidans* and *At. ferrivorans*.

Occasionally at the beginning of some winters, a period of mixing and total homogenization was observed in entire water column, being this process favoured by dry autumns. The pit lake recovered the chemical stratification after intense episodes of rainfall (strong inflow of runoff). An unusual mixing process happened during summer 2009 as a result of intense evapoconcentration that took place in the upper layer.

High average concentrations of SO_4 (8.5 g/L), Mg (1.0 g/L) and metals (Fe 760 mg/L, Al 230 mg/L, Mn 88 mg/L and Cu 29 mg/L) were measured in the homogeneous pit lake during the winter mixing. In this process the dissolved oxygen is introduced from surface to depth, but it is rapidly consumed by the bacterial oxidation of ferrous iron, decreasing the Fe(II)/Fe(III) ratio. This ability is normal in these types of microorganisms as could be checked during the winter mixing of entire water column in November 2008 or partial mixing of summer 2009, in which had a decrease of the Fe(II) and a increase of the Fe(III) as a result of aerobic bacterial oxidation. These bacterial species have revealed metabolic versatility, being able to reduce ferric iron in anoxic conditions. This ability is less common but it was registered in the anoxic bottom layer during stratification periods (Fe(II) increased and Fe(III) dropped). Extremophile bacteria respond to changes in environmental conditions and its versatility seems to control the evolution of the redox species of iron in the bottom layer of this pit lake.

https://doi.org/10.1180/S0026461X00006502 Published online by Cambridge University Press

Deep ground water migration in Brazilian Federal District based on isotope geochemistry

R.V. SANTOS*, W. PACHECO AND L.H. MANCINI

Instituto de Geociências, Universidade de Brasília, Campus Darcy Ribeiro, 70910-900 Brasília – DF (*correspondence: rventura@unb.br)

The young capital of Brazil is placed geographically in the Brazilian Central Plains, where the average altitude is close to a 1,000 m above sea level. The area includes drainages that flow to three of the most important river basins of the country: the Paraná, the Amazon, and the São Francisco river basins. Because population has already reached more than 2 million people and continues to grow, policy makers increasingly use groundwater reservoirs.

In order to evaluate the geochemical stability of these reservoirs, we performed an 18 month detailed monitoring of is $\delta^{13}C$, $\delta^{18}O$, δD and $^{87}Sr/^{86}Sr$ isotopic composition. The isotopic data revealed two main behaviors of these reservoirs: 1) those that present a narrow range of isotopic variation; and 2) those that present a wide range of isotopic variation. While the former were interpreted as isotopic equilibrated water-host rock reservoirs, the later were interpreted as reservoirs that did not reached isotopic equilibrium due to the young age of their waters. We further show that isotopic fluctuation observed in these reservoirs may be related to changes in hydrostatic pressure induced by seasonal variations of rainfall amount.

Biogeochemical and microbial controls of ^{129}I mobility in groundwater

PETER H. SANTSCHI[1], ROBIN BRINKMEYER[1], KATHLEEN A. SCHWEHR[1], SAIJIN ZHANG[1], CHEN XU[1], HSIU-PING LI[1] DANIEL I. KAPLAN[2], CHRIS YEAGER[2] AND KIMBERLY A. ROBERTS[2]

[1]Texas A&M – Galveston, Galveston, Texas
[2]Savannah River National Laboratory, Aiken, South Carolina

Due to its long half-life (17 My), high mobility, and biophilic properties, ^{129}I, a major by-product of nuclear fission, is one of the three major risk drivers at nuclear disposal sites. In aquatic environments, iodine (I), mainly exists as I^-, IO_3^- and organic iodine (OI). Field and laboratory batch and column studies were established to understand the inter-conversion of I species in an ^{129}I-contaminated plume located in F-area of the Savannah River Site (SRS), by determining speciated ^{129}I and stable ^{127}I using GC-MS [1]. These studies demonstrated that the mobility of I species greatly depended on the I concentration used [2, 3]. It was found that bacteria isolates can accumulate I^- at environmentally relevant concentrations (0.1 μM I^-); some isolates were also found to oxidize I^- to IO_3^- [*4*]. When the hypothesis that I^- mobility can be controlled through an engineered barrier system was tested, results showed that while the majority of I (as ^{127}I and ^{129}I) existed as I^- near the source term, iodide transformed into iodate and organo-I downgradient [5], and was removed through the formation of immobile particulate OI and partly released as mobile OI [6], depending on aromaticity and relative hydrophobicity; the greater the aromaticity, the greater the uptake of iodine [7].

[1] Zhang *et al*. (2010) *ES&T* **44**, 9042–9048. [2] Schwehr *et al*. (2009) *ES&T* **43**, 7258–7264. [3] Zhang *et al*. (2011) *ES&T* submitted. [4] Li *et al*. (2011) *Appl*. *Environ*. *Microbiol*. 77 2153–2160. [5] Kaplan *et al*. (2011) *ES&T* **45**, 489–496. [6] Otosaka *et al*. (2011) *Sci*. *Tot*. *Environ*. submitted. [7] Xu *et al*. (2011a,b) *GCA, ES&T*, submitted.

https://doi.org/10.1180/S0026461X00006502 Published online by Cambridge University Press

Low oxygen fugacity mantle derived auriferous fluids for Archaean Orogenic Gold deposit of Ajjanahalli, Chitradurga Schist belt, Dharwar Craton, India

S. SARANGI[1]*, A. SARKAR[2], V. BALARAM[3] AND R. SRINIVASAN[3]

[1]Department of Applied Geology, ISM-Dhanbad, India (ssarangi2@Rediffmail.com)
[2]Dept of Geology and Geophysics, IIT-Kharagpur, India
[3]National Geophysical Research Institute, Hyderabad

The BIF hosted Ajjanhalli gold deposit of Chitradurga Schist Belt, Dharwar Craton, India has been grouped under Orogenic type of gold deposit in an Archaean set up [1]. Recently magma/mantle origin has been proposed [2] for the source of CO_2 rich aurifereous fluids based on $\delta^{13}C$ values of carbonates (-5.1±1.4‰) and the fluid (-5.81±1.14‰). We present here the REE compositions of same carbonates from the auriferous quartz-carbonate veins (QCVs) and compare them with our previous obtained isotope data to understand the source of the mineralising fluid.

Both the chondrite and PAAS normalized REE plots of the carbonates of QCVS shows distinct positive Eu anomaly. As positive Eu anomaly is seen under low oxygen fugacity condition of fluids [3], we propose that the auriferous fluids responsible for gold minerlisation at Ajjanhalli could be from a oxygen depleted source. The $\delta^{13}C$ values of carbonates of these carbonates have also indicated a mantle or a felsic magmatic source of auriferous fluids [2]. Though felsic magma source has also been believed for the ultimate source of auriferous fluids [4], positive Eu anomaly of QCVs goes against such a possibility as granitic magma generated hydrothermal fluids could have shown a negative Eu anomaly. We therefore suggest that auriferous fluids could be from a mantle reservoir under a low oxygen fugacity condition.

Since the Orogenic gold deposit at Ajjanahalli deposit is spatially located on a crustal scale shear zone [1] possibility of a mantle derived auriferous fluids cannot be ruled out.

[1] Kolb *et al*. (2004) *Econ. Geol*. **99**, 743–759. [2] Sarangi *et al*. (2009) *GCA*.73, A1158. [3] Drake *et al*.(1975)*GCA*.39, 689–712. [4] Ridley & Diamond (2000) *Soc Econ Geol Rev*, **13**, 141–162.

Oxygen isotopes in perovskites from kimberlites

CHIRANJEEB SARKAR[1]*, C.D. STOREY[2], C.J. HAWKESWORTH[3] AND R.S.J. SPARKS[1]

[1]Department of Earth Sciences, University of Bristol, Bristol, BS8 1RJ, UK (*correspondence: C.Sarkar@bristol.ac.uk)
[2]School of Earth & Environmental Sciences, University of Portsmouth, Portsmouth, PO1 3QL, UK
[3]University of St Andrews, Scotland, KY16 9AJ, UK

Isotopic data (Sr, Nd and Hf) obtained from groundmass perovskites ($CaTiO_3$) within kimberlites have been shown to more accurately reflect the unaltered signature, which has besieged whole rock studies. However, recent studies have questioned their suitability to represent primary kimberlite magma. *In situ* trace elements along with Sr and stable O isotope data have been employed to assess the effects of contamination on perovskites from Orapa and Wesselton kimberlite. Crustal contamination had a minimal role as the samples have an extended range in La/Yb and Sr/Yb rather than scatter around low values. Moreover, lack of any perovskites with elevated $\delta^{18}O$ also suggests minimal interaction with upper crustal material.

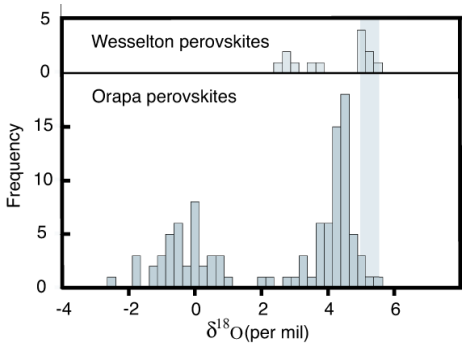

The $\delta^{18}O$ values from Orapa perovskites show two distinct peaks (around +3.6‰ and -0.6‰). Wesselton perovskites in contrast are clustered around $\delta^{18}O$ values of +4‰. Perovskite in equilibrium with the mantle has lower $\delta^{18}O$ than other common upper mantle minerals. One group of Orapa perovskites and the Wesselton perovskites are interpreted to reflect the $\delta^{18}O$ of uncontaminated upper mantle derived kimberlite magma (4.2‰). The negative $\delta^{18}O$ values from the second group of Orapa perovskites are attributed to crystallisation of perovskite after magma degassing, rather than to crustal assimilation, magma mixing, cooling or hydrothermal alteration. The Wesselton sills, however, did not suffer significant degassing, at least to the extent to deplete the magma in ^{18}O.

https://doi.org/10.1180/S0026461X00006502 Published online by Cambridge University Press

Synthesis of lithium ion-sieves using biogenic birnessite as a precusor

K. SASAKI, E. MORIOKA AND Q. YU

Department of Earth Resource Engineering, Kyushu University, Fukuoka, Japan (keikos@mine.kyushu-u.ac.jp)

Lithium (Li) is regarded as one of the most important elements in advanced industries, and its concentration in geothermal water is around 10 mg/L at the maximum corresponding to about 50 times larger than in seawater [1]. In the present work, synthesis of lithium ion-sieve was investigated using biogenic Mn oxides. Biogenic Mn oxides were produced by a Mn-oxidizing fungus, *Paraconiohyrium sp*.WL-2 strain at pH 6.5 [2].

After biogenic birnessite was suspended in LiCl solution, the solid phase was obtained by evaporation at 80 °C for 24 hours and then calcined at 450 °C for 4 or 8 hours. The calcined product was washed with 0.1 mol/L HCl to exchange with Li^+ to obtain a sorbent as a template for Li^+ ions. To compare with biogenic birnessite, several types of synthesized Mn oxides, that is, acidic birnessite, ramsdellite, Mn_3O_4, cryptomelane, were investigated as the starting materials in the same manner.

Based on XRD results, $LiMn_2O_4$ was detected in three products of five before acid washing, that is, derived from biogenic birnessite, acidic birnessite and ramsdellite. The minimum calcination time was required to obtain a pure $LiMn_2O_4$ phase using biogenic birnessite as a starting material. XRD peaks assigned to $LiMn_2O_4$ were maintained even after Li^+ ions were extracted by acid washing.

While products from acidic birnessite sorbed little Li^+, the products from biogenic birnessite and ramsdellite sorbed Li^+ more effectively. Some release of Mn^{2+} was observed during sorption of Li^+ ions on the product derived from ramsdellite. Products derived from biogenic birnessite showed the most effective performance to sorb Li^+ ions.

Very alkaline condition is required to synthesize ramsdellite, while biogenic birnessite can be produced around neutral pH values. Therefore, biogenic birnessite is a promising geomimetics as starting materials for synthesis of the effective lithium ion-sieves.

[1] Yoshinaga, T. *et al*. (1982) *Proc NZ Geotherm Workshop* Pt **2**, 329–332. [2] Sasaki, K. *et al*. (2008) *Mater. Trans*. **49**, 605–611.

Sorption of Sr^{2+} on hydroxyapatite from calcined fish bones at different temperatures

K. SASAKI*, S. TSURUYAMA, S. MORIYAMA AND T. HIRAJIMA

Kyusyu University, Fukuoka 819-0395, Japan (*coresspondance: keikos@mine.kyushu-u.ac.jp, s-tsuruyama09@mine.kyushu-u.ac.jp, s-moriyama09@mine.kyushu-u.ac.jp, hirajima@mine.kyushu-u.ac.jp)

Hydroxyapatite was produced by calcination of fish bones at different temperatures (400- 1100 °C). Higher calcination temperatures reduced the organic matter content but also provided better crystallized hydroxyapatite and larger crystal sizes with less lattice strain. Higher calcination temperatures also decreased the specific surface area and increased the ion-exchange capacity hydroxyapatite. Sorption of Sr2+ as a surrogate for radionuclides was investigated with hydroxyapatite calcined at different temperatures. These results demonstrated that lattice strain affects ion-exchange properties at nano-domain level relatively more as compared to its effects on the surface area.

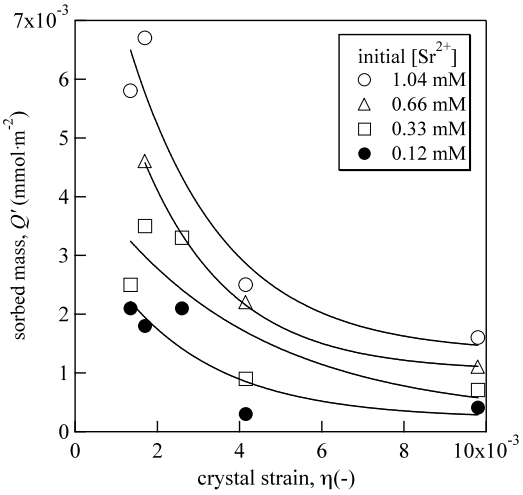

Figure 1: Sorption capacity of Sr^{2+} on hydroxyapatite with different lattice strain.

https://doi.org/10.1180/S0026461X00006502 Published online by Cambridge University Press

Study of deep subsurface microbial community under changing redox conditions using quantitative method

Y. SASAKI[1]*, T. ASANO[2], Y. AMANO[3], T. SATO[1], T. IWATSUKI[3] AND H. YOSHIKAWA[1]

[1]Geological Isolation Research and Development Directorate, Japan Atomic Energy Agency, Tokai, Ibaraki, Japan (*correspondence: sasaki.yoshito@jaea.go.jp)
[2]Environmental Business Division, Bio-Business Promotion Department, CHUGAI TECHNOS Corporation, Nishi-Ku, Hiroshima, Japan.
[3]Geological Isolation Research and Development Directorate, Japan Atomic Energy Agency, Horonobe, Hokkaido, Japan

Microbial activity is one of controlling factor for geochemical condition and the change during excavation and backfilling of underground facility. This study aims to evaluate the role of microbes on geochemical evolution around underground facility. We investigate microbial community and redox condition in the borehole drilled from 140m depth gallery of underground research laboratory (URL) in Horonobe area of Hokkaido, Japan.

Redox potential (ORP_{obs}) of groundwater changed from oxidized condition (+180mV) to reducing condition (-480mV) in 10 days. Total microbial count also decreases from $6.6x10^5$ cells/ml to $3.2x10^4$ cells/ml. Quantification analysis using both 16S rRNA and functional genes with real-time PCR shows that the biomass decreased constantly; domain bacteria (16S rRNA), Nitrate reducers (*nirS*), denitrifires (*nosZ*), Metal reducers (Geobacteraceae 16S rRNA) and Methane oxidizers (*pmoA*). On the other hand, the biomass increased in 5 days and then decreased or be maintained approximately-constant. ; domain archaea (16S rRNA), nitrate reducers (*nirK*), sulfate reducers (*dsr*), methanogens (*mcrA*). The change corresponded with redox potential change. These groups would have ecological relationship. Microbial community quickly changes according with redox condition change in deep subsurface.

This study was performed as a part of the 'Project for Assessment Methodology Development of Chemical Effects on Geological Disposal System' funded by the Ministry of Economy, Trade and Industry of Japan.

Air quality over India: Weekly periodicities and long term trends

S.K. SATHEESH[1,2]*, K. KRISHNA MOORTHY[3], S.S. BABU[3], N. SRIVASTAVA[1] AND V. VINOJ[4]

[1]Centre for Atmospheric and Oceanic Sciences, Indian Institute of Science, Bangalore-560012, India (*correspondence: profsks@gmail.com)
[2]Divecha Centre for Climate Change, Indian Institute of Science, Bangalore-560012, India
[3]Space Physics Laboratory, Vikram Sarabhai Space Centre, Thiruvananthapuram-695022, India
[4]Pacific Northwest National Laboratory, Richland, WA 99352, USA

Air quality degradation is emerging to be an issue of major concern in India. This is mainly attributed to unplanned urbanization and industrial growth. Central Pollution Control Board is executing a nation-wide programme of ambient air quality monitoring. This network consists of 342 monitoring stations covering 127 cities in India. In addition, Indian space Research Organisation (ISRO) is maintaining 33 climate observatories across the country namely ARFINET (Aerosol Radiative Forcing over India Network). In this study, we have used multi-year observations of particulate mass (PM) concentration, aerosol black carbon (BC) mass concentration and aerosol optical depth (AOD) from these network observatories to make assessment of ambient air quality over India and its radiative impact. It has been observed that both column AOD and ground-level measurements (BC and PM) exhibit a weekly cycle with low aerosol concentrations on weekends. In comparison to the weekdays, the weekend reductions of AOD, BC and PM were ~15%, 25% and 24%, respectively. Aerosol trends indicates conflicting trends at different regions of India, thereby reflecting the complex factors behind the impact of growth on environment. While an increasing trend in aerosol has been observed in many cities, some cities show a decreasing trend during the last few years. Aerosol radiative impact assessment was made using ground-based radiometers and is compared with that simulated by radiative transfer models (which employ measured aerosol microphysics). One striking inference from this effort is the large discrepancy between observed and modelled aerosol surface radiative impact. Potential sources of such discrepancies are discussed in this presentation. The CHIMERE chemistry-transport model was used to simulate PM, BC and AOD over India and are compared with measurements. Evaluation of CHIMERE output shows that while diurnal and seasonal trends are captured reasonably by the model, absolute magnitudes differ substantially.

https://doi.org/10.1180/S0026461X00006502 Published online by Cambridge University Press

U-Th-Pb analyses by eximer laser ablation/ICP-MS on MG Brazilian xenotime

KEI SATO[1]*,
MIGUEL A.S. BASEI[1]; CESAR M. FERREIRA[2];
WALTER M. SPROESSER[1]; SILVIO R.F. VLACH[1];
WOLDEMAR IVANUCH[3]; ARTUR T. ONOI[1]

[1]Instituto de Geociencias, USP-Brasil
(*correspondence: Kei.Sato@usp.br)
[2]Universidade Federal de Ouro Preto, DEGEO, MG, Brasil
[3]Universidade Estadual do Rio de Janeiro, DGPI, RJ, , Brasil

Measurements

Several fragments of MG xenotime were mounted in epoxy disk (2.54 cm). Temora, FC and GJ standards were used as reference. The analytical conditions were: RF = 1200 Watts, Cooling gas = 15 L/min, Aux gas = 0.70 L/min, Sample gas flow = 0.75 L/min. Detector configuration: $^{202}Hg = IC_3$, $^{204}Hg + ^{204}Pb = IC_4$, $^{206}Pb = L_4$, $^{207}Pb = IC_6$, $^{208}Pb = L_3$, $^{232}Th = H_2$ and $^{238}U = H_4$, where IC = MIC, L (low) and H (high) are Multi Faraday Cups. The intensity to ^{80}Ar for stable condition was around 10V (aux gas =0.77 L/min and He gas = 0.65 L/min). The Laser analytical conditions to get the best ablation rate were: wavelength = 193 nm, Energy = 6mJ, Repetition rate = 10Hz, He gas flow = 0.65 L/min, spot size = 38 mm.

Results

The MG crystal shows Th concentration ranging from 300 to 2000 ppm with low common Pb ($^{204}Pb/^{206}Pb$ ratio <0.0001). The Th/U ratio ranges from 0.9 to 4.5. The GJ show low ^{232}Th intensity (~2 mV) but high ^{238}U (150 mV) intensity while MG shows high ^{232}Th (150mV) and normal ^{238}U intensity (90mV). Also the $^{232}Th/^{238}U$ ratios on GJ zircon standard range from 0.012 to 0.022, while in the MG ratio are much higher ranging from 0.7 to 4.7. The ^{232}Th intensity on GJ zircon standard range from 0.7 to 3 mV, while MG presents 130 mV (gray portions) to 900 mV (brown portions). Electron microprobe analyses, indicate high contents of Dy_2O_3 (3 – 6%), Er_2O_3 (3-4%), Yb_2O_3 (2-3%) and Lu_2O_3 (0.3 – 0.8%) for MG. The $^{206}Pb/^{238}U$ weighted average age of 445.8 +-4.5 Ma using GJ1 as standard, is lower than the TIMS age of 492Ma (1). This difference must be investigate but here it is suggested to be related to matrix effect.

Conclusions

The MG xenotime present a high U content, permitting precision measurements which is very helpful for the beam focusing during the LA-ICP-MS pre-adjustment set up. Therefore its high REE and Th concentrations, require matrix corrections of several percent for data from most zircon samples.

[1] Fletcher *et al*. (2004) *Chemical Geology* **209**, 295–314.

Effects of non-supercritical CO_2 on leaching of potential microbial substrates from macromolecular organic matter

PATRICK SAUER*, CLEMENS GLOMBITZA AND JENS KALLMEYER

University of Potsdam Institute for Earth- and Environmental Sciences Karl-Liebknecht-Straße 24, 14476 Potsdam, Germany (*correspondence: sauer@geo.uni-potsdam.de)

The storage of CO_2 in underground reservoirs is discussed controversly in the scientific literature and the public. The worldwide search for suitable storage formations also considers coal bearing strata. In addition, injection of CO_2 into coal formations is already applied for enhanced gas recovery of coal bed methane. Nevertheless, processes resulting from increased CO_2 concentration especially in organic matter rich formations are rareley investigated.

Depending on reservoir pressure and temperature, the injected CO_2 will dissolve in the porewater causing a decrease in pH [1] and resulting in acidic formation waters.

Recent investigations outlined the importance of potential substrates (e.g. low molecular weight organic acids) stored in organic-rich litologies such as coals [2]. Huge amounts of these substrates are chemically bound to the macromolecular matrix and may be liberated by hydrolysis within the acidic porewater. Therfore, injection of CO_2 into coal formations may result in an enhanced nutrient supply for microbial metabolism.

To study the effects of high dissolved CO_2 concentrations on macromolecular organic matter, we developed an inexpensive, high-pressure high-temperature incubation system. It allows not just controlling hydrostatic pressure and temperature but also the concentration of dissolved gases. Furthermore the system can be used for both static and flow through experiments and also allows subsampling during the experiment without depressurization.

We will present results from leaching experiments of low molecular weight organic acids such as formate and acetate with CO_2 saturated water at variing temperature and pressure conditions on coal samples of different thermal maturity.

[1] Meyassami *et al*. (1992) *Biotechnol. Progess* **8**, 149–154.
[2] Glombitza *et al*. (2009) *Org. Geochem*. **40**(2), 175–185.

https://doi.org/10.1180/S0026461X00006502 Published online by Cambridge University Press

Aerosol particle phase state measurement technique using a low pressure impactor

E. SAUKKO*, H. KUULUVAINEN AND A. VIRTANEN

Department of Physics, Tampere University of Technology, Tampere, FI-37720, Finland
(*correspondence: erkka.saukko@tut.fi)

The phase state of aerosols has impact on the behaviour of atmospheric aerosols. Recently published results show that the atmospheric biogenic SOA particles can adopt amorphous solid phase [1]. Existing methods to resolve solvent absorption induced phase change, such as tandem differential mobility analysis rely on the size change of particles related to solvent uptake.

To study the particle phase and phase change induced by size-preserving processes e. g oxidation, a new method has been developed. The method relies on impaction of particles on a smooth substrate and subsequent counting of bounced particles by condensation particle counter [2].

An example data of bounce probability with varying relative humidity is given in Figure 1. An ammonium sulphate aerosol was cycled through the system and an almost step-like transition was seen on the bounce probability at around 80% relative humidity. This corresponds well with the known deliquescence relative humidity of 80% [3].

The bounce probability can not at present be quantitatively linked to mechanical properties of particles, but it is qualitatively informative. The method has been applied on nebulised laboratory aerosols as well as on SOA.

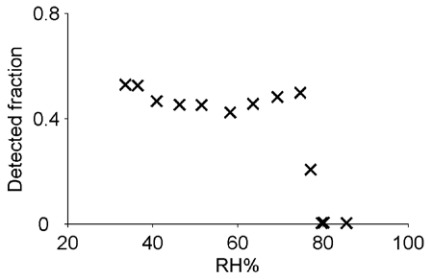

Figure 1: Fraction of 91nm ammonium sulfate particles detected after impaction with varying humidity

This work was supported by the Maj and Tor Nessling foundation.

[1] Virtanen, A. *et al*. (2010) *Nature* **467**, (7317) 824–827. [2] Saukko *et al*. (2011) To be submitted to *Atmos. Meas. Tech*. [3] Mikhailov, E. S. *et al*. (2009) *Atmos. Chem. Phys*. **9**, (24) 9491–9522.

Gold mobility in the mantle: Constraints from sulfides in pyroxenites and lherzolites

J.E.J. SAUNDERS*, N.J. PEARSON AND SUZANNE Y. O'REILLY

GEMOC/CCFS, Macquarie University, NSW, 2109, Australia
(*correspondence: james.saunders@mq.edu.au)

Sulfides are the host for gold in the mantle [1], yet there is a scarcity of reliable Au analyses for sulfides from different mantle rock types. As a result, the geochemical behaviour of Au in the mantle is still poorly understood. In this study Au has been measured along with major and trace elements in sulfides in the well-characterised peridotite and pyroxenite xenoliths from Qilin, southeastern China. The peridotites are spinel and amphibole-spinel lherzolites, and the pyroxenites are basaltic melts that have re-equilibrated to spinel and garnet websterites in the upper mantle [2].

Pyrrhotite with very limited variability in major-element geochemistry is the dominant sulfide in the pyroxenites. The sulfides in the lherzolites include polyphase assemblages of mainly monosulfide solid solutions (MSS) with minor millerite, hazlewoodite and cubanite. The lherzolite-hosted sulfides have substantial variation in Fe, Ni and Cu contents. Interstitial and enclosed sulfides in these samples are mineralogically and chemically identical.

There are significant differences in the Au content of the pyroxenite- and lherzolite-hosted sulfides. Most pyroxenite sulfides have Au concentrations below lower limits of detection (<200 ppb), whereas the Au concentrations in lherzolite-hosted sulfides are several times higher than detection limits. There is no systematic difference between the Au content of sulfides in samples that have been modally metasomatised (amphibole-bearing), and sulfides in amphibole-free samples.

The lherzolites are quite fertile (equivalent to ~10% melt removal [3]), but there is no consistent trend in the PGEs (average Pd_{PUM}/Os_{PUM} = 1.49). However Au in these samples does appear to be depleted compared with the PGEs (average Au_{PUM}/Os_{PUM} = 0.25). This trend in the lherzolites strongly contrasts with the Au/Os ratio in the pyroxenites, where Au is relatively enriched. This comparison between Au in pyroxenite- and lherzolite-hosted sulfides suggests that Au can be transported by melts, and these melts may play a significant role in Au enrichment in the mantle.

[1] Mitchell & Keays (1981) *GCA* **45**, 2425–2442. [2] Xu *et al*. (1996) *Lithos* **38**, 41–62. [3] Guo *et al*. (1999) *J. Petrol*. **40**, 1125–1149.

https://doi.org/10.1180/S0026461X00006502 Published online by Cambridge University Press

Silicon isotopes in granitoid rocks

PAUL S. SAVAGE[1]*, R. BASTIAN GEORG[2], HELEN M. WILLIAMS[3], KEVIN W. BURTON[1], ALEX N. HALLIDAY[1] AND BRUCE W. CHAPPELL[4]

[1]Department of Earth Sciences, Oxford University, Oxford, UK (*correspondence: Paul.Savage@earth.ox.ac.uk)
[2]WQC, Trent University, Peterborough, Ontario, Canada
[3]Department of Earth Sciences, Durham University, Durham, UK
[4]Earth and Environmental Sciences, University of Wollongong, NSW, Australia

Granites (and other felsic lithologies) constitute ~50% of the mass of the upper continental crust [1] and play a major role in global weathering [2], yet little information exists on their Si isotopic composition and systematics. In principle, S-type granites (that is, those with a pelitic sedimentary affinity [3]) should be isotopically light, as weathering enriches sediment in the lighter Si isotopes, whereas 'igneous' granites (I- and A-type) should be isotopically heavier. Previous work [4] reveals relatively large Si isotopic variation in granitoid rocks, but no systematic differences between granite types - however, the large uncertainties associated with these data makes interpretation difficult.

Here we revisit this problem and provide a Si isotopic perspective on granite petrogenesis with the benefit of high-precision techniques. We have analysed a representative suite of over 30 I-, S- and A-type granitoid samples and mineral separates, using a HF-free alkali fusion method and high-resolution MC-ICP-MS [5].

The data fall between δ^{30}Si = -0.41 and -0.11 ± 0.06‰ (2 s. d. external precision), although the variation within each batholith is small, providing evidence of a strong source control. However, Si isotopes do not distinguish between I- and S-type granites; both groups display a similar range of isotopic compositions. In contrast, the data for A-type granites are more restricted and comparable to extrusive felsic material [6]. A strong negative correlation with initial $^{87}Sr/^{86}Sr$ provides evidence that Si isotopic variation in both I- and S-type granites can be explained by contamination of an 'igneous' source region magma by an enriched (high Rb/Sr) end-member, possessing a light δ^{30}Si signature, such as sediment derived from continental crust.

[1] Wedepohl (1995) *Geochim. Cosmochim. Acta*, **59 (7)** 1217–1232. [2] Wollast & Mackenzie (1983) In, *Silicon Geochemistry & Biogeochemistry*, Academic Press, 39–76. [3] Chappell & White (2001) *Aust. J. Earth Sci.* **48**, 489–499. [4] Ding *et al.* (1996) *Silicon Isotope Geochemistry*, Geological Publishing House, Beijing. [5] Georg *et al.* (2006) *Chemical Geology* **235**(1-2), 95–104. [6] Savage *et al.* (2011) *Geochim. Cosmochim. Acta,* in review.

Volcanic ashes as the source of dissolved calcium in seawater

A.V. SAVENKO* AND V.S. SAVENKO

Moscow M.V. Lomonosov State University, 119991, Moscow, Russia
(*correspondence: Alla_Savenko@rambler.ru)

The geochemical balance of carbon in the modern ocean indicates that 487 million ton of C_{org} annually oxidizes and form Ca–Mg carbonates. The reaction of carbonate formation requires 1 628 million ton of Ca (Mg) from silicates. Volcanic terrigenous ashes coming into the ocean possess of great specific surface and can pretend to the role of significant source of labile Ca (Mg). It was tested experimentally.

Variable amounts of ashes were placed into artificial 35‰ seawater containing no borates and salts of weak acids with the exceptions of carbonate. Hermetically closed contents were mixed during a month, and filtered through 0.22 μm filters. Values of pH, Alk, and concentrations of Ca, Mg, and Si were determined both in filtrates and the initial seawater.

Concentrations of calcium and silicon in all experiments increase in direct relation to the solid/water mass ratio (table). Maximal calcium mobilization was observed for the Koryaksky volcano ashes containing 2.1% S_{tot}. High sulfur content in this sample accounted for dramatic pH and Alk reduction. But pH and Alk reduction was observed also in the experiments with low-sulfur ashes from Kamchatka. This indicates that other reactions may affect acid-base equilibrium. Magnesium concentration except the Karymsky volcano ashes also increases with the solid/water mass ratio increase, but lesser than calcium concentration. Dissolved calcium and magnesium coming into the ocean can possibly bind dissolved inorganic carbon formed by oxidation of C_{org} of continental runoff in the ocean.

Volcano	Mass of ash, g/l	pH	ΔAlk	Δ[Ca]	Δ[Mg]	Δ[Si], μM
			meq/l			
Koryak-sky, 2.1% S	10	7.17	–0.80	4.39	0.17	94.4
	20	6.79	–1.48	8.89	0.51	143.0
	50	5.92	–2.30	21.55	1.82	263.5
Ksudach, 0.022% S	10	7.56	–0.22	0.34	0.09	86.9
	20	7.45	–0.42	0.57	0.14	128.6
	50	7.24	–0.84	1.03	0.26	211.2
Karymsky, 0.085% S	10	7.49	<0.02	0.11	<0.02	26.4
	20	7.43	–0.16	0.23	<0.02	43.4
	50	7.32	–0.38	0.34	<0.02	86.4
Eyjafjalla-jökull, 0.076% S	10	7.61	0.10	1.14	0.57	89.3
	20	7.60	0.14	1.82	0.88	125.4
	35	7.61	0.19	3.19	1.08	155.6

Table 1: Variation of seawater composition at the interaction with volcanic ashes.

https://doi.org/10.1180/S0026461X00006502 Published online by Cambridge University Press

Tracing deep slab recycling via study of boron isotopes of volcanic rocks from hotspot (OIB) settings

I.P. SAVOV[1,2]*, S.B. SHIREY[2], S. TONARINI[3], J.G. RYAN[4] AND E. HAURI[2]

[1]University of Leeds, School of Earth and Environment, Leeds LS2 9JT, United Kingdom (*correspondence: i.savov@see.leeds.ac.uk)
[2]DTM-Carnegie Institution of Washington, 5241 Broad Branch Road, Washington DC 20015, USA.
[3] Istit.Geosci.Georisorse, CNR, Via Moruzzi 1, Pisa, Italy
[4]Geology Department, University of South Florida, 4202 E.Fowler Ave, SCA 528, Tampa, FL 33620, USA

Boron and B isotopes have potential to be among the best tracers of fluids and crustal components in the deep mantle because isotopically light B, strongly fractionated at the slab or isotopically heavy B, imprinted in the wedge could be recycled. Analytical challenges in basaltic rocks are presented by low B concentrations, and only limited high precision B isotope ratios are reported for OIB volcanic suites [1, 2]. Hence B and B isotopes have not been widely used to quantify potential slab and crustal contributions to hotspot magmas. Here we report LA-ICP-MS and TIMS δ^{11}B ratios and SIMS B concentrations for OIB lavas from key hotspot sites representing end-member components of the various mantle reservoirs. The B contents are always low (generally <5 ppm) and the δ^{11}B ratios are as follows: Society Isl. (+1.3 to -7.7‰; n=10); French Polynesia-Samoa Isl. (+2.8 to -9.1‰; n=10); Mt.Erebus/McMurdo Group/Crary Mts. (+2.3 to –10.4 ‰; n=10); St.Helena Isl. (+19 to -3.8‰; n=5); Reunion Isl. (-1.4 to -10.2‰; n=2) and Gough Isl. (-3.9 to -8.1‰; n=7). Interestingly, our new B and B isotope dataset often shows large deviations from currently accepted intraplate B and B isotope values for the deep mantle [3]. We shall evaluate the impact of processes such as assimilation of seafloor-altered basement and ancient subduction-related metasomatism as possible causes for the observed isotope variations. The overall negative B isotope results, combined with mantle-like Sr and Nd isotope ratios, indicate very sufficient and large volume B losses during the initial (shallower) stages of subduction, confirming the fluid mobile nature of this important slab tracer.

[1] Turner *et al*. (2007) *Nature* **447**, 702–705. [2] Tanaka & Nakamura (2005) *Geochim.Cosmochim Acta* **69**, 3385–3399. [3] Chaussidon & Marty (1995) *Science* **269**, 383–386.

Seasonal dynamics of sulfide oxidation processes in Tokyo Bay dead zone sediment

M. SAYAMA

National Institute of Advanced Industrial Science and Technology (AIST), Tsukuba 305-8569, Japan (m.sayama@aist.go.jp)

Sulfide (H_2S) pool in Tokyo Bay dead zone sediment changed dramatically according to the season (Fig. 1). In early fall with hypoxic bottom water, sediment surface was covered with *Beggiatoa* massively, indicating biological H_2S oxidation with NO_3^-. During winter with oxic bottom water, ascorbate-extractable-iron oxide (Asc-Fe(III)), that reflects ferrihydrite (high reactivity towards H_2S, insulative), showed a seasonal maximum, indicating chemical H_2S oxidation with Fe(III). During late fall, oxalate-extractable-Fe(III) (Oxa-Fe(III)), that reflects magnetite (low reactivity towards H_2S, conductive), showed a remarkable increase with a unique pH signature, pH maximum at oxic-anoxic interface (Fig. 2). Those results suggest that the main process for H_2S oxidation during transition period from hypoxic to oxic bottom water was probably bioelectrochemical reactions with O_2. H_2S oxidation processes in Tokyo Bay dead zone sediment are dynamically shifting in response to O_2 conditions in the bottom water.

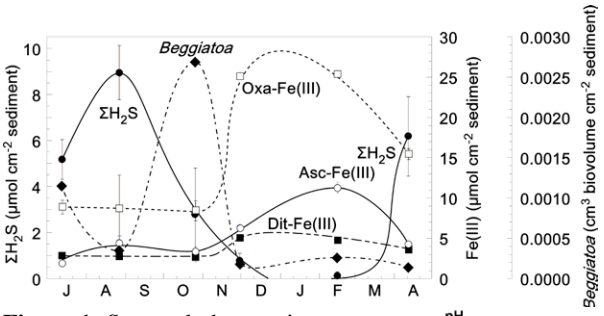

Figure 1: Seasonal changes in depth integrated (0-30mm) pool size of H_2S, *Beggiatoa* and iron oxides in Tokyo Bay dead zone sediment.

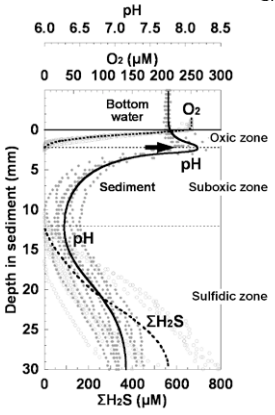

Figure 2: Microprofiles of O_2, pH and H_2S at sediment-water interface during transition period from hypoxic to oxic bottom water (November 30) in Tokyo Bay dead zone sediment.

https://doi.org/10.1180/S0026461X00006502 Published online by Cambridge University Press

The role of impurity atoms in forming cation vacancies in the pyrrhotite

A.M. SAZONOV* AND V.V. ONUFRIENOK

Siberian Federal University, Krasnoyarsk, Russia
(*correspondence: anatoly.sazonov@yandex.ru)

Synthetic pyrrhotites (Fe_nS) not containing interstitial atoms in the crystal structure and natural pyrrhotites of the 'Blagodatny' mine containing interstitial point defects have been investigated in the stable phase The phase and chemical composition was monitored by using the methods of X-ray diffraction (XRD) and X-ray spectrum analysis (XRS).

As a result of comparison of the crystal structure and the phase composition of the synthesised samples with natural pyrrhotites the influence of the inclusion atoms on the concentration of cation vacancies has been established.

The influence of impurity atom on the concentration of the cationic vacancies was considered on the basis of calculating the thermodynamic potentials using the Bose-Einstein quantum statistics. The theoretical calculations were compared with X-ray analysis data (Table 1).

The results of the X-ray analysis (XRS and XRD)		The results of the theoretical calculations of the number of defect on point of lattice		
S/Fe ratio	defects mass, %	sum of defects	impurity atom	cationic vacancies
1.130	0.160	0.1038	0.0020	0.1018
1.140	0.168	0.1185	0.0021	0.1164
1.147	0.151	0.1284	0.0021	0.1213
1.154	0.176	0.1234	0.0022	0.1212
1.152	0.143	0.1326	0.0022	0.1304
1.160	0.166	0.1389	0.0023	0.1366
1.158	0.155	0.1366	0.0024	0.1342
1.164	0.177	0.1412	0.0025	0.1387
1.164	0.178	0.1411	0.0026	0.1385
1.157	0.186	0.1363	0.0028	0.1335
1.180	0.415	0.1529	0.0062	0.1467

Table 1. Results of theoretical calculations on the basis of X-ray analysis of samples (XRS and XRD).

As it is shown in the table, tendency to increase of concentration cationic vacancies with increase impurity atom is calculated on the basis of experimental results.

The influence of S on silicate melt structure: An experimental and spectrocospic approach

B. SCAILLET[1]*, Y. MORIZET[2], I. DI CARLO[1] AND M. PARIS[3]

[1]Institut des Sciences de la Terre d'Orléans, UMR CNRS 6113, 1a rue de la Férollerie, 45071 Orléans (France) (*correspondence: bscaille@cnrs-orleans.fr)

[2]Laboratoire de Planétologie et Géodynamique de Nantes (LPGN), UMR CNRS 6112, 2 rue de la Houssinière, 44300 Nantes (France)

[3]Institut des Matériaux Jean Rouxel (IMN), UMR CNRS 6502, 2 rue de la Houssinière, 44300 Nantes (France)

Sulfur is one important volatile element after C and H in magmatic systems, however its effects on silicate melt structure and magmatic physical properties are poorly addressed. We present preliminary result of the effect of sulfur on silicate melt structure based on an experimental approach and spectroscopic measurments.

Glasses of HPG8 and An-Di eutectic compositions were synthesised at 300 MPa and 1250°C and under oxidising conditions (ΔFMQ+3.0) using IHPV. Starting compositions were equilibrated with a fluid phase composition: S (0 to 5 wt.%) and H_2O (5 wt.%). Recovered glasses were characterised using EMPA to determine S solubility, FTIR for H_2O solubility, Raman and Solid State NMR for glass structure.

S solubility determined in glasses changes from 0 to 1100 ppm and 0 to 8700 ppm for HPG and An-Di, respectively. The increase in S solubility is accompanied by the decrease in the H_2O content from ~5 to 4 wt.% H_2O. S is directly correlated to the initial S content traducing the change in the fluid phase composition.

Analyses of fluid inclusions suggest S is present as SO_2 and metallic S in HPG and An-Di glasses and additional H_2S has also been identified in some inclusions for An-Di glasses. The S speciation within the glasses is only represented by $M^{n+}SO_4$ groups (M^{n+} is Ca^{2+} in An-Di, Na^+ in HPG) consistent with the oxidising conditions of the experiments.

Raman and NMR analyses of the glass structure show subtle changes upon S dissolution. We observe 1) a slight polymerization with increasing S content, 2) a decrease in ^{VI}Al in An-Di and 3) a change in the H environments with increasing S content. The observed changes may be the result of decreasing H_2O content. However, the subtles changes remain very small suggesting that S will produce only minor changes to the melt strucutre in comparison to H_2O effect. Hence, the change in magmatic viscosity upon S dissolution is likely to be small.

https://doi.org/10.1180/S0026461X00006502 Published online by Cambridge University Press

Subducted serpentinites are the boron reservoirs for arc magmatism

MARCO SCAMBELLURI[1] AND SONIA TONARINI[2]

[1]Dipartimento per lo studio del territorio e delle sue Risorse, Università di Genova, Corso Europa 26, Genova - Italy
[2]Istituto di Geoscienze e Georisorse-CNR, Pisa, Italy

Serpentinites are key players in volatile and fluid-mobile element cycles in subduction zones. Their dehydration represents the main event for fluid and element flux from slabs to mantle, though no direct proof of this fact yet exists. For this purpose, B isotopes are known markers of fluid-assisted element transfer during subduction. Until recently, the altered oceanic crust has been considered the main ^{11}B reservoir for arc magmas, which largely display positive $\delta^{11}B$. However, slab dehydration below fore-arcs transfers ^{11}B to the overlying hydrated mantle and leaves the residual mafic crust very depleted in ^{11}B below sub-arcs. The ^{11}B-rich composition of serpentinites candidate them as the heavy B carriers for subduction. Here we present high positive $\delta^{11}B$ of Alpine high-pressure (HP) serpentinites recording subduction metamorphism: we show a connection among serpentinite dehydration, release of ^{11}B-rich fluids and arc magmatism. In general, the $\delta^{11}B$ of these rocks is heavy (16‰ to + 24‰ $\delta^{11}B$). $^{87}Sr/^{86}Sr$ ranges from 0.7044 to 0.7065, i.e. lower than oceanic serpentinites formed from seawater. Our data suggest two implications. 1st, the analyzed HP serpentintes are ^{11}B reservoirs for subduction. They maintain high ^{11}B down to a first fluid release event, thus the $\delta^{11}B$ of olivine-veins, that fingerprint the composition of released fluids, justify the positive values observed in many arc lavas. Fluids released by dehydration of such HP serpentinites by full antigorite breakdown should have up to + 20‰ $\delta^{11}B$. The comparable ^{11}B fingerprint of serpentintes, their fluids and arc lavas provides a strong link between serpentinite subduction and arc magmatism. 2nd, the combination of δD, $\delta^{11}B$, $^{87}Sr/^{86}Sr$ of the HP serpentinite apparently favour their location above the subducting slab. This implies that serpentinites were formed by low-T fluids likely arising from a subducting lower plate.

A new Br isotope analytical protocol: Constraints on the global Br cycle

BRUCE F. SCHAEFER

GEMOC, Earth and Planetary sciences, Macquarie University, Sydney NSW, 2109, Australia

Bromine possesses a chemistry broadly comparable to that of Cl and F, however its heavier mass and lower abundance results in slightly different behaviours in the geochemical cycling. Hence it is disproportionately enriched in sea water with respect to Cl, and unlike F possesses isotopes which may be fractionated by geological processes. These isotopes are ^{79}Br (50.686%) and ^{81}Br (49.314%).

Br can be considered to be a 'hydrophile' element, and hence its behaviour is in many ways analogous to that of water. Therefore environmental (low temperature) aqueous processes, particularly transpiration, weathering and evaporation are likely to produce fractionations in $\delta^{81}Br$ of the order of ~3.5‰ [1]. These signatures may be inherited by hydrous fluids derived from subducted slabs in regions where extensive hydrothermal alteration and/or carbonate deposits are present in the downgoing slab.

This study has developed new chemical extraction, and most significantly, new mass spectrometric protocols for Br isotopes on silicates and waters using N-TIMS methodologies. Existing CF-IRMS methodologies offer internal precision of ~0.3‰ (1SD, [1]), whereas N-TIMS measurements of laboratory HBr and seawater standards produce external reproducibility of <0.07‰ (1SD) over a 6 month period with internal precision typically <0.06‰ (1SD) on single analyses.

Southern Hemisphere Pacific Ocean Water (SHPOW) records $^{81}Br/^{79}Br$ significantly lower (0.9627) than the IUPAC canonical ratio (0.9729; a difference of ~10‰).

Protocols for mitigation of PO_3^- polybaric interferences on $^{79}Br^-$ will also be presented, as will $\delta^{81}Br$ data for depleted Island Arcs Tholeiites.

[1] Shouaker-Stash *et al*. (2005) *Anal*. *Chem* **77**, 4027–4033.

https://doi.org/10.1180/S0026461X00006502 Published online by Cambridge University Press

High-precision ^{10}Be-dating of moraines and the exploration of pro-glacial bedrock as climate archive using the new *in situ* ^{14}C/^{10}Be tool

JOERG M. SCHAEFER[1], IRENE SCHIMMELPFENNIG[1], BRENT GOEHRING[2], ROBERT C. FINKEL[3] AND DYLAN H. ROOD[4]

[1]Lamont-Doherty Earth Observatory/Columbia University, Palisades, NY-10964, USA
[2]Department of Geosciences, Pennsylvania State University, University Park, Pennsylvania, USA
[3]Earth and Planetary Science Department, University of California-Berkeley, Berkeley, California, USA
[4]Lawrence Livermore Natl Lab, Ctr Accelerator Mass Spectrometry, Livermore, CA 94550 USA

Methodological and analytical progress in cosmogenic nuclide techniques has surged in recent years, fueled in part by the CRONUS inititatives. One example is the increase in sensitivity of the ^{10}Be and the *in situ* ^{14}C methods that affords new perspectives on glacier fluctuations in response to past climate change. Moraine records around the globe can now be dated with unprecedented precision and pro- and subglacial bedrock can be explored as climate archive for past warm periods.

Here we present published and unpublished glacier chronologies from southern and northern mid-latitudes. The chronologies show centennial resolution of past glacier advances. The proglacial bedrock data yield complementary informations about periods of smaller-than-today glaciers.

We discuss the climatic implications of these data sets, focusing on (i) the chemical and analytical protocols behind this advance, (ii) the high internal consistency of the chronologies and the underlying reasons, and (iii) perspectives towards further methdo progress and its relevance for climate science.

Modeling of alteration processes in the Ringelbach granitic research catchment (Vosges, France)

T. SCHAFFHAUSER, B. FRITZ, F. CHABAUX, B. AMBROISE, A. CLÉMENT AND Y. LUCAS

LHYGES, Université de Strasbourg/EOST, CNRS, France (thiebaud.schaffhauser@etu.unistra.fr)

A geochemical modeling approach has been used to characterize the nature of weathering processes occuring within the Ringelbach granitic catchment (Vosges, France). The main springs were regularly sampled over the 2004-2006 period and analysed for major and trace element concentrations and Sr and U isotope ratios. Water samples from two 150-m deep boreholes drilled within the watershed were also used and analysed for this study; Geochemical characteristics of the waters are systematically different among the springs (depending on their elevation along a same slope) and deep boreholes (Chabaux *et al*. this issue).

The coupled transport/reaction model KIRMAT [1, 2] allows us to discuss and constrain the origin of such a systematic geochemical variation. The KIRMAT model combines geochemical reactions and one dimension mass transport equations to simulate the reactive transport of a fluid through a rock along a given water pathway. It was also designed to incorporate ideal solid solutions for the precipitation of clay minerals [3]. In the case of the Ringelbach weathering, the model simulates the transport of rainwaters along a 1-D water pathway crossing the different weathering levels of the granitic bedrock, from the surface saprolite level to the deep fresh granite. The long-term simulations (30ky) lead to weathering mineralogical sequences and to porosity evolution of the granitic bedrock consistent with field observations. They also point out that the geochemical characteristics of the water samples collected on the Ringelbach catchment depend on both the lithological level in wich the waters circulate and on the duration of the water transfert within each lithological level. The latter is certainly a key parameter to be further addressed in future studies.

[1] F. Gérard, B. Fritz, A. Clément, J.L. Crovisier (1998) *Chemical Geology* **151**, 247–258. [2] Y. Lucas, A.D. Schmitt, F. Chabaux, A. Clément , B. Fritz, P. Elsass, S. Durand (2010) *Applied Geochem*. **25**, 1644–1663 [3] B. Fritz, A. Clément, Y. Amal, & C. Noguera (2009) *GCA* **73**, 1340–1358.

https://doi.org/10.1180/S0026461X00006502 Published online by Cambridge University Press

Formation of seconday minerals A lysimeter approach

F. SCHÄFFNER[1]*, D. MERTEN[1], G. DE GIUDICI[2], P.C. RICCI[2] AND G. BÜCHEL[1]

[1]Friedrich-Schiller-University, Jena, Germany (*correspondence: franziska.schaeffner@uni-jena.de)
[2]University of Cagliari, Cagliari, Italy

Heavy metal contamination of large areas due to uranium mining operations poses a serious long-term environmental problem. In Ronneburg, in eastern Thuringia, Germany, leaching of low grade uranium bearing ores (uranium content < 300g/t) proceeded from 1972 to 1990 using acid mine drainage (AMD; pH 2.7-2.8) and diluted sulphuric acid (10g/l). Secondary mineral phases like birnessite, todorokite and goethite occure as natural attenuation process associated with enrichment of heavy metals, especially Cd, Ni, Co, Cu and Zn due to a residual contamination even after remediation efforts.

To reveal the processes of secondary mineral precipitation in the field a laboratory lysimeter approach was set up under similar conditions than in the field. Homogenated soil from the field site and quartz were used as substrates. Water supply was just from the bottom by a mariott´s bottle using contaminated groundwater from the field. Evaporation processes were accepted to allow continuous flow of water. This leads to precipitation of epsomite and probably aplowite on the top layer equal to field investigations. *In situ* measurements of redox potentials showed in general high oxidizing conditions (200-750 mV) due to different redox couples in the groundwater. After 4 weeks first secondary minerals became visible. Although Eh/pH data does not support formation of manganese minerals, SEM-EDX data show microorganisms in organic rich phases together with the occurrence of manganese, oxygen and nickel, indicating manganese oxides enriched in nickel. Infrared (IR) spectroscopy give hints for todorokite of being the secondary manganese mineral. Soil water samples were used for monitoring behavior of metals within the lysimeter. Hence saturation indices (SI) for different secondary minerals were calculated with PHREEQC. Clay minerals (e.g. kaolinite, illite) show SI values up to 5 indicating precipitation. This is coincided with a nearly completely depletion of aluminum in the soil water after entering the lysimeter and XRD measurements. The SI of goethite also shows oversaturation with respect to the soil solution. SEM-EDX analyses and IR spectroscopy confirm the formation of goethite. Data revealed that the formation of goethite is mainly dominated by Eh/pH processes in this system and that heavy metals like Zn and U could be enriched.

Are Large Igneous Provinces net-sinks for CO_2?

MORGAN F. SCHALLER[1], JAMES D. WRIGHT[1] AND DENNIS V. KENT[1,2]

[1]Earth and Planetary Sciences, Rutgers University, Piscataway, NJ (*correspondence: schaller@rutgers.edu)
[2]Lamont Doherty Earth Observatory, Palisades, NY

Continental flood basalts are subaerially erupted Large Igneous Provinces (LIPs), often covering significant continental areas with millions of cubic kilometers of lava. Recent evidence from the Central Atlantic Magmatic Province (CAMP) record in the Eastern North American (ENA) Newark Rift Basin demonstrated that LIPs may result in a transient doubling of atmospheric pCO_2, followed by a ~300 ky falloff to near pre-eruptive concentrations (*1*). We use the pedogenic carbonate paleobarometer in the corollary Hartford Basin to confirm findings in the Newark, and to test the million-year scale effect of the CAMP eruptions.

We find that the Hartford basin pCO_2 record is consistent with observations from the Newark, where a ~4400 ppm pCO_2 peak is identified just after each volcanic episode. The significantly longer post-extrusive Portland formation of the Hartford Basin shows a fourth CO_2 pulse to ~4500 ppm, about 250 ky after the last lava recorded in the ENA section, which may correlate to a later basalt in the Central High Atlas Basin of Morocco. The Hartford record also shows a rapid post-eruptive decrease in pCO_2, reaching pre-eruptive background concentrations of ~2000 ppm in <~300 ky, consistent with observations from the Newark Basin. Furthermore, the Hartford post-extrusive section exhibits a long-term decrease in pCO_2 to levels below the pre-CAMP background over the subsequent 1.5 My following the final apparent episode of eruptions.

We use a simple geochemical carbon-cycle model to demonstrate that the rapidity of these decreases, and the fall to concentrations below background may be accounted for by a 1.5-times amplification of continental silicate weathering due to the presence of the CAMP basalts themselves. If basalt has 10-times the chemical reactivity of continental crust, such an amplification would require eruption of lavas over an aerial extent of ~8.3 x10^6 km^2, well within independent estimates of the CAMP at 1.1 x 10^7 km^2. Together, these results indicate that continental flood basalts result in an extreme short-term perturbation of the carbon system, followed by a long-term decrease in pCO_2 to below pre-eruptive levels, implying they may have an overall net-cooling effect on global climates.

[1] M. F. Schaller, J. D. Wright, D. V. Kent (2011) *Science* **331**, 1404.

https://doi.org/10.1180/S0026461X00006502 Published online by Cambridge University Press

Alkaline mantle melts pinpoint late Triassic thinning of the Southern Alpine lithosphere (Ivrea Zone, Italy)

U. SCHALTEGGER[1]*, O. MÜNTENER[2], A. ULIANOV[2], M. OVTCHAROVA[1], I. PEYTCHEVA[1,3], M. ANTOGNINI[4] AND F. GIRLANDA[4]

[1]Earth and Environmental Sciences, University of Geneva, Switzerland (*correspondence: urs.schaltegger@unige.ch)
[2]Mineralogy and Geochemistry, University of Lausanne, Switzerland
[3]Bulgarian Academy of Sciences, Sofia, Bulgaria
[4]Museo Cantonale di Storia Naturale, Lugano, Switzerland

Following granulite facies metamorphism and abundant mafic magmatism in the Permian lower crust, the European – Adriatic continental crust thermally equilibrated prior to upper Triassic to lower Jurassic rifting and exhumation. During this process, decompressional partial melts from the asthenosphere intruded into the lower continental crust and locally triggered partial melting and rejuvenation of isotopic systems. Such features have been described from the Ivrea zone [1, 2].

We studied Na-rich peralkaline leucocratic pegmatoid lenses within the ultramafic Finero body (N-Italy/S-Switzerland) at the eastern end of the Ivrea zone. These pegmatoids are composed of nepheline, plagioclase, biotite, zircon, apatite, sodalite and corundum. High-precision U-Pb ID-TIMS age determinations on single crystals, fragments and on a transect through a one centimeter sized zircon, combined with *in situ* laser ablation ICP-MS data, as well as initial Hf isotopes provide evidence that zircon grew episodically between 210 and 190 Ma from melts originating from an enriched mantle source. Variations in trace element composition and in age - up to 2 million years within one zircon crystal - are compatible with a first emplacement of plagioclase/albite and nepheline megacrystal bearing pegmatoids that are subsequently brecciated by a K, REE and trace element rich, fluid-saturated liquid. Both liquids are zircon saturated. The pulsed zircon growth is interpreted to reflect episodes of enhanced crustal stretching and thinning, producing a low-percentage of mantle melting. Our data may explain why the granulite-facies parageneses in the Ivrea zone have been locally overprinted and rejuvenated, solving the decennial controversy on the age of the regional granulite-facies event.

[1] Schaltegger & Brack (2007) *Int. J. Earth Sci.* **96**, 1131–1151. [2] Quick *et al.* (2009) *Geology* **37**, 603–606.

Estimating stable isotope signatures of core formation

EDWIN A. SCHAUBLE

UCLA, Los Angeles CA 90095 USA

The geochemical separation of isotopes at equilibrium is a process driven by material dynamics, chiefly the zero-point energy of vibrations (phonons). Isotopic signatures caused by this process might be useful for understanding the composition and conditions of formation of the Earth's core, as well as metal-silicate segregation elsewhere in the solar system [1-5]. This presentation will discuss recent progress in using first-principles models to understand isotopic fractionation caused by dissolution into metal alloys at high temperatures and/or pressures, as well as complementary techniques including spectroscopy-based modeling, experiments, and empirical calibration. Estimates of H, C, N, O, Si, S and Cr isotope fractionations in iron-rich metallic melts are calculated with density functional theory, via models of iron-rich crystals with bonding environments analogous to liquid alloy, e.g. dhcp-FeH, Fe_3C-cohenite and $Fe_{15}Cr$. Alloying atoms in these crystals are completely coordinated by iron. Equilibrium fractionation is assumed to be driven by the reduction of vibrational frequencies when heavy isotopes are substituted – though mass-independent fractionation may become significant for very heavy elements (e.g. platinum group elements, Pb). Quasiharmonic methods approximate the effects of high pressure and thermal expansion – in the case of silicon-isotope fractionation it appears that pressure effects of bond compression and increased cation coordination in silicate melts roughly cancel each other along the mantle liquidus. Stronger pressure effects are possible for other elements. The calculations suggest that iron alloys will usually be depleted in heavy isotopes, relative to other planetary materials, by as much as ~100‰/amu at 2000 K in the case of D/H fractionation between FeH and water, or as little as ~0.1‰/amu in the case of $^{53}Cr/^{52}Cr$. Isotopic signatures appear to be largest for light elements (H >> C, N, O > Si > S, Cr), and at low temperatures. All of the light-element systems studied could show isotopic separations large enough to measure, suggesting that significant core partitioning could perturb the bulk silicate Earth isotopic composition. Experimental and empirical determinations of Si-isotope and C-isotope fractionations broadly agree with theoretical models.

[1] Georg *et al.* (2007) *Nature* **447**, 1102. [2] Rustad & Yin (2009) *Nature Geoscience* doi: 10.1038/ngeo546. [3] Polyakov (2009) *Science* **323**, 912. [4] Ziegler *et al.* (2010) EPSL **295**, 487–496. [5] Moynier (2011) *et al. Science* **331**, 1417.

https://doi.org/10.1180/S0026461X00006502 Published online by Cambridge University Press

Modeling isotopic signatures of nebular chlorine condensation

EDWIN A. SCHAUBLE[1] AND ZACHARY D. SHARP[2]

[1]UCLA, Los Angeles CA 90095 USA
[2]University of New Mexico, Albuquerque NM 87131 USA

Recent measurements of $^{37}Cl/^{35}Cl$ in bulk chondrites and the silicate Earth suggest a relatively homogenous distribution of chlorine isotopes[1], but significant variation has been found in other planetary samples. In order to assess the potential for stable chlorine isotope ratio measurements to constrain the origin and transport of chlorine in chondritic parent bodies and other planetary precursors, and more broadly in minerals and ices, we calculated equilibrium $^{37}Cl/^{35}Cl$ isotope fractionations between gas-phase HCl and the crystalline phases $HCl.3H_2O$, NaCl (halite), KCl (sylvite) and $Na_4Al_3(SiO_4)_3Cl$ (sodalite) using a combination of experimental vibrational frequencies and electronic structure (DFT) models. Sodalite is estimated to have ~0.7‰ lower $^{37}Cl/^{35}Cl$ than HCl at ~950 K, the expected 50% condensation point for silicate-hosted chloride. This fractionation is in the same direction, but somewhat smaller than, the ~1.3‰ $^{37}Cl/^{35}Cl$ depletion observed in primitive sodalite inclusions in Allende[1]. Calculated halite-sodalite fractionation at 1098 K is also of the same sense but smaller than an experimental calibration (0.02‰ vs. 0.3‰) [1]. In contrast, $HCl.3H_2O$ hydrate is predicted to have 3-6‰ higher $^{37}Cl/^{35}Cl$ than coexisting HCl gas in equilibrium at temperatures relevant to low- pressure gas/crystal partitioning (roughly 140-160 K). This enrichment in ice is opposite in sense to what would be expected in a general rapid condensation process — more mobile ^{35}Cl-bearing molecules with weaker H-Cl bonds should react faster and thus ^{35}Cl should be enriched in the rapid condensation product. It is also opposite in sense to predicted and observed equilibrium isotope fractionation between HCl vapor and liquid water [2], but may overlap fractionation associated with disequilibrium evaporation. These results suggest that it may be possible to distinguish between icy [3] and silicate sources of chloride to planets and planetary precursors, so long as chlorine condensation in not quantitatively complete. Acid hydrate-derived high $^{37}Cl/^{35}Cl$ signatures, if found, could additionally indicate a post-condensation origin of chlorine-bearing minerals in chondrite minerals, and would be consistent with correlated high chlorine abundances and hydration in CI chondrites.

[1] Sharp *et al*. (2007) *Nature* **446**, 1062–1065.[2] Sharp *et al*. (2010) *GCA* **74**, 264–273, Schauble *et al*. (2003) *GCA* **67**, 3267–3281. [3] Zolotov & Mironenko (2007) *LPSC* #2340.

Modes of interaction between inorganic engineered nanoparticles and biological and abiotic surfaces

G.E. SCHAUMANN[1]*, P.M. ABRAHAM[1], A. DABRUNZ, R. SCHULZ[1] AND L. DUESTER[1,2]

[1]University Koblenz-Landau, Institute of Environmental Sciences, Germany
(*correspondence: schaumann@uni-landau.de)
[2]Department of Aquatic Chemistry, Federal Institute of Hydrology, Koblenz, Germany

Engineered nanoparticles are subjected to various aging and transformation pathways when they are emitted into the environment. One important pathway is connected to their attachment to biological or inorganic surfaces (e.g. planktonic invertebrates, plant leaves, biofilms or soil and sediment particles).

In this study the attachment of $n\text{Ag}^0$ and $n\text{TiO}_2$ to daphnia, plant leaves and organic as well as to inorganic model surfaces was studied, with the objective to understand the physicochemical interactions, in order to examine a possible link between (eco)toxicological effects and the attachment of the nanoparticles.

Surface-nanoparticle interactions were investigated in ecotoxicological test systems and in laboratory sorption experiments. The model surfaces were chosen to cover a wide range of intermolecular interactions considering van-der Waals interactions as well as proton donor and acceptor interactions. Samples were analysed quantitatively by ICP-MS and qualitatively by microscopic techniques (optical microscopy, environmental scanning electron microscopy and atomic force microscopy including nanomechanical properties).

In ecotoxicological test systems, attachment of nanoparticles to *Daphnia magna* occurred in large nanoparticle clusters and inhibited the molting of inidividuals. The deposition mechanism is in these systems determined by aggregation processes. In contrast, sorption of individual nanoparticles occured from stable suspensions. The sorption coefficient was determined by the chemical nature of the model surfaces as well as by the surfaces accessible for the nanoparticles.

The current results show that attachment is determined by an interplay between physicochemical nanoparticle-surface interactions, colloidal stability and physical characteristics.

https://doi.org/10.1180/S0026461X00006502 Published online by Cambridge University Press

Growth conditions of stalagmites derived from noble gas concentrations in fluid inclusions

Y. SCHEIDEGGER[1,2], N. VOGEL[1,2], S. FIGURA[1], M. BRENNWALD[1], R. WIELER[2], D. FLEITMANN[3] AND R. KIPFER[1,2]

[1]Eawag, Water Resources and Drinking Water, Dubendorf, Switzerland
[2]ETH Zurich, Institute for Geochemistry and Petrology, Zurich, Switzerland
[3]Geological Insitute, University of Berne, Switzerland

Stalagmites are increasingly used as climate archives to reconstruct past climate conditions over long time intervals and in wide ranges of continental regions. We analysed noble gases in 43 holocene samples from 2 tropical stalagmites (D1, P3) from Socotra Island, Yemen. Kr and Xe concentrations in many of the samples are explained as binary mixtures of noble gases from air-saturated fluid inclusion water and atmospheric noble gases released from air inclusions ('excess air'). After 2-component deconvolution, equilibrium concentrations of noble gases in the fluid inclusion water are calculated, from which in turn noble gas temperatures (NGTs) are deduced [1]. NGTs are assumed to reflect the ambient cave temperature at the time of the last gas exchange.

Many NGTs in D1 and P3 agree with the modern cave temperature (28°C). However, we observe relatively large NGT variations over short timescales, which cannot reflect actual cave temperature variations. We attribute these variations to changing conditons during air-water partitioning between inclusion water and the local cave atmosphere. An occasional enrichment in CO_2 around the stalagmite would lower the partial pressures of Kr and Xe and thus reduce their equilibrium concentrations in the inclusion water leading to spuriously high NGTs.

Our analyses also provide a record of the water content and allow to determine the amount of excess air in the samples. D1 shows a statistically significant regime shift at ~1.5 ka BP (see [2] for age model) both in the water content and in the amount of excess air. The regime shift coincides with the most negative excursion in the $\delta^{18}O$ record of the calcite [2]. Thus, growth conditions of stalagmite D1 changed dramatically at this time, possibly in response to a reduced drip rate, which lead to a major change in the amount of air and water inclusions incorporated in the stalagmite.

[1] Kipfer *et al*. (2002) *Rev. Mineral. Geochem*. **47**, 615–700. [2] Fleitmann *et al*. (2007) *Quart. Sci. Rev*. **26**, 170–188.

Chromium isotopes in Saanich Inlet sediments and waters

K. SCHEIDERICH[1]*, C. HOLMDEN[1] AND R. FRANCOIS[2]

[1]Saskatchewan Isotope Lab, Univ. of Saskatchewan, Saskatoon, SK S7N 5E2, Canada (*correspondence: kas373@mail.usask.ca, ceh933@mail.usask.ca)
[2]Earth and Ocean Sciences, Univ. of British Columbia, Vancouver, BC V6T 1Z4, Canada (rfrancoi@eos.ubc.ca)

Saanich Inlet is a classic locality for study of anoxic sedimentation and sulfidic water column processes. Organic-rich sediments from the inlet are enriched in Cr relative to the detrital background. Water column sulfide develops in the summer months as a result of stratification and high primary productivity and restricted deep water renewal. Thus, Saanich Inlet provides an excellent opportunity to uncover the modern behaviour of Cr isotopes, which show promise as a tool for paleoenvironmental analysis with respect to redox cycling. Cr isotopes are fractionated through reduction of soluble Cr(VI) to relatively insoluble Cr(III), enriching the Cr(III) in the lighter Cr isotopes. This study will be the first to assess the fractionation between Cr in contemporaneous waters and sediments in an anoxic setting.

Preliminary results for total Cr in the water of Saanich Inlet (100 m depth) show a $\delta^{53}Cr$ of +0.30‰ (normalized to SRM 979), with a total Cr concentration of 0.11 μg/L. This is a lower concentration than open ocean seawater (North Atlantic Seawater; 0.26 μg/L), suggesting that there may be removal of Cr from the water column. At the time of collection (August 2010), the water column was sulfidic below ~80 m depth. Open ocean Cr [1] has a $\delta^{53}Cr$ of +0.45 to +0.71‰, which suggests that Cr in the sulfidic water column of Saanich Inlet is being reduced and removed to the sediments. The Cr leached from the organic component of Saanich sediments was -0.17‰, while bulk marine sediments average -0.03‰ [2]. This system does not conform to the results of groundwater and laboratory experiments performed by others, which yielded large fractionation factors of ~+3.5‰ and predicted sedimentary $\delta^{53}Cr$ values of ~-3‰. One possibility is that reduction goes to completion on only a small fraction of the available Cr, perhaps facilitated by water column particulates or processes operating at the sediment-water interface.

[1] Bonnand, Parkinson, James, Fehr, & Connelly (2010) PP11A-1428, Fall AGU. [2] Schoenberg, Zink, Staubwasser, & von Blanckenburg (2008) *Chem. Geol*. **249**, 294–306.

https://doi.org/10.1180/S0026461X00006502 Published online by Cambridge University Press

The biogeochemistry of phytosiderophores in the rhizosphere in relation to Fe uptake

W. SCHENKEVELD[1], E. OBURGER[2], M. DELL'MOUR[3], C. STANETTY[3], M. WALTER[3], S. HANN[3], M. PUSCHENREITER[2] AND S. KRÄMER[1]*

[1]Universität Wien, Dept. of Environmental Geosciences Althanstraße 14, 1090 Wien, Austria (*correspondence: stephan.kraemer@univie.ac.at)
[2]University of Natural Resources and Applied Life Sciences, Dept. of Forest and Soil Sciences, Tulln, Austria
[3]University of Natural Resources and Applied Life Sciences, Dept. of Chemistry, Wien, Austria

Phytosiderophores (PS) are naturally occuring chelators, which are exuded by graminaceous plant species for the sake of iron acquisition (Strategy II) [1]. PS are highly efficient in mobilizing Fe from soil [2], and upregulation of PS exudation is the key iron deficiency stress response mechanism for graminaceous plants [1].

Despite the extensive research on the mechanism of action of PS, the understanding of the biogeochemistry of PS in the rhizosphere is still limited. The vast majority of studies have been carried out under conditions quite remote from those present in the rhizosphere (e.g. with hydroponic systems).

A lack of adequate analysis and sampling techniques, the complicated acquisition of PS from root exudates and the biodegradation of PS by rhizosphere microorganism are among the principal problems, prohibiting a more detailed study of PS in relation to soil-grown plants.

Our research project addresses several of these issues, amongst others through synthesis of PS ligands, development of new analytical methods suitable for measuring PS and metal-PS complexes in soil solution, and application of novel rhizosphere sampling techniques with rootboxes and microsuction cups.

The overall aim of the projects is an integral quantification of the source and sink terms determining PS concentrations in the rhizosphere. Both reaction kinetics and thermodynamic equilibrium aspects will be considered. Processes that will be examined include adsorption, desorption, mobilization of iron and other metals from the soil, biodegradation, PS exudation and PS-facilitated iron uptake.

[1] Marschner *et al*. (1986) *J. Plant Nutr*. **9**, 695–713.
[2] Krämer *et al*. (2006) *Adv. Agron*. **91**, 1–46.

Hydrothermally induced changes of electrical rock conductivity and permeability in porous feldspar-rich materials

A. SCHEPERS* AND H. MILSCH

Deutsches GeoForschungsZentrum, 14473 Potsdam, Germany (*correspondence: schepers@gfz-potsdam.de)

Due to the extraction of heat during geothermal energy production from deep sedimentary reservoirs, dissolution and/or precipitation reactions may be induced which potentially alter the pore space properties of the reservoir rocks. In this study hydrothermal batch and flow-through experiments were conducted with feldspar-rich porous materials at temperatures up to ~160°C, under hydrostatic pressure conditions, and durations up to 4 months to investigate the influence of such reactions on electrical rock conductivity (σ_r) and permeability (k).

Sample materials were feldspar-rich Rotliegend sandstone samples and granular analogue materials composed of quartz, K-feldspar, and plagioclase grains. The temperature range applied in the experiments pertains to a low enthalpy geothermal energy production scenario. The starting fluids ranged from deionised H_2O to 2 mol/L $NaCl_{aq}$ solutions. σ_r was continuously monitored while k was measured at irregular intervals throughout the flow-through experiments. In the batch experiments electrical fluid conductivity (σ_f) was measured at irregular intervals.

Chemical fluid analyses were performed on the resulting fluids with respect to the major ions of the system H^+, Na^+, Al^{3+}, Si^{4+}, K^+, Ca^{2+}, OH^-, Cl^-, and SO_4^{2-}. Aliquots of the solid materials were characterised prior and after the experiments with XRD, BET, Hg-porosimetry, SEM, and EMPA. Sub μm sized structures on altered grains were also investigated with TEM. One sandstone sample was analysed with X-ray CT with a resolution of ~2 μm prior and after a flow-through experiment to image the pore space *in situ*.

Dissolution features were common on the altered solid materials while precipitates were rarely observed. Precipitates were sub μm sized amorphous particles occurring mainly on plagioclase surfaces. The transient increases of concentrations of dissolved ionic species, of σ_f, and σ_r indicate a kinetically controlled dissolution process. Concurrently k decreases in the course of the flow-through experiments. The k decrease is mainly due to thermo-mechanical effects but may also result from the observed dissolution and precipitation reactions which lead to an alteration of the geometrical properties of the pore space.

https://doi.org/10.1180/S0026461X00006502 Published online by Cambridge University Press

The speciation of Au, Ag, Hg, Th and U in peat polluted by acid mine drainage

I.N. SCHERBAKOVA*, E.V. LAZAREVA, M.A. GUSTAYTIS AND S.M. ZHMODIK

Institute of Geology and Mineralogy SB RAS, Pr. Koptug, 3, Novosibirsk, 630090, Russia (*correspondence: sherbachok@ngs.ru)

The peat substance is one of the more popular natural sorbents that is used to recovery of elements from aqueous solutions including other similar materials. Ursk's sulfide-bearing waste piles (Ursk, Kemerovo region, Russia) have been formed more 50 years ago. The wastes of the cyaniding primary Cu-Zn-polymetallic ores and these of the oxidation zone have been dumped as a two piles. The natural stream draining the waste piles has been transformed in acid mine drainage (AMD). The wastes have not been fixed and hence ravine's swampy territory below the tailings piles have been covered with the derived waste matter. The interactions between the bog peat substances, AMD and wastes pore solutions have occurred for 50 years. It have been established the elements precipitation and concentration on peat substance. The Zn, Cu, Pb, Zn concentrations in peat samples are comparable to these in the wastes. The ore contained 4 ppm of Au. The contains of Au in waste covering the peat substance range from 0.2 to 1.7 ppm. It have been obtained that the concentrations of Au in the peat that is contacting with sulfide-bearing waste are 0.3-14.3 ppm. The Fe hydroxides, sulfides, jarosite, gypsum are established there.

The speciation of Au, Ag, Hg, Th and U in peat material has been determined using the selective extraction technique. It have been identified the following elements forms in peat substances: the water-soluble forms, these associated with organics/sulfides and with the Fe(III) hydroxides/oxides and residue. The part of all being studied elements is partially attributed to the water-soluble compounds (0.1 Au, 0.6 Hg, 0.08 Th, 0.5 U ppm). Gold is partly presented as organ-complexes ore sulfides (up to 1.4 ppm). In places where the gold concentration is in reaches 10 ppm, it appears mostly in the native form. The submicrometer gold Cu-bearing grains are observed among secondary minerals of Fe and are formed on the detrital material. Silver may enters as isomorphic admixture in the jarosite and mainly presets in contamineted peat as Fe(III) hydroxides/oxides fraction. Mercury as organ-complexes and/or as the secondary sulfide of Hg has been registered in peat samples. The major unit of U is associated with organic material and Th is with residual fraction.

This work was supported by the RFBR 11-05-01020, SB RAS Integrative Project #31 and IGM SB RAS grant #2.

Organic and inorganic $scCO_2$-rock interactions – Results from laboratory experiments

ANN-KATHRIN SCHERF*, HANS-MARTIN SCHULZ, ANDREA VIETH-HILLEBRAND AND KETZIN-GROUP

German Research Centre for Geosciences – GFZ, Telegrafenberg, 14473 Potsdam (*correspondence: scherf@gfz-potsdam.de)

Mineralogical changes in the reservoir in the cause of CO_2 injection and its propagation may provide information on e.g. CO_2-induced geochemical interactions and are of great importance for the estimation of potential risks of geological CO_2 storage. To overcome the gap of direct observations, experimental studies at simulated reservoir conditions are an important tool to study all types of potential CO_2-fluid-rock interactions *ex situ* on mineral phases or real reservoir samples.

In this broad experimental study, our aim was to examine the role of supercritical CO_2 ($scCO_2$) on the mobilization of organic compounds from mineral phases as well as the changes in elemental and mineralogical composition of reservoir and cap rock samples due to the defined temporal exposure to $scCO_2$ under variing p-T-conditions. For this purpose several flow-through experiments using $scCO_2$ have been performed [1] on real rock samples of different lithologies from an real CO_2 storage site: the Ketzin site in Germany.

$ScCO_2$-extracts as well as untreated and $scCO_2$-treated rock samples were analysed using a variety of organic and inorganic geochemical, mineralogical and microscopic techniques to detect changes compared to untreated twin samples.

Generally, organic matter mobilization – mainly the low molecular weight organic acids formate and acetate - occurred linearly within the first 8 hours, then continued with decreasing extraction yields. XRD and XRF analyses revealed no quantitatively distinguishable changes in elemental and mineralogical composition between $scCO_2$-treated and untreated twin samples. However, SEM images indicated blastesis and corrosion effects on mineral surfaces as well as a partly loss / destruction of primary cements due to the exposure to $scCO_2$.

[1] Scherf *et al*. (2011) *Energy Procedia* **4**, 4524–4531.

https://doi.org/10.1180/S0026461X00006502 Published online by Cambridge University Press

Re-Os constraints on gold mineralisation events in the Neo-archaean Storø supracrustal belt, Southern West Greenland

ANDERS SCHERSTÉN[1], KRISTOFFER SZILAS[2], ROBERT A. CREASER[3], TOMAS NÆRAA[2], JEROEN VAN GOOL[4] AND CLAUS ØSTERGAARD[5]

[1]Department of Earth and Ecosystem Sciences, Lund University, Sölvegatan 12, SE-223 62 Lund, Sweden (anders.schersten@geol.lu.se)
[2]Geological Survey of Denmark and Greenland, Øster Voldgade 10, 1350 Copenhagen K, Denmark
[3]Department of Earth and Atmospheric Science, University of Alberta, Edmonton, Alberta, T6G 2E3, Canada
[4]Scandinavian Highlands Holding A/S, Horsholm Kongevej 11, 2970 Horsholm, Denmark
[5]21st North, Kullinggade 31, DK-5700 Svendborg, Denmark

The Storø supracrustal belt in Godthåbsfjord, southern West Greenland, hosts gold mineralization that is associated with arsenopyrite along a contact between lithological units and along the axial plane of a large fold core. Here we present new arsenopyrite Re-Os and zircon U-Pb data to constrain the age of the debated Storø gold deposit. Arsenopyrite from a stratiform mineralisation yield a 2.71 ±0.05 Ga isochron and model ages for highly radiogenic arsenopyrite form a bimodal distribution with peaks at 2.66 Ga and 2.71 Ga respectively. The older population combined with the isochron result yields a weighted mean of 2.707 ±0.008 Ga (MSWD = 0.57, n=4). A 2.64 ±0.02 Ga isochron from arsenopyrite from the axial plane of the fold core indicate a two-stage mineralisation process. The 2.64 ±0.02 Ga isochron is in perfect agreement with U-Pb zircon data (Nutman *et al*. 2007. Prec. Res. 159, 19-32), which are best explained by orogenic mineralisation during amphibolite facies metamorphism along structural weak planes. The initial $^{187}Os/^{188}Os$ value of 0.56 ±0.16 for the 2.64 ±0.02 Ga isochron indicates a crustal source for the metals, whereas the initial $^{187}Os/^{188}Os$ = -0.1 ±0.6 for the 2.71 ±0.05 Ga isochron remains unconstrained. Nevertheless, these data are best explained by relatively short crustal residence times of less than 0.1 Ga, wherein the Os, and associated metals, were extracted from the mantle after 2.8 Ga, and in which the 2.64 ±0.02 Ga stage formed by mobilisation of an earlier mineralisation around 2.72 Ga. Such a model is corroborated by detrital zircon constraints, which imply that volcanism and the first mineralisaton stage is ≤2.8Ga. Finally, the ~2.63 Ga amphibolite facies metamorphic event in the Storø supracrustal belt was important for the redistribution of gold bearing sulphide minerals.

Marcasite in clastic sediments – Formative processes and deep time stability

JUERGEN SCHIEBER AND MICHAEL CHESHIRE

Department of Geological Sciences, Indiana University, Bloomington, Indiana 47405, (jschiebe@indiana.edu)

Marcasite occurs in marine and brackish water shale, claystone, and sandstone units from multiple locations and ages (Proterozoic through Eocene). Textural observations, such as differential compaction around marcasite concretions, indicate that these marcasites formed during early diagenesis in surface sediments. In marine shales and sandstones, textural studies suggest that marcasite precipitation is intimately associated with corrosion and destruction of framboidal pyrite for the former, and with destruction of reworked early diagenetic pyrite concretions for the latter. Marcasite formation in association with pyrite destruction is consistent with a scenario whereby earlier formed diagenetic pyrite is re-oxidized in surface environments to produce the low-pH conditions required for marcasite formation.

In brackish water claystones, marcasite occurs as radial fibrous masses along the margins of burrows that penetrated into reducing sediments. Soil science research that associates marcasite formation with water-logged acid sulfate soils in coastal settings suggests that this marcasite as well formed because oxidation of pre-existing iron sulfides provided favorable conditions for marcasite growth.

Marcasite concretions from both marine and brackish water settings show multiple generations of marcasite growth, and $\delta^{34}S$ values were measured from successive generations in micro-drilled samples and by ion-probe. The data show the lowered $\delta^{34}S$ values indicative of microbial sulfate reduction in surface sediments, as well as a wide range of $\delta^{34}S$ values suggestive of variable degrees of system closure (marine) and salinity fluctuations (brackish).

The studied samples range from approximately 50 million to 1.6 billion years in age and were all collected from unmetamophosed sediments. Marcasite is considered metastable and thought to invert to pyrite over time. Our observations indicate that this conversion proceeds very slowly at low temperatures (<200ºC). In general, partial conversion of marcasite to pyrite is minor to absent for fine grained sediments (shales and claystones), and common and completed to various degrees in sandy sediments.

https://doi.org/10.1180/S0026461X00006502 Published online by Cambridge University Press

High precision Ca isotope analysis using MC-ICPMS and TIMS

M. SCHILLER*, C. PATON AND M. BIZZARRO

Centre for Star and Planet Formation, Natural History Museum of Denmark, University of Copenhagen, DK-1350 Copenhagen, Denmark (*correspondence: schiller@snm.ku.dk)

Calcium is a refractory lithophile element and a major rock-forming constituent of rocky planets. Whereas most Ca isotopes are synthesized during hydrostatic and explosive nucleosynthesis in massive stars, the synthesis of ^{48}Ca is unique, as it is only efficiently produced in a low entropy environment most likely achieved in a type-Ia supernova [1]. Thus, high-precision Ca isotope measurements of meteorites and their components allow for a better understanding of the nature of the various stellar sources that contributed matter to the nascent solar system.

However, there are several challenges for the precise measurement of Ca isotopes. The natural abundance of the six stable isotopes (40, 42, 43, 44, 46 and 48) of Ca varies by a factor of >24000 (40 to 46), providing an obstacle for the simultaneous measurement of all Ca isotopes. In addition, there is a 20% mass difference between ^{40}Ca and ^{48}Ca, which produces a large mass dispersion beyond the geometry of either of the mass spectrometers used in our study. To overcome these issues we used a combination of TIMS and MC-ICPMS, where the low mass range (40-44) was measured using a Triton TIMS, while the overlapping high mass range (42-48) was measured using a Neptune MC-ICPMS. To precisely analyse ^{46}Ca using the MC-ICPMS we measured in high-resolution ($m/\Delta m \sim 6500$) and at total beam intensities of >5000 V. To further avoid direct isobaric interferences from Ti and Sr, we also established an improved chemical separation of Ca effectively eliminating especially Ti and Sr.

Repeated analyses of rock standards relative to the NIST SRM915b Ca-standard demonstrate that our approach allows the measurement of ^{40}Ca/^{44}Ca, ^{43}Ca/^{44}Ca, ^{46}Ca/^{44}Ca and ^{48}Ca/^{44}Ca to 50, 2.5, 50 and 12 ppm (2 sd), respectively, when normalized to ^{42}Ca/^{44}Ca. This represents a 100-fold improvement compared to previous studies for the less abundant isotopes of Ca. Using this improved resolution, we have re-investigated the extent of Ca-isotope heterogeneity in the solar protoplanetary disk by analyzing a suite of strategically-selected inner solar system objects.

[1] Meyer (1998) *Phys. Rep.* **227**, 257–267.

Inhibition of calcite dissolution kinetics during direct liming of acid surface waters

M. SCHIPEK* AND B.J. MERKEL

TU Bergakademie Freiberg, Chair of Hydrogeology, 09596 Freiberg, Germany (*correspondence: schipek@geo.tu-freiberg.de)

Dissolution kinetics of pure calcite is well investigated, e.g. [1, 2]. But, composition of natural carbonates, as well as the constituents in mine waters, have a strong influence on the solution kinetics and may inhibit dissolution processes during lake liming.

The reactivity of synthetic marble powder and industrial products was investigated. Significant differences in reactivity was obvious at $p_{CO2} > 3.8 \bullet 10^{-4}$ atm. Ions typical for acid mine drainage (e.g. Mn^{2+}, Cd^{2+}, SO_4^{2-}) do have different effects on the kinetic of carbonate dissolution. Manganese ions (c = $8.98 \bullet 10^{-4}$ mmol/L) inhibit calcite dissolution. Experiments with 5-times excess of calcite results in 66.4% of dissolved calcium compared to experiments without inhibitor. Providing a surplus of calcite particles (20-times excess) results in 92.7% of the equilibrium concentration and a significant time-shift in reaching equilibrium (20, 000 min instead of 12, 000 min).

Cadmium has as well a significant influence on dissolution and kinetics. Only 58.2% of the calcium concentration was reached with cadmium as inhibitor (c = $7.65 \bullet 10^{-6}$ mmol/L) compared to the dissolution in pure water. Using carbonate 20 times in excess revealed a slightly higher dissolution reaction (63.8%).

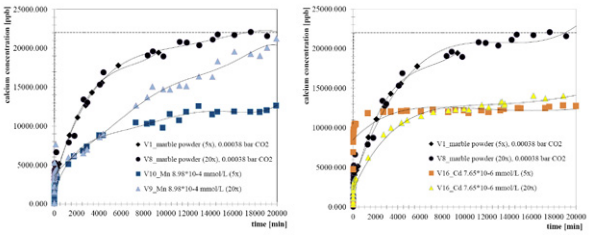

Increased CO_2 partial pressure might be used to compensate inhibtion by material impurities and/or water constituents.

[1] Plummer *et al.* (1978) *American Journal of Science* **278**(2), 179–216. [2] Dreybrodt *et al.* (1996) *Geochim Cosmochim Acta* **60**(18), 3375–3381.

https://doi.org/10.1180/S0026461X00006502 Published online by Cambridge University Press

The microbiology and biogeochemistry of sulfidic mine dumps

AXEL SCHIPPERS

Federal Institute for Geosciences and Natural Resources (BGR), Geomicrobiology, Stilleweg 2, 30655 Hannover, Germany (axel.schippers@bgr.de)

The microbiology and the relevant biogeochemical processes in the dumps and heaps are reviewed and have to be understood for improving copper heap leaching operations and to develop and control countermeasures for the formation of acid mine drainage (AMD). Pyrite or pyrrhotite oxidation is the most relevant biogeochemical process in sulfidic mine waste dumps and heaps and different techniques have been applied to measure reaction rates: column experiments, humidity cells, heat flow measurements, or oxygen consumption measurements. Acidophilic Fe(II)-and sulfur-oxidizing microorganisms are most relevant for metal sulfide oxidation. Anaerobic biogeochemical processes in sulfidic mine dumps and heaps are Fe(III)- and sulfate reduction, but little is known about the reaction rates. Fe(III)-reducing microorganisms dissolve Fe(III)(hydr)oxides and may thereby release adsorbed or precipitated metals. Sulfate-reducing microorganisms precipitate and immobilize many metals. Mainly culturing approaches were used to study the microbial communities in sulfidic mine dumps and heaps. More recently, molecular biological techniques have been applied to investigate the microbial diversity and to quantify and monitor particular microorganisms.

[1] Schippers, A. *et al*. (2010) *Hydromet*. **104**, 342–350.

Bioremediation strategies to inhibit salt-enhanced stone weathering

MARA SCHIRO[1]*, ENCARNACION RUIZ-AGUDO[1], FADWA JROUNDI[2], MARIA TERESA GONZALEZ-MUÑOZ[2] AND CARLOS RODRIGUEZ-NAVARRO[1]

[1]Dept. Mineralogy and Petrology, Univ. of Granada, Spain (*correspondence: mschiro@gmail.com)

[2]Dept. Microbiology, Univ. of Granada, Spain

Salt weathering is an important mechanism contributing to the degradation and loss of carved stone and historic stone buildings. Stone monuments in the presence of salt and water, suffer from salt-enhanced physical and chemical weathering. It has been observed that weathering rates of rocks in nature, as well as building stones, are slowed down by naturally occurring or artificially produced patinas. These tend to be bacterially produced, durable mineralized coatings that lend some degree of protection to the underlying stone surface [1].

Our research shows that bacterially produced carbonate coatings can be quite effective at reducing both physical and chemical weathering of stone by soluble salts. The calcite-producing-bacteria used in this study were isolated from stone monuments in Granada, Spain [2] and cultivated in an organic-rich culture medium on a variety of artificial and natural substrates (including limestone, marble, sandstone, quartz, calcite single crystals, glass cover-slips, and sintered porous glass). Scanning electron microscopy (FESEM) was used to image bacterial calcite growth and biofilm formation. *In situ* atomic force microscopy (AFM) enabled calculation of dissolution rates of untreated and treated surfaces. 2D-XRD showed the mineralogy and crystallographic orientation of bacterial calcium carbonate.

Results indicate that bacterially produced calcite crystals form a coherent, mechanically resistant surface layer in perfect crystallographic continuity with the calcite substrate (self-epitaxy). These calcite biominerals are more resistant to chemical weathering by salt-enhanced dissolution, apparently due to the incorporation of organics (bacterial exopolymeric substances, EPS). Conversely, on silicate substrates, non-oriented vaterite forms, leading to limited protection. Organic films formed on treated substrates appear to promote salt crystallization at reduced supersaturation [3], thus reducing salt crystallization pressure and minimizing physical damage. These preliminary results indicate that bacterial treatments have tremendous potential to protect built cultural heritage.

[1] De Muynck *et al*. (2010) *Ecol. Eng*. **36**, 118–136. [2] Jimenez-Lopez *et al*. (2007) *Chemosphere* **68**, 1929–1936. [3] Ruiz-Agudo *et al*. (2006) *Cryst. Growth Des*. **6**, 1575–1583.

https://doi.org/10.1180/S0026461X00006502 Published online by Cambridge University Press

Mineral assemblages and metamorphic history of granulites in the Rychleby Mts., Bohemian Massif

KATEŘINA SCHLÖGLOVÁ*, SHAH WALI FARYAD, DAVID DOLEJŠ AND HELENA KLÁPOVÁ

Institute of Petrology and Structural Geology, Charles University, Albertov 6, 128 43 Praha 2, Czech Republic (*correspondence: schloglo@gmail.com)

Relics of high-pressure metamorphic rocks are preserved in various crustal and mantle segments of the Variscan orogen in central Europe. These rocks may provide important insights into early stages of plate convergence and burial as well as exhumation mechanisms. We use mineral assemblages and chemistry to reconstruct the pressure-temperature (*P-T*) paths of high-pressure granulites in the Rychleby Mts., Bohemian Massif. Mafic granulites consist of garnet, omphacite, kyanite, two feldspars, and quartz with accessory rutile and zircon. The peak assemblage was partly replaced by pargasitic amphibole and biotite during exhumation. Garnet grains are zoned from $Gr_{36}Py_{10}Alm_{54}$ (core) to $Gr_{20}Py_{38}Alm_{42}$ (rim), and host inclusions of phengite, omphacite, unmixed feldspars, kyanite, and rutile. Omphacite composition varies from $Di_{44}Hd_{14}Jd_{42}$ (inclusions in garnet) through $Di_{63}Hd_{20}Jd_{17}$ (porphyroblasts) and $Di_{63}Hd_{24}Jd_{13}$ (symplectitic intergrowths with plagioclase). Reintegrated composition of the feldspar porphyroblasts is $Or_{43}Ab_{53}An_{04}$. Felsic granulite variety is composed of garnet, kyanite, two feldspars, quartz, accessory rutile, and zircon. Garnet preserves zoning from $Gr_{32}Py_{10}Alm_{68}$ (core) to $Gr_{25}Py_{24}Alm_{51}$ (rim), and it contains inclusions of phengite, sometimes replaced by biotite and zoisite. We have applied various univariant equilibria in order to estimate the *P-T* conditions of inclusion entrapment, porphyroblast growth as well as matrix recrystallization during exhumation. The phengite-garnet pairs indicate pre-peak temperatures of 840-860 °C. Ternary feldspar solvus and Zr concentrations in rutile (with a maximum at 1400-1900 ppm Zr) indicate 830-910 and 850-890 °C, respectively. The corresponding pressure, constrained by garnet-omphacite-kyanite-quartz and garnet-feldspar-kyanite-quartz equilibria, ranges between 15 and 18 kbar. Exchange equilibria between omphacite and garnet reveal peak temperatures as high as 950-980 °C, followed by decompression to 900 °C and 14 kbar associated with the formation of amphibole. Crystallization of biotite, at the expense of garnet, occurred near 740 °C possibly after a melt loss, which facilitated preservation of peak mineral assemblages. The reconstructed pressure-temperature path is consistent with extrusion of bimodal calc-alkaline igneous suite from orogenic root.

Biochemical characterization of single weathering hyphae of *Paxillus involutus* using CLSM and synchrotron based μFTIR

A. SCHMALENBERGER[1,2], A.W. BRAY[3], A.L. DURAN[4,1], J.R. LEAKE[4,1], S.A. BANWART[1], L. TATIC[1], G. CINQUE[5], M.D. FROGLEY[5], J. FILIK[5], J. PIJANKA[5], S. BONNEVILLE[3], L.G. BENNING[3] AND M.E. ROMERO-GONZALEZ[1]*

[1]Cell-Mineral Research Centre, The University of Sheffield, Broad Lane, Sheffield, UK (*correspondence: m.e.romero-gonzalez@sheffield.ac.uk)
[2]Life Sciences, The University of Limerick, Ireland
[3]School of Earth and Environment, University of Leeds, UK
[4]Animal and Plant Sciences, The University of Sheffield, UK
[5]Diamond Light Source Ltd, Didcot, UK

The mycelium of symbiotic ectomycorrhizal fungi (EM) increases nutrient uptake by the plants through fungal secretion of low molecular weight organic acids that can accelerate mineral dissolution. This EM weathering with pine trees plays a key role in nutrient mobilization processes and pedogenesis. Here we report first insights into the chemical variability of the weathering mycelium when studied on a micrometer scale using Confocal Laser Scanning Microscopy (CSLM) and synchrotron based micro Fourier Transform Infrared (μFTIR) spectroscopy.

Pine seedlings ectomycorrhizal with *Paxillus involutus* were grown in microcosms containing wells with olivine, quartz, basalt, granite and limestone. CLSM analysis of EM hyphae with the molecular probe SNARF4F in contact with basalt and limestone revealed a pH below or at 4.6 while the pH of EM in contact with granite identified pH values that varied from pH 4.6 to 6.5 with variations observed within single cells. Chemical μFTIR maps of single hyphae at a resolution of 5x5 μm identified variabilities within the spatial distribution of lipids, amides and carbohydrates. Particular distinctions in intensities of carbohydrates and lipids were discovered on a single cell level.

We conclude that mineralogy has a significant impact on the biochemistry of colonizing symbiotic EM mycelia, individual hyphae and cells. Earlier studies showed that exudation of oxalate is increased in the presence of basalt and limestone[1] and here we report the corresponding biochemical changes that take place on a single hypha scale.

[1] Schmalenberger, A. *et al*. (2010) *Geochim. Cosmochim. Ac*. **74**(12), A923.

https://doi.org/10.1180/S0026461X00006502 Published online by Cambridge University Press

Growth- and post-growth behavior of major and trace elements in garnets, a case study

ALEXANDER SCHMIDT, MATTHIAS KONRAD-SCHMOLKE AND PATRICK J. O'BRIEN

Department of Earth & Environmental Science, University of Potsdam (alexander.schmidt@geo.uni-potsdam.de, mkonrad@geo.uni-potsdam.de, obrien@geo.uni-potsdam.de)

The distribution of major and trace elements in the mineral garnet plays an important role in the interpretation of ages deduced by e.g. Lu-Hf and Sm-Nd garnet geochronology. A common understanding is that Lu and other heavy rare earth elements (HREE) have high partition coefficients for garnet, hence will be enriched in early formed garnet cores, while on the other hand light rare earth elements (LREE), such as Sm, will be incorporated during late growth into garnet rims. Further, distribution patterns of HREE in garnet are important indicators for processes during metamorphism as they might point to episodic and multi-generation garnet growth, as well as to mineral reactions producing distint enrichment peaks during garnet growth (e.g. amphibole- & epidote-out reactions).

In this study we investigate these distribution patterns of major and trace elements in a variety of garnets from chemically different host rocks, and discuss the influence of e.g. diffusion on the preservation of growth zoning.

The first results show that nearly all single-generation garnets indeed preserve element distribution profiles with an enrichment of Lu and other HREE in garnet cores. Interestingly diffusion often seems to play a negligible role for the HREE compared to the major elements. Distinct Lu peaks in garnet cores do on the one hand correspond to well-preserved Mn peaks, but also Lu enrichments together with flat Mn patterns are observed, which indicates that Lu (and presumably other HREE) are less prone to diffusional resetting compared to e.g. the major elements. One of the major aims of this study will be to constrain how explicitly diffusion can influence and alter major and trace element distribution profiles in garnets and how these are interrelated with each other. With this information it hopefully will be non-ambiguous to interpret geochronological data of garnets from the Lu-Hf and Sm-Nd isotope systems.

Role of fluid flow conditions on denitrification rates in sediments during managed groundwater recharge

CALLA M. SCHMIDT[1]*, ANDREW T. FISHER[1], ANDREW J. RACZ[1], BRIAN S. LOCKWOOD[2] AND MARC LOS HUERTOS[3]

[1]University of California, Santa Cruz, Santa Cruz, California 95064 (*correspondence: cschmidt@ucsc.edu)

[2]Pajaro Valley Water Management Agency, Watsonville, California 95076

[3]California State University, Monterey Bay, Seaside, California 93955

We measured *in situ* denitrification during infiltration through saturated sediments to develop a mechanistic understanding of controls on denitrification rates. Sampling and measurements were completed below a managed aquifer recharge pond, providing strong constraints on initial nitrate and carbon concentrations, flow rates, and other controlling parameters. Co-located thermal measurements were used to determine flow rates with time, and chemical and isotopic methods were used to assess denitrification progress. Zero order denitrification rates of 3 to 300 μmol L^{-1} d^{-1} were measured during infiltration. Denitrification was not detected at times and locations where the infiltration rate exceeded a threshold of approximately 0.9 m d^{-1}. Pore water profiles of oxygen and nitrate concentrations indicated a deepening of the redoxocline at higher flow rates, which reduced the thickness of the zone favorable for denitrification. Below the threshold infiltration rate, denitrification rates were positively correlated with infiltration rates, suggesting that for a given set of sediment characteristics an optimal range in infiltration rate exists for achieving maximum nitrate load reduction. This study has implications for managing water resources to achieve the greatest possible nitrate load reduction by denitrification in both natural and manipulated settings including recharge ponds, wetlands, and hyporheic zones in streams.

https://doi.org/10.1180/S0026461X00006502 Published online by Cambridge University Press

Zircon as a Raman spectroscopic pressure sensor

C. SCHMIDT[1], M. STEELE-MACINNIS[2] AND M. WILKE[1]

[1]Deutsches GeoForschungsZentrum (GFZ), Telegrafenberg, 14473 Potsdam, Germany (hokie@gfz-potsdam.de, max@gfz-potsdam.de)

[2]Department of Geosciences, Virginia Tech, Blacksburg, VA 24061, USA (mjmaci@vt.edu)

Experiments using diamond-anvil cells have been crucial in understanding minerals and fluids at high pressure (*P*) and temperature (*T*) because sample properties can be studied *in situ*. Pressure in these cells must be determined indirectly, e.g. from the shift in wavenumber of a Raman line of a phase inside the sample chamber. The 464 cm^{-1} Raman line of quartz has frequently been applied as pressure sensor because of its fairly large shift with *P* ($\partial\nu/\partial P$ ~9 cm^{-1}/GPa) and relatively small shift with *T* ($\partial\nu/\partial T$ ~-0.014 cm^{-1}/K) [1]. However, its use is limited by phase transitions and high solubility of quartz in many fluids and melts. In such situations, zircon represents an option because it is stable over a larger range in *P*, *T*, and fluid composition (e.g. [2]).

In this study, we calibrate the shifts in wavenumber of the ν_3-SiO_4 (~1008 cm^{-1}) Raman band of fully crystalline synthetic zircon with *T* and *P*. The relationship between wavenumber and *T* from 22 to 950 °C is described by the equation ν (cm^{-1}) = $7.26*10^{-9}*T$ (°C)^3 - $1.58*10^{-5}*T$ (°C)^2 - $2.893*10^{-2}*T$ (°C) + 1008.64. At ~25 °C, the $\partial\nu/\partial P$ slope to 6.6 GPa is 5.69 cm^{-1}/GPa, and that to 2 GPa is 5.81 cm^{-1}/GPa. The latter does not significantly change with temperature, as determined using a Bassett-type hydrothermal diamond-anvil cell [3], with the pressure based on the EoS of H_2O [4]. The observed $\partial\nu/\partial P$ slopes are 5.88 cm^{-1}/GPa for the 700 and 600 °C isotherms, and 6.08 cm^{-1}/GPa along the 500 °C isotherm. The zircon pressure sensor was used to obtain isochores for aqueous fluids with 6 wt% $NaAlSi_3O_8$, 16 wt% $Na_2Si_2O_5$, 28 wt% $Na_2Si_{1.3}O_{3.6}$, or 64 wt% $Na_2Si_3O_7$ to 800 °C and 1.43 GPa. Except of the experiment with H_2O + 6 wt% $NaAlSi_3O_8$, these isochores were at significantly higher pressures (by up to ~700 MPa) than calculated from the liquid-vapor homogenization temperature using the EoS of H_2O [4]. The actual sample temperature should be well known for accurate determination of *P* using this sensor ($\partial\nu/\partial T$ ~-0.038 cm^{-1}/K).

[1] Schmidt & Ziemann (2000) *Am. Mineral.* **85**, 1725–1734. [2] Finch & Hanchar (2003) *Rev. Min. Geochem.* **53**, 1–25. [3] Bassett *et al.* (1993) *Rev. Sci. Instrum.* **64**, 2340–2345. [4] Wagner & Pruß (2002) *J. Phys. Chem. Ref. Data* **31**, 387–535.

Fractionated enrichment of Zr-Hf and Nb-Ta in ferromanganese crusts

K. SCHMIDT, MICHAEL BAU AND ANDREA KOSCHINSKY

Jacobs University Bremen, Earth and Space Sciences, 28759 Bremen, Germany (k.schmidt@jacobs-university.de)

The very slow growth rate of and the high adsorption capacity attracting dissolved elements from seawater makes marine hydrogenetic ferromanganese (Fe-Mn) crusts generally suitable for the investigation of environmental and paleooceanographic conditions in the past. However, a detailed unterstanding of enrichment processes and possible fractionation mechanisms of elements and isotopes during the accumulation of the crusts is required. Here we report on the distribution of the geochemical twin elements Zr-Hf and Nb-Ta in ferromanganese crusts from the Northern and Southern Central Pacific, the Eastern North Atlantic and from the hydrothermal vent field Logatchev-1. Recent studies [e.g. 1] dealing with the distribution of Zr-Hf and Nb-Ta in the Pacific Ocean show a fractionation of these elements relative to chondritic values throughout the water column, with distinct signatures in different water masses. Our investigated depth profiles of ferromanganese crusts cover up to 20 Ma and are characterized by highly variable distributions of Zr, Hf, Nb, and Ta, accompanied by changing and fractionated Zr/Hf and Nb/Ta ratios. The Zr/Hf ratios in crust surfaces are always lower compared to the range of Zr/Hf ratios in modern deep seawater. Thus, ferromanganese crusts do not inherit the Zr/Hf (and Nb/Ta) signature of the water mass at the location of crust formation and the ratios cannot be used as paleooceanographic tracers. The elements are almost exclusively bound to the Fe oxyhydroxide fraction of the crust and are probably enriched via surface precipitation. While the Fe oxyhydroxide colloids and particles accumulating in the crusts may have formed away from the crust location and would then carry a different, integrated signal [2], the always lower than seawater Zr/Hf ratios in the crusts also indicate the preferred enrichment of Hf relative to Zr during accumulation in the crust and thus a fractionation of the dissolved seawater Zr/Hf ratio. Seawater data for Nb-Ta are scarce, but a preferential enrichment of Nb in the Fe-Mn crusts can be suggested. The different particle reactivity of the geochemical twin elements is related to the different electron structure causing differences in complex stabilities and the type of chemical bonding. Further, the contribution of hydrothermal Hf to the marine Hf budget will be discussed.

[1] Firdaus, M.L. Minami, T. Norisuye, K. & Sohrin, Y. (2011) *Nature Geoscience* **4**, 227–230. [2] Bau, M. & Koschinsky, A. (2006) *Earth & Planetary Science Letters* **241**, 952–961.

https://doi.org/10.1180/S0026461X00006502 Published online by Cambridge University Press

Centennial-scale sea surface temperature and salinity change in the Florida Straits during the early Holocene

M.W. SCHMIDT[1]*, W. WEINLEIN[1], F. MARCANTONIO[2] AND J. LYNCH-STIEGLITZ[3]

[1]Department of Oceanography, Texas A&M University, College Station, TX 77843, USA (*correspondence: schmidt@ocean.tamu.edu)
[21]Department of Geology and Geophysics, Texas A&M University, College Station, TX 77843, USA
[3]School of Earth and Atmospheric Sciences, Georgia Institute of Technology, Atlanta, GA 30307

Previous studies showed that sea surface salinity (SSS) in the Florida Straits [1] as well as Florida Current transport [2] covaried with changes in North Atlantic climate over the past two millennia. However, little is known about earlier Holocene variability in the Florida Straits. Here, we combine Mg/Ca-paleothermometry and stable oxygen isotope measurements on the planktonic foraminifera *G. ruber* (white variety) from Florida Straits sediment core KNR166-2 JPC51 (24° 24.70′N, 83° 13.14′W, 198m deep) to reconstruct a high-resolution (~35 yr/sample) early to mid Holocene record of sea surface temperature and $\delta^{18}O_{SEAWATER}$ ($\delta^{18}O_{SW}$, a proxy for SSS) variability. In addition, we also measured Ba/Ca ratios in the same shell material as a proxy for riverine input into the Gulf of Mexico over the same time interval. After removing the influence of global $\delta^{18}O_{SW}$ change due to continental ice volume variability, our $\delta^{18}O_{SW}$ record suggests early Holocene surface salinity enrichments caused by increased evaporation/precipitation ratios in the Florida Straits associated with periods of reduced solar output [3], increased ice rafted debris in the North Atlantic [4] and the development of more permanent El Niño conditions in the eastern equatorial Pacific [5]. When considered with previous high-resolution reconstructions of early Holocene tropical atmospheric circulation changes, our results provide evidence that solar output variability over the Holocene can have a significant impact on the global tropical hydrologic cycle.

[1] Lund & Curry (2006) *Paleoceanography* **21**, PA2009. [2] Lund *et al*. (2006) *Nature* **444**, 601–604. [3] Reimer *et al*. (2004) *Radiocarbon* **46**, 1029. [4] Bond *et al*. (2001) *Science* **294**, 2130–2136. [5] Marchitto *et al*. (2010) *Science* **330**, 1378–1381.

Rare earth element variation in hydrothermal Fe-oxide Cu-Au systems

ANDREAS SCHMIDT MUMM AND CRISTIANA CIOBANU

School of Earth and Environmental Sciences Cooperative Research Centre for Deep Exploration Technologies, The University of Adelaide Adelaide, South Australia 5005 (andreas.schmidtmumm@adelaide.edu.au, Cristiana.ciobanu@adelaide.edu.au)

Mineral deposits of Cu-sulphides and gold paragenetically associated with hematite and magnetite may also contain variable, in some cases economic levels of uranium and rare earth elements. The size of these deposits, e.g. Olympic Dam with an ore body in excess of 3x5x2km implies large, crustal scale fluid processes. Alteration of the host rock of these deposits is variable but distinct alteration mineral facies can be distinguished. The commonly identifed regional geochemical footprint of these REE anomalous deposits is a pronounced sodic alteration (albitisation) with accompanying formation of calc-silicate / magnetite / Fe-amphibole breccias and metasomatism. On the depositional side of the mineralising system we can distinguish two types of alteration asociated with Cu and Au mineralisation: i) a pyrite/magnetite dominated assemblage with pronounced potassic (biotite, K-spar) alteration and a predominance of chalcopyrite ± bornite, locally and variably overprinted by hematite + bornite + covellite + chalcocite. ii) a hematite dominated assemblage with bornite + covellite + chalcocite and much less chalcopyrite. Gold content appears related to sulphide abundance but Au rich zones with low sulphide grades are present. The different alteration/mineralisation zones have distinct REE patterns. The regional albitisation zone, which is seen as the source region of the metal components displays a path of initial depletion of LREE followed by an overall REE depletion as the involved rock is progressively converted to an albitite. Intermediate sections dominated by magnetite / biotite / K-spar alteration can have intense enrichment of REE including the formation of discrete RE minerals (allanite) but this appears to be most related to a late stage of the mineralising process. A pronounced enrichment of the REE occurs in the hematite / sericite dominated section, with REE rich barite and fluorite as well as RE minerals such as bastnaesite, florencite, monazite and xenotime. On the mineral grain scale enrichment of REE and U is pronounced in the hematite / sericite dominated part of the system.

https://doi.org/10.1180/S0026461X00006502 Published online by Cambridge University Press

Growth rate effect on Sr/Ca and Mg/Ca partitioning between calcite and fluid: *In situ* data

A.K. SCHMITT[1]*, R.I. GABITOV[1], A. SADEKOV[2] AND A.LEINWEBER[1]

[1]University of California, Los Angeles, CA, 90095, USA (*correspondence: axel@oro.ess.ucla.edu)
[2]University of Edinburgh, Edinburgh, *EH9 3JW, UK*

Sr/Ca and Mg/Ca (Me/Ca) abundances in speleothems, foraminifera, coccolith, and mollusks have been extensively used as paleotemperature proxies. However, inconsistencies exist between different Me/Ca-temperature calibrations which imply disequilibrium exchange of Sr/Ca and Mg/Ca between fluid and calcite, thereby jeopardizing their use as paleoclimate proxies unless the overriding physico-chemical and biological effects on elemental partitioning can be calibrated.

This study complements existing experimental data on Sr and Mg partitioning that are mostly based on bulk analysis of calcite precipitated at different rates. In our alternative approach, the advancing rate of the crystal surface was determined by sequentially spiking calcite-precipitating fluids with rare earth element (REE) dopants. *In situ* secondary ion mass spectrometry (SIMS) analyses of Me/Ca were performed on single crystals of experimentally grown calcite at relative external reproducibilities for both ratios of ~1 % (1s. d.). REE patterns reveal concentric domains of calcite growth. The growth rate of calcite generally decreases with time - i.e. crystal rims advanced at slower rates than cores. Fluids were sampled periodically for Me/Ca, dissolved inorganic carbon, and pH.

SIMS profiles across individual calcite crystals displayed depleted Sr/Ca and elevated Mg/Ca at crystal rims relative to interiors. The partition coefficient of Sr/Ca ($K_d^{Sr/Ca}$) increases by ~100±2% with increasing growth rate over the range of 1 to 8 μm/day (at 25°C). In contrast, $K_d^{Mg/Ca}$ decreases by ~33±16% over the same range.

Our results suggest that Sr (Mg) are enriched (depleted) in the near-surface region of calcite relative to the bulk crystal lattice. This observation is consistent with previous *in situ* data and the surface entrapment model [1, 2], which underscores that Sr/Ca and probably Mg/Ca in natural carbonates are not a direct proxy for marine and terrestrial temperature, and require corrections for the dependency of partitioning behavior on crystal growth rate.

[1] Gabitov & Watson (2006) *G-cubed* **7**, 11. [2] Watson (2004) *Geochim. Cosmochim. Acta* **68**, 1473–1488.

Zircon rim response to metamorphic and hydrothermal regime-change

D.A. SCHNEIDER[1] AND A.K. SCHMITT[2]

[1]Earth Sciences, University of Ottawa, Canada, K1V 6N5
[2]Earth & Space Sciences, University of California-Los Angeles, USA 90095

A significant advance in zircon geochronology is the recognition of different types of neoblastic growth and recrystallization during tectonism and mineral-fluid interaction. Such domains can form in zircon and other accessory minerals as a consequence of alteration and dissolution-precipitation processes across a range of P-T conditions, and as low as ~200 °C particularly when in the presence of fluids. Distinct chemical and isotopic signatures associated with these alteration regimes can reveal valuable geological information regarding the timing and source of fluid influx, as well as mineral-fluid interaction at the sub-grain level. Application of SIMS depth-profiling now permit unparalleled spatial resolution analysis (down to ~0.2 μm) of these thin alteration zones. Complementary LA-ICPMS depth-profiling allows detection of geochemical changes accurately down to ~5 μm. Depth-profiling of unpolished zircon or other accessory crystal species measures changes in radiogenic (U-Pb), stable isotopic ($\delta^{18}O$) and chemical (REE) signatures that translate into concentration-depth profiles as drilling progresses into the crystal's interior. One application is to resolve the source and timing of fluid-flow responsible for lode Au deposits of the Canadian Abitibi Province. Depth-profiling techniques successfully uncovered <3 μm alteration domains in wall-rock zircon, occurring as light REE-enriched "rims", and Th/U and ^{18}O values suggest that alteration involved limited crustal recycling. Zircon rim ages are significantly younger than host rock ages, and correlate to intensely mineralized and deformed quartz-carbonate-Au shear veins. Subsequent zircon alteration correlating to thin, shallow-dipping and less altered and mineralized vein networks occurred 20 m.y. later, and represents a late hydrothermal fluid pulse at the end of retrograde metamorphism. A similar approach revealed an episode of Eocene metamorphism (metasomatism?) in the western Cyclades of the Aegean, an area known for iron- and sulfide-ore skarn deposits. A dominant zircon population had a spongy structure created by complete recrystallization of the pre-existing crystal, possessing low Th/U and flat and depleted HREE patterns, and yielding Eocene ages with $\delta^{18}O$ ~7‰. Detailed pre- and post-analytical imaging is necessary to document crystal structures and mineral outgrowths. Depth-profiling on zircon is a successful, yet nascent application for the dating of mineral deposits and fluid flow.

https://doi.org/10.1180/S0026461X00006502 Published online by Cambridge University Press

A multi-component reactive transport model assessment of microbial processes and trace metal cycling across a gradient in sulfate reduction rates along the California Margin

A. SCHNEIDER MOR[1], C. STEEFEL[2] AND K. MAHER[1]

[1]Department of Geological and Environmental Sciences, Stanford University, Stanford, CA, 94305, USA (*correspondence: ayaschm@stanford.edu).
[2]Earth Sciences Division, Lawrence Berkeley National Laboratory Berkeley, CA 94720 USA

Sediments and pore water from 4 ODP Leg 167 sites along the California Margin (1011, 1017, 1018 and 1020) were used to compare biogeochemical processes across a gradient of sulfate reduction (SR) rates with the purpose of studying the processes that control these rates and how they affect trace metal redistribution. Measurements of the trace element composition of pore water and sediment along with $\%CaCO_3$, %biogenic silica, wt% carbon and $\delta^{13}C$ of Total Organic Carbon (TOC) were used to constrain the multicomponent reactive transport model CrunchFlow. The rates of sulfate reduction, methanogenesis and anaerobic methane oxygenation (AMO) were constrained by fitting the model to the measured concentration profiles. The sites are distinguished by the depth of AMO: a shallow zone is observed at sites 1018 (14 to 19 mcd) and 1017 (23 to 27 mcd), while deeper zones occur at sites 1011 (45 to 55 mcd) and 1020 (97 to 113 mcd). In general, the sulfate reduction rates are faster (on the order of $9\text{-}9.9*10^{-17}$mol/L/yr) for the shallow zones, compared to $1\text{-}1.4*10^{-17}$ mol/L/yr for the deeper zones. AMO rates are also faster at the shallow belt $2*10^{-7}$ mol/L/yr compared to $3*10^{-8}$ mol/L/yr at the deeper sites. Sites with shallow sulfate reduction zones appear to have high rates of AMO resulting in high alkalinity concentrations close to the sediment-water interface. The dissolved metal ion concentrations also varied between the sites, with Fe (0.01-7uM) and Mn (0.01-57uM) concentrations highest at Site 1020 (water depth 3000m) and lowest at site 1017 (water depth 950m). The highest Fe and Mn concentrations occurred at various depths, with no direct correlation to sulfate reduction and alkalinity maximum values. Modeling of the dissolved and solid SiO_2, Ca, Mg, K, Mn and Fe is used to establish the relationship between the biogeochemical reactions and trace metal variations and to better constrain the parameters that influence the trace metal distributions in the sediment column.

Dissolved reactive mangenese at pelagic redoxclines

B. SCHNETGER[1]* AND O. DELLWIG[2]

[1]Institute for Chemistry and Biology of the Marine Environment, University of Oldenburg, Germany (*correspondence: schnetger@icbm.de)
[2]Marine Geology Section, Leibniz Institute for Baltic Sea Research, Rostock, Germany

Experiments with suboxic freshwater and seawater suggest a dissolved reactive manganese fraction (dMn_{react}) that completely oxidizes within 36 h, mainly by microbial activity. The fast redox cycle of Mn drives the 'Mn pump' transporting metals into anoxic basins. A difference method can be used to determine dMn_{react}. One aliquot of a water sample is directly filtered and represents the total dissolved Mn. A second aliquot is aged under atmospheric oxygen and app. 20°C and filtered after 36 h representing the residual dissolved Mn(II). The concentration of dMn_{react} is calculated as difference of both aliquots.

Application to the Black Sea revealed dMn_{react} profiles comparable to published Mn(III) patterns analysed with a polarographic method. Both methods show that the upper part of the suboxic zone consists exclusively of dMn_{react} or Mn(III). dMn_{react} is a half quantitative measure of dissolved M(III), an unknown fraction of i) autocatalytic oxidation of dissolved Mn(II) by readily produced MnO_x and ii) microbial Mn(II) oxidation. Thus, the present method helps to assess the full potential for oxidation of dissolved Mn within an aquatic environment. The method has the advantage that sample preparation can be easily done on site, followed by analysis of dissolved Mn by conventional methods in the lab.

dMn_{react} was also detected in the Landsort Deep (Baltic Sea) with values distinctly increasing from the outer regions towards the central part (max. 3 μM). Similar to the Black Sea, dMn_{react} concentrations increase in the suboxic transition zone separating oxygenated and H_2S containing waters. In contrast, almost no dMn_{react} was present in the Gotland Basin (Baltic Sea). Pronounced lateral currents and turbulence in the Gotland Basin prevent the formation of a stable suboxic zone, a prerequisite necessary for accumulation of dMn_{react}. Such intrusions supply trace amounts of O_2 and H_2S thus causing either immediate oxidation/reduction of dMn_{react} or deteriora–tion of its stabilising ligands.

Analysis of dMn_{react} in the seasonally anoxic Lake Dagow (Germany) revealed maximal concentration of 6 μM. This value significantly exceeds the level of the Landsort Deep most likely due to the stable stratification of this lake during sampling.

https://doi.org/10.1180/S0026461X00006502 Published online by Cambridge University Press

Decoupled evolution of temperature and precipitation in Western Germany during the Last Interglacial reconstructed from a precisely dated speleothem

D. SCHOLZ[1,2]*, D. HOFFMANN[2,3], C. SPÖTL[4], P. HOPCROFT[5], A. MANGINI[6] AND D.K. RICHTER[7]

[1]Institute for Geosciences, University of Mainz, Germany (*correspondence: scholzd@uni-mainz.de)
[2]Bristol Isotope Group (BIG), School of Geographical Sciences, University of Bristol, United Kingdom
[3]CENIEH, Burgos, Spain
[4]Institut für Geologie und Paläontologie, Leopold-Franzens-Universität, Innsbruck, Austria
[5]Bristol Research Initiative for the Dynamic Global Environment (BRIDGE), School of Geographical Sciences, University of Bristol, United Kingdom
[6]Heidelberger Akademie der Wissenschaften, Germany
[7]Institute for Geology, Mineralogy and Geophysics, Ruhr-University Bochum, Germany

We present high-resolution $\delta^{18}O$, $\delta^{13}C$ and trace element profiles for stalagmite HBSH-1 from Hüttenbläserschacht-höhle, western Germany. The major part of the sample grew between 130 and 80 ka providing a climate record with decadal to centennial resolution for Marine Isotope Stage (MIS) 5. The record shows three growth interruptions during this period coinciding with the Greenland Stadials suggesting that stalagmite growth in this area is a very sensitive proxy for cool and dry conditions in the northern hemisphere.

We interpret stalagmite $\delta^{18}O$ as a proxy for past temperature changes, whereas stalagmite $\delta^{13}C$ rather reflects changes in the hydrologic balance. The $\delta^{13}C$ record shows three pronounced negative peaks during MIS 5, and the timing of those is in agreement with MIS 5e, 5c and 5a. This suggests warm and relatively humid climate in western Germany for these phases.

During the Last Interglacial, the evolution of $\delta^{18}O$ and $\delta^{13}C$ is opposite. Whereas the $\delta^{18}O$ signal suggests the warmest conditions around 125 ka followed by a gradual decrease, the $\delta^{13}C$ signal indicates wetter conditions towards the end of the Last Interglacial. This 'decoupling' of temperature and humidity during MIS 5e is also visible in a series of snapshot simulations performed using the general circulation model FAMOUS. The decoupling is probably related to the change in solar insolation, which influences the atmospheric dynamics and storm activity in the region.

Mumia vera – vera mumia?

BARBARA M. SCHOLZ-BÖTTCHER[1]*, ARIE NISSENBAUM[2] AND JÜRGEN RULLKÖTTER

[1]ICBM, University of Oldenburg, D-26111 Oldenburg, Germany (*correspondence: bsb@icbm.de)
[2]Dep. Environmental Science and Energy Research, Weizmann Institute of Science, Rehovot 76100, Israel

The drug *mumia vera* has a long tradition not only in Arabian but also in ancient European medicine. The knowledge in antiquity of the curativeness of asphalt combined with the belief in the magics of death made *mumia vera* a precious ingredient of medications with a very broad spectrum of indications. Since the 16th century it was even used as paint pigment. The export of mummies is supposed to have started in the 12th century and the drug was still available in 1924. Because the export of mummies was banned by the Arabs since the 17th century a more or less macabre market of substitutes developed.

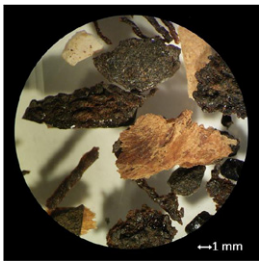

Figure 1 Reflected-light microscopy of the sample analysed

A small amount of ground *mumia vera* from a pharmaceutical vessel of the early 18th century was analysed on a molecular level. A number of diverse particles were hand-picked under the microscope and analysed separately via CP-pyrolysis GC-MS. Extracts were analysed by GC-MS. The ingredients of all particles exhibited a close relation to authentic ancient mummy material and published data in this field [1, 2, 3]. Besides fibres of linen and wood as well as embalming material (cedrium, pistacia turpentine, beeswax, Dead Sea asphalt) pieces of most probably human tissue and a wax-like substance (possibly a kind of adipocere) were found. Some inconsistencies in the data point to a mixture of material most plausibly due to occasional refilling of the vessel. Genuine mummy material milled as a whole obviously was used as medicine in the present case.

[1] Koller *et al*. (2005) *Archaeometry* **47**, 609–628.
[2] Buckley & Evershed (1999) *Analyst* **124**, 443–452.
[3] Rullkötter & Nissenbaum (1988) *Naturwissenschaften* **75**, 618–62.

https://doi.org/10.1180/S0026461X00006502 Published online by Cambridge University Press

Experimental constraints on Ag isotope fractionation during planetary core formation

M. SCHÖNBÄCHLER[1]*, K.J. THEIS[1] AND B.J. WOOD[2]

[1]SEAES, The University of Manchester, M13 9PL, UK (*correspondence: m.schonbachler@manchester.ac.uk)
[2]Department of Earth Sciences, University of Oxford, Parks Road, Oxford, OX1 3PR, UK

A recent study [1] proposes a heterogeneous accretion scenario for the Earth, which is for the first time based on isotopic constraints from the short-lived Pd-Ag, Mn-Cr and Hf-W decay systems. The study concludes that the Earth inherited the major part of its moderately volatile element depletion from its building blocks. The model also requires a late addition of volatile-rich material while core formation was still active. These findings are in good agreement with work based on elemental abundances of the BSE (Bulk Silicate Earth) and partitioning experiments (e.g. [2]) as well as dynamic models of the accretion and planet formation [3]. The late addition of volatile-rich material is mainly required by the Pd-Ag decay system to explain the identical Ag isotope compositions but different Pd/Ag ratios of CI chondrites and BSE.

The need for a late volatile-rich addition can be relaxed by proposing that the true BSE Ag isotope composition is more radiogenic (~ +1.2 epsilon^{107}Ag/^{109}Ag) than the measured value (-2.2 ± 0.7 [1]), because the latter was modified by extraction of light Ag into the Earth's core. To explore this possibility, we performed experiments on mixtures of silicate, sulphide and metal in a piston-cylinder apparatus at 1.5 GPa and 1800 K. Metal and silicate phases of the run products were manually extracted and analysed for Ag isotopes on a MC-ICPMS following the protocol of [4]. The Ag isotope compositions obtained for metal and silicates were identical within the analytical uncertainty (± 0.5 epsilon). This demonstrates that Ag isotope fractionation is negligible at the investigated conditions. Isotope fractionation generally decreases with T^{-2} at the temperature range considered for metal-silicate equilibration in a deep magma ocean. Therefore it is likely that Ag isotopes do not fractionate at conditions predicted for terrestrial core formation (higher T and P). Moreover, the experimental results also show that Ag partitioning into the metal increases with sulphur content.

[1] Schönbächler *et al*. (2010) *Science* **328**, 884. [2] Wood *et al*. (2008) *GCA* **72**, 1415. [3] O'Brien *et al*. (2006) *Icarus* **184**, 36. [4] Schönbächler *et al*. (2007) *Int. J. Mass Spec*. **261**, 183.

Evidence of mantle heterogeneity underneath slow-spreading ridges? Case study at 45°N mid-Atlantic ridge

N SCHROTH[1]* AND B.J. MURTON[2]

[1](*correspondence: ns2r07@noc.soton.ac.uk)
[2](bramley.murton@noc.soton.ac.uk)

Axial volcanic ridges (AVR) are a ubiquitous feature along mid-oceanic ridges. Although numerous studies have been performed on their structure and volcanic activity, many questions still remain unanswered, e.g. do AVR basalts have a common parental magma, and are the basalts derived from different magma chambers erupting at different times?

During cruise JC24 in 2008, nearly 300 basaltic samples were collected with the ROV ISIS in order to answer some of these questions.

A large dataset has now been compiled and some preliminary results will be presented. Rare earth element (REE) data coupled with trace element data of 30 samples revealed three different groups of samples. Group I is charaterized by low La/Yb, incompatible element concentrations between normal and enriched mid-oceanic ridge basalt (N- and E-MORB). Group III has highly elevated La/Yb ratios, and a pattern of incompatibles that is more enriched in light REE than E-MORB. Group II lies in between but shows clear gaps to both other groups.

As REEs are not available for all samples yet, the incompatible and alteration-resistant elements Nb-Zr-Y were used to extend the grouping to a further 230 samples analysed by XRF. The results are coherent with the REE groupings. In addition, groups II and III could be subsequently split into subgroups.

The most enriched samples occur on (1) flat-topped volcanoes, situated off-AVR, (2) in the median valley near these volcanoes, (3) in the median valley walls on the western side as well as in the western axial floor, and (4) at the northern tip of the main AVR structure. Group II occurs on the axial floor north and west of the AVR, in the western median valley wall, and at the northern and southern tips of the AVR.

It is the aim of this study to reveal connections between volcanic structures, as well as to define the various melt sources.

Wider implications of this study are insights into the magma storage and plumbing underneath the AVR, and a detailed geochemical map of a (typical) mid-Atlantic ridge segment.

https://doi.org/10.1180/S0026461X00006502 Published online by Cambridge University Press

Lessons to learn from amino acid distribution in POM of Lake Baikal

CARSTEN J. SCHUBERT[1], JUTTA NIGGEMANN[2], MICHAEL STURM[1], BENTE LOMSTEIN[3] AND MATTHEW D. MCCARTHY[4]

[1]Eawag, Swiss Federal Institute of Aquatic Science and Technology, SURF, Kastanienbaum, Switzerland (carsten.schubert@eawag.ch)
[2]Forschungsgruppe der Max-Planck-Gesellschaft - Marine Geochemie - Carl von Ossietzky Universität, Oldenburg, Germany
[3]Department of Biological Sciences, Section for Microbiology, University of Aarhus, Aarhus, Denmark
[4]Ocean Sciences Department, University of California, Santa Cruz,

Lake Baikal offers a unique opportunity to study water column processes in a freshwater system with conditions similar to oceanic systems. With a maximum water depth of ~1640 m, Lake Baikal is the deepest lake on Earth and due to efficient vertical mixing, oxygen concentrations are high throughout the water column.

Furthermore, although Lake Baikal receives considerable input of suspended particles via rivers, primary production in the surface waters is the major source of carbon and energy for organisms in deeper water layers and in the sediments.

Sediment trap material from Lake Baikal, collected at 18 different water depths (50-1350 m), has been investigated for total hydrolysable amino acids (THAA) and amino acid D- and L-enantiomers. The THAA flux decreased by 50% in the upper 500 m and remained constant below this depth, indicating that organic matter (OM) degradation was mostly restricted to the upper water column.

We additionally measured nitrogen isotopes on THAA (POM) from different water depths that allowed for determination of source and food web changes.

The dependence of ^{222}Rn air-water partitioning on water temperature and water salinity

MICHAEL SCHUBERT AND ALBRECHT PASCHKE

Helmholtz Centre for Environmental Research – UFZ, Permoserstr. 15, 04318 Leipzig, Germany

Radon (^{222}Rn) is used as natural aquatic tracer for many applications. A prominent example is its use as indicator for submarine groundwater discharge (SGD) processes.

On-site radon-in-water detection is performed by means of a mobile radon-in-gas monitor and radon extraction from the water into a closed circulating air volume. For converting the detected radon-in-air concentration into radon-in-water values the water/air partition coefficient ($K_{w/air}$) needs to be known.

$K_{w/air}$ depends on two water parameters that are easily attainable on site: temperature and salinity. Possible values for $K_{w/air}$ cover a range between about 0.50 (cold fresh water) and 0.03 (hot saline water). The temperature dependence of $K_{w/air}$ applies for all environments (terrestrial and marine) and is generally taken into consideration. The 'salting out' of radon, however, is often underestimated or not accounted for at all, potentially leading to an erroneous data interpretation.

Theoretical considerations that are based on reported data as well as on an extensive own dataset resulted in the easily applicable equation shown below. The equation allows for uncomplicated consideration of the dependence of $K_{w/air}$ on both, temperature (T [K]) *and* salinity (S [‰]) (see Fig. 1).

$$\ln\beta = -56.90 + 92.49\left(\frac{100}{T}\right) + 22.24\ln\left(\frac{T}{100}\right) + S\left\{-0.219 + 0.138\left(\frac{T}{100}\right) - 0.022\left(\frac{T}{100}\right)^2\right\}$$

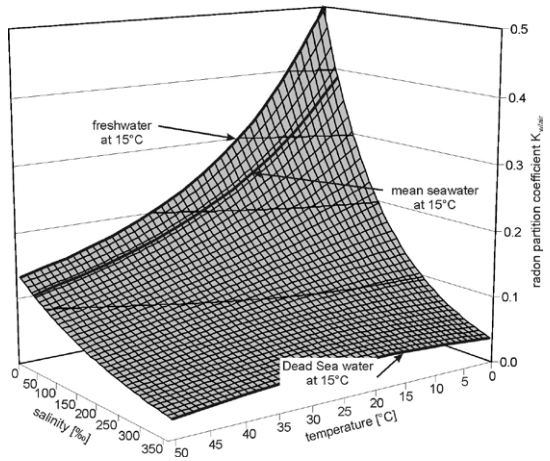

Figure 1: Dependence of the air/water partitioning coefficient ($K_{w/air}$) of radon on water temperature and salinity (*cf.* Eq. 1)

https://doi.org/10.1180/S0026461X00006502 Published online by Cambridge University Press

Exploring micro-scale stable isotope variations using femtosecond laser ablation MC-ICP-MS

J.A. SCHUESSLER AND F. VON BLANCKENBURG

German Research Centre for Geosciences GFZ, Section 3.4, Earth Surface Geochemistry, Potsdam, Germany (jan.schuessler@gfz-potsdam.de)

We present advancements in micro-scale analyses of non-traditional stable isotopes using a second generation custom build femtosecond laser ablation system coupled to a multicollector ICP mass spectrometer.

The heart of our laser ablation system is based on the latest generation Ti-Saphire regenerative amplifier system *Spectra Physics Solstice*, which produces 100 fs infrared (IR) laser pulses with up to 3.7 mJ/pulse. Non-linear optics are used to convert the fundamental IR wavelength into the UV with a wavelength of 196 nm and an adjustable pulse energy of up to of 0.1 mJ/pulse. The system provides full control on laser parameters, such as spot size, energy density, pulse width, repetition rate (continuous from 1 to 1000 Hz) and beam shape. The spot size can be varied from 10 to 100 μm in diameter with energy densities on the sample between 0.1 and 50 J/cm^2.

The laser beam is delivered to the sample (thin sections or polished blocks contained in a He-flushed sample cell) through a fully automated and computer controlled microscope stage, modified with UV optical components to focus the laser beam and visualise the sample surface. Special emphasis in the construction was given to high quality optical imaging of the sample, while maintaining an optimum laser beam quality.

A custom-designed software allows integrated control on laser parameters, sample positioning and observation, as well as fully automated analyses through a synchronised operation with a *Thermo Neptune* MC-ICP-MS, equipped with a *Neptune Plus Jet Interface* for increased sensitivity.

We will present results on optimized analytical conditions for stable isotopes measurments of Fe, Si, and Mg at the micro scale in various matrices, such as minerals, glasses, and soils.

Climate change and the KISS principle

R.D. SCHUILING[1]*, O. TICKELL[2] AND S.A. WILSON[3]

[1]Institute of Geosciences, Utrecht University, the Netherlands (*correspondence: schuiling@geo.uu.nl)
[2]Oxford Climate Associates/Kyoto2 (oliver.tickell@kyoto2.org)
[3]Dept. Geological Sciences, Indiana University, Bloomington (siowilso@indiana.edu)

Mineral carbonation is the logical answer to rising CO_2 levels. The CO_2 is captured in a safe and sustainable way and returned to the rock record as solid carbonates. The recipe is simple and straightforward:

-select an abundant material that weathers easily (olivine or serpentine)

-mine and mill this material

-spread it in a favorable climate for weathering

Instead of leaving it at that, and follow the KISS principle (Keep It Simple, Stupid), most researchers try to develop techniques to speed up the carbonation. This costs extra energy and money. This is a major reason why the storage of CO_2 in abandoned oil and gas fields, or in saline aquifers is still the favored mitigation strategy. Mineral carbonation has been overlooked, mainly because researchers have made it too complicated in their attempts to speed up the reaction.

There is no need to speed up the reaction, as olivine grains of 100 μm weather and capture CO_2 in a few years in a suitable climate. Extrapolation of abiotic experiments suggests that weathering is not fast enough. Outside the laboratory the role of biotic factors like mycorrhizal fungi on land or lugworms on tidal flats has been demonstrated, which speed up the weathering reaction by factors of ten to almost one thousand. Crushed serpentinite mine tailings in British Columbia are known to weather fifty times faster than basaltic tuffs in even the most favorable climate for weathering.

For the global C-cycle it makes no difference where the CO_2 is captured, as the atmosphere is a well mixed reservoir on the timescale of a few months. Capturing and storing of CO_2 from flue gases is too expensive. The separation step alone costs already considerably more than straightforward enhanced weathering.

The strategy for enhanced weathering relies upon olivine mined in the wet tropics. This material is milled and the grains are spread over the surrounding area. The whole operation (mining, milling and transport) will cost around 10 Euro/ton of captured CO_2. Negative effects on the environment are unlikely.

https://doi.org/10.1180/S0026461X00006502 Published online by Cambridge University Press

Nanocalcite as a model for biogenic, geological calcite

L. SCHULTZ*, M.P. ANDERSSON, D. OKHRIMENKO, K.N. DALBY AND S.L.S STIPP

Nano-Science Center, Department of Chemistry, University of Copenhagen, Denmark (*correspondence: lschultz@nano.ku.dk)

Many geological systems, including chalk, limestone, and calcareous sandstone, contain sub-µm (nano), biogenic calcite formed by organisms long ago. These systems are intimately linked to environmental and economic interests (e.g. aquifers and petroleum reservoirs). Many geochemical research studies seek to understand the transformation (e.g. growth/dissolution) and reactive influence of calcite on pore fluids. For model system calcite, studies typically use commercial samples or calcite synthesized from super-saturated solutions of Ca^{2+} and CO_3^{2-}. The particle size of these types is generally much larger than biogenic calcite, and industrial calcite often contains trace amounts of the chemicals used during the manufacturing process or for ensuring good storage properties.

We explored an alternative method for synthesizing nanocalcite by carbonating a Ca $(OH)_2$ slurry using gaseous CO_2. This method has been used for industrial product improvement, but the use of nanocalcite as a model research system with high purity and surface area has not been explored.

Surface- and bulk-sensitive techniques, including X-ray photoelectron spectroscopy (XPS), infrared spectroscopy (IR), and X-ray diffraction (XRD), indicate negligible contamination from unreacted hydroxyl or trace metals. Further, there was no evidence of other $CaCO_3$ polymorphs, vaterite or aragonite. SEM showed agglomerations of nanostructured particles and the BET method quantified specific surface area in the range from 13-16 m^2/g. IR spectra of industrial calcite, geological calcite (chalk) and nanocalcite displayed distinctly different peak widths, in the order of nanocalcite < chalk < industrial calcite. This indicates that nanocalcite has a relatively high degree of crystallinity and few defects.

This study shows that nanocalcite might improve research results in studies that seek to understand processes in ultrafine geological calcite. Ongoing work will use nanocalcite to more effectively analyze recrystallization rates and surface reaction/adsorption phenomena that are important to aquifer and oil reservoir applications.

Timing of early solar system homogenization from p-process ^{180}W heterogeneities

T. SCHULZ[1,2]* AND C. MÜNKER[1]

[1]Institut für Geologie und Mineralogie, Universität Köln, Germany

[2]Department of Geological Sciences, University of Vienna, Austria (*correspondence: toni.schulz@univie.ac.at)

Introduction

Collapse and subsequent formation of the solar system may have been triggered by a nearby supernova. This can explain the injection of freshly synthesized short-lived radionuclides into the young solar system and can also account for the presence of nucleosynthetic isotope anomalies in meteorites. In order to trace the mixing history of nuclides in the early solar system, we performed the first analyses of one of the rarest isotopes in the solar system, p-process ^{180}W (ca. 0.1 % relative abundance).

Methods and Results

Measurements were conducted using a Neptune ICP-MS, equipped with high sensitivity 10^{12} Ohm resistors. For most analyzed iron meteorites, clearly resolvable ^{180}W excesses (up to +7 $\varepsilon^{180}W$-units) were measured, whereas metals from chondrites and IAB iron meteorites overlap with the terrestrial value. There are distinct ^{180}W abundance variations between different groups of iron meteorites.

Discussion and Conclusion

Our first data provide clear evidence for an increasing homogenization of the early solar system by decreasing ^{180}W anomalies with decreasing age, suggesting mixing-timescales in the order of several million years. As most asteroidal parent bodies accreted and differentiated during this time span parent nuclides of short lived decay systems may not have been homogeneously distributed in the early solar system.

Because the production of ^{180}W requires distinct stellar environments, multiple supernovae explosions may have affected the early solar system, thus further weakening the astrophysical view that protostars have formed in relative isolation from their molecular cloud neighbours [1].

[1] L.W. Looney, J.J. Tobin, B.D. Fields (2006) *APJ* **652**, 1755.

https://doi.org/10.1180/S0026461X00006502 Published online by Cambridge University Press

Could bacterial residues be an important source of SOM? – A case study from a glacier forefield

CHRISTIAN SCHURIG[1]*, RIENK SMITTENBERG[2], JÜRGEN BERGER[3], ERIKA KOTHE[4], ANJA MILTNER[1] AND MATTHIAS KÄSTNER[1]

[1]Helmholtz Centre for Environmental Research –UFZ, Environmental Biotechnology, Leipzig, Germany (*correspondence: christian.schurig@ufz.de)
[2]ETH Zürich, Geology Department, Zürich, Switzerland (smittenberg@erdw.ethz.ch)
[3]Max Planck Institute for Developmental Biology, Electron Microscopy Unit, Tübingen Germany
[4]Friedrich Schiller University of Jena, Microbial Phytopathology, Jena, Germany

Recently, stocks of soil organic matter (SOM) have been shown to decrease in European soils and also worldwide, which compromises soil fertility and enhances emissions of carbon dioxide to the atmosphere. However, the general structure of SOM, and thereby the mechanisms behind its genesis and loss, remain unclear.

In this framework, microbial biomass is generally regarded to be of low importance for SOM formation. In particular on freshly exposed surfaces, however, bacteria colonize barren mineral surfaces faster than fungi or higher plants. Moreover, recent results indicate that bacterial cell wall fragments frequently occur on soil mineral surfaces and also accompany the microbial colonization of previously clean and sterile activated carbon surfaces after incubation in groundwater. Hence, we hypothesized that, at least, in the initial stages of soil formation bacteria and their fragments may play an important role in particulate SOM formation bearing in mind that most dead organic matter entering the soil is processed by bacteria.

This hypothesis was proven by tracing the development of SOM in a chronosequence with samples from the forefield of a receding glacier (Damma-glacier, Canton Uri, Switzerland) by scanning electron microscopy and other methods. The initially barren mineral surfaces have been shown to be rapidely covered with microbial residues as soil age increases. Moreover, this data compares well to growing C/N-ratios, water contact angles and fatty acid contents in earlier deglaciated samples.

Iron isotope fractionation in soil solutions of a Gleysol

STEPHAN SCHUTH[1,2]* AND TIM MANSFELDT[1]

[1]Department of Geosciences, Soil Geography/Soil Science, University of Köln, Germany
[2]Institute for Mineralogy, Leibniz University Hannover, Germany (*correspondence: s.schuth@mineralogie.uni-hannover.de)

Analyses of Fe isotope compositions in a Gleysol with petrogleyic properties from NW Germany yielded bulk δ^{57}Fe values of +0.29‰ (Ah horizon, Fe_{total} ca. 50 g/kg) to –0.30‰ (Bg horizon, Fe_{total} ca. 320 g/kg). A special feature of this Gleysol is a local massive enrichment of Fe (hydr)oxides (comprising mostly goethite and ferrihydrite). In contrast to the overlying CrBg and Bg horizons, the 2Cr horizon which developed from glaciofluvial sands, is characterized by a relatively high δ^{57}Fe value of +0.22‰, but lowest total Fe amounts (ca. 7 g/kg).

To evaluate the relationship of Fe isotope composition of the four horizons and their soil solution, we sampled the soil solution at different depths during spring and autumn. Water of a nearby stream and Fe-rich precipitates in the stream sediments were additionally sampled.

The Fe isotope composition and Fe concentration of the soil solution strongly varied with both depth and abundance of Fe (hdr)oxides, but revealed little seasonal effects. We observed extremely low δ^{57}Fe values of –2.8‰ and Fe concentrations of ca. 3 mg/L in the soil solution of the CrBg horizon. In contrast, the soil solution obtained from the underlying sandy 2Cr horizon is characterized by δ^{57}Fe values of –1.5‰ and high Fe concentrations of up to 60 mg/L. The water of the adjacent stream showed δ^{57}Fe values of –0.03‰, whereas the Fe-rich precipitates in the stream bed are marked by a high δ^{57}Fe value of +0.55‰.

We conclude that the low δ^{57}Fe values in the soil solution are the result of preferential adsorption and precipitation of heavy Fe isotopes on abundant Fe (hydr)oxide phases in the CrBg horizon. The Fe-poor 2Cr horizon lacks this capability, therefore, higher δ^{57}Fe values and Fe concentrations are observed in its soil solution. For the Fe-rich precipitates of the stream, preferred removal of heavy Fe isotopes during precipitation entailed high δ^{57}Fe values.

https://doi.org/10.1180/S0026461X00006502 Published online by Cambridge University Press

Evaluation of lake biomarkers as indicator of environmental changes along a climatic gradient in Cameroon

VALÉRIE SCHWAB-LAVRIČ[1]*, YANNICK GARCIN[2], DIRK SACHSE[2], GILBERT TODOU[3], OLIVIER SÉNÉ[4], JEAN-MICHEL ONANA[4], GASTON ACHOUNDONG[4] AND GERD GLEIXNER[1]

[1]Max-Planck-Institut für Biogeochemie, Jena, Germany (*correspondence: vschwab@bgc-jena.mpg.de)
[2]DFG-Leibniz Center for Surface Process and Climate Studies, Institut für Erd- und Umweltwissenschaften, Universität Potsdam, Germany
[3]École Normale Supérieure, University of Maroua, Cameroon
[4]National Herbarium of Cameroon, IRAD, Yaoundé, Cameroon

Small crater lakes that have not been exposed to anthropogenic impacts are considered as sensitive recorders of environmental conditions. Here, we studied changes in lipid composition of sediments and water particles organic matter (POM) from lakes, and soils from lake catchments collected in Cameroon along a large environmental gradient (rainfall of ~ 4000 to 700 mm per year) to evaluate sedimentary lipids as indicators of local and regional environmental changes in the tropics.

Large abundances of an unresolved complex mixture and bacterial lipids in water POM, higher relative concentration of terrestrial refractory lipids in deeper water POM as well as differences in compound distributions and abundances between sedimentary and aquatic lipids indicate intense degradation of primary autochthonous organic matter throughout the water column. No characteristic changes in the distribution patterns of the major compounds, short- and long-chain *n*-alkanes, *n*-alkenes, alcohols and fatty acids, in the studied samples along the environmental gradient indicate that distribution of these source-specific biomarkers may not be appropriate to reconstruct ecosystem changes in tropical fossil records. In sediments, tetra- and penta-cyclic triterpenoids, principally consisting of brassicasterol and mainly terrestrial plants-derived stigmasterol and β-sitosterol, increase in abundance with rainfall. Campesterol is identified only in the drier zones. C_{32}-C_{34} botryococcenes usually associated with the freshwater *B. braunii* algae were found in soils and lake sediments of the rainiest site. A possible terrestrial contribution of these compounds to lake sediments in this environment will be discussed.

$PM_{2.5}$ chemical composition at rural background site in Central Europe

J. SCHWARZ[1]*, J. KARBAN[1], V. HAVRÁNEK[2], E. CHLUPNÍČKOVÁ[3] AND J. SMOLÍK[1]

[1]Institute of Chemical Process Fundamentals AS CR, Prague, Czech Republic (*correspondence: schwarz@icpf.cas.cz)
[2]Institute of Nuclear Physics AS CR, Řež at Prague, CR
[3]Czech Hydrometeorological Institute, Prague, CR

$PM_{2.5}$ mass and its chemical composition was studied from Feb 2009 to Mar 2010 at Czech rural backgroud site Košetice. The site is located about 80 km SE from Prague and it is part of EMEP, EUSAAR, and ACTRIS networks. Samples were taken 24 hours each 6th day, in total, 70 samples were analyzed. Besides gravimetry, water soluble ions (IC), elements (PIXE), OC/EC (TOT method) and levoglucosan (GC-MS) were analyzed.

The mass closure was calculated between $PM_{2.5}$ mass and analyzed species. The concentration of crustal elements (Al, Si, Ca, Ti, Fe, Mn were recalculated to their oxides, OC (corrected for positive sampling artifact) and EC were converted to OM resp. EC mass using factor 1.6 resp. 1.1. Using these factors the total analyzed mass was equal to 90% of $PM_{2.5}$ mass determined using gravimetry in average. A resulting average chemical composition of $PM_{2.5}$ mass at Košetice site is shown in the Fig. 1.

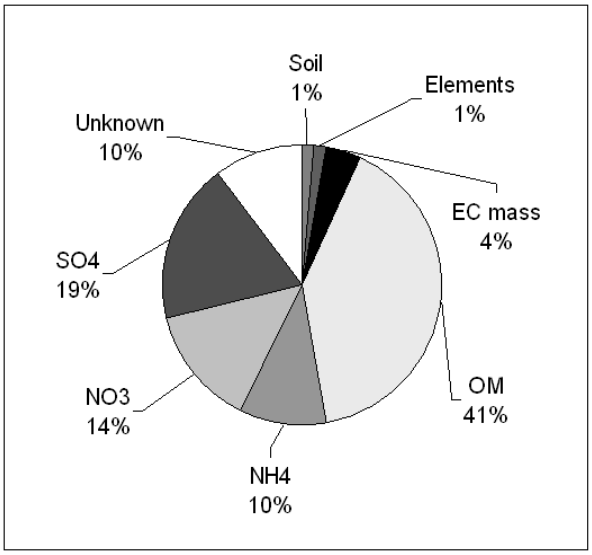

Figure 1: Average composition of PM2.5 at Košetice

$PM_{2.5}$ was dominated by OM and secondary inorganic ions. We thank for support to GA CR by grant No.205/09/2055.

https://doi.org/10.1180/S0026461X00006502 Published online by Cambridge University Press

The Ligurian ophiolite: An analogue to marine serpentinite-hosted hydrothermal systems

E.M. SCHWARZENBACH*, G.L. FRÜH-GREEN AND S.M. BERNASCONI

ETH Zurich, Department of Earth Sciences, Zurich Switzerland
(*correspondence: esther.schwarzenbach@erdw.ethz.ch)

Carbonate-veined mantle sequences in ophiolites exposed on continents show strong similarities to oceanic core complexes and to moderate temperature, peridotite-hosted hydrothermal systems found along slow-spreading ridges. Serpentinization processes associated with exposure of mantle rocks at the ocean floor thereby play a fundamental role in the global marine bio-geochemical cycles and in mass transfer between seawater and the oceanic lithosphere. Here we present a mineralogical and C and S geochemical study of serpentinites and ophicalcites from an ophiolitic sequence in the Northern Apennine (Italy) and compare this sequence to calcite-veined serpentinites from the Iberian Margin and serpentinites from the basement of the Lost City Hydrothermal Field. The comparison between ancient and modern peridotite-hosted hydrothermal systems provides constraints on fluid pathways, fluid fluxes, redox conditions and microbial activity and their time-integrated changes.

The Northern Apennine ophiolites include serpentinites and ophicalcites that are bounded by shear zones that form domal structures and are characterized by distinct talc-amphibole-chlorite alteration assemblages, which strongly resembles the damage zones associated with detachment faults along ocean ridges. The serpentinites and ophicalcites record multiple phases of seawater infiltration, with initiation of serpentinization above ~300°C and calcite precipitation at temperatures < ~150°C. The sulfide mineralogy is dominated by pentlandite, pyrrhotite, pyrite, millerite and siegenite, which reflects fairly oxidizing conditions and corresponds to redox-gradients typically found in oceanic serpentinites. The sulfur isotope signatures also indicate a multiphase history of fluid-rock interaction, but show a strong influence from microbial activity, similar to signatures in serpentinites from the Iberian Margin. Field and mineralogical observations show a strong relation of the Northern Apennine ophiolite to an oceanic setting near a mid-ocean ridge associtiated with detachment faults. In addition, the results of our study suggest that major fault zones strongly influence fluid circulation in these hydrothermal systems and control the incorporation of both carbon and sulfur from seawater.

Base metal ore deposits and marine mineral resources: Rare metal sources for sustainable energies?

U. SCHWARZ-SCHAMPERA

Federal Institute for Geosciences and Natural Resources, 30655 Hannover, Germany.

The progress in modern electronic technologies and the need for the use of renewable energies both increase the worldwide demand for metals and metalloids that are critical in high-technology products. There is significant and increasing demand for trace elements like indium, gallium, tellurium, selenium, molybdenum, cadmium, but also for major commodities like nickel, cobalt, copper. The group of so-called 'electronic metals' is already an integral part in most technical houseware and office products i.e., computers, notebooks, televisions, cell phones. New technologies and the need for renewable energy concepts in times of global climate changes lead to growing markets in photovoltaic industries. All major worldwide economies face a 20% - target of energy production from renewable energies until 2020. High-efficiency thin-film devices base on metals like indium, gallium, cadmium, tellurium, selenium, molybdenum; their substitution by keeping the high efficiency remains undeveloped. The market situation for these trace elements is tight and demand increases by an increasing number of industrial consumers. Production comes from known ore deposits on land and requires suitable and qualified technical facilities for the recovery of these trace components as by-products from conventional base metal concentrates. Few land-based ore deposits are known to host and produce these trace metals. Production increase, however, is limited due to restrictions on the production of the main commodities, metallurgical constraints, and limited refining capacities. A number of additional ore deposits, however, are capable to meet the demand if more scientific and technical effort is laid on the by-products. As a potential future source, marine mineral resources like manganese nodules, manganese crusts, and polymetallic massive sulfides are locally highly enriched in these trace metals and may define additional reserves. Enrichment factors, elevated concentrations, the mineralogical control, and ore characteristics in base metal deposits represent favourable conditions for the recovery of these metals. The actual production and demand situation is presented for the most important 'electronic metals' and the enhanced potential of ore deposits and marine resources in the future supply is discussed.

https://doi.org/10.1180/S0026461X00006502 Published online by Cambridge University Press

Revisiting the age of the Merensky Reef, Bushveld Complex

JAMES S. SCOATES[1], COREY J. WALL[1], RICHARD M. FRIEDMAN[1] AND KEVIN R. CHAMBERLAIN[2]

[1]Pacific Centre for Isotopic and Geochemical Research, University of British Columbia, Vancouver BC, V6T1Z4 (Canada, jscoates@eos.ubc.ca)

[2]Department of Geology and Geophysics, University of Wyoming, Laramie WY, 82071, USA

The giant Paleoproterozoic Bushveld Complex in the Kaapvaal craton of South Africa may have been emplaced and crystallized in a relatively short period of time [1], perhaps as little as a few million years, followed by rapid cooling [2]. Determination of the absolute duration of Bushveld-related magmatism requires careful application of the single-grain chemical abrasion ID-TIMS, or CA-TIMS, U-Pb zircon method. We recently reported a CA-TIMS zircon age for a sample of the PGE-rich Merensky Reef (West Mine, Rustenburg Section) in the Western Limb of the Bushveld Complex with a weighted mean $^{207}Pb/^{206}Pb$ age of 2054.4 ± 1.3 Ma (2σ, decay constant errors not included, n = 6) [3]. Use of the EARTHTIME ^{205}Pb-^{233}U-^{235}U tracer and synthetic U/Pb standard solutions now allow for assessing intra- and inter-laboratory reproducibility. We provide a new U-Pb age for zircon from a sample of the Merensky Reef in the Eastern Limb of the complex (Farm Driekop), 2055.30 ± 0.61 Ma (MSWD = 0.43, n= 10), and a revised age based on new analyses for our sample of the reef from the Western Limb, 2056.13 ± 0.70 Ma (MSWD = 0.44, n = 8). All ages were Th-corrected using Th/U = 3, characteristic of the B-1 and B-2 marginal rocks related to the Upper Critical Zone [4]. Compiled results for analyses of the 2000 Ma EarthTime standard solution are 1999.75 ± 0.47 Ma (MSWD = 0.42, n = 18). Analyses conducted at Wyoming by CA-TIMS, with EARTHTIME tracer and standard solutions, on zircon from the Western Limb sample yield a preliminary age of 2056.1 ± 1.1 Ma (MSWD = 0.096, n = 6). This interlaboratory comparison reveals that the crystallization age of the Rustenburg Merensky Reef sample is slightly older than the age reported in [3], although within analytical uncertainty. These results demonstrate the contemporaneity of these Merensky Reef samples, separated by ~300 km, and the potential for distinguishing magmatic events within the Bushveld Complex different in age by 1-2 million years.

[1] Cawthorn & Walraven (1998) *J. Petrol.* **39**, 1669–1687. [2] Nomade *et al.* (2004) *J. Geol. Soc. London* **161**, 411–420. [3] Scoates & Friedman (2008) *Econ. Geol.* **103**, 465–471. [4] Barnes *et al.* (2010) *Econ. Geol.* **105**, 1491–1511.

Tracking Archean seawater trace metal inventories through multi-proxy analysis of euxinic black shales

C.T. SCOTT[1]*, N. PLANAVSKY[2], B. KENDALL[3], B. WING[1], A. BEKKER[4], A.D. ANBAR[3] AND T.W. LYONS[2]

[1]McGill University, Montreal, QC H3A 2A7, Canada (*correspondence: clinton.scott@mcgill.ca, boswell.wing@mcgill.ca)

[2]University of California, Riverside, CA 92521, USA (planavsky@gmail.com, timothyl@ucr.edu)

[3]Arizona State University, Tempe, AZ 85287, USA (brian.kendall@asu.edu, anbar@asu.edu)

[4]University of Manitoba, Winnipeg, MT R3T 2N2, Canada (bekker@cc.umanitoba.ca)

Seawater concentrations of biologically significant and redox-sensitive trace metals have varied through time, reflecting intimate coupling of geological and biological processes in the Earth System. Euxinic black shales, organic carbon-rich mud rocks deposited beneath sulfidic bottom waters, are commonly enriched in such trace metals. Recent work focusing on Mo enrichments have demonstrated the potential to use geochemical analyses of euxinic black shales to track temporal trends in the concentrations of other trace metals in seawater [1].

Multiple episodes of euxinic deposition have recently been identified in the Archean [2-4]. In this study we compare the enrichments of a suite of biologically relevant trace metals (Fe, Mo, Cu and Zn) from Archean euxinic black shales in order to identify temporal trends in their relative abundance in seawater. To strengthen our arguments for faithful preservation of seawater chemistry and to facilitate comparison between Archean shales, as well as comparisons to euxinic shales deposited throughout Earth history, we present our study in the context of additional redox proxies, including TOC, Fe speciation, multiple S isotope analyses and Re-Os systematics.

[1] Scott *et al.* (2008) *Nature* **452**, 456–459. [2] Reinhard *et al.* (2010) *Science* **326**, 713–716. [3] Kendall *et al.* (2010) *Nature Geoscience* **3**, 647–652. [4] Scott *et al.* (2011) *Geology* **39**, 119–132.

https://doi.org/10.1180/S0026461X00006502 Published online by Cambridge University Press

Seasonal variations in microbial carbon cycling in freshwater wetland sediments identified through rate assays, lipid biomarkers, and porewater geochemistry

KATHERINE E. SEGARRA[1], VLADIMIR SAMARKIN[1], MARCOS Y. YOSHINAGA[2], FLORENCE SCHUBOTZ[2,3], VERENA B. HEUER[2], KAI-UWE HINRICHS[2] AND SAMANTHA B. JOYE[1]*

[11]Department of Marine Sciences, The University of Georgia, Athens, GA, USA(*correspondence: mjoye@uga.edu)
[2]Marum, Center for Marine Environmental Sciences and Department of Geosciences, Leobener Str., 28359 Bremen, University of Bremen, Germany
[3]Department of Earth, Atmospheric and Planetary Sciences, MIT, Cambridge, USA

Freshwater wetlands account for about 25% of the annual methane emissions to the atmosphere. A potential positive feedback exists between global warming and the production of this powerful greenhouse gas in sediments. This study explored seasonal variations in the dominant pathways (e.g. methanogenesis) of terminal metabolism in coastal, freshwater wetland sediments from three distinct biogeographic provinces. Through geochemical profiles, microbial rate assays, and lipid biomarker analyses, we assessed seasonal variability in the biogeochemical functioning in coastal Florida, Georgia, and Maine. We evaluated the role of temperature and other seasonal factors on rates and pathways of methane production and consumption, as well as sulphate reduction, acetogenesis, and acetate oxidation, through radiotracer rate assays. Intact polar membrane lipid analyses revealed distinct microbial communities at the three sites which varied with season and depth. The combination of microbial activities, sediment porewater geochemistry, and lipid biomarker analysis provides insight into seasonal fluctuations in microbial-mediated carbon mineralization in freshwater sediments.

Tracing sedimentary pyrite oxidation during managed aquifer recharge

S. SEIBERT[1,2]*, G. SKRZYPEK[2], C. DESCOURVIERES[1], C. HINZ[2] AND H. PROMMER[1,2]

[1]CSIRO Land and Water, Wembley, Australia (*correspondence: simone.seibert@csiro.au)
[2]The University of Western Australia, Crawley, Australia

Oxidation of sedimentary pyrite is often one of the main drivers affecting groundwater quality during managed aquifer recharge [1, 2]. In cases where this leads to the depletion of the sedimentary buffering capacity, groundwater acidification and particularly the associated mobilisation of heavy metals and metalloids (e.g. arsenic) can significantly deteriorate groundwater quality [3, 4]. Data and techniques that allow for a detailed identification and quantification of the mineral reactions are therefore crucial to assess and predict such adverse water quality changes.

The present study examines the feasibility of using stable sulphur isotope analysis as a supporting tool for tracking and characterising pyrite oxidation processes during an aquifer storage and recovery experiment in Perth, Western Australia. During the experiment pyrite oxidation was triggered by the injection of potable aerobic water into a well characterised heterogeneous, anaerobic aquifer. Stable sulphur isotope signals ($\delta^{34}S$) were analysed for sedimentary sulphur species and for aqueous sulphate concentrations in both the ground- and the injectant water in addition to extensive hydrochemical monitoring.

The collected data, including the $\delta^{34}S$ value was interpreted by geochemical and reactive transport modelling. The models were specifically adapted to incorporate all reactions and isotope fractionation processes that affect the evolution of $\delta^{34}S$ in the groundwater and the sediments.

The observed $\delta^{34}S$ data from the monitoring wells indicate that the released sulphate is characterised by a successively changing $\delta^{34}S$ signal during the injection phase. These observed $\delta^{34}S$ trends are thought to result from a highly variable $\delta^{34}S$ composition of the pyrite, which was most likely caused by isotopic fractionation associated with the sulphate reduction that occurred during and/or after the deposition of the sediments.

[1] Prommer & Stuyfzand (2005) *EST* **39**, 2200–2209. [2] Descourvieres *et al*. (2010) *Appl. Geochem*. **25**, 261–275. [3] Jones & Pichler (2007) *EST* **41**, 723–730. [4] Wallis *et al*. (2010) *EST* **44**, 5035–5041.

https://doi.org/10.1180/S0026461X00006502 Published online by Cambridge University Press

Mineralogy, geochemistry and age of greisen mineralization in the Li-Rb-Cs-Sn-W deposit Zinnwald, Erzgebirge, Germany

TH. SEIFERT[1]*, PETYA ATANASOVA[1], JENS GUTZMER[1] AND JÖRG PFÄNDER[2]

[1]TU Bergakademie Freiberg, Division of Economic Geology and Petrology, D-09596 Freiberg, Germany, (*correspondence: thomas.seifert@mineral.tu-freiberg.de)
[2]TU Bergakademie Freiberg, Division of Tectonophysics, Argon lab, D-09596 Freiberg, Germany

The Erzgebirge (Krušné hory) is a world class area for Li-Rb-Cs-F-Sn-W-Bi greisen mineralization, which is associated to late-Variscan, postcollisional 'small intrusion' Li-F granites in space and time [1]. A typical example is the Zinnwald/Cínovec Li-Rb-Cs-Sn-W deposit, which is hosted by the Cínovec-Zinnwald granite cupola and Teplice rhyolite. Sn-W(-Li) mining was active for about 700 years until 1990. The exposed intrusion (1.3 x 0.3 km) is composed of a Li-F-granite which in part is strongly greisenized by high-temperature fluids [1, 2]. The flat dipping quartz-zinnwaldite-topaz-fluorite cassiterite greisen ore bodies in the German part of the Zinnwald deposit have a thickness of up to 25 m and resources of about 50 kt Li, 19.5 kt Rb, 1 kt Cs, 6.7 kt Sn, and 2.7 kt W [3]. Three representative zinnwaldite-rich quartz-Li-mica-topaz-fluorite-cassiterite greisen samples with a total weight of 30 t were taken in two levels of the old mining area. The average bulk geochemistry and the range of 16 greisen subsamples indicate the high concentrations of rare elements and fluorine: Li (3290, 490-6990 ppm); Rb (2320, 440-4900 ppm); Cs (67, 13-160 ppm); Sn (1620, 50-13.900 ppm); W (140, 25-390 ppm); Nb (90, 52-153 ppm); F (2.7, 0.36-4.3 wt.%); Th (38, 22-85 ppm). The geochemical signature (e.g., relatively high Li, Rb, Cs, F, Nb, Sn) of the greisen and Li-F granite show similar trends [1, 3]. Seven Li-mica separates have been dated by Ar-Ar in Freiberg (ALF) using laser step heating techniques and an ARGUS multicollector noble gas mass spectrometer. Ages are interpreted as near-formation ages of Li-mica and range between 312.6 ± 2.1 Ma and 314.9 ± 2.3 Ma (2σ external).

[1] Seifert & Kempe (1994) Zinn-Wolfram-Lagerstätten und spätvariszische Magmatite des Erzgebirges. Beih. z. European *Journal of Mineralogy* **6**, 125–172. [2] Štemprok (1960) On the genesis of the ore deposit of Cínovec. Report Inter. Geol. Congress, Session XXI, 43–53. [3] Seifert & Gutzmer (2010) Li-rich Sn(-W-polymetallic) deposits in Saxony. Freiberger Forschungsforum, TU BA Freiberg, June 2011, Session FK **3**, "Lithium for Li-Ion Batteries - Resources & Recovery".

Analysis of iodine, bromine and chlorine in marine sediments and carbonate nodules by ICP-MS

T. SEKIYA[1]*, Y. MURAMATSU[1], H. ANZAI[1], R. MATSUMOTO[2], H. TOMARU[2] AND S. AIZAWA[3]

[1]Department of Chemistry, Gakushuin University, Mejiro 1-5-1, Toshima, Tokyo, Japan (*correspondence: 10142014@gakushuin.ac.jp Yasuyuki.muramatsu@gakushuin.ac.jp)
[2]Department of Earth and Planetary Science, University of Tokyo, Bunkyo, Tokyo, Japan
[3]Department of Chemistry and Chemical Biology, Gunma University, Gunma, Japan

Halogens are thought to be useful in the geochemical studies of rock and sediment formation. However, their analyses are difficult due to their low abundances, specifically Br and I. There are lack of reliable analytical results also for standard rocks. Therefore, we have examined separation procedures of Cl, Br and I from sediments and sedimentary rock samples by pyrohydrolysis. Halogens evaporated by pyrohydrolysis collected in trap solutions. The concentrations of Br and I were determined by ICP-MS and that of Cl was measured by ion-chromatograpy.

Using the developed methods, we have analysed Cl, Br and I in various standard rock samples. The analytical results agreed well with certified values. New data for standard rocks (e.g. JMS-1, JMS-2, JCp-1, JCt-1), in which the concentrations were not known, were also obtained.

We also analyzed sediments and carbonate nodules collected from methane hydrate areas in Japan Sea. In these areas, high iodine concentrations were observed in pore waters in the sediments. We also analysed Br and Cl for comparison.

Results obtained for these elements in solid phase of the sediments were in the ranges: Cl: 5000-10000 ppm, Br: 40-150 ppm, I: 10-200 ppm. High iodine concentrations are characterized by methane hydrate areas. Concentrations of Br and I showed the decreasing tendency with depth. Markedly high values of I in surface sediment was observed. This suggested that I was accumulated by the deposition of organic matters from seawater and also by the fixiation in oxic layer of the sediments from pore water. The concentrations of Cl, Br and I in carbonate nodules were about 100 ppm, 7 ppm, 4.6 ppm. I in carbonate nodules was found to be highly concentrated from pore water compared with Br. The I/Br ratios in carbonate nodules were much higher than those in pore water and solid phase of the sediments. Concentratian mechanisms of the iodine is being examined now.

https://doi.org/10.1180/S0026461X00006502 Published online by Cambridge University Press

Identifying the when and where of oil generation using platinum, palladium, osmium and rhenium geochemistry

D. SELBY[1], A.J. FINLAY[1] AND M.J. OSBORNE[2]

[1]Department of Earth Sciences, Durham University, Durham, DH1 3LE, UK (david.selby@durham.ac.uk, a.j.finlay@durham.ac.uk)

[2]BP International Centre for Business & Technology, Building H, Chertsey Rd., Sunbury-on-Thames, Middlesex, TW16 7LN, UK

Understanding the timing and source of petroleum generation permits more successful oil exploration and recovery. Traditionally, oil source rock identification uses organic chemical analysis of light oil fractions. However, common processes such as biodegradation preferentially removes light hydrocarbons from petroleum compromising traditional oil to source fingerprinting techniques. We therefore developed a new geochemical technique, which not only absolutely dates oil generation through Re–Os geochronology, but also enables the identification of source units through the comparison of ^{187}Osmium/^{188}Osmium at the time of generation (Os_g) and Platinum/Palladium (Pt/Pd) ratios in oils and their potential source units. We demonstrate the applicability of this method in the well understood United Kingdom Atlantic Margin (UKAM) petroleum system and then apply it to identify the source of the West Canadian Tar Sands (WCTS).

Our data yields a Re–Os age of 68±13 Ma (MSWD=20) for oils of the UKAM, indistinguishable from published basin models. Furthermore, the Os_g and Pt/Pd values of these oils are indistinguishable from those of the known source rock, demonstrating that Os_g and Pt/Pd values can be used to identify oil source. When applied to the WCTS, comparison of Pt/Pd and Os_g values with the three potential source units suggests that the dominant source unit is the late Jurassic Gordondale Fm. with only minor inputs from other sources (e.g. Devonian-Mississippian Exshaw Formation).

Unlike traditional organic geochemistry, Pt/Pd and Os_g fingerprinting is not rendered ineffective by biodegradation allowing oil source correlation in previously unsuitable petroleum systems and the deduction of migration pathways. Combining Re–Os geochronology with Pt and Pd geochemistry has identified the Gordondale Fm. as the source of the WCTS. This now permits both spatial and temporal constraints on petroleum systems to be established and therefore provide a significant tool for petroleum system exploration and development.

Bio-Au nanoparticles on archaeal and bacterial S-layers

S. SELENSKA-POBELL[1]*, T. REITZ[1], A.GEISSLER[1], M.L. MERROUN[2] AND T. HERRMANNSDÖRFER[3]

[1]Institute of Radiochemistry, HZDR, D-01328 Dresden, Germany (*correspondence: s.selenska-pobell@hzdr.de)

[2]Microbiology Dept., University of Granada, Granada, Spain

[3]Dresden High Magnetic Field Laboratory, HZDR, Dresden

Gold nanoparticles with substantially different properties were produced by using two alternative S-layer templates. The first one was a bacterial template, representing sheets of the S-layer of *Bacillus sphaericus*; the second one was in a form of empty cells (ghosts) consisting of the so-called SlaA-layer of the thermoacidophilic archaeon *Sulfolobus acidocaldarius*. The archaeal SlaA-layer is resistant not only to high temperatures and acidity but also to detergents, that allowed to purify the SlaA-layer-ghosts keeping the shape of the cells. The production of the Au nanoparticles was performed according to [1, 2] in a two-step procedure by using DMAB as a reducing agent.

We demonstrate that the SlaA-ghosts of *S. acidocaldarius* serve as a very efficient template for complete reduction of Au(III) to Au(0). In the case of using S-layer sheets of *B. sphaericus* only 40 % of the added Au(III) was reduced to Au (0) [2]. The size of the archaeal bio-Au nanoparticles was about 2.5 nm, while those of the bacterial ones was about 4 nm. The most striking property of the archaeal bio-Au nanoparticles is, however, that they are paramagnetic, in contrast to the bacterial ones and also to bulk gold, which are diamagnetic. As demonstrated by SQUID magnetometry, the archaeal bio-Au possesses an unusually large magnetic moment of about 0.1 μ_B/Au atom. HR-TEM combined with EDX analysis revealed that the archaeal Au nanoparticles are bound to sulfur atoms. The latter originate from the thiol groups of the cystein amino acid residues which are characteristic for the SlaA-layer of *S. acidocaldarius* but absent in the S-layer of *B. sphaericus*. Surprisingly, the magnetic moment of the archaeal bio-Au nanoparticles is substantially larger than the ones observed for thiol capped, chemically produced Au nanoclusters [3]. We suggest that the unusual shape and the biochemical characteristics of the SlaA-ghosts are responsible for the observed extraordinary properties of the archaeal bio-Au.

[1] Merroun *et al*. (2007) *Mat. Sc. Tech*. **27**, 188–192.
[2] Jankovski *et al*. (2010) *Spectroscopy* **24**, 177–181, 2010.
[3] Crespo *et al*. (2004) *Phys. Rev. Lett*. **93**, 087204.

https://doi.org/10.1180/S0026461X00006502 Published online by Cambridge University Press

Combined U-Pb zircon dating and apatite trace element compositions applied to Paleozoic tephrochronology

BRYAN K. SELL[1]* AND SCOTT D. SAMSON[2]

[1]Sec. Earth & Envir. Sci., Univ. of Geneva, 1205, Geveva, Switzerland (*correspondence: Bryan.Sell@unige.ch)
[2]Dep. of Earth Sci., Syracuse Univ., Syracuse, NY 13244, USA, (sdsamson@syr.edu)

The global utility of a stratigraphic section that records important Earth history events requires a robust geological timescale. This could be accomplished either by establishing highly precise and accurate ages for the the section in question or by accurately correlating strata in the section of interest to those regions where a well-developed time scale has already been established. For pre-Cenozoic rocks the challenge of developing independent age constraints for any given section of rock increases with age.

An anomalously high abundance of tephra in the Late Ordovician of eastern North America and Scandinavia presents a unique opportunity to test aspects of the importance of high-precision U-Pb zircon geochronology combined with the utility of crystal-chemistry based tehprochronology. Specifically, high-precision ages combined with robust crystal chemical data can be assessed in view of its ability to help understand aspects of the Great Ordovician Biodiversification Event, end-Ordovician mass extinctions, various oceanic carbon isotope events, and the end-Ordovician glaciation. A few of the widespread tephra possibly derive from the largest known eruptions in the Phanerozoic, which may have triggered important biotic and climatic responses. Tephrostratigraphic correlation of these large eruptive units has been challenging beyond several 100's of square kilometers because the tephra are heavily altered and span different depositional and tectonic settings. Volcanogenic apatite trace element concentrations (Mg, Cl, Mn, Fe, Y, and Ce) have been successfully applied to these tephra correlation problems in the eastern U.S. and between North America and Europe. This apatite trace element tephrochronologic approach has been invaluable for investigating several chronostratigraphic schemes related to Ordovician biostratigraphy, chemostratigraphy, and sequence stratigraphy. Our new U-Pb zircon and apatite trace element data shows that there is some significant disparity in previously assumed temporal relationships, particularly between widely spaced locations.

Exoplanet atmospheres: From hot to habitable worlds

FRANCK SELSIS[12]

[1]Université de Bordeaux, Observatoire Aquitain des Sciences de l'Univers, BP 89, F-33271 Floirac cedex, France (selsis@obs.u-bordeaux1.fr)
[2]CNRS, UMR 5804, LAboratoire d'Astrophysique de Bordeaux, BP 89, F-33271 Floirac cedex, France

Current observational techniques allow us to detect a broad variety of extrasolar planets. In some cases we can measure properties such as the planetary radius, mass and temperature and constrain the structure, molecular composition and dynamics of their atmospheres. The diversity of observed exoplanets is extraordinary in terms of planetary system architectures, physical conditions and chemical compositions. I will present several striking cases that illustrate this diversity.

At two extremes of the known sample of exoplanets are hot gas giants, whose atmospheres constitute a puzzle for both physicists and chemists, and potentially "habitable" worlds which, despite very exotic properties, could host liquid water. I will focus on these two types of atmospheres and show that their modeling is a challenging but extremely rich subject. I will then discuss the prospects for the next step of exoplanet characterization.

https://doi.org/10.1180/S0026461X00006502 Published online by Cambridge University Press

A chlorine isotope view of mantle metasomatism via slab fluids/melts

J. SELVERSTONE* AND Z.D. SHARP

Dept of Earth & Planetary Sciences, University of New Mexico, Albuquerque, NM 97131 USA
(*correspondence: selver@unm.edu)

We use Cl, H and O stable isotope geochemistry to investigate fluid/melt infiltration of the Finero peridotite (Ivrea Zone) in a shallow mantle wedge setting (1.2-1.6 GPa, ~900°C, Perple_X modelling). Unaltered samples from the Balmuccia peridotite have typical mantle δ^{37}Cl values of -0.4±0.3‰ and provide a reference frame for the metasomatized rocks. Four lithologies from Finero (1: spinel harzburgites with minor amph ± phlog, 2: harzburgites with abundant phlog ± amph, 3: amph segregations, and 4: phlog segregations) have δ^{37}Cl values between –2.0 and +2.1‰ (Fig. 1). We also report preliminary chlorine isotope data from HP/UHP rocks (hydrothermally altered oceanic crust, serpentinites with rodingite dikes, and Mn-rich and calcmica schists) that represent likely subduction inputs (Fig. 1). The isotopic variability recorded at Finero cannot be reconciled with metasomatism by a single fluid. Three principal components describe the sample variability: (A) endmember peridotite, (B) a low δ^{37}Cl, high δD, and high δ^{18}O component (melt derived from subducted sediment), and (C) a high δ^{37}Cl, δD, [Cl], and [K] component (high-salinity fluid likely released from altered oceanic crust). Preserved cm-scale isotopic heterogeneities indicate channelized infiltration of fluid/melt at different times and from different slab source rocks. Small-scale fluid release events – not just large-scale serpentinite dehydration – are thus important in chemical transfer from subducted slabs to the mantle wedge.

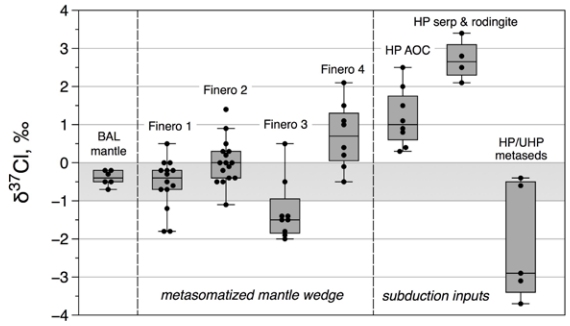

Figure 1: Box-and-whisker plot of δ^{37}Cl values from unaltered mantle peridotite (BAL), metasomatized Finero rocks, and various HP and UHP rocks from the western Alps.

Correlation of δ^{13}C and PGE contents in magmatic ores

D.V. SEMENOVA*, V.A. PONOMARCHUK AND V.V. RYABOV

Sobolev Institute of Geology and Mineralogy SB RAS, 630090 Novosibirsk, Acad. Koptyug av., 3, Russia
(*correspondence: semenovadina@gmail.com)

Typically, the spatial association of rare metals, including PGE, with the organic matter is regarded as an argument to the important role of organic matter in ore formation. As an example, ore deposit in black shales is given [1]. However, there are also many sedimentary basins with low metal concentrations. Thus, ore mineralization occurences in black shales are not a reliable criterion for genetic connection: mineralization – organic matter. Mineralized geological formations with low contents of reduced carbon are best suited to reveal such relations.

The example of correlation between the isotopic composition of carbon, it's content and PGE concentrations in the ores of one of the deposits of the northwestern Siberian platform is presented in this study. Carbon isotope composition were determined using Thermo Finnigan 253 mass spectrometer with specially-constructed line [2]. Special attention was paid for the signal from neutral C0 species (graphit, solid solution C) in the isotopic analysis. The contents of this carbon in the samples range from 15 to 80 ppm. δ13C values were mainly in the range of -21 to -26, 5 ‰. In rare cases, heavier isotope values were obtained for graphite: -12; -13, 5; -14, 5‰. Data have shown that there is no correlation between carbon contents and PGE concentrations (correlation coeffcient is 0.45). However, the comparison of PGE contents in ores and carbon isotope values (C0) has shown the complete linear dependence (the correlation coefficient is 0.94) between them: the weighting of carbon isotope composition was accompanied by the increasing of PGE contents in the same samples. Such a weighting of carbon isotope composition was noted earlier by Ryabov *et al*. [3]. The most possible explanations of the results is that platinum group elements are transfered by specific organometallic compounds rather than the whole organic matter.

[1] Coveney *et al*. (2003) *Ore Geol. Rev*. **24**, 1–5. [2] Semenova & Ponomarchuk (2009) *Geochim. Cosmochim. Acta* **73**, A1193. [3] Ryabov *et al*. (2010) *Geochim. Cosmochim. Acta* **74**, A895.

https://doi.org/10.1180/S0026461X00006502 Published online by Cambridge University Press

Petrogenesis of mantle peridotites from the Kizildag ophiolite (SE Turkey): Implications from mineral composition

A.D. SEN[1], I. UYSAL[1], M. GODARD[2], U. BAGCI[3] AND M. KALIWODA[4]

[1]Karadeniz Technical University, Department of Geological Engineering, 61080-Trabzon, Turkey (*correspondence: ahmetds@gmail.com)
[2]Géosciences Montpellier, Universite Montpellier 2 - cc60Place Eugene Bataillon, 34095-Montpellier, France
[3]Mersin University, Department of Geological Engineering, 33342-Çiftlikköy/Mersin, Turkey
[4]Mineralogical State Collection Munich, LMU, D–80333, München, Germany

Kizildag (Hatay, SE Turkey) ophiolitic complex is one of the best maintained Tethyan lithospheric remnants of Turkey ophiolites. Mantle tectonites from the Kizildag ophiolite contains spinel with Cr# 0.47-0.61 which indicates that they are residue of ~23-30% of partial melting of primitive upper mantle, and are similar to the supra subduction zone peridotites. Pyroxenes have lower content of Al ($Al_2O_3^{Cpx}$=1.61-2.77 wt%) and Ti (TiO_2^{Cpx}<0.25), and also indicate the respectively high degree of depletion. Clinopyroxene from the twelve peridotite samples of Kizildag ophiolite complex analyzed by LA-ICP MS for their trace and REE contents. Clinopyroxenes from mantle tectonites show LREE enrichment (Sm_N/Lu_N=0.04-0.78) and nearly horizontal HREE (Er_N/Lu_N=0.49-1.32) patterns. There is a negative correlation between Sm/Yb vs. Yb contents of clinopyroxenes, which consistent with the hydrous partial melting and fluid-melt enrichment trend. There is also a negative correlation between Yb content in clinopyrexene and Cr# of spinel. The depleted composition of incompatible elements and LREE enriched pattern known as an evidence for mantle-melt interaction. There is a good correlation between Cr# of spinel and HREE concentration of clinopyroxenes. However, chondrite-normalized Ce concentrations $(Ce)_N$ of clinopyroxene in mantle tectonites of Kizildag ophiolite is higher (0.10-0.13ppm) than the abyssal peridotites. The mineral chemistry results indicate that the mantle tectonites shows higher degree of partial melting than abyssal peridotites. Subducting oceanic lithosphere produces LREE-enriched melt and/or fluids and this is resulted with the higher melting. These evidences indicate an arc magmatism i.e. a suprasubduction zone setting fort he genesis of Kizildag ophiolite.

Human impact on global element cycles

I.S. SEN* AND B. PEUCKER-EHRENBRINK

Woods Hole Oceanographic Institution, Woods Hole, MA 02540, USA (*correspondence: isen@whoi.edu)

Material flow caused by human actions has become a major component of the Earth's biogeochemical cycles. In order to constrain the effect of human activity on global elemental cycles, Klee and Graedel [1] quantified the magnitude of anthropogenic activities on 77 of the naturally occuring elements. Their study compiled estimates of natural (weathering of continental crust, net primary production, element mobilized through sea spray) and anthropogenic (mining, biomass burning, and fossil fuel combustion) element fluxes and determined the role of humans on global elemental cycles. While Klee and Graedel [1] assessed the role of a number of important natural and anthropogenic processes, their assessment was not comprehensive. For instance, global dust fluxes [2] and losses to and gains from the extraterrestrial environment were not considered.

Here we revisit the Klee and Graedel [1] study and add important sources (chemical flux contributions from volcanoes and aeolian dust, input of extraterrestial matter) that affect global elemental cycles. In addition, we updated chemical inventories and fluxes for a range of processes.

Our calculation shows a substantial change from the original Klee and Graedel [1] study. Geochemical cycle of 22 elements are dominated by human actions. Biogeochemical cycle of gold, platinum, palladium, rhenium and iridium are dominated by anthropogenic activities, followed by chromium, antimony, copper, mercury, rhodium, lead, bismuth, tin, tellurium, cesium, arsenic, tungsten, iron, silver, nickel, indium and uranium.

[1] Klee & Graedel (2004) *Annu. Rev. Environ. Resour.* **29**, p. 69–107. [2] Cakmur *et al.* (2006) *J. Geophys. Res.* **111**, D06207, doi: 10.1029/2005JD005791.

https://doi.org/10.1180/S0026461X00006502 Published online by Cambridge University Press

Assessments of the anthropogenic radiative forcing over the Amazon Basin: Aerosols and land-use change

E.T. SENA*, S.P. CAMARA, F.F. FRIGERI, A.L. CORREIA AND P. ARTAXO

Institute of Physics, University of São Paulo, R Matão, Trav R, 187, 05508-090, São Paulo/SP, Brazil (*correspondence: elisats@if.usp.br, spinc@if.usp.br, felipef@if.usp.br, acorreia@if.usp.br, artaxo@if.usp.br)

Man-made biomass burning activities that occur yearly in the Amazon send large amounts of smoke to the atmosphere, and alter the landscape by converting forested areas into pastures and cropland. This work addresses the radiative forcing (RF) of the smoke aerosol and of the land cover change in Amazonia, seeking to quantify their climatic impact over the Earth System.

The cloud-free direct RF due to biomass burning aerosols was derived from the CERES sensor (Clouds and the Earth's Radiant Energy System) [1] flux retrievals over the Amazon from 2000 to 2009, considering the peak of the burning season from August to September. The Amazon Basin was divided in 0.5° latitude-longitude grid cells according to [2], and the broadband shortwave (0.3 to 5.0 μm) radiation flux was regressed against the aerosol optical depth to determine the radiative flux under clean (no aerosol) conditions, F_{cl}. The direct RF was derived by subtracting from F_{cl} the flux under average aerosol conditions. The resulting aerosol RF shows large spatial and temporal variations, with an average of -10.4±4.4 W/m^2 in a basin-wide scale, during the biomass burning season from 2000 to 2009. In local spatial scales and across the solar spectrum this figure can vary significantly. For instance, over the city of Alta Floresta, Brazil (-9.9°N, -56.0°E) for the 2007 burning season the cloud-free spectral direct aerosol RF was estimated as -57 W/m^2 at 440 nm, -17 W/m^2 at 675 nm, +11 W/m^2 at 870 nm, and +6 W/m^2 at 1020 nm.

The RF due to land-use (albedo) change was estimated for clean (no aerosol) conditions over the state of Rondonia, Brazil, an area that has been heavily deforested since the 70's. Surface reflectance retrievals from MODIS (Moderate Resolution Imaging Spectroradiometer) were used to select study areas, and the RF was computed as the difference between the CERES radiative flux at the top of the atmosphere above forests and over nearly bare-ground deforested patches. The albedo land-use change RF was -22±3 W/m^2, a figure that can be compared to the direct aerosol RF, but in the Amazon these deforestation patches correspond to a nearly permanent modification of the surface albedo that also changes the local radiation budget.

Studies of the indirect (i.e. mediated by clouds) aerosol forcing over the Amazon Basin are currently under way and they will help throwing in one more puzzle piece to the set above, depicting key factors that define the human RF over the Amazon.

[1] Wielicki *et al*. (1996) *Bull. Amer. Meteor. Soc*. **77(5)**, 853-868. [2] Patadia *et al*. (2008) *J. Geophys. Res* **113**, D12214.

Osmium isotope signatures in peridotites from the ultra-slow spreading SWIR and RTJ

R. SENDA[1]*, H. SATO[2], K. NAKAMURA[1], H. KUMAGAI[1] AND K. SUZUKI[1]

[1]Japan Agency for Marine-Earth Science and Technology, Yokosuka, 237-0061 Japan (*correspondence: rsenda@jamstec.go.jp)

[2]School of Business Administration, Senshu University, Kawasaki, 214-8580 Japan

The ridge magmatic systems are the places where crust directly forms. They provide information on how different crust forms depending on variable spreading rates associated with amount of melt supply and the source of the supplied melts. The central part of the Southwest Indian Ridge (SWIR), known as an ultra-slow spreading system (14-16 mm/yr) was investigated. We had two cruises of R/V Hakuho-Maru in 2008 (KH07-4 Leg2) and 2010 (KH09-5 Leg4) R/V Hakuho-Maru and dredged aphyric to porphyritic basalts, peridotites, metamorphic and sedimentary rocks from 17 sites from 34E to 40E along SWIR. We also sampled peridotites from the Rodriguez Triple Junction (RTJ) where three ridge system, the Central Indian Ridge, the Southeast Indian Ridge and SWIR meet together (YK05-16 Leg1 at 2005 by R/V Yokosuka and Shinkai 6500).

The Re-Os isotope systematics were investigated to identify the source of basalts and peridotites. One of the major advantages using Re-Os system is that they are relatively robust to secondary effects, e.g. sea water alteration and mantle metasomatism. The Os isotope ratios of peridotites from SWIR and from RTJ are $^{187}Os/^{188}Os$ = 0.1239-0.1307, which are in the range of those reported as abyssal peridotites. The Os isotope ratios of spinels from SWIR, however, indicate more depleted signature; around $^{187}Os/^{188}Os$ = 0.121, compared to the primitive upper mantle ($^{187}Os/^{188}Os$ = 0.1296, [1]) and peridotites from SWIR of this study and [2]. Such mismatches of Os isotope ratios between the spinels and the peridotites have been also reported even within a hand specimen level [2]. The time of Rhenium depletion (T_{RD}) ages were estimated as around 1Ga for these spinels, which show that the host peridotites of spinels experienced melt extraction at least around 1Ga even they were recovered from the currently active ridge.

[1] Meisel *et al*. (2001) *GCA* **65**, 1311–1323. [2] Standish *et al*. (2001) *Geochem, Geophys. Geosyst*. **3**, 2001GC000161

https://doi.org/10.1180/S0026461X00006502 Published online by Cambridge University Press

Molybdenite deposition in Bingham Canyon deposit: Role of sulfur, redox and pH chemistry in magmatic-hydrothermal fluids

JUNG HUN SEO, MARCEL GUILLONG AND CHRISTOPH A. HEINRICH

ETH Zurich, Institute of Geochemistry and Petrology, 8092 Zurich, Switzerland

The Bingham Canyon porphyry deposit shows a distinct metal zonation of 1) shallow Cu-Au mineralization (Cu-stage) and 2) deeper Mo mineralization (Mo-stage) occurring in a separate vein set that truncates earlier Cu-Au veins.

In deep low-grade Cu-stage quartz veins, we found high concentrations of Cu, S, and Mo in the fluids, whereas in low-grade Mo-stage veins, we found rather lower Cu, but similar concentrations of S and Mo, compared to the input fluids of the Cu-stage. Sulfur concentrations in intermediate density (ID) type inclusion in deep low-grade Cu-stage samples are similar to their Cu concentration, whereas ID-type inclusions in low-grade Mo-stage veins have S contents in excess over their Cu content. Compared to the P-T conditions of the Cu-precipitation stage (90-260 bars and 320-430 °C), the Mo-precipitating fluids extended to higher pressures and temperatures of 140-710 bars and 360-580 °C.

Mass-balance calculation and vapor/brine partitioning data indicate that the mass of vapor phase exceeded that of brine by about 9/1 and more than 70% of Mo, Cu, and S (by mass) were deposited by the vapor phase in both mineralization stages.

High Mo contents (max. 0.0054 Mo/Na in ID; 380 μg/g Mo in brine) in the hydrothermal fluids were maintained from the early Cu-stage to the late Mo-stage, suggesting that Mo concentration in the fluids may not be the decisive factor for the separate Cu & Mo precipitations in Bingham Canyon deposit. Instead, the metal separation may be explained by a reduction in redox and a pH increase in the fluids from evolving source region. This is indicated by 1) the stoichiometry of chalcopyrite and molybdenite precipitation reactions, 2) a difference in the Fe/Mn ratio in fluids of the two (Cu and Mo) veining stages, 3) incipient muscovite alteration along high-temperature molybdenite veins, and 4) an increasing vapor/brine partition for Mo.

We suggest that the early Cu-stage fluids were slightly oxidized, allowing efficient Cu-Fe sulfides precipitation and thereby consume much of the dissolved S. By contrast during the later Mo-stage, the fluids were more reduced and acidic, thereby allowing selective saturation of molybdenite as the first precipitating sulfide.

Uranium interactions with bacterial communities from contaminated soils in Chernobyl

C. SERGEANT[1]*, N. THEODORAKOPOULOS[2], L. PIETTE[2], M.H. VESVRES[1], C. LE MARREC[3], R. CHRISTEN[4], F. COPPIN[5], L. FEVRIER[5], A. MARTIN-GARIN[5], C. BERTHOMIEU[2] AND V. CHAPON[2]

[1]University Bordeaux/CNRS UMR5797, 19 chemin du Solarium, BP120, 33175 Gradignan, France (*correspondence: sergeant@cenbg.in2p3.fr)

[2]LIPM, UMR 6191, CEA Cadarache, Bât 185, 13108 Saint Paul Lez Durance, France (virginie.chapon@cea.fr)

[3]Institut Polytechnique de Bordeaux/INRA UMR 1219, 210 chemin de Leysotte, 33882 Villenave d'Ornon, France (clehenaff@enscbp.fr)

[4]University Nice-Sophia-Antipolis/CNRS UMR 6543, Parc Valrose, 06108 Nice, France(richard.christen@unice.fr)

[5]LRE, IRSN, CE Cadarache, Bât 186, 13108 Saint Paul Les Durance, France (arnaud.martin-garin@irsn.fr)

Following the Chernobyl accident in 1986, vegetation, contaminated soil and other radioactive debris were shortly buried *in situ* in trenches. The present work describes the analysis of the structure of the bacterial communities that have been evolving in this environment for more than 20 years. Comparison of the diversities found in soil samples exhibiting contrasted radionuclides content is a prerequesite to point out the potential role of microorganisms in radionuclide migration in soils.

Bacterial communities were examined using a genetic fingerprinting method that allowed a comparative profiling of the samples (DGGE), with universal and group-specific PCR primers. Our results indicate that a long term exposure to radionuclides did not lead to extinction of bacterial diversity in Chernobyl soils.

A collection of aerobic and anaerobic culturable isolates was also assembled. A phylogenetic analysis of 250 heterotrophic aerobic isolates revealed that 5 phyla are represented: *Beta-, Gammaproteobacteria, Actinobacteria, Bacteroidetes* and spore-forming *Firmicutes*, the last being largely dominant [1].

Eleven representative fast-growing strains, related to diverse genera, were exposed to uranium. In each case, bacteria/uranium interactions exhibited different kinetics, suggesting that underlying mechanisms (biosorption, accumulation, precipitation) could be different.

[1] Chapon *et al*. (2011) *Applied Geochem* (under revision)

https://doi.org/10.1180/S0026461X00006502 Published online by Cambridge University Press

Biomineralization of Fe^{II}-Fe^{III} green rust in γ-FeOOH coated sand column under saturated flow conditions

A.-S. SERGENT, K. HANNA, P.P. REMY AND F. JORAND*

LCPME UMR 7564 CNRS- Nancy-University, Jean Barriol Institute, 405 rue de Vandoeuvre, 54600 Villers-lès-Nancy, France
(*correspondence: jorand@pharma.uhp-nancy.fr)

The synthesis of Fe(II)–Fe(III) green rusts (GR) in environmental and engeneering systems is a challenging project due to the higher reactivity of GR towards a panel of organic or inorganic pollutants. While the biomineralization and stabilization of GR have been well described in batch reactor from ferric oxide respiration by *Shewanella putrefaciens* [1, 2] or mixed cultures of bacteria [3, 4], their formation routes as a main secondary iron mineral under flow-through conditions remain undescribed.

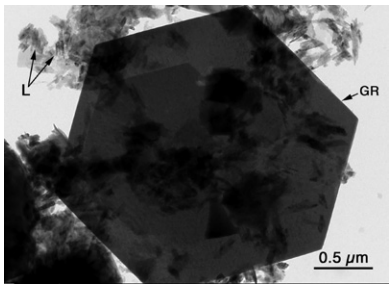

Figure 1: Picture of a green rust (GR) crystal obtained in a lepidocrocite (L) sand packed column incoculated with *S. putrefaciens* and fed with formate as electron donor.

Formation of both GR and magnetite was observed in a lepidocrocite-coated sand packed column at a flow rate of 0.1 mL/min. However, GR was the dominant secondary mineral when silicate was present in the injected feed solution (Fig.1). In this latter case, untransformed lepidocrocite was still present in the sand packed column. This behavior could be explained by the sorption of dissolved silicate on the lepidocrocite surface, which might hinder the reactive sites and so limit the bioreduction extent. On the other hand, the interactions of dissolved Si with the lateral faces of the GR crystals could stabilize the GR structure, thus preventing its transformation into magnetite.

[1] Zegeye *et al*. (2010) *Geobiology* **8**, 209–222. [2] O'Loughlin *et al*. (2010) *Environ. Sci. Technol*. **44**, 4570–4576. [3] Blöthe & Roden (2009) *Appl. Environ. Microbiol*. **75**, 468–473. [4] Jorand *et al*. (2011) *Sci. Total Environ*. **406,** 2586-2596

Hg (II) sequestration by ettringite-type phases. A geochemical modeling and EXAFS study

S. SERRANO[1], D. VLASSOPOULOS[2], B. BESSINGER[3] AND P.A. O'DAY[1]

[1]University of California, Merced CA USA
[2]Anchor QEA, LLC., Portland OR USA
[3]S.S. Papadopulos & Associates, Inc., Portland OR USA

Sequestration of Hg by ettringite-type phases (Ca_6 [Al $(OH)_6]_2$ $(SO_4)_3 \cdot 26H_2O$), formed during hydration of Portland-type and super-sulfate cements, as a potential method for sediment remediation was investigated theoretically with a kinetic-equilibrium model and experimentally in co-precipitation (Hg+Al+SO_4+Ca and Hg+Fe+SO_4+Ca systems) and substrate-amended (quartz, clay, and/or sediment) batch experiments in aqueous NaCl solutions. Geochemical modeling predicted formation of ettringite and calcium-silicate-hydrate (C-S-H) gels as a function of reaction time, corroborating XRD results for amendment batch experiments. XRD patterns of the co-precipitation products showed Al-ettringite and gypsum as the main mineral phases in the Hg+Al+SO_4+Ca and Hg+Fe+SO_4 +Ca systems, respectively. Extraction results indicated that <20% of added Hg was associated with the exchangeable fraction in both co-precipitation and substrate-amended batch experiment. XAS and electron microprobe characterization of the Hg co-precipitation and cement hydration products suggests physical micro-encapsulation of Hg in ettringite as a polynuclear chloromercury calcium precipitate. Hg XAS analysis of the solid products in the Hg+Fe+SO_4+Ca system indicated Hg sorption on ferrihydrite as the main retention mechanism. These results revealed that, in the presence of Cl^-, Hg immobilization in cement systems is kinetically controlled by Hg-Cl complexation and precipitation of cement hydration products. However, in high Fe systems, Hg retention predominantly as the Hg $(OH)_2$ species, is controlled by fast sorption equilibrium on ferrihydrite.

https://doi.org/10.1180/S0026461X00006502 Published online by Cambridge University Press

Experimental study of mineral equilibria in the system Li_2O-K_2O-Al_2O_3-SiO_2-HF-H_2O (with topaz) at 400°C and 100 MPa

T.V. SETKOVA*, YU.B. SHAPOVALOV AND V.S. BALITSKY

Institute of Experimental Mineralogy, Academica Osipyana Street 4, Moscow distr. 142432, Chernogolovka, Russia (*correspondence: setkova@iem.ac.ru)

The experimental study of mineral equilibria in the system Li_2O-K_2O-Al_2O_3-SiO_2-HF-H_2O was carried out to determine influence of composition of solution (lithium content) on genesis of greisen deposits.

Topaz one of the major indicators of F-bearing minerals participating in most of the studied reactions. Experiments were performed in autoclaves in gold ampules with self-sealing shutter by a technique of monovariant reaction. This technique is based on change of topaz grain weight. All the mineral phases participating in the reaction were placed together into ampoules. The topaz was used as rounded grain whereas other components of reactions were added as powder. As a result influence of lithium on shift of topaz stability field on the diagram $\lg_{(mHF)}$ - $\lg_{(mKF)}$ established earlier [1] for modeling system K_2O-Al_2O_3-SiO_2-HF-H_2O has been estimated. At low concentration of LiF and high concentration of HF in the solution the line limiting the topaz field for monovariant equilibrium topaz-AlF_3 moves downwards to the axis $\lg_{(mHF)}$. Muscovite stability field is replaced by lepidolite field at relatively high concentration of LiF and low concentration HF in the solution. Absence of potassium in the solution leads to formation of the lithium-bearing alumina-fluoride phase.

[1] Shapovalov Yu.B. (1988) *The collection of articles on physical & chemical petrology*, V.15. P.160-167 (in Russian)

Krypton and xenon in air bubbles from ice cores as tracers of past ocean temperature

JEFFREY P. SEVERINGHAUS[1] AND KENJI KAWAMURA[2]

[1]Scripps Institution of Oceanoggraphy, CA 92093-0244
[2]National Institute for Polar Research, Tokyo, Japan

The heavy noble gases krypton and xenon are quite soluble in liquid water, with a strong temperature-dependence of the solubility. Because the total inventory of these gases in the ocean-atmosphere system is constant, an increase in the oceanic inventory must be accompanied by a complementary decrease in the atmospheric inventory. Dinitrogen (N_2) gas is much less soluble and so its atmospheric inventory is little affected by ocean temperature change. Sources and sinks of N_2 may be neglected due to the great abundance of this gas in the atmosphere, and the fact that the entire denitrifiable inventory of N comprises less than 0.01% of the atmospheric pool. Thus the ratios Kr/N_2 and Xe/N_2 in the past atmosphere should predominantly reflect past ocean temperature change. These parameters may be estimated from measurements of trapped air composition in ice cores, making appropriate corrections for gravitational settling and thermal fractionation that occurred in the snow layer (firn) at the ice core site. Measurements are done by classical dual- dynamic-inlet electron impact mass spectrometry on air melt-extracted from 1 kg of ice, and encompass the krypton isotope pair $^{86}Kr/^{82}Kr$ and $^{15}N^{14}N$ for the purpose of making the gravity and thermal corrections.

This new proxy reflects mean ocean temperature change, albeit slightly weighted toward the cold end of the temperature distribution due to the greater solubility of these gases in cold water. Because the ocean's heat and gas burdens are set at the outcrop where air-sea equilibration last occurs, and they travel through the ocean interior nearly adiabatically and conservatively, there is no time lag between changes in ocean heat content and changes in atmospheric noble gas burden. Consideration of the solubilities and relative volumes of the reservoirs leads to the prediction that a 1˚C warming will produce a +0.5‰ increase in atmospheric Kr/N_2. Current measurement precision is around 0.2‰ for a 1-kg piece of ice, suggesting a precision of about 0.4˚C for this proxy. Reconstructions over the past glacial cycle suggest a glacial mean ocean temperature about 3˚C colder than present, with a rapid warming of about 2˚C between 18-15 ka. This was a time period of rapid atmospheric CO_2 increase, consistent with the hypothesis that atmospheric CO_2 lowering in the glacial episodes was caused by sequestration in a poorly ventilated, dense, cold deep water layer.

https://doi.org/10.1180/S0026461X00006502 Published online by Cambridge University Press

Enhanced *in situ* methanogenesis and microbial community analysis of coal beds

JOEL R. SEVINSKY AND WILLIAM R. MAHAFFEY*

Luca Technologies, Golden, CO 80129 USA
(*correspondence: bill.mahaffey@lucatechnologies.com)

Biogenic methane has enormous potential as a sustainable energy source and is found in a wide variety of subsurface, anaerobic, hydrocarbon bearing environments. The Powder River Basin in Wyoming, USA is an area previously shown to be an active 'geobioreactor', or an area where active *in situ* methanogenesis occurs as determined by coal conversion to methane in laboratory experiments, the presence of metabolic intermediates in coalbed methane formation waters, and the ability of the consortia present in these waters to convert the metabolites to methane. Understanding the composition and metabolism of the methanogenic consortia has been one of several key steps in commercializing the process of sustainable biogenic methane production.

In order to identify the microbes present in these methanogenic consortia, we performed microbial community analysis using error-correcting barcode pyrosequencing analyzed with the QIIME bioinformatic pipeline. This involved hundreds of samples collected from different locations within a set geographical area over several years. We used both bacterial and archaeal specific primers to amplify these distinct populations from our DNA samples. The QIIME pipeline was used for library demultiplexing, OTU picking, alignment, taxonomic identification, and statistical analysis of community structure using Unifrac. Spotfire was used for visualization of QIIME results with metadata from the formation.

Here we demonstrate the large scale areal and temporal sampling for community analysis of coalbed methane (CBM) wells within a discrete but large area of the Powder River Basin. Temporal consists of the baseline state, followed by a bio-stimulation phase (i.e. Restoration) and enhanced methane production phase. Under baseline conditions, we find distinct bacterial and archaeal populations that vary by coal, water chemistry, and time. Community profile signatures help determine the areas of greatest methanogenic potential and identify patterns of ground water recharge, water movement, and potential metabolic bottlenecks. Data will be presented showing increased gas production over pre-restoration decline curves, the period of enhanced methane production and the observed changes in the microbial community structure associated with enhanced gas generation.

An Exafs and *ab initio* study of aquated Cd^{2+} and chlorocadmium(II) complexes up to 300°C

T.M. SEWARD[1], K.H. LEMKE[2], C.M.B. HENDERSON[3], J.M. CHARNOCK[3] AND S.A. SADJADI[2]

[1]Victoria University of Wellington, New Zealand (terry.seward@vuw.ac.nz)
[2]University of Hong Kong, Hong Kong, kono@hku.hk
[3]University of Manchester, UK

The hydrothermal transport and deposition chemistry of cadmium in the Earth's crust is still poorly known. X-ray absorption spectroscopy and quantum chemical calculations can provide fundmental insight on a molecular level into the formation/stability and hydration of the geochemically relevant Cd(II) complexes.

We have measured the EXAFS of aqueous cadmium nitrate, perchorate and chloride solutions up to 300°C and at the equilibrium saturated vapour pressure using an X-ray optical cell employing silica glass windows. In dilute nitrate solutions ((0.01m Cd $(NO_3)_2$/0.01m HNO_3), Cd^{2+} is coordinated to 6 water molcules over the temperature range from 25 to 250°C. There is a small electrostrictive contraction of the Cd-water distance from 2.27 to 2.23Å with increasing temperature as the water solvent properties change at conditions along the two phase curve. In more concentrated nitrate and perchorate solutions (1.00m), the mono-, di- and trinitato- and monoperchoratocadmium (II) ion pairs were detected. The stepwise formation of chlorocadmium (II) complexes was also studied from 25 to 300°C in solutions having HCl concentrations from 0.001 to 3.00m. For example, in 3.00m HCl, the $CdCl_4^{2-}$ species predominated over the entire temperature range with the Cd-Cl distance remaining essentially constant at 2.46-2.45Å.

The computational part of the study was designed to provide further insight into the nature of Cd^{2+} hydration as well as to the coordination and hydration of the cadmium chloride complexes. We performed a systematic survey of the equilibrium geometries of $CdCl_m$ $(H_2O)_n$ for m=0-4 and n=0-11. We employed the cc-pVnZ (PP) (n=D, T) correlation consistent basis set for Cd, cc-pV (d+n)Z (n=D, T) for Cl and cc-pVnZ (n=D, T) for H and O (abbreviated as VnZ (PP) (n=D, T). Geometry optimisations for the various hydrated complexes were performed at the RHF and the results thereof then applied as starting geometries for subsequent MP2 level calculations. In the case of Cd $(H_2O)_6^{2+}$ for example, the optimal Cd-O distance is 2.28Å. If 7 waters are constrained to the first shell, then the distance extends to 2.35Å, however, this geometry with $7H_2O$ is unstable.

https://doi.org/10.1180/S0026461X00006502 Published online by Cambridge University Press

Composition modeling of pollution of groundwater by usage of geoelectrical and hydrogeochemical studies

MAHDI SHABANKAREH[1], A. GHASEMI[2] AND S. AFSHARI[3]

[1]ACECR, IUT branch, Isfahan University of thech, Isfahan, Iran (*correspondence: shabankareh@mi.iut.ac.ir)
[2,3]ACECR, IUT branch, Isfahan University of thech, Isfahan, Iran

Now a day, the use of indirect methods of measurement and detection of groundwater contamination due to high speed and lower cost is interested. Among the geophysical methods are very important. in this project was trying, with sampling of groundwater resources and their chemical analysis and Select the appropriate method, and the effect of trace pollutants using the results in comparison to groundwater modeling with integrated studies and hydrogeochemical and geoelectical was acting.

Thirteen profiles with the schlumberger array with south to north in the direction have been picked in study area. General review of the main geoelectrical sections are shown four layers and in some places raise up to six layers. To achieve good picture of the situation in depth, plans are extracted in different depths. These maps are identified manner and distribution of lateral variations of electrical resistance of geological formations.

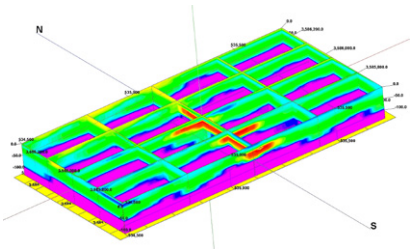

Figure 1: fence of 3d resistance modeling

10-meter depth Plan trend shows a noticeable decrease in the amount of resistivity is observed, especially in the south, it's the main zone of contamination, probably. These studies with samples from 69 water wells were investigated fully consolidated.

Discussion of Results

Results showed that the electrical resistance of contamination zone is lower than usual about the same sedimentary unit which is caused by the effect of pollutants. Based on field observations in the vicinity of this area there are water channel which converted this area to a washed zone that contaminations can penetrate into the soil with infiltrated water.

Geochemical zoning analysis based on 'Axes Level' innovative method

MAHDI SHABANKAREH[1], SEYED HASAN TABATABAEI[2] AND ZAHRA PIRMORADIAN[3]

[1]ACECR, IUT Branch, Isfahan University of Tech., Isfahan, Iran (shabankareh@mi.iut.ac.ir)
[2]Mining Engineering Department, Isfahan University of Tech., Isfahan, Iran (tabatabaei@cc.iut.ac.ir)
[3]Mining Engineering Department, Isfahan University of Tech., Isfahan, Iran
(*correspondence: syscadmi@sepahan.iut.ac.ir)

Primary Geochemical halo and alteration zones around ore deposits with the phenomenon formation of ore deposits in a relationship are genetic. So that the diagnosis clear boundary between alteration regions and geochemical alteration halo not be always possible. Observations have shown that spatial distribution (longitudinal, lateral and vertical) halo is complicated and controlled by several variables, such as differences in the mobility of elements which can be function of temperature, pressure, physicochemical specificities enclosing rock, etc.

These zonings can be classification of the use geochemical zoning, with the mineral solutions to flow instruments are matched. This can be useful as a guide in determining the direction and mineralization activity center used to be. Numerical methods in analyzing series of zoning are used in the primary halo, are:

1- Grigorian Method: Based on put data normalized data in a certain interval and compare their changes in shapes. [1]

2- Solovov method (gravity center): gravity center of halo for a two-element ratio is obtained. [1] This more comprehensive than the Gregorian method but has two problems: Effect of torque and weakness in analyzing horizons with different distances. 'Axis level' method was developed to correct these problems by using integral of the halo surface in Perpendicular direction of geochemical profiles. The aim of this method is effecting of halo shape to obtain the center of gravity.

This is similar to the mean value theorem in integral and led to obtain a gravity axe for vertical halo, this axe is called 'Axe Level'. Geochemical element zoning is the result of sorting axes levels.

https://doi.org/10.1180/S0026461X00006502 Published online by Cambridge University Press

High pressure and temperature silicon isotope fractionation between metal and silicate

A. SHAHAR[1]*, V. HILLGREN[1], E. YOUNG[2], L. DENG[1], Y. FEI[1], C. MACRIS[2] AND R.B. GEORG[3]

[1]Geophysical Laboratory, Carnegie Institution of Washington, Washington D. C (*correspondence: ashahar@ciw.edu)
[2]Department of Earth and Space Sciences, UCLA, CA
[3]Water Quality Centre, Trent University, Peterborough, ON

The Si stable isotope fractionation between metal and silicate has been investigated experimentally in order to better constrain the amount of silicon present in the Earth's core. Experiments at 1800°C were conducted at 1 GPa, while those at 2000 and 2200°C were performed at 7 GPa. All experiments were in MgO capsules so that no silicon was lost during the run and the three-isotope technique was used to demonstrate equilibrium. The isotope analyses were measured by laser ablation MC-ICPMS as spatial resolution is a key parameter in analyzing experiments.

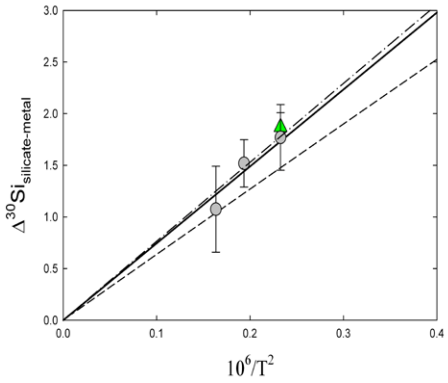

The temperature dependent silicon isotope fractionation is $\Delta^{30}Si_{silicate\text{-}metal} = 7.45\pm0.41*10^6/T^2$ shown in the figure above, experimental data points shown in circles along with best fit line (solid) and theoretical curve (dashed, [2]). The current experiments have: 1. duplicated our previous results [1] performed in a graphite capsule (triangle in figure above), demonstrating that several weight percent carbon in iron metal does not change the silicon isotope fractionation factor, as predicted; 2. shown that the silicon stable isotope fractionation between metal and silicate is insensitive to the structure and composition of the silicate as the fractionation between silicate melt and olivine is insignificant; and 3. shown that there is no pressure effect on isotope fractionation between 1 and 7 GPa (to within analytical uncertainty).

[1] Shahar *et al*. 2009 *EPSL* **228**, 228–234. [2] Georg *et al*. 2007 *Nature* **447** 1102–1106.

Nature and characteristics of metasedimentary rocks in Northern Sanandaj-Sirjan Zone

FATEMEH SHAJARI

School of Geology, College of Science, University of Tehran, Tehran, Iran (f.shajari@yahoo.com)

Upper Permian-Lower Trias sediments from the Sanandaj-Sirjan zone (SSZ) in western Iran record a cycle of Neotethyan oceanic basin opening and closure when the Central Iranian block separated from Gondwana and Arabia. Their studies could determine constraints of the geotectonic evolution of the area. The sediments were metamorphosed under mid-to-upper greenschist-facies conditions due to subsequent northeastward convergence of the oceanic domain below the Iran. Geochemical analysis implied that the studied metasedimentary rocks have relatively uniform chemical composition which may indicate differing from similar sedimentary rocks [1]. Davoudian *et al*. [2] however reported eclogite lenses from a locality near north of Shahrekord which indicate high pressure metamorphism in the SSZ and tectonic processes such as shearing leading to their exhumation during following continent–continent collision.

The granular and lepidoblastic to lepido-granoblastic textures are seen in the slates and phyllites, respectively. Andalusite and garnet are the major porphyroblasts in the schists. These rocks are composed of biotite, muscovite, quartz and feldspars. The schistosity of rocks is oriented in the NW-SE direction.

Major element data has a narrow range and enrichment in Al_2O_3, all of which can be interpreted as a reflection of a pelitic provenance. It is supported by low Cr and Ti concentrations that prevent a mafic source. In addition high aboundances of S-type granitoids that are penetrated into this metasedimentary country rocks reveal partial melting of metapelites to produce these felsic rocks.

[1] Ahadnejad, Hirt, Valizadeh & Bookani (2011) *Geologica Carpatica* doi: 10.2478/v10096-011-0004-5. [2] Davoudian, Genser, Dachs & Shabanian (2008) *Mineralogy & Petrology* **92**, 393–413.

https://doi.org/10.1180/S0026461X00006502 Published online by Cambridge University Press

Keep and touch – Dust and mineral iron utilization by the marine diazotroph *Trichodesmium*

Y. SHAKED[1,2]*, M. RUBIN[2,3] AND I. BERMAN-FRANK[3]

[1]Inst of Earth Sciences, Hebrew Univ., Jerusalem, Israel (*correspondence: yshaked@vms.huji.ac.il)
[2]Interuniversity Inst. for Marine Sciences, Eilat, Israel (formaxrubin@yahoo.com
[3]Faculty of Life Sciences, Bar Ilan Univ., Ramat Gan, Israel (irfrank@mail.biu.ac.il)

Oceanic blooms of *Trichodesmium*, a filamentous N_2 fixing cyanobacterium, provide ~50% of the new nitrogen sources to subtropical and tropical areas, fueling primary production and influencing nutrient flow and biogeochemical cycling of organic and inorganic matter. *Trichodesmium's* extensive surface blooms require large inputs of iron that are partly supplied by aeolian dust sources. Yet the processes and mechanisms associated with dust acquisition are currently poorly defined. Here we explore how natural populations and laboratory cultures of *Trichodesmium* collect, process, and utilize iron from synthetic iron oxides and desert dust. Using a combination of uptake and dissolution experiments with microscopic observations, we find that, similar to most phytoplankton, solid-phase iron has to dissolve prior to its acquisition by *Trichodesmium*. We show that, unlike other studied phytoplankton, *Trichodesmium* apply cell-surface processes that accelerate the rate of dissolution of iron from iron oxides and mineral dust particles, and thereby increase cellular iron uptake rates. Natural puff colonies are particularly effective in dissolving dust, probably due to efficient dust trapping by the intricate colony morphology, followed by active centering and packaging of the dust within the colony core (Fig. 1). Thus, colony formation in *Trichodesmium* provides an advantageous strategy for iron acquisition from particulate sources such as dust.

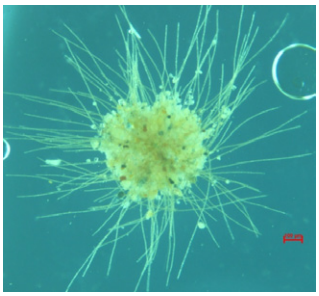

Figure 1: Active centering of dust by puff-shaped natural *Trichodesmium* colony, enabling it to dissolve and acquire iron from dust.

An experimental study on the effect of melt composition on partitioning behavior of copper in magmatic - hydrothermal systems

L.B. SHANG*, H. LI AND W.L. FAN

Institute of Geochemistry, CAS, 46 Guanshui Rd. Guiyang, 550002, China
(*correspondence: shanglinbo@vip.gyig.ac.cn)

Copper is one of the major ore metals in porphyry-type deposits. It has been proposed that metals in those deposits are magmatically derived. The essential feature of the magmatic-hydrothermal model is the separation of mental-rich aqueous fluid from silicate melt. Experimental studies on the partitioning of copper between granitic melt and aqueous fluids have demonstrated the importance of complexing agents, especially chloride, in the transport of copper. However, few experimental data are available concerning the role of melt composition in magmatic-hydrothermal process.

The present study was conducted to evaluate the effect of melt composition on the partitioning behavior of copper. We investigated experimentally the fluid/melt partitioning of copper in the systems synthetic haplogranite gel -H_2O-HCl at 1kbar, 850 °C with Ni-NiO buffer by using rapid-quench cold seal bombs. Experimental data show that the partition coefficient of copper $D_{Cu}^{fluid/melt}$ linearly increases with increasing HCl concentration. That agrees with results of other researchers, who interpreted this behavior as the result of the formation of CuCl complexes in the fluids. $D_{Cu}^{fluid/melt}$ show a strong melt compositon dependence, increasing from 1.28 to 10.09 with the molar $(Na_2O+K_2O)/Al_2O_3$ of melt varying from 1.56 to 0.83, and increasing from 1.35 to 22.18 with the molar Na/K of melt varying from 0.58 to 2.56. The data presented here suggest increasing partition of copper in peralkaline, especially K-rich, granitic melt phase. It implies that, like the fluids, the changes of melt composition also have great effects on the partitioning behavior of copper between aqueous fluids and silicate melt.

https://doi.org/10.1180/S0026461X00006502 Published online by Cambridge University Press

Nanoscale study of exopolymeric substance-mediated uranium biomineralization

PAUL P. SHAO[1]*, DANIEL S. ALESSI[1], MALGORZATA STYLO[1], JOHN R. BARGAR[2] AND RIZLAN BERNIER-LATMANI[1]

[1]Ecole Polytechnique Fédérale de Lausanne (EPFL), Lausanne, Switzerland (*correspondence: paul.shao@epfl.ch)

[2]Stanford Synchrotron Radiation Lightsource (SSRL), Menlo Park, CA, USA

Bacterially-mediated biogenic reduction of soluble hexavalent uranium U(VI) into a less-soluble U(IV) product is among the planned bioremediation strategies at uranium-contaminated sites in the U.S. The primary product of this reduction is thought to be uraninite (UO_2), a highly insoluble crystalline nanoparticulate. While uraninite forms under certain conditions, recent research has shown formation of another U(IV) species under different conditions. *Shewanella oneidensis* MR-1, an intensely studied bacterium for its remediation properties, produces UO_2 under simple aqueous solutions (sodium bicarbonate). In the presence of moderate or high concentrations of alkaline earth cations such as Ca^{2+}, the same bacterium will form U(IV) diffusely distributed on cell biomass and biopolymers, termed monomeric U(IV) [1].

There is electron microscopy evidence that exopolymeric substances (EPS) play a role in the formation of UO_2 [2]. Moreover, EPS-deficient mutants appear to produce less UO_2 than the wild-type, confirming that prediction.

Here, we present a combined microscopic and spectroscopic approach to address the changes in U biomineralization as a function of medium. Using scanning transmission X-ray microscopy (STXM) coupled to near edge X-ray absorption fine structure (NEXAFS), we acquired carbon speciation and actinide elemental maps of *S. oneidensis* wild-type and mutant each generating either UO_2 or monomeric U(IV). In concert, we also provide cryo-preserved, low-dose transmission electron microscope (TEM) images of the reducing bacteria thin-sectioned to display ultrastructure features. The specificity of the association of UO_2 and monomeric U(IV) with biomolecules was demonstrated with these approaches suggesting the importance of individual biomolecules in controlling biomineralization products.

[1] Bernier-Latmani *et al*. (2010) *Environ. Sci. Technol*. **44**, 9456–9462. [2] Marshall *et al*. (2006) *PLoS Biol*. **4**, 1324–1333.

Modelling the free energy of adsorption of persistent organic pollutants at clay mineral-water interfaces

T.V. SHAPLEY* AND S.C. PARKER

Department of Chemistry, University of Bath, Bath, BA2 7AY, UK (*correspondence: t.v.shapley@bath.ac.uk)

Clay minerals represent a cheap alternative for the remediation of pollutants. The clay mineral bentonite has been shown experimentally to adsorb organic pollutants [1] and heavy metal ions [2]. Here we applied computational techniques to model the adsorption of a range of organic molecules, more specifically polyhalogenated compounds (PHCs), on the clay minerals montmorillonite and pyrophyllite. Montmorillonite, a dioctahedral smectite, is the principal constituent of bentonite, while pyrophyllite is the template for all dioctahedral smectites.

The CLAYFF [3] and GAFF [4] force fields were applied to the clay surface and organic molecules, respectively. The interatomic potentials were derived using simple mixing rules and TIP3P/FS [5] water was used in solvated systems. DFT-D2 calculations using the VASP code [6] were carried out to confirm the potential model. PMF free energy calculations were undertaken using the DL_POLY_2.0 code [7]. Further free energy calculations, steered molecular dynamics, umbrella sampling and metadynamics used the PLUMED software plug-in [8].

Our results show that the simple model for the interatomic potentials had good agreement with DFT-D2 calculations. Adsorption energies for montmorillonite were dependent on the counter ions. The free energy techniques all gave comparable results. However, metadynamics was both consistently accurate and less computationally demanding than the other methods. In general, for similarly structured PHCs the adsorption energy increased with the number of chlorine substituents. Even in simple systems the differences are significant, for example the free energies of adsorption for benzene and hexachlorobenzene on the surface of pyrophyllite were -9.6 and -38.6 $kJmol^{-1}$, respectively.

[1] Hassanien *et al*. (2010) *J. Haz. Mat*. **178**, 94–100. [2] Hamidpour *et al*. (2010) *J. Haz. Mat*. **181**, 686–691. [3] Cygan *et al*. (2004) *J. Phys. Chem. B* **108**, 1255–1266. [4] Wang *et al*. (2004) *J. Comp. Chem*. **25**, 1157–1174. [5] Wu *et al*. (2006) *J. Chem. Phys*. **124**, 024503. [6] Kresse & Furthmuller (1996) *Phys. Rev B* **54**, 11169–11186. [7] Smith & Forester (1996) *J. Mol. Graph*. **14**, 136–141. [8] Bonomi *et al*. (2009) *Comp. Phys. Comm*. **180**, 1961–1972.

https://doi.org/10.1180/S0026461X00006502 Published online by Cambridge University Press

Relationship between incidence of esophageal cancer in Maravehtapeh region (Northeast of Iran - Golestan province) and concentration of trace elements in sediments

NEDA SHARIFI SOLTANI[1] AND FARID MOORE[2]

[1]Department of Geoscience, Shiraz University, Shiraz-Iran (*correspondence: N.sharifi09@gmail.com)
[2]Department of Geoscience, Shiraz University, Shiraz-Iran (*correspondence: Moore@susc.ac.ir)

Esophageal cancer is one of the ten most common cancer and the eighth cause of death in the world. In Iran annually about 51,000 new cases of cancer occur. Most organs of men and women involved in is gastrointestinal tract which about 6500 cases are esophageal cancer. Since the distribution of Esophageal squamous cell cancer (esophageal cancer belt) matches loess deposits of the world which is extended from north of China to north east of Iran, Therefore , likely there is a close relationship between loess deposits and this endemic disease.

Sediment samples of study area were taken from 50 stations in 'atrak' river basin. Trace elements results from ICP-MS analysis in the 'ACME' laboratory-Canada were studied.To obtain extent of external factors (Anthrapogenic impacts), 'Enrichment factor' and 'Muller's geoaccumulation index' was calculated which the amount of enrichment factor was mainly between 0.5-2.5 that shows concentration of elements not affected by anthrapogenic factors and the amount of geoacuumulation index was between -0.5-0.5 which also shows no significant pollution. Results of Analysis of varience 'Anova' test which is investigated the statistical relation of formation 'five formations in study area' with concentration of trace elements, shows concentration of Selenium is directly related with the type of formation since with 95 percent confidence level, there is a signicant difference in amount of Se in different formations especially loess deposits which have the least Se concentration. Considering that Se deficiency in body can enhance esophageal cancer risk, recommneded in future studies measuring of Se concentration in water samples and blood serum of residents of this area.

Mobilization of multi-walled carbon nanotubes in consecutive imbibition and drainage events

PRABHAKAR SHARMA[1] AND DENIS M. O'CARROLL[2]

[1]Department of Earth Science, Uppsala University, Villavägen 16, Uppsala, 75236 Sweden (prabhakar.sharma@geo.uu.se)
[2]Department of Civil and Environmental Engineering, The University of Western Ontario, London, ON, Canada (docarroll@eng.uwo.ca)

Carbon nanotubes (CNTs) are important engineered nanoparticles with unique and beneficial properties. As a result CNTs has been used in a wide range of commercial products including electronics, optical devices and drug delivery leading to their disposal in the natural environment. Literature studies have investigated the mobility of CNTs in saturated porous media under differing physical and chemical conditions. However CNT transport in temporally changing porous media water content has not been investigated thus far (a common scenario with rainfall/infiltration events in the vadose zone). This study investigated the mobilization of multi-walled CNTs (MCNTs) in repeated wetting and drying cycles with varying flow rates and ionic strength of the inflow solution. Imbibition-drainage-imbibition cycle experiments suggest that MCNTs mobilization increased with increase in flow rates. MCNTs mobilization occurred only with first imbibition events at low ionic strengths however less mobilization happened for higher ionic strength inflow solution in the first imbibition cycle and additional MCNTs were found in the outflow solution in second imbibition cycle, using low ionic strength solution. This observation was likely due to the attachment forces between MCNTs and sand surface. Most of the MCNT mobilization occurred during liquid-gas interface movement with less chance of MCNTs to jump the energy barrier at higher ionic strength solution experiments. As a result less detachment of MCNTs occurred from the sand surface.

https://doi.org/10.1180/S0026461X00006502 Published online by Cambridge University Press

The Cl isotope composition of the mantle revisited

Z.D. SHARP[1], J. SELVERSTONE[1] AND J.A. MERCER[1]

Dept. Earth & Planet. Sci. Univ. New Mexico, Albuquerque, NM 87131 (zsharp@unm.edu)

Published estimates for the δ^{37}Cl value of the mantle range from less than -3‰ to +5.7‰. We combine new data from mantle-derived materials with new chondritic and lunar data to refine the δ^{37}Cl value of the mantle to between -0.5 and 0.0‰ (SMOC). Samples include basalts from Hawaii, Iceland and New Mexico (δ^{37}Cl = -0.15±0.15‰, *n*=7), peridotites from Balmuccia, Italy (-0.25±0.16‰, *n*=5), and Cl-bearing diamonds from Canada (-0.05‰). The δ^{37}Cl values of our new and previously published data (Sharp *et al*. Nature, 2007; Science, 2010) average -0.15±0.35‰ (*n* = 26), indistinguishable from the lowest lunar sample (δ^{37}Cl = -0.7‰), the average of type 3 chondrites (δ^{37}Cl = -0.5‰; Mercer *et al*. LPSC 2011) and evaporites (~ 0‰).

Although Cl isotope variations do exist in contaminated mantle (John *et al*. EPSL, 2010), the large published range for the primitive mantle is explained by analytical artefacts. Published TIMS data are unreliable, yielding high δ^{37}Cl values (Nakamura *et al*. LPSC 2011). A published SIMS value for 'archived' MORB (< -3‰, Layne *et al*. Geol. 2009) has a Cl content an order of magnitude lower than corresponding standards, explaining the anomalously low value. Low mantle estimates from gas source mass spectrometry (Bonifacie *et al*. Science, 2008) are also likely artefacts of small sample size; their observed systematic decrease in δ^{37}Cl value with size is not seen in our work, presumably because we use a more sensitive continuous-flow method. We do see a sharp drop off to δ^{37}Cl values of < -3‰ for peak areas less than 200mV· sec, but larger replicates of the same mantle samples always give δ^{37}Cl values close to 0‰. The similarity of the crustal and mantle reservoirs explains the lack of secular variation in crustal samples, obviates the need for a fractionation mechanism between mantle and crust and defines a homogeneous inner solar system reservoir.

The Cl isotope composition of the Moon and Mars

Z.D. SHARP[1], C.K. SHEARER[2], F.M. MCCUBBIN[2] AND C.B. AGEE[1,2]

[1]Dept. Earth and Planet. Sci., U. New Mexico, Albuquerque, NM, USA 87131

[2]Institute of Meteoritics, U. New Mexico, Albuquerque, NM, 87131, USA

The bulk Earth and the least altered carbonaceous chondrites have Cl isotope compositions (δ^{37}Cl values) close to 0‰ (Sharp *et al*. Nature, 2007; Mercer et al, LPSC, 2011). In contrast, Cl isotope variations on Mars, and especially the Moon, are extreme – Apollo samples range from near 0‰ (the Earth value) up to 24‰ (Sharp *et al*. Science, 2010 and unpublished). We interpret the high δ^{37}Cl values as a result of degassing of metal chlorides. On Earth, Cl volatilizes from basaltic melts as HCl (g) with no apparent Cl isotope fractionation. In the absence of H_2O, Cl volatilizes as metal chlorides, which leads to the preferential loss of ^{35}Cl, and an ever-increasing δ^{37}Cl value of the residual Cl in the melt. The δ^{37}Cl value is a function of both the H/Cl ratio and total Cl content. The lowest and Earth-like δ^{37}Cl value is found as surface coatings of lunar glass beads which have the highest H- and lowest Cl-contents (Saal *et al*. Nature, 2007) of all measured samples. The highest δ^{37}Cl values are found in KREEP basalts (McCubbin *et al*. GCA in press), which formed in melts with high Cl contents. These results are consistent with a chemical divide between H and Cl. Cl is lost by HCl volatilization until either Cl or H is consumed, leaving the other element in excess. The low δ^{37}Cl samples (74002, 36) fall on the high H/Cl side of the chemical divide, the high δ^{37}Cl value samples lie on the low H/Cl side. If initial Cl contents are low, Cl vaporization will be minimal because Cl saturation of the melt may be only slightly overstepped. We conclude that the Moon was generally anhydrous (10s of ppb H), but anomalous eruptive samples (lunar glass beads) with high H- and low Cl-contents existed and are manifest as low δ^{37}Cl samples.

In contrast to the Moon, Martian meteorites range from -3‰ to +2‰ (*n*= 8). All shergottites have negative δ^{37}Cl value and all cumulates have positive δ^{37}Cl values. Only near-surface effects are known to fractionate Cl isotopes. The different Cl isotope compositions of Martian samples are explained by near-surface contamination or volatile loss.

https://doi.org/10.1180/S0026461X00006502 Published online by Cambridge University Press

Organic matter photochemistry: Singlet oxygen precursor lifetimes

CHARLES M. SHARPLESS

Department of Chemistry, University of Mary Washington, Fredericksburg, VA 22401 (csharple@umw.edu)

Background

Dissolved organic matter (DOM) photochemistry plays a key role in pollutant fate and carbon cycling [1, 2]. Central to this are various reactive intermediates whose production and reactions can alter the DOM. These include $^1O_2$, O_2^- and H_2O_2, e (aq)$^-$, •OH, and triplet DOM states (^{3}DOM*) [3]. Various evidence suggests that ^{3}DOM* is the $^1O_2$ precursor.

$$^1\text{DOM} + h\nu \rightarrow {}^1\text{DOM}^* \rightarrow {}^3\text{DOM}^* \quad (1)$$

$$^3\text{DOM}^* + {}^3O_2 \rightarrow {}^1\text{DOM} + {}^1O_2 \quad (2)$$

Intersystem crossing from the excited singlet forms ^{3}DOM* which then transfers energy to O_2. Despite many studies on $^1O_2$ production, the photophysical properties of ^{3}DOM* are not well known. This work uses the O_2 dependence of $^1O_2$ quantum yields (Φ_{1O2}) to estimate the yields and lifetimes of ^{3}DOM* as a function of wavelength. Experiments employed a Xe lamp, bandpass filters, and fufuryl alcohol as a $^1O_2$ probe. Buffered D_2O was used as a solvent to increase the $^1O_2$ lifetime, allowing for extensive experimentation.

Results and Discussion

Figure 1 displays data for Suwannee River OM at 370 nm. The asymptote above 0.5 mM O_2 shows that all ^{3}DOM* precursors to $^1O_2$ are being trapped and that their quantum yield is 0.025. The ratio of the intercept to slope of the inverse linear plot equals the lifetime of ^{3}DOM* multiplied by the total rate constant for its quenching by and energy transfer to O_2. Assuming a total value of 10^{10} M^{-1} s^{-1} for these processes yields a ^{3}DOM* lifetime of 6.5 µs, which is also found at 313 and 415 nm. Other samples have similar lifetimes that are also invariant with wavelength. However, the quantum yields vary by more than two-fold. This suggests that Φ_{1O2} is controlled by absolute yields of ^{3}DOM* rather than its decay kinetics.

Figure 1: Φ_{1O2} (370 nm) versus [O_2] for Suwannee River Organic Matter, pD 6.0. Inset: linearized inverse plot.

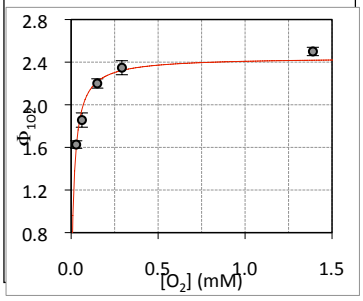

[1] Guerard *et al*. (2009) *Environ. Sci. Technol*. **43**, 8587–8592. [2] Xie *et al*. (2004) *Environ. Sci. Technol*. **38**, 4113–4119. [3] Blough & Zepp (1995) in *Active Oxygen in Chemistry*, Blackie Academic, 280–333.

Dissolution-precipitation as a possible mechanism of C-O-H fluid/melt segregation in the deep mantle

A. SHATSKIY[1,2], K.D. LITASOV[1,2] AND E. OHTANI[1]

[1]Tohoku University, Sendai, Japan (shatskiy@m.tains.tohoku.ac.jp, klitasov@m.tains.tohoku.ac.jp, ohtani@m.tohoku.ac.jp)
[2]IGM SB RAS, Novosibirsk, Russia

Trace amounts of fluid dispersed in the mantle cannot be easily removed from the crystalline framework if that insoluble in the fluid. However, at the mantle conditions water and carbonates are excellent silicate solvents. Hence, the migration of a fluid droplet through a solid may proceed by a combination of dissolution and deposition of the solid at the forward and rear faces of the fluid/melt droplet respectively, and solute flow across the droplet. The driving force for this process is a concentration gradient of solid silicate in the fluid. This can be caused by temperature gradient, differences in stable and metastable phase solubilities, and stress.

In this study we measured MgO-SiO_2 diffusion in the $K_2Mg(CO_3)_2$ (KMC), $K_2Mg(CO_3)_2 2H_2O$ (KMCH), and H_2O at 17 and 24 GPa. The summary of obtained data is shown in the figure below along with available literature data on diffusion in the silicate and carbonate melts and water fluid.

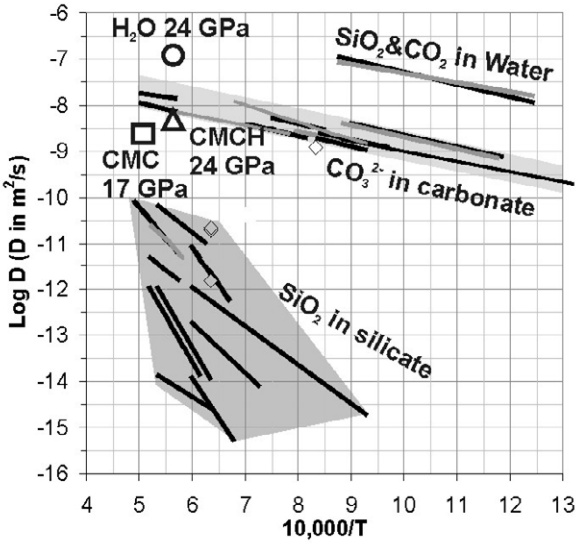

Based on obtained results we estimate stress drived fluid migration rate. For example, at low mantle conditions (2000 K and 25 GPa) migration rate of 10-µm inclusion of hydrous fluid estimated to be 1-2 km/y at 10 MPa stress level.

https://doi.org/10.1180/S0026461X00006502 Published online by Cambridge University Press

Deep crust of the Siberian craton evidence from xenolith

V.S. SHATSKY[1]*, V.G. MALKOVETS[1], L. BUZLUKOVA[1], W.L. GRIFFIN[2], E.A. BELOUSOVA[2] AND S.Y. O'REILLY[2]

[1]V.S. Sobolev Institute of Geology and Mineralogy, Siberian Branch Russian Academy of Sciences, Novosibirsk, 630090, Russia (*correspondence: shatsky@igm.nsc.ru)
[2]GEMOC National Key Centre, Macquarie University, Sydney, 2109, Australia (wgriffin@els.mq.edu.au)

Deep-seated xenoliths hosted in kimberlite pipes (Udachnaya, Leningradskaya, Yubileynaya, Komsomolskaya, Botuobinskaya, Zapolyarnaya) from the Siberian craton include mafic and felsic garnet granulite, two-pyroxene granulites, gneisses, and amphibolite. Calculated equilibration temperatures range from 600 to 850 °C at pressures from 8 to 1.4 GPa. Garnet granulites give the highest temperatures (710-850 °C) and pressures (9-14 GPa) and amphibolites the lowest; felsic granulites fall between these two groups. The mafic xenoliths are picrobasaltic to basaltic in bulk chemical composition. The chondrite-normalised REE patterns for the mafic granulite xenoliths vary from flat to LREE-enriched (La_N/Yb_N=8.6-18.8); some have slight positive Eu-anomalies. Garnet granulite xenoliths with low REE contents and positive Eu-anomalies are interpreted as cumulates. The bulk compositions of felsic granulites and gneisses vary from andesite to rhyodacite. Zircon LAM-ICPMS dating shows several episodes in the formation of the deep crust of Siberian craton. Zircons from mafic granulites are metamorphic and have concordant ages from 1.78 to 1.97 Ga. Most zircon grains from felsic granulites show oscillatory zoning in BSE images; some show core-rim structure, in which the cores have oscillatory zoning. The age of 2.95 Ga obtained from zircon in felsic xenoliths of the Botuobonskay pipe is the oldest age recorded in the xenolith suite. Magmatic zircons from the Zapollyarnay pipe yielded NeoArchean ages of 2.71 Ga.

Primary biological organics in ambient PM in the Southeastern U.S.

S. SHAW[1], G. CASUCCIO[2], E. EDGERTON[3], T. LERSCH[4], A. ROHR[5] AND P. THORNE[6]

[1]Electric Power Research Institute, 3420 Hillview Avenue, Palo Alto, CA, 94306, USA (*correspondence: sshaw@epri.com)
[2]R. J. Lee Group, 350 Hochberg Rd., Monroeville, PA, 15146, USA (gcasuccio@rjlg.com)
[3]Atmospheric Research & Analysis, Inc., 410 Midenhall Way, Cary, NC, 15146, USA (eedgerton@atmospheric-research.com)
[4]R. J. Lee Group, 350 Hochberg Rd., Monroeville, PA, 15146, USA (tlersch@rjlg.com)
[5]Electric Power Research Institute, 3420 Hillview Avenue, Palo Alto, CA, 94306, USA (arohr@epri.com)
[6]University of Iowa, University Research Park, 126 IREH, Iowa City, IA 52242-5000, USA (peter-thorne@uiowa.edu)

Primary biological organic particles (or bioaerosols) are released by, or composed of, biological organisms. These can include fungal spores, microbes, pollen, or other materials. Little is known about the contributions of such biological materials to ambient particulate matter (PM), though indications are that in highly vegetated regions a substantial amount of organic PM mass could be due to such sources. Large areas of natural wilderness exist in the Southeastern U.S., and even the urban areas in the region are known to be heavily impacted by biological emissions.

Therefore a field campaign was launched at one urban (Atlanta, GA) and one rural site (Yorkville, GA) in fall 2009 and spring 2010 to quantify the amount of bioaerosols in both PM2.5 and PM10-2.5. Particle mass, elemental carbon (EC), organic carbon (OC), bioaerosol fragments, and several biochemical markers (endotoxin, protein, and β-D-glucans) were measured through established and modified sampling methods. The methods and method testing will be described, and preliminary results on the contributions of bioaerosol to particle organic carbon will be provided. For example, scanning electron microscopy demonstrated that bioaerosols accounted for 60-70% of the organic carbon mass in PM10-2.5.

This analysis will help to determine the amount and sources of organic PM mass (in particular the importance of primary biological particles to PM), and to investigate potential impacts of naturally emitted PM on human health.

https://doi.org/10.1180/S0026461X00006502 Published online by Cambridge University Press

Proxy validation from the culturing perspective: A top down approach

T.J. SHAW[1]*, M. MYRICK[1], T. RICHARDSON[2] AND L. HILL[1]

[1]Department of Chemistry and Biochemistry, University of South Carolina, Columbia SC 29208 (*correspondence: shaw@chem.sc.edu, myrick@chem.sc.edu, hill@chem.sc.edu)

[2]Department of Biological Sciences, and Marine Science Program, University of South Carolina, Columbia SC 29208 (richardson@biol.sc.edu)

Laboratory culture experiments offer promise for proxy validation under controlled environmental conditions. Long term culture experiments for benthic foraminifera have proved useful for validation of proxy metal uptake as distribution coefficients [1]. Culture experiments have also helped discern ontogenic variation and feeding effects from environmental variations [2]. However the time and culture reservoir size required for such experiments are daunting [3].

Cultures of planktonic species offer a much more practical approach to proxy identification and validation. Small cultures can be maintained under nearly constant environmental conditions. A new instrumental method allows for the analysis of plankton cultures on a cell by cell basis [4]. Measurable differences in cell physiology occur as a function of macro and micro nutrient concentrations. Results from *E. huxleyi* indicate evidence for variations in the Mg incorporation into pigment porphyrins. This technology is being developed to for field-based instruments and holds promise for tracking signals through the water column as material alters prior to burial.

[1] Havach, Chandler, Wilson-Finelli, & Shaw (2001) *Geochim. Cosmochim. Acta.* **65**, 1277–1283. [2] Hintz, Chandler, Bernhard, McCorkle, Havach, Blanks, & Shaw (2004) *Limnol. Oceanogaphyr, Methods* **2**, 160–170. [3] Hintz, Shaw, Chandler, Bernhard, McCorkle, & Blanks (2006) *Geochi.t Cosmochim. Acta* **70**(8), 1964–1976. [4] Hill, Richardson, Profeta, Shaw, Hintz, Twining, Lawrenz, & Myrick (2010) *Rev. Sci. Instrum.* **81**, article 013103.

Genesis of platinum mineralization in gabbro-dolerites of Pay-Khoy (Russia, Nenets autonomous district)

R.I. SHAYBEKOV

Institute of Geology Komi SC UB RAS, Syktyvkar, Russia, 54 Pervomayskaya st (*correspondence: shaybekov@geo.komisc.ru)

Platinum mineralization of dolerites of Pay-Khoy anticlinorium is superimposed on magmatic sulfide mineralization; therefore the formation record of PGE-mineralization has been reviewed by us within the framework of the genesis of sulfide mineralization at late magmatic and hydrothermal stages.

Based on the formation conditions, the PGE enrichment in Pay-Khoy gabbro-dolerites can be distinguished at: 1) isomorphic inclusions in magmatogene sulfides; 2) forming intrinsic minerals from residual fluid melt after crystallization of main sulfide minerals; 3) resedimented in the form of late chalcogenides during postmagmatic transformations. Our observations show that the highest thermal PGE form in the Pay-Khoy gabbro-dolerites represents microinclusions of platinum in sulfides. At decreasing temperature the intrinsic PGE minerals formed, predominantly palladium ones, and gradually the number of corresponding mineral phases increased.

Thus, the platinoids in Pay-Khoy gabbro-dolerites are nonuniformly distributed between three mineral associations: 1) early (magmatic) chalcopyrite-pentlandite-pyrrothine; 2) intermediate (magmatic) sulfide-telluride-sulfoarsenide; 3) late (hydrothermal) arsenide-telluride.

The work was made with the support of the program of the presidium RAS №09-П-5-1006 and SC-7198.2010.5.

https://doi.org/10.1180/S0026461X00006502 Published online by Cambridge University Press

Rates of oxidation in CSPV experiments involving H_2O-bearing mafic magmas

THOMAS SHEA* AND JULIA E. HAMMER

SOEST, Univ. Hawaii, 1680 East-west rd., Honolulu, HI, 96822, USA (*correspondence: tshea@hawaii.edu)

A difficulty in performing experiments on near-liquidus hydrous mafic melts in gas-medium cold-seal pressure vessels (CSPV) is the tendency for H_2O in the fluid phase to dissociate and H_2 to diffuse through capsule material, leading to progressive oxidation of sample material. Consequences include premature stabilization of Fe-Ti oxide phases and commensurate deviation of the liquid line of descent toward silica enrichment. Methodologies commonly employed to mitigate the oxidation problem, not without their own drawbacks, include incorporating CH_4 into the pressurizing gas, limiting run duration to 24 hours, enclosing samples in Au-alloy capsules, and incorporating solid buffering assemblages to serve as indicators of fO_2 excursion. Using the Co-Pd-O system as an fO_2 sensor [2], we examined the rate of oxidation of basaltic andesite at 1010 ºC and P_{H2O}=150 MPa pressurized with a mixture of Ar and CH_4. Our time-series reveals that oxidation occurs at very high rates of 3-4 log units within 48h. Both the variability of fO_2 and magnitude of dehydration-oxidation are considered unacceptable for phase equilibrium work. Incorporation of additional CH_4 serves only to offset the progressive oxidation trend toward a lower absolute range in fO_2. However, incorporation of a substantial mass of Ni metal powder as an O_2 getter to the outer capsule successfully (a) prevents oxidation within 48h, and (b) stabilizes fO_2 at the NNO buffer.

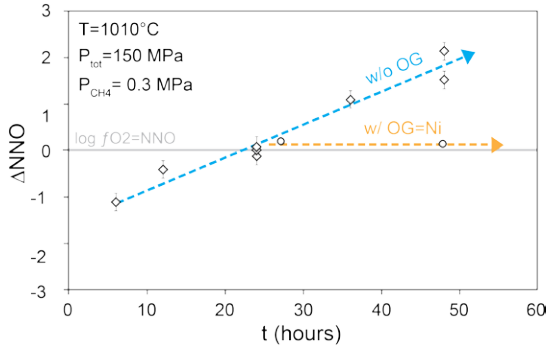

Figure 1: Rates of fO_2 variation in basaltic-andesite

[1] Berndt *et al*. (2002) *Am. Mineral* **87**, 1717–1726.
[2] Taylor *et al*. (1992) *Am. Mineral* **77**, 284–295.

The chemistry of some minerals from the Shir-Kuh granitoidic batholith, South-West of Yazd, Central Iran

M. SHEIBI[1]* AND A. NÉDÉLEC[2]

[1]Faculty of earth Science, Shahrood University of Technology, Shahrood, Iran (*correspondence: Sheibi58@gmail.com)
[2]University of Toulouse, LMTG/OMP, 14 Ave E. Belin, 31400 Toulouse, France (nedelec@lmtg.obs-mip.fr)

The S-type granitoidic batholith of Shir-Kuh (135 Ma) which is part of central Iran is located in SE of Yazd and consists of three main granodioritic, monzogranitic and leucogranitic units. The systematic changes in the composition of plagioclase reveal that the granodiorite is a calcic core plagioclase-rich, the monzogranite a differentiated melt, and the leucogranite a late residual melt. Totally, all biotites have high Al^{VI} (3.2 to 6.2 apfu) which is characteristic of peraluminous granites. The high almandine component of garnet is similar to those in other peraluminous plutons and, in particular, to the magmatic garnets. Muscovite appears as both primary and secondary-looking grains. Monazite occurs as two types of chemically crystals: monazite and brabantite [CaTh $(PO_4)_2$]. The observed homogeneous grains of Th and U poor monazite and tiny microcrystals of brabantite inside the apatite indicate dissolving apatite during anatexis. Little hematite (less than 10%) composition which included within restite biotite consists with the idea that the Shir-Kuh granite is generated from the sedimentary source materials contained graphite. Considering the mineral assemblages presented in the batholith, the fact that some biotite may represent restite and the mean temperature of 820°C in agreement with the zircon saturation thermometry, such liquids may have formed at a temperature 750 to 850°C by dehydration melting of biotite.

https://doi.org/10.1180/S0026461X00006502 Published online by Cambridge University Press

Paleosol constraints on atmospheric CO_2 levels in the Archaean and Proterozoic

N.D. SHELDON

Dept. of Geological Sciences, University of Michigan, 1100 N. University Avenue, Ann Arbor, MI 48109, USA

Precambrian atmospheric pCO_2 levels were previously estimated using simple thermodynamic models based upon the mineral assemblages in paleosols and BIFs [1–3]. However, thermodynamic approaches often require unreasonable or poorly constrained assumptions, and their results are highly dependent on the quality of the thermodynamic data available. In particular, re-evaluation of the paleosol thermodynamic model using more recent thermodynamic data [4] demonstrates that that approach [1] is unreliable and does not provide a significant contraint for atmospheric pCO_2 reconstruction.

As an alternative, a new model based upon paleosol mass-balance during weathering has been proposed [4]. The paleosol mass-balance model gives replicable results from multiple and widely distributed contemporaneous paleosols from the Paleoproterozoic (~2.2 Ga ago [4]) and Mesoproterozoic [4–5], and gives results that are consistent with independent proxies based on microfossils [6–7]. The pCO_2 curve generated by this method spans from 2.7–0.96 Ga ago [4, 5, 8] and indicates that: 1) late Archean and early Paleoproterozoic pCO_2 levels were similar, suggesting no significant change in response to the Great Oxidation Event; 2) from at least 2.7–1.8 Ga ago, pCO_2 levels were broadly consistent at 20–40 times pre-industrial levels; 3) between 1.8 and 1.1 Ga ago, there was a significant drop in pCO_2 to less than 10 times pre-industrial levels, coincident with a change in calcification and stromatolite abundance in the oceans. Climate model results using the paleosol-derived pCO_2 values indicate consistently equable conditions from 2.7–0.96 Ga ago and are also permissive of a Paleoproterozoic 'snowball' Earth event, which suggests that the paleosol mass-balance model provides a quantitatively valuable constraint on Archaean and Proterozoic pCO_2 levels.

[1] Rye *et al*. (1995) *Nature* **378**, 603–605. [2] Ohmoto *et al*. (2004) *Nature* **429**, 395–399. [3] Rosing *et al*. (2010) *Nature* **464**, 744–749. [4] Sheldon (2006) *Precambrian Research* **147**, 148–155. [5] Mitchell & Sheldon (2010) *Precambrian Research* **183**, 738–748. [6] Kah & Riding (2007) *Geology* **35**, 799–802. [7] Kaufman & Xiao (2003) *Nature* **425**, 279–282. [8] Driese *et al*. (in press) *Precambrian Research*.

Effect of helium on structure of SiO_2 glass probed by Raman spectroscopy

G. SHEN[1] AND P. LAZOR[2]*

[1]High Pressure Collaborative Access Team, Geophysical Laboratory, Carnegie Institution of Washington, Argonne, IL 60439, USA (gshen@ciw.edu)

[2]Department of Earth Sciences, Uppsala University, 75236 Uppsala, Sweden (*correspondence: peter.lazor@geo.uu.se)

SiO_2 glass represents a prototypical network-forming glass whose structure can be understood in terms of a continuous network of corner shared SiO_4 tetrahedra, with a high degree of intermediate range order. Numerous studies on structure and compressibility have been performed on SiO_2 glass under high pressure due to its importance as a model geological component, and an increased interest on polyamorphism of glasses and liquids.

In this work, SiO_2 glass was subjected to helium in diamond anvil cell at pressures up to 20 GPa. Micro-Raman measurements were performed in the back-scattering geometry utilizing argon-ion laser excitation. Single-stage, high throughput spectrometer equipped with an EM-CCD detector were used for data collection. Comparison of the evolution of Raman bands of SiO_2 glass upon compression with and without [1, 2] helium loading strongly supports incorporation of helium in the voids of SiO_2 glass structure. This is signified by a less profound narrowing of the inter-tetrahedral angle distribution, as revealed by the spectral widths of band corresponding to the symmetric bending motion of Si-O-Si linkage. Similar effect is seen in the Raman spectra of a recovered sample at ambient pressure. The shape of the corresponding Raman band is largely restored, although signs of local angular distortions remain.

The Raman results on the incorporation of helium are corroborated by a parallel x-ray diffraction study on the structure factor and compressibility [3]. Comparing these observations to the findings of other studies suggest that the effect of helium on the structure and compression of SiO_2 glass is unique. The strong effect of dissolved helium may have implications in Earth's evolution models and is also important in interpreting the high-pressure experiments in general because helium is widely used as a pressure medium.

[1] Hemley *et al*. (1986) *Phys. Rev. Lett*. **57**, 747–750. [2] Sugai & Onodera (1996) *Phys. Rev. Lett*. **77**, 4210–4213. [3] Shen *et al*. (2011) *PNAS* **108**, 6004–6007.

https://doi.org/10.1180/S0026461X00006502 Published online by Cambridge University Press

Partial melting and element transfer during continental subduction-zone metamorphism: Geochemical insights from leucosome within UHP eclogite in the Dabie orogen

YING-MING SHENG* AND YONG-FEI ZHENG

School of Earth and Space Sciences, University of Science and Technology of China, Hefei 230026, China (*correspondence: ymsaint@ustc.edu.cn)

Mineralgraphic observations, elemental and isotopic analyses of major and accessory minerals as well as simultaneous *in situ* LA-ICPMS analyses of zircon trace elements and U-Pb isotopes were carried out on a polymineralic leucosome (rutile + garnet + phengite + epidote + kyanite + quartz) and its host UHP eclogite from the Dabie orogen. The results are integrated to decipher the partial melting of UHP eclogite and its associated mass transfer during continental subduction-zone metamorphism. Multiphase inclusions mainly containing quartz + K-feldspar + K-rich melt ± plagioclase ± other silicate/carbonate minerals were found in garnet and epidote from both the leucosome and eclogite, indicating that the leucosome-forming fluid is a hydrous melt that is rich in K, Al and Si. Oxygen isotope analyses yield temperatures of 570-700ºC for quartz–garnet and quartz-kyanite pairs. The same minerals from the two rocks give nearly consitent $\delta^{18}O$ and δD values, suggesting that the hydrous melt was directly derived from *in situ* partial melting of the host eclogite. In comparison with the host eclogite, the leucosome is remarkably rich in phengite and epidote, indicating that the hydrous melt is associated with distinct LILE and LREE transport. Garnet and rutile in the leucosome show distinct higher contents of HREE (2.2-5.7 times) and Nb-Ta (1.8-2.0 times) than the host eclogite, indicating that these normally fluid-immobile elements are also active during partial melting of UHP eclogite. The LA-ICPMS analyses show that most zircons from the leucosome are metamorphic in origin, while the all zircons in the eclogite are residue of magmatic origin. This suggests that Zr as an incompatible element is preferrentially partitioned into the partial melt. Zircon U-Pb dating gives protolith ages of 774±45 Ma for the eclogite, and metamorphic ages of 217±2 Ma and 210±2 Ma for the leucosome. Thus, the leucosome is interprated to have formed via the partial melting of UHP eclogite during exhumation of the deeply subducted continental crust. In this regard, fluid flow and element transfer in the continental subduction zone occurred in the stage of exhumation rather than subduction.

The effects of silver nanoparticles on wastewater biofilms

Z. SHENG AND Y. LIU*

Department of Civil and Environmental Engineering, University of Alberta, Edmonton, AB, T6G 2W2, Canada (*correspondence: yang.liu@ualberta.ca)

The goal of research

The objective of this research is to understand the potential effects of silver nanoparticles (Ag-NPs) on biological wastewater treatment processes.

Methods adopted

Molecular biology techniques (polymerase chain reaction — denaturing gradient gel electrophoresis, PCR-DGGE) were used to analyze the effects of Ag-NPs on wastewater biofilms, which reveals the response of various genera in the complex biofilm microbial community. Electron microscopy was also used to examnie the uptake of Ag-NPs into the biofilms.

Results and discussion

It was found that intact wastewater biofilms were highly tolerant to Ag-NPs. With an application of 200 mg Ag/L Ag-NPs for 24 h, no significant reduction of bacteria in the biofilms was detected. PCR-DGGE studies showed that microbial susceptibility to Ag-NPs is different for each genus. For instance, sulfur oxidizing bacteria *Thiothrix* sp. are more sensitive to Ag-NPs than other bacteria in the biofilms. Ag-NPs are quickly sorbed to the biofilms during incubation and trapped in extracellular polymeric substances (EPS) in the biofilms. This can be an important reason for the high tolenrance of wastewater biofilms to Ag-NPs. After the removal of loosely bound EPS, the viability of wastewater biofilms was reduced when treated under the same conditions (200 mg Ag/L Ag-NPs, 24 h).

https://doi.org/10.1180/S0026461X00006502 Published online by Cambridge University Press

Metal complexation in hydrothermal fluids: Insights from *ab initio* molecular dynamics

DAVID M. SHERMAN[1]* AND YUAN MEI[1,2]

[1]School of Earth Sciences, University of Bristol, Bristol BS8 1RJ, UK (*correspondence: dave.sherman@bris.ac.uk)
[2]School of Earth and Environmental Sciences, University of Adelaide, Adelaide SA 5000, Australia

Complexation of metals by Cl^- and HS^- ligands in hydrothermal fluids is a fundamental process in the evolution of the Earth's crust and the formation of ore deposits. Current thermodynamic models of complexation equilibria under hydrothermal conditions depend on extrapolations of experimental data using equations of state based on the Born model of solvation. Thermodynamic parameters for aqueous species are often provisional estimates based on systematic correlations between fundamental properties such as entropy, volume, ionic radius etc. Computational molecular simulations, however, can be used to test current thermodynamic models, predict metal speciation, and even estimate thermodynamic properties. For a condensed fluid, molecular dynamics simulations can be used to sample the configurational degrees of freedom in order to predict properties as a function of pressure and temperature. Simulations of dilute solutions, however, require very large systems (1000's of atoms) and very long (> 1 ns) simulation times; such calculations are only practical by treating the atomic interactions using classical two- or three-body interatomic potentials. However, classical potentials seem to be unreliable for describing metal-ligand interactions, especially for transition metals and metalloids such as Sn^{+2}, Au^{+3}, Cu^{+2} and Cu^+. 'Ab initio molecular dynamics' treats the molecular motions classically but the atomic interactions quantum mechanically. Although these simulations are only practical for systems with 100's of atoms over short times (< 100 ps), they are giving fundamental new insights on metal speciation in hydrothermal fluids. Here, we describe simulations of Cu, Zn, Sn, Au, and Ni in NaCl- and HS-bearing aqueous fluids up to 350 °C. We show that predicted structures and speciation are in close agreement with experiment. Based on our simulations, we propose that the major driving force for metal complexation in hydrothermal fluids is the change in translational entropy between reactants and products. Entropies and free energies of complex formation can be estimated using thermodynamic integration and metadynamics. Applications of these techniques to Zn-Cl and Cu-Cl-HS stability constants will be presented.

Collection and determination of suspended particulate trace metals: The US GEOTRACES Intercalibration cruises

R.M. SHERRELL[1]*, H. PLANQUETTE[2], M. PAUL FIELD[1], J.K.B. BISHOP[3], T. WOOD[3], P. LAM[4], B. TWINING[5] AND P. MORTON[6]

[1]IMCS, Rutgers Univ., New Brunswick, NJ 08901 USA (*correspondence: sherrell@marine.rutgers.edu)
[2]School of Ocean & Earth Science, NOCS, Univ. of Southampton SO14 3ZH, UK (h.planquette@noc.soton.ac.uk)
[3]Univ. of California, Berkeley, CA 94720-4767 USA (jkbishop@berkeley.edu)
[4]Marine Chemistry and Geochemistry, WHOI,Woods Hole, MA 02543 USA (pjlam@whoi.edu)
[5]Bigelow Laboratory for Ocean Sciences, West Boothbay Harbor, ME 04575 USA (btwining@bigelow.org)
[6]Department of Oceanography, Florida State Univ., Tallahassee, FL 32306-4320 USA (pmorton@fsu.edu)

As part of the GEOTRACES Intercalibration and Methods Development effort, we have been working to optimize techniques for the accurate and precise determination of suspended particulate trace metals (TMs) from full water column profiles in various oceanic regimes. The goal has been to determine the best particle collection and analysis methods for future GEOTRACES ocean basin sections and to carry out laboratory intercalibration to arrive at community consensus on analytical methods and results. We will present results from the Atlantic and Pacific Intercalibration cruises (IC1 and IC2; 2008-09), with a focus on the feasibility of accurate and precise determination key Geotraces TMs as well as other TMs on small volume (~10L) samples collected from rosette-mounted Go-Flo bottles. We will summarize our findings with respect to filter type, practical performance, blanks and potential artifacts such as dissolved metal adsorption. Details of the filtration methodology will be described, with an important emphasis on minimizing element-dependent particle settling artifacts and determining appropriate procedural blanks. Digestion methods for particulate samples will be evaluated and results from an interlaboratory intercalibration exercise will be presented, with a summary of ICP-MS analytical approaches. Results for samples collected using 5-10L Go-Flo bottle samples will be compared with parallel samples collected with large-volume *in situ* pumps.

https://doi.org/10.1180/S0026461X00006502 Published online by Cambridge University Press

Manganese precipitation and the removal of zinc from No Cash Creek, Keno Hills, Yukon, Canada

B.L. SHERRIFF[1], B. JOHNSON[2] AND S. DAVIDSON[3]

[1]Department of Geological Sciences, University of Manitoba, Winnipeg, MB, Canada, R3T 2N2 (*correspondence: BL_Sherriff@umanitoba.ca)

[2]InTerraLogic Inc.4715 Innovation Dr, Suite 110, Fort Collins, CO 80525, U.S.A

[3]Access Consulting Group, #3 Calcite Business Centre151 Industrial Road, Whitehorse, Yukon Y1A 2V3Canada

No Cash Creek is a natural stream that receives water from the 500-level adit of the historic No Cash Mine (1948 to 1988). The adit discharge water and stream sediments contain elevated concentrations of Mn, Fe and Zn which decrease rapidly downstream in cascading (aerated) and additionally in a quiescent peat bog environment.

Optical microscopy showed that there were coatings around lithic grains and plant fragments in stream sediments within 600 m of the adit. EMP BSE images and element mapping of the lithic coatings show concentric bands rich in Mn and Zn (Fig. 1).

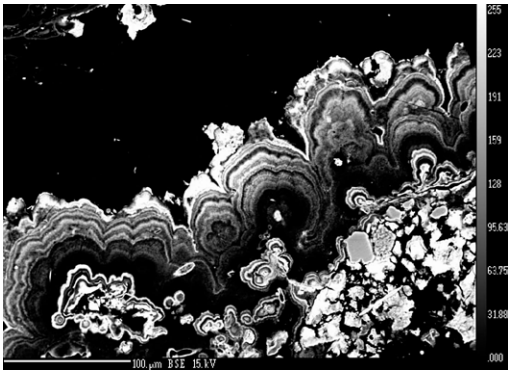

Figure 1: Mn-rich coating on a lithic grain

Initial data show that the average concentration of Mn and Zn varies within one sample with type of mineral substrate from 23 wt. % Mn and 6 wt. % Zn around pyrite to 9 wt. % Mn and 4 wt. % Zn around sphalerite. Mafic lithic fragments also have higher Mn and Zn than silicic grains. There is also considerable variation across one coating (Fig.1) from 30 to 12 wt. % Mn and 8 to 4 wt. % Zn although the Mn:Zn ratio remained constant at 3.1 (st. dev. 0.5).

Coatings around wood contain predominantly Fe with <30 wt. % Fe and <3 wt. % Zn. There is no apparent relationship between the concentration of Fe and Zn.

In conclusion, the major process removing Zn from the water of No Cash Creek is coprecipitation with or absorption on Mn-rich coatings around lithic grains.

Hotspot: The Snake River geothermal drilling project

JOHN W. SHERVAIS

Dept Geology Utah State University, Logan Utah 84322-4505 (john.shervais@usu.edu)

The Snake River Plain (Idaho, USA) represents the track of deep-seated mantle hotspot that has thinned the lithosphere and fueled the intrusion of up to 10 km of hot basaltic magma into the lower and middle crust. The heat from these intrusions, and from rhyolites formed by the basalt, drives the high heat flow and high geothermal gradients observed in deep drill holes from throughout the Snake River Plain [1-3]. Heat flow in the SRP tends to be high along the margins of the plain (80-100 mW/m^2-s) and low in shallow drill holes along the axis of the plain (20-30 mW/m^2-s). However, deep drill holes (>1 km) along the axias of the plain are characterized by high heat flows and high geothermal gradients below about 500 m depth [2]. This discrepancy is caused by the Snake River aquifer – a massive aquifer system that extends under the plain. Thermal gradients through the aquifer are static until the base of the aquifer is reached, then rise quickly at deeper levels in the crust. Below the aquifer along the axis of the plain, heat flow values are comparable to heat flow values along the margins of the plain or higher (75-110 mW/m^2-s [2]). Bottom hole temperatures for wells along the margins of the plain near Twin Falls are typically around 30-60°C at 400-600 m depth [4] and as high as 120°C at 2800 m depth in the axial region of the plain [2].

The Snake River Geothermal Drilling Project is jointly funded by the US Department of Energy (DOE) and by International Continental Drilling Program (ICDP). Our goal is to evaluate geothermal potential in three settings: (1) the high sub-aquifer geothermal gradient associated with the intrusion of mafic magmas and the release of crustal fluids from the associated wall rocks, (2) the valley-margin settings where surface heat flow may be driven by the up-flow of hot fluids along buried caldera ring-fault complexes, and (3) in the western SRP graben. Drilling is currently in progress.

[1] Blackwell (1978) *Geol Soc Am Memoir* **152**. [2] Blackwell (1989) *Tectonophysics* **164**, 323–34. [3] Lewis & Young (1989) USGS *Water-Resources Investigations Report* **88**–4152. [4] Baker & Castelin (1990) Idaho Dept. Water Resources, *Water Information Bulletin* No. **30**, Part 16.

https://doi.org/10.1180/S0026461X00006502 Published online by Cambridge University Press

Geological characteristics of the Hukeng tungsten deposit, Jiangxi Province, South China

GUODONG SHI, MAOYAN MA, JUN LIU, HAIJIAO YOU, YOUFEI GUAN AND YONG ZHAN

The Civil Engineering School, Anhui University of Architecture, P.R. China (gdshi@aiai.edu.cn)

Hukeng tungsten deposit, located in Wugongshan metallogenic belt in central part of Jiangxi Province, South China, is one large scale quartz vein type wolframite deposit, which is in the south margin of Hukeng granite intrusion, covering the area of 6 km^2.

The strata exposed in the Hukeng ore district belong to the Sinian Laohutang formation and Likeng formation, and are composed of slightly metamorphic sericite phyllite, phyllitic siltstone and phyllitic sandstone. Two groups of faults are well developed in the Hukeng ore district, NE and NW faults separately, which are all composed of silicated breccia and mylonite and control the formation of the Hukeng tungsten deposit. There developed the Hukeng muscovite granite stock ($\gamma^{52\ (2)c}$) with age of 151.6±2.6 [1], where developed the wolframite-bearing quartz veins. The muscovite granites are with high content of garnet, developing silicification and greisenization generally and associated with W, Zn Bi and S mineralization. Wall rock alteration in the Hukeng deposit includes silicification, potassic feldsparization, fluoritization and hornfelsic alteration.

In this deposit, more than 310 ore veins with WO_3 grades from 0.1% to 2.5% have been recognized. These ore veins distribute in Xinsheng'ao sector, Hukeng sector and Xijialong sector. Ore types are mainly wolframite quartz ores, wolframite-fluorite quartz ores and wolframite-sulfide quartz ores. Ore minerals in this deposit are mainly wolframite and pyrite, secondly sphalerite and chalcopyrite, with minor amounts of molybdenite, chalcocite, cubanite, bismuthinite and native bismuth. The ore textures mainly include idiomorphic texture, hypautomorphic texture and poikilitic texture, and the ore structures include massive structure, banding structure and compound structure of massive and banding. Based on cross-cutting relationships of the ore veins, mineral assemblages, paragenetic sequence and ore fabrics, the ore-forming process can be divided into three mineralization stages: quartz-wolframite stage, quartz-fluorite-wolframite stage and quartz-pyrite-sphalerite-wolframite stage.

This research was financially supported by the Doctoral Fund of Anhui University of Architecture of China (No.K02415).

[1] Liu *et al*. (2008) *Acta Petrologica Sinica* **24**(08), 1813–1822.

Experimental test of the CO self-shielding model for the early Solar System's oxygen isotope evolution

X.-Y. SHI[1], Q.-Z. YIN[2], Z. LUO[1], H. HUANG[1] AND C.-Y. NG[1]

[1]Dept. Chemistry, Univ. California, Davis, CA, USA
[2]Dept. Geology, Univ. California, Davis, CA, USA

We designed a laboratory experiment to test the carbon monoxide self-shielding (COSS) model advanced to explain the oxygen isotope distribution in the early Solar System materials [1-3]. Our unique 'windowless' vacuum ultra-violet (VUV) ultra high resolution laser photodissociation and photoionization mass spectrometry is designed to mimic the solar nebular photochemistry environment and experimentally verify if the CO photodissociation at VUV wavelengths (90-110 nm) would produce the expected mass independent oxygen isotope fractionation as predicted in the recently revived self-shelding model [1-3]. This model has been invoked to explain the peculiar oxygen isotope distribution observed in early solar system materials and has a specific prediction for the Sun's oxygen isotope composition [4], a top science priority of NASA's GENESIS mission.

However, the first experimental test of COSS model by [5] using the Advanced Light Source (ALS) at Lawrence Berkeley National Laboratory (LBNL), poses a serious question on the COSS model, although the validity of [5] were immediately challenged by [6-8]. The significance of COSS model for the early solar system warrants a second opinion with closer experimental scrutiny. If the COSS model stands the test of experimental verification, it has major implications for the origin and transport of water in the Solar System that governs the ultimate habitablility of planets.

Our VUV laser system can generate 4-5 orders of magnutide higher optical resolution, with brightness more than 6 orders of magnitude greater than the broadband synchrontron light source at ALS at LBNL. This will ensure higher signal-to-noise ratios when studying weak transitions or transitions of less abundant isotopologues, such as $^{13}C^{17}O$. Our initial finding supports a 'slope-1' ^{16}O depletion line as the COSS model postulates and observed in the early solar system material and now observed in the Sun [9].

[1] Clayton, R. N. (2002) *Nature* **415**, 860. [2] Yurimoto & Kuramoto (2004) *Science* **305**, 1763. [3] Lyons & Young (2005) *Nature* **435**, 317. [4] Yin, Q.-Z. (2004) *Science* **305**, 1729. [5] Chakraborty *et al*. (2008) *Science* **321**, 1328. [6] Lyons *et al*. (2009) *Science* **324**, 1516a. [7] Federmann & Young (2009) *Science* **324**, 1516b. [8] Yin, Q.-Z. *et al*. (2009) *Science* **324**, 1516c. [9] McKeegan *et al*. (2011) *Science* (in press)

https://doi.org/10.1180/S0026461X00006502 Published online by Cambridge University Press

Evolution mechanism of groundwater environmental factors under artificial recharge

SHI XU-FEI[1,2] AND ZHANG WEN-JING[1,2]

[1]College of Environment and Resources, Jilin University, Changchun 130026, China
[2]Institute of Water Resources and Environment, Jilin University, Changchun 130026, China

Research Content

In order to study the effect of artificial recharge on the groundwater quality, the mixed effect of artificial recharge water and groundwater was studied by use of mathematical simulation. The evolution of the groundwater environment and characteristics of elements was studied by analysising the correlation of different amount of recharge water, temperature, redox conditions and pH, which provided basis for environmental control in indoor simulated experiment.

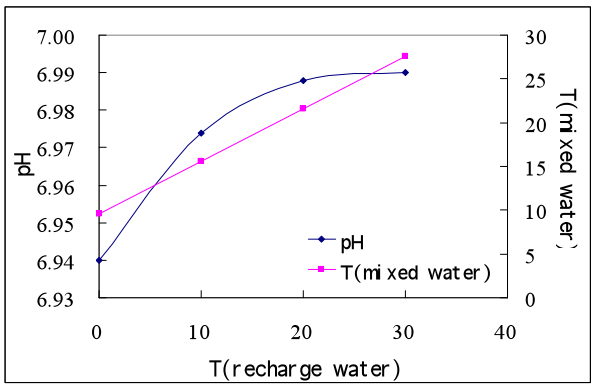

Figure 1: Curve of T of recharge water vs pH and T of mixed water (Recharge water:Groundwater=6:4)

Results

The artificial recharge water will not lead to catastrophe or decrease of water quality in aquifer, and it will improve water quality in aquifer to some extent. The influence sphere of temperature, redox conditions and pH in different artificial recharge conditions was determined.

Discussion on radioactively environmental problems during phosphorite mining and processing in Longmenshan area

SHI ZE-MING, NI SHI-JUN AND ZHANG CHENG-JIANG

Department of Geochemistry, Chengdu University of Technology, China (shizm@cdut.edu.cn, nsj@cdut.edu.cn, zcj@cdut.edu.cn)

Longmenshan area is the main phosphorite producing zone in Sichuan province, with abundant phosphorite resources which are mostly reservoired in strata of upper Sinian, lower Cambrian and upper Devonian. The phosphorites are neritic sedimentary deposits characterized by containing less high-grade ore, more lean ore and harmful impurities unevenly distributed. There are two major phosphorite mines in studied area: Qingping and Jinhekou mines. And the phosphorus chemical enterprises in Sichuan province are mainly located in the Tuojiang basin.

Phosphorites, especially the marine facies phosphorites are widely distributed and strongly accumulated in uranium. Most of phosphorites have high radioactive uranium contents. Owing to phosphorite mining and processing in Longmenshan area, the Chengdu plain, especially in Tuojiang basin, has higher level in radioactive element content. The primary source tracing results show that average content of uranium in phosphorites is 31.0mg/kg, much higher than the background value, and nearly 10 times of uranium content in wall rock. And the average content of uranium in phosphate fertilizer is 20.9 mg/kg, about 7 times of that in wall rock. Phosphorite mining and processing are main causes for the high radioactive elements contents in this region.

The uranium content analysis on the main river water of Tuojiang basin, Mianyuan River and Shitingjiang River, shows that the average uranium content in water is up to 1.90 ng/ml of Mianyuan River, and 0.79 ng/ml of Shiting River. Both of the values are much higher than the average level (0.309 ng/ml) of rivers all over the world.

The uranium content study on the horizontal and vertical profile of soil in the vicinity of phosphogypsum dumps in phosphate fertilizer plant shows that phosphogypsum dumping has great impact on the soil radioactive level with uranium diffusion more than 2km width in horizontal and 50cm depth in vertical.

https://doi.org/10.1180/S0026461X00006502 Published online by Cambridge University Press

Pb sources of bivalves from Western Canada, Mexico and Hawaii

A.E. SHIEL, A.C. BYRNE AND D. WEIS

PCIGR, EOS, Univ. of British Columbia, Vancouver, BC V6T 1Z4, Canada (ashiel@eos.ubc.ca)

Bivalves from British Columbia (Canada), Hawaii (US) and Baja California (Mexico) show human-related trace metal input that we track with Pb isotope 'fingerprinting'.

Oysters from both Desolation Sound (BC mainland) and Barkley Sound (west coast of Vancouver Island) have relatively low Pb contents (0.05–0.22 μg g^{-1} dry weight) with Pb isotopic signatures (^{206}Pb/^{207}Pb = 1.1483–1.1744) indicating large contributions from anthropogenic sources. The Pb isotopic ratios can be explained by mixing of modern anthropogenic Pb emissions with natural Pb end-members (e.g. Coast Plutonic Complex [1]). The Pb isotopic signatures of the BC oysters are also consistent with those of BC atmospheric aerosols (recorded by lichens [2]) and road dust collected from highways in the lower BC mainland [3]. More specifically, Desolation Sound oysters have higher Pb contents and lower ^{206}Pb/^{207}Pb values than those from Barkley Sound. The lower ^{206}Pb/^{207}Pb ratio exhibited by the BC mainland oysters is attributed to contributions of anthropogenic Pb emissions from a source that is characteristically unradiogenic (low ^{206}Pb/^{207}Pb), potentially emissions from ore smelting in a nearby facility [4].

The Pb isotopic signature (1.1652 for ^{206}Pb/^{207}Pb) of Hawaiian oysters (Honolulu Harbor) is comparable to that exhibited by BC oysters, despite significantly higher Pb concentration (5.7 μg g^{-1} dry weight). Lead contents (0.07–0.42 μg g^{-1} dry weight) of Mexican bivalves (Baja California) are within the range of those of BC bivalves with Pb signatures (^{206}Pb/^{207}Pb = 1.1788–1.2088) closer to natural values.

The similarity between the Pb isotopic compositions of bivalves from BC, Hawaii and Mexico suggests comparable anthropogenic Pb sources across the NE Pacific, e.g. from unleaded motor gasoline and diesel fuel. Even with the low Pb levels found in some bivalves (e.g. BC oysters), Pb isotopes can be used to identify emissions from industrial processes and consumption of fossil fuels as important Pb sources.

[1] Cui and Russell (1995) *GSA Bull* **107**, 127–138.
[2] Simonetti *et al*. (2003) *Atmos Environ* **37**, 2853–2865.
[3] Preciado *et al*. (2007) *Water Air Soil Poll* **184**, 127–139.
[4] Shiel *et al*. (2010) *Sci Total Environ* **408**, 2357–2368.

Structure and petrology of the mantle beneath Hawaii constrained by seismic discontinuity imaging and mineral phase relations

S.-H. SHIM[1], Q. CAO[1], R.D. VAN DER HILST[1] AND M.V. DE HOOP[2]

[1]Massachusetts Institute of Technology
[2]Purdue University

Hawaiian volcanoes has been regarded as the archetype of the surface representation of deep mantle plume. Yet, the structure and chemisty of the plume remain uncertain. Our GRT imaging of velocity discontinuities combined with phase relations studied in mineral physics provides new constraints on the structure and petrology of the mantle between 200 and 1000 km depths.

While only small topographic changes were found directly beneath Hawaii, large depth variations of the *410*, *520*, and *660* discontinuities were found up to 2,000 km west of Hawaii. The deepening of the *410* and *520* discontinuities are consistent with high-temperature response of the α-to-β and β-to-γ transformations due to their positive Claepyron slopes. Westward from Hawaii the *660* discontinuity changes from anomalously shallow to anomalously deep, suggesting a lateral transition from the post-spinel to a post-garnet transformation (in pyrolitic mantle) across a high temperature anomaly near the base of the transition zone. The large spatial scale of *660* topography (compared to *410*) is consistent with a regional-scale boundary layer and ponding of hot material at 660-km depth.

Our images also reveal reflectors at 300 and 800 km depths and splitting of the *520* discontinuity. Splitting of the *520* discontinuity can occur if the host rock is significantly enriched with Ca and Si. The *300* discontinuity can be related to a silica transition, requiring Si-enrichment. The *800* discontinuity can be related to either the post-stishovite transformation or post-garnet transformation in an Al, Si-rich rock. Therefore, these structures indicate significant presence of non-pyrolitic components in the top 1000 km of the mantle beneath Hawaii, and the composition that is responsible for these structures is likely basaltic. Our study provides first seismic evidence for the significant existence of recycled components in the mantle beneath Hawaii.

https://doi.org/10.1180/S0026461X00006502 Published online by Cambridge University Press

Nature of mantle heterogeneities

S.-H. SHIM, R.D. VAN DER HILST, B. GROCHOLSKI, K. CATALLI, Q. CAO AND X. SHANG

Massachusetts Institute of Technology

Seismic studies have revealed discontinuous changes and lateral variations in velocities at different depths in the mantle. While temperature variation is an important factor, the interpretation of some large-scale mantle structures requires compositional variation. However, the composition of the heterogeneities remains unclear (e.g. primordial or recycled).

Our high-resolution seismic GRT imaging revealed discontinuities at 300, 540, 800 km depths beneath Hawaii [1]. The silica phase transitions can explain the shallower discontinuities. The post-stishovite transition in an Al-rich rock or the post-garnet transition in a Si-rich rock can explain the deeper discontinuity. We also found splitting of the *520* discontinuity (to 520 and 540), which can be related to the exsolution of $CaSiO_3$ perovskite in a Ca-rich rock. These suggest a significant amount of recycled materials (e.g. basalt) in the upper mantle beneath Hawaii.

In the mid-mantle, Fe^{3+} in perovskite [2] and Fe^{2+} in ferropericlase [3] undergo high spin to low spin transitions. Although these transitions are unlikely to cause seismic discontinuities, the spin transition of Fe^{3+} in perovskite may change the bulk sound speed of Al-rich heterogeneities (such as basalt) at 1700-2000 km depth, where lateral variations in bulk sound speed have been documented seismically [4].

The effects of Al in the lowermost mantle would make the perovskite-to-postperovskite boundary seismologically undetectable in pyrolite [5, 6]. Our new experiments reveal that the boundary is seismically detectable in harzburgite and basalt due to element partitioning with ferropericlase and silica, implying that the observation of the D″ discontinuity is related to a significant presence of recycled materials in the lowermost mantle [6].

This series of studies implies that differentiated rocks (e.g. basalt) injected into the mantle by subducting slabs may exist over the entire depth range of the mantle and survive over geologic time scales.

[1] Cao *et al*. (2011) in review. [2] Catalli *et al*. (2010) *EPSL*. [3] Badro *et al*. (2003) *Science*. [4] Trampert *et al*. (2004) *Science*. [5] Catalli *et al*. (2009) *Nature*. [6] Grocholski *et al*. (2011) in review.

Electrolyte ion adsorption at the hematite/water interface: A cryogenic X-ray photoelectron spectroscopy study

KENICHI SHIMIZU*, ANDREI SHCHUKAREV, PHILIPP KOZIN AND JEAN-FRANÇOIS BOILY

Department of Chemistry, Umeå University, Sweden
(*correspondence: kenichi.shimizu@chem.umu.se)

Cryogenic X-ray photoelectron spectroscopy was used to probe monovalent ions (Na^+, K^+, Rb^+, Cs^+, NH_4^+, F^-, Cl^-, Br^-, I^-) associated to the hematite/water interface. Our findings revealed coexisting cations and anions both below and above the isoelectric point of hematite. Surface loadings tend to follow the trend in the ionic radii of both alkali metal and halide ions. Chloride loadings are largely unaffected by the identity of the associated alkali metal ion. Sodium loadings are, on the other hand, considerably affected along the halide series (Fig. 1). Sorption of ammonium ion occurs by hydrogen bonding to surface hydroxyl groups, a mechanism shifting the pK_a of NH_4^+ from 9.3 in water to 8.4 at the interface.

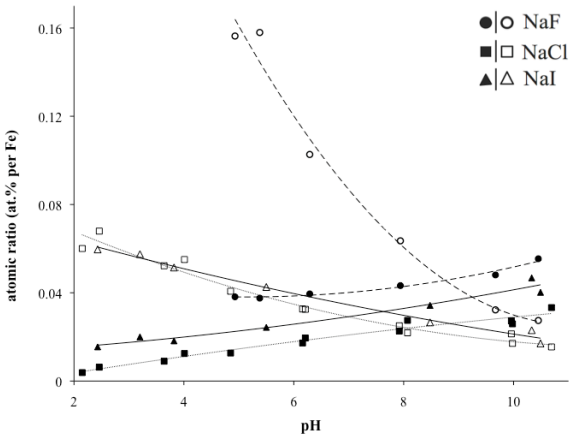

Figure 1: Surface loadings of electrolytes sodium (closed symbols) and halide (open symbols) ions (I=50 mM).

https://doi.org/10.1180/S0026461X00006502 Published online by Cambridge University Press

Geochemical study of fresh volcanic glasses from ~145Ma Shatsky Rise

K. SHIMIZU[1]*, J-I. KIMURA[1], Q. CHANG[1] AND T. SANO[2]

[1]IFREE, JAMSTEC, Yokosuka, Kanagawa, 237-0061, Japan (*correspondence: shimmy@jamstec.go.jp)

[2]National Museum of Nature and Science, Tokyo 169-0073, Japan

Shatsky Rise is a Late Jurassic-Early Cretaceous large oceanic plateau located in the northwestern Pacific. It consists of three major massifs: Tamu, Ori and Shirshov Massifs from southwest (older) to northeast (younger), forming along the trace of a triple junction at a mid oceanic ridge. The Rise is 1000km × 200km in size. During the IODP Exp. 324 (Sept.-Nov., 2009) five sites were drilled on Shatsky Rise, two on Tamu Massif (Sites U1347 and U1348; east flank and north flank), two on Ori Massif (Sites U1349 and U1350; summit and east flank) and one on Shirshov Massif (Site U1346; summit). Unaltered fresh volcanic glasses were sampled from all sites except for Site U1349. Glass is preserved as thin rims of lava flow margins or fragments in volcanic breccias. All glasses (115 samples) are sub-alkalic (tholeiitic) basalts, with MgO and SiO_2 contents ranging from 8.5 to 5 wt% and from 48.5 to 52 wt%, respectively. Three types of magmas (normal-Ti, low-Ti and high-Nb) are identified in this study. Assuming that source of these magmas was depleted MORB source mantle [1], the trace element patterns of the normal-Ti magmas suggest that they formed at deeper depths within the garnet stability field (~3GPa), whereas the low-Ti and high-Nb magmas may have formed at shallower depths, where spinel was stable (~1 GPa). Glasses with high Nb/U from Site U1348 and high-Nb type from Site U1350 indicate that the magmas of Shatsky Rise require more than one mantle source. Deep mantle melting and multiple sources for these magmas are different from N-MORB and are important factors to constrain for genesis of Shatsky Rise.

[1] Mahoney *et al*. (2005) *Geology* **33**, 185–188.

Large regional variations in F/Cl ratios for the MORB source mantle

N. SHIMIZU

Woods Hole Oceanographic Institution (nshimizu@whoi.edu)

Fluorine (F) and Chlorine (Cl) are highly incompatible in mantle-basalt systems (Dalou *et al*. 2011) and their abundances in basaltic melts are generally unaffected by solubility limits (e.g. Carroll and Webster, 1994). These features could make their abundance ratio (F/Cl) in mid-ocean ridge basalts (MORBs) a good additional tracer for elucidating how heterogeneity of the MORB source mantle has evolved. Using analytical procedures developed with a Cameca IMS 1280 at Woods Hole Oceanographic Institution, F and Cl concentrations in glasses of basaltic compositions are determined routinely with precisions of ±10% (2σ) for F and ±5% (2σ) for Cl. Based only on melt inclusion data obtained here and in literature (~220) from EPR (Siqueiros FZ, Saal *et al*. 2002; JdF Axial, Helo *et al*. 2011), MAR (17°N, FAMOUS, 23-27°N, 33°S), and Gakkel Ridge (Shaw *et al*. 2010), it is found that F/Cl ratios display non-overlapping clusters for regions, and subgroups of a region: F/Cl = 10±1 for MAR (17°N, 23-27°N, a subgroup of FAMOUS), consistent with the north Atlantic average value of Schilling *et al*. (1980). F/Cl = 5±1 for Gakkel and a subgroup of JdF, and samples from 33°S MAR and a subgroup of JdF and FAMOUA possess F/Cl=2.5±0.5. In contrast, the Siqueiros dataset display distinctly high and variable F/Cl (14 – 80). It is evident that the observed variations are not produced directly by seawater-related mechanisms, and that no single F and Cl composition can be assigned to the MORB source mantle, suggesting local as well as regional heterogeneity due to incorporation of lithologies with diverse F/Cl fractionation prehistories. It is also noticeable that the range of F/Cl in MORBs is significantly different from that for arc magmas (< 0.5, e.g. Le Voyer *et al*. 2010).

https://doi.org/10.1180/S0026461X00006502 Published online by Cambridge University Press

Effect of thickness of oceanic lithosphere on chemical composition of OIBs: Implication for origin of the South Pacific magmatism

G. SHIMODA

Geological Survey of Japan, National Institute of Advanced Industrial Science and Technology, Tsukuba 305-8567, Japan (h-shimoda@aist.go.jp)

The northwest Pacific Ocean is known to contain a large number of Cretaceous seamounts and several oceanic plateaus and rises. These seamounts, plateaus and rises may have formed during the large-scale magmatic event in the South Pacific that is still active in the present-day French Polynesia region. Although it is unclear whether the Cretaceous seamounts and plateaus were produced by the same process that is now operate in the South Pacific, distinct isotopic signatures of the Cretaceous seamounts can be traced back to the magmas of the South Pacific, suggesting that single process has been active since the Cretaceous [1].

In order to examine the geochemical connection between the Cretaceous seamounts and present-day ocean islands, elemental ratios are determined for fluid-immobile incompatible elements (La/Yb, Nb/Zr, Ta/Zr, Th/Nb and Th/Ta). A notable geochemical feature of these ratios is a correlation between the elemental ratios and 'relative age' that can be an index of the thickness of lithosphere beneath hot spots. In addition, there are no systematic difference in the elemental ratios between the Cretaceous seamounts and present-day ocean islands. As the thickness of oceanic lithosphere is a function of square root of its age, these correlations suggest importance of tectonic environment to determine the chemical composition of the magmas. Other important geochemical feature is that the elemental ratios of mid-ocean ridge basalts (MORBs) from the East Pacific Rise (EPR) may not be on these trends. This observation could imply that source material of the EPR MORBs is different from that of the seamounts and islands. Since the source material of EPR MORBs can have a representative composition of upper mantle beneath the South Pacific, this difference could imply the material flow from the deep mantle. Therefore melting of mantle plume from the lower mantle, which melting condition depends on thickness of lithosphere, can be a plausible origin of the magmatism in the South Pacific.

[1] Konter,. Hanan, Blichert-Toft, Koppers, Plank & Staudigel (2008) *EPSL* **275**, 285–295.

Geochemical characteristics of black slate-hosted uranium deposits in the Okcheon Metamorphic Belt, Korea

DONGBOK SHIN*, SUJEONG KIM AND MINA CHOI

Kongju Nat'l Univ. 314-701, Korea (*correspondence: shin@kongju.ac.kr)

Carboneceous black slates in the Okcheon Metamorphic Belt of South Korea are thin beds known for their low grade U mineralization accompanying rare elements such as Ba, V, and Mo. U mineralization is distinctly concentrated in coalish slates which are imbedded in the black slates. Coalish slates show highly disturbed pattern in their texture unlike black slates, and contain quartz vein and sulfide minerals such as pyrite and pyrrhotite. Chondrite-normalized REE patterns of 36 samples for both of the rock types show that coalish slates are more enriched in HREE compared to black slate, and the total REE contents are higher in coalish slate (231 ppm) than in black slate (159 ppm). These petrographical as well as geochemical features strongly suggest that U mineralization in the black slate was related with post depositional hydrothermal activity. U also shows strongly positive correlation with V, Cu, and Mo, indicating that they were precipiated together during the hydrothermal process. Sulfur isotope compositions of black slate are low in values from -19.5 to 1.5‰, implying organic sulfur from sedimentary process, and those of coalish slate range from 7.3 to 9.0‰, possibly by metamorphism or hydrothermal process. As for carbon isotope, black slate ranges from -16.8 to -3.8‰ and coalish slate from -15.8 to -4.6‰. The wide range of carbon isotope reflects the mixture of organic carbon with calcite carbon from seawater origin. On the contrary, oxygen isotope compositons of the two rock types are narrow in range and similar to each other (14.6 to 15.5‰ for black slate and 14.9 to 18.5‰ for coalish slate), implying that oxygens are from calcite of seawater origin. Thus it seems like that the rare elements listed above would have been remobilized to participate in the formation of coalish slate after they were originally introduced to black shale under reduced condition.

https://doi.org/10.1180/S0026461X00006502 Published online by Cambridge University Press

Introduction of three granitoid types with different origins from ophiolitic mélange of Nain (Central Iran)

N. SHIRDASHTZADEH[1]*, R. SAMADI[2] AND G. TORABI[3]

[1]Department of Geology, Faculty of Science, University of Isfahan, Iran (*correspondence: nshirdasht@sci.ui.ac.ir)
[2]Department of Geology, Science and Research Branch of Isalamic Azad University, Tehran, Iran
[3]Department of Geology, Faculty of Science, University of Isfahan, Iran

Introduction

Mesozoic ophiolte melange of Nain is located in Central East Iranian microcontinent. Field studies and petrography indicate presence of three types of granitoids (plagiogranites, high-K granites, and tonalites) with different origins in ophiolitic mélange of Nain. Three granitoid types are different in mineralogy and are including of: (1) Plagiogranites (containing Qtz+Pl+Amp±Prh±Chl) (Mineral abbrevations from [1]); (2) high-K granites (including of Qtz+Pl+Or+Ms+small magmatic Grt (Alm) grains); (3) tonalites that are seen as intruded dikes in the amphibolitic rocks, containing Qtz+Pl+Amp+ small metamorphic Grt (Alm-Sps) grains ±Prh.

Discussion

Plagiogranites are indicated by [2] to be originated of differentiation of primary basalt. Mineral chemistry of garnets in high-K granitoids (almandine) show they have an igneous origin formed through melting of high Ca-Al sedimentary rocks. Garnets in tonalites (almandine-spessartine) have formed by regional metamorphic processes occurred after formation of tonalites (based on Fig. 11 in [3] and Table 1). In Breif, (1) plagiogranites are the final products of primary basalt differentiation, (2) high-K granites have formed through melting of sediments and (3) tonalites have been resulted by some degrees of partial melting and anatexis of their host amphibolite.

Rock Type	High K-granite		Tonalite	
Pyrope	5.63	5.94	13.66	13.71
Almandine	76.07	75.82	45.35	45.76
Grossular	2.28	2.11	4.54	5.20
Spessartine	16.02	16.09	36.40	35.25

Table 1: End members percent of garnets.

[1] Kretz (1983) *Am Min* **68**(1/2), 277–279 [2] Rezai (2006) *M.Sc.Thesis University of Isfahan, Iran* 139. [3] Harangi *et al*. (2001) *J Pet* **42**(10), 1813–1843.

3 Ga onset of the supercontinent cycle: SCLM and crustal evidence

STEVEN B. SHIREY[1], STEPHEN H. RICHARDSON[2] AND MARTIN J. VAN KRANENDONK[3]

[1]DTM-Carnegie Institution of Washington, 5241 Broad Branch Rd, NW, Washington, DC 20015 USA
[2]Department of Geological Science, University of Cape Town, Rondebosch, 7700, South Africa
[3]Geological Survey of Western Australia, 100 Plain St, East Perth, WA 6004, Australia

A full understanding of the formation and evolution of the continents requires the use of constraints from both the subcontinental lithospheric mantle (SCLM) and crust. Significant differences exist globally between >3.2 Ga versus <3.0 Ga crust and SCLM. We propose that this time is a boundary between different geodynamic regimes on Earth and the start of the supercontinent (Wilson) cycle [1, 2].

To characterize the SCLM through time, we use geochronological studies of sulfide and silicate inclusions in diamonds from more than 20 kimberlites on 4 cratons [3]. Diamonds >3.2 Ga contain exclusively peridotitic (harzburgitic) silicate and sulfide inclusions whereas diamonds <3.0 Ga contain predominantly eclogitic silicate and sulfide inclusions. Similarly, >3.0 Ga kimberlite-borne eclogite xenoliths are largely absent in the SCLM rock record, whereas they are common thereafter.

Archean crust also records major differences across the 3.0–3.2 Ga interval. Prior to 3.2 Ga, crust grew by vertical accretion over upwelling mantle in long-lived plateaux floored by extremely depleted residual harzburgitic SCLM or via slab melting and crustal imbrication over shallow subduction zones (e. g West Greenland) [4], whereas lateral accretion, allochthonous greenstone belt growth and calcalkaline magmatic products of mantle wedge melting emerge only after 3.2 Ga [5].

This temporal and geochemical change can perhaps best be explained as the result of a step-wise change in the tectonic style of the planet from rapid mantle convection, small plates, shallow subduction, and localized recycling >3.2 Ga, followed by large plates, steep subduction, and full upper mantle recycling <3.0 Ga. These geodynamic changes would have had profound effects on mantle depletion, crustal growth, and geochemical cycles.

[1] Shirey *et al*. (2010) *EOS Trans AGU* U33A-0009. [2] Van Kranendonk *et al*. (2010) *Precamb Res* **177**, 145–161.[3] Gurney *et al*. (2010) *Econ Geol* **153** 689–712.[4] Van Kranendonk (2011) *Am J Sci* **310**, 1187–1209.[5] Smithies *et al*. (2005) *Earth Planet Sci Lett* **231**, 221–237.

https://doi.org/10.1180/S0026461X00006502 Published online by Cambridge University Press

Magma storage conditions of Mutnovsky volcano, Kamchatka

T.A. SHISHKINA[1]*, R.R. ALMEEV[1], R.E. BOTCHARNIKOV[1], F. HOLTZ[1] AND M. PORTNYAGIN[2]

[1]Institute of Mineralogy, Leibniz University of Hannover, Callinstrasse 3, 30167, Hannover, Germany (*correspondence: t.shishkina@mineralogie.uni-hannover.de)
[2]IFM-GEOMAR, Kiel, Germany

Mutnovsky is a typical island-arc tholeiitic volcano, located in the southern part of the Eastern Volcanic Front of Kamchatka (Russia). This active volcano hosts a hydrothermal field, one of the largest in Kamchatka, providing an excellent example of modern interaction of magmatic and hydrothermal systems. Investigations of the magma storage conditions such as depth, temperature, volatile budget and redox state beneath Mutnovsky volcano are crucial to understand the input and the role of magmatic component in the course of magma-hydrothermal interactions. We investigated these conditions experimentally and with the help of melt inclusion study.

To evaluate the magma storage conditions, two sets of crystallizaton experiments at 100 and 300 MPa have been performed using the most magnesian basalt of Mutnovsky as a starting composition [1]. The mineral phenocryst assemblage of Mutnovsky basalts (Ol, Pl, CPx, and Mt) was succesfully reproduced at 100 MPa (1025-1100°C, 0.5–3.5 wt.% H_2O) and at 300 MPa (1000-1075°C, 1.5–5.0 wt.% H_2O). The mineral phenocryts compositions in the experimental runs and in Mutnovsky basalts were similar. Compositions of experimental residual glasses saturated with Ol+Pl+CPx+Mt assemblage reproduce well the natural liquid line of descend and confirm a genetic link between primitive and more evolved eruptive products of Mutnovsky volcano.

Olivine-hosted melt inclusions from basaltic tephra (50-55 wt.% SiO_2; 4-6.5 wt.% MgO) contain 1.7-2.7 wt.% H_2O and 0-180 ppm CO_2. According to our experimental data on H_2O-CO_2 solubility in Mutnovsky basalt [1], these volatile abundances correspond to shallow depths (pressures below 110 MPa). The values of S^{+6}/S^{-2} in melt inclusion obtained by XANES correpond to the range of logfO_2 between QFM+0.9 and QFM+1.7 (QFM is quartz-faylite-magnetite buffer).

Our study confirms the presence of a shallow magma reservoir beneath Mutnovsky volcano at about 3 km depth. The phenocrysts in lavas could, however, crytallize at different depths in magmatic conduit during a polybaric crystallization (starting at least from 300 MPa).

[1] Shishkina *et al*. (2010) *Chem. Geol*. **277**, 115–122.

The generation of geochemical asymmetry in MORB around Iceland by radially symmetric plume flow under an asymmetric ridge system

O. SHORTTLE AND J. MACLENNAN*

Department of Earth Sciences, University of Cambridge, Cambridge CB2 3EQ, UK (*correspondence: jcm1004@cam.ac.uk)

Geochemical asymmetry in Mid-Ocean Ridge Basalt (MORB) around Iceland was first recognised almost forty years ago and similar spatial patterns of MORB compositions been reported from a number of other plume-influenced ridges. Basalts from the Kolbeinsey Ridge to the north of Iceland are depleted in incompatible trace elements and have low $^{87}Sr/^{86}Sr$ and high $^{143}Nd/^{144}Nd$ when compared with basalts from the Reykjanes Ridge to the south. Previous models that have attempted to account for this asymmetry have typically been based upon the presence of asymmetry in the compositional field, temperature field or flow field in the Icelandic plume. Here we instead propose that the geochemical asymmetry around Iceland is controlled by asymmetry in the geometry of the ridge system. The presence of such geochemical asymmetry does not require radial asymmetry in the plume composition, temperature or flow field other than that imposed by the plate spreading.

Geophysical observations indicate that the plume conduit is centred under south-eastern Iceland. If mantle flows radially in the plume head from this position, then it will arrive at the Reykjanes Ridge without passing under a fully developed spreading system and will therefore have barely been melted before it rises and melts in the corner flow under the Reykjanes Ridge. In contrast, radial plume head flow dictates that the mantle that rises and melts under the Kolbeinsey ridge has travelled through the deep parts of the melting region under the Northern Volcanic Zone of Iceland. While only modest extents of melting may occur in the deep part of the melting region, it is likely that this melting preferentially extracts magma from enriched, fusible heterogeneities in the mantle. Therefore, the mantle rising under the Kolbeinsey Ridge may already have been stripped of an enriched geochemical signature by small extents of melting during transit under the Northern Volcanic Zone. Simple quantitative models of this depletion of mantle flowing radially in the deepest parts of the melting region are able to match the first order observations from Iceland and other plume-influenced ridges such as the Galápagos.

https://doi.org/10.1180/S0026461X00006502 Published online by Cambridge University Press

Analysis of thermal phases in Canaanite ceramic 'Metallic Ware' using FT-IR spectroscopy

SHLOMO SHOVAL[1] AND YITZHAK PAZ[2]

[1]Geology Group, Department of Natural Sciences, The Open University of Israel, The Dorothy de Rothschild Campus, 1 University Road, POB 808, Raanana, Israel (shovals@openu.ac.il)

[2]Institute of Archaeology, Tel-Aviv University, Tel-Aviv, Israel

Early Bronze Age (EBA) ceramic 'Metallic Ware' from the North Canaan was analyzed using FT-IR spectroscopy and applying of curve fitting and second derivative techniques. The Metallic Ware is hard, highly fired pottery which resounds with a distinctive metallic ring when struck. The spectroscopic analysis is advantageous in analysis of amorphous and short-range ordered thermal phases lacking of XRD peaks. The applying the spectral analysis improves the identification of the individual phases in the composition of the pottery. The results demonstrate that the ceramic 'Metallic Ware's are composed of non-calcareous or poorly-calcareous ceramics. The spectra demonstrate that the vessels are composed mainly of meta-clay. The type of the meta-clay in the composition of the pottery is identified by the location of the main SiO stretching band using curve fitting and second derivative techniques. Most of the ceramic 'Metallic Ware's contain mixtures of metakaolinite and meta-smectite. The appearance of both phases, indicates that calcareous raw materials contained smectite and kaolinite, were used for manufacture of the 'Metallic Ware'. It seems that the presence of smectite in the raw material enable sintering at lower firing temperature.

Study of geochemistry, geochronology and petrogenesis of the Early Paleozoic granites in South China

L.S. SHU* AND Y. ZHANG

State Key Laboratory for Mineral Deposits Research, School of Earth Sciences and Engineering, Nanjing University, Nanjing, China (lsshu2003@yahoo.com.cn)

This paper shows results of petrology, geochemistry, zircons U-Pb dating and *in situ* Hf isotope. Geochemically, the A/CNK values have an average of 1.16; the REE compositions show higher ΣREE contents, enrichment in LREEs, depletion in Eu and REE patterns; the trace element spider diagrams are enrichment in Rb, Th, U and depletion in Ba, Sr, Nb, Ti. Zircons mostly exhibit euhedral and high Th/U values, an average of 1.08. The zircons from thirty plutons yielded rather similar U-Pb concordia ages from 436±6 Ma to 441±4 Ma, corresponding to Llandovery Epoch of Silurian. Several xenocrysts yielded the U-Pb ages around 700 Ma, implying that a breakup event took place during Neoproterozoic. *In situ* Lu–Hf isotopic analysis shows that all the εHf (t) value of zircons are negative, and their model ages (TDM2) values indicate that the Silurian granitic magma came from the recycle of Meso-Paleoproterozoic basement. Researches suggest that an intracontinental tectono-magmatic event took place during the Early Paleozoic, which is characterized by folding and thrusting, leading to crustal shortening and thickening. The high geothermal temperature from thickening crust and accumulation of producing high-heat radioactive elements will gradually soften crustal rocks and cause a partial melting, forming peraluminous granitic magma. Under the post-orogenic extensional and de-pressure condition, these granitic magma rose and emplaced in the upper crust, leading to development of S-type plutons.

https://doi.org/10.1180/S0026461X00006502 Published online by Cambridge University Press

Compositions of phyllosilicates from the TAG hydrothermal system at 26°N on the Mid-Atlantic Ridge as guide to subseafloor entrainment of seawater: Results from ODP Leg 158

L. SHU, W. BACH, A. KLÜGEL AND N. JÖNS

Fachbereich Geowissenschaften, Universität Bremen, Klagenfurter Straße, 28359 Bremen (liping@uni-bremen.de, wbach@uni-bremen.de, akluegel@uni-bremen.de, njoens@uni-bremen.de)

The TransAtlantic Geotraverse (TAG) hydrothermal system east of Mid-Adlantic Ridge at 26°N in a water depth of 3670 m is one of the largest known massive sulfide accumulations on the seafloor (2.7 million tonnes of sulfide; [1]). Anhydrite is an ideal tracer in active hydrothermal systems, but (unlike phyllosilicates) it dissolves after hydrothermal activity has ceased. Phyllosilicate compositions can provide useful constraints on sub-seafloor seawater entrainment, which supplement and extend the record in gangue. Calibrating the phyllosilicate record of fluid evolution against that of anhydrite in the TAG subseafloor may hence provide us with a useful tool in studying fluid mixing in hydrothermal stockwork zones underlying ancient volcanigenic massive sulfide deposits.

Results from trace element concentrations indicate that the paragonite patterns are fairly uniform and – compared to N-MORB – show positive Ba, U, Pb, Sr anomalies. In contrast, chlorite patterns are variable and can be divided into 3 different types: chlorite type A occurs in a breccia from the peripheral part of the upflow zone and in the deepest part of Holes 957E and 957C. Type A shows negative Sr and Ba anomalies and positive U and Pb anomalies. Chlorite type B occurs throughout Holes 957E and 957C in the central part of the mound, but is lacking in samples from the periphery of the upflow zone. Type B shows no or small Sr anomalies but positive U, Ba, and Pb anomalies. Chlorite type C occurs in alteration halos of basalt from underneath the mound. It shows no significant U anomalies, but negative Ba anomalies and large positive Pb anomalies.

The results suggest that the different chlorite pattern types relate to sub-seafloor fluid flow dynamics, which are variably dominated by (i) seawater entrainment and heating, (ii) mixing of seawater and hydrothermal fluid, and (iii) pooling and conductive cooling of hydrothermal fluids.

[1] Hannington, M.D. de Ronde, C.E.J. & Petersen, S. (2005) *Economic Geology* **100**, 111–141.

Ultra-depleted eclogites: Residues of TTG melting

Q.SHU[1,2]* AND G.P. BREY[1]

[1]Univ. Frankfurt, Germany
[2] China University, Beijing
(*correspondence: shu@em.uni-frankfurt.de)

Eclogites from the Bellsbank diamond mines (SA) fall into categories A and B of Coleman [1]. We collected eclogites from a coarse concentrate dump from the present day production. These fall into three groups, one in A (Mg-rich) and two groups B1 (Fe-rich) and B2 (Ca-rich). They are derived from a temperature range between 850 to 1050°C (A and B1) and 1050 to 1150°C (B2). All xenoliths have exceptionally fresh and clear clinopyroxenes. REE patterns from A and B1 show the ultra-depleted character in their REE patterns which were LREE depleted in both cpx and grt. However, the LREE up to Sm were reenriched in most cases disturbing the Sm-Nd system. Both phases have extremely high εH with one sample giving the highest εHf ever measured with 13753 in garnet and 6518 in cpx. Such values require a long time integrated history with very high Lu/Hf in the bulk rock. We suggest that the eclogites are derived in the early Archean from picritic to basaltic protoliths of low pressure origin, which were subsequently subducted and partially molten with not much time delay. The products of the partial melting process should be TTG melts according to experimental work (e.g. [2]). The partial melting generated the high Lu/Hf ratios in the residue which are necessary to reach such extreme high εHf values as found in our rocks. The higher temperature Group B2 eclogites have positive Eu anomalies which indicate a low pressure origin as plagioclase cumulates. These eclogites still have higher εHf as most known eclogites and may also have been involved in the partial melting process. Lu-Hf grt-cpx two-point isochrones give eruption ages around 120 Ma for samples with T > 950°C; lower-T samples give increasing ages with decreasing temperature. The Sm-Nd isotope system does not give any consistent information on the origin of the rocks because of subrecent addition of LREE to the rocks.

[1] Coleman *et al*. (1965) *JGSA Bull*. **76**. [2] Rapp *et al*. (2002) *Nature* **425**.

https://doi.org/10.1180/S0026461X00006502 Published online by Cambridge University Press

Active methanogenesis in the subsurface during development process

Y.H. SHUAI*, S.C. ZHANG, J.K. MI AND M. LIU

PetroChina Research Institute of Petroleum Exploration & Development, Beijing, China
(*correspondence: yhshuai@petrochina.com.cn)

Methanogenic biodegradation of organic matter provides us prospects of methane resource artificially generated continuously in the subsurface anaerobic condition. Unfortunately, this process is such a long period in the geological condition that human being can not wait for. However, several cases in China demostrate methanogenesis process could be very quick.

Examples presented in this article are related to the biodegradation of heavy oil components and the significant change of the associated gas characteristics. The first example is from Liaohe depression, Bohaiwan basin. Biodegradated gases were produced widely in the west of the depression, from 1300~1600 m, with temprature ranging from 45 °C to 60 °C. Accompanied crude oil had been biodegraded heavily above 4 degree biodegradation. During producing stage less than a decade, the dryness (C_1/C_{1+}) of gas became higher and higher from 0.92 to 0.97. Based on meterial balance method, about 80 percent of producing gas should be neogenicly generated. The second example is from Songliao Basin, Northeastern China. The dry coefficient of associated natural gas increased from the beginning 85% (40 years ago) to present 95%. And content of non-hydrocarbon components, such as H_2S and CO_2, slightly increases, too. The similar trend happened in the another field, Liuzhuang field of Jinhu depression in the Subei basin, Eastern China. Differently, the dryness of associated gas has been stable at 98 %, but the stable carbon isotope ratio of CH_4 varied from -51.2 ‰ to -53.6 ‰.

All those cases demonstrate that biogenic methane could be generated in amazing rates. Once appropriate conditions provided, the interesting geomicrobes can give us whatever we want.

Supported by PetroChina Innovation Fund (2009D-5006-01-01)

Mineral chemistry of the skarn type ores from Furong Tin deposit in Hunan Province, P.R.China

Y. SHUANG[1,2]*, J. CHEN[1,2] AND H. LI[1,2]

[1]Chongqing Key Laboratory of Exogenic Minerallization and Mine Environment, Chongqing Institute of Geology and Mineral Resources, Chongqing 400042, China
(*correspondence: shy0124@yahoo.com.cn)
[2]Chongqing Research Center of State Key Laboratory of Coal Resources and Safe Mining 400042, China

Tin in skarns forms a significant part of the total Sn resource of South China. The Furong tin polymetallic deposit in the central Nanling region, South China is dominantly composed of skarn type ores hosted in Carboniferous and Permian strata and Mesozoic A-type granitic intrusions. In this study, mineral chemistry research has been carried out on skarn ores from No. 19 ore lode using microscope and EPMA analysis, in order to constrain the tin mineralization condition of skarn in Furong deposit.

Primary skarns in Furong deposit are mainly consisting of grossular-andradite, baicalite, ferro-edenite, malayaite, and minus idocrase, wollastonite, cassiterite formed under oxidizing conditions. The garnet and ferro-edenite are characterized with high Sn concentration (0.22~0.73%), distinctly higer than those formed under reducing conditions [1]. Accordingly, the primary skarn formed under oxidizing conditions. In this case, tin dominantly occurs as Sn^{4+} and entered the crystal lattices of skarn minerals.

Under the alteration of the F-, Cl- and Sn-riched ore-forming solution exsolved from biotite granite magma, the primary skarn was regressive metamorphosed to form hydrothermal minerals and ores. Along the endo-contact zones of the granite and the carbonate wallrock, the primary skarns were altered to type Ⅰ ores with the association of cassiterites + phlogopite + fluorite + magnetite, which mainly related to the hydrothermal fluids exsolved from biotite granite. The association of tremolite, diopside, chlorite, sulphide, i.e. Type II ores was formed along the exo-contact zones of the biotite granite, which was significantly influenced by the fluid from wallrock.

This research project was financially supported by the National Natural Science Foundation of China (41003024).

[1] Chen *et al*. (1992) *Ore Geol. Rev*. **7**, 225-248.

https://doi.org/10.1180/S0026461X00006502 Published online by Cambridge University Press

The impact of heavy metals concentration on soil biological properties in Kintyre Pb mining area, Jamaica

N. SHUKUROV[1], CLAION ROBINSON[2], PAUL WRIGHT[2] AND G. LALOR[2]*

[1]Institute of Geology & Geophysics, Academy of Sciences of Uzbekistan, 49, N.Khodjibaev Str., Tashkent-100041, Uzbekistan (nosirsh@yahoo.com)

[2]International Centre for Environmental and Nuclear Sciences, University of the West Indies, Mona, Kingston 7, Jamaica, West Indies (*correspondence: glalor@uwimona.edu.jm)

Soil contamination with heavy metals occurs as a result of both anthropogenic and natural activities. Heavy metals could have long-term hazardous impacts on the health of soil ecosystems and adverse influences on soil biological processes. Soil microorganisms are recognized as sensors towards any natural and anthropogenic disturbance occurring in the soil ecosystem. Similarly, soil nematodes are also considered as one of the important soil biota and frequently influenced by HM contamination. The total number of nematode individuals has recently been used to investigate changes in soil biota composition in response to environmental stresses. This study was conducted within the Kintyre Pb mining area. Soil sampling plots are located in the Hope River valley, in the foothills of the Port Royal Mountains near to the Kingston. Mining was discontinued in the late 19th century, leaving a legacy of superficial tailings and crushed ore. These materials have been dispersed into the surrounding areas. HM concentrations, soil pH, soil moisture content (SM), total number of nematode individuals (TotalNem) and nematode community structure were studied. 18 soil samples (0-10 and 10-20 cm) from 3 sampling plots with different pollution levels (low (<100 mg/kg), moderate (300-700 mg/kg) and very high (>1000 mg/kg) concentration) were sampled in triplicate. Airdrieyed soils samples were sieved trough 2mm mesh and HM, TotalNem, SM, pH were determined in subsamples. TotalNem was significantly lower ($p<0.05$) in soil samples with high concentration of HM from the soil sampling plot C than in soils with low and moderate HM content from the soil sampling plots A and B. No significant differences were observed SM and pH between soil layers and sampling plots. TotalNem patterns confirmed that the concentration of heavy metals had a significant impact on nematodes. The soil nematodes were sensitive to Pb, Cd and Zn as an indicator of soil pollution with HM and can be used within the Environmental assessment projects.

A Chinese antimony smelting site and possibility for its phytoremediation

SHURKHUU TSERENPIL* AND LIU CONG-QIANG

State Key Laboratory of Environmental Geochemistry, Institute of Geochemistry, 550002 Guiyang, PR China (*correspondence: tserenpil.sh@gmail.com)

Anthropogenic sources such as mining operations and smelting plants are great contributors to antimony (Sb) accumulation in the environment. Sb is considered a non-essential element and is toxic to most living organisms at elevated concentrations. Chinese Sb vein-type ore deposits account for 55% of the world's resources of Sb [1], and the country has been the global dominant in its production for over 10 decades. As a consequence, water and soil as well as fauna and flora within Sb mining and smelting areas are significantly contaminated by this metalloid and co-occurring elements [2-5]. Its anthropogenic release is mainly to the land; therefore, it is crucial to investigate the fate of Sb within the soil system in the smelting areas where its release is often very high and land needs to be cleaned up.

Discussion of results

Soils were sampled at uncultivated, cultivated and fallow farmland in the vicinity of a Sb smelter in Guangxi Zhuang, China. Topsoils at all the sites were heavily polluted by metals including Sb, Pb and As; and their concentrations were measured at 410-3330 $mg \cdot kg^{-1}$, 410-3690 $mg \cdot kg^{-1}$ and 200-460 $mg \cdot kg^{-1}$, respectively. However, the elevated concentrations of Hg (0.11-0.30 $mg \cdot kg^{-1}$) may be occurred both naturally and anthropogenically at the sites studied. This study showed that aerosol particles from Sb smelter can result in severe pollution of the local environment by toxic metals and pose a high risk via agricultural plants. Dissoluble proportion of Sb was insignificant (0.70-1.63%) compared to its deposition in the surface soils; however, water extractable amounts produced a slightly reduced germination rate on wheat seed with a lighter weight. Sb(III) adsorption on the smelting site soil was studied in order to examine its mobilization in pH changes; furthermore, to determine an optimal pH for higher Sb mobility that could facilitate plant uptake. The adsorption maximum (56 $ml \cdot g^{-1}$) appeared at pH of 3, while it was 10-17 $ml \cdot g^{-1}$ at pH of 6-7 which showed anion sorption may be dominant in Sb sorption onto bulk soil. It is therefore suggested that to maintain soil pH near neutral will increase Sb concentration in the soil water solution and it will enhance the feasibility of the phytoremediation.

[1] Wu (1993) *Ore Geology Review* **8**, 213–232. [2] Fu *et al*. (2011) *Microchem. J* **97**, 12–19. [3] He (2007) *Environ. Geochem. Health* **29**, 209–219. [4] Tserenpil &Liu (2011) *Microchem. J* **98**, 15–20. [5] Wang *et al*. (2010) *J. Soil Sediments* **10**, 827–837.

https://doi.org/10.1180/S0026461X00006502 Published online by Cambridge University Press

The effect of iron-oxidizing bacteria on the stability of the gold-thiosulfate complex

J. SHUSTER[1]*, A. SMITH[1], T. BOLIN[2] AND G. SOUTHAM[1]

[1]Department of Earth Sciences, The University of Western Ontario, London, ON CANADA N6A 5B7 (*correspondence: jshuster@uwo.ca)
[2]CMC-XOR-Sector 9, Advanced Photon Source, Argonne Laboratory, Argonne, IL USA 60439

Acidophilic iron oxidising bacteria, enriched from a Rio Tinto river sample collected approximately 7 km SW of Nerva, Spain, precipitated colloidal gold when exposed to 2 μM to 20 mM Au $(S_2O_3)_2^{3-}$. Growth of the consortium produced soluble ferric iron and colloidal, ferric iron-oxide mineral precipitates. A range of gold (I) thiosulfate solutions reacted with the whole cultured system and with each component system separately (i.e. bacteria, spent media, mineral precipitates) immobilized gold from solution within several hours. Transmission electron microscopy and scanning electron microscopy demonstrated that the immobilization of gold occurred differently by the three components in the microbial system. When each separate constituent was exposed to 20 mM gold: bacteria precipitated 30.78% gold in the form of 5 nm colloids concentrated along the cell envelope; the colloidal, iron-oxide minerals precipitated 26.26% gold as 5 nm colloids that reduced and replaced the acicular iron-oxide filaments extending outward from the particles; and spent media, devoid of residual organics and solid iron oxides precipitated 99.51% gold as 200 nm to 2 μm gold sulfide colloids and aggregates. In a chemical control experiment, gold did not react with soluble ferrous iron under the same experimental conditions. This suggests that stripping electrons from organic material and a role for ferric iron in destabilising the gold thiosulfate complex were critical to colloidal gold formation. Analysis of whole culture systems exposed to 2 mM gold using XANES/EXAFS demonstrated that gold (I) was immobilized and reduced to a gold sulfide and elemental gold, respectively. The direct immobilisation of gold by these iron oxidising bacteria and the indirect immobilization of gold by biologically-mediated, iron oxide precipitates suggests an active and passive role the biosphere has in influencing the mobility of gold as soluble complexes or as colloids. Understanding the biogeochemistry of gold interception and accumulation within a geologic temporal setting would provide insight into dispersal of gold in natural weathering systems where weathering of gold bearing metal sulfides occurs.

Mercury stratigraphy: A proxy for volcanogenic CO_2 buildup in Neoproterozoic snowball Earth and volcanism in the K-T transition

A.N. SIAL[1], L.D. LACERDA[2], C. GAUCHER[3]; V.P. FERREIRA[1], L. CHIGLINO[1], M.S. CAMPOS[1]; M.V. NASCIMENTO-SILVA[1] AND W.S. CEZARIO[1]

[1]NEG-LABISE, Dept. Geol. UFPE, Recife, Brazil (*correspondence sial@ufpe.br)
[2]LABOMAR, UFC, Fortaleza, Ceará, Brazil
[3]Fac. Ciencias, Univ. Republica, Montevideo, Uruguay

Mercury tends to concentrate in sediments deposited right after major glacial events [1] as a result from leaching of volcanogenic Hg from land surface and accumulation along argillaceous sediments. Wherever geological background of Hg is negligible, its concentration in sediments may be useful for investigation of climatic changes.

Volcanism is assumed to be responsible for CO_2 build up in the atmosphere during Snownall Earth event with subsequent greenhouse effect, ice melting and cap carbonate deposition [2]. Intense volcanism witnessed the Cretaceous-Tertiary transition [3] and was, perhaps, responsible for dramatic climatic change.

We have used Hg as a proxy of volcanism intensity and CO_2 buildup during snowball events in Neoproterozoic cap carbonates in NE Brazil. Localities where carbonates are in sharp – but not erosional – contact with basal diamictites (earliest stages of aftermath of glacial events) and show $\delta^{13}C$ values ~ –5‰ were analyzed. Hg contents are usually over 10 times higher than background values (<1 ngg^{-1}), occasionally reaching values > 200 ng g^{-1}. Hg contents in cap carbonates of the Sergipano Belt and Ubajara Basin are similar to those in carbonates deposited coevally to volcanic activity elsewhere. This study supports mantle-origin for the CO_2 in cap carbonates, transferred to the atmosphere by volcanism.

In three drill-hole cores in carbonate rocks that register the K-T transition (KTB) in the Paraiba Basin, NE Brazil, Hg increases (4 ngg^{-1}) in the early Danian right after the KTB. Hg spikes predating the KTB register volcanism before this transition. Hg shows stratigraphic variation synpathetic with $\delta^{13}C$ and $\delta^{18}O$ stratigraphies.

This study supports Hg stratigraphy as possible tracer of dramatic climatic changes as those in Neoproterozoic snowball Earth events and in the KTB.

[1] Santos *et al*. (2001) *Radiocarbon* **43**, 801–808.
[2] Hoffman & Schrag (2002) *Terra Nova* **14**, 129–155.
[3] Sheth (2005) *Gondwana Research* **8**, 109–127.

https://doi.org/10.1180/S0026461X00006502 Published online by Cambridge University Press

The effects of road salt influx on the geochemical cycling of Woods Lake, Kalamazoo, MI

R.J. SIBERT, C.M. KORETSKY*, C. SNYDER, A. MACLEOD AND S. BARONE

Dept of Geosciences, Western Michigan University, Kalamazoo, MI 49008
(*correspondence: carla.koretsky@wmich.edu)

The seasonal application of road deicing salts in densely populated areas can exacerbate eutrophication, and change the seasonal geochemical/mixing cycles of urban lakes through the gradual elevation of chloride concentrations. Elevated chloride levels in hypolimnetic waters may lead to persistent density and redox stratification (i.e. meromixis), stable anoxia in bottom waters, and a decrease in biological diversity. Therefore, the goal of this study is to examine the influence of road salt influx on the geochemical and physical mixing cycles of Woods Lake, a small, kettle lake in urban Kalamazoo, MI (Z_{max} ~13 m). Water samples were collected monthly between May and July 2010, and approximately twice a month between August 2010 and March 2011 at 1 m intervals using a van Dorn sampler. Temperature, pH, conductivity, and dissolved oxygen (DO) values were obtained *in situ* using a YSI 650MDS/600QS multiparameter sonde. Laboratory samples were analyzed colorimetrically for Fe^{2+}, total alkalinity, ΣNH_4^+, ΣPO_4^{3-}, ΣH_2S, and Mn^{2+}, by IC for Cl^- and SO_4^{2-}, and by ICP-OES for major ions and trace metals (Mg, Ca, K, Na, Zn, Ni, Co, Cu, and Pb). The data indicate that temperature varies seasonally in a predictable manner; typical summer and fall thermal stratification is antecedent to inverse wintertime stratification, punctuated by a transition period of thermal homogeneity (November) within the water column. However, analyses of redox sensitive species (i.e. Fe^{2+}, Mn^{2+}, ΣPO_4^{3-}, ΣH_2S, etc) show that Woods Lake displays persistent redox stratification and hypolimnetic anoxia throughout the entire sampling period. For example, maximum Fe^{2+} concentrations are >290 μM in fall and >250 μM in winter below 9 m, indicative of the relative persistence and magnitude of hypolimnetic anoxia. Conductivity profiles indicate the presence of a chemocline that varies from ~8 m in the spring, summer, and fall, to ~10 m in the winter. Conductivity and Cl^- data correlate strongly throughout the sampling period, typically with an $R^2 > 0.95$. Concentrations are more than one hundred times higher than those found in rural lakes of the same region. These data imply persistent hypolimnetic anoxia and redox stratification, presumably due to nutrient and road salt inputs, and that both fall and spring turnover events never fully reach completion.

Radiocarbon depression in aquatic foodwebs of the Colorado River, USA: Coupling between carbonate weathering and the biosphere

J.O. SICKMAN*, M.A. ANDERSON, D.M. LUCERO, J. MCCULLOUGH AND W. HUANG

Department of Environmental Sciences, University of California, Riverside CA 92521
(*correspondence: jsickman@ucr.edu)

The ^{14}C content of living organisms is generally considered to in isotopic equilibrium with the atmosphere. We measured substantial radiocarbon depression of organisms within planktonic and benthic foodwebs of Copper Basin Reservoir, a short residence-time lake at the intake to the Colorado River Aqueduct in California, USA. All levels of the foodweb, had depressed radiocarbon content with inferred 'age' of ca. 1100 to 1200 radiocarbon years ($\Delta^{14}C$ range: -137 to -151‰, Figure 1).

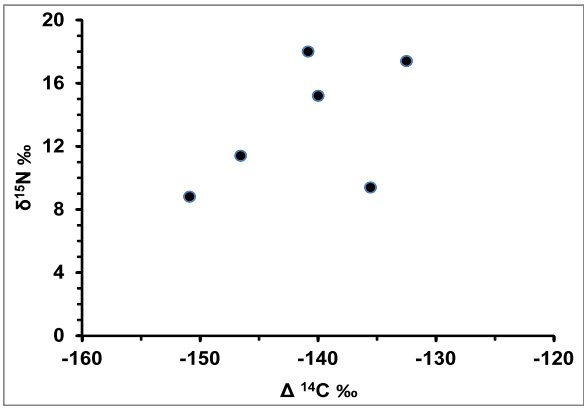

We presume that 'dead' carbon from carbonate weathering entered into the foodweb via photosynthesis, depressing the ^{14}C content of organisms below that of the atmosphere. A two-component mixing model incorporating carbonate weathering and atmospheric CO_2, shows that 15-17% of the carbon in the aquatic foodwebs of Copper Basin is derived from weathering of carbonate minerals in the Colorado River basin. Worldwide, only a few cases of radiocarbon depression have been reported for aquatic ecosystems and the degree of ^{14}C depression in the Colorado River is much larger than that observed in the Arctic or deep ocean environments.

https://doi.org/10.1180/S0026461X00006502 Published online by Cambridge University Press

Geochemistry of Paleocene volcanism and oceanic island arc affinities of the Chagai Arc, Balochistan, Pakistan

REHANUL HAQ SIDDIQUI[1], MUHAMMAD ASIF[2] KHAN AND MUHAMMAD QASIM JAN[3]

[1]GeoscienceAdvance Research Laboratories, Geological Survey of Pakistan, Shahzad Town, Islamabad Pakistan
[2]National Centre of Excellence in Geology University of Peshawar, Pakistan
[3]National Centre of Excellence in Geology University of Peshawar, Pakistan

The main exposures of the Paleocene lava flows occur in an east-west trending subduction related magmatic belt known as Chagai arc in the western part of Pakistan.

The Paleocene lava flows are mainly represented by basalts (49.22-52.46 wt. % SiO_2) and basaltic-andesite (52.75-53.90 wt. % SiO_2. The petrochemical studies show that these are mainly medium to low -K oceanic island arc tholeiites. The trace element patterns show enrichment in LILE and depletion in HFSE relative to N-MORB. The primordial mantle-normalized trace element patterns show marked negative Nb anomalies with positive spikes on Ba and Sr which strongly confirm their island arc signatures, which is further supported by flate-slightly LREE enriched chondrite-normalized REE patterns. These volcanics have lower average $^{87}Sr/^{86}Sr$ ratio (0.70446), which is more consistent with a depleted mantle source and closely correlate with oceanic island arcs rather than continental margin type arcs. The average trace element ratios including Zr/Y (2.25), Ti/V (15.47), La/Yb_N (1.62), Ta/Yb (0.03) and Th/Yb (0.24) of these volcanics are more consistent with oceanic island arc tholeiite rather than analogous rocks of the continental margins type arcs.

Eruptive history and chemical evolution of the Acigöl volcanic field, central Anatolia, Turkey, based on geochemical and isotopic (Sr-Nd-Pb, $\delta^{18}O$) constraints and ion microprobe zircon analysis

W. SIEBEL[1], A.K. SCHMITT[2], M. DANIŠÍK, [3] F. AYDIN[4] AND E. KIEMELE[1]

[1]University of Tübingen, Germany
[2]UCLA, USA
[3]University of Waikato, New Zealand
[4]University of Nigde, Turkey

The Acigöl volcanic field has been interpreted as a thermally growing system, where smaller magma pulses coalesced into a large, interconnected silicic magma reservoir [1]. We established a high temporal resolution chrono-stratigraphic framework for rhyolitic volcanism at Acigöl from zircon U-Th disequilibrium and (U-Th)/He dating combined with thermometry and O-Sr-Nd-Pb isotopic data. In contrast to previous dating [2], we found that zircon crystallized in only two pulses corresponding to separate eruptions in the eastern and western Acigöl field during Mid- (~150–200 ka, group I) and Late Pleistocene (~20–25 ka, group II) times, respectively. For group II zircons, resolvable differences exist between interior (average: 30.7±0.9 ka; 1σ error) and rim (21.9±1.3 ka) crystallization ages. These translate into radial crystal growth rates of ~10^{-13} – 10^{-14} cm/s. Rim crystallization ages and (U-Th)/He eruption ages (24.2±0.4 ka) overlap within age uncertainty. Compositionally, group I lavas are less evolved (SiO_2 = 71–73 wt.%), than group II lavas (SiO_2 = 74–75 wt.%). Within each group, compositional variability is small, and Nd-Pb isotope ratios are fairly homogeneous. Group II rhyolites have $\delta^{18}O$(zircon) overlapping mantle values (5.56 ± 0.16 ‰), whereas group I rhyolites are slightly more enriched in ^{18}O, consistent with some crustal material input. By contrast, group II rhyolites have markedly more radiogenic $^{87}Sr/^{86}Sr$ ratios (0.7065–0.7091) compared to those of group I (0.7059–0.7065). The correlation between hydration (loss on ignition data) and $^{87}Sr/^{86}Sr$ in the group II lavas indicates that Sr was added during post-eruption alteration by wind-blown material. Isotope constraints preclude the possibility that the rhyolite magmas formed by partial melting of any known regional crystalline basement rocks. Despite the longevity of rhyolite volcanism at Acigöl, and trends from group I to group II rhyolites of progressive depletion in compatible trace elements and decreasing zircon saturation temperatures, evidence for brief zircon residence is consistent with autochthonous crystallization in small discrete magma batches rather than in a fully interconnected magma reservoir.

[1] Druitt TH et al. (1995), *J Geol Soc, London* **152**, 655-667
[2] Bigazzi G, et al. (1993), *Bull Volcanol* **55**, 588-595

https://doi.org/10.1180/S0026461X00006502 Published online by Cambridge University Press

Molybdenum isotope fractionation during soil formation: A new proxy?

C. SIEBERT[1], J. PETT-RIDGE[2], S. OPFERGELT[1,3], K. BURTON[1] AND A.N. HALLIDAY[1]

[1]Dept. Earth Sciences, Univ. of Oxford, Oxford, UK (*correspondence: christopher.siebert@earth.ox.ac.uk)
[2]Dept. Crop and Soil Science, Oregon State University, OR 97331, USA (julie.pett.ridge@gmail.com)
[3]Earth and Life Inst., Univ. catholique de Louvain, Louvain-la-Neuve, Belgium (sophie.opfergelt@uclouvain.be)

Over the last decade molybdenum has become one of the most investigated tracers for redox conditions in the oceans. However, little is known about the processes controlling the isotope composition of the riverine inputs to the oceans. Several recent studies [1, 2] have shown that many river waters have a heavy Mo isotopic composition. However, crustal rocks are in general close to zero and therefore fractionation of Mo isotopes must occur during weathering or transport. This study has investigated the behavior of Mo isotopes under different weathering conditions. Results from a soil climate gradient from Hawaii show that redox conditions during soil formation can control Mo isotope compositions in soils. Reducing soil profiles have light isotope compositions whereas oxidizing profiles are heavy. This general isotope behavior is confirmed by results from soil profiles from Iceland. Here reducing layers within the profiles show marked negative isotope excursions. In general oxic profiles show positive isotope compositions increasing with depth and organic C content. In addition these profiles show that fractionation relative to the source rock is dependent on the degree of weathering, i.e. relatively un-weathered profiles do not show isotope fractionation. Sequential extractions confirm that organic matter plays a crucial role in fractionating molybdenum isotopes in soils. These observations together with the generally heavy isotope composition of rivers indicate that the current mass balance of molybdenum in Earth surface processes might not be in steady-state. In addition, our data open interesting possibilities for the use of molybdenum isotopes as a paleo-proxy for soil processes. Finally, our data show that interpretations of the marine sedimentary record are difficult as long as we do not understand changes in the molybdenum input over time.

[1] Archer & Vance (2008) *Nature Geosciences* **1**, 599.
[2] Pearce *et al*. (2010) *EPSL* **295**, 104–114.

Diamond anvil cell applied to the geochemistry of Earth's core formation

JULIEN SIEBERT[1,2], JAMES BADRO[2], DANIELE ANTONANGELI[1,2] AND FREDERICK J. RYERSON[2]

[1]IMPMC, Université Pierre et Marie Curie, UMR CNRS 7590, 4 place jussieu, 75005 Paris, France
[2]IPGP, 1 rue jussieu, UMR CNRS 7154, 75005, Paris, France
[3]Lawrence Livermore National Laboratory, 7000 East Avenue, Livermore, California, 94550, USA

The abundances of siderophile elements in the Earth's mantle bear the imprint of the core formation in the early Earth. Thermodynamic expressions used to constrain the metal-silicate partitioning behavior of siderophile elements are mainly established from large volume press experiments that do not cover the full range of potential P-T conditions for core-mantle equilibrium. The diamond anvil cell is the only static technique capable of achieving required P-T conditions but until now its capabilities to perform quantitative metal-silicate partitioning experiments at extreme conditions has been untapped. We use protocols that effectively link high P-T diamond anvil cell with analytical techniques such as focused ion beam device (FIB); NanoSIMS; electron microprobe; transmission electron microscopes; and *in situ* synchrotron X-ray diffraction measurements allow us to obtain quantitative data on element partitioning at superliquidus conditions above 30 GPa and 3000 K. Here we present our advances in both experimental and analytical methods. We look at the partitioning of 6 siderophile elements (Ni, Co, Cr, V, Mn, and Nb) that have been extensively studied at lower P-T conditions and constrain the solubility of light elements (Si and O) at these extreme conditions. Experiments were conducted between 35-75 GPa and 3100-4400 K. We then update expressions that describe the partitioning behavior of these elements to address the validity of proposed core formation models (i.e. single-stage core formation model and continuous core formation model).

https://doi.org/10.1180/S0026461X00006502 Published online by Cambridge University Press

Ore processing and metallurgy technologies applied to soil washing: Feasibility studies in the Linares area (Andalucía, Spain)

C. SIERRA[1], D. JIMÉNEZ-GÁMEZ[1], J. MENÉNDEZ-AGUADO[1], E. AFIF[1], J. MARTÍNEZ[2], J. REY[2] AND J.R. GALLEGO[1]*

[1]Environmental Biotechnology and Geochemistry Group. University of Oviedo. C/Gonzalo Gut. S/N, 33600-Mieres (Asturias), Spain (*correspondence: jgallego@uniovi.es)

[2]Escuela Politécnica Superior de Linares, Universidad de Jaén, 23700 Linares (Jaén, Spain)

For centuries, an important mining industry was developed in the area of Linares (Andalucía, Spain). This activity produced a large quantity of waste materials, which were accumulated in the surrounding of the exploitation and ore processing sites, affecting the qulity of several Ha. of soil [1]. In this work, we have assessed the viability of physical separation of toxic elements, given that soil washing is a suitable remediation technique to reduce the volume of contaminated soil [2, 3]. On this purpose, we have conducted a feasibility study by means of chemical analyses, and a detailed edaphic and mineralogic characterization of the soils, followed by grain-size, gravimetric, and magnetic separation pilot-scale tests.

Chemical analyses revealed anomalous concentrations of Sb, Cu, Ag, Cd, Mn, Pb and Zn, exceeding both natural backgrounds and the maximum levels permitted by Spanish environmental laws. In this context, we propose an approach based on similar ore processing and metallurgy strategies to those used in the past to recover Pb and other metals in the study area [4]. Thus, wherever geochemical data indicated that the contaminants are predominantly present as free minerals (areas mainly related with mining waste), a treatment by means of grain-size classification methods is feasible. On the other hand, in soils with ancient metallurgy affection, the contaminants are more uniformly distributed in all size fractions; therefore the complexity is higher, and as a consequence, other treatments such as hydrodynamic separation (hydrocycloning), or magnetic separation (HGMS) are needed to complement grain-size classification.

[1] Martínez *et al*. (2008*) Appl. Geochem*. **23**, 2324–2336. [2] Mann (1999) *J Hazard Mater*. **66**, 119–136. [3] Sierra *et al*. (2010) *J Hazard Mater*. **180**, 602–608.[4] Dermont *et al*. (2008*) J Hazard Mater*. **152**, 1–31.

Thermal stability of soils and the detection of use-induced changes

CHRISTIAN SIEWERT

University of Applied Sciences Dresden, Pillnitzer Platz 2, D-01326 Dresden, Germany (cs@csiewert.de)

Several investigations on soils are currently focused on sustainable land use. However, there are still no common laboratory method to distinguish soils from carbon containing substrates (CCS). This makes the detection and evaluation of use-induced soil changes not easy.

We tried to fingerprint natural soils using thermogravimetry. The goal was to create a reference base for easier detection of use-induced soil changes with a simple detection method. For this purpose, over 150 samples under natural vegetation were collected and analysed from natural parks, biosphere reserves and other protected regions in US, Europe, South America and Russia.

Using different statistical approaches, it was not possible to directly derive common characteristics of natural soils from peaks or curves from thermogravimetric data.

But, the thermal mass loss allows a reliable detection of organic carbon, nitrogen, clay and carbonates in soils with high accuracy [1]. Further, typical relationships were found to exist between mass losses in distinct temperature areas in soils under natural vegetation.

For example, nearly all natural soils characterised by a correlations between mass losses around 125 °C and 525 °C with high coefficient of determination (0.7 – 0.9). This correlation can easily be explained by the long term influence of clay minerals on water sorption (mass losses around 125 °C) and on accumulated of humic substances [2] (mass losses around 525 °C). In contrast, CSS are ususally a result of shorter time periods or prevalence of non biotic processes. Additional water binding by plant residues can modify mass losses aroun 125 °C and disturb the correlation. At 525 °C the decay of black carbon has a similar effect.

Further investigations should clarify to what extend the correlations found in natural soils can be used to distinguish soils from carbon containing substrates and to detect influences of cultivation, fertilization and other land use technologies.

[1] Siewert, C. (2004) *Soil Sci. Soc. Am. J.* **68**, 1656–1661. [2] Rasmussen, P. E. Keith, W. T. Goulding, J. R. Brown, P. R. Grace, Henry Janzen, H. Körschens, M. (1998) *Science* **282**, 893–896.

https://doi.org/10.1180/S0026461X00006502 Published online by Cambridge University Press

Analysis of organic biomarkers in single Precambrian oil-bearing fluid inclusions using ToF-SIMS

SANDRA SILJESTRÖM[1,2]*, JUKKA LAUSMA[1], HERBERT VOLK[3], SIMON GEORGE[4], PETER SJÖVALL[1], ADRIANA DUTKIEWICZ[5] AND TOMAS HODE[1]

[1]Department of Chemistry and Materials Technology, SP Technical Research Institute of Sweden, 501 15 Borås, Sweden (*correspondence: sandra.siljestrom@sp.se)
[2]Stockholm University, Stockholm, Sweden
[3]CSRIO Earth Science and Resource Engineering, North Ryde, Australia
[4]Macquarie University, Sydney, Australia
[5]University of Sydney, Sydney, Australia

Organic biomarkers are valuable sources of information on the biodiversity and environment of early Earth. However, with organic biomarkers, especially in old samples, there are often problems of syngeneity and many of the most ancient biomarkers are suspected of being younger contamination.

A type of sample where biomarkers are better constrained in the rock is oil-bearing fluid inclusions, especially if single inclusions can be analysed. However, most inclusions, including Precambrian oil-bearing fluid inclusions are so small (less than 10 μm) that analyzing single ones with conventional techniques is not possible. Therefore, we have developed an approach employing time-of-flight secondary ion mass spectrometry (ToF-SIMS) to selectively open individual oil-bearing inclusions by C_{60}^+ ion etching, and to subsequently analyse their content. Using this approach steranes and hopanes could be detected in single Ordovician oil-bearing inclusions (15-30 μm) from the Siljan impact structure in Sweden.

Now the developed approach has been applied on Precambrian samples. Four different oil-bearing fluid inclusions trapped in a 1.43 Ga sandstone from the Roper Superbasin in Australia were opened and analysed with ToF-SIMS. The ToF-SIMS spectra of the oil in the different inclusions were similar to each other indicating that the same oil was trapped in all inclusions. In addition, the ToF-SIMS spectra contained peaks that could be assigned to alkanes, cycloalkanes, aromatic moities, steranes and hopanes.

With further development and if applied on other Precambrain samples this approach could help answering questions regarding early evolution of life on Earth.

The impact associated to wastewaters treatment plant discharges into a fluvial system (Central Portugal)

A. SILVA, N. CARVALHO, P. ALMEIDA, N. OLIVEIRA, I.M.H.R. ANTUNES, A. FERREIRA AND T. ALBUQUERQUE

Polytechnic Institute of Castelo Branco, 6000-243 Castelo Branco, Portugal (teresal@ipcb.pt)

The Ocreza River is an important fluvial system in inner central Portugal, which originates in the Gardunha Chain at 1160 meters high and stretching for about 80 km before flowing into the Tagus river. It has several creeks and tributaries along which there are several communities dedicated mostly to agriculture and livestock activities. The impact of several wastewaters treatment plants discharges on water quality must be characterized, monitored and, mostly controlled as it has a crucial role on local communities' welfare.

This paper focuses on the Alcains and Castelo Branco wastewaters treatment plants which discharges into the Líria River, an Ocreza's tributary. Twenty georeferenced water samples were collected between the wastewaters treatment plants discharges and the Ocreza river confluence. Secondary inflows were identified and sampling performed at approximately equal distances and, were conducted during three different hydrological periods in 2010: rainy winter (January), intermediate conditions (March) and dry season (June). The following chemical parameters were analyzed: biochemical oxygen demand (BOD), dissolved oxygen concentration (DO), dry residue, P_{total}, N_{total}; pH, temperature and microbiological parameters. The dissolved oxygen concentration (DO), biochemical oxygen demand (BOD) and microbiological parameters were used as indicators to the presence of organic matter in the body of water, and consequentlty as parameters for evaluating the environmental pollution.

The QUAL2kw software was used to construct a water quality model performing a coupled hydrodynamic and water dispersion model to simulate the pollution in the Ocreza River due to sewage effluent. The model's fair calibration is demonstrated by the simulation consistent results with field observations and demonstrate that the model has been correctly calibrated. The model is suitable for evaluating the environmental impact of sewage effluent on Ocreza River from the wastewaters treatment plant inflows, allowing feasibility studies of different treatment schemes and the development of specific monitoring activities.

https://doi.org/10.1180/S0026461X00006502 Published online by Cambridge University Press

Recognition of mucilage and microbial events on the Early–Late Pliensbachian (Lusitanian Basin, Portugal)

R.L. SILVA[1]*, L.V. DUARTE[1], J.G. MENDONÇA FILHO[2], F.S. DA SILVA[2], T.F. SILVA[2] AND M.J. COMAS-RENGIFO[3]

[1]IMAR-CMA and DCT, UC, 3000, Coimbra, Portugal (*correspondence: ricardo.silva@student.dct.uc.pt)
[2]LAFO, UFRJ, 21949-900, Rio de Janeiro, Brazil
[3]UCM-CSIC, 28040, Madrid, Spain

In the Lusitanian Basin (Portugal), the Early–Late Pliensbachian interval (c. a. 186 Ma, Early Jurassic) is characterized by the deposition of organic-rich marl–limestone hemipelagic alternations on a north-westerly dipping low-energy carbonate ramp [1]. The aim of this work is to present the characterization of these organic-rich facies at a basinal scale, supported by the combination of Sedimentology, Stratigraphy and Paleontology with Geochemistry, Organic Petrography, Palynofacies and Biochemistry.

Several well defined black shales (*s. l.*) are observed throughout the studied sections, where TOC values reach up to 26.3 wt.%. From the integration of the available data, we suggest that these black shales correspond to mucilageneous agreggates and/or microbial biofilm events, whose origin is related with palaeoceanographic and palaeoclimatic changes. Modern and fossil examples show that massive mucilage and microbial outbreaks can have severe effects on the biota [e.g. 2, 3] and that their preservation can be an important factor in influencing several elemental cycles and their major disturbances [e.g. 4].

It has been evoked that the Late Pliensbachian corresponds to a widespread organic matter preservation interval (Late Pliensbachian OMPI), linked to the complex chain of events that ultimately led to the Toarcian Oceanic Anoxic Event [5]. Our data highlights the relationship between microbial development and contemporaneous palaeoenvironmental changes and adds valuable information to understand their role in the modern world.

This work is a contribution to project PTDC/CTE-GIX/098968/2008 (FCT-Portugal, COMPETE/FEDER).

[1] Duarte *et al*. (2010) *Geol Acta* **8**(3), 325–340. [2] Danovaro *et al*. (2009) *PLoS ONE* **4**(9), e7006. [3] Castel & Rodgers (2009) *Environmental Geosciences* **16**(1), 1–23. [4] Gorin *et al*. (2009) *Terra Nova* **21**, 21–27. [5] Silva *et al*. (2011) *Chem Geol* **283**, 177–184.

The interaction between Central and South America from Sr-isotope chemostratigraphy of Cenozoic coral reef sucessions

J.C. SILVA-TAMAYO[1]*, C. MONTES[1], A. CARDONA[1], C. JARAMILLO[1], G. BAYONA[2], V. RAMIREZ [3], E. NIÑO[3], M. DUCEA[4], A. SIAL[5] AND V. ZAPATA[1]

[1]Smithsonian Tropical Research Institute (* correspondence: jsilvatamayo@yahoo.com)
[2]Corporacion Geologica Ares
[3]Ecopetrol
[4]University of Arizona
[5]Stable Isotope Laboratory, LABISE

The interaction between Central America and South America has been extensively studied due to important implications that the separation of the Caribbean and Pacific oceans may have in terms of oceanography, ecology (i.e. connectivity) and global climate. Timing the exact closure of the Panama Isthmus has remained difficult due to the lack of a well-constrained chronostratigraphic framework for the Panamanian-Colombian area. The Panama Basin is the main tectonic feature separating the Chorotega and Choco-Darien Blocks [1]. Previous investigations have suggested a connection between western Panama and North America at ca 19 Ma; implying disconnection between the Chorotega and Choco-Darien during that time [2]. However, recent geochronologic investigations along eastern and western Panama have suggested a tectonic interaction between Central America – South America at ca 23 Ma [3, 4].

The Darien Formation in the Choco-Darien Block consists of Eocene-Oligocene collisional arc-related volcanics. Exquisitely well-preserved coral reef patchy carbonate successions nonconformably overlay the Darien Formation. Sr-isotope chemostraigraphic data and calcareous nanoplankton suggests a depositional age between 23.3 and 13.65 Ma. The depositional age of such carbonate successions that cover the latest arc record in eastern Panama provides a unique temporal framework for the beginning of Panama-Northern South America tectonic interaction and the resulting Cenozoic paleoceanographic, paleoclimatic and paleobiologic changes in the neotropics.

[1] Coates *et al*. (2004) *Geol. Soc. Am. Bul*. **116**, 1327–1344. [2] Kirby *et al*. (2008) *PloS ONE* **3**(7) e2791. [3] Farris *et al*. (submitted) *Geology*. [4] Montes *et al*. (Submitted)

https://doi.org/10.1180/S0026461X00006502 Published online by Cambridge University Press

Novel denitrifier method for measuring ^{15}N and ^{18}O of nitrate

H. SILVENNOINEN[1], J. ZHU[1]*, PT. MØRKVED[2], L. BAKKEN[1], J. MULDER[1] AND P. DÖRSCH[1]

[1]Norwegian University of Life Sciences, 1432 Ås, Norway (*correspondence: jing.zhu@umb.no)
[2]Institute for Energy Technology, 2007 Kjeller, Norway

The 'Denitrifier Method' using *Pseudomonas aureofaciens* to convert NO_2^- and NO_3^- quantitatively to N_2O, first devised by Sigman & Casciotti *et al*. [1, 2] has become a state-of-the-art method for nitrate preparation prior to IRMS analysis of ^{15}N & ^{18}O. This method is, however, relatively laborious and requires numerous successive steps of culturing, purging and concentration, all of which increase the risk of contamination by non-sample NO_3^- or N_2O. Moreover, the viability of the used *P. aureofaciens* cultures typically remains unreported, making it difficult to assess fractionation biases through incomplete NO_2^- and NO_3^- conversion. Here we present a novel denitrifier method that uses *Paracoccus denitrificans* (a complete denitrifier) to remove any NO_3^- and N_2O background from the growth medium before culturing *P. aureofaciens*. We found that *P. aureofaciens* cultures growing oxically in sterilized *P. denitrificans* treated medium can be switched successfully to anoxic respiration in the presence of 20 mM NH_4^+ with the sample NO_2^- and NO_3^- as the sole electron acceptor. This significantly shortens preparation times and reduces the risk of contamination (Tab. 1). We successfully tested the method for water samples with pH as low as 4 and for soil extracts containing 0.5 M KCl. First results applying the novel method to pore water samples from an N-saturated subtropical forest in southwest China will be presented.

	Precision (nmol)	^{15}N accuracy (‰)	^{18}O accuracy (‰)	Duration (days)
Original	20	0.4	20	10
New	≤ 25	1.9	7.9	3

Table 1: Comparison of the original with the newly developed denitrifier method

[1] Sigman *et al*. (2001) *Analytical Chemistry* **73**, 4145–4153.
[2] Casciotti *et al*. (2002) *Analytical Chemistry* **74**, 4905–4912.

Large sulfur isotope fractionation does not require disproportionation

MIN SUB SIM*, SHUHEI ONO AND TANJA BOSAK

Department of Earth, Atmospheric, and Planetary Sciences, Massachusetts Institute of Technology, Cambridge, MA 02139, United States (*correspondence: mssim@mit.edu, sono@mit.edu, tbosak@mit.edu)

Microbial sulfate reduction (MSR) controls the partitioning of sulfur isotopes among various sulfur reservoirs, leaving a sedimentary sulfur isotope record that is used to track the oceanic budgets of oxidants, the progressive oxygenation of Earth's surface, and the evolution of microbial metabolisms through geologic history. Although previous environmental studies and models suspected that MSR alone could produce sulfur isotope offset between sedimentary sulfides and sulfates as large as ~ 75‰, all culture studies to date reported enrichment factors for MSR ($^{34}\varepsilon$) smaller than 47‰. ^{34}S fractionation larger than 47‰ and its relationship to ^{33}S fractionation ($^{33}\lambda$) were thus thought to indicate active microbial disproportionation and oxidative recycling of sulfur.

A pure, actively growing culture of the recently isolated marine sulfate reducing bacterium (DMSS-1) produces sulfide depleted in ^{34}S by 6 to 66‰. The largest isotope effects occur during the very slow growth of cultures grown on glucose, a recalcitrant organic substrate. The large isotope effects and the associated $^{33}\lambda$ values produced by DMSS-1 during sulfate reduction approach the equilibrium value between sulfate and sulfide at low temperatures (<40 °C). These findings bridge the long-standing discrepancy between the upper limit for $^{34}\varepsilon$ in laboratory cultures and the corresponding observations in nature and indicate that near-equilibrium $^{34}\varepsilon$ and $^{33}\lambda$ do not unambiguously record the stepwise oxygenation of Earth's surface environment. Instead, the strong dependence of $^{34}\varepsilon$ on the availability and quality of natural organic matter suggests that temporal or regional changes in the sulfur isotope systematics may reflect the changing nature of organic material that fueled sulfate reduction during the Proterozoic and the Phanerozoic.

https://doi.org/10.1180/S0026461X00006502 Published online by Cambridge University Press

Iron distribution in the clay of weathering crust of Katalambinskoe ore field

Y.S. SIMAKOVA*, V.P. LIUTOEV AND A.Y. LYSIUK

Institute of Geology of RAS , Syktyvkar. 167982, Russia
(*correspondence: yssimakova@rambler.ru)

Samples of the so-called structureless clays from mature weathering crust of Katalambinskoe ore field have been studied. Kaolinizated white clay and ocher brown clay characterized using infrared (IR), EPR and Mössbauer spectroscopy. X-ray diffraction (XRD) study indicates that raw materials consists of low-ordered kaolinite (up to 70%), well-ordered muskovite and minor relics of initial chlorite. Major impurities in ocher clay are goethite, lepidocrocite, magnetite and uncrystallized iron oxide.

Kaolinite substituted muscovite and paragonite in the initial rocks. IR spectra in the region of stretching vibrations of OH groups are also indicated presence of structurally imperfect kaolinite. Chemical analysis of the kaolinizated sample show content Fe_2O_3 = 3, 10%, FeO = 0, 35%, in ocher sample - Fe_2O_3 = 20, 64% and FeO = 0, 44%, respectively.

Mossbauer spectrum of white kaolinizated clay can be described by a superposition of two doublet of three-and ferrous iron. According to [1], the doublet can be attributed to the octahedral position of ferric iron in the kaolinite structure. High linewidth of the doublet of ferric iron indicates a low ordering kaolinite. Ferrous doublet has parameters typical of octahedral cis-positions in muscovite present in the samples according to the x-ray analysis. It accounts for about 15% of the total iron content in the sample.

Sextet structure shows the presence in the brown clay of the two magnetically ordered phases, characterized by the values of magnetic hyperfine fields 500 and 470 kOe. It should be noted that the doublet spectrum can be observed in goethite, if present by nanoscale particles. According to X-ray analysis is goethite is the dominant Fe-containing phase.

Thus, in the process of weathering crust Katalambinskoe ore field iron can form oxide-hydroxide secondary phases and enter the structure of usually iron-free phyllosilicates (ex. kaolinite).

[1] Castelein *et al*. (2002) *J. Eur. Ceramic Soc*. **22**, 1767–1773.

Biogeochemical footprint of the Ta-, and Nb-bearing carbonatite, Blue River Area, British Columbia, Canada

GEORGE J. SIMANDL[1,2], ROBERT FAJBER[1] AND COLIN E. DUNN[3]

[1]British Columbia Geological Survey, Victoria, BC, Canada
[2]University of Victoria, School of Earth and Ocean Sciences, Victoria, BC, Canada
[3]Consulting Geologist/Geochemist, Sidney, BC, Canada

This orientation survey demonstrates that coniferous trees are suitable sampling media in the exploration for carbonatites and related rare earth elements (REE), Ta, Nb, and phosphate deposits.

Twenty four samples of twigs with needles from Subalpine Fir (Fir) and White Spruce (Spruce) were collected over the Upper Fir carbonatite and surrounding amphibolites and paragneisses. Twigs and needles were analyzed separately. Twigs were milled using a Wiley mill. The resulting pulps were digested in HNO_3, then Aqua Regia and then analyzed by ICP-MS/ICP-ES. Needles were ashed, digested in Aqua Regia and then submitted for ICP-MS/ICP-ES analysis.

Light rare earth elements (LREE), Y, Zr and P in both twigs and needles are good exploration vectors for carbonatite-related REE and apatite mineralization. The highest concentrations of LREE are detected directly over carbonatites or fenites. Concentrations of heavy rare earth elements (HREE) are near or below the detection limit. Tantalum is found in detectable concentrations only in spruce twig samples spatially related to carbonatite. Detectable Ta concentrations range from 0.001 to 0.003 ppm. Niobium concentrations range from 0.02 to 0.24 ppm in Spruce twigs, 0.005 to 0.071 ppm in Spruce needles (dry weight normalized), and 0.012 ppm to 0.030 ppm in Fir needles (dry weight normalized).

Spruce twig data show a positive correlation between Fe, REE and Zr; Nb correlates positively with Fe, Ti, Ce, and Nd. Fir twigs were not analysed. Spruce needle data suggest strong positive correlations between P, Mg and Ti, as well as Nb and REE, and Zr and Fe, and a moderate positive correlation exists between P and Ca. There are not enough Fir needle samples for formal statistical analysis, however, strong positive correlations are suspected between Fe and REE, Fe and Ti, and P and Zr.

https://doi.org/10.1180/S0026461X00006502 Published online by Cambridge University Press

Rare Earth Elements (REE) recovery as a by-product of fertilizer production from sedimentary Phosphate deposits – Conceptual evaluation

LAURA SIMANDL[1]*, GEORGE J. SIMANDL[2,3] AND ROBERT FAJBER[2]

[1]St-Michaels University School, 3400 Richmond, Victoria, British Columbia, Canada, V8P 4P5 (*correspondence: laura.simandl@smus.bc.ca)
[2]British Columbia Ministry of Energy and Mines, Victoria, British Columbia
[3]University of Victoria, School of Earth and Ocean Sciences, Victoria, BC, Canada

Worldwide, phosphate deposits are classified into three main categories: a) phosphorites (sedimentary phosphate deposits), b) apatite-rich igneous rocks and related residual deposits, and c) modern and ancient guano accumulations. Marine phosphorites are the most significant in terms of global phosphate production, reserves and resources. Phosphorites average approximatley 460 ppm total rare earth elements (∑REE), are enriched in REE relative to typical shale (207 ppm ∑REE), and can contain more than 1600 ppm of ∑REE. Total concentration and proportions of individual REEs within phosphorites vary substantially.

Currently, China produces the vast majority of the world's REE supply. Rapid increases in internal demand for REE have motivated the Chinese government to introduce limits and taxes on REE exports. The resulting insecuirty regarding global REE supply created a rise in REE prices. The world's REE demand for 2010 was estimated at 125 000 tonnes. Assuming average REE content of 460 ppm ∑REE in phosphorite, the world's phosphate production of 170 million tonnes represents over 70 000 tonnes of contained REE.

Considering the phosphorites of the Fernie Formation in British Columbia (Canada), at current REE prices, a tonne of phosphate rock has an 'in the ground value' of more than US$ 160. This is more than the current market value of high-quality commercial phosphorite concentrate (approximately US$ 130-150). The above rudimentary considerations indicate that at current REE prices, the economic viability of REE recovery as a by-product of phosphate mining should be re-evaluated.

In situ SXRF determination of trace element abundances in aqueous fluid at 1 - 3 GPa and 300 – 500°C: Applications to subduction zone element cycling

A. SIMON[1], L. TANIS[1], O. TSCHAUNER[1], M. FRANK[2], P. CHOW[3], Y. XIAO[3], G. SHEN[3] AND J. HANCHAR[4]

[1]Department of Geoscience, High Pressure Science and Engineering Center, University of Nevada Las Vegas, Las Vegas, USA
[2]Department of Geoscience, Northern Illinois University, DeKalb, IL, USA
[3]HPCAT, Advanced Photon Source, Carnegie Institute of Washington, Argonne, IL, USA
[4]Department of Earth Sciences, Memorial University of Newfoundland, Canada

Interpreting trace-element variability in arc magmas that are hypothesized to have an aqueous fluid signature is predicated on having a quantitative understanding of the aqueous fluid-mediated trace-element transfer at PT conditions attending slab-sediment devolatilization. Experimental efforts to quantify the element-scavenging potential of aqueous fluid (s) were historically performed ex situ by recovery-type experiments. Here, we report further development of a synchrotron-based hydrothermal diamond anvil cell technique that allows *in situ* quantitative determination of trace element abundances in aqueous fluid at PT conditions appropriate for slab devolatilization. Notably, *in situ* reversals can be performed. The technique was developed by measuring the dissolution of YPO_4 (xenotime), a proxy for the behavior of heavy rare earth elements (HREE), in aqueous fluid at 1 to 3 GPa and 300 to 500°C. Yttrium concentrations and pressure were measured *in situ* by using synchrotron X-ray fluorescence (SXRF) and X-ray diffraction (XRD) of gold, respectively. Yttrium standards were measured in the same sample chamber as xenotime experiments, and a multi-point standard calibration curve was used to calculate Y abundances in the fluid in the xenotime dissolution experiments. This ensures a constant fluorescence excitation volume for the standards and the unknowns. The new data indicate that Y (HREE) concentrations in aqueous fluid are relatively constant at 300 to 500°C and 1 to 3 GPa, suggesting that increasing temperature, at a given pressure, does not increase the HREE-scavenging ability of aqueous fluid. These data have important implications for HREE recycling in subduction zone environments.

https://doi.org/10.1180/S0026461X00006502 Published online by Cambridge University Press

Balancing of geological acidity and buffering potentials of Mid German lignite open casts by long-term experiments

A. SIMON[1], N. HOTH[1], J. RASCHER[2] AND P. JOLAS[3]

[1]TU Bergakademie Freiberg Akademiestraße 6, 09596 Freiberg (andre.simon@ tu-freiberg.de)
[2]GEOmontan, Am St. Niclas Schacht 13, 09599 Freiberg
[3]MIBRAG mbH, Glück-Auf-Straße 1, 06727 Theißen

Problem and Solution

Open cast lignite mining induces sulphide weathering associated with Acid Mine Drainage - phenomena (mobilisation of acidity, sulphate, heavy metals). This partial weathering of sulphides is embedded in hydro-geochemical buffering reactions. Essential buffers are carbonates, aluminium/ iron hydroxides and aluminium silicates. Especially the carbonate buffering is important [1].

For sustainable strategic activities to reduce the acidification of ground waters by the lignite dump sites Peres and Schleenhain (Germany, South of Leipzig/Saxony), it is essential to evaluate the acidification and buffer potentials of the overburden units. These investigations need to consider the applied mining technology [2].

In long-term experiments (>500d), wet samples of forefield drillings of the five aquifers and some aquiclude units were exposed to weathering (T = 10 °C).

These tests shows clearly that the Oligocene aquifers (Aquifer 2 and 3) are the main problem sediments. The low pH values are coupled to a high acidity, iron and sulphate release. In contrast the glacial marly till contributes by buffering carbonates.

The subsequent buffering tests with aquifer 2 and 3 material in combination with the glacial till sediments, shows a clear effective buffering with increasing addition of glacial till. A release of iron and heavy metals can be completely prevented for longer times. The detailed investigation of the already existing water phase of the dump site Peres confirms the buffering effect by these carbonates.

Therefore the overburden dumping technology will be even more directed to the effective buffering by mixing the problematic materials with the buffering tills.

[1] Hoth (2004) Schriftenreihe für Geowissenschaften, Heft **15**, 214 S. ISBN 3–937040-10-2. [2] Rascher *et al*. (2006) Lithofazielle Modellierung tertiärer Fazieseinheiten in Bergbaufolgelandschaften. i. A. Sächs. Landesamt f. Umwelt u. Geologie, 1–102, Freiberg.

Ca isotopes of Central American arc basalts lack carbonate component

J.I. SIMON[1], S.T. BROWN[2] AND D.J. DEPAOLO[2]

[1]KR, NASA Johnson Space Center, Houston, TX 77058, USA (Justin.I.Simon @NASA.gov)
[2]Center for Isotope Geochemistry, Unversity of California and Lawrence Berkeley National Laboratory, Berkeley, CA 94720, USA

Subduction of sediment fundamentally represents a loss of continental crust and a gain of relatively enriched components to the mantle. Provided that possible mixing end members can be defined, stable Ca isotope signatures provide a powerful probe for identifying various sources in volcanic arc magmas. For example, marine carbonates are enriched in light Ca isotopes by about -0.2 to > -1.0‰ [1], relative to igneous rocks and should clearly implicate subducted sediment. Here we present Ca isotopic compositions for basalts from along the active Central American volcanic arc front that represent the range of trace element signatures indicative of various amounts of sediment recycling through the subduction zone (e.g. based on Ba/La values).

In an attempt to balance sedimentary input and arc volcanic output across the Nicaraguan margin [2] compared sediment input (i.e. high Ba/La) in arc magmas to offshore sedimentary drill cores, concluding that over the last ~20 Ma as much as 75% of the modern sedimentary column has been subducted. Despite measuring samples with trace element signatures that imply large amounts of subducted carbonate, we find no resolveable evidence for a low $^{44}Ca/^{40}Ca$ component. In detail, arc basalts from Guatemala, Honduras, and Nicaragua range from 0.04 to -0.18‰ in $^{44}Ca/^{40}Ca$ (mantle=0 scale). These nearly indistiguishable results are somewhat surprising given the fact that $CaCO_3$ has ≥4 times more Ca than the basalts. Mass balance shows that ~2-10% carbonate should produce resolvable effects.

Several potential reasons for the missing Ca isotopic signal are considered, including that: (1) subducted carbonate has an isotopic composition similar to mantle Ca, cf. [1], (2) subducted carbonate is largely dolomite, and/or (3) the record found in the drill cores is not representative of subducted sediment in the modern arc. Our new Ca isotope data imply that, at least for the Nicaraguan volcanic arc, trace element geochemistry may be less well understood than we believe. This is supported by the fact that the highest $\delta^{18}O$ values are associated with low Ba/La [3], and not the high Ba/La values typically correlated with increasing fluids from the slab.

[1] Fantle, M. and D.J. DePaolo (2007) *GCA* **71**, 2524–2546. [2] Plank, T. *et al*. (2002) *Geology* **30**, 1087–1090. [3] Vogel, T.A. *et al*. (2006) *JVGR* **156**, 217–228.

https://doi.org/10.1180/S0026461X00006502 Published online by Cambridge University Press

The influence of melt structure on the partitioning of trace elements

S. SIMON[1] *, M. WILKE[1], S. KLEMME[2], W.A. CALIEBE[3] AND K.O. KVASHNINA[4]

[1]GFZ, German Research Centre For Geosciences, Potsdam, Germany (*correspondence: ssimon@gfz-potsdam.de)
[2]Westfälische Wilhelms-Universität, Münster, Germany
[3]Deutsches Elektronen-Synchrotron, Hamburg, Germany
[4]European Synchrotron Radiation Facility, Grenoble, France

Partitioning of trace elements between melt and crystal is a versatile tool to reconstruct the origin of igneous rocks, thus it is essential to understand the controlling parameters. It is generally accepted that the partitioning of trace elements (TE) is controlled by T, p, fO_2 and crystal chemistry (e.g. [1]). Several studies have also proposed a significant influence of the melt composition and thus melt structure on TE partitioning [2 – 4]. Particularly, Prowatke & Klemme's results [4] on TE partitioning between melt and titanite, which varied over several orders of magnitude, suggest a strong control of the melt composition and thus melt structure. To date there is no clear understanding of the relationship between melt structure and element partitioning. Ponader & Brown [5] report already that coordination of some rare earth elements (REE) in quenched melts changes with the degree of polymerization of the melts, this was used to explain differences in chemical partitioning. However they did not provide a direct correlation between the analysis of the element coordination and partitioning data.

In this study, different melt compositions were taken from Prowatke & Klemme [4], doped with selected REE (0.5 wt%, 2 wt%) and synthesized as glasses. EXAFS was used to get information about coordination and radial distances to the neighboring atoms of the REE in the glasses. Resonant Inelastic X-ray Scattering (RIXS) provides information about the electronic structure and was used to derive further constraints on the coordination. The measured EXAFS spectra show small variation in the distance to the first oxygen neighbours to the different glasses. The RIXS and high resolution XANES indicate only slight differences in site symmetries. Although only preliminary, our results show that the strong difference in element partitioning correlates only with rather small changes in the TE coordination.

[1] Blundy & Wood (2003) *Earth Planet. Sci. Lett.* **210**, 383–397. [2] Watson (1976) *Contrib. Mineral. Petrol.* **56**, 119–134. [3] Ryerson & Hess (1978) *Geochim. Cosmochim. Acta* **42**, 921–932. [4] Prowatke & Klemme (2005) *Geochim. Cosmochim. Acta* **69**, 695–709. [5] Ponader & Brown (1989) *Geochim. Cosmochim. Acta* **53**, 2893–2903.

Formation of carbonate minerals during magmatic/hydrothermal alteration of volcanic rocks at Unzen volcano, Japan

A. SIMONYAN[1]*, S. DULTZ[1,2], H. BEHRENS[1], J. FIEBIG[3] AND K. VOGES[1]

[1]Institute for Mineralogy, Leibniz University of Hannover, Callinstr. 3, 30167 Hannover (*correspondence: simonian@mineralogie.uni-hannover.de)
[2]Institute of Soil Science, Leibniz University of Hannover, Herrenhäuser Str. 2, D-30419 Hannover
[3]Institute for Geosciences, J.W. Goethe University of Frankfurt, Altenhöferallee 1, D-60438 Frankfurt am Main

The alteration processes of dacitic and andesitic rocks of Unzen volcano are characterized by almost complete substitution of amphibole phenocrysts with two types of carbonates (up to 20 wt.%), quartz, muscovite and chlorite. In this study we investigate the main factors responsible for the alteration of porous volcanic rocks at Unzen.

It is determined that unaltered dacite has pores in the range from 100 nm to 10 μm, whereas the most frequent pore sizes for coherent altered dacites are observed in the range between 30 and 400 nm. All samples are characterized by interconnected porosity.

The unaltered amphiboles exhibit a homogeneous oxygen isotopic composition, with $\delta^{18}O$ vs VSMOW varying between 6.6 and 7.0‰, pointing to their primary magmatic origin. The oxygen isotopic composition of carbonates substituted amphiboles ranges from 6.0 to 9.1‰ vs VSMOW and their carbon isotopic composition varies between –4.7 and –6.4‰ vs VPDB. It implies that magmatic CO_2 and primary silicates provide the main sources for the carbonate carbon and carbonate oxygen, respectively. Hydrogen isotope composition of unaltered amphiboles shows typical magmatic signatures (δD=-48‰) without any evidence for late- or post-magmatic contamination by meteoric waters.

A series of hydrothermal fluid/rock interaction experiments in different systems, i.e. dacite or pure amphibole + H_2O, $H_2C_2O_4 \cdot 2H_2O$, $Ag_2C_2O_4$, Pl, $CaCO_3$ in different proportions were conducted at temperatures from 300 to 700°C and at pressures from 100 to 300 MPa, respectively. The first analyses of the experimental products show that amphiboles participate in exchange reactions with fluid with the formation of new mineral phases, e.g. $CaSiO_3$, however the size of produced phases was too small for proper identification. Raman spectra confirm that carbonates are indeed present as secondary phases in altered amphiboles (<5μm), providing constraints on the carbonation reactions.

Further experiments are required to reproduce natural mineral assemblages and to determine typical conditions for carbonate formation in Unzen conduit.

https://doi.org/10.1180/S0026461X00006502 Published online by Cambridge University Press

Do ^{226}Ra-^{230}Th isochrons provide realistic crystallization ages?

KENNETH W.W. SIMS[1]*, SYLVAIN PICHAT[2], MARK REAGAN[3], PHILLIP KYLE[4], NELIA DUNBAR[4], JANNE BLICHERT-TOFT[2,]

[1]Dept of Geology and Geophysics, University of Wyoming, Laramie,, WY, USA (ksims7@uwyo.edu)
[2]Laboratoire de Sciences de la Terre, Ecole normale superieure de Lyon Fr (pichat@ens-lyon.fr, blicher@ens-lyon.fr)
[3]Department of Geoscience, University of Iowa Iowa City, IA, USA (mark-reagan@uiowa.edu)
[4]N.M.B.G/E&ES Department, New Mexico Tech, Socorro, NM, 87801, USA (kyle@nmt.edu, nelia@nmt.edu)

In this contribution we investigate the timescales of magma genesis, melt evolution, crystal growth rates and magma degassing in the Mt Erebus magmatic system using measurements of ^{238}U-^{230}Th-^{226}Ra-^{210}Pb-^{210}Po; ^{232}Th-^{228}Ra-^{228}Th and ^{235}U-^{231}Pa-^{227}Ac. These are the first measurements of ^{231}Pa-^{227}Ac in volcanic samples and thus this is the first data set to present the entire suite of relevant ^{238}U, ^{235}U and ^{232}Th decay series nuclides in a volcanic system. Our sample suite consists of 22 historic bombs, ranging from 1972-2005; and 5 anorthoclase megacrysts separated from historic bombs for the years 1984, 1989, 1993, 2004, 2005. These samples ^{238}U-^{230}Th and ^{230}Th-^{226}Ra are significant and uniform over the 36 year historical record. The anorthoclase megacrysts and phonolite glass show complimentary ^{226}Ra/^{230}Th disequilibria. In all samples, ^{210}Pb/^{226}Ra are in secular equilibrium for both phases. For phonolite glass separates ^{227}Ac/^{231}Pa is also unity. For the phonolite glass ^{228}Ra/^{232}Th is in equilibrium, whereas in the anorthoclase megacrysts ^{228}Ra/^{232}Th is significantly greater than unity..

Instantaneous crystal fractionation, with long magma residence time (> 100 years, < 3 kyrs, depending on D_{Ba}/D_{Ra}), can account for the ^{238}U-^{230}Th-^{226}Ra-^{210}Pb and ^{235}U-^{231}Pa-^{227}Ac systematics. However, the significant ^{228}Ra/^{232}Th disequilibria in the anorthoclase megacrysts preclude this simple interpretation. To account for this apparent discrepancy we have developed an open-system, continuous crystallization model, which incorporates both nuclide in-growth and decay during crystallization and recharge. Our model can successfully reproduce all of the measured ^{238}U- ^{235}U- and ^{232}Th- decay series disequilibria. More importantly, this model shows that when the timescale of crystallization is comparable to the half-life of ^{226}Ra, the simple ^{230}Th-^{226}Ra isochron techniques typically used in most U-series studies likely provide erroneous ages.

Dissolved ^{230}Th-^{232}Th dynamics in the Eastern Tropical Pacific Ocean

AJAY K. SINGH[1], FRANCO MARCANTONIO[1] AND MITCHELL LYLE[2]

[1]Department of Geology & Geophysics, Texas A& University, College Station, TX 77843, USA (*correspondence: asingh1@neo.tamu.edu)
[2]Department of Oceanography, Texas A&M University, College Station, TX 77843, USA

We present data for dissolved ^{230}Th and ^{232}Th concentrations in seawater from nine depth profiles along a transect (~85°W) from about 7°N to 8°S in the eastern tropical Pacific Ocean. Our sampling sites cover the highly productive regions of the Pacific cold tongue close to the equator, and less productive regions of the Panama and Peru Basins. Dissolved ^{230}Th is thought to be scavenged onto sinking particles, and reversible exchange between dissolved and particulate phases takes place throughout the water column. As a result vertical dissolved ^{230}Th profiles should show a linear increase in ^{230}Th concentration with increasing water column depth.

Filtered (dissolved fraction of ^{230}Th-^{232}Th) and unfiltered (dissolved and particulate fraction of ^{230}Th-^{232}Th) seawater samples have been processed following established protocols developed by GEOTRACES. Our data thus far show little evidence for a linear increase in the concentration of dissolved ^{230}Th with depth, and the observed vertical structure may be related to either water mass or particle flux effects. Dissolved ^{230}Th concentrations range from 0.25 to 1.46 dpm/1000L for filtered samples. Dissolved ^{232}Th concentrations are low and range from 0.002 to 0.007 dpm/1000 L for filtered samples. While concentrations of ^{230}Th are slightly higher in the unfiltered samples, ^{232}Th concentrations are ususally much higher in the unfiltered samples (up to 170% higher), compared to those concentrations in the filtered samples. The greatest differences between filtered and unfiltered Th concentrations occur in the bottommost samples. Our preliminary results also indicate that that there is a concentration gradient along the transect—higher concentrations of ^{230}Th are found in the low-particle-flux Peru Basin while very low concentrations of ^{230}Th have been determined in profiles closer to the Panama Basin. Like the ^{230}Th data, the ^{232}Th concentrations are highest the further south in the transect. However, in contrast to the ^{230}Th concentrations, there is little structure in the ^{232}Th concentrations, which vary little with depth.

https://doi.org/10.1180/S0026461X00006502 Published online by Cambridge University Press

Grain size analysis of sediments of Thar Dessert, India to infer sedimentary environment

CHANDER KUMAR SINGH, RINA KUMARI AND SAUMITRA MUKHERJEE

School of Environmental Sciences, Jawaharlal Nehru University, New Delhi-110067

Grain size is a fundamental descriptive measure of sediment and sedimentary rock. Grain size parameters are useful for recognizing sedimentary environments as dune, river, beach marine and others of continental shelf through graphical, moment and statistical methods. Bivariate plots between various statistical grain size parameters can be successfully used for distinction of such environments. The statistical grain size parameters were treated using different statistical tools such as factor and discriminatory analysis to decipher the depositional history of the sediments of the study region. The analysis suggests that the deposits are not unequivocally aeolian, but contain sediments contributed by marine, shallow marine, fluvial, aeolian and lacustrine processes. Fluvial and fluvio-lacustrine deposits formed the base for the aeolian deposition in the region. SEM analysis of grains are a type of caliche formation in which fine grained calcareous sediments has reached near surface by capillary action and deposited. Angular outlines and features such as high relief, sharp edges and articulate steps were observed in the grains. The results of bivariate plots of mean (phi), moment mean and discriminant analysis does not show any specific trend of grain size for different geomorphic environments however these functions states that the sedimentary depositional environment in the study area has been mainly controlled by fluvial and marine activities but the importance of aeolian action also can not be ignored.

Geochemistry and mineralogy of Tertiary sedimentary rocks from Kerala, South India – Implications to REE behaviour under intense chemical weathering

PRAMOD SINGH* AND C.G. LAKSHMIDEVI

Department of Earth Sciences, Pondicherry University, Pondicherry 605014, India
(*correspondence: pramods@yahoo.com)

The Tertiary sedimentary rocks of Kerala along the south-west coast of India are mainly divided into three formations, Vaikom, Warkala and Quilon. This research evaluates the clay mineral and geochemical compositions including the rare earth elements (REE) of the mudstones and sandstones from two sedimentary sections of Warkala formation from the Karuchal and the Warkala region. The high CIA values ranging between 97 and 99 for Karuchal area and between 85 and 98 for Warkala area suggests that these sediments are extremely weathered. Further Kaolinite as the dominant clay in rocks from Karuchal section and Kaolinite / Gibbsite as the dominant clay in rocks from Warkala section also corroborate higher degree of weathering. All elements except Al, Ti and Ni exhibit depletion in comparison to UCC. The chondrite normalised REE pattern exhibit high degree of fractionation, ((Ce/Yb)n ranging between 30 and 67 for sediments of Karuchal section; (Ce/Yb)n ranging between 14 and 50 for sediments of Warkala section. On normalizing with all the probable source rocks exposed in the area, the REE plot of the sediments exhibit LREE enrichment and HREE depletion. This indicates that the higher (Ce/Yb)n ratios are not because of source, but due to the loss of HREE and residual enrichment of LREE bearing phases. This suggests mobilisation and removal of HREE from the system under extreme chemical weathering. Our finding has important implications as REE is commonly accepted to reflect the nature of exposed continental crust [1].

[1] McLennan, Nance & Taylor (1980) *Geochim. Cosmochim. Acta* **44**, 1833–1839.

https://doi.org/10.1180/S0026461X00006502 Published online by Cambridge University Press

Sustainable water resource management in Eastern Punjab using remote sensing and GIS to demarcate water potential zones

RAVI PRAKASH SINGH[1], C.K. SINGH[2] AND S. MUKHERJEE[3]

[1](singhravi004@gmail.com)
[2](chanderkumarsingh@gmail.com)
[3](saumitramukherjee3@gmail.com)

Water is a fluctuating resource making it difficult to measure in time and in space. To demonstrate the efficiency of the geographic information system (GIS) for groundwater management, information on the parameters controlling groundwater such as lithology, geomorphology, soil type, land use and land cover and lineament analysis were analyzed. IRS LISS-III and Landsat satellite data of the area was used to infer information on the geologic lineaments and geomorphology. To identify linear features i. e lineament enhancement and directional filtering was performed on single bands of Landsat images. Thematic maps for geology, slope, soil, geomorphology and lineament were prepared and integrated in GIS by assigning the weights and ranking to various parameters controlling the occurrence of groundwater to generate the groundwater potential map for the study area. The results indicate that the floodplain of river and its adjoining areas have very good groundwater potential, whereas the steeply sloping area in the northern part having high relief and slope possesses poor groundwater potential. The groundwater potential zones were obtained by weighted overlay method using the spatial analysis module in ArcGIS 9.0. The southern part of the study area showed highest decline in water level in last 3 decades. Thus a holistic water resource management strategy needs to be developed for this part of the district. The floodplain of the river in the area holds potential for further groundwater development as these areas belong to good class in GPI map.

Toward a self-consistent pressure scale: Elastic moduli and equation of state of MgO and Ringwoodite by simultaneous X-ray density and Brillouin sound velocity measurements at high-P and high-T

STANISLAV SINOGEIKIN[1,2]*, DMITRY LAKSHTANOV[2,3], VITALI PRAKAPENKA[4], CARMEN SANCHEZ-VALLE[2,5], JINGUING WANG[2,5], GUOYIN SHEN[1,4] AND JAY BASS[2]

[1]HPCAT and Geophysical Lab, Carnegie Institution of Washington, USA
(*corresponcence: ssinogeikin@ciw.edu)
[2]University of Illinois at UC, Geology Dept., USA
[3]BP Exploration Operating Company Ltd, Sunbury, UK
[4]GSECARS, The University of Chicago, Chicago, IL, USA
[5]Institute for Mineralogy and Petrology, ETH Zurich, CH

Accurate phase diagrams and PVT equations of state (EOS) of materials strongly depend on the PVT calibrations of standard materials (e.g. MgO, NaCl, Au, Pt), which currently do not predict identical pressures at the same experimental conditions. MgO is one of the simplest and most studied materials and is a common pressure standard, although its accurate high-PT EOS is still uncertain. The direct way of obtaining a self consistent pressure scale is by measuring acoustic velocities (Vp and Vs) and density simultaneously. Such P-V-T-Vp-Vs measurements allow one to determine the pressure directly, without resort to a separate calibration standard.

Recently, as part of a major COMPRES initiative, we have constructed a Brillouin spectrometer at GSECARS, APS, which allows accurate simultaneous sound velocity and lattice parameter measurements at high P and high T. Such measurements were performed on single crystal MgO in diamond cells. At each PT we measured the unit cell parameters and the acoustic velocities in several crystallographic directions, and directly obtained all three single crystal, and isotropic adiabatic bulk (Ks) and shear (μ) elastic moduli.

In addition we demonstrate that successful P-V-T-Vp-Vs measurements can be performed on certain polycrystalline materials, e.g. Ringwoodite (gamma-Mg_2SiO_4). The results of these experiments and implications for a self consistent P-V-T (-Vp-Vs) pressure scale will be presented and discussed.

https://doi.org/10.1180/S0026461X00006502 Published online by Cambridge University Press

In situ Fe-Mg isotopic analysis of zoned olivines

C.K. SIO[1], N. DAUPHAS[1], F.-Z. TENG[2], R.T. HELZ[3] AND M. CHAUSSIDON[4]

[1]Origins Laboratory, Dept. of the Geophysical Sciences, The University of Chicago (ksio@uchicago.edu)
[2]Dept. of Geosciences and Arkansas Center for Space and Planetary Sciences, The University of Arkansas
[3]Uinted States Geological Survey, Reston, VA
[4]CRPG, Vandoeuvre lès Nancy, France

Chemical diffusion profiles in zoned olivines may be used to infer the thermal history of the system surrounding them. However, diffusive transport is not the only way to produce a chemical gradient. An olivine that crystallized rapidly may produce a similar zoning pattern.

Fe and Mg isotopic analyses of bulk olivines reveal that isotopes can be used to recognize chemical diffusion in olivines [1-3]. Chemical diffusion can induce large isotopic fractionations because light isotopes always diffuse faster than their heavier counterparts [4-5]. At equilibrium, little isotopic fractionation is expected given the high temperatures of magmatic systems.

Olivines in Kilauea Iki lave lake have large chemical zoning profiles and lighter iron isotopic compositions than the bulk basalts [1]. Teng *et al*. [1] showed that in these olivines, the isotopic compositions are correlated by a slope of -3.3 in a plot of $\delta^{56/54}$Fe vs. $\delta^{26/24}$Mg, in close agreement to the predicted slope of -2.7 for binary diffusion [2]. Here we provide definite evidence that diffusive transport is responsible for the light Fe isotopic compositions measured in olivines in Kilauea Iki lava lake.

A zoned olivine ~4 mm in size was microdrilled in two orthogonal traverses for Fe and Mg isotopic measurements. Isotopic compositions were measured by MC-ICPMS. Profiles are observed with iron isotopic compositions ranging from -1.2 ‰ in the core to to -0.2 ‰ in the rim ($\delta^{56/54}$Fe deviations from IRMM-014). The variations can be explained by diffusion of Fe into olivine following magmatic evolution towards more Fe-rich and Mg-poor compositions.

In situ Fe and Mg isotopic measurements in olivines can help identify grains that are affected by chemical diffusion. These olivines may be used as tools for diffusion-based geothermometry.

[1] Teng F-Z *et al*. (2008) *Science* **320**, 1620–1622. [2] Dauphas *et al*. (2010) *Geochim. Cosmochim. Acta* **74**, 3274–3291. [3] Teng F-Z *et al*. (2011) 42nd LPSC Abstract #2660. [4] Richter *et al*. (2009) *Geochim. Cosmochim. Acta* **73**, 4250–4263. [5] Roskosz *et al*. (2006) *Earth Planet. Sci. Lett*. **248**, 851–867.

Potentially toxic metal bearing mineral phases in total suspended particles from Budapest, Hungary

P. SIPOS[1], E. MÁRTON[2], T. NÉMETH[1], V. KOVÁCS KIS[3], Z. MAY[4] AND Z. SZALAI[5]

[1]HAS Institute for Geochemical Research, Budapest, Hungary (sipos@geochem.hu)
[2]Paleomagnetic Laboratory, Eötvös Loránd Geophysical Institute, Budapest, Hungary
[3]HAS Research Institute for Technical Physics and Materials Science, Budapest, Hungary
[4]HAS Institute of Materials and Environmental Chemistry, Budapest, Hungary
[5]HAS Geographical Research Institute, Budapest, Hungary

Total suspended particles (TSP) in the urban air can be both inhaled and ingested so causing health damage due to their size, shape or toxic components. In this study mineralogical (XRD, AEM), geochemical (XRF) and magnetic (MS) analyses were performed to characterize the mineral phases containing potentially toxic metals in TSP from three sampling sites in Budapest. The samples represent wide range of physico-chemical properties. Their particles are generally below 50 μm with a maximum frequency at around 10-12 μm. Between 45 and 80% of their particles belong to the PM10 fraction. They show significant enrichment in several potentially toxic metals with concentrations 1342-19 046 mg/kg for Zn, 434-3597 mg/kg for Pb, 394-699 mg/kg for Zn and 38-144 mg/kg for As. Their main mineral components reflects the geological characteristics of the sampling areas. Additionally, large amount of magentite (up to 15%) and amorphous organic matter, as well as gypsum and halite was also found in the samples.

The most important toxic metal bearing mineral phases are spherular or xenomorphic magnetite particles containing 2-3 wt% Pb and Zn. These magentite particles often form aggregates and are closely associated with soot and/or clay minerals. In samples with high magnetite content toxic metal-free magnetite spherules up to a few micrometer size also appear. The magnetic analyses showed that the sizes of the magnetite particles is rarely below 30 nm. Clay minerals and mica particles may also contain significant amount of Zn (up to 5wt%). Additionally, ZnO and $ZnCO_3$ particles were also found in the sample with highest Zn content. Magnetite particles are resistant to weathering releasing its toxic components slowly to the environment, while layer silicates may be the source of mobile toxic metals in these samples. The study was financially supported by the OTKA (K 76317 and K 75395).

https://doi.org/10.1180/S0026461X00006502 Published online by Cambridge University Press

Pyroxene and olivine exsolution textures in majoritic garnets from the Mir kimberlitic pipe (Yakutia)

E.A. SIROTKINA*, A.V. BOBROV, V.K. GARANIN, A.V. BOVKUN, B.B. SHKURSKII AND D.V. KOROST

Geological Faculty, Moscow State University, Moscow, Russia (*correspondence: katty.ea@mail.ru, archi3@yandex.ru)

Majoritic garnets are widely abundant as inclusions in diamonds worldwide [1]. Pyroxene exsolution textures were registered in garnets from mantle xenoliths in kimberlites [2, 3], as well as in rocks of ultrahigh-pressure metamorphic complexes [4], which provides evidence for their crystallization at pressures >7–8 GPa. We studied three large (>5 mm) garnet xenocrysts (Samples 317, 559 and 563) from the Mir pipe (Yakutia) containing regularly oriented pyroxene and olivine lamellae with angles of 71–72° between them. Garnets of all samples are pyrope-rich (75.1–78.6 mol %), with medium CaO (4.5–5.8 wt %) and low Cr_2O_3 (up to 0.59 wt %) concentrations. Clinopyroxene lamellae are enriched in diopside component (89.9–94.4 mol %). Olivines are characterized by the high Mg# (up to 0.96) and extremely high NiO concentration (1.6 wt % in Sample 559; 2.79 wt % in Sample 317). According to the data of 3D X-ray tomography using a scanner SkyScan1172 and 3D analysis (CT-An software), garnet (Sample 317) contains 9 vol % pyroxene and 0.5 vol % olivine lamellae. Calculation of the compositions of primary garnets demonstrated that Si content in them exceeded 3 f. u. (3.084 in Sample 317; 3.088 in Sample 559; 3.094 in Sample 563) providing evidence for incorporation of majoritic component. The formation of such garnets occurred at pressures >7.5 GPa and high temperatures (Ni in majoritic garnet and olivine). Subsequent decrease of *PT* parameters to 3.0–3.1 GPa and 950–1000°C [5] resulted in pyroxene and Ni-olivine exsolution in former majoritic garnet.

Support: RFBR (09-05-00027), MD (534.2011.5).

[1] Stachel (2001) *EJM* **13**, 883–892. [2] Haggerty & Sautter (1990) *Science* **248**, 993–996. [3] Sautter *et al*. (1991) *Science* **252**, 827–830. [4] van Roermund & Drury (1998) *Terra Nova* **10**, 295–301. [5] Simakov & Taylor (2000) *Intern. Geol. Rev.* **42**, 534–544.

Effects of organic ligands and temperature on the kinetics and mechanisms of olivine carbonation

O. SISSMANN*[1,2], D. DAVAL[3], I. MARTINEZ[1], F. BRUNET[4], N. FINDLING[4] AND F. GUYOT[1,5]

[1]IPGP, Université Paris Diderot, CNRS, France (*correspondence: sissmann@ipgp.fr)
[2]Laboratoire de Géologie, ENS-CNRS, France
[3]Lawrence Berkeley National Laboratory, CA, USA
[4]ISTerre, CNRS, Université J. Fourier, Grenoble, France
[5]IMPMC, Paris, France

The slow dissolution kinetics of Mg-rich silicates has become a critical issue for the geologic CO_2 sequestration in basic rocks. Previous batch carbonation studies on San Carlos olivine performed in CO_2 saturated water (at 90°C and PCO_2= 280 bar) have focused on the role that secondary phases, such as amorphous silica layers (SiO_2 (am)), have on the transport of reactants from and to the reactive surfaces. The fluid composition remained roughly constant over the duration of the experiment, close to saturation with respect to amorphous silica and with a $[Mg^{2+}]/[SiO_2$ (aq)] ratio close to stoechiometric release, suggesting a passivation of the olivine surface by the silica layer.

In order to accelerate the dissolution process, organic ligands such as citrate and acetate were added to the solutions and tested at 1M and 0.1M concentrations in similar batch experiments. An intrinsic increase of the dissolution rate of olivine was expected prior to the formation of a passivating silica layer.

Preliminary results confirm this idea since Mg was released in non-stoechimoetric proportions with respect to SiO_2 (aq) (found to be in equilibrium with SiO_2 (am)).

Similarly, a slight increase of temperature (from 90°C to 120°C) accelerated the reaction kinetics as well, possibly impacting the textural properties of SiO_2 (am). Current TEM investigations are directed to confirming a possible link between the observed increase of the rate and textural properties of secondary phases. In addition, because carbonate minerals have a retrograde solubility, thermodynamical modelling suggests that this temperature increase should allow the fluid to reach saturation with respect to carbonates before reaching saturation with respect to SiO_2 (am). Enough Mg can therefore be released to initiate the formation of carbonates before the silica precipitates and passivates the olivine surface.

https://doi.org/10.1180/S0026461X00006502 Published online by Cambridge University Press

Impact of the earthworm *Lumbricus terrestris* on arsenic mobility and speciation in soil

T. SIZMUR[1]*, M.J. WATTS[2], G.D. BROWN[3], B. PALUMBO-ROE[2] AND M.E. HODSON[1]

[1]Soil Research Centre, University of Reading, RG6 6DW, UK (*correspondence: t.p.sizmur@reading.ac.uk, m.e.hodson@reading.ac.uk)
[2]British Geological Survey, NG12 5GG, UK (mwatts@bgs.ac.uk, bpal@bgs.ac.uk)
[3]Dept. Chemistry, University of Reading, RG6 6AB, UK (g.d.brown@reading.ac.uk)

Earthworms can be found living in arsenic contaminated soil. Generally earthworm activity increases the mobility and bioavailability of contaminants [1]. Using soil collected from Devon Great Consols containing 1150 mg As kg^{-1} we have investigated how the secretion of earthworm mucus and the passage of soil through the earthworm gut impacts mobility and speciation of As.

Lumbricus terrestris were cultivated in the As-contaminated soil and the casts collected. Water soluble As increased from 1.6 mg kg^{-1} in the bulk soil to 18 mg kg^{-1} in the casts. Casts were then aged and this effect was still present 56 days after soil excretion. Analysis indicated that these changes were due to release of As(V) from soil particles during the digestion process as a result of increases in pH and increased concentrations of disolved organic carbon. No reduction of As(V) to As(III) was detected despite passage of the As through the anoxic rear-gut of the earthworm.

Solutions of earthworm mucus were produced by washing earthworms with deionised water. These solutions were then used as an extractant for the As-contaminated soil. At low mucus concentrations As extraction was reduced relative to deionised water due to formation of ternary complexes between the amino acids present in the mucus, As and surfaces of Fe oxyhydroxides. However, at higher mucus concentrations increased pH and dissolved organic carbon effects dominated resulting in increased extraction of As.

The mobilisation of As (and other elements) from contaminated soils in the environment by cast production and mucus secretion may allow for accelerated leaching or uptake into biota which is under-estimated in current risk assessments based on analysis using soils in the absence of soil biota.

[1] Sizmur & Hodson (2009) *Environ. Pollut.* **157**, 1981–1989.

Continental subduction, slab breakoff and eduction: End-member processes for UHP rock histories

ELENA SIZOVA, TIBAULT DURETZ AND TARAS GERYA

Institute of Geophysics, Swiss Federal Institute of Technology, Sonneggstrasse 5, 8092 Zurich, Switzerland (taras.gerya@erdw.ethz.ch)

We conducted a set of numerical experiments to study the evolution of a subduction–collision system subject to spontaneous slab breakoff. The study takes into account complex rheological behaviour including plasticity, viscous creep and Peierls creep and mineralogical phase transformations including UHP melting. A limited number of contrasting geodynamic scenarios were observed that combine several previously suggested end-member tectonic processes such as continental subduction, multiple crustal stacking, oceanic slab delamination and breakoff, plate eduction, ductile crustal extrusions and buoyant partially molten trans-lithospheric plumes. In the explored parameter space, breakoff depth can range from 40 to 400 km with Peierls creep in the cold subducted mantle been a key mechanism for slab necking. We also found that melting of crustal materials at ultrahigh pressure metamorphic (UHPM) conditions can trigger the exhumation of high temperature-ultrahigh pressure metamorphic (HT-UHPM) rocks. In the model, the generation of temperatures high enough for anatexis during subduction is due to the continental crust and associated sediments coming into contact with hot asthenospheric mantle of the wedge at ultrahigh pressure conditions. The consequent enhanced buoyancy of the melt-bearing crustal and associated sedimentary materials drives the subsequent exhumation of the HT-UHPM rocks from mantle depths to mid-to-lower crustal levels. Exhumation occurs by a thermally induced slab-parallel ductile extrusion of melt-bearing crustal materials along the interface between the stagnant subducted slab and the mantle wedge. The up to 1000 C peak temperatures achieved in the experiments at UHPM conditions are the highest obtained so far in experiments using numerical models; they are similar to many natural HT-UHPM rocks. The sensitivity studies suggest that some other mechanisms proposed previously for the exhumation of UHPM rocks including multiple crustal stacking, plate eduction, trans-lithospheric crustal plumes and channel flow are mainly controlled by the oceanic slab age and length and by the incoming passive margin geometry. Indeed, all these exhumation processes typically result in colder P-T paths with the coldest (<500 C) peak temperatures been produced by the eduction-driven exhumation.

https://doi.org/10.1180/S0026461X00006502 Published online by Cambridge University Press

Trace elements and lead isotopes in moldavites: Source material fractionation or variable parent lithologies mixing?

ROMAN SKÁLA[1]* AND LADISLAV STRNAD[2]

[1]Institute of Geology ASCR, v.v.i., Rozvojová 269, 16500 Praha 6, Czech Republic (*correspondence: skala@gli.cas.cz)

[2]Faculty of Science, Charles University, Alberov 6, CZ12800 Praha 2, Czech Republic (lada@natur.cuni.cz)

Samples and data collection

Contents of selected minor and trace elements and lead isotope composition have been determined for 16 moldavites from South Bohemian (4), West Moravian (5) and Cheb Basin (7) partial strewn fields. Data were measured using ICP-MS technique from solution following the protocol of Strnad *et al*. [1].

Results

After normalizing the measured values to average element contents for moldavites from the South Bohemian partial field it appeared that the moldavites from Cheb Basin differ from those from South Bohemia and Moravia. They are highly enriched in Zn, Ba, Pb, and U while they display significant depletion in Cr and Ni. Moravian moldavites display either no or significantly less differences when compared to South Bohemian moldavites.

Chondrite-normalized REE contents overlap existing literature data. HREE tend to be enriched in Moravian samples whereas the samples from the Cheb Basin appear to be depleted in HREE compared to the moldavites from the South Bohemian field. Concentrations of LREE remain more or less invariant among all regions.

In the plot $^{208}Pb/^{206}Pb$ *vs*. $^{206}Pb/^{207}Pb$ the moldavites from the Cheb Basin are clearly separated from the rest of the samples analyzed; samples from South Bohemia and Moravia do not differ.

Conclusions

The data collected do not corroborate idea of selective source material fractional vaporization, or that of selective condensation neither the hypothesis of Engelhardt *et al*. [2] explaining the formation of moldavites by preferential trapping of large ions into early condensates. We assume that measured composition reflects the lithological variability of the target area instead.

[1] Strnad *et al*. (2005) *GGR* **29**, 303–314. [2] Engelhardt von W. (2005) *GCA* **69**, 5611–5626.

Nitrogen isotope fractionation during the oxidation of substituted anilines by manganese oxide

MARITA SKARPELI-LIATI[1,2], MARTIN JISKRA[2], WILIAM A. ARNOLD[3], CHRISTOPHER J. CRAMER[4] AND THOMAS B. HOFSTETTER[1,2]*

[1]Eawag, Swiss Federal Institute of Aquatic Science and Technology, CH-8600, Dübendorf, Switzerland (*correspondence: thomas.hofstetter@eawag.ch)

[2]Institute of Biogeochemistry and Pollutant Dynamics, ETH Zurich, CH-8092 Zurich, Switzerland

[3]Department of Civil Engineering University of Minnesota, Minneapolis, MN 55455

[4]Department of Chemistry and Supercomputing Institute, University of Minnesota

Primary aromatic amino groups are often the position of initial attack during the mineral-catalyzed oxidative transformation processes of soil and groundwater contaminants. Here, we explored the N isotope fractionation associated with the oxidation of substituted anilines as a diagnostic tool for identifying the initial oxidation steps of such degradation processes. Apparent ^{15}N-kinetic isotope effects, $AKIE_N$, were determined for oxidation of various substituted anilines in suspension of manganese oxide (MnO_2) and compared to reference oxidation experiments in homogeneous solution and at electrode surfaces, as well as to density functional theory calculations of intrinsic KIE_N for electron and hydrogen atom transfer reactions.

Spectroscopic characterization of MnO_2-particles as well as the investigation of co-solute effects on mineral reactivity showed that despite complex reaction kinetics of contaminant disappearance, substituted aniline oxidation occurred in one elmentary, isotope-sensitive reaction step. Owing to the partial aromatic imine formation after one- electron oxidation and corresponding increase in C–N bond strength, $AKIE_N$ -values were *inverse*, substituent-dependent, and confined to the range between 0.992 and 0.999 in agreement with theory. However, $AKIE_N$-values became *normal* once the fraction of cationic species prevailed owing to ^{15}N-equilibrium isotope effects, EIE_N, of 1.02 associated with N atom deprotonation. The observable $AKIE_N$-values are substantially modulated by the acid/base pre-equilibria of the substituted anilines and isotope fractionation may even vanish under conditions where normal EIE_N and inverse $AKIE_N$ cancel each other out. Our work suggests that the observed pH- and substituent-dependent trends of N isotope fractionation provide a new line of evidence for the identification of oxidative degradation processes of substituted primary aromatic amines.

https://doi.org/10.1180/S0026461X00006502 Published online by Cambridge University Press

Solubility and toxicity of hydroxylapatite (hap) nanoparticles (nps): Implications for nanobiomaterial safety

KYRIAKI SKARTSILA, SUPERB MISRA AND EVA VALSAMI-JONES

Natural History Museum, London UK (kyrs@nhm.ac.uk)

Nanotechnology has the potential to solve many of modern society's problems, notably in medicine and the environment. Although an increase in interest in regulating risks from nanotechnologies is evident in recent years, research and regulation of risks lag behind the driving forces of intellectual curiosity and commercial potential. The aim of this work is to contribute to a better understanding of the risks of nanotechnology and ultimately to their control. We specifically focus on the reactivity and the potential toxicity of HAP NPs, which are used in many medical innovations.

A variety of HAP NPs were synthesised selected on the basis of their biocompatibility and particle size. Full detailed physicochemical characterisation was carried out in parallel. The synthesis method was then optimised to provide control over crystal growth, agglomeration, particle size and shape mainly by investigating the effect of synthesis parameters such as: synthesis temperature, pH, maturation time, concentration of the capping agent, drying and calcination temperature.

The reactivity/chemical stability of the nanoHAPs was assessed by solubility experiments, which showed that solubility exponentially increases as the grain size decreases. This is in agreement with the modified version of the Kelvin equation, which describes the prediction that solubility is dependent on the particle size and is expected to increase exponentially as particles get smaller. Furthermore, these experiments showed that solubility correlates well with the crystallinity of nanoHAPs.

Protein adsorption studies were carried out as a proxy for toxicity; high proportion of protein adsorbed indicates better biocompatibility, and therefore less likelihood for toxicity. These experiments showed that more protein was absorbed by the smallest, least crystallised and non-functionalised HAP NPs, suggesting that these are the most biocompatible nanoHAPs.

Flux rates for water and carbon during greenschist facies metamorphism

ALASDAIR SKELTON

Department of Geological Sciences, Stockholm University, 106 91 Stockholm, Sweden (alasdair.skelton@geo.su.se)

The time-averaged flux rate for a CO_2-bearing hydrous fluid during greenschist facies regional metamorphism was estimated to $10^{-10.2 \pm 0.4}$ $m^3 . m^{-2} . s^{-1}$. This was evaluated by combining 1) Peclet numbers obtained by chromatographic analysis of the propagation of reaction fronts in 33 metamorphosed basaltic sills in the SW Scottish Highlands (Fig. 1), 2) empirical diffusion rates for CO_2 in water obtained by Wark & Watson (2003), and 3) calculated time-averaged metamorphic porosities. The latter were calculated using an expression obtained by combining estimated Peclet numbers with the empirical porosity – permeability relationships obtained by Wark and Watson (1998) and Price *et al*. (2006) and Darcy's law. This approach yielded a time-averaged metamorphic porosity of $10^{-2.6 \pm 0.2}$ for greenschist facies conditions. The corresponding timescale for metamorphic fluid flow was $10^{3.6 \pm 0.1}$ years. By using mineral assemblages to constrain fluid compositions, I further obtained a time-averaged annual flux rate for carbon of 0.5-7 mol-C. $m^{-2} . yr^{-1}$. This matches measured emission rates for metamorphic CO_2 from orogenic hot springs. These fluxes significantly exceed estimated rates of CO_2 drawdown by orogenic silicate weathering and therefore indicate that orogenesis is a source rather than a sink of atmospheric CO_2.

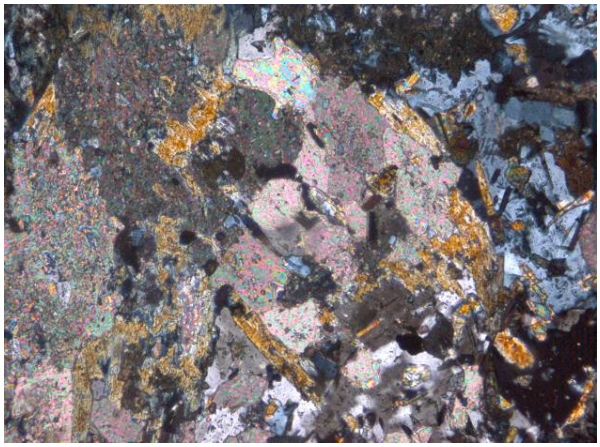

Figure 1: Photomicrograph (in XPL) showing replacement of amphibole by calcite: evidence of carbon transfer, preserved in a metabasaltic sill from the SW Scottish Highlands.

https://doi.org/10.1180/S0026461X00006502 Published online by Cambridge University Press

Tracing episodic magma accretion by zircon $^{18}O/^{16}O$ isotopes and U-Pb dating in the Adamello batholith, Italy

A. SKOPELITIS[1]*, I. BINDEMAN[2], A. ULIANOV[3], P. BRACK[4] AND U. SCHALTEGGER[1]

[1]University of Geneva, 1205 Geneva, Switzerland (*correspondence: Alexandra.Nowak@unige.ch)
[2]University of Oregon, OR 97403, USA
[3]University of Lausanne, 1015 Lausanne, Switzerland
[4]ETH, 8092 Zürich, Switzerland

Styles and timescales of batholith formation still remain a matter of debate. There is growing evidence that batholiths are not formed by a single ascent of magma but by accretion of multiple batches. In the latter case, are they derived from the same source or different ones, and do they suffer similar degrees of contamination?

In order to answer these questions, we study tonalites from the Adamello batholith (33-43 Ma) localized in the northern Italian Alps. Previous studies mainly based on cooling ages highlighted a younging of magmatic activity towards the north [1, 2, 3], which is confirmed by our new U-Pb zircon LA-ICP-MS dating. Isotopic compositions of both Sr and O indicated increased contribution from higher $\delta^{18}O$, more radiogenic supracrustal sources in the same direction [4]. We present new data from a $^{18}O/^{16}O$ isotope study on small quantities of freshest and refractory separates of quartz, amphibole, titanite and zircon, and best estimate $\delta^{18}O$ magma values [5]. The data confirm increasing crustal contamination towards the north indicated by elevated $\delta^{18}O$ values up to 7‰ in zircon. H isotope ratio is strongly negative (-97‰) for the amphibole in the most northerly sample suggesting an assimilation of hydrothermally-altered rocks or an assimilation of marine sediment. We will quantify the contamination by AFC modelling using geochemistry, whole rock and mineral isotopes. As a preliminary conclusion, the Adamello batholith was formed by different pulses over ca 10 m. y. coming from different in $\delta^{18}O$ magma reservoirs with contrasting oxygen isotope compositions, due to their different depth in a $^{18}O/^{16}O$ zoned crust.

[1] Callegari & Brack (2002) *Mem. Sci. Geol.* **54**, 19–49. [2] Schaltegger *et al.* (2009) *Earth Planet. Sci. Lett.* **186**, 108–218. [3] Del Moro *et al.* (1983) *Mem. Soc. Geol. It.* **26**, 261–284. [4] Cortecci *et al.* (1979) *Contrib. Mineral. Petrol* **68**, 421–427. [5] Bindeman (2008) *Rev. Min. Geoch.* **69**, 445–478.

Melting of carbonaceous sediments in subduction zones

S. SKORA* AND J. BLUNDY

Dept of Earth Sciences, University of Bristol, BS8 1RJ, UK (*correspondence: Susanne.Skora@bristol.ac.uk, Jon.Blundy@bristol.ac.uk)

The terrestrial carbon cycle is of immense interest to geoscientists as it has important consequences for, inter alia, Earth's climate, diamond formation, carbonatite volcanism and mantle metasomatism. Subduction zones provide the major geotectonic settings where surficial carbon can enter the Earth, and potentially return via arc volcanism. To date, experimental phase equilibria studies as well as thermodynamic calculations suggest that carbonates behave in a refractory manner under most subduction zone conditions in the slab. This stands in contrast to observations from nature, namely that CO_2 is released in arc volcanoes. Stable isotopic characteristics further suggest that most arc carbon is sediment-derived.

The suggested limited release of CO_2 at sub-arc depths, either by melting or by decarbonation, poses a great challenge to explain the high arc-flux of CO_2. This study aims to test the hypothesis that calcareous lithologies melt more readily at sub-arc conditions in the presence of external water, similarly to the melting behaviour of non-calcareous lithologies.

Two different calcareous lithologies were picked from the southern Lesser Antilles arc – one containing approx. 5% and one with approx. 35% carbonate. Initial experiments at 900°C, 3 GPa, 10% added water have yielded very high degrees of silicate melts, despite the fact that previous experimental studies have placed the solidus at temperatures >900°C at 3 GPa (fluid-absent conditions). This suggests that the fluid-saturated solidus in carbonaceous sediments has not been adequately constrained by the available fluid-absent experiments. In addition to glass, experimental run products contain either garnet + phengite + rutile + carbonate (5% carbonate lithology) or zoisite + quartz + rutile + carbonate (35% carbonate lithology). We will further investigate under which conditions CO_2 can be transported into the overlying mantle wedge.

https://doi.org/10.1180/S0026461X00006502 Published online by Cambridge University Press

The 1.86-1.84 Ga magmatism in the Western East European Craton (Lithuania): Implications for a convergent continental margin

G. SKRIDLAITE[1]*, M. WHITEHOUSE[2], S. BOGDANOVA[3] AND L. TARAN[4]

[1]Nature Research Centre, Vilnius, Lithuania (*correspondence: skridlaite@geo.lt)
[2]Swedish Museum of Natural History, Stockholm, Sweden
[3]Department of Geology, Lund University, Sweden
[4]Belarussian Research and Geological Exploration Institute

The East European Craton in western Fennoscandia was mostly formed by the accretion of distinct terranes at c. 1.8 Ga. TTG magmatic rocks in the age range 1.86-1.84 Ga are abundant in the crystalline crust of S, central and NW Lithuania. In the south, TTG rocks compose the large Randamonys massif. A Zm347 tonalite yielded an 1859±5Ma concordia age, while a Vr268 diorite was dated at 1848±6 Ma. A strongly deformed 7Gr granitic rock in adjacent NW Belarus gave a similar 1844±8 Ma igneous age. In central Lithuania, the Glv99 igneous mafic granulites display magmatic 1839±15 Ma and metamorphic 1809±9 Ma ages. The nearby Grz105 gneissic granite was intruded at c. 1837±6 Ma, while the Kz65 granite further north was emplaced at 1844±5 Ma [1]. The area to the south and west of the above described rocks in Lithuania and in N Poland is dominated by younger c. 1.83-1.79 Ga magmatic rocks. The fragments of a c. 1.83-1.82 Ga volcanic island arc in Sweden [2], N Poland and Lithuania [3] compose a considerable part of this younger domain.

The distribution of 1.86-1.84 Ga magmatic arc-related rocks in Lithuania likely delineates fragments of a convergent continental margin. It continues northwestwards across the Baltic Sea into south-central Sweden, and southwards to N Poland and NW Belarus.

[1] Motuza *et al*. (2008) *Geologija* 1(61) 1–16. [2] Mansfeld *et al*. (2005) *GFF* **127**, 149–157. [3] Wiszniewska *et al*. (2005) *Min. Soc. of Poland- Special Papers* **26**, 104–108.

Abnormal (Y+REE)-enriched zircon from the pegmatite dike (Gridino, the Belomorian province, Fennoscandian shield)

S.G. SKUBLOV[1]*, O.L. GALANKINA[1] AND S.G. SIMAKIN[2]

[1]Institute of Precambrian Geology and Geochronology, Russian Academy of Sciences, St. Petersburg 199034, Russia (*correspondence: skublov@gmail.com)
[2]Jaroslavl Branch of Institute of Physics and Technology, Russian Academy of Sciences, Jaroslavl 150055, Russia (simser@mail.ru)

Zircon can contain naturally U and Th up to 10 wt% and several thousands of ppm of REE. The maximum known contents of REE (up to 98, 154 ppm) was found in zircons from Bidoudouma stream close to Oklo, Gabon [1].

We found abnormal (Y+REE)-enriched zircon in the thin pegmatite dike cutting precambrian eclogites (village Gridino, the Belomorian province, Fennoscandian shield, see outcrop photo in [2]). Zircon core ($^{207}Pb/^{206}Pb$-age 2685 Ma) is captured eclogite protolith with regular REE distribution. Rim is characterized by high contents of REE (61, 280–96, 760 ppm), Y (55, 360–84, 800 ppm) and distinctly positive Ce anomaly. U and Th contents are not so high – maximum 2230 and 90 ppm, respectively.

Age of rim crystallization is svecofennian (1875 Ma) following high-pressure metamorphism event

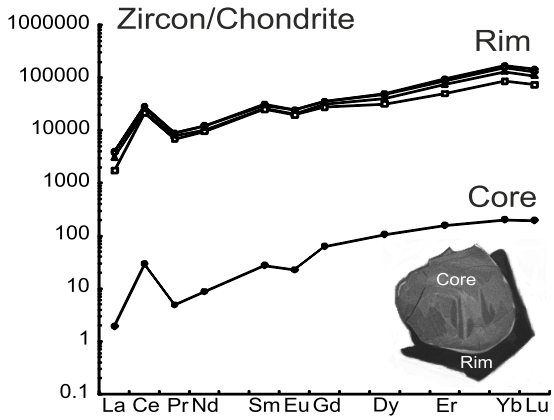

Figure 1: REE patterns for zircon core and rim (insert is CL image)

[1] Horie *et al*. (2006) *Phys. Chem. Earth* **31**, 587–592. [2] Hölttä *et al*. (2008) *Episodes* **31**, 13–19.

https://doi.org/10.1180/S0026461X00006502 Published online by Cambridge University Press

Nanoparticle bioremediation: Application of solid phase capture

R.L. SKUCE*, D.J. TOBLER, M.R. LEE AND V.R. PHOENIX

Department of Geographical and Earth Sciences, University of Glasgow, UK
(*correspondence: rebecca.skuce@ges.gla.ac.uk)

The use of engineered nanoparticles continues to expand rapidly. As this intensifies, so does the environmental risk posed if they are released into the environment. This is of particular concern due to the potential toxicity of some nanoparticles. As it stands, we are poorly prepared to deal with nanoparticle pollution and thus remediation strategies must be developed. Here ureolysis-driven calcium carbonate precipitation by the urease positive bacterium *Sporosarcina pasteurii* is investigated as a means of removing nanoparticles from aquatic systems. This technology has been investigated for the solid phase capture of radionuclide and trace element contaminants in groundwater systems [1]. However its potential to capture nanoparticles has yet to be examined.

Batch experiments showed the successful removal of highly stable organo-metallic nanoparticles at concentrations up to 10mg/l (the highest concentration tested thus far). Over 90% of nanoparticles were captured within 24 hours and capture efficiency appeared to be inversely proportional to calcite precipitation rate. As calcite precipitated, the nanoparticles became trapped within the growing calcite crystal. As the calcite-nanoparticle composite continued to grow, it adhered to surfaces (such as the edge of the reaction flask, or the edge of a pore space), immobilizing the nanoparticles from solution. Nanoparticles are believed to act as nucleation sites for the precipitating calcite. First order reaction kinetics were calculated to determine reaction rate constants, and in particular, S_{crit}, the critical saturation required for nucleation. This technology has the potential for application in contaminated groundwaters and soils as an *in situ* remediation technique for nanoparticle pollutants.

[1] Warren, L.A. Maurice, P.A. Ferris (2001) *N.P.F.G.* **18**, 93–115.

Testing a geochemical tracer tool in New Zealand water

ANGELA T. SLADE[1]*, N.R. WARNER[2], A. VENGOSH[2] AND BRANDON WHITEHEAD[1]

[1]School of Environment, The University of Auckland, 23 Symonds Street, Auckland 1142, New Zealand, (*correspondence: a.slade@auckland.ac.nz)
[2]Division of Earth and Ocean Sciences Nicholas School of the Environment, Duke University, Durham, NC 27708,

Deteriorating water quality along the Tarawera River, in Kawerau (New Zealand), is thought to be correlated to the solid and liquid waste disposal practices of the local pulp and paper mill in conjunction with naturally occurring geothermal discharge in the area. Due to high concentrations of boron in the liquid from both of these sources this study investigates the use of this element as a tool to assist in improving the management of the waterways and water quality in the region.

Comprehensive scientific studies that have been conducted for over 20 years have identified boron as a successful natural tracer for use in water bodies in different parts of the world. [1-3] Drawing on this information we executed a temporal water quality survey to assess the consistency of boron isotope composition values at a localised scale. This survey included monthly sampling over a six-month period spanning the wet and dry seasons. The water samples were a selection of pond, river, ground (shallow and deep zones), and geothermal, coupled with leachate and aeration pond water from a pulp and paper solid waste site. The boron concentration data and isotope ratios were established using ICP-MS and negative TIMS, respectively.

This paper discusses: 1) the effectiveness of boron isotope composition values as signatures for water; 2) the reliability of these signatures as a tool for water quality and management purposes; 3) the level to which sampling, analytical and environmental anomalies have influenced the results.

[1] Vengosh *et al*. (2005) *Water Resources Research* **41**, 1–19. [2] Barth *Water Resource* (1998) **32**, 685–690. [3] Tonarini *et al*. *Isotopes in Environmental & Health Studies* (2009) **45**, 169–183.

https://doi.org/10.1180/S0026461X00006502 Published online by Cambridge University Press

Factors affecting detrital zircon age distribution – Natural samples and experimental approach

J. SLAMA* AND J. KOSLER

Centre for Geobiology and Department of Earth Science, University of Bergen, Allegaten 41, N-5007 Bergen, Norway (*correspondence: jiri.slama@geo.uib.no)

We have investigated some of the factors that affect the accuracy of detrital zircon age provenance studies. The main goal was to quantify the effects of individual factors in the deviation of the measured detrital age spectra from the real zircon age distribution in the sediment and in the sediment source. The analysis has been carried out in a natural catchment in the Scottish Highlands representing simple two-component source system and on samples of synthetic sediment prepared on purpose for this study using zircon-free quartz sand and known number of zircon grains of known age distribution. Our results suggest that the zircon fertility of the source rocks and physical parameters of zircon grains represent the most important factors affecting the distribution of zircon age populations in the stream sediments. It can account for a several-fold difference between the ratio of the rocks in the source area and abundance of zircon in the sediment. Additional age biases can be introduced during sample preparation and data processing. The sample preparation and selection of zircons from the mineral concentrate may result in preferential loss of small grains and enhancement of the age component represented by larger grains. This can, together with the preference for larger grains during handpicking, cause several-fold difference compared to the real age distribution in the sediment sample. These factors appear to be more important for the reproducibility of zircon age spectra than is the number of zircon grains analyzed per sample. Even the most abundant age population in the sample may deviate by tens of percent from its real content in the sediment after hundred or more analyses have been done. The complex relations between proportion of zircon age populations in the source, sediment and analyzed sample make it difficult to relate the peak intensity in the age spectra to the sediment quantity contributed from different sources. At all times, the analytical limits of the dating techniques must be considered when evaluating potential overlap of zircon populations that are closely spaced in time. Although the visualization of U-Pb data in probability density plots is commonly used for comparison between samples, the detrital zircon age spectra must always be interpreted relative to the volume of individual age populations, not to the intensities of the age peaks.

Fluoride removal by calcite – Stirring rate/temperature effects

S.B. SLEAP, B.D. TURNER*, K. KRABBENHOFT AND S.W. SLOAN

Centre for Geotechnical and Materials Modelling, The University of Newcastle, N.S.W., 2308, Australia (*correspondence: Brett.Turner@newcastle.edu.au, Scott.Sleap@newcastle.edu.au, Kristian.Krabbenhoft@newcastle.edu.au Scott.Sloan@newcastle.edu.au)

Fluoride contamination of groundwater due to anthropogenic activities remains a major concern for many industries worldwide. The effects of stirring rate and temperature on the removal of fluoride by calcite have been studied in order to determine the most efficient and cost effective method of remediating such contamination.

The kinetics of calcite dissolution and precipitation in aqueous solution has been the subject of numerous investigations. However, little study has been undertaken on heterogeneous systems where mass transport processes and surface reactions determine rates. Aleksey, *et al*. [1] have noted that traditional thermodynamic approaches to determine equilibrium are problematic and there is a need for a kinetic approach to solving these problems. The effects of stirring and temperature on the heterogeneous calcite/F systems are the focus of this study.

A series of free drift experiments were conducted in a controlled temperature (CT) room at 20°C, 30°C and 40°C, with P_{CO2} in equilibrium with the atmosphere ($P_{CO2} \approx 10^{-3.5}$). Calcite was added to potassium fluoride solutions and stirred at 0, 200 and 300rpm using an overhead stirrer. The results in Table 1 have been determined by fitting the experimental data to the non-linear Hill 1 function ($r^2 > 0.98$).

RPM	Temp	Minutes	RPM	Temp	Minutes
300	40°C	5,143	0	40°C	13,224
300	30°C	9,196	0	30°C	24,250
200	40°C	11,287	0	20°C	138,169
200	30°C	22,330			

Table 1: Time (min) to reach equilibrium F removal

The results clearly demonstrate that a greater rate (dF/dt) of fluoride removal is possible with increased stirring rate and temperature. Early in the reaction <200 minutes dissolution is largely a function of a surface reaction as mixing has little effect on the rate [2]. In the latter part of the reaction, stirring rate has a significant effect, consequently hydrodynamic transport effects dominate [2].

[1] Alekseyev *et al*. (1997) *Geochimica et Cosmochimica Acta*. **61**, 1125–1142. [2] Plummer & Parkhurst (1979) *Chemical Modelling in Aqueous Systems*.

https://doi.org/10.1180/S0026461X00006502 Published online by Cambridge University Press

Minerals of Pt_3Sn-Pd_3Sn-Pd_3Pb-Pd_3As-Pd_3Sb system in PGE-Cu-Ni and PGE ores of the Norilsk region

S.F. SLUZHENIKIN AND A.V. MOKHOV

IGEM RAS, Staromonetny 35, Moscow 119017 Russia (*correspondence: nlo_s@mail.ru)

All minerals of the system – rustenburgite Pt_3Sn, atokite Pd_3Sn, zvyagintsevite Pd_3Pb, guanglinite Pt_3As and unnamed mineral with Pd_3Sb composition were found in Norilsk ores. A wide isomorphizm between Pt and Pd is established in the system, in particular within Pt_3Sn-Pd_3Sn series. The minerals very often contain Au as an admixture up to 6 wt.% (Fig. 1). An almost complete isomorphism between Sn, Pb, As и Sb is found. Chemical isomorphism is expressed in terms of zonal occurrences of the minerals during successive growth and replacement.

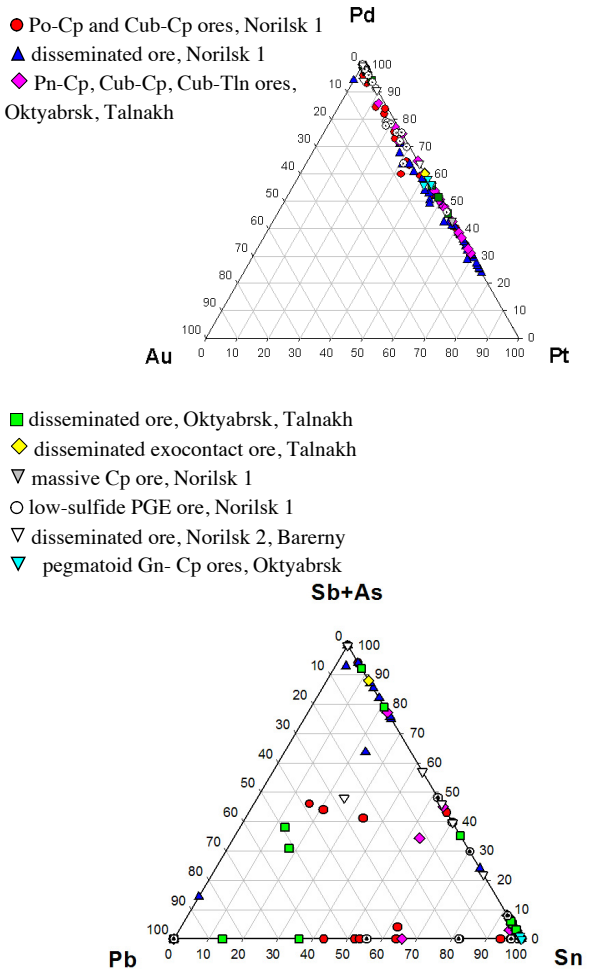

Figure 1: Chemical composition of Pt_3Sn-Pd_3Sn-Pd_3Pb-Pd_3Sb-Pd_3As minerals from Norilsk ore.

Does aerosol alter entrainment mixing in warm cumulus?

J.D. SMALL[1,2], H.H. JONSSON[3] AND P.Y. CHUANG[1]

[1]Earth and Planetary Sciences, University of California Santa Cruz, Santa Cruz, CA, 95064, USA (*correspondence: pchuang@ucsc.edu)

[2]NASA/JPL, Pasadena, CA, 91109, USA (Jennifer.Small@jpl.nasa.gov)

[3]Center for Interdisciplinary Remotely Piloted Studies (CIRPAS), Naval Postgraduate School, Marina, CA, 93933, USA (hjonsson@nps.edu)

We analyze the cloud microphysical response to entrainment mixing in warm cumulus clouds observed from the CIRPAS Twin Otter during the GoMACCS field campaign near Houston, TX in summer 2006. Cloud drop size distributions and cloud liquid water contents from the Artium Flight phase-Doppler interferometer in conjunction with meteorological observations are used to investigate the degree to which inhomogeneous versus homogeneous mixing is preferred as a function of height above cloud base, distance from cloud edge, and aerosol concentration. Using four complete days of data during which 101 non-precipitating cloud penetrations (minimum 300 m in length), we find that inhomogeneous mixing primarily explains liquid water variability in these clouds.

While theory predicts the potential for aerosol to affect mixing type via changes in drop size, over the range of aerosol concentrations experienced (moderately polluted rural sites to highly polluted urban sites), the observations, while consistent with this hypothesis, do not show a statistically significant effect of aerosol on mixing type. Instead we find two non-aerosol effects primarily control the microphysical response to entrainment mixing. First, we show that there is a tendency for mixing to be more homogeneous towards cloud top, which we attribute to the combination of increased turbulent kinetic energy and cloud drop size (due to condensational growth) with altitude which together cause the Damköhler number to increase by a factor of between 10 and 30 from cloud base to cloud top. Second, we find that cloud edges appear to be air from cloud centers which have been diluted solely through inhomogeneous mixing. We give plausible explanations for this second effect, but none thus far has been demonstrated using the observations.

Lastly, we discuss the possible ramifications of these observations on other key cloud properties, in particular warm rain formation and cloud albedo.

https://doi.org/10.1180/S0026461X00006502 Published online by Cambridge University Press

Formation of diamond from oxidized fluids/melts: δ^{13}C-N SIMS study of an eclogitic diamond from the Jericho kimberlite, Canada

K.A. SMART*, T. CHACKO, T. STACHEL, R.A. STERN AND K. MUEHLENBACHS

Dept. of Earth and Atmospheric Sciences, Univ. of Alberta, Edmonton, AB, Canada
(*correspondence: kasmart@ualberta.ca)

Diamonds are key to understanding the sources, speciation and cycling of carbon in the mantle, and together this information is crucial for the study of mantle redox processes. The carbon isotope composition of diamond provides essential information on both the source and redox-state dependent speciation of C reservoirs involved in diamond growth. Growth models are commonly based on xenocrystic diamonds sampled from kimberlites and usually represent mixed populations and multiple growth events. In contrast, *in situ* studies of single growth zones in individual diamonds are better suited for building diamond growth models. Here we present the results of a coupled CL-imaging and SIMS δ^{13}C-N study of a single, 0.5cm diamond from an eclogite xenolith from the Jericho kimberlite, Canada.

CL images of the diamond show a relatively homogeneous core mantled by oscillatory dark and light growth layers towards the rim. SIMS analyses of carbon isotope composition and nitrogen content in the core show systematic and coupled variations: N decreases rimwards from ~5000 to 1000 ppm and δ^{13}C increases from -4.1 to -2.7‰ in the same direction. We interpret these systematic co-variations to reflect fractional crystallization of diamond from a single melt/fluid pulse. Moreover, the coupled rimward enrichment in ^{13}C and depletion in N indicate diamond formation from an oxidized growth medium where N behaved compatibly in diamond relative to the medium. Modelling the core zone growth shows that the initial δ^{13}C value of the diamond-forming fluid/melt was between -2.3 and 0‰ (depending on temperature and C speciation, e.g. CO_3^{2-} or CO_2). The carbon source therefore was either subducted carbonates (δ^{13}C~0‰) that had undergone partial decarbonation causing ^{13}C depletion or primary mantle fluids/melts (-5‰) that had undergone extensive C fractionation prior to precipitation of the diamond investigated here. We favor a model where the carbon was sourced from a carbonatite-like medium, potentially derived from subducted sediments, as the host eclogites themselves have evidence for crustal protoliths and interaction with carbonatite-like metasomatic agents[1].

[1] Smart K.A. *et al*. (2009) *EPSL* **284** 527–537.

Biotic dissolution of Tl(I)jarosite by *Shewanella putrefaciens* CN32

C.M. SMEATON*, B.J. FRYER AND C.G. WEISENER

Great Lakes Institute for Environmental Research, University of Windsor, ON, Canada
(*correspondence: smeato3@uwindsor.ca)

Jarosites (MFe$_3$ (SO$_4$)$_2$ (OH)$_6$) are precipitated in the Zn industry to scavenge iron, alkali metals and sulfate ions during base metal processing and often contain toxic metals such as Pb, Ag and Tl. During this process, large volumes of jarositic wastes are produced and often confined to large repositories. Despite the toxicity of Tl, few studies exist on the abiotic and biotic dissolution of thallium mineral phases. In this study we examined the dissolution of synthetic Tl (I)-jarosite (TlFe$_3$ (SO$_4$)$_2$ (OH)$_6$) by *Shewanella putrefaciens* CN32 using batch experiments under anaerobic circumneutral conditions.

ATP, Fe and Tl concentrations were measured over time and showed increased Fe(II) and Tl in inoculated versus control samples (Fig 1). Tl concentrations in inoculated samples increased by a factor of 2 compared to control samples (Fig 1). In contrast to previous studies with Pb and Ag-jarosite, SEM images of *S. putrefaciens* CN32 did not show precipitation of Tl nanoparticles associated with the cell surface thus suggesting an alternative mechanism for Tl detoxification [1, 2].

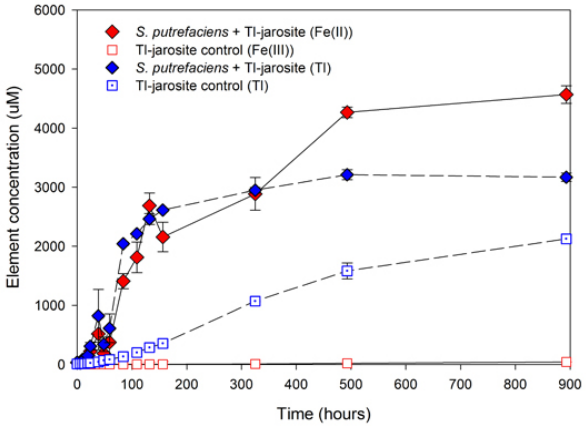

Figure 1: Fe and Tl release over time

[1] C.M. Smeaton *et al*. (2009) *Env. Sci. Tech*. **43**, 8091–8096.
[2] C.G. Weisener *et al*. (2008) *Geomicrobiology* Journal, **25**, 415- 421.

https://doi.org/10.1180/S0026461X00006502 Published online by Cambridge University Press

Volcanism on Methana (W Aegean arc): Magma mixing, crustal contamination & mantle sources

I. SMET[1]*, E. DE PELSMAEKER[1], M. ELBURG[1], F. VANHAECKE[2] AND T. ANDERSEN[3]

[1]Department of Geology and Soil Science, Ghent University, 9000, Belgium (*correspondence: ingrid.smet@ugent.be)
[2]Department of Analytical Chemistry, Ghent University, 9000, Belgium
[3]Department of Geosciences, University of Oslo, Norway

The peninsula of Methana represents the westernmost active centre of the (continental) South Aegean arc. Volcanism started about 1.1 Ma ago and the last eruptive phase is as young as 2200 years. Volcanic deposits are mostly andesitic to dacitic lava domes and flows with abundant mafic enclaves, but two volcanic centres also show volumetrically important pyroclastic deposits [1].

The many mafic enclaves in the lavas suggest that magma mingling has been important. Evidence for magma mixing includes a poor correlation between modal mineralogy and silica content, and the common occurrence of disequilibrium assemblages (such as biotite, zircon, quartz + olivine). Major and trace element concentrations of different lava flows and domes show a large variability, seemingly unrelated to silica content. $^{87}Sr/^{86}Sr$ ratios are variable (0.705-0.708), and the correlation with silica content is poor.

Enclosed xenoliths are mostly carbonates (and a few silicates) and are restricted to the two volcanic centres that also show pyroclastic activity. $^{87}Sr/^{86}Sr$ isotope ratios of these volcanics increase with increasing Sr concentration, suggesting carbonate assimilation. Interestingly, carbonate contamination is only observed in the pyroclast-bearing centres, and could therefore be responsible for their more explosive behaviour, as already suggested for Merapi volcano in Indonesia [2].

One lava flow displays a combination of the highest Sr concentrations (530 ppm, versus 200-350 ppm for the other volcanic deposits) and the lowest $^{87}Sr/^{86}Sr$ ratios (0.705). Similar volcanics have been found on the islands of Aegina and Nisyros, and point towards variations in mantle sources.

[1] V. Dietrich *et al*. (1995) Geological Map of Methana Peninsula (Greece) 1,25000, ETH, Zurich, Switzerland.
[2] J. Chadwick *et al*. (2007) *J. Petrol*. **48**, 1793–1812.

Uranium in tap and groundwater – Indications for anthropogenic origin

G. SMIDT[1]*, M. BIRKE[2], L. ERDINGER[3], M. SCHÄF[3], F. KNOLLE[4], A. KOSCHINSKY[1] AND E. SCHNUG[5]

[1]Intergrated Environmental Studies, Jacobs University Bremen, Campus Ring1, D-28759 Bremen, Germany (*correspondence: g.smidt@jacobs-university.de)
[2]Federal Institute for Geosciences and Natural Resources, Wilhelmstr. 25-30, D-13593 Berlin
[3]University Hospital Heidelberg, Dept. of Medical Microbiology and Hygiene, Im Neuenheimer Feld 324, D-69120 Heidelberg
[4]GeoPark Harz, Braunschweiger Land – Ostfalen, Grummetwiese 16, D-38640 Goslar
[5]Technical University - Faculty 2 Life Sciences, Pockelsstraße 14, D-38106 Braunschweig

Uranium (U) is a natural chemo- and radiotoxic heavy metal. The exposure of humans to U is mainly determined through uptake by drinking water. This paper reports on the U content in 4251 tap waters and 350 groundwaters from Germany collected by several research groups over the last 5 years and discusses the possible origin of U. This database is by far the largest available in the country and it represents data of drinking water to which 76% of the entire German population has access. The mean U concentration was 1.61 μg/L U, the median 0.50 μg/L U. 25.2% of all samples had U concentrations below the detection limits, which accounts for water to which 41.0% of the entire population has access. 24% of samples were above 2 μg/L U, 4.4 above 10 μg/L U, representing a population of 10.2 and 0.28%, respectively. The regional distribution of U concentrations follows the geological structures reported for mineral waters, however in contrasts to this clear evidences for anthropogenic influence through agricultural activities were found in drinking and groundwaters of areas with intense cropping productions in southern and northern Germany. Soil analyses show the high mobilisation capacity of fertilizer-derived U from arable soils in comparison to unfertilized control sites.

https://doi.org/10.1180/S0026461X00006502 Published online by Cambridge University Press

Processes of heavy metals immobilization in mires

BEATA SMIEJA-KRÓL[1]*, BARBARA FIAŁKIEWICZ-KOZIEŁ[2] AND JERZY WIEDERMANN[3]

[1]University of Silesia, 60 Będzińska, 41-200 Sosnowiec, Poland (*correspondence: beata.smieja-krol@us.edu.pl)
[2]Mickiewicz Univ., Dzięgielowa 27, 61-680 Poznań, Poland (basiafk@amu.edu.pl)
[3]Institute for Ferrous Metallurgy, 12 Miarki, 44-100 Gliwice, Poland (J.Wiedermann@imz.pl)

Long time mining and smelting activities have produced a widespread regional anomaly in Pb, Zn and Cd concentration in soils of Silesia region, southern Poland. Two mires: Bagno Bruch (BB) and Bagno Mikołeska (BM), located within the anomaly, were chosen to study processes of heavy metals immobilization in acid, water-logged and peat accumulating ecosystems.

The chemical analyses of peat were conducted using ICP-MS method. The solid samples (inorganic particles and peat) were investigated using FESEM.

A narrow peat layer, highly enriched in Pb, Zn and Cd, were detected at depth between 9 and 27 cm below the mires surface. The contaminated layer contained 460-1190 mg/kg of Pb, 1037-2371 mg/kg of Zn and 11.92 - 62.6 mg/kg of Cd. Above and below the layer, metal concentrations were several times lower, reaching values of 0.3-8.0 mg/kg Pb, 22-73 mg/kg Zn and 0.1-0.5 mg/kg of Cd in the deeper (below 50 cm), pre-industrial peat layer.

The study shows that an important part of the contaminants are immobilized in inorganic particles. In the contaminated layer, the fly-ash particles, originated from dust deposition, comprise up to 1.7% by volume of dry peat. The formation of authigenic (Zn, Cd)S (up to 1.1% by vol.), barite (~0.5% by vol. in BB, not found in BM), and traces of PbS, indicates the importance of secondary processes, like microbial activity, in metals distribution and immobilization.

The research was funded by the grant N N304 319136 from the Polish Ministry of Science and Higher Education.

Deformation of garnet in eclogite: Dominant mechanisms and the active role of fluids

M.A. SMIT[1], E.E. SCHERER[1], T. JOHN[1] AND A. JANSSEN[1,2]

[1]Institut für Mineralogie, Westfälische Wilhelms-Universität, Corrensstrasse 24, D-48149, Münster, Germany (m.a.smit@uni-muenster.de)
[2]Institute for Transuranium Elements, European Commision Joint Research Center, Hermann-von-Helmholtz-Platz 1, D-76344, Eggenstein-Leopoldshafen, Germany

The response of subducting rocks to stress under different physicochemical conditions is crucial to predicting the evolution of slab strength and the generation of earthquakes. Experiments on mafic rock rheology [1, 2] suggest that prograde metamorphism to eclogite should not significantly change bulk-rock viscosity. Yet, field evidence demonstrates a dramatic, but temporary competence loss as a result of such reaction [3]. This discrepancy underscores the need for further study into the relationship between fluid-flow, mineral reactions, and rheological properties of eclogite.

Garnet fabrics are particularly enigmatic features that sometimes indicate very efficient deformation of this mineral under conditions where it is expected to remain rigid. To investigate this, we compared the textural and microstructural characteristcs of garnet in an eclogite mylonite (Caledonian eclogites, Norway) to those of garnet that crystallized statically in a high-pressure seismic melt (Zambian eclogites).

In contrast to the static garnet crystals, mylonite garnet is flattened parallel to the main foliation. The grains exhibit foliation-perpendicular fractures, random crystallographic orientations, and abundant dissolution features, indicating mass transfer away from the grain boundaries. The grains accomodated large strains by intergranular pressure solution in the presence of fluid at high pressure.

This study shows that fluid-wetted grain boundaries occur in eclogite at depth and that these play a crucial role in the rheological weakening of such rock. Seismic imaging monitors the slab depth at which such weakening occurs as a distinct perturbation, beyond which slab coherrence is strongly reduced [4]. Even though fluid invasion may be only short-lived [5] and eclogites should rigidify when fluids exit the system, the temporary competence loss of these rocks could have a great impact on slab dyanmics.

[1] Mackwell *et al*. (1998) *JGeophRes* **103**, 975–984. [2] Jin *et al*. (2001) *Geology* **29**, 667–670. [3] Austrheim (1987) *EPSL* **81**, 221–232. [4] Rondenay *et al*. (2008) *Geology* **36**, 275–278. [5] Camacho *et al*. (2005) *Nature* **435**, 1191–1196.

Fractionation of a hydrous arc magma: The origin of adakitic and alkaline signatures at Savo volcano, Solomon Islands

D.J. SMITH[1]*, M.G. PETTERSON[1], A.D. SAUNDERS[1], G.R.T. JENKIN[1] AND J. NADEN[2]

[1]Geology Dept., University of Leicester, Leicester, LE1 7RH, UK (*correspondence: djs40@le.ac.uk)
[2]British Geological Survey, Keyworth, Nottingham, NG12 5GG, UK

Savo, Solomon Islands, is a historically active volcano dominated by sodic, alkaline lavas and pyroclastic rocks with up to 7.5 wt % Na_2O, and high Sr arc-like trace element chemistry. The petrogenetic history of the erupted suite suggests high water contents in the parental melts, favouring: a) the early fractionation of oxides; b) early, abundant crystallisation and differentiation of hornblende; and c) limited extraction of feldspar. Instead, it shows pseudo-closed system crystallisation; plagioclase forms but does not fractionate, so although crystals record formation in a melt of decreasing Sr, whole rock Sr increases with magmatic evolution [1].

Early amphibole fractionation and limited plagioclase fractionation contribute to an adakite-like geochemical signature of the Savo suite. Previous authors have noted this [2], but in the case of Savo, the adakite signature is a consequence of the fractionation history. The sodic, alkaline nature can also be attributed to feldspar; whole rock Na increases with SiO_2 as albite is retained. Na/K increases by biotite fractionation.

Much of the magma's water load appears to be released prior to eruption; Savo's eruptive style is that of dome formation, and pyroclastic rocks are all crystalline and non-vesicular. Fluids are released to a hydrothermal system [3] with the potential to form economic mineralisation. The oft-made linkage between 'adakitic' magmatism and economic copper and gold mineralisation (see [4] for review and criticism) may instead be an association between mineralisation and hydrous parental magmas.

[1] Smith, Petterson, Saunders, Millar, Jenkin, Toba, Naden & Cook (2009) *Contrib. Mineral. Petrol.* **158**, 785–801. [2] Schuth, Munker, Konig, Qopoto, Basi, Garbe-Schonberg & Ballhaus (2009) *J. Petrol.* **50**, 781–811. [3] Smith, Jenkin, Naden, Boyce, Petterson, Toba, Darling, Taylor & Millar (2010) *Chem. Geol.* **275**, 35–49. [4] Richards & Kerrich (2007) *Econ. Geol.* **102**, 537–576.

Understanding bioavailability of iodine in soils of Northern Ireland

H.E. SMITH[1,2]*, E.L. ANDER[2], E.H. BAILEY[1], N.M.J. CROUT[1], M.J. WATTS[2] AND S.D.YOUNG[1]

[1]School of Biosciences, Biology Building, University of Nottingham, University Park, Nottingham NG7 2RD
[2]British Geological Survey, Kingsley Dunham Centre, Keyworth, Nottingham NG12 5GG
(*correspondence: plxhes@nottingham.ac.uk)

The impact of soil-iodine dynamics on the availability of iodine to plants has been investigated, with a focus on uptake to grass as pasture from a range of soil types in Northern Ireland. The aim of the work was to determine how the availability of iodine to plants is dependent on soil properties. A predictive model of iodine behaviour based on the findings will take into account location, soil type and seasonal changes within Northern Ireland as a case study. The model may ultimately be useful in predicting human and animal populations at risk of iodine deficiency diseases.

The transformations and dynamics of ^{129}I added as either $^{129}I^-$ or $^{129}IO_3^-$ to soils have been followed. Results indicate rapid transformation of inorganic iodine into organic forms, with ultimate incorporation into soil organic matter via formation of intermediates e.g. HOI or I_2. Rates of incorporation are highly dependent on physico-chemical parameters including soil pH, organic matter content and major oxide composition. Rate of transformation to organic forms depends upon initial iodine speciation. Iodide is lost more rapidly (minutes-hours) than iodate (hours-days), especially in soils with high organic matter. In all cases initial incorporation has been demonstrated by size exclusion chromatography to be in the low molecular mass humic substances.

The ultimate speciation and location of iodine in soil will affect the amount potentially available to plants, which therefore depends strongly on both the speciation of iodine and soil properties.

https://doi.org/10.1180/S0026461X00006502 Published online by Cambridge University Press

Monogenetic basaltic volcanoes represent extraction rather than melting events

I.E.M. SMITH[1]*, L.E. MCGEE[1], S.J. CRONIN[2], M. BEBBINGTON[2] AND J.M. LINDSAY[1]

[1]School of Environment, University of Auckland, PB92019, Auckland, New Zealand (*correspondence: ie.smith@auckland.ac.nz)

[2]Institute of Natural Resources, Massey University, Palmerston North, NZ (S.J.Cronin@massey.ac.nz, m.bebbington@massey.ac.nz)

Magmas from very small basaltic systems (volumes <0.1 km3) leak from the mantle on time scales of 10^4- 10^6 years to form fields of small volcanoes each resulting from a single short-lived eruption sequence. Because magma volumes are small and rise quickly they do not fractionate within the crust or assimilate components from it. Hence, their chemical compositions and variability reflect the interplay of processes deep in the system. The range of chemical compositions displayed by individual eruptions shows the diversity of these processes. Do these small magma batches represent discrete melting events or instead extraction episodes tapping long-lived (10^4 year) zones of partial melting? In the Auckland Volcanic Field N.Z. paleo-magnetic measurements [1] correlated with the ~ 31 ka Mono Lake magnetic excursion identify five eruptions of alkali basalt magmas from depths of ~80km within a time interval of a few hundred years. The chemical composition erupted in each event cannot be related to the others by fractionation processes. Heat flux constraints suggest that these discrete magma batches cannot represent distinct melting events. Rather they represent separate extraction events from a continuous but heterogeneous melt zone. Their near simultaneous eruption along with the overall pattern of volcanic activity at Auckland indicates that such extraction events may be driven by plate boundary related tectonic processes occurring over 600 km away.

[1] Cassata *et al*. (2008) *EPSL* **268**, 76–88.

Australasian sea surface temperatures over the past millennium

MARITA SMITH[1]*, JOCHEN BROCKS[1], PATRICK DE DECKKER[1], RAQUEL LOPES DOS SANTOS[2] AND STEFAN SCHOUTEN[2]

[1]Research School of Earth Sciences, The Australian National University, Canberra, ACT 0200, Australia (*correspondence: marita.smith@anu.edu.au)

[2]Department of Marine Biogeochemistry and Toxicology, Royal Netherlands Institute for Sea Research, P.O Box 59, 1790 AB Den Burg, Texel, The Netherlands.

The 'hockey-stick' temperature increase of the 20th century has instigated concern for a global warming trend. In order to investigate this temperature increase, it is necessary to derive high-resolution temperature records that span the last millennium. Currently, data from this period is sourced almost exclusively from the Northern Hemisphere, predominantly from terrestrial records. There is a considerable lack of temperature records for the Southern Hemisphere, making analysis of hemispheric and global trends in temperature changes difficult.

Marine sediments can often represent a continous geological record of climate through the gradual deposition of organic matter on the sea floor over time. Biomarkers are organic compounds produced by living organisms that have extraordinary preservation potential in sediments. The most useful biomarkers are resistant to diagenesis and can be readily linked to a characteristic group of producing organisms [1]. The lipids of some haptophyte marine algae (alkenones) and marine Crenarchaeota (glycerol dialkyl glycerol tetraethers) in the sedimentary record are biomarkers that may be converted to sea-surface temperature via the $U^{K'}_{37}$ [2] and TEX_{86} [3] proxies, respectively.

Here, we present a record of sea-surface temperature using multicores sourced from near the Australian east coast (at ~1, 000 m depth) utilising the combined capacities of these biomarker proxies. This is the first temperature record to span the past millennium in the Southern Hemisphere and provides an important means of palaeoenvironmental inference for hemispheric and global climatic trends during this period.

[1] Brocks & Pearson (2005) *Molecular Geomicrobiology* **59**, 233–258. [2] Brassell *et al*. (1986) *Nature* **320**, 129–133. [3] Schouten *et al*. (2002) *Earth & Planetary Science Letters*, **204**, 265–274.

https://doi.org/10.1180/S0026461X00006502 Published online by Cambridge University Press

Mercury isotope fractionation in layered roasted ore waste

ROBIN S. SMITH[1,2]*, JAN G. WIEDERHOLD[1,2], ADAM D. JEW[3], GORDON E. BROWN JR.[3], BERNARD BOURDON[4] AND RUBEN KRETZSCHMAR[1]

[1]Institute of Biogeochemistry and Pollutant Dynamics, ETH Zurich, Switzerland (*correspondence: robin.smith@env.ethz.ch)
[2]Isotope Geochemistry, ETH Zurich, Switzerland
[3]Department of Geological & Environmental Sciences, Stanford University, Stanford, CA 94305, USA
[4]ENS Lyon and CNRS, France

High concentrations of mercury (Hg) can often be found in the environment around inactive Hg mines. During mine operation, rock containing the primary ore mineral HgS was crushed and heated in furnaces to temperatures of ~ 700 °C (calcination). Most of the resulting elemental Hg vapor was condensed and collected and the remaining mine tailings (calcines) were piled on site. This removal process was not complete and significant amounts of Hg remained in the calcines. Large pieces of calcine often exhibit a characteristic internal layering, with dark-grey cores, light-grey outer rims, and red outer surface layers. The speciation of the Hg-bearing compounds in these wastes determines the solubility, volatility, and thus mobility of the remaining Hg [1, 2].

Various environmental processes fractionate the stable Hg isotopes via mass-dependent (MDF) and/or mass-independent fractionation (MIF); however, the controlling mechanisms are not fully understood. These isotopic signatures provide a promising new tool for further understanding Hg transformations and emissions from highly contaminated mining sites. Here we report stable Hg isotope results for different layers in calcine cobbles collected at the inoperative New Idria Hg mine, San Benito County, CA, USA.

Differently colored layers in the calcines were carefully separated, powdered, and digested following either total or sequential procedures [3]. Isotopic analyses were performed on a Nu Plasma MC-ICP-MS with cold vapor introduction.

Our analyses revealed significant concentration gradients across the different layers, with higher Hg concentrations in outer rims and lower concentrations in inner regions. In all sequential extractions, the 12M HNO_3 soluble fraction displayed the highest Hg concentration. In general, bulk calcine samples were isotopically heavier than ore and unroasted ore wastes, and significant MDF δ^{202}Hg gradients existed from isotopically heavy centers to lighter rims. These findings suggest that incomplete roasting of ore rocks led to pronounced Hg isotope gradients which were presumably caused by kinetic effects during diffusive processes.

[1] Kim *et al*. (2003) *ES&T* **37**, 5102–5108. [2] Jew *et al*. (2011) *ES&T* **45**, 412–417. [3] Bloom *et al*. (2003) *Anal. Chim. Acta* **479**, 233–248.

Toward establishing precise chronologies for the integration of Late Pleistocene palaeoclimate archives: An example from Suigetsu SG06, Japan

V.C. SMITH[1], D.F. MARK[2], R.A. STAFF[1], S.P.E. BLOCKLEY[3], C. BRONK RAMSEY[1], C. BRYANT[4], T. NAKAGAWA[5], K.H. KIM[6], A. WEH[7], K. TAKAMURA AND T. DANHARA

[1]Research Laboratory for Archaeology, University of Oxford, UK (victoria.smith@rlaha.ox.ac.uk)
[2]Scottish Universities Environmental Research Centre (SUERC), UK (d.mark@suerc.gla.ac.uk)
[3]Centre for Quaternary Research, Royal Holloway, UK
[4]NERC Radiocarbon Facility-Environment, UK
[5]Department of Geography, University of Newcastle, UK
[6]Ewha Womans University, South Korea
[7]SELFRAG AG, Kerzers, Switzerland
[8]Beppu Geothermal Laboratory, Kyoto University, Japan
[9]Kyoto Fission-track Co., Ohmiya, Kita-ku, Kyoto, Japan

To further understand abrupt climate changes, and any geographical leads and lags, it is important to precisely correlate high-resolution terrestrial, marine and ice core archives from around the globe. This requires improved dating techniques and methods for correlating these sedimentary archives. Volcanic ash (tephra) layers provide ideal markers to synchronise records over regional areas, and $^{40}Ar/^{39}Ar$ eruption ages can provide direct temporal constraints. Here we discuss the methodology used to obtain high-precision $^{40}Ar/^{39}Ar$ age of a tephra within the SG06 Suigetsu archive.

The 73 m-long SG06 core from Lake Suigetsu, Japan provides continuous record of sedimentation spanning the last ~150 kyrs [1] and represents one of the most important Late Pleistocene palaeoclimatic records. SG06 is annually layered (varved) down to ~65 kyrs and contains numerous terrestrial plant macrofossils, from which a varve chronology and radiocarbon analyses are currently being paired to generate a wholly terrestrial radiocarbon calibration dataset that extends to the older limit of the radiocarbon analytical method (see [1]). We present our $^{40}Ar/^{39}Ar$ ages along with the varve and ^{14}C chronology to show that it is possible to get accurate and precise ages of eruption units that are near the young limit of the $^{40}Ar/^{39}Ar$ method.

[1] Nakagawa *et al*. (2011) *Quaternary Science Reviews*, in press.

https://doi.org/10.1180/S0026461X00006502 Published online by Cambridge University Press

The scale factor in the ectomycorrhizal fungal weathering debate

M.M. SMITS[1], Z. BALOGH-BRUNSTAD[2], L. SACCONE[3], H. WALLANDER[4] AND J.V. COLPAERT[1]

[1]Centre of Environmental Science, Hasselt University, Belgium (mark.smits@uhasselt.be)
[2]Hartwick College, Oneonta, NY, 13820 USA
[3]H.H. Wills Physics Laboratory, University of Bristol, UK
[4]Microbial Ecology, Lund University, Sweden

Ectomycorrhizal fungal weathering research has a long history, but with the launch of the term 'Rock-eating Fungi' this research topic attracted increased attention. There is growing evidence that ectomycorrhizal fungi do interact with soil minerals. Carefully designed laboratory experiments show increased mineral dissolution rates in the presence of ectomycorrhizal fungi. Even at the scale of the individual hyphae we gain more insight in the mechanisms of fungal-mineral interactions via sophisticated (ultra)-microscopic and spectroscopic techniques. But the basic question whether ectomycorrhizal fungi have a significant contribution to soil mineral weathering, remains unanswered.

Over the past decades several reviews have been published, some advocating and others opposing the role and significance of ectomycorrhizal fungi in soil mineral weathering. Most of the arguments used in this debate are scale-dependent. The ignorance of the importance of scale has hindered communication and better insight into each other arguments. Key points in the arguments opposing ectomycorrhizal weathering are that mineral dissolution is expected to be mainly driven by water or proton-metal exchange reactions and not through the formation of organic-metal complexes due to extremely low concentrations of organic chelators in soil solutions. Key points in the arguments in favour of ectomycorhizal weathering are that fungi act at the scale of individual hyphae, creating isolated water pockets with probably very dinstict chemistry and showing hyphal-mineral contact interactions.

It is important to realize that in ectomycorrhizal plants, the fungal partner is the main interface between plant and soil. Recent studies show that fungal hyphae preferentially colonize some minerals over others, implicating that plant/fungal interactions with minerals take place in a nonrandom fashion. But fungal hyphae only cover <5% of the mineral surfaces. The scale and heterogeneity of weathering actions should be acknowledged before drawing conclusions in relation to the relevance for the actual soil mineral weathering process.

Excess argon systematics under HP-LT conditions: A tracer for metamorphic fluid connectivity?

A.J. SMYE[1]*, C.J. WARREN[2], M.J. BICKLE[1] AND T.J.B. HOLLAND[1]

[1]Department of Eath Sciences, University of Cambridge, UK (*correspondence: as859@cam.ac.uk)
[2]Department of Earth and Environmental Sciences, The Open University, Milton Keynes, UK

UV laserprobe single-grain fusion apparent $^{40}Ar/^{39}Ar$ ages of phengite from a gl + jd bearing blueschist of the Tauern Window, Eastern Alps range between 35.35 ± 0.37 Ma and 43.67 ± 0.50 Ma (1σ). These ages are between 2—11 Ma older than the age of blueschist-facies metamorphism determined by U—Pb allanite [1] and Rb—Sr [2] multi—mineral geochronlogy. Pseudosection calculations show that the phengite grew close to peak pressure conditions of ~10 kbar at 450° C, before Barrovian metamorphism (~7 kbar, 550°C) at ca. 30 Ma [3]. The anomalously old $^{40}Ar/^{39}Ar$ phengite ages show that the sample contains excess ^{40}Ar, i.e. ^{40}Ar decoupled from parent ^{40}K. Concentrations of excess ^{40}Ar vary on the mm—cm lengthscale.

The incompatible nature of Ar means that high concentrations of fluid—borne Ar are required to facilitate partitioning of Ar into mica. Numerical modelling of Ar diffusion in phengite provides an estimate of the expected $^{40}Ar/^{39}Ar$ age for a mica following the Tauern PTt path. We show that the measured 'older' apparent ages may be reproduced by: 1. an open rock volume, where Ar is fluid—borne within an interconnected grain boundary reservoir, 2. a closed system in which the Ar concentration of the grain boundary reservoir is controlled by metamorphic porosity and whole—rock K_2O content, or 3. a temporal variation between these two end-member scenarios. Collectively, these calculations show that, provided an independent constraint on the timing of mica growth exists, excess ^{40}Ar contamination can be used to investigate degrees of fluid flow and fluid pathway connectivity during a metamorphic cycle.

[1] Smye *et al*. *In Press EPSL*. [2] Glodny *et al*. (2005) *Contrib*. *Mineral*. *Petrol*. **149**, 699—712. [3] Inger & Cliff (1994) *J*. *Met*. *Geol*. **12**, 695—707.

https://doi.org/10.1180/S0026461X00006502 Published online by Cambridge University Press

Hydrous phases in the lower mantle

JOSEPH R. SMYTH AND DAVID A. BROWN

Department of Geological Sciences, University of Colorado, Boulder CO 80309 USA (smyth@colorado.edu, davanbro@colorado.edu)

Dehydration of subducting lithospheric slabs to less than 200 ppmw H_2O in the upper mantle is virtually impossible given the stability of nominally hydrous phases such as serpentine, 10Å phase, phase A, chondrodite, and clinohumite. Velocity models of the transition zone are consistent with significant hydration (> 1000 ppmw H_2O), but not with a dry pyrolite composition. It seems likely then that transition zone is relatively hydrous and that slabs penetrating the TZ are also hydrous. Where slabs push through 660 km into the lower mantle the fate of the water depends on the H solubility in $MgSiO_3$-perovskite, periclase, akimotoite, and majoritic garnet as well as the nominally hydrous phase D.

FTIR studies indicate relatively low solubility of H in perovskite and periclase [1]. However, we have synthesized $MgSiO_3$-perovskite with up to 2000 ppmw H_2O as measured by SIMS. It is, however, as yet unclear if the H is in the structure or as inclusions. We have measured up to 3000 ppmw H_2O in majoritic garnet where hydration may be associated with Mg octahedral vacancies. Phase D ($MgSi_2H_2O_6$) is a nominally hydrous phase stable to depths up to 1500km. We have synthesized Phase D in silica-excess and Mg-excess compositions as well as aluminous compositions. Phase D has a high bulk modulus but a relatively low density so that hydrous slabs penetrating 660 km may be buoyant [2]. Further experimental work is required for a meaningful constraint on possible H contents of the lower mantle.

[1] Bolfan *et al*. *(2002) Geophys. Res. Lett* **30**, GL0178182.
[2] Hushur *et al*. (2011) *JGR* in press.

Hot summers in the Western United States during the Late Cretaceous and Early Cenozoic

KATHRYN E. SNELL[1]*, JEFFREY THOMPSON[1], BRADY FOREMAN[2], BRIAN WERNICKE[1], C. PAGE CHAMBERLAIN[3], JOHN EILER[1] AND PAUL KOCH[4]

[1]California Institute of Technology, Pasadena, CA (*correspondence: ksnell@caltech.edu)
[2]University of Wyoming, Laramie, WY
[3]Stanford University, Palo Alto, CA
[4]University of California Santa Cruz, Santa Cruz, CA

Understanding how seasonal temperatures on land respond to global greenhouse climate conditions is important for predicting effects of climate change on ecosystem structure, agriculture and distributions of natural resources. Fossil floral and faunal assemblages suggest winter temperatures in middle and high latitude continental interiors during the Cretaceous and early Cenozoic were at or above freezing, whereas terrestrial summer temperature estimates are uncertain. Carbonate clumped isotope (Δ_{47}) temperature estimates from lacustrine and paleosol carbonates appear to be generally biased toward summer temperatures in middle and high latitudes. Though problematic for reconstructing mean annual temperature (MAT), this bias presents an opportunity to reconstruct terrestrial summer temperatures and, through comparison with paleobotanical data, estimate past terrestrial seasonality.

Here, we compile MAT estimates from paleoclimate and paleoelevation studies in the western United States. We then compare these data with existing [1, 2] and new Δ_{47} temperature estimates from Late Cretaceous – Present lacustrine and paleosol carbonates from the western United States. In this compilation, land temperatures are warm during the Late Cretaceous, reach an apex during the early-middle Eocene and then cool to the present (sharply from the late Miocene to Pleistocene). Both MAT and summer temperature estimates are warmer than modern MAT and summer temperature estimates at the study sites throughout the Cenozoic and Late Mesozoic. Summer temperatures from low paleoelevation sites during the Late Cretaceous to the Early Eocene are relatively warm (~30 – 40°C), though these values may include a few degrees of radiant solar heating of the surface. Regardless, these data suggest that at middle latitudes, both winters and summers in continental interiors may warm substantially under greenhouse climate conditions.

[1] Passey *et al*. (2010) *PNAS* **107**, 11245–11249.
[2] Huntington *et al*. (2010) *Tectonics* **29**, TC3005.

https://doi.org/10.1180/S0026461X00006502 Published online by Cambridge University Press

Anthropogenic contributions of ^{129}I and ^{85}Kr to global reservoirs: Current distribution patterns and projected increases

G.T. SNYDER[1]*, J.E. MORAN[2] AND A. ALDAHAN[3,4]

[1]Rice Universtiy, Houston, TX, 77003, USA
(*correspondence: gsnyder@rice.edu)
[2]California State Univ. East Bay, Hayward, CA 94542, USA
(*correspondence: jean.moran@csueastbay.edu)
[3]Uppsala University, SE-75236, Uppsala, Sweden
(*correspondence: ala.aldahan@uaeu.ac.ae)
[4]United Arab Emirates Univ., Al Ain, United Arab Emirates

^{129}I and ^{85}Kr are two isotopes whose presence in global surface reservoirs is due primarily to nuclear reprocessing activities. A knowledge of the partitioning of these isotopes in surface reservoirs is critical to our understanding of how release and storage of these isotopes should be handled presently and in the future.

Long-lived ^{129}I (half-life=15.6 Myr) partitions primarily into shallow soil and seawater. While its residence time in the atmosphere is short, repeated cycling of iodine between surface waters and the atmosphere has resulted in its distribution far from point sources. Downwelling of surface waters in the North Atlantic presently transports ^{129}I to deep waters which provide a temporary sink for anthropogenic iodine. In contrast, the relatively short-lived ^{85}Kr (half-life=10.76 yr) partitions primarily into the atmosphere and its dispersal is a result of wind patterns in the troposphere. We compare the present distribution of these two isotopes and model their increase into the future when the bulk of nuclear reprocessing is projected to move from Western Europe to Asia. We also discuss the effect of speciation of ^{129}I and stable ^{127}I in the environment, and disequilibrium between these two isotopes.

Combined use of Raman, ToF-SIMS and AFM imaging for characterizing the surface reactivity of sea salts

S. SOBANSKA*, M. CHOËL, M. MOREAU AND J. BARBILLAT

LASIR/CNRS University of Lille 1, Bât C5, 59655 Villeneuve d'Ascq Cedex, France
(*correspondence: sophie.sobanska@univ-lille1.fr)

Sea salt particles are typically emitted in the atmosphere through by breaking waves and bursting bubbles at the ocean surface where Cl^-, Na^+, Mg^{2+}, K^+ and SO_4^{2-} are the most abundant ions. It is well established that sea salts can react with gaseous species to form complex aerosols [1, 2]. Such reactive uptakes on the surface of particles during their atmospheric residence time can significantly alter their optical properties and affect their ability to act as cloud condensation nuclei. In addition, some products may be photochemically active at solar wavelengths and may affect the oxidative properties of the atmosphere [3]. Finally, in the marine atmosphere fatty acids (FA) are known to be present as particles and/or as a coating on sea salt particles which could influence sea salt reactivity [4]. *In situ* observation of the atmospheric processing of the surface of particles can be performed in laboratory by Raman microspectrometry (RMS) and Atomic Force Microscopy. The combined use of both techniques is a powerful tool to determine the morphology and the distribution of molecular species within individual micrometer-size particles [5]. Moreover, the first layers at the surface of particles (few nm) can be analyzed using Time-of-Flight Secondary Ion Mass Spectroscopy (Tof-SIMS) [6]. In this study, laboratory experiments were conducted to simulate heterogeneous reaction at the surface of sea salt particle (NaCl) coated with FA and exposed to gaseous pollutants (NO_2). As expected, formation of nitrate salts on the surface of NaCl was evidenced and influence of FA demonstrated at the surface scale. Finally, by using RMS imaging in the UV range (266 nm and 325 nm), the photochemistry of formed nitrates and influence of FA on their photo-reactivity was also studied. This work demonstrated the the potential of the combination of RMS, AFM and ToF-SIMS imaging for studying the heterogeneous chemistry of the particle surfaces.

[1] Finlayson-Pitts (2003) *Chem. Rev.* **103** (12) 4801–4822. [2] Rossi (2003) *Chem. Rev.* **103**, 4823–4882. [3] Roca *et al.* (2008) *J. Phys. Chem. A*, **112**, (51) 13275–13281. [4] Stemmler *et al.* (2008) *Atmos. Chem. Phys.* **8**, 5127–5141. [5] Scolaro *et al.* (2009) *J. Raman Spectrosc.* **40** (2) 157–163 [6] Gaspar *et al.* (2004) *Appl. Surf. Sci.* **231–232** 520–523.

https://doi.org/10.1180/S0026461X00006502 Published online by Cambridge University Press

Mineral composition of sediments of the Southern Baltic Sea and their heavy metals content

K. SOBCZAK[1]*, J. BEŁDOWSKI[2] AND M. MICHALIK[1]

[1]Institute of Geological Sciences, Jagiellonian University, ul. Oleandry 2a, 30-063 Kraków, Poland (*correspondence: katarzyna.sobczak@uj.edu.pl, marek.michalik@uj.edu.pl)

[2]Marine Chemistry and Biochemistry Department Institute of Oceanology, Polish Academy of Sciences, Powstańców Warszawy 55, 81–712 Sopot, Poland (hyron@iopan.gda.pl)

Samples of sediments were collected from eight cores in three areas of the southern Baltic Sea (the Gulf of Gdańsk, Bornholm Deep and the Odra Bank) from three different depths (0-3cm, 25-28cm and 35-38cm).

Mineral and chemical composition of sediments was studied using XRD, SEM-EDS, ICP-MS, and ICP-AES methods. Chemical composition of leachates from sequential extraction was also determined.

Samples from the Gulf of Gdańsk are dominated by silty fraction, samples from the Odra Bank represent fine to medium sands with abundant shell fragments, sediments from Bornholm Deep are mainly clay. Quartz predominates in all samples. In silty samples framboidal piryte is present; halite and gypsum occurs only in few of them. Clay minerals occur in low amount in silty samples. Ilmenite, zircon and Fe compound are common in sand, but appear sporadically in silt samples.

Geoaccumulation index (Igeo = ln (Cn/1.5×Bn); Cn-measured concentration, μg/g, Bn - geochemical background value, μg/g) indicates strong to very strong Cd pollution in three surface samples. Other factors revealed pollution by As, Cd, Mo and Hg. Variation of concentration of heavy metals occurs in profiles, e.g. Hg and Cd are concentrated in uppermost samples but As and Mo concentration increase downward. Results of sequential extraction suggest significant diversity of metals speciation in sediments.

Crustal recycling: New findings and challenges

A.V. SOBOLEV[1,2,3]

[1]ISTerre, University J. Fourier BP 53, 38041 Grenoble Cedex 9, France (alexander.sobolev@ujf-grenoble.fr)

[2]Max Planck Institute for Chemistry, Postfach 3060, 55020 Mainz, Germany

[3]Vernadsky Institute of Geochemistry, RAS, 119991 Moscow, Russia

Since Hofmann and White's paper [1] crustal recycling via subduction and convection is a widely accepted explanation for the heterogeneity of OIB sources. Recycled crust has been recognized even in the sources of MORB (e. g [2, 3]). However, there are still no common view on the amount, composition and ages of recycled materials in both parts of the mantle.

In this paper I review recent approaches for estimating the contents and ages of recycled crust in the sources of OIB, LIP and MORB. In particular, I discuss the ability of olivine phenocrysts to record the magma source mineralogy in their concentrations of Ni, Mn, Fe, Zn, Co, Sc and Ca. I show that adiabatic decompression of deep-sourced mantle magmas and the presence of garnet in their sources do not compromise the ability of olivine to register olivine-free source lithologies.

Large datasets of new olivine compositions and published high-precision analyses [3, 4] suggest the common presence of olivine-free pyroxenite produced by melting and reaction of oceanic crust in the sources of OIB, LIP and MORB. The proportions of pyroxenite-derived melt commonly correlate with trace element and isotope data from bulk rocks [5, 6] indicating binary mixing of melts from peridotitic and pyroxenitic sources. High amounts of recycled oceanic crust are associated with high excess mantle temperatures and high depths of melt generation, in agreement with the high density and melt productivity of a garnet-rich source [3].

The ages of recycled oceanic crust estimated from correlation of bulk-rock $^{187}Os/^{188}Os$ ratios and the proportions of pyroxenite-derived melt [5] or from the $^{86}Sr/^{87}Sr$ of ancient recycled seawater [7] are in the range of 1.0-0.2 Ga. This implies a time-scale of general mantle circulation of a few centimetres per year.

[1] Hofmann, A. W. & White, W. M. (1982) *EPSL* **57**, 421–436. [2] Hirschmann, M. M. & Stolper, E. M. (1996) *CMP* **124**, 185–208. [3] Sobolev, A.V. *et al*. (2007) *Science* **316**, 412–417. [4] Sobolev, A.V. *et al*. (2009) *Petrology* **17**, 253–286. [5] Sobolev, A.V. *et al*. (2008) *Science* **321**, 536. [6] Gurenko, A. A. *et al*. (2009) *EPSL* **277**, 514–524. [7] Sobolev, A.V. *et al*. (2011) *Nature* (in press)

https://doi.org/10.1180/S0026461X00006502 Published online by Cambridge University Press

Heterogeneities in the mantle plume: Spatial scales and ages

A.V. SOBOLEV[1,2,3], A.W. HOFMANN[2], K.P. JOCHUM[2], D.V. KUZMIN[2] AND B. STOLL[2]

[1]ISTerre, University J. Fourier BP 53, 38041 Grenoble Cedex 9, France (alexander.sobolev@ujf-grenoble.fr)
[2]Max Planck Institute for Chemistry, Postfach 3060, 55020 Mainz, Germany
[3]Vernadsky Institute of Geochemistry, RAS, 119991 Moscow, Russia

Recycling of oceanic crust through subduction, mantle upwelling, and remelting in mantle plumes is a widely accepted mechanism to explain ocean island volcanism. However, neither time scales of this process nor spatial scales of the resulting mantle heterogeneities are well understood.

We report data on trace elements, $^{87}Sr/^{86}Sr$, $^{207}Pb/^{206}Pb$, and $^{208}Pb/^{206}Pb$ ratios for 138 melt inclusions in olivine phenocrysts from single lava of Mauna Loa shield volcano, Hawaii, indicating enormous mantle source heterogeneity. The variations in isotopic compositions and trace element ratios far exceed all known ranges for Hawaiian shield stage volcanoes. The variation range is highest for melt inclusions trapped in the most magnesian olivines. This is consistent with the interpretation that melt inclusions in early olivine phenocrysts yield information on the compositions of unmixed parental melts, while lavas and inclusions in more evolved olivine are mixtures of these melts.

We show that highly radiogenic strontium ($^{87}Sr/^{86}Sr$=0.7081± 0.0006, 2σ) in severely Rb-depleted melt inclusions matches the isotopic composition of 200-650 Ma old seawater. We infer that such seawater must have contaminated the Mauna Loa source rock, prior to subduction, imparting a unique 'time stamp' on this source. Small amounts of seawater-derived strontium in plume sources may be common but can be identified clearly only in ultra-depleted melts originating from generally highly (incompatible-element) depleted source components.

We also show that the Sr-rich component of Mauna Loa lavas is particularly unradiogenic ($^{87}Sr/^{86}Sr$ < 0.7030), supporting the suggestion that it corresponds to plagioclase cumulate gabbros from recycled oceanic crust (Sobolev et al, Nature, 2000).

Enormous isotope heterogeneity of melts mixed in a single plumbing system favours small-scale mantle source heterogeneity preserved in the mantle plume. The presence of 200-650 Ma old oceanic crust in the source of Hawaiian lavas implies a time-scale of general mantle circulation with an average rate of about 2 (± 1) cm/a, a much faster rate than previously thought.

Modeling relationships between a mantle plume, a large igneous province and a mass extinction

S.V. SOBOLEV[1], A.V. SOBOLEV[2,3], D.V. KUZMIN[3], N.A. KRIVOLUTSKAYA[3], A.G. PETRUNIN[1], N.T. ARNDT[2], V.A. RADKO[3] AND YU.R. VASILIEV[3]

[1]GFZ, German Research Centre for Geosciences, 14473 Potsdam, Germany (*correspondence: stephan@gfz-potsdam.de)
[2]ISTerre, University J. Fourier BP 53, 38041 Grenoble Cedex 9, France (alexander.sobolev@ugf-grenoble.fr)
[3]Vernadsky Institute of Geochemsitry, RAS, 119991 Moscow, Russia

Large Igneous Provinces (LIPs) are known for their rapid production of enormous volumes of magma, for dramatic thinning of the lithosphere and for their links to global environmental catastrophes. Controversy surrounds even the basic idea that LIPs form through melting in the heads of thermal mantle plumes. The Permo-Triassic Siberian Traps – the type example and the largest continental LIP, is located on thick cratonic lithosphere and was synchronous with the largest known mass-extinction event. However, there is no evidence of pre-magmatic uplift nor of a large lithospheric stretching of the basaltic sequence, predicted above a plume head. Moreover, estimates of magmatic CO_2 degassing from the Siberian Traps are considered insufficient to trigger climatic crises leading to the hypothesis that the release of thermogenic gases from the sediment pile caused the mass extinction.

Here we present petrological evidence for a large amount (15 wt%) of dense recycled oceanic crust in the head of the plume and developed a thermomechanical model that predicts no pre-magmatic uplift and requires no lithospheric extension. The model employs source-composition and temperature [1, 2] petrological constraints, non-linear elasto-visco-plastic rheology [3] and pressure- and temperature-dependent melting of a heterogeneous mantle. The model implies extensive plume melting and heterogeneous delamination of the thick cratonic lithosphere during a few hundred thousand years. The model also suggests that massive CO_2 and HCl degassing from the plume could *alone* trigger the Permian-Triassic mass extinction and predicts it happening *before* the main volcanic phase.

[1] Sobolev, A.V. *et al*. (2009) *Petrology* **17**, 253–286. [2] Sobolev, A.V. *et al*. (2009) *Russian Geology & Geophysics* (2009) **50**, 999–1033. [3] Sobolev, S.V. & Babeyko, A.Y. (2005) *Geology* **33**, 617–620

https://doi.org/10.1180/S0026461X00006502 Published online by Cambridge University Press

The effect of pressure on tetrahdral tilting in feldspars

L.M. SOCHALSKI-KOLBUS* AND R.J ANGEL

Dept. Of Geosciences, Virginia Tech, Blacksburg, VA 24060, USA (*correspondence: lsochals@vt.edu, rangel@vt.edu)

Feldspars are framework aluminosilicates that comprise approximately 60 percent of the Earth's crust. The defining features of the feldspar framework are corner-sharing TO_4 tetrahedra connected into chains of 4-rings that run parallel to a-axis and b-axis. These 4-rings are connected by their corners and form a 'double-crankshaft' chain parallel to the d (100).

The response of the feldspar structure to pressure is very anisotropic with approximately 60-70% of the volume compression attributed to the length of the crystallographic direction d (100) [1]. It is of interest to undermine the details of this anisotropy and to predict thermodynamic properties and phenomena such as elastic softening for petrologic and geophysical investigations. Previous attempts to predict structural behavior of feldspars have been focused on individual T-O-T angles [2, 3], but this has been unsuccessful in describing structural reasons for either changes or the thermodynamic properties. Megaw (1974) [4] proposed a model that considers four independent tilt systems derived and 2 of the four tilt systems effect the length of the d (100).

Single crystal X-ray diffraction was performed on an ordered plasioclase crystal of 20% anorthite content and structures were determined from 0 – 9.221 GPa. The effect of high pressure on these four different tilt systems have been studied on Na-rich plagioclase from this study and previously measured samples from 0 - 37 % anorthite. I found that 3 of the 4 tilt systems change similarly until 5-6 GPa. After this pressure range, these three tilt systems change behavior. Interestingly, these are the approximate pressures that there is elastic softening seen in the volumes for Na-rich feldspars. The systematics found from this current study are being investigated to see if tetrahedral tilting is a useful tool for predicting the thermodynamic properties and behavior of feldspars at high pressure.

[1] Johnson (2007) *MS Thesis, VT.* [2] Downs *et al.* (1994) *Am. Min.* **79**, 1042-1052. [3] Baur *et al.* (1996) *J. Sol. St. Chem.* **121**, 12-23. [4] Megaw (1974) *The Feldspars: Chapt. 6,* 87-113.

A new statistical method for modeling mixing of mantle end-members for global MORB and OIB isotopic data

R. A. SOHN [1]* AND K.W.W. SIMS[2]

[1]Woods Hole Oceanographic Institution, 360 Woods Hole Rd., MS #24, Woods Hole, MA, 02543 (*correspondence: rsohn@whoi.edu)

[2]Dept of Geology and Geophysics, University of Wyoming Laramie, Wy, 82070 (ksims7@uwyo.edu)

Long-lived isotopic ratios have been used to identify reservoirs of chemically distinct material in the Earth's interior, typically labeled DMM, EM1, EM2 and HIMU [1, 2]. We have developed a new statistical method that allows us to find best-fitting mixing curves and surfaces for binary and ternary systems, respectively, and we apply this method to global compilations of isotopic ratios ($^{87}Sr/^{86}Sr$, $^{143}Nd/^{144}Nd$, $^{206}Pb/^{204}Pb$, $^{207}Pb/^{204}Pb$, $^{208}Pb/^{204}Pb$) for MORB and OIB samples in order to rigorously test various mixing hypotheses. The method also allows us to refine isotopic ratio estimates for the putative mantle end-member components, and quantify the misfit between a given dataset and an arbitrary mixing model.

We find that the global suite of MORB data requires at least three end-member components, one of which is DMM, a second that is similar to EM1 but with distinct Pb isotopes defined by samples from the South Atlantic, and a third that is similar to, but nevertheless distinct from, HIMU, defined by samples from the equatorial Atlantic. The global suite of OIB data, on the other hand, requires at least five end-member components, four of which appear to mix with the common component FOZO [3, and references therin]. Some OIB sample sets (e.g. Hawaii, Iceland), however, are difficult to distinguish statistically from the MORB field.

Our mixing analysis focuses on finding the simplest model that fits the MORB and OIB isotopic data and is consistent with the wider body of geochemical evidence. This type of rigorous statistical method is indispensable for analyzing large amounts of complex geochemical data, and it provides an objective means for discriminating between competing models of mantle mixing through formal hypothesis testing.

[1] Zindler & Hart (1986) *Ann. Rev. Earth & Planet. Sci.* **14**, 493–571. [2] Hart, S. R. (1988) *EPSL* **90**, 273–296. [3] Hart *et al.* (1992) *Science* **256**, 517–520.

https://doi.org/10.1180/S0026461X00006502 Published online by Cambridge University Press

Protracted history of continental subduction at the southern edge of the Maya Block, central Guatemala: Petrological and geochronological evidences

L.A. SOLARI[1]*, A. GARCÍA CASCO[2], J.K.W. LEE[3] AND A. ORTEGA-RIVERA[4]

[1]Centro de Geociencias, UNAM, Juriquilla, 76001 Querétaro, Mexico (*correspondence: solari@servidor.unam.mx)
[2]Departamento de Mineralogía y Petrología, Universidad de Granada, 18002 Granada, Spain (agcasco@ugr.es)
[3]Department of Geology, Queen's University, Kingston, Ontario, K7L 3N6, Canada (lee@geol.queensu.ca)
[4]ERNO, Instituto de Geología, UNAM, 83000 Hermosillo, Son., México (amabel@servidor.unam.mx)

The Rabinal Granite Suite is an anatectic S-type composite pluton which fringes the southernmost North America Plate margin in Central Guatemala. It is a Kfs-Pl-Ms-Qtz granite-granodiorite, showing increasing deformation along its southern margin where it is crosscut by the dextral, Late Cretaceous, top-to-NE Baja Verapaz Shear Zone. Previously considered as Devonian-Mississippian in age, it has been recently dated at 562-453 Ma. LA-ICPMS U-Pb and Ar-Ar geochronology, combined with microprobe mineral chemistry, allow precising its P-T-time history. U-Pb zircon ages indicate a crystallization age of 471 +3/-5 Ma (Middle Ordovician), as well as abundant cores inherited from the metapelitic source with main density peak distributions at 700, 806, 900, 996, 1376 Ma. Laser total fusion Ar-Ar analyses of magmatic muscovite (Si= 6.2-6.4 atoms per 20 O and 4 OH) indicate cooling at various times during the mid-late Paleozoic. The petrologic conditions of the Ordovician metamorphism, partial melting of a metapelitic protolith and seggregation-ascent-crystallization of the granitic melt occurred along a clockwise P-T-t path at intermediate P, with maximum P of 8 kbar (ca. 25 km) during prograde metamorphims and peak T of 750 °C (at mid-crustal levels, 5-7 kbar). This evolution is interpreted as the result of a tectonic cycle related to the initial opening of the Rheic Ocean. A second clockwise path at high-P is indicated by high silica muscovite (Si= up to 7.0 atoms pfu), with peak P of ca 10 kbar at ca. 330 °C. This second event did not recrystallize the U-Pb clock in zircons, but it is clearly recorded by a main peak of laser total fusion Ar-Ar analyses on high Si muscovite grains yielding an average of 70.09 ± 0.5 Ma. This latest Cretaceous stage is related to subduction of the North America plate margin (cover and pre-Mesozoic basement) below the Caribbean Plate and ensuing collision with the Caribbean volcanic arc.

Evolution of magma oceans

V.S. SOLOMATOV

Washington Univ., St. Louis, MO, 63130, USA (slava@wustl.edu)

Lord Kelvin's vision of the early molten Earth has been reincarnated after the samples returned by the Apollo missions presented evidence that the Moon might once have been molten. This evidence led to a hypothesis of a lunar magma ocean. The idea of an early molten Earth - the terrestrial magma ocean hypothesis - was developed not long after and rapidly gained a broad acceptance [1]. Magma oceans or magmaspheres of various types on Earth as well as on other terrestrial planets have been proposed [2-8]. The growing list of extrasolar planets now includes planets which currently are likely to be at least partially molten [9]. The hypothesis of magma oceans is undoubtedly among the most important building blocks in the modern narrative of planetary formation and evolution. The major challenge in describing the evolution of magma oceans is that we have to deal with the extreme conditions of planetary interiors where the material properties and global dynamics are poorly understood [10, 11]. Answers to even basic questions concerning whether solid phases sink or float in magma oceans, how long it takes magma oceans to crystallize and where chemical equilibriation occurs have been eluding researchers for decades. Yet, these questions are critical for the interpretation of geochemical data, for the understanding of how magma oceans lead to the current planetary structures and to the current dynamic regimes of planetary interiors including the existence of plate tectonics on Earth [12].

[1] Warren (1985) *Ann. Rev. Earth Planet. Sci.* **13**, 201–240. [2] Sleep (2000) *JGR* **105**, 17563–17578. [3] Elkins-Tanton *et al.* (2005) *JGR* **110**, E12S01. [4] Labrosse *et al.* (2007) *Nature* **450**, 866–869. [5] Reese & Solomatov (2006) *Icarus* **184**, 102–120. [6] Albarede & Blichert-Toft (2007) *C. R. Geoscience* **339**, 917–927. [7] Reese *et al.* (2007) *JGR* **111**, E04S04. [8] Brown & Elkins-Tanton (2009) *EPSL* **286**, 446–455. [9] Leger *et al.* (2009) *A&A* **506**, 287–302. [10] Abe (1997) *PEPI* **100**, 27–39. [11] Solomatov & Stevenson (1993) *JGR* **98**, 5375–5418. [12] Sleep (2007) *Treatise on Geophysics* **9**, 145–169.

https://doi.org/10.1180/S0026461X00006502 Published online by Cambridge University Press

Mobility of elements from cesium formate residue emplaced on pegmatite tailings

P. SOLYLO* AND B. L. SHERRIFF

[1]Department of Geological Sciences, University of Manitoba, Winnipeg, MB, Canada, R3T 2N2 (*correspondence: patrick_solylo@hotmail.com)

A unique Cesium Products Facility (CPF) manufactures a cesium-formate drilling mud from pollucite ore at a pegmatite mine in SE Manitoba, Canada. The CPF is a closed system, with the waste slurry discharged to containment cells. When a cell is full, the Cs-rich slurry is dewatered, and the residue is dry-stacked on neutral tailings in a hydrogeologically closed tailings management area. This study concentrated on the geochemical and mineralogical reactions occurring within the residue pile and the underlying tailings to determine the mobility of Cs and other residue-related elements including Rb, Sr, Ba and Li.

Drill cores were extracted from the residue and tailings. The mobility of residue-related elements was examined through mineralogical observations, sequential extraction and porewater analysis.

The residue contains an order of magnitude more Cs (up to 2 wt. %) than the tailings (up to 0.3 wt. %). Sequential extraction results showed that 47% of the total Cs in the residue is mobile under natural conditions, compared with only 24% in the tailings. The stable forms of Cs in the residue are pollucite, feldspar and formate with sulphate and carbonate being the mobile forms. The Cs being released into the tailings does not appear to be re-precipitating in secondary phases. Cesium is predominantly in pollucite in the tailings. Rb, Sr, Ba and Li are all immobile in both the residue and the tailings in feldspar, lepidolite and barite.

Earth's early atmospheric density revealed from Archaean raindrop imprints

SANJOY M. SOM[1]*, DAVID C. CATLING[2] AND ROGER BUICK[2]

[1]NASA Ames Research Center, Moffett Field, CA 94035, USA (*correspondence: sanjoy.m.som@nasa.gov)
[2]University of Washington, Seattle, WA 98195, USA (dcatling@u.washington.edu)
[3]University of Washington, Seattle, WA 98195, USA (buick@ess.washington.edu)

The Archaean atmosphere has been investigated dominantly by numerical models that typically assume a total atmospheric pressure of ~1 atm [1-3]. However, barometric pressure may have been different, owing to the negligible presence of oxygen in the atmosphere [4], and the resulting difference in the redox-sensitive cycling of the other major gas, nitrogen.

We have developed a new method that uses lithified raindrop imprints as a proxy for atmospheric density. We consider the physics that determine the morphology of raindrop imprints preserved in tuff of the ~2.7 billion year old Ventersdorp Supergroup of South Africa [5]. Volume and surface area of raindrop imprints are a function of raindrop size and terminal velocity, the latter being dependent upon air density, whereas maximum raindrop size is not.

We experimentally determine the relationship between imprint volume and surface area as a function of raindrop size in wet ash (10% moisture by weight) from the 2010 Eyjafjallajokull event (Iceland) and Pahala (Hawaii), as modern analogs to the Ventersdorp tuff. We are then able to place an upper bound on the late Archaean atmospheric density, which has previously had no such observational constraint.

[1] Kasting (1987) *Precambrian Res* **34**, 205–229. [2] Haqq-Misra *et al*. (2008) *Astrobiology* **8**, 1127–1137. [3] Domagal-Goldman *et al*. (2008) *EPSL* **269**, 29–40. [4] Bekker *et al*. (2004) *Nature* **427**, 117–120. [5] Van der Westhuizen *et al*. (1989) *Sediment Geol* **61**, 303–309.

https://doi.org/10.1180/S0026461X00006502 Published online by Cambridge University Press

'WEERTMAN' cracks: A possible mechanism for near sonic speed diamond extraction from the Earth´s mantle

H. SOMMER[1]*, K. REGENAUER-LIEB[2,3], O. GAEDE[3], H. JUNG[1] AND B. GASHAROVA[4]

[1]School of Earth and Environmental Sciences, Seoul National University, Seoul, 151-747 Korea (*correspondence: info@holgersommer.de)
[2]School of Earth & Geographical Sciences, The University of Western Australia, Perth, Western Australia 6009, Australia
[3]CSIRO Exploration & Mining, PO Box 1130, Bentley, WA 6102, Australia
[4]ANKA/Inst.Synchotron Radiation, Forschungszentrum Karlsruhe GmbH, Hermann-von-Helmholtz-Platz 1, Eggenstein-Leopoldshafen, D-76344 Germany

'Weertman' cracks are two-dimensional liquid-filled cracks, which can move with a velocity close to Rayleigh-wave speed driven by the buoyancy or gravitational potential energy of the fluid and external stress fields. Therefore 'Weertman' cracks would be a potential transport mechanism for the diamond bearing kimberlitic-melt from the Earth's mantle to the Earth's surface. Arguments for the formation of 'Weertman' cracks are threefold: i) The geometry of kimberlite pipes resembles the shape predicted by 'Weertman' cracks; ii) Like Weertman cracks kimberlites themselves never develop an explosive stage besides the phreatomagmatic eruption due to contact with groundwater close to the Earth's surface; the melt often gets trapped near the Earth's surface; iii) The speed for the uplift of the diamonds from >150 km depth must be larger than 800 km/h to explain preservation of diamonds. The question to be answered is: What method can be used to confirm the formation of 'Weertman' cracks? Here we show that OH-diffusion profiles in nominally water free minerals, recorded from quenched diamondiferous host rock, are indicative for near sonic speed diamond extraction from the Earth´s mantle. This unforeseen discovery shows that 'Weertman' cracks are the only possible transport mechanism for diamonds from the Earth's mantle to the surface. Further, our findings show that the observed breadths of kimberlite pipes are surprisingly short, given the fact that the magma ascends from depths is in order of up to ~330 m/s. The ascent rates of kimberlites are of high economic interest, because if the diamonds are to long in contact with the kimberlitic melt they start to dissolve within a few minutes.

This research was supported by the Mid-career Researcher Program through an NRF grant funded by the MEST (No. 3345-20100013) and is a contribution to UNESCO IGCP 557.

Provenance discrimination of plants from three bedrock types using strontium isotopes and chemical analysis

B.Y. SONG[1], G. MUKESH[2], W.J. SHIN[2], M. CHOI[2] AND K.S. LEE[2]*

[1]Graduate School of Analytical Science and Technology, Chungnam National Univ (songby10@kbsi.re.kr)
[2]Korea Basic Science Institute, Ochang Center, Chungbuk 363-883, Korea (*correspondence: kslee@kbsi.re.kr)

This study is to assess the inter–lithological variations in the stable Sr isotopes that define an ecosystem/ habitat nutrient cycle and their signature in the aboveground vegetation. Five plant species, *Acacia sp*., *Zelkova serrata*, *Prunus serrulata*, *Capsicum annuum*, *Zea mays* and *Allium fistulosum* commonly found growing on granite, limestone and basalt formations were selected. Our hypothesis is based on the two facts-one the $^{87}Sr/^{86}Sr$ ratios depends on geological regime and this ratio varies significantly from one geological formation to another [1]. Second plants display particularly strong isotopic signals because they construct their tissues from such small molecules [2]. Based on these premise this natural phenomenon can be put into use to explain inter–lithological differences and effects of these inter–lithological variations on plant nutrient physiology.

Preliminary analsysis shows that $^{87}Sr/^{86}Sr$ ratios of tree leaves and fruit vegetables varied according to bedrock types in which they grow. $^{87}Sr/^{86}Sr$ ratios of plant leaves and vegetables well reflected the geological characteristics of three regions where they were grown.

[1] Faure (1986) *Principles of Isotope Geology*, Wiley. [2] Marshall *et al*. (2007) *Sources of variations in the stable isotope composition in plants*. Blackwell Publishing.

https://doi.org/10.1180/S0026461X00006502 Published online by Cambridge University Press

Integrated model to simulate and predict fate and transport process of contaminant in vadose zone

LINRUI SONG[1], JING ZHANG[2]* AND HUILI GONG[3]

[1]The Key Laboratory of Resource Environment and GIS of Beijing, Capital Normal University, Beijing 100048, P.R. China

[2]The Key Laboratory of Resource Environment and GIS of Beijing, Capital Normal University, Beijing 100048, P.R. China (*correspondence: maggie2008zj@yahoo.com)

[3]College of Resource Environment and Tourism, Capital Normal University, Beijing 100048, P.R. China

Interaction between surface water and groundwater is always a hot research topic in geochemistry, ecohydrology and interdisciplinary sciences. It's better to reveal the law of contaminant behavior in the regional water cycle process coupling of surface water and groundwater simulation, and also provide a good basis for the comprehensive consideration in environment changes effected by nature and anthropogenic. Vadose zone is the bond linking of surface water and groundwater, therefore, the physical mechanism of integrated model will be greatly enhanced considering the dynamics of vadose zone water movement. In this research, the rural plain area in the Capital City of China, Beijing with water eco-system protection function has been selected as the study location which experiences period of drought and wetness annually. Based on the use of traditional field survey techniques combined with remote sensing technology to access to the model parameters, this research will discuss the comparison between two surface - groundwater integrated models (MIKESHE and IHM) to simulate and predict the fate and transport process of nitrogen loading in the study area.

Under the auspices of National Natural Science Foundation of China (No.40901026) & Supported by Beijing Municipal Science & Technology New Star Project Funds (No.2010B046)

The molybdenum isotopic indication of low-medium temperature hydrothermal ore-forming systems: A case study on the Dajiangping pyrite deposit, Western of Guangdong Province, China

SONG SM[1], HU K[1], WEN HJ[2] AND ZHANG YX[2]

[1]State Key Laboratory for Mineral Deposits Research, School of Earth and Engineering, Nanjing University, Nanjing 210093, China

[2]Institute of Geochemistry, Chinese Academy of Sciences, Guiyang 550002, China

We present molybdenum isotope data from 12 hydrothermal syndepositional silicalite and carbonaceous slate samples from the Dajiangping pyrite deposit in western Guangdong Province, South China. The $\delta^{97/95}$Mo values from Orebody III range from -0.02‰ to 0.29‰, with an average of 0.18‰. In contrast, the composition values from Orebody IV display a larger variation from -0.70‰ to 0.62‰, especially the five samples from the main ore bed all show strong negative values. Orebody III is likely to have been deposited from submarine exhalative hydrothermal fluids under a relatively strong reducing environment and Orebody IV may have also been influenced by hydrothermal superimposition in a more oxidized disequilibrium condition. The $\delta^{97/95}$Mo values of Orebody IV are clearly negative, together with the values increasing stratigraphically upward in the ore beds, suggesting that the metallogenic environment of Orebody IV could be present dynamic fractionation in this restricted environment. Microorganisms including organic matter and replacement and/or adsorption of Fe-Mn oxides might influence the Mo isotopic fractionation in the ore-forming fluids.

https://doi.org/10.1180/S0026461X00006502 Published online by Cambridge University Press

Structural controls on surface hydroxyl reactivity in iron hydroxides

XIAOWEI SONG* AND JEAN-FRANÇOIS BOILY

Department of Chemistry, Umeå University, Sweden (*correspondence: xiaowei.song@chem.umu.se)

Mineral surfaces are populated with distinct types of hydroxyl groups displaying various catalytic roles with respect to gases, solvents and solutes. Knowledge of the types and distributions of hydroxyl groups on minerals with different surface structures is essential for gaining molecular-scale resolution of these processes.

This work provides Fourier transform infrared (FTIR) spectroscopic signatures of hydroxyl groups present on surfaces of FeOOH minerals, including lath- and rod-shaped lepidocrocite (γ), (nano) goethite (α) and akaganéite (β).

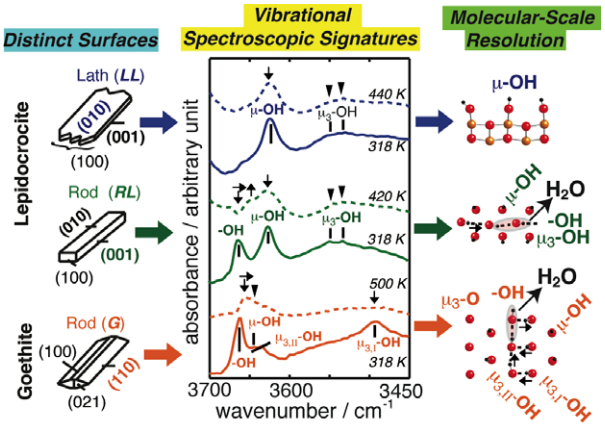

Figure 1: Synopsis of FTIR work, assisted by MD simulations, used to identify surface species and reactivity.

Our combined FTIR and molecular dynamics studies of these FeOOH surfaces enabled the extraction of unique spectroscopic signatures for distinct hydroxyl groups. Individual responses of these groups to variations in proton loadings and temperature provide experimental validation to previous theoretical accounts on their reactivity. These efforts now provide new possibilities for probing important gas-phase adsorption processes. They should moreover lay foundations for interfacial studies involving water.

La-Ce and Sm-Nd isotope geochemistry of felsic granulite in the Jirisan complex, Yeongnam Massif, Korea

YONG-SUN SONG[1], SEUNG-GU LEE[2]*, YOSHIHIRO ASAHARA[3] AND TSUYOSHI TANAKA[3]

[1]Department of Earth Environmental Sciences, Pukyong National University, Pusan 608-737, Korea (yssong@pknu.ac.kr)

[2]Geological Research Division, Korea Institute of Geoscience and Mineral Resources, Daejeon 305-350, Korea (sgl@kigam.re.kr)

[3]Department of Earth and Environmental Sciences, Nagoya University, Nagoya 464-8601, Japan (asahara@eps.nagoya-u.ac.jp, tanaka@eps.nagoya-u.ac.jp)

REEs contain two long-lived decay systems, the ^{147}Sm-^{143}Nd and ^{138}La-^{138}Ce decay systems, which provide us with the information on ages and initial ratios that helps us understand their origin and history. Hence, the application of the La-Ce and Sm-Nd isotope systematics in petrogenetic studies has enabled an estimation of the light rare earth element (LREE) patterns in source materials of the rocks.

We report La-Ce and Sm-Nd isotopic data of highly evolved granites with the composition of major and rare earth element from the felsic granulite, which occurs at the Jirisan Complex in the Yeongnam Massif, Korea. Based on the Ce and Nd isotopic data, we also discuss the REE geochemistry of source material of the Jirisan felsic granulite. The felsic granulite shows three different types of chondrite-normalized REE pattern: one is a tetrad REE pattern of M-type with a large negative Eu anomaly, another is a W-type tetrad REE pattern, and the third is an REE pattern of crustal type showing an LREE-enriched and HREE-depleted pattern. U-Pb zircon and Rb-Sr whole rock ages are 1874 Ma and 1831±36 Ma (2σ) with initial 0.7028±0.0097, respectively. However, Sm-Nd isotopic system from these rocks shows error-chron ages from 1235 Ma to 1570 Ma suggesting that Sm-Nd isotopic system might have been disturbed by specific geochemical processes related to the formation of the tetrad REE patterns. Nevertheless, initial Ce-Nd isotopic values show that all three types were derived from the isotopically similar source materials. Our data also indicate that La-Ce and Sm-Nd isotopic system may be useful in understanding REE fractionation between rock and its source material.

https://doi.org/10.1180/S0026461X00006502 Published online by Cambridge University Press

Direct observation of chemical modification of Asian Dust particles during long-range transport

YOUNG-CHUL SONG, HAE-JIN JUNG, HYEKYEONG KIM AND CHUL-UN RO*

Department of Chemistry, Inha University
(*correspondence: curo@inha.ac.kr)

In our previous works [1-3], it was clearly demonstrated that the combined use of quantitative energy-dispersive electron probe X-ray microanalysis (ED-EPMA), known as low-*Z* particle EPMA, and attenuated total reflectance FT-IR (ATR-FT-IR) imaging technique had the great potential for detailed characterization of individual aerosol particles. In this work, individual Asian Dust particles collected during an Asian dust storm event occurred on Nov. 11, 2002 in Korea were characterized by the combined use of low-*Z* particle EPMA and ATR-FT-IR imaging technique. By the combined use of the two single-particle analytical techniques on the same individual particles, it was observed that Asian Dust particles had experienced extensive chemical modification during long-range transport, through heterogeneous reactions with nitrogen or sulfur oxide species resulting in nitrate and/or sulfate formations, respectively. On the basis of information on their morphology, elemental concentrations, and functional groups of individual particles available from the two analytical techniques, overall 109 individual particles were classified into four particle types: Ca-containing (38%); $NaNO_3$-containing (30%); silicate (23%); and miscellaneous particles (9%). Among overall 41 Ca-containing particles, the numbers of particles containing nitrate, sulfate, and both are 14, 8, and 17, respectively, whereas the number of unreacted $CaCO_3$ particles is just 2, clearly demonstrating that the Asian Dust particles had extensively experienced heterogeneous reactions during long-range transport. The combined use of the two single particle analytical techniques could provide detailed information on their physicochemical characteristics of individual Asian Dust particles, and thus the identification of airborne amorphous phase calcium carbonate particles and nitrite species in aerosol phase, and mineralogy of silicate particles on a single particle basis could be performed.

[1] Ryu & Ro (2009) *Anal. Chem.* **81**, 6695–6707. [2] Jung & Ro (2010) *Anal. Chem.* **82**, 6193–6202. [3] Song & Ro (2010) *Anal. Chem.* **82**, 7987–7998.

The gully nitrogen migration and flux at northern China city

YUJIA SONG AND HUIQING LIU*

School of Urban and Environment Science, Northeast Normal University, 130024, Changchun, China
(ccssf0431@163.com,
*correspondence: jlsongyujia@126.com)

Research Object and Results

Yitong River at a representative northern China city, Changchun, was selected as research object. We quantitatively investigated the migration path and flux of nitrogen at gully region in the city under rapid urbanization process.

The results showed that at Yitong River basin, the total nitrogen input flux was 188 kg/hm^2, following the sequence of fertilizer input> biological immobilization> feed> atmospheric deposition. the total nitrogen output flux was 102.5kg/hm^2, following the sequence of products> waste output> denitrification> surface runoff. the net nitrogen storage was 85.5kg/hm^2. The migration path and flux of nitrogen were obviously by human activities, showing an imbalance of input and output and a tendency of nitrogen accumulation and pollution.

Discussion of Results

Nitrogen migration is a combined effect from meteorology, hydrology, topography and agricultural practices, among which rainfall is the key driving force [1]. The material input and migration directly impact nutrient loss [2].

Under the background of globalization, the nitrogen migration and the biogeochemical processes become extremely complex due to the coupling effects from interfering and natural factors [3], the knowledge about nitrogen source and destination is still very limited, China is localized at monsoon area, where the highest rate of environmental change occurs. Thus, long-term monitoring and modeling regarding entire watershed ecosystem as a whole and quantitative analysis of the coupling mechanism of human activity and natural processes are required. This will provide theoretical support for the healthy evolution and development of cities.

[1] M.Mihara (2001) *Journal of Agricultural Engineering Research* **78**, 209–216. [2] H. Tiessen (1995) *Phosphorus & the Global Environment* **2**, 135–142. [3] R. W. Howarth *et al.* (1996) *Biogeochemistry* **35**, 75–139.

https://doi.org/10.1180/S0026461X00006502 Published online by Cambridge University Press

Mechanisms of Cd sorption to montmorillonite (Na-SWy-2) clay affected by ionic strength and microbial ligand

Z. SONG[1], B.A. BUNKER[1] AND P.A. MAURICE[2]

[1]Department of Physics, University of Notre Dame, Notre Dame, IN 46556, USA (*correspondence: zsong@nd.edu)
[2]Department of Civil Engineering and Geological Sciences, University of Notre Dame, Notre Dame, IN 46556, USA

Many microorganisms exude low molecular weight organic ligands known as siderophores to acquire nutrient Fe; these ligands may also affect the fate and transport of other metals. In this study, we investigated the effects of pH, ionic strength, and the siderophore desferrioxamine B (DFOB) on Cd sorption to montmorillonite using batch experiments, Extended X-ray Absorption Fine Structure (EXAFS) analysis, and X-ray Diffraction (XRD) measurements to monitor changes in montmorillonite 001 d-spacing upon sorption.

The extent of Cd sorption to montmorillonite increased with increasing pH and decreasing ionic strength. The presence of DFOB inhibited Cd sorption at pH < ~7 and enhanced Cd sorption at pH > ~7. Sorption densities ranged from 1.1 (11% sorption) to 10.0 (100% sorption) μmol sorbed/gram of clay. EXAFS analysis showed that the detailed sorption mechanism varied as a function of pH, ionic strength and DFOB concentration (0 or 1.0 mM). In the absence of DFOB, at low pH (~5.0 for samples in 0.1M $NaNO_3$ and ~5.0 and ~7.5 for samples in 0.01M $NaNO_3$), EXAFS showed that Cd sorbed outer-spherically; at higher pH (~7.5 and ~8.5 for samples in 0.1M $NaNO_3$ and 8.5 for samples in 0.01M $NaNO_3$), Cd sorbed as a mixture of inner-sphere and outer-sphere complexes. In the presence of DFOB, at pH ~5.0, Cd sorbed outer-spherically; at pH ~7.5 and 8.5, Cd sorbed as a mixture of inner-sphere and outer-sphere Cd-DFOB complexes. Furthermore, the ratio between inner-sphere and outer-sphere sorption increased with both pH and ionic strength. XRD measurements indicate that layer spacing did not vary substantially as a function of Cd concentration, ionic strength, or pH. However, in the presence of DFOB, the d-spacing expanded by ~ 2Å, which is consistent DFOB absorption. This study demonstrates that Cd sorption to swelling clay can involve a complex interplay of mechanisms depending upon environmental conditions.

Experimental fluid-rock interaction simulating brine reinjection in greywacke-hosted reservoirs of the Taupo Volcanic Zone, New Zealand

R. SONNEY AND B.W. MOUNTAIN*

GNS Science, Wairakei Research Centre, 114 Karetoto Rd, Taupo 3377, New Zealand (*correspondence: b.mountain@gns.cri.nz)

A high temperature-pressure fluid-rock interaction apparatus has been used to simulate greywacke - brine interaction at 154ºC and 27 bars using a continuously-flowing fluid. The experiment was designed to reproduce the scenario where reinjection brine is disposed in a fractured greywacke aquifer; a typical lithology at New Zealand geothermal power plants. The fluid used was an actual reinjection brine from an operating plant, containing ~3400 mg/kg of total dissolved solids including SiO_2 (960 mg/kg), Na (799 mg/kg), K (131 mg/kg), Cl (1027 mg/kg) and SO_4 (423 mg/kg). In order to remove atmospheric oxygen contamination, the fluid was degassed first with ultrapure N_2 followed by a H_2S:N_2 mixture (1:100) for 20 minutes. The final pH of the fluid was 6.8 at room temperature. For the simulation, 24 g of crushed, seived and ultrasonically-cleaned greywacke (1-2 mm) was placed in the core holder of the flow-through apparatus. At room temperature and 1 ml/hr of brine flow (one week duration), the reacted fluid attained a pH of 7.8 and contained elevated concentrations of Ca and Mg (77 and 6 mg/kg, respectively). This is attributed to calcite dissolution. After a temperature increase to 154ºC, the reacted fluid remained oversaturated with respect to amorphous silica but a loss of 240 mg/kg of SiO_2 was observed. Of the other dissolved species: Mg, Ca, Sr, Al, Mn, and Fe showed a significant decrease; while Li, Na, K, As, and the anions showed no measurable change. Variation of flow rate (0.5 ml/hr) showed little change in effluent chemistry suggesting partial equilibrium with some mineral phases. SEM examination of the run products at the entry point of the brine showed a complete overgrowth of amorphous silica on all mineral surfaces. Reacted material at the exit point of the fluid did not show extensive silica overgrowths indicating removal of polymerised silica nanospherules early during water-rock interaction. Partial equilibrium with a secondary phase containing Ca-Mg-Fe suggests a possible control on fluid composition by calcite and/or clay minerals. This was observed in previous experiments using distilled water. These results show that the silica phase precipitating at these conditions in the geothermal aquifer is amorphous silica.

https://doi.org/10.1180/S0026461X00006502 Published online by Cambridge University Press

Geochemical fingerprint of an Oligocene to Miocene arc segment in Eastern Mindanao (Philippines)

IRIS SONNTAG[1,3]*, ROBERT KERRICH[2] AND STEFFEN HAGEMANN[3]

[1]CSIRO, ARRC, Kensington, WA 6151, Australia (*corrospondence: Iris.Sontnag@csiro.au)
[2]University of Saskatchewan, Saskatoon, Canada S7N 5E2
[3]CET, University of Western Australia, Nedlands, WA 6009, Australia

The Oligocene to Miocene arc segment in central Eastern Mindanao (Philippines) is part of the Philippine Mobile Belt (PMB) and is related to the low sulfidation epithermal Co-O mine. The PMB constits of the Paleogene volcanic Philippine arc and accreted crustal framgents from the Eurasian plate [1]. This sudy of the Co-O magma suite addresses the geochemical fingerprint of this arc segment, inlcuding the nature of the mantle wedge, involement of subducted material such as sediment or crustal fragments (form the Eurasian plate) and relationships between geotectonic setting and ore forming processes.

The Co-O magma series displays typical island arc geochemical patterns highlighted by the conjunction of LREE-enrichment with depletion of Nb, Ta and Ti. The igneous rocks are dominantly calc-alkaline magma series (andesites and dacites), with some tholeiitic trends for basaltic rocks. There are no significant enrichment of LILE or LREE when compared to younger Pliocene magmas of the Philippines. Nb contents and Zr/Nb ratios (x-y) of the basalts are comparable to other primitive arc magmas in the Pacific (e.g. Marianas) signifying a MORB-like mantle wedge. Th/Ce values below 0.1, and Th/La ratios similar to the Marianas (that are close to mantle values), rule out sediment melting or seamounts on the slab. This magma series involved thin arc crust in an intraocenaic arc setting related to a potentially intermediate to steep dipping subduction zone in an extensional to neutral geochtectenic remige, without addition of rifted fragments or continental crust. The Co-O gold mine has relatively high base metal contents and is comparable to other low sulfidation deposits genereated in a neutral geochtectonic arc regime and is potentially in transition to a porphyry deposits, in contrast to bimodal volcanism in back-arc regimes [cf. 2]. However, the low to medium K Co-O magma series varies partly from other arc magma series related to low sulfidation epithermal systems due to its lack of ‘crustal contamination’.

[1] Pubellier *et al*. (1991*) J Southeast Asian Earth Sci* **6**, 239–248. [2] John (2001) *Econ Geol* **96**, 1827–1853.

Origin of nepheline-normative primitive magmas in island arcs

F. SORBADERE[1]*, P. SCHIANO[1], N. METRICH[2]

[1]Clermont Université, Université Blaise Pascal, Laboratoire Magmas et Volcans, Clermont-Ferrand, France (*correspondence: F.Sorbadere@opgc.univ-bpclermont.fr)
[2]Institut de Physique du Globe, Sorbonne, Paris-Cité, Univ. Paris Diderot, Paris, France

Here we address the question of the origin of Si-undersaturated arc magmas, although they are rarely emitted on Earth surface, through a systematic on major and trace elements in primitive olivine-hosted melt inclusions. Samples are Mg-rich basalt to ankaramite lavas and lapilli scoriae from different volcanic arcs (Vanuatu, Lesser Antilles, Indonesian, Luzon and Aeolian arcs).

Melt inclusions display trace element patterns typical of arc-related calk-alkaline basalts, with variable enrichments in LILE, Sc (20 to 90 ppm), and La/Yb or Nb/Y ratios ranging from 1 to 18, and from 0.1 to 0.3, respectively. In CMAS projections, the melt inclusions delineate a trend linking two well-defined end-members strongly or poorly enriched in diopside component.

As a whole, the melt inclusions provide snapshots of instantaneous melts recording a compositional diversity of primitive magma batches, which requires the multi-stage mixing between melts generated by partial melting of peridotite and amphibole-bearing clinopyroxene-rich lithologies. This hypothesis is also supported by trace element models including Sc and incompatible element ratios, where melt inclusions form mixing trend between the two lithologies. We conclude that amphibole-bearing clinopyroxenite, occuring as metasomatic segments in the upper mantle of island arcs [1, 2], could be a suitable source for Ne-normative, Di-rich melt inclusions found in arc environments [3-7]. The progressive melting of these lithologies and surrounding peridotite could account for the geochemical characteristics of the studied melt inclusions.

[1] Pilet *et al*. (2008) *Science* **320**, 916–919. [2] Pilet *et al*. (2009) *Contrib*. *Mineral*. *Petrol*. **5**, 621–643. [3] Gioncada *et al*. (1998) *Bull*. *Volcanol*. **60**, 286–306. [4] Métrich *et al*. (1999) *EPSL* **167**, 1–14. [5] Schiano *et al*. (2000) *G3* **1**, n°5, 1018. [6] Médard *et al*. (2006) *J*. *Petrol*. **47**, 481–504. [7] Elburg *et al*. (2007) *Chem*. *Geol*. **240**, 260–279.

https://doi.org/10.1180/S0026461X00006502 Published online by Cambridge University Press

Ni speciation and isotope fractionation in marine ferromangenese deposits

JEFFRY V. SORENSEN[1], BRANDY M. TONER[1], BLEUENN GUEGUEN[2,3] AND OLIVIER ROUXEL[2,3]

[1]University of Minnesota, St Paul, MN, USA (toner@umn.edu, sore0317@umn.edu)
[2]Université de Brest, IUEM, Plouzané, France (bleuenn.gueguen@univ-brest.fr, orouxel@univ-brest.fr)
[3]IFREMER, Département Géosciences Marines, Plouzané, France

Marine ferromanganese deposits have slow deposition rates and laminar growth habits. Variations in major and trace element speciation and isotopic composition of successive layers within the crusts have the potential to retain information regarding ocean chemical conditions. It is thought that Ni can incorporated into the structure of marine ferromanganese deposits such that the Ni is retained over time [1],[2]. The goal of this study is to explore Ni isotope systematics in marine ferromanganese deposits as a tracer for metal sources and chemical conditions at the time of Ni sorption.

Our study pairs stable isotopic fractionation measurements (via MC-ICP-MS [3]) with synchrotron X-ray spectroscopy techniques to identify the local coordination environment of sorbed Ni. This is accomplished by using laboratory generated 2-line ferrihydrite, goethite, and hexagonal-birnessite that have had Ni sorbed under a suite of pH values and Ni concentrations. We're also investigating a range of natural marine deposits such as ferromanganese nodules and crusts from different oceanic basins.

Preliminary findings show that: (1) initial aqueous Ni concentration can affect the fractionation of sorbed isotopes, and (2) pH can influence both the structural location of Ni sorption as well as the fractionation of Ni isotopes. Mineral surface charge and structural properties likely control the extent of Ni isotope fractionation. We hypothesize that in a natural deposits, mineralogy together with Ni sources and enrichment conditions are important parameters controlling Ni isotope signatures.

[1] Peacock & Sherman (2007) *Chemical Geology* **238**, 94–106. [2] Manceau, Tamura, & Marcus (2002) *American Mineralogist* **87**, 1494–1499. [3] Gueguen *et al*. (2011) *Geophysical Research Abstracts* **13**, EGU2011-6890

Early Paleozoic granites in the Jiamusi terrane of the Central Asian fold belt

A.A. SOROKIN[1]*, A.B. KOTOV[2], Y.B. SAL'NIKOVA[2] AND N.M. KUDRYASHOV[3]

[1]Institute of Geology and Nature Management, Blagoveshchensk, Relochny, 1, Russia (*correspondence: sorokin@ascnet.ru)
[2]Institute of Precambrian Geology and Geochronology, St.Petersburg, Russia
[3]Geological Institute of the Kola Sc., Apatity, Russia

In the structure of the eastern part of the Central-Asian fold belt a series of continental blocks (terranes) is distinguished. These are: the Argun, Mamyn, Bureya, Jiamusi blocks (terranes) composed of granitoids of different ages but their age has being remained disputable for quite a long time. At present a series of age datings are obtained (U-Pb method). Basing on that datings we can say with certainty that the Early Paleozoic granitoids are widely developed in this terrane.

In the northeastern part of the Jiamusi terrane we obtained the age of 480±4 Ma granites of Sutara massif, the age of 471±10 Ma of leucogranites of the Kabala massif and the age of 461±5 Ma of quartz syenites of the Durilovsky massif.

Similar age values are also given for granites in the south Jiamusi terrane [1] and for granites in the Argun, Mamyn, Bureya terranes [2-5]. In this connection it cannot be excluded that all above mentioned Early Paleozoic granitiods belong to a single orogenic belt.

Thise study was supported by RFBR (Gr.No 10-05-00172), FEB RAS (Gr.No 09-I-ONZ-09, 09-II-SB-08-007).

[1] Wilde *et al*. (2003) *Prec. Res* **122**, P. 311–327. [2] Sorokin *et al*. (2004) *GCA* **73**, Iss. 13. Suppl. **1**, A1254. [3] Sorokin & Kudryashov (2004) *GCA* **68**, Iss. 11. Suppl. 1. A685. [4] Sorokin *et al*. (2004) *Petrology* **12**, 367–376. [5] Sorokin *et al*. (2010) *Doklady Earth Sciences* **431**, 299–303.

https://doi.org/10.1180/S0026461X00006502 Published online by Cambridge University Press

Geochemical features of the Amur River sediments in its middle reaches

O.A. SOROKINA

Institute of Geology and Nature Management FEB RAS, Russia, Relochniy 1, Blagoveshchensk, Amur Region, Russia (library@ascnet.ru)

The Amur River is one of the largest rivers of the East Asia. The main channel and tributaries of the Amur River cross the geological units of different ages.

A distribution of rare earth elements in the studied samples of the bottom sediments of the Amur River is moderately differentiated ([La/Yb] n=9.6-14.9). A characteristic feature of their distribution is also an enrichment in LREE relatively to MREE and comparatively gentle graph in the in the field of MREE and heavy HREE which is supported by the ratios of [La/Sm]n=3.3.-4.1 and [Gd/Yb]=1.1-2.2. All spectra of rare earth elements have moderately expressed negative Eu anomaly (Eu/Eu*=0.7-0.9) (Fig.1).

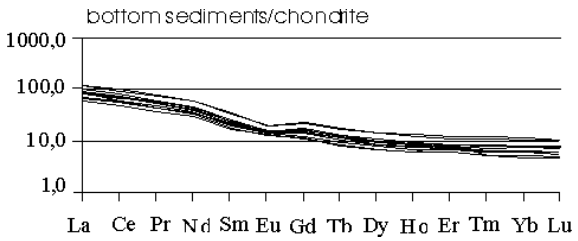

Figure 1: The rare earth elements' distribution in the bottom sediments of the Amur river. The composition of chondrite is used according to [1].

In comparison with the composition of the upper continental crust the bottom sediments under study are at a definite degree depleted in such elements as Sc (3.7 – 9.0 ppm), Cu (8-22ppm), Nb (9-13 ppm), Ta (0.21-0.37 ppm), Y (9-17 ppm). The concentration of Zn (50-75 ppm), Rb (82-109 ppm), Sr (290-350 ppm), Pb (15-24 ppm), W (1.1-2.2 ppm), Th (5.2-11.9 ppm), U (1.0-5.4 ppm), REE correspond to the level of those in the upper continental crust while the concentrations of Ba (550-840 ppm), V (63 – 81 ppm), Cr (63-80 ppm), Co (12-14 ppm), Ni (31-43 ppm), Zr (190-309 ppm) a bit higher than their crust values.

It was established that the most probable sources of the bottom sediments in the studied section of the Amur River were siliceous acid magmatic or metasedimentary rocks.

[1] McDonough, Sun S-s. (1995) *Chemical Geology*. **120**, 223–253.

Systematic underestimation of the oxidation state of MORB glasses

PAOLO A. SOSSI[1,2]* AND HUGH ST.C. O'NEILL[2]

[1]Department of Geology and Geophysics, University of Adelaide, Adelaide, SA 5000, Australia

[2]Research School of Earth Sciences, Australian National University, Canberra, ACT 0200, Australia (*correspondence: paolo.sossi@anu.edu.au)

The $Fe^{3+}/\Sigma Fe$ of a magma and its fO_2 are related by:

$$Fe^{2+}O + 0.25\ O_2 = Fe^{3+}O_{1.5}$$

This dependence has been calibrated using a wide range of silicate melt compositions equilibrated at known fO_2 and analysed by wet chemistry ([1], [2]) and Mössbauer. Analyses of large sets of natural MORB glasses by wet chemistry (e.g. [3], [4]) report tight distributions around $Fe^{3+}/\Sigma Fe \approx 0.1$, corresponding to the relative oxidation state $\Delta QFM \approx -0.5$. However, recent determinations of $Fe^{3+}/\Sigma Fe$ on MORB glasses by XANES ([5], [6]) consistently return more oxidised values, about 0.16, correponding to $\Delta QFM \approx +0.5$.

The wet chemistry method [7] relies on the complete oxidation of Fe^{2+} to Fe^{3+} by reduction of V^{5+} to V^{4+}. However, it does not discriminate between Fe^{2+} and other reduced species. One such species, S^{2-}, is present in MORB glasses at $\sim 10^3$ ppm, but not in the glasses used to establish the $Fe^{3+}/\Sigma Fe$- fo_2 relationship.

To test the effect of S^{2-} during wet chemistry, a series of Fe-free glasses with the An-Di eutectic composition were prepared using CO_2-CO-SO_2 gas mixtures to produce S^{2-} ranging from 0 to 4500 ppm [8]. These glasses were subjected to the procedure of ref. [7]. The results establish that S^{2-} is fully oxidised during dissolution to S^{6+} (i.e. sulfate) according to the reaction:

$$S^{2-} + 8V^{5+} = 8V^{4+} + S^{6+}$$

From the reaction stoichiometry, 1000 ppm S^{2-} is equal to 2 wt% Fe_2O_3, which is more than enough to account for the discrepancy in the $Fe^{3+}/\Sigma Fe$ of MORB between wet chemistry and XANES. Determination of S and its speciation in basalts is essential to understanding their redox state, since degassing of S as SO_2 will tend to further reduce basalts with S^{2-} but oxidise basalts with S^{6+} [9].

[1] Kilinc *et al*. (1983) *Contrib. Min. Pet*. **83**, 136–140. [2] Kress & Carmichael (1991) *Contrib. Min. Pet*. **108**, 82–92. [3] Christie *et al*. (1986) *EPSL* **79**, 397–411. [4] Bézos & Humler (2005) *GCA*, **69**, 711–725. [5] Berry *et al*. (2003) *Am. Min*. **88**, 967–977. [6] Kelley & Cottrell (2009) *Science,* **325**, 605–607. [7] Wilson (1960) *Anal*. **85**, 823–827. [8] O'Neill & Mavrogenes (2002) *J. Pet*. **43**, 1049–1087. [9] Metrich & Clocchiatti (1996) *GCA* **60**, 4151–4160

https://doi.org/10.1180/S0026461X00006502 Published online by Cambridge University Press

Searching for ancient crusts: Integrating Pb isotopes in plagioclase with Hf isotopes in zircon

A.K. SOUDERS[1]*, P.J. SYLVESTER[1] AND J.S. MYERS[2]

[1]Department of Earth Sciences, Memorial University, St. John's, NL A1B 3X5, Canada (*correspondence: kate.souders@mun.ca)

[2]Department of Applied Geology, Curtin University, Perth, WA 6845, Australia

The composition of the Earth's early crust is a topic of much interest in geology today. We present *in situ* analyses by LA-MC-ICPMS for the Pb isotope compositions of preserved igneous plagioclase (An 75-89) megacrysts and the Hf isotope compositions of BSE-imaged domains of zircon grains from 21 samples from two anorthosite complexes in southwestern Greenland, Fiskenæsset and Nunataarsuk, which represent two of the best-preserved Archean anorthosites in the world. *In situ* LA-ICPMS U-Pb geochronology of the zircon grains suggests that the crystallization age of the Fiskenæsset complex is 2936 ± 13 Ma (2σ, MSWD = 1.5) and the Nunataarsuk complex is 2914 ± 6.9 Ma (2σ, MSWD = 2.0). Initial Hf isotope compositions of zircon grains from both anorthosite complexes fall between depleted mantle and a less radiogenic crustal source with a total range up to 5 ε_{Hf} units. In terms of Pb isotope compositions of plagioclase, both anorthosite complexes share a depleted mantle end member yet their Pb isotope compositions diverge in opposite directions from this point: Fiskenæsset toward a high-μ, more radiogenic Pb crustal composition and Nunataarsuk toward low-μ, less radiogenic Pb, crustal composition. By using Hf isotopes in zircon in conjunction with Pb isotopes in plagioclase we are able to constrain both the timing of mantle extraction of the crustal end member and its composition. At Fiskenæsset, the depleted mantle melt interacted with an Eoarchean (~ 3600 – 3800 Ma) mafic crust with $^{176}Lu/^{177}Hf$ ~ 0.026. At Nunataarsuk, the depleted mantle melt interacted with a Hadean (~ 4200 Ma) mafic crust with $^{176}Lu/^{177}Hf$ ~ 0.032. Using our new *in situ* approach, contamination of mantle derived magma by ancient mafic crust has been discovered in both the Fiskenæsset and Nunataarsuk anorthosite complexes of Greenland. The isotope data presented here suggest the survival of Hadean and Eoarchean crust until ~ 2900 Ma. There is potential that this old mafic crustal could be preserved at the surface within the Nunataarsuk and Fiskenæsset regions today.

REE and isotope (Sr, S, Pb) geochemistries to constrain the genesis of the F-(Ba-Pb-Zn) ores of the Zaghouan District (NE Tunisia)

F. SOUISSI[1]*, N. JEMMALI[1], R. SOUISSI[1] AND J-L. DANDURAND[2]

[1]Institut national de recherche et d'analyse physico-chimique. 2026 Sidi Thabet, Tunisia (*correspondence: souissi_foued@yahoo.fr)

[2]Université de Toulouse, UPS (OMP), LMTG, 14 Avenue E. Belin, 31400 Toulouse Cedex, France

The F-(Ba-Pb-Zn) ore deposits of the Zaghouan District, which are located in NE Tunisia, occur as open space fillings or stratabound orebodies, hosted in Jurassic, Cretaceous and Tertiary layers. Ore fluids are hydrothermal (80 to 200°C) brines (10 to 30 wt % NaCl equiv.). The chondrite-normalized REE patterns may be split into three groups: (i) 'Normal marine' patterns characterizing the wallrock carbonates; (ii) REE patterns sloping to the right-hand side, with small negative Ce and Eu anomalies, characteristic of the early ore stages; (iii) Bell-shaped REE patterns displaying LREE depletion, as well as weak negative Ce and Eu anomalies, characterizing fluids of subsequent stages. The $^{87}Sr/^{86}Sr$ ratios, show that the Sr of the epigenetic carbonates (dolomite, calcite) and ore minerals (fluorite, celestite) is more radiogenic than that of the country rocks. The uniformity of this ratio throughout the District, provides evidence for the isotopic homogeneity and, consequently, the identity of the source of the mineralizing fluids. The $\delta^{34}S$ values of barite associated to mineralizations, are close to the $\delta^{34}S$ of Triassic sea water (17%). The $\delta^{34}S$ values of sulphide minerals show a wide range for galena (-13.6 to +11.4%), but restricted for sphalerite (-2.6 to +2.1%). However, considered individually, each deposit is characterized by a restricted range of $\delta^{34}S$ values for both sulphides, which requires that reduction took place in closed systems. The more negative $\delta^{34}S$ values are assigned to bacterial reduction, while the more positive are assigned to thermo-chemical reduction of Triassic sulphates. Taking account of the homogeneity in the Pb-isotope composition of galenas, a single upper crustal source for base-metals is accepted. The Late Paleozoic basement seems to be the more plausible source for F-Pb-Zn concentrated in the deposits. The formation of the Zaghouan District ore deposits is considered as the result of the Zaghouan Fault reactivation during the Upper Miocene period.

https://doi.org/10.1180/S0026461X00006502 Published online by Cambridge University Press

Binge/purge oscillations of the thawing Fennoscandian Ice Sheet revealed by ε_{Nd} and biomarkers

G. SOULET[1,2]*, G. MENOT[1], G. BAYON[2], F. ROSTEK[1], E. PONZEVERA[2], G. LERICOLAIS[2] AND E. BARD[1]

[1]CEREGE, Univ. Aix-Marseille, CNRS, IRD & Collège de France, Technopole de l'Arbois BP80, 13545 Aix en Provence cedex 4, France (*correspondence: soulet@cerege.fr)

[2]Ifremer, centre de Brest, Géosciences Marines, 29280 Plouzané cedex, France

At its maximum extent, the FIS advanced into the watershed of the Dnepr River, one of the main rivers feeding the former Black Sea 'Lake'. As a consequence, the Black Sea basin potentially represents a suitable location to investigate the dynamics of the FIS retreat and its impacts on global/regional climate and European hydrographical reorganizations in the context of the Last Deglaciation.

Here, we report high-resolution geochemical data from a core retrieved in the Black Sea. We combine the use of Nd isotopes in clay fraction (ε_{Nd}) and bulk XRF-Ti/Ca as tracers for sediment provenance, together with biomarkers as tracers for river runoff (BIT-index) and boreal soil leaching (C_{25}-alkanes). During Heinrich Event 1 (HE1), four drastic periods of Deglacial Water Pulses (DWPs) occurred as unequivocally revealed by the biomarkers. Concomitantly, ε_{Nd} signatures clearly demonstrated that the DWPs were generated by the thawing FIS. Each period of DWPs (~200 yr in duration) occurred repeatedly every 200 yr, displaying a peculiar cyclic-like pattern. By analogy with MacAyeal [1]'s model, we propose a binge-purge model to explain the observed cyclicity: the binging period requiring a continuous FIS retreat, the purging period involving regional interactions between the formed proglacial lakes and the atmosphere.

[1] MacAyeal (1993) *Paleoceanography* **8**, 775–784.

Impact of aerosols on the equilibrium response of the climate system

GABRIELA SOUSA SANTOS* AND ISABELLE BEY

Institute for Atmospheric and Climate Science & Center for Climate Systems Modeling, ETH Zurich (*correspondence: gabriela.sousa-santos@env.ethz.ch)

Aerosols have both a direct and indirect effect on climate. The first effect arises from the aerosol scattering and absorption of radiation in the atmosphere. The indirect effect relates to their influence on cloud properties.

In the present study, we investigate the equilibrium response of the climate system to two scenarios of primary emissions of black carbon, organic carbon, sulfur dioxide, benzene, toluene, and xylene correspondent to 1850s and today conditions. We use the fully-unified aerosol-climate model ECHAM5-HAM coupled to a mixed layer ocean (MLO)[1, 2, 3]. Using a MLO coupled to the climate-aerosol model allows us to diagnose the aerosol impact in a comprehensive manner. The emissions were taken from the ACCMIP (Atmospheric Chemistry & Climate Intercomparison Project) [4], an inventory developed for the next IPCC assessment.

We will show results of several equilibrium simulations with a focus on the response of the hydrological cycle to aerosol effects, like impacts on water vapour, sensible heat fluxes, precipitation minus evaporation patterns, convective mass fluxes, etc. Preliminary results indicate that the aerosol forcing of black carbon, organic carbon, and sulfur dioxide from 1850s to present day resulted in a global mean surface cooling of 0.9K, a reduction in global mean precipitation of 0.11mm/d (3.41%), and an increase in cloud cover of 1.1%.

[1] Lohmann *et al*. (2007) *Atmos. Chem. Phys*., **7**:3425446. [2] Roeckner *et al*. (1995) In R.J. Charlson and J. Heintzenberg, editors, *Aerosol forcing of climate*, chapter **18**. John Wiley & Sons. [3] Stier *et al*. (2005) *Atmos. Chem. Phys*., **5**:1125-1156. [4] Lamarque *et al*. (2010), *Atmos. Chem. Phys*., **10**:7017-7039.

https://doi.org/10.1180/S0026461X00006502 Published online by Cambridge University Press

A 50-year record of PGEs in Antarctic snow

TSEREN-OCHIR SOYOL-ERDENE[1], YOUNGSOOK HUH[1]*, SUNGMIN HONG[2] AND SOON DO HUR[3]

[1]School of Earth and Environmental Sciences, Seoul National University, Seoul, Korea (soyoloo@snu.ac.kr, *correspondence: yhuh@snu.ac.kr)

[2]Department of Oceanography, Inha University, Incheon, Korea

[3]Korea Polar Research Institute, Incheon, Korea

Antarctic snow preserves an atmospheric archive that enables the study of global atmospheric changes and anthropogenic disturbances from the past. We report atmospheric deposition rates of platinum group elements (PGEs) in Antarctica during the last ~50 years based on determinations of Pt, Ir and Rh in snow samples collected from Queen Maud Land, East Antarctica to evaluate changes in the global atmospheric budget of these noble metals. The 50-year average PGE concentrations in Antarctic snow were 17 fg g^{-1} (4.7–76 fg g^{-1}) for Pt, 0.12 fg g^{-1} (<0.05–0.34 fg g^{-1}) for Ir and 0.71 fg g^{-1} (0.12–8.8 fg g^{-1}) for Rh. The concentration peaks for Pt, Ir and Rh were observed at depths corresponding to volcanic eruption periods, indicating that PGEs can be used as a good tracer of volcanic activity in the past. A significant increase in concentrations and crustal enrichment factors for Pt and a slight enhancement in enrichment factors for Rh were observed after the 1980s. This suggests that there has been large-scale atmospheric pollution for Pt and probably Rh since the 1980s, which may be attributed to the increasing emissions of these metals from anthropogenic sources such as automobile catalysts and metal production processes.

Geochemistry and distribution of total heavy mineral concentrations of beach sediments of the Sakarya Delta (SW-Black Sea)

K. SÖZERI*, M. ERGIN, Z. KARAKAŞ AND B.D. ESER

Ankara University, Faculty of Engineering, Department of Geological Engineering/Affiliated with Geological Research Center for Fluvial, Lacustrine and Marine Studies (AGDEJAM), Tandoğan, Ankara, Turkey 06100 (*correspondence sozeri@eng.ankara.edu.tr, ergin@eng.ankara.edu.tr, karakas @eng.ankara.edu.tr, Basak.Eser.Dogdu@eng.ankara.edu.tr)

This study aims to investigate geochemistry and total heavy mineral distributions of marine beach sediments of the Sakarya Delta (SW-Black Sea, Turkey) where some higher metal contents were reported in sediments and related to possible occurrences of beach placers. With support of TÜBİTAK (Project No: 108Y333) and Ankara University-Sci. Res. Pro. Of. (Project 20070745007HPD), 48 surficial sediment samples were collected from the coastal beaches of Sakarya Delta representing modern shoreline and backshore sub-environments. In addition to geomorphological field observations, multielement and grain size analysis as well as total heavy mineral determinations are performed. Multielement geochemistry was carried out using ICP-MS method. Preliminary results showed that beach bulk sediments of the Sakarya Delta generally contained similar amounts of Ti, Pb, U, Mg and Sn compared with average rock composition of Earth's crust. The concentrations of As (6-24 ppm), Sb (0, 3-2, 1ppm), Ca (2-9 ppm), Cr (17-3999 ppm) were comparatively higher whereas Cu (6-27 ppm), Mo (0, 1-0, 7 ppm), Sn (0, 4-5, 2 ppm), Y (5-27 ppm), Nb (4-36 ppm) and Ta (0, 3-2, 5 ppm) contents are lower. Elements Cr, Fe, Mn, Co, Ni, Nb, Y and Ce reached their highest concentrations in sediments collected close to the Sakarya River mouth. The total heavy mineral concentrations of the bulk sediments are generally low, with except of 3 samples which contained highest total heavy mineral concentrations (70-95 %). The locations of these 3 samples were also aligned to or towards the river mouths.

https://doi.org/10.1180/S0026461X00006502 Published online by Cambridge University Press

Recycling elements from the slab to arc crust: Insights from element mass balance of the Izu arc system

CARL SPANDLER

School of Earth & Environ Sci, James Cook University, Townsville, Australia (Carl.Spandler@jcu.edu.au)

One of the most important processes leading to formation of continental crust is element transfer from subducting lithosphere to newly-formed arc crust. Despite extensive study of HP/UHP metamorphic rocks that represent paleo subducted slabs and experiments to replicate subduction zone conditions, little consensus has been reached on the nature of the mass transfer agents (e.g. aqueous fluid or hydrous melt), or the efficiency of the recycling process. Here, I use a mass balance of K and Ce in the Izu arc system as an alternative approach to resolving recycling processes in subduction zones. Potassium and Ce are enriched in arc lavas and are controlled by phengite and allanite/monazite in subducted crustal rocks. The extensive stability of these phases in the slab means K and Ce in slab fluids should be buffered to beyond sub-arc depths [1, 2].

The Izu arc was chosen for this study as the subducting Pacific slab is relatively cold and has been well characterised for chemical composition [3]. The ~50 Ma tectonic and magmatic history of the arc is well constrained, and the volume and composition of the arc crust can be accurately determined thanks to an excellent ash record, numerous seismic profiles of the arc and exposure of mid/lower arc crustal sections in the Tanzawa plutonic complex, Honshu.

Rates of arc crustal growth are calculated to be 130 - 200 km^3 km^{-1} strike length m. $y.^{-1}$. Comparing the composition of this crust (corrected for mantle input and subduction erosion) to subduction inputs reveals that 50 to 90% of the K and 10 to 15% of the Ce is recycled from the subducting plate back to the arc crust. Using experimentally-determined solubility relations [1, 2], these fluxes would require all of the available water in the sub-arc crust plus a 0.1 - 0.7 km column of slab serpentinite if the mass transfer agent is a hydrous slab melt. By contrast, excessive volumes of slab serpentinite (6 - 60 km thick column!) are required to provide the water needed if the transport agent is an aqueous fluid. These results confirm slab melts to be the dominant mass transfer agent in the Izu subduction zone and highlights the importance of subducted serpentinite as a water source for arc magmatism.

[1] Plank *et al*. (2009) *Nature Geoscience* **2**, 611–615.
[2] Hermann & Rubatto (2009) *Chem. Geol*. **265**, 512–526.
[3] Plank *et al*. (2007) *Geochem. Geophys. Geosys*. **8**, Q04I16.

How to safely store water samples prior to stable hydrogen and oxygen isotope analyses?

JORGE E. SPANGENBERG

Institute of Mineralogy and Geochemistry, University of Lausanne, CH-1050 Lausanne, Switzerland (Jorge.Spangenberg@unil.ch)

Safe storage of water samples between sampling and their stable hydrogen and oxygen isotope analyses (determination of δ^2H and $\delta^{18}O$ values) is still a topic of concern in hydrological studies. Water sorption and the diffusive transfer of water molecules through organic polymeric material may entail an isotopic fractionation [1]. A methodological study of variation of δ^2H and $\delta^{18}O$ values of waters stored in different type of bottles was performed.

A set of sixteen botlles of eleven different organic polymers (plastics), including low and high density polyethylene (LDPE and HDPE), polypropylene (PP), polycarbonate (PC, polyethylene terephthalate (PET), and high resistance Teflon® (PFA) from different size (10 to 500 mL) and wall thickness (0.20 to 1.50 mm) were completely filled (no headspace) with the same bottled water coming from a single natural spring (Evian® water, Evia-les-Bains, France) and were properly closed. Additionaly, 16 narrow neck bottles of amber glass were filled with the same water for comparison. All the water-filled bottles (n = 16 x 12 = 192) were stored at room temperature, and were opened one after the other over a period of time ranging from 0 to 659 days between 17 November 2008 and 7 September 2010. Immediately after the bottles have been opened, two 10 mL glass vials were filled, and stored at +4°C prior to analysis. The δ^2H and $\delta^{18}O$ values of all the water samples were determined using Cr-reduction in a Thermo Fisher Scientific H-Device and CO_2–equilibration in a Gas Bench II, respectively. Changes of up to +5‰ for δ^2H and +1.5‰ for $\delta^{18}O$ values were measured, depending on the type of plastic bottle. The carbon and hidrogen isotope compositions of the different plastic materials range from –33.3 to –27.5‰ and –108.1 to –71.7‰, respectively. The PET and PC plastics have $\delta^{18}O$ values ~22.5‰.

[1] Spangenberg & Vennemann (2008) *Rapid Commun. Mass Spectrom*. **22**, 672–676.

https://doi.org/10.1180/S0026461X00006502 Published online by Cambridge University Press

Particulate Organic Carbon deposition offshore Taiwan following typhoon Morakot

ROBERT SPARKES[1,2]*, NIELS HOVIUS[2], ALBERT GALY[2], VASANT KUMAR[1] AND JAMES LIU[3]

[1]Department of Materials Science and Metalluryy, University of Cambridge, UK (*correspondence: rbs26@cam.ac.uk)
[2]Department of Earth Sciences, University of Cambridge, UK
[3]Institute of Marine Geology and Chemistry, NSYSU, Taiwan

Woody debris and petrogenic carbon can be exported by hyperpycnal discharge from the fluvial and shallow-marine system, and stored on geological timescales in basins, but offshore storage of fresh Particulate Organic Carbon (POC) and the efficiency of burial of petrogenic carbon are poorly constrained. We present a case from Taiwan, where riverine fluxes are known [1].

Following Typhoon Morakot (2009, up to 3m rainfall), eight sediment cores totalling 191 cm were collected from turbidites in the Kaoping submarine canyon at depths up to 976 m, and from the neighbouring slope. Coarse, modern woody debris was present in 32% of core samples, exclusively within the sandy parts of turbidites. Total Organic Carbon concentrations were highest in slope deposits, averaging 0.59%, and in sandy canyon deposits. Canyon and floodplain samples had similar distributions of isotopic values, suggesting mixing of two endmembers. One is a combination of fresh woody debris and recycled coal-grade material from sedimentary rocks in the hinterland. The other is higher-grade carbonaceous material including graphite, likely from the central mountain belt. The river signal was fully preserved in the canyon. Slope deposits had a lighter ^{13}C signature indicating marine organic carbon input.

Raman spectroscopy suggests that high-grade graphite and low-grade material were sourced from Plio-Pleistocene deposits in the western foreland, whilst intermediate-grade graphitic material was sourced from the central mountain belt. High-grade graphite metamorphic conditions are not exposed in Taiwan: this material must have survived at least two cycles of erosion and deposition.

[1] West *et al*. (2011) *Limnology & Oceanography* **56**(1), 77–85.

Time-resolved metal(loid) reactivity at biogeochemical interfaces

DONALD L. SPARKS[1]*, MATTHEW GINDER-VOGEL[2] AND GAUTIER LANDROT[3]

[1]Delaware Environmental Institute, University of Delaware, Newark, DE 19716, USA (*correspondence: dlsparks@udel.edu)
[2]University of Delaware, and Calera Corporation, Los Gatos CA 95032 USA (mginder-vogel@calera.com)
[3]University of Delaware, and Lawrence Berkeley National Lab, Berkeley, CA 94720 USA (GJLandrot@lbl.gov)

The rates of important chemical processes at biogeochemical interfaces including ion exchange, sorption, and redox can occur over wide time scales. Ex- situ batch and flow techniques offer high elemental sensitivity, but their time resolution is not adequate to capture rapid reaction rates that often comprise a significant portion of many processes such as sorption and oxidation-reduction. Measurement of rapid, initial rates of environmentally important reactions at the mineral/water interface is critical in determining reaction mechanisms. Until recently, experimental techniques with sufficient time resolution and elemental sensitivity to measure initial rates were very limited. Some techniques such as pressure-jump methods can capture rapid reactions on millisecond time scales, but the rate parameters are indirectly measured and reaction mechanisms can only be inferred. Ideally, one would prefer to follow reaction rates in real-time, in situ, and at the molecular scale to definitively determine reaction mechanisms. In this presentation the use of *in situ* synchrotron-based, quick scanning X-ray absorption spectroscopy (Q-XAS), at sub-second time scales, is applied to measure the initial oxidation of As(III) and Cr(III) by hydrous manganese oxide [1], [2]. Results indicate that with these techniques, chemical kinetics are being measured. The rapid kinetic techniques are coupled with synchrotron-based XAS and XRD, and a stirred-flow technique, to provide a comprehensive assessment of As(III) and Cr(III) oxidation kinetics and mechanisms on hydrous manganese oxide over a range of temporal scales [3], [4].

[1] Ginder-Vogel, Landrot, Fischel & Sparks (2009) *PNAS* **106**(38), 16124–16128. [2] Landrot, Ginder-Vogel & Sparks (2010) *Environ. Sci. Technol.* **44**(1), 143–149. [3] Lafferty, Ginder-Vogel & Sparks (2010a) *Environ. Sci. Technol.* **44**, 8460–8466. [4] Lafferty, Ginder-Vogel, Zhu, Livi & Sparks (2010b) *Environ. Sci. Technol.* **44**, 8467–8472.

https://doi.org/10.1180/S0026461X00006502 Published online by Cambridge University Press

Rapid age determination of oysters using shell Mg/Ca ratios

BILL SPENCE[1], DAVID P. GILLIKIN[2], DAVID H. GOODWIN[3], DAMON BYRNE[2], PETER ROOPNARINE[4] AND LAURIE ANDERSON[5]

[1]CETAC Technologies, Manchester, UK (bspence@cetac.com)
[2]Union College, Dept of Geology, Schenectady, NY (gillikid@union.edu, byrned@garnet.union.edu)
[3]Denison University, Dept of Geosciences, Granville, OH (goodwind@denison.edu)
[4]California academy of Sciences, Invertebrate Zoology & Geology, San Francisco, CA (proopnarine@calacademy.org)
[5]Louisiana State University, Geology and Geophysics, Baton Roughe, LA (glande@lsu.edu)

Magnesium to calcium (Mg/Ca) ratios exhibit a strong temperature dependence in foraminifera and corals, but not in bivalve mollusks. Various studies have reported Mg/Ca-temperature relationships with R2 values ranging from 0.8 to 0.3, and significantly different relationships for bivalves growing at different salinities was reported. However, this poor temperature correlation does not render Mg/Ca data useless. A weak temperature dependence would allow time (seasons and years) to be determined along the growth axis of shells. This would provide information about age, growth rate and also allow other proxies to be aligned with time. Previous studies have shown that Mg/Ca ratios can indeed by used for this purpose in a gastropod and pen shell (Pinna); these studies hand drilled powders from the shells and analyzed them using wet chemistry, which is relatively time consuming. Line scans using laser ablation systems can cover several centimeters of shell in a few minutes. If line scans could be used to put calendar dates on shell material it would allow very rapid assessment of the aforementioned variables. We test this method on the resilifer of two oyster species (Crassostrea gigas and C. virginica) using a CETAC LSX-213 laser ablation system coupled to a PE Elan 6000 DRC ICP-MS. Shells of both species exhibit annual cyclicity in Mg/Ca ratios using spot and line scan laser sampling, which matches the seasonal cyclicity determined using stable oxygen isotopes. Elemental maps will be generated to determine the distribution of Mg over the resilifer. Our preliminary results suggest that line scans offer a rapid technique for determining age, growth rate and timing of shell growth in oyster reslifers.

Super-Si garnet breakdown kinetics and implications for craton evolution

D. SPENGLER*, Y. NISHIHARA AND K. FUJINO

Ehime University, Matsuyama 790-8577, Japan (*correspondence: spengler@geo.uni-potsdam.de, yunishi@sci.ehime-u.ac.jp, fujino@sci.ehime-u.ac.jp)

Decompression experiments have shown that super-Si garnet (Grt) decomposes to Grt + pyroxene (Pyx) with specific micro-structures [1, 2]. They support that natural analogues (found in mantle xenoliths, diamond inclusions, massif peridotites) record up to several hundreds of kilometre exhumation - all believed to apply to contrasting geological scenarios including mantle convection, kimberlite magmatism and plate tectonics [2-4].

Here we used glass powder with a 'pyrolite minus olivine' composition for polycrystalline dry super-Si Grt synthesis (18 GPa, 1600 °C, 2.3 h) and subsequent decompression (10 GPa, 1450 °C, 0-12 h). All recovered samples have a granular coronitic texture of new Grt+Pyx surrounding relic super-Si Grt cores. Quantified XRD spectra show transformed volumes are similar, ~40%. The mineral chemistry (EDS) of breakdown products differs from that of corresponding equilibrium minerals synthesised along with each decompression experiment. In contrast, most natural analogues are chemically equilibrated requiring that volume diffusion exceeded initial breakdown. Modelling of Si-Al interdiffusion in Grt suggests that grains below 10 μm in size or lamellae spacing are able to chemically equilibrate at temperature-time conditions corresponding to those of both kimberlite eruption and ultra-high pressure metamorphism at convergent plate margins. Larger sizes and spacings require upper mantle residence for equilibration.

Results show that super-Si Grt transformation during decompression occurred partially and within the first minutes, but barely continued during the experiments. By implication, natural analogues record a multi stage process: fast decomposition during decompression (corona formation) before volume diffusion (chemical equilibration and lamellae formation) during sub-continental lithospheric mantle (SCLM) residence before final exhumation to the Earth's surface by different geological processes. Given the affinity of super-Si Grt breakdown microstructure occurrence to Archaean areas at global scale, models for craton stabilisation demand the inclusion of processes suitable for: (1) cargo through the upper mantle, like mantle convection/plumes, and (2) SCLM growth in the Grt-peridotite stability field. Shallower stages would have erased the microstructural record.

https://doi.org/10.1180/S0026461X00006502 Published online by Cambridge University Press

Zircon from kimberlites of the Nyurbinskaya pipe as indicator of kimberlite emplacement and lithosphere evolution

Z.V. SPETSIUS[1], E.A. BELOUSOVA[2], W.L. GRIFFIN[2], S.Y. O'REILLY[2] AND A.S. IVANOV[1]

[1]Scientific Investigation Geology Enterprise, ALROSA Co Ltd, Mirny, Yakutia, 678170, Russia (spetsius@cnigri.alrosa-mir.ru)

[2]GEMOC ARC National Key Centre, Department of Earth and Planetary Sciences, Macquarie University, NSW, 2109, Australia (elena.belousova@mq.edu.aTu)

About 300 zircon grains have been recovered from the kimberlite concentrate of the Nyurbinskaya pipe with the aim of finding mantle zircons that would allow estimation of the age of kimberlite emplacement. We evaluated the kimberlitic or crustal origin of individual zircon grains using a two-step approach. The first step included the preparation of mounts, collecting cathodoluminescense images of the zircons, electron microprobe analysis of major elements and LAM-ICPMS analysis of trace elements. These data identified zircons with low content of U (<50ppm) and Y (1-150ppm) and low Nb/Ta (<3) ratio of probable mantle (kimberlitic) origin and zircons of crustal origin with increased Y and U content.

The second step involved U-Pb dating and Hf-isotope analysis. The largest population, consisting of crustally-derived zircons, defines a U-Pb age peak at ca 2700 Ma, probably representing the Archean age of the lower crust below the Nakynsky kimberlite. This main population shows a range of εHf (t) values of 3.2 to -14.6 and T_{DM} crustal model ages between 3.6 and 2.7 Ga, and suggests that at least 70% of the deep crust was formed from 3.2-2.8 Ga ago. The minor age population represented by the kimberlite zircons of the Nurbinskaya pipe gave a weighted mean $^{206}Pb/^{238}U$ age of 381±7 Ma, which is considered as the best estimate for the kimberlite emplacement. The zircons of this younger age population have a narrow range of εHf(t) values of -33.5 to -34.5 and T_{DM} crustal model age of 3.2 Ga.

Are aliphatic monomers of grasses and herbs useful biomarkers for vegetation shifts?

S. SPIELVOGEL[1,2] *, J. PRIETZEL[2], N. DECHAMPS[2], L. BECKER[3] AND G. GUGGENBERGER[3]

[1]Universität Koblenz-Landau (*correspondence: spielvogel@uni-landau.de)

[2]Technische Universität München

[3]Leibniz Universität Hannover

Each plant species has a unique aliphatic composition. The aliphatic monomer composition of differrent grasses and herbs was analyzed to investigate wheter the pattern can be traced back after decay and transformation into soil organic matter (SOM).

We analyzed the aliphatic monomer pattern (e.g. Alkanols, Alkanoic acids, Alkanes) of dominant grasses and herbs as well as of soil samples derived from four different regions where recently vegetation shifts took place or are assumed to have taken place (Bayerischer Wald and Limestone Alps, Germany; Bagé, Brazil; Qinghai, Tibet). Our aim was to develop a robust classification model for SOM source and vegetation history using these biomarkers. The data on the composition of the aliphatic monomers of the grasses and herbs were analyzed with three different classification models (linear, non-linear and binary), to find the best model to classify the different plant species. Based on the discriminant equations obtained, soil samples were classified and the performances of the three classification models were compared.

We yielded a series of monomers corresponding to previously reported hydrolysates [1, 2, 3], that discriminated significantly among the different grass and herb species. Hence, all tested classification models discriminated sufficently among the grass and herb species. Between 56% and 85% of the cases were classified correctly, depending on the respecitve site, the training set and the used model. However, the aliphatic pattern in soils is subjected to changes during decomposition of the plant material and the different biomarker monomers exhibited different turnover rates. Thus, only a multivariate binary classification model that did not rely on quantitative properties and compound ratios was sufficient to classify in average 67% of the soil samples correctly, depending on their decomposition status.

[1] Nierop *et al*. (2006) *Plant Soil* **286**, 269–285. [2] Feng & Simpson (2007) *Org. Geochem.* **38**, 1558–1570. [3] Otto & Simpson (2007) *J. Separat. Sci.* **30**, 272–282.

https://doi.org/10.1180/S0026461X00006502 Published online by Cambridge University Press

Rates of crystal nucleation and growth from inversion of natural crystal size distributions

VÁCLAV ŠPILLAR* AND DAVID DOLEJŠ

Institute of Petrology and Structural Geology, Charles University, 128 43 Praha 2, Czech Republic (*correspondence: vaclav.spillar@seznam.cz)

Magmatic textures provide sensitive record of physical processes and variables during magma solidification. Quantitative characterization of texture is thus a useful tool for interpreting the thermal regime and rates of crystal nucleation and growth. Here we show that different pairs of nucleation and growth rate functions can result in textures having identical crystal size distributions (CSD). In order to eliminate such ambiguity of CSDs, we use time variation in crystallinity as an additional constraint leading to unique nucleation and growth rates. While the nucleation rate strongly depends on the CSD slope, curvature and fluctuations, the character of growth rate curve is more related to changes in crystallinity. When crystallinity increases quasi-linearly with time, the growth rate diverges to very high values at the beginning and the end of crystallization, due to small area of solid-liquid interface. That is, the growth rate is slowest at moderate crystallinities, when the crystal surface area is largest. This transient behavior also facilitates approach to equilibrium. When we employ relevant thermal cooling model and bracket the total crystallization by liquidus and solidus temperatures, we can estimate the total crystallization time, and scale all rate functions into real units. Estimated rates of crystal growth are inversely proportional to magma chamber size, and increase non-linearly from its interior to the margin. Application to solidification time and CSDs of the Hawaiian lava lakes results in growth rates of about 10^{-11} cm s^{-1}, which is in good agreement with natural observations. The growth rates can be converted to crystallization time for any grain size of interest. In log-linear CSDs, the growth time of the most abundant grain size varies from ~1/10 of the characteristic cooling time for crystals in the pluton interior to ~1/400 for those near the contacts. Relative growth times thus depend on neither a CSD slope nor a magma body size. The changes in crystal size with time allow us to predict the distance of movement due to action of gravitational forces. The crystal travel distance increases quadratically with the magma chamber size, rendering the crystal settling to be most efficient in large reservoirs. For kilometer-sized bodies we predict that a crystal moves across half of a magma chamber even in viscous magmas, up to 10^9 Pa. s.

Stability and breakdown of $Ca^{13}CO_3$ melt combined with formation of ^{13}C -diamond in static experiments up to 80 GPa and 4000 K

A.V. SPIVAK[1]*, YU.A. LITVIN[1] AND L.S. DUBROVINSKY[2]

[1]Institute of Experimental Mineralogy RAS, 142432, Chernogolovka, str. Akademition Osip'yan 4 (*correspondence: spivak@iem.ac.ru)

[2]Bayerisches Geoinstitut, Universitat Bayreuth, Universitatsstraße 30, D-95447 Bayreuth

PT conditions of $Ca^{13}CO_3$ melting, stability of the melts, and their decomposition by the reaction $Ca^{13}CO_3$ = CaO + $^{13}CO_2$ (fluid) are investigated at static pressures of 8.5 – 80.0 GPa and temperatures of 1900 – 4000 K with the use of diamond anvil cell and laser heating. The occurrence of $^{13}CO_2$ is accompanied by formation of ^{13}C-diamond (above 11 GPa) and ^{13}C-graphite (below 11 GPa) that is indicative for the $^{13}CO_2$ breakdown to ^{13}C and O_2. Another 'solution-melt' mechanism of isotope-pure ^{13}C-diamond synthesis was realized in melts of the carbonate $Ca^{13}CO_3$ - ^{13}C-graphite (metastable phase) system in the multianvil press at pressures 8.5 and 20 GPa and temperatures up to 2500 K. It was first found in static high pressure experiment that melting of Ca carbonate is congruent over a wide 11.0 – 80.0 GPa pressure interval at temperatures up to 3400 K. It is also important that the phase region for the Ca carbonate melts is sufficiently wide extending from 2300 to 3500 - 3800 K at the 20.0 – 80.0 pressure range. Of particular interest is the first experimental evidence for diamond formation in the two-phase region CaO + CO_2 (fluid). The use of isotope-distinguished carbonate $Ca^{13}CO_3$ in the diamond anvil cell experiments gives an unambiguous evidence that ^{13}C-diamond has been formed from $Ca^{13}CO_3$ melt by a two-stage decomposition reaction: (1) $Ca^{13}CO_3$ (melt) = CaO + $^{13}CO_2$ (fluid) and (2) $^{13}CO_2$ (fluid) = ^{13}C (diamond) + O_2.

The results are applied to the construction of PT phase diagram for the $CaCO_3$ join (of the CaO – C – O_2 system) up to 80 GPa and 4000 K. The melting and decomposition relations of the $CaCO_3$ join as well as accompanying processes of diamond formation are applied and discussed in the context of the problem of natural 'super deep' diamonds origin in carbonate-rich growth media of the transition zone and lower mantle of the Earth.

Support: Grants of RF President MK-913.2011.5, RAS Presidium P 02, RFBR 10-05-00654 and 11-05-00401.

https://doi.org/10.1180/S0026461X00006502 Published online by Cambridge University Press

Aerosol mass spectrometer constraint on the global secondary organic aerosol budget

D.V. SPRACKLEN[1]*, J.L. JIMENEZ[2], K.S. CARSLAW[1], D.R. WORSNOP[3], M J. EVANS[1], G. W. MANN[1], Q. ZHANG[4], M.R. CANAGARATNA[3], J. ALLAN[5], H. COE[5], G. MCFIGGANS[5], A. RAP[1] AND P. FORSTER[1]

[1]School of Earth and Environment, University of Leeds, Leeds, LS2 9JT, UK (*correspondence: dominick@env.leeds.ac.uk)
[2]Department of Chemistry and Biochemistry, and CIRES, University of Colorado, Boulder, CO, USA
[3]Aerodyne Research, Billerica, MA, USA
[4]Department of Environmental Toxicology, University of California, Davis, CA, USA
[5]Centre for Atmospheric Science, School of Earth, Atmospheric and Environmental Sciences, University of Manchester, Manchester, UK

The budget of atmospheric secondary organic aerosol (SOA) is very uncertain, with recent estimates suggesting a global source of between 12 and 1820 Tg (SOA) a^{-1}. We used a dataset of aerosol mass spectrometer (AMS) observations and a global chemical transport model to produce top-down constraints on the SOA budget. We treated SOA formation from biogenic (monoterpenes and isoprene), lumped anthropogenic and lumped biomass burning volatile organic compounds (VOCs) and varied the SOA yield from each precursor source to produce the best overall match between model and observations. Organic aerosol observations from the IMPROVE network were used as an independent check of our optimised sources. The optimised model has a global SOA source of 140 ± 90 Tg (SOA) a^{-1} comprised of 13 ± 8 Tg (SOA) a^{-1} from biogenic, 100 ± 60 Tg (SOA) a^{-1} from anthropogenically controlled SOA, 23 ± 15 Tg (SOA) a^{-1} from conversion of primary organic aerosol (mostly from biomass burning) to SOA and an additional 3 ± 3 Tg (SOA) a^{-1} from biomass burning VOCs. We used a dataset of 14C observations from rural locations to estimate that 10% of our anthropogenically controlled SOA is of urban/industrial origin, with 90 Tg (SOA) a^{-1} (90%) most likely due to an anthropogenic pollution enhancement of SOA from biogenic VOCs.

Differentiation of impact-melt sheets: Evidence from Manicouagan with implications for the Moon

J.G. SPRAY*, C.D. O'CONNELL-COOPER AND L.M. THOMPSON

Planetary and Space Science Centre, University of New Brunswick, Fredericton, NB E3B 5A3, Canada (*correspondence: jgs@unb.ca)

Introduction

Recent exploration drilling of the late Triassic, ~80-90 km rim-diameter Manicouagan impact structure, Canada, has yielded ~18 km of core from 38 locations, three holes of which are >1.5 km deep [1]. This new data provides unprecedented insight into the internal structure and composition of a relatively large crater. Complemented by an ongoing 10-year (2006-2016) ground-based research project (the Manicouagan Impact Research Program: MIRP), the goal is to better understand impact crater tectonics and the formation and evolution of impact melt bodies. This is being achieved through training undergraduate, MSc and PhD students, in collaboration with PDFs and Research Scientists, as well as colleagues working internationally.

Impact melt characteristics – new revelations

The drilling program has revealed that the Manicouagan impact melt sheet is not of uniform thickness (previously considered ~300 m thick), but includes considerably thicker sections: up to ~1000 m of clast-poor impact melt, underlain by ~400 m of clast-rich impact melt [2]. These thicker sections of melt comprise a monzodioritic Lower Zone (~500 m), a quartz monzodioritic Middle Zone (~250 m) and a quartz monzonite Upper Zone (~275 m). This is only the second impact structure known to unequivocally exhibit differentation (previously, Sudbury was the sole exemplar). Geochemical investigation of the thicker melt sheet sections indicates that they formed via fractional crystallization [2].

Impact melt sheet-footwall relations

Drilling results, coupled with field work, have revealed that the interface between the impact-melt sheet and footwall is not flat, but exhibits more complex 'topography', which strongly implicates the presence of fault-controlled structure [3]. This new evidence allows the construction of hypothetical cross-sections, which provide insight into central peak and terrace collapse formation mechanisms for complex craters on Earth, the Moon, Mars and beyond.

[1] Spray *et al*. (2010) *Planet. Space Sci*. **58**, 538–551.
[2] O'Connell-Cooper & Spray (in press) *JGR Solid Earth*.
[3] Spray & Thompson (2008) *Met. Plan. Sci*. **43**, 2049–2057.

https://doi.org/10.1180/S0026461X00006502 Published online by Cambridge University Press

On modeling H^+ and U transport behavior in an acidic plume

N. SPYCHER[1]*, S. MUKHOPADHYAY[1], D. SASSEN[1], H. MURAKAMI[1], S. HUBBARD[1], J. DAVIS[1], AND M. DENHAM[2]

[1]Lawrence Berkeley National Lab., Berkeley, CA 94720, USA (*correspondence: nspycher@lbl.gov)
[2]Savannah River National Lab., Aiken, SC 29808, USA

A nearly 1 km long acidic plume has developed under the F-Area at the U.S. Department of Energy Savannah River Site, South Carolina, from the disposal of low-level acidic radioactive waste solutions into seepage basins overlying relatively permeable, mostly sandy sediments. The disposal operations lasted for about 35 years until 1990, when the seepage basins were solidified and capped. Since then, the groundwater pH in the plume has remained mostly in the 3–3.5 range despite the end of disposal operations and fast groundwater velocities, although U concentration adjacent to the basins has been decreasing exponentially.

Here, we report on exploratory geochemical and reactive transport modeling investigations conducted to assess the relative roles of surface protonation and mineral precipitation in slowing down the rebound of pH at this site, as well as U transport behavior downgradient of the disposal basins. The modeling work is integrated with investigations of 'reactive facies', which aim at identifying specific types of sediments with unique properties affecting reactive transport, then correlating these sediment types with lithologic facies and their associated geophysical signatures for estimation of reactive properties over plume scales.

One- and two-dimensional reactive transport simulations were conducted considering Al and Fe mineral dissolution and precipitation, as well as H^+ and U surface complexation models from the literature. Simulations indicate that H^+ sorption reactions on goethite and kaolinite (primary minerals at the site besides quartz) could buffer pH at the site for long periods of time. The precipitation of Al silicates, hydroxides, and/or hydroxy sulfates could also strongly impede pH rebound at the site. Although the pH is computed to rebound quite slowly, U concentrations could potentially decrease at comparatively much faster rates from dilution with clean recharge water. Simulations results are most sensitive to reactive surface areas, to relative rates of reaction versus acidic discharge, to relative rates of mineral precipitation and dissolution, and to the type of implemented sorption models and parameters. The model sensitivity to heterogeneous fields of permeability and reactive surface areas derived from the reactive facies investigations is also investigated.

Biomineralization and growth mechanism of morphologically controlled strontium carbonate

B. SREEDHAR[1]*, CH. SATYA VANI[1], D. KEERTHI DEVI[1] AND G. PARTHASARATHY[2]

[1]Indian Institute of Chemical Technology (CSIR), Hyderabad-500 607, India (*correspondence: sreedharb@iict.res.in)
[2]National Geophysical Research Institute (CSIR), Hyderabad-500606 (drg.parthasarathy@gmail.com)

Biomineralization is a growing discipline in modern earthscience and is attracting much attention as it helps us (i) to synthesis marine carbonates with required morphology, composition and structure and (ii) to understand and quantify the controlling factors which affects the microbial mineralization in deep marine environments.[1, 2] The biological systems are very effective at controlling crystal growth, especially polymers have been successfully developed to control crystallization of inorganic particles in aqueous solutions. In this work we report the synthesis of araganite type strontium carbonate super structures using Gum acacia and also discussed the growth mechanism of the carbonates.

Gum acacia is a branched polysaccharide containing carbohydrates, amino acids, gulcuronic acid and a glycoprotein complex. The functional groups (-OH) present in arabinose and rhamnose and (-COOH) of glucuronic acids play a crucial role in the growth and formation of metal carbonates whereas the proteinaceous core with amino acids (-NH_2) stabilize the formed metal carbonates and play a key role in mimicking the biomineralization process. The crystallization involves the formation of different hierarchical structures like rice grain, doughnut shaped, flower shaped, hexagonal rods and cross shaped which have never been seen before in natural biominerals. Proteins and polysaccharides with complicated patterns of various functional groups in GA selectively adsorb on to the metal ion thereby hindering the crystal growth, followed by the mesoscale self-assembly of nanometer-scale building block into hierarchical superstructures. The key reaction of CO_2 with Sr^{2+} ions entrapped within GA polymer leads to the growth of beautiful structures of strontianite. Structural characterization of the synthesized materials was investigated by XRD, SEM, EDAX, TEM, TGA-MS and FT-IR.

[1] Porter SM. (2007) *Science* **316**, 1302. [2] Sanchez-Roman. M. *et al*. (2011) *Chemical Geology* **281**, 143.

https://doi.org/10.1180/S0026461X00006502 Published online by Cambridge University Press

Fe and S isotope compositions of hydrothermal sulfides from the Northern Lau Basin

B. Sreenivas[1]*, D. Ray[2], A.L. Paropkari[2], A. Mazumdar[2], B. Vijaya Gopal[1], L. Surya Prakash[2], G. Balu[1] and Y.J. Bhaskar Rao[1]

[1]National Geophysical Research Insitute (CSIR), Hyderabad 500007, India (*correspondence: bsreenivas@ngri.res.in)
[2]National Institute of Oceanography (CSIR), Dona Paula, Goa 403004, India

Massive sulfides belonging to the extinct hydrothermal field of the North Lau Basin were studied for their Fe and S isotope compositions. Sulfide samples belonging to pedestal slab, peripheral chimneys (remnants of white smokers) and oxide precipitates filling the hollows of pillowed basalts were studied. Detailed mineralogical and geochemical studies on the same set of samples indicated the similarites between the Lau hydrothermal field and the Trans-Atlantic Geotraverse (TAG) active mound [1]. The sulfides of pedetal slab mainly consisting chalcopyrites and pyrites with minor barite and sphalerite show $\delta^{34}S$ values between 8.4 to 9.6 ‰ (V-CDT). The major constituent of sulfides belonging to peripheral chimney is sphalerite, whlie pyrite and chlcopyrite being minor. The $\delta^{34}S$ values range from 5.5 to 8.3 ‰. These $\delta^{34}S$ values are very similar to those of TAG hydrothermal sulfides [2]. Such high $\delta^{34}S$ values for TAG hydrothermal sulfides were interpreted as a result of mixing of sulfur of sulfate reduction origin and that of the hydrothermal fluids. The high $\delta^{34}S$ values in case of Lau Basin also corroborate the influence of sulfate reduction. The sphalerite-rich sulfides of the peripheral chimney have slightly depleted $\delta^{34}S$ values when compared to the pedestal slab indicating increased effect of hydrothermal solutions in them.

The $\delta^{56}Fe$ values of samples belonging to pedesatl slab show a range between -0.3 to -1.1 ‰ (IRMM-014), while those of the peripheral chimney vary from -0.6 to -1.7 ‰. The oxide precipitates show maximum fractionation in Fe isotope compositions having $\delta^{56}Fe$ values of -0.8 and -3.0 ‰. Among the oxide precipitates, the MnO-rich top layer is characterized by lowest $\delta^{56}Fe$ value indicating the influence of temperatures. Further, role of redox conditions can be envisaged in controlling Fe isotope compositions based on the correlation between $\delta^{56}Fe$ and Ce anomalies.

[1] Paropkari, A.L. *et al*. (2010) *J. Asian Earth Sci*. **38**, 121–130. [2] Gemmell, J.B. & Sharpe, R. (1998) in Herzig *et al*. (eds) *Proc. ODP Sci. Results* **158**, pp. 71–84.

Assessment of heavy metal contamination in surface water of Ranipet industrial area, Tamil Nadu, India

S. Srinivasa Gowd and M. Ramakrishna Reddy

Dept. of Geology & Geoinformatics and Earth Sciences, Yogi Vemana University, Kadapa-516003, A.P., India (ssgowd@hotmail.com)

Environmental geochemical studies were carried out in and around Ranipet industrial area, Tamil Nadu, India to find out the extent of chemical pollution in surface and groundwater due to waste disposal from tannery industries. Ranipet is located at 79°19′ – 79°22′ E longitude and 12°53′ – 12°57′ N latitude, about 120 km from Chennai on Chennai-Bangalore highway and it is chronic polluted area and one of the biggest exporting centers of tanned leather. It is one of the biggest exporting centers of tanned leather in India. The total number of industries located in and around Ranipet town are 240 tanneries along with ceramic, refractory, boiler auxiliaries plant, and chromium chemicals.

Studies were carried out to find out the contamination of surface water bodies due to industrial effluents. The results reveal that the surface water in the area is highly contaminated showing very high concentrations of some of the heavy / toxic metals like Cadmium ranging from 0.2 to 401.4 μg/L (average of 51.1 μg/L), Chromium 2.4 1308.6 (average of 247.2 μg/L), Copper 2.1–535.5 μg/L (average of 95.5 μg/L), Nickel 1.6–147.0 μg/L (average of 36.7 μg/L), Lead 6.4–2034.4 μg/L (average of 467.8 μg/L) and Zinc 20.8–12718.0 μg/L (average of 3760.4 μg/L). The concentration levels of these metals are much above the permissible limits in surface water and are health hazards especially for the people working in the tannery industries. It was observed that the people in the area are seriously affected and suffering from occupational diseases such as asthma, chromium ulcers and skin diseases. Distribution of metals, their contents at different locations, and their effects on human health are discussed in this paper.

https://doi.org/10.1180/S0026461X00006502 Published online by Cambridge University Press

Mineral growth and dissolution from rare event methods

ANDREW G. STACK

Oak Ridge National Laboratory. (stackag@ornl.gov)

Computational theory and hardware have advanced sufficiently to allow in-depth examination of free energy landscapes for complex, geologically important reactions. Here, we used two rare event theories, metadynamics and reactive flux, to probe the attachment and detachment of barium ions to the [120]-oriented monomolecular step on barite and compare these reaction rates and mechanisms to those measured experimentally. This reaction was chosen because attachment and detachment of barium ions to these step-edges is thought to be rate limiting and barite scale has been found to inhibit production of oil and geothermal energy in some cases.

Using metadynamics, we found that detachment and attachment of ions does not occur directly to and from solution, but several intermediate states are observed. Starting from a barium kink site making five bonds to three surface sulfates, detachment first proceeds to a bidentate state containing two bonds to two surface sulfates, followed by an inner-sphere adsorbed species (making one bond), then an outer-sphere adsorbed species before completely dissolving.

Reactive flux calculations of the transitions between each of these states revealed that moving from the inner-sphere adsorbed species to outer-sphere adsorbed is limiting the rate of detachment. For attachment, the transition from inner-sphere adsorbed to the bidentate species is rate limiting. Arrehenius activation energies of each of these rate limiting steps were calculated by performing the reactive flux calculations at multiple temperatures. The activation energies and rate constants, compare favorably to those measured experimentally by atomic force microscopy in the case of dissolution.

The implications this study are two-fold. Firstly, the observation of multiple intermediates states implies that mineral growth and dissolution reactions can lead to pools of labile or recalcitrant material in variou states of adsorption onto mineral surfaces. This addresses the longstanding issue of non-steady state dissolution rates. Secondly, the ability to quantitatively probe complex reaction mechanisms on surfaces accurately will be a powerful technique in addressing mineral reactivity and mechanisms.

This research was sponsored by the Division of Chemical Sciences, Geosciences, and Biosciences, Office of Basic Energy Sciences, U.S. Department of Energy.

A multi-isotope study for identifying groundwater movement near disturbed salt domes: Case study Stassfurt, Germany

S. STADLER[1], H. HOLLAENDER[2], J. SUELTENFUSS[3], C. JAHNKE[4] AND A. BOHN[4]

[1]Federal Institute for Geosciences and Natural Resources (BGR), Hanover, Germany
[2]State Authority of Mining, Energy and Geology (LBEG), Hanover, Germany
[3]University of Bremen, Germany
[4]Brandenburg University of Technology (BTU) Cottbus, Germany

An area of the German part of the Southern Permian basin affected by anthropogenically induced subrosion was investigated for its potential for ongoing salt dissolution induced by groundwater movement. A set of environmental tracers supported by hydrochemical analyses was applied to establish aquifer fingerprints of the covering layers (Quaternary and Triassic) and of flooded parts of the mining area (Zechstein), and revealed prevailing mixing components: A modern groundwater component was identified by the presence of ^{3}H and $^{3}He_{tri}$ which indicates young apparent groundwater ages (0 - 50 a) in the covering layers. Using this, percentages of modern water could be derived for each sample. The presence or absence of ^{14}C in the samples represents an age classification between the modern groundwater component (<50 a) given above, and an old groundwater component (apparent groundwater ages <50 000 a). The trends derived from radiocarbon could generally be validated by low $^{4}He_{rad}$ contents in samples from the modern groundwater component and elevated $^{4}He_{rad}$ contents in the old groundwater. Contact between meteoric water and Zechstein salts could be identified by the presence or absence of Permian crystallization water from the dissolution of e.g. Carnallite and/or Kieserite in the samples. We developed a conceptual model of groundwater flow and interactions between groundwater of the different aquifers in the studied area and discuss potential implications for ground subsidence.

https://doi.org/10.1180/S0026461X00006502 Published online by Cambridge University Press

High-pressure calibration of the oxygen fugacity recorded by garnet bearing peridotites

VINCENZO STAGNO, CATHERINE A. MCCAMMON AND DANIEL J. FROST

Bayerisches Geoinstitut, Universität Bayreuth, D-95440, Germany (vincenzo.stagno@uni-bayreuth.de)

The oxygen fugacity within the Earth's upper mantle below ~50 km depth can be measured by performing oxy-thermobarometry determinations on garnet bearing mantle xenoliths. The commonly used equilibrium includes the $Fe_3Fe_2Si_3O_{12}$ garnet component. A knowledge of the mantle oxidation state is important in order to understand the speciation of heterovalent elements and C-O-H-bearing volatile-rich phases.

To date, measurements have shown that the upper mantle (>250 km depth) is typically characterized by a heterogeneous fO_2 between -1 to -5 log units relative to the FMQ oxygen buffer. This range mainly arises from the pressure dependence of the employed oxybarometer, which drives the fO_2 to lower values with increasing pressure.

The aim of this study was to investigate the iron oxidation state of garnet equilibrated with carbonate and graphite/diamond in a typical peridotite mantle assemblage in order to test the current oxythermobarometer at high pressure. Experiments were performed using a layer of garnet sandwiched between oxygen buffering carbon/carbonate bearing assemblages, which fixed the oxygen fugacity at known values at pressures between 3 and 7 GPa and temperature of 1100-1600 °C. Several configurations were tested either in the presence of natural Cr-bearing garnets or hydrous conditions and empolyong both relatively reduced and oxidized starting materials. fO_2 was measured using a sliding redox sensor assemblage empolying Fe-Ir alloy. Using these measurements a re-evaluation of the oxy-thermobarometer calibration was performed. Redox profiles for cratonic mantle were reexamined with implications for carbon speciation in the mantle.

Assessment of carbon needs to renew soil fertility

FOTINI E. STAMATI[1]*, NIKOLAOS P. NIKOLAIDIS[1] AND JERALD P. SCHNOOR[2]

[1]Department of Environmental Engineering, Technical University of Crete (TUC), University Campus, 73100, Chania, Greece (*correspondence: fotini.stamati@enveng.tuc.gr)

[2]Department of Civil and Environmental Engineering, 4105 Seamans Center, The University of Iowa, Iowa City, Iowa 52242

Conversion of natural to agricultural ecosystems induces SOM losses due to changes in land management practices and reductions in litter input. The average rate of soil organic carbon (SOC) stock decline after the conversion of a native land to cropland decreases in time [1] and depends on the previous landuse type (forest, grassland, shrubland), and the decomposition regime (determined by climatic conditions, size of the carbon litter input, texture and other factors). SOC can be depleted by 50% in about 5 years in the tropics and 50 years in temperate ecoregions. On the basis of soil resilience and sustainability of agriculture, the adoption of appropriate agricultural practices for the maintenance of carbon in croplands is a win-win situation because they will prevent erosion and contribute to inherent soil and product quality, biodiversity, fertility, water quality, and agricultural economy [2]. Monitoring field data and modeling exercises are essential for the assessment of the turnover of different carbon pools in order to optimize organic input strategies for carbon sequestration in stable forms so as maintain soil structure and fertility [3]. In this work, grassland to cropland and forest to cropland conversions under different climatic regimes were modeled with ROTH-C. Chronosequence literature data for dryland steppes [4], temperate grasslands [5], mediterranean shrublands [6] and forests in the tropics [7] were used for the modeling. The methodological approach for model caibration and estimation of uncertainty presented by Stamati *et al.* (2011) [4] was followed. Appropriate carbon addition under different climatic regimes and soil textures are suggested for sustainable agricultural practices (carbon sequestration, HUM increase).

[1] Mann (1986) *Soil Sci.* **142**, 279–288. [2] Lal (2004) *Science* **304**, 1623–1627. [3] Nikolaidis (2011) *Applied Geochem.* (In Press) [4] Li *et al.* (2009) *Land Degrad. Develop.* **20**, 176–186. [5] Olson *et al.* (2005) *Soil Till. Res.* **81**, 217–225. [6] Evrendilek *et al.* (2004) *J. Arid Environ.* **59**, 743–752. [7] Ashagrie *et al.* (2007) *Soil Till. Res.* **94**, 101–108. [8] Stamati *et al.* (2011) *J. Environ. Qual.* (In review)

https://doi.org/10.1180/S0026461X00006502 Published online by Cambridge University Press

Experimental determination of the hydrous basalt liquidus

C.C. STAMPER[1]*, J.D. BLUNDY[1], E. MELEKHOVA[1] AND R.J. ARCULUS[2]

[1]Department of Earth Sciences, University of Bristol, Bristol, BS8 1RJ, UK. (*correspondence: c.stamper@bristol.ac.uk)

[2]Research School of Earth Sciences, The Australian National University, Canberra, Australia

A series of experimental liquidus determinations have been carried out on a hydrous primitive basalt at a range of lower crustal pressures. The starting composition replicates the major element chemistry of an olivine picrite from South East Mountain, Grenada, Lesser Antilles with 15.3 wt % MgO and Mg# = 73. The island is known for erupting primary mantle melts, and products of the arc volcanism from Grenada yield evidence for magmatic water contents of ≤ 6.4 wt % H_2O [1].

The ulimate aim of this experimental series is to map out the topology of the hydrous basalt liquidus. The position of the liquids relative to a mantle adiabat determines the amount of superheating experienced by a magma as it ascends to lower pressures. This in turn has implications for the manner in which mantle-derived melts interact with the crust.

Equilibrium experiments are being conducted using both piston cylinder and TZM apparatus at pressures ≤ 1.7 GPa and water contents of 2.5 and 5.0 wt % at fO_2 = NNO. Experiments on the most hydrous starting composition are ongoing and have bracketed the liquidus between temperatures of 1265-1280°C at 1.3 GPa and 1250-1280°C at 1.7 GPa.

These experiments are also being used to explore phase relations at high temperatures and investigate the potential for multiple saturation points. At 1.7 and 1.3 GPa the liquids phases are olivine, clinopyroxene and Cr-rich spinel.

A further objective of this project is to extend the P-T range of experiments in an attempt to recreate the assemblages found in cumulate xenoliths from Grenada.

[1] Bouvier, Métrich & Deloule (2010) *Geochem. Geophys. Geosyst.* **11**, Q09004.

Effects of diagenesis in Triassic limestone of Opolskie Voivodesip

K. STANIENDA

Institute of Applied Geology, Silesian University of Technology, 44-100 Gliwice, Poland (Katarzyna.Stanienda@polsl.pl)

Introduction

During Middle Triassic time (Muschelkalk) the SW part of Poland was situated in the SE part of the Germanic Epicontinental Sea. Full profile of Lower Muschelkalk was found in the SW part of Poland (area of Silesia- Opolskie Voivodesip). Formation contains strata of Gogolin Beds, Górażdże Beds, Terebratula Beds and Karchowice Beds [1, 2]. The effects of destructive and constructive diagenesis were observed in Triassic limestone of Opolskie Voivodesip.

Discussion of Results

The effects of destructive diagenesis are longitudinal channels created by sea organisms and micritic coats in marginal areas of allochemes and peloides. Effects of eogenetic stage of constructive diagenesis are: first generation cement (micritic, orthosparitic and palisade), Mg- calcite, early diagenetic dolomite and clay minerals. During mesogenetic stage pseudosparitic, mosaic cement (second generation cement) was formed. It fills in the space in the rock between allochemes and builds together with the micritic cement the rock mass of limestone poor in allochemes. Neomorphic processes like transformation of aragonite into low magnesian calcite, recrystallization of calcite crystals which build the trochites of Crinoideas, recrystallization and agradation of crystals which build the cement and dissolution which caused the formation of stylolites fill in with the iron compounds, were also going during the mesogenetic stage. Telogenetic stage characterized by karst processes, dedolomitization and silification. Effects of karst processes are karst funnels and karst formations present in some areas of strata. During dedolomitization dolomite pseudomorphs were formed. During silification processes small pores in rocks were filled in with quarz or chalcedony and silica concretions, which create special levels in some limestone strata, were formed.

Project was financed from capital of National Center of Science.

[1] Bodzioch A. (1990) International workshop field seminar the Muschelkalk- sedimentary environment, facies & diagenesis, 9–11. [2] Szulc J. (2000) *Annales Societatis Geologorum Poloniae* **70**, 1–48.

https://doi.org/10.1180/S0026461X00006502 Published online by Cambridge University Press

Collection and measurements of reservoir fluids properties – 'Today and tomorrow'

ARTUR STANKIEWICZ[1], MICHAEL O'KEEFE[2], FARSHID MOSTOWFI[3], JOHN RATULOWSKI[3], MALCOLM ATKINSON[4] AND SACHIN SCHARMA[5]

[1]Schlumberger, Clamart, France (astankiewicz@slb.com)
[2]Schlumberger Wireline, London, UK (mokeefe@slb.com)
[3]Schlumberger, DBR, Edmonton (fmostowfi@slb.com)
[4]Schlumberger, Aberdeen, UK (matkins@slb.com)
[5]Schlumberger, Geoservices, France (ssharma@slb.com)

Representative analyses of properties of hydrocarbon and non-hydrocarbon fluids in the petroleum industry strictly depend on the quality of the sub- or surface sampling. The exploration & appraisal activities in challenging pressure and temperature environments, as well as difficult fluids such as heavy oils, very high levels of H_2S or CO_2 require a completely new approach. Development and implementation of new technologies is a must, not a luxury.

Experience shows that the majority of non-representative data coming from laboratories are directly due to poor sampling practices and/or inadequate technologies employed. Recent improvements in sampling tools, include innovative approaches to prevent scavenging of H_2S, or absorption of mercury species, utilizing exotic metarials such as Inconel 725, and inert coatings such as Dursan. The increased working range of sampling/analytical equipment is reaching pressures of 1700 bar (25 kpsi) and temperatures of 200°C.

Recent years have also witnessed increased focus on *in situ* measurements at downhole conditions, or as close to the wellsite as possible. Evolution of optical absorption spectroscopic tools such as LFA (Live Fluid Analyzer) led to developemnts of 'downhole laboratories' employing Grating Spectrometer technology, such as IFA (InSitu Fluid Analyzer) providing critical data on fluid properties (C_1, C_2, C_{3-5}, C_{6+}, CO_2, Gas-Oil Ratio, density, viscosity) in real time. The live water pH is now possible, both in the reservoir as well as in the laboratory. Breakthroughs in the mud gas logging are included an unprecedented leap from qualitative/comodity tools to quantiative fluid facies evalaution while drilling in C_{1-6} range, including application of GC/MS and laser MS technologies for the methane stable isotope measurements.

The need for *in situ* measurements requires miniaturization and operational robustness. This article will discuss the latest advances in sampling and measurements along the fluid value chain – from the reservoir to laboratory.

Cadomian igneous rocks from Europe's Variscan belt, Lazovo complex

J. STATELOVA[1]*, A.V. QUADT[2], P. MACHEV[3] AND S. GEORGIEV[4]

[1]GI-BAS, Bulgaria (*correspondence: js@geology.bas.bg)
[2]IGMR, ETH-Zurich, Switzerland (vonquadt@erdw.ethz.ch)
[3]Sofia University, Bulgaria (machev@gea.uni-sofia.bg)
[4]Geological survey of Norway (georgiev@colostate.edu)

The geochemical and the age information contained in the Cadomian/Pan-African orogeny elements in Europe helps to identify portions of the Neoproterozoic-Cambrian plate boundaries [1]. In the Balkanides several types of such elements are known: some of the protolithes of Srednogorie high-grade metamorphic series - intermediate and acid igneous rocks ~590-620 Ma old [2]; Cherni Vrah ophiolite complex - ~560 Ma [3]; and 550 to 1100 Ma old inherited zircon cores detected in all high-grade metamorphic rocks.

We studied one of the easternmost exposures of the Variscan belt in the Balkanides in Tvarditsa mountain. The metamorphites of Lazovo complex cover wide areas of its southern slopes and host the pre-Triassic Tvarditsa pluton [4]. GPA geothermobarometry shows that amphibolite facies conditions were reached [5] in Variscan times [6].

The metamorphites in the eastern parts of Lazovo complex formed over intermediate to basic igneous protholites containing lense- and layer-shaped bodies of pyroxenites. They had different pre-Varsican metamorphic history compared to the garnet-bearing and the two-mica gneisses in the western parts of the complex [5]. The eastern part gneisses studied form thick layers of distictive composition, not related to metamorphic differentiation. They preserve field and geochemical evidence of their magmatic origin. Their trace-element composition suggests subduction-oriented source.

The zircons from the gneisses sudied and from the metapyroxenites have slightly elongated to rounded shapes. They display growth and sector zoning corresponding to igneous conditions of crystallisation. The U-Pb ages of the zircons obtained by LA-ICP-MS cluster at around 600 Ma.

Our data constrain for the first time the protholith age of Lazovo complex metamorphites and allow better correlation with the Neoproterozoic terrains in Eastern Europe.

[1] Murphy (2006) *Prec. Res.* **147**, 305–319. [2] Carrigan *et al.* (2006). [3] von Quadt *et al.* (1998) *C. R. ABS.* **51**(1–2), 81–84. [4] Ivanov *et al.* (1974) *Rev. BGS* **48**(2), 1–24 [5] Statelova, Machev (2006) *Proc. CBGA* **18**, 598–691. [6] Statelova (2006) BGS Conf. 189–192.

https://doi.org/10.1180/S0026461X00006502 Published online by Cambridge University Press

Tracing magma chambers in the lab: A case study on Lascar volcano

A. STECHERN[1]*, M. BANASZAK[2], R.E. BOTCHARNIKOV[1], F. HOLTZ[1] AND G. WÖRNER[2]

[1]Institute for Mineralogy, Leibniz University of Hannover, Germany (*correspondence: a.stechern@mineralogie.uni-hannover.de)
[2]Geowissenschaftliches Centrum Göttingen, Abt. Geochemie, Göttingen, Germany

Lascar volcano is a calc-alkaline stratovolcano located in the Central Volcanic Zone (CVZ), Northern Chile and represents the most active volcano in this area. The activity of Lascar is characterized by extensive lava flows, domes, and pyroclastic deposits such as the most recent eruption in 1993. Present activity is restricted by vigorous degassing from the open vents. The composition of erupted rocks of Lascar range from poorly porphyritic mafic andesites to dacites.

In this study we combine geochemical analyses with high P-T experiments to investigate possible depth of storage from the pre-eruptive conditions of crystallization on the one hand, as well as the role of magma-mixing and differentiation during magma ascent on the other.

Well-established geo-thermo- and barometers were used to characterize the crystallization conditions of the recent 1993 eruption. Results give evidence for a large temperature interval of crystallization from ~ 850 to 1050°C and pressures between 400 to 500 MPa. Oxygen fugacity was in the range of 1.0 to 2.0 log units above the Ni/NiO oxygen buffer. The analyses of melt inclusions are dacitic to rhyolitic in compositions with rather small concentrations of chlorine, fluorine and sulfur, indicating that the evolved magma was largely degassed.

The major element compositions of Lascar lavas indicate significant changes in the magmatic processes with the alternation of mixing- and fractionation-dominated stages. The compositional variation of deeper magmas (~ 1.3 ± 0.3 GPa) can be reconciled with magma mixing models. The compositional variations of most lavas erupted in 1993 and of a few older samples correspond to crystal fractionation trends, which have been reproduced experimentally at 300 to 500 MPa. Experimental data, geochemical trends and thermo-barometric data indicate that the pre-eruptive depth of the youngest magmas (< 7.1 ka) is rather shallow (~ 500 ± 200 MPa). A possible interpretation of these results is that magma storage in upper crustal levels is mostly dominated by fractional-crystallization whereas deeper magma chambers show clear evidence for magma-mixing processes.

Upscaling pore scale carbonate precipitation rates to the continuum scale

C.I. STEEFEL[1]*, C. NOIRIEL[2], L. YANG[1] AND J. AJO-FRANKLIN[1]

[1]Lawrence Berkeley National Laboratory, One Cyclotron Road, Berkeley, CA 94720, USA (*correspondence: CISteefel@lbl.gov)
[2]Université de Lille, France (catherine.noiriel@univ-lille1.fr)

An integrated approach combining experimental reactive flow columns and continuum-scale reactive transport modeling has been used to compare microscopic and bulk (upscaled) rates of carbonate mineral precipitation. The experiments consisted of the injection of supersaturated, carbonate-rich solutions into calcite packs. Bulk rates of precipitation based on the change in chemistry over the length of the column were compared with spatially resolved determinations of carbonate precipitation using X-ray synchrotron imaging at the micron scale. These data are supplemented by well-stirred reactor experiments to evaluate the rate of precipitation as a function of solution supersaturation in the absence of transport effects. Results indicate good agreement between rates determined with fluid chemistry and with microtomography. The distribution of calcite precipitates shows a nonlinear spatial profile, with the greatest accumulation near the column inlet. Precipitation is greatest on Iceland spar seeds, with crystal morphology of the new precipitates suggesting growth via a 2D heterogeneous nucleation mechanism.

Using the rates of precipitation as a function of supersaturation determined in the well-stirred flowthrough reactors, it is possible to match the spatially-resolved microtomographic data with a continuum reactive transport model *if the generation of new reactive surface area is accounted for*. The experimentally-determined value of 0.90 m^2/g for the specific surface area of the neoformed calcite, added to the initial calcite surface area of 0.012 m^2/g, results in good agreement with the continuum model. The approach used here also demonstrates that it is possible to determine upscaled reactive surface area in porous media if the intrinsic rate (per unit surface area mineral) is known.

https://doi.org/10.1180/S0026461X00006502 Published online by Cambridge University Press

Nickel isotope anomalies: Neutron-rich or neutron-poor?

R.C.J. STEELE[1*,2], T. ELLIOTT[1], C.D. COATH[1] AND M. REGELOUS[1,3]

[1]Bristol Isotope Group, Dept Earth Sciences, University of Bristol. Bristol, UK (*correspondence: r.steele@bristol.ac.uk)
[2]Natural History Museum, Cromwell Road, London UK
[3]GeoZentrum Nordbayern, Universität Erlangen-Nürnberg, Erlangen, Germany

The solar system is a mixture of many different nucleosynthetic sources. Numerous studies have investigated the nucleosynthetic origins of the solar system by examining isotopic anomalies in meteorites [e.g. 1]. Isotopic anomalies in the most neutron-rich isotopes of Ca, Ti, Cr in primitive meteorites have been interpreted as incomplete-mixing of a highly neutron enriched nucleosynthetic source into the early solar system [2-4]. This source has been variously hypothesised to be a type Ia supernova [5], type II supernova [6] or an AGB star [7]. However, nearly all of the reported measurements of these anomalies have employed normalisation to a pair of lighter-isotopes, assumed not to be anomalous. Hence, in these cases the inference of a neutron-rich anomaly is a point of interpretation since the anomaly could equally well reside on one of the normalising isotopes.

More recently, Ni has been added to the list of elements exhibiting apparent anomalies in its most neutron-rich isotopes, ^{62}Ni and ^{64}Ni [8, 9, 10]. We have made further measurements of Ni isotopes in bulk meteorites, both mass-independently (internally-normalised) and mass-dependently (double-spike), to yield absolute Ni isotope ratios that will better constrain the nucleosynthetic environment from which this incompletely mixed component arose. Preliminary results suggest that, in fact, the anomalies reside on ^{58}Ni and not on ^{62}Ni or ^{64}Ni. If these findings of neutron-poor anomalies are confirmed, they have far-reaching implications for the nucleosynthetic sources of the Ni isotopic anomalies and the identification of the nucleosynthetic sources of the solar system in general.

[1] Reynolds *et. al.* (1964) *JGR,* **69** 3263–3281. [2] Lee *et. al.* (1978) *ApJL,* **220** L21-L25. [3] Heydegger *et. al.* (1979) *Nature*, **278** 704–707. [4] Birck *et. al.* (1984) *GRL*, **11** 943–946. [5] Meyer *et. al.* (1996) *ApJ*, **462** 825–839. [6] Hartmann *et. al.* (1985) *ApJ*, **297** 837–845. [7] Lugaro *et. al.* (2004) *MEMSAI,* **75** 723–728. [8] Birck *et. al.* (1988) *EPSL,* **90** 131–134. [9] Regelous *et. al.* (2008) *EPSL*, **272** 330–338. [10] Steele *et. al.* (2010) *LPSC,* **41** 1984.

Silica speciation in aqueous sodium silicate solutions

M. STEELE-MACINNIS[1], C. SCHMIDT[2] AND R.J. BODNAR[1]

[1]Department of Geosciences, Virginia Tech, Blacksburg VA 24061 USA (mjmaci@vt.edu, rjb@vt.edu)
[2]Deutsches GeoForschungsZentrum GFZ, Telegrafenberg, 14473 Potsdam, Germany (hokie@gfz-potsdam.de)

Aqueous alkali silicate fluids can significantly contribute to the mobility of high field-strength elements in the lower crust and upper mantle [1]. The speciation of silica in these fluids is important for understanding the transport of such elements as alkali-silica complexes. Speciation of aqueous fluids and melts in the Na_2O-SiO_2-H_2O system has been previously studied *in situ* for one composition on the H_2O-NS4 join [2]; here, we investigate silica speciation of fluids over a range of compositions in the Na_2O-SiO_2-H_2O system.

The speciation of dissolved silica in aqueous sodium silicate solutions has been studied *in situ* up to 600°C and 2 GPa using Raman spectroscopy and a Bassett-type hydrothermal diamond-anvil cell [3]. Starting materials were either aqueous NaOH solution plus quartz, or water plus sodium silicate glass (NS2 and NS3), yielding bulk compositions from 10 to 70 wt% SiO_2 and various Na/Si ratios. Composition was determined from the dimensions of the sample chamber and the quartz or glass chip, and the densities of the individual phases. The cell was heated until all phases except zircon were dissolved to yield a single fluid phase, which permitted analysis at known fluid composition. Pressure in the cell was determined from the shift in wavenumber of the ν_3-SiO_4 (~1008 cm^{-1}) band of zircon [4].

The assignment of Raman bands to particular dissolved species remains somewhat elusive, so the interpretation is partly qualitative. The main trends observed in Raman spectra of fluids with increasing SiO_2/H_2O ratio include 1) decrease in the intensity of the ~770 cm^{-1} band (monomer); 2) increase in the intensity of the ~1050 cm^{-1} band (assigned to bridging oxygen Si-O stretch [2]); and 3) increase in spectral contributions at ~550-600 cm^{-1} and ~830-1000 cm^{-1}, which have been assigned to Q^n species [*e.g.* 2]. These trends are interpreted to represent increasing polymerization. Opposite trends, interpreted to indicate decreasing polymerization, are observed with increasing Na/Si ratio.

[1] Manning *et al.* (2008) *EPSL* **272**, 730–737. [2] Mysen (2009) *Geochim. Cosmochim. Acta* **73** 5748–5763. [3] Bassett *et al.* (1993) *Rev. Sci. Instr.* **64**, 2340–2345. [4] Schmidt *et al.* (2011) *MinMag,* this volume.

https://doi.org/10.1180/S0026461X00006502 Published online by Cambridge University Press

Structure and function of microbial communities associated with low-temperature hydrothermal venting and formation of barite chimneys at Loki's Castle vent field

I.H. STEEN[1]*, I.H. THORSETH[2], I. ROALKVAM[1], H. DAHLE[1], R. STOKKE[1] AND R.B. PEDERSEN[2]

[1]Department of Biology, Centre for Geobiology, University of Bergen, Norway (*correspondence: ida.steen@bio.uib.no)
[2]Department of Earth Science, Centre for Geobiology, University of Bergen, Norway

Structure and function of microbial communities associated with barite chimneys in a low-temperature diffuse venting area at the Loki's Castle black smoker vent field at the Arctic Mid-Ocean Ridge (AMOR) were studied by 454-pyrosequencing of PCR amplified 16S rRNA gene sequences and total community cDNA (270 356 reads). White microbial mats present on the barite chimneys, and associated with sibolignid tubeworms directly on the seafloor, where dominated by Sulfurimonas comprising 86-96% of the rRNA-tags. mRNA-tags indicated that vent fluids rich in H_2S (and barium) discharged into the sulfate-rich seawater supported a chemolithoautotrophic lifestyle where reduced sulfur species were oxidized by oxygen or nitrate. CO_2-fixation proceeded via the rTCA-cycle. Scanning electron microscopy revealed that large amounts of thread-like extracellular polymeric material in the microbial mats acted as nucleation points for barite biomineralization. Anaerobic methanotrophs (ANME) of the ANME-1 clade (26%), and the GOM-arc1 group (14.3%) were dominating in the white chimney barite whereas the black flow channel harbored the most diverse microbial community including taxa such as Planctomycetales, 13.5%; Thiotrichales, 10.5%; Thaumarchaeota (MG 1.1. a), 9.4%; Pseudomonadales 7.2%; and Methylococcales, 3.5%. Hence, indicating methane (aerobic/anaerobic), sulfur and ammonia oxidation and heterotrophic metabolisms as dominating processes.

High pressure and high temperature effect on the structural stability of smectites doped with rare earth elements

V.F. STEFANI[1], R.V. CONCEIÇÃO[2] AND N.M. BALZARETTI[1]

[1]Physics Institute, UFRGS, Porto Alegre – RS, Brazil. (vicentestefani@hotmail.com, naira@if.ufrgs.br)
[2]Geoscience Institute, UFRGS, Porto Alegre – RS, Brazil. (rommulo.conceicao@ufrgs.br)

Smectites are phyllosilicates with high cation exchange capacity (CEC) in the interlayers. For these and other features, smectites have been used in various parts of the world as secondary barriers for possible leak of liquids that contain radioactive elements in definitive deposits of nuclear waste disposal. In such case, radioactive cation could be captured by smectite through cationic exchanges. However, very little is known about the stability of smectite under high pressures and high temperatures (HPHT). Preliminar studies developed by our group in dioctahedral calcium smectites showed that the smectite structure is stable, remaining dioctahedric after processing up to 7.7 GPa and at room temperature. This work intends to replace the calcium of the smectite for heavy rare earth elements (REE) using the CEC characteristic of the smectite. We have achieved a cation exchange in smectite using La^{+3} as REE so far. Results in SEM/EDS showed that there was not more evidence of calcium in the sample after CEC procedures; on the other hand, a large amount of lanthanum was present. Our next step is to submit La-rich smectite under extreme conditions of pressure and temperature in order to investigate the structure and chemical changes. To achieve high pressures, hydraulic presses with boards of anvils with toroidal profile and diamond anvil cell (DAC) is being used. SEM, X-ray diffraction and FTIR in situ analysis will be performed on all samples.

https://doi.org/10.1180/S0026461X00006502 Published online by Cambridge University Press

The stability and structure of Mg^{2+} bicarbonate and carbonate ion pairs – An experimental and theoretical study

ANDRI STEFANSSON[1], KONO LEMKE[2], PASCALE BÉNEZÉTH[3] AND JACQUES SCHOTT

Institute of Earth Sciences, University of Iceland, Sturlugata 7, 101 Reykjavík, Iceland

The chemistry of Mg^{2+} in aqueous CO_2 solutions is of fundamental importance, both with respect to the reaction mechanism of magnesium carbonate precipitation and in relation to sequestration of CO_2 by carbonate mineralization.

In order to get insight into the coordination and stability of Mg^{2+} bicarbonate and carbonate ion pairs, a combined experimental and theoretical study was conducted. Potentiometric titration and UV-Vis-IR spectrophotometric measurements on dilute solutions were conducted and the stability constants for the $MgHCO_3^+$ and $MgCO_3$ (aq) complexes derived *in situ* at 10-100°C. In addition, density functional calculations were conducted on the hydration environment around the Mg^{2+}, HCO_3^- and CO_3^{2-} and on the respective complexes.

The aquated Mg^{2+} ion is octahedral coordinated. Upon substitution of HCO_3^- or CO_3^{2-} with first shell waters, the coordination changed to five fold with important implication for further reactions and magnesium carbonate mineralization. At neutral to alkaline pH values, the $MgHCO_3^-$ and $MgCO_3$ (aq) ion-pair contribute significantly to the CO_2 speciation in magnesite saturated to supersaturated solutions. Moreover, with increasing temperature, their stabilities increase. However, under alkaline conditions and with increasing temperatures, the solutions become brucite saturated limiting the availability of Mg^{2+} in solution for carbonate mineralization and ion-pair formation.

Fluids on the loose – Capturing meaningful geochronology in sulfides

HOLLY J. STEIN[1,2]

[1]AIRIE Program, Department of Geosciences, Colorado State University, Fort Collins, CO 80523-1482, USA (hstein@cnr.colostate.edu)

[2]Geological Survey of Norway, 7491 Trondheim, Norway

For generations, economic geology students have been taught to tackle the world's giant ore deposits. If you aren't studying an economically important deposit at an operational mine, the value of your work may be perceived as less important. This approach to understanding the non-unique pandemic phenomenon of metal-carrying, sulfur-bearing, and sulfide-precipitating fluids in the crust has stymied our progress in ore geology. We cannot glean crucial and fundamental relationships by simply acquring more and more data from massively chaotic environments fraught by full-time chemical and physical disequilibrium. If we want to understand *how* fluids are transferred in the Earth's crust, *where* fluids originate and *why* they migrate, and how these fluids relate to the observed and unseen rock record, we must turn our attention to locations where fluids have left their simple and indelible mark in the geologic history. This is readily accomplished through study of small metallic-mineral occurrences, and in particular by application of Re-Os geochronology and tracer studies. Dating of many small sulfide-bearing deposits gives us detailed histories of terrane-scale fluid migration events, be they external additions or metamorphic rearrangements of existing volatiles.

As geoscientists we have no truly robust means to correlate through space without the component of time. Without absolute dating, we have no frame of reference beyond immediately visible stacking or cross-cutting relationships. Re-Os studies of sulfides in the Earth's crust have taught us that (1) the duration of large porphyry-style mineralization is an unimportant question as it is different for every deposit and every district and will not help us find ore, (2) the age of sulfide mineralization should not be shoe-horned to agree with associated U-Pb ages for obvious reasons, and (3) excluding true porphyry-style deposits, the mineralization process, in its entirety, commonly spans tens of millions of years.

If you want to understand the ore giants in the world, step back and be sure you understand the less complicated varieties first. Less is more. Good questions demand the right analytical approach. Though easy access to geochemical data tempts us to adopt the get-more-data approach, this will not lead to clarity of understanding.

https://doi.org/10.1180/S0026461X00006502 Published online by Cambridge University Press

North Atlantic influence on rainfall in the Dead Sea – Sahel watersheds: Implication for abrupt Holocene climate fluctuations

M. STEIN[1], Y. KUSHNIR[2] AND E.J. KAGAN[1,3]

[1]Geological Survey of Israel, 30 Malkhe Israel St., Jerusalem, 95501, Israel, (motis@vms.huji.ac.il)
[2]Lamont-Doherty Earth Observatory, Columbia University, NY, 10964, USA, (kushnir@ldeo.columbia.edu)
[3]Institute of Earth Sciences, The Hebrew University, Jerusalem, 91904, Israel, (elisa.kagan@mail.huji.ac.il)

Observations of 19th and 20th century precipitation in the Dead Sea watershed region display a multidecadal, anti-phase relationship to North Atlantic (NAtl) sea surface temperature (SST) variability, such that when the NAtl is relatively cold, Jerusalem experiences higher than normal precipitation and vice versa. This association is underlined by a negative correlation to precipitation in the sub-Saharan Sahel and a positive correlation to precipitation in western North America, areas that are also affected by multidecadal NAtl SST variability. These observations are consistent with broad range of Holocene hydroclimatic fluctuations from the epochal, to the millennial and centennial time scales, as displayed by the Dead Sea and Sahelian lake levels and by direct and indirect proxy indicators of NAtl SSTs. On the epochal time scale, the gradual cooling of NAtl SSTs throughout the Holocene in response to precession-driven reduction of summer insolation is associated with previously well-studied wet-to-dry transition in the Sahel and with a general increase in Dead Sea lake levels from low stands after the Younger Dryas to higher stands in the mid- to late-Holocene. On the millennial and centennial time scales there is also evidence for an antiphase relationship between Holocene variations in the Dead Sea and Sahelian lake levels and with proxy indicators of NAtl SSTs. However, the records are punctuated by abrupt lake-level drops and extensive expansion of the desert belt at ~8.1, 3.3 and 1.4 ka cal BP, which appear to be in-phase and which occur during previously documented abrupt major cooling events in the Northern Hemisphere. The catastrophic aridity at 3.3 ka cal BP caused probably the collapse of the late Bronze cultures at the Levant, Mediterranean and Nileland. It sends an important message for the future of modern human culture.

Si isotope signatures in soils by UV femtosecond laser ablation

G. STEINHOEFEL[1], J. BREUER[2], F.V. BLANCKENBURG[1], I. HORN[3], D. KACOREK[4] AND M. SOMMER[5]

[1]GFZ Potsdam, Germany (grit.steinhoefel@gfz-potsdam.de, fvb@gfz-potsdam.de)
[2]University of Hohenheim, Germany (breuer@lachemie.uni-hohenheim.de)
[3]Leibniz University of Hannover, Germany (i.horn@mineralogie.uni-hannover.de)
[4]Warsaw University of LifeSciences-SGGW, Poland (danuta_kaczorek@sggw.pl)
[5]ZALF Müncheberg, Germany (sommer@zalf.de)

Si isotope fractionation during weathering is now commonly mapped at the catchment scale. But we still lack an understanding of the processes that set isotope ratios. These take place at the mineral/pore water interface. We present the first Si isotope data of the principle Si pools in soils determined by a UV femtoseond laser ablation system coupled to a multicollector inductively coupled plasma mass spectrometer (MC-ICP-MS). This approach provides the opportunity to obtain precise and accurate data (1) on bulk sample materials as fused glass beads or pressed powder pellets, (2) at the mineral scale in thin sections and (3) for solutions after Si separation and evaporation. We investiagted two immatured Cambisol profiles developed on paragneiss and sandstone in the Black Forest (Germany), respectively, after the last-glacial maximum. Bulk soils show a largely uniform signature in both soil profiles, which is close to those of primary feldspar and quartz with δ^{30}Si value of around -0.4‰. Clay formation is associated with limited Si mobility and hence preserves the original Si isotope signature of parental minerals. Organic-rich environments can promote intense weathering, which lead to high Si mobilization during clay formation together with significant negative isotope signatures down to -1.0‰ in topsoils. Biogenic minerals, i.e. phytoliths, exhibit negative Si isotope signature of about -0.4‰, which is in the range measured for different European tree species. Their impact in bulk soil signatures is negligible but is likely important for the dissolved Si pool. These results can now be used to reconstruct weathering and Si transport processes in soils to identify the source of dissoved Si in soil and river waters, which are commenly enriched in heavy Si isotopes.

https://doi.org/10.1180/S0026461X00006502 Published online by Cambridge University Press

Failure of density functional theory for ground state calculations on TiO_2

GERD STEINLE-NEUMANN[1], VOJTECH VLČEK[1], EVA HOLBIG[1] AND XIANG WU[1,2]

[1]Bayerisches Geoinstitut, Universität Bayreuth, 95440 Bayreuth, Germany
[2]School of Earth and Space Sciences, Peking University, Beijing 100871, China

Electronic structure computations based on density functional theory (DFT) is playing an increasingly important role in the study of material properties, including high pressure properties that are relevant for Earth's interior. The success of DFT-based computations has been limited by the failure of standard implementations of DFT to properly describe the transtion metal-bearing oxides and silicates that are of great importance in the Earth's mantle, especially for Fe-bearing compounds.

There is less appreciation of DFT failures for lighter transition metal-bearing materials. For SiO_2 it is documented that with the local density approximation (LDA) stishovite is predicted stable over quartz which is corrected by the introduction of the generalized gradient approximation (GGA) [1]. However, experimental structural parameters and physical properties of quartz are better reproduced by LDA [1]. Similarly, and not well documented, for TiO_2 DFT in any approximation predicts rutile stable over anatase, in conflict with calorimetry [2].

We have revisited the relative stability of TiO_2 anatase and rutile, as well as other crystalline phases, with highly accurate all-electron methods and various approximations to exchange and correlation, and confirm that rutile is always found stable over anatase. Also, computing harmonic zero point motion energy for the two phases from linear response phonon computations does not stabilize anatase. However, a strong anharmonic character of rutile lattice vibration is revealed that warrants further studies.

High pressure phase relations are better reproduced within DFT, and a proper sequence of high pressure phase stability is reproduced [3]. Zero pressure bulk moduli are all below 240 GPa, sugessting that there are no superhard phases of TiO_2. Higher coordination of high pressure phase leads to stronger localization of the Ti 3d states.

[1] Haman (1996) *Phys. Rev. Lett.* **76**, 660. [2] Ranade *et al.* (2002) *Proc. National Academy of Sciences* **99**, 6476. [3] Wu *et al.* (2010) *J. Phys. Cond. Matter* **22**, 295501.

Detection of airborne radionuclides released during the nuclear accident at Fukushima Daiichi over Europe

P. STEINMANN[1]*, O. MASSON[2], R. GURRIARAN3, H. WERSHOFEN[4] AND RO5 COMMUNITY MEMBERS[5]

[1]Federal Office of Public Health, 3003 Bern, Switzerland (*correspondence: philipp.steinmann@bag.admin.ch)
[2]IRSN, 13115 Saint Paul lez Durance, France
[3]IRSN, 91400 Orsay, France
[4]PTB, 38116 Braunschweig, Germany
[5]"Ring of 5 (Ro5)" is an informal group dedicated to the survey of artificial radioacitvity in the atmosphere

Atmospheric release of radioactivity after the nuclear accident at Fukushima Daiichi started on the 12th of March 2011. Within approximately 10 days contaminated air masses reached Europe. The long range transport resulted in a dilution of the activity concentrations in the air by a factor on the order of 10000 times compared to concentrations reported from Japan. With levels of some tens of mBq m^{-3} at the most, there has been no health safety risk in Europe. The dispersion of the radioactive traces over Europe were followed through the analyses of filters of more than 140 high-volume samplers. Rapid exchange of data was granted through the participation of many laboratories in a network called "Ring of Five (Ro5)" which is an informal information club started in 1983 for this very purpose.

Switzerland was situated at the edge of a corridor with higher levels and saw comparatively low maximum total ^{131}I activities of around 2 mBq m^{-3}. At the end of March the activity ratios of gaseous ^{131}I/particulate ^{131}I recorded in Switzerland were around 4 to 6, while the activity ratio of particulate $^{131}I/^{137}Cs$ was roughly 10. Samples taken with airplanes in the upper troposphere as well as samples from a high altitude station at Jungfraujoch (3500 m a.s.l.) allowed to assess the vertical mixing of the radioactive traces. Temporal evolution of isotopic ratios such as $^{132}Te/^{137}Cs$ or $^{136}Cs/^{137}Cs$ helped to estimate the duration of the major emissions as well as the composition of the source term.

In Switzerland atmospheric deposition of radioactivity was very low with only a few Bq m^{-2} for ^{131}I. This lead to spurious contamination of grass and leafy vegetables (up to a few Bq kg^{-1} fresh weight). Again, at these levels there has been no food safety risk.

https://doi.org/10.1180/S0026461X00006502 Published online by Cambridge University Press

Interactions of phosphate and phosphonate with the calcite surface

J. STELLING*, A.K. NOTHSTEIN AND T. NEUMANN

Karlsuhe Institute of Technology (KIT), Institute of Mineralogy and Geochemistry, D-76131 Karlsruhe, Germany (*correspondence: stelling@kit.edu)

Crytsal growth mechanisms of calcite have been studied in detail in the past [1, 2]. The ability of calcite to adsorb P as phosphate from raw, sea and artificial water [3, 4] has been investigated intensively to recover P as a valuable nutrient [5]. Moreover, a detailed understanding of the interaction between phosphonates and calcite is of great interest for large–scale application as scale inhibitor, dispersant or chelating agent [6]. To date, understanding atomic–level processes that govern the kinetics of calcite growth with respect to phosphate and phosphonate anions is still incomplete.

As part of the ReCaWa joint project (Reactivity of Calcite/Water Interfaces), we investigate the sorption and coprecipitation processes of phosphate and phosphonate on calcite surfaces from (super)saturated calcite solutions. Solutions were prepared from p. a. grade chemicals ($CaCl_2$, $NaHCO_3$) in double distilled water (18.2 MΩ·cm), with pH adjusted to 8.2 and I=0.1 mol/L. Phosphate (H_3PO_4, $Na_3PO4{\cdot}6H_2O$) or phosphonate (etidronic acid, HEDP) were added in concentrations from 3–1000 μmol/L and 10–25 μmol/L, respectively. For batch experiments differing amounts precipitated calcium carbonate or limestone powder with varying specific surface area (SSA) and crystal morphology were added to the solutions. Additional and upcoming coprecipitation experiments under strongly defined conditions are performed using a mixed flow reactor (MFR) to allow coprecipitation of homogeneous phosphate or phosphonate containing calcite onto the calcite seed powder.

Experimental results show that phosphate uptake is a function of SSA and formation of HEDP precipitates dependent on the calcite morphology, respectively. Forthcoming analytical work includes the identification of different fixation mechanisms and phosphorus–containing phases using XRD and XAFS spectroscopy at grazing incidence.

[1] Morse *et al*. (2007) *Chem. Rev*. **107**, 342–381. [2] Larsen *et al*. (2010) *Geochim. Cosmochim. Acta* **74**, 2099–2109. [3] Donnert *et al*. (1999) *Environ. Technol*. **20**, 735–742. [4] Song *et al*. (2006) *Chemosphere* **63**, 236–243. [5] Gilbert (2009) *Nature* **461**, 716–718. [6] Nowack (2003) *Water Res*. **37**, 2533–2546.

Geochemistry of lamprophyres in rare-metal districts related to granitoids

M. ŠTEMPROK[1]*, TH. SEIFERT[2] AND D. DOLEJŠ[1]

[1]Faculty of Science, Charles University, 12843 Praha 2, Czech Republic (*correspondence: miroslav.stemprok@natur.cuni.cz)

[2]Technical University Bergakademie, 09596 Freiberg, Germany

Lamprophyres occur occasionally in mafic-silicic dyke suites of rare-metal (RM) granitoids in Paleozoic provinces of Western and Central Europe, Central Kazakhstan, the Altai, and in Mesozoic provinces of Transbaikalia, Yakutia, Chukotka and Alaska, which host RM (Sn, W, Nb, Ta, Mo, Be) mineralization. We evaluate 190 whole-rock chemical analyses of lamprophyres and variable sets of trace elements in order to uncover any genetic relationships between the melts derived from metasomatized upper mantle and enrichment in RM and alkalies. The lamprophyres correspond to minettes and kersantites with minor spessartites, and have 40-65 wt. % SiO_2, 0.8-9.6 wt. % K_2O, up to 17.8 wt. % MgO, and up to 1450 ppm Cr and 515 ppm Ni. The highest molar $MgO/MgO+FeO^{TOT}$ ratios up to ~0.75 indicate no substantial modification by fractionation or crustal assimilation. The Zr-Hf and U-Th ratios are not decoupled, and the Nb-Ta ratios approach the primitive mantle values. However, absolute concentrations of these elements, which are also considered to be the least mobile in aqueous fluids, show large to extreme enrichments: Zr (27-1420 *vs*. 190 ppm in calc-alkaline lamprophyres [1], 193 ppm in the upper continental crust [2]), Hf (3.5-36 *vs*. 5.2 ppm [1], 5.3 ppm [2]), U (0-29 *vs*. 3 ppm [1], 2.7 ppm [2]), Th (4-75 *vs*. 9 ppm [1], 10.5 ppm [2]), Nb (2-150 *vs*. 13 ppm [1], 12 ppm [2]), Ta (0-16 *vs*. 0.9 ppm [1], 0.9 ppm [2]). These levels in lamprophyres of the RM districts exceed the average abundances of some elements in calc-alkaline lamprophyres or in the differentiated upper continental crust by one to two orders of magnitude. They are also systematically enriched in F (0.04-2.85 *vs*. 0.11 wt % [1]), Rb (43-1490 *vs*. 70 ppm [1]), Cs (2.4-122 *vs*. 3 ppm [1]), Li (14-447 *vs*. 44 ppm [1]), and Sn (1-417 *vs*. 2 ppm [1]) partly due to superimposed greisenization. However, the overall enrichment pattern of lamprophyres and mineralized granites suggests that the source of some components in RM districts can be traced to mantle-derived melts, as previously proposed for the Cornubian province [1].

[1] Rock (1991) *Lamprophyres*. Blackwell, 285 pgs. [2] Rudnick & Gao (2003) *Treatise on Geochemistry* **3**, 1–64.

https://doi.org/10.1180/S0026461X00006502 Published online by Cambridge University Press

Experimental study of monazite/melt partitioning

A.S. STEPANOV, J. HERMANN AND D. RUBATTO[1]

The Australian National University, Research School of Earth Sciences, Canberra, Australia

Monazite (LREE, Th)PO_4 is a common accessory mineral and the major host of LREE, Th and U in the Earth's continental crust. Monazite is stable to high temperatures and pressures and is thus a key phase for trace element redistribution during partial melting of crustal rocks. We performed monazite-melt partitioning experiments in a piston-cylinder press over the temperature range 750 to 1200°C and pressures of 10-50 kbar. The starting composition was a synthetic granite mix with about 8 wt% H_2O that was doped with trace elements corresponding to 0.5-3 wt. % of monazite.

Experiments at temperature >800°C and pressure <30 kbar produced melt with monazite. At lower temperatures quartz and plagioclase also formed. At higher pressures, kyanite, coesite, jadeite, apatite, zircon and epidote group mineral start to crystallize. Monazite was produced in all experiments and formed small grains (<5μm across). Laser ablation-ICP-MS analyses of monazite-melt mixes were performed and the monazite composition was calculated using regression analysis. The concentration of some elements was also obtained with Electron Microprobe analysis. These analyses were in good agreement with the monazite compositions obtained by the regression method.

The LREE and Th concentrations of melts coexisting with monazite strongly increase with increasing temperature. The melt composition has less influence on these concentrations. Monazite solubility decreases by 30-40 % with increasing pressure. REE, Th, U, Y and As strongly partition into monazite, whereas other trace elements (Li, Be, B, Sc, Ti, V, Mn, Sr, Zr, Nb, Ba, Hf, Ta, Pb) have monazite/melt partition coefficients lower than 10. Monazite has the highest preference for LREE from La to Nd, with a decrease in partition coefficients for Sm, MREE and HREE. Difference in partitioning of of LREE and HREE tend to decreases with increase of temperature and decrease with increase of pressure. Th partition coffecients are 30 % higher than those for LREE and are indipendent of pressure and temperature. Partition coefficients for U are much lower than for Th and LREE.

The new experimental data provide a basis for calculation of factionation of LREE, Th and U during fractional cristalization and melting in the presence of monazite at crustal conditions and in subduction zones.

Aerosol, clouds, precipitation, radiation, and climate; A global perspective

GRAEME L. STEPHENS

Jet Propulsion Laboratory California Institute of Technology 4800 Oak Grove Dr Pasadena, CA, 91109

The cloud systems of our planet fundamentally shape our climate in the way they affect the flow of radiation in and out of the planet and in the way they connect key processes together to form the hydrological cycle. Despite the many years of cloud observations from space, we have not gained much insight into these key roles. Information about cloud particle size from satellite radiometers, for example, has been derived now for more than two decades but we still have not convincingly determined if this information is in fact related to real cloud physical properties. Nevertheless correlation between this remote sensing particle size information and aerosol content now serves as a basis for parameterization of the so-called indirect effects in climate models, a key tuning knob of climate model sensitivity. Similarly we have also observed precipitation from space for many years but have not been able to tie these observations to actual cloud physical processes and thus precipitation observations alone offer little real insight into how precipitation is likely to be shaped by the broader environment in which it forms. In this talk, we demonstrate that new observations now available for Earth orbiting satellites, when combined together, are advancing our understanding of the processes that connect aerosol, cloud and precipitation together and in turn provide a unique view on how these processes alter the planet's radiation balance. New insights on the effects of aerosol on cloud physical properties will be described as well as how these in turn affect both the water and energy balance of planetary cloud systems. The relevance of these new insights to the climate system and climate change will be emphasized.

https://doi.org/10.1180/S0026461X00006502 Published online by Cambridge University Press

Evidence for the formation of a fluorapatite surface layer on nano-sized hydroxyapatite after the exposure to an aqueous solution

VANESSA STERNITZKE*, RALF KAEGI, JANET G. HERING AND C. ANNETTE JOHNSON

Eawag, Swiss Federal Institute of Aquatic Science and Technology, 8600 Dubendorf, Switzerland (*correspondence: vanessa.sternitzke@eawag.ch)

Hydroxyapatite (Ca_{10} $(PO_4)_6$ $(OH)_2$; HAP) is the main constituent of bones and teeth [1]. Its ability to take up fluoride is applied in dental care [2] but also for drinking water purification [3]. Even though much research has been performed on fluoride uptake on HAP [e.g. 4], it is not fully understood how deeply fluoride incorporates into the HAP crystal.

It is believed that fluoride adsorbs to the HAP surface and exchanges for the hydroxide to form the less soluble fluorapatite (Ca_{10} $(PO_4)_6F_2$; FAP) [5]. The uptake capacity of fluoride on the HAP crystal is controlled by the exposure time and pH of the system [4]. A simultaneous formation of fluorite (CaF_2) cannot be ruled out when calcium and fluoride achieve saturation concentration [6]. However, a dissolution of CaF_2 in favour of FAP recrystalization is likely.

Batch studies were performed at 25 °C to investigate the uptake of fluoride as function of pH and initial fluoride concentration on synthetic HAP over an equilibration time of 28 days.

The reacted solids were investigated by Fourier Transform Infrared Spectroscopy (FTIR), which provided estimates on weight percentages on FAP formation on HAP after 28 days. Nano Secondary Ion Mass Spectroscopy (NanoSIMS) and Transmission Electron Microscopy (TEM) analysis gave additional information for a thin layer of FAP on HAP crystals.

To our knowledge it is the first time that the presence of a fluoridated surface layer on a nano-sized HAP crystal was qualitatively *and* quantitatively determined by micro- and spectroscopic analyses.

[1] Elliott (1969) *Calcified Tissue Res.* **3**, 293–307. [2] Driessens (1973) *Nature* **243**, 420–421. [3] Bregnhoj (1995) *PhD Thesis*, University of Denmark. [4] Lin *et al.* (1981) *Colloids & Surfaces* **3**, 357–370. [5] McCann (1952) *J. of Biol. Chem.* **201**, 247–258. [6] Christoffersen *et al.* (1995) *Caries Res.* **29**, 223–230

Ice formation on atmospheric mineral dust particles

OLAF STETZER, ANDRÉ WELTI, LUIS LADINO AND FELIX LÜÖND

ETH Zurich, Institute for Atmospheric and Climate Science, 8092 Zurich, Switzerland (*correspondence: olaf.stetzer@env.ethz.ch)

Mineral dust particles are known to be efficient catalysts for the formation of ice in clouds. In recent field studies by our group at the Jungfraujoch in the Swiss Alps a good correlation of the concentration of ice nuclei with the concentration of large particles during Saharan Dust events at this location was found [1]. Similar results are available from other groups as well e.g. [2].

However, the influence of size, shape, chemical composition, and the modifications of some of these parameters through anthropogenic emissions of pollutants to the atmosphere on the formation of ice is still mostly unknown and needs to be investigated further. This is complicated by the fact that ice in clouds may form via different pathways or mechanisms (immersion freezing, deposition freezing, contact freezing) and the parameters determining their efficiency in forming ice are different.

In our lab we investigate these different ice nucleation mechanisms with individual experiments for the different mechanisms using mineral dust aerosols. In this paper, our recent results on the ice nucleation properties of mineral dust particles for immersion freezing, and contact freezing are presented and compared.

The analysis of the immersion freezing data is done by calculations based on classical nucleation theory (CNT) assuming different assumptions regarding the properties of the mineral dust aerosols. From this analysis, the presence of so-called active sites can be deduced at which the nucleation process takes place preferably [3]. CNT also predicts that ice nucleation is a statistical process and therefore time dependant. To proof this, we conducted a special set of experiments where the residence time in the nucleation chamber is varied between 3 and 19 seconds. The results are again analysed and compared against CNT calculations as explained above and suggest, that immersion freezing is indeed time dependant where the frozen fraction increases with residence time.

[1] Chou *et al.* (2010) *ACPD*, **10**, 23705–23738. [2] Klein *et al.* (2010) *ACPD*, **10**, 10211–10221. [3] Lüönd *et al.* (2010) *JGR Atmospheres*, **115** D14201.

https://doi.org/10.1180/S0026461X00006502 Published online by Cambridge University Press

Uranium(VI) complexation with lactate and citrate in dependence on temperature (7-65°C)

ROBIN STEUDTNER, KATJA SCHMEIDE AND GERT BERNHARD

Helmholtz-Zentrum Dresden-Rossendorf, Institute of Radiochemistry, P.O. Box 510119, D-01314 Dresden, Germany (r.steudtner@hzdr.de)

After disposal in nuclear waste repositories the chemical and migration behavior of actinides depends on many factors. It is estimated that maximum temperatures in the near field of a repository could reach 300°C in dependence on the waste forms [1] and the host rock [2]. Thus, for the long-term safety assessment, knowledge of the interaction of actinides such as uranium with inorganic and organic ligands at elevated temperatures is required. The amount of organic matter in a repository can be separated in humic substances and in low molecular weight organic substances. A not negligible component of low molecular weight organic substances is the group of carboxylic acid. For example, citric acid is used in nuclear reprocessing [3] and acetic, lactic and formic acid were identified in rock extracts and pore water of Opalinus Clay [4]. Reliable experimental data on the complexation of U(VI) in solution at elevated temperatures are still needed.

Therefore, we studied the U(VI) complexation by lactic acid (pH 3) and citric acid (pH 0-10) in the temperature range from 7 to 65°C. Species distribution and complex formation constants were determined by means of UV-Vis and time-resolved laser-induced fluorescence spectroscopy. In the U(VI) lactate system, we identified the formation of 1:1- and 1:2-complexes. In the presence of citrate, we could characterize five U(VI) complexes in dependence on pH value. The complex formation between U(VI) and these both ligands was found to be endothermic and entropy-driven. The complex stability constants of the U(VI) complexes increase with increasing temperature. This could lead to an increased mobility of U(VI) at higher temperatures.

[1] Rao, Jiang, Zanonato, Di Bernardo, Bismondo & Garnov (2002) *Radiochimica Acta* **90**, 581–588. [2] Warwick, Hall, Zhu, Dimmock, Robbins, Carlsen & Lassen (1997) *Chemosphere* **35**, 2471–2477. [3] Dodge & Francis (1997) *Environmental Science & Technology* **31**, 3062–3067. [4] Courdouan, Christl, Meylan, Wersin & Kretzschmar (2007) *Applied Geochemistry* **22**, 2926–2939.

Early differentiation of terrestrial planets: The relative importance of big impactors and small impactors

DAVID J. STEVENSON

Caltech 150-21, Pasadena CA 91125 USA (djs@gps.caltech.edu)

Planetary accretion arises through discrete events but is often treated as if those events were so frequent and large in number as to produce a continuum (a mass flux and characetristic time interval of accretion). Although there have also been published models that study the effects of discrete large impacts, insufficent attention has been paid thus far to the differences that arise for delivering material through a large number of small bodies and delivering the same mass (at the same epoch) as a small number of large bodies (e.g. Earth or Moon-sized giant impactors). The nature of the impacts is different in respect of the depth to which melting takes place, the extent to which equilibrium is establised between core forming materials and mantle materials, and the pressure range of equilibration. As a result, two accretion scenarios that involve identical sequences (timing and size) of imapct events can have different outcomes (different Hf/W inferred chronologies, different mantle siderophile inventories, different initial core T, etc) according as to the physical models one uses to describe the outcome of different sized impacts. Contrary to what some of the current literature implies, this is *not* merely the issue of the timing of the last giant impact since multiple giant impacts can be responsible for a large fraction of the mass delivery. It is also true that one cannot ignore the background 'drizzle' of smaller bodies (implied by the dynamic friction in the Nice models for example). I will describe semi-quantitatively the range of outcomes according as to the range of possible accretion histories for the terrestrial planets in general but with particular emphasis on Earth. This will also require an update of our current understanding of the mechanisms of core formation and the nature of melting curves and magma oceans in the deep mantle.

https://doi.org/10.1180/S0026461X00006502 Published online by Cambridge University Press

The strontium stable isotope composition of seawater during glacial intervals

E. STEVENSON[1], K.W. BURTON[1], F. MOKADEM[1], I.J. PARKINSON[2], P. ANAND[2] AND E. HATHORNE[3]

[1]Present Address: Department of Earth Sciences, Oxford University, Parks Road, Oxford, OX1 3PR, UK
[2]Department of Earth and Environmental Sciences, The Open University, Milton Keynes, MK7 6AA, UK
[3]IFM-GEOMAR, Leibniz Institute of Marine Sciences, University of Kiel, D-24148, Kiel, Germany

The strontium ($^{88}Sr/^{86}Sr$) stable isotope composition of seawater reflects input from continental weathering and hydrothermal exchange at mid-ocean ridges, and output in carbonate sediments. It has been suggested that increased weathering of shelf carbonates accompanying the low sea levels during the last glacial maximum (LGM) will have enhanced the flux of light Sr (from carbonates) to the oceans. However, temperature and species dependent fractionation of Sr stable isotopes during incorporation into marine carbonate has to be quantified in order to accurately reconstruct past seawater compositions.

This study presents high-precision $\delta^{88}Sr$ data, obtained using double-spike TIMs technique. Present-day seawater yields a $\delta^{88}Sr$ composition of 0.356±0.007 ($2\sigma_m$) with no resolvable difference between Pacific, Atlantic and Indian Oceans. *Globigerinoides sacculifer* from sites in the South Atlantic, covering a temperature range of ~10°C, show no systematic variation with temperature. Both *G. sacculifer* and *G. menardii* show systematic variations with growth rate (shell size) with heavier compositions in the larger size fractions. By contrast, *G. aequilateralis* and *G. ruber* show with no systematic variation with shell size. Preliminary $\delta^{88}Sr$ data for *G. ruber* covering the last 70 kyr indicate that there was no resolvable change in the $\delta^{88}Sr$ composition of seawater across the LGM and deglaciation. In this case the postulated enhanced weathering of shelf carbonates during glacial intervals [1], delivering light Sr isotopes to the ocean may not have been as significant as predicted [2] or else was offset by increased production and preservation of carbonates, driving seawater to heavier $\delta^{88}Sr$ values. Alternatively the very long residence time of Sr in the oceans may simply buffer the changes in input or output such that no changes are resolved at the level of precision of this study.

[1] Stoll, H. M. & Schrag, D. P. (1998) *Geochim. Cosmochim. Acta* **67**, 1107–1118. [2] Krabbenhoft *et al*. (2010) *Geochim. Cosmochim Acta* **74**, 4097–4109.

Pb and Sr isotopes and the provenance of the painting materials in 19th century Canada

R.K. STEVENSON[1]*, E.A. MOFFATT[2] AND M-C. CORBEI[2]

[1]GEOTOP and SCTA, UQAM, PO Box 8888, St. Centre-Ville, Montreal, QC H3C 3P8 (*correspondence: stevenson.ross@uqam.ca)
[2]Conservation Science Division, Canadian Conservation Institute, Department of Canadian Heritage, 1030 Innes Road, Ottawa, ON K1A 0M5

Introduction

Cornelius Krieghoff was a 19th century Canadian artist (1815-1872) of winter landscapes and depictions of aboriginal and rural Quebec life. Like many pre-20th century artists, Krieghoff used a pigment known as lead white composed of a synthetic analogue of hydro-cerussite, often with lead carbonate impurities. Krieghoff used lead white in the preparation layer on the canvas and as a white pigment (either alone or in mixtures to lighten other colours). Calcium carbonate was often added as an extender. Samples of lead white and other Pb-bearing pigments of 15 Krieghoff works painted between 1844 and 1871 were also analysed for Pb and Sr isotopes to provide constraints on pigment sources.

Results

The bulk of the lead isotope data yield isotopic compositions that are consistent with data obtained from lead white in European paintings of the same or earlier periods [1, 2]. However, a few samples yielded lead isotope compositions that were more suggestive of a North American origin. The Sr isotope ratios of the samples range from values consistent with Palaeozoic carbonates to values in excess of present day seawater.

[1] Keisch & Callahan (1976) *Archaeometry* **18**, 181–193. [2] Fortunato *et al*. (2005) *Analyst* **130**, 898–906.

https://doi.org/10.1180/S0026461X00006502 Published online by Cambridge University Press

Origin of dissolved metals in produced water from the Devonian Marcellus shale, USA: Sr isotope systematics

BRIAN W. STEWART[1,2]*, ELIZABETH C. CHAPMAN[1,2], ROSEMARY C. CAPO[1,2], RICHARD W. HAMMACK[1], KARL T. SCHROEDER[1] AND HARRY M. EDENBORN[1]

[1]US DOE-National Energy Technology Laboratory, 626 Cochrans Mill Rd., Pittsburgh, PA 15236

[2]University of Pittsburgh, Department of Geology & Planetary Science, Pittsburgh, PA 15260 (*correspondence: bstewart@pitt.edu)

The horizontal drilling and hydrofracturing techniques used for extraction of natural gas from shales of the Marcellus Formation (USA) lead to production of significant volumes of high-TDS (total dissolved solids) waters that have interacted with the source shale and potentially adjacent units. Determining the source of these dissolved salts and understanding local and basinal variations in TDS have direct relevance to exploration methodologies and water management and reclamation.

A series of flowback waters have been collected from drilling operations in a geographic region spanning ~375 km, from northeastern to southwestern Pennsylvania. Most $^{87}Sr/^{86}Sr$ values fall within a narrow range, from 0.7101 to 0.7112; samples from two adjacent wells in Westmoreland County, Pennsylvania, define a second grouping (0.7120-0.7121). This bimodal distribution of flowback values could be a result of hydrofracturing water interacting with different producing members of the Marcellus Formation, or lateral (facies) variations in the isotopic composition of formation salts. The relatively tight clustering of values among geographically distant sites argues against variable influxes of brines from adjacent formations. Marcellus flowback waters contain notably elevated levels of barium and strontium (up to 12, 000 and 5, 000 mg/L, respectively, for the samples in this study). The Ba/Sr ratios of the flowback fluids measured here also vary systematically with geographic location, The combination of Ba/Sr and $^{87}Sr/^{86}Sr$ provide a method for uniquely identifying regional variations in flowback waters.

The $^{87}Sr/^{86}Sr$ ratios of Marcellus waters measured here fall well above Phanerozoic seawater values. Thus, while the Marcellus brines may have a significant seawater component, this has clearly been augmented by a high-$^{87}Sr/^{86}Sr$ source, possibly originating from dissolution of radiogenic minerals within the shale. Ongoing leaching studies of core material from the Marcellus Formation and adjacent units will provide additional insight into the origins of salts in Marcellus waters.

Evolution of andesite magma systems; Egmont Volcano, New Zealand

R.B. STEWART[1]*, A.V ZERNACK[1], M.B. TURNER[2], R.C. PRICE.[3], I.E.M. SMITH[4] AND S.J. CRONIN[1]

[1]Volcanic Risk Solutions, INR, Massey University, PB 11222, Palmerston North 4442, New Zealand (*correspondence: r.b.stewart@massey.ac.nz)

[2]GEMOC ARC. National Key Centre, Department of Earth and Planetary Sciences, Macquarie University, NSW, 2109. Australia

[3]Faculty of Science and Engineering, University of Waikato,PB3105, Hamilton , New Zealand

[4]School of Environment, University of Auckland, PB 92019, Auckland 1142, New Zealand

A major issue in andesite magmas genesis is explaining disequilibrium crystal, matrix glass and whole rock compositions. Taranaki/Egmont is a high-K andesite volcano in the western North, Island, New Zealand, with a 200, 000 year eruption record. Thirteen recently identified and dated pre-7 ka debris avalanche deposits record the magmatic evolution of the Taranaki volcanic system. Clast compositions show a gradual enrichment in K_2O and LILE with time to high-K andesites in the Holocene. Pre-100 ka magmas include relatively primitive basalts and basaltic andesites and mineral chemistry indicates crystallisation within the lower crust or mantle. Modal rock compositions become more silicic in younger units, and the appearance of late-stage low-pressure mineral phases (high-Ti hornblende, biotite and Fe-rich orthopyroxene), suggests an increase in more evolved magmas with time. Six compositionally distinct Holocene magma batches erupted on 1500-2000 year timescales, synchronous with variations in eruptive frequency in which the largest volume (>0.5 km^3) events erupt the most evolved magmas. We suggest that andesite magmas were generated within a lower crustal 'hot zone' [1]. Matrix glasses in both xenoliths and lavas/tephras are mostly dacitic to rhyolitic in composition and, in younger lavas have a high K_2O content. These glasses may represent some of the partial melts from the 'hot zone'[2]. The disequilibrium observed in the andesites is due to the mixing of these diverse components. A complex and dispersed magma assembly and storage system developed in the upper crust where the magmas were further modified by fractional crystallisation and magma mixing and mingling [2].

[1] Annen *et al*. (2006) *J Petrol* **47**, 505–539. [2] Turner *et al*. (2011) *Geological Society of America Bulletin* (accepted for publication).

https://doi.org/10.1180/S0026461X00006502 Published online by Cambridge University Press

Contrasting halogen geochemistry of barren and mineralized breccias of the Sudbury Igneous Complex, Ontario

R.C. STEWART[1]*, J.J. HANLEY[1] AND D.E. AMES[2]

[1]Department of Geology, Saint Mary`s University, Halifax, Canada (*correspondence: stewcraig@gmail.com)
[2]Geological Survey of Canada, 601 Booth Street, Ottawa, Ontario, K1A 0E8, Canada

The potential for the halogen elements (Cl, Br, I) to be used as geochemical indicators for contact-style Ni-Cu-PGE mineralization along the lower contact of the Sudbury Igneous Complex (SIC) has been investigated. Two environments - one barren, and the other containing economic magmatic sulphide ore systems - were compared. The studied host rocks to these deposits are polymict igneous-textured breccias, formed by partial melting of the Archean country rocks (gneisses).

No significant differences in bulk major and trace element geochemistry of rocks between the environments aside from the halogen elements were observed. Two major differences in halogen geochemistry were recognized:

First, mineralized breccias show marked enrichment in I. This is thought to have resulted from the leaching of I from brecciated sulphides by hydrothermal fluids released during contact metamorphism and partial melting of the country rocks, and is unique to those breccias that host sulfides. The anomalous I can be detected for distances of up to several 100 metres from mineralized samples. This observation is consistent with experimental studies which show that I is the most compatible halogen in sulfide liquids [1] leading to I enrichment in environments where sulfide liquids crystallize.

Second, analysis of the soluble fraction (from fluid inclusions) of the halogens reveal that two distinct fluid end-members were trapped in the matrix of the breccias during their crystallization (as mixtures in primary fluid inclusions): a high Cl^-/Br^- fluid phase of probable magmatic origin (exsolved from the SIC), and a low Cl^-/Br^- fluid phase derived from fluid released during dehydration of hydrous minerals in the country rocks. Mineralized breccias contain a much higher proportion of the non-magmatic fluid end-member. This would suggest that footwall partial melting was a critical component to deposit development, possibly promoting sulfide saturation in this local environment or the transportation of ore metals in high salinity fluids of non-magmatic origin (e.g. groundwater, metamorphic fluid).

[1] Mungall & Brenan (2003) *Can. Min.* **41**, 207–220.

Sources and input mechanisms of hafnium and neodymium in surface waters of the Atlantic sector of the Southern Ocean

T. STICHEL[1,2]*, M. FRANK[1], J. RICKLI[3], B. HALEY[1], E. HATHORNE[1], C. JEANDEL[4] AND C. PRADOUX[4]

[1]IFM-GEOMAR, Wischhofstr. 1-3, 24148 Kiel, Germany
[2]now at SOEST, University of Hawaii 1680 East-West Rd, Honolulu, USA (*correspondence: tstichel@hawaii.edu)
[3]Bristol Isotope Group, University of Bristol, Parks Road, United Kingdom
[4]LEGOS, 14 av. Edouard Belin, Toulouse 31400, France

The first combined dissolved hafnium (Hf) and neodymium (Nd) isotope and concentration data from surface waters of the Atlantic sector of the Southern Ocean are presented here. The samples were collected along the Zero Meridian (ZM), in the Weddell Sea (WS) and in the Drake Passage (DP) during RV Polarstern expedition ANTXXIV/3 and ANTXXIII/3 in the frame of the International Polar Year (IPY) and the GEOTRACES program. The distribution of Hf and Nd concentrations is overall similar. However, at the northernmost station located 200 km southwest of Cape Town a pronounced increase of the Nd concentration is observed, whereas the Hf concentration at the same time is at its minimum indicating lower amounts of Hf than of Nd released by weathering of the Archean cratonic rocks of South Africa. From the southern part of the Subtropical Front (STF) to the Polar Front (PF) Hf and Nd show the lowest concentrations (<0.12 pmol/kg and 10 pmol/kg, respectively), most probably due to the low terrigenous flux in this area and scavenging of Hf and Nd by biogenic opal. In the vicinity of landmasses the Hf and Nd isotope composition is clearly labelled by terrigenous inputs. Near South Africa Nd isotope values as low as $\varepsilon_{Nd} = -18.9$ indicate unradiogenic inputs supplied via the Agulhas Current. To the south the Nd isotope compositions are relatively radiogenic ($\varepsilon_{Nd} \sim -8$ to -8.5) towards the STF, within the Antarctic Circumpolar Current, in the Weddell Gyre and the Drake Pasage. Near the volcanic Antarctic Peninsula the isotopic data show significant increases to $\varepsilon_{Hf} = 6.1$ and $\varepsilon_{Nd} = -4.0$. implying an enhanced release of Nd and Hf. The Hf isotope compositions in the study area only show a small range between $\varepsilon_{Hf} = 6.1$ and 2.8. The new data show that Hf can be a sensitive tracer for prevailing physical weathering conditions, which is not the case for Nd. Neodymium isotopes show a factor of five larger range than Hf isotopes, which confirms Nd isotopes to be a sensitive tracer for the provenance of weathering inputs to surface waters of the Southern Ocean.

https://doi.org/10.1180/S0026461X00006502 Published online by Cambridge University Press

Rapid seawater circulation through animal burrows in mangrove forests — A significant source of saline groundwater to the tropical coastal ocean

T.C. STIEGLITZ[1]*, J.F. CLARK[2] AND G HANCOCK[3]

[1]School of Engineering & Physical Sciences, James Cook University, Townsville, QLD, Australia (*correspondence: Thomas.Stieglitz@jcu.edu.au)
[2]Earth Science, UCSB, Santa Barbara, CA, USA (jfclark@geol.ucsb.edu)
[3]CSIRO Land and Water, Canberra, ACT, Australia (gary.hancock@csiro.au)

A common approach for quantifying rates of submarine groundwater discharge (SGD) to the coastal ocean is to use geochemical tracers such as ^{222}Rn and short lived radium isotopes, which are naturally enriched in groundwater relative to seawater and have well understood chemistries within the marine environment. They occur in both fresh (continental) and saline (marine) groundwaters and thus the water source is often ambiguous. Here, we present a detailed investigation into the tidal circulation of seawater through animal burrows using ^{222}Rn and isotopes of radium in the Coral Creek mangrove forest, Hinchinbrook Island, Queensland, Australia. The study was conducted at the end of the dry season in a creek with no freshwater inputs. Significant export of radionuclides and salt from the forest into the creek indicates continuous tidally driven circulation through the burrows. Results demonstrate that the forest sediment is efficiently flushed, with a water flux of about 30 L/m^2/ day of forest floor, which is equivalent to flushing about 10% of the total burrow volume per tidal cycle. Importantly, annual average circulation flux through mangrove forest floors are of the same order as annual river discharge in the central GBR. However, unlike the river discharge, the tidal circulation should be relatively stable throughout the year. This work documents the importance of animal burrows in maintaining productive sediments in these systems, and illustrates the physical process that supports large exports of organic and inorganic matter from mangrove forests to the coastal zone. It also illustrates the importance of considering saline groundwater sources when interpreting SGD radionuclide tracers in the coastal ocean.

Observationally constrained estimates of carbonaceous aerosol transport and radiative effects

PHILIP STIER[1]*, ZAK KIPLING[1], J.P. SCHWARZ[2,3] AND D.W. FAHEY[2,3]

[1]Department of Physics, University of Oxford, Oxford, UK (*correspondence: philip.stier@physics.ox.ac.uk)
[2]Cooperative Institute for Research in Environmental Sciences, University of Colorado, Boulder, USA
[3]Chemical Sciences Division, Earth System Research Laboratory, NOAA, Boulder, USA

Atmospheric aerosols play an important role in the global climate system. Carbonaceous aerosols stand out through their potential to warm (through absorption and semi-direct effects) and cool (through scattering and indirect effects) climate, depending on their microphysical properties and regional distribution. Current global aerosol models vary drastically in simulated abundance, transport and radiative properties of carbonaceous aerosols and show significant biases when compared to observations [1].

To advance our understanding of uncertainties in global models we utilise observational profile data obtained during the HIPPO aircraft campaigns [2] to constrain the remote transport in two microphysical aerosol climate models, ECHAM-HAM [3, 4] and HadGEM-UKCA [5]. In addition to mass concentrations, the SP2 instrument retrieves information about the mixing state of black carbon, providing constraints on the structural representation in microphysical models. In synergy with absorption optical depth retrievals from the AERONET sun-photometer network, such observations provide a unique constraint on transport and abundance of carbonaceous aerosols.

Comparison of the standard and observationally constrained setups will demonstrate the reduction of uncertainty in the simulated radiative effects. Nudged simulations using sector-specific emission inventories will allow quantifying sectoral contributions and the additivity of the individual contributions to the total carbonaceous radiative effects.

[1] Koch, D *et al*. (2009) *Atmos. Chem. Phys.* **9**, 9001–9026. [2] Schwarz, J.P. *et al*. (2010) *Geophys. Res. Lett.* **37**, L18812, doi: 10.1029/2010GL044372. [3] Stier, P. *et al*. (2005) Atmos. Chem. Phys. **5**, 1125–1156. [4] Stier, P *et al*. (2007) *Atmos. Chem. Phys.* **7**(19), 5237–5261. [5] Mann, G.W. *et al*. (2010) *Geosci. Model Dev*. (3), 519-551.

https://doi.org/10.1180/S0026461X00006502 Published online by Cambridge University Press

The ash that closed Europe's airspace: Part II, the physical aspects of the Eyjafjallajökull ash

S.L.S. STIPP[1]*, T. HASSENKAM[1], S. NEDEL[1], N. BOVET[1], HEM C.P.[1], BALOGH Z.I.[1], K. DIDERIKSEN[1], E.S. EIRIKSDOTTIR[2], H.A. ALFREDSSON[2], N. OSKARSSON[2], B. SIGFUSSON[3], G. LARSEN[2] AND S.R. GISLASON[2]

[1]Nano-Science Centre, Department of Chemistry, University of Copenhagen, Denmark (stipp@nano.ku.dk)
[2]Institute of Earth Sciences, University of Iceland, Reykjavik, Iceland (sigrg@raunvis.hi.is)
[3]Reykjavik Energy, Iceland

On 14 April 2010, when meltwaters from the Eyjafjallajökull glacier mixed with hot magma, an explosive eruption sent unusually fine-grained ash into the jet stream. It quickly dispersed over Europe. Previous airplane encounters with ash had resulted in sand blasted windows and particles melted inside jet engines, causing them to fail. Therefore, air traffic was grounded for several days. Concerns also arose about health risks from fallout, because ash can transport toxic elements such as fluoride, aluminium and arsenic. For this study, we compared samples of the initial explosive ash with ash from the later, more typical eruption. Using nanotechniques, custom-designed for studying natural materials, we explored the physical and chemical nature of the ash to determine if fears about health and safety were justified and we developed a protocol that will serve for assessing risks during a future event [1].

We used atomic force spectroscopy (AFS) to map the adhesion properties on individual ash particles. With X-ray photoelectron spectroscopy (XPS), we determined the composition of nanometer scale salt coatings. By oscillating an atomic force microscopy cantilever, to which a single ash particle had been glued, we could measure the mass of adsorbed salts with picogram (pg; 10^{-12} g) resolution. The particles of explosive ash that reached Europe in the jet stream were especially sharp and hard, therefore abrasive, over their entire size range, from submillimeter to tens of nanometers. Edges remained sharp, even after 2 weeks of abrasion in stirred water suspensions. From the composition of the particles, we could predict that they would soften and melt at temperatures typical of a jet engine (1500 to 2000 °C).

This paper is the second of a two part presentation, where the first part, by Sigurdur Gislason, focuses on the Eyjafjallajökull eruption, grain size distribution and soluble salt coatings.

[1] Gislason S.R. *et al*. (2011) *PNAS*, **108**, 7307-7312

Biogeochemical cycling of cadmium in the Tasman Sea: Constraints from cadmium isotopes

C.H. STIRLING[1,2,*], M. GAULT-RINGOLD[1,2], E. BREITBARTH[1] AND E.C.V. BUTLER[3]

[1]Department of Chemistry, University of Otago, New Zealand (*correspondence: cstirling@chemistry.otago.ac.nz)
[2]Centre for Trace Element Analysis, University of Otago, New Zealand
[3]CSIRO Wealth from Oceans Flagship, Hobart Laboratories, Australia

The biogeochemical cycling of cadmium (Cd) is likely to be an important component of the ocean's biological pump, yet the processes controlling its uptake are poorly understood. Stable isotopes of Cd offer the potential to provide new insights into the distribution and cycling of marine Cd, as sizeable 0.1%-level isotopic fractionation in seawater has been demonstrated due to biological uptake by marine phytoplankton [1, 2]. Furthermore, Cd isotopes may prove to be a reliable proxy for past and present nutrient utilization in the oceans. However, the limited results to date reveal the complex interplay of biological uptake, particle 'scavenging', and the mixing of different water masses. Additional datasets are, therefore, required to gain insight into the processes that govern the marine distribution of Cd.

Using multiple-collector inductively coupled plasma mass spectrometry (MC-ICPMS) combined with double spiking techniques, we report the Cd isotopic composition and concentration of depth profile samples collected along a longitudinal transect in the Tasman Sea during the SS01/2010 ('PINTS') voyage — a GEOTRACES Process Study. The sampling transect extended southwards from the sub-tropical Pacific Ocean to the Southern Ocean, characterised by a strong longitudinal gradient with respect to the supply of trace metal-bearing dust, phytoplankton biomass, and oceanic temperature. The Cd isotopic and concentration water column signatures are interpreted in the context of other trace metals and macronutrients that potentially colimit marine phytoplankton growth, as well as oceanographic parameters, such as phytoplankton biomass. These data help elucidate the sources and biogeochemical cycling of Cd in the Tasman Sea, the validity of the Cd/Ca paleonutrient proxy, and the potential of Cd isotopes as a proxy of past nutrient utilization in the oceans.

[1] Ripperger *et al*. (2007) *EPSL* **265**, 229–245.
[2] Abouchami *et al*. (2011) *EPSL*, in press.

https://doi.org/10.1180/S0026461X00006502 Published online by Cambridge University Press

Depth- and pressure dependent permeability in the upper continental crust — Data from the Urach 3 geothermal well

INGRID STOBER

Mineralogy Geochemistry, University of Freiburg, Germany (ingrid.stober@uni-freiburg.de)

The 4500 m deep research borehole 3 at Urach (South Germany) has been extensively used for hydraulic testing of the crystalline basement since the late seventies. The data permit a general interpretation of the hydraulic properties of the crystalline continental upper crust at different depth intervals. The gneissic basement contains an interconnected fluid-filled fracture system.

Low-pressure hydraulic tests show that the basement on a larger scale can be described as a homogeneous, isotropic aquifer and this characteristic hydraulic behavior persists at least several hundred meters away from the borehole. This demonstrated homogeneity of the aquifer (or fluid reservoir), together with the highly saline water in an interconnected system of copious fractures is characteristic of the continental upper crust in general. On a smaller scale, however, the fractures, crossing the uncased sections in the borehole, define the flow-behavior locally. So, at the beginning of a hydraulic test the pressure data show the influence of wellbore storage and skin, followed by a linear and a bilinear flow-period, and later on by a pseudo-radial flow-period. The transmissivity of the bulk rock can be derived from the data of the pseudo-radial flow-period.

The complete set of test data shows that in the crystalline basement permeability decreases with depth. There is also evidence for pressure dependent hydraulic phenomena, in paricular permeability is found to vary with pressure.

Numerous high-pressure tests, some with well-head pressures of > 600 bar were carried in the Urach 3 borehole. The test data clearly show a P-dependence of permeability. During hydraulic tests with well-head pressures above 176 bar permeability of the crystalline basement increases dramatically, showing the elastic reaction of the rock due to pressure. At pressures below 176 bar the hydraulic data show no significant elastic reaction of the rock. A mathematical description of the pressure dependent increase of transmissivity has been derived from the data.

How do mineral substrates affect calcite nucleation and growth?

G.J. STOCKMANN[1,2]*, E.H. OELKERS[2], D. WOLFF-BOENISCH[1] AND N. BOVET[3]

[1]Institute of Earth Sciences, University of Iceland, Sturlugata 7, 101 Reykjavík, Iceland (*correspondence: gjs3@hi.is)

[2]Geochimie et Biogéochimie Experimentale, LMTG/CNRS, Université de Toulouse, 14 Avenue Edouard Belin, 31400 Toulouse, France (oelkers@get.obs-mip.fr)

[3]NanoScience Center, University of Copenhagen, Universitetsparken 5, 2100 Copenhagen Ø, Denmark

Calcite was precipitated in flow-through experiments at 25 °C from supersaturated aqueous solutions in the presence of seeds of calcite and six different silicates: augite, basaltic glass, enstatite, labradorite, olivine, and peridotite. The aim of the experiments was to determine how calcite nucleation and growth depends on the identity and structure of the growth substrate. Calcite saturation was achieved mixing a $CaCl_2$-rich solution with a $NaHCO_3$-Na_2CO_3 buffer in a mixed-flow reactor containing 0.5-2 grams of mineral grains. This led to a calcite saturation index of 0.6 and pH 9.1 for the reactive solution inside the reactor.

Although chemical conditions, flow rate and temperature were identical for all experiments, the onset of calcite nucleation and the amount of calcite being precipitated depended on the identity of the substrate. With calcite as the growth substrate, new calcite crystals formed instantaneously. Calcite nucleated relatively rapidly on olivine, enstatite, and peridotite (mainly composed of Mg-olivine). Scanning Electron Microscope images showed silicate crystals to be almost completed covered with calcite coatings at the end of the experiments. Less calcite growth was found on labradorite and augite, and least on basaltic glass. In all cases, calcite precipitation occurs on the mineral substrate and not adjacent to them.

These findings indicate that calcite nucleation and its subsequent growth depends on the crystal structure of the silicate substrate. Orthorhombic silicate minerals (olivine and enstatite) are the easiest for trigonal calcite to nucleate on. Monoclinic augite and triclinic labradorite show intermediate behavior, whereas basaltic glass with its non-ordered crystal structure is the least favorable platform for calcite growth. The results have implications for CO_2 mineralization in ultramafic and basaltic rocks [1] indicating that trigonal carbonates easier precipitate on crystalline rather than glassy rocks, but even glass surfaces can serve as a substrate for calcite nucleation.

[1] Oelkers *et al*. (2008) *Elements* **4**, 333–337.

https://doi.org/10.1180/S0026461X00006502 Published online by Cambridge University Press

A new methodology for an improved description of radionuclide retardation in safety assessments

M. STOCKMANN[1]*, V. BRENDLER[1], J. SCHIKORA[1], U. NOSECK[2] AND J. FLÜGGE[2]

[1]Helmholtz-Zentrum Dresden-Rossendorf, D-01328 Dresden, Germany (*correspondence: m.stockmann@hzdr.de)
[2]GRS Braunschweig, D-38122 Braunschweig, Germany

Conceptual model

In safety assessments usually the K_d concept with temporally constant values is applied to describe the radionuclide retardation in the far field of a repository.

In this study, the existing transport program r³t [1] used for large model areas and very long time scales has been improved. Implementing the smart K_d concept based on surface complexation allows to consider the impact of varying geochemical conditions.

The new methodology describes the sorption of radionuclides as a function of selected, important environmental parameters E_i such as pH, pCO_2, ionic strength, concentration of the cations Ca^{2+} and Al^{3+} and presence of characteristic mineral phases. The Gorleben site as a potential repository site in Germany has been selected as an exemplary case of application for a proof-of-concept.

Most of the individual parameters E_i were not available in r³t so far. Thus the transport of the respective substances as well as equations describing pH and concentrations of ions as a function of accessible mineral phases had to be implemented. Then the reactive transport model r³t can call pre-calculated K_d values for selected sediments for each time-space point. They are stored in a multidimensional matrix depending on the real geochemical conditions. Figure 1 shows the frequency distribution of the pre-calculated smart K_d values for Am^{3+} and UO_2^{2+}.

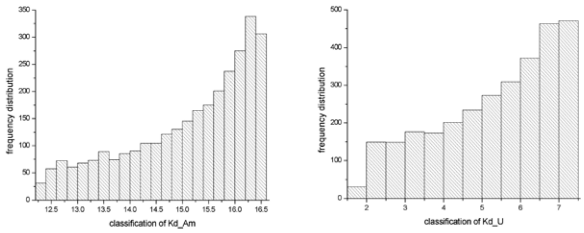

Figure 1: Frequency distribution of the pre-calculated K_d values for Am^{3+} and UO_2^{2+} (in m³/kg).

[1] Fein (2004) *Report GRS-192*.

Combined NanoSIMS and TEM *in situ* analysis of pristine matrix material of ALHA 77307 and Acfer 094

A.N. STOJIC[1]*, F.E. BRENKER[1] AND P. HOPPE[2]

[1]Goethe Universitaet, Institut fuer Geowissenschaften, 60438 Frankfurt/Main, Germany (stojic@em.uni-frankfurt.de)
[2]Max-Planck Institute for Chemistry, P.O. Box 3060, 55020 Mainz, Germany

Only a few structural studies on presolar silicates and oxides exist [1]. Commonly the NanoSIMS mapping technique is used to identify presolar grains in the meteoritic matrix from a polished thin section. To extract these presolar grains for further TEM analysis, a complex and risky lift out procedure by FIB is needed [1], reducing the availability of such grains for structural studies. In contrast, Argon Ion Slicing (ArIS), a recently introduced TEM sample preparation technique in geosciences, yields super large electron transparent areas of up to 40, 000 μm^2 [2]. The availability of extremely large thin foils makes a substantial change in the sequence of procedure steps possible, i.e. preparation of a large thin foil first, followed by the NanoSIMS scan on the previously obtained thin foil (Fig.1). No additional sample preparation for TEM is required once the grains are identified by NanoSIMS.

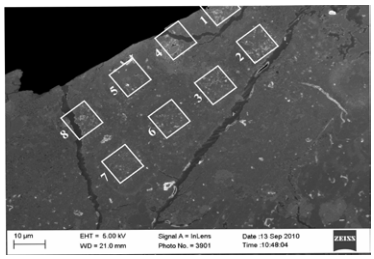

Figure 1: Thin foil section of ALHA 77307 with NanoSIMS scan windows indicated

Pieces of Acfer 094 and ALHA 77307 were ArIS treated until large electron transparent areas were obtained. These TEM thin foils were scanned for oxygen isotope ratios with a Cameca NanoSIMS 50. Based on large O-isotopic anomalies we detected 2 presolar grains (both silicates) out of 8 ion images (10 x 10 μm^2) in ALHA 77307, and 7 presolar grains (6 silicates and one oxide) out of 22 ion images (same size) from Acfer 094.

[1] Vollmer *et al*. (2009) *ApJ* **700**, 774–782. [2] Stojic & Brenker (2010) *Eur. J. Mineral*. **22**, 17–21.

https://doi.org/10.1180/S0026461X00006502 Published online by Cambridge University Press

Multimethod characterisation of nanoparticles in the environment

BJORN STOLPE[1]*, JAMIE LEAD[1], DAN LAPWORTH[2], STEPHANIE HANDLEY-SIDHU[1], JULIA FABREGA[3], TAMARA GALLOWAY[3], JESSICA POOLE[4], CORRINE WHITBY[4] AND IAN COLBECK[4]

[1]Shool of Geography Earth and Environmental Science, University of Birmingham, B15 2TT, UK (*correspondence: b.stolpe@bham.ac.uk, s.handley-sidhu@bham.ac.uk)
[2]British Geological Survey, Oxfordshire, OX10 8BB, UK (djla@bgs.ac.uk)
[3]School of Biosciences, University of Exeter, EX4 4PS, UK (t.s.galloway@exeter.ac.uk)
[4]Dept of Biological Sciences, University of Essex, Colchester, CO4 3SQ, UK (colbi@essex.ac.uk)

A range of techniques for the characterisation of nanoparticles will be presented, and their feasibility in studies of nanoparticle toxicity and environmental behaviour will be discussed. Techniques are often complimentary in the information they provide, and a multimethad approach is therefore recommended for nanoparticle characterisation. Results will be presented from the following studies, carried out at the Facility for Environmental Nanoparticle Analysis and Characterisation (FENAC) at the University of Birmingham:

1. Iron-rich and organic nanoparticles in anoxic groundwater, characterised under oxygen-free conditions by atomic force microscopy (AFM), transmission electron microscopy (TEM), scanning electron microscopy with energy-dispersive X-ray diffraction (SEM-EDX) and field-flow fractionation (FFF).
2. Biogenic hydroxyapatite – relation between metal uptake and particle size/surface area, determined by X-ray diffraction (XRD), BET-surface area measurements, SEM, DLS and zeta-potential measurements.
3. ZnO nanoparticle dissolution and toxicity to marine invertebrates - dependency on particle size and morphology, characterised by TEM, AFM, dynamic light scattering (DLS), zeta-potential measurements and nano-tracking analysis (NTA).
4. Nanoparticle impact on bioremediation of hydrocarbons in aquatic ecosystems - relation to particle size and chemistry, determined by DLS, FFF, TEM and XRD.

Pore scale heterogeneity of porous media influencing the spatial and temporal distribution of microbial metabolic activity

KONSTANTIN STOLPOVSKY[1], MEHDI G. GHARASOO[2] AND MARTIN THULLNER[2]

[1]Department of Earth Sciences – Geochemistry, Utrecht University, the Netherlands (k.stolpovsky@geo.uu.nl)
[2]Department of Environmental Microbiology, UFZ – Helmholtz Centre for Environmental Research, Leipzig, Germany (mehdi.gharasoo@ufz.de, martin.thullner@ufz.de)

Microbial activity plays a crucial role in the cycling of carbon, nutrient elements and contaminants in the environment. This includes porous environments like soils or aquifers. These bacterial habitatats are often characterized by a high temporal variability of substrate supply, and by a high spatial heterogeneity of the porous matrix at the pore scale. As a consequence, microbial growth conditions and the resulting microbial redox activity in natural porous media environments may differ from typical laboratory setups used to study microbial behaviour. Pore scale heterogeneities and the resulting transport regime can lead to highly complex distribution patterns of substrates and the corresponding microbial growth conditions including the frequent occurrence of stress periods for the microbial population. Microorganisms can respond to such stress periods by switching from an active into an inactive or dormant state, and the corresponding microbial abundance and substrate degradation dynamics may exhibit rather complex temporal and spatial patterns.

This study considers an extended modelling concept for the growth and degradation activity of microbial species able to switch between two different physiological states. This concept is implemented into a pore network model which allows simulating the changes of microbial growth conditions in heterogeneous porous media. The model is used to study the impact of pore scale heterogeneities on the distribution and activity of microorganisms in such media and to determine the biodegradation capacity of the microbial population.

https://doi.org/10.1180/S0026461X00006502 Published online by Cambridge University Press

Sources, sinks, and reactivity of electrophilic groups within natural organic matter

A.T. STONE* AND P.M. FLANDERS

Geography and Environmental Engineering, Johns Hopkins Univ., Baltimore, MD 21218, USA (*correspondence: astone@jhu.edu)

Carbonyl and carboxylate ring substituents are believed to be present in high abundance within natural organic matter (NOM). Their potential impact on the reactivity of dihydroxybenzene/benzoquinone functionalities has not, however, been addressed. Owing to their electron-withdrawing nature, carbonyl and carboxylate ring substituents raise the redox potential necessary for oxidizing dihydroxybenzenes to corresponding benzoquinones. Carbonyl- and carboxylate-substituted benzoquinones generated in this way are far more electrophilic than unsubstituted analogs, and hence capable of Michael-type adduct formation with a wider range of oxygen-, nitrogen-, and sulfur-donor nucleophiles. Heightened electrophilicity also raises rates of competitive hydration reactions.

We have observed these phenomena in experiments employing low MW NOM surrogates. MnO_2 (pyrolusite) readily oxidizes acetoxyhydroquinone to acetoxy-p-benzoquinone and gentisate to carboxy-p-benzoquinone. Unlike unsubstituted p-benzoquinone, p-benzoquinones possessing electron-withdrawing groups rapidly hydrate. Adduct yields increase substantially as the nucleophile concentration is increased, a reflection of more successful competition relative to the hydration pathway.

Benzoquinones are one sub-class of conjugated ene carbonyls capable of Michael-type adduct formation. It is possible that oxidation reactions, e.g. by manganese(III, IV) oxyhydroxide crusts within oxic sediments, generate other reactive, transient electrophiles. Knowledge of their sources and sinks may improve our understanding of elemental and functional group incorporation into NOM.

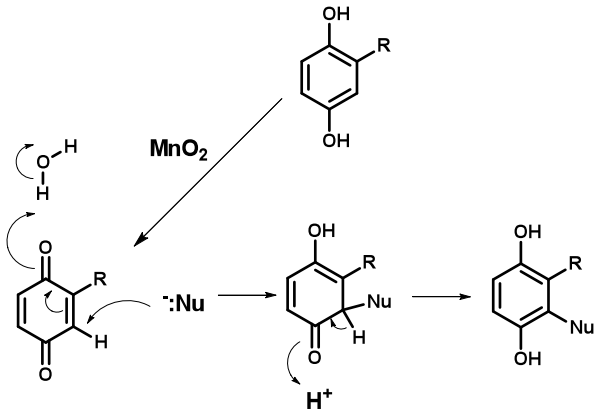

Cosmogenic nuclide measurements of Pleistocene glacial erosion

JOHN STONE*, ZACHARY PLOSKEY, BERNARD HALLET AND MARC JAFFREY

Dept of Earth and Space Sciences, University of Washington, Box 351310, Seattle, WA, 98195, USA (*correspondence: stn@uw.edu, zploskey@uw.edu, hallet@uw.edu, mjaffrey@uw.edu)

Glacial erosion plays a crucial role in landscape evolution at high altitudes and high latitudes, at the nexus between mountain building, surface processes and climate. Yet we lack a quantitative basis for incorporating glacial erosion into numerical models of these processes, and have few specific estimates of glacial erosion over 10^5-10^6 year timescales. We have developed a method of measuring past glacial erosion rates using cosmogenic nuclide depth profiles in bedrock. We are using this to determine glacial erosion histories, improve glacial erosion laws, and incorporate these into geomorphic process models.

Cosmogenic nuclide measurements on rock and soil surface samples have been widely used to estimate erosion rates in continuously exposed landscapes. Conversely, measurements on glaciated bedrock have been used primarily to date ice retreat, or, where such ages are compromised by prior exposure, to identify the sites as areas of limited glacial erosion. However, because the survival of nuclides produced beneath glaciated surfaces depends on subsequent glacial erosion, depth profiles accumulate information about the cumulative erosion history. Nuclide concentrations, concentration gradients and ratios are all sensitive to the history of exposure and erosion; we can use inverse methods to recover long-term average erosion rates of glaciated landforms from these data. Published cosmogenic nuclide measurements from glaciated bedrock surfaces suggest that these methods will be widely applicable to the study of mid- to late-Pleistocene erosion beneath glaciers and ice sheets.

https://doi.org/10.1180/S0026461X00006502 Published online by Cambridge University Press

Observational and modeling study of the relationship between aerosols and super-cooled cloud fraction

TRUDE STORELVMO[1], ULRIKE LOHMANN[2] AND YONG-SANG CHOI[3]

[1]Yale University, New haven, CT, USA (trude.storelvmo@yale.edu)
[2]ETH-Zurich, Zurich, Switzerland (ulrike.lohmann@env.ethz.ch)
[3]Ewha Womans University, Seol, Korea (ysc@ewha.ac.kr)

Recent observational and modeling studies indicate that aerosols may have a strong effect on Earth's energy budget via their influence on mixed-phase clouds. Global climate studies have predicted aerosol interaction with mixed-phase clouds to warm the current climate, but estimates are uncertain because mixed-phase cloud processes in GCMs are highly parameterized and have to date been poorly constrained by satellite data. Here, we present global and regional distributions of the frequency of supercooled cloud water and its link to aerosols from two global climate models (GCMs), compared to a new satellite data set. Both GCMs link ice formation at temperatures between -40 and 0 degrees C to the simulated concentrations of aerosols with ice nucleating ability (IN), assigning different freezing efficiencies to the different insoluble aerosol species (mineral dust, bio-aerosols and soot). Consequently, both models generally simulate an anti-correlation between aerosol abundance and supercooled liquid water in clouds, a finding that was recently qualitatively confirmed by satellite observations. By studying the relationship between aerosols and the supercooled cloud fraction (SCF) from the GCMs and from the NASA spaceborne lidar instrument CALIOP (cloud-aerosol lidar with orthogonal polarization), we get strong indications of how aerosols may influence mixed-phase clouds. We argue that with the new validation of SCF and its link to aerosols, GCM estimates of aerosol effects on climate via their influence on mixed-phase clouds may become more reliable.

The magmatic, metamorphic, mineralisation and plate tectonic evolution of continents

CRAIG D. STOREY[1]* AND MARTIN P. SMITH[2]

[1]School of Earth and Environmental Sciences, University of Portsmouth, PO1 3QL, UK (*correspondence: craig.storey@port.ac.uk)
[2]School of Environment and Technology, University of Brighton, BN2 4GJ (martin.smith@brighton.ac.uk)

Around 60% of continental crust was formed by the end of the Archaean and since then some form of plate tectonics has driven periods of supercontinent formation (at c.2.7 Ga, 1.9 Ga, 1.1 Ga and 0.35 Ga). Net growth of new crust declined in the Proterozoic and Phanerozoic and at the same time there has been a change in the mode of subduction from predominantly flat in the Archaean to progressively steeper towards the present day. This, along with the gradual cooling of the Earth, has resulted in marked changes in the preserved magmatic, metamorphic and mineralisation record. The first appearance of high-pressure metamorphic rocks, implying either overthickened crust or subduction, occurs in the Late Archaean around 2.7 Ga. There is a step-change in the magmatic products of subduction at the Archaean-Proterozoic transition from dominantly TTG through sanukitoid to calc-alkaline (basalt-andesite-diorite-rhyolite) as the main mode, which is most likely a result of a change in subduction angle and the development of a mantle wedge. This marks the onset of a form of modern plate tectonics. Whilst subduction magmas have been continuously produced they have also been continuously destroyed at continental margins, except at times when supercontinents formed, leading to pronounced peaks in crystallisation ages of detrital zircons. World-class ore deposits also correlate with the supercontinent cycle. During the Palaeoproterozoic (c.2.4-2.1 Ga) there was a period of anomalously low net continental growth followed by a peak of growth and mineralisation at c.1.9-1.8 Ga. We show how Fe-Oxide and related Cu and Au deposits can be linked to this cycle by measurement of Nd isotopes within titanite. The results imply that fertile mafic crust was incubated on the margins of the Archaean craton in the early Palaeoproterozoic but mineralisation did not occur until an arc was initiated at the margin and hence provided a heat and fluid source for mobilisation and concentration of the metals. The implication is that the formation and preservation of new continental crust is related to plate tectonics and the supercontinent cycle, which in turn controls the concentration and preservation of world-class ore deposits.

https://doi.org/10.1180/S0026461X00006502 Published online by Cambridge University Press

The mid-depth $\Delta^{14}C$ anomaly during termination 1, Do hydrothermal vents play a role?

LOWELL D. STOTT[1]* AND AXEL TIMMERMANN[2]

[1]Department of Earth Sciences, University of Southern California, Los Angeles, 90089 (stott@usc.edu)
[2]Department of Oceanography, University of Hawaii at Manoa, 1000 Pope Road, Marine Sciences Building, Honolulu, HI 96822 (axel@hawaii.edu)

The ~-190‰ drop in surface ocean and atmosphere $\Delta^{14}C$ during the last glacial termination cannot be explained entirely by ^{14}C production change and thus appears to require a flux of ^{14}C-depleted carbon into the upper ocean/atmosphere or a repartitioning of carbon in the ocean. A deglacial $\Delta^{14}C$ stratigraphy from deep Pacific cores does not exhibit a -190‰ decline as observed in upper ocean records during the 'Mystery Interval' [1]. There are large benthic ^{14}C-age excursions in several deglacial records from intermediate water depth cores at low latitudes but not in higher latitude cores [2]. These observations lead us to consider whether the flux of ^{14}C-depleted carbon from hydrothermal sites in the Pacific played a role in the Mystery Interval $\Delta^{14}C$ changes. Recent studies document liquid CO_2 and CO_2-rich fluids accumulationin in sediments that blanket active vents. The storage and net flux of CO_2 from the sediments is regulated by a CO_2-hydrate cap at the sediment/water interface. The temperature dependence of CO_2 hydrate stability is a possible mechanism for affecting storage and release of CO_2 and CO_2-rich fluids from sediments. We explore a hypothesis where hydrothermal systems act as a 'capacitor' for CO_2 storage-release. CO_2-hydrate stability expands upward to shallower depths during glaciation, reducing the net flux of ^{14}C-depleted CO_2 to the ocean. During deglaciation, CO_2-hydrate stability deepens, releasing ^{14}C-depleted CO_2 from sediment reservoirs. A ~3ºC temperature increase at intermediate depths in the Pacific during T1 would have lowered the hydrate stability horizon several hundred meters and released ^{14}C-depleted carbon to the upper ocean/atmosphere. This would explain why abyssal water masses were not anomalously old during the last glacial and why the -190‰ decrease in $\Delta^{14}C$ during the Mystery Interval is not observed at deep water sites.

[1] Broecker, W. & S. Barker (2007) *Earth & Planetary Science Letters* **256**(1-2), 90–99. [2] Stott. L & Timmerman. A (2011) *Hypothesised link between glacial/ interglacial atmospheric CO_2 cycles and storage/release CO_2 – rich fluids from the deep sea*. AGU Geophysical monograph series: Understanding the causes, mechanisms and extent of abrupt climate change.

Sampling the Earth's mantle

A. STRACKE

Westfälische Wilhelms Universität, Institut für Mineralogie Corrensstrasse 24, 48149 Münster, Germany (stracke.andreas@uni-muenster.de)

The Earth's mantle is isotopically highly heterogeneous, certainly on the kilometer scale of the melting region, but perhaps even on a smaller scale. During partial mantle melting and melt extraction, instantaneous melts from a range of depths are mixed to different extents, eventually forming the melts sampled by oceanic volcanism. Mixing of partial melts from a range of different source components has an averaging effect that biases the isotopic composition of the melts compared to those of their mantle sources. The isotopic composition of oceanic basalts hence reflects only a limited extent of the isotopic heterogeneity present in the mantle.

The relative amount of melt mixing is reflected in the correlations between isotope ratios and different trace element parameters. For OIB, where melt extraction occurs over a short depth interval underneath a thick oceanic lithosphere, little melting of refractory, depleted mantle components occurs. Consequently, melts from the enriched mantle components do not become significantly diluted, resulting in few correlations between isotope and trace element ratios, but also a close correspondence of enriched melt and average enriched source signatures. In ridge-related settings, in the absence of a thick oceanic lithosphere, the depleted mantle components melt to a large extent, and the enriched melts are diluted significantly during partial melting and melt extraction. Melts from the enriched source components, however, still dominate the final erupted melt and obscure the true extent of mantle depletion in mid ocean ridge basalts (MORB). Hence the depleted components of the Earth's mantle are expected to be isotopically more extreme than even the most depleted MORB.

Care must be taken, therefore, to extrapolate the isotopic variation observed in oceanic basalts directly to mantle heterogeneity. Before attributing the isotopic signatures of the basalts directly to those of the mantle, it needs to be understood how partial melting samples and averages heterogeneous source components. Only then can we infer the distribution of heterogeneous source components, their size, mineralogical, chemical and isotopic composition, which is a prerequisite for inferring the origin of the various heterogeneous materials in the Earth's mantle.

https://doi.org/10.1180/S0026461X00006502 Published online by Cambridge University Press

Pb concentrations, stable isotopes and ^{210}Pb in seawater, phytoplankton, zooplankton, sardines, anchovy from the Gulf of Lion

EMILIE STRADY[1], ALAIN VERON[1], JEAN FRANCOIS CHIFFOLEAU[2] AND OLIVIER RADAKOVITCH[1]

[1]University Paul Cezanne, CEREGE laboratory, Aix en Provence, France (strady@cerege.fr, radakovitch@cerege.fr, veron@cerege.fr)
[2]IFREMER, LBCM, Nantes, France (jfchiffo@ifremer.fr)

Introduction

The COSTAS project aims at understanding the trophic transfer of metallic contaminants through seawater, phytoplankton, zooplankton, sardine and anchovy populations in the Gulf of Lion (NW Mediterranee). Its originality is to combine the ecology of the trophic web and the biogeochemistry of the metallic contaminants. We present here preliminery results of bioaccumulated lead in each compartment at four stations, which were emphasized by analysing for the first time and in the same samples ^{210}Pb activity as a proxy of natural lead and $^{204, 206, 207, 208}$ Pb stable isotopes as proxy of anthropogenic Pb in the environment.

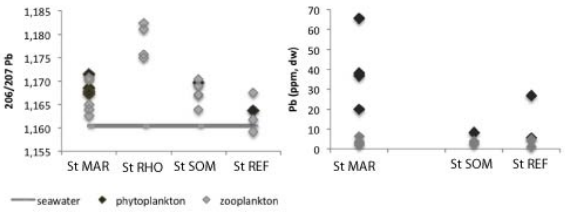

Figure 1: preliminary $^{206/207}$Pb and Pb concentrations in seawater, phytoplankton and zooplankton in the Gulf of Lion.

Results and discussion

Higher Pb concentrations in phytoplankton than in zooplankton (Fig 1) confirm the low ability of Pb to bioaccumulate in zooplankton. Pb isotopes ratios show different signatures among stations, despite constant Pb concentrations, close to the seawater signal in station far from the coast (St REF) and close to the radiogenic signal (1.175) in the Rhone station (St RHO). Emphasis on the relation between isotopes signals, Pb concentrations and plankton size/species will conduct to better understand the assimilation of Pb by plankton.

Review on biogeochemistry of microbial coal-bed methane

DARIUSZ STRĄPOĆ[1,2,3]

[1]Dariusz BioGeoChem LLC, Houston, TX 77077 USA (strapoc@gmail.com)
[2]Indiana University, Bloomington, IN 47405, USA
[3]Formerly: ConocoPhillips, Houston, TX 77079 USA

Microbial methane accumulations have been discovered in multiple coal-bearing basins over the past two decades. Such discoveries were originally based on unique biogenic signatures in the stable isotopic composition of methane and carbon dioxide. Basins with microbial methane contain either low-maturity coals with predominantly microbial methane gas or uplifted coals containing older, thermogenic gas mixed with more recently produced microbial methane. Recent advances in genomics have allowed further evaluation of the source of microbial methane, through the use of high-throughput phylogenetic sequencing and fluorescent in situ hybridization, to describe the diversity and abundance of bacteria and methanogenic archaea in these subsurface formations. However, the anaerobic metabolism of the bacteria breaking coal down to methanogenic substrates, the likely rate-limiting step in biogenic gas production, is not fully understood. Coal molecules are more recalcitrant to biodegradation with increasing thermal maturity, and progress has been made in identifying some of the enzymes involved in the anaerobic degradation of these recalcitrant organic molecules using metagenomic studies and culture enrichments. In recent years, researchers have attempted lab and subsurface stimulation of the naturally slow process of methanogenic degradation of coal [1].

Discussion includes description of (i) how occurrences of microbial methane accumulations in coal beds are identified through the use of geochemical tools such as stable isotopes; (ii) geological and hydrogeological constraints of such accumulations; (iii) the origin and composition of coal as the substrate and implications to microbial methane formation; (iv) methods of analysis of microbial metabolic pathways and microbial communities involved in biodegradation of various moieties of coal's organic matter; (v) attempts of stimulation of enhanced microbial methane generation in coals.

[1] Strapoc *et al*. (2011) *Annu. Rev. Earth Planet. Sci* **39** 617-656

https://doi.org/10.1180/S0026461X00006502 Published online by Cambridge University Press

Challenges to predicting the fate of emerging classes of organic micropollutants in subsurface environments

TIMOTHY J. STRATHMANN[1]*, MICHAEL MACHESKY[2], KEVIN FINNERAN[3] AND TIAS PAUL[1]

[1]Univ. Illinois, Dept. Civil & Environ. Engr., Urbana, IL 61801 USA (*correspondence: strthmnn@illinois.edu)
[2]Illinois State Water Survey, Champaign, IL 61820 USA
[3]Clemson Univ., Environ. Engr. Earth Sci., Anderson, SC 29625 USA

Widespread detection of emerging micropollutants (e.g. antibiotics, hormones, personal care products) in soil and aquatic environments has raised serious concerns that necessitate improved understanding of processes controlling their environmental fate. However, existing models and reaction mechanisms are inadequate for predicting the fate of micropollutants that possess complex structures and functional groups not usually present in more commonly studied contaminants. Here, we describe recent efforts to characterize processes and mechanisms contributing to the fate of two widely detected classes of antibiotic micropollutants (sulfonamides, fluoroquinolones). First, we describe a novel microbially mediated-abiotic transformation mechanism for the antibiotic sulfamethoxazole (SMX) in subsurface environments. Rapid dissipation of SMX is observed in iron-reducing soil microcosms, and mechanistic studies demonstrate that SMX transformation occurs via abiotic reactions of sorbed Fe(II) with an isoxazole group in the SMX structure, a moiety not previously reported to be amenable to reductive transformation in soil environments.

The complex poly-ionogenic structures of some micropollutants have complicated efforts to predict sorption and speciation in subsurface environments. For example, the unique characteristics of zwitterionic fluoroquinolone (FQ) structures (presence of both positively and negatively charged groups) lead to complex electrostatic interactions with charged surfaces that cannot be accounted for by isotherm or point-charge surface complexation models. Here, we describe the application of a charge-distribution (CD) surface complexation model for zwitterionic species sorbing to variably charged oxide minerals. Model formulation includes functional group-specific inner- and outer-sphere bonding interactions with mineral surfaces, in accordance ATR-FTIR spectroscopic observations. CD model predictions agree closely with measurements of FQ sorption to three oxide soil minerals (TiO_2, α-FeOOH, and γ-AlOOH) collected over a wide range of pH, ionic strength and FQ concentrations.

Multiple sulfur isotopic evidence for multiple origins of late Archean and early Paleoproterozoic sediment-hosted pyrite, Quadrilátero Ferrífero of Minas Gerais

H. STRAUSS[1]*, A.R. CABRAL[2], A. CORDING[1] AND N. KOGLIN[3]

[1]Institut für Geologie und Paläontologie, WWU Münster, 48149 Münster, Germany (*correspondence: hstrauss@uni-muenster.de)
[2]Technische Universität Clausthal, Lagerstätten und Rohstoffe, 38678 Clausthal-Zellerfeld, Germany
[3]Julius-Maximilians-Universität Würzburg, Institut für Geographie und Geologie, 97074 Würzburg, Germany

Multiple sulfur isotopes were measured in different types of pyrite (detrital, framboidal, euhedral, finely disseminated) from a late Archean to early Proterozoic metasedimentary succession in the Quadrilátero Ferrífero of Minas Gerais, southern São Francisco craton, Brazil. Samples derive from the Moeda Formation, a coarse clastic, metaconglomeratic unit, and carbonaceous phyllite of the Batatal Formation. The Moeda Formation rests unconformably on Archean greenstone rocks and is conformably overlain by the Batatal Formation. The depositional age for both sedimentary units is bracketed between 2580 and 2420 Ma [1].

Multiple sulfur isotope results display distinct differences between the type of pyrite and the stratigraphic position of the host metasedimentary rocks. This offers the potential for resolving pyrite provenance and formation, for distinguishing prevailing metabolic pathways, and identifying the overall oxidation state of Earth's atmosphere.

All pyrite samples show clear mass-independently fractionated sulfur isotopes, defining a slope of -1 in a $\Delta^{36}S/\Delta^{33}S$ plot. This confirms previously published data and underlines the interpretation of a low atmospheric oxygen abundance [2]. Combining $\delta^{34}S$ and $\Delta^{33}S$, detrital and euhedral pyrite from the Moeda metaconglomerate exhibit largely positive values of $\Delta^{33}S$ (up to +8‰). In contrast, framboidal pyrite from the Moeda Formation has negative multiple sulfur isotope values. Pyrite from the overlying Batatal Formation displays also mostly negative $\delta^{34}S$ and $\Delta^{33}S$ values. These results indicate at least two different metabolic pathways archived: microbial turnover of elemental sulfur and sulfate reduction.

[1] Hartmann *et al*. (2006) *J. South Amer. Earth Sci.* **20**, 273–285. [2] Johnston (2011) *Earth Sci. Rev.* **106**, 161–183.

https://doi.org/10.1180/S0026461X00006502 Published online by Cambridge University Press

Fluid-enhanced crystallization to generate high-S apatite of silicic magmas: Evidence from Pinatubo and other calc-alkaline systems

MARTIN J. STRECK[1]*, ASHLEY VAN HOOSE[1], CINDY BRODERICK[2] AND FLEURICE PARAT[3]

[1]Department of Geology, Portland State Univ., Portland, OR 97207, USA (*correspondence: streckm@pdx.edu)
[2]Department of Mineralogy, Univ. of Geneva, Geneva 1205, Switzerland (Cindy.Broderick@unige.ch)
[3]Géosciences Montpellier, Univ. Montpellier 2, Montpellier cedex 5, France (Fleurice.Parat@gm.univ-montp2.fr)

We consider high-S apatites to be apatites with ≥0.7 wt.% SO_3. High-S apatites of magmas with rhyolitic melt are of particular interest because experimental data suggest that such apatites are 'over enriched' in S relative to equilibrium crystal-melt partitioning processes. In Pinatubo dacite, 29% of all investigated apatites (N=69) include high-S concentrations. Conversely, the dominant apatite populations of silicic oxidized magmas are medium- (0.3-0.6 wt.% SO_3) and low-S (<0.3 wt.% SO_3) apatites (also at Pinatubo), which are consistent with crystallization from melt at or below S saturation at various temperatures.

Explanations for high-S apatites range from inheritance (from mafic magmas or country rock) to S exchange between apatite and anhydrite as a consequence of close petrographic association of both phases in systems containing anhydrite (e.g. at Pinatubo). The compositional fingerprint (e.g. REE, Sr) ties high-S apatites to the same melt environment as the dominant populations, and thus makes inheritance unlikely. Finding low-S apatite inclusions in anhydrite in conjunction with the lack of consistent rimward enrichment of S of anhydrite-hosted apatites, argues against S exchange between these two phases.

To generate high-S apatite, we envision a process that we call 'fluid-enhanced crystallization,' whereby the high-S signal is controlled by the presence of a S-rich fluid adjacent to a growing apatite while other compositional characteristics are mostly controlled by the silicate melt. This process would be consistent with observed reverse S zonation towards the rim, small scale and strong changes in S content within single grains, occurrence of low- to high-S apatites as inclusions together in single host minerals, and compositional similarity among low- to high-S apatites. At Pinatubo the existence of such S-rich fluid is corroborated by S isotopes of anhydrite as well as growth features of anhydrite. A suitable source for S-rich fluids would be fluids derived from degassing underplated mafic magmas.

Post-collisional magmatism during Variscan orogeny: The Furcatura pluton (Danubian domain, Romanian Southern Carpathians)

C. STREMTAN[1], J. RYAN[1], V. ATUDOREI[2] AND I. CHERATA[3]

[1]Dept. of Geology, University of South Florida, Tampa, US (cstremta@mail.usf.edu)
[2]Dept. of Earth and Planetary Sciences, University of New Mexico, Albuquerque, US
[3]Dept. of Geology, "Babes-Bolyai" University, Cluj-Napoca, Romania

Exploratory geochronological data indicate that the Furcătura pluton (312 ±2.8 Ma) was emplaced during the Hercynian orogeny. This late stage magmatism is essentially granitic/granodioritic, lacking associated basic rocks. Furcatura pluton (FP) is remarkably heterogeneous, showing wide ranges for most of the petrographical and geochemical parameters. The metaluminous to slightly peraluminous (average A/CNK of 1.04) granitoids are high-K (K_2O/Na_2O of 0.51-1.63) calc-alkaline, while some samples have shoshonitic affinity (maximum K_2O of 5.61). They lack significant Eu anomalies (average Eu/Eu* of 0.94) and have subparallel REE patterns, with ΣREE ranging from 51.11 to 203.7. The heterogeneous character of the FP is further reflected in the $\delta^{18}O$ values of the quartz separates, ranging from 7.37 to 11.59‰, with the highest values measured in the late magmatic aplitic veins. In conventional discrimination diagrams, as well as reflected by their trace elemental compositions, FP granitoids show both I- and S-type granite features. Geochemical evidence suggests the pluton was derived from a heterogeneous, primarily (lower?) crustal source, with subordinate additions of mantle-derived melts (e.g. low Nb/U and Ce/Pb). However, based on available data, contributions from a previously subduction-enriched mantle component can not be completely ruled out. Therefore, the FP granitoids may provide clues for deciphering the processes involved in the production of post-collisional magmas.

https://doi.org/10.1180/S0026461X00006502 Published online by Cambridge University Press

Study of candidate matrix-matched calibration standards for geological applications by nuclear and laser ablation based methods

VLADIMÍR STRUNGA[1], VLADIMÍR HAVRÁNEK[2], JAN KUČERA[2], VIKTOR KANICKÝ[1], TOMÁŠ VACULOVIČ[3], ALEŠ HRDLIČKA[3], ZDENĚK MORAVEC[3], DALIBOR VŠIANSKÝ[1], JIŘÍ PINKAS[3], MILOŠ KLÍMA[4] AND JINDŘICH KYNICKÝ[5]

[1]Department of Geological Sciences, Masaryk University, Kotlářská 2, 611 37 Brno (strunga@sci.muni.cz)
[2]Nuclear Physics Institute of the ASCR, Řež 130, 250 68 Řež
[3]Department of Chemistry and CEITEC MU, Masaryk University, Kotlářská 2, 611 37 Brno
[4]Department of Physical Electronics, Masaryk University, Kotlářská 2, 611 37 Brno
[5]Department of Geology and Pedology, Mendel University of Agriculture and Forestry, Zemědělská 3, 61300 Brno

Laser ablation with induction coupled mass spectroscopy (LAICPMS) and laser induced breakdown spectroscopy (LIBS) became widely used in geological sciences. For quantification procedure of methods based on laser ablation, the matrix matched standards are required. Such standards, are largely lacking, especially for geological applications. We aimed at filling this gap by analyzing minerals, rocks, fused powdered rocks, sol-gel derived and plasmochemically deposited mineral analogues to identify possible candidate materials. The homogeneity and trace elements contents of the above mentioned materials were examined using μ-PIXE, LAICPMS-screening and by PIXE/PIGE/INAA techniques. Major/minor elements were studied using EPMA. PIGE is capable to detect some light elements that are not detectable by X-ray spectroscopic methods. INAA provides reliable informations about trace element composition of examined materials, with favourable detection limits compared with the majority of common analytical techniques.

Work has been supported by SAMAS MUNI/G/0124, GAPT MUNI/E/0139, MSM 0021622410, CZ.1.05/1.1.00/02.0068, and GACR P207/11/0555.

Constraints on Earth outgassing history from Ar isotope composition of Devonian atmosphere

FINLAY M. STUART AND DARREN F. MARK

Isotope Geosciences, Scottish Universities Environmental Research Centre, East Kilbride G75 0QF, UK

The noble gases have long been used to show that the terrestrial atmosphere resulted from the outgassing of the Earth's interior rather than capture of the solar nebula during accretion. The primordial and radiogenic isotopes of the noble gases combine to make them a powerful tool for determining the time and tempo of Earth outgassing. Our understanding of the outgassing history of the Earth is largely derived from measurements of He, Ne, Ar and Xe isotope in samples of modern mantle, crust and atmosphere. Despite several attempts [1] there has been no unequivocal measurement of the isotopic composition of noble gases in ancient atmosphere.

We have now determined the Ar isotope composition of pristine samples of the 404 Ma Rhynie chert using a new multi-collector mass spectrometer and a low blank laser extraction technique. $^{40}Ar/^{36}Ar$ are systematically lower than the modern air value, and are not accompanied by non-atmospheric $^{38}Ar/^{36}Ar$ ratios. We conclude that the Rhynie chert has captured Devonian atmosphere-derived Ar. The data indicate that the $^{40}Ar/^{36}Ar$ of Devonian atmosphere was at least 3 % lower than the modern air value. Thus the Earth's atmosphere has accumulated at least $5 \pm 0.2 \times 10^{16}$ moles of ^{40}Ar in the last 400 million years, at an average rate of $1.24 \pm 0.06 \times 10^{8}$ mol ^{40}Ar/year. This overlaps the rate determined from ice cores for the last 800, 000 years [2] and implies that there has been no resolvable temporal change in outgassing rate since the mid-Palaeozoic. The new data require outgassing early in Earth history, and suggest that pristine samples of Archaean and Proterozoic chert may prove useful as palaeo-atmosphere tracer.

[1] Turner, G. (1989) *J. Geol. Soc. London* **146**, 147–154.
[2] Bender, M. *et al.* (2008) *Proc. Nat. Acad. Sci.* **105**, 8232–8237.

https://doi.org/10.1180/S0026461X00006502 Published online by Cambridge University Press

Glaciers: A window into anthropogenic perturbation of the global carbon cycle

ARON STUBBINS[1†], E. HOOD[2], P.A. RAYMOND[3], G.R. AIKEN[4], R.L. SLEIGHTER[1], P.J. HERNES[5], D. BUTMAN[3], P.G. HATCHER[1], R.G. STRIEGL[4], P. SCHUSTER[4], H.A.N. ABDULLA[1] AND R.G.M. SPENCER[6]

[†] Skidaway Institute of Oceanography, Savannah, GA, USA
[1]Old Dominion University, Norfolk, VA, USA
[2]University of Alaska Southeast, Juneau, AK, USA
[3]Yale University, New Haven, CT, USA
[4]USGS, 3215 Marine Street, Boulder, CO, USA
[5]University of California, Davis, CA, USA
[6]Woods Hole Research Center, Falmouth, MA, USA

Glacier-derived dissolved organic matter (DOM) provides a significant source of ancient, yet highly bioavailable C to downstream ecosystems. The remnants of ancient peatlands and forests since overrun by glaciers have been invoked as a source of this ancient, labile DOM. Here we challenge this hypothesis, demonstrating that DOM exported from glaciers is predominantly anthropogenic and enters glaciers in a pre-aged form. C-containing aerosols, mainly from biomass and fossil fuel burning, are the original source of this aged-glacier DOM. Once deposited on glacier surfaces, aerosol DOM is exported downstream, providing an energy subsidy to aquatic ecosystems. As deposition of combustion products is a global phenomenon, we propose that all ecosystems are receiving this ancient, labile C subsidy. In vibrant ecosystems, the labile DOM windfall is presumably rapidly processed, its signal lost and impact masked. In frigid glacier environments, these inputs stand out, making glaciers sentinel ecosystems for the study of perturbation to global biogeochemical cycles through anthropogenic deposition. This deposition is predicted to increase in the future as emissions of combustion derived aerosols accelerates along with industrial growth.

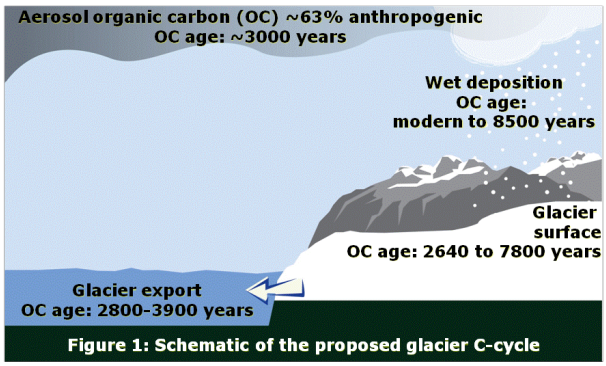

Figure 1: Schematic of the proposed glacier C-cycle

Climatically driven changes in sediment supply on the SW Iberian shelf since the Last Glacial Maximum

R. STUMPF[1]*, M. FRANK[1], J. SCHÖNFELD[1] AND B.A. HALEY[1,2]

[1]Leibniz Institute of Marine Sciences (IFM-GEOMAR), Wischhofstraße 1-3, 24148 Kiel, Germany (*correspondence: rstumpf@ifm-geomar.de)
[2]College of Oceanic & Atmospheric Sciences, 104 Ocean Admin. Bldg., Corvallis, OR 97331-5503, USA

The assemblage of marine sediments on the SW Iberian shelf reflects various ambient particle sources that have undergone significant changes as a function of prevailing weathering and transport regimes since the Last Glacial Maximum (LGM). The relatively rapid, decadal scale Mediterranean overturning circulation permits mixing of suspended particles from the entire Mediterranean Sea. They are entrained into the suspended particulate matter (SPM) carried by Mediterranean Outflow Water (MOW), which enters the Eastern North Atlantic through the Strait of Gibraltar and spreads at intermediate water depth in the Gulf of Cadiz and along the Portuguese continental margin. Further major sediment sources that have potentially contributed to the budget of SPM along the flow path of MOW on the SW Iberian shelf are North African dust and river transported particles from the Iberian Peninsula. In order to reconstruct climate and circulation driven changes in the supply of sediments from these sources over the past ~23 000 years, radiogenic Nd, Sr, and Pb isotope records of the clay-size sediment fraction were produced from three gravity cores in the Gulf of Cadiz (577 m) and on the Portuguese shelf (1745 m, 1974 m). These records were supplemented by time series of clay mineral abundances and clay mineral ratios from the same set of samples. Contrary to expectations, the transition from the LGM to the Holocene was not marked by very strong changes of the source areas of the sediments deposited on the SW Iberian shelf. However, the Heinrich stadial 1 and the African Humid Period are marked by significantly different isotopic records. The data also suggest that the continental chemical weathering regime changed with prevailing climate conditions and supplied the SW Iberian shelf with variable clay mineral abundances from essentially the same source rocks.

https://doi.org/10.1180/S0026461X00006502 Published online by Cambridge University Press

High methane oxidation rates in ferruginous lake Matano

A. STURM[1], S.A. CROWE[2], C.A. JONES[2], K.L. LESLIE[1], D.E. CANFIELD[2], S. NOMOSATRYO[3], A. MUCCI[4] AND D.A. FOWLE[1]

[1]Dept. of Geology, University of Kansas (arsturm@ku.edu)
[2]NordCEE, Syddansk Universitet, Odense Denmark
[3]Research Center for Limnology, Indonesian Institute of Sciences (LIPI), Cibinong-Bogor, Indonesia
[4]Earth and Planetary Sciences, McGill University, Montréal, Canada

Lake Matano is the 8th deepest lake on the planet and is the world's largest known ferruginous basin [1]. This ancient lake is persistently stratified, and beyond its high Fe content, it is characterized by extremely low SO_4^{2-} and very high CH_4 concentrations. It has been proposed that CH_4 consumption in the lake occurs via a novel pathway in which CH_4 oxidation is coupled to the reduction of Fe and Mn (hydr)oxides [1]. To investigate the pathways of CH_4 consumption, we monitored methane oxidation rates with a ^{14}C-CH_4 tracer, both with and without the addition of a suite of electron acceptors including Fe and Mn (hydr)oxides. Our initial measurements yield volume specific rates as high as 0.8 μmol l^{-1} d^{-1}, comparable to modelled rates from C isotope and CH_4 concentration profiles [1]. Our measured rates, without added electron donor, are 7 orders of magnitude higher than those reported for the Cariaco Basin [2] and approximately 10 to 50 times higher than in Big Soda Lake, Nevada [3]. Considering the ultra-oligotrophic nature of Lake Matano, these are remarkably high rates. Electron acceptor addition experiments are in progress and these results will be discussed. Our results to date clearly show that CH_4 is an important component of the C cycle in Lake Matano and by extension ferruginous systems in general.

[1] Crowe *et al*. (2011) *Geobiology* **9**, 61–78. [2] Ward *et al*. (1987) *Nature* **327**, 226–229. [3] Iversen, Oremland & Klug (1987*) Limnol Oceanogr*. **32**, 804–814.

Laboratory experiments and modeling of CO_2 dissolution in water for carbon sequestration

M. STUTE[1,2]*, D. FERNANDEZ DE LA REGUERA[1] AND J.M. MATTER[1]

[1]Lamont-Doherty Earth Observatory, Palisades, NY 10964
[2]Barnard College, New York, NY 10027
(*correspondence: martins@ldeo.columbia.edu)

The injection of CO_2 gas in the dissolved phase is an alternative to that of supercritical CO_2 if the depth of the formation is <800m, or where immediate solution trapping is desired because of safety concerns. The most efficient way to dissolve CO_2 in water is downhole in order to take advantage of the increased hydrostatic pressure. We conducted experiments in a 100m long 'well' set up in the staircase of a Manhattan building to study the dynamics of the dissolution process. CO_2 was added at the top of the well with a sparger and the dissolution process was monitored downstream by image processing technology.

The experimental results reveal that bubble size and density decrease along the flow path as expected. However, the rate of dissolution decreased along the flow path with bubbles dissolving rapidly initially and extremely slowly afterwards. As the bubbles decrease in size, they became harder to dissolve, due to effects of rigidity of the gas-liquid interface and the presence of low solubility gases in the water and gas. The degree of dissolution could be considerably enhanced by using a passive mixer or an active downhole submersible pump. The dissolution process was simulated using the Darcy-Weisbach equation and a one-dimensional multi-gas numerical gas exchange model. Besides CO_2, common impurities such as N_2, O_2, noble gases, H_2, H_2S and gas tracers (SF_6 and SF_5CF_3) were included in the model. Extrapolation of the model parameters to real-world injection scenarios (e.g. the Carbfix pilot project in Iceland [1]) illuminate the role that the dissolved gas composition, the purity of the CO_2, and temperature play in controlling the efficiency of CO_2 dissolution for storage in geologic formations.

[1] Gislason *et al*. (2010*) Int. J. Greenh. Gas Con*. **4**.

https://doi.org/10.1180/S0026461X00006502 Published online by Cambridge University Press

Geochemical and biological controls on the product of microbial U(VI) reduction

MALGORZATA STYLO[1]*, DANIEL S. ALESSI[1], BENJAMIN USTER[1], JUAN S. LEZAMA-PACHECO[2], JOHN R. BARGAR[2] AND RIZLAN BERNIER-LATMANI[1]

[1]Environmental Microbiology Laboratory, Ecole Polytechnique Federale de Lausanne, EPFL, Lausanne CH 1015, Switzerland (*correspondence: malgorzata.stylo@epfl.ch)

[2]Stanford Synchrotron Radiation Lightsource, Menlo Park, CA 94025, USA

Bioremediation of the uranium-contaminated subsurface involves the reductive transformation of soluble U(VI) species to less mobile U(IV) species by the *in situ* stimulation of indigenous microorganisms. The U(IV) mineral uraninite, $UO_{2(s)}$, is considered the most desirable product of bioreduction due to its low solubility and high stability under reducing conditions. However, the formation of uraninite may be inhibited under certain geochemical conditions, leading to the formation of biomass-associated U(IV) complexes, referrred to as monomeric U(IV).

In this study we examine the role of medium composition and extracellular polymeric substances (EPS) as inhibitors or promoters of uraninite precipitation. Uranium L_{III} edge X-ray absorption spectroscopy and a wet chemical extraction technique are used to differentiate between U(IV) species. It was previously reported that under controlled conditions in a simple medium containing bicarbonate and PIPES buffer at pH 6.8 (BP), the reduction of U(VI) by *Shewanella oneidensis* led to the formation of uraninite. In contrast, in a more complex Widdel Low Phosphate (WLP) medium, contaning numerous salts, the reduction by the same bacterium led to the formation of monomeric U(IV).

The results show that varying concentrations of NaCl (i. e, ionic strength alone) cannot acount for the molecular U(IV) production observed in WLP medium. The presence of phosphate or calcium ions in the medium has a larger influence on the U(VI) bioreduction product, leading to an increase in monomeric U(IV) formation. Moreover, bacterial EPS production indirectly affects U(IV) speciation. The product of U(VI) reduction in BP medium by a mutant of *Shewanella oneidensis* deficient in EPS production was richer in monomeric U(IV) than that of the wild-type under the same conditioon.

This work begins to explore the complexity of the factors influencing the product of U(VI) reduction. More in-depth investigation of the biological and geochemical factors influencing uranium bioreduction is warranted.

Analysis on environmental and economic sustainable development

SU HAO[1]* AND XU WEN-LAI[2]

[1]School of Economics & Management, Southwest Jiaotong University, ChengDu, 610031, PR China (*correspondence: shenyuren007@sina.com)

[2]College of Environment and Civil Engineering, Chengdu University of Technology, Chengdu 610059, China

Eco-environment is the basis for social and economic development, and the two have the unity of opposites. Depletion of natural resources for eco-development will inevitably affect the environment. Today, the deteriorating eco-environment makes human beings aware that the past social economic development was at the expense of the eco-environment. Human beings must seek coordinated development of soc-economy and the eco-environment.

Now take Chengdu city as an example, we have researched the region's vertical coordination of ecological environment and social economic development from 2001 to 2010. This research employed the method of Principal Component Analysis (PCA) to determine the ecological environment and socio-economic index weight. Based on the index weight, we set up the established evaluation model for sustainable development. And we found the regional ecological environment and socio-economic interaction law. From 2001 to 2010, social and economic development level of Chengdu were steadily rising, and the ecological environment of the ten years were basically flat, no improving. During the ten years, the construction of the ecological environment was far behind the social and economic development.

Funding: The Fundamental Research Funds for the Central Universities (SWJTU10XS38).

[1] Cui GY. (2010) *Geochimica et Cosmochimica Acta*. **12**, A199-A199. [2] Xu WL. (2010) *Geochimica et Cosmochimica Acta*. **12**, A1162-A1162.

https://doi.org/10.1180/S0026461X00006502 Published online by Cambridge University Press

Quantitative identification of reservoir fluid properties and boundary shifts by laser-induced fluorescence

JIN SU[1,2], SHUICHANG ZHANG[1,2], GUANYOU ZHU[1,2], BIN ZHANG[1,2] AND XIAOMEI WANG[1,2]

[1]Research Institute of Petroleum Exploration and Development, PetroChina, Beijing 100083, China
[2]State Key Lab of Oil Recovery Elevation, Research Institute of Petroleum Exploration and Development, PetroChina, Beijing 100083, China

In an oil-gas reservoir with multi-stage structural movement, both hydrocarbons and reservoir bitumen may have suffered from multi-stage mixture, alteration and deconstruction, which results in difficulties to reconstruct migration and adjustment histories of hydrocarbons due to many factors that affect the reconstruction. However, direct evidence for different phases of hydrocarbon migration, variations in oil-gas properties and shifts of oil-water boundaries could be obtained from fluid inclusions of oil-gas reservoirs, which can record primary components and temperature-pressure conditions of hydrocarbon migration and charge. Thus, the present study uses quantitative assessment parameters, such as fluorescence strength and maximum emission waves of organic fluid inclusions, to characterize variations related with oils, gases and water in reservoirs so as to reconstruct adjustment processes of hydrocarbon reservoirs.

The Tarim Basin in China has experienced multi-cycle structural activities, and several developed petroleum systems are vertically superimposed or horizontally distributed in the basin. the present research quantitatively investigates fluorescence characteristics of reservoir sandstones, delineates the difference in fluorescence characteristics for oil-bearing or condensate-bearing reservoirs using λmax (maximum radiofluorescence wave length) and △λ (a wave length between 2/1 I_{max}), quantitatively analyzes the relationship between the primary oil-water boundary when hydrocarbon charge occurred and the present-day boundary, deduces reasons resulting in the elevation of oil-water boundaries based on structural evolution, and particularly, distinguishes dominant migrating pathways from all the oil-bearing reservoir beds according with the comparison of I_{max} (maximum radiofluorescence intensity) between present-day and old reservoirs. Therefore, the laser-induced fluorescence quantitative analysis can also play a significant role in investigating variations in paleo-oil-water boundaries, determining paleo-oil-column height, demonstrating oil saturation and wettability of reservoirs, and simulating displacement pressure of reservoirs as well.

Biodegradation of petroleum hydrocarbon in shallow groundwater from carbon and sulfur isotope evidence

SU XIAO-SI, LV HANG* AND ZHANG WEN-JING

Jilin University, Changchun, China, 130021
(*correspondence: lvhangmail@163.com)

Biodegradation is one of main natural attenuation processes in petroleum hydrocarbons contaminated groundwater [1]. Carbon and sulfur isotopes may have been markedly kinetic-fractionated during biodegradation process [2], which provides a powerful tool to reveal mechanism of petroleum hydrocarbons biodegradation. In an oilfield area in Northeast China, oil-bearing saline water moves upward and infiltrates into the shallow groundwater resulting from the accident and the area of groundwater-contaminated plume is about 8000m^2. Concentration of Total Petroleum Hydrocarbons (TPHs), dissolved Inorganic Carbon (DIC) and dominant terminal electron accepters or donators, $\delta^{13}C_{DIC}$ and $\delta^{34}S_{SO42-}$ have been analyzed.

Analytical results show that the spreading direction of contaminated plume is controlled by groundwater flow. And the concentrations of SO_4^{2-} and pH increase along groundwater flow in the central line of the plume while TPH and DIC decrease. The $\delta^{13}C_{DIC}$ values of the uncontaminated groundwater range between -9.5 and 8.0‰$_{PDB}$, while the contaminated is characterized by a significant depletion of ^{13}C with $\delta^{13}C_{DIC}$ of -18.3~-18.5‰$_{PDB}$. Furthermore, the concentration of DIC is negatively correlated with the value of $^{13}C_{DIC}$. It is deduced that the increase of DIC results from the biodegradation of petroleum hydrocarbon in groundwater. Meanwhile, the ^{34}S in the contaminated groundwater with the $\delta^{34}S_{SO42-}$ of 25.0‰ ~ 48.1‰$_{CDT}$ is depleted to the uncontaminated groundwater with the $\delta^{34}S_{SO42-}$ of 19.2‰ ~13.9‰$_{CDT}$. The Rayleigh model calculation [3] shows that the biodegradation of petroleum hydrocarbon with the bacterial sulfate reduction has occurred in the contaminated aquifers.

[1] Christof Bolliger *et al*. (1999) *Biodegradation* **10**, 201-217. [2] Knöller K *et al*. (2002) *South American Symposium on Isotope Geology* **5**, 438–440. [3] Ian Clark *et al*. (1997) *Environmental Isotopes in Hydrogeology* 145–147.

https://doi.org/10.1180/S0026461X00006502 Published online by Cambridge University Press

The alteration sequence of PGM in the gossan of the Aguablanca Ni-Cu-(PGE) sulphide deposit, SW Iberia

S. SUÁREZ[1]*, H.M. PRICHARD[2], F. VELASCO[1], P.C. FISHER[2] AND I. MCDONALD[2]

[1]UPV/EHU. Dep. Mineralogy & Petrology. Barrio Sarriena s/n 48940 Spain (*correspondence: saioa.suarez@ehu.es)
[2]Cardiff University. School of Earth and Ocean Sciences. Main Building. Park Place. Cardiff CF10 3AT (UK)

The gossan outcrops overlying the Aguablanca magmatic deposit [1] (situated in the Ossa-Morena Zone in SW Iberia) host significant total PGE contents of up to 5 ppm, with Pt and Pd dominant over Rh, Os, Ir and Ru. A detailed survey of the PGE distribution was carried out in this gossan in order to understand the processes that change primary magmatic PGM during weathering in an oxidising, low-T environment. PGE were investigated in host relic PGM (by SEM-EDS) and as traces in the host Fe-oxides and oxyhydroxides that form the gossan (by LA-ICP-MS) [2].

The study showed a gradual alteration of the PGM and release of PGE during the gossan formation, including: (i) initial breakdown of the already slightly altered, primary PGM [3] (24% of the total PGM located); (ii) formation of partially oxidised Pt-Pd-phases (3%), with a composition close to 'Pt_2O' and "(Pt, Pd)O'; (iii) formation of numerous oxidised Pt- and Pd-(±Cu-Fe, Bi-Te)-phases (68%), with a composition usually close to "$(Pt, Pd)O_2$" and "$(Pt, Pd)_3O_4$". Palladium-rich hydroxides were also identified. These phases all appear to have formed from alteration of earlier PGM to form pseudomorphs. Among them, Pt-rich PGM are more frequent and always appear better preserved than Pd-rich PGM; (iv) formation of Fe-Ni-Cu-(±Pt-Pd)-oxides (5%), mainly in patches that may include relic precursor PGM; and lastly, (v) incorporation of PGE into ferruginous supergene products, with a greater dispersion of Pd than for the other PGE. LA-ICP-MS analyses showed that Pt, Ir and Rh in oxides are mainly located close to sulphide relicts. In contrast, Pd accompanied by Cu, Ni, Bi or Te, occur widely distributed within the different generations of Fe-oxides.

These observations suggest that the sequence of alteration of igneous PGM in a gossan is likely to be one of PGE-oxide formation followed by dispersion of the PGE into the Fe-oxides. This work adds to the understanding of the evolution of PGM in the surface environment.

[1] Tornos *et al*. (2006) *Miner Deposita* **41**, 737–769.
[2] Suárez *et al*. (2010) *Miner Deposita* **45**, 331–350.
[3] Ortega *et al*. (2004) *Can Mineral* **42**, 325–350.

Late-Cretaceous alkaline continental magmatism associated with Deccan Continental Flood Basalt sequences of Saurashtra in Western India

D.V. SUBBA RAO*, E.V.S.S.K. BABU, G.VIDYASAGAR AND B.MADHUKAR

National Geophysical Research Institute, Hyderabad, India (*correspondence: dvsubbarao@ngri.res.in)

The Saurashtra region in Western India consists of seven volcano-plutonic complexes (plugs) occurring within the Deccan Continental Flood Basalts of WDVP. The three major plugs occurring at Junagadh (Girnar), Barda and Alec Hills pipe-like igneous intrusions located along the E-W trending Narmada-Son lineament. Alkaline magmatism is represented by lamprophyres and nepheline syenites forming as minor composite intrusions which are spatially and temporally related and occur chiefly within the diorites in the upper part of the Girnar Complex. Nepheline syenite is generally cream coloured, spotted black and pinkish red with pyroxene and nepheline respectively and consists of a granitoid aggregate of alkali feldspar, nepheline, sodalite, cancrinite and aegerine. In lamprophyric sills, Cpx occurs as microphenocrysts of small rounded to prismatic crystals which show the characteristic oscillatory zoning (X_{Mg} = 0.65–0.77) and amphiboles which are of calcic variety (X_{Mg} = 0.48 to 0.65). X_{An} in plagioclase varies from 25 to 96. These alkaline rocks have higher concentration of total alkalies (8.0 to 14.57wt %), Al_2O_3 (22.2wt %), LILE and ΣREE as well as highly fractionated REE patterns. The available data suggest that they are products of fractionation of an alkali basic magma from which early crystallization of lamprophyres took place under high PH_{20} conditions followed by nepheline syenites which crystallized at lower PH_{20} under relatively dry conditions from the residual liquids. The occurrence of high MgO dykes (olivine tholeiites, Opx bearing pyroxenite dykes and ankaramite dyke), the essexite pluton and deep-seated lineaments coupled with the presence of strong positive gravity anomalies in the Saurashtra region reflect prevalence of an underlying sub-surface high density component in the Girnar and most of the other plugs in the region.

https://doi.org/10.1180/S0026461X00006502 Published online by Cambridge University Press

Volume and ionic conductivity measurements of H_2O ice at high pressure and temperature

E. SUGIMURA[1]*, T. KOMABAYASHI[1], K. OHTA[1], K. HIROSE[1,], N. SATA[2], Y. OHISHI[3] AND L.S. DUBROVINSKY[4]

[1]Dept. of Earth and Planet. Sciences, Tokyo Tech., 2-12-1 Ookayama, Meguro, Tokyo 152-8551, Japan (*correspondence: sugimura@geo.titech.ac.jp)
[2]Inst. for Research on Earth Evolution, Japan Agency for Marine-Earth Science and Technology, 2-15 Natsushima-cho, Yokosuka, Kanagawa 237-0061, Japan
[3]Japan Synchrotron Radiation Research Institute, 1-1-1 Kouto, Sayo, Hyogo 679-5198, Japan
[4]Bayerisches Geoinstitut, Universität Bayreuth, Bayreuth 95440, Germany

We examined isothermal volume (V) compression of H_2O ice based on *in situ* x-ray diffraction measurements at 33-79 GPa and 873 K, and its ionic conductivity at 20-60 GPa up to 920 K using impedance spectroscopy (IS) technique. High pressure (*P*) and temperature (*T*) conditions were generated by using an externally-heated diamond anvil cell. The anomalous volume reduction likely due to the hydrogen bond symmetrization was observed at 50-53 GPa and 873 K, while the previous study at room temperature reported that the highly compressible phase associated with the symmetrization is present at 40-60 GPa. There is no volume discontinuity in the isothermal compression, which contadicts the proposed first order *P-T* boundary between ice VII and superionic ice [2, 3]. In addition, *in situ* IS measurements shows that the ionic conductivity of ice monotonically increases with increasing *T*, and exhibits superionic conduction (>10^{-1} S/cm) above 580-720 K at 20-60 GPa, which is the first experimental evidence of the superionic conduction in H_2O ice at high pressure. This suggests that superionic ice appears at sufficiently lower *P-T* than the proposed triple point.

Combining above results with the existing planetary isentropes [4], superionic H_2O ice is stable at *P-T* conditions corresponding to the interiors of Neptune and Uranus, the ice giants. The presence of superionic ice in these planets possibly accounts for the non-dipolar and non-axis symmetric structure of their magnetic fields.

[1] Sugimura *et al*. (2008) *PRB* **77**, 214103. [2] Lin *et al*. (2005) *GRL* **32**, L11306. [3] Goncharov *et al*. (2009) *J. Chem. Phys*. **130**, 124514. [4] de Pater *et al*. (2001) in *Planetary Sciences*, Cambridge University Press, New York.

The system SiO_2-H_2O revisited: Equation of state to very high temperatures and pressures including critical behavior

MIROSLAV ŠULÁK* AND DAVID DOLEJŠ

Institute of Petrology and Structural Geology, Charles University, 128 43 Praha 2, Czech Republic (*correspondence: miroslav.sulak@natur.cuni.cz)

The system SiO_2-H_2O represents a simple model for metasomatism and hydrous melting in the lower crust and upper mantle. In this binary, the upper critical end point (UCEP), where complete miscibility between concentrated aqueous fluids and hydrous silicate melts occurs, is located at 1100 °C and 9.5 kbar [1], near the geothermal subduction gradient with important consequences for aqueous devolatilization *vs*. melt generation in the subducting slab. We have derived a new equation of state for aqueous silica, which combines intrinsic thermal properties of SiO_2 units with volumetric contributions resulting from solvent compression in the hydration sphere. The concentration scale is mole fraction, which enables the difference between standard states at infinite dilution and pure substance to be linked *via* excess energy of mixing represented by symmetric Margules term (*W*). In addition, the pressure-temperature locus of the UCEP provides two additional constraints on energy-composition relationships, thus reducing the effective number of independent parameters of the equation of state. The Gibbs energy of SiO_2 (aq) has the form: $\Delta G = a + bT + cT\ln T + dP + eT\ln\rho_w$, where ρ_w is the density of aqueous solvent at pressure and temperature of interest. The thermal part is assembled from constant enthalpy, entropy, and heat capacity, whereas the pressure term employs constant volume of the unhydrated species. Additional contribution arises from the pressure-volume work necessary to compress solvent molecules from bulk density to the density in hydration shell due to electrostriction, and it is related to solvent volumetric properties only [2]. The model was calibrated by 342 experimental quartz solubilities at 25-1100 °C and 0.001-20 kbar and ranging from 9 ppm to 70 wt.%, yielding a = -963.5 kJ mol^{-1}, b = 844.3 J K^{-1} mol^{-1}, c = -124.1 J K^{-1} mol^{-1}, d = 2.26 J bar^{-1} mol^{-1}, e = -16.65 J K^{-1} mol^{-1}, and W = 29.1 kJ mol^{-1}, with overall accuracy of 1.3 kJ mol^{-1}. In contrast to previous studies, our new model is capable of addressing SiO_2 behavior in dilute aqueous fluids and hydrous melts, including their supercritical mixtures.

[1] Kennedy *et al*. (1962) *Am. J. Sci*. **260**, 501–521. [2] Dolejš & Manning (2010) *Geofluids* **10**, 20–40.

https://doi.org/10.1180/S0026461X00006502 Published online by Cambridge University Press

Agriculture's impact on the Si cycle by accelerated biomineralisation

LEIGH SULLIVAN[1,2] AND JEFFREY PARR[1,2]

[1]Southern Cross University, Australia (*correspondence: leigh.sullivan@scu.edu.au)
[2]Plantstone Pty Ltd, 90 Zouch Rd Stoney Chute 2480

Biogenic silica plays a major role in the global cycling of silicon [e.g. 1] and in processes such as mineral weathering, soil acidification, and regulation of atmospheric CO_2. Phytoliths form by silicon biomineralisation within plants (especially grasses) and constitute a major pool of biogenic silica. Biogenic silica production rates reported for natural vegetation communities have a mean of ~70 $kgSiO_2ha^{-1}yr^{-1}$ [e.g. 2, 3, 4], but vary widely from only 2 $kgSiO_2ha^{-1}yr^{-1}$ to up to 1, 380 $kgSiO_2ha^{-1}yr^{-1}$ for a tropical bamboo forest [5]. This data indicate a global silica phytolith production rate of ~1 billion tons of SiO_2yr^{-1} prior to agricultural development.

However, many agricultural crops and pastures are based on silica-accumulating grass species that produce silica phytoliths far in excess of that produced by most natural vegetation communities. For example, silica phytolith production rates in grass crops such as rice, wheat, sugar cane and bamboo are usually an order of magnitude greater than those observed for most natural vegetation communities [6, 7, 8] and can be over 3, 000 kg per ha^{-1} yr^{-1} [8].

Accelerated silicon biomineralisation consequent of agriculture not only results from higher silicon uptake within such crops but also by the increased biomass produced by agricultural practices such as fertilisation and irrigation.

Further factors that impact the global silicon cycle from this process include: 1) the large area being cultivated annually with high silica phytolith producing crops and pastures (e.g. ~0.7 billion ha under cereal crops alone), and 2) the slow turnover rates of silica phytoliths (e.g. >300 yrs under tropical rainforests [4] and grasslands [3]).

The results presented here show that agriculture, by greatly accelerating the production of biogenic silica from the cultivation of high silica phytolith producing plants, has considerably impacted the silicon cycle with implications for other silicon-associated geochemical processes. Such implications are explored in this paper.

[1] Derry *et al.* 2005. *Nature*, **433**, 728–731. [2] Cornelis *et al*. 2010. *Biogeochem*. ***97***, *231–45*.[3] Blecker *et al.* 2006. *Global Biogeochem. Cyc.* **20**, 3023. [4] Alexandre et al, 1997. *Geochim. Cosmochim. Acta,* **61**, 677–82. [5] Meunier et al, 1999. Geology, **27**, 835–87. [6] Parr *et al*. 2009. *Sugar Tech* **11**, 17–21. [7] Parr & Sullivan (In press) *Plant & Soil*. [8] Parr *et al*. 2010. *Global Change Biol*. **16**, 2661–7.

2575 Ma age of Nuvvuagittuq metamorphic garnet

N.C. SULLIVAN[1], E.F. BAXTER[1] AND S.J. MOJZSIS[2]

[1]Dept. of Earth Sciences, Boston University, Boston, MA (norasull@bu.edu, efb@bu.edu)
[2]Dept. of Geological Sciences, University of Colorado, Bolder, CO (mojzsis@colorado.edu)

The recent discovery of pre-3.75 Ga metasedimentary rocks in the Nuvvuagittuq supracrustal belt (NSB) of northern Quebec, Canada, provides a new suite of rocks to further our understanding of Eoarchean Earth process. The NSB includes a CaO-poor (cummingtonite) amphibole, plagioclase, biotite, quartz and garnet-bearing mafic schist. The exact age and history of this rock is being debated: associated zircon ages give a minimum age of 3.77 Ga [1], and a $^{146}Sm/^{142}Nd$ isochron suggests that the NSB includes components as old as ca. 4.28 Ga [2].

Garnet Sm-Nd geochronology is a valuable tool to elucidate the tectonic and metamorphic histories of mafic rocks; recent improvements in sample preparation have improved both the accuary and precision with which we are able to date the growth of garnet [3]. Although garnet dating in the cummingtonite amphibolite rocks will not resolve the age debate, it will tell us when the most recent garnet-forming metamorphic event occured at which time Nd isotopes were last mobilzed and exchanged among metamorphic phases.

After crushing and hand picking a visually clean garnet separate we performed partial dissolutions to remove micro-inclusions. Using a three step sequence of acids: concentrated HF, concentrated $HClO_4$, and 7N HNO_3, acid-cleansed garnets showed high $^{147}Sm/^{144}Nd$ ratios (~6.0) indicating that low Sm/Nd micro-inclusions were eliminated. However, replicate preparations produced significant scatter in the isochron towards older apparent ages indicative of contamination from an older inherited high Sm/Nd inclusion phase (likely zircon). Adding a fourth aqua regia step to the partial dissolution sequence cleansed the garnet of these contaminants yielding slightly higher $^{147}Sm/^{144}Nd$ (~6.1) and a robust three point garnet-matrix isochron age of 2574.70 ± 0.72 Ma (MSWD=0.77). This new age represents the youngest age associated with the NSB and implies the terrane underwent a final greenschist-amphibolite grade heating event after the final ca. 2.7 Ga crustal growth episode documented by metamorphic overgrowths on zircons [4].

[1] Cates & Mojzsis (2007) *EPSL* **255** 9–21. [2] O'Neil *et al*. (2008) *Science* **321**, 1828–1831. [3] Pollington & Baxter (2011) *Chemical Geology* **281**, 270–282. [4] Cates & Mojzsis (2009) *Chemical Geology* **261**, 98–113.

https://doi.org/10.1180/S0026461X00006502 Published online by Cambridge University Press

Slab-derived halogens and noble gases with a marine pore-fluid signature

H. SUMINO[1]*, C.J. BALLENTINE[2], R. BURGESS[2], S. ENDO[3], K. YOSHIDA[4], T. MIZUKAMI[5], G. HOLLAND[6], S. WALLIS[3] AND T. HIRAJIMA[4]

[1]GCRC, University of Tokyo, Tokyo 113-0033, Japan (*correspondence: sumino@eqchem.s.u-tokyo.ac.jp)
[2]SEAES, University of Manchester, Manchester M13 9PL, UK
[3]Department of Earth and Planetary Sciences, Graduate School of Environmental Studies, Nagoya University, Nagoya 464-8602, Japan
[4]Department of Geology and Mineralogy, Graduate School of Science, Kyoto University, Kyoto 606-8502, Japan
[5]Department of Earth Science, Graduate School of Environmental Studies, Kanazawa University, Kanazawa 920-1192, Japan
[6]Lancaster Environment Centre, Lancaster University, Lancaster LA1 4YQ, UK

Subduction volcanism is generally considered to form a 'subduction barrier' that efficiently recycles volatile components contained in subducted slabs back to the Earth's surface. Nevertheless, subduction of sediment and seawater-dominated pore fluids to the deep mantle has been proposed to account for the non-radiogenic elemental abundance and isotopic pattern of heavy noble gases (Ar, Kr, Xe) in the convecting mantle [1]. To verify whether and how subduction fluids preserve a seawater signature, we determined noble gas and halogen compositions of the exhumed mantle wedge peridotite and eclogite from the subduction-related Sanbagawa metamorphic belt, southwestern Japan, in which relicts of slab-derived water are contained as hydrous mineral inclusions or aqueous fluid inclusions.

The observed noble gas and halogen compositions of the peridotite [2] and eclogite samples shows striking similarites with marine pore fluids, challenging a popular concept that the water flux into the mantle wedge occurs only by hydrous minerals in altered oceanic crust and sediment. These results indicate that subduction and closed system retention of marine pore fluid occurs to depths of at least 100 km, necessitating a reassessment of the dominant transport mechanism and source of water in subduction zones. Further subduction of a small amount of marine pore fluid can account for the heavy noble gas composition observed in the convecting mantle.

[1] Holland & Ballentine (2006) *Nature* **441**, 186–191.
[2] Sumino *et al*. (2010) *EPSL* **294**, 163–172.

Temperature controls of sulphur isotope fractionation during sulphate reduction by *Thermodesulfobacterium* and *Desulfovibrio* strains

JIA-LIN SUN[1], LI-HUNG LIN[1], SAUL-WOOD LIN[2], JIE-WEI SHIU[2] AND PEI-LING WANG[2]

[1]Department of Geosciences, National Taiwan University
[2]Institute of Oceanography National Taiwan University

Sulphate reducers are known to fractionate sulphur isotopes during dissimilatory sulphate reduction. Unravelling the factors controlling the fractionation pattern would be essential to identify the contribution of each enzymatic pathway at the cellular level, interpret the isotopic signatures in geological materials, and track the sulphur cycling in natural occurrences. This study examined the sulphur isotope fractionation patterns catalyzed by a thermophilic *Thermodesulfobacterium*-related strain and a mesophilic *Desulfovibrio gigas* over wide temperature ranges.

The *Thermodesulfobacterium*-related strain grew between 34 and 85 °C with an optimal temperature at 72 °C and the highest cell-specific sulphate reduction rate at 68 °C. The isotope fractionation ($\varepsilon^{34}S_{sulphate\text{-}sulphide}$) ranged between 9.1 and 25.7 ‰ over temperatures ranging from 51 to 77 °C. The fractionations remained at high levels for the growth above 55 °C and decreased significantly for the growth at 51 °C. The *D. gigas* grew between 10 and 45 °C with an optimal temperature at 36 °C and high cell-specific sulphate reduction rates between 30 and 36 °C. The isotope fractionation ranged between 8.5 and 52.0 ‰ over temperatures ranging from 19 to 39 °C and peaked at 24 °C. The relationships between the fractionation and temperature for two strains in this study in part resembled those previously reported for *Archaeoglobus*-related strains but distinct from those for *D. desulfuricans*, *T. indicus* and *Desulfobacterium autotrophicum*, suggesting that the isotope fractionation is controlled by the complex combinations of contribution from individual pathways. Measurements of multiple isotopes are warranted to reconcile the modelled uncertainty.

https://doi.org/10.1180/S0026461X00006502 Published online by Cambridge University Press

Soil water movement traced by oxygen isotope in the Mu Us sandy land, North China

SUN JIANG*, RAO WENBO, SUN XUE

Institue of Isotope Hydrology, School of Earth Sciences and Engineers, Hohai University, Nanjing, 210098, China (*correspondence: taiyangfeng23@126.com)

Soil water is very important to plant growth because of arid climate in the Mu Us sandy land. However, knowledge on soil water movement of this region is little till now. In this study, oxygen isotope compositions of soil water in the dune profiles at Henan Village are investigated and then soil water movement is explored.

Two dune profiles with the depth of 3.75m are bored at a about 12 h interval before and after a thunderstorm in the same site at Henan where average annual precipitation is about 400mm but average annual evaporation is up to 2000mm [1]. Soil water is extracted from samples after they are sent to the laboratory by the vacuum-distillation apparatus and then is analyzed for $\delta^{18}O$ via MAT253.

$\delta^{18}O$ value of soil water changes greatly between -0.96 and -7 in the upper part with the depth of about 1.8m but fluctuates constantly within a narrow range of -6 ~ -8 in the lower part of the first profile (before thunderstorm). $\delta^{18}O$ value of soil water also has a large variation from -2.87 to -7.54 in the upper part and a similarly narrow range in the lower of the second profile (after thunderstorm). The isotopic data have three implications: (1) the evaporation only impact water isotope in the upper profile with the 1.8m depth; (2) the thunderstorm event carries more negative oxygen isotopic composition into the upper profile; (3) since soil water in the lower profiles has $\delta^{18}O$ value more positive than that of local groundwater [2], they seem not to be of same origin. In addition, the average infiltration rate of this precipitation is about 15cm per hour through calculation.

As a result, the precipitation infitration is only limited to the 1.8m depth under the land surface although there is a large amount of the precipitation for the thunderstorm event in a short time. It is thus inferred that vertical infiltration of the precipitation through the dunes might have little recharge to groundwater.

[1] Yang Yuncheng *et al*. (2005) *Acta Geoscientica Sinica* **26**, 289–292. [2] Hou Guangcai *et al*. (2007) *Journal of Jilin University (Earth Science Edition)* **37**, 255–260.

Geochronology of continental volcanic-type gold mineralization in East Tianshan, Western China: Constraints from Ar-Ar isotope of Shiyingtan gold deposit

SUN JINGBO[1]*, CHEN WEN[1], LI HUAQIN[1], JI HONGWEI[2,1] AND LI JIE[2]

[1]Laboratory of Isotope Geology, Institute of Geology, CAGS, Beijing, 100037 China (*correspondence: jingbo95003@126.com)

[2]China University of Geosciences (Beijing), Beijing, 100029 China

The East Tianshan area in northwest China locates on the boundary between Tarim plate and Kazakhstan-Junggar plate. Both plates had experienced a complicated breakup and collision since late Precambrian, accompanied by large-scale thrust and continental volcanism [1]. Previous studies suggested two stages of continental volcanism: the first stage occurred between Late Carboniferous and Early Permian with isotopic age of 310~290Ma; the second stage occurred between Late Permian and Early Triassic with isotopic age of 260~240Ma. The Shiyingtan gold deposit locates in the extensional tectonic-magmatic belt of Queleage in East Tianshan area, composing mainly of NO.I, NO.II, NO.III ore bodies, with ores held by both gold-bearing quartz veins and altered andesite. Andesite, hornblende andesitic dacite, amygdaloidal andesite, volcanic breccia agglomerate lava and volcanic breccia of Permian are the exposed strata within mined area.

In order to study the metallogenic epoch of Shiyingtan gold deposit, altered andesite ores were sampled from NO.I ore body, from which sericite is extracted for ^{40}Ar-^{39}Ar isotope dating analysis by step-heating, yielding a plateau age (Tp) of 304.2±1.3Ma and isochron age (Ti) of 304.7±4.9Ma (initial ratio of $^{40}Ar/^{36}Ar$=292±10). This mineralization age of 304Ma in Shiyingtan gold deposit is in great concordance with the age of ore-bearing volcanic rocks, deposition of gold occurred in extensional tectonic stage of post-orogenic between late Carboniferous Kazakhstan-Junggar and Tarim plates, developing in the extensional area of shear flank.

This work was supported by the Science and Technology Research Project of China (No.: 2007CB411306; 200911043-13; 1212011120293).

[1] Li *et al*. (2004) *Geological Publishing House*.

https://doi.org/10.1180/S0026461X00006502 Published online by Cambridge University Press

Geochemical characteristics of the Shaxi-Changpushan porphyry Cu-Au deposit: Significance to ore formation

S.C. SUN, S.G. HE AND F. JIANG*

Institute of Disaster Prevention Science & Technology, Yanjiao, 101601, Beijing, China (grg@fzxy.edu.cn)

Introduction

The Shaxi-Changpushan porphyry copper (gold) deposit is located in the northwestern Luzong volcanic basin. It also belongs to the north of the middle and low part of the Yangtze iron and copper metallogenic zone with the multiple location of faults, where Fanshan-Tongling deep fault and Tan-Lu fault belt come through the whole mineralization region and result in serious rock deformation in Jurassic [1].

Methods and Results

Basd on geochemical studies and literatures [2-10], including chemical analysis on bulk rocks, rare earth and trace element studies, fluid inclusion, S and O isotopic analysis, we present significant proofs for the copper-(gold) mineralization in Shaxi porphyry copper-gold deposit. The sulfur isotope dada show that the magma has the characteristics of deep source. Compared with the other large and supper-large porphyry copper deposits in China and the adjacent copper mineralized areas, ore-forming processes and conditions were analyzed. Our study indicates that the ore-forming fluids and materials were dominated with the magmatic origin, whereas the meteoric water played small role in the ore-forming processes. There are great potentialities to form a large porphyry copper deposit from the point view of tectonic evolution and geochemical characteriscs in Shaxi-Changpushan Cu-Au ore district.

[1] Chang Y.F. *et al*. (1991) *Geol. Pub. House,* Beijing. [2] Yang X.Y. & Lee I.S. (2005) *N. Jb. Mineral. (Abh.)* **181**, 223–243. [3] Yang X.Y. *et al*. (2002) *N. Jb. Mineral. (Abh.)* **177**, 293–320. [4] Yang X.Y. *et al*. (2006) *J. Geol. Soc. India*, **67**, 475–494. [5] Zhou T.F. *et al*. (2007) *Ore Geol. Rev*. **31**, 279–303. [6] Yang X.Y. *et al*. (2007a) *Acta Geol. Sinica*, **76**, 477–487. [7] Yang X.Y. *et al*. (2007b) *J. Geol. Soc. India*, **70**, 235–251.[8] Lan X.H. *et al*. (2009) *Chinese J. Geochemistry*, **28**, 28–43.[9] Ling M.X. *et al*. (2010) *Econ. Geol*. **104**, 303–321. [10] Yang, X.Y. *et al*. (2011) *Inter. Geol. Rev*. http://dx.doi.org/10.1080/00206810903211906.

Oceanic Anoxic Events and Cenozoic large scale molybdenum mineralization

WEIDONG SUN[1], CONGYING LI[1,3], HONG ZHANG[1,3], XING DING[2], MINGXING LING[2] AND WEI-MING FAN[1]

[1]Key Laboratory of Mineralogy and Metallogeny, Guangzhou Institute of Geochemistry, Chinese Academy of Sciences, P. O. Box 1131, Guangzhou, PR China

[2]Key Laboratory of Isotope Geochronology and Geochemistry, Guangzhou Institute of Geochemistry, Chinese Academy of Sciences, P. O. Box 1131, Guangzhou, PR China

[3]Graduate University of the Chinese Academy of Sciences, Beijing 100049, PR China

Half of the world's Mo reserve is hosted in Cenozoic porphyry-copper (Cu)-molybdenum (Mo) and porphyry-Mo deposits along the west coast of the American continents with nearly no Mo porphyry deposits along the west coast of the Pacific Ocean. In contrast, most Mo deposits in Eastern Asia are located along the Qinling-Dabie orogenic belt and in Northeastern China. Here we show that the large scale Mo mineralization along the west coast of the American continents is mainly due to the partial melting of Mo enriched sediments formed during oceanic anoxic events (OAEs) in the Jurassic and the Cretaceous. Porphyry-Cu-Mo deposits in the American continents are formed through partial melting of Mo-rich OAE sediments carried by flatly subducted oceanic crust in the east Pacific. High-fluorine (F) porphyry-Mo deposits are mostly located in the Colorado mineral belt (COMB), which are formed through direct partial melting of high grade metamorphosed Mo-rich OAE sediments in backarc settings, induced by the roll back of the flatly subducted east Pacific slab. Most low-F porphyry-Mo deposits have closer spatial relationship with porphyry-Cu-Mo deposits and are formed through partial melting of metamorphosed OAE sediments induced by arc magmas. In contrast, Mo porphyry deposits in Eastern Asia belong to low-F type, likely formed through partial melting of metamorphosed Mo rich sediments. Molybdenum deposits in Northeastern China were likely also due to Mo rich sediments formed during OAEs, whereas those from the Qinling orogenic belt were likely related to sediments formed in Triassic backarc settings.

https://doi.org/10.1180/S0026461X00006502 Published online by Cambridge University Press

Extraction time for soil water of desert sand used in stable isotope analysis

SUN XUE*, RAO WENBO AND SUN JIANG

Institue of Isotope Hydrology,School of Earth Sciences and Engineers, Hohai University, Nanjing, 210098, China (*correspondence: sunxue217@yahoo.cn)

Vacuum distillation has been widely used to extract soil water for stable isotopic analysis in studies of water cycle Distillation time is very crucial to complete soil water extraction. In this study, experiments of extracting water from dune sand of the Chinese desert are carried out to determine optimal extraction time.

Seven 30g sand samples with 10% moisture and known water isotopes are prepared and the distillation temperature is set at 105°C for the experiments of soil water extraction. The samples are vacuum-distilled for 4min, 8min, 12min, 16min, 20min, 25min and 30min, respectively (Fig. 1). Extracted water is analyzed for δ^2H and $\delta^{18}O$ by MAT253.

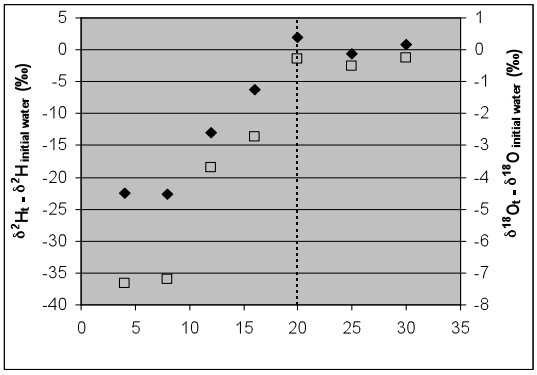

Figure 1: Isotopic variation of water extracted from sand samples.

As shown Fig.1, δ^2H_t-$\delta^2H_{initial}$ and $\delta^{18}O_t$-$\delta^{18}O_{initial}$ gradually increase with time. They arrive to zero (‰) at 20min and then tend to be constant. This result indicates it need take at least 20min to completely extract soil water from desert sands. For different types of soils, the extraction time is distinct [1]. To be on the safe side, we suggest 28min for extracting water from sands in the Chinese deserts. Certainly, water extraction of over 30min is insignificant. Our conclusion agree well with West *et al*. (2006) [2].

[1] Landon *et al*.(1999) *Journal of Hydrology* **224**, 45–54. [2] West *et al*. (2006) *Rapid Commun. Mass Spectrom* **20**, 1317–1321.

Episodic events of the Western North China Craton and North Qinling Orogenic Belt, in central China: Revealing by detrital zircon U–Pb ages

YONG SUN, CHUNRONG DIWU, HONG ZHANG, QIAN WANG, ANLIN GUO AND LONGGANG FAN

State Key Laboratory of Continental Dynamics, Department of Geology, Northwest University, Xi'an, 710069, China (diwuchunrong@163.com)

Detrital zircon U-Pb geochronology serves as a proxy to study of crustal evolution and provenance discrimination. In order to unravel episodic events and their tectonic relationship of the North China Craton (NCC) and North Qinling Orogenic Belt (NQOB), detrital zircons from modern river sands and metasedimentary rocks are collected and dated by LA-ICPMS. Although the western NCC (Ordos terrane) is covered by Mesozoic-Cenozoic basin sediments, the U-Pb dating results have shown that the age populations of detrital zircons from the western NCC with prominent U–Pb age peaks at 2475 Ma and 1850 Ma, which indicates the western NCC (Ordos terrane) also has early Precambrian basement similar to the eastern and central craton. In addition, a significant number of early Paleozoic (520-400 Ma) zircons have bee found in the western NCC, which is quiet different from the eastern NCC and is considered to be related to the collision between the NQOB and the NCC.

The age spectra of detrital zircons from the NQOB presents a complex age pattern, which reveals four major age groups of Neoarchean (2.6–2.4 Ga), Neoproterozoic (1.0–0.85 Ga), early-middle Paleozoic (450-350 Ma) and early Mesozoic (250–170 Ma). As indicated by the U-Pb isotopic data that the NQOB could be an independent terrane at least prior to the Neoproterozoic and once a portion of the Grenville orogenic belt during the 1.2-0.8 Ga with a peak of ~1.0 Ga. In other words, the NQOB has its unique geological evolution history obviously different from those of the NCC and the Yangtze Craton. The complete collision between the NQOB and the NCC perhaps took place at Paleozoic (450-400 Ma).

https://doi.org/10.1180/S0026461X00006502 Published online by Cambridge University Press

Predicting reservoir fluid properties using absolute concentrations of canned cutting gas components

YONGGE SUN

Department of Earth Science, Zhejiang University, Hangzhou 310027, P.R. China

The canned cutting gas data are the most frequently used geochemical approach to characterize reservoir fluid properties during petroleum exploration. Traditionally, canned cutting gas analyses are semi-quantitative and usually reported as C_1 through C_5 normalized, therefore increasing the uncertainty in respect to fluid prediction. Here, we developed a quantitative method for canned cutting gas analyses, and together with their carbon isotopic compositions and molecular parameters to identify reservoir fluid types and barriers.

The canned cuttings are received from the well site. Samples are routinely analyzed at intervals varying from 10 to 30m. A known volume of cuttings are homogenized with water in a gas-tight blender and a sample of head space is analyzed for methane, ethane, propane, butane and pentane. For absolute concentrations of cutting gas components, an internal standard is chosen and the relationship of GC response factor between standard and aimed gas components is constructed. By adding known amount standard into canned cutting system before GC analysis, absolute concentrations of canned cutting gas components can be calculated and reported as μmol.

If neglecting the lose of gas during drilling and transport to surface, degassing efficiency is the most important factor to influence absolute concentrate of gas components, which strictly depends on temperature and its holding time and rock characters. Here, temperature and its holding time are investigated and the results show that concentration of gas components goes up with an increase of temperature up to 60°C and then keep stable, while the holding time is a not a significant factor where there is almost no change from 30min to 60min. Stable carbon isotopic compositions of gas components are less affected by degassing efficiency and this is in agreement with the observation by GeoMark.

A case study from the Panyu low-uplift of Baiyun depression, South China Sea is presented. Quantitative data, integrated with DST results, preliminary criteria can be made to define whether the oil and/or gas reservoir identified by normal logging is a commercial pay zone, and therefore for further DST planning.

This work was supported by NSFC Project 40972093.

Experimental study of solution-mineral interaction in the Qisanba uranium deposit, NW-China

SUN ZHANXUE[1], ZHOU YIPENG[2] AND LIU JINHUI[2]

[1]Laboratory of National Defence Key Discipline of Radioactive Geology and Exploration Techniques (East China Institute of Technology), Fuzhou, Jiangxi 344000, China (*correspondence: zhxsun@ecit.edu.cn)

[2]Key Laboratory of Nuclear Resources and Environment (East China Institute of Technology), Ministry of Education, Nanchang, Jiangxi 330013, China (ypzhou@ecit.cn)

Introduction

The Qisanban U deposit is hosted by a sandstone aquifer with groundwater whose TDS ranging roughly from 8-12 g/L. All the past pilot acid and alkaline *in situ* leach uranium mining tests failed due to serious chemical plugging during the mining processes. To develop a new solution mining technique, leaching test of uranium ores in ammonium bicarbonate solution was carried out. The TDS of the solution was maintained around 2 g/L by dilution using fresh water, and the pH was kept as 6.0-6.3 by pumping CO_2 into the solution.

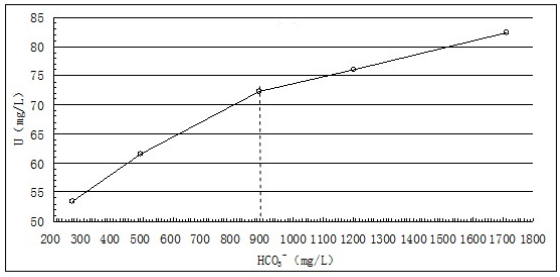

Figure 1: Uranium vs. HCO_3^- concentration of the solution

Result and discussion

The experiments showed that uranium can be leached effectively from the ores in ammonium bicarbonate solution without any chemical plugging. A new bicarbonate solution uranium mining technique based on groundwater dilution may be proposed.

This work is financially supported by the NSFC under the Project No. 40872165.

https://doi.org/10.1180/S0026461X00006502 Published online by Cambridge University Press

First finds of 'Alloclasite' (Fe,Co,Ni) AsS in Ni sulphides of Bangur Gabbro, Orissa, India

P.V. SUNDER RAJU

National Geophysical Research Institute (A Council of Scientific and Industrial Research) Hyderabad, India-500606 (perumala.raju@gmail.com)

The diarsenides and sulfarsenides of Fe, Co and Ni have a widespread geological occurrence; they exhibit complex paragenetic and compositional relations, and are commonly associated with economically important minerals, such as PGM and gold. We found mineral phase consist of enriched amounts of (Fe, Co, Ni) (As, S) $_2$ phases in Ni-S phases of Bangur gabbro in Orissa. The age of Bangur Gabbro is ~3.1 Ga. The eastern part of the Indian Shield is composed of a high-grade metamorphic terrain known as the Chhotanagpur Craton in the north and a granite- greenstone terrain known as the Singhbhum Craton in the south. The latter is mainly composed of several granitoid batholiths, which are largely surrounded and intervened by supracrustal rocks. Both Bangur and Baula (21°15'38' to 21°16'55' North and 86°.19'14' to 86°20'10' East) in the eastern part of Indian shield have been studied earlier by earlier workers [1], but petrological data (i.e. magma evolution and ore forming processes) are scanty. We report here the presence of mineral phase consists of (Fe, Co, Ni) (As, $S)_2$. There is complete solid solution series exist between alloclasite- cobaltite- gresdorffite. The observed assemblages and solid solution agree well with experimental data on Fe-Co-Ni-As-S system.

[1] Mondal, S.K. (2009) *J Geol Soc India* **73**, 36–51.

Aerosol optical properties and direct radiative effect over India based on satellite remote sensing measurements

ANU-MAIJA SUNDSTRÖM[1]*, PEKKA KOLMONEN[2], LARISA SOGACHEVA[2], EDITH RODRIGUEZ[2], MERI HANNUKAINEN[1], KSENIA ATLASKINA[1] AND GERRIT DE LEEUW[1,2,3]

[1]P.O. Box 64, 00014 University of Helsinki, Finland (*correspondence: anu-maija.sundstrom@helsinki.fi)
[2]Finnish Meteorological Institute, Climate Change Unit, Erik Palmen Aukio 1, 00101, Helsinki, Finland
[3]TNO, Utrecht, The Netherlands

Aerosols affect Earth's radiation budget directly by scattering and absorbing solar radiation, and indirectly by modifying the microphysical properties of clouds. However, large uncertainties still exist in current estimates of the aerosol effects on climate, mainly due to aerosols strong temporal and spatial variation (e.g. [1]). India is one of the world's most populated countries. Along with the continuously increasing population and economic growth the increase of the anthropogenic pollutants is evident. Large emissions of aerosol and precursor gases transported from these regions can have significant impacts on air quality and climate on both regional and global scales.

In this work a measurement-based approach is applied to study the aerosol optical properties and to estimate the aerosol direct radiative effect over India. To assess this, observations from satellite instruments, such as AATSR (Along Track Scanning Radiometer onboard ENVISAT) and CALIOP (Cloud-Aerosol Lidar with Orthogonal Polarization onboard CALIPSO) are used along with a radiative transfer code. The data consists of observations between 2006 and 2010. Preliminary results show e.g. that over areas with elevated aerosol optical depths the fine particles can account for over 80% of the total aerosol extinction.

[1] Yu, Kaufman, Chin, Feingold, Remer, Anderson, Balkanski, Bellouin, Boucher, Christopher, DeCola, Kahn, Koch, Loeb, Reddy, Schulz, Takemura & Zhou (2006) *Atmos.Chem. Phys.* **6**, 613–666.

https://doi.org/10.1180/S0026461X00006502 Published online by Cambridge University Press

W-Sn ores of the Svetloye deposit: Mode of formation from isotope, fluid inclusion and modeling studies

T.M. SUSHCHEVSKAYA[1], A.JU. BYCHKOV[3], A.V. IGNATIEV[2], S.S. MATVEEVA[3], J.A. POPOVA[3], N.I. PRISYAGINA[1] AND T.A. VELIVETSKAYA[2]

[1]Vernadsky Institute of Geochemistry RAS, Moscow, Russia (tms@geokhi.ru)
[2]Far East Geological Institute, Vladivostok, Russia
[3]Moscow StateUniversity

Large Svetloye W-Sn deposit (Chukotka, North- East of Russia) is located in the apical part of a leucogranite stock. The deposit is composed of a series of quartz veins among the flyschoid rocks (T_{1-2}), cut by the dikes (K_1). The veins are dominated by the quartz- wolframite- cassiterite- arsenopyrite-muscovite mineral assemblage. The later sulfide and quartz-fluorite –calcite assemblages are of limited development. Fluid inclusion study showed, that productive mineral association was formed by aqueous low-salinity sodium chloride fluids at T 350-270°C, P 0, 5-1, 0 kbar. The remarkable low salinity (<5% mass) was cryometrically found for the earliest magmatic fluids from primary magmatic fluid inclusions and fluid phase of melt inclusions in quartz from leucogranites of the stock. W and/or Sn ore formation was accompanied by increasing in alkalinity and degree of oxidation of fluids. Boiling of ore-forming fluids was rather typical of the central part of the deposit. Isotopic (H, O, Ar) study of minerals [1] and oxygen isotope zonality of host granites witness to precipitation of cassiterite-wolframite ores presumably from magmatic fluids strongly diluted with meteoric waters, interacted with wall rocks.

Analysis of possible role of main factors of W-Sn precipitation, such as cooling, boiling, interaction with wall rocks and mixing of genetically different fluids have been modelled with the help of HCh software package [2]. Natural data are best consistent with model of mixing of ore-forming solutions with exogenic fluid, reequilibrated with host rocks, as it was found for the Sn-W Iultin deposit, situated in the same ore province [3].

[1] Sushchevskaya T. *et al*. (2000) *Geochem. Int*. **38**. Suppl. 2 .P. 123. [2] Shvarov Ju. Bastrakov E. (1999) *Australian. Geol. Surv*. org. 56p. [3] Sushchevskaya T.M. Bychkov A.Ju. (2010) *Geochem. Int*. **48**. P.1246.

Strontium stable isotope variations in lunar basalts

CHELSEA N. SUTCLIFFE[1], KEVIN W. BURTON[1], IAN J. PARKINSON[2], DAVID COOK[1], BRUCE L.A. CHARLIER[2] FATIMA MOKADEM[1] AND ALEX N. HALLIDAY[1]

[1]Department of Earth Sciences, University of Oxford, South Parks Road, Oxford OX1 3AN, UK
[2]Department of Earth and Environmental Sciences, The Open University, Walton Hall, Milton Keynes, MK7 6AA, UK

In the terrestrial environment strontium (Sr) stable isotopes may experience significant fractionation, both at low- and high-temperatures, involving carbonate precipitation [1] and plagioclase crystallisation [2], respectively. Recent data for lunar basalts suggests that these rocks may possess light Sr stable isotope compositions ($\delta^{88}Sr$ = +0.16±0.07) [2] relative to mantle derived terrestrial basalts ($\delta^{88}Sr$ = +0.30±0.07) [2, 3]. However, few samples have been analysed thus far, and at the ±50 ppm precision of these measurements, obtained using an MC-ICP-MS [2, 3], such variations cannot be clearly resolved.

This study presents high-precision (±10 ppm) double spike TIMs data for $^{87}Sr/^{86}Sr$ and $^{88}Sr/^{86}Sr$ for a suite of lunar basalts and anorthosites. These data confirm the light Sr stable isotope compositions observed previously for lunar rocks [2] but also demonstrate that there are significant and resolvable variations in $\delta^{88}Sr$ ranging from +0.348 for a lunar norite to +0.151 for a high-Ti Mare basalt. These variations, taken with those for evolved terrestrial basalts, are most simply explained by the preferential incorporation of the heavy isotopes of Sr into plagioclase with a fractionation factor of ~1.0002 for $^{88}Sr/^{86}Sr$ [2]. These results clearly indicate that for the Moon primary igneous processes alone can produce significant variations in $\delta^{88}Sr$, without the recycling that may occur on Earth.

[1] Fietzke, J. & Eisenhauer A. (2006) *Geochem. Geophys. Geosyst*. **7**, Q08009. [2] Charlier, B.L.A. *et al*. (2011) *Earth Planet. Sci. Lett*. Submitted. [3] Moynier, F. *et al*. (2010) *Earth Planet. Sci. Lett*. **3-4**, 359–366.

https://doi.org/10.1180/S0026461X00006502 Published online by Cambridge University Press

^{129}I as an oceanographic tracer in the Japan Sea

T. SUZUKI[1]*, M. MINAKAWA[2], S. OTOSAKA[3] AND O. TOGAWA[3]

[1]Japan Atomic Energy Agency, Aomori 035-0053, Japan (suzuki.takashi58@jaea.go.jp)
[2]National Research Institute of Fisheries Science, Kanagawa 236-8648, Japan
[3]Japan Atomic Energy Agency, Ibaraki 319-1195, Japan

Introduction

Iodine-129 is a natural occurring radionuclide with a half life of 15.7 Ma. During last six decades, ^{129}I has also been released in the environment by nuclear weapons testing and the operation of nuclear fuel reprocessing plants.

The Japan Sea is a semi-enclosed marginal sea. The turnover time of water was reported about a few hundred years which was much shorter than that of the Pacific Ocean. Some of long-lived artifical radionuclides, therefore, would be useful tracers to study the oceanic circulation in the Japan Sea. In this paper, we summarize our recent studies of the Japan Sea using ^{129}I.

Experimental

To investigate the potential of ^{129}I as oceanographic tracer in the Japan Sea, seawater samples were collected at 7 stations by cruises of R/V Soyo-Maru and T/S Osyoro-Maru in 2007. Iodine isotopic ratios were measured by an accelarator mass spectrometry at the Mutsu Office of the Japan Atomic Energy Agency.

Results and Discussion

1. Fractions of ^{129}I source in surface seawater were estimated using a natural isotopic ratio and fission yield. This estimation suggests that ^{129}I in surface seawater consists of natural occurring (2%), weapons testing (10%) and reprocessing plants (88%) [1].
2. The averaged surface concentration of ^{129}I in a subarctic circulation was higher than that in a subtropical circulation. Taking account of the location and the total amount of ^{129}I released from reprocessing plants in EU, this different concentration would indicate that ^{129}I released from those plants is supplied to the Japan Sea.
3. The concentration of ^{129}I in the Japan Sea bottom water (JSBW) was higher than that of the natural level. This result indicates anthropogenic ^{129}I is transported vertically by winter convection [2] and the turnover time of the JSBW is estimated to be about 200 years.

[1] Suzuki et al, (2008) *Nucl. Instr. & Meth.* **268**, 1229–1231.
[2] Suzuki et al, (2009) *Qua. Geochrono.* **3**, 268–275.

Selenate reduction by iron-reducing bacteria isolated from Bangladesh soil

Y. SUZUKI[1]*, R. OYAMA[1], H. SAIKI[1], K. TANAKA[2] AND T. OHNUKI[3]

[1]School of Bioscience and Biotechnology, Tokyo University of Technology, 1404-1 Katakura-cho, Hachioji, Tokyo 192-0982, Japan (*correspondence: yosuzuki@bs.teu.ac.jp)
[2]Institute for Sustainable Sciences and Development, Hiroshima University, 1-3-1 Kagamiyama, Higashi-Hiroshima, 739-8530 Japan
[3]Advanced Research Center, Japan Atomic Energy Agency, Tokai, Ibaraki 319-1195, Japan

Introduction

Microbial reduction of highly soluble selenate and selenite to insoluble elemental selenium is an important phenomenon affecting the mobility of selenium and useful to remediation of Se-contaminated soils. Previously, we had reported the selenite reduction by *Shewanella putrefaciens* [1]. In this study, we examined the selenate reduction by iron-reducing bacteria isolated from Bangladesh soil.

Experimental

Soils from Samta Village, Jessore, Bangladesh were used to start an enrichment culture with H_2 as a potential electron donor and Fe(III)-EDTA as a electron acceptor (Fe-medium). The enrichment was purified by serial dilution with Fe-medium. Analysis of 16S rRNA sequence of the isolate was conducted. Selenate reducing ability of the isolate was examined in an anaerobic medium containing 5 mM Na_2SeO_4 with a gas phase of H_2-CO_2 (80:20). Effect of iron on the selenate reduction was investigated in media containing 5 mM Na_2SeO_4 and 0-20 mM Fe(III)-EDTA. Precipitates occurred in the media were analysed by XANES spectroscopy.

Results and Discussion

An iron-reducing bacterium, designated L1, was isolated by the serial dilution. Results of 16S rRNA analysis showed that L1 is a novel species and close to *Desulfotomaclum guttoideum* and *Clostridum celerecrescens*. L1 grew in the medum with 5 mM selenate. Cell density of L1 increased with reduction of selenate to selenite, meaning that the bacterium respires selenate. Followed by the selenate reduction, selenite was reduced to elemental selenium forming red precipitates. In the presence of Fe(III), the red precipitates were initially formed and later they turned black precipitates. The XANES analysis indicated that the red and black precipitates contained Se (0) and Se (-II), respectively.

[1] Suzuki *et al*. (2010) *GCA* **74**, A1011.

https://doi.org/10.1180/S0026461X00006502 Published online by Cambridge University Press

Cathodoluminescence of quartz as a reflection of the evolution of the Teplice Caldera

KATEŘINA ŠVECOVÁ[1], KAREL BREITER[2] JAROMÍR LEICHMANN[1]

[1]Department of Geological Sciences, Masaryk University, Kotlářská 2, CZ-61137 Brno, Czech Republic (175727@mail.muni.cz) (leichman@sci.muni.cz)
[2]Institute of Geology AS CR, v. v. i., Rozvojová 269CZ-165 00 Praha 6, Czech Republic (breiter@gli.cas.cz)

The late-Variscan Altenberg-Teplice Caldera (ATC) is situated in the Eastern Krušné Hory Mts./Erzgebirge on both sides of the Czech-German border. The studied borehole Mi-4, situated in the western part of the ATC, crossed all volcanic units of the caldera fill in the thickness of 950m.

According to Breiter *et al*. [1], the ATC consits of five volcanic phases. Two oldest units composed of the basal rhyolites (BR) and overlying dacites (DC) are calc-alkaline in character and may probably represent a product of high-degree melting of a immature material of the lower crust. Three younger units of Teplice rhyolite (TR1-3) are high-K calc-alkaline in character, significantly enriched in Rb, Th and HREE. This younger part of the ATC should be interpreted as a product of low-degree high-temperature melting of much more evolved crustal material.

The inner structure of quarz crystals was studied using cathode luminescence with hot-cathode (HC 2) and scanning luminescence (microprobe CAMECA SX100). Quartz grains from the ATC show intensive zonning in both modes of observations. The oldest unit, BR is charakteristic with nearly violet luminescence with weak zonning. In many cases these are just fragments of much larger grains and there are carbonate veins going trough the quartz. In DC unit have quarz grains dark blue luminiscence and no zonning. Quartz grains in three younger units TR1-3 have blue luniscence in hot CL with dark center and lighter margins. Significantly more intensive zonation appears in scanning luminescence. Very tiny zones symetrically rimm the core, dissolution of individual zones could be often documented. Some grains appears as fragments only. Majority of grains were corroded during their evolution. This has resulted in sometimes very bizarre shapes of grains. Quartz grains from the uppermost extrusive unit, rhyolite lava (TR3) are mostly rounded (2 mm diam.), often with granophyric overgrowth.

[1] Breiter, K. Novák, J. K. Chlupáčová, M. (2001) Chemical Evolution of Volcanic Rocks in the Altenberg-Teplice Caldera. *Geolines* **13**, 17–22.

Surface complexation evidence that amino acids prefer special sites on oxide surfaces

D.A. SVERJENSKY[1]*, R.M. HAZEN[2], D. AZZOLINI[1], N. LEE[1] AND K. KLOCHKO[2]

[1]Johns Hopkins University, Baltimore, MD 21218 USA (*correspondence: sver@jhu.edu)
[2]Geophysical Laboratory, Carnegie Institution of Washington, Washington, DC 20015 USA

Adsorption data for a variety of amino acids on rutile, amorphous titanium dioxide and hydrous ferric oxide covering wide ranges of pH, ionic strength and surface loading have been analyzed with the extended triple-layer model (ETLM), ATR-FTIR spectroscopic studies and quantum chemical approaches [1-4]. The results provide a consistent picture of the surface speciation of amino acids on oxides. The ETLM analysis requires a surface site density of 3.0 sites/nm^2. Each amino acid adsorbs in at least two ways to oxide surfaces: at low surface loadings, a species 'lying down' on the surface; at high surface loadings, a species 'standing up' on the surface. We focus here on glutamic acid (H2Glu) and dihydroxyphenylalanine (DOPA or H3DP) on rutile. At the highest loadings, about 0.47 sites/nm^2 are occupied by the 'standing up' Glu attached through the distal carboxylate to a surface functional group >TiO (OH^{2+}). The attachment consists of one inner-sphere bond and one H-bond. The amount of Glu adsorbed corresponds to about 16% of the total site density. However, this type of attachment cannot take place on the ideal (110) face of rutile which overwhelmingly predominates on our rutile sample in SEM pictures. The reason is that groups such as >Ti $(OH)_2$ or >Ti (OH)O are not present on the ideal (110) face. They are present on (111) or (101), suggesting that at least 16% of the (110) surface in our sample consists of (111) or (101) structures that contain the special functional groups that Glu prefers. A similar conclusion applies to DOPA. At high loadings, DOPA attaches to two Ti as (>TiOH^{2+})>TiHDP- with one inner-sphere bond and one H-bond from the two phenolic groups on the DOPA the separation of which (2.78 A) almost exactly matches the two >TiOH groups (2.77 A), but only when these are exposed on the (101) plane. Overall, the ETLM analysis indicates that both Glu and DOPA at high loadings prefer special functional groups that are not available on the ideal (110) plane, implying that most amino acid adsorption is on steps on (110) surfaces of rutile and similar structures on other oxides. HRTEM studies are underway to test this suggestion.

[1] Jonsson *et al*. (2009) *Langmuir* **25**, 12127–12135. [2] Parikh *et al*. (2011) *Langmuir* **27**, 1778–1787. [3] Bahri *et al*. (2011) *Env. Sci. Technol*. DOI: 10.1021/es1042832. [4] Sverjensky *et al*. (2008) *Env. Sci. Technol*. **42**, 6034–6039.

https://doi.org/10.1180/S0026461X00006502 Published online by Cambridge University Press

Trace element analysis in quartz by using laser ablation ICP-MS: A tool for deciphering magma evolution

M. SVOJTKA*, L. ACKERMAN AND K. BREITER

Institute of Geology, Academy of Sciences CR, 16500 Praha 6, Czech Republic (*correspondence: svojtka@gli.cas.cz)

Quartz is one of the most abundant mineral in the Earth's continental crust and is a common and most resistant rock-forming mineral in silica-oversaturated rocks. During post-magmatic and metamorphic alterations, trace elements are relatively stable in quartz crystal lattice. We have used laser ablation ICP-MS technique to (1) evaluate the chemical composition of igneous quartz from two comagmatic granitic and rhyolitic suites and (2) correlate cathodoluminiscence internal structures and trace element patterns in quartz to define relations of element chemistry and zonation.

Internal structure of quartz grains was studied by cathoduluminiscence (CL) on the electron microprobe. Trace element (Li, Be, B, Rb, Sr, Ba, Pb, Ge, Al, P, Ti, Cr, Mn) concentrations were measured using a New Wave UP-213 laser ablation system connected with sector-field single collector ICP-MS (Thermo Element 2). Laser was fired at repetition rate of 20 Hz and energy of 8-10 J/cm^2. All data were calibrated against the external standard NIST SRM612 glass and silica contents were used for internal standardization. Time-resolved signal data were processed using the Glitter software; caution was taken to constrain the signal to chemically homogeneous parts of the crystals and to avoid any inclusions and inhomogenities that can be potentially present in the analysed.

Our pilot samples were taken from the late-Variscan magmatic system of the A-type in eastern Krušné hory Mts. (N Bohemian Massif). The rhyolite samples from borehole Mi-4 represent evolution of the Altenberg-Teplice caldera, whereas the granite sample from borehole CS-1 document vertical zonality of the comagmatic Cínovec pluton.

Cathodoluminescence images of quartz grains (crystals and their fragments) from the rhyolite show distinct domains with a characteristic bright and dark luminiscence: the cores are dark (poor in Ti, and enriched in Al and Ge), whereas rims are bright (rich in Ti and poor in Al). Quartz grains from granites are homogeneous, without any CL zonation. Evolution from the deeper protolithionite to the upper zinnwaldite granite is documented by increase of Al, Ge, B, Sr, Ba, and decrease of Ti-contents in quartz.

Computer simulation of clay mineral – biomolecule interactions

JACOB B. SWADLING[1], PETER V. COVENEY[1]* AND H. CHRISTOPHER GREENWELL[2]

[1]Centre for Computational Science, Department of Chemistry, University College London, WC1H 0AJ, UK (*correspondence: p.v.coveney@ucl.ac.uk)

[2]Department of Earth Science, Durham University, Durham, DH1 3LE, UK

We show simulations of various 25-mer sequences of single stranded RNA, in bulk water and with aqueous montmorillonite clay [1]. Over timescales of only a few nanoseconds, specific RNA sequences fold to characteristic secondary structural motifs, which do not form in the corresponding bulk water simulations. Our simulations show that, in aqueous Ca^{2+} environments, RNA can tether to the clay surface through a nucleotide base leaving the 3′ end of the strand exposed, providing a mechanism for the regiospecific adsorption and elongation of RNA oligomers on clay surfaces.

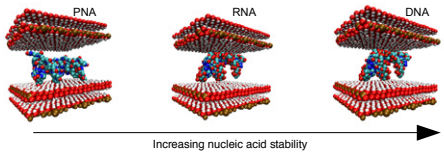

We study the structural stability of three different nucleic acids, intercalated at varying degrees of hydration within a magnesium aluminum layered double hydroxide (LDH) mineral host and free in aqueous solution [2]. The nucleotides investigated are ribose nucleic acid (RNA), deoxyribose nucleic acid (DNA), and peptide nucleic acid (PNA), all in duplex form. Our simulations show that DNA has enhanced Watson-Crick hydrogen-bonding when intercalated within the LDH clay layers, compared with intercalated RNA and PNA, whilst the reverse trend is found for the nucleic-acids in bulk water. The tendency for LDH to alter the stability of the three nucleic acids persists for higher temperature and pressure conditions. These results suggest that a mineral based origin of life may have favored DNA as the information-storage biomolecule over potentially competing RNA and PNA, providing a route to modern biology from the RNA world.

[1] J. B. Swadling, P. V. Coveney, & H. C. Greenwell. (2010) *J. Am. Chem. Soc.* **132**, 13750–13764. [2] J. B. Swadling, P. V. Coveney, & H. C. Greenwell. (2010, submitted).

https://doi.org/10.1180/S0026461X00006502 Published online by Cambridge University Press

Chronology of fluvial incision in the upper Ganges inferred from *in situ* cosmogenic isotopes

Z. SWANDER[1]*, A. DOSSETO[1], D. FINK[2] AND C. MIFSUD[2]

[1]GeoQuEST Research Centre, School of Earth and Environmental Sciences. University of Wollongong. Wollongong, NSW, Australia (*corresponence: zjs785@uow.edu.au, tonyd@uow.edu.au)

[2]Australian Nuclear Science and Technology Organization. Lucas Heights, NSW, Australia (fink@ansto.gov.au, cxm@ansto.gov.au)

Although past climatic cycles are well constrained, little is known about their effect on catchment erosion and sediment transport. For instance, what is the role of climate variability on river aggradation/degradation cycles in tectonically active settings? The Alaknanda River, one of the two major tributaries of the Ganges River, constitutes an ideal area for studying this question. From its glacial headwaters sourcing sediment from 7, 000+ meter peaks, fueled by meltwater and the summer monsoon that annually brings the river to sustained flood levels; the Alaknanda River transports a tremendous volume of sediment to the fertile floodplain and the delta of the Ganges River. Sediment transport dynamics has fluctuated in the past with episodes of fluvial aggradation and incision. Recently, Ray and Srivastava (2010) have used OSL dating to provide a chronology of the episodic formation of river terraces, showing that it occurred during two phases: between 45 and 25 ka, and between 18 and 11 ka. A detailed knowledge of fluvial incision chronology is still lacking. Cosmogenic radionuclides (CRN) ^{10}Be and ^{26}Al can be used to determine how long a bedrock surface has been exposed to cosmic rays at the Earth's surface. This can be used to quantify the timing of fluvial incision through bedrock or overlying sediments. With this aim in mind, we have collected bedrock samples along the Alaknanda River at strategic sites. Results will inform on the timing of fluvial incision in this catchment, which when combined to the chronology of river aggradation, will provide a detailed understanding of river dynamics in the lower Himalayas. By comparing these results to regional climatic records, we will be able to identify the role of climate on catchment dynamics in a tectonically active environment.

Ray & Srivastava (2010) *Quaternary Science Reviews* **29**, 2238–2260.

Regulation of atmospheric pCO_2 by the North Pacific Ocean since the last interglacial

GEORGE E.A. SWANN[1] AND ANDREA M. SNELLING[2]

[1]School of Geography, University of Nottingham, University Park, Nottingham, NG7 2RD, UK (*correspondence: george.swann@nottingham.ac.uk)

[2]NERC Isotope Geosciences Laboratory, British Geological Survey, Keyworth, Nottingham, NG12 5GG, UK (asnel@bgs.ac.uk)

The large 80-100 ppmv variations in atmospheric pCO_2 documented in ice-cores from Antarctica over glacial-interglacial cycles provide an essential forcing mechanism in driving the climate system. Existing research on the terrestrial biosphere as well as the low latitude and Southern Oceans are capable of explaining c. 50% of this variability when invoking mechanisms including deep water upwelling, stratification and the biological pump. Evidence is presented here, using new diatom oxygen, silicon and carbon isotope data, that changes in the strength of the North West Pacific Ocean biological pump and the regional halocline also played a key role in acting as both a net sink and source of CO_2 between MIS 5e and MIS 4.

Methods

δ^{18}O and δ^{30}Si were analysed following a combined step-wise fluorination procedure with measurements made on a Finnigan MAT 253 with an analytical reproducibility of 0.4‰ and 0.06 ‰ respectively [1]. Diatom δ^{13}C was analysed using a Costech elemental analyser linked to an Optima mass spectrometer via cold trapping with an analytical reproducibility of 0.3‰.

Results/Discussion

Whereas the regional water column is characterised by an inefficient biological pump and significant ventilation of CO_2 to the atmosphere in MIS 5e, a more efficient siliceous pump during MIS 5b-c led to a reduction in such exchanges. Both intervals culminate with increased meltwater input, establishing a stratification boundary and inhibiting further productivity as well as large scale ventilation of CO_2. Such changes would have helped drive the climate system through the MIS 5 sub-stages and into the last glacial period.

[1] Leng & Sloane (2008) *Journal of Quaternary Science* **23**, 313–319.

https://doi.org/10.1180/S0026461X00006502 Published online by Cambridge University Press

A microbially-mediated deep terrestrial nitrogen cycle at Henderson Mine, CO

ELIZABETH D. SWANNER* AND ALEXIS S. TEMPLETON

Department of Geological Sciences, University of Colorado, Boulder, CO 80309, USA
(*correspondence: swanner@colorado.edu)

The existence of life in deep terrestrial subsurface rocks has been established at multiple sites, yet few studies have investigated the origin of nutrients that support such life. At Henderson Mine, CO, subsurface fluids drain from boreholes at 3000' depth, supporting a diverse microbial community based on 16S rRNA gene surveys. The fluids of several boreholes contain nitrogen in multiple oxidation states, including NH_4^+ at 5-100 μM. Fluid mixing trends show a correlation between NH_4^+ and degree of water-rock interaction, and so we ask whether subsurface NH_4^+ is sourced geologically or biologically. As this Mo deposit developed from partial melting of the lower crust, it is plausible that a sedimentary source of nitrogen was mineralized into NH_4^+, which then substituted for K^+ in silicate minerals in the stockworks. We used FTIR microscopy to detect and quantify NH_4^+ in from biotites and other mineral phases. We also investigate whether biological nitrogen fixation of N_2 supplies the microbial community with NH_4^+. In the borehole fluids with the highest NH_4^+ (~100 μM), we amplified the *nifH* gene from DNA extracts of filtered fluids, but not from borehole fluid DNA where NH_4^+ concentrations were lower. We use a phylogenetic and quantitative PCR-based approach to evaluate whether *nifH* belongs to the novel phylum of bacteria first detected in these samples, the Henderson candidate division.

Our geochemical calculations predict that nitrification (NH_4^+ and NO_2^- oxidation) is favorable in the high NH_4^+ borehole, and so we next asked whether nitrifiers were present. The DNA from the high-NH_4^+ borehole fluid was the only sample to contain 16S rRNA sequences from archaea and the bacterial genus *Nitrospira*. From this sample, we amplified the gene for archaeal ammonium oxidation, *amoA*, but not the bacterial version of the gene, suggesting that archaeal ammonium oxidizers (AOA) are better adapted to this environment. Finally, we amplified a novel *nxrB* gene encoding the beta subunit of nitrite oxidoreductase specific to nitrite-oxidizing *Nitrospira*. Amplification of genes for nitrogen fixation and nitrification support the existence of a subsurface nitrogen cycle. The ubiquity of Mo in enzymes of the nitrogen cycle may dictate the energy sources utilized by microbes in this subsurface Mo mine.

Is there really a mixing-zone stable carbon and oxygen isotope signal?

PETER K. SWART

Division of Marine Geology and Geophysics, Rosenstiel School of Marine and Atmospheric Sciences, University of Miami, Miami Fl 33149 (pswart@rsmas.miami.edu)

A number of distinctive changes in $\delta^{13}C$ and $\delta^{18}O$ signals of carbonates in response to different diagenetic phenomena have been proposed. For example, sub-aerial exposure surfaces are typically characterized by extreme depletions in the $\delta^{13}C$ and a slight enrichment in $\delta^{18}O$, the vadose zone is characterized by constant and depleted $\delta^{18}O$ values, but wildly varying $\delta^{13}C$, the freshwater phreatic zone possesses negative $\delta^{13}C$ values which are not so variable as the vadose zone, the mixing-zone is characterized by a co-varying trend from negative to positive $\delta^{13}C$ and $\delta^{18}O$ values, and finally the marine phreatic zone has values of both $\delta^{13}C$ and $\delta^{18}O$ which are fairly positive. In this presentation the interpretation of the co-varying trend in the mixing-zone is questioned. Instead it is proposed that this trend really represents a range of varying amounts of recrystallization taking place in the freshwater phreatic zone. The significant change in interpretation is based on observations from several deep cores in the Bahamas which have penetrated shallow-water carbonates which were deposited and sub-aerially exposed during the numerous sea-level changes during the Pleistocene. During the last glacial period sea level fell at least 120 m below its present position. Based on present interpretation of the co-varying stable C and O isotopic record at this level no freshwater water lens would have been present. Clearly a significant freshwater lens was present extending downwards as much as 40 m, coincidently corresponding to the zone of covariation between the C and O isotopes.

https://doi.org/10.1180/S0026461X00006502 Published online by Cambridge University Press

The Archean anorthosite-monzogranite magmatic association of the Narryer Gneiss Terrane, Western Australia

P.J. SYLVESTER[1] *, A.K. SOUDERS[1], J.L. CROWLEY[2] AND J.S. MYERS[3]

[1]Department of Earth Sciences, Memorial University, St. John's, NL A1B 3X5, Canada (*correspondence: psylvester@mun.ca)
[2]Department of Geosciences, Boise State University, 1910 University Drive, Boise, Idaho 83725-1535 USA
[3]Department of Applied Geology, Curtin University, Perth, WA 6845, Australia

The Narryer Gneiss Terrane is located in the Yilgarn Craton, Western Australia [1]. A layered anorthosite-gabbro-ultramafic intrusion called the Manfred Complex [2] is exposed just northeast of Mount Narryer. The complex is about 3.73 Ma old based on U-Pb zircon geochronology [3]. It is engulfed and disrupted by two banded granite gneisses. Meeberrie gneiss is mainly derived from monzogranites that have U–Pb zircon ages of 3.68–3.60 Ga [3, 4], although minor components are as old as 3.73 Ga [5]. Dugel gneiss formed from younger monzogranite to syenogranite magmas emplaced at 3.38–3.35 Ga [3, 4, 5]. Because the Manfred Complex is older than all but one component of the gneisses, it has been thought to be unrelated to the major magmatic events that produced the monzogranitic intrusions.

We have sampled additional anorthositic rocks from the Narryer Gneiss Terrane and determined their ages by LA-ICPMS U-Pb zircon geochronology. These rocks include anorthosite, leucogabbro, gabbro, amphibolite and peridotite. Anorthosites and leucogabbros located near 7 Mile Bore, north of the Jack Hills give ages of 3.73-3.63 Ga, similar to the ages for the Meeberrie gneiss, whereas northeast of Mount Dugel, north of Billabidy well, leucogabbros formed at about 3.3 Ga, similar to ages for the Dugel gneiss. Northwest of Mount Dugel, the anorthosites formed at about 3.5 Ga; this age is similar to tonalitic to monzogranitic protoliths of the Eurada gneiss, emplaced at 3.49–3.44 Ga [5].

The correspondence of ages of anorthosites and monzogranites in the Narryer Gneiss Terrane suggests that these rocks may represent a previously unrecognized, but distinctive magmatic association of the Archean.

[1] Williams & Myers (1987) *WA Geol. Surv. Rpt.* **22**, 32 pp. [2] Myers (1988) *Prec. Res.* **38**, 309-323. [3] Kinny *et al.* (1988) *Prec. Res.* **38**, 325-341. [4] Myers & Williams (1985) *Prec. Res.* **27**, 153-163. [5] Nutman *et al.* (1991) *Prec. Res.* **52**, 275-300.

Most recent developments in AMS technologies

H.-A. SYNAL, T. SCHULZE-KÖNIG, M. SEILER, M. SUTER, CH. VOCKENHUBER AND L. WACKER

Laboratory of Ion Beam Physics, ETH Zurich, Schafmattstr. 20, 8093 Zurich, Switzerland (synal@phys.ethz.ch)

In charge state 1+, molecular interferences can be efficiently suppressed in multiple collisions of ions with stripper gas atoms or molecules. This made a new class of AMS spectrometers possible using compact acceleration systems at terminal voltages of about 500 kV. At ETH an even more compact spectrometer was developed using a vacuum insulated high voltage platform operated at 200 kV (MICADAS). Such systems can be regarded as state-of-the-art, matching the requirements of high performance radiocarbon dating.

Recent investigations performed at ETH to explore the basic principle behind the detection technique in particular of radiocarbon at even lower energies has opened novel opportunities to further reduce size and complexity of radiocarbon detection systems. Here, the use of He as a stripper is the key to minimize energy and angular straggling in connection with charge exchange and molecule dissociation processes. Dissociation cross section of mass 14 molecules in He gas have been found to be fairly constant at energies between 40 and 100 keV and are sufficiently large to reduce the intensity of molecular beams extracted from a graphite target by 10-11 orders of magnitude. Another important fact is the high yield of charge state 1+ at energies as low as 45 keV where values of more than 75% have been observed.

In a proof-of-principle experiment, using ions at 45 keV as they are extracted from the source and a molecule dissociation unit kept at ground potential, the feasibility of radiocarbon dating measurements over the entire ^{14}C dating range have been demonstrated.

Apart form radiocarbon, He as stripper gas has also striking advantages for other radionuclides. In particular, the detection of actinides in charge state 3+ at stripping energies of about 300 keV will become possible at unparalleled efficiencies.

https://doi.org/10.1180/S0026461X00006502 Published online by Cambridge University Press

The role of volcano-plutonic complex for simulation of origin of rare-metal granites from Transbaikalia, Russia

L.F. SYRITSO (BADANINA)[1]*, V.S. ABUSHKEVICH[2], E.V. BADANINA[1] AND E.V. VOLKOVA[1]

[1]St. Petersburg State University, Department of Geochemistry, University emb. 7/9, St.-Petersburg, 199034, Russia (*correspondence: Liudmila_Syritso@mail.ru)
[2]Institut of Geology of Precambrian RAS, St. Petersburg

The composition of rocks, melts (on the basis of melt inclusions study), isotopic-geochemical and geochronological characteristics (Rb-Sr and Sm-Nd isotopic systems) of rare-metal granites and accompanying sub-volcanic rocks in the ore clusters of Transbaikalia (Orlovka, Etyka, Shumilovka Li-F granites – Ta deposits, Scherlovaya Gora granites, greisen and rhyolite – Sn-W deposit, Bukuka – vein-greisen W deposit) were studied [1-3]. Close age interval of its formation, a similarity of geochemical specialization, crustal isotope-geochemical characteristics with signs of depleted of finite terms of series of differentiation allow us to consider the association of acid rock as a co-genetic volcanic-plutonic complexes. [4]. Dedicated rock types - ongonites, rhyolites, ongorhyolites, trachyrhyodacites – differentiates by the P-T regimes of crystallization, by the specialization of volatile, by the concentration levels of trace elements in the melts, by the isotopic and geochemical characteristics. These indicators reflect the levels of origin of melts, their degree of differentiation and extent of mantle-crust interaction. Ascertained shift of the isotopic compositions of late members of the series of differentiates toward depleted is reflected in a reduction of IR_{Sr} and, on the contrary, increasing of $^{147}Sm/^{144}Nd$ and values of ε_{Nd} (T), and occurs simultaneously with the accumulation of trace elements. Such situation may be explained by additional juvenile (depleted) component in the form of fluid phase with mantle characteristics produced by plume processes of Northeast Asian hot mantle field [5].

[1] Abushkevich V.S. Syritso L.F. (2007) *Nauka*, **147**. [2] Badanina *et al*. (2010) *Petrology* **18**, 139–167. [3] Badanina *et al*. (2008) *Petrology* **16**, 299–311. [4] Syritso *et al*. (2011) *Petrology* (in press). [5] Yarmoluk V.V. Kovalenko V.I. (2003*) Petrology*. **11**, 556–586.

Kinetics of Fe-isotope exchange with pyrite at hydrothermal conditions

DREW D. SYVERSON[1], W.C. SHANKS, III[2] AND W.E. SEYFRIED JR.[1]

[1]Department of Geology and Geophysics, University of Minnesota, Minneapolis, MN 55414 (syve0063@umn.edu, wes@umn.edu)
[2]U.S. Geological Survey, 973 Denver Federal Cent, Denver, CO 80225 (pshanks@usgs.gov)

The lack of data for the rates of Fe mass transfer between hydrothermal fluids and Fe-bearing minerals presents a challenge to the interpretation of subseafloor alteration processes at mid-ocean ridges (MORs). Field studies have relied on observations made from experiments performed at ambient conditions and also equilibrium theoretical models to understand the processes and mechanisms of sulfide precipitation/recrystallization [1-3]. Quantification of rates of isotopic exchange will add constraints to the chemical and isotopic evolution of hydrothermal vent fluids and minerals.

The rate of Fe-isotopic exchange between pyrite and hydrothermal fluid ($FeCl_{2\,(aq)}$) was examined at 350C, 500 bars using an isotopically enriched ^{57}Fe tracer at pyrite saturation equilibrium. The experimental design took advantage of liquid sulfur hydrolysis to buffer redox and pH, ensuring that pyrite is the only Fe-bearing mineral in the system exchanging with the hydrothermal fluid. The degree of Fe-isotopic exchange between $FeCl_{2\,(aq)}$-pyrite rapidly approached ~100% within days ($2.14*10^{-6}$ mmol/s). The low pH (in situ) and conditions of high dissolved sulfur may facilitate isotope exchange, as has been reported for sulfur isotope systematics [4] at similar chemical and physical conditions.

Speciation of the measured concentrations of dissolved ΣCl, H_2S, H_2, ΣFe^{++}, ΣSO_4^{--} and pH indicate that the fluid is saturated with respect to pyrite. Moreover, measured dissolved H_2 is in excellent agreement with that predicted from phase equilibria calculations, confirming that full equilibrium was achieved. The reaction quotient for $S^0 + H_2 \Leftrightarrow H_2S$ equilibrium was also determined ($\log K_{eq} \sim 4.1$).

The rapid rate of isotopic exchange between pyrite and fluid at acidic, high temperature systems, such as back-arc basins, implies that sulfide minerals may record the effects of short term temporal isotopic/chemical perturbations.

[1] Rickard, D. (1997) *Geochim. Cosmochim. Ac.* **61**, 115–134. [2] Rouxel *et al*. (2008) *Chem. Geol*. **252**, 214–227. [3] Polyakov & Soultanov (2011) *Geochim. Cosmochim. Ac.* **75**, 1957–1974. [4] Ohmoto & Lasaga (1982) *Geochim. Cosmochim. Ac.* **46**, 1727–1745.

https://doi.org/10.1180/S0026461X00006502 Published online by Cambridge University Press

Effects of prolonged volcanic activity of the Paraná continental flood basalts on the paleogeography, salt geochemistry and presalt oil resources of the South Atlantic rift

PETER SZATMARI

Petrobras Rio de Janeiro Brazil

The recent discovery and intense exploration of giant oil deposits in Early Cretaceous presalt sediments of the South Atlantic rift offshore Brazil (Santos, Campos and Espírito Santo Basins), adjacent to the Paraná Continental Flood Basalt province, has thrown a new light on the complex interaction between continental flood basalts, rift evolution, and rift lake chemistry. Rifting started in the uppermost Jurassic to lowermost Cretaceous with the deposition of fluvial, fresh water lacustrine and then saline lacustrine terrigenous sediments. The continental Paraná flood basalts were dated onshore at 134.6±0.6 Ma (Thiede and Vasconcellos, 2010, *Geology*), possibly related to the Valanginian Weissert Oceanic Anoxic Event. Offshore, basalt volcanism in the rift continued intermittently to 115 Ma, intercalating with presalt sediments. The flood basalts, associated with dikes, sills, and thermal uplift, blocked the entrance of sea water from the south into the southward widening rift. The main source of sediments changed from Proterozoic granites and Paleozoic sandstones to basalts. Farther out into the rift lake, terrigenous sediments gave place to the deposition of thick lacustrine limestones, dolomites, and Mg-silicates from solutions rich in Ca, Mg and silica supplied by the eroding basalts. In latest Aptian time, the entry and repeated desiccation of sea water under an arid climate led to the deposition of stratified salt, several km thick. Ca- and Mg-rich solutions from the eroding basalts, interacting with basin brines, caused the halite to be interlayered with the Ca-Mg chloride tachyhydrite. The subsequent leaching of the carbonates by CO_2 degassing from the basalts was essential to create the high-permeability oil reservoirs sealed by salt.

Mesoarchaean suprasubduction zone ophiolite in the Tartoq Group, SW Greenland

KRISTOFFER SZILAS[1], VINCENT J. VAN HINSBERG[2] AND ALEXANDER F.M. KISTERS[3]

[1]Geological Survey of Denmark and Greenland, Øster Voldgade 10, 1350 Copenhagen, Denmark (ksz@geus.dk)
[2]University of Oxford, South Parks Road, Oxford, UK
[3]Stellenbosch University, Matieland 7602, South Africa

The Tartoq Group comprises supracrustal rocks of dominantly volcanic origin in several discrete fault-bounded blocks. The main lithological units include: pillow lavas, dykes, gabbros, and serpentinites. Peak metamorphic conditions range from greenschist facies to upper amphibolite and lower granulite facies.

LA-ICP-MS U/Pb zircon age dating of an orthogneiss sheet that was intrusive into the supracrustal rocks yield a minimum age of 2.996 ± 0.006 Ga for the Tartoq Group.

The mafic metavolcanic rocks are dominated by tholeiitic basaltic compositions (MgO = 6-10 wt.% and FeO^T = 12-14 wt.%). They possess negative primitive mantle-normalised Nb-anomalies (Nb_N/La_N = 0.5-0.8). Pillow lavas, dykes and gabbros have similar flat chondrite-normalised REE patterns (La_N/Sm_N = 0.8-1.0), which together with serpentinite cumulate/mantle, indicate that they form a co-magmatic assemblage resembling that of an ophiolitic ocean floor sequence. La, Y, and Nb values are similar to those of modern back-arc basalts and Th/Yb vs. Nb/Yb also indicates a subduction zone component in the source of the volcanic sequence. The serpentinites have SCLM-like PGE patterns.

The structural relations combined with geochemical, and metamorphic data suggest that the Tartoq Group is a slab of Mesoarchaean suprasubduction zone oceanic crust, which after shallow subduction, was emplaced in an exhumation wedge, retrogressed by fluid input, imbricated with marginal orthogneisses, and folded and thrust into several tectonic slices and slabs with the orthogneisses.

https://doi.org/10.1180/S0026461X00006502 Published online by Cambridge University Press

Arsenic speciation and sequential extraction studies

T. SZOCS AND A. BARTHA

Geological Institute of Hungary, Stefánia út 14., 1143 Budapest, Hungary (szocst@mafi.hu, bartha@mafi.hu)

Shallow groundwater speciation studies were carried out using a field separation method in two regions of Hungary. Sequential extractions using the Tessier *et al*. [1] method was applied to evaluate the arsenic content distribution in each fractions. The speciation studies showed a redox environment which can promote remobilization under reductive conditions at almost each site. The sequential extractions revealed that a relatively high proportion of the arsenic could be found in the very stable residual fraction, which was also detected in other regions and by other methods (Routh and Hjelmquist [2]). At these sites the arsenic content of the groundwater was lower than at sites where the arsenic is in the more easily leachable form.

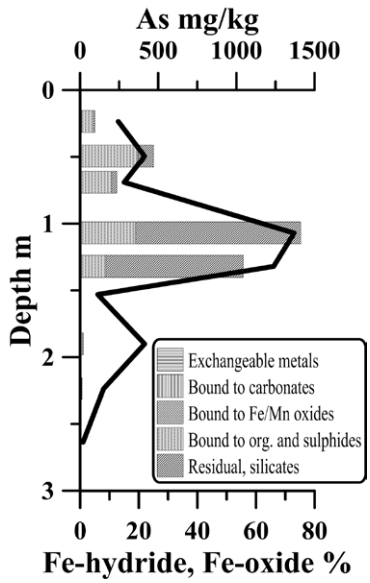

Figure 1: Distribution of arsenic in the extracted fractions versus depth**.**

This study was financed by Hungarian National Research Fund grant K67967.

[1] Tessier *et al*. (1979) *An. Chem*. **51**(7), 844-851. [2] Routh & Hjelmquist (2011) *Appl. Geoch*. **26**, 505–515.

https://doi.org/10.1180/S0026461X00006502 Published online by Cambridge University Press

Immobilization of arsenic released from excavated rocks affected by hydrothermal alteration

C.B. TABELIN* AND T. IGARASHI

Laboratory of Groundwater and Mass Transport, Hokkaido University, Sapporo 060-8628, Japan (*correspondence: carlito@trans-er.eng.hokudai.ac.jp, tosifumi@eng.hokudai.ac.jp)

New Method for the Disposal of Excavated Rocks Containing Arsenic

We have developed the adsorption-layer system as a simple and effective disposal method for disposing excavated rocks containing toxic elements like arsenic (As). This system is composed of a bottom adsorption layer and a low-permeability soil cover that incase the altered rock. The low-permeability soil cover lowers the water infiltration rate while the adsorption layer scavenges As leached out from the rock.

Discussion of Results

The altered rock sample used in this study was collected from a tunnel project in Hokkaido, Japan, and is composed of silicate minerals (*e.g.* quartz and plagioclase), calcite (minor mineral) and pyrite (trace mineral). Sequential extraction showed that the rock was capable of releasing as much as 18.4 mg of As per kg of altered rock. Based on these results, we conservatively estimated the amounts of natural and artificial adsorbents required to capture all of the leachable As content of the rock and tested these calculations through column experiments. All four adsorbents when used in the bottom adsorption layer effectively lowered the As released from 185 μg/L to below the drinking water standard of 10 μg/L (Figure 1). These results indicate that the adsorption-layer system is an effective countermeasure for the disposal of excavated rocks enriched in As.

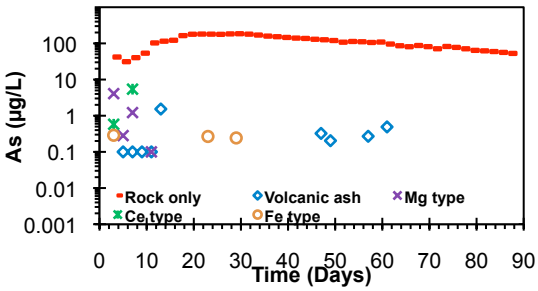

Figure 1: Evolution of As concentration in the effluent with and without adsorption layer. Missing points denotes concentrations below the detection limit of ICP-AES+Hydride generation.

Towards past climate reconstruction of speleothems by atmospheric sampling LA-ICPMS

D. TABERSKY[1], I. DE MADDALENA[1], M.B. FRICKER[1], R. DIETIKER[1], D. FLEITMANN[2] AND D. GÜNTHER[1]*

[1]ETH Zurich, Department of Chemistry and Applied Biosciences, Laboratory of Inorganic Chemistry (*correspondence: guenther@inorg.chem.ethz.ch)

[2]University of Bern, Institute of Geological Sciences and Oeschger Centre for Climate Change Research

Trace elemental distributions in paleoclimatic archives such as stalagmites represent a precious source of information on past climate variability. Analytical procedures play a pivotal role in the assessment of monthly to sub-annual trace metal variations in these paleoclimate archives [1]. The analysis of stalagmite samples requires a method that allows for the quantification of major and minor trace elements in high spatial resolution. This demand can be addressed by laser ablation combined with detection by inorganic mass-spectrometry.

Classically, airtight ablation cells are utilized for laser ablation strategies. Following the tradition of sealed cell designs, a *low dispersion high capacity laser ablation cell* was developed [2]. However, even such a cell is restricted to samples less than 25 cm in length and therefore, it cannot host the majority of stalagmite samples without modification. Large samples have to be broken or cut into smaller pieces, which unfortunately leads to the destruction of many years of valuable information. Atmospheric sampling rudiments enabled by recent developments [3] and/or quasi-closed cell designs [4] promise to overcome this limitation and provide full-scale climatic records.

This study investigated potential sample inlet systems by computer modeling of gas flow characteristics of new sample-transportation device geometries. Based on the results of computational flow dynamics, prototype inlet systems were built and characterized. Results are compared to those obtained by large closed cell approaches. Further, the newly developed method was applied to investigate seasonal trace element variations in a stalagmite sampled from Sofular Cave in northwestern Turkey.

[1] Fairchild *et al.* (2006) *Earth-Sci Rev* **75**, 105. [2] Fricker *et al.* (2011) *Int J Mass Spectrom*, doi: 10.1016/j.ijms.2011.01.008. [3] Kovacs *et al.* (2010) *J Anal Atom Spectrom* **25**, 142. [4] Asogan *et al.* (2009) *J Anal Atom Spectrom* **24**, 917.

https://doi.org/10.1180/S0026461X00006502 Published online by Cambridge University Press

FT-ICR/MS and quantum chemical studies of aqueous polyoxometalates

M.A. TACZKOWSKA[1], K.H. LEMKE[1]*, S.A. SADJADI[1] AND T.M. SEWARD[2]

[1]Department of Earth Sciences, University of Hong Kong, Pokfulam Road, Hong Kong, SAR (*correspondence: kono@hku.hk)

[2]SGEES, Victoria University of Wellington, Wellington, New Zealand

Mass spectrometric and quantum chemical studies of aqueous oxometalates, for instance, polyoxotungstate and polyoxomolybdate clusters, provide a suitable means of delivering molecular-scale information on the speciation, distribution and abundance of such moieties in crustal fluids. This study presents Fourier transform ion cyclotron resonance (FT-ICR) mass spectrometric data pertaining to the stability of polyoxomolybdate and polyoxotungstate clusters as well as mixed polymolybdotungstate clusters. We also report theoretical geometries and energies of the above clusters using B3LYP/aug-cc-pVDZ level theory in combination with SDD ECPs for W and Mo. Ion cluster experiments have been conducted on a Bruker 7T FT-ICR mass spectrometer with electrospray ionization capability. The mass spectrometer has also been modified to include a leak valve system used to introduce solvents and conduct solvation studies of ion clusters. Ion clusters generated from electrosprayed aqueous solutions containing Na_2MoO_4 and Na_2WO_4 salts (1-50mM) include the polyoxomolybdates $[Na_{2m+1}Mo_mO_{4m}]^+$ ($m \leq 11$), polyoxotungstates $[Na_{2n+1}W_nO_{4n}]^+$ ($n \leq 20$), and the mixed polymolybdotungstates $[Na_{2\,(m+n)+1}Mo_mW_nO_{4\,(m+n)}]^+$ ($m+n \leq 5$) (see below). We also identified several gas-phase polyoxometalates with magic numbers (abundance anomalies) as well as pure and mixed doubly- and triply-charged polyoxometalate clusters. Thermodynamic data obtained for the stepwise solvation of individual polyoxometalate clusters with H_2O will be presented and compared with hydration energies obtained from quantum chemical calculations.

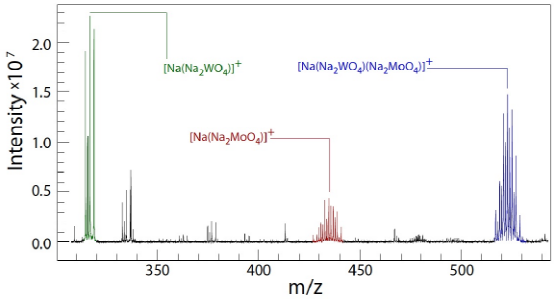

Figure 1: Positive-ion ESI-MS of aqueous Na_2MoO_4/Na_2WO_4 solution.

Mineralogy of the sodic-calcic hydrothermal alteration host rocks of the Esfordi, Choghart and Chadormalu magnetite-flourapatite deposits, Bafq area, Central Iran

S. TAGHIPOUR[1], A. KANANIAN[2] AND J. DONOVAN[3]

[1]School of Geology, College of science, University of Tehran, Tehran, Iran (taghipour@khayam.ut.ac.ir)

[2]School of Geology, College of science, University of Tehran, Tehran, Iran (taghipour@khayam.ut.ac.ir)

[3]CAMCOR, University of Oregon, Eugene, Oregon, 97403, USA (donovan@uoregon.edu)

The Esfordi, Choghart and Chadormalu Ap-Mt deposits are located in the bafq area, Central Iran. Flourapatite is one of the most important mineral in the studied area. This mineral is formed in primary and secondary generations. On the basis of the EPMA analysis, flourapatite is characterized by high CaO (54-57), P_2O_5 (40-43) and minor amount Na_2O, SiO_2, F, Cl contents. Amphibole is the major mineral in the igneous rocks, sodic-calcic alteration and mineralization zones. This mineral has been found both phenochryst and needle inclusions in the apatite, magnetite, plagioclase and quartz minerals. The phenochryst of amphibole has altered to the brown biotite, chlorite and calcite. Chemically, two different amphiboles occur in the sodic-calcic alteration zone. The first type is edenite to ferro-edenite in the contact of igneous rocks, which has replaced by altered bodies. It has Na+K > 0.5 %, Mg# values 0.46 and highest Ti, AlVI values. The second type amphibole occurs in the sodic-calsic alteration zones and commonly replaced edenite with Na+K<0.50 and Mg# values of 0.67. The composition of them is between actinolite to magnesiohornblende. Also amphibole is a very important mineral in the mineralization zone. Chemically, it is actinolite to ferro-actinolite with average Mg# values of 0.57. On the basis of the palagioclase-amphibole geothermometer (Holland and Blundy 1994) this assemblage has formed in the 525-549° C and 1.2-1.7 kbar pressures, so evolution of the main hydrothermal process has occur in the shallow crust levels.

[1] Holland, T and Blundy, J., (1994) Non-ideal interactions in calcic amphiboles and their bearing on amphibole–plagioclase thermometry. *Contributions to Mineralogy and Petrology* **116**, 443–447.

https://doi.org/10.1180/S0026461X00006502 Published online by Cambridge University Press

Direct measurement of Ce^{3+}/Ce^{4+} and Eu^{2+}/Eu^{3+} in Hadean zircons by XANES

NICHOLAS D. TAILBY[1]*, DUSTIN TRAIL[1], NICOLE L. CATES[2], STEPHEN J. MOJZSIS[2], ELIZABETH BELL[3], T. MARK HARRISON[3] AND E. BRUCE WATSON[1]

[1]Department of Earth & Environmental Sciences and New York Center for Astrobiology, Rensselaer Polytechnic Institute, Troy, NY 12180, USA (*correspondence: tailbn@rpi.edu)
[2]Department of Geological Sciences, University of Colorado Boulder, Colorado 80309, USA
[3]Department of Earth and Space Sciences and Institute of Geophysics and Planetary Physics, UCLA, California 90095, USA

Normalized REE profiles in zircon, ancient or modern, have been used as an indicator of environmental conditions. In this regard, excursions from an otherwise smooth trend among the lanthanides (i.e. positive Ce anomalies and negative Eu anomalies) are thought to be related to changes in valence ratios in response to the intrinsic oxygen fugacity of the system in which the host zircon crystallized. REE partitioning systematics and the magnitude of anomalies are generally not considered in conjunction with direct measurement of valence ratios of Ce or Eu within zircon, which requires very specialized instrumental capability.

We present Ce L_{III}-edge and Eu L_{III}-edge XANES spectra from ancient Jack Hills and Acasta Gneiss zircon grains. These analyses represent the first attempt to directly constrain valence in ancient grains, where trace element concentrations can be as low as 2 ppm for Eu and 7 ppm for Ce. Jack Hills grains studied here (4.0-4.1 Ga), show distinct positive Ce anomalies but indicate only minimal Ce^{4+} in XANES (<20%). Zircon grains from the Acasta Gneiss (3.6-3.9 Ga), by contrast, show domains with variable Ce^{4+} content (40-100%). The variable valence ratios of the two populations, by virtue of not being dominated by a single species, suggests that no dominant process resets valence over geological timescales and that considerable information may be obtained from a combined study of REE profiles and associated valence speciation in zircon.

Intracrystal microstructures in alkali feldspars from apparently fluid deficient felsic granulites: A chemical and TEM study

L. TAJCMANOVA[1], R. ABART[2], R. WIRTH[3], G. HABLER[2], LUIZ F.G. MORALES[3] AND D. RHEDE[3]

[1]IMP-ETHZ, Zürich, Switzerand
[2]Department of Lithosphere Research, Vienna, Austria
[3]Helmholtzzentrum, GFZ, Potsdam, Germany

Samples of apparently ‘dry’ high-pressure felsic granulites from the Bohemian Massif (Variscan belt of Central Europe) contain large perthites with several generations of exsolution features. The contacts between the orthoclase-rich host and the plagioclase precipitates of the first generation and the contact between the orthoclase-rich host and large kyanite, quartz and garnet inclusions is lined with a thin rim of albite This albite was formed at a late stage of the petrogenetic history related to fluid infiltration and associated albitization. In the vicinity of the large inclusions the plagioclase precipitates of the first perthtite generation become significantly depleted and the perthite microstructure coarsens composed dominantly of tweed orthoclase.

The primary exsolutions probably formed by spinodal decomposition at around 850-900°C during the high pressure stage (16-18 kbar). The second generation of albite-rich precipitates was formed at around 600-500°C. TEM investigations revealed that the interfaces between the second generation plagioclase lamellae and the orthoclase rich host are coherent or semi coherent. The formation of albite linings at phase boundaries and of patch perthite produced incoherent interfaces. The patch perthites, albitization and secondary coarsening in the vicinity of large inclusions developed below 400°C contemporaneously with fluid infiltration in the course of deuteric alteration.

https://doi.org/10.1180/S0026461X00006502 Published online by Cambridge University Press

Constraining the P-T conditions of melting in stromatic migmatites from Ronda (S. Spain)

L. TAJCMANOVA[1], O. BARTOLI[2], B. CESARE[3]* AND A. ACOSTA-VIGIL[4]

[1]IMP-ETHZ, Zurich, Switzerland
[2]Dipartimento di Scienze della Terra, Univ. Parma, Italy
[3]Dipartimento di Geoscienze, Univ. Padova, Italy
(*correspondence: bernardo.cesare@unipd.it)
[4]IACT, CSIC, Granada, Spain

We have studied fine-grained stromatic metatexites occurring c. 400 m below the contact with the Ronda peridotite (Ojén unit, Betic Cordillera, SE Spain). These rocks contain Qtz + Pl + Kfs + Bt + Fib + Grt + Ms + Ap + Gr ± Ilm and have a main foliation defined by alternating layers of biotite and fibrolite and thin (~ 0.5 cm) leucosomes. Garnet occurs in very low modal amount (<1%). Muscovite is an armored inclusion or texturally retrograde.

Microstructural evidence of melting in the migmatites includes *pseudomorphs* after melt films, euhedral feldspars, and *nanogranite* inclusions in garnet. Remelted nanogranites show granitic compositions. The latter microstructure demonstrates that garnet crystallized in the presence of melt.

We have constructed two pseudosections: one for the bulk rock in the MnNCKFMASHT system, and the other for the composition of the remelted nanogranite inclusions in the NCKFMASH system. Calculated isopleths for chemical parameters of garnet (X_{Mg}, X_{Grs}), biotite (X_{Mg}, X_{Ti}) and plagioclase (An content) in the Qtz-Pl-Kfs-Bt-Grt-Sil-melt field match the actual values in the rock. The *P-T* conditions of equilibration were estimated at 4.5-4.8 kbar, 680-700 °C. These *P-T* conditions overlap with the low-T tip of the melt field in the pseudosection for the nanogranite composition. They are also consistent with the complete experimental remelting of nanogranites at 700°C.

These results indicate that nanogranites represent the anatectic melt generated at, or soon after, muscovite melting, and that garnet is able to trap melt inclusions also at temperatures lower than those of biotite breakdown melting.

Projection of future climate change by aerosols along the Representative Concentration Pathways (RCPs) with a global climate model

TOSHIHIKO TAKEMURA

Research Institute for Applied Mechanics, Kyushu University, 6-1 Kasuga-koen, Kasuga, Fukuoka 816-8580, Japan (toshi@riam.kyushu-u.ac.jp)

Projection of climate change in the 21st century due to aerosols is simulated by an aerosol global climate model, SPRINTARS [1-4], along the emission scenarios of the Representative Concentration Pathways (RCPs) in this study. SPRINTARS is coupled to an atmosphere-ocean general circulation model, MIROC, developed by the Atmosphere and Ocean Research Institute (AORI)/University of Tokyo, National Institute for Environmental Studies (NIES), and Japan Agency for Marine-Earth Science and Technology (JAMSTEC) [5]. It includes the radiation, cloud, and precipitation processes related with the aerosol direct, semi-direct, and indirect effeects of main tropospheric aerosols (black carbon (BC), organic matter, sulfate, soil dust, and sea salt) as well as the transport processes. The model treats not only the aerosol mass mixing ratios but also the number and mass concentrations of cloud droplets and ice crystals as prognostic variables. All RCPs' scenarios (RCP2.6, RCP4.5, RCP6.0, and RCP8.5) which are used in climate simulations for the Fifth Assessment Report of the Intergovenmental Panel on Climate Change (IPCC AR5) are applied in this study. Sulfate aerosols, which have the negative direct radiative forcing and a role of cloud condensation nuclei, are gradually decreasing almost over the globe, on the other hand, BC aerosols, which have the positive direct radiative forcing and a role of ice nuclei, are still increasing. Therefore the total aerosol effects on the climate system may be largely different between 20th and 21st centuries.

We would like to thank the contributors of development of SPRINTARS and MIROC. This study is partly supported by the Funding Program for Next Generation World-Leading Researchers in Japan.

[1] Takemura *et al*. (2000) *J. Geophys. Res.* **105**, 17853–17873. [2] Takemura *et al*. (2002) *J. Clim.* **15**, 333–352. [3] Takemura *et al*. (2005) *J. Geophys. Res.* **110**, doi: 10.1029/2004JD005029. [4] Takemura *et al*. (2009) *Atmos. Chem. Phys.* **9**, 3061–3073. [5] Watanabe *et al*. (2010) *J. Clim.* **23**, 6312–6335.

https://doi.org/10.1180/S0026461X00006502 Published online by Cambridge University Press

Where life meets rocks: Understanding P cycling during the early phases of soil formation

F. TAMBURINI[1]*, S.M. BERNASCONI[2], V. PFAHLER[1], E. BÜNEMANN[1] AND E. FROSSARD[1]

[1]Group of Plant Nutrition, Inst. of Agricultural Sciences, ETH Zürich, Eschikon 33, 8315 Lindau, Switzerland (*correspondence: federica.tamburini@ipw.agrl.ethz.ch)
[2]Geological Institute, ETH Zürich, Sonneggstrasse 5, 8092 Zürich, Switzerland (stefano.bernasconi@erdw.ethz.ch)

Deglaciated forefields are natural environmental laboratories where the interactions betweeen life and the inorganic realm can be investigated. The forefield of the Damma glacier, located in the Swiss Alps, has been extensively studied in the framework of a multidisciplinary project (BigLink) aiming at a better understanding of the initial phases of soil formation and development. A key aspect is to determine how nutrient availability changes along the chronosequence and which are the processes driving these changes. While the influence of soil development on the distribution of phosphorus (P) forms in soil is known, still little information is available on the rates and relative importance of the processes driving these changes. Here, we present data on the stable isotopic signature of oxygen bound to P in phosphate (δ^{18}O-P) extracted from soils (between 12 and 300 years old) and plants sampled along the chronosequence.

We performed a sequential extraction of P from soils of different age including a resin extraction (plant available P), an hexanol extraction (microbial P) and an HCl extraction (as a proxy for mineral P). We also extracted P from monocotylendon grasses. All P pools were then analyzed for their δ^{18}O-P. We also measured δ^{18}O in water from soils and plants, and soil phosphatase. The mineral pool bears the signature of igneous material and shows no significant change along the sequence. The isotopic signatures of the plant available and microbial P pools are more variable and already at the very first site, they show a significant deviation from the parent material, being close to temperature-dependent equilibrium with water. Phosphorus extracted from grasses shows even heavier values and reflect equilibration with leaf water.

Phosphate from plant residue and, to a lesser extent, organic matter mineralization contribute to the plant available P pool. But overall, our data suggest P is rapidly cycled in the soil by the microbial community, starting very early in the soil development.

Sources and cycling of nitrogen in the Gulf of Trieste (N. Adriatic Sea)

S. TAMŠE[1]*, P. MOZETIČ[2] AND N. OGRINC[1]

[1]Jožef Stefan Institute, Jamova 39, 1000 Ljubljana, Slovenia (*correspondence: samo.tamse@ijs.si)
[2]Marine Biological Station Piran, National Institute of Biology, Fornače 41, 6330 Piran, Slovenia

The sources of nitrate were determined using the stable isotope approach in the Slovenian part of the Gulf of Trieste and its main river tributaries Rižana and Dragonja. The sampling was performed in May, August and November 2010. At both river mouths impacts on the nitrogen cycle from municipal sewage or agriculture were observed through elevated nitrate concentrations and $\delta^{15}N_{NO3}$ values. This was most probably due to leaching of organic fertilizers from agricultural land and was more pronounced in August in Rižana and in November in Dragonja. Mixing along the salinity gradient was the main control on the spatial variations in isotopic composition of nitrate in the investigated part of the Gulf of Trieste. The relation between the isotopic composition of nitrate and its concentration showed that nitrate at most marine sampling locations was the result of mixing between its marine and terrestrial origins. In May, a strong terrestrial influence of river Rižana was observed at locations 'K 0 m' and 'ERI2 0.3 m' (Bay of Koper) with more negative $\delta^{13}C_{POC}$ values. The impact of nitrification was observed in November at all sampling locations at depths from 10 – 20 m. The correlations between $\delta^{15}N_{PN}$ and NO_3^- concentration indicated that NO_3^- assimilation was a major source of N in particulate organic matter (POM) in all sampling months. The low values of fractionation factors ε (0.4‰, 1.1‰ and 1.4‰), compared to other studies, were probably the consequence of different phytoplankton species and different growth conditions. The carbon isotopic mass balance calculation of POM revealed high contributions of allochthonous OM from freshwater inflows in May. The proportion of allochthonous vs. autochthonous OM decreased with depth. On the other hand the POM in August and November was mainly of autochthonous origin. In November a higher contribution of allochthonous OM was observed only at the surface.

https://doi.org/10.1180/S0026461X00006502 Published online by Cambridge University Press

Mantle diapir or mantle wedge plume of NW Rota-1 volcano, Mariana arc

Y. TAMURA[1]*, O. ISHIZUKA[2], R.J. STERN[3], H. SHUKUNO[1], H. KAWABATA[1], R.W. EMBLEY[4], Y. HIRAHARA[1], Q. CHANG[1], J. –I. KIMURA[1], Y. TATSUMI[1], A. NUNOKAWA[1] AND S.H. BLOOMER[5]

[1]IFREE, JAMSTEC, Yokosuka 237-0061, Japan (*correspondence: tamuray@jamstec.go.jp)
[2]Geological Survey of Japan, AIST, Tsukuba 305-8567, Japan (o-ishizuka@aist.go.jp)
[3]University of Texas at Dallas, TX 75080-3021, USA
[4]PMEL, NOAA, Newport, OR 97365-5238
[5]Oregon State University, Corvallis, OR 97331

COB and POB

We found near-primitive and phenocryst-poor lavas from NW Rota-1 volcano in the Mariana arc. These magnesian basalts are petrographically distinct cpx-olivine basalt (COB) and plagioclase-olivine basalt (POB). Fo content of olivines and Cr# of spinels are higher in COB than in POB. Moreover, COB is lower in Zr/Y and Nb/Yb and TiO_2, Al_2O_3, Na_2O, P_2O_5, Nb, Ta, Zr, Hf, HREE and Y than POB both at MgO = 8 wt. % and at estimated primary magmas, suggesting that COBs formed from higher degrees of mantle melting. COB has Ba/Nb, Th/Nb, $^{87}Sr/^{86}Sr$, $^{208}Pb/^{206}Pb$ and $^{207}Pb/^{206}Pb$ that are higher than for POB, and also have steeper light REE-enriched patterns and lower $^{143}Nd/^{144}Nd$, indicating that COB has a greater subduction component than POB. $^{176}Hf/^{177}Hf$ values between COB and POB are the same and Hf behavior in COB and POB is similar to those of Zr, Y and HREE, suggesting that Hf is not included in the subduction component, which produced the differences between COB and POB.

Mantle Diapir or mantle wedge plume

These estimated subduction components suggest flush melting of subducting sediment of the uppermost part of the slab at the temperature between phengite-out and monazite-out temperature (~900 °C) and rutile-out and garnet-out (~1000 °C) [1]. We suggest that high temperature at the base of mantle wedge (>1000 °C) combined with slab-derived metasomatic agents (hydrous sediment addition) ultimately lead to enough partial melting and buoyancy to initiate diapiric ascent. Degrees of mantle melting of primitive COB and POB are ~24 % and 18 %, respectively. Diapiric ascent of hydrous peridotite mixed heterogeneously with sediment melts may be responsible for the NW Rota-1 basalts.

[1] Skora & Blundy (2010) *Journal of Petrology* **51**, 2211–2243.

General depositional features of the carbonate platform gas reservoir of the Lower Triassic Jialingjiang Formation in the Sichuan Basin of Southwest China: Moxi gas field of the central basin

XIUCHENG TAN[1,2]*, LING LI[2], HONG LIU[2], BING LUO[2], YAN ZHOU[2], JIAJIE WU[2] AND XIONG DING[1,2]

[1]State Key Laboratory of Oil and Gas Reservoir Geology and Exploitation. Southwest Petroleum University, Chengdu, Sichuan 610500, China (*correspondence: tanxiucheng70@163.com)
[2]School of Resource and Environment, Southwest Petroleum University, Chengdu, Sichuan 610500, China

The general depositional features of the carbonate platform gas reservoir of the Lower Triassic Jialingjiang Formation in the Sichuan Basin of southwestern China were addressed based on a case study of the representative second member of the Formation (termed as Jia 2) in the Moxi gas field of the central basin. The features mainly include depositional setting, lithology, depositional structure, depositional sequence and reservoir space. These results lead to a conclusion that the Jialingjiang reservoir (the second member in particular) is not of a tidal flat deposition in an intertidal (to supratidal) environment as previously suggested but of restricted and evaporative carbonate platform deposition in a subtidal environment. The tidal-flat like (i.e. platform flat) facies occur only in the Jia 2^2-B layer. Moreover, the restricted-evaporative carbonate platform facies can be divided into 5 sub-facies and 23 micro-facies, of which the facies of grain shoal and dolomitic flat are relatively favorable for reservoir development. Their depositional model, distribution and evolution were further tentatively suggested, as the facies are subject to paleo-tomography and sea level variations. These results provide supplement to the present hot studies of the Permian-Triassic gas reservoir geology in China, as the Jialingjiang Formation has been investigated much less in comparison with the underlying Lower Triassic Feixianguan and Upper Permian Changxing formations.

https://doi.org/10.1180/S0026461X00006502 Published online by Cambridge University Press

Specific sorption of Th(IV), Np(V) and U(VI) on biogenic Mn oxide

K. TANAKA[1]*, Y. TANI[2] AND T. OHNUKI[3]

[1]Institute for Sustainable Sciences and Development, Hiroshima University, Higashi-Hiroshima, 739-8530 Japan (*correspondence: kt0830@hiroshima-u.ac.jp)
[2]Institute for Environmental Sciences, University of Shizuoka, Shizuoka 422-8526, Japan
[3]Advanced Science Research Center, Japan Atomic Energy Agency, Tokai 319-1195, Japan

Intoroduction

Sorption of radioactive elements on mineral surfaces is one of important processes which retard their migration in natural environments. Manganese(IV) oxide has attracted much attention because of its strong sorption property. Recently, it is accepted that the formation of Mn oxide is microbially mediated in most of Mn oxide deposits. Therefore, we investigated the sorption behavior of actinides on biogenic Mn oxide.

Methods

Sorption experiments of Th(IV), Np(V) and U(VI) on biogenic and synthetic Mn oxides were carried out in 10 mmol/L NaCl solution. We used *Acremonium* sp. strain KR21-2, a Mn-oxidizing fungus, to prepare biogenic Mn oxide [1]. Abitic Mn oxide (δ-MnO_2) was synthesized according to Villalobos *et al*. [2]. The biogenic or synthetic Mn oxide was put into 10 mmol/L NaCl solution. Then, stock solution containing ^{232}Th(IV), ^{237}Np(V) and ^{238}U(VI) was added to the NaCl solution. Solutions aftter sorption experiments were sampled by filtration with a 0.2 μm filter to measure actinide concentrations using an ICP-MS.

Results and Discussion

Sorption experiments showed that Th(IV) and U(VI) were strongly sorbed on synthetic Mn oxide. Neptunium(V) was also strongly sorbed on synthetic Mn oxide. In contrast, Np(V) was not sorbed on biogenic Mn oxide at all. Uranium(VI) was sorbed less on biogenic Mn oxide than on synthetic Mn oxide. Difference of the sorption behavior of Np(V) and U(VI) between biogenic and synthetic Mn oxides may be caused by the difference of their sorption properties. Sorption of Th(IV) on biogenic Mn oxide decreased with increasing pH. Thorium(IV) sorbed on biogenic Mn oxide was desorbed into solution phase with increasing time. This is possibly due to complexation of Th(IV) with organic ligands released from fungal cells.

[1] Tanaka *et al*. (2010) *GCA* **74**, 5463–5477. [2] Villalobos *et al*. (2003) *GCA* **67**, 2649–2662.

Re-evaluation of the B isotopic fractionation between $B(OH)_3$ and $B(OH)_4^-$ using methods beyond harmonic level

MAO TANG, QI LIU AND YUN LIU*

State Key Laboratory of Ore Deposit Geochemistry, Institute of Geochemistry, Chinese Academy of Sciences, Guiyang 550002, China (Liuyun@vip.gyig.ac.cn)

Since Hemming and Hanson (1992), B isotopic signature of carbonates has been used as a proxy to indicate the paleo-pH value of seawater and paleo-pCO_2 up to at least 13 Ma. This largely depends on the isotopic fractionation factor between B $(OH)_3$ and B $(OH)_4^-$ (e.g. Spivack *et al*. 1993; Sanyal *et al*. 1995; Palmer *et al*. 1998; Pearson and Palmer, 1999; Sanyal *et al*. 2000; Palmer and Pearson, 2003). However, the B isotope proxy was questioned recently for the unclear mechanisms of B incorporation into carbonates especially using NMR techniques (e.g. Klochko *et al*. 2009). Furthermore, the fractionation factor between B $(OH)_3$ and B $(OH)_4^-$ is not completely established. Kakihana and Kotaka (1977) suggested 1.019 at 25 °C, but subsequent theoretical studies suggested a larger value (e.g. Liu and Tossell, 2005; Zeebe, 2005; Rustad and Bylaska, 2007). Klochko *et al*. (2006) measured the fractionation factor between B $(OH)_3$ and B $(OH)_4^-$ using pH-shift method. Their new value is 1.0272 ± 0.0006 in seawater at 25 °C. Their pure water result contains much larger uncertainty (2 per mil at 25 °C and about 5 per mil at 40 °C). Rustad *et al*. (2010) investigated the fractionation factor in pure water through a series of computational quantum chemistry methods. They found DFT methods could not produce a fractionation factor close to the experimental value (1.031), and extrapolated MP2 results were also significantly different. Their results raised questions about the suitability of DFT methods to deal with B species in solution.

In this study, we use theoretical methods beyond harmonic approximations to study B isotope fractionation. Large anharmonic effects are found for some B-bearing compounds. This is the first study to show that B isotope fractionation is affected significantly by its anharmonicity. B isotope system hence becomes another which requires theoretical treatments beyond harmonic approximations. Unfortunately, all the previous studies including our previous work (Liu and Tossell, 2005) used Bigeleisen-Mayer equation which is purely based on harmonic approximations to deal with B isotope fractionation. Those previous results therefore need to be re-evaluated.

https://doi.org/10.1180/S0026461X00006502 Published online by Cambridge University Press

Separation of arsenate and phosphate for the measurement of the isotope composition of the oxygen in arsenate

X.TANG[1], Z. BERNER[1] AND S. NORRA[1,2]

[1]Institute of Mineralogy and Geochemistry, Karlsruhe Institute of Technology 76131, Germany
[2]Institute of Geography and Geoecology, Karlsruhe Institute of Technology, Karlsruhe 76131, Germany

The investigation of the isotopic composition of oxygen in As-oxyanions may offer some new insights into the development of arsenic enriched groundwaters [1]. A basic analytical requirement is, however, the quantitative separation of the various dissolved oxyanionic species which may coexist in the water. Among the several potentially interfering oxianions the separation of phosphate and arsenate appears to be a challenging task due to their very similar chemical behavior.

In this study, tests were carried out using the anion exchange resin Amberlite IRA-400. 250 mL of solution containing 15mg/L of phosphate and 1 mg/L of arsenate was mixed with 1 g of resin, and stirred with 500 rpm at 21°C for 2 hours. It was found that IRA-400 adsorbed both arsenate and phosphate to 99.9%. Subsequently, experiments were carried out to strip selectively arsenate and phosphate. Using 1 mol/L CH_3COOH, HCl and HNO_3 arsenate was desorbed to 66.3%, 91.1% and 95.8%, respectively, but in the same time also some phosphate went into solution (60.1%, 4.9% and 5.0%, respectively). At lower pH (2 mol/L HCl or 2 mol/L HNO_3) the concentration of phosphate in the leachate was below detection limit, and 99% of the arsenate was released from the resin.

Because for the isotope analysis arsenate is precipitated as Ag_3AsO_4, the presence of large amounts of Cl^- ions in solution is disadvantageous due to the coprecipitation of AgCl. Therefore, for isotopic work 2 mol/L HNO_3 appears to be an optimal desorption agent for the selective release of arsenate and phosphate from Amberlite IRA-400. After the desorption experiments the resin could be regenerated under alkaline conditions by using 1 mol/L NaOH.

[1] Berner Z. Tang X. Norra S. Oxygen isotopy of arsenate/arsenite, A novel approach to constrain the source of As in groundwater. Goldschmidt 2010, A84.

Mineral CO_2 sequestration in mine waste rock: Column experiments

E.K. TANGWA[1*,2], I.F. WALDER[2] AND A. LUNDKVIST[3]

[1]Depart. of Geology, Univ. Tromso, 9037, Tromso, Norway (*correspondence: elvis.k.tangwa@uit.no)
[2]Kjeoy Research and Education Center, 8412 Vestbygd, Norway (ifwalder@kjeoy.no)
[3]LKAB, Kiruna Sweden, SE-98186 Kiruna

Basic silicates are the main source releasing Ca, Mg and possibly Fe for carbonate mineral formation. This paper presents the results from column experiments using two waste rocks: type 1 and type 2 from the Kiruna iron mine, Sweden. The main objective of the test is to understand reactions rates and conditions necessary to scale up these experiments.

Ten columns holding 5-6 kg of these waste rocks, including a column with actinolite rich material, have been running at ~18ºC, for 6-15 months, with water flow rates (0.3-2 ml/min). The columns are continously injected with 2-3 ml/min CO_2, except one control column. The two types of waste rocks have similar chemistry and mineral composition (plagioclase + actinolite + quartz + biotite + muscovite + calcite + pyrite ± aptite); however, type 2 waste rock has a significantly higher magnetite content. Water samples have been collected weekly for all columns and regularly analyzed for major cations and anions, alkalinity and pH.

The main sources of cations are actinolite and calcite. Calcium concentration is relatively high (250-100 mg/l), during the first months possibly due to calcite dissolution and later due to actinolite dissolution. Magnesium and iron is low and indicates secondary mineral formation. Type 2 waste rocks have a high neutralizing capacity, with pH slowly dropping from 8 to about 5.5-6. Element release rate for the control column (no CO_2) is 1-2 orders of magnitude less than the other columns, indicating that carbonic acid is a effective leaching agent. There is a moderate to strong positive correlation between Ca, Mg and K release rate and pH and HCO_3^-. Mass loading depends upon flow rate; however there is higher element concentrations in column with a lower flow rate. Up to 70% of the calcium has been removed within the first 14 months of leaching.

https://doi.org/10.1180/S0026461X00006502 Published online by Cambridge University Press

Sensitive, high-resolution measurement of volatile organic compounds dissolved in seawater using proton transfer reaction-mass spectrometry

HIROSHI TANIMOTO[1]*, SOHIKO KAMEYAMA[1], SATOSHI INOMATA[1], URUMU TSUNOGAI[2], ATSUSHI OOKI[1], YOKO YOKOUCHI[1], SHIGENOBU TAKEDA[3], HAJIME OBATA[4], ATSUSHI TSUDA[4] AND MITSUO UEMATSU[4]

[1]National Institute for Environmental Studies, 16-2 Onogawa, Tsukuba, Ibaraki 305-8506, Japan (*correspondence: tanimoto@nies.go.jp)
[2]Faculy of Science, Hokkaido University, N10 W8, Kita-ku, Sapporo, Hokkaido 060-0810, Japan
[3]Faculty of Fisheries, Nagasaki University, 1-14 Bunkyo-machi, Nagasaki, Nagasaki 852-8521, Japan
[4]AORI, University of Tokyo, 5-1-5 Kashiwanoha, Kashiwa, Chiba 277-8564, Japan

We developed an equilibrator inlet-proton transfer reaction-mass spectrometry (EI-PTR-MS) method for fast detection of volatile organic compounds (VOCs) including dimethyl sulfide (DMS) and isoprene dissolved in seawater. Dissolved VOCs extracted by bubbling pure nitrogen through the sample was continuously directed to the PTR-MS. DMS reached equilibrium with an overall response time of 1 min, and the detection limit was 50 pmol per Liter at 5-s integration [1]. The EI-PTR-MS instrument was deployed during a research cruise in the western North Pacific Ocean. Comparison of the EI-PTR-MS results with results obtained by means of membrane tube equilibrator-gas chromatography/mass spectrometry agreed reasonably well on average. EI-PTR-MS captured temporal variations of dissolved DMS and isoprene concentrations, including elevated peaks associated with patches of high biogenic activity. These results demonstrate that EI-PTR-MS was effective for highly time-resolved measurements of VOCs in the open ocean [2]. Further measurements will improve our understanding of the biogeochemical mechanisms of the production, consumption, and distribution of VOCs in the ocean surface.

[1] Kameyama, Tanimoto, Inomata, Tsunogai, Ooki, Yokouchi, Takeda, Obata, & Uematsu (2009) *Anal. Chem.* **81**, 9021–9026. [2] Kameyama, Tanimoto, Inomata, Tsunogai, Ooki, Takeda, Obata, Tsuda, & Uematsu (2010) *Marine Chem.* **122**, 59–73.

Oxygen isotope geochemistry beneath paleofumaroles

D. TANNER*, J.A. MAVROGENES AND R.W. HENLEY

RSES, Australian National University, ACT 0200, Australia (*correspondence: dominique.tanner@anu.edu.au)

Little is known about the chemical processes operating beneath fumaroles. However recent detailed documentation of sulfosalt assemblages has shown that mineral deposits such as El Indio, Chile and Summitville, Colorado contain quenched sulfosalt melt assemblages. Thus, these deposits provide a snapshot into the fracture-controlled plumbing systems hundreds of metres beneath paleo-solfatara. Independent temperature estimates suggest deposition of quartz and sulfosalts at ~ 675°C. This study focuses on the oxygen isotopic composition of euhedral quartz crystals (~200 microns in diameter) grown within sulfide/sulfosalt melt.

In situ stable isotope microanalyses of quartz separates from sulfosalt assemblages were performed using the SHRIMP II at the Australian National University. Intricate zonation of aluminium concentration in quartz (~2 micron growth bands) was mapped using the electron microprobe, and then targeted using a 20 micron spot on SHRIMP II.

Preliminary results indicate that the $\delta^{18}O$ of quartz crystals from the El Indio and Summitville deposits exhibit a wide range in isotopic compositions (3.7‰-17.1‰) – with variation of up to 11‰ within an individual crystal.

We interpret the heavy oxygen which exceeds the values of the 'magmatic water box' to be evidence of kinetic fractionation during hydrous silica deposition and subsequent dehydration.

https://doi.org/10.1180/S0026461X00006502 Published online by Cambridge University Press

Rogue hafnium isotopes in Lac de Gras kimberlites, Canada: Ultradeep vs. shallow mantle processes

S. TAPPE[1]*, D.G. PEARSON[1], B.A. KJARSGAARD[2], G.M. NOWELL[3] AND D. DOWALL[3]

[1]Department of Earth and Atmospheric Sciences, University of Alberta, Edmonton, Canada (*correspondence: tappe@ualberta.ca)
[2]Geological Survey of Canada, Ottawa, Canada
[3]Earth Sciences, Durham University, Durham, UK

The Hafnium isotope compositions of kimberlites and related rocks tend to fall significantly below the terrestrial Nd-Hf isotope array, which is primarily defined by the compositions of oceanic basalts. Previous models suggested that this peculiar feature may fingerprint isolated ancient oceanic crust within the kimberlite magma source region [1], invoking the mantle transition zone as a viable source location. Based on new Nd-Hf isotope data for Greenland kimberlites [2], it was recently argued that departure from the terrestrial array can be equally well explained by interaction between convective mantle-derived carbonate-rich melts and phlogopite-rich metasomes residing in lower reaches of cratonic lithosphere.

Here, we present an extensive geochemical and Sr-Nd-Hf isotope data set for fresh 75-to-45 Ma hypabyssal kimberlites from the Lac de Gras area, central Slave craton, Canada. Although the Lac de Gras kimberlites mineralogically resemble South African Group-I kimberlites, their Sr-Nd isotope compositions are transitional between kimberlites and orangeites. Epsilon Hf ranges between -15 and +5 at relatively restricted epsilon Nd (-5 to 0), and these isotope systematics define a near vertical array that is at an even wider angle to the terrestrial Nd-Hf isotope array than the South African kimberlites. Furthermore, in data closely filtered to eliminate the effects of crustal contamination, there are pronounced negative correlations between the $^{176}Hf/^{177}Hf$ ratios and proxies of phlogopite-rich metasomes such as K_2O and TiO_2, which suggests that, similar to the Greenland kimberlites, the Lac de Gras proto-kimberlite magmas aquired 'rogue' Hf isotope compositions through interaction with long-term enriched mantle lithosphere. Based on the observation that the 'steep' Lac de Gras kimberlite Nd-Hf isotope array runs towards the unradiogenic metasomatic G10 garnet compositions from the Slave lithospheric mantle, we speculate that rogue Hf isotope compositions of Lac de Gras kimberlites may be linked to ancient fluid metasomatism that also facilitated diamond growth within the Slave cratonic lithosphere.

[1] Nowell *et al*. (2004) *Journal of Petrology* **45**, 1583–1612.
[2] Tappe *et al*. (2011) *EPSL* **305**, 235–248.

Geochemical constraints on petrogenesis and geotectonic setting for Silurian basalts of the Prague Synform (Bohemian Massif)

Z. TASÁRYOVÁ[1,2]*, V. JANOUŠEK[1,2], J. FRÝDA[1,2], Š. MANDA[1,2], P. ŠTORCH[3] AND J. TRUBAČ[1,2]

[1]Faculty of Sciences, Charles University, Albertov 6, Praha 2, 128 43, Czech Republic (*correspondence: zuzana.tasaryova@geology.cz)
[2]Czech Geological Survey, Klárov 3, Praha 1, 118 21, Czech Republic
[3]Institute of Geology, Academy of Sciences, Rozvojová 269, Praha 6, 165 00, Czech Republic

Similar to the other peri-Gondwanan terranes, the Prague Synform preserves the evidence of intense basic volcanic activity during Silurian. Studied alkaline basaltic volcanism was controlled by deep-seated faults, both parallel and perpendicular to the longitudinal axis of the synform, providing ascent paths for mantle-derived magmas.

The basalts are characterized by steep REE patterns [1] (La_N/Yb_N~3.5–13.5; Gd_N/Yb_N~1.8–3.6) lacking Eu anomalies, high LILE abundances, low Zr/Nb ratios (5.4–12), positive Ti anomalies in NMORB-normalized spiderplots, $^{87}Sr/^{86}Sr_{425}$ of 0.7028–0.7046 and positive ε_{425} values (+6.9 to +4.3), i.e. characteristics transitional between EMORB and OIB. Correlations of Sr and Nd isotopic data with independent geochemical parameters (e.g. mg#, 1/Sr, 1/Nd, Zr/Nb) document a general contamination (AFC) trend during Silurian. Nevertheless, temporal shifts from evolved to more primitive basaltic compositions are obvious within individual fault-related volcanic centres.

These features require primary melt generation by a low degree of partial melting of a garnet peridotite. The incompatible element ratios suggest within-plate setting, transitional between that of OIB and CRB [2]. Temporal progression from evolved to more primitive basaltic compositions could be explained in terms of diminishing crustal contamination of mantle-derived magmas. Given the geochemical variation in basalts and the well documented existence of Neoproterozoic continental basement, the geotectonic setting for the Prague Synform in the Silurian time can be characterized by progressive attenuation and rifting of continental lithosphere due to asthenosphere upwelling.

This study was funded by Grant Agency of the Czech Republic (P210-10-235).

[1] Boynton (1984) In, Henderson (ed.) *Rare Earth Element Geochemistry*, Elsevier, 63–114. [2] Agrawal *et al*. (2008) *Int. Geol. Review* **50**, 1057–1079.

https://doi.org/10.1180/S0026461X00006502 Published online by Cambridge University Press

Elemental and isotopic composition of cultured scleractinian corals

I. TAUBNER[1]*, F. BÖHM[1], J. FIETZKE[1], A. EISENHAUER[1], D. GARBE-SCHÖNBERG[2] AND J.EREZ[3]

[1]Leibniz Institute of Marine Sciences, IFM-GEOMAR, Kiel, 24148, Germany (*correspondence: itaubner@ifm-geomar.de)
[2]Institute of Geosciences, Christian-Albrechts-Universität, Kiel, 24118, Germany
[3]Institute of Earth Sciences, The Hebrew University of Jerusalem, 91904, Israel

Scleractinian corals are known for strong vital effects with respect to stable isotope and trace element incorporation. Nevertheless, they have successfully been used as proxy recorders for a variety of environmental parameters, including pH and temperature. Understanding the processes inducing 'vital effects' is essential for a successful application of these proxies.

To investigate the effects of pH and temperature, a branching scleractinian coral of the genus *Pocillopora* was grown under controlled laboratory conditions in natural seawater at (i) a temperature range from 22 to 28°C at constant pH; and (ii) a pH range from 7.8 to 8.3 at constant temperature. Samples were analyzed for boron, oxygen, carbon, and calcium isotopes, as well as Sr/Ca and Mg/Ca ratios.

Covariation of coral Mg/Ca and Sr/Ca with ambient carbonate ion concentration and temperature was recently explained by Cohen *et al*. [1] and Gaetani *et al*. [2] with a Rayleigh distillation model where the efficiency of cation utilization in a calcifying fluid increases with $CaCO_3$ saturation and temperature. This model implicitly predicts a significant positive correlation of the skeletal calcium isotopic composition with seawater pH and temperature.

The Rayleigh model can quantitatively explain the relatively high Ca isotope ratio observed in coral aragonite. However, no significant change in Ca isotope ratios was observed, neither with temperature nor pH. While Mg/Ca ratios increase with temperature as expected with the Rayleigh model, they show only 10% of the predicted Mg/Ca variations for the investigated pH range. Furthermore Sr/Ca showed no change with pH whereas Sr/Ca vs. temperature displayed a steeper slope than expected for inorganic aragonite precipitation [3]. Consequently, our data suggest that simple application of the Rayleigh model cannot explain the proxies incorporated to our cultured corals.

[1] Cohen *et al*. (2009) *G3* **10**, 1-12. [2] Gaetani *et al*. (2011) *GCA* **75**, 1920-1932. [3] Dietzel *et al*. 2004 *Chem. Geol*. **203**, 139-151.

Characteristics of arsenic distribution in the Holocene sediment deposits of South-Western Bangladesh

M. TAUHID-UR-RAHMAN[1], A. MANO[1], K. UDO[1], Y. ISHIBASHI[2] AND Y.H. HAN[2]

[1]DCRC, Tohoku University, Japan, (liton2005@gmail.com)
[2]Dept. of CEE, Tajago University, Japan

The geochemistry of aquifer sediments coupled with the groundwaters of Kalaroa, south-western Bangladesh was studied with the object of elucidating As distribution to investigate its sorption and mobility. The role of the channel slope and sediment diameter on the sediment depositional process has been revealed evidently by the observations obtained from the borehole lithology. Results showed that trapped As on sediment matrix could be a function of the sediment diameter, its surface area and relative radio-carbon age. These observations were corroborated significantly with the findings obtained from laboratory leaching and adsorption tests. It was found that the brown clay which has the smallest particle diameter could adsorb as much as 98% of As from the contaminated groundwater (500 μg/L) while relatively lower As (74%) was captured by the medium grained particles having relatively larger diameters and smaller areas. Based on the adsorption capability, the sediment types may be ranked such as; brown clay > black clay > very fine sand > fine sand >medium sand. Presence of As was also observed to be greatly dependent on the availability of its (As) carrier minerals particularly Fe and Al oxides along the aquifer depth. The two younger sediment types such as brown clay and very fine sand were observed as the main sources in releasing the As into the groundwater, as they have contained organic carbon that may be sufficient enough to get decomposed under the microbial activities. The positive correlations that were obtained for As with Fe, Al, HCO_3, and DOC from the groundwater analysis strongly support such As release mechanism.

https://doi.org/10.1180/S0026461X00006502 Published online by Cambridge University Press

Late Paleocene sea surface cooling in Southeast New Zealand

K.W.R. TAYLOR[1]*, C.J. HOLLIS[2], L. HANDLEY[1,3], H.E.G. MORGANS[2], E.M. CROUCH[2], S. SCHOUTEN[3] AND R.D. PANCOST[1]

[1]Organic Geochemistry Unit, School of Chemistry, University of Bristol, Cantock's Close, BS8 1TS, UK (*correspondence: kyle.taylor@bris.ac.uk, luke.handley@gmail.com, r.d.pancost@bris.ac.uk)

[2]Geological and Nuclear Sciences, P.O Box30-368, Lower Hutt, NZ (c.hollis@gns.cri.nz, h.morgans@gns.cri.nz, e.crouch@gns.cri.nz)

[3]Department of Marine Biogeochemistry and Toxicology, Royal Netherlands Institute for Sea Research, P.O. Box 59, 1790 AB Den Burg, Texel, Netherlands (stefan.schouten@nioz.nl)

A particularly intriguing aspect of the Paleocene is the apparent dramatic enrichment of ^{13}C in the carbon isotopic composition of the ocean-atmosphere reservoir at c. 60-57 Ma, which is associated with isotopic evidence for cooling [1]. Increases in organic content and siliceous microfossil abundance offshore New Zealand suggest an associated increase in oceanic productivity [2]. However, it is uncertain if these signals are a local response to global cooling or are due to other factors, such as regional oceanographic changes or sea level changes. To address this uncertainty, we have developed sea surface temperature records (SST) to evaluate the magnitude of cooling across a range of sites, with particular focus in the southwest Pacific region.

Here we construct SSTs from mid-Waipara River, NZ (c. 55°S) and the eastern margin of the Campbell Plateau (ODP site 1121, 62°S) across the Paleocene using TEX_{86}. We find a general cooling trend of c. 3°C correlated to the onset of the Paleocene Carbon Isotope Maximum (PCIM) from 60.5 to 58 Ma. A similar trend is also apparent in preliminary data from Paleocene strata at Bass River, New Jersey, USA (c. 27°N). Moreover, we reveal a more pronouced cooling interval in the uppermost 13 m of the 83 m thick Paleocene strata at Mid-Waipara coincident with elevated TOC and isotopically heavy organic carbon ($\delta^{13}C$>-25‰), indicating an enhanced local response to climate changes. We reconstruct biomarker records to investigate ecological changes associated with cooling at Mid-Waipara, and use compound specific carbon isotope analysis of higher plant biomarkers to interrogate carbon cycle dynamics.

[1] Zachos, J. *et al*. (2001) Science **292**. [2] Hollis, C. J. (2006) *Eclogae Geologicae Helvetiae* **99** (Suppl. S)

Mycorrhizal weathering through space and time: Implications for the long-term carbon cycle

L.L. TAYLOR[1], S.A. BANWART[2], J.R. LEAKE[1] AND D.J. BEERLING[1]

[1]Animal and Plant Sciences, University of Sheffield, UK (*correspondence: L.L.Taylor@sheffield.ac.uk)

[2]Cell-Mineral Research Centre, Kroto Institute, University of Sheffield, UK

Several recent hypotheses strongly link plants and their fungal symbionts to the long-term carbon cyle via their impact on the release of calcium and magnesium from silicate minerals: (a). Primary productivity controls the nature, extent and rate of biological weathering [1]; (b). Mycorrhizal fungi direct this weathering activity toward nutrient-rich minerals more effectively than roots [2]; (c). The evolution of ectomycorrhizal fungi could have contributed to CO_2 drawdown in the Cretaceous [3]. In contrast to the ancestral arbuscular-mycorrhizal fungi, ectomycorrhizal fungi can exude copious amounts of organic acids and they prevent most of the host root system from interacting directly with the soil [2]. In models of the long-term carbon cycle [4], plant weathering and response to changes in atmospheric CO_2 are usually represented by empirical functions. We have previously integrated simple yet rigorous rate laws into such a model to test the third hypothesis (c), but we used global mean temperatures along with a simplistic empirical function to represent net primary productivity [3]. We now continue to explore the effects of weathering by plants and mycorrhizal fungi through geological time, linking our weathering model to the Hadley Centre general circulation model [5] and the Sheffield Dynamic Global Vegetation Model [6] to produce weathering and primary productivity maps for the modern day and for several Mesozoic and Cenozoic timeslices. Comparison of our results with published observations provides support for hypotheses (a) and (b).

[1] Brantley *et al*. (2011) *Geobiology* **9**, 140–165. [2] Taylor *et al*. (2009) *Geobiology* **7**, 171–191. [3] Taylor *et al*. (2011) *Am. J. Sci*. in review.[4] Berner (2006) *Geochim. Cosmochim. Acta* **70**, 5653–5664. [5] Gordon *et al*. (2000) *Climate Dynamics* **16**, 147–168.[6] Beerling & Woodward (2001) *Vegetation & the Terrestrial Carbon Cycle,* Cambridge University Press.

https://doi.org/10.1180/S0026461X00006502 Published online by Cambridge University Press

Time resolved luminescence of framework silicates

R.P TAYLOR[1,2]*, J.F.W. MOSSELMANS[1], A.A. FINCH[2] AND P.D. QUINN[1]

[1]Diamond Light Source, Didcot, OX11 0DE, UK (*correspondence: rpt5@st-andrews.ac.uk)
[2]Dept. of Earth Sciences, St Andrews, KY16 9AL, UK (aaf1@st-andrews.ac.uk)

The development of the new Time Resolved X-ray Excited Optical Luminescence (TR-XEOL) facility at the i18 microfocus beamline at the Diamond Light source allows the comparison of time resolved luminescence data collected at this facility to be compared with data collected from Photoluminescence (PL) and cathodoluminescence excitation. The presentation shows results from luminescent centres in the blue and ultra-violet regions from a number of framework silicates including feldspar, quartz and sodalite. Our results show differences between XEOL Photoluminescence and Cathodoluminescence spectra which provide insights into the physical nature of the centres causing the light emitted.

We show lifetime measurements for UV and blue centres XEOL. Many samples show differences in the lifetime between pulsed laser and pulsed X-ray excitation with the X-ray excitation showing significant increases in decay lifetimes. Samples typically display a doubling of the value of the shortest lifetime component. We hypothesise that the differences in the lifetimes of the emissions probe the nature of the absorption and energy transfer mechanism within the mineral. The luminescence signal can be analysed both by energy to differentiate between alternative emission pathways and as a time resolved signal to probe the mechanisms involved in absorption, energy transfer, and other factors affecting the relaxation lifetimes. We make preliminary inferences on the physical nature of the centres involved in UV-blue luminescence in framework silicates. Fig 1 shows a XEOL spectra from RT51 a single crystal Anorthite feldspar Alaska (Smithsonian Institute) fitted with a single exponential.

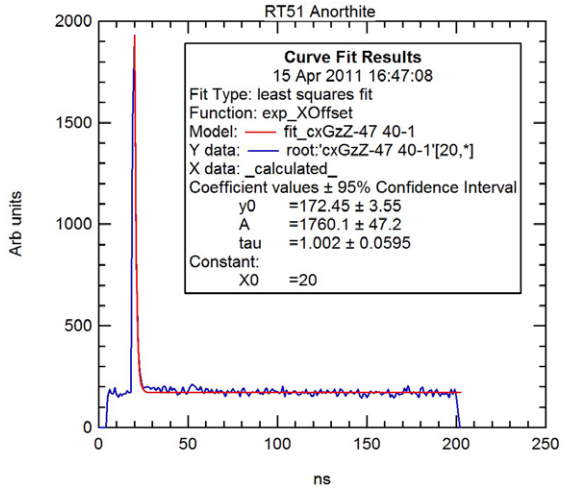

Calculated stability of osumilite, sapphirine and biotite in K_2O-FeO-MgO-Al_2O_3-SiO_2-H_2O-TiO_2-O (KFMASHTO)

K. TAYLOR-JONES[1]*, R. POWELL[2] AND T.J.B. HOLLAND[1]

[1]Department of Earth Sciences, University of Cambridge, Cambridge, CB2 3EQ, United Kingdom (*correspondence: kat32@cam.ac.uk)
[2]School of Earth Sciences, University of Melbourne, Victoria 3010, Australia.

With the advent of the new Holland & Powell internally-consistent thermodynamic dataset [1], in the form of the initial release of the dataset (tc-ds61. txt) on http://www. esc. cam. ac. uk/people/academic-staff/tim-holland, and http://www. metamorph. geo. uni-mainz. de/thermocalc/, calculation of the stability of osumilite, sapphirine and biotite can be undertaken in a much improved way. This has necessitated the development of new activity-composition (a-x) relations for the minerals as the underpinning relationships from the dataset generation have changed, as well as recognition of shortcomings in earlier models. The osumilite a-x model is a major reworking of the previously used one. The sapphirine a-x model is built on our recent work [2], with changes relating to the way sapphirine end-members are now incorporated in the dataset. Dataset annite, and the attendant a-x model for biotite, takes account of the fact that 'annite' in experiments contains significant ferric iron. We present calculated pressure-temperature projections (petrogenetic grids) for quartz-saturated systems at high and ultrahigh temperature crustal conditions in K_2O-FeO-MgO-Al_2O_3-SiO_2-H_2O (KFMASH), K_2O-FeO-MgO-Al_2O_3-SiO_2-H_2O-O (KFMASHO), and K_2O-FeO-MgO-Al_2O_3-SiO_2-H_2O-TiO_2-O (KFMASHTO), and calculated compatibility diagrams, to illustrate the phase equilibria.

[1] Holland & Powell (2011) *Journal of Metamorphic Geology* **29**, 333-383. [2] (2010) *Journal of Metamorphic Geology* **28**, 615-633.

https://doi.org/10.1180/S0026461X00006502 Published online by Cambridge University Press

Nd isotopic compositions in the central Indian Ocean

HIROFUMI TAZOE[1]*, HAJIME OBATA[2], HISAO NAGAI[3] AND TOSHITAKA GAMO[2]

[1]Institute of Radiation Emergency Medicine, Hirosaki University(*correspondence: tazoe@cc.hirosaki-u.ac.jp)
[2]Atmosphere and Ocean Research Institute, the University of Tokyo
[3]College of Humanities and Sciences, Nihon University

Nd isotopic composition in seawater is controlled by input from surrounding terrestrial sources, boundary exchange process, lateral transportation, and mixing water masses. During global thermohaline circulation, the Indian Ocean receives deep waters originated from the Southern Ocean, and its warm and salty surface waters return to the Atlantic Ocean via Southern Ocean. Low-salinity waters of the North Pacific origin are injected at the eastern side of the Indian Ocean via the Indonesian Throughflow. The fingerprints of the Pacific waters might be traced in the intermediate water in the southeastern Atlantic Ocean. On the other hand, Nd isotope data are too scarce to precisely describe Nd isotopic signatures of the main water masses in the Indian Ocean. In this study, vertical profiles of Nd isotopic compositions in the ceantral Indian Ocean are presented.

Seawater samples were obtained both with Teflon coated X-type Niskin samplers with CTD-carosel multi-sampling system and the PVC large volume sampler during R/V Hakuho-Maru KH-09-5 cruise (2009. 11. 6 - 2010. 1. 12). From each 10L of seawater, rare earth elements (REEs) were preconcentrated by Fe coprecipitation. After removal Fe by di-isopropyl ether, REEs were purified with ion exchange resin. Further Nd separation was performed by TRU Resin and Ln Resin (Eichrom Tec.). Nd isotopic compositions were measured by thermal ionization mass spectrometer (Finnigan MAT 262).

In the sampling station, ER-10 (19°59′ S, 72°33′E, 4343m), of the central Indian Ocean, wide ranges of Nd isotopic composition were observed. The ε_{Nd} values decreased from surface (ε_{Nd} = -5.7) to high salinity Subantarctic Mode Water at 600 m depth (ε_{Nd} = -9.3). Antarctic Intermediate Water showed also relatively low ε_{Nd} values, though the water mass between 1000 m and 1500 m depth, whose salinity and oxygen concentration were low, had higher ε_{Nd} values (-6.3 - -5.9). This radiogenic Nd signal could be derived from the Indonesian Throughflow and affect the Nd compositions of Antarcitc and Atlantic intermediate water.

Ubiquitous subaerial weathering during emersion of the Fortescue Late Archean igneous province, Western Australia

Y. TEITLER[1]*, P. PHILIPPOT[1], M. GERARD[2], F. FLUTEAU[1] AND G. LE HIR[1]

[1]IPGP, Université Paris 7-Denis Diderot, 1 rue Jussieu, Paris, France (*correspondence: teitler@ipgp.fr)
[2]IMPMC, 4 place Jussieu, Paris, France (martine.gerard@impmc.jussieu.fr)

The 2.77Gy old Mount Roe paleosol at Whim Creek, Fortescue Group, Western Australia, is a reference weathering profile, used for constraining maximum concentrations of atmospheric oxygen and greenhouse gases (CO_2, CH_4) during the Late Archean. Inferences on Early Earth atmospheric composition, however, are based on the interpretation of reconstructed chemical profiles which are not supported by direct mineralogical observations. This in turn resulted in a number of controversies that remain to be solved. The Whim Creek paleosol occurs at the top of a vesicular, subaerial basaltic flow exposed along two km-scale outcrops located about 5 km away from each other. It mainly consists of fresh footwall basalt progressively grading to a 5 meters thick brecciated chloritic-rich zone showing evidence of corestone weathering, overlain by a 5 to 20 meters thick sericitic-rich zone. Clastic sediments are often inter-bedded between the top sericite zone and the overlying basaltic flow. This is consistent with a significant time gap between deposition of footwall and hanging wall lava flows, a required condition to develop a thick weathering profile. Similar weathering profiles have been identified both along the same stratigraphic level some 100 km away from the Whim Creek locality (Sherlock River) and in the younger 2.74 Gyr old Kylena Formation. This indicates that basalt weathering was a long-lasting process of wide geographic influence.

Meter scale blue-greenish titanite-rich bodies containing primary weathering-related phyllosilicates (Berthierine, Smectite) were found as hard cores within the sericite zone at both Whim Creek and Sherlock River localities. In addition, remnants of bedded-parallel diaspore/pyrophyllite deposits containing carbonaceous material were found in the Whim Creek sericite zone. Field and petrological investigations indicate that both the phyllosilicates and diaspore horizons predate sericitization.

These occurrences are the first relic testimony of the original weathering profiles documented in rocks older than 2.2 Gyr, thus representing unvaluable new means for inventorying the Late Archean paleoclimatic conditions.

https://doi.org/10.1180/S0026461X00006502 Published online by Cambridge University Press

U-Pb and Lu-Hf isotopic constraints on the genesis of a Variscan two-mica granite from Carrazeda de Ansiães

R.J.S. TEIXEIRA[1], A.M.R. NEIVA[2], M.E.P. GOMES[3] AND T. ANDERSEN[4]

[1,3]Department of Geology, UTAD, Apartado 1013, 5001-801 Vila Real, Portugal (rteixeir@utad.pt, mgomes@utad.pt)
[2]Department of Earth Sciences, University of Coimbra, 3000-272 Coimbra, Portugal (neiva@dct.uc.pt)
[4]Dep. of Geosciences, Univ. of Oslo, PO Box 1047 Blindern, N-0316 Oslo, Norway (tom.andersen@geo.uio.no)

The Carrazeda de Ansiães area is located in the Portuguese sector of the Central Iberian Zone and is characterized by abundant S-type granites. LAM-ICPMS U-Pb geochronology confirms that one of those granites (Cabeça Boa granite) has been emplaced during the last ductile deformation phase (D_3) of the Variscan orogeny, showing an age of 327 ± 3 Ma. LAM-ICPMS Hf isotope data of the magmatic zircons show a wide range of negative εHf_t values (from -8 to -4), indicating that they could have been derived from heterogeneous crustal anatectic melts. Detrital zircons from a host chlorite phyllite yield a major group of Neoproterozoic ages (561 – 574 Ma), but there are also Mesoproterozoic, Paleoproterozoic and Neoarchean ages. The inherited zircon cores from the granite superficially match the age pattern of the host metasediment. Furthermore, a significant number of inherited zircon cores from the granite has εHf_t values similar to those of the detrital zircons of the chlorite phyllite, suggesting that this metasediment could have been one of the sources involved in the genesis of the granite. However, the average εHf_{320} for the detrital zircons is ca. -19 and is much more evolved than the magmatic zircons with average εHf_{320} (ca. -6), supporting that the melt was not exclusively controlled by the detrital zircons. Therefore, a more juvenile melt source, possibly indicated by the tonalite enclaves in the granite, must also have been involved in its genesis. So, the detrital zircons are interpreted as a contaminant during ascent and emplacement and not a source for the melt. The U-Pb isotope data of detrital zircons of the chlorite phyllite indicate that its maximum depositional age is ca. 578 Ma. The presence of Mesoproterozoic zircons (ca. 1.1 – 1.2 Ga) in the chlorite phyllite argues in favour of a peri-Amazonian location of its Neoproterozoic/Early Paleozoic depositional basin, close to West Avalonia. A West African Craton provenance could also be admitted, if a long distance river transportation of Mesoproterozoic zircons, from the southwest Baltica or Arabian–Nubian Shield, is considered.

PGE perspective on Early Cretaceous oceanic anoxic event: Pacific vs. Tethyan domains

M.L.G. TEJADA[1,2], K. SUZUKI[2], A. ISHIKAWA[2,3], T. NOZAKI[2], R. SENDA[2], G. RAVIZZA[4] AND J.I. KIMURA[2]

[1]NIGS, Univ of the Phils, Quezon City, 1101 Philippines
[2]IFREE, Japan Agency for Marine-Earth Science and Technology, Yokosuka, 237-0061 Japan
[3]ESA, The Univ of Tokyo, Tokyo, 153-8902 Japan
[4]SOEST, Univ of Hawaii, Honolulu, HI, 96822 USA

Mapping of the Os isotope composition of organic-rich sediments formed in Early Cretaceous oceans, Tethys (Gorgo a Cerbara, Italy) and Pacific (DSDP Site 463 and ODP Site 1207B), supports the global occurrence of oceanic anoxic event OAE 1a. In this study, PGE abundances of the same sedimentary sections, together with their Os isotope composition are used to investigate whether or not a meteorite impact had caused the changes in marine conditions that led to oceanic acidification and oxygen depletion at that time. Alternatively, was it the massive volcanism of the Ontong Java Plateau, in southwest Pacific Ocean that solely led to the early Cretaceous global marine anoxia?

In both oceans, based on results from the Selli Level horizon at Gorgo a Cerbara and its equivalent at Site 463, a negative excursion of the seawater Os isotope composition coincides with the OAE1a interval. These results suggest input of unradiogenic Os into the oceans, attributable to both mantle and meteoritic materials. However, no meteoritic signature is evident from the abundances and the inter-element ratios of the PGEs for both sections. The Ir abundance at Site 463 section is 24-285 ppt and fall within the range for that of Gorgo a Cerbara, which are lower than the values for other known large impact horizons. Selli Level-equivalent horizon including the interval that yielded the highest concentration of Re and other PGEs at Site 463 have non-chondritic Os/Ir and Pt/Ir values of 1.5-41 and 14-76, (vs. chondritic values of 1.03 and 2.0). At both sites, PGE abundances and interelement ratios point to a massive volcanic eruption, during the emplacement of the Ontong Java Plateau (+Manihiki and Hikurangi plateaus), as the most likely explanation for the seawater Os isotope excursions coinciding with the anoxia event in both Tethyan and Pacific oceans 120 m. y. ago.

https://doi.org/10.1180/S0026461X00006502 Published online by Cambridge University Press

The bullets weathering in microscale

V. TEJNECKÝ[1*], O. DRÁBEK[1], P. DRAHOTA[2], S. BAKARDJIEVA[3], J. JEHLIČKA[2] AND L. BORŮVKA[1]

[1]Department of Soil Science and Soil Protection, Czech Univrsity of Life Sciences in Prague, 165 21 Prague 6 - Suchdol, CZ (*correspondence: tejnecky@af.czu.cz, drabek@af.czu.cz, boruvka@af.czu.cz)

[2]Institute of Geochemistry, Mineralogy and Mineral Resources, Charles University, Albertov 6, 128 43 Prague 2, CZ (drahota@natur.cuni.cz, jehlicka@af.czu.cz)

[3]Institute of Inorganic Chemistry of the ASCR, v.v.i, Husinec-Řež 1001, 250 68 CZ (bakardjieva@uach.cz)

Shooting ranges represent places of extreme point source contamination. It endangers the natural environment and especialy soil by release of risk elements (RE) e.g. Pb, Sb, Zn, Cu, Ni, Sb a Ag. This study monitors the loosening of selected RE from bullets and their fate in the soil.

Bullets' weathering represents RE input into soil; in monitored shooting range it was max. 7 g Pb kg^{-1}. The bullet with mantle, collected from shooting mound, was studied by Scanning electron microscopy (SEM) with EDAX detection. The bullet core is composed almost solely of Pb (Figure 1a). Other parts of the bullet have far more diverse composition and serve as another source of RE (Cu, Zn) in soil. Generally, the mantle is made of Fe with inner and outer Cu coating. The observed bullet is surrounded by coroded mantle and a mixture of iron oxides - detected by Raman spectroscopy. The remaining Cu layer can be seen inside of the mantle (Figure 1b) and in a mixture of coroded mantle and newly created Fe-oxides (Figure 1c). X-ray powder diffraction detected these newly formed Fe oxides and whewellit in the bullets surroundings and on the mantle surface. The Fe oxides and whewellit can serve as RE sorbent. A possible RE mobilisation was examined by BCR extraction.

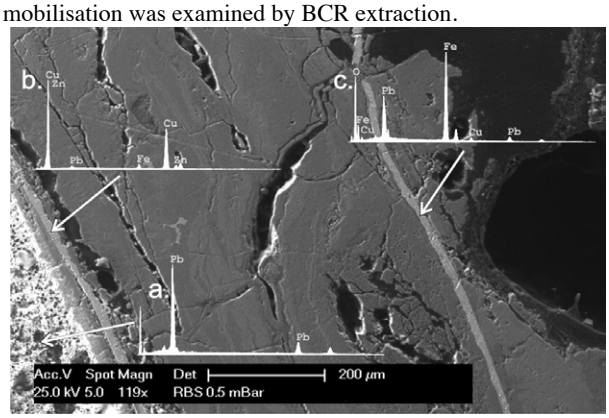

Figure 1: SEM image of bullet mantle with EDAX analysis.

The geochemical properties of manganese occurences of Isparta, Turkey

Y. TEKER[1] AND M. KUŞCU[2]

[1]Disaster and Emergency Management Presidency, Ankara, Turkey (yelizteker@gmail.com)

[2]Süleyman Demirel Üniversity, Department of Geological Engineering, Isparta, Turkey (mkuscu@mmf.sdu.edu.tr)

The manganese occurences of Isparta are located in Bağıllı, Havutlu and İmrezi areas. Havutlu manganese occurence and Bağıllı manganese occurence are found in Tesbihli formation of Ladinian (Triyassic), İmrezi manganese occurence is found in Ispartacay formation of Triyassic-Jurassic. Manganese mineralizations are seen generally cutting radyolarite in stockwork, lenticular and normal vein forms. Pyrolusite, psilomelane, braunite, todorokite, cyrptomelane, rhodochrozite, manganese phosphide, jacobsite, manganocalcite, pyrite, magnetite, hematite and goethite are determined as ore minerals in the manganese occurences.

In the manganese occurences, average composition is 20.19 % MnO, 2.98 % Fe_2O_3 and 70.63 % SiO_2. The diagrams prepared by using trace elements show that manganese mineralizations are determined in the hydrogenetic area and this also supported with the ratio of Fe/Mn of mineralizations.

https://doi.org/10.1180/S0026461X00006502 Published online by Cambridge University Press

Copper speciation in organic wastes by X-ray absorption spectroscopy

M. TELLA[1]*, S. CHATAING[1], B. COLLIN[2], M.A. DIOT[2], M.N. BRAVIN[3] AND E. DOELSCH[1]

[1]CIRAD, UPR Recyclage et risque, F-34398 Montpellier, France (*correspondence: marie.tella@cirad.fr)
[2]CEREGE, CNRS-UPCAM UMR6635, F-13545 Aix en Pce, France
[3]CIRAD, UPR Recyclage et risque, F-97408 Saint-Denis, La Réunion, France

The benefits of the use of organic wastes as fertilizers and soil amendments should be assessed together with potential environmental and toxicological impacts due to the presence of trace elements. The knowledge of trace elements speciation is essential to better understand their behavior after the spreading of organic wastes on soils and to predict their bioavailability. The present work aimed at studying speciation of copper (Cu) in various organic wastes (sewage sludge, composts and animal manure), which exhibit moderate to high levels of copper (24 to 340 mg kg^{-1} dry matter). These wastes were selected because they are commonly used in several countries as fertilizer or soil amendment (Réunion-France, Magacascar, Senegal). Size fractionation was first performed to account for the complexity of wastes and X-ray absorption spectroscopy (XAS) has been combined with different analytical approaches to determine speciation.

Organic wastes exhibited a fairly large enrichment in Cu in smaller solid fractions (0.2-20 μm) in comparison with raw wastes (130 to 1 900 mg kg^{-1} dry matter). X-ray Near-Edge Structure Spectroscopy (XANES) spectra were recorded on smaller solid fractions and analyzed by linear combination fitting (LCF) of references spectra. Analyses of pre-edge and inflexions in the absorption edge of spectra indicated that Cu is present in both Cu(I) and Cu(II) oxidation states. Therefore, LCF results showed that all small fractions are well fitted by different amounts of Cu(I)-S and Cu(II)-O in both octahedral and axial elongated octahedral (~square planar) geometries (Table 1).

	Cu(I)-S	Cu(II)-O	
		octahedral	square planar
Sewage sludge	60%	40%	≤10%
Composts	30%	40%	30%
FF-MSWC	≤10%	40%	60%

Table 1: LCF results for small size fractions of wastes (FF-MSWC=fine fraction from municipal solid waste composts)

In conclusion, Cu possesses its own chemical status and environments for each type of organic wastes, which could lead to different mobility after spreading on land.

Origin of Miocene volcanic rocks from Eskisehir, NW Anatolia, Turkey

S. TELSIZ[1]*, A. TEMEL[1] AND A. GOURGAUD[2]

[1]Hacettepe University, Geological Engineering Department, 06800 Beytepe, Ankara, Turkey (*correspondence: stelsiz@hacettepe.edu.tr)
[2]Université Blaise Pascal, OPGC, Laboratoire CNRS 'Magmas et Volcans' 5 rue Kessler-63038, Clermont-Ferrand Cedex, France

Volcanic rocks from Eskisehir region containing pyroclastic products (deposits) and lavas/domes with basaltic and andesitic composition occurred in Early-Late Miocene age (19.5-7.9 Ma) based on Ar-Ar radiometric dating. Volcanic products in the region have both alkaline and calcalkaline characteristics; and their composition range from tephrite to ryholite. It was determined that the samples of 19.5-16.8 Ma age and basaltic trachyandesite to ryholitic composition with 0.703885-0.710988 and 0.512317-0.512489 $^{87}Sr/^{86}Sr$-$^{143}Nd/^{144}Nd$ isotopic ratios and low Nb/La<1 values were derived from a subduction zone and/or a lithospheric source enriched by crustal contamination process. On the other hand, it was concluded that the younger samples (13.6-7.9 Ma) with trachybasalt and tephritic composition with 0.703470-0.703505 and 0.512884-0.512930 isotopic ratios and high Nb/La>1 values were generated from an asthenospheric source with a low degree of partial melting, in the absence of crustal and lithospheric contribution.

https://doi.org/10.1180/S0026461X00006502 Published online by Cambridge University Press

Olivine and pyroxene surface reactivity during H_2-generation

ALEXIS S. TEMPLETON[1], LISA E. MAYHEW[1], THOMAS P. TRAINOR[2], PETER ENG[3] AND THOMAS M. MCCOLLOM[4]

[1]Department of Geological Sciences, University of Colorado, Boulder, CO 80309, USA (templeta@colorado.edu)
[2]Department of Chemistry, University of Alaska, Fairbanks, AK 99775, USA
[3]Consortium for Advanced Radiation Sources, University of Chicago, Chicago IL 60637
[4]Laboratory for Space Physics, University of Colorado, Boulder, CO 80309, USA

The hydrothermal alteration of ultramafic rocks is commonly invoked as a key source of H_2 available for subsurface lithoautotrophic microbial communities. At a mechanistic level, H_2 generation is intimately related to changes in the oxidation state of Fe and the temperature-dependent partitioning of Fe into secondary phases such as serpentine, Fe-rich brucite and magnetite. However, few experimental studies have directly examined the dynamic links between solid-phase Fe speciation and the extent of H_2-generation during multi-stage serpentinization reactions.

We will present a series of hydrothermal experiments designed to measure microscale changes in distribution and speciation of Fe during electron transfer reactions between olivine and pyroxene surfaces and saline fluids. Polished slabs and powders of olivine and pyroxene have been suspended in flexible Au/Ti reaction cells at 230°C-300°C, and the serpentinization reactions have been arrested after a few days, a few weeks and a few months to measure progressive changes in mineral surface chemistry as H_2 is evolved. Surface-sensitive X-ray scattering and spectroscopic measurements have been combined to measure the growth of new mineral phases (e.g. lizardite detected by surface X-ray diffraction), to determine the redistribution of Fe and Si within the reaction interface (using reflectivity and total external reflection X-ray fluorescence measurements), and to measure changes in the speciation and oxidation state of Fe (using surface-sensitive Fe XANES analyses). In particular, we are monitoring the formation of Fe(II)-brucite and Fe(II)/(III)-bearing serpentine during incipient reactions, and the subsequent formation of magnetite, as $[H_2]$ variably increases.

To date, little information exists regarding the rates and mechanisms of olivine serpentinization below 200°C. However, we will also speculate about how our interfacial measurements could be used to probe changes in surface-controlled electron transfer processes when H_2-consuming microorganisms colonize olivine and pyroxene surface under highly reducing conditions.

Extracellular electron transfer in microbial environments

L. TENDER

Center for Bio/Molecular Science and Engineering, Naval Research Laboratory, Washington DC, USA (leonard.tender@nrl.navy.mil)

Dissimilatory metal-reducing bacteria (DMRB), such as Geobacter and Shewanella spp., occupy a distinct metabolic niche in which they acquire energy by coupling oxidation of organic fuels with reduction of insoluble extracellular electron acceptors (i.e., minerals). Their unique extracellular electron transfer (EET) capabilities extend to reduction of anodes (electrodes maintained at sufficiently positive potentials) on which they form persistent, electric current generating biofilms. This capability makes DMRB useful as anode catalysts in microbial fuel cells (MFCs) for alternative energy generation and degradation of organic wastes. One hypothesis describing the mechanism of EET by Geobacter and Shewanella spp. involves superexchange in which electrons are conducted by a succession of electron transfer reactions among redox proteins associated with the outer cell membranes, aligned along pilus-like filaments (e.g. pili), and/or throughout the extracellular matrix. Here theory is presented, previously developed to describe superexchange within abiotic redox polymers, to describe superexchange within DMRB biofilms grown on anodes. This theory appears to apply to recent *ex situ* measurements of electrical conductivity by individual pilus-like filaments of S. oneidensis MR-1 and G. sulfurreducens DL1, referred to as microbial nanowires. Microbial nanowires have received much recent attention because they are thought by some to impart electrical conductivity to DMRB biofilms and because of the prospect of microbe-produced conductive nanomaterials. This theory appears to apply to preliminary *in situ* demonstration of electrical conductivity of an anode-grown G. sulfurreducens DL1 biofilm. Characterization by cyclic voltammetry is also presented of glassy carbon BMAs (biofilm modified anodes) of DL1 (a wild type strain), KN400 (a variant that generates higher current density), and mutant strains in which outer membrane c-type cytochromes S or Z (OmcS, OmcZ) were deleted. These BMAs were characterized at 1) state of transition from planktonic cells grown utilizing fumarate as their electron acceptor to anode bound cells utilizing the anode as their electron acceptor; 2) during biofilm growth; 3) when fully grown; and 4) when fully grown under non-turnover condition after subsequently starved of acetate. The results indicate interesting aspects of EET by G. sulfurreducens DL1.

https://doi.org/10.1180/S0026461X00006502 Published online by Cambridge University Press

New insights into mantle and crustal processes from high-temperature magnesium isotope fractionation

F.-Z. TENG[1]*, W.-Y. LI[2] AND S.-A. LIU[2]

[1]Department of Geosciences & Arkansas Center for Space and Planetary Sciences, University of Arkansas, Fayetteville, AR 72701, USA (fteng@uark.edu)

[2]School of Earth & Space Science, University of Science & Technology of China, Hefei, Anhui 230026, China

Equilibrium isotope fractionation generally decreases with increasing temperature and is expected to be insignificant at high temperatures. By contrast, kinetic isotope fractionation associated with chemical diffusion and Soret effect can be extremely large at high temperatures as shown by recent experiments. However, the extent to which kinetic isotope fractionation may occur in nature remains uncertain.

Here we report large high-temperature kinetic Mg isotope fractionation in zoned olivines and equilibrium Mg isotope fractionation among mantle and crustal minerals. Significant Mg isotope fractionation (>0.4 ‰ variation in $^{26}Mg/^{24}Mg$) was found in over 60 olivine grains from Hawaii, which reflects isotope fractionation associated with inter-diffusion of Mg and Fe during magmatic differentiation. Large Mg isotope fractionation, up to 1.1 ‰ in $^{26}Mg/^{24}Mg$, was found between coexisting garnet and omphacite in 5 orogenic eclogites, and between coexisting spinel, cpx, opx and olivine in 13 mantle peridotites. The large inter-mineral isotope fractionation reflects equilibrium partitioning of Mg isotopes between coexisting minerals as evidenced by the temperature-dependent isotope fractionation, lack of mineral zoning, and absence of intra-mineral isotopic variations, as well as equilibrium oxygen isotope fractionation among these minerals. The direction of inter-mineral equilibrium Mg isotope fractionation among these mantle and crustal minerals agrees with theoretical predictions, suggesting that inter-mineral Mg isotope fractionation is primarily controlled by the Mg-O bond strength, with stronger bonds favoring heavier Mg isotopes.

Our results demonstrate that both equilibrium and kinetic isotope fractionation can occur during high-temperature geological processes, with great potential applications. Kinetic isotope fractionation associated with chemical diffusion can be used to identify diffusive transport in zoned minerals, which is key for using chemical zoning to constrain magmatic timescales. Large equilibrium Mg isotope fractionation among mantle and crustal minerals can potentially be used as a high-precision geothermometry in mantle and crustal geochemistry.

Solvent effect on the precipitation of Mg-carbonate

HENRY TENG AND JIN WANG

Dept. Chemistry, The George Washington University, Washington, DC 20052 (hteng@gwu.edu)

Low temperature synthesis of anhydrous magnesite continues to be an outstanding geochemical problem despite our improved understanding in the Mg-CO_3 system (e.g. formation of various hydrated forms and basic hydromagnesites). Presently, the prevalent hypothesis for the lack of magnesite crystallization under ambient conditions seems to focus on the strongly hydrated Mg^{2+} ions (compared to Ca^{2+}). It is hypothesized that the robust hydration shell around Mg^{2+} lowers the cation's activity and provides a barrier for the access of CO_3^{2-}. We intend to explore the possibility of magnesite crystallization in the presence of alcohol which could potentially replace H_2O or dislodge the water cage around Mg^{2+}. We hypothesize that (1) the presence of alcohol in water will distort or weaken the rigid water shell around magnesium ions due to the change in solvent dielectric properties and the water-alcohol interactions to facilitate the interaction of Mg^{2+} and CO_3^{2-}; and (2) dry conditions in pure alcohol may lead to the formation of anhydrous magnesite. We found that $MgCl_2$ and guanidine carbonate (GC) can be used as reactants since both show workable solubility in methanol (me).

Four batches of reactions have been carried out between $MgCl_2$ and GC in water and methanol (Mg-aq + GC-aq; Mg-me +GC-aq; Mg-aq + QC-me; Mg-me + QC-me). The presence of methanol in water greatly accelerates the precipitation, but none of four batches led to the formation of magnesite. FT-IR and XPS revealed the presence of CO_3 in the products, but XRD analysis identified either amorphous phases or could not be matched with the diffraction patterns of any known Mg-CO_3 salts in the database. The sample synthesized in the presence of water were found to be amorphous nanoparticle aggregates, while that formed in pure methanol exhibits a well-crystallized thin platelet assembly morphology. It appears that methanol is able to facilitate Mg-CO_3 crystallization, but the presence of minute amount of H_2O in solvent or in air still found a way to be incorporated in the crystal structure, confirming the high affinity of Mg^{2+} toward water molecules.

https://doi.org/10.1180/S0026461X00006502 Published online by Cambridge University Press

Phytoavailability and bioaccumulation of vanadium in the soil in Panzhihua Region, S.W. China

YANGUO TENG[1], JIE YANG[1] AND ZHENGQI XU[1,2]

[1]College of Water Sciences, Beijing Normal University, Beijing 100875, China (teng1974@163.com)
[2]Department of Geochemistry, Chengdu University of Technology, Chengdu 610059, China (xuzhengq@163.com)

Vanadium is a ubiquitous trace metal in the environment, which is an essential trace element for living organisms, but the excessive content is harmful to human beings, animals and plants. A biogeochemical investigation of vanadium in the soil was carried out in Panzhihua region, SW China.

The content of vanadium was detected in different land-use districts soil. The total content of vanadium in different land-use districts characterized that: smelting area (range 208.1-938.4 mg/kg, average 532.1 mg/kg) > mining area (range 111.6-591.2 mg/kg, average 312.7 mg/kg) > urban park (range 94.0-183.6 mg/kg, average 119.8 mg/kg) ≈ agricultural area (range 71.7-227.2 mg/kg, average 113.0 mg/kg).

Based on improved BCR sequential extraction, the chemical speciation of vanadium (acid-soluble, reducible, oxidisable and residual) were determined. In the soil from four different land-use districts, the fraction of vanadium in each sequential extraction characterized that residual > oxidisable ≥ reducible > acid-soluble.

The phytoavailable content of vanadium was characterized that: the polluted areas (mining area 18.8-83.6 mg/kg, smelting area 41.7-132.1 mg/kg and the unpolluted area (agricultural area 9.8-26.4 mg/kg, urban park 9.9-25.2 mg/kg); while the phytoavailable proportion of vanadium was characterized that: the polluted areas (mining area 6.50-24.30%, smelting area 6.89-24.54%) and the unpolluted area (agricultural area 8.39-21.15%, urban park 8.20-23.72%).

In study area, The concentrations of vanadium in beet leaf samples were in the range of 6.5-42.8 mg/kg, and in mongo leaf samples were in the range of 3.0-22.7 mg/kg. In addition, the content of vanadium in samples in urban park was slightly lower than that of other three areas. The biological adsorption coefficient (BAC) of vanadium in study area showed that vanadium was weak or intermediate accumulated by plants. A pot experiment showed that alfalfa had strong metal adaptability and high accumulation of vanadium.

This study is granted by China Natural Science Foundation (No.41073068) and Doctoral Program of Specialized Research Fund for University (20090003110021).

Megacryst compositional heterogeneities in plagioclase ultraphyric basalts (PUBs)

F.J. TEPLEY, III*, A. LANGE, A. BURLEIGH, R. NIELSEN AND A. KENT

College of Earth, Ocean and Atmospheric Sciences, Oregon State University, Corvallis, OR 97331, USA (*correspondence: ftepley@coas.oregonstate.edu) (langea@geo.oregonstate.edu, burleian@onid.orst.edu, nielsenr@geo.oregonstate.edu, kentad@geo.oregonstate.edu)

Plagioclase ultraphyric basalts (PUBs) are common in many oceanic tectonic settings particularly along slow to intermediate spreading ridges; however, the nature of their petrogenesis remains unclear. We have examined samples from the South West Indian Ridge (SWIR; ultraslow), Juan de Fuca Ridge (JdF; slow to moderate) and the Blanco Transform (pull apart), and more generally the global distribution of PUBs and their chemistries. Our work focuses on measuring major- and trace-element compositions and *in situ* Sr-isotopic compositions of plagioclase, and hosted melt inclusions, with the goal of documenting the extent to which the phenocrysts represent a coherent suite of genetically related material, and of understanding the dynamics of magma storage, transport and evolution within the oceanic crust.

Analyses of plagioclase and their hosted melt inclusions from all three study sites demonstrate both unchanging intra-grain compositions and considerable inter- and intra-grain variability in major- and trace-element compositions. Preliminary *in situ* Sr-isotopic data shows minimal differences between crystal and host glass. For those exhibiting compositional variability, each plagioclase megacryst analyzed appears to have a distinct history representing a complex crystal cargo, each crystal of which may have experienced a different petrogenetic history.

Globally, the distribution of PUBs is limited to ridges with ultraslow to moderate rates of spreading. Accumulated data suggest that PUB host glasses show a similar range in composition as global MORB glasses. For example, a plot of K_2O/TiO_2 versus MgO shows that there is no preferred liquid composition for PUB as compared to worldwide MORB glasses.

We believe that the compositional heterogeneites exhibited in PUB megacrysts are a result of complex crystallization histories involving melts of varying composition, changes in the physical conditions of crystal growth, and complex crystal exchange mechanisms.

https://doi.org/10.1180/S0026461X00006502 Published online by Cambridge University Press

The behavior of vanadium between water and basalt

MASASHI TERADA AND SHIKAZONO NAOTATSU

3-14-1, Hiyoshi, Kouhokuku, Yokohama, Kanagawa, Japan (tera.masa1106dgmail.com, sikazono@applc.keio.ac.jp)

In the surrounding area of Mt. Fuji, central Japan, it has been reported that vanadium concentration is relatively high (0.05-0.1 (mg/l)) in ground water and river water, due to the dissolution of vanadium from basalt. This concentration is 50 to 100 times high compared to the normal concentration of vanadium in natural waters. However a compositional relationship between surface waters and rocks has not been reported. The reason is vanadium is usually not considered as a contaminant in the water. Therefore, this study experimentally examines the behavior of vanadium in ground water and basalt interaction, and the migration behavior of vanadium in ground water in the surrounding area of Mt. Fuji based on the experimental study. In the experiment, the basalt samples of different ages were used and the experiment on the dissolution and adsorption of vanadium from the basalt was performed. The behavior of vanadium dissolved in aquifers in Mt. Fuji area was considered. The results of the dissolution adsorption experiments showed that the dissolved vanadium species in water were affected by pH and dissolved oxygen. In addition, the vanadium in basalts is considered to be contained in magnetite, in pyroxene and in the volcanic glass and to have adsorbed onto each minerals surface. The extraction experiment of vanadium from them revealed the existing chemical forms of vanadium are different in different basalt samples.

Application of NICA-Donnan model to modelling of Eu(III) solubility in the presence of deep groundwater humic substances

M. TERASHIMA*, M. OKAZAKI, K. IIJIMA AND M. YUI

Gelogical Isolation Research and Development Directorate, Japan Atomic Energy Agency, 4-33 Muramatsu, Tokai-mura, Naka-gun, Ibaraki 319-1194, Japan (*correspondence: terashima.motoki@jaea.go.jp)

Modelling of radionuclide bindings by deep groundwater humic substances (HSs) is a key subject for assessing the carrier effects of HSs on migration of radionuclides in geological disposal system of high level radioactive waste. The NICA-Donnan model of which generic parameters are prepared [1, 2] is one of the most useful models for the modelling of metal-ion bindings by soil and surface water HSs in a variety of solution conditions. However, its applicability to the deep groundwater HSs has yet to be elucidated. In this study, to clarify the applicability of the NICA-Donnan model and its generic parameters, the Eu(III) solubility simulated by the model and parameters were compared to the experimentally obtained solubility in the presence of HSs isolated from deep groundwaters at the depth of 250 to 500 m in Horonobe area, Hokkaido, Japan.

The solubility experiments showed the results that apparent solubility of Eu(III) were not enhanced in the presence of the deep groundwater HSs (i.e. fulvic acids or humic acids), while the solubility was enhanced in the presence of Aldrich humic acid. The NICA-Donnan model and its generic parameters successfully simulated the solubility enhancement by the Aldrich humic acid. However, they could not simulate the apparent solubility in the presence of the deep groundwater HSs. These results suggest that the NICA-Donnan model and/or its generic parameters cannot be applied to the modelling of trivalent radionuclide bindings by the deep groundwater HSs in the Horonobe area. Based on the Eu(III) binding characters of HSs, the reason on the disagreements between the experiments and the simulations will be discussed.

This study was partly funded by the Ministry of Economy, Trade and Industry of Japan.

[1] Milne *et al*. (2001) *Environ. Sci. Technol* **35**, 2049–2059.
[2] Milne *et al*. (2003) *Environ. Sci. Technol* **37**, 958–971.

https://doi.org/10.1180/S0026461X00006502 Published online by Cambridge University Press

Transition of a pyrrhotites to antiferromagnetic state induced by cation vacancies

A.V. TEREHOVA *, V.V. ONUFRIENOK AND A.M. SAZONOV

Siberian Federal University, Krasnoyarsk, Russia (*correspondence: VOnufriynok@yandex.ru)

Pyrrhotites have the NiAs crystal structure in which a fraction of cation sites is unoccupied. The temperature (T_0) at which the total magnetic moment of the two sublattices is zero (antiferromagnetic) depends on the chemical composition. It can change from 558 K ($Fe_{10}S_{11}$) to 593 K (Fe_7S_8). Accordingly, concentration of vacancy: from 9.1% to 12.5 %.

There was studied the dependence of the magnetization on the temperature of the pyrrhotite samples after being synthesized at 1273 K. The synthetic pyrrhotites were investigated with a thermoballistic apparatus in a field of $10^6/4\pi$ A/m. The phase and chemical composition was monitored by using the methods of X-ray diffraction (XRD).

The influence of concentration vacancies on the temperature to transition of the pyrrhotites to the antiferromagnetic state was considered on the basis of calculating the magnetic moment of the two sublattices using the molecular field method. Integral of the exchange interaction: $J_{11} = 6.55 \cdot 10^{-21}$ joules; $J_{22} = 5.21 \cdot 10^{-21}$ joules, $J_{12} = J_{21} = 6.52 \cdot 10^{-21}$ joules. For pyrrhotites ($Fe_{10}S_{11}$- Fe_7S_8) the Neel point $T_N = 593$ K (pyrrhotites transition temperature to the paramagnetic state).

samples temperature	Concentration of cation vacancies, %				
	9.1	9.9	10.7	11.6	12.5
T_0, K	¶548	¶568	¶578	¶588	¶593
	#558	#578	#588	#593	#593
Specific magnetization of the samples; $\sigma \cdot 10^{-7}$, T $\cdot m^3/kg$					
T = 293 K	#13.70	#14.91	#16.26	#17.84	#19.05
¶ as calculated; # the experimental data					

Table 1. Temperature to transition of pyrrhotites to the antiferromagnetic state (if the inequality $T_0 < T_N$).

As it is shown in the table, tendency to decreasing of temperature to transition pyrrhotites to the antiferromagnetic state with increasing concentration of cation vacancies is observed both experimental data and the theoretical calculation results.

Zeolitization of aluminosilicate waste materials in soil as a tool for soil remediation

R. TERZANO

Dept. of Agro-forestry and Environmental Biology and Chemistry (Di.B.C.A.), University of Bari, I70126 Bari, Italy (r.terzano@agr.uniba.it)

Zeolites are largely used in soil remediation technologies by exploiting their well-known high cation exchange capacity. Beside this property, zeolites possess large pores and internal cavities. Such pores can be used to trap scarcely soluble heavy metal (HM) precipitates, thus chemically reducing their solubility and physically isolating the contaminant at the microscopic level.

Zeolite synthesis can be easily promoted in soil at low temperatures by adding Si- and Al-containing materials in alkaline conditions. As a consequence of this process HM are stabilized as micro or nano clusters of oxides and hydroxides trapped inside the structure of crystalline zeolites or physically and chemically immobilized by amorphous 'geopolymers' [1-4].

In this process, waste materials such as coal fly ash, blast furnace slag, building wastes, glass and aluminum refuses can be profitably employed, together with cheap alkali reagents (e.g. NaOH, KOH, lime).

The process has been successfully applied to Cu [2], Cd [4], Ni [5] and Cr(VI) polluted soils.

Promoting zeolite synthesis in soil can be a promising methodology to effectively stabilize HM in polluted sites, especially in combination with other physico-chemical or biological remediation processes.

[1] Terzano *et al*. (2005) *Appl. Clay Sci*. **29**, 99–110.
[2] Terzano *et al*. (2005) *Environ Sci Technol* **39**, 6280–6287.
[3] Terzano *et al*. (2006) *Appl. Gochem*. **21**, 993–1005.
[4] Terzano *et al*. (2007) *Appl. Clay Sci*. **35**, 128–138.
[5] Belviso *et al*. (2010) *Chemosphere* ***78***, 1172–1176.

https://doi.org/10.1180/S0026461X00006502 Published online by Cambridge University Press

Mineral weathering and mobilization of trace metals in the rhizosphere: The role of root exudates

R. TERZANO[1]*, L. MEDICI[2], T. MIMMO[3], N. TOMASI[4], R. PINTON[4] AND S. CESCO[3]

[1]Di.B.C.A., Bari Univ., 70126 Bari, Italy (*correspondence: r.terzano@agr.uniba.it)
[2]I.M.A.A.–C.N.R., 85050 Tito Scalo (PZ), Italy
[3]Fa.S.T., Bolzano Free Univ., 39100 Bolzano, Italy
[4]Di.S.A., Udine Univ., 33100 Udine, Italy

The mobilization of trace elements in the soil-plant system takes place essentially in the rhizosphere, where roots are intimately in contact with soil. In the rhizosphere, conditions such as pH modification, changes in red-ox potential, high concentrations of organic ligands (either of vegetal or microbial origin), and the modulation of soil-enzyme and microorganism activities, can strongly influence and modify the biogeochemical cycles of several elements, thus causing changes in their availability for plant nutrition.

One class of these elements is composed by the trace metals; some of them are essential for plants even if in small concentrations and are amongst the micronutrients, such as Fe, Zn, Mn. Trace-metal solubility and availability can be influenced, among other factors, by the presence in soil of organic complexing agents that can induce metal mobilization from stable mineral phases. Among these compounds, root exudates such as low molecular weight organic acids (e.g. citric acid, malic acid, oxalic acid), phenolic compounds (e.g. flavonoids), siderophores, can be cited. These molecules can strongly contribute to mineral weathering in rhizosphere and, therefore, to the mobilization of trace metals. The mobilized trace metals, in function of the element and of its concentration, can be either essential nutrients or toxic elements for plants.

Within this context, the objective of this research is to study the mineral weathering processes occurring in the rhizosphere, with particular attention addressed toward the processes involved in trace-metal mobilization and the role of natural organic chelating agents, such as low molecular weight organic acids, phenolic compounds and siderophores. Possible synergic or competitive effects, using pure chemicals as well as exudates collected from plants, on trace-metal solubilization and on mineral weathering occurring among these compounds are being evaluated.

This research is supported by Italian M.U.R.S.T. (FIRB RBFR08L2ZT).

Plio-Pleistocene evolution of water mass exchange and erosional input in the Fram Strait

CLAUDIA TESCHNER[1], MARTIN FRANK[1], BRIAN HALEY[2], MARCUS CHRISTL[3], CHRISTOPH VOGT[4] AND JOCHEN KNIES[5]

[1]IFM-GEOMAR, Wischhofstr.1-3, Kiel, Germany (cteschner@ifm-geomar.de)
[2]COAS, OSU, Corvallis, OR 97331-5503, USA
[3]Laboratory of Ion Beam Pysics, ETH Zurich, Switzerland
[4]FB Geowissenschaften, University of Bremen, Germany
[5]Geological Survey of Norway, NO-7491 Trondheim, Norway

We determined the isotopic composition of neodymium (Nd), lead (Pb) and beryllium (Be) of past seawater to reconstruct water mass exchange and erosional input between the Arctic Ocean and the Norwegian-Greenland Seas (NGS) over the past approximately 5 Myr. For this purpose, sediments of ODP site 911 (leg 151) from 900 m water depth on Yermak Plateau in the Fram Strait were leached to extract the isotopic composition of past bottom water from early diagenetic metal oxide coatings on the sediment particles [1].

Nd isotope signatures extracted from site 911 agree well with the present day deep water εNd signature of -11.8 ± 0.4 [2]. Overall the Nd isotope composition was more radiogenic in the core section older than 2.7 Ma (εNd = -9 to -10) and then progressively decreased to less radiogenic values (εNd = -11 to -12) similar to the present isotopic composition. $^{206}Pb/^{204}Pb$ ratios evolved from 18.7 to more radiogenic values around 19.2 between 2 Ma and today.

The εNd data indicate that mixing of water masses from the Arctic Ocean and the NGS has controlled the Nd isotope signatures of deep waters on the Yermak Plateau since the onset of the Northern Hemisphere Glaciation (NHG). In contrast, the $^{206}Pb/^{204}Pb$ of deep waters in the Fram Strait appears to have been dominated by glacial weathering inputs from old continental landmasses, such as Greenland or parts of Svalbard since 2 Ma. The changes in the εNd and $^{206}Pb/^{204}Pb$ were similar to those found for the central Arctic Ocean and the North Atlantic (derived from Fe-Mn crusts).

A record of cosmogenic ^{10}Be normalized to ^{9}Be in the same leaches shows a strikingly similar short term variability to those of εNd and $^{206}Pb/^{204}Pb$ suggesting that all three isotope systems have been influenced by the same process controlled by the extent of continental ice sheets and the associated weathering inputs.

[1] Gutjahr *et al*. (2007) *Chemical Geology* **242**, 351–370.
[2] Andersson *et al*. (2008) *GCA* **72**, 2854–2867.

Atmospheric dust input to the Northern Gulf of Aqaba

N. TEUTSCH[1]*, O. TIROSH[2], A. TZIPORI[2], U. DAYAN[3] AND Y. EREL[2]

[1]Geological Survey of Israel, Jerusalem, 95501 Israel (*correspondence: nadya.teutsch@gsi.gov.il)
[2]Institute of Earth Sciences, Hebrew University of Jerusalem, Israel
[3]Department of Geography, Hebrew University of Jerusalem, Israel

Atmospheric dust is considered a major source of nutrients to the open sea and major oceanic gyres. However, the contribution of airborne material to the nutrient budget of coastal marine environments was usually neglected because their supply from continental surface runoff was considered adequate. The Gulf of Aqaba situated at the north of the Red Sea is located in an extremely arid region with practically no runoff input, and therefore provides an ideal site to investigate the role of airborne dust in nutrient budget. The major objectives of this study are to quantify the role of atmospheric dust in the nutrient balance of the oligotrophic waters of the Gulf of Aqaba and to characterize the atmoshperic dust input associated with different synoptic conditions.

Suspended dust samples were continuously collected ca. every ten days for almost four years in the northwestern corner of the Gulf of Aqaba, on the pier of the Interuniversity Institute for Marine Sciences, Eilat, Israel. After collection, samples underwent sequential dissolution in order to dissolve first water-soluble salts, then carbonates and oxides, and finally Al-silicates. Dust load vary seasonally from low values in the summer to higher values in the fall, varying values in the winter and highest values in the spring. Major element chemistry points to the main phases extracted at each leaching stage and trace elements are mainly associated with the major elemental trends. Occasionally the dust samples contained elevated concentrations of anthropogenically-emitted metals (e.g. Pb, Zn, Cu) that could be attributed to changes in synoptic conditions. Elemental ratios point to seasonal and synoptic-control on the sources of the dust which in turn determine the solubility of the dust.

Tropical hydrologic cycle variability in the Florida Straits during Marine Isotope Stages 2 and 3

T.R. THEM II[1]*, M.W. SCHMIDT[1] AND J. LYNCH-STIEGLITZ[2]

[1]Department of Oceanography, Texas A&M University, College Station, TX 77843, USA (*correspondence: theo1085@tamu.edu)
[2]School of Earth and Atmospheric Sciences, Georgia Institute of Technology, Atlanta, GA, 30332, USA

Reconstructions of North Atlantic salinity variability during the last deglacial suggest that major reorganizations in the tropical hydrologic cycle are linked to North Atlantic Meridional Overturning Circulation (AMOC) and high-latitude climate change [1, 2]. However, it remains unclear if the same mechanisms are responsible for the abrupt climate oscillations during Marine Isotope Stages (MIS) 2 and 3. Here, we generate high-resolution records of sea surface temperature (SST) and $\delta^{18}O_{SEAWATER}$ ($\delta^{18}O_{SW}$, a proxy for surface salinity) from 20-39 ka ago by combining Mg/Ca paleothermometry with $\delta^{18}O$ measurements in shells from the surface-dwelling foraminifera *Globigerinoides ruber* in Florida Margin cores KNR166-2-JPC26 (24°19.61'N, 83°15.14'W; 546 m depth; 18-240 cm/kyr sed. rate) and JPC29 (24°16.93'N, 83°16.24'W; 648 m depth; 8-20 cm/kyr sed. rate). As an additional proxy of salinity variability resulting from riverine input into the Gulf of Mexico, we also measure Ba/Ca ratios in the same *G. ruber* shell material. Finally, benthic $\delta^{18}O$ values in the same cores were measured as a proxy for changes in Florida Current transport, based on the procedures outlined in [3, 4]. Our initial results show that increased Ba/Ca ratios (increased riverine influence), decreased $\delta^{18}O_{SW}$ values (fresher surface salinity) and increased benthic $\delta^{18}O$ values (suggesting increased Florida Current transport) correlate with the abrupt onset of interstadial phases in the NGRIP $\delta^{18}O_{ICE}$ record.

[1] Schmidt *et al*. (2004) *Nature* **428**, 160–163. [2] Carlson *et al*. (2008) *Geology* **36**, 991–994. [3] Lynch-Stieglitz *et al*. (2011) *Paleoceanography* **26**, PA1205. [4] Lynch-Stieglitz *et al*. (in prep)

https://doi.org/10.1180/S0026461X00006502 Published online by Cambridge University Press

Post-depositional thermal history of the 4364–3060Ma zircon-bearing metasandstones of the Illaara and Maynard Hills granite greenstone belts, Western Australia

E.R. THERN[1]*, F. JOURDAN[2], N.J. EVANS[3], B.J. MCDONALD[3], M. DANISIK[3], R.A. FREW[2] AND D.R. NELSON[4]

[1]DIAP, Curtin Univ., Perth, WA, Australia (*correspondence: eric@thern.org)
[2]WA Argon Isotope Facility, Curtin Univ., Perth, Australia
[3]CSIRO ESRE, Perth, Australia
[4]School of Natural Sciences, Univ. of Western Sydney, Australia

The post-depositional thermal history (spanning 3060Ma to 26Ma) of the ca. 3060Ma Illaara and Maynard Hills granite greenstone belt metastandstones (peak metamorphism of upper greenschist facies) is characterized by a combination of SHRIMP U-Th–Pb, Ar/Ar and (U-Th)/He geochronology.

Ar/Ar multi-grain tourmaline results defining two plateau ages of ~2940Ma on a cross-cutting quartz-tourmaline vein provide a minimum depositional age for the metasandstones. Post depositional stratiform qtz-tourmaline veins are a common occurrence in Archean quartzites, and can be useful in assigning minimum depositional ages and timing of hydrothermal fluids.

SHRIMP U-Th–Pb data of >275 rutile analyses from 8 metasandstone samples reveal a complex history of events between deposition of metasandstones (ca. 3060 Ma) and the subsequent folding, thrusting and granitic intrusions (ca. 2730-2630 Ma, regional D1 to D3 events). Some individual rutile grains yield multiple dates which span from before the maximum depositional age of the quartzite at ca. 3060Ma to the last major metamorphic and granitic event at ca. 2630Ma. These rutiles exhibit weakly defined core-rim younging profiles which represent multiple stages of metamorphic growth or Pb-loss reset events. These results suggest that under protracted greenschist metamorphic conditions rutile can retain signatures of multiple thermal events and even retain some of their original detrital characteristics.

Ar/Ar plateau ages on muscovites from both greenstone belts show that late to post deformation planar-foliation recrystalization at ca. 2605Ma (possibly coeval with the end of D3) marks the end of high-grade tectono-thermal events.

(U-Th)/He on zircon at ca. 230Ma defines exhumation and temperatures <180C for these metasandstones, similar to fission track results throughout the Yilgarn. Goethite (U-Th)/He ages of 26Ma are likely coeval with Fe-rich meteoric fluid influx and associated zero-age Pb-loss and Fe enrichment in metamict zones of both rutile and zircon within the metasandstones.

Past ocean temperatures and coupled U/Th and ^{14}C measurements from deep-sea corals

NIVEDITA THIAGARAJAN, JESS ADKINS AND JOHN EILER

Department of Geological and Planetary Sciences California Institute of Technology 1200 E California Blvd, Pasadena, CA 91125

Deep-sea corals are a unique archive in paleoceanography. They have large banded skeletons that allow for high resolution records and have a high uranium content allowing for accurate calendar ages independent of radiocarbon age measurements. One problem with using deep-sea corals for long records is that it is difficult to date a large numbers of corals accurately and precisely. Unlike sediment cores, fossil fields of corals have no inherent stratigraphy and each individual coral must be separately dated.

Here we present the results of 'reconnaissance radiocarbon age analyses' made at NOSAMS on 519 *Desmophyllum dianthus* (*D. dianthus*) collected from the New England Seamounts and South of Tasmania. We will also present the results of 80 more deep-sea corals measured on the Gas-Source AMS also at NOSAMS in WHOI. We find that the coral populations respond to rapid climate change events and are sensitive to climatically driven changes in thermohaline circulation, productivity, $[O_2]$ and $[CO_3^{2-}]$.

Once dated however, their use as a paleoceanographic archive is complicated by the isotope and trace-metal disequilibria in their skeletons relative to co-existing seawater. However two tracers that overcome these vital effects are paired U-series and radiocarbon dates and clumped isotope measurements. Here we will present preliminary data of YD and H1 corals from the New England Seamounts collected from 1000-2600m of water depth in the North Atlantic where all three tracers are measured in the same corals.

We find that the temperature profile of the ocean during both the YD and H1 coral population is constant with depth. The average potential temperature of the Younger Dryas profile is 1.6 ± 0.5°C while the average potential temperature of the Heinrich 1 profile is 3.1±0.9°C. If one outlier in the H1 profile is removed the average temperature becomes 2.3±0.5°C. We will discuss implications for salinity gradients in the water column during these time periods as well changes in the circulation of the ocean.

https://doi.org/10.1180/S0026461X00006502 Published online by Cambridge University Press

Using ToF-SIMS to study biomarkers

V. THIEL[1]*, M. BLUMENBERG[1], C. HEIM[1], J. LAUSMAA[2], T. LEEFMANN[1], J. REITNER[1], S. SILJESTRÖM[2] AND P. SJÖVALL[2]

[1]Geowissenschaftliches Zentrum, Universität Göttingen, Abt. Geobiologie, Goldschmidtstr. 3, D-37077, Göttingen, Germany (*correspondence: vthiel@gwdg.de)
[2]SP Technical Research Institute of Sweden, Chemistry and Materials Technology, Box 857, SE-501 15 Borås, Sweden

Time-of-flight secondary ion mass spectrometry (ToF-SIMS) is a technique designed to analyze the composition and lateral distribution of molecules and chemical structures on surfaces. A beam of high-energy ions (primary ions) bombards the sample surface, resulting in the emission of secondary ions from the outermost molecular layers of the sample. Analysis of these ions with respect to mass yields a mass spectrum which contains chemical information about the sample surface. During the measurement, the primary ion beam is scanned over a selected analysis area and individual mass spectra are recorded from each raster point within this area. The acquired data can then be used to produce (i) ion images, which show the signal intensity of selected secondary ions across the analysis area, and (ii) mass spectra from selected regions of interest on the sample surface.

These capabilities have generated much interest in the use of ToF-SIMS for the characterization of lipids and other organic biomolecules at the microscopic (μm-) level (see [1] and [2] for reviews). Here we introduce static ToF-SIMS imaging mass spectrometry as a tool for organic geochemical analyses. After describing the ToF-SIMS analysis principles, experiments on selected sample types relevant in geobiology and organic geochemistry are reported, namely soft (microbial cell matter, sediments), hard (microbialites), and liquid (fluid inclusions) samples. This presentation aims to put the potential of ToF-SIMS for organic biomarker approaches up for discussion, considering not only the strengths, but also current drawbacks and limitations for which further development would be beneficial for the field.

[1] Winograd & Garrison (2010) *Annual Review of Physical Chemistry* **61**, 305–22. [2] Thiel & Sjövall (2011) *Annual Review of Earth & Planetary Sciences* **39**, 125–156.

Raison d'être of X-ray spectromicroscopy for geochemistry

JUERGEN THIEME[1], JULIA SEDLMAIR[2], MAREIKE MATHES[2], JOERG PRIETZEL[3] AND JOHN COATES[4]

[1]NSLS-II, Brookhaven National Laboratory, Building 817, Upton, NY-11973, USA (jthieme@bnl.gov)
[2]Institute for X-Ray Physics, University of Goettingen, Friedrich-Hund-Platz 1, 37077 Goettingen, Germany
[3]Lehrstuhl fuer Bodenkunde, Technische Universitaet Muenchen, 85350 Freising-Weihenstephan, Germany
[4]Dept. for Plant and Microbial Biology, University of California, Berkeley, CA-94720, USA

X-ray microscopy in the sub-keV X-ray energy range uncovers structures down to 10 nm size, at higher X-ray energies structure sizes down to 30 nm can be imaged. The technique is capable of imaging specimens directly in aqueous media. X-ray microscopy images can be used for tomographic reconstructions of thick samples. By choosing the used X-ray energy appropriately, it is possible to perform spectro-microscopy studies. X-ray fluorescence can be used as a highly sensitive method to identify trace elements. Comprising, the combination of microscopy and spectroscopy is a powerful tool for addressing key questions in many scientific areas, e.g. to study structures in the environment showing dimensions on the nanoscale. Applications to scientific issues in geochemistry, geomicrobiology, and in soil and environmental sciences will be used to show the significance of this tool for science. X-ray images show the appearance of structures on the nano- and microscale. X-ray tomography conveyed morphological changes of humic substances due to biologically induced redox changes. Using the spectromicroscopy potential, the distribution of organic and inorganic components in such samples has been studied. NEXAFS spectra have been analyzed for major chemical constituents. This reveals e.g. the influence of extraction methods on the properties of humic sub-stances. Spectromicroscopy allows the study of carbon nanotubes and their influence on the environment. X-ray fluorescence spectromicroscopy studies of the spatial distribution, the chemical state of sulfur and its co-localization with iron in soils were performed. X-ray spectroscopy and spectromicroscopy has been used to study the release of sulfur from war debris from World War II into urban soils, an issue of rising importance.

https://doi.org/10.1180/S0026461X00006502 Published online by Cambridge University Press

The double effect of Mg on the long-term alteration rate of a nuclear waste glass

B. THIEN[1,3]*, N. GODON[1] AND A. AYRAL[2]

[1]Comissariat à l'Energie Atomique, Laboratoire d'Etude du Comportement à long terme des Materiaux, 30207 Marcoule, France

[2]Institut Européen des Membranes, cc047-UM2, Place Eugène Bataillon, 34293 Montpellier, France

[3]Paul Scherrer Institut, Laboratory for Waste Management, 5232 Villigen, Switzerland

(*correspondence: bruno.thien@psi.ch)

During their aqueous alteration, AVM French nuclear glasses exhibit a large range of behaviour, in spite of a small range of composition. AVM glasses alteration rates are controlled by two phenomena: (i) precipitation of secondary phases, mostly aluminous hectorites [1], and (ii) diffusion of water across a more or less protective gel layer. Magnesium contained in these glasses enhances the precipitation of these secondary phases, leading to a partial or total dissolution of the gel layer. This dissolution increases the glass alteration rates. On the other hand, Mg also incorporates in the gel, increasing his passivation properties [2]. The predominance of one of these two phenomena depends on the initial composition of the glass and on the initial composition of the solution (Fig. 1).

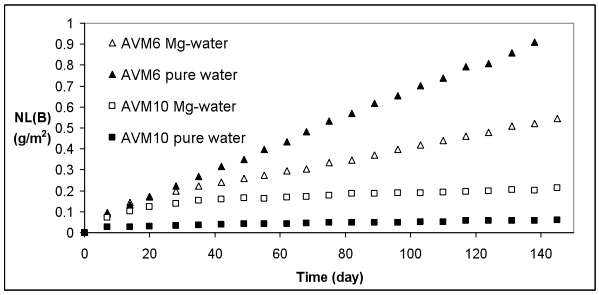

Figure 1: Quantities of altered glass for 2 different AVM glasses, AVM 6 and AVM 10, leached in pure water and in Mg-water.

[1] Thien *et al*. (2010) *Appl. Clay Sci.* ***49***, 134–141. [2] Thien (2010) *PhD Thesis*, University of Montpellier.

Magma sources at Eyjafjöll and adjacent South Iceland central volcanoes

MATTHEW THIRLWALL*, CHRISTINA MANNING AND DAVE LOWRY

Dept of Earth Sciences, Royal Holloway, University of London, Egham TW20 0EX, UK

(*correspondence: m.thirlwall@es.rhul.ac.uk)

We present Pb-Sr-Nd-Hf-O isotopic data for Quaternary transitional basaltic rocks of the six central volcanoes of the South Iceland flank zone. These are amongst the deepest melts in Iceland based on high Dy/Yb and low Na_2O/TiO_2. Each volcano shows limited ranges in isotopic composition, but Eyjafjöll Sr-Nd-Hf-O data lie systematically between Heimaey at more depleted isotopic compositions to the SW, and Katla and Tindfjöll at more enriched compositions to the E and N respectively. A tight $^{143}Nd/^{144}Nd$ – $\delta^{18}Ool$ correlation at Eyjafjöll extends from the mantle-like $\delta^{18}O$ of Heimaey to +4.2‰ values in Katla and Hekla olivines. Detail provided by double-spike Pb data shows however that Katla eruptives are not a possible enriched mixing end-member as they have relatively elevated ^{208}Pb, and indeed 3 or more mixing components would be required to explain the Pb isoopic compositions of Eyjafjöll and Tindfjöll eruptives.

The Nd-O isotopic correlation at Eyjafjöll is present in samples from several interglacial stages and could only result from crustal contamination if Eyjafjöll was underlain by an early Quaternary basement of hydrothermally-altered Katla-like volcanics. Given that the bulk of Katla has developed more recently than Eyjafjöll, this seems implausible. The +4.2‰ olivine $\delta^{18}O$ observed at Katla, Hekla, and in some Tindfjöll and Eyjafjöll lavas, is consistent with the value proposed in Icelandic low-$\delta^{18}O$ mantle [1]. It is associated also with low K/Nb and low Na_2O/TiO_2 suggesting that it is co-hosted with recycled oceanic crust that in the flank zone is most effectively tapped by deep melts.

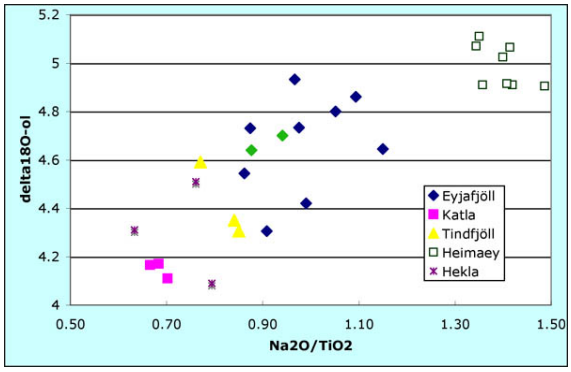

[1] Thirlwall *et al*. (2006) *Geochim. Cosmochim. Acta* **70**, 993.

https://doi.org/10.1180/S0026461X00006502 Published online by Cambridge University Press

Sea-water ^{231}Pa and ^{230}Th measurements, understanding the proxy in the S.E. Atlantic?

A.L. THOMAS AND G.M. HENDERSON

Department of Earth Sciences, South Parks Road, Oxford, OX1 3AN (*correspondence: alext@earth.ox.ac.uk)

A recent paleo record of ^{231}Pa/^{230}Th from the South Atlantic [1], has been interpreted as evidence for reversed flow of deep water at the last glacial maximum relative to the modern circulation. The ability of the ^{231}Pa/^{230}Th proxy to accurately reflect past paleoceanographic conditions is crucial to the interpretation of such down core records, and this accuracy has been questioned in another recent study [2], using an inverse approach to test whether paleo data is consistent with modern circulation. Currently, our understanding of the controls on sedimentary ^{231}Pa/^{230}Th, limits the robustness of our interpretations of this proxy. We present new ^{231}Pa and ^{230}Th measurements from the South Atlantic, collected on a UK-GEOTRACES cruise (D357; GA10) at 40°S, and compare to local sedimentary data to shed light on the regional controls on sedimentary ^{231}Pa/^{230}Th and hence asses the robustness of down core interpretations. By comparison with data from elsewhere in the Atlantic this data indicates the role of water masses and processes such as boundary scavenging on the ^{231}Pa/^{230}Th proxy and therefore points to the robustness of the proxy for past reconstruction.

[1] Negre *et al*. (2010) *Nature* **468**, 84–88. [2] Burke *et al*. (2011) *Paleoceanography* **26** PA1212.

Pre-Sturtian euxinia and ocean chemistry: Evidence from the Coppercap Formation in Northwest Territories, Canada

K. THOMAS[1], C. HALLMANN[1], F. MACDONALD[2], R. SUMMONS[1] AND S. ONO[1]

[1]Massachusetts Institute of Technology, Cambridge, MA (katthomas@mit.edu, hallmann@mit.edu)

[2]Harvard University, Cambridge, MA (fmacdon@fas.harvard.edu)

The mechanisms that lead to the onset of the Late Proterozoic global glaciations are yet unresolved but can be correlated through globally observed chemostratigraphical changes [1]. In interpreting the geochemical evidence from this time period, critical analysis of global versus regional effects [2] comes into play in determining the true extent of marine euxinia. Here we present a geochemical record of paired carbonate associated sulfate ($\delta^{34}S_{CAS}$) and pyrite ($\delta^{34}S_{pyr}$), organic carbon ($\delta^{13}C_{org}$) and carbonate ($\delta^{13}C_{carb}$) along with lipid biomarker analysis of the Coppercap Formation in the Northwest Territories, Canada, which was deposited just prior to the onset of the Sturtian glaciation.

Trimethylarylisoprenoids carotenoid-derived lipids indicative of purple and green sulfur bacteria were found throughout the section and indicate persistent euxinia in the shallow sediments deposited in a syn-rift basin. We observe an average $\Delta^{34}S_{CAS\text{-}Pyr}$ of ~ 25‰ which is typical for Neoproterozoic deposits [3] [4]. Increased burial of organic carbon and sedimentary sulfide is implicated from an isotopic shift in $\delta^{13}C_{carb}$ and $\delta^{34}S_{CAS}$. Severe euxinic conditions mid-section is evidenced from increased concentrations of arylisoprenoids and which coincides with a ~15‰ increase in $\delta^{34}S_{CAS}$, showing an interplay between more restricted conditions and marine ingressions. The implications of these geochemical signals and biomarker distributions are placed into a context of the onset of the Late Proterozoic glaciations.

[1] F. Macdonald *et al*. (2010) *Science* **327** 1241–1243. [2] D. Johnston *et al*. (2010) *EPSL* **290** 64–73. [3] M. Hurtgen *et al*. (2005) *EPSL* **203** 413–429. [4] D. Fike *et al*. (2006) *Nature* **444** 744–747.

https://doi.org/10.1180/S0026461X00006502 Published online by Cambridge University Press

Negative sulfur-MIF anomalies in metasomatized eclogites from Siberia

E. THOMASSOT[1], C. ROLLION-BARD[1], D.G. PEARSON[2], N. ASSAYAG[3] AND M. FIALIN[3]

[1]CRPG/CNRS, Vandoeuvre-lès-Nancy, France
[2]University of Alberta, Edmonton, AB, Canada
[3]IPG–Paris et Université Paris VI, France

Sulfur Mass Independent Fractionations (S-MIF), likely formed in the Archean atmosphere, are preserved in sedimentary rocks formed prior to 2.5 Ga [1]. Their recyclage into the mantle has been identified in metasedimentary sulfides included in diamonds, which carry significant S-MIF [2, 3]. However in both metasediments and diamond inclusions, most S-MIF values (carried by insoluble S-species) are positive, whereas the material balance of sulfur cycled from Archean atmosphere to sedimentary reservoirs requires that the average of all S-MIF is 0. Despite this requirement, the record of a negative S-MIF reservoir (likely dissolved in the oceans) is mostly absent, with only barite and sulfide of hydrothermal origin having these characteristics but representing a quite modest reservoir in size. Here we present a detailed petrological study coupled with *in situ* S-isotope measurements in 4 sulfides (~500μm in diameter) extracted from a mantle eclogite xenolith from the Mir kimberlite (Siberia). They consist of complex assemblages of (1) classic mantle sulfides (intergrowths of pyrrhotite and pentlandite) with (2) K-rich sulfides (djerfisherite) invaded by (3) veinlets of alteration-related minerals (mainly chlorite), resulting from multi-stage metasomatic processes [4]. Because of this complexity, we performed *in situ* multiple S-isotope measurements using a new Caméca ims 1280-HR2, allowing precise measurement with a spatial resolution < 20 μm, with precision for $\Delta^{33}S$ better than ±0.1 ‰.

Despite mineralogical heterogeneities, $\delta^{34}S$ in each sulfide has a narrow range (± 0.9 ‰). Most suprisingly, they show significant, exclusively negative MIF, ranging from 0 to -0.42‰ (±0.1 ‰, n=18). Metasomatic djerfischerite rims show smaller isotopic anomalies which cannot be clearly distinguished outside of uncertainty. We interpret the negative $\Delta^{33}S$ in the primary sulfides as reflecting an imprint of hydrothermal circulation in Archean oceanic crust. The smaller anomalies in the rims may reflect later reequilibration during modal metasomatism. Hence the signature appears to be evidence of a more widespread reservoir with negative $\Delta^{33}S$ that may balance the Archean S-MIF budget. The new S isotope data also provide further support for subducted oceanic crust as the protoliths of Siberian eclogites.

[1] Farquhar *et al*. (2000). [2] Farquhar *et al*. (2002). [3] Thomassot *et al*. (2007). [3] Misra *et al*. (2004).

Extreme ^{15}N-enrichments in 2.72-Gyr-old sediments: Evidence for a turning point in the nitrogen cycle

C. THOMAZO[1]*, M. ADER[2] AND P. PHILIPPOT[3]

[1]UMR CNRS 5561 Biogéosciences, Université de Bourgogne, Dijon, France
(*correspondence: christophe.thomazo@u-bourgogne.fr)
[2]Equipe de géochimie des isotopes stables, Institut de Physique du Globe de Paris, Sorbonne Paris Cité, Université Paris Diderot, UMR 7154 CNRS, F-75005 Paris, France
[3]Equipe de geobiosphère actuelle et primitive, Institut de Physique du Globe de Paris, Sorbonne Paris Cité, Université Paris Diderot, CNRS, F-75005 Paris, France

Although nitrogen is a key element in organic molecules such as nucleic acids and proteins, the timing of the emergence of its modern biogeochemical cycle is poorly known. Recent studies suggests the establishment of a complete aerobic N biogeochemical cycle at about 2.68 Gyr. Here, we report new bulk nitrogen isotope data for the 2.72 billion-year-old sedimentary succession of the Tumbiana Formation (Pilbara Craton, Western Australia). The nitrogen isotopic compositions vary widely from +8.6‰ up to +50.4‰ and are inversely correlated with the very low $\delta^{13}C$ values of associated organic matter defining the Fortescue excursion (down to about -56‰).

We argue that the main driver of this exceptional high $\delta^{15}N$ values is the isotope fractionation associated with microbial ammonia oxidation, the produced nitrite and nitrate being totally converted to gaseous N_2O or N_2 by denitrification. The expression of this isotope fractionation in the rock record suggests that a small increase in oxidant availability allowed water column colonization by ammonia oxidizing micro-organisms, but was too limited to allow ammonium to be fully used up. The subsequent decrease of $\delta^{15}N$ values down to modern values 5 ±3‰ by 2.6 Gyr probably reflects a redox increase of at least part of the water column, leading to the establishment of a chemocline interface (localized either in the water column or in the sediment) where ammonium is quantitatively oxidized by denitrification as in modern environments. This study allows us to date precisely the onset of the oxidative part of the nitrogen cycle at 2.72 Gyr. We see the first evidence for ammonium oxidation, nitrification, and denitrification, which implies an increase in the availability of electron acceptors and probably oxygen in the Tumbiana depositional environment, 300 million years before the oxygenation of the Earth's atmosphere.

https://doi.org/10.1180/S0026461X00006502 Published online by Cambridge University Press

Uranium series analysis of 2006 Augustine volcanics: An investigation into the timescales of magmatic processes

J.A. THOMPSON* AND M.K. REAGAN

University of Iowa, Iowa City, Iowa 52245
(*correspondence: jennifer-cash@uiowa.edu)

The frequent eruptions (5 eruptions in the last century) and the narrow range of erupted products (dacites to andesites) in conjunction with excellent documentation of the 2006 eruption by the Alaskan Volcano Observatory (AVO) make Augustine an ideal location for investigating the time-scales of magma mixing and differentiation. Toward this end, a set of 17 representative samples of the 2006 eruption were analyzed for ^{238}U, ^{230}Th, ^{226}Ra, and ^{210}Pb abundances, as well as major and trace element concentrations.

All samples from Augustine have consistent excesses of (^{230}Th) over (^{238}U). Similar excesses in other andesitic lavas have been explained by slab or lower crustal melting with residual garnet, or differentiation from basalt generated by melting mantle in the presence of garnet or Al-rich pyroxene. We prefer the latter explanation based on documentation for basaltic parental magmas (Larsen *et al*. 2010), and a lack of evidence for garnet fractionation with differentiation. Variations in ($^{230}Th/^{232}Th$) values vary independently of SiO_2 concentrations, suggesting that the mixtures of melts and crystals making up the differentiated magmas have average ages as high as 54 Ka.

Our most mafic sample (an enclave with 53 wt % SiO_2) has ($^{226}Ra/^{230}Th$) = ~1.2. With increasing concentrations of SiO_2, the ($^{226}Ra/^{230}Th$) values decrease to ~1 at SiO_2 ~ 56 wt. %, increase to 1.45 at SiO_2 ~ 59 wt %, then decrease to ~1 in samples with >61 wt. % SiO_2. These data suggest that three magmas mingled and mixed during the 2006 eruption: basaltic andesites with Ra excesses generated by mantle melting; a 59 wt % SiO_2 magma with Ra excesses generated from incongruent melting of youg plutonic materials, and 61-62 wt % SiO_2 andesites with relatively long crustal residence times.

Excesses of (^{210}Pb) over (^{226}Ra) were measured in the most mafic and silicic samples at Augustine, whereas intermediate samples had either equilbrium ($^{210}Pb/^{226}Ra$) or small ^{210}Pb deficits. The excesses in the basaltic andesites were likely generated during degassing within a compositional boundary layer. Excesses in high silica samples were likely produced by localized degassing through porous networks of vesicles.

Best practices for ensuring consistent coral geochronology

W.G. THOMPSON

113A Clark Lab, MS # 23, Woods Hole Oceanographic Institution, Woods Hole, MA 02543

The goal of geochronology is to supply an accurate timescale for earth processes, and U-Th coral dating has been sucessfully used to infer the history of sea level change. However, it is widely acknowledged that U-Th coral geochronology is strongly impacted by diagenetic artefacts over much of its practical dating range [1]. Improved understanding of the major diagenetic processes producing significant artefacts in coral ages has inspired a vigorous debate over best practices in coral geochronology [2]. Traditional approaches rely on screening criteria to identify corals that have behaved as a closed system, while newer approaches seek to quantify and correct for the diagenetic processes directly. Regardless of the preferred approach for U-Th age interpretation, it is clear that differences in screening criteria and assumptions about the oceans past uranium isotope ratio have considerable influence on the conclusions inferred from U-series coral data. Using new and existing data, and fundamental statistical analysis, we demonstrate the sensitivity of U-Th coral geochronology to small differences in age interpretation practices. Furthermore, we suggest simple and practical steps that can be taken now to make the interpretation of coral ages more objective and consistent; a fundamental goal of geochronology.

[1] Thompson, Andersen, Dutton & Siddall (2010) *PAGES News* **18**, 39–40. [2] Andersen, Gallup, Scholz, Stirling & Thompson (2009) *PAGES News* **17**, 54–56.

https://doi.org/10.1180/S0026461X00006502 Published online by Cambridge University Press

Volatile short lived iodocarbons from biotic and abiotic sources affecting atmospheric chemistry

U.R. THORENZ*, M.KUNDEL, J. BOSLE AND T. HOFFMANN

Johannes Gutenberg-University, Institute for Inorganic and Analytical Chemistry, Duesbergweg 10-14, 55128 Mainz (*correspondence: ute.thorenz@uni-mainz.de)

Atmospheric Iodine chemistry in the lower troposphere gained more attention in the last decade, because of its ozone depleting capacity [1]. The oxides formed during this reaction may also undergo further oxidation and form polyoxides which then play a role in new particle formation [2]. Precursors of both reactions are iodocarbons found in the marine atmosphere. These Iodocarbons are emitted by different macroalgae [3] and are also produced by abiotic reactions [4]. The investigation of both release pathways is the aim of the presented study.

The method developed uses thermodesorption gas chromatography negative chemical ionisation mass spectrometry TD-GC-NCI-MS. Using the negative ionisation mode the method detection limits were reduced by on order of magnitude compared to electron impact. (LOD: Iodomethane 2.01 pg, Iodethane 0.98 pg, Iodchloromethane 0.26 pg, Iodbromomethane 7.37 pg, Diiodmethane 8.61 pg)

To investigate the biotic release pathway we treated different algae species with various ozone mixing ratios and measured iodocarbon and inorganic iodine release of the algae. We found a correlation on ozone concentration and iodine as well as organo-iodine release. A good correlation was found for iodine release and place of growth, meaning that algae growing above or in the intertidal zone release less iodine than algae in the sublittoral zone.

dT investigate the abiotic pathways of forming iodocarbons a chamber experiment was done using particulate HOI and fulvic acid. The particles were formed by an atomizer and crossed a chamber with a residuance time of 160 seconds. Even after this short reaction time the formation of iodomethan was seen.

[1] Read *et al*. (2008) *Nature* **453**, 1232–1235. [2] O'Dowed *et al*. (2002) *Nature* **417**, 632–636. [3] Nightingale *et al*. (1995) Limnol. Oceanogr. **40**, 680–689. [4] Carpenter *et al*. (2005) *Environ. Sci. Technol*. **39**, 8812–8816.

Rapid changes in North Atlantic deep ocean circulation during the MIS 5a/4 glacial inception

D.J.R. THORNALLEY[1]*, S. BARKER[1], I.R. HALL[1] AND G. KNORR[2]

[1]School of Earth and Ocean Sciences, Cardiff University, Park Place, Cardiff, CF10 3AT, UK (*correspondence: ThornalleyDJ@cf.ac.uk, BarkerS3@cf.ac.uk, Hall@cf.ac.uk)

[2]Alfred Wegener Institute, Bussestrasse 24, D-27570 Bremerhaven, Germany (Gregor.Knorr@awi.de)

Earth's climate during the Plio-Pleistocene epoch has been characterised by oscillations between glacial and interglacial conditions, thought to be related to changes in the Earth's orbit, as well as feedbacks including variations in atmospheric CO_2 and ice albedo. Detailed examination of the last glacial termination (and earlier terminations) has revealed that millennial-scale changes, probably involving variation in the Atlantic meridional overturning circulation (AMOC), play a critical role in the mechanism of glacial termination. Conversely, very little is known about the AMOC during the onset of glacial conditions and the associated millennial-scale variability.

Here, we investigate North Atlantic deep ocean circulation during the Marine Isotope Stage 5a to 4 glacial inception ~70, 000 years ago, an interval which contains Dansgaard-Oeschger events 19 and 20 and also marks the onset of full glacial conditions, involving a rapid lowering of sea-level an abrupt decrease in atmospheric CO_2. Using a range of geochemical and sedimentological methods applied to marine sediment cores, we present high resolution (100-200 year) proxy reconstructions of deep water circulation and chemistry from depth transects in both the eastern and western North Atlantic. The chronology of the cores is tightly constrained, enabling us to examine the precise timing of deep ocean chemistry and circulation changes with respect to the decrease in sea-level and atmospheric carbon dioxide.

https://doi.org/10.1180/S0026461X00006502 Published online by Cambridge University Press

Strontium behaviour during bioreduction in nitrate impacted sediments

C.L. THORPE[1], G.T.W. LAW[1], I.T. BURKE[2], J.R. LLOYD[1], S. SHAW[2] AND K. MORRIS[1]*

[1]Research Centre for Radwaste and Decommissioning, SEAES, University of Manchester, M13 9PL, UK (*correspondence: kath.morris@manchester.ac.uk)
[2]School of Earth and Environment, University of Leeds, LS2 9JT, UK

^{90}Sr is a contaminant at nuclear sites, has a ~30 year half life and has high potential mobility in ground waters. Here, we explored the behaviour of Sr^{2+} during sediment bioreduction under varying pH and NO_3^- amendments. During NO_3^- reduction, enhanced Sr^{2+} sorption to sediments occurred as alkalinity developed as a result of OH^- and HCO_3^- formation during denitrification [1, 2]. During development of metal reducing conditions, Sr^{2+} was then re-released to solution in microcosms with a final pH < 9 suggesting that Sr^{2+} had been preferentially sorbed to Fe(III)-bearing mineral phases during NO_3^- reduction and reductive dissolution of Fe(III)-phases was controlling Sr^{2+} solubility. In microcosms with a final pH > 9, Sr^{2+} was retained on sediments throughout bioreduction presumably to its association with stable carbonate phases which become oversaturated at high pH. Further investigation of these systems with X-ray absorption spectroscopy, electron microscopy and modelling indicated that that at pH < ~9, Sr^{2+} forms outer sphere complexes in the sediment whilst at pH > ~9, incorporation into carbonate phases is possible. Overall, Sr^{2+} behaviour during bioreduction is complex with high pH bioreducing conditions showing potential for co-treating Sr^{2+} with a range of radioactive contaminants.

[1] Thorpe *et al*. (In review) *Geomicro J*. [2] Law *et al*. (2010) *Environ. Sci. Tech*. **44**, 150–155.

Rb-Sr and Sm-Nd isochron ages of the Dongmozhazhua and Mohailaheng Pb-Zn ore deposits in Yushu area, southern Qinghai and their geological implications

TIAN SHIHONG[1,2]*, HOU ZENGQIAN[3], YANG ZHUSEN[1], LIU YINGCHAO[3] AND SONG YUCAI[3]

[1]Institute of Mineral Resources, CAGS, Beijing 100037, China (*correspondence: s.h.tian@163.com)
[2]Key Laboratory of Metallogeny and Mineral Assessment, MLR, Beijing 100037, P.R. China
[3]Institute of Geology, CAGS, Beijing 100037, China

Dongmozhazhua and Mohailaheng Pb-Zn deposits in Yushu area of Qinghai Province are representative Pb-Zn deposits in the Cu-Pb-Zn polymetallic mineralization belt of the northern part of the Nujiang-Lancangjiang-Jinshajiang area, which are in the front belt of Yushu thrust nappe system. The ages of the Dongmozhazhua deposit have been determined by the Rb-Sr isochron method for sphalerite; whereas, the ages of the Mohailaheng deposit have been determined by the Rb-Sr isochron method for sphalerite and the Sm-Nd isochron method for fluorite. The age of Dongmozhazhua deposit is 35.015 ± 0.034 Ma ($(^{87}Sr/^{86}Sr)_0$= 0.7088072 ± 11) for sphalerite. The age of Mohailaheng deposit is 32.22 ± 0.36 Ma ($(^{87}Sr/^{86}Sr)_0$=0.70851380 ± 89) for sphalerite and 31.75 ± 0.28 Ma ($(^{143}Nd/^{144}Nd)_0$= 0.51236150 ± 54) for fluorite with an average of 32 Ma. Combined with geological and geochemical data, it is concluded that the Dongmozhazhua and Mohailaheng deposits formed during the same geological event and the metals have the same source. Together with regional mineralization geological setting, a possible tectonic model for metallogeny of Dongmozhazhua and Mohailaheng Pb-Zn deposits has been established. These two ages are close to the ages of the Pb-Zn deposit in Lanping basin of the southern part of the Nujiang-Lancangjiang-Jinshajiang area and in Tuotuohe basin of the northern part of the Nujiang-Lancangjiang-Jinshajiang area, indicating that it is possible that the narrow 1000 km-length belt controlled by thrust nappe system in the eastern and northern margins of Tibetan plateau would be a giant Pb-Zn mineralization belt.

This work was supported by grants (Contracts No. 2006BAB01A08, 1212010818096, 2011CB403104, U0933 6051, 2009CB421007, 2009CB421008).

https://doi.org/10.1180/S0026461X00006502 Published online by Cambridge University Press

Speciation and thermodynamic properties of Manganese(II) and Nickel(II) chloride complexes in hydrothermal fluids: *In situ* XAS study

YUAN TIAN[1]*, JOËL BRUGGER[2], WEIHUA LIU[3], BARBARA ETSCHMANN[2], STACEY BORG[3], DENIS TESTEMALE[4], BRIAN O'NEILL[1] AND YUNG NGOTHAI[1]

[1]School of Chemical Engineering, The University of Adelaide, Australia (*correspondence: yuan.tian01@adelaide.edu.au)
[2]School of Earth and Environmental Sciences, The University of Adelaide, Australia
[3]CSIRO Earth Science and Resource Engineering, Australia
[4]Institut Néel, Département MCMF, France

Aqueous Mn (II) and Ni (II) chloride complexes play an important role in Mn/Ni transport and deposition in hydrothermal ore-forming systems. Understanding metal transport and deposition relies on our knowledge of the metal speciation transported in hydrothermal fluids and thermodynamic properties of each species.

Synchrotron based XAS technique was used to measure *k*-edge spectra of Mn (II) and Ni (II)-bearing solutions with increasing temperature and salinity. Mn (II) and Ni (II) exhibit similar XANES spectral evolutions to other divalent transition metals, which reveals that octahedral species predominante at room temperature, while tetrahedral species become more important with increasing temperature and sanility. *Ab initio* XANES simulations and EXAFS refinements determined the structure of predominant end-member species $M(H_2O)_6^{2+}$ and $MCl_3(H_2O)^-$ and demonstrated that fully chlorinated complex MCl_4^{2-} is not stable in hypersaline brines (M = Mn, Ni). This result, together with previous studies of aqueous chloride complexes of Fe (II)[1] and Co (II)[2] revealed the difference in the two pairs of transition metals to form high order chloride complexes: Mn-Fe and Ni-Co. The former member forms $MCl_3(H_2O)^-$ at high temperature and high salinity while latter member forms fully chlorinated complex under the same conditions. XANES spectra were used to calculate formation constants and thermodynamic properties of $MCl_3(H_2O)^-$ species which can explain the strong fractionation between the proposed couple metals in hydrothermal systems.

[1] Testemale *et al*. (2009) *Chemical Geology* **264**, 295–310. [2] Liu *et al*. (2011) *Geochim. Cosmochim. Acta* **75**, 1227–1248.

Craton destabilization and alkaline magmatism in equatorial East Africa

JOHN V. TIBERINDWA[1,2], KLEMENS LINK[1], ERASMUS BARIFAIJO[2] AND STEPHEN F. FOLEY[1]

[1]Geocycles Research Centre and Institute for Geosciences, University of Mainz, 55099 Mainz Germany
[2]Department of Geology, Makarere University, Kampala, Uganda

Several types of alkaline magmatism are typically related to specific locations on and around cratons. Diamond-bearing kimberlites are restricted to craton centres, many lamproites occur around craton edges, and ultramafic lamprophyres are associated with areas where cratons are rifted. The Tanzanian craton is an example of a craton at an intermediate stage of destabilization. It is supported by warm upwelling mantle and its surface is at an elevation of >1, 100m. However, unravelling the petrogenesis is complicated by the confluence of cratonic magmatism with the East African Rift. We have reassessed alkaline magmatism around the Tanzanian craton and find a negative correlation between K/Na ratios in rocks and distance from the craton. Potassium-rich rocks have generally been associated with the western rift branch because of the occurrence of kalsilite-bearing volcanic rocks there, but also occur at the eastern edge of the craton. The association of potassium with cratons is attributed to melting at >140 km depth to form mixed source regions containing phlogopite pyroxenite and peridotite. In the western branch of the rift, the base of the lithosphere is interpreted to plunge to deeper levels towards the north beneath a saddle of cratonic lithosphere that links the Tanzanian and Congo cratons [1]. K/Na of magmas decreases towards the south where melting occurs closer to the surface. Here, amphibole rather than phlogopite is involved in melting. In southern Kenya (eastern rift), olivine phenocrysts have high Ni contents that are interpreted to indicate melting of a different type pyroxenite, namely garnet pyroxenites that are also found as xenoliths [2]. Due to the combination of craton destabilization and continental rifting, the pattern of magmatism around the Tanzanian craton shows a great variety of contemporaneous magmatism which is similar to that stretched over more than 1, 200 million years during several stages in the Labrador Sea rift [3].

[1] Link *et al*. (2010) *Int. J. Earth Sci*. **99**, 1599–1611. [2] Kaeser *et al*. (2009) *Contrib. Mineral. Petrol*. **157**, 453–472. [3] Tappe *et al*. (2007) *Earth Planet. Sci. Lett*. **256**, 433–454.

https://doi.org/10.1180/S0026461X00006502 Published online by Cambridge University Press

Peering through the diagenetic window for Archean phototrophs

M.M. TICE[1]*, J. CAI[1], C.-T. LEE[2] AND D.R. LOWE[3]

[1]Department of Geology & Geophysics, Texas A&M Univ., College Station, TX 77843 (*correspondence: mtice@geos.tamu.edu, jjcc@neo.tamu.edu)
[2]Department of Earth Science, Rice Univ., Houston, TX 77005 (ctlee@rice.edu)
[3]Department of Geological & Environmental Sciences, Stanford Univ., Stanford, CA 94305 (drlowe@stanford.edu)

Because Fe^{2+} can be oxidized by several environmentally-relevant pathways, it is not currently known what process produced banded iron formations prior to the oxygenation of the atmosphere [1]. In contrast, Mn^{2+} is not known to be oxidized by anoxygenic organisms and is not as photochemically reactive as Fe^{2+}. It has therefore been suggested that sedimentary Mn(IV) minerals should be regarded as the geologic marker of oxygenic photosynthesis [2]. Unfortunately, these minerals are some of the first electron acceptors to be reduced during sedimentary diagenesis [3], so their absence in sedimentary rocks of a given age does not necessarily indicate the absence of oxygenic photosynthetic bacteria at that time. Seeing through the window of diagenetic metal reduction is therefore critical to reconstructing a manganese proxy record of the evolution of oxygenic photosynthesis.

Diagenetic carbonate minerals in hematitic cherts of the 3.26 Ga Fig Tree Group preserve a range of rare earth element (REE) distributions with end-members consistent with minimally modified seawater (superchondritic Y/Ho and no middle REE enrichment) and sedimentary pore fluids in iron-reducing diagenetic zones (chondritic Y/Ho and middle REE enrichment). Low Mn/Fe ratios and seawater-like REE distributions are present in ankerite in deep-water hematitic banded iron formation. Ankerite and dolomite in shallow-water jaspers preserve elevated Mn/Fe ratios that correlate inversely with degree of diagenetic alteration inferred by REE distributions. No primary Mn(IV) minerals have been observed in any of these rocks. We show that this pattern is most consistent with a lack of Mn(IV) minerals prior to diagenetic alteration and the absence of oxygenic phototrophs during deposition of Fig Tree banded iron formation.

[1] Dietrich, Tice & Newman (2006) *Current Biology* **16**, R395-R400. [2] Kopp, Kirschvink, Hilburn & Nash (2005) *PNAS* **102**, 11131–11136. [3] Canfield & Thamdrup (2009) *Geobiology* **7**, 385–392.

Dating granites from the Erzgebirge by different methods – A comparison

M. TICHOMIROWA[1] AND J. PFÄNDER[2]

[1]Institute of Mineralogy, TU Bergakademie Freiberg, D-09599 Freiberg, Germany
[2]Institute of Geology, TU Bergakademie Freiberg, D-09599 Freiberg, Germany

Granites from the Erzgebirge mark the final stage of the Variscan Orogeny. Therefore, they are important time marks to unravel the evolution of late and post-orogenic processes. Until now, there is still a large scatter of ages obtained at different laboratories and by different methods for these igneous rocks. The granites display very distinct geochemical and petrological patterns. 'Early' granites were almost undifferentiated and consist mainly of biotite granites. 'Later' granites were strongly differentiated and appear as two-mica granites or Li-mica granites. Some of the 'latter' granites belong to fluorine-rich varieties. In addition to geochemical magmatic differentiation, many granites were severely overprinted by hydrothermal activity which was often related to ore-forming processes. Multiple overprint processes may hamper precise and accurate dating of such granites because of the possible disturbance of dating systems.

Recently, an age difference of about 9 (±3) Ma was established between two granite suites belonging to the 'early' and 'late' stage by the single zircon evaporation method [1]. We present new age data (Pb/Pb on zircon, U/Pb SHRIMP on zircon, U/Pb conventional dating, Rb/Sr on mineral separates, Ar/Ar on mica) for these and further granite suites from the Erzgebirge (Eibenstock, Aue-Schwarzenberg, Kirchberg, Bergen, Frauenstein). The data will be discussed in light on duration of igneous processes as well as on precision of dating methods.

[1] Tichomirowa & Leonhardt (2010) *Z. Geol. Wiss.* **38**, 99–123.

https://doi.org/10.1180/S0026461X00006502 Published online by Cambridge University Press

Effects of Louisville seamount subduction: Geochemical evidence from central Tonga-Kermadec arc volcanoes

C. TIMM[1], I.J. GRAHAM[1], M.I. LEYBOURNE[1], C.E.J. DE RONDE[1] AND J. WOODHEAD[2]

[1]GNS Science, PO Box 30-368, Lower Hutt, New Zealand
[2]School of Earth Sciences, The University of Melbourne, Melbourne, Victoria 3010, Australia

Alkaline Louisville seamount lavas and volcaniclastics were subducted beneath the Tonga arc since ~4 Ma, while the locus of seamount-arc intersection moved southward with time. Presently, Louisville material is subducting beneath the northern Kermadec/southern Tonga arc nearby the arc volcanoes Monowai, 'U', 'V'. Basalts recovered from all three volcanoes during the NZAPLUME III expedition show MORB-type REE patterns with enrichments of LILE and negative Nb anomalies. Lavas from Ata Island (located ~250 km N of 'V') however have higher La/Sm, Sm/Yb (and Th/Yb) than lavas from Monowai, 'U' and 'V', suggesting the input of fluid-immobile elements, such as LREE, MREE and Th from the slab into the mantle wedge beneath Ata Island. Conversely more radiogenic Sr and Pb isotopic compositions are found in lavas from volcano 'U' and 'V', consistent with input of fluid-transported Sr and Pb from subducted Louisville material beneath these volcanoes. Because dehydration of the slab requires lower temperatures than melting, we suggest that both the higher fluid-immobile, more to less incompatible element ratios (and slightly lower $^{143}Nd/^{144}Nd$) in the Ata Island lavas, and the higher Sr and Pb isotopic composition in the 'U' and 'V' lavas may reflect the influence of subducting Louisville material transported to the mantle wedge via aqueous fluids and hydrous melts and/or bulk mixing at different locations and times.

[1] Turner, S.P. *et al*. (1997) *Geochimica et Cosmochimica Acta* **61**, 4855–4884.

A paradox between Mg and Li isotope ratios during weathering

E.T. TIPPER[1,2], D. CALMELS[2], J. GAILLARDET[2], P. LOUVAT[2], F. CAPMAS[2] AND B. DUBACQ[1]

[1]Dept. of Earth Sciences, University of Cambridge, UK (ett20@cam.ac.uk)
[2]IPGP-Université Paris 7, Paris, France

The sources and processes that release mineral-bound (Mg) to solute Mg during chemical weathering are surprisingly under-constrained, but are critical for a complete understanding and quantification of its global biogeochemical cycle and chemical weathering. Magnesium isotope ratios ($^{26}Mg/^{24}Mg$ expressed as $\delta^{26}Mg$) in the river waters of the Mackenzie basin show in excess of 1‰ variability. In suspended sediments $\delta^{26}Mg$ values show in excess of 3‰ variation and correlate with the Ca/Mg ratio, a strong indication that the rock composition is controlled by a mixture of carbonate and silicate minerals. Riverine $\delta^{26}Mg$ values do not show the same control. Rather, they show coherent trends suggesting that Mg isotopes are more likely controlled by process-related fractionation. In particular, we highlight a linear positive covariation (R^2=0.81) between Li ($^7Li/^6Li$) and Mg isotope ratios in the rivers waters of the Mackenzie Basin and in four of the world's largest rivers. This is therefore representative of the average processes occurring at a global scale. Li is not present in appreciable quantities in carbonate rocks, but Mg can be. Therefore Mg isotope ratios are not being dominated by processes linked to carbonate dissolution. Li isotopes have often been interpreted in term of process controlled fractionation linked to silicate weathering and clay and previous work has demonstrated that during weathering, Mg and Li isotopes show opposite discrimination. Waters are often enriched in the light isotope of Mg and the heavy isotope of Li compared to the rocks they drain. The data present a paradox because any covariation between $^7Li/^6Li$ and $^{26}Mg/^{24}Mg$ would be anticipated to show a negative slope, rather than the positive slope observed. This paradox could be very simply resolved by interpreting the isotopic compositions as mixtures of different water bodies (such as groundwaters and surface waters for example) but this is not supported by concomitant variation in Mg/Li ratios. Modelling results show that the co-variation is more likely related to fractionation linked to clays. Coupled modelling of Mg and Li enables both the fractionation factors associated with such processes to be estimated, and the proportion of Mg that is incorporated into secondary phases, enhancing our current understanding of solute Mg at spatial scales from the critical zone to the continental scale rivers.

https://doi.org/10.1180/S0026461X00006502 Published online by Cambridge University Press

On the thermal and dynamic requirements for mantle melting

M. TIRONE* AND J. GANGULY

Department of Geosciences, Univ. of Arizona, Tucson, 85721 AZ, USA (*correspondence: max.tirone@gmail.com)

Our understanding of the petrological geodynamics of the Earth's mantle can be improved by numerical simulations supported by a comparison of the results with observable quantitites. Melting in the upper mantle is the end-product of dynamic and petrological processes. The description of these processes is usually based on several simplifying assumptions. However, a more realistic approach should consider the complex interplay among the petrological and dynamical aspects. Here we present a multistage numerical procedure to characterize the thermal and dynamic conditions of the mantle that ultimately control the melting process as a function of time and space during mantle upwelling. (1): A parameterized mantle convection model is used in conjuction with a thermodynamic approach and an optimized mineralogically dependent viscosity model to determine the thermal structure of the mantle from top to bottom using several constraints such as the melting temperature requirement to generate komatite magmatism in the Archean and plume melting in more recent time. (2): The viscosity and the thermodynamic models and the thermal state at the CMB from the thermal history study are then applied to model the geodynamic evolution of a thermal plume. (3): The thermal and dynamic evolution at shallow depth (but below the mantle solidus) is then used to constrain the melting process which is investigated using a coupled two-phase flow model and a thermodynamic formulation for melt that is modified from pMELTS.

The whole procedure illustrates the interconnection among a wide range of factors, such as thermal history, CMB temperature, mantle viscosity, thermal structure of plumes, evolution and composition of melt.

Here stage (3) is applied to the case of melting under a moving plate (e.g. Hawaii) which is discussed in some details. In particular it is shown how the thermal and dynamic interaction of the plume with the lithosphere affects the melt distribution and composition and how it is related to the various stages of magma emplacement. A source component of melt detected by the model is clearly provided by the lithospheric mantle. Pyroxenite cumulates are obtained by partial crystallization of underplated melt. Bathymetry appears to be correlated with the thermal erosion of the lithosphere.

Influence of glass composition on Si and Ca isotope measurements by SIMS

L. TISSANDIER*, C. ROLLION-BARD AND G. CARO

CRPG/CNRS, BP 20, 54501, Nancy, France (*correspondence: tix@crpg.cnrs-nancy.fr)

Isotopic data obtained by *in situ* mass-spectrometry are affected by instrumental mass fractionation effects related to the nature of the sample. This 'matrix effect' can cause large deviations from the real value and needs to be accurately evaluated in order to obtain precise stable isotope ratios. To constrain these matrix effects, we measured Ca and Si isotopes in a series of silicate glass standards spanning a wide compositional range ($7 < SiO_2 < 72$; $0 < Al_2O_3 < 56$; $0 < CaO < 50$; $0 < MgO < 32$; in wt%). Measurements were performed on a CAMECA IMS1270 at the CRPG/CNRS, Nancy France. We used a multicollection mode, and the different isotopes were measured on Faraday cups. Regardless of the composition of the glass, internal precision was better than 0.1‰, and external reproducibility ranges between 0.15 and 0.35‰ (2σ). The isotopic compositions of Ca and Si in these samples were also measured by TIMS and ICPMS, respectively.

In these different standard glasses, Ca and Si isotopic signatures show a clear compositional dependence. To a first order, instrumental mass fractionation is controlled by the silica content of the glass. However, smaller effects can also be observed for samples with identical silica content, e.g. when substituting Ca for Mg. These results show that the degree of polymerization of the glass is the key parameter for understanding these matrix effects, but it has to be completed by other factors considering the nature of the different constituing elements. Based on these results, we derived a new empirical law, linking compositional parameters to the degree of polymerization of the glass and instrumental fractionation. In Fe-free compositions, instrumental mass fractionation, spanning more than 20‰ in $\delta^{30}Si$ and $\delta^{44}Ca$, can be accurately corrected using this method. After correction, the dispersion of the results is less than 1‰ around the mean value, and this correction is much more successful than other proxies previously used (SiO_2 content, NBO/T,...). Correcting instrumental fractionation effects in glasses containing Fe is more complex since this element can occur in several oxidation states in glasses.

https://doi.org/10.1180/S0026461X00006502 Published online by Cambridge University Press

Hydrogeochemistry, groundwater quality and pollution potential studies of Satna City, Madhya Pradesh, India

R.N.T. TIWARI RABINDRA

Department of Geology, Government P.G. Science College, Rewa – 486001 Madhya Pradesh, India (rntiwari03@rediffmail.com)

Hydrogeochemical investigations were carried out in Satna City (Latitude 230 58' : 240 30'N, Longitude 80 0 21' : 81 0 23') Madhya Pradesh, India. In the study area, Limestones of Bhander Group, Vindhyan Supergroup (Neoproterozoic) are exposed. A total of 30 groundwater samples were collected during Post-monsoon season of 2010 and subjected to analysis for chemical characteristics. The main hydrochemical facies are Ca-Mg-HCO_3 and Ca-Mg-SO_4 –cl types. As per classification, most of the samples are normal chloride, normal carbonate, moderate to very hard in nature. The concentration of sulphate was higher due to gypsum bands associated with shale formation. In few samples concentration of fluoride exceeds maximum permissible limit (>1.5 mg/l) due to fluorite bearing mineral associated with aquifer. The concentration of nitrate in groundwater samples of the area is also exceeded beyond the permissible limit of 45mg/l. The consumption of water having nitrate concentration in excess of 100 mg/l may reduce the oxygen carrying capacity of the blood, particularly in infants causing infantile methemoglobinaemia. The analytical results reveal that most of the samples containing high nitrate also have high chloride and potash. In the absence of a possible geogenic source of chloride in the area, application of nitrogen rich fertilizer seem to be possible source. The comparison of analysed data with WHO (1984) and ISI (1991) indicate that groundwater samples of the area are more or less suitable for drinking.

Besides these, pollution potential has been estimated by DRASTIC modeling which suggests that the area is highly susceptible to pollution. A proper attention and water quality programme is needed to check the groundwater pollution.

EBSD Study of Lattice Preferred Orientation (LPO) of the harzburgite NWA 5480

B.J. TKALCEC* AND F.E. BRENKER

Goethe University, Geoscience Institute, 60438 Frankfurt, Germany (*correspondence: tkalcec@em.uni-frankfurt.de)

Classified as belonging to the Howardite-Eucrite-Diogenite (HED) group of achondrites, the olivine-rich diogenite Northwest Africa 5480 is thought to represent an ultramafic cumulate formed within a magma chamber in the upper mantle of the differentiated asteroid 4 Vesta, or a Vesta-like body [1]. Dominated by olivine (57 vol%) and orthopyroxene (42 vol%) NWA 5480 has further been classified a harzburgite [2], whereby the distribution of olivine and orthopyroxene is very heterogeneous, with some areas displaying up to 90% of either of the two minerals. In this study, structural analysis was performed on the olivine grains of NWA 5480 using electron backscatter diffraction (EBSD), which allows us to measure and visualize the crystallographic orientation of the crystal axes to discover any lattice preferred orientation (LPO) [3]. The sample was categorized into two regions for targeted analysis: (a) Zone A, dominated by coarse-grained olivine, and (b) Zone B, dominated by orthopyroxene-olivine schlieren. A total of 1361 EBSD crystallographic orientation measurements of coarse-grained olivine were recorded from 58 sites (each site covering 1 mm2) within Zone A and a total of 148 measurements of finer-grained olivine were recorded from 20 sites within Zone B. Only EBSD measurements with a mean angular deviation (MAD) of <1 were accepted and recorded. The EBSD results of Zones A and B display pronounced yet distinctly differing LPOs, suggesting two separate deformation processes and/or events. A comparison with olivine LPO in terrestrial cumulates and deformed mantle peridotites illustrates the unlikeliness that the olivine LPO from Zone A of NWA 5480 was formed through cumulation or compaction processes. In contrast, a distinct similarity to the olivine LPO formed by pencil glide ((0kl)[100] glide system), typical of plastic deformation in the terrestrial mantle, causes us to consider alternative formation processes for NWA 5480, including the feasibility of convection within the Vestan mantle.

[1] McSween Jr. H. (2010) *Space Sci Rev* DOI 10.1007/s11214-010-9637-z. [2] Beck, A. & McSween, H.Y. Jr. (2010) *Meteoritics & Planetary Science* **45**, 850–872. [3] Prior, D. *et al*. (1999) *Amercian Mineralogist* **84**, 1741–1759.

https://doi.org/10.1180/S0026461X00006502 Published online by Cambridge University Press

Splittings, satellites and fine structure in the soft X-ray spectroscopy of the actinides

J.G. TOBIN

Lawrence Livermore National Laboratory, Livermore, CA, USA, (Tobin1@LLNL.Gov)

Despite the limitations imposed by their sometimes high levels of radioactivity, there has recently been remarkable progress in the soft X-ray spectroscopy of the actinides, particularly that of Plutonium (Pu) and Uranium (U). For example, synchrotron-radiation-based X-ray absorption spectroscopy (XAS) and X-ray photoelectron spectroscopy (XPS) played important roles in the progress of the understanding of Pu electronic structure, [1-5] leaving only the last issue of electron correlation before a complete understanding is achieved. [6] Two examples of the manifestations of the large spin-orbit splitting in the 5f states are (1) the large disparity in the 4d branching ratios of Pu and U (Fig 1.), and (2) the presence of the pre-peak structure in U and its absence in Pu. Even more recently, we have begun experiments upon the important nuclear fuel system UO_2, [7-9] which also exhibits strong electron correlation. [7] Our new measurements using Resonant Inverse Photoelectron Spectroscopy (RIPES) and X-ray Emission Spectroscopy (XES) [10] indicate new satellite structure, to complement that already observed in XPS [9] and XAS. [7, 8]

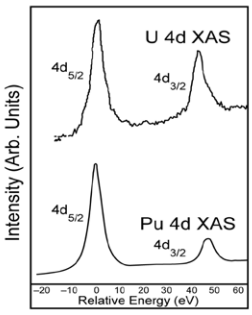

Figure 1 Comparison of the 4d XAS in elemental U and elemental Pu. From Ref 5.

Lawrence Livermore National Laboratory is operated by Lawrence Livermore National Security, LLC, for the U.S. Dept of Energy, Natl Nuclear Security Admin. under Contract DE-AC52-07NA27344. This work was supported by the DOE Office of Science, Office of Basic Energy Science, Division of Materials Science and Eng.

[1] J.G. Tobin *et al*. (2003) *Phys. Rev. B* **68**, 155109. [2] K.T. Moore *et al*. (2003) *Phys. Rev. Lett*. **90**, 196404. [3] G. van der Laan *et al*. (2004) *Phys. Rev. Lett*. **93**, 097401. [4] J.G. Tobin *et al*. (2005) *Phys. Rev. B* **72**, 085109. [5] J.G. Tobin *et al*. (2008) *J. Phys. Cond. Matter* **20**, 125204. [6] S.W. Yu *et al*. (2008) *J. Phys. Cond. Matter* **20**, 422202. [7] S.-W. Yu *et al*. (2011) *Phys. Rev. B* **83**, xxxxxx. [8] G. Kalkowski *et al*. (1987) *Phys. Rev. B* **35**, 2667. [9] S.-W. Yu & J.G. Tobin, (2011) *J. Vac Sci. Tech. A* **29**, 021008. [10] J.G. Tobin *et al*. (2011) *Phys. Rev B* **83**, 085104.

Plugging of porous media and rock fractures using ureolysis-driven calcite precipitation

D.J. TOBLER* AND V.R. PHOENIX

School of Geographical and Earth Sciences, University of Glasgow, Glasgow, G12 8QQ, UK (*correspondence: dominique.tobler@glasgow.ac.uk)

Ureolysis-driven calcite precipitation has shown great potential in a wide range of applications, including solid-phase capture, concrete crack remediation, soil stabilisation and carbon sequestration. Here, this process is investigated as a means of reducing the primary porosity and/or secondary fracture porosity of host rocks surrounding nuclear waste repositories in order to control or prevent radionuclide transport. Several studies have used simple sand column experiments to determine the best approach to plug pore spaces between grains; however, a field deployable approach that ensures a homogenous and stable seal has not yet emerged. Furthermore, there is no study that assessed the potential of this method to seal rock fractures. This is important as the hydraulic regime in fractures is very different compared to grain porosity.

Here, flow-through experiments in various media (sand columns, fractured / non-fractured rock cores) were carried out to examine the potential of ureolysis–driven calcite precipitation to seal primary and secondary porosity effectively and homogenously. The 'plugging efficiency' was examined as a function of varying injection strategies, flow rate, urea and Ca^{2+} concentration and the addition of a grout (e.g. silica nanoparticles). The temporal change in porosity was monitored by the decrease in hydraulic conductivity, and the local spatial distribution of the calcite fill was quantified using scanning electron microscopy.

Results from sand column / sandstone rock core experiments show that under continuous flow conditions, a gradient in calcite fill developed along the flow path of the column / core. In contrast, static conditions (i.e. no flow) permitted the reaction to occur homogenously throughout the column / core resulting in a stable plug. Note that under both static and continuous flow conditions, new bacteria needed to be injected every 1-2 days due to embedment of the bacteria within the forming precipitates. Initial results from fractured rock core experiments indicate that bacteria less likely 'attach' to fracture surfaces, which significantly lowers rates of ureolysis and calcite precipitation within the fracture. The use of a saline fixative and varying flow rates will be tested to increase the reaction yield.

https://doi.org/10.1180/S0026461X00006502 Published online by Cambridge University Press

A variably enriched mantle wedge and contrasting melt types during arc stages following subduction initiation in the southwest Pacific

ERIN TODD[1], JAMES B. GILL[2] AND JULIAN A. PEARCE[3]

[1]Dept. of Earth and Planetary Sciences, University of California, Santa Cruz, USA (todd.erin@gmail.com)
[2]Dept. of Earth and Planetary Sciences, University of California, Santa Cruz, USA (jgill@pmc.ucsc.edu)
[3]School of Earth, Ocean and Planetary Sciences, Cardiff University, Cardiff, CF10 3YE, UK (PearceJA@cardiff.ac.uk)

Mantle sources at the initiation of Vitiaz arc magmatism in the SW Pacific (≥45Ma) have isotope ratios similar to the mantle currently underlying the Havre Trough and adjacent back-arc basins. The early Vitiaz melt source was not only a mixture of depleted mantle plus small amounts of slab-derived component, but also includes an enriched FOZO component that makes it 'Pacific' in character. This old enriched component anchored SW Pacific arcs untils opening of the Lau Basin. Preferential melting of the enriched component leaves a more depleted residue. The Vitiaz nascent- and proto-arc, preserved in subaerial Eocene to lower-Oligocene rocks in Viti Levu, Fiji and 'Eua, Tonga, are similar in age and magma types to the earliest Izu-Bonin-Mariana (IBM) arc. Like IBM, Yavuna and 'Eua basalts range from boninitic to tholeiitic in composition. 'Eua is LREE-depleted whereas Yavuna ranges from LREE-depleted to LREE-enriched. The early arc was characterized by extreme variations in HFSE and HREE, reflecting large variations in percent melting, extending to very high degree melting necessary to generate low boninitic trace-element concentrations. Early bonintic melts have a more enriched quality (isotopically and in LREE/HREE) than tholeiitic melts. The end of Yavuna arc magmatism coincides with formation of the South Fiji Basin (SFB) (~20-30 Ma). Rocks of the Yavuna Group are unconformably overlain by late Oligocene to early Miocene rocks of the Wainimala Group, so 'second arc' edifices were at least in part deposited on Eocene to early Oligocene arc basement. Yavuna and Wainimala rocks show similar ranges for $^{143}Nd/^{144}Nd$ but variation in $^{176}Hf/^{177}Hf$ defines an array steeper than the Mantle Array in Hf-Nd isotope space. Higher $^{176}Hf/^{177}Hf$ ratios for Wainimala rocks indicate a more depleted source mantle than existed prior to SFB spreading.

Magmatic evolution of lunar highland rocks estimated from trace elements of plagioclase in regolith

S. TOGASHI[1], N.T. KITA[2], A. TOMIYA[1] AND Y. MORISHITA[1]

[1]Geological Survey of Japan, AIST, Tsukuba 305-8567, Japan (*correspondence: s-togashi@aist.go.jp)
[2]Department of Geoscience, University of Wisconsin, Madison 1215 W. Dayton Street, Madison, WI 53706-1692, USA (noriko@geology.wisc.edu)

SIMS analyses of plagioclases and the host magma

The SIMS trace element analyses of plagioclases in lunar regolith are performed in order to estimate compositions of host magmas of FAN and Mg-suite rocks. We reexamined partition coefficients of trace elements between plagioclase and magma by taking account of the compositional dependence. The estimated host magmas of FAN have low Ba (48-115ppm), Sr (90-152ppm), and TiO_2 (0.5 to 1.3%).

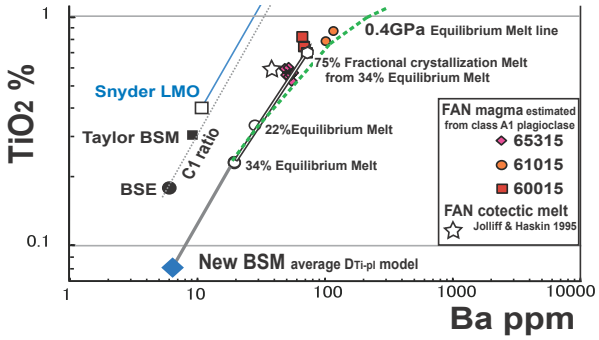

Figure 1: The estimated host magmas of FAN. Snyder LMO [1], Taylor BSM [2], FAN cotectic melt [3]

Model for FAN magma evolution

We developed an igneous evolution model for magmas of FAN and Mg-suite rocks by using phase relations based on MELTS program. We propose a new Bulk Silicate Moon (BSM) model with high Al_2O_3 (6.1%), sub-chondritic Sr/Al and Ti/Ba ratios and chondritic Sr/Ba ratios. High degrees (22-34% or more) of equilibrium melting of the BSM could produce the primary FAN magma under high pressure (0.4-3GPa), whether the BSM is partially or totally molten at the initial stage.

[1] Snyder *et al*. (1992) *GCA* **56**, 3809–3823. [2] Taylor (1982) *Planetary science*. 481p. [3] Jolliff & Haskin (1995) *GCA* **59**, 2345–2374.

https://doi.org/10.1180/S0026461X00006502 Published online by Cambridge University Press

Transformation of iodide to organic iodine in soil-water system

Y.S. TOGO[1,2] AND Y. TAKAHASHI[1]

[1]Hiroshima University, Hiroshima 739-8526, Japan (yoko-togo@aist.go.jp, ytakaha@hiroshima-u.ac.jp)
[2]National Institute of Advanced Industrial Science and Technology, Ibaraki 305-8567, Japan

Iodine is an important trace element for human beings according to the following reason: (i) iodine deficiency is one of the world's most prevalent disease, (ii) radioactive iodine can be released by the use of nuclear energy. To predict iodine behavior in natural systems, speciation of iodine is essential because mobility of iodine is different among each species. In this study, we determined chemical forms of iodine in soil and pore water using X-ray absorption near edge structure (XANES) and high performance liquid chromatography (HPLC)-ICP-MS, respectively.

Materials and methods

Soil and pore water samples were collected at five depths: 0, 3, 6, 9, and 12 cm under flooded condition in Yoro area, Chiba, Japan. Brine water, which contained I^-, was supplied from top of the soil column. Iodine concentration in soil samples were determined by alkaline extraction method [1]. Chemical forms of iodine in soil were deterined by K-edge XANES (SPring-8, BL01B1) [2]. Iodine mapping of soil grain was obtained at beamline 37XU (SPring-8) by a micro-XRF technique. Iodide, iodate, and organic iodine in pore water were separaterly detected by HPLC-ICP-MS using anion exchange column and size exclusion column. Soil incubation experiments were performned using soil collected at 3 cm depth (soil : Milli-Q water = 1 : 1) under oxic and unoxic conditions.

Results and Discussion

Concentration of iodine in soil was highly correlated with that of organic carbon content. According to XANES and micro-XRF, iodine in soil exists as organic iodine at any depths. On the other hand, pore water collected at a 0–6 cm depth containing 50–60% of organic iodine bound to dissolved organic matter and the rest was I^-. At a 9–12 cm depth, 98% of iodine was I^- in the aqueous phase. The distribution coefficient of organic iodine in the soil-water system was more than 10-fold greater than that of iodide. Soil incubation experiments demonstrated that dissociation of iodine from organic iodine to I^- occurred under anoxic condition. Mobility of iodine is strongly affected by organification of iodine under oxic condition and dissociation from organic matter as I^- under anoxic condition.

[1] Yamada *et al*. (1996) *Soil Sci. Plant Nutr*. **42**, 859–866.
[2] Shimamoto & Takahashi (2008) *Anal. Sci*. **24**, 405–409.
[3] Shimamoto *et al*. *Environ. Sci. Technol*. in press.

Comparison of ^{4}He and ^{14}C dating, noble-gas temperatures and stable isotope (δ^2H, δ^{18}O) data for groundwater in stratified aquifers (Tomsk-7, S.E. Siberia)

I.V. TOKAREV[1]*, R. KIPFER[2,3], Y. TOMONAGA[2], M.S. BRENNWALD[2] AND E.A. VERESCHAGINA[1]

[1]IEG RAS, Sredniy 41, of. 519, Saint-Petersburg, 199004 (*correspondence: tokarevigor@gmail.com)
[2]Eawag, Swiss Federal Institute of Aquatic Science and Technology, CH-8600 Dübendorf
[3]Institute of Geochemistry and Petrology, Swiss Federal Institute of Technology (ETH), CH-8092 Zürich

The groundwater of six stacked aquifers in the south-eastern part of Siberia near the former Tomsk-7 nuclear research facility has been studied.

Groundwater ages were estimated by ^{4}He concentrations and ^{14}C-activities, and paleoclimate conditions were reconstructed using dissolved noble gas concentrations (and the corresponding noble-gas temperatures) in combination with stable isotope data (δ^2H, δ^{18}O) [1, 2].

^{4}He ages of the four lower aquifers vary from 2 to 15 ka, and increase with depth and along the flow path with increasing distance from the recharge area. Depleted δ^2H, δ^{18}O as well as noble-gas concentrations based recharge temperatures of 0.5-2 °C indicate that the water infiltrated during cold climate state. Such cold climate conditions prevailed in the studied region between 5 and18 ka BP.

In general, ^{14}C-ages for the four lower aquifers are consistent with the He-ages (6-33 ka), whereby the ^{14}C ages tend to be higher than He-ages. The estimation of the ^{14}C-ages is quite robust as the aquifer matrix hardly contains any carbonates. The age difference can be explained by uncertainties in the calculation of the He-ages, which is strongly depends on the assumed aquifer porosity. The mean porosity is only vaguely known due the interbedding of sands and clays.

A strong shift of δ^2H and δ^{18}O data in the upper aquifer layers indicates that these layers were temporarily frozen during the Younger Dryas.

In conclusion, stable isotopes, noble-gas temperatures, and dating show consistent results and can be used to analyze groundwater dynamics on large time scales and to validate conceptual and numerical groundwater models.

[1] Tokarev *et al*. (2009a) *Water Res*. **36**, (2) 206–213.
[2] Tokarev *et al*. (2009b) *Water Res*. **36**, (3) 339–350.

https://doi.org/10.1180/S0026461X00006502 Published online by Cambridge University Press

Geochemical modeling for boron removal by a permeable reactive barrier using magnesium oxide

C. TOKORO[1]*, J. KURAMI[1], S. MORIYAMA[2] AND K. SASAKI[2]

[1]Waseda University, Tokyo 169-8555, Japan (*correspondance: tokoro@waseda.jp, nightmarev.dtk@akane.waseda.jp)

[2]Kyusyu University, Fukuoka 819-0395, Japan (s-moriyama09@mine.kyushu-u.ac.jp, keikos@mine.kyushu-u.ac.jp)

Geochemical models for boron removal by magnesium oxide was constructed from experimental results obtained in batch test [1]. Partial dissolution of magnesium oxide, precipitation of brucite and MgB $(OH)_5$, and complex ion formation of MgB $(OH)_4^+$ were considered. First order kinetics were also considerd for precipitation or disolution of these minerals. These models successfully expressed experimental results of pH and concentration of boron/magnesium ion in solution.

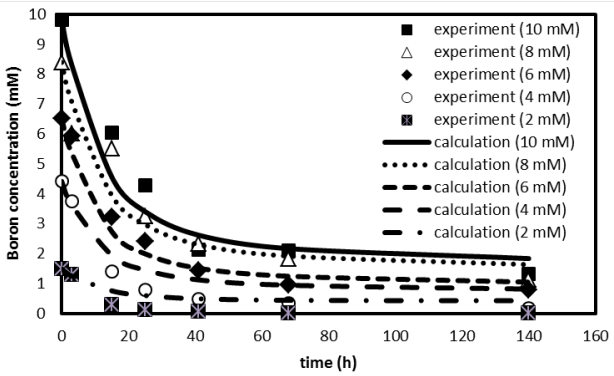

Figure 1: Comparison between experimental data and geochemical model analysis for boron concentarion change over time.

The above model was also confirmed to fit to the observed data in continuous column tests in combination with one dimensional advection-diffusion equation. This model is practically useful to predict the long term performance of PRB to treat borate using MgO for several decades.

[1] Sasaki *et al*. (2011) *J. Hazard. Mater* **185**, 1440–1447.

Physicochemical controls on adsorbed water film thicknesses in unsaturated porous media

TETSU K. TOKUNAGA

Earth Sciences Division, Lawrence Berkeley National Laboratory, Berkeley, CA 94720, USA (tktokunaga@lbl.gov)

Large volumes of Earth's subsurface contain pores with water present as wetting films residing between mineral surfaces and a nonwetting fluid. These variably water-saturated environments include soils, deep unsaturated rock formations, and deep reservoirs containing hydrocarbons and CO_2. Water in these environments is retained by both capillarity and adsorption, with the adsorptive component most sensitive to solution chemistry and interfacial properties at both solid-water and water-fluid (gas, immiscible liquid, or supercritical fluid) interfaces. It is important to understand how the thickness of adsorbed water films varies with system properties because film thickness can control flow and transport within the aqueous phase, and because reactions at mineral surfaces are strongly influenced by the contacting fluid phase. The thickness of films is dependent on the component of the wetting phase chemical potential denoted the matric potential in soils and the disjoining (capillary) potential in deep reservoirs. The Derjaguin-Landau-Verwey-Overbeek (DLVO) theory combines electrostatic and van der Waals contributions to predict water film potential versus thickness relations, and is frequently applied in studies of mineral-water-mineral and mineral-water-hydrocarbon systems. However, adsorbed water films confined between mineral surfaces and nonwetting fluid phases are not present over the full range of disjoining potentials because a pore scale dependent threshold capillary pressure needs to be exceeded to allow coexisitence of both fluid phases in pores. In this study, capillary scaling [1] is used to predict ranges of matric (disjoining) potentials within which adsorbed water films can exist in gas-water-mineral systems and in supercritical CO_2-water-mineral systems [2]. We then apply DLVO models to calculate adsorbed water film thicknesses in these systems [3]. These calculations predict that under many conditions found in the subsurface, thicknesses of adsorbed water films are less than 20 nm. Moreover, the calculations predict a very wide range of potentials over which thicknesses of adsorbed films are less than 2 nm.

[1] Miller & Miller (1956) *J. Appl. Phys.* **4**, 324–332.
[2] Tokunaga (2009) *Water Resour. Res.* **45**, W06415.
[3] Tokunaga (in review, *Water Resour. Res.*)

https://doi.org/10.1180/S0026461X00006502 Published online by Cambridge University Press

Mantle degassing rates and gas loss from atmosphere: A view from xenology

I. TOLSTIKHIN[1]*, B. MARTY[2] AND A. HOFMANN[3]

[1]Geological Institute, RAS, Apatity, and Space Research Institute, RAS, Moscow, Russia (*correspondence: igor.tolstikhin@gmail.com)
[2]CRPG-CNRS, 54501 Vandoeuvre-Les-Nancy, France
[3]Max-Planck-Institut für Chemie D-55128 Mainz, Germany

To understand evolution of gas species of the Earth - atmosphere system, ^{244}Pu-^{238}U-Xe systematic is crucial and must be included in any model related to gas loss / gain by the Earth reservoirs. The initial ^{244}Pu/^{238}U = 0.01 in meteorites and terrestrial zircons [1] is known; correspondingly the closed-system ^{136}Xe (Pu)/^{136}Xe (U)= 40. These ratios, bulk silicate earth [^{238}U] = 38 ppb, present day ^{136}Xe (Pu) / ^{136}Xe (U) ≤ 0.2, proposed for the mantle [2, 3], and amount of ^{136}Xe (Pu) ≤ 0.05 tmol in the atmosphere, constrain the evolution of terrestrial volatiles.

(1) The MORB-source mantle (one reservoir model is considered) has been degassed severely, so that only about 0.01% of the initially available Xe has survived 4.5 Gyr long degassing [4, 5]). Recent degassing models based on U-Th-He and K-Ar systems, e.g. [6], postulate a low degassing and are inconsistent with this constraint. (2) This model predicts a late time for the atmosphere closure to Xe loss, about 4 Gyr ago, and simultaneous loss of other gases, which seems highly improbable. Introducing into the deep earth an early, small, less-degassed, nearly-isolated reservoir allows reconciliation of observed and modelled noble gas abundances in the Earth [5].

[1] Turner *et al*. (2007) *EPSL* **261**, 491–499. [2] (Kunz *et al*. (1998) *Science* **280**, 877–880. [3] Caffee *et al*. (1999) *Science* **280**, 877–880. [4] Tolstikhin & Marty (1998) *Chem. Geol*. **147**, 27–52. [5] Tolstikhin *et al*. (2006) *Chem. Geol*. **226**, 79–99. [6] Gonnermann & Mukhopadhyay (2009) *Nature* **459**, 560–564.

Albitite related to iron oxide mineralization: Melt inclusion evidence for a magmatic origin

C.M. TOMÉ[1]*, F. TORNOS[1] AND M. WÄLLE[2]

[1]Instituto Geológico y Minero de España, Madrid, Spain (*correspondence: c.tome@igme.es)
[2]Institut of Geochemistry and Petrolgy, ETH, Zurich, Switzerland

Albitite is an uncommon rock present in very different geological settings. The dominant mineralogy consists almost entirely by albite and quartz with some other accessories but, despite its simple mineralogy, this rock is of unclear origin. A metasomatic source is dominantly proposed, especially for the albitite related to iron oxide, W-Sn and Nb-Ta-Zr-REE-rich mineralization. There are only few studies that propose a magmatic origin for this rock, usually in ophiolitic complexes. In this study we describe some large intrusive mesozonal bodies of porphyritic albitite related to magnetite mineralization in the Ossa Morena Zone (SW Spain) and we report the existence of true silicate melt inclusions in this type of rocks. These melt inclusion data indicate that the rocks are primary and not metasomatic in origin.

Crystallized silicate melt inclusions in phenocrysts of quartz in both fresh or slightly altered albitite were analyzed by LA-ICPMS. Melt inclusion show an 'albitic' composition with SiO_2 (72%), Al_2O_3 (13%) and Na_2O (8%) as major elements. In agreement with the compatibility model, trace elements such as Sr, Ba, V, Zr, P and other major elements like Ti and Mg are compatible with the bulk-mineralogy of the rock whereas incompatible elements as well as ore metals stay in the residual melt represented by the melt inclusions. The quartz phenocrysts also show some sporadic magnetite blebs coexisting with the silicate melt inclusions, suggesting the existence of an iron oxide melt phase segregated from the silicate melt and related to the formation of the mineralization.

This melt inclusion study toghether with the field relationships and the petrography demonstrates that not all the albitite related to iron oxide mineralization is a consequence of the pervasive sodic alteration of previous plutonic rocks but also product of highly differenciated felsic magmas. We also adress the posible link between these melts and the formation of magmatic and hydrothermal magnetite mineralization.

https://doi.org/10.1180/S0026461X00006502 Published online by Cambridge University Press

Experiments on the wetting properties of precious metal-rich sulfosalt melts against MSS

ANDREW G. TOMKINS

School of Geosciences, Monash University, Clayton 3800 Victoria, Australia (andy.tomkins@monsh.edu)

In a significant proportion of magmatic sulfide ore deposits, Pt, Pd, Au and Ag (precious metals), correlate strongly with As, Bi, Sb and Te. In these deposits, the majority of the precious metals can be locked in platinum-group minerals (PGM). The majority of these PGM consist of Pt and Pd complexed with one or more of the semi-metals As, Sb, Bi and Te. In addition, domains rich in non-PGM sulfarsenides, such as gersdorffite and nickeline, with very high precious metal concentrations are found within some ores. These observations imply that these semi-metals play a critical role in controlling the distribution of precious metals in some deposits.

Piston cylinder experiments have been used to study the wetting behavior of As-rich sulfosalt melts against monosulfide solid solution (MSS). This is important information because the wetting propoerties of a melt against its solid crystal framework control melt migration processes; a wetting melt requires about an order of magnitude less volume than a non-wetting melt to form an interconnected permeable melt network, which allows melt migration.

Experiments show that range of As-rich melt compositions wet MSS, including those that contain significant proportions (1 – 45%) of precious metals. Interestingly, sulfosalt melts that are extremely Au-rich or Pt-rich (> ~40% Au; > ~ 50% Pt + 5% Au) do not wet MSS. These results imply that if a late stage As-rich sulfosalt melt is able to form either through magma contamination with something like carbonaceous shale (which tend to be As-rich), or simply through fractionation of the sulfide melt (many sulfosalt minerals crystallise at lower temperatures than MSS) it should preferentially partition incompatible Bi, Sb, Te, Pt, Pd, Au and Ag. Furthermore, where the proportion of As-rich sulfosalt melt exceeds ~ 0.2% of the rock volume, an interconnected melt drainage network will be able to form along MSS crystal triple junctions. Because sulfarsenide melt is significantly more dense than MSS, it would then be able to drain downwards, further scavenging precious metals. The greater the length of this melt migration pathway, the more effective the enrichment in precious metals. Ultimately, very precious metal rich sulfosalt melt accumulations can form by this mechanism. When such a sulfosalt melt fractionates as it migrates, a spectrum of PGM would result.

Noble gases in the sediment pore water as proxies for physical transport processes and past environmental conditions in Lake Van?

Y. TOMONAGA[1]*, M.S. BRENNWALD[1] AND R. KIPFER[1,2]

[1]Eawag, Swiss Federal Institute of Aquatic Science and Technology, CH-8600 Dübendorf, Switzerland (*correspondence: tomonaga@eawag.ch)

[2]Institute of Geochemistry and Petrology, Swiss Federal Institute of Technology (ETH), CH-8092 Zurich, Switzerland

Since many decades unconsolidated sediments in lakes and oceans have been proposed as a potential archive for noble-gas records to reconstruct past environmental conditions in lakes and oceans. In addition, the accumulation of non-atmospheric noble-gas isotopes allows tracing the geochemical origin and transport processes of the pore fluids. For instance, the abundance of terrigenic He isotopes reflects the residence time and transport dynamics of the pore fluids in the sediment. The $^{3}He/^{4}He$ ratio of terrigenic He can be used to constrain the geochemical origin of the pore fluids. However, methods for reliable noble-gas analysis in sediment pore water have been developed only recently.

Lake Van (Turkey) is one of the largest terminal lakes and the largest soda lake on Earth. The physical conditions of the lake are known to react sensitively to changes in the hydrological cycle and the environmental conditions of the lake catchment. Therefore the noble-gas records in the sediments of Lake Van have a great potential as an archive for palaeoenvironmental research. Also, the basin of Lake Van is situated in a tectonically active region characterized by the presence of major faults and volcanos. The lake is known to accumulate mantle fluids. Noble-gas isotopes are therefore useful to study the origin and transport processes of terrigenic fluids in the sediment pore space and their release into the water body.

In this study we present noble-gas data measured in the pore water of sediment samples collected in Lake Van. On the one hand, data from short cores taken at different sites throughout the lake basin will be discussed. Furthermore, we intend to present first results from the noble-gas samples taken from a 220 m long core during the 2010 ICDP drilling operations of the PALEOVAN project.

https://doi.org/10.1180/S0026461X00006502 Published online by Cambridge University Press

Iron microbial mat formation from deep continental brines

BRANDY M. TONER[1]*, LINDSEY J. BRISCOE[1], F. MARC MICHEL[2], SCOTT C. ALEXANDER[3], E. CALVIN ALEXANDER JR.[3] AND JEFFREY A. GRALNICK[4]

[1]Department of Soil, Water and Climate, University of Minnesota, St. Paul, MN, USA (*correspondence: toner@umn.edu)
[2]Geological and Environmental Sciences, Stanford University, Stanford, CA, USA
[3]Department of Earth Sciences, University of Minnesota, Minneapolis, MN, USA
[4]Department of Microbiology, BioTechnology Institute, University of Minnesota, St. Paul, MN, USA

Iron oxidizing microorganisms are distributed globally and have been identified as major contributors to iron cycling and mineral formation from diverse geochemical settings – freshwater seeps to deep-sea vents – where ever opposing iron(II)-oxygen gradients prevail. A study of iron microbial mat formation from deep continental groundwaters along anoxic-oxic boundaries has been undertaken. The goals of the research are to define microbial niches created at acute geochemical gradients, and determine how microbial activity alters the mineralogy of mat deposits.

Iron microbial mat processes occur at 700 m depth where anoxic brines emerge from exploratory boreholes into an oxic, mined environment (Soudan Underground Mine State Park, Soudan, MN, USA) within a 2.7 Ga Banded Iron Formation. These sodium-calcium chloride brines are characterized by 100 mS conductivity, pH 6+, -650 mV oxidation-reduction (redox) potential, and total dissolved iron concentrations of 100 mg/L. As the brines equilibrate with the atmosphere in shallow flow channels over ~100 m distance, the pH decreases to 2.8, redox potential increases to +50 mV, and total dissolved iron decreases to less than 40 mg/L. Along these gradients, iron mat formations with diverse facies characteristics and mineralogy are observed.

For minerals from the first 100 m of the channels, iron 1s extended X-ray absorption fine structure spectroscopy and X-ray scattering measurements reveal the presence of akaganeite in all samples, as well as a transition from a biogenic iron oxyhydroxide to ferrihydrite/goethite. Scanning electron microscopy of critical point dried samples shows that microbial biomass is a substantial component of the mat at 0.3 m from the borehole where low redox potential is observed. From this low redox area, cultured isolates from the genus *Marinobacter* and genus *Idiomarina* were obtained. In seeps having lower conductivity, different cultivars and minerals are observed. These results point to salinity as an important factor in the geomicrobiology of the iron mats.

Late Cretaceous hydrocarbon seep carbonates from Kardoi village, Tibet, China

HONGPENG TONG[1,2], YOUYAN BIAN[1,2], DONG FENG[1] AND DUOFU CHEN[1]*

[1]Key Laboratory of Marginal Sea Geology, Guangzhou Institute of Geochemistry, CAS, Guangzhou 510640, China (*correspondence: cdf@gig.ac.cn)
[2]Graduate University of the Chinese Academy of Sciences, Beijing 100049, China

One of the most common signs of the hydrocarbon seeps is the precipitation of carbonates close to the seafloor. Ancient hydrocarbon seeps are increasingly recognized, and occur in a variety of different marine settings and on different regional scales. However, such hydrocarbon seeps are rarely found in ancient strata of the mainland China. Here, we report two isolated carbonate bodies that have been interpreted to represent hydrocarbon-seep deposits. These deposits are in the upper Cretaceous strata at the southern and the northern Kardoi village of Xigaze, Tibet, China. The upper Cretaceous strata here consist of turbidites of a forearc basin, which has been uplifted into Yarlung Zangbo suture zone. The seep carbonates at the southern Kardoi section are about 30 vol% of the strata, occurring as nodules and chimneys while the seep carbonates at the northern Kardoi section mainly occur as nodules and account for about 10 vol% of the turbidite strata. Carbonate rocks from both sections are mainly composed of calcite, in sharp contrast to the host rocks which primarily are felsic minerals. The matrix of the carbonates mainly consists of micritic calcite. Framboid pyrites are frequently observed in the matrix. The carbonates exhibit $\delta^{13}C$ values as low as -32‰ relative to the V-PDB standard, suggesting that they are predominantly hydrocarbon derived, probably thermogenic methane. Overall, the carbonate fabrics and isotope signatures provide unequivocal evidences for a seep origin of the Xigaze deposits. Additional geochemical, mineralogical and petrographic studies of all micritic carbonates are underway. The obtained results will be used for constraining the controlling processes of the two geographically separated southern and northern sections.

We thank Prof. Chi-yue Huang (GIG) for helpful discussion. This work was partially supported by the NSFC (40872079 and 40725011) and Guangzhou Institute of Geochemistry of CAS (GIGCX-07-13).

https://doi.org/10.1180/S0026461X00006502 Published online by Cambridge University Press

Topographic confocal Raman microscopy. Established methods – Novel concepts – New possibilities

J. TOPORSKI AND T. DIEING

(jan.toporski@witec.de, thomas.dieing@witec.de)

Confocal Raman microscopy has found increasing relevance over the past years in various field of application in geo- and/or geobiology research. The benefit of obtaining molecular, compositional information on the submicron-scale in three dimensions is of tremendous use yet thus far slightly alleviated by that “large” topography in the range of hundreds of micron or millimeters could not be analyzed without sample pretreatment, i.e. cutting or polishing to obtain a sufficiently flat surface. The new technique of Topographic Confocal Raman Imaging now allows analysis of rough surfaces or tilted samples.

The core element of this imaging mode is an integrated sensor for optical profilometry. Large-area topographic coordinates from the profilometer measurement are correlated with the large-area confocal Raman imaging data. This allows confocal Raman imaging along inclined or rough samples with the true surface held in constant focus while maintaining high level of confocality. The profilometry capabilities of True Surface Imaging mode allows scan ranges of up to 50x100 mm with a spatial resolution on the order of 100 nm vertically and 10 μm laterally. Measuring distances of 10 mm and more provide flexibility for variable sample size requirements. In combination with AFM, the profilometer can even be used as a pre-inspection tool to determine topographic features of interest for high-resolution AFM investigations on large samples.

The potential and examples for Geoscience applications will be shown.

Revisiting the influence of particle size on the equilibrium composition

D. TOPPING[1,2]* AND G. MCFIGGANS[1]

[1]Centre for Atmospheric Science, University of Manchester, UK (*correspondence: david.topping@manchester.ac.uk)
[2]National Centre for Atmospheric Science, University of Manchester, UK

Introduction

Atmospheric aerosol particles can comprise many thousands of largely unidentified compounds with a wide range of properties. The size of an aerosol particle influences the equilibrium composition and phase state for a given set of ambient conditions and availability of semi-volatile material. Incorporating the influence of curvature in theoretical constructs can be complex. Unfortunately, basic absorptive equilibrium partitioning models largely neglect the influence of curvature, leading to errors in predicted composition and volatility for conditions in which size is likely to play an important role: new particle formation in the atmosphere or unseeded experiments in smog chambers.

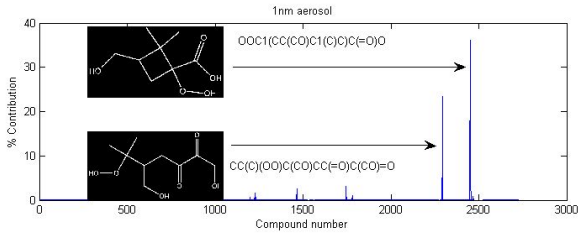

Figure 1: Example of identification of top two compounds contributing to the condensed phase abundance for a 2nm diameter aerosol.

Discussion of Results

In this study we present application of a partitioning model that explicitly accounts for impact of curvature on the equilibrium position for particles of any size and comprised of an unlimited number of compounds. Using results from state-of-the-art gas phase degradation models and property predictive techniques, we are able to explore generalised relationships between, for example, expected aerosol functionality and particle size (e.g. Figure 1). A discussion of the caveats behind this approach is given, along with pitfalls of not explictly accounting for aerosol size in previously applied predictive frameworks with potential impacts of subsequent aerosol properties.

https://doi.org/10.1180/S0026461X00006502 Published online by Cambridge University Press

Provenance and grain size effects of siliciclastic sediments in the Dead Sea basin from Pb-Sr-Nd isotopes and trace chemistry

A. TORFSTEIN[1], S.L GOLDSTEIN[1,2] AND M. STEIN[3]

[1]Lamont-Doherty Earth Observatory, Columbia University (adi.torf@ldeo.columbia.edu)
[2]Department of Earth and Environmental Sciences, Columbia University (steveg@ldeo.columbia.edu)
[3]Geological Survey of Israel, Israel (motis@vms.huji.ac.il)

The history of the late Quaternary Dead Sea basin (DSB) hypersaline lakes is closely coupled with orbital and millenial scale climate change in the Northern Hemisphere. In addition, these water bodies were the terminal sink for proximal Cenozoic carbonate bedrock and eolian material originating from the Sahara, suggesting that the deconvolution of the sediment source end members can provide quantitative constraints on the flux of pluvial and eolian material to the DSB during different climate stages.

We present Pb-Sr-Nd isotopic compositions combined with trace and minor element concentrations of siliciclastic sediments deposited over the last 70 ka in Lake Lisan, the last glacial Dead Sea. For each sample, analyses were performed on three grain size fractions of carbonate free material (>20um, 20-5um, <5um).

Significant differences are observed between the composition of the grain size fractions, whereby relative to the two coarse grain size populations, the <5um fraction displays more radiogenic values of $^{87}Sr/^{86}Sr$ (0.7106-0.7125, compared to 0.7087-0.7096 in the coarse fractions) and $^{206}Pb/^{204}Pb$ (18.26-18.93, consistantly higher than coeval coarse fractions), while $^{143}Nd/^{144}Nd$ values in all grain sizes overlap within a range of ~0.5120-0.5123. In addition, the <5um fraction is relatively enriched in lithophilic elements such as Zr, Nb, Pb, and Be.

While the range of lead isotopic compositions corresponds to values measured in proximal bedrock and thus monitors local sources, $^{87}Sr/^{86}Sr$ compositions deviate toward the composition of eolian end member sources, providing distinct constraints on the flux of airbone particles to this area during the late Quaternary. We will present a record of temporal and long term variations in the sediment end member fluxes and compare them to regional climate records. These will further be considered in the context of the grain size distribution and its effect on the chemical and isotopic composition of the samples.

Biogenic supergene galena-rich ore in the Las Cruces deposit, Spain

FERNANDO TORNOS[1], NIEVES G. MIGUELEZ[1], FRANCISCO VELASCO[2] AND JUAN CARLOS VIDEIRA[3]

[1]Instituto Geológico y Minero de España. Rios Rosas 23, 28003 Madrid (Spain) (*correspondence: f.tornos@igme.es)
[2]Universidad del Pais Vasco, Leioa, Spain (francisco.velasco@ehu.es)
[3]Cobre Las Cruces SA (juancarlos.videira@cobrelascruces.com)

The Las Cruces deposit, within the Iberian Pyrite Belt, is one of the richest copper deposits worldwide, shows a well developed supergene alteration zone developed on a steeply dipping primary volcanic-hosted massive sulfide deposit of late Devonian age. The supergene alteration zone formed in the interphase between the basement, including the massive sulfides, and a 150 m thick sequence of Tertiary marl, which hosts a confined aquifer; this gossan probably replaces a former subaerial goethite-rich one that was similar to the other ones found in the IPB. It has several horizons including an upper siderite-hematite zone (red gossan), an intermediate galena-siderite-iron sulfide zone (black rock), a barren coarse pyrite zone and a deep chalcocite zone. The black rock includes skeletal crystals of galena intergrown with siderite and fine grained greigite. Galena shows a mat-like distribution and both the sulfur and carbon isotopes are consistent with a biogenic derivation. The rock shows abundant textures indicative of microbial activity, including forms that resemble fossil microbes and a distribution of the galena controlled by possible microbial mats. Galena shows widespread skeletal growth and both the sulfur and carbon isotopes are consistent with a biogenic derivation; sulfur isotopes values in galena are remarkably high (>19‰) and different from the near 0‰ values of the bulk of the mineralization while $\delta^{13}C$ isotopes in siderite are between -33 and -42‰. Finally, the rock shows abundant textures indicative of microbial activity.

Our interpretation is that the former subaerial gossan hosted during burial major heterotrophic microbial activity that coupled reduction of sulfate carried by the aquifer with oxidation of hydrocarbons or methane accumulated below the sedimentary cap, a process that was enhanced by the heat advected by deep circulating fluids.

https://doi.org/10.1180/S0026461X00006502 Published online by Cambridge University Press

Sediment diagenesis modelling in a AMD contaminated reservoir

E. TORRES[1]*, R.M. COUTURE[2], B. SHAFEI[3], C.R. CÁNOVAS[4], P. VAN CAPELLEN[2] AND C. AYORA[1]

[1]IDAEA-CSIC, Jordi Girona 18-26, 08034, Barcelona, Spain (*correpondence: ester.torres@idaea.csic.es)
[2]Earth and Environmental Sciences, University of Waterloo, 200 University Ave. West, Waterloo, ON, Canada
[3]School of Earth and Athmospheric Sciences, GA, Institute of Technology, 311 First Drive, Atlanta, Georgia, USA
[4]Department of Geodynamics, University of Huelva, Avda Fuerzas Armadas s/n 21071 Huelva, Spain

The Sancho water reservoir is located in the Odiel Basin, Huelva (SW Spain) in the Iberian Pyrite Belt. The Basin has been mined intensively during the last century. While the mines are now abandoned, the Basin is still heavily contaminated by acid mine drainage (AMD).

The reservoir has a pH of ~4, with high SO_4 (200 ppm) and heavy metal concentrations in the water column. A monomictic behaviour forces the reservoir to mix in winter, which oxigenates the bottom waters. Solid and aqueous phases analyses show that the sediment acts as a sink of trace elements (e.g. As, Cd, Pb) during oxic conditions and as a source for them during anoxic conditions at the bottom.

Quantitative transport-reaction modelling of sediment diagenesis has been performed by improving on the apporoach outlined in Couture *et al*. [1]. The model has been modified by including: $FeCO_3$ as a new phase, pH and porosity functions with depth, and two organic matter (OM) pools. Due to the monomictic behaviour of the reservoir non-steady-state boundary conditions were imposed as a function of time for O_2, as an error function, and for the Fe $(OH)_3$ (s) flux, because of its dependence on the O_2 concentration. The reaction network includes three primary reactions discribing the degradation of OM via oxic respiration, iron and SO_4 reduction. The secondary reactions considered are the oxidation of pore water Fe(II) by O_2, and of H_2S by O_2 and Fe $(OH)_3$ (s).

The Fe $(OH)_3$ (s) and SO_4 are reduced in the upper few cm, releasing Fe^{2+} and H_2S which precipitate as FeS and pyrite. Excess of Fe^{2+} precipitates as $FeCO_3$. Under anoxic conditions solute concentrations on sediment pore water increase due to the absence of oxygen. Owing to the time-dependent O_2 function implemented in the model, we obtain a periodic response for the years simulated which allow us to reproduce the complex features of the measured sedimentary profiles.

[1] Couture *et al*. (2010) *Env. Sc. Tech*. **44(1)** 197–203.

Hydrogeochemical analysis of the Sahl-Abad playa brines (East of Iran)

H.A. TORSHIZIAN*, M.JAVANBAKHT, H. MOLLAIE AND M.R. KETABDARI

Islamic Azad University, Mashhad Branch (*correspondence: h.torshizian@yahoo.com)

The Iranian playas are one of the important playa zones in the world. The study area is located in the North of Birjand in the East of Iran. From hydrogeochemical point of view, the brines of this playa is of the Na- Ca- Mg- K-Cl- SO4 series, with the PH ranging from neutral to slightly alkaline. The concentration of some the above ions are very high in these brines, which is due to the composition of parent rocks in the surrounded area. The evaporate minerals within the brines are NaCl and CaSO4. On the basis of chemical composition of the brines especially their trace element (concentration of Br less than 27ml and ratio of Cl to Br which is more than 290) and concentration of Gypsum and Halite in sediments, a meteoric origin (meteoric water of first order of neutral group) is suggested for these brines.

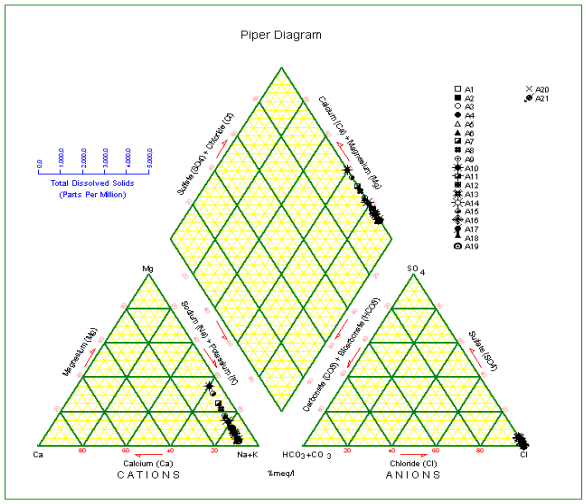

Figure 1: Piper diagram of the Sahl Abad playa brines

https://doi.org/10.1180/S0026461X00006502 Published online by Cambridge University Press

Oxygen isotope modification through assimilatory sulfur cycling

ROSALIE TOSTEVIN[1], ALEXANDRA V. TURCHYN[1]*, ALISON G. SMITH[2], MARIA ZORI[2], CHRISTOPHER J. HOWE[3] AND DAVID J. LEA-SMITH[3]

[1]Department of Earth Sciences, Downing Street, University of Cambridge (*correspondence avt25@cam.ac.uk)
[2]Department of Plant Sciences, Downing Street, University of Cambridge
[3]Department of Biochemistry, Tennis Court Road, University of Cambridge

Isotope modification of oxygen isotopes in sulphate in natural environments is widely understood to be dominated by microbially mediated exchange with water during dissimilatory sulphate reduction, and possible abiotic exchange with water at high temperatures and pressures in hydrothermal systems. Here we show a separate mechanism that can also modify the oxygen isotope composition of sulphate ($\delta^{18}O_{SO4}$) in natural environments, through *assimilatory sulphur cycling*. We define this as the assimilation of sulphur into proteins and biomolecules during cellular growth and its return to the extracellular sulphur pool during cellular turnover. Oxygen isotopes in sulphate are replaced during this cycling and thus this process might be an important, and as yet unconstrained factor in understanding the variability of the $\delta^{18}O_{SO4}$ in natural environments. The cyanobacterium *Synechococcus* sp. PCC7002 and the diatom *Phaeodactylum tricornutum* were grown separately in pure culture and the sulphate in the media was monitored for changes in oxygen isotopes relative to a sterile control flask. The media used contained 3mM sulphate and water with $\delta^{18}O_{H2O}$ of 40‰. The $\delta^{18}O_{SO4}$ increased significantly over the period of cell growth (3 weeks). Replicate experiments in media with sulphate concentrations of 30mM (similar to marine environments) show smaller but analytically resolvable changes in the $\delta^{18}O_{SO4}$ over the period of cell growth. Our results suggest that the $\delta^{18}O_{SO4}$ of marine sulphate could be significantly modified by assimilatory sulphur cycling in regions of high biological productivity, and may be a novel proxy for constraining total carbon turnover in an ecosystem.

Tungsten isotopic anomalies in Archean komatiites

M. TOUBOUL*, I.S. PUCHTEL AND R.J. WALKER

Dept. of Geol. Univ. of MD, College Park, MD 20742, USA (*correspondence: mtouboul@umd.edu)

Late or heterogeneous accretion, early mantle differentiation, and/or core-mantle interaction are processes that could have created subtle ^{182}W isotopic heterogeneities within Earth's mantle (where $^{182}Hf \rightarrow {}^{182}W + \beta^-$; $t_{½} = 9$ Myr). To facilitate the search for such effects, we have developed a new ultra-high precision measurement protocol using a *Triton* thermal ionization mass spectrometer, allowing us to resolve ^{182}W anomalies at a ±6 ppm level. Here, we present ultra-high precision W isotopic compositions and W abundances of Archean komatiites from Komati, Weltevreden, Belingwe, Kostomuksha and Vetreny.

Within each komatiite sequence, W abundances are generally correlated with proxies for lava differentiation. In some samples, however, W clearly shows open system behaviour, indicated by large enrichments that are accompanied by enrichments in U and Re. This is likely due to post-eruption alteration and highlights the care that must be taken when examining W isotopes in altered rocks. Of greatest note, Kostomuksha samples exhibit ^{182}W excesses relative to the modern upper mantle, ranging from +12 to +35 ppm. A plot of $\varepsilon^{182}W$ *vs.* 1/W defines a binary mixing line that extrapolates to an ambient terrestrial composition ($\mu^{182}W = 0$), as would be expected due to the variable open-system behaviour of W identified in some samples.

The positive ^{182}W anomaly in the mantle source of the Kostomuksha komatiites is inconsistent with incorporation of a core component, as was initially suggested to explain the $^{186, 187}Os$ enrichments that are also present in the system. Our results, therefore, indicate that the Kostomuksha source included a primordial component characterized by high Hf/W, Re/Os and Pt/Os. The short half-life of ^{182}Hf requires that this reservoir was created within the first ~50 Ma of the Solar System. We speculate that this reservoir represents a product of metal-silicate partitioning at the base of a deep magma ocean and is consistent with reduced metal-silicate D values observed at high P/T for Pt and Re. This component would have contributed highly radiogenic ^{182}W, ^{187}Os and ^{186}Os, but its low elemental abundances would have been largely eliminated by mixing with mantle re-enriched in moderately and highly siderophile elements via late accretion. The generation of these komatiites at 2.8 Ga attests to the long-lived nature of the reservoir, and highlights the evident sluggish mixing of the mantle, even during the Hadean.

https://doi.org/10.1180/S0026461X00006502 Published online by Cambridge University Press

A hydrogen rich Early Earth?

H. TOULHOAT[1]*, V. BEAUMONT[1]*, V. ZGONNICK[2], N. LARIN[3] AND V.N. LARIN[3]

[1]IFP New Energy, 1 & 4 Avenue de Bois Préau, 92852 Rueil-Malmaison Cedex, France. (*correspondence: valerie.beaumont@ifpen.fr)
[2]Ukrainian Association for Hydrogen Energy, Nogina St. 14/23, Krivoy Rog, 50014, Ukraine
[3]Russian Academy of Science, Schmidt Institute of Physics of the Earth, B.Gruzinskaya St. 10, 123995, Moscow, Russia
[4]Lomonosov Moscow State University, Leninskiye Gory, 119991, Moscow, Russia

V.N. Larin (1993) [1] proposed that the chemical differentiation in the solar system was driven by the magnetic field of the Protosun, which induced a magnetic zoning of the ionized solar nebula matter. This hypothesis is geochemically supported by a correlation between the Log of the chemical element abundances of the Earth outer geospheres relative to the Sun, and the first ionization potential of these elements.

The observed correlation is theoretically reappraised in the present paper and is interpreted as a Boltzmann distribution, which is proportional to the distance to the Protosun. The model is succesfully tested for the observed solar normalized chemical compositions of the Earth, Mars and chondrites; poorly convincing results are obtained for Venus in absence of reliable data for low abundance elements.

The comparison of the abundance of a given element in the Earth's crust with the average abundance predicted from the proposed model is further interpreted as reflecting the geochemical radial differentiation of the Earth. Using a simple thermochemical model, we propose that the radial distribution of hydrogen on Earth is a function of the chemical affinities of major Earth forming elements with hydrogen.

This model provides insights for hydrogen abundance on Earth. Notably, the inner Earth would have been and still could be hydrogen rich. Although most of this hydrogen have escaped to atmosphere and space through the thorough degassing of the mantle, it is reasonable to suggest, in the perspective given by our model, that very large amounts still reside in the core.

[1] V.N. Larin (1993) *Hydridic Earth*. Ed. C. W. Hunt. Polar Publishing. 247 p.

Anions in clay materials: A case study for multi-scale modeling approaches

C. TOURNASSAT

BRGM, French Geological Survey, 45060, Orléans, France

Swelling property in water endows clay materials with a very low hydraulic conductivity and transport of water and solutes in these media is mainly diffusive, with diffusion coefficients that are much smaller than in bulk water. As a consequence, clay materials are recognized as efficient barriers for waste confinements. For instance, bentonites are already used by solid-waste-disposal operators in the form of compact and/or geosynthetic clay liners while engineered bentonite barriers and natural clay formations are foreseen for radioactive waste confinement in deep geological repositories. Clay material physical and chemical properties result from their small size (typically $< 2\mu$m) and structural specificities. Recent developments of computationnal and spectrometric techniques enabled to probe these properties down to the molecular scale, providing accurate descriptions of processes taking place at the solid/water interface. However, for engineering applications, clay properties must be characterised at a large spatial scale (1m-100m) using macroscopic descriptions and often empirical parameters enabling predictive modelling on extended timescales (typically 100 000 years for radwaste repositories). Making the link between these spatial and temporal scales is of paramount importance to assess the robustness of long term predictive modelling results through a detailed justification for the necessary modelling simplifications.

The present talk will focus on anions distribution and mobility in montmorillonite and illite clay materials that are representative of natural clay formation mineralogy. Illite and montmorillonite structures have an excess of negative charge that is compensated by cations adsorption in their interlayer space and on their outer surface. Conversely, anions undergo weak or no specific adsorption and are repelled from the negative surface, a phenomenon called anion exclusion. While this process can be adequately predicted by theoretical models on simple static systems (e.g. clay suspension in 1:1 electrolytes), its quantitive prediction on complex systems (compact clay material, multispecies electrolytes) remains problematic as well as its impact on macroscopic anion diffusion parameters. We will review models available from the nano- to the macroscopic scale in order to (i) highlights recent improvements in our understanding of anion distribution and mobility in clay materials and (ii) to identify remaining gaps to be elucidated.

https://doi.org/10.1180/S0026461X00006502 Published online by Cambridge University Press

Halogen compositions in kimberlites and their constituent minerals

C. TOYAMA[1]*, Y. MURAMATSU[1], J. YAMAMOTO[2], H. SUMINO[3], S. NAKAI[3] AND I. KANEOKA[3]

[1]Gakushuin University, Tokyo, 171-8588, Japan (*correspondence: 09242003@gakushuin.ac.jp, yasuyuki.muramatsu@gakushuin.ac.jp)
[2]Kyoto University, Oita, 874-0903, Japan
[3]University of Tokyo, Tokyo, 113-0032, Japan

Introduction

Studies on the isotope and element compositions in kimberlites will provide important information to estimate chemical environment of the Earth's mantle. We had analyzed major and trace elements in kimberlites from South Africa and China. However, some kind of data about chemical compositions of kimberlites are still lacking. Especially, data of halogen elements are very limited. In this study, we analyzed concentrations of halogen elements (Cl, Br, I) in kimberlites and their constituent minerals from six regions, and considered the characteristics and their origin of each area.

Samples and method

Samples analyzed are 34 kimberlites collected from South Africa, China, Greenland, Brazil, Canada and Russia. For the determination of halogen, we used the pyrohydrolysis method combined with ICP-MS [1].

Results and Discussion

The results show that concentrations of Cl, Br and I in kimberlite samples are higher than those in common ultra-mafic rocks. Markedly high Br concentrations (>10ppm) are found in some kimberlite samples from China and Russia, while iodine concentrations in some samples from South Africa, Greenland, Canada and Brazil are relatively high (>0.1ppm). The I/Br ratios (about 1×10^{-1}) in kimberlites obtained for South Africa, Greenland, Canada and Brazil are very similar and relatively high, and they are similar to those in chondrite (CI), peridotite and basalt. The I/Br in kimberlites possibly shows the characteristics of halogen in the mantle where kimberlite magmas were formed. In case of Chinese and Russian kimberlite samples, the I/Br ratios (about 2×10^{-3}) are significantly low suggesting that they are associated with materials having low I/Br ratio, which might have been influenced by seawater (I/Br ratio: 1×10^{-3}).

[1] Muramatsu & Wedepohl (1998) *Chemical Geology* **147**, 201–216.

UV-VIS absorbance, fluorescence and concentration of dissolved organic carbon (DOC) of sea-surface microlayer samples collected at Okinawa, Japan

Y. TOYAMA[1], Y. MIYAGI[2] AND T. ARAKAKI[2]*

[1]Graduate School of Engineering and Science, University of the Ryukyus, 1 Senbaru Nishihara-cho Okinawa Japan 903-0213 (k108406@eve.u-ryukyu.ac.jp)
[2]Faculty of Science, University of the Ryukyus, 1 Senbaru Nishihara-cho Okinawa Japan 903-0213 (*correspondence: arakakit@sci.u-ryukyu.ac.jp)

Introduction

The sea-surface microlayer (SML) covers the ocean surface, and SML has been operationally defined as roughly the top 1 to 1000 micrometer of the ocean surface. SML controls transfer of chemical substances between the ocean and atmosphere, influencing the chemical compositions of atmospheric aerosols that occur in breaking waves. Since solar radiation reaching the ocean surface is relatively strong, compared to the underlying bulk seawater, photochemical reactions on the ocean surface could induce significant chemical changes which in turn change chemical compositions of atmospheric aerosols. This study tries to elucidate the photochemical properties of SML by measuring the UV-VIS absorbance, fluorescence and concentration of dissolved organic carbon (DOC).

Discussion of Results

We collected coastal SML samples around Okinawa Island, Japan. Okinawa Island is located in semi-tropical region and parts of the island coast are covered with coral reefs and parts of the island are heavily affected by human activities. We selected 10 sampling sites represending different environmental conditions, i.e. close to residence area or relatively remote area. We used a glass plate method to collect SML samples, and at the same location and time bulk seawater samples were collected about 10-cm below the surface with high density polyethylene bottles.

Results showed that enrichment factors (EF), defined as ratio between SML and bulk seawater, of absorbance (at 300 nm) and DOC were ca 1.0 to 2.4 and 1.0 to 1.8, respectively. Based on the fluorescence measurements, it is suggested that humic acid-like compounds and aromatic amines were concentrated in the SML, compared to the bulk seawater. We further discuss impacts of human activities on photochemical properties of SML around Okinawa Island.

https://doi.org/10.1180/S0026461X00006502 Published online by Cambridge University Press

Dating of submarine hydrothermal deposits by ESR and U-series methods

S. TOYODA[1]*, F. SATO[1], S. NAKAI[2], A. TAKAMASA[2] AND J. ISHIBASHI[3]

[1]Department of Applied Physics, Okayama University of Science, Japan (*correspondence: toyoda@dap.ous.ac.jp)
[2]Earthquake Research Institute, Univesity of Tokyo, Japan (snakai@eri.u-tokyo.ac.jp)
[3]Graduate School of Earth and Planetary Science, Kyushu University, Japan (ishi@geo.kyushu-u.ac.jp)

As interests in submarine massive sulfides as mineral resources increase, geochronological study of submarine ore deposits becomes more important. Formation of a large ore body requires long-time duration of hydrothermal activity. Moreover, a systematic geochronological study to reveal mineralization stages and sequences would provide an important key to explore submarine ore deposits. We focused on a chronological study of barite ($BaSO_4$) and developed an application of electron spin resonance (ESR) dating of barites. Barite is a sulfate mineral commonly occurred in submarine ore deposits, sometimes including substantial amount of radium that substitutes barium.

As a sample, we used a massive ore deposit collected from a submarine active hydrothermal field (in the southern Mariana backarc basin). This deposit grew rather horizontally to a few meters in length and about 15 cm in a diameter. A piece of slice with thicknees of about 5 cm was taken from the middle part of the deposit and cut into 13 pieces. Each piece was crushed and barite and spharelite were extracted by chemical and magnetic methods.

The ESR signal due to SO_3^- radical was observed in barite. The signal intensity increased with gamma ray dose. By extrapolating the dose response to the zero ordinate, the accumulated natural doses were obtained. The concentration of radium was obtained by the low background gamma ray spectroscopy using a gemanium semiconductor detector. The natural dose rates were calculated from the value. The ESR ages were obtained by dividing the accumulated natural doses by dose rates.

U-series ages were also obtained for these pieces using sulfide mineral mainly composed of sparelite and pyrite by mass spectroscopy. The ages were calculated from the disequiliburium between ^{234}U and ^{230}Th.

The ages obtained by these two methods were consistent within 30 %. The ages for these 13 pieces were grouped into two, one about 2500 years and the other about 1300 years.

The oxidation state of Hadean melts and implications for the composition of Earth's early atmosphere

DUSTIN TRAIL*, E. BRUCE WATSON AND NICHOLAS D. TAILBY

Department of Earth & Environmental Sciences and New York Center for Astrobiology, Rensselaer Polytechnic Institute, Troy, NY 12180, USA (*correspondence: traild@rpi.edu)

Zircon is an exceptionally durable mineral that retains primary chemistry for most elements from the time of igneous crystallization. Zircons are the only known terrestrial solids dating from the first 500 Ma of Earth history, and thus present a unique opportunity to constrain intensive petrological variables from Hadean (i.e. >3.85 Ga) melts that would otherwise be inaccessible. We report an experimental calibration that makes it possible to evaluate the oxygen fugacity of terrestrial melts prior to the Archean based on the incorporation of heterovalent Ce into zircon. Zircons were grown in a piston cylinder apparatus at 1 GPa and 900 to 1300ºC from hydrous silicate melts (~72 wt% SiO_2) doped with La, Ce and Pr (±P). The melt Ce^{4+}/Ce^{3+} ratio was controlled throughout the duration of the experiments by buffering the oxygen fugacity at values broadly covering the range observed in terrestrial and lunar magmas.

Application of this calibration to zircons from the Bishop Tuff magma chamber, mid-ocean ridge basalt residuals, and lunar grains yields average calculated oxygen fugacities broadly consistent with independent estimates. Furthermore, our results show that Hadean zircons crystallized in melts having average oxygen fugacities within error of the fayalite-magnetite-quartz buffer, including zircons with chemical characteristics consistent with an origin from a mantle-derived melt. The oxidation state of Hadean magmas may yield critical constraints on the speciation of volatile gases entering the atmosphere in the Hadean; results of our calibration are most consistent with H_2O, CO_2, SO_2, and N_2 gaseous species as early as 200 Ma after solar system formation.

https://doi.org/10.1180/S0026461X00006502 Published online by Cambridge University Press

Geochemistry and PGE mineralogy of chromitite seams of the eastern Bushveld complex, South Africa

M. TREDOUX[1]*, F. ZACCARINI[2], G. GARUTI[2], J. KOTKE-LEVIN[1] AND C. GAUERT[1]

[1]Geology Dept, Univ. of the Free State, PO Box 339, Bloemfontein, 9300 South Africa (*correspondence: mtredoux@ufs.ac.za)
[2]Department of Applied Geosciences and Geophysics, University of Leoben, A - 8700 Leoben, Austria

With the increasing interest in chromitites of the Bushveld complex as platinum-group element (PGE) ores, the need to characterize these layers and their PGE mineralization has grown. This is particularly true for the eastern limb, which in general has been under-explored relative to the western limb.

The whole-rock PGE geochemistry of the eastern limb chromitites was investigated in the 1980s [1, 2]. These studies indicated that the PGE concentrations in the chromitites increased with continued fractional crystallisation. It was also found [2] that the Pt/Pd ratio remains constant right up to, and including, the Merensky reef.

This geochemical investigation was based on borehole core samples, comprising a complete section through the Middle Group (MG) chromitite layers in the central part of the eastern limb [3]. The mineralogical study was supplemented by data from Lower Group (LG) and MG chromitite xenoliths which were associated with the Onverwacht and Tweefontein dunite pipes [4]. The whole rock PGE patterns of all the layers show the same positive Rh anomaly which typically is displayed by the UG2 chromitite. The MG layers display an increase of the HT-PGE (Os, Ir and Ru) relative to the LT-PGE (Pt, Pd and Rh) with stratigraphic height. The individual groups both correlate positively with the Cr_2O_3 concentration.

High magnification ore microscopy and back-scattered electron imaging indicate that very fine-grained (generally ≤10 μm) laurite is by far the major PGE mineral. The laurite composition does not vary significantly from the bottom of the LG to the top of the MG layers, indicating constant S fucacity. This is in contrast with the Upper Group (UG) layers, in which a great variation of PGE minerals is found. A peculiarity of the MG layers is that laurite is often associated with rutile.

[1] Lee & Tredoux (1986) *Econ Geol* **81**, 1087. [2] Lee & Parry (1988) *Econ Geol* **83**, 1127 [3] Kottke-Levin *et al.* (2009) *Appl Earth Sci (Trans Inst Min Metall B)* **118**, 111. [4] Zaccarini *et al.* (2002) *Can Min* **40**, 481.

Trace element mobility during spheroidal weathering of dolerite dykes from central Portugal

M.J. TRINDADE[1,3], F. ROCHA[2,3]*, M.I. PRUDÊNCIO[1,3] AND M.I. DIAS[1,3]

[1]Technological and Nuclear Institute, EN 10, 2686-953 Sacavém, Portugal
[2]Geoscience Dept., Aveiro University, 3810-193 Aveiro, Portugal (*correspondence: tavares.rocha@ua.pt)
[3]GeoBioTec Research Center, Aveiro University, Portugal

This study focused in an outcrop of central Portugal where several dolerite dykes, intercalated in granite, show a characteristically well developed spheroidal weathering pattern, forming concentric shells of decayed rock. The trace element mobility during weathering of four rounded boulders of decomposition, from three dolerite dykes, is analyzed. Each of them was separated in a clay-rich external shell, two intermediate shells and a core. Their chemical and mineralogical composition was obtained by neutron activation analysis and X-ray diffraction, respectively.

Primary minerals (Ca-plagioclase, augite and biotite) predominate over secundary phases (chlorite, smectite, kaolinite and talc) in the inner parts of the boulders. The more external shells present abundant clay minerals, especially smectite, being the primary minerals accessory or inexistent.

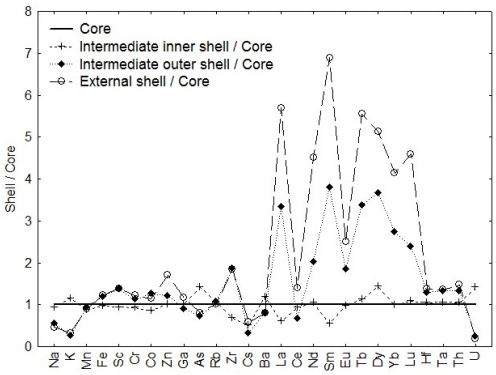

Figure 1: Chemical variability in one rounded boulder.

Weathering promoted the release of REE^{3+} from primary phases, mobilization by meteoric waters, and incorporation in secondary phases, especially smectite, the most abundant clay mineral. Ce and minor Eu were retained, causing negative anomalies. Hf, Ta, Th, Zr, Fe, Sc and Zn were also mobilized into secundary phases. The impoverishment of the outer shells in Na, K, Cs, Ba and U shows they were mobilized out of the system during alteration.

https://doi.org/10.1180/S0026461X00006502 Published online by Cambridge University Press

Re-Os isotopes and redox-sensitive elements of the Himalayan black shales: Implications to marine anoxia near the Pc-C boundary

GYANA RANJAN TRIPATHY* AND SUNIL KUMAR SINGH

Physical Research Laboratory, Ahmedabad-380009, India (*correspondence: gyana@prl.res.in, sunil@prl.res.in)

Present study attempts to determine the timing and its implications related to changes in the redox state of seawater at around the Pc-C boundary using Re-Os isotopes and redox-sensitive elements of black shales sampled from a underground phosphrite mine (Maldeota, Dehradun) just overlying the Pc-C bounadry in the Lower Tal formation of the Lesser Himalaya, India. The measured $^{187}Re/^{188}Os$ ratios of these shales vary widely (51 to 137), but linearly with that of $^{187}Os/^{188}Os$ (1.363 to 2.116). Following the bivariate approach that used by Singh *et al*. [1], the $^{187}Re/^{188}Os$-$^{187}Os/^{188}Os$ systematics of these shales provided a depositional age of 541±8 (2σ) Ma with an initial $^{187}Os/^{188}Os$ value of 0.90±0.02 (2σ). The Re-Os age of black shales obtained in this study is quite consistent with the reported radiometric ages for Pc-C boundary at other locations of the world.

Geochemical compositions of black shales deposited near the Pc-C boundary is observed to be different than that of the overlying sequences of black shales. The average Al-normalizied values of organic carbon (C_{org}/Al) and redox-sensitive elements (Re/Al, Os/Al, V/Al, Cr/Al, Cu/Al) of these shales are found to be significantly higher compared to that of black shales [1] overlying ~3 m above [2], but separated by a phosphrite sequence from these shales. This enrichment of C_{org} and trace elemental ratios in the black shales deposited at 541 Ma indicates a highly euxinic seawater near the Pc-C boundary. The inferences from this study of reducing seawater chemistry at the Pc-C boundary can find application in understanding the causative factors of the Cambrian explosion of life. For example, the highly euxinic state of seawater could have imposed a mass extinction [3], which subsequently led to large diverfication in biology resulting into Cambrian explosion of life.

[1] Singh, Trivedi & Krishnaswami (1999) *Geochim. Cosmochim. Acta* **63**, 2381–2392. [2] Sharma, Rao, Azmi, Gopalan & Pantulu (1992) *Curr. Sci.* **62**, 528–530. [3] Kimura & Watanabe, *Geology* **29**, 995–998.

Non-isothermal dehydroxylation kinetics of common sheet-like phases and their informational value

R. TRITTSCHACK* AND B. GROBÉTY

Dept. of Geosciences, Univ. of Fribourg, 1700 Fribourg, Switzerland (*correspondence: roy.trittschack@unifr.ch)

Studying the decomposition kinetics by thermal analyses (e.g. Thermogravimetry, Differential Thermal Analysis, Differential Scanning Calorimetry) of rock forming minerals have a long tradition in Earth Sciences. Often observed rate laws have been used for mechanistic interpretation of the reactions. Classical approaches (Avrami, Time to a Given Fraction TGF) focus on model fitting techniques to extract single values of the apparent activation energy E_a and the 'rate determing step' is derived from the value of the exponent in the Avrami equation. From the physico-chemical point of view such interpretations are for most reactions commonly wrong and have often been critisised especially in the chemistry literature [1-3].

Isoconversional treatment of model-free non-isothermal datasets give, in contrast to the classical methods, E_a as a function of α. Variation of E_a with α are a clear sign that the reaction rate is determined by more than one parallel or sequential step and that classical treatment is not feasible. In such a case, mechanistic interpretation of the kinetic experiments is only possible in combination with information gained from simulations (Density-functional-theory (DFT) models [4, 5]) or *in situ* diffraction and spectroscopic methods.

Here, the dehydroxylation kinetics of two natural occuring phases, lizardite and brucite, are taken as examples for contrasting behaviour of the rate determining reaction step. Lizardite dehydroxylation illustrates a highly dynamic and predominantly increasing evolution of E_a with α [6] indicating that several different steps become rate determining, whereas brucite dehydration evolves with a nearly constant E_a indicating that only one step is rate determining over the entire reaction progress. The possible rate determining steps will be discussed.

[1] Galwey (2004) *Thermochim. Acta.* **413**, 139–183. [2] Vyazovkin & Wight (1997) *Annu. Rev. Phys. Chem.* **48**, 125–149. [3] Vyazovkin (2000) *New. J. Chem.* **24**, 913–917. [4] Molina-Montes *et al*. (2008) *J. Phys. Chem. B* **112**, 7051–7060. [5] Churakov *et al*. (2004) *J. Phys. Chem. B* **108**, 11567–11574. [6] Trittschack & Grobéty (submitted) *Eur. J. Mineral*.

https://doi.org/10.1180/S0026461X00006502 Published online by Cambridge University Press

Crustal CO_2 liberation at Merapi, Indonesia: An earthquake trigger?

V.R. TROLL[1], D.R. HILTON[2], J.P. CHADWICK[3], E.M. JOLIS[1], L.M. SCHWARZ-KOPF[4], M. ZIMMER[5], L.S. BLYTHE[1] AND F.M. DEEGAN[1]

[1]Dept. Earth Sci (CEMPEG), Uppsala University, Sweden (valentin.troll@geo.uu.se)
[2]Geosci. Res. Division, Scripps Inst. Oceanography, USA
[3]Dept. Petrol (FALW), The Netherlands
[4]GeoDocCon, Konradsreuth, Germany
[5]GeoForschungsZentrum, Potsdam, Germany

On May 26th, 2006, the magnitude 6.4 Yogyakarta earthquake occurred along a splay of the Opak River Fault system, with hypocentres at 10-15km depth [1]. Prior to 2006, variation of fumarole carbon isotope ratios was limited ($\triangle\delta^{13}C_{2001\text{-}2004}$ = 0.5‰ ± 0.3l) with an average baseline value of -4.1‰ ±0.2 (vs, PDB). This value is typical of subduction zones [2]. Carbon dioxide collected after the earthquake showed a dramatic increase from the baseline to $\delta^{13}C$ = –2.4‰. In 2007 and 2008, $\delta^{13}C$ values returned to background levels. This rise coincided with an increase in eruptive intensity and volcano seismicity by a factor of 3-5 for several weeks after the earthquake [1]. High carbon isotope gas values, such as those observed in 2006, are not produced by decompression- or fractionation induced degassing in either open or closed system mode [3], suggesting an addition of CO_2 from a non-magmatic, high-$\delta^{13}C$ source. The increase in $\delta^{13}C$ in 2006, its transient duration, the crustal depth of the earthquake hypocentres, and the link with eruptive and seismic intensity are all consistent with addition of CO_2 from mid- to upper-crustal depths. Such additions of crustal CO_2 to subduction zone baseline fluxes may modify volatile budgets of ascending magmas at Merapi considerably [4]. Therefore, CO_2 liberation from long-term crustal storage reservoirs, such as the thick limestone basement underneath Merapi, may be a process that is triggered and/or amplified by external mechanisms such as seismic events. We thus envisage a chain of events whereby earthquake and volcano interact in a positive feedback loop. We conclude that crustal volatiles intensify ongoing eruptions and that late-stage volatile addition may potentially trigger explosive eruptions independently of magmatic recharge and fractionation processes and may even be a key factor in promoting regional seismic activity.

[1] Walter *et al*. (2008) *Geoch. Geoph. Geos*. **9**, 1–9. [2] Hilton *et al*. (2002) *Rev. Mineral. Geochem*. **47**, p. 319–370. [3] Holloway & Blank (1994) *Rev. Mineral. Geochem*. **30**, 187–230. [4] Deegan *et al*. (2010) *J. Petrol*. **51**, 1027–1051.

Noble gases as tracers to determine the effective diffusivity in the sediment porewater of Lake Hallwil

M.TRÖSCH[1], Y. TOMONAGA[1]*, C.P. HOLZNER[1] AND R. KIPFER[1,2]

[1]Eawag, Swiss Federal Institute of Aquatic Science and Technology, CH-8600 Dübendorf, Switzerland (*correspondence: tomonaga@eawag.ch)
[2]Institute of Geochemistry and Petrology, Swiss Federal Institute of Technology (ETH), CH-8092 Zurich, Switzerland

Noble-gas concentrations in surface waters and sediment porewater are often found at atmospheric equilibrium according to the local temperature and salinity conditions prevailing in water body during gas partitioning with the atmosphere. As noble gases are chemically inert, deviations of the measured noble-gas concentrations from the expected solubility equilibrium concentrations can be interpreted in terms of physical transport processess.

Since 1985 an artificial aeration system is installed at the bottom of Lake Hallwil, a medium-sized eutrophic lake in Switzerland, to foster the water circulation and to prevent anoxic conditions in its hypolimnion. Starting from 2002 the aeration system has been enhanced in order to inject oxygen-enriched gas into the water body during the summer period. The enrichment in oxygen is achieved by pumping atmospheric air through large volumes of molecular sieves. The same process is also responsible for a significant enrichment in light noble-gas species (i. e, He, Ne, and Ar) in the injected gas phase.

The small bubbles injected at low pumping rates during summer completely dissolve into the water column producing a characteristical noble-gas excess pattern. This noble-gas excess is expected to diffuse from the water column into the sediments. Therefore, noble gases have the potential to be used directly as tracers to determine the effective diffusivity of solutes in the sediment pore space under quasi-natural conditions and to allow to quantify the overall injected gas / O_2 mass over large time scales.

In this work we present noble-gas concentrations measured in the water column and in the sediment porewater of Lake Hallwil over the last five years. Based on these data we modelled the diffusive transport of He, Ne, and Ar in the sediment column to quantify diffusive transport and the O_2 injection into Lake Hallwil.

https://doi.org/10.1180/S0026461X00006502 Published online by Cambridge University Press

Boron isotope systematics of pH regulation in cold-water corals and resilience to ocean acidification

J.A. TROTTER[1]*, M.T. MCCULLOCH[1,2], P. MONTAGNA[3,4], M. LÓPEZ CORREA[5], M. TAVIANI[4] AND G. FÖRSTERRA[6]

[1]The UWA Ocean Institute and School of Earth and Environment, The University of Western Australia, Crawley 6009, Australia (*correspondence: julie.trotter@uwa.edu.au)
[2]ARC Centre of Excellence in Coral Reef Studies, UWA
[3]LSCE, Av. de la Terrasse, 91198, Gif-sur-Yvette, France
[4]ISMAR-CNR, via Gobetti 101, I-40129 Bologna, Italy.
[5]GeoZentrum Nordbayern, 91054 Erlangen, Germany
[6]Huinay Scientific Field Station, Casilla 1150, Puerto Montt, Chile

Cold-water corals are thought to be especially vulnerable to CO_2-driven climate change and ocean acidification because they live close to the aragonite saturation horizon, which is now rapidly shoaling as anthropogenic CO_2 penetrates into the deep oceans. Due to the sensitivity of calcification to saturation state, this may not only lead to decreased calcification rates but also dissolution of deep-sea calcifiers.

Here we report boron isotopic measurements of cold-water corals representing a wide range of deep-sea and shallow-water environments. These zooxanthellate aragonite corals are all found to have relatively high $\delta^{11}B$ compositions, lying significantly above the seawater borate equilibrium curve. The internal pH of the solitary coral *Desmophyllum dianthus*, determined from the measured $\delta^{11}B_{carb}$ compositions, defines a highly correlated linear array with seawater pH. This relationship, indicative of internal (extracellular) up-regulation of pH at the site of calcification [1], corresponds to a differential pH (ΔpH) of ~0.7 to 0.8 units above ambient seawater. As a consequence the aragonite saturation state of the calcifying fluid is increased approximately two to five-fold, facilitating calcification in low pH environments. This contrasts with the hyper-calcifying tropical zooxanthanlate corals that operate within a significantly lower range of ΔpH values from 0.3 to 0.4 units [1], indicating the importance of temperature on the kinetics of inorganic calcification. These new observations suggest that the effect of declining carbonate saturation state in the deep-oceans may be partially offset by the combined effects of biological up-regulation of internal pH and enhanced rates of calcification from higher ocean temperatures.

[1] Trotter *et al*. (2011) *Earth Planet Sci Lett*. **303**, 163–173.

Origin and composition of LLSVPs in the lowermost mantle

REIDAR G. TRØNNES

Natural History Museum, Univ. Oslo, Norway (*correspondence: r.g.tronnes@nhm.uio.no)

The structure of the lowermost mantle (D") is dominated by spherical harmonics degree-2 variation with two anti-podal Large Low Shear-Velocity Provinces (LLSVPs) [1]. Their locally steep margins may be favourable sites for the generation of mantle plumes, giving rise to large igneous provinces, and even kimberlites, with ages covering the last 540 Ma [2-4]. The LLSVPs are probably thermochemical piles with sufficient density to resist thermal buoyancy and destruction. Steep margins could be promoted by elevated bulk modulus of the pile material [2].

The piles may be enriched in meta-basaltic material with high density caused by high Fe/Mg ratio in perovskite and high bulk modulus associated with the presence of stiff silica minerals and absence of soft ferropericlase [5, 6]. Peridotite or komatiite with elevated Fe/Mg may be alternative materials in the piles. The origin and age of the LLSVPs are probably linked to the nature of the material. Accumulation of basaltic rocks from subducted slabs could occur slowly in the plume generation zones near the LLSVP-margins over 3-4 Ga [7]. Emplacement of komatiitic or peridotitic material with elevated Fe/Mg, however, could have occurred early, either during the final solidification of a lowermost mantle magma ocean [8, 9] or by sinking of solidified material from a melt accumulation zone (by buoyancy) at 400 km depth [10]. Melting in hot Hadean or Archean plumes may have been widespread at 20-25 GPa where the peridotite solidus is at relatively low T [11, 12]. The psedo-invariant melt compositions at $p > 15$ GPa are poorly constrained and may be relatively silica-rich at 23-30 GPa, where ferropericlase is the liquidus phase [11-13]. A systematic melting study of a range of simplified compositions will provide further insights.

[1] Dziewonsky *et al*. (2010) *EPSL* **299**, 69–79. [2] Garnero & McNamara (2008) *Science* **320**, 626–628. [3] Torsvik *et al*. (2006) *GJI* **167**, 1447–1460. [4] Torsvik *et al*. (2010) *Nature* **455**, 352–356. [5] Hirose *et al*. (2005) *EPSL* **237**, 239–251. [6] Irifune & Tsuchia (2007) *Treatise Geophys*. **2**, 33–62. [7] Trønnes (2010) *Mineral. Petrol*. **99**, 243–261. [8] Labrosse *et al*. (2007) *Nature* **450**, 866–869. [9] Stixrude *et al*. (2009) *EPSL* **278**, 226–232. [10] Lee *et al*. (2010) *Nature* **463**, 930–933. [11] Herzberg & Zhang (1996) *JGR* **101**, 8271–8295. [12] Trønnes & Frost (2002) *EPSL* **197**, 117–131. [13] Ito *et al*. (2004) *PEPI* **143–144**, 397–406.

https://doi.org/10.1180/S0026461X00006502 Published online by Cambridge University Press

Sulphate reduction induced by hydrogen under hydrothermal conditions

L. TRUCHE[1]*, G. BERGER[2] AND P. CARTIGNY[3]

[1]G2R, Univ. de Lorraine, Vandoeuvre-Lès-Nancy, France (*correspondance: laurent.truche@g2r.uhp-nancy.fr)
[2]CNRS, IRAP, 14 av. E. Belin, 31400 Toulouse, France
[3]IPGP, Univ. Paris Diderot, France

Abiotic redox reactions induced by hydrogen are of prior importance in numerous fields of investigation in geoscience where hydrogen is produced either naturally or indirectly via industrial activities: e.g. nuclear waste storage [1], underground storage of hydrogen [2], hydrogen generation during serpentinization and related redox reaction [3], early earth, termochemical sulphate reduction (TSR) [4].

In this experimental study we focus on sulphate reduction induced by hydrogen under hydrothermal conditions. We provide kinetic data as a function of temperature (125°C-300°C), pH, hydrogen pressure, sulphate speciation (HSO_4^-, $MgSO_4°$, $CaSO_4°$), surface catalysts or additional electron donor (Hastelloy C273, Ni (0), Fe (0), magnetite). This parametric approach on simplified systems allow us to probe the reaction mecanism and to discriminate electron donors: i.e. native metal, mixte oxide, atomic hydrogen or H_2. In addition, we provide kinetic data that can be apply in numerical simulations. In presence of these catalysts, the reaction rate is one to two order of magnitute higher than in diphasique systems [4] i. e: aqueous sulphate + dissolved hydrogen. However, low pH are required in presence of Hastelloy or Ni (0) to reduced sulphate within hours in the temperature range 250-300°C. Under these conditions hydrogen is not necessary but the reaction rate is enhanced in its presence. We suppose that hydrogen radicals generated by alloy or metal corrosion are the main electron donors. In presence of magnetite, the reaction occurs at low temperature (125°C) but only under restricted conditions: low sulfate concentration, pH around magnetite PZC and hydrogen partial pressure. We further reveale that sulphide reaction initiation is not a necessary condition providing that these catalytic surfaces are present in the system.

The results of this study are discussed in the light of kinetic data and reaction pathways obtained in previous studies using hydrocarbons as electron donor instead of H_2.

[1] Truche *et al*. (2009) *GCA*, **73**, 4824–4835. [2] Panfilov (2010) *Transp. in Porous Media*, **85**, 841–865. [3] Fu *et al*. (2007) *GCA*, **71**, 1982–1998. [4] Truche *et al*. (2010) *GCA*. **74**, 2894–2914.

Platinum-group elements in basaltic rocks from the Etendeka province in N.W. Namibia

R.B. TRUMBULL*, J.K. KEIDING AND K. HAHNE

GeoForschungsZentrum Potsdam, Telegrafenberg, D-14473 Potsdam, Germany (*correspondence: bobby@gfz-potsdam.de)

The continental flood basalts and intrusive rocks of the Paraná – Etendeka Large Igneous Province have been reasonably well studied, giving a good foundation for more specific questions. One aspect of special interest in LIPs and their mantle source (s) concerns the behavior of platinum group elements (PGE). These elements and their isotopes can help distinguish mantle components (lithospheric, asthenospheric, deep-mantle) and they have obvious economic significance. Some Phanerozoic flood basalt provinces are associated with important Cu-Ni-PGE ore deposits (Emeishan, Siberia), whereas others appear to lack them (Karoo, Deccan and Paraná-Etendeka). Whether this difference relates to conditions in the magma source region or to the nature of crustal assimilation is debated, but sulfur is seen to play a critical role.

We present new PGE concentration data for lavas, dolerite dikes and gabbroic intrusions from the southern Etendeka region of Namibia. The rocks represent the low-Ti magma series, with examples from both tholeiitic and alkaline groups. MgO contents range from 5 to 18 wt.%. PGE concentrations were measured on 5g samples by Ni-sulphide fire assay followed by ICPMS. The results give very low values compared with basalts from other LIPs, with 1 to 6 ppb total PGE, but in agreement with a previous study of Karoo and Etendeka rocks [1]. Primitive mantle-normalized PGE concentrations are below 1 and PGE abundance patterns show moderate to high fractionation (Pt/Ir = 5-30). Ratios of Cu/Pd are high (10^4 to 10^5). There appear to be no systematic differences in abundance or PGE patterns in the tholeiitic vs. alkaline magma series.

The low PGE contents in these rocks may relate to retention of sulphides in the mantle source as argued by [1] or to removal by sulphide saturation of the magma during ascent and evolution. Bulk-rock ratios of chalcophile-lithophile trace elements (e.g. Cu-Zr) in the samples suggest the latter but additional evidence will come from analyses of S and trace elements in olivine-hosted melt inclusions.

[1] Maier *et al*. (2003) *Contributions to Mineralogy & Petrology* **146**, 44–61.

https://doi.org/10.1180/S0026461X00006502 Published online by Cambridge University Press

Sea floor methane emissions in continental shelves and the role of anaerobic methane oxidation

IANA TSANDEV[1], PIERRE REGNIER[1,2], ANDREW DALE[3] AND ANDY RIDGWELL[4]

[1]Faculty of Geosciences, Utrecht University, Utrecht, the Netherlands
[2]Department of Earth and Environmental Sciences, Unversité Libre de Buxelles, Brussels, Belgium
[3]Leibniz-Institut für Meereswissenschaften (IFM-GEOMAR), Kiel, Germany
[4]School of Geographical Sciences, University of Bristol, Bristol, UK

Fluxes of methane from sea floor gas hydrates are a key forcing of Earth's climate. If this methane is oxidized aerobically, such as in a ventilated water column or the oxic part of the sediment, it results in loss of seawater dissolved inorganic carbon (DIC) and alkalinity (ALK) and $CaCO_3$ dissolution. The effect can be opposite if anaerobic oxidation of methane takes place, eg. throughout the reduced part of the sediment column, releasing alkalinity and inducing carbonate precipitation. In this study we identify shelf environments known for high methane hydrate concentrations and model the sediment column with a 1-D biogeochemical reaction network simulator (BRNS) of sedimentary dynamics. Upper boundary conditions on the sediment are extracted from an Earth system model of intermediate complexity – GENIE – through steady state fields of the relevant tracers (organic matter flux to the seafloor, bottom water oxygen content, etc.). We further impose bottom boundary upward advective fluxes of methane on the sediment column based on hydrate dissolution estimates. We identify the pathways of methane transformation – aerobic vs. anaerobic. We find that upon methane hydrate destabilization, anaerobic methane oxidation (AOM) can significantly reduce the efflux of methane to the overlying water and build up DIC and ALK inventories in the sediment porewaters, pushing the system toward carbonate precipitation. This results in increased effluxes of DIC and ALK to the overlying seawater. The magnitude of the AOM effect is, however very sensitive to the assumed rate of anaerobic methane oxidation in the sediment.

Biogeochemical impact of long-range transported dust over Northern South China Sea

S.-C. TSAY[1]*, S.-H. WANG[1,2] AND N.C. HSU[1]

[1]Goddard Space Flight Center, NASA, Greenbelt, Maryland, USA (*correspondence: si-chee.tsay@nasa.gov, christina.hsu@nasa.gov)
[2]Oak Ridge Associated Universities, Oak Ridge, Tennessee, USA (sheng-hsiang.wang-1@nasa.gov)

Transpacific transport and impact of Asian dust aerosols have been well documented (e.g. results from ACE-Asia and regional follow-on campaigns), but little is known about dust invasion to the South China Sea (SCS). On 19-21 March 2010, a fierce Asian dust storm affected large areas from the Gobi deserts to the West Pacific, including Taiwan and Hong Kong. As a pilot study of the 7-SEAS (Seven South East Asian Studies) in the northern SCS, detailed characteristics of long-range transported dust aerosols were first observed by a comprehensive set of ground-based instruments deployed at the Dongsha islands (20°42′52″ N, 116°43′51″ E). Aerosol measurements such as particle mass concentrations, size distribution, optical properties, hygroscopicity, and vertical profiles help illustrate the evolution of this dust outbreak. Our results indicate that these dust particles were mixed with anthropogenic and marine aerosols, and transported near the surface. Satellite assessment of biogeochemical impact of dust deposition into open oceans is hindered by our current inability in retrieving areal dust properties and ocean colors over an extensive period of time, particularly under the influence of cloudy conditions. In this paper, we analyze the changes of retrieved Chlorophyll-a (Chl-a) concentration over the northern SCS, considered as oligotophic waters in the spring, from long-term SeaWiFS measurements since 1997. Over the past decade, six long-range transported dust events are identified based on spatiotemporal evolutions of PM_{10} measurements from regional monitoring stations, with the aid of trajectory analysis. Multi-year composites of Chl-a imagery for dust event and non-dust background during March-April are applied to overcome insufficient retrievals of Chl-a due to cloudy environment. Due to anthropogenic modification within a shallow boundary layer off the densely populated and industrial southeast coast of China, the iron ion activation of deliquescent dust particles enhances the efficiency of fertilization for biological productivity. Compared to the West Pacific, the marine ecosystem in the northern SCS is much more susceptible to the biogeochemical impact of long-range transported Asian dust.

https://doi.org/10.1180/S0026461X00006502 Published online by Cambridge University Press

Multimegabar phase relations of major Earth and planetary materials

TAKU TSUCHIYA*, H. DEKURA, A. METSUE AND Y. KUWAYAMA

Geodynamics Research Center, Ehime Univ. Matsuyama 790-8577, Japan

Recent improvements in detection methods have allowed for the discovery of terrestrial exoplanets with 1–10 times Earth's mass, so-called 'super-Earths'. However, their interior is currently highly unclear, because understanding of the ultrahigh-pressure phase relations of major Earth and planetary materials is still quite limited. Those should be clarified before developing models of the internal structures of such objects. In this study, we tried to establish the ultrahigh-pressure and temperature phase relations of some silicates by means of *ab initio* techniques.

It has been known that silica (SiO_2) shows a sequential phase evolution from quartz, coesite, stishovite, $CaCl_2$, α-PbO_2 and pyrite (modified fluorite) with elevating pressure. However, further denser phases are still underdetermined, although studies on some low-pressure analogs have suggested an orthorhombic cotunnite phase as the final high-pressure phase. After examining several dense structure types with AX_2 compound, we successfully discovered a new phase transformation of pyrite type SiO_2 at multi-megabar condition to an unexpected hexagonal structure, which possesses high and relatively regular nine-fold coordinated Si. Similar phase transitions were also predicted in other dioxide compounds, and we finally succeeded in identifying one of them experimentally.

Then, we investigated high-pressure stabilities of some important silicate compounds ($MgSiO_3$ and $CaSiO_3$) and elucidated that the new phase change in silica could initiate breakdown of these silicates to oxide mixtures in the conditions relevant to the mantle of super-Earths and the core of giant planets. Thsy would lead to various complexities in their internal structures. Our calculations show that relatively large density jump is expected associated with the breakdown of $MgSiO_3$ post-perovskite, while the breakdown of $CaSiO_3$ yields an metallic oxide phase. Based on the results, we try to make a standard internal structure model of terrestrial exoplanets.

Research supported by JSPS Grant-in-Aid for Scientific Research Grants 20001005 and 21740379 and the Ehime Univ G-COE program 'Deep Earth Mineralogy'.

Subduction cycling of C-O-H volatiles from sediment melting

K. TSUNO[1]*, R. DASGUPTA[1], L. DANIELSON[2] AND K. RIGHTER[2]

[1]Department of Earth Science, Rice University, Houston, TX, 77005, USA (*correspondence: Kyusei.Tsuno@rice.edu)
[2]NASA-Johnson Space Center, Houston, TX, 77058, USA

Sediment subduction is a key mechanism of crustal recycling and mantle-exosphere exchange of C-O-H fluids. Thus high pressure melting systematics of C-O-H bearing pelite is important. While experimental data on the melting relations of alumina-rich pelites became recently available to 23.5 GPa [1, 2], those of alumina-poor pelites are limited to 3 GPa [3, 4]. To completely understand the deep cycling of water and carbon dioxide via sediment subduction, we performed new melting experiments on a silica and alumina-poor, water-undersaturated and carbonate-saturated pelite up to 7 GPa.

Piston cylinder and multi-anvil experiments are performed at 3-7 GPa and 800-1150 °C using a model pelite composition containing 1 wt.% H_2O and 5 wt.% CO_2 in Au capsules. We bracketed the solidus temperatures, at 800-850 °C at 3 GPa, at 900-1000 °C at 5 GPa, and <1100 °C at 7 GPa. Cpx, garnet, and coesite are present in all the experiments, and subsolidus phases also include rutile, phengite, and $calcite_{ss}$ at 3 GPa and 800 °C and joined by kyanite at 5 GPa and 900 °C. The near-solidus melts at 3 GPa, 850 °C are hydrous rhyolite, whereas those at 5 GPa, 1000 °C and 7 GPa, 1100 °C are K-rich carbonatitic. At 5 GPa and 1100 °C, both silicate and carbonatite melts were present. The phengite-out boundary is located between 850 and 900 °C at 3 GPa and 1000 and 1100 °C at 5 GPa, and phengite was not present at 7 GPa and 1100 °C. The solidus constrained in our study is 50-100 °C lower than the previous experiments on pelitic compositions [1, 2].

Comparison of our melting boundaries with thermal models of slab surface temperatures suggests that water-undersaturated, carbonated pelite solidus is located near the *P-T* trajectories of warm subduction zones. Hence subducting pelite in cold to intermediate subducting zones likely survives melting-induced devolatilization up to ~200 km. Hot subduction, on the other hand, may lead to supply of K-rich carbonatitic melt flux to deep sub-arc mantle wedge.

[1] Thomsen & Schmidt (2008) *EPSL* **267**, 17–31. [2] Grassi & Schmidt (2011) *J. Petrol.* **52**, 765–789. [3] Tsuno & Dasgupta (2011) *Contrib. Mineral. Petrol.* **161**, 743–763. [4] Tsuno & Dasgupta (submitted) *EPSL*.

https://doi.org/10.1180/S0026461X00006502 Published online by Cambridge University Press

Accumulation of trace elements in paddy soil and dry land under different geological background

C.L. TU[1], T.B. HE[2]*, C-Q. LIU[1] AND Y.C. LANG[1]

[1]State Key Laboratory of Environmental Geochemistry, Institute of Geochemistry, Chinese Academy of Sciences, Guiyang 550002, China

[2]Agricultural college, Guizhou University, Guiyang 550025, China (*correspondence: hetengbing@163.com)

To establish a rational farming mechanism, it is essential to know the relative contributions of both natural and anthropogenic sources to the trace elements in agricultural soil. Our results indicate that the difference of physicochemical properties in natural soils derived from three types of geological parent material is significant ($p<0.01$), but there are no significant differences between trace element contents. Trace element concentrations in most agricultural soils are far beyond natural soils and most of paddy soils have higher trace element contents than dry land soils, which indicates that anthropogenic input strongly influenced trace elements in agricultural soil and more seriously the paddy soil. In dry land, the basic physicochemical properties of soils are similar to those of natural soils derived from same geological parent material. Trace element contents exhibit high relationships with soil pH, C/N and physical clay (<0.01mm) ($p<0.05$). The soil derived from carbonate rock has relative high contents of trace elements and alkaline condition of the soil make the significant enrichments of Cd, Cr and Hg in dry land. The soil derived from red residua has the highest values of Pb and As contents in dry land, partly because the type of soil has amount of physical clay which could weaken the mobility of trace elements. In the paddy field, the differences of paddy soils derived from different parent materials are fading slowly due to numerous times of irrigation and drainage. The key difference is that most of paddy soils derived from carbonate rocks show neutral to alkaline, others show neutral to acidic in paddy fields. Traced element contents have just a pronounced relationship with cation exchange capacity (CEC) ($p<0.05$). With exception of Cr and Hg in paddy soil derived from carbonate rock, different geological background didn't significantly influence the trace element contents.

This work is financially supported by the Foundation of Chinese Academy of Sciences (KZCX2-XB2-08) and National Natural Science Foundation of China (41003009)

Transport and aggregation behavior of quantum dots and model nanoparticles in soil environments: Role of soil chemistry and biofilms

NATHALIE TUFENKJI[1]*, IVAN R. QUEVEDO[1] AND SHWETA TRIPATHI[1]

Department of Chemical Engineering, McGill University, 3610 University Street, Montreal, Quebec, H3A 2B2 Canada (*correspondence: nathalie.tufenkji@mcgill.ca)

Recent reports underline the potential environmental risks linked to the 'nano' revolution, yet little is known regarding the fate and impacts of engineered nanomaterials following their release in natural soils and groundwaters. To better understand the transport and fate of these materials in natural environments, a growing number of experimental studies are being conducted. Studies of nanoparticle transport in soils commonly involve laboratory-scale packed column experiments and more recently, deposition experiments using a quartz crystal microbalance (QCM). Such experimental investigations of nanoparticle transport and deposition provide valuable insights into their migration behavior and, hence, potential risks linked with the release of these materials in the natural environment.

Ongoing studies in our laboratory are aimed at examining the transport and aggregation behavior of commercial quantum dots (QDs) and model polystyrene latex nanoparticles in natural and model soil environments. Well-controlled experiments are conducted over a wide range of soil porewater chemistries to understand the role of salt concentration, ion valence and dissolved macromolecules on nanoparticle transport and stability. Moreover, the mobility of the nanoparticles in the presence of soil biofilms is evaluated using laboratory-scale column studies. Transport and deposition studies are complemented with physicochemical characterization of the nanoparticles and collector surfaces using several techniques (e.g. Kelvin probe force microscopy (KPFM), dynamic light scattering (DLS), transmission electron microscopy (TEM), confocal laser scanning microscopy (CLSM) and laser Doppler velocimetry (LDV)). Taken together, this data is used to interpret the stability of the quantum dots and model nanomaterials in soil environments.

https://doi.org/10.1180/S0026461X00006502 Published online by Cambridge University Press

Primary and secondary water content heterogeneity in volcanic glasses

H. TUFFEN[1], J.M. CASTRO[2], J. OWEN[1] AND J.S. DENTON[3]

[1]Lancaster Environment Centre, Lancaster University, UK (h.tuffen@lancaster.ac.uk, j.owen2@lancaster.ac.uk)
[2]Institut für Geowissenschaften, Johannes Gutenberg University Mainz, Germany (castroj@uni-mainz.de)
[3]Los Alamos National Laboratory (jo.denton@yahoo.com)

Spatial heterogeneities in the dissolved water content within volcanic glasses are generated by diffusive degassing and crystallization of melts, as well as subsequent post-eruptive hydration of quenched glasses. Characterization of the resultant water diffusion gradients using micro-analytical techniques such as SIMS or synchrotron FTIR allows us to model the timescale of water diffusion and thus key pre-, syn- and post-eruptive processes. We present a variety of micro-analytical data to illustrate three sources of water content heterogeneity within rhyolitic glasses.

Firstly, enrichment of water in glass surrounding spherulites reflects its expulsion during growth of anhydrous mineral phases. Our diffusion models have placed new constraints on spherulite growth rates within obsidian flows [1]. Secondly, we have found strong water enrichment adjacent to perlitic fractures in subglacially erupted obsidian lavas [2]. Diffusion and cooling models show that perlitisation starts at ~400 °C and occurs over timescale of days [3]. Finally, we have used SIMS analysis to overcome the hydration problem and successfully measure the dissolved magmatic water content of pumices [4]. This provides new insight into magma storage and degassing prior to an exceptionally violent eruption.

[1] Castro *et al*. (2009) *Chem Geol* **268**, 272–280. [2] Tuffen H *et al*. (2010) *Earth Sci Rev* **99**, 1–18. [3] Denton JS *et al*. in prep, *Geology*.[4] Tuffen H *et al*. in prep, *EPSL*.

Studies of near surface redox transitions in crystalline rocks in Sweden and Greenland

E.-L. TULLBORG[1]*, H. DRAKE[2], J. SUKSI[3] AND J. SMELLIE[4]

[1]Terralogica AB, P.O. Box 4140, SE-443 14 Gråbo, Sweden (*correspondence: evalena@terralogica.se)
[2]School of Natural Science, Linnaeus University, SE-391 82 Kalmar, Sweden
[3]Laboratory of Radiochemistry, Department of Chemistry, P.O. Box 55, FIN-00014 University of Helsinki
[4]Conterra AB, P.O. Box 8180, SE 104 20 Stockholm

Oxidising groundwater conditions in the near surface of crystalline rock usually change to reducing in the upper 100 m of the bedrock. To detect the depth of this redox transition zone only from groundwater considerations may be difficult because of flow changes and mixing with time. More useful is to use a combination of different geochemical analyses of redox sensitive elements (e.g. Ce, U) in fracture coating samples. These data, together with mapped changes in fracture mineralogy with depth (especially the presence or absence of minerals like Fe-oxyhydroxides and Fe-sulphides), have been shown to mirror the switch from oxidising to reducing conditions [1, 2, 3]. In addition, U-series isotopes can provide time constraints on redox changes contributing to mobilisation and deposition of uranium.

The present study compares new results from close to the ice margin in Greenland (Greenland Analogue Project [4].) with results from two coastal Swedish sites (Äspö and Laxemar) [2, 3]. One of the key questions for the long term safety of a repository for spent nuclear fuel is whether the intrusion of glacial meltwater can maintain its oxidising character to repository depth (~500 m). If that is the case, mineralogical and geochemical evidence should be observed, especially in fracture material from the Greenland drill cores.

The comparison of results shows that although evidence of oxidation (e.g. breakdown of pyrite and formation of Fe-oxyhydroxide) are documented to greater depth in the Greenland drill cores than at Äspö and Laxemar, it does not exceed 100 m. Also, positive Ce anomalies (indicating Ce^{4+}) are recorded to greater depth in the Greenland drill cores (~ 40 m) compared with Äspö and Laxemar (10-15 m), although still not very deep. Uranium isotopes indicate a transition from mobilisation to deposition in accordance with the other redox indicators, albeit the patterns are complex and the uranium content in the Greenland samples is very low.

[1] Tullborg *et al*. (2008) *Appl Geochem* **23**, 1881–1897. [2] Landtröm *et al*. (2001) SKB R-01-37. [3] Drake *et al*.(2009) *Appl Geochem* **24**, 1023–1039.
[4] www.skb.se/GAP.

https://doi.org/10.1180/S0026461X00006502 Published online by Cambridge University Press

Wetting of mineral surfaces – Molecular dynamics simulation

DANIEL TUNEGA[1,2], ROLAND ŠOLC[1], HASAN PAŠALIĆ[2], MARTIN H. GERZABEK[1] AND HANS LISCHKA[2]

[1]Institute of Soil Research, University of Natural Resources and Life Sciences, Vienna, Peter-Jordan-Strasse 82, A-1190 Vienna, Austria (*correspondence: daniel.tunega@boku.ac.at) (rsolc@boku.ac.at, martin.gerzabek@boku.ac.at)

[2]Institute for Theoretical Chemistry, University of Vienna, Währinger-Strasse 17, A-1090 Vienna, Austria (hans.lischka@univie.ac.at, hasan.pasalic@univie.ac.at)

Wettability of minerals is primarily related to an energetic characteristic of surfaces affecting processes as adhesion, friction, detergency, biofilm growth, etc. The wetting ability of a solid surface is mainly determined by its chemical composition, structure and topography [1]. The solid-liquid contact angle method is often used to characterize wettability of surfaces and to determine its surface free energy.

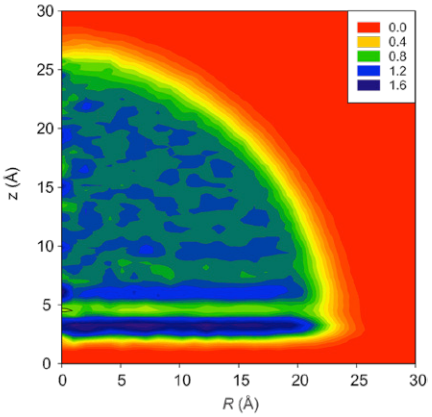

Figure 1: Visualization of water density profile (in g/cm3) of water droplet on the (001) tetrahedral kaolinite surface calculated for last 2 ns of MD simulation.

In order to elucidate structural and compositional factors affecting hydrophilic/hydrophobic character of minerals, interactions of water nanodroplets with basal surfaces of selected minerals (particularly kaolinite, goethite and lepidocrocite) were investigated by means of classical molecular dynamics simulations at room temperature. From the evolution and shape of the nanodroplet on the surfaces it was possible to characterize hydrophobic/hydrophilic character of studied surfaces.

[1] Bachmann, J. *et al*. (2000) *Soil Sci. Soc. Am. J.* **64**, 564–567.

Single particle ICP-MS for detection of engineered nanoparticles in environmental samples

JANI TUORINIEMI[1]*, GEERT CORNELIS[1], STEFAN GUSTAFSSON[2] AND MARTIN HASSELLÖV[1]

[1]Department of chemistry, University of Gothenburg. Kemivägen 10 412 96 Gothenburg, Sweden (jani.tuoriniemi@chem.gu.se, geert.cornelis@chem.gu.se, martin.hassellov@chem.gu.se)

[2]Department of Applied Physics, Chalmers University of Technology, 412 96 Gothenburg, Sweden (stefan.gustafsson@chalmers.se)

Nanoparticles are used in increasing quantities in a vast number of products and concerns have been raised about possible harmful effects on health and environment. In order to study their fate and transport in different environmental compartments, methods that are sensitive, selective and capable of detecting extremely low concentrations of engineered nanoparticles among a high background concentration of natural nanoparticles need to be developed.

The established methods in trace metal analysis fail to distinguish between different types of particles, and other techniques (e.g. electron microscopy) can not provide quantitative information on a routine basis.

Single particle ICP-MS has showed promising potential for element-specific particle detection, by detecting particles as single intense spikes [1]. In this study, the technique is developed for complex environmental matrices and the capabilities and limitations of the technique for analysis and size estimation are explored.

Au and Ag standard nanoparticle suspensions have been used to show that an optimal dwell time exists between 1 and 10 ms for a specific nanoparticle size - background concentration combination where the spread in spike intensities is minimized, the sensitivity with respect to concentration is maximized while the (spike) signal-to-noise-ratio is kept high enough to detect the smallest particles in the sample. It was also possible to simultaneously measure the size and number concentrations of e.g. Ag nanoparticles, and the background concentration of dissolved silver, because nanoparticle spike intensities are independent from the dissolved signal.

Finally, application of the method to spiked natural waters and real treated waste water as well as road runoff is presented.

[1] C. Degueldre, P-Y Farvarger S. Wold (2006) *Analytica chimica acta* **555**, 263-268.

https://doi.org/10.1180/S0026461X00006502 Published online by Cambridge University Press

Isotopic composition of the Early Precambrian crust of the South-Western Siberian Craton: Implications for crustal growth and mantle-crustal interaction through time

OLGA TURKINA

Institute of Geology and Mineralogy SB RAS, Novosibirsk, Russia (turkina@igm.nsc.ru)

Isotopic Sm-Nd whole-rock and Lu-Hf zicon analysis is a powerful approach for tracing crustal growth and evolution through time. New isotopic data on Early Precambrian metamorphic complexes and granitoids from the south-western Siberian Craton are used to constrain main stages of crustal growth via magmatism and to trace mantle-crustal interaction during lithosphere evolution.

The oldest crust of the south-western Siberian Craton consists of Paleoarchaean (3.3-3.4 Ga) TTG and felsic granulite complexes. The isotopic signatures (ε_{Nd} from +3.1 to -1.0 and ε_{Hf}=2.1-3.3) suggest involvement of pre-3.3 Ga crust in their formation. Felsic metamagmatic and granitoid complexes were formed through a time interval from 2.9 to 1.85 Ga and are mostly characterized by negative ε_{Nd} values suggesting their crustal-derived genesis. The ε_{Nd} values decrease through time but deviate from the isotopic evolution trend of the Paleoarchaean crust. The higher ε_{Nd} values are indicative of mantle contribution to the genesis of the felsic rocks. Both, the T_{Hf} (DM) of 3.0-3.2 Ga and ε_{Hf} from -1.6 to +2.4 of the 2.7 Ga felsic metavolcanics, confirm involvement of older crustal and mantle sources in their formation. The studied mafic metamagmatic associations vary in age from ca. 3.4 to 2.6 Ga. The Paleo- and Mesoarchaean amphibolites compositionally correspond to tholeiitic basalts. Their flat REE patterns $(La/Yb)_n$=0.6-1.4) and ε_{Nd} values (1.1-4.4) suggest derivation from depleted mantle. On the contrary, the Neoarchean (2.6-2.7 Ga) mafic granulites, which protoliths correspond to subduction-related basalts, are mostly enriched in LREE and possess variable ε_{Nd} (+3.9 to -0.2) and ε_{Hf} (7.2-2.2). These features suggest contamination of their mantle sources by crustal material probably via sediment subduction. Thus, the available isotopic data provide evidence of mantle-crustal interaction during the Early Precambrian evolution of the south-western Siberian Craton. Contribution of mantle sources in the formation of felsic rocks is traced during the whole Early Precambrian, while the reverse proccess of recycling of crustal material into the mantle are marked in the Neoarchaean mafic rocks only.

Rapid assembly of an 'S-type' batholith in New Zealand: The plutonic equivalent of a supereruption?

R. TURNBULL[1]*, A. TULLOCH[1] AND J. RAMEZANI[2]

[1]GNS Science, Private Bag 1930, Dunedin, New Zealand (*correspondence r.turnbull@gns.cri.nz)

[2]Dept. Earth, Atmospheric and Planetary Sciences, MIT, USA

Plutonic bodies are an integral part of most orogenic belts and reflect the plumbing system by which mantle and lower crustal melts are fractionated and crust is formed. A critical step in understanding the formation of the Earth's crust is investigating the physical and chemical processes that lead to the formation of large-volume silicic caldera-forming magmatic systems.

Recent research has suggested that some plutons were produced by incremental growth and solidification over several millions of years and therefore do not retain large volumes of eruptible magma at any stage in their construction. In contrast, caldera-forming eruptions require rapid accumulation of large volumes of silicic magma.

We present preliminary high-precision U-Pb ID-TIMS geochronology from the Devonian Karamea Suite in western New Zealand that suggest the entire suite of 'S-type' granites was emplaced within ~2.1 Ma The Karamea magma flux rates (~85-125km^3/km arc/Ma)[1] are comparable to, or in excess of, those estimated for volcanic 'flare-up' events (supereruptions) which are typically associated with large volumes of silicic magma. We hypothesise that the Karamea high magma production rates required intimate interaction between voluminous hot asthenospheric magma and the lowermost sialic crust, necessitating emplacement within an extensional intra-arc setting similar to that observed in the active Taupo Volcanic Zone of New Zealand. Detailed O- and Hf-isotopic studies in zircon, and geochemical characterisation of mafic end members of the suite will allow us to test these hypotheses, and also to determine the relative contributions of juvenile and recycled continental crust to magma generation.

[1] Tulloch *et al*. (2009) *GSA Bulletin*. **121**, 1236–1261.

https://doi.org/10.1180/S0026461X00006502 Published online by Cambridge University Press

Dissolved metals and As from metal mine waste - Laboratory vs. field determination

A.J.M. TURNER*, C.B. BRAUNGARDT AND J.S. RIEUWERTS

University of Plymouth, Drake Circus, Plymouth. PL4 8AA (*correspondence: alison.turner@plymouth.ac.uk)

Leachates from aged mine waste tips at two abandoned metal mines in south west England were investigated in order to determine the scale and mechanisms of ecotoxic element release and assess the advantages and limitations of field and laboratory methods. Tip drainage waters were sampled in streams and shallow groundwater and master variables were determined *in situ*. In the laboratory, mine waste samples were extracted in batch experiments (acetic acid, MilliQ H_2O and $MgCl_2$) and the European dynamic up-flow percolation test (CEN TS14405). A range of metals, metalliods and anions was analysed in water samples and mineralogy (XRD, SEM-EDX) and particle size of mine waste was determined.

Waste tip material contained a small proportion (<5%) of primary sulphide ore minerals, and Pb, Cu, Zn, Mn and As were associated with abundant secondary Fe phases and clays. Fractional release of elements from the mine waste was generally observed in column and field leachates. At low concentrations (<5 μmol L^{-1}), selective metal adsorption onto secondary Fe phases was implied in the order of affinity of Pb>Cu>Mn>Zn>Cd> Ni.

Under oxic conditions, element release from the waste material was controlled by the interplay of dissolution and sorption processes. Column and batch extractions with MilliQ H_2O provided a good approximation of metal concentrations observed in the field when the L:S ratio was representative of field conditions, i.e. low and high L:S ratio for perched water tables within tips and shallow groundwaters, respectively. However, metal and As behaviour at the solid-solution interface was very sensitive to pH change. Leachate As concentrations were higher in the field (up to 380 μmol L^{-1}, pH 5.0-5.3) than in the laboratory experiments (up to 41 μmol L^{-1}, pH 4.0-4.5), reflecting the greater mobility of oxyanions at higher pH values. Conversely, Pb concentrations were lower in the field (up to 2.8 μmol L^{-1} pH 3.2-5.6) compared to laboratory leachates (up to 81 μmol L^{-1}, pH 1.9-2.6). Batch extractants that amend the eluent pH also resulted in descrepancies between field and batch leachates. This highlighted the importance of maintaining pH conditions representative of field pore waters in column and batch extractions. Nevertheless, when applied to representative samples, carefully constrained laboratory experiments can aid the prediction of pollutant fluxes in the field.

Fluoride removal from solution by calcite — pCO_2 sorption kinetics

B.D. TURNER*, S.B. SLEAP, K. KRABBENHOFT AND S.W. SLOAN

Centre for Geotechnical and Materials Modelling, The University of Newcastle, 2308, NSW Australia (*correspondence: brett.turner@newcastle.edu.au) (Scott.Sleap@ newcastle.edu.au, Kristian.**Krabbenhoft**@newcastle.edu.au, Scott.Sloan@newcastle.edu.au)

Effective remediation modeling and design depends on the ability to predict the rate at which a pollutant will be removed from a system. It is important therefore, to model the sorption *rate* rather than equilibrium sorption. Here we establish the time dependence of F sorption under various conditions.

The kinetics of fluoride removal by calcite as a function of pCO2 (mol%), initial fluoride concentration and calcite surface area were analysed according to pseudo- first and second order reaction kinetics. If pseudo-second order kinetics are applicable, a plot of t/q_t against t should be a linear relationship, from which the initial sorption rate constant (h), can be determined from the slope and intercept of the plot.

Free drift experiments were carried out in a constant temperature room utilizing a gas glovebox connected to commercially prepared CO_2/N_2 mixtures. Solutions of F (as KF) were equilibrated in the CO_2/N_2 atmosphere prior to the addition of calcite of known mass and size (<150 μm & +1.18-2.36mm). pH and F^- ion selective electrodes were used to follow the reaction in at one minute intervals.

It was found that the pseudo-second order reaction kinetic model provided the best correlation to the data in all cases (r^2>0.99). Plots of the sorption rate constant (log (h)) vs pCO_2 show that for the same initial [F], the <150μm fraction (larger SA) has a larger rate constant as larger SA dissolves quicker. Particles with the same SA however show a significant difference in the sorption rate with changes in initial [F]. The fact that h increases with increasing [F]. is surprising given that previous findings[1] show the larger the initial concentration the slower the reaction rate as it takes longer to reach equilibrium

The major advantage of these results is the possibility of obtaining generalized predictive expressions which can be used directly to derive the amount of fluoride removed at any given concentration, pCO_2 and reaction time without the necesstity of developing complicated theoretical models.

[1] Plazinski, W. *et al*. (2009) *Advances in Colloid and Interface Science* **152**(1-2), 2–13.

https://doi.org/10.1180/S0026461X00006502 Published online by Cambridge University Press

Direct evidence for the nature and timing of sub-arc mantle metasomatism

SIMON TURNER[1], JOHN CAULFIELD[1], MICHAEL TURNER[1], PETER VAN KEKEN[2], RENE MAURY[3], MIKE SANDIFORD[4] AND GAELLE PROTEAU[5]

[1]GEMOC, Department of Earth and Planetary Sciences, Macquarie University, Sydney 2109, Australia
[2]Department of Geological Sciences, University of Michigan, MI 48109-1005, USA
[3]UMR CNRS 6538 Donaines Oceaniques, Universite de Bretagne Occidentale, Brest, France
[4]School of Earth Sciences, University of Melbourne, VIC 3010, Australia
[5]Universite Pierre et Marie Curie, Laboratoire de Petrologie, 4 Place Jussieu, Paris cedex 05, France

Subduction delivers sediment and hydrated oceanic lithosphere into the convecting mantle. Some of these materials are involved in magma generation and returned to the surface as arc volcanism. The remainder continues into the deeper mantle contributing to long-term heterogeneity that may be later sampled by mantle plumes. In order to understand the global cycling of volatiles in subduction zones it is essential to understand the physical and chemical processes of fluid release and melting. Unique upper mantle samples from Batan Island (Philippines) have incompatible trace element and radiogenic isotope characteristics typical of their host lavas. Here we show that they also preserve extreme U-Th-Ra disequilibria. These do not result from either host magma contamination, steady-state diffusion in the mantle or subsequent crustal level processes. Rather, they provide the first direct evidence that such signatures in arc lavas originate in the mantle and that contributions from both wet sediment melts (between 8 kyr and 10's kyr ago) and aqueous fluids (<< 8 kyr) were separately delivered from the slab. The samples also us to estimate the amounts of water (≥ 625 ppm) that may be returned to the asthenosphere, perhaps to be stored at the seismic transition zone.

Life as the catalyst of mineral weathering in acidic forest ecosystem

M-P. TURPAULT[1]*, S. UROZ[1,2], C. CALVARUSO[1,2], C. COLLIGNON[1,2], L. MARESCHAL[1], P. FREY-KLETT[2] AND C. LEPLEUX[1,2] .

[1]INRA-BEF 54280 Champenoux, France (*correspondence: turpault@nancy.inra.fr)
[2]IAM –INRA-Univ. Nancy, 54280 Champenoux, France (uroz@nancy.inra.fr)

In our temperate regions, forests ecosystems developed on acidic soils are characterized by a low nutrient-content and an absence of fertilization. In this context, the life (plant, fungi, bacteria) is strongly dependent on the nutrients input coming from soil mineral weathering and atmospheric deposits. However, what do we know about the relative contribution of biotic and abiotic reactions on the mineral weathering process? What is the stability of soil mineral in time? Are there mineral weathering hot spots into the soil? Who are the actors involved in mineral weathering? Our present knowledge highlights that mineral dissolution is increased in the upper soil horizons where life is intense and the organic matter mineralised. Preliminary analyses also show that a large proportion of fine-size minerals evolves during the seasons in relation with the environmental conditions. Notably, the soil under the influence of the tree root systems (ie rhizosphere) appears as an important mineral weathering hot spot due to intense biological activities (root and associated microbes), which take place in. Despite its small size (ca. 1% of soil), it contributes up to half of the weathering flux. Recent results showed an enrichment of efficient mineral weathering bacteria in the rhizosphere, suggesting a functional complementation between the trees and their associated microbes. Future challenges will be to identify the abiotic and biotic parameters impacting weathering reactions, and to develop models integrating life. Multidisciplinary approaches combining isotopic and genetic tools as well as biogeochemistry and ecology are needed.

https://doi.org/10.1180/S0026461X00006502 Published online by Cambridge University Press

Single crystal Sr-isotope data of Ferrar lavas and sills determined by LA-MC-ICPMS

JAN F. TYMPEL[1], MICHAEL ABRATIS[1], AXEL GERDES[2] AND LOTHAR VIERECK-GOETTE[1]

[1]Institute of Geosciences, Friedrich-Schiller-Universitaet Jena, Germany

[2]Institute of Geosciences, Goethe-Universitaet Frankfurt am Main, Germany

The emergence of the Mid-Jurassic Ferrar Large Igneous Province (LIP) in North Victoria Land (NVL), East-Antarctica, which preceded the Mesozoic disintegration of the supercontinent Gondwana, constitutes an apposite example of rapidly emplaced large-scale in- and extrusive magmatic successions within the continental lithosphere. The emplacement commenced with shallow sill intrusions into partly unconsolidated epi- and volcaniclastic sediments of a preexisting sedimentary basin (Transantarctic Basin) chiefly composed of Triassic to Jurassic fluvial strata, forming a potent and up to several hundred meters thick continuous igneous succession that is capped by the Kirkpatrick flood basaltic andesite series.

Strontium isotope ratios ($^{87}Sr/^{86}Sr$) determined by *in situ* Laser Ablation Multi Collector Inductively Coupled Mass Spectrometry (LA-MC-ICP-MS) on single plagioclase phenocrysts show characteristically radiogenic (crustal) values between 0.7094 and 0.7117 as is characteristic of the Ferar LIP and distinguishing from the Karoo LIP. Within this range, lithologically and geochemically distinct rock units display systematically different isotope ratios: shallowly intruded andesite sills and associated cross-cutting dykes show the most radiogenic values ($^{87}Sr/^{86}Sr$ = 0.7112 - 0.7117), local pillow lavas of basaltic andesite composition and flows show intermediate ratios ($^{87}Sr/^{86}Sr$ = 0.7103 - 0.7106) and orthopyroxene rich lava flows feature the lowest ratios ($^{87}Sr/^{86}Sr$ = 0.7094 - 0.7097). Moreover, stratigraphically young high-Ti Kirkpatrick andesite lavas exhibit significantly lower Sr isotope ratios than underlying low-Ti flow counterparts. These systematic variations in isotope ratios could indicate different degrees of crustal assimilation of the respective magmas.

Measured isotope ratios of Sr and Rb ($^{87}Sr/^{86}Sr$ vs. $^{87}Rb/^{86}Sr$) from most rock samples allow for plotting well defined isochrones, which are in fair agreement with previously published crystallization ages averaging around 180 Ma. Method-related dating uncertainties, however, complicate chronologic interrelations between the petrographically distinct units.

Heinrich events on the Irish Atlantic margin: Insights from the Pb isotopic composition of ice-rafted feldspar

S. TYRRELL[1]*, L.T. TOMS[1,2] AND P.D.W. HAUGHTON[1]

[1]UCD School of Geological Sciences, University College Dublin, Belfield, Dublin 4, Ireland (*correspondence: shane.tyrrell@ucd.ie)

[2]PetroStrat Ltd., Tan-y-Graig, Conwy, Wales, LL32 8FA, United Kingdom (lee.toms@petrostrat.com)

Understanding the provenance of ice-rafted debris (IRD) constrains the delivery of material from the ice margin into the marine environment and provides insight into the coupling between ice sheet instability, ocean circulation and the climate system. Six distinct IRD-rich horizons from the Last Glacial are recognized in the North Atlantic deep marine record. These horizons, termed 'Heinrich layers', are linked with binge-purge ice-cycles of the Laurentide (LIS) ice-sheet and associated with Bond-Cycle (~10ka) rapid cooling. These layers bracket other, less-significant, ice-rafting events which are potentially coupled with millennial-paced Dansgaard-Oeschger oscillations.

The Pb isotopic composition of K-feldspar, measured *in situ* using LA-MC-ICPMS, provides a powerful means of linking ice-rafted debris back to its basement source/s. In the North Atlantic region, Pb isotopes in basement rocks have been shown to vary at a scale appropriate to distinguishing ice sheet sources. Specifically, unradiogenic Pb K-feldspar compositions are indicative of derivation from the LIS or Greenland ice-sheet (GIS), whereas more radiogenic compositions suggest sourcing from the British-Irish ice sheet (BIIS).

K-feldspar Pb analyses have been obtained from IRD-bearing horizons in two well-characterised gravity cores on the eastern margins of the Rockall Basin, offshore western Ireland. These include data from 'Grey Bands', a lithologically distinct facies and likely 'Heinrich layer' equivalent. The results show that LIS/GIS sources dominate the 'Grey Bands' whereas BIIS sources mainly contributed the non-'Grey Band' IRD, supporting correlation of 'Grey Bands' with Heinrich events. The data also illustrate that the Bond-Cycle paced forcing, which may have led to increased ice calving on the LIS, had little or no apparent impact on the stability of the BIIS. Furthermore, this approach has allowed for the identification of a Heinrich-like layer in the older (~250ka; MIS 8) glacio-marine record west of Ireland.

https://doi.org/10.1180/S0026461X00006502 Published online by Cambridge University Press

Lead sources in Lower Silesia (S.W. Poland): Isotopic study of soils, basement rocks and anthropogenic materials

R. TYSZKA[1]*, A. PIETRANIK[2], J. KIERCZAK[2], V. ETTLER[3] AND M. MIHALJEVIČ

[1]**Wroclaw University of Environmental And Life Sciences**, C.K. Norwida 25/27, 50-375 Wroclaw, Poland (*correspondence: rafal.tyszka@up.wroc.pl)

[2]University of Wroclaw, Cybulskiego 30, 50-205 Wroclaw, Poland

[3]Charles University, Albertov 6, 128 43, Prague 2, Czech Republic

At present, water and atmosphere is contaminated by heavy metals derived from different sources. The main challenge is to identify these sources and estimate their contributions. In environmental studies isotopic ratios of $^{206}Pb/^{207}Pb$ and $^{208}Pb/^{206}Pb$ are routinely used to track Pb contamination in these sources, because at the first approach, the anthropogenic Pb has lower $^{206}Pb/^{207}Pb$ and higher $^{208}Pb/^{206}Pb$ than the lithogenic one.

In this study we characterize Pb isotopic ratios of various lithogenic backgrounds and anthropogenic materials in Lower Silesia, SW Poland. The area comprises several important mining and smelting sites, mainly of Cu ores, and coal mines. We also provide isotopic data for soil profiles developed on different geological units, in contaminated and uncontaminated sites, in order to characterize interactions between anthropogenic and lithogenic materials in the area.

Samples of basement rock, ore, coal, slag, fly ash and soil were collected from different parts of Lower Silesia. Anthropogenic materials from Lower Silesia have uniform $^{206}Pb/^{207}Pb$ of ca. 1.18 with Pb concentrations varying from 3 to over 10000 ppm. On the other hand, $^{206}Pb/^{207}Pb$ in natural rocks varies from 1.17 to 1.38 and the Pb concentration is generally low, below 30 ppm.

The soil profiles formed on natural bedrock are characterized by increase in Pb concentration from the bottom to the top of each profile, which is correlated with decrease in $^{206}Pb/^{207}Pb$ and are good records of contamination by antropogenic airborne material. The uppermost soil horizons (A and O) contain from 40 to 70% of anthropogenic Pb and deeper horizons may contain up to 10% of anthropogenic Pb. The source of this Pb is best approximated by coal burning.

https://doi.org/10.1180/S0026461X00006502 Published online by Cambridge University Press

Lead, zinc and antimony leaching from glass-works fly ash in simple organic acids

M. UDATNY[1]*, M. MIHALJEVIC[1] AND L. STRNAD[2]

[1]Institute of Geochemistry, Mineralogy and Mineral Resources, Faculty of Science, Charles University, Albertov 6, 128 43 Prague, Czech Republic (*correspondence: martinudatny@seznam.cz)

[2]Laboratories of Geological institutes, Faculty of Science, Charles University, Albertov 6, 128 43 Prague, Czech Republic

The release of hazardous elements from anomalous geomaterials represent risk for the environment. In our research, we focused on exogenic alteration of fly ash (FA) originating from glass-works in Svetla nad Sazavou (Czech Republic). This factory produces glass with high amounts of PbO. FA from electrostatic filter contains elevated concentrations of Pb, Zn and Sb. The main mineral phases of this material detected by X-ray diffraction are calcite $CaCO_3$ (79%), witherite $BaCO_3$ (10%), quartz SiO_2 (6%) and senarmontite Sb_2O_3 (5%). Small amount of FA may be emitted from factory and can settle in the surrounding environment (soil).

Low-molecular-weight organic acids (citric, acetic and oxalic in concentration of 0.5 mmol/L), simulating soil-like environments and deionised water, were used to test possible mobilization of risk elements from the FA. The leaching experiments were carried out at liquid-to-solid (L/S) ratio of 10 (1 g of FA in 10 ml of leaching medium). The solutions were shaked in ten different times (0.5 to 1440 hours). Leachates were analyzed by inductively coupled plasma mass spectrometry (ICP-MS).

Lead, Zn and Sb exhibit different kinetic leaching curves corresponding to different behaviour of cations (Zn, Pb) and anion (Sb). The concentration of Zn in leachate initially increased, then rapidly decreased and subsequently wery slowly increased. The Pb concentration increased rapidly at the beginning and then very slowly decreased due to possible sorption on present and newly formed phases. Concentration of Sb in leachate increased during all the experiment, which can be attributed to the slow dissolution of senarmontite. Large differences between four leaching solutions were not observed. The leaching is fastest in the citric acid solution. The initial pH were about 3.3–4.0 for organic acids and about 5.6 for deionised water). All the leachates reached the pH value about 10, which corresponds to the equilibrium with calcite present in the FA.

Newly discovered MIL 090030, MIL 090032, and MIL 090136 nakhlites: Paired with MIL 03346?

A. UDRY AND H.Y. MCSWEEN, JR.

Department of Earth and Planetary Sciences, University of Tennessee, Knoxville, TN, 37996, US

Here we present the petrology of newly discovered (2009-2010) meteorites: MIL 090030, MIL 090032 and MIL 090136 from Miller Range, Antarctica. Our aim is to test the hypothesis [1, 2] that these meteorites are paired with nakhlite MIL 03346, which underwent less equilibration and faster cooling that the other nakhlites, and so originate from the top of the nakhlite cumulate pile [3].

The mineralogy of these nakhlites is dominated by cumulus euhedral augite and less-abundant cumulus olivine. They also display a fine-grained albitic intercumulus matrix composition, which exhibits fayalite-magnetite filaments, and skeletal ilmenite. Pyroxene displays a 10 μm Fe-rich rim, suggesting reequilibration with intercumulus matrix. Iddingsite has been observed, representing the aqueous alteration product of olivine. Pyroxene cores have a composition of Wo_{40} and En_{36}, and pyroxene rims have an average composition of $Wo_{32\text{-}40}$ and $En_{8\text{-}12}$. Olivine has a composition of $Fo_{35\text{-}42}$, and interstitial olivine has a composition $>Fa_{90}$, which are similar to those of MIL 03346 [3].

Similarities in mineral compositions, abundances, and textures infer that these nakhlites are paired with MIL 03346. Major and trace elements combined with CSD analyses, will determine the location of these three nakhlites within the cumulate pile and further assess the possibility of a pairing with nakhlite MIL 03346. This enables the petrologic variability to be constrained within a much larger sample of MIL 03346.

[1] Righter K. (2010) *Antartic Meteorite Newsletter* **33**, 2. [2] Corrigan C. M. *et al*. (2001) *LPSC* **42**, #2657. [3] Day J. M. D. *et al*. (2005) *Met & Pl. Sc*. **41**, 581–606.

https://doi.org/10.1180/S0026461X00006502 Published online by Cambridge University Press

'Hidden' metals and minerals: How to detect nanocompounds

S.S. UDUBASA[1]*, G. UDUBASA[1], S. CONSTANTINESCU[2] AND N. POPESCU-POGRION[2]

[1]Univ. of Bucharest, Fac. of Geology & Geophysics, Bucharest, Romania (*correspondence: sorin.udubasa@gmail.com)

[2]National Institute of Materials Physics, Magurele-Bucharest, Romania

Mining waste dumps provide materials suitable to investigate the fate of some metals and minerals during processing/alteration by meteoric waters. Such materials contain commonly all the minerals of the primary ores. It has been proven that, in addition, some minerals or compounds at nanometric scale can form within the waste dumps. Such minerals we can call 'hidden', as they escape the routine investigation by mineralogical methods. Their identification relies on structural techniques such as TEM/SAED, NGR (Mössbauer), XRD etc.

A waste dump in the Leaota Mts., South Carpathians, Romania, has been selected for detailed investigations. The material was produced by exploration of several types of ores, i.e. a combination of pentametallic ores (Ag-Co-Ni-Bi-U) and gold + Cu-Pb-Zn ores. Note that the waste dump is about 50-60 years old.

Attempts were made for the uptake of metals by using *Zea mays* and *Trifolium repens* planted on waste dump materials and neutral soils artificially enriched in metals (Au, U, Cu, As). Good results were obtained in both experiments. Significant enrichment factors of metals (plants vs. starting substratum) were obtained in both cases and both plants, plus surprisingly by analysing also *Alnus incana*, a spontaneously grown tree on the waste dump [2].

The 'hidden' compounds of nanometric size were identified in all the samples analysed: Au, Au-Ag alloys, Ag_2CO_3 (probably the first occurrence under natural conditions), maghemite, wüstite, pseudobrookite, lavendulan, and an amorphous phase, on which the silver carbonate develops. Such nanocompounds are likely to facilitate the metals uptake by plants as the nano-sized compounds show a greater bioavailability as compared to the crystalline (larger size) equivalents [1, 3].

The search for nanocompounds in plants and a deeper investigation of the amorphous phase are in progress.

[1] Hochella (2008) *Elements* **4**, 373–379. [2] Udubasa *et al*. (2010) *Rev. Roum. Geol./Rom. J. Geology*, **53–54** (in press). [3] Waychunas & Zhang (2008) *Elements* **4**, 381–387.

Ultraviolet Spectra of $^{32/33/34/36}SO_2$; implications for the Archaean atmosphere

YUICHIRO UENO[1], SEBASTIAN DANIELACHE[2], SHOHEI HATTORI[2], MATTHEW JOHNSON[3] AND NAOHIRO YOSHIDA[2]

[1]Tokyo Institute of Technology, Meguro, Tokyo 152-8551, Japan (ueno.y.ac@m.titech.ac.jp)

[2]Tokyo Institute of Technology, Midori-ku, Yokoyama, 226-8502, Japan

[3]University of Copenhagen, DK-2100, Denmark.

Photodissociation of SO_2 is known to yield mass independent fractionation of sulfur isotopes (S-MIF). The MIF recored in the Archaean sedimentary rocks can be an important tracer for the atmospheric chemistry at that time, though wavelength dependency of the MIF by SO_2 photolysis is still poorly understood. We newly determined the ultraviolet absorption cross sections of not only $^{32}SO_2$, $^{33}SO_2$ and $^{34}SO_2$ but also $^{36}SO_2$ from 190 to 220 nm with a resolution of 4 cm^{-1}. The spectra of the ^{32}S, ^{33}S and ^{34}S samples are in agreement with our previously published spectra [1]. The cross sections of the isotopically enriched species (>98% for all the four isotopologues) were corrected based on the isotopic composition of the samples used for the measurements. The absorption spectra show rich vibrational structure and the positions and widths of the peaks change with isotopic substitution in a complex fashion.

The results show that the mass independent fractionation observed during broadband photolysis is product of the change in the amount of red shifting of the heavier isotopologues as suggested by our previous analyses [1, 2].

We will discuss the implications for the chemical composition of the Archaean atmosphere and its evolution based on our calculated wavelength dependency of mass independent fractionation factors for ^{33}S and ^{36}S.

[1] Danielache *et al*. (2008) *J Geophys Res* **113**, D17314.
[2] Ueno *et al*. (2009) *PNAS* **106**, 14784–14789.

https://doi.org/10.1180/S0026461X00006502 Published online by Cambridge University Press

A novel application of (U-Th)/He geochronology to constrain the age of small, young meteorite impact craters: A case study of Monturaqui crater, Chile

I. UKSTINS PEATE[1], M.C. VAN SOEST[2] AND J.-A. WARTHO[2]

[1]Geoscience, 121 Trowbridge Hall, Univ. Iowa, Iowa City IA 52242 (Ingrid-Peate@uiowa.edu)

[2]Noble Gas Geochem. & Geochron. Labs, School of Earth and Space Exploration, Arizona State University, Tempe AZ 85287

Small and young impact structures have been commonly dated by methods such as thermoluminescence, ^{14}C, short-lived extinct radionucleide and cosmogenic techniques. However, (U-Th)/He dating is a low temperature radiometric technique that could potentially bridge the gap between the previously mentioned methods and common geochronological techniques employed on larger impact structures to yield precise impact formation ages. Here we report (U-Th)/He apatite and zircon single crystal ages from the small and young Monturaqui impact structure. The very small size of this crater will act as an ultimate test for the applicability of the low temperature (U-Th)/He technique for dating very small, young impact structures.

We selected two samples of impactite from the Monturaqui crater, representing different lateral sampling areas from the ejected material. A total of 10 zircons and 22 apatite grains were analyzed, and yielded a total of 10 successful zircon ages, and 12 successful apatite ages. The zircon (U-Th)/He ages range from 0.662 to 197.3 Ma and the apatite (U-Th)/He ages range from 0.616 to 61.5 Ma. This age fits well with the previous age range estimates for Monturaqui, and the range is interpreted to reflect a set of partially to completely reset (U-Th)/He ages, which yielded 2 reset apatite ages and 1 reset zircon age, which give a mean age of 663 ± 90 ka.

The results of this study show that the (U-Th)/He dating method has the potential to yield accurate ages for even very small impact structures, like Monturaqui: 663 ± 90 ka. Many of the grains are only partially reset, requiring analysis of a large number of grains to obtain an accurate age, similar to detrital dating studies.

Calorimetry in soil sciences: An unique approach

HAMEED ULLAH*, JOSE A. SIMONI AND CLÁUDIO AIROLDI

Instituto de Quimica, Universidade Estadual de Campinas, Campinas, São Paulo, Brazil (*correspondance: hameedchemist@yahoo.com)

All physical, chemical and biological processes are accompanied by changes in energy which means, heat. This makes calorimetry one of the most suitable techniques to study all these process [1]. In Soil study, microorganism, microbial biomass and organic matter are the most important parameter of soil quality [2] and they could be evaluated, at the same time, using Calorimetry, more generally by ITC and DSC.

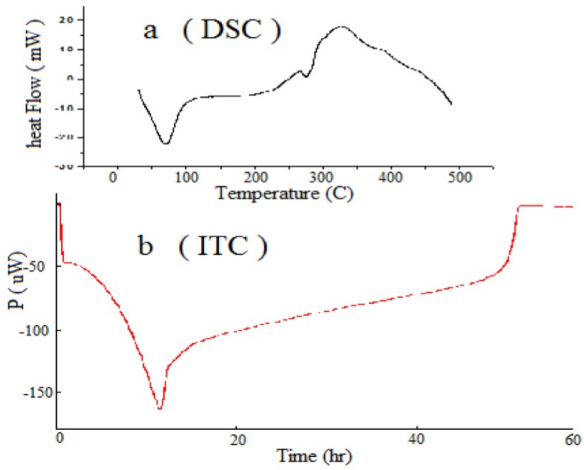

Figure 1: DSC (a) and ITC (b) curves of soil sample

In this study we have evaluated the use of Isothermal microcalorimetry (ITC) to study the effects of soil aging and influence of different experimental conditions on the glucose degradation of Brazilian soil. We also study the influence of the green house effect on the soil metabolism using ITC (Fig.1b). Differential Scanning Calorimetry used to study various properties (organic matter etc) of the soil understudy (Fig.1a). [1] Barros, N.; Salgado, J. and Feijóo, S, (2007) Thermochimica Acta **58**, 11. [2] Sposito, G (1989), The Chemistry of Soils., Oxford University Press, New York, pp, 43

https://doi.org/10.1180/S0026461X00006502 Published online by Cambridge University Press

Oxygen and carbon isotope signatures of high-latitude Permian to Jurassic calcitic fossils from southern hemisphere

C.V. ULLMANN[1]*, H.J. CAMPBELL[2] AND C. KORTE[1]

[1]Københavns Universitet, Øster Voldgade 10, 1350 København K, Denmark (*correspondence: cu@geo.ku.dk)
[2]GNS Science, 1 Fairway Drive, Avalon 5010, New Zealand

Oxygen and carbon isotope values of calcitic fossils have been frequently used for characterization of palaeo-environments and for attempts to estimate temperature of past seawater. Fossil shell and skeletal remains of low-Mg-calcite are most suitable for this purpose because of their resistance to diagenesis and to resetting of their primary geochemical signals. Studies of samples from high palaeolatitudes are of particular interest of their potential to quantify past palaeotemperature gradients.

In the present study, brachiopods, bivalves and belemnites were sampled from Permian to Jurassic successions in New Zealand and New Caledonia that were deposited at palaeolatitudes higher than 60°S in marine forearc environments with sedimentation dominated by volcanogenic siliciclastics. The good temporal resolution, based on New Zealand stages, minimizes errors in stratigraphic correlation to low latitudes. The quality of samples was checked by scanning electron microscopy (SEM) with complementary trace element evaluation (ICP-OES) currently in progress. These screening techniques are used for evaluation of postdepositional alteration of samples as well as for detection of potential vital effects and ecological impacts.

A preliminary evaluation of about 1200 $\delta^{18}O$ and $\delta^{13}C$ values shows distinct temporal fluctuations based on the upper envelopes of the trends [cf. 1]. The overall carbon isotope trend is in good agreement with the low-latitude datasets, including its rapid increase of ~4 ‰ during the early Late Triassic [2] that is therefore likely of global nature. The early and middle Permian and the late Jurassic high-latitude $\delta^{18}O$ values are heavier if compared to their low-latitudes counterpart. The Triassic values, on the other hand, do not show any clear difference between high- and low-latitudes, indicating a diminished pole-to-equator sea surface temperature gradient at these times.

[1] Korte *et al*. (2008) *Palaeogeogr. Palaeocl.* **269**, 1–16.
[2] Korte *et al*. (2005) *Palaeogeogr. Palaeocl.* **226**, 287–306.

Long-term forecast of acidity load from overburden substrate into a mining pit lake: An integrated approach

K.-U. ULRICH[1]*, I. GUDERITZ[1], B. HEINRICH[1], L. WEBER[2], K.-H. POKRANDT[2] AND C. NITSCHE[1]

[1]BGD Soil & Groundwater Laboratory, 01219 Dresden, Germany (*correspondence: kulrich@bgd-gmbh.de)
[2]LMBV Lausitzer & Mitteldeutsche Bergbauverwaltungs-gesellschaft mbH, 04356 Leipzig, Germany

Open-cast lignite mining in Germany left behind hundreds of lakes most of which are strongly acidic and do not meet water quality standards set for recreational use and water management purposes. To estimate future expenses and develop appropriate reclamation technologies, the authority in charge (LMBV) needs a reliable prediction of the lake water chemistry including the loads of acidity and alkalinity. By combining field and bench experiments with appropriate models, the most relevant physicochemical processes were identified and reliable data collected to determine crucial model parameters that enable a long-term forecast of net acidity load from the lake bed into the water of Lake Zwenkau, a pit lake of $176 \cdot 10^6$ m^3 currently being filled. The results demonstrate that the release of acidity is mainly by molecular diffusion of protons following ion exchange within the submerged overburden substrate (~5 km^2). Similar release rates were found in both a 10-month field test and bench experiments under controlled conditions. While during the five-year period of lake filling the overburden substrate contributes by only ten percent to the overall load of net acidity, this source of acidity will dominate over other sources like groundwater recharge beyond the filling period.

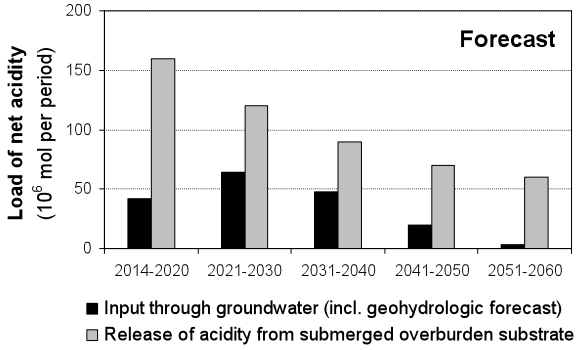

Without technical treatments, the discharge of net alkalinity from natural groundwater may not balance the net acidity of the pit lake before the 2051-60 decade.

https://doi.org/10.1180/S0026461X00006502 Published online by Cambridge University Press

Weathering effects on the mineralogical and geochemical composition of the New Caledonia ophiolite

MARC ULRICH[1]*, MANUEL MUÑOZ[1], STEPHANE GUILLOT[1], CATHERINE CHAUVEL[1], DOMINIQUE CLUZEL[2] AND CHRISTIAN PICARD[3]

[1]Institut des Sciences de la Terre (ISTerre), CNRS, Université Joseph Fourier, France (* correspondence : marc.ulrich@ujf-grenoble.fr)
[2]PPME, Université de la Nouvelle-Calédonie, Nouméa, Nouvelle-Calédonie
[3]Chrono-Environnement, Université de Franche Comté, Besançon, France

Since its complete obduction (at ~34 Ma), the New Caledonia ophiolite has experienced strong weathering due to tropical conditions. This alteration is expressed as laterization affecting the serpentinized peridotites located at the upper part of the massif. This weathering does not macroscopically affect the serpentinites located in the lower part of the ophiolite, but previous studies showed that these serpentinites display anomalous chemical composition relative to the others (silica enrichment, strong Ce negative anomaly).

Our study focuses on the determination of the processes responsible of (a) the chemical variability of the serpentinites and (b) the formation of new mineral phases in the different parts of the ophiolitic sequence. First, mineral phases (including the polymorphs of serpentine) were identified by Raman spectrometry. Second, the relationship between mineral phases in finely-divided assemblages were characterized using an original method, based on micro-beam X-ray fluorescence mapping of cm-scale samples. Third, the chemical exchanges between the different parts of the ophiolitic sequence were estimated from the compositions of major elements and REE in serpentinites, peridotites and laterites.

Our results demonstrate that the chemical and mineralogical transformations of the basal serpentinite are directly linked to the laterization process occurring at the top of the ophiolite. Laterization leads to leaching of silica, magnesia (~80g/100g of protolith) and REE. Only the cerium, which is immobile in oxidyzing conditions, remains immobile in the laterites. Leached elements are transported by percolation of meteoric fluids to the bottom of the ophiolitic sequence where they accumulate and precipitate by supersaturation. New phases such as magnesite and amorphous silica are formed. In the laterites located at the top of the sequence, the leaching process leads to the concentration of transition metals of economical interests such as iron and nickel.

Determining the porosity of analcime by X-ray reflectometry

VASILY ULYASHEV

Institute of Geology Komi SC UB RAS, Syktyvkar, Russia, 54 Pervomayskaya st (*correspondence: vaskom77@mail.ru)

X-ray reflectometry represents the method of research based on measurement of reflective ability in x-ray range of lengths of waves and using the phenomenon of full external reflexion of X-rays. The given technique last years is used in chemistry, the physicist and materials technology for definition of physical and geometrical properties of surfaces, thin films and multilayered structures.

In the presented work as a method x-ray reflectometry porosity of a mineral - analcime Na_2 $[Al_2Si_4O_{12}]$ (H_2O) $_2$ is investigated. Reflectogram the given mineral is on fig. 1.

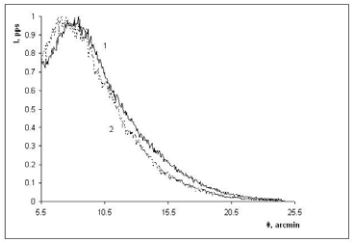

On reflectogram we find a critical angle for each curve *($\theta_{exp.\,cur.}$)* which corresponds to a point with the intensity equal to half of the maximum size (I = 0.5). From fig. it is visible that a critical angle initial mineral: *$\theta_{exp.\,cur}$ = 11, 9 argmin*. For this purpose, what to define porosity it would be necessary to know still a critical angle calculated theoretically under the formula of Frenelja *$\theta_{theor.\,cur}$ = 13, 37 argmin*.

Knowing experimental and theoretical critical calculate angles porosity under the formula $P = 1–(\theta_{exp.cur}/\theta_{the.cur.})^2$ [1].

Porosity of the initial sample has made *21 %* (an error *of 1 %)*.

Let's consider reflectogram annealed analcime (a curve 2). In drawing distinctions of curves 1 and 2 are well visible. Annealing has led to displacement critical angle towards smaller corners (*$\theta_{exp.\,cur}$ = 11, 5 argmin)*. Porosity annealed a mineral has made *27 %*.. Thus, annealed has led to porosity increase. At present while there is no strict explanation of this effect. It is possible to assume that during time annealed there was a partial phase transition in surface mineral areas. It can be assumed that during annealing occurred partial phase transition in the surface region of the mineral.

[1] A.A. Lomov, V.A. Bushuev, V.A. Karavansky. (2000) *Kristallografija* **45**(5), 915–920.

https://doi.org/10.1180/S0026461X00006502 Published online by Cambridge University Press

Transboundary problems of water resources quality in the Selenga river basin

I.D. ULZETUEVA*, D.TS.-D. ZHAMYANOV, B.O. GOMBOEV AND V.V. KHAKHINOV

Baikal Institute of Nature Management SB RAS, 8, Sakhyanova Str., Ulan-Ude, 670047, Russia (*correspondence: idulz@mail.ru, dabaj18@yahoo.com)

The Selenga river basin is occupies the territory of 447060 km^2 and it is devided by two countries – Russia and Mongolia. 67 % of territory is situated in Mongolia, 33 % - in Russia [1].

From 2007 to 2009 years the Baikal Institute of Nature Management together with Korea Environment Institute, Institute of Geoecology of Mongolian Academy of Sciences have carry outed 3 scientific expeditions in the territory of Selenga river basin (in territory of Russia and Mongolia) within the scope of the International project 'Integrated water management model on the Selenge river basin' for social and economic information collection and water sampling.

We studied the identification of the general content of 15 microcomponents (Fe, Cu, Mn, Zn, As, Mo, Al, Pb, U, Cd, Ni, Co, Cr, Ag, Au) in 30 samples in water objects of the Selenga river basin: 16 from which are selected in territory of Mongolia, on river Selenga inflows – Orkhon, Tuul, Kharaa, 14 in Republic of Buryatia (Russian Federation) – in waters the river Selenga, and on its inflows – Uda, Dzhida, Modonkul.

The investigated waters of the Selenga river basin are alkalescent and low-mineralized, concerning to hydracarbonate class of calcium group and have a favorable oxygen mode. Reduction of concentration of the main ions downstream the river is connected with effect of dilution by waters of inflows which have a smaller mineralization.

Results of researches of the Selenga river basin water quality have shown that the basic pollutants are metals: copper, iron, zinc, arsenic, aluminium, manganese, molybdenum, uranium.

Almost all water objects do not correspond to the requirements of water objects quality of fishery purpose (in Russia the rivers of fishery purpose have the highest standards on water quality, the river Selenga in the territory of Russia is the water object of fishery purpose). The Most polluted rivers are Tuul, Kharaa, Modonkul which basins are the most influenced by industrial regions, and also mining enterprises.

[1] *The Ecosystems of Selenga basin*.–Moscow, Nauka, 2005.

Release mechanisms of Sr and Cs from the weathered Hanford sediments

W. UM[1,2]* AND H-S CHANG[3]

[1]Pacific Northwest National Laboratory, Richland, WA, USA (*correspondence: wooyong.um@pnl.gov)
[2]Pohang University of Science and Technology, South Korea
[3]Savannah River Ecology Laboratory, Aiken, SC, USA

Introduction

Various aspects of the acute effects of the released high level radioactive waste on sediments, including mineral weathering and contaminant transport have been extensively investigated at the Hanford Site. However, the long-term behavior of radionuclides in the contaminated sediment after the removal of the caustic source is not as well studied. Sediment pore water is expected to return to conditions of circumneutral pH and low ionic strength after long times, but the possibility exists that radioactive contaminants sequestered in the impacted sediments might be remobilized by the change in subsurface geochemical conditions.

Results and Discussion

The leaching behavior and release mechanisms for Sr and Cs from the unsaturated columns packed with the two weathered Hanford sediments was modeled using the CrunchFlow code, which represented the reaction network as a combination of mineral dissolution/precipitation and ion exchange reactions. The leach tests were conducted using background Hanford pore water with focus on the first 200 pore volumes. The weathered sediments were prepared by reaction for 6 months with a synthetic Hanford tank waste leachate containing stable Sr and Cs (10^{-5} and 10^{-3} molal representative of LOW- and HIGH-weathered sediments, respectively) as surrogates for ^{90}Sr and ^{137}Cs. The mineral composition of the weathered sediments shows that zeolite (chabazite-type) and feldspathoid (sodalite and cancrinite) are the major byproducts. However, the amount of secondary minerals in the sediments varied depending on the weathering conditions. Reactive transport modeling indicated that the leaching behavior of Cs was controlled by ion exchange, while Sr release was affected primarily by dissolution of the secondary minerals. The release of K, Al, and Si at later times in the leaching experiment using the HIGH-weathered sediment indicates additional dissolution of a more crystalline mineral (cancrinite-type). A two-site ion-exchange model successfully simulated the behavior of Cs release in the LOW-weathered sediment column. However, a three-site ion-exchange model was needed to describe Cs release in the HIGH-weathered sediment column.

https://doi.org/10.1180/S0026461X00006502 Published online by Cambridge University Press

Petrological implications of temporal and spatial variations in magma chemistry of the Quaternary Tendurek shield volcano, Eastern Anatolian Collision Zone, Turkey

E. UNAL[1]*, M. KESKIN[2], V.A. LEBEDEV[3], E.V. SHARKOV[3], M. LUSTRINO[4] AND M. MATTIOLI[5]

[1]YYU, Dept. of Geol. Engineering, Zeve Campus, Van, Turkey (*correspondence: esinunal@yyu.edu.tr)
[2]Istanbul Univ., Dept. of Geol. Engineering, Avcilar, Istanbul, Turkey (keskin@istanbul.edu.tr)
[3]RAS, IGEM, Staromonetny per., 35, Moscow, Russia
[4]Università degli Studi di Roma La Sapienza, Dipartimento di Scienze della Terra, P.le A. Moro, 5, 00185 Roma, Italy
[5]Università degli Studi di Urbino 'Carlo Bo', Dipartimento di Scienze Geologiche, Italy

The Quaternary Tendürek Volcano is one of the largest eruption centers of the Eastern Anatolia with a summit elevation of 3538 m and a footprint area of 650 km^2. It is a shield volcano consisting of lavas ranging in composition from tephrites through benmoreites/phonolites to trachytes. The young volcanism of the region is thought to be related to the continent-continent collision taken place after the closure of the Neo-Tethys Ocean. The Tendürek volcano is of special importance, because it is one of the rare places in Eastern Anatolia where calc-alkaline and potassic alkaline volcanism coexisted.

Lavas of the Tendürek volcano are classified on the SiO_2 versus K_2O diagram as medium K / high K and shoshonitic series. Medium to high potassic basalts, trachy-basalts, tephrites and basaltic-trachyandesites basically follow a partial melting trend on La vs. La/Yb diagram in contrast to the trachy-andesites, phonotephrites, tephriphonolites, phonolites, and trachytes of the shoshonitic series aligning along a fractional crystallization trend. The high-SiO_2 shoshonitic rocks (i.e. phonolites) uniformly contain lower concentrations of TiO_2 (0.52-1.17 %), MgO (0.46-1.05 %) and CaO (1.01-2.93 %) and high values of K_2O (3.95-5.16 %). The high-SiO_2 phonolitic lavas have a more pronounced enrichment in incompatible elements, such as Rb, Th, La and Nb, in comparison to those in the other shoshonitic rocks. The aforementioned differences in the chemical compositions of these two groups of shoshonitic rocks may reflect variations in the fractional crystallization process which involved clinopyroxene and plagioclase during the petrogenesis of the potassic rocks.

The global climate impact of civil aviation

NADINE UNGER

School of Forestry and Environmental Studies, Yale University, New Haven, CT 06511, USA (nadine.unger@yale.edu)

Aircraft emissions affect climate change through increasing carbon dioxide (CO_2) but also a host of other short-lived non-CO_2 effects that are complex, involve impacts that are both warming and cooling and are unique to this sector. Previous assessments of aviation climatic impacts have used a segmented approach whereby each effect was calculated separately and the effects summed. Integrated approaches using newly available Earth System models that allow simulation of more realistic interactions between effects are now possible and give different results. Here, we apply the NASA GISS Earth System Model to reassess the net radiative forcing on 20- and 100-year timescales due to year 2006 emissions from civil aviation including the effects on ozone, methane, sulfate, black carbon, water vapor and CO_2. A new hourly resolution aviation emissions inventory that was developed using the Federal Aviation Administration's Aviation Environmental Design Tool is applied. The model includes interactive tropospheric and stratospheric chemistry, full coupling between gas-phase chemistry and aerosols in the exhaust and background atmosphere. The sensitivity of the ozone climate impact to altitude of emission injection is examined for aircraft emissions and compared to other major anthropogenic surface sources of precursors. The climate impact of global desulfurization of jet fuel is examined. Global mean temperature response to aviation emissions is compared relative to the impacts of other major economic sectors.

https://doi.org/10.1180/S0026461X00006502 Published online by Cambridge University Press

Metasedimentary rocks as indicators of crustal growth

L.N. URMANTSEVA* AND O.M. TURKINA

Institute of Geology and Mineralogy SB RAS, Novosibirsk, Russia (*correspondence: urmantseva@gmail.com)

Results of Sm-Nd isotopic analyses and U-Pb dating on metasedimentary rocks of two main basement uplifts of western part of the Siberian Craton (illustrated by paragneisses of Angara-Kan granulite-gneiss block of the Yenisey Ridge and Irkut granulite-gneiss block of the Sharyzhalgai Uplift) were summarized to constrain provenance of metasediments, time of sedimentation and finally to determine stages of crustal growth.

Sm-Nd model ages of rocks under consideration (T_{Nd} (DM)=2.4-3.1 Ga for the Sharyzhalgay Uplift and 2.4-2.8 Ga for Angara-Kan block) indicate presence of the Archean and Paleoproterozoic sources in the provenance [1, 2]. As regarding U-Pb data on zircons there are three detrital core age groups (≥2.7, 2.3, 1.95-2.0 Ga) in rocks of the Sharyzhalgai Uplift and cores varying in age from ~2.6 to ~1.9 Ga in rocks of the Angara-Kan block [3, 4]. The age of metamorphic rims of ca. 1.85-1.86 Ga in both cases determines the upper boundary of sedimentation and together with the youngest core ages brackets sedimentation time between 1.85 and 1.95 Ga for the Irkut block and 2.0-1.9 and 1.86 Ga for Angara-Kan block.

Potential source areas for ancient mainly Neoarchean material might be rocks of the exposed basement of south-west margin of the Siberian Craton. Presence of juvenile Paleoproterozoic crust in source area is indicated by minimal values of model Nd ages of paragneisses in common with prevail Paleoproterozoic detrital zircon cores. These Paleoproterozoic juvenile crustal sources may have been presented by buried basement of western part of the Craton, where model Nd ages of 2.3-2.4 Ga for granites and 2.8-3.4 Ga for gneisses were determined by Kovach *et al*. [5].

Finally, examined Sm-Nd and U-Pb isotopic data allow to identify derivation of detritus from buried and exposed basement of the Siberian Craton and determine the Archean and Paleoproterozoic stages of crustal growth within the Siberian Craton.

[1] Turkina & Urmantseva (2009) *Lithology & Mineral Resources* **44**(1), 43–57. [2] Nozhkin *et al*. (2008) *Dokl. Earth Sci*. **432A**(9), 1495–1500. [3] Urmantseva & Turkina (2009) *Acta Geol. Sinica* **83**(5), 875–883. [4] Urmantseva (2010) *IAGR Conf. Series* **9**, 18–19. [5] Kovach *et al*. (2000) *Petrology* **8**(4), 353–365.

Nanoscale observations of dolomite dissolution

M. UROSEVIC[1]*, E. RUIZ-AGUDO[1], C.V. PUTNIS[2], C. CARDELL[1], A. PUTNIS[2] AND C. RODRIGUEZ-NAVARRO[1]

[1]Dept. Mineralogy and Petrology, University of Granada, Fuentenueva s/n, 18071 Granada, Spain (*correspondence: maja@ugr.es)

[2]Institut für Mineralogie, Universität Münster, Corrensstrasse 24. D-48149, Münster, Germany

The dissolution of carbonate minerals plays a fundamental role in a large spectrum of geological and biological processes as e.g. the global carbon cycle, and biomineralization. Moreover the understanding of carbonate dissolution is essential in the preservation of the Cultural Heritage and building stone. Among other carbonates, calcite ($CaCO_3$) and magnesite ($MgCO_3$) dissolution has been thoroughly investigated over a range of environmental conditions and solution compositions. In contrast, there is a significant lack of understanding of the molecular-scale reaction mechanisms of dolomite ($CaMg(CO_3)_2$) [1]. In this work we present a systematic *in situ* Atomic Force Microscopy (AFM) study of dolomite dissolution in the pH range 3 to 10 aimed to unravel the nanoscale processes governing dolomite-fluid interactions. Dolomite dissolution under neutral to alkaline pH seems to be controlled by the removal of dolomite layers by spreading and coalescence of shallow etch pits, nucleated at point defects or in defect-free areas. Overall dolomite dissolution rate (R_{AFM}) values were nearly pH-independent in the range 5 to 10 (7-$9 \cdot 10^{-13}$ mol·cm^{-2}·s^{-1}), while a slight increase in R_{AFM} values was observed at pH < 5 (10-$17 \cdot 10^{-13}$ mol·cm^{-2}·s^{-1}). At all pHs (and particularly at pH < 5) the formation of a Mg-rich surface precipitate (most probably nesquehonite) was detected. Our results suggest that the mechanism of dolomite dissolution inferred solely from measurements of the solution chemistry could be misestimated as a consequence of the precipitation of such a secondary phase, particularly at acidic pHs.

[1] Ruiz-Agudo *et al*. (2011) *Chem. Geol*. **281**, 364–371.

https://doi.org/10.1180/S0026461X00006502 Published online by Cambridge University Press

Enhancing the bioavailability of subbituminous coal

M.A. URYNOWICZ[1]* AND Z. HUANG[2]

[1]Coalbed Natural Gas Center of Excellence, University of Wyoming, Laramie, WY 82071, USA (*correspondence: murynowi@uwyo.edu)
[2]University of Wyoming, Laramie, WY 82071, USA

Recent scientific discoveries suggest that much of the coal bed natural gas (CBNG) within the Powder River Basin, located in Wyoming and Montana, was generated by anaerobic microbial systems within the coal seams long after the initial process of coalification. This type of natural gas, referred to as secondary biogenic natural gas, relies on the active biological conversion of coal-derived constituents into methane. Secondary biogenic CBNG can also be found in numerous other coal fields located throughout the world. Interest in secondary biogenic natural gas has grown significantly in recent years with the realization of its vast potential and the significant benefits that this energy source has over fossil fuels.

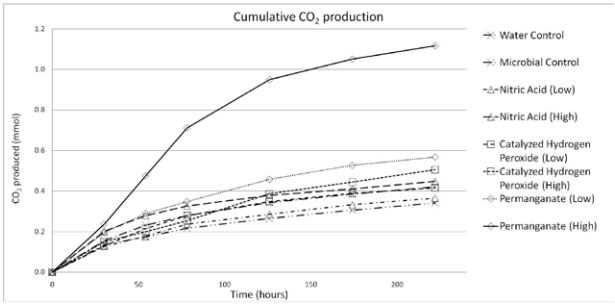

Figure 1: Cumulative CO_2 production.

The aim of this study was to evaluate several conventional groundwater remediation technologies including *in situ* chemical oxidation with permanganate and catalyzed hydrogen peroxide, and acid treatments for enhancing the biodegradability of coal. Although dissolved organic carbon was increased with each method, only the permanganate treatment resulted in a significant increase in coal bioavailability (Figure 1).

Enhanced shelf sediment weathering during glacial periods damps pCO_2 reduction: A negative feedback

H. USHIE[1]* AND K. MATSUMOTO[2]

[1]AORI, University of Tokyo, Chiba 277-8564, Japan (*correspondence: ushie@aori.u-tokyo.ac.jp)
[2]Geology and Geophysics, University of Minnesota, Minneapolis, MN 55455, USA (katsumi@umn.edu)

In the past 800 thousand years and before industrialization, the largest variations in atmospheric CO_2 concentration (pCO_2) occurred in connection with the glacial cycles that characterized Earth's climate over this period [1]. The mechanisms responsible for the glacial-interglacial pCO_2 changes have remained unresolved. One curious feature of at least the last four glacial-interglacial cycles is that pCO_2 reached about the same upper limit of 280 ppm during peak interglacial periods and about the same lower limit of 180 ppm during peak glacial periods. Here, we show using a numerical model of earth system [2] that enhanced shelf sediment weathering during glacial sea-level low stand will tend to raise pCO_2 and thus stabilize it from further reduction. This is contrary to the so-called shelf nutrient hypothesis [3], which proposed that increased weathering of nutrients (e.g. phosphate) would enhance the organic carbon pump of the ocean and thus reduce pCO_2. We demonstrate that weathering of exposed continental shelves would in fact raise pCO_2 because not all nutrients from weathering will be utilized by biology but more importantly because the spatial distributions of carbon and phosphate from weathering become decoupled in such a way that carbon is preferentially stored in the upper ocean and phosphate in the deep ocean. An extension of this finding suggests that the preferential dissolution of phosphate in shelf sediments during interglacial high stand would tend to enhance biological production and thus stabilize pCO_2 from further increase. The impact of sea level-driven continental shelf exposure and submersion on CO_2 is therefore a negative feedback that helps explain both the upper and lower limits of pCO_2 over the Pleistocene.

[1] Luthi *et al*. (2008) *Nature* **453**, 379–382. [2] Matsumoto *et al*. (2008) *Geosci. Model Dev*. **1**, 1–15. [3] Broecker (1982) *Prog. Oceanog*. **11**, 151–197.

https://doi.org/10.1180/S0026461X00006502 Published online by Cambridge University Press

Experimental and numerical investigations of the formation of felsic asteroidal crust

T. USUI[1]*, J.H. JONES[1] AND H. SENSHU[2]

[1]KR, NASA/JSC, Houston, TX 77058, USA
(*correspondence: tomohiro.usui@nasa.gov)
[2]PERC, Chiba Institute of Technology, Chiba, Japan

Achondrites exhibit a diverse set of petrographical and geochemical features that individually reflect distinct environments during differentiation processes on their parent asteroids. Our study reports on experimental and numerical investigations that constrain the formation of felsic asteroidal crust recorded in paired achondrites GRA 06128 and GRA 06129 (GRAs).

GRAs are characterized by high abundances of sodic plagioclase, resulting in alkali-rich, felsic, whole-rock compositions. Geochemical studies suggest that the GRAs originate from a partial melt from a volatile-rich asteroid that did not segregate metallic core. We performed partial melting experiments on a synthetic, alkali-bearing, H-chondrite composition under a wide range of fO_2 conditions (IW-1 to IW+2). The experiments suggest that fO_2 conditions significantly influence the compositions of partial melts. Partial melts at IW-1 are distinctly enriched in SiO_2 (up to 70 wt%) and depleted in FeO contents relative to those of >IW melts (~39-47 wt% SiO_2). The silica-enriched, reduced (IW-1) melts are characterized by high alkali contents, resulting in silica-oversaturated compositions. In contrast, the silica-depleted, oxidized (>IW) melts, which are also enriched in alkali contents, have distinclty silica-undersaturated compositions. These experimental results suggest that alkali-rich, felsic, asteroidal crusts as represented by GRAs should originate from a low-degree (F = <15 %, T = <1050 °C), relatively reduced (~IW-1) partial melt from a parent body having near-chondritic compositions.

We also perfomed numerical simulations for the thermal evolution of a GRAs parent body by assuming ^{26}Al and ^{60}Fe with the CAI canonical values as dominant heat sources. The numerical investigations suggest that a GRAs parent body should have accreted 0.7-1.2 Myr after CAI and reached a size of 18–50 km in radius in order to satisfy both chronological and experimental constraints of GRAs. This implies that a planetesimal that possesses a felsisc crust produced by low-degree partial melting would have intermediate characteristics regarding the size and/or timing of accretion between chondrite and highly differentiated achondrite parent bodies.

Thermodynamic consequences of the injection of CO_2-H_2S gas mixtures in sulfur-rich hydrocarbon reservoirs

RAKHIM UTEYEV[1], LAURENT RICHARD[2]*, AURÉLIEN RANDI[1] AND JACQUES PIRONON[1]

[1]Nancy-Université, G2R, 54506 Vandoeuvre-lès.Nancy cedex, France (rakhim.uteyev@g2r.uhp-nancy.fr, aurelien.randi@g2r.uhp-nancy.fr, jacques.pironon@g2r.uhp-nancy.fr)
[2]Amphos21, Passeig. de García i Fària 49-51, 08019 Barcelona, Spain
(*correspondence: laurent.richard@amphos21.com)

Many petroleum basins around the world, among which the recently discovered giant oil and gas fields of the Northern Caspian Sea, are characterized by very high H_2S contents. In order to overcome the tremendous environmental challenge associated with the exploitation of these petroleum and natural gas reserves, the capture on the platforms and reinjection inside the reservoirs of CO_2-H_2S gas mixtures has been proposed. If these gas mixtures are out of chemical equilibrium with the water-rock-gas-hydrocarbon systems at depth, predicting the occurrence of such reactions as the formation and destruction of organic sulfur compounds, or the precipitation of elemental sulfur in the reservoirs is of major importance for the oil industry.

Activity diagrams and temperature – log $f\,H_2S_{(g)}$ diagrams have been constructed to determine the relative stabilities of H_2S, hydrocarbons, organic sulfur compounds, and elemental sulfur at temperatures and pressures typical of petroleum reservoirs. The diagrams suggest that thiacycloalkanes and thiophenes may react with H_2S to produce hydrocarbons and elemental sulfur, while benzo- and dibenzothiophenes should not react with H_2S due to their higher stability.

Experiments have been conducted at 150°C and 500 bar in sealed autoclaves, in which various classes of organic sulfur compounds were reacted with H_2S in the presence of water. In accord with the thermodynamic predictions, thiacycloalkanes and thiophenes reacted with H_2S, while benzo- and dibenzothiophenes did not. Elemental sulfur was formed only in the reactions involving the thiophenes, which we interpret in terms of the potential for reduction (electron transfer) which is higher in the case of the thiophenes. In contrast, no hydrocarbons were detected at the end of the experiments. Dithiacycloalkanes were produced instead. Group additivity estimates of the thermodynamic properties of dithiacycloalkanes suggest that these compounds may be stable under the conditions of the experiments.

https://doi.org/10.1180/S0026461X00006502 Published online by Cambridge University Press

Podiform chromitites from the Turkish ophiolites: An overview to the mineralogy of Platinum-group elements

İ. UYSAL[1]*, F. ZACCARINI[2], G. GARUTI[2], M. KALIWODA[3], R. HOCHLEITNER[3], R.M. AKMAZ[4] AND S. SAKA[1]

[1]Karadeniz Technical University, Dept. Geol. Eng. Trabzon, Turkey (*correspondence: iuysal@ktu.edu.tr)
[2]University of Leoben, Dept. Appl. Geol. Sci. Geophysics, Leoben, Austria
[3]Ludwig Maximillian University, Mineralogische Staatssammlung, Münich, Germany
[4]Zonguldak Karaelmas University, Dept. Geol. Eng., Zonguldak, Turkey

Podiform chromitites of Mesozoic ophiolites of the Western Mediterranean Tethys represent a major source of chromium, and are considered a potential target for platinum group elements (PGE) exploration. Turkey is one of the major chromite producers in the world, ranking 4th in exports. Most of the Turkish chromitites occur in the mantle tectonite unit of supra-subduction zone ophiolites. In this contribution we have summarized the results of investigation obtained on several Turkish Cr- and Al-rich podiform chromitites [Muğla (SW Turkey), Eskişehir, Bursa (NW Turkey), Kop Mountains (NE Turkey), Kahramanmaraş, Malatya, and Gaziantep (SE Turkey)] with special regard to their mineralogy of platinum group elements (PGE). About 450 PGM grains, generally less than 15 μm in size, have been identified in all the investigated chromitites. They occur in fresh (84%) and altered chromite crystals (6%), along cracks and fissures (8%) of the chromite and, rarely, in the silicate matrix (2%) generally composed of secondary silicates, such as chlorite and serpentine. The PGM form single phase crystals or they are part of polyphasic grains composed of other PGM, base metals sulphides and silicates. The PGM containing IPGE (Os, Ir, Ru) are the most abundant phases (96% of all PGM) compared to the PPGE (Rh, Pd, Pt) bearing PGM (4%). The IPGE bearing PGM are composed of laurite-erlichmanite serie (74%), native osmium (8%), unidentified Ru-Fe phases (6%), native iridium (4%), irarsite (3%), unidentified Ir phases (2%) and native ruthenium (1%). Very rare (up to 2%) kashinite, cuproiridsite, ruarsite, and unidentified Os phase have also been identified. A total of 20 grains of PPGE phases have been found in all the localities, and most of them are Pt-Fe alloys (40%), accompanied by platinum (20%), hollingworthite (20%) and unidentified Pt (10%), Rh (5%) and Pd (5%) phases. These results confirm a strong predominance of PGM containing IPGE over PPGE, as typical for mantle hosted ophiolitic chromitites.

https://doi.org/10.1180/S0026461X00006502 Published online by Cambridge University Press

Arsenate precipitation: An alternative fate of As in soils contaminated with mine-related wastes

K. VACA-ESCOBAR[1] AND M. VILLALOBOS[1,2]*

[1]Environmental Bio-Geochemistry Group, Chemistry School
[2]Earth Sciences Graduate Program, Geology Institute, UNAM, Coyoacan, CU, Mexico 04510, D.F
(*correspondence: mariov@geologia.unam.mx)

Introduction

Arsenic and heavy metals are highly abundant elements in soils contaminated with mining and metallurgical wastes [1]. The final fate of arsenic in aerated environments is usually reported as As(V) bound to iron oxide surfaces [2]. However, we have found evidence of an alternative mechanism as insoluble heavy metal arsenates [3]. In this work we investigate the conditions that favor one mechanism over the other by both modeling and experimental methods. We applied a triple layer surface complexation modeling scheme [4] simultaneously with arsenate precipitation equilibra to predict the speciation expected as a function of total As/Fe ratios, and pH in a simple goethite /Pb(II)/ carbonate system, and compared the results with experimental data under selected conditions.

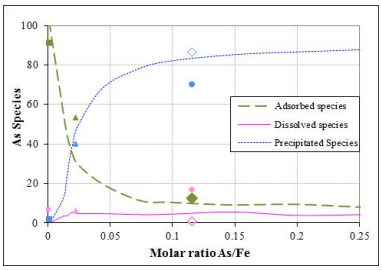

Figure 1: As(V) species distribution in goethite/Pb(II)/ carbonate systems. Model and experimental results at pH 7.

Discussion of Results

Adsorption processes only prevail at very low As/Fe ratios, and precipitation as Pb(II) arsenate quickly becomes predominant (Fig. 1). Modeling results as a function of pH will also be presented.

[1] Vaughan (2006) *Elements* **2**, 71–75. [2] Foster *et al*. (1998) *Am. Mineral* **83**, 553–568. [3] Villalobos *et al*. (2010) A*quat. Geochem*. **16**, 225–250. [4] Salazar-Camacho & Villalobos (2010) *Geochim. Cosmochim. Acta* **74**, 2257–2280.

Microbial and photochemical mineralization of dissolved organic carbon from big rivers

A.V. VÄHÄTALO[1,2] AND H. AARNOS[2]

[1]Coastal Zone Research Tem, Aronia Research and Development Institute, Novia University of Applied Sciences and Åbo Akademi University (anssi.vahatalo@helsinki.fi)
[2]Department of Environmental Sciences, University of Helsinki (hanna.aarnos@helsinki.fi)

We addressed the potential for microbial and photochemical mineralization of dissolved organic carbon (DOC) from ten big rivers. In order to quantify the direct photochemical mineralization of DOC to CO_2, the sterile-filtered river waters were irradiated with an artificial solar radiation until photochemical reactions photobleached chromphoric dissolved organic matter (CDOM) completely. For the assessment of biological mineralization of DOC, irradiated waters and their dark controls received nutrients and indigenous microbes from rivers. The concentration of DOC was followed over one year to quantify the amount of DOC consumed by microbes. Photochemical reactions mineralized DOC directly to CO_2 and also produced biologically available photoproducts. The magnitude of photoreactive DOC depended on the magnitude of CDOM. A part of DOC was resistant to photoreactions but was decomposed with low rate by microbes.

https://doi.org/10.1180/S0026461X00006502 Published online by Cambridge University Press

The first data about the concentrations REEs in waters from weathering zone of Berezitovoe gold deposit (Priamurye, Russia)

ELENA A.VAKH, ALEKSANDR S. VAKH AND NATALIA A. KHARITONOVA

Far East Geological Institute FEB RAS, Russia, Adasea@mail.ru

The Beresitovy gold deposit located in the northeastern Amur gold province in the downstream basin of the Khaikta River. In 2007, two mining companies: Berezitovy Mine Ltd. and High River Gold Mines Ltd., started to mine this deposit. Geologically, the deposit is localized in a southeast part of the North Asian craton, in a zone of its joint with formations of northern frame Tukuringra-Dzhagdinsky terrein Mongolo-Ohotsky zone. Two formations of sediments (granites and ore–metasomatic rocks) occur in the deposit. Main minerals bearing REEs are allanit, monatsit - (Ce), chervandonit - (Ce).

In this study we present the preliminarily results of investigation the content and distribution of REEs in the bedrock and water from weathering zone of deposit. Our data indicate that the content of REEs in bedrock of Berezitovoe deposit can reach up to 230 ppm and the content of LREEs is at about 90% of total REEs. All types of bedrock display of strong negative Eu amonalies.

The surface water of area is enriched in total REEs (1, 4 ppm), although the content of LREEs is higher in 8-10 times then HREEs. Drainage water is yellow, dark -yellow color with TDS up to 10 g/l and pH varies from 3, 0 to 4, 5. This water belongs to Mg-K-SO_4 type and content a huge amount of REEs (up to 16, 1 ppm). The concentration LREEs is higher then HREEs as well. It is established that drainage water is a selective accumulation of middle REEs.

Comparison of REEs content in bedrocks, ore and surface water is appeared the similarity of their profiles.

Speleothem record of permafrost in Siberia and aridity in Mongolia during the last 450 kyr

A. VAKS[1]*, O.S. GUTAREVA[2], S.F.M. BREITENBACH[3], E. AVIRMED[4], A.M. KONONOV[2], A.V. OSINZEV,[5] AND G.M. HENDERSON[1]

[1]Department of Earth Sciences, University of Oxford, Oxford, United Kingdom (*correspondence: Anton.Vaks@earth.ox.ac.uk)

[2]Institute of Earth's Crust, Russian Academy of Science, Siberian Branch, Irkutsk, Russia

[3]Swiss Federal Institute of Technology Zurich, Geological Institute, Zurich, Switzerland

[4]Institute of Geography, Mongolian Academy of Sciences, Ulaanbaatar, Mongolia

[5]Arabica Speleological Club, Irkutsk, Russia

We have used speleothems from six caves along a north-south transect in Eastern Siberia and the Mongolian Gobi Desert (60°22′N - 42°50′N) to track the evolution of permafrost and desert aridity. The studied caves are located in various climate zones: from the southern boundary of continuous permafrost, through the discontinuous/island permafrost, to the dry Gobi Desert.

More than 90 horizons of 22 speleothems were dated by U-Th method. The youngest speleothem age in the northernmost cave was 404 ± 32 kyr, corresponding to interglacial Marine Isotopic Stage (MIS) 11, while eleven other horizons in six speleothems from this cave were older than the ~500 kyr U-Th dating limit. These results suggest that MIS-11 in Eastern Siberia was warmer than today, causing brief permafrost degradation at 60°N, followed by re-establishment and continuous permafrost since then. Between 56°N and 52°N speleothem ages clustered into the warmest intervals of interglacial MIS-11, 9, 7, 5 and 1, showing intermittent melting of the permafrost. This data provides constraints on glacial-interglacial migrations of the southern boundary of continuous permafrost in Eastern Siberia during the last 450 kyr. No speleothem deposition younger than 500 kyr was found in the Gobi Desert, showing that arid conditions prevailed during this entire period.

The year-round monitoring of $\delta^{18}O$ and δD values of cave water and atmospheric precipitation in the city of Irkutsk and nearby cave shows that $\delta^{18}O$ and δD values of rain and snow are in direct relationship with temperature throughout the year, and $\delta^{18}O$ and δD values of the cave water reflect the weighted annual average of precipitation. Ongoing work is making use of these observations to create stable isotope records of the Siberian speleothems.

https://doi.org/10.1180/S0026461X00006502 Published online by Cambridge University Press

Mantle source components of the Early Cretaceous to Paleogene mafic tholeiitic and alkaline magmatism in Rio and related mantle metassomatism processes

S.C. VALENTE

Geosciences Dept., UFRuralRJ, Seropédica, RJ, 23890-00, Brazil (sergio@ufrrj.br)

The Early Cretaceous (*c*. 132 Ma) to Paleogene (*c*. 55 Ma) mafic magmatism in Rio is mostly represented by tholeiitic dolerites and ultramafic and alkaline lamprophyres, respectively [1]. The tholeiites are often regular, long, tens of metres-thick, vertical, ENE-trending intrusions with remarkably uniform textures and structures. In contrast, the ultramafic and alkaline lamprophyre dykes are generally less than one metre thick and display variable textures, structures and morphologies. Litogeochemical and Sr-Nd-O isotopic data show that the least evolved tholeiitic dolerites seem not to represent contaminated melts and are likely to be related to a predominantly asthenospheric, plume source similar in composition to Tristan da Cunha lavas. Small contributions (~10%) from the overlying subcontinental lithospheric mantle may have imprinted lithospheric signatures in the least evolved dolerites such as negative Nb anomalies. The Paleogene alkaline dykes comprise a strongly undersaturated suite including ultramafic and alkaline lamprophyres and sodic agpaitic phonolites. Sr-Nd isotope data point to a contribution of asthenospheric mantle sources for the generation of the alkaline dykes likely to be related to the Trindade plume. Heat conduction and advection from the plume triggered the melting of the readly fusible, volatile-rich, mafic potassic parts of the overlying subcontinental lithospheric mantle beneath Rio, leading to the generation of the most primitive ultramafic ultrapotassic lamprophyres. Major and trace element characteristics of the ultrapotassic ultramafic lamprohyres (*e.g*. CaO/Al_2O_3 <1; $(La/Nb)_N$~0.9) and their Sm-Nd model DM ages (496-660 Ma) indicate that the Late Proterozoic enrichment process of the subcontinental lithospheric mantle seems to have been unrelated to subduction processes but largely controlled by the migration of high H_2O/CO_2 silicate melts from the underlying asthenosphere.

[1] Valente (1997) *PhD* thesis, QUB, UK. 400pp.

Lunar zircon: Primitive $\delta^{18}O$ of dry evolved and mafic magmas

J.W. VALLEY*, M.J. SPICUZZA AND T. USHIKUBO

WiscSIMS, Dept. of Geoscience, Univ. Wisconsin, Madison, WI, 53706, USA
(*correspondence: valley@geology.wisc.edu)

Oxygen isotope ratios of zircons from the Moon have been measured *in situ* by SIMS [1], including grains from: quartz monzodiorite (n=4; 4, 294 Ma [2]), impact melt (n=1), breccia and shocked norite (n=2), and Apollo 12 (n=6) and 14 (n=3) regolith. Zircons from regolith may represent lithologies not found at Apollo landing sites. Some zircons have K-feldspar ± silica as inclusions or infilling cracks, suggesting they represent extreme differentiates of mafic magmas, similar to zircons in lunar granophyre [2]. The average $\delta^{18}O$ for lunar zircons ranges from 5.19 to 5.82 ‰ (ave. = 5.59 ±0.33‰, 2SD). Trace element concentrations of these zircons, also measured by SIMS, are: Ti 37-170 ppm; P 425-1120 ppm; Y 780-2850 ppm; total REE 485-1780; Hf 10, 500-12, 750 ppm; Th 4-38 ppm; and U 12-108 ppm [1].

The $\delta^{18}O$ (whole rock) values of mare basalts range from 5.33 to 5.81: 5.69 ±0.17 (2SD, n=23) for low-Ti and 5.54 ± 0.26‰ (n=15) for high-Ti basalts [3, 4]. The low variability allows comparison with zircons from other samples. The average basalt has the same $\delta^{18}O$ as igneous zircons: $\Delta^{18}O$ (WR-Zrc) ~ 0. This WR-Zrc fractionation contrasts with samples from Earth, where $\Delta^{18}O$ (WR-Zrc) ~ 0.0612 (wt.% SiO_2) –2.50‰ [5]. For instance, unaltered MORB $\delta^{18}O$ (WR) values average ~ 5.6-5.7, while $\delta^{18}O$ (Zrc) values average 5.2 ±0.5 (n=197) for gabbro and plagiogranite from ocean crust: $\Delta^{18}O$ (WR-Zrc) ~0.5 [6]. Thus $\Delta^{18}O$ (WR-Zrc) values on the Moon deviate significantly from relations on Earth.

In general, values of $\delta^{18}O$ (Zrc) vary negligibly during closed system magmatic differentiation because $\Delta^{18}O$ (WR-Zrc) correlates to $\delta^{18}O$ (WR); both increase for siliceous rocks with high $\delta^{18}O$ minerals (Qt, Flds). However, in detail, variable T will change this relation and the best explanation of the lunar results is that magmatic T's were significantly higher due to low water content. High crystallization T for lunar zircons is supported by values of [Ti] in lunar zircons (37-170 ppm) that are significantly higher than in terrestrial igneous zircons (0.2-30 ppm) [7]. We thus infer a low water content of these highly evolved lunar melts and that mafic parent magmas on the Moon were significantly drier.

[1] Spicuzza *et al*. (2011) *LPSC*, abst 2455. [2] Meyer *et al*. (1996) *Met. Plan. Sci*. **31**, 370–387. [3] Spicuzza *et al*. (2007) *EPSL* **253**, 254–265. [4] Liu *et al*. (2010) *GCA* **74**, 6249–6262. [5] Lackey *et al*. (2008) *J Pet* **49**, 1397–1426. [6] Grimes *et al*. (2011) *CMP* **161**, 13–33. [7] Fu *et al*. (2008) *CMP* **156**, 197–215.

https://doi.org/10.1180/S0026461X00006502 Published online by Cambridge University Press

The role and effect of boron during the crystallization of $CaCO_3$

B. VALLINA-ANTUÑA[1,2], J.D. RODRIGUEZ-BLANCO[1], J.A. BLANCO[2] AND L.G. BENNING[1]

[1]School of Earth and Environment, University of Leeds, LS2 9JT, United Kingdom (beatrizvallina@gmail.com)
[2]Departamento de Fisica, Universidad de Oviedo, E-33007 Oviedo, Spain

Boron (B) is a crucial element in carbonate biominerals and its isotopic signature is used as a paleo-acidity proxy and to reconstruct atmospheric CO_2 levels through time [1, 2]. Most studies however, focused on compositional or isotopic analyses of natural marine carbonates, but the mechanisms of boron incorporation or the role and effect that $[B]_{aq}$ plays during the nucleation and growth of the various calcium carbonate polymorphs is still unknown. Therefore the aim of this research was to quantitatively assess the crystallization pathways of $CaCO_3$ polymorph in the presence of $[B]_{aq}$ and to mimic B/Ca ratios in modern seawater.

The experiments were performed at 10-30°C in stirred reactors by mixing equimolar solutions of $CaCl_2$ and Na_2CO_3 doped with 0-25mM of $[B]_{aq}$. Reactions were followed for between ten minutes and eight hours, while simultaneously recording changes in pH as a direct proxy for the crystallization reactions. At regular time intervals solid and solution aliquots were collected and characterized by XRD, SEM, FTIR or wet-chemical analysis.

The results show that in the presence of $[B]_{aq}$ the initial amorphous calcium carbonate (ACC) remained stable for up to 5 minutes, while at equivalent conditions with no $[B]_{aq}$ the transformation to vaterite begins after ~1 minute [4]. However, after the full ACC breakdown, the crystallization pathways vary dramatically as a function of temperature and $[B]_{aq}$, concentration compared to the pure system [2]. For example, at 30°C and 10mM $[B]_{aq}$, the ACC to calcite transformation via vaterite was ~ 25% faster compared to the pure system. Furthermore, when 25mM of $[B]_{aq}$ were added, the initial ACC transformed directly to calcite in less than 10 minutes with no vaterite intermediate. Overall our experiments revealed that the effect of temperature was inverse to that of the B/Ca ratio in solution. The effects were also reflected in the variations in polymorph distribution as a function of time and in the changes in morphologies of the various $CaCO_3$ polymorphs at the conditions tested.

[1] Hemming *et al*. (1995) *Geochim Cosmochim Acta* **59**, 371–279. [2] Paris *et al*. (2010) *Geology* **38**, 1035-1038. [3] Rodriguez-Blanco *et al*. (2011) *Nanoscale* **3**, 265-271. [4] Bots *et al*. *Min Mag* (this volume)

New characterization of uranium mineralogy in Ukrainian ores

A.A. VALTER[1] AND K.B. KNIGHT[2]

[1]Institute of Applied Physics, Nat. Acad. Sci. Ukraine, Sumy, 40030, Ukraine (avalter@iop.kiev.ua)
[2]Lawrence Livermore National. Lab., (knight29@llnl.gov)

The economically significant uranium ores of Ukraine form one of the largest uranium ore reserves in Europe. Concentrated in the central Ukrainian shield, these ore bodies (~1, 8 Ga, inferred from U-Pb analyses [1]), are associated with albitites in granites. Carbonates, iron oxides and Ca-Fe garnets are found genetically associated with uranium minerals, while albite and other alkali silicates formed during earlier stage metasomatic processes. Albite has been altered at the margins adjacent to the uranium minerals from low to high albite. We present preliminary work characterizing primary uranium ores in Ukraine, as part of a larger effort to develop a database of nuclear materials for Ukraine.

We have studied uranium minerals from representative samples of the Severinskoje (I), Michurinskoje(II), and Vatutinskoje (III) deposits, as well as from the Adabash fracture zone mineralization (IV), using mineralogy and gamma spectrometry [2]. This study presents new X-ray diffraction (powder and single grains), SEM and TEM characterizations, and microprobe study of the principal U-minerals present:

Uraninite (IV), a_0=0, 542 nm, forming cubic crystals up to 0, 5 mm. Average composition is Na_2O 5, 6%; SiO_2 0, 8%; CaO 1, 74%; PbO 23%; U_3O_8 72, 4%. U, Ca, Pb appear to be associated with the host crystal matrix, while Na, Si and trace elements are concentrated in solid inclusions (up to 0, 5 mm). *Coffinite (I, II, III)* forms elongated crystals up to 0, 1 mm. Average composition is Al_2O_3 0, 9%; SiO_2 15%; CaO 2, 5%; Fe_2O_3 1, 4%; U_2O_3 65%. *Brannerite (II, III)* forms elongated, needle-like crystals up to 0, 1 mm. Average composition is PbO 6, 17%; UO_2 39, 18%; CaO 3, 15%; SiO_2 2, 31%; TiO_2 24, 49%; FeO 2, 08%. This mineral occurs intergrown with an unknown silicate mineral (mixture) with composition ~ (Ca, Pb, U)(Ti, Fe)$_2$Si$_3$O$_{11}$. *Ca-Uraninite (I)* ~CaU_2O_6, is cubic, a_0 = 5, 37 nm. This is possibly a new mineral variety. It forms in thin veins (~20 um thick) and globules (~1 um). *Ca-boltwoodite (I)* occurs as thin veins of plate-like crystals up to 20 um in diameter. The boltwoodite powder XRD pattern suggests a disordered layered structure, possibly representing a new mineral variety. The relative composition is U:Si:(Na+K+$Ca_{0,5}$) ≈ 1:1:1.

This work performed under the auspices of the U.S. Department of Energy by Lawrence Livermore National Laboratory under Contract DE-AC52-07NA27344.

[1] Belevtsev *et al*. (1995) *Naukova Dumka,* 396p (in Russian). [2] Valter *et al*. (2007) *Prob. Atom. Sci. Tech*. **5**, 69–75.

https://doi.org/10.1180/S0026461X00006502 Published online by Cambridge University Press

Re-Os in pyrite as a constraint on the timing of HP metamorphism during the Tianshan orogeny (NW China)

D. VAN ACKEN[1], R.A. CREASER[1], W. SU[2] AND J. GAO[2]

[1]University of Alberta (vanacken@ualberta.ca, rcreaser@ualberta.ca)

[2]Chinese Academy of Sciences (suwen@mail.igcas.ac.cn, gaojun@mail.igcas.ac.cn)

The Tianshan mountain belt in Central Asia is situated between the Junggar and Tarim basins. Because of its large extension of over 2500 km of length and complex geological history, it is a key piece to understand the tectonic evolution of Eurasia. Paleozoic collision resulted in the closeure of the Paleo-Asia ocean and amalgamation of small continental fragments. Dating of metamorphic units within the Tianshan is important to understand the timing of its tectonic evolution throughout the Phanerozoic.

Collision between the Yili-Central Tianshan and Tarim-Karakum plates in the southwestern Tianshan is recorded by eclogites embedded in greenschist and blueschist-facies metapelites, in the high-pressure, low-temperature belt in the Southern Tianshan, NW China. The majority of ages obtained with Sm-Nd, Ar-Ar, and U-Pb time the peak of metamorphism in the Late Carboniferous around 345 Ma, while younger Ar-Ar and Rb-Sr ages around 310 Ma are interpreted as mica cooling ages or recrystallization due to fluid flow. Younger U-Pb ages of about 225 – 230 Ma suggest later peak metamorphism, and thus a later continental collision, or resetting of the U-Pb system during the Triassic.

New Re-Os data, obtained on pyrite mineral separates from eclogites from the western Tianshan HP-LT belt, confirm the older Carboniferous ages. Sulfides from three eclogite samples yield ages between 310 and 380 Ma, with large uncertainties up to 100 Ma resulting from the few data points per sample available. These ages likely represent sulfide formation or recrystallization during eclogite-facies metamorphism, and provide independent evidence for Carboniferous ages of eclogite formation.

The similar ages yielded by isotope systems hosted in silicates and sulfides from Tianshan eclogite confirm a) Carboniferous ages for the eclogite-facies metamophism during the Tianshan orogeny and b) the potential of the Re-Os system to date sulfide formation in metamorphic rocks. However, ages obtained in this manner may represent ages of sulfide formation by fluid flow or remobilization during later stages of metamorphism, and thus needs to be compared with independent, silicate mineral-hosted isotope chronometers.

Metal pollution assessment in sediment of the Talar River, N. Iran

M. VANAEI, A. MAGHSOUDI, A.S. SAEEDI AND M. NAJJARAN

In the Ghaemshahr Area the Lenth of the Tallar River Separated to 8 sample site and 112 Samples Collected from Sediment and For the Distingoition of Geogenic Pollution for each sample, 1 gr of sample was digested with the solution of $HF+HC_lO_4+HNO_3$ but in the Antropogenic Pollution the sample was digested with the solution Acetic Acid, hydroxileamine, Hydrocloride and hydrogenproxide and then Analized with Atomic Abasorbtion Method

The Enrichment Ratio and Geo-accumulation Index has been Calculated and Evalutated the Degree of Contamination Metals (Zn, V, Sn, Pb, Ni, Cu, Cr, Co, Cd, Ag, Fe) In the Sediment of the Talar River.

According to the contamination categories, the Ag has been Enriched and show very high absorption and Cd in the 1, 2, 4, 5, 7 Site and Sn in the 2, 4, 6, 7 Site Shows Intense to Very High Absorption.

Degree of Geo-accumolation Index Show that the Ag in the 1, 2, 3, 4, 5, 7, 6 Sites has been Enriched and Show Heavily Contaminated and Cd in the 1 Site and Sn in the 2, 5 Site Shows Heavily Contaminated.

In the Dogol Railway Station to Orim Village the Cd, Ag and Sn Contain of High Level of Antropogenic Contamination and Fe Contain of Low Level of Antropogenic Contamination and in the Babolsar-Bahmanir site Cd, Ag and V Contain of High Level of Antropogenic Contamination and Fe Contain of Low Level of Antropogenic Contamination

Activity Minning (Coal and Fluorite) and Depo of Coal in the Upper part of River Very Affected the Absorption and Contamination but in the Downstream, Realize of Industry and Urban Sewage very Affected the Absorption and Contamination

https://doi.org/10.1180/S0026461X00006502 Published online by Cambridge University Press

Causes and consequences of isotopically heavy dissolved molybdenum in rivers

DEREK VANCE[1]*, ANDREW R. KEECH[1], ALAN MATTHEWS[2] AND COREY ARCHER[1]

[1]Bristol Isotope Group, School of Earth Sciences, University of Bristol, Wills Memorial Building, Bristol, BS8 1RJ, UK (*correspondence: d.vance@bristol.ac.uk)

[2]Institute of Earth Sciences, Hebrew University of Jerusalem, 91904 Israel

The molybdenum (Mo) isotopic composition of the dissolved load of rivers is isotopically heavy relative to likely average continental crust. Two key aspects of this finding are not understood. The first is the origin of this isotopic fractionation. The second is the degree to which the riverine dissolved load reflects the delivery of Mo isotopes from the continents to the oceans. Both of these issues are crucial to the intrepretation of oceanic Mo isotope records, and to their use as redox indicators. Here we address both these issues, the first using new data from soil profiles that constrain processes by which Mo and its isotopes are released during weathering, and the second through data and models that have implications for the release of Mo from riverine particulate material in estuaries and shallow seas.

We have studied Mo isotope systematics in a range of soil chronosequences, and the data suggest that the behaviour of Mo and its isotopes in the weathering environment is dependent on an array of controls. In one key chronosequence from Scotland, however, there is a previously un-heralded role implied for biological processes. In these soils, there is pronounced retention of Mo in organic material at the top of the profile, that becomes more pronounced as the soil ages. In these soils Mo isotope retention/release in/from soils is controlled by both Fe-Mn oxides and organic material. These data are consistent with recent findings that Mo is limiting in many terrestrial ecosystems and that soil bacteria take up the light isotope.

A key issue for oceanic Mo isotope records is the isotopic composition of the input from the continents. The heavy dissolved load of rivers presents some severe problems for models of the Mo isotope mass balance in the modern oceans. Recent data from continental margin settings, however, particularly those that are marginally sub-oxic, suggests that diagenetic reactions could release the light particulate Mo washed into the oceans as the counterpart of the heavy dissolved load. The implications of this suggestion for the oceanic Mo isotope budget will be explored.

GEOTRACES intercalibration results for Nd isotopes and REE on seawater and particulate samples

TINA VAN DE FLIERDT[1], KATHARINA PAHNKE[2] AND GEOTRACES INTERCALIBRATION PARTICIPANTS

[1]Department of Earth Science and Engineering, Imperial College London, South Kensington Campus, London, SW7 2AZ, UK

[2]Department of Geology and Geophyscis, University of Hawaii, Honolulu, HI 96822, USA

One of the key activities during the initial phase of the international GEOTRACES program was an extensive international intercalibration effort for all trace elements and isotopes (TEIs) targeted by the program, to ensure that results from different cruises and from different labs can be compared in a meaningful way. Two intercalibration cruises sailed in 2008 and 2009 to enable systematic testing of sampling equipment and methods, and to collect large amounts of homogenous seawater samples to check whether results for dissolved and particulate TEIs obtained by different laboratories are accurate and reproducible.

Here we present the results from the intercalibration efforts on neodymium isotopes and rare earth elements in seawater and marine particulates. For seawater, we obtained Nd isotope results from 11 different laboratories on duplicate seawater samples from two different water depths (2000m and 15m) at the Bermuda Atlantic time series study site (BATS). Average ε_{Nd} values are -13.1 ± 0.6 and -9.1 ± 0.6. This is a very satisfactory result for the community, as individual labs typically achieve external reprodibilities of $^{143}Nd/^{144}Nd$ measurements between 0.2 and 0.4 ε units (2 σ standard deviation). In an attempt to test whether the spread in reported isotope ratios is due to differenct protocols used for pre-concentration and ion chromatography, or rather due to different methods applied on the mass spectrometry end, we distributed an isotopic standard of unknown composition to all labs. Averaged results from all laboratories reveal a very similar external reproducibility of 60 ppm (2σ SD) on $^{143}Nd/^{144}Nd$, indicating that mass spectrometry is the main variable in achieving accurate and precise Nd isotope ratios.

We will furthermore present Nd isotope results on systematic shipboard filtration tests, a comparison of different sampling systems, as well as intercalibration results for Nd isotopes in marine particulates and REE patterns in seawater and particulates. While the community is definitely ready for Nd isotope measurements in seawater, the analyses of marine particulates seems to require a common methodology to provide comparable results.

https://doi.org/10.1180/S0026461X00006502 Published online by Cambridge University Press

Crystallization of low-K calc-alkaline igneous rocks at lower crustal pressures

G. VAN DEN BLEEKEN[1]*, O. MÜNTENER[1] AND P. ULMER[2]

[1]Institute of Mineralogy and Geochemistry, University of Lausanne, Switzerland (*correspondence: g.vandenbleeken@opgc.univ-bpclermont.fr, othmar.muntener@unil.ch)

[2]Institute for Mineralogy and Petrology, ETH Zürich, Switzerland (peter.ulmer@erdw.ethz.ch)

We will present phase relations and compositions from high-pressure equilibrium crystallization experiments on low-K calc-alkaline rocks saturated in H_2O. The wider rationale of this study is to advocate the role of crystal fractionation in the lower crust of subduction-related magmatic arcs, as an alternative to the more conventional partial melting of amphibolites [1]. Furthermore, we aim to clarify the role of epidote (+Na-mica) during igneous crystallization near the solidus, and its potential effect on derivative granitic rock compositions by comparing our results with studies on natural sodium-rich granitoids [2].

As starting materials, we use a powdered natural paragonite+epidote+garnet-bearing mafic rock derived from the lower crust of the Kohistan paleo-island arc, and a trace-element-doped gel of similar composition. Experimental pressure and temperature were varied in the near-solidus domain (1.0-1.6 GPa; 650-800 °C), representing conditions relevant for deep arc crust formation. All experimental runs were buffered at NNO.

First results show that amphibole occurs in all runs, garnet is present at pressures above 1.0 GPa, and plagioclase is present in all runs except where epidote is present. As minor phases, rutile or ilmenite, and quartz are observed. In accordance with the addition of ~15 wt% water, coexisting liquids were saturated in H_2O, as indicated by the occurrence of 'bubbles'. Close to the solidus at 1.2 GPa, plagioclase disappears and an amphibole+garnet+rutile+ epidote+quartz assemblage coexists with vapour and hydrous melt. On a water-free basis (EMP analyses recalculated to 100 wt%), the glasses have high silica contents (~70-76 wt%) and low amounts of total alkali (~1.1-1.5 wt%), placing them into the dacite and rhyolite fields on the TAS diagram.

More experimental and analytical work is underway, and we will present a comprehensive set of data on phase relations, major-element compositions and element partitioning at the Conference.

[1] Brown & Rushmer (2006.) *Cambridge University Press*.
[2] Petford & Atherton (1996) *J. Pet.* **37**, 1491–1521.

How deep is deep? Plant biogeochemistry for detecting deep mineralisation

B.G. VAN DER HOEK*, S.M. HILL AND ROBERT C. DART

Deep Exploration Technologies Cooperative Research Centre, School of Earth & Environmental Sciences, University of Adelaide, Australia, 5005 (*correspondence: benjamin.vanderhoek@adelaide.edu.au)

Transported and potentially deep regolith extends across much of Australia, presenting a challenge for mineral explorers using traditional surface geochemical exploration techniques. Plant biogeochemistry is emerging as a valuable supplementary tool in exploration programs within these environments.

The application of plant biogeochemistry involves the chemical analysis of plant material (subaerial), where the elements are sourced from the regolith via the roots. Accumulation of elements in plant material is dependant on the element and its bioavailability. Element concentrations in plants are typically orders of magnitude lower than in geochemical material and exhibit different element associations.

Plant material has been analysed from the Tunkillia Au-prospect in the Gawler Craton, South Australia. Extensive exploration drilling has defined a biomodal distribution of Au – low concentrations at near-surface, a depletion zone, and primary mineralisation at depths exceeding 40 m. Gold concentrations in a variety of plant species have been up to 20 times background levels of plants in the region.

At Tunkillia, a large plant biogeochemistry and down-hole geochemistry dataset is integrated with isotope and soil biota analysis. This assists modelling of the vertical transportation of elements and limitations of plant root systems that access deep into the regolith profile.

https://doi.org/10.1180/S0026461X00006502 Published online by Cambridge University Press

Carbonation of steel slag II

SIEGER R. VAN DER LAAN[1]*, CHRISTIAN LIEBSKE[1], HANS KOBESEN[2], ELEANOR J. BERRYMAN[3], ANTHONY E. WILLIAMS-JONES[3] AND ARTACHES A. MIGDISOV[3]

[12]TATA Steel RD&T, Ceramics Research Centre, TATA Steel Europe OSF2, IJmuiden, The Netherlands (*correspondence: sieger.van-der-laan@tatasteel.com)
[3]Department of Earth and Planetary Sciences, McGill University, Montreal, Quebec, Canada

One of the options that the steel undustry has to mitigate some of its CO2 emissions is mineral carbonation of steel slag, a by-product of the steel refining process. Our study investigates reactions taking place during dissolution and carbonation of steel slag, with the aim of determining optimal conditions for conversion. A H_2O-CO_2 fluid is pumped through slag grains (2 – 3 mm) in a flow-through reactor at elevated pressure, and temperatures of 125 to 200°C, as described in a companion abstract [1]

The starting steel slag contains ~50 wt% CaO in larnite (Ca_2SiO_4), srebrodolskite ($Ca_2Fe_2O_5$) and free lime. In addition, there is an inert phase, Mg-wuestite ((Fe, Mg)O)). After an experiment, entire cross sections of slag grains were analysed by SEM-EDS spectral imaging. Based on the information in the images, the volume proportions and distribution of reactant and product minerals were quantified using in-house developed PARC (PhAse Recognition & Characterization) software. This method reliably reproduces bulk compositions of solids as confirmed with XRF analysis [2]. The PARC results were used to calculate the mass balance between starting material, reacted slag and fluid and, in conjunction with the fluid chemistry, helped reconstruct the reaction path.

[1] Berryman *et al*. (2011) Goldschmidt Conference, this issue. [2] van Hoek & van der Laan (2011) Goldschmidt Conference, this issue

δD of alkenones as proxy for paleo sea surface salinity

M.T.J. VAN DER MEER[1]*, S. KASPER[1], A. BENTHIEN[2], J. BIJMA[2], R. ZAHN[3], J.S. SINNINGHE DAMSTÉ[1] AND S. SCHOUTEN[1]

[1]NIOZ, BGC, PO Box 59, 1790 AB Den Burg, The Netherlands (*correspondence: Marcel.van.der.Meer@nioz.nl)
[2]AWI, PO Box 12 01 61, D-27515 Bremerhaven, Germany
[3]ICREA and UAB, E-08193 Bellaterra (Cerdanyola), Spain

Culture studies of haptophyte algae showed that there is a strong correlation between the fractionation factor $\alpha_{alkenones\text{-}growth}$ water and salinity [1]. with less fractionation at higher salinities. Based on these results, paleosalinities of the Black Sea and the Eastern Mediterranean have been reconstructed using the δD of alkenones [2, 3].

However, there has been some debate about whether analyzing the C_{37} alkenones together is appropriate for reconstructing paleosalinity since there is a relatively large difference in the δD of the $C_{37:2}$ and $C_{37:3}$ alkenones, respectively [4-6]. To examine this potential problem we analyzed the $C_{37:2}$ and $C_{37:3}$ alkenones of the original Schouten *et al*. [1] *E. huxleyi* samples separately and found an increasing difference in δD between the $C_{37:2}$ and $C_{37:3}$ alkenone with decreasing temperature and, therefore, decreasing relative abundance of the $C_{37:2}$ alkenone. These results suggested that for the purpose of reconstructing paleo SSS it might be better to analyze the C_{37} alkenones together rather than the separate isomers.

To test this δD paleo sea surface salinity proxy in open marine settings it was applied to assess Agulhas current variability during the transition from Marine Isotope Stage (MIS) 6 to 5 and MIS 2 to 1. The reconstructed paleo SSS show a substantial shift to lower salinities during both deglaciations in agreement with reconstructions based on oxygen isotopes and Mg/Ca of planktonic foraminfera. These results indicate the potential of this proxy in open marine settings where salinity shift are relatively small.

[1] Schouten *et al*. (2006) *Biogeosciences* **3**, 113–119. [2] van der Meer *et al*. (2007) *EPSL* **262**, 594–600. [3] van der Meer *et al*. (2008) *EPSL* **267**, 426–434. [4] D'Andrea *et al*. (2007) *Anal. Chem*. **79**, 3430–3435. Schwab & Sachs (2009) *Org. Geochem*. **40**, 111–118. [6] Wolhowe *et al*. (2009) *Biogeosciences* **6**, 1681–1694.

https://doi.org/10.1180/S0026461X00006502 Published online by Cambridge University Press

The age and origin of the Limpopo sub-continental lithospheric mantle

Q.H.A. VAN DER MEER[1], M. KLAVER[1], L. REISBERG[2], B. DAVIDHEISER[1] AND G.R. DAVIES[1]*

[1]VU Amsterdam, De Boelelaan 1085, 1081HV Amsterdam, The Netherlands (*correspondence: gareth.davies@falw.vu.nl)
[2]CRPG, 15 rue Notre-Dame de Pauvres, B.P. 20, 54501 Vandoeuvre-lès-Nancy, France

The Limpopo Mobile Belt (LMB) represents the suture zone between the Kaapvaal and Zimbabwe cratons, but the timing of the collision is still highly debated. Mantle tomography indicates a clear continuation of subcratonic mantle beneath LMB and the adjacent cratons. The origin of both the crust and lithospheric mantle of the LMB is also the subject of controversy and a Zimbabwean, Kaapvaal and allochtonous origin have all been proposed.

The Venetia kimberlite cluster is located within the central zone of the mobile belt and mantle xenoliths from the diamond mine provide an excellent opportunity to address the origin of LMB. We present an extensive petrology-geochemical dataset on a selection of Venetia peridotitic xenoliths, including 24 Re-Os isotope analyses.

Whole rock and mineral major element analyses of garnet-harzburgites and lherzolites indicate that the Venetian lithospheric mantle underwent up to 50% melt depletion, at least partially in the absence of garnet and by implication <70km. The depleted residue was subsequently re-enriched in silica and incompatible elements by subduction-related and asthenospheric melts. The mode of whole rock rhenium depletion ages is 2.6 Ga, which is significantly younger than both the Zimbabwe and Kaapvaal cratons.

Based on combined Os-Nd-Hf isotope systematics of the xenoliths we argue that the majority of the SCLM beneath LMB stabilised at ~2.6 Ga in a separate terrain, which is coeval with major crust forming recorded by zircon Hf and U-Pb model ages

Patterns of cosmogenic age distributions for Late Quaternary moraines in Tibet

J. VAN DER WOERD[1], E. KALI[2], M.-L. CHEVALIER[3], J. LIU-ZENG[4], A.-S. MÉRIAUX[5], P. TAPPONNIER[6], G. HILLEY[7], H. LI[3], R.C. FINKEL[8] AND F.J. RYERSON[9]

[1]IPGS-EOST, UMR 7516, CNRS/Université de Strasbourg, 5, Rue Descartes 67000 Strasbourg, France (jeromev@unistra.fr)
[2]Université de Lyon 1, Lyon, France
[3]CAGS, Beijing, China
[4]ITPR-CAS, Bejing, China
[5]U. of Newcastle, UK
[6]EOS, Singapore
[7]Stanford University, Stanford, CA, USA
[8]U. of California, Berkeley, CA, USA
[9]LLNL, CA, USA

Uncertainties in moraine exposure ages have been recognized as a difficulty when trying to reconstruct past climate changes or comparing moraine exposure ages with known paleo-climate proxys such as $\delta^{18}O$ variations. Many moraines have been dated although the number of samples on each moraine vary widely and may often be too small to assess the true geological scatter of the dated landform. Here we present cosmogenic age distributions for moraines of Tibet and present various explanations to explain the shape of the distributions for moraines dated with large numbers of samples. While it is true that the more samples are dated the more complexity may arise just by adding more information to the data set, it is also true that by targeting to few samples complex depositional or post-depositional processes may be completely overlooked. We focus on moraines deposited in comparable glacial setting from the last glacial maximum and before, and will show that similar geomorphologies are not necessarily correlated with age but most probably to similar glacier ice dynamics. Distributions of ages need to be explained by some independent assessment of depositional or post-depositional model, that can be further tested by the addition of observations, such as, for instance, the relative ages of inset moraines, or the amount of cumulated tectonic offset when available. True and independent moraine age assessments are preferable whenever possible, but it is noticeable that some patterns of ages can be recognized over large sets of data covering large areas of Tibet that argue for at least some synchronous glacial advances and moraine retreats, that with no surprise do correlate with global climate variations.

https://doi.org/10.1180/S0026461X00006502 Published online by Cambridge University Press

Satellite-based estimates of fine particulate matter during the Moscow wildfires of 2010

AARON VAN DONKELAAR[1]*, RANDALL V. MARTIN[1,2], ROB LEVY[3], ARLINDO DA SILVA[4], MICHAL KRZYZANOWSKI[5], NATALIA CHUBAROVA[6], EUGENIA SEMUTNIKOVA[7] AND AARON COHEN[8]

[1]Dept. of Physics and Atmospheric Science, Dalhousie University, Halifax, Nova Scotia, Canada (*correspondence: aaron.van.donkelaar@dal.ca, randall.martin@dal.ca)
[2]Harvard-Smithsonian Center for Astrophsyics, Cambridge, Massachusetts, USA
[3]NASA Goddard Space Flight Center, Greenbelt, Maryland, USA (robert.c.levy@nasa.gov)
[4]Global Modeling and Assimilation Office, NASA Goddard Space Flight Center, Greenbelt, Maryland, USA (arlindo.m.dasilva@nasa.gov)
[5]WHO European Centre for Environment and Health, Bonn, Germany (mkr@ecehbonn.euro.who.int)
[6]Geography Dept., Moscow State University, Moscow, Russia (chubarova@imp.kiae.ru)
[7]State Environmental Organization, Mosecomonitoring, Moscow, Russia (info@mosecom.ru)
[8]Health Effects Institute, Boston, MA, USA (acohen@healtheffects.org)

Acute exposure to high levels of fine particulate matter ($PM_{2.5}$), such as emitted by the Moscow wildfires in summer 2010, are associated with serious adverse health effects, yet the location and scale of such events often make *in situ* monitoring difficult. Recent satellite retrieval developments have the potential to monitor surface pollution during these events. We estimate daily $PM_{2.5}$ concentrations using satellite observations during the Moscow fires. We increase the coverage of aerosol optical depth (AOD) retrieved from the Moderate Resolution Imaging Spectroradiometer (MODIS) by relaxing the operational cloud screening criteria which can mistake extreme aerosol events for cloud. This relaxed product shows excellent agreement with coincident operational retrievals (r^2=0.994; slope = 1.010) and increases coverage during the fires by 21.3%. We relate MODIS AOD to $PM_{2.5}$ using a chemical transport model (GEOS-Chem) and find good agreement with $PM_{2.5}$ values estimated from *in situ* PM_{10}. We find that the relationship between AOD and $PM_{2.5}$ is insensitive to uncertainties in biomass burning emissions. Satellite-derived and *in situ* values both indicate peak daily mean $PM_{2.5}$ of ~600 μg/m^3 on August 7, 2010 around Moscow, with a potential ~400 excess deaths during the fires.

Growth rate of giant gypsum crystals

A.E.S. VAN DRIESSCHE[1], J.M. GARCÍA-RUÍZ[1], K. TSUKAMOTO[2], L.D. PATIÑO[1] AND H. SATOH[2]

[1]LEC, IACT, CSIC - U.Granada, 18100 Granada, Spain
[2]Department of Mineralogy, Petrology and Economic Geology, Tohoku University, Sendai 980-8578, Japan

Mineralogical processes taking place close to equilibrium, or with very slow kinetics, are difficult to quantify precisely. The determination of ultra slow precipitation rates should reveal characteristic timing associated to processes that are important at geological scale. We designed a high-resolution phase-shift interferometer to measure growth rates of crystals at very low supersaturation values. To test this technique, we selected the giant crystals of gypsum of Naica ore mines

(Mexico), a challenging subject in mineral formation. They are formed by a self-feeding mechanism driven by solution-mediated anhydrite-gypsum phase transition, and are the result of an extremely slow crystallization process close to equilibrium [1]. To calculate the formation time of these crystals we measured the growth rates of the {010} face of gypsum growing from current waters from Naica at different temperatures. The slowest measurable growth rate was found at 55 °C, being 1.4±0.2x10^{-5} nm/s, the slowest value measured for a crystal growth process. At higher temperatures growth rates increase exponentially due to decreasing gypsum solubility and higher kinetic coefficient [2]. At 50 °C neither growth nor dissolution was observed indicating that growth of giant crystals of gypsum occurred at Naica between 58 °C and current temperature of Naica waters, confirming formation temperatures determined from fluid inclusion studies. Our results demonstrate the usefulness of applying advanced optical techniques in laboratory experiments to gain a better understanding of crystal growth processes occurring at a geological time scale.

[1] García-Ruiz *et al*. (2007) *Geology* **35**, 327–330. [2] Van Driessche *et al*. (2010) *Cryst. Growth Des*. **10**, 3909–3916.

https://doi.org/10.1180/S0026461X00006502 Published online by Cambridge University Press

Effect of low-molecular-weight organic acids on thallium mobility in soil – A model rhizosphere solution approach

A. VANĚK*, I. GALUŠKOVÁ AND M. KOMÁREK

Czech University of Life Sciences Prague, 16521 Prague, Czech Republic (*correspondence: vaneka@af.czu.cz)

The kinetic batch leaching of Tl-bearing mineral soil in 500 μM solutions of citric, oxalic and acetic acid was performed to simulate the release of Tl in the rhizosphere-like environment. The obtained data demonstrate that low-molecular-weight organic acids significantly contribute to soil alteration accompanied by the release of lithogenic Tl (if present). The highest mobilization rates for Tl were observed after 0.5 h of leaching (with maximal values obtained for oxalate) followed by a substantial decrease. Thallium extractability in the organic acid solutions was up to 2.8-fold higher compared to water. Based on the experimental and speciation modeling data, Tl release is mainly pH-driven and can be attributed to acid ion exchange and/or acid leaching, as the formation of Tl-LMWOA complexes is negligible. The main Tl solubility-controlling phases predicted include illite and the identified Mn (III, IV) oxide due to their ability to efficiently sorb Tl^+ on the mineral surfaces from which Tl can be potentially mobilized. The role of primary silicates (i.e. orthoclase and muscovite) in the total process of Tl mobilization seems to be of lesser importance because the supposed alteration/dissolution of these phases during LWMOA leaching was limited.

A geochemical reference (baseline) for the natural geogenic variation in Pb isotope ratios in sedimentary soils

P.F.M. VAN GAANS[1]*, N. WALRAVEN[2], G. VAN DER VEER[3], S.P. VRIEND[3], B.J.H. VAN OS[4] AND G.TH. KLAVER[1]

[1]Deltares, Utrecht, the Netherlands (*correspondence: pauline.vangaans@deltares.nl, gerard.klaver@deltares.nl)
[2]GeoConnect, Castricum, the Netherlands (n.walraven@geoconnect.nl)
[3]Universiteit Utrecht, Utrecht, the Netherlands
[4]Rijksdienst voor het Cultureel Erfgoed, Amersfoort, the Netherlands (b.van.os@cultureelerfgoed. nl)

Given the wide historic to recent use of lead, enhanced Pb concentrations in soils may pose serious problems. The Pb isotopic composition (Pb-ic) can be used to distinguish natural from anthropogenic Pb and to appoint anthropogenic Pb sources. Often, a local reference is used to establish the natural geogenic Pb-ic, with which to compare the observed ratios in contaminated soils. However, Pb-ic is known to depend on soil type and show high spatial variability. Here we go for a regional approach, using as reference a set of 342 samples of sand and clay subsoils in the Netherlands. The combined geogenic Pb isotope ratios ($^{206}Pb/^{207}Pb$, $^{208}Pb/^{207}Pb$ and $^{206}Pb/^{208}Pb$) are empirically modelled, through regression with geochemical proxies as predictors.

Total concentrations of Al and Zr, as measured by XRF, were found to be suitable, mutually independent predictors of the geogenic Pb isotope variability. To eliminate the effects of outliers and high variability, we used a robust trimmed least squares regression, based on a core dataset containing the 70% of the data having the smallest absolute regression residuals. For this core dataset, the percentage of variance explained is about 70%. The model grasps the main trends displayed in the measured data: a) an apparent age range within both sands and clays, tending towards higher ^{208}Pb with increasing apparent age, and b) a clear shift towards lower ^{207}Pb from sands to clays. The Zr content is hypothesized to represent the proportion of U-Th containing 'parent' minerals to Pb containing 'daughter' minerals; the Al content represents the proportion of secondary minerals.

The regional reference allows prediction of the baseline Pb-ic where no local reference is avaialble, e.g. in topsoils that differ in lithology from their subsoil or where subsoil Pb contamination is suspected. Otherwise the regional reference is as suitable as a local subsoil reference.

https://doi.org/10.1180/S0026461X00006502 Published online by Cambridge University Press

Characterization of Fe(0) electro-coagulation reaction products using synchrotron-based techniques

C.M. VAN GENUCHTEN[1]*, J. PEÑA[2], S.E.A. ADDY[1], G. SPOSITO[1,2] AND A.J. GADGIL[1,2]

[1]University of California, Berkeley, Berkeley, CA (*correspondence: cmvangenuchten@berkeley.edu)
[2]Lawrence Berkeley National Laboratory, Berkeley, CA

Electrocoagulation (EC) using Fe (0) electrodes is a promising technology capable of cheaply and efficiently removing arsenic from drinking water. In EC, an electric current is applied to Fe (0) electrodes inserted into pumped groundwater contaminated with arsenic. Electrolysis of the Fe (0) anode leads to the *in situ* formation of iron (oxyhydr)oxides, which form surface complexes with arsenic. Of concern in such systems are common groundwater constituents (PO_4^{3-}, SiO_2, Ca^{2+}, Mg^{2+}), which can influence the structure of the generated precipitates in both subtle and complex ways. To assess the influence of these ions, synchrotron-based techniques were used to characterize EC precipitates generated in chemically varying electrolytes. Electrolytes were chosen to clarify the individual effect of strongly-adsorbed ions (0.5mM Na_2HPO_4, 0.75mM SiO_2) and weakly-adsorbed ions (1mM $CaCl_2$, 1mM $MgCl_2$, 2mM NaCl) on the removal of 1μM As(V) at pH 7.5. The As K-edge XANES and EXAFS spectra of precipitates generated in the Na_2HPO_4 electrolyte differed in both phase and line shape from those of precipitates generated in the NaCl and $CaCl_2$ electrolytes. These differences likely reflect a change in the adsorbent structure due to sorption of the surface-poisoning PO_4^{3-} oxyanion. The Fe K-edge EXAFS spectra and PDFs of similar samples will be presented to provide complementary views of the adsorbent structure (phase, crystallite size, and degree of FeO_6 octahedral polymerization) in instances where variations in the As K-edge spectra were observed. These results provide an important molecular-scale understanding of arsenic removal during EC.

On the way to medical diagnosis based on the isotopic analyis of metabolically relevant transition metals

L. VAN HEGHE[1]*, E. ENGSTRÖM[2], I. RODUSHKIN[2], A. VERSTRAETE[3], H. VAN VLIERBERGHE[4], C. CLOQUET[5] AND F. VANHAECKE[1]

[1]Department of Analytical Chemistry, Ghent University, Krijslaan 281-S12, Ghent, Belgium (*correspondence: lana.vanheghe@ugent.be)
[2]ALS Scandinavia, Aurorum 10, 977 75 Luleå, Sweden
[3]Department of Clinical Chemistry, Ghent University, De Pintelaan 185, Ghent, Belgium
[4]Department of Gastroenterology and Hepatology, Ghent University, De Pintelaan 185, Ghent, Belgium
[5]CRPG/CNRS, BP 20, 54501, Vandoeuvre-Nancy, France

Although modern medicine already has many sophisticated tools for the diagnosis of a large variety of diseases, there are still diseases for which diagnosis is difficult or can only be accomplished at a later stage of progression. New diagnostic tools are therefore highly needed for drawing unequivocal conclusions or start medicating people at an earlier stage.

A promising approach for diagnosis is the isotopic analysis of elements the metabolism of which is affected by the disease (e.g. Fe)[1]. Next to Fe, also Zn and Cu are important transition metals because of their great catalytic, structural and regulating importance in the human body [2].

These non-radiogenic elements show natural variations in isotopic composition due to isotope fractionation. As a result, we aim at developing a minimally invasive method, based on isotopic analysis using MC-ICPMS. In the method developed for this purpose Cu, Fe and Zn were isolated from blood within the same chromatographic separation with quantitative recovery, thus avoiding the effect of on-column isotope fractionation. External precisions for this method are 0.02; 0.05 and 0.03 ‰ (2s) for δ^{56}Fe, δ^{66}Zn and δ^{65}Cu, respectively. A first sample set comes from supposedly healthy human volunteers (reference population, including vegetarians and 'omnivorous) to investigate the dependence of isotope composition and nutrition. Whole blood from patient populations will be investigated at a later phase.

[1] Krayenbuehl (2005) *Blood* **105**, 3812–3816. [2] Walravens (1979) *Western J of Medicine* **130**, 133–142.

https://doi.org/10.1180/S0026461X00006502 Published online by Cambridge University Press

Towards a quantitative record of Archaean ocean water chemistry: An element partitioning approach

VINCENT J. VAN HINSBERG[1]*, KRISTOFFER SZILAS[2] AND BERNARD J. WOOD[1]

[1]Department of Earth Sciences, University of Oxford, United Kingdom (*correspondence: V.J.vanHinsberg@gmx.net)
[2]Geological Survey of Denmark and Greenland - GEUS, Copenhagen, Denmark

The composition of the Archaean ocean is of interest for two reasons in particular: 1. Ocean water is the reaction product of processes operating on the surface of the early Earth and in its interior, and its composition thus allows for insights into, and constraints on these processes, including the nature of Archaean plate tectonics; and 2. Ocean water is the likely medium in which life originated and developed, and knowledge of its composition, and changes therein over time provides insights into the inorganic forcing on life's evolution.

Qualitative information on the composition of the early Earth ocean has been obtained from the mineralogy and compositions of marine sediments preserved in the geological rock record. Banded Iron Formations, in particular, appear a viable source of information on changes in (trace) element abundance [1]. At present, it is not possible to translate this qualitative record into actual concentrations, and information is furthermore restricted to a small suite of elements, which severely limits the information that can be gained.

In this contribution, we present an approach that uses the lattice-strain theory systematics in element partitioning to reconstruct *quantitative* information on water chemistry from the composition of minerals. Although this approach can be applied to marine sediments, we use it here on samples of altered ridge basalts (greenstones), which are an indirect source of information on ocean water chemistry, because the interaction between ocean water and fresh oceanic crust at the ridges has a dominant control on the composition of the ocean. Combining experimentally determined mineral - fluid partition coefficients for chlorite and plagioclase at appropriate conditions, with the compositions of these minerals in well-preserved Archaean greenstones, we are able to track the evolving composition of the early Earth ocean.

[1] Konhauser, Pecoits, Lalonde, Papineau, Nisbet, Barley, Arndt, Zahnle & Kamber (2009) *Nature* **458**, 750-754.

Innovative low kV X-ray microanalysis of submicron particles using PARC algorithms

CORRIE J.G. VAN HOEK* AND SIEGER R. VAN DER LAAN

TATA Steel RD&T, Ceramics Research Centre, IJmuiden, The Netherlands
(*correspondence: corrie.van-hoek@tatasteel.com)

One of the challenges in microanalysis is to get accurate qualitative and quantitative analysis on the smallest phases present in a sample. Using PARC (**P**h**A**se **R**ecognition and **C**haracterization) algorithms as developed at CRC, we can arrive at the theoretical resolution using a FEG-SEM equipped with X-ray microanalysis equipment as will be shown in this paper.

The analytical spatial resolution for microanalysis is dictated by the SEM acceleration voltage, and the average atomic number of the phases present in the specimen. The challenge is finding the proper spot in a sample where the best analysis (without contaminated signal from the surrounding), can be obtained of the smallest phase for a given analytical condition.

The PARC approach simply circumvents manual selection of spots by including ALL pixels of an image field in the spectral image (SI) dataset. PARC software sorts all pixels of the SI dataset according to the phases they represent. The pixel populations can than be automatically cleaned from contaminant signals, leaving pure spectra for ZAF corrected quantification. The quality of analysis subsequently can be assessed from the resulting phase stoichiometry. In addition, phase area proportions and phase chemistry can be combined to reproduce the bulk composition of the sample material. We will show that using PARC in combination with FEG-SEM-EDS good stoichiometric analysis can be obtained on samples with crystals of less than 500 nm, even for trace phases.

Several PARC applications will be presented during this conference.

https://doi.org/10.1180/S0026461X00006502 Published online by Cambridge University Press

H_2O and CO_2 devolatilization in subduction zones: Implications for the global water and carbon cycles

PETER VAN KEKEN[1]*, BRAD HACKER[2], ELLEN SYRACUSE[3] AND GEOFF ABERS[4]

[1]University of Michigan, Ann Arbor, MI, USA (*correspondence: keken@umich.edu)
[2]University of California, Santa Barbara, CA, USA
[3]University of Wisconsin, Madison, WI, USA
[4]Columbia University, Palisades, NY, USA

Subduction of sediments and altered oceanic crust functions as a major water and carbon sink. Upon subduction the water and carbon may be released by progressive metamorphic reactions. Quantification of the volatile release from subducting slabs is important to determine the provenance of volatiles that is released by the volcanic arc and to constrain the flux of water and carbon to the deeper mantle. In recent work we used a global set of high resolution thermal models of subduction zones to predict the flux of H_2O from the subducting slab [1] which provides a new estimate of the dehydration efficiency of the global subducting system. It is found that mineralogically bound water can pass efficiently through old and fast subduction zones (such as in the western Pacific) but that warm subduction zones (such as Cascadia) see nearly complete dehydration of the subducting slab. The top of the slab is sufficiently hot in all subduction zones that the upper crust dehydrates significantly. The degree and depth of dehydration is highly diverse and strongly depends on (p, T) and bulk rock composition. On average about one third of subducted H_2O reaches 240 km depth, carried principally and roughly equally in the gabbro and peridotite sections. The present-day global flux of H_2O to the deep mantle translates to an addition of about one ocean mass over the age of the Earth. We extend the slab devolatilization work to carbon by providing an update to Gorman *et al*. [2], who quantified the effects of free fluids on CO_2 release. We use the new high resolution and global set of models to provide higher resolution predictions for the provenance of CO_2 release to the mantle wedge.

[1] van Keken, Hacker, Syracuse, Abers, J. (2011) *Geophys. Res*. [2] Gorman *et al*. (2006) *Geochem. Geophys. Geosyst*.

Geology, age and origin of the oldest terrestrial rocks and minerals

MARTIN J. VAN KRANENDONK

Geological Survey of Western Australia, 100 Plain St., East Perth, WA 6004 Australia (martin.vankranendonk@dmp.wa.gov.au)
School of Earth and Environment, The University of Western Australia, Crawley WA 6009 Australia

Earth's mineral and rock record extends back to an astonishing 4.4 Ga. The earliest history (4.4–4.03 Ga, 'The Hadean') is represented by zircon crystals and isotopic evidence from younger rocks of buried and/or vanished sources of this age [1, 2]. In the Archean, increasing amounts of crust are preserved from 4.03–3.5 Ga, but only as high-grade gneiss terrains with little primary sedimentary or volcanic material. Strangely, these rocks contain little or no evidence for meteorite bombardment at this time. Nevertheless, these remnants contain important clues to crust-forming processes and tantalising hints of the earliest biosphere. After 3.5 Ga, better-preserved crustal remnants yield more robust clues to early Earth processes and biosphere components.

Debate continues on the nature of early crust formation processes, specifically whether plate tectonics (of any kind) operated in early (or even middle) Earth history. Hadean crust may have been thick and basaltic, crystallised from a magma ocean and locally intrenally differentiated to form tonalite [3]. The early Archean was characterised by two types of crustal growth mechanisms, as on modern Earth [4]: 1) plateau formation over zones of upwelling mantle, forming thick welts of autochthonous crust affected by internal differentiation (e.g. East Pilbara Terrane, Pilbara Craton); 2) subduction-accretion in zones with voluminous arc-like magmatism and crustal imbrication (e.g. Western Greenland). By 3.1 Ga, modern-style (i.e. steep) subduction had commenced locally [5], and a significant proportion of the continental crust may have formed by 3.0 Ga, starting the supercontinent cycle.

[1] Wilde *et al*. (2001) *Nature* **409**, 175–178. [2] O'Neil *et al*. (2008) *Science* **321**, 1828–1831. [3] Kemp *et al*. (2010) *Earth Planet Sci. Lett*.296, 45–56. [4] Van Kranendonk (2011) *Am. J. Sci*. **310**, 1187–1209. [5] Smithies *et al*. (2005) *Earth Planet Sci. Lett*. **231**, 221–237.

https://doi.org/10.1180/S0026461X00006502 Published online by Cambridge University Press

Freeze-fry cycles in the Paleoproterozoic Turee Creek Group, Western Australia

MARTIN J. VAN KRANENDONK[1]*, AIVO LEPLAND[2] AND KOSEI E. YAMAGUCHI[3,4]

[1]Geological Survey of Western Australia, 100 Plain St., East Perth WA, 6004 Australia (*correspondence: martin.vankranendonk@dmp.wa.gov.au)
[2]Geological Survey of Norway, 7491 Trondheim, Norway
[3]Dept. Chemistry, Toho University, 2-2-1 Miyama, Funabashi, Chiba 274-8510, Japan
[4]NASA Astrobiology Institute

Previous research has suggested a Paleoproterozoic Snowball Earth consisted of up to three glaciations from 2.42–2.22 Ga, coincident with the timing of the inferred rise in atmospheric oxygen [1, 2]. Supporting geological and isotopic data from North America, Fennoscandia, and South Africa are supported by the occurrence of glacial rocks in the Turee Creek Group (TCG), Australia, and their geochemical characteristics [3, 4].

New $\delta^{13}C$ and $\delta^{18}O$ isotope data on bedded and stromatolitic dolomites, combined with previously available results [5] - recast in the light of corrected stratigraphic assignation - suggest that three freeze-fry cycles are recorded in the TCG. The first cycle is preserved in the lowest Kungarra Formation, reflected by a decrease and subsequent increase in $\delta^{13}C$ upsection, from 0-2‰→-6‰→0‰, associated with a decrease in $\delta^{18}O$ from 0→-4‰. Part of a second cycle is recorded in rocks of the glaciomarine Meteorite Bore Member and immediately overlying rocks of the upper Kungarra Formation ($\delta^{13}C$ from -2.5 to -6‰→-1‰, and $\delta^{18}O$ from 0 to -3→-12‰), whereas a third cycle is recorded in rocks of the overlying Kazput Formation ($\delta^{13}C$ from -3→1‰, and $\delta^{18}O$ from 0→-16→5‰).

The low-grade TCG carbonates are considered to have escaped significant post-depositional resetting. $\delta^{18}O$ variability and trends are interpreted to reflect changes in the temperature of basinal diagenetic fluids across cooling and warming periods, while mantle-like $\delta^{13}C$ values support periodic global collapse of the biosphere.

[1] Kirschvink *et al*. (2000) *PNAS* **97**, 1400–1405. [2] Papineau, Mojzsis & Schmitt (2007) *Earth Planet. Sci. Lett*. **255**, 188–212. [3] Martin (1999) *GSA Bull*. **111**, 189–203 [4] Williford *et al*. (2011) *Geochim. Cosmochim. Acta* (in press). [5] Lindsay & Brasier (2002) *Precambr. Res*. **114**, 1–34.

Ion diffusion in argillaceous materials

L.R. VAN LOON

Paul Scherrer Institut, 5232 Villigen PSI, Switzerland

Molecular diffusion is the dominant transport process of radionuclides which needs to be considered when evaluating the safety of radioactive waste repositories in argillaceous host rocks. The diffusive behaviour of radionuclides depends both on the properties of the porous medium and on the diffusing species.

Clay minerals (notably montmorillonite and illite) have a permanent negative surface charge which attracts cations and repulses anions leading to the formation of a diffuse double layer (DDL). The net positive charge of the DDL compensates the negative charge of the clay surface [1]. In the case of the diffusion of neutral species, no interaction between the electrostatic field and the species occurs and diffusion can be described by Fick's law [2]. The concentration gradient in the pore water is the driving force for diffusion of neutral species. In this case, only geometrical factors such as constrictivity and tortuosity are important. In the case of charged species, the situation is different. Because cations are attracted by the negative surface charge, the concentration gradients in the DDL and in the interlayers of the clay grains are larger than in the free pore water and consequently the diffusive flux is also larger. The electrostatic field thus enhances cation diffusion. Unlike cations, anions are repulsed from the surface leading to anion exclusion from the interlayers and the DDL. Anion exclusion leads to a lower accessible porosity for the anions, resulting in lower diffusive fluxes. All factors directly influencing the DDL thus also affect the diffusive behaviour of cations and anions.

This study gives an overview of the state-of-the art of knowledge on diffusion processes in dense argillaceous materials. Focus will be on tracer diffusion of ion exchanging cations, anions and neutral species in a constant electrolyte background and in different argillaceous materials [3]. The diffusive behaviour of cations which.. sorb via surface complexation is expected to be different and a brief outlook on current activities will be discussed.

[1] Appelo, Van Loon & Wersin (2010) *Geochim. Cosmochim. Acta* **74** 1201–1219. [2] Van Loon, Soler & Bradbury (2003) *J. Contam. Hydrol*. **61** 73–83. [3] Glaus, Frick, Rossé & Van Loon (2010) *Geochim. Cosmochim. Acta* **74** 1999–2010.

https://doi.org/10.1180/S0026461X00006502 Published online by Cambridge University Press

A predictive model for cation diffusion in periclase

JAMES A. VAN ORMAN AND KATHERINE L. CRISPIN

[1]Department of Geological Sciences, Case Western Reserve University (james.vanorman@case.edu, klc24@case.edu)

Understanding rates of diffusion in periclase is essential for understanding chemical transport in Earth's lower mantle. Cation diffusion through periclase is faster than through any other major crystalline phase in the lower mantle, and thus provides an upper limit on the bulk diffusive transport that is possible in the absence of fluids.

The variation in diffusivity among different cations is controlled by their ionic properties, including size, charge, polarizability and electron configurations. No clear relationships among ionic properties and diffusivity have previously been recognized in periclase, despite the existence of a large diffusion database. The trends are obscured by variations in diffusivity that are likely due to the variable chemical purity of the MgO crystals used in the experiments. Here we take advantage of constraints provided by diffusion and ionic conductivity studies on doped MgO crystals to compare the cation diffusion data at a common vacancy concentration. Clear trends emerge between diffusivity and ionic size, charge, polarizability and crystal field stabilization energy. These trends are parameterized to provide a predictive expression for cation diffusion rates in periclase over a broad range of conditions relevant to Earth's lower mantle.

^{40}Ar-^{39}Ar geochronology and PT estimations on garnet-hornblende-muscovite-plagioclase schists from the Kheis Belt, South Africa

V. VAN SCHIJNDEL* AND D.H. CORNELL

Department of Earth Sciences, The University of Gothenburg, SE-40530, Sweden
(*correspondence: valby.van.schijndel@gvc.gu.se)

The Kheis Belt on the western margin of the Kaapvaal Craton, South Africa, is often referred to as a thin-skinned fold and thrust belt. However, Humphreys *et al*. [1] indicated that the schists of the Palaeoproterozoic Groblershoop Formation within the Kheis Belt reached equilibrium conditions between 600-700°C and 8-11 kBar. The schists of this study contain a main mineral assemblage of grt+hbl+plag+musc+epi+qtz with accessory chlorite, biotite, ilmenite and rutile. The peak metamorphic mineral assemblage is represented by grt+hbl+musc and the plagioclase has an Ab content of 0.83. The garnet and hornblende have inclusions of quartz, epidote and ilmenite, indicating a greenschist facies mineralogy assemblage. This is oldest assemblage preserved in the sample. Preliminary modeled results, obtained by equilibrium phase diagrams based on bulk composition were calculated for the NaCaKFMASH system with the program Theriak/Domino [2, 3]. These diagrams indicate that the garnet and hornblende growth started at 520°C and 9.5-10 kBar. An increase in Mg in the rims of the garnets points to a prograde reaction. PT conditions went up during garnet growth and reached a possible maximum at 660°C and 12.5 kBar. At higher temperatures kyanite becomes stable and this is not present in the samples. It is unlikely that the temperature reached above 660°C. Retrograde chlorite postdates all other minerals. 40Ar-39Ar dating on both muscovite and hornblende gave 1147±4 Ma and 1141±3 Ma. These ages are related to the Namaqua Orogeny and the agreement between the cooling ages of muscovite and hornblende arguments for a rapid uplift. Therefore are these ages thought to represent cooling ages that can be directly correlated with the peak metamorphic conditions.

[1] Humphreys *et al*. (1991) *S. Afr. J. Geol*. **94**, 170–173.
[2] De Capitani (1994) *European Journal of Mineralogy,* **72**.
[3] De Capitani (1994) *Jahrestagung der Deutschen Mineralogischen Geselleschaft* **6**, 48.

https://doi.org/10.1180/S0026461X00006502 Published online by Cambridge University Press

Monitoring nutrients cycles at catchment scale

T.P. VAN TOL[1] AND B. VAN DER GRIFT[2]*

[1]Alterra, Wageningen University and Research Centre, P.O. Box 47, NL-6700 AA Wageningen, The Netherlands (dorothee.vantol-leenders@wur.nl)
[2]Deltares, P.O. Box 85467, NL-3508 TA Utrecht, The Netherlands (*correspondence: bas.vandergrift@deltares.nl)

In The Netherlands, the high concentration of nitrogen and phosphorus has an adverse affect on the quality of our surface water. The abundant growth of algae, water plants and reed is a recurring problem in Summer. Furthermore, the discharge of nutrient-rich water into the sea is a real threat to the marine ecosystem. Unfortunately, the origin and fate of all these nutrients often remains unclear.

The total nutrient concentration in surface water is determined by a range of sources, transport routes and chemical or biological processes. Nutrient cycles at a watershed scale are therefore very complex. To come up with solutions to improve the water quality it is very important to gain insight into the origin of the sources, their transportation time and what happens en route. In four typical watersheds in the Nederland's we studied the biogeochemical cycling of nitrogen en phosphorus at regional scale. The main goal of the project is to understand the relationship between long term changes in nutrient surplus and the quality of the surface water. The four watersheds are: a sandy with high loads of nutrients due to intensive cattle breeding, a more natural sandy area, a clay polder and a polder with peat soil. Each area has it own characteristics regarding the sources and transport route for nutrients. For this study we analysed soil, groundwater, sediment and surface water quality on several locations. The surface water quality and quantities were monitored continuously in the period 2004-2010. Combined with data collected on nutrient loads this resulted in an extensive dataset to study biogeochemical cycling of nitrogen and phosphorus in the soil-groundwater-surface water system at regional scale. A combined soil-groundwater-surface water model is used to predict the effectiveness of different source or transport route oriented measures to improve the quality of the surface water.

One of the major findings is the importance of sediments in the binding and relase of phosphorus when transported form groudnwater to surface water and the rol of sulfate in this proces.

Uranyl coordination chemistry on magnesite and brucite surfaces: Polarisation dependent EXAFS

A. VAN VEELEN[1]*, G.T.W. LAW[1], A.J. SMITH[1], J.R. BARGAR[2], J. ROGERS[2] AND R.A. WOGELIUS[1]

[1]University of Manchester, School of Earth, Atmospheric and Environmental Sciences, Oxford Road, Manchester, M13 9PL, United Kingdom (*correspondence: arjen.vanveelen@postgrad.manchester.ac.uk)
[2]Stanford Synchrotron Radiation Laboratory, PO Box 4349, Stanford, CA 94309, USA

Previous studies have examined uranium uptake by calcium carbonate minerals (calcite and aragonite) under conditions pertinent to both natural and anthropogenically perturbed systems. However, research on uranyl uptake by magnesium-rich minerals such as magnesite [$MgCO_3$], brucite [$Mg(OH)_2$], nesquehonite [$MgCO_3 \cdot 3H_2O$] and hydromagnesite [$Mg_5(CO_3)_4(OH)_2 \cdot 4H_2O$] has not, to the best of our knowledge, been previously conducted. Such experiments will improve our understanding of the mobility of uranium and other actinides in natural lithologies such as dolomitic limestones or mafic igneous emplacements, as well as provide key information applicable to nuclear waste repository strategies involving Mg-rich phases. Thus, experiments with minerals powders were used to determine the partition coefficients and coordination of UO_2^{2+} during adsorption and coprecipitation with magnesite, brucite nesquehonite and hydromagnesite. A second set of experiments used single crystal magnesite (10.4) cleavage surfaces and MgO(111) surfaces engineered and hydroxylated to be equivalent to the $Mg(OH)_2$(00.1). Here EXAFS measurements were made at $\chi = 0^o$ and $\chi = 90^o$ in order to use the polarisation of the incident beam to unequivocally determine adsorbate and coprecipitate structures. The selected minerals were reacted with uranyl chloride at three different concentrations (500, 50 and 5 ppm) above and below solubility boundaries of schoepite ($UO_2(OH)_2 \cdot H_2O$) at pH 8 and $PCO_2 = 10^{-3.5}$ atm. K_d values for Mg carbonate phases were comparable to or exceeded those published for calcium carbonates. EXAFS results showed clear polarisation dependence of surface uranyl. The spectra demonstrated consistently that the uranyl molecule is preferentially oriented with the axial oxygens perpendicular to the mineral surface. This implies the creation of local rutherfordine-like regions which may polymerise at high uranyl activities into a thin film.

https://doi.org/10.1180/S0026461X00006502 Published online by Cambridge University Press

Nanoscale structural variation in pyrobitumen of the 2.0 Ga Zaonega Formation, Karelia, Russia

M.A. VAN ZUILEN[1]*, D. FLIEGEL[2], R. WIRTH[3], A. LEPLAND[4], Y. QU[5], A. SCHREIBER[3], A.E. ROMASHKIN[6] AND P. PHILIPPOT[1]

[1]Institut de Physique du Globe, 75005 Paris, France (*correspondence: vanzuilen@ipgp.fr)
[2]National Institute of Nutrition and Seafood Research, [5]004 Bergen, Norway
[3]GeoForschungsZentrum Potsdam, Telegrafenberg [1]4473 Potsdam, Germany
[4]Geological Survey of Norway, 7491 Trondheim, Norway
[5]Centre for Geobiology, University of Bergen, 5007, Bergen, Norway
[6]Institute of Geology, Karelian Science Centre [1]85610 Petrozavodsk, Russia

Alteration and especially remobilization of organic material and carbonic fluids in Archean rocks has led to many controversies regarding early life. It is therefore important to establish the detailed changes that occur when carbonaceous materials are affected by metamorphism. A case study is presented here of carbonaceous matter that occurs in sediments of the 2.0 Ga old Zaonega Formation, Karelia, Russia. Petroleum generation and contact-metamorphism caused by intersecting magmatic bodies, regional greenschist-facies metamorphism, and circulation of silicate-saturated fluids, led to complex mixtures of silicious and bituminous materials. Raman spectroscopy and transmission electron microscopy on pyrobitumen-rich samples revealed two significantly distinct carbon allotropes; 1) graphitic films representing highly ordered carbon, and 2) variously oriented nm-scale crystallites representing strongly disordered carbon that comprises the bulk pyrobitumen matrix. This clear bimodal distribution in structural order cannot be related to a simple temperature- or pressure-induced graphitization process, and requires additional effects that caused annealing of sp2-bound carbon crystallites. Potential effects include variations in graphitizing precursor materials, local stress and strain caused by mineral authigenesis or gas bubble growth, and reorganization of graphitic clusters by hydrothermal fluid circulation. The details of these effects and their implications for the general alteration and remobilization process of organic structures in the Archean rock record will be discussed.

Evaluation of chromium reductive immobilization and oxidative re-mobilization in flow-through aquifer sediment columns

CHARULEKA VARADHARAJAN*, PETER S. NICO, LI YANG, MATTHEW A. MARCUS, RUYANG HAN, MARKUS BILL, JOERN LARSEN, APRIL VAN HISE, SERGI MOLINS, CARL STEEFEL, MARK CONRAD, EOIN L. BRODIE AND HARRY R. BELLER

Earth Sciences Division, Lawrence Berkeley National Laboratory, 1 Cyclotron Road, Berkeley, CA (*correspondence: cvaradharajan@lbl.gov)

Remediation of chromium contamination typically involves reducing the toxic and soluble hexavalent form, Cr(VI), to the relatively harmless and mostly immobile trivalent state, Cr(III). The objective of the overall project is to identify the biogeochemical mechanisms that control *in situ* chromium reduction and oxidation.

In the initial phase of the experiment, reduction under anaerobic conditions was observed for over 12 months by subjecting flow-through columns containing homogenized sediments from the Hanford 100H site to different dominant electron acceptors, i.e. NO_3^-, Fe(III), and SO_4^{2-}, in the presence of Cr(VI) and lactate. Cr(VI) was depleted in the effluent solutions of the nitrate-treated columns, all of which exhibited denitrifying conditions, as well as in some of the sulfate-amended columns where fermentative conditions were dominant. However, only a small amount of Cr(VI) was removed under other electron-accepting conditions. Spectroscopic analysis of the column sediments showed that most of the chromium was precipitated as mixed phase Cr-Fe hydroxides.

In the second phase of the study, the denitrifying and fermentative columns were subjected to oxidizing conditions that are expected to be prevalent once the bioremediation is completed (with nitrate and O_2 present). Preliminary results show that the chromium precipitated in the denitrifying columns was more readily mobilized under the oxidizing conditions, suggesting that fermentative conditions promote more sustained Cr(VI) remediation.

https://doi.org/10.1180/S0026461X00006502 Published online by Cambridge University Press

LA-ICPMS U-Pb ages of Paleo- and Mesoproterozoic granites in Bolivia

G.L. VARGAS-MATOS[1], M.C. GERALDES[1], R. MATOS[2] AND W. TEIXEIRA[3]

[1]UERJ, Faculdade de Geologia. Rua Sao Francisco Xavier 524, Rio de Janeiro (RJ), 22241-000, Brazil
[2]UMCLA. Universidad Mayor San Andreas. La Paz, Bolivia
[3]USP. Universidade de Sao Paulo. Sao Paulo (SP) Brazil

Proterozoic granites of Bolivia new U-Pb zircon ages indicate an important change in chronostratigraphy of Bolivian Precambrian. The age of the Correreca Granite (1894 ± 13 Ma and 1925 ± 32 Ma) suggest an important magmatic event which spatial distribution is bounded on the north by the San Diablo shear zone, defining the oldest terrain with distinct geological story from other areas of the Bolivian pre-Cambrian. The San Pablo granite (ascribed as the Lomas Manechi magmatic event) yielded 1617 ± 14 Ma, in agreement with the ages of the literature (1.67-1.62 Ga). The results of isotopic granitoids of Cachuela, Motacusal and Talcoso (San Ignacio orogeny), present U/Pb age between 1307 and 1333 Ma, suggesting an important period of generation of granitoids in the Bolivian pre-Cambrian.

The Sunsas magmatism presents predominantly crustal sources and presents temporal variation between 1071 Ma and 1047 Ma (Granites Naranjito, Taperas, Primavera and El Carmen).

The data here reported suggest a geological evolution for the Bolivian pre-Cambrian composed of four episodes of magmatism represented by the Correreca event, followed by San Pablo event. The younger San Ignacio event is represented by magmatic arc with important participation of older continental crust. Finally, the magmatism Sunsas is comprised of anarogenic (type A) and crustal rocks (S-type) representing an important collisional period in the SW Amazonian craton.

Petrology of lamprophyres as a result of the study of minerals

ELENA VASYUKOVA

IGM SB RAS, av. ak. Koptyuga, 3, Novosibirsk, Russia (lenav@inbox.ru)

Lamprophyres of the Chuya complex are one of the biggest displays of the alkali high potassium early mezozoic magatism of the Gorny Altay. Within this region dikes distributed unevenly, according to the fault zones and fractures. We have studied two largest and most saturated dikes local areas – South Chuya and Yustyd. The choice of these two areas is linked to the fact, that they are con fined to two distinct fault systems, located in the different host rocks and associated with the different ore disttricts. In addition, rocks of different areas vary in the degree of carbonatization, phenocrysts and structural-textural features.

Petro- and geocemical characteristics of rocks from different local habitats were so similar, that alowed to assert a single maternal source. Phenocrysts of pyroxen, phogopite, containing cromium and possibly olivine suggest, that the parental melt was high-Mg and its geochemical characteristics indicate the involvement of enriched mantle. Trends in harker variation diagrams, morphology (type 'dike-in-dike') – all this dose not in contradict the hypothesis on the formation of the dikes as a result of fractionation. Studies of minerals have confirmed this suggestion. Most informative for petrological studies in this rocks are phlogopites and apatites. The composition of plogopites reflects changes in the content of major elements, and apatites – of rare elements. In addition, their constituent volatiles significantly influenced the composition of the fluid phase of the rockforming melt. Study of their composition, relationships and restoration of the sequence of crystallization of minerals allowed to assume a model of formation of the Chuya lamprophyre complex, explain the differents between the two dikes areas.

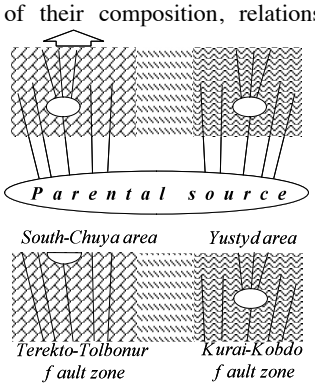

The ultimate hypothesis is that the dikes South Chuya area formed at great depths directly from the source dyke Yustyd area are the result of crystallization of fractionated melt in the hypabyssal parts of the lithosphere, and associating with lamprophyre syenite massif is an intermediate chamber.

https://doi.org/10.1180/S0026461X00006502 Published online by Cambridge University Press

Eu(III) interactions with calcium carbonate

AIKATERINI I. VAVOURAKI[1]*, ÁGELES FERNÁNDEZ-GONZÁLEZ[2], MANUEL PRIETO[2] AND PETROS G. KOUTSOUKOS[1]

[1]Department of Chemical Engineering, University of Patras, Greece (*correspondence: kvavouraki@chemeng.upatras.gr)
[2]Department of Geology, Universidad de Oviedo, Spain

Understanding the interactions of radionuclides with mineral phases is important for the long-term storage safety of nuclear waste deposits which depends strongly on their interactions with the minerals. Calcite is a candidate mineral for use in nuclear waste repositories. Model studies involve nonradioactive trivalent lanthanides. In the present work Eu(III) interactions with calcite were investigated using two crystallization techniques which could yield complementary information. Counter-diffusion of (Ca^{2+}, Eu^{3+}) and (Na^{+}, CO_3^{2-}) ions was achieved through a porous silica hydrogel [1] in a U-shaped tube and aqueous solutions supersaturated with respect to calcite were prepared by mixing equimolar $CaCl_2$ and Na_2CO_3 solutions. The range of Eu(III) concentration was 10^{-2} – 50 mM. In the case of gels, Eu(III) was introduced into the sodium silicate solution used for the preparation of the silica gel to avoid formation of Eu(III) oxides. Crystals of calcium carbonate polymorphs in the presence of Eu(III) were formed in less than a month in the silica gel. Crystal growth proceeded and was finalized past a time period of one year. Additional crystallization experiments were carried out by vapor diffusion using the sitting drop crystallization method on a 'crystallization mushroom' [2]. Calcium carbonate precipitated in droplets containing $CaCl_2$: $(NH_4)_2CO_3$ ratio of 2.5 in the presence of Eu(III) concentration of 4 – 10 mM. The calcium carbonate polymorphs formed in the presence of Eu(III) were examined by Scanning Electron Microscope (SEM-EDS) and with electron microprobe (EMP) analysis. The extent of incorporation of Eu(III) into the calcium carbonate crystal structure is discussed in the perspective of using this mineral as a host for radionuclide disposal.

[1] Prieto M. Fernández-González A. Putnis A. & Fernández-Díaz L. (1997) *Geochim. Cosmochim. Acta* **61**, 3383–3397. [2] Hernández-Hernández A. Rodríguez-Navarro A.B. Gómez-Morales J. Jiménez-Lopez C. Nys Y. & García-Ruiz J.M. (2008) *Cryst. Growth Design* **8**, 1495–1502.

Bacterial and fungal communities colonizing mercury sulfide surfaces

A.I. VAZQUEZ-RODRIGUEZ[1]*, C.M. SANTELLI[2], S.C. BROOKS[3] AND C.M. HANSEL[1]

[1]School of Engineering and Applied Sciences, Harvard University, Cambridge, MA USA (*correspondence: avazquez@fas.harvard.edu)
[2]Department of Mineral Sciences, Smithsonian Institution, Washington, DC USA
[3]Environmental Sciences Division, Oak Ridge National Laboratory, Oak Ridge, TN USA

Soils and sediments, where mercury (Hg) can exist as Hg sulfide minerals (HgS), represent major reservoirs of Hg in aquatic environments. Due to their low solubility, primary and authigenic HgS (e.g. cinnabar and metacinnabar) have historically been considered insignificant sources of soluble Hg(II) to the environment. Recently however, the solubility of HgS was shown to be greatly enhanced in the presence of a natural microbial consortium [1]. The mechanisms for this enhanced solubility have yet to be assessed. Moreover, bacteria and fungi capable of colonizing HgS surfaces in the environment have not been identified, yet their proximity and association with the mineral makes them likely key players in effecting chemical changes that can impact dissolution.

To this end, we assessed the microbial diversity on HgS surfaces in the Hg-contaminated sediments and floodplain soils of the East Fork Poplar Creek in Oak Ridge, TN. Cinnabar and metacinnabar mineral sections were incubated at various depths, and hence redox conditions, in the creek channel, bank, and floodplain. Other metal sulfides, namely pyrite (FeS_2) and sphalerite (ZnS), were also incubated to distinguish the host metal effects on the colonizing community composition. Composition and diveristy were determined after 6 weeks of incubation, via pyrosequencing using bacterial (16S rRNA) and fungal (ITS) primers.

Our results reveal a high diversity of microorganisms colonizing all the metal sulfide surfaces. The microbial community composition and phylogenetic diversity vary as a function of the host metal within the sulfide, as well as between the HgS polymophs, cinnabar and metacinnabar. Oxidation rinds are observed on metacinnabar surfaces, the extent of which decreases with depth within the sediment. These communities have been cultivated and are being investigated for their ability to solubilize HgS. The results from this study will have large implications on the role that microbial communities play in the dissolution of HgS phases and hence mobility of Hg within the environment.

[1] Jew A.D. *et al*. (2007) AGU Fall Meeting.

https://doi.org/10.1180/S0026461X00006502 Published online by Cambridge University Press

On the origins of prebiotic carbon containing rocks in the early Earth

ARON VECHT

Aron Vecht and Associates, London NW4 2AG, England (phosphors@vecht.com)

In 2007, we suggested that a paradigm shift was required to alter the generally accepted view of the organic origin of the carbon in earliest rocks [1]. To explain the distribution of deposits of methane (as hydrates), natural gas, oil, oil-tars, carbonatites as well as carbonates, we proposed the existence of stable minerals at depth which reacted when exposed to water and/or oxygen nearer the surface. We termed such rocks 'reactive minerals'. We chose carbides as examples e.g. Calcium Carbide or Aluminium Carbide. These would yield acetylene and methane respectively when exposed to water. These would in turn form carbonates under oxidizing conditions, or hydrocarbons and even graphite when exposed to a reducing environment. Under high temperatures carbonates would yield oxides while hydrocarbons would form carbon dioxide. We suggested that the existence of a considerable range of carbon containing compounds found in prebiotic rocks was not consistent with their organic origin.

More recently, evidence has been presented to support our suggestions.

1. The existence of a range of carbonate magma intrusions [2].
2. More detailed studies of ^{13}C to ^{12}C ratio. This was originally assumed to be evidence for the organic origin of carbonate deposits [3], however, more recently this conclusion has been questioned.

The oldest carbon containing rocks showing the existence of living systems is based on Stomatoporoids and Prokarryotic cell structures. These are based on Chlorophyll and DNA systems respectively. Clearly such complicated organic structures must have developed from other organic synthetic systems. Thus Miller-Urey type systems [4] or Fischer-Tropsh catalytic reaction [5] have been proposed. Such complicated processes are unlikely to explain the large carbon containing deposits found with wide distribution. The simple carbon compounds we propose are much more likely to result in the variety and distribution of the range and extent of carbon compounds found on Earth.

The relationship between the earliest organic species and the earliest carbon containing rocks need considerable further study. Many assumptions are made without detailed information. Unfortunately, although detailed isotopic studies of the oldest rocks have been reported, the extent of carbon present (or absent) has so far been overlooked [6].

[1] A. Vecht Goldschmidt Conference Abstract A1060 (2007) [2] D.K. Bailey J. (1993) *Geol Soc* **150**, 637. [3] H.D. Holland (1984) *'The Chemical Evolution of the Atmosphere & Oceans'* P.356 et seq. [4] S.L. Miller & H.C. Urey (1959) *Science* **130**, 3370.= [5] F. Fischer & H. Tropsch, Brentstoff (1923) *Chem.* **4**, 276 & 7 97 (1926). [6] M.G. Jackson *et al.* (2010) *Nature* **446**, 853

Power law behavior in continental crustal heat production and its implications to the thermal regime of the continents

NIMISHA VEDANTI, RAVI P. SRIVASTAVA, O.P. PANDEY AND V.P. DIMRI

National Geophysical Research Institute, Council of Scientific and Industrial Research, Hyderabad- 500606, India (nimisha@ngri.res.in)

The nature and distribution of radiogenic crustal heat production is directly related to the temperature-depth regime in the continental lithosphere. It depends upon the amount of Uranium, Thorium and Potassium present in the rock. It is a primary source of heat flow and contributes to as much as 50% to the observed heat flow at the surface. In the absence of direct sub-surface measurements, number of heat production models have been proposed, which includes widely used exponential model in which heat production diminishes exponentially with depth [1, 2], however this has not been the case. Our detailed study of the fractal behavior in the deep crustal heat production data from some of the prominent continental crustal section across the globe like Kaapvaal craton (south Africa), Baltic shield (Russia) and Dharwar craton (India) etc. exhibits inherent power law behavior in the deep continental heat production data, rather than exponential as has hitherto been believed [3]. This would mean that in case of power law distribution model, decay of heat production with depth within the crust will be slower. Consequently, more heat flow would be generated by heat producing elements within the crust and thus heat flow input from the mantle would be comparatively lower. This would affect rheological behavior of the crust. In comparison to exponential model, power law distribution conforms much better with geological observations and rock types, where metamorphic grade gradually increases with depth till Moho is reached and corresponding lithologies changes from felsic, to mafic. Thus, fractal models can be considered more realistic in defining the decay of heat producing elements with depth within the differentiated crust. Present findings will have significant impact in the estimation of lithospheric temperature-depth distribution.

[1] Lachenbruch, A.H(1968) *J.Geophys.Res.* **73**, 6977-6989. [2] Lachenbruch, A.H(1970) *J.Geophys.Res.* **75**, 3291-3300. [3] Vedanti,N.et al. (2011) *Nonlin. Process.Geophys.* **18**, 119–124.

https://doi.org/10.1180/S0026461X00006502 Published online by Cambridge University Press

Discovering environmentally-critical nanomineralogy: Highly reactive Mn-oxyhydroxide nanofiber nucleation and growth catalyzed by nanohematite

HARISH VEERAMANI[1]*, URS DIPPON[2], MITSUHIRO MURAYAMA[1], RACHEL HENDERSON[1], ANDREAS KAPPLER[2] AND MICHAEL F. HOCHELLA, JR.[1]

[1]Department of Geosciences, Virginia Tech, Blacksburg, VA 24061, USA (*correspondence: harish@vt.edu)
[2]Geomicrobiology, Center for Applied Geoscience (ZAG) Eberhard-Karls-University of Tübingen, Germany

Manganese oxides typically form by the oxidation of aqueous Mn(II) catalyzed by mineral surfaces and are non-specific but potent redox-active mineral components commonly found in the environment. They therefore participate in a wide array of reactions with organic and inorganic compounds. They often exhibit high sorptive reactivities and capacities exceeding those exhibited by iron oxides. When present, they can play a key role in the mobility and bioavailability of important aqueous ions.

The present study investigates abiotic Mn(II) oxidation catalyzed by nanoparticulate hematite in the presence of molecular oxygen in batch reactors. The kinetics of the reaction is studied as a function of the hematite particle size and the presence of organic ligands. The effect of organic ligands on the morphology of Mn-oxides is also studied.

Surface-area normalized rate constants suggest differences in reactivity of hematite depending on its particle size. The end product of Mn(II) oxidation, a higher valent manganese oxyhydroxide identified as the mineral hausmannite, has been characterized by employing a suite of analytical techniques including high-resolution TEM, EELS mapping, SAED and SEM. The resultant Mn-oxyhydroxides have a unique nanosized, fiber-like morphology. SEM analyses were used to describe the formation and growth of Mn-oxyhydroxides fibers over time. Mössbauer analysis on nanoparticulate hematite after complete Mn(II) oxidation indicate small detectable amounts of Fe(II) suggesting hematite reduction and resorption of ferrous iron.

These findings suggest that the formation of Mn-oxides can be influenced by the bulk mineralogical and geochemical composition of the surrounding environment, as well as by the interfacial solute–solid nanochemistry of the solid-phase oxidant. This study further signifies the relevance of low-temperature interfacial geochemistry in the formation and the transformation of environmentally pertinent nanominerals.

Arsenic partition in redox gradients systems with iron and sulfur presence

A.S. VEGA, S.E. ACEVEDO, E. LEIVA, P. RÍOS, G.E. PIZARRO AND P.A. PASTEN*

Department of Hydraulic and Environmental Engineering Pontificia Universidad Catolica de Chile Santiago Chile (*correspondence: ppasten@ing.puc.cl)

In many cases the fate of arsenic (As) is controlled by its interaction with iron (Fe) and sulfur (S) species at the mineral-water interface. Although redox gradients are ubiquitous in aqueous systems, fewer controlled experimental studies have been performed on As-Fe-S systems. The interaction between diffusion-limited transport and the kinetics/equilibrium of chemical reactions was studied using redox gradient columns and batch sorption/coprecipitation experiments. The column was filled with a glass porous media, 1 mM $FeCl_2$ and 0.1 mM As(III) or As(V). Boundary redox conditions were controlled at each end (oxygen saturated water and 3 mM sulfide). Batch experiments used ferrihydrite and mackinawite as models for Fe and Fe/S precipitation under oxic and anoxic environments, respectively. A PHREEQC model was calibrated with the results from the batch experiments and it was used to assess As especiation scenarios in the column. Arsenic (0.1 mM) is effectively removed from solution by reaction with ferrihydrite (As(V): 99% As(III): 98%) and mackinawite (As(V): 45% As(III):93%) at oxic and anoxic conditions, respectively. Similar As removal from solution was observed when mackinawite and ferrihydrite were formed before and after As was added to the solution. The only exception was when mackinawite reacted with As(V). In the redox gradient column As is immobilized at oxic (pe = 0.3) and anoxic (pe = -3) conditions, whereas at intermediate redox potentials As is mobile (see Figure 1), showing that Fe and S have a buffer effect on the fate of As. The PHREEQC model shows that equilibrium conditions are not attained in the column.

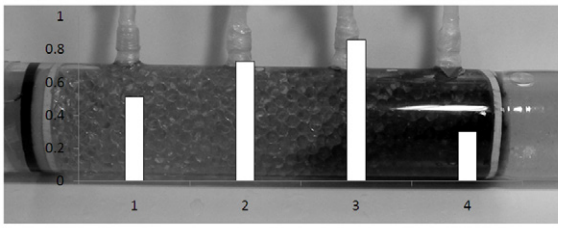

Figure 1: Redox gradient column. At the oxic boundary As immobilization on Fe oxides was favoured while As immobilization on Fe-S minerals was favoured at the anoxic boundary. Bars depict the As concentration in solution.

Fondecyt 1100943/2010

https://doi.org/10.1180/S0026461X00006502 Published online by Cambridge University Press

Exploration of interactions involving human tooth enamel and dental composites using vertical scanning interferometry

MANUEL VEGA-ARROYO[1,2], S. RAY TAYLOR[2], ROLF S. ARVIDSON[1]*, HEIDI B. KAPLAN[3], GENA D. TRIBBLE[2] AND ANDREAS LUTTGE[1]

[1]Department of Earth Science MS-126, Rice University, Houston TX 77005, USA (*correspondence: rsa4046@rice.edu)
[2]University of Texas Health Science Center at Houston – Dental Branch, Houston, TX 77030, USA
[3]Department of Microbiology and Molecular Genetics, University of Texas Medical School, Houston, TX 77030, USA

Although methacrylate resin-based dental composites are now used in the restoration of ~70% of the 120 million cavities (carious lesions) treated every year in the US, these materials have a limited service-life, requiring replacement after less than ~6 years (40% of a conventional amalgam). This replacement is most commonly necessitated because of secondary caries. Although the origin of these lesions at resin composite restoration sites is as yet unclear, they may be localized by leakage via microgaps between the cavosurface wall and the restoration. These microgaps result from shrinkage accompanying acrylate polymerization, thus yielding a protected microenvironment for growth of oral flora and subsequent chemical attack of the tooth (hydroxyapatite dissolution), and possibly the resin as well.

We present preliminary experimental results using restored teeth analyzed by vertical scanning interferometry (VSI, Fig. 1). VSI allows precise quantification of the geometry of the microgap environment and changes developing therein. Although the distribution of microgap volume is heterogeneous, the data clearly reveal the potential for micro-environments. Ongoing experiments include analysis of the chemical and mechanical response of these materials to imposed thermal and mechanical stresses, and *in vitro* analysis of microbial populations and attendant biofilm development.

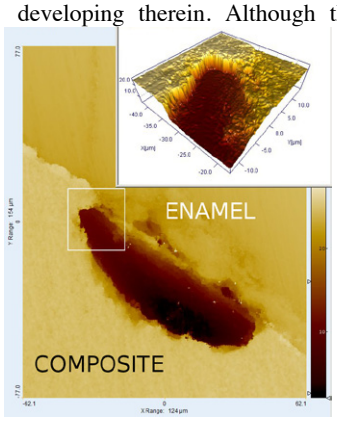

Figure 1: Microgap development at tooth-composite boundary.

Grain-supported flow at magma transfer zones

N. VEGAS[1]*, J. RODRIGUEZ[2], J.M. TUBIA[1], J.J. ESTEBAN[1] AND J. CUEVAS[1]

[1]Dpt. Geodinamica, Univ. Pais Vasco, UPV/EHU, E48940, Spain (*correspondence: nestor.vegas@ehu.es)
[2]Dpt. Mineralogía-Petrología, Univ. País Vasco, UPV/EHU, E48940, Spain

Before extruding in volcanic systems, magma suffers a continued evolution during ascent from its source. Fingerprints of this magma transfer through the lithosphere are recorded by microstructures and textures in plutonic rocks.

At the most internal parts of the Variscan chain, high-K plutonic suites were emplaced following the roots of the orogen [1]. This singular high-K and Mg association of rocks (vaugnerites, appinites, redwitzites or durbachites) is related with vertical extrusion of lithosferic-mantle derived, high-K and Na melts [2, 3].

A widespread feature of these high-K suites is the development of sphene-centred ocellar textures in some synplutonic intrusions affected by mingling processes. The structural and petrological study of these textures indicates that they formed as an effect of Reynolds dilatancy in highly crystallised crystal mushes affected by grain-supported flow [4]. Fabrics deduced from field and ASM studies indicate oblate strain and compressive regime. These conditions favoured the vertical movement of hyperdense crystal mushes with non-newtonian behaviour. The strain partitioning in these magma transfer zones will promote melt migration to upper structural levels. Moreover, it will enhance the mingling process, fauvoring the large lithological variation observed in these suites.

[1] Ferre & Leake (2001) *Lithos*. [2] Janousek & Holub (2007) *Proc. Geologists' Assoc*. [3] Lexa *et al*. (2011) *J metam Geol* [4] Vegas *et al*. (2011) *J Geol*.

https://doi.org/10.1180/S0026461X00006502 Published online by Cambridge University Press

Intracratonic carboniferous granites in the Paleoproterozoic crust of Lithuania: New SHRIMP U-Pb zircon ages

I. VEJELYTE[1]*, K. YI[2], M. CHO[3] N. KIM[2] AND T. LEE[2]

[1]Vilnius Univ., D. of Hydrogeology and Engineering Geology (*correspondence:irma.vejelyte@gf.vu.lt), Lithuania
[2]Korean Basic Science Institute, Ochang, South Korea
[3]Seoul National University, Seoul, South Korea

Employing a Sensitive High-Resolution Ion Microprobe at Korea Basic Science Institute, we found Carboniferous granite previously unknown in the Paleoproterozoic crust of western Lithuania. The granite sample was recovered from a deep drill hole, Girkaliai-2, which is situated 3 km to the east of the Baltic Sea, within the Telsiai deformation zone. In the drill core, the analyzed granite forms a 10-cm wide dyke intruding the Paleoproterozoic charnockitic rocks. It is medium to fine-grained and consists of K-feldspar, plagioclase, biotite, and quartz. Accessory phases include monazite, zircon and opaque minerals. The contact between the granite and the host charnockite is straight and sharp. Two groups of zircon grains have been recognized in the granite. Zircons of major group are prismatic in shape and show concentric and oscillatory zoning characteristic of magmatic growth. Their U/Pb ratios are 0.81-2.15, and the U contents are 57-156 ppm. A weighted mean $^{206}Pb/^{238}U$ age of 349.1±5.7 Ma (MSWD=3.2) was obtained from 12 spots. The second group of zircons yielded concordant U-Pb ages of 2042, 1880, 1846, 1726, 1630, and 1455 Ma. These grains represent xenocrysts entrapped from various country rocks during the granite emplacement. Our U-Pb zircon ages demonstrate that the Paleoproterozoic crust in western Lithuania has been affected by Early Carboniferous magmatism. The Girkaliai granitic dyke is similar to the 355 Ma diabase dykes in the eastern Baltic offshore [1], and the ca. 350 Ma alkaline-carbonatite intrusions in Poland such as Elk, Pisz and Tajno. Thus, all of these Carboniferous ages are attributed to the intracratonic magmatism associated with Paleozoic rifting in the East European craton [2]. This is a contribution to the project 'Precambrian rock provinces and active tectonic boundaries across the Baltic Sea and in adjacent areas' of the Visby Programme (the Swedish Institute).

[1] Motuza *et al*. (1994) *Geologija* **16**, 16–20. [2] Wiszniewska *et al*. (2010) *Abst. Vol. of Goldschmidt Conf.*

Microbial sulphur isotope fractionation in a Mars analogue environment at Rio Tinto, SW Spain

ESTHER VELASCO[1,2]*, PAUL MASON[2], PIETER VROON[1], WILFRED RÖLING, RICARDO AMILS[3,4] AND GARETH DAVIES[1]

[1]Faculty of Life and Earth Sciences, VU University of Amsterdam, The Netherlands (*correspondence: esther.velasco@falw.vu.nl)
[2]Department of Earth Science, Utrecth Unversity, The Netherlands
[3]Centro de Astrobiologia, Madrid, Spain
[4]CBM-SO, Autonoma University of Madrid, Spain

Sulphur isotopes are likely to be a key in future tool for the detection of past or present life on Mars, where abundant sulphate minerals are present. To investigate the link between the activity of sulphate reducing microorganisms and sulphur isotope fractionation, we incubated sediment from a modern hyper-acidic, Fe-rich subareal environment at Rio Tinto, SW Spain. This site has been frequently used as a geochemical analogue of Mars.

Sediments were sampled from the upper part of the Rio Tinto (Marismilla) as wel as the estuary (Moguer). Laboratory incubation were carried out at 30°C using an artificial input solution with sulphate in excess and following techniques developed by Stam *et al*. [1]. The experiments were performed with an input solution at pH 7 and pH 3 and electron donors were provided by the natural substrate. Duplicate reactors were incubated for a total of 10 weeks. Initial data indicate moderate sulphate reduction rates of between 5 and 90 nmol cm^{-3} h^{-1} in Marismilla and between 5 and 45 nmol cm^{-3} h^{-1} in Moguer, independently of pH. Outflow solutions showed pH close to 7, regardless of inflow pH of 7 or 3, suggesting buffering within the sediment. Sulphur isotope fractionation was extreme in the Moguer estuary, extending beyond the maximun of 47‰ as predicted by the standard Rees model [2] of microbial sulphur isotope fractionation, suggesting that additional fractionation is possible [3] or indicating multiple cycles of reduction and oxidation of sulphate within the reactors. And inverse correlation between sulphate reducing rates and isotope fractionation was observed.

[1] Stam, M.C. *et al*. (2010) *Chemical Geology* **278**, 23–30. [2] Rees, C.E. (1973) *GCA* **37**, 1141–1161. [3] Brunner, B. Bernasconi, S.M. (2005) *GCA* **69**, 4759–4771.

https://doi.org/10.1180/S0026461X00006502 Published online by Cambridge University Press

Mineral metastability and effective bulk composition: The effect of grain sizes and modal mineral amounts

S.O. VERDECCHIA[1]*, J. RECHE[2], E.G. BALDO[1], E. SEGOVIA-DIAZ[3] AND F.J. MARTINEZ[2]

[1]CICTERRA (CONICET-UNC). Av. Veléz Sarsfield 1611, X5016CGA Córdoba, Argentina (*correspondence: sverdecchia@gmail.com)

[2]Departament de Geologia, Universitat Autónoma de Barcelona, 08193 Bellaterra, Spain

[3]Dpto. de Petrología y Geoquímica, CSIC-Universidad Complutense, 28040 Madrid, Spain

Large staurolite porphyroblasts (up to 2 cm) were recognized in quartz-mica schist of the Sierra de Ancasti (west-central Argentina) [1] with the mineral association: Crd-And-St-Grt-Bt-Ms-Pl-Qtz-Chl-Op. Textural relations suggest that the assemblage St-Grt-Bt was present in the metamorphic peak. Growth of late And or Crd porphyroblast is recognized as well. Two post-peak textural domains were indentified: a) St being replaced by And without Crd, and b) Crd rich domains lacking And. A P-T pseudosection in the MnNCKFMASH system using XRF bulk composition allowed to estimate conditions of 590°C and 5.2kb for the St-Grt-Bt assemblge but post-peak textures and mineral compositions where not predictable. We assumed that the original XRF bulk composition was not valid during post-peak conditions not only because the cores of metastable porphyroblasts such as staurolite could have been isolated and excluded of the effective bulk composition [2] (EBC), but also, because heterogeneous distribution of staurolite could have affected the local EBC. Accordingly, post-peak textural relations (~580°C-3.5kb) developed during decompression were modeled using two bulk compositional domains defined on the basis of observed differences in staurolite mode. Two extreme cases were modelled: a) St poor - Crd rich domains lacking And; b) And + St rich domains lacking Crd. Results approximate real compositions and modal amounts observed in both post-peak textural domains. Thus, variation of EBC and generation of EBC domains through the PT path is a critical factor to consider for correct interpretation of metamorphic mineral and textural evolution and particularly for discrimination between polymetamorphic and single metamorphic episodes.

[1] Willner (1983) In Aceñolaza *et al*. 1983 (eds) *Münst. Fors. zur Geol. und Pälaont*. **59**, 31–100. [2] Stüwe (1997) *Contrib. Mineral. Petrol*. **129**, 43–52.

Evaluation of contaminant transport parameters at Leningrad Atomic Power Plant drain area

E.A. VERESCHAGINA

SpbSU, Saint-Petersburg, 199178 (ea.grigorieva@gmail.com)

The Leningrad Atomic Power Plant (Leningrad APP) drain area was studied. A hydrological study has been performed to demonstrate how contaminant transport proceeds in case of hypothetical disasters.

Gridded Surface Subsurface Hydrologic Analysis (GSSHA) model was chosen for the simulation of radionuclide and chemical transport. GSSHA is a physics based, fully distributed, hydrologic and sediment transport model. The distributed nature of the model confers significant potential advantages for the analysis of non-point source pollutant fate and control.

Precipitations falling on the watershed contain specified concentrations of contaminants for hypothetical disasters at Leningrad APP. As rainfall accumulates on the land surface, ponded surface water infiltrates, providing a source of contaminants into the soil column, and move as surface runoff to adjacent territory. Concentrations of contaminant are affected by decay and transformations.

The most part of the water ponded on the land surface infiltrates, removing contaminants. Water that infiltrates is assumed to contain the same concentration of dissolved contaminants as the ponded water. Infiltration was simulated using traditional Hortonian Green and Ampt (GA) approach.

Additionally, field experiments for testing the values of the Green and Ampt infiltration equation parameters were done for prevailing at the drain area soil types. The determined parameters were the effective capillary suction and the effective hydraulic conductivity.

Comparison of the model outputs with the experimental data indicates that the model can successfully describe cumulative infiltration in different soil types and contaminant transport.

https://doi.org/10.1180/S0026461X00006502 Published online by Cambridge University Press

Using rare earth elements (REE) for tracing water masses

MARC VERHEUL[1] AND GERARD KLAVER[2]

[1]Deltares, Utrecht, The Netherlands (marc.verheul@deltares.nl)
[2]BRGM, Orleans, France (G.klaver@brgm.fr)

Rare earth elements are a group of elements consisting of scandium, yttrium and the lanthanides. The concentrations in Dutch ground and surface water are low, at sub ppb (μg/kg) level, but measurable with an optimised ICP-MS. The lanthanides show chemically nearly identical behaviour, which results in concentrations with a constant ratio between the different elements, although the absolute concentrations can vary by more than two orders of magnitude. The measured concentrations need to be divided by the levels in a reference clay mineral, yielding a flat line for samples with a clayey signature. Water with a calciferous influence is enriched with the heavier REE compared to the lighter REE. The slope can be expressed by the quotient of the sum of the normalised ytterbium and lutetium values and the sum of the normalised lanthanum and praseodymium values. The gadolinium anomaly (an enrichment) is caused by the application of gadolinium as a contrast agent during medical MRI-scans. This last anomaly is a clear indication of anthropogenically influenced (ground) water.

Due to absence of topography and constant water substraction in the polderareas of the Netherlands, the hydrological system can be extremely complex locally. With REE-profiles and by combining all the characteristics of these REE-profiles, it is possible to make a water balance in these complex hydrological systems.

A simple method for *in situ* zircon U-Th-He dating

PIETER VERMEESCH AND ANDY CARTER

Department of Earth and Planetary Sciences, Birkbeck, University of London (p.vermeesch@ucl.ac.uk)

In situ U-Th-He dating of zircon by laser ablation offers significant advantages over the current practice of whole grain degassing and dissolution:

1. It dramatically increases sample throughput. Grains of zircon are notoriously hard to dissolve. Measuring their U and Th content requires dissolution in hydrofluoric acid at high temperature and pressure using a Parr bomb for up to 72 hours. In contrast, measuring the U and Th content by LA-ICP-MS can be done in a matter of minutes.
2. The process of in-situ measurements of U and Th content of grains yields U-Th-Pb ages as a by-product. Thus, in-situ dated zircon crystals are double-dated by default, offering exciting new research opportunities for detrital geochronology.

We here propose a simple four step procedure to measure *in situ* U-Th-He ages without the need to know any absolute concentrations or ablation pit volumes:

1. Polish and mount two sets of grains in indium: a standard of known U-Th-He age, and the sample of interest, whose age is unknown.
2. Ablate the grains with a UV laser and measure the raw helium signal (e.g., in units of mV or Hz) of the unknown sample along with helium measurements of the age standard.
3. Measure the U and Th signals of the standard and the unknown by EMPA, SIMS, or LA-ICP-MS in the same order as the helium measurements.
4. Given the known age of the standard and its raw U and Th signals, calculate the expected He signal of the standard. Dividing the measured by the expected He signal yields a 'gain factor' K. The U-Th-He age of the unknown is then obtained by applying this same gain factor to its raw He signal.

This new method eliminates the need for interferometric microscopy to measure ablation pit volume, largely avoids the challenges of measuring absolute U and Th concentrations by ICP-MS, and has relatively few sources of analytical uncertainty, potentially resulting in improved precision and accuracy over alternative analytical procedures.

https://doi.org/10.1180/S0026461X00006502 Published online by Cambridge University Press

Modelling Li isotope signatures of waters altering a basaltic glass in under-saturated conditions

A. VERNEY-CARRON[1], N. VIGIER[1] AND R. MILLOT[2]

[1]CRPG-CNRS, Vandœuvre lès Nancy, France
[2]BRGM, Orléans, France

In order to use lithium isotopes as tracers of silicate weathering, it is necessary to constrain the Li isotope fractionation caused by weathering processes (especially, mineral dissolution and secondary phase formation) as a function of environmental parameters.

Preferential uptake of ^{6}Li during the formation of clay minerals was quantified by several studies (e.g. [1]). Concerning leaching, experiments with a Li-rich basaltic glass in under-saturated conditions have shown that the δ^7Li values of the leachates are lower than the fresh basaltic glass value during the early stages [2]. This was explained by a 2-step model: (1) Li is released in solution by diffusion, which leads to the formation of a leached layer. As ^{6}Li is lighter than ^{7}Li, the ratio of the diffusion coefficients of both isotopes (a=D_7/D_6) is lower than 1. Thus, the solution is enriched in ^{6}Li and the leached layer in ^{7}Li. (2) The dissolution of the leached layer tends to increase the solution δ^7Li value. D_7/D_6 is also found to correlate with temperature.

In order to model natural data, D_7/D_6, but also the relative contribution of diffusion and dissolution rates has to be estimated. At T < 20°C, D_7/D_6 is nil. However, it can be significant for hydrothermal fluids. Using diffusion and dissolution rates at high T°, the model shows that the high dissolution rate masks the kinetic effect due to diffusion. In any case, the only way to produce δ^7Li values in solution greater than that of the fresh mineral is to preferentially incorporate ^{6}Li into the secondary phases formed during the alteration.

[1] Vigier *et al*. (2008) *GCA* **72**, 780–792. [2] Verney-Carron *et al.* (2011) *GCA* (in press)

The Pb age of the Earth from Neoarchean galenas

J. VERVOORT[1]*, J. BLICHERT-TOFT[2] AND F. ALBARÈDE[2]

[1]School of Earth and Environmental Sciences, Washington State University, Pullman, WA, USA 99164 (*correspondence: vervoort@wsu.edu)
[2]Ecole Normale Supérieure, 69007 Lyon, France

Pb isotopes have provided the earliest estimates for the age of the Earth [1-3] and still provide important absolute age constraints on Earth's formation. Recent age determinations using the Pb isotope composition of the bulk silicate Earth range from 50 to 150 Ma after solar system formation [4-8]. Variation in present-day Pb isotope compositions in the silicate Earth, however, contribute to the uncertainty in these age determinations. Here we use the Pb isotope composition of galenas in volcanogenic massive sulfide (VMS) deposits in the Superior Province, Canada to determine the Pb age of the Earth. All deposits are Neoarchean (~2.7 Ga) and are derived from juvenile, mantle-derived volcanic rocks, as evidenced by their Nd and Hf isotopic compositions. Pb isotopes in the galenas are time invariant and thus provide a snapshot of the Neoarchean mantle from which they are ultimately derived.

A plausible scenario for Earth's Pb evolution is that it began with a low μ in the solar nebula and increased progressively during accretion to the current value of ~ 8 for the silicate Earth [4-8]. Using a low average μ from 4.56 to 4.52 Ga (< 0.7) with an increase to its current high μ at 4.52 Ga, the galena Pb trend is nearly coincident with the 2.7 Ga Geochron. With these parameters there is no Pb paradox at 2.7 Ga. The timing of this process, however, is dependent on the early stage of Pb evolution on Earth: If μ was lower during Earth's formation, the bulk of Pb loss occurred earlier; if μ was higher, integrated Pb loss occurred later, but with maximum of ~4.48 Ga. Our estimate for the Pb age of the Earth of ~4.52 Ga is older than the range of ages based on the present-day silicate Earth. This age most likely dates Pb loss to the core [4-8] or to space during accretion [9], and may have been finally punctuated by a moon forming impact.

[1] Holmes (1946) *Nature* **157**, 680–684. [2] Houtermans (1946) *Naturwissenschaften* **33**, 185–186. [3] Patterson (1956) *GCA* **10**, 230–237. [4] Allegré *et al*. (1995) *GCA* **10**, 1445–1456. [5] Galer & Goldstein (1996) *AGU Monogr*. ***95***, 75–98. [6] Halliday (2004) *Nature* **427**, 505–509. [7] Wood & Halliday (2005) *Nature* **437**, 1345–1348. [8] Allègre *et al*. (2008) *EPSL* **267**, 386–398. [9] Albarède *et al*. (2011) *MinMag*, this volume.

https://doi.org/10.1180/S0026461X00006502 Published online by Cambridge University Press

Arsenic mobility in coal-combustion ashes mixed with agricultural soil

V. VESELSKÁ[1]*, K. PEŤKOVÁ[1], R.M. BOLANZ[2], J. MAJZLAN[2], Ľ. JURKOVIČ[1], B. LALINSKÁ[3], E. HILLER[1] AND O. ĎURŽA[1]

[1]Department of Geochemistry, Comenius University, Bratislava, 842 15 Bratislava, Slovakia (*correspondence: veselska@fns.uniba.sk)
[2]Institute of Geosciences, Friedrich-Schiller University, Jena, Germany
[3]Department of Mineralogy and Petrology, Comenius University, Bratislava, 842 15 Bratislava, Slovakia

In this study, we focus on the influence of coal combustion residues (ashes) on soils. Ashes with elevated As content were buried in soils when a dam of an ash impoundment of the Nováky power plant (Slovakia) failed in 1965; subsequently, the ashes were covered by agricultural soil. In order to assess the arsenic mobility, we performed leaching studies with distilled water, ammonium nitrate, and acid ammonium oxalate solutions on ash-soil samples collected in three various depths intervals (0-30, 20-60 and 40-100 cm) at various locations in the 1965 ash spill.

Mild extractions with H_2O and 1 M NH_4NO_3 show that there is a potential to contaminate the surrounding environment with As due to relatively high concentrations of As measured in the leachates. However, in both extractions, the released As concentrations represent only a small percentage of the As_{TOT} (5.3% and 0.3%, respectively).

Oxalate-extractable As fraction (73% of the As_{TOT}) should be associated with the poorly crystalline Fe, Al, and Mn oxide phases, which represent 17%, 14%, and 63% of the total element concentrations in the samples, respectively. It could be assumed that released amounts of Si_{OX} (484- 21, 319 mg/kg) and Al_{OX} (10.04-22, 984 mg/kg) support a possibility of silicate leaching from amorphous glasses in this extraction step.

Single extractions were complemented with magnetic separation of heavy fraction, X-ray diffraction and electron microprobe analyses of ash-soil mixture. These studies show, that the magnetic fraction of the soils contains an average value of 0.15 wt% As and 0.08 wt% As in the non-magnetic fraction. In depths of > 40 cm, there were significant positive correlations between As and total Fe (r=0.71), as well as As and total Al (r=0.78). Positive correlation of r=0.94 was also found for As-Ca, indicating that Fe, Al, and Ca-rich minerals control the distribution of As and retain this element in the soils.

This study was supported by the project VEGA No. VEGA 1/1034/11.

From compositional to P-T-deformation-t(relative age)-redox maps at the thin section scale

OLIVIER VIDAL, PIERRE LANARI, BENOIT DUBACQ, MANUEL MUNOZ AND ERIC LEWIN

Linking deformation with metamorphic conditions requires spatially continuous estimates of pressure (P) and temperature (T) conditions at least in two dimensions (P–T maps) that can be superposed to the observed structures of deformation at different scales.

We have developed an approach and a package of matlab scripts to produce EMP quantitative X-ray maps of composition at the thin section scale. These maps of mineral composition can be combined with a multi-equilibrium approach involving phyllosilicates to calculate P–T-deformation-t (relative age)-Fe^{2+}/Fe^{3+} maps, even for samples free of low variance parageneses. Various application examples show that in metapelites metamorphosed at < 550 °C, the composition of phyllosilicates does not change significantly by lattice diffusion with varying P and T. Different compositions of phyllosilicate grains coexisting metastably in the same thin section are therefore indicative of different P-T conditions of crystallization that were achieved at different times. The nucleation of new phyllosilicate grains with different compositions during P–T variation is activated by deformation, so that the location of the different phyllosilicate generations characteristic of different P–T conditions is correlated to the microstructures. In addition to historical information about the P–T and deformation history, the P–T-deformation-t-Fe^{2+}/Fe^{3+} maps highlight the evolution of redox condition and the heterogeneity of rheology at the thin section scale.

https://doi.org/10.1180/S0026461X00006502 Published online by Cambridge University Press

Interaction of Se(IV)/Se(VI) species with granitic rock: Understanding of retention processes

K. VIDENSKA[1]*, V. HAVLOVA[2], M. GALIOVA[3] AND V. HAVRANEK[4]

[1]ICT Prague, Technická 5, 166 28 Prague 6, Czech Rep. (*corespondence: katerina.videnska@vscht.cz)
[2]NRI Rez plc., Husinec-Rez 130, 250 68 Rez, Czech Rep
[3]Masaryk University, Kotlářská 2, 61137 Brno, Czech Rep
[4]INP CAS, Husinec-Rez 130, 250 68 Rez, Czech Rep

Introduction

The fission product ^{79}Se belongs between radionuclides considered in safety assessment of radioactive waste geological repository, namely due to relative long half life ($3.56 \cdot 10^5$ yrs), anionic form in solution and biogenic character.

Modelling

According to modelling (the Geochemist´s Workbench) Se can be present at –II, 0, +IV and +VI oxidation states under granitic water conditions. Se (0) stability field would increase with increasing concentration of Se.

Experimental

Se(IV) and Se(VI) as anionic species are not usually supposed to be strongly bound on mineral surfaces [1]. Series of batch sorption experiments with crushed granitic rock revealed different sorption properties of selenite Se(IV) and selenate Se(VI), with favourable attraction of Se(IV). The higher oxidation state of selenium and large grain size significantly decreased K_D–values.

Discussion

In order to identify potential retention mechanisms, LA-ICP-MS and PIXE measurement were performed on surface of granitic samples after contact with Se(IV) or Se(VI) solution. Surface maps revealed trend of Se increased concentration in presence of Fe.

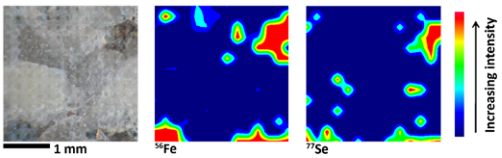

Figure 1: LA-ICP-MS surface map of granite sample after contact with 2.10^{-5} M Se(IV) solution.

The research was funded by Czech Ministry of Trace and Industry under contract No. FR-TI1/362. MG acknowledge support from the MSMT (MSM 0021622412).

[1] Carbol & Enquist (2007) *SKB* R 97–13.

Seawater-derived REY and HFSE systematics in Archean BIFs

S.VIEHMANN[1,4]*, J.E. HOFFMANN[1,2], C. MÜNKER[2], B.W. ALEXANDER[3,4] AND M. BAU[4]

[1]Steinmann Institut, Universität Bonn, Germany (*correspondence: fumi@uni-bonn.de)
[2]Geologisch-Mineralogisches Institut, Universität zu Köln, Germany
[3]Inorganic Ventures Inc., Christiansburg, VA, USA
[4]Jacobs Universität Bremen, School of Engineering & Science, Bremen, Germany

The HFSE and REE-Y patterns of Banded Iron Formations (BIFs) can be used to place constraints on the trace element composition of Archean seawater [e.g. 1]. Here we report the first high-precision HFSE (Nb, Ta, Zr, Hf) and REE (Lu, Sm, Nd) concentration data for separated chert and magnetite mesobands of ca. 3.7 Ga old BIFs from Isua (SW Greenland) and ca. 2.7 Ga old BIFs from the Temagami Formation (Superior Province, Canada), all obtained by isotope dilution. Other trace element measurements were performed using Quadrupole ICP-MS.

PAAS-normalized REY signatures of both Archean BIFs are comparable to modern and other Archean seawater patterns (e.g. [2]) and show seawater-like positive La, Y, Gd anomalies. Positive Eu anomalies suggest an enhanced hydrothermal input in Archean oceans, and the constant lack of negative Ce anomalies indicates anoxic seawater conditions [3].

Superchondritic ratios of Nb/Ta and Zr/Hf in magnetite bands of the Isua BIFs (40.2 - 59.2; 44.9 - 53.7) point toward lower Nb/Ta and Zr/Hf ratios of Isua cherts (19.2 - 32.5; 31.3 - 46.1). Temagami BIFs display the same characteristic with superchondritic Zr/Hf ratios in magnetite samples (38.1 - 47.1) contrary to subchondritic Zr/Hf ratios in cherts (18.9 - 28.5). By contrast magnetite and chert layers of Temagami BIFs exhibit uniform Nb/Ta ratios (14.1 - 27.0). Compared to compositions of modern aqueous [e.g. 4] and hydrothermal reservoirs, HFSE ratios of the Archean BIFs lie between those fields. Therefore different depositional environments for Isua and Temagami BIFs are favoured and also a different behaviour of both geochemical twins (Nb-Ta and Zr-Hf) in different water depths and water masses of Archean seawater is suggested.

[1] Bau M. Alexander B. (2009) *Precam. Res.* **174**, 337-346. [2] Planavsky N. *et al.* (2010) *GCA* **74**, 6387–6405. [3] Bau M. Koschinsky A. (2009) *Geochem. J.* **43**, 37–47. [4] Firdaus M.L. *et al.* (2011) *Nature Geosc.* **4**, 227–230.

https://doi.org/10.1180/S0026461X00006502 Published online by Cambridge University Press

Iron isotope signature of Paleoproterozoic banded iron formation from Quadrilátero Ferrífero, Minas Gerais, Brazil

L.C. VIEIRA[1]*, F. POITRASSON[1,2], R.I.F. TRINDADE[3] AND F.F. ALKIMIM[4]

[1]Instituto de Geociências, Universidade de Brasília, Campus Darcy Ribeiro, 70904-970 Brasília-DF, Brazil (*correspondence: lucieth@unb.br)
[2]Laboratoire Géosciences Environnement Toulouse, IRD-CNRS, 14-16, av. E. Belin, 31400 Toulouse, France
[3]Instituto de Astronomia Geofísica e Ciências Atmosféricas, Cidade Universitária, Rua do Matão 1226, Universidade de São Paulo, 05508-090 São Paulo-SP, Brazil
[4]Departamento de Geologia, Campus do Morro do Cruzeiro, Universidade Federal de Ouro Preto, 35400-000 Ouro Preto-MG, Brazil

The iron cycle study provides important insights into the early Earth System evolution history. The Precambrian record is marked by Banded Iron Formation (BIF) occurrences, which are the product of chemical precipitation from seawater, which were subsequently affected by diagenetic and metamorphic processes.

In Central Brazil, the Quadrilátero Ferrífero region comprises a large occurrence of Paleoproterozoic BIF with approximately 7000 km^2, which hosts one of the largest iron ore deposits in the world. Some samples of the Quadrilátero Ferrífero's BIF were used in a preliminary investigation on the iron isotope signature recorded by these deposits.

We have analyzed a suite of samples by MC-ICP-MS using the nickel doping technique. Thirty three analyses of the Milhas hematite standard gave a δ^{57}Fe value of 0.766±0.088‰ (2SD), relative to the IRMM-14 standard. On the USGS BIF reference rock we obtained δ^{57}Fe = 0.903±0.042 (2SE, n=6). Both values agree within uncertainties with previously published values. Our results on the Quadrilatero Ferrifero show large δ^{57}Fe variations, between -1.493± 0.034‰ and -0.061±0.12‰. These different δ^{57}Fe values were obtained for BIF samples which have different mineralogical associations. Samples with the lightests δ^{57}Fe correspond to siliceous BIF whereas all other samples, are BIFs intermingled with carbonates. Such an isotopic range extending towards very light δ^{57}Fe values have only been found in 2.5-2.7 Ga age BIFs, like those of the Quadrilátero Ferrífero.

Biogeochemical characterization of geothermal fluids

ANDREA VIETH-HILLEBRAND, ALEXANDRA VETTER, ANKE SACHSE, STEFANIE HENNE, SIMONA REGENSPURG AND KAI MANGELSDORF

GFZ German Research Centre for Geosciences, Telegrafen-berg, D-14473 Potsdam (vieth@gfz-potsdam.de)

Biogeochemical investigations on deep geothermal fluids are relatively rare, but are of great importance to characterize the geochemical origin of the fluid as well as the potential that biological processes will effect the working reliability of geothermal plants.

To characterize the natural variability in the inventory of dissolved organic carbon (DOC) compounds in geothermal fluids, samples from different geothermal plants in numerous geothermal regions of the world have been screened for the qualitative and quantitative composition of the DOC using size-exclusion chromatography. The characterization of the DOC as well as inorganic anions are valuable to evaluate if microbial processes will be relevant in the geothermal system as the DOC and several inorganic anions like nitrate and sulfate represent potential nutrients for the microbial ecosystem. The changes in composition of the microbial ecosystem in geothermal plants and heat storage systems were also characterized by bacterial membrane phospholipid fatty acids (PLFA) composition.

Here, we will present recent results on the screening of the DOC in selected geothermal fluids from a variety of geothermal plants and heat storage systems as well as the monitoring of fluid chemistry and PLFA composition in heat storage systems present in the North German Basin.

Samples from a solar assisted heat storage located in a quaternary freshwater aquifer in 15 to 30 m depth clearly show that the composition of the microbial ecosystem changes with respect to the seasonal changes of charge and discharge of heat. In wintertime, the PLFA composition of the indigenous microbial community showed an adaptation of the cell membrane during the discharge mode, when temperature decreases from 50 to 13.7°C during time of heat extraction.

One deep heat storage in the North German Basin (1250 m depth) where surplus heat from a gas and steam cogeneration plant is stored in summertime and which is used in wintertime for district heating shows changing PLFA patterns that clearly indicate different composition of the microbial communities on the warm and cold side.

https://doi.org/10.1180/S0026461X00006502 Published online by Cambridge University Press

Isotopic tracing of lithium sources in the Seine River, Paris (France)

N. VIGIER[1], J. GAILLARDET[2], P. LOUVAT[2] AND J. CHEN[2]

[1]CRPG-CNRS, Nancy Université, 15 rue Notre-Dame-des-Pauvres B.P. 20 F-54501 Vandœuvre lès Nancy
[2]IPGP, CNRS, 75252 Paris, France

Li isotopes have recently been used for tracing chemical erosion of silicate lithologies in present-day river basins and in the past, through oceanic records. Silicate weathering is a significant sink of atmospheric CO_2, but classical methods are insufficient for determining alteration rates and control laws with sufficient precision to be used in modeling of geochemical cycles and climate at large scale.

Most of the published studies show that dissolved lithium mainly come from silicate lithologies, even in mixed lithology basins (e.g. Kisakurek *et al*. 2005). However, recently a couple of sudies have also shown that anthropogenic input might impact the Li isotopic composition of natural waters. Indeed, some rain waters display unusually high δ^7Li and fertilizers may also be highly enriched in ^{7}Li (Millot *et al*. 2010). Analyses of commercial solutions show that their δ^7Li are particularly high relative to the range estimated for natural systems (Tomascak, 2004).

In order to estimate the order of magnitude of Li contamination of natural waters from anthropogenic sources, the Seine River in Paris, the largest urban area in France, has been sampled at various seasons. Li isotopes were measured in the filtered fractions (<0.2µm) by MC-ICP-MS, after the Li separation procedure described in Vigier *et al*. (2009).

The δ^7Li measured in the dissolved fractions of the Seine River range between 8.6‰ and 14.2‰. This range is within that determined for rivers located far from human activity. However, these values are low when compared to the published values for carbonate and evaporite lithologies (~30‰). This may mean that, even in a basin dominated by this kind of lithology, dissolved Li mainly comes from minor silicate phases. This is consistent with the low Li levels in carbonates. Another possibility is that anthropogenic inputs are significant and have on average a low δ^7Li in the Paris area. Some streams draining rooves and roads display a wide range of δ^7Li (from 25‰ to -17‰), with an average of 7‰. A positive correlation between δ^7Li and discharge in the Seine waters does suggest a role of anthropogenic components, such as for Zn (Chen *et al*. 2008). More investigation is needed in order to better determine the isotope composition of each potential endmember.

FTIR study of OH-OD exchange in Fe-free ringwoodite-wadsleyite samples

E. VIGOUROUX[1], J. INGRIN[1], N. BOLFAN-CASANOVA[2] AND D. FROST[3]

[1]UMET - UMR CNRS 8207 - Université Lille 1 – Cité Scientifique, 59655 Villeneuve d'Ascq, France (eric.vigouroux@ed.univ-lille1.fr, jannick.ingrin@univ-lille1.fr)
[2]LMV - UMR CNRS 6524 - Université Blaise Pascal – 5 rue Kessler, 63038 Clermont-Ferrand, France
[3]BGI – Bayreuth University– Universitatsstrasse, 95447 Bayreuth, Germany

Mantle ringwoodite and wadsleyite may incorporate large amount of H in their structure (up to several wt % H_2O). A good knowledge of hydrogen diffusion in these mineral phases and its relationship with their electrical conductivity is critical to estimate the real amount of water present in the transition zone. We synthesized ringwoodite and wadsleyite in multi-anvil presses up to 21 GPa and 1100 °C from forsterite powder surrounded by a small amount of brucite. The grain size of the ringwoodite samples ranged between 30 and 70 μm, while wadsleyite samples had grains sizes smaller than 20 μm. The samples incorporated moderate amount of water in the range of 0.1 to 0.2 wt% H_2O as confirmed by FTIR analyses performed on double face polished thin slices of few hundred microns.

In order to measure H diffusion rate in ringwoodite, we annealed a 106 μm thick slice for up to 80 hours in a OD enriched atmosphere at 400°C and we followed step by step the OH-OD exchange by FTIR. The main OH band in ringwoodite, the OH broad band at 3120 cm^{-1}, decreased rapidly but no equivalent OD band was produced. It suggests that, in ringwoodite, the mobility of H linked to this defect, is high and the removing of hydrogen from the crystals are not limited by D self-diffusion (ringwoodite was not destabilized even after 80 hours annealing, as confirmed by Raman and FTIR analyses). The effective diffusion coefficient through the thin section is of the order of 2 10^{-14} m^2s^{-1}, and the corresponding intra-crystalline diffusion coefficient is around 3 10^{-15} m^2s^{-1} assuming an average grain size of 40 μm. These results are ten times faster than the diffusion coefficient in wadsleyite extrapolated at 400°C from the experiments of Hae *et al*. 2006 performed in wadsleyite [1].

[1] Hae *et al*. (2006) *Earth Planet Sci Let* **247**, 141–148.

https://doi.org/10.1180/S0026461X00006502 Published online by Cambridge University Press

Estimation of mass discrimination in MC-ICP-MS Nd isotope analysis using generalized power law

B. VIJAYA GOPAL, B. SREENIVAS AND Y.J. BHASKAR RAO

National Geophysical Research Institute (CSIR), Hyderabad 500007, India (bvijayagopal@ngri.res.in)

The multi collector Inductively Coupled Plasma Mass Spectrometer (MC-ICP-MS) is known for large mass discrimination when compared to Thermal Ionization Mass Spectrometer (TIMS), but remains time-independent. An exponential law is routinely used to correct for this mass discrimination in MC-ICP-MS analysis. Although, this resulted in precisions of < 50 ppm when compared to TIMS analysis, the fringe isotope ratios, eg. $^{150}Nd/^{144}Nd$ seems to deviate by > 500 ppm. Thus, a generalized power law (GPL; [1]) was introduced. Applying GPL for Nd isotope analysis of JMC Nd, it was shown that an exponent variable (n) of -0.23 is more effective in correcting the measured Nd isotope ratios using Nu Plasma MC-ICP-MS [2]. Also it was observed that variable n for various instruments generally ranges between -0.2 and -0.5. In this work, we estimated the n value for Nd isotope compositions of JNd_i measured on Nu HR MC-ICP-MS and found that GPL with a n value of -0.19 is more effective (Fig. 1). This value of n appears similar to the one obtained by Wombacher and Rehkamper [2].

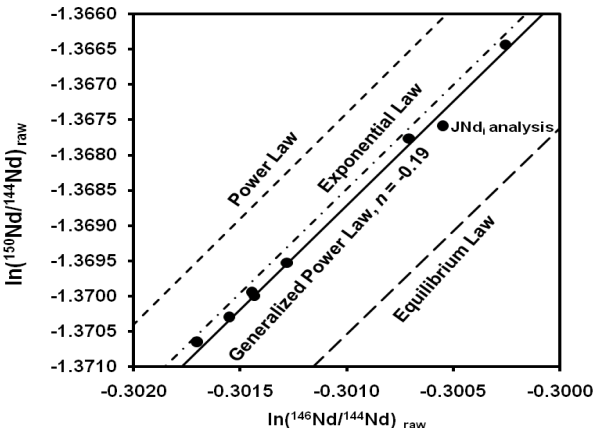

Figure 1: Analysis of JNd_i with various laws for correction

[1] Maréchal, C.N. Télouk, M & Alberède, F. (1999) *Chem. Geol.* **156**, 251–253. [2] Wombacher, F & Rehkämper, M. (2003) JAAS, **18**, 1371–1375.

REE distribution for the Arkachan large intrusion-related Gold deposit: Evidence for fluid origin

O.V. VIKENT'EVA*, G.N. GAMYANIN AND N.S. BORTNIKOV

IGEM RAS, Moscow 119017, Russia (*correspondence: ovikenteva@rambler.ru)

The Arkachan gold deposit is located in the tin metallogenic zone of Mesozoic Verkhoyansk belt (400 km to the North of Yakutsk) and hosted by sandstones and siltstones $C_{2\text{-}3}$-P_1. There is granite intrusion 2 km beneath the deposit. REE were determined by ICP-MS for unaltered and altered host rock, for quartz and carbonate and for fluid inclusions.

The REE total content increases from unaltered to altered host rocks from 90 to 200 ppm and from 170 to 830 ppm for sandstones and siltstones, respectively. All studied host rocks, ore carbonate and quartz are enriched in LREE, but carbonates from altered terrigenous rocks has La/Yb<1. Host rock alteration produced by acidic high temperature fluids and REE distribution were controlled by the sorption. Role of the complexation is increased at ore quartz and carbonate precipitation. Values of tetrad effect, more pronounced for the third tetrad are 1.2-1.5. Distinct negative Eu anomaly (Eu/Eu*=0.4-0.7) prevails in the rocks and minerals (Fig.1).

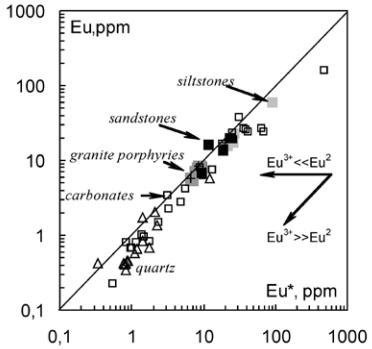

Figure 1: Plot of chondrite-normalized Eu concentrations versus calculated Eu^*_n values, where $Eu^*_n=(Sm_n(Tb_n \cdot Eu_n)^{½})^{½}$.

Fluids with deficient of Eu derived from granitic plutons. The Eu/Eu* values for the some samples, e.g. for late quartz, are 1-1.4, specified by a relatively reduced hydrothermal fluid with $Eu^{3+}<<Eu^{2+}$. The inverse relationship of ∑REE and of Eu/Eu* indicates a substantial role of magmatic fluid in the formation of the altered rocks. The hydrothermal fluids of the Arkachan deposis are known to be a mixture of H_2O+CO_2+NaCl with salinity of 3.7 to 26.3 wt % NaCl-equv. leaving chloride as the most likely candidate for the REE-transporting agent. LREE depletion of the siderite might be a result of the mineralogical control.

https://doi.org/10.1180/S0026461X00006502 Published online by Cambridge University Press

Ore-magmatic hydrothermal systems of massive sulphide deposits of Southern Urals: Melt and fluid inclusion data

I.V.VIKENTYEV[1]*, V.S.KARPUKHINA[2], V.B.NAUMOV[2] AND A.Y. BORISOVA[3,4]

[1]IGEM RAS, Moscow 119017, Russia (*correspondence: viken@igem.ru)
[2]GEOKHI RAS, Moscow 119991, Russia (naumov@geokhi.ru)
[3]GET-OMP, Toulouse 31400, France (borisova@lmtg.obs-mip.fr)
[4]Geological Department, MSU, Moscow 119899, Russia

According to existing models [1], the formation of the volcanogenic massive sulphide (VMS) deposits of the Urals is related to shallow chambers of acidic magma. The ore bodies are hosted by locally altered felsic rocks. All economic VMS deposits are located at some lithostratigraphic levels corresponding to two major and a few local stages of Lower Silurian and Middle Devonian volcanism. Melt inclusions (MI) and high density fluid inclusions (FI) in quartz phenocrysts were studied in 200 samples of dacite, rhyodacite and rhyolite.

Two main types of MI have been discovered: the most widespread devitrified inclusions, and rarely found glasses, some of them contain the ore globules of magnetite and also sulphides, represented by pyrrhotite, pentlandite, chalcopyrite and bornite, defined by electron microprobe. Melting of glasses occurred at 600-720°C, homogenization at 850-1130°C, whereas devitrified inclusions at 750-820°C and 950-1210°C accordingly. MI were analyzed for major elements and F, Cl by electron microprobe and H_2O by secondary ion microprobe. The concentrations of volatiles in the MI are (in wt%) are H_2O up to 6.5, Cl up to 0.28, F up to 0.42 contents; the average content of sulfur is 0.025 wt%.

FI in quartz phenocrysts are round to negative crystal shaped, from 25 to 100 μm, with gas bubbles from 8 to 40 μm. The homogenization of the FI occurred at 124-250°C in liquid phase. The freezing temperatures of FI range from -14 to -37°C. Salinities are from 1.2 to 6.2 wt% NaCl, density of aqueous fluids from 0.80 to 0.94 g/cm^3, calculated pressure from 680 to 850 MPa. Micro-Raman investigation demonstrated a presence of liquid H_2O only. Evaluated by LA-ICP-QMS at GET [2] contents in the magmatic fluid are**:** Cu 0.03-2.1 wt%, Zn 0.008-1.7 wt%, K 0.08-2.0 wt%, Fe 0.1-1.3 wt%, B 40-1600 ppm, Ba 20-2200 ppm, Sn 4-1600, Pb 14-740 ppm, Ag 4-200 ppm, Au 4-8 ppm.

[1] Baranov *et al*. (1988) *Proc. 7th IAGOD Symp,* 449–460. [2] Borisova *et al*. (2010) *Geostand. Geoanal. Res,* **34**, 245–255.

Alterations to nanoparticle associated proteins

P.J. VIKESLAND, M.S. HULL, M. CHAN, R. KENT AND P. PATI

Virginia Tech, Blacksburg, VA 24061, USA (pvikes@vt.edu, mahull@vt.edu, mychan@vt.edu, ronkent40@gmail.com, param@vt.edu)

Engineered nanoparticles are often either purposely stabilized with proteins or acquire a protein 'halo' while in geologic or biologic media. The presence of this protein coat is generally thought to stabilize nanoparticles and make them resistant to aggregation and deposition phenomena. Our work has systematically examined the gold nanoparticle/protein interface in an effort to quantify the strength and stability of these interactions and to define the chemical and morphological transformations of the protein coat. Bovine serum albumin (BSA) was chosen as a representative protein and gold nanoparticles serve as a model nanoparticle system. Gold is an ideal model nanoparticle since it can be readily produced as monodisperse suspensions of varying size and variable surface functionality. Furthermore, gold is amenable to a number of surface plasmon enabled spectroscopies that facilitate quantitative evaluation of the protein/gold interface.

This presentation will highlight studies conducted to 1) quantify BSA binding to gold nanoparticle surfaces, 2) evaluate how BSA conformation changes in response to variations in solution chemistry, 3) determine the stability of the BSA coating under flow conditions, and 4) elucidate the chemical and biological reactivity of the BSA coating. These experiments collectively rely upon UV-Vis measurements of changes in the surface plasmon band location and intensity, surface enhanced Raman spectroscopy to evalate changes in BSA conformation and chemistry, and deposition and flow-cell AFM studies that define the stability of the BSA-gold nanoparticle interaction.

The current work has led to an improved understanding of protein/nanoparticle interactions and has helped define the chemical and morphological transformations that surface associated proteins are subject to. The collected results have important implications on the ultimate fate, transport, and toxicity of nanoscale particles released to aquatic environments.

https://doi.org/10.1180/S0026461X00006502 Published online by Cambridge University Press

Optimizing the use of magnetite from an iron mine for reduction of aqueous Cr(VI)

M. VILLACÍS-GARCÍA[1] AND M. VILLALOBOS[1,2]*

[1]Environmental Bio-Geochemistry Group, Chemistry School
[2]Earth Sciences Graduate Program, Geology Institute, UNAM, Coyoacan, C. U., Mexico 04510, D.F
(*correspondence: mariov@geologia.unam.mx)

Introduction

Magnetite is an inverse spinel ferrite that contains in its structure both Fe^{3+} and Fe^{2+} [1], and may therefore act as a reducing agent. This behavior has been applied in remediation of contaminated water with oxydized metal species that upon chemical reduction become immobile [2]. In this paper we present an investigation using natural samples of this mineral from an Fe mine deposit in Mexico towards the reduction of Cr(VI) to Cr(III), with the final aim to understand the geochemical conditions of optimal performance for applying it to real pollution scenarios. The most important problem to solve for optimal implementation, is the rapid surface passivation of the mineral due to complete oxidation of superficial Fe^{2+}, which results in very low Cr(VI) reduction yields.

Methodology

Investigations were performed with magnetite of various particle sizes, both natural and synthetic. Batch experiments were performed with a solid concentration of 6 g L^{-1} and concentrations of Cr(VI) of 5-10 mg L^{-1} and up to 50 mg L^{-1}. Mixtures of magnetites with low amounts of Fe (0) were also investigated, which presumably replenish superficial magnetite Fe(II) [3].

Discussion of Results

The reduction capacity of magnetite increased with decreasing particle size, but the overall reduction rates and yields were relatively low. Small weight percentages of Fe (0) (1-5%) mixed with magnetite, which in the absence of magnetite showed no reduction capacity, significantly increased both rates and yields. We report the optimization of the magnetite/Fe (0) ratio as a function of particle size, and pH, and confirmed the surface-mediated reduction mechanism.

[1] Liu *et al*. (2006) *Mater. Lett*. **60**, 2979–2983. [2] Kendelewicz *et al*. (2000) *Surf. Sci*. **44**, 55–60. [3] Coelho *et al*. (2008) Chemosphere **71**, 90–91.

A unified surface structural model for ferrihydrite: Proton, electrolyte, and arsenate adsorption

M. VILLALOBOS[1]* AND J. ANTELO[2]

[1]Environmental Bio-Geochemistry Group, Chemistry School, and Earth Sciences Graduate Program, Geology Institute, UNAM, Coyoacan, CU, Mexico 04510, D.F
(*correspondence: mariov@geologia.unam.mx)
[2]Soil Science and Agricultural Chemistry Dept., University of Santiago de Compostela, Spain

Introduction

Ferrihydrite (FH) is a common hydrous ferric oxide nanomineral of 'young' formation in aqueous geochemical environments. Its small particle sizes (1.5-5 nm) [1, 2] expose a very high specific surface area at the mineral/water interface, and this may have considerable influence on the transport and fate of a variety of trace and major elements through diverse sorption processes. In particular, arsenate anions show a very high affinity for FH, and their fate in contaminated environments is almost invariably associated to Fe(III) oxide surfaces [3, 4]. The extremely small FH nanoparticles, which show high particle aggregation when dried, preclude experimental determination of important surface parameters for the thermodynamic description of its adsorption behavior. In the present work we have compiled eight sets of published acid-base surface titration data for synthetic preparations of FH across a wide range of particle sizes, and two sets of arsenate adsorption data, and unified their description through a face-distribution site-density model developed previously for goethite.

Discussion of Results

We show that the surface proton charge behavior of FH in conjunction with its As(V) adsorption behavior may be adequately described using the affinity constants derived for goethite, by assuming the FH surface to be composed predominantly of a surface site configuration equal to that of the (010) goethite face (*Pnma* space group). Also, through the applied model the available specific surface area of each FH preparation in aqueous suspension may be successfully derived, showing values between 330 and 1120 m^2/g. The implications of the results reported here are highly relevant for predictive purposes of FH surface reactivity in general.

[1] Murphy *et al*. (1976) *J. Colloid Interface Sci*. **56**, 270–283. [2] Janney *et al*. (2000) *Clay Clay Min*. **48**, 111–119. [3] Arai *et al*. (2006) *ES&T* **40**, 673–679. [4] Slowey *et al*. (2007) *Appl. Geochem*. **22**, 1884–1898.

https://doi.org/10.1180/S0026461X00006502 Published online by Cambridge University Press

Variation of silica and diatoms in Wagner and Consag Basins in the North part of California Gulf, Mexico

RUTH ESTHER VILLANUEVA-ESTRADA[1]*, ALEJANDRO ESTRADAS-ROMERO[1], ROSA MARÍA PROL-LEDESMA[1], MARÍA EUGENIA ZAMUDIO-RESENDIZ[2], DAYAN RODRÍGUEZ[1], EZEQUIEL TOBON[1] AND RENTERIA JAZMIN[1]

[1]Instituto de Geofísica, Universidad Nacional Autónoma de México (*correspondence: ruth@geofisica.unam.mx)
[2]Instituto de Ciencias del Mar y Limnología. Universidad Nacional Autónoma de México

In this work we present preliminary results about the abundance and species richness of diatom in sediments related with the chemistry of pore water. The oceanographic cruise (WAG-02) was done at the end of July 2010 in the Wagner and Consag basins of the Northern part of Gulf of California. The study area is characterized by pockmarks, mud volcanoes and gas vents at depths of 65 to 150 m approximately [1].

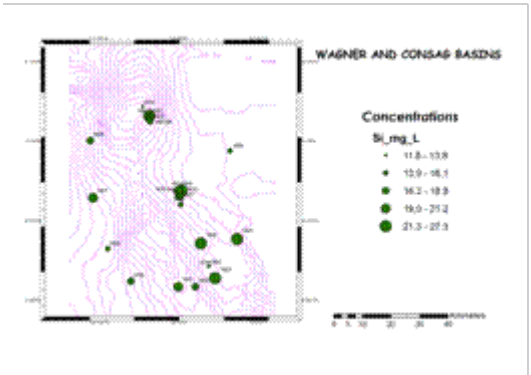

Figure 1: Spatial distribution of silica concentrations in pore water.

Discussion of Results

The presence of silica in the Wagner Fault could be high productivity waters in the zone, dissolution of minerals and the hydrothermal activity.

[1] Canet, C. *et al*. (2010) *Sedimentary Geology* **228**, 292–303. [2] Battarbee, R.W. (1986) 527–570.

Os isotopes in sulfides from xenoliths of the Campos de Calatrava Volcanic Field, Central Spain

C. VILLASECA[1], J.M GONZÁLEZ-JIMÉNEZ[2], W.L. GRIFFIN[2], E. ANCOCHEA[1], F. GERVILLA[3], S.Y O´REILLY[2], N.J. PEARSON[2] AND E. BELOUSOVA[2]

[1]Dpt. Petrology and Geochemistry, UCM-CSIC, Madrid, Spain (granito@geo.ucm.es, eancochea@geo.ucm.es)
[2]GEMOC ARC National Key Centre, Sydney, Australia (jose.gonzalez@mq.edu.au., bill.griffin@mq.edu.au, sue.oreilly@mq.edu.au, npearson@mq.edu.au, elena.belousova@mq.edu.au)
[3]Dpt. Mineralogy & Petrology, University of Granada, Spain (gervilla@ugr.es)

The Campos de Calatrava Volcanic Field (CCVF) comprises more than 200 volcanic centers with ultra-potassic to more Na-rich alkaline magmas that intruded the easternmost branch of the Hercynian Iberian Massif, in central-south Spain, ca. 8.7-0.7 Ma ago. Small lherzolite-wherlite xenoliths are embedded in pyroclastic deposits of volcanic centers. These xenoliths are spinel-bearing varieties; garnet is absent in the lherzolite suite. The presence of interstitial volatile-rich minerals (i.e. amphibole and phlogopite) and the distribution of trace elements in them suggest mantle metasomatism by subduction-related melts [1].

Fe-rich monosulphide solid solution (Fe-rich Mss) (<16.67 at% Ni) is the only sulphide present in the xenoliths. *In situ* LA-MC-ICPMS analyses reveal that sulfides included in primary silicates are Os-poor (<15 p. p. m.), making it difficult to obtain precise Re-Os isotope data. In contrast, sulfides sitting in open fractures or included in metasomatic silicates have higher Os contents (up to 89 p. p. m.). The Re-Os data show large variations in $^{187}Os/^{188}Os$ (0.1142-0.1241) and $^{187}Re/^{188}Os$ (0.02-0.12). T_{MA} and T_{RD} (Re depletion) model ages, compared with PUM at the present day, range from 1.0 to 2.3 Ga and from 0.75 to 2.1 Ga respectively. One grain has $^{187}Os/^{188}Os$ = 0.1270 and $^{187}Re/^{188}Os$ = 0.05; T_{MA} and T_{RD} are 0.4 and 0.35 Ga.

The differences in Re-Os systematics of sulfides reflect a probable metasomatism at 1 Ga ago. This metasomatic event is also recognised in Nd T_{DM} ages from spatially associated gabbros of the Hercynian orogen in central Spain (Fernández-Suárez *et al*. 2011).

[1] Villaseca, C. *et al*. (2010) *Geol. Soc. London Special Publ*. **337**, 125–152. [2] Fernandez-Suárez *et al*. (2011) *Lithos* doi: 10.1016/j.lithos.2010.09.010.

https://doi.org/10.1180/S0026461X00006502 Published online by Cambridge University Press

Novel insights into the ion sorption properties of calcite in aqueous solutions using cavity ring-down spectroscopy

A. VILLEGAS-JIMÉNEZ[1]*, R.M. HAZEN, [1] AND D.A. SVERJENSKY[2]

[1]Carnegie Institution of Washington, Geophysical Laboratory, Washington, D.C. 20015, USA (*correspondence: adriano@gl.ciw.edu)
[2]Johns Hopkins University, Earth and Planetary Sciences, Baltimore, MD 21218, USA

Despite significant advances on the elucidation of the structure of the calcite-water interface, much controversy still surrounds some of its most fundamental physical-chemical properties [e.g. the pH of the isoelectric point, the point of zero net surface charge, the proton and lattice-derived ion sorption properties]. This is largely due to the lack of suitable experimental approaches allowing a rigorous characterization of calcite surface equilibria over expanded compositional ranges. Electrokinetic techniques do not allow direct probing of surface reactions whereas conventional wet-chemical approaches (batch and titration) fail to control or monitor $CO_{2\ (g)}$ exchange across the air-water interface which leads to large uncertainties in the computed (ad)sorption data. Recently, a novel titraton protocol that addreses this difficulty was developed and tested over a relatively wide range of chemical conditions [1]. The new data was interpreted in terms of the following $2H^+/Ca^{2+}$ ion exchange equilibrium:

$$(\equiv CaCO_3)_{2(exc)} + 2\ H^+ \Leftrightarrow \equiv Ca(HCO_3)_{2(exc)} + Ca^{2+}$$

If true, this mechanism may impact the aqueous speciation of carbonate-rock systems with restricted $CO_{2\ (g)}$ ventilation via the buffering of pH and calcite dissolution. It follows that a careful verification of this reaction is warranted. To this end, and to gain further insight into the ion sorption properties of $CaCO_{s3\ (s)}$ in aqueous solutions, we are conducting new titrations of high-purity, additive-free, synthetic calcite and aragonite powders over a broader range of conditions using a novel titration approach that allows, for the first time, a reliable monitoring of the chemistry of the $CaCO_{3\ (s)}$-$H_2O_{\ (l)}$-$CO_{2\ (g)}$ system. Accurate pCO_2 measurements are obtained via a gas-recirculation device and a last-generation cavity ring-down laser spectrometer which avoids interferences from water vapor with negligible sample perturbation, a notable advantage over IR spectrometer-based strategies. Our approach yields very high-quality data suitable for the calibration of ion sorption models for $CaCO_{3\ (s)}$ surfaces.

[1] *Phys. Chem. Chem. Phys.* (2009) **11**, 8895–8912.

Molybdenum isotopes in the altered oceanic crust, a novel proxy for recycling?

F. VILS[1]*, T. ELLIOTT[1], M. WILLBOLD[1], M. HARRIS[2], C. SMITH-DUQUE[2], R. COGGON[3] AND D. TEAGLE[2]

[1]University of Bristol, BS8 1RJ Bristol, United Kingdom (*correspondence: flurin.vils@bristol.ac.uk)
[2]National Oceanography Centre Southampton, University of Southampton, SO14 3ZH Southampton, United Kingdom
[3]Imperial College London, SW7 2AZ, United Kingdom

During movement of the oceanic crust away from mid-ocean ridges, hydrothermal alteration of the oceanic crust results in a distinct elemental and isotopic signal. The change in isotopic composition compared to unaltered MORB is an important tracer for the involvement of fluids released from the altered oceanic crust at the base of arc volcanoes during subduction. Any isotopic system not fractionated during dehydration reaction and inert to diffusion is therefore a valuable tracer to shallow or deep recycling of subducted material. Recent studies showed that Mo isotopes could be such a novel proxy [1, 2, 3] as measured Mo isotope values in arc and ocean island basalts differ significantly from mantle values (estimated to be similar to continental crust 0‰ $\delta^{97/95}$Mo). This study investigates the change in Mo isotopes through the altered oceanic crust to better constrain the input into the subduction zone.

Samples of the altered oceanic crust across the Pacific Ocean have been measured for Mo isotopes and Mo concentrations (ODP Sites 1179, 1301, 1256). Combined the studied samples show a decreasing down-hole trend varying over 1‰ $\delta^{97/95}$Mo. The heavier isotope ratio in the upper part of the crust might be the source region for the heavy isotope ratio seen in the Mariana arc [2] and the lighter isotope ratio further down-hole might be the source for the light isotope ratio seen in ocean islands basalts [1, 3]. To further constrain this down-hole trend over a complete section of the altered oceanic crust (through pillow basalts, sheeted dyke complex, and gabbros), additional Mo isotope and concentration measurements on the deepest ODP hole (Site 1256) are currently in process.

[1] Willbold *et al.* (2009) GCA **73 suppl.** A1444. [2] Freymouth *et al.* (2011) this volume. [3] Lai *et al.* (2011) this volume.

https://doi.org/10.1180/S0026461X00006502 Published online by Cambridge University Press

Heavy metals and arsenic in the soils in the area of Narva power plants: Distribution and controlling factors

L.-E. VINNE*, L. BITYUKOVA AND H. SCHVEDE

Institute of Geology at Tallinn University of Technology, Tallinn, Estonia
(*correspondence: liis-erliken.vinne@gi.ee)

Two world's largest oil shale-fired thermal power plants located in the North-eastern Estonia are the main sources of air pollution in Estonia. Up to 50 ths tonnes of combustion ashes are emitted to the atmosphere annually.

Oil shale contains most of the naturally occurring chemical elements at least in trace amounts. Trace species may be realised during combustion and can pose an environmental and human risk. Soils have been considered as one of the main recipients of pollutants.

To evaluate potential hazard of contamination in the area influenced by the Narva Power Plants the geochemical mapping was carried out. Geochemical maps created basing on the ICP-MS data for major and trace elements allow illustrating spatial distribution of elements studied and outline the areas with uncommon concentrations in the soils. Well-defined areas with the highest values of elements are observed generally along the seacoast zone and to the east of the Narva region that reflect the incorporation of the Lower Ordovician shale bedrock naturally enriched in potentially toxic elements.

Mobility and availability of arsenic and heavy metals in soils was evaluated by the two-steps (milliQ water and sodium acetate) sequential extraction. The results showed that heavy metals and arsenic are leached in low quantities and attributed generally to mineral phase in the soils. The water soluble fractions are negligible (<1%). The Na-acetate extractable concentrations of Cd, Co, Cr, Pb and Zn are much higher than those obtained using water extraction. Extractability of elements depending on pH, grain size composition and soil types also as elements contribution from very various parent materials will be discussed in the presentation.

Thermodynamics of solid solutions of carbonates with non-isostructural end-members: The prediction of solubility limits with the single defect method

V.L. VINOGRAD[1], M.I. LUCHITSKAIA[2] AND B. WINKLER[2]

[1]Institute of Energy and Climate Research (IEK6), Forschungszentrum Jülich, 52425, Germany (v.vinograd@fz-juelich.de)
[2]Institute of Geosciences, University of Frankfurt, Frankfurt a.M., 60438, Germany

Carbonates are considered as sorbents for various contaminants dissolved in aqueous solutions. Numerous studies suggested that carbonates can retain significant amounts (up to thousands of ppm) of SO_4^{2-}, SeO_4^{2-}, $HAsO_3^{2-}$, HPO_4^{2-}, CrO_4^{2-}, while concurrent spectroscopic and surface diffraction studies have shown that these anions, indeed, replace CO_3^{2-} units of the carbonates. The question is, can these experimental results be considered as a proof for the formation of thermodynamically stable solid solutions? Our approach to the problem is based on the assumption that the solute components obey Henry's law. This is equivalent to assuming that the enthalpy of mixing of a diluted solid solution can be approximated as a linear function of the mole fraction of the solute. The extrapolation of this line to 100% of the solute component allows defining the enthalpy of the virtual (solute) end-member, which within the same assumption forms a perfectly ideal solution with the host. We have been able to calculate the total energies of virtual end-members from the total energy of the host (carbonate) and the energies of supercells of the host with a single CO_3^{2-} unit replaced by an anion of the solute end-member. The energies were calculated from first principles. The standard enthalpies of the virtual end-members were then calculated relative to reference compounds with the same composition, whose standard thermodynamic properties are well defined. Our calculations predict vanishingly small concentrations of SO_4^{2}, SeO_4^{2-}, $HAsO_3^{2-}$ and HPO_4^{2-}. This suggests that carbonate 'solid solutions' formed by co-precipitation with these components are not stable in the thermodynamic sense. Experimental approaches to testing this hypothesis are discussed.

https://doi.org/10.1180/S0026461X00006502 Published online by Cambridge University Press

Thermodynamics of rutile- and α-PbO_2-type solid solutions from quantum-mechanical calculations

V.L. VINOGRAD[1] AND B. WINKLER[2]

[1]Institute of Energy and Climate Research (IEK6), Forschungszentrum Jülich, 52425, Germany (v.vinograd@fz-juelich.de)
[2]Institute of Geosciences, University of Frankfurt, Frankfurt a.M., 60438, Germany

Recent progress in analytical techniques sensitive to ppm-range concentrations attracted the interest of petrologists to geothermobarometry based on trace element partitioning between various minerals [1]. Current approaches for the calibration of such geothermobarometers are purely phenomenological. Indeed, the thermodynamic mixing properties of solid solutions, whose concentration ranges do not exceed 1000 ppm, cannot be easily measured and thus typically are not known. We propose to use atomistic model simulations for the calibration and extrapolation of such geothermobarometers. In this report we will present the results of density functional theory based simulations of TiO_2-SiO_2 and TiO_2-ZrO_2 solid solutions with rutile and a-PbO_2-type structures obtained using the double-defect method [2]. The results will be discussed in relation to Zr-in-rutile thermometry and Si-in-rutile barometry. The pressure effects of Ti-in-quartz and Ti-in-zircon thermometers have also been modeled.

[1] T. Zack, R. Moraes, A. Kronz (2004) *Contrib. Mineral. Petrol.* **148**, 471–488. [2] V.L. Vinograd, B. Winkler (2010) *Reviews in Mineralogy & Geochemistry* **71**, 451–475.

Factors affecting the physical phase state of SOA particles from biogenic and anthropogenic precursors

A. VIRTANEN[1]*, E. SAUKKO[1], A. LAMBE[2], P. MASSOLI[3], T. ONASCH[3], J. WRIGHT[2], D.R. CROASDALE[2], A. LAAKSONEN[4], P. DAVIDOVITS[2] AND D. WORSNOP[3]

[1]Tampere University of Technology, Department of Physics, P.O.Box 692, 33101 Tampere, Finland (*correspondence: annele.virtanen@tut.fi)
[2]Boston College, Department of Chemistry, 2609 Beacon Street, Chesnut Hill, MA 02467-3860, USA
[3]Aerodyne Research, 45 Manning Road, Billerica, MA 08121-3976, USA
[4]Finnish Meteorological Institute, P.O. Box 503, 00101 Helsinki, Finland

SOA formation and properties are widely studied to clarify the role of SOA in radiative forcing and climate. However, very limited information is available on the morphology and phase state of SOA particles. Verifying the physical phase state of SOA particles gives new and important insight into their formation and growth process and essential information on their implications in the atmosphere [1, 2].

According to our recent results [3], pine derived SOA particles in chamber conditions as well as atmospheric SOA particles formed in boreal forest can be amorphous solid in their physical state at least several hours after their formation. However, it is not known yet how general the observation is and what the atmospheric implications are.

In this study we have investigated the physical phase state of SOA particles formed in Boston College flow tube from various precursor VOCs representing both biogenic and anthropogenic sources. In addition, the phase change was investigated as a function of particle oxidation level (O:C) and flow tube SO_2 concentrations.

According to our results the solid phase is the dominating phase state of formed SOA in the case of both biogenic and anthropogenic precursors at least up to relative humidity (RH) values of 55-70%. At higher RH values the humidity induced phase transition takes place and particles liquefy. We find that the O:C ratio of particles as well as chamber SO_2 concentration have an effect on the phase of SOA particles.

[1] Zahardis *et al.* (2007) *Atmos. Chem. Phys.* **7**, 1237-
[2] Zobrist *et al.* (2008) *Atmos. Chem. Phys.* **8**, 5221-
[3] Virtanen *et al.* (2010) *Nature*, **467**, 467.

https://doi.org/10.1180/S0026461X00006502 Published online by Cambridge University Press

The delivery of organic material to the early solar system

R. VISSER[1]*, E.F. VAN DISHOECK[2,3], S.D. DOTY[4] AND E.A. BERGIN[1]

[1]Dept. of Astronomy, University of Michigan, 500 Church Street, Ann Arbor, MI 48109-1042, USA (*correspondence: visserr@umich.edu)
[2]Leiden Observatory, Leiden University, P.O. Box 9513, 2300 RA Leiden, the Netherlands
[3]Max-Planck-Institut für Extraterrestrische Physik, Giessenbachstrasse 1, 85748 Garching, Germany
[4]Dept. of Physics and Astronomy, Denison University, Granville, OH 43023, USA

The solar nebula, in which the Earth and all other solar-system bodies were formed, was a complex chemical mixture of gas and dust. In order to fully understand the nebula's chemical composition at the time the solid bodies were formed, one has to go back in time and retrace the chemistry to the molecular cloud that collapsed to form the solar nebula. Here we present recent astrochemical observations and models that aim to do just that [1, 2, 3]. The main focus is on water and on simple organic compounds like methanol (CH_3OH) and dimethyl ether (CH_3OCH_3), which are tracers of the organic complexity that likely aided the eventual formation of life. The models predict that water and simple organics were already formed abundantly at an early time. As the parent molecular cloud collapsed and evolved into the early solar system, changes in density, temperature and radiation led to further chemical processing. The abundances of several key species in this simulated solar nebula match those observed in comets [4], but others are off by orders of magnitude. We discuss what both the good and the poor matches mean for the delivery of organic material to the Earth and elsewhere.

[1] Jørgensen *et al*. (2009) *Astron. Astrophys*. **507**, 861–879. [2] Visser *et al*. (2009) *Astron. Astrophys*. **495**, 881–897. [3] Visser *et al*. (2011) *Astron. Astrophys*. submitted. [4] Bockelée-Morvan *et al*. (2000) *Astron. Astrophys*. **353**, 1101–1114.

Raman spectroscopy of endoevaporitic microbial communities from the Atacama Desert

PETR VÍTEK[1]*, HOWELL G.M. EDWARDS[2], JAN JEHLIČKA[1], ELIZABETH CARTER[3], CARMEN ASCASO[4] AND JACEK WIERZCHOS[4]

[1]Institute of Geochemistry, Mineralogy and Mineral Resources, Charles University in Prague, Albertov 6, 128 43 Prague 2, Czech Republic (*correspondence: vitek2@natur.cuni.cz)
[2]Centre for Astrobiology and Extremophiles Research, School of Life Sciences, University of Bradford, Bradford BD7 1DP, United Kingdom
[3]Vibrational Spectroscopy Facility, School of Chemistry, University of Sydney, Sydney, NSW 2006, Australia
[4]Museo Nacional de Ciencias Naturales, CSIC, c/ Serrano 115 dpdo., 28006 Madrid, Spain

Geobiological systems with emphasis on halite and gypsum crusts from the Atacama Desert, one of the driest places on Earth, were studied. Raman spectroscopic analysis revealed variations in pigment composition within various endolithic colonies, allowing in some cases suggestions to be made about survival strategies.

Scytonemin, an effective extracellular UV-protectant, was found in cyanobacterial colonies within halite and gypsum crust from the hyperarid core of the Atacama Desert using Raman spectroscopy. The amount of scytonemin present differed depending on the particular microhabitat. Substantial differences are proposposed to reflect a variable biosynthesis due to the amount of light available inside the halite and gypsum crust.

Raman spectroscopic analyses of the endoevaporitic colonies from Ca-sulphate exhibited systematic variations in carotenoid composition together with the presence/absence of a phycobiliprotein signal (indicative for cyanobacteria). The cyanobacterial signal was accompanied by two clearly distinguishable ν(C=C) carotenoid bands at ~1516 and 1498 cm^{-1}, pointing to carotenoids of different chain length. Within the colonies living closer to the surface, scytonemin was also identified. The Raman signal of algal colonies from near the rock surface exhibited a ν(C=C) carotenoid band at ~1525 cm^{-1} accompanied by chlorophyll, whereas the same carotenoid band obtained from red algae is shifted towards lower wavenumbers with the spectra lacking chlorophyll.

Fast Raman mapping of the green algal colonies exhibited great potential of the method for the study of endolithic communities in their original habitats.

https://doi.org/10.1180/S0026461X00006502 Published online by Cambridge University Press

Readily available acidity in schwertmannite

CHAMINDRA VITHANA[1,2]*, LEIGH SULLIVAN[1,2], RICHARD BUSH[1,2] AND ED BURTON[1,2]

[1]Southern Cross GeoScience, Southern Cross University, Australia (*correspondence: c.vithana.10@scu.edu.au)
[2]CRC CARE, Building X, University of South Australia, Mawson Lakes SA 5095, Australia

Introduction

Schwertmannite and jarosite are considered as less soluble ironhydroxy sulfate minerals which are present in highly acidic environments (pH < 3). These minerals release acidity in the long run as they weather by hydrolysis [1]. However, 1M KCl extraction of soil samples (Clarence and Quartz) spiked with those two minerals showed that schwertmannite has some acidity that may be readily available.

Results and Discussion

Unlike jarosite, schwertmannite released acidity during 1M KCl extraction. It was found that the measured acidity in schwertmannite added samples was ~1/3 of the expected total inherent acidity (Figure 1). This acidity release was also associated with the release of surface bound sulfate from schwertmannite. It was found that ~30% of sulfate in schwertmannite was able to be release by 1M KCl, an amount that matches other observations [2].

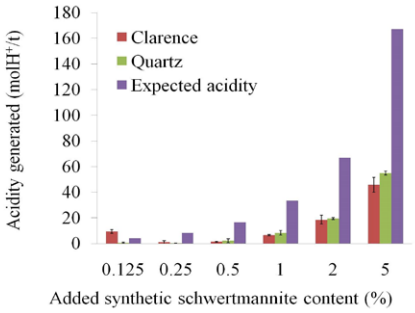

Figure 1: Acidity generated vs expected acidity

[1] Ahern *et al*. (2004) Queensland Acid Sulfate Soils Manual. [2] Bigham *et al*. (1990) *Geochim. Cosmochim. Acta* **54**, 2743–2758.

Dust from copper smelters in the Zambian Copperbelt

M. VÍTKOVÁ[1]*, V. ETTLER[1], F. VESELOVSKÝ[2], B. KŘÍBEK[2] AND O. ŠEBEK[3]

[1]Institute of Geochemistry, Mineralogy and Mineral Resources, Charles University in Prague, Albertov 6, 128 43 Prague 2, Czech Republic (*correspondence: vitkova3@natur.cuni.cz, m.vitkova@seznam.cz)
[2]Czech Geological Survey, Geologická 6, 152 00 Prague 5, Czech Republic
[3]Laboratories of the Geological Institutes, Charles University in Prague, Albertov 6, 128 43, Prague 2, Czech Republic

Smelting activities in the Copperbelt Province (Zambia) have produced huge amounts of various wastes. Dust particles emitted during the ore and slag processing pose high risk of environmental pollution in this area [1, 2]. Three types of dusts identified as possible sources of contamination were studied: (A1) dust from slag crushers, (A2) fly ash trapped by filters originating from processing of the slags and (B) electrostatic precipitator dust from smelting of Cu and Co-rich ores. Bulk chemical analyses and mineralogical investigation using XRD, SEM/EDS and TEM were performed. The samples were enriched with various levels of metals and metalloids. Maximum concentrations of 256 g Cu/kg (B), 8.9 g Co/kg (A1), 4.7 g Pb/kg (A2) and 19.8 g Zn/kg (A2) were determined. Based on XRD analysis, the composition of dust A1 generally corresponds to silicate slags [3] with dominating Ca-Fe pyroxenes, quartz (SiO_2), fayalite (Fe_2SiO_4) and cuprospinel ($CuFe_2O_4$). Calcite ($CaCO_3$), Ca-Fe pyroxenes and quartz represented the main phases of fly ash A2 with minor ZnS and elemental Cu and a significant portion of amorphous/glassy fraction. Chalcanthite ($CuSO_4 \cdot 5H_2O$), magnetite (Fe_3O_4) and delafossite ($CuFeO_2$) dominated in dust B. Detailed mineralogical investigations revealed the presence of Cu sulphides in the studied samples and possible substitutions of metals in the pyroxene structure. Elevated concentrations of Cu, Co and Zn were detected in the silicate glass. *In situ* weathering processes may result in the release of contaminants into the environment (e.g. soils) depending on the stability of phases present in the dust.

[1] Kříbek *et al*. (2010) *J. Geochem. Explor*. **104**, 69–86. [2] Pettersson & Ingri (2001) *Chem. Geol*. **177**, 399-414. [3] Vítková *et al*. (2010) *Mineral. Mag*. **74**(4), 581–600.

https://doi.org/10.1180/S0026461X00006502 Published online by Cambridge University Press

Sedimentary and chemical weathering fluxes at the outlet of the granitic Strengbach catchment (Vosges massif, Eastern France)

DANIEL VIVILLE*, FRANÇOIS CHABAUX, PETER STILLE, MARIE-CLAIRE PIERRET, SOPHIE GANGLOFF AND SYLVAIN BENARIOUMLIL

EOST-LHYGES (CNRS/Uni. Strasbourg), 1, rue Blessig, F-67084 Strasbourg Cedex, France (*correspondence: dviville@unistra.fr)

Understanding the relationship between chemical weathering and physical erosion rates is an important issue of Surface and Environmental Science. The determination of the relationships and parameters controlling chemical weathering and physical erosion can be achieved, among others, by comparing weathering and erosion fluxes measured at the outlet of small experimental watersheds. Astonishing is the fact, that numerous studies of chemical weathering fluxes exist and that only a few focused on erosion fluxes. This is for instance the case for the Strengbach catchment, for which geochemical budgets have been established since the mid 80ties but physical erosion rates only since very recently.

The aim of this study is to assess the physical erosion rate of the granitic Strengbach catchment (0.8 km^2, Vosges Massif, Eastern France) with the dissolved flux carried by the streamlet.

The results show that the erosion rate (about 5 T. km^{-2}. yr^{-1}) is at least equivalent to the chemical weathering rate and could be twice depending on the weathering rate retained corrections (atmospherical, biological). They also indicate that the erosion rate based on the lonely suspended matters calculation induces an underestimation of about 30%.

On the basis of this work, it appears that the weathering and erosion budgets determined on the Strengbach catchment do not differ significantly from other granitoids catchments studied previously.

Marine Mo isotope inventory: The role of igneous rock weathering

A.R. VOEGELIN[1]*, TH.F. NÄGLER[1], N. NEUBERT[2], T. PETTKE[1], M. STEINMANN[3] AND O. POURRET[4]

[1]Institut für Geologie, Universität Bern, Switzerland (*correspondence: voegelin@geo.unibe.ch)
[2]Institut für Mineralogie, Leibniz Universität Hannover, Germany
[3]UMR 6249 Chrono-Environment, Université de Franche-Compté, France
[4]HydrISE, LaSalle Beauvais, 60026 Beauvais cedex, France

The marine isotope inventory strongly depends on fractionation processes during continental rock weathering and subsequent river transport. Concerning molybdenum (Mo), the riverine contribution accounts for the largest part of the marine budget (e.g. [1]). Models of oceanic Mo cycling thus strongly depend on understanding continental processes causing Mo isotope fractionation.

This study investigates the effect of igneous crustal rock weathering on aquatic $\delta^{98/95}$Mo signals by comparing stream water and bedrock (basalt, granite, gneiss) Mo isotope data to results of laboratory leach experiments. Stream waters analyzed here are enriched in the heavy isotopes, a result in line with findings of previous studies [2-4]. To date, weathering of magmatic rocks has not been associated with resolvable Mo fractionation, as their $\delta^{98/95}$Mo show little variability ($\delta^{98/95}$Mo = -0.1 to 0.3‰, [5]). Incongruent mineral weathering and/or adsorption/resorption processes are the most likely factors to have caused the observed signals, while soil retention and adsorption of light Mo to the particulate load play a secondary role. This interpretation, based on water and bedrock samples, is supported by data of bedrock leach experiments, where leach solutions show a moderate fluctuation in $\delta^{98/95}$Mo between 0.5 and 1‰. This is nearly identical to the variability found in the stream waters (0.6-1.1‰). Sulfide oxidation was proposed to be an important factor controlling stream water Mo isotopic composition in a catchment underlain by sedimentary rocks [4]. Considering that silicate rocks may contain sulfides with variable isotope signatures, their incongruent dissolution could generate the observed aqueous $\delta^{98/95}$Mo signals.

[1] McManus *et al*. (2002) *Geochem. Geophys. Geosyst.* **3**, 1078. [2] Archer & Vance (2008) *Nature Geosci*. **1**, 597–600. [3] Pearce *et al*. (2010) *EPSL* **295**, 104–114. [4] Neubert *et al*. (2011) *EPSL* **304**, 180–190. [5] Siebert *et al*. (2003) *EPSL* **211**, 159–171.

https://doi.org/10.1180/S0026461X00006502 Published online by Cambridge University Press

Nanoparticulate Fe(III)-precipitates forming by Fe(II) oxidation in water

A. VOEGELIN*, S. SCHWARZ, S.J. HUG AND R. KAEGI

Eawag, Swiss Federal Institute of Aquatic Science and Technology, CH-8600 Duebendorf, Switzerland (*correspondence: andreas.voegelin@eawag.ch)

The oxidation of dissolved Fe(II) at oxic/anoxic boundaries leads to the precipitation of nanoparticulate Fe(III)-phases that profoundly impact the biogeochemical cycling of Fe and the fate of other major and trace elements in environmental systems. Despite the importance of Fe(III)-precipitates as immobilizing sorbents or colloidal carriers for contaminants and nutrients, numerous questions relating to their formation, their structural diversity and resulting differences in reactivity remain to be resolved.

Own recent work on Fe(III)-precipitates formed in aerated Fe(II)-containing aqueous solutions at pH 7 indicated the importance of Fe(III)-phosphates [1, 2]: At molar dissolved P/Fe (II) ratios >0.5, we observed exclusive formation of amorphous Fe(III)-phosphates that also incorporated substantial amounts of Ca. At P/Fe(II) <0.5, we concluded from X-ray absorption spectroscopy data that Fe(III)-phosphate formed until P was depleted, followed by the formation of other F(III)-phases (Si-rich hydrous ferric oxide at Si/Fe > 0.5, 2-line ferrihydrite at Si/Fe ~0.2-0.5, or lepidocrocite at Si/Fe <0.2) [1]. Electron microscopy data suggested that the different Fe(III)-phases became mixed in nanoparticles with diameters of a few 10-100 nm [2].

In continuing work, we aim (i) to resolve the composition and structure of Fe(III)-phosphates and the mode of cation and anion incorporation (Ca versus Mg, phosphate versus arsenate), (ii) to evaluate the transformation of different types of fresh precipitates during aging, and (iii) to assess how the different types of fresh Fe(III)-precipitates and their aging products affect other major and trace elements in aquatic systems. This work is based on controlled laboratory experiments in synthetic aqueous solutions, complemented by studies on real systems such as diagenetic Fe accumulations in lake sediments or As-removal units for drinking water treatment.

[1] Voegelin *et al*. (2010) *Geochim. Cosmochim. Acta* **74**, 164–186. [2] Kaegi *et al*. (2010) *Geochim. Cosmochim. Acta* **74**, 5798–5816.

The partitioning of volatile elements between metal and silicate at high pressures and temperatures

A.K. VOGEL[1]*, D.C. RUBIE[1], D.J. FROST[1] AND H. PALME[2]

[1]Bayerisches Geoinstitut, Universität Bayreuth, D-95440 Bayreuth, Germany (*correspondence: antje-kathrin.vogel@uni-bayreuth.de)

[2]Forschungsinstitut und Naturmuseum Senckenberg, D-60325 Frankfurt, Germany

Volatile elements are depleted in the Earth´s mantle and in nearly all other solid objects of the inner solar system (Moon, Mars, meteorites), most probably because they failed to condense at high temperatures. In some cases evaporation before or during accretion may also have occurred. Many of these elements were additionally affected by core formation. To disentangle primary depletion and depletion by core formation and to provide additional clues for the processes of core formation we studied the metal - silicate partitioning behaviour of the volatile siderophile elements Sn, Pb P, Cu and Ge, covering a range of 650 K in condensation temperatures.

Experiments were performed over a pressure and temperature range of 10.5 GPa to 23 GPa and 2273 K to 2673 K respectively using a multianvil apparatus. The oxygen fugacity varied from -2.0 to -2.4 log units relative to the iron-wüstite-buffer. The starting materials consisted of 3 parts (by weight) silicate (peridotitic composition) and 1 part (by weight) metal, with the latter consisting of 95 wt% Fe, and 1 wt% of P_2O_5, Cu, GeO_2, SnO and Pb_3O_4 respectively. To consider the effect of S one experiment was performed with 10wt% S added as FeS to the metal phase of the starting material. Analyses of the metal phases were performed with an EPMA, the compositions of the silicate phases were analyzed by LA-ICP-MS.

The volatile elements Sn and Pb are similarly depleted in the Earth´s mantle, which requires similar effective partition coefficients ($D^{met/sil}$) during core formation. However, at low pressures the partition coefficients of Sn and Pb differ by up to two orders of magnitude. Our results show that the liquid metal – liquid silicate partition coefficients of Sn and Pb converge with increasing pressure, indicating that equilibration pressures of at least 30 GPa were necessary to avoid fractionating them in the Earth´s mantle.

We found that 10 wt.% S in the metal phase has hardly any influende on the $D^{met/sil}$ of Pb but lowers the value for Sn by about 0.6 orders of magnitude.

https://doi.org/10.1180/S0026461X00006502 Published online by Cambridge University Press

Isotope reference materials for present and future isotope research

JOCHEN VOGL* AND WOLFGANG PRITZKOW

BAM Federal Institute for Materials Research and Testing, Berlin, Germany (*correspondence: jochen.vogl@bam.de)

The variation of isotope abundance ratios is increasingly used to unravell natural and technical questions. In the past the investigation and interpretation of such variations was the field of a limited number of experts. With new upcoming techniques and research topics in the last decades, such as provenance and authenticity of food, the number of published isotope data strongly increased. The development of inductively coupled plasma mass spectrometers (ICPMS) from an instrument for simple quantitative analysis to highly sophisticated isotope abundance ratio machines influenced this process significantly. While in former times only experts in mass spectrometry were able to produce reproducible isotope data, nowadays many laboratories, never been in touch with mass spectrometry before, produce isotope data with an ICPMS. Especially for such user isotope reference materials (IRM) are indispensible to enable a reliable method validation. The fast development and the broad availability of ICPMS also lead to an expansion of the classical research areas and new elements are under investigation. Here all users require IRM to correct for mass fractionation or mass discrimination or at least to enable isotope data related to a common accepted basis. Despite this growing interest suitable IRM are still lacking for a number of isotope systems such as magnesium.

For all isotope abundance ratio applications reference materials are necessary either for correction of mass fractionation/mass discrimination, for method validation or to provide a common accepted basis. The production of these urgently needed IRM, however, has stagnated within the past decades. Reasons might be that the scientific relevance often has not been realized; time and effort seemed not in balance with the scientific gain. Recently the situation has changed slightly, as researcher at NIST resumed their work and BAM and NRC started working on IRM.

The needs for present research on isotope variations are being considered and are compared to the limitations of current isotope reference materials within this presentation. The resulting disagreement between both is being discussed and solutions will be provided.

Geochemical consequences of thermomechanical processes in subduction zones. Implications for crustal making processes

KATHARINA VOGT[1], TARAS GERYA[1,2] AND ANTONIO CASTRO[3]

[1]Swiss Federal Institute of Technology (ETH-Zurich), 8092 Zurich, Switzerland
[2]Moscow State University, 119899 Moscow, Russia
[3]University of Huelva, 21071 Huelva, Spain

We have analyzed the dynamics of crustal growth processes at active continental margins based on a 2D coupled petrological-thermomechanical numerical model of an oceanic-continental subduction zone. The model includes spontaneous slab retreat and bending, dehydration of subducted crust, aqueous fluid transport, partial melting, melt extraction and melt emplacement in form of both extrusive volcanics and intrusive plutons.

Our results show that the rate of crust formation and the composition of newly formed crust are strongly depended on the degree of rheological weakening induced by fluids percolating from the subducting slab and upwards propagating melts. Subsequently we could identify the following geodynamic regimes: (i) stable arcs (ii) compressional arcs with plume development and (iii) extensional arcs.

Crust formation in stable arc settings is characterized by flattened intrusions and low crustal growth rates. At first dacitic melts are produced due to partial melting of the slab nose, followed by flux melting of wet peridotite. In compressional arcs the emplacement of hybrid plumes adds additional material to the continantal crust. Partially molten rock melanges composed of basalts and sediments accumulate at asthenospheric depth forming plumes, which rise through the mantle prior to emplacement. We have calculated the isotopic initial ratios of Sr and Nd in the plume during the simulations, showing that the geochemical signature varies strongly with the basalt/(basalt+sediment) fraction in the plume. These signatures are transferred to andesitic magmas and finally confirm the geochemical signatures of the continental crust.

Crustal growth in extensional arc settings is accomplished by decompression melting of dry peridotite, leading to elevated crustal growth rates.

https://doi.org/10.1180/S0026461X00006502 Published online by Cambridge University Press

Experimental weathering of micas in acid soils conditions: Contribution of boron isotopes

A. VOINOT[1,2] *, D. LEMARCHAND[1], M-P. TURPAULT[2] AND F. CHABAUX[1]

[1]LHYGES, CNRS-UDS, Strasbourg, France (*correspondence: alexandre.voinot@etu.unistra.fr)
[2]BEF, INRA, Champenoux, France

Soil minerals evolve by contact with weathering agents (protons, organic acids and ligands) supplied by atmospheric inputs or produced by coexisting living organisms. Determination of their relative contribution and seeing if they interact with soil minerals through different mechanisms is a key step toward identification of the pedogenic processes in action and soil sustainability.

In order to test if different weathering agents can induce specific and traceable mechanisms (dissolution vs. transformation), we lead a series of laboratory experiments intended to investigate the behavior of phyllosilicate minerals in contact with 3 different chemical reactants: HCl (protons), citric acid (organic acids) and siderophores (ligands). These experiments were performed at 2 different pH conditions (pH3 and pH4.5) for 37 days at 20°C in a continuous flow system. Biotite was selected as test mineral because it is a common and reactive mineral in soils. To trace weathering reactions, we monitored the boron chemical and isotopic compositions in the outflowing solutions. The choice of B as weathering proxy is based on its balanced distribution between minerals sites (interlayers and tetrahedral sites). Moreover, each of these sites have distinct B isotopic signatures [1], in line with the large isotopic fractionation generated by weathering reactions [2].

Comparison of B and major elements in solution reveals that all experiments conducted at pH3 and citric acid at pH4.5 lead to predominant dissolution reactions. By contrast, reactions conducted at pH4.5 with HCl and siderophores show a large removal of isotopically fractionnated boron, indicating a predominant contribution of interlayer sites and a large transformation (vermiculitization) of the biotite.

[1] L. B. Williams *et al*. (2001) *Geochimica et Cosmochimica Acta* **65**, 1769–1782. [2] D. Cividini *et al*. (2010) *Geochimica et Cosmochimica Acta* **74**, 3143–3163.

Proterozoic magmatism

O. VOLCAN

oasisvolcan@yahoo.com

Proterozoic magmatism along the margin of the Yangtze Block is extensive and provides important evidence in the plate tectonic reconstructions for the Proterozoic.The wangcang area on the northwestern margin of the Yangtze Block consists of complex Archean to early Proterozoic crystalline basement and a suite of high-grade metamorphic rocks surrounded by late Neoproterozoic to Phanerozoic sedimentary covers.In the the northwestern margin of the Yangtze craton there were found many bodies as tectonic blocks of greenshist rocks, which were named Hekou Formation. Single- grains zircon U–Pb TIMS dating of andesite-dacite indicates that the Hekou Formation erupted at 882 ± 69 Ma. This is a new time for volcanics rocks found along the margin of the Yangtze Block.

https://doi.org/10.1180/S0026461X00006502 Published online by Cambridge University Press

Spatial pollution gradients in Central Europe after 25 years of decreasing industrial emissions

P. VOLDRICHOVA[1,2]*, M. NOVAK[1], L. ERBANOVA[1], E. PRECHOVA[1], F. VESELOVSKY AND V. BLAHA[1]

[1]Department of Geochemistry, Czech Geological Survey, Geologicka 5, 152 00 Prague 5, Czech Republic (*correspondence: petra.voldrichova@geology.cz)

[2]Department of Analytical Chemistry, Faculty of Science, Charles University in Prague, Albertov 6, 128 43 Prague 2, Czech Republic

Industrial pollution in the Czech Republic (Central Europe) peaked in the mid-1980s. Soft coal combustion in the north of the country was one of the largest sources of many trace elements for the atmosphere and ecosystems. Introduction of more advanced technology in the 1990s led to a steep decrease in nationwide industrial emission rates of pollutants. In the mid-1980s, the Northern Czech Republic was 4 to 10 times more polluted than the Southern Czech Republic, which is less industrialized. In 2009, we established a new network of 10 monitoring stations near the borders between the Czech Republic, Germany, Austria and Poland. Samples of vertical and horizontal atmospheric deposition (snow and ice accretions, respectively) are collected each winter (Oct. 15- April 15). Monitoring sites are situated on mountaintops at an elevation of 1000 m. All samples are treated in a clean laboratory (class 7). Concentration of 19 elements (Al, As, Bi, Be, Cu, Co, Cr, Cd, Fe, Mn, Ni, Pb, Sb, Sc, Ti, Th, U, V, and Zn) is determined using SF ICP MS. Preliminary data from 2009 suggest that, for most of the environmentally relevant elements, spatial pollution gradients differ from previous decades. For example, for arsenic (As) and lead (Pb), the eastern part of the country (Jeseniky and Beskydy Mts.) exhibits the highest pollution loads. At the same time, the northern and southern part of the country show lower pollution loads. The northern part of the country, situated near a cluster of coal-burning power plants, experienced a faster decrease in pollution rates over the past 25 years than the south; its current atmospheric deposition is not significantly higher than in the south. For antimony (Sb), all 10 sites have similar atmospheric inputs. For zinc (Zn), the highest concentrations in atmospheric input were found in the northwest. Novohradske Mts. (south) have similar Zn inputs as Jizerske Mts. (north). Overall, pollution levels are up to 20 times lower compared to the late 1980s. They are more site-specific, and reflect temporal changes in operation of distant vs. local point sources of pollution.

The Paleozoic $\delta^{88/86}Sr_{seawater}$ record – Quantifying carbonate production rates at mass extinction events

H. VOLLSTAEDT[1]*, A. EISENHAUER[1], F. BÖHM[1], J. FIETZKE[1], A. KRABBENHÖFT[1], V. LIEBETRAU[1], J. FARKAŠ[2] AND J. VÉIZER[3]

[1]Leibniz-Institut für Meereswissenschaften (IFM-GEOMAR), Wischhofstr. 1-3, D-24148 Kiel, Germany (*correspondence: hvollstaedt@ifm-geomar.de)

[2]Czech Geological Survey, Geologicka 6, 152 00 Praha 5, Czech Republic

[3]University of Ottawa, Dept. of Earth Sciences, 140 Louis Pasteur, Ottawa, Canada K1N 6N5

Within the Phanerozoic Eon strata boundaries are often associated with the extinction of marine organisms. The reasons for these events are still discussed and a quantification of observed changes in the marine carbonate system is missing.

Strontium (Sr) is one of the most important divalent cations in calcium carbonate minerals and a carrier of important proxy information. In terms of the Sr output flux of the ocean ($\delta^{88/86}Sr_{seawater}$: ~0.39‰), isotopically light carbonates ($\delta^{88/86}Sr_{carbonates}$: ~0.15 – 0.25‰) represent the major Sr sink. Consequently, variations in Sr/Ca and paired $^{87}Sr/^{86}Sr$-$\delta^{88/86}Sr$ values are a suitable tool to investigate the global carbonate budget throughout Earth's history including the biotic turnover of calcifying organisms at stratigraphic boundaries. Latter processes are expected to have a large influence on Sr geochemistry and isotope composition of seawater.

We measured paired $^{87}Sr/^{86}Sr$-$\delta^{88/86}Sr$ ratios of ~120 modern and Paleozoic marine brachiopod samples which were screened for diagenetic alteration prior to the measurement. Reproducibility of double spike-derived $\delta^{88/86}Sr$ based on an international coral carbonate standard (JCp-1) is 0.019‰ (2SD, n=26).

We observe major drops in $\delta^{88/86}Sr_{seawater}$ of 0.05 – 0.15‰ at mass extinction events which coincide with a decrease of 10-50% in the number of marine genera [1]. This emphasizes the strong coupling of the carbonate system to $\delta^{88/86}Sr$ of seawater. In contrast, $\delta^{44/40}Ca_{seawater}$ changes are much less pronounced at these biotic turnovers. Furthermore, excursions in $\delta^{13}C_{carbonate}$ at strata boundaries are related to changes in the organic carbon production rather than to the carbonate production.

By taking changes in $^{87}Sr/^{86}Sr$, $\delta^{88/86}Sr$ and Sr/Ca into account we are able to make quantitive statements on the Sr input and output fluxes of the ocean at the major Paleozoic mass extinction events, including the Permian/Triassic boundary.

[1] Sepkoski (1997) *J. of Paleontology* **71**, 533–539.

https://doi.org/10.1180/S0026461X00006502 Published online by Cambridge University Press

Unconventional matrices prevent novel isotopes turning traditional

F. VON BLANCKENBURG[1], J. BOUCHEZ[1], M. GUELKE-STELLING[2], M. OELZE[1], C. OSTERTAG-HENNING[3], J. SCHUESSLER[1] AND G. STEINHOEFEL[1]

[1]Earth Surface Geochemistry at GFZ German Centre for Geosciences, Potsdam, Germany (fvb@gfz-potsdam.de)
[2]KIT, Mineralogy and Geochemistry, Karlsruhe, Germany
[3]Bundesanst. Geowiss. Rohstoffe BGR, Hannover, Germany

Do 'non'-traditional isotopes still deserve their prefix? It only takes a look at your preferred stable isotope systems compilation to realise that variations are largest in the biosphere and its geologic derivatives. Hence, to move the field into the next decade, and beyond the Geosciences, we need to develop tools to cater for matrices that are by any geological standard non-traditional. Here we review progress on this effort from our laboratories' past years work.

Biomedical

Metal isotopes are superb tools to trace the process and timing humans metabolize nutrients. Each human bears a distinct stable Fe isotope signature in its blood, which is identical to that in muscle tissue and that of blood plasma, suggesting that this characteristic ratio is set when Fe is received by the transferrin molecule during intestinal absorption.

Plant Physiology and human nutrition

Higher plants induce substantial fractionation of Mg, Si, Ca, Fe, and Zn isotopes. Fe isotope fractionation has been shown to differ between grasses and non-grasses, where the former are enriched in light Fe through reduction in soils, and the latter take up unfractionated complexed Fe(III). Plants induce similar fractionation as metals are being moved through their tissue.

Crude oil

First results of various types of crude oil yielded surprisingly heavy Fe isotope compositions, tracing bacterial iron oxidation/reduction processes during oil biodegradation in the reservoirs.

Weathering at the micrometer scale

The large diversity of weathering and biotic products in soils requires detection of their isotope variability at the micro-scale. We have now developed a second-generation UV-femtosecond laser ablation system, and measure novel stable isotopes in bulk soil (as fused glass beads or powder pellets), at the mineral scale in thin sections, individual phytoliths, and by ablating fluids after element separation and evaporation.

The challenge to all these cases is to (1) develop taylor-made matrix-suited methods; (2) demonstrate that the analyses are free of artefacts, requiring reference materials; (3) understand the underlying processes - the ultimate aim.

The ^{10}Be(meteoric)/^{9}Be ratio as a tracer of weathering and erosion

F. VON BLANCKENBURG*, H. WITTMANN AND N. DANNHAUS

Earth Surface Geochemistry at GFZ German Centre for Geosciences, Potsdam, Germany
(*correspondence: fvb@gfz-potsdam.de)

We provide a systematic framework to derive weathering and erosion rates from the ratio of the meteoric cosmogenic nuclide ^{10}Be to stable ^{9}Be, suggested to serve as proxy for weathering and erosion over the late Cenozoic [1].

In a weathering zone some of the ^{9}Be, present in silicate minerals, is released and partitioned between a reactive phase (adsorbed to clay and hydroxide surfaces), given the high partition coefficients at intermediate pH, and to a minor degree into the dissolved phase in pore waters. The combined mass flux of both phases is defined by the soil formation rate times a mineral dissolution rate – and is hence proportional to the chemical weathering rate. The surface of the weathering zone is continuously exposed to fallout of meteoric ^{10}Be. This ^{10}Be percolates into the weathering zone where it mixes with dissolved ^{9}Be. Both isotopes may exchange with the adsorbed Be, given that equilibration rates of Be are fast relative to soil residence times. Hence a ^{10}Be/^{9}Be (reactive) ratio results from which the ^{9}Be weathering flux can be calculated given that the delivery rate of ^{10}Be is now often known. If the loss of ^{10}Be into the dissolved phase is furthermore small, the ratio of ^{10}Be (reactive) to that of the residual mineral-bound ^{9}Be provides a physical erosion rate.

We have tested this approach in sediment of the Amazon and Orinoco basin, and compared it to dissolved Be isotope data [2]. The reactive Be was extracted from sediment by combined hydroxylamine and HCl leaches. In the Amazon trunk stream, the Orinoco, Apure, and La Tigra river ^{10}Be/^{9}Be (dissolved) agrees well with ^{10}Be/^{9}Be (reactive), showing that in most rivers these two phases also equilibrate. ^{10}Be/^{9}Be ratios range from 5×10^{-9} for the Brazilian shield rivers to 2×10^{-10} for the Beni river draining the Andes, corresponding to denudation rates of 0.01mm/yr for the shields and 0.5mm/yr for the Andes, compatible with denudation rates from *in situ*-produced cosmogenic ^{10}Be [3]. 10-50% of the ^{9}Be was mobilised from bedrock.

Once delivered to the ocean, this riverine Be, be it dissolved or reactive, will eventually drive ^{10}Be/^{9}Be ratios of ocean water and disclose global weathering rates.

[1] Willenbring & von Blanckenburg (2010) *Nature* **465**. [2] Brown, E. *et al*. (1992) *Geochim Cosmochim Acta* **56**. [3] Wittmann *et al*. (2011) *Geol Soc. Am. Bull*. **123**.

https://doi.org/10.1180/S0026461X00006502 Published online by Cambridge University Press

Apatite composition of Southern Germany volcanoes: Clues to origin and magmatic evolution

A. VON DER HANDT[1] AND M.K. RAHN[2]

[1]Geowissenschaftliches Institut, University of Freiburg 79104 Freiburg, Germany
[2]Swiss Federal Nuclear Safety Inspectorate (ENSI), 5200 Brugg, Switzerland

Volcanic activity in SW Germany has focussed along the Upper Rhine graben (with volcanic centres at Kaiserstuhl and Odin's Forest). In addition, eruptive centres are also found far away from known tectonic lines in the Urach and Hegau areas. Dating of these rocks reveals an extended period of activity along the Upper Rhine graben (60-15 Ma [1]), while activity in isolated centres was relatively short (Kaiserstuhl: 16-19 Ma [1, 2], Hegau: 15-7 Ma [3, 4]), Urach: 17-? Ma [5]).

Apatite is a common mineral in many of the eruptive products, which are mostly of mafic to ultramafic as well as carbonatitic composition. Previous studies on these apatites (e.g. Rahn and Selbekk 2008) have shown that their composition is variable with respect to Si and S (replacing P) as well as OH and Cl (replacing F). Thus the question arises whether apatite could be used as an indicator of magmatic evolution and whether there are clear differences to be found, which allow a distinction between the Kaiserstuhl, Hegau and Urach eruptive centres on the basis of apatite composition.

In order to evaluate the compositional evolution, apatites from the Kaiserstuhl and Hegau were dated using the fission track technique. Dated samples were analysed by means of EPMA and SIMS to obtain major and trace element data and check for sample internal variation. Both, Kaiserstuhl and Hegau volcanics show a large compositional range from F-rich to OH-rich chemistry, with Cl-endmember lower than 5%. Apatites close to OH endmember are restricted to samples from the Hegau. A clear distinction of sources is possible on the basis of Sr, Zr and REE element contents. Hegau apatites show a wider spread in magmatic REE fractionation, together with flatter chrondrite REE patterns. Combination of age and compositional data allows to clearly attribute distant tuff layers to the Hegau, while no such layers show Kaiserstuhl characteristics. Erupted material from the Hegau has faced up to 80 km of westward air transportation.

[1] Keller *et al*. (2002) *SMPM* **82**, 121–130. [2] Kraml *et al*. (2006) *Geostand. Geoanal. Res*. **30**, 73–86. [3] Schreiner (1992) *Geol. Landesamt BW*, 290p. [4] Rahn & Selbekk (2008) *Swiss J. Geosc*. **100**, 371–381. [5] Kröchert *et al*. (2009) *Zeitschr. deut. Ges. Geowissensch*. **160**, 325–331.

Chemical speciation of Fe-rich colloids and nanoparticles in the Southern Ocean

B.P. VON DER HEYDEN[1]*, A.N. ROYCHOUDHURY[1] AND S.C.B. MYNENI[2]

[1]Dept. of Earth Sciences, Stellenbosch University, Stellenbosch 7602, South Africa (*correspondence: bvon@sun.ac.za)
[2]Dept. of Geosciences, Princeton University, Princeton, NJ 08544, USA

Iron is an important nutrient and limits the productivity in the Southern Ocean. Previous biogeochemical studies largely focused on the size-dependent Fe-pools in ocean water with little attention to the chemical speciation of iron. As a result, molecular level factors affecting the bioavailability of particle-bound iron are largely unexplained.

Using clean techniques, samples were collected along two transects between Cape Town, Antarctica and the South Georgia Islands. Iron particles were trapped on 0.2μm filters and subsequently analyzed in their pristine state using *in situ* L-edge XANES spectroscopy and high-resolution scanning transmission X-ray microscopy. Chemical speciation of the discreet, quasi-spherical particles was accomplished through a combination of the spectral shape analysis and the quantitave parameterization of the L_3-edge splitting.

From these spectroscopic analyses, particles in Southern Ocean could be classified into five broad categories including ferric oxides, magnetite, other mixed valence species and at least two ferrous species. A distinct spatial variation in iron speciation was also evident with ferric species predominating in the mid-latitudes (32°S- 55°S) and ferrous-rich species more common in the high latitudes. A number of mixed-valence species, including magnetite, made up a significant proportion of the particles found to the north of the Polar Front. Proximal to the African- and South Georgian shelves, Al-substitution, a solubility-depressing effect, was observed to occur in the ferric species. The substituted Al in iron oxides displayed a gibbsite-like structure.

We are currently evaluating the cause of this spatial and chemical variability, which may be attributed to the particle source, and to a range of processes including photochemical response and biological interactions. However, it is clear that such variability in speciation will have a profound impact on Fe solubility and iron-ligand interaction, thereby influencing the Fe-pool that is bioavailable.

https://doi.org/10.1180/S0026461X00006502 Published online by Cambridge University Press

Clay mineralogy and chemical environment of an Aptian lacustrine succession in North-Eastern Brazil

W. VORTISCH[1]*, V.H. NEUMANN[2], R. GRATZER[1] AND D. ROCHA[2]

[1]Montanuniversität Leoben, 8700 Leoben, Austria (*correspondence: Walter.Vortisch@unileoben.ac.at, gratzer@unileoben.ac.at)

[2]Universidade Federal de Pernambuco, Dep. de Geologia, Recife, Brazil (neumann@ufpe.br, dunaldson@msn.com)

The studied core was drilled in the Jatobá Basin, which is underlain and surrounded by the crystalline basement of the Borborema Province (NE Brazil).

113 samples were analysed by X-ray diffractometry, 17 of which were selected for clay mineral analysis. Sandstones were also studied by polarising microscopy and scanning electron microscopy.

Petrographically, 5 lithotypes can be defined: (1) generally silty grey shales, (2) grey marly shales to shaly marls, (3) generally fine-grained, argilaceous sandstones (4) micritic limestones, occasionally with a minor content of dolomite, (5) dolostone (dolomite > calcite).

In many of the shales, expandable clay minerals are dominant among the clay mineral suite (predominantly illite-smectite), followed by illite, kaolinite and chlorite.

In contrast to the shales, sandstones can contain considerable amounts of smectite, besides illite and minor proportions of kaolinite and chlorite. Quartz and feldspars are usually main components. Calcite is sometimes present. Some of the sandstones show high contents of unweathered biotite, often marking sedimentary structures like ripple crossbedding as dark layers.

The presence of chlorite and biotite as clastic components, indicate mild regional weathering, and/or fast erosion and transport to the lacustrine basin. Smectite occurring in the sandstones indicates volcanic activity.

The ocurrence of dolomite is uncommon for lacustrine freshwater environments. Freshwater conditions are indicated by oxygen isotopes [1] and ostracods. The occurrence of dolomite together with high organic matter content and intensive bacterial activity may explain lacustrine dolomite formation without evaporitic conditions.

[1] Gratzer *et al*. (2011) Stable isotopes of organics & inorganics of Aptian lacustrine sediments in northeastern Brazil. This volume.

Constraining subannual variability in river chemistry and hydrology with $^{87}Sr/^{86}Sr$: A case study in the Fraser River basin, Canada

B.M. VOSS[1,2]*, B. PEUCKER-EHRENBRINK[1], T.I. EGLINTON[1,3], S.L. GILLIES[4], S. MARSH[4], A. JANMAAT[4], B. DOWNEY[4], J. FANSLAU[4], H. FRASER[4] AND G. MACKLAM-HARRON[4]

[1]WHOI, MS 25, Woods Hole, MA 02543, USA (*correspondence: bvoss@whoi.edu)

[2]MIT, Cambridge, MA 02139, USA

[3]ETH, Zürich 8092, Switzerland

[4]UFV, Abbotsford V2S-7M8, Canada

River systems present a significant challenge to quantification of global elemental fluxes among atmospheric, terrestrial, and marine reservoirs, as aquatic passageways exhibit complex processing and storage of material on timescales driven by local and distant climatic and geophysical cycles [1-3]. The Fraser River basin in southwestern Canada has three important features making it ideal for testing geochemical approaches to tackling these issues: 1) its moderate size and temperate climate are neither exceptional nor insignificant among global rivers; 2) a spectacular diversity of bedrock geology and vegetation allow for discrimination of sources of transported material; and 3) its modest industrial footprint allows for assessment of relatively unperturbed processes. Three recent field campaigns at low, medium, and high water flow have generated a broad dataset of informative geochemical parameters. Dissolved $^{87}Sr/^{86}Sr$ signatures of major tributaries and daily discharge data form the backbone of a preliminary attempt to model the geochemical variability of exported material across the hydrograph. Over one full year of time series sampling near the Fraser mouth has demonstrated that subannual variability in dissolved $^{87}Sr/^{86}Sr$ is significant and mirrors temporal and spatial changes in the hydrology of the basin. Extending this approach to other elemental fluxes of interest and other river basins will vastly improve global biogeochemical budgets and the potential to predict future changes.

[1] Aufdenkampe *et al*. (2011) *Front Ecol Environ* **9**(1), 53–60. [2] Rossi *et al*. (2009) *J Hydrol* **377**, 237–244. [3] Milliman & Syvitski (1992) *J Geol* **100**, 525–544.

https://doi.org/10.1180/S0026461X00006502 Published online by Cambridge University Press

Review of geochemical problems and mitigation during the production of geothermal reservoirs

FRANCOIS-D. VUATAZ AND NIELS GIROUD

Laboratory for Geothermics - CREGE, University of Neuchatel, CH-2000 Neuchatel, Switzerland (francois.vuataz@unine.ch)

Introduction

In many geothermal fields worldwide, production and reinjection of hot brines modify the temperature and pressure conditions around the wells. This induces geochemical processes within the reservoir and/or along the well casings and the surface pipelines. Some geothermal fluids are relatively benign even at high temperature, whereas others can cause numerous problems due to either a high salinity or a high content of particular gases or dissolved solids. Permeability decrease, well and pipeline partial plugging or metal corrosion are the main consequences of these chemical processes. If they are not taken seriously into consideration and solved, the outcome can be a production decrease, a high maintenance cost, or even the loss of a well.

Mineral scaling

Due to the high solubility of silica at high temperature, silica scaling is a frequent problem in geothermal plants. Amorphous silica precipitates after flashing or cooling of the fluid in surface pipelines or reinjection wells. Silica can be removed from the fluid and exploited commercially as a by-product. Carbonate scaling occurs in carbonate reservoirs and CO_2-rich fluids. Other minerals can form scales, such as anhydrite, sulphides and oxides.

Metal corrosion

Various types of corrosion are observed on well casings and surface pipelines, due to dissolved H_2S and CO_2, high chloride content or gas exsolution. Numerous laboratory experiments on the corrosion processes have been performed, but the results often differ from on-site monitoring experiments of the corrosion processes.

[1] Ngothai Y. Yanagisawa N. Pring A. Rose P. O'Neill B. & Brugger J. (2010) *Proc. Australian Geotherm. Ener. Conf. Adelaide*. [2] Gunnarsson I. & Arnórsson S. (2005) *Geothermics* **34**, 320–329. [3] Reyes A. G. Trompetter W. J. Britten K. & Searle J. (2003) *J. Volcanol. Geotherm. Res.* **119**, 215–239.

Liquid carbonates investigated by First-principles Molecular Dynamics simulations

R. VUILLEUMIER[1]*, A. SEITSONEN[2], N. SATOR[3] AND B. GUILLOT[3]

[1]Ecole Normale Superieure, Departement de Chimie, UMR 8640 CNRS-ENS-UPMC, 24, rue Lhomond, 75005 Paris, France (*correspondence: rodolphe.vuilleumier@ens.fr)

[2]Physikalisch Chemisches Institut, Universität Zürich, Winterthurerstrasse 190, CH-8057 Zürich, Switzerland (Ari.P.Seitsonen@iki.fi)

[3]Laboratoire de Physique Théorique de la Matière Condensée, Université Pierre et Marie Curie (Paris 6), UMR CNRS 7600, case courrier 121, 4 place jussieu, 75252 Paris cedex 05, France (sator@lptmc.jussieu.fr, guillot@lptmc.jussieu.fr)

The Earth mantle is mainly composed of silicates and its carbon contents is very low, of the order of 10 to 500 ppmw [1]. However carbon and its oxidized forms as carbonates and CO_2, likely play a crucial role in the dynamics and chemical differentiation of the mantle. The onset of partial melting at about 300km deep in the mantle, corresponds to the formation of liquid carbonates or carbonatites. In the astenosphere, the observed electrical conductivity anomalies [2] could originate from carbonatitic magmas exhibiting a very large conductivity, about 100 to 100 000 times that of olivine. However the physical and chemical properties of carbonatites at mantle conditions are poorly known and some theoretical guidance could be useful in this context.

We present a First-principles Molecular Dynamics simulation study of liquid $CaCO_3$. Its structural and transport properties have been investigated in the (T, P) range 1000-2000K and 0-6 GPa. Diffusion constants are found in good agreement with available data on viscosity [3]. Surprisingly CO_3^{2-} units diffuse nearly as fast as the Ca^{2+} cations. Because of the fast dynamics into the melt it was also possible to estimate the ionic conductivity. For the investigated thermodynamic conditions, we found an ionic conductivity close to 100 S. m^{-1}, in agreement with the available experimental data [2]. The local structure around the CO_3^{2-} anions has been studied in details and appears to be quite complex, sharing some similarities with the crystalline polymorphs calcite and aragonite. Simulation data on vibrational spectroscopy of liquid $CaCO_3$ will also be presented.

[1] R. Dasgupta & M. M. Hirschmann (2010) *Earth & Planetary Science Letters* **298**, 1. [2] F. Gaillard *et al*. (2008) Science **322**, 1363. [3] D. P. Dobson *et al*. (1996) *Earth & Planetary Science Letters* **143**, 207–215.

https://doi.org/10.1180/S0026461X00006502 Published online by Cambridge University Press

A low sulphur epithermal gold mineralisation in Kisacik-Ayvacik area (Çanakkale-Turkey)

ALAADDIN VURAL[1], DOĞAN AYDAL[2] AND İBRAHIM AKPINAR[1]

[1]Gumushane University, Engineering Faculty, Geological Engineering Department, Baglarbasi, 29100, Gumushane, Turkey (*correspondence: vural@gumushane.edu.tr) (hiakpinar@gumushane.edu.tr)

[2]Ankara University, Engineering Faculty, Geological Engineering Department, 06100, Tandoğan, Ankara, Turkey (aydal@ankara.edu.tr)

Kısacık-Ayvacık area is located in northern part of Küçükkuyu (Çanakkale), town within Biga Peninsula, northwestern Anatolia, Turkey. In general, throughout the area magmatic rocks and ultramafic rocks, sporadically at their contacts, are seen.

The purpose of this work is to investigate the occurrences conditions, types, places of gold enrichment and probing the genetics of gold enrichment in Kısacık-Ayvacık area along with outlining alteration distribution, petrographic and ore mineralogy features of the rocks in the region. In general, Pre-Tertiary rock units of Kazdağı Group and ophiolitic melange, and Tertiary magmatic rocks consisting altered haematitized-silicified andesite, rhyolite, ignimbrite, quartz porphyry and pyroclastic rocks are present. These rocks have subalkaline composition, nevertheless showing a calcalkaline tendency.

The gold mineralizations in Kısacık-Ayvacık area are observed within altered volcanic rocks of dacite, andesite and tuffs. These rocks have galena, pyrite, chalcopyrite, graphite, and haematite minerals and mineralisation of invisible gold enrichment. Gold values in studied volcanic rocks changes between 40 ppb-8500 ppb. Occurences temperatures of gold mineralizations change between 190 °C and 290 °C, salinity 0-7 % NaCl and S isotope values are mostly near zero. Consequently, these values imply a low-sulphidized epithermal type gold mineralization in the study area.

Application of experimental mineralogy to the description of new platinum-group minerals

A. VYMAZALOVÁ[1]*, M. DRÁBEK[1] AND F. ZACCARINI[2]

[1]Czech Geological Survey, Geologicka 6, 152 00 Prague 5, Czech Republic (*correspondence: anna.vymazalova@geology.cz)

[2]University of Leoben, Peter Tunner Str.5, A8700 Leoben, Austria (federica.zaccarini@unileoben.ac.at)

According to [1] there are more that 500 platinum-group (PG) phases termed as unidentified and require complete or clearer identification to be approved as new mineral species, in particular crystallographic characterization is often missing. One of the significant tools enabling the better characterisation of a natural phase can be an application of a synthetic material. The advantage is that the synthetic PG-phases are prepared in a required amount, under controlled chemical and physical parameters, such as chemical composition and temperature. The synthetic PG-phase can be thus applied as a comparative and descriptive material of a natural analogue. Such approach has been used in case of description of milotaite (PdSbSe) [2] or pašavaite ($Pd_3Pb_2Te_2$) [3]. The synthetic material should display the identical optical and physical (microhardness and reflectance) properties and chemical identity with natural sample. Significant role plays the structural identity of natural and synthetic material that has to be also proved. Electron back-scattering diffraction (EBSD) study can be applied to support structural identity. Furthermore the Raman spectroscopy, a nondestructive, structurally sensitive technique, suitable for grains of small mineral size (less than 10 microns) such of those of PGM is a sufficient method to prove structural identity.

[1] Daltry & Wilson (1997) *Min. Petrol* **60**, 185–229. [2] Paar *et al.* (2005) *Can. Miner.* **43**, 689–694. [3] Vymazalová *et al.* (2009) *Can. Min.* **47**(1), 53–62.

https://doi.org/10.1180/S0026461X00006502 Published online by Cambridge University Press

Focusing of upward fluid migration due to mineral grain size variation

I. WADA[1]*, M.D. BEHN[1], E.M. PARMENTIER[2] AND A.M. SHAW[1]

[1]Woods Hole Oceanographic Institution, Woods Hole, MA, 102543, USA (*correspondence: iwada@whoi.edu, mbehn@whoi.edu, ashaw@whoi.edu)
[2]Brown University, Providence, RI, 02912, USA (em_parmentier@brown.edu)

In this study, we use numerical models to quantify the effect of mineral grain size on the migration path of aquous fluids in the mantle wedge. Grain size affects grain-scale permeability of the mantle and fluid migration, which is an important factor that controls the location of hydrous melting in the wedge. By coupling a subduction zone thermal model with a laboratory-derived grain size evolution model, we predict that the spatial variation in grain size in the flowing part of the mantle wedge is large; grain size increases from 10–100 μm in the shallowest part of the region beneath the forearc to a few cm in the hottest part of the mantle beneath the arc. Based on our preliminary modeling results, we find that aqueous fluids that migrate into the shallow fine-grain-size region become trapped in the down-going mantle due to low permeability and dragged downdip until permeability becomes high enough for the fluids to migrate upward. Thus, the grain size distribution can play an important role in controlling the location of hydrous melting by focusing the upward fluid migration. We plan to further develop our model by incorporating the effect of dynamic pressure gradients and accounting for the variation in fluid influx at the wedge base. Our modelling results will then be compared with the locations and degrees of hydrous melting inferred from geophysical and geochemical data for various arcs worldwide.

Metal-silicate partitioning of Mo and W at high pressures and temperatures: Applications to core formation on Earth and Mars

J. WADE[1] AND B. J. WOOD[2]

[1]Dept of Earth Sciences, University of Oxford, South Parks Rd, Oxford, OX1 3AN. (*Jon.Wade@earth.ox.ac.uk)
[2]Dept of Earth Sciences, University of Oxford, South Parks Rd, Oxford, OX1 3AN. (Bernie.Wood@earth.ox.ac.uk)

In order to place better constraints on the conditions of core formation on Earth and other terrestrial planetary bodies we have performed experiments to determine the partitioning of Mo and W between liquid Fe-rich metal and liquid silicate at pressures of 1.5-24 GPa and temperatures of 1803-2723K. Experiments performed in MgO capsules at 1.5 GPa/1923 K indicate that Mo is in the +4 oxidation state in the silicate at oxygen fugacities >2 log units below the IW (Fe-FeO) buffer. In contrast W^{6+} is the dominant tungsten oxidation state in the silicate at 1.9-3.2 log units below the IW buffer

Mo metal/silicate partitioning is strongly dependent on pressure and silicate melt composition, but temperature has no detectable effect. In contrast, we find that W partitioning is strongly dependent on silicate melt composition and temperature, but the role of pressure is minor.

Applying these and earlier results to the Earth and Mars indicates that the Mo content of the terrestrial mantle is consistent with core segregation at pressures of 20-40 GPa, in agreement with earlier work on Ni and Co partitioning. The Mo content of silicate Mars is about half that of silicate Earth and is consistent with much lower pressures of core formation (~11 GPa) on the smaller planet. In contrast to these results, the W content of silicate Mars (~50 ppb) is insensitive to conditions of core formation while that of silicate Earth (~12 ppb) is inconsistent with a single stage of core formation at any pressure. Since metal-silicate partitioning of W is strongly influenced by light element (S, Si, O) contents of the metal, we consider it likely that the “light” element in the core is largely responsible for the inconsistency in core-mantle partitioning of this element.

https://doi.org/10.1180/S0026461X00006502 Published online by Cambridge University Press

REE and stable isotope constraints on formation of metamorphic quartz veins: A case study from the Rhenish Massif (Germany)

T. WAGNER[1]*, A.J. BOYCE[2], J. ERZINGER[3]

[1]Geochemistry and Petrology, ETH Zurich, Switzerland (*correspondence: thomas.wagner@erdw.ethz.ch)
[2]Scottish Universities Environmental Research Center, Glasgow, UK
[3]GeoForschungsZentrum, Potsdam, Germany

We have investigated fluid-rock reactions during formation of metamorphic quartz veins in the fold-and-thrust belt of the Rhenish Massif (Germany). The veins record two assemblages that were formed in an evolving fluid-rock system, which are (1) massive vein filling (elongate-blocky quartz, chlorite, apatite, albite) and (2) open space filling (euhedral quartz crystals, carbonates, sulfides). We performed a detailed REE and stable isotope study of vein minerals, altered wall rocks and precursor host rock metapelites. The REE and oxygen isotope data of vein quartz and altered wall rocks, combined with mass balance analysis, support that local mobilization of material was dominant during formation of the early massive vein assemblage, but that contributions from advecting fluids were also important. The strong shift in K/Na ratios in altered wall rocks and model fluid temperatures that are higher (350-400 °C) than estimates for the host rocks point to substantial fluid advection. Formation of the veins can be explained by a crack-flow-seal model, with multiple repetition of vein opening, fluid advection and vein sealing events. Each cycle was initiated with vein opening, resulting in enhanced permeability and considerable fluid advection and hydrothermal alteration of wall rocks. Conditions during each cycle evolved towards a decrease in fluid advection, coupled with substantial diffusional leaching of silica and precipitation in the veins. The formation of the later open space filling assemblage records transition from an advection- to a diffusion-dominated regime. This is supported by vein mineral and fluid inclusion textures recording conditions of undisturbed mineral growth, fluid inclusion data that point to a thermally equilibrated state (150-200 °C), and stable isotope data that demonstrate a local source for the vein minerals.

From anoxia to oxic conditions in the aftermath of oceanic anoxic event 2 (Late Cretaceous)

M. WAGREICH

University of Vienna, Center for Earth Sciences, Althanstrasse 14, 1090 Vienna, Austria, (michael.wagreich@univie.ac.at)

Sections in the Ultrahelvetic units of the Eastern Alps (Austria) record oceanic anoxic event 2 (OAE 2) at the distal European continental margin of the western Tethys [1, 2]. Upper Cenomanian marl-limestone cycles are overlain by black, organic-rich (5% TOC, kerogen type II) layers, followed by Lower/Middle Turonian light grey to reddish marly limestones. Carbon isotope values display the well documented positive shift. The appearance of red-colored carbonates (CORB - Cretaceous Oceanic Red Beds) indicates a total time span of about 1.5 my for oxic bottom waters to become dominant. Orbital cycles of 400 kyr and 100 kyr frequencies are identified. Benthic foraminifera associations indicate repeated phases of enhanced organic matter flux and less aerated bottom waters during the transitional interval [3]. Sedimentation of red layers was controlled by periods of well oxygenated bottom waters, reduced sedimentation rates and degradation of organic matter in the underlying sediments. Principal component analysis of carbonate chemical data showed that the development of red coloured pelagic sediments is accompanied by a shift towards highly oligotrophic conditions in the surface ocean as well as a decrease in hydrothermal activity [4].

Higher up in the section, red limestone-marl cycles are present. Enhanced input of nutrient- like trace metals during episodes of higher volcanic activity is inferred, terrigeneous elements (Al, Li, Rb, Be) decrease upwards. Iron speciation data for marl and limestone layers attest to oxic early diagenesis during marl deposition compared to limestone episodes. Low sediment accumulation rates (2.5 mm/ka) are reconstructed. Geochemistry and stable isotope data indicate a highly oligotrophic environment with efficient recycling of organic matter and nutrients in the upper water column. Nutrient availability varied and resulted in periods of higher primary production. Iron oxides cause the red color in CORBs. The main fraction of iron in CORB sediments is fixed in silicate lattices and immobile.

[1] Neuhuber *et al*. (2007) *PPP* **251**, 222-238. [2] Wagreich *et al*. (2008) *Cret. Res*. **29**, 965-975. [3] Wendler *et al*. (2009) *SEPM Spec. Publ*. **91**, 209-221. Neuhuber & Wagreich (2011) *Sediment. Geol*. **235**, 72-78.

https://doi.org/10.1180/S0026461X00006502 Published online by Cambridge University Press

Uniform Os isotopic composition in early-formed planetesimals

R.J. WALKER

Dept. of Geology, University of Maryland, College Park, MD 20742, USA (rjwalker@umd.edu)

The isotopic compositions of some elements, such as W, Ru and Mo, vary among early-formed planetesimals. These variations likely reflect incorporation of different proportions of matter from diverse nucleosynthetic sources, and could be the result of accretion from a poorly mixed nebula, accretionary processes that favored isotopically distinct components, and/or late injection of isotopically diverse matter to the nascent Solar System. Constraints placed on the level of isotopic variability among early-formed planetesimals for additional elements with different chemical characteristics and nucleosynthetic origins may help to elucidate the dominant processes. Osmium is an important element to add to this list as it is one of the most refractory elements, yet is volatile in oxidized forms. Further, separate *s*- and *r*-process enriched components have been shown to exist in low metamorphic grade chondrites. Although, bulk chondrites show no measureable Os isotopic anomalies, early formed iron meteorites are also fertile hunting grounds. Isotopic anomalies for a number of elements are present in irons. For Os, certain irons from groups IAB, IIAB, IIIAB, IVA and IVB also show well resolved anomalies in ε^{190}Os, ε^{189}Os and ε^{186}Os$_i$. These anomalies, however, differ from anomalies observed in components extracted from chondrites, and are attributed to variable exposure of the irons to cosmic rays. Of note, each of the major iron groups contains at least one member with no resolved Os isotopic anomalies. We conclude that Os was homogeneously distributed on the scale of planetesimal accretion within the current level of resolution (~ ±5 ppm for ε^{190}Os). This contrasts with heterogeneity in other siderophile elements, such as W, Ru and Mo. Given that W and Os are similarly refractory, this may indicate that anomalies present for other elements in irons resulted from selective incorporation of mineralogic hosts, rather than large scale nebular heterogeneity.

Nuclear forensic analysis of trinitite at high spatial resolution

C.M. WALLACE*, A. SIMONETTI, AND P.C. BURNS

Department of Civil Engineering and Geological Sciences, University of Notre Dame, Notre Dame, IN 46556, USA (*correspondence: cwallac1@nd.edu)

The world's first atomic bomb, the Trinity "gadget" was detonated on July 16, 1945. The explosion resulted in partial melting of the surrounding desert sand, which subsequently fused into blast-melt glass known as trinitite. Recent investigations of trinitite have been conducted using a variety of analytical techniques, including EMPA, SEM, SIMS, XRF, and light microscopy [1,2]. This study includes preliminary results from optical microscopy, SEM, and laser ablation inductively coupled plasma mass spectrometry (LA-ICP-MS). Optical microscopy was used in order to "map" thin sections of trinitite and distinguish remnant crystalline grains and inclusions from the surrounding glassy matrix. SEM was conducted on samples prior to thin sectioning in order to image surface morphology. Quantitative spot analyses were subsequently performed via LA-ICP-MS in order to determine the trace element/radionuclide compositions of different phases. The LA-ICP-MS results to date confirm the "supergrade" nature of the plutonium and the presence of a natural uranium tamper in the Trinity device. In addition, plutonium-rich areas are characterized by higher REE abundances and correlate negatively with the fission product ^{137}Cs. Trace element abundances are extremely variable within individual crystal grains (hundreds of microns). The relationship between Pb isotope ratios and Pu abundances is somewhat ambiguous, i.e. they do not correlate positively in all of the trinitite phases. Future work will include isotopic analysis using a LA-multi-collector-ICP-MS instrument configuration.

[1] Fahey *et al*. (2010) *PNAS* **107**, 20207-20212. [2] Eby *et al*. (2010) *Geology Today* **26**, 180-185.

https://doi.org/10.1180/S0026461X00006502 Published online by Cambridge University Press

Incorporation of ^{90}Sr into alkaline altered sediments

S.H. WALLACE[1], S. SHAW[1], K. MORRIS[2], J.S. SMALL[3] AND I.T. BURKE[1]*

[1]School of Earth and Environment, University of Leeds, Leeds, UK (*correspondence: I.T.Burke@leeds.ac.uk)
[2]School of Earth, Atmospheric and Environmental Science, University of Manchester, Manchester, UK
[3]National Nuclear Laboratory, Risley, Warrington, UK

The use of cementitious materials is ubiquitous at nuclear facilities and in radioactive waste packaging. Water in contact with fresh cement produces a highly alkaline solution dominated by K and Na hydroxides causing localised areas of high pH groundwater at the concrete/soil interface. Silicate minerals within sediments and clay barrier materials are known to alter to zeolite and feldspathoid phases under these conditions. The effect of alkaline pore fluid induced weathering reactions on the mobility of radionuclides is not well understood, especially with respect to potentially highly soluble fission products such as ^{90}Sr (as Sr^{2+}).

Here we used 20 $g.L^{-1}$ batch experiments containing sediments representative of the UK Sellafield nuclear site in a pH 13.5 high ionic strength cement-based leachate to investigate Sr^{2+} sorption as a function of time. Experiments initially contained 20 ppm Sr^{2+} (spiked with 30 $Bq.mL^{-1}$ ^{90}Sr tracer) and were sampled from 2 days up to one year (one experiment was aged for one year at 70°C). Change in Sr speciation within sediments was determined using X-ray absorption spectroscopy and sequential extraction techniques.

At 2 days 72.6±8.6% ^{90}Sr was removed from solution, which rose to 93.8±3.3% at 10 days but then decreased to 81.8% after a year. In the 70°C aged sample sorption increased to 98.0±2.5%. This suggests that initial alteration enhances Sr sorption but further recrystallisation releases some sorbed Sr. Sequential extractions show that the majority (65-75%) of ^{90}Sr remains in the $MgCl_2$ exchangeable fraction even after one year. In the 70°C aged sample, 25.2±5.8% ^{90}Sr was found to be residual. EXAFS analysis revealed two Sr-O-Si(Al) bond distances at 3.69 and 3.84 in a 10 day sample and at 3.57 and 3.83 Å in a one year sample, consistent with weak Sr sorption to aluminosilicate phases. EXAFS spectra from a 70°C aged sample contain evidence for a single Sr-O-Si(Al) bond distance at 3.45 Å consistent with Sr incorporation in a neoformed feldspathoid phase such as cancrinite. These results indicate that alkaline altered sediments could be a sink for ^{90}Sr in the environment, however even after alteration ^{90}Sr may remain exchangeable with other ions in solution.

Reactive transport modelling to quantify arsenic mobilization and capture during aquifer storage and recovery of potable water

ILKA WALLIS[1,2], HENNING PROMMER[2,3], THOMAS PICHLER[4], VINCENT POST[1] AND CRAIG SIMMONS[1]

[1]Flinders University / NCGRT, South Australia
[2]CSIRO Land & Water, Australia
[3]University of Western Australia
[4]University of Bremen, Germany

Aquifer storage and recovery (ASR) is an artificial recharge technique which is increasingly used as a water management tool to augment depleted groundwater resources. ASR is a critical component of the long-term water supply plan in various regions, including Florida and Australia. However, under particular, site-specific conditions the viability of ASR as a safe and cost-effective water resource may be impacted by elevated arsenic concentrations that are detected during recovery of the injectant. This study describes a conceptual and process-based reactive transport model of the coupled physical and geochemical mechanisms controlling the fate of arsenic during ASR. The conceptual/numerical model assumes that (i) arsenic is initially released following pyrite oxidation triggered by the injection of oxygenated water (ii) then largely complexed to neo-formed hydrous ferric oxides before (iii) being released again during recovery as a result of both dissolution of hydrous ferric oxides and displacement from sorption sites by competing anions. Multi-cycle hydrochemical data from an affected site where oxic, potable water was injected into a reducing pyrite-containing storage zone were used to evaluate the model. For this site a detailed assessment of the partitioning of arsenic among mineral phases, surface complexes and aqueous phases during injection, storage and recovery is given, together with an evaluation of temporal and areal extent of arsenic mobilization and capture.

https://doi.org/10.1180/S0026461X00006502 Published online by Cambridge University Press

Physico-chemical and mineralogical transformations of fluid fine tailings (FFT) associated with the Alberta oil sands end pit lakes

G.E. WALSHE*, M. CHEN, E. CHI FRU AND C.G. WEISENER

GLIER, University of Windsor, Windsor, Ontario, Canada (gwalshe@uwindsor.ca; chen112h@uwindsor.ca; echifru@uwindsor.ca; weisener@uwindsor.ca)

Traditional methods used to extract bitumen involve caustic hot water digestion and flotation, which produce a fine tailing slurry consisting of water, sand, fines residual bitumen and naphtha products [1]. The current practice is to store the tailings in large settling basin to allow the solids to settle out by gravity forming a denser unconsolidated mass termed fluid fine tailings (FFT). To date little information exists on the biogeochemical nature of the newly processed FFT product prior to deposition and the evolution of the material during long term storage in settling basins.

Discussion and Results

During the development of the material significant changes in pore water geochemistry and the associated *in situ* development of AVS are observed, giving rise to the depostion of proto-iron sulfides (Fig. 1). The chemical evolution of porewater and head water was tracked over a period of 6 months. The significance of changes observed will be discussed in terms of the biotic versus physico-chemical processes.

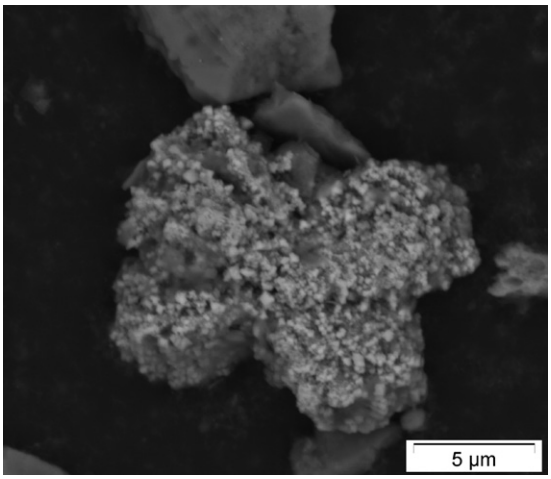

[1] Chalaturnyk et al. (2002) *Petroleum Science and Techonolgy,* **20,** 1025-1046

Highly oxidized species in TSR-altered oils

C.C. WALTERS[1]*, K. QIAN[1], C. WU[1], A.S. MENNITO[1], AND Z. WEI[2]

[1]Exxonmobil Research & Engineering, 1544 Route 22 East, Annandale, NJ 08801 (*correspondence: clifford.c.walters@exxonmobil.com)

[2]Exxonmobil Exploration Co., 233 Benmar, Houston TX 77060

Thermochemical sulfate reduction (TSR) involves a complex series of redox reaction that occur typically in hot (>120°C) carbonate reservoirs whereby petroleum is oxidized by sulfate forming H_2S, CO_2, and a sulfur-rich insoluble solid. It is well documented that oils altered by TSR are enriched in organosulfur species, primarily thiophenic, that form as a consequence of the primary sulfate reduction reaction and back reactions with produced H_2S or other low valance state sulfur species. In contrast, enrichment in partially oxidized hydrocarbons has not been reported in TSR-altered oils, which typically have low Total Acid Numbers (TAN < 0.2).

Oils from onshore Alabama were analyzed by negative ion electrospray ionization Fourier transform ion cyclotron resonance mass spectrometry (NESI-FTICR-MS). The suite includes oils at varying extent of TSR-alteration as well as oils of equivalent thermal maturity that have not subjected to TSR-alteration. Although the total amount of oxygen species is low in all samples, their relative distribution varies in a systematic manner. With increasing extent of TSR, 1O and 2O species, which dominate unaltered oils, are replaced with species containing additional oxygen atoms. Hydrocarbons and organosulfur species with 5 to 8 oxygen atoms are detected only in the most TSR-altered oils.

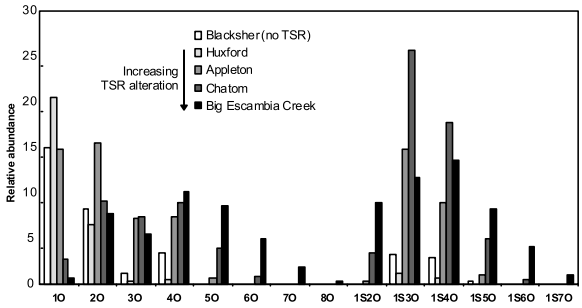

The distributions of the Ox and SOx species appears to accurately reflects the extent of TSR and are particularly useful in deciphering the geohistory of reservoirs where H_2S and light hydrocarbons have migrated in from off-structure.

https://doi.org/10.1180/S0026461X00006502 Published online by Cambridge University Press

The evolution dynamics of chemical mantle reservoirs – 3D numerical results

U. WALZER[1]* AND R. HENDEL[2]

[1]Institut für Geowissenschaften, Friedrich-Schiller-Universität Jena, Humboldtstr. 11, 07743 Jena, Germany (*correspondence: u.walzer@uni-jena.de)

[2]Institut für Geowissenschaften, Friedrich-Schiller-Universität Jena, Humboldtstr. 11, 07743 Jena, Germany (roland.hendel@uni-jena.de)

A dynamic 3-D spherical-shell model for the chemical evolution of the Earth's mantle is presented. Chemical differentiation, convection, stirring, and thermal evolution constitute an inseparable dynamic system. Our model is based on the solution of the balance equations of mass, momentum, energy, angular momentum, and four sums of the number of atoms of the pairs ^{238}U-^{206}Pb, ^{235}U-^{207}Pb, ^{232}Th-^{208}Pb, and ^{40}K-^{40}Ar. Similar to the present model, the continental crust of the real Earth was not produced entirely at the start of the evolution but developed episodically in batches. The details of the continental distribution of the model are largely stochastic, but the spectral properties are quite similar to the present real Earth. Some preliminary results have been published in [1]. The modeled present-day mantle has no chemical stratification but we find a marble-cake structure. If we compare the observational results of the present-day proportion of depleted MORB mantle with the model then we find a similar order of magnitude. The MORB source dominates under the lithosphere. In our model, there are nowhere pure unblended reservoirs in the mantle. It is, however, remarkable that, in spite of 4500 Ma of solid-state mantle convection, certain strong concentrations of distributed chemical reservoirs continue to persist in certain volumes, although without sharp abundance boundaries. It is interesting to compare these results with the survival of primitive blobs in the lower mantle proposed by Becker *et al*. [2]. Finally we present results regarding the numerical method, implementation, scalability and performance.

[1] U. Walzer and R. Hendel. Mantle convection and evolution with growing continents. *J. Geophys. Res.* **113**:B09405, doi:10.1029/2007JB005459, 2008. [2] T. W. Becker, J. B. Kellogg, and R. J. O'Connell. Thermal constraints on the survival of primitive blobs in the lower mantle. *Earth Planet. Sci. Lett.* **171**:351–365, 1999

Wettability alteration upon reaction with $scCO_2$: Pore scale visualization and contact angle measurements

JIAMIN WAN*, YONGMAN KIM AND JONGWON JUNG

Earth Sciences Division, Lawrence Berkeley National Laboratory, Berkeley, CA, 94720 USA (jwan@lbl.gov, ymkim@lbl.gov, jjung@lbl.gov)

The interfacial forces among reservoir mineral substrates, brine and supercritical (sc) CO_2 can greatly affect the distribution of $scCO_2$ injected in geological formations for its sequestration. When brine and $scCO_2$ contact with a substrate, the equilibrium configuration among the three interfacial tensions determines the wetting property (contact angle) of the substrate. The contact angle together with the pore size distribution determines the distribution of capillary entry pressures for porous media. Therefore, contact angles in the mineral-brine-$scCO_2$ system control the pore-scale advance of the $scCO_2$-brine interface during injection, structure trapping of CO_2 at reservoir-caprock boundaries, and residual trapping of $scCO_2$ at later stages of geologic sequestration. The wetting behavior of $scCO_2$ in contact with caprocks is especially important because it is a primary factor controlling CO_2 leakage from reservoirs to the land surface and atmosphere. Although CO_2 is commonly assumed to be the non-wetting phase in the current predictive models for CO_2 storage capacity, recent studies have begun to show that the wettability of caprock minerals can be altered in the presence of $scCO_2$ under pressures and temperatures representative of geological storage conditions. Understanding is critically needed on how and to what degrees chemical reactions and physical processes in the deep reservoirs affect the wetting properties of rock surface. Such understanding will enable more reliable estimates of CO_2 residual saturations and capillary threshold pressures needed for predicting larger scale system behavior.

We studied silica wettability alteration within single pores containing brine and $scCO_2$ under flow conditions, using engineered transparent micromodels. The process of $scCO_2$ injection into an initially brine saturated silica porous network (pore throat and body sizes are 30 and 120 μm, respectively) was conducted under controlled P and T. We observed (1) the CO_2 phase entering pores, displacing brine, and leaving initially smooth brine films coating silica pore walls with the contact angle θ close to zero, and (2) over longer times (CO_2 diffused into brine films), the brine films contracted into small brine-droplets as a result of decreased wettability (increased θ). At steady state, the θ values of these brine-droplets are 49° ±10° for the 1.0 M, and 70° ±7° for 5.0 M NaCl. We hypothesize that neutralization of the silica surfaces resulting from brine film acidification by CO_2 is responsible for the observed wettability alteration.

https://doi.org/10.1180/S0026461X00006502 Published online by Cambridge University Press

Quantifying electron flow in the sulfidation of lepidocrocite

M. WAN[1], C. SCHRÖDER[1,2] AND S. PEIFFER[1,*]

[1]Department of Hydrology, University of Bayreuth, Bayreuth Germany (moli.wan@uni-bayreuth.de; *correspondence: s.peiffer@uni-bayreuth.de)
[2]Center for Applied Geoscience, Eberhard Karls University, Tübingen, Germany

The interaction between sulfide and ferric (oxyhydr)oxides exerts control on electron flow and ultimately the sulfur cycle in many anoxic groundwater, soil and marine systems. In most situations it leads to pyrite formation, the pathway still being researched [e.g. 1]. To identify the intermediate products and to quantify the electron flow during the reaction we used Mössbauer spectroscopy, TEM, wet chemsitry analyses and a novel technique to determine polysulfides.

We reacted synthetic lepidocrocite enriched in the Mössbauer-sensitive isotope ^{57}Fe and dissolved sulfide at neutral pH in an anoxic glove box. The solid fraction was extraced at different time steps (15 min, 2hrs, 48 hrs, 72 hrs and one week), frozen and analyzed with Mössbauer spectroscopy. Both iron and sulfur species were measured with wet chemistry analysis methods in parallel runs. Polysulfides were derived with Trifluoromethanesulfonate and measured by HPLC with UV-Dector.

Mössbauer spectra showed the formation of pyrite after 48 hrs. Mackinawite and magnetite were identified as intermediate products and confirmed TEM observations by Hellige *et al*. [1]. The spectra also provided evidence for Fe-deficient FeS phases such as pyrrhotite. Wet chemistry analysis shows polysulfides form in the first few minutes, accompanying with the formation of elemental sulfur. Most of them are surface associated. With the knowledge on the distribution of Fe between its oxidation states, mineral phases and dissolved species and the determination of polysulfides we can quantify the electron flow along the reaction path to pyrite formation.

[1] Hellige *et al*. (2011) *Geochim. Cosmochim. Acta* in review.

A thermogravimetric study of thermally treated silica nanoparticles

QUAN WAN[1]*, YI XIAO[1] AND GEORGE BARAN[2]*

[1]Institute of Geochemistry, Chinese Academy of Sciences, Guiyang, Guizhou, 550002, P.R. China (*correspondence: wanquan@vip.gyig.ac.cn, grbaran@temple.edu)
[2]College of Engineering, Temple University, Philadelphia, Pennsylvania 19122, USA

Silica is the most abundant mineral in the earth's crust. The surface chemistry of silica often plays a critical role in many earth processes, for example weathering of rocks. When the size of silica particles approaches the nanoscale or when they contain nanoscale pores, the surface area of the silica particles increases dramatically and this can fundamentally affect several properties of interest. Using a combination of dehydration (heating 2hrs at 200°C), dehydroxylation (heating 2hrs at 400, 600 or 800°C) and rehydroxylation (boiling overnight in water), we thermally treated three different types of silica particles, *i.e*. AA-05 (spherical , diameter ~ 500 nm) synthesized via the Stöber process, N-2329 (spherical , diameter ~ 75 nm) synthesized through water glass route, and V-258 (irregular, median size ~700 nm) ground glass [1]. Samples were characterized by thermogravimetric analysis (TGA), pycnometry, elemental analysis and scanning electron microscopy (SEM). We found that heating 2hrs at 200°C removed physically absorbed water, while heating at higher temperature incrementally removed surface silanol groups. Boiling overnight in water resulted in partial recovery of silanol groups. However dehydroxylation became irreversible for samples treated at over 400°C inconsistent with the Zhuravlev model [2]. Our results also indicated that AA-05 Stöber silica was nanoporous with a lower density (1.9 g/cm^3) than that (2.2 g/cm^3) of the fully condensed N-2329 which was obtained through the water glass route. The considerable carbon content (~ 2wt%) in AA-05 was also consistent with incomplete condensation during Stöber synthesis. Both AA-05 and N-2329 showed better thermal stability than did V-258, which melted at 800°C. The increased density of AA-05 after treatment at 600 and 800°C suggested that the nanopores in Stöber silica begin to collapse at 600°C.

[1] Wan *et al*. (2010) J Therm Anal Calorim **99,** 237-243. [2] Zhuravlev (2000) *Colloid Surface A* **173**, 1-38.

https://doi.org/10.1180/S0026461X00006502 Published online by Cambridge University Press

Carbon biogeochemical cycle in the impounded Wujiang River, China

B. WANG[1,*], C. Q. LIU[1] AND F. WANG[2]

[1]Chinese Acad Sci, Inst Geochem, State Key Lab Environm Geochem, Guiyang 550002, Peoples R China (*correspondence: baoliwang@163.com) (liucongqiang@vip.skleg.cn)

[2]Shanghai Univ, Sch Environm & Chem Engn, Inst Appl Radiat, Shanghai 201800, Peoples R China (fswang@shu.edu.cn)

Wujiang River is a major hydropower source for China□s massive West-to-East Power Transmission Project. A series of reservoirs were constructed along it and now it becomes a typical impounded river. We have seasonally determined the $\delta^{13}C$ values of dissolved inorganic carbon (DIC), particulate organic carbon (POC), and phytoplanktonic carbon (PPC), and related hydro-chemical parameters to understand the carbon biogeochemical cycle in the impounded Wujiang River.

Soil organic matter and aquatic phytoplankton are the possible contributors of riverine POC. $\delta^{13}C_{PPC}$ showed a perfect linear relationship with $\delta^{13}C_{POC}$, suggesting that POC was mainly derived from phytoplankton. With the development of reservoir after damming, riverine heterotrophic ecosystem is transformed to autotrophic one, and phytoplankton becomes the dominant contributor of POC. pH values in the reservoir waters were generally larger than 8, indicating a predominance of bicarbonate in DIC. HCO_3^- concentrations decreased while the $\delta^{13}C_{DIC}$ and $\delta^{13}C_{POC}$ increased in the surface water of the reservoirs. And with the increase of phytoplanktonic biomass, algae assimilate more inorganic carbon and thereby exhibit more positive $\delta^{13}C$ value. So, photosynthesis is one of the main processes that affect $\delta^{13}C_{DIC}$ and $\delta^{13}C_{POC}$ in the surface water. Compared to the surface water before dam, DIC in release water showed the deficit in ^{13}C when thermal stratification developed. Release water is from deep water of reservoir and $\delta^{13}C_{DIC}$ values decrease with water depth as photosynthesis declines and respiration increase. Thus, respiration, which makes the DIC pool enriched in ^{12}C, is the other main process affecting $\delta^{13}C_{DIC}$ in the reservoirs. Compared to DIC, POC showed larger fluctuations in $\delta^{13}C$ values because phytoplankton had more influences on $\delta^{13}C_{POC}$ than that on $\delta^{13}C_{DIC}$ during the transformation of inorganic carbon into organic carbon. Our results demonstrated that river damming has important impacts on riverine carbon biogeochemical cycling.

Multiple generations of granitic magma in the West Kunlun, NW China: Implications for crustal melting and mantle-crust interaction at an active continental margin

C. WANG[1,2]*, L. LIU[2], W.Q. YANG[2], Y.T. CAO[2], R.S. LI[1] AND S.P. HE[1]

[1]Xi'an Center of Geological Survey, China Geological Survey, Xi'an 710054, P R China (*correspondence: wangc-mail@163.com)

[2]State Key Laboratory of Continental Dynamics, Department of Geology, Northwest University, Xi'an 710069, P R China

Active margins along accretionary orogens are considered to be major sites of the formation of juvenile continental crust [1], but subduction processes also produce crustal recycling and differentiation rather than growth [2]. West Kunlun is a large accretionary orogen formed by long-standing subduction, arc-continent collision and closure of Paleo-Tethys between the south margin of the Tarim Block and western portion of the Himalayan-Tibetan orogen from the early Paleozoic to the early Mesozoic. Two major granitoid belts based on geochronology data were identified, the early Paleozoic suite and the early Mesozoic suite. Mafic magmatic enclaves are abundant in most of these granitoids. There is a strong mantle component to these rocks, and imply production of the rock series has involved mixing between mantle and crustal magma components. The source characterstics of granites and zircon Hf isotope characteristics indicated that the West Kunlun granitic magma was formed on the base of continental crust. Recycling of older continental crust, and of Mesoproterozoic crust in particular, appears to be an important process in the evolution of the orogenic continental crust of West Kunlun between early Paleozoic and Mesozoic. There is not of pronounced new crust formed and formation of the West Kunlun orogen in the outboard of the ancient Tarim margin related with Paleo-Tethys subduction. Such processes may represent an advancing orogen.

This work is supported by the National Science Foundation of China (Grant No.40902022, 40972128) and Natural Science Foundation of Shannxi Province, China (Grant No. 2010JM5007)

[1] Condie (2007). *GSAM* 200, 145-158. [2] Plank (2005). *J. Petrol*. 46, 921-944.

https://doi.org/10.1180/S0026461X00006502 Published online by Cambridge University Press

13α(*n*-alkyl)-tricyclic terpanes: A series of biomarkers for the unique microbial mat ecosystem in the middle Mesoproterozoic (1.45~1.30Gyr) North China Sea

C. WANG*, M. WANG, J. XU, Y. LI, Y. YU, J. BAI, T. DONG, X. ZHANG, X. XIONG AND H. GAI

State Key Laboratory of Oil Science and Prospecting, China Univ. of Petroleum, Beijing, 102249, China (*correspondence: wchj333@126.com)

Anoxygenic photosynthesis may have modulated Proterozoic oxygen production and sustained an intermediate redox state in the oceans for the Earth's middle age [1, 2]. A special biomarker assembly indicates that a unique prokaryotic microbial mat ecosystem may have contributed to the major primary production in the middle Mesoproterozoic (1.45~1.30Gyr) North China sea [3]. However, we know little about the microbial structures of the Mesoproterozoic microbial mats. Here, we report for the first time that the series of 13α(n-alkyl)-tricyclic terpanes (C_{18}~C_{33}) (13αNATTs) occurs in the organic-rich shales from this middle Mesoproterozoic sequence, including Hongshuizhuang Fm, Tieling Fm and Xiamaling Fm. We infer the long straight-chain substitution (up to C_{15}) in 13αNATTs to be originally of n-alkyl-substituted chain, while not of demethylated isoprenoid chain [4]. This scenario is probably just like that of hopanes. Thus, 13αNATTs may have originated from prokaryotes, given the robust evidence of steranes being undetectable in the shales [3].

The fact that 13αNATTs have not been detected from the post-Mesoproterozoic sedimentary sequences in China, may suggest that 13αNATTs could be a unique series of biomarkers for some special Mesoproterozoic prokaryotes, which probably disappeared from the late geological record. The remaining key question is to reveal what kinds of prokaryotes may have contributed to 13αNATTs?

[1] Johnston *et al*. (2009) *PNAS* **106**, 16925–16929. [2] Lyons *et al*. (2009) *PNAS* **106**, 18045–18046. [3] Wang (2010) *GCA* **74**, A1099-A1099. [4] Wang and Simoneit (1995) *Chem. Geol*. **120**, 155–170.

Phase equilibrium of the Cd-bearing quaternary reciprocal system at 298 K

WANG CHUNLEI[1], HUANG YI[1,2]*, ZOU FANG[1] AND NI SHIJUN[1,2]

[1]Department of Geochemistry, Chengdu University of Technology, Sichuan, PRC (*correspondence: huangyi@cdut.cn)

[2]Applied Nuclear technigues in Groscience Key Laboratory of Sichuan Proviance, PRC

Solid-Liquid Equilibrium of reciprocal quaternary system K^+, Cd^{2+}//Cl^-, SO_4^{2-}-H_2O at 298 K were studied by an isothermal solution saturation method. Experimental results indicate that there are seven univariant curves F_2E_2, F_4E_2, E_2E_1, F_3E_1, E_1E_3, F_5E_3, F_1E_3, three invariant point: : E_1, E_2 and E_3 and five crystallization fields in the reciprocal quaternary system. There is double salt $Cd_3KCl_7{\cdot}4H_2O$ existing in the reciprocal quaternary system. The crystallization zones of equilibrium solid phases are K_2SO_4 ($F_2E_2F_4$), KCl ($F_4E_2E_1F_3$), $CdCl_2{\cdot}H_2O$ ($F_5E_3F_1$), $Cd_3KCl_7{\cdot}4H_2O$ ($F_3E_1E_3F_5$), $3CdSO_4{\cdot}8H_2O$ ($F_1E_3E_1E_2F_2$), respectively. The point E_1 represents the equilibrium of three solid phase KCl, $Cd_3KCl_7{\cdot}4H_2O$, and $3CdSO_4{\cdot}8H_2O$. The eutectic point E_2 represents the equilibrium of three solid phase K_2SO_4, KCl and $3CdSO_4{\cdot}8H_2O$. The other eutectic point E_3 represents the equilibrium of three solid phase $Cd_3KCl_7{\cdot}4H_2O$, $CdCl_2{\cdot}H_2O$ and $3CdSO_4{\cdot}8H_2O$. Potassium Sulfate has the biggest crystallization fieldwhile Cadmium Chlorine has a smaller crystallization region than others.

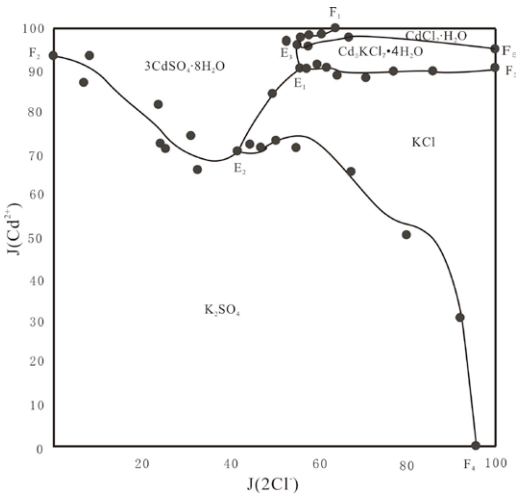

https://doi.org/10.1180/S0026461X00006502 Published online by Cambridge University Press

Integrated development and management of water resources: A typical area in China

DONG WANG[1]*, JICHUN WU[1], LACHUN WANG [2] AND YUN LIANG SHI

[1]Department of Hydrosciences, School of Earth Sciences and Engineering, State Key Laboratory of Pollution Control and Resource Reuse, Nanjing University, Nanjing 210093, China (*correspondence: wangdong@nju.edu.cn)

[2]School of Geographic and Oceanographic Sciences, Nanjing University, Nanjing 210093, China

It is unfortunate that problems with water are considered to grow worse in the coming decades. Water Scarcity is one of the most pervasive problems afflicting people throughout the world. According to the World Water Council, human beings have access to less than eight-tenths of one percent of the total water on our blue planet.Although freshwater is a renewable natural resource, its circulation rate is determined by climate system, human activities, etc., and there is an upper limit to the volume of freshwater natural resource.

More intense droughts in the past decade, affecting an increasing number of people, have been linked to higher temperatures and decreased precipitation, but are also frequently a consequence of the misunderstanding of water resources. The increased exposure to potential hazards has led to more awareness of intergraded groundwater and surfacewater development and management, especially in Karst area, which have complicated hydrologic and hydrogeologic conditions.

Houzhai Catchment is a typical Karst area in Guizhou Province in the southwest of China. A conceptual Karst streamflow model is established, whose parameters are calibrated and determined by Genetic Algorithm. According to three indexes (Relative Error, Cross-correlation Coefficient and Deterministic Coefficient), the results show that the proposed model can simulate and forecast the special runoff yield and flow concentration process of this typical Karst area, which is useful to improve the evaluation method and promote growing awareness of the need for properly integrated development and management of water resources.

This study was supported by the National Natural Science Fund of China (No. 41071018, 41030746, 40725010, and 40730635), the Skeleton Young Teachers Program and Excellent Disciplines Leaders in Midlife-Youth Program of Nanjing University.

Effects of soil environment on activity of rare earth elements: Implications for land utilization

D.Y. WANG[1], Y.F. LI[1], Y. Y. YANG[1], Y. SHANG [2] AND M. WANG [1]

[1]College of Earth Sciences, Jilin University, Changchun 130061, China (wang_dy@jlu.edu.cn, yfli@jlu.edu.cn, yyyang10@mails.jlu.edu.cn, wangmeng880716@163.com)

[2]Land Surveying and Mapping Institute of Shandong Province, Jinan 250013, China (rulyshang@yahoo.com.cn)

Rare earth elements (REEs), as an agent for increasing products, have been widely used in agricultural processes. However, how do the soil environments affect the activity of REEs in the soil? It is one of the hotly-discussed issues in the land utilization. This paper reports the total REE contents of 40 surface soil samples and available REE contents of 20 samples from the Yanbian region in the eastern Jilin Province, NE China analyzed using ICP-MS. The total REE contents range from 95.7 to 266 ppm, yielding a weighted mean value of 150 ppm, which is lower than the average REE content (187 ppm) of soil in China. The available REE contents for 20 samples vary from 18.5 to 118 ppm, yielding a weighted average value of 56.8 ppm. The average REE activity indexes in the soil, i.e., available REE contents/total REE contents, are between 23.2% and 46.5% (average 37.9%). Correlation analyses done by SPSS software indicate that the total and available contents of Yb and Lu exhibit evidently positive correlations while these of other REE have extremely remarkable positive correlations. The activity indexes of Y, Sm, Gd, Er, Tm, Yb, and Lu show evidently positive correlations with pH values in soil. Additionally, the difference of REE activity indexes between different types of soils also occurs. Compared with the similar studies of Hainan province, southern China where the climatope, soil type and soil physical and chemical properties are different from the Yanbian area, REE activity index in the soils from NE China is evidently low, suggesting that the climatope, soil type, and soil physical and chemical properties have important affects on REE activity in soil. Therefore, it is of important implications for scientifically using land, protecting soil environment, and maintaining agro-ecosystems to understand and utilize relationship between soil environment and REE activation in them.

https://doi.org/10.1180/S0026461X00006502 Published online by Cambridge University Press

Late Triassic bimodal magmatism in the Lesser Xing'an-Zhangguangcai Range, NE China: Constraints on the timing of transformation of Paleo-Asian ocean into circum-Pacific ocean tectonic systems

F. WANG, W.L. XU *, E. MENG, F.H. GAO AND H.H. CAO

College of Earth Sciences, Jilin University, Changchun 130061, China (jlu-wangfeng@sohu.com; *correspondence: xuwl@jlu.edu.cn)

The Lesser Xing'an-Zhangguangcai Range, NE China, is located in the eastern section of Central Asian Orogenic Belt (CAOB) [1]. Geochronological and geochemical data of Triassic igneous rocks from the region provide constraints on the timing of the transformation of the Paleo-Asian tectonic system into the circum-Pacific system. LA-ICP-MS and SIMS zircon U-Pb dating results for two basalts, one gabbro, two rhyolites, and one dacite indicate that they formed during the Late Triassic (208-228 Ma). The mafic rocks have SiO_2 = 48.97-51.89 wt.%, TFe_2O_3 = 7.86-10.13 wt.%, K_2O = 1.05-1.72 wt.%, Mg# [Mg/(Mg+Fe^{2+})] = 0.54-0.63, Cr=107-405 ppm, Ni=44-102 ppm, whereas felsic rocks have SiO_2 = 73.60-75.69 wt.%, TFe_2O_3 = 0.69-1.19 wt.%, K_2O = 4.10-4.36 wt.%, Mg# = 0.05-0.23, suggesting a typical bimodal igneous association. In addition, these mafic rocks are characterized by enrichment in LREEs and LILEs, depletion in HREEs and HFSEs (such as Nb, Ta, Ti), and weak Eu anomalies (0.87-1.05), whereas felsic rocks exhibit strongly depletion in Sr, P, Ti, enrichment in Th, U, K, and relatively obvious negative Eu anomalies (0.61-0.65). The above findings, combined with the coeval A-type rhyolites in eastern Heilongjiang and Jilin provinces [2], imply that they formed under a post-collisional extensional envirnment related to the final collision between the North China Craon and the Siberia Craton in the Late Permian and/or Early Triassic. Meanwhile, this finding also suggests that the subduction of the Paleo-Pacific plate beneath the Eurasian continent could took place after the Late Triassic.

This research was financially supported by research grants from the Natural Science Foundation of China (Grant 41072038) and the Geological Survey of China (Grants 1212010070301 and 1212010611806).

[1] Sengör *et al*. (1993) *Nature* **364**, 299–307. [2] Xu *et al*. (2009) *J. Asian Earth Sci*. **34**, 392–402.

Genetic and functional properties of uncultivated Miscellaneous Crenarchaeota Group (MCG): Implication from the metagenome analysis

FENGPING WANG[1]*, JUN MENG[2], YANPING ZHENG[1,2], DAN QIN[2,], JUN XU[1] AND XIANG XIAO[1],

[1]State Key Laboratory of Microbial Metabolism and State Key Laboratory of Ocean Engineering, Shanghai JiaoTong University, Shanghai, 200240, People's Republic of China (*correspondence: fengpingw@sjtu.edu.cn)

[2]The School of life science, Xiamen University, 361005, People's Republic of China

The MCG Archaea is one of the most predominant Archaeal groups in various environments. Till present, no member of MCG has been cultivated or characterized, and its ecological roles and evolutionary position remain obscure. Within this study, the genetic potential and physiology of MCG and its evolutionary relationship with other archaeal members were analyzed and inferred based on metagenomic analysis. Comparisons of gene organizations and similarities around the 16S rRNA genes of available MCG Fosmid and Cosmid clones found completely no synteny, demonstrated big genetic variations within groups of MCG. A topoisomerases IB gene (TopIB) was found in a MCG Fosmid genome fragment, TopIB phylogenetic analysis placed MCG within the newly postulated archaeal Phylum-Thaumarchaeota. Functions of some genes on the genome fragment were tested by in-vitro expression. Gene involved in protocatechuate degradation and chemotaxis were found in a genome fragment, suggesting a role of this group of archaea in protocatechuate degradation. The up-expression of 4-carboxymuconolactone decarboxylases was observed when the sediment was amended with protocatechuate, further supporting the idea of MCG group as protocatechuate degrader.

https://doi.org/10.1180/S0026461X00006502 Published online by Cambridge University Press

Study on diagenetic environments of calcite veins hosted in marine carbonate rock in middle Yangtze region of Southern China

WANG FURONG[1,2], HE SHENG[1,2] AND YANG XINGYE[2]

[1]Key Laboratory of Tectonics and Petroleum Resources Ministry if Education, China University of Geosciences, Wuhan 430074, China
[2]Faculty of Earth Resources, China University of Geosciences, Wuhan 430074, China

Thin slices suggest that calcite veins hosted in marine carbonate rock of appearing locating in middle Yangtze region of southern China develop two crystal forms including radiaxial calcite and isometric structure calcite in Triassic, and isometric structure calcite can be identified of calcite veins in Permian and Ordovician. And some calcite veins develop double-crystal pattern.

Cathodeluminescence document that different structure calcite veins show different luminous intensity in Triassic which can identified three periods of calcite veins, and luminous intensity has no different between calcite veins and surrouding rocks in Permian and Ordovician with medium orange to dark light.

Carbon-oxygen isotopes of calcite veins show that The range of $\delta^{13}C$ is -6.76 ‰ ~ 4.01‰(PDB), $\delta^{18}O$ is -17.95‰ ~ -5.67‰(PDB) in calcite veins, which indicates that calcite veins deposit in marine phreatic environment and mixing phreatic environment. Calcite veins in Triassic are sedimentary origin, and part of calcite veins in Permian and Ordovician suffer latter diagenesitc fluid dissolution. Fluid generating from organic-matter maturation effect the information of calcite veins in Permian to some degree.

Tectonothermal evolution of the Triassic flysch in the Songpan-Garzê orogen, Eastern Tibetan plateau

H. WANG[1], M. RAHN[2], J. ZHOU[3], X. TAO[4]

[1]School of Earth and Space Sciences, Peking University, China (*correspondence: hjwang@pku.edu.cn)
[2]Swiss Federal Nuclear Safety Inspectorate (ENSI), 5200 Brugg, Switzerland
[3]Chinese Academy of Geological Sciences, China
[4]College of Earth Sciences, Chengdu University of Technology, China

Low temperature metamorphic indicators give an insight into the tectonothermal evolution of the Triassic flysches in the Songpan-Garzê orogen, eastern Tibetan plateau. The Triassic flysches experienced large-scale folding, faulting and a thermal overprint from diagenesis to lower greenschist facies. Maximum metamorphic conditions were 380 ± 25ºC and low to intermediate pressures. Iso-thermal zones mapped with illite crystallinity (IC) describe following relationships between thermal zones and fold axes, faults and strata boundaries: i) anchizonal boundaries run across strata boundaries and fold axes indicating the main folding of the flysches occurred prior to metamorphism; ii) large-scale faults make boundary offsets in thermal zones suggesting the structural movement along the Longmenshan (LMS) and the Xianshuihe faults took place after low grade metamorphism.

From NW to SE, the Triassic flysches in the Songpan-Garzê orogen show a complex pattern. From this pattern a general increase in grade towards the LMS fault belt and across the LMS fault belt, greenschist facies rocks on its NW side are juxtaposed to diagenetic rocks in the Sichuan basin on its SE side. This juxtaposition is marked by IC jumps of 0.23ºΔ2θ in SW of LMS, 0.40ºΔ2θ in the Middle and 0.66ºΔ2θ in NE of LMS. Across the Xianshuihe fault, the truncated IC zones within the flysches suggest a total offset of roughly 60 km due to post-metamorphic sinistral strike-slip.

Compression at the end of the Triassic induced by the interaction of the South China, North China and the North Tibetan blocks caused the closure of the Paleotethys ocean and led to folding of the flysches within the Songpan-Garzê basin. Very low to low grade metamorphism may have been caused by the increase in thermal gradient due to large-scale magmatic activity in the Jurassic. FT ages reveal Early to mid-Cretaceous exhumation. Finally the India–Asia collision caused the formation of the Longmenshan fault and the Xianshuihe strike-slip fault in the early Tertiary and disturbed the distribution of metamorphic zones.

https://doi.org/10.1180/S0026461X00006502 Published online by Cambridge University Press

3.84 Ga crustal material in Dunhuang Block, Gansu Provence, China

HONG-LIANG WANG,XUE-YI XU ,TAO ZHU, TING LI AND ZHI-PEI LI

Xi'an Center of Geological Survey (Xi'an Institute of Geology and Mineral Resource), CGS, Xi'an,shaanxi 710054, China

Crustal materials formed in the early period of solid earth (≥3.8Ga) are few reserved in the world. We get magma crystallization age 3841±16 Ma from metamorphic amphobolite of Dunhuang block rock recently (Fig. 1, Table.1), which is the oldest crustal material had been detected in Dunhuang block, and early earth material found in metamorphic basic volcanics is also rare in the world yet. This metamorphic basic volcanics belong to sub-alkaline volcanics and tholeiite series with $SiO_2 = 47.94\times10^{-2} \sim 49.32\times10^{-2}$. We also get metamorphic zircon ages of ~3.5Ga and 3.3Ga, consistent with previous Sm-Nd age 3487Ma. It indicates that Archean basement exist in Dunhuang block. This new result has important significance for exploreing and studyting the age、properties and growth characteristic, and developing comparison study between Dunhuang block and Huabei craton.

Figure 1: CL images and ages of zircons for amphibolite of Dunhuang rock group

Samp.	$^{207}Pb/^{206}Pb$	1σ	$^{207}Pb/^{235}U$	1σ	$^{206}Pb/^{238}U$	1σ
23	3841	16	3842	6	3845	17
24	3820	15	3608	65	3240	14
16	3496	16	3311	6	3015	13
34	3332	17	3332	7	3331	16

Table 1: older zircon U-Pb data for amphibolite from Dunhuang rock group(Ma)

This study was supported by China territorial resources survey project (No.1212010610319) and the National Natural Science Foundation of China (No.40773044).

Implications of fault spilling gases in searching active ruptures

HUALIN WANG[1], GUODONG ZHENG[2], JIQIANG WANG[1], CHAO HU[1] AND XIA LIU[1]

[1]Shandong Institute of Seismic Engineering, Jinan 250021, China

[2]Key Laboratory of Petroleum Resources Research, Institute of Geology and Geophysics, CAS, Lanzhou 730000, China

The seeped gases as called as fault spilling gases may contain abundant information about the geological processes in the deep Earth, and also be significant in searching and studying on the spatial distribution and activity of faults. In this paper, a systematic study was performed on the Yishu tectonic zone, the Haiyuan tectonic zone for an Ms8.5 earthquake in 1920, the Tancheng tectonic zone for an Ms8.5 earthquake in 1668, the Xanshuihe tectonic zone, and several active faults in the Shandong flatlands and some major results were summarized as the followings.

1, the concentration of Rn and Hg and their variation degree of fault spilled gas could be used as sensitive index to evaluate the activity of faults connection. Higher concentration of Rn and lower Hg may indicated stronger stress accumulation and poorer connection of faults, lower concentration of Rn and higher Hg may indicated lower stress accumulation and better connection of faults, and lower concentrations of both Rn and Hg may indicate poorer stress accumulation and poorer connection of faults.

2, the measurement of fault spilled gas has been implied well in searching active faults in the flatlands area. The Rn measurement of fault spilled gas combined with engineering drilling profiles to the Yidu fault zone, the Shuangshan-Lijiazhuang fault zone, and the Heze fault zone for the Ms7.0 earthquake in 1937 was successful to identify all the locations and displacement of faults, and their activity times.

3, the measurement of fault spilled gas can be also used well in the geometric and kinetic studies of faults. The structural pivot area, the pull-apart area and the compression area of strike-slip faults could be located according to the distribution pattern of geochemical surroundings from the measurement of fault spilled gas, which may supply a fast and simple method to study on the geometric and kinetic properties of faults and used successfully to the Haiyuan seismic fault zone and the Xianshuihe fault zone.

https://doi.org/10.1180/S0026461X00006502 Published online by Cambridge University Press

Assessment of heavy metal pollutions from lead-zinc mining activities in the North River Basin, China

J. WANG[1], J. LIU[1], Y.H. CHEN[1]*, T.F. XIAO[2], C.L. WANG[3], X.P. LI[1] AND J.Y. QI[4]

[1]School of Environmental Science and Engineering, Guangzhou University, Guangzhou 510006, China (*correspondence: chenyheng@eyou.com)
[2]Insititute of Geochemistry, Chinese Academy of Sciences, Guiyang 550002, China (xiaotangfu@vip.gyig.ac.cn)
[3]Guangdong Provincial Academy of Environmental Science, Guangzhou 510045 (wangchunlin1982@163.com)
[4]South China Institute of Environmental Sciences, MEP, Guangzhou 516005, China (qjyyjq78@163.com)

Chemical analysis of 120 samples of surface sediments and 82 samples of surface water around the lead-zinc ore mining area in the North River Basin (upper part of the Pearl River Delta), South China was performed in order to (i) determine the contamination levels of heavy metals (Tl, As, Cd, Cr, Cu, Hg Ni, Pb and Zn) by means of Inductively Coupled Plasma Mass Spectrometry (ICP - MS); (ii) identify potential sources of the heavy metals; and (iii) to identify those processes that determine the spatial variability of the heavy metals between the source areas and some distant locations in downstream direction. Among the examined elements, high contents of Tl, As, Cd, Cu, Pb and Zn were found in the sediments from the mainstream and feeders of the North River close to the mining area. We interpret the most likely sources of the heavy metal contamination in the sediments are wastewater discharges, mineral tailing materials and dust depositions resulting from the excessive mining activities, since the heavy metal distribution in the basin generally shows a decreasing trend from the location closest to the mining sites towards the downstream directions, and most importantly because the heavy metal contents are mostly related to the Tl contents. Thallium, as a rare element is seldom found in the normal environmental settings but is highly concentrated in the lead-zinc ore minerals in this area. Thus, the good relationships between the Tl contents and the contents of other heavy metals signify that Tl could be used as a special environmental tracer to track, and eventually to quantify the heavy metal contaminations from mining activities of ore specifically bearing Tl. This work enhances our understanding of heavy metal contaminations around a mining site. The local environmental protection and future mineral resources exploitation activities might also benefit.

This work is supported by NSFC (No. 40930743).

The characteristics of generation and distribution of CO_2 gas pools in Songliao Basin, China

J.H WANG[1], X. LUO[2], L.H HOU[3] AND Y.WANG[4]

[1]Research Institute of Petroleum Exploration and Development, Beijing, China (284174762@qq.com)
[2]Research Institute of Petroleum Exploration and Development, Beijing, China
[3]Research Institute of Petroleum Exploration and Development, Beijing, China (lhhou@petrochina.com.cn)
[4]Research Institute of Petroleum Exploration and Development, Jilin Oil Company, songyuan, China (wangy1@petrochina.com.cn)

There are so many gas pools with high CO_2 component are distributed in volcanic reservoir. It also indicates that the CO_2 in CO_2 gas pools are mainly of magma origin by the analysis of the characteristics of gas components, carbon isotope composition of CO_2 and helium isotope composition of He in 10 of CO_2 gas pools in Songliao Basin. The main characters of CO_2 gas pools are $\delta^{13}C_{CO2} > -8‰$ and R/Ra=1.9~7.2. Geological background and analysis of fluid inclusion indicate that the CO_2 in Changling, De hui and Gu long etc fault depression are mainly forming lately. The reasons are following. The first is that the fluid inclusions of CO_2 are late period fluid inclusions which are banded occurrence in cracks of transecting quartz grain or transecting widen quartz. Their homogenization temperatures are 120~140°C. So, the forming stage of CO_2 may be mainly between 72Ma and 48 Ma. The formation and distribution of CO_2 are relatives with many kinds of faults including lithosphere faults, crust fractures, basement rifts and overburden faults especially relatives with NE-NNE deep faults which have strike slip motion in late stage. These kinds of faults mainly controlled depression formation in early stage and had NE-NNE left-lateral strike slip motion in late stage. Also, volcanic erupted with amazing amount of CO_2 in this stage and the faults became the channel of the CO_2 migration and then prompted the formation of CO_2.

https://doi.org/10.1180/S0026461X00006502 Published online by Cambridge University Press

High-pressure behavior of CaF_2 nanocrystals

J.S. WANG, C.L MA, J HAO, D ZHOU AND Q.L CUI*

State Key Laboratory of Superhard Materials, Jilin University, Changchun 130012, PR China
(*correspondence: cql@jlu.edu.cn)

The alkaline-earth fluoride CaF_2 is a well-known face-centered- cubic ionic minerals, and has long been used as mineralogical models for the behavior of ionically bonded minerals in the Earth's mantle [1]. It is widely accepted that the actualization of nanosized materials have opened doors for finding new properties with respect to their macroscopic counterparts. Although there are many high-pressure studies on bulk CaF_2, pressure induced structural phase transitions in nanoscale system has rarely been reported [2, 3].

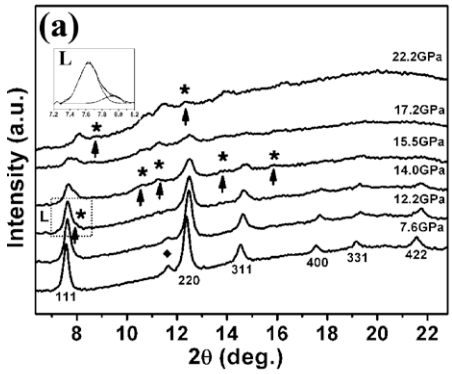

High-pressure behavior of nanocrystalline CaF_2 samples with an average grain size of 8 nm have been studied by *in situ* synchrotron radiation x-ray diffraction. A pressure-induced fluorite structure to orthorhombic $PbCl_2$-type structure transition starts at 14.0 GPa, and phase transition is sluggish. The orthorhombic phase of nanocrystalline CaF_2 is stable up to 46.5 GPa. The enhancement of transition pressure in CaF_2 nanocrystals as compared with the corresponding bulk material is mainly caused by the surface energy difference between the phases involved.

[1] Abby Kavner (2008) *Phys. Rev. B* **77**, 224102. [2] X. Wu, S. Qin & Z. Y. Wu (2006) *Phys. Rev. B* **73**, 134103. [3] E Morris, T Groy & K Leinenweber (2001) *J. Phys. Chem. Solids* **62**, 1117.

Elastic properties of hydrous and anhydrous mantle minerals at high pressure

J. WANG AND J.D. BASS*

Geology Department, University of Illinois, 1301 W Green Street, Urbana, IL 61801 USA
(*correspondence: jaybass@uiuc.edu)

Anyhdrous and hydrous forms of wadsleyite and ringwoodite, high-pressure phases of $(Mg,Fe)_2SiO_4$ +- H_2O, are major constituents of the transition zone of Earth's mantle, and are likely abundant in many subducting slabs. Therefore, the seismic properties of these phases are essential to understand the chemical and thermal state of these regions, as well as the seismic signature of water in the mantle to 660 km depth. We have measured the acoustic wave velocities of several key anhydrous and hydrous forms of these minerals up to transition zone pressures by Brillouin spectroscopy on samples compressed in a diamond anvil cell. Hydrous samples contained roughly 2% by weight of H_2O. These experiments allow us to assess the effects of pressure, Fe and H_2O on the elastic properties of these phases. These measurements should provide insight on key questions such as the olivine content and hydration state of the transition zone. It appears that one of the critical issues in addressing the effects of hydration on these phases is the accurate measurement of water content. Our results indicate that determinations of the structurally-bound hydrogen content by SIMS and IR spectroscopy on these samples can vary greatly.

https://doi.org/10.1180/S0026461X00006502 Published online by Cambridge University Press

Primordial ages of lithospheric mantle vs ancient relicts in the asthenospheric mantle: *In situ* Os perspective

KUO-LUNG WANG[1]*, S.Y. O'REILLY[2], W.L. GRIFFIN[2], N.J. PEARSON[2], V. KOVACH[3] AND V. YARMOLYUK[4]

[1]Institute of Earth Sciences, Academia Sinica, Taipei, Taiwan (*correpsondence: kwang@earth.sinica.edu.tw)
[2]GEMOC, Macquarie University, Sydney, Australia
[3]IPGG, Russian Academy of Sciences, St. Petersburg, Russia
[4]IGEM, Russian Academy of Sciences, Moscow, Russia

Recent studies have shown that volumes of ancient depleted material can survive in the convecting asthenospheric mantle for long periods so that the use of Os model ages of mantle xenoliths to constrain the age of lithospheric mantle events should be approached with caution. In this study, we use *in situ* Os-isotope dating on sulfides in peridotitic xenoliths from cratonic (Tok, Russia) and off-craton (Tariat and Dariganga, Mongolia) settings of the Neoproterozoic-Phanerozoic Central Asia Orogenic Belt (CAOB) to examine lithosphere formation. A few Tok sulfides yield an apparent isochron indicating an age of 3.2 Ga. The high initial $^{187}Os/^{188}Os$ (0.117) of the apparent isochron suggests that it represents a mixing line, possibly involving an Archean component. In Tariat, both T_{MA} ages from the least-disturbed sulfides ($^{187}Re/^{188}Os<0.07$) and T_{RD} ages from higher-Re/Os sulfides yield model ages ranging from 0.5 to 3.0 Ga, with peaks around 1.7-1.5, 1.2 and 0.7-0.5 Ga. These ages suggest that SCLM beneath the Tariat region existed at least by Proterozoic time, and that some domains are Archean. The Os model ages are well-correlated with crustal events recorded in the overlying Precambrian Tarvagatay Terrane. It would be a remarkable coincidence if sulfides derived from randomly selected fragments of refractory materials in the convecting asthenospheric mantle would combine to give such a systematic correlation. We therefore prefer the simplest interpretation: the sulfide Os ages in the Tok and Tariat peridotites record major events that affected the crust+SCLM. The oldest of these events may record major melt extraction, and the later ones metasomatic events. Sulfides in Dariganga peridotites also have Mesoproterozoic Os model ages. Although Proterozoic crustal events have not been reported in this region so far, Proterozoic Nd model ages for basement rocks around the Xilinhot region in the vicinity of the Dariganga Plateau (B. Chen, pers. comm.) suggest that a Precambrian crustal terrain should be expected and might be found by studies of deep-crustal xenoliths in the Dariganga region.

The geochemistry of fluid inclusions in Yimen Sanjiachang copper deposits

LEI WANG[1], RUN-SHENG HAN[1], GUO TANG[1], YI-DUO HU[2] AND JIAN-GUO HANG[1]

[1]Kunming University of Science and Technology; Southwest Institute of Geological Survey, Geological Survey Center for Non-ferrous Mineral Resources, Kunming, China, 650093 (*correspondence: cumtwl1983@yahoo.com.cn)
[2]Kunming Vocational and Technical College of Industry, Kunming, China, 650302

Sanjiachang copper deposits including three copper deposits of Shishan copper deposit, Caiyuanhe copper deposit and Fengshan copper deposit[1]. Shishan Copper deposit is a diagenesis - weak reworked deposit Fengshan copper deposit is a strongly reworked deposit which controlled by diapir structure[2], Caiyuanhe copper deposit is a transitional type of the first two deposits, The fluid inclusions have significant differences of the three copper deposits with the following characteristics: From Shishan copper Caiyuanhe copper deposit Fengshan copper deposit Inclusions size are increase(1.5μm-2.15μm), and number are increase, pure liquid inclusions in order to reduce and liquid inclusions in order to increase, Fengshan copper found gas inclusions (about 15%) and a small amount of NaCl sub-inclusions. From Shishan copper Caiyuanhe copper deposit Fengshan copper deposit gangue mineral homogenization temperatures are gradually increasing there are two homogenization temperature range of 113.4 ~ 194.3 °C (95% of this range) and 220 ~ 320 °C in Fengshan copper deposit-hishan copper depost salinity inclusions have the feature of high K^+ content, low Na^+ content, Caiyuanhe copper deposit and Fengshan copper depost have the feature of high Na^+ content , low K^+ content [2], Fengshan copper has two salinity content range of 4-10% and 12-18%.

The results show that from Shishan copper deposit - Caiyuanhe copper deposit - Fengshan copper deposit is gradually enhanced the role of structural transformation, Fengshan copper mineralization has the characteristics of two and the main ore mineralization in the low temperature of 113.4 ~ 194.3 °C.

Granted by the project of the State Crisis Mine (20089 943) and the Distinguishing Discipline of KUST (2008).

[1] Tian Yulong *et al* (2000). *Acta Mineralogica Scinica* **20**, 73-79. [2] Lei Wang *et al* (2010). *Geochimica Et Cosmochimica Acta* **74**, A1104-A1104.

https://doi.org/10.1180/S0026461X00006502 Published online by Cambridge University Press

Microecology perspective and environmental impact of coal mine sulfur-bearing waste dump

L.L. WANG[1]*, M. YUE[2] AND L.L. WANG[1]

[1]School of Resources and Environmental Engineering, Hefei University of Technology, Hefei 230009, China (wangllhfut@gmail.com)
[2]Hefei University, Hefei 230022, China

Coal mines in Chian are mostly located in the north. Below the coal layer, there is a fracture-karst aquifer with strong anisotropy often used as drinking water source for local inhabitants[1-2]. Mining has caused environmental pollution. Some studies involve flow and solute transportant in fractured media[3-7]. Others pay attentions to the pollution control from sources [8]. In this study, by hydrogeological survey, sampling and testing in the sulfur-containing waste dump of the mining area in Sitai mine, Shanxi Province, the content of the material and its environmental characteristics were analyzed. The advantage of microbial flora in the sulfur-containing waste dump and its colony structure were discussed. The 16S rDNA of the special microorganisms was determined; The role of microorganisms and kinetic parameters in the weathering process of sulphide were studied.

The pH values of leaching water in the yard of sulfur containing waste dump were around 2.5, the color of leaching filtrate were almost reddish-brown.

The 9 strains which isolated from the acid water belonged to two species: *Acidiphilium sp.* and *Acidithiobacillus ferrooxidans*, they were the advantage microbial flora in this environment.

The initial pH of liquid phase, temperature, solid-liquid ratio and particle sizes of mining rocks would affect the behavior of microorganisms in the process of pyrite weathering.

When microorganisms and culture medium were coexist, the pyrite oxidation rate reached 3.14 mmol.d-1.L-1, it was 28.55 times of the control group. the release regularities of As, Cu, Zn, Ni, Pb influenced obviously by microorganisms.

[1] Qian *et al*. (2006) *Hydrogeol. J*. **14**: 1192-1205. [2] Qian *et al*. (2009) *Hydrogeol. J*. **17**: 1749–1760. [3] Zhou *et al*. (2004) *Int. J. Rock Mech. Min. Sci*. **41**:402. [4] Qian *et al*. (2005) *J. Hydrol.* **311**: 134-142. [5] Qian *et al*.(2007) *J. Hydrol.* **339**: 206-219. [6] Qian *et al*. (2011) *Hydrol. Process*. **25**: 614-622. [7] Qian *et al*. (2011) *J. Hydrol.* **399**: 246-254. [8] Qian *et al*.(2010) *Geochim.Cosmochim. Acta* **74**: 837-837.

Precious metal (Pt, Pd, and Au) in Fengshan porphyry Cu-Mo deposit, China

MINFANG WANG[1,2]

[1]Faculty of Earth Resources, China University of Geosciences, Wuhan, Hubei, 430074, China (wang_minfang@163.com)
[2]State Key Laboratory of Geological Processes and Mineral Resources, China University of Geosciences, Wuhan, Hubei, 430074, China

Nine hand specimen and four flotation concentrates have been analyzed (Table 1).

Sample	Type	Au ppb	Pt ppb	Pd ppb
FS50	intrusive rock	11	0.137	0.165
FS94	altered rock	4	0.234	0.288
FS57	altered rock	10	0.389	3.907
FS4	ore, skarn	1480	0.037	3.095
FS9	ore, skarn	531	0.204	17.979
FS45	ore, skarn	310	0.099	0.403
FS64	ore, skarn	402	0.07	1.314
FS8	ore, porphyry	28	1.765	13.888
FS36	ore, porphyry	220	0.175	6.877
SC	sulfide concentrate	897	15.9	13
CFC	copper flotation concentrate	6070	21.8	32
MFC	molybdenum flotation concentrate	2360	81.4	32
CMFC	copper-molybdenum flotation concentrate	12	1.3	1

The results show that concentrate samples have the highest content of precious metal and almost are 1-2 orders of the magnitude higher than ore samples, while the rock samples are the poorest. Meanwhile, the porphyry ore samples have the higher content of Pd, Pt and Au than in the skarn ore samples. PGE enrichment in porphyry deposits probably requires a mantle source region, liberation of mantle sulfides during partial melting in the source region, and an oxidized melt that effectively prohibits the formation of magmatic sulfides during fractionation.This study clearly demonstrates the potential for further research.

https://doi.org/10.1180/S0026461X00006502 Published online by Cambridge University Press

Contrasting microbial communities and geochemical patterns reflect different styles of methane oxidation and methanogenesis in terrestrial mud volcanoes

PEI-LING WANG[1], LI-HUNG LIN[2], TING-WEN CHENG[2], YUNG-HSIN CHANG[2], WEN-JING LAI[1], JING-YI TSENG[1], WEN-YU TSAI[2] AND CHIH-HSIEN SUN[3]

[1]Institute of Oceanography, National Taiwan University
[2]Department of Geosciences, National Taiwan University
[3]Exploration and Development Research Institute, CPC Corporation Taiwan

Hydrocarbon seeps and mud volcanoes are ubiquitous in marine and terrestrial environments where gaseous fluids with unconsolidated sediments ascend along fractures tapping into potential gas or petroleum reservoirs in deep subsurface. Although extensive geochemical and microbiological studies have been conducted on marine settings, terrestrial counterparts remain poorly constrained.

This study combined molecular screening of 16S rRNA and functional genes, and geochemical analyses of porewater, sediment and gas collected from mud volcanoes distributed in eastern and southwestern Taiwan to determine how microbial communities respond to various methane fluxes and geological contexts. Our findings indicated that mud volcano systems in both regions were characterized by stratified geochemical characteristics and community assemblages resembling or contrasting those in marine settings in several aspects. In particular, anaerobic methanotrophy was linked to different electron accepting processes (sulfate versus iron reduction) in different regions, suggesting various affinities of functional expression on the presence of specific minerals. The proliferation of anaerobic methanotrophy is apparently decoupled from the supply of deeply-sourced methane but strongly dependent on the in-situ methanogenesis controlled by the fermentative production of specific methanogenic precursors. Microbial communities compartmentalized into different depth intervals collectively enable less than 40% of methane inventory emitted to atmosphere. Contrasting patterns of metabolic and geochemical stratification reflect microbial communities thriving on inherited minerals and geochemical disequilibria induced by the interaction between the upward transport of gaseous, reducing, diluted fluids and the downward infiltration of oxidizing, solute-enriched fluids subjected to surface evaporation.

Potential-pH diagram for the V-Cl-H_2O system at high chlorine concentration

R. L. WANG[1], Y. ZENG[1,2]* AND S. H. ZHANG[1]

[1]Department of Geochemistry, Chengdu University of Technology, Chengdu, 610059 China;
[2]Mineral Resources Chemistry Key Laboratory of Sichuan Higher Education Institutions, Chengdu 610059, China (*correspondence: zengyster@gmail.com)

Vanadium, widely distributed in the nature, is essential to human and closely related to human health. While the total amount of vanadium in human body gathers to a certain degree, it shows middle-high toxicity. The toxicity of vanadium depends on its species and valence, which are mainly due to pH value, potentials, the total concentration of vanadium, and the kinds of coexistent ions in the solution. Moreover, the toxicity of vanadium increases with increasing oxidation state.

Under natural environmental conditions in soil and water, vanadium dominantly exists in either +4 or +5 oxidation state as aquatic species of vanadyl(VO_3^{2-}) or vanadate(VO_4^{3-}), respectively. Under weak reducing conditions, vanadyl(V^{IV}) species is stable, while in oxidizing conditions, vanadate (V^{V}) is stable across almost the entire pH range. VO_3^{2-} and VO_4^{3-} can coexist depending on the redox potential and pH value of the solution and concentration.

In this paper, the potential and pH value of the V-Cl-H_2O system at $C_{T(Cl)}$ = 1.0 mol·L^{-1} are determined by using a concentration comparison method. Based on the measured data, the preliminary predominance diagrams were constructed. A Comparison between the predominance diagrams for the V-Cl-H_2O system with $C_{T(Cl)}$ = 1.0 mol·L^{-1} at different vanadium concentrations ($C_{T(V)}$ = 1.0×10^{-3} mol·L^{-1} and $C_{T(V)}$ = 1.0×10^{-5} mol·L^{-1}) [1],[2] has been done. It is shown that the location and size of the advantage regional of vanadium ion VO_2^+, $H_2VO_4^-$, VO_4^{3-} are similar. Under the conditions with pH 0.00-5.68, and Eh 0.5-0.9 V, the area of VO^{2+} advantage region is decreased at $C_{T(V)}$ = 1.0×10^{-5} mol·L^{-1}. At Eh value of 0.0-0.5 V, the $HV_2O_5^-$ advantage region is replaced by VO^+ with pH 3.68-14.00.

The authors acknowledge the support of the Program for New Century Excellent Talents in University (NCET-08-0900)

[1] Zeng, Y.; Ma, M. R. (2009) *Acta Phys.-Chim.Sin,* , **25**: 955. [2] Wu, J.M.; Zeng, Y. (2007) *Acta Phys.-Chim.Sin,* , **23**: 1141.

https://doi.org/10.1180/S0026461X00006502 Published online by Cambridge University Press

The temporal and spatial variations of N_2O saturations in a eutrophic lake

SHILU WANG

Laboratory of Environmental Geochemistry, Institute of Geochemistry, Chinese Academy of Sciences (wangshilu@mails.gyig.ac.cn)

Much of the N_2O emitted from aquatic ecosystems is anthropogenically derived [1]. However, there remains considerable uncertainty in the magnitude of anthropogenic N_2O emitted from aquatic environments and how N_2O emissions respond to increasing loads of anthropogenic N and eutrophication in general. In this study, N_2O saturations were examined in the ecologically heterogeneous, eutrophic lake, Lake Taihu, in eastern China. I found that anthropogenically-enhanced inorganic nitrogen N inputs act as a limited primary control on the spatial distribution of N_2O saturations in heavily eutrophied parts of the lake only and that overall, lake N_2O production and emission are not raised as significantly as expected due to high N input [2]. A distinct diurnal pattern of N_2O saturations is displayed in July, which is controlled by biogeochemical processes [3]. While large-scale changes (~25-fold) in N_2O fluxes in Lake Taihu are a function of variable N loading, biogeochemical processes concerning O_2 and N transformation at the sediment-water interface have significant (~twofold) impacts on the regulation of N_2O production over very short time scales.

This work was supported by the major projects on control and rectification of water body pollution (2009ZX07101-013).

[1] Seitzinger (2000) *Chemosphere, Glob. Chang. Sci.***2**, 267-279. [2] Wang S (2009) *Sci. Total Envir.* **407**, 3330-3337. [3] Wang S (2010) *J. Environ. Qual.* **39**, 1858-1863.

The dissolving and driving process in Qarhan salt lake, China

WANG WENXIANG[1]*, LI WENPENG[2] AND HAO AIBING[3]

[1]China University of Geoscience, Beijing, 100083, China (*correspondence: hiwangwenxiang@126.com)

[2]China Institute of Geo-Environment Monitoring, Beijing, 100081, China

[3]China Geogical Survey, Beijing, 100037, China

Qarhan salt lake is located in Qaidam Basin, Qinghai Province, China. There are about 3 million tons of solid potassium resources in Qarhan salt lake[1]. About half of the solid resources are of low grade. We can't exploit the low grade resource directly.

The solid potassium can be dissolved and transferred to liquid state by mixed with solution in low potassium concentration. We use water from Seniehu lake as the solution to carry on the research.The experiment area is 1 km^2. 35 monitoring wells are set up in order to obtain data of the saline water level and composition. There is a recharge trench on one side of the experiment area and a drainage thench on the other side. The low potassium solution comes into the experiment area from the recharge trench. During the flowing process, the concentration of potassium resolution becomes high. In the end, the high potassium solution flows out of the experiment area through the drainage trench.

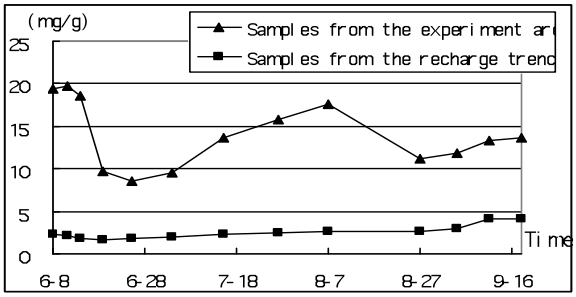

Figure 1: Potassium concentration duration curve

The result shows that solution with low potassium concentration can essily dissolve the solid potassium. However, the concentration of sodium must not be too high.[2]

[1] Li Wenpeng (1993) Journal of Hebei College of Geology 16, 254-263. [2] Wang Wenxiang (2010) *Mineral Deposits* **29**, 697-703.

https://doi.org/10.1180/S0026461X00006502 Published online by Cambridge University Press

U–Pb zircon, geochemical and isotopic constraints on age and origin of Cretaceous granites from the North Qinling, central China and implications for interaction between crust and mantle

XIAOXIA WANG[1]*, TAO WANG[2], QIUJU QI[3] AND SHAN LI[2]

[1]Institute of Mineral and Resource, Chinese Academy of Geological Science, Beijing 100037, China (*xiaoxiawang@hotmail.com)
[2]Institute of Geology, Chinese Academy of Geological Science, Beijing 100037, China
[3]China University of Geosciences, Beijing 100083, China

Zircon U-Pb dating, geochemical and isotopic (Nd, Sr, Hf) analyses for two granitoid plutons have been carried out in the different blocks of the North Qinling. Zircon dating by LA-ICP-MS for the Lantian granite in the southern margin of the North China Block and Muhuguan granite in the North Qinling orogen yields ages of 133±1 Ma and 150±1Ma, respectively. The samples studied from the Lantian granite contain zircons mostly having xenocrystic cores. The inherited zircons have Paleoproterozic ages. Both granites exhibit similar mineralogical, chemical and isotopic characteristics. They have metaluminous to peraluminous compositions (A/CNK ratios 0.9 to 1.05) and display K_2O/Na_2O ratios of 0.9 to 1.5. In terms of trace elements, they show an enrichment of LREE and medium fractionation between LREE and HREE (La_N/Yb_N ratios 16 to 33). Compared with the primordial mantle, distinct negative anomalies of P and Ti, and slight negative anomalies of Ba and Nb are observed in both granite plutons. They are further characterized by low $\varepsilon_{Nd}(t)$ of −11.8 to −18.3 and $\varepsilon_{Hf}(t)$ of −23.4 to −5.7 for the Liantian granite and low $\varepsilon_{Nd}(t)$ of −7.6 to −11.4 and $\varepsilon_{Hf}(t)$ of −17.4 to −7.3 for the Muhuguan granite. We interpret these Cretaceous granites as partial melting of old crust, mixed with juvenile mantle component and suggest the basement of the North Qinling with more juvenile composition from the southern margin of North China block to Shangdan suture.

Particle size effects in bioleaching of uranium waste ore

WANG XUEGANG[1,2,3]*, SUN ZHANXUE[3] AND LIU JINHUI[3]

[1]State Key Laboratory Breeding Base of Nuclear Resources and Environment, East China Institute of Technology, Nanchang, JX 330013, P. R. China (*correspondence:xuegangwang@yahoo.com.cn)
[2]Key Laboratory of Radioactive Geology and Exploration Technology Fundamental Science for National Defense, East China Institute of Technology, Fuzhou, JX 344000, P. R. China
[3]Department of Civil and Environmental Engineering, East China Institute of Technology, Fuzhou, JX 344000, P. R. China (zhxsun@ecit.cn, liujh@ecit.cn)

The effect of mineral paricle size on the bioleaching of uranium from the 721 Uranium Mine Shan-nan deposit waste ore, located in the Jiangxi Province, south of China, was investigated. A mixed bacteria, which isolated from the uranium mine ores and the predominant bacteria were *Acidithiobacillus ferrooxidans* and *Leptospirillium ferriphilum,* was applied into the column bioleaching test. The uranium leaching effect in different particle size uranium ore were shown in table 1.

particle size (mm)	U content (%)	Slag U content (%)	Leaching rate(%)
>25	0.0289	0.00258	10.73
20-25	0.0141	0.00098	30.49
15-20	0.0161	0.00089	44.72
10-15	0.0330	0.00093	71.81
5-10	0.0332	0.00069	79.21
2-5	0.0403	0.00068	83.13
1-2	0.0434	0.00058	86.63
<1	0.0479	0.00057	88.10

Table 1: The leaching rate of different particle size

As can be seen from table 1, with the waste uranium ore particle size decreasing, the leaching rate was increasing. Decreasing the particle size from 25mm to 1mm the uranium leaching rate enhanced from 10.73% to 88.1%. While the particle size less than 15mm fraction leaching rate was over 71.81%, also the particle size greater than 15mm fraction leaching rate less than 44.72% , which adverse to uranium bioleaching. Consider the actual process, recommended crushed ore to -15mm can be obtained better effect.

Project supported by the National High-tech R&D Program of China (863 Program) (No.2007AA06Z120) and International Cooperation Projects of China (No. 2008DFA71760).

https://doi.org/10.1180/S0026461X00006502 Published online by Cambridge University Press

From solids to liquids: A coordinated approach for studying dynamic processes in the deep Earth using large-volume apparatus and synchrotron radiation

YANBIN WANG

Center for Advanced Radiation Sources, The University of Chicago, 5640 S. Ellis Ave., Chicago, IL 60637, USA (wang@cars.uchicago.edu)

For the past fifteen years, we have been developing synchrotron-based large-volume high pressure (LVP) techniques at the GeoSoilEnviroCARS (GSECARS) sector of the Advanced Photon Source (APS) for a better understanding of the thermodynamic state, the dynamic processes, and the evolution of the Earth and other planets. The technical and scientific developments have enabled us to conduct coordinated studies on materials in both the solid and liquid states under simultaneously high pressure and high temperature conditions. In this presentation I will discuss the following dynamic aspects of recent scientific studies: (1) rheological properties of earth materials at high pressure and temperature, using the deformation DIA (D-DIA) – recent results on olivine deformation will be used as an example, (2) textural evolution in multi-phased materials under large shear deformation using the high-pressure x-ray tomographic microscope (HPXTM) – applications of such studies on mantle dynamics will be discussed, (3) in-situ high-pressure tomographic studies on Fe-S melt segregation from silicate using HPXTM and new constraints on the timing of formation of the Earth's core, and (4) new development for melt studies, including fusion curve, structure, density, and elasticity, aiming at a "complete suite" of physical properties for a better understanding of melt physics. A brief discussion on future prospect will also be presented.

Quantitative ^{2}H NMR as site-specific $^{2}H/^{1}H$ probe to study organic matter

Y. WANG[1], G.D. CODY[1], C.M.O'D. ALEXANDER[2] AND M.L. FOGEL[1]

[1]Geophysical Laboratory, Carnegie Institution of Washington (ywang1@ciw.edu, gcody@ciw.edu, mfogel@ciw.edu)

[2]Department of Terrestrial Magnetism, Carnegie Institution of Washington (alexander@dtm.ciw.edu)

Recent studies show that the biosynthetic fractionation between fatty acids and water can vary by up to 500‰, depending on biological and environmental factors that include: species, metabolic pathways, aridity, and salinity. These variations are poorly understood, which has restricted the specificity of biomarker $\delta^{2}H$ records and thus their use as paleoenvironmental and geobiological proxies. Direct detection of the site-specific ^{2}H distribution via ^{2}H NMR provides a powerful means for investigating these variations and the underlying mechanisms. Unlike approaches that employ chemical/thermal fragmentation and IRMS measurements, ^{2}H NMR is non-destructive, applicable to almost all types of organic molecules, and free of isotopic fractionation. Similar to the advent of compound-specific isotope analyses, it has the potential to open a new door to the study of organic materials that will benefit a broad range of biogeochemical and low-temperature geochemical studies.

Historically, ^{2}H NMR experiments on natural samples have been difficult due to the scarcity of the ^{2}H nucleus and its low receptivity to radio frequency radiation which together lower the sensitivity by ~$7x10^{5}$ times compared to ^{1}H NMR. Furthermore, the ^{2}H NMR spectra is complicated by the quadrupolar interaction of the ^{2}H nuclei. We have successfully developed a solid state ^{2}H NMR experimental protocol to significantly amplify the signal-to-noise ratio and yield simplified, purely isotropic spectra.

With this method, we studied the site-specific ^{2}H distribution in residual organic matter from two carbonaceous chondrite meteorites and a bituminous coal. Combined with ^{1}H NMR spectra and bulk $^{2}H/^{1}H$ analyses, we derived the $\delta^{2}H$ values for aliphatic and aromatic sites and the $^{2}H/^{1}H$ fractionation factor between these groups, which provide a unique basis for coupling the $^{2}H/^{1}H$ distribution to the chemical history of chondrites. In an on-going study, we investigated H isotope exchange rates by incubating pristane, cumene, and anthracene, separately, with clay minerals soaked in ^{2}H-enriched water. Liquid state ^{2}H NMR was used to study the efficiency of ^{2}H substitution at methyl, methylene, methine, and aromatic sites. The results will improve our understanding of the influences on H isotopic composition of sedimentary organic matter and petroleum.

https://doi.org/10.1180/S0026461X00006502 Published online by Cambridge University Press

Nd-Sr-Pb isotopic and elemental geochemistry of silicalites from the sulphide ore deposit in the Guangdong region, China

WANG YINXI[1], LI HUIMING [1] ,WANG YUANYUAN [2], CHEN YIJUN[1], ZHANG MENGQUN[1] AND WANG HENIAN [2]

[1]Center of Modern Analysis, Nanjing University, Nanjing 210093, China
[2]Nanjing Institute of Geology and Paleontology, Academy of Sciences, Nanjing 210008, China.
[3]Dept.of Earth Science, Nanjing University, 210093, China

Silicalite is well developed and is present as layers, thin layer or siliceous band in the banded ores. The Dajiangping pyrite deposits lie on the Yunfu County of Guangdong .region, China. is a super-large pyrte ore deposite.

The silicalite is mainly coposed of microlitic and cryptocrystalline quartz. SiO_2 is the essential chemical composed of the silicalite, ranging from 81.50% to 94.32%, together with Al2O3 content between 0.45% and 9.44%, CaO< 0.12% and MgO<0.36%. The contents of FeO, MnO, K_2O and Na_2O are commonly low. The isotopic characters of the Dajiang pyrite orebody are: εNd(t) =-12 ~ -13, $(^{87}Sr/^{86}Sr)I$ = 0.73085 ~ 0.73104, $(^{206}Pb/^{204}Pb)I$ =18.467 ~ 18.485, $(^{207}Pb/^{204}Pb)I$ =16.239 ~ 16.384 and $(^{208}Pb/^{204}Pb)I$ =39.805 ~ 39.873. Because of the isotopic characteristic of Sr-Nd-Pb in the whole rock, these evidences reflect the character of crust source but not that of magmatic source region.

The dertermination of Dajiangping pyrite deposit indicates that the Precambrian continental rift massive sulphide ore deposit is also an important kind of deposit in South China basides. Evidently, the above-mentioned Sr-Nd-Pb isotopic geochemistry reflecte the crust source r of the Dajiang pyrite deposits.

This work is granted by the National Natural Science Foundation of China (No. 40872028) and by the Analysis Testing Foundation of Nanjing University

[1] *Wang Henian*,et al. (1997). *Chinese Science Bulletin*, Vol. **42**, 23:1983-1985

Rb-Sr and Sm-Nd isotopic ages of Sulphide deposits in the Guangdong region, China

WANG YINXI[1], LI HUIMING [1], WANG YUANYUAN [2], HU XIN[1], LIU DI[1], TAO XIANCONG[1] AND WANG HENIAN [3]

[1]Center of Modern Analysis, Nanjing University, Nanjing 210093, China (*correspondence: yxwang@nju.edu.cn)
[2]Nanjing Institute of Geology and Paleontology, Academy of Sciences, Nanjing 210008, China.
[3]Dept.of Earth Science, Nanjing University, 210093, China

The Dajiangping pyrite deposits lie on the Yunfu County of Guangdong .region, China. is a super-large pyrte ore deposite.

Rb-Sr and Sm-Nd isotope ages were measured by using VG354 mass spectrometer at Modern Analysis Centre, Nanjing University and the analytical procedures were discussed and given in detailed by Wang(1)

The Rb-Sr and Sm-Nd dating of the orebody give the ages of 630.1±7.3Ma and 637.5±6.9Ma,respectively. The ages slightly approximate the age in ferred from the occurrence of the later Proterozoic algae. This may be related to the subsequent geological effect on the Rb-Sr and Sm-Nd isotope system of the Dajiangping pyrite orebody. Because of the good linearity of Rb-Sr and Sm-Nd internal isochron between the whole rock, these evidences reflect the character of well-ditributed source. Evidently, the above-mentioned Rb-Sr and Sm-Nd isotopic ages reflecte the ages of the Dajiang pyrite deposits.

The silicalites ages of deposits in this are 630.1±7.3Ma and 637.5±6.9Ma, belonging to the later Proterozoic epoch. The dertermination of Dajiangping pyrite deposit indicates that thePrecambrian continental rift massive sulphide ore deposit is also an important kind of deposit in South China basides . The Dajiangping pyrite deposit is similar to the famous Proterozoic super-large depostis in the world. The ages determination of Dajiangping pyrite deposit bed plays an important role in confirming the agesof the Yunkai Group.

This work is granted by the National Natural Science Foundation of China (No. 40872028) and by the Analysis Testing Foundation of Nanjing University

[1] *Wang Yinxi et al*. (1992). *Chinese Science Bulletin* **37**, 36-39

https://doi.org/10.1180/S0026461X00006502 Published online by Cambridge University Press

Nd-Sr isotopic geochemistry of fossils from the bottom of Cambrian in the Yunnan, Sichuan and Xinjiang region, China

YINXI WANG*,[1], YUANYUAN WANG , JIEDONG YANG[1] AND HUIMING LI[1]

[1]Center of Modern Analysis, Nanjing University, Nanjing 210093, China (*correspondence: yxwang@nju.edu.cn)
[2]Nanjing Institute of Geology and Paleontology, Academy of Sciences, Nanjing 210008, China.

This paper the results of Rb-Sr and Smi-Nd isotopic date fromphosphatic fossils and collophanites collected from three important Precambrian-Cambrian boundary section in China.The samples under study were collected from three important sections in China, namely, the Meishucun section at Yunnan Province, the Maidiping section at Sichuan province and the Wushi section at Xinjiang Uygur Autonomous Region.

$\varepsilon_{Nd(}$(T) and $^{87}Sr/^{86}Sr$ values of small shelly fossils from maidiping section are -6.5 to -7.1 and 0.709624 to 0.709812, respectively. $\varepsilon_{Nd(}$(T) and $^{87}Sr/^{86}Sr$ values of small shelly fossils from Meishucun section are -6.1 to -7.1 and 0.709310 to 0.709700, respectively. $\varepsilon_{Nd(}$(T) and $^{87}Sr/^{86}Sr$ values of small shelly fossils from Kalpin section are -6.1 to -6.5 and 0.709436 to 0.709576, respectively. $\varepsilon_{Nd(}$(T) and $^{87}Sr/^{86}Sr$ values of small shelly fossils from three section are very similar.

The palaeoseawater in the three areas of China was co-oceanic during the Precambrian-Cambrian transitional period, with an average $\varepsilon_{Nd(}$(T) value of -6.6 ± 0.5. The Nd model age of the tested samples is about 1.8Ga, which represents the mean age of the continental source sres surrounding China's seawater.

This work is granted by the National Natural Science Foundation of China (No. 40872028) and by the Analysis Testing Foundation of Nanjing University

[1] *Yang Jiedong et al..* (1989). *Chinese Science Bulletin,* Vol. **34**, 63

Surfacial geochemical features of elements in Qinghai-Tibet Plateau

WANG YONGHUA[1] AND WANG MINGQI[2]

[1]Chengdu center, China Geological Survey, Sichuan, China 610082
[2]China University of Geosciences, Beijing, China

Qinghai-Tibet Plateau in China covers the area about 2,400,000km^2. Different landscapes including high-cold mountain, high-cold lake and swamp plateau, desert, deep velley are developed in the area. National geochemical mapping results show that there are typical distribution patterns of elements in different terrains.

High-cold mountain landscape, which is about 900,000km^2, over 4,000m hight and less than 0°C annual temperature, is situated in the heart of the plateau. Most elements including Ag, Au, Ba, Be, Bi, Cd, Co, Cr, Cu, F, Hg, La, Li, Mn, Mo, Nb, Ni, P, Pb, Sn, Sr, Th, U, V, Y, Zn, Zr, SiO_2, Al_2O_3, TFe_2O_3, MgO and Na_2O in the stream sediments are quite close to the average value of the whole area and only As, B, Sb, W and K_2O are slightly enriched .

High-cold lake terrain is over 800,000km^2, 4500m hight, 100-400mm rainfall and 0°C-4°C annual tempreture. Most elements including Cr, La, Li, Nb, P, Sn, Sr, V, Zr, Al_2O_3, TFe_2O_3, Ag, B, Ba, Be, Bi, Cd, Co, F, Hg, Li, Mn, Mo, Ni, Pb, Th, U, W, Y, Zn, K_2O, MgO, Na_2O in the terrain are decreased and only CaO is strongly enriched and As, Sb, Sr are slightly encreased.

Desert is widespread in west part of China and over 800,000km^2 in the plateau, in which annual rainfall is less than 400mm and the annual temperature is about 0 °C. The many elements like As, B, Cd, Hg, Li, Ni, Sb, Ti, U, V, W, Zn, Ag, Be, Bi, Co, Cr, Cu, F, La, Mn, Mo, Nb, P, Pb, Sn, Th, Y, Zr, TFe_2O_3 in the terrain are low than the average value of whole plateau; but Ba, Sr, CaO, MgO, Na_2O and K_2O are increased.

Deep valley landscape, which is 640,000 km^2 and over 1500m relief, is distributed around the plateau. The average contents of most elements including Ag, Au,Be, Cd, Co, Cr, Cu, F, Hg, Mn, Mo, La, Li, Mn, Mo, Nb, Ni, P, Pb, Sn, Th, Ti, U, V, W, Y, Zn, Zr, Al_2O_3, Tfe_2O_3 and K_2O in the terrain are much higher than that in whole plateau.

https://doi.org/10.1180/S0026461X00006502 Published online by Cambridge University Press

n-Alkan-2-ones of lacustrine sediments and its climate significance in Linxia Basin, NE Tibetan Plateau, NW China

YONGLI WANG[1,2], XIAOMING FANG[2], YUANMAO LI[1], DAXIANG HE[1], YINGQIN WU[1], HUI YANG[1] AND YOUXIAO WANG[1]

[1]Key Laboratory of Petroleum Resources Research, Institute of Geology and Geophysics, Chinese Academy of Sciences, Lanzhou 730000, China

[2]Center of Basin-Mountain System and Environ-ment, Institute of Tibetan Plateau Research, Chinese Academy of Sciences, Beijing 100085, China (correspondence:Fangxm@itpcas.ac.cn)

Abundant n-alkan-2-ones were detected in all samples and the distribution ranging was from C17 to C31 in the lacustrine sediments of Maogou section in the Linxia Basin, NE Tibetan Plateau, NW China. The maxima peaks of C27, C29 and C31 were especially obvious and the odd carbon number predominance was remarkable from C25 to C31. The different maxima peaks of n-alkan-2-one from relative higher to lower carbon-numbered compounds were changed obviously and six climate stages could be identified in entire depositional section. Abundant isoprene-ketones (i.e., isomeric C18 ketones, iKC18) were detected in all samples. The relative abundance of isoprene-ketones for MG5 and MG8 to MG11 were higher, while that for MG1 to MG4 and MG6 to MG7 were lower. The isoprene-ketone can be regarded as recorder of temperature changes of the sedimentary environment. The higher abundance of isoprene-ketones indicates the low temperature of the sedimentary environment. The greatest change showed for MG7 to MG8 when the relative abundance of isoprene-ketones increased sharply, indicating the climate turned to cold condition at ~8Ma suddenly. Another obvious change in the relative abundance of isoprene-ketones was higher in MG5 indicating a cold condition at ~13Ma.

Based on the distribution characteristics of these biomarkers, we suggest that they record information related to climate change.

Supported by grants No. KZCX2-YW-Q05-05, XDA05120204, KZCX2-EW -104(2), NSFC No.40672123 and 2005CB422001.

Water hydrogen and oxygen isotope composition characterization in the tea ditch of Anxian, China

WANG YONGLI, NI SHIJUN AND ZHANG CHENGJIANG

[1]Department of Geochemistry, Chengdu University of Technology, Sichuan Province, (wangyl@cdut.edu.cn, nsjl@cdut.edu.cn, zcj@cdut.edu.cn)

This paper studies isotopic composition in the Chayuan Gou of Anxian area. The results showed that the water body δD is between -68 ‰ ~ -54 ‰, $\delta^{18}O$ in between -11 ‰ ~ -8 ‰; Sample put above global rainfall line and distribute in two different area(ChuBa Gou water area, Chayuan Gou water area). these show the groundwater and surface water originated in the meteoric waters of supply; according to $\delta^{18}O$ isotopic composition water Supplies elevation are about 1400 ~ 1500m.

ChuBa Gou water system and Chayuan Gou water system has different hydrogen and oxygen isotopic composition, the front is enrich lighter isotopes and the later is enrich heavy isotopes. S15 isotopic composition of spring water showed that the groundwater come from different two type groundwater mixing, the mixing ratio of 3:2.

https://doi.org/10.1180/S0026461X00006502 Published online by Cambridge University Press

Mechanism of uranium accumulation in a mining-impacted acidic peatbog

Y. WANG[1]*, M. FRUTSCHI[1], V. PHROMMAVANH[2], M. DESCOSTES[2] AND R. BERNIER-LATMANI[1]

[1]Ecole Polytechnique Fédérale de Lausanne (EPFL), Environmental Microbiology Laboratory (EML), Station 6, CH-1015 Lausanne, Switzerland (*correspondence: yuheng.wang@epfl.ch)

[2]AREVA NC - Business Group Mines, Direction R&D, BAL 3720C, Tour AREVA, 1, place Jean Millier, 92084 Paris La Défense Cedex, France

Uranium can accumulate in peatbogs from both natural and anthropogenic sources [1, 2]. An acidic peatbog located in central France was affected by historical uranium mining activities as well as by continued uranium leaching from granite rocks. As a result, this site displays areas, referred to as hotspots, in which uranium concentration can reach up to 4,000 mg/kg [3]. The first-order question for this site is the mechanism leading to this remarkable accumulation. Microbially-driven reductive immobilization is a possible route but so is the complexation of U(VI) by solid phase organic matter that is abundant in the peat soil.

In order to unravel this mechanism and to evaluate the impact of proposed remediation strategies, extensive depth-resolved sampling of soil and porewater have been carried out at hotspots as well as at U-free background areas. Core samples were analyzed for chemical composition, mineralogy and uranium speciation using a combination of x-ray diffraction, gamma spectrometry, sequential chemical extractions, electron microscopy of petrographic sections, cryo electron microscopy of plunge-frozen samples and bulk and micro-scale X-ray absorption spectroscopy. Moreover, the microbial community present in the soil was characterized phylogenetically and probed for its metabolic potential for U(VI) reduction. Additionally, porewater physico-chemical parameters (e.g., pH, Eh, DO, Fe(II), SO_4^{2-}, sulfide, U, Mn(II), major inorganic cations and anions, TOC, TIC) were obtained from the same spots to allow correlation of the water and soil characteristics as a fucntion of depth. This approach is the basis for a delineation of the redox transition from oxic to anoxic and the corresponding microbial activity in each redox zone and provides the information needed to understand the mechanism of accumulation of U in this site.

[1] Krachler and Shotyk (2004). *J Environ Monit* **6**, 418-426. [2] Regenspurg *et al*. (2010). *Geochim Cosmochim Acta* **74**, 2082-2098. [3] Moulin (2008). PhD, Ecole Centrale de Paris.

Modeling hydrogen and carbon isotopes of thermogenic gases from different kerogens in closed system

YUNPENG WANG[1], CHANGYI ZHAO[2] ,HONGJUN WANG[2] AND JINZHONG LIU[1]

[1]SKLOG, Guangzhou Institute of Geochemistry, Chinese Academy of Sciences, Guangzhou 510640, China

[2]RIPED of PetroChina, Beijing 100083, China

For better characterizing the hydrogen and carbon isotopes of thermogenic gases, we studied three selected lacustrine, marine and terrigenous kerogen (coal) samples using gold-tube closed system. We found the obvious fractionation mutation of hydrogen isotope at higher conversion rate for lacustrine and marine kerogen. How to model the isotopic variation is a key issue. Here, we take Rayleigh's method proposed by Rooney (1995) [1], and the isotopic variation was modeled by using two Rayleigh's functions and the results are showing in Fig. 1. In Rayleigh's function, we fitted the experimental results through adjusting the initial isotope compositions of the gas precursors (δ_0) and fractionation factors (ε=1000(α-1), α is the ratio of reaction rates of isotopes). It is clear that there exist variations for evolution trend of lacustrine and marine kerogen while conversion rate (F) reaches around 0.6, but the variation is not obvious for coal in comparison. Figure 1 suggests that the initial isotope and fractionation factor changed for type I/II kerogen. Inspecting the generation and cracking record, we found these variations are corresponding to the onset temperature of massive secondary cracking of heavy hydrocarbons to methane. This study implies that the secondary cracking of oil in closed system will chang the hydrogen and carbon isotopes of thermogenic gases.

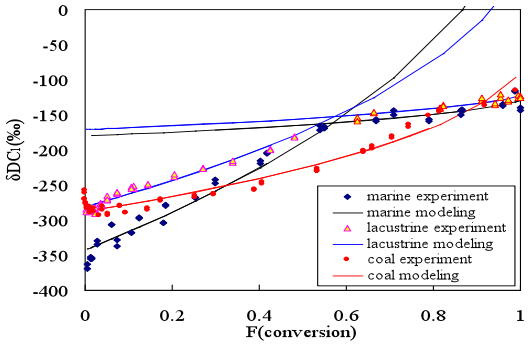

Figure 1: The experimental and modeling results

[1] Rooney *et al*. (1995) *Chem. Geology*. **126**, 219–232.

https://doi.org/10.1180/S0026461X00006502 Published online by Cambridge University Press

Fractionation of highly siderophile elements, selenium and tellurium in peridotites from the Baldissero and Balmuccia peridotite massifs, Ivrea Zone (Northern Italy)

Z. WANG*, H. BECKER AND T. GAWRONSKI

Freie Universität Berlin, Institut für Geologische Wissenschaften, Malteserstrasse 74-100, D-12249 Berlin, Germany (*correspondence: zaicongwang@gmail.com)

Peridotites from the Ivrea Zone (Northern Italy) are known for their excellent preservation and absence of low temperature alteration features. We have determined abundances of highly siderophile elements (HSE), Se and Te, and $^{187}Os/^{188}Os$ in depleted and fertile spinel lherzolites and a harzburgite (loss on ignition <1 %) from the Balmuccia and Baldissero massifs in order to study the behaviour of elements such as Au, Re, Se and Te that are otherwise easily affected by alteration processes. The lherzolites (Al_2O_3=2.0-3.1 %) have absolute and relative abundances of Os, Ir and Ru (Os/Ir=1.13±0.04, Ru/Ir = 2.02±0.08, n=10), consistent with typical mantle lherzolites. Incompatible HSE are relatively depleted (e.g., Re/Ir = 0.04±0.02, Au/Ir= 0.30±0.10, Pd/Ir=1.90±0.40). Balmuccia peridotites show limited variation and Baldissero peridotites larger scatter, with a harzburgite showing the lowest abundances of incompatible HSE and chalcophiles. All samples show a systematic depletion pattern in CI chondrite normalized diagrams with Pd > Au > Re, but no systematic variation with lithophile tracers exist. Se concentrations of lherzolites range between 54 and 89 ng/g and Te contents from 12 to 18 ng/g, resulting in Se/Te (4.2-7.3) below CI chondrite values. Initial $\gamma Os_{(300Ma)}$ (-2.3 to +2.0) are consistent with the notion that the last partial melting event occurred during the Phanerozoic. The data on lherzolites can be explained by moderate degrees of partial melting and control of partitioning by sulphide-silicate equilibrium with $D_{Re}<D_{Au}<D_{Pd}$ and $D_{Se}<D_{Te}$.

In situ stable isotopic detection of anaerobic oxidation of methane in Monterey Bay cold seeps via integrated cavity ouput spectroscopy

SCOTT D. WANKEL[1]*, MANISH GUPTA[2], J. BRIAN LEEN[2], ROBERT PROVENCAL[2], VIMAL PARSOTAM[2] AND PETER R. GIRGUIS[3]

[1]Department of Earth and Planetary Sciences, Harvard University, Cambridge, MA 02138 (*correspondence: sdwankel@fas.harvard.edu)
[2]Los Gatos Research, Inc., Mountain View, CA 94041
[3]Department of Organismic and Evolutionary Biology, Harvard University, Cambridge, MA 02138

Anaerobic methane oxidation (AOM) plays an important role in the global methane cycle by governing the release of CH_4 from anoxic sediments into the global ocean and ultimately the atmosphere. Thus, gaining an accurate understanding of both the distribution of CH_4 sources and the occurrence of AOM as well as the spatial and temporal variability of cycling pathways is critical. Environmental analyses of methane stable isotopic composition ($\delta^{13}C_{CH4}$) provide just such an indicator of CH_4 source, whether biogenic or thermogenic, as well as a spatial and temporal integrator of microbial cycling pathways, such as AOM. Here we present results from several deployments of a newly developed *in situ* methane stable isotope analyzer (Off-Axis ICOS) capable of measuring $\delta^{13}C_{CH4}$ to full ocean depths. Deployments to cold seep environments (960m) in Monterey Canyon (California) revealed a distinct separation between $\delta^{13}C_{CH4}$ in advecting fluids relative to sediment pore fluids. Multiple visits to two sites revealed $\delta^{13}C_{CH4}$ in advecting fluids ranging from -70.2 to -63.8‰, while fluids sampled from adjacent pushcore holes exhibited higher $\delta^{13}C_{CH4}$ (-64.2 to -50.2‰). While advective flux of CH_4 from the central seep orifice is substantial, these data implicate the importance of AOM in consuming a minimum of 57 to 70% of the diffusive flux of CH_4 in the surrounding sediments.

https://doi.org/10.1180/S0026461X00006502 Published online by Cambridge University Press

Crustal accretion on mid-ocean ridges revealed through volatile concentrations in olivine-hosted melt inclusions

V.D. WANLESS*, A. SHAW AND M. BEHN

Department of Geology and Geophysics, Woods Hole Oceanographic Institution, Woods Hole, MA 02543, USA (*correspondence: dwanless@whoi.edu)

We present volatile (H_2O, CO_2, Cl, S, and F) and major element data from melt inclusions in olivines found in crustal xenoliths and crystal clots from the fast-spreading East Pacific Rise to determine the depths of crystallization on mid-ocean ridges (MOR). The melt inclusions are generally, more primitive compared to the host glasses, with MgO concentrations ranging from 7.5 to 11.5 wt% and 6.6 to 8.4 wt%, respectively. Vapor saturation pressures calculated from equilibrium CO_2-H_2O concentrations suggest crystallization depths ranging from the crust-mantle transition (~6 km bsf) to above the seismically imaged, shallow melt lens (~600 m bsf). Minimum pressures estimates indicate that most of the melt inclusions (~70%) cluster between 1 and 2.5 km, consistent with crystallization in the shallow melt lens. However, the remaining melt inclusions show minimum equilibration pressures deeper than 2.5 km, implying that olivine crystallization beneath fast-spreading centers is not limited to the shallow melt lens.

Vapor-saturation pressures are also used to determine how volatile and major element concentrations vary with depth in the ocean crust. In general, volatile concentrations are much more variable in the upper 4 km of crust compared to the lower crust. For instance, Cl concentrations in melt inclusions formed in the upper crust range from 10 to 66 ppm, compared to only 42 to 51 ppm in melt inclusions formed deeper in the crust. This may result from higher degrees of fractional crystallization and/or increased fluid-rock interaction in the shallow crust. Major elements show no systematic variations with depth; however, more evolved olivines (Fo <86) are restricted to pressures within the shallow crust.

Several models have been proposed for crustal accretion beneath MORs (e.g., gabbro glacier or stacked sills), however there is no consensus on how the lower crust is formed at MORs or the depths over which crystallization occurs. Our volatile data imply that crystallization on fast-spreading ridges occurs throughout the crust, favoring models of in-situ crystallization or stacked sills and is inconsistent with a purely top-down, gabbro glacier model for lower crustal accretion on fast-spreading MORs.

A role of plant biomass-derived black carbon in electron transfer processes?

T. WANZEK[1], M. KEILUWEIT[1,2], D.PIERSON,[1] J. BAHAM[1] AND M. KLEBER[1]*

[1]Oregon State University, Department of Crop and Soil Science, Corvallis, OR 97331 (*correspondence: Markus.Kleber@oregonstate.edu)

[2]Lawrence Livermore National Laboratory, Physical and Life Sciences Directorate, Livermore, CA 94550

Recent work by Roden *et al*. [1] has provided strong evidence for a role of aromatic compounds in providing solid-state electron shuttles for electron transfer between bacteria and metal oxide surfaces. Historically, such materials are considered to be part of operationally defined "humic" substances [2] and are thought to result from "humification", i.e., from processes of secondary synthesis in the course of organic matter decomposition. However, there is increasing evidence that soils and sediments are subject to large imports of aromatic carbon on a global scale [3,4] through vegetation fires and additions of industrial black carbon. Future additions of aromatic carbon to soils are expected to rise in the wake of the evolving "Biochar" movement [5].

Up to one fifth of oxygen-containing functional groups on industrial black carbon can have quinonic functionality [6], and a number of studies suggest that quinone functionalities within natural organic matter can be a suitable electron transfer mediator for iron bioreduction and contaminant degradation [7]. It has been determined that the efficiency of quinone redox mediators is controlled by their reduction potential, stability towards side reactions and kinetic reactivity in electron transfer reactions [7].

Here we take a first step towards identifying a potential role of plant biomass-derived black carbon in generating aromatic compounds with the ability to serve as electron transfer media. Titrations and spectroscopic information were used to test the hypothesis that redox potentials of chars vary as a function of quinone group abundance. Grass and wood chars generated across a range of heat treatment temperatures [8] allowed us to represent the varying amounts of oxygenated surface groups known to occur in natural chars.

[1] Roden *et al*. (2010). *Nature Geoscience* **3**:417-421. [2] Lovley *et al*. (1996). *Nature* **382**:445-448. [3] Schmidt & Noack. (2000). *Global Biogeochem. Cycles* **14**:777-793. [4] Rodionov *et al*. (2010). *Global Biogeochem. Cycles* **24**:Gb3013. [5] Lehmann J. (2007). *Nature* **447**:143-144. [6] Studebaker *et al*. (1956). *Ind. & Eng. Chemistry* **48**:162-166. [7] Uchimiya & Stone. (2009). *Chemosphere* **77**:451-458. [8] Keiluweit *et al*. (2010). *ES&T* **44**:1247-1253.

https://doi.org/10.1180/S0026461X00006502 Published online by Cambridge University Press

Modelling phase behaviour in the geological storage of carbon dioxide

O. WARR[1]*, C.J. BALLENTINE[1] AND A. MASTERS[2]

[1]SEAES, University of Manchester, M13 9PL, UK (*correspondence: oliver.warr@postgrad.manchester.ac.uk)
[2]CEAS, University of Manchester, M13 9PL, UK

Global warming is currently accepted as a key issue facing man. One potentially viable solution is carbon dioxide sequestration in shallow aquifers [1] where carbon dioxide is expected to exist as a supercritical phase above an underlying water phase [2]. It is essential therefore that this binary phase system is fully understood. One technique is to use trace inert proxies (i.e. noble gases) which can coexist as solute particles within both phases, the partitioning of which is affected by the extent of phase interactions (groundwater contact) and the magnitude/rate of carbon dioxide dissolution. These proxies can therefore be used to yield essential information on these processes [3].

It is however imperative that noble gas partitioning between the two phases is well constrained. We are constructing a Gibbs-Ensemble Monte Carlo simulation to model this binary phase system which will include noble gas tracers to generate the partitioning coefficients for all noble gases for the wide range of conditions expected in storage sites. This simulation simultaneously samples the molecular configurations in both water-rich and carbon dioxide-rich phases. Particles are exchanged between the two systems. At steady state the two phases are at thermodynamic equilibrium and the corresponding compositions and overall densities can be calculated. Models selected for water [4] and carbon dioxide [5] have already been extensively tested across the temperatures and pressure ranges of interest (40-150 Bar, 320-360 K) with average simulated densities being within 1.1% and 5% respectively of experimental values and thus are considered sufficiently accurate thermodynamically for incorporation into the model. Further ground-truthing for the model is being provided by lab experiments under simulated shallow aquifer conditions. We present the current progress in creating this model and discussion of the challenges which have arisen as a result of modelling such a complex system.

[1] IPCC (2005) [2] Holloway & Savage (1993) *Energy Convers. Mgmt* **34**, 925-932. [3] Ballentine & Burnard (2002) *RiMG* **47** 481-538. [4] Berendsen *et al.* (1987) *J. Phys. Chem* **91**, 6269-6271. [5] Zhu *et al.* (2009) *Chin. J Chem. Eng.* **17**, 268-272.

Mantle heterogeneity constraints from abyssal peridotite sulfide Pb and Os isotopic compositions

JESSICA M. WARREN[1]* AND STEVEN B. SHIREY[2]

[1]Geological and Environmental Sciences, Stanford University (*correspondence: warrenj@stanford.edu)
[2]Department of Terrestrial Magnetism, Carnegie Institution of Washington

Convection over the history of the Earth has led to multiple cycles of mantle depletion and enrichment, which are preserved as ancient chemical compositional anomalies in the oceanic mantle. Studies of long-lived radiogenic isotopes in basalts, such as Pb, have indicated signficant mantle heterogeneity in both the depleted upper mantle and the mantle source of ocean island basalts. The basalt data array defines a ~2 Ga age that has been interpreted as recording mixing of ancient subducted slabs with depleted mantle.

In contrast to basalts, abyssal peridotites from oceanic ridges have the potential to constrain the sub-kilometer lengthscale of mantle variability. Analysis of Pb isotopes in peridotites has been limited by the very low concentration of Pb in these residues of mantle melting. We have employed a technique for the determination of Pb and Re-Os isotopes and concentrations in peridotite sulfides using a modified version of the Re-Os technique for sulfide inclusions in diamonds.

The Pb and Re-Os isotopic composition of 21 sulfide grains were determined for abyssal peridotites from the Gakkel and Southwest Indian Ridges. Concentrations of Pb and Os in sulfides are correlated, with a correlation coefficient of ~0.8. The relatively lower mantle normalized concentrations of Pb (27, for an average of 4 ppm) with respect to Os (470, for an average of 1.6 ppm) indicates that Pb is much less compatible in sulfide during mantle melting than previously thought. Sulfide Pb concentrations are so low that sulfides cannot be the main reservoir of mantle Pb, storing only ~2%, with the remainder hosted in silicates.

Sulfide Pb isotopic compositions extend to unradiogenic values that plot to the left of the geochron and cover a wider range than associated basalts. Pb and Os isotopic compositons are correlated, also with a coefficient of ~0.8. The Re-Os data in sulfides fall along a 2 Ga model age, similar to the age given by the Pb-Pb system for the same sulfides. Multiple grains from the same peridotite have different isotopic compositions and elemental concentrations. Taken together, these results indicate that the mantle is heterogeneous down to the sub-sample lengthscale, with the Pb-Os correlation requiring that these heterogeneities were created by prior ridge melting events at ~2 Ga.

https://doi.org/10.1180/S0026461X00006502 Published online by Cambridge University Press

Suspended floc: Links between microbial ecology, FeOOH and trace element dynamics

L.A.WARREN*, A.V.C. ELLIOTT AND J.M. PLACH

SGES, McMaster University, 1280 Main St West, Hamilton ON L8S4K1 Canada
(*correspondence: warrenl@mcmaster.ca)

The linkages between microorganisms and geochemical processes in environmental systems hinge on ecological relationships associated with the microbial consortia involved. These ecological relationships are often highly cooperative and macroscopically structured to enable microscale redox cycling not favourable under bulk system conditions. Suspended floc, highly microbially active, trace element (TE) rich and interactive with bulk aqueous solution, are poorly studied with respect to microbial-mineral-TE biogeochemistry. Characterization of suspended floc TE abundance and partitioning for Ag, As, Cu, Ni and Co across six variably impacted aquatic ecosystems identify floc to be a key TE sequestration sedimentary compartment, concentrating TE ~55x above that of surficial bed sediments. Further, floc TE-geochemical partitioning patterns were conserved across systems, with amorphous Fe oxyhydroxides (FeOOH) consistently as the most important sorbent phase for TE retention, irrespective of physcio-chemical conditions or TE involved. Results indicate that floc TE uptake is biologically linked to floc microbial components. Floc organic concentration directly predicts floc FeOOH concentration while imaging analysis shows bacterial exopolymeric substances (EPS) fibrils, a major floc constituent, to be heavily mineralized. Thus while floc FeOOH are the dominant floc TE sequestration phase, EPS and microbial constituents are the critical foundation underpinning floc TE behaviour through their structural role in floc FeOOH occurrence, ultimately creating a distinctly different solid than bed sediments with differing controls on TE uptake. Further, the enrichment of both iron reducing and iron oxidizing microorganisms from all flocs collected across a spectrum of systems widely variant in [O_2] and pH indicate previously unconstrained Fe cycling occurs at the floc scale that is controlled by floc ecology, not by system geochemistry. These results add to the growing evidence that ecological partnership enables consortial microbes to "sidestep" geochemical constraints predicted to occur at the bulk scale.

Carbonation of artificial silicate minerals: Passive removal of atmospheric CO_2

C-L. WASHBOURNE[1]*, P. RENFORTH[2] AND D.A.C. MANNING[1]

[1]School of Civil Engineering and Geosciences, Newcastle University, NE1 7RU, United Kingdom (*correspondence: carla-leanne.washbourne@ncl.ac.uk)
[2]Department of Earth Sciences, University of Oxford, Oxford, OX1 3AN, United Kingdom

Artificial silicate minerals present an accessible source of material for enhanced weathering. Silicate 'wastes' may perform carbon sequestration through *in situ* carbonation of calcium (Ca) and magnesium (Mg) phases. Maximum carbon (C) capture potential using artificial silicates is 190-332Mt C a^{-1} [1]. Soil engineering, promoting CO_2 sequestration by inclusion of these reactive mineral substrates, has the potential to capture a portion of the C turnover of the global pedologic system; 75 Gt C a^{-1} [2][3][4].

Stable isotope data ($\delta^{13}C$, $\delta^{18}O$) confirm that >50-90% of C in pedogenic carbonates, formed on artificial silicates, is atmospherically derived. Field observations and laboratory data demonstrate that anthropogenic soils accumulate 20-30 kg C m^2 as carbonates (≥organic carbon content in natural soils). Flow-through experiments (25°C, 1 atm.) using fresh basic steel slag show pH buffered at ~11.6 as Ca leaches at a rate of $\log_{10}$-8.9 – $\log_{10}$-9.3$mol^{-1}sec^{-1}cm^{-2}$, several orders of magnitude faster than 'natural' silicates. Once portlandite ($Ca(OH)_2$) has been consumed pH is reduced to ~9.1 and calcium carbonate precipitation continues.

Effective, low-energy field-scale implementation of mineral carbonation through soil engineering could assuage current constraints on economic performance [5][6][7]. Proof of principle for carbonation of artificial silicates in engineered soils has been demonstrated [4]; proof of field scale feasibility will be demonstrated though continued empirical and experimental observation including extensive analysis of carbon in urban soils at the Science Central development site, Newcastle upon Tyne, UK.

[1] Renforth *et al*. (2011), *Environ Sci Technol* **45** *(6) 2035-41* [2] Schlesinger *et al*. (2000), *Biogeochem*, **48**; 7-20 [3] Manning (2008), *Min Mag*, **72**; 639-649 [4] Renforth *et al*. (2009), *Applied Geochem*, **24** (9) 1757-1764 [5] Butt *et al*. (1997), *Global Warming International Conference*, Columbia NY. [6] Huijgen *et al*. (2005), *Environ Sci and Technol* **39**: 9676-9682 [7] Lackner *et al*. (1997), *Energy Conversion and Management* **38**: S259-S264

https://doi.org/10.1180/S0026461X00006502 Published online by Cambridge University Press

Pathways of dissolved organic matter in the subterranean estuary: Evaluation of organic geochemical tracers

HANNELORE WASKA[1]*, MICHAEL SEIDEL[1], THORSTEN DITTMAR[1] AND GUEBUEM KIM[2]

[1]Max Planck Research Group for Marine Geochemistry, ICBM, University of Oldenburg, Germany (*correspondence: hwaska@mpi-bremen.de, mseidel@mpi-bremen.de, tdittmar@mpi-bremen.de)
[2]Environmental and Marine Biogeochemistry Laboratory, School of Earth and Environmental Sciences, Seoul National University, South Korea (gkim@snu.ac.kr)

The mixing zone of fresh terrestrial groundwater and recirculating seawater in a coastal permeable aquifer, the so-called "subterranean estuary", is a powerful bioreactor which determines the fate of dissolved compounds as they are transported into the ocean via submarine groundwater discharge (SGD). Dissolved organic matter (DOM) plays a crucial role in driving microbial remineralization processes, and through its breakdown contributes to the groundwater nutrient pool. Until recently, DOM in the subterranean estuary was mostly determined as bulk dissolved organic carbon, providing limited information on sources and degradation states. Studies of chromophoric DOM (CDOM) and biomarkers such as lignin provide information on DOM origin. Other traditional parameters, such as amino acid D/L ratios and degradation indices, and stable isotopic composition (e.g. $\delta^{13}C$), can be used to track the processing of DOM. Emerging analytical techniques, e.g. ultra-high resolution Fourier-transform ion cyclotron resonance mass spectrometry (FT-ICR-MS), improve our understanding of the chemical composition of DOM by providing molecular fingerprints. We investigated two intertidal subterranean estuaries, in Hampyeong Bay along the Yellow Sea coast of South Korea and on Spiekeroog Island, a barrier island in the German Wadden Sea. The major objective was to characterize pathways of DOM as it travels through the aquifer. In Hampyeong Bay, amino acid and CDOM data pointed to a mostly marine DOM source, whereas on Spiekeroog, $\delta^{13}C$ values indicated both a marine and a terrestrial DOM source. Molecular fingerprinting showed that a large amount of DOM was processed in the aquifer of Spiekeroog Island, whereas several components were passing the subterranean estuary unaltered, possibly forming a source of refractory DOM.

Is your clean lab full of zinc?

L.E. WASYLENKI[1]*, E.B. WILKES[2] AND A.D. ANBAR[3]

[1]Dept. of Geological Sciences, Indiana University, 1001 East Tenth Street, Bloomington, IN 47405-1405 USA (*correspondence: lauraw@indiana.edu)
[2]Dartmouth College, Hanover, NH 03755 USA
[3]School of Earth and Space Exploration and Dept. of Chemistry and Biochemistry, Arizona State University, Tempe, AZ 85287 USA

Contamination of samples with extraneous zinc is likely much more common and severe than many metal isotope geochemists expect. Bottles, tubes, pipette tips, and especially disposable gloves are often produced with Zn stearate as the mold release agent. By far the largest amount of zinc is introduced by gloves. Dilute HCl will effectively rid other items of Zn, but gloves cannot be cleaned easily, and their use can lead to surface contamination throughout the lab.

We recently conducted experiments in which dissolved Zn was partly adsorbed onto Mn-oxide particles. The dissolved and adsorbed pools were separated by filtration, and isotope ratios were analyzed by MC-ICP-MS. A commercial ICP solution was both our standard ($\delta^{66/64}Zn = 0$) and the source of Zn in the experiments. When gloves were worn for sample handling, blanks contained as much as 150 ng Zn, and both the dissolved and adsorbed pools came out enriched in heavy isotopes relative to the starting pool, in apparent violation of mass balance. Without gloves, blanks were lower, but still variable, and mass balance was more closely satisfied. Zinc leached from two brands of allegedly low-zinc vinyl gloves was +10‰ relative to our standard ($\delta^{66/64}Zn$). We conclude that glove Zn in our lab contaminated our samples, even when gloves were not worn for sample processing.

We were only able to see clear evidence of contamination because (1) we had an expectation of mass balance, and (2) we happened to use a standard strongly enriched in light isotopes relative to our gloves. We caution others who measure unknown, natural samples that most natural samples are similar in isotopic composition to the gloves we measured and to JMC-Lyon Zn, which is becoming an accepted Zn isotope standard. Knowing whether variable amounts of glove zinc are contaminating samples is therefore a challenge. We recommend very careful monitoring of blanks and column chemistry yields, and we plan to designate and clean a glove-free workspace within the clean lab for further zinc isotope work.

https://doi.org/10.1180/S0026461X00006502 Published online by Cambridge University Press

Raman spectroscopic insight into structural changes in berlinite with high pressure and temperature

ANKE WATENPHUL[1]* AND CHRISTIAN SCHMIDT[2]

[1]Deutsches Elektronen-Synchrotron DESY, Notkestr. 86, 22603 Hamburg, Germany (anke.watenphul@desy.de) (* correspondence: anke.watenphul@desy.de)
[2]Deutsches GeoForschungsZentrum (GFZ), Telegrafenberg, 14473 Potsdam, Germany (hokie@gfz-potsdam.de)

Berlinite ($AlPO_4$) and α-quartz are structural isotypes, which are related to each other by the coupled substitution 2 Si = Al + P. The SiO_4 tetrahedra along the *c*-axis in α-quartz are replaced in berlinite by alternating AlO_4 and PO_4 tetrahedra. This preferred ordering results in a doubled *c* unit-cell parameter. The frequencies of Raman modes of berlinite and α-quartz are very similar because the atomic masses of Al + P are almost the same as that of two Si atoms [1]. However, detailed inspection reveals a greater complexity in the Raman spectrum of berlinite [2]. To obtain more information on the relationships to the berlinite structure, we studied the strong A_1-Raman lines at 462 and the 1111 cm^{-1} at temperatures up to 800 °C and pressures up to 10 GPa.

The positions of both bands shift in the opposite direction with pressure (*P*) and, likewise, with temperature (*T*). The 1111 cm^{-1} Raman line is accompanied by a less intense band at 1104 cm^{-1}. With increasing *P*, the 1111 cm^{-1} band shifts towards lower wavenumbers and that at 1104 cm^{-1} to higher wavenumbers. Both lines thus display the same frequency at about 1.4 GPa at 23 °C. With further increase in *P*, they become fully separated above 5 GPa. Both Raman lines originate from stretching vibrations of the PO_4 tetrahedra. The opposed behavior with pressure is tentatively interpreted as being caused by the alternate succession of the AlO_4 and PO_4 tetrahedra along the *c*-axis, which permits a different compression/extension of the P-O1 and P-O2 distances.

The results also indicate the great potential of berlinite as a pressure sensor for diamond-anvil cell experiments, including studies at elevated *T*. A relative shift, defined by the difference of the shifts in the wavenumber between the 462 and the 1111 cm^{-1} lines with *P* and *T*, can be used as pressure gauge. Moreover, this sensor may be applicable at higher pressures than α-quartz [3] because no high-pressure polymorph isomorphic to coesite or stishovite is known.

[1] Scott (1971), *Phys. Rev. B* **4**, 1360-1366. [2] Gregora *et al.* (2003) *J. Phys.: Condens. Matter* **15**, 4487–4501. [3] Schmidt & Ziemann (2000), *Am. Mineral.* **85**, 1725-1734.

Effect of ionic strength on Ca isotope and Sr incorporation into calcite

J. WATKINS[1]*, D.J. DEPAOLO[1,2], F.J. RYERSON[3] AND M. GONZALES[4]

[1]Univ. of California-Berkeley, Berkeley, CA 94720, USA (*correspondence: jwatkins@berkeley.edu)
[2]Lawrence Berkeley National Laboratory, Berkeley, CA 94720, USA
[3]Lawrence Livermore National Laboratory, Livermore, CA 94550, USA
[4]The Pennsylvania State, University Park, PA 16802, USA

Chemical reactions in nature lead to stable isotope variations in part because diffusivities and reaction rates are mass-dependent. For crystals grown from aqueous solution, there is no general theory that relates reaction rate to mass, but the contribution of isotope-specific reaction rates to the net isotope composition of a mineral must be related to processes occurring at the mineral-fluid interface.

Laboratory experiments have shown that the Ca isotope composition ($\delta^{44}Ca$) of calcite precipitated from aqueous solution varies considerably (up to 1.5‰) and correlates with the crystal growth rate (*R*). Generally, inorganic calcite precipitation experiments yield calcite crystals that are enriched in the light isotope of Ca relative to the parent solution. The degree of light isotope enrichment correlates with Sr/Ca in calcite. These observations indicate that variations in $\delta^{44}Ca$ in calcite reflect a mass dependence on reaction rate coefficients (*k*) and that the physical process responsible for mass discrimination is also responsible for trace element discrimination. We postulate that dehydration/rehydration kinetics of Ca^{2+} and Sr^{2+} and/or the presence of impurities on the mineral surface are controlling the kinetic isotope and trace element effects. If true, the presence of other ions (e.g. NH_4^+) in solution should perturb the stability of the hydration shell of Ca^{2+} and Sr^{2+} and also interfere with their incorporation into the mineral lattice.

We present results from inorganic calcite precipitation experiments using two solutions that differ in ionic strength (*I*=0.095 vs. *I*=0.485 mol/l). In low ionic strength experiments, we observe correlations between $\delta^{44}Ca$, Sr/Ca and *R* that are in excellent agreement with results from a previous study that used a similar parent solution composition (Tang *et al.*, *GCA*, 2008). In our initial experiments at high ionic strength, values of $\delta^{44}Ca$ vs. *R* and Sr/Ca vs. *R* lie off the previous trends, but $\delta^{44}Ca$ and Sr/Ca co-vary such that $\delta^{44}Ca$ vs. Sr/Ca is relatively independent of solution composition. Additional experiments are underway and results will be discussed in the context of molecular-scale processes - and their liquid composition-dependence – controlling isotopic and trace element incorporation into minerals.

https://doi.org/10.1180/S0026461X00006502 Published online by Cambridge University Press

Sum Frequency Vibrational Spectroscopy (SFVS) of water and hydroxyls on the corundum ($1\bar{1}02$) surface: Acid-base properties from direct observation of protonation states

G. A. WAYCHUNAS[1]*, J. SUNG[2] AND Y. R. SHEN[2]

[1]Earth Sciences Division, LBNL, Berkeley, CA 94720, USA (*correspondence: gawaychunas@lbl.gov

[2]Physics Department, UC Berkeley, Berkeley, CA 94720 USA

SFVS is a powerful tool for quantitative measurement of protonated functional groups on mineral surfaces, especially when used in a phase-sensitive mode [1]. This is demonstrated for the corundum ($1\bar{1}02$) interface where the orientation and nature of surface hydroxyls on the dry protonated surface can be obtained and compared with models for the surface termination derived from crystal truncation rod (CTR), X-ray reflectivity (XRR) measurements, and with the most likely functional group assignments [2]. Hydroxyl orientations are determined from pole-figure type measurements of the magnitude of the non-linear optical susceptibility for each band, and the polar orientation (up-down with respect to the z-direction) is determined from measurements of the imaginary part of the susceptibility. A scheme for describing the hydrogen bonding among these protonated groups is found to be consistent with surface symmetry and the particular vibrational frequencies observed. The addition of water to the interface alters the hydrogen bonding of the hydroxyls and introduces water-functional group hydrogen bonding [3]. Direct measurement of the SFVS hydroxyl and water band amplitudes as a function of pH can be used to test the expected pKa values for the functional groups, and hence link interfacial acid-base properties to precise molecular surface entities and their protonation states.

This research has been in part supported by the Division of Chemical Sciences, Geosciences and Biosciences, Office of Basic Energy Sciences, U.S. Department of Energy.

[1] Shen & Ostroverkhov (2006) *Chem. Rev.* **106**, 1140-1154. [2] Sung *et al.* (2011) *J. Amer. Chem. Soc.* **133**, 3846-3853. [3] Sung *et al.* (in review, *J. Amer. Chem. Soc.*)

Evolution of the lower crust from S. Mexico: Constraints from Lu-Hf isotopes and U-Pb ages in zircon

B. WEBER[1]*, E. SCHERER[2], K. MEZGER[3] AND J. RUIZ[4]

[1]CICESE, 22860 Ensenada B.C., México (*correspondence: bweber@cicese.mx)

[2]Mineralogie, WWU, D-48149 Münster, Germany

[3]Geologie, Uni Bern, CH-3012 Bern, Switzerland

[4]Geosciences, Univ. Arizona, Tucson AZ, 85721 USA

Unraveling the origin and tectonic evolution of lower continental crust is often complicated by granulite facies metamorphism that obscures petrogenetic features and resets isotopic systems. In order to reconstruct the assemblage of ancient supercontinents (like Rodinia), it is crucial to understand the evolution of individual crustal blocks, its relations, and its position with respect to the cratons. Four isolated lower crustal complexes of mid-Proterozoic (Grenville) age also referred to as "Oaxaquia" [1] are exposed in E and SE Mexico. Oaxaquia was interpreted in terms of arc magmatism, followed by backarc rifting, and migmatization, predating AMCG (anorthosite-mangerite-charnockite-granite) intrusions and granulite facies metamorphism [2].

U-Pb zircon dating by laser ablation MC-ICPMS and single-grain Lu-Hf analysis by solution MC-ICPMS was applied to elucidate crustal growth and igneous history of Oaxaquia. Typical Oaxaquia rocks include AMCG suite rocks as well as arc-type migmatites and orthogneisses, all of which having zircon cores at ~1.2 Ga, additional igneous growth zones migmatite zircons, and granulite facies rims at ~1.0 Ga. Hafnium isotopes of typical Oaxaquia rocks display little variations yielding $T_{DM(Hf)}$ model ages from 1.50 to 1.65 Ga [3]. Significant differences could be observed in zircons from E Mexico orthogneiss (Huiznopala) with $T_{DM(Hf)}$ at ~1.8 Ga [3]. New detailed laser dating of such zircons revealed mostly ~1.4 Ga and older zircon cores, surrounded by ~1.2 Ga igneous zones, indicating melting of crustal precursors different from typical Oaxaquia.

The results lead to a new model in which typical Oaxaquia evolved as juvenile arc in the early mid-Proterozoic. Continental crustal slices, probably from the continental arc of Amazonia, were thrusted over or attached to the Oaxaquia oceanic arc, which was then buried and partially melted to produce AMCG rocks prior to the collision with Baltica during the final stage of Rodinia assemblage.

[1] Ortega-Gutiérrez *et al.* (1995) *Geology* **23**, 1127-1130. [2] Keppie *et al.* (2003) *Precambrian Res* **120**, 365-389. [3] Weber *et al.* (2010) *Precambrian Res* **182**, 149-162.

https://doi.org/10.1180/S0026461X00006502 Published online by Cambridge University Press

Airborne measurements of volcanic particles and gases with small aircrafts — Examples of measurements in the Eyjafjallajökull ash plume over Germany and Iceland

K. WEBER[1]*, J. ELIASSON[2], A. VOGEL[1], C. FISCHER[1], M.F. MEIER[3], B. GROBÉTY[3] AND D. DAHMANN[4]

[1]University of Applied Science, 40474 Düsseldorf, Germany (*correspondence: konradin.weber@fh-duesseldorf.de)
[2]University of Iceland, 107 Reykjavik, Iceland
[3]University of Fribourg, 1700 Fribourg, Switzerland,
[4]IGF, 44789 Bochum, Germany

During the 2010 eruption period of the Eyjafjallajökull the University of Applied Sciences of Duesseldorf and the University of Reykjavik performed several measurement flights with small aircraft in the volcanic plume. Whereas the University of Applied Sciences mapped the distal plume over Germany, the University of Iceland explored the airspace over western Iceland and near the Eyjafjallajökull, partly entering the volcanic plume boundary directly.

The use of the small piston-motor driven research aircraft in the special situation of volcanic plumes has several advantages over jet engine driven research aircrafts:

The piston-motor driven aircraft are robust enough to operate even at elevated ash concentration levels.

The small aircrafts allow a low cruising speed during the measurements and have thus the advantage of delivering results with a high spatial resolution.

The low possible aircraft cruising speed during the measurements simplifies the intake of even bigger ash particles into the measurement systems.

Small aircraft allow a very cost effective operation.

The aircraft were equipped with optical particle counters (OPCs) for on-line in-situ results. Moreover, the German aircraft was equipped with a DOAS system for SO_2 and a NDIR analyzer for CO_2 measurements.

The measurement flights revealed that the ash plume over Germany had a very inhomogeneous structure. Sub-plumes and different vertical plume layers could be identified. Regional elevated SO_2 concentrations could be detected. Peak ash particle concentrations of more than 330 μg/m3 could be found during the measurement flights over northern Germany, whereas the flights over Iceland showed low concentrations outside the plume, but values of about 2000 μg/m3 within the boundary of the plume.

A "cradle to grave" analysis of geothermal arsenic in a lowland river system

J.G. WEBSTER-BROWN[1]*, N.J. WILSON[2], A.F. HEGAN[3], H.K. CHRISTENSON[1] AND P.J. SWEDLUND[4]

[1]Waterways Centre for Freshwater Management, University of Canterbury, Christchurch, New Zealand (*jenny.webster-brown@canterbury.ac.nz, hannah.christenson@pg.canterbury.ac.nz)
[2]University of Bayreuth, Bayreuth, Germany (nathaniel.wilson@uni-bayreuth.de)
[3]SEAES, University of Manchester, United Kingdom. (aimee.hegan@manchester.ac.uk)
[4]Department of Chemistry, University of Auckland, New Zealand (p.swedlund@auckland.ac.nz)

In the central North Island of New Zealand, arsenic is released from geothermal hotsprings into the large lowland Waikato River, and thereafter into the Tasman Sea. Aspects of arsenic geochemistry in the geothermal fluids, and in the river and its lake waters, have been previously studied but a catchment-scale analysis of factors affecting geothermal arsenic on its journey to the sea has highlighted the importance of biological as well as geochemical processes.

Evidence for biological interactions with arsenic occurs on a different timescale to that typically used to identify geochemical interactions. For example, when arsenic is released into the surface environment via the Champagne Pool hot spring at Waiotapu, it occurs predominantly as arsenite ion. In the outflow arsenic is immediately exposed to a regime of decreasing temperature, attended by increasing oxygen and periodic influxes of H_2S from small fumeroles, favouring oxidation to arsenate ion or removal as orpiment (As_2S_3) respectively. However, diurnal variations in arsenic concentrations in the outflow confirm the influence of photosensitive microorganisms, evidently through their intervention in dissolved sulphide-sulphate equilibria. Similarly, after discharging into the Waikato River, geothermal arsenic appears to be most immediately controlled by adsorption to the iron oxide component of SPM. However, long term adsorption experiments under light/dark conditions, and a more detailed assessment of the competitive adsorption of important diatom nutrients; silica and phosphate, indicate that arsenic concentration is not regulated simply by the availability of iron oxide adsorption sites. In a river such as the Waikato, enriched in both geothermal silica and agricultural phosphate, diatom growth and decay also influences arsenic speciation and mobility.

https://doi.org/10.1180/S0026461X00006502 Published online by Cambridge University Press

Thermophilic anaerobic oxidation of methane performed by novel microbial consortia

G. WEGENER[1,2], K. KNITTEL[1], T. HOLLER[1], V. KRUKENBERG[1], F. WIDDEL[1] AND A. BOETIUS[1,2,3]

[1]Max Planck Institute for Marine Microbiology, Bremen, Germany
[2]MARUM, Center for Marine Environmental Sciences, Bremen, Germany
[3]Alfred Wegener Insitute for Polar and Marine Research, Bremerhaven, Germany

The anaerobic oxidation of methane with sulfate (AOM) controls the emission of the greenhouse gas methane from the ocean floor and is performed by microbial consortia of archaea (ANME) associated with bacterial partners [1]. So far, *in vitro* propagation of AOM was documented for temperatures up to approx. 25°C, but the presence of molecular ANME markers in hydrothermal sediments suggests higher temperature ranges for this process [2, 3]. In natural enrichments from Guaymas Basin hydrothermal sediments we show *in vitro* propagation of AOM up to 70°C with a growth optimum of 50°C and doubling times of around 60 days. We performed microbiological experiments and genetic, microscopic and mass spectrometric analyses to characterize the key agents in thermophilic AOM. The hot Guaymas enrichments are dominated by filamentous ANME-1 archaeal cells, which form individual sheaths around their bacterial partners. These belong to the deep-branching HotSeep-1 cluster which closest relatives are thermophilic sulfur reducers, e.g. *Desulfurella*. So far the interaction between these novel ANME-1 types and their bacterial partners is not resolved, but the highly structured consortia support previous hypotheses of an obligate syntrophic partnership. Furthermore, our results indicate that AOM might be more widespread than previously assumed including hot subsurface sediments and gas reservoirs [4,5] .

[1] Knittel & Boetius (2009) *Annu Rev Microbiol* [2] Teske *et al* (2002) *AEM* [3] Schouten *et al* (2003) *AEM* [4] Speed & Clayton (1975) *Geology* [5] Werner *et al* (1988) *Chem Geol*

Spinels under elevated pressures and temperatures – A synchrotron study

M. WEHBER[1]*, C. LATHE[2] AND F. SCHILLING[3]

[1]DESY/HASYLAB, Notkestrasse 85, 22607 Hamburg, Germany (*correspondence: michael.wehber@desy.de)
[2]Helmholtz-Centre Potsdam, GFZ German Research Centre for Geosciences, Telegrafenberg, 14473 Potsdam, Germany (christian.lathe@desy.de)
[3]KIT Karlsruhe Institute for Technology, Institute for Applied Geosciences, Kaiserstrasse 12, 76131 Karlsruhe, Germany (frank.schilling@kit.edu)

Spinels have the general formula AB_2O_4 and crystallize in the cubic spacegroup Fd-3m. They play important roles in geosciences and technical applications. The aim of this study was to make simultaneous high-pressure/high-temperature (HP/HT) measurements to find out how the thermal expansion behave under high pressure.

In this study, the three different spinels magnetite ($FeFe_2O_4$), franklinite ($ZnFe_2O_4$) and gahnite ($ZnAl_2O_4$) were investigated with energy-dispersive powder XRD using two different multi-anvil-presses at HASYLAB. Isothermal experiments were performed up to 15 GPa using MAX200x, thermal experiments up to 5 GPa and 1100 K using MAX80. Diffraction data were evaluated with the Rietveld-method to obtain the cell parameter of the sample and the pressure medium. Pressure-volume-data were fitted to second and third order Birch-Murnaghan equation of state to obtain the bulk moduli of each sample. In addition, the thermal expansion coefficient were calculated at different pressures.

Evaluation of the HP measurements yielded the following bulk moduli. For magnetite: $K_{T2nd} = 187(6)$ GPa, $K_{T3rd} = 184(7)$ GPa with $K' = 4.5(2)$, for franklinite $K_{T2nd} = 180(5)$ GPa, $K_{T3rd} = 178(6)$ GPa with $K' = 4.6$ and for gahnite $K_{T2nd} = 207(7)$ GPa, $K_{T3rd} = 204(9)$ GPa with $K' = 4.9$. HP/HT experiments showed a linear pressure dependence of the thermal expansion at least up to 5 GPa ($-1.3*10^{-6}$ $(KGPa)^{-1}$ for magnetite, $-1.7*10^{-6}(KGPa)^{-1}$ for franklinite and $-3.0*10^{-6}(KGPa)^{-6}$ for gahnite). There seems to be an additional connection to the iron content of the spinels whereat the increase of the iron content decreases the slope of the pressure dependence.

https://doi.org/10.1180/S0026461X00006502 Published online by Cambridge University Press

On the fluid-mobility of molybdenum, tungsten, and antimony in subduction systems

H. WEHRMANN*[1], R. HALAMA[2], D. GARBE-SCHÖNBERG[2], K. HOERNLE[1,3], G. JACQUES[1], K. HEYDOLPH[1,3], J. MAHLKE[1,3] AND K. SCHUMANN[1,3]

[1]Sonderforschungbereich 574, IFM-GEOMAR, Kiel, Germany (*hwehrmann@ifm-geomar.de)
[2]Sonderforschungbereich 574, Institute of Geosciences of the University of Kiel, Germany
[3]IFM-GEOMAR, Kiel, Germany

Molybdenum (Mo) and tungsten (W) have long been regarded as being more or less immobile during slab fluid-induced arc magma generation. Here we characterize about 180 samples of young, predominantly mafic to intermediate tephras and lavas for their Mo, W, and antimony (Sb) concentrations, to examine the fluid-mobility of these elements in subduction systems. Samples were taken along the active arcs of the Chilean Southern Volcanic Zone (SVZ) and the Central American Volcanic Arc (CAVA). When relating Mo, W, and Sb to trace element ratios typically used to constrain the involvement of subduction fluids in magma formation, such as Ba/La or U/Th, Mo, W, and Sb are enriched in the most fluid-influenced, highest-degree melts. W/Mo ratios correlate positively with Pb/Ce, which is established to reflect a recent subduction signal or assimilation of crustal material with an ancient subduction signature, suggesting that subduction processes promote enrichment of W over Mo. This is well expressed at the SVZ and most of the CAVA; while few OIB-type rocks from Central Costa Rica form an opposite trend. Moreover, Mo/W ratios co-vary with Cl contents derived from melt inclusions, indicating that the relative degree of mobilization responds to the composition of the subduction fluid. To evaluate the mobility of Mo, W, and Sb during metamorphism in the slab, eclogites with no or minor metasomatic overprint and a fluid-induced overprint in an eclogite-blueschist sequence were investigated. None of the three elements shows a systematic variability related to metasomatism and the minor variations are interpreted to reflect protolith heterogeneity. This suggests that Mo, W and Sb remain relatively immobile up to depths of 70 km in the subduction zone.

Long-term development of diagenetic signals of past sulfate-methane transition zones in subseafloor sediments

L. M. WEHRMANN[1]*, C. MÄRZ[2], P. MEISTER[1], C. OCKERT[3], B. BRUNNER[1], N. GUSSONE[3], B.M.A. TEICHERT[3] AND T.G. FERDELMAN[1]

[1]Max Planck Institute for Marine Microbiology, Bremen, Germany (*correspondence: lwehrman@mpi-bremen.de, pmeister@mpi-bremen.de, bbrunner@mpi-bremen.de, tferdelman@mpi-bremen.de)
[2]Newcastle University,UK (christian.maerz@newcastle.ac.uk)
[3]University Münster, Germany (charlotte.ockert@uni-muenster.de, Nikolaus.Gussone@uni-muenster.de, barbara.teichert@uni-muenster.de)

Anaerobic oxidation of methane (AOM) coupled to sulfate reduction in the sulfate-methane transition zone (SMTZ) leaves prominent diagenetic carbon and sulfur signatures in pore-water and solid-phase chemistry that are preserved over geological time scales. We report on the evolution of these signals in the sediments of Site U1341 drilled during Integrated Ocean Drilling Program (IODP) to the Bering Sea to a depth of 600 meters below seafloor (mbsf). At this site, present-day microbial activity associated with organic carbon mineralization is comparably low as evidenced in low dissolved inorganic carbon (DIC) concentrations, and a minor decrease in sulfate concentrations in the top 50 mbsf. Strong decrease of sulfate concentrations below 140 mbsf mirrored by pronounced ^{34}S-sulfate enrichment at the depth of minimum sulfate concentrations suggest that the extent of microbial sulfate reduction was high in this sediment interval deposited during a period of elevated primary productivity in the water column between 2.48 and 2.56 Ma. Elevated sulfate reduction rates drove sulfate to depletion and facilitated the onset of methanogenesis, AOM and the installation of a SMTZ. Rates of these processes apparently declined as a consequence of decreased availability of organic carbon during later time periods. This interpretation is consistent with ^{34}S-enriched pyrite, ^{13}C-depleted dolomite phases and barium depletion to detrital background in distinct sediment intervals. Close examination of the diagenetic pore-water and solid-phase signals, however, revealed that their relative positions in the sedimentary sequence considerably diverge. Also, pore-water DIC, sulfate, Ca and Mg concentrations and isotope profiles do not covary systematically. Our results suggest variable responses of diagenetic signals produced by past SMTZs in the pore-water and sediment over prolonged time scales.

https://doi.org/10.1180/S0026461X00006502 Published online by Cambridge University Press

Seawater pH records from a fringe coral reef in southern Hainan Island, the Northern South China Sea: Implications for ocean acidification

GANGJIAN WEI[1], LUHUA XIE[1], WEIZHONG WU[1], WENFENG DENG[1] AND MALCOLM T. MCCULLOCH[2]

[1]State Key Laboratory of Isotope Geochemistry, Guangzhou Institute of Geochemistry, Chinese Academy of Sciences, Guangzhou 510640, China

[2]School of Earth Environment, The University of the Western Australia, WA 6009, Perth, Australia

The observations for seawater pH time-series have been conducted since 2008 in Luhuitou coral reef, fringed to Sanya in the southern Hianan Island, the northern South China Sea (SCS). Diurnally cycles are the most significant variations for seawater pH on coral reef, with amplitudes up to 0.3~0.6 in general. High pH generally occur at noon (12 am ~ 2 pm), while low pH generally occur at mid-night (0 am ~ 2 am). The pH variations are highly correlated to those of dissolved inorganic carbon (DIC) and dissolved oxygen (DO) concentrations in seawater, as well as $\delta^{13}C$ of DIC and sea surface temperature (SST). This suggests that such seawater pH changes are mainly controlled by photosynthesis and respirations of the bio-mass on coral reef. Seasonal seawater pH variations on this coral reef are of ~0.3, and an ~0.1 pH decrease trend from 2008 to 2010 can be figured out. Such variation patterns apparently correlate to changes in atmospheric CO_2 concentration, but the variation amplitudes are significantly larger than that contributed from the increaseing pCO_2. Ecosystem decline on this coral reef possibly resulted from rapid urbanization in this region may account such seawater pH decrease.

A seasonal-resolution seawater pH record from 1980 to1996 has also been recontructed by the $\delta^{11}B$ of a *Porites* coral rom this reef. No decline trend of seawater pH has been observed during this period. Periodical variation with an apparent 10-yr period is clearly presented in this record, which is similar to that from the Great Barrier Reefs of Australia [2]. This indicates that natural variations for seawater pH with large annual amplitude (0.1~0.3) are generally observed on coral reefs in the west Pacific. Such variations are comparable to the predicted ocean acidification trend in the following centary (0.3~0.4 for global ocean: [1]).

[1] Caldeira and Wickett, 2003 *Nature*, , **425**:365. [2] Wei *et al*., 2009 *Geochim. Cosmochim. Acta*, , **73**:2332–2346

Deltaic landforms and stratigraphic controls on groundwater arsenic

B. WEINMAN[1]*, S.L. GOODBRED[2], A. VAN GEEN[3] AND A.K. SINGHVI[4]

[1]Univ of Minnesota, St. Paul, MN 55108, USA (*correspondence: bweinman@umn.edu)

[2]Vanderbilt Univ., Nashville, TN 37235, USA

[3]Lamont Doherty Earth Observatory, Pallisades, NY 10964, USA

[4]Physical Research Laboratory, Ahmedabad 380-009, India

Sediment deposits can have physical (hydraulic conductivity and anisotropy) and chemical (diagenetic) effects on biogeochemical cyclings. In Asian deltas, our sedimentological work shows that groundwater arsenic heterogeneity can be explained by an aquifer's depositional history. In Bangladesh, variable thicknesses of the floodplain's mud-capping (0-13m) allows for differential flushing in the shallow aquifer [1]. In turn, this allows for differential groundwater arsenic concentrations over 10's of meter distances, supporting more of a physical (flushing) control on arsenic by the sediments. In Vietnam, there is a more "chemical" type of sedimentary control, with higher groundwater arsenic sourced in Holocene sands, while lower arsenic is seen in water from Pleistocene units. This is different than the more "physical" sedimentary control observed in Bangladesh, indicating more of a reactive-transport or chemical (weathering) control by the sediments [2, 3].

Despite these differing chemical and physical effects on groundwater arsenic by their host sediments, one commonality between these and other arsenic-prone regions is that abandoned-channel facies consistently serve as local depocenters for muds and/or Holocene sand units, which both correlate to higher groundwater arsenic. This raises an ancillary concern about hydroelectric and other river-diverting projects, which can leave downstream areas starved for both sediments and water [4,5]. In the case of groundwater arsenic, we see these types of diversions as potentially mimicking the natural waning associated with the abandonment by a river, leaving a potential for new landforming events favoring higher arsenic concentrations in the groundwater.

[1] Weinman *et al*. (2008) *GSA Bulletin* **120**,1567-1580. [2] White & Brantley (2003) *Chemical Geology* **202**, 479-506. [3] Davis *et al*. (2004) *Eos* **85**(44), 449,455. [4] Vorösmarty *et al.* (2009) *Bull. Atomic Sci* **65**(2), 31-34. [5] Khalequzzaman (1994) *Nat Hazards* **9**, 65-80.

https://doi.org/10.1180/S0026461X00006502 Published online by Cambridge University Press

Isotopic fractionation of Cu in plants

CHARLOTTE WEINSTEIN*[1], FREDERIC MOYNIER[1], KUN WANG[1], RANDAL PANIELLO[1], JULIEN FORIEL[1] AND SYLVAIN PICHAT[2]

[1]Department of Earth and Planetary Sciences, Washington University in St. Louis, 1 Brookings Dr., St. Louis, MO 63130, USA (*correspondence: cbweinstein@wustl.edu)
[2]Laboratoire de Sciences de la Terre, Ecole nomale superieure de Lyon, 46 allee d'Italie, 69007 Lyon, France

Knowledge of the copper cycle in the plant-soil-water system is needed in order to better constrain proper plant micronutrient nutrition, control pollution, and determine sustainable soil management practices. Here, we will report the Cu isotopic compositions of different components (seeds, germinated seeds, leaves, and stems) of the dicot, lentil (*Lens culinaris*), and of two monocots, Virginia wild rye (*Elymus virginicus*) and hairy-leaved sedge (*Carex hirsutella)*. The isotopic measurmeents were done by multi-collection inductively coupled plasma-mass spectrometry at Washington University following the procedure described in [1,2,3]. Our data are reported in permil deviation (δ^{65}Cu) from the standard, NIST 976. The isotopic compositions of these plants (δ^{65}Cu≈ -0.43,-0.41) are systematically enriched in the lighter isotope of Cu (^{63}Cu) in comparison to the soil in which they grow (δ^{65}Cu≈ +0.19), suggesting a preferential uptake of ^{63}Cu into the plant. Furthermore, different components within the plants themselves are isotopically fractionated. The shoots (stems, leaves and seeds) are systematically lighter than the underground parts of the plants and the Cu isotopic compositions of individual leaves become lighter in correlation with their heights on the plant. These results are similar to what has been observed for Zn isotopes, which are assumed to be transported through plants by means of diffusion and kinetic fractionation across cell membranes [4]. Because of this similarity, we suggest that the same transport mechanisms (diffusion and transport through cell membranes) are also responsible for the observed isotopic fractionation of Cu. Furthermore, the Cu isotopic variations measured in plants are similar in magnitude to the differences previously measured in various soils, and therefore should be taken into account in order to accurately interpret the isotopic compositions of Cu in soils.

[1] Marechal *et al*. (1999) *Chem Geol*, **156**, 251-273. [2] Moynier *et al*. (2006) *Geoch. Cosmo. Acta*, **70**, 6103-6117. [3] Moynier *et al*. (2010) *Geoch. Cosmo. Acta* **74**, 799-807. [4] Moynier, F. *et al*. (2009) *Chem. Geol*., **267**, 125-130.

ULVZ as repository for the enriched component in the Hawaiian source

D. WEIS[1], M.O. GARCIA[2], J.M. RHODES[3], M. JELLINEK[1] AND J.S. SCOATES[1]

[1]PCIGR, EOS, University of British Columbia, Vancouver BC, V6T1Z4, Canada (dweis@eos.ubc.ca)
[2]Geology & Geophysics, Univ. Hawai'i, Honolulu, HI 96822
[3]Geology & Geography, Univ. Massachusetts, Amherst, MA 01003, USA

The origin, scale and location of mantle heterogeneities have been debated for over 50 years. Improved analytical precision for radiogenic isotopes, combined with statistical data analysis, allow for more detailed investigations into the geochemical variations of basalts related to mantle plumes and for modeling of the shallow and deep plume conduit and structure. Identification of two clear geochemical trends (Loa and Kea) among Hawaiian volcanoes [1, 2] in all radiogenic isotope systems [3], together with the recurrence of similar isotopic signatures at >350 kyr intervals, has implications for the dynamics and internal structure of the Hawaiian mantle plume [4] and for the scale of heterogeneities in the deep mantle. Recent isotopic data for over 850 samples from the shield, post-shield and rejuvenated stages on Hawaiian volcanoes indicate source differences between the Loa- and Kea-trend volcanoes that are maintained throughout the ~1 Myr activity of each volcano and that extend back in time on all the Hawaiian Islands (to ~5 Ma). Hawaiian post-shield and rejuvenated lavas have more Kea-like geochemical characteristics than the underlying shield lavas with only two exceptions. Loa-trend volcanoes have more heterogeneous compositions than Kea-trend volcanoes in all isotopic systems by a factor of ~1.5 and present an EM-component (most expressed in Ko'olau) as well as different geochemical trends with time (increase of Pb isotopic ratios in Loa). The Loa-Kea distinction reflects differences in the plume source, at the core-mantle boundary, where the Mauna Loa side of the Hawaiian plume samples a more heterogeneous source that may correspond to the northeast end of the Pacific ultra-low velocity zone (ULVZ). Kerguelen, an EM-I oceanic island, is located on the eastern end of the ULVZ African anomaly. We infer that these deep velocity anomalies at the CMB are the repositories for EM components brought to the surface by strong mantle plumes.

[1] Tatsumoto (1978) *Earth Planet. Sci. Lett*. **38**, 63-87. [2] Abouchami *et al*. (2005) *Nature* **434**, 3401-06. [3] Weis (2010) Abs V41F-01 Fall AGU Meeting. [4] Farnetani & Hofmann (2009, 2010) *Earth Planet. Sci. Lett*. **282**, 314-322; **295**, 231-240.

https://doi.org/10.1180/S0026461X00006502 Published online by Cambridge University Press

Bacterial physico-chemical controls on As-Pb iron hydroxy sulfates in reduced environments

C.G. WEISENER[1]*, C.M. SMEATON[1], G.E. WALSH[1], A.M.L. SMITH[2,3,4], E.C. FRU[1] AND B.J. FRYER[1]

[1]Great Lakes Institute for Environmental Research, University of Windsor, ON, Canada (*weisener@uwindsor.ca)
[2]Dept. of Mineralogy, The Natural History Museum, Cromwell Road, London, SW7 5BD, UK
[3]Davy Faraday Research Laboratory, The Royal Institution of Great Britain, 21 Albemarle Street, London, UK
[4]Dept. of Earth and Planetary Sciences, Birkbeck, University of London, Malet Street, London, WC1E 7HX, UK

We recently demonstrated the intracellular precipitation of Pb by *Shewanella putrefaciens* CN32 during the reductive dissolution of Pb-jarosite [1]. In the present study, we build upon earlier research which focused on the abiotic dissolution of Pb-As-jarosite [2]. In this study we examine the reductive dissolution of Pb-As-jarosite ($PbFe_3(AsO_4)(SO_4)(OH)_6$) by bacteria under anaerobic circumneutral conditions. Microbial biomass, SEM, ATP, [Pb] and solution chemistry including As and Fe speciation were monitored over time to assess the influence of *S. putrefaciens* on As-Pb jarosite. The work will discuss the rates of Fe reduction versus As reduction and the fate of Pb providing new insight into Pb, Fe and As biogeochemical cycling in reduced environments.

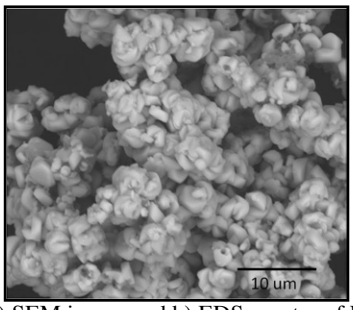

Figure 1: a) SEM image and b) EDS spectra of Pb-As-jarosite

[1] C.M. Smeaton *et al*., (2009) *Env. Sci. Tech*. **43**, 8091-8096. *Journal*, **25**, 415- 421. [2] A.M.L. Smith *et al*., (2006) *Chemical Geology*, **229**, 344-61.

High-Mg carbonatitic HDFs, kimberlites and the SCLM

Y. WEISS[1]*, W.L. GRIFFIN[2], D.R. BELL[3] AND O. NAVON[1]

[1]The Institute of Earth Sciences, the Hebrew University of Jerusalem, Israel (*yakov.weiss@mail.huji.ac.il)
[2]GEMOC, Macquarie University, NSW, Australia
[3]School of Earth and Space Exploration, Arizona State University, AZ, USA

Trace-element patterns of high-Mg carbonatitic high-density fluids (HDFs) trapped in Siberian fibrous diamonds are similar to those of Group I kimberlites, but are slightly more fractionated. The patterns of both are comparable in shape to the average pattern of peridotite xenoliths from the sub-continental lithospheric mantle (SCLM) [1].

Possible scenarios for explaining these similarities include mixing, fractionation and melting:

1) Adding 2.5% of kimberlitic magma or 0.7% of the Siberian high-Mg HDFs to a highly depleted peridotite closely reproduces the SCLM pattern.
2) The formation of the high-Mg HDFs through fractionation of kimberlitic magma calls for 70% crystallization of olivine, pyroxene garnet and carbonate. However, the alkalis and Ba of the calculated fluid are too low and the middle to heavy REE, Zr, Hf, Ti and Y are too high compared to the Siberian high-Mg HDFs.
3) Simple batch melting of 0.5% of a source with average SCLM modal abundance and trace-element composition closely reproduces the trace-element pattern of the Siberian high-Mg HDFs. Higher degrees of melting (~2%) of the same source yield patterns similar to those of Group I kimberlite.

High-Mg HDFs in diamonds from Kankan, Guinea have major-element compositions comparable to that of the Siberian high-Mg carbonatitic HDFs. However, they are depleted in K, Rb, Cs, Nb and Ta and enriched in Ba, Th, U and LREE relative to the Siberian ones. These differences closely correspond to those between the patterns of Group II and Group I kimberlites, respectively. Extending the melting scenario to the Kankan HDFs and Group II kimberlites, the two can be produced by 0.2 and 1% melting of SCLM that carries phlogopite (0.3% and 0.1%, respectively) and a trace of rutile.

Whether it is mixing, melting or combination of both, the new constraints indicate a very close genetic relation between high-Mg carbonatitic HDFs, kimberlites and the average SCLM.

[1] McDonough (1990) *EPSL* **101**, 1-18.

https://doi.org/10.1180/S0026461X00006502 Published online by Cambridge University Press

Photolysis of iron(III) carboxylato complexes — Quantum yield determination and reactivity simulation in clouds and atmospheric particles

C. WELLER, A. TILGNER AND H. HERRMANN

Leibniz-Institut für Troposphärenforschung, 04318, Leipzig, Germany (weller@tropos.de)

Iron is always present in the atmosphere in concentrations from ~10^{-9} M (clouds, rain) up to ~10^{-3} M (fog, particles). Sources are mainly mineral dust emissions. Iron complexes are very good absorbers in the UV-Vis actinic region and therefore photo-chemically reactive. Iron complex photolysis can be an in important degradation pathway for organic compounds with the ability to bind iron.

Absorption spectra and Fe^{2+} quantum yields of iron(III) coordination compounds with oxalate, malonate, succinate, glutarate, tartronate, tartrate, glyoxalate and pyruvate were experimentally determined. Complex solutions were irradiated in a 1 cm quartz cell by excimer laser flash photolysis at wavelengths of 308 and 351 nm or by Hg(Xe) lamp photolysis at 436 nm (for Fe(III) oxalate system). Photochemically produced Fe^{2+} was spectroscopically detected at 510 nm as $[Fe(phenanthroline)_3]^{2+}$.

Measured quantum yields of malonate and glutarate complexes are in the range of $0.02 < \Phi < 0.05$, while succinate, tartrate, pyruvate, glyoxylate and tartronate complexes show values between $0.12 < \Phi < 1.21$. The measured overall quantum yields include contributions from secondary thermal reactions. Furthermore, in some systems a dependence of the measured quantum yield on the amount of the incident photons was determined. In the case of oxalate, a dependence of the quantum yield on the initial concentration of iron(III) oxalato complexes was observed. A kinetic simulation of the reaction system after the photolysis was performed for oxalate, succinate, glyoxalate and tartrate complexes to characterize the influence of secondary thermal reactions on the quantum yield.

A tropospheric chemistry simulation with the multi-phase chemistry mechanism CAPRAM (Chemical Aqueous Phase RAdical Mechanism) involving the photolysis of the studied complexes and subsequent reactions of the resulting fragments showed that Fe(III) complex photolysis represents a major sink for the ligands oxalate, tartronate, tartrate and pyruvate in addition to the oxidation via free radicals.

Technical and policy challenges in deep vadose zone remediation of metals and radionuclides

DAWN M. WELLMAN AND MICHAEL J. TRUEX

Pacific Northwest National Laboratory, Richland, Washington 99354; (dawn.wellman@pnl.gov, mj.truex@pnl.gov)

Deep vadose zone contamination is a significant issue in many regions of the world, although much of the focus has been on arid and semiarid regions where that zone is thickest. Contamination in deep vadose zone environments is isolated from exposure such that direct contact is not a factor in its risk to human health and the environment; rather, movement of contamination from the deep vadose zone to the groundwater creates the potential for exposure and risk to receptors. Therefore, while the deep vadose zone is not necessarily considered a resource requiring restoration, limiting flux from contaminated vadose zone is key for protection of groundwater resources and down-gradient receptors. However, technical challenges complicate the decision process for deep vadose zone remedial actions.

Remediation of metal and radionuclide contamination in the deep vadose zone is complicated by heterogeneous contaminant distribution and the preferential saturation-dependent flow in heterogeneous sediments. Thus, efforts to remove contaminants have generally been unsuccessful; and as a result, the magnitude of contaminant discharge (mass per time) from the vadose zone to the groundwater must be maintained low enough by natural attenuation (e.g., adsorption processes or radioactive decay) or through remedial actions (e.g., contaminant mass or mobility reduction) to meet the groundwater concentration goals.

Contaminant transport mechanisms through the vadose zone can attenuate the overall contaminant flux to the groundwater, and vadose zone contamination may not necessarily require remediation if the natural flux results in sufficiently low contaminant concentrations in the groundwater. In some cases, remediation to control transport, enhance attenuation mechanisms, or remove contaminants may be needed to limit flux so groundwater or surface water protection standards are maintained. This presentation reviews major processes viable for deep vadose zone metal and radionuclide remediation that form the practical constraints on remedial actions.

https://doi.org/10.1180/S0026461X00006502 Published online by Cambridge University Press

Lithium self-diffusion in $LiAlSi_2O_6$ glass and single crystals

A.-M. WELSCH[1]* H. BEHRENS[1], I. HORN[1], S. ROSS[1], P.J. VULIĆ[2], D. MURAWSKI[1] AND A. KREMENOVIĆ[2]

[1]Institut für Mineralogie, Leibniz Universität Hannover, Callinstr. 3, 30167 Hanover, Germany, (*correspondence: a.m.welsch@mineralogie.uni-hannover.de)

[2]Department of Crystallography, University of Belgrade, Đušina 7, 11000 Belgrade, Serbia

Understanding the mechanisms of lithium diffusion is of great interest for geo- and material sciences. Optimizing the performance of Li-bearing solid media has a significant impact in developing new technologies. Knowledge of kinetic Li-isotopic fractionation leads to better understanding of geological processes in which lithium geochemistry plays a major role.

Our ongoing research is aimed to investigate Li diffusion in aluminosilicate media. In the scope of this study, spodumene ($LiAlSi_2O_6$) like materials were selected as representative model system since lithium, as the only mobile species, migrates through a static aluminosilicate network. Crystalline and glassy materials are compared in order to determine the effect of structural order on Li-diffusion. Glasses were produced by melting of oxide and carbonate mixtures as well as by melting natural spodumene. Natural crystals are from different pegmatites worldwide. Synthetic single crystals were obtained in a slow crystallization process using a flux method. The samples were tested by impedance spectroscopy for ionic conductivity in the range between 1 Hz to 10 MHz at temperatures up to 940 K. Additionally, lithium self-diffusion coefficients were determined by diffusion couple experiments using two halves with same base composition but different Li isotopic abundancies. Li isotope profiles were measured using UV fs laser ablation coupled with ICP-MS. Raman spectroscopy aided in better understanding the local structural features which coordinate lithium migration.

Ionic conductivity was found to be 6 - 7 orders of magnitude slower in natural spodumene crystals than in the glasses while the activation energy for Li conduction is about the same for both materials (0.66 kJ/mol for the glass, 0.76. kJ/mol for the crystal). This implies that the barrier for Li-migration is not sensitive to structural order in aluminosilicate materials. Comparison of Li isotope diffusion data and dc ionic conductivity yields a correlation factor of 0.5 for Li-diffusion in $LiAlSi_2O_6$-glasses.

Basin evolution, lithofacies palaeogeography and manganese mineralization in Heqing basin, Yunnan province, Southwest of China

XING-PING WEN[1], RUN-SHENG HAN[1,2] AND XIAO-FENG YANG[3]

[1]Faculty of Land Resource Engineering, Kunming University of Science and Technology, Kunming, 650093, P. R. China (wfxyp2008@gmail.com)

[2]Southwest Institute of Geological Survey, Geological Survey Center for Non-ferrous Mineral Resources, Kunming, 650093, P. R. China

[3]Research Center for Analysis and Measurement, Kunming University of Science and Technology, Kunming, 650093, P. R. China

Heqing basin is located in the northwest of Yungui plateau, southwest of China, a geological conjunction zone of three tectonic units separated by Jinshajiang, Honghe and Xiaojinhe-Lijiang fault belts. Heqing manganese deposit is situated in southwestern margin of Heqing basin. The Songgui formation of the Late Triassic series is the principal ore-host strata, composed mainly of mudstone, limestone and siltstone [1].

Heqing sedimentary manganese deposit formation is associated with Heqing basin evolution. The lithofacies paleogeography of Heqing basin is reconstructed. Sedimentary facies and palaeogeography of the Late Permian Changxingian ages reveal littoral deposits in Heqing manganese deposit. Then the sea level is continuously elevated in the Middle Triassic Ladinian age. Sedimentary facies and palaeogeography of the Late Triassic Carnian age expose shallow sea platform marginal bank facies in Heqing manganese deposit, which is beneficial to accumulation of ore-forming minerals under more stable geological and physicochemical conditions. In the Late triassic Norian age, the region marine regression lead to littoral deposits facies in Heqing manganese deposit, which terminates mineralization.

This study was jointly supported by the crisis of resource exploration mining project, China (20089943) and the innovation team of ore-forming dynamics and prediction of concealed deposits, KMUST, Kunming, China (2008).

[1] Fan, Delian and Yang, Peiji. (1999), *Ore Geology Reviews* **15**, 1-13.

https://doi.org/10.1180/S0026461X00006502 Published online by Cambridge University Press

Biogeochemical patterns and processes in buoyant, deep-sea hydrothermal plumes

KATHLEEN WENDT[1], KARTHIK ANANTHARAMAN[2], JOHN A. BREIER[3], GREGORY J. DICK[2], KATRINA J. EDWARDS[4], PETER R. GIRGUIS[5], JEFFRY V. SORENSEN[1], JASON SYLVAN[4] AND BRANDY M. TONER[1,*]

[1]University of Minnesota, St. Paul, MN, USA, (*corresponding: toner@umn.edu)
[2]University of Michigan, Ann Arbor, MI, USA
[3]Woods Hole Oceanographic Institution, Woods Hole, MA, USA
[4]University of Southern California, Los Angeles, CA, USA
[5]Harvard University, Cambridge, MA, USA

Along the global mid-ocean ridge, sub-seafloor hydrothermal circulation results in the exchange of heat and chemical species between seawater and the ocean crust. The resulting thermally and geochemically altered fluids are vented at the seafloor. The mixing of cold, oxic deep-ocean waters with hydrothermal fluids creates plumes with physically and chemically dynamic features. Hydrothermal plumes represent a globally distributed interface where marine hydrothermal circulation exerts its biogeochemical influence on elemental budgets of ocean basins.

The goal of the present study is to describe the microbiological niches created by physical and geochemical gradients in plumes. One of our central hypotheses is that microorganisms respond to and alter the geochemistry of hydrothermal plumes. To achieve this goal and test our hypothesis, a field study was undertaken at the Eastern Lau Spreading Center (ELSC). While multiple vent sites along the ELSC are included in the larger study, here we report on an integrated, biogeochemical investigation of a single buoyant plume within ABE vent field.

A series of replicate sample sets were collected by *in situ* filtration at 0.5m, 40m, 200m within a buoyant plume using the *ROV JASON*. Above plume background and near bottom background sample sets were also collected. Hydrothermal plume particles in sample replicates or splits have been queried for bulk geochemistry, particle-by-particle mineralogy, and microbial community composition. These three data streams are being evaluated individually to characterize the geochemical and microbiological changes throughout the plume with respect to above and below plume backgrounds. In addition, an iterative and integrated analysis is being used to compare: (1) calculated mineralogy to direct measurements; and (2) predicted energy yields from chemoautotrophy to observed microbial composition.

Biogeochemical cycling of iron, sulfur and carbon in the nutrient-rich meromictic acid pit lake Cueva de la Mora (Spain)

K. WENDT-POTTHOFF[1]*, M. KOSCHORRECK[1], M. DIEZ ERCILLA[2] AND J. SÁNCHEZ ESPAÑA[2]

[1]UFZ – Helmholtz Centre for Environmental Research, Department Lake Research, D-39114 Magdeburg, Germany (*correspondence: katrin.wendt-potthoff@ufz.de)
[2]Instituto Geológico y Minero de Espana (IGME), 28003 Madrid, Spain

Cueva de la Mora is a meromictic, nutrient-rich acid pit lake with pronounced vertical gradients of physicochemical parameters in the chemocline and monimolimnion [1]. We studied microbial activity, abundance and biomass, and biogeochemical cycling of iron, sulfur and carbon to find out if (1) the high nutrient content influenced alkalinity-producing microbial processes compared to other acid pit lakes, and (2) if sediments in the shallow, mixed and the deep, stagnant parts of the lake exhibited biogeochemical differences related to meromixis. We hypothesized that redox cycling was more intense in the mixed part and higher amounts of reduced components would accumulate in the stagnant part.

Several biogeochemical reaction rates were higher than in typical acid pit lakes and fell rather within the range of neutral or weakly acidic lakes, probably a consequence of nutrient levels. Anaerobic processes occurred mainly in the sediments, and methanogenesis was negligible for the carbon budget of the lake. Sediments from the mixed and stagnant parts of the lake differed markedly. Mixolimnetic sediments showed high iron and sulfate reduction rates, and they appeared to undergo substantial recycling, as supported by reactive Fe(II) and Fe(III) profiles, relation between sulphate reduction and accumulation of reduced sulphur, and viable counts of iron and sulphur reducing and oxidising bacteria. Monimolimnetic sediments exhibited lower anaerobic microbial activities, and surprisingly accumulated more Fe(II) than mixolimnetic sediments, but less carbon and reduced sulfur. This might be explained by a strong separation of the monimolimnetic water body, resulting in comparably less input of energy (light) and allochthonous matter. The effect of alkalinity-generating microbial processes is not sufficient to neutralize the lake within a few decades.

[1] Sánchez España J, López Pamo E, Diez M, Santofimia E (2009), *Mine Water Environ* **28**:15-29

https://doi.org/10.1180/S0026461X00006502 Published online by Cambridge University Press

Tracing N_2O transformation pathways in a lake ecosystem by N_2O isotopomer analysis

C.B. WENK[1]*, H.J.R. BLEES[1], K. KOBA[2], K.L. CASCIOTTI[3], C.J. SCHUBERT[4], M. VERONESI[5], C.V. FREYMOND[1], H. NIEMANN[1], J. ZOPFI[6] AND M.F. LEHMANN[1]

[1]Insitute of Environmental Geosciences, University of Basel, Switzerland (*correspondence: christine.wenk@unibas.ch)
[2]Faculty of Agriculture, Tokyo University of Agriculture and Technology, Japan
[3]Department of Environmental Earth System Science, Stanford University, USA
[4]Swiss Federal Institute of Aquatic Science and Technology (Eawag), Switzerland
[5]Institute of Earth Sciences, University of Applied Sciences of Southern Switzerland, Switzerland
[6]Laboratory of Microbiology, University of Neuchâtel, Switzerland

In terrestrial and aquatic ecosystems, N_2O can be produced through two pathways: nitrification and incomplete denitrification. The measurement of the stable isotopic and isotopomeric composition of N_2O can help determine the relative importance of these processes in net N_2O production. To date, relatively little is known about the role of lakes as N_2O source to the atmosphere, and N_2O isotopomer dynamics in lakes have barely been studied.

Lake Lugano (South Basin) is a monomictic, eutrophic lake, where high bottom water N_2O concentrations are observed (900nM; 100x equilibrium saturation). Sediment core incubations with ^{15}N-labeled substrates suggest that sedimentary denitrification is the main N_2O source. These incubation data, however, appear to conflict with water column observations. A N_2O concentration maximum at the aerobic/anaerobic interface, together with the intramolecular distribution of ^{15}N (SP of ~33‰) in N_2O suggests that N_2O in the water column is mainly produced by nitrification. The investigated redox-transition zone is a net sink for NO_x, and N_2O gradients suggest N_2O reduction just below this zone. Yet, isotopomeric signatures that were previously assumed to be characteristic for N_2O production by denitrifying organisms were not observed. Our results raise doubts about the general validity of previously reported N_2O isotopomer effects from laboratory experiments for lake ecosystems.

Spins deep in the Earth

RE NATA WENTZCOVITCH

Department of Chemical Engineering and Materials Science, Minnesota Supercomputing Institute, University of Minnesota, MN, USA, 55403

There has been much interest in spin crossovers found in 2003 and 2004 in the most abundant minerals of Earth's lower mantle ((MgFe)O and (MgFe)(Si,Fe)O_3-perovskite) under pressure. Spin crossovers depend on thermodynamic conditions and a full understanding of this problem requires its investigation as function of pressure and temperature. There are several controversies, especially in the perovskite systems, and surprises are revealed by electronic structure calculations. The geophysical consequences of these crossovers are yet to be fully understood. I will review recent progress in the study of spin crossovers and give an overview of this phenomenon and its potential implications for the Earth.

Research carried out in collaboration with H. Hsu, K. Umemoto, P. Blaha,. Research supported by the MRSEC Program of NSF under Award Number DMR-0212302 and DMR-0819885, and by NSF/ATM-0428774, EAR-0810212, and EAR-1047629.

https://doi.org/10.1180/S0026461X00006502 Published online by Cambridge University Press

The Santa Quitéria Batholith, NE Brazil: A mantle–crust interaction

E. WERNICK[1]*, S.A. ZINCONE[2] AND T.J.S. SANTOS[2]

[1]Instituto de Geociências, UNESP, Rio Claro, SP, Brazil (*correspondence: wernick@uol.com.br)
[2]Instituto de Geociências, UNICAMP, Campinas, SP, Brazil

Granitoid magmatism is an important tool for the characterization of mantle-crust interaction, a process which extremes are represented by M- type (mantelic) and S- type (crustal) granites. The huge (~15.000km^2) Brasiliano Santa Quitéria batholith (SQB) from the Borborema Province, state of Ceará, NE Brazil, comprises mainly high-K/shoshonitic megaporphyritic/evengrained monzodiorites, monzogranites and granites. Its long lasting (650-470 Ma.) magmatic evolution reflects part of the closure of the Pharusian Ocean and the collision between the Amazonas, São Luiz, São Francisco and West Congo cratons. 90 Sm-Nd data for SQB rocks [1-4] show that their parent magma represents an isotopic mixture of a juvenile mantelic component with older, mainly Paleoproterozoic, crustal rocks. The geological, petrographic and geochemical evidences for the mixture change from the syncolissional, via the syntranscurrent, to the late magmatic stage of the batholith, the last one related to the regional relaxing and collapsing of the orogen.

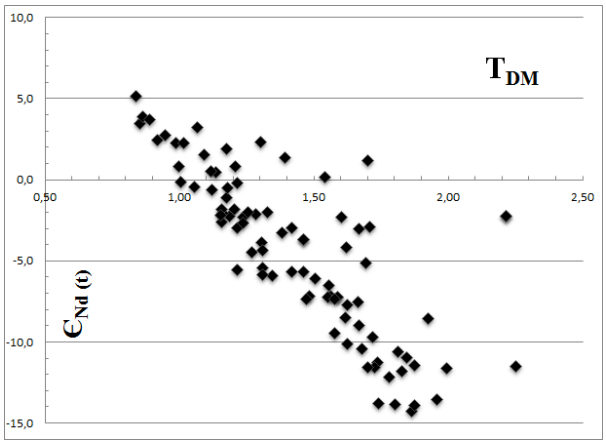

[1] Fetter (1999) Ph.D. thesis, Kansas University, USA, 164p.
[2] Castro (2004) Ph.D. thesis. USP, Brazil, 221 p.
[3] Teixeira (2005) Master Dissertation, UNB, Brazil, 128p.
[4] Santos *et al*. *unpublished*.

Probing the silicon isotope signature of supply limited chemical weathering in the Cordillera Central of Costa Rica

A. JOSHUA WEST[1,2], SOPHIE OPFERGELT[1], RACHAEL JAMES[3], PHILIP POGGE VON STRANDMAN[4] AND KEVIN BURTON[1]

[1]University of Oxford, Department of Earth Sciences, South Parks Road, Oxford OX1 3AN, UK
[2]University of Southern California, Department of Earth Sciences, Los Angeles, CA, 90089, USA; (correspondence: joshwest@usc.edu)
[3]National Oceanography Centre Southampton, European Way, Southampton, SO14 3ZH, UK
[4]University of Bristol, Department of Earth Sciences, Queen's Road, Bristol, BS8 1RJ, UK

The fractionation of silicon isotopes during tropical, supply-limited weathering remains incompletely understood, a key missing link in being able to use the Si isotope system to infer the rates and character either of primary mineral weathering, or of biogeochemical cycling of Si. Samples of rock, soil, vegetation, and water from La Selva Biological Preserve, on the flanks of Volcan Barva in the Cordillera Central of Costa Rica, provide the opportunity to (i) better constrain the isotopic signature of dissolved Si associated with supply-limited weathering, and (ii) understand the mechanisms generating the observed isotopic characteristics in these settings. We collected samples from La Selva and analysed these samples for δ^{30}Si by MC-ICP-MS. Si-isotope analyses of samples from La Selva confirm that weathering in tropical, supply-limited environments generates the isotopically lightest dissolved Si that has been observed in stream and river waters measured globally. Streams with significant groundwater contribution, with flowpaths through less altered volcanic bedrock, have significantly higher isotopic compositions, reflecting primary mineral weathering. Analysis of bedrock and soils, including clay separates from soils, indicates that this light isotopic composition of dissolved Si is a consequence of the dissolution of clay minerals formed during previous weathering cycles. Contemporary weathering processes in the soil at La Selva are associated with precipitation of even lighter neo-formed clays, driving the bulk soil to increasingly light Si isotope ratios. Weathering of secondary minerals in such locations, as confirmed in this study, may complicate interpretation of the variability in dissolved riverine Si isotopes over large spatial scales and long temporal scales.

https://doi.org/10.1180/S0026461X00006502 Published online by Cambridge University Press

Mo isotope signature of OAE 1a: New insights from the Western Tethys

S. WESTERMANN[1]*, D. VANCE[1], C. ARCHER[1] AND S. ROBINSON

[1]Bristol Isotope Group, School of Earth Sciences, University of Bristol, Wills Memorial Building, BS8 1RJ, UK (*correspondence: stephane.westermann@bristol.ac.uk)
[2]University College London, Gower Street, London,WC1E 6BT (stuart.robinson@ucl.ac.uk)

Oceanic anoxic events (OAEs) record profound and rapid changes in the chemistry of the world ocean. Quantifying the oxygenation state of the oceans through OAEs is of fundamental importance to understanding the global perturbation of the carbon cycle observed during these events. The aim here is to trace global redox change in the wolrd ocean through the early Aptian anoxic event (OAE 1a, Selli event), one of the most significant and widespread black shale events of the Cretaceous.

We selected the Gorgo a Cerbara section (Italy), where evidence of euxinic conditions has recently been provided by biomarkers [1-2], and investigated the redox-sentive trace element (RSTE) distribution and the molybdenum (Mo) isotopes variations through the section.

All RSTE measured present similar behaviour, with a low background level contrasted by maxima in concentrations within the Selli level. A relatively good correlation is observed between total organic carbon (TOC) values and RSTE accumulation, suggesting well-developped anoxia. However, Mo isotopes show surprisingly negative values through the section. An increasing trend in $\delta^{98/95}$Mo is observed before the Selli interval, with values ranging from -0.89 up to 0.06 ‰. Then, $\delta^{98/95}$Mo values remain more or less constant fluctuating around -0.23 ‰, but with a shift towards more negative values within the Selli level. This trend is interrupted by a positive peak to 0.13 ‰, corresponding to samples with the highest Mo content (up to 94 ppm).

The RSTE behaviour indicates variations in the oxygenation state of the western Tethys, reaching anoxic/euxinic conditions during OAE 1a. However, the light $\delta^{98/95}$Mo values suggest that the redox conditions may not have been fully euxinic. Iron speciation measurments will be performed to further investigate the redox conditions during the deposition of the Selli interval, and its relationship to sedimentary Mo isotope evolution.

[1] Pancost, R. *et al*. (2004). *Journal of the Geological Society* 161, 353–364. [2] van Breutel *et al*. (2007). *Paleoceanography* 22, PA1210.

Melting and melt/rock reaction of sulphides in Middle Atlas spinel peridotite xenoliths

K.J. WESTNER*[1], N. WITTIG[1,2], R. KLEMD[1], H. BRÄTZ[1] AND I. OSBAHR[1]

[1]GeoZentrum Nordbayern, Mineralogie & Endogene Geodynamik, Universität Erlangen, Schlossgarten 5(a), 91052 Erlangen(*correspondence: katrin.westner@geo.stud.uni- erlangen.de)
[2]National High Magnetic Field Laboratory & Department of Earth, Ocean, and Atmospheric Science, FSU, 1800 E. Paul Dirac Drive, Tallahassee, FL 32310, USA

The major and siderophile and chalcophile trace element composition (n=25) in sulphides (58 analyses) and Fe-hydroxides (7 analyses) of seven spinel-facies peridotite xenoliths from the Moroccan Middle Atlas was determined at the University of Erlangen by electron microprobe and in-situ LA-ICP-MS. The sulphide assemblage comprises monosulphide solid solution, pentlandite and minor isocubanite. Sulphides occur as: (i) inclusions (eu- to subhedral) in primary silicates, usually associated with sulphide melt trails; (ii) anhedral grains on silicate grain boundaries, and (iii) within silicate glass in discrete melt pockets formed during the ascent of the xenoliths. Variably pervasive alteration of sulphides to hydroxides is generally associated with cracks in the peridotite matrix. Three PGE patterns were identified – often within the same sample and irrespective of the petrographic occurrence: [a] IPGE > PPGE; [b] no PGE fractionation and [c] PPGE > IPGE. Hydroxides show nearly identical PGE patterns with similar PGE abundances to their host sulphides. Relatively incompatible chalcophile elements correlate with the degree of PGE fractionation. The presence of such PGE fractionation ([a] & [c]) on thin-section scale is consistent with mantle melting experiments [1], which predict residual IPGE-rich sulphides and (trapped) PPGE-rich melt blebs. The close proximity of interstitial and enclosed grains with these patterns suggests contemporaneous sulphide-silicate crystallisation due to melt-rock reaction of olivine and pyroxene, hence trapping sulphide melt as inclusions and leaving potentially earlier residual IPGE-rich sulphides intact. Whole rock major and siderophile trace elements and Os isotopes are also in accordance with coupled sulphide-silicate introduction [2]. Our results allow deciphering the mobility and transport of upper mantle sulphide melts, which is a crucial prerequisite for understanding the generation of crustal noble metal deposits.

[1] Bockrath *et al*. (2004) *Science* **305**, 1951-1953. [2] Wittig *et al*. (2010) *Lithos* **115**, 15-26.

https://doi.org/10.1180/S0026461X00006502 Published online by Cambridge University Press

Noble gases and halogens in Icelandic basalts

B. WESTON*, R. BURGESS AND C.J. BALLENTINE

SEAES, The University of Manchester, Manchester, U. K. (*bridget.weston@postgrad.manchester.ac.uk)

We present noble gas and halogen data from a suite of samples taken from across Iceland. Iceland combines hotspot volcanism, a spreading ridge and abundant sub-glacially erupted basaltic sampes. This combination allows for samples which erupted under high enough presssures to retain a measurable noble gas content, and also display signatures representing interaction between ocean island and mid-ocean ridge basalt mantle sources. In terms of the isotopic composition of the light noble gases, this interaction has been the subject of a number of studies. However, the elemental heavy noble gas composition of Icelandic basalts has been less well investigated. Studies are hampered by the large, isotopically atmospheric component typically found in Icelandic sub-glacial samples; this late-stage contamination can swamp other signatures. In addition, the degassing process results in both elemental fractionation and loss of the noble gases. Taking full account of both these processes is crucial to resolving the elemental noble gas composition of Iceland's source mantle: Evidence for volatile recycling, volatile sources during the Earth's history and the nature of different mantle source zones are just a few topics that require elemental data as well as isotopic.

Isotopic neon and argon ratios show mixing between air and mantle components, allowing corrected abundances of krypton and xenon to be calculated: Although isotopically indistinguishable from air, these are elementally non-atmospheric, allowing the fit of the data to degassing models to be assessed. We use a variation on the model of Gonnermann and Mukhopadhyay to define possible degassing trends for these samples [1]. Known mantle production ratios for $^{4}He/^{40}Ar$ and $^{4}He/^{21}Ne$ then allow limits to be placed on elemental ratios from Iceland's source mantle.

In contrast to the noble gas analyses, elemental fractionation is not apparent in the halogen data; for example, I/Cl ratios are consistently close to the bulk earth value of 72 x 10^{-6} across a broad range of samples [2]. However, halogen concentrations vary widely, with the highest values found towards central Iceland. Combined with the noble gas results, this data can provide an insight into the halogen composition of the different mantle sources interacting at Iceland.

[1] Gonnermann and Mukhopadhyay (2007) *Nature* **449**, 1037-1040. [2] Burgess *et al*. (2002) *EPSL* **197**, 193-203.

C-solubility in magmas at low fO_2

D.T. WETZEL[1]*, M.J. RUTHERFORD[1], S.D. JACOBSEN[2], E.H. HAURI[3] AND A.E. SAAL[1]

[1]Dept. of Geological Sciences, Brown University, Providence RI 02912 (*correspondence: Diane_Wetzel@brown.edu)
[2]Dept. of Earth and Planetary Sciences, Northwestern University, Evanston, IL 60208 (steven@earth.northwestern.edu)
[3]DTM Carnegie Institute of Washington, DC 20015 (hauri@DTM.ciw.edu)

Available evidence suggests that in the absence of water, carbon is the element responsible for generating the gas phase that drives fire-fountain eruptions in low oxidation-state magmas [1, 2]. For example, recent experiments show that C forms a CO-rich gas phase in ascending lunar picritic magmas at 40 MPa [3]. Indigenous H (H_2O), discovered in a range of lunar picritic glasses [4], affects this conclusion. Our study was designed to determine the solubility and speciation of C in H-bearing graphite-saturated picritic magmas and the effect of H on the initial gas phase generated.

Experimental A15 green glass samples were pre-set at IW, enclosed in graphite, and run in an IHPV. C and H contents determined by SIMS show 3-150 ppm C and 6-140 ppm H at lower pressures and up to 1400 ppm C and 1250 ppm H at 1 GPa. Carbon in the green glass has a strong positive correlation with pressure. Analyses also show a positive correlation between dissolved C and H in the experimental glasses. Raman spectroscopy indicates CH_4 present in the melt, which confirms the observed trend between C and H in the glasses. These results are consistent with experiments on Na-silicate [5] and haplobasaltic [6] melts. Magmatic C contents greater than ~20 ppm will cause the first gas phase to form from C-H (CH_4) species saturation assuming H contents were in the range 200-1000 ppm. Thermodynamic models [7] predict a CH_4- and H_2-rich gas phase in equilibrium with a reduced melt at P>40 MPa and CO-rich gas at lower pressures.

[1] Sato M. (1976) *PLSC 7th*, p.1323-25. [2] Fogel R.F. and Rutherford M.J. (1995) *GCA,* **59**, 201-15. [3] Nicholis M.G. and Rutherford M.J. (2009) *GCA,* **73**, 5905-17. [4] Saal A.E. *et al*. (2008) *Nature*, **454**, p.192-95. [5] Mysen *et al*. (2009) *GCA,* **73**, 1696-1710. [6] Ardia P. *et al*. (2011) *LPSC XLII,* Abst. #1659. [7] Zhang C. and Duan Z. (2009) *GCA,* **73**, 2089-2102.

https://doi.org/10.1180/S0026461X00006502 Published online by Cambridge University Press

Diatom Si isotope variations from the Atlantic Sector of the Southern Ocean (ODP Site 1093) record environmental changes of the last 170 ka

F. WETZEL[1]*, A. SHEMESH[2], B.C. REYNOLDS[1]

[1]Institute of Geochemistry and Petrology, Department of Earth Sciences, ETH Zurich, Switzerland (*correspondence: wetzel@erdw.ethz.ch)

[2]Department of Environmental Sciences & Energy Research, The Weizmann Institute of Science, Rehovot, Israel

A number of recent studies utilized silicon isotopes to trace changes in the biogeochemical cycling of silicon in the paleocean [1, 2]. The main controling process on this cycle is the uptake of silicon by opal-precipitating phytoplankton. Accounting for about 60% of the oceanic primary production, diatoms link the dissolved silicon (nutrient) pool and oceanic CO_2 uptake from the atmosphere. Since the Southern Ocean plays a key role in ocean circulation and deep-sea ventilation, its underlying opal-rich sediments are particularly suitable for studying the link between atmospheric CO_2 variations and phytoplankton nutrient utilization. The degree of surface silicon utilization is to a first order a function of nutrient supply from below and should be reflected in the diatom silicon isotope composition. In combination with carbon isotope ($\delta^{13}C$), nitrogen isotope ($\delta^{15}N$) and micronutrient (esp. Fe) information it is possible to reconstruct the efficiency of the biological pump that determines whether the surface ocean acts as a net source or sink for atmospheric CO_2.

Here, we present down-core (0-170 ka) silicon isotope variations of diatoms from the Atlantic Sector of the Southern Ocean (OPD Site 1093) and examine the impact of glacial-interglacial climate change on the degree of silicon isotope utilization. The results show that the degree of silicon isotope utilization during interglacial periods is different from that of peak glacial periods. During peak glacial periods, silicon utilization is inefficient at a time where an efficient biological pump is assumed to draw down additional atmospheric CO_2, implying a more complex relationship between silicon in frustules and nutrients contributing to organic tissues. In addition, ambiguity exists as to whether the increased efficiency in the biological pump during glacials was, as commonly believed, a contributor to the low atmospheric CO_2 concentrations or a consequence and therefore 'only' a positive feedback.

[1] Ellwood *et al*. (2010) *Science* **330**:1088-1091; [2] Hendry *et al*. (2010) *EPSL* **292**:290-300;

The extent of oceanic anoxic events revealed by correlated Mo- and U isotope records

S. WEYER[1]*, C. MONTOYA-PINO[2], G.W. GORDON[3], B. VAN DE SCHOOTBRUGGE[2], W. OSCHMANN[2], J. PROSS[2] AND A.D. ANBAR[3]

[1]Institut für Mineralogie, Leibniz Universität Hannover, 30167 Hannover, Germany (*correspondence: s.weyer@mineralogie.uni-hannover.de)

[2]Institut für Geowissenschaften, Universität Frankfurt, 60431 Frankfurt a. M., Germany

[3]School of Earth and Space Exploration, Arizona State University, Tempe, Arizona 85287, USA

Isotopic signatures of redox-sensitive trace metals in black shales (e.g. Mo and U) have become a frequently used tool to estimate the extent of anoxic or euxinic conditions in ancient oceans [1-5]. A disadvantage of these tools is that they are sensitive to local redox conditions or other effects [4-6]. Here we show that combining Mo- and U isotopes provide a much more robust approach.

We studied black shales from and around both the Cretaceous OAE2 (Demerara Rise, Central Atlantic ocean) and the early Jurassic T-OAE (Dotternhausen, Germany, and Truc de Balduc, France) and compared our results with those from "recent" sapropels of the Black Sea (unit I and unit II). Samples from all investigated units display a distinct negative correlation of Mo- and U isotope records. This coupling of Mo- and U isotopes is likely generated during black shale formation under variable (redox) conditions.

Samples from the OAE2 and those from below- and above OAE2 together define a single trend of Mo- versus U isotopes. Individual trends are defined by sample suites from different subzones of the lower Toarcian (during- and slightly after the T-OAE). All these trends are significantly shifted towards lighter isotope compositions compared to the trend defined by Black Sea samples, except samples from the *bifrons* zone (the youngest lower Toarcian) which display almost modern Mo- and U isotope records. Our findings indicate significant enhancement of seafloor anoxia (5-10-fold compared to present) during both OAE2 and T-OAE. For both periods, enhancement of seafloor anoxia exceeded the duration of the OAEs, as defined by their $\delta^{13}C_{org}$ excursions.

[1] Arnold *et al*. (2004), *Science* **304**, 87-90; [2] Pearce *et al*. (2008), *Geology* **36**, 231-234; [3] Kendall *et al*. (2009), *GCA* **73**, 2534-2558; [4] Gordon *et al*. (2009), *Geology* **37**, 535-538; [5] Montoya Pino *et al*. (2010); *Geology* **38**, 315-318; [6] Poulson *et al*. (2006) *Geology* **34**, 617-620.

https://doi.org/10.1180/S0026461X00006502 Published online by Cambridge University Press

Occurence of reduction induced sulfide saturation in oxidised arc magmas

TARUN H.E. WHAN*, JOHN A. MAVROGENES AND RICHARD J. ARCULUS

Research School of Earth Sciences, Australian National University, ACT Australia 0200
(*correspondence: tarun.whan@anu.edu.au)

It has been previously well documented that solubility of sulfur in silicate melts increases by order of magnitude as the sulfate $(SO_4)^{2-}$ compared to the sulfide (S^{2-}) species [1]. Also established is magnetite saturation, the first phase to appear on the liquid line of decent during fractional crystallisation that subtracts significant amounts of total Fe and also lowers the Fe^{3+}/Fe^{2+} of the residual magma, may trigger reduction in the evolving silicate melt [2]. This process of reduction induced sulfide saturation (RISS) can lead to a melt attaining sulfide saturation in a closed system, without the need of any external input i.e., crustal assimilation of sulfur or an enriched slab component.

We have explored the details of the processes subsequent to magnetite saturation in arc magmas. For example, preliminary analysis of melt inclusions contained within titanomagnetite separated from a suite of subaqueous quenched volcanic glasses from the Pual Ridge recovered during Marine National Facility Voyage (FR08-1991), while confirming predicted Cu and S abundances at peak enrichment of these elements, require some finite amount of magnetite fractionation before sulfide saturation is achieved.

Relatively oxidised sulfate-saturated, representative basaltic andesite compositions doped with a suite of chalcophile trace elements, have been experimentally equilibrated under reducing conditions to simulate RISS. The experiments yield Cu-Ag-Au rich sulfides, experimentally validating for the first time the plausibility of this process in evolving arc magmas.

[1] Jugo, P. J., R. W. Luth & J. P. Richards (2005a). *Journal of Petrology* **46**(4): 783-798. [2] Jenner, F. E., O'Neill, H. ST. C., Arculus, R. J., Mavrogenes, J. A. (2010) *Journal of Petrology* **51**(12): 2445- 2464.

Fluid pressure versus rock pressure: Their influence on metamorphic reactions

JOHN WHEELER[1], SERGIO LLANA-FUNEZ[2] AND DAN FAULKNER[1]

[1]School of Environmental Sciences, University of Liverpool, Liverpool, L69 3GP, UK
(*correspondence: johnwh@liv.ac.uk)
[2] Departamento de Geología, Universidad de Oviedo, calle Arias de Velasco s/n, 33005 Oviedo, Spain

In the upper part of the Earth aqueous and other fluids interact physically and chemically with their surroundings, naturally or during fluid disposal and extraction. Differences between rock and fluid pressure are common in the upper few km of the crust. Pressure affects chemical equilibrium: so how do these two different pressures affect chemical processes? Despite the fundamental nature of this question, there are no agreed answers and systematic tests are lacking. Here we discuss results from a set of experiments on gypsum dehydration, where confining and fluid pressure are independently varied.

Because they involve significant volume change, dehydration reactions are sensitive to pressure. Most dehydration reactions involve a net volume increase; hence in confined conditions overpressure develops unless the fluid can drain away. Thus, porosity and permeability development are key processes in nature and experiment. In addition, when confining pressure is greater than fluid pressure, the solids may compact. Reaction, fluid flow and compaction will all influence the evolving fluid pressure field and feedbacks are inevitable. Despite this we show how we can distinguish the effects of reaction rate from those of other processes.

We have run an extensive set of experiments on gypsum dehydration (to bassanite) and, in parallel, have developed a numerical model for dehydration. We show two results.

1. Experiments show that the rate of gypsum dehydration is strongly influenced by pore fluid pressure and not by confining pressure. This means that, even as the bassanite becomes the dominant load supporting phase, the confining pressure it supports is not influencing the thermodynamics of the reaction.

2. Experiments and the numerical model both show that under some conditions a reaction *front* develops, separating unaltered gypsum from substantially reacted regions. Such fronts, if they develop, exert a strong influence on behaviour in experiments and will equally influence natural systems.

https://doi.org/10.1180/S0026461X00006502 Published online by Cambridge University Press

Liposome study of MtrABC: A Porin cytochrome electron transport system from *Shewanella oneidensis*

G.F. WHITE*, M.J. EDWARDS, N.A. BAIDEN, A. HALL, J.N. BUTT, D.J. RICHARDSON AND T.A. CLARKE

University of East Anglia, Norwich NR4 7TJ, UK (*correspondence: gaye.white@uea.ac.uk)

S. Oneidensis are able to respire in the absence of oxygen because they can use oxidised metals, external to the cell, as terminal electron acceptors. This involves electron transfer across the bacterial cell envelope to the surface of minerals such as Fe(III) and Mn(IV) oxides. Genetic knockout studies have identified a suite of proteins associated with electron transport through the outer membrane [1]. This includes the MtrABC complex. Studies of these proteins led to the putative model for Porin-Cytochrome Electron Transport (PCET) shown in Fig. 1 below [2, 3].

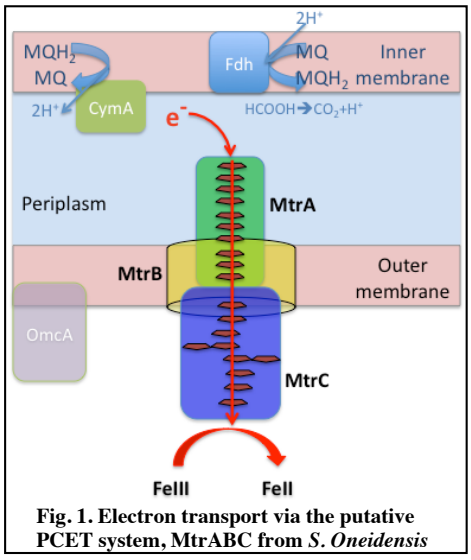

Fig. 1. Electron transport via the putative PCET system, MtrABC from *S. Oneidensis*

In this model the decaheme cytochromes MtrA and MtrC meet inside the transmembrane sheath, MtrB. The 20 hemes are closely aligned allowing electrons to flow through the MtrAC "wire". To test this model, we have inserted MtrABC into liposomes containing a hydrophyllic electron source, reduced methyl viologen, that also acts as a redox indicator. We describe the development of this technique and present our investigations into PCET via MtrABC across a lipid bilayer to a range of soluble and insoluble minerals.

[1] Myers *et al*. (2002) *App. Env. Microbiol*. **68**, 2781-2793. [2] Ross *et al*. (2007) *App. Env. Microbiol*. **73**, 5797-5808. [3] Hartshorne *et al*. (2009) *PNAS*. **106**, 22169-22174.

Correlated uranium concentration, radiation damage, and increased SHRIMP U/Pb ages of zircon

LLOYD T. WHITE* AND TREVOR R. IRELAND

Research School of Earth Sciences, The Australian National University (*correspondance: lloyd.white@anu.edu.au)

SHRIMP U-Pb age calibrations require an accurate calibration of the observed ion ratios. Previous work has shown that there is a correlation between highly elevated uranium concentrations (>3000 ppm) and an increase in apparent age [1]. This "high uranium effect" has been attributed to U, Pb gain or loss, matrix-dependent sputtering, and changes in secondary ionisation effeciency of different species. If this process is systematic, then it may be possible to obtain a calibration that will allow correction of high U spots and allow comparison with more normal zircon.

We report results from SHRIMP I, II and RG analyses of several samples of varying uranium concentration and age (~20 Ma, ~50 Ma, ~100 Ma and ~180 Ma). Our results suggest that the "high uranium effect" can vary between different geometries of SHRIMP (i.e. I, II and RG) and may (at least in part) relate to how the machine is calibrated. It also appears that the "high-uranium effect" is more pronounced in the older zircons.

Raman spectroscopy was used to analyse some of the zircons that had been analysed previously with SHRIMP. This was done so that the uranium concentration and U/Pb age was known for each Raman analysis. The Raman results suggest that the correlation between uranium concentration and age is complex, but implies that the older apparent ages obtained from SHRIMP are related to zircons that have lost some, or all of their crystalline structure. Thus, the "high-uranium effect" is more problematic in older zircons because of accumulated radiation damage, which will also promote Pb redistribution.

[1] Williams & Hergt (2000), *Beyond 2000: New Frontiers in Isotope Geoscience*, Woodhead, Hergt, & Noble (eds), Lorne, Abstract Proceedings, p. 185-188.

https://doi.org/10.1180/S0026461X00006502 Published online by Cambridge University Press

Implications of a non-chondritic Earth for terrestrial heat production and geodynamics

WILLIAM M. WHITE AND JASON PHIPPS MORGAN

Dept. of Earth & Atmospheric Sciences, Cornell University, Ithaca, NY 14853 USA (wmw4@cornell.edu, jp369@cornell.edu)

Previous geochemical estimates of terrestrial radiogenic heat production were based on the assumption that refractory lithophile elements, such as the REE, U, and Th are present in the Earth in chondritic relative proportions (the "modified chondritic Earth' model). However, $^{142}Nd/^{144}Nd$ ratios in modern terrestrial materials imply that the Sm/Nd ratio in the Earth, or at least the observable part of it, that is about 6% higher than chondritic, and hence the Earth is non-chondritic, even for ratios of refractory lithophile elements. The most likely explanation is that a low Sm/Nd igneous protocrust that formed as as the Earth accreted was lost through collisional erosion. A protocrust 6% enriched in Nd relative to Sm would have been more strongly enriched in the more highly incompatible elements K, U, and Th. Calculations based on a model of protocrust formation and collisional erosion that satisfy both Sm-Nd and Lu-Hf isotopic constraints imply U and Th concentrations in the bulk silicate Earth (BSE) about 40% lower than in the 'modified chondritic Earth' model. Asumming a K/U = 13800 for the BSE, the K concentration is 30% lower than previously believed. This corresponds to a terrestrial heat production of 11.9 TW, compared to estimates ranging from 16 to 20 TW based on 'modified chondritic Earth' model. Of this, some 5 to 10 TW of heat production is in the continental crust, leaving <6 TW of heat production in the mantle. For comparison, recent estimates of U, Th, and K in the depleted mantle imply heat production in the range of 0.6–1.0μW/kg; if the depleted mantle occupies the entire mantle, this translates into mantle heat production of 3-4 TW. Mantle heat losses are roughly 33 TW, hence the mantle Urey ratio (ratio of heat production to heat loss) is in the range of 0.09 to 0.19. At present, heat generated by viscous dissapation of the gravitational energy released by sinking slabs is 12 to 15 TW, and <5 TW is released by the cooling core. Of this energy, only a fraction, 3.8 to 4.8 TW can produce new gravitational power to drive convection and plate tectonics. Thus gravitational energy is being consumed at a much higher rate than it is being regenerated. This is a clear indication that the present rate of slab subduction is not sustainable and that the mantle is in a phase of faster than normal slab subduction and plate spreading.

Hygroscopic and CCN properties of marine aerosol

J.D. WHITEHEAD[1]*, J.D. ALLAN[1], N. GOOD[2] AND G. MCFIGGANS[1]

[1]Centre for Atmospheric Science, SEAES, The University of Manchester, Oxford Road, Manchester, M13 9PL, UK (*correspondence: James.Whitehead@manchester.ac.uk).

[2]Centre for Atmospheric and Instrumentation Research, University of Hertfordshire College Lane, Hatfield, AL10 9AB, UK

The impact of marine aerosols on cloud properties is the subject of active research due to the high level of uncertainty associated with their effect on the climate. In order to quanitify these effects more accurately, it is important to measure and understand aerosol water uptake, which can vary greatly with particle size and composition. The tools available for this task include the Hygroscopicity Tandem Differential Mobility Analyser (HTDMA) and the Cloud Condensation Nuclei counter (CCNc), however consistency between the aerosol water uptake derived with these instruments can be affected by the composition in particular due to the presence of organic components [1].

Both instruments were operated at Mace Head, during winter 2010 and summer 2011. The site's location on the west coast of Ireland makes it ideal for sampling air masses from over the North Atlantic without significant local anthropogenic influence. During the winter, the aerosol particles in the clean marine air at this location consist largely of inorganic components, so it is expected that reconciliation between the hygroscopic and CCN properties of the aerosols will be straightforward. Owing to hotly-debated impacts of the contribution of organic aerosol components to droplet activation and to the expected higher summertime contribution to primary marine particulate of biogenically derived organic matter [2], reconciliation of aerosol water uptake derived with each instrument presents additional challenges. This can be examined with reference to aerosol composition data from an Aerosol Mass Spectrometer (AMS) simultaneously operating at the same location.

Recent progress with the analysis and comparison of the winter and summertime data will be presented and discussed in the context of previous marine experiments.

[1] Good *et al*. (2010) *Atmos. Chem. Phys*. **10**, 3189-3203. [2] Yoon *et al*. (2007) *J. Geophys. Res*. **112**, doi:10.1029/2005JD007044.

https://doi.org/10.1180/S0026461X00006502 Published online by Cambridge University Press

Quadruple sulfur isotope determination by SIMS: Limitations, progress and prospects

M.J. WHITEHOUSE

Swedish Museum of Natural History, Stockholm, Sweden (martin.whitehouse@nrm.se)

The discovery of mass independent fractionation effects in sulfur isotopes leading to what is commonly referred to as "anomalous" or "MIF" sulfur has revolutionised our understanding of the evolution and interaction of sulfur reservoirs. Of the four naturally occurring sulfur isotopes, variations in the abundance of ^{33}S and ^{36}S may be produced by upper atmosphere photo-catalysed reactions acting on SO_2. The distinctive and irreversible signatures preserved in sulfides or sulfates in the geological record are key to understanding the evolution of Earth's atmosphere [1], and provide important tracers in geobiological [2] and ore-forming processes [3]. Recent studies have also investigated ^{36}S abundance as a potential tracer of the MIF process [4].

Among the various methods available to measure sulfur isotopes, secondary ion mass spectrometry (SIMS) combines high-spatial and -volume resolution with a precision adequate for many studies, as well as the ability to efficiently analyse a large number of *in situ* targets. To date, SIMS studies have been limited to the three most abundant isotopes, ^{32}S, ^{33}S and ^{34}S, all of which may be measured simultaneously using Faraday cups (FC's) with typical precision on $\delta^{33}S$ (and $\Delta^{33}S$) and $\delta^{34}S$ of <0.2‰ (1σ). The low abundance of ^{36}S (ca. 0.02%) however presents a significant analytical challenge to SIMS. Under typical analytical conditions used for triple-sulfur isotope analysis, a ca. 10^9 cps ^{32}S will be accompanied by only 2 x 10^5 cps ^{36}S which is too low to yield acceptable precision using FC's. Furthermore, the ~5-10-fold signal increase needed to reach such precision can only be achieved with a considerable loss of spatial resolution. An alternative approach is to measure ^{36}S in a pulse-counting electron multiplier (EM) but the small Hamamatsu EM's on the IMS1270/80 experience significant gain drift at high count rates. Nonetheless, with appropriate within and between run drift correction, usable internal precision on $\Delta^{36}S$ of ~0.5‰ (1σ) can be achieved with spatial resolution <10 μm, as will be demonstrated with case studies from both early- and late-Archean sulfides. Lower noise FC amplifiers or substitution of a more robust EM can eventually improve precision.

[1] Farquhar & Wing (2003) *EPSL* **213**, 1-13. [2] Kamber & Whitehouse (2007) *Geobiology* **5**, 5-17. [3] Bekker *et al* (2009) *Science* **326**, 1086-1089. [4] Shen *et al*. (2009) *EPSL* **279**, 383-391

Geomicrobiology of hyperalkaline Cr(VI) contaminated land

ROBERT A. WHITTLESTON[1], IAN T. BURKE[1], DOUGLAS I. STEWART[2] AND R.J.G. MORTIMER[1]

[1]School of Earth and Environment, University of Leeds, Leeds, LS2 9JT, UK

[2]School of Civil Engineering, University of Leeds, Leeds, LS2 9JT, UK

Chromium in the form of its carcinogenic anion, chromate, has been entering the soils beneath a chromite ore processing residue (COPR) disposal site in the north of England for over 100 years, as a hyper alkaline (pH 13.5) liquor. This study reports the findings of a multi-disciplinary investigation into the biogeochemical processes occurring within the subsurface that influence contaminant fate.

The soil immediately beneath the waste was found to have a pH of 11→12.5, and contain 0.3→0.5% w/w chromium, and 45→75% of the microbially available iron is Fe(II). The soil pH and Cr concentrations were found to decrease with distance from the waste. XAS and (S)TEM analysis indicated that Cr is present throughout the soils as a mixed Cr(III)-Fe(III) oxy-hydroxide phase, resistant to air oxidation. This suggests that the elevated soil Cr content is due to reductive precipitation of Cr(VI) by Fe(II), producing a stable long term host for Cr(III). 16s rRNA community analysis of the soil immediately beneath the waste found a microbial population dominated by *Proteobacteria*, *Firmicutes* and *Bacteriodetes* species. Addition of this soil to alkaline Fe(III) containing growth media (pH=9.2) produced a consortium of iron reducing microorganisms dominated by the *Firmicutes* species, particularly *Anaerobranca*, *Anaerovirgula* and *Tissierella*.

Microcosm experiments demonstrated the capacity of COPR affected soil to abiotically remove all Cr(VI) from COPR leachate within 40 days. Amendment of the pH (~pH 9) resulted in the development of a cascade of microcrobially mediated terminal electron accepting processes, reaching Fe(III) reduction after complete Cr(VI) removal. A *Firmicutes* dominated population (73%) was identified in the pH amended microcosm systems during Fe(III) reduction, with *Dethiobacter sp* dominant, but *Anaerobranca sp* also present.

This work suggests that abiotic reductive precipitation of Cr(VI) by microbially produced Fe(II) can be effective at preventing the spread of chromium from COPR waste sites.

https://doi.org/10.1180/S0026461X00006502 Published online by Cambridge University Press

Lithium and its isotopes in Central European Rivers

U. WIECHERT[1]*, C.V. ULLMANN[1,2], D. UHLIG[1], T. PFAHL[1], M. RICKING[1] AND H. BECKER[1]

[1]Freie Universität Berlin, Germany (*correspondence: wiechert@zedat.fu-berlin.de)
[2]University of Copenhagen, Denmark

Lithium isotopes are a promising new means to study silicate weathering. To date most lithium isotope work on river systems has been done on ocean islands [1] or remote regions of, for example, the Himalayas [2] where human influence on rivers is minor. In this study we present lithium abundances and isotopic ratios for the central European rivers Danube, Elbe, and Rhine. The catchments of these rivers are highly populated, densely industrialised, and affected by a highly developed farming industry. The goal of this ongoing project is to identify major processes and anthropogenic sources which control lithium and its isotopes in central European rivers. The investigated waters show lithium concentrations (dissolved load) between ~2 and 22 µg/l and δ^7Li from +4 to +22 ‰ relative to L-SVEC. Some Danubian and upper Rhine waters have lithium abundances close to 2 µg/l and high δ^7Li up to +22 ‰. Similar concentrations (0.2-4.0 µg/l) and δ^7Li ~+23 ‰ are reported for more pristine river systems worldwide [3] indicating that lithium in the upper Danube and upper Rhine is largely controlled by silicate weathering. The catchments of the lower Elbe, in particular waters of the river Saale, are characterized by high lithium concentrations and ^{7}Li/^{6}Li. These waters have also high sulfate concentrations and δ^{34}S up to +8.5 ‰ CDT indicating a contribution from Permian evaporites. This is reasonable because evaporites have been mined in the region for more than a century. Samples from the river Elbe near Dresden, all Rhine and Danube samples show a good correlation between lithium isotope ratios and silicon fraction in the dissolved load (r^2 = 0.7). The highest molar fractions of silicon are connected to low δ^7Li ~5 ‰ and δ^{34}S ~3.4 ‰ in catchments of the river Elbe near Dresden. This is consistent with very intense weathering or a distinct style of weathering probably related to oxidation of sulfides and formation of highly acidic waters in old mining districts of the Erzgebirge.

[1] Pogge von Strandmann *et al*. (2008) *EPSL* **274**, 462-471; [2] Kisakurek *et al*. (2005) *EPSL* **237**, 384-401. [3] Huh *et al*. (1998) *GCA* **62**, 2039-2051.

Shale gas potential of the Upper Jurassic strata in the central part of the Polish Lowlands

D. WIĘCŁAW* AND P. KOSAKOWSKI

AGH University of Science and Technology, Al. Mickiewicza 30, 30-059 Krakow, Poland (*correspondence: wieclaw@agh.edu.pl)

The Upper Jurassic strata, rich in organic matter, are regarded as the main source rock of the large hydrocarbon accumulations in the Nowegian sector of the North Sea [1]. Also in Poland the Kimmeridge and Tithonian strata were subject of a large-scale exploration. In numerous wells only oil and gas shows were recorded. [2]. Our present study shows a new point of view on the posibility of shale gas accumulation in these strata. The investigations were conducted in the central part of the Polish Lowlands where the analysed strata are covered by thick Cretacous deposits.

In total, 126 samples (66 from the Kimmeridgian and 60 from the Tithonian strata, respectively) were collected. Rock-Eval pyrolysis indicates a large diversity in the total organic carbon (TOC) content, from 0.14 to 6.6 wt% (median 1.1 wt%) and from 0.19 to 10.2 wt% (median 1.6 wt%) in the Kimmeridgian and Tithonian strata, respectively. The total hydrocarbon content in the analysed rocks is not high and medians equal 1.32 and 4.2 mg HC/g rock, respectively. Hydrocarbon potential of the Kimmeridgian strata is usually low with the median value of 121 mg HC/g TOC indicating the presence of gas-prone kerogen, whereas for the Tithonian strata, the median of this index equals 272 mg HC/g TOC (mixed gas- and oil-prone kerogen). Maturity of organic matter corresponds with the initial phase of “oil window”. The BasinMod® 1-D modelling revealed that the generation of hydrocarbons from the Upper Jurassic source rocks occurred in the Late Cretaceous time. This process was interrupted by inversion on the Polish Lowlands.

In the selected areas of the Polish Lowlands the Kimmeridgian and Tithonian strata have generated sufficient amount of hydrocarbons to saturate rock and can be considered as a potential shale gas source.

The investigations were financed by the Ministry of Science and Higher Education (Project No. N307 3141 39).

[1] Justwan & Dahl (2005) *Proc. 6th Petrol. Geol. Conf.*, 1317-1329. [2] Karnkowski (1999) *Oil and gas deposits in Poland*, 380pp.

https://doi.org/10.1180/S0026461X00006502 Published online by Cambridge University Press

Primary shape and nanomechanical properties of natural Fe-colloids studied by AFM and SEM

A.K. WIECZOREK*, A. FRITZSCHE AND K.U. TOTSCHE

Institut für Geowissenschaften, Hydrogeologie, Friedrich-Schiller-Universität Jena, Burgweg 11, D-07749 Jena, (*correspondence: arkadiusz-krzysztof.wieczorek@uni-jena.de)

Natural colloids and nanoparticles are involved in a multitude of biogeochemical and physicochemical processes and act as mobile reactive carriers [1]. Interactions with each other and with the immobile phase not only affect hydraulic properties, but may change geometric, mechanic and physicochemical properties of the pore network and its interfaces. Of particular importance are the nanoparticulate mineral-organic mixed phases, formed either by the way of heterogeneous nucleation, sorption or co-precipitation [2][3]. We studied natural colloids sampled from soils subjected to redoximorphosis combining Scanning Electron Microscopy, Energy-Dispersive X-ray Spectroscopy and Atomic Force Microscopy. We identified three types of material, i.e. bulky Fe-aggregates, linear-aligned Fe-aggregates and flat, circular, soft and adhesive patches, presumably pure organic in nature. The majority belongs to the bulky-type with mean sizes around 50nm. Yet they are formed of much smaller subunits. The linear-aligned aggregates, presumable representing the subunits of the bulky aggregates, have mean diameters around 20 nm with large variety of lengths. They seem to be “chained” along linear structures, which we hypothesize to be of biotic origin. Thus, biotic material may be important in the geometric structuring of the aggregation process of natural colloids.

[1] Totsche & Kögel-Knabner (2004) *Vadose Zone Journal* **3(2)**, 352-367. [2] Eusterhues *et al*. (2008) *Environ. Sci. Technol*. **42**, 7891–7897. [3] Eusterhues *et al*. (2011) *Environ. Sci. Technol*. **45**, 527–533.

Sequential extractions as a tool to investigate stable metal isotope fractionation between soil pools

JAN G. WIEDERHOLD[1,2]*, BERNARD BOURDON[2,3] AND RUBEN KRETZSCHMAR[1]

[1]Institute of Biogeochemistry and Pollutant Dynamics, ETH Zurich, Switzerland (*correspondence: wiederhold@env.ethz.ch)

[2]Isotope Geochemistry, Institute of Geochemistry and Petrology, ETH Zurich, Switzerland

[3]ENS Lyon and CNRS, France

Stable isotope ratios contain information about sources and transformations in the biogeochemical cycle of metals in the environment. The recent development of high-precision methods to resolve metal isotope fractionation (e.g., Fe, Hg) now allows to apply these new isotope tracers to a variety of natural systems and sample matrices including soils. Biogeochemical metal cycling in soils plays an important role in chemical weathering processes, nutrient dynamics, and the fate of pollutants in terrestrial ecosystems.

The stable isotope signature of bulk soil samples can be assessed relatively easily by analysing total digest solutions. However, metals in soil samples are often present in various "pools" which can have very different histories and chemical properties. Thus, valuable information on isotopic differences between soil pools and fractionation between them is lost by analyzing only the isotope signature of bulk samples. Sequential chemical extractions are an established tool to separate metal pools from natural samples. However, the application of sequential extractions in stable isotope studies bears the risk of introducing fractionation artifacts during the extraction procedure. Thus, a careful method development is required to assess the suitability of specific extraction steps.

Here, we present iron isotope (δ^{56}Fe) and mass-dependent (MDF) and mass-independent (MIF) mercury isotope (δ^{202}Hg, Δ^{199}Hg) data from sequential extractions of different environmental samples measured by MC-ICP-MS. Newly-developed extraction methods were able to trace the evolution of secondary iron phases in young initial soils from a granitic glacier forefield, revealing that the imprint of a kinetic isotope effect during silicate weathering is preserved in pedogenic minerals. Mercury isotope ratios of sequential extracts from contaminated mine samples demonstrated that isotopically-distinct Hg pools exist within different tailing materials, exhibiting strong positive MDF and small negative MIF signatures in the more soluble extraction steps relative to the bulk isotopic composition. Future applications as well as potential limitations and pitfalls of sequential extraction methods in metal isotope studies will be discussed.

https://doi.org/10.1180/S0026461X00006502 Published online by Cambridge University Press

Life at the dry limit: Microbial colonization of evaporites in the Atacama Desert

J. WIERZCHOS[1]*, A. DE LOS RÍOS[1], A.F. DÁVILA[2], S. VALEA[1], B. CÁMARA[1], O. ARTIEDA[3] AND C. ASCASO[1]

[1]MNCN-CSIC, 28006 Madrid, Spain (*correspondence: j.wierzchos@mncn.csic.es)
[2]SETI Institute, Mountain View, CA 94043-2172, USA (adavila@seti.org)
[3]Universidad de Extremadura, 10600 Plasencia, Spain (oartieda@unex.es)

The hyper-arid core of the Atacama Desert is considered the driest region on Earth, one of the most challenging environments for life, and a Mars analog, due mainly to water scarcity. While Atacama soils are essentially lifeless, we have shown that hygroscopic halite crusts are colonized by endolithic communities composed of cyanobacteria, heterotrophic bacteria and archaea [1, 2]. The interior of the crusts provides shelter against extreme temperatures and UV radiation, and facilitates cell hydration through mineral deliquescence [3]. We also found that microporous and translucent gypsum crusts represent another evaporitic habitat for life in Atacama. This substrate is colonized by endolithic and hypoendolithic free living algae, fungi, cyanobacteria and heterotrophic bacteria, as well as by epilithic lichens [4]. The colonization of gypsum crusts appears to be controlled by atmospheric water potential. Based on our work in Atacama, we propose that putative Martian microorganisms withdrew to similar evaporitic micro environments as the planet dried out [5]. As such, evaporitic deposits would be primer targets for the search for life.

[1] Wierzchos *et al*. (2006) *Astrobiol*. **6**, 415-422. [2] De los Ríos *et al*. (2010) *Int*. *Microb*. **13**, 79-89. [3] Dávila *et al*. (2008) *J*. *Geophys*. *Res*. **113**, G01028. [4] Wierzchos *et al*. (2011) *Geobiol*. **9**, 44-60. [5]. Dávila *et al*. (2010) *Astrobiol*. **10**, 617-628.

Trace element mobilisation in a natural analogue CO_2 storage site

MAX WIGLEY*, MIKE BICKLE, NIKO KAMPMAN, BENOIT DUBACQ AND HAZEL CHAPMAN

Dept. Earth Sciences, Downing Street, Cambridge CB2 3EQ, UK (*correspondence: mmw36@ cam.ac.uk)

Natural analogues present a unique opportunity to study fluid-mineral interactions and transport processes that may occur in geological CO_2 storage systems [1,2]. Near Green River, Utah, USA, regionally extensive portions of the red-bed Entrada sandstone have been locally bleached white/yellow by low temperature diagenetic fluids [3]. Fluid inclusion studies [3], field relationships and modelling suggest that the fluid responsible for the bleaching is a low Eh-pH, CO_2-rich brine, containing variable amounts of methane.

Analyses reveal systematic patterns of trace element mobilisation and transport resulting from CO_2-promoted oxide dissolution (Fig. 1). Trace metals and REE concentrations are enriched at the transition from bleached to red facies. Element distribution is controlled by partitioning between the fluid and secondary minerals (carbonate, oxide, and clay phases), that precipitate as geochemical fronts propagate through the host rock. These fronts separate reduced, acidic fluid from oxidized groundwater.

Modelling suggests that bleaching results from dissolution of hematite from the red sandstones by a reaction of the form:

$$20Fe_2O_3 + 64CO_2 + 5CH_4 + 19H_2O + 11H^+ = 30Fe^{+2} + 59HCO_3^- + 10FeHCO_3^+,$$

in which CO_2 and a small fraction of methane complex the iron in solution. This reaction combined with Eh-pH diagrams suggest the precipitation of an iron-bearing carbonate and/or iron oxide phase, consistent with petrological observations.

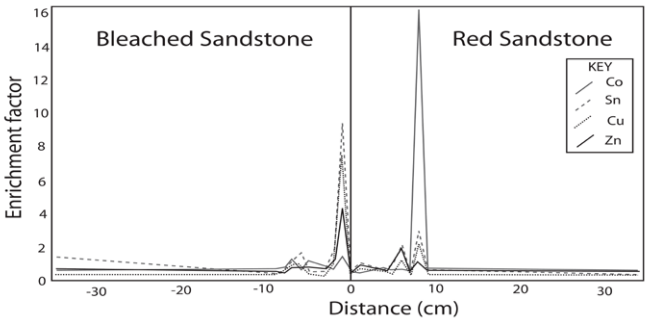

Figure 1. Plot of enrichment factor of metals relative to unaltered Entrada sandstone, versus distance from the bleached-unbleached contact.

[1] Moore *et al* (2005), *Chem*. *Geol*. **217**, 365-385. [2] Kampman *et al* (2009), *Earth Planet*. *Sci*. *Lett*. **284**, 473-488. [3] Kampman (2010), PhD thesis.

https://doi.org/10.1180/S0026461X00006502 Published online by Cambridge University Press

Chemical composition of biomass used in co-combustion with coal in Polish power-plants

W. WILCZYŃSKA-MICHALIK[1]*, R. GASEK[1] AND M. MICHALIK[2]

[1]Institute of Geography, Pedagogical University, ul. Podchorążych 2, 30-085 Kraków, Poland (*correspondence: wmichali@up.krakow.pl; rgasek@ap.krakow.pl)

[2]Institute of Geological Sciences, Jagiellonian University, ul. Oleandry 2a, 30-063 Kraków, Poland; (marek.michalik@uj.edu.pl)

Biomass is considered as important non-fossil renewable energy source. Potential biomass resources in Poland are estimated to be around 30 millions Mg per year and the share of biomass in electricity production and other applications is increasing systematically. Lack of complex life cycle assessment studies is the reason that real environmental value of biomass usage as fuel is not fully understood.

Concentration of major and trace elements in biomass is very important in prediction of technological problems during combustion and usage of combustion co-products as well as their environmental impact. Composition of biomass is related to many factors, e.g.: type of biomass, age of plant, growth process, fertilizers and pesticides used, soils composition and contamination, atmospheric pollution of plantation area, harvesting, transportation and storage.

The study is based mineralogical (optical and electron microscopy, XRD) and chemical analyses of samples of biomass used in power-plants in southern Poland.

The content of mineral component is low. Mineral particles can be considered as detrital (i.e. introduced by water or wind during plant growth) and anthropogenic (introduced during harvesting, transportation, storage and processing).

Chemical variation of studied samples of biomass is significant (e.g. Ca from 0.1 to 1.1wt%; P from 0.2 to 0.89wt%; Al from <0.01 to 0.09wt%; Na from <0.001 to 0.106wt%; K from 0.05 to 2.4wt%; S from <0.01 to 0.22wt% and for selected trace elements: Mn from 7 to 333 ppm; Pb from 2.9 to 25.6 ppm; Zn from 8.3 to 79.4 ppm; Cu from 2.2 to 25.2 ppm; Mo from 0.03 to 0.72 ppm; Hg from <1 to 21 ppb). The content of several trace elements is within the range comparable with Polish coals (e.g. Mn, Cr, Cu, Ni, Pb, Zn).

Significant differences in chemical composition of various types of biomass suggest that it is possible to expect different behaviour during combustion and different environmental impact. It also suggests that careful blending of biomass may be important.

Hydrothermal alteration and Ni sulphide formation in the Bon Accord Ni-oxide body, Barberton, South Africa

ANTJE WILDAU[1]*, A.E. WILLIAMS-JONES[2] AND MARIAN TREDOUX[1]

[1]Department of Geology, University of the Free State, Bloemfontein, 9300, South Africa (*correspondence: antje@geologie-leipzig.de)

[2]Department of Earth and Planetary Sciences, McGill University, Montreal, QC, H3A 2A7, Canada

The Bon Accord deposit is a 3.5Ga Ni-oxide body in the Barberton Greenstone Belt, South Africa. This small, lens-shaped orebody (6 x 3 x 0.35 m) was discovered in 1920, and mined out in the 1960s. The Ni concentration ranged from 35wt.% NiO in the center to 10wt.% NiO at the rim. The deposit has attracted considerable attention because of its very unusual mineralogy (e.g., bonaccordite, cochromite, nimite, liebenbergite, willemseite, trevorite). The orebody is hosted by a talc-carbonate-serpentinite and is located in the contact metamorphic aureole of a younger granite. The genesis of the deposit is unknown and the two main hypotheses that have been advanced for its formation are controversial. One of these is that the deposit is the product of a meteorite impact and the other is that it is an oxidized body of nickel-iron from the Earth's core.

Petrographic and geochemical studies of the Bon Accord deposit show the influence of hydrothermal fluids. In the centre of the deposit, there are relicts of primary liebenbergite (Ni_2SiO_4), which was serpentinized and later altered to willemseite ($(Ni,Mg)_3Si_4O_{10}(OH)_2$). The rest of the orebody is completely devoid of liebenbergite (Ni_2SiO_4) but much richer in népouite ($Ni_3Si_2O_5(OH)_4$) and willemseite ($(Ni,Mg)_3Si_4O_{10}(OH)_2$). The outer parts contain abundant millerite (NiS) and heazlewoodite (Ni_3S_2), plus a number of Ni-arsenide and Cu-sulphide minerals (10 vol.%), whereas the centre is almost devoid of Ni-sulphide minerals (<1vol.%), These minerals occupy cracks in the ferroan trevorite ($NiFe_2O_4$) and nickeloan magnetite ($(Ni,Fe)_3O_4$). In some places, the secondary minerals replace these oxides.

The mineralogical and textural relationships described above are consistent with alteration of the primary silicate minerals by reactions of the type:

2 liebenbergite + H_2S + H_2O → millerite + népouite

These observations suggest that the Bon Accord deposit formed from Ni-rich komatiite that was altered by circulating hydrothermal fluids, forming secondary sulphide minerals.

https://doi.org/10.1180/S0026461X00006502 Published online by Cambridge University Press

A comparision of mm scale resolution techniques for sediment core analysis

D. WILHELMS-DICK[1]*, T. HANEBUTH[1], U. RÖHL[2], T. WESTERHOLD[2], M. KRIEWS[3], H. RÖMMERMANN[3] AND S. KASTEN[1]

[1]Bremen University, Postfach 330 440, 28334 Bremen, Germany (*correspondence: wilhelms@uni-bremen.de)
[2]Marum, Postfach 330 440, 28334 Bremen, Germany
[3]Alfred Wegener Institute for Polar and Marine Research, Postfach 120161, 27515 Bremerhaven, Germany

To study high-frequency variability in the Arabian Monsoon intensity, laminated sediments from the oxygen minimum zone (200-1200m) of the Arabian Sea offer a high-resolution climate archive [1]. The chemical signature which is used to reconstruct past climate can be obtained using several different analysing techniques. In the presented study a 5.3 m long sediment core from the northern Arabian Sea (GeoB12309-5: 24:52.3°N; 62:59.9°E, 960 m water depth), covers the past 4,900 cal yrs BP. The XRF core scanner data show highly varying signals in the upper 1.6 m core depth. Based on these results and radiograph images, samples were taken for LA-ICP-MS and ICP-MS/OES analysis.

The big advantages of analysing a sediment core via XRF core scanning are non-destruction and speed, but only relative variations for chemical elements are obtained and not element concentrations. The LA-ICP-MS methods is quasi non-detructive, you obtain element concentrations but is more time consuming. The most precise, but also most time consuming methods for main and trace element analysis are the ICP-MS/OES techniques after full acid digestion.

Results from all 3 methods show similar chemical patterns at distinct sediment structures (e.g. turbidites) for Ca, Rb and Sr. However, the comparability between the 3 methods is worse for Al, K, Ti, Fe and Zr. The particle size, water content of the sediment and surface roughness highly influences the XRF method, to some extent also the LA-ICP-MS technique. These results suggest that the soft sediment cores including its overall quality and surface conditions limit the ability of the sub-mm scale XRF scanning method to receive reliable data for Ca, Rb and Sr. However, the LA-ICP-MS technique as it was used here shows problems with long term drift, hence making it very difficult to accurately compare the 3 high resolution methods. Due to the relatively large amount of sediment digested, the ICP-MS/OES method delivers the most accurate results which are assumed to best serve as input data for frequency analysis.

[1] Von Rad *et al*. (1999) *Quat. Res*. **51**, 39-53.

Zircon solubility in Na-Si-Al-O-H fluids by *in situ* SR-XRF analysis

M. WILKE[1], C. SCHMIDT[1], J. DUBRAIL[1], K. APPEL[2] AND M. BORCHERT[2]

[1]Deutsches GeoForschungsZentrum GFZ, Potsdam, Germany (max@gfz-potsdam.de)
[2]Deutsches Elektronen-Synchrotron, Hamburg, Germany

The geochemical budget of high-field-strength elements (HFSE, i.e., Ti, Zr, Hf, Nb and Ta) in rocks is largely controlled by accessory phases such as zircon or rutile. Thus, the mobility of HFSE during processes in the Earth's crust and mantle is closely linked to solubility and stability of these phases. Fluid composition appears to be the most important parameter because it may drastically affect the complexation of HFSE. Earlier studies ([1],[2]) on rutile report enhanced solubility for aqueous fluids with $Na_2Si_3O_7$ (NS3) or $NaAlSi_3O_8$. Complexing of Ti with alkalies and silica (siloxan groups) dissolved in the fluid has been suggested as an important mechanism to explain these high solubilities. A similar mechanism for enhanced solubility can be expected for the zircon-hafnon series.

Synthetic zircon was equilibrated with fluids containing $Na_2Si_3O_7$, $Na_2Si_3O_7$ + 5 wt% Al_2O_3, or $NaAlSi_3O_8$ at *T* up to 750 ˚C and *P* up to 1.5 GPa using hydrothermal diamond-anvil cells. The Zr content of the fluids was determined *in situ* at *P* and *T* by confocal synchrotron radiation μXRF analysis at beamline L, HASYLAB. At *P* of 450–950 MPa and *T* of 500–750°C, Zr concentrations range from 20 to 90 ppm in H_2O + 10 wt% NS3 fluids. In H_2O + 18 wt% NS3 solutions, they increase to 200 to 500 ppm and drop to 100–150 ppm upon addition of Al. The highest concentrations of up to 1000 ppm were measured in fluids containing 30 wt% NS3. At constant NS3 content, the Zr concentration generally decreases with P and increases with T. One experiment with zircon *and* hafnon was done to measure Zr-Hf fractionation. At a NS3 content of 27 wt%, a molar Hf/Zr ratio of 2.7 was determined, which indicates significant Hf-Zr fractionation in these fluids. For a fluid with 6 wt% $NaAlSi_3O_8$ at ~1.45 GPa and 600°C, the XRF signal was at the detection limit, i.e. ~1 ppm Zr or below. These solubility data are qualitatively consistent with those on rutile ([1],[2]) and indicate strong differences in Zr speciation with *P*, *T*, and fluid composition. They represent another example for which efficient complexation of HFSE by siloxan-like units in the fluid is indicated (see also ref. [3]).

[1] Manning *et al*. (2008) *Earth Planet. Sci. Lett*. **272**, 730-737. [2] Antignano & Manning (2008) *Chem. Geol*. **255**, 283-293. [3] Dubrail *et al*. (2011) *MinMag*, this volume.

https://doi.org/10.1180/S0026461X00006502 Published online by Cambridge University Press

Compound-specific isotopic evidence of paleoenvironmental change Lake El'gygytgyn, NE Russia

K. WILKIE*, S.T. PETSCH, S. BURNS AND J. BRIGHAM-GRETTE

Dept. of Geosciences, University of Massachusetts, Amherst, MA, USA (*correspondence: kwilkie@geo.umass.edu)

Recent successful drilling operations at Lake El'gygytgyn, NE Russia have recovered sediment cores back to 3.6Ma, representing the longest time-continuous sediment record of past climate change in the terrestrial Arctic. Compound-specific isotopic analysis of sedimentary lipids from this remote basin spanning the last 120ka allows reconstruction of past hydrological conditions, thereby providing a powerful tool for reconstructing past Arctic climate changes.

The hydrogen isotopic composition of lipid biomarkers was determined from previously obtained Lake El'gygytgyn sediment cores and compared with other multi-proxy evidence of past climate change within the lake basin. Here we present δD measurements of individual sedimentary fatty acids representing aquatic and terrestrial sources (e.g. aquatic, δD_{AQ}: nC_{20}, nC_{22}; terrestrial, δD_{TER}: nC_{30}) over the past 120 ka. The δD_{AQ} record shows little variation on glacial-interglacial cycles, possibly due to perennial ice cover during full glacial conditions and/or changes in aquatic community structure and aquatic organic matter sources. The data from terrestrial components show significant variation (up to 70‰) between glacial-interglacial intervals as well as variation on millenial timescales (~200 yr resolution). The most negative δD_{TER} values occur during glacial conditions (i.e. the Last Glacial Maximum and MIS 4) while enriched values are observed during interglacial intervals (i.e. most notably during the Holocene and MIS 5e). Preliminary reconstruction of the isotopic composition of precipitation from these results allows for comparision with the δD ice core records from both Greenland and Antarctic to assess high latitude environmental change and global teleconnections. Initial comparison of these records shows high fidelity with speleothem records from Hulu and Dongge caves [1] as well as with δD_{GRIP} [2] and δD_{VOSTOK} [3] records.

[1] Wang *et al*. (2005), *Science* **308**, 854-857. [2] Masson-Delmotte *et al*. (2005), *Science* **309**, 118-121. [3] Petit *et al*. (1999), *Nature* **399**, 429-436.

The W isotopic composition of the Hadean mantle – Evidence for the late heavy bombardment

M. WILLBOLD[1], T. ELLIOTT[1] AND S. MOORBATH[2]

[1]University of Bristol, School of Earth Sciences, Wills Memorial Building, Queens Road, Bristol, BS8 1RJ, United Kingdom

[2]University of Oxford, Department of Earth Sciences, South Parks Road, Oxford, OX1 3AN, United Kingdom

The contrasting behaviour of its daughter and short-lived ($t_{1/2}$ ~9Ma) parent has made the ^{182}Hf-^{182}W system invaluable in determining the timescales of planetary core formation. However, Hf is also considerably less incompatible than W in many melting and crystallisation scenarios in purely silicate systems. Thus the ^{182}Hf-^{182}W pair has also been used with success in examining the evolution of the silicate portion of planetessimals. Recent $\varepsilon^{142}Nd$ data demonstrate that Hadean mantle fractionation events are recorded in the isotopic signatures of samples from Isua, Greenland. Notably one interpretation of terrestrial ^{142}Nd-^{143}Nd systematics invokes the formation of an enriched, deep reservoir within the first 30Ma of Earth History. It has further been suggested that the contrast between $\varepsilon^{142}Nd$ in the most ancient Greenland samples and present day mantle (~20ppm) is a result of partial remixing between this hidden reservoir and convecting mantle after ~3.5Ga. If so, the Greenland samples derived from mantle that pre-dates this event would be expected to show a difference in $\varepsilon^{182}W$ relative to modern mantle.

We have made high-precision (<5ppm; 2σ) $\varepsilon^{182}W$ measurements on some Isua samples. These document significant differences between these samples and modern mantle values (~13ppm). In contrast to previous studies [1,2] our analyses are considerably more precise and we are the first to document significant differences. However, the magnitude of the difference in our $\varepsilon^{182}W$ is smaller than predicted for a remixing scenario of early enriched reservoir with the convecting mantle that can account for the difference in $\varepsilon^{142}Nd$ between Isua and present mantle. We thus re-emphasise the conclusions of [1], that this change in $\varepsilon^{142}Nd$ with time does not provide good evidence for the existence of an early enriched reservoir. We further note that the addition of ~0.5% of primitive chondritic material after core formation, as suggested by the late veneer model, is sufficient to account for the lowering of $\varepsilon^{182}W$ from values we report in the Isua samples to present-day.

[1] Iizuka, T. *et al*. (2010) *Earth and Planetary Science Letters* **291**, 189-200. [2] Moynier, F. *et al*. *Proceedings of the National Academy of Sciences* (2010) **107**, 10810-10814.

https://doi.org/10.1180/S0026461X00006502 Published online by Cambridge University Press

From thermochronometric ages to exhumation rates

S.D. WILLETT[1], M.T. BRANDON[2], M. FOX[1] AND F. HERMAN[1]

[1]Geological Institute, ETH, 8092 Zurich, Switzerland
[2]Yale University, New Haven, CT, USA

To render a thermochronometric age into a more useful exhumation rate, it is necessary to process that age through a thermal model. We present a set of analytical and numerical thermal modelling methods of increasing complexity; which we feel are as simple as possible, while still retaining the essential physics of the thermal processes. We consider first the simple case of converting a single age into an exhumation rate. We include the dependence of the closure temperature on cooling rate (Dodson, 1973) and the upward advection of heat and derive some simple, analytical expressions relating exhumation rate to age through the kinetic parameters of the thermochronometric system, first, by assuming the geothermal gradient has been constant in time, and, second, using the transient analytical solution for an advecting halfspace. The second problem we consider is the effects of topographic relief on the closure isotherm. We calculate the mean depth to a closure isotherm using the solution described above, and then use spectral methods to calculate topography on this isotherm in response to topography of the surface. Finally, we consider the problem of spatially-varying exhumation rate. For this problem we combine the approaches given above, calculating perturbations to isotherms using spectral methods, combined with 1-D models of heat advection and diffusion. The 1-D models are linked by imposing a spatial correlation structure on the exhumation rate, which is otherwise free to vary in space and time. This approach provides an efficient method to "invert" a large number of thermochronometic ages, distributed in space and elevation, providing maps of time-varying exhumation rate. We illustrate each of these methods with data from the European Alps.

Novel approaches to organic aerosol chemical characterization

B.J. WILLIAMS[1]*, Y. ZHANG[1], R. MARTINEZ[1], K.S. DOCHERTY[2,3], I.M. ULBRICH[2], J.L. JIMENEZ[2], S.V. HERING[4], N.M. KREISBERG[4], A.H. GOLDSTEIN[5], AND D.R. WORSNOP[6]

[1]Washington University, St. Louis, MO 63130, USA (*correspondence: brentw@seas.wustl.edu)
[2]University of Colorado and CIRES, Boulder, CO 89309, USA
[3]Alion Science and Technology, Research Triangle Park, NC 27709, USA
[4]Aerosol Dynamics Inc., Berkeley, CA 94710, USA
[5]University of California, Berkeley, CA 94720, USA
[6]Aerodyne Research Inc., Billerica, MA 01821

In recent years several new approaches have been introduced to improve the chemical characterization of atmospheric organic aerosol (OA). Here, we highlight two techniques, the thermal desorption aerosol gas chromatograph (TAG) for automated in-situ molecular level OA speciation [1], and the high resolution time-of-flight aerosol mass spectrometer (AMS), which in addition to inorganic speciation, measures total fine OA mass concentrations and determines O/C, H/C, and N/C elemental ratios [2]. While each technique has its strengths, the TAG system is not capable of complete OA analysis without prior chemical derivatization, and the AMS is not capable of separating individual compounds. Here, we will describe recent efforts to create a combined TAG-AMS system to provide measurements of total OA, elemental ratios, and individual compounds. Finally, we discuss our efforts to develop novel data analysis approaches. Positive matrix factorization (PMF) has been used to deconvolve timeseries of AMS mass spectra [3] and timeseries of TAG source-marking compounds [4] into major components contributing to atmospheric OA concentrations. The desire to have combined TAG-AMS input parameters for a single PMF analysis have inspired novel measurement ideas that will be introduced here.

[1] Williams *et al*. (2006) *Aerosol Sci Technol* **40**, 627-638. [2] DeCarlo *et al*. (2006) *Anal Chem* **78**, 8281-8289. [3] Ulbrich *et al*. (2009) *Atmos Chem Phys* **9**, 2891-2981. [4] Williams *et al*. (2010) *Atmos Chem Phys* **10**, 11577-11603.

https://doi.org/10.1180/S0026461X00006502 Published online by Cambridge University Press

Isotopic evidence for internal oxidation of the Earth's mantle during accretion

HELEN M. WILLIAMS[1,2]*, BERNARD J. WOOD[1], JON WADE[1], DANIEL J. FROST[2] AND JAMES TUFF[1]

[1]Department of Earth Sciences, The University of Oxford, South Parks Road, Oxford OX1 3AN, UK

[2]Department of Earth Sciences, Durham University, Science Labs, Durham DH1 3LE, UK (*correspondence: h.m.williams2@durham.ac.uk)

[3]Bayerrishes Geoinstitut, Universität Bayreuth, D-95440 Bayreuth, Germany

The Earth's mantle is currently oxidised and out of chemical equilibrium with the core. Why this should be the case, and why the Earth's mantle should be oxidised relative to other terrestrial planets is poorly understood. It has been proposed that the oxidised nature and high ferric iron (Fe^{3+}) content of Earth's mantle was produced internally by disproportionation of ferrous iron (Fe^{2+}) into Fe^{3+} and metallic iron by perovskite crystallisation during accretion [1]. Here we show that there is a substantial Fe isotope fractionation between experimentally equilibrated metal and perovskite, which can account for the heavy Fe isotope compositions of terrestrial basalts relative to equivalent samples derived from Mars and Vesta [2,3] as the latter are too small to stabilise perovskite. Mass balance calculations indicate that all of the mantle's Fe^{3+} could have been generated from a single disproportionation event, which is consistent with complete dissolution of perovskite in the lower mantle during the Moon-forming giant impact. The similar Fe isotope compositions of terrestrial and lunar basalts [2,3] is consistent with equilibration between the mantles of the Earth and Moon in the aftermath of the giant impact [4] and suggests that the heavy Fe isotope composition of the Earth's mantle was established prior to, or during the giant impact. The oxidation state and ferric iron content of the Earth's mantle was therefore plausibly set by the end of accretion, and is decoupled from later volatile additions [5], tectonic plate recycling and the rise of oxygen in the Earth's atmosphere at 2.45 Ga [6].

[1] Frost, D. J. *et al*., (2004). *Nature* **428** (6981), 409 [2] Poitrasson, F. *et al*., (2004). *EPSL*. **223** (3-4), 253 [3] Weyer, S. *et al*., (2005). *EPSL* 240 (2), **251** [4] Pahlevan, K. and Stevenson, D. J., (2007) *EPSL*. **262** (3-4), 438. [5] Schonbachler *et al*., (2010) *Science* **328** (5980), 884. [6] Kump, L. R., (2008) *Nature* **451** (7176), 277.

Characterization of elemental sulfur reducing bacteria using transmission electron microscopy and their impact on sulfur isotope fractionation

KENNETH H. WILLIAMS[1]*, MICHAEL J. WILKINS[2]*, ALICE C. DOHNALKOVA[2], JENNIFER L. DRUHAN[1], AND MARK E. CONRAD[1]

[1]Lawrence Berkeley National Laboratory, Berkeley, CA, 94720, USA (*khwilliams@lbl.gov)

[2]Pacific Northwest National Laboratory, Richland, WA, 99352, USA (*michael.wilkins@pnl.gov)

The process of elemental sulfur (S^0) reduction by a microorganism isolated from an acetate-stimulated aquifer at the Department of Energy's Rifle Integrated Field Research Challenge (IFRC) site in Rifle, Colorado (USA) was studied using a combination of transmission electron microscopy (TEM) and isotopic techniques. Results were compared to those obtained using the well-characterized S^0 reducer *Geobacter sulfurreducens*. The site isolate was obtained from Rifle groundwater using acetate and S^0 flowers as the electron donor and acceptor, respectively. Based on 16S rRNA analysis, the isolate was most closely related to the β-proteobacterium *Azospira orzyae* (syn *Dechlorosoma suillum*). TEM revealed the isolate to be a curved rod with a single polar flagellum. Finely particulate S^0 granules (<5nm) were observed along the outer membrane as aqueous sulfide concentrations reached peak values of ca. 1200μM. Prolonged growth resulted in an abundance of aggregated filaments bound within a sulfur-rich matrix; their biogenesis and relation to cell growth remains unknown. Microbial reduction of S^0 coupled to oxidation of acetate may lead to significant deviations in the $\delta^{34}S$ values of sulfide relative to $\delta^{34}S$ values of S^0.

Such studies are critical for understanding the process of sulfur reduction in reduced environments, hypothesized to enable prolonged U(VI) immobilization at the Rifle IFRC site. Research at the site has identified significant accumulation of S^0 accompanying oxidation of aqueous sulfide by Fe(III)-oxide minerals, with the process generating an abundant electron acceptor capable of supporting the activity strains implicated in enzymatic U(VI) reduction (e.g. *Geobacter)* following exhaustion of reactive Fe(III) minerals. These results will enable incorporation of rates of microbial S^0 reduction and $\delta^{34}S$ fractionation within reactive transport models describing biogeochemical processes at the Rifle site and provide additional insights into sulfur cycling pathways.

https://doi.org/10.1180/S0026461X00006502 Published online by Cambridge University Press

Atomistic simulation of oxygen transport in actinide oxides and at their interfaces

N.R. WILLLIAMS[1]*, S.C. PARKER[1] A. DEVEY[2] AND M. READ[2]

[1]Department of Chemistry, University of Bath, Bath BA2 7AY, United Kingdom (*correspondence: n.r.williams@bath.ac.uk)
[2]AWE, Aldermaston, Reading, RG7 4PR (mark.read@awe.co.uk, anthony.devey@awe.co.uk)

Actinides such as uranium and its oxides are receiving increasing attention because of the interest in nuclear fuels not least because of awareness of issues associated with CO_2 emissions, security of energy supply and waning fossil fuel reserves. This also has implications on the storage of these materials in both the long and short term. Computational methods provide a complementary route for studying the corrosion of nuclear fuels and transport through the environment.

We used computer simulation techniques, using both potential-based and electronic structure methodologies to investigate the structure and stability of the surfaces and interfaces, primarily of uranium dioxide as well as the factors controlling oxygen transport through the materials. The electronic structure simulations used the VASP code [1] using GGA+U method, but are further complicated by the magnetic contribution of the 5f electrons. The correct ground state and properties are obtained by correctly controlling the orbital occupation matrices [2]. The interatomic potentials were derived to reproduce the calculated and experimental properties and used to evaluate the grain boundary structures as a function of temperature using molecular dynamics with the DL_POLY code [3].

A number of grain boundary structures were investigated we found that at high temperatures but below the melting point that UO_2 undergoes a fast ion transition where oxygen becomes highly mobile. The grain boundaries showed enhanced diffusivity, displaying fast ionic conduction at significantly lower temperatures than observed in the bulk crystal.

In summary a number of computational techniques have been utilised to investigate actinides such as uranium and their oxides. Increased understanding of the intrinsic disorder present in these oxides and its effect on corrosion offers significant benefits for the safe storage and handling of nuclear fuel materials.

[1] Kresse & Furthmuller (1996), *Phys. Rev. B*, **54**, 11169-11186. [2] Devey (2011) *J. Nucl Mater* doi:10.1016/j.jnucmat.2011.03.012 [3] Smith and Forester (1996) *J. Mol Graph* **14**, 136-141

Transitional oxygenation recorded in the Paleoproterozoic Turee Creek Group, Western Australia

KENNETH H. WILLIFORD[1]*, MARTIN J. VAN KRANENDONK[2], TAKAYUKI USHIKUBO[1], REINHARD KOZDON[1] AND JOHN W. VALLEY[1]

[1]NASA Astrobiology Inst., WiscSIMS, Dept. of Geoscience, Univ. Wisconsin, Madison, WI 53706 USA, (*correspondence: kwilliford@geology.wisc.edu)
[2]Geol. Surv. Western Australia, Perth, WA 6004, Australia

In situ, multiple sulfur isotope data from pyrite in the glaciomarine Meteorite Bore Member of the Paleoproterozoic Turee Creek Group, Western Australia, indicate deposition during a transitional stage in the rise of atmospheric oxygen. Abundant detrital pyrite in one diamictite layer exhibits a range of $\Delta^{33}S$ (–3.6 to 11.6‰) encompassing the entire known range for the Archean. Small, but significant, S-MIF ($\Delta^{33}S$ from –0.8 to 1.0‰) is preserved in authigenic pyrite throughout the section. A >90‰ range in $\delta^{34}S$(Py) (–45.5 to 46.4‰ VCDT) is strong evidence for vigorous microbial sulfate reduction under non-sulfate limited conditions, an indication that oxidative continental weathering of sulfides was sufficient before and during deposition to deliver a large quantity of sulfate to the ocean. Multiple generations of pyrite were observed, distiguished by their isotopic and minor element compositions. Sharp gradients in $\delta^{34}S$ (30‰ over <4 μm; defined by 3 μm spots) constrain the degree of sulfur diffusion during metamorphism and thus the time-temperature history of the unit. This is the first observation of such a large range in $\delta^{34}S$ together with significant S-MIF, and it reveals a chapter in the history of atmospheric oxygenation heretofore unknown from similarly age-constrained glacial deposits in North America [1] and South Africa [2]. The new data highlight the critical role of microbial sulfate reduction in the oxidative transition and are consistent with the proposal by Zahnle *et al*. [3] that increasing seawater sulfate led to the shutdown of the Archean methane greenhouse, curtailing the preservation of S-MIF. However, the suggestion that S-MIF disappears completely before continental glaciation [3] is not supported by our data or those from North America [1] and South Africa [2], and details of the Great Oxidation Event remain to be elucidated.

[1] Papineau *et al*. (2007) *EPSL* **255**, 188-212. [2] Guo *et al*. (2009) *Geology* **37**, 399-402. [3] Zahnle *et al*. (2006) *Geobiology* **4**, 271-283.

https://doi.org/10.1180/S0026461X00006502 Published online by Cambridge University Press

High-resolution metabolomics reveals unusual *N*-methyl *lyso* phosphatidylethanolamines as abundant and strain-specific lipids in acid mine drainage biofilms

P. WILMES[1]*, C.R. FISCHER[2], B.P. BOWEN[3], B.C. THOMAS[4], R.S. MUELLER[4], V.J. DENEF[4], N.C. VERBERKMOES[5], R.L. HETTICH[5], T.R. NORTHEN[3] AND J.F. BANFIELD[6]

[1]Department of Earth and Planetary Science, University of California, Berkeley, CA 94720, USA; present address: Public Research Center – Gabriel Lippmann, Belvaux L-4422, Luxembourg (*correspondence: wilmes@lippmann.lu)

[2]Department of Earth and Planetary Science, University of California, Berkeley, CA 94720, USA; present address: Ginkgo Bioworks, Boston, MA 02210, USA (curt@ginkgobioworks.com)

[3]GTL Bioenergy Division and Life Sciences Division, Lawrence Berkeley National Laboratory, CA 94720, USA (bpbowen@lbl.gov, trnorthen@lbl.gov)

[4]Department of Earth and Planetary Science, University of California, Berkeley, CA 94720, USA (bcthomas@berkeley.edu, rmueller@berkeley.edu, vdenef@berkeley.edu)

[5]Chemical Sciences Division, Oak Ridge National Laboratory, Oak Ridge, TN 37830, USA (verberkmoesn@ornl.gov, hettichrl@ornl.gov)

[6]Department of Earth and Planetary Science, and Department of Environmental Science, Policy and Management, University of California, Berkeley, CA 94720, USA (jbanfield@berkeley.edu)

High-resolution untargeted metabolomics was applied to 14 distinct biofilm samples retrieved from the air-solution interface of acid mine drainage (AMD) solutions within the Richmond Mine (Iron Mountain, Redding, CA). Among the detected metabolites, we identified and characterized a group of *lyso* phosphatidylethanolamine lipids which were highly abundant. The unusual polar head group structure of these molecules is similar to lipids found in phylogenetically unrelated acidophilic chemoautolithotrophs and may be related to the affinity of these lipids for iron and calcium ions. Correlations of *lyso* phospholipid and strain-resolved protein abundance patterns suggest a link between the *lyso* phospholipids and the UBA-type substrain of *Leptospirillum* group II. By combining high-resolution molecular "omic" technologies, we demonstrat Focusing of upward fluid migration due to mineral grain size variation

e the ability to identify cryptic but organism-specific small molecules that may be of paramount importance to biogeochemical processes occurring in mining impacted environments.

A spatial perspective on Nd isotope records from the Western Indian Ocean: Evidence for a 'boundary exchange' control?

D.J. WILSON*, A.M. PIOTROWSKI AND A. GALY

Department of Earth Sciences, University of Cambridge, Cambridge, CB2 3EQ (*correspondence: david.wilson@esc.cam.ac.uk)

Reconstructing past water mass mixing using Nd isotopes relies upon the quasi-conservative behaviour of this tracer. In contrast, recent studies in the modern oceans have demonstrated that 'boundary exchange' [1] and/or reversible scavenging [2] may be important processes in the Nd cycle. 'Boundary exchange' in particular would complicate our interpretation of down core Nd isotope records, since any significant addition of Nd from sediments would make the proxy behave non-conservatively. However, modelling studies at a global scale [3, 4] have been unable to distinguish between advection and 'boundary exchange' as the dominant control on the Nd isotopic distribution of seawater.

In this study, using 10 sediment cores from the deep western Indian Ocean, we address the importance of 'boundary exchange' from the Madagascar and Mascarene Plateau margins. Deep water ε_{Nd} composition is reconstructed using foraminiferal coatings, which agree within error with bulk sediment leachates. Holocene core tops located along the south-to-north flow path of Circumpolar Deep Water (CDW) record different ε_{Nd} values. Cores nearest to the inflow record an ε_{Nd} of -8.6, which shifts to -11.3 near Madagascar and -7.1 near Mascarene. Comparison to detrital ε_{Nd} in the same cores suggests a control by local sedimentary inputs from Madagascar and the Mascarene Plateau. This allows a first attempt to quantify 'boundary exchange' along this margin and potentially to reconstruct past changes. Cores to the south of the Madagascan margin (i.e. upstream in deep water flow) appear to record the changing advected composition of CDW across Termination I, whereas marginal sites record offset ε_{Nd} values and reduced glacial-interglacial variability. This underlines the importance of deciphering 'boundary exchange' before inferring global ocean circulation changes from Nd isotope records. Additionally, it may provide insight into temporal changes in the inputs, and therefore budget, of REE's and other particle-reactive elements in the oceans.

[1] Lacan & Jeandel (2005), *EPSL* **232**, 245-257. [2] Siddall *et al*. (2008), *EPSL* **274**, 448-461. [3] Arsouze *et al*. (2007), *Chem. Geol*. **239**, 165-177. [4] Jones *et al*. (2008), *EPSL* **272**, 610-619.

https://doi.org/10.1180/S0026461X00006502 Published online by Cambridge University Press

Tracing changes in the East Asian Monsoon using the Mg isotope record in a loess-paleosol sequence from Luochuan, China

JOSH WIMPENNY[1], QING-ZHU YIN[1]*, DARREN TOLLSTRUP[1], LIE-WEN XIE[2] AND JIMIN SUN[2]

[1]Department of Geology, University of California, Davis, CA
[2]Institute of Geology and Geophysics, Chinese Academy of Sciences, Beijing, China

We present Mg isotope data from a loess-paleosol sequence from Luochuan in the central Chinese Loess Plateau. The alternating loess-paleosol layers result from changes in climate and weathering intensity; loess layers representing cooler, drier periods when the winter monsoon was strong, while paleosol layers form during warmer, wetter periods with a stronger summer monsoon. Bulk δ^{26}Mg analyses show that both loess and paleosol layers are enriched in the light isotopes of Mg relative to the bulk continental crust. On average, loess layers contain lighter δ^{26}Mg values than the paleosol, with average values of -0.57‰ ± 0.19 (2σ), and -0.37‰ ± 0.18 (2σ) respectively. These light δ^{26}Mg values are a direct result of high amounts of carbonate in the sediment layers (up to ~15%) and the fact that carbonate is enriched in light Mg relative to silicates. The higher chemical weathering intensity subjected to the paleosol layers means more carbonate has been leached away, hence the remaining sediment is isotopically heavier than the loess layers where more carbonate remains. The high amplitude changes in δ^{26}Mg related to alternating loess-paleosol layers at Luochuan closely match changes in other weathering tracers including magnetic susceptibility, grain size and Na/Ca ratios. This suggests that all of these proxies are controlled by the same process, i.e. changing climate related to changes in northern hemisphere circulation. In addition, our δ^{26}Mg analyses also record a longer term change in chemical weathering, manifested as a shift to more positive δ^{26}Mg values ~500 to 900Ka. This coincides with the approximate timing of a strengthening in the summer monsoon and a reduction in the seasonality of precipitation. Thus, Mg isotopes record weathering changes on two different timescales in Chinese loess, that have implications for our understanding of how the East Asian Monsoon may have behaved over the last 2.6Ma. We suggest that the sensitivity of Mg isotopes to the presence of carbonate, and to the formation of secondary silicates makes the Mg system a powerful tool that can be used to enhance our understanding of past weathering processes.

Carbon isotopes in DIC trace benthic and pelagic processes in tidal areas of the North Sea

VERA WINDE[1], PETER ESCHER[1], NICOLE KOWALSKI[1], OLAF DELLWIG[1], BERND SCHNEIDER[1], MATTHIAS SCHULTZ[1], PHILLIP BÖNING[2], JUSTUS E.E. VAN BEUSEKOM[3], GERD LIEBEZEIT[2] AND MICHAEL E. BÖTTCHER[1]*

[1]Leibniz IOW, D-18119 Warnemünde, Germany. (*michael.boettcher@io-warnemuende.de)
[2]ICBM, CvO University of Oldenburg, D-26382 Wilhelmshaven/ D-26111 Oldenburg, Germany
[3]AWI Wadden Sea Station Sylt, D-25992 List, Germany

We investigate the spatial gradients and temporal dynamics of the dissolved inorganic carbonate system in tidal areas of the North Sea. We aim for an understanding of the impact of benthic processes on the production of alkalinity and its subsequent export to the open North Sea, as well as the role of benthic processes, e.g. the interaction (destruction, formation) of surface pore waters with sedimentary calcium carbonate. These processes in turn have the potential to modify the pore water and the bottom water composition that exchanges with the shallow North Sea. The benthic and pelagic processes may change in the future as the North Sea is facing increasing atmospheric CO_2 pressures, and decreasing pH and changes in nutrient inventories are expected.

Water column and pore water samples were taken at different seasons, during tidal cycles and on transects through different tidal basins of the German Wadden Sea (Jade Bay, Sylt, Spiekeroog) for measurements of alkalinity, DIC, pH, salinity, temperature, δ^{13}C(DIC), besides major and trace elements. The carbonate system demonstrates significant tidal, and spatial, as well as seasonal variations in the water column. Such variabilities reflect mixing processes with freshwater via coastal tributaries and the influence of benthic and pelagic (e.g. primary production) processes, changing with season. Results from the East-Frisian Wadden Sea are compared to measurements in the North-Frisian Wadden Sea system. Locally, pore waters in sandy sediment, influenced by upward methane fluxes and AOM, reveal steep physico-chemical gradients. Low-tide drainage of anoxic pore waters leads to the liberation of ^{12}C-enriched DIC, TA, nutrients and (H_2S, CH_4).

Field data will be integrated in a modelling environment of the North Sea carbonate system. Research is supported by BMBF within the BIOACID project, IOW, AWI, and ICBM.

https://doi.org/10.1180/S0026461X00006502 Published online by Cambridge University Press

100-year record of $^{236}U/^{238}U$ in coral as a step towards establishing ^{236}U as oceanic tracer

S. WINKLER[1]*, P. STEIER[1], J. CARILLI[2]

[1]Faculty of Physics, University of Vienna, 1090 Wien Austria (* correspondence: stephan.winkler@univie.ac.at)
[2]Institute for Environmental Research, Australian Nuclear Science and Technology Organisation

Since uranium is known to behave conservatively in ocean waters, ^{236}U has great potential in application as oceanic tracer. Approximately 600kg of ^{236}U ($t_{1/2}$=23.4Ma) were introduced into the oceans by atmospheric nuclear weapon testing [1]. A resulting initial average $^{236}U/^{238}U$ ratio of $5{\cdot}10^{-9}$ is expected for the oceanic mixed layer. This ratio is significantly higher than the expected natural pre-nuclear background, which is expected to be at 10^{-14} levels [2].

In order to place first experimental constraints the input term from global stratospheric fall-out we established a year-by-year record of $^{236}U/^{238}U$ for a core from the Caribbean Sea. The selected core was taken in 2006. It has shown well-defined annual banding structure under X-ray and stretches back more than 100 years, therefore covering the interesting period of global stratospheric fall-out.

We used the exceptional sensitivity and ultra-low background for ^{236}U of the Vienna Environmental Research Accelerator's Accelerator Mass Spectrometry system for this measurement and find a $^{236}U/^{238}U$ signature of $(1.84{\pm}0.08){\cdot}10^{-9}$ for the fall-out peak. Furthermore we set a first experimental upper limit of $4{\cdot}10^{-12}$ on the pre-anthropogenic $^{236}U/^{238}U$-ratio in ocean surface waters.

[1] Sakaguchi *et al*. (2009) *Science of the Total Environment* **407**(14), 4238-4242. [2] Steier *et al*. (2008) *NIM B* **266**(10), 2246-2250.

Aeolian iron flux in the South-Western Ross Sea, Antarctica

V.H.L. WINTON[1,2]*, M.-A. MILLET[3], N.A.N. BERTLER[1,2] G.B. DUNBAR[1], B. DELMONTE[4] AND P. ANDERSSON[5]

[1]Antarctic Research Centre, Victoria University of Wellington, PO Box 600, Wellington (*correspondence: holly.winton@vuw.ac.nz)
[2]GNS Science Ltd, PO Box 31 321, Lower Hutt
[3]School of Geography, Environment and Earth Sciences, Victoria University of Wellington
[4]Dipartimento di Scienze dell'Ambiente e del Territori Università degli Studi di Milano-Bicocca, Milano, Italy
[5]Laboratory for Isotope Geology, Swedish Museum of Natural History, PO Box 50 007, 104 05 Stockholm

Each summer the waters in the south-western Ross Sea experience vast phytoplankton blooms. This phenomenon is thought to be stimulated by the addition of bio-available Fe in an otherwise Fe-limited environment. Amongst all the potential Fe sources, input from aeolian dust, which has accumulated on sea ice and is released to the ocean in summer as the sea ice melts, is heavily underestimated. The south-western Ross Sea provides an excellent example to study this biogeochemical process.

The amount of bio-available Fe supplied to the ocean depends on a number of factors including, but not limited to; the dust flux into the ocean, particle size distribution and its Fe content. However, none of these parameters are well constrained in the south-western Ross Sea region and, as a result, the significance of this Fe source in the biogeochemical cycle of plankton growth remains to be quantified.

Dust is shown to be sourced locally based on: a) elevated regional dust flux for the region which is higher by orders of magnitude than predicted in global dust distribution models [1] and in the Antarctic Plateau [e.g. 2]; b) Sr and Nd isotopic signature matching local potential source rocks. The regional dust flux for particles <10 μm in size (the potentially bio-available fraction) is ~0.08 g/m^2/yr. Fe-solubility measurements are currently being completed on the 0.4-10 μm size fraction following the leaching protocol of Aguilar-Islas *et al*. [3]. This will allow us to quantify the amount and estimate its importance for aeolian Fe-fertilisation for bio-productivity in this region.

[1] Mahowald *et al*. (2005) *Global Biogeochem. Cycles* **19,** GB4025. [2] Delmonte *et al*. (2004) *Earth Planet. Rev*. **66**, 63-87. [3] Aguilar-Islas *et al*. (2010) *Marine Chem*. **120**, 25-33.

https://doi.org/10.1180/S0026461X00006502 Published online by Cambridge University Press

Quantification of H in olivine: Direct calibration of FTIR and SIMS by ERDA

A.C. WITHERS[1]*, M.M. HIRSCHMANN[1], H. BUREAU[2] AND C. RAEPSAET[3]

[1]Department of Earth Sciences, University of Minnesota, Minneapolis, MN 55455, USA (*correspondence: withers@umn.edu)

[2]IMPMC, UMR CNRS 7590, Campus Jussieu, 4 place Jussieu, 75252 Paris, France

[3]Laboratoire Pierre Süe, CEA-CNRS, UMR9956, CEA Saclay, 91191 Gif sur Yvette, France

Experimental studies show that varying the H content of olivine has a marked effect on rheology and electrical conductivity, such that the H content of olivine can be said to control tectonic processes and to affect the observable properties of the mantle [1,2]. In order to apply experimental results to the Earth, we need to be able to measure accurately the H content of olivines in experiments. Calibrations for the commonly used infrared (FTIR) and ion probe (SIMS) techniques rely on just a handful of truly independent measurements of natural olivines by ^{15}N nuclear reaction analysis [3]. Moreover, it has been suggested, on the basis of comparative SIMS measurements, that the infrared absorption coefficient (k) for OH stretching bands in high pressure olivines could be greater by as much as a factor of 3 than that derived from natural samples [4], implying that H contents have been underestimated in many experimental studies.

We used elastic recoil detection analysis (ERDA) to determine k for OH bands in Fo_{90} olivines with 240-2000 ppm H_2O, synthesised at 3-10 GPa in multianvil experiments that were optimised for growth of large, homogeneous crystals. On the basis of 20 ERDA and >200 FTIR analyses of olivines from 7 experiments, the H content (in ppm H_2O) is given by 0.120±0.008×total integral absorption, corresponding to an integral extinction coefficient of 45,000 L/(mol·cm^2), i.e. k is ~35% *smaller* than the value previously derived for natural olivines. This implies that the H contents of experimental olivines have in fact been generally *overestimated*.

The samples that were analysed using ERDA are used as SIMS standards, thereby providing a direct calibration that avoids the baseline uncertainties that are inherent to FTIR. Direct calibration of SIMS using high pressure experimental samples allows for improved high accuracy analysis at high spatial resolution.

[1] Hirth & Kohlstedt (1996) *EPSL* **144**, 93-108 [2] Karato (1990) *Nature* **347**, 272-273 [3] Bell *et al*. (2003) *JGR* **108**, 2105 [4] Kovács *et al*. (2010) *Am Min* **95**, 292-299

W-Os isotope systematics in IVB iron meteorites

N. WITTIG AND M. HUMAYUN

National High Magnetic Field Laboratory & Dept. of Earth, Ocean, & Atmospheric Science, Florida State University, Tallahassee, FL 32310, USA. (wittig@magnet.fsu.edu)

^{182}Hf-^{182}W dating implies contemporaneous condensation of the earliest solar system solids (CAIs) and magmatic differentiation of planetesimals (i.e., iron meteorite groups) [1]. IVB iron meteorites exhibit $\varepsilon^{182}W$ (-3.56±0.1) lower than CAIs ($\varepsilon^{182}W$ -3.28±0.2). The initial W isotope signature of CAIs may have been reset by metamorphism of chondrites [2] while IVB irons need to be corrected for thermal neutron capture due to galactic cosmic ray (GCR) exposure. Although GCR corrections have become more sophisticated, determining the true ^{182}W deficit remains problematic [3].

Using Os isotopes as *in situ* neutron dosimeters [4], we re-evaluated the degree of GCR modification of $\varepsilon^{182}W$. Our IVB $\varepsilon^{182}W$ data is derived from a more complete sampling of the IVB group (including Iquique, Weaver, Kokomo), but using smaller samples than [4-5]. MC-ICP-MS measurements (NEPTUNE™) of W isotopes were performed on 10-20ng aliquots using an Apex™ introduction system and Jet Ni sampler and X skimmer cones. The reproducibility of $\varepsilon^{182}W$ for NIST SRM 3163 is ±0.14ε (2σ, n=142) and ±0.32ε (2σ, n=19, 10-25ng) if a smaller, random standard population is considered to capture the analytical uncertainty expected from our IVB set. Since Tlacotepec has systematically lower $\varepsilon^{182}W$, the average $\varepsilon^{182}W$ (-3.31±0.22, 2σ) of IVBs is calculated for n=9 samples, excluding Tlacotepec. Our IVB average $\varepsilon^{182}W$ is more radiogenic than previously reported [1-3,5-6] but with larger analytical uncertainty. Importantly, our $\varepsilon^{182}W$ IVB average is identical to the most recent CAI value [1].

By using Tlacotepec with its large GCR-induced ^{182}W-^{190}Os shift as an anchor point, the Os-W isotope data of this group can be projected towards $\varepsilon^{190}Os$ of 0 [4] to yield a pre-irradiation $\varepsilon^{182}W$ of -2.95. This $\varepsilon^{182}W$ allows for ~4 Myr of accretion and planetesimal differentiation for IVBs and reconciles current models of solar system formation with the W isotope record. A follow-up higher-precision W-Os isotope study from the same digestions is underway.

[1] Kleine *et al*. (2009), *GCA* **73**, 5150–5188. [2] Humayun *et al*. (2007), GCA 71, 4609-4627. [3] Markowski *et al*. (2006), *EPSL* **250**, 104–115. [4] Huang & Humayun (2008), *LPSC XXXIX* (**1168**). [5] Qin *et al*. (2008), *EPSL* **273** 94-104. [6] Markowski *et al*. (2006), *EPSL* **242** 1-15.

https://doi.org/10.1180/S0026461X00006502 Published online by Cambridge University Press

Analysis of As and Sb in samples from Turtle Pits hydrothermal field using new standard material

C.C. WOHLGEMUTH-UEBERWASSER[1]*, S. SCHUTH[2], J. BERND[3] AND F. VILJOEN[1]

[1]Paleoproterozoic Mineralization Research Group (PPM), Department of Geology, University of Johannesburg, PO Box 524, Auckland Park 2006, South Africa (*correspondence: cora@geoinventio.de)

[2]Institut für Mineralogie, Leibniz Universität Hannover, Callinstr. 3, 30167 Hannover, Germany (s.schuth@mineralogie.uni-hannover.de)

[3]Institut für Mineralogie, Universität Münster, Corrensstr. 24, 48149 Münster, Germany (jberndt@uni-muenster.de)

New sulfide standard material was produced for the analysis of As, Sb, Se and Te in sulfides with LA-ICP-MS. The sulfide was synthesized from metal powders and elemental S. Trace metal concentrations are around 30 ppm and were added as chloride solutions. Reaction to sulfide powders proceeded in evacuated silica glass tubes at 973 K, then sintered in a piston–cylinder press for 4 hours at 2 GPa and 1373 K. About one third of the sulfide pellet was analysed with solution quadrupole ICP-MS for bulk trace metal concentrations. A part of the remainder was polished and analysed with an ArF excimer laser coupled to an Element 2 ICP-MS at the Universität Münster. Homogeneity given as 2-sigma relative standard deviation of 20 randomly distributed spot analyses is <7.6% for all trace elements.

The newly obtained standard material was used for the quantitative analysis of a pyrite sample from the Turtle Pits hydrothermal field by LA-ICP-MS. This allows for the spatial resolution of trace element distribution within the sample. Averages of 18 single spot analyses result in As concentrations of 140 – 2000 ppm and Sb contents of 1 – 60 ppm, with no obvious correlation of these two elements. In contrast, within single laser spectra from pyrite a strong correlation between As and Sb has been observed. As arsenic is assumed to be substituted non-stoichiometrically into the pyrite lattice, it seems obvious that in the sample under investigation, Sb is also substituted into the pyrite lattice and that it does not merely occur within inclusions as suggested in previous studies.

Analyses of coexisting sphalerite reveal higher Sb contents of up to 160 ppm, relative to pyrite. The ablation spectra are marked by abrupt elevations in the intensity of Sb which is probably caused by Sb-rich inclusion.

Primary phases in peridotites of the Ślęża ophiolite (SW Poland)

P. WOJTULEK[1], J. PUZIEWICZ[1]* AND T. NTAFLOS[2]

[1]Univ. Wrocław, Poland (*correspondence jacek.puziewicz@ing.uni.wroc.pl

[2]Univ. Wien, Austria (theodoros.ntaflos@univie.ac.at)

The peridotitic members of the Variscan Ślęża Ophiolite (SW Poland) are part of the complete ophiolitic sequence. WR trace element and REE patterns of gabbroic/basaltic ophiolite member show MORB affinity [1].

The peridotites are serpentinized but aggregates of olivine ± clinopyroxene ± spinel are preserved in the central part of the outcrop (Radunia Hill). Olivine ($Fo_{91.8 - 92.6}$) contains 0.2 – 0.4 wt % NiO. Clinopyroxene (mg# 0.92 – 0.94, Cr_2O_3 0.9 – 1.2, Al_2O_3 2.7 – 3.4, Na_2O <0.03 wt. %) is in places altered into clinopyroxene II (mg# 0.95 – 0. 97), chromian magnetite (Cr usually between 0.10 and 0.80 atoms pfu, C=3). Isolated grains of olivine and chromian magnetite occurring in serpentine groundmass are less magnesian ($Fo_{89.3 - 90.5}$), and rich in Cr, respectively. The whole-rock REE contents are below detection limits of ICP-MS method.

The mineral composition of the aggregates suggests dunitic composition of the protolith. Highly magnesian content of olivine is probably the record of depletion typical for MORB mantle. Clinopyroxene possibly is the result of late melt infiltration. Serpentinization obviously decreases forsterite content in olivine, thus the chemical composition of phases occurring in relics may be not representative for the primary mineral composition.

[1] Pin *et al*. (1988) *Lithos* **21**, 195-209.

https://doi.org/10.1180/S0026461X00006502 Published online by Cambridge University Press

A fractal aggregate model of Early Earth organic hazes: UV shielding with minimal antigreenhouse cooling

E.T. WOLF[1,2]*, F. TIAN[1] AND O.B. TOON[1,2]

[1]Laboratory for Atmospheric and Space Physics, University of Colorado, UCB 392, Boulder, CO 80309 (*correspondence: eric.wolf@colorado.edu)

[2]Department of Atmospheric and Oceanic Sciences, University of Colorado

The Archean Earth (3.8 to 2.5 billion years ago) was probably enshrouded by a Titan-like photochemical haze composed of fractal aggregate hydrocarbon aerosols. In this study a three-dimensional fractal aggregate model of the early Earth photochemical haze is explored and compared with the standard liquid drop haze model used in earlier studies [1]. Fractal aggregate microphysical processes are modeled using the method introduced by Cabane *et al*. [2]. The optical properties of the aerosols are determined using a mean-field approximation of multiple scattering by fractal aggregates composed of identical spheres [3]. Early Earth fractal hazes are found to be optically thick in the ultraviolet wavelengths while remaining relatively transparent in the mid-visible wavelengths. At an annual production rate of 10^{14} grams per year and an average monomer radius of 50 nanometers, the haze has global mean effective optical depths of τ_{uv} = 11.2 and τ_{vis} = 0.5. Such a haze would provide a strong shield against UV light while causing only minimal antigreenhouse cooling. Protected by a strong UV shield, photolytically unstable greenhouse gases such as CH_4 and NH_3 may have been able to build up to high concentrations helping warm the young Earth despite the faint young Sun. Our findings reopen the hypothesis of Sagan and Mullen [4] that the young Earth may have been home to a reducing atmosphere.

[1] J.D. Haqq-Misra *et al*. (2008) *Astrobiology* **8(6)**, 1127. [2] M. Cabane *et al*. (1993) *Planet. Space Sci*. **41(4)**, 257. [3] R. Botet *et al*. (1997) *Applied Optics* **36(33)**, 8791 [4] C. Sagan, G. Mullen (1972) *Science* **177**, 52.

Magma physical properties affect isotope variations in volcanic rocks: The example of high-T rhyolites

J.A. WOLFF*[1], B.S. ELLIS[1] AND F.C. RAMOS[2]

[1]School of Earth and Environmental Sciences, Washington State University, Pullman, WA 99164, USA (*correspondence: jawolff@mail.wsu.edu)

[2]Dept. of Geological Sciences, New Mexico State University, Las Cruces, NM 88003, USA

Volcanic rocks often exhibit internal heterogeneity in radiogenic isotopes. Isotopic disequilibrium between co-existing phenocrysts, phenocrysts and matrix, and isotopic zoning within single crystals ("crystal isotope stratigraphy") has been demonstrated in basalts, andesites, dacites, rhyolites and alkaline magmas. High-temperature "Snake River type" rhyolites appear to be an exception. Despite the occurrence of Snake River Plain rhyolites in a region of isotopically highly variable crust and mantle, and significant differences from rhyolite unit to rhyolite unit, internally they are near-homogeneous in $^{87}Sr/^{86}Sr$. Little or no zoning is found within feldspar phenocrysts, and feldpsars within a single unit are tightly grouped. Some units show minor contrasts between phenocrysts and matrix. In contrast, associated basalts and lower-T rhyolites in the same area represent different types of magmas that passed through the same crustal column, and have the relatively large internal $^{87}Sr/^{86}Sr$ variability exhibited by common volcanic rocks.

High temperature rhyolitic magmas possess a unique combination of temperature and melt viscosity. Although they are typically 200°C hotter than common rhyolites, the effect on viscosity is offset by lower water contents (~2 wt%), hence their melt viscosities are in the same range as common, water-rich, cool rhyolites (10^5 – 10^6 Pa s). However, the high magmatic temperatures dictate that cation diffusion rates are 2 – 3 orders of magnitude greater than in common rhyolites. We hypothesize that this combination of characteristics promotes Sr isotopic homogeneity: viscosities that are too high to permit crystal transfer and magma mixing on timescales shorter than those required for diffusive homogenization of Sr between phenocrysts and matrix (100 – 1000 years). This is untrue for the vast majority of magmas, in which either crystal transfer is rapid (<< 100 years) due to low melt viscosities (basalts and intermediate magmas), or else Sr diffusion rates are so slow that the equilibration time is longer than the lifetime of the system (high-silica minimum melt rhyolites: 10^5 – 10^6 years).

https://doi.org/10.1180/S0026461X00006502 Published online by Cambridge University Press

High–temperature hydrothermal activity in the lower oceanic crust: Petrological and geochemical evidence for fluid pathways in the Oman Ophiolite

P.E. WOLFF[1]*, D. GARBE–SCHÖNBERG[2], J. KOEPKE[1] AND K. STREUFF[2]

[1]Institute for Mineralogy, Leibniz University of Hannover, Callinstr. 3, 30167 Hannover, Germany (*correspondance: e.wolff@mineralogie.uni–hannover.de)
[2]Institute of Geosciences, Christian–Albrecht–University of Kiel, Ludewig–Meyn–Str. 10, 24118 Kiel, Germany

The Oman ophiolite is regarded as best example for fast–spreading oceanic crust on land. Petrological findings indicate that multiple intrusions of gabbroic sills play a significant role for the formation of the deep plutonic crust at fast–spreading oceanic ridges [1], a model which requires a substantial cooling of the deep oceanic crust, probably by seawater–derived high–temperature hydrothermal circulation [e.g.,2]. In this study we present petrological and geochemical data for veins and zones formed by hydrothermal alteration within the lower layered gabbro sequence of the Samail ophiolite in Oman (Wariyah, Wadi Tayin Massiv).

Veins and alteration zones of mm to m scale within an unaltered olivine gabbro record high (>800°C), medium (~600°C), and low temperature (~350–500°C) hydrous alteration indicating possible fluid pathways for hydrothermal circulation. Petrological results show mineral assemblages typical for predicted interaction between olivine gabbro and seawater–derived fluid [3]. High temperature veins display mineral assemblage of olivine + plagioclase + pyroxenes + pargasitic amphibole ± oxides. Decreasing temperature result in a change in alteration paragenesis, where hydrous minerals become more abundant. The typical medium temperature mineral assemblage is plagioclase + clinopyroxene + chlorite + magnesiohornblende ± oxides followed by low temperature veins mainly consitsting of epidote + prehnite + actinolite/tremolite.

Geochemical micro–analyses of sub–mm veinlets and adjacent host rocks show systematic enrichment of fluid mobile elements (e.g., LREE, Eu, Mo, W) in these veins and indicate possible element mobility during hydrothermal activity. These preliminary results suggest that hydrothermal circulation at very high temperatures exists.

[1] Kelemen (1997), *Earth Planet. Sci. Lett.* **146**, 475-488. [2] Bosch (2004), *J. Petr.* **45**, 1181-1208. [3] McCollom and Shock, *J. Geophy. Res.* **103**, 547-575.

Can seawater promote *in situ* mineral sequestration?

D. WOLFF-BOENISCH[1]*, S. WENAU[2], E.H. OELKERS[3] AND S.R. GISLASON[1]

[1]Institute of Earth Sciences, University of Iceland, Sturlugata 7, 101 Reykjavik, Iceland (*correspondence: boenisch@raunvis.hi.is)
[2]MARUM – Centre for Marine Environmental Sciences, University of Bremen, Leobener Straße 28359 Bremen, Germany
[3]Géochimie et Biogéochimie Experimentale, GET/CNRS, Université de Toulouse, 14 Avenue Edouard Belin, 31400 Toulouse, France

Dissolution of mafic and ultramafic rocks in the presence of CO_2 is of great current interest due to the potential for carbon storage in basaltic and/or peridotitic rocks. This storage method involves converting gaseous or supercritical CO_2 into carbonate minerals for its safe, long-term storage. In-situ carbonatization of CO_2 faces a major challenge in that huge quantities of water are required to dissolve CO_2 to promote reactions. This challenge might be overcome by using seawater for the dissolution of CO_2 during its injection.

To assess the possible use of seawater during carbon storage efforts, steady-state silica release rates (r_{Si}) from basaltic glass and crystalline basalt of same chemical composition and dunitic peridotite have been determined in far-from-equilibrium dissolution experiments at 25°C and pH 3.6 in a) artificial seawater solutions under 4 bar pCO_2, b) varying ionic strength solutions, including acidified natural seawater, c) acidified natural seawater of varying fluoride concentrations, and d) acidified natural seawater of varying dissolved organic carbon concentrations. Glassy and crystalline basalts exhibit similar r_{Si} in solutions of varying ionic strength and cation concentrations. Rates of all solids increase by 0.3-0.5 log units in the presence of 4 bar pCO_2 compared to atmospheric CO_2 pressure. At atmospheric CO_2 pressure, basaltic glass r_{Si} were most increased by the addition of fluoride to solution whereas crystalline basalt rates were most enhanced by the addition of organic ligands. In contrast, peridotite rates are unaffected by either the addition of fluoride or organic acids. Most significantly, Si release rates from the basalts are found to be not more than 0.6 log units slower than corresponding peridotite rates at all conditions considered in this study. This rate difference becomes negligible in seawater suggesting that CO_2-charged seawater injected into basalt might be nearly as efficient for mineral sequestration as injection into peridotite.

https://doi.org/10.1180/S0026461X00006502 Published online by Cambridge University Press

Water structure at the structurally heterogeneous calcite surface

M. WOLTHERS[1,2,*], D. DI TOMMASO[2], Z. DU[2] AND N.H. DE LEEUW[2]

[1]Department of Earth Sciences, Utrecht University, P.O. Box 80021, 3508 TA Utrecht, The Netherlands. (*correspondence: wolthers@geo.uu.nl)

[2]Department of Chemistry, University College London, 20 Gordon Street, London WC1 H0AJ, United Kingdom.

The calcite surface has been subject of numerous simulation studies. These studies have generally focused on simulations of perfectly flat calcite surfaces, and in particular the dominant (10-14) face. In both natural environments and in experiments, the calcite surface is of course not atomically flat, and surface roughness is expected to have an effect on the reactivity of the surface sites. Indeed, it has been shown that trace elements differentially incorporate into the calcite surface depending on surface structure [1], while this differential reactivity is not at all captured in the current macroscopic surface chemical models [2,3]. The aim of this work is to obtain information on the interactions of water molecules with the different surface sites present in etch pits and on growth terraces at the calcite (10-14) surface. Results show that the local environment around the structurally distinct sites differs significantly, with the formation of more calcium–water bonds and H-bridges at less-coordinated sites, while the bond length of the metal-hydroxyl site does not vary with position at the surface. Temperature changes over the range of 300 to 340 K does not affect the local environment of the surface groups.

The information obtained in this study is crucial for the improvement of the existing macroscopic surface model for the reactivity of calcite [2]. This mineral surface structural model for calcite was developed using the Charge Distribution MUltiSite Ion Complexation (CD–MUSIC) modelling approach [4] to describe the chemical structure of carbonate mineral-aqueous solution interfaces. The high sensitivity of the model toward parameters describing hydrogen bridging and bond lengths at the mineral-water interface, currently limits the predictive application of the calcite CD–MUSIC model.

[1] Paquette and Reeder (1995) *Geochim. Cosmochim. Acta* 59, 735-749. [2] Wolthers M. *et al.* (2008) *Am. J. Sci.* 308, 905-941. [3] Villegas-Jiménez *et al.* (2009) *Geochim. Cosmochim. Acta*, 73, 4326-4345. [4] Hiemstra and Van Riemsdijk (1996) *J. Colloid Interf. Sci.* 179, 488-508.

Mass-independent Cd isotope fractionation during evaporation

FRANK WOMBACHER

Universität zu Köln, Institut für Geologie und Mineralogie, 50674 Köln, Germany (fwombach@uni-koeln.de)

Modern mass spectrometry is capable to reveal mass-independent isotope fractionations (MIF) for many heavy elements [1].

Here, we investigate mass-independent Cd isotope fractionations that result from the evaporation of liquid Cd into vacuum. Three residues from evaporation display large mass-dependent Cd isotope fractionations with $1000\ln\alpha$ ranging from -23.2 to -48.3 ‰ for $^{110}Cd/^{114}Cd$ relative to the starting material [2]. These samples were repeatedly analyzed at high precision using a Neptune MC-ICP-MS, with ion beam intensities typically larger than 20V for ^{114}Cd and analysis times of about 30 minutes. Deficits ranging from 8 to 28 ppm were well resolved for $^{111,113,116}Cd/^{114}Cd$. The accurate quantification of the MIF requires that the mass-dependence of the evaporation induced isotope fractionation is accurately corrected. This was facilitated using the generalized power law and normalization to $^{110}Cd/^{114}Cd$ of the starting material. Note, that the mass-dependence for evaporation was found to be intermediate between that expected to describe kinetic and equilibrium fractionation [2, 3].

MIF for ^{111}Cd, ^{113}Cd and ^{116}Cd scales with deviations from a trend between nuclide mass and mean-squared nuclear charge radii defined by the other five Cd isotopes, thus suggesting that the MIF is due to nuclear volume effects. The preferential evaporation of ^{111}Cd, ^{113}Cd and ^{116}Cd may result from their more tightly bond 5s electrons that are thus not as easily delocalized and hence form weaker metallic bonds in the liquid. Our results are in accord with previous work [4] on the evaporation of Hg, another group 12 element.

[1] Epov *et al.* (2011) *JAAS* advanced article. [2] Wombacher *et al.* (2004) *Geochim. Cosmochim. Acta* **68**, 2349–2357. [3] Young *et al.* (2002) *Geochim. Cosmochim. Acta* **66**, 1095-1104. [4] Estrade *et al.* (2009) *Geochim. Cosmochim. Acta* **73**, 2693–2711.

https://doi.org/10.1180/S0026461X00006502 Published online by Cambridge University Press

Episodic estuarine hypoxic events: Integrating the biogeochemistry, hydrology and climate on a sub-tropical floodplain, Eastern Australia

V.N.L. WONG[1]*, S.G. JOHNSTON[1], S. WALSH[2], S. MORRIS[2], E.D. BURTON[1], R.T. BUSH[1], L.A. SULLIVAN[1], P.G. SLAVICH[2]

[1]Southern Cross GeoScience, Southern Cross University, Lismore, NSW 2480, Australia (*correspondence: vanessa.wong@scu.edu.au)

[2] NSW Department of Trade and Investment, Regional Infrastructure and Services, Wollongbar, NSW 2477, Australia

Globally, the frequency, magnitude and spatial extent of anthropogenically-induced coastal hypoxic events is increasing [1]. Episodic hypoxia in riverine and estuarine systems can follow high-flow events such as floods or the release of environmental allocations. These events can result in complete deoxygenation of the water column and significant effects on aquatic organisms and ecosystem function. This study integrates the biogeochemical, hydrological and climatic processes from four flood events on two sub-tropical floodplains in eastern Australia [2,3].

We found that a key driver of hypoxia was the extensive modification of floodplain surface hydrology through the construction of drainage networks. Backswamp basins were originally natural storage basins for floodwaters, supporting large areas of wetland vegetation. Drier conditions, due to drainage, has shifted vegetation assemblages from wetland-dominant species to flood-intolerant species. When inundated, senescent vegetation provides a source of labile carbon which rapidly consumes oxygen from the overlying waters, producing anoxic water with high oxygen demand. Carbon metabolism during these events is strongly coupled with microbially-mediated reduction of accumulated Fe and Mn oxides commonly found on coastal floodplains. These redox sensitive species provide a geochemical signature to identify the sources and causes of estuarine hypoxic events. Whilst anoxic floodwaters were previously retained in backswamp wetland basins during the flood recession phase, these waters are now exported rapidly to the main channel.

Post-flood hypoxic events frequently occur in summer, especially when long, dry periods are followed by rapid, intensive rainfall. These events will most likely increase in frequency and magnitude as a result of climate change due to more frequent and hotter summer floods.

[1] Diaz & Rosenberg (2008) *Science* **321**, 926-929. [2] Johnston *et al*. (2003) *Mar. and Fresh. Res*. **54**, 781-795. [3] Wong *et al*. (2010) *Estuar. Coast. Shelf Sci*. **87**, 73-82.

Stable isotopes ratio in nitrate: A tool to unravel the biogeochemistry of nitrate in an estuarine environment

W.W. WONG[1]*, P.M. COOK[1], M.R. GRACE[1] AND I. CARTWRIGHT[2]

[1]Water Studies Centre, Monash University, Clayton, Melbourne 3800, Australia (*correspondence: weiwen.wong@monash.edu)

[2]School of Geosciences, Monash University, Clayton, Melbourne 3800, Australia

Port Philip Bay is a large coastal embayment in temperate south eastern Australia, with a population in excess of 4 million in the local catchment. Like other coastal waters, the bay is typically nitrogen limited and hence there is much interest in identifying sources and sinks of this nutrient within catchments and estuaries surrounding the bay.

This study was carried out in the Werribee estuary, one of the major estuarine systems within Port Philip Bay. Werribee estuary is eutrophic with nitrate concentrations exceeding 1mgN/L during base flow conditions. There are a number of potential sources of nitrogen to the estuary including treated sewage effluent, market gardens, groundwater and the Werribee River. We aimed to distinguish the sources and transformation processes of nitrate in this estuarine environment using a multidisciplinary approach, focussing on stable isotopes and radon measurements.

Monthly sampling of surface water and groundwater was carried out over a 12 month period. Our preliminary results showed that (i) there was a positive correlation between $\delta^{15}N\text{-}NO_3$ and $\delta^{18}O\text{-}NO_3$ with a 2:1 $\delta^{15}N{:}\delta^{18}O$ gradient in both surface and groundwaters suggesting that denitrification was occurring and led to considerable transformation of the isotope signatures from their sources values within groundwater and surface waters. (ii) There was a strong correlation between nitrate and radon concentrations (R^2=0.79) at a site in the upper estuary consistent with nitrate derived from groundwater. (iii) The $\delta^{15}N$ and $\delta^{18}O$ of nitrate were +18±4‰ and +11±4‰ respectively when nitrate concentrations in surface waters exceeded 0.2mgN/L, which was consistent with the signatures observed in ground water with high nitrate concentrations (>10mgN/L) beneath the market gardens.

https://doi.org/10.1180/S0026461X00006502 Published online by Cambridge University Press

Influence of cyanide on granite weathering

N. WONGFUN[1]*, M. PLÖTZE[2], H. BRANDL[3] AND G. FURRER[1]

[1]Inst. of Biogeochemistry and Pollutant Dynamics, ETH Zürich, Zürich 8092, Switzerland (*correspondence: nuttakan.wongfun@env.ethz.ch)
[2]Inst. for Geotechnical Engineering, ETH Zürich, Zürich 8093, Switzerland
[3]Inst. of Evolutionary Biology and Environmental Studies, University of Zürich, Zürich 8057, Switzerland

Availability of nutrients in the glacier forefield is usually very low. Mobilization of nutrients from rock through weathering processes plays an important role to overcome this limitation [1]. Microorganisms and plants modify their local environment by various exudates including cyanide [2], which is a crucial agent during the initial period of colonization and soil formation.

To elucidate the effect of cyanide on dissolution of granite minerals, the samples were collected from the Damma glacier area (Central Alps, Switzerland) at approximately 2,500 m a.s.l. After crushing and sieving, materials with size fraction <63 μm (surface area=1.55 m^2/g) were selected for abiotic dissolution experiment. Batch experiments were carried out with a solid/liquid ratio of 10 g/L in the absence or presence of cyanide under oxic conditions at 22±1 °C, I=0.01, pH range of 5-7 for 24 hours.

Among the elements released from granite, enhanced Fe concentrations were observed in presence of cyanide. This applies particularly with increasing pH, suggesting that deprotonated cyanide becomes more important for the formation of Fe compleses. Iron cyanide complexes presence at high concentrations in particular at pH above 6 [3] and allow high concentrations of dissolved Fe. The dissolved Al concentrations were considerably lower than those of Fe due to precipitation of secondary phases (e.g. gibbsite and kaolinite).

[1] Bernasconi *et al*. (2008) *MinMag* **72**, 19-22. [2] Frey *et al*. (2010) *AEM* **76**, 4788-4796. [3] Meeussen *et al*. (1992) *ES&T* **26**, 1832-1838.

Accretion and initial differentiation of the Earth

B.J. WOOD

Department of Earth Sciences, University of Oxford, South Parks Road, Oxford OX1 3AN, U.K. (berniew@earth.ox.ac.uk)

A large number of moon- to Mars-sized planetary embryos with different metal/silicate/volatile ratios are believed to have formed around the young sun in ~1 M.yr. As Earth accreted from such embryos through a succession of impacts, the metallic core segregated and there was some loss of the most volatile elements. The chemical and isotopic composition of silicate Earth provides most evidence for these processes. Depletions of silicate Earth, relative to primitive meteorites, in elements known to have entered the core (e.g Mo, W, Ni, Co) place constraints on the physical conditions of accretion. Short and long-lived chronometers (^{182}Hf-^{182}W, ^{238,235}U-^{206,207}Pb, ^{205}Pb-^{205}Tl, ^{107}Pd-^{107}Ag) enable estimates of the timing of core formation, the influence of the moon-forming impact and the history of volatile accretion to the Earth. If we begin with the assumptions that core segregation was continuous during accretion and that metal and silicate fully equilibrated, simultaneous consideration of the depletion factors of a large number of elements in silicate Earth lead to the following general conclusions: (1) The average pressure of core segregation on Earth was high >30 GPa, implying depths of >800 km. (2) Earth began as a small, strongly reduced body and became more oxidised as it grew. (3) Si (~5%) and S (~2%) are major components of the "light" element in Earth's core. Relaxing the assumption of full equilibration (ie allowing for the addition of metal to the core without reaction with the mantle) and allowing for the influence of S and Si on partitioning does not significantly alter these conclusions.

The ^{182}Hf-^{182}W age of Earth's core [1], may be used in combination with other short- and long-lived radioactive systems to show (1) Moderately volatile elements were predominantly added to Earth towards the end of accretion [2] and (2) The fractionation of U from Pb at ~100 M.yr after the origin of the solar system is consistent with Pb extraction in a small amount of core material added during the moon-forming giant impact.

[1] Kleine, T., Munker, C., Mezger, K., & Palme, H., Rapid accretion and early core formation on asteroids and the terrestrial planets from Hf-W chronometry. *Nature* **418** (6901), 952-955 (2002). [2] Schönbächler, M., Carlson, R.W., Horan, M.F., Mock, T.D., & Hauri, E.H., Heterogeneous accretion and the moderately volatile element budget of Earth. *Science* **328**, 884-887 (2010).

https://doi.org/10.1180/S0026461X00006502 Published online by Cambridge University Press

Core formation and volatile element addition to the Earth

B.J. WOOD[1] AND M. REHKÄMPER[2]

[1]Dept of Earth Sciences, University of Oxford, South Parks Road, Oxford, OX1 3AN; U.K.
[2]Dept of Earth Science & Engineering, Imperial College, London SW7 3AZ; U.K.

It is well known that the Pb isotopic composition of the silicate Earth indicates a fractionation of U from Pb at ~100 M.yr after the origin of the solar system. This fractionation has recently been ascribed to entry of Pb into the core (e.g.[1]) on an Earth with low U/Pb, and to late addition of Pb and other moderately volatile elements to an Earth which initially had very high U/Pb [2]. Use of extinct radioactive systems, combined with an understanding of volatile element partitioning into the core can elucidate the relative timings of core formation and volatile addition [3]. We have determined the metal-silicate partitioning of moderately volatile elements Ag, Pb, Tl, Mn and Cr in order to use the extinct systems ^{107}Pd-^{107}Ag, ^{205}Pb-^{205}Tl and ^{53}Mn-^{53}Cr in conjunction with ^{182}Hf-^{182}W and ^{238,235}U-^{206,207}Pb to investigate core formation and volatile element addition to the growing Earth.

Tl, which is chalcophile but only weakly siderophile at low pressure is found to become as siderophile as Pb at pressures >20 GPa. This means that, given the high pressures of core formation indicated by refractory siderophile element (Ni, Co, Mo etc) abundances in the mantle, the ^{205}Pb-^{205}Tl system is consistent with core formation being the principal reason for the low Pb and Tl abundances (relative to lithophile elements of similar volatility) in silicate Earth. Ag is moderately siderophile at all pressures while Mn and Cr are similar to one another in having weak siderophile character. When considered together the 3 short-lived systems are consistent with addition of moderately volatile elements during the principal period of core formation with timescale constrained by the ^{182}Hf-^{182}W system. ^{53}Mn-^{53}Cr and ^{107}Pd-^{107}Ag indicate that accreted materials became more volatile rich as accretion progressed with major addition of volatiles during the last 30-60% of accretion.

[1] Wood, B.J. & Halliday, A.N., (2010) *Nature* **465**, 767-771. [2] Albarède, F., (2009) *Nature* **461**, 1227-1233. [3] Schönbächler, M., Carlson, R.W., Horan, M.F., Mock, T.D., & Hauri, E.H., (2010) *Science* **328**, 884-887.

Controls on early biomineralisation: Oxygen and competition

R.A. WOOD[1]*, A.R. PRAVE[2], K-H. HOFFMANN[3], S.W. POULTON[4], J.W. LYNE[1], M.O. CLARKSON[1] AND S. KASEMANN[5]

[1]School of Geos., Univ. of Edinburgh, EH9 JW, UK (*correspondence: Rachel.Wood@ed.ac.uk)
[2]Dept. of Earth Sci, Univ. of St Andrews, KY16 9AL, UK
[3]Geol. Survey of Namibia, Windhoek
[4]School of Civil Eng. and Geosciences, Newcastle Univ, NE1 7RU, UK
[5]Dept. of Geosciences, University of Bremen, 28334 Bremen, Germany.

Animals require oxygen, and so the first appearance of metazoans during the Ediacaran (580-543 Ma) has been linked to the widespread development of oxygenated oceanic conditions [1, 2, 3]. However, the nature of ocean redox chemistry through this period is complex, with deeper water anoxia persisting in certain areas [4]. In addition, few studies have directly documented the nature of ocean chemistry at locations that coincide with palaeontological evidence for major biological innovation [3]. Thus, the precise environmental context for early animal evolution, particularly the rise of biomineralisation, remains unclear. Here, we present a high resolution reconstruction of carbon isotope and ocean redox dynamics, as recorded in sedimentary rocks deposited from ~553-549 million years ago in the Zaris Sub-Basin of the Nama Group, Namibia. The succession spans deep distal to shallow proximal carbonate settings, and coincides with the first appearance of skeletal metazoans. Iron-sulphur systematics demonstrate that oxic conditions developed only intermittently in the shallowest waters where the first skeletal metazoans are preserved, while deeper waters remained consistently anoxic and iron-rich (ferruginous). Thus, late Ediacaran surface-water oxygenation was unstable, inferring that the first skeletal metazoans developed in short-lived habitats. The opportunistic ecologies and characteristically simple biomineralisation styles of Ediacaran taxa are likely to be a direct consequence of these dynamic redox conditions.

[1] Knoll et al. (1999) Science, 284, 2129–2137 [2] Fike *et al*. (2006) *Nature,* **444**, 744-747 [3] Canfield *et al*. (2007) *Science,* **315,** 95-99 [4] Canfield *et al*. (2008) *Science,* **321**, 949-952.

.

https://doi.org/10.1180/S0026461X00006502 Published online by Cambridge University Press

Testing boundary exchange of Nd isotopes in the Eastern tropical Pacific Ocean

STELLA WOODARD[1]*, FRANCO MARCANTONIO[2], DEBORAH THOMAS[1] AND MITCHELL LYLE[1]

[1]Department of Oceanography, Texas A&M University, College Station, TX 77843, USA (*correspondence: swoodard@ocean.tamu.edu)
[2]Department of Geology & Geophysics, Texas A&M University, College Station, TX 77843, USA

We investigate the possibility of boundary exchange as a mechanism for altering the Nd isotopic composition of seawater along the eastern margin of the equatorial Pacific Ocean by analyzing Nd isotopes and concentrations in seawater and sediment collected along a transect in the Panama and Peru Basins during the Fall of 2010. The region plays an important role in the global carbon cycle due to enhanced productivity, upwelling and venting of CO_2 rich waters and is affected by enhanced precipitation and riverine runoff. In addition, the area is interesting in terms of intermediate water circulation with the confluence of NPIW and AAIW near the equator at depths of ~500-1000m.

Seawater dissolved $^{143}Nd/^{144}Nd$ and [Nd] profiles were determined for five locations (see map) and compared with the Nd isotopic composition of biogenic apatite (thought to reflect bottom water εNd) and lithogenic material isolated from the tops of five multi-cores (see map). Preliminary data from seawater collected at site WC13 show a decrease in εNd from -2.1 at 500m to -3.4 at 2750m water depth.

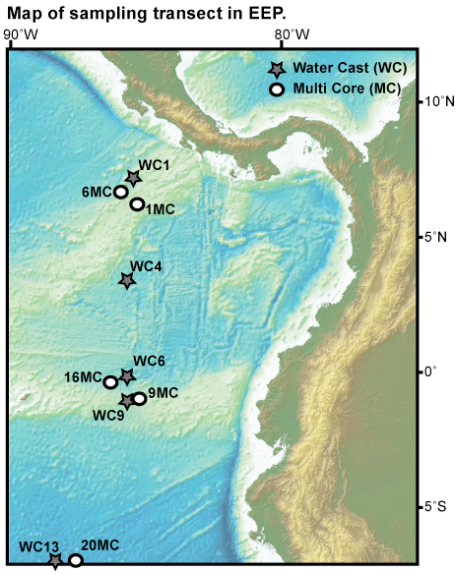

Minor effect of physical size sorting on iron solubility of transported mineral dust

M.T. WOODHOUSE, Z.B. SHI, K.S. CARSLAW, M.D. KROM, G.W. MANN AND L.G. BENNING

School of Earth and Environment, University of Leeds, Leeds, United Kindom (m.woodhouse@see.leeds.ac.uk)

Observations show that the fractional solubility of Fe (FS-Fe, defined as the ratio of dissolved to total Fe) in dust aerosol increases from ~0.1% in regions of high dust mass concentration and up to 80% in remote oceanic regions where concentrations are lowest [1, 2]. Here, we combined laboratory geochemical measurements with global aerosol model simulations to test the hypothesis that the increase in FS-Fe is due to physical size sorting during dust transport. We determined the FS-Fe in size-fractionated dust generated from two representative Saharan dust source samples using a customized dust re-suspension and collection system. The results show that the FS-Fe is size-dependent and ranges from 0.1-0.8%. The size-resolved FS-Fe data were then combined with simulated (size-resolved) dust mass concentration data from a global aerosol model, GLOMAP, to calculate the FS-Fe of dust aerosol over the tropical and subtropical North Atlantic Ocean. We found that the calculated FS-Fe in the dust aerosol increased from ~0.1% at high dust mass concentrations (e.g., >100 $\mu g\ m^{-3}$) to ~0.2% at low concentrations (<1 $\mu g\ m^{-3}$) due to physical size sorting alone. These values are one to two orders of magnitude smaller than those observed on cruises across the tropical and sub-tropical North Atlantic Ocean [1, 3] under an important pathway of Saharan dust plumes for similar dust mass concentrations. Even when the FS-Fe of the sub-micrometer size fractions (0.18-0.32 μm, 0.32-0.56 μm, and 0.56-1.0 μm) in the model were increased by a factor of 10 over the measured values, the calculated FS-Fe of the dust was still more than an order of magnitude lower than that measured in the field. Therefore, the physical sorting of dust particles alone is unlikely to be an important factor in the observed inverse relationship between the FS-Fe and the atmospheric mineral dust mass concentrations. These results suggest that processes such as chemical reactions and/or mixing with combustion particles are the main mechanisms to cause the increased FS-Fe in long-range transported dust aerosols.

[1] Baker, A., Jickells, T., (2006) *Geophys Res Lett*, **33**, L17608; [2] Mahowald N. *et al*., (2005) *Global Biogeochem Cycle*, **19**, GB4025; [3] Buck, C. *et al*., (2010) *Mar Chem*, **120**, 14-24.

https://doi.org/10.1180/S0026461X00006502 Published online by Cambridge University Press

Structural systematics of Mg-Fe^{2+}-bearing spinels and spinelloids

A.B. WOODLAND[1]*, R.J. ANGEL[2] AND M. KOCH[3]

[1]Inst. für Geowissenschaften, Univeristät Frankfurt, Altenhöferallee 1, 60438 Frankfurt, Germany (*correspondence: woodland@em.uni-frankfurt.de)
[2]Dept. of Geosciences, Virginia Tech, Blacksburg, VA, 24060, U.S.A.
[3]Inst. für Geowissenschaften, Universität Heidelberg, Im Neuenheimer Feld 234-6, 69120 Heidelberg, Germany

Spinels and struturally related spinelloids have been synthesised in the geologically relevant system M_2SiO_4-$MFe^{3+}{}_2O_4$, where M = Mg and Fe^{2+} at 1100-1200°C and 3 to 16 GPa. Starting materials were mixtures of Fe_3O_4 and pre-synthesised olivine solid solutions. Unit-cell parameters were determined by Rietveld refinement of powder diffraction patterns containing Si as an internal standard.

Spinel exhibits a range in composition, which requires consideration of four endmembers: ringwoodite, Fe-ring-woodite, magnetite and magnesioferrite. As expected, the cell parameter decreases with increasing M_2SiO_4 content. A least squares fit to the dataset (n=53) suggests ideal or near ideal behaviour in this quaternary system. The derived molar volume for $MgFe_2O_4$ ($V° = 44.51(12)$ cm^3) implies a degree of inversion of x = 0.78 [1], although this was not explicitly accounted for in the fit.

Spinelloid II exhibits only a limited compositional range with nMg ≤ 0.26 cpfu. Molar volumes decrease with increasing Mg content. Single-crystal refinements indicate that Mg preferentially resides on the M3 site, which is the octahedral site containing the bridging oxygen of the T_3O_{10} tetrahedral group.

Compared with Mg-free [2] spinelloid III, the incorporation of Mg causes a systematic reduction in volume. Aweighted least squares fit yields $V°_{Fe3O4} = 45.04(6)$ cm^3, $V°_{Fe2SiO4} = 42.89(10)$ cm^3 and $V°_{Mg2SiO4} = 40.9(4)$ cm^3, assuming ideal mixing (non-ideality is not statistically significant). Mg prefers the M2 site, which is attached to the bridging oxygen of the T_2O_7 group.

The volume behaviour of spinelloid V is similar to the other spinelloids, except that the volume reduction from Mg addition is not so clearly defined. This could be due to changing ordering of i) Fe^{3+} and Si on the TO_4 and T_2O_7 sites, and/or ii) Mg, Fe^{2+} and Fe^{3+} across the octahedral sites. A weighted least squares fit yields $V°_{Fe3O4} = 44.96(4)$ cm^3, $V°_{Fe2SiO4} = 42.53(8)$ cm^3 and $V°_{Mg2SiO4} = 40.3(3)$ cm^3 for the theoretical endmembers, assuming ideal mixing.

[1] O'Neill *et al*. (1992) *Am Min* **77**, 725-40, [2] Woodland, Angel (2000) *Contrib Mineral Petrol* **139**, 734-47.

F, Cl and S contents of olivine-hosted melt inclusions from picritic dike rocks, Etendeka, NW Namibia

L. WORGARD[1]*, , R.B. TRUMBULL[2], J. K. KEIDING[2], I.V. VEKSLER[2,3], M. WIEDENBECK[2], T. WENZEL[1] AND G. MARKL[1]

[1]Universität Tübingen, Wilhelmstr. 56, D-72074 Tübingen, Germany (*correspondance: linda.worgard@uni-tuebingen.de)
[2]GeoForschungsZentrum Potsdam, Telegrafenberg, D-14473 Potsdam, Germany
[3]Technical University Berlin, Department of Mineralogy and Petrology, Ackerstrasse, 71-76, D-13355 Berlin, Germany

Volatile contents and their evolution during magma differentiation are important to understand for better assessment of their role during volcanic eruptions and for estimation of atmospheric loading. Furthermore volatiles have shown potential to be used to put constraints on different mantle sources. Here we present for the first time F, Cl and S concentrations of olivine-hosted melt inclusions analyzed by SIMS from picritic dikes from the southern Etendeka region, NW Namibia.

The analyzed host olivines are Mg-rich (Fo_{84-93}) and their re-homogenized (and post-entrapment corrected) melt inclusions contain between 10 and 18 wt.% MgO and show SiO_2 contents of 45-52 wt.% and thus range from basalt to komatiite in composition.

F concentrations in the analyzed melt inclusions vary from 200 to 450 ppm, Cl varies from 5 to 40 ppm and S from 10 to 1100 ppm. F and S concentrations increase with decreasing forsterite content of the host olivine, whilst Cl does not. F/Cl ratios are variable and range from 4 to 45, with the highest values presumably being influenced by degassing prior to melt inclusion entrapment and/or post entrapment leaking. Most F/Cl ratios and low Cl/K ratios (≤ 0.3) indicate a depleted mantle source for these picritic dikes [1-3], which is consistent with earlier Sr and Nd isotope work of [4]. We plan to compare the volatile contents of the melt inclusions with that of the corresponding whole rocks (analyzed by pyrohydrolysis) in order to further constrain the significance of potential degassing processes.

[1] Stroncik & Haase (2004), *Geology* **32**, 945-948. [2] Michael & Cornell (1998), *Journal of Geophysical Research* **103**, 18, 325-18, 356. [3] Pyle & Mather (2009), *Chemical Geology* **263**, 110-121. [4] Thompson *et al* (2001), *Journal of Petrology* **42**, 2049-2081.

https://doi.org/10.1180/S0026461X00006502 Published online by Cambridge University Press

Computational modelling of water and amino acid adsorption at corundum structured oxide surfaces

L. WORONYCZ[1]*, T.V. SHAPLEY[1], C. ARROUVEL[2], D. COSTA[3] AND S.C. PARKER[1]

[1]Department of Chemistry, University of Bath, Bath, Somerset, BA2 7AY, United Kingdom (*correspondence: L.Woronycz@bath.ac.uk)

[2]Universidade Federal de Sergipe, São Cristóvão, SE 49.100-000 Brazil

[3]LPCS, ENSCP Chimie Paris Tech, Paris, France.

The interactions between biomolecules and inorganic surfaces play an important role in many natural environments and hence it is essential to understand the nature of the chemical interaction between the biomolecule and the surface, the resulting biomolecule conformation and the influence of other surface species notably water. This can be achieved by using atomistic simulation techniques and we have focused on the corundum structured oxide α-Cr_2O_3 and compared with the structural analogues of α-Fe_2O_3 and α-Al_2O_3.

We have used a combination of simulation techniques to investigate the surfaces and surface adsorption. These include potential-model based techniques using the static lattice code METADISE [1] for generating the initial structures of the surfaces and the molecular dynamics code: DL_POLY [2] on incorporation of water. The interatomic potentials were then tested with DFT using VASP [3].

The results from both interatomic potentials and DFT show that the {10.2} and {00.1} surfaces are the most stable and energetically prefer dissociative adsorption. The adsorption energies are in reasonable accord, for example DFT predicts -0.75 eV on the {10.0} surface compared to -0.84 eV. The DFT studies on the different forms (neutral, anionic and cationic) of glycine (Gly) 1, lysine (Lys) and glutamic acid (Glu) have been used to test and develop the potential models. The results show that the neutral amino acid molecules become anionic on adsorption at low coverage on anhydrous Al_2O_3 and Cr_2O_3. An oxido-amino acid complex is formed with the creation of an iono-covalent bond M-O(C). Finally, the results show that hydroxylation of the surfaces clearly modify amino acid adsorption.

[1] Watson *et al*. (1996), *J. Chem. Soc. Farad. Trans*,. **92**, 433-438. [2] Smith and Forester (1996) *J. Mol Graph* **14**, 136-141 [3] Kresse & Furthmuller (1996), *Phys. Rev. B*, **54**, 11169-11186.

Magnesium isotope fractionation in a hardwood forest of Southern Québec, Canada

S. WORSHAM[1]*, C. HOLMDEN[1] AND N. BÉLANGER[2]

[1]Saskatchewan Isotope Laboratory, University of Saskatchewan, Saskatoon, Canada (*correspondence: srw039@mail.usask.ca, ceh933@mail.usask.ca)

[2]Université du Québec à Montréal, Montréal, Canada (belanger.nicolas@teluq.uqam.ca)

Magnesium (Mg) is an essential macronutrient for plants, acting as the coordinating cation for chlorophyll as well as serving other important metabolic functions. Recent laboratory studies have demonstrated mass dependent fractionation of Mg within plants [1,2], while there is only one confirmation of plant fractionation in the field to date [3]. Our study builds on previous work through an investigation of Mg isotope fractionation in a forested ecosystem. Broader questions motivating this work include the potential impact of forest Mg cycling on the signature of the continental weathering flux of Mg delivered to the oceans by river flow.

Mg isotope fractionation is being examined in a forested first order catchment in southern Québec, Canada, dominated by sugar maple (*Acer saccharum)* and characterized by soils developed from granite, mangerite and anorthosite. Thus far, we observe fractionation coupled with the uptake of Mg into maple trees from the soil pool as well as significant internal plant fractionation. Preliminary δ^{26}Mg (^{26}Mg/^{24}Mg) values for the study plot exhibit an overall fractionation range of 1.15‰ (23% of reported terrestrial variation). Most interesting is considerable fractionation associated with the degradation of chlorophyll during leaf senescence. We believe translocation of light chlorophyll-bound Mg back into the tree accounts for this finding, driving whole leaf δ^{26}Mg to higher values prior to litter fall. Measured δ^{26}Mg values of senescent leaves and litter range from –0.88±0.10‰ to –1.32±0.09‰. Analyses of soil water and stream water samples during low and high flow indicate that Mg isotope values in the stream may be influenced by fractionation during plant uptake; however, a lithology driven (particularly silicate weathering [4]) control is still under investigation. With this presentation, we will review the progress made to date on factors influencing Mg isotope fractionation in a forested catchment.

[1] Black *et al*. (2008) *Environ. Sci. Technol*. **42,** 7831-7836. [2] Bolou-Bi *et al*. (2010) *Geochim. Cosmochim. Acta* **74,** 2523-2537. [3] Tipper *et al*. (2010) *Geochim. Cosmochim. Acta* **74,** 3883-3896. [4] Tipper *et al*. (2006) *EPSL* **250**, 241-253.

https://doi.org/10.1180/S0026461X00006502 Published online by Cambridge University Press

Carbonate-associated sulfate: A seawater proxy with potential and weaknesses

T. WOTTE[1]*, H. STRAUSS[1] AND G.A. SHIELDS[2]

[1]Institut für Geologie und Paläontologie, WWU Münster, D-48149 Münster, Germany (*correspondence: thomas.wotte@uni-muenster.de)

[2]Department of Earth Sciences, University College London, London WC1E 6BT, UK

It is generally considered that the sulfate ion is incorporated into the carbonate lattice during precipitation, consequently called carbonate-associated sulfate (CAS). Even if the mechanism of incorporation as well as the potential effects that diagenesis might have on the sulfur isotopic composition of CAS are not completely understood, it is regarded as a powerful proxy for reconstructing the primary seawater sulfate sulfur composition. Both, analytical and diagenetic aspects can affect the isotopic composition of CAS and have to be carefully considered when talking about carbonate-associated sulfate in the context of primary seawater composition. Bacterial sulfate reduction, particularly under sulfate limiting conditions in the pore water realm, causes ^{34}S-enrichment in the residual dissolved sulfate. On the other hand, sulfide oxidation results in ^{34}S-depleted sulfate. If incorporated, both would alter $\delta^{34}S_{CAS}$.

When extracting the original CAS signal it is essential that any other sulfates, which could influence this primary information, are removed. Otherwise, a mixed δ^{34}S signal is generated, composed of primary and secondary sulfate sulfur, that does not represent the sulfate sulfur isotopic composition of the paleo-seawater. Various methods of CAS extraction were developd, using different chemicals (e.g., NaCl, NaOCl, H_2O_2) or only deionised water to exclude non-CAS, organic sulfur, and metastable sulfides. These different methods result in variations in $\delta^{34}S_{CAS}$, but, no thorough calibration or comparison between the methods is presently available.

Based on comprehensive leaching procedures and detailed data sets comparing several extraction methods for CAS, we are able to identify the sources of secondary sulfate which has the potential to affect the primary CAS isotopic signal during extraction. Further, we determined the effect of pyrite oxidation on CAS by using δ^{34}S data generated from chromium-reducible sulfur (CRS). The aim of our research is to establish a rigid protocol for CAS extraction that enables the interpretation of sulfur isotope data from carbonate-associated sulfate as a true seawater proxy.

Petrologic significance of high-precision zircon U-Pb dates from the Skaergaard intrusive complex

J.F. WOTZLAW[1]*, I.N. BINDEMAN[2], U. SCHALTEGGER[1], C.K. BROOKS[3] AND H.R. NASLUND[4]

[1]Earth Sciences, University of Geneva, Switzerland (*correspondence: joern.wotzlaw@unige.ch)

[2]Geological Sciences, University of Oregon, Eugene, USA

[3]Natural History Museum, Univ. Copenhagen, Denmark

[4]Geological Sciences, SUNY, Binghamton, USA

The Skaergaard intrusion (East Greenland) has long been regarded as a type example of a layered intrusion that essentially evolved by closed-system fractional crystallization. Late-stage ferrodiorites, however, are depleted with respect to ^{18}O ($\delta^{18}O_{magma}$ ~3-4 ‰), recording incorporation of meteoric water derived oxygen into the magma prior to final solidification [1]. Incorporation of meteoric water into these late-stage differentiates requires either devolatilization of hydrated stoped blocks or remelting after subsolidus hydrothermal alteration. Such processes probably operated on timescales of ~100 ka and are thus potentially resolvable by high-precision ID-TIMS U-Pb geochronology.

We present high-precision zircon U-Pb dates for low-δ^{18}O ferrodiorites from the Sandwich Horizon (SH), a normal-δ^{18}O pegmatite from the lower zone of the layered series and the tholeiitic Basistoppen sill, that was emplaced ~200 m above the SH shortly after solidification of the Skaergaard magma [2]. Weighted mean ^{206}Pb/^{238}U zircon dates of statistically equivalent clusters yield precise crystallization ages for the normal-δ^{18}O pegmatite and the Basistoppen sill that overlap within subpermil uncertainty. In contrast, ^{206}Pb/^{238}U zircon dates from the SH do not form a statistically equivalent cluster. We interpret the observed scatter to reflect 321 ± 182 ka of crystallization. Notably, the youngest zircon from the SH is 125 ± 84 ka younger than the age of intrusion of the Basistoppen sill. This requires that either the SH was still molten or was remelted after emplacement of the Basistoppen sill. If the latter interpretation is correct, it would support models for the generation of late-stage low-δ^{18}O magmas that involve remelting induced by intrusion of the Basistoppen sill. These results demonstrate the potential of high-precision U-Pb geochronology for resolving complex histories of Cenozoic intrusions.

[1] Bindeman, I.N., Brooks, C.K., McBirney, A.R. & Taylor, H.P. (2008), *J. Geol.* **116**, 571-586. [2] Naslund, H.R. (1986), *Contrib. Mineral. Petrol.* **93**, 359-367.

https://doi.org/10.1180/S0026461X00006502 Published online by Cambridge University Press

Extracellular electron transport by the Gram-positive species *Thermincola potens*

K. WRIGHTON[1], H. CARLSON, R. MELNYK[1], K. BYRNE-BAILEY[1], J. THRASH[1], J. BIGI[2,3], J. REMIS[4], D. SCHICHNES[5], M. AUER[4], C. CHANG [2,3] AND J. COATES[1]*

[1]Department of Plant and Microbial Biology, University of California, Berkeley CA (*correspondance: jdcoates@berkeley.edu)
[2]Department of Chemistry, University of California, Berkeley
[3]Howard Hughes Medical Institute, University of California, Berkeley
[4]Life Sciences Division, Lawrence Berkeley National Laboratory
[5]College of Natural Resources Biological Imaging Facility, University of California, Berkeley

Despite their importance in iron redox cycles and bioenergy production, the underlying physiological, biochemical, and genetic mechanisms of extracellular electron transfer by Gram-positive bacteria remain insufficiently understood. We investigated respiration by *Thermincola potens* strain JR of the insoluble electron acceptors Fe(III) oxyhydroxide and anode surface. This isolate, a member of the Firmicutes, was obtained from the anode surface of a microbial fuel cell [1]. We found no evidence for soluble redox-active components secreted into the surrounding medium based on cyclic voltammetry measurements in conjunction with medium replacement experiments. Confocal microscopy revealed highly stratified biofilms in which cells contacting the electrode surface were disproportionately viable relative to the rest of the biofilm. There was also no correlation between biofilm thickness and power production, suggesting cells in contact with the electrode were primarily responsible for current generation. These data, along with cryo-electron microscopy experiments, support contact-dependent electron transfer by *T. potens* strain JR from the cell membrane across the 37 nm cell envelope to the cell surface. Furthermore, we present physiological and genomic evidence that direct extracellular electron transfer is mediated by *c*-type cytochromes. Taken together, our findings provide the first evidence to implicate direct extracellular electron transfer by Gram-positive bacteria and identify *c*-type cytochromes as a potential molecular conduit for charge transport.

[1]. Wrighton, K.C., Agbo, P., Warnecke, F., Weber, K.A., Brodie, E.L., DeSantis, T.Z., Hugenholtz, P., Andersen, G.L., & Coates, J.D. (2008). *ISME Journal* **2**, 1146-1156.

Fluid inclusion study of Haojiahe sandstone-type copper deposit, Yunnan province, China

HAI-ZHI WU, RUN-SHENG HAN AND PENG WU

Kunming University of Science and Technology, Southwest Institute of Geological Survey, Geological Survey Center for Non-ferrous Mineral Resources, Kunming, 650093, China (*correspondence: haizhiwu664@yahoo.com.cn)

Haojiahe sandstone-type copper deposit is located in the Chuxiong red bed basin, Yunnan province, China. Two dominant stages of fluid, rock-forming period and reworked mineralization period, are recorded in the gangue minerals of different types of ore.

The rock-forming period of fluid inclusions, mainly aqueous inclusions, can be observed in calcite and quartz cement and secondary enlargement of quartz in disseminated and lamellar ores. The homogenization temperatures range from 84.1 to 162.3ºC, with peak values between 122 and 146℃; and the salinities are from 3.3 to 14wt%$NaCl_{eq}$, with peak values between 5.5 and 7.5wt%$NaCl_{eq}$. The analytic results got by Laser Raman Spectroscopy, show that the gas components were mainly H_2O, SO_2 and CO_2, suggesting a relative oxidizing environment.

The reworked mineralization period of fluid inclusions, including aqueous inclusions and some hydrocarbon inclusions, can be observed in quartz paragenetic with copper minerals in banding or vein ores. The homogenization temperatures range from 145.5 to 227.2℃, with peak values between 170 and 200℃; and the salinities are from 4.5 to 15.2wt% $NaCl_{eq}$, with peak values between 7 and 9.5wt%$NaCl_{eq}$. The gas components were H_2O, CH_4, C_2H_6, CO and CO_2, suggesting a relative reducing environment.

Results of this study show the fluid evolution have experienced increased temperature, increased salinity and a environmental change from oxidizing to reducing.

Granted jointly by the project of State Crisis Mine (20089943) and the Distinguishing Discipline of KUST (2008).

https://doi.org/10.1180/S0026461X00006502 Published online by Cambridge University Press

Fluorine partitioning between hydrous minerals and aqueous fluid at 1 GPa and 770 – 850 ˚C

J. WU* AND K.T. KOGA

Laboratoire Magmas et Volcans, Clermont Université, BP 10448, Université Blaise Pascal, CNRS, IRD, Clermont-Ferrand, France
(*correspondence: j.wu@opgc.univ-bpclermont.fr)

Mechanisms of volatile transfer from subducting slab to melting region beneath arc volcanoes are probably the least undrestood process of arc magma genesis. Fluorine, which suffers minimum degassing in arc primitive melt inclusions, retains the information of magma genesis at the depths. It is our interest to understand geochemical behavior of F along with other trace element, and to characterize volatile transfer from the slab to the mantle. Experimentally determined solubility of F in aqueous fluid, and partition coefficients of F between fluid and minerals provide first order information about the character of the volatile-transporting agent. Here, we report experimentally determined the solubility of F in aqueous fluid. The solid starting materials contain 5% or 1.9% F, and an approximately same amount of pure water was added right before an experiment. The experiments are conducted at 1GPa and from 770 to 850°C, for the duration of 3 to 13 days, in gold capsule, with Ni/NiO buffer, using piston cylinder high-pressure apparatus. After quenching, the liquid part is retrieved into a known volume of deionized water for the liquid analysis and the solid part is measured by an electron microprobe. We also calculate the fluid composition with mass-balance.

All samples are equilibrated with hornblende, a humite group mineral, and fluid. With mass-balance calculation a range of partition coefficents are determined: D(fluid /hornblende) = 0.13-0.42; D(fluid/norbergite) = 0.02-0.04; D(hornblendes/norbergite) = 0.13-0.17. The D_F are constant over the temperature range within their uncertainties. Furthermore, F anions are preferentially incorporated into the humite group minerals than hornblende, and nearly all OH site of nobergite are occupied by F in our system. The concentration of F in the fluid is 0.22-0.78 wt% based on mass-balance, and direct analyses of fluids are under way. The F/H_2O values are 10-100 times larger for primitive arc melt inclusions (0.05-0.81) than for ours (0.0024-0.0085). This suggests either 1) drastic water loss in arc melt incusions, or 2) presence of fractionation phases other than ones in this study.

Advances and challenges in the study of mechanisms on salinization and contamination of deep groundwater in the North China Plain

J. F. WU*, Y. YANG, Y. ZHANG AND X. B. ZHU

Department of Hydrosciences, School of Earth Sciences and Engineering, Nanjing University, Nanjing 210093, China
(*correspondence: jfwu@nju.edu.cn)

Groundwater in deep aquifers is the main water source of households, industry and agriculture in the North China Plain (NCP). However, information on degradation of groundwater quality is often seen in this region, which poses a great threat to the intersts of society or ecosytems. This presentation reviews the recent advances in the study on mechanism of deep groundwater quality degradation over the last several decades in the NCP: salinization due to shallow saline groundwater intrusion and contamination by man-made sources. In general, degradation and deterioration of deep grouindwater quality found in the NCP was deductively explained by groundwater over-exploitation and mis-management, but the mechanism of groundwater quality degradation is largely unknown so far. As a consequence, further investigation is needed to uncover the mechanism of salinization and contamination of deep groundwater resource. Due to the compexity of the aquifers, some techniques developed for fractured rock systems [1, 2] may be used as a reference in highly heterogeneous porous aquifers, and the confronting issues and challenges can be summarized as: (i) how to address the heterogeneity of alluvial deposits including aquifers and aquitards [3]; (ii) how to characterize the spatial and temporal extent and intensity of downward salinity intrusion of shallow saline groundwater [4]; (iii) how to delineate the chemical and biochemical processes of man-made sources in aquifers [5]; and (iv) how to understand the apparent scale-effects on different hydrogeological parameters at a regional scale under field conditions [6, 7]. (Grant Nos. 2010CB428803 and 41072175)

[1] Zhou *et al*. (2004) *Int. J. Rock Mech. Min. Sci*. **41**(3), 402-402. [2] Qian *et al*. (2006) *Hydrogeol. J*. **14**, 1192-1205. [3] Rojas *et al*. (2010) *Water Resour. Res*. **46**, W08520. [4] Song *et al*. (2007) *Hydrogeol. Eng. Geol*. **34**(1): 44-46. [5] Singhal & Islam (2008) *J. Contam. Hydrol*. **96**, 32-47. [6] Qian *et al*. (2007) *J. Hydrol*. **339**, 206-215. [7] Chen *et al*. (2009) *Journal of Hydrodynamics* **21**(6): 820-825.

https://doi.org/10.1180/S0026461X00006502 Published online by Cambridge University Press

Geochemical anomaly pattern in the Haojiahe sandstone-type copper deposit, Yunnan, China

PENG WU*, RUNSHENG HAN AND JING LI

Kunming University of Science and Technology; Southwest Institute of Geological Survey, Geological Survey Center for Non-ferrous Mineral Resources, Kunming 650093, China (*correspondence: wupeng8104@yahoo.com.cn)

Haojiahe deposit controlled by the Upper Cretaceous (K_2mx_2) is the typical one of sandstone-type copper deposits in the Chuxiong Basin. Ore-bodies (average grade: Cu 1.5%) are located in the interface between purple bed and grey bed. From purple bed to grey bed, the ore mineral zonality is hematite, chalcocite, bornite, chalcopyrite and pyrite.

Ore-forming elements association is Cu, Ag, As, Hg. The average contents of copper ores $\sum$REE=119.19×10^{-6}, LREE/HREE=8.93, δEu=0.74, δCe=0.95. Chondrite-normalized REE distribution patterns show oblique to the HREE side with the poor Eu and enrichment in LREE. From oxidized zone to transitional zone (purple bed→copper ore→grey bed), $\sum$REE and δCe decrease gradually with the increase of δEu. The geochemical characteristics well indicate the change of oxidation and reducing environment [1, 2]. These are probably related to the water-rock interaction or infiltration metasomatism.

The vertical zonation of indicator elements in K_2mx_2 from the top to the bottom is Zn, Cs→Pb, Tl, Mo→Cu, Ag, As→Sb, Hg, Co and the transversal zonation from grey belt to purple belt is Mo, Pb→Cu, Hg, Ag→Cu, Ag, As, Sb, Hg.

Geochemical anomaly pattern has been established, that is, the anomaly of Zn, Pb, Mo appears above the orebodies (average distance: Zn 30m, Mo 10m),and the anomaly of Sb, Hg, Co under the orebodies. The anomaly of Cu, Ag and the ratio of Cu/Ag>170, Cu/(Pb+Zn)>10, Cu/(As+Sb+Hg)>180 are concomitant with rich orebodies; the anomaly of Pb, Zn, Co, (Ni) and Cu/Ag<128, Cu/(Pb+Zn)<9, Cu/(As+Sb+Hg)<8 implies barren. The contents of Cu, Ag, As, Hg and the ratio of dual elements increase longitudinally, and it shows that the copper minealization is enhanced gradually. This pattern provides an important basis for the depth ore-forming prognosis.

Granted jointly by the Basic Applied Research Foundation of Yunnan Province (2010ZC013) and the Distinguishing Discipline of KUST (2008).

[1] Alex C. Brown (2006). *Journal of Geochemical Exploration* **89**, 23-26. [2] El Desouky (2008). *Ore Geology Reviews* 3**4**, 561-579.

Origins and sources of CO_2 in natural gas in Eastern Sichuan Basin, China

XIAOQI WU

PetroChina Research Institute of Petroleum Exploration & Development, Beijing 100083, China (wuxiaoqi@petrochina.com.cn)

The eastern Sichuan Basin in China is well-known for the development of H_2S-bearing gas fields such as Puguang, and the natural gas generally contains CO_2. High-content CO_2 was thought to accompany high-content H_2S, and this might be one of the proofs of TSR (Thermochemical Sulfate Reduction) [1]. The CO_2 contents of natural gas from eastern Sichuan Basin vary from 0% to 32.04%, and gas samples with low-content (<2%) and 6%-10% CO_2 account for 61.6% and 20.0% of the total respectively.

The $\delta^{13}C_{CO2}$ values vary from -23.4‰ to 3.3‰, and 34.4% of the samples have low $\delta^{13}C_{CO2}$ values (<-12‰) which are in accordance with those of typical organic CO_2 [2], and they are mainly with low contents of CO_2 (<3%). The corresponding H_2S contents are very low or zero. This type of CO_2 was derived from the oxidation of organic matters. However, the other type of CO_2 displays large $\delta^{13}C$ values (>-8.3‰) and shares similar carbon isotopic characteristics with inorganic CO_2 [2] and reservoir carbonates [1], and differs dramatically from that of TSR origin [3]. In this case, no obvious relation exists between the CO_2 and H_2S contents, so it does between the CO_2 and TSR as study by Huang *et al*. [4]. Under the precipitation in the deep-burial period, CO_2 generated during the TSR was mainly transformed into secondary calcite, which demonstrated low $\delta^{13}C$ values (-18.2‰~-10.3‰) [1].

Inorganic CO_2 can be divided into mantle-derived origin and decomposition or dissolution of carbonates [2]. The helium in the natural gas was crustal derived due to the low R/Ra ratios (<0.036) without significant contribution from the mantle. The temperature required for decomposition of carbonates was too high to reach for the deep-buried carbonate reservoirs. In consideration of substaintial uplift in late Jurassic, CO_2 with large $\delta^{13}C$ values was mainly derived from the dissolution of reservoir carbonates under the effect of acidic fluid.

[1] Zhu *et al*. (2005) *Sci China -Earth Sci* **48**, 1960-1971. [2] Dai *et al*. (1996) *AAPG Bull* **80**, 1615-1626. [3] Worden *et al*. (1995) *AAPG Bull* **79**, 854-863. [4] Huang *et al*. (2010) *Sci China-Earth Sci* **53**, 642-648.

https://doi.org/10.1180/S0026461X00006502 Published online by Cambridge University Press

The distribution of biomarkers and the geological significance of the severely biodegraded crude oil in Gudao reservoir

YINGQIN WU[1,2], YONGLI WANG[1], TIANZHU LEI[1], JIANG CHANG[1], YOUXIAO WANG[1] AND YANQING XIA[1]*

[1]Key Laboratory of Petroleum Resources Research, Institute of Geology and Geophysics, Chinese Academy of Science, Lanzhou 730000, China (*correspondence: yqxia@lzb.ac.cn)

[2]Graduate School of the Chinese Academy of Sciences, Beijing 100049, China (wuyingqin001@163.com)

Biodegraded crude oil in China are distributed widely and make up a certain portion of heavy-oil resources. An unresolved complex mixture (UCM) of hydrocarbons isolated from a biodegraded crude oil of the Gudao reservoir in the Shengli Oilfield, China. Some of the hydrocarbons were identified using GC-MS. The result showed that the hydrocarbons expect for tricyclic terpanes, steranes, hopanes, 25-norhopanes, were completely depleted in saturated fraction, as well as hydrocarbons expect for triaromatic steranes and few methylnaphthalenes, methylphenanthrenes, chrysene series in the aromatic fraction, which indicate that severe biodegradation occurred in this reservoir. Relatively abundant pentacyclic terpane characterized by high concentration of norhopane and gammacerane, low content of Ts and Tm, the "L"-type and asymmetrical "V"-type distribution of regular steranes and 4-methylsteranes, and high maturity as revealed by sterane and terpane parameters, suggesting aerobic depositional environment with a salt and stratified water body. Furthermore, The results also showed that the magnitude of "UCM" hump existed in the aromatic fraction is apparently larger than that of "UCM" hump existed in the saturated fraction, which implied that the biodegradation rate for aromatic hydrocarbons is parallel or even exceed that of saturated hydrocarbons and the alteration occurred in this reservoir was associated with biodegradation with water-washing.

Supported by grants No. KZCX2-YW-Q05-05, XDA05120204, KZCX2-EW -104(2), NSFC No.40672123 and 2005CB422001.

Determination on nitrate use capacity in plants via isotope tracer

YANYOU WU* AND KUAN ZHAO

IAE, Jiangsu University, Zhenjiang, 212013, China (*correspondce: yanyouwu@ujs.edu.cn)

Materials and Treatments

Broussonetia papyrifera (BP) and *Morus alba* (MA) seedlings were cultured in the modified Hoagland nurient solution adding different concentrations (0, 20, 60 g L^{-1}) of polyethylene glycol (PEG, simulating drought) (pH5.5). *Orychophragmus violaceus* (OV) seedlings were cultured in the modified Hoagland nurient solution adding different concentrations (0, 2.5, 10 mM) of $NaHCO_3$ (BC) (pH 8.2). The sole nitrate N was potassium nitrate with 16.99‰ of the $\delta^{15}N$. The sole ammonium N was $NH_4H_2PO_4$ with -1.21‰ of the $\delta^{15}N$. The $\delta^{15}N$, net photosynthetic rate (Pn, μmol $m^{-2}s^{-1}$) and N content (Cn, mg g^{-1}) of the third or fourth fully expanded leaf were measured. The proportion (f_B) of nitrate to total inorganic N was calculated by a two-component mixing model. The nitrate use capacity (NUC, mg $m^{-2}h^{-1}$) in plants was calculated by the formula: $NUC= 90CnPnf_B$.

Results and discussion

From Table 1, we can found that OV under high concentration BC had the greatest NUC, MA under drought stress the least. Even under drought stress, BP had a great NUC. The great NUC of BP and OV under the Karst drought or high concentration bicarbonate resulted in their adaptability to Karst environment, partly. The plants of the adaptability to Karst environment alternately use nitrate and ammonium N under Karst environment.

PS-T	$\delta^{15}N$	Pn	f_B	NUC
MA-PEG/0	-2.41	6.3	0.11	1.59
MA-PEG/20	-1.51	1.0	0.15	0.40
MA-PEG/60	-1.53	0.1	0.15	0.03
BP-PEG/0	-1.25	2.8	0.17	1.04
BP-PEG/20	3.19	2.9	0.38	2.39
BP-PEG/60	2.91	3.9	0.37	3.10
OV-BC/0	12.73	3.9	0.84	6.28
OV-BC/2.5	15.95	2.1	0.99	4.77
OV-BC/10	16.08	3.3	1.00	7.10

Table 1: NUC of several species of plants under different treatment (PS=plant species, T=treatment).

This work was supported by NSFC (No. 40973060, No.31070365).

https://doi.org/10.1180/S0026461X00006502 Published online by Cambridge University Press

Tectonic evolution of the Qinling-Tongbai-Dabie orogenic belt

YUAN-BAO WU[1] AND YONG-FEI ZHENGB[2]

[1]State Key Laboratory of Geological Processes and Mineral Resources, Faculty of Earth Sciences, China University of Geosciences, Wuhan 430074, China (*correspondence: yuanbaowu@cug.edu.cn)

[2]CAS Key Laboratory of Crust-Mantle Materials and Environments, School of Earth and Space Sciences, University of Science and Technology of China, Hefei 230026, China

The Qinling-Tongbai-Dabie-Sulu orogenic belt marks the suture between the North and South China Blocks in Central China, forming one of the most important orogens in the eastern Asia. Although it has been extensively studied for more than 20 years, there are hot controversies about the location and number of sutures and the timing of arc-continent and continent-continent collisions during the convergence between the North and South China Blocks. The Dabie-Sulu orogenic belt is characterized by the occurrence of Triassic UHP eclogite-facies metamorphic rocks. On the other hand, there are Paleozoic events of arc-continent collision in the Qinling-Tongbai orogenic belts that were subsequently followed by the Triassic process of continental collision. Rifting occurred at the northern part of the Yangtze Block, synchronous with the middle Paleozoic collision, and was followed by the opening of the Paleo-Tethyan ocean during the Late Paleozoic. These indicate that the Qinling-Dabie-Sulu orogen is a typical multiple evolution orogen, including the Early to Middle Paleozoic continental subduction and collision, the Silurian extension and rifting in relation to the opening of the Paleo-Tethyan ocean during the Late Paleozoic, and the Triassic continental material subduction, HP-UHP metamorphism and subsequent exhumation. Therefore, it is a complex orogenic belt on the time and location of arc-continent and continent-continent collisions between the North and South China blocks, and the amalgamation of the two continental blocks along the Qinling-Tongbai-Dabie-Sulu orogenic belt is a multistage process that spans about 300 Ma.

Composition and structure of the 3.65 Å phase: A DHMS with exclusively six-fold coordinated Si

B. WUNDER*, R. WIRTH, M. KOCH-MÜLLER AND S. JAHN

GFZ German Research Centre for Geosciences, Section 3.3, Telegrafenberg, 14474 Potsdam, Germany (*correspondence: wunder@gfz-potsdam.de)

Dense Hydrous Magnesium Silicates (DHMS) are suggested to be important hosts and carriers of water under hydrous conditions of the Earth´s mantle and in subduction zones. Therefore, their study is central to the understanding of the Earth´s deep water cycle. The so-called 3.65 Å phase, named after the *d*-value of its prominent X-ray reflection, is the least well-characterized phase of the DHMS family, as neither its chemical composition nor its structure are well constrained.

In our recent study [1], the 3.65 Å phase was synthesized in the system MgO-SiO_2-H_2O at 10 GPa and 425 °C for 77 hours run duration in a multi-anvil press from a gel plus excess water. The composition of the 3.65 Å phase was determined to be $MgSi(OH)_6$ by combining results from SEM-, TEM-, EMP-, IR- and Raman-analysis. Powder XRD combined with Rietveld refinement revealed the 3.65 Å phase to be isostructural with δ-$Al(OH)_3$. Its structure can be described as an A-site vacant perovskite with probably long-range random distribution of Si and Mg at octahedral sites. The 3.65 Å phase represents beside phase D the second DHMS with exclusively six-fold coordinated Si.

The H-positions could not be determined by the powder XRD Rietveld refinement. Therefore, the apparent orthorhombic space group – either *Pnam* with protons in unordered configuration, or $P2_12_12_1$ with ordered H-positions – was ambiguous. Preliminary first-principles DFT-calculations predict the structure with $P2_12_12_1$ or monoclinic $P2_1$ symmetry with ordered Mg and Si as the most stable structure at ambient conditions.

The 3.65 Å phase is stable at pressures above about 9.0 GPa and decomposes above about 500 °C due to the reaction 3.65 Å phase = high-clinoenstatite + water. This limited P-T-stability together with its high water content of 35 wt.% makes it a rather unrealistic phase in the Earth´s mantle. If at all, the 3.65 Å phase might only exist under hydrous conditions in very limited areas, i.e., in the coldest parts of old and extremly fast subducted slabs, e.g., Tonga.

[1] Wunder *et al*. (2011) *Am. Mineral*., in press, DOI: 10.2138/am.2011.3782.

https://doi.org/10.1180/S0026461X00006502 Published online by Cambridge University Press

Exploring carbonate aquifers and their susceptibility for metal release during CO_2 leakage

A. WUNSCH[1]*, A.K. NAVARRE-SITCHLER[1], R.M. MAXWELL[2] AND J.E. MCCRAY[1]

[1]Environmental Science and Engineering Division, Colorado School of Mines, Golden, CO 80401, USA (*correspondence: awunsch@mines.edu)

[2]Geology and Geological Engineering Department, Colorado School of Mines, Golden, CO 80401, USA

Metal transport resulting from potential CO_2 leakage into freshwater aquifers is a major concern accompanying carbon sequestration operations. Acidity resulting from dissoluton of leaked CO_2 into aquifer waters may result in release of metals from aquifer minerals. Carbonate aquifers have the ability to buffer increased acidity through calcite and dolomite dissolution, and are therefore theoretically "safer" than non-buffering aquifers. However, carbonate minerals are rarely found as pure phases in nature, often containing impurities in the solid phase. These impurities substitute for either calcium or carbonate in the crystal lattice. Buffering of acidity requires dissolution of carbonate minerals, resulting in potential release of trace elements. Whole-rock analysis of natural carbonate rock samples show solid-phase concentrations of Pb and Cr on the order of several ppm, and of Ba, Co, Ni, Rb, Sc and Zn on the order of tens or hundreds of ppm. Prediction of the behavior of these metals through modeling is difficult, as there are several models of co-precipitation and dissolution in solid solutions. Simple stoiciometric dissolution predicts very different release behavior of these metals from calcite dissolution at various CO_2 partial-pressures. For example, at low P_{CO2}, cobalt concentrations in solution are as high as 776 ppb, and decrease with increasing P_{CO2}, whereas barium concentrations in solution increase with increasing P_{CO2}, following a trend similar to that of calcium. In this work, batch dissolution experiments are combined with SEM and electron microprobe analyses, to investigate dissolution rates and equilibrium release of metals from carbonate rocks and to determine their solid-phase source.

Uncovering the key processes involved in manganese biogeochemical cycling in the Ocean

K. WUTTIG[1], M. HELLER[1] AND P. CROOT[2]

[1]IFM-Geomar, Kiel, Germany (kwuttig@ifm-geomar.de, mheller@ifm-geomar.de)

[2]Plymouth Marine Laboratory, Plymouth, United Kingdom (pecr@pml.ac.uk)

Mn forms a critical part of many redox enyzmes most notably for photosynthesis, where as part of Photosystem II it converts H_2O to O_2. Many marine organisms also contain Mn superoxide dismutases (SOD), that act as part of the intracellular defences against reactive oxygen species (ROS) and in particular rapidly convert superoxide (O_2^-) into O_2 and H_2O_2. While laboratory studies have shown that the growth of marine phytoplankton is reduced for some species at the low Mn concentrations found in open ocean seawater, currently there is little evidence from fieldwork to suggest Mn limitation occurs, but this possibility remains, particularly for the Southern Ocean.

The supply of Mn to the open ocean is predominantly via the deposition of aeolian dust and subsequent dissolution of Mn(II) from the particles. The released Mn(II) is slowly oxidized (via biota or chemically) to insoluble MnO_2 which precipitates out of the water column. In the sunlit ocean, H_2O_2 can reduce MnO_2 back to Mn(II) completing a redox cycle. New work by a number of groups suggest that transient Mn(III) species, intermediate in the cycling between Mn(II) and MnO_2 may play an important role in both the Mn and Fe biogeochemical cycles in surface waters. In coastal waters Mn(II) can diffuse from reducing sediments with subsequent mixing into the photic zone.

In this presentation we will present data for Mn concentrations, speciation and kinetic reactivity from two research cruises in the Tropical Atlantic (M83-1 and MSM17-04) and from a dust deposition experiment performed in trace metal clean mesocosms in the Mediterranean (DUNE2). We will use our combined dataset to determine the predominant source of Mn to shelf waters in the Mauritanian upwelling region and the adjacent open ocean in the Tropical Atlantic, which are impacted by both Saharan dust and potentially coastal sedimentary sources that are advected offshore by the upwelling waters. Finally we will examine the evidence for Mn(III) in the euphotic zone of the open ocean and the implications this had for Mn biogeochemical cycling in the ocean.

https://doi.org/10.1180/S0026461X00006502 Published online by Cambridge University Press

XANES investigation of selenium speciation in silicate glasses

JEREMY L. WYKES, HUGH ST. C. O'NEILL AND JOHN A. MAVROGENES

Research School of Earth Sciences, Australian National University, Acton, ACT, 0200, Australia

The speciation of sulfur in silicate melts as a function of oxygen fugacity is an important factor in volcanic degassing and ore deposition. Due to the large number of electrons involved in the 2- to 6+ transition, sulfur changes from 2- to 6+ over a very narrow fO_2 interval, <2 log units. The 4+ valence state of sulfur does not appear to be an important species in silicate melts. Selenium lies directly below sulfur in group 16 of the periodic table and is considered to display similar geochemical behavior. However, differences in redox speciation between sulfur and selenium, either in the fO_2 of Se^{2-} to Se^{6+} relative to S^{2-} to S^{6+} transitions, or the existence of a Se^{4+} stability field will result in fractionation of Se from S in magmatic systems [1].

We have conducted high pressure, high temperature experiments under controlled fO_2 conditions to investigate the speciation of Se in silicate melts. Oxide mixes of basaltic composition were doped with 500 to 2500 ppm Se and equilibrated in Pt or graphite-Pt capsules at 1400°C for 36 hours. Chemical potential of oxygen was controlled by the addition of Ru-RuO_2, PtO_2 and the presence of graphite, to produce experiments reflecting reduced (graphite ≈ FMQ-2.2; [2]), oxidising (Ru-RuO_2 ≈ hematite-magnetite at 1400°C) and very oxidising conditions (PtO_2 produces O_2 gas phase).

Quenched glasses were recovered from the piston-cylinder experiments and the selenium K-edge XANES (X-Ray Absorption Near Edge Structure) spectra were collected in fluorescence mode at the Australian National Beamline Facility at the Photon Factory, Tsukuba, Japan.

Glasses from each redox condition produced a distinct Se K-edge spectra, with the absorbtion edge energy increasing with increasing fO_2. The spectra are interpreted to represent Se^{2-}, Se^{4+} and Se^{6+}. Thus, at moderate to high fO_2, selenium exhibits distict redox speciation to sulfur, with the existence of a significant stability field for Se^{4+}, and the Se^{2-} to Se^{4+} transition will occur over a larger fO_2 range than S^{2-} to S^{6+}. We suggest that Se^{6+} is not an important species in silicate metls at geologically relevant oxygen fugacities.

[1] Jenner, O'Neill, Arculus, Mavrogenes (2010) *Journal of Petrology* **51**, 2445-2464. [2] Médard, McCammon, Barr, Grove (2008) *American Mineralogist* **93**, 1838-1844.

Geochemical evidence of source and process controls on Mid-Miocene silicic volcanism in the Idaho-Oregon-Nevada Region, USA

A. WYPYCH* AND W.K. HART

Geology Dept., Miami University, Oxford, OH 45056, USA (*correspondence: wypycha@muohio.edu)

In this study we report results of a geochemical and petrological investigation of Mid-Miocene silicic volcanism in the Idaho-Oregon-Nevada (ION) region aimed at examining models of continental crust formation and modification in the northwestern US. In the late Oligocene to Miocene portions of the northwestern US underwent extension accompanied by bimodal (mafic and silicic) volcanism [1,2]. The ION region resides in the northernmost Basin and Range Province on a "transitional" lithosphere between Mesozoic accreted lithosphere to the west and Precambrian Wyoming Craton to the east as marked by Sr isotopic composition (0.704 and > 0.706 respectivly). It is characterized by bimodal, silicic (~16 to ~13 Ma) and mafic (~17 to 15 Ma) volcanism temporally related to the main volumes of Columbia River flood basalt activity to the north. Mantle upwelling behind an active magmatic arc, mafic magma intrusion into crust, melting of heterogeneous lithosphere and mixing of the melts from heterogeneous sources are contributing to the ION region bimodal volcanism and its continuation in time and space to the NE (Snake River Plain-Yellowstone) and the NW (High Lava Plains-Newberry) [1,3,4].

To investigate the heterogeneity and spatial and temporal relationships between off craton, "transitional", and on craton sources and reservoirs five ION volcanic centers are investigated. We conducted petrological, geochemical and Sr, Nd and Pb isotopic analyses on 23 whole rock-glass separate pairs and Hf isotopic analyses on the glass separates [3]. In addition to the influence of sptaillay and temporally heterogeneous source regions open system behavior in crustal storage chambers plays an important role in ION area silicic magma evolution. This is evident from feldspar dissolution textures and differences in trace element and isotopic compositions between whole rock and glass separate pairs.

[1] Brueseke et al. (2008) *Bull. Volc.* **70**, 343-360. [2] Scarberry et al. (2010) *Tectonophys.* **488**, 71–86. [3] Nash et al. (2006) *Earth Plant. Sci. Lett.* **247**, 143-156. [4] Christiansen and McCurry (2008) *Bull. Volc.*, **70**, 251-267.

https://doi.org/10.1180/S0026461X00006502 Published online by Cambridge University Press

Generating Kermadec Arc SMS deposits: Roles of magmatic volatiles

R.J. WYSOCZANSKI[1]*, M.R. HANDLER [2], C.I. SCHIPPER[3], J. CREECH[2], M.D. ROTELLA[2], C.J.N. WILSON[2] AND R.B. STEWART[3]

[1]NIWA, PO Box 14901, Wellington, New Zealand (*correspondence: r.wysoczanski@niwa.co.nz)
[2]SGEES, Victoria University, Wellington, New Zealand
[3]INR, Massey University, Palmerston North, New Zealand

Seafloor massive sulphide (SMS) deposits in oceanic subduction zones, such as the Kermadec Arc/Havre Trough (KAHT), are a valuable commodity and may be viable as a precious metal source. The ultimate source, however, of S and metals in SMS deposits is unknown. Here, we present elemental data, including volatiles (H, C, S, Cl) of basalts from along the southern KAHT to address the relationship between magmatic composition and hydrothermal venting. The findings are as follow:

1. Back-arc melt inclusion (MI) water contents (~2.5 wt. %) are similar to the hydrothermally active arc, implying that the lack of back-arc hydrothermal activity is not due to lower magmatic water contents. Slab-derived fluid components do not differ between the southern and middle portions of the Kermadec Arc, implying that subduction of the thick Hikurangi Plateau crust in the south (cf. normal oceanic crust in the north) does not enrich the mantle in fluids.

2. SO_3 contents do not correlate with slab-derived components, suggesting that little S is added to the mantle source from the slab. S degasses as sulphate, resulting in more reduced rock compositions, which then interact with hydrothermal fluids. Pressures from H_2O contents of MIs imply that the magma chambers of arc front volcanoes that are hydrothermally inactive are deeper than for hydrothermally active volcanoes.

3. Basalt compositions from hydrothermally active arc front volcanoes do not significantly differ from those with no activity. This implies that factors other than magmatic composition determine the location and extent of hydrothermal activity.

4. Concentrations/ratios of metals in basalt magmas require metal enrichment over magmatic compositions to produce SMS deposits in the order Pb>Zn>>Cu. This may occur via crustal scavenging or magmatic fluid additions. Elemental ratios in chalcopyrite-bearing chimneys can, however, be achieved from basalt magmas by fractionation to evolved compositions.

https://doi.org/10.1180/S0026461X00006502 Published online by Cambridge University Press

Study on main sources of the sulfur in acid rain in Jiangxi province, China

F. XIA[1], J.-Y. PAN[1], FAN. XIA[2], S.-H. CHEN[1], H.-M. PENG[1] AND P. LIU[1]

[1]State Key Laboratory Breeding Base of Nuclear Rersources and Environmental, East China Institute of Technology, Nanchang 330013, China (xf730@163.com)

[2]Shanghai Environmental Monitoring Centre, Shanghai 200030, China (xiahoufan@sohu.com)

The main sources of sulfur in rain water include bio-organic sulfur and anthropogenic sulfur in Jiangxi province, China.

We analyzed the sulfur isotopic composition of rain water from Nanchang City in this paper. The results indicated that the sulfur isotopic composition possesses a seasonal variation trend. It is discussed individually that the different sulfur sources of rain water with the principle of mass balance, the relative contribution of the biogenic and the anthropogenic to sulfur source of acid rain in Nanchang each can be calculated quantitatively. In summer and autumn, the sulfur in rain water comes mainly from bio-organic sulfur, In winter and spring,the sulfur in rain water dominantly originates from anthropogenic sulfur (Fig.1). The sulfur in rain water from the sea may be very small in percentage.

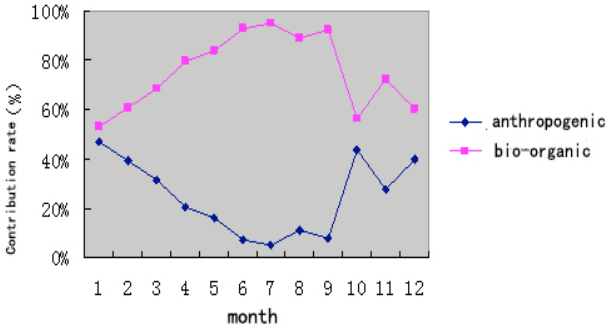

Figure 1: Two main sulfur sources' relative contribution to the precipitation in Jiangxi province

This research was jointly supported by the National natural Science Foundation of China (Grant No. 40963004).

Multistage growth of garnet in UHP metagranite in the Dabie orogen

QIONG-XIA XIA, YONG-FEI ZHENG, XIAO-NAN LU

CAS Key Laboratory of Crust-Mantle Materials and Environments, School of Earth and Space Sciences, University of Science and Technology of China, Hefei 230026, China (qxxia@ustc.edu.cn)

Garnet is a common mineral in subduction-zone metamorphic rocks, and its growth and reworking can be linked to metamorphic P-T conditions. We performed a combined study of major and trace elements by means of EMP and LA-ICPMS analyses on garnet from UHP metagranite in the Dabie orogen. Three stages of garnet growth are deduced from the major element zonation based on the assumption that Ca contents and Fe/Mg ratios in metamorphic garnet are indicative of metamorphic pressure and temperature, respectively. The first stage of growth (Grt-I) occurs in the core of skeletal garnets, which is characterized by the homogeneously low X_{Grs} values and Fe/Mg ratios, indicative of the highest temperature but the lowest pressure. It is a residue of magmatic garnet that most likely nucleates in the stage of protolith granite formation. The second stage of growth (Grt-II) occurs in the mantle and core of garnets, which is indicated by the increased X_{Grs} values and Fe/Mg ratios, corresponding to continuous increase in temperature and pressure till peak pressure and thus garnet growth during the prograde subduction. The third stage of growth (Grt-III) occurs in the rims of all garnets, which is suggested by slightly decreased X_{Grs} values and Fe/Mg ratios in response to a pressure decrease but a temperature increase till peak temperature. These rims overgrew subsequent to the peak pressure with continuous heating during the initial exhumation. REE distributions in the three stages of garnets are also different from each other. Both Grt-I and Grt-II exhibit steep MREE-HREE patterns with high HREE contents, with obvious negative Eu anomalies and high REE contents for Grt-I. Grt-III displays obviously lowered REE contents compared to those for Grt-I and Grt-II, with two subtypes of MREE-HREE patterns: steep (IIIa) and plat MREE-HREE patterns (IIIb). Therefore, the garnet from low-T/UHP metagranites displays obvious multiple stages of growth during continental collision. Nevertheless, the highest pressure occurs in the cores or mantles whereas the maximum temperature occurs in the rims, suggesting that the peak pressure did not occur at the peak temperature during the continental collision. Thus the "hot" exhumation is recorded in the garnets from the low-T/UHP granitic gneiss. This provides a thermal condition for dehydration melting of the deeply subducted continental crust.

https://doi.org/10.1180/S0026461X00006502 Published online by Cambridge University Press

Diffusive anisotropy in low-permeability Ordovician sedimentary rocks from the Michigan basin in southwest Ontario

Y. XIANG[1], T. AL[1,*], L. CAVÉ[1,2] AND D. LOOMER[1]

[1]Department of Earth Sciences, University of New Brunswick, Fredericton, New Brunswick, Canada (*correspondence: TAL@UNB.CA)

[2]Present Address: Environment Canterbury, Christchurch, New Zealand

Diffusive anisotropy and its scale-dependence were investigated using samples from the Upper Ordovician Georgian Bay Formation (shale and thin interbeds or 'hardbeds' of limestone and siltstone) and Middle Ordovician argillaceous limestone from the Michigan Basin of southwest Ontario, Canada. Effective diffusion coefficients (D_e) were determined for iodide (I^-) and tritiated water (HTO) tracers on paired cm-scale subsamples oriented normal (NB) and parallel to bedding (PB). Measurements were conducted using X-ray radiography and through-diffusion methods. The D_e values range from 4.8×10^{-13} to 5.3×10^{-12} $m^2 \cdot s^{-1}$ for shale, 2.1×10^{-13} to 1.3×10^{-12} $m^2 \cdot s^{-1}$ for limestone, and 4.1×10^{-14} to 5.6×10^{-13} $m^2 \cdot s^{-1}$ for siltstone interbeds within the Georgian Bay shale formation. The sample-scale anisotropy ratios ($D_{e\text{-}PB}$: $D_{e\text{-}NB}$) for D_e values obtained using I^- tracer are 0.9 to 4.8, and the anisotropy ratios for HTO tracer are in the range of 1.1 to 7.0. A formation-scale anisotropy ratio of 8.0 was calculated for the Georgian Bay Formation from the ratio of the arithmetic to the harmonic mean of D_e data measured at the sample scale and weighted for the thickness of interbedded siltstone/limestone and shale units.

The influence of porosity distribution on diffusive anisotropy has been investigated using one-dimensional spatially-resolved profiles of I^--accessible porosity obtained from radiography experiments, and the use of $AgNO_3$ for fixation of I^- tracer in the pores, allowing for SEM visualization of I^--accessible pore networks. The porosity profiles generally display greatest heterogeneity in the direction normal to bedding. The SEM imaging suggests that diffusion pathways are preferentially oriented parallel to bedding in the shale, and that diffusion occurs dominantly within the argillaceous component of the limestone but fine clay-filled voids in the limestone are also accessible for diffusive transport.

Characteristics and prediction of high quality coal measure source rocks in Oligocene Yacheng Formation of Qiongdongnan Basin, Northwestern South China Sea

J. XIAO[1,2]*, H. WANG[1,2] AND B. ZHU[2]

[1]Faculty of Earth Resources, China University of Geosciences, Wuhan 430074, China (*correspondence: xj0930@cug.edu.cn)

[2]Key Laboratory of Tectonics and Petroleum Resources (CUG), Ministry of Education, Wuhan 430074, China (wanghua1@cug.edu.cn, zhubei@cug.edu.cn)

The coal measure strata of marine-terrigenous facies in Oligocene Yacheng Formation are the major source rocks of Qiongdongnan Basin. Through comprehensive studies, main characteristics of this set of coal measure source rocks can be concluded as following: (1) they consist chiefly of coals, carbonaceous mudstones and dark mudstones with relatively high organic matter abundance and type II_2-III kerogen. Among them, coals have been most noticed because of the highest organic carbon abundance (19.9-95.9%) and hydrocarbon-generating potential (14.3-142.8mg/g), (2) the drilling and logging data shows that coals are developed in multiple seams with thin single seam thickness and unstable plane distribution, and their logging responses are high neutron porosity, high acoustic interval transit time, high resistivity, low natural gamma ray, and low lithology density, (3) coal seams in Yacheng Formation mostly form by the gelatification and are deposited in the peat swamp environments of braided river delta plain, fan delta plain, and upper intertidal zone and supratidal zone in tidal flat, and (4) the relatively gentle paleotopography and the approximately equivalent sedimentary rate and subsidence rate are the two key control factors of the development of coal measure strata. According to the above conclusions, three favorable development areas of high quality coal measure source rocks in Yacheng Formation are predicted, including Yacheng area of western Qiongdongnan Basin, northeastern slope and southern slope of the basin.

This research is financially supported by National Natural Science Foundation of China (No. 40702023), Key Laboratory of Tectonics and Petroleum Resources (CUG), Ministry of Education (No. TPR-2009-16), CAS Key Laboratory of Marginal Sea Geology, Guangzhou Institute of Geochemistry (No. MSGL09-03), and Key Lab of Submarine Geosciences, SOA (No. KLSG0801).

https://doi.org/10.1180/S0026461X00006502 Published online by Cambridge University Press

Biogeochemical characteristics and environmental effects of low-molecular-weight organic acids in lacustrine ecosystem

M. XIAO[1] AND F.C. WU[2]*

[1]The State Key Laboratory of Environmental Geochemistry, Institute of Geochemistry, Chinese Academy of Sciences, Guiyang 550002, China (xiaomin@mails.gyig.ac.cn)
[2]Chinese Research Academy of Environmental Sciences, Beijing, 100012, China
(*correspondence: wufengchang@vip.skleg.cn)

Low molecular weight organic acids (LMWOAs), are generally considered as the important immediate products during the conversion of anaerobic organic substance (carbohydrates, fats, proteins, etc.) into CH_4 and CO_2, and closely related to lacustrine regional environmental evolution [1, 2]. In this research, the composition and contents of LMWOAs were determined, temporal-spatial variation trends and their contributions to dissolved organic carbon (DOC) were investigated in overlying waters of two plateau lakes in China: Lake Hongfeng (HF) and Lake Dianchi (DC) where two sampling sections were set as P1 and P2. Total organic acids (TOAs) were on average 6.55 μmol·L^{-1} in HF, 7.98 and 6.54 μmol·L^{-1} in DC, which can contribute to total DOC approximately 7.47%, 2.67% and 2.48%, respectively. This study identified 5 key organic acids such as lactic, acetic, pyruvic, sorbic and oxalic acid. The results show that pyruvic acid in these two lakes was confirmed as the major component among LMWOAs with the average concentrations of 2.35 μmol·L^{-1} in HF, 3.82 and 3.35 μmol·L^{-1} in DC. The sources and behaviors of LMWOAs during the photoradiation on lacustrine dissolved organic matter were also discussed. Differential physicochemical parameters indicated that the increasing-decreasing and decreasing-increasing diurnal variation trends of TOAs at two sampling sections in DC were dependent on autochthonous biological and photochemical activity. TOAs in HF decreased with time, mainly due to strong microbial assimilation and mineralization in hypolimnion. LMWOAs' photochemical production from allochthonous humus and consumptiom in epilimnion of HF basically leveled off with time except for significant increase at 18:00, indicative of their direct terrestrial import. The increase of pyruvic acid in epilimnion in HF at night reflected a photoradiation hysteresis effect, and resulted from great algal decomposition. Various hydrochemical conditions revealed that massive algal cover in DC and thermal stratification in HF primarily controlled the profile behavior of decrease and increase for LMWOAs. This research would benefit for management and eco-regulation of lacustrine aquatic environment.

[1] Boschker *et al*. (2001) *FEMS Microbiol Ecol* **35**, 97-103
[2] Xiao *et al*. (2009) *J Hydrol* **365**, 37-45

Redefine Bulunkuole group in eastern Pamirs syntaxis and its signification – From the evidence of LA-ICP-MS isotope dating of detrital zircon

PEI-XI XIAO, XIAO-FENG GAO, LEI KANG, ZENG-CHAN DONG, LEI GUO AND REN-GANG XI

Xi'an Center of Geological Survey (Xi'an Institute of Geology and Mineral Resource), CGS, Xi'an, Shaanxi 710054, China (xaxpeixi@163.com)

The Bulunkuole Group is riching in iron ore Paleoproterozoic mesometamorphic rock series distributing in the eastern Pamirs syntaxis. According to sedimentary formation, metamorphism, ore-bearing potential and isotope dating, we disassemble these high pressure rock association (metamorphosed in 220Ma) which is composed of granulite, spinel olivine, garnet pyroxenolite from Bulunkuole Group, belong to the part of Kangxiwar tectonic mélange; The rock series of alterative volcanic rock folding alterative detrital rock (age is 522Ma) belongs to Ordovician. In fact, the Bulunkuole Group is composed of alumina rich gneiss and schist, gneiss and schist folding quartzite and griotte, schist and calc-silicate rock folding metavolcanite and iron ore depsits from bottom to top, and it is intruded by early Palaeozoic (506-542 Ma) acidic to intermediate rocks. There are four peak values of age region: 2.7-2.1Ga, 1700-554Ma, 536-344Ma and 302-230Ma in age frequency diagram according to 127 isotope data of detrital zircon (Fig 1). The zircons of the first peak value (2.7-2.06Ga) show the characteristic of magmatic origin, the others were metamorphic origin(or recrystallization). In consequence, the Bulunkuole Group should formed in Paleo-Mesoproterozoic (from 2.14-2.06Ga to 1.14Ga).

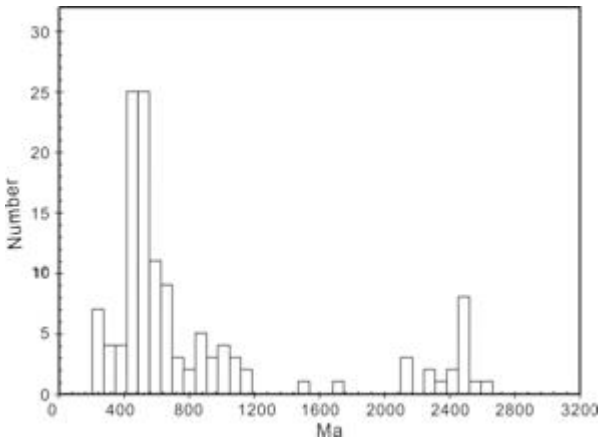

Figure 1 Age frequency diagram of detrital zircons from the Bulunkuole Group

https://doi.org/10.1180/S0026461X00006502 Published online by Cambridge University Press

Effects of melt percolation on platinum group elements and Re-Os systematics of peridotites from the Tan-Lu fault zone, eastern North China Craton

YAN XIAO AND HONG-FU ZHANG

Institute of Geology and Geophysics, Chinese Academy of Sciences (xiaoyan@mail.iggcas.ac.cn, hfzhang@mail.igcas.ac.cn)

Concentrations of PGE and Re-Os isotopic compositions were determined for a suite of variably metasomatised peridotite xenoliths from Cenozoic Beiyan volcanoes within the Tan-Lu fault zone, eastern North China Craton. The majorities of Beiyan peridotites have flat chondrite-normalized PGE patterns whereas their total PGE contents range between 0.97 and 61.4 ppb, which was reduced by more than 90% from lherzolite, cpx-rich lherzolite to wehrlite, probably because intergranular sulfides were completely removed by silicate melt. Meanwhile, Beiyan peridotites have low and variable Re (0.0002-0.5118ppb) and Os (0.194-10.4ppb) abundances and high $^{187}Os/^{188}Os$ (0.12167-0.14978) ratios. The $^{187}Os/^{188}Os$ ratios in some wehrlites are much higher than the value of the primitive mantle. The high $^{187}Os/^{188}Os$ ratios have also been observed in peridotites found in other localities within the Tan-Lu fault zone such as Shanwang and Nüshan. This could be the result of the addition of radiogenic Os during the melt percolation. Extremely low Os abundances in Beiyan peridotites suggest that Os may behave as an incompatible element during melt percolation and could mobilize with the dissolution of sulfides. The suprachondritic $^{187}Os/^{188}Os$ ratios in peridotites within the Tan-Lu fault zone relative to those away from the Tan-Lu fault zone indicate that the Tan-Lu fault zone as a melt infiltrating channel had played an important role in the radiogenic Os enrichment induced by the melt percolation. This could be the reason for the Os isotopic heterogeneity observed in eastern NCC.

Octanol-water partition coefficient (K_{OW}): Is it a good measure of hydrophobicity of nanoparticles?

Y. XIAO AND M. WIESNER*

Duke University, Civil & Environmental Engineering, Durham, NC 27708, USA (*correspondance: weisner@duke.edu)

Hydrophobicity, as one of the key properties of NPs, plays a significant role in the fate, transport and bioavailability of NPs. Octanol-water partition coefficient (K_{OW}) is a traditional measure of hydrophobicity of organic compounds, and has been recently applied to NPs. However, due to the larger size, NPs may not diffuse freely between the phases, which may undermine the fundamental assumption of the application of K_{OW}. Based on thermodynamic models, we hypothesize: (1) partitioning of NPs is controlled by both hydrophobicity and size; (2) amphiphilic NPs with larger size are more likely to stay at the liquid-liquid interface rather than in the bulk phase.

We conducted the K_{OW} measurement using shake-flask method for seven different NPs in aqueous suspensions, including aqueous C_{60} (aqu-C_{60}), tetrahydrofuran-C_{60} (THF-C_{60}), fullerol, nano-gold coated with citrate (Au-Ci), nano-silver coated with PVP (Ag-PVP), citrate (Ag-Ci) and gum arabic (Ag-GA). The hydrophobicity of these NPs was determined in Rose Bengal adsorption experiments. According to our results, the NPs that exhibited greater hydrophobicity showed larger K_{OW}. We also measured the K_{OW} of Au-Ci and aqu-C_{60} NPs aggregates with different size (10 ~ 100 nm). Our results showed that as size increased, K_{OW} of aqu-C_{60} increased, however, K_{OW} of Au-Ci was not dependent on size. Dark field microscopy revealed that Au-Ci NPs with size less than 30 nm mainly remained in bulk water phase; while the majority of Au-Ci NPs with size around 100 nm were accumulated near the water-octanol interface. These results may be due to the amphiphilic property (K_{OW}=0.38) and larger size of Au-Ci NPs, which might elevate the attachment energy of particles to the interface and consequently the attachment became irreversible. Overall, our study demonstrated that size, in addition to hydrophobicity, is an important factor to determine the partitioning of NPs. The current application of K_{OW} as a measure of hydrophobicity for NPs is inherently flawed and needs further investigation.

https://doi.org/10.1180/S0026461X00006502 Published online by Cambridge University Press

Li isotopic composition of subduction-related leucogranites: Source tracking and tectonic implications

YILIN XIAO,[1]* LIJUN XU[1], YONGJUN GAO[2], SHUGUANG LI[1], HE SUN[1] AND HAIOU GU[1]

[1]School of Earth and Space Sciences, University of Science and Technology of China, Hefei, 230026, China (ylxiao@ustc.edu.cn)

[2]Department of Earth and Atmospheric Sciences, University of Houston, Houston, TX 77204, USA

We report lithium (Li) elemental and isotopic data for a suite of leucogranitic and gneissic rocks (presumed protolith of the leucogranites) from the boundary between the North China craton (NCC) and the South China plate (SCP), which represents an important repository for understanding the Mesozoic thinning processes of the NCC. The leucogranites have very low Li concentrations (around 1-8 ppm) but extremely heavy isotopic compositions (from 8.6 to 16.1). Overall, Li concentrations and isotopic compositions of the leucogranites are different from those of associated rocks from adjacent areas, including granites (δ^7Li =2.7-3.8) and gneisses (δ^7Li = 0.8-6.5) from North Dabie, garnet-bearing gneisses (δ^7Li =2.2-4.2) from South Dabie, as well as those of their host rock–the Archean gneisses (δ^7Li =-0.6 to 0.0), but are similar to those of garnet-bearing gneisses (δ^7Li =1.2- 22.5) from the Sulu area. Based on Li isotope data, with the combination of mineralogical (e.g., garnet) and other geochemical data, we suggest that the leucogranites resulted from the partial melting of the subducted gneisses from the Sulu area. Such an observation is very important for providing constraints on the subduction direction of the SCP during the Triassic UHP metamorphic event.

Trace element redistribution in oceanic crust during subduction-zone metamorphism – Evidence from Western Tianshan, China

YUANYUAN XIAO[1]*, YAOLING NIU[1,2], HUAIKUN LI[3], HUICHU WANG[3], JON DAVIDSON[1] AND XIAOMING LIU[4]

[1]Durham University, UK (yuanyuan.xiao@durham.ac.uk; yaoling.niu@durham.ac.uk; j.p.davidson@durham.ac.uk);

[2]Lanzhou University, China;

[3]Tianjin Institute of Geology, China (tjlhuaikun@cgs.gov.cn; tjwhuichu@163.com);

[4]Northwest University, China (xmliu@nwu.edu.cn)

Constraining the geochemical consequences of subduction-zone metamorphism (SZM) is important for understanding subduction-zone magamism, crustal growth and the origin of mantle compositional heterogeneity. For this purpose, we have conducted a detailed trace element study on ultra-high pressure metamophic (UHP) rocks of both basaltic and sedimentary protoliths from Western Tianshan, China using *in situ* LA-ICP-MS.

We found that during SZM, phengite, and to a lesser extent, paragonite, are major hosts of all the Ba, Rb and Cs. Paragonite also hosts some Sr and Pb. Epidote group minerals host 95% of LREEs, Th, U, Pb and Sr, 60% of MREEs and 30% of HREEs. Garnet preferentially hosts HREEs relative to progressively lighter REEs. Rutile and titanite host essentially all the Ti, Nb and Ta. Titanite also hosts some Sr, Pb and REEs. Retrograde albite can host some Sr and Ba. Glaucophane and (sodic-)calcic amphiboles, omphacite and chlorite contain very low contents of these incompatible elements (except Li). In addition, analyses of coexisting paragonite and clinozoisite, preserved as lawsonite pseudomorphs in garnet, show $Kd^{clinozoisite/paragonite}$ for Pb and Sr to be ~ 20 and 4-10 respectively.

Because lawsonite, epidote, garnet, titanite and rutile are stable over a large P-T range during SZM and can exchange REEs, Th, U and HFSEs among each other, these elements are largly redistributed in the newly-formed minerals without significant loss from the system, explaining their relatively immobile nature. Sr and Pb may have been mobilized as shown by their decrease towards rims of prograde clinozoisite, which is also consistent with the insignificant correlations of bulk-rock Sr and Pb with immobie HFSEs. Ba, Cs and Rb are mobile in rocks of basaltic protolith and could have been re-enriched by late infiltrated fluids (e.g., some retrograde mica crystals have very high Ba, Cs and Rb), whereas these same elements may be immobile in rocks of sedimentary protolith, reflecting stronger protolith controls on elemental behavior.

https://doi.org/10.1180/S0026461X00006502 Published online by Cambridge University Press

Mobilization and re-distribution of major and trace elements during extreme weathering of basalt in Guangzhou Province, South China

XIAO ZHONGFENG[1,2] AND ZHAO XIMEI[1,2]

[1]Shandong Provincial Key Laboratory of Eco-Environmental Science for Yellow River Delta, Binzhou 256603, China (xzfazxm@163.com)

[2]Binzhou University, Binzhou 256603, China

Chemical weathering is one of the most important processes that change the chemical composition of the Earth's surface. Weathering products are easily carried out of weathering profiles and deposited in lakes and oceans as the main lithogeneous component in sediments. Therefore, the mobilization and re-distribution of elements during chemical weathering may influence the chemical composition of sediments. Generally, sedimental compositions can be used to trace the provenance of sediments and to reconstruct paleoclimate record [1]. Comprehensive understanding of the behavior of elements during chemical weathering may help to better explain the records found in sediments(Ma et al, 2007; Wei et al, 2004)

Major elements of a laterite profile developed on Neogene basalts in Guangzhou Province, South China were reported in this study. The results indicate that most of the elements have been mobilized and transferred downwards along the profile by aqueous solution. conservative elements during incipient chemical weathering, such as Fe, Ti, Zr, Hf, Nb and Ta, the removals are up to 25–43% in the upper profile. Al, Mn，Ti were significantly enriched in the middle (2-3m) profile, this may indicate there has an paleo-water level. All the REEs are remarkably enriched in the middle and the lower profile.

All the characters of the maior and trace elements are similar as it in the weathering profile of basalt in Hainan island mentioned in Ma *et al*. (2007). These may indicated that the basalt in south China underwent the same process of weathering conditions.

[1] M. Zabel *et al*. Late Quaternary climate changes in central Africa as inferred from terrigenous input to the Niger fan, *Quatern. Res*. **56** (2) (2001), pp. 207–217.

Impact of water-level fluctuations on concentration trends of petroleum contaminants in pipeline leakage area

SU-XIAOSI[1,2] ,WANG-WEI[1,2]* AND ZHENG-ZHAOXIAN[1,2]

[1]Key Laboratory of Groundwater Resources and Environment, Ministry of Education, Jilin University, Changchun, 130021, China (*correspondence:wangwei_wangwei@126.com)

[2]Institute of Water Resources and Environment, Jilin University, Changchun, 130021, China

Overview of Case Study

Monitored natural attenuation is one of the most commonly used remediation technologies which means that groundwater contamination was reduced to safety range by the effect of natural degradation and dilution. In typical area of certain oilfield of china, after the leakage oil cleaning up□most of the high level contamination areas ofgroundwater are at pipeline leakage site and sewage infiltration area. Detected from continuous 12 months monitoring, the TPH□Total petroleum hydrocarbons□ concentration of groundwater show tow types of correlation with water-level fluctuations. Firstly, at the border of pollution plume, water-level fluctuations are positive correlation with TPH concentrations that as the water level raises, The TPH concentration increases in January to June. Secondly, at the middle of pollution plume, water-level fluctuations were always positive correlation with TPH concentrations during the whole monitoring period.

Discussion of Results

The monitoring results show that attenuation of petroleum hydrocarbon contamination did not show a simple exponential or linear law with water-level fluctuations [1]. These results demonstrate that the TPH concentration at the high level (0.1-0.2mg/l), convection-dispersion is main process of monitored natural attenuation, and it is affected by water-level fluctuations significantly. Meanwhile at the low level (0.1-0.2mg/l),adsorption and biodegradation are the main process, which shows Linear attenuation characteristics. All the results indicate that in the study area, if the petroleum hydrocarbon contamination is higher than threshold (0.1-0.2mg/l), it would be appropriate to apply active remediation projects to local groundwater remediation, when lower than the threshold monitored natural attenuation will be more suitable.

[1] Alan E. Kehew, Patrick M. Lynch. *Environ Earth Sci*. Published on line :08 June, 2010.

https://doi.org/10.1180/S0026461X00006502 Published online by Cambridge University Press

Granitic porphyry dykes in the Qitianling batholith, Hunan Province, South China: Evidence for the multistage mineralization

LEI XIE*, RUCHENG WANG, JINCHU ZHU AND WENLAN ZHANG

State Key Laboratory for Mineral Deposits Research (Nanjing University), School of Earth Sciences and Engineering, Nanjing University, Nanjing 210093, China (*correspondence: xielei@nju.edu.cn)

The Qitianling Sn deposit, Hunan Province, China, is famous for its super-large reserves. Two granitic dykes enriched in Sn at Qitianling are subvolcanic counterpart of Sn-bearing granites. Textural relationships provide evidence for a quenched silicate melt with phenocrysts, consisting of albite, quartz, K-feldspar, and zinnwaldite. The porphyry tin deposit arises from abundant cassiterite and rutile enriched in W and Nb. An affinity with Qitinaling (amphibole-) biotite granites arises from the geochemistry and their compositions are quite similar to each other. It is highly evolved, strongly peraluminous and enriched in W, Sn, Nb, Ta, Li and F. The melt belongs to the residual melt throughout the fractional crystallization. Analyses of zircon proved the high evolution of the source. Different textures of cassiterite grains provided the magmatic and hydrothermal process. The result of geochronological work shows the zircon U-Pb age of the dyke of 147.15 ± 0.45 Ma, providing that it belongs to the third stage of Qitinaling magmatism. The formation of a porphyry tin deposit is believed to be one of the last events at Qitianling. This super hypabyssal intrusive mass contains cryptoexplosive breccia. The occurrence at depth of a hidden granitic body could be the source of the granitic dykes. Therefore the fine-grained Qitinaling felsic dykes is appropriate recorder for the concealed granitic body and mineralization. The late-stage mineralization related to the fine-grained granitic dyke is believed to be distinguished important in the multi-stage mineralization.

Response of Antarctic Intermediate Water to weaker Atlantic Meridional Overturning Circulation during the last deglaciation

RUIFANG XIE[1]*, FRANCO MARCANTONIO[1] AND MATTHEW W. SCHMIDT[2]

[1]Texas A&M University, Department of Geology and Geophysics, MS 3115, College Station, Texas 77843 (*correspondence: xie_1984@tamu.edu, marcantonio@geos.tamu.edu)

[2]Texas A&M University, Department of Oceanography, MS 3146, College Station, Texas 77843 (schmidt@ocean.tamu.edu)

The modes of ocean circulation in response to climate change have been a subject of intense interest. During the last deglaciation, cold periods such as the Younger Dryas (YD) and Heinrich 1 (H1) are thought to be coincident with significant reductions in North Atlantic Deep Water (NADW) formation. Yet, the role that Antarctic Intermediate Water (AAIW) played during these cold events is still poorly constrained. Benthic Cd/Ca data from sediment cores in the Florida Straits suggest a reduced contribution of AAIW in the North Atlantic western boundary current during the YD [1]. However, ε_{Nd} evidence in sediment cores from Tobago basin and Brazil margin suggests a greater influence of AAIW in the North Atlantic during YD and H1 [2].

In this study, we measure Nd radiogenic isotope ratios of the authigenic Fe-Mn hydroxides in two sediment cores, KNR166-2-26JPC (546 m water depth) and KNR166-2-31JPC (751 m water depth), within the Florida Straits in an effort to investigate the waxing and waning of AAIW during the last deglaciation. Both cores are located within the Florida Current, which under modern conditions represents a mixture of recirculated North Atlantic subtropical gyre water and Southern origin waters. Our preliminary results for both cores show significantly less radiogenic ε_{Nd} values during the YD than during the Holocene (~1 epsilon unit for 26JPC and ~0.6 epsilon units for 31JPC). We interpret the lower ε_{Nd} during the YD as signifying a decreased input of Southern-sourced waters arriving at these sites, in agreement with the study of Came et al.[1]. Additional high-resolution Nd isotope analyses of Florida Straits sediments deposited during earlier Heinrich Events and the Last Glacial Maximum will be presented in an effort to constrain the role of intermediate waters during periods of reduced NADW formation.

[1] Came et al. (2008) *Paleoceanography* **23**, PA1217 [2] Pahnke et al. (2008) *Nature Geoscience* **1**, 870-874

https://doi.org/10.1180/S0026461X00006502 Published online by Cambridge University Press

Study on decision support system for water pollution control of ShaYing River

XIAOYAN XIE[1]*, LIANGMIN GAO[2] AND XIAOQING LIU[2]

[1]School of Mechanical Engineering, An Hui University of Science and Technology, Huainan 232001, China (*correspondence: xyxie@aust.edu.cn)
[2]School of Earth and Environment, An Hui University of Science and Technology, Huainan 232001, China

According to the survey on water quality, hydrology, geography of ShaYing River, water pollution situation is analyzed. Aiming at this serious problem, the present situation of water pollution is analysed, the decision support system of ShaYing River water pollution control is analyzed completely and studied. From the standpoint of development process, functional design, framework and modularization design, using GIS technology and object-oriented programming language Visual Basic, the system with visual interface is exploited with MapObjects of GIS and database. Intelligent management of ShaYing River water pollution control come true, the system achieves functions of inputting information , treating data , searching information, thematic maps, water quality evaluation and water quality prediction, which can help data management, searching and assistant decision for water environment. It will provide a powerful tool and intelligent decision information for ShaYing River's water environment management in the future.

Research supported by Study on Water Pollution Control Decision Support System of the Lower Shaying River valley (No. 2008ZX07010-003-04)

The geochemical characteristics of the Mashan complex, Guangxi, and its geological implications

Z. XIE*, B. WANG, J.F. CHEN AND Z. LI

School of Earth and Space Sciences, University of Science and Technology of China, Hefei, 230026 (*correspondence: zxie@ustc.edu.cn)

Previous Nd isotope studies about the Mesozoic granitoid intrusions in South China suggested that some bodies formed a southwest-northeast belt with low Nd model ages (T_{DM}) in range of 1.7-1.2 Ga, lower than those of adjacent intrusions. It is also suggested that their magma sources and formation progresses should be related to the crustal extension and asthenosphere upwelling.

The detailed geochemical and geochronological studies about the Mashan complex, Guangxi suggest one possibility that the the magma source of the low T_{DM} intrusions was derived from the partial melting of the Neoproterozoic juvenile mantle. The complex includes diabase porphyrite, diorite porphyrite, syenite porphyry, quartz-syenite porphyry and granite porphyry. Their zircon SHRIMP U-Pb ages are in range of 154-148 Ma, indicating that the complex was formed in a short time. The major and trace element compositions of these rocks suggest that they were derived from one mantle source without Nb, Ta negative anomaly. The $\varepsilon_{Nd}(t)$ of diabase is +2.3, T_{DM}(II) is 0.7 Ga, those of diorite and syenite are +5.9~-+2.6 and 0.7~0.5 Ga, those of quartz-syenite are +0.4 and 0.9 Ga, and those of granitic rocks are -0.3~-2.4 and 1.1~1.0 Ga. The zircon $\delta^{18}O$ of diabase is 6.2‰, that of diorite is 5.7‰, which are close to the mantle value of 5.6‰, however, those of granitic and quartz-syenite are 7.2‰ and 7.5‰, respectively, suggesting that the quzrtz-syenite and granites were slightly contaminated by crustal rocks. The zircon Hf model ages of the grains with ages in 160-140 Ma are mainly in range of 1500-600 Ma calculated by felsic crust, and form a peak value at 1000 Ma.

It is conlcuded that the complex was derived from the partial melting of juvenile lithosphere mantle formed in the Neoproterozoic, triggered by the lithosphere extension and asthenoshphere upwelling. After that, the magma was experienced strongly fractional crystallization. However, the granitic magma was contaminated by crustal materials, which may differentiated from the mantle during the Neoproterozoic and remelted in about 175-160 Ma. It should not be ruled out the contribution of the asthenosphere to the basic rocks.

This study is supported by funds from the Natural Science Foundation of China (40873002, KZCX2-EW-QN508).

https://doi.org/10.1180/S0026461X00006502 Published online by Cambridge University Press

REE deposits in China

CHENG XU[1]*, JINDRICH KYNICKY[2] AND ANTON R. CHAKHMOURADIAN[3]

[1]Laboratory of Orogenic Belts and Crustal Evolution, Peking University, Beijing 100871, China (*correspondence: xucheng1999@hotmail.com)
[2]Mendel University of Agriculture and Forestry, Brno, Czech Republic (jindrak@email.cz)
[3]University of Manitoba, Winnipeg, Manitoba, Canada (chakhmou@cc.umanitoba.ca)

Rare earths are relatively abundant in the Earth's crust, but discovered minable concentrations are less common than for most other ores. China, the United States, Russia, India, Malaysia and Brazil constitute the largest percentage of the world's rare earth economic resources. The REE deposits in China are mainly related with carbonatite-alkaline complexes, weathered granite and placer (Fig. 1). The Bayan Obo is largest LREE deposit in the world, and its reserves are more than 13500 Mt. LREE deposits in carbonatite-alkaline complexes from Panxi region (West China) and Miaoya (Central China) are also large. The weathered granite-type REE deposits in South China are characterized by REE, especially HREE adsorption in clay minerals. The origin of Bayan Obo deposit is disputed, including carbonatite magmas, sediment, and carbonatite-derived fluid mixing sediment [1]. Studies suggested that the anomaly high REE compositions in mantle source and mineral fractional crystals and carbonate cumulate processes are key cases for the REE deposit formation related with carbonatite-alkaline rocks [1, 2]. The weathered REE deposits in South China were formed by leaching granites, and REE adsorbed by clay minerals. The precondition requires the granites contain abundant REE minerals. But how the granite can produce the primary REE minerals is not clear. Granite is quite normal rock in world, but not all of them can supply sufficient REE for mineralization. It is necessary to study the primary granite magma type REE deposits.

[1] Xu et al. (2008) *Lithos* **106**, 12-24. [2] Xu et al. (2010), *Lithos* **118**, 145-155.

Re-Os geochronology of black shale from the Barents Sea: Refining the Triassic time scale

G. XU[1,2], J.L. HANNAH[1,2], H.J. STEIN[1,2], A. MØRK[3,4], B. BINGEN[2] AND B.A. LUNDSCHIEN[5]

[1]AIRIE Program, Colorado State University, Fort Collins, CO 80523-1482 USA (Guangping.Xu@colostate.edu)
[2]Geological Survey of Norway, NO-7491 Trondheim, Norway
[3]SINTEF Petroleum Research, NO-7465 Trondheim, Norway
[4]Norwegian University of Sciences and Technology, NO-7491 Trondheim, Norway
[5]Norwegian Petroleum Directorate, NO-4003 Stavanger, Norway

Stage boundaries in the currently accepted Triassic time scale differ by as much as 8 Ma from those in a proposed "alternate" Triassic time scale [1]. Re-Os isochron ages combined with biostratigraphy for black shales from Kong Karls Land, Spitsbergen, and Svalis Dome in the Barents Sea help resolve these differences.

Drill core samples of black shales of the upper Ladinian Botneheia Formation next to the Kong Karls Land (easternmost Svalbard archipelago) [2], inferred to be near the Ladinian-Carnian boundary, yield a precise Model 1 Re-Os isochron age of 239.2 ± 0.4 Ma. Another section from 8 meters deeper in the same drill core yields a less precise but nominally younger age of 237.1 ± 2.3 Ma, though the two ages overlap within uncertainty. The black shale section from a nearby drill core [2], inferred to be the Carnian Tschermakfjellet Formation, yields a Model 1 age of 228.9 ± 1.4 Ma. In a previous study at Svalis Dome in the Barents Sea [3], a Re-Os isochron age of 239.3 ± 2.7 Ma was determined for the Botneheia Formation, shown by palynology to be uppermost Anisian. Together these results suggest a very short duration for the Ladinian Stage (a few million years), and support the "Alternate Time Scale for the Triassic" proposed by Ogg et al. [1], where the Ladinian Stage is from 240.5 to 236.8 Ma.

Our results affirm the utility of the Re-Os chronometer for dating black shales and correlating paleogeographically separated regions in absolute time.

This work is funded by Petromaks - NFR 180015/S30

[1] Ogg et al. (2008) *The concise geological time scale*. Cambridge University Press, 177 pp. [2] Riis et al. (2008) *Polar Research* **27**: 318-338. [3] Xu et al. (2009) *EPSL* **288**: 581-587.

https://doi.org/10.1180/S0026461X00006502 Published online by Cambridge University Press

Structure and stability of nickel hydroxide at high T-P conditions

H. XU[1]*, D.D. HICKMOTT[1], J. ZHANG[2], Y. ZHAO[2], S.C. VOGEL[2] AND L.L. DAEMEN[2]

[1]EES Division, Los Alamos National Laboratory, EES-14, MS-H805, Los Alamos, NM 87545, USA (*correspondence: hxu@lanl.gov)
[2]LANSCE Division, Los Alamos National Laboratory, LANSCE-LC, MS-H805, Los Alamos, NM 87545, USA

Nickel hydroxide, $Ni(OH)_2$, belongs to the CdI_2-type, layered hydroxide family $M(OH)_2$ (M = Mg, Ca, Ni, Co, etc.) and is of interest from the crystal-chemical viewpoint, as it provides a model structure for studying hydrogen-mediated interatomic interactions. $M(OH)_2$ phases are also interesting for studying Earth's deep water cycle. Though uncommon in the deep Earth, they are present as component units in the structures of many hydrous minerals (such as hydrous magnesium silicate phase E), which are potential hosts for water in the mantle. In addition, $Ni(OH)_2$ is a cathode material in Ni-based rechargeable alkaline batteries. Thus studying the structure and stability of $Ni(OH)_2$ at various conditions is of significance both geologically and for its practical applications.

In this study, using *in situ* time-of-flight neutron and energy-dispersive synchrotron X-ray diffraction, we have examined the structure and stability of nickel hydroxide at temperatures up to 623 K and/or pressures up to 8 GPa. To avoid the large incoherent scattering of neutrons by hydrogen, a deuterated sample $Ni(OD)_2$ was synthesized and used for neutron experiments. For synchrotron experiments, both $Ni(OH)_2$ and $Ni(OD)_2$ were measured, allowing studying the H/D isotopic effects. Rietveld analysis of neutron data and peak fitting of synchrotron patterns allowed determination of coefficients of thermal expansion, bulk moduli and other thermoelastic parameters. Moreover, the atomic positions and atomic displacement parameters, particularly of D, have been obtained, and the role of hydrogen-mediated interatomic interactions in the mechanisms of compression, thermal expansion and phase stability of nickel hydroxide are discussed. These results are also compared with those of other $M(OH)_2$ phases to determine the structural and stability systematics of the $M(OH)_2$ family.

Recycling of lower continental crust in an intra-continental setting: Mineral chemistry and oxygen isotope insights from websterite xenoliths in the North China Craton

W.L. XU[1,2], Q.J. ZHOU[1], F.P. PEI[1], D.B. YANG[1], S. GAO[2], W. WANG[1] AND H. FENG[1]

[1]College of Earth Sciences, Jilin University, Changchun 130061, China (xuwl@jlu.edu.cn, perplesky@126.com, peifp@jlu.edu.cn, yangdebin@jlu.edu.cn, wangwei@jlu.edu.cn, hfeng@263.net)
[2]State Key Lab of Geological Processes and Mineral Resources, China University of Geosciences, Wuhan 430074, China (sgao@263.net)

A suite of websterite xenoliths entrained by the Early Cretaceous Feixian basalts in the eastern North China Craton provide direct evidence for recycling of dense lower continental crust in an intracontinental setting. Petrographic observations indicate that olivines within the xenoliths are replaced by orthopyroxenes, which in turn are replaced by clinopyroxenes. The $\delta^{18}O$ values of olivines from websterite xenoliths vary from 7.1 ‰ to 7.6 ‰ (±0.4‰, 2SD). The Ni contents of the orthopyroxenes and clinopyroxenes in the websterites are much higher than those of mantle-derived harzburgite and lherzolite xenoliths within the Early Cretaceous high-Mg diorites, and of phenocrysts within the Late Cretaceous basalts. Clinopyroxenes in the websterite xenoliths have high $^{87}Sr/^{86}Sr$ ratios (0.70862–0.70979). These findings, together with high initial $^{86}Sr/^{87}Sr$ ratios (0.70977–0.70990) and low Nd(t) values of the host basalts (–13.1 to 13.4) [1], indicate that the melt, which modified the lithospheric mantle, could be derived from partial melting of the delaminated eclogitic continental crust. Therefore, our study shows that the intracontinental recycling of lower continental crust is a key factor not only to result in chemical and isotopic enrichment in the subcontinental lithospheric mantle [2], but also to result in compositonal variations of intracontinental basalts [1, 3].

This research was financially supported by National Basic Research Program of China (2009CB825005) and the NSFC (90814003 and 90714010).

[1] Gao *et al*. (2008) *Earth Planet. Sci. Lett*. **270**, 41–53. [2] Xu *et al*. (2008) *Earth Planet. Sci. Lett*. **265**, 123–137. [3] Liu *et al*. (2008) *Geochim Cosmochim Acta* **72**, 2349–2376.

https://doi.org/10.1180/S0026461X00006502 Published online by Cambridge University Press

Geochemistry and petrogenesis of the Carboniferous-Permian granitic magmatism in Tianshan, Northwestern China

XUE-YI XU[1], HONG-LIANG WANG[1,2], PING LI[1], JUN-LU CHEN[1] AND WANG NING[1]

[1]Xi'an Center of Geological Survey (Xi'an Institute of Geology and Mineral Resource), CGS, Xi'an, Shanxi 710054, China

[2]State Key Laboratory of Continental Dynamics, Department of Geology, Northwest University, Xi'an, Shanxi 710069, China)

The Carboniferous-Permian grantic magmatism developed strongly in Tianshan orogenic belt , which are composed of various rock types in diversified geodynamic settings. It not only concludes diorite, monzogranite, tonalite, plagiogranite of calc-alkaline series, but also syenite, quartz syenite, albitophyre of alkaline series. Via comparison of petrogenesis, geochemistry, and magma- processes of granitic rocks , the granitic rocks related to different tectonic units can show that the granitic rocks formed during the period of Carboniferous-Permian are mainly calc-alkali series. The Carboniferous-Permian granitic rocks developed in Eastern Tianshan and Bogda rift zone, containing more MgO, TiO_2, Na_2O and less K_2O, Nb, and Th than the granitic rocks developed in ancient micro-terrain and its edge, means a different source. The granitic rocks in the rift zone formed by the mixing processes of the crust and mantle, containing different degrees of crust-derived components, usually are closely related to intermediate-acid volcanics. However, the granitic rocks developed in ancient micro-terraint mainly show strong information about crust source. The chemical composition of granitic rocks formed in the same tectonic settings but developed in different regions also is different. For example, the Tomor Peak granitic rocks developed in Western Tianshan, and the Kuruktag granitic rocks developed in the south of Central and Eastern Tianshan are all formed by crust source. But the former rocks possesses more Mg, K, Nb, Sr and less Zr, Ba than the latter. This shows some differences of crustal components added in Eastern Tianshan and western sections. Moreover, the positive εNd value of granitic rocks developed in the study region may be caused by partially melting of mantle-derived volcanic rocks.

This study was supported by the National Natural Science Foundation of China (Grant No. 40872061)

Geochemical characteristic contrast of heavy metals between sulphide mines and oxide mines

ZHENGQI XU[1,2,*], SHIJUN NI[2], YANGUO TENG[1] AND CHENGJIANG ZHANG[2]

[1]College of Water Science, Beijing Normal University, Beijing, 100875, China (*correspondence: xuzhengq@163.com)

[2]Department of Geochemistry and Nuclear Resource Engineering, Chengdu University of Technology, Chengdu, 610059, China

Sulphide mines have always been the concerns of people because of their various forms and the resultant environmental problems, whereas oxide mines are paid less attention and not studied much because they do not cause obvious environmental problems. However, the potential environmental problems caused by oxide mines can not be ignored. The author chooses Panzhihua V-Ti-Magnetite, a famous oxide mine in China, as the subject of research. The geochemical characteristics of heavy metals in various environmental media (such as water, soil, and atmosphere) during the process of mining are systematically studied by using the above media as research carriers and employing the analyzing methods of ICP-MS and ICP-AES.

The results show that the geochemical characteristics of heavy metals in the sulphide mines and oxide mines have both similarity and difference. The biggest differences are: the content of chalcophile elements in environmental media of sulphide mines is far higher than that in oxide mines; the worst pollution of oxide mines is caused by atmosphere dust and heavy metals, while the worst pollution of sulphide mines is caused by acid mine drainage. The similarity between the two mines is that their morphological features are same.

Moreover, compared with the sulphide mines, the geochemical characteristics of the oxide mines are: it is mainly polluted through atmosphere circulation; its primary pollution medium is lithometeor; its most remarkable environmental problem is heavy metal pollution and geologic disasters. The oxide mine has potential geochemical hazards, which always break out with change of physical and chemical conditions.

https://doi.org/10.1180/S0026461X00006502 Published online by Cambridge University Press

Environmental effects of the Zarand coal mines and coal washing plant in Kerman Province, Southeast Iran

ABDOLMAJID YAGHUBPUR AND BAHAREH HAKKAKZADEH

Tarbiat Moallem Univ. 49 Mofateh Av. Tehran , Iran. (ayaghubpur@yahoo.com)

The Zarand coal mines are located 80 Km northwest of Kerman, southeast Iran. The coal seams are situated in a large synclinal structure and the age of the coal based on their fossil contents is late Triassic to early Jurassic. Several openings in this mining area are presently operating with various names such as Pabdana, Babnizu, Khomrud, etc. In the vicinity of the Zarand coal mines there is a coal washing plant that reduces the amounts of coal ash to 10-12 percent. The excess amounts of the ashes are sent to a pool that was constructed near the plant.

At present more than 6 million tons of waste materials are piled up in the dumping areas and the sedimentary basins near the coal washing plant. Every year the amounts of the additional wastes are estimated to be more than 400000 tons.

In this investigation water, soil, mines wastes of the coal washing plant (ancient and recent), coal concentrates, and the coals from various active and abandoned mines were sampled. After accurate sampling, the samples were precisely prepared for laboratory examinations.

The results of different chemical analyses on the waste materials of the coal washing plant indicated that the amounts of As Pb, Cu, Fe, K, Mn, Mg, Ni and Ca are higher than the standard amounts of these elements in the coal mining industries of other parts of the world. The amounts of As, Cu, Fe, Mo, Mn, Pb and Zn are also high in the coal samples of the of the coal mines. The abundance of these elements in coal during mining and coal washing processes could be considered as the source of contamination of soils and water(underground) in the mining areas. So, the water from the wells located in the areas downwards the coal washing plant are contaminated with the several toxic and semi toxic elements and should not be used for drinking purposes.

Direct (U-Th)/He dating of native metals

O.V. YAKUBOVICH[1], S.Z. YAKOVLEVA[2], E.B. SALNIKOVA[2], A.B. KOTOV[2] AND YU.A. SHUKOLYUKOV[1,2]

[1]Saint-Petersburg State University, department of Geology, Universitetskaya emb. 7/9, Saint-Petersburg, 199034, Russia (cubiko@mail.ru)

[2]Institute of Precambrian geology and geochronology, Russian Academy of Science, Makarova emb. 2, Saint-Petersburg, 199034, Russia (xekrarne@gmail.com)

Relatively quick migration of helium from crystal structures has been known for a long time. However, there is a group of minerals – native metals – where the stability of helium is anomalously high: (a) native metals have the highest volume density, therefore helium migration is hindered in comparison with other minerals; (b) helium, due to its very low solubility in metals, assembles in atomic clusters - "bubbles" of nanometre size. Migration of helium "bubbles" as a whole from the crystal structures needs relatively high temperature near the melting point of metals [1].

Native metals contain ~10^{-7} g/g of uranium in average. Nevertheless, the concentration of radiogenic helium in native metals is sufficient for detection.

In our work we used the following experimental setup: mass-spectrometer complex MSU-G-01-M ("Spektron-Analit", Russia) with a constant magnetic field. The sensitivity of the spectrometer for ^{4}He determination is ~10^{5} atoms. It allows us to reliably detect radiogenic ^{4}He in the samples of microgram weight. The concentration of U was determined by the isotope dilution analysis with ^{235}U tracer. The results of U analyses in parallel aliquots are reproduced within the accuracy of 0.5%. The blank level did not exceed 1 pg of U. Isotopic composition of U was determined on Finnigan MAT-261 multicollector mass-spectrometer.

Due to a strong heterogenity of uranuim distribution in native gold we have performed the measurements of uranium and helium concentrations in a single gold granule. In order to avoid uranium loss during the helium extraction, the gold sample was put in a sealed pumped out quartz tube.

We are going to discuss the first results and draw a conclusion about the possibility of using (U-Th)/He method for the direct dating of native gold and other native metals.

This work is supported by RFFI and Carl Zeiss company

[1] Shukolyukov, Yakubovich, Rytsk (2010), *Doklady Earth Sciences*, **430**,1, 243-247

https://doi.org/10.1180/S0026461X00006502 Published online by Cambridge University Press

Modeling of the role of organic matter in the carbonate system seasonal changes in the Barents Sea

EVGENIY YAKUSHEV AND KAI SØRENSEN

Norwegian Institute for Water Research, Gaustadalleen 21, Oslo, 0349, Norway, (eya@niva.no)

This work aimed in studying of the role of seasonality of the biogeochemical processes of organic matter production and decay in the seasonal changes of the carbonate system (pH, pCO2, aragonite saturation). Data received at a transect Tromsø – Spitsbergen with a Ferrybox equipped SOOP vessel was used for verification. A 2D simplified vertical model was used to parameterize the hydrophysical processes of at a Coast-Open Arctic section. The biogeochemical processes were parameterized using OxyDep, simplified biogeochemical model aiming time scales seasonal and larger, that considered inorganic nutrient (NUT), dissolved (DOM) and particular (POM) organic matter and biota (BIO). Dissolved inorganic carbon (DIC) and alkalinity (Alk) were considered as independent model parameters. DIC changes were correlated with NUT using Redfield ratio, Alk was changed in the marine boundary of the modeled transect. The carbonate system equilibration was considered as a fast process and calculated at every time step using an iteration procedure. The carbonate system modeling was described on the base of standard approach. According to the model estimates the summer formation of DOC and POC and their further destruction can play a compatible role in the carbonate system seasonal dynamics. Modeled seasonal variations of pH (~0.2) are close to the observed ones t, i.e. 7.94-7.99 in February and 8.04-8.16 in August (pH(Tot)).The received results allowed to demonstrate that the upper layer water pCO2 varies from 480 ppm in winter to minimum values of 280 ppm during the OM production period. Therefore summer invasion of CO2 should be replaced by winter evasion.

Decompression melting in tectonics: Where's the melt?

C. YAKYMCHUK[1], F. KORHONEN[2] AND M. BROWN[1]*

[1]Laboratory for Crustal Petrology, Department of Geology, University of Maryland, College Park, MD 20742, USA (*correspondence: mbrown@umd.edu)

[2]Department of Applied Geology, Curtin University, Perth, WA 6845, Australia

The presence of melt in the continental crust influences tectonics. Using petrogenetic grids and pseudosections for fertile bulk compositions, multiple authors have invoked decompression across hydrate-breakdown melting reactions as an important factor enhancing exhumation and the development of gneiss domes, and in the production of late orogenic granites. However, the amount of melt that can be produced during decompression is strongly dependent on the fertility of the crust at the *T* of interest and the melt generated may be quite small if, as expected, melt is lost each time the melt fraction reaches the melt connectivity transition (MCT) at 7 mol% (~7 vol%). Thermodynamic modeling of an average amphibolite facies metapelite was undertaken in the NCKFMASHTO system using THERMOCALC and the Holland & Powell dataset to investigate decompression across the major melt-producing reactions following prograde heating and episodic melt loss. The modeling places constraints on the quantity of melt that can be produced from progressively more residual rocks during decompression. *P–T* pseudosections were calculated for isobaric heating at 1.2 GPa followed by decompression to 0.4 GPa at 750°C, 820°C, and 890°C. Melt was periodically removed from the system at the *P–T* conditions where the melt fraction reached the MCT (85 % of the available melt is extracted); a new bulk composition was obtained and a new *P–T* pseudosection was calculated. For isothermal decompression at 750°C, the protolith produces ~20 mol% total melt; ~8 mol% melt is produced prior to crossing the field where melting associated with Ms + Qtz breakdown is initiated and Kfs starts to grow, and an additional ~6 mol% is produced at $P < 0.5$ GPa. For isothermal decompression at 820°C, the residual composition produces ~3 mol% melt to 0.6 GPa and another ~13 mol% melt within the Crd stability field to 0.4 GPa. At 890°C, isothermal decompression occurs at ~5°C above the elevated solidus in the most residual composition, which produces ~3 mol% melt. These results demonstrate that integrating melt loss into model *P–T* paths involving prograde heating and suprasolidus decompression yields lower quantities of melt during the decompression segment than commonly invoked. Based on these results, tectonic and petrogenetic models that require decompression melting may need re-evaluation.

https://doi.org/10.1180/S0026461X00006502 Published online by Cambridge University Press

Sulfur supplied by basaltic magma injection into the magma feeding system of Asama volcano, central Japan – A melt inclusion study

Y. YAMAGUCHI

Shinshu Univ. Matsumoto, 390-8621, Japan (yoshia_ygutti@d4.dion.ne.jp)

Asama volcano is situated at the junction of the volcanic fronts of the North Japan arc and the Izu-Mariana arc. Most of the erupted materials have andesitic whole-rock compositions. However, previous melt inclusion studies found no sign of primary andesitic melt and revealed that basaltic liquid formed a part of the ejecta [1].

For four eruption events of Asama volcano in the past 23,000 years, I here discuss a large sulfur supply by basaltic magma injections into the Asama magma system, based on microprobe analyses of olivine-hosted melt inclusions from the following eruption events; Itahana Brown Pumice fall (23 ka), Scoria in Komoro Pumice flows (11 ka), 1783 (Tenmei) Pumice fall (1783 AD), 2004 scoria fall (2004 AD).

In the evolution of Asama volcano, basaltic magma is believed to have been repeatedly injected into a long-lived crystal-rich felsic reservoir beneath the volcano [2]. The major phenocrysts (plagioclase, ortho- and clinopyroxene, and Fe-Ti oxides) were principally derived from the felsic magma and trapped sulfur-poor felsic melt inclusions (SiO_2 66-76wt%, S <400 ppm). In contrast, olivine (>Fo_{80}), a rare phenocryst in most cases, was derived from basaltic magma, trapping sulfur-rich mafic melts of basalt-basaltic andesite composition (SiO_2 48-65wt%, S <3600 ppm) before the mixing.

Olivine phenocrysts commonly include crystalline phases of esseneitic ($CaFe^{3+}AlSiO_6$) clinopyroxene, pargasitic amphibole, and a spinel solid solution (magnetite-hercynite-chromite), suggesting a high oxygen fugacity and hydrous conditions of the basaltic magma. Measured S-Kα wavelength shifts for the trapped melt indicate that the dominant sulfur-bearing species is SO_4^{2-} (> NNO + 1), with a corresponding high sulfur solubility in the magma. In most of the trapped melts, however, this primary high sulfur concentration was decreased by extensive early sulfide precipitation and distillation by vapor-boiling before the melt entrapment. High sulfur concentration is recorded in the composition of some pre-boiling, and the most mafic melt inclusions (SiO_2 48-53wt%). Basaltic magmas are expected to transport more than 3000 gram sulfur/tons of magma from the mantle source region into the felsic reservoir beneath Asama volcano.

[1] Anderson (1982) *JGR* **87,** 7047-7060. [2] Aramaki & Takahashi (1992) *IAVCEI Commission on Explosive Volcanism,* 1-60.

Noble gas isotopic compositions of mantle xenoliths in a kimberlite

JUNJI YAMAMOTO[1], MARK D. KURZ[2], HIDEMI ISHIBASHI[3] AND JOSHUA CURTICE[2]

[1]Institute for Geothermal Sciences, Kyoto University, Noguchibaru, Beppu 874-0903, Japan (*correspondence: jyama@bep.vgs.kyoto-u.ac.jp)

[2]Woods Hole Oceanographic Institution, Woods Hole, MA 02543, USA

[3]University of Tokyo, Tokyo 113-0032, Japan

Oceanic island basalt (OIB) provides an important window into the heterogeneous Earth's interior. The terrestrial inventory of radiogenic noble gas nuclides such as ^{40}Ar implies that the OIB source is less degassed (e.g., [1]). Assuming a K content and $^{40}Ar/^{36}Ar$ of OIB source, we can evaluate non-radiogenic ^{36}Ar content of the source, which enables us to assess the degassing state of the Earth's interior. Mantle-derived xenoliths entrained by OIB magma are potentially useful to consider a pristine feature of OIB magma because the OIB magma might have been captured in a source mantle of the xenoliths during ascent of the magma. Kimberlite is regarded as OIB erupted at continents (e.g., [2]). Mantle xenoliths in kimberlite are often metasomatized by the host kimberlite and could inherit the noble gases.

Here we report noble gas isotopic compositions of nine mantle xenoliths in a kimberlite erupted in Siberia at 380 Ma. The xenoliths are appropriate samples to explore the kimberlite magma because they are well metasomatized by the kimberlite magma. The noble gas isotopic compositions are all dominated by both radiogenic nuclides and atmospheric components. Firstly we corrected the atmospheric contribution to $^{40}Ar/^{36}Ar$ using an assumed relationship with a solar-like end-member of Ne. Then we corrected the effect of radiogenic addition to He and Ar isotopic ratios as follows. Assuming that the mantle xenoliths originally had homogeneous noble gas isotopic compositions, the present radiogenic noble gas isotopic compositions of the xenoliths are mainly caused by subsequent addition of radiogenic nuclides. Thus $^{3}He/^{4}He$ and $^{40}Ar/^{36}Ar$ of nine xenoliths corrected for the radiogenic contribution should converge into the original compositions. Actually, subtraction of ^{4}He and ^{40}Ar from the measured $^{3}He/^{4}He$ and $^{40}Ar/^{36}Ar$ at a rate of measured $^{4}He/^{40}Ar^*$ shows a converged point with $^{40}Ar/^{36}Ar$ of ~1800 and $^{3}He/^{4}He$ of ~50 Ra in a diagram of $^{3}He/^{4}He$ vs. $^{40}Ar/^{36}Ar$. Combination of the $^{40}Ar/^{36}Ar$ with a K content of OIB source will elucidate degassing state and layered structure of the Earth's interior.

[1] Allègre *et al*. (1996) *Geophys. Res. Lett*. **23**, 3555-3557. [2] Sumino *et al*. (2006) *Geophys. Res. Lett*. **33**, L16318.

https://doi.org/10.1180/S0026461X00006502 Published online by Cambridge University Press

Behavior of rare earth elements during chemical alteration of deep granitic rocks at Tono, Central Japan

Y. YAMAMOTO[1]*, Y. TAKAHASHI[2], H. SAKAMI[2], T. MIZUNO[1], K. AMANO[1], K. HAMA[1] AND H. SHIMIZU[2]

[1]Japan Atomic Energy Agency, Gifu 509-6132, Japan (*correspondence: yamamoto.yuhei@jaea.go.jp, mizuno.takashi@jaea.go.jp, hama.katsuhiro@jaea.go.jp, amano.kenji@jaea.go.jp)

[2]Hiroshima Univ., Hiroshima 739-8526, Japan (ytakaha@hiroshima-u.ac.jp, hiro-shim@mm.em-net.ne.jp)

Behavior of rare earth elements (REEs) in deep subsurface (from 85 to 1010 meter below ground level) during groundwater–granite interaction was investigated using chemical analysis of bulk rock and microscopic observation. It was revealed that REEs provide information on chemical alteration of granite even in the early stage of alteration, when the chemical index of alteration (CIA) using major element composition does not reflect the effect. REE patterns of granite with higher phosphorous concentration show a steeper slope in the lighter REE part relative to patterns of granite with lower phosphorous concentration. The relationship between the relative shape of REE patterns and phosphorous concentration suggests that phosphate minerals play a significant role in the release and incorporation of REEs at depth in granite, as they do in the surface environment. Allanite also plays a role as a REE host phase in granite indicated by the similarities in the relative shape of REE patterns, especially those with steep slopes. The steep slope in REE patterns corresponds to fresh granite, whereas the gentle slope in REE patterns corresponds to relatively altered granite in terms of chemical alteration. Change in the REE host minerals as granite alteration progress has an effect on the relative shape of the REE pattern of granite. Slope of REE pattern of granite can be explained using the patterns of accessory minerals. Presence of the accessory minerals and their alteration were also observed by electron microscopic analysis. Our results demonstrate that, during granite alteration, behavior of REEs in deep subsurface depends on dissolution and precipitation of accessory minerals, similar to the behavior in surface environments. REE pattern of granite is sensitive to the early stage of granite alteration, suggesting that the relative shape of REE pattern can be used as an indicator of the weak water–rock interaction in deep subsurface.

D/H exchange of hydrogen on fatty acids

ATSUKO YAMANAKA*, AKIKO S. GOTO AND TAKASHI KORENAGA

Department of Applied Chemistry, Graduate School of Science and Engineering, Tokyo Metropolitan University, Tokyo 192-0397, Japan (*correspondence: yamanaka-atsuko@ed.tmu.ac.jp)

Compound-specific stable isotope analysis of biomarkers has been employed in a number of geochemical studies as a powerful tool to track delivery of organic matter and to reconstruct climates and ecosystems in the geological past. Stable hydrogen isotopic composition of lipid molecules such as fatty acids has been employed as an effective tool to understand modern to paleo environments. In this study, to further evaluate the reliability of hydrogen isotope information (δD) of H-C bounds on organic compounds, we examine the isotope exchanges on fatty acids in phospholipid bilayer of pseudo cell membranes that exposed with 0 to 50% of D_2O at room temperature or 85ºC for 12 hours. Exchange of D/H is the maximum when 50% D_2O is used, in which increase of δD values is between 93 and 328‰. These results indicate that hydrogen isotopes are clearly exchanged even hydrogen on C-H bound in fatty acids and that its magnitude may depend on type of fatty acids (chain-length and unsaturation degree) and state of bilayers (gel vs liquid crystal). Based on these results, we roughly estimated that hydrogen isotopic composition should be change by up to a maximum 0.0099‰ when it is expected in water with enrichment in D by 100‰ for 12 hours.

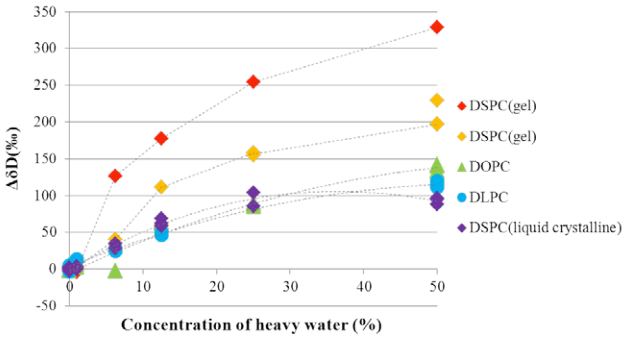

Figure 1: Change in δD value with respect to difference concentration of heavy water.

https://doi.org/10.1180/S0026461X00006502 Published online by Cambridge University Press

Pressure-induced phase transitions and electron spin state changes of iron bearing spinels

T. YAMANAKA[1]*, A. KYONO[1], S. KHARLAMOVA[2], V. STRUZHKIN[1], H-K, MAO[1,2] AND R.J. HEMLEY[1]

[1]Geophysical Laboratory, Carnegie Institution of Washington, Washington, DC 20015, USA (*correspondence tyamanaka@ciw.edu)

[2]High Pressure Collaboration Access Team, Carnegie Institution of Washington, Argonne, IL 60439, USA

High-pressure phase transitions of iron bearing spinel compounds in the earth crust attract a large attention in order to understand strong electronic correlation such as charge transfer, electron hopping, electron high-low spin transition, Jahn-Teller distortion and charge disproponation in the lower mantle or subduction zone. To prove the Jahn-Teller transition and electron spin state change of Fe_3O_4, Fe_2TiO_4, $FeCr_2O_4$ and Fe_2SiO_4, we executed a series of the diffraction studies of these polycrystalline and single-crystal and X-ray emission study (XES) using DAC and SR facilities at ambient temperature and Raman spectroscopic study under high pressures up to 90GPa.

Fe_2TiO_4 and $FeCr_2O_4$ show the transformation from cubic (*Fd3m*) to tetragonal ($I4_1/amd$) with c/a<1.0 and transform to orthorhombic (*Cmcm*) due to the Jahn-Teller effect of Fe^{2+} ($3d^6$) at the tetrahedral site[1]. The transition to orthorhombic post-spinel structure at high pressures is confirmed in these whole solid solutions. The transition pressures decrease from 27GPa (Fe_3O_4) to 12GPa (Fe_2TiO_4) with increasing Ti content.

XES reveals the spin transition between high spin (HS) and low spin (LP). The transition pressures of Fe_5O_4, Fe_2TiO_4, Fe_2SiO_4 are 22GPa, 18GPa and over 80GPa, respectively. The HP-LP transition induces their structure transitions due to the enormous reduction in iron ionic radius. A new further high-pressure phase (*Pmma*) of Fe_2TiO_4 was found. Rietveld analyses of the powder diffraction data have been conducted and the bulk modulus of each phase was observed.

[1] T. Yamanaka, T. Mine, S. Asogawa and Y. Nakamoto (2009 *Physical Review* B **80**, 134120

Boron contents and isotope compositions of oceanic crusts from the Oman and Troodos ophiolites

K. YAMAOKA[1]*, S. MATSUKURA[2], T. ISHIKAWA[3] AND H. KAWAHATA[2]

[1]Geological Survey of Japan, National institute of Advanced Industrial Science and Technology, 1-1-1 Higashi, Tsukuba, Ibaraki 305-8567 Japan (*correspondence: k.yamaoka@aist.go.jp)

[2]Atmosphere and Ocean Research Institute, The University of Tokyo, 5-1-5 Kashiwanoha, Kashiwa, Chiba, 277-8564 Japan

[3]Kochi Institute for Core Sample Research, JAMSTEC, 200 Monobe Otsu, Nankoku, Kochi, 783-8502 Japan

Boron is excellent tracer for elucidating crustal recycling in subduction zones because of the high concentration of boron in the upper part of the slab and the high mobility of boron during dehydration of the slab. However, fundamental data for vertical distribution of boron in hydrothermally altered oceanic crust are still limited. In this study, boron contents and isotopic compositions were determined for complete section of the oceanic crusts in the Oman and Troodos ophiolite.

Although the boron contents of rocks decreased with depth in both the oceanic crusts, altered rocks from deep section showed obvious boron enrichment relative to fresh rocks. The pillow lavas in the Troodos ophiolite, which have been weathered on the seafloor for ~80 Myrs, was highly enriched in boron (>100 ppm), supporting that boron inventory of pillow lava section strongly depends on the crustal age. The $\delta^{11}B$ of rocks in the Oman ophiolite systematically increased with depth and negatively correltate with the $\delta^{18}O$ values, suggesting that the $\delta^{11}B$ values are eccentially controlled by alteration temperature. On the othre hand, the $\delta^{11}B$ profile in the Troodos ophiolite didn't show clear increase trend.

The boron contents for the bulk oceanic crusts of the Oman and Troodos ophiolites are estimated to be 3.6 ppm and 12 ppm, respectively. About 8‰ of $\delta^{11}B$ was estimated for both the bulk oceanic crusts. In contrast to previous views, hydrothermally altered gabbro section can be a large sink of boron. This boron-enriched, high-$\delta^{11}B$ lower oceanic crust may impact on the estimate of the $\delta^{11}B$ value for fluids librated from the subducted oceanic slab, which is believed to largely control the $\delta^{11}B$ values of arc magmas generated in the mantle wedge.

https://doi.org/10.1180/S0026461X00006502 Published online by Cambridge University Press

Constraining timing of brittle deformation – A case study from fault zones in Toki Granite, Japan

S. YAMASAKI[1]*, H. ZWINGMANN[2], A. TODD[2], K. YAMADA[1], K. UMEDA[1] AND T. TAGAMI[3]

[1]Tono Geoscience Center, Japan Atomic Energy Agency, 959-31 Toki, Gifu, 509-5102, Japan (*correspondence: yamasaki.seiko@jaea.go.jp)
[2]CSIRO ESRE, Bentley, WA 6102, Australia
[3]Earth and Planetary Sci., Kyoto Univ., Kyoto, 606-8502, Japan

Early studies [e.g. [1]] highlighted the potential for determining the timing of near-surface brittle deformation using isotopic dating of authigenic illites in fault gouge. However, it has remained difficult owing to the possibility of contaminantion. In recent years, precise size separation combined with mineral characterization of gouge samples has demonstrated the suitability of illite K-Ar dating for constraining the timing of brittle deformation [e.g. [2]].

We present K-Ar age data from two gouge samples collected from a fault in the Cretaceous Toki granite, central Japan. The fault occurs sub-vertically along the wall of a shaft, and the minimum age of the fault deformation is estimated as ~20 Ma, as the Miocene sedimentary formation is not displaced by the fault. The samples were collected from the gouge zone at the depth of 252.9 and 403.7 m. The gouge samples were separated into four grain-size fractions (<0.1, <0.4, <2, 2-6 μm) and characterized by XRD, SEM, and TEM.

The fine fractions give younger K-Ar ages, suggesting enrichment in more recently grown authigenic illites. The finest fractions (<0.1 μm) give ages of 46 ±1 and 43 ±1 Ma (±2 sigma). The K-Ar ages of the fractions with no detectable contamination from detrital K-bearing minerals range from 53 to 43 Ma. This range is consistent with the stability field of illite and the main temperature field of brittle deformation (<300°C) within the cooling history of the host granite body of the fault, which was evaluated by apatite and zircon fission-track and K-Ar biotite ages from the host rock.

[1] Lyons and Snellenburg (1979), *Geol. Soc. Amer. Bull.* **82**, 1749-1752. [2] Zwingmann *et al.* (2010) *Chem. Geol.* **275**, 176-185.

Effects of pH and coexisting ions on hydrodynamic size of various humic substances evaluated by flow field flow fractionation

Y. YAMASHITA*, S. TANAKA, S. NAGASAKI AND T. SAITO

Department of Nuclear Engineering and Management, University of Tokyo, 7-3-1 Hongo, Bunkyo-ku, Tokyo, Japan (*correspondence: yyamashita@n.t.u-tokyo.ac.jp)

Humic substances (HSs) can behave as carriers for heavy metals and radionuclides in soil and aquatic environments. Understanding their molilities is essential for the fate of toxic ions. In the present study, we determined the hydrodynamic properties of the several IHSS standard HSs and evaluated the effects of pH and coexisting ions on their sizes by flow field flow fractionation (Fl-FFF) that provides a continuous and less-invasive size fractionation under wide ranges of chemical conditions.

We used the asymmetrical Fl-FFF system (AF2000 FOCUS, Postnova Analytics) with a UV-VIS detector at the wavelength of 255 nm and a fluorescence detector at the excitation/emission wavelength of 255/475 nm to obtain the fractogram of HSs.

Fig shows the fractrgrams of Suwannee river humic acid (SHA) and Elliot Soil humic acid (EHA) at pH 9.1, 7.0 and 5.5, respectively. SHA shows monomodal fractograms at all pH investigated. In addtion, the modal hydrodynamic diameters of SHA at both pH 5.5 and 9.1 are larger than that at pH 7.0, indicating that the intramolecular electrostatic repulsion between their deprotonated functional groups causes the expansion of SHA molecules at the basic condition, while intermolecular coagulation occurs at the acidic condition because of a decrease of the negative charge. On the other hand, EHA exhibits the bimodal size distributions at pH 7.0 and 5.5. This implies that some fractions EHA can easily coagulate by a pH decrease and that others hardly coagulte. We will present the pH-dependent fractograms of other HSs together with the effects of mono-, di- and trivalent cations.

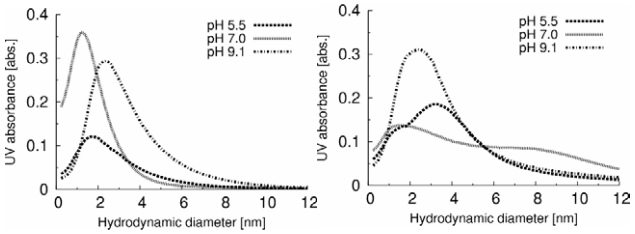

Figure 1 The fractgrams of SHA and EHA at various pH.

https://doi.org/10.1180/S0026461X00006502 Published online by Cambridge University Press

Tin isotope analysis for an archaeological application

E. YAMAZAKI[1], S. NAKAI[2]* AND T. SAITO[3]

[1]Tokyo Institute of Technology, Tokyo 152-8551, Japan (yamazaki.e.aa@m.titech.ac.jp)
[2]Earthquake Research Institute, University of Tokyo, Tokyo 113-0032, Japan (*correspondance: snakai@eri.u-tokyo.ac.jp)
[3]National Museum of Japanese History, Chiba 285-8502, Japan (saito@rekihaku.ac.jp)

Sn isotopes was proposed to verify recycling of bronze products[1]. In order to evaluate recycling by Sn isotopes, we need an assumption that raw materials of tin ore (cassiterite) have uniform Sn isotopic composition independent of regional differences. Recently, Haustein *et al*.[2] reported a series of Sn isotopic data for cassiterite samples and observed the largest significant variation of the isotopic composition (about 0.6 ‰ per mass). In this study, we investigated the variation of Sn isotopic compositions for cassiterite samples mainly in Japan. Prior to this challenge, we developed a new method to decompose cassiterite samples[3] and analyze their Sn isotopic compositions.

We analyzed 7 cassiterite samples from Japanese deposits and one cassiterite from Peru. And we found a linear correlation that follow a mass dependent fractionation in the cassiterite samples. Sn isotopic variation in Japanese cassiterites was limited to be within ±0.16‰ per mass. Such an isotopic fractionation presumably reflect differences in mineralization environment of cassiterite, such as precipitation processes and redox reactions. However, the classification of deposit types and Sn isotopic ratio seem to have no correlation. Therefore, more information is required to explain the observed Sn isotopic fractionation in cassiterite. On the other hand, in our preliminary experiments, bronze artifact from China shows fractionation of ±0.7‰ per mass [3], which exceeds the range of mass fractionation observed in the cassiterite samples. Therefore, Sn isotopes might be useful in detecting recycling. We are also planning to analyze these bronze artifacts again and to verify isotopic fractionation.

The author thanks Dr. Shunso Ishihara for providing cassiterite samples.

[1] Budd *et al*. (1995) *Israel Jour. Chem*. **35**, 125-130. [2] Haustein *et al*. (2010) *Archaeom*. **52**, 816-832. [3] Caley (1932) *JACS*, **54**,3240-3243. [4] Nakai & Saito (2002) *Geochim. Cosmochim. Acta,* **66**, A545.

Paleoenvironmental reconstructions of the Yangtze Sea, South China, through the Ordivician and Silurian transition

YAN DETIAN

Key Laboratory of Tectonics and Petroleum Resources of Ministry of Education, China University of Geosciences, Wuhan 430074, China (*correspondence: yandetian@cug.edu.cn)

The Yangtze Sea covering the Yangtze Craton in the South China received deposits mainly of black shale, with some shell limestone interlayers during the Late Ordovician and Earily Silurian periods [1]. Sedimentary facies and isopach data indicate that several highlands, either emerging or submerging, developed in the Yangtze Sea. Both Chemical Index of Alteration (CIA) and Chemical Index of Weathering (CIW) changes indicated a moderate chemistry weathering in the Late Ordovician under cold and dry climate, and suggested a peri-glacial period [2]. Before and after the peri-glacial period, climate of the Yangtze Sea was characterized by warm and humid condition [3, 4].

A series of geochemical data implied that deep water mass above the submerging highland differed from shallow water mass in redox. The deep water mass, represented by samples from the Wangjiawan section located in Yichang, was characterized by reduction with DOP > 0.45 and FeHR/FeT > 0.38 in most time of the Late Ordovician to Early Silurian, excepting in the peri-glacial period that showed an oxidation with DOP <0.45 and FeHR/FeT < 0.38. On the other hand, the shallow water mass, represented by samples from the Sanjiaguan section located in Yichang, was characterized by oxidation with DOP <0.45 and FeHR/FeT < 0.38, quite similar to that of the deep water in the peri-glacial period.

The $\delta^{13}C$ of sedimentary organic carbon data showed positive excursion in the peri-glaical period in both deep and shallow water sections [5]. It might reflect the "high-low-high" changes in organic productivity. It is the high organic productivity and reduction of the deep water that have promoted deposition of hydrocarbon source rocks in the Yangtze Sea, South China.

[1] Chen *et al*. (2004) *Palaeogeogr. Palaeoclimat. Palaeoecol*. **204**, 353-372. [2] Brenchley *et al*. (1994) *Geology* **22**, 295-298. [3] Brenchley *et al*. (1995) *Mod. Geol*. **20**, 69-82. [4] Yan *et al*. (2010) *Geology* **37**, 599-603. [5] Yan *et al*. (2009) *Palaeogeogr. Palaeoclimat. Palaeoecol*. **274**, 32-39.

https://doi.org/10.1180/S0026461X00006502 Published online by Cambridge University Press

Stimulation of the anaerobic oxidation of pyrite by activators at neutral pH in the presence of nitrate

R. YAN[1], A. KAPPLER[2], H.-H. RICHNOW[3] AND S. PEIFFER[4]*

[1]Department of Hydrology, University of Bayreuth, 95440 Bayreuth, Germany
[2]Geomicrobiology Group, Center for Applied Geosciences, Eberhard-Karls-University Tuebingen, 72076 Tuebingen, Germany
[3]Department of Isotope Biogeochemistry, Helmholtz Centre for Environmental Research, 04318 Leipzig, Germany
[4]Department of Hydrology, University of Bayreuth, 95440 Bayreuth, Germany
(*correspondence: S.Peiffer@uni-bayreuth.de)

Denitrification coupled to pyrite oxidation is a major process that has been observed in many groundwater aquifers, although a direct reaction between nitrate and pyrite could not be detected [1, 2].Our understanding of the mechanisms of this redox process is, however, still limited. Since Fe(III) is detected as a well-known oxidant for pyrite in the presence of oxygen even at neutral pH [3], we postulate that electron transfer is being mediated through this reaction also in the presence of nitrate as terminal electron acceptor. Microbial catalysis by bacteria, such as Fe(II) oxidizing or sulfide reducing bacteria, is considered to affect the denitrification and pyrite oxidation rates significantly. Therefore, bacteria are supposed to simulate the electron transfer from pyrite to nitrate.

The goal of the work is to understand the mechanism of the anaerobic oxidation of pyrite coupled to nitrate reduction in anoxic groundwater sediments. To this end batch experiments have been set up in which synthesized pyrite is exposed to nitrate-dependent Fe(II)-oxidizer strain BoFEN1 [4] testing the effect of Fe(II), Fe(III), and ferrihydrite as chemical activators. These batch experiments are separated into abiotic and biotic conditions to individually assess the pure chemical and microbial stimulation. First results from these epxeriments will be presented in this conference.

[1] Jorgensen *et al*. (2009) *Environmental Science & Technology* **43**(13): 4851-4857. [2] Schippers & Jorgensen (2001) *Geochimica Et Cosmochimica Acta* **65**(6): 915-922. [3] Peiffer & Stubert (1999) *Geochimica Et Cosmochimica Acta* **63**(19-20): 3171-3182. [4] Kappler *et al*. (2005) *Geobiology* **3**(4): 235-245.

Effect of soil sand on ^{13}C CP-MAS NMR spectra quality

I.H. YANARDAĞ*, A. FAZ, M.A. MUÑOZ, A. BÜYÜKKILIÇ YANARDAĞ AND R. GALLARDO

Technical Univ. of Cartagena, Sustainable Use, Management and Reclamation Soil and Water Research Group. Cartagena Spain.
(*correspondence: ibrahim.yanardag@upct.es)

Under semiarid climate condition such as Spain, soil consist of low organic matter concentrations therefore low organic compound effects on spectra quality and their organic fraction is often excluded from characterization by means of solid-state ^{13}C NMR spectroscopy **[1]**. That's way quantitative interpretation of such spectra becomes difficult and sometimes impossible. The aim of this study is to compare the effects of soil sand on ^{13}CP-MAS NMR spectra quality soil C mass balance in similar soil, in Albacete region, South-East Spain.

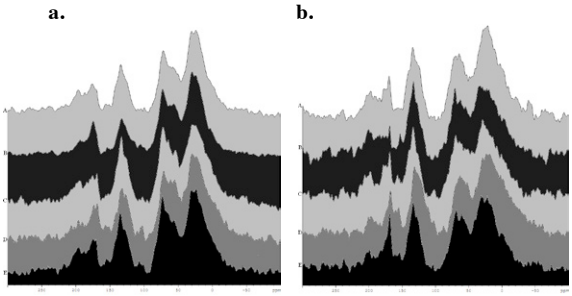

Figure 1. ^{13}C NMR results **a.** with sand **b.** without sand.

The result presented (Figure 1) that there were significantly differences between O-Alkyl, Aromatic and Phenolic groups with removal sand from soil, but this treatment was not significantly effected on Alkyl, Methoxyl and Carboxyl groups in functional groups of organic matter.

Consequently the peaks of NMR spectra became more pronounced with removal of sand from the soil in Aromatic, Phenolic and Carboxyl groups of soil organic matter.

[1] Gonçalves *et al*. (2003) *Geoderma* **116** (2003) 373– 392.

https://doi.org/10.1180/S0026461X00006502 Published online by Cambridge University Press

Quantitative exploration of the system $MgCl_2$-H_2O using cryogenic Raman spectrum

YANG DAN[1,2]* AND XU WENYI[1,2]

[1]Institute of Mineral Resources, CAGS, Beijing 100037, China (*correspondence:yangd_2004@yahoo.com.cn)
[2]Key Laboratory of Metallogeny and Mineral Assessment, MLR, Beijing 100037, P.R. China

The fluid is play a very important role in geological processes. With respect to hydrothermal deposits, the composition and nature of ore-forming fluids is the key to understanding the mechanism of mineralization. Raman spectroscopy can not analyze the ions such as Na^{+}, Ca^{2+}, Mg^{2+} and so on, but these ions are common in ore-forming fluids.

In this paper, we obtained Raman spectrum of $MgCl_2$ standard solutions with different concentrations (Fig.1). This experimental condition is rapidly cooling to -180°C and slow warming to observe hydrate formation process (that is manifested as a darkening of the vision in the microscope), and finally, rapidly cooling down to -180°C. Through the analysis of peak parameters, we has founded two quantitative relationships: (1) the peak intensity ratio (I_{3514}/I_{3090} and I_{3401}/I_{3090} and I_{3464}/I_{3090}) and concentration; (2) the total integration area of $MgCl_2$ hydrate peaks (the total integration area of 3401、3464、3514cm^{-1})and the concentration. These findings are important to quantitatively analyze the $MgCl_2$ by Raman spectroscopy in natural inclusions.

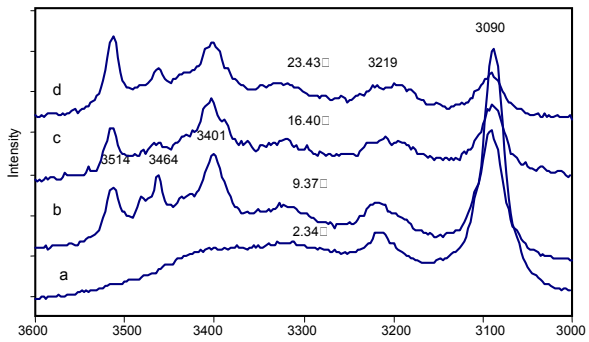

Figure 1 Raman spectrum of $MgCl_2$-H_2O with different concentrations at -180°C(experimental conditions as described in the text; 3401、3464、3514$cm^{-1}$is $MgCl_2$ hydrate peaks, 3090cm^{-1} is ice peak)

Chronology of detrital zircons from Jurassic sandstones in Western Shandong Province, China: Constraints on the nature of the Tan–Lu Fault Zone

D.B. YANG[1,2], W.L. XU[1], Y.G. XU[2] AND F.P. PEI[1]

[1]College of Earth Sciences, Jilin University, Changchun 130061, China (yangdb@jlu.edu.cn, xuwl@jlu.edu.cn, peifp@jlu.edu.cn)
[2]Key Laboratory of Isotope Geochronology and Geochemistry, Guangzhou Institute of Geochemistry, Chinese Academy of Sciences, Guangzhou 510640, China (yigangxu@gig.ac.cn)

It has been controversial when the large-scale sinistral strike-slip of the Tan–Lu Fault Zone occurred, while LA-ICP-MS U-Pb dating data of the detrital zircons from the Jurassic sandstones in the western Shandong Province provides constraints on this issue. The dating results indicate that the detrital zircons from the Early-Middle Jurassic Fangzi Formation in the Mengyin and Zhoucun basins have age populations of 2452, 1950-2050, 1755, 431, 315, 282, 227, 171 Ma, and 2494, 1844, 322, 273, 223, 159 Ma, respectively, whereas ones from the Middle-Late Jurassic Santai Formation in the Mengyin and Pingyi basins are dominated by the 2519, 1883, 277, 191, 150 Ma, and 2558, 607, 181, 137 Ma, respectively. The former suggests that the sedimentary rocks from the Fangzi Formation formed after 159-171 Ma, the latter implies that deposition of the Santai Formation took place after 137-150 Ma. In addition, the detrital zircons with ages of 218-244 Ma (mean=225±3 Ma, MSWD=0.6, n=22) from the Early-Middle Jurassic Fangzi Formation display typical growth zoning and have high Th/U ratios (generally >0.51), suggesting a magmatic origin. These Triassic detrital zircons are in age similar to emplacement ages (205-225 Ma) of post-collisional Shidao complex within the Sulu Orogen. Based on the regional geology, it is suggested that the latter is the only source of the Triassic detrital zircons. Therefore, we conclude that the Sulu Orogen had located in the present position during the Middle-Late Jurassic, i.e., the large-scale sinistral strike-slip movement of the Tan–Lu Fault Zone did not happen in the Early Cretaceous.

This work was financially supported by the NSFC (41002018, 90814003), the Ph.D. Programs Foundation of the Ministry of Education of China (20100061120002), and the Basic Scientific Research Foundation of Central Universities of China (200903026).

https://doi.org/10.1180/S0026461X00006502 Published online by Cambridge University Press

Pb, C, H, O and S isotope geochemistry of the Maoping carbonate-hosted Pb-Zn(-Ag-Ge) deposit in Northeast Yunnan province, China

G.S. YANG[1]*, Y. ZHANG[1], R.S. HAN[1,2] AND P. WU[1,2]

[1]Kunming University of Science and Technology, Kunming 650093, China (*correspondence: ygs0080009@163.com)
[2]Kunming University of Science and Technology, Southwest Institute of Geological Survey, Kunming 650093, China

In order to trace the sources of the ore metals and ore-forming fluids of the large-sized carbonate-hosted Maoping Pb-Zn(-Ag-Ge) deposit, Pb, C, H, O and S isotopic compositions of the deposit are presented in this paper.

The Pb isotopic ratios of the ores range from 18.340 to 18.914 for $^{206}Pb/^{204}Pb$, 15.510 to 15.796 for $^{207}Pb/^{204}Pb$ and 38.845 to 39.573 for $^{208}Pb/^{204}Pb$, which are similar to those of the host carbonate rocks and the Emeishan basalts, indicating that these rocks may have provided metals to the ore fluid. The $\delta^{34}S$ values of the ores show a total range from 7.96‰ to 24.1‰, most of which are between 10‰ and 16‰, indicating that the sulfur should be derived from the sedimentary strata. The $\delta^{13}C_{PDB}$ values of the gangue minerals range from-1.1‰ to -3.7‰, indicating that the carbon of the ore-forming fluid was derived from the mixture of the crust-source carbon in the strata and deep-source carbon. The fluid inclusions δD values of the sphalerite, pyrite and calcite range from -37‰ ~ -49‰, -42‰ ~ -61‰, and -45‰ ~ -64‰ , the corresponding $\delta^{18}O_{SMOW}$ values range from -9.0‰ ~ 3.4‰, -6.8‰ ~ -12.7 ‰ and 14.9‰ ~ 18.8‰. The calculated $\delta^{18}O_{H2O}$ values of calcite range from 5.2‰ to 9.7‰, if the formation temperature is 200°C. These data indicate that the ore-forming fluids were likely a mixture of magmatic hydrothermal fluid and metamorphic water, and had water-rock interaction and isotope exchange with the underlain ore-bearing strata during their ascending process from the depth.

Genesis of barite in eclogite from the main-hole of the Chinese Continental Scientific Drilling (CCSD)

H. YANG[1], L-F. ZHANG[2]* AND F-L. LIU[1]

[1]Institute of Geology, Chinese Academy of Geological Sciences, Beijing 100037, China (hyang@cags.ac.cn, lfl0225@sina.com)
[2]School of Earth and Space Sciences, Peking University, Beijing 100871, China (*correspondence: lfzhang@pku.edu.cn)

Barite was found as an accessory mineral in eclogite from the main-hole core (in the depth intervals of 0~700 m) of CCSD. It is a diagnostic mineral of fluid activity, which is uncommon to be found in metamorphic rocks. The presence or absence of this mineral helps to constrain interpretation of the redox conditions [1]. Strontium-isotope analyses have been used to constrain the genesis of barite and thus make it possible to supply the origin information of related fluid.

Barite in eclogite has various occurrences during the metamorphic process. (1) UHP metamorphic eclogite-facies stage. Barite mainly exists as mineral inclusions in garnet, omphacite and the aggregates of K-feldspar ± albite + Quartz. It is rich in Sr, and the $SrSO_4$ content is about 45 mol%. (2) Early retrograde stage. Barite (0~20 mol% $SrSO_4$) was preserved among the mineral grains and dispersing in symplectite composed of clinopyroxene and albite. It is associated with allanite, epidote, hyalophane, celsian, K-feldspar. (3) Retrogressive amphibolite-facies stage. Barite (<5 mol% $SrSO_4$) exists as the oxidized outmost rim of pyrite. The Sr content in barite almost decreases during the retrogressive process. Barite together with the associated minerals constrain the change of redox conditions throughout the there metamorphic stages, which is oxidition-reduction-oxidition.

Barite separated from eclogite samples have $^{87}Sr/^{86}Sr$ values of 0.70621~0.71043. It shows that barite is mainly originated from the continental crust and may be precipitated from the fluid exsoluted from the continental crust during the plate exhumation.

[1] Hanor (2000) *Rev. Min. Geochem.* **40**, 193-275.

https://doi.org/10.1180/S0026461X00006502 Published online by Cambridge University Press

In situ diamonds and moissanite in podiform chromitites of the Luobusa and Ray-Iz ophiolites, Tibet and Russia

J.-S. YANG[1] AND P.T. ROBINSON[2]

[1]Institute of Geology, Chinese Academy of Geological Sciences, 26 Baiwanzhuang Road, Beijing, 100037, China (yangjingsui@yahoo.com.cn)

[2]Department of Earth Sciences, Dalhousie University, Halifax, Nova Scotia, Canada, B3H, 4J1, (p.robinson@ns.sympatico.ca)

Podiform chromitites and peridotites of several ophiolites, including the Luobusa and Donqiao bodies of Tibet, the Semail ophiolite of Oman and the Ray-iz ophiolite of Russia, contain various combinations of deep mantle minerals, such as diamond, coesite, moissanite, base-metal and PGE alloys and native elements. These are associated with a range of crustal minerals, including zircon, corundum, kyanite, sillimanite, almandine garnet and rutile. Most of these minerals have been recovered from heavy mineral separates but in-situ grains of diamond, moissanite and corundum occur in podiform chromitites of the Luobusa and Ray-Iz ophiolites. Coesite, possibly after stishovite, from the Luobusa ophiolite is intergrown with kyanite on the rim of an Fe-Ti alloy grain recovered from chromitite. The in-situ diamonds, moissanite and corundum consist of euhedral to subhedral grains about 200-500 μm across, enclosed in small, irregular to spherical patches of carbon hosted in chromite grains. Both the diamonds and moissanite are characterized by having exceedingly low C isotopic values (mean $\delta^{13}C$ = -28), much lower than typical kimberlite diamonds. The in-situ UHP minerals in chromite grains suggest that at least some of the chromite crystallized at depth. Based on the occurrence of these minerals in widely separated ophiolites of variable age, we suggest that diamonds and associated minerals may be common in the upper oceanic mantle.

Gabbroic xenoliths in Pleisto-Holocene alkali basalts from Jeju Island, South Korea

KYOUNGHEE YANG

Dept. of Geological Sciences, Pusan National University, Busan, 609-735, South Korea (yangkyhe@pusan.ac.kr)

Gabbroic xenoliths occur in Pleisto-Holocene alkali basalts from Jeju Island, Korea, consisting of plagioclase + clinopyroxene + orthopyroxene. The coarse grain size (up to 3 mm), moderate mg# of pyroxenes (70-77) and textural features (e.g., poikilitic) indicate that gabbroic xenoliths are cumulates of igneous origin. Clinopyroxene from these xenoliths is constantly enriched in REEs with smooth convex-upward patterns, as expected for cumulus minerals formed from a melt enriched in incompatible-trace elements. Strikingly similar major and trace element variations and patterns of constituent minerals between gabbroic xenoliths and the host basalt indicate that cumulates are genetically related to the host basalt, but more evolved. The xenoliths crystallized at the margins in a volatile-rich roof environment of magma reservoirs, which had emplaced above the present Moho estimates beneath Jeju Island, suggesting the presence of ancient high-level magma storage reservoir beneath hotspot or plume-impacted areas. Following consolidation of the xenolith lithologies, volatile- and incompatible-elements enriched melt infiltrated through grain boundaries, and metasomatized the anhydrous cumulate phases, producing amphiboles. This volatile-enriched melt, as metasomatic agents, could have resulted from initially anhydrous to volatile-saturated compositions, being evolved by fractional crystallization. The studied xenoliths appear to represent cumulus remnants of melt compositions leading to more evolved rocks which related with the prior volcanism in the southern part of Jeju Island. It is noteworthy that this metasomatism is a relatively young event at the continental margin near the back arc basin (East Sea) in the Western Pacific.

https://doi.org/10.1180/S0026461X00006502 Published online by Cambridge University Press

Ore-forming age and origin of the Donggou porphyry Mo deposit in the Eastern Qinling orogenic belt, central China

LI YANG[1], F. CHEN[2] AND X.-Y. ZHU[1]

[1]Institute of Geology and Geophysics, Chinese Academy of Sciences, Beijing 100029, China
[2]School of Earth and Space Sciences, University of Science and Technology of China, Hefei 230026, China

The Qinling orogenic belt geologically consists of four tectonically juxtaposed zones, from south to north, the northern margin of the Yangtze Craton, South Qinling terrain, North Qinling terrain, and the southern margin of the North China Craton. The gigantic Mo-bearing metallogenic belt of East Qinling is mainly situated in the southern margin of the North China Craton and extends east-western from the Jinduicheng Mo deposit in west to the Tangjiaping Mo deposit in east. Previous studies have shown that the Mo mineralization in East Qinling occurred in three periods: 233-221 Ma, 148-138 Ma and 131-112 Ma, origin of the molybdenum ore-forming and related geodynamic setting but are still debated.

In this study, we report U-Pb zircon and Re-Os molybdenite ages and Sr-Nd-Pb isotopic compositions of the Donggou porphyry molybdenum deposit, being one of the superlarge deposits in this molybdenum mineralization belt. It is spatially associated with the fine-grained Donggou granite porphyry, and hosted in the Mesoproterozoic rhyolite, andesite, and tuffaceous siltstone of the Xiong'er Group. Re-Os molybdenite dating results constrain two stages of the Mo mineralization in an interval of 3 Ma. Zircon U-Pb ages demonstrate the earlier Mo mineralization was almost simultaneous with the formation of the host Donggou granitic porphyry. Geochemically, this porphyry belongs to A-type granite, being enriched in contents of LILEs (such as K, Rb, Th and U) and HFSEs (such as Nb, Ta and Zr), strongly depleted in contents of Ba, Sr, Eu and Ti, and high Ga/Al ratios. Whole-rock Sr-Nd-Pb isotopic compositions of the porphyry implies that the Mo-bearing magma were derived from crustal material by partial melting in an intra-continental extensional environment.

Modeling of co-metabolic Cr(VI) reduction under denitrifying conditions

L. YANG, S. MOLINS, C.I. STEEFEL, AND H.R. BELLER

Lawrence Berkeley National Laboratory, Berkeley CA 97020 USA, (LYang@lbl.gov, SMolins@lbl.gov, CISteefel@lbl.gov, HRBeller@lbl.gov)

Bioremediation of chromium contamination in groundwater often relies on *in situ* reductive immobilization strategies mediated by indigenous microbial communities stimulated with the injection of an organic electron donor. Depending on the presence of electron acceptors, a series of biogeochemical reactions and parallel abiotic geochemical reactions can occur, resulting in a complex network of enzymatic and indirect reaction pathways.

We used a reactive transport model [1] to interpret the rate of chromate reduction in a flow-through column experiment using natural Hanford 100H aquifer sediment into which a solution containing chromate, nitrate, and lactate was injected. The model includes biomass growth and decay, and thermodynamic limitations on reaction rates [2]. Further, we implemented a formulation that accounts for co-metabolic reduction of Cr(VI) based on previous studies on a pseudomonad isolated from the Hanford 100H aquifer [3]. Analysis of the experimental results indicate that the chromate reduction rates increased with the increasing denitrification rates, which is consistent with a co-metabolic mechanism. The reactive transport modeling agrees with this observation and was used to quantify the efficiency of the process. Model results also illuminate a change in reaction pathways as the nutrient ammonium was depleted, with the apparent result that another nitrogen source (i.e., nitrate) was used instead. Further, a kinetic conversion of nitrite to N_2 was needed to reproduce the observed pH behavior.

[1] Li, Steefel, Williams, Wilkins & Hubbard (2009) *Environ. Sci. Technol.* **43**, 5429-5435. [2] Jin & Bethke (2003) *Appl. Environ. Microbiol.* **69**, 2340-2348. [3] Han, Geller, Yang, Brodie, Chakraborty, Larsen & Beller (2010) *Environ. Sci. Technol.* **44**, 7491-7497.

https://doi.org/10.1180/S0026461X00006502 Published online by Cambridge University Press

Geochemical characteristics of heavy metals in soil profile from an old metalliferous mining area in China

L.S. YANG , Y.H. LI* AND H.R. LI

Institute of Geographical Sciences and Natural Resources Research, CAS, Beijing 100101, China (*correspondence: yhli@igsnrr.ac.cn)

Factors affecting the geochemical behavior of HMs

Heavy metals (HMs) is a major concern due to its potentially adverse impacts on public health [1, 2]. In mining areas, the essential of the natural pedogenesis is the elemental recombination and migration [3]. However, the process can be greatly accelerated by human mining activities.

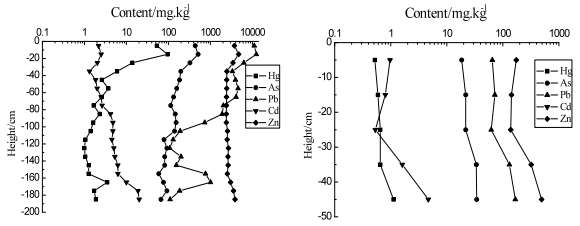

Figure 1: Vertical distribution of HMs in the soil profile. (Left-soil from mining area; Right-soil from control site)

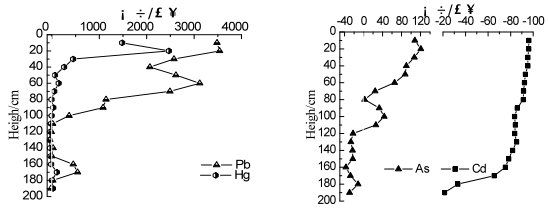

Figure 2: Migration ratio (Δ) of HMs in comparison with Fe.

Discussion of Results

The migration features of the major elements revealed that the soil from the mining area finished the primary process of chemical weathering characterized by leaching of Ca, and initiated the secondary process accompanying by leaching of K. Except the element Cd, other HMs such as Pb, Hg and As were enriched (Figure 2). It might be caused by both the pedogenesis and human mining activities. Extensive human mining activities made a major contribution to the accumulation of HMs in top soil.

[1] Li *et al*. (2009) *Environ Geochem Health* **31**, 617-628. [2] Ji *et al*. (2009) *Acta Scientiae Circumstantiae* **29**, 1094-1102. [3] Chen *et al*. (2008) *J. Geogr. Sci*. **18**, 341-352.

Computational studies of structural, magnetic, and spectroscopic properties of actinide species

PING YANG

W.R. Wiley Environmental Molecular Science Laboratory, Pacific Northwest National Laobratory, Richland, WA, 99352, USA. (ping.yang@pnl.gov)

The complicated electronic structure of actinide complexes leads to their versatility of chemical reactivity, spectral and magnetic properties, and dynamical behavior. We will show that first-principle computational chemistry modeling can be used as an effective tool to provide insight into these properties. Recent theoretical and spectroscopic studies indicate that variations of orbital character in bonding interactions are connected with differences in chemical reactivity. In this study, we applied density functional theory (DFT) to probe the electronic structure of the ground state of actinide complexes. We found that calculations provide a quantitatively accurate microscopic picture of the bonding interactions of the actinide-ligand bonds. Based on the understanding of fundamental bonding interactions, we will discuss the magnetic and dynamic properties. We found that time-dependent density functional theory (TD-DFT) correctly reproduces the experimental spectroscopic results, lending confidence to characterize the transition nature of excitations. These fundamental findings provide a solid foundation towards a more complete and accurate understanding of the physico-chemical properties of actinide complexes in the natural environment.

This research is supported by the DOE Basic Energy Sciences Heavy Element Program. Part of the computing was performed using the MSCF in the EMSL, a national scientific user facility sponsored by the Department of Energy's Office of Biological and Environmental Research located at Pacific Northwest National Laboratory.

https://doi.org/10.1180/S0026461X00006502 Published online by Cambridge University Press

Are the silicate reference glasses BAM-S005 A and B suitable for *in situ* microanalysis?

Q.C. YANG[1]*, K.P. JOCHUM[1], B. STOLL[1], U. WEIS[1] AND M. WIEDENBECK[2]

[1]Max-Plank-Institut für Chemie, Postfach 3060, 55020 Mainz, Germany (*correspondence: Qichao.Yang@mpic.de)
[2]Deutsches GeoForschungsZentrum, 14473 Potsdam, Germany

BAM-S005 Type A and B from the Federal Institute for Materials Research and Testing (BAM, Germany) are soda-lime reference glasses certified for bulk analysis. In order to test whether these glasses are also suitable for microanalysis, we have assessed the homogeneity of major and trace elements, including the 22 certified trace elements using LA-ICP-MS, EPMA and SIMS [1]. The results show that all major elements and most trace elements are homogeneously distributed. Possible exceptions are Se and Cl which might be heterogeneously distributed.

Figure 1 shows our LA-ICP-MS results for BAM-S005-A calibrated against the new reference values for NIST 610 [2] following ISO guidelines. All data agree within uncertainty limits with the BAM certified reference values. Figure 1 also shows our LA-ICP-MS data using the 14 years old NIST 610 values [3] for calibration. Under this calibration, significant differences for As, Cd, Mo, Sn, Sb, expecially for Se and Cl, are observed.

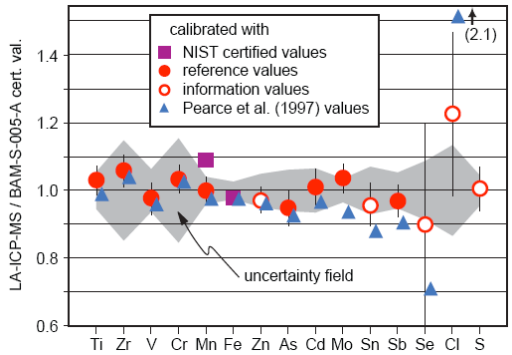

Figure 1: Normalized LA-ICP-MS data for BAM-S005-A using different calibration procedures [2, 3]. Uncertainties include the analytical error of LA-ICP-MS and the uncertainties of the NIST reference values.

[1] Yang *et al*. (2011) *Geophys Res Abs* **13**, EGU2011-7533. [2] Jochum *et al*. (2011) *GGR* (in press). [3] Pearce *et al*. (1997) *Geostandard Newslett* **21**, 115-144.

Geochemical constraints on the sediment source-to-sink process of the Changjiang (Yangtze) River

S. Y. YANG*, C. LI, Q. WANG AND J.Q. SHAO

State Key Lab. of Marine Geology, Tongji Uni., Shanghai 200092, China (*correspondence: syyang@tongji.edu.cn)

As the largest river originated from the Himalayan-Tibetan Plateau, the Changjiang delivers huge amount of terrigenous matter into East Asian marginal seas, which exerts a great control on marine sedimentation and biogeochemical cycle. The sediment source-to-sink (S2S) process of the Changjiang is significantly different from those of well-known MARGINS sites and widely-documented island rivers such as the Kaoping River in Taiwan, because of its complicated provenance geology, weathering regime and rapidly increasing human impacts on the drainage system.

We have systematically investigated the sediment S2S process of the Changjiang river system by using various geochemical proxies including REE and Sr-Nd isotopic compositions and detrital zircon chemistry. Source rock compositions and chemical weathering intensities in the drainage basin account for the compositional variations of the modern Changjiang sediments. The bulk Sr-Nd isotopic compositions and age spectrum of zircon provide good constraints on sediment recycling and evolution of weathered upper continental crust in the Yangtze Craton. Geochemical composition of the sediment into the sea is complicated by hydrodynamic sorting and changing sediment suppliers in relation to variability of monsoon-induced precipitation in the river basin. The Three Gorges Reservoir also complicates the sediment S2S process and changes river geochemistry.

Despite spatial and seasonal variations in geochemical compositions are clearly registered in the modern Changjiang sediments, the proxies for deciphering sediment provenance and chemical weathering intensity can be established for the study of river-sea interaction and paleoenvironmental reconstruction at different temporal scales.

This work was supported by NSFC research fund (Grant No: 41076018).

https://doi.org/10.1180/S0026461X00006502 Published online by Cambridge University Press

Two episodes of the Early Cretaceous magmatic activity in the Gan-Hang Rift, South China: *In situ* zircon U-Pb dating

SHUI-YUAN YANG, SHAO-YONG JIANG*, YAO-HUI JIANG AND KUI-DONG ZHAO

State Key Laboratory for Mineral Deposits Research, School of Earth Sciences and Engineering, Nanjing University, Nanjing 210093, China (*correspondence: shyjiang@nju.edu.cn)

Results of *in situ* zircon U–Pb ages using high-precision dating methods (SHRIMP or LA-ICP-MS) are reported for magmatic activity in the Gan-Hang Rift, South China. The Gan-Hang Rift, trending at least 450 km in a NE-SW direction, is a part of a Mesozoic BRP (Basin and Range Province) in southeastern China, and is an important magmatic zone composed of both volcanic-intrusive complex and A type granites.

Zircon U–Pb dating of the volcanic-intrusive complex from Xiangshan basin, Center Jiangxi Province, provides insights into the extrusive and intrusive activity at Xiangshan, which took place within a short time span (135–137 Ma) [1-2]. SHRIMP zircon U–Pb dating for two A type granitic plutons (Tongshan and Damaoshan plutons) and a diabasic dike in the northwest of the Gan-Hang Rift shows that the granitic plutons and diabasic dike were emplaced in the Early Cretaceous (122–129 Ma) [3]. A zircon U–Pb dating on a newly discovered A-type granitic pluton in Baijuhuashan (126±3 Ma), western Zhejiang Province, was carried out recently [4]. Our new study concerns a volcanic-instrusive complex in Xinlu basin, western Zhejiang Province, which produced zircon U–Pb ages of 134–135 Ma. All these *in situ* zircon U–Pb dating results indicate that two major episodes of magmatic activity occurred in the Gan-Hang Rift. The first stage (134-137Ma) generated the volcanic-intrusive complex, which marked the onset of the extension. With ongoing extension the crust and lithospheric mantle became progressively thinned and formed the second stage of granitic plutons between 122 Ma and 129 Ma. These A-type magma in the Gan-Hang Rift were likely generated with the peak episode of an extensional tectonic regime during the Cretaceous in South China, perhaps corresponding to the rollback of the Pacific plate.

[1] Yang *et al*. (2010) *Sci China Earth Sci* **53,** 1411-1426. [2] Yang *et al*. (2011) *Miner Petrol* **101,** 21-48. [3] Jiang *et al*. (2011) *Lithos* **121,** 55-73. [4] Wong *et al*. (2009) *Lithos* **112,** 289-305.

Halogen profiles of pore waters from gas hydrate potential area offshore of SW Taiwan

T.F. YANG[1]*, H.-C. CHEN[1], H.-W. CHEN[1], W.-L. HONG[1], P.-C. CHUANG[1], N.-C. CHEN[1], S. LIN[2], S.-H. CHUNG[3] AND Y. WANG[3]

[1]Department of Geosciences, National Taiwan University, Taipei 106, Taiwan (*correspondence: tyyang@ntu.edu.tw)

[2]Institute of Oceanography, National Taiwan University, Taipei 106, Taiwan (swlin@ntu.edu.tw)

[3]Central Geological Survey, MOEA, New Taipei City 235, Taiwan (chung@moeacgs.gov.tw, wangys@moeacgs.gov.tw)

Variations of halogen concentra-tions (Cl^-, Br^- and I^-) and ammonium (NH_4^+) in pore water of marine sediments of selected sites were studied to help understanding the fluid source and the pathway of sulfate reduction in the potential gas hydrate area of offshore SW Taiwan, where has been characterized with very high methane flux [1, 2, 3, 4]. According to the concentration profiles (I^-, Br^-, CH_4, SO_4^{-2}, NH_4^+), we can classify those studied sites into four groups. In group-1, which represents background group, concentrations show no clear variations with depth. In group-2, rapid reduction of sulfate and significant increase in NH_4^+ and/or CH_4 are observed. In group-3, CH_4, I^-, Br^- and NH_4^+ all increase with increasing depth. Unlike group-2, NH_4^+ concentration increases faster than those in group-2. In group-4, the CH_4 concentration increases at depth, while there are only very low I^-, Br^- and NH_4^+ concentrations. Those category except group-1 indicated the mixing of in situ and deep source fluids.

Based on the stoichiometry ratio between sulfate consumption and DIC increasing from the profiles of the studied coring sites, we can summary the pathway of sulfate reduction for group-2 to -4 as followings: For group 2, which could represent the majority sites in offshore SW Taiwan, sulfate is mainly consumed by AMO process with methane from the depth. For group-3, sulfate is consumed by decomposition of local organic matters with very few fluid input from depth. For group-4, almost all sulfates are consumed by AMO process.

[1] Chuang *et al*. (2006) *Terr. Atmos. Ocean. Sci*., **17**, 903-920. [2] Yang *et al*. (2006) *Terr. Atmos. Ocean. Sci*., **17**, 933-950. [3] Yang (2008) *Geofluids* **8**, 219-229. [4] Chuang *et al*. (2010) *Geofluids* **10**, 497-510.

https://doi.org/10.1180/S0026461X00006502 Published online by Cambridge University Press

Application of nano-powders in the sewage treatment

XIAOJING YANG AND LEI JI

School of Energy and Environment, Xihua University, Chengdu 610039,China(yangfmrl@sina.com)

A certain amount of nano-powders have been added in different concentrations of chemical oxygen demand (COD) of water samples and putting a certain period of time. The change of water turbidity, conductivity and chemical oxygen demand (COD) were used as the criterion of sewage purification. The chemical oxygen demand (COD) of experimental sewage solution is 500mg/L、1500mg/L、2000mg/L、3000mg/L and 5000mg/L respectively. The barium titanate nano-powders and activated carbon nano-powders, the size of 200nm, were added in these solutions and laid up for seven days. The experimental results showed that activated carbon nano-powders and barium titanate nano-powders did not affect on the conductivity of water samples obviously.

The barium titanate nano-powders can significantly reduce the turbidity of water samples. The turbidity of water samples changed from 123 to 9 degree when the weight ratio of barium titanate nano-powders were from 0.25%; 0.5%; 0.75% to 1% respectively. However, the purification of the chemical oxygen demand (COD) was not effective. When the chemical oxygen demand (COD) is not high, purifying rate of sewage is about 45%. When the chemical oxygen demand (COD) exceed 1650 mg/L, purifying rate of sewage is only 25%. If the content of barium titanate nano-powders increased, purifying rate did not change obviously.

The effect of activated carbon nano-powders on the turbidity and chemical oxygen demand (COD) of sewage was obvious. The turbidity of water samples changed from 123 to 13 degree and the purifying rate of chemical oxygen demand (COD) from 60% to 95% when the weight ratio of activated carbon nano-powders were from 0.25%; 0.5%; 0.75% to 1% respectively. Even the chemical oxygen demand (COD) exceed 5000mg/L, the purifying rate of of chemical oxygen demand (COD) of sewage can reach 92% and a high concentration of chemical oxygen amount of (COD) could be reduced to meet the requirement of waste water discharge standards during some period.

Platinum-Group Element mineralization in black shales in Xinjiang, China

Y.Q. YANG [1], Y.Y. ZHAO [2] AND F. PIRAJNO[3]

[1]State Key Laboratory of Geological Processes and Mineral Resources, Beijing 100083, China (dxqy8@cugb.edu.cn)

[2]Institute of Mineral Resourcesof Chinese Academy of Geological Sciences, Beijing 100037, China (yuanyizhao2@sina.com)

[3]School of Earth and Environment, The University of Western Australia, 35 Stirling Highway, Crawley, WA 6009, Australia

Geological Setting

Black shales are favorable host rocks for many types of ore deposits. Among them gold and PGE are very important deposits to black shales. There exists vast areas of the black shales in Xinjiang of China, which distribute among Tianshan Mountains, Tarim Basins and Beishan districts. The mains bearing-ore strata are Sawayaertun formation at SW Tianshan and Heijieshan formation at East Tianshan (Fig.1).

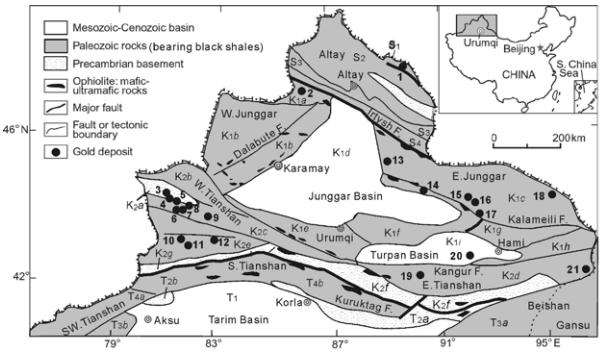

Figure 1 The sketch map of structures and rocks

Although PGE ore deposits have not yet discovered in Xinjiang at present, but many exceptionally vestiges of PGE to be demonstrated [1], and had discovered gold ore deposits related with black shales, such as Sawayaertun Gold deposit. Up on flood plain sediment, a geochemical province of Pt and Pd of a content of 0.8 ng/g is delineated at East Tianshan .

Forming Conditions

Hercynian-Indosinian tectono-magmatism under a post-collision extensional environment provided heat and metal extracted from basement rocks and mafic body.Shear zones control the metallic fluid,such as Muruntau gold deposit in Uzbekistan, located in the southwest Tianshan mountains and hosted in Early Paleozoic black carbonaceous shales [2].

[1]Wang X, *et al*. (2007) *Geological bulletin* **26**, 1519-1530.
[2] Graupner T. *et al*. (2000) *Mineralogical Magazine* **64**, 1007-1016.

https://doi.org/10.1180/S0026461X00006502 Published online by Cambridge University Press

Rb-Sr dating of the Wangpingxigou Pb-Zn deposit, China

JUN-MING YAO[1]*, YAN-JING CHEN[1,2], TAI-PING ZHAO[1] AND XIANG-HUI LI[3]

[1]Key Laboratory of Mineralogy and Metallogeny, Guangzhou Institute of Geochemistry, CAS, Guangzhou 510640, China (yaojunming@gig.ac.cn)

[2]Key Laboratory of Orogen and Crust Evolution, PKU, Beijing 100871, China (yjchen@pku.edu.cn)

[3]Laboratory for Radiogenic Isotope Geochemistry, Institute of Geology and Geophysics, CAS, Beijing 100029, China

Unlike their big brothers, SEDEX and MVT types of Pb-Zn ore deposits which are distinguished for their large reserves and stable occurrence and have long been the focus of scientific research and industrial exploration, vein-type Pb-Zn deposits are often ignored for the small scales and diverse occurrence. However, in the last few years, numerous vein-type Pb-Zn deposits have been discovered in the East Qinling orogenic belt, which include several large to super-large Pb-Zn ore deposits, such as Wangpingxigou, Tieluping and Lengshuibeigou etc. These vein-type Pb-Zn deposits possess important economic value and huge exploration potentials.

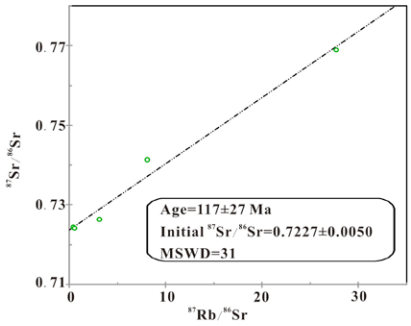

Figure 1: The Rb-Sr isochron age of single-grain sphalerite from Wangpingxigou Pb-Zn deposit, Henan province.

The single-grain Rb-Sr analytical technique was employed on sphalerite to date the Pb-Zn mineralization of the Wangpingxigou deposit. Five sphalerite grains from sulfide ores yield an Rb-Sr isochron age of 117 ± 27 Ma with the initial 87Rb/86Sr value of 0.7227 ± 0.0050 (Figure 1), significantly higher than those of Yanshanian intermediate-felsic porphyries and granite plutons. This age agrees with the Re-Os model age (116 ± 1.7 Ma) of Donggou Mo deposit located in Waifangshan district. This suggests that the Mo-Au polymetallic deposits in Waifangshan area were formed in the same period.

Quantitative research on nanopores of coal using atomic force microscope

SUPING YAO*, KUN JIAO AND MIAOCHUN LI

State Key Laboratory for Mineral Deposits Research (Nanjing University), School of Earth Sciences and Engineering, Nanjing University, Nanjing 210093, China (*correspondence: spyao@nju.edu.cn)

Atomic Force Microscope (AFM) is a new approach to nanopore structure study and porosity measuring by observing the nanopores of coal directly and processing the quantitative measurement of pore structure parameter.

AFM could study the surface nature of samples under contact mode using several methods. The section analysis could characterize the nanopore geometry, the grain analysis could study the nanopore distribution of coal, and the parameters got from bearing analysis are important in porosity measurement. A large amount of nanopores with different shapes shows in anthracite (Sample QS), the section analysis shows that the diameter and the depth of the largest pore in the analized area is 354.4nm and 13.5nm respectively, while those of the smallest pore is 33.2nm and 1.6nm respectively. The statistic data of scanning area (Table.1) implies that the number of pores in anthracite is 5 times more than gas coal, the Pore Area / Total Area ratio of anthracite is also higher. However, the average pore size of anthracite is abviously smaller than gas coal. The hydrocabon generation process of coal with the increase of coalification degree (maturity) could account for the increase of pore size.

The high resolution imaging and quantitative analysis of advantage of AFM could be utilized to pore structure reasearch, quantitative pore size analysis and porosimetry, which could help to understand the nanopore generation, pore geometry and adsorption mechanism.

Sample	Ro (%)	Pore Acount (/mm^2)	Average Pore Size (nm^2)	Total Pore Area (μm^2)	Pore/ Total Area (%)
Spm	0.67	5.33×10^5	71816	1915	3.83
CX	0.72	5.55×10^5	74829	2090	4.18
QS	2.47	2.57×10^6	23871	3075	6.15
SX	4.34	3.32×10^6	19441	3230	6.46

Table 1 Quantitative analysis data of coal (scanning area 50000 μm^2)

https://doi.org/10.1180/S0026461X00006502 Published online by Cambridge University Press

New geochemical and geochronological constraints for the origin of Orhaneli-Dursunbey volcanic rocks, NW Anatolia (Turkey)

O.S. YARAR*, O. KAMACI AND S. ALTUNKAYNAK

Department of Geology, Istanbul Technical University, 34469, Maslak, Istanbul, Turkey, (*correspondence: serhatyarar@gmail.com)

An extensive volcanism constructed through multiple eruptions of basic to silicic magmas developed during the Late Cenozoic in NW Anatolia (Turkey). New radiometric age and geochemical data are presented from the volcanic activity in the study area which is situated between the towns of Orhaneli (Bursa) and Dursunbey (Balıkesir). The felsic lavas are volumetrically more dominant than mafic lavas.Volcanism in the region began with felsic pyroclastic rocks and rhyolitic-rhyodasitic lavas. K/Ar radiometric age data obtained from rhyolite lavas indicates that their age varies from 19.4 to 19.0 Ma corresponding to the Early Miocene. According to their mode of occurrences, pyroclastic rocks of felsic phase may be divided into two groups; the pryoclastic fall deposits and the pyroclastic flow deposits. The pyroclastic fall deposits are represented by pumice fall, pumice-ash, ash and ash-block fall deposits. The pyroclastic flow deposits may also divided into two subgroups; ash-block deposit and ignimbrites. Our field observations indicate that the volcanic rocks were formed from a number of small vents which set along approximately NNE-SSE trending fault zones by the plinian/sub-plinian eruptions. Felsic volcanism was followed by transitional basalts, basaltic andesite lavas with the age of 18.7 to 17.5 Ma as the last products of volcanism in the Orhaneli-Dursunbey volcanic field.

Geochemically, the volcanic association is high-K calc-alkaline in nature and show similar characteristics to post-collisional volcanic rocks. Both volcanic suites exposed in Orhaneli and Dursunbey area display a gap in silica concentrations. Trace element characteristics and Sr-Nd isotope data indicate that coexisting mafic and felsic magmas derived from lithospheric mantle source yielding depleted but LILE-enriched compositions, with subsequent contamination. Basic parental magmas of mafic and intermediate volcanic rocks were generated from EM1-type mantle previously modified by subduction, whereas felsic volcanic rocks were produced by assimilation of silicic crust and combined fractional crystallization (AFC).

Rates and mechanisms of hydration in crystalline crust

BRUCE W.D. YARDLEY*[1], HANS-PETER NABEIN[2] AND WILHELM HEINRICH[2]

[1]School of Earth & Environment, University of Leeds, Leeds LS2 9JT, UK, (*correspondence: b.w.d.yardley@leeds.ac.uk)

[2]Deutsches GeoForschungsZentrum (GFZ), D-14473 Potsdam, Germany (hans-peter.nabein@gfz-potsdam.de)

A free water phase in crystalline rocks of the mid to lower crust fulfils two roles: it enhances deformation while present, but participates in hydration reactions that lead to its consumption. The precise rate of hydration has important implications for crustal rheology as it determines whether the continental crust normally contains free water. We have investigated hydration rates for powdered enstatite-oligoclase-quartz under mid-crustal conditions of 400ºC and 300 MPa and find that c. 2.0E-07 g H_2O is consumed per m^2 enstatite surface per second. This rate is comparable to the rates of hydration of andalusite + K-feldspar from Schramke *et al*. [1].

Such rates are dependent on calculated surface areas, which may change during the run. We therefore carried out a series of experiments using 4mm diameter cores of fine grained (100-200 microns) basaltic hornfels. These hydrated too slowly for accurate weight loss measurements, consistent with only the outer surface of the cylinder being effectively reactive. This result validates the approach in earlier work [2], in which we calculated that water films with a half width of 100 μm can only persist for periods of a few tens of years under these conditions.

Experiments with hollow cores resulted in marked segregation as product minerals grew as well-formed crystals creating vein-like material in the available space.

[1] Schramke *et al*. (1986) *American Jl Sci* **287**, 517-59. [2] Yardley *et al*. (2010) *Geofluids* **10**, 234-40.

https://doi.org/10.1180/S0026461X00006502 Published online by Cambridge University Press

Redox profile through the Siberian craton: Fe K-edge XANES determination of Fe^{3+}/Fe^{2+} in garnet from peridotite xenoliths of the Udachnaya kimberlite

G.M. YAXLEY[1]*, A.J. BERRY[2], V.S. KAMENETSKY[3], A.B. WOODLAND[4], D. PATERSON[5], M.D. DE JONG[5] AND D.L. HOWARD[5]

[1]Research School of Earth Sciences, The Australian National University, Canberra ACT 0200, Australia (*correspondence: greg.yaxley@anu.edu.au)
[2]Department of Earth Science and Engineering, Imperial College London, UK
[3]ARC Centre of Excellence in Ore Deposits, University of Tasmania, Hobart TAS 7001, Australia
[4]Institut für Geowissenschaften, Universität Frankfurt, Frankfurt/M, Germany
[5]Australian Synchrotron, Clayton VIC 3168, Australia

In cratonic lithosphere the oxygen fugacity (fO_2) of peridotite is expected to broadly decrease with increasing depth. However metasomatic events may locally perturb this trend, often leading to oxidation [1,2].

We have investigated the fO_2-depth variation in the Siberian Craton using a suite of fresh garnet lherzolites from the Udachnaya East kimberlite. Garnet $Fe^{3+}/\sum Fe$ was detemined using XANES spectroscopy [3] on the X-ray Fluorescence Microscopy beamline of the Australian Synchrotron.

Thermobarometry established that the samples range in pressure from 3.9-7.1 GPa and lie along a typical cratonic geotherm. Several samples exhibit evidence for metasomatic enrichment, with elevated abundances of Ti, Zr and Y in garnet and clinopyroxene, broadly consistent with an earlier study of another Udachnaya xenolith suite [4]. Others are less or unaffected by metasomatism, with very low abundances of these elements.

$\Delta \log_{10}[fO_2]^{FMQ}$ [52] varies from -2.5 to -5.9 log units and broadly decreases with increasing pressure. The metasomatised samples all derive from P > 5 GPa and most exhibit a resolvable shift to fO_2 values ≈1.5-2.0 log units higher than the unmetasomatised ones, at given pressure.

[1] Woodland & Koch (2003) *EPSL* **214**, 295-310. [2] McCammon *et al*. (2001) *Contrib Mineral Petrol* **141**, 287-296. [3] Berry *et al*. (2010) *Chem Geol* **278**, 31-37. [4] Ionov *et al*. (2010) *J. Petrol*. **51**, 2177-2210. [5] Gudmundsson & Wood (1995) *Contrib Mineral Petrol* **119**, 56-67.

Assessment of heavy metal contamination in soils around Gebze industrial area, NW-Turkey

GÜLTEN YAYLALI-ABANUZ

Department of Geological Engineering, Karadeniz Technical University, 61080, Trabzon, Turkey (gultenyaylali@yahoo.com)

Soil contamination poses a serious risk to human health, particularly in densely populated areas. Pollution from industries activities can be introduced into the food chain via soil, plant and water and threatens human health. Increase in heavy metal pollution in the soils of Gebze (Turkey) due to intense industrialization and urbanization has become a serious environmental problem. There are two large organized industrial zones in Gebze; the Gebze Organized Industrial Zone (GOIZ) and the Dilovası Organized Industrial Zone (DOIZ). This region hosts several industrial facilities which are the main source for hazardous wastes which include paint, plastic, electric, metal, textile, wood, automotive supply industry, food, cosmetics, packing, machinery, and chemicals. Soil samples were collected from these two industrial zones and analyzed for their metal contents. Results of the analysis show that the soils are characterized by high concentrations of Cd, As, Pb, Zn, Mn, Cu, Cr and Hg. Since concentrations of other elements do not exceed the permissible levels, they are not evaluated. Concentrations are 0.05-176 mg/kg of Cd, 10-1161 mg/kg of Cr, 7.87-725 mg/kg of Cu, 1.50-65.60 mg/kg of As, 17.07-8469 mg/kg of Pb, 1.96-10000 mg/kg of Mn, 29.5-10000 mg/kg of Zn, and 9-2721 µg/kg of Hg. Application of factor, cluster and correlation analysis showed that heavy metal contamination in soils originates from industrial activities and heavy traffic which are of anthropogenic origin. Contaminations in soils were classified as geoaccumulation index, enrichment factor, contamination factor, and contamination degree. Integrated pollution index (IPI) values indicate that heavy metal pollution levels of soils collected from industrialization sites are greater than those from distal parts of industrialization. Spreading of hazardous wastes from industrial facilities in the study area via rain or wind is the main source of soil pollution. In addition, traffic-related metal pollution is also observed. In order to mitigate the impact of environmental pollution, factory wastes must be reliably disposed.

https://doi.org/10.1180/S0026461X00006502 Published online by Cambridge University Press

Nb/Ta fractionation resulted by fluid-rock interaction in subducted oceanic crust

KAI YE, SHUN GUO, YI, CHEN AND JINGBO LIU

State Key Laboratory of Lithospheric Evolution, Institute of Geology and Geophysics, Chinese Academy of Sciences, Beijng 100029, China

Nb/Ta ratios in the silicate Earth reservoirs (Earth's mantle and crust) are almost all subchondritic and thus document a clear deficit of Nb relative to Ta in the silicate Earth, known as the terrestrial Nb–Ta paradox. One proposed solution is a hidden reservoir of subducted eclogitic oceanic crust with superchondritic Nb/Ta ratios in the Earth's lowermost mantle. However, many high-pressure experiments demonstrate that the melts and fluids equilibrating with the eclogite commonly have higher Nb/Ta ratios than the residue rutile-bearing eclogites, and recent observations proved that natural eclogites commonly have subchondritic Nb/Ta ratios, suggesting that the down going subducted oceanic crust could not be the superchondritic Nb/Ta reservoir. We reported here data of Nb/Ta ratios of natural eclogites and internal HP veins from Dabieshan UHP terrane. The host eclogites have chondritic Nb/Ta ratios (19-21), but some of the HP veins, which crystallized from the UHP fluids released from the host eclogites have superchondritic Nb/Ta ratios (35-38). Our data demonstrate that UHP fluid-rock interactions in subducted oceanic crust resulted in great Nb/Ta fractionation with UHP fluid have much higher Nb/Ta ratios than the residue solid eclogite, and the superchondritic Nb/Ta reservoir are expected in the mantle wedge which reacted with the high Nb/Ta fluid.

Oxygen triple-isotope evidence for enhancement of CO_2 sequestration efficiency by diatom-diazotroph assemblages in a giant river plume

LAURENCE Y. YEUNG[1,2], WILLIAM M. BERELSON[1], EDWARD D. YOUNG[2], MARIA G. PROKOPENKO[1], EDWARD J. CARPENTER[3] AND PATRICIA L. YAGER[4]

[1]Dept. of Earth Sciences, University of Southern California, Los Angeles, CA 90089, USA

[2]Dept. of Earth and Space Sciences, University of California, Los Angeles, CA 90095, USA (lyyeung@ucla.edu)

[3]Romberg Tiburon Center and Dept. of Biology, San Francisco State University, Tiburon, CA 94920, USA

[4]Dept. of Marine Sciences, University of Georgia, Athens, GA 30602, USA

The Amazon river outflow influences biogeochemistry hundreds to thousands of kilometers from the river mouth, out to the western region of the oligotrophic tropical North Atlantic (TNA). This dynamic and evolving "plume" is characterized by a significant CO_2 undersaturation in surface waters associated with biological new production.

Observations and inverse modeling suggest that the TNA is typically a carbon source to the atmosphere of ~2.5 Tmol C yr^{-1} [1,2]. Net production in the Amazon plume, however, reverses the normal TNA surface condition, removing up to 1.7 Tmol C yr^{-1} from the atmosphere [3]. ANACONDAS (NSF OCE-0934095) hypothesized that this efficient biological pump is driven by an unusual assemblage of diatoms and diazotrophic (N_2-fixing) cyanobacteria; our team studied the carbon cycling and ecology of the plume during its maximum extent in May-June 2010 on the *R/V Knorr*.

We present new *in situ* net-community and gross primary production data from the expedition. We observe a peak enhancement in export production efficiency over a narrow sea-surface salinity window (S = 32–33 psu) using the O_2/Ar and oxygen triple-isotope (i.e., $^{17}\Delta$) methods. This striking increase in export production coincides with similar increases in biological carbon drawdown and counts of *Hemiaulus hauckii*, a diatom often found in symbiosis with the diazotroph *Richelia intracellularis*. These data support the diatom-diazotroph assemblage mechanism for enhancing new production and carbon sequestration in tropical river plumes. The strength of this CO_2 sink is likely sensitive to changes in tropical hydrology and terriginous runoff over time.

[1] Takahashi *et al*. (2002), *Deep-Sea Res. II* **49**, 1601-1623. [2] Mikaloff-Fletcher *et al*. (2007), *Global Biogeochem. Cycles* **21**, GB1010. [3] Subramaniam *et al*. (2008), *Proc. Nat. Acad. Sci. USA* **105**, 10460-10465.

https://doi.org/10.1180/S0026461X00006502 Published online by Cambridge University Press

Spatial prediction of soil organic carbon using digital soil mapping techniques in Slovakia

YUSUF YIGINI*, PANOS PANAGOS AND LUCA MONTANARELLA

European Commission Joint Research Centre 21027 Ispra (VA) Italy (*correspondence: yusuf.yigini@jrc.ec.europa.eu, panos.panagos@jrc.ec.europa.eu, luca.montanarella@jrc.ec.europa.eu)

High-resolution and continuous soil maps are an essential prerequisite for precision agriculture and many environmental studies. Conventional, sample-based soil mapping is costly and time consuming, and the data collected are available only for discrete points in any landscape. Thus, sample-based soil mapping is not reasonably applicable for large areas like countries. Due to these limitations, geostatistical techniques can be used to map soil properties. Soil organic carbon (SOC) is one of the most important parameters shaping soil environment and it plays a key role in determining soil quality. Spatial prediction of soil organic carbon in a large scale has an important role in environmental studies and field practices for both soil quality and carbon sequestration. This study was conducted to interpolation of point data to produce continuous map of soil organic carbon content in Slovakia. The measured point data were extracted from LUCAS (Land Use/Cover Area Frame Survey) results for Slovakia region. The regression kriging approach is applied and Corine Land Cover (CLC), SRTM 90m, European Soil Database (ESDB), climate and land management data were used as covariates. Finally, the soil organic carbon prediction map was produced in raster format at a spatial resolution of 100×100m.

Geochemistry and $^{40}Ar/^{39}Ar$ geochronology of adakite-like porphyries in NW Turkey: Implications for slab breakoff induced adakitic magmatism

M. YILDIZ* AND S. ALTUNKAYNAK

Department of Geological Engineering, Istanbul Technical University, 34469, Istanbul, Turkey (myildizitu@gmail.com)

A number of plutons and porphyries emplaced into the Izmir-Ankara suture zone (IASZ), which marks the collision zone between Anatolide-Tauride platform and Sakarya continent in NW Turkey. This study focuses on the geochemistry and geochronology of Adakite-like porphyries exposed in the IASZ.

Adakite-like porphyries are spatially and temporally associated with Eocene plutons that are intrusive into ophiolitic and blueschist rocks along the IASZ. The plutons range in age from 54 to 48 Ma and include granodiorite, quartz diorite, and syenite. They are medium- to high-K calcalkaline in composition and are predominantly metaluminous I-type granitoids. Geochemical compositions and Nd-Sr isotope systematics indicate that these plutons represent the products of hybrid magmas evolved from partial melting of subduction modified lithospheric mantle and, through assimilation, fractional crystallization of these melts at crustal levels.

Adakitic rocks are represented by rhyolite and dacite porphyries. They are peraluminous, and exhibit adakitic characteristics. They have high SiO_2, Al_2O_3, Na_2O contents, Sr/Y and La/Yb ratios and low Y, Yb contents, and display enrichments of LILE and LREE, depletion of HFSE and lack of Eu anomaly. Our $^{40}Ar/^{39}Ar$ ages are 53.7 to 54 Ma for the adakite-like porphyries.

These geochemical features, timing and nature of Adakite-like porphyries and geology of the region indicate that, collectivelly, adakitic magmatism was not formed above an actively dehydrating subducted slab but are consistent with a magmatism that is more typical of intraplate tectonic settings. We suggest that adakite-like porphyries likely formed by as a result of interaction between crustal and lithospheric mantle melts. These partial melts requere increased heat flow at about 54 Ma. High heat flow could have occurred by slab breakoff that is compatible with the geodynamic evolution of the region. As a consequence of slab breakoff, upwelling asthenospheric mantle would raise the geothermal gradient beneath the suture zone.

https://doi.org/10.1180/S0026461X00006502 Published online by Cambridge University Press

Genesis of ultramafic related magnesite in Northwest Turkey along the Izmir-Ankara Suture: A stable isotope study

ASUMAN YILMAZ AND MUSTAFA KUSCU

[1]Aksaray University, Geology Department, 68100, Aksaray, Turkey
[2]Suleyman Demirel University, Geology Department,32260, Isparta, Turkey

The magnesite occurrences of Eskisehir area (Süleymaniye, Margı, Tutluca), which are hosted by Alpine type ultramafic rocks, have been studied, in order to elucidate the origin of water, carbon and are compared with similar magnesite occurring in Turkey and other countries. Süleymaniye magnesite occurences have δ ^{13}C (PDB) values ranging from -2,71 ‰ to -7.69 ‰; Margı magnesite occurrences δ ^{13}C (PDB) values ranging from -7.59 ‰ to -11.24 and Tutluca magnesite occurences have δ ^{13}C (PDB) values ranging from -8.69 ‰ to -10.4 ‰. Süleymaniye magnesite occurrences have havier isotopic value of others. They have similar δ ^{18}O (SMOW) isotopic values ranging from 27.35 δ ^{13}C ‰ to 30.78 ‰. Petrographic, mineralogic and isotopic data indicate that magnesite precipitation of Eskisehir area in near surface environment at low P and T.

Critical review of Hf-W and U-Pb clocks for terrestrial core formation

Q.-Z. YIN[1], C.-T. LEE[2], J. BLICHERT-TOFT[3] AND F. ALBARÈDE[3]

[1]Univ. of California, Davis, CA, USA (qyin@ucdavis.edu)
[2]Rice University, Houston, TX 77005, USA
[3]Ecole Normale Supérieure de Lyon, 69007 Lyon, France

Since the discovery of radiogenic ^{182}W in the Earth's mantle in 2002, the extent to which the incoming accreting bodies (impactor) isotopically equilibrated with the proto-Earth before the two cores merged to form Earth's core has been hotly debated. Resolving this issue is critical for interpreting Hf-W constraints on terrestrial core formation and the origin of the Earth and Moon. Models of accretion highlight that either (i) the Hf-W age of terrestrial core formation is well constrained between 10-30 Myr [1] as long as the degree of metal-silicate equilibration is between 40-100% [2], or that (ii) the Hf-W systematics constrains the degree of equilibration to 40% and do not constrain timing at all [2]. In the latter case, the U-Pb system has been used to argue for a much later time of core formation [3].

Problems with the late core formation model are as follows. (a) the Moon and the Bulk Silicate Earth (BSE) have nearly identical O, Cr and W isotopes [4], which is difficult to explain if the impactor and the proto-Earth equilibrated only to 40%. (b) Coudpled ^{142}Nd-^{182}W modeling suggests that silicate differentiation would occur before core-mantle segregation [5]. (c) The basic premise of using U-Pb systematics of the BSE to estimate timing of core formation may be incorrect. Ref. [6] emphasized the fact that the BSE, as represented by oceanic basalts, lies to the right of the geochron in Pb-Pb space. In order to resolve this "paradox", ref. [6] computed a model age for the BSE and suggested a 100-200 Myr age for Pb segregation to the core, but because Canyon Diablo troilite was assumed to represent the core, these model ages are minimum estimates for the timing of Pb segregation. In ref. [7], we show that Pb segregation could have been much later, but instead of the core, Pb segregation may have been controlled by sulfide-silicate differentiation associated with the formation of continents. (d). Finally, the similar ^{182}W of the Earth and Moon [4] does not necessarily imply that the Earth-Moon system formed after ^{182}Hf had decayed (>60Myr) because both bodies are still radiogenic compared to chondrites. The key question is whether Hf/W ratios for BSE and the Moon are distinguishable?

[1] Yin *et al*. (2002) *Nature*, **418**, 949. [2] Rudge *et al*. (2010) *Nature Geo*. **3,** 439. [3] Wood and Halliday (2010) *Nature*, **465**, 767. [4] Touboul *et al*. (2007) *Nature,* **450**, 1206. [5] Moynier *et al* (2010) *PNAS*, **107**, 10810. [6] Allegre *et al*. (1995) *GCA*, **59**, 1445. [7] Lee *et al*. (this meeting).

https://doi.org/10.1180/S0026461X00006502 Published online by Cambridge University Press

Early degassing of the Earth

REIKA YOKOCHI

The University of Chicago, 5734 South Ellis Avenue, Chicago, IL 60637 (yokochi@uchicago.edu)

Some of noble gas isotopes are produced by radioactivities having different half-lives: the β-decay of ^{129}I produces ^{129}Xe with $T_{1/2}$ = 15.7 Myr, the spontaneous fission of ^{244}Pu produces $^{131\text{-}136}$Xe with $T_{1/2}$ = 82 Myr, and the still active decay of ^{238}U also produces ^{4}He and $^{131\text{-}136}$Xe by spontaneous fission with $T_{1/2}$ = 4.45 Gyr. Argon-40 is also produced by the β-decay of ^{40}K with $T_{1/2}$ = 1.27 Gyr. These contrasted production rates of noble gas isotopes allow investigation of terrestrial degassing during the accretional period, the Hadean, and from the Archean to present (e.g. [1-9]).

The xenon isotopic composition of the mantle-derived rocks suggests an extended degassing history of the Earth during Hadean, which can be modeled assuming the degassing to be a first-order rate process, i.e. the amount of noble gas extracted from the mantle is proportional to its total amount in the mantle reservoir [9]. In the model, it was assumed that the mangle degassing decreased gradually as expected for a progressively cooling Earth. The efficiency of degassing was estimated to be 1.2×10^{-8} duing Hadean in this model [9], whereas the degassing efficiency of the mantle at present is $0.6\text{-}3.8 \times 10^{-11}$ based on the recent global ^{3}He flux estimate [2]. We investigate how the transition between these two modes of degassing occurred using radiogenic noble gas isotopes.

[1] M.L. Bender, B. Barnett, G. Dreyfus, J. Jouzel and D. Porchelli (2008) *PNAS* 105 (**24**) 8232-8237. [2] D. Bianchi, J.L. Sarmiento, A. Gnanadesikan, R.M. Key, P. Schlosser and R. Newton (2010) *EPSL* **297**, 379-386. [3] M.W. Caffee, G.B. Hudson, C. Velsko, G.R. Huss, E.C.J. Alexander, A.R. Chivas (1999) *Science* **285**, 2115– 2118. [4] J. Kunz, T. Staudacher and C. Allegre (1998) *Science* **280**, 877– 880. [5] B. Marty (1989) *EPSL* **94**, 45-66. [6] M. Ozima, F.A. Podosek, G. Igarashi (1985) *Nature* **315**, 471– 474. [7] T. Staudacher and C.J. Allegre (1982) *EPSL* **60** 389– 406. [8] G.W. Wetherill (1975) *Annu. Rev. Nucl. Sci.* **25**, 283–328. [9] R. Yokochi and B. Marty (2005) *EPSL* **238**:17-30

Hydrothermal alteration in the Vargeão basaltic impact structure (South Brazil)

E. YOKOYAMA[1,2]*, A.NEDELEC[2], R.I.F TRINDADE[1], G. BERGER[3] AND D.BARATOUX[3]

[1]IAG, University of São Paulo, São Paulo, Brazil (*correspondence: elder@iag.usp.br, rtrindad@iag.usp.br)

[2]GET- OMP, University Paul Sabatier, Toulouse, France (nedelec@lmtg.obs-mip.fr)

[3]IRAP-OMP, University Paul Sabatier, Toulouse, France (baratoux@dtp.obs-mip.fr; gilles.berger@lmtg.obs-mip.fr)

The Vargeão impact structure

Hypervelocity impact phenomena are of primary importance in the evolution of solid bodies of the Solar System[1]. But craters on basaltic rocks, which are the best analogs for the surface of other planets and satellites, are rare on Earth. The 12 km wide Vargeão, which is a well-preserved complex structure formed on basaltic flows of the Serra Geral Formation (about 133-131 Ma) [2]. At Vargeão, the impact-related materials are chiefly represented by centimeter breccia-veins that are found in all lithologies (basalts and ryodacites). We conducted a detailed petrological study (petrography, microprobe, SEM and XRD) on these veins.

Results

Our results show that the veins were strongly affected by the post-impact hydrothermal fluids. The hydrothermal alteration varies geographically in the structure. On the rim area this alteration consists of total or partial substitution of the melt matrix by quartz, calcite and iron oxides. At the central area, the alteration mineral assembly is composed of quartz, iron oxides, zeolites and rarely calcite. Usually, the alteration shows a zoned setting, which also varies locally. At some outcrops on the rim area, we also observed the occurrence of disseminated native copper. Clay minerals (smectites) were observed in all samples and are probably related to weathering. The post-impact hydrothermalism on basaltic craters and their possible implications for the evolution of planetary bodies surface will be discussed.

[1] French (1998) *LPI Contribution*, Houston, **954**, 120 pp [2] Kazzuo-Vieira *et al.* (2009) *Rev. Bras. Geof.* **27**(3),375-388

\

https://doi.org/10.1180/S0026461X00006502 Published online by Cambridge University Press

Influence of microbiology and photochemistry on iodine cycling

L. YOKOYAMA[2], K. WAGENER[1] AND A. DE L.R. WAGENER[1]*

[1]Departamento de Quimica, PUC-Rio, 22453-900 RJ, Brazil (*correspondence: angela@puc-rio.br)
[2]Escola de Quimica, UFRJ, 21941-909 RJ, Brazil

Investigation of microalgae, bacteria and photochemistry influence on the cycling of iodine in seawater was carried out. Axenic cultures of *Tetraselmis sp*. and natural bacteria found in seawater were prepared and samples were collected over 54h at 3 and 6h interval, respectively. Determinations included I^-, IO_3^-, O_{dis}, NO_3^-, NO_2^-, NH_4^+, DOC, pH, I in biomass, biomass growth and chorophylls.

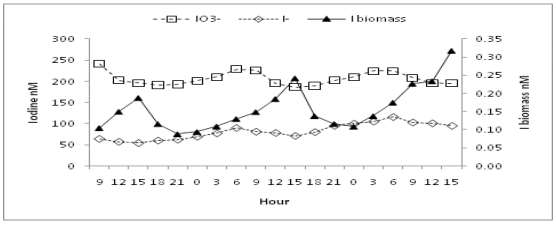

Figure 1: I^-, IO_3^- and I in biomass (*Tetraselmis sp*)

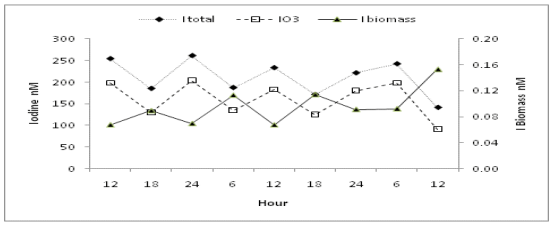

Figure 2: IO_3^-, I total and I biomass (bacteria culture)

Discussion and results

Dissolved iodine was absorbed during photosynthesis of *Tetraselmis* and released in respiration. A net production of 52 nM of I^- occurred while ΔIO_3^- was < 4 nM. The shift by 3h in oscillations of IO_3^- and O_{dis} indicates partipation of the former in enzymatic reactions as suggetesd by [1].Significant correlations between I^- concentration and primary production were found. Sorption of iodine seems to involve I^- and organic I and may involve compounds that act storing energy. This would explain the liberation of I^- at night. Iodate showed cyclic variation in the bacteria culture with 12 hours amplitude. A significant activity of nitrifying and denitrifying bacteria was observed.

[1] Wait & Truesdale (2003), *Mar Chem* **81**, 137-148

Reactive transport analysis on chemical weathering of a porous rhyolite

T. YOKOYAMA

Department of Earth and Space Science, Osaka University, 1-1 Machikaneyama, Toyonaka, Osaka 560-0043, Japan (tadashi@ess.sci.osaka-u.ac.jp)

Reaction and transport in chemical weathering of a porous rhyolite from Kozushima, a volcanic island in Japan, were studied. The mass balance in the rhyolite can be described by the following reaction-transport equation:

$$\partial c/\partial t = R_d(1-c/c_{eq})A/\Phi + D\partial^2 c/\partial x^2 - v\partial c/\partial x \qquad (1)$$

where c is the concentration (dissolved Si), t time, x depth from the surface of the rock, R_d dissolution rate (far from equilibrium), c_{eq} equilibrium concentration, A reactive surface area, Φ porosity, D apparent diffusion coefficient, and v fluid flow rate. Each of the parameters in eq. (1) has been determined by the laboratory experiments designed to simulate natural condition. The dissolution rate of Si and hydraulic conductivity of the rhyolite were measured by flowing pure water into a rock coulmn under a constant water head. The apparent diffusion coefficient of dissolved Si was determined by a through diffusion experiment [1]. Reactive surface area was measured by BET method. The depth profiles of the concentration of dissolved Si and dissolution rate calculated by eq. (1) (Fig. 1) reveal that an average dissolution rate for a depth of 1 m is ~2E−18 mol Si cm^{-2} sec^{-1}. The dissolution rate of the rhyolite during 52,000 years of weathering has been estimated by the field based study to be ~6E−19 mol Si cm^{-2} sec^{-1} [2]. The calculated dissolution rate is within one order of magnitude of the field rate.

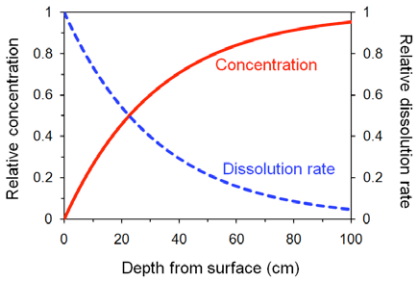

Figure 1: Depth profiles of the concentration of dissolved Si and dissolution rate.

[1] Yokoyama & Nakashima (2005) *Eng. Geol.* **80**, 328-335.
[2] Yokoyama & Banfield (2002) *Geochim Cosmochim Acta* **66**, 2665-2681.

https://doi.org/10.1180/S0026461X00006502 Published online by Cambridge University Press

Evaluation of in-house metallic standard for siderophile elements using fs-LA-ICPMS

T.D. YOKOYAMA*, T. IMAI[2], Y. UCHIYAMA[2], T. SUZUKI[3], T. YOKOYAMA[1], M. TAKEYAMA[4], E. TAKAHASHI[2] AND T. HIRATA[1]

[1]Dept. Earth and Planet. Sci., Kyoto Univ., Kyoto 606-8502, Japan (*correspondence: yokoyama@kueps.kyoto-u.ac.jp)
[2]Dept. Earth and Planet. Sci., Tokyo Ins. Tech., Tokyo 152-8551, Japan
[3]IFREE, Japan Agency for Marine Sci. and Tech., Yokosuka 237-0061, Japan
[4]Dept. Metallurgical Engin., Tokyo Ins. Tech., Tokyo 152-8551, Japan

Siderophile elements were preferentially distributed into the metallic phase or metallic core during the planetary formation sequence. Abundance data for siderophile elements can provide key information concerning the chemical evolution of metallic core or metallic phase in the meteoritic parent. However, pricise determination of the siderophile elements in the metallic samples have been retarded by the analytical difficlty mainly due to poor analytical precision or sensitivities achieved by the conventional laser ablation-ICP-mass spectrometry[1]. However, most of commercially available standard materials for elemental analysis does not cover many siderophile elements. To overcome this, we have prepared the in-house calibration standard material of Fe-Ni metal for determination of siderophile elements using femtosecond laser ablation ICP-mass spectrometry. The in-house metallic standard was prepered through arc melting technique from a mixture of high purity Fe, Ni and 20 siderohile and chalcophile elements powders, and heating treatment to minimize the elemental heterogeneity. The nominal concentrations of trace elements were 150 μg/g. The resulting metal button was subsidized to evalation of major and trace element abundance using EPMA and the fs-LA-ICPMS. The abundance data for both the major elements and trace elements reveraled that the abundance for trace elements did not vary measurably within the analytical precisions achived here. In this precision, we will present the abundance data. In this presentation, we will present the abundance data for several iron meteorites to comparing the previously reported value. Availability of in-house metallic standard for meteoritic metals will be discussed in this presentation.

[1] Hirata and Kon (2008) *Anal. Sci.*, **24**, 345-353.

Effect of oxidation state on arsenic and selenium incorporation into calcite

Y. YOKOYAMA* AND Y. TAKAHASHI

Hiroshima University, Hiroshima 739-8526, Japan (*correspondence: yoshiyuka@hiroshima-u.ac.jp)

The influences of oxidation state on arsenic (As) and selenium (Se) coprecipitation with calcite were evaluated with the information of their oxidation states both in water and calcite, and thermodynamic stability in water. To assess these reaction quantitatively, As and Se distribution coefficients (K_d) into calcite were determined using reproducible experimental system of their partition at low precipitation rates such as in natural systems.

The XAFS measurements showed that calcite selectively incorporated pentavalent As (arsenate) rather than trivalent As (arsenite)[1], and tetravalent Se (selenite) was selectively incorporated rather than hexavalent Se (selenate). Molecular geometries of dissolved selenite and selenate are similar to that of arsenite and arsenate, respectively. However, there was no relationship in their incorporation behavior into calcite. Interestingly, the XANES analysis detected arsenate and selenite in calcite precipitated only from arsenite or selenate spiked systems, respectively. Moreover, our cyclic voltammetric measurement observed arsenate stabilization in solution containing calcium ion indicating the shift of arsenite/arsenate redox boundary. These phenomena are associated with high stability of calcium arsenate and calcium selenite complexes compared with those for arsenite and selenate, respectively. Considering the abundance of calcium in natural water, the valence change effects by calcium is important as a (geo)chemical reaction which may have been overlooked so far. Hence, we conclude that the factor controlling incorporation behavior of As and Se into calcite is the stabilities of their complexes with calcium ion. These thermodynamic properties should be explained by quantum chemical approaches. In view of the valence change effects by calcium, ratios of their net K_d into calcite were determined at pH ~7 : $K_{As(V)}/K_{As(III)}$ was >2500 and $K_{Se(IV)}/K_{Se(VI)}$ was 150.

Immobilization of As and Se with calcite in groundwater are of great interest for remediation of contaminated drinking water such as in Bangladesh and for inhibition of ^{79}Se migration from nuclear waste repositories, respectively. Therefore, the present findings should provide some insights into those concerns because As and Se oxidation states are variable in subsurface environment.

[1] Yokoyama *et al.* (2009) *Chem. Lett.* **38,** 910-911.

https://doi.org/10.1180/S0026461X00006502 Published online by Cambridge University Press

Silicic acid removal as calcium or magnesium silicate from geothermal water

KOTARO YONEZU[1], YOHEI KAWABATA[1], KOICHIRO WATANABE[1] AND TAKUSHI YOKOYAMA[2]

[1]744 Motooka, Nishi-ku, Fukuoka 819-0395 Japan, (yone@mine.kyushu-u.ac.jp)
[2]6-10-1 Hakozaki, Higashi-ku, Fukuoka 812-8581 Japan

Geothermal energy is one of the most probable clean energy in Japan; however the total power supply from geothermal energy has recently plateaued due to short lifetime of reinjection well caused by siliceous deposit from geothermal water. Removal of silicic acid as calcium or magnesium silicate is investigated towards an effective utilization of geothermal energy.

Sample solutions were prepared to be an initial Ca/Si or Mg/Si molar ratio = 1.4 to 4.0 (Si concentration: 400 ppm). The solutions were magnetically stirred and the pH was maintained at 11 or 12 with NaOH solution. At appropriate intervals, an aliquot of the suspensions was filtered using a 0.45 μm membrane filter. At an initial Ca/Si or Mg/Si ratio = 2.1, silicic acid in the solution can be effectively removed within 1 h. The precipitates are identified as calcium silicate or amorphous magnesium silicate by XRD patterns. In addition to removal of silicic acid, simultaneous removal of boron coprecipitated with silicate was investigated (B concentration: 40 ppm). In the case of calcium silicate, around 50 % of boron can be removed. In contrast, almost all boron can be removed from the solution by magnesium silicate. ^{11}B NMR result showed that boron coprecipitated with magnesium silicate exists as 4-coordinated, suggesting that the coprecipitated boron may be incorporated by substitution of Si with B.

Advantages of this removal method are realization of longer lifetime implement at geothermal power plant and simultaneous removal of hazardous elements. The treatment of enormous amount of silicate removed from geothermal water remains an issue to be solved.

Christina River Basin Critical Zone Observatory: Carbon-mineral interactions from molecular to basin scales in the Anthropocene

KYUNGSOO YOO[1], ANTHONY K. AUFDENKAMPE[2], CHUNMEI CHEN[3] AND DONALD L. SPARKS[3]

[1]Dept. of Soil, Water, and Climate, University of Minnesota, St.Paul, MN.USA. (*correspondence: kyoo@umn.edu)
[2]Stroud Water Research Center, Avondale, PA. USA. (aufdenkampe@stroudcenter.org)
[3]University of Delaware Environmental Institute, DE, USA. (cmchen@udel.edu and dlsparks@udel.edu

Over the last several decades, biogeochemical studies on terrestrial carbon cycle have converged on a consensus that tight association of organic matter (OM) with minerals through physical occlusion or surface complexation is crtical in lengthening the turnover time of carbon (C).

The primary goal of the Christian River Basin Critical Zone Observatory (CRB-CZO) is to scale up C-mineral interactions that occur at molecular and mineral grain scales to soil profiles to hillslopes and finally to basin scales. While small (nano to mineral grain) scale characterizations of C-mineral interactions are being made, physical movment of OM and minerals –such as soil mixing at soil profile scale, physical erosion and deposition in watershed scales, and stream turbulence in streams – is investigated as responsible for their contacts. Chemical weathering of minerals and minerals' interaction with water are considered as processes that generate the surface area and reactivity of minerals where OM could be complexed. Additionally, biological cycling of OM prepares OM's chemical affinity to minerals.

Preliminary analyses suggest that the extents of physical contacts between OM and minerals – which are required for C-mineral complexation – are indeed limited by their physical movements and that these movements are highly sensitive to land use types. Furthermore, eroded minerals from agricultural fileds appear to complex C during their fluvial transit. The preliminary data support the core assumptions of our hypothesis that accelerated erosion and deposition in agricultural and constructional watershed may generate greater amount of mineral-complexed C.

In the end, we expect that our intensive field sampling and installation of wireless sensor network and data management toward testing our hypothesis should build our CRB-CZO as an excellent resource for entire scientific community.

https://doi.org/10.1180/S0026461X00006502 Published online by Cambridge University Press

Uranium and radium isotope ratio at Korean hot spring water

YOON YEOL YOON, SEUNG GU LEE, SOO YOUNG CHO, KIL YONG LEE AND TAE JONG LEE

Korea Institute of Geoscience and Mineral Resources, Gwahang-no 92, Yuseong-gu, Daejeon, 305-350, Korea (yyyoon@kigam.re.kr, sgl@kigam.re.kr, sycho@kigam.re.kr, kylee@kigam.re.kr, megi@kigam.re.kr)

The hydrological characteristics of the groundwater were affected by surrounding geology and water-rock interaction. To understand hydrogeology, various applications of isotope geochemical techniques for geothermal investigations have been applied.

Uranium and Radium are natural radionuclides and they have isotopes. To understand water-rock interaction and hot spring water environments ^{234}U, ^{238}U, ^{226}Ra, and ^{228}Ra were analyzed using extractive radiochemistry and LSC measurements.

Uranium isotope was extracted with HDEHP and counted with LSC. Radium isotopes were separated using Ba coprecipitation and ^{226}Ra was counted with LAC and ^{228}Ra was analyzed with HPGe γ-detector. Among them ^{228}Ra is below detection limit.

Sample	U(μg/L)	$^{234}U/^{238}U$	Ra-226 (Bq/L)
SCHS	1.50	1.0	<0.003
DGHS	5.03	0.69	<0.003
BAHS	0.04	-	<0.003
BKHS	<0.01	-	0.005
MGHS	0.68	1.17	0.010
DRHS	3.58	1.50	0.006
HYHS	0.68	1.06	0.145
DSHS	0.17	-	<0.003
ASHS	5.94	0.80	<0.003
YSHS	49.7	0.71	<0.003
PDHS	0.01	-	0.031
SAHS	0.07	-	0.014
PCHS	1.39	1.0	<0.003
GHHS	0.011	-	<0.003

Table 1. Uranium and radium istope values in Korean hot spring water.

[1] Ammar (2010) *J. Environ. Radioact.* **101**, 681-691. [2] El-Reefy (1997) *J. Chem. Tech. Biotechnol.* **69**, 271-275. [3] Nakano-Ohta (2007) *J.nucl.Radiochem. Sci.* **8**, 143-148. [4] Vasile (2010) *Appl. Radiat. Isotop.* **68**, 1236-1239.

Relative B-Li-Cl compositions: Capability and limitation to direct observation of deep geofluid

K. YOSHIDA[1]*, Y. SENGEN[1], S. TSUCHIYA[1], K. MINAGAWA[1], T. KOBAYASHI[2], T. MISHIMA[3], S. OHSAWA[3] AND T. HIRAJIMA[1]

[1]Kyoto University, Oiwake-cho, Sakyo-ku, Kyoto, Japan. (*correspondence: yoshikem@kueps.kyoto-u.ac.jp)
[2]Chiba University, Yayoi-cho, Inage, Chiba, Japan
[3]IGS, Kyoto University, Noguchibaru, Beppu, Japan

Some recent studies invoked that the variation of some fluid soluble light elements, e.g., Li, B and Cl, are capable of suggesting fluid generation depths [1, 2]. To evaluate this idea, we mesured relative B-Li-Cl compositions of fluid inclusions in quartz veins intercalated with basic/pelitic schists and eclogites of the Sambagawa belt, Japan, as foliation parallel quartz veins are capable of preserving the characteristics of syn-metamorphic fluid inclusion [3].

Li/B ratio of the crush-leached fluid extracted from quartz veins intercalated with basic schists and eclogites from Wakayama and Besshi area show a positive correlation with peak *P-T* conditions of their host rocks [4]. However, some fluid samples extracted from quartz veins hosted in pelitic schists from Besshi area have much higher Li/B ratios than those of the basic schist of the same metamorphic grade [5]. Hydrochemical facies of those samples are characterized by the dominance of Na-Cl or Na/K-HCO_3. Optical and SEM-CL observation indicate that those quartz veins are deformed with various degrees and most of them show polygonal texture. On the other hand, most crush-leached fluid extracted from quartz veins of Asemi-gawa area show discrete Li/B value. Their hydrochemical facies are characterized by the dominance of Ca-HCO_3, which is known as the characteristics of pore fluid in near surface fracture of continental crust [6], and quartz veins have strongly deformed fabric.

These results suggest that deformation during the exhumation stage, accompanied with fluid infiltration, can severely modify the compositions of fluid trapped in the corresponding veins. Despite that there are several problems in using fluid inclusions in quartz veins as a means to investigate geofluid activity, hydrochemical facies of the crush-leached fluid and quartz fabric can be clues to find the syn-metamorphic fluid.

[1] Scambelluri *et al.* (2004) *EPSL* **222**, 217-234. [2] Ohsawa *et al.* (2010) *Jour. Hot Spr. Sci.* **56**, 295-319. [3] Nishimura *et al.* (2008) *Jour. Min. Pet. Sci.* **103**, 94-99. [4] Sengen *et al.* (2009) *Abst. Ann. Meeting of JpMS, Sapporo*. [5] Yoshida *et al.* (2011) *Jour. Min. Pet. Sci.* in printing. [6] Bucher & Stober (2010) *Geofluids* **10**, 241-253.

https://doi.org/10.1180/S0026461X00006502 Published online by Cambridge University Press

Carbon isotope evolution in magmatic systems by CO_2 fluxing

SHUMPEI YOSHIMURA[1]* AND MICHIHIKO NAKAMURA[2]

[1]Natural History Sciences, Hokkaido University, Sapporo 060-0810, Japan (*correspondence: shumpyos@ep.sci.hokudai.ac.jp)
[2]Department of Earth Science, Tohoku University, Sendai 980-8578, Japan (nakamm@m.tohoku.ac.jp)

Simple degassing models often fail to explain the high CO_2/H_2O ratio of melt inclusions and obsidian pyroclasts. This suggests that the fluxing of a deep-derived CO_2-rich fluid is common in crustal magmatic systems (e.g., [1]). This process, called "CO_2 fluxing", is believed to be a combination of the advective flow of a CO_2-rich fluid through a magma column and the resulting volatile exchange. However, other processes, such as closed-system equilibrium degassing under the presence of a buffering CO_2-rich fluid [2] and disequilibrium open-system degassing [3], can explain such data. In this study, we show that carbon isotope ($\delta^{13}C$)–CO_2 systematics may discriminate these processes.

We present a theoretical framework of carbon isotope evolution caused by CO_2 fluxing based on a reactive transport model. We assumed that a CO_2-rich fluid with a constant CO_2/H_2O ratio and a constant $\delta^{13}C$ value is introduced into a magma column and flows upward through the column, exchanging volatile components chemically and isotopically with the melt. The governing equations consist of an advection equation, the solubility law of CO_2-H_2O and an equation of isotope equilibration. The equilibrium volatile exchange is assumed at each level of the column.

The calculations show that initial carbon isotope distribution is immediately modified as the fluxing proceeds. When the first incremental of the introduced fluid reached the top of the column, the $\delta^{13}C$ value was almost constant along the column, whereas CO_2-H_2O concentrations were still changing towards entire equilibrium between the magma and the introduced fluid. These results are in contrast to those for other processes such as equilibrium degassing where $\delta^{13}C$ decreases as degassing proceeds, or disequilibrium degassing where $\delta^{13}C$ is expected to increase because $^{12}CO_2$ may diffuse faster than $^{13}CO_2$.

[1] Métrich & Wallace (2008) *Reviews in Mineralogy and Geochemistry* **69**, 363–402. [2] Newman *et al*. (1988) *J. Volcanol. Geotherm. Res*. **35**, 75–96. [3] Gonnermann & Manga (2005) *Earth Planet. Sci. Lett*. **238**, 1–16.

Temperature dependence of Mg isotope fractionation in deep-sea coral: Paleoceanographic implication as a new proxy for water temperature

TOSHIHIRO YOSHIMURA[1'2]*, MASAHARU TANIMIZU[3], MAYURI INOUE[1], ATSUSHI SUZUKI[4], NOZOMU IWASAKI[5] AND HODAKA KAWAHATA[1]

[1]Atmosphere and Ocean Res. Inst., The University of Tokyo, 5-1-5 Kashiwanoha, Kashiwa 277-8563, Japan (*Correspondence: yoshimura@aori.u-tokyo.ac.jp)
[2]Graduate School of Frontier Science, The University of Tokyo, Kashiwa 277-8564, Japan
[3]Kochi Inst. for Core Sample Res., JAMSTEC, Kochi, Japam
[4]Geological Survey of Japan, AIST, Tsukuba, Japam
[5]Usa Marine Biological Institute, Kochi Univ., Kochi, Japam

This study presents magnesium isotopic composition and its temperature dependence of high Mg biogenic calcium carbonates to evaluate their potential proxy of paleo seawater temperature. Degrees of Mg isotope fractionation compared to present seawater were measured in deep-sea coral. The mean $\delta^{26}Mg$ value of deep-sea corals was –2.5‰. Moreover, Mg isotope fractionation in deep-sea coral showed a clear temperature dependence from 2.5 to 19.5 °C. The observed temperature dependence of Mg isotope fractionation in deep-sea coral skeletons allows potential application of Mg isotopes of high-Mg calcite to an environmental proxy for water temperature, and one possible way for robust temperature reconstruction is a multi-proxy approach which provides complementary and more robust temperature data using traditional and non-traditional temperature proxies. The mean $\delta^{26}Mg$ value of large benthic foraminifera which are also composed of high-Mg calcite was -2.34‰. Deep-sea coral and benthic foraminifera both plot on the same regression line within uncertainty. Deep-sea corals and benthic foraminifera also showed similar Mg isotope fractionation factor to inorganically precipitated calcite, and the slope of temperature dependence in Mg isotope fractionation is similar to that for an inorganically precipitated calcite speleothem. Moreover, Mg concentrations and the relationship between Mg/Ca and temperature were also similar between deep-sea corals and inorganically precipitated calcite. Taking into account elemental partitioning and the calcification rate of biogenic CaCO3, the similarity among inorganic minerals, deep-sea corals and benthic foraminiferas may indicate a strong mineralogical control on Mg isotope fractionation for high-Mg calcite.

https://doi.org/10.1180/S0026461X00006502 Published online by Cambridge University Press

Laboratory-based conductivity structure in the mantle transition zone

T. YOSHINO[1], A. SHIMOJUKU[1] AND T. KATSURA [2]*

[1]Institute for Study of the Earth's Interior, Okayama Univ., 682-0193 Misasa, Japan (tyoshino@misasa.okayama-u.ac.jp, simojuku@misasa.okayama-u.ac.jp)
[2]Bayerisches Geoinstitut, Univ. Bayreuth, 95440 Bayreuth, Germany (*correspondence: tomo.katsura@uni-bayreuth.de)

It is essential to assess the species and amount of volatile components in the mantle for understanding its dynamics and evolution. For this reason, we studied conductivity of the upper-mantle minerals as a function of temperature and incorporated water content. Our measurements on hydrous olivine, wadsleyite and ringwoodite demonstrated that, although the water incorporation to these minerals increases their conductivity, this effect is relatively small. In contrast, other research groups claimed significantly larger effects. Our measurement was criticized due to lack of impedance spectroscopy for wadsleyite although we adopted this method for olivine and partly ringwoodite. For this reason, we reinvestigated conductivity of hydrous wadsleyite by means of impedance spectroscopy.

Our measurement demonstrated that conductivity of a fluid phase released from hydrous wadsleyite masks that of wadsleyite itself above 1000 K. It was also found that the impedance arcs in the Nyquist plot are significantly distorted when the fluid phase is released, probably because impedance arcs of the grain boundary fluid and reaction on the electrodes overlap with each other. The measurement results given by our conventional low frequency method and impedance sprectroscopy show excellent agreement. These observations prove appropreateness of our previous conclusion.

We constructed a laboratory-based conductivity model of the upper mantle using our experimental data. This model shows the following features. The conductivity jump at 410-km depth is very small even if it exists. In contrast, the conductivity jump at 520-km depth is remarkable. There is no evidence from conductivity for presence of water in the mantle transition zone beneath the Pacific Ocean. Very high amount of water (0.5 %) would be required to explain the high conductivity beneath the Philippine Sea if it is explained by hydration of the upper-mantle minerals.

In situ iron isotope analyses of pyrites from 3.5 to 3.2 Ga sedimentary rocks of the Barberton Greenstone Belt, Kaapvaal Craton

KAZUMI YOSHIYA[1], YUSUKE SAWAKI[2], TAKAZO SHIBUYA[2], SHINJI YAMAMOTO[3], TSUYOSHI KOMIYA[3], SHIGENORI MARUYAMA[1] AND TAKAFUMI HIRATA[4]

[1]Dept. of Earth and Planetary Sci., Tokyo Institute of Technology, Japan (yoshiya.k.aa@m.titech.ac.jp)
[2]Japan Agency for Marine-Earth Sci. & Tech., Japan
[3]Dept. of Earth Sci. and Astro., Komaba, Univ. Tokyo, Japan
[4]Dept. of Geology and Mineralogy, Kyoto Univ. Japan

The Barberton Greenstone Belt (BGB), South Africa consists of volcano-sedimentary successions and sedimentary rock sequences deposited between 3.5 and 3.2 Ga, and is subdivided into three groups: the Onverwacht, Fig Tree, and Moodies Groups. Several putative morphological fossils (filamentous and sphere type) and trace fossils were reported from the Hooggenoeg and Kromberg Formations in the Onverwacht Group [1,2,3]. On the other hand, isotopic data suggest the activities of sulphate-reducing bacteria and photosynthetic bacteria at 3.4 Ga [4]. Dissimilatory iron reduction (DIR) is also considered to be one of the earliest metabolisms on Earth [5], but the previously reported oldest isotopic evidence for the DIR by bacteria is from 2.9 Ga [6]. We report the in-situ iron isotope analysis of individual pyrites in sedimentary rocks from the BGB, using femtosecond laser ablation multi-collector ICP-MS technique (fs-LA-MC-ICP-MS) [7]. We obtained a large variation of iron isotope data from -1.9 to +3.6 ‰ in δ^{56}Fe values, from 94 pyrite grains in 16 samples: five cherts from the Hooggenoeg Formation, eight cherts from the Kromberg Formation, one sandstone from the Fig Tree Group, and three sandstones from the Moodies Group. The δ^{56}Fe values of pyrite from Hooggenoeg Formation show positive values, whereas those from the Kromberg Formation show wide variation from positive to negative values. The negative δ^{56}Fe values of pyrites with a nadir down to -1.9 ‰ in the Kromberg Formation indicates DIR by bacteria. This result shows that the activity of iron-reducing bacteria can date back to, at least, the middle Archean.

[1] Engel *et al*. (1968), *Science* **161**, 105-108. [2]Walsh and Lowe (1985) *Nature* **314**, 530–532. [3] Furnes *et al*. (2004), *Nature* **304**, 578–581. [4] Kakegawa and Ohmoto (1999), *Precam. Res*. **96**, 209–224. [5] Lovley (2004), Origins, Evolution, and Biodiversity of Microbial Life. pp. 301–313. [6] Yamaguchi *et al*. (2005) *Chem. Geo*. **218**, 135-169. [7] Nishizawa *et al*., (2010), *GCA*. **74**, 2760-2778.

https://doi.org/10.1180/S0026461X00006502 Published online by Cambridge University Press

Geological characteristics of black shale series in southern Anhui Province

HAIJIAO YOU[1,2], YONG ZHAN[1,2] AND YOUFEI GUAN[1,2]

[1]China Gezhouba Group Corporation, P.R. China (youhaijiao@yahoo.cn)
[2]Anhui University of Architecture, P.R. China

The black shale series in southern Anhui are developed widely. The southern Anhui area is located in the northeast margin of Lower Yangtze block and adjacent to Jiangnan uplift zone. The occurrence of Paleozoic strata is relative complete, and the Lower Cambrian shale black shale series are relatively well developed in Hetang Formation and Huangbailing Formation that locate on both sides of Jiangnan deep-fault zone. The area developed the Sinian and Early-Middle Triassic sedimentary cover, late Yanshanian intrusions, NE Jura-type folds and a series of the NE tthrusting (sliding) nappe structure, and suffered multi-stage tecteonic movements with a polycyclic feature of magmatic activities.

Lower Cambrain Hetang Formation and Huangbailing Formation are the primary strata of black shale series, and they are different on lithology and thickness. Then former is divided into three parts from bottom to top on lithology: the lower part is carbonaceous siliceous mudstone member intercalating with limestone, composing of Si-bearing carbonaceous shale, carbonaceous limestone, calcipulverite and phosphatic nodule with obvious rhythm, and the middle part is carbonaceous mudstone member that comprises carbonaceous mudstone, siliceous mudstone and silty carbonaceous mudstone, intercalating with a layer of fine-grained calcipulverite, and the carbonaceous materials are enriched to form stone coal layer in the lower section of the middle part, and the upper part is mudstone member with horizontal laminar, mostly composed of gray calcareous mudstone and carbonaceous mudstone with obvious horizontal laminar. The later is also divided into three parts: the lower part is black carbonaceous siliceous shale member with lentoid stone coal layer at the bottom, and the middle part is gray medium-bedded calcipulverite and black carbonaceous shale, and the upper part is yellow green mudstone with silty shale. The thickness of Huangbailing Formation is more than Hetang Formation's.

The middle members of Hetang Formation and Huangbailing Formation both have poly-metallic enrichment layer where enriched useful elements (Ni, Mo, Au, Ag, etc.), rare elements (Cd, Se, Ti, Cs, etc.) and radioactive elements (U, Th, etc.). Therefore, the systematic study on black shale series in the area has important theoretical significance and potential economic value.

This research was financially supported by the Natural Science Foundation of Anhui Provincial Education Department of China (NO.KJ2010A070).

Microbial dolomite in Cambrian stromatolites of Tarim basin, northwest China

XUELIAN YOU

Institute of Geology and Geophysics, Chinese Academy of Sciences, Beijing 100029, China (youxuelian007@gmail.com)

Microbial mediation is the only proven mechanism to precipitate experimental dolomite under Earth's surface conditions [1]. Proving a biogenic microbial origin for ancient stromatolites is very difficult, but there are dumbbell dolomite with nanoglobule texture within micritic dolomite crystal (Fig 1A) and aggregates of nanoglobules dolomite (Fig 1B) in dark stromatolitic laminae in a inter-supratidal of the lower sabkha deposits. Nanoglobules (indicated by red arrows in Fig 1A) are 50–90 nm in diameter and aggregates of nanoglobules (indicated by black arrows in Fig 1B) are 100–160 nm (large globules).

The characteristic texture, morphology and sizes in diameter are very similar to the results of dolomite precipitation in anerobic or aerobic culture experiments [2, 3]. These results reveal that these observed may be microbial signatures preserved in the rock record .

These results provide microbial tracers evidences in Cambrian dolomite stromatolites which are proposed a microbial dolomite origin.

This work is granted by the National major Science and Technology Project of China (No. 2008ZX05008-003)

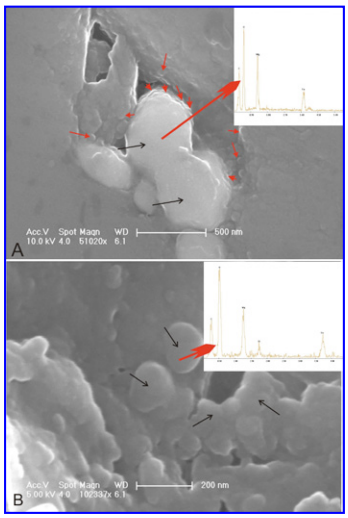

Figure 1: SEM photomicrographs of microbial dolomite

[1] Vasconcelos C *et al*. (1995) *Nature* **377**, 220-222. [2] Bontognali T *et al*. (2008) *Geology* **36**, 663-666. [3] Sánchez-Román M *et al*. (2008) *Geology* **36**, 879-882.

https://doi.org/10.1180/S0026461X00006502 Published online by Cambridge University Press

Study of evolution model of Triassic K-rich brine in Sichuan Basin

ZHOU YOU[1] AND ZHANG HANG[2]

[1]key lab of Geomathematics of Sichuan province, chengdu sichuan China, 610059 (*correspondence: zhouyou06@cdut.cn)

[2]Chengdu university of technology , chengdu sichuan China, 610059 (zhanghang@cdut.edu.cn)

Sichuan Basin has rich brine resources in China. It has 2000 years of mining history of Salt in it's southwest mine.

This paper forms the ancient brine hydrogeological conditions, and establishes the Sichuan basin evolution model of K-rich brine. This paper argues that causes of K-rich brine in eastern Sichuan and western Sichuan is not entirely consistent.K-rich Brine formation process in Triassic can be summarized as follows:

1. Early and Middle Triassic, Sichuan Basin become marginal sea with seawater intrusion. Water salinity increased and the initial potassium concentrated. In the end of Early Triassic, the submarine volcanic eruption formed about 1 m thick mung bean rock, and provided a wealth of potassium resources.

2. Indo-China movement in the end of Middle Triassic, almost the entire Sichuan Basin rised above the sea surface. Triassic strata was impact of erosion and denudation. Original sedimentary brine was poured and mixed by leaching water.

3. Late Triassic Basin decreased, seawater intrusion until the Cretaceous. In this period, basin accumulated a thick layer of sediment over 1000m. Original sedimentary brine was deep closed and metamorphism. Rock salt, mung bean rock and plaster provided potassium and water.

4. In the end of Cretaceous, Sichuan movement maked the basin to rise again and also to make the basin have a large number of drapes and fractures,which have become reservoir space of K-rich brine. Sichuan movement has also brought deep hydrothermal which Contain potassium and other elements. K-rich Brine Enriched in the fornix trap structure, formed Brine deposits

In Sichuan basin, K-rich brine was found in eastern Sichuan and western Sichuan. PL4 well in western Sichuan, Boron content is up to 4767.6mg/l, and potassium content is 49.95g/l. The content is about twice the eastern C25 well. This paper argues that PL4 well is deeply influenced by the deep hydrothermal than C25 well, and East Tethys seawater had supply the western basin in the end of Middle Triassic. This view was support by trace element and isotope geochemistry.

[1] Wangyunpu (1982), study of brine formation [M] [2] Linyaoting (2009), *Salt Lake Research*, **17**(1),6-12

High mass resolution gas-source mass spectrometry

E.D. YOUNG[1]*, D. RUMBLE III[2] , P. A. FREEDMAN[3], E.A. SCHAUBLE[1] AND W. GUO[2]

[1]Department of Earth and Space Sciences, UCLA, Los Angeles, CA 90095 (eyoung@ess.ucla.edu)

[2]Geophysical Laboratory, Carnegie Institution of Washington, Washington DC, 20015

[3]Nu Instruments Ltd., Wrexham, UK

Conventional gas-source isotope ratio mass spectrometers are fully capable of measuring the relative abundance of the rare $^{13}C^{18}O^{16}O$ isotopologue (m/e ~ 47) in CO_2. Abundances of rare isotopologues of other gases are promising tracers of provenance in geochemistry and atmospheric chemistry, but measurements are not possible at present due to the limitations imposed by gas-source mass spectrometers on the market today. A critical step forward is an increase in the mass resolving power (MRP) of these instruments.

We have begun a project to build a high-MRP gas-source isotope ratio mass spectrometer designed expressly for the purpose of resolving rare isotopologues of a variety of gases, including those of CH_4. The latter have driven the design in large part because of the difficulty in resolving $^{13}CDH_3$ from $^{12}CD_2H_2$ (m/Δm = 6178) together with the great potential that these species would have in establishing the provenance of CH_4.

We utilize the so-called "Matsuda" post-ESA lens arrangement for minimizing aberrations. The design maximizes MRP while minimizing vertical dispersion along the flight path. With a magnetic sector radius of 800 mm the anticipated MRP is ~ 30,000 to 40,000 with acceptable sensitivity. This is sufficient for flat-top peak resolution of a wide variety of rare isotopologues of gases that include CH_4, O_2, N_2O, SO_2, among others. An example calculation of the effect of MRP on separating mass-18 isotopologues of CH_4 is presented in the figure below. Results show that an MRP approaching 30,000 is required for flat-top resolution of $^{18}CH_4$ species.

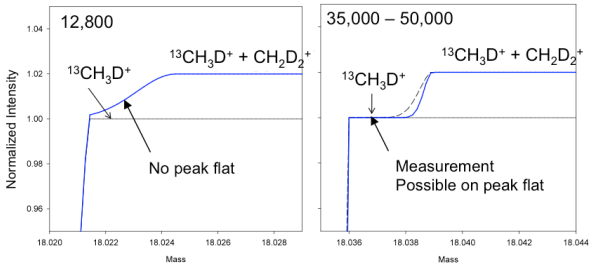

https://doi.org/10.1180/S0026461X00006502 Published online by Cambridge University Press

Assessment of the geochemical processes and environmental pollution in the Trincomalee bay, Sri Lanka

SANSFICA M. YOUNG[1]*, A. PITAWALA[2] AND H. ISHIGA[1]

[1]Department of Geosciences, Shimane University, 690-8504, Matsue, Japan

[2]Department of Geology, University of Peradeniya, Peradeniya, Sri Lanka

Trace and major elements of surface sediments in bay environment are often used to study the geochemical processes, environmental issues, transportation of weathered products. The Trincomalee bay can be divided into three parts as for sediment distribution; Koddiyar Bay (KB), Thanmbalagam Bay (TB) and Inner Harbor (IH). Surface samples from all three areas have been collected and XRF analysis was carried out to determine As, Pb, Zn, Cu, Ni, Cr, V, Sr, Y, Nb, Zr, Th, Sc, Fe_2O_3, TiO_2, MnO, CaO, P_2O_5 and total sulphur contents. Geographical Information System (GIS) maps for ratio plots Th/Zr was used to consider heavy mineral (HM) accumulation and dilution and the surface distribution of Th and Zr individually to further explain many HM faces involved. The GIS maps for other individual elements also were used to explain the geochemical processes within the bay area upon the input of the river sediments and also the pollution activities.

Th/Sc-Zr/Sc shows that the sediments are of andesite to rhyolite in composition, while the KB shows Zr enrichment. Cr/V-Y/Ni shows a Cr dilution with carbonates while the Cr-Ni shows a quartz dilution in the IH indicating marine influence. Environmental contamination of Cu, Pb As, Zn is seen in the IH due to the harbour and in the KB and TB with natural issues.

Weighting stream sediment geochemical samples as exploration indicator of deposit-type

M. YOUSEFI[1], A. KAMKAR-ROUHANI[1] AND E.J.M. CARRANZA[2]

[1]Mining Department, Shahrood University, Iran (*correspondence: m.yousefi.eng@gmail.com, kamkarr@yahoo.com)

[2]Faculty of Geo-Information and Earth Observation (ITC), University of Twente, Netherlands (carranza@itc.nl)

Factor analysis has been widely used for classification of stream sediment geochemical data in mapping of prospective areas for certain type of mineral deposits [1, 2]. However, interpretation of the results of factor analysis remains challenging in terms of selecting the factor (or association of elements) that best predicts the location of known mineral deposits of a certain type. Here, we used stepwise factor analysis to recognize and omit non-predictive geochemical elements from the data to elicit the best factor representing the presence of mineral deposits of the type being examined. Then, to obtain a geochemical mineralization probability index of mineral deposits of the type sought X ($GMPI_X$) for each stream sediment geochemical sample, we used multivariate and logistic regression analyses sequentially. The generalized model of $GMPI_X$ for mineral deposits of the type sought (X) is

$$GMPI_X = \frac{e^{\alpha_0+\alpha_1 y_1+\alpha_2 y_2+\cdots+\alpha_n y_n}}{1+e^{\alpha_0+\alpha_1 y_1+\alpha_2 y_2+\cdots+\alpha_n y_n}},$$

where $y_1, y_2,\ldots,y_n$ are 'predictor' elements of the deposit-type of interest, which were obtained from the results of stepwise factor analysis; $\alpha_1, \alpha_2,\ldots, \alpha_n$ are multivariate regression coefficients. The values of $GMPI_X$ range between 0 and 1. These values can be mapped to delineate areas upstream of geochemical samples where mineral deposits of the type sought are likely present. Successful application of the proposed methodology is demonstrated for fluorite deposits in a study area in Iran.

[1] Reimann *et al*. (2002) *Applied Geochemistry* **17,** 185-206.
[2] *Helvoort et al*. (2005) *Applied Geochemistry* **20,** 2233-2251.

https://doi.org/10.1180/S0026461X00006502 Published online by Cambridge University Press

Oxidative weathering of black shale: A long-term humidity cell test

C.X. YU[1]*, M. ÅSTRÖM[1], P. PELTOLA AND H. DRAKE

School of Natural Science, Linnaeus University, 39182 Kalmar, Sweden (*correspondence: changxun.yu@lnu.se)

Weathering of black shale is of large envionmental interest, and is characterized by oxidation of sulfide minerals (mainly pyrite) and organic matter [1]. When oxidized large amount of trace elements could be liberated and subsequently transferred into the broader environment. Here we present a long-term humidity cell test of non-weathered black shale (NBS) and weathered black shale (WBS). The NBS and WBS was leached for 137 (66 leaching cycles) and 53 weeks (40 leaching cycles), respectively.

BET surface area of NBS increased by 26 %, which is mainly contributed by euhedral pits caused by the oxidation of pyrite embedded in the illite matrix (Fig. 1a). XRD analyses confirmed that the amount of pyrite decreased from ~4.3% to 2.8% during the experiment. As a result, large proportions (27% to 61%) of Co, Ni, Cd, Zn, Mn, U and Cu have been leached from NBS, whereas the proportions leached of As, Cr, Ba, Pb and V were lower than 2.3%. Major cations Fe and Al in NBS leachates showed significant correlation with S after cycle 32 at pH 5.5, implying that their behaviours were controlled by common sulphate minerals thereafter. The pore-rich grains of leached NBS, structured by a silicate matrix (illite and quartz) resistant to the oxidative weathering, were characterized by abundant precipitation of siderite and/or gypsum within pores and schwertmannite coating onto their surface (Fig. 1a). Three types of encrustations were identified in both leached NBS and WBS: schwertmannite with minor amount of Fe^{3+} phosphate (Fig. 1b), Fe^{3+} phosphate and apatite. These encrustations have strong affinity for trace elements occurred as negative charged aqueous species (e.g $H_2AsSO_4^-$), providing potential filters for natural trace element cyling.

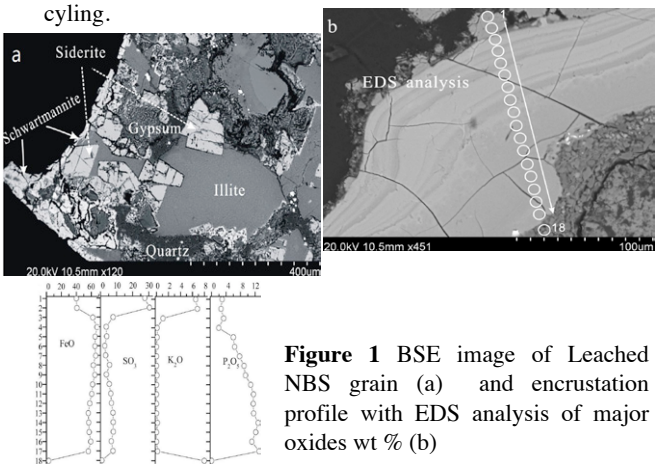

Figure 1 BSE image of Leached NBS grain (a) and encrustation profile with EDS analysis of major oxides wt % (b)

[1] Lavergren *et al*. (2009) *Appl Geochem* **24**, 59–369.

Assessing impact of aerosol intercontinental transport on regional air quality and climate: What satellites can help

HONGBIN YU[1,2]

[1]Earth System Science Interdisciplinary Center, University of Maryland, College Park, MD 20740, USA
[2]Laboratory for Atmospheres Research, NASA Goddard Space Flight Ceneter, Greenbelt, MD 20771, USA (Hongbin.Yu@nasa.gov)

Mounting evidence for intercontinental transport of aerosols suggests that aerosols from a region could significantly affect climate and air quality in downwind regions and continents. Current assessment of these impacts for the most part has been based on global model simulations that show large variability. The aerosol intercontinental transport and its influence on air quality and climate involve many processes at local, regional, and intercontinental scales. There is a pressing need to establish modeling systems that bridge the wide range of scales. The modeling systems need to be evaluated and constrained by observations, including satellite measurements. Columnar loadings of dust and combustion aerosols can be derived from the MODIS and MISR measurements of total aerosol optical depth and particle size and shape information. Characteristic transport heights of dust and combustion aerosols can be determined from the CALIPSO lidar and AIRS measurements. CALIPSO lidar and OMI UV technique also have a unique capability of detecting aerosols above clouds, which could offer some insights into aerosol lofting processes and the importance of above-cloud transport pathway. In this presentation, I will discuss our efforts of integrating these satellite measurements and models to assess the significance of intercontinental transport of dust and combustion aerosols on regional air quality and climate.

https://doi.org/10.1180/S0026461X00006502 Published online by Cambridge University Press

Formation of the oldest rocks in the Cathaysia Block, Southern China

JIN-HAI YU[1,2], SUZANNE Y. O'REILLY[2], LIJUAN WANG[1,2] AND W.L. GRIFFIN[2]

[1]State Key Laboratory for Mineral Deposits Research, School of Earth Sciences and Engineering, Nanjing University, Nanjing 210093, China

[2]GEMOC ARC National Key Centre, Department of Earth and Planetary Sciences, Macquarie University, Sydney, N.S.W. 2109, Australia

Precambrian basement in the Cathaysia Block of South China is mainly found in the Wuyishan area (southern Zhejiang and northwestern Fujian Provinces). The Badu Complex which is the oldest rock in the area consists of various mets-sedimentary rocks and was intruded by Paleoproterozoic (1.88-1.86 Ga) granites. CL images, U-Pb dating results and trace element compositions of zircons from the high-grade metamorphic rocks in the Badu Complex indicate that inherited zircon cores are of magmatic origin and predominantly formed ca. 2500 Ma ago, while the rims overgrew at 1886-1882 Ma and 252-234 Ma. Although some zircon cores have Paleoproterozoic ages similar to the rims, the similarity in the trace element and Hf-isotopic compositions between these Paleoproterozoic cores and those Neoarchean cores suggests that these zircon cores underwent intense Pb-loss resulting from late high-grade metamorphism. The unimodal age (~2.5 Ga) distribution of detrital zircons and positive εHf(t) of most Neoarchean zircons (Fig. 1) suggests that the detritus of these sedimentary protoliths probably came from a proximal volcanic arc, implying that they were deposited in an arc basin and almost synchronously with ~2.5 Ga volcanism. These are the oldest rocks in the Cathaysia Block found so far. The combination of zircon U-Pb ages and Hf-isotope data suggests that both generation of juvenile crust and reworking of 2.8 Ga and 3.5-3.3 Ga crust occurred at ~2.5 Ga.

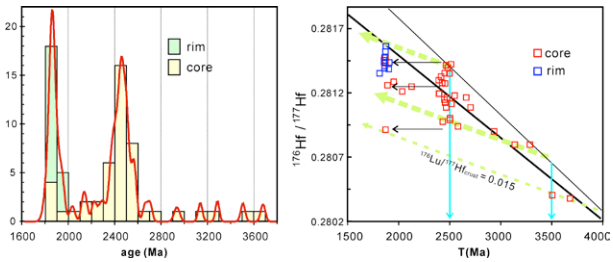

Strong ~1.9 Ga thermal event only involved the reworking of older crust material without the input of juvenile crust.

Geochemical characters and LA-ICP-MS zircon U-Pb dating of the Lenglonglin volcanic rocks in North Qilian tectonic belt

JI-YUAN YU, XIANG-MIN LI, GUO-QIANG WANG AND PENG WU

Xi'an Center of Geological Survey(Xi'an Institute of Geology and Mineral Resource), CGS, Xi'an, haanxi 710054. China (yujiyuan111@163.com)

The Qilian Orogen is divided into the Northern, Central and Southern Qilian. Lenglonglin area of Menyuan is located in the east segment of Northern Qilian and is composed of volcanic rocks and little acid volcanic rocks. Geochemical analyses show that Lenglonglin rocks have SiO_2 ranging from 48.94 to 60.97 wt %, K_2O/Na_2O less than 1, SiO_2-Nb/Y and SiO_2 - FeOT/MgO diagram shows the samples belong entirely to the tholeiitic series. Low Ti and high Al,Fe indicating that they are typically characterized as is land arc volcanic rocks. These monzogranites are depleted in HFSE, such as Ta, Nb and Ti, such as enriched in LILE, such as K, Th, Rb and Ba, with total REE contents ranging from 9.88 to 42.21 ppm and ∑LREE/ ∑HREE ratios of 0.81-5.70. The Chondrite-normalized REE patterns of these volcanic rocks is weak negative Eu anomalies (δEu = 0.58-1.10), These results with the accepted Kermadec island volcanic of New Zealand is very similar.At the same time, Zr/Y-Zr、Ti-Zr、Tb-Th-Ta*2 and Hf/3-Th-Ta indicate that these volcanic rocks could represent typical land arc volcanic rocks. In order to limit accurate formation time of Lenglongling volcanic rocks in the east segment of North Qilian orogenic belt by LA-ICP-MS U-Pb isotope dating technique, combined with cathodoluminescence image(CL) study, was used to determine the zircons from Lenglongling Dacite. Two main populations of zircons from Lenglongling Dacite obtained, giving an average $^{206}Pb/^{238}U$ ages of 460. 17±0.92Ma and 203.2Ma±3.8Ma. With the relevantdata synthesized, Lenglongling Intermediate-Basic volcanic rocks were considered to form in the Middle Ordovician, It was transformated by the Yanshan collision orogeny. These new data have important significance for further research on the tectonic evolution and the ore prospecting directions in the east segment of the north Qilian orogenic belt .

This study is supported by China Geological Survey survey project (No. 1212010010405 and No.1212010818090)

https://doi.org/10.1180/S0026461X00006502 Published online by Cambridge University Press

Structural effect of Zn^{2+} on biogenic Mn oxides: EXAFS analysis of solid residues after concomitant immobilization

QIANQIAN YU[1]*, KEIKO SASAKI[1], TSUYOSHI HIRAJIMA[1], KAZUYA TANAKA[2] AND TOSHIHIKO OHNUKI[2]

[1]Department of Earth Resources Engineering, Kyushu University, Fukuoka, Japan (q-yu09@mine.kyushu-u.ac.jp)
[2]Advanced Science Research Center, Japan Atomic Energy Agency, Ibaraki, Japan

Manganese oxides which are thought to be the potential scavenger of trace metals are commonly believed to be biogenic origin. Zn^{2+} in aquatic phase can be immobilized in Mn oxide phase during the biotic oxidation of Mn^{2+}. The amounts of immobilized Zn^{2+} were around twice in microbial Mn^{2+} oxidation in the presence of Zn^{2+} than in simple sorption of Zn^{2+} on biogenic Mn oxides which was produced in advance (Fig. 1). Analysis of Zn K-edge EXAFS spectrum for the solid residue after the concomitant immobilization of Zn^{2+} suggests that Zn atoms are coordinated to O atoms via triple-corner sharing (TC) at Mn vacant site in tetrahedral coordination. The XRD patterns showed that it belongs to poorly crystalline birnessite, its crystal size was calculated to less than 100 nm by Scherrer equation, and there is a lack of stacking in c axis. The measurement of zeta potential for the solid residue after the concomitant immobilization of Zn^{2+} indicated that the surface charge was more negative compared with fresh biogenic birnessite. XAFS/EXAFS analysis revealed that it contains less Mn(III) contents and larger numbers of vacant sites than fresh biogenic birnessite. Co-existence of Zn^{2+} influences Mn oxide formation during bio-oxidation, resulting in poorly crystallized birnessite and other types of Mn oxides which can be commonly found in the natural environments.

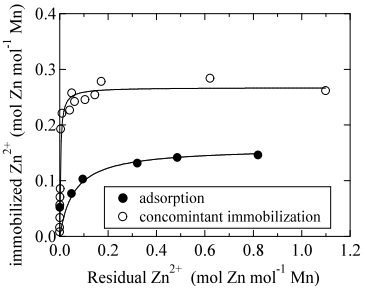

Figure 1: Sorption isotherms of Zn^{2+} on biogenic birnessite (●), and in concomitant immobilization with microbial oxidation of Mn^{2+} ions (○) at 25 °C and pH 6.5.

Metastable phase equilibria for the aqueous system containing lithium, rubidium and chloride at 298.15 K

X. D. YU[1], Y. ZENG[1,2]*, J.Q. ZHANG[1], J.Y. YANG[3]

[1]Department of Geochemistry, Chengdu University of Technology, Chengdu, 610059, China; (*correspondence: zengyster@gmail.com)
[2]Mineral Resources Chemistry Key Laboratory of Sichuan Higher Education Institutions, Chengdu, 610059, China;
[3]Development & Comprehensive Utilization of Marine Sedimentary Brine Sichuan Provincial Key Laboratory, Chengdu, 610059, China

The Pingluoba underground brine (Southwest China), belongs to the marine sedimentary deep brine. The components of the brines are sodium, potassium, lithium, borate, and the rare alkaline elements rubidium and cesium. However, the utilization of the underground brine scarcely has been reported because of a lack of relative solubilities and metastable phase diagram. The system containing lithium, rubidium and chloride is one of the subsystems of the underground brine and has not been reported. In this paper, the metastable equilibria of this system were studied at 298.15 K using an isothermal evaporation method.

Figure 1 is the metastable phase diagram of the system at 298.15 K. The diagram consists of one invariant point, two univariant curves and two crystallization fields. No double salt or solid solution is formed in this system at 298.15 K. The invariant point E is cosaturated with $LiCl{\cdot}H_2O$ and RbCl, and the mass fraction of its equilibrium solution is *w*(LiCl) 29.74 % and *w*(RbCl) 23.21 %. $LiCl{\cdot}H_2O$ is the only crystallization form of lithium chloride at 298.15 K.

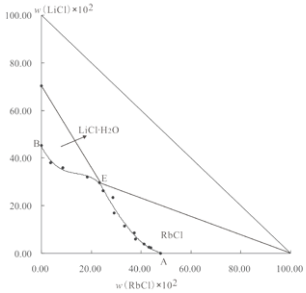

Figure 1: Metastable phase diagram of the system containing lithium, rubidium and chloride at 298.15 K

The authors acknowledge the support of the Project of the China Geological Survey (1212010011809), the Program for New Century Excellent Talents in University(NCET-08-0900), and the Research Fund from the Development & Comprehensive Utilization of Marine Sedimentary Brine Sichuan Provincial Key Laboratory (2009-230).

https://doi.org/10.1180/S0026461X00006502 Published online by Cambridge University Press

Water contents in the Cenozoic subcontinental lithospheric mantle beneath the Cathaysia block, SE China

Y. YU[1,2]*, X.S. XU[1,2], W.L. GRIFFIN[2] AND S.Y. O'REILLY[2]

[1]State Key Laboratory for Mineral Deposits Research, School of Earth Sciences and Engineering, Nanjing Univ., Nanjing 210093, China (*correspondence: yao.yu@mq.edu.au)

[2]GEMOC, Department of Earth and Planetary Sciences, Macquarie University, NSW 2109, Australia

Refractory subcontinental lithospheric mantle (SCLM) is produced by the removal of partial melts from mantle rocks; this process includes the removal of H_2O. The nature and stability of the SCLM are also strongly influenced by hydrous melts and fluids, which affect the physical and chemical properties of mantle minerals and rocks.

Our recent work has focussed on determining the H_2O contents of peridotite xenoliths from the Cathaysia block, SE China using Fourier transform infrared spectrometry (FTIR). The xenoliths consist mainly of nominally anhydrous minerals (NAMs, e.g., olivine, pyroxene) and are direct samples that may reflect the actual H_2O budget of SCLM.

The homogeneity in H_2O distribution within single pyroxene grains, equilibrium partitioning of H_2O between cpx and opx ($D_{cpx/opx} \approx 2.3$) and correlations between H_2O contents and major elements suggest that the xenoliths preserve the H_2O contents of their mantle source. The average whole-rock water contents calculated from mineral modes is 60±20 ppm. This is much higher than the H_2O contents of peridotites from the North China Craton (average 26±17 ppm). However, it is still low compared to other SCLM inferred from typical cratonic (122±54 ppm) and off-cratonic (81±40 ppm) peridotites.

This medium-dry SCLM can be explained by the refertilization of old lithospheric mantle which has undergone multiple geological events through time, e.g., hydration due to paleo-Pacific plate subduction and massive H_2O extraction during large-scale Late Mesozoic magmatism in SE China. The redox state is another factor in controlling the H_2O contents in the SCLM. This is supported by the negative correlations between pyroxene H_2O contents and spinel $Fe^{3+}/\sum Fe$ in xenoliths from Niutoushan (Mg#<90). This locality lies astride the Changle–Nan'ao fault, which facilitated the infiltration of peridotites by oxidized fluids or melts rising from the subducting Pacific plate.

Automated fitting of XRD profiles of interstratified phyllosilicates

HONGJI YUAN* AND DAVID L. BISH

Dept of Geol. Sciences, Indiana University, Bloomington, IN 47405 USA (*correspondence: honyuan@indiana.edu)

Phyllosilicate minerals are common constituents of soils and many rocks, but quantitative analysis of such materials using X-ray diffraction (XRD) is difficult due to the presence of interstratification within many phyllosilicates. Interstratification refers to the occurrence of two or more types of layers in a single crystallite (also termed "coherent scattering domain"). Diffraction from interstratified phyllosilicate minerals has been successfully modeled, and several software codes (e.g., NEWMOD [1], Diffax [2] and Sybilla [3]) have been developed. However, these programs rely on trial-and-error methods, making the results sensitive to user input. FITMOD, an automated parametric fitting program based on Reynolds' [6] methodology and incorporating recent progress in the structures of phyllosilicate minerals, has been developed [4]. The downhill simplex method [5] was applied in FITMOD to minimize the discrepancies between experimental and simulated XRD profiles by simultaneously varying all adjustable model parameters including the chemical composition (e.g., cation content) and structure (e.g., proportion of the two components, crystal-size distribution, stacking order). Both previously simulated and experimental XRD profiles were used to evaluate the performance of FITMOD in terms of the goodness of fit (R_{wp}, R_p), accuracy, as well as efficiency. Fits to simulated profiles yielded values of R_{wp} as low as <0.3%. Very good fits to experimental profiles were also obtained, with results in excellent agreement with previously published data. Importantly, final results were quite insensitive to starting model parameters, and the method allows fitting with minimal operator intervention.

[1] Reynolds (1985) Hanover, New Hampshire, USA. [2] Treacy *et al*. (1991) *Proc. Math. and Phys. Sci*. **433**, 499–520. [3] Aplin *et al*. (2006) *Clays and Clay Minerals*, **54**, 500-514. [4] Yuan and Bish (2010) *Clays and Clay Minerals*, **58**,727-742. [5] Nelder and Mead (1965) *Computer Journal*, 7, 308-313. [6] Reynolds (1980) Chap. 4 in Brindley & Brown, *Crystal Structures of Clay Minerals and their X-ray Identification*.

https://doi.org/10.1180/S0026461X00006502 Published online by Cambridge University Press

K-feldspar glasses syntheses for external calibration of *in situ* Pb isotope analysis using LA-MC-ICPMS

H.L. YUAN*, J.Y. SONG, K.Y. CHEN, M.N. DAI, Z.A. BAO AND G.F. HE

State Key Laboratory of Continental Dynamics, Department of Geology, Northwest University, Xi'an, 710069 (*correspondence: sklcd@nwu.edu.cn)

Laser ablation Quadruple and multiple collector ICP-MS (LA-Q&MC-ICPMS) is one of the most important analytical technique in terms of in situ analysis of trace elements and isotopic compositions. Matrix matched standards could impair the obstacles of precise measurements including fractionation and matrix effect. Lead isotopic composition of K-feldspar is one of the important ways to trace the history of rock formation and evolution [1]. However, there is no appropriate external standard for in situ Pb isotope analyses using LA-MC-ICPMS. This work describes the synthesis of K-feldspar glasses with a high temperature furnace. The final experimental conditions of the synthesis are melting the 1300mesh K-feldspar powders at 1680 ºC for 2 hours followed by liquid nitrogen quenching. The surface glasses are slightly heterogeneous due to lead evaporation at high temperature while the inside of the glasses are homogenous. The lead isotopic compositions of the glasses are 1.90779 ± 0.00009 ($^{208}Pb/^{206}Pb$,2s), 0.75899 ± 0.00004 ($^{207}Pb/^{206}Pb$, 2s), 20.909 ± 0.002 ($^{206}Pb/^{204}Pb$, 2s), 15.871 ± 0.002 ($^{207}Pb/^{204}Pb$, 2s) and 39.888 ± 0.005 ($^{208}Pb/^{204}Pb$, 2s), and the RSD are 0.007%, 0.008%, 0.016%, 0.016% and 0.021% (Fig. 1), respectively. The results show that the synthesized K-feldspar glasses could be potentially served as external calibration standard for in situ lead isotope measurements.

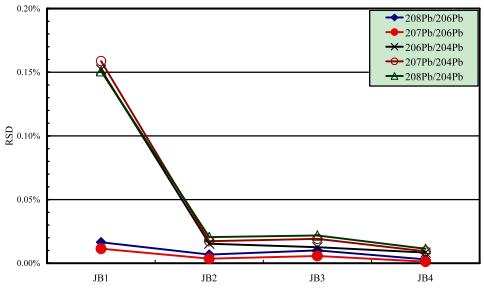

Figure 1 Relative standard deviation of Pb isotope ratio of synthesized K-Feldspar glasses

[1] Gagnevin *et al*., *Geocheim. Cosmochim. Acta,* (2005), **69**(7): 1899-1915

The zircon fission track constraint on the mineralizing ages of the Jiapigou gold deposits, Northeastern China

WANMING YUAN, JUN DENG AND ZHIXIN HUANG

State Key Laboratory of Geological Processes and Mineral Resources, China University of Geosciences, Beijing, 100083, China

The Jiapigou gold district is located at the north margin of the North China Craton, and its evolution is closely related to the Siberian Plate in the north, Yangtze Craton in the southeast and Pacific Plate in the east. The gold deposits belong to quartz vein type and are close related to a NE shear zone and the magmatic activities.

Samples for zircon fission track analyses were collected from different ores and alteration rocks. A total of 12 zircon samples were successfully analyzed. All the sample fission track ages have $P(\chi^2)$ values >5% and all grains counted belong to a single population of ages. The zircon ages range between 78 Ma and 158 Ma and centralize at 4 age groups of 158-152 Ma, 126-116 Ma, 108-98 Ma and 88-78 Ma.

A lot of homogenization temperature values of the metallogenic fluid inclusions from different ore deposits mainly range from 180 °C to 280 °C. This temperature could represent the mineralization temperature of the research gold deposits. The zircon fission tracks have a retention temperature of about 250 °C. Apparently, the zircon fission track ages can represent metallogenic ages in the gold districts.

Therefore, the 4 zircon age groups for different ores and alteration rocks could indicate the 4 epochs of gold mineralization. This could be confirmed by some geological evidences, such as, the different alteration cycle, the multiple periods of intrusions, coincident other thermochronological data and so on.

https://doi.org/10.1180/S0026461X00006502 Published online by Cambridge University Press

Migration and speciation of heavy metals in stream sediments of a mining-influenced basin, China

XUYIN YUAN, QUAN LIU AND QI ZHANG

School of the Environment, Hohai University, Nanjing 210098, China (*correspondence: yxy_hjy@hhu.edu.cn)

Tongling mine, located in the lower reaches of Yangtze River, is a multi-metal deposit with dominant Cu. Size fraction, the metal concentrations (Cu, Pb, Zn, Cr, Cd) and speciation, the acidic extractable metals (oxalic acid) were determined in order to investigate the impact of mining on stream sediments.

The enrichment factors (EFs) of heavy metals in the sediment nearby mine area were Cd(585) > Cu(289) >> Zn(81.9) >Pb(34.8) > Cr (2.3). The EFs of sediment in the site adjacent the Yangtze River decreased with Cd(15.3) > Pb(7.9) > Cu(5.4) > Zn (2.2) > Cr(1.3). It is indicated that heavy metals in sediments decrease obviously by transportation of about ten kilometers. The proportions of clay decreased and sand increased in sediments, which also altered the metal speciation in sediment by transportation. The oxidizable fraction (B2) decreased and the residual fraction (B4) increased for Cu. The exchangeable fraction (B1) and the reducible fraction (B3) of Cr descended. The significant variations of Pb speciation presented in the sediments. B1 and B2 ascended, but B4 descended. B3 notably increased and B4 decreased for Cd. The geochemical fractions of Zn showed the stable proportions in sediments of different sites. The acidic extractable fractions (oxalic acid) of five metals in sediments revealed different peculiarities. The proportion of extractable Cu decreased and the proportion of extractable Cr increased with distance from the mine site. But the proportions of extractable Zn, Pb, Cd showed less fluctuations during migration.

The stream sediments show different metal attenuation and removable metal variations during the transportation. These variations of metals depend on sediment size, mineral components and geochemical properties of metals.

Selenite reduction by *Bacillus L*

Y.-Q. YUAN[1,2], J.-M. ZHU[1]*, L. LEI[1,2], C.-Q. LIU[1] AND H.-B. QIN[1,2]

[1]The State Key Lab. of Environmental Geochemistry, Inst. of Geochemistry, CAS, Guiyang 550002, China (*correspondence: zhujianming@vip.gyig.ac.cn)

[2]Graduate University of Chinese Academy of Sciences, Beijing 100049, China.

A bacterium was isolated and purified from the selenium(Se)-high carbonaceous mudstone of Enshi, China. It was named as YTB-BL(*Bacillus L.*) in our lab. In order to investigate its potential tolerance and reduction for selenium oxyanions. This strain was inoculated in liquid medium (yeast extract and glucose)containing 5, 25, 100, 300, 500 and 800 mM of sodium selenite and selenate under aerobic, anaerobic and facultative anaerobic conditions, respectively. The results showed that this strain can be resistant to the SeO_3^{2-} and SeO_4^{2-} concentration of as high as 800 mM in the above three conditions. However, the doubling time(DT)of the strain was increased from 100.3h to 219.7h when SeO_3^{2-} concentration was changed from 500 mM to 800 mM under facultative cultivation, so did under the other two conditions. But this bacterium grew fastest under aerobic condition. Furthermore, it was able to reduce the soluble selenite anion(SeO_3^{2-}) to red elemental selenium(Se^0), which were present nanospheres distributed around or within the cells. The averagely transformed efficiency of Se^{+4} to Se^0 by YTB-BL was approximately 57% in the liquid medium containing 5-25 mM of sodium selenite. YTB-BL is a special kind of strain with wide adaptative and higher resistant selenite-reducing abilities, which would provide the better chance for microbial remediation of Se polluted areas.

The study was supported by the Knowledge Innovation Program of the Chinese Academy of Sciences (KZCX2-YW-JC101) and the National Natural Science Foundation of China (40721002, 40973085, 40573050).

https://doi.org/10.1180/S0026461X00006502 Published online by Cambridge University Press

Whole-rock chemostratigraphy of diverse magma series in the Tertiary alkaline volcanics of Trabzon-Giresun area, NE Turkey

C. YÜCEL*, M. ARSLAN, İ. TEMIZEL AND E. ABDIOĞLU

Department of Geological Engineering, Karadeniz Technical University, 61080-Trabzon, Turkey
(*correspondence: cyucel@ktu.edu.tr)

The Tertiary volcanics of the Trabzon-Giresun area have a narrow extend lying along the Black Sea coast in NE Turkey as a part of Eastern Pontide Tertiary Volcanic Province (EPTVP) [1]. Petrochemically, the volcanics can be divided into mildly alkaline group with medium to high-K, and moderately alkaline group with sodic-potassic in characters. The mildly alkaline group contains two sub-suites as basalt, trachy-basalt and basaltic trachy-andesite (BTB) suite croping out as dikes and sills, lava flows-pillow lavas and breccias, and trachyte and trachy-andesite (TT) suite croping out as dikes and domes. The moderately alkaline group consists of basanite-tephrite (BT) suite croping out as brecciated lavas and breccias [2]. Major oxide and trace element versus SiO_2 variation plots suggest fractionation of common mineral phases such as cpx+olivine+Fe-Ti oxide in the BTB suite, plagioclase±sanidine+biotite+Fe-Ti oxide in the TT suite, and cpx+Fe-Ti oxide+apatite in the BT suite.

N-type MORB normalized trace element patterns exhibit subduction signatures with enrichment in LILE (Sr, K_2O, Rb, Ba), Th and Ce and depletion in Zr, Y, Nb, Ta and TiO_2 contents. The chondrite-normalized REE patterns show two diversing trends with moderately enriched (La_N/Lu_N=2.27-7.95) for mildly alkaline, and highly enriched patterns (La_N/Lu_N=29-49) for moderately alkaline volcanics The patterns have also concave shape with marked light REE enrichment and heavy REE depletion, implying effect of significant clinopyroxene fractional crystallization during the evolution of the mafic volcanic suites. Volcanic facies, chemostrigraphy and whole-rock petrochemistry of the Trabzon-Giresun area Tertiary alkaline volcanics reveal that there might have been diversing parental magmas derived from different degrees of partial melting of enriched lithospeheric mantle which was modified by paleo-subduction induced fluids and/or melts.

[1] Arslan, M. (2003) *Geology and Mining Potential of Eastern Black Sea Region Symposium Proceedings, Trabzon,* 103-105. [2] Yücel *et al*. (2010) *4th National Geochemistry Symp. Proceedings Book, Elazığ,* 31-32.

Metals and As in mine tailings drainage systems: Mobility and removal

N.V. YURKEVICH* AND O.P. SAEVA

Trofimuk Institute of Petroleum Geology and Geophysics SB RAS, Koptyug av., 3, Novosibirsk, Russia, 630090
(*correspondence: YurkevichNV@ipgg.nsc.ru)

Sulfide-bearing mill wastes are sources of high concentrations of acid, soluble metals and As. These are serious problems for ore mining areas such as the Kemerovo and Cheljabinsk regions in Russia. Contents of Cu, Zn, Cd, Pb, As, and Sb in wastes of the Belovo Zn-processing and the Karabash Cu-smelting plants are 2-3 orders of magnitude higher than the content of continental crust. Main mineral forms are pyrite FeS_2, chalcopyrite $CuFeS_2$, sphalerite ZnS, arsenopyrite FeAsS and scorodite $FeAsO_4*2H_2O$. High dissolved metals, As and Sb concentrations are found in drainage waters and influenced rivers; their concentration often exceeds Maximum Permissible Concentrations and background levels. Concentrations of metals, As and Sb in bottom sediments of the affected rivers are elevated a hundred meters below the input of drainage. These sediments become a source of secondary contamination.

Field experiments were conducted on the wastes – natural water interaction. Results of the experiments showed that 10-86 % of elements contained in the wastes pass into solution. Two groups of elements can be defined by their leaching behavior: relatively immobile – Sb, Pb, and Fe (10-16 %), and elements that are readily leached – As (67 %), Zn (70 %), Cd (71 %), and Cu (86 %). Leachates were used as influent to additional columns that tested limestone and a mixture of natural clay as geochemical barriers. The decrease in elements mobility in the clay and limestone columns is consistent with the accumulation detected in bottom sediments in the Belovo settling pond. In both the column and natural environment, Cd, As, and Sb is adsorbed on Fe (III) hydroxides at pH > 4 in oxidizing waters; changes of conditions to lower pH result in transfer of adsorbed elements into solution. An alternative to adsorption in oxic systems elements mobility is also decreased by the formation of sulfides and arsenides ($CuFe_2S_3$, Cu_3BiS_3, $NiAs_2$, $Ni_{11}As_8$, $Cu_9Sb_8S_{21}$, $CoAs_3$).

In addition, we propose electrochemical method for the treatment of high mineralized acid drainage (pH = 3.5, total concentration of Al, Cu, Zn, Cd, Pb, Fe, As, and Sb up to 10 g/L and sulfate-ion concentration up to 20 g/L) which is based on addition of metallic aluminium and allow to reach concentrations of elements in solution by 2-3 orders of magnitude lower then initial.

https://doi.org/10.1180/S0026461X00006502 Published online by Cambridge University Press

Modeling of column experiments – Influence of glass micro balls

VRATISLAV ŽABKA, IVAN BRUSKÝ AND JAN ŠEMBERA

Institute of Novel Technologies and Aapplied Informatics Technical University of Liberec, Studentska 2, 46117 Liberec, Czech Republic (ivan.brusky@tul.cz)

Our paper is focused on modeling of a laboratory experiment using the software package The Geochemist's Workbench. We simulate a column experiment in which water solution flows trough a porous soil. The subjects of our interest are the interactions between water solution and porous soil. In some in-situ decontamination technologies, sinking-in reagents are used to be used. Column experiments are important for preparation and verification of such decontamination activities.

To verify the experiment configuration we decided to begin with the simplest case of the column experiment: the flowing water solution is pure distilled water and the porous medium is inert glass micro balls. Even in such a simple experiment we could observe unexpected change of pH of water solution after passage through the column. We try to understand this observation and simulated in mentioned software.

The results of the study will be presented.

Platinum group minerals (PGM) in chromite lode deposits from the Sulawesi ophiolite belt

F. ZACCARINI[1]*, A. IDRUS [2], G. GARUTI[1], O.A.R. THALHAMMER[1] AND F.M. MEYER[3]

[1]University of Leoben, Dept. Appl. Geol. Sci. Geophysics, Leoben, Austria(*correspondence: federica.zaccarini@unileoben.ac.at)

[2]Gadjah Mada University·Dept. Geol, Eng., Yogyakarta, Indonesia

[3]RWTH Aachen University, Inst. Min. Econ. Geol., Aachen, Germany

Some localities in Indonesia including Borneo and Sulawesi host PGM-bearing podiform (ophiolite)-type chromitites. Borneo is the locality type of two platinum group minerals (PGM), the rare vincentite and laurite, the most common Ru minerals. These PGM have been found in placers, however, data on the occurrence of PGM in lode deposits of Indonesian Archipelago are very poor. We present a mineralogical investigation on lode chromite deposits and associated PGM from the Sulawesi ophiolite belt. The investigated chromitites were sampled in the South and Southeast Arms of Sulawesi. According to the #Cr (0.51-0.88), in both the localities chromite composition varies from Cr-rich to Al-rich. TiO_2 is low in the Southeast Arm chromitites (0.07-0.28 wt%), whereas in the South Arm chromitites its values are comprised between 0.08 up to 0.55 wt%. Small PGM, 1 to 10 μm in size, have been found in both the localities and in Cr- and Al-rich chromitites. The most abundant PGM is laurite that occur included in fresh chromite or in contact with chlorite along cracks of the chromite. Laurite forms polygonal crystals and it occurs as single phase or in association with amphibole, chlorite, Co-pentlandite, apatite and other PGM. Small grains of irarsite (less than 3 μm) have been found associated with small blebs of awaruite and Co-pentlandite in the chromite gangue composed of chlorite. One grain (2 μm in size) containing Ru and Fe was found in the rim of a laurite occurring with Co-pentlandite in the chromite crack, filled with chlorite. The results suggest that the studied chromitites could have crystallized from different melts varying in composition from MORB formed in back-arc setting (Al-rich) to boninites related with subduction zone (Cr-rich). The bimodal composition and the anomalous enrichment in TiO_2 observed in some chromitites, may also indicate vertical zoning due to the fractionation of a single magma batch during its ascent, implying accumulation of Cr-rich chromitites at deep mantle levels and formation of the Al-rich ones close to the Moho-Transition Zone. All the laurite are considered to be magmatic in origin, i.e. entrapped as solid phases during the crystallization of chromite. Irarsite possibly represents a low temperature exolution product.

https://doi.org/10.1180/S0026461X00006502 Published online by Cambridge University Press

Challenges in the identification of redox reactive Fe(II) mineral phases in suboxic aquifer sediments

J.M. ZACHARA, T. PERETYAZHKO, J.P. MCKINLEY, CHONGXUAN LIU AND A.R. FELMY

Pacific Northwest National Laboratory, Richland, WA, USA

The kinetics of ^{99}Tc(VII) reduction, as the pertechnetate anion [$^{99}TcO_4^{2-}$ = 10^{-6} mol/L], were investigated in a series of suboxic aquifer sediments from the U.S. DOE, Hanford site exhibiting an average pH = 8. Reaction rates varied markedly displaying half-lives ranging from 2 to 110 d. Rate constants did not normalize to extractable Fe(II) concentration. The heterogeneous reaction products, as identified by EXAFS analysis, were adsorbed ^{99}Tc(IV) clusters (n = 2-4) that did not vary in size with reduction rate. Iron was not observed in the second coordination sphere. The Fe mineralogy of the sediments was investigated using a combination of chemical extraction, x-ray diffraction, variable temperature Mossbauer spectroscopy, and analytical electron microscopies; revealing the presence of a complex Fe(II) mineral suite containing variable concentrations of pyroxenes, siderite, Fe(II)-phyllosilicates (smectites, illites, and mica), and magnetite. Direct correlations between ^{99}Tc reaction rates and Fe(II) mineralogy were not evident. The most reactive sediment was titrated with higher levels of ^{99}Tc (10^{-4} mol/L), with the distribution of Fe(II) mineral phases monitored by Mossbauer spectroscopy after ^{99}Tc(VII) reaction. Spectral peak positions for siderite at 4.5 K decreased during titration from 29% to 6% of the total area, transforming to those of Fe(III) oxide, providing presumptive evidence that siderite was one of several reactive phases. Additionally, ^{99}Tc(VII)-oxidized sediment was screened by digital autoradiography to identify ^{99}Tc(IV)-containing mineral phases. These phases were manipulated for analysis by electron microprobe and micro-x-ray diffraction. A significant fraction of the ^{99}Tc(IV)-containing phases were Fe-micas as observed in a previous investigation with sediments from another location. Residual siderite did not appear to contain ^{99}Tc(IV). We conclude with a discussion of: i.) the challenges involved in the identification of redox active phases using macroscopic and microscopic techniques and ii.) kinetic versus thermodynamic controls on redox reactivity in mineralogically heterogeneous subsurface sediments.

Evaluation of rock properties and rock structures in the micron-range with sub-micron X-ray Computed Tomography

G. ZACHER[1]*, M. HALISCH[2], O. BRUNKE[1] AND T. MAYER[1]

[1]GE Sensing & Inspection Technologies GmbH, Niels-Bohr-Str. 7, 31515 Wunstorf, Germany

[2]Leibniz Institute for Applied Geophysics, Stilleweg 2, 30655 Hannover, Germany

In recent years high resolution X-ray Computed Tomography (CT) for geological purposes contribute increasing value to the quantitative analysis of rock properties. Especially spatial distribution of minerals, pores and fractures are extremely important in the evaluation of reservoir properties. The possibility to visualize a whole plug volume in a non-destructive way and to use the same plug for further analysis is undoubtedly currently the most valuable feature of this new type of rock analysis and will be a new area for routine application of high resolution X-ray CT in the near future.

The paper outlines new developments in hard- and software requirements for high resolution CT. It showcases several geological applications.

The results were performed with the phoenix nanotom and recently phoenix nanotom m, the first 180 kV nanofocus CT system tailored specifically for extremely high resolution scans of samples up to 240 mm in diameter and weighing up to 3 kg with voxel-resolutions down to <300 nm. These characteristics with respect to spatial resolution principally allow CT measurements which valuably complement many absorption contrast setups at synchrotron radiation facilities (Withers 2007 [1]; Brunke *et al*. 2008 [2]; Kastner *et al*. 2010 [3]).

[1] Brunke *et. al*. (2008) „Comparison between x-ray tube-based and synchrotron radiation-based μCT" in Developments in X-Ray Tomography VI, edited by Stuart R. Stock, *Proceedings of SPIE*, Vol. **7078**. [2] Withers (2007) "X-ray nanotomography", *Materials Today,* **10(12)**, 26-34. [3] Kastner *et. al*. (2010) "A comparative study of high resolution cone beam X-ray tomography and synchrotron tomography applied to Fe- and Al-alloys", in *NDT & E Int*. vol **43**, pages 599-605.

https://doi.org/10.1180/S0026461X00006502 Published online by Cambridge University Press

Robust trace element analysis of rutile by LA-ICP-MS

T. ZACK* AND M. BARTH

Institut für Geowissenschaften, Universität Mainz, Germany (*correspondence: zack@uni-mainz.de)

Several recent studies reporting trace element results for rutile by LA-ICP-MS using spot sizes as large as 40 μm. However, even Q-ICP-MS are sensitive enough to have a suitable signal-to-background ratio for a number of important trace elements in most natural rutiles (*e.g.*, V, Cr, Fe, Zr, Nb, Sn, Hf, Ta, W and U) at spot sizes of only 10 μm. Here, counting statistics give errors better than 5% for Zr concentrations on the 100 ppm level (translating to analytical errors in metamorphic temperatures of only a few °C). Still, the level of accuracy is so far unknown at such small spot sizes mostly due to a lack of suitable rutile standards.

Recently, we have proposed to use three natural (R10, R19, Diss) and one synthetic (Sy) rutiles as secondary mineral standards [1]. These minerals are sufficiently homogeneous and analyzed by several techniques (EMP, SIMS, ID-MC-ICP-MS) for a range of trace elements to test LA-ICP-MS performances. Therefore, we have run several LA-ICP-MS profiles with variable spot sizes (10-40 μm) along the same EMP and SIMS profiles as reported in [1].

Most importantly, it is found that spot size differences can have a severe effect on calculated rutile concentrations for such small spots. For example, calculated Zr concentrations for rutile systematically deviate by 40% between 10 and 40 μm. This makes it an absolute neccessity to always use identical spot sizes at such small scales. Furthermore, it can be demonstrated that an accuracy of <10% is reached for most trace elements for the rutile standards R19 and Diss when R10 is used as a matrix matched standard under the exact same analytical conditions.

The demonstration of an accuracy of <10% for 10 μm spot analysis for rutile by LA-ICP-MS significantly opens up the field of rutile geochemistry. In Mainz, with the help of a fast-washout large format cell and automization, we routinely use such small spot sizes for rutile trace element analysis with a sample throughput of >60 samples/hour. Applications are found *e.g.*, in pre-scanning for high-U detrital rutiles suitable for U/Pb dating [2] and fine-scale Nb diffusion profiles [3].

[1] Luvizotti *et al* (2009) *Chem Geol* **261**, 346-369, [2] Zack *et al* (in press) *Contr Min Petrol*, [3] Cruz-Uribe *et al*, *MinMag*, this volume

Effect of plant-microbial associations on weathering of basalt, granite, schist, and rhyolite

DRAGOS ZAHARESCU[1]*, KATERINA DONTSOVA[12], JON CHOROVER[12], TRAVIS HUXMAN[13], RAINA MAIER[2] AND JULIA PERDRIAL[2]

[1]B2 Earthscience, The Univ. of Arizona, Tucson, AZ, USA, (zaharescu@email.arizona.edu, dontsova@email.arizona.edu, chorover@cals.arizona.edu)

[2]Dep. of Soil, Water & Environmental Science, The Univ. of Arizona, Tucson, AZ, USA (rmaier@ag.arizona.edu, jnperdri@email.arizona.edu)

[3]Dep. of Ecology and Evolutionary Biology, Univ. of Arizona, Tucson, AZ, USA, (huxman@email.arizona.edu)

The goal of this study was to measure how plant–microbe interactions affect the initial weathering of four distinct rock types (basalt, granite, schist, and rhyolite) and the extent to which this weathering results in chemical denudation versus biomass accumulation or re-precipitation of dissolution products. This initial phase of experiment focused on denudation. We hypothesised that the presence of plants will increase weathering but decrease denudation (i.e., we will see more mineral transformation but less element loss from system in the presence versus absence of plants). To achieve research objectives, we conducted a series of environmentally–controlled, greenhouse experiments that involved measuring plant uptake, mineral transformation and chemical denudation in basalt (35.9% An64 plagioclase, 6.5% diopside, 11.9% forsterite, and 45.7% basaltic glass), granite (28.8% quartz, 31.1% K-feldspar, 32.8% albite, and 7.2% muscovite), rhyolite (32.6% quartz, 15.9% albite, and 51.5% K-feldspar in crystalline form, plus yet unquantified glass fraction), and schist (23.8% quartz, 22.8% K-feldspar, 14.2% albite, 7.6% amphibole, and 31.7% biotite), as affected by presence and growth of microbiota and vascular plants. The experiments also included plant-free (but microbially-colonized) and abiotic (sterile) controls. Buffalo Grass (Buchloe dactyloides) and Ponderosa Pine (Pinus ponderosa) were employed as model plant species. Plants were grown in 4 cm (diameter) by 30 cm (length) Plexiglas columns filled with granular study materials. Columns were equipped with micro-suction cup solution samplers to collect soil solution. Solution was analysed to deptermine pH, cations and metals, anions, and aqueous phase organic matter chemistry. Concentrations of low molecular weight organic acids in soil solution and drainage water were also determined.

https://doi.org/10.1180/S0026461X00006502 Published online by Cambridge University Press

Did the glacial Atlantic overturning circulation run backwards?

R. ZAHN[1]*, I.R. HALL[2], G.M. HENDERSON[3], P. MASQUÉ[1] AND A.L. THOMAS[3]

[1]Universitat Autònoma de Barcelona, Institut de Ciència i Tecnologia Ambientals, Departament de Física, 08193 Bellaterra, Spain (*correspondance: rainer.zahn@uab.cat)
[2]School of Earth and Ocean Sciences, Cardiff University, Cardiff CF10 3AT, U.K.
[3]Department of Earth Sciences, University of Oxford, Oxford OX1 3AN, UK

Recently Pa/Th profiles from the South Atlantic were published [1] that display structures very different from Pa/Th profiles in the North Atlantic. It was argued that these profiles indicate i) deep waters leaving the glacial Southern Ocean had a Pa/Th fingerprint not much different from that of NADW today, due to extensive Pa scavenging; ii) a basin-scale meridional Pa/Th gradient developed in the glacial Atlantic that run opposite to that of today, reflecting a more substantive northward flow of "southern sourced water" (SSW). This concept, in our view, reconciles an apparent conflict between εNd measured on Fe-Mn oxide coatings on planktonic foraminifera at the Bermuda Rise and Pa/Th data at the same location: the first indicating northward flowing SSW at the LGM while the second supposedly reflecting southward flowing "northern source water" (NSW) [2].

We borrow the provocative title from the conveners because it reflects the debate over how far we can take the proxy records. The interplay between NSW and SSW is reflected by a suite of proxy data e.g., stable carbon isotopes ($\delta^{13}C$), Pa/Th and nutrient-based trace element ratios (Cd/Ca). Pa/Th profiles are scarce and meridional gradients must be mapped using Pa/Th from a range of different water depths while gas-exchange normalized $\delta^{13}C_{as}$ suggests a prominent role of SSW in the glacial AMOC. Taking all evidence at face value suggests the glacial AMOC received a stronger water mass contribution from the southern hemisphere oceans. At the same time several questions arise: does scavenging of Pa in the Southern Ocean outcompete lateral advection and so depleting the water column of Pa? Do radiogenic isotope and nutrient-based proxies uniquely identify water mass end members? How robustly do the proxies reflect the AMOC in the past, including physical near-bottom flow speeds? These questions are not easy to answer but they help refine the direction of future work.

[1] Negre *et al*. (2010) *Nature* **468**, 84-88. [2] Roberts *et al*. (2009) *Science* **327**, 75-78.

Xenon the magnificent

KEVIN ZAHNLE

NASA Ames Research Center, Moffett Field CA 94035 (Kevin.J.Zahnle@NASA.gov)

Xenon is the heaviest noble gas and the heaviest gas likely to be found in a primoridal atmosphere. It would seem to be the least likely gas to escape. Yet there is probably more evidence for massive Xe escape from Earth than for any other element save helium. Nonradiogenic atmospheric Xe is strongly mass fractionated (by about 4% per amu) compared to any of its plausible solar system sources. By contrast, Kr is only mildly fractionated, if at all. Xenon is also relatively underabundant with respect to Kr.

Radiogenic Xe also suggests escape. Radiogenic ^{129}Xe (from ^{129}I decay, half-life 15.7 Myr) is present in the atmospheres of Earth and Mars but at less than 1% the qunatity expected given the primoridal abundance of ^{129}I, Radiogenic Xe from spontaneous fission of ^{244}Pu (half-life 82 Myr) is also notably underabundant. The upper limit on fissogenic ^{136}Xe in air is about 1 part in 6 of Earth's cosmic complement from ^{244}Pu. This is an upper limit because it depends on U-Xe (rather than solar Xe) being the primordial Xe of Earth. U-Xe makes modeling Earth's Xe much easier, but it has not otherwise been seen in the solar system.

For Xe escape to explain the dearth of fission Xe in air, escape must have taken place late enough in Earth's story that ^{244}Pu was extinct. The mechanism would have affected Xe but not Kr or Ar. One possibility is that Xe escaped as an ion, probably in polar winds of hydrogen and hydrogen ions channelled by planetary magnetic fields. This can occur because Xe, alone among the noble gases, is more easily ionized than hydrogen. Thus Xe will tend to be present oin the H-H+ wind as Xe+, whilst the other noble gases would be neutral. Because of the Coulomb force, at 2000 K and 1% H ionization, diffusivity of Xe^+ is 3 orders of magnitude lower than that of neutral Xe or Kr. The Xe^+ ions are therefore dragged to space by the protons. Under these circumstances fractionating hydrodynamic escape can apply uniquely to xenon among the noble gases over a wide range of hydrogen escape fluxes.

https://doi.org/10.1180/S0026461X00006502 Published online by Cambridge University Press

The solubility of Au and Cu in andesite melts

ZOLTAN ZAJACZ[1,2], PHILIP A. CANDELA[1], PHILIP M. PICCOLI[1], MARKUS WÄLLE[2] AND CARMEN SANCHEZ-VALLE[2]

[1]Laboratory for mineral deposits research, University of Maryland, College Park, MD, USA, (zoltan.zajacz@erdw.ethz.ch)

[2]Institute of Geochemistry and Petrology, ETH Zürich, 8092 Switzerland

We conducted experiments in MHC cold seal vessels at 1000 ºC and 200 MPa to study the solubility of Cu and Au in andesite melts as a function of the Cl and S content of the silicate melt and oxygen fugacity of the system. A gold activity of 0.99 and a Cu activity of 0.01 were imposed by using AuCu alloy capsules.

At an fO_2 of NNO-0.2, the solubility of Au shows a positive linear correlation with the S concentration in the melt, and increases from 41±8 ng/g (1σ) in a S-free melt to 1547±52 ng/g in a melt with 344±20 μg/g S, a condition near pyrrhotite saturation. Chlorine has a relatively minor positive effect on Au solubilty; a S-free andesite melt with 1.00±0.01 wt% Cl contained only 112±20 ng/g Au.

The effect of fO_2 on the solubility of Au is significant, leading to 0.18±0.04 log unit increase in Au solubility for 1 log unit increase in fO_2 in a S-free, Cl-bearing melt, which is approximately consistent with +1 valence of Au in the silicate melt. In S-bearing melts, the effect of fO_2 on gold solubilty is further complicated by the following (or a similar) reaction: $Au+FeS(melt)+H_2O(melt)=AuSH(melt)+FeO(melt)+0.5H_2(g)$ Accordingly, a maximum in Au solubility is observed just at the low fO_2 end of the S^{2-}/S^{6+} transition, however, it is much smaller than that shown by Botcharnikov *et al*. (2011) [1].

The apparent solubility of Cu at an fO_2 of NNO-0.2 and aCu of 0.01, ranges between 45±1 and 78±1 μg/g and shows a weak positive correlation with the S and Cl concentration in the melt. Moderate excess solubitly over that predicted assuming a dominant $CuO_{0.5}$(melt) species is observed in S-bearing experiments in the fO_2 range of the S^{2-} to S^{6+} transition and above. Variation in the K_2O/Na_2O and FeO/Na_2O ratios in the melt did not siginificantly affect Au and Cu solubilites.

Model volatile/melt parition coefficients of Cu and Au suggest that volatiles exsolving from andesite magmas are efficient at extracting Au, but inefficient at extracting Cu.

[1] Botcharnikov, Linnen, Wilke, Holtz, Jugo & Berndt (2011), *Nature Geoscience* **4**, 112-115.

Cryogenic cave carbonates – A new tool for estimation of former permafrost depths

K. ŽÁK[1]*, M. FILIPPI[1], R. ŽIVOR[1] AND D.K. RICHTER[2]

[1]Institute of Geology AS CR, v.v.i., Rozvojová 269, 165 00 Praha 6, Czech Republic (*correspondence zak@gli.cas.cz, filippi@gli.cas.cz, zivor@gli.cas.cz)

[2]Ruhr-University Bochum, Institute of Geology, Mineralogy and Geophysics, Universitätsstr. 150, 44801 Bochum, Germany (detlev.richter@rub.de)

Geochemical processes in the Earth's critical zone largely depend on the presence or absence of a permafrost (perennially frozen ground, i.e. soil and rock remaining at or below 0 °C for at least two consecutive years, [1]). While the areal extent and depth of present-day permafrost zone are relatively well known [1], the extent, duration, and depth of permafrost during Pleistocene glacials are much less understood. Here we present a new tool for the estimation of former permafrost minimum depth based on the occurrence of a specific type of secondary carbonate in caves.

Cryogenic cave carbonate (CCC) is a unique type of secondary carbonate formed in caves during freezing of common calcium bicarbonate water by the expulsion of dissolved load by the growing ice. CCCs can be identified based on their typical morphology and occurrence, by U-series dating fitting into glacials, and especially by specific C- and O-isotope geochemistry, which proves their formation during water freezing [2, 3, 4]. CCCs were formed at the transitions from glacials to interglacials or from stadials to interstadials and occur as accumulations of loose crystals and crystal aggregates on the cavity bottom, where they were deposited after melting of the ice filling of the cavity. CCCs show a unique isotope composition with $\delta^{18}O$ values down to -25 ‰ (PDB), and $\delta^{13}C$ values up to +6 ‰.

We collected data for all known CCC occurrences in a belt parallel to the southern edge of the Weichselian continental glaciation (southern Poland, Slovakia, Czech Republic, central Germany), dated them by U-series method, and evaluated their depths under the surface. When using data from isolated cavities only, which cannot be cooled by air circulation, a minimum Weichselian permafrost depths in this belt can be estimated at 30–70 m under the surface (the study was supported by the project GA CR P210/10/1760).

[1] French (2007) *The periglacial environment*, 3rd ed., 458 p. [2] Žák *et al*. (2004) *Chem. Geol*. **206**, 119-136. [3] Richter & Riechelmann (2008) *Internat. J. Speleology* **37**, 119-129. [4] Žák *et al*. (2008) *Quat. Internat*. **187**, 84-96.

https://doi.org/10.1180/S0026461X00006502 Published online by Cambridge University Press

A combined Earth-Moon Si isotopes model to track rocks petrogenesis

T. ZAMBARDI AND F. POITRASSON

Géosciences Environnement Toulouse, CNRS– UPS – IRD, France. (zambardi@get.obs-mip.fr)

Silicon is after oxygen the second most abundant element in the Earth's crust. As such, its stable isotope variations in geological materials may represent important mass transfer between terrestrial reservoirs. Despite early analytical limitations and although Si isotopes were not expected to fractionate significantly during high temperature magmatism, studies conducted more than 15 years ago [1, 2] hinted that Si isotope compositions of granitoids may be heavier than that of mafic igneous rocks.

In this study, we determined the silicon isotope signatures of a set of igneous terrestrial rocks that includes andesites, monzogranites, granites of different types, as well as 8 lunar samples including basalts and highlands anorthosites. Analytical methods involved alkaline fusion of the powdered samples, cationic exchange chromatography and high resolution MC-ICP-MS in the wet plasma mode. Long-term (3 years) external reproducibility for $\delta^{30}Si$ and $\delta^{29}Si$ was given by repeated measurements of BHVO-2. It yielded 2 standard deviations (2SD) of 0.076‰ and 0.047‰, respectively, for individual measurements.

A comparison between lunar and terrestrial bulk igneous rocks reveals that Si isotope composition become slightly, thought significantly enriched in heavy isotopes as a function of felsic mineral abundances. We interpret this in terms of global planetary differentiation processes. However, the terrestrial trend is more scattered, which reveal the occurrence of sources and processes that do not exist on the Moon, probably because they involve water. Terrestrial andesites may be isotopically heavier than other lunar and terrestrial igneous rocks with similar silicon contents whereas S-type granites are isotopically much lighter than other granite types. These results are interpreted as the influence of seawater or hydrothermal fluids on andesitic sources and the occurrence of sediments containing the products of aqueous weathering in S-type granite protoliths. The fact that Si is a major element in igneous rocks, but not a major constituent of water like O, makes its isotopic composition likely more robust against alteration and weathering of the studied rocks, yet delivering significant information in terms of source of the magmatic bodies studied.

[1] Douthitt (1982) *Geochim. Cosmochim. Acta* **46**, 1449-1458. [2] Ding *et al.* (1996) *Geol. Publish. House, Beijing, China*, 125 pp.

Melting condition and evolution of fissural volcanism in the island of Faial (Azores archipelago)

VITTORIO ZANON[1], ANGELO PECCERILLO[2] AND JOSÉ MANUEL PACHECO[1]

[1]Centro de Vulcanologia e Avaliação de Riscos Geológicos, Universidade dos Açores, Rua Mãe de Deus 9500-501, Ponta Delgada, Portugal (Vittorio.VZ.Zanon@azores.gov.pt)

[2]Dipartimento di Scienze della Terra, Univeristà di Perugia, Piazza Università, 1 06100 Perugia, Italy (peccean@unipg.it)

Two WNW-ESE-trending fissure zones, which are separated by NNW-SSE transtensional faults, are the expression of the regional extensional tectonics in the island of Faial. Several monogenetic centres and a large stratovolcano were generated along these faults.

Erupted magmas are nepheline- to hypersthene normative basalts to hawaiites, generated at about 2110-1600 MPa (~63 km deep, in the spinel facies) and 1367-1407°C.

Mafic rocks of the westernmost fissure zone have lower MgO and HREE, and higher Na_2O, P_2O_5, TiO_2, Zr, Nb, Th, LILE and LREE than those from the easternmost fissure zone. All these differences are related to slightly different melting degrees (between 3 and 5%), which also reflect the different silica saturation degrees. However, near-primary melts of these two fissure zones show LILE contents, particularly Ba, which are among the highest in the whole Atlantic area. This feature, together with the common presence of fluid inclusions in many ultramafic xenoliths sampled, evidence the occurrence of a metasomatic event prior to mantle source melting.

Hawaiites evolved from basalts by 18-25% fractional crystallization of Mg-olivine, diopside and Ca-plagioclase, at 560-700 MPa (~17-21 km deep). There is no evidence for magma ponding at intracrustal depths.

Fractionation of mafic phases generated cumulate layers at the crust-mantle boundary. Ascending basaltic melts sampled these olivine-and-clinopyroxene bearing layers to generate ankaramites which show MgO content lower than primary melts. These peculiar lithologies crop out along the western margin of the stratovolcano, possibly along faults that directly tapped the cumulate layers.

https://doi.org/10.1180/S0026461X00006502 Published online by Cambridge University Press

Release of silica from micas by alkaliphilic anaerobes

D. G. ZAVARZINA[1]*, A. V. SAVENKO[2], N. I. CHISTYAKOVA[3], A. A. SHAPKIN[3] , T. N. ZHILINA[1] AND G.A. ZAVARZIN[1]

[1]Winogradsky Institute of Microbiology RAS, Moscow 117312, Prospect 60-letiya Oktyabrya 7/2, Russia (*correspondence: zavarzinatwo@mail.ru)

[2,3] Lomonosov Moscow State University,

[2] Geographic and [3]Physics Depart., Leninskie Gory, Moscow 119992, Russia

Soda deposits are formed at the final stages of continental CO_2-weathering. It could occur under alkaline conditions either chemically, which seems favorable, or biotically. There are two main groups of alkaliphilic microbial agents that act in anaerobic conditions on the water-rock contact: a) fermentative hydrolytic decomposers of particulate organic matter, e.g. cellulose, capable to produce organic acids as the products of metabolism; b) respiratory anaerobes, utilizing dissolved compounds with external electron acceptors.

We studied the interaction of pure cultures of microbes with biotite and glauconite during 165 days under alkaline conditions at pH 9.5 and total mineralization was 15 g/l. Mössbauer spectroscopy, IR-specrtoscopy and solubility of micas in water were used for the investigation of the solid phase. Fermentation products were recorded during the bacterial growth.

Following combinations were studied: (i) chemical alkalinolysis of micas under sterile conditions; (ii) biotic alkalinolysis of micas by alkaliphilic *Clostridium alkalicellulosi* [1], which produces organic acids and ethanol from cellulose; (iii) biotic alkalinolysis by alkaliphilic dissimilatory iron-reducer *Geoalkalibacter ferrihydriticus* [2] with acetate as an electron donor; (iiii) combined binary culture of *Cl. alkalicellulosi* and *G. ferrihydriticus* with cellulose as organic substrate.

Release of silica under experimental conditions for the both minerals was as following: (i) no release; (ii) no release; (iii) release of silica, formation of new soluble phase; (iiii) release of silica, formation of new soluble phase.

It is proposed that the anaerobes with respiratory metabolism are more effective than fermentative in bioweathering of rock-forming minerals as micas with release of silica. Chemical weathering even under most favorable conditions is far less pronounced than microbe-mineral interactions.

[1] Zhilina *et al*. (2005) *Microbiology,* **74**, 642-653. [2] Zavarzina *et al*. (2006) *Microbiology*, **75**, 775-785.

Evidence for evolution of growth media in superdeep diamonds from Sao-Luis (Brasil)

D.A. ZEDGENIZOV[1]*, A.L. RAGOZIN[1], V.S. SHATSKY[1], H. KAGI[2], S. ODAKE[2], W.L. GRIFFIN[3] D. ARAUJO[3] AND O.P. YURYEVA[1]

[1]V.S. Sobolev Institute of Geology and Mineralogy, 3 Koptyuga ave., 630090, Novosibirsk, Russia (*correspondence: zed@igm.nsc.ru)

[2] Geochemical Research Center, Graduate School of Science, University of Tokyo, Tokyo 113-0033, Japan

[3]GEMOC ARC National Key Centre, Macquarie University, NSW 2109, Australia

Diamonds from Sao-Luis (Brazil) are known to be originated from the depths of transition zone and lower mantle [1]. In this study we consider some aspects of the composition and evolution of growth media for diamonds from this locality.

CL imaging has revealed the complex growth history for most diamonds, reflecting their formation in several stages. Nitrogen content in an individual diamonds varies from several to 500 ppm. An apparent tendency for the 3107 cm^{-1} peak intensity to increase with increasing the nitrogen content gives support to the idea that the conditions favouring the incorporation of nitrogen in these diamonds might also favour the incorporation of hydrogen. Specific feature of diamonds from Sao-Luis is extremely high nitrogen aggregation state (90-100 %B1). The set of luminescence centers N3, H3, H4, 490.7 is typical for all diamonds. Radiation-induced centers with peaks at 536 and 576 nm are often observed.

The total range of carbon isotope composition in diamonds studied by SIMS makes up from -3.3 to -20.3 ‰ of $\delta^{13}C$. Some diamonds show local variations of $\delta^{13}C$ between different growth zones (up to 7 ‰).

The dominant inclusions in studied diamonds are CaSi-perovskite and AlSi-phases. MgSi- and CaTi-perovskites, ferropericlase, native iron, coesite and zircon have also been found. Raman shift of coesite peak show high residual pressure (>3 GPa at ambient temperature).

FTIR study of some microinclusion-bearing diamonds showed that water and carbonates are not major components of diamond-forming fluids. LA-ICPMS bulk composition has significant enrichment in Ca, Fe and Al and strong depletion in Mg. Trace elements show general enrichment in Ti and V and depletion in Sr, LREE and Ni. Most probable source for such environments might be fluids from deeply subducted rocks of metasomatized oceanic lithosphere.

[1] Kaminsky *et al*. (2001) *Contrib. Miner. Petrol*. **140**, 734-753.

https://doi.org/10.1180/S0026461X00006502 Published online by Cambridge University Press

Mobility of trace elements in ombrotrophic peat bogs

LEONA ZEMANOVA[1]*, MARTIN NOVAK[1], PETRA PACHEROVA[1], ARNOST KOMAREK[2]

[1]Czech Geological Survey, Geologicka 6, 152 00 Prague 5, Czech Republic (*correspondence: leona.zemanova@geology.cz)

[2] Faculty of Mathematics and Physics, Charles University, Sokolovska 83, 186 75 Prague 8, Czech Republic

The geochemical cycles of many trace elements have been altered by human activity. Peat bogs are often used as an archives of past pollution. Concentration patterns of individual elements downcore can be recalculated into rates of historical atmospheric deposition. However, vertical mobility of trace elements in the petlands could "smear out" the historical record. We performed a peat transplant experiment to test the mobility/immobility of six trace elements (Mn, Fe, Pb, Zn, Cu and Ti), buried in organic soil. Three replicated cores from a peat bog situated in a heavily polluted area in northern Czech Republic were transplanted into a peat bog situated in unpolluted southern Czech Republic, and vice-versa. After 18-months, peat cores were excavated, taken to the laboratory and analyzed. Two different patterns were observed. The first group of elements (Fe, Mn) was characterized by convergence of concentration patterns to their host site, regardless of whether the host site was originally richer or more deficient in these elements. The second group of elements (Pb, Zn, Cu, Ti) was resistant to change during the transplant experiment, with concentration patterns unchanged. Our transplant experiment showed that not just lead but also copper and zinc could be used in retrospective peat pollution studies because there was no evidence of post-depositional mobility.

Concurrence of Mid-Miocene high Sr/Y granite and leucogranite in the Yardoi gneiss dome, Tethyan Himalaya, Southern Tibet

LINGSEN ZENG[1]*, LI-E GAO[1], KEJIA XIE[2] AND GUYUE HU[1]

[1]Institute of Geology, Chinese Acadmy of Geological Sciences, Beijing 100037 (*correspondence: zls1970@gmail.com)

[2]Institute of Tibetan Research, Chinese Academy of Sciences, Beijing 100085

We report a new suite of porphyric granite and leucogranite in the Yardoi gneiss dome (YGD) in the easternmost of the Northern Himalayan Gneiss Domes (NHGD), south of the Yarlung-Tsangpo suture. SHRIMP and LA-ICP-MS zircon U/Pb dating show that the porphyric granite dikes (PGD) and garnet-bearing leucogranites (LG) formed at ~17.7 Ma to ~20.0 Ma and at ~17.1 Ma, respectively. Both suites of granite have high Na/K (>1.30) ratios. The PGDs are characterized by (1) high Sr (>450 ppm), low Rb (<95 ppm) and Y (<6 ppm), and high Sr/Y (>86) ratios; (2) no Eu anomalies; and (3) low initial $^{87}Sr/^{86}Sr$ ratios (<0.7098) and higher ε_{Nd} (>-8.5) values. In contrast, the LGs have (1) lower Sr (<130 ppm) and higher Rb (92-130 ppm); (2) pronounced negative Eu anomalies with Eu/Eu*<0.55; and (3) relatively higher Sr ($^{87}Sr/^{86}Sr(t)$=0.7136-0.7148) and unradiogenic Nd ($\varepsilon_{Nd}(t)$=-7.7~-11.1). These data demonstrate that these Mid-Miocene granites have major and trace element and radiogenic isotope compositions similar to those of >35 Ma granites[1,2], but significantly different from those granites of similar ages in the High Himalya as well as in the NHGD[3]. High Sr/Y and relatively unadiogenic Sr isotope compositions in the PGDs could be derived from partial melting of mafic materials formed during previous compressional thickening event which was triggered by the input of juvenile heat and material associated with the Miocene E-W extension. An AFC process (plagioclase fractional crystallization and comtamination by crustal materials) could be a primary factor leading to the formation of these LGs. Concurrence of high Sr/Y granites and leucogranites in NHGD indicates that the Miocene rifting could have played an important but previously unrecognized role in producing the Himalayan leucogranite.

Supported by SinoProbe-2 and NSFC (41073024).

[1] Zeng *et al*. (2009) *Chin Sci Bull* **54**, 104-112. [2] Zeng *et al*. (2011) *EPSL* **303**, 251-266. [3] Zhang *et al*. (2004) *EPSL* 228, 195–212

https://doi.org/10.1180/S0026461X00006502 Published online by Cambridge University Press

Organic geochemistry characteristics for mudstones in the Permian Zhesi Formation, Eastern Inner Mongolia, China: A new instance showing good hydrocarbon potential in the marine strata

X.P. ZENG*, X.L. PENG, N. LIU AND C. CHEN

College of Earth Sciences, Jilin University, Changchun, 130061, China
(*correspondence: zengxiangpeng111@yahoo.cn)

More and more instances show that the marine strata has an effiective hydrocarbon potential as the terrestrial one did. And the study on the characteristics of organic geochemistry of the Permian Zhesi Formation in eastern Inner Mongolia provides an opportunity to achieve a breakthrough in marine petroleum exploration in northeastern China. The thickness of the mudstones in the Zhesi Formation is about 1000 m and 30 dark mudstone outcrop samples were collected. The values of TOC are distributed in 0.3%~1.67% (average 0.81%). 90% of the values are greater than 0.5% which is taken as the lower limit of the abundance of organic matter, while 20% of the values exceed 1.0%. It suggests that the source rocks are up to the medium-good hydrocarbon potential. The kerogen type is mainly II_2 and the highest pyrolysis temperatures are in the range of 469~549°C. Ro values are between 2.5% and 4.28%. The source rocks are in high to over mature stages. It is worth noting that the geochemical index of the outcrop samples in the study area are similar to the core ones in the Zhesi Formation, Songliao Basin which have been proved to have a good hydrocarbon potential. Therefore the outcrop mudstones in the eastern Inner Mongolia should be considered to be of a good hydrocarbon generated prospect.

This research was financially supported by the Natural Science Foundation of China (40972075) and the Strategic Research Center of Oil & Gas Resources (14B09XQ1201).

Phase equilibrium for the aqueous system containing ammonium, magnesium and chloride at 323.15 K

Y. ZENG[1,2]*, X. D. YU[1], J. Y. YANG[3] AND J. HONG[1]

[1]Department of Geochemistry, Chengdu University of Technology, Chengdu, 610059, China (*correspondence: zengyster@gmail.com)
[2] Mineral Resources Chemistry Key Laboratory of Sichuan Higher Education Institutions, Chengdu, 610059, China;
[3] Development & Comprehensive Utilization of Marine Sedimentary Brine Sichuan Provincial Key Laboratory, Chengdu, 611530, China

Phase equilibrium and phase diagram can give basic data for crystallization process. In the technology of exploit potassium from Pingluoba underground brine (Sichuan, China), magnesium ion accumulates in the mother liquid to form an aqueous system containing magnesium, ammonium and chloride. In this paper, the solubility of the system was measured using an isothermal solution method at 323.15 K.

Figure 1 is the phase diagram of the system at 323.15 K. The diagram consists of two invariant points, three univariant curves and three crystallization fields corresponding to single salts $MgCl_2 \cdot 6H_2O$, NH_4Cl and the double salt $NH_4Cl \cdot MgCl_2 \cdot 6H_2O$. The incommensurate invariant point E_1 is saturated with salts NH_4Cl and $NH_4Cl \cdot MgCl_2 \cdot 6H_2O$, and the mass fraction of its equilibrium solution is w (NH_4Cl) 7.27 % and w ($MgCl_2$) 25.87 %. The other invariant point E_2 is saturated with salts $MgCl_2 \cdot 6H_2O$ and $NH_4Cl \cdot MgCl_2 \cdot 6H_2O$, and the mass fraction of its equilibrium solution is w (NH_4Cl) 0.30 % and w ($MgCl_2$) 35.98 %. Results show that the salt $MgCl_2$ has salting out effect to the salt NH_4Cl.

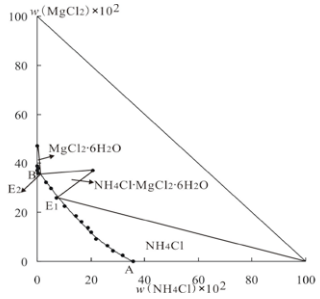

Figure 1 Phase diagram of the system containing ammonium magnesium and chloride at 323.15 K

The authors acknowledge the support of the Project of the China Geological Survey(1212010011809), the Research Fund from the Development & Comprehensive Utilization of Marine Sedimentary Brine Sichuan Provincial Key Laboratory (2009-230).

https://doi.org/10.1180/S0026461X00006502 Published online by Cambridge University Press

S isotope investigation of a redox-stratified system dominated by chemotrophic sulfide oxidation

AUBREY L. ZERKLE[1,2], JENNIFER L. MACALADY[3], DANIEL S. JONES[3] AND JAMES FARQUHAR[1]

[1]Dept. of Geology and ESSIC, University of Maryland, College Park, MD, USA
[2]Currently at School of Civil Engineering and Geosciences, Newcastle University, Drummond Building, Newcastle upon Tyne, NE1 7RU, UK, (aubrey.zerkle@ncl.ac.uk)
[3]Dept. of Geosciences, Pennsylvania State University, University Park, PA, USA

Anoxic and sulfidic conditions seem to have been common in parts of stratified Precambrian oceans. The fate of sulfide in these systems would presumably have depended on the availability of oxidants and the depth of the redox interface. Before widespread oxygenation of the surface oceans, sulfide in shallow waters reaching the photic zone would have been oxidized by anoxygenic phototrophs. Increasing oxygenation of surface waters would have driven the redox interface deeper into the ocean (and eventually into the sediments), where chemotrophic oxidation utilizing newly available oxidants (e.g., O_2 and NO_3^-) would have taken over. We are using multiple S isotopes to examine S cycling processes and resulting isotope signatures in biofilms dominated by chemotrophic S-oxidizing organisms in the sulfidic Frasassi cave system (central Italy). Fractionations between sulfide and S^0 in these biofilms are larger than those previously measured in the laboratory, and vary with stream chemistry, with larger fractionations occurring at higher O_2/H_2S. Mass balance models of sulfate, sulfide, and S^0 isotope values point to a complex sulfur cycle within the biofilms. Fractionations between sulfate and sulfide plot outside the range of $\delta^{34}S$ vs $\Delta^{33}S$ published for natural systems dominated by sulfate reduction, and could provide a fingerprint for oxidative S cycling in modern (and potentially ancient) environments.

Density and apparent molar volume of binary electrolyte aqueous solutions at elevated temperatures

D. ZEZIN*, T. DRIESNER AND C. SANCHEZ-VALLE

Institute of Geochemistry and Petrology, ETH Zurich, Clausiusstrasse 25, 8092 Zurich, Switzerland (*correspondence: denis.zezin@erdw.ethz.ch; thomas.driesner@erdw.ethz.ch, carmen.sanchez@erdw.ethz.ch)

Essentially all aqueous fluids encountered in geothermal and hydrothermal environments represent multicomponent electrolyte mixtures. Quantitative modeling of geothermal reservoir processes therefore requires thermodynamic properties of such solutions. While experimental data are available for most pure electrolyte solutions, the properties of multi-electrolyte solutions are largely unstudied at elevated temperatures and pressures above the vapour pressure saturation curve. This lack of experimental data precludes the derivation of accurate pressure dependencies in thermodynamic models of excess thermodynamic properties of aqueous species in geothermal fluids.

We present the results of an experimental study on the volumetric properties of binary electrolyte solutions at temperatures up to 300 °C and pressures up to 400 bar over a wide range of compositions and ionic strengths. We used a vibrating-tube densimeter to measure the relative density of aqueous solutions containing mixtures of alkali and alkali earth chlorides. Pressure, temperature and composition dependence of density and other derived properties of binary mixtures were constrained. Mean apparent molar volumes of the electrolyte solutions were calculated from the experimental data and compared to various mixing models from the lterature. The data will be used in the ongoing development and/or parameterization of models for the calculation of excess thermodynamic properties (Hingerl *et al.*, this conference). The results of this study will permit a quantitative modeling of the properties of complex aqueous solutions and simulation of fluid-rock interaction processes occurring in geothermal systems.

https://doi.org/10.1180/S0026461X00006502 Published online by Cambridge University Press

The solubility of gold in water-hydrogen sulphide vapours

D. ZEZIN[1]*, A. MIGDISOV[2] AND A.E. WILLIAMS-JONES[2]

[1]Institute of Geochemistry and Petrology, ETH Zurich, Clausiusstrasse 25, 8092 Zurich, Switzerland (*correspondence: denis.zezin@erdw.ethz.ch)
[2]Department of Earth & Planetary Sciences, McGill University, Montreal, H3A 2A7 Canada

Although the formation of high-suphidation epithermal deposits of Au has generally been attributed to hydrothermal mobilization of ore components by saline aqueous liquid, pressure-temperature conditions favour the domination of vapour over liquid in these magmatic hydrothermal ore-forming systems. In view of this and the longevity of many magmatic-hydrothermal systems, it is reasonable to consider the possibility, that vapour rather than liquid may be the principal ore fluid for high-sulphidation epithermal deposits. To test this hypothesis, we have experimentally investigated the solubility of gold in H_2O-H_2S gas mixtures. The speciation and stability of gold species were evaluated in gas-only system at temperatures from 300 to 400 °C and pressures up to 265 bar, with hydrogen fugacity constrained by the reaction $H_2+S=H_2S$. Results of the experiments demonstrate that Au can be dissolved in significant concentrations in aqueous vapours. As the fugacity of gold increases with the fugacity of H_2S (in both pure H_2S gas and H_2O-H_2S mixtures), it follows that formation of stable volatile sulphide species and their solvation by H_2S ($AuS(H_2S)_n$) control the solubility of gold in the gas phase. Moreover, as the solubility of Au in the vapour phase increases with the fugacity of H_2O, it also follows that gold solubility is enhanced by formation of species hydrated by H_2O molecules, $AuS(H_2O)_m$. These results provide strong evidence that H_2S plays an important role in the vapour transport of gold.

The relative importance of solvation/hydration of sulphide and chloride complexes was assesed for vapours of composition similar to those of natural low-density magmatic-hydrothermal fluids. As these vapours are mostly water rich, gold will be transported in the vapour dominantly as hydrated gold complexes. The data on the stoichiometry and stability of gold species presented in this study represent an important contribution to our knowledge of the chemical properties of volatile metal species. Equally important, they permit accurate modeling of vapour-related processes involved in the mobilization, transport and deposition of gold in magmatic hydrothermal systems, notably those of epithermal environments.

Water resources issues in the basin of transboundary Selenga river

D.TS.-D. ZHAMYANOV, I.D. ULZETUEVA, V.S. BATOMUNKUEV AND E.D. SANZHEEV

Baikal Institute of Nature Management SB RAS, 8, Sakhyanova Str., Ulan-Ude, 670047, Russia, (*correspondence: dabaj18@yahoo.com)

According to the United Nations, in the world is more than 260 rivers belonging by several states. Within their basins it is formed about 80 % of a world river flow and lives about 40 % of a world's population [1].

The Selenga river basin is located in the centre of the Euroasian continent, in a zone of a world watershed of Arctic and Pacific oceans basins and closed basin of the Central Asia. In the landscape relation the Selenga river basin is situated in contact area of taiga and steppe natural zones that predetermines development in this territory the natural environment, which is characterised by a high level of a biological variety and hypersensibility to external influences.

The intergovernmental border divides the Selenga river basin into 2 inadequate parts: its prevailing top part is situated in the territory of Mongolia, bottom – in the Russian Federation. The river Selenga – the main inflow of lake Baikal, the importance and uniqueness of which natural characteristics are recognised by the world community as object of the World natural heritage of UNESCO and are legislatively fixed only at the Russian level. Now the Russian-Mongolian relations in the field of protection of water resources are regulated on the basis of the intergovernmental Agreement for protection and use of transboundary waters (1995).

In a boundary control point in 1992-2008 years Fe, Cu, Zn, phenols and nitrogen were constantly marked above permitted standard content. The greatest values of concentration of polluting substances are marked in 1997, 2001, 2002, 2004 years. Thus in separate years presence of pesticides and mercury was fixed, which are according to the Russian requirements is inadmissible for lake Baikal basin. In 2010 for the lake Baikal the government of the Russian Federation enters even more rigid acceptable exposure standards.

The basic sources of pollution are treatment facilities of big cities of Mongolia and Republic of Buryatia (Russian federation) (Ulaanbaator, Darkhan, Erdenet, Ulan-Ude, Gusinoozersk, Zakamensk), and also the mining enterprises (especially gold mining) in Selenga river basin.

[1] Danilov-Danilyan, 2006.

https://doi.org/10.1180/S0026461X00006502 Published online by Cambridge University Press

Whether has platinum group elements (PGE) enriched in sulfide-rich black shale series in Southern Anhui Province?

YONG ZHAN[1,2], HAIJIAO YOU[1,2], YOUFEI GUAN[1,2], GUODONG SHI[2] AND MAOYAN MA[2]

[1]China Gezhouba Group Corporation, P.R.China (787545119@qq.com)
[2]Anhui University of Architecture, P.R. China

The PGE enriched in black shale series can be found in many places in China, such as Yunnan, Guizhou, Hunan, Gansu, as well as in Shanxi Province. In southern Anhui Province, the Early Cambrian black shale series are developed widely. But whether has PGE enriched in sulfide-rich black shale series is unclear.

The black shale series in southern Anhui Province, belonging to Lower Yangtze depression area, located in the Jiangnan deep-fault zone and suffered multi-stage tectonic movements, where magmatic activities show a polycyclic feature. The black shale series of Hetang Formation in southern Anhui is very stable in the whole Yangtze region and it's sequence corresponds with Niutitang Formation in western Hunan and Guizhou. The black shale series in southern Anhui mainly develop carbonaceous chert, carbonaceous shale, Si-bearing carbonaceous mudstone with the horizontal laminar, rhythmic bedding, wavy bedding, striped bedding and water ripple structure and contain star-shaped pyrite and pyrite aggregates in term of laminar distribution locally. The black shale series belongs to marine hydrothermal deposit that represents an abnormal marine sedimentation, and the sediment environment changes from the anoxic reducing environment in early stage to the half-reduction-oxidation environment in late stage [1]. PGE distribute in black shale series in Hunan-Guizhou region, especially in Ni-Mo sulfide ore bed, and spots of PGE can be found in part. The content of Re (Pd) is $1030\sim5550\times10^{-9}$, up to 10280×10^{-9}; Os content is $60\sim150\times10^{-9}$, up to 190×10^{-9}; Pt content is $50\sim580\times10^{-9}$, up to 690×10^{-9}[2].

The black shale series in southern Anhui is the same as Hunan-Guizhou in sequence, geological features, geochemical characteristics and genesis, so there is a great probability for enrichment and metalogeny of PGE in black shale series in southern Anhui. And the black shale series in southern Anhui should be given a systematic study.

This research was financially supported by the Natural Science Foundation of Anhui Provincial Education Department of China (NO.KJ2010A070).

[1] Xu *et al*. (2009) *Acta Petrologica Et Mineralogica* **28**(2), 118-128. [2] Liu. (2002) *Jilin Geology* **21**(4),1-8.

Hydration crystallization process in mafic-felsic mixing magmatic system: A case study from the Dabie orogen (East-central China)

C. ZHANG[1,2]*, F. HOLTZ[1] AND C. MA[2]

[1]Institute of Mineralogy, Leibniz University of Hannover, Callinstr 3, D-30167 Hannover, Germany (*correspondence: c.zhang@mineralogie.uni-hannover.de)
[2]State Key Laboratory of Geological Processes and Mineral Resources, Faculty of Earth Sciences, China University of Geosciences, 430074 Wuhan, China

Hydration crystallization processes, which refer to hydrous minerals-forming reactions in the late stages of magma evolution, have essential influence on the evolution and composition of solid phases and liquids of hydrous magmas as well as on the evolution of water content in residual melts. For quantitatively modeling igneous systems involving hydrous crystllization processes, the knowledge of physico-chemical conditions, i.e. X, T, P, $a\mathrm{H_2O}$, $f\mathrm{O_2}$, prevailing in magmas is a prerequisite.

The Liujiawa intrusion is an igneous complex located at the eastern boundary of the Dabie orogen, consisting of mafic and felsic components of distincitive origins. We identified five lithologically different parts: amphibole-rich cumulate, biotite-pyroxene gabbronorite, diorite, dioritic porphyry and granite. Geochemical data indicate that the gabbronorites ressemble the most primitive basaltic magmas, while the granites represent continental crust-derived magmas. Fractional crystallization and magma mixing processes have generated other lithologies. The low An content (<An60) of plagioclase and the crystallization sequence (opx prior to cpx) indicate a water content lower than 2.8 wt% H_2O in the parental melts. Biotite (16 wt%) is the only hydrous mineral in the gabbronorite, except for trace amounts of amphibole, while biotite is absent in the amphibole-rich cumulate (amphibole 48 wt%). In the diorite, a clear evidence of magma mixing is given by helminthoid clinopyroxene relics in the core of euhedral amphiboles. Textural and chemical data indicate that biotite and amphibole formed from incongruent hydration reactions of orthopyroxene and clinopyroxene, respectively. Continuous formation of amphibole at various T-P-$a\mathrm{H_2O}$ conditions are revealed by systematically varying chlorine and Al concentrations. To summarize, hydrous crystallizations, as part of the vertical evolution of intracontinental magmatism, are responses to various physico-chemical conditions, and the fractionation including hydrous minerals have significant contributions to the petrological and geochemical characteristics of final rocks.

https://doi.org/10.1180/S0026461X00006502 Published online by Cambridge University Press

Mineralization features and metallogeny of polymetallic deposit in black shale series in Southwest China

CHENGJIANG ZHANG , ZHENGQI XU AND SHIJUN NI

Chengdu University of Technology, Chengdu, 610059, China (*correspondence: xuzhengq@163.com)

Black shale series is widely distributed in the Late Sinian-Early Cambrian in Southwest China. Its lithologic characters are: carbonaceous shale or slate, carbonaceous dolomite, siliceous dolomite, silicalite and phosphorite. It is accompanied with mineralization and enrichment of Mo, V, U, Hg and P. Its mineralization features and metallogeny are studied through systematic sampling and analysis.

The mineralization features are: (1) Black shale series is the source bed, in which the contents of U and other metal elements are higher. (2) Uranium mineralization is accompanied with the features of multi-elements. At present, the mainly found types include: U-P, U-Hg, U-Mo, U-V and U-Au. (3) Uranium mineralization occurs near the center of submarine hydrothermal venting-flowing of black shale series. At some special geological positions, such as the center of submarine hydrothermal venting-flowing, Mo, Ni and U, as well as platinum group elements, concentrate and mineralize. (4) Uranium mineralization in black shale series is obviously related with the transformation effect in the later period and is the necessity for the forming of large and rich uranium deposit in black shale series in Southwest China. There are apparent proofs for the later transformation effect on uranium mineralization in black shale series. For example, in Baimadong Uranium Deposit and Jinsha Uranium Deposit in Guizhou Province, the stratohorizons with uranium of higher content are all accompanied with fault structure, tectonic breccia and hydrothermal alteration of silicification.

Metallogeny of U-Polymetallic deposit in Black Shale Series in Southwest China mainly undergoes the following stages: 1) Early enrichment: Primary enrichment of Uranium of higher content (uranium anomaly) in the depositing and diagenetic period of black shale series is the prelude of metallization of Uranium deposit in Southwest China. 2) Later transformation effect: Transformation of the shallow fluid causes the re-enrichment of Uranium (uranium ore occurrence, small or middle-scale uranium deposit); 3) Superimposed mineralization: Superimposition and transformation of the deep fluid causes the formation of rich and large ore (large-scale Uranium deposit).

Geochronology and Sr-Nd-Pb-Hf isotopic compositions of gabbroic intrusions adjacent to Southern Shang-Dan Suture Zone in the Qinling orogen, central China

CHENG-LI ZHANG*, LIANG LIU AND LEI LI

State Key Laboratory of Continental Dynamics, Northwest University, Xi'an, 710069, China (*correspondence: clzhang@nwu.edu.cn)

Shang-Dan Suture Zone (SDSZ) is a main tectonic boundary between North and South Qinling belts in Qinling Oregon, central China, and marked by a discontinuous tectonic lens of island-arc volcanic-sedimentary rocks, which were intruded by gabbroic intrusions to south side of SDSZ in east Qinling. The U-Pb zircon age, Hf and whole-rock Sr-Nd-Pb isotopes for the gabbros are reported in order to assess their source signatures and tectonic settings.

The U-Pb ages of 478±11Ma and 434.7±4.4Ma have been obtained from Fushui and Ziyu gabbroic intrusion, respectively. Both of them have quite similar Pb isotopic compositions, of which the initial $^{206}Pb/^{204}Pb$ ratios of Fushui gabbros rang from 18.1154 to 18.3353 and the Ziyu gabrros from 18.0195 to 18.0851. However, the Fushui gabbros has much high initial $^{87}Sr/^{86}Sr$ (0.70785~0.71191) and negative $\varepsilon_{Nd}(t)$ (-5.43~-2.79), showing a relatively enriched mantle reservoir with DMM and EM2 signatures. In contrast, Ziyu gabbros possess low initial $^{87}Sr/^{86}Sr$ (0.70353~0.70426) and positive $\varepsilon_{Nd}(t)$ (+3.98~+4.19), displaying a slightly depleted mantle source. In addition, Ziyu gabbros posses a wide ranges of $\varepsilon_{Hf}(t)$=-39~+10, evidently indicating contamination resulted by the continental materials during transfer through crust. Furthermore, both gabbros are characterized by the island-arc magmas with a relatively enriched LILE, poor HFSE and evident depletion of Nb, Ta and Ti. Thus, we infer that both gabbroic intrusions have resulted from subduction-related processes during early Paleozoic, and the mantle source changes from the Fushui to Ziyu intrusions present subduction of the ancient Qinling oceanic crust during 478Ma and break off of the Qinling oceanic plate around 435Ma due to arc-continent collision.

This research project was supported by the National Key Basic Science Research Project of China (2009CB825003).

https://doi.org/10.1180/S0026461X00006502 Published online by Cambridge University Press

Geogical significations of Qiatekaer Cu-Ni-Sulfide mineralized occurrence in West Kangguer ductile shear belt, Jueluotage area, Eastern Tianshan, Northwest China

D.Y. ZHANG, T.F. ZHOU*, F. YUAN AND Y. FAN

School of Resources and Environmental Engineering, Hefei University of Technology, Hefei 230009, China (*correspondence: tfzhou@hfut.edu.cn)

Geology and geophysics of the Qiatekaer occurrence

The Qiatekaer Cu-Ni occurrence is located in the east section of Kangguer deductile shear belt, eastern section of Jueluotag tectonic belt, Eastern Tianshan, Xinjiang, China. which have the same geological setting as the Cu- Ni deposits in the east part. The mafic dyke out crops in Qiatekaer area was found sulfides such as pyrite and pentlandite, and Ni concentration of some mineralized gabbros reach more than 400ppm, and Cu-Ni mineralized abnormalities are obviously indentified by geophysical methods such as gravity, magnetism and CSAMT [1].

Discussion

Geological characters indicate that Qiatekaer area has large potential to form Cu-Ni deposits, and there are obvious Cu-Ni sulfide mineralization judged by geochemical and geophysical characters[2, 3]. The identification of Qiatekaer Cu-Ni sulfide mineralized occurrences gives good direction to further explorer Cu-Ni deposits along the Kangguer deductile shear belt, which extends more than 500 kilometers.

The research is sponsored by the National Key Basic Science Research project of China (2007CB411304), the National Natural Science Foundation of China (41040025, 40772057), the Program for New Century Excellent Talents in University (NCET-10-0324) and the Anhui Provincial Natural Science Foundation for Distinguished Young Scholars (Grant No. 08040106907, 04045063).

[1] Hao (2010) 305 Conferrence Report, Tianjin (in Chinese). [2] Su BX(2010) PhD thesis 1-237 (in Chinese). [3] Li *et al*. (2006) *Acta Geoscientica Sinica* **27** (5), 424-446 (in Chinese).

Microanalysis of trace element in Fe oxide and sulphides using LA ICP-MS and EMPA

DEXIAN ZHANG[1,2,3]*, BRIAN RUSK[3], NICK OLIVER[3] AND TAGEN DAI[1,2]

[1]School of Geosciences and Info-physics, Central South University, Changsha, Hunan Province, China,410083 (*correspondence: Dxzhang303@gmail.com)

[2] Key Laboratory of Metallogenic Prediction of Nonferrous Metals, Ministry of Education,China,410083

[3]Economic Geology Research Unit, School of Earth and Environmental Sciences, James Cook University, Townsville, QLD, Australia

Our aims are to investingate the trace element concentrations and distributions in natural Fe oxides and sulfides using LA ICP-MS combined with EMPA,which are predominantly important in the study of ore genesis, economic geology of ore deposit.

In our study we analysed 267 individual magnetite and 139 pyrite in 48 samples using a GeoLas 193 nm excimer laser ablation system coupled to a Varian 820-MS series ICP-MS, and conducted elemental maps on 12 magnetite grains and sulphides grains on a Jeol JXA8200 super-probe at the Advanced Analytical Center (AAC) at James Cook University. The laser system parameters are :repetition rate:10 Hz, laser beam energy: 8J/cm^2, analysis time: 65 (30s measurement of background (laser off) and 35s analysis signal), external standard: NIST SRM 610, 612 and Mass -1, the internal standard: Fe.

EMPA trace element maps indicate that magnetite is not zoned with respect to trace element distribution, so we can use analysis limited spot on magnetite to represent the whole concentration of individual grain. The typical detection limits for a 45 micron spot are Li (1.62 ppm), Na (518ppm), Mg (0.58 ppm), Al (0.93 ppm), Si (80 ppm), K (1.41 ppm), Ca (18.39 ppm), Ti (0.17 ppm), V (0.03 ppm), Cr (1.13 ppm), Mn (0.29 ppm), Fe (5.73 ppm), Co (0.03 ppm), Ni (0.89 ppm), Cu (0.28 ppm), Zn(0.96 ppm), Ga (0.55 ppm)), Ge (0.82 ppm), As (0.17ppm), Mo (0.03 ppm), Ag (0.01 ppm), In (0.08 ppm), Sn (0.11 ppm), Sb (0.03 ppm), Ba (0.29 ppm), W (0.005 ppm), Au (0.004 ppm), Pb (0.01 ppm), Bi (0.003 ppm), Th (0.001 ppm)

The results suggests that LA ICP-MS combined with EMPA is a effective and powerful tools to investigate the trace element concentration and distribution in Fe oxides and sulphides.

https://doi.org/10.1180/S0026461X00006502 Published online by Cambridge University Press

Simulating foam transport in the vadose zone at the continuum scale

Z. FRED ZHANG[1]*, MARK D. WHITE[1] AND MARTIN W. FOOTE[2]

[1]Energy and Environment Directate, Pacific Northwest National Laboratory, Richland WA 99352 USA (*correpondence: fred.zhang@pnl.gov)
[2]MSE Technology Applications, Inc., Butte, MT 59701 USA

The nuclear wastes residing in the deep vadose zone at the Hanford Site near Richland, WA, USA, threaten the underlying groundwater [1]. To immobilize the contaminants, aqueous and/or gaseous amendments may be carried by foam and injected into the contamination region. Foam is an emulsion-like, two-phase system in which gases are dispersed in a liquid and separated by thin liquid films. Foam has a very low density and a very high apparent viscosity. The transport of foam in the vadose zone is complex in that the number of lamellae present governs foam flow characteristics such as viscosity, relative permeability, and interactions between injected and residential fluids. We have developed a simulation capability into the STOMP numerical simulator [2] to model the transport of foam and the amendments contained in foam. Bench-scale lab experiments were conducted by injecting pre-generated foam into an initially unsaturated system containing one or more types of sediments. Soil water content and foam pressure were measured with time at multiple locations. The Figure below shows the simulated moisture-content distribution during the injection of foam into a two-dimensional flow cell. Further work is warranted for better understanding the foam transport mechanism in the vadose zone and parameterizing the model.

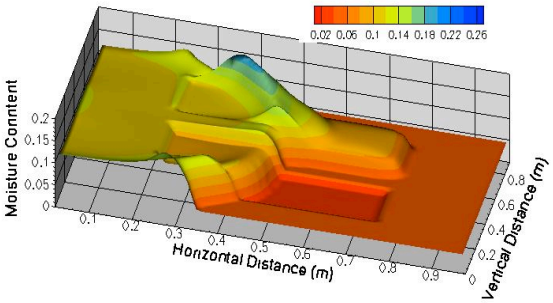

Figure 1: Simulated moisture content distribution during the injection of foam.

[1] United States Department of Energy (2010), DOE/RL-2010-89, Revision 0. [2] White and Oostrom (2006), PNNL-15782, Pacific Northwest National Laboratory.

The significance of Cenozoic magmatism from the Eastern margin of the Eastern Himalayan syntaxis

HONGFEI ZHANG, FABIN PAN, WANGCHUN XU, LAISHI ZHAO AND YONGHAO YE

State Key Laboratory of Geological Processes and Mineral Resources, China University of Geosciences, Wuhan 430074, China (hfzhang@cug.edu.cn)

Previous studies show that the adakitic rocks have magma crystallization ages between 10~18 Ma in central Gangdese belt (west of 92°E) and 22~26 Ma in eastern Gangdese (east of ~ 94°E) [1,2,3,4]. It seems that the magma crystallization ages for the Gangdese adakitic magmatism tend to an increased variation from west to east. However, whether this variational trend extend to far eastern Gangdese is uncertain because previous work on the far eastern Gangdese adakitic magmatism lacks high-precision geochronological data. If the age variational trend for the adakitic magmatism is true, an interesting issue is what continental dynamic process taken place along the Gangdese belt.

We carried out an integrated study of U-Pb zircon dating, geochemistry and Sr-Nd-Hf isotopes for two granitoid intrusions in Motou area, the eastern margin of the eastern Himalayan syntaxis. U-Pb zircon dating shows their magma crystallization ages of ~28 Ma. These granitoids have adakitic geochemical signatures. Our result further confirms the age variation of the adakitic magmatism along the Gangdese belt. We suggest that the adakitic magmatism resulted from break-off of the subducted Indian continental slab and a westward propagation model for the slab break-off can account for the age variation and magma generation.

[1] Chung *et al*., 2009. *Tectonophysics*, v. **477**, p. 36-48. [2] Ji *et al*., 2009. *Chemical Geology*, v. **262**, p. 229-245. [3] Xu *et al*., 2010. *Lithos*, v. **114**, p. 293-306. [4] Zhang *et al*., 2010, *Contributions to Mineralogy and Petrology*, v. **160**, p. 83-98.

https://doi.org/10.1180/S0026461X00006502 Published online by Cambridge University Press

Modeling of hyporheic zone of surface water - groundwater with 3S technology

JING ZHANG[1]*, HUILI GONG[2] AND XIAOJUAN LI[3]

[1]The Key Laboratory of Resource Environment and GIS of Beijing, Capital Normal University, Beijing 100048, P. R. China (*correspondence: maggie2008zj@yahoo.com)
[2]College of Resource Environment and Tourism, Capital Normal University, Beijing 100048, P.R. China
[3]College of Resource Environment and Tourism, Capital Normal University, Beijing 100048, P.R. China

Hyporheic zone of surface water - groundwater is a mixture of surface water and ground water zone where the biogeochemical activities in the region are very strong. Moreover, this zone is mainly affected by natural factors and human factors. The physical, chemical and biological processes are often occurs within the hyporheic zone, and affect the water movement, solute transport processes and the process of biological activities. Massive algae blooms are one of the biggest problems that rivers/lakes/coasts face today in China. For example, before the Beijing 2008 Olympic Games opening, Qingdao Olympic Sailing Venue, the green algae covers a third of the sea off the city of Qingdao. Algae are often caused from high nitrogen containing components of untreated waste, and nitrogen is a detergent and the main ingredient in plant fertilizer. The hope Green Olympic Games and current situation make so many Chinese people unease. Rapid development of computer technology and geo-information technology provides an objective basis for truly integrated cross-disciplinary. Global Earth Observation System of aerospace, aviation and ground coordination with multi-temporal and spatial resolution has been more and more widely applied in geochemical, hydrological, ecological and environmental studies. With the advanced development of 3S technology (Remote Sensing, Geographic Information System, Global Positioning System), monitoring, measuring and modeling biogeochemical processes and its ecological function in hyporheic zone of groundwater and surface water is more visualized and reliable. This talk will focus on an overview of application of 3S on biogeochemical processes in hyporheic zone of groundwater and surface water in China with some preliminary modeling studies [1].

[1] Under the auspices of National Natural Science Foundation of China (No.40901026) and Supported by Beijing Municipal Science & Technology New Star Project Funds (No.2010B046).

Recycling subcontinental plagioclase-rich lower crust in the North China craton

JUN-BO ZHANG[1,2], WEN-LI LING[1,2]*, YONG-SHENG LIU[1,2], SHAN GAO [1,2], TIMOTHY KUSKY[1], ZI-WAN CHEN[1,2], XIAO-FEI QIU[1] AND MENG CHE[1]

[1]State Key Laboratory of Geological Processes and Mineral Resources, China University of Geosciences, Wuhan 430074, China (*correspondence: lingwenli2008@126.com)
[2]Faculty of Earth Sciences, China University of Geosciences, Wuhan 430074, China

Foundering of eclogitic lower crust into the convecting mantle has been proposed to explain the unusually evolved chemical composition of Earth's continental crust. However, whether the granulitic lower crust is also removable remains unclear due to its relatively lower density. Here, we report a geochemical study of distinct phenocrystal clinopyroxene and silicic melt inclusions hosted by early Cretaceous high-Mg andesite (HMAs) from Shandong province, eastern North China craton, which suggests recycling of plagioclase-rich lithologies. Three types of clinopyroxenes are recognized. Type I and II clinopyroxenes show normal- and reverse zonation, respectively, and both are featured by clear negative Eu anomalies in their cores. Type III clinopyroxene occurs in a remnant poikilitic texture with a high-Mg# core, but with no Eu anomaly, and encloses low-Mg# olivine grains. Both olivine and clinopyroxene crystals of the andesite contain high-Si and low-Mg melt inclusions, which are enriched in alkali metals and have low Eu/Eu*, showing a nature akin to their host clinopyroxenes and HMAs. It is thus suggested that the HMAs were derived from lower-degree melting of recycling plagioclase-rich lithologies. These rocks are interpreted as granulitic lower crust returned into the convecting mantle, which then interacted with mantle peridotite via partial melting. If so, our scenario also provides a critical guide for making high-Mg andesite and continental crust and that the granulitic component input could play a key role in the subcontinental mantle heterogeneity.

https://doi.org/10.1180/S0026461X00006502 Published online by Cambridge University Press

A LA-ICP-MS study of garnet from the Nihe iron deposit, Anhui Province, China

LEJUN ZHANG*, TAOFA ZHOU, YU FAN, FENG YUAN, LING MA AND BING QIAN

School of Resources and Environment Engineering, Hefei University of Technology, P.R. China (*correspondence: zljzhang@163.com)

The Luzong volcanic basin is located at the central part of the Middle and Lower Yangtze River area and contains numerous important Cu-Au-Fe deposits. The Nihe iron deposit is a newly discovered large scale iron deposit in the western part of the Luzong volcanic basin. In the contact zone of the diorite porphyry intrusion and the trachyandesite of Zhuanqiao Formation occur anumbers of garnet in the Nihe iron deposit. This study presents LA-ICP-MS data for garnets from the Nihe iron deposit, discusses the factors controlling incorporation of trace elements into garnets, and strengthens the potential of garnet trace elements geochemistry as a tool to help understand the evolution of hydrothermal fluids.

Garnets from the Nihe iron deposit range from $Adr_{48}Grs_{52}$ to almost pure andradite (Adr>99). LA-ICP-MS data show that the garnet have detectible Zr, V, U, Sc, Nb, Th, Zn, Ga, Cr, Ge, Hf, Sr, Ta, Pb and REE (∑442~1301ppm, avg. 812ppm). All the garnets are show typical LREE-enriched and HREE-depleted patterns, with a strong positive Eu anomaly. Incorporation of trace element into garnet is in part controlled by its crystal chemistry, with a coupled substitution mechanism(eg. $[X^{2+}]$ VIII -1$[REE^{3+}]$ VIII +1 $[Si^{4+}]$ IV -1 $[Z^{3+}]$ IV +1). Variations in textural, optical features and geochemistry of the garnet are largely controlled by fluid composition. Garnet composition and zonation record the history of the hydrothermal fluid and can be used to identify fluid changes in physicochemical properties.

This research was supported by funds from the National Natural Science Foundation of China (Grant No. 40830426, 40803015), Research Fund for the Doctoral Program of Higher Education (Grant No. 20100111110010), Deep Exploration Technology and Experimentation (SinoProbe-03)and the Science Research Project of CODES, Centre of the Excellence in Ore deposits, University of Tasmania (Grant No. CODES2009 P2. N3).

Formation mechanism of foliated (garnet-bearing) granites of the Tongbai-Dabie orogenic belt: Evidence from the Mamiao cross section

L. ZHANG[1]*, Z. ZHONG[1], H. ZHANG[1] AND W. SUN[2]

[1]State Key Laboratory of Geological Processes and Mineral Resources, Faculty of Earth Sciences, China University of Geosciences (Wuhan), Wuhan 430074, P. R. China (*correspondence: lizhang@cug.edu.cn)

[2]Key Laboratory of Isotope Geochronology and Geochemistry, Guangzhou Institute of Geochemistry, the Chinese Academy of Sciences, Guangzhou, 510640, China

High pressure (HP) metamorphic rocks are important for understanding the genesis of the foliated (garnet-bearing) (FGB) granites in the Tongbai-Dabie orogenic belt. Based on a study on geochemistry of HP metamorphic rocks and FGB granites from the Mamiao cross section in the Tongbai-Dabie orogenic belt, the relationship between these rocks are discussed. The regular pattern of variation trends of elemental compositions of the HP metamorphic rocks, as well as the similarity in the isotopic compositions suggests the continuous evolutional relationship of retrograde metamorphism between the HP rocks. The changes in elemental compositions between HP gneisses and FGB granites are significantly different from variations of elemental compositions occurred during the retrograde metamorphism of HP eclogites. These differences in geochemistry presented in this study and previous studies suggest that there is no continuous evolutional relationship of retrograde metamorphism between the FGB granites and the HP metamorphic rocks. The magma source of the FGB granites was most likely from retrograded metamorphism and depressional partial melting of the UHP gneisses.

This research was supported by NSFC of China (No. 40873044) and the Chinese National Key Project for Basic Research (No.2006CB403502).

https://doi.org/10.1180/S0026461X00006502 Published online by Cambridge University Press

Kinetic experiments of some silicate mineral dissolutions in water from a subcritical to a supercritical state

RONGHUA ZHANG, SHUMIN HU AND XUETONG ZHANG

Institute of Mineral Resources, Chinese Academy of Geological Sciences, Lab.Geochemical Kinetics. Baiwanzhuang road 26, Beijing 100037 (zrhhsm@pku.edu.cn)

Measurements of steady-state dissolution rate of pyroxene, quartz, garnet, albite and actinolite in water were performed using flow through reactor (well mixed) from a subcritical to a supercritical state at temperatures from 25 to 435°C at 23-33 MPa. Minerals used in experiments are collected through microscope, cleaned and analyzed chemically. Usually, all reactive solutions were undersaturated with respect to the mineral. A few secondary product phases were found on the reacted surface. The kinetic experiments indicate that the measured dissolution rates of the minerals at T ≤300°C coincide with previous experiments of quartz, diopside and albite published in literatures. The dissolutions are stoichiometric, when the release ratio of molar concentrations of metal M_i versus molar concentration of Si in outlet solutions $\Delta Mi/\Delta Si$ is identical to the stoichiometric number N_i in solid. The stoichiometric dissolution of pyroxene in water is present at near 200°C, and it for albite in water is at 300°C. Dissolution rates (r_{Si}) for quartz, diopside, hedenbergite, albite, garnet in water were found to increase with increasing T from 25 to 300°C. Experiments indicate that the rates of pyroxene and albite decrease with increasing T from 300 to 400°C. The maximum release rates of Si for those minerals are reached at 300°C. The maximum rates for quartz are at about 374°C. The different metals of the minerals often behave the different release rates. Usually, the release rates of Na, Ca, Mg, Fe, Al of minerals are often higher than Si at T<300°C, and the metal M_i-H^+ exchange reactions are faster at low temperature. The hydrolysis of Si-O-Si bond and metal ion-H^+ exchange reactions at T< 300°C are different from reactions at T ⩾ 300°C. Because, the effects of water solvent properties (lowering density and dielectric constant within the region from a sub-critical to supercritical state, hydrogen networks of water molecules break) affect dissolution rates, e.g., dissolution rates of Si vary with 1/dielectric constant.

Note: This project is supported by the projects of 2010G28, 2008ZX05001-003-006, K1006, SinoProbe-07-02-03, SinoProbe-03-01-2A.

Melting of juvenile lithospheric mantle: Geochemical evidence from Neoproterozoic mafic-ultramafic rocks in South China

SHAO-BING ZHANG*, RONG-XIN WU AND YONG-FEI ZHENG

School of Earth and Space Sciences, University of Science and Technology of China, Hefei 230026, China (*correspondence: sbzhang@ustc.edu.cn)

While many studies deal with the fate of ancient SCLM, less attention has been paid to the fate of juvenile lithospheric mantle. We present a geochemical study of a Neoproterozoic mafic-ultramafic complex in the eastern Jiangnan orogen, South China. Harzburgite is significantly depleted in Ca and Al, suggesting significant melt extraction; gabbro and spilite have low contents of TiO_2 and P_2O_5. While all the mafic rocks show the arc-like patterns of REE and trace element distribution, the harzburgite is complementary to the mafic rocks in the spidergrams. Zircon U-Pb dating on the gabbro gave three groups of ages at 891±13 Ma, 824±3 Ma and 764±19 Ma, respectively. The 891±13 Ma zircons are less common and unzoned or weakly zoned in CL images, which are interpreted as residues from magma source. The 824±3 Ma zircons are dominant and show clear magmatic zoning, representing crystallization age of the gabbro. The 764±19 Ma ages result from reworking of the collision orogen in response to supercontinent breakup. The harzburgite, troctolite and gabbro have positive $\varepsilon_{Nd}(t)$ values of 3.29 to 5.69 and lower initial $^{87}Sr/^{86}Sr$ ratios of 0.7033 to 0.7059, whereas the spilites show neutral $\varepsilon_{Nd}(t)$ values of -1.24 to 0.40 and higher initial $^{87}Sr/^{86}Sr$ ratios of 0.7039 to 0.7068. In particular, the gabbro rich in zircons has the highest $\varepsilon_{Nd}(t)$ values of 5.69 and the youngest Nd model age of 1.03 Ga. Lu-Hf isotope analyses on the zircons from the gabbro gave positive $\varepsilon_{Hf}(t)$ values of 10.2 to 12.1 at t = 824 Ma and Hf model ages of 0.90 to 0.98 Ga Ma. The positive $\varepsilon_{Hf}(t)$ and $\varepsilon_{Nd}(t)$ values as well as the small differences between the magma crystallization age and the Hf-Nd model age for the gabbro indicate its derivation from partial melting of an isotopically depleted mantle source. Along with available data in the Jiangnan orogen which suggests the postcollisional tectonic setting, it is concluded that the mafic-ultramafic rocks were derived from partial melting of the juvenile lithospheric mantle that probably formed by arc-continent collision at about 900 Ma, and underwent partial melting at about 820 Ma. Therefore, the gabbro and spilite represent the melts, whereas the harzburgite would be the restites after melt extraction. This provides geochemical evidence for anatexis of juvenile lithospheric mantle in the postcollisional regime.

https://doi.org/10.1180/S0026461X00006502 Published online by Cambridge University Press

Phase equilibrium of the Cd-bearing systems at 298 K: $Cd^{2+}//Cl^-$, SO_4^{2-}, NO_3^--H_2O quaternary system

ZHANG SHIPENG[1], HUANG YI[2,3]* AND NI SHIJUN[3]

[1]College of Materials and Chemistry & Chemical Engineering, Sichuan, PRC

[2]Department of Geochemistry, Chengdu University of Technology, Sichuan, PRC (*correspondence: huangyi@cdut.cn)

[3]Applied Nuclear technigues in Groscience Key Laboratory of Sichuan Proviance, PRC

Solid- Liquid Equilibrium of quaternary system $Cd^{2+}//Cl^-$, SO_4^{2-}, NO_3^--H_2O at 298 K were studied by an isothermal solution saturation method. Experimental results indicate that there are three univariant curves BE, AE and CE, one invariant point E and three crystallization fields in the quaternary system. The quaternary system belongs to a simple type, and there're no double salts or solid solution existing. The crystallization zones of equilibrium solid phases are $CdCl_2·H_2O$, $CdSO_4·H_2O$, and $Cd(NO_3)_2·8H_2O$, respectively. The composition of the invariant point is $CdCl_2·H_2O$, $CdSO_4·H_2O$, and $Cd(NO_3)_2·8H_2O$, respectively. The physico-chemical properties of solution in the quaternary system show regular changes along with the increased cadmium concentration. The results indicated that $Cd(NO_3)_2·8H_2O$ possessed the highest solubility among those three salts, which means a strong transfer of Cd ion and a high pollution risk of soil environment. And the solubility of $CdSO_4·H_2O$ would be restrained as the salts existing together.

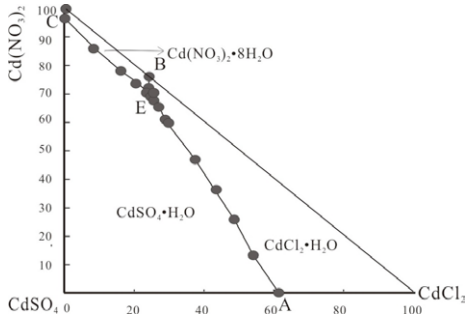

A simulation study of hydrocarbon gas generation from Fischer–Tropsch synthesis with varying carbon source and hydrogen in a gold tube system

ZHANG SHUICHANG, MI JINGKUI AND HE KUN

Key Laboratory for Petroleum Geochemistry, China National Petroleum Corporation

The Fischer–Tropsch synthesis (FTS) is a widely accepted mechanism for the formation of abiogenic gases, but the experimental results from different laboratories vary considerably and can rarely match the natural occurrence [1-3]. Our FTS experiments were conducted in a sealed gold tube on Fe and Ni catalysts using graphite and CO_2 with distinctive isotopic composition as the starting material by reduction in pure hydrogen at 400 °C and 50 MPa for 2-60 h. Results show that synthesis between gaseous phase carbon (CO_2) and H_2 is easier than solid phase carbon (graphite) counterpart and ^{13}C depleted CO_2 is more reactive than ^{13}C enriched CO_2. After short reaction time carbon isotopic compositions of hydrocarbons from all three FTS experiments decrease in $\delta^{13}C$ values of C_2 to C_4 alkanes with respect to CH_4, showing so-called inverse trend. With increasing reaction time, synthesis was gradually shifted to thermal cracking. ^{13}C depleted gas from thermal cracking mixed with ^{13}C enriched residual gas leads to partial reversal and normal isotopic distribution among C_1-C_4 alkanes. Hydrocarbon gases from the FTS will finally decompose to carbon and hydrogen if reaction time is longer enough.

FTS experiments running under laboratory condition from low to high temperature differs from abiogenic synthesis of hydrocarbons in natural systems, which is a cooling process from high to low temperature either under aqueous hydrothermal or volcanic intrusion condition. Hydrocarbons generated from the FTS experiments may be decomposed via thermal cracking and isotopic composition among gaseous components can show all possible distribution patterns. FTS-type natural reactions occur under certain PT condition and hydrocarbon gases generated have no further decomposition and may hold a fixed "inverse" isotopic distribution. This may explain the controversial isotopic distribution patterns observed from varying FTS experiments.

[1] Charlou *et al*. (1998) *GCA* **62**(13), 2323-2333. [2] McCollom etal. (2006) *EPSL* **43**(1-2),74-84. [3] Taran *et al*. (2010) *GCA* **74**, 6112-6125.

https://doi.org/10.1180/S0026461X00006502 Published online by Cambridge University Press

Reactive transport modeling of carbon sequestration in volcanogenic sandstone formations

SHUO ZHANG[1]*, DONALD J. DEPAOLO[2] AND TIANFU XU[3]

[1]307 McCone Hall, University of California, Berkeley, CA 94720-4767, USA (*correspondence: shuozhang@berkeley.edu)

[2]475 McCone Hall, University of California, Berkeley, CA 94720-4767, USA (depaolo@eps.berkeley.edu)

[3]Earth Sciences Division, Lawrence Berkeley National Laboratory, University of California, Berkeley, CA 94720, USA (Tianfu_Xu@lbl.gov)

Geological storage of carbon dioxide in deep saline formations can decrease the accumulation of CO_2 in the atmosphere, and thus slow down global warming. Most injected CO_2 remains for a long time as either a separate supercritical phase or in solution in brine; both forms constitute increased risk of leakage back to the surface or other environmental impacts. Mineralogical trapping of injected CO_2 is more secure but usually very slow. For standard sandstones (quartzite and arkose) investigated so far, it takes up to 10000 years to achieve 5 percent CO_2 mineralization [1]. Volcanogenic sandstones have relatively high reaction rates and larger amounts of reactive minerals, which means that if they were used for storage, there could be a larger fraction of CO_2 mineralized in a shorter time. However, porosity and permeability tend to decrease with increase of volcanic rock fragments (VRF) in sandstones, which limits the rate of CO_2 injection. We have attempted to quantitatively evaluate these tradeoffs to assess the feasibility of using volcanogenic sandstone to achieve highly secure CO_2 storage. We determined relationships between VRF percent, porosity, permeability and CO_2 injection rate from available geological data, and used TOUGHREACT to evaluate the trade-off between higher reactivity and lower porosity and permeability. Preliminary results show that roughly 5% VRF is optimal, and can result in almost complete CO_2 mineralization, but this depends on the magnitude of reactive surface area (RSA) specified. Varying RSA between 2 cm^2/g and 50 cm^2/g changes the fraction mineralized from 13% to almost 100% at 1000 years. Baseline simulations were done with a 1-D model. A corresponding 2-D radial model shows a slight increase of mineralized CO_2 due to a larger interface between the CO_2 plume and saline water.

[1] Audigane, P., *et al*. (2007) *American Journal of Science* **307**(7): p. 974-1008.

Biomethylation potential of mercury depends on the kinetics of HgS precipitation

T. ZHANG, H. HSU-KIM* AND M.A. DESHUSSES

[1]Duke University, Civil & Environmental Engineering, Durham, NC 27708, USA (*correspondance: hsukim@duke.edu)

Monomethylmercury (MeHg) is an extreme neurotoxin that accumulates in food webs and poses a significant risk to human health. In natural aquatic systems, the predominant mechanism of MeHg production is microbial methylation of inorganic mercury (Hg) by sulfate-reducing bacteria (SRB). MeHg production rates are largely controlled by the availability of Hg species for uptake into SRB and the productivity of those microbes. In sediments, sulfide controls Hg speciation due to its high abundance and strong affinity to bind Hg^{2+}. Previous studies have demonstrated that natural organic matter (NOM) interferes with the precipitation of $HgS_{(s)}$ by preventing aggregation of HgS nanoparticles that are formed during the initial stages of precipitation. We hypothesize that bioavailable Hg concentration is related to the kinetics of HgS precipitation, and not necessarily to equilibrium speciation of Hg in sulfidic porewater.

We conducted methylation bioassays using pure cultures of two methylating SRB, *Desulfobulbus propionicus* (1pr3) and *Desulfovibrio desulfuricans* (ND132). The bacterial cultures were exposed to three different forms of Hg-sulfides, including dissolved $Hg(NO_3)_2$ and Na_2S, humic-coated HgS nanoparticles (<30 nm), and metacinnabar particles (>1000 nm), which were formulated to represent three different 'aging' states of mercury in sulfidic sediments. Our results showed that methylation rates were greatest with the dissolved Hg-sulfide treatment. In the treatments with HgS nanoparticles, MeHg production was observed at a rate that was significantly faster than the metacinnabar treatment. These results may be due to: 1) the relatively poor crystallnity of HgS nanoparticles compared to bulk minerals that are inherently less soluble; 2) the larger extent of nanoparticle-bacteria surface contact that allows nanoparticulate Hg to be spatially more accessible for the methylating bacteria than micro-scale metacinnabar. Moreover, methylation potential appeared to decrease as HgS nanoparticles 'aged' (16 hrs~1 week), which may be attributed to the enhanced crystallinity of nanoparticles during aging. Overall, our study points to a new paradigm for modeling aqueous mercury speciation in anaerobic environments and the bioavailability of inorganic mercury to methylating bacteria.

https://doi.org/10.1180/S0026461X00006502 Published online by Cambridge University Press

The bioleaching effect of agitation speed on low-grade chalcopyrite ore under the combined catalysis

W. M. ZHANG[1,2] *

[1]State Key LaboratoryBreeding Base of Nuclear Resources and Environment, East China Institute of Technology, Nanchang 330013, China
(*correspondence: wmzhang@ecit.cn)
[2] School of Civil and Environmental Engineering, East China Institute of Technology, Fuzhou 344000, China

Chalcopyrite is the most important copper mineral. It is, however, relatively recalcitrant to chemical and bacterial oxidation because of its special crystal structure and electrochemistry in contrast to many other copper minerals. It is essential to find some desirable methods to enhance chalcopyrite bioleaching. The purpose of this work is to study the bioleaching of agitation speed on low-grade chalcopyrite ore under the combined catalysis

The low-grade chalcopyrite ore used in this study was obtained from Yongping Copper Mine, SE-China. The particle size was less than 5 mm. The chemical composition is as follows: 0.40% Cu, 14.12% Fe, 13% S. The chemical phase analysis showed that chalcopyrite is 0.38% and the other copper minerals 0.02%. The mixed *Acidithiobacillus ferrooxidans* and *Acidithiobacillus thiooxidans* used in this study were isolated from acid mine drainage at Yongping Copper Mine. Leaching experiments were carried out in 10 L plastic drum with 800 ml 9K + S medium without Fe^{2+}, 200 ml inoculation, 25%(W/V) pulp density, 3.0 g/L activated carbon, 2.0 mg/L Ag^{+}, 8.0 g/L Fe^{2+} and 1.20 pH (the pH values were controlled within 1.50 with sulphuric acid during the bioleaching processes). The agitation speeds were 120, 150, 180, 240 and 300 rpm ,respectively.

The results show that the agitation speed has a great effect on the bioleaching of low-grade chalcopyrite ore under combined catalysis of activated carbon, Ag^{+} and Fe^{2+}. The agitating speed of 300 rpm is most beneficial to the dissolution of copper, in this case, the leaching rate of copper reaches 84% after 456 h leaching, which is 37% higher than that at 120 rpm. It is found that it is more favorable to the bioleaching of low-grade chalcopyrite ore if the redox potential is controlled at 580-620 mV.

Variation of hydro-chemistry in lower reaches of the Chinese Golmud-river and its effects on the groundwater

ZHANG WENJIE AND TAN HONGBING

School of Earth Sciences and Engineering, Hohai University, Nanjing, 210098

Major chemical compositions of Golmud-River in Qinghai, China have been measured in order to understand the spatial changeable characteristics and uncover their formation mechanism. In the lower reaches, the river is divided into two dominate tributaries of west river and east river. The principal chemical compositions of Golmud-River change significantly after it flows into alluvial-pluvial fan through Golmud city. With respect to the upper reaches, the chemical composition of west river changes slightly while the TDS of the east river increases greatly with an average of 1566.028 mg/L and reaches to a peak value of 2956.160mg/L in the same geological features. In order to figure out this abnormal variation, hydrological characteristics of the two rivers are researched. TDS of West River varies from 360.061 mg/L in the upper reaches to 552.166 mg/L in the lower reaches. Such characteristic indicates that chemical compositions of West River are principally dominated by dissolution of weathered chemical components along the river course. In contrast, the sharp rise of TDS of east river could arise owing to fluctuations of groundwater table which is about 1~3m and higher than groundwater critical evaporation depth. Moreover, groundwater table has been rising with the ascending of water leakage since the completion of hydropower station in upper reaches. Consequently, a large amount of salts are carried upward to the surface and greatly accumulated under strong evaporation. Hence, a conclusion can be drawn that significant high salinity of East River originates from soil salinization which is due to groundwater table ascending and strong evaporation.

https://doi.org/10.1180/S0026461X00006502 Published online by Cambridge University Press

Influence of humic acids on pyrene sorption by carbon nanotubes

XIAORAN ZHANG, MELANIE KAH AND THILO HOFMANN*

Department of Environmental Geosciences, University of Vienna, Althanstrasse 14, 1090 Vienna, Austria (*correspondence: thilo.hofmann@univie.ac.at)

Understanding the interactions between organic contaminants and carbon nanotubes (CNTs) is essential for evaluating the materials' potential environmental impact and their application as sorbent. Although a great deal of work has been published in the past years, data are still limited in terms of compounds, concentrations, and conditions investigated. This can be mainly explained by limitations associated with the generally-applied batch sorption test set ups. The present study focuses on the effects of humic acids (HA) on the sorption of organic contaminants onto CNTs. The presence of HA may have two opposite effects on sorption. On one hand, competition between HA and organic contaminants can result in a decrease in sorption to CNTs. On the other hand, HA are known to disperse CNTs and we showed in a previous study that sorption capacity is directly related to surface area. The presence of HA may thus increase sorption of organic contaminants through an increase in the available surface area. The balance between these phenomena remains unclear as classical separation techniques (e.g. centrifugation or filtration) are not adequate to efficiently separate the CNTs and liquid phase under conditions where CNTs are partially dispersed. We previously validated a passive-sampling method to study sorption of PAHs. The method is applicable to dispersed CNTs and we here use it to investigate the influence of HA on the sorption of pyrene. Sorption isotherms were determined over a wide concentration range. Changes in isotherm shapes were interpreted in terms of sorption mechanisms for a range of HA concentrations (0-200 mg/L).

Changes in the sorbent properties as a function of HA concentration are essential to understand and distinguish the various processes involved. CNTs settling behaviour, size distribution in suspension and particle diameter in the supernatant were determined by UV-vis spectrometer, particle size analyzer (CIS-100) and dynamic light scattering, respectively. Preliminary results confirmed the strong dispersing effect of HA on CNTs. The size range of CNTs decreased from 0-60 μm down to 0-8 μm in suspensions containing 0 and 200 mg/L HA, respectively. The speed of settling also decreased dramatically with increasing HA concentration, but after 2 d, particles remaining in the supernatant had similar diameters for all HA concentrations (200 nm), as compared to the control without HA (650 nm). Together with the isotherm analysis, these results will allow a better understanding of the interactions between organic contaminants and CNTs in complex environmental matrices.

Chemical sensors based on Zr/ZrO_2 electrode for measurement of pH in a subcritical to supercritical aqueous water

XUETONG ZHANG, RONGHUA ZHANG AND SHUMIN HU

Institute of Mineral Resources, Chinese Academy of Geological Sciences, Lab.Geochemical Kinetics. Baiwanzhuang road 26, Beijing 100037 (zrhhsm@pku.edu.cn)

A Zr/ZrO_2 oxidation electrode was fabricated for in situ measurement of pH values in aqueous solutions at elevated temperatures. Combined with an Ag/AgCl reference electrode, the Zr/ZrO_2 sensor responded rapidly and precisely to the pH of the solutions over a wide range of temperatures. The Zr/ZrO_2 electrode was made by oxidizing Zr metal wire with a Na_2CO_3 melt to produce a thin film of ZrO_2 on the Zr wire surface. The nanostructure of the ZrO_2 thin film was characterized using high-resolution transmission electron microscopy (HRTEM) observations. The nature of the nanostructured ZrO_2 thin film on the Zr of the Zr/ZrO_2 electrode plays a vital role in the construction of Zr/ZrO_2 chemical sensors, particularly when the electrode is utilized for in-situ measurement of the electrochemical parameters of aqueous solutions at high temperatures and pressures.

Electric probe analyses of the ZrO_2 thin films revealed that the Zr/ZrO_2 interface is divided into 5 zones from the outermost zone to the center: 1) prismatic and oxygen-rich ZrO_2 zone; 2) ZrO_2; 3) oxygen-rich Zr; 4) oxygen-bearing Zr; 5) Zr metal. Especially, the outermost oxygen-rich ZrO_2 zone of the films is composed of nanometer-sized monoclinic crystals.

The experimental measurements of the Zr/ZrO_2 sensor potential against an Ag/AgCl reference electrode indicate that the sensor potential responds linearly with the pH of NaCl-HCl-H_2O (and NaCl-NaOH-H_2O) over the temperature range from 20 to 200°C. The slope of the potential versus pH plot at 200°C is close to the theoretical value of the Nernstian slope for the test solution at electrochemical equilibrium. The Zr/ZrO_2 sensor is expected to find use for in situ measurement of pH in aqueous fluids in natural processes over a wide temperature range, especially for hydrothermal vent fluids at mid-ocean ridges.

This project is supported by the project of 2010G28, 2008ZX05001-003-006, K1006, SinoProbe-07-02-03, SinoProbe-03-01-2A.

https://doi.org/10.1180/S0026461X00006502 Published online by Cambridge University Press

On the quantification of OC and EC and their isolation for radiocarbon measurement by a modified thermal/optical method

Y.L. ZHANG[1,2,3]*, N. PERRON[2,4], A.S.H. PRÉVÔT[2], L. WACKER[5] AND S. SZIDAT[1,3]

[1]Department of Chemistry and Biochemistry, University of Bern, Berne, Switzerland (yanlin.zhang@dcb.unibe.ch)
[2]Paul Scherrer Institut (PSI), Villigen, Switzerland
[3]Oeschger Centre for Climate Change Research, University of Bern, Berne, Switzerland
[4] Now at: Devision of Nuclear Physics, Lund University, Lund, Sweden
[5]Lab. of Ion Beam Physics, ETH Hönggerberg, Zurich, Switzerland

Carbonaceous aerosols, which comprise the large fractions of elemental carbon (EC) and organic carbon (OC), badly affect climate and human health. However, there is a large uncertainty about detailed apportionment and quantification of its sources due to the large number of origins and chemical compounds associated with the aerosols. Radiocarbon (^{14}C) measurements of EC and OC allow an improvement in carbonaceous aerosol source apportionment, leading to a full and unambiguous distinction and quantification of the contributions from non-fossil and fossil sources (Szidat, 2009). The principle technique of thermal-optical analysis (TOA), which employs laser light absorption to distinguish EC from the pyrolyzed OC, is widely accepted for determination of OC and EC concentrations. However, the challenge of TOA methods lies in physically differentiating the OC and EC. Early removal of EC in the inert phase (He) and the formation of char due to pyrolysis of OC can lead to large errors in ^{14}C measurements of OC and EC, if using the conventional protocols such as IMPROVE, EUSAAR-2 and NIOSH. Here, we present a new protocol including four-stage thermal treatments optimized for isolating OC, mixture of refractory OC and non-refractory EC and refractory EC for ^{14}C measurement. In our protocol, the charring was found to be significantly reduced to less than 5% when analyzing the water-extracted filters under pure O_2 mode (65ml/min) for summer and winter filters from Gothenburg (Sweden), Moleno and Zurich (Switzerland). And both charring carbon and refractory OC could be evolved completely before native EC throughout the analysis. OC and EC together with other carbonaceous fractions could be isolated for ^{14}C measurement by the present TOA method. Furthermore, a new TOA protocol for OC/EC determination including pure O_2 pre-treatment was developed to reduce the uncertainty in EC determination from charring and light-absorbing organic compounds (also called "brown carbon") compared to other protocols.

[1] Szidat, *Science* **323**, 470-471 (2009). [2] Ruff *et al*., *Radiocarbon* **49**, 307-314 (2007).

Degassing history of Earth

YOUXUE ZHANG

Department of Geological Sciences, University of Michigan, Ann Arbor, MI 48109-1005, USA (youxue@umich.edu)

"*Once upon a time, there were few data but many models. Now, there are many data but no models.*"

Noble gas isotopes have provided much of our understanding of Earth's early history [1-3]. Various degassing models have been developed, including degassing of the whole mantle, degassing of all gases at similar relative rate [1], solubility-controlled degassing [2], and steady-state degassing models [4]. This report will evaluate various degassing models with recent data. For example, helium outgassing flux has been lowered by more than a factor of two based on sophisticated ocean general circulation models [5], which also impacts on the estimated degassing flux of carbon. Years of measurements and progress have allowed isotopic ratios of various mantle reservoirs being pieced together [6]. For example, $^{129}Xe/^{130}Xe$ in OIB mantle is found to be lower than that in MORB mantle [7]. Missing Xe has been found to be a non-issue [8]. Nucleogenic ^{21}Ne production rate relative radiogenic ^{4}He has been revised [9-10], which leads to an interesting neon paradox that nucleogenic ^{21}Ne production in the whole silicate Earth is barely enough to supply nucleogenic ^{21}Ne in air. Although non-nucleogenic mantle neon is solar, nonradiogenic mantle argon is atmospheric [11]. Nonradiogenic mantle helium is commonly thought to be similar to Jupiter. For Kr and Xe, the jury is still out. I will address what the new data mean in terms of Earth's degassing, whether the new data can be modeled consistently, or whether we are now suffering from too many data.

[1] Allegre *et al*. (1986/87) *EPSL* **81**, 127-150. [2] Zhang & Zindler (1989) *J. Geophys. Res.* **94**, 13719-13737. [3] Zhang (1998) *Geochim. Cosmochim. Acta* **62**, 3185-3189. [4] Pocelli & Wasserburg (1995) *Geochim. Cosmochim. Acta* **59**, 4921-4937. [5] Bianchi *et al*. (2010) *EPSL* **297**, 379-386. [6] Jackson *et al*. (2009) *EPSL* **287**, 519-528. [7] Graham (2002) *Rev. Mineral. Geochem.* **47**, 247-317. [8] Zhang (2002) *Earth-Sci. Rev.* **59**, 235-263. [9] Yatsevich and Honda (1997) *J. Geophys. Res.* **102**, 10291-10298. [10] Leya and Wieler (1999) *J. Geophys. Res.* **104**, 15439-15450. [11] Raquin *et al*. (2009) *EPSL* **287**, 551-558.

https://doi.org/10.1180/S0026461X00006502 Published online by Cambridge University Press

Anaerobic cultivation and degradation capability evaluation of microorganisms in petroleum-contaminated groundwater at low temperature

YULING ZHANG, XIAOSI SU*, SHENGYU ZHANG AND HUANCHI JIN

Key Lab of Groundwater Resources and Environment, Ministry of Education, Jilin University (*correspondence: lingling29@126.com),
(State major projects for water pollution control and treatment Technology 2008ZX02707-007)

In this study, water and soil samples were collected from the shallow groundwater in vertical direction of a petroleum contaminated site in the northeast of China. Cultivation research of anaerobic microorganisms and microbial degradation test of TPH were carried out using 0# diesel oil as the sole carbon source. Microorganisms were enriched in the four traditional culture media by anaerobic pyrogallic acid method [1,2].

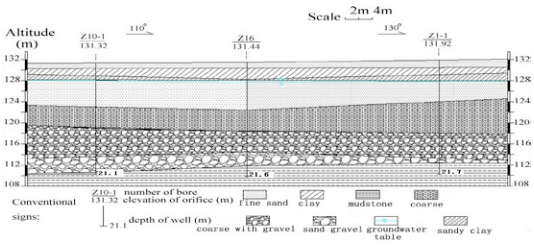

Figure 1: Hydrogeologic profile of petroleum-contaminated site

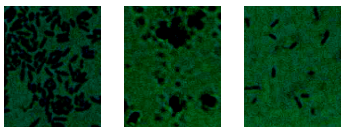

Figure 2: Morphology of three kinds strains which had the most degradation effect on TPH under the microscope

Discussion of results

Species and relative density of microorganisms were heterogeneous in different layers of groundwater after 10 days' cultivation at 10°C. All of these strains had a certain extent of degradation effect on TPH in oxygen limited environments under low temperature, with three kinds of which had a degradation efficiency of more than 60%.

[1] Zhang Yu-Ling *et al*. (2008) *Journal of Harbin Institute of Technology* **40,** 1481-1484. [2] Zhang Lan-Ying *et al*.(2007) *Chemical Research in Chinese Universities* **23,** 1-4.

Characteristic and the formation conditions of chlorite in granite-type uranium ore-field, South China

ZHANSHI ZHANG[1,2]*, GUOLIN GUO[1] AND ZHENPING JIANG

[1]Key Laboratory of Radioactive Geology and Exploration Technology Fundamental Science for National Defense, East China Institute of Technology, Fuzhou, Jiangxi, 344000, China (*correspondence: zhszhang@ecit.cn)

[2]Key Laboratory of Nuclear Resources and Environment (East China Institute of Technology), Ministry of Education, Nanchang, 330013, China

Granite-type uranium deposits were the most important uranium mining deposit type in China currently. Chloritization was one of the most developed hydrothermal alterations during the uranium mineralization, and also developed before and after the mineralization. Quarry operation had proven that chloritization-type-ore not only the important supplement of the traditional silicification-type-ore but also a new high-grade type ore. Three representative granite-type uranium ore fields in South China had selected in this study. Based on the field investigation, representative chloritization-uranium-ore had been sampled. Separating of clay minerals, XRD analysis and electron probe microanalyser(EPMA) had been employed to study the characteristic and the formation condition of the chlorite.

It is revealed the assemblage type of clay minerals were chlorite-illite or illite-chlorite types. Chlorite distributed in the rocks either in pseudomorph of biotite or vermiform and flaky conglomeration in veins. Brunsvigite and Ripidolite had been distinguished based on the chemical composition based on EPMA analyze, magnesium and iron chemical composition of chlorite varied greatly, chlorite was mostly derivated from the argillaceous rock based on nAl/n(Al+Mg+Fe) value, escept some from the magnesium-rich fluid which might announce that there were some chlorite and even the chloritezation-type-ore had be contaminated by Mafic-rich fluid. The formation temperature varied in 163□287°C had been calculated. The temperature of chlorite which related to the formation of uranium deposit is higher than the chlorite which formatted before and after the uranium mineralization. And the temperature is closed to the temperature of uranium deposit. The chlorite formed under reduction condition. Dissolve-precipitation and dissolve-transfer-precipitation were the formation mechanism.

This work was supported by the National Natural Science Foundation of China (Grant No: 40972068 and No: 40772068).

https://doi.org/10.1180/S0026461X00006502 Published online by Cambridge University Press

Hydrogen isotope fractionation in marine algae: Salinity effect

ZHAOHUI ZHANG[1,*], WEIMING GONG[1] AND KUNSHAN GAO[2]

[1]Department of Earth Sciences, Nanjing University, 22 Hankou Road, Nanjing, 210093, China. (*correspondence: zhaohui@nju.edu.cn)

[2]State Key Laboratory for Marine Environmental Sciences, Xiamen University, Xiamen, 361005, China

With the advance of GC-IRMS technology, compound-specific hydrogen isotopes of algal biomarkers have been widely used in hydrology reconstruction in paleoceanography. However, the salinity effect on hydrogen isotope fractionation in marine algae remains largely unclear. We have cultured five different species of myarine algae, Prymnesiophyceae *Emiliana huxleyi* (CCMP 1516), Prymnesiophyceae *Geophyrocapsa oceanica* (CCMP 2051), Dinophyceae *Prorocentrum minimum* (CCMP 1329), *Navicula climacosphenae bootyh*, Coscinodiscophyceae *Thalassiosina pseudomanh* (CCMP 1335) in artificial sea water with different salinities while keeping other parameters the same. Cell density was measured on a Z2 Coulter® Particle Count and Size Analyzer. Algal biomarkers are analyzed for structure identification on GC-MS and measured for hydrogen isotope ratio on GC-IRMS. Salinity effect in hydrogen isotope fractionation will be discussed.

ID-TIMS zircon U-Pb age of Yulonggou intrusive rocks and its geological significance in South Qilian Mountains, NW China

ZHAO-WEI ZHANG[1,2], WEN-YUAN LI[1], YONG-BAO GAO[1,2] AND ZHOU-PING GUO[1]

[1]Xi'an Center of Geological Survey(Xi'an Institute of Geology and Mineral Resource), CGS, Xi'an, Shaanxi 710054, China

[2]Chang'an University,Xi'an,Shaanxi 710054,China (zhaoweiz@126.com)

Yulonggou intrusive rocks, belongs to Riyueshan-Hualong basic-ultrabasic rocks belt, the belt has developed a number of intrusive rocks related closely with copper-nickel mineralization, it is great significance for the emplacement time and mineralization characteristics of basic-ultrabasic rocks to guide prospecting in Hualong area. The paper reports partial achievements of magmatic type copper-nickel ore resources potential evaluation in Hualong county, Qinghai Province, mainly by fieldsurvey and research on Yulonggou intrusive rocks on the process of the project, and obtained the zircon U-Pb age of 442.4±1.6 Ma(MSWD=0.059) rock formation in Yulonggou by ID-TIMS. Its petrology and geochemistry characteristics analysis and regional comparative research showing Yulonggou intrusive rocks is a ferruginous series ultrabasic-basic complex rocks, and has good magmatic differentiation and high abundance of useful elements that Ni、Cu、Co, so it is a favorable ore formation intrusive rocks; The age of 440 Ma, is conversion period from subduction orogeny to collision orogeny in the whole of Qilian Mountains, and into the stage of orogenic with the closure of Laji Mountain small ocean basin, form Yulonggou basic-ultrabasic intrusive rocks in extensional environment of post-collision. Contacting information of other intrusive rocks in Riyushan-Hualong basic-ultrabasic rocks belt, all the intrusive rocks may be formed in the same period, and have specific dynamic mechanism and evolution process. This extensional rifting event has a very close relationship with the mineralization, so the research has very important practical significance.

This study was supported by China Geological Survey project (No. 1212010911032, 1212011121088 and 1212011121092)

https://doi.org/10.1180/S0026461X00006502 Published online by Cambridge University Press

Elastic anomalies due to spin state transitions in cobaltate perovskites: Analogue behaviour for Fe^{2+} in $(Mg,Fe)SiO_3$

ZHIYING ZHANG[1]*, JOHANNES KOPPENSTEINER[2], WILFRIED SCHRANZ[2] AND MICHAEL A. CARPENTER[1]

[1]Department of Earth Sciences, University of Cambridge, Downing Street, Cambridge CB2 3EQ (*correspondence: zz254@cam.ac.uk)
[2]Faculty of Physics, University of Vienna, Strudlhofgasse 4, A-1090, Vienna, Austria

$(Mg,Fe)(Si,Al)O_3$ perovskites with orthorhombic *Pnma* structure and (Mg,Fe)O are the principal minerals of the Earth's lower mantle. Fe^{2+} undergoes spin state transitions at high pressure and high temperature, which have important effects on the physical properties of the lower mantle. Fe^{2+} in (Mg,Fe)O changes from high spin state to low spin state with increasing pressure, leading to large changes in the bulk modulus and small changes in the shear modulus. However, the influence of spin state transitions on $(Mg,Fe)(Si,Al)O_3$ are less clear. There are still controversies about the nature of the stable spin configuration at high pressure and high temperature, the extent of the effect of spin state transitions on elastic properties and so on. It is hard to investigate the elastic moduli and acoustic dissipation at high pressure and high temperature. Therefore, analogue materials have been made use of. Co^{3+} is isoelectronic with Fe^{2+}, and undergoes spin state transitions as a function of temperatue at ambient pressure. We have investigated elastic anomalies and acoustic dissipation associated with spin state transitions of Co^{3+} in $NdCoO_3$ and $GdCoO_3$ perovskites (orthorhombic, *Pnma*) using resonant ultrasound spectroscopy at high frequencies (0.1-1.5 MHz) and dynamic mechanical analysis at low frequencies (0.1-50 Hz). Strain analysis based on lattice parameter data from the literature shows that the spin state transitions are accompanied by significant variations in shear strain due to the change in ionic radius of Co^{3+}. Spin state/strain coupling via octahedral tilting leads to the renormalization of shear modulus. In $NdCoO_3$, the shear strain is small, and thus the coupling is weak. The temperature dependence of the shear modulus scales semi-quantitatively with an empirical spin order parameter. On the other hand, large shear strain and strong coupling occurs in $GdCoO_3$, and large softening of the shear modulus by up to ~35% has been observed, accompanied by enhanced acoustic dissipation. The large shear strain associated with octahedral tilting in $(Mg,Fe)SiO_3$ at high pressure suggests similar elastic behaviour as in $GdCoO_3$.

Structure and mineralization characteristics of Kangding gold orefield, Sichuan Province, China

ZHANG ZHIJUN[1 2], DENG JUN[1], GONG QINGJIE[1] AND WANG QINGFEI[1]

[1]China University of Geosciences, Beijing, 100083
[2]Tianjin North China Geological Exploration Bureau, Tianjin, 300170

The Kangding gold orefield, located in the north part of the 'kangding complex' block and Sanjiang ore cluster area, has great potential in mineral resources. Based on the geological settings, the gold deposits in the study area are divided into two series : one series is in Kangding complex and the other is in the Xiaojin area with arc-shaped structures. Orefield structure, ore deposit geochemistry and metallogenic model are studied and compared between the two series. The rocks mainly contain amphibolite, granite, granulite, and basic dikes. The Kangding complex has experienced the formation of the basement from Neoarchean to the Paleoproterozoic, the Neoproterozoic magmatic activities (between 860-750Ma.) with the mountain of the main body, Mesozoic Indo-Chinese - Yanshanian magmatic activity, as well as the Cenozoic Himalayan magmatic activities. Magmatic activities are closely related to the formation of gold mineralization. Kangding complex is characterized by two layers which are crystalline basement and fold basement. It is a mixture of metamorphic and magmatic complex, and is the product of regional metamorphism, deformation and partial melting of magmatic rocks since Proterozoic.

https://doi.org/10.1180/S0026461X00006502 Published online by Cambridge University Press

Characteristics of metallogenetic fluids and genesis of Nongping gold-copper deposit in Eastern Yanbian, Northeastern China

H.L.ZHAO, Y. S. REN*, N. JU AND H. WANG

College of Earth Sciences, Jilin University, Changchun 130061, China (*correspondence: renys@ jlu.edu.cn)

Nongping is another porphyry deposit besides Xiaoxinancha large-scale gold-copper deposit in Yanbian area, Northeastern China. It experienced such four stages as sulfides, quartz-sulfides, quartz-sulfides-bismuthinite and quartz-melnikovite-tourmaline stage. And the quartz-sulfide-bismuthinite stage is the main gold mineralizing stage.

The petrographic and microthermometric studies on the fluid inclusions in quartz grains from sulfides-bearing quartz vein formed in the main mineralizing stage show that there are five types of the primary inclusions: (I) gas-liquid, (II) CO_2-bearing three-phase, (III) multiple phases, (IV) pure gas and (V) pure aqueous phase. The metallogenic fluid is of high-moderate temperature (homogenization temperature ranges from 237.8 to 399.4 °C, mainly in the range of 310 ~ 370 °C). The salinity of fluid inclusions is 1.39~12.3wt% and 33.32 ~ 42.03wt%. Different types of inclusions are closely accompanied, with roughly accordant homogenization temperatures and significantly different salinity. These characteristics indicate that the metallogenetic fluids experienced fluid boiling. The laser Raman spectroscopic analysis shows that the main components gas phase of the metallogenetic fluids are H_2O and CO_2, with a small amount of CH_4.

Nongping gold-copper deposit and Xiaoxinancha large-scale gold-copper deposit develop the same kinds of inclusions with similar homogenization temperatures, and they both experienced fluid boiling in the formation of deposits [1,2]. Combined with metallogenic geological conditions and mineralization, a conclusion can be drawn that both two deposits are derived from the same magmatic and mineralization events under alike tectonic settings. At the end of the early Cretaceous, thanks to the subduction of the Pacific Ocean slab to the Eurasia plate, large copper-gold mineralization took place under the background of lithospheric extension.

[1] Li *et al*. (1995) *Mineral Deposits*. **14**(2), 151-166. [2] Zhao *et al*. (2008) *Journal of jilin university (earth science edition)*.**38** (3),384-388

High-resolution carbon and oxygen isotopic record through the transition from OAE1a to ORB1 in the Mudurnu section, central Turkey

KUI-DONG ZHAO[1], SHAO-YONG JIANG[1]*, XIU-MIAN HU[1], İSMAIL ÖMER YILMAZ[2] AND HONG-FEI LING[1]

[1]State Key Laboratory for Mineral Deposits Research, School of Earth Sciences and Engineering, Nanjing University, Jiangsu, 210093, P. R. China (*correspondence: shyjiang@nju.edu.cn)

[2]Department of Geological Engineering, Middle East Technical University, 06531 Ankara, Turkey

Change in oceanic sedimentation from Cretaceous black organic carbon-enriched deposits (Oceanic Anoxic Events) to predominantly oceanic red beds (ORBs) occurred widely in the Tethys. Few attentions have been given to the transition and environmental changes from the Selli Level (OAE1a) to the Oceanic Red Bed 1 (ORB1).

High-resolution carbon and oxygen isotope curves derived from the early Aptian hemipelagic sediments cropping out at Mudurnu, central Turkey, reveals isotopic excursion and recovery through the transition from the OAE1a to ORB1. Comparison with the standard reference $\delta^{13}C$ curve of the Alpine Tethys shows that the overall character of the excursion through OAE1a is clearly reproduced in central Tethys. A sharp negative $\delta^{13}C$ excursion (1.5‰) followed by an abrupt and prolonged positive $\delta^{13}C$ excursion (3.5‰) and black shale deposition through OAE1a. $\delta^{18}O$ values also show sharp negative excursion synchronous with $\delta^{13}C$ before OAE1a, implying that the onset of OAE1a might be related with rapid influx of CO_2 into the atmosphere from volcanogenic and/or methanogenic sources. Aftermath the OAE1a, $\delta^{13}C$ values keep high value and last for a long time (>1.0 myr), then decrease gradually to normal values until the appearance of ORB1. The recovery of carbon isotope last for longer than 1myr. Gradually intensifying of bottom circulation and increasing in dissolved oxygen in bottom waters is the most probable the cause for the transition from OAE1a to ORB1.

https://doi.org/10.1180/S0026461X00006502 Published online by Cambridge University Press

Component and structure of manganese dominant mineral of Co-rich crusts from West Pacific

ZHAO LEI[1] YANG HUA[1] AND ZHAO XIAOYI[2]

[1]China University of Geosciences (Beijing), 100083 (zhaolei51yh@yahoo.com.cn)
[2]Hebei Province Geophysics Investigation Institude

West Pacific is one of the most enriched regions of Co-rich crust. This study selected a multilayered-structure crust, and sampled from an enrichment belt of the main manganese mineral. The component of the manganese- dominant mineral is MnO_2 with water and a lot of other element (Fe, Ca, Na, Mg, etc.), its formula can be writing as $MnO_2 \bullet XH_2O$ (with Fe, Ca, Na, Mg, and other elements). As it is completely different from vernadite, but its structure and stability similar with δ -MnO_2 ; for close intergrowth with iron hydroxide, XRD values are larger with the 0.24~0.245 nm and the 0.14~0.143 nm than vernadite. The name is proposed for the marine δ -MnO_2 . Marine δ -MnO_2 has layer-structure even with tunnel structure, and has good structural stability. When heated to 400 °C , its crystal structure remains basically unchanged. Marine δ -MnO_2 changes into Mn_2O_3 (γ -Mn_2O_3) around 550 °C , then changes into Mn_3O_4 around 804 °C . The temperature of 804 °C is lower 146 °C than the temperature of 950 °C reported by a literature, the structural stability may be related to the metal ions contained. The manganese-dominant mineral of Cobalt-rich crusts in this area is δ -MnO_2 , for the three main manganese minerals of todorokite, birnessite and δ -MnO_2 in deep seas, δ -MnO_2 is the most thorough oxidized mineral, the O/Mn are 1.74~1.87,1.87~2.00,1.99. This shows that the crusts underwent the strong oxidative environments and agrees with the enrichment characteristic of the REE.

Identification of marine manganese minerals should use many means, and the peak of XRD should be determined according to the standard of marine manganese minerals. Considering different stabilities and structures between marine manganese minerals and the terrestrial counterparts, we should use a new naming system for marine manganese minerals: marine 1 nm mineral, marine 0.7 nm manganese mineral marine δ -MnO_2.

[1] F. Jean, C. Cachet, L. T. Yu. (1997) Structural changes induced by chemical reduction of various MnO2 species, *Journal of Applied Electrochemistry*, **27**: 635-642

Fe isotope evidence for mantle metasomatism in the lithospheric mantle of the Eastern China

X.M. ZHAO[1]*, H.F. ZHANG[1] AND X.K. ZHU[2]

[1]State Key Laboratory of Lithopheric Evolution, Institute of Geology and Geophysics, Chinese Academy of Sciences, Beijing 100029, China (*correspondence: xinmiao312@mail.iggcas.ac.cn, hfzhang@mail.iggcas.ac.cn)
[2]Institute of Geology, Chinese Academy of Geological Sciences, Beijing 100037, China (xiangkun@cags.net.cn)

To further constrain the iron isotopic composition of the terrestrial mantle and investigate the behavior of iron isotope during mantle processes, we have determined the Fe isotopic composition of Cenozoic alkali basalts and peridotite xenoliths entrained in Mesozoic and Cenozoic basalts from eastern China by high-resolution MC-ICP-MS.

Results from alkali basalts show a limited Fe isotopic variation, with δ^{57}Fe ranging from 0.169‰ to 0.241‰. By contrast, both the mantle peridotites and their mineral separates from the North China Craton exhibit an extremely large Fe isotopic variation with δ^{57}Fe ranging from -1.002‰ to 0.258‰. This may reflect heterogeneous Fe isotopic compositions of the lithospheric mantle beneath the North China Craton. An average δ^{57}Fe (-0.028‰) calculated from all the mantle xenoliths in this study is obviously lower than the average value (0.198‰) of δ^{57}Fe for the Cenozoic alkaline basalts, similar to the previous observation that the basalts generally have heavier Fe isotopes than the mantle peridotites. In individual minerals, δ^{57}Fe of the olivines (-0.968 to 0.154‰) are systematically lighter than those of the coexisting pyroxenes (-0.718 to 0.169‰ for orthopyroxene and -0.642 to 0.304‰ for clinopyroxene, respectively). The phlogopite of apparently metasomatic origin has the heaviest iron isotopic composition amongst the mineral phases with δ^{57}Fe of 0.302 to 0.376‰. This Fe isotope disequilibrium between mineral phases and an extremely Fe isotope variation in these peridotites, in particularly for the wehrlites, were probably produced by the multistage melt-peridotite interactions, consistent with the petrological observation that some of the xenoliths analyzed such as wehrlites were the products of highly mantle metasomatism. Analogous positive correlations between δ^{57}Fe and other major and trace element indicators of metasomatism such as CaO and Rb further support the above suggestion.

These characters suggest that mantle metasomatism or melt-rock interaction can significantly modify Fe isotopes and play an important role in producing Fe isotopic heterogeneity of the lithosphere mantle.

https://doi.org/10.1180/S0026461X00006502 Published online by Cambridge University Press

The effect of post-depositional fluids on Edicaran sedimentary carbonate in South China

YAN-YAN ZHAO* AND YONG-FEI ZHENG

School of Earth and space science, University of Science and technology of China, Hefei 230026, China (*correspondence: yyanzhao@ustc.edu.cn)

The post-depositional fluid flow in carbonates can alter the primary geochemical signatures, leaving detectable signatures in the chemical sedimentary rocks. The geochemistry of veins or cements is essential to understanding the origin of post-depositional fluids. We carried out a detailed study that combines the conventional and laser methods of analyzing C-O isotopes and trace elements in Ediacaran carbonates of the Lantian formation at Piyuancun in South China. Different components of carbonates (calcite, dolomite and bulk carbonate) and different microfacies (wallrock and veins) were analyzed, respectively. The results are used to examine the primary geochemical signatures and geometry of post-depositional fluid flow. All carbonate components show $\delta^{18}O$ values of -18.48 to -12.78‰ and $\delta^{13}C$ values of -10.28 to -7.02‰ (both relative to PDB). The $\delta^{18}O$ values for all carbonate components are almost consistent, but dolomites have slightly higher $\delta^{13}C$ values than the calcite and bulk carbonate. The different components of carbonate have preserved their primary geochemical signatures based on isotope fractionations between calcite and dolomite. Thus, the dolomite would probably precipitate from the same water as the calcite. The veins can be divided into Groups A and B based on their $\delta^{18}O$ values of –17.2 to –11.3‰ and –23.7 to –18.1‰, respectively. Nevertheless, $\delta^{13}C$ values for all the veins and wallrock fall in the same range from –10.6 to –8.9‰. Group A veins have different $\delta^{18}O$ values and REE patterns from the corresponding wallrock, indicating that these veins and wallrock are not in equilibrium with each other and vein-forming fluids are of external origin. There is no correlation between $\delta^{18}O$ and $\delta^{13}C$ values for these veins and wallrock, suggesting that the wallrock was not altered by diagenesis. The low $\delta^{18}O$ values for these veins indicate that the vein-forming fluids were derived from continental deglacial meltwater subsequent to the Gaskiers iceage. Group B veins have similar $\delta^{18}O$ and $\delta^{13}C$ values to the corresponding wallrock. Their REE patterns are almost similar to those of the wallrock except a small difference in HREE. These features indicate that vein-forming fluids are similar to those of wallrock and thus of internal origin. The precipitation water for these veins and wallrock is probably related to seawater. Therefore, the post-depositional effects of diagenetic fluids are recorded by the vein-wallrock compositions.

Zinc isotopes in the Southern Ocean – A tracer of biogeochemical cycling?

Y. ZHAO[1]*, D. VANCE[1] AND W. ABOUCHAMI[2]

[1]Bristol Isotope Group, School of Earth Sciences, University of Bristol, Wills Memorial Building, Bristol BS8 1RJ, UK (*correspondence: y.zhao@bristol.ac.uk)

[2]Max Planck Institute for Chemistry, P.O. Box 3060, 55020 Mainz, Germany (wafa.abouchami@mpic.de)

Zinc (Zn) is an important trace metal micronutrient in the marine realm. Dissolved Zn concentrations show extreme variation in the ocean, probably due to both biological uptake and regeneration as well as abiotic processes. Zn isotopes may be useful in tracking this biogeochemical cycling. Here we report the first Zn isotopic data for the Southern Ocean, using a newly developed analytical approach. Our samples derive from the IPY/Geotraces ANT-XXIV/III cruise (Atlantic sector, Southern Ocean), whose main objective was to study the biogeochemistry of trace metals in the Fe-limited Southern Ocean. Our study is focused on the distribution and isotopes of dissolved Zn across the major frontal systems along the Greenwich Zero Meridian, including 3 depth profiles and 11 samples across a surface transect.

Much higher Zn concentrations were found at the surface of the southern ACC and the Weddell Gyre (WG) relative to that of Sub-Antarctic Front (SAF). The WG depth profile showed a local Zn (and Si) concentration maximum in the upper 200m. Zn and Si concentrations show tight linear correlations at any one site. Surface waters, however, showed a monotonically poleward decreasing trend of Zn/Si. Heavy $\delta^{66}Zn$ was found in the surface waters of the southern ACC and WG. Anomalously low $\delta^{66}Zn$ at around 50m depth has been noted in two of the three depth profiles in this study. In surface waters $\delta^{66}Zn$ is fairly constant except for a pronounced fall in at the Polar Front Zone (PFZ) co-incident with a drop in concentration.

These Zn isotope variations are consistent with biological uptake of light isotopes in the photic zone. Isotopically light Zn at around 50m is consistent with findings of similarly light Zn in the shallow sub-surface at other locations, and may highlight the role of shallow recycling of cellular Zn as an important process in the oceanic Zn cycle.

https://doi.org/10.1180/S0026461X00006502 Published online by Cambridge University Press

Gas accumulation rules of volcanic rocks of deep formations in Songliao Basin, Northeast China

Z.H. ZHAO[1]*, G.H. JIAO[1], P. SUN[1], X.S. JUAN[1], J.X. XIAO[2], X.H. JIANG [1] AND H.Q. BAI[1]

[1]Langfang Branch of Petroleum Exploration and Development Research Institute, Petrochina, Langfang 065007 (*correspondence: zehui_zhao@pku.org.cn)
[2]School of Energy Resources, China University of Geosciences (Beijing), Beijing 100083 (xiaojx@cugb.edu.cn)

Deep formations of Songliao basin are defined as between basement and second member of Quantou formation in lower Cretaceous, including later Jurassic Huoshiling formation, early Cretaceous Shahezi formation, Yincheng formation, Denglouku formation and 1-2 members of Quantou formation. Songliao basin was made up of groups separated fault depressions in Shahezi age of early Cretaceous.

The volcanic rocks in Yincheng formation and Huoshiling formation, are the major reservoirs for deep gas. By the means of systematically analyzing the form conditions, accumulation patterns and exploration prospects of the deep gas, it is suggested that the deep volcanic gas reservoirs are characterized by the short distant migration for gas, locating around main trough and along the fault. The existence of deep volcanic gas pool is controlled by source rocks. High quality volcanic reservoirs controlled by lithology, by lithofacies, by fracture and diagenesis, take controls of the extent of the gas pool. The locations and high production of volcanic gas pools are controlled by faults. Generally, the source rocks, reservoirs and faults all make the contribution to the formation of volcanic gas pool. From the point of view of the forming conditions of deep volcanic gas pools, it is suggested that the beneficial tectonic zone with both development of the source rock and the volcanic reservoir are the favorable exploration zone.

A 4 million year record of paleo-erosion rates from the Qilian Shan, China

ZHIJUN ZHAO[1] AND DARRYL E. GRANGER[2]*

[1]College of Geographical Sciences, Nanjing Normal University, Nanjing 210046, China (zhaozhijun@njnu.edu.cn)
[2]Dept. of Earth and Atmospheric Sciences, Purdue University, West Lafayette, Indiana, 47907 USA (*correspondence: dgranger@purdue.edu)

It has been proposed that mountain erosion rates increased rapidly at 2-4 Ma due to climate change, based partly on sediment accumulation rates in central Asia [1]. This idea has been recently supported by paleo-erosion rates from the Tien Shan determined from ^{10}Be in basin sediments, which suggest that erosion rates in these mountains doubled near 2 Ma [2]. To test the hypothesis that this represents a regional climatic signal, we constructed a 4 Ma record of paleo-erosion rates from the Qilian Shan, at the northeastern topographic boundary of the Tibetan Plateau.

We analyzed 22 samples for ^{10}Be to determine paleo-erosion rates from the Laojunmiao (LJM) section exposed in an anticline near the city of Yumen. A subset were also analyzed for ^{26}Al. The LJM section has previously been dated by magnetostratigraphy [3]. After accounting for changes in sedimentation rates, we observe no clear change in source area erosion rates from 4 Ma to 1.2 Ma; however, erosion rates increase by an order of magnitude during a discrete interval extending from 1.2-0.8 Ma, subsequently returning to near the background rate. The interval of rapid erosion is found immediately above a regional unconformity.

Our erosion rate record indicates that climate change across the Plio-Pleistocene boundary did not strongly influence erosion in the sparsely glaciated Qilian Shan. Although we cannot exclude that climate change near the Middle Pleistocene transition may have driven the rapid erosion we observe, we prefer the explanation that rapid erosion is a transient response to a tectonic uplift and fault activity near the range front, as evidenced by the regional unconformity. Rapid erosion and sedimentation rates observed elsewhere, such as the Tien Shan [2], may therefore be a local response to either glaciation or uplift, rather than indicators of a global response to climate variability.

[1] Zhang, P., and Molnar, P. (2001) *Nature* **410**, 891-896. [2] Charreau *et al*. (2011) *Earth Plan. Sci. Lett*. **304**, 85-92. [3] Fang, X.M. *et al*. (2005) *Science in China D* **48**, 1040-1051.

https://doi.org/10.1180/S0026461X00006502 Published online by Cambridge University Press

Origin of postcollisional mafic-ultramafic rocks in the Dabie orogen: Implications for recycling of the deeply subducted continental crust

Z.-F. ZHAO* AND Y.-F. ZHENG

School of Earth and Space Sciences, University of Science and Technology of China, Hefei 230026, China (zfzhao@ustc.edu.cn)

Recycling of the deeply subducted continental crust has bearing on crust-mantle interaction during its subduction to mantle depths, which is known to cause ultrahigh-pressure (UHP) metamorphism in the stability fields of coesite and diamond. UHP metamorphic slices are generally considered as an exhumed product from the mantle depths, which provides a reference to the recycled crust. However, it is critical to find petrological and geochemical records that bear the recycling of deeply subducted continental crust and the consequent crust–mantle interaction in continental subduction zones.

The Dabie orogen was built by the Triassic continental collision between the South and North China Blocks, with subduction of the continental crust to mantle depths. It is intriguing whether the recycled continental crust is recorded in postcollisional mafic igneous rocks. Whole-rock major–trace element and Sr-Nd isotopes and zircon Hf isotopes were determined for postcollisional mafic-ultramafic rocks of Early Cretaceous age in the orogen. The results show arc-like patterns of trace element distribution, high initial $^{87}Sr/^{86}Sr$ ratios of 0.7065 to 0.7077 and very negative $\varepsilon_{Nd}(t)$ values of −19.9 to −15.3 for whole-rock. Zircon Hf isotope analyses gave negative $\varepsilon_{Hf}(t)$ values of −26.3±0.6 to −7.0±0.5 with two-stage Hf model ages of 1.62 to 2.83 Ga. These trace element and radiogenic isotope compositions are similar to those in UHP rocks, suggesting that the mafic-ultramafic rocks were derived from an enriched mantle source with incorporation of crustal component. It may be generated by interaction between the subcontinental lithospheric mantle and the felsic melt derived from the subducting continental crust. In other words, there would be melt-peridotite reactions during the continental deep subduction, forming the orogenic lithospheric mantle composed of peridotite, pyroxenite and hornblendite. Partial melting of the orogenic lithospheric mantle gave rise to the postcollisional mafic-ultramafic rocks, recording the recycling of continental crust in the continental subduction zone.

The evolution of the Tarim Craton in Archean and Proterozoic: Zircon U–Pb and Hf isotopic evidence from the Kuruktag area, NW China

B.H. ZHENG[1]*, W.B. ZHU[1], L.S. SHU[1], H.L. WU[1] AND J.W.HE[1],

[1]State Key Laboratory for Mineral Deposits Research, Department of Earth Sciences, Nanjing University, Nanjing 210093, P.R. China (*correspondence: zhengbihai@gmail.com)

The Tarim Craton is one of the three major cratons in China. Compared with Yangtze Craton and North China Craton, only limited age data of the basement rocks in Tarim have been published. Presently, there is still great uncertainty about the formation and crustal growth of the Tarim Craton. Kuluktag Uplift is located in the northeast of Tarim Basin. Basement rocks crop out widely in Kuluktag and are unconformably overlain by Sinian strata. Three Proterozoic detrital zircon samples (F3, F7, F10) and one Neoproterozoic Granite sample (F4) have been collected and LA-ICPMS U-Pb zircon dating as well as Hf isotopic analysis have been carried out. The results show that the granite sample was formed in ca. 832Ma, probably related to the break of Rodinia Supercontinent. The three detrital zircon samples reveal identical age spectra. Two events are recorded: 1) Ca. 2000Ma metamorphism, which caused the reworking of old crustal materials; 2) Tectonic activity between ca. 2350Ma to ca. 2750Ma, which involved both juvenile and old crustal materials. Two stage model ages of all four samples vary from ca. 3.8Ga to ca.2.5Ga, indicating the crustal growth of Tarim Craton lasted from the Paleoarchean to the earliest Palaeoproterozoic, which is comparable with Yangtze and North China Cratons.

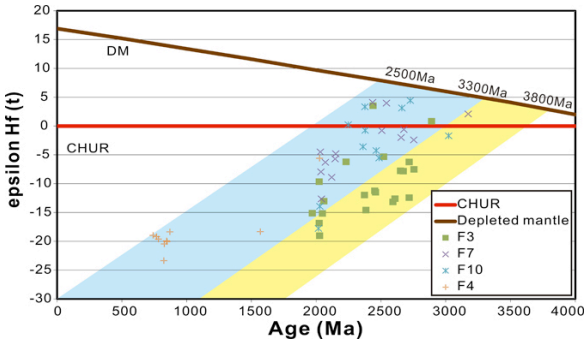

Figure 1: Diagram of εHf(t) values vs. $^{207}Pb/^{206}Pb$ ages for zircons of samples from Kuruktag, NE Tarim in this study.

https://doi.org/10.1180/S0026461X00006502 Published online by Cambridge University Press

Influence of major hydraulic projects on saltwater intrusion in the Yangtze River estuary

ZHENG MAOHUI[1*], LIU SHUGUANG[1,2] AND JIANG SIMIN[2]

[1]Shanghai Institute of Disaster Prevention and Relief, Tongji University, Shanghai 200092, China (*correspondence: zmh@tongji.edu.cn)

[2]Department of Hydraulic Engineering, Tongji University, Shanghai 200092, China (jiangsimin@tongji.edu.cn)

To understand the influence of the Three Gorges Project (TGP) and South-to-North Water Diversion Project (SNWDP) on saltwater intrusion in Yangtze River estuary, a depth-averaged 2D numerical model, loosely coupled with geographic information system (GIS), is developed to compute and analyze the hydrodynamics and salinity field about the estuary water. The model is validated through observed data. Then combined simulations under multiple hydrologic conditions considering different regulation schemes of the hydraulic projects as well as varied tidal ranges in the outer sea are carried out. Furthermore, the numerical output is rendered dynamically in GIS environment, and the distribution behaviours and variation trend of salinity are analyzed. The result shows that the salinity of north branch is higher than that of south branch (fig.1), and the change of salnity is mostly affected by river discharge. The maximum water diversion scheme of 1000 m^3/s of SNWDP will aggravate saltwater intrusion, while the increased discharge of TGP in dry season will restrain saltwater intrusion in the estuary.

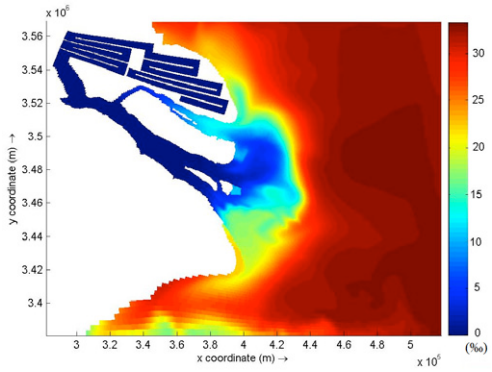

Figure 1: simulated salinity field of Yangtze River estuary in dry season

This study is supported by Key Laboratory of Yangtze River Water Environment, Ministry of Education (YRWEF08003) and partly supported by Nation Natural Science Foundation of China (41001217) .

Methodology and foreground of metalloprotein

PEI-XI ZHENG[1] AND YAN ZHOU[2]

[1]College of EarthSciences, Jilin University, Changchun China 130061

[2]Center of Test Science and Experiment Jilin University Changchun China 130026

Metalloproteins is proposed as a new omics to follow genomics, proteomics and metabolomics. Researchs on metalloproteins not only answer the question of the chemical compose of metals and proteins, but also pioneer a new way for probing into the mechanisms of life substances such as metalloproteins in life activity. In Metalloproteins, metalloenzymes and othe metalcontaining biomolecules are defined as “Metallomes”. Syntheses and metabolic functions of genes and proteins cannot be performed without the aid of various metal ions and metalloproteins. The main research targets of metallomics are to identify the metallomes and elucidate their biological or physiological functions in biosystem. Chemical speciation analysis is a key technology in metalloproteins study.

Some new trends in the study of metalloproteins and metalloenzymes have been described from aspects of metal ions-related diseases (especially the neurodegenerative diseases), the roles of metalions in folding, aggregation and assembly of proteins, the design and reconstruction of metallochaperons and metalloproteins, interactions between metalloproteins and DNA.

Now, metallomics is focused on analytical techniques and methods, particularly the so-called hyphenated techniques which combine a high-resolution separation technique (gel electrophoresis/laser ablation, chromatography or capillary electrophoresis) with a highly sensitive detection method as elemental (inductively coupled plasma, ICP) or molecular (electron spray ionization (ESI) or matrix-assisted laser desorption/ionization (MALDI)) mass spectrometry, or nuclear X-ray fluorescence/absorption spectrometry. The applications of these advanced analytical methods in the identification of metallo-/phosphor-/seleno-proteins, probing of relationships between structure and function of metalloproteins, and study of clinically used metallodrugs will be selectively outlined, along with their advantages and limitations.

https://doi.org/10.1180/S0026461X00006502 Published online by Cambridge University Press

Nd-isotope evolution in the Cretaceous Gault and chalk seas (Albian–Maastrichtian)

XINYUAN ZHENG[1]*, HUGH C. JENKYNS[1], GIDEON M. HENDERSON[1], DAVID WARD[2] AND ANDREW S. GALE[3]

[1]Department of Earth Sciences, University of Oxford, South Parks Road, OX1 3AN, UK (*correspondence: xinyuanz@earth.ox.ac.uk)
[2]Crofton Court, 81 Crofton Lane, Orpington, Kent, BR5 1HB, UK
[3]School of Earth and Environmental Sciences, University of Portsmouth, Burnaby Road, PO1 3QL, UK

Nd isotopes recovered from Cretaceous fossil fish teeth can promote understanding of ocean circulation during this Period [e.g. 1-2], but this goal is limited by the sparsity of available data. This study presents a new time-series of Nd isotopes obtained from fish teeth collected mainly from the Gault Clay and English Chalk in the UK, spanning ~ 110 – ~ 67 Ma.

ε_{Nd} values range from ~ -8 to ~ -12.5 in the mid- to Late Cretaceous. The data show a clear decreasing trend from ~ -9 to ~ -10.5 from the early Albian to late Albian. Data from the Cenomanian–Turonian range from ~ -8.5 to ~ -11, and then reach the lowest values of ~ -12.5 in the Santonian and early Campanian, and finally recover to ~ -9 in the Maastrichtian.

Comparison with weathering proxies allows this effect to be deconvolved from circulation changes. For example, the parallel increase in the Nd-isotope and Sr-isotope ratios [3] from the early Campanian to Maastrichtian supports the idea that this increasing trend in the Nd-isotope record reflects the reorganization of ocean circulation; otherwise the enhanced global continental weathering, as indicated by Sr isotopes, should have driven the Nd isotopes in the opposite direction.

Interestingly, the low Nd-isotope values found in the Santonian and early Campanian in our record happened coincidently with major changes in Nd isotopes in the South Atlantic [2]. This coincidence in timing might suggest that changes of ocean circulation patterns in the NW European area are caused not only by local processes, but are also related to large-scale reorganization of ocean circulation induced by global tectonic movements.

[1] Pucéat *et al*. (2005), *EPSL* **236**(3-4), 705-720. [2] Robinson *et al*. (2010), *Geology* **38**(10), 871-874. [3] McArthur *et al*. (2001), *J. Geol*. **109**, 155-170.

Growth of zircon and rutile during continental subduction-zone metamorphism: A case study of UHP eclogite in the Dabie orogen

Y.-F. ZHENG*, X.-Y. GAO, R.-X. CHEN AND T.S. GAO

CAS Key Laboratory of Crust-Mantle Materials and Environments, School of Earth and Space Sciences, University of Science and Technology of China, Hefei 230026, China (*correspondence: yfzheng@ustc.edu.cn)

Both time and temperature of zircon formation can be directly dated by the U-Pb chronometer and the Ti-in-zircon thermometer, respectively. However, difficulty is encountered for rutile due to the effects of high common Pb on the U-Pb dating and pressure variable on the Zr-in-rutle thermometer. This is particularly so for Dabie-Sulu UHP eclogites of China, which gave consistently lower Zr-in-rutile temperatures than known estimates. Nevertheless, a combined study of zircon and rutile enables tight constraints on P-T-t path of continental subduction-zone UHP eclogites. We measured the Zr content of rutile by both EMP and LA-ICPMS for low-T/UHP eclogit in the Dabie orogen. Zircon U-Pb isotopes and trace elements were analyzed by LA-ICPMS, yielding U-Pb ages of 242±4 Ma and Ti-in zircon temperatures of 713±17°C for Group I zircons, and U-Pb ages of 226±2 Ma and Ti-in-zircon temperatures of 681±12°C for Group II zircons. The Zr-in-rutile temperatures were calculated and interpreted based on possible P-T-t paths for the eclogite. Most inclusion and matrix rutiles yield Zr-in-rutile temperatures of 574 to 658°C at 2.5 GPa and 593 to 680°C at 3.3 GPa. This suggests that these rutiles would grow below and at the peak pressure during continental subduction. A few inclusion rutiles give high temperatures of 719-757°C at 2.0 GPa, consistent with their growth at the peak temperature during HP eclogite-facies recrystallization in response to the "hot" exhumation. Thus, the Zr-in-rutile thermometry is capable of providing metamorphic temperatures for rutile growth provided if petrological and geochronological constraints are available on their P-T-t paths. Although the secondary Zr loss of rutile could be enhanced by fluid-assisted recrystallization, the slow rate of Zr diffusion in rutile makes it impossible as an efficient mechanism for a considerable change in rutile Zr content at the eclogite-facie conditions. Therefore, the remarkable differences in Zr content and thus in temperature between the different occurrences of rutile suggest that many rutiles did not grow at peak P-T conditions. In other words, the Zr-in-rutile temperatures can be used to indicate rutile growth in the different stages of continental subduction-zone metamorphism.

https://doi.org/10.1180/S0026461X00006502 Published online by Cambridge University Press

Formation of anhydrous amorphous calcium carbonate and implication for biomineralization

GEN-TAO ZHOU[1]*, YE-BIN GUAN[1] AND QI-ZHI YAO[2]

[1]School of Earth and Space Sciences, University of Science and Technology of China, Hefei 230026, P. R. China (*correspondence: gtzhou@ustc.edu.cn)

[2]School of Chemstry and Materials, University of Science and Technology of China, Hefei 230026, P. R. China

Amorphous calcium carbonate (ACC) has been found as a transiently stabilized precursor in biomineralization in a variety of organisms, and is thought to play a role in the biological control over the subsequent crystallization. However, transient and stable phases of ACC differ in their structure and composition. Stable ACC contains structural water at a ratio of 1:1, while transient ACC is an anhydrous phase, and usually is in a syncytic membrane-delineated environment. Despite the fact that little is known about the formation and stabilization of biogenic ACC, it has been shown that certain macromolecules and/or other additives, such as magnesium and phosphate, may be determinant factors in the processes. To the best of our knowledge, nevertheless, no anhydrous ACC has been successfully synthesize in vitro even in the presence of the macrobiomolecules extracted from biogenic anhydrous ACC. Herein, a biomimetic mineralization process was applied to synthesize $CaCO_3$ by use of phosphatidylcholine (PC) as a model mineralization modifier. The present results show that PC is capable of inducing formation of the unusual anhydrous ACC, and the anhydrous ACC can transform into calcite with the follow-up mineralization. It implies that membrane lipid can exert significant effect on the formation and transient stabilization of anhydrous ACC bound by the membrane. Moreover, an intriguing phenomenon is that there is a large amount of ACC exclusively overlying on the surface of the secondary calcite during the subsequent mineralization. Therefore, the secondary calcite may function as an "organic-inorganic composition substrate", facilitating ACC deposition to its surface. This finding may indicate that even though the biogenic crystalline $CaCO_3$ and ACC intimately contact each other in organism, it does not means the exclusive origin of the crystalline polymorph from ACC. In contrast, the crystalline polymorph may facilitate the formation of ACC. Our results may provide a new insight into biomineralization mechanism of $CaCO_3$.

Geochemical character and tectonic implication of the Fuling composite pluton in Southern Anhui Province

ZHOU JIE[1,2], JIANG YAOHUI[2] AND XING GUANGFU[1]

[1]Nanjing Institute of Geology and Mineral Resource, Nanjing 210016, China

[2] State Key Laboratory for Mineral Deposits Research, Department of Earth Sciences, Nanjing University, Nanjing 210093, China

The Fuling composite granite located in the South of Anhui Province, is one of a tungsten-bearing granites in the east of Jiangnan orogenic belt. It crops out over an area of approximatedly 145km^2. The complex intruded into Precambrian to Cambrian siliceous shale, siliceous mudstone and limestones, with NE-SW direction. The complex is composed of 4 rock unites, the earliest units consists of spotted feldspar granite, the earlier units of feldspar granite, the later porphyraceous feldspar granite, and the last fine grain feldspar granite, named Jingkanling body, Yulongchuan body, Xiaochangxi body, and Fanzhengjian body respectively. Petrochemical data show that these granites are metaluminous to peraluminous and have high-silica (SiO_2>71%), total alkalis (Na_2O+K_2O = 5.72 to 10.75wt.%), rare elements (total REE = 99.14 to 533.86ppm) and Fe*(FeOt/(FeOt+MgO) = 0.83 to 0.97). In trace elements, they are enriched in Rb, Th, U, Zr, Hf and depleted in Ba, Sr, and Ti. Compared to the Xiaochangxi pluton and Fanzhengjian pluton, the Jingkanling pluton and Yulongchuan plutons are more depleted in Nb,Ta. $(La/Yb)_N$ ratios of the late granite unit lower than the early, average value is 11.93, 7.84, 5.15, 6.92 respectively. New LA-ICPMS zircon U-Pb dating suggests that the crystallization age of the Yulongchuan body is 127Ma, belonging to late Yanshan periods. Isotopically, Fangzhengjian granite has negative $\varepsilon_{Nd}(t)$(-5.5~ -5.91), and T_{2DM} values is between 1.35Ga to 1.4Ga. Petrographic, elemental and Sr-Nd isotopic characteristics indicate that the pluton belongs to an A_2 type granite. Fuling granite intrusion is enlongated in a NE-SW orientation, which is consistant with the distribution of regional Late Yanshanian granites in the coastal area and is parallel to the NE trending Jixi fault. A-type granites generally form in extensional tectonic environments regardless of the origin of the magma source. Combined with other A-type granites in the NE Yangtze Block, it can be concluded that Fuling A-type granite was derived by partial melting of metasediments in the back-arc extension environment, trigged by the subduction of the Pacific plate.

https://doi.org/10.1180/S0026461X00006502 Published online by Cambridge University Press

The comparsion of Mo isotope and paleo-oxygenation parameters in black shales from Upper Yangtze marine sediments

LIAN ZHOU, JIE SU, HU ZHAOCHU, HUANG JUNHUA, ZHAO LAISHI

State Key Laboratory of Geological Processes and Mineral Resources, China University of Geosciences, Wuhan 430074, China

This paper investigates the high-solution of Mo isotopes and uses trace-element analyses for fresh and representative black shales and siliceous shales collected from the transition between the Late Ordovician and the Early Silurian at the Wangjiawan section in Yichang and the Late Permian Dalong Formation in the Shangsi Section of Sichuan. The applicability of different geochemical parameters used as paleo-oxygenation indices are also compared. The preliminary results show that V/(V+ Ni), U_{auth}(auth U), V/Cr, Ce_{anom} and U/Th have a scattered variation range, but most samples plot within the suboxic-anoxic fields. The suboxic-anoxic environment was dominant during the deposition and formation of the two anoxic facies. These redox indicators show little correspondence to the δ^{98}Mo values. The U/Mo ratio can be used as a potential proxy for the paleo-redox conditions due to the possibility that Mo is enriched relative to U at different redox gradients during early diagenesis. This evidence is more significant for the euxinicity condition and corresponds to positive δ^{98}Mo (>1.5‰) values with low U/Mo ratios. This evidence is likely related to the depositional conditions near the boundary between anoxic and euxinic environments, which are characterised by low bioturbation or water circulation. Other samples reveal a wide scatter of U/Mo ratios and δ^{98}Mo <1.5‰. These results are likely due to punctuated improvements in oxygenation with intense bioturbation or water circulation, which led to the redistribution of trace element.

This study has been supported financially by the National Natural Science Foundation of China (Nos. 41073007, 40821061, 90714010) and MOST Special Fund from the State Key Laboratory of Geological Processes and Mineral Resources and the Fundamental Research Funds for the Central Universities.

Study on glaciochemical and microparticle characteristics of three snow pits in East Antarctica

L.Y. ZHOU[1]*, Y.SH. LI[2] AND S. JIANG[2]

[1]The key Laboratory of Coast & Island Development of Ministry of Education, School of Geographic and Oceanographic Sciences, Nanjing University, 210093, China (*correspondence:liyazhou@nju.edu.cn)

[2]Polar Research Institute of China, 200129, China

In the Antarctic summer of 1998/1999, the third Chinese Trans-Antarctic inland glaciological scientific expedition successfully entered Dome A area and extended its research to the site of 79°16'S, 77°00'E, 3,931 m.a.s.l, 1,128km away from Zhongshan station. We present the glaciochemical and microparticle characteristics of three snow pits which were drilled at the 1128km(DAP1), 1000km(DAP2) and 800km(DAP3) site along the investigation route.

From the dating results of the three snow pits, we come to a conclusion that the DAP1 snow pit, which was 3.3m deep, represented the whole sediments from 1987 to 1998; while DAP2 snow pit which was 2.1m deep represented a 7-year long sediment from 1992 to 1998 and DAP3 snow pit of 2.4m deep represented a 8-year long sediment from 1991 to 1998. Comparing the different radius part of the microparticles in the snow pits, we find that they are well linear related which implicates that the main source of the microparticles is the remote continents and the local factors have weak influence on them. The concentration of microparticles also coincides with the accumulation rate, that is, high microparticle concentrations agree with high accumulation.

From the glaciochemical analysis results, we find that the concentration of calcium in the snow pits changes smoothly, which implicates that it is from the deposit of the remote continents and the local influence is not evident. But for DAP3 snow pit, the calcium concentration slightly fluctuates for the unknown local causes. The sulfate in the snow pit exhibits a noticable wave crest for the eruption of Pinatudo volcano in 1991, which verifies the preciseness of the snow pit dating. What's more, the precipitation calculated by the snow pits well agree with the trend of global warming. The snow pit contains instructive information on the sedimentary characteristics and the climate change.

This study was granted by the National Natural Sciences Foundation of China (No.40703019, 40773074, 40906098).

https://doi.org/10.1180/S0026461X00006502 Published online by Cambridge University Press

Instantaneous release nuclide diffusion and migration simulation in fracture medium

N.Q. ZHOU[1] S. ZHAO[1] AND Y.Q. TANG[2]

[1] Dept. of Hydraulic Engineering, Tongji University, Shanghai, 200092 China (nq.zhou@tongji.edu.cn)
[2] Nuclear Industry of China Geotechnical Engineering Co. Ltd, Shijiazhuang, 050021 China

Most nuclear power plants are built on the bedrock foundations in China. The safety of nuclear power plant is an important matter. A magnitude 9.0 earthquake hit Japan's northeastern Honshu island on March 11, 2011. Fukushima nuclear power plant was disabled, releasing numerous uranium and radiocative ^{131}I dangerous contaminant into the environment. ^{131}I and ^{137}Ce have been detected in China.

The purpose of this work is to introduce nuclude diffusion and migration in fracture medium. Qian *et al* once studied contaminants migration in fracture medium [1,2]. Nuclide has its characteristics, such as attenuation, absorption, dilution, and so on. The experiment can be only carried out in laboratory. ^{131}I is used to simulate nuclide migration, its radiocative half-life is 8.3 days. According to the geological conditions of Zhejiang Sanmen Nuclear Plant, China, the lithology is tuff sandstone and andesite basalt on Unit 1 and Unit 2 reactor blocks. The fracture distributions are investigated on the field. Based on the statistical results, random fractures are generated using Monte Carlo method [3]. Li *et al* studied ^{85}Sr, ^{134}Se and ^{60}Co absorption equilibrium resperctively [4]. Iodine absorption coefficient is measured, then the diffusion and migration equation is established about include instantaneous release.

The research results show that: Instantaneous release of radionuclides in fracture medium is mainly diffusion and adsorption at the preliminary stage. When the adsorption reaches saturation, diffusion and migration of radionuclides play major roles. With the increase of radionuclide migration distance and the lapse of time, the decay will become more obvious and the impact will gradually disappear beyond a certain distance.

This study was supported by the National Science Fund of China (41072208) and Kwang-Hua Fund for College of Civil Engineering, Tongji University.

[1] Qian *et al*.(2007) *J. Hydrol*. **339**: 206-219. [2] Qian *et al*. (2011) *Int. J. Rock Mech. Min. Sci*. **48**:132-140. [3] Zhou *et al*. (2004) *Int. J. Rock Mech. Min. Sci*. **41**:402. [4] Li *et al*. (2003) *Radiation protection bulletin*. **23(2)**: 27-31(in Chinese).

Carbon isotope of residual gas in the source and reservoir rocks in the Northeastern Sichuan Basin

S.X. ZHOU[1], J. LI [1,2], B.Z. WANG [1,2], S.P. LIU[1,2] AND H.K. ZHANG[1,2]

[1]Key Laboratory of Petroleum Resources Research□Institute of Geology and Geophysics, CAS, Lanzhou, 730000 (*correspondence:sxzhou@lzb.ac.cn)
[2]Graduate University of CAS, Beijing, 1000049

There are many large gas fields in the northeastern part of Sichuan Basin, but their origin and source are not clear due to limited information obtained from chemical compositions of accumulated gas. In this study, carbon isotopic signatures of residual hydrocarbon gas and CO_2 in different source rocks, reservoir rocks and solid bitumens have been measured and gas-source correlation have been done in this area.

Our results show that various source rocks in different geological period have different isotopic composition of residual gas. Methane in the Precambrian and Cambrian mudstones range from -34.1‰ to -39.4‰ with ethane -27.1‰ to -37.3‰, while other source rocks isotopic signatures are $\delta^{13}C_{C1}$=-30.2 ~ -32.6‰ for Ordovician , $\delta^{13}C_{C1}$=-30.9 ~ -31.8‰ for Silurian, $\delta^{13}C_{C1}$=-35.5‰ for Permian and $\delta^{13}C_{C1}$= -34.5‰ for Triassic, and ethane isotopic values in these source rocks lighter than -28‰ indicate that gases in various marine source rocks are derived from sapropelic organic matter except Permian source rock.

Residual gas in Precambrian solid bitumens are -30.6 ~ -34.9‰ for methane and -30.1‰ for ethane, while gas in the Lower Triassic and Upper Permian reservoir formations containing solid bitumens display methane $\delta^{13}C$ values between -32.5‰ and -36.1‰ lighter than methane values of gas in the reservoirs, ethane $\delta^{13}C$ values between -20.7‰ and -26‰ heaver than ethane values in natural gas, and $\delta^{13}C$ values of CO_2 between -8.6‰ and -13.6‰. It is conclusion that some natural gases maybe relate to Silurian source rocks, and thermochemical sulfate reduction (TSR) is not obvious in reservoirs.

This work was supported by partly by the Key Project of Chinese Academy of Science (grant KZCX2-YW- Q05-03-05) , the National Special Projects of Science and Technology (2008ZX05018-001-05) and the Chinese National Major Fundamental Research Developing Project (2011CB201103).

https://doi.org/10.1180/S0026461X00006502 Published online by Cambridge University Press

Analysis of Poyang Lake water body dissolved inorganic carbon isotopic tracing and its carbon source contribution

ZHOU WEN-BIN[1,2], HU CHUN-HUA[1,2]*, JIANG JIAN-HUA[1,2], GUO CHUN-JING [1,2] AND LOU QIAN [1,2]

[1]School of Environmental and Chemical Engineering, Nanchang University, Nanchang, 330031, China (*correspondence: chhu@ncu.edu.cn)

[2]Key Laboratory of Lake Poyang Environment and Resource Utilization, Ministry of Education, Nanchang University, Nanchang, 330029, China

In recent decades, intensifying global climate changes caused by the greenhouse effect have led to recognition of the importance of the global carbon cycle. The key to the research on this phenomenon is the identification of the source of CO_2, its variations, and its response to human activities. Lake is sensitively responding to regional and global climate changes, being a rather considerable carbon source [1-2]. During the high- and low-water periods of 2009 and 2010, water samples from the Poyang Lake region and the estuary of five rivers were collected. We analyzed the correlation of the temporal and spatial distribution of dissolved inorganic carbon (DIC). We also examined the carbon flux in the lake and the contribution of its three major carbon sources to the flux. Results show that the DIC content in the high-water period is higher than that during the low-water period. In contrast, the value of $\delta^{13}C$ DIC is positive in the low-water period and negative in the high-water period; the monthly DIC carbon flux in Poyang Lake is 2.822t–268.428t, and its mean is 135.836t. The largest contributor (73.07% contribution rate) to the carbon flux in Poyang Lake is the CO_2 water vapor exchange. The second largest contribution (15.53% contribution rate) is the river input. Weathering of rocks with dissolved carbonate is the major mechanism controlling the DIC source and the $\delta^{13}C$ DIC composition. The changes in seasonal rainfall runoff are the main factors.

[1] Yu H & Li N. (2008) *Environmental Science and Technology* 21(2), 1-5. (in Chinese). [2] Kling G.W *et al*. (l99l) *Science* 251, 298-301.

Predicting CO_2 EOR and geological sequestration processes with artificial noble gas tracers

Z. ZHOU[1]*, M.J. BICKLE[2], A. GALY[2], H.J. CHAPMAN[2], N. KAMPMAN[2], B. DUBACQ[2], M. WIGLEY[2], O. WARR[1], T. SIRIKITPUTTISAK[1], P. HANNAH[3] AND C.J. BALLENTINE[1]

[1]University of Manchester, M13 9PL, UK (*correspondence: zheng.zhou@manchester.ac.uk)

[2]Department of Earth Sciences, University of Cambridge, UK

[3]Full-Spectrum Monitoring, LLC, USA

Naturally occurring noble gas isotopes provide one of the best tools to study gas-fluid-mineral interaction [1]. By injecting and studying artificial noble gas tracers in CO_2 EOR or potential sequestration reservoirs, hydrological modelling can be established to quantify the multi-phase flow of fluids and determine the flow path and flow rate of fluids. This will enable further understanding of gas-aqueous fluid-mineral reactions and kinetics.

We present preliminary results from an artificial noble gas tracer study in a commercial CO_2 EOR reservoir located in Wyoming, USA. We constructed a continuous tracer injection system which consisted of two HPLC pumps, three high pressure cylinders and a wireless remote system monitoring temperature, pressure and weight in real time. Over 9 days, we injected 2 STP litres of ^{3}He and ^{129}X each directly into the EOR CO_2 injection stream. Based on the analysis of background $^{3}He/^{4}He$ and $^{129}Xe/^{132}Xe$ (0.07Ra and 0.98 respectively), our predicted spiked $^{3}He/^{4}He$ and $^{129}Xe/^{132}Xe$ ratios for the mass of injected CO_2 are 49.54Ra and 11.64 respectively. The wellhead injector fluid and 4 production wells surrounding the injector were sampled from September 2010 to February 2011.

Preliminary results show that the highest $^{3}He/^{4}He$ and $^{129}Xe/^{132}Xe$ ratios in the injected CO_2 stream reached 49.0Ra and 23.94 respectively and establish the tracer input function. ^{3}He tracer was detected in all producing fluid samples from 4 monitoring wells. Spike breakthrough is consistent with the reservoir geology with the wells updip of the injector seeing tracer arrival earlier than those located downdip of the injector. Spike breakthrough in wells updip of the injector correlated with the well temperature which was an indication of the CO_2 breakthrough, but in the wells downdip of the injector spike came through, most probably, dissolved in the water phase. $^{3}He/^{4}He$ ratio is at a much lower level than the injected ratio and reflect the magnitude of reservoir fluid and CO_2 interaction.

[1] Gilfillan *et al*. (2009) *Nature* **458**, 614-618.

https://doi.org/10.1180/S0026461X00006502 Published online by Cambridge University Press

Re-Os geochronology of black shales from the Neoproterozoic Doushantuo Formation, Yangtze platform, South China

BI ZHU[1,2], HARRY BECKER[2], SHAO-YONG JIANG[1]*, DAO-HUI PI[1] AND MARIO FISCHER-GÖDDE[2]

[1]State Key Laboratory for Mineral Deposits Research, School of Earth Sciences and Engineering, Nanjing University, Jiangsu, 210093, P. R. China (*correspondence: shyjiang@nju.edu.cn)

[2]Freie Universität Berlin,Institut für Geologische Wissenschaften, Malteserstr. 74-100, D-12249 Berlin, Germany

Re-Os geochronometer is a useful tool in dating organic-rich sedimentary rocks like black shale. Precise Re-Os chronology also provides constraints on temporal variation in Os isotopic composition of seawater, which reflects the relative dominance of radiogenic Os from weathering of upper continental crust and unradiogenic Os from alteration of oceanic crust or dissolution of cosmic dust.

In this study, we carried out Re-Os isotopic analysis of black shale samples from the fossil-bearing Miaohe member (Doushantuo Formation IV) at Jiulongwan section and from Doushantuo Formation II at Baiguoyuan section in Three Gorge area, South China. A Re-Os isochron age of 593±17 Ma (MSWD=1.0) with initial Os ratio of 0.88±0.13 for the basal Miaohe Member was obtained by using a CrO_3-H_2SO_4 dissolution technique. This age falls in the range of precise U-Pb zircon ages of 551 Ma from the top and 635 Ma near the base of the Doushantuo Formation, respectively. The minimum age difference of ~25 Ma between the base of the Miaohe member and the 551 Ma old tuff on the top of the Miaohe member means very low sedimentation rates during black shale deposition (< 0.5 m/Ma). By the same technique, samples from Doushantuo Formation II at Baiguoyuan section only gave an imprecise age of 582±58 Ma (MSWD=1.8) with an initial Os of 0.54±0.05, which is comparable to the initial Os (0.62±0.03) for the 608 Ma Ediacaran Old Fort Point Formation in western Canada (Kendall *et al*. 2004). The increase in initial Os ratio from 0.54 for the lower Doushantuo Formation to 0.88 for the upper Doushantuo Formation is consistent with the secular increase of $^{87}Sr/^{86}Sr$ in the late Neoproterozoic ocean, and may result from enhanced continental weathering rates during the Ediacaran due to continental convergence of East and West Gondwana and subsequently the formation of a Transgondwana Supermountain.

Recent advances in kinetics of water-rock interaction and applications to geological carbon sequestration

CHEN ZHU[1]*, FAYE LIU[1] AND PENG LU[1,2]

[1]Department of Geological Sciences, Indiana Univeristy, Bloomington, IN 474705, USA (*correspondence: chenzhu@indiana.edu)

[2]Now at the Carela Corporation

Recent laboratory experiments, field, and modelling studies on the kinetics of water-rock interactions have shown that the rates of dissolution and precipitation reactions are strongly inter-dependent or coupled [e.g., 1, 2, 3]. Numerous laboratory experiments have measured the dissolution rates at conditions far from equilibrium. However, reactions in batch and column experiments and in the field proceed in the near equilibrium region because of the low solubility of aluminosilicates. In the near equilibrium region, the Gibbs free energy term in the rate equations reduce the overall reaction rates. In the case of feldspar dissolution, slow clay precipitation effectively reduces feldspar dissolution rates by orders of magnitude. The implication is that a reaction network is operating, and a system geochemistry approach is necessary for studies of kinetics in geological systems.

When water-rock interaction theories are applied to geological carbon sequestration, the rate of fluid flow also plays a significant role on reaction rates. Recently, we conducted multi-phase reactive flow and transport modelling to simulate large scale CO_2 injection (a million tons per year for 100 years) into Mt. Simon sandstone, a major deep saline reservoir in the Midwest of USA [4]. The results indicate that most of the injected CO_2 remains within a radius of 2500 m lateral distribution. Four major trapping mechanisms and their spatial and temporal variations are evaluated in our simulations: hydrodynamic, solubility, residual, and mineral trapping. In our model, the replenishing water continues to dissolve CO_2 long after the injection, which results in total dissolution of hydrodynamically trapped CO_2 at the end of 10,000 years. In contrast, most previous models neglected the regional flow after injection and hence artificially limited the extent of geochemical reactions as if in a batch system. Consequently, a supercritical CO_2 plume (hydrodynamic trapping) would persist after 10,000 years.

[1] Zhu ., AE Blum, DR Veblen (2004) *WRI-11* (eds. R B Wanty and RRI Seal), **v2**., pp. 895-899. [2] Zhu, C, and Lu, P, *GCA* **v73**, p.3171-3120. [3] Zhu, C, Lu, P, Zheng, Z, Ganor, J, *GCA* **v74**, 3963-3983. [4] Liu, F, P Lu, C Zhu, Y Xiao (2011) T*he International Journal of Greenhouse Gas Control*, v.**52**(2), 294-307.

https://doi.org/10.1180/S0026461X00006502 Published online by Cambridge University Press

Kinetic study of brucite carbonation

CHEN ZHU[1], LIANG ZHAO[1]*, XIONG GAO[1], JUNFENG JI[1], JUN CHEN[1] AND H. HENRY TENG[1,2]

[1]Department of Earth Sciences, Nanjing University, Nanjing, Jiangsu, 210093, PRC (*correspondence:zhaoliang@nju.edu.cn)
[2]Department of Chemistry, the George Washington University, Washington, DC, 20052, USA

Increasing evidence suggests that the widespread used of fossil fuels has led to a rapid increase in carbon dioxide concentration in atmosphere. One method to prevent CO_2 in the atmosphere from rising to unacceptable levels is carbon dioxide sequestration. Of all the options proposed so far, mineral carbonation is the one that offers advantages in the stablity of the final products and hence the elemination of legacy issues. However, this approach faces the problem of slow reaction kinetics and the difficulty of recycling leaching agents used to extract cations [1].

We present an experimental study of mineral carboation using NH_4Cl solution as leaching agent and brucite as raw material. The acidic environment resultant from caused by NH_4^+ hydrolysis facilitates mineral dissolution and the release of NH_3, which will be collected as a base agent for pH adjustment during the carbonate process and form NH_4Cl again. Recycle use of the leaching agent lowers the total cost and increases the commercial potential of the process. Furthermore, most magnesium-rich layer silicon minerals have similar structures and brucite-like magnesium-oxygen octahedral layers exist between silicon-oxgen tetrahedrons, it is reasonable to believe that brucite and magnesium-rich layer silicon minerals have similar dissolution mechanism.

Kinetic experiments show that the convertion-time followed the Avrami model, and that the reaction rate increased with increasing temperature and ammonium chloride concentration, decreasing solid/liquid ratio, and particle size. The following mathematical equation is found to fit the relationship between the reaction constant(k) and various experimental parameters:

$$k=5.22\times10^{5}C^{0.12}(S/L)^{-0.22}D^{-0.31}e^{-5710/T}.$$

The reaction activiation energy calculated by the Arrhenius equation 47.47kJ/mol, in agreement with the reported value for surface controlled brucite dissolution [2].

[1] Sipilä*et al*. (2008) *Greenhouse Issues* **90**, 3-4. [2] Huang *et al*. (2009) *The Chinese Journal of Process Engineering* **9**, 1121-1126 (in chinese).

Large area multi-stage quasi-layer petroleum accumulation in carbonate reservoirs in Tazhong area, Tarim Basin

ZHU GUANGYOU[1,2], ZHANG SHUICHANG[1,2], WANG YU[1,2] AND SU JIN[1,2]

[1]Research Institute of Petroleum Exploration and Development, PetroChina, Beijing 100083, China
[2]State Key Lab of Oil Recovery Elevation, Research Institute of Petroleum Exploration and Development, PetroChina, Beijing 100083, China

Tazhong area is an important exploration domain in the Tarim basin with abundant petroleum. Ordovician carbonate reservoir is the major exploration target. The formation and distribution of those reservoirs were major controlled by high energy sedimentary facies, dissolution and faults. Reef-shoal complex in the Lianglitage Formation in Upper Ordovician and karst weathering crust reservoir in the Yingshan Formation in Lower Ordovician were both distributed quasi-layered in large area. The Hydrocarbons were complex accumulated in multi-layer. Those reservoirs were composed of carbonate rocks with low porosity and low permeability, and buried in 4500~6500m depth with intensive heterogeneity. The spatial distribution of effective reservoirs controlled the occurrence of hydrocarbon and accumulated in large area, which showed an integral enrichment characters.

Detailed oil-source rock correlation indicates that the crude oils were mix-oils originated from both Cambrian source rocks and Ordovician source rocks, nevertheless, the natural gases were major oil-crack gases from Middle-Lower Cambrian sources. The analysis of accumulating process shows that the Tazhong area experienced three stages of hydrocarbon accumulation. The first stage occurred in the Late Caledonian tectonic cycle and the hydrocarbons originated from Cambrian-lower Ordovician source rocks, and were severely degraded in the Early Hercynian tectonic movements in large areas. The second stage occurred in the Late Hercynian tectonic cycle which was the most important hydrocarbon charging stage, the oils and gases were from Middle-Upper Ordovician source rocks. The third stage occurred in the late Himalayan tectonic cycle, Cambrian oil-crack gases began to generated in depth, charged into Ordovician reservoirs along faults, gas-washed the oil pools and then formed condensate gas reservoirs which is now extensively occurred in Tazhong area.

https://doi.org/10.1180/S0026461X00006502 Published online by Cambridge University Press

Geochronology, geochemistry and ore-forming fluid characteristics of the Shijinpo gold deposit in Beishan belt, NW China

JIANG ZHU, XINBIAO LV*, CHAO CHEN AND YALONG MO

Faculty of Earth Resources, China University of Geosciences, Wuhan, 430074, China
(*correspondence: Lvxb_01@163.com)

The Shijinpo gold deposit is one of numerous lode gold deposits in the Beishan orogenic belt, southern margin of the Altaids, northwestern China. Gold mineralization is hosted in the early Devonian granite and consists primarily of auriferous quartz veins that confined to the EW-trending faults. Ore-related hydrothermal alteration is dominated by sericite + quartz + sulfide assemblages in close proximity of gold veins. Pyrite is the predominant sulfide mineral, variably coexisting with minor amounts of chalcopyrite, sphalerite, and galena. Gold occurs mostly as free gold enclosed in or filling microfractures of pyrite and quartz. Native gold is present coexisting with Au-bearing tellurides consisting mainly of petzite.

Measured $\delta^{34}S$ values for sulfide minerals range from 8.32‰ to 10.33‰, indicating a deep-seated sulfur source most likely of magmatic origin. Calculated $\delta^{18}O$ values for the ore fluid range from +2.7‰ to +3.3‰ and the corresponding δD values range from -95‰ to -99 ‰, compatible with mixing of magmatic and meteoric components. Fluid inclusion studies suggest that gold veins were deposited at intermediate temperature conditions (150 to 320°C) from aqueous or aqueous-carbonic fluids with moderate salinity (4.65 to 12.16 wt% NaCl equiv). The ore-forming fluid is assumed to undergo boiling at high temperature triggered by fracturing and then mixed with the ground water. Laser incremental heating $^{40}Ar/^{39}Ar$ analysis of hydrothermal sericite yield an plateau age at 364.6 ± 3 Ma (2σ), suggesting that the gold veining took place in the late Devonian.

Combining these observations with the regional geology we propose that the Shijinpo gold deposit was formed during compressional to transpressional processes in a subduction-related setting.

Mechanisms of nitrogen dissipation in an N-saturated subtropical forest in Southwest China

J. ZHU*, P. DÖRSCH, H. SILVENNOINEN AND J. MULDER

Norwegian University of Life Sciences, 1432 Ås, Norway
(*correspondence: jing.zhu@umb.no)

Published N budgets for N-saturated watersheds in subtropical SW China suggest significant N retention, despite low forest growth, P deficiency and high soil acidity [1]. To characterize mechanisms of N dissipation in these systems, we applied state-of-the-art field and laboratory methodologies to a headwater catchment at Tieshanping (TSP), SW China, (4.04 g N m^{-2} a^{-1} atmogenic deposition, 61% of which in form of NH_4^+ and 0.57 g N m^{-2} a^{-1} effusion in stream water mostly as NO_3^-). We explored spatiotemporal patterns of N_2O emission and ^{15}N and ^{18}O natural abundances of NO_3^- *in situ* and characterized nitrification and denitrification and their gaseous product stoichiometries by laboratory incubation.

Highest N cycling rates and N_2O emissions were found during the wet season (summer), with marked variations between wet and dry years. N_2O emissions during summer were driven mainly by rain episodes. Soils on the hillslopes showed higher denitrification and N_2O emission rates than a perturbed groundwater discharge zone (GDZ) which had less organic carbon. The spatial pattern of denitrification was consistent with NO_3^- concentration profiles and natural abundance signatures. Laboratory experiments confirmed that organic carbon is the limiting factor for N-removal by denitrification in this ecosystem and that the different landscape elements harbour denitrifier communities with distinct N_2O product stoichiometries, explaining part of the variation in observed N_2O emissions. Nitrification in the hillslopes was found to be unbalanced, producing significant amounts of nitrite which decomposed rapidly to NO and N_2O at low native pH (4.0), indicating chemodenitrification from incomplete NH_4^+ oxidation as a potentially important additional source for N_2O. Estimated annual N_2O emission for 2009 and 2010 was 0.29 g N m^{-2}, equivalent to appr. 8.5% of the annual N input. To close the N budget of the watershed, a field ^{15}N labelling experiment was conducted to assess total gaseous losses including N_2.

[1] Chen XY and Mulder J. (2007). *Science of the Total Environment* **378**: 317-330

https://doi.org/10.1180/S0026461X00006502 Published online by Cambridge University Press

The first observation of Chang'E-2 gamma-ray spectrometer

M.H. ZHU[1], T. MA[2], J. CHANG[2], W.-H. IP[1,3], Z. TANG[1] AND A. A. XU[1]

[1]Macau University of Science and Technology, Taipa, Macau
[2]Purple Mountain Observatory, Nanjing, China
[3]National Central University, Jhongli, Taiwan

Gamma-ray measurement coming from the lunar surface is a powerful method to infer its composition of material in the top several tens of centimeters. While gamma ray lines are remotely measured in orbit, chemical elements can be identified in light of the energies from which they were emitted, and concentrations can be estimated based on their fluxes.

Chang'E-2 spacecraft was launched to the Moon (100 km, circle polar orbit) at 1st, Oct., 2011, with a gamma-ray spectrometer (CE2-GRS) as one of its scientific payloads. CE2-GRS using a large $LaBr_3$ (Ce) crystal as its main detector is expected to provide global elemental maps of the lunar surface (e.g., Th, K; Mg, O, Al, Ca, Si, Fe, Ti). It employs a big cup-shape CsI (Tl) crystal to suppress the Compton effects and reduce the background gamma rays from the spacecraft materials interacted with GCRs. Gamma-rays are recorded as 512 channel-spectrum every 3 seconds in the range of 0.3 to 10 MeV with the energy resolution of ~ 4% fwhm@662 keV.

CE2-GRS has about 4-days background measurements in its cruise period. The spectrum shows higher quality than that from past scintillation detectors for the lunar gamma-ray remote measurement. From the background spectra, self-activity peaks of $LaBr_3$ crystal (from ^{138}La and ^{227}Ac decay chain generation) can be found clearly. Elements (O, K, Mg, Al, and Ti) from the spacecraft body, the fuels, and instruments were also identified. Potassium map (cps, 5°×5°) was obtained using first three-month measurements. Since the higher spatial resolution (~ 150 km × 150 km), the derived map can show the potassium distribution on the Moon clearly.

Absolute calibration will be carried out based on the spatial response function. Comparisons with that of Lunar Prospector, Kaguya, and Chang'E-1 will be investigated to see if the new potassium could indicate some interesting, new science.

A Paleoproterozoic tectonothermal event recorded in Precambrian basement rocks of the Kuluketage uplift, Northeastern Tarim, China

W.B. ZHU, H.L. WU, L.S. SHU AND D.S. MA

State Key Laboratory for Mineral Deposits Research, Department of Earth Sciences, Nanjing University, Nanjing 210093, People's Republic of China, (zwb@nju.edu.cn)

The Kuruktag uplift is located to the north of the Tarim Block. The Neoarchaean to early Neoproterozoic basement rocks are unconformably overlain by the middle Neoproterozoic to Phanerozoic sedimentary cover. The Precambrian basement rocks also crop out in the Korla region, at the western end of the Kuruktag uplift, whose ages are uncertain because of the paucity of reliable isotopic data. These basement rocks, including gneisses, amphibolites, marbles and schists, were subjected strongly deformed and metamorphosed to amphibolite facies.

Four garnet-bearing schists were collected for zircon U–Pb dating and Hf-isotope analyses. CL images display that most zircon grains occur as relatively dark and rounded crystals and are homogeneous in texture, indicative of metamorphic origin. The samples give four metamorphic zircon ages of 1844Ma, 1847Ma, 1850Ma and 1867Ma, respectively. The metamorphic zircon age of ~1.85 Ga obtained in this study indicate that an important tectonothermal event occurred at the end of the Paleoproterozoic in the Tarim Block. Lu–Hf isotopic analysis on these zircons gives Hf model ages ranging from 2.9 to 3.5Ma, indicating that the late Paleoproterozoic metamorphism and tectonism of the Tarim Block represent an overprint on an Archaean basement. These data imply a Paleoproterozoic orogeny in the northern Tarim.

This episode of Precambrian tectonothermal event is broadly coeval with those seen in many continents around the world such as Baltica, Laurentia, Northern Finland, Northern Fennoscandian Shield, Amazonia, North China and India, etc., which is coincident with the timing of the orogeny associated with the amalgamation of the Columbia super-continent, suggesting that the Tarim Block was the part of this supercontinent.

https://doi.org/10.1180/S0026461X00006502 Published online by Cambridge University Press

Origin and fractionation of heavy metals of sediments in the drinking water source of Beijing

ZHU XIANFANG[1] AND JI HONGBING[1,2]*

[1]The Key Laboratory of Metropolitan Eco-Environmental Processes, College of Resource Environment and Tourism, Capital Normal University, Beijing 100048 China (xf_zhu@126.com, *correspondence: hongbing.ji@yahoo.com)

[2]State Key Laboratory of Environmental Geochemistry, Institute of Geochemistry, Chinese Academy of Sciences, Guiyang 550002, China

The Miyun Reservoir, the only one surface drinking water source of Beijing, incepted kinds of pollutants from rivers, agricultural production, mining activity, tailing and so on. Four sediment cores (35cm per core) were collected from Miyun Reservoir and cut into slices of 5 cm each core. Samples were subjected to a total digestion technique and analyzed by ICP-OES for Cr, Pb, Cd, Co, Cu, Mn, Ni, Ti, V and Zn, and by AFS for As and Hg. The seven-step sequential extraction technique was determined the distribution of speciation for heavy metals (except As and Hg). The results revealed the contents of heavy metals were not apparent enrichment compared with the shale standard. Most of heavy metals decreased while the depth increased. The results showed that the main fraction for most of heavy metals was residual phase. Additionally, the extractive phase of Cd was higher and reached 60%, the following was Ni, Co, Zn and Pb.

The origin of heavy metals was identified by multivariate analysis with total content. The results of correlation analysis revealed obvious correlation between heavy metals. Cu, Mn and V were highly correlated among them ($r>0.800$; $p<0.01$), Cr and Ni were also identified, whereas As and Ti were less correlated with Cu, Mn and V ($r>0.500$; $p<0.01$). The correlation coefficients were not as high as among Hg, Co and other heavy metals. PCA showed there were five principal components. PC1 included Ti, Cd, Cu, Mn and V, PC2 were Cr and Ni, PC3 were As and Zn, PC4 was Hg, and PC5 was Co. Therefore, the five principal components represented five primary origins of heavy metals, which were erosion of rocks, industrial and mining, agricultural production and domestic sewage, atmospheric deposition and secondary pollution of water environment, respectively. The results provided scientific basis for protection of drinking water source of Beijing.

This study was supported by the program of “One Hundred Talented People” of the CAS

Isotope fractionation of transition metals by higher plants

X.K. ZHU[1], S.Z. LI[1], Y.M. LUO[2] AND L.H. WU[2]

[1]Lab Isotope Geol., MLR, Inst. Geol., CAGS, Beijing, China (xiangkun@cags.ac.cn; blueoceain@yahoo.com.cn)

[2]Inst. Soil Sci., CAS, Nanjing, China

Transition metals such as Fe, Cu and Zn are present as trace elements in organisms, but are essential for life. Thus variations in transition metal isotope composition may be important in tracing the interaction between geosphere and biosphere, to trace the pathways of these elements into and within biological system. A prerequest for these applications is an adequate undersdanding of the the mass fractionation of these isotopes during steps of biological uptake and translocation . Here we report the result of a case study for sotope fractionations of Fe, Cu, Fe and Zn by higher plant using a Cu accumulator *Elsholtzia splendens*.

Elsholtzia splendens growth-experiments were carried out in green house and in soils with different chemical properties, namely: copper contaminated soil collected from natural envirioment □denoted as CK□, CK with addition of sulphur powder, CK with addition of EDDS, and CK with addition of both EDDS and sulhpur. Soils, roots, stems and leaves were measured for Cu, Fe and Zn isotope ratios using Nu Plasma HR MC-ICPMS after digestion and chemical purification. The results display some prominant features, taking Cu isotopes as an example: 1) relative to soils, the plants show overall lighter isotope enrichment, implying significant isotope fractionation occurred during Cu uptaking of the root from the soil and light Cu isotope were taking preferentially; 2) from soil to root to stem, Cu isotope composition become progressively lighter, indicating stepwise mass fractionation during Cu uptaking and translocating; 3) relative to stems, leaves enrich heavy Cu isotope by *ca*.0.3‰, suggesting a change in Cu transport mechanism from stems to leaves, and showing that heavy Cu isotope can be preferentially taken at some stage during biological processes; 4) the extent of light isotope enrichment of the plant relative to soil varies with the chemical property of the soil, and the light Cu isotope enrichment is enhanced by the addition of EDDS.

The results presented above enhance our knowledge about mass fractionation proccesses of transition metal isotopes in higher plants significantle.

https://doi.org/10.1180/S0026461X00006502 Published online by Cambridge University Press

Mining-induced groundwater environmental impact assessment at Shuyang county, Jiangsu Province, China

X.B. ZHU, J.C. WU, J.F. WU AND X. YUAN

Dept. of Hydrosciences, School of Earth Science and Engineering, Nanjing University (zxb@nju.edu.cn)

The phosphorite was found at Tangzhuang village, Shuyang county, Jiangsu province. It is about 2.2km^2. It's can be used and planned to be exploited in the future. Groundwater environment would be impacted heavily by exploiting phosphorite because the phosphorite is deep below the subsurface. The groundwater level should be reduced to the bottom elevation of the phosphorite. So, the huge cone of depression, which result in the subsidence, would be developed.

There is the phreatic aquifer and the confined aquifer in the study area. The hydrogeologic conceptual model was generalized and the numerical model of groundwater flow was built with the MODFLOW module in GMS software. The dewatering of deposit was caculated, 4100m^3/d for the upright well used for workers to get inside the exploitation platform and 13054^3/d for the exploitation channel. The drawdown is computed at the same time. The maximum drawdown is 60m for the confined auqifer and 4m for the phreatic aquifer.

The effect of phosphorite exploitation on the groundwater environment is obvious. Some engineering measures are suggested to be implemented to reduce the effect. Pumping well planned to be built to supply drinking water for people around the study area. Grouting convrete boreholes are suggested to be constructed to cut off the water exchange between the phreatic and the confined aqufer. The effect of exploitation and the subsidence due to dewatering of deposit can be controlled with these engineering measures.

The research was financially supported by National Natural Science Foundation of China (No.40702038 and No. 40725010)

Zircon ages and Hf isotopic feature of Neoproterozoic metamorphosed sedimentary rocks in the South Qinling terrain, China

X.-Y. ZHU [1,2], F. CHEN [2], S.-Q. LI [2] AND L. YANG [1]

[1]Institute of Geology and Geophysics, Chinese Academy of Sciences, Beijing, 100029, China

[2]School of Earth and Space Sciences, University of Science and Technology of China, Hefei, 230026, China

The Qinling orogenic belt, being part of the central orogenic belt in China, was resulted from the North China and South China blocks in early Mesozoic. The Shangnan-Danfeng tectonic zone is an inner suture, which separates this belt into the North and South Qinling terrains. Neoproterozoic sedimentary-volcanic sequences widely distributed in South Qinling have been considered to be basement rocks. Characteristic Neoproterozoic magmatic events (~750 Ma) were recorded in zircons from magmatic and low-grade metamorphic rocks in the South Qinling terrain and the South China block, interpreted as an indicator for close tectonic connection of both terrains in Neoproterozoic [1, 2].

This study presents results of zircon situ Lu-Hf and U-Pb isotopic analysis of low-grade metamorphic sedimentary-volcanic sequences in the South Qinling terrain. Most detrital zircons are euhedral to subhedral, implying a short transportation of material after weathering. Detrital zircon populations with oscillatory zonation of magmatic origin yield U-Pb ages mainly clustering at ~850 Ma and ~1890 Ma. Two zircon groups are characterized by distinguishable Hf isotopic feature, having negative initial εHf values of around -8.4 and positive initial εHf values of around +3.6, respectively. The atypical Neoproterozoic magmatic activity of ~850 Ma in the South Qinling terrain basement, similar to those along the northwestern and south eastern margins of South China block, are probably related to an earlier stage of the break-up of Rodinia supercontinent [3, 4].

[1] Chen *et al*. (2006) *JAES* **28**, 99-115. [2] Yu *et al*. (2008) *Precam. Res* **164**, 1-15. [3] Ling *et al*. (2001) *Phs. Chem. Earth* (A) **26**, 805-819 [4] Li *et al*. (2010) *Am. J. Sci* **310**, 951-980

https://doi.org/10.1180/S0026461X00006502 Published online by Cambridge University Press

Abnormal positive $\delta^{13}C$ values of carbonate in Lake Caohai, Southwest China and their possible paleoenvironmental significances

Z. ZHU [1,2,3], J. CHEN [1]*, S. REN [2] AND Y. LI [2]

[1]The State Key Laboratory of Environmental Geochemistry, Institute of Geochemistry, Chinese Academy of Sciences, Guiyang 550002, China (*correspondence: chenjingan@vip.skleg.cn)

[2]Chongqing Key Laboratory of Exogenic Minerallization and Mine Environment, Chongqing Institute of Geology and Mineral Resources, Chongqing 400042, China

[3]Chongqing Research Center of State Key Laboratory of Coal Resources and Safe Mining 400042, China

Carbon source inputs, CO_2 exchanges between atmosphere and lake water, as well as lacustrine productivity are commonly considered as the main controls on the $\delta^{13}C$ values of lake authigenic carbonates. Generally, $\delta^{13}C$ values of carbonates in most lakes are lower than +5‰, few are up to +13‰ [1]. Here, stable carbon isotopes were measured on bulk carbonates from a short sedimentary core in Lake Caohai, Guizhou Province, southwest China. The results showed that $\delta^{13}C$ values vary between -14.25‰ and +23.10‰, which is the largest carbon isotope variations discovered so far in carbonates from lacusrine sediments, and some $\delta^{13}C$ values are the most positive values up to +23.10‰, more positive than previously reported values. On the basis of combination with oxygen isotope and carbonate contents proxies, we suggested that the carbon isotope composition of carbonate from Lake Caohai was controlled by photosynthesis/ respiration of aquatic plants, and the input of bacteria to carbon isotope fractionation of organic matter may be responsible for the abnormal positive $\delta^{13}C$ values in Lake Caohai [2,3]. Therefore, more attention should be paid on the carbon isotope composition of carbonates in Lake Caohai in future research.

This work is financially supported by the National Natural Sciences Foundation (40673068) and the National Key Funds of China (2006CB403201).

[1] Blas *et al*. (1999) *Earth* ***Planet. Sci. Lett.*** 171**, 253 - 266.** [2] Teranes *et al*. (2005) *Limnol. Oceanogr*. **50**, 914 - 922. [3] Hollander *et al*. (2001) *GCA* **65**, 4321 - 4337

Al diffusion in olivine: An experimental study

IRINA ZHUKOVA*, HUGH O'NEILL AND IAN CAMPBELL

Research School of Earth Scuance, National Australian University, ACT 2000 (*correspondence: irina.zhukova@anu.edu.au)

Al content in olivine is temperature dependent [1] and diffusion is thought to be very slow [e.g. 2].

We performed a series of experiments of Al diffusion in San Carlos olivine and synthetic forsterite at 1300ºC and log fO2 = -0.7; -5.7 and atmosphere pressure. In order to provide an inside into mechanism of alumina substitution into olivine, activities of SiO_2, MgO and Al_2O_3 were buffered in all runs. Four mineral associations were used: (a) forsterite – periclase – spinel; (b) forsterite – spinel – sapphirine; (c) forsterite – sapphirine – cordierite; (d) forsterite – cordierite – enstatite and the results analysed by LAICPMS. Each profile was fitted to a one – dimensional diffusion model in a semi-infinite medium with a source reservoir maintained at constant concentration.

The concentration of Al at the interface in equilibrium with the high silica activity buffer (d) is 5 times higher than in case of the low silica activity buffer (a), changing from 50 ± 12 ppm to 220 ± 30 ppm. The solubility of Al in S.C.O. is 2 - 4 times higher than in forsterite (430 ± 50 ppm). These concentrations are 2-4 times lower then those calculated from olivine-spinel geothermometer (940 ± 170 ppm) [1] and obtained by partitioning experiments (755 ± 25 ppm) [3] at temperature of interest.

High rate diffusion of Al in S.C.O. and forsterite was obtained: $\log D_{Al/Fo} = -15.6 \div -13.2$ (m^2/s) and $\log D_{Al/Ol} = -15.1 \div -14.4$ (m^2/s). No dependence of Al diffusion rate on oxygen fugacity has been observed. The rate of Al diffusion was strongly controlled by activity of major cations (Si, Mg): there are 2 order of magnitude difference between diffusion coefficients of Al in forsterite in low and high silica activity experiments: $\log D_{Al/Fo(a)} = -15.5 \pm 0.1$ (σ) (buffer *a* with activities of $a_{SiO2} = 0.01$ and $a_{MgO} = 1.00$) compare to $\log D_{Al/Fo(c)} = -13.3 \pm 0.1$ (σ) (buffer *d* with activities of $a_{SiO2} = 0.58$ and $a_{MgO} = 0.14$). This difference suggests that the mechanism of Al substitution into the olivine lattice requires an ochtohidral site vacansy.

[1] Wan, et. al (2008) *American Mineralogist* 93, 1142-1147; [2] Spandler & O'Neill (2010) *Contrib Mineral Petrolr* 159, 791-818; [3] Agee & Walker (1990) *Contrib Mineral Petrol* 105, 243-254.

https://doi.org/10.1180/S0026461X00006502 Published online by Cambridge University Press

The characteristic of lithology and facies and reservoir of volcanic rock in Songliao Basin, China

ZHUO SHENGGUANG[1]*, WANG XIANBIN[2] AND YANG GUIFANG[3]

[1] Zhuo Shengguang,Northeast University at Qinhuangdao, China (*correspondence: zoe200200@163.com)
[2]Key Lab of Petrol Resources Research, CAS, Lanzhou (xbwang@lzb.ac.cn)
[3]Northeast Petroleum University at, Qinhuangdao, China (sgzhuo@sina.com)

Yingcheng formation is rich in volcanic rock.in Songliao Basin,China.Volcanic lithofacies consists of eight types; such as fallout facies, effusion facies, base surges facies, pyroclastics flow facies, lahar facies, eruption-sedimentary facies,sub-volcanic rock facis and sub-explosive breccia facies. Volcanic apparatus make up of layered volcano, micro-shield volcano and cone volcano. Lithology of volcanic rock is mainly middle acid volcanic rock (dacite, rhyolite, middle acid brecciated tuff and tuff), belonging to the calc-alka-line series of subalkaline series. The eruptive and overflow facies have better reservoir capacity, the reservoir capacity of volcanic rocks has largely been affected by volcanic condensation diagenesis, tectonism, solution and fluid activity.the volcanic rocks reservoir commonly with the porosity of 6.3% ~ 10.8 % and permeability of about $0.55\times10^{-3}\mu m^2$ ~ $122.0\times10^{-3}\mu m^2$.The most of effective reservoir are the upper phase or external phase of volcanic facies belts, usually being layers or thin layers of 10-20m.The pores of volcanic reservoir could be classified into four types: 1) primary pores of original rocks, 2) diagenetic pores, 3) diagenetic fractures, 4) secondary tectoclases and weathered fractures. Types 2) and 3) are the most effective reservoir space which were formed in volcanic eruption process of cooling and aftercooling.

U-Pb age, geochemical and Hf-O isotopic constraints on magma source of the I-type calc-alkaline Baimaxueshan Batholith (SW China): Implications for crustal recycling at a convergent margin

J.-W. ZI[1,2]*, P.A. CAWOOD[1,3], W.-M. FAN[2], E. TOHVER[1], Y.-J. WANG[2] AND T.C. MCCUAIG[1]

[1]School of Earth and Environment, University of Western Australia, Crawley, WA 6009 Australia (*correspondence: zijianw@gmail.com)
[2]Guangzhou Institute of Geochemistry, Chinese Academy of Sciences, Guangzhou 510640, China
[3]Department of Earth Sciences, University of St. Andrews, KY169AL, Fife, Scotland, UK

The late Permian to Tiassic is a critical period of the development of the eastern Paleo-Tethys, and corresponds with ocean closure and arc accretion onto the margin of Asia. Mafic enclaves and host granitoids from the Baimaxueshan batholith within the Sanjiang Orogen, SW China, document the tectonomagmatic history of accretion. SHRIMP U-Pb analyses on zircons from the mafic enclaves and host granitoids bracket their crystallization ages into the range of ca. 253-248 Ma, and establish that the mafic and felsic magmas were coeval. The granitoids have calc-alkaline, metaluminous I-type character, and show features of magma mixing between mafic and felsic melts. Whole-rock elemental and Sr-Nd isotopic systematics are compatible with an infracrustal origin for the felsic melt, whereas the mafic enclaves may represent relicts of magmas derived from partial melting of subduction-modified ancient lithospheric mantle triggered by fluids/melts released from the descending slab. The elevated *in situ* zircon $\delta^{18}O$ values shown by both the mafic enclaves (9.23 ± 0.2‰ (VSMOW)) and host rocks (8.70 ± 0.09‰) require a considerable input of high-$\delta^{18}O$ supracrustal components through subduction or underthrusting to the sub-arc mantle wedge, which also explains the enriched Sr-Nd and zircon Hf isotopic ratios ($\varepsilon_{Hf}(t)$ = -10 ± 1) displayed by the enclave samples. This together with zircon Hf depleted mantle model ages (T_{DM}^{C}= 1.53 to 2.52 Ga) peaked in the Mesoproterozoic imply that crustal growth processes largely involved reworking of pre-existing lithosphere rather than accretion of juvenile asthenosphere-derived materials.

https://doi.org/10.1180/S0026461X00006502 Published online by Cambridge University Press

Application of lithogeochemistry for regional scale mapping of geothermal prospectivity in Sabalan volcano, North West of Iran

M. ZIAEI, M.ZIAII, A.KAMKAR AND M. ASGHARI

Faculty of Mining and Geophysics, Shahrood University of Technology; Shahrood, Iran, (mziaii@shahroodhut.ac.ir)

Many different techniques are suggested for geothermal (convective systems) exploration including geological mapping, magnetic, gravity, hot spring, geochemical sampling, seismic and well logging methods. Geothermal systems are usually characterized by indicative geological features that may not be implied or easily be described by only one analytical method. The methodology presented here provides combined applications of several different methods in order to generate regional scale mapping of geothermal prospectivity in Sabalan volcano located in North West of Iran. The relation of the geothermal occurrences (18 geothermal occurrences used as training points) to evidential maps is assessed by means of the logistic regression as a data driven method. Six evidential maps were used derived from maps of (1) gravity, (2) magnetic, (3) geology, (4) zone proximal to hydrothermal alteration, (5) zones proximal to faults, (6) geochemical multiplicative zonality (V_z). The first five evidential maps are selected based on previous research works. Sixed evidential map is selected based on geochemical zonality anomaly.

According to geochemical studies As, Sb, Hg, Bi and B are typically enriched in geothermal areas. Thus V_z can be introduced as a geochemical evidential map for geothermal exploration.

At least seven sub-areas (in which two areas have been explored and exploited) can be recommended for follow up exploration work based on favorability map. The results indicated that, integration of V_z evidential map with other maps used as spatial evidence is important in filtering-out false selected areas.

[1] Carranze, E.J.M., Wibowo, H., Barritt, S.D. and Sumintadireja, P. (2008) Spatial data analysis and integration for regional-scale geothermal potential mapping, West Java, Indonesia, *Geothermics*, pp.267-299.

Geochemistry of mantle microxenoliths from Zagadochnaya kimberlite (Yakutia, Russia)

L. ZIBERNA[1]*, P. NIMIS[1], A. ZANETTI[2], N.V. SOBOLEV[3] AND A. MARZOLI[1]

[1]University of Padua, Department of Geosciences, Italy (*correspondence: luca.ziberna@studenti.unipd.it; paolo.nimis@unipd.it, andrea.marzoli@unipd.it)
[2]IGG-CNR, Pavia, Italy (alberto.zanetti@unipv.it)
[3]V.S. Sobolev Institute of Geology and Mineralogy, Novosibirsk, Russia (sobolev@uiggm.nsc.ru)

The Zagadochnaya kimberlite is a barren type-II kimberlite, which contains Cr-diopside, pyrope garnet (Grt) and spinel xenocrysts, as well as eclogite and grospydite xenoliths [1], but no discrete peridotite xenoliths. We have investigated Grt grains and associated minerals. Some Grts (groups A, B) and associated Cr-diopsides (similar to subgroups IIa, IIb of [2]) show evidence of an early metasomatic event and variations in LHREE/HREE ratios compatible with a model of percolative fractional crystallization of kimberlite melts [3]. Other Grts (group C) exhibit strongly sinusoidal CI-normalized REE patterns, typical for cratonic Grt-peridotites produced by metasomatism of strongly refractory harzburgites. Most of group B and C Grts show secondary domains rich in Cr-diopside + Cr-spinel ± phlogopite. In these domains the Grts are (Ca, Cr)-depleted, are enriched in almost all incompatible elements, and show humped CI-normalized REE patterns (max at Eu). Low Ti/Zr ratios (~ 10) and presence of phlogopite in these domains suggest an origin by reaction with a melt of type-II kimberlite affinity. Based on Ca concentration profiles across Grt zoning, this late-stage event took place less than 10^4 years before the Zagadochnaya kimberlite eruption, i.e. it was probably related to the same magmatic stage of the host kimberlite.

[1] Sobolev *et al*. (1968) *J Petrol* **9**, 253-280. [2] Nimis *et al*. (2009) *Lithos* **112**, 397-412. [3] Burgess & Harte (2004) *J Petrol* **45**, 609-634.

https://doi.org/10.1180/S0026461X00006502 Published online by Cambridge University Press

Silicon and oxygen isotopes: The maturation of lacustrine diatoms

K. ZIEGLER[1]*, J.P. DODD[2], Z. D. SHARP[2], A.J. BREARLEY[2] AND E.D. YOUNG[1]

[1]Department of Earth and Space Sciences & Institute of Geophysics and Planetary Physics, University of California, Los Angeles, CA 90095, USA. (*correspondence: kziegler@ess.ucla.edu).

[2]Department of Earth and Planetary Sciences, University of New Mexico, Albuquerque, NM 87131, USA.

Oxygen and silicon isotope values of recent (antemortem, post-mortem) and Pleistocene lacustrine diatoms from the Valles Caldera (New Mexico) provide the opportunity to study 420 ka of opal maturation at the same location.

The $\delta^{18}O$ (SMOW) values, obtained by laser-fluorination [1], indicate significant reequilibration, with an increase in $\delta^{18}O$ value from <22‰ to >29‰ within 0.5 yrs after death. This is consistent with growth under oxygen isotopic disequilibrium followed by post-mortem equilibration with lake water. While no structural changes go with the alteration, differences in element compositions also imply exchange between water and diatom. Wholesale reequilibration of $\delta^{18}O$ ratios requires Si-O bond breaking. We measured the $\delta^{30}Si$ values of the same diatoms to see if Si also undergoes isotope exchange. $\delta^{30}Si$ values were obtained by MC-ICPMS [2].

The $\delta^{30}Si$ values (NBS-28) of all ante-mortem and post-mortem diatoms range from -1.0 to -2.6‰, and -0.4 to -1.9‰, respectively. A specific subset of diatoms was collected in spring, and the same population sampled 0.5 and 1.5 years post-mortem. The $\delta^{30}Si$ values increase from -2.4 to -1.9 to -0.4‰, indicating a possible maturation trend. The large ante-mortem range can also be explained by variable relative inputs from processes affecting the $\delta^{30}Si$ values of lake water (diatom [3] and clay [4] formation removes ^{28}Si from water).

Middle Pleistocene (interglacial) lacustrine diatoms from the Valles Caldera have even higher $\delta^{30}Si$ values of +0.3 to +0.7‰. The trend from low to high $\delta^{30}Si$ ratios mimics the $\delta^{18}O$ changes (at a smaller scale). Interglacials correlate with more positive $\delta^{30}Si$ values in marine diatoms [5]. We infer that Pleistocene Valles Caldera diatoms had higher initial $\delta^{30}Si$ values than modern ones, and additionally that exchange processes during burial caused further opal maturation.

The combined silicon and oxygen isotope study of such a system improves our understanding of the potential for using Si isotopes as paleoclimate proxies.

[1] Dodd & Sharp (2010), *GCA* **74,** 1381-1390. [2] Ziegler *et al*. (2010), *EPSL* **295**, 487-496. [3] De La Rocha *et al*. (1997), *GCA* **61**, 5051-5056. [4] Ziegler *et al*. (2005), *GCA* **69,** 4597-4610. [5] De La Rocha *et al*. (1998), *Nature* **395**, 680-683.

Silicon and oxygen isotope values of cherts and their precursors

K. ZIEGLER[1,2]*, J. MARIN-CARBONNE[1], K.D. MCKEEGAN[1] AND E.D. YOUNG[1,2]

[1]Department of Earth and Space Sciences, University of California, Los Angeles, CA 90095, USA. (*correspondence: kziegler@ess.ucla.edu).

[2]Institute of Geophysics and Planetary Physics, University of California, Los Angeles, CA 90095, USA.

We measured $\delta^{30}Si$ and $\delta^{18}O$ ratios in two sets of recent cherts and their precursors in order to evaluate the use of cherts as proxies for environmental conditions at their formation, and to constrain diagenetic transitions. This work has implications for models for Archean cherts formation.

In a handsample from the Miocene Monterey Formation [1, 2], both cristobalitic chert and biogenic, marine opal-A precursor are present. Magadi chert is modern, inorganic, quartzose chert formed from chemically precipitated magadiite [3, 4]. Both precursor-to-chert transitions are due to dissolution-precipitation processes. Monterey chertification is due to later diagenetic water [1, 2], and Magadi chertification occurs at the surface in the same system as magadiite [3, 4].

$\delta^{30}Si$ values were analyzed by MC-ICPMS (Neptune™), $\delta^{18}O$ values of cherts by ion microprobe (Cameca 1270), and precursor $\delta^{18}O$ values were taken from literature [1, 3].

The $\delta^{18}O$ values of the Monterey opal (37‰) and chert (28-34‰) suggest temperatures of 15°C and 48±8°C, respectively [1]. The $\delta^{30}Si$ values of the chert and opal are 0.0‰ and 1.4‰, respectively. Diatom formation increases the $^{30}Si/^{28}Si$ of the aqueous phase [5], and high diatom $\delta^{30}Si$ values are expected in highly productive oceans. Later chert-forming diagenetic water, equilibrated with Monterey Shale [1], is expected to have more negative $\delta^{30}Si$ values [6], and explains the lower $\delta^{30}Si$ value of the chert.

In contrast, the inorganic magadiite and magadi chert have similar $\delta^{18}O$ (33-38‰ [3, 4] and 38‰, respectively) and $\delta^{30}Si$ values (-0.2 and -0.5‰, respectively). The isotopic similarity demonstrates that no fractionation attends this chertification, as both phases form from the same silicon and oxygen source (hot springs [3, 4]).

$\delta^{30}Si$ ratios of cherts record the last chertification event, which can imprint different $\delta^{30}Si$ values onto its precursor. This needs to be considered for paleoclimate reconstructions.

We thank Jim Boles (UCSB) for providing the samples.

[1] Murata *et al*. (1977), *AJS* **277**, 259-272. [2] Pisciotto (1981), *Sedimentology* **28**, 547-571. [3] O'Neil & Hay (1973), *EPSL* **19**, 257-266. [4] Behr & Röhricht (2000) *Int J Earth Sci* **89**, 268-283. [5] De La Rocha *et al*. (1997), *GCA* **61**, 5051-5056. [6] Ziegler *et al*. (2005), *GCA* **69,** 4597-4610.

https://doi.org/10.1180/S0026461X00006502 Published online by Cambridge University Press

On the multitude of niches for bacteria and archaea in an acidic biofilm

S. ZIEGLER[1], K. DOLCH[1], J. MAJZLAN[2] AND J. GESCHER[1]*

[1]Department of Microbiolgy, Albert-Ludwigs University Freiburg, Germany (*correspondence: johannes.gescher@biologie.uni-freiburg.de)
[2]Department of Mineralogy, Friedrich Schiller University Jena, Germany

We studied a microbial snottite biofilm in an abandoned pyrite mine. The organisms that build up the biofilm grow at pH about 2.3 and sulphate concentrations of up to 200 mM. The microorganisms are dependent on the oxidative dissolution of pyrite as the primary energy source and on CO_2 as the primary carbon source. We assessed the microbial diversity in the consortium using restriction fragment length polymorphism and subsequent sequencing. As expected, organisms belonging to the genera *Leptospirillum* represented the majority of bacterial species. Interestingly, we could furthermore identify archaeal sequences that are most closely related to the ARMAN (Archaeal Richmond Mine Acidophilic Nanoorganisms) group [1] as well as to so far uncultured members of the Thermoplasmatales. Using oxygen profiling we determined that the high oxygen demand of the microorganisms lead to a drop from 100% to 0% oxygen within 700 μm. Hence the internal part of the biofilm seems to be anoxic. Interestingly, we could show that bacteria populated the biofilm mostly at the oxygenated vicinity. MAR FISH experiments, using $^{14}CO_2$ revealed that this is also the center of primary production. However, archaea populated the anoxic core only. Currently, we investigate the archaeal niche in the biofilm.

[1] Baker *et al*. (2006) *Science* **314**: 1933-1935.

Developing a comprehensive approach to chamber studies of secondary organic aerosol formation

P. J. ZIEMANN*, A. MATSUNAGA, S. AIMANANT, G. YEH AND Y. B. LIM

Air Pollution Research Center, University of California, Riverside, CA 92521, USA (*correspondence: paul.ziemann@ucr.edu)

Much of what is currently understood about the chemical and physical processes involved in the atmospheric oxidation of organic gases and particles and the formation of secondary organic aerosol (SOA) has been obtained from experiments carried out in environmental (smog) chambers. Achieving a level of understanding from such studies that is sufficient for extrapolating results to the atmosphere (with confidence) and the development of accurate models of SOA formation requires the acquisition of detailed information on a variety of gas and particle properties and processes, such as gas and particle-phase reaction kinetics, gas and particle composition, particle phase, compound vapor pressures, and gas-particle-wall interactions. Obtaining such data is a challenge, but in this talk I will show examples of studies carried out in our laboratory on selected aerosol-oxidant and VOC-oxidant systems in which this goal is close to being achieved. I will demonstrate that by using a diverse array of measurement techniques including mass spectrometry, nuclear magnetic resonance spectroscopy, gas and liquid chromatography, spectrophotometry (with and without compound derivatization), traditional elemental analysis, pycnometry, temperature-programmed thermal desorption, and scanning mobility particle sizing it is possible to develop full, quantitative mechanisms of organic gas and aerosol chemical reactions and models of SOA formation. Doing so, however, requires a more comprehensive approach to chamber studies that acknowledges the obvious: “The atmosphere does not have walls.”

https://doi.org/10.1180/S0026461X00006502 Published online by Cambridge University Press

The hafnium and neodymium isotopic composition of seawater in the tropical Atlantic Ocean

M. ZIERINGER[1]*, T. STICHEL[1,2] AND M. FRANK[1]

[1]IFM-GEOMAR, Wischhofstrasse 1-3, 24148 Kiel, Germany (*correspondence: mzieringer@ifm-geomar.de)
[2]SOEST, University of Hawaii 1680 East-West Rd, Honolulu, HI 96822, USA

The combination of radiogenic isotopes of hafnium (Hf) and neodymium (Nd) has been used to investigate present and past changes of ocean circulation patterns and continental weathering regimes. We present the first combined full water column Hf and Nd isotopic compositions and concentrations in seawater of the western Atlantic Ocean, as well as Hf and Nd isotopic and concentration data in surface waters of the tropical Atlantic Ocean between the Canary Islands and the northeastern coast of Brazil. Samples were collected during GEOTRACES cruise A11 (Meteor M81/1) from Las Palmas (Canary Islands) to Port of Spain (Trinidad and Tobago) in spring 2010.

Hf concentrations in surface waters range between a maximum of 0.67 pmol/kg north of 20°N off the coast of NW Africa and in the area of the Canary Islands and a minimum of 0.20 pmol/kg off the northeastern coast of Brazil. Surface waters with reduced salinities (< 33.6 psu) due to freshwater input by the Amazon river also show low Hf concentrations. Nd concentrations show a similar distribution pattern with a maximum off the coast of Mauritania (27 pmol/kg) and a minimum in the Amazon plume (14 pmol/kg). Elevated concentrations provide evidence of inputs from partial dissolution of dust from the Sahara region and from ocean island wheathering, which is also reflected in more radiogenic Hf and Nd isotope compositions [1]. Low concentrations of Hf and Nd in the Amazonas plume are most likely caused by particle scavenging induced by high productivity.

Deep-water samples show the highest Hf concentrations in UNADW in the area of the Canary Islands (0.93 pmol/kg), as well as in UNADW in the western basin. Nd concentrations range between a minimum of 12 pmol/kg in SACW and a maximum of 34 pmol/kg in AABW. Lower Hf concentrations in LNADW and AABW indicate an oceanic residence time of Hf shorter than that of Nd.

The isotopic distribution of Hf and Nd in the same samples reflect inputs via dust, the Amazon river, and weathering inputs from the volcanic Canary islands, as well as intermediate and deep water mass mixing.

[1] Rickli *et al*. (2009), *EPSL* **280**, 118-127.

Connection of atmospheric stability and aerosol and gaseous polutants concentration

N. ZIKOVA[1,2]* AND V. ZDIMAL[1]

[1]Department of Aerosols and Laser Studies, Institute of Chemical Process Fundamentals of the ASCR, Prague, Czech Republic (*correspondence: zikova@icpf.cas.cz)
[2]Department of Meteorology and Environment Protection, MFF UK, Prague, Czech Republic

Our aim is to find suitable criteria to asses an atmospheric stability without direct measurements in order to estimate relationships between meteorological conditions and concentration of aerosol particles (measured by SMPS) and gaseous pollutants (O_3, NO_2 and SO_2). An aerological method, a synoptical method and NWP models' CAPE values are applied.

Aerological method and CAPE were found to be suitable methods for description of atmosperic stability. Synoptical method shows mainly origin of air masses.

The strongest relationships between aerosol particles and stability was found for acumulation mode particles, weaker for particles under 50 nm in diameter.

A negative correlation for acumulation mode particles shows "dilution" of atmosphere during unstable conditions, whereas during stable conditions the aerosol acumulates.

Similar relatioship is between gaseous polutants and stability (apart from concentrations of NO_2).

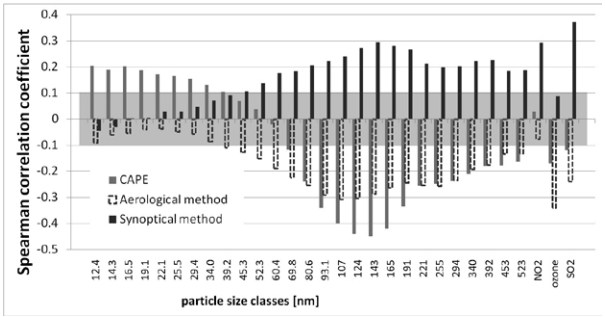

Figure 1: Dependencies between aerosol concentration in different sizes, gaseous pollutants concentrations and atmospheric stability described by the three tested methods.

[1] Zikova N. (2010) *WDS'10 Proceedings of Contributed Papers: Part III – Physics*, Matfyzpress, pp. 97–102. Ack: GACR P209/11/1342 and SVV-2011-263308.

https://doi.org/10.1180/S0026461X00006502 Published online by Cambridge University Press

Possible rhenium fractionation during standard Re-Os dissolution and chemical separation procedures

A. ZIMMERMAN[1], S. GEORGIEV[1,2], G. YANG[1], H. STEIN[1,2] AND J. HANNAH[1,2]

[1]AIRIE Program, Colorado State University, USA
[2]Geological Survey of Norway, 7491 Trondheim

A recent curiosity-driven experiment revealed surprising apparent fractionation of rhenium isotopes during standard Re-Os chemical procedures for Carius tube digestion and elemental separation. A non-standard $^{185}Re/^{187}Re$ ratio of ~0.602 was measured from a standard Re solution after Carius tube digestion and anion exchange chromotography. A replicate produced a similar, though not identical ratio. These surprising results led to a series of quantitative tests to identify procedure(s) that may have led to Re fractionation.

In the original experiments, Re standard solution, Os standard solution, and inverse *aqua regia* were digested in Carius tubes at 250 ºC for 12 hours. The Os was extracted using chloroform-HBr solvent extraction. The isolated Os underwent microdistillation and was measured for its isotopic composition (IC). Os IC ratios matched expected values. After solvent extraction, the Re was collected via anion exchange chromotography and purified using a single bead clean-up. The final measured $^{185}Re/^{187}Re$ was 0.601608 versus the expected value of 0.597393. The replicate yielded an IC of 0.599062. Additional tests of Re standard solution loaded directly onto exchange columns and directly onto single beads yielded similarly elevated ratios.

Given such results, a more detailed experiment excluded the Carius tube digestion and loaded diluted Re standard solution directly on the anion exchange columns. One mL fractions were collected as the Re eluted from the column. Half of each 1 mL aliquot was loaded directly onto Pt filaments for IC measurements whereas the second half underwent single bead cleaning prior to IC measurement. Re was only found in the first three of seven 1 mL splits. Only the third 1 mL fraction produced ratios significantly different than the expected ratio. In all cases, the single bead-treated and straight-off-the-column Re IC ratios matched, thereby showing that Re fractionation does not occur during the single bead clean-up procedure.

Given the apparent lack of Re fractionation in the most recent experiment, which bypassed the Carius tube step, a final experiment utilizing the Carius tube digestion along with step-wise column collection is being conducted. This experment should replicate the orignal inquiry and also help identify if and when Re fractionation occurs.

Risk element sorption in soil amended by urban particulate matter

D. ZIMMERMANNOVÁ[1], J. SZÁKOVÁ[1]*, M. KOMÁREK[1] AND J. SYSALOVÁ[2]

[1]Czech University of Life Sciences, CZ-165 21 Prague 6, Czech Republic (*correspondence: szakova@af.czu.cz)
[2]Institute of Chemical Technology, CZ-166 28 Prague 6, Czech Republic (Jirina.Sysalova@vscht.cz)

Introduction

Our previous experiment showed that although the element contents in dust samples exceeded significantly those in soil, the element contents in plants were not affected by single-rate soil amendment with the rural dust sample [1]. Therefore, we tested the potential effect of urban particulate matter (PM) amendment to two soils differring in their physicochemical parameters (rate: 0.6 g of PM per 1 kg of the soil) on sorption characteristics described by Freundlich and Langmuir isotherms.

Soil	E	K_L	S_{max} (mmol/kg)
Chernozem	0.978	15.6	86.1
Chernozem+PM	0.959	13.6	81.4
Fluvisol	0.963	1.93	137
Fluvisol+PM	0.939	1.09	165

Table 1. Parameters derived from the fitting of the sorption isotherms of Cd with the Langmuir equation

Discussion of the results

Whereas the Freundlich isotherms did not indicate any effect of PM addition to the soils, the Langmuír isotherm allowed us to estimate the potential behavior of the PM in the soil. The results for Cd are summarized in Table 1. The PM added to the Chernozem did not lead to substantial changes in sorption characteristics. On the contrary, the presence of PM in the Fluvisol increased the number of potential sorption sites in the soil. However, the results of the approximation showed a lower affinity of Cd for the Fluvisol and a better stability and a lower bioavailability of Cd in the Chernozem. The results are supported by the decreasing Cd contents in both lettuce and chard biomass growing in PM amended Fluvisol compared to the unamended one.

[1] Száková, J., Sysalová, J., Tlustoš, P.: (2005): *Plant Soil Environ*. **51**, 376. Financial support for these investigations was provided by GAČR Project No. 521/09/1150.

https://doi.org/10.1180/S0026461X00006502 Published online by Cambridge University Press

From Archean to Cambrian: Isotopic crustal evolution of the Borborema Province, NE Brazil

S.A. ZINCONE[1]*, E. WERNICK[2] AND T.J.S. SANTOS[1]

[1] Instituto de Geociências, UNICAMP, Campinas, SP, Brazil (*correspondence: teozincone@gmail.com)
[2] Instituto de Geociências, UNESP, Rio Claro, SP, Brazil

Crustal accretion occurs mainly by the input of calc-alkaline granitoids in the cores of pericontinental and intraoceanic orogens. The added magmas are mainly hybrid, a mixture of a mantle derived component with older crustal rocks as the result of the underplating of major amounts of mafic magma beneath the continental crust. The Santa Quitéria Batholith, Borborema Province, is a good example of the mixing of a juvenile Brasiliano component with older, mainly Paleo-proterozoic, crustal material [1]. One consequence of this growth process must be a systematic change in the crustal isotopic composition through time. This assumption is confirmed by 307 Sm-Nd data for Archean, Paleo- and Neoproterozoic rocks from the northern Borborema Province [1-7] which show a systematic change of the $^{144}Nd/^{143}Nd_{(t)}$ values with time.

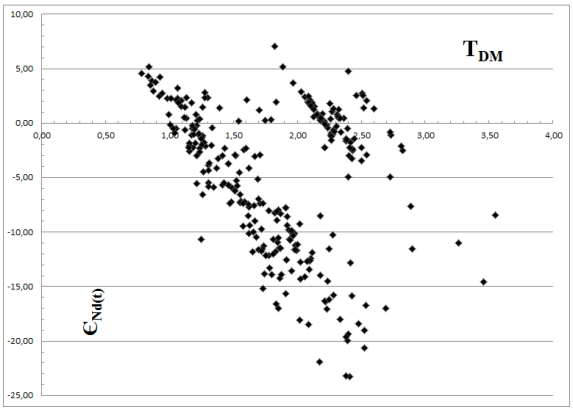

[1] Wernick *et al*. (2011) *MinMag*, this volume. [2] Fetter (1999) Ph.D. thesis, KU, USA, 164p. [3] Castro (2004) Ph.D. thesis. USP, Brazil, 221 p. [4] Arthaud (2007) Ph.D. thesis. UNB, Brazil, 164p. [5] Martins (2008) *Gondwana Research*, **15**, 71-85. [6] Torres (2006) *Rev. de Geologia*, **19(2)**, 163-176. [7] Nogueira (2004) Ph.D. thesis. UNESP, Brazil, 123p.

Plastic deformations in zircon and their influence on its chemical composition

T.F. ZINGER[1], N.S. BORTNIKOV[2] AND E.V. SHARKOV[2]

[1]IPGG RAS, St-Petersburg, Russia (tzinger@mail.ru)
[2]IGEM RAS, Moscow, Russia (bns@igem.ru; sharkov@igem.ru)

We studied 150 grains of zircon from 8 gabbro samples, dragged at 4 sites in axial part of the MAR, Markov Deep, 6ºN, during 10th cruise of R/V "Academic Ioffe" (2001-2002) and 22nd cruise of R/V "Professor Logachev" (2003). This part of the MAR represents typical oceanic core complex (OCC), where altered lower crustal gabbros and serpentinized mantle peridotites expose on seafloor. These rocks were undergone by different tectonic deformations, including plastic flowage. The zircon in gabbros along with host rocks were undergone by plastic creep at 815 to 680ºC (Ti-in-zircon thermometry).

During deformations zircon was enriched by diversity of rare elements (U, Th, Hf, Pb, P and Y) and REE. We suggest that it was linked both with appearance of deformation-related crustal-plastic microstructures in zircon, which enhanced diffusion of these components, and circulation of intergranular fluid as demonstrated processes of delution and redeposition of the zircon material with appearance of secondary small pyramidal zircons on another side of the crystal. Nature of this high-temperature fluid is not clear yet: it can be residual fluid, formed under solidification of host-gabbros, or result of involving of fluids, circulated in upper oceanic lithosphere, under it heating by these intrusions; most likely both factors were setting in motion. Introducing U, Th and Hf into zircon crystals can change their original isotopic systematics and influence on results of their isotopic dating.

https://doi.org/10.1180/S0026461X00006502 Published online by Cambridge University Press

Chemical models for formation of clay-rich layered rocks in the Mawrth Vallis region, Mars

M.YU.ZOLOTOV[1]* AND M.V.MIRONENKO[2]

[1]School of Earth and Space Exploration, Arizona State University, Tempe, AZ 85287, USA (*correspondence: zolotov@asu.edu)

[2]Vernadsky Institute of Geochemistry and Analytical Chemistry, Russian Academy of Sciences, 19 Kosygin Str., Moscow 119991, Russia

Clay minerals have been detected in ancient martian terrains with the near-infrared orbital spectroscopy [1,2]. In the Mawrth Vallis region, a prospective landing site for the MSL rover in 2012, minerals are observed within the following stratified sequence of layered rocks (from the top): silica and kaolinite, montmorillonite-like Al-rich clays, a Fe^{2+} phyllosilicate, Mg/Fe smectites, and sulfates [2-6]. We use three numerical models to explore a formation of these rocks through alteration of a fragmented basaltic material by a downward percolation of H_2SO_4-rich fluids. One model assumes a decrease in the solution to rock ratio with depth. In another model, the downward fluid migration is considered. In both models, fluids reach chemical equilibrium with rocks. In the third model, kinetics of mineral dissolution is considered along with fluid percolation. The modeling is performed for 0 ºC and pressure from 0.006 to 1 bar. The system was either open or closed with respect to CO_2 and O_2.

The modeling reproduces the observed silica-kaolinite-montmorillonite-smectite sequence of dominated minerals. In the models, the sequence reflects neutralization of fluids with depth. Open system models also lead to formation of goethite and/or hematite, and carbonates form in association with smectites (saponite). In closed systems, zeolites and Fe^{2+}-chlorites occur with smectites, and Fe^{2+}-chlorite rich rocks form between layers rich in montmorillonite and smectites. The latter result is consistent with observations, though the upper part of the martian profile also agrees with an open-system acid alteration. Modeled Ca sulfates coexist with clay minerals, and more soluble sulfates could form through evaporation of neutralized fluids accumulated in the lower part of the stratigraphic sequence.

[1] Poulet *et al*. (2005) *Nature* **438**, 623-627. [2] Mustard *et al*. (2008) *Nature* **454**, 305-309. [3] Wray *et al*. (2008) *Geophys. Res. Lett*. **35**, L12202. [4] Bishop *et al*. (2008) *Science* **321**, 830-833. [5] McKeown *et al*. (2009) *J. Geophys. Res*. **114**, E00D10. [6] Wray *et al*. (2010) *Icarus* **209**, 416-421.

Study on the phase equilibrium of the quaternary system Cd^{2+}, K^+, $Na^+//SO_4^{2-}$-H_2O at 298 K

FANG ZOU[1], HUANG YI[1,2]*, NI SHIJUN[2] AND ZENG YING[3]

[1]Department of Geochemistry, Chengdu University of Technology, Sichuan, PRC (*correspondence: huangyi@cdut.cn)

[2]Applied Nuclear technigues in Groscience Key Laboratory of Sichuan Proviance, PRC

[3] College of Materials and Chemistry & Chemical Engineering, Sichuan, PRC

Solid- Liquid Equilibrium of quaternary system Cd^{2+}, K^+, $Na^+//$ SO_4^{2-}-H_2O at 298 K were studied by an isothermal solution saturation method. Experimental results indicate that there are five univariant curves E_1F_1, E_1F_4, E_1E_2, E_2F_2 and E_2F_3, two invariant points E_1, E_2 and four crystallization fields in the quaternary system. The system belongs to a quaternary system, and there is a double salt ($Na_2SO_4{\cdot}3K_2SO_4$) existing. The crystallization zones of equilibrium solid phases are K_2SO_4 ($E_1F_1MF_4$ field), $Na_2SO_4{\cdot}3K_2SO_4$ ($E_1E_2F_3F_4$ field), $Na_2SO_4{\cdot}10H_2O$ ($E_2F_2AF_3$ field), and $CdSO_4{\cdot}H_2O$ ($E_2F_1BF_2$ field), respectively. The composition of the invariant point E_1 is K_2SO_4, $Na_2SO_4{\cdot}3K_2SO_4$ and $CdSO_4{\cdot}H_2O$, respectively. The composition of the invariant point E_2 is $Na_2SO_4{\cdot}3K_2SO_4$, $Na_2SO_4{\cdot}10H_2O$ and $CdSO_4{\cdot}H_2O$, respectively. The physico-chemical properties of solution in the quaternary system show regular changes along with the increased cadmium concentration. $CdSO_4$ possessed the highest solubility among those three salts, which means a strong transfer of Cd ion and a high pollution risk of soil environment.

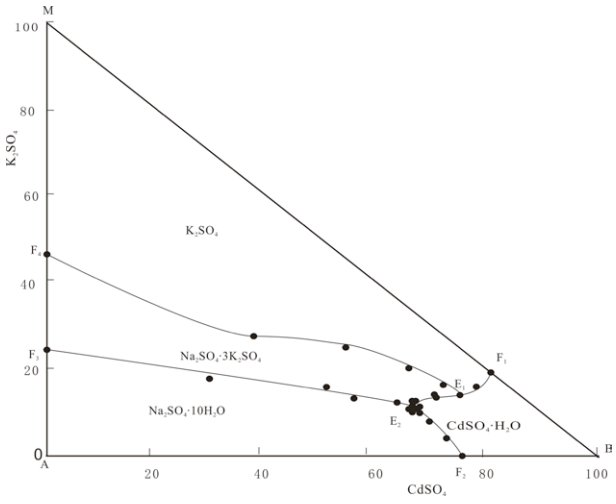

https://doi.org/10.1180/S0026461X00006502 Published online by Cambridge University Press

Geochemistry and metallogenesis of fluid in Liuju sandstone-bound copper deposit, Dayao, Yunnan, China

ZOU HIAJUN[1,2,*], HAN RUNSHENG[2], YAO ZHIHUA[1] AND LIU MENGQIONG[3]

[1]Yunnan Copper Industry Group, Kunming, Yunnan, P.R.China 650051 (*correspondence: zouhaijunlmq@yahoo.com.cn)
[2]Kunming University of Science and Technology, Kunming, Yunnan, P.R.China 650093
[3]Yunnan Architecture Engineering Design Institute, Kunming ,China P.R.China, 650041

11 typical samples are purple or bleached sandstone and ores, from K_2ml_1 (main orebody hosting bed), K_2ml_2, K_2md and K_1p in Liuju Sandstone-bound Copper Deposit, Dayao, Yunnan, China. Quartz and minor calcite were used for making fluid inclusion tests.

The original inclusions mainly are in vapor-liquid phase. Their generation period features are apparent. The original and secondary inclusions in bleached sandstone respectively represent main metallization stage (forming stratiform chalcocite orebody) and reforming stage. The ones in quartz veins respectively represent minor metallization stage (forming veiny chalcopyrite orebody) and later reforming stage. The ore-forming fluid could be two medium-low salinity fluid of organic material-bearing, medium-temperature to medium-low- temperature, reducing fluid and a little organic material-bearing, oxidizing fluid. 70% uniform temperature numbers of fluid inclusions assemble between 200°C and 100°C. The fluid belongs to NaCl-H_2O system, in which, beside agglutinates, the salinity is less than 12%. The component test results of the original quartz inclusions by La-ICP-MS show the fluid in main metallization stage is of H_2O-SO_2-CO_2-CH_4 (C_3H_8-C_2H_6) - HSO_4^- - HCO_3^- type, and the fluid in secondary metallization stage is of H_2O-SO_2-CO_2-N_2-CO-CH_4- HSO_4^- type.

Research results indicate the fluid metallogenesis mode may be described as: the forming and reforming movements of the Daxueshan Anticline provided power and energy (heat energy) for metallization, which drove deep-seated organic matter-bearing and reducing fluid to go up and cycle, with superficial oxidizing infiltrating fluid, to extract ore-forming material from the source beds. Because of the physical-chemical conditions changing in the high permeability and porosity of sandstone beds at the gently inclined wing of the Anticline, oxidation-reduction reactions occurred in the fluids which led to form the deposit.

Robust aerosol indirect effects inferred from remotely-sensed cloud properties acquired during VOCALS

PAQUITA ZUIDEMA[1], DAVID LEON[2] AND DAVID PAINEMAL[3]

[1]U. of Miami/RSMAS, 600 Rickenbacker Cswy, Miami, FL 33149, USA, (pzuidema@rsmas.miami.edu)
[2] U of Wyoming, Laramie, WY, 82071, USA (leon@uwyo.edu)
[3] U. of Miami/RSMAS, 600 Rickenbacker Cswy, Miami, FL 33149, USA, (dpainemal@rsmas.miami.edu)

One wealth of the VOCALS field experiment in the southeast Pacific stratocumulus region is a unique dataset on cloud properties acquired through a suite of airborne remote sensors. This includes a lidar, a cloud radar and a radiometer providing cloud liquid water paths. All are valuable individually, but in combination form a powerful suite capable of extending aircraft assessments of aerosol-cloud-precipitation impacts beyond what can be done with in-situ measurements. The cloud liquid water path dataset also allows for the statistically-robust examination of thin clouds, which cloud radars and satellites have difficulty characterizing. For this presentation the new cloud liquid water path dataset is described, compared to adiabatically-derived values, and aerosol indirect effects — co-variations with cloud liquid water path, precipitation, and cloud albedos — are assessed. In keeping with the theme session, comparisons to similarly-derived satellite properties will be made to opine on satellite assessments but done on larger spatial scales.

https://doi.org/10.1180/S0026461X00006502 Published online by Cambridge University Press

Effects of grid size in interpolating of geochemical data

RENGUANG ZUO[1,2]

[1]State Key laboratory of Geological Process and Mineral Resources, China University of Geosciences, Wuhan, 430074, China (zrguang@cug.edu.cn)
[2]State Key laboratory of Geological Process and Mineral Resources, China University of Geosciences, Wuhan, Beijing, 100083, China

Grid size is one of important uncertainty sources in interpolating of geochemical data. We explore the grid size how to influence geochemical mapping using a case study located in the western Gangdese belt, Tibet (China). This study area measures about 19,375 km^2 and comprises of 921 stream sediment samples with a density 0.05 sample point per km^2 corresponds to the scale of about 1:500, 000. The selection of grid size is influenced by the density of samples or mapping scale(i.e., The denser the sample points, the larger the scale of mapping, and the smaller the grid size), and the structure of point patterns (i.e., distance between the sampled points, and the range of spatial dependence). Generally, the gird size should be smaller than a given size which makes >95% of the closest point pairs not fall into the same grid. The grid size is also larger than a given grid size because finer grid cell do not make sense as it will be hard to visualize or print them at this scale of work [1]. The resulting of neighbour nearest distance between point pairs shows that the average spacing between the closest point pairs is 2.18 km, and 5% probability smallest distance is 1.09 km, which makes >95% point not fall into the same grid. The original dataset is divided into two parts namely testing dataset and training dataset. The testing dataset contains randomly selected samples, which are 5% of the total number of samples, and the remaining 95% samples are used for interpolating data. Six grid sizes namely 1.1 km, 1.3 km, 1.5 km, 1.7 km, 1.9 km, 2.1 km are selected to interpolate Cu data using inverse distance weighted method (IDW) with the same parameters. The results indicate that 1.7 km is the optimal grid cell size in this study because the interpolating Cu map has the maximum value of standard deviation, and the difference between Cu true value and interpolated value has the lower mean and relative lower standard deviation.

[1] Hengl (2006), *Computers & Geosciences* **32**, 1283-1298.

Technical methods of barriers of near-surface disposal of very low level radioactive waste

RUI ZUO, JINSHENG WANG AND YANGUO TENG

College of Water Sciences, Beijing Normal University, Beijing 100875, China, (zr@bnu.edu.cn)

The caused environmental pollution problems by nuclear are very urgent, any country treats it with caution. Under existed technologies, geological disposal is recognized as the most effective method. For security and efficient, the very low level radioactive waste (VLLW) is separated from the medium-low-level radioactive waste, and the design of the repository could meet the environmental requirements without very strict geological condition, however, the barrier material of the VLLW repository still is key to radioactive waste disposal. A candidate site, which was for the disposal of VLLW in Southwestern China, was built in the terraces of alluvial valley. We focused on the multiple geological barrier system on the near-surface geological disposal. The multiple barrier technology is reflected at natural barriers (natural geological body) and engineering barriers (material). For the absorption of the barrier, batch tests and column experiments methods were applied for the influencing factors and mechanism of adsorption.

The disposal site was on a narrow but long river terraces at the interchange of two rivers, the groundwater table in the site was generally 5-6m. ^{90}Sr were selected as the typical nuclides. The barriers in the wall and bottom of repository (basin-shaped) were selected. The fine particle (d<1mm), which is from the site, was used for the barrier material in the wall, attapulgite mixed with gravel was used for the bottom barriers. The sorption characteristics and influencing fators of ^{90}Sr in the two barrier material were measured by batch tests, results show that the selected fine particle (d<1mm) for ^{90}Sr have a certain adsorption, the orders of distribution coefficient in the 10^2. And from the results, the K_d value of the fine particle and the attapulgite was 40-80 and 100-120, respectively, and there was a great influence of pH value, content of CO_3^{2-}, and initial concentration on sorption. In addition, modified (acid treated, sonicated and baked) attapulgite was researched for the sorption capacity, the concentration of hydrochloric acid at 1M, or ultrasonic time of 10min, or the temperature at 600°C, the adsorption of nuclear improved significantly.

This study is supported by “the Fundamental Research Funds for the Central Universities”.

https://doi.org/10.1180/S0026461X00006502 Published online by Cambridge University Press

Luminescent properties of natural copper and silver iodide

L.A. ZYRYANOVA, N.N. BOROZNOVSKAYA AND K.V. TOLOCHKO

Tomsk State University, Tomsk, Russia

Studies have been performed on the structural characteristics and roentgenoluminescence spectra (RL) of copper and silver iodides from the zone of oxidation of the Rubtsovsk polymetallic deposit (Rudnyi Altai). The investigation on the RL characteristics of the natural Cu and Ag iodides has demonstrated their dependence on the Cu/Ag-ratio and the structural type of a mineral. It has been established that the RL spectra of the cubic marshite (Cu, Ag)I, miersite (Ag, Cu)I and hexagonal iodargyrite (AgI) differ in the intensity and spectral composition of the emission in the wave length range of 400-800 nm. The correlation has been discovered between the silver content entering the minerals of the (Cu, Ag)I - (Ag, Cu)I series and the RL intensity in the range of 600-800 nm. The shift of emission bands in the range of 600-800 nm from iodargyrite to miersite and farther to marshite into the long-wave zone has been established. In the iodargyrite RL spectra, the short-wave RL band (420-450 nm) has been found, the emission character of which coincides with the excitonic luminescence of 2*H* and 4*H* polytypes of AgI.

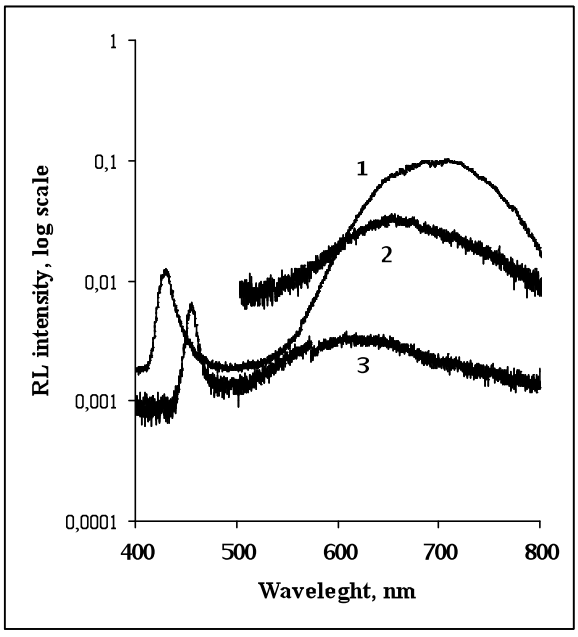

Fig. 1: Roentgenoluminescence spectra (RL) of copper and silver iodides: 1 – marshite, 2 – miersite, 3 – iodargyrite

These researches have been supported by the Ministry of Education and Science of Russia.

https://doi.org/10.1180/S0026461X00006502 Published online by Cambridge University Press

Deconstructing the nuclear accident at the Fukushima-Daiichi Plant: What went wrong and what are the prospects for recovery?

EDWARD BLANDFORD

Center for International Security and Cooperation Stanford University, (edb3@stanford.edu)

The recent large-scale industrial accident at the Fukushima-Daiichi Nuclear Power Plant was the culmination of three inter-related factors: external natural hazard assessment and site preparation, the utility's approach to risk management, and the fundamental reactor design. The reactor accident was initiated by a magnitude 9 earthquake followed by an even more damaging tsunami. However, it was othe inability to remove the decay heat in the reactor core that led to core meltdown and radioactive release. A review of the timeline of the major Fukushima accident sequences will be given. The plant first experienced a station blackout (i.e. loss of all offsite and onsite power) due to flooding of backup critical emergency cooling equipment. The lack of an ultimate heat sink led to the fuel overheating. Subsequently, the generation of hydrogen through steam oxidation of the fuel cladding led to chemical explosions causing significant structural damage.

The focus of this talk is on the engineering aspects of the reactor accident and the prospects for local environmental recovery. Radionuclide measurements in space and time provide important evidence for the exact evolution of fuel damage leading to partial core melting in multiple units. A review of the spent nuclear fuel pools is given where isotopic water composition and visual inspection images provide important evidence for the condition of the spent nuclear fuel.

While it will be several months to a year before we will be in a position to learn most of the lessons from this tragedy, several conclusions about preventative design, mitigation actions, and emergency response have been drawn by international organizations

While the public health impact appears to have been low, the economic and nearby environmental consequences are severe, There is no doubt that land restoration will take over a decade and perhaps much longer. A review is given of actions taken by the Japanese government for land recovery in areas such as decontaminating top soil and local farmland as well as highly radioactive water used during 'feed and bleed' cooling of the core.

The role of the Geochemical Society of Japan for mitigating the Fukushima accident and its aftermath

MITSURU EBIHARA

Department of Chemistry, Graduate School of Science and Engineering Tokyo Metropoolitan University, (ebihara-mitsuru@tmu.ac.jp)

A huge earthquake (M 9.0) and coupled tsunami on March 11, 2011 yielded enormous damage in the area from north Kanto to whole Tohoku district. Besides direct disaster caused by earthquake and tsunami, equally serious accident happened at Fukushima Daiichi nuclear power plant of Tokyo Electric Power Company. By this accident, nuclear power reactors couldn't been controlled properly, and eventually radioactive materials were released from the nuclear power reactors and dispersed over rather wide area. Consequently, agricultural materials, drinking water and food were contaminated with radioactive nuclides. It was urgent to figure out how radioactive materials were spread not only in the area close to the nuclear reactors but also over surrounding, rather wide district. Such information must release the uneasiness for public people and objectively predict the possible influence caused by radioactive material over agricultural products for people engaging in agriculture.

To grapple with this task promptly as well as effectively, scientists belonging to the Geochemical Society of Japan, the atmospheric and oceanic section of the Japan Geoscience Union and the Japan Society for Nuclear and Radiochemical Sciences were allied and presented a proposal for comprehensive and systematic survey of radioactive materials in the environment to the ministry of Education, Science, Culture and Technology (MEXT). In this proposal, aerosol, rain, soils and underground water samples are to be collected as systematically as possible and as wide as possible for the sampling area. Besides such an action, we discussed with nuclear physicists to work together in collecting soil samples in Fukushima prefecture systematically and measuring radioactivity precisely under controlled counting protocol, making contour maps of individual radionuclides. Such a collaborative project was eventually supported by the government and officially started in early June, being continued for three months. The data thus obtained are to be opened to the governmental sector as well as to the public including scientific communities in due course so that national and international academic societies can utilize these data for scientific discussion.

https://doi.org/10.1180/S0026461X00006502 Published online by Cambridge University Press

Geochemistry of the long term evolution of the used nuclear fuel/water interaction

BERND GRAMBOW

SUBATECH, Ecole des Mines, Université de Nantes, CNRS-IN2P3, 4, r Alfred Kastler, 44307 Nantes, France

Options for stabilizing the failed reactors in Fukushima are to create a sarcophage or to remove the fuel debris for safe geological disposal. In either case interaction of the molten and re-solidified damaged fuel (corium =UO_2-ZrO_2-Zr-Fe_2O_3..) will occur with natural waters leading to certain radionuclide release. Very little is known on the interaction of this material under natural geochemical conditions. In the absence of more pertinent data, and since in corium the UO_2/ZrO_2 seems to be a tetragonal solid solution, one may use the large knowledge from used fuel/water interaction to obtain some insight in potential radionuclide release controls.

A very large experimental and theoretical database has been collected since 30 years on used nuclear fuel/water interaction in the context of deep geological disposal options in clay rock, granite and salt. Current understanding and model uncertainties were recently assessed in the just finished European MICADO project. Detailed parametric studies of dissolution and radionuclide release behavior have allowed identifying key dissolution mechanism. The comparison of spent fuel behavior to that of natural uraninite as well as to pure UO_2 and Pu doped UO_2 gave important insight into radiation effects on fuel behavior over geological time. Two radionuclide release terms can be distinguished: a rapid release of a few percent of the inventories of volatile fission products such as Cs-135, Cs-137, I-131 and I-129 from fracture surfaces and grain boundaries in the fuel and a much slower release governed by the dissolution of the fuel matrix. The latter process concerns the release characteristics of matrix bound radionuclides, mainly the actinides, Sr and the rare earth elements. Fuel surface oxidation states are of fundamental importance for fuel matrix dissolution. The gamma and alpha radiation fields may create local oxidizing conditions at the fuel surface, accelerating fuel dissolution. The radiolytical enhancement of fuel dissolution is counteracted in geological disposal by the presence of hydrogen. Estimated times needed under natural water conditions for complete fuel matrix dissolution are in the range of 10000 yr under oxic conditions and in the range of millions of years under reducing conditions.

The fraction of matrix bound radionuclides will be lower and the labile fraction will be higher in the fuel debris of Fukushima than in ordinary spent fuel since high temperatures lead to stronger volatilization. Even though reducing conditions might have prevailed in the initial stages of fuel melt-down in the accident (large oxygen potential buffer capacity of melted metal Zirconium and presence of hydrogen) the beneficial long-term effect of hydrogen is unlikely to occur in Fukushima debris since hydrogen is expected to escape and oxidizing conditions will prevail.

Atmospheric dispersion of the Fukushima effluents

A. MATHIEU[1*], J.P.BENOIT[1], D.DIDIER[1], J.GROELL[1], I.KORSAKISSOK[1], D.QUÉLO[1], E.QUENTRIC[1], O.SAUNIER[1], M.TOMBETTE[1], V.WINIAREK[2], M.BOCQUET[2]

[1] Institute of Radiation Protection and Nuclear Safety, BP 17, 92262, Fontenay-aux-Roses, France, (*correspondance: anne.mathieu@irsn.fr)

[2] Université Paris-Est, CEREA, joint laboratory Ecole des Ponts ParisTech and EDF R&D, Champs-sur-Marne, France

In case of an accidental situation involving radioactive material, government agencies have to provide, in support of the public authorities, a scientific estimation of the emission and of its consequences for human health and environment. The technical crisis centre of IRSN has a special focus on atmospheric dispersion since it's the first contribution to radiation exposure. IRSN operates a complete modelling platform which links a release of radioactive material to its consequences. The evolution of atmospheric and ground activity is computed by using an estimation of the source term and the state of the atmosphere. Atmospheric dispersion is modelled using a Gaussian puff model at small scale, and a Eulerian long-range transport model at large scale.

Following the earthquake and tsunami that hit Japan on March 11, 2011, IRSN has monitored in real time, the state of the Dai-ichi nuclear power plant as well as simulated the atmospheric dispersion of estimated releases. The talk will present the atmospheric dispersion of the plume simulated through the Japanese territory as well as the American and European continents. The relevance of the simulations will be assessed by comparisons with measurements. Uncertainties about the source term and the meteorological conditions will be discussed. Finally, the use of atmospheric dispersion model, inverse modelling and data assimilation techniques to narrow uncertainties on the source term will be illustrated.

https://doi.org/10.1180/S0026461X00006502 Published online by Cambridge University Press

Measurement of radioactivity of aerosol at a few sites in Japan after the Fukushima Daiichi Accident

S. NAGAO[1*], M. KANAMORI[2], T. TOKUNARI[2], K. HAYAKAWA[3], A. TORIBA[3], T. KAMEDA[3], Y. HAMAJIMA[1], M. INOUE[1] AND M. YAMAMOTO[1]

[1]Low Level Radioactivity Laboratory, Inst. of Nature and Environ. Technol., Kanazawa Univ., Nomi, Ishikawa 923-1224, Japan,
(*correspondance: nagao37@staff.kanazawa-u.ac.jp)
[2]Graduate School of Natural Sci. and Technol., Kanazawa Univ., Kakuma, Ishikawa 920-1192, Japan
[3]Inst. of Medical, Pharmaseutical and Health Sciences, Kanazawa Univ., Kakuma, Ishikawa 920-1192, Japan

Nuclear accident at the Fukushima Daiichi Nuclear Power Plant (NPP) was occurred after the 2011 Tohoku Earthquake and Tsunami. About 370-630 PBq of radionuclides was released from the Fukushima Daiichi NPP, according to the estimation by Nuclear Safety Commission (NSC) of Japan and Nuclear and Industrial Safety Agency (NISA). To understand migration behaviour of radionuclides in atmosphere, we have to monitor radioactivities of ^{131}I, ^{134}Cs and ^{137}Cs of aerosol samples in Japan temporally and spatially.

We have been collected aerosol samples using a high volume air sampler at Wajima and Nomi in Ishikawa Prefecture, Japan before the Fukushima Daiichi NPP accident. To realize transport processes of radionuclides from the Fukushima Daiichi, the filter samples collected at above sites, about 400 km far from the Fukushima Daiichi NPP, were measured for radioactivities of ^{131}I, ^{134}Cs and ^{137}Cs using ultra-low background Ge detection system at the Ogoya Underground Laboratory of Kanazawa University.

The presentation will be reported for the radioactivities of ^{131}I, ^{134}Cs and ^{137}Cs at the Ishikawa sites from March to May in 2011, before and after the Fukushima accident. We also show temporal variations in radioactivities of these radionuclides at a few sites in Japan, reported by Japanese scientists as preliminary data, and discuss the migration of these radionuclides in atmosphere on the basis of the spatial variations.

Seismological investigations of the March 11, M9, Tohoku-oki earthquake

JEROEN RITSEMA

Department of Geological Sciences, University of Michigan

On March 11, 2011, a shallow, M9 earthquake with an epicenter roughly 160 km offshore struck the Fukushima prefecture in Japan. The ensuing tsunami was responsible for 20,000 fatalities, widespread damage along the Honshu coast, and the flooding of the Fukushima Dai-ichi nuclear power station, a crisis that is still unfolding. Yet, from a seismological point of view, the response to the earthquake has been a success. Thanks to the enormous investment in seismological and geodetic infrastructure by scientists from Japan and around the world, the earthquake magnitude, faulting mechanism, depth, extent along the Japan Trench, and, hence, its tsunami-generation potential was fully understood within 30 minutes after the earthquake occurred.

The Tohoku-oki earthquake was a classic mega-thrust (i.e. reverse) earthquake. It ruptured a fault plane on the plate interface that is dipping 14 degrees to the west. The largest slip was concentrated at shallow depth near the trench which explains the exceptionally large tsunami. Every large earthquake holds surprises and Tohoku-oki was not an exception. Before March 11, the seismic record suggested that M7.5 to M8.2 earthquakes break small patches of the plate interface along the Japan Trench south of Sendai. Given this experience, the magnitude of the Tohoku-oki earthquake was unexpectedly high. Moreover, the Tohoku-oki earthquake was spatially compact. It ruptured only a 200x100 square km area of the plate interface. Just west of the trench, slip on the fault plane exceeded 60 m. This is the largest fault offset ever reported.

The Tohoku-oki earthquake has been analyzed by a large number of scientists around the world. An open-access special issue of the journal “Earth, Planets, and Space” appeared in June. Articles in this issue are already providing a detailed and remarkably consistent picture of the many complex facets of the Tohoku-oki earthquake. In this presentation, I will summarize these investigations and place the earthquake in a historical context.

https://doi.org/10.1180/S0026461X00006502 Published online by Cambridge University Press

Present situation of radioactive contamination in soil by the Fukushima Dai-ichi accident

M.YAMAMOTO[1]*, T. TAKADA[1], N. NAGAO[1], M. HOSHI[2], K. ZUMADIOV[2], T. SHIMA[3], M. FUKUOKA[3], S. KIMURA[4]

[1]Kanazawa Univ., LLRL, Ishikawa, Japan,
*Correspondance: pluto@llrl.ku-unet.ocn.ne.jp
[2]Hiroshima Univ., Hiroshima, Japan
[3]Osaka Univ., Osaka, Japan
[4]Dokkyo Medical Univ., Tokyo, Japan

On 11 March 2011, A Great East Japan Earthquake of magnitude 9.0 happened, and generated a series of large tsunami waves in the east coast of Japan. By these events, Tokyo Electric Power Company (TEPCO) Fukushima Dai-ichi Nuclear Power Plants (units 1, 2, 3 and 4) suffered major damage, and significant amounts of radionuclides were released into the environment. Monitoring efforts performed so far have shown that dangerous contamination is mostly localized in a narrow band within 40 km of the plant, stretching to the northwest. The Japanese Government announced that the serious accident of TEPCO's Fukushima Daiichi Nuclear Power Plant was ranked up to Level 7, the most serious accident according to INES, the same level as that in the case of Chernobyl Nuclear Power Plant in the Soviet Union on April 26, 1986.

To understand the components of radionuclides released, their levels and distributions, some soil core samples up to a depth of 30 cm were taken at the zone within 20-30 km from the plant in the end of March. The samples were cutted every 5 cm in depth. Another one soil sample (0-5 cm in depth) was also collected at the ca. 1.7 km point (outside the premises) west from of the plant in April. These samples were subjected to the measurements of γ-ray emitting radionuclides and Pu isotopes

As a result, volatile radionuclides such as ^{131}I,^{134,137}Cs and so on were mainly detected with various levels, showing serious contamination in the NW from the plant. The distribution reflected the role of wind pattern and rainfall in washing out radionuclides to the ground. Small amounts of Pu isotopes (^{239,240}Pu and ^{238}Pu) were detected for all of the surface soil (0-5 cm) from zone within 20-30km, but their activity ratios of ^{238}Pu/^{239,240}Pu were around 0.03, indicating the origin of global fallout Pu. Only one sample collected from 1.7 km close the plant showed a little higher ratio of ca 0.06. Thus, currently, Pu release was negligibly small and volatile nuclides ^{131}I,^{134,137}Cs, etc. were responsible for a large share of released radioactivity. There are some spots of higher contamination called "Hot Spot".

A preliminary overview of studies on dispersals of radionuclides from Fukushima nuclear power plants

NAOHIRO YOSHIDA

Department of Environmental Chemistry and Engineering, Tokyo Institute of Technology, Japan

The Tohoku Japan earthquake occurred on 11th March, 2011, accompanied by huge tsunami which attacked all coastal areas in northeastern Japan and caused the accdidents of Fukushima Daiichi nuclear power plant. Some nuclear reactors lost their control almost entirely or partly, and the fission products and feasible neutron activated nuclides in the reactors have been dispersing in environment.

To promote a study on disperse of the radionuclides in order to prevent further unnecessary dose for people, many scientists have gathered and started monitoring, mapping, and model simulation of disperse of radionuclides in local and large covering areas as well. This is a preliminary overview of studies on dispersals by many motivated collaborators.

Radionuclides are found to be strong tracers of atmospheric and oceanic movement with time stamps of some with their different half-lives to distinguish different emission phenomena, direct and/or rebound transport, and dry and/or wet deposition. The distribution of radionuclides in time and space is highly localized, which may be determined by their accumulation and diffusion because of distance, topography, wind direction, precipitation, surface runoff, marine gires and currents. Their occurrences, however, are sometimes difficult to be explained straightforward because of the unknown source processes and their strength, their physical and chemical forms in the atmosphere and the oceans, their transformation through chemistry, the size distribution of dusts on which they are absorbed, dry and/or wet deposition on the surface soil, and their chemistry and transport after deposition.

Some scientific programs have started and will continue before and even after the cease of the nuclear plant crisis, to obtain knowledge on the ongoing radioactive pollution, to understand and to predict their distributions, and for the unexpected similar future accidents. This is a great challenge for the scientists in this research field, geochemistry and not necessarily limited to isotope geochemists nor any scientists, but to human beings. Further international collaborations would be much appreciated in any fields of study with different time and space scales.

https://doi.org/10.1180/S0026461X00006502 Published online by Cambridge University Press

A

Aagaard, P. 398
421
1638
Aarnos, H. 2056
Aarons, S. 398
Abart, R. 1981
Abbaci, K. 1751
Abbas, Z. 1126
Abbaslou, H. 399
Abbasnia, H. 399
Abbott, L. 400
Abdelfadil, K. 400
Abdioğlu, E. 2237
Abdulla, H. 401
Abdurrachman, M. 401
Abe, K. 1425
Abe, M. 1392
Abe, N. 402
Abed Esfahany, A. 1773
Abedi, A. 1178
1179
Abedi, N. 402
Abedian, N. 1486
Abers, G. 2069
Abiven, S. 403
764
Abouchami, W. 403
883
1664
2266
Abraham, P.M. 404
1810
Abramov, O. 1485
Abramovich, S. 1082
Abrams, J. 404
Abratis, M. 405
2043
Abreu, I. 629
Abrikosov, I. 1664
Abrosimova, N. 405
Abtahi, A. 399
Abushkevich, V. 1976
Acero, P. 406
918
Acevedo, S. 2077
Achoundong, G. 1829
Achterberg, E. 576
1007
Aciego, S. 398
Ackerman, L. 406
1605
1972
Ackermann, S. 546
Acosta-Vigil, A. 495
1982
Adam, J. 407
Adams, P. 407
Addy, S. 2067
Ader, M. 798
1280
1473
1794
2007
Adhikari, R.R. 408
Adkins, J.F. 408
504
704
880
1286
1735
2003
Adlakha, E. 409
Adler, A. 1006
Adler, M. 490
Aeschbacher, M. 409
938
1790
Aeschbach-Hertig, W. 410
583
867
1156
Afanasiev, P. 1751
Afanasiev, V. 1221
Affek, H. 410
802
Afif, E. 1873
Afonin, I. 411
Afshari, S. 1843
Agee, C. 411
1848
Agnihotri, R. 1431
Agostini, C. 412
Agostini, S. 412
Agranier, A. 973
1101
1507
Agrinier, P. 413
628
798
944
1644
Ague, J. 501
810
Aguilera, A. 1796
Ahadnejad, V. 413
735
Ahlberg, E. 1126
Ahmadi, G.A. 414
Ahmady Birgani, H. 414
Ahmed, A. 447
Ai, Z. 1447
Aiglsperger, T. 415
Aiken, G. 1054
Aimanant, S. 2285
Airo, M-L. 1357
Airoldi, C. 2047
Aiuppa, A. 415
Aizawa, S. 1833
Ajo-Franklin, J. 1931
Aka, F. 1420
Akai, R. 416
Akaryalı, E. 418
Akçay, M. 416
1776
Akce, M.A. 1133
Akhiani, M. 713
Akinfiev, N. 502
1670
Akinin, V. 1553
1554
Akizawa, N. 417
Akmaz, R.M. 2055
Akob, D.M. 417
825
Akpınar, A. 418
Akpınar, İ. 2105
Aksoy, E. 418
Al, T. 1171
2189
Alakangas, L. 419
Alam, M. 1648
Alavi Tabaee, F. 419
Albarède, F. 420
475
535
973
1283
2082
2220
Albayrak, M. 606
Albrecht, H. 1377
Albrecht, N. 928
Albuquerque, T. 1567
1874
Alcicek, M.C. 1165
Alcorta, M. 1191
Aldahan, A.A. 1048
1902
Alday, F. 1749
Alekhin, Y. 420
421
Alemu, B.L. 398
421
Aleon, J. 422
Alessi, D. 422
484
520
1846
1958
Alewell, C. 799
Alexander, B.W. 2084
Alexander, Calvin 2022
Alexander, Conel O'D. 796
1124
2126
Alexander, D. 1721
Alexander, S. 2022
Alfarra, M.R. 423
Alfredsson, H.A. 423
920
920
1945
Al-Hamdan, M. 1345
Ali, G. 1006
Ali, M.A. 1534
Alieva, V. 814
Alizade Paeen Afrakaty, E. 1482
Alkimim, F.F. 2085
Allan, A. 424
1408
Allan, J. 1924
2154
Allard, T. 1579
Allègre, C.J. 424
685
1294
1460
1686
Allen, Carlton 944
Allen, Charlotte M 425
1079
Aller, R.C. 1752
Alletti, M. 425
597
1572
Allison, N. 426
Almeev, R. 426
548
871
1073
1596
1864
Almeida, A. 1352
Almeida, P. 1567
1874
Almogi-Labin, A. 427
464
815
1082
1500
1589
Alpermann, T. 427
Alphonse, V. 1440
Alt, K.W. 585
Alt-Epping, P. 428
Alterskjær, K. 428
Althoff, F. 429
Altmaier, M. 591
1194
Altunkaynak, S. 1138
2216
2219
Alvarez, F. 1704
Alvarez, P. 652
Álvarez-Iglesias, P. 438
Álvarez-Valero, A. 1239
Alves, C.F. 1423
Amachi, S. 429
Amalberti, J. 430
Amanda, M. 826
Amano, K. 2202
Amano, Y. 1800
Ambroise, B. 637
1807
Amelin, Y. 1074
1137
Amend, J. 430
1460
1669
Ames, D.E. 1942
Amils, R. 2079
Amini, M. 515
Ammann, M. 431
Amor, K. 431
Amor, M. 1453
Amouroux, D. 814
Amundson, R. 432
1543
An, Y. 432

https://doi.org/10.1180/S0026461X00006502 Published online by Cambridge University Press

Ananatharaman, K. 2146
Anand, P. 1941
Anand, R. 1332
..... 1705
Anawar, H.M. 433
Anbar, A. 433
..... 1168
..... 1373
..... 1501
..... 1660
..... 1746
..... 1778
..... 1831
..... 2135
..... 2151
Ancochea, E. 2090
Ander, L. 1897
Andersen, C. 434
Andersen, M.B. 434
..... 1008
Andersen, T. 1895
..... 1993
Anderson, A. 435
Anderson, F.S. 435
Anderson, L. 1921
Anderson, Melissa 436
Anderson, Michael 1870
Anderson, Robert 436
..... 437
..... 462
..... 994
Anderson, Robert S 1270
Anderson, S. 1270
Andersson, J. 1629
Andersson, M. 437
..... 565
..... 1827
Andersson, P. 431
..... 1267
..... 2167
Andrade, A. 438
Andrade, C. 1499
Andrault, D. 438
..... 547
..... 1630
André, Laurent 1272
André, Luc 743
Andreae, M.O. 439
..... 1117
..... 1664
Andreani, M. 439
Andreas, E.L. 738
Andreeva, I. 440
Andreiev, A. 440
Andreiev, O. 440
Andres, A.S. 1462
Andrews, A. 441
Andrews, G. 1733
Andrews, M.Y. 441
Andronicos, C. 650
Angel, R. 442
..... 1905
..... 2177
Angeles, C. 1671
Angert, A. 442
Anguelova, M.D. 738
Anma, R. 1573
Annen, C. 443
Annersten, H. 516
..... 1614
Anoshkina, J. 443
Anovitz, L. 444
Anquetil-Deck, C. 1042
Anselmetti, F.S. 1540
Antao, S. 1326
Antelo, J. 444
..... 2089
Antler, G. 445
Antognini, M. 1809
Antonangeli, Daniele 561
..... 1498
..... 1872
Antonangeli, Daniele 1721
Antonopoulos, D. 1259
Antunes, M. 445
..... 1567
..... 1874
Antúnez, G.N. 1747
Anzai, H. 1515
..... 1833
Aoki, K. 1782
Aoyagi, N. 1781
Aoyama, A. 872
Apelt, S. 1202
Apostel, C. 763
Appel, K. 787
..... 1630
..... 2160
Appleby, P. 1196
April, R. 446
Aquilina, A. 1011
Arafin, S. 446
Arai, S. 417
..... 447
..... 1087
..... 1089
Arakaki, T. 2028
Arakawa, Y. 447
Aranovich, L. 448
Araujo, D. 1213
..... 2244
Araújo, M.D.F. 1499
Araujo, P. 491
Arce, F. 444
Archer, C. 448
..... 464
..... 657
..... 1163
..... 1720
..... 2061
..... 2149
Archer, D. 887
Archer-Nicholls, S. 1439
Arcilla, C. 613
Arcis, H. 449
Arculus, R.J. 449
..... 1107
..... 1370
..... 1381
..... 1436
..... 1529
..... 1668
..... 1929
..... 2152
Ardia, P. 450
Areias, M.D.C. 1717
Arenholz, E. 1609
Argyraki, A. 450
Arienzo, I. 451
..... 1499
Arienzo, M. 451
Arik, F. 452
..... 1582
Arkadakskiy, S. 452
Arkimaa, H. 1357
Arlinghaus, H. 1728
Armstrong, F. 1434
Armstrong, L. 453
Armstrong, Richard 724
..... 954
..... 1037
Armstrong, Robin 771
Armytage, R. 453
Arndt, N.T. 454
..... 646
..... 788
..... 881
..... 1076
..... 1282
..... 1292
..... 1904
Arneth, A. 1205
..... 1683
..... 1727
Arnold, G.L. 1373
..... 1723
Arnold, W.A. 454
..... 1887
Arrouvel, C. 2178
Arslan, M. 460
..... 793
..... 817
..... 950
..... 2237
Artaxo, P. 455
..... 1838
Artemieva, I.M. 455
Artieda, O. 2158
Aruguete, D. 1031
Arvidson, R.S. 456
..... 1255
..... 1371
..... 2078
Arz, H. 797
Arzamastsev, A. 456
Arzamastseva, L. 456
Arzilli, F. 457
Asadi-Haroni, H. 419
..... 722
..... 911
..... 1390
Asael, D. 457
Asahara, Yoshihiro 1910
Asahara, Yuki 458
Asahi, H. 1782
Asano, T. 1800
Ascaso, C. 2094
..... 2158
Aseri, A. 458
Asgariyan, H. 800
Asghari, A.A. 2283
Ashchepkov, I. 459
..... 777
..... 930
..... 1085
AshckenaziI-Polivoda, S. 1082
Ashfaque, K.N. 1534
Ashi, J. 1079
Ashley, G.M. 1384
Asimow, P.D. 411
..... 459
..... 901
Askari, N. 1179
Aslan, Z. 460
Assayag, N. 628
..... 786
..... 1261
..... 2007
Assonov, S. 875
Asta, M.P. 918
Astilleros, J.M. 450
..... 1155
..... 1497
Åström, M. 419
..... 460
..... 517
..... 780
..... 1421
..... 1424
..... 2231
Atanasova, P. 1833
Atkinson, M. 1930
Atlas, R. 461
Atlaskna, K. 1968
Attal, M. 1229
Attenkofer, K. 915
Atudorei, V. 1954
Aubaud, C. 682
Audetat, A. 521
..... 834
..... 1065
..... 1302
..... 1322
Audry, S. 461
..... 1728
Auer, M. 2180
Aufdenkampe, A. 1147
..... 1279
..... 2224
Auffan, M. 1304
..... 1751
Aulbach, S. 462
Aumont, B. 575
Auque, L.F. 918
Auro, M. 462

https://doi.org/10.1180/S0026461X00006502 Published online by Cambridge University Press

Austrheim, H. 509
..... 1277
..... 1650
..... 1651
..... 1676
Austrins, L. 1208
Auzende, A-L. 561
..... 848
Avagyan, A. 1777
Avalos-Perez, A. 677
Avanzinalli, R. 448
Avery, B. 1180
Avigad, D. 1497
Avino, R. 622
Avirmed, E. 2057
Avni, Y. 1426
Awadh, S.M. 463
Awalt, M. 574
Awasthi, N. 525
Ayala-Luis, K. 463
..... 1064
Ayalon, A. 410
..... 487
Aydal, D. 2105
Aydin, F. 1871
Aydin, Ü. 452
Aydınçakır, E. 464
Ayers, J.C. 1344
Ayora, C. 1380
..... 2025
Ayral, A. 2005
Ayrault, S. 1300
..... 1668
Aysal, N. 1176
Azaroual, M. 1272
..... 1601
Azevedo, M.D.R. 1423
Azrieli, I. 464
Azzolini, D. 1350
..... 1971

B

Babechuk, M.G. 465
Babiel, R. 914
Babu, E.V.S.S.K. 1606
..... 1960
Babu, S.S. 1800
Baburek, J. 1486
Bach, W. 544
..... 1011
..... 1125
..... 1134
..... 1437
..... 1548
..... 1699
..... 1702
..... 1866
Bachet, M. 511
Bachmann, O. 465
..... 564
..... 1067
Baciu, C. 466
Backman, J. 455
Badallo, S. 1773
Badanina, E. 466
..... 1976
Badanina, I. 1394
Badger, M. 467
Badot, P-M. 683
Badro, J. 467
..... 697
..... 769
..... 1498
..... 1721
..... 1872
Badruzzaman, A.B.M. 1534
Baek, D-Y. 468
Baek, K. 468
..... 1285
Baek, M-H. 1597
Baero, W. 469
Baese, R. 469
Bağcı, U. 1837
Baghbani, S. 1774
Bagus, P. 470
Baham, J. 2132
Baharifar, A.A. 1179
Bai, H. 2267
Bai, J. 2114
Bai, M. 432
Bai, Z-J. 470
Baiden, N. 2153
Bailey, E. 1897
Bailey, Ken 1444
Bailey, Kevin 1361
Baitsch Ghirardello, B. 471
Bajda, T. 471
Bakardjieva, S. 1994
Baker, A. 640
..... 641
..... 1007
Baker, D. 745
Baker, E. 1370
Baker, J. 694
..... 1408
..... 1409
..... 1473
Baker, K. 472
Bakken, L. 775
..... 1876
Bakker, R.J. 500
..... 580
..... 774
..... 1014
Bakun-Czubarow, N. 472
Balakrishnan, S. 1430
Balan, E. 533
Balan, S. 498
Balaram, V. 1798
Balci, N. 473
Balco, G. 473
Baldeyrou-Bailly, A. 869
Baldo, E.G. 2080
Baldwin, S. 852
..... 1250
Balen, D. 474
..... 1631
Balint, I. 1481
Balitsky, V. 1841
Ballentine, C.J. 400
..... 474
..... 648
..... 1038
..... 1140
..... 1277
..... 1502
..... 1683
..... 1963
..... 2133
..... 2150
..... 2274
Ballhaus, C. 420
..... 475
..... 858
..... 878
..... 1005
..... 1169
..... 1275
Balogh, Z. 920
..... 1945
Balogh-Brunstad, Z. 475
..... 1167
..... 1530
..... 1900
Baltensperger, U. 476
..... 1013
Balter, V. 476
Balthasar, K. 538
Baltrūnas, D. 783
Balu, G. 1926
Balvin, A. 1036
Balzer, N. 605
Balzer, W. 477
Banakar, V. 1387
Banaszak, J. 1462
Banaszak, M. 477
..... 1043
..... 1931
Bandeira, C. 1385
Bandini, A. 593
..... 1643
Bandura, A. 1378
Banerjee, D. 478
..... 789
Banfield, J. 2165
Banik, N.L. 478
Banks, D.A. 1718
Banks, J. 479
Bannon, D. 479
Banwart, S.A. 441
..... 472
..... 553
..... 581
..... 695
..... 1455
..... 1817
..... 1990
Bao, C. 480
Bao, L-R. 1318
Bao, Z. 2235
Baran, G. 2112
Baratoux, D. 2221
Baratoux, L. 480
Barba-Brioso, C. 840
Barbanson, L. 813
Barbante, C. 481
Barbecot, F. 481
Barber, A. 904
Barbero, L. 482
..... 1176
..... 1416
Barbillat, J. 1902
Barclay, J. 519
Barconnot, P. 1122
Bard, E. 482
..... 490
..... 553
..... 1456
..... 1758
..... 1789
..... 1917
Bardelli, F. 483
..... 756
Barden, H. 798
Baresi, L. 483
Bargar, J.R. 422
..... 484
..... 520
..... 549
..... 913
..... 1306
..... 1464
..... 1649
..... 1846
..... 1958
..... 2072
Barger, M. 484
Barifaijo, E. 2011
Barkan, E. 1371
Barkay, T. 690
..... 1596
Barker, Abigail 485
..... 516
Barker, Amanda 777
Barker, G. 1667
Barker, S. 2009
Barkman, J. 485
..... 590
Barkmann, W. 477
Barkusky, D. 1081
Barley, M. 486
..... 1217
Barling, J. 486
Bar-Matthews, M. 410
..... 464
..... 487
..... 979
Barmet, P. 1013
Barmettler, K. 1238
Barnes, E. 487
Barnes, J. 432
..... 488
Barnes, Sarah-Jane 488
..... 506
..... 723
..... 1607
Barnes, Stephen 489
..... 489
Barnett, G. 411
Barone, S. 1870
Baroni, M. 490

https://doi.org/10.1180/S0026461X00006502 Published online by Cambridge University Press

Baronnet, A. 1535
Bar-Or, I. 490
Barou, F. 746
Barr, J. 1303
Barrenechea, J.F. 1645
Barrie, C. D. 880
Barrie, Craig 879
Barrie, L. 1159
Barriga, F. 707
Barros, F. 491
Barros, N. 491
..... 1456
Barrott, J.J. 492
Barrow, M. 492
Barrows, C. 913
Barry, P. 493
..... 1023
Barry, T. 1610
Bartels, A. 493
Barth, A.R. 494
Barth, J.A.C. 494
..... 1518
Barth, M. 572
..... 1219
..... 1753
..... 2240
Bartha, A. 1978
Bartoli, O. 495
..... 1982
Barton, L. 1428
Barton, R.N.E. 492
Bartz, W. 495
Basak, C. 1412
Basei, M. 496
..... 1801
Baskar, R. 1693
Baskar, S. 1252
..... 1693
Baskaran, M. 496
..... 1176
..... 1416
Bass, J. 1792
..... 1883
..... 2120
Bassinot, F.M. 685
..... 1460
Bassot, S. 1760
Basu, S. 497
..... 1469
Batchelor, D. 897
Bates, R. 846
Bates, S. 1168
Bates, T. 497
..... 1770
Batina, N. 677
Batista, E.R. 1414
Batista, M.J. 1645
Batomunkuev, V. 2248
Battaglia-Brunet, F. 558
..... 1601
Battani, A. 498
..... 1647
Bau, M. 498
..... 1250
..... 1819
..... 2084
Baudron, P. 681
Bauer, K. 499
Bauer, S. 499
Baumgartner, L. 854
..... 1303
Baumgartner, M. 500
..... 774
Baumgartner, P. 593
..... 1643
Baxter, A. 500
Baxter, E. 485
..... 501
..... 611
..... 779
..... 1962
Baykara, M.O. 1165
Bayon, G. 501
..... 674
..... 1917
Bayona, G.A. 623
..... 1492
..... 1875
Bayova, A. 556
Bazarkina, E. 502
Be'eri-Shlevin, Y. 1155
Bea, S.A. 502
..... 1697
Beam, J.P. 503
..... 521
Bearup, L. 503
Beaufort, L. 553
Beaumont, V. 2027
Bebbington, M. 1898
Bebout, G. 1118
..... 1437
Beccaluva, L. 528
Bechgarrd, K. 989
Bechtel, A. 943
Beck, A.R. 504
Beck, H.P. 1157
..... 1504
Beck, M. 551
Beck, P. 1493
Becker, H. 469
..... 504
..... 851
..... 900
..... 2131
..... 2156
..... 2275
Becker, L. 1922
Becker, T. 1200
Becker, U. 505
..... 1056
Becker, V. 1518
Beckmann, S. 505
Bedard, L.P. 506
Beer, Julia 506
Beer, Jurg 512
Beerling, D.J. 441
..... 581
..... 1586
..... 1990
Begaudeau, K. 507
Begg, G. 946
Behar, F. 507
Behn, M. 1166
..... 2106
..... 2132
Behrends, T. 508
Behrens, H. 493
..... 843
..... 908
..... 1192
..... 1880
..... 2145
Behrens, M. 1365
Beier, C. 508
..... 866
..... 906
..... 962
..... 974
..... 1439
Beig, G. 1779
Beinlich, A. 509
..... 1651
Bekker, A. 509
..... 1217
..... 1647
..... 1663
..... 1831
Békri, S. 794
Bélanger, N. 2178
Belets'ka, Y. 1526
Belitz, K. 1252
Belkin, H. 770
Bell, A. 510
Bell, D. 1102
..... 2143
Bell, E. 982
..... 1981
Bell, K. 510
..... 965
Bellefleur, A. 511
Beller, H. 1680
..... 2073
..... 2210
Bellieni, G. 614
..... 1457
Belline, J.B. 511
Bellouin, N. 1682
Belmaker, R. 512
Belousova, E. 771
..... 1497
..... 1850
..... 1922
..... 2090
Belova, D. 512
Belyatsky, B. 1292
..... 1466
Bełdowski, J. 1903
Bénard, A. 513
..... 513
Benarioumlil, S. 2096
Bender, M. 514
Bender Koch, C. 1064
Ben Dhia, H. 819
Benedetti, M.F. 1129
Benedix, G. 1128
Bénézeth, P. 511
..... 899
..... 1934
Benisek, A. 946
Benner, S. 1207
Bennett, V. 514
..... 1108
Benning, L.G. 553
..... 559
..... 576
..... 581
..... 1741
..... 1748
..... 1790
..... 1817
..... 2059
..... 2176
Benoit, D. 859
Benoit, M. 1451
Bensalah, M. 1423
Benthien, A. 2063
Bento dos Santos, T. 632
Benzerara, K. 515
..... 524
..... 561
..... 587
..... 698
Bérail, S. 1788
Berelson, W.M. 882
..... 1415
..... 2218
Beresford, S. 847
Berg, M. 515
Berg, P. 666
Berg, S. 516
Bergenholtz, J. 1126
Berger, A. 516
..... 1102
Berger, E. 517
Berger, G. 2034
..... 2221
Berger, J. 1828
Berger, T. 517
Bergin, E.A. 2094
Bergmann, U. 798
Beriozkin, V. 1224
Berkana, W. 518
Berkesi, M. 518
..... 961
Berlo, K. 519
..... 974
Berman-Frank, I. 1845
Bermingham, K. 519
Bernabeu, A. 438
Bernard, S. 515
..... 520
..... 524
..... 1291
Bernasconi, S.M. 1269
..... 1455
..... 1830
..... 1983
Berndt, J. 1046
..... 1220
..... 2169
Berner, C. 475
Berner, U. 1002
Berner, Z. 1082
..... 1986

https://doi.org/10.1180/S0026461X00006502 Published online by Cambridge University Press

Bernhard, G. 1940
Bernier-Latmani, R. 422
484
520
768
1649
1846
1958
2130
Berninger, U-N. 899
Bernini, D. 521
Bernstein, H.C. 521
Bernstein, S. 1489
Berntsen, T. 1683
Berresheim, H. 635
1580
Berry, A. 522
600
778
1124
1557
2217
Berryman, E. 522
2063
Berstein, H. 503
Berthe, G. 523
Berthold, C. 1148
Berthomieu, C. 1839
Bertier, P. 523
Bertler, N. 2167
Bertrand, H. 614
1457
Bertrand, S. 524
Bettenhausen, C. 1053
Beucher, C. 1737
Beulig, F. 825
Bevacqua, D. 1561
Bey, I. 1917
Beyeler, J.D. 1722
Beyer, A. 417
Beyssac, O. 515
524
Bezos, A. 968
Bhadury, P. 912
Bhaskar Rao, Y.J. 1926
2087
Bhatia, M. 525
Bhutani, R. 525
1430
Bi, X.W. 526
1057
1059
Bialek, J. 635
1580
Bian, H. 526
666
Bian, N. 527
Bian, Y. 527
2022
Bianchini, G. 528
717
Bibikova, E. 528
Bicer, E. 1582
Bickle, M. 529
643
786
1140
1411
1900
2158
2274
Bickmore, B. 529
Biczok, J. 1039
Biddanda, B. 496
Bieresdorfer, R. 1434
Biester, H. 1723
Bigi, J. 2180
Bijma, J. 2063
Bilici, Ö. 530
Bill, M. 673
693
1045
2073
Billen, M. 1097
Bindeman, I.N. 530
806
1614
1661
1889
2179
Bindi, L. 540
Bingen, B. 907
2196
Binnie, S. 1543
Birck, J.L. 936
Bird, D. 1120
1659
1724
Bird, L. 874
Birgersson, M. 999
Birke, M. 1895
Bíró, L. 1655
Birot, D. 1218
Bischoff, A. 1046
1759
Bischoff, J. 1753
Bish, D. 2234
Bishop, J. 1855
Bityukova, L. 2092
Bizimis, M. 1553
1554
Bizzarro, M. 531
692
1607
1815
Bjerrum, C.J. 970
1297
1765
Black, J. 531
Blackburn, T. 532
Bladotskaya, E. 1788
Blaettler, R. 532
Blaha, V. 2100
Blair, N. 1295
Blakeman, R. 879
Blamart, D. 1706
1744
Blanc, G. 948
Blanchard, M. 533
Blanchet, C. 533
Blanchon, P. 1040
Blanco, J.A. 2059
Bland, P.A. 1128
Blard, P.H. 473
534
1122
1276
Blättler, C.L. 534
730
Bleeker, W. 1485
Blees, H.J.R. 2147
Blees, J. 535
Blichert-Toft, J. 420
485
528
535
590
805
941
973
1044
1283
1704
1881
2082
2220
Bloch, E. 536
Blockley, S. 1899
Blodau, C. 506
Blondes, M. 536
Bloomer, S. 1984
Blough, N. 537
742
Blowes, D. 537
1673
Blowes, K. 1673
Bluhm, H. 1510
Bluhm, K. 538
Blum, A. 604
Blum, Joel 922
1210
Blum, Jurgen 1228
Blum, W. 1265
1455
Blumberger, J. 1757
Blume, J. 538
Blumenberg, M. 780
2004
Blundy, J. 443
771
843
1201
1640
1725
1889
1929
Blusztajn, J. 1094
Blythe, L. 516
1121
2032
Bo, Y. 1367
Bobadilla, H. 539
Bobos, I. 539
Bobrov, A. 540
1885
Bodnar, R.J. 495
540
620
770
817
826
1197
1204
1245
1281
1489
1932
Boekhout, F. 541
Boers, R. 541
Boetius, A. 1110
2139
Boffa Ballaran, T. 542
1256
1591
Bogatko, S. 542
Bogdanova, S. 1890
Bogush, A. 543
Böhm, E. 543
Böhm, F. 544
803
844
870
1195
1699
1989
2100
Bohn, A. 1927
Bohnert, E. 1458
Boichu, M. 1572
Boily, J-F. 544
1232
1860
1910
Boiron, M-C. 645
1362
1718
Bojakowska, I. 545
1281
Bokuniewicz, H. 545
1695
Boland, D. 546
689
Bolanz, R. 546
2083
Bolarinwa, A.T. 547
Bolea, E. 895
Bolfan, N. 547
Bolfan-Casanova, N. 438
2086
Bolin, T. 1869
Bolívar, J.P. 482
1176
1416
Bollasina, M. 1478
Bollmann, J. 764
Bolte, T. 548
Bolton, A. 1409
Bolton, E. 441
Boman, A. 460
Bonadiman, C. 548
1451

https://doi.org/10.1180/S0026461X00006502 Published online by Cambridge University Press

Bonazza, M. 781
Bond, Daniel 1346
Bond, David 970
Bondár, M. 743
Bone, S. 549
Bones, D. 549
Bong, Y-S. 550
..... 1282
Bonhoure, J. 550
Bonifacie, M. 413
..... 551
..... 798
Bonilla, C. 1295
Böning, P. 551
..... 2166
Bonn, B. 552
Bonnand, P. 552
Bonnet, M-P. 1653
Bonnet, N. 553
Bonneville, S. 553
..... 576
..... 1817
Bonnin, D. 1389
Bontemps, S. 647
Bookman, R. 1500
Boothman, C. 1189
..... 1351
Boparai, H. 1208
Borah, R.R. 1780
Boraso, R. 690
Borch, T. 1271
Borchert, M. 1630
..... 2160
Bordas, F. 740
Boreham, C. 1194
Borer, P. 1069
Borg, G. 554
Borg, S. 2011
Borges, M. 554
Borghini, G. 555
Borglin, S. 693
Borisova, A.Y. 466
..... 1087
..... 2088
Borisover, M. 555
Bormann, B. 1167
Borngässer, G. 883
Boromand, Z. 1496
Borovička, J. 556
Boroznovskaya, N. 556
..... 2292
Borrmann, S. 981
Borschneck, D. 1290
..... 1751
Bortnikov, N. 662
..... 2087
..... 2288
Bortnikova, S. 405
Borůvka, L. 573
..... 1994
Bosak, T. 479
..... 557
..... 1876
Bosbach, D. 846
..... 1262
Bosch, D. 557
..... 1490
..... 1777
Boschi, C. 558
Bosle, J. 1254
..... 2009
Bossy, A. 558
Bostock, H. 1408
Botcharnikov, R.E. 559
..... 1864
..... 1931
Bots, P. 559
..... 1741
..... 1748
Botta, C. 1751
Böttcher, M.E. 741
..... 1356
..... 1522
..... 2166
Bottero, J.Y. 1290
..... 1304
..... 1751
Bottjer, D. 1415
Bottke, W. 560
..... 1043
Bouby, M. 1047
Bouchet, R. 1283
..... 1704
Bouchez, J. 560
..... 2101
Bouchez, T. 1434
Boudad, L. 911
Bougiatioti, A. 1532
Bougoure, J. 1164
..... 1634
Bouhifd, M.A. 453
Boulard, E. 561
Boulart, C. 647
..... 1490
Boulet, B. 1106
Boullemant, A. 926
Bouman, C. 561
..... 593
..... 1351
Bourbonnais, A. 1293
Bourdet, J. 562
Bourdon, B. 562
..... 694
..... 752
..... 851
..... 1024
..... 1025
..... 1199
..... 1220
..... 1675
..... 1714
..... 1759
..... 1899
..... 2157
Bourg, I.C. 563
..... 841
..... 1035
Bourgeade, P. 683
Bourles, D. 490
..... 563
..... 697
..... 1122
..... 1276
Bourrand, J-J. 1261
Bousquet, R. 1559
Bousserrhine, N. 1440
Bouvet, N. 920
Bouvet de Maisonneuve, C. 564
Bouvier, A. 564
..... 565
..... 1128
Bouzid, M. 1353
Bouzouggar, A. 492
Bovet, N. 565
..... 715
..... 1266
..... 1426
..... 1565
..... 1945
..... 1946
Bovkun, A. 1885
Bowen, Benjamin 2165
Bowen, Brenda 566
Bowen, G. 566
..... 567
Bower, D. 567
Bowers, G. 568
Bowler, G. 467
Bowles, N. 944
Bowman, J. 568
Bown, P. 914
..... 1737
Bowring, S. 485
..... 532
Boyanov, M.I. 569
..... 598
..... 1259
..... 1556
..... 1766
Boyce, Adrian 879
..... 1277
..... 2107
Boyce, A. J. 880
Boyce, J. 569
Boyet, M. 513
Boyle, E. 570
..... 852
..... 1286
Boyle, R. 1474
Bozau, E. 570
Bożęcki, P. 571
Bozkaya, G. 571
Bozovic, M. 572
Bracciali, L. 572
Brachert, T. 589
Brack, P. 583
..... 1889
Brad, B. 1840
Bradley, A.S. 573
..... 1121
Bradley, R.S. 853
Bradová, M. 573
Bradtmiller, L. 574
Braida, M. 781
Brake, S. 828
Brandao, M. 1455
Brandl, H. 2174
Brandl, P.A. 574
..... 1703
Brandon, M. 2162
Brandon, W.C. 1041
Brański, P. 1281
Brantley, S.L. 575
..... 1015
..... 1313
Brassell, S. 876
Bratton, J. 1462
Brätz, H. 2149
Braucher, R. 563
..... 697
..... 1122
Brauer, A. 1685
Bräuer, P. 575
Braun, J-J. 1728
Braungardt, C. 576
..... 1738
..... 2041
Brauns, M. 609
Bravin, M.N. 1129
..... 1995
Bray, A.W. 553
..... 576
..... 1817
Brearley, A. 1291
..... 2284
Breecker, D. 577
Brehme, M. 577
Breier, J. 2146
Breit, G. 810
Breitbarth, E. 1945
Breitenbach, S. 2057
Breiter, K. 894
..... 1971
..... 1972
Breitkreuz, C. 736
Brekhofskikh, V. 679
Brendlé, J. 1047
Brendler, V. 582
..... 1947
Brenker, F.E. 1947
..... 2015
Brenna, M. 578
..... 578
Brennecka, G.A. 565
..... 579
Brennenstuhl, K. 801
Brenner, M. 498
Brennwald, M.S. 532
..... 579
..... 1074
..... 1379
..... 1675
..... 1811
..... 2018
..... 2021
Brens, R. 580
Breu, J. 1409
Breuer, J. 1935
Breuer, M. 1757

https://doi.org/10.1180/S0026461X00006502 Published online by Cambridge University Press

Brey, G. ... 1364
... 1866
Brey, M. ... 580
Briais, A. ... 973
Brickner, I. ... 1008
Bridge, J. ... 581
... 695
Brigham-Grette, J. ... 2161
Bril, H. ... 699
... 948
... 949
Brinkmeyer, R. ... 1797
Brinza, L. ... 581
Briois, V. ... 1290
Briscoe, L. ... 2022
Brito, A. ... 1717
Britz, S. ... 582
Broad, K. ... 451
Brocks, J.J. ... 582
... 953
... 1283
... 1898
Bröder, L. ... 583
Broder, M. ... 1523
Broderick, C. ... 583
... 1954
Brodholt, J. ... 431
... 697
Brodie, E.L. ... 1431
... 2073
Broecker, W. ... 1425
Brogioli, R. ... 584
Bromhal, G.S. ... 806
Bronk Ramsey, C. ... 1899
Brooks, B. ... 932
Brooks, C.K. ... 2179
Brooks, P. ... 1621
Brooks, S.C. ... 569
... 1045
... 2075
Brookshaw, D. ... 584
... 1351
Broom-Fendley, S. ... 585
Brophy, J. ... 566
Broska, J. ... 585
Brosse, E. ... 498
Brounce, M. ... 586
Brouwer, J. ... 586
Brovkin, V. ... 887
Brown, Andrew ... 553
... 599
Brown, Ashley ... 1351
Brown, D.A. ... 1901
Brown, E. ... 1312
Brown, Geoffrey ... 1886
Brown, Gordon E. ... 524
... 587
... 678
... 1120
... 1464
... 1503
... 1668
... 1706
... 1899
Brown, J. ... 1123
Brown, K. ... 587
Brown, M. ... 2200
Brown, Sandra ... 1071
Brown, Shaun ... 1680
... 1879
Brownlee, S. ... 588
Brtnicky, M. ... 1260
Bruand, E. ... 588
... 1672
Bruce, L. ... 1221
Brugger, J. ... 1447
... 1707
... 1707
... 2011
Brugger-Schorr, C. ... 589
Brügmann, G. ... 589
Bruguier, F. ... 1700
Bruguier, O. ... 557
... 1490
... 1777
Brulc, J. ... 1259
Brumsack, H-J. ... 551
... 741
... 797
... 1419
Bruneel, O. ... 1503
Brunelli, D. ... 1453
... 1605
Brunet, F. ... 1885
Brüning, S. ... 856
Brunner, B. ... 2140
Brunstein, D. ... 1122
Bruský, I. ... 2238
Bryan, S. ... 590
... 1402
Bryanskaya, A. ... 1278
Bryant, C. ... 1023
... 1277
... 1899
Bryce, J.G. ... 485
... 528
... 590
Brydson, R. ... 1350
Bryson, J. ... 626
Brzezinski, M. ... 1737
Bube, C. ... 591
... 1458
Büchel, G. ... 417
... 1808
Bucher, K. ... 591
Buchet, N. ... 553
Buchko, I. ... 592
Büchner, J. ... 592
Buchs, D. ... 593
... 1643
Buchs, N. ... 593
Budd, D. ... 594
Budwill, K. ... 594
Budzinski, H. ... 1434
Buenemann, E. ... 1983
Buffett, B. ... 595
Bugaï, D. ... 1760
Bugler, M. ... 1052
Buharova, O. ... 443
Buhl, D. ... 1195
Bui, E. ... 595
Bui, T.H. ... 1314
... 1616
Buick, R. ... 1907
Buikin, A. ... 596
Buisman, C.J.N. ... 933
... 964
Bukhanovski, N. ... 555
Bukowiecki, N. ... 476
Bulanova, G. ... 1213
Bull, I. ... 1088
Bullen, T. ... 596
Bulusu, S. ... 2087
Bunker, B. ... 1766
... 1912
Bura-Nakić, E. ... 597
... 677
Burchard, M. ... 949
Bureau, H. ... 561
... 848
... 2168
Bureau, S. ... 893
Bureć-Drewniak, W. ... 1247
Burg, A. ... 938
Burger, E. ... 974
Burgess, K. ... 1628
Burgess, R. ... 400
... 474
... 648
... 1683
... 1963
... 2150
Burghardt, D. ... 1101
Burgisser, A. ... 425
... 597
... 1572
Bürgmann, H. ... 627
Burgos, W. ... 598
... 598
... 1123
... 1271
Burke, A. ... 599
... 1735
... 1736
Burke, I.T. ... 599
... 2010
... 2109
... 2155
Burkhardt, C. ... 600
... 1024
Burleigh, A. ... 1998
Burnard, P. ... 688
... 1376
Burnham, A. ... 600
Burns, D. ... 601
Burns, P. ... 2108
Burns, S.J. ... 853
... 2161
Burov, E. ... 601
Burrows, J. ... 1727
Burrows, S. ... 1042
Burruss, R. ... 562
... 602
Burstein, Y. ... 410
Burton, E.D. ... 602
... 678
... 1163
... 2095
... 2173
Burton, K.W. ... 423
... 603
... 716
... 742
... 1571
... 1609
... 1803
... 1872
... 1941
... 1969
... 2148
Buschaert, S. ... 1647
Bush, R.T. ... 602
... 678
... 1163
... 2095
... 2173
Busigny, V. ... 603
... 1280
Buss, H. ... 604
Butler, E. ... 1945
Butler, I. ... 1256
Butler, J. ... 882
Butt, J. ... 604
... 680
... 1757
... 2153
Butterfield, D. ... 1269
... 1370
Butterfield, N. ... 605
Buxmann, J. ... 605
Buyukkilic-Yanardag, A. ... 606
Buyukutku, A. ... 606
Buzek, F. ... 1550
Bychkov, A. ... 607
... 1660
... 1969
Byerly, B. ... 607
Byrne, A.C. ... 1859
Byrne, D. ... 1921
Byrne, J. ... 608
... 686
Byrne-Bailey, K. ... 2180
Bytchkov, A. ... 1098

C

Cabezas-Calvo-Rubio, F. ... 681
Cabidoche, Y-M. ... 742
Cabral, A.R. ... 609
... 609
... 1292
... 1953
Cabral, R. ... 610
Cabral Pinto, M.M.S. ... 610
Cabri, L. ... 1094
Caby, R. ... 557
Cacho, I. ... 614
Caddick, M. ... 501
... 611
... 779
Cadkova, E. ... 1215

https://doi.org/10.1180/S0026461X00006502 Published online by Cambridge University Press

Caffee, M. 1543
Cagnati, A. 781
Cai, G.S. 1059
Cai, Jindang 2012
Cai, Jin Gong 611
..... 760
Cai, X. 612
Cai, Yuan Feng 611
..... 612
Cai, Yue 1006
Calas, G. 587
..... 613
..... 885
..... 1389
..... 1503
..... 1579
Caldeira, R. 1355
Calderón, M. 539
Calibo, M. 613
Caliebe, W.A. 1880
Calin, N. 1076
Caliro, S. 622
Callegaro, S. 614
..... 745
Calmels, D. 1023
..... 1411
..... 2013
Calov, R. 887
Calvaruso, C. 2042
Calvo, E. 614
..... 1616
Cama, J. 621
Cámara, B. 2158
Camara, S. 1838
Cameron, E. 1704
Cameron, V. 615
Campbell, G. 615
Campbell, H.J. 2048
Campbell, I.H. 425
..... 1079
..... 2281
Campbell, K. 484
..... 616
Campbell, S. 1006
Campos, M. 616
..... 1869
Campos, T. 679
Campredon, B. 617
Canagaratna, M. 617
..... 1924
Candela, P.A. 2242
Canet, C. 1671
Canfield, D.E. 618
..... 706
..... 970
..... 1123
..... 1616
..... 1663
..... 1957
Canion, A. 1068
Cannat, M. 968
Canonica, S. 1790
Cansu, Z. 618
Cantoni, M. 1721
Cao, H. 619
..... 1614
..... 2116
Cao, Jian 619
Cao, Jun 1063
Cao, Q. 1859
..... 1860
Cao, X. 620
..... 1482
Cao, Y.t 2113
Cao, Yu-Ting 1342
Capasso, G. 630
Capmas, F. 2013
Capo, R. 1942
Capobianco, R. 620
Cappelli, C. 621
Capponi, G. 1393
Cappuyns, V. 1029
Caraballo, M. 1380
Caracas, R. 621
Carbone, C. 622
Cardace, D. 1460
Cardell, C. 1767
..... 2052
Cardellini, C. 622
Cardinal, D. 743
..... 1594
Cardona, A. 623
..... 1492
..... 1875
Caricasole, P. 401
Caricchi, L. 443
..... 1444
Carignan, J. 683
..... 818
Carilli, J. 2167
Carley, T. 623
Carlson, H. 2180
Carlson, Richard 624
..... 624
..... 777
..... 1044
..... 1085
..... 1093
..... 1340
..... 1556
..... 1642
Carlson, Ross P. 503
..... 521
..... 625
Carlson, W. 625
Carlut, J. 911
Carniel, L. 626
Caro, G. 2014
Carpenter, E.J. 2218
Carpenter, L. 640
Carpenter, M.A. 626
..... 2263
Carranza, E.J.M. 2230
Carrasco, G. 627
Carrasquillo, A. 705
Carreira, P. 630
Carrico, C. 1633
Carrilho Lopes, J. 1795
Carroll, M.R. 412
Carroll, S. 1698
Carslaw, K. 1924
..... 2176
Carstens, D. 627
Carter, A. 2081
Carter, E. 2094
Carter, L. 1408
..... 1409
Cartigny, P. 628
..... 682
..... 1261
..... 2034
Cartwright, I. 2173
Cartwright, Julia A 628
Cartwright, Julyan H.E. .. 1644
Carvalho, Á. 629
Carvalho, C. 707
Carvalho, F. 629
Carvalho, M.R. 630
Carvalho, N. 1567
..... 1874
Carvalho, P. 630
Carvalho, R. 1383
Casareto, B.E. 468
..... 872
..... 1143
..... 1160
Casas-Ruiz, M. 482
..... 1176
..... 1416
Casciotti, K.L. 2147
Casiot, C. 1503
Cassata, W. 631
Cassidy, M. 631
Castilhos, Z. 491
Castillo, A. 647
Castro, A. 2098
Castro, Jonathan 2038
Castro, Juan 1540
Castro, P. 632
Castro Georgi, J. 814
Casuccio, G. 1850
Catalan, G. 626
Catalano, J. 632
..... 868
Cataldi, K. 1860
Cates, N. 633
..... 1388
..... 1481
..... 1485
..... 1981
Cathelineau, M. 1718
Cathey, H. 548
Cathles, L. 650
..... 1613
Catling, D. 1651
..... 1907
Catrouillet, C. 633
Cauët, E. 542
Caulfield, J. 2042
Cauquoin, A. 634
Cavalcante, R. 634
..... 864
..... 1328
Cave, L. 2189
Cawood, P.A. 755
..... 993
..... 2282
Ceburnis, D. 635
..... 1580
..... 1727
Celep, S. 848
Çelik Karakaya, M. 635
..... 1149
Cempírek, J. 1049
..... 1052
..... 1207
..... 1551
Cenki-Tok, B. 603
..... 812
Censi, P. 1697
Centeno, J. 636
Čepička, I. 779
Cerdan, O. 1686
Ceriani, A. 745
Cerli, C. 636
..... 1134
Cerrato, J.M. 484
..... 913
Cesare, B. 495
..... 1982
Cesco, S. 2001
Cetiner, Z. 637
Ceuleneer, G. 1490
Cezario, W. 1869
Chabaux, F. 637
..... 681
..... 683
..... 886
..... 1455
..... 1617
..... 1641
..... 1724
..... 1807
..... 2096
..... 2099
Chabbi, A. 1788
Chacko, T. 1894
Chaduteau, C. 1280
Chadwick, J. 1627
..... 2032
Chadwick, O. 935
Chae, B.G. 1287
Chae, S-H. 820
Chaerun, S.K. 638
Chagneau, A. 638
Chaka, A. 1581
Chakhmouradian, A. 677
..... 1260
..... 2196
Chakraborty, A. 639
Chakraborty, S. 834
Chalapathi Rao., N.V. 639
Chalikakis, K. 1464
Chalmers, N. 1021
Chalupníčková, E. 1829
Chamberlain, C.P. 1493
..... 1901
Chamberlain, K. 1831
Champan, H. 2158
Chan, C. 640

https://doi.org/10.1180/S0026461X00006502 Published online by Cambridge University Press

Chan, M. 2088
Chance, R. 640
641
1007
Chandra, U. 641
Chaneac, C. 1389
Chaneva, S. 642
Chang, C. 2180
Chang, He 1592
Chang, Hyunshik 2050
Chang, J 2183
Chang, Jin 2278
Chang, Q. 978
1861
1984
Chang, S-C. 642
Chang, X.Y. 643
Chang, Yuan-Pin 1352
Chang, Yung-Hsin 2123
Chapman, E. 1942
Chapman, H. 643
1140
1411
2274
Chapman, M. 829
Chapman, P. 644
Chapon, V. 1839
Chappaz, A. 1373
Chappell, A. 595
Chappell, B.W. 1108
1803
Charehsaz, N. 414
Charette, M. 525
Charlet, L. 483
756
841
902
1194
1602
1637
Charlier, B. 1969
Charlou, J.L. 644
1218
1623
Charmoille, A. 1264
Charnley, S. 1513
Charnock, J. 1608
1842
Charpentier, J. 645
Charreau, J. 1276
Charrier, R. 1756
Chataing, S. 1995
Chaudhri, N. 1156
Chaurand, P. 1290
1304
1751
Chaussidon, M. 645
646
1362
1404
1479
1884
Chauvel, C. 646
788
893
1292
2049
Chaux, L. 647
Chavagnac, V. 647
1490
Chavarria, K. 693
Chavrit, D. 474
648
Chazot, G. 1261
Che, X. 648
Checa, A.G. 1644
Chefetz, B. 1657
Chelnokov, G. 1178
Chemtob, S. 649
Chen, B. 649
Chen, Chao 620
2277
Chen, Chen 650
Chen, Chen 2246
Chen, Chunmei 2224
Chen, Dan-Ling 650
1342
Chen, Duofu 527
2022
Chen, Fukun 651
816
1316
1637
2210
2280
Chen, Fuwen 1111
Chen, G. 651
1345
Chen, H 401
Chen, Hongey 1024
1411
Chen, Hsiao-Chi 2213
Chen, Hsin-Wei 652
Chen, Hsuan-Wen 2213
Chen, Jian-Chang 652
Chen, Jiangfeng 2195
Chen, Jiawei 652
Chen, JingYing 653
Chen, Jiu-Bin 653
Chen, Jiubin 2086
Chen, Jun 1867
Chen, Jun 1111
1400
2276
Chen, Jun-Lu 654
1315
2198
Chen, Kai Loon 654
Chen, Kaiyun 2235
Chen, Kuikui 931
1374
Chen, Meng 2253
Chen, Michael 2110
Chen, Min-Te 1352
Chen, Nai-Chen 2213
Chen, Nan 643
Chen, Q. 432
655
Chen, R-X. 655
658
2270
Chen, S-H 2188
Chen, Sheng-Han 656
Chen, T.Y. 656
1056
Chen, W. 657
1111
1311
1964
Chen, X. 657
Chen, Yang 783
1111
Chen, Yan-Jing 2215
Chen, Yi 658
1341
2218
Chen, Yijun 2127
Chen, Yi-Xiang 658
891
Chen, Yong-Heng 1341
2119
Chen, Yongsheng 659
Chen, Youwei 526
Chen, Zhou 659
Chen, Zi-Wan 1332
2253
Cheng, C. 660
Cheng, D-H. 660
Cheng, H. 753
853
Cheng, J. 661
Cheng, T-W. 1330
2123
Cheng, Xiang 1310
Cheng, Xu 677
Cheong, C-S. 1109
Cherata, I. 1954
Cherchi, C. 661
Cherkasova, E. 662
Chernyshev, I. 662
Cheshire, M. 1814
Chesnyuk, A. 764
Chetelat, B. 1317
Chevalier, M-L. 2064
Chew, D. 663
Chhabra, P. 617
Chi, B.M. 1113
Chia, C. 1293
Chialvo, A. 663
Chiaradia, M. 541
614
918
1420
1457
1708
Chiessi, C. 948
1020
Chiffoleau, J.F. 1952
Chi Fru, E. 2110
2143
Chiglino, L. 664
1869
Chikaraishi, Y. 664
Childress, L. 1295
Chilom, G. 665
Chin, E. 665
1283
Chin, M. 526
666
Chiodini, G. 620
622
Chiogna, G. 1744
Chipman, L. 666
Chiriac, R. 1493
Chirico, R. 1013
Chirita, P. 667
Chistyakova, N. 2244
Chistyakova, S. 667
Chittleborough, D. 1118
Chiu, H-Y. 668
Cho, D-L. 1288
Cho, H.-R. 1131
Cho, M. 2079
Cho, S.Y. 668
2225
Cho, Y.C. 1287
Choël, M. 1902
Choi, Jong-A 1185
Choi, Jung-Yoon 1109
Choi, Man-Sik 1282
Choi, Mina 1862
Choi, Minseok 1184
1908
Choi, Sang-Hoon 669
Choi, Seon-Gyu 669
Choi, Sung Hi 670
Choi, Y-S. 1950
Chollet, M. 670
Chon, H.T 671
Chong, G. 432
Chopping, C. 671
Chorover, J. 672
970
1621
1621
1696
1749
2240
Chou, I-M 562
1058
Chourey, K. 1360
Chovan, M. 1201
Chow, P. 1878
Chowdhury, A. 1208
Chrastny, V. 672
1550
Christen, R. 1839
Christensen, J.N. 673
1680
Christenson, H. 2138
Christiansen, K. 1408
1409
Christl, I. 1625
Christl, M. 673
1018
2001
Christopoulou, D. 1602
Christov, C. 1272
Chu, B. 1367
Chu, N-C. 674

https://doi.org/10.1180/S0026461X00006502 Published online by Cambridge University Press

Chu, X. 674
..... 1168
Chuang, Patrick 1893
Chuang, Pei-Chuan 2213
Chubarova, N. 2065
Chugaev, A.V. 662
..... 1176
Chung, C-W. 1771
Chung, San-Hsiung 2213
Chung, Sun-Lin 668
..... 1338
Churakov, S. 675
..... 675
Ciabeghodsi, A. 676
Cicconi, M.R. 676
..... 676
..... 676
..... 921
Ciglenečki, I. 597
..... 677
Cihlarova, H. 677
..... 1260
Cikurel, H. 938
Cinque, G. 1817
Ciobanu, C. 1820
Ciobanu, G. 1402
Ciobotă, V. 1360
Cipriani, A. 555
Ciren, P. 1216
Ciric, A. 937
Cismasu, A.C. 678
..... 1464
Civetta, L. 451
..... 1121
..... 1499
Claesson, S. 528
Claeys, P. 753
Claff, S.R. 678
Clague, D. 1100
Claire, M. 831
Clark, B. 679
Clark, I. 1171
..... 1484
Clark, James 714
Clark, Jordan 1944
Clarke, Amanda 985
Clarke, Antony 679
Clarke, T. 604
..... 680
..... 1757
..... 2153
Clarkson, M. 2175
Class, C. 555
..... 680
..... 1035
Claude, C. 681
..... 681
Cleaves, Henderson J. 1228
Cleaves, H. James 1202
..... 1287
Clement, Alain 737
..... 1547
..... 1807
Clement, Amy 451
Cliff, J.B. 1298
..... 1506
Clift, P. 682
Clog, M. 682
Cloquet, C. 683
..... 818
..... 2067
Cluzel, D. 2049
Cluzel, N. 1211
Coates, J. 2004
..... 2180
Coath, C. 860
..... 1932
Cobert, F. 683
Cochran, J.K. 1752
Cockell, C.S. 1655
Cockerton, A.B. 684
Cody, G. 684
..... 2126
Coe, A. 756
..... 1091
Coe, H. 872
..... 1924
Coelho, D. 794
Coetsee, L. 1169
Coffin, R.B. 1752
Cogez, A. 685
Coggon, R. 2091
Cohen, Aaron 2065
Cohen, Anthony 756
..... 1091
Coke, C. 685
Coker, V. 608
..... 686
Çolak, D.N. 1776
Colakoglu, A.R. 686
Colarco, P. 687
Colbeck, I. 1948
Cole, D. 444
..... 663
Cole-Dai, J. 1114
Coleman, D. 687
Coleman, M. 413
Coleman Wasik, J.K. 688
Coles, B. 1267
..... 1271
Colic, J. 1472
Colin, A. 688
Colin, F. 681
Collerson, K. 689
Collignon, C. 2042
Collin, B. 1995
Collinet, G. 832
Collins, G. 701
Collins, R. 546
..... 689
Collinson, M.E. 1052
Collon, P. 1191
Colman, A. 527
Colombani, J. 1585
Colombo, M. 690
Colpaert, J. 1900
Coltorti, M. 548
..... 690
..... 1451
Colussi, A. 811
..... 1034
Colvin, V. 859
Coma, R. 1616
Comas, M. 1356
Comas-Rengifo, M.J. 1875
Conceição, R.V. 626
..... 691
..... 910
..... 1299
..... 1933
Conde, L. 1665
Condie, K. 691
..... 1557
Condon, D. 692
..... 1021
Conil, S. 1301
Connan, S. 635
Connelly, J. 692
Conrad, M.E. 673
..... 693
..... 708
..... 782
..... 1045
..... 1680
..... 2073
..... 2163
Conrad, S. 1032
Conrad, T. 1000
Constantinescu, S. 2046
Contreras Quintana, S. 1450
Cook, C. 693
Cook, D. 1969
Cook, M. 807
Cook, P. 2173
Cooke, D. 1491
Cooper, G. 694
Cooper, L. 694
Cooper, N. 463
Cooper, R. 728
Copley, J. 1011
Coppin, F. 1839
Corbeil, M-C. 1941
Cordani, U. 1355
Cording, A. 1953
Cordova, E. 1103
Corfu, F. 630
..... 685
..... 695
..... 1743
Corgne, A. 561
..... 848
Corinne, C. 1389
Corkhill, C. 644
..... 695
Cormier, L. 613
Cornelis, G. 2039
Cornelis, J-T. 696
Cornell, D. 1690
..... 2071
Coronado, F. 1233
Correia, A. 1838
Correia, G.G. 696
Correia, P. 1329
Corselli, C. 738
Corsetti, F. 1415
Corum, M. 536
Corvini, P. 1300
Cosca, M. 593
..... 1643
Cosmidis, J. 515
Cossart, E. 697
Costa, D. 2178
Costa, F. 564
Costanza, A. 768
Costin, D. 466
Côté, A. 697
Cottam, M. 585
Cottrell, E. 586
Couder, E. 698
Couradeau, E. 698
Courtin-Nomade, A. 558
..... 699
..... 948
..... 949
Cousineau, M. 699
Coutaud, A. 700
..... 1654
Couto, H. 700
..... 701
Couto, J.M. 701
Couture, R.M. 702
..... 1480
..... 1602
..... 2025
Coveney, P. 1972
Cox, R. 702
Crabtree, J. 703
Craddock, P. 703
Craine, J.M. 838
Cramer, C.J. 1887
Crane, E. 882
Crapster-Pregont, E. 1006
Crean, D. 686
Creaser, R.A. 462
..... 1028
..... 1168
..... 1292
..... 1814
..... 2060
Creech, J. 2187
Crespo-Feo, E. 1645
Criddle, C. 569
Criscenti, L. 704
Crispin, K. 2071
Crispini, L. 1393
Cristina, V-P. 1738
Croasdale, D.R. 2093
Crocket, K.C. 704
Croiset, N. 1601
Cronin, S.J. 578
..... 578
..... 1531
..... 1898
..... 1943
Croot, P.L. 538
..... 705
..... 1003
..... 2185
Cross, E. 705
Cross, J. 706
Crosson, W. 1345
Crosta, X. 1594
Croteau, M-N. 596

https://doi.org/10.1180/S0026461X00006502 Published online by Cambridge University Press

Crouch, E. 1593, 1990
Crout, N. 1897
Crowe, S.A. 706, 1123, 1312, 1957
Crowley, James 1975
Crowley, John 981
Crowley, Q. 935, 1377
Crudeli, D. 738
Crummy, J. 707
Cruz, Miguel 708
Cruz, M[a] Inês 707
Cruz-Uribe, A. 708
Cuadros, J. 1463
Cucchi, F. 1465
Cudahy, T. 1275
Cuello, G. 841
Cuesta, E. 1416
Cuevas, J. 2078
Cui, B. 709
Cui, Guang-Yao 1360
Cui, Guangyao 709
Cui, Q. 1374, 2120
Cui, Z.L. 836
Cuif, J-P. 1744
Cumming, V. 710
Cummings, P. 1378, 1666
Cummins, R. 1121
Cuney, M. 809, 1718
Cunha, F. 1328
Cunningham, H.S. 710
Curl, E. 488
Curtice, J. 2201
Curtius, H. 1262
Cusack, M. 711
Cuthbert, M. 1713
Cuthbert, S. 1683
Cutting, R. 686
Cypionka, H. 505
Czerny, J. 1259
Czuppon, G. 711

D

D'Alessio, M. 717
D'Antonio, M. 1499
Daae, F.L. 712
Dabiri, R. 1487
Dabrunz, A. 1810
Dachs, E. 946
Daemen, L. 2197
Dage, D. 1103
Dahl, T. 712, 970
Dahle, H. 712, 1933
Dahmann, D. 2138
Dahou, S. 1010
Dahrazma, B. 713
Dai, L-Q. 713
Dai, M. 2235
Dai, N. 714
Dai, T. 2251
Dai, Y. 1346, 1482
Daines, S. 714
Dalai, T.K. 715
Dalby, K.N. 715, 1565, 1569, 1827
Dal Corso, J. 716, 1667
Dale, A. 2035
Dale, C.W. 716, 759, 1086, 1381, 1552, 1610
Dall'Osto, M. 1580
Dallai, L. 558, 717
Dallas, J. 1473
Dalla Vecchia, E. 520
Dal Maso, M. 718, 1181
Dalton, C. 718
Daly, J.S. 719
Damashek, J. 1416
Damdinov, B. 719
Damdinova, L. 720
Damdinsuren, N. 968
Damian, C. 1101
Dammshäuser, A. 705
Dana, K. 402
Dandurand, J-L. 1916
Dang, H. 720
Danhara, T. 1899
Dani, N. 626
Daniel, I. 670, 721, 1639
Daniel, P. 2132
Danielache, S. 2046
Danielson, L. 2036
Danisik, M. 816, 1871, 2003
Dannhaus, N. 2101
Danyushevsky, L. 721, 954, 1445, 1608
Darabi Gholestan, F. 722
Daraktchiev, M. 1701
Daraoui, A. 722
Darbha, G. 849
Dardenne, K. 846
Dare, S. 723
Darling, J. 812
Dart, R.C. 1549, 2062
Darton, R. 1362
Das, Sarah 525
Das, Satadal 723
Dasgupta, R. 724, 1283, 1302, 1793, 2036
Dasgupta, S. 828
Da Silva, A. 957, 2065
da Silva, F.S. 1875
Da Silva Filho, A. 724
Datta, S. 991, 1528
Daugherty, S. 1673
Daughney, C. 725
Daumit, K. 705
Dauphas, N. 600, 703, 725, 1663, 1884
Daus, B. 1147
Daval, D. 726, 1784, 1885
David, J. 1647
David, M. 826
Davidheiser, B. 2064
Davidovits, P. 2093
Davidson, J. 1132, 2192
Davidson, S. 1856
Davies, A. 726
Davies, Gareth 2064, 2079
Davies, Geoff 727, 727
Davies, R. 726
Dávila, A.F. 2158
Davis, A. 728, 1361
Davis, C. 467
Davis, F. 728
Davis, J. 484, 729, 945, 1925
Davis, S. 1128
Davoudian Dehkordi, A.R. 729
Davranche, M. 1410, 1613
Dawson, K.S. 730
Day, C.C. 492, 730
Day, J. 560, 610, 731, 1508
Dayal, A.M. 1397, 1606
Dayan, U. 2002
de Andrade, V. 1712
Deane, G. 1770
de Baar, H. 1664, 1725
Debaille, V. 731, 788
De Bardon De Segonzac, C. 633
De Beer, D. 889, 1694
Debure, M. 732, 870
DeCarlo, P. 1013
Decesari, S. 825, 1587
Decesary, S. 1727
Dechamps, N. 1922
Declercq, J. 732
DeConto, R. 1586
Decrée, S. 733
De Deckker, P. 1898
Deditius, A. 733
Deegan, F.M. 594, 734, 1121, 1614, 2032
Deek, A. 734
Deerberg, M. 561, 969
Deering, C. 465, 986
Deevong, P. 1626
Deevsalar, R. 735
Deflandre, B. 1276
de Garidel-Thoron, T. 553
Degering, D. 735
De Giudici, G. 1808
Dehner, C. 853, 1209, 1428
de Hoop, M. 1859
Deibel, C. 1191
Deja, E. 736
Déjeant, A. 829
de Jong, J. 1664, 1725
de Jonge, M. 522, 2217
Dekas, A. 1574
Dekayir, A. 1464
de Koker, N. 521, 736, 1536
Dekura, H. 737, 2036
Delacour, A. 439
Delalande, M. 737
De Lange, G.J. 738, 940, 1009
Delaye, J-M. 613
Del Campillo, M.C. 1789
de Leeuw, G. 738, 1968
de Leeuw, J. 739
De Leeuw, N. 2172
Delgado-Bonal, A. 1418
Delgardio, J. 1068
Delikan, A. 739
Dell´Mour, M. 1812
Dell'Abate, M.T. 740
Della Puppa, L. 740

https://doi.org/10.1180/S0026461X00006502 Published online by Cambridge University Press

Dellinger, M. 1644
Dellwig, O. 741
1356
1522
1822
2166
Delmonte, B. 1629
2167
de los Ríos, A. 2158
Deloule, E. 547
733
741
847
1084
1211
1412
1458
Delvaux, B. 696
698
742
Del Vecchio, R. 537
742
Delvigne, C. 743
De Maddalena, I. 1979
DeMenocal, P. 574
Demény, A. 711
743
Demichelis, R. 744
744
Demidova, T. 786
De Min, A. 745
Demir, Y. 745
De Moor, M. 1023
Demouchy, S. 547
746
Demuth, F. 1476
Den Auwer, C. 1010
Denef, V. 2165
Deng, B. 746
Deng, H. 747
1618
Deng, Jie 1482
Deng, Jun 2235
2263
Deng, L. 747
1844
Deng, W. 2141
Deng, Y-T. 1621
Denham, M.E. 673
1925
Deniz, K. 748
1133
Dennis, K. 802
Dentener, F. 748
Denton, J. 2038
Deonarine, A. 1054
DePaolo, D.J. 749
782
880
1035
1539
1879
2136
2257
De Pelsmaeker, E. 1895
De Putter, T. 733
Derbeko, I. 749
Dere, A. 575
Derenne, S. 750
Derimian, Y. 1152
de Ronde, C. 2013
Derrey, I.T. 750
Derrien, D. 1709
Derry, L. 751
deRuiter, P. 751
1455
de Saint-Blanquat, M. 443
Desaunay, A. 752
Deschamps, P. 1628
1647
1728
Descostes, M. 2130
Descourvieres, C. 1832
Deshusses, M.A. 2257
de Souza, G. 752
1715
Desrochers, K. 1673
Desrochers, S. 753
Dessert, C. 881
Devau, N. 907
Devey, A. 2164
Devey, C. 805
Devilliers, A. 759
De Vivo, B. 770
1197
De Vleeschouwer, D. 753
Dewaele, S. 733
Dewers, T. 1527
De Windt, L. 732
DeWit, M. 876
Dey, S. 754
De Yoreo, J. 880
1056
1539
Dhankhar, R. 754
Dhuime, B. 528
Dhuime, Bruno 755
993
Dia, A. 1410
1613
Diamond, L.W. 428
Dias, Á. 707
Dias, M.I. 1408
2030
Dias, P. 1740
Dias, R. 1305
Di Carlo, I. 1805
Dick, G. 2146
Dickie, I. 1210
Dickinson, W. 755
Dickson, A. 756
Dickson, J. 1641
Dickson, T. 1358
Dideriksen, K. 920
1945
Didier, M. 756
Diedrich, T. 757
Diehl, T. 666
Dieing, T. 2023
Diekrup, D. 757
Diemar, G. 1375
Diener, A. 758
Dierssen, H. 477
Dietiker, R. 1979
Dietman, B.J. 758
Dietrich, M. 1560
Dietrich, W. 1543
Dietze, V. 952
1030
Dietzel, M. 870
1038
1538
1560
Diez Ercilla, M. 2146
DiGiovine, B. 1191
Dijkstra, A.H. 759
1552
Dikmen, S. 759
Dilek, Y. 760
876
Dimier, A. 1518
Dimond, C. 1692
Dimri, V. 2076
Di Muro, A. 1458
Dinelli, E. 622
1233
Ding, F. 611
760
Ding, G-C. 1671
Ding, L. 761
Ding, T. 761
889
Ding, Xing 1965
Ding, Xiong 1984
Dingwell, D.B. 676
762
Dini, A. 558
762
Dino, R. 1385
Diot, M.A. 1995
Dipple, G.M. 502
982
Dippold, M. 763
Dippon, U. 763
1147
1658
2077
Ditchburn, R. 755
Di Tommaso, D. 2172
Dittmar, T. 403
764
1541
2135
Dittrich, M. 764
1312
Dittrich, T. 765
Diwu, C. 765
1966
Dixneuf, S. 766
Dixon, D. 766
Dixon, J. 767
Diz, P. 767
Do, T.A. 454
Dobias, J. 768
Dobosz, A. 768
Dobrzhinetskaya, L. 769
1095
Dobson, D. 431
769
Do Cabo, V. 770
Docherty, K. 2162
Dodd, J. 2284
Doelsch, E. 1290
1304
1995
Doherty, A. 540
770
Doherty, C. 1006
Dohmen, R. 771
805
834
Dohnalkova, A. 865
1796
2163
Dolch, K. 2285
Dolejs, D. 521
831
1014
1817
1923
1937
1961
Dolgopolova, A. 771
Dolin, V. 772
Domagal-Goldman, S. 831
Domingos, R.F. 1635
Dommen, J. 1013
Donahue, N. 772
Donaldson Hanna, K. 944
Donard, O.F.X. 814
814
1788
Donat, J. 627
Dong, H. 598
1098
Dong, Shaohua 526
Dong, Shuofei 773
Dong, T. 2114
Dong, Y. 1374
Dong, Z-C. 1144
2190
Donis, D. 1110
Donnadieu, Y. 1291
Donoghue, K. 773
Donovan, J. 1980
Dontsova, K. 2240
Donval, J.P. 644
1218
Doppler, G. 500
774
Dorea, C. 1550
Dória, A. 774
1717
Dörsch, P. 775
1876
2277
Dorta, L. 584
775
1220
dos Santos Pinheiro, G.M. 1653
Dosseto, A. 776
1516
1973

https://doi.org/10.1180/S0026461X00006502 Published online by Cambridge University Press

Dosso, L. ... 776
... 968
... 1261
... 1498
Doty, S.D. ... 2094
Doucet, L-S. ... 513
... 777
... 930
... 1085
Douglas, P. ... 799
Douglas, T. ... 777
Doulati, F. ... 1099
Douvalis, A. ... 924
Dowell, D. ... 1988
Downes, H. ... 770
... 778
Downey, B. ... 2103
Downs, R. ... 994
Doyle, P. ... 778
Døssing, L. ... 706
Drábek, M. ... 2105
Drábek, O. ... 573
... 1994
Dragovic, B. ... 501
... 779
Drahota, P. ... 779
... 1391
... 1468
... 1994
Drake, H. ... 517
... 780
... 1421
... 2038
... 2231
Dreier, A. ... 780
Drenzek, N. ... 799
Dreossi, G. ... 781
Drevnick, P.E. ... 688
Drew, D. ... 835
Drewitt, J. ... 1098
Driese, S. ... 577
Driesner, T. ... 781
... 1026
... 2247
Droop, G. ... 1608
... 1683
Drouet, T. ... 698
Druhan, J. ... 782
... 2163
Druschel, G. ... 782
Druteikienė, R. ... 783
Du, K. ... 783
Du, S. ... 784
Du, Xin ... 784
Du, Xingxing ... 827
Du, Z. ... 2172
Duan, J. ... 1115
Duan, R-C. ... 1332
Duan, Z. ... 785
Duarte, E. ... 1700
Duarte, L.V. ... 696
... 785
... 1875
Dubacq, B. ... 786
... 1140
... 2013
... 2083
... 2158
... 2274
Dubessy, J. ... 518
... 1654
Dubinin, A. ... 786
... 1240
... 1726
Dubinsky, E. ... 693
Dubois, E. ... 1409
DuBois, J. ... 853
... 1209
... 1428
Dubrail, J. ... 787
... 1778
... 2160
Dubrovinsky, L.S. ... 787
... 1654
... 1664
... 1923
... 1961
Ducea, Mihai ... 1875
Ducea, Mihai ... 623
... 1756
Duchemin, C. ... 788
Duchêne, S. ... 1412
Dudas, F. ... 532
Duester, L. ... 1810
Dufek, J. ... 465
... 788
... 1067
Dufey, J. ... 696
Duffaut-Espinosa, L. ... 627
Duke, J. ... 766
Dulnee, S. ... 789
Dultz, S. ... 1880
Dumale, Jr., W. ... 789
Dümig, A. ... 790
Dumitras, D-G. ... 1076
Dunbar, G. ... 2167
Dunbar, N. ... 805
... 1572
... 1881
Dungan, M. ... 564
... 694
... 1132
Dunham-Cheatham, S. ... 1766
Dunkl, I. ... 790
Dunkley, D.J. ... 980
... 1087
Dunn, B. ... 531
Dunn, C. ... 1877
Duo, T. ... 612
Dupont, C. ... 791
Dupraz, C. ... 791
Dupraz, S. ... 1453
... 1473
Dupré, B. ... 1573
Duque, J.F. ... 623
Duran, A.L. ... 1398
... 1817
Durance, P. ... 1097
Durant, A.J. ... 792
Duretz, T. ... 1886
Durmus, E.S. ... 792
... 1570
Dursun, T. ... 793
Ďurža, O. ... 2083
Düster, L. ... 1202
Dutkiewicz, A. ... 1874
Dutrow, B. ... 793
Dutton, A. ... 794
Duvail, M. ... 794
Dybowska, A. ... 757
Dyda, R.Y. ... 1134
Dyment, J. ... 493
... 1007
Dymshits, A. ... 540
Dyriw, N. ... 449
Dziejowski, J.E. ... 795

E

Eadington, P. ... 562
Eagling, J. ... 796
Ebel, D.S. ... 796
Eberl, D. ... 1098
Ebinger, C. ... 941
Ebrahimi, S. ... 797
Echegoyen-Sanz, Y. ... 570
Ecke, F. ... 1548
Eckert, J. ... 441
Eckert, S. ... 797
... 1419
Eckert, W. ... 490
... 1140
Eckhardt, J.-D. ... 538
Edenborn, H. ... 1942
Edgar, K. ... 914
Edgerton, E. ... 1850
Edinei, K. ... 1299
Edinger, E. ... 1653
Edkymish, A. ... 959
Edwards, H.G.M. ... 1107
... 2094
Edwards, K. ... 2146
Edwards, L.R. ... 853
Edwards, M. ... 604
... 680
... 1757
... 2153
Edwards, N. ... 798
Edyvean, R. ... 472
Eeckhout, S. ... 921
Egal, M. ... 1503
Eggenkamp, H. ... 798
Eggins, S. ... 1143
... 1619
Egli, M. ... 799
Eglinton, T. ... 799
... 836
... 1734
... 1775
... 2103
Egorov, A. ... 1745
Ehlert, C. ... 800
... 942
Ehrenfreund, P. ... 1228
Ehrig, K. ... 1375
Ehya, F. ... 800
Eichhubl, P. ... 826
Eickmann, B. ... 801
Eidner, S. ... 801
Eigl, R. ... 802
Eikenberg, J. ... 992
... 1714
Eiler, J. ... 530
... 551
... 569
... 628
... 649
... 802
... 850
... 1358
... 1535
... 1901
... 2003
Eiriksdottir, E. ... 920
... 920
... 1945
Eisenhauer, A. ... 544
... 803
... 828
... 844
... 870
... 1018
... 1195
... 1326
... 1699
... 1989
... 2100
Eisenhauer, T. ... 451
Eisner, J. ... 803
Eissenstat, D. ... 1015
Ekholm, M. ... 1664
Ekman, A. ... 813
Ela, W. ... 1749
El Aref, M. ... 1783
Elbaz-Poulichet, F. ... 1503
Elburg, M. ... 1895
Eldad, S. ... 1657
El Gammal, E.S. ... 804
Elghorfi, M. ... 804
Eliasson, J. ... 2138
Elkins, L. ... 805
Elkins-Tanton, L. ... 560
Ellam, R.M. ... 1442
Elliott, A. ... 2134
Elliott, T. ... 448
... 805
... 805
... 867
... 1264
... 1651
... 1687
... 1932
... 2091
... 2161
Ellis, Ben ... 806
... 1614
... 2170
Ellis, Brian R. ... 806
Ellmies, R. ... 770
Elming, S-Å. ... 1083
Elmore, A. ... 807
El-Naggar, M. ... 1538

https://doi.org/10.1180/S0026461X00006502 Published online by Cambridge University Press

Elphick, S. 1256
Elsayed, O.F. 807
Elser, J. 1660
1746
Eltgroth, S. 1286
Elzinga, E.J. 808
1061
Emami, M.H. 1179
1486
Emanuel, H. 476
Emblanch, C. 1464
Embley, R. 1370
1984
Emeis, K-C. 808
Emerson, S. 809
Emetz, A. 809
Emmanuel, S. 810
Emre, H. 618
Emsbo, P. 810
Enami, S. 811
1034
Endo, S. 1963
Enea, F.C. 811
Eng, P. 1996
Engelbrecht, J.P. 812
1105
Engelen, B. 505
Engi, M. 812
Engling, G. 656
Engström, A. 813
Engstrom, D.R. 688
Engström, E. 2067
Ennaciri, A. 804
813
Enzmann, F. 1095
Enzweiler, J. 491
Epov, V. 814
Epova, E. 814
Erba, E. 738
Erbacher, J. 1002
Erban, V. 1103
1605
Erbanova, L. 815
2100
Erdinger, L. 1895
Erdmann, M. 548
Erel, Y. 1426
1589
2002
Eremets, M. 856
Erez, J. 803
815
844
1009
1195
1989
Ergin, M. 792
1570
1918
Erhardt, A. 816
Eric, S. 1289
Erickson, M. 1537
Eriksson, P. 1429
Eroglu, S. 816
Ersoy, B. 759
Ersoy, H. 817
Ervens, B. 1727
Erzinger, J. 2107
Esbensen, K.H. 506
Escartin, J. 968
Escauriaza, C. 1295
Escher, P. 2166
Escoto, M.O. 1747
Eser Dogdu, B. 792
1570
1918
Espahbod, M.R. 800
Esposito, R. 540
620
817
Esteban, J.J. 2078
Estes, M. 1345
Estes, S. 1345
Esteve, I. 698
Estévez Rodríguez, M.D. 606
Estradas-Romero, A. 2090
Estrade, N. 818
Etayo-Serna, F. 893
Etou, M. 818
1481
Etoubleau, J. 1261
1508
Etschmann, B. 1707
2011
Ettler, V. 819
1239
1468
2044
2095
Eturki, S. 819
Eun, S-H. 820
Eusterhues, K. 820
1344
1712
Evans, D. 530
821
Evans, J. 947
Evans, K. 821
822
1506
Evans, M. 1924
Evans, N. 2003
Evans, S. 1040
Evans, V. 1351
Evershed, R. 1088
1328
Eves, A. 711
Evins, L.Z. 822
Evrard, C. 823
Evstigneeva, T. 823
1691
Ewart, T. 689
Ewing, Robert 1338
Ewing, Rodney 505
733
Ewing, S. 432
Ewing, T. 824

F

Fabbrizio, A. 1535
Fabian, K. 1438
Fabisch, M. 825
Fabrega, J. 1948
Facchini, M.C. 635
825
1587
1727
Faccini, B. 1451
Fagel, N. 842
Fahey, D. 1944
Fahlman, B. 492
Fairall, C.W. 738
Fairchild, I. 552
Faiz, M. 826
Fajber, R. 1877
1878
Fakih, M. 1440
Falck, H. 436
Falguères, C. 911
Fall, A. 826
Fallick, A.E. 1001
1082
1152
1452
1714
Falloon, T. 721
Falteisek, L. 779
Falter, J. 1438
Fan, H-R. 827
1055
Fan, Q. 827
1315
Fan, Weiming 1965
2282
Fan, Wenling 1845
Fan, Yu 2251
2254
Fan, Yukun 1048
Fandeur, D. 587
Fang, J. 828
Fang, X. 2129
Fang, Y. 642
Fanghänel, T. 1194
Fanslau, J. 2103
Fantle, M. 828
Farber, D. 1792
Farges, F. 1300
Farkas, J. 829
1550
2100
Farmer, E. 829
Farmer, G.L. 830
Farnetani, C. 1035
Farnsworth, C. 830
Farnsworth, S. 626
Farquhar, J. 831
1140
1619
1663
1742
2247
Farrant, A. 1718
Faryad, S.W. 831
1817
Fat'yanov, O.V. 459
Fathabadi, G. 1496
Fathordoobadi, S. 1749
Faucon, M.P. 832
Faul, K. 1686
Faulhaber, A. 1633
Faulkner, D. 2152
Faure, G. 1543
Favas, P. 832
1665
1665
Favier, V. 1122
Favreau, E. 674
Fawcett, S. 1777
Fayek, M. 1579
Faz, A. 1750
Faz Cano, A. 606
2206
Fazelvalipour, Arash 833
Fazelvalipour, Ardalan 833
Federico, L. 1393
Fedortchouk, Y. 833
Fedotova, A. 528
Fehn, U. 834
1704
Fei, H. 834
Fei, Y. 747
835
1071
1844
Feig, S. 1210
Feijoo, S. 491
Fein, J. 1766
Feinberg, J. 588
Feineman, M. 708
835
Feingold, G. 679
Feinstein, S. 1082
Feiznia, S. 414
Fekete, A. 1016
Feldmann, H. 883
Fellhauer, D. 1194
Felmy, A. 1173
1173
2239
Fendorf, S. 1207
1306
1464
Feng, D. 527
2022
Feng, H. 2197
Feng, S. 836
Feng, Xiaojuan 799
836
Feng, Xin-Bin 653
Fenn, M. 1670
Fenn, T. 837
Fenter, P. 632
837
1378
Fenton, C. 1537
Ferdelman, T.G. 1450
2140
Fernandes, Firmino 1622
Fernandes, Flavia 774
Fernandes, Lina 838
Fernandes, Luis 1299
Fernandes, P. 554
1355
1740

https://doi.org/10.1180/S0026461X00006502 Published online by Cambridge University Press

Fernandez, C. 1462
Fernández, J.M. 838
..... 839
Fernández, R. 839
Fernandez-Caliani, J.C. 840
Fernández Davila, A. 917
Fernandez de la Reguera, D. 1957
Fernández-Díaz, L. 840
..... 1497
Fernández-González, Á... 2075
Fernandez-Gonzalez, A... 1669
Fernández-González, Á..... 840
Fernandez-Gonzalez, A... 1116
Fernández-Guallart, E. 1616
Fernandez-Martinez, A. 841
..... 1130
Fernández-Ondoño, E. 1540
Fernández Sanfrancisco, O. 1356
Ferot, A. 547
Ferraro, A. 1021
Ferrasse, J-H. 1290
Ferrat, M. 773
Ferreira, A. 1567
..... 1874
Ferreira, Cesar 1801
Ferreira, Claudia 841
Ferreira, N. 632
Ferreira, P. 1717
Ferreira, V. 616
..... 842
..... 1869
Ferreira da Silva, E.A. 610
..... 1408
Ferreira Lima, B.A. 1653
Ferrier, K.L. 1722
Ferris, D. 1114
Ferry, J. 551
Fevrier, L. 1839
Fialin, M. 2007
Fiałkiewicz-Kozieł, B. 842
..... 1896
Fiebig, J. 1880
Fiege, A. 843
..... 1396
Field, L. 843
Field, M.P. 1855
Field, P.R. 844
Fietz, S. 1029
Fietzke, J. 544
..... 803
..... 844
..... 1195
..... 1687
..... 1989
..... 2100
Fifield, K. 1760
Figuła, A. 471
Figura, S. 1811
Fike, D. 845
..... 850
..... 1459
Filella, M. 845
Filik, J. 1817
Filip, J. 1207
Filippi, M. 1391
..... 2242
Finch, A. 426
..... 1505
..... 1991
Finck, N. 846
Findling, N. 1493
..... 1885
Finessi, E. 825
..... 1587
Fink, D. 1973
Finkel, R.C. 1543
..... 1807
..... 2064
Finlay, A. 846
..... 1834
Finneran, K. 1953
Fintor, K. 847
Fiol, S. 444
Fiorentini, G. 690
Fiorentini, M.L. 486
..... 489
..... 847
Fiquet, G. 561
..... 848
Firat Ersoy, A. 848
..... 849
..... 956
Fischer, Christian 1449
..... 2138
Fischer, Cornelius 849
..... 1371
Fischer, Curt 2165
Fischer, S. 850
Fischer, T. 1023
Fischer, W. 845
..... 850
Fischer-Gödde, Mario 504
..... 851
Fischer-Gödde, Mario 2275
Fisher, A. 1818
Fisher, C. 1629
Fisher, K. 1612
Fisher, P. 723
..... 1960
Fitoussi, C. 851
Fitton, J.G. 1442
Fitts, J.P. 806
Fitzgerald, M. 598
Fitzgerald, P. 852
Fitzsimmons, J. 852
Flamerich, R. 766
Flanagan, J.B. 1105
Flanders, P. 1949
Flanner, M. 1683
Fleckenstein, J.H. 506
Fleisher, M. 436
..... 437
..... 462
Fleitmann, D. 853
..... 1244
..... 1811
..... 1979
Fletcher, I. 1511
..... 1696
Fliegel, D. 1200
..... 2073
Flis, J. 853
Floess, D. 854
Flora, O. 1465
Flores, K. 593
..... 1643
Florian, P. 1535
Flossmann, A. 854
Flügge, J. 1947
Fluteau, F. 1291
..... 1992
Flynn, G. 855
Foden, J. 855
Foerstendorf, H. 856
..... 1513
Fogaren, K. 921
Fogel, M. 2126
Fohlmeister, J. 1693
Foley, S. 856
..... 981
..... 2011
Folsom, J. 625
Fölster, J. 1212
Fomba, K.W. 857
Fomin, I. 857
Fones, G. 1006
Fonseca, Raúl O. C. 475
..... 858
..... 1275
Fonseca, Rita 707
Fontaine, G. 1220
Foote, E. 944
Foote, M. 2252
Ford, D. 1718
Foreman, B. 1901
Foriel, J. 2142
Fórizs, I. 1165
Form, A. 1687
Formolo, M.J. 1723
Formoso, M.L.L. 511
Fornace, K. 570
Forster, P. 1924
Forsterra, G. 2033
Forsyth, D. 1772
Fort, M. 697
Fortes, A.D. 946
Fortin, D. 699
..... 858
Fortner, J. 859
Fortney, J. 693
Fossen, H. 1213
Foster, G.L. 859
..... 960
..... 1009
..... 1415
..... 1476
..... 1687
Foster, James H. 932
Foster, John 1037
Foster, L. 860
..... 1687
Foster, T. 793
Fottova, D. 815
..... 1550
Fouquet, Y. 644
..... 674
..... 823
..... 1218
..... 1261
..... 1508
Fourie, D. 981
Fourre, E. 860
..... 1218
Foustoukos, D. 1287
Fowle, D. 706
..... 1303
..... 1957
Fox, M. 2162
Fox, P. 484
..... 729
Fralick, P. 1217
Fram, J. 921
France, L. 547
France-Lanord, C. 683
..... 861
..... 1276
..... 1369
Franchi, I.A. 1469
Francis, D. 407
..... 1556
Francisco, G. 406
Francois, R. 1333
..... 1811
Francu, J. 861
..... 1205
Frandsen, C. 862
..... 915
Frank, A.H. 1495
Frank, E. 862
Frank, Mark 435
..... 1878
Frank, Martin 533
..... 656
..... 800
..... 863
..... 897
..... 942
..... 989
..... 1018
..... 1233
..... 1575
..... 1943
..... 1956
..... 2001
..... 2286
Frank, R. 492
Franke, K. 1022
Franke, M. 863
Franklin, R. 1346
Franz, G. 1026
..... 1363
Franz, J. 942
Franz, L. 1354
Franzen, M. 634
..... 864
..... 1328
Fraser, D. 864
Fraser, H. 2103

https://doi.org/10.1180/S0026461X00006502 Published online by Cambridge University Press

Freda, C. 516
... 594
... 734
... 1121
... 1422
... 1614
Fredrickson, J. 604
... 680
... 865
... 1757
Freedman, P. 2229
Freeman, C. 1491
Freeman, K.H. 730
... 874
... 1377
... 1384
Freeman, S. 1339
Frei, D. 1452
Frei, R. 403
... 516
... 616
... 706
... 1765
Freitag, S. 679
Freitas, Maria Da Conceição 1499
Freitas, M. C. 433
Freitas, S. 1354
Freiwald, A. 1491
Frenz, M. 1244
Frenzel, P. 1117
Frerichs, Janin 865
Frerichs, Joshua 1433
Freslon, N. 501
Freund, H.-J. 470
... 866
Freund, S. 866
Freundt, F. 867
Frew, A. 2003
Frew, R. 898
Frey, F. 1451
Freyer, G. 1068
Frey-Klett, P. 2042
Freymond, C.V. 2147
Freymuth, H. 867
Frezzotti, Maria Luce 495
Frezzotti, Massimo 781
Fricker, M.B. 1979
Friedman, R. 1039
... 1831
Friedrich, L. 868
Frierdich, A. 632
... 868
Frigaard, N-U. 702
Frigeri, F. 1838
Frings-Meuthen, P. 1019
Frith, M. 1762
Fritz, B. 637
... 737
... 869
... 1547
... 1807
Fritzsche, A. 869
... 2157
Frogley, M. 1817
Fröjdö, S. 460
Fröllje, H. 797
Frondini, F. 622
Frosini, D. 781
Frossard, A. 497
... 1770
Frossard, E. 1983
Frost, D.J. 542
... 1256
... 1551
... 1590
... 1591
... 1763
... 1928
... 2086
... 2097
... 2163
Fruchter, N. 870
Frugier, P. 732
... 870
Früh-Green, G. 1269
... 1830
Frutschi, M. 2130
Frýda, J. 1988
Fryer, B.J. 1894
... 2143
Fu, S.M. 643
Fuchs, P. 871
Fuchs, Sebastian 897
Fuchs, Sebastian 871
Fuchser, J. 403
... 764
Fuentes-Lopez, E. 872
Fueri, E. 493
Fujii, N. 1564
Fujimura, H. 468
... 872
... 1143
... 1160
Fujino, K. 1921
Fukami, Y. 873
Fukuyama, M. 873
Fulda, B. 874
Fulthorpe, R. 764
Fulton, J. 874
... 1377
Fulton, S. 583
Funk, S.P. 875
Füri, E. 875
... 1007
Furman, T. 941
... 1531
Furmann, A. 876
Furnes, H. 760
... 876
Furrer, G. 2174
Fußwinkel, T. 877
Futter, M. 877
... 1212
Fuzzi, S. 1727

G

Gäb, F. 878
Gabelica, Z. 759
Gabitov, R. 878
... 1821
Gable, C. 793
Gabrielsen, R.H. 1743
Gadgil, A. 2067
Gaede, O. 1908
Gaeta, M. 1422
Gaetani, G. 879
Gagan, M. 1143
Gagnevin, D. 879
... 880
Gagnon, A. 880
Gago-Duport, L. 767
... 917
Gai, H. 2114
Gaillard, F. 881
... 971
... 1076
... 1504
Gaillardet, J. 560
... 861
... 881
... 1023
... 1609
... 2013
... 2086
Gaillou, E. 882
Gaines, R. 882
Gajos, N. 1366
Galankina, O. 1890
Galbiatti, H. 1292
Galbraith, E. 1093
Gale, Allison 718
Gale, Andrew 2270
Gale, J.D. 744
... 744
Galeczka, I. 883
Galeotti, S. 1586
Galer, S.J.G. 403
... 431
... 585
... 883
... 1019
... 1664
Galera Monge, T. 1356
Galindez, J.M. 884
Galindo-Uribarri, A. 1104
Galiová, M. 1242
... 2084
Galkova, O. 543
Gall, L. 884
Gallagher, K. 805
Gallardo, R. 2206
Gallego, J.R. 885
Gallego-Urrea, J. 1126
Gallet, S. 646
Galloway, T. 1948
Galoisy, L. 613
... 885
Galoyan, G. 1777
Galuskova, I. 2066
Galvez, M. 515
Galy, A. 886
... 897
... 1024
... 1050
... 1140
... 1411
... 1562
... 1920
... 2165
... 2274
Galy, V. 799
... 836
... 1023
... 1369
Gamble, J.A. 1442
Gamo, T. 570
... 1992
Gamyanin, G. 2087
Ganbavale, G. 1402
Gane, J. 986
Ganeshram, R. 1640
Gangloff, S. 886
... 2096
Ganguly, D. 1695
Ganguly, J. 536
... 2014
Ganne, J. 480
Ganopolski, A. 887
Ganor, J. 1754
Gantt, B. 887
... 1457
Gao, B. 888
Gao, E.G. 761
... 888
Gao, F. 2116
Gao, H. 889
Gao, Jianfei 761
... 889
Gao, Jun 2060
Gao, K. 2262
Gao, Lei 890
... 1309
Gao, Liangmin 890
... 891
... 2195
Gao, Li-E 2245
Gao, Lin 649
Gao, R. 1273
Gao, S. 1060
... 1340
... 1344
... 1348
... 1454
... 2197
... 2253
Gao, T. 2270
Gao, Xiang 620
Gao, Xiao-Feng 1144
... 2190
Gao, Xiao-Ying 891
... 2270
Gao, Xiong 2276
Gao, Xubo 892
Gao, YongBao 892
... 2262
Gao, Yongjun 2192

https://doi.org/10.1180/S0026461X00006502 Published online by Cambridge University Press

Gaona-Narvaez, T. 893
Garanin, V. 1395
..... 1885
Garbarino, G. 438
..... 848
Garbe-Schönberg, D. 426
..... 966
..... 990
..... 1012
..... 1096
..... 1560
..... 1661
..... 1989
..... 2140
..... 2171
Garcia, M.O. 601
..... 998
..... 1642
..... 2142
Garcia-Arostegui, J-L. 681
García Casco, A. 1906
Garcia-Guinea, J. 1004
García-Martínez, M.J. 885
Garcia-Olivares, A. 1015
García Ruiz, J.M. 1576
..... 2065
Garcin, M. 1731
Garcin, Y. 1829
Garcon, M. 646
..... 893
Gardenová, N. 894
Gardner, M. 500
Garg, S. 894
..... 995
Garijo Marcos, D. 895
Garnier-Zarli, E. 1440
Garric, J. 1751
Garrido, C.J. 1401
..... 1586
Garrido, F. 895
..... 1004
Garuti, G. 415
..... 896
..... 1214
..... 2030
..... 2055
..... 2238
Gasek, R. 896
..... 1463
..... 2159
Gasharova, B. 1662
..... 1675
..... 1908
Gaspar, A. 1016
Gasparon, M. 1652
Gasser, D. 588
Gatebe, C. 1077
Gates, A. 604
..... 680
Gattacceca, J.C. 897
Gaucher, C. 616
..... 664
..... 1869
Gauert, C. 897
..... 2030
Gault, A. 898
Gault-Ringold, M. 898
..... 1945
Gaupp, R. 1783
Gautam, M. 1282
..... 1908
Gautason, B. 899
Gautheron, C. 1383
Gauthier-Lafaye, F. 1106
Gautier, Q. 899
..... 1430
Gavanji, N. 900
Gavrieli, I. 938
Gavrilov, Y. 756
Gawęda, A. 1470
Gawronski, T. 900
..... 2131
Gayer, E. 901
Gaynullova, O. 1745
Gazel, E. 901
Gazze, Salvatore A. 1146
Gazze, Salvatore A 1398
Geantet, C. 1751
Gebauer, D. 744
Gebbie, G. 902
Gee, M. 784
Geerlings, P. 542
Gehin, A. 483
..... 902
Gehlen, M. 1459
Gehrels, G. 903
Geibert, W. 903
..... 1007
..... 1053
..... 1640
Geiger, F. 1127
Geilert, S. 904
Geisler, T. 1190
..... 1298
..... 1455
Geissler, A. 1351
..... 1834
Geldmacher, J. 1019
..... 1221
..... 1516
Gelinas, Y. 904
Gellissen, M. 905
..... 928
Genc, S.C. 905
..... 1176
Genin, A. 1008
Génin, J-M. 906
Genoni, L. 781
Genske, F.S. 906
Gente, P. 1507
Georg, B. 742
..... 1548
..... 1571
Georg, R.B. 1803
..... 1844
George, A. 446
George, S. 1874
GeorgeOna-Nguema, G. . 1276
Georgiev, S. 907
..... 1930
..... 2287
Geotraces Intercalibration Participants, ... 2061
Geraki, T. 1608
Geraldes, M.C. 2074
Gérard, E. 698
..... 1453
Gerard, F. 907
Gerard, M. 1992
Gerdes, A. 541
..... 592
..... 770
..... 908
..... 1103
..... 1156
..... 1339
..... 1364
..... 1468
..... 1474
..... 1497
..... 1690
..... 1708
..... 2043
Gerdts, G. 1541
Gerlach, F. 1081
Germerott, S. 908
Gerringa, L. 1664
..... 1725
Geršl, M. 909
Geršlová, E. 909
Gersonde, R. 436
..... 994
Gertner, I. 909
Gervasoni, F. 910
Gervilla, F. 934
..... 2090
Gerya, T. 471
..... 910
..... 1393
..... 1886
..... 2098
Gerzabek, M.H. 2039
Gescher, J. 1720
..... 2285
Gessner, K. 936
Geyer, S. 1488
Ghaleb, B. 481
..... 911
..... 1617
Ghanbari, M. 1483
Gharasoo, M. 1948
Ghasemi, A. 1843
Ghavami-Riabi, R. 722
..... 911
..... 1390
Gherardi, J-M. 1333
Ghinet, C. 1076
Ghosh, D. 912
Ghosh, P. 1693
Ghosh, S. 912
Giammar, D. 484
..... 913
Giannakis, G. 1595
Gianoncelli, A. 1388
Gibbons, A. 1032
Gibbon-Walsh, K. 913
Gibbs, S. 914
Gibert, E. 481
Gibson, B. 1673
Giehl, C. 914
Gieré, R. 915
..... 1030
..... 1137
Giese, R. 1703
Giesler, R. 1569
Giffaut, E. 756
Gil, C. 767
Gilabert, J. 681
Gilbert, A. 1314
Gilbert, B. 915
..... 1757
Gilbert, P. 916
Gilbert, S. 1445
Gilfillan, S. 916
Gill, B. 1373
Gill, J. 917
..... 1189
..... 1692
..... 2017
Gillet, P. 1721
Gilli, A. 1540
Gillies, S. 2103
Gillikin, D.P. 1921
Gillow, J. 679
Gil Lozano, C. 917
Gima, S. 1143
Gimeno, M.J. 918
Gimmi, T. 675
Gin, S. 732
..... 870
..... 1700
Ginder-Vogel, M. 1920
Gingras, M. 1631
Giordano, G. 706
Giosan, L. 799
Giraldez, I. 840
Girardeau, J. 918
Girardi, C. 1476
Girguis, P.R. 919
..... 1121
..... 2131
..... 2146
Girlanda, F. 1809
Girnth, A-C. 919
Giroud, N. 2104
Gislason, Sigurdur 1945
..... 2171
Gislason, Sigurdur R. 423
..... 883
..... 920
..... 920
..... 951
..... 1569
..... 1571
Giuli, G. 676
..... 921
Gkritzalis-Papadopolous, A. 1591
Gladding, T. 1655
Glaser, B. 763
Glatzel, P. 921
Glazer, B. 921
Glazner, A. 1475

https://doi.org/10.1180/S0026461X00006502 Published online by Cambridge University Press

Glazyrin, K. 542
1664
Gleason, A. 1406
Gleason, J. 398
922
1210
Gleixner, G. 1081
1117
1368
1829
Gliwicz, T. 545
Gloaguen, E. 1452
Glockzin, M. 741
Glombitza, C. 922
1801
Glover, A. 1011
Glover, C. 546
689
Glud, R. 666
Gnauk, T. 857
981
Gniese, C. 865
1154
Gnos, E. 1102
Go, Y-H. 923
Gocmez, G. 923
Godard, M. 1334
1635
1837
Goddard, W. 924
1034
Goddéris, Y. 1573
Godel, B. 489
Godelitsas, A. 450
924
1155
Godon, N. 2005
Godoy, J.M. 1764
Goehring, B. 1807
Goel, G. 925
Goessler, W. 1584
Goettlicher, J. 925
1201
Goffredi, S. 926
Gogot, J. 926
Gökgöz, A. 1165
Golanoski, K. 537
742
Goldberg, T. 927
Goldblatt, C. 927
1474
Golden, J. 994
Goldfarb, R.J. 1542
Goldhaber, M. 928
Golding, S. 486
1465
Goldmann, A. 928
Goldsmith, J. 1753
Goldstein, A. 2162
Goldstein, S.L. 555
1132
1491
1589
2024
Golobocanin, D. 1472
Golovin, A. 777
1085
Golubev, Y. 929
929
Golubeva, Y. 929
Gombiner, J. 1006
Gomboev, B. 2050
Gomes, C. 841
1358
Gomes, E. 832
Gomes, Marcia E.B. 511
Gomes, Maria 685
1418
1993
Gomez, J. 918
Gómez-Garrido, M. 606
Gómez-Pugnaire, M.T. 1401
1586
Gomi, H. 1027
Goncalves, J. 1628
Gonçalves, M. 930
1387
1645
Goncalves, R. 1385
Goncharov, A. 930
Gondar, D. 444
Gondikas, A. 931
1054
Gong, J. 657
Gong, L. 931
1374
Gong, Q. 2263
Gong, W. 2262
Gonnermann, H.M. 932
Gonzales, M. 2136
González, A.G. 932
1795
González, F.J. 933
Gonzalez, P. 933
Gonzalez-Alvarez, I. 934
González-Dávila, M. 932
1795
González Fairén, A. 917
Gonzalez-Jimenez, J.M. 934
2090
Gonzalez-Muñoz, M.T. 1816
González-Toril, E. 1796
Good, N. 423
2154
Goodbred, S. 2141
Goodenough, K. 935
1377
Goodfellow, B. 935
Goodhue, R. 554
1355
Goodwin, D.H. 1921
Goodwin, T. 1603
Gooseff, M. 598
Gopel, C. 936
Gorbachev, N. 1226
Gorbatsevich, F. 1604
Gorby, Y. 1538
Gorczyk, W. 936
Gordanic, V. 937
Gordon, G. 1501
2151
Gordon, J. 764
Gordon, S.M. 937
Goren, O. 938
Gorin, G.E. 1585
Gorski, C. 938
Goss, A. 1161
Gostic, R. 939
Goto, A. 939
2202
Goto, T. 1368
Gou, L. 940
Goudeau, M-L. 940
Gould, D. 537
Gourgaud, A. 1995
Gourlan, A.T. 1460
Gouze, P. 1635
Govil, P.K. 1378
Grace, M. 2173
Graham, D. 590
941
973
Graham, I. 755
2013
Grail, Q. 1713
Gralnick, J. 941
2022
Grancher, D. 1122
Grange, M. 942
Granger, D. 2267
Granieri, D. 622
Grant, K. 1611
Graser, P. 1429
Grass, G. 1707
Grassa, F. 630
Grasse, P. 800
863
942
989
Grassian, V. 943
Grassl, H. 1627
Grathwohl, P. 1744
Gratzer, R. 943
2103
Gray, D. 1705
Gray, W. 587
Gréau, C. 944
Grebenshchikova, V. 814
Green, A. 1574
Green, D. 872
1229
Green, H. 769
1095
Green, S. 1068
Greene, J. 1191
Greenhagen, B. 944
Greenwell, C. 864
1972
Greenwood, R. 716
Grégoire, M. 741
1084
1427
1451
1677
Gregory, C. 1696
Gregory, K. 945
Grémare, A. 1791
Greneche, J-M. 902
Greskowiak, J. 945
Grevel, K-D. 946
1391
Grew, E. 947
994
Grice, S.M. 1016
Griffin, W.L. 934
946
1051
1182
1395
1528
1558
1850
1922
2090
2121
2143
2232
2234
2244
Griffioen, J. 947
Grimes, C. 1155
Grimes, S.T. 1052
Grinenko, V. 596
Groat, L.A. 947
1474
Grobéty, B. 1449
2031
2138
Grocholski, B. 1860
Grocke, D.R. 1023
1661
Groeneveld, J. 948
Grosbois, C. 558
948
Gross, J. 949
Grossin-Debattista, J. 1434
Group, K. 1813
Gruau, G. 1410
1613
Gruiz, K. 599
Gründger, F. 1244
Grunert, P. 1038
Grybos, M. 949
Gu, A.Z. 661
Gu, C. 1590
Gu, H. 2192
Gu, P-Y. 997
Gu, Xiaochun 1307
Gu, Xiaoxi 784
Guan, Ye-Bin 2271
Guan, Youfei 950
1342
1857
2228
2249
Guan, Yunbin 649
850
1535
Gucer, M.A. 460
950
Gückel, K. 1513
Gudbrandsson, S. 951
Guderitz, I. 2048

https://doi.org/10.1180/S0026461X00006502 Published online by Cambridge University Press

Gudkov, A. 951
Guedes, A. 629
..... 952
..... 1716
..... 1740
Gueguen, B. 1914
Guéguen, F. 952
Guelke-Stelling, M. 953
..... 2101
Guendouz, A. 1628
Gueneli, N. 953
Guenne, A. 1434
Guenther, A. 997
..... 1727
Guenther, D. 1220
Guenther, F. 1117
Guérin, O. 906
Guerrot, C. 938
Guest, R. 1588
Guggenberger, G. 1922
Guicharnaud, R. 1571
Guilderson, T. 807
Guillon, S. 1644
Guillong, M. 559
..... 954
..... 1445
..... 1839
Guillot, B. 430
..... 971
..... 2104
Guillot, S. 2049
Guimaraes, I. 724
..... 954
Guitreau, M. 1485
Gulecal, Y. 955
..... 1460
Gul Karaguler, N. 473
Güllü, B. 955
..... 1133
Gulmez, F. 905
Gultekin, F. 848
..... 849
..... 956
Gun, J. 1140
Günay, A. 759
Gunay, K. 686
Günther, D. 583
..... 584
..... 775
..... 1979
Guo, A. 765
..... 956
..... 1966
Guo, C-J. 1054
..... 2274
Guo, D. 1322
Guo, G. 2261
Guo, J-L. 891
..... 1454
Guo, Lei 1144
..... 2190
Guo, Liang 1021
Guo, S. 658
..... 1341
..... 2218
Guo, W. 2229
Guo, X. 411
Guo, Yangyang 956
Guo, Yonghai 972
Guo, Yun 957
Guo, Zhaojie 1308
Guo, Zhouping 2262
Gupta, M. 2131
Gupta, P. 957
Gupta, S 773
Gupta, Sanchayan 684
Gurioli, L. 958
Gurriaran, R. 1936
Gurugubelli, B. 958
Gussone, N. 519
..... 959
..... 1118
..... 2140
Gustafsson, J.P. 959
Gustafsson, S. 2039
Gustaytis, M. 1813
Gutareva, O. 2057
Gutierrez, V. 918
Gutjahr, M. 543
..... 960
..... 1687
Guttman, J. 938
Gutzmer, J. 765
..... 979
..... 1655
..... 1791
..... 1833
Guyader, V. 644
..... 1218
Guyot, F. 561
..... 1453
..... 1473
..... 1885
Guzman, M. 960
Guzmics, T. 518
..... 961
Gwalani, L. 711
Gwanmesia, G. 1326
Gwynn, J.P. 1048
Gysel, M. 476
Gysi, A. 961

H

Ha, J. 587
Ha, N.T. 515
Haase, K.M. 508
..... 574
..... 866
..... 906
..... 962
..... 990
..... 1246
..... 1703
Haber, T. 1694
Habicht, K. 702
Habler, G. 1981
Hache, M. 1154
Hacker, B.R. 937
..... 962
..... 1166
..... 1189
..... 1260
..... 2069
Haderlein, S.B. 1117
..... 1574
Hadj Ammar, F. 1628
Hädrich, A. 963
Haeckel, M. 1010
..... 1326
Haertig, C. 1648
Haese, R. 963
Haest, M. 1275
Haflidason, H. 1732
Hageman, S. 964
Hagemann, S. 1913
Hagiwara, S. 818
Hahm, D. 1600
Hahm, W.J. 1722
Hahn, B.C. 1766
Hahn, T. 1655
Hahne, K. 2034
Haigis, V. 964
..... 1098
Hain, M.P. 965
Hakala, J. 497
..... 718
Hakkakzadeh, B. 2199
Halama, R. 965
..... 966
..... 1118
..... 2140
Halbach, P. 1459
Halden, N. 868
Haley, B.A. 1943
..... 1956
..... 2001
Halfpenny, A. 1442
Halisch, M. 2239
Hall, A. 680
..... 2153
Hall, I. 2009
..... 2241
Hall, P. 966
Hall, R. 585
Halldorsson, S. 1023
Haller, M. 1573
Hallet, B. 1949
Halliday, A.N. 742
..... 884
..... 967
..... 1325
..... 1539
..... 1571
..... 1673
..... 1803
..... 1872
..... 1969
Hallmann, C. 2006
Halverson, G. 855
..... 1072
Hama, K. 2202
Hamada, M. 967
..... 1752
Hamada, S. 1161
Hamamura, N. 968
Hamelin, B. 681
..... 1628
..... 1647
Hamelin, C. 776
..... 968
..... 1498
Hamilton, D. 969
Hamilton, J. 423
Hamilton, V.E. 969
Hammack, R. 1942
Hammarlund, E. 970
Hamme, R. 809
Hammer, J. 589
..... 958
..... 1852
Hammond, C. 970
Hammond, S.J. 1381
Hammor, D. 557
Hammouda, T. 971
Han, J. 1168
Han, M-S. 1109
Han, Run-Sheng 971
..... 1062
..... 1307
..... 1312
..... 1592
..... 2121
..... 2145
..... 2180
..... 2182
..... 2208
..... 2290
Han, Ruyang 2073
Han, Yeongcheol 972
Han, Y.h. 1989
Han, Yong 972
Hanan, B. 590
..... 776
..... 973
Hanano, D. 487
Hanchar, J. 1629
..... 1878
Hancock, G. 1944
Händel, M. 417
..... 869
..... 973
Handler, M. 974
..... 1473
..... 2187
Handler, R. 1757
Handley, H. 974
..... 1439
Handley, L. 1593
..... 1990
Handley-Sidhu, S. 975
..... 1039
..... 1713
..... 1948
Hanebuth, T. 2160
Hanemann, R. 975
Hanfland, C. 903
Hanfland, M. 542
Hang, Z. 2229
Hanger, B. 522

https://doi.org/10.1180/S0026461X00006502 Published online by Cambridge University Press

Hanilçi, N. 745
Hanke, A. 636
Hanke, F. 1167
Hanley, J.J. 409
976
1174
1290
1634
1942
Hann, S. 1812
Hanna, K. 1840
Hannah, J.L. 907
976
2196
2287
Hannah, P. 2274
Hannah, T. 1305
Hannington, M. 1100
1257
Hannukainen, M. 1968
Hans, U. 1199
Hansel, C.M. 977
1280
1298
1796
2075
Hansen, B.T. 1200
Hansen, Hans Christian B. 463
1064
Hansen, Heidi Elisabeth 977
Hansteen, T.H. 844
1687
Hanyu, T. 978
Hao, A. 2124
Hao, J. 1374
2120
Haraguchi, D. 978
Harald, M. 1703
Hardcastle, T. 1350
Hardy, B. 696
Harigane, Y. 1087
Häring, M. 979
Harlavan, Y. 979
1497
Harley, S. 1377
Harlov, D. 980
Harms, B. 831
Harper, D. 970
Harpold, A. 1621
Harries, D. 980
1256
Harris, C. 594
981
1121
1614
Harris, E. 981
Harris, James Arthur 1016
Harris, Jeffrey W. 1533
Harris, M. 2091
Harris, S. 1305
Harrison, A.L. 982
Harrison, R. 588
1438
Harrison, T.M. 878
982
1981
Harsh, J. 1641
Hart, D. 704
Hart, S. 983
1094
Hart, W.K. 2186
Hartmann, J. 983
984
984
1495
Hartmann, L.A. 1624
Hartnett, H. 985
1746
Hartog, N. 985
Hartung, E. 986
Harvey, C.F. 1534
Harvey, J. 603
986
Hasalová, P. 987
Hashemi, S.M. 987
Hashimoto, K. 1524
Hashizume, K. 988
Hasiotis, S. 828
Hasni, S. 638
Hasozbek, A. 988
Hassan, M.Q. 1648
Hassellöv, M. 1126
2039
Hassenkam, T. 920
989
1426
1530
1945
Haszeldine, R.S. 916
Haszeldine, S. 1001
Hatcher, P.G. 401
507
Hathorne, E. 989
1233
1941
1943
Hatipoglu, E. 848
849
956
Hatipoglu, Z.N. 990
Hatløy, V. 907
Hattendorf, B. 584
1220
Hatton, P-J. 1709
Hattori, R. 1314
Hattori, S. 1079
2046
Hauff, F. 990
1012
1032
1096
1661
Haug, G.H. 965
1748
Haug, J. 991
Haug, T. 1528
Haughton, P. 2043
Hauri, E. 991
1594
1642
1648
1804
2150
Häusler, K. 741
Hausmann, B. 1626
Haussler, W. 1409
Hautot, S. 971
Havelcová, M. 861
992
Havlova, V. 992
2084
Havránek, V. 1829
1955
2084
Hawkesworth, C.J. 528
755
993
993
1108
1152
1268
1798
Hawley, N. 496
Hay, M. 729
945
Hayes, C. 994
Haynes, H. 1550
Hazemann, J-L. 721
1290
1639
Hazen, R.M. 684
994
1202
1287
1350
1971
2091
Hazen, T. 693
995
He, D. 995
He, G. 2235
He, H. 1089
He, J. 2268
He, K. 996
1461
He, M. 996
1329
He, P. 1434
He, Sheng 1317
2117
He, Shigen 761
888
1965
He, Shi-Ping 997
2113
He, Tengbing 2037
He, Tong 1111
He, Z. 709
Headley, J. 492
Heald, C. 997
Heald, S. 865
1609
Heaman, L. 462
1556
Heath, J. 1527
Heaton, D. 998
Heberling, F. 998
Hebert, C. 1721
Heck, S. 998
Hedlund, T. 999
Hedrich, S. 1119
Hedström, M. 999
Heeschen, K. 1000
1730
Hefter, J. 1521
Hegan, A. 2138
Heggie, G. 486
Hegoda, C. 834
Heidbuechel, I. 1621
Heighton, L. 742
Heim, C. 2004
Heim, M. 695
Heimsath, A. 432
Hein, J.R. 1000
1655
Heinemann, A. 844
Heinemann, N. 1001
Heinrich, B. 2048
Heinrich, C.A. 409
1226
1839
Heinrich, W. 1709
2216
Heister, K. 1001
1046
1671
Hejazi, S.H. 1773
Held, P. 585
Heldt, M. 1002
Helffrich, G. 1002
Hélie, J-F. 753
Hellebrand, E. 958
1764
Heller, M.I. 705
1003
2185
Hellevang, H. 398
421
1003
1065
1638
Hellige, K. 508
Hellmann, R. 726
Helmhart, M. 895
1004
Helms, J.R. 1004
Helmy, H. 475
1005
1169
Hélouis, T. 1752
Helz, G. 1005
Helz, R. 1884
Hem, C. 920
1612
1945
Hembury, D. 1006
Hemley, R. 2203

https://doi.org/10.1180/S0026461X00006502 Published online by Cambridge University Press

Hemming, S. 642, 693, 1006
Hemmings, A. 680
Hemond, C. 493, 973, 1007, 1101, 1261, 1507
Hendel, R. 2111
Henderson, D. 1191
Henderson, G.M. 492, 534, 692, 730, 903, 1007, 1020, 1045, 1053, 1371, 2006, 2057, 2241, 2270
Henderson, M. 1842
Henderson, R. 2077
Hendrickson, C. 1739
Hendry, K.R. 1008, 1736
Hendy, E. 1008
Henehan, M. 1009
Henjes-Kunst, F. 770
Henkel, S. 1723
Henley, R. 1429, 1987
Henne, S. 2085
Hennekam, F.M. 1009
Hennet, L. 1098
Hennig, C. 478, 1010
Henriques, R. 1761
Henry, D. 793
Hensen, C. 1010, 1326, 1356
Hentscher, M. 1011, 1702
Hepburn, L. 1011
Herbert, R. 1012
Herbrich, A. 1012
Hergt, J. 1608
Hering, J.G. 830, 1939
Hering, S. 2162
Heringa, M. 1013
Herman, F. 2162
Hermann, J. 824, 1013, 1229, 1311, 1413, 1646, 1938
Hermanska, M. 1014
Herms, P. 1014
Hernandez, A. 1116
Hernandez, E. 1700
Hernandez, L.B. 1685
Hernandez, R. 610
Herndon, E. 1015
Herndon, S. 705
Hernes, P.J. 1134
Hernlund, J. 1027, 1547, 1689
Herrero, C. 1015
Herrin, J.S. 628
Herrmann, A.M. 1016
Herrmann, H. 575, 857, 981, 2144
Herrmann, M. 963
Herrmanndoerfer, T. 1834
Hertkorn, N. 1016
Hertzberg, J. 1017
Herut, B. 427, 445, 1500, 1532, 1769
Hervé, F. 539
Hervig, R.L. 450
Herwartz, D. 1017, 1365
Herwehe, L. 598
Herzberg, C. 901
Hesselbo, S.P. 1225
Hettich, R. 1360, 2165
Hettmann, K. 1018
Heuer, L. 1018
Heuer, V. 963, 1832
Heumann, A. 451
Heuser, A. 1019
Hewitt, M. 492
Heydolph, K. 1019, 2140
Hibberson, W. 1229
Hibbert, K. 1020
Hickey, B. 1020
Hickey-Vargas, R. 580
Hickmott, D. 2197
Hicks, S. 1279
Hidalgo Staub, R. 1244
Hierro, A. 482, 1176
Hiess, J. 1021
Higgins, J. 514
Higgins, S.R. 1784
Highwood, E. 1021
Higuchi, H. 1143
Higuchi, T. 468, 872, 1160
Hilary, D. 459
Hildebrand, H. 1022
Hill, A. 844
Hill, L. 1851
Hill, S.M. 758, 1118, 1443, 1480, 1549, 2062
Hillaire-Marcel, C. 1022, 1653
Hillamo, R. 825
Hillel, P. 695
Hillenbrand, C-D. 960
Hiller, E. 1051, 2083
Hilley, G. 935, 1493, 2064
Hillgren, V. 1844
Hilton, D. 493, 594, 1007, 1023, 1252, 2032
Hilton, R.G. 886, 1023, 1024, 1050
Hin, R.C. 1024
Hindersmann, I. 1025
Hindshaw, R. 1025
Hingerl, F. 1026
Hinrichs, K-U. 963, 1702, 1832
Hinsinger, P. 907, 1129
Hintelmann, H. 653
Hinton, R. 860
Hinz, C. 1832
Hiorth, A. 1445, 1446, 1613
Hippler, D. 1026
Hirahara, Y. 978, 1984
Hirai, K. 789
Hirai, M. 1544
Hirajima, Takao 1963, 2225
Hirajima, Tsuyoshi 1503, 1799
Hirao, N. 458
Hiraoka, N. 1547
Hirata, D. 1573
Hirata, T. 1027, 1159, 1562, 1564, 2223, 2227
Hiroaki, I. 1105
Hirose, Katsumi 1182
Hirose, Kei 458, 1027, 1215, 1547, 1961
Hirsch, L. 1554
Hirschmann, M.M. 450, 728, 1028, 2168
Hnatyshin, D. 1028
Ho, H.H. 1029
Ho, S.L. 1029
Ho, T-Y. 1030, 1284
Hoàng-Hòa, T.B. 915, 1030
Hoareau, G. 1490
Hobbs, B. 936
Hochella, M.F. 1031, 1042, 2077
Hochleitner, R. 2055
Hochstetler, D. 1744
Hode, T. 1874
Hodell, D. 1031
Hodson, M.E. 581, 1886
Hoefen, T. 1305
Hoehn, E. 1074
Hoenisch, B. 1619
Hoeprich, P.D. 1431
Hoernle, K. 990, 1012, 1019, 1032, 1096, 1236, 1661, 2140
Hoeschen, C. 1512
Hofacker, A. 1032
Hofer, M. 579
Hoffman, C. 2175
Hoffmann, D. 1823
Hoffmann, G. 1129
Hoffmann, J.E. 1033, 2084
Hoffmann, K.H. 1152
Hoffmann, Martin 1033
Hoffmann, Michael 811, 1034
Hoffmann, T. 1254, 2009
Hofhansl, F. 1495
Hofmann, Albrecht W. 555, 1034, 1035, 1393, 1904, 2020
Hofmann, Amy E 1035
Hofmann, Axel 743, 1776

https://doi.org/10.1180/S0026461X00006502 Published online by Cambridge University Press

Hofmann, T. 1450
..... 1533
..... 2259
Hofstetter, T.B. 938
..... 1887
Hohl, S. 1036
Hokr, M. 1036
Holben, B. 1152
Holbig, E. 1936
Holden, A. 1037
Holden, J. 1100
Holden, P. 1037
..... 1086
Holland, G. 1038
..... 1963
Holland, H. 509
Holland, T. 1900
..... 1991
Holländer, H. 1927
Höllen, D. 1038
..... 1560
Holler, T. 2139
Holliday, K. 638
..... 1039
Hollings, P. 1039
Hollis, C. 1593
..... 1990
Holm, P.M. 485
Holmden, C. 828
..... 1040
..... 1811
..... 2178
Holmes, W. 1265
..... 1691
Holtz, F. 493
..... 548
..... 559
..... 1073
..... 1596
..... 1864
..... 1931
..... 2249
Holzheid, A. 905
..... 1270
Holzkamper, S. 1693
Holzner, C.P. 2032
Homoky, W. 1007
Homolova, V. 1040
Hon, R. 1041
Honda, M. 1169
Hong, J. 2246
Hong, Soon Gyu 1600
Hong, Sungmin 972
..... 1918
Hong, Wei 1041
Hong, Wei-Li 2213
Hooda, A. 754
Hooker, J.J. 1052
Hoose, C. 1042
Hopcroft, P. 1823
Hopf, J. 1042
Hopkins, M. 1043
..... 1485
Hoppe, P. 981
..... 1209
..... 1947
Hoppert, P.D.M. 780
Hoppmans, E.C. 1540
Hora, J.M. 1043
Horan, M. 1044
Horiguchi, K. 1044
Horikawa, K. 1782
Horita, J. 551
..... 1045
Horn, I. 1279
..... 1935
..... 2145
Horn, M. 1737
Horn, W. 1190
Horner, T. 1045
Horng, M.J. 1024
..... 1411
Hornibrook, E. 1328
Horsfield, B. 520
Horstmann, M. 1046
Horstwood, M.S.A. 572
..... 1021
Horwath, W. 1327
Höschen, C. 1001
..... 1046
Höss, P. 1047
Hoth, N. 1154
..... 1879
Hou, K. 1047
..... 1320
Hou, L.H. 1369
..... 2119
Hou, X. 1048
Hou, Z.Q. 1347
..... 2010
Hough, R. 1048
..... 1332
Houghton, J. 1049
House, C. 1574
Houzar, S. 1049
..... 1052
..... 1207
Hövelmann, J. 509
Hovis, G. 1050
Hovius, N. 886
..... 1024
..... 1050
..... 1411
..... 1920
Hovorič, R. 1051
Hovorka, S. 916
Howard, D. 522
..... 2217
Howard, K.A. 1334
Howe, C.J. 2026
Howe, R.C.T. 1146
Howell, D. 1051
Hrazdil, V. 1052
Hrdlička, A. 1955
Hren, M.T. 1052
Hršelová, P. 1049
..... 1207
Hruska, J. 1234
Hsieh, A. 903
Hsieh, B. 1567
Hsieh, P-S. 1268
Hsieh, Y-T. 1053
Hsu, N.C. 1053
..... 2035
Hsu-Kim, H. 931
..... 1054
..... 2257
Hu, Chao 2118
Hu, Chaoyong 1348
Hu, Chun-Hua 1054
..... 2274
Hu, D. 682
Hu, F-F. 827
..... 1055
Hu, G. 2245
Hu, J. 1055
Hu, K. 1909
Hu, Qiaona 1056
Hu, QinHong 892
Hu, Rong 1056
Hu, Rui-Zhong 526
..... 1057
Hu, Shou Zhi 1057
..... 1317
Hu, Shui-Ming 1361
Hu, Shumin 1058
..... 2255
..... 2259
Hu, W. 1058
Hu, Xiaojia 956
Hu, Xiaoxiao 612
Hu, Xiao Yan 1059
Hu, Xin 2127
Hu, Xiu-Mian 2264
Hu, Xuefei 1345
Hu, Yandi 1130
Hu, Yi-Duo 2121
Hu, Yuan 1618
Hu, Yung-Jin 1545
Hu, Yu-Zhao 1059
Hu, Z. 1060
..... 1348
..... 2272
Hua, R. 1060
Huang, Fang 1061
Huang, Fengxian 1374
Huang, Haiping 1567
Huang, Huang 1857
Huang, Jen-How 1061
..... 1658
Huang, Jian 1062
Huang, Jian-Guo 1062
..... 2121
Huang, Jing 674
Huang, Jing-Li 1063
Huang, Junhua 1063
..... 2272
Huang, Lin 1361
Huang, Li-Zhi 1064
Huang, P. 1064
Huang, Ruifang 1065
Huang, Ru-Jin 1254
Huang, Shanshan 1065
..... 1565
Huang, Shichun 966
..... 1451
Huang, Shipeng 1066
Huang, W. 1870
Huang, X. 1060
Huang, Y. 1066
..... 2114
..... 2256
..... 2289
Huang, Zaixing 2053
Huang, Zhigang 1067
Huang, Zhixin 2235
Hubbard, S. 1925
Huber, C. 465
..... 788
..... 1067
Huber, F.M. 1047
Hublet, G. 731
Hudáčková, N. 1468
Hudgins, T. 1511
Hudon, P. 1068
Hudson, G. 434
Hudson, J. 1358
Huertas, J. 621
Huettel, M. 660
..... 666
..... 1068
Huff, W. 1069
Hug, S. 1069
..... 1534
..... 2097
Hughen, K. 524
Huh, Y. 972
..... 1070
..... 1918
Huisman, A. 1070
Hull, A. 467
Hull, M. 2088
Hulshof, A. 537
Humayun, M. 728
..... 2168
Hummel, M. 1042
Hummer, D. 1071
Hund, S.V. 1071
Hunt, C. 1667
Hunt, S.A. 1469
Hunter, J. 705
Hunter, K. 898
Hur, H. 1357
Hur, S.D. 972
..... 1918
Hurel, C. 617
Hürlimann, N. 1072
Hurowitz, J. 649
Hurtgen, M. 1072
..... 1126
Hurtig, N.C. 1073
Husen, A. 1073
Hussam, A. 1534
Husted, S. 814
Hutcheon, I. 939
..... 1095
Huxman, T. 2240
Huxol, S. 1074
Huyskens, M. 1074
Hwang, Jeong 1075
Hwang, Jin-Ju 1109
Hwang, Jinyeon 1075
Hwieh, Y-T. 1007
Hyatt, N. 695

https://doi.org/10.1180/S0026461X00006502 Published online by Cambridge University Press

Hypr, D. 909
Hyun, H-N. 923
Hyvönen, E. 1357

I

Iacono-Marziano, G. 1076
1504
Iacovino, K. 1572
Iancu, A.M. 1076
Ibrahim, R. 1401
Ibrahim, T. 1734
Icenhower, J. 1077
Ichikawa, H. 1158
Ichoku, C. 1077
Idrus, A. 494
1078
2238
Igarashi, T. 1979
Iglesias-Briones, M.J. 767
Ignatiev, A. 1969
Ignotti, E. 1354
Igor, T. 951
Iguchi, A. 1085
Ihlenfeld, C. 1303
Iijima, K. 1999
Iizuka, R. 1078
Iizuka, T. 425
1074
1079
Ijiri, A. 1079
1782
Ikeda, M. 1080
Ikehara, M. 1782
Ikehata, M. 1080
Ilangovan, D. 1081
Ilanko, T. 1572
Ilgner, B. 679
Illerhaus, B. 1081
Illing, C.J. 1082
1578
Illner, P. 1082
Ilton, E. 470
1173
Imai, T. 2223
Imfeld, G. 807
Imoto, H. 789
Inácio, M. 1083
Inagaki, F. 1079
Inanli, F. 1069
Indoitu, R. 1152
Ingri, J. 1083
1548
Ingrin, J. 741
1084
2086
Ingrisch-Ertel, W. 676
Innocent, C. 1617
Inomata, S. 1987
Inoue, A. 1084
Inoue, C. 1423
1561
Inoue, M. 1085
2226
Inskeep, W.P. 503
521
968
1104
1232
Ionescu, D. 1694
Ionov, D.A. 459
513
513
777
805
930
1085
Ip, W-H. 2278
Ireland, Thomas 1663
Ireland, Trevor 1037
1086
2153
Irvine, K. 1719
Irving, T. 1199
Isaac, C. 1039
Ishibashi, H. 2201
Ishibashi, J. 2029
Ishibashi, Y. 1989
Ishiga, H. 2230
Ishii, H. 1547
Ishikawa, A. 1086
1993
Ishikawa, T. 1158
1258
2203
Ishimaru, S. 1087
Ishizuka, O. 1087
1984
Ishuk, N. 543
Isla, E. 1791
Ismail, S.S. 1088
Isozaki, Y. 1145
Isseven, T. 905
Istok, J. 1103
Itai, T. 968
Ito, A. 1088
Ito, H. 1089
Ivanic, T.J. 1529
Ivanochko, T. 1441
Ivanov, Alexander 1922
Ivanov, Alexei 1089
Ivanov, S. 951
Ivanova, T. 1224
Iwai, K. 1793
Iwamori, H. 1090
1090
1258
Iwane, K. 1561
Iwanuch, W. 496
1801
Iwasaki, N. 2226
Iwatsuki, T. 1800
Izokh, O. 1091
Izon, G. 1091

J

Jabbar, T. 1092
Jablonska, M. 1092
Jaccard, S. 1093
Jackova, I. 1550
Jackson, I. 1326
Jackson, M. 610
624
966
1093
1094
1219
Jackson, R. 1484
Jackson, Samuel 1146
Jackson, Simon 1094
Jackson, V. 766
Jacob, D. 1095
Jacobs, J. 1213
Jacobsen, B. 1095
Jacobsen, Stein 829
Jacobsen, Steven 2150
Jacobson, A. 777
1096
Jacques, G. 1096
2140
Jadamec, M. 1097
Jaffrey, M. 1949
Jagadamma, S. 1433
Jagoutz, O. 471
1097
Jahn, B-M. 646
1391
Jahn, S. 964
1098
1231
1652
2184
Jahnke, C. 1927
Jahren, J. 1003
Jaisi, D. 1098
Jak, H.G. 1168
Jakobsson, M. 922
Jakub, T. 1988
Jakubowski, T. 1099
Jalayeri, H. 1099
1178
Jalowitzki, T.L.R. 910
James, R. 552
2148
Jamieson, H. 898
Jamieson, J. 1100
Jamtveit, B. 509
1100
Jan, M.Q. 1871
Jang, E-S. 1600
Janin, M. 1007
1101
Janmaat, A. 2103
Janneck, E. 1101
Janney, P. 1102
Janots, E. 1102
1263
1651
Janousch, M. 422
Janoušek, V. 1103
1551
1988
Jansen, M. 985
Jansik, D. 1103
Janssen, A. 1896
Janzen, M. 1104
Jaramillo, C. 1875
Jardine, A. 1696
Jardine, P. 1045
Jaroń, I. 1247
1281
Jarrett, R. 1705
Jarvis, A. 599
Jaupart, C. 1403
1638
Javad PoorgohardiI, M. 399
Javanbakht, M. 2025
Jay, Z. 1104
Jayanty, R.K.M. 812
1105
Jayawardana, D.T. 1105
Jayne, J. 705
Jeambrun, M. 1106
1296
Jean, M. 1106
Jean-Baptiste, P. 860
1218
1623
Jeandel, C. 1125
1943
Jeandel, E. 1518
Jeanloz, R. 1406
Jeanson, A. 1010
Jedidi, N. 819
Jedlička, R. 831
Jeffries, T. 1566
Jehlicka, J. 1107
1994
2094
Jellinek, M. 2142
Jemmali, N. 1916
Jeng, F-S. 1337
Jenkin, G. 1897
Jenkyns, H.C. 534
2270
Jenner, F. 449
1107
1558
Jennings, E. 1108
Jensen, K.A. 822
Jensen, M. 1171
1484
Jensen, S. 775
Jeon, H. 1108
Jeong, G-Y. 1185
Jeong, Jaein 1599
Jeong, Jong-Tae 1597
Jeong, Yong Seok 1286
Jeong, Youn-Joong 1109
Jephcoat, A. 453
Jerome, R. 1289
Jerram, D.A. 1164
Jerzykowska, I. 1109
Jessell, M.W. 480
Jessen, G. 1110
Jettestuen, E. 1613
Jew, A. 1899
Jezek, J. 1468
Jézéquel, D. 603
1280
Jheong, W-W. 1286
Ji, Hongbing 1110
2279

https://doi.org/10.1180/S0026461X00006502 Published online by Cambridge University Press

Ji, Hongwei 657
..... 1111
..... 1311
..... 1964
Ji, J.F. 611
..... 783
..... 1111
..... 1323
..... 1400
..... 2276
Ji, L. 2214
Ji, X. 1112
Jia, D. 1112
Jia, G. 1113
Jiang, C. 1191
Jiang, F. 1113
..... 1965
Jiang, Ganqing 1168
..... 1778
Jiang, Guo-Hao 1057
Jiang, J-H. 1054
..... 2274
Jiang, Shao-Yong 2213
..... 2264
..... 2275
Jiang, Simin 2269
Jiang, Su 1114
..... 2272
Jiang, W. 1361
Jiang, Xiaohua 2267
Jiang, Xiao-Hui 827
Jiang, Xin 1114
Jiang, Y-H. 2213
..... 2271
Jiang, Z.Y. 661
Jiao, G. 2267
Jiao, J-G. 1115
Jiao, K. 1115
..... 2215
Jickells, T. 640
Jilbert, T. 1116
Jimenez, A. 1116
..... 1497
Jimenez, J-L. 617
..... 1924
..... 2162
Jimenez-Diaz, A. 1766
Jiménez-Espejo, F.J. 1739
Jiménez-Gámez, D. 1873
Jimoh, M.T. 547
Jin, B. 1117
Jin, H. 2261
Jiskra, M. 1887
Jitaru, P. 832
Jo, H-J. 1109
Joachimski, M. 1246
Jochum, K.P. 475
..... 1017
..... 1117
..... 1275
..... 1904
..... 2212
Johannesson, K. 991
..... 1528
Johengen, T. 496
John, C. 1128
John, T. 1014
..... 1118
..... 1277
..... 1759
..... 1896
Johnson, A. 1118
Johnson, Barrie 1119
Johnson, Brent 1856
Johnson, C. Annette 1939
Johnson, Clark M 1043
Johnson, G. 1119
Johnson, I. 1561
Johnson, K. 1101
Johnson, Mark 841
Johnson, Matthew 887
..... 1120
..... 2046
Johnson, N. 1120
Johnson, T. 1480
Johnsson, A. 989
Johnston, D.T. 1121
..... 1663
Johnston, S. 602
..... 1163
..... 2173
Jolas, P. 1879
Jolis, E.M. 734
..... 1121
..... 1614
..... 2032
Jollivet, P. 613
Jomelli, V. 1122
Jonczy, I. 1122
Jones, Adele M. 995
Jones, Adrian P. 497
..... 1469
Jones, Camille 1753
Jones, CarriAyne 1123
..... 1957
Jones, Daniel 1123
..... 2247
Jones, David 845
Jones, Jesse 1124
Jones, John 1124
..... 2054
Jones, L. 1572
Jones, M. 920
..... 1125
Jones, Tessa 708
Jones, Tony 1588
Jonkers, H. 1784
Jöns, N. 1125
..... 1134
..... 1437
..... 1866
Jonsson, C. 1126
Jonsson, H. 1893
Joo, Y.J. 1126
Jorand, F. 1840
Jordan, D. 1127
Jordan, G. 899
Jorge, F. 455
Jorge, R.C.G.S. 1740
Jorgensen, B. 1204
Jorge Pedro, G. 406
Joschko, M. 1081
Joseph, S. 1293
Joshi, R.K. 1127
..... 1435
Joulian, C. 558
Jourdan, A-L. 1128
Jourdan, F. 1128
..... 2003
Jouvin, D. 1129
Jouzel, J. 634
..... 1129
Jovanovic, D. 937
Joye, S.B. 1832
Joyner, D. 693
Jørgensen, B.B. 1450
Jørgensen, S.L. 712
Jroundi, F. 1816
Ju, N. 1710
..... 2264
Judith, H. 1354
Juillot, F. 587
..... 1503
..... 1668
Jun, Y-S. 1130
..... 1130
Jung, E.C. 1131
Jung, Hae-Jin 1911
Jung, Haemyeong 1131
..... 1598
..... 1650
..... 1662
..... 1675
..... 1908
Jung, I-H. 1068
Jung, J. 2111
Jung, Stefan 1432
..... 1577
Jung, Sung Yun 1188
Jurányi, Z. 476
Juřička, D. 1132
Jurkovič, Ľ. 1051
..... 2083
Jweda, J. 1132

K

Kabengi, N. 1706
Kaczorek, D. 1935
Kadik, A. 1133
..... 1394
Kadioğlu, Y.K. 748
..... 955
..... 1133
..... 1222
Kaegi, R. 1534
..... 1939
..... 2097
Kaestner, M. 1828
Kagan, E. 1935
Kagi, H. 1078
..... 2244
Kah, M. 2259
Kahl, W-A. 1134
Kahn, R. 1077
Kaiser, K. 636
..... 1134
..... 1203
Kajdas, B. 1135
Kakegawa, T. 1579
Kakonyi, G. 1388
..... 1747
Kakuk, B. 451
Kalangi, A. 567
Kalbitz, K. 636
..... 1203
Kali, E. 2064
Kalinichev, A. 1135
..... 1136
Kalinowski, B. 419
..... 1424
Kaliwoda, M. 1837
..... 2055
Kallmeyer, J. 408
..... 922
..... 1136
..... 1801
Kalmykov, S. 1632
..... 1745
Kalogerakis, N. 1496
..... 1595
Kaltenbach, A. 1137
Kaltenmeier, R. 1137
Kalvoda, J. 1223
Kamaci, O. 1138
..... 2216
Kamber, B.S. 465
..... 1138
..... 1633
..... 1755
Kamenetsky, V. 559
..... 1139
..... 1169
..... 1375
..... 2217
Kameyama, S. 1987
Kamga, A.W. 401
..... 507
Kaminski, U. 1030
Kaminsky, F. 1139
Kamkar, A. 2283
Kamkar-Rouhani, A. 2230
Kämpf, H. 1243
Kampman, N. 786
..... 1140
..... 2158
..... 2274
Kamyshny, A. 1140
Kan, J. 1279
Kananian, A. 1141
..... 1980
Kanao, T. 1119
Kanayama, K. 1087
Kandeler, E. 1001
Kandler, N. 1092
Kanduč, T. 1141
Kaneko, M. 1142
Kaneoka, I. 1142
..... 2028
Kaneshima, S. 1002
Kaneshiro, A. 1143
Kang, H. 468
..... 1597
Kang, Jung Ok 1143
Kang, Jung-Yoon 1144

https://doi.org/10.1180/S0026461X00006502 Published online by Cambridge University Press

Kang, K-G. 923
Kang, Lei 1144
Kang, Lei 1342
2190
Kang, M. 483
902
Kang, S-A. 1188
Kani, T. 1145
Kanický, V. 894
1242
1955
Kantor, I. 1792
Kanzaki, Y. 1145
Kao, S-J. 1050
Kaotekwar, A.B. 1146
Kapitulcinova, D. 1146
Kaplan, D.I. 1797
Kaplan, H.B. 2078
Kaplan, L. 1147
Kappler, A. 763
1147
1148
1234
1453
1509
1658
2077
2206
Karadag, M.M. 1582
Karageorgis, A. 450
Kara Gülbay, R. 1148
Karakas, Z.S. 792
1570
1918
Karakaya, N. 635
1149
Karakus, A. 1566
Karapurkar, S.G. 1431
Karaseva, O. 512
Karato, S-I. 1149
1587
Karban, J. 1829
Karcher, M. 1048
Karimzadeh, L. 1150
Karki, B. 736
1150
Karl, T. 1151
Karlicek, D. 781
Karlsson, T. 999
1151
Karnieli, A. 1152
Karnland, O. 999
Karpoff, A-M. 1296
Karpukhina, V. 2088
Karunakaran, C. 1730
Kasama, T. 588
Kasemann, S. 805
1152
2175
Kashiv, Y. 1191
Kashiwabara, T. 1153
Kashyap, N.R. 1153
Kasper, S. 2063
Kassahun, A. 1154
Kasten, S. 1723
2160
Kästner, M. 1476
Kaszuba, J. 671
1527
Katayama, T. 1154
Kato, Souichiro 1524
Kato, Susumu 1524
Kato, Y. 1154
1553
Katsev, S. 764
1312
Katsikopoulos, D. 1155
1669
Katsnelson, M. 1664
Katsura, T. 834
2227
Katz, J. 915
1757
Katzir, Y. 1155
Katzlberger, C. 1092
Kaudse, T. 1156
Kaufman, A.J. 757
Kauliich, B. 1388
Kaur, P. 1156
Kausch, M. 1157
Kautenburger, R. 1157
1504
Kavner, A. 531
1689
Kawabata, H. 978
1189
1984
Kawabata, Y. 2224
Kawagucci, S. 1079
1392
Kawahata, H. 1085
1158
2203
2226
Kawai, K. 1158
Kawakami, T. 1159
Kawamura, Kenji 1841
Kawamura, Kimitaka 1159
Kawamura, R. 1160
Kawana, K. 1160
Kawasaki, K. 554
Kawasaki, T. 1161
Kay, S. 1161
Kaya, S. 587
Kayama, M. 1162
1543
Kayzar, T. 1661
Kazahaya, K. 1258
Kazemi Mehrnia, A. 1162
Kazil, J. 679
Kazmierczak, J. 1237
Keech, A.R. 434
1163
1720
2061
Keene, A. 1163
Keene, W. 497
1770
Keerthi Devi, D. 1925
Keevil, H. 1595
Kefi, S. 751
Kegler, P. 905
1270
Keiblinger, K.M. 1495
Keiding, J.K. 1164
2034
2177
Keil, T. 1477
Keiluweit, M. 1164
1634
2132
Keith-Roach, M. 796
1165
1738
Kele, S. 1165
Kelemen, P. 937
1166
1166
Keller, C.K. 1167
Keller, D. 446
Keller, L. 517
Keller, N. 1370
Kelley, D. 1100
Kelley, K. 586
1396
1630
1648
Kelley, S. 1167
Kelly, C. 1231
Kelly, S. 569
Kelokaski, M. 511
Kemner, K.M. 569
598
1259
1556
1766
Kemp, T. 993
Kempe, S. 1237
Kempl, J. 1168
Kendall, B. 433
757
1168
1778
1831
Kendelewicz, T. 587
Kendrick, M. 1169
Kennedy, Ben 986
Kennedy, Bianca 1169
Kennedy, M. 1170
1170
Kennell, L. 1171
Kennett, B. 1171
Kenney, J. 1172
Kent, A. 1611
1998
Kent, D.V. 424
1808
Kent, P. 1378
Kent, R. 2088
Keppens, E. 753
Keppler, F. 429
Keppler, H. 521
1172
1322
Kerestedjian, T. 934
Kerisit, S. 1173
1173
1338
Kerr, A. 1020
Kerr, M. 1174
Kerrich, R. 934
1174
1397
1779
1913
Kersten, F. 1175
Kersting, A. 1064
1175
Keskin, M. 905
1176
2051
Kesler, S. 733
1193
Kessel, R. 1198
Ketabdari, M.R. 2025
Ketterer, M. 1176
Kettler, R. 1177
Khakhinov, V. 2050
Khalaf, E.E.D.A.H. 1177
Khalili, A. 889
1450
Khalo-Kakai, R. 911
Khan, Maudood 957
Khan, Muhammad Asif 1871
Kharghani, M. 713
Kharitonova, N. 1178
2057
Kharlamova, S. 2203
Khatib, M.M. 668
Khazaii, M. 1178
1179
Khezri, M. 1486
Khodaian Chegeni, Z. 1179
Khodri, M. 1122
Khosh, M. 777
Khoury, H.N. 1180
Kido Soule, M. 1249
Kieber, D. 497
Kieber, R. 1180
Kiemele, E. 1871
Kiendler-Scharr, A. 718
825
1181
1587
Kienel, U. 1748
Kienzler, B. 591
1458
Kierczak, J. 736
949
1181
2044
Kiflawi, I. 1182
Kikawada, Y. 1182
Kikuchi, S. 1183
1392
Kil, Y. 1183
Kilburn, M.R. 1298
1585
Kilcoyne, D. 684
Killick, D. 837
Kilpatrick, A. 1754

https://doi.org/10.1180/S0026461X00006502 Published online by Cambridge University Press

Kim, Bojeong 1031
Kim, Byung-Gon 820
..... 1187
Kim, C. 1706
Kim, Deug-Soo 1184
Kim, Dong Woo 669
Kim, Goeun 1184
Kim, Guebuem 2135
Kim, Hyang Mi 1600
Kim, HyeKyeong 1911
Kim, I. 1285
..... 1599
Kim, Jae Gon 1287
Kim, Jinwook 1098
Kim, Jiyeon 1185
..... 1284
Kim, Ju-Yong 1206
Kim, Kangjoo 1185
Kim, Kee-Hyun 1186
Kim, Kyoung-Ho 923
..... 1600
Kim, Kyoung-Woong 1206
Kim, Kyu Han 1899
Kim, Man-Hae 1187
Kim, Minjoong 1599
Kim, N. 2079
Kim, Sang-Tae 1186
Kim, Sang-Woo 1187
Kim, Seok-Hwi 1185
Kim, Seung-Sep 1600
Kim, Sujeong 1862
Kim, T-K. 1288
Kim, Yeongkyoo 1185
..... 1284
Kim, Yongman 2111
Kim, Yoo-Jun 1187
Kim, Young Jae 1188
..... 1188
..... 1285
Kimber, R. 1189
..... 1351
Kimura, J-I. 978
..... 1189
..... 1861
..... 1984
..... 1993
Kimura, T. 1781
King, A. 728
King, C.L. 1589
King, Helen 1190
King, Hubert 1190
Kinnaird, J. 1619
Kinoshita, N. 1191
Kipfer, R. 532
..... 579
..... 1074
..... 1379
..... 1675
..... 1811
..... 2018
..... 2021
..... 2032
Kipling, Z. 1944
Kirchenbaur, M. 494
..... 1191
Kirchner, C. 1192
Kirchner, J.W. 1722
Kirf, M. 1192
Kirk, J. 1193
Kirk, M. 1416
Kirkpatrick, R.J. 568
..... 1136
Kiro, Y. 1193
Kirpotin, S. 461
Kirsch, R. 1194
Kirschvink, J. 850
Kirste, D. 1194
Kirste, J. 1195
Kisakürek, B. 803
Kisi, E. 626
Kisters, A. 1977
Kita, N.T. 568
..... 2017
Kitagawa, H. 1628
Kitajima, K. 1155
..... 1231
..... 1656
..... 1769
Kitanidis, P.K. 1744
Kısakürek, B. 1195
Kjarsgaard, B.A. 1610
..... 1988
Klaminder, J. 877
..... 1196
Klammer, D. 1038
Klápová, H. 1817
Klasa, J. 1196
..... 1677
Klaver, G. 2066
..... 2081
Klaver, M. 2064
Kleber, M. 1164
..... 1634
..... 2132
Klebesz, R. 540
..... 1197
Klebow, B. 1197
Kleerebezem, R. 1784
Klein, F. 1011
..... 1134
..... 1198
..... 1437
Klein-BenDavid, O. 1198
Kleine, B. 1199
Kleine, T. 600
..... 1024
..... 1199
..... 1245
..... 1759
Kleinert, S. 1147
Kleinhanns, I.C. 1200
Kleist, E. 718
..... 1181
Kleja, D.B. 959
Klemd, R. 1118
..... 1200
..... 1575
..... 2149
Klemme, S. 1200
..... 1880
Klevenz, V. 1225
Klíma, M. 1955
Klimant, I. 666
Klimko, T. 1201
Klimm, D. 1694
Klimm, K. 1201
Klitzke, S. 1202
Klochko, K. 1202
..... 1287
..... 1971
Kloess, G. 897
..... 1195
..... 1694
Kloppmann, W. 938
Klotzbücher, T. 1203
Kluge, T. 410
Klügel, A. 544
..... 871
..... 1203
..... 1699
..... 1866
Klump, V. 496
Klunder, M. 1007
Klüpfel, L. 938
Klyukin, Y. 540
..... 1204
Knab, N. 1204
Knaeble, A. 1537
Knauss, K.G. 726
..... 1784
Knesl, I. 1205
..... 1239
Knies, J. 2001
Knight, K. 939
..... 2059
Knipping, J. 493
Knittel, K. 2139
Knolle, F. 1895
Knope, K. 766
Knorr, G. 2009
Knorr, W. 1205
Knowles, E. 1206
Ko, J-I. 1206
Ko, K. 668
Ko, M-S. 1206
Koba, K. 1544
..... 2147
Kobayashi, S. 1793
Kobayashi, T. 2225
Kobchenko, M. 1100
Kobesen, H. 2063
Kocar, B. 1207
Koch, C. 463
Koch, J. 775
Koch, M. 2177
Koch, P. 1901
Koch-Müller, M. 2184
Kock, D. 865
Kocourková, E. 1207
Kocur, C. 1208
Kodaira, S. 1208
Kodama, J-I. 1368
Kodolányi, J. 1209
Koehler, I. 1148
Koehn, K. 1209
Koele, N. 1210
Koening, A. 1732
Koepke, J. 1073
..... 1192
..... 1210
..... 1560
..... 2171
Kofukuda, D. 1145
Koga, K.T. 670
..... 1211
..... 1752
..... 2181
Kogarko, L. 596
..... 1211
Kögel-Knabner, I. 790
..... 820
..... 1001
..... 1046
..... 1512
..... 1671
Kogiso, T. 1212
Koglin, N. 1953
Köhler, M. 735
Köhler, P. 404
..... 983
Köhler, S.J. 877
..... 1212
..... 1538
Kohlmann, F. 1213
Kohlstedt, D. 746
Kohn, S. 1213
Kokaly, R. 1305
Kokfelt, T.F. 990
Kolaylı, H. 530
Kolejka, V. 909
Kolesnikov, A.I. 1756
Kollegger, P. 1214
Köllner, K.E. 627
Kolmakov, Y. 1214
Kolmonen, P. 1968
Komabayashi, T. 1215
..... 1961
Komarek, A. 2245
Komárek, M. 672
..... 740
..... 1215
..... 2066
..... 2287
Komatsu, K. 1078
Komiya, T. 1168
..... 2227
Kömürcü, M.İ. 418
Komuro, K. 1162
Kon, Y. 1027
Kondragunta, S. 1216
Koneev, R. 1216
Kong, F-M. 1320
Konhauser, K. 1148
..... 1217
..... 1266
..... 1481
..... 1631
..... 1733
König, S. 494
..... 1036
..... 1217
..... 1514

https://doi.org/10.1180/S0026461X00006502 Published online by Cambridge University Press

Konikow, L. 1218
..... 1462
Konn, C. 644
..... 1218
Kononov, A. 2057
Konovalenko, S. 556
Konrad-Schmolke, M. 1219
..... 1652
..... 1818
Konter, J. 1094
..... 1219
Kontinen, A. 1389
Kontolaimakis, G. 1496
Kooijman, E. 1220
Koornneef, J. 1220
Kopp, C. 1448
Koppensteiner, J. 2263
Koppers, A. 1094
..... 1219
..... 1221
Kopylova, M. 1221
Koralay, T. 1133
..... 1222
Korenaga, J. 1775
Korenaga, T. 939
..... 2202
Korepanova, O. 1620
Koretsky, C. 484
..... 1222
..... 1223
..... 1381
..... 1870
Korhonen, F. 2200
Kořínková, D. 1223
Korkmaz, S. 1148
Korobova, E. 1224
..... 1746
Koroleva, O. 1224
Korost, D. 1885
Korte, C. 1225
..... 1765
..... 2048
Kosakowski, G. 1026
Kosakowski, P. 2156
Koschinsky, A. 498
..... 1000
..... 1225
..... 1819
..... 1895
Koschorreck, M. 2146
Kosler, J. 977
..... 1470
..... 1892
Köster, J. 797
Kostka, J. 1045
..... 1068
Kostylew, J. 1226
Kostyuk, A. 1226
Kotelnikov, Alexey 1227
Kotelnikov, Alexey 1227
Kotelnikova, Z. 1227
Kothe, E. 1828
Kotková, J. 1228
Kotler, J.M. 1228
Kotloski, N. 941
Kotov, A. 1785
..... 1914
..... 2199
Kotova, O. 1658
Kotronakis, M. 1496
Kotsev, T. 1238
Kottke-Levin, J. 2030
Kouba, C. 1229
Koutsoukos, P. 2075
Kovach, V. 2121
Kovacs, I. 1229
Kovács, J. 1230
Kovacs, R. 775
Kovács Kis, V. 1884
Kovalenker, V. 1230
Kowalski, N. 2166
Kowalski, P. 1231
Kowsmann, R. 1764
Kozaily, J. 1098
Kozdon, R. 1231
..... 1656
..... 2164
Koziel, S. 594
Kozin, P. 1232
..... 1860
Kozubal, M. 503
..... 1232
Kraal, P. 1116
Krabbenhöft, Andre 883
Krabbenhöft, André 803
..... 870
..... 2100
Krabbenhoft, K. 1892
..... 2041
Kraemer, S.M. 1533
..... 1625
..... 1789
Kraft, S. 1233
Kraitzer, T. 938
Kralj, M. 1233
Kram, P. 1234
..... 1455
Krämer, S. 1812
Krämer, U. 1234
Krantz, D. 1462
Kranz, S.A. 1235
Krasheninnikov, S. 1235
Krasnova, E. 1236
Krasnova, T. 909
Krause, J. 589
Kreidenweis, S. 1633
Kreisberg, N. 2162
Kreissig, K. 1018
..... 1267
..... 1271
Krejsek, Š. 1236
Kremenovic, A. 2145
Kremer, B. 1237
Kremleva, A. 1237
Krepski, S. 640
Kretzschmar, R. 874
..... 1025
..... 1032
..... 1033
..... 1061
..... 1238
..... 1269
..... 1625
..... 1658
..... 1899
..... 2157
Kretzschmar, T. 1238
Kribek, B. 861
..... 1205
..... 1239
..... 2095
Krieger, U. 549
..... 1070
..... 1402
Kriegsman, L. 1239
Kriews, M. 2160
Krikun, E. 1240
Kristjansson, J.E. 428
..... 1042
Krivolutskaya, N. 1240
..... 1258
..... 1904
Krivovichev, S. 1241
Krmíček, L. 1241
..... 1242
Krmíčková, M. 1242
Kroeger, K. 1462
Kroener, A. 691
Krol, M. 1208
Kroll, J. 705
Krom, M. 1532
..... 2176
Kromer, B. 1242
Kronrod, V. 1257
Kronz, A. 880
..... 1043
Krot, A. 1243
Krueger, S. 1237
Krüger, J.C. 1243
Krüger, M. 505
..... 865
..... 1244
Kruger, T. 1362
Krüger, Y. 1244
Kruijer, T. 1245
Krukenberg, V. 2139
Krukowski, E. 1245
Krumm, S. 1246
Krumman, M. 969
Krzeminska, E. 1246
Krzemiński, L. 1246
Krznarić, D. 677
Krzyzanowski, M. 2065
K-Schmolke, M. 811
Ksienzyk, A. 1213
Kuba, N. 1160
Kubicki, J. 1378
..... 1721
Kubrová, J. 556
Kučera, J. 1955
Kucera, M. 1009
Kucharzyk, J. 545
..... 1247
Kudrass, H. 1369
Kudryashov, N. 1247
..... 1914
Kudun Yozgat, K. 1248
Kuduon, J. 1036
Kuehl, J. 693
Kuepper, F.C. 1248
Kuesel, K. 1344
Kuhn, G. 436
..... 960
Kuiper, K. 1501
Kujawinski, E. 525
..... 1249
Kukuła, A. 1249
Kula, J. 1250
Kulaksiz, S. 498
..... 1250
Kulenbekov, Z. 1251
Kulik, D. 1026
..... 1251
Kullerud, K. 1525
Kulmala, M. 455
..... 718
Kulmer, O. 589
Kulongoski, J. 1252
Kumagai, H. 1838
Kumar, Abhinav 1252
Kumar, Alok 525
Kumar, C. 1728
Kumar, N. 1378
Kumar, Ranjit 1253
Kumar, R. Vasant 1920
Kumari, K.M. 1253
Kumari, R. 1253
..... 1882
Kumke, M. 801
Kummer, N.A. 1254
Kump, L. 457
..... 1217
Kundel, M. 1254
..... 2009
Kunes, J. 1255
Kung, J. 1326
Kunz, M. 699
Kupiainen, K. 1683
Kurami, J. 2019
Kurganskaya, I. 1255
..... 1371
Kurlanda, H. 1256
Kurnosov, A. 542
..... 1256
..... 1591
Kurnosova, I. 1224
Kurovskaya, N. 1366
Kurz, M. 1094
..... 2201
Kurzweil, F. 1257
Kuşcu, M. 1994
..... 2220
Kusebauch, C. 1277
Küsel, K. 417
..... 825
..... 963
..... 1360

https://doi.org/10.1180/S0026461X00006502 Published online by Cambridge University Press

Kushiro, I. 1782
Kushmaro, A. 490
Kushnir, Y. 1935
Kuskov, O. 1257
Kusky, T. 2253
Kusuda, C. 1258
Kusy, D. 472
Kuuluvainen, H. 1802
Kuvylin, A. 1224
Kuwayama, Y. 2036
Kuypers, M. 889
..... 1450
..... 1477
Kuzmann, E. 906
Kuzmin, D. 1240
..... 1258
..... 1393
..... 1904
..... 1904
Kuzmina, O. 1258
Kuzyakov, Y. 763
Kuzyura, A. 1566
Kvashnina, K.O. 787
..... 1880
Kwaśniak-Kominek, M. ... 1259
Kwiecien, O. 532
Kwitko-Ribeiro, R. 609
Kwon, K. 549
Kwon, M.J. 1259
..... 1556
..... 1766
Kylander-Clark, A. 962
..... 1260
Kyle, P. 1572
..... 1881
Kynicky, J. 677
..... 1132
..... 1236
..... 1260
..... 1955
..... 2196
Kyono, Atsuchi 2203
Kyono, Atsushi 567

L

Laaksoharju, M. 1424
Laaksonen, A. 2093
Laan, P. 1725
Labanieh, S. 1261
Labat, D. 1573
Labbe, M. 1756
Labidi, J. 1261
Labille, J. 1751
Labolle, F. 683
Laborda, F. 895
Labrosse, S. 1027
Labs, S. 1262
Lacerda, L. 1869
Lach, P. 645
..... 1362
Lachner, J. 673
Lackey, J.S. 1262
Lackner, K. 1263
Lacks, D. 925
Lacrampe-Couloume, G. . 1038
..... 1314
Ladino, L. 1939
Lafay, R. 1263
Lafortune, S. 1264
La Fuente, S. 1233
Lagane, C. 1728
Lagneau, V. 944
..... 1353
Lahajnar, N. 808
Lahann, R. 566
Lahaye, Y. 1211
Lahr, D. 557
Lahr, J. 1459
Lai, W-J. 2123
Lai, Y.J. 805
..... 1264
Lair, G. 1265
..... 1455
Lajeunesse, E. 881
Lakshmanan, S. 1265
Lakshmidevi, C.G. 1882
Lakshtanov, D. 1883
Lakshtanov, L. 512
..... 1266
Lalinská, B. 1201
..... 2083
Lalonde, K. 904
Lalonde, S. 1217
..... 1266
..... 1631
..... 1733
Lalor, G. 1868
Lam, P.J. 1267
..... 1562
..... 1855
Lambe, A. 2093
Lambelet, M. 1267
Lamberti, W. 1190
Lamendella, R. 693
Lamy, F. 1029
Lan, C-Y. 1268
Lan, T-G. 827
..... 1055
Lan, V.M. 515
Lanari, P. 2083
Lanc, P. 1037
..... 1086
Lancaster, P. 1268
Lancelot, J. 1760
Landais, A. 860
..... 1129
Landi, P. 412
Landrot, G. 1920
Lang, S. 1269
Lang, Y-C. 1339
..... 2037
Lange, A. 1998
Lange, H. 775
Lange, R. 411
Langenhorst, F. 980
..... 1042
..... 1438
Langer, G. 1235
Langmuir, C. 694
..... 718
..... 1132
..... 1274
..... 1600
Langner, H.W. 1494
Langner, P. 1269
Langston, A. 1270
Lanson, B. 1493
Lapanje, A. 1731
Lapides, I. 555
Lapitsky, S. 420
Laplante, K. 1304
Laporte, D. 1211
Lapworth, D. 1948
Laquire, C. 1180
Lara, L.E. 1096
Larikova, T. 1270
Larin, N. 2027
Larin, V.N. 2027
Larner, F. 1271
LaRoche, J. 1623
Larsen, J. 2073
Larson, L. 598
..... 1123
..... 1271
Larssen, G. 920
..... 1945
Larter, S. 1272
..... 1567
Lartiges, B. 861
Laskov, C. 1117
..... 1574
Lassin, A. 1272
Lassiter, J. 607
..... 1273
..... 1761
Laszlo, I. 1216
Lathe, C. 1510
..... 2139
Latypov, R. 667
..... 1273
Lau, W. 1274
Laubach, S.P. 826
Laubier, M. 1274
Lauerwald, R. 984
..... 1495
Laukamp, C. 1275
Laurenz, V. 475
..... 1275
Lauretta, D. 517
Lausmaa, J. 1874
..... 2004
Lauterjung, J. 1510
Lavé, J. 534
..... 1276
..... 1369
Laverman, A. 1276
..... 1421
..... 1590
Lavik, G. 889
Lavkulich, L.M. 1071
Law, G.T.W. 1351
..... 2010
..... 2072
Lawson, M. 1277
Layne, G. 1277
..... 1759
Lazar, B. 512
..... 870
..... 1278
..... 1769
Lazar, L. 466
Lazareva, E. 543
..... 1278
..... 1813
Lazareva, O. 1279
Lazarov, M. 1279
Lazor, P. 1853
Lazzeri, M. 533
Lead, J. 975
..... 1948
Leake, J.R. 441
..... 581
..... 1398
..... 1817
..... 1990
Leal, S. 952
Leanni, L. 1276
Lear, C. 859
Learman, D. 1280
Lea-Smith, D. 2026
Leat, P. 1610
Leavitt, W.D. 1121
Lebeau, O. 1280
Lebedev, V.A. 1176
..... 2051
Le Cadre, E. 907
Le Campion, P. 1453
Lech, D. 1281
Lechtenfeld, O. 673
Leck, C. 1413
Leclerc, E. 1301
..... 1751
Lecumberri-Sanchez, P. .. 1281
Ledevin, M. 1282
Ledru, M.P. 1122
Leduc, C. 681
Lee, A-R. 1282
Lee, B. 1130
Lee, Carina 1283
Lee, Choon Oh 1287
Lee, Cin-Ty 420
..... 665
..... 1283
..... 1302
..... 1365
..... 2012
..... 2220
Lee, D-C. 652
..... 873
..... 1030
..... 1284
Lee, Giehyeon 1289
..... 1525
Lee, Gyeongmin 1284
Lee, Hajung 1285
..... 1599
Lee, Hao-Yang 668
Lee, Hea Youn 671

https://doi.org/10.1180/S0026461X00006502 Published online by Cambridge University Press

Lee, Hyo Eun 1188
..... 1188
..... 1285
Lee, Hyojeong 567
Lee, Hyomin 1075
Lee, Jae-Sung 1186
Lee, James KW 1906
Lee, Jeong-Ho 1286
Lee, Ji-Hoon 865
Lee, Jin-Su 1206
Lee, Jong-Mi 570
..... 1286
Lee, Jung Hwa 1287
Lee, Kil Yong 668
..... 2225
Lee, Kwang-Sik 550
..... 1184
..... 1282
..... 1908
Lee, Martin 1891
Lee, Minhee 468
..... 1285
..... 1597
..... 1598
..... 1599
Lee, N. 1287
..... 1971
Lee, Sang Soo 837
Lee, Seung Gu 1288
..... 1910
..... 2225
Lee, Seung Ryeol 1288
Lee, Sung-Woo 1649
Lee, Tae-Ho 2079
Lee, Tae Jong 1288
..... 2225
Lee, Typhoon 652
Lee, Yeonjin 1289
Lee, Young Jae 1188
..... 1188
..... 1285
Lee, Young Mi 1600
Leefmann, T. 2004
Leen, J.B. 2131
Lees, J. 1737
Lefevre, G. 1289
Lefort, D. 1290
Lefort, S. 1509
Le Gal La Salle, C. 1760
Legros, S. 1290
..... 1450
Le Guillou, C. 1291
Le Hir, G. 1291
..... 1992
Lehman, S. 590
..... 1402
Lehmann, Benjamin 1292
Lehmann, Bernd 609
..... 609
..... 639
..... 1292
Lehmann, J. 1293
Lehmann, M.F. 535
..... 734
..... 1293
..... 1540
..... 2147
Lehn, G. 777
Le Houedec, S. 1294
Lehsten, V. 1205
Lehtipalo, K. 718
Lei, L. 2236
Lei, T.Z. 2183
Leichmann, J. 1971
Leinweber, A. 1821
Leinweber, P. 1294
Leipe, T. 741
Leithold, E. 1295
Leiva, E. 1295
..... 2077
Le Losq, C. 1296
..... 1535
Lemarchand, D. 1296
..... 1724
..... 2099
Le Marrec, C. 1839
Lemke, K. 1297
..... 1842
..... 1934
..... 1980
Lemon, S. 446
Le Munier, M. 1434
Lenardic, A. 1557
Lenehan, C. 1707
Lenniger, M. 1297
Lenting, C. 1298
Lentini, C. 1298
Lenton, T. 714
..... 1299
..... 1474
Lentz, D. 436
Lenz, Conny 1356
Lenz, Cristine 691
..... 1299
Lenz, M. 1300
Leon, D. 2290
Le Pape, P. 1300
Lepland, A. 1301
..... 1449
..... 1682
..... 1714
..... 2070
..... 2073
Lepleux, C. 2042
Lequy, É. 1301
Lerchbaumer, L. 1302
Lericolais, G. 1917
le Roex, A. 680
le Roux, V. 1283
..... 1302
Lersch, T. 1850
Lerssi, J. 1357
Lesher, C. 925
Leslie, K. 1303
..... 1957
Leuthold, J. 1303
Lev, O. 1140
Levard, C. 678
..... 1304
..... 1706
Leveille, R. 1304
Levenson, Y. 815
Levin, L. 1574
Le Voyer, M. 1535
Levy, R. 1152
..... 2065
Lewan, M. 1305
..... 1305
Lewandowska, R. 1306
Lewicka, Z. 859
Lewin, E. 1102
..... 2083
Lewis, A. 423
Lewis, E.R. 738
Lexa, O. 831
..... 1103
Leya, I. 1245
Leybourne, M. 2013
Lezama-Pacheco, J.S. 422
..... 484
..... 520
..... 913
..... 1306
..... 1464
..... 1649
..... 1958
Li, Baosheng 1326
Li, Bo 856
Li, Bo 1307
Li, Chao 1647
Li, Chao 1307
..... 2212
Li, Chao-Yang 1350
Li, Chuanxin 1308
Li, Chusi 470
Li, Congying 1965
Li, Da 1308
Li, Daoji 890
..... 1309
Li, F. 1374
Li, Gaojun 1309
Li, Guanglai 1060
Li, Haibin 1112
Li, Haibing 2064
Li, Hairong 2211
Li, Hang 661
..... 1310
..... 1867
Li, Henan 659
Li, Hm 2128
Li, Hongyan 1310
Li, Hsiu-Ping 1797
Li, Huaikun 2192
Li, Huaqin 1111
..... 1964
Li, Hui 783
Li, Hui 1845
Li, Huijuan 1311
Li, Huimin 526
Li, Huiming 2127
..... 2127
Li, Huiyin 1110
Li, Jiang 1345
Li, Jie 657
..... 1111
..... 1311
..... 1964
Li, Jing 2273
Li, Jing 1312
..... 2182
Li, Jiying 1312
Li, Jun 1459
Li, Jun 1114
Li, Jun 1323
Li, K. 659
Li, Lei 2250
Li, Li 1313
Li, Ling 1313
..... 1984
Li, Long 1038
..... 1314
Li, M. 2215
Li, Na 1314
Li, Ni 1315
Li, Pengwei 1063
Li, Ping 654
..... 1315
..... 2198
Li, Ping 1343
Li, Q-L. 1316
Li, R.s. 2113
Li, Ruzhong 659
Li, Shan 2125
Li, Shizhen 2279
Li, Shuang Qing 651
..... 1316
..... 2280
Li, Shuguang 2192
Li, Shui Fu 1057
..... 1317
Li, Siliang 1317
Li, T. 1315
..... 2118
Li, Wang-Ye 1997
Li, Wei 1321
Li, Wenpeng 2124
Li, WenYuan 892
..... 2262
Li, Xiang-Hui 2215
Li, Xiang-Min 1318
..... 2232
Li, Xiang-Ping 2119
Li, Xian-Hua 1316
Li, Xiao-Dong 1318
..... 1343
Li, Xiao-Hui 1319
Li, Xuefang 1319
Li, Xu-Ping 1320
Li, Yan 1359
Li, Yanhe 1320
Li, Yanxia 1321
..... 1329
Li, Yiquan 1112
Li, Yong 1168
Li, Yonghua 1321
..... 2211
Li, Yongli 2114
Li, Yuan 1322

https://doi.org/10.1180/S0026461X00006502 Published online by Cambridge University Press

Li, Yuansheng 1114
..... 2272
Li, Yuefen 1322
..... 2115
Li, Yunxia 1347
Li, Zhen 1681
Li, Zheng Wen 1323
Li, Zheng-Xiang 1350
Li, Zhi 2195
Li, Zhi-Pei 2118
Li, Zhiqiang 945
Li, Zhiyang 1113
Li, Zibo 1323
Liang, J. 1324
Liang, Yan 1324
Liang, Yu-Hsuan 1325
Liao, F. 1325
Liao, L. 718
Liao, Z. 1350
Licht, O. 491
Lichtschlag, A. 1110
Lichwa, J. 717
Liebermann, R. 1326
Lieberwirth, I. 1477
Liebetrau, V. 803
..... 1010
..... 1326
..... 2100
Liebezeit, G. 2166
Liebrand, D. 1136
Liebscher, A. 850
..... 1709
Liebske, C. 2063
Lienhard, D. 549
Liermann, H-P. 1407
..... 1630
Likhanov, I. 1327
Liles, G. 1327
Lilley, M. 1269
..... 1370
Lillis, P. 710
Lim, H. 693
Lim, K. 1328
Lim, Y. 2285
Lima, A. 1452
Lima, Edmilson 1329
Lima, Enjôlras 634
..... 864
..... 1328
..... 1329
Lima, M. 1329
Limmer, D. 682
Lin, Chu-Ching 1596
Lin, Chunye 1321
..... 1329
Lin, I-Jhen 668
Lin, In-Tian 1411
Lin, J. 1600
Lin, L-H. 1330
..... 1963
..... 2123
Lin, Saulwood 1963
..... 2213
Lin, Shi Guo 1323
Lin, W. 1268
Lindeboom, R. 1330
Lindegren, M. 1331
Lindsay, C. 1402
Lindsay, J. 1439
..... 1898
Lindsay, M. 537
..... 1673
Ling, H-F. 657
..... 1056
..... 1308
..... 1331
..... 2264
Ling, M. 1965
Ling, W-L. 518
..... 1332
..... 1681
..... 2253
Link, K. 2011
Linnemann, U. 592
Linnen, R. 458
..... 559
..... 648
Lintern, M. 1332
..... 1705
Lipenkov, V. 860
Lippmann-Pipke, J. 1333
..... 1341
Lippold, H. 1341
Lippold, J. 543
..... 1333
Liqin, Z. 1334
Lishka, H. 2039
Lissenberg, C.J. 1334
Lissner, H. 1335
..... 1648
Litasov, K. 540
..... 1335
..... 1395
..... 1849
Little, M. 1603
Little, S. 1336
Little, T. 852
Littler, K. 1737
Litvin, Y. 540
..... 1133
..... 1336
..... 1566
..... 1923
Liu, A. 649
Liu, Bing-Xiang 651
Liu, Bo 1450
Liu, Changhong 1337
Liu, Chia-Mei 1337
..... 1361
Liu, Chongxuan 945
..... 1173
..... 1338
..... 2239
Liu, Chuan-Zhou 1338
Liu, Cong-Qiang 1317
..... 1318
..... 1339
..... 1343
..... 1868
..... 2037
..... 2113
..... 2236
Liu, Di 2127
Liu, Di 1055
Liu, Faye 2275
Liu, Feng 1320
Liu, Fulai 1339
..... 2208
Liu, Haixia 1309
Liu, Haozhe 1340
Liu, Hong 1313
..... 1984
Liu, Hui 643
Liu, Huiqing 1911
Liu, James 1050
Liu, James T. 1920
Liu, Jia 1084
Liu, Jianshe 1345
Liu, Jingao 1340
Liu, Jingbo 658
..... 1341
..... 2218
Liu, Jinhui 651
..... 1967
..... 2125
Liu, Jinzhong 2130
Liu, Juan 1609
Liu, Juan 1341
..... 2119
Liu, Jun 1342
..... 1857
Liu, Li 1617
Liu, Liang 650
..... 1342
..... 2113
..... 2250
Liu, Lianwen 1323
Liu, Lizhen 1343
Liu, Mei 1867
Liu, Mengqiong 2290
Liu, Min-Wu 1115
Liu, Na 1617
..... 2246
Liu, Nan 728
Liu, P 2188
Liu, Peng 1673
Liu, Qi 1349
..... 1985
Liu, Quan 2236
Liu, Quin 636
Liu, Shaopeng 2273
Liu, Sheng-Ao 1997
Liu, Shentai 620
Liu, Shugen 746
Liu, Shuguang 2269
Liu, T. 1343
Liu, Wei 1304
Liu, Weihua 1447
..... 2011
Liu, Xi 747
Liu, Xia 2118
Liu, Xiaoming 650
..... 765
..... 1332
..... 1344
..... 1681
..... 2192
Liu, Xiaoqing 2195
Liu, Xiatao 1329
Liu, Xinran 1344
Liu, Xinyu 657
Liu, Xue-Yan 1318
Liu, Yajie 1345
Liu, Yang 569
Liu, Yang 1345
Liu, Yang 1854
Liu, Yanrong 1346
Liu, Ying 1346
..... 1367
Liu, Ying Chao 1347
..... 2010
Liu, Yong 1347
Liu, Yongsheng 1060
..... 1348
..... 2253
Liu, Yu 1316
Liu, Yuegao 620
Liu, Yuhui 1348
Liu, Yuming 1349
Liu, Yun 1319
..... 1349
..... 1985
Liu, Yu-Ping 1350
Liu, Zhi 1447
Liu, Zhongfang 567
Liu-Zeng, J. 2064
Livens, F. 1189
..... 1351
Livi, K. 1350
Livingston, J. 1701
Llamas, J.F. 885
Llana-Funez, S. 2152
Llorens, I. 1668
Lloyd, J.R. 584
..... 608
..... 686
..... 1189
..... 1351
..... 2010
Lloyd, N. 969
..... 1351
Lo, C-H. 668
Lo, L. 1352
Lobo, J. 1352
Lobst, R. 400
Lochte, K. 538
Locke, S. 1588
Lockwood, B. 1818
Löfgren, S. 1212
Loges, A. 1353
Lohan, M. 1007
Lohmann, K. 1052
Lohmann, U. 1413
..... 1950
Loiacono, S. 1460
Loiselet, C. 498
Lomas, M. 1734
Lomstein, B. 1825
Long, P. 484
..... 1556
Long, X. 783
Longeville, S. 1409
Longmire, P. 1353
Longnecker, K. 1249

https://doi.org/10.1180/S0026461X00006502 Published online by Cambridge University Press

Longo, F. 415
Longo, K. 1354
..... 1750
Longo, M. 1354
lo Nigro, G. 438
Lonitz, K. 1554
Loomer, D. 2189
Loope, D. 1177
Lopes, G. 1355
Lopes, J.M. 1355
Lopes dos Santos, R. 1898
López, R. 444
Lopez, V. 1766
Lopez Correa, M. 1491
..... 2033
López Fernández, M. 1356
Lopez-Garcia, P. 698
Lopez-Moreno, S. 1741
López-Pamo, E. 1796
Lopez-Rodriguez, C. 1356
López Sánchez-Vizcaíno, V. 1401
..... 1586
Lorenz, E. 1357
Lorenz, J. 877
Lorenzen, J. 533
Loring, J.S. 1569
Los Huertos, M. 1818
Losos, Z. 1207
Lou, Q. 2274
Loughlin, S. 707
Loukola-Ruskeeniemi, K. 1357
Loun, J. 1391
Lourenço, Alexandre 701
Lourenço, Ana 1358
Lourenço, N. 1383
Louvat, P. 560
..... 603
..... 881
..... 1129
..... 2013
..... 2086
Love, A. 583
Love, G.D. 1647
..... 1723
Lovell, T. 566
Lovett, G. 1210
Lövgren, L. 999
..... 1331
..... 1530
Lowe, Donald 2012
Lowe, Douglas 1439
Lowry, D. 2005
Lowry, G. 652
..... 931
..... 945
..... 1706
Lowry, Z. 1305
Loy, A. 1626
Loyd, S. 1358
Lu, A. 1114
..... 1359
Lu, D. 1066
Lu, F. 1110
Lu, G-H. 1330
Lu, H. 1115
Lu, Jianjun 1359
Lu, Jun-Fu 709
..... 1360
Lu, L.F. 611
Lu, P. 2275
Lu, Shang Shong 518
..... 1332
Lu, Shipeng 1360
Lu, Siming 1614
Lu, Xiao-Nan 2188
Lü, Xinbiao 620
..... 1447
..... 1482
Lu, Y-C. 1337
..... 1361
Lu, Z-T. 1361
Luais, Beatrice 645
Luais, Béatrice 1362
..... 1412
Luan, F. 598
..... 1271
Lubansky, A. 1362
Lucas, A. 1363
Lucas, R. 877
Lucas, Y. 1807
Lucassen, F. 1363
Lucchetti, G. 622
Lucero, D. 1870
Luchitskaia, M.I. 2092
Luchs, T. 1364
Lüders, T. 505
Lüders, V. 1281
..... 1364
Luffi, P. 937
..... 1283
..... 1365
Luguet, A. 494
..... 858
..... 1365
Luis Francisco, A. 406
Lukanin, O. 1366
Lukens, C.E. 1722
Lukesova, V. 1428
Lukman, S. 1781
Lukšienė, B. 783
Lund, S.P. 1163
Lundin, L. 1455
Lundkvist, A. 1986
Lundschien, B.A. 2196
Lundstrom, Craig 1366
Lundstrom, Craig 925
Luo, Beiping 1402
Luo, Bing 1984
Luo, J.L. 1367
Luo, L. 1367
Luo, M. 1048
Luo, P. 1368
Luo, S. 1368
Luo, X. 1369
..... 2119
Luo, Yiming 1333
Luo, Yun 632
Luo, Z. 1857
Lüönd, F. 1939
Lupker, M. 861
..... 1276
..... 1369
Luppold, F.W. 1002
Lupton, J. 941
..... 1370
Luque, F.J. 1645
Luquot, L. 1635
Lustrino, M. 2051
Luth, R.W. 875
Luther, G. 1370
..... 1382
Lutoev, V. 1877
Luttge, A. 456
..... 1077
..... 1255
..... 1371
..... 2078
Lützenkirchen, J. 1251
Luz, B. 1371
Lv, H. 1959
Lv, K. 1372
Lv, W. 432
Lv, X. 2277
Lvov, S. 1378
Lybrand, R. 1696
Lyle, M.W. 1136
..... 1401
..... 1881
..... 2176
Lyle, P. 1442
Lynch-Stieglitz, J. 1820
..... 2002
Lyne, J. 2175
Lyons, J. 1372
Lyons, T.W. 433
..... 457
..... 603
..... 674
..... 1168
..... 1217
..... 1373
..... 1647
..... 1705
..... 1723
..... 1778
..... 1831
Lysiuk, A. 1877

M

Ma, Changqian 2249
Ma, Chi 569
..... 1535
Ma, Chunli 1374
..... 2120
Ma, D. 2278
Ma, G. 931
..... 1374
Ma, J. 1057
Ma, Lei 1375
Ma, Liang 2254
Ma, Maoyan 950
..... 1342
..... 1857
..... 2249
Ma, Ming-Chao 1114
Ma, P-L. 1695
Ma, Rui 1706
Ma, Rui 945
Ma, Tao 2278
Ma, Teng 892
Ma, Z-P. 1318
Maacha, L. 804
..... 813
Maas, R. 578
..... 1039
..... 1375
Mabery, S. 1431
Mabry, J. 1376
Macalady, D. 1376
Macalady, J.L. 730
..... 1123
..... 1377
..... 2247
Macaskie, L. 975
..... 1039
..... 1713
Macdonald, F. 557
..... 1749
..... 2006
MacDonald, J. 1377
Machender, G. 1378
Machesky, M. 1378
..... 1666
..... 1721
..... 1953
Machev, P. 1930
Machida, S. 1379
Mächler, L. 1379
Macias, F. 1380
Mackelprang, R. 693
Mackensen, A. 948
Mackizadeh, M.A. 1141
..... 1380
Macklam-Harron, G. 2103
MacLean, L. 615
..... 706
Maclennan, J. 1546
..... 1764
..... 1765
..... 1864
MacLeod, A. 1381
..... 1870
MacLeod, C.J. 1334
Mácová, D. 861
Macpherson, C.G. 1381
MacRae, C. 1440
Macris, C. 1382
..... 1844
Madden, A. 1031
Madeira, J. 1423
Madeleine, G. 1354
Mader, M. 494
Mäder, U. 839
Madhukumar, B. 1960
Madison, A. 1382
Madland, M.V. 1445
..... 1446
..... 1613
Madureira, P. 944
..... 1383
Maeda, S. 1422

https://doi.org/10.1180/S0026461X00006502 Published online by Cambridge University Press

Maeder, U. 884
Maejima, Y. 1425
Maenhout, W. 1152
Maerschalk, C. 698
Magand, O. 490
Magee, C. 1383
Maghsoudi, A. 2060
Magill, C.R. 1384
Magna, T. 519
..... 959
..... 977
..... 1118
..... 1384
..... 1385
..... 1520
..... 1551
Magnier, C. 1385
Magnin, V. 1700
Mahaffey, W. 1842
Mahan, K. 532
Mahdavi, A. 1386
Maher, K. 708
..... 1120
..... 1229
..... 1386
..... 1822
Mahesh, B. 1387
Mahlke, J. 1096
..... 2140
Mahoney, J. 508
Mahy, G. 832
Maia, F. 1387
Maia, M. 973
..... 1101
Maiden, A. 1388
Maier, A. 1388
..... 1485
Maier, R. 970
..... 2240
Maier, W.D. 488
..... 489
..... 813
..... 862
..... 1389
Maillard, E. 807
Maillot, F. 1389
..... 1503
..... 1668
Majkut, J. 1390
Majlesi, M.J. 1390
Majzlan, J. 546
..... 580
..... 946
..... 1201
..... 1391
..... 2083
..... 2285
Makabe, A. 1544
Maki, K. 1027
..... 1159
..... 1391
Mäkie, P. 1392
Makishima, A. 1693
Makita, H. 1183
..... 1392
Makovicky, E. 1790
Malamoud, K. 1393
Malatesta, C. 1393
Maldonado, A. 933
Malec, J. 1239
Maletz, J. 976
Malik, Z.A. 1394
Malikova, N. 1409
Malitch, K. 1394
Malkovets, V. 1395
..... 1850
Mallik, A. 724
Mallmann, G. 1442
..... 1557
Maloof, A. 1072
Malov, A. 1395
Malta, M. 629
Malthe-Sørenssen, A. 1100
Mamontov, E. 1378
Mancini, Lucia 516
Mancini, Luis 1797
Manda, Š. 1988
Mandaliev, P. 1238
Mandell, A. 1699
Mandeville, C. 843
..... 1396
Manecki, M. 471
..... 853
..... 1259
Manetti, P. 412
Mangasini, F. 1023
Mangelsdorf, K. 2085
Mangini, A. 543
..... 853
..... 1252
..... 1396
..... 1693
..... 1764
..... 1823
Manhoven, G. 887
Mani, D. 1397
Manikyamba, C. 1397
Manikyamba, M. 1779
Mankasingh, U. 1398
Mann, G. 1924
..... 2176
Manning, Christina 1398
..... 2005
Manning, Craig 787
..... 1382
..... 1399
..... 1399
Manning, D. 1711
..... 2134
Manning, P. 798
Mano, A. 1989
Mansaray, Z. 1140
Mansfeldt, T. 1025
..... 1400
..... 1424
..... 1828
Mantovani, F. 690
Manuela, F. 1751
Mao, C. 1400
Mao, H-K. 2203
Mao, J. 1004
Marandi, R. 1099
Marcaillou, C. 439
Marcano, M. 1511
Marcano, N. 1567
Marcantonio, F. 1401
..... 1820
..... 1881
..... 2176
..... 2194
Marchesi, C. 1401
..... 1586
Marchesi, M. 1233
Marchitto, T. 590
..... 1402
Marchlewski, T. 471
Marcolli, C. 1402
Marcus, M.A. 688
..... 1267
..... 2073
Marecal, V. 1076
Maréchal, J.C. 1728
Maresch, W.V. 949
Mareschal, J-C. 1403
..... 1638
Mareschal, L. 2042
Marescotti, P. 622
Margus, M. 677
Maria Jose, G. 406
Mariani, E. 769
..... 1377
Marignac, C. 733
Marillo Sialer, E. 1403
Marin-Carbonne, J. 1404
..... 2284
Marincea, S. 1076
Marinozzi, M-C. 1453
Mark, D. 806
..... 1404
..... 1501
..... 1899
..... 1955
Markič, M. 1141
Markl, G. 750
..... 1018
..... 1353
..... 1405
..... 1405
..... 1698
..... 2177
Marks, M.A.W. 750
..... 914
..... 1018
..... 1405
..... 1698
Marks, S. 925
Marler, B. 946
Marley, S. 1191
Marlow, J 1574
Marlow, Jeffrey 1406
Marmier, N. 617
Maron, P-A. 1788
Marquardt, C. 478
Marquardt, H. 1406
..... 1407
..... 1407
Marquardt, K. 1406
..... 1407
Marques, J.M. 630
Marques, R. 1408
Marr, J. 1408
..... 1409
Marritt, S. 604
Marry, V. 1409
Marsac, R. 1410
Marschall, H. 805
..... 811
..... 1108
..... 1410
Marsh, S. 2103
Marshall, A. 1739
Marshall, B. 1305
Marske, J. 601
..... 998
Marti, D. 1244
Martin, A. 992
Martin, Candace E. 1411
..... 1589
Martin, Caroline 1411
Martin, Céline 1412
Martin, E. 1412
Martin, F. 399
Martin, L. 1413
Martin, Maria 1413
Martin, Mirko 1101
Martin, Pamela 527
Martin, Patrick 1007
Martin, Randall 2065
Martin, Richard L 1414
..... 1414
Martindale, R. 1415
Martinek, K. 861
..... 1205
Martinez, C.E. 1015
Martínez, F.J. 2080
Martinez, I. 1885
Martinez, Jean-Michel 1653
Martínez, Julián 1873
Martinez, P. 1750
Martinez, R. 2162
Martinez, Z. 1660
Martínez-Botí, M.A. 1415
Martinez-Garcia, A. 1029
Martinéz García, M. 1356
Martínez-Ramos, C. 1416
Martínez-Ruiz, F. 1356
..... 1739
Martinez-Vincente, D. 681
Martin-Garin, A. 1839
Martini, A. 1416
Martinovic, M. 1472
Martín-Peinado, F.J. 1417
..... 1742
..... 1747
Martins, D. 930
Martins, G. 1717
Martins, H. 1417
Martins, J.M.F. 752
..... 1527
Martins, Línia 1423
Martins, Lisa 1418
Martins, Z. 1228
Martin-Torres, F.J. 1418
Márton, E. 1884

https://doi.org/10.1180/S0026461X00006502 Published online by Cambridge University Press

Marty, B. 688
..... 875
..... 1376
..... 1674
..... 2020
Maruoka, T. 699
..... 1086
Maruyama, S. 1158
..... 2227
Marx, C. 573
Marx, T. 410
März, C. 741
..... 1419
..... 2140
Marzocchi, U. 1419
Marzoli, A. 614
..... 745
..... 918
..... 1354
..... 1420
..... 1457
..... 2283
Mashukov, A. 1420
Mashukova, A. 1420
Masion, A. 1290
..... 1304
..... 1751
Maskenskaya, O. 1421
Mason, O. 693
Mason, P.R.D. 642
..... 1421
..... 1480
..... 1742
..... 2079
Masotta, M. 1422
Masque, P. 903
..... 2241
Masquelin, H. 1299
Mass, T. 1008
Massey, M.S. 1306
..... 1464
Massiot, D. 1535
Massoli, P. 2093
Masson, O. 1936
Masson-Delmotte, V. 1129
Mastalerz, M. 876
Masters, A. 2133
Masuda, H. 1422
Masuda, S. 1423
Mata, J. 1383
..... 1423
Matern, K. 1424
Mather, K.A. 1610
Mather, T. 519
Mathes, M. 2004
Mathez, E.A. 1607
..... 1619
Mathias, P. 1703
Mathur, R. 1467
Mathurin, F. 1424
Matos, R. 2074
Matos, V. 554
Matsuda, J-I. 447
..... 1044
Matsukura, S. 1158
..... 2203
Matsumoto, K. 2053
Matsumoto, R. 1515
..... 1833
Matsunaga, A. 1633
..... 2285
Matsuzaki, H. 1084
..... 1425
..... 1515
Matter, A. 853
Matter, J. 1425
..... 1957
Matthews, A. 410
..... 464
..... 979
..... 1426
..... 2061
Matthiesen, J. 1426
Mattielli, N. 731
..... 788
..... 805
..... 842
..... 1594
Mattinson, J. 1021
..... 1427
Mattioli, M. 2051
Matusiak-Małek, M. 1249
..... 1427
..... 1677
Matveeva, S. 607
..... 1969
Matys, E. 557
Matys Grygar, T. 1428
Matzel, J. 1095
Mauri, F. 533
Maurice, P. 853
..... 1209
..... 1428
..... 1912
Maurrasse, F.J-M.R. 893
Maury, R. 2042
Mavimbela, P. 1429
Mavrogenes, J.A. 449
..... 1107
..... 1429
..... 1529
..... 1987
..... 2152
..... 2186
Mavromatis, V. 1430
Maxfield, P. 1328
Maxwell, R. 503
..... 2185
May, C. 1165
May, Z. 1884
Maya, J.M. 1430
Maya, M.V. 1431
Mayali, X. 1431
Mayanovic, R. 435
Mayer, Adam 1432
Mayer, Adriano 681
..... 1464
Mayer, Bernhard 1432
Mayer, Bernhard 923
..... 1119
..... 1286
..... 1670
Mayer, Kristin 1229
Mayer, K Urlich 502
Mayer, T. 2239
Mayer, U. 1037
..... 1697
Mayes, M. 1433
Mayes, W. 599
Mayhew, L. 1433
..... 1996
Maynard-Casely, H. 1793
Mayo, J. 859
Mazaheri, S.A. 1434
Mazdab, F. 568
Mazeas, L. 1434
Mazeh, S. 442
Mazhari, S.A. 1435
Mazumdar, A. 1127
..... 1435
..... 1615
..... 1926
McAlpine, S. 1436
McArthur, J.M. 1436
McCallum, C. 1437
McCammon, C. 547
..... 1590
..... 1928
McCarthy, M. 1825
McCausland, P.J.A. 1099
McCave, N. 1646
McClelland, J. 777
McCollom, T. 1437
..... 1996
McComish, J. 846
McCray, J. 503
..... 1527
..... 2185
McCuaig, T.C. 2282
McCubbin, F. 1848
McCulloch, M. 1143
..... 1438
..... 1491
..... 2033
..... 2141
McCullough, J. 1870
McDaniel, G. 1686
McDonald, B. 2003
McDonald, I. 1389
..... 1960
McDonough, W.F. 531
..... 965
McEnroe, S. 1438
McFadden, K. 1168
McFarlane, C. 436
Mcfiggans, G. 423
..... 872
..... 1439
..... 1924
..... 2023
..... 2154
McGee, D. 574
McGee, L. 1439
..... 1898
McGloin, M. 1440
McGlone, M. 1210
McGlynn, S. 1574
McGoldrick, P. 1647
McGovern, P.J. 1766
Mcheik, A. 1440
McIntosh, G. 1441
McIntosh, J. 1141
..... 1416
..... 1621
McIntosh, W. 1572
McIntyre, D.L. 806
McKay, G. 1469
McKay, J. 1441
McKee, G.A. 401
Mckeegan, K. 878
..... 2284
McKenna, A. 1739
McKenna, C. 1442
McKercher, K.B. 1411
McKibbin, S. 1442
McKinley, J. 865
..... 2239
McLean, K. 1097
McLean, N. 1021
McLennan, Scott 1443
McLennan, Stephanie M. 1443
McLoughlin, N. 1206
McMahon, S. 1444
McManus, J.F. 1444
..... 1484
McMaster, T.J. 475
..... 581
..... 1146
McMeeking, G. 1021
McMillan, M. 994
McPhie, J. 1375
McSween, H.Y. 2045
Mead, R. 1180
Meakin, P. 1757
Mechati, M. 557
Medaris Jr., L.G. 1769
Medici, L. 2001
Meerts, P. 832
Mees, F. 733
Meeus, C. 698
Meffre, S. 1375
..... 1445
Megawati, M. 1445
..... 1446
Mehay, S. 1269
Méheut, M. 1446
Mehta, V. 913
Mei, W. 1346
..... 1447
Mei, Y. 1447
..... 1855
Meibom, A. 769
..... 1448
..... 1448
Meier, M.F. 1449
..... 2138
Meireles, C. 632
Meisel, T. 1403
Meister, D. 1449
Meister, P. 1450
..... 2140
Meisterjahn, B. 1450
Melack, J. 1719
Melchiorre, M. 1451

https://doi.org/10.1180/S0026461X00006502 Published online by Cambridge University Press

Melekhova, E. 1929
Meleney, P. 1451
Meleshyn, A. 1197
Melezhik, V.A. 1082
..... 1449
..... 1452
..... 1714
Melgunov, M. 1278
Melhorn, T. 569
Meli, S. 495
Melleton, J. 1452
Melton, E.D. 1453
Memarzadeh, M. 1390
Menand, T. 443
Mende, K. 1778
Mendez, J. 767
Mendonça Filho, J.G. 696
..... 785
..... 1875
Menegon, L. 1525
Menéndez-Aguado, J. 1873
Ménez, B. 1453
..... 1473
..... 1605
Meng, E. 1454
..... 2116
Meng, F-X. 1454
Meng, J. 2116
Menguy, N. 561
..... 885
..... 1579
Menneken, M. 1455
Mennito, A. 2110
Menon, M. 1455
Menon, S. 499
Ménot, G. 553
..... 1456
..... 1789
..... 1917
Mentel, T.F. 718
..... 1181
Menuge, J.F. 879
..... 880
Menzies, M. 706
Mercadier, J. 809
..... 1718
Mercat, C. 1106
Mercer, J. 1848
Mercier, J.C. 507
Mercier-Bion, F. 1289
Meredyk, S. 1653
Mériaux, A-S. 2064
Merino, A. 1456
Merkel, B. 1251
..... 1254
..... 1648
..... 1815
Merle, R. 918
..... 1420
..... 1457
Merlini, M. 542
Merroun, M. 1356
..... 1834
Merschel, G. 498
Merten, D. 417
..... 1808
Mertz, D. 805
Mertzimekis, T. 924
Mesfioui, R. 401
Meskhidze, N. 887
..... 1120
..... 1457
Mesko, G. 642
..... 1006
Messina, A. 770
Metcalf, J. 852
Metelka, V. 480
Métrich, N. 1396
..... 1458
..... 1913
Metsue, A. 2036
Metz, V. 591
..... 1458
..... 1754
Metzger, J.G. 1459
Meunier, J-D. 681
Mevel, C. 968
Meyer, C. 942
Meyer, G.N. 1537
Meyer, J. 1101
Meyer, M. 1010
..... 1078
..... 1459
..... 2238
Meyer, V. 666
Meyerdierks, A. 1669
Meyer-Dombard, D. 430
..... 1460
Meynadier, L. 424
..... 685
..... 1294
..... 1460
Meysman, F. 1694
Mezger, K. 403
..... 519
..... 959
..... 1220
..... 1461
..... 2137
Mezouar, M. 438
Mi, J. 996
..... 1461
..... 1867
..... 2256
Mibe, K. 1715
Mic, A.C. 1782
Michael, H. 1462
..... 1462
Michael, P. 1366
Michalak, P. 1552
Michalik, M. 896
..... 1109
..... 1135
..... 1463
..... 1903
..... 2159
Michalski, J. 1463
Michard, G. 603
Michau, N. 737
..... 1730
Miche, H. 1464
..... 1751
Michel, F.M. 678
..... 1306
..... 1464
..... 2022
Michel, L. 577
Michelini, M. 1465
Michelot, J-L. 523
..... 1300
..... 1628
..... 1760
Michler, A. 849
Michot, L.J. 1730
Micoulaut, M. 971
Middag, R. 1725
Middleton, A. 1465
Mietto, P. 716
Mifsud, C. 1973
Migdisov, A. 522
..... 871
..... 1073
..... 1353
..... 1466
..... 2063
..... 2248
Migdisova, N. 1466
Miguelez, N.G. 1467
..... 2024
Mihailova, B. 1467
Mihaljevic, M. 819
..... 1239
..... 1428
..... 1468
..... 2044
..... 2045
Mihalopoulos, N. 1532
Mikami, M. 1144
Mikes, T. 1468
Mikhail, S. 497
..... 1469
Mikhlin, Y. 1745
Miklesh, D. 1312
Miklius, A. 932
Mikouchi, T. 1469
Míková, J. 1470
Mikulski, S. 472
..... 1470
Mikutta, C. 1033
..... 1238
..... 1269
..... 1471
..... 1658
Milanović, I. 677
Militzer, B. 1471
Miljevic, N. 1472
Milke, R. 736
..... 961
Millar, I. 935
Miller, Calvin 623
Miller, Cass 587
Miller, Chris 567
Miller, D. 1385
Miller, Mark 1187
Miller, Mette 702
Miller, Samuel 1416
Miller, Sarah 590
Miller, Scott 852
Millero, F.J. 1472
Millet, Marc-Alban 424
..... 1439
..... 1473
..... 2167
Millet, Maurice 952
Millo, C. 1473
Millonig, L.J. 1474
Millot, R. 1731
..... 2082
Mills, B. 1474
Mills, C. 928
..... 1305
Mills, D. 1123
Mills, H.J. 1723
Mills, Rachel 1007
..... 1011
Mills, Ryan 687
..... 1475
Mills, S. 1475
Milne, A. 1007
Milsch, H. 1812
Miltner, A. 1476
..... 1828
Milton, A. 1476
Milucka, J. 1477
Mimmo, T. 2001
Min, J. 957
Minagawa, K. 2225
Minakawa, M. 1970
Minambres, L. 1633
Minami, M. 1477
Ming, Y. 1478
Mintz, J. 577
Miranda, R. 1423
Mironenko, M. 2289
Mironov, N. 1478
..... 1661
Mishima, T. 2225
Mishra, B. 569
Mishra, H. 811
..... 1034
Mishra, R.K. 1479
Misiti, V. 1121
Misra, S. 1888
Mita, Y. 1479
Mitamura, M. 1422
Mitchell, C. 1480
Mitchell, D. 1118
Mitchell, K. 702
..... 1480
Mitchell, R.H. 961
Mito, S. 1477
Mitsunobu, S. 1183
..... 1392
Mittlefehldt, D.W. 628
Miura, M. 447
Mixa, P. 1103
Miyagi, L. 1406
Miyagi, Y. 2028
Miyairi, Y. 1425
Miyajima, N. 1438
Miyajima, Y. 1087
Miyamoto, M. 1469
Miyazaki, A. 1481

https://doi.org/10.1180/S0026461X00006502 Published online by Cambridge University Press

Miyazaki, J. 1392
..... 1544
Miyazaki, K. 1391
Miyazaki, Takashi 978
..... 1523
Miyazaki, Tsuyoshi 789
Mizukami, T. 1963
Mizuno, T. 2202
Mloszewska, A. 1481
Mo, Y. 1482
..... 2277
Mochida, M. 1160
Modabberi, S. 419
Modini, R. 1770
Moeini, A. 1482
Moeller, K. 1483
Moeser, C. 1157
Moffatt, E. 1941
Moghaddasi, S.J. 1483
Mohajjel, M. 1179
Mohamed, K.J. 1484
Mohammadi, S.S. 668
Mohapatra, R. 1484
Möhler, O. 1042
Moine, B.N. 513
Moita, P. 1485
Mojzsis, S. 633
..... 862
..... 1043
..... 1217
..... 1388
..... 1481
..... 1485
..... 1759
..... 1962
..... 1981
Mokadem, F. 603
..... 1941
..... 1969
Mokhov, A. 1893
Mokhtari, M.A.A. 1486
Mokrushin, A. 1247
Molina, I. 1572
Molinari, M. 1486
..... 1601
Molins, S. 1487
..... 2073
..... 2210
Mollaei, H. 1487
..... 2025
Mollenhauer, G. 1029
Möller, A. 1559
..... 1753
Moller, N. 1488
Möller, P. 1488
Monahan, C. 635
..... 1580
Moncada, D. 540
..... 1489
Mondal, S.K. 1489
Money, C. 576
Monie, P. 1490
Monks, P. 423
Monnin, C. 647
..... 1490
Monnington, A. 1491
Montagna, P. 1438
..... 1491
..... 2033
Montanarella, L. 418
..... 2219
Montarges-Pelletier, E. 1730
Montecinos, P. 1492
Monteiro, J.P. 1738
Montes, C. 623
..... 1492
..... 1875
Montes-Hernandez, G. 1263
..... 1493
..... 1547
Montlucon, D. 799
..... 836
Montoya-Pino, C. 797
..... 2151
Moon, Sang Ho 1075
Moon, Seulgi 1493
Moorbath, S. 2161
Moore, F. 1494
..... 1542
..... 1847
Moore, J.N. 1494
Moore, K. 454
Moore, T. 922
Moorthy, K.K. 1800
Moosavi, Z. 797
Moosdorf, N. 984
..... 984
..... 1495
Mooshammer, M. 1495
Mopper, K. 1004
Moradi, K. 1636
Moradian, Marzieh 1496
Moradian, Mohsen 1496
Moraes, A. 1329
Moraetis, D. 1496
Morag, N. 1497
Morales, J. 1497
Morales, L. 1981
Moran, J.E. 1902
Morard, G. 561
..... 670
..... 1498
Morata, D. 1568
Moravec, Z. 1955
Morbidelli, A. 1699
..... 1763
Moreau, M. 1902
Moreau-Fournier, M. 725
Moreira, D. 698
Moreira, M. 944
..... 1383
..... 1498
..... 1770
Moreira, S. 1499
Moreno García, A. 1356
Moresi, L. 1097
Moretti, R. 451
..... 1296
..... 1499
Mor-Federman, T. 1500
Morgan, D.J. 553
..... 707
..... 1500
Morgan, J.L.L. 1501
Morgan, L. 1404
..... 1501
Morgan, S. 1521
Morgan, W. 1021
Morgans, H. 1990
Morgunova, A. 1502
Mori, R. 921
Mori, Y. 1391
Moriarty, R. 1502
Morie, S. 679
Moriguti, T. 1693
Morikawa, N. 1258
..... 1422
Morin, G. 533
..... 587
..... 1389
..... 1503
..... 1579
..... 1668
Morioka, E. 1799
Morishita, T. 1089
Morishita, Y. 2017
Moritz, A. 904
Moriyama, S. 1503
..... 1799
..... 2019
Morizet, Y. 507
..... 1504
..... 1805
Moron, S.E. 1492
Morono, Y. 1079
Moros, M. 741
Moroz, T. 1659
Morris, A. 1054
Morris, K. 1351
..... 2010
..... 2109
Morris, S. 2173
Morrison, G. 1388
Morrison, J. 928
Morsilli, M. 690
Mortimer, G. 1143
Mortimer, R. 2155
Morton, D. 1283
Morton, P. 627
..... 1855
Möser, C. 1504
Moser, D. 568
..... 1556
Mosher, H. 1505
Mosselmans, F.W. 581
..... 778
..... 1505
..... 1608
..... 1991
Mostowfi, F. 1930
Mothersole, F. 1506
Motoki, A. 1573
Motoyama, H. 972
Mouchel-Vallon, C. 575
Moucka, F. 1506
Mougel, B. 1507
Mountain, B.W. 1912
Moureau, J. 560
Mousavi, S.Z. 1507
Moussa, N. 823
..... 1508
Moussallam, Y. 1572
Mouzakis, K. 1527
Movilla, J. 1616
Mowlem, M. 1591
Moynier, F. 1508
..... 2142
Mozetič, P. 1983
Mørk, A. 2196
Mørkved, P.T. 1876
Mørup, S. 862
Mpodozis, C. 1161
Mucci, A. 706
..... 1382
..... 1509
..... 1616
..... 1957
Mudd, S. 1229
Muddu, S. 1728
Mudelsee, M. 853
Muehe, E.M. 1147
..... 1234
..... 1509
Muehlenbachs, K. 899
..... 1894
Mueller, H.J. 1510
Mueller, K. 1510
Mueller, M. 569
Mueller, P. 1361
Mueller, R. 2165
Muenker, C. 475
Mugler, C. 1623
Muhling, J. 1511
..... 1696
Mukasa, S. 670
..... 975
..... 1511
Mukhamadiyarova, R. 420
..... 421
Mukherjee, S. 1253
..... 1882
..... 1883
Mukhopadhyay, Sujoy 901
..... 1512
..... 1630
Mukhopadhyay, Sumit 1925
Mulakaluri, N. 1620
Mulch, A. 499
..... 1468
Mulder, J. 1876
..... 2277
Mulholland, D. 1653
Mulitza, S. 1020
Müller, A. 1655
Müller, C.W. 1001
..... 1046
..... 1512
Muller, David 1293
Müller, Dietmar 1032
Müller, Katharina 1513
Müller, Konrad 857
Müller, M. 1195

https://doi.org/10.1180/S0026461X00006502 Published online by Cambridge University Press

Müller, W. 821
Mumma, M. 1513
Munemoto, T. 1514
Munes, J.C. 630
Munhá, J.M. 1355
Munir, A.K.M. 1534
Münker, C. 494
..... 1033
..... 1036
..... 1191
..... 1514
..... 1827
..... 2084
Munnik, F. 609
Munoz, A. 1741
Munoz, M. 439
..... 547
..... 2049
..... 2083
Munoz Garcia, M.A. 2206
Muñoz Gonzalez, A. 1515
Muñoz-Jolis, E. 516
..... 594
Munroe, P. 1293
Müntener, O. 1072
..... 1303
..... 1692
..... 1809
..... 2062
Murakami, H. 1925
Murakami, M. 458
Murakami, T. 1145
..... 1514
Muramatsu, Y. 429
..... 1084
..... 1425
..... 1515
..... 1704
..... 1833
..... 2028
Murawski, D. 2145
Murayama, M. 2077
Murphy, B. 914
Murphy, D. 400
..... 689
..... 1516
Murphy, J. 921
Murphy, M. 1516
Murray, T. 835
Murrell, M. 805
Murthy, N.N. 1603
Murton, B.J. 493
..... 1007
..... 1824
Murty, K.S. 1517
Murzin, V. 1204
Muschalle, T. 1154
Musetto, A. 1462
Mussi, A. 1744
Muszyński, A. 1552
Muto, S. 1547
Mutschler, T. 538
Mutterlose, J. 1002
Myers, J. 1916
..... 1975
Myers, K. 1462
Myhre, G. 1517
Mykhaylov, V. 809
Myneni, S. 1518
..... 1762
..... 2102
Myrick, M. 1851
Myrold, D. 1634
Myrttinen, A. 1518
Mysen, B. 1519
..... 1519
Myska, O. 1520

N

N'Sungani, P. 1490
Na, U-S. 1184
Naafs, D. 1521
Naba, S. 480
Nabein, H-P. 2216
Nabelek, P. 1521
Naden, J. 1897
Nadimi, A. 1773
Nadine, M. 698
Nagahara, H. 1522
..... 1782
Nagai, H. 1992
Nagaishi, K. 1258
Nagasaki, S. 1781
..... 2204
Nagashima, K. 1243
Nagel, B. 808
Nagel, T.J. 1033
Nagle, A. 1772
Nägler, T.F. 1292
..... 1522
..... 2096
Nagy, K. 837
Naidoo, T. 1523
Naik, B.G. 1435
Naik, H. 1431
Nair, S. 1523
Naira, M.B. 1933
Najjaran, M. 2060
Najman, Y. 572
Najorka, J. 773
Nakada, R. 1524
Nakagawa, T. 1899
Nakai, S. 978
..... 2028
..... 2029
..... 2205
Nakamatsu, Y. 1142
Nakamura, E. 1628
..... 1693
Nakamura, Kentaro 1392
..... 1838
Nakamura, Koichi 1079
Nakamura, M. 2226
Nakamura, R. 1524
Nakamura, Takashi 1085
Nakamura, Toshio 1288
Nakanishi, T. 1191
Nakano, S. 1078
Nakaya, S. 1422
Nakayama, K. 1553
Nakayama, T. 1044
Namgung, S. 1525
Naqvi, S.W.A. 1431
Naraoka, H. 988
Narkiewicz, W. 1247
Nascimento, R. 616
Nascimento-Silva, V. 1869
Nasdala, L. 1051
Nash, B. 548
Nasipuri, P. 1525
Naslund, H.R. 2179
Nasr Esfahani, A.K. 1526
Nastos, P. 924
Natali, C. 528
Natland, J.H. 426
..... 1073
Naumann, R. 1333
Naumko, I. 1526
Naumov, V. 2088
Navarre-Sitchler, A. 503
..... 1527
..... 2185
Navarro-Ochoa, C. 707
Navel, A. 1527
Navon, O. 1182
..... 1528
..... 2143
Navrotsky, A. 1756
Nayak, G. 838
Nazarchuk, N. 809
Næraa, T. 1814
Neal, A. 991
..... 1528
Neal, C. 1385
..... 1529
Nebel, O. 449
..... 1461
..... 1529
Nebel-Jacobsen, Y.J. 1529
Nebera, T. 556
Neck, V. 591
Nedel, S. 920
..... 1945
Nédélec, A. 1852
..... 2221
Negev, I. 938
Negrich, K. 1530
Negrila, C. 1786
Nehrke, G. 1235
Neidhardt, J. 820
Neilson, R. 1034
Neiva, A. 445
..... 630
..... 1993
Nekrasov, S. 607
..... 1660
Nelin, C. 470
Nelson, D. 2003
Nelson, H. 1530
Nelson, W. 1531
Nemati, R. 1141
Nemchin, A.A. 942
..... 1298
..... 1455
Němeček, K. 573
Nemeth, K. 1531
Németh, T. 1655
..... 1884
Nenes, A. 1532
..... 1532
Neo, N. 1379
Nestola, F. 1533
Nesvorny, D. 560
Neubauer, E. 1533
Neubert, N. 1522
..... 2096
Neufelder, R. 566
Neumann, A. 1534
Neumann, C. 506
Neumann, R.B. 1534
Neumann, T. 538
..... 758
..... 1937
Neumann, U. 1148
Neumann, V. 943
..... 1329
..... 2103
Neusser, G. 1406
Neuville, D.R. 430
..... 1296
..... 1535
Neves, L. 1418
..... 1622
Newbold, J.D. 1147
Newcombe, M. 1535
Newman, D. 1377
Newton, R.J. 716
..... 986
Nezbeda, I. 1536
Ng, C-Y. 1857
Ng, N.L. 617
Ngothai, Y. 2011
Ngwenya, B. 1256
Ni, H. 1536
Ni, J. 2250
Ni, S. 1858
..... 2114
..... 2129
..... 2198
..... 2256
..... 2289
Nicholas, S. 1537
Nico, P. 1164
..... 1634
..... 1709
..... 2073
Nicolic, N. 1558
Niedermann, S. 1333
..... 1537
Niedermayr, Andrea 1538
Niedermayr, Anrea 870
Nielsen, Lars Peter 1419
..... 1538
..... 1636
..... 1729
Nielsen, Laura 1539
Nielsen, Mark 919
Nielsen, Mike 1056
Nielsen, R. 1998
Nielsen, S. 1539
..... 1673
Nielsen, T. 1643

https://doi.org/10.1180/S0026461X00006502 Published online by Cambridge University Press

Niemann, H. 535
..... 1540
..... 2147
Nieto, J.M. 1380
Nieto, O. 1540
Nietzsche, S. 1360
Niggemann, J. 764
..... 1541
..... 1825
Niggemann, S. 925
Nightingale, M. 1119
Nikiforov, A. 1571
Nikogosian, Igor 642
..... 1541
Nikogosian, Igor 1240
Nikolaeva, I. 607
..... 1089
Nikolaeva, K. 471
Nikolaidis, N.P. 418
..... 1455
..... 1496
..... 1595
..... 1928
Nikolenko, E. 1542
Niles, P. 1463
Nilsson, A. 587
Nimis, P. 1354
..... 1533
..... 2283
Nimmo, F. 1763
Ninagawa, K. 1162
..... 1543
Nino, H. 1875
Niroomand, S. 1542
Nishido, H. 1162
..... 1543
Nishihara, Y. 1921
Nishiizumi, K. 1543
Nishimura, T. 789
Nishiyama, N. 1544
Nishizawa, M. 1544
Nisida, Y. 1479
Nissenbaum, A. 1823
Nitsche, C. 2048
Nitsche, H. 1545
Nitschke, U. 766
Nitzsche, K. 1669
Niu, J.Y. 1545
Niu, Y. 2192
Nixon, S. 1546
Njuguna, J. 1751
Noble, R. 1705
Noble, S. 1021
Noble, T. 1646
Nobre Silva, I. 1451
..... 1546
Noguchi, T. 1392
Nogueira, A. 1794
Nogueira, P. 1795
Nogueira, R. 1717
Noguera, C. 1547
..... 1601
Noiriel, C. 1931
Nolte, N. 1200
Nomaki, H. 1392
Nomosatryo, S. 1957
Nomura, M. 1182
Nomura, R. 1547
Nonnotte, P. 1508
Noordmann, J. 1548
Nordblad, F. 1548
Nordstrom, D.K. 616
..... 1549
Nordt, L. 577
Noret, A. 481
Norisuye, K. 570
Norman, M. 601
Normington, V. 1549
Noronha, F. 629
..... 952
..... 1716
..... 1740
Norra, S. 1986
Norris, M. 1550
Northen, T. 2165
Northway, M. 1021
Norton, N. 1068
Noseck, U. 582
..... 1947
Nosova, F. 1650
Nothstein, A.K. 1937
Noureddine, H. 1440
Noury, P. 1751
Novak, Martin 672
..... 815
..... 829
..... 1455
..... 1520
..... 1550
..... 2100
..... 2245
Novák, Milan 1391
..... 1551
Novakova, T. 1428
Novell, T. 496
Novella, D. 1551
Novikova, M. 448
Novotná, J. 1132
Nowak, K. 1476
Nowak, Marcus 914
..... 1148
Nowak, Monika 1552
Nowell, G.M. 1552
..... 1988
Nowicki, K. 435
Nozaki, T. 1553
..... 1993
Ntaflos, T. 459
..... 1249
..... 1427
..... 1553
..... 1554
..... 1677
..... 2169
Nuijens, L. 1554
Numata, M. 1481
Nunes, J. 1383
Nunokawa, A. 1984
Nunoura, T. 1544
Nutman, A. 514
Nyrow, A. 1778

O

O'Brien, D. 1699
..... 1763
O'Brien, E. 1451
O'Brien, P.J. 1219
..... 1228
..... 1555
..... 1818
O'Brien, R. 1167
O'Carroll, D. 1208
..... 1847
O'Connell, T. 1667
O'Connell-Cooper, C. 1924
O'Connor, T. 1361
O'Day, P. 895
..... 1004
..... 1555
..... 1621
O'Dea, S. 914
O'Dowd, C. 635
..... 825
..... 1580
..... 1727
O'Keefe, M. 1930
O'Leary, J. 879
O'Loughlin, E.J. 569
..... 1259
..... 1556
..... 1766
O'Neil, J. 407
..... 1481
..... 1556
O'Neill, B. 2011
O'Neill, C. 1051
..... 1557
O'Neill, H. 1107
..... 1124
..... 1229
..... 1442
..... 1557
..... 1558
..... 1646
..... 1915
..... 2186
..... 2281
O'Reilly, S.Y. 934
..... 946
..... 1051
..... 1395
..... 1558
..... 1802
..... 1850
..... 1922
..... 2090
..... 2121
..... 2232
..... 2234
O'Rourke, H. 719
O'Sullivan, G. 796
O'Dowd, C. 738
Oalmann, J. 1559
..... 1753
Oates, C. 1303
Obata, H. 570
..... 1987
..... 1992
Oberli, F. 600
..... 976
..... 1634
Oberthur, T. 804
..... 1552
..... 1575
Obst, M. 763
Oburger, E. 1812
Och, L. 657
..... 1308
Ocheltree, T. 1528
Ockert, C. 2140
Odake, S. 2244
Odusi, O.O. 547
Oelkers, E.H. 732
..... 757
..... 920
..... 951
..... 1125
..... 1430
..... 1559
..... 1946
..... 2171
Oelmann, Y. 1767
Oelze, M. 1560
..... 2101
Oeser, M. 1560
Ofner, J. 605
Ogawa, N. 664
Ogawa, Y. 1423
..... 1561
Ogrinc, N. 1983
Oh, J. 1075
Oh, S.G. 1285
Ohishi, Y. 458
..... 1215
..... 1961
Ohkouchi, N. 664
Ohkura, T. 1425
Ohmoto, H. 1561
Ohnemus, D.C. 1267
..... 1562
Ohno, T. 1562
Ohnuki, T. 1563
..... 1970
..... 1985
..... 2233
Ohsawa, S. 2225
Ohsumi, T. 1563
Ohta, K. 1027
..... 1961
Ohta, T. 1288
Ohtani, E. 540
..... 1335
..... 1849
Ohwada, M. 1258
Oi, M. 1564
Oi, T. 1182
Okabayashi, K. 1422
Okabayashi, S. 1027
..... 1564
Okada, Makoto 1782
Okada, Moritami 1479
Okaue, Y. 818
..... 1772
Okazaki, M. 1999

https://doi.org/10.1180/S0026461X00006502 Published online by Cambridge University Press

Okazaki, Y. 1782
Okhrimenko, D. 1565
..... 1827
Økland, I. 1565
Okoemova, V. 1566
Okrusch, M. 1156
Oksuz, N. 1566
Oldenburg, T. 1567
Olías, M. 482
..... 1176
Oliveira, J. 629
Oliveira, L.C. 785
Oliveira, N. 1567
..... 1874
Oliver, B. 2239
Oliver, N. 2251
Oliveri, E. 1697
Oliveros, V. 1568
..... 1756
Olivier, T. 513
Olivo, G.R. 768
Ölmez, E. 923
Olsen, N. 708
Olsen, P. 1568
Olsson, J. 1569
Olsson, R. 1569
Omoregie, E. 1602
Onal, Z. 792
..... 1570
Onana, J-M. 1829
Ona-Nguema, G. 587
..... 1503
Onasch, T. 2093
Ong, R. 613
Ono, S. 479
..... 1570
..... 1876
..... 2006
Onodera, J. 1782
Onoi, A. 1801
Onstott, T.C. 1333
Onufrienok, V. 1571
..... 1805
..... 2000
Ooki, A. 1987
Oomori, T. 468
..... 872
..... 1143
Opfergelt, S. 742
..... 1571
..... 1872
..... 2148
Oppenheimer, C. 425
..... 597
..... 1572
Ord, A. 936
Oren, A. 1107
..... 1572
Orgogozo, L. 1573
Orhan, H. 739
Orihashi, Y. 910
..... 1379
..... 1573
Orphan, Victoria 1406
Orphan, Victoria J 1574
Orsetti, S. 1574
Orsi, G. 451
..... 1121
..... 1499
Ortega, L. 1645
Ortega Rivera, A. 1906
Ortiz, J.e. 885
Ortiz, J. Eugenio 933
Ortiz, Joseph 1402
Osbahr, I. 1575
..... 2149
Osborne, A. 1575
Osborne, M. 1834
Oschmann, W. 2151
Osinzev, A. 2057
Oskarsson, N. 920
..... 1945
Osmaston, M. 1576
Ossorio Peralta, M. 1576
Ostendorf, J. 1577
Oster, J. 1386
Osterc, A. 1577
Østergaard, C. 1814
Österlund, L. 1392
Ostertag-Henning, C. 908
..... 1000
..... 1578
..... 1728
..... 1730
..... 2101
Ota, Y. 1578
Otake, T. 1579
Othmane, G. 1579
Otosaka, S. 1970
Ott, U. 628
..... 1099
Otte, K. 1580
Oulehle, F. 1520
Ovadnevaite, J. 635
..... 1580
Overholt, W. 1068
Ovtcharova, M. 1303
..... 1692
..... 1809
Owada, S. 978
Owen, Jacqueline 2038
Owen, Justine 1543
Oxford, G. 1581
Oyama, R. 1970
Oyan, V. 1176
Ozaki, K. 1581
Ozawa, H. 458
..... 848
..... 1547
Ozawa, K. 1522
..... 1782
Oze, C. 1753
Özkan, A.M. 1582
Özkul, M. 1165
Öztürk, A. 1582
Öztürk, C. 1583

P

Pacáková, I. 1584
Pacevski, A. 1279
Pacheco, F.A.L. 1584
Pacheco, J.M. 2243
Pacheco, W. 1797
Pacherova, P. 2245
Pachon-Rodriguez, E.A. . 1585
Pack, A. 928
Pacton, M. 1585
Padrón-Navarta, J.A. 1401
..... 1586
Pagani, M. 799
..... 1586
Paglione, M. 825
..... 1587
Pahlevan, K. 1587
Pahnke, K. 2061
Paige, D. 944
Painemal, D. 2290
Pakhomova, A. 1241
Pakhomova, S. 1588
Palace, V. 868
Palacios, C. 1704
Palacz, Z. 1588
Palastanga, V. 1116
Palchan, D. 1589
Palesskii, S. 1089
Palessky, S. 459
Palin, J.M. 1411
..... 1589
Palke, A. 1590
Pallud, C. 1157
..... 1276
..... 1421
..... 1590
Palmans, A. 1228
Palme, H. 905
..... 928
..... 1763
..... 2097
Palmer, Martin 631
..... 1006
..... 1476
..... 1591
Palmer, Matthew 1007
Palumbo-Roe, B. 1886
Pamato, M.G. 1591
Pan, F. 2252
Pan, G. 1592
Pan, J-Y. 2188
Pan, P. 1592
Panagos, P. 418
..... 1455
..... 2219
Panahdar, F. 729
Panahi, K. 1507
Pancost, R.D. 467
..... 716
..... 1328
..... 1593
..... 1990
Pandey, O.P. 1593
..... 2076
Pang, K-N. 668
Paniello, R. 1508
..... 2142
Panizzo, V. 1594
Pankhurst, R. 771
Panov, N. 1152
Pantoja, S. 524
Papanastassiou, D. 1040
Papineau, D. 1594
Parada, M. 842
Paradis, S. 1595
Paranychianakis, N. 1595
Parat, F. 1596
..... 1954
Pardo, R. 1191
Pardo-Igúzquiza, E. 1739
Pareti, S. 1642
Parikh, M. 1596
Paris, E. 676
..... 921
Paris, G. 560
Paris, M. 1805
Parise, J. 1326
Park, Changyong 632
..... 837
Park, Chan-Soo 1183
Park, Chan-Young 1185
Park, Chung-Kyun 1597
Park, G. 1075
Park, Jinyoung 468
..... 1597
Park, Jun-Cheul 820
Park, Jung-Woo 669
Park, Minho 1597
..... 1598
Park, M.r. 1131
Park, Munjae 1598
Park, R. 1599
Park, Sanghee 1598
..... 1599
Park, Seong-Sook 1600
Park, Soo-Oh 1188
..... 1285
Park, Sung-Hyun 1600
Parker, S.f. 1756
Parker, Stephen 703
..... 930
..... 1486
..... 1601
..... 1846
..... 2164
..... 2178
Parkinson, I. 552
..... 603
..... 1609
..... 1941
..... 1969
Parman, S.W. 1552
Parmentier, Marc 2106
Parmentier, Marc 1601
Paropkari, A.L. 1926
Parr, J. 1962
Parrish, R.R. 572
..... 1718
Parshotam, L. 1602
Parsons, C. 1602
Parsons, M. 898
..... 1603
Parsotam, V. 2131
Parth, V. 1603

https://doi.org/10.1180/S0026461X00006502 Published online by Cambridge University Press

Parthasarathy, G. 641
..... 1593
..... 1604
..... 1604
..... 1780
..... 1925
Pašalić, H. 2039
Pašava, J. 1605
Pascarelli, S. 435
..... 547
..... 787
Paschke, A. 1825
Pasieczna, A. 1247
Pasini, V. 1453
..... 1605
Passey, B. 551
..... 802
Pastén, P. 1295
..... 2077
Pastukhov, M. 814
Paterson, D. 522
..... 2217
Pati, J.K. 1606
Pati, P. 2088
Patil, D. 1397
..... 1606
Patiño, L.D. 2065
Patnaik, J.K. 1252
Paton, C. 531
..... 1607
..... 1815
Patten, C. 1607
Pattrick, R. 584
..... 608
..... 686
..... 1608
Paul, B. 1608
Paul, M. 1191
Paul, T. 1953
Payne, C. 1473
Payne, J. 1611
Payne, T. 546
..... 689
Paytan, A. 816
Paz, Y. 1865
Peacock, C. 599
Pearce, A. 782
Pearce, Carolyn 1608
..... 1609
..... 1757
Pearce, Christopher 1125
..... 1609
Pearce, J. 1610
..... 2017
Pearson, A. 490
..... 573
Pearson, G.D. 716
..... 1086
..... 1365
..... 1381
..... 1552
..... 1610
..... 1988
..... 2007
Pearson, N.J. 934
..... 946
..... 1051
..... 1395
..... 1558
..... 1611
..... 1802
..... 2090
..... 2121
Peate, D. 1611
Peccerillo, A. 2243
Pecha, M. 903
Pécheyran, C. 1788
Pečiulytė, D. 783
Pecoits, E. 1217
..... 1266
..... 1481
Pedentchouk, N. 1612
Pedersen, C. 1612
Pedersen, G.K. 1297
Pedersen, J. 1613
Pedersen, R.B. 707
..... 712
..... 801
..... 977
..... 1483
..... 1565
..... 1933
Pedersen, T. 1441
Pedro, L. 406
Pédrot, M. 1613
Pedroza, K. 1614
Peggy, O. 1840
Pegoraro, A. 602
Pei, F. 619
..... 1454
..... 1614
..... 2197
..... 2207
Peiffer, S. 506
..... 508
..... 1615
..... 2112
..... 2206
Peketi, A. 1435
..... 1615
Peláez, A.I. 885
Pelegri, J.L. 1015
Pelejero, C. 614
..... 1616
Pellerin, A. 1616
Pelletier, J. 1696
Pelletier, M. 1730
Pellin, M. 728
Pelt, E. 1617
Peltek, E. 1278
Peltola, P. 517
..... 1421
..... 2231
Peña, J. 2067
Pena, L. 614
Peng, H-M. 2188
Peng, J. 526
Peng, P. 1113
..... 1368
Peng, Xiaolei 1617
..... 2246
Peng, Xiu Hong 747
..... 1618
Peng, Y. 1618
Peng, Z. 1701
Penman, D. 1619
Penn, R.L. 454
Penniston-Dorland, S. 1437
..... 1619
Pentcheva, R. 1580
..... 1620
..... 1684
Perchuk, A. 1502
..... 1620
Perdrial, J. 1621
..... 2240
Perdrial, N. 1621
Pereira, A.C. 696
..... 1418
..... 1622
Pereira, V. 1083
Pereira, Z. 1355
Peres, P. 1622
Peretyazhko, T. 865
..... 2239
Perez, A. 1704
Perez, F. 1218
..... 1623
Pérez, N. 932
..... 1795
Pérez-Cruzado, C. 1456
Perez Holmberg, J. 1126
Perner, M. 1225
..... 1623
Pernet-Fisher, J. 1624
Perre, E. 531
Perrier, R. 697
Perrillat, J-P. 561
..... 1793
Perrino, C. 1642
Perron, N. 2260
Perron, T. 532
Perrot, V. 814
Perry, C. 1403
..... 1638
Perry, S. 852
Persson, P. 422
..... 1151
..... 1172
..... 1392
..... 1569
Pertille da Silva, J. 1624
Peru, K. 492
Perugini, D. 1625
Pesch, M-L. 1625
Pester, M. 1626
Pester, N. 1626
Petaev, M. 1243
Petäjä, T. 718
Peter, T. 1070
..... 1402
Peters, C.A. 806
Peters, K. 1627
Peters, M. 801
..... 1560
Peters, N. 1572
Peters, S. 1627
Petersen, J. 1628
Peterson, M. 1511
..... 1628
Petersson, A. 1629
Petit, J.R. 490
..... 860
..... 1629
Petitgirard, S. 1630
Peťková, K. 2083
Pető, M. 1630
Petr, Š. 1988
Petrakaki, N. 450
Petrash, D. 1631
Petrinec, Z. 474
..... 1631
Petrov, V. 1632
Petrunin, A. 1632
..... 1904
Petrus, J.A. 1633
Petsch, S. 1416
..... 2161
Pettenati, M. 938
Petters, M. 1633
Petterson, M. 1897
Pettke, T. 954
..... 976
..... 1198
..... 1634
..... 2096
Pett-Ridge, Jennifer 1164
..... 1431
..... 1634
Pett-Ridge, Julie 1872
Peuble, S. 1635
Peucker-Ehrenbrink, B. 799
..... 1837
..... 2103
Peuget, S. 613
Peulen, T-O. 1635
Peyravi, S. 1636
Peytcheva, I. 1809
Pfaff, K. 1698
Pfaffenberger, L. 1013
Pfahl, T. 2156
Pfahler, V. 1983
Pfänder, J. 816
..... 979
..... 1833
..... 2012
Pfeffer, C. 1636
Pfister, C. 527
Pham, C. 1637
Pham, T.H. 1637
Pham, V.T.H. 398
..... 1638
Phaneuf, C. 1403
..... 1638
Phil, H. 826
Philippot, P. 1291
..... 1639
..... 1992
..... 2007
..... 2073
Phillips, D. 1169

https://doi.org/10.1180/S0026461X00006502 Published online by Cambridge University Press

Phillips, R. 1339
Phipps-Morgan, J. 2154
Phoenix, V. 1265
1550
1691
1891
2016
Phrommavanh, V. 2130
Pi, D. 1350
2275
Piasecki, S. 907
Piazolo, S. 1051
1650
Picard, A. 721
1639
Picard, C. 2049
Picardal, F. 639
876
Piçarra, J.M. 1355
Piccoli, P.M. 2242
Piceno, Y. 693
Pichat, S. 1333
1881
2142
Pichavant, M. 1572
Pichevin, L. 1640
Pichler, T. 2109
Pick, T. 1695
Pickle, R. 1772
Pickles, J. 1640
Pidgeon, B. 942
Pieczka, A. 947
Pielichowskiaze, K. 1751
Piepenbrock, A. 763
Pierce, Elizabeth 693
Pierce, Eric 1077
1641
Pierce, J. 407
Pierret, M-C. 1641
1724
2096
Pietranik, A. 736
1181
2044
Pietrodangelo, A. 1642
Pietruszka, A. 601
998
1642
Piette, L. 1839
Pijanka, J. 1817
Pik, R. 1276
Pilbeam, L. 1643
Pilet, S. 593
1643
Pili, E. 1644
Pimblott, S. 1608
Pimentel, M. 616
Pina, C.M. 1644
Piña, R. 1645
Piñero, E. 1356
Pinkas, J. 1955
Pinto, A. 1645
Pinto, K. 1492
Pinto de Abreu, M. 1383
Pinton, R. 2001
Piotrowski, A.M. 897
1646
1734
2165
Pirajno, F. 2214
Pirard, C. 1013
1646
Pirmoradian, Z. 1843
Pironon, J. 2054
Pirre, M. 1076
Pisapia, C. 1647
Pitawala, A. 1105
2230
Pitcairn, I. 1199
Pizarro, G. 1295
2077
Pizarro, O. 645
Plach, J. 2134
Planavsky, N. 603
1217
1266
1373
1647
1778
1831
Planer-Friedrich, B. 1104
1254
1648
Plank, T. 1648
1768
Planquette, H. 1855
Plante, A.F. 838
839
Plathe, K. 1649
Platon, T. 1214
Platt, S. 1013
Platt, U. 605
Platte, A. 925
Plechov, P. 513
857
Plechova, A. 1649
Plessen, B. 1125
1364
Ploskey, Z. 1949
Plotkina, J. 1785
Plotnikova, I. 1650
Plötze, M. 2174
Plumlee, G. 1305
Plümper, O. 509
1650
1651
Plymale, A. 865
Podladchikov, Y. 854
1118
Pogge von Strandmann, P. 805
1651
2148
Poh, S.C. 1652
Pohl, F. 858
Pöhle, M. 1652
Pointing, M.D. 730
Poirier, A. 753
926
1653
Poitrasson, F. 1653
2085
2243
Pokhilenko, N. 1085
1395
Pokrandt, K-H. 2048
Pokrovski, G.S. 502
1654
1654
Pokrovsky, O.S. 461
700
1573
1654
Pokryszka, Z. 1264
Polacsek, T.K. 1655
Poland, M. 932
Polerecky, L. 1477
1694
Polgári, M. 1655
Poli, S. 495
Polizzotto, M.L. 1534
Poll, C. 1001
Pollehne, F. 741
Polley, G. 1619
Pollington, A. 501
611
1656
Pollok, K. 834
980
1042
1656
Polozov, A. 1076
Polubesova, T. 1657
Polya, D. 1277
Polyak, L. 922
Polyakov, V. 1657
Pombo, S.A. 1658
Ponaryadov, A. 1658
Ponomarchuk, V. 1659
1836
Ponomareva, V. 1661
Ponton, C. 799
Ponzevera, E. 501
674
1101
1508
1917
Poole, J. 1948
Pop, C. 466
Pope, E. 1659
Popescu-Pogrion, N. 2046
Popova, J. 1660
1969
Poppitz, W. 427
Porcelli, D. 431
453
1267
Porcher, C. 1299
Poreda, R. 916
Poret-Peterson, A. 1660
Porter, S. 1661
Portnyagin, M. 426
1235
1236
1478
1649
1661
1864
Possnert, G. 1048
Post, J. 882
Post, V. 945
2109
Post, W.M. 1433
Posth, N. 1147
1148
Postma, O. 1501
Potgieter, J. 1662
Potts, M. 467
Potysz, A. 1181
Poulton, S.W. 615
831
927
1091
1308
1419
1651
1662
1663
Pourcelot, L. 1106
1137
Pourmand, A. 725
1663
Pourovskii, L. 1664
Pourret, O. 550
633
647
832
2096
Powell, C. 1664
Powell, R. 1991
Power, I.M. 982
Pozzi, J-P. 911
Prabhakar, B.C. 1153
Pradoux, C. 1943
Prakapenka, V. 1792
1883
Prakash, O. 1068
Prasad, M.N.V. 1665
Prata, A.J. 792
Pratas, J. 832
1665
1665
Pratt, A.R. 768
Prave, A. 1152
2175
Prazeres, C. 1645
Prechova, E. 1550
2100
Preda, M. 963
Predota, M. 1378
1666
Prelevic, D. 572
1666
Prendergast, A. 1667
Prenni, A. 1633
Preston, P. 679

https://doi.org/10.1180/S0026461X00006502 Published online by Cambridge University Press

Preto, N. 716
..... 1667
Prévôt, A. 1013
..... 2260
Priadi, C. 1668
Price, Richard 1668
..... 1943
Price, Roy E. 1330
..... 1669
Prichard, H. 686
..... 723
..... 1960
Prieto, M. 1116
..... 1669
..... 2075
Prieto, X. 1702
Prieto-Rubio, M. 840
Prietzel, J. 1712
..... 1922
..... 2004
Principato, S. 738
Pringle, M. 1451
Prinzhofer, A. 1788
Prisyagina, N. 1969
Pritzkow, W. 2098
Probst, A. 1641
Prochaska, W. 580
Proemse, B. 1432
..... 1670
Proenza, J. 415
Prokofiev, V. 1670
Prokopenko, M.G. 882
..... 2218
Prokushkin, A. 1573
Prol-Ledesma, R.M. 1671
..... 2090
Prommer, H. 945
..... 1832
..... 2109
Pronin, N. 1650
Pronk, G.J. 1001
..... 1671
Proskurowski, G. 1269
Pross, J. 2151
Prosser, G. 1794
Proteau, G. 2042
Protsko, O. 1672
Proupin, J. 491
Prouty, N. 1732
Proux, O. 1290
..... 1304
..... 1668
Provencal, R. 2131
Provenzano, C. 691
Proyer, A. 1672
Prudêncio, M.I. 1408
..... 2030
Prunier, J. 1653
..... 1724
Prytulak, J. 805
..... 1539
..... 1673
Ptacek, C. 537
..... 1673
Puchol, N. 1276
Puchtel, I.S. 1020
..... 1674
..... 2026
Pujol, M. 1674
..... 1675
Pulford, I. 1550
Purchase, M. 1675
Purdie, P. 1189
Purton, J. 703
Purtschert, R. 583
..... 1361
Puschenreiter, M. 1812
Pushkarev, E. 896
Pushkarev, Y. 1676
Putlitz, B. 1303
..... 1692
Putnis, A. 586
..... 1190
..... 1196
..... 1656
..... 1676
..... 1677
..... 1767
..... 2052
Putnis, C.V. 1196
..... 1656
..... 1676
..... 1677
..... 1767
..... 2052
Puzenat, E. 1751
Puziewicz, J. 1249
..... 1427
..... 1677
..... 2169
Pyle, D. 519
Pystin, A. 1678
Pystina, Y. 1678

Q

Qafoku, O. 1609
Qi, Jian-Ying 2119
Qi, Jun 1679
Qi, Q.J. 2125
Qi, Z. 427
Qian, B. 2254
Qian, K. 2110
Qian, Y. 666
Qiang, W. 1966
Qin, D. 2116
Qin, H. 1679
..... 2236
Qin, L. 1680
Qin, Y. 1320
Qing, C. 747
..... 1618
Qiu, H. 1680
Qiu, J-S. 1681
Qiu, X.F. 518
..... 1681
..... 2253
Qiu, Z-L. 1316
Qu, X. 1434
Qu, Y. 1682
..... 2073
Quaas, J. 1627
..... 1682
Quantin, C. 1300
Quas-Cohen, A. 1683
Quattrochi, D. 1345
Quazi, S. 764
Quevedo, I. 2037
Quigley, D. 744
Quinn, Patricia 497
..... 1683
Quinn, Paul D. 581
..... 1505
..... 1991
Quinn, T. 1770
Quirico, E. 1493
Quiroga, C. 1684

R

Raatikainen, T. 825
Rabbia, O.M. 1685
Racek, M. 831
Rach, O. 1685
Racz, A. 1818
Rad, S. 1686
..... 1731
Radakovitch, O. 681
..... 1952
Raddatz, J. 1491
Rademacher, L. 1686
Radko, V. 1904
Radtke, M. 609
Rae, J.W.B. 859
..... 960
..... 1009
..... 1020
..... 1687
Raepsaet, C. 2168
Rafols, J. 613
Ragazzola, F. 844
..... 1687
Ragnarsdottir, K.V. 1398
..... 1455
Ragozin, A. 2244
Rahaman, W.R. 1688
Rahn, M. 2102
..... 2117
Rai, N. 1688
Rai, S.K. 1689
Rainey, E. 1689
Raisbeck, G. 634
Raiteri, P. 744
..... 744
Raith, J. 1690
Rajagopalan, V. 1593
Rajmohan, N. 870
Rakhmonkulova, S. 1690
Rakotoarisoa, O. 699
..... 949
Ralph, J. 994
Ramakrishna Reddy, M. . 1926
Ramamurthy, P.B. 1606
Ramanan, B. 1691
Ramaswamy, V. 1478
Ramdohr, R. 1691
Ramette, A. 1110
Ramezani, J. 2040
Ramirez, Carlos 1023
Ramírez, Cristóbal 1692
Ramirez, D.A. 1492
Ramirez, V. 1875
Ramos, F. 1692
..... 2170
Ramos, V. 1573
Rampone, E. 555
Ramsay, R. 711
Ranaweera, L. 1693
Řanda, Z. 556
Randi, A. 2054
Ranea Robles, P. 1356
Rangarajan, R. 1693
Rantica, E. 1642
Rantzsch, U. 1694
Rao, A. 1694
Raoof, B. 764
Rap, A. 1924
Rapaglia, J. 1695
Rasa, I. 1162
Rasch, P. 1695
Rascher, J. 1879
Rasmussen, B. 1511
..... 1696
Rasmussen, C. 839
..... 1696
Raso, M. 1697
Rasouli, P. 1697
Rate, A. 784
..... 1363
Ratschbacher, B. 1698
Ratschbacher, L. 937
Ratulowski, J. 1930
Rau, G. 1698
Raub, T. 850
Raucsik, B. 1230
Raudsepp, M. 1595
Rausch, Svenja 544
..... 1548
Rausch, Svenja 1699
Raven, K. 1484
Ravizza, G. 1993
Ravna, E.J.K. 1525
Ray, C. 717
Ray, D. 1926
Ray, James 1621
Ray, Jessica 1130
..... 1130
Ray, Jyotiranjan 525
Raymond, S. 1699
Read, M. 2164
Reagan, M.K. 1087
..... 1700
..... 1714
..... 1881
..... 2008
Rebenack, C. 893
Rebiscoul, D. 1700
Reche, J. 2080
Reddy, C. 1604
Reddy, M.N. 1378
Redeker, K. 1602
Redemann, J. 1701
Redfern, S. 1701
Redlich, A. 779

https://doi.org/10.1180/S0026461X00006502 Published online by Cambridge University Press

Reeburgh, W. 1702
Reeder, R. 1357
Reese, B.K. 1723
Rees-Owen, R. 1593
Reeves, E. 1702
Regelous, M. 508
..... 574
..... 866
..... 962
..... 1246
..... 1703
..... 1932
Regenauer-Lieb, K. 1662
..... 1675
..... 1908
Regenspurg, S. 479
..... 577
..... 1703
..... 2085
Regis, D. 812
Regnier, P. 2035
Reguir, K. 677
..... 1260
Rehkamper, M. 927
..... 1018
..... 1267
..... 1271
..... 2175
Rehm, K.E. 1191
Reich, M. 733
..... 1704
Reich, T. 1223
Reiche, M. 1360
Reiche, S. 914
Reichmann, H.J. 1407
Reid, F. 693
Reid, J. 549
Reid, M. 1704
Reid, N. 1705
Reimer, T. 1742
Rein, E. 907
Reinfelder, J. 690
Reinhard, Christopher 433
..... 457
..... 1373
..... 1647
Reinhard, Christopher 1705
Reinhold, J. 1081
Reinholz, U. 609
Reinoso-Maset, E. 1165
Reinsch, B. 931
..... 1706
Reisberg, L. 614
..... 1420
..... 1457
..... 1706
..... 2064
Reith, F. 615
..... 1707
..... 1707
Reitner, J. 2004
Reitsma, M. 1708
Reitz, A. 1010
..... 1326
Reitz, T. 1834
Relvas, J. 707
Remer, L. 1152
..... 1701
..... 1708
Remis, J. 2180
Rempel, K. 1709
Remusat, L. 1291
..... 1709
Remy, P-P. 1840
Ren, Y.S. 1710
..... 2264
Renard, F. 1493
Renberg, I. 1196
René, M. 1710
Renema, W. 821
Renforth, P. 1711
..... 2134
Renne, P.R. 588
..... 631
..... 1442
..... 1711
..... 1712
Rennert, T. 820
..... 869
..... 973
..... 1424
..... 1712
Rennie, V. 445
..... 1713
Renock, D. 505
Renshaw, J. 975
..... 1039
..... 1713
Rentería, J. 2090
Resing, J. 1370
Restrepo-Moreno, S. 1492
Reubi, O. 694
..... 1714
Reuschel, M. 1714
..... 1794
Reverdatto, V. 1327
Revil, A. 1538
Revsbech, N.P. 1419
Rey, D. 438
Rey, J. 1873
Reynard, B. 1715
Reynard, L.M. 534
..... 730
Reynaud, S. 870
Reynolds, Ben 752
..... 1025
..... 1715
..... 2151
Reynolds, Brian 1455
Reysenbach, A-L. 968
Rezvani Khalilabad, M. 1716
Rezvukhin, D. 1395
Rhede, D. 1363
..... 1981
Rhodes, J.M. 601
..... 2142
Ribeiro, C. 1716
Ribeiro, D. 1717
Ribeiro, H. 629
..... 952
..... 1716
..... 1740
Ribeiro, M.D.A. 774
..... 1717
Ribes, M. 1616
Ricci, P.C. 1808
Ricco, A.J. 1228
Rice, J. 665
Richard, A. 1718
Richard, L. 2054
Richards, D. 692
..... 1718
Richardson, D. 604
..... 680
..... 1757
..... 2153
Richardson, S. 1863
Richardson, T. 1851
Richey, J. 1719
Richnow, H-H. 865
..... 1244
..... 2206
Richter, A. 1495
Richter, D.K. 1823
..... 2242
Richter, F. 1719
Richter, K. 1720
Rickaby, R. 1045
Ricking, M. 2156
Rickli, J. 434
..... 1720
..... 1943
Ricolleau, A. 1721
Ridgwell, A. 860
..... 2035
Ridley, M. 1378
..... 1721
Riebe, B. 722
Riebe, C.S. 776
..... 1722
..... 1722
Riedel, T. 1723
Riedinger, N. 1373
..... 1723
Riesemeier, H. 609
Rieuwerts, J. 2041
Rigby, M. 1429
Righter, K. 2036
Rihs, S. 1724
Riipinen, I. 407
Riishuus, M. 434
..... 1724
Rijkenberg, M. 1725
Riker, J. 1725
Riley, M. 1713
Rillard, J. 1726
Rimskaya-Korsakova, M. 1240
..... 1726
Rimstidt, J.D. 620
Rinaldi, M. 635
..... 1727
Rinne, J. 1727
Rinnen, S. 1728
Rinnert, E. 823
Rios, P. 1295
..... 2077
Riotte, J. 1728
Ripley, E. 773
..... 1729
Risgaard-Petersen, N. 1419
..... 1538
..... 1636
..... 1729
Risse, A. 1000
..... 1728
..... 1730
Rittweger, J. 1019
Ritz, K. 1016
Rivard, C. 1730
Rivé, K. 1686
..... 1731
Rivera, M.B. 840
Rivera, N. 1621
Rizzo, D. 782
Rizzo, G. 1794
Rizzo, L. 455
Rman, N. 1731
Ro, C-U. 1911
Roalkvam, I. 1732
..... 1933
Roark, E.B. 1732
Robbins, L. 1733
Roberge, J. 706
Robert, F. 645
..... 750
..... 1404
Robert, G. 1733
Roberts, H. 527
Roberts, J. 1734
Roberts, K.A. 1797
Roberts, Natalie 1734
Roberts, Nick 1735
Robertson, D. 1191
Robin, E. 948
Robinson, C. 1868
Robinson, L.F. 462
..... 599
..... 704
..... 1008
..... 1484
..... 1735
..... 1736
Robinson, Paul T 1736
..... 2209
Robinson, Peter 1438
Robinson, R. 1737
Robinson, S. 1737
..... 2149
Robson, T. 1738
Roca, A. 1747
Rocha, C. 1738
Rocha, D. 943
..... 2103
Rocha, F. 1408
..... 2030
Roden, E. 639
Rodenburg, J. 1388
Rodger, A. 1275
Rodgers, R. 1739
Rodrigo-Gámiz, M. 1739
Rodrigues, A. 952
..... 1740

https://doi.org/10.1180/S0026461X00006502 Published online by Cambridge University Press

Rodrigues, B. 554
1740
Rodríguez, D. 2090
Rodriguez, Javier 2078
Rodríguez, Jose 1873
Rodriguez, Jose 526
Rodríguez, Jose Antonio 491
Rodriguez-Blanco, J.D. 559
1741
1748
1790
2059
Rodriguez-Hernandez, P. 1515
1741
Rodriguez-Navarro, C. 1767
1816
2052
Rodríguez-Tovar, F.J. 1417
1739
1742
Rodushkin, I. 2067
Roerdink, D.L. 1742
Roesch, N. 1237
Roetting, T. 1380
Roffeis, C. 1743
Rogers, A.D. 969
Rogers, J. 2072
Rogers, K. 711
Rogers, N. 941
Roghi, G. 716
1667
Röhl, U. 2160
Rohovec, J. 556
779
Rohr, A. 1850
Rohrbach, Arno 475
Rohrbach, Arno 1743
Rojik, P. 861
1205
Rolfe, S. 472
Roling, W. 2079
Rolland, Y. 1490
1777
Rolle, M. 1117
1744
Rollion-Bard, C. 646
1744
2007
2014
Rols, J-L. 700
1654
Romanchenko, A. 1745
Romanchuk, A. 1745
Romaniello, S. 1501
1660
1746
Romanov, S. 1224
1746
Romanova, I. 1516
Roman-Ross, G. 1602
Romer, R.L. 400
572
1010
1243
1281
Romero, A. 1741
Romero-Freire, A. 1747
Romero-Gonzalez, M. 644
695
1747
1817
Romero Viana, L. 1748
Römmermann, H. 2160
Roncal-Herrero, T. 559
1741
1748
Rood, D. 1807
Rooney, A. 1749
Roopnarine, P. 1921
Root, Robert 970
Root, Robert 1749
Rory, M. 1492
Rosales, R.M. 1750
Rosario, N. 1354
1750
Rose, A. 689
894
1751
Rose, J. 1290
1304
1751
Rose, P.S. 1752
Rose-Koga, E.F. 610
1211
1752
Rösel, D. 1753
Rosell-Mele, A. 1029
Rosenbauer, R. 1120
1753
Rosenberg, Y.O. 1754
Rosenqvist, J. 1378
1754
Rosenthal, A. 1229
Rosiere, C. 1217
Rosing, M.T. 1489
1659
Rosner, M. 1125
1702
1755
Ross, I. 1747
Ross, K.C. 1755
Ross, N.L. 1756
Ross, S. 2145
Ross, Steve 1732
Rossberg, A. 789
1194
1513
Rossel, P. 1756
Rossman, G. 649
Rosso, K. 632
915
1173
1609
1757
1757
Rost, B. 1235
1758
Rostek, F. 1758
1917
Rostron, B. 452
Roszjar, J. 1759
Rotella, M. 2187
Rotenberg, B. 794
Roth, A. 1759
Rothe, J. 478
998
Rother, G. 444
1245
1527
Rouai, M. 1464
Rouchon, V. 1385
Rouff, A. 1760
Rough, M. 1616
Rousseau, L. 911
Rousseva, S. 1455
Routh, J. 912
1252
1693
Routier, T. 647
Roux, C. 1760
Rouxel, O. 457
1217
1266
1508
1914
Rouzaud, J-N. 1709
Rovira, P. 1761
Rowe, M. 1611
1700
1761
Roy, R. 1431
Roychoudhury, A. 1762
2102
Rozanov, A. 1762
Rozsypal, C. 1718
R S, S. 525
Ruan, J. 1348
Ruban, A.V. 1664
Rubatto, D. 812
824
1938
Ruberg, S. 496
Rubie, D.C. 1763
2097
Rubin, K. 1763
1764
Rubin, M. 1845
Rubio, B. 438
Rubio Ordóñez, A. 685
Ruby, C. 906
Ruckelshausen, M. 1764
Rudge, J. 1765
Rudnick, R.L. 965
1340
Rudy, M. 495
Rueda, G. 1029
Ruggieri, G. 558
Ruggieri, N. 1029
Ruhl, M. 1765
Rui, X. 1766
Ruiz, Javier 1766
Ruiz, Joaquin 837
1193
2137
Ruiz, L. 1728
Ruiz-Agudo, Encarnacion 1677
1767
1816
2052
Ruiz-Agudo, Encarnación 1196
Ruiz Cánovas, C. 2025
Rullkötter, J. 1823
Rumble, D. 2229
Rumpel, C. 1788
Rupp, J. 566
Ruppenthal, M. 1767
Ruprecht, P. 1768
Rusch, D. 1104
Rusciadelli, G. 690
Rushmer, T. 407
1768
Rushton, T. 1561
Rusk, B. 2251
Russak, A. 1769
Russell, A. 1769
Russell, J. 1006
Russell, L. 497
1770
Russell, P. 1701
Russoniello, C. 1462
Rutgers v. d. Loeff, M. 673
Ruth, A.A. 766
Rutherford, M. 991
2150
Ruzié, L. 944
1770
Ryabchikov, I.D. 1771
Ryabenko, E. 942
Ryabov, V. 1089
1659
1836
Ryan, C. 489
1332
Ryan, Jeffrey 1804
1954
Ryan, Joseph 1077
1771
Ryan, Joseph 1054
Ryb, U. 1426
Rychanchik, D. 1452
Ryder, C. 1021
Ryder, J. 1221
Ryerson, F. 749
1872
2064
2136
Ryu, I. 1185
Ryu, J-S. 1096
1184
Ryzhenko, B. 662
1366
Rzepa, G. 571
1259

S

Saal, A. 974
991
1535
1628
1772
2150

https://doi.org/10.1180/S0026461X00006502 Published online by Cambridge University Press

Sabita, A. 1772
Sabokkhiz, F. 1773
Saccone, L. 475
1398
1900
Sachan, H.K. 1689
Sachse, A. 2085
Sachse, D. 1685
1748
1829
Sadeghian, M. 900
1773
1774
1774
Sadekov, A. 1821
Sadiklar, M.B. 745
Sadjadi, A. 1842
Sadjadi, S. 1297
1980
Saeedi, A.S. 2060
Saenz, J. 1775
Saeva, O. 2237
Safari, M. 1435
Sagawa, T. 1143
Sageman, B. 1126
Sager, M. 671
Sager, W. 1775
Sağlam, E.S. 1776
Saha, L. 1606
1776
Sahakyan, L. 1777
Sahami, A. 1777
Sahle, C. 1778
Sahoo, P.K. 1185
Sahoo, S.K. 1778
Sahu, S.K. 1779
Saiano, F. 1697
Said, N. 1779
Saiki, H. 1970
Saikia, B.J. 1780
1780
1781
Saini, G. 640
Saint-Macary, H. 1290
Sainz-Díaz, C.I. 1644
Saito, M. 462
Saito, Takumi 1781
2204
Saito, Tomoyuki 818
Saito, Tsutomu 2205
Sajedian, E. 1494
Saka, S. 2055
Sakai, K. 1085
Sakai, R. 1782
Sakai, S. 1782
Sakami, H. 2202
Sakamoto, I. 1087
Sakamoto, T. 1782
Sakamoto, Y. 1579
Sakellariadou, F. 1783
Sakulchiacharoen, N. 1208
Sakuma, H. 1080
Sal`nikova, Y. 1914
Salama, W. 1783
Salanne, M. 1409
Salaun, P. 913
Saldi, G.D. 726
1559
1784
Salehikhoo, F. 1313
Salek, S. 1784
Salgado, J. 491
1456
Salhi, E. 1790
Saliot, P. 1622
Salmon, E. 401
507
Salmon, U. 1363
Salnikova, E. 1785
2199
Salt, L. 1725
Salzano, R. 1642
Samadi, R. 1785
1863
Samarkin, V. 1832
Samide, A. 1786
Sample, J. 1786
Sampson, B. 1271
Samson, S. 1835
Samsonova, A. 1787
Samuel, H. 1787
Sanabria, G. 1788
Sanaullah, M. 1788
Sanborn, M. 565
Sánchez, J. 885
Sánchez-Alcala, I. 1789
Sánchez Espana, J. 2146
Sánchez-Pastor, N. 840
Sanchez-Valle, C. 1883
2242
2247
Sanchi, L. 1789
Sand, K. 1790
Sander, A. 691
Sander, M. 409
938
1790
Sander, P.M. 1017
Sander, S. 1225
Sanders, R. 1007
Sandiford, M. 2042
Sandler, A. 427
Sandmann, D. 1791
Sañé, E. 1791
Sang, L. 1792
Sang, S-H. 1792
Sanloup, C. 1793
San Miguel, E.G. 1416
Sano, T. 426
1073
1775
1861
Sano, Y. 988
1578
1793
Sansjofre, P. 1794
Sansone, F. 921
Sansone, M.T.C. 1794
Sant'Ovaia, H. 629
774
841
952
1358
1716
1795
Santana-Casiano, J.M. 932
1795
Santelli, C.M. 1796
2075
Santofimia, E. 1796
Santos, G.M. 1764
Santos, J.F. 1485
Santos, R. 1797
Santos, S. 634
Santos, T. 2148
2288
Santschi, P.H. 1797
Sanwani, E. 638
Sanzheev, E. 2248
Sappok, A. 705
Saracco, G. 1464
Sarangi, S. 1798
Sarda, P. 430
Sari, E. 473
Sarkar, A. 1798
Sarkar, C. 1798
Sarmiento, J. 1390
Sarnthein, M. 1687
Sarr, A. 1788
Sasaki, K. 1503
1799
1799
2019
2233
Sasaki, Y. 1800
Saslow, S. 1127
Sassen, D. 1925
Sata, N. 1961
Satheesh, S.K. 1800
Sato, F. 2029
Sato, H. 1838
Sato, K. 496
1801
Sato, Takeshi 1208
Sato, Tomofumi 1800
Satoh, H. 1190
2065
Sator, N. 430
971
2104
Satya Vani, C. 1925
Sauer, P. 1801
Sauheitl, L. 763
Saukko, E. 1802
2093
Saunders, A. 1897
Saunders, J. 1802
Saunders, K. 843
Savage, P.S. 1803
Savaşçın, M.Y. 412
Savenko, A. 1803
2244
Savenko, V. 1803
Savina, M. 728
Savov, I.P. 707
966
986
1804
Savoye, S. 523
Sawaki, Y. 1168
2227
Sawicka, J. 1723
Sawyer, G. 1572
Saxena, P.R. 1603
Sayama, M. 1804
Sayer, A. 1053
Sayili, İ.S. 1583
Sayit, K. 973
Sayle, D. 1486
Sazonov, A. 1571
1805
2000
Scaillet, B. 425
881
921
1076
1572
1805
Scambelluri, M. 1393
1806
Scarchilli, C. 781
Scarsi, P. 1023
Schaefer, B.F. 906
1516
1806
Schaefer, J.M. 1807
Schäf, M. 1895
Schäfer, J. 948
Schäfer, T. 478
638
849
1047
Schäffer, A. 1476
Schaffer, B. 1350
Schaffhauser, T. 637
1807
Schäffner, F. 417
1808
Schaller, M. 1568
1808
Schaltegger, U. 541
583
1303
1708
1809
1889
2179
Schaperdoth, I. 1377
Schardt, C. 1459
Schauble, E. 1018
1382
1446
1809
1810
2229
Schaumann, G.E. 404
1810
Scheer, L. 1509
Scheffler, M. 1620
Schefuss, E. 799

https://doi.org/10.1180/S0026461X00006502 Published online by Cambridge University Press

Scheidegger, Y. 1811
Scheiderich, K. 1811
Scheinost, A.C. 478
..... 789
..... 1194
Schenk, V. 469
..... 1014
Schenkeveld, W. 1812
Schepers, A. 1812
Scherbakova, I. 1813
Scherer, E. 1896
..... 2137
Scherer, M. 1757
Scherf, A-K. 1813
Scherstén, A. 1629
..... 1814
Schettler, G. 1709
Schiano, P. 1913
Schichel, T. 989
Schichnes, D. 2180
Schieber, J. 639
..... 1814
Schiedung, H. 1400
Schiemenz, A. 1324
Schikora, J. 1947
Schild, D. 478
..... 591
Schiller, M. 531
..... 755
..... 1607
..... 1815
Schilling, F.R. 1510
..... 2139
Schilling, J-G. 805
Schimmelmann, A. 876
Schimmelpfennig, I. 1807
Schipek, M. 1254
..... 1815
Schipper, I. 2187
Schippers, A. 1816
Schiraldi, B. 807
Schiro, M. 1816
Schlegel, Melissa 1416
Schlegel, Michel 667
Schlieker, M. 1458
Schlöglová, K. 1817
Schmahl, W.W. 1580
Schmalenberger, A. 553
..... 1817
Schmandt, B. 1761
Schmeide, K. 1940
Schmidt, A. 1818
Schmidt, B. 493
Schmidt, Calla 1818
Schmidt, Caroline 763
..... 1453
Schmidt, Christian 787
..... 1778
..... 1819
..... 1932
..... 2136
..... 2160
Schmidt, D. 467
..... 860
..... 1687
Schmidt, K. 498
..... 1819
Schmidt, Mark 1010
Schmidt, Matthew W. 1017
..... 1820
..... 2002
..... 2194
Schmidt, Max W. 475
..... 912
..... 1024
..... 1097
..... 1743
Schmidt, Michael W.I. 403
Schmidt, Moritz 638
..... 837
Schmidt Mumm, A. 1820
Schmidt-Rohr, K. 1004
Schmitt, Anne-Désirée 683
Schmitt, Axel 530
..... 633
..... 878
..... 1736
..... 1821
..... 1821
..... 1871
Schmitt, C. 1191
Schmitt-Kopplin, P. 1016
Schneider, B. 2166
Schneider, D. 1821
Schneider, H. 944
Schneider, J. 1364
Schneider, T. 867
Schneider-Mor, A. 1386
..... 1822
Schnetger, B. 551
..... 741
..... 797
..... 1419
..... 1522
..... 1822
Schnitzler, J-P. 1727
Schnoor, J.P. 1928
Schnug, E. 1895
Schoemann, V. 1725
Schoenberg, R. 1483
Schofield, D. 935
Schofield, P. 581
..... 778
..... 1196
Scholes, J. 472
Scholl, A. 778
Schöll-Barna, G. 743
Scholten, J. 1738
Scholz, D. 1117
..... 1823
Scholz, F. 1010
..... 1326
Scholz-Böttcher, B. 1823
Schönbächler, M. 1824
Schöne, G. 1101
Schönfeld, J. 1956
Schöpa, A. 443
Schott, J. 511
..... 757
..... 899
..... 1430
..... 1559
..... 1934
Schouten, S. 533
..... 1540
..... 1593
..... 1898
..... 1990
..... 2063
Schraepler, R. 1228
Schrag, D. 802
Schram, N. 1037
Schranz, W. 2263
Schreiber, A. 520
..... 2073
Schreiter, I. 494
Schrenk, M. 430
Schröder, C. 1148
..... 2112
Schroeder, F. 1201
Schroeder, K. 1942
Schroth, N. 1824
Schubert, C.J. 535
..... 627
..... 734
..... 1110
..... 1192
..... 1825
..... 2147
Schubert, M. 1825
Schubotz, F. 1832
Schuessler, J.A. 1826
..... 2101
Schuhmacher, M. 1622
Schuiling, R. 1826
Schüler, M. 1477
Schulte, P. 494
Schultz, L. 1827
Schultz, M. 2166
Schulz, A. 865
Schulz, H-M. 520
..... 1244
..... 1813
Schulz, Marjorie 604
..... 935
Schulz, Michael 738
Schulz, R. 1810
Schulz, T. 1514
..... 1827
Schulze, N. 1195
Schulze-König, T. 1975
Schulz-Vogt, H.N. 919
Schumacher, J. 1410
Schumann, K. 1096
..... 2140
Schurig, C. 1828
Schuth, Stephan 494
..... 1217
..... 1400
..... 1828
..... 2169
Schuth, Stephan 1036
Schvede, H. 2092
Schwab-Lavrič, V. 1829
Schwaiger, L.K. 1545
Schwalb, A. 1117
Schwartz, S.E. 738
Schwarz, Jaroslav 1829
Schwarz, Joshua 1944
Schwarz, S. 2097
Schwarzenbach, E. 1830
Schwarzenbach, R.P. 409
..... 1790
Schwarz-Kopf, L. 2032
Schwarz-Schampera, U. 1830
Schwehr, K.A. 1797
Schwieters, J. 561
..... 969
..... 1351
Schwinger, M. 722
Sciare, J. 1727
Scoates, J. 1546
..... 1831
..... 2142
Scott, A. 1350
Scott, C. 1373
..... 1647
..... 1705
..... 1831
Scott, G. 588
Scott, R. 1191
Scott, S. 882
Scott, T. 860
Seabourne, C. 1350
Seabra, A. 1292
Sebek, O. 819
..... 1468
..... 2095
Seddique, A.A. 1422
Sedlazeck, P. 915
Sedlmair, J. 2004
Seewald, J. 1702
Segarra, K. 1832
Segovia-Diaz, E. 2080
Seibert, S. 1832
Seidel, M. 2135
Seifert, T. 400
..... 765
..... 1791
..... 1833
..... 1937
Seifert, W. 592
Seiler, M. 1975
Seinfeld, J. 617
Seitsonen, A. 2104
Sejkora, J. 1049
Seki, O. 1782
Sekine, T. 1543
Sekiya, T. 1833
Sekiyama, T.T. 1144
Selby, D. 710
..... 846
..... 1661
..... 1749
..... 1834
Selenska Pobell, S. 1834
Sell, B. 1835
Sellers, W. 798
Selsis, F. 1835

https://doi.org/10.1180/S0026461X00006502 Published online by Cambridge University Press

Seltmann, R. 771
Selverstone, J. 1836
1848
Šembera, J. 2238
Semenova, D. 1659
1836
Sempere, T. 541
Semutnikova, E. 2065
Sen, A.D. 1837
Şen, C. 464
Sen, I. 1837
Sena, E. 1838
Senda, R. 978
1838
1993
Séné, O. 1829
Sengen, Y. 2225
Senshu, H. 2054
Seo, Jieun 669
Seo, Jung Hun 1290
1839
Sephton, M.A. 1228
Sepúlveda, J. 524
Sequeira, A. 632
Serebryakov, N. 530
Sergeant, C. 1839
Sergeev, D.S. 759
Sergent, A-S. 1840
Serikov, I. 1554
Serlegi, G. 743
Serrano, E. 1616
Serrano, S. 895
1004
1555
1840
Setidjaji, L.D. 1078
Setkova, T. 1841
Severinghaus, J. 1841
Severmann, S. 797
Sevinsky, J. 1842
Seward, T. 1297
1842
1980
Seyfried, W. 1626
1976
Seyler, P. 1653
Shabanian Boroujeni, N. 729
Shabankareh, M. 1843
1843
Shafei, B. 2025
Shahar, A. 747
1469
1844
Shajari, F. 1844
Shaked, Y. 1845
Shakouri, B. 800
Shamsh, P. 958
Shang, J. 1338
Shang, L. 1845
Shang, X. 1860
Shang, Y. 2115
Shanks, W.C. 1976
Shao, H. 1130
Shao, J. 2212
Shao, P. 1846
Shao, Y. 1144
Shapkin, A. 2244
Shapley, T. 1846
2178
Shapovalov, Y. 1841
Sharifi, N. 1847
Sharkov, E.V. 1176
2051
2288
Sharma, M. 1548
Sharma, N.C. 1781
Sharma, Pooja 641
Sharma, Prabhakar 1847
Sharma, S. 1930
Sharp, J. 520
Sharp, Z. 1810
1836
1848
1848
2284
Sharpless, C. 1849
Shatskiy, A. 540
1335
1849
Shatsky, V. 1850
2244
Shavorskiy, A. 1510
Shaw, A. 2106
2132
Shaw, Samuel 500
559
1741
1748
2010
2109
Shaw, Stephanie 1850
Shaw, T. 1851
Shaybekov, R. 1851
Shcheka, S. 834
Shcherbinina, E. 756
Shchukarev, A. 1860
Shea, T. 958
1852
Shearer, C. 1848
Sheibi, M. 1774
1774
1852
Shekari, S. 900
1774
Sheldon, N.D. 1052
1853
Shelef, E. 935
Shellnutt, J.G. 1391
Shemesh, A. 2151
Shen, C-C. 1165
1352
Shen, G. 1853
1878
1883
Shen, J.J-S. 652
Shen, R. 2137
Sheng, R. 1307
Sheng, Y-M. 1854
Sheng, Z. 1854
Shepherd, M. 1683
Sherman, D.M. 1336
1447
1855
Sherrell, R. 1855
Sherriff, B. 1856
1907
Shervais, J. 1106
1856
Sherwood, N. 520
Sherwood Lollar, B. 1038
1314
1333
Sheth, H. 525
Shevalier, M. 1119
Shevchenko, V. 1683
Shevko, A. 1089
Shi, G. 950
1342
1857
2249
Shi, L. 604
680
1757
Shi, Xian 1322
Shi, Xiaoying 1778
Shi, Xiaoyu 1857
Shi, Xufei 1858
Shi, Y. 2115
Shi, Zeming 1858
Shi, Zongbo 1532
2176
Shibata, H. 1314
Shibata, T. 1159
Shibuya, T. 2227
Shiebi, M. 1773
Shiel, A.E. 1071
1080
1859
Shields, G. 657
1308
2179
Shikazono, N. 895
1154
1561
1564
1999
Shim, S-H. 1859
1860
Shimizu, H. 2202
Shimizu, Kenichi 1860
Shimizu, Kenji 1073
1861
Shimizu, Nobu 1511
Shimizu, Nobumichi 513
610
843
879
1211
1396
1752
1861
Shimoda, G. 1862
Shimojuku, A. 2227
Shin, D. 1109
1862
Shin, J.K. 1188
Shin, W-J. 550
1184
1282
1908
Shinmen, K. 1085
Shinozuka, Y. 1701
Shipway, B. 844
Shirai, K. 1793
Shirdashtzadeh, N. 1785
1863
Shirey, S. 462
1531
1804
1863
2133
Shirkhani, K. 402
Shirokova, L. 461
Shiryaev, A. 1745
Shishkina, T. 1864
Shiu, J-W. 1963
Shkurskii, B. 1885
Shock, E. 1746
Shojaei, B. 1526
Shore, J. 665
Shorttle, O. 1864
Shoval, S. 1865
Shu, D. 1168
Shu, Liangshu 1865
2268
2278
Shu, Liping 1866
Shu, Q. 1866
Shuai, Y. 1867
Shuang, Y. 661
1867
Shufelt, N. 782
Shukolyokov, Y. 2199
Shukuno, H. 1984
Shukurov, N. 1690
1868
Shuller, L. 505
Shumlyanskyy, L. 528
Shurkhuu, T. 1868
Shuster, D.L. 473
631
1722
Shuster, J. 1869
Shutcha, M. 832
Shuttleworth, S. 1094
1351
Sial, A. 616
664
842
1869
1875
Siame, L. 563
697
Sibert, R. 1870
Sicart, J.E. 1122
Sickman, J. 1870
Siddiqui, R.H. 1871
Siebe, C. 1121
Siebel, W. 651
816
1316
1871

https://doi.org/10.1180/S0026461X00006502 Published online by Cambridge University Press

Siebert, Christian 1488
Siebert, Christopher 884
..... 1325
..... 1571
..... 1872
Siebert, J. 561
..... 848
..... 1498
..... 1721
..... 1872
Siegert, M. 1244
Siemens, J. 878
Sierau, B. 1413
Sierra, C. 1873
Siewert, C. 1873
Sigfússon, B. 920
..... 920
..... 1945
Sigman, D.M. 965
Siitauri-Kauppi, M. 511
Sikes, E. 807
Sikl, J. 1520
Siklósy, Z. 743
Silantyev, S. 776
..... 1236
Silin, D. 1487
Siljanen, H. 775
Siljeström, S. 1874
..... 2004
Silva, A. 1567
..... 1874
Silva, C.A. 1492
Silva, E. 1083
Silva, F. 954
Silva, M.M.V.G. 445
..... 610
Silva, P. 1485
Silva, R.L. 696
..... 785
..... 1875
Silva, T.F. 1875
Silva Filho, A. 954
Silva Tamayo, J.C. 1875
Silveira, F. 691
Silveira, M. 508
Silvennoinen, H. 1876
..... 2277
Sim, M.S. 1876
Simakin, Sergei 1240
Simakin, Sergey 1890
Simakova, Y. 1877
Simandl, G.J. 1595
..... 1877
..... 1878
Simandl, L. 1878
Simeone, R.J. 1041
Siminchuk, S. 1420
Simionovici, A. 1282
Simmons, C. 2109
Simões, P. 1417
Simon, Adam 510
..... 1878
Simon, André 1879
Simon, D.F. 1635
Simon, E. 1101
Simon, J. 1124
..... 1879
Simon, R. 924
..... 925
Simon, S. 964
..... 1880
Simonelli, L. 1778
Simonetti, A. 1568
..... 2108
Simoni, J.A. 2047
Simonucci, C. 1760
Simonyan, A. 1880
Sims, K.W.W. 805
..... 1714
..... 1881
..... 1905
Sinclair Smith, F. 1713
Sindern, S. 1078
..... 1459
Singer, B.S. 1043
Singer, J. 568
Singh, A. 1401
..... 1881
Singh, C.K. 1253
..... 1882
..... 1883
Singh, P. 1394
..... 1882
Singh, Ram 446
Singh, Ravi Prakash 1883
Singh, S.K.S. 1688
..... 1689
..... 2031
Singha, K. 598
Singhvi, A. 2141
Sinha, B. 981
Sinha, R. 773
Sinninghe Damsté, J.S. 1540
..... 2063
Sinogeikin, S. 1883
Sinton, J. 1094
..... 1764
Sio, C.K. 1884
Sipilä, M. 718
Sipos, P. 1884
Siqueira, R. 1354
Sircombe, K. 755
Sirikitputtisak, T. 1140
..... 2274
Sirotkina, E. 1885
Sissmann, O. 1885
Sitnikova, M. 770
Sivan, O. 445
..... 490
..... 1769
Sizmur, T. 1886
Sizova, E. 1886
Sjöberg, S. 1530
Sjovall, P. 1874
..... 2004
Skála, R. 1887
Skarpeli-Liati, M. 1887
Skartsila, K. 1888
Skelton, A. 1199
..... 1888
Skinner, K. 569
Skinner, L. 1687
Skipper, N. 864
Sklar, L. 1722
Skopelitis, A. 1889
Skora, S. 1889
Skov, H. 1683
Skrabal, S. 1180
Skridlaite, G. 1890
Skrzypek, G. 1832
Skublov, S. 1890
Skuce, R. 1891
Skulan, J. 1501
Skyllberg, U. 1151
Slade, A. 1891
Slama, J. 1892
Slater, G. 1038
..... 1314
Slavich, P. 2173
Sleap, S. 1892
..... 2041
Sleep, B. 1208
Sleighter, R.L. 401
Slepkov, A. 602
Sloan, B. 1265
Sloan, S. 1892
..... 2041
Sloan, W.T. 701
..... 1691
Slomp, C.P. 738
..... 1116
Slowik, J. 1013
Sluijs, A. 914
Sluzhenikin, S. 1893
Small, James 1168
Small, Jennifer 1893
Small, Joe 2109
Smalla, K. 1671
Smalley, M. 864
Smart, K.A. 1610
..... 1894
Smart, P. 1718
Smeaton, C.M. 1894
..... 2143
Smellie, J. 2038
Smet, I. 1895
Smethie, W. 1371
Smidt, G. 1895
Smieja-Król, B. 1896
Smit, M. 1220
..... 1896
Smith, Adrian M L 2143
Smith, Alison G. 2026
Smith, Alyssa 1869
Smith, Andrew J. 2072
Smith, Andy 778
Smith, C. 1213
..... 1640
..... 1718
Smith, D. 1897
Smith, H. 1897
Smith, I.E.M. 578
..... 578
..... 1439
..... 1531
..... 1898
..... 1943
Smith, Joanne 886
Smith, Joseph P. 1752
Smith, L. 782
Smith, Marita 1898
Smith, Martin 1950
Smith, R. 1899
Smith, S. 1501
Smith, V. 594
..... 706
..... 1899
Smith, William 1601
Smith, William 1506
Smith-Duque, C. 2091
Smits, M.M. 475
..... 1900
Smittenberg, R. 790
..... 1828
Smolík, J. 1829
Smye, A. 1900
Smyth, J.R. 1901
Snehota, M. 717
Snell, K. 1901
Snelling, A. 1973
Snider, J. 679
Snowdon, L. 1272
Snyder, C. 1870
Snyder, G.T. 1704
..... 1902
Soares, M.A. 1431
Sobanska, S. 1902
Sobczak, K. 1903
Sobolev, A. 1240
..... 1258
..... 1292
..... 1393
..... 1661
..... 1903
..... 1904
..... 1904
Sobolev, N.V. 2283
Sobolev, S. 1632
..... 1904
Sochalski-Kolbus, L. 1905
Soderholm, L. 766
..... 837
Soejono, I. 1103
Soeller, C. 1041
Sofo, J. 1378
Sogacheva, L. 1968
Sohn, R. 1905
Sohn, Y.K. 578
..... 578
Sohnel, T. 1441
Solari, L. 1906
Solc, R. 2039
Soler, A. 1233
Solomatov, V. 1906
Solomon, D. 1293
Solylo, P. 1907
Som, S. 1907
Sommer, H. 1662
..... 1675
..... 1908
Sommer, M. 1935
Somoza, L. 933
Song, B-R. 1908

https://doi.org/10.1180/S0026461X00006502 Published online by Cambridge University Press

Song, C-K. 1187
..... 1599
Song, J. 2235
Song, L. 1909
Song, M. 1402
Song, P. 919
Song, Sheng-Rong 1337
..... 1361
Song, Sm 1909
Song, W. 677
Song, X. 1910
Song, Yong-Sun 1910
Song, Young-Chul 1911
Song, Yucai 2010
Song, Yujia 1911
Song, Z. 1912
Sonmez, M.S. 473
Sonnenthal, E. 708
..... 1680
Sonney, R. 1912
Sonntag, I. 1275
..... 1913
Soonsin, V. 1402
Sorbadere, F. 1913
Sorensen, J. 1914
..... 2146
Sorokin, A. 1914
Sorokina, O. 1915
Sossi, P. 855
..... 1915
Sosson, M. 1777
Souders, K. 1916
..... 1975
Souissi, F. 1916
Souissi, R. 1916
Soulet, G. 1917
Soultanov, D. 1657
Sousa Santos, G. 1917
Southam, G. 615
..... 1707
..... 1869
Southwell, M. 1180
Sowa, K. 1793
Soyol-Erdene, T-O. 1070
..... 1918
Sozeri, K. 792
..... 1570
..... 1918
Sørensen, K. 2200
Špaček, P. 406
Spahr, S. 1574
Spandler, C. 1668
..... 1919
Spangenberg, J.E. 1919
Sparkes, R. 886
..... 1050
..... 1920
Sparks, D.L. 1279
..... 1920
..... 2224
Sparks, S. 443
..... 1798
Spence, B. 1921
Spencer, E.C. 1756
Spengler, D. 1921
Spera, F. 590
Spetsius, Z. 1395
..... 1922
Speziale, S. 1406
..... 1407
Spicuzza, M. 1769
..... 2058
Spiegelman, M. 1035
Spielhagen, R.F. 656
Spielvogel, S. 1922
Spikings, R. 541
..... 1708
Špillar, V. 1923
Spiro, B. 773
Spivak, A. 1923
Spormann, A. 587
Sposito, G. 549
..... 563
..... 841
..... 1637
..... 2067
Spötl, C. 1823
Spracklen, D. 997
..... 1924
Spray, J. 1924
Spriggs, G. 939
Sproesser, W. 1801
Sprung, P. 1245
Spycher, N. 1925
Sracek, O. 1207
..... 1239
Sreedhar, B. 1593
..... 1925
Sreenivas, B. 1606
..... 1926
Srikarni, C. 1606
Srinivasa Gowd, S. 1926
Srinivasan, B. 525
..... 1394
Srinivasan, R. 1798
Srivastava, N. 1800
Srivastava, R.P. 2076
Srncik, M. 802
Sruoga, P. 835
Ssemmanda, I. 589
Stachel, T. 462
..... 1051
..... 1894
Stack, A. 1927
Stadler, S. 1000
..... 1730
..... 1927
Stadnitskaia, A. 1540
Staff, R. 1899
Stagno, V. 1928
Stalker, L. 1194
Stam, M. 1421
Stamati, F.E. 1496
..... 1928
Stamper, C. 1929
Stanetty, C. 1812
Stanienda, K. 1929
Stanjek, H. 523
Stankiewicz, A. 1930
Stannek, L. 780
Starchenko, S. 1676
Starinsky, A. 1193
Starr, D. 1510
Statelova, J. 1930
Staude, S. 1405
Staudigel, H. 1094
..... 1206
Stebbins, J. 678
..... 1590
Stechern, A. 1931
Stedry, R. 1468
Steefel, C.I. 782
..... 839
..... 884
..... 1077
..... 1487
..... 1822
..... 1931
..... 2073
..... 2210
Steele, A. 567
Steele, J 1574
Steele, Joshua 1406
Steele, R. 1932
Steele-MacInnis, M. 1819
..... 1932
Steen, I.H. 1732
..... 1933
Steenbergh, A.K. 1116
Steenrod, S. 526
Stefani, V.F. 1933
Stefano, C. 1511
Stefanovsky, S. 1241
Stefansson, A. 961
..... 1934
Steier, P. 802
..... 1092
..... 2167
Steiger, M. 946
Stein, H.J. 907
..... 976
..... 1470
..... 1934
..... 2196
..... 2287
Stein, Mordechai 512
..... 1278
..... 1589
..... 1935
..... 2024
Stein, Moti 870
..... 1935
..... 1935
..... 1935
Stein, R. 1521
Steinborn, J. 1648
Steinhoefel, G. 1935
..... 2101
Steininger, R. 925
..... 1201
Steinle-Neumann, G. 1936
Steinmann, M. 633
..... 647
..... 2096
Steinmann, P. 1936
Stelling, J. 1937
Stemig, A. 454
Stemprok, M. 1937
Stengel, C. 515
Stengel, D.B. 635
..... 766
Stenni, B. 781
..... 1129
..... 1465
Stepanov, A. 1938
Stepanova, M. 1550
Stephan, T. 728
Stephens, G. 1938
Stern, D. 1426
Stern, Richard 1051
..... 1894
Stern, Robert 1189
..... 1984
Sternemann, C. 1778
Sternitzke, V. 1939
Stetzer, O. 1939
Steudtner, R. 1940
Stevens, R. 1667
Stevenson, D. 712
..... 1940
Stevenson, E. 1941
Stevenson, R. 753
..... 1941
Stewart, Bob 2187
Stewart, Brian 1942
Stewart, D. 2155
Stewart, R. Craig 1942
Stewart, Robert B. 1943
Stibilj, V. 1577
Stichel, T. 863
..... 1943
..... 2286
Stieglitz, T. 1944
Stier, P. 1627
..... 1944
Stille, P. 637
..... 683
..... 886
..... 952
..... 1030
..... 1617
..... 1641
..... 2096
Stilson, T. 1555
Stimac, I. 673
Stipp, S.L.S. 423
..... 437
..... 475
..... 512
..... 565
..... 715
..... 920
..... 989
..... 1266
..... 1426
..... 1530
..... 1565
..... 1569
..... 1612
..... 1790
..... 1827
..... 1945

https://doi.org/10.1180/S0026461X00006502 Published online by Cambridge University Press

Stirling, C. 898
..... 1137
..... 1945
Stixrude, L. 736
Stober, I. 1946
Stocchero, M. 1587
Stockmann, G.J. 1946
Stockmann, M. 582
..... 1947
Stohl, A. 1683
Stojic, A.N. 1947
Stokes, D. 1770
Stokke, R. 1732
..... 1933
Stoll, B. 475
..... 1117
..... 1904
..... 2212
Stolow, A. 602
Stolpe, B. 975
..... 1948
Stolper, E. 569
..... 1535
Stolpovsky, K. 1948
Stolze, K. 1513
Stone, A. 1949
Stone, J. 473
..... 1949
Stone, W. 847
Storelli, N. 702
Storelvmo, T. 1950
Storey, C. 528
Storey, Craig 755
..... 811
..... 1108
..... 1268
..... 1798
..... 1950
Stosch, H.-.G. 538
Stosnach, H. 1405
Stott, L. 1951
Stracke, A. 1220
..... 1432
..... 1765
..... 1951
Strady, E. 1952
Stramma, L. 863
..... 942
Strąpoć, D. 1952
Strathmann, T. 1953
Stratmann, A. 1419
Straub, K.L. 1789
Strauss, H. 757
..... 801
..... 1082
..... 1257
..... 1449
..... 1560
..... 1714
..... 1953
..... 2179
Streck, M.J. 1596
..... 1954
Streets, D. 666
Strekopytov, S. 1271
Stremtan, C.C. 1954
Streuff, K. 2171
Stricker, C. 928
Strickland, A. 1231
..... 1656
..... 1769
Stringfellow, W. 693
Strnad, L. 1468
..... 1887
..... 2045
Stroncik, N.A. 1333
Stroth, C. 1728
Strunga, V. 1955
Struzhkin, V. 2203
Strzepek, R. 898
Stuart, F. 1955
Stubbins, A. 1956
Stubbs, J. 422
..... 484
..... 520
Stuber, N. 1021
Stuewe, K. 588
Stumpf, R. 1956
Stumpf, T. 638
..... 1039
Stunitz, H. 1525
Sturchio, N. 837
..... 1361
Sturm, A. 1957
Sturm, M. 1825
Stute, M. 1425
..... 1957
Styles, M. 935
Stylo, M. 484
..... 1846
..... 1958
Su, G. 890
Su, Hao 1958
Su, Hui 1679
Su, Jie 2272
Su, Jin 1959
..... 2276
Su, W. 2060
Su, X-S. 784
..... 1959
..... 2261
Suárez, S. 1960
Subba Rao, D.V. 1960
Subramanian, S. 1728
Suda, S. 1633
Suess, E. 1648
Sugimoto, N. 1187
Sugimura, E. 1961
Sugiura, N. 1578
Sui, J. 827
Suksi, J. 2038
Šulák, M. 1961
Sullivan, L.A. 678
..... 1962
..... 2095
..... 2173
Sullivan, N. 1962
Sullivan, R. 1633
Sültenfuss, J. 1927
Sümegi, P. 743
Sumino, H. 474
..... 769
..... 1963
..... 2028
Summering, J. 1164
Summons, R.E. 1082
..... 1377
..... 1775
..... 2006
Sun, Chao 1322
Sun, Chih-Hsien 2123
Sun, H. 2192
Sun, Jia-Lin 1963
Sun, Jiang 1964
Sun, Jianling 1367
Sun, Jimin 2166
Sun, Ji-Min 1318
Sun, Jingbo 657
..... 1111
..... 1311
..... 1964
Sun, P. 2267
Sun, Q. 1058
Sun, R. 785
Sun, S.C. 888
..... 1965
Sun, W. 1324
..... 1965
..... 2254
Sun, Xia 1348
Sun, Xue 1966
Sun, Y 773
Sun, Yong 765
..... 1966
Sun, Yongge 1967
Sun, Yu 1361
Sun, Zhangxu 651
Sun, Zhanxue 888
..... 1967
..... 2125
Sundal, A. 398
Sundby, B. 1382
..... 1509
Sunder Raju, P.V. 1968
Sundström, A-M. 1968
Sung, J. 2137
Sung, Y.H. 1285
Suparka, E. 401
Surya Prakash, L. 1926
Sus, F. 992
Sushchevskaya, N. 1466
Sushchevskaya, T. 1660
..... 1969
Sutcliffe, N. 1969
Suter, M. 1975
Suto, K. 1423
..... 1561
Sutterasak, T. 1083
Sutton, G. 1705
Suvorova, E. 484
..... 520
..... 768
Suzuki, A. 1085
..... 2226
Suzuki, K. 978
..... 1212
..... 1553
..... 1661
..... 1838
..... 1993
Suzuki, Takashi 1970
Suzuki, Toshihiro 1027
..... 1212
..... 2223
Suzuki, Y. 468
..... 872
..... 1143
..... 1160
Suzuki, Yoshinori 1970
Sval'nov, V. 786
Švecová, K. 1971
Sverjensky, D. 994
..... 1202
..... 1287
..... 1350
..... 1971
..... 2091
Svirskaya, N. 1240
Svisero, D. 496
Svojtka, M. 406
..... 1223
..... 1972
Swadling, J. 1972
Swander, Z. 1973
Swann, G. 1973
Swanner, E. 1974
Swanson, R.L. 1752
Swanson-Hysell, N. 1072
Swart, H. 1169
Swart, P. 451
..... 1974
Swayze, G. 1305
Swedlund, P. 725
..... 1441
..... 2138
Sweeney, R. 1640
Swennen, R. 1029
Sýkorová, I. 861
..... 992
Sylvan, J. 2146
Sylvester, P.J. 663
..... 1275
..... 1916
..... 1975
Symons, D. 554
Synal, H-A. 1975
Syracuse, E. 2069
Syritso, L. 466
..... 1976
Sysalová, J. 2287
Syverson, D. 1976
Szabó, C. 518
..... 711
..... 961
Száková, J. 1584
..... 2287
Szalai, Z. 1884
Szatmari, P. 1977
Szidat, S. 2260

https://doi.org/10.1180/S0026461X00006502 Published online by Cambridge University Press

Szilas, K. 1814
..... 1977
..... 2068
Szocs, T. 1731
..... 1978

T

Ta, C. 1707
Tabasi, S. 1179
Tabatabaei, S.H. 1843
Tabelin, C. 1979
Tabersky, D. 1979
Taboada Castro, T. 1329
Tachibana, S. 1782
Taczkowska, M. 1980
Tada, R. 1080
Taffs, R. 625
Tagami, T. 2204
Taghipour, B. 1380
..... 1386
..... 1494
Taghipour, S. 1141
..... 1980
Tahata, M. 1168
Tailby, N. 1981
..... 2029
Tajcmanova, L. 1981
..... 1982
Tajika, E. 1581
Takahashi, E. 967
..... 2223
Takahashi, H. 1258
Takahashi, K. 1782
Takahashi, M. 1258
Takahashi, N. 1208
Takahashi, T. 978
Takahashi, Yoshio 1153
..... 1183
..... 1392
..... 1524
..... 2018
..... 2202
..... 2223
Takahashi, Yui 1561
Takahasi, S. 1080
Takahata, N. 988
..... 1578
..... 1793
Takai, K. 1079
..... 1183
..... 1392
..... 1524
..... 1544
Takamasa, A. 2029
Takano, Y. 664
Takao, K. 1010
Takao, S. 1010
Takashima, T. 1524
Takaya, Y. 1154
..... 1553
Takazawa, E. 805
Takeda, S. 1987
Takemura, K. 1899
Takemura, T. 1982
Takeuchi, M. 1477
Takeyama, M. 2223
Tamaki, K. 1379
Tamburini, F. 1983
Tamše, S. 1983
Tamura, A. 417
..... 1087
..... 1089
Tamura, N. 699
..... 948
Tamura, Y. 1984
Tan, H. 2258
Tan, Q. 666
Tan, Xin 432
Tan, Xiucehng 1984
Tanaka, K. 1970
..... 1985
..... 2233
Tanaka, R. 1693
Tanaka, S. 2204
Tanaka, Taichu Y. 1144
Tanaka, Tsuyoshi 1477
..... 1910
Tang, Guo 2121
Tang, Guo-Qiang 1316
Tang, M. 1985
Tang, R. 1447
Tang, Xiaodong 1191
Tang, Xiaohui 1986
Tang, Y. 2273
Tang, Z. 2278
Tangwa, E. 1986
Tani, K. 1087
Tani, Y. 1985
Tanimizu, M. 1153
..... 1258
..... 1379
..... 2226
Tanimoto, H. 1987
Tanis, E. 1878
Tannennberger, M. 1362
Tanner, D. 1987
Tao, R. 835
Tao, Xiancong 2127
Tao, Xiaofeng 2117
Tao, Xiaowan 1066
Tappa, M. 687
Tappe, S. 1610
..... 1988
Tappero, R. 1528
Tapponnier, P. 2064
Taran, L. 1890
Taran, O. 1278
Tarasenko, I. 1178
Tarits, P. 971
Tartarotti, P. 1794
Tasáryová, Z. 1988
Tasnadi, F. 1664
Tateno, S. 1547
Tatsumi, Y. 978
..... 1984
Tatyanin, G. 411
Taubner, I. 844
..... 1195
..... 1989
Tauhid-Ur-Rahman, M.D. 1989
Taviani, M. 780
..... 1491
..... 2033
Taylor, J. 811
Taylor, K. 1593
..... 1990
Taylor, Lawrence 569
Taylor, Lyla 581
..... 1990
Taylor, Rex 631
Taylor, Richard 1505
..... 1991
Taylor, S.R. 2078
Taylor-Jones, K. 1991
Tazoe, H. 1992
Teagle, D. 474
..... 648
..... 2091
Tebo, B. 1382
..... 1649
Tegner, C. 434
Teichert, B. 2140
Teitler, Y. 1291
..... 1992
Teixeira, R. 685
..... 1993
Teixeira, W. 2074
Tejada, M.L. 613
..... 1993
Tejero, R. 1766
Tejnecký, V. 573
..... 1994
Teker, Y. 1994
Telfeyan, K. 991
..... 1528
Tella, M. 1995
Telling, N. 608
..... 686
Telsiz, S. 1995
Temel, A. 990
..... 1995
Temel, M. 955
Temizel, İ. 2237
Tempest, K. 809
Templer, S. 479
Templeton, A. 1206
..... 1433
..... 1437
..... 1974
..... 1996
Templeton, J. 1006
Tender, L. 1996
Teng, F-Z. 1884
..... 1997
Teng, H.H. 1997
..... 2276
Teng, Y. 1998
..... 2198
..... 2291
Tepley Iii, F. 1998
Terada, M. 1999
Terashima, M. 1999
Terehova, A. 1571
..... 2000
Terrinha, P. 1423
Terzano, R. 2000
..... 2001
Teschner, C. 2001
Testemale, D. 721
..... 1639
..... 1668
..... 2011
Teutsch, N. 464
..... 2002
Thaler, C. 1473
Thalhammer, O. 1214
..... 2238
Thaw, S.H. 643
Theis, K.J. 1824
Them, T. 2002
Theodorakopoulos, N. 1839
Thern, E. 2003
Therrien, F. 699
Thiagarajan, N. 2003
Thiam, H.N. 643
Thiel, V. 2004
Thiele-Bruhn, S. 1294
Thieme, J. 1344
..... 2004
Thien, B. 1724
..... 2005
Thill, A. 1304
Thirlwall, M. 585
..... 776
..... 1398
..... 2005
Thomas, A.L. 1007
..... 1020
..... 2006
..... 2241
Thomas, Björn 775
Thomas, Bob 935
Thomas, Brian 2165
Thomas, Burt 1120
..... 1753
Thomas, D. 2176
Thomas, E. 860
Thomas, I. 944
Thomas, J.B. 1040
Thomas, K. 2006
Thomas, R. 466
Thomas, W. 1238
Thomassot, E. 462
..... 1362
..... 2007
Thomazo, C. 2007
Thompson, Aaron 1621
Thompson, Alan 501
Thompson, I. 500
Thompson, Jeffrey 1901
Thompson, Jennifer 2008
Thompson, Lauren 1180
Thompson, Lucy 1924
Thompson, W.G. 2008
Thomson, J. 738
Thorenz, U. 1254
..... 2009
Thornalley, D. 2009
Thorne, P. 1850
Thornton, S. 472

https://doi.org/10.1180/S0026461X00006502 Published online by Cambridge University Press

Thorpe, C.L. 1351
..... 2010
Thorseth, I.H. 712
..... 801
..... 1065
..... 1483
..... 1565
..... 1933
Thrash, C. 2180
Thrilwall, M. 1624
Thullner, M. 1948
Thyberg, B. 1003
Tian, F. 2170
Tian, Shi Hong 1347
..... 2010
Tian, Shihong 761
Tian, Y. 2011
Tiberg, C. 959
Tiberindwa, J. 2011
Tice, M. 2012
Tichomirowa, M. 2012
Tickell, O. 1826
Tiedemann, R. 948
..... 1029
..... 1175
..... 1575
Tietz, O. 592
Tilgner, A. 575
..... 2144
Tillmann, R. 718
..... 1181
Tilton, G. 590
Timm, C. 2013
Timmermann, A. 1951
Timms, N. 942
Tindle, A. 1610
Tipper, E. 1562
..... 2013
Tirone, M. 2014
Tirosh, O. 2002
Tishin, P. 411
Tissandier, L. 2014
Titov, A. 1659
Tiwari Rabindra, R.N. 2015
Tjallingii, R. 533
Tkachev, S. 1792
Tkalcec, B. 2015
Tlustoš, P. 1584
Tobin, J.G. 2016
Tobler, D. 1891
..... 2016
Tobón, E. 2090
Todd, A. 2204
Todd, E. 2017
Todd, J. 821
Todou, G. 1829
Togashi, S. 2017
Togawa, O. 1970
Togo, Y. 2018
Tohver, E. 2282
Tokarev, I. 1787
..... 2018
Toki, T. 1079
..... 1392
Tokoro, C. 978
..... 2019
Tokunaga, T. 2019
Tolan, M. 1778
Toli, K. 924
Tollerud, H. 828
Tollstrup, D. 665
..... 1692
..... 2166
Tolochko, K. 2292
Tolosana-Delgado, R. 790
Tolstikhin, I. 2020
Tom, L. 693
Tomaru, H. 1515
..... 1833
Tomasi, N. 2001
Tomasini, J. 1723
Tomé, C.M. 2020
Tomiya, A. 2017
Tomkins, A.G. 684
..... 822
..... 1440
..... 1475
..... 2021
Tomlinson, E. 706
Tommasi, A. 746
Tomonaga, Y. 532
..... 2018
..... 2021
..... 2032
Toms, L. 2043
Tonarini, S. 1804
..... 1806
Toner, B.M. 688
..... 1537
..... 1914
..... 2022
..... 2146
Tong, H. 527
..... 2022
Tonolla, M. 702
Toon, O.B. 2170
Tootell, D. 1588
Toporski, J. 2023
Topping, D. 1439
..... 2023
Torabi, G. 1863
Tordesillas, A. 1768
Tordiff, J. 1673
Torfstein, A. 2024
Tornos, F. 1467
..... 2020
..... 2024
Torrent, J. 1789
Torres, E. 2025
Torres, O. 1708
Torres, T. 885
..... 933
Torshizian, H.A. 399
..... 2025
Toselli, A. 842
Tossell, J. 1349
Tostevin, R. 2026
Totsche, K.U. 417
..... 820
..... 869
..... 973
..... 1335
..... 1344
..... 1712
..... 2157
Touboul, M. 1759
..... 2026
Toucanne, S. 501
Toufaily, J. 1440
Toulhoat, H. 2027
Toulkeridis, T. 966
Tournassat, C. 2027
Toyama, C. 2028
Toyama, Y. 2028
Toyoda, S. 1162
..... 2029
Trail, D. 1485
..... 1981
..... 2029
Trainor, T. 1996
Trang, J. 882
Trang, P.T.K. 515
Traoré, D. 681
Trappitsch, R. 728
Travis, B. 793
Trebosc, J. 1744
Trebotich, D. 1487
Tredoux, M. 1005
..... 1169
..... 2030
..... 2159
Trejtnarová, H. 992
Tremaine, P. 449
Tremblay, L. 904
Tremblay, M. 1006
Trent, A. 986
Treu, F. 1465
Triantafyllidis, T. 538
Tribble, G.D. 2078
Tricot, G. 1744
Trindade, M. 2030
Trindade, R.I.F. 1794
..... 2085
..... 2221
Tripathi, P. 1593
Tripathi, S. 2037
Tripathy, G.R. 2031
Tripati, A. 1358
..... 1786
Trittschack, R. 2031
Trivitayanurak, W. 407
Troch, P. 1696
Trofimovs, J. 631
Troll, V.R. 485
..... 516
..... 594
..... 734
..... 1121
..... 1614
..... 1627
..... 2032
Trösch, M. 2032
Trots, D.M. 1256
..... 1591
Trotta, M. 768
Trotter, J. 1438
..... 1491
..... 2033
Troyer, L. 1271
Trønnes, R. 2033
Truche, L. 1047
..... 2034
Truex, M. 2144
Trumbull, R.B. 1164
..... 1736
..... 2034
..... 2177
Tsai, W-Y. 1330
..... 2123
Tsandev, I. 2035
Tsanev, V. 1572
Tsay, S-C. 2035
Tschauner, O. 1878
Tschegg, C. 1553
..... 1554
Tse, J. 1778
Tseng, J-Y. 2123
Tsuchida, S. 1392
Tsuchiya, J. 737
Tsuchiya, M. 664
Tsuchiya, S. 2225
Tsuchiya, T. 737
..... 1158
..... 2036
Tsuchiya, Y. 1425
Tsuda, A. 1987
Tsukamoto, K. 1190
..... 2065
Tsukui, K. 1006
Tsuno, K. 724
..... 2036
Tsunogai, U. 1079
..... 1987
Tsuruyama, S. 1799
Tsushima, S. 856
Tsyrenov, B. 720
Tu, C-L. 1339
..... 1343
..... 2037
Tubia, J.M. 2078
Tubrett, M. 663
Tucker, G. 1270
Tufenkji, N. 2037
Tuff, J. 2163
Tuffen, H. 519
..... 2038
Tullborg, E-L. 780
..... 2038
Tulloch, A. 2040
Tunega, D. 2039
Tuoriniemi, J. 2039
Tupinambá, M. 609
Turchyn, A.V. 445
..... 1031
..... 1713
..... 2026
Türk, T. 494

https://doi.org/10.1180/S0026461X00006502 Published online by Cambridge University Press

Turkina, O. 2040
..... 2052
Turnbull, R. 986
..... 2040
Turner, A. 2041
Turner, B. 1892
..... 2041
Turner, M. 1943
..... 2042
Turner, S.P. 906
..... 974
..... 1516
..... 2042
Turo, L. 1771
Turpault, M-P. 1301
..... 2042
..... 2099
Tütken, T. 585
..... 1017
Tuttas, D. 561
..... 593
..... 969
Tutunaru, B. 1786
Tüysüz, N. 1248
Tuysuz, O. 905
Twining, B. 1855
Tyagi, M. 675
Tyler, P. 1011
Tympel, J.F. 2043
Tyrrell, S. 2043
Tyszka, R. 2044
Tzipori, A. 2002

U

Uchiyama, Y. 2223
Udatny, M. 2045
Udisti, R. 781
Udo, K. 1989
Udry, A. 2045
Udubasa, G. 2046
Udubasa, S.S. 2046
Udvardi, B. 1229
Uematsu, M. 1987
Uemura, R. 1160
Ueno, Y. 2046
Uesugi, J. 417
Uesugi, K. 1212
Ugalde, C. 1191
Uhlig, D. 2156
Újvári, G. 1230
Ukelis, O. 1518
Ukstins Peate, I. 1611
..... 2047
Ulbrich, I. 2162
Ulfbeck, D. 531
..... 1607
Ulianov, A. 541
..... 1072
..... 1708
..... 1809
..... 1889
Ullah, H. 2047
Ullmann, C.V. 1225
..... 1551
..... 2048
..... 2156
Ulmer, P. 676
..... 1072
..... 1220
..... 2062
Ulrich, A. 1037
Ulrich, K-U. 2048
Ulrich, M. 2049
Ulyashev, V. 2049
Ulzetueva, I. 2050
..... 2248
Um, W. 2050
Umeda, G. 531
Umeda, K. 2204
Umino, S. 1087
Unal, E. 1176
..... 2051
Underschultz, J. 1194
Unger, N. 2051
Ünlü, T. 1583
Unsworth, C. 1271
Unsworth, S. 1379
Urbano, L. 1049
Urmantseva, L. 2052
Urosevic, M. 1767
..... 2052
Uroz, S. 2042
Urusov, V. 1241
Urynowicz, M. 2053
Ushie, H. 2053
Ushikubo, T. 2058
..... 2164
Ushioda, M. 967
Uspenskaya, T. 786
Ussler, W. 926
Uster, B. 1958
Usui, T. 1124
..... 2054
Usuki, T. 1268
Utembe, S. 1439
Uteyev, R. 2054
Utsunomiya, S. 733
..... 1142
Utton, C. 695
Uysal, I. 745
..... 1837
..... 2055
Uysal, T. 1465

V

Vaca Escobar, K. 2056
Vaculovič, T. 894
..... 1242
..... 1955
Vafeidis, A. 1695
Vagner, T. 1477
Vähätalo, A. 2056
Vakh, A. 2057
Vakh, E. 2057
Vaks, A. 2057
Valea, S. 2158
Valencia, V. 623
Valente, S. 2058
Valentim, B. 952
..... 1716
..... 1740
Valley, J. 568
..... 1155
..... 1231
..... 1656
..... 1769
..... 2058
..... 2164
Vallina, B. 2059
Valsami-Jones, E. 757
..... 1196
..... 1888
Valt, M. 781
Valter, A. 2059
van Acken, D. 2060
Vanaei, M. 2060
van Aken, H. 1725
van Beek, P. 1053
Van Bergen, M.J. 642
..... 904
..... 1296
..... 1541
Van Bergen, P. 448
van Berk, W. 570
van Beusekom, J.E.E. 2166
Van Cappellen, Philippe 1296
..... 1421
..... 1480
..... 1532
..... 1590
Van Cappellen, Philippe 702
Vance, D. 434
..... 464
..... 615
..... 657
..... 960
..... 1163
..... 1336
..... 1415
..... 1720
..... 2061
..... 2149
..... 2266
Van De Flierdt, T. 693
..... 704
..... 1267
..... 2061
van de Moortèle, B. 670
..... 1715
Van den Berg, R. 719
van den Berg, S. 913
Van den Bleeken, G. 2062
van den Bogaard, P. 1032
..... 1096
Van den Boorn, S. 448
..... 1675
van der Grift, B. 947
..... 2072
van der Hilst, R. 1859
..... 1860
van der Hoek, B. 2062
Vanderkluysen, L. 508
..... 985
van der Laan, G. 608
..... 686
van der Laan, S. 522
..... 1725
..... 2063
..... 2068
van der Meer, M. 2063
van der Meer, Q. 2064
van der Veer, G. 2066
Van der Weijden, C.H. 1584
Van Der Weijden, R. 964
van der Woerd, J. 2064
van de Schootbrugge, B. 2151
Van de Valk, J. 1673
van Dishoeck, E.F. 2094
van Dongen, B. 798
van Dongen, J. 1228
van Donkelaar, A. 2065
Van Driessche, A.E.S. 1576
..... 2065
Vanek, A. 672
..... 2066
van Gaans, P. 985
..... 1455
..... 2066
van Geen, A. 1402
..... 2141
van Geldern, R. 494
..... 1518
van Genuchten, C. 2067
van Gool, J. 1814
Vanhaecke, F. 1895
..... 2067
van Heerden, E. 1333
Van Heghe, L. 2067
van Heuven, S. 1725
van Hinsberg, V. 1977
..... 2068
van Hoek, C. 1725
..... 2068
van Hoose, A. 1954
Van Hullebusch, E. 1300
van Keken, P. 1189
..... 2042
..... 2069
Vankeuren, M. 1006
Van Kranendonk, M.J. 1301
..... 1863
..... 2069
..... 2070
..... 2164
vanLier, J.B. 1330
Van Loon, L. 2070
van Loosdrecht, M. 1784
Van Meir, N. 1760
Vanne, J. 1357
Van Orman, J. 925
..... 991
..... 2071
van Os, B. 2066
Van Pinxteren, D. 981
Van Rampelbergh, M. 753
van Riemdijk, W. 1455
van Schijndel, V. 2071
van Soest, M. 2047
Vantelon, D. 1730
van Tol, D. 2072
van Veelen, A. 2072

https://doi.org/10.1180/S0026461X00006502 Published online by Cambridge University Press

Van Vlierberghe, H. 2067
van Westrenen, W. 1461
..... 1688
..... 1793
van Zuilen, M. 1639
..... 1682
..... 2073
Varadharajan, C. 2073
Varga, A. 1230
Varga, G. 1230
Vargas, G. 1704
Vargas-Matos, G. 2074
Varley, N. 1714
Vasconcelos, C. 551
..... 1585
Vasiliev, P. 1566
Vasiliev, Y. 1904
Vasiliu, M. 766
Vasyukova, E. 2074
Vauchez, A. 1490
Vaughan, D. 584
..... 608
..... 686
Vaughan, M. 1701
Vavouraki, A. 2075
Vazquez, J. 530
Vazquez-Rodriguez, A.I. .. 2075
Vecht, A. 2076
Vedanti, N. 2076
Veeramani, H. 520
..... 2077
Vega, A. 2077
Vega-Arroyo, M. 2078
Vegas, N. 2078
Veizer, J. 2100
Vejdani, Y. 833
Vejelyte, I. 2079
Veksler, I.V. 1164
..... 2177
Velasco, E. 2079
Velasco, F. 1467
..... 1960
..... 2024
Velikoslavinsky, S. 592
Velivetskaya, T. 1969
Velu, V. 1695
Venera, Z. 1103
Vengosh, A. 1891
Vennemann, T. 499
VerBerkmoes, N. 2165
Verbruggen, N. 832
Verchovsky, A.B. 497
..... 596
..... 1469
Vercouter, T. 1579
Verdecchia, S.O. 2080
Verdeny, E. 903
Vereschagina, E. 2018
..... 2080
Verheul, M. 2081
Verheyden, S. 753
Vermeesch, P. 2081
Vermeulen, K-J. 985
Vermooten, S. 947
Verney-Carron, A. 2082
Veron, A. 1952
Veronesi, M. 535
..... 2147
Verplanck, E. 830
Verstraete, A. 2067
Vervoort, J. 623
..... 993
..... 1523
..... 2082
Veryovkin, I. 728
Veselovsky, F. 1239
..... 2095
..... 2100
Veselská, V. 2083
Vestreng, V. 1683
Vesvres, M-H. 1839
Vetter, A. 2085
Vidal, Olivier 2083
Vidal, Olivier 869
Videira, J.C. 1467
..... 2024
Videnska, K. 2084
Vidovic, M. 937
Vidyasagar, G. 1960
Viehmann, S. 2084
Vieira, L.C. 1653
..... 2085
Viereck-Goette, L. 405
..... 975
..... 2043
Viers, J. 700
..... 1573
Viet, P.H. 515
Vieth-Hillebrand, A. 1813
..... 2085
Vigh, T. 1655
Vigier, N. 2082
..... 2086
Vigouroux, E. 2086
Vijaya Gopal, B. 1606
..... 1926
..... 2087
Vikent'eva, O. 2087
Vikentyev, I. 2088
Vikesland, P. 2088
Viladkar, S. 1393
Vilas, F. 438
Viljoen, F. 2169
Villa, I. 1501
Villacís - García, M. 2089
Villalobos, M. 2056
..... 2089
..... 2089
Villanueva, M. 491
Villanueva-Estrada, R.E. 1671
..... 2090
Villaseca, C. 2090
Villegas-Jimenez, A. 2091
Villieras, F. 1730
Vils, F. 2091
Vinha, M. 630
Vinne, L-E. 2092
Vinningland, J.L. 1613
Vinograd, V.L. 2092
..... 2093
Vinoj, V. 1800
Violette, A. 1728
Viollier, E. 597
..... 603
..... 1276
Virtanen, A. 1802
..... 2093
Visser, R. 2094
Vítek, P. 1107
..... 2094
Vithana, C. 2095
Vitkova, M. 2095
Vittecoq, B. 1686
Viville, D. 1641
..... 2096
Vivit, D. 604
Vlach, S. 1801
Vladimir, S. 1289
Vlassopoulos, D. 1555
..... 1840
Vlcek, L. 444
..... 663
..... 1378
Vlcek, V. 1936
Vockenhuber, C. 673
..... 1975
Voegelin, Andrea R. 1292
..... 2096
Voegelin, Andreas 830
..... 874
..... 1032
..... 1534
..... 2097
Vogel, Andreas 1449
..... 2138
Vogel, Antje Kathrin 2097
Vogel, N. 1811
Vogel, S. 2197
Voges, K. 1880
Vogl, J. 1755
..... 2098
Vogt, C. 2001
Vogt, K. 2098
Voinot, A. 2099
Volcan, O. 2099
Voldrichova, P. 1550
..... 2100
Volk, H. 1874
Völker, C. 404
Volkova, E. 1976
Vollat, B. 1751
Vollstaedt, H. 803
..... 2100
von Blanckenburg, F. 767
..... 953
..... 1560
..... 1826
..... 1935
..... 2101
..... 2101
von der Handt, A. 2102
von der Heyden, B. 1762
..... 2102
von der Kammer, F. 1450
..... 1533
Vondrasek, R.C. 1191
von Eynatten, H. 790
von Gunten, U. 1790
Vonhof, H. 1364
Von Netzer, F. 505
von Quadt, A. 1930
Voronin, V. 543
Vortisch, W. 943
..... 2103
Voss, B. 799
..... 2103
Voßmeyer, A. 1723
Voutsadaki, S. 1496
Vriend, S. 2066
Vroon, P.Z. 904
..... 1168
..... 2079
Vrublevskii, V. 1227
Všianský, D. 1955
Vuataz, F-D. 2104
Vuille, M. 1122
Vuilleumier, R. 2104
Vuilleumier, S. 807
Vulic, P.J. 2145
Vuoriainen, S. 1357
Vural, A. 2105
Vvedenskaya, I. 1726
Vymazalová, A. 2105

W

Wacey, D. 1585
Wacker, L. 1975
..... 2260
Wada, I. 2106
Wade, J. 2106
..... 2163
Wadhwa, M. 565
..... 579
Waelbroeck, C. 1129
Waerenborgh, J.C. 1408
Wagener, A. 2222
Wagener, K. 2222
Wagner, G. 1195
Wagner, M. 1626
Wagner, Thomas 877
..... 1026
..... 1353
..... 2107
Wagner, Thomas 927
..... 1091
..... 1170
Wagnon, P. 1122
Wagreich, M. 2107
Waight, T. 1643
Waite, D. 546
..... 689
..... 894
..... 995
Wakabayashi, T. 1562
Wake, B. 1007
Wakeham, S. 1775
Walder, I. 1986
Walker, D. 1768
Walker, Richard 560
Walker, Richard J. 731
..... 1340
..... 1674
..... 2026
..... 2108

https://doi.org/10.1180/S0026461X00006502 Published online by Cambridge University Press

Walker, S. 766
Wall, C. 1831
Wall, F. 770
1566
Wallace, C. 2108
Wallace, P. 1648
Wallace, S. 2109
Wallander, H. 475
1900
Wälle, M. 877
2020
2242
Waller, C. 411
Waller, L. 1345
Wallis, I. 2109
Wallis, S. 1963
Wallmann, K. 1010
Wallner, G. 802
1092
Wallschläger, D. 702
Walraven, N. 2066
Walsh, J. 1701
Walsh, K. 1699
Walsh, S. 2173
Walshe, G.E. 2110
2143
Walter, Martin 1812
Walter, Michael 453
1213
1444
Walters, C. 2110
Walther, S. 554
Walzer, U. 2111
Wan, J. 673
2111
Wan, M. 2112
Wan, Q. 2112
Wanek, W. 1495
Wang, Baoli 2113
Wang, Baozhong 2273
Wang, Bin 2195
Wang, Chao 649
Wang, Chao 997
1342
2113
Wang, Chunjiang 2114
Wang, Chunlei 2114
Wang, Chun-Lin 2119
Wang, Deborah L. 1545
Wang, Dong 1310
2115
Wang, Dongyan 1322
2115
Wang, Feng 619
971
1454
1614
2116
Wang, Feng-Ping 2116
Wang, Furong 2117
Wang, Fushun 2113
Wang, Gangsheng 1433
Wang, Guangcai 972
Wang, Guo-Qiang 2232
Wang, Hailong 1695
Wang, Hejing 2117
Wang, Henian 2127
2127
Wang, Hongjun 2130
Wang, Hong-Liang 654
765
2118
2198
Wang, Hua 2189
Wang, Hualin 2118
Wang, Hui 1710
2264
Wang, Huichu 2192
Wang, J. 1124
Wang, Jiang Hai 1057
Wang, Jianwei 1136
Wang, Jin 1341
2119
Wang, Jin 1997
Wang, Jing Hong 1369
2119
Wang, Jingshu 1374
2120
Wang, Jinguing 1883
2120
Wang, Jin-Jin 1059
Wang, Jinsheng 2291
Wang, Jiqiang 2118
Wang, Kun 2142
Wang, Kuo-Lung 1268
2121
Wang, Lachun 2115
Wang, Lei 1062
2121
Wang, Lijuan 2232
Wang, Lijun 1677
Wang, Lingling 2122
Wang, Linjun 957
Wang, Luhong 1340
Wang, Lulu 2122
Wang, Meng 2114
2115
Wang, Minfang 2122
Wang, Mingnian 709
Wang, N. 2198
Wang, O. 1673
Wang, Pei-Ling 1330
1963
2123
Wang, Ping 1309
Wang, Qingfei 2263
Wang, Quan 2212
Wang, R.l. 2123
Wang, Ru Cheng 648
2194
Wang, Sheng-Hsiang 2035
Wang, Shilu 2124
Wang, Tai-Tien 1337
Wang, Tao 2125
Wang, Wei 2197
Wang, Weiguo 666
Wang, Weijia 709
Wang, Wenxiang 2124
Wang, WuYi 1321
Wang, Xianbin 2282
Wang, Xiangqin 996
Wang, Xiaofang 1367
Wang, Xiao-Lan 1059
Wang, Xiaolin 1058
Wang, Xiaoming 1375
Wang, Xiao Xia 2125
Wang, Xinqiang 1778
Wang, Xiuyu 1527
Wang, Xudong 1060
Wang, Xue Gang 2125
Wang, Xue-Kun 971
Wang, Yanbin 2126
Wang, Yanxin 892
Wang, Ying 2126
Wang, Ying 2119
Wang, Yingge 587
Wang, Yinxi 2127
2127
2128
Wang, Yonghua 2128
Wang, Yongli 612
Wang, Yongli 2129
2183
Wang, Yongli 2129
Wang, You Xiao 2183
Wang, Yu 2276
Wang, Yuanyuan 2127
2127
2128
Wang, Yuejun 2282
Wang, Yuheng 1389
1503
2130
Wang, Yunpeng 2130
Wang, Yunshuen 2213
Wang, Zaicong 2131
Wang, Zhengrong 441
Wang, Zhilin 472
Wang, Zimeng 913
Wanger, G. 1538
Wankel, S. 2131
Wanless, V.D. 2132
Wanzek, T. 2132
Ward, A. 1771
Ward, D. 2270
Warden, A. 1305
Warmada, I.W. 1078
Warner, N. 1891
Warr, O. 1140
2133
2274
Warren, C. 1167
1900
Warren, J. 731
2133
Warren, L. 2134
Wartho, J-A. 2047
Warzinski, R.P. 806
Waseda, A. 1524
Washbourne, C-L. 1711
2134
Washton, N. 1771
Waska, H. 2135
Wasylenki, L. 2135
Watanabe, K. 2224
Watanabe, T. 1793
Watanabe, Y. 1561
Watenphul, A. 2136
Watkins, J. 749
2136
Watson, A. 1474
Watson, B. 485
878
Watson, D. 569
1045
Watson, E.B. 1040
1981
2029
Watts, M. 1886
1897
Watzin, M. 782
Waworuntu, J. 1777
Waychunas, G. 841
915
1130
2137
Weare, J.H. 1488
Webb, L. 852
Webb, S. 484
1433
1796
Weber, B. 2137
Weber, C. 523
Weber, Karrie 1177
Weber, Konradin 1449
2138
Weber, L. 2048
Weber, P.K. 1431
1634
Webster, J. 510
Webster-Brown, J. 2138
Wegener, G. 2139
Weh, A. 1899
Wehber, M. 1510
2139
Wehrer, M. 1335
Wehrli, B. 1192
Wehrmann, H. 1096
2140
Wehrmann, L. 2140
Wei, G. 2141
Wei, K-Y 1352
Wei, W. 2193
Wei, Xiaofei 1313
Wei, Xinglin 1060
Wei, Z. 2110
Weigand, W. 427
Weijma, J. 933
964
1330
Weinberg, R. 987
Weiner, T. 442
Weingartner, E. 476
Weinlein, W. 1820
Weinman, B. 1229
2141
Weinstein, C. 2142
Weinstein, Y. 1193

https://doi.org/10.1180/S0026461X00006502 Published online by Cambridge University Press

Weis, D. 486
487
731
1071
1080
1451
1546
1859
2142
Weis, U. 475
1117
2212
Weisener, C.G. 1894
2110
2143
Weiss, D.J. 773
1129
1271
Weiss, H. 907
Weiss, S. 478
Weiss, W. 1002
Weiss, Y. 1182
1528
2143
Welander, P. 1377
Weldeab, S. 1233
Weller, C. 2144
Wellman, D. 1103
2144
Welsch, A.-M. 2145
Welti, A. 1939
Wen, H. 1909
Wen, S. 1307
Wen, X-P. 2145
Wenau, S. 2171
Wendt, K. 2146
Wendt-Potthoff, K. 2146
Wengorsch, T. 426
Wenk, C.B. 535
1293
2147
Wenk, H-R. 1406
Wenk, J. 1790
Wentzcovitch, R. 2147
Wenzel, T. 877
1405
2177
Wenzhöfer, F. 666
1110
Werner, R. 990
1012
1032
1236
Wernick, E. 2148
2288
Wernicke, B. 1901
Wershofen, H. 1936
Weryer, S. 1783
Wesolowski, D. 1378
1666
West, A.J. 1415
2148
West, J. 567
Westall, F. 1282
Westerhold, T. 1136
2160
Westermann, S. 2149
Westervelt, D. 407
Westner, K. 2149
Weston, B. 474
648
2150
Westrenen, W.V. 1168
Wetmore, K. 693
Wetzel, D. 2150
Wetzel, F. 2151
Weyer, S. 543
797
1279
1548
2151
Whan, T. 2152
Wheeler, J. 1377
2152
Whitaker, T. 435
Whitby, C. 1948
White, A. 604
White, G. 680
2153
White, L. 2153
White, M. 2252
White, N. 599
1546
White, S. 970
White, T. 575
1377
1455
White, W. 650
2154
Whitehead, B. 1891
Whitehead, J. 2154
Whitehill, A. 1570
Whitehouse, M.J. 594
719
734
1102
1138
1277
1301
1405
1614
1629
1714
1752
1759
1890
2155
Whiteside, J. 1568
Whittington, A. 1733
Whittleston, R. 2155
Widdel, F. 1477
2139
Widerlund, A. 1083
Wiechert, U. 469
1551
2156
Więcław, D. 2156
Wieczorek, A.K. 869
2157
Wiedenbeck, M. 521
834
2177
2212
Wiederhold, J. 1025
1899
2157
Wiedermann, J. 1896
Wieler, R. 600
1245
1675
1811
Wierzbicki, R. 452
Wierzchos, J. 2094
2158
Wieser, Martin 410
Wieser, Michael 1432
Wiesner, M. 2191
Wigley, M. 786
1140
2158
2274
Wignall, P.B. 716
Wijbrans, J. 1501
Wilcke, W. 1767
Wilcken, K. 1339
Wilczynska-Michalik, W. 896
1463
2159
Wild, M. 666
Wildau, A. 2159
Wilde, S. 993
1696
Wildenschild, D. 587
Wildt, J. 1181
Wilhelms-Dick, D. 2160
Wilke, M. 787
964
1778
1819
1880
2160
Wilkes, E. 2135
Wilkes, H. 1685
Wilkie, K. 2161
Wilkins, M. 2163
Wilkinson, J. 844
Wilkinson, Jamie 1028
Wilkinson, K.J. 1635
Wilkinson, M. 1001
Willbold, M. 867
1264
2091
2161
Willett, S. 2162
Williams, B. 2162
Williams, H.M. 884
1020
1803
2163
Williams, I.S. 1108
1246
Williams, J-P. 1766
Williams, K. 484
729
1556
2163
Williams, N. 2164
Williams, Q. 689
Williams, Terry 1211
Williams, Trevor 693
Williams, W. 1361
Williams-Jones, A.E. 522
871
1073
1353
1466
2063
2159
2248
Williford, K. 2164
Williford, R. 1771
Wilmes, P. 2165
Wilsky, F. 1200
Wilson, A. 1589
Wilson, C. 424
694
2187
Wilson, D. 2165
Wilson, J. 1738
Wilson, M. 707
Wilson, N. 2138
Wilson, P. 1009
Wilson, R. 837
Wilson, S.A. 502
1826
Wimpenny, J. 665
2166
Winbjörk, H. 1012
Wind, B. 1831
Winde, V. 2166
Wing, B. 699
1314
1616
Winkel, L.H.E. 515
Winkler, B. 2092
2093
Winkler, R. 860
Winkler, S. 802
2167
Winton, V.H. 2167
Wirick, S. 855
Wirth, R. 520
1005
1095
1981
2073
2184
Wirth, S.B. 1540
Wiseman, C. 1031
Wiszniewska, J. 1246
Withers, A.C. 450
724
2168
Wittebroodt, C. 523
Wittig, N. 2149
2168
Wittmann, H. 2101
Wobrock, W. 854

https://doi.org/10.1180/S0026461X00006502 Published online by Cambridge University Press

Wogelius, R.A. 798
2072
Wohlgemuth-Ueberwasser, C.C. 1005
2169
Wohling, D. 583
Wojtulek, P. 2169
Wolf, E. 2170
Wolfe, A. 1505
Wolfe, C.J. 932
Wolff, E. 1210
1560
Wolff, J. 806
1692
2170
Wolff, P.E. 2171
Wolff-Boenisch, D. 576
883
951
1946
2171
Wolf-Gladrow, D. 404
983
1235
Wolthers, M. 2172
Wombacher, F. 2172
Wong, Vanessa 2173
Wong, Victor 705
Wong, W.W. 2173
Wongfun, N. 2174
Wood, B.J. 1539
1824
2068
2106
2163
2174
2175
Wood, R. 2175
Woodard, S. 2176
Wooden, J. 568
623
1155
Woodfield, B.F. 1756
Woodhead, Jon 1138
Woodhead, Jonathon 692
1169
1608
2013
Woodhouse, M. 2176
Woodland, A. 522
2177
2217
Woodruff, L. 1537
Woodward, M. 1007
Worgard, L. 2177
Wörner, G. 451
477
1043
1062
1931
Woronycz, L. 2178
Worsfold, P. 796
1165
Worsham, S. 2178
Worsnop, Douglas 718
Worsnop, Douglas R. 617
705
825
1580
1924
2093
2162
Wotte, T. 2179
Wotzlaw, J-F. 2179
Woycheese, K. 1460
Wright, James 1808
Wright, Justin 2093
Wright, P. 1868
Wrighton, K. 2180
Wu, Chang-Zhi 1710
Wu, Chunping 2110
Wu, Cindy 693
Wu, D. 1343
Wu, Fengchang 2190
Wu, Fu-Yuan 1288
1316
1338
1340
Wu, Hailin 2268
2278
Wu, Hai-Zhi 2180
Wu, Jia 2181
Wu, Jiajie 1984
Wu, Jianfeng 2181
2280
Wu, Jichun 2115
2280
Wu, L. 1112
Wu, P. 1312
2180
2182
2208
2232
Wu, Q.H. 643
Wu, R-X. 2255
Wu, T-W. 1391
Wu, Wei-Min 569
Wu, Weizhong 2141
Wu, Xiang 1936
Wu, Xiaoqi 2182
Wu, Yanyou 2183
Wu, Ying 799
1016
Wu, Y. Q 2183
Wu, Yuanbao 2184
Wu, Yunjun 480
Wunder, B. 2184
Wunsch, A. 2185
Wuttig, K. 538
2185
Wyche, K. 423
Wykes, J. 2186
Wypych, A. 2186
Wysoczanski, R. 424
974
2187

X

Xi, R-G. 1144
2190
Xia, F 2188
Xia, Fan 2188
Xia, Qiong-Xia 2188
Xia, Qunke K 741
1084
Xia, Yiben 957
Xia, Y. Q 2183
Xia, Yuan 2280
Xiang, M. 1313
Xiang, Y. 2189
Xiao, Jianxin 2267
Xiao, Jun 2189
Xiao, M. 2190
Xiao, P-X. 1144
2190
Xiao, S. 1168
Xiao, T-F. 2119
Xiao, X. 2116
Xiao, Yan 2191
Xiao, Yao 2191
Xiao, Yi 2112
Xiao, Yilin 1062
2192
Xiao, Yuanyuan 2192
Xiao, Yuming 1878
Xiao, Z. 2193
Xiaosi, S. 2193
Xie, H. 1776
Xie, K. 2245
Xie, Lei 2194
Xie, Lie-Wen 665
2166
Xie, Luhua 2141
Xie, R. 2194
Xie, S. 1348
Xie, X. 2195
Xie, Y. 1041
Xie, Zhi 2195
Xie, Zhouqing 1142
Xin, H. 1293
Xin, X. 1110
Xing, G. 2271
Xiong, X. 2114
Xiong, Y. 637
Xiu, Z. 652
Xu, A. 2278
Xu, Chen 1797
Xu, Cheng 1260
2196
Xu, Chuanyu 1216
Xu, D. 472
Xu, Guangping 907
2196
Xu, Gui-Wen 470
Xu, H. 2197
Xu, Jin 2114
Xu, Jun 1457
2116
Xu, Li 525
Xu, Lijuan 2192
Xu, Lingling 1345
Xu, Linshu 480
Xu, M. 1784
Xu, Sheng 1339
Xu, Shujuan 2267
Xu, Tao 1367
Xu, Tianfu 2257
Xu, Wangchun 2252
Xu, Wen Lai 1958
Xu, Wen-Liang 619
1454
1454
1614
2116
2197
2207
Xu, Wenyi 2207
Xu, Xisheng 2234
Xu, Xue-Yi 654
1315
2118
2198
Xu, Y. 2207
Xu, Z. 1998
2198
2250
Xue, Y. 1337
Xue, Z. 1267

Y

Yager, P.L. 2218
Yaghubpur, A. 2199
Yagi, T. 1078
Yakovleva, Sofia 2199
Yakovleva, Sonya 1785
Yakubovich, O. 2199
Yakushev, E. 2200
Yakymchuk, C. 2200
Yalcinalp, B. 817
Yamada, Keita 1314
Yamada, Kunimi 2204
Yamaguchi, I. 1159
Yamaguchi, K. 1561
2070
Yamaguchi, Yasuhiko 1079
Yamaguchi, Yoshiaki 2201
Yamakawa, M. 1564
Yamamoto, J. 2028
2201
Yamamoto, Masahiro 1524
Yamamoto, Masatsugu 401
Yamamoto, S. 1158
2227
Yamamoto, Y. 2202
Yamanaka, A. 2202
Yamanaka, Takamitsu 2203
Yamanaka, Toshiro 1392
Yamaoka, K. 1158
2203
Yamasaki, S. 2204
Yamashita, Y. 2204
Yamasoe, M. 1750
Yamauchi, R. 1182
Yamazaki, D. 834
Yamazaki, E. 2205
Yamazaki, T. 1221
Yan, C. 1276
Yan, D. 2205
Yan, L. 1089
Yan, R. 2206
Yanardag, I.H. 606
2206
Yang, C. 1369

https://doi.org/10.1180/S0026461X00006502 Published online by Cambridge University Press

Yang, Dan 2207
Yang, Debin 2197
..... 2207
Yang, Gang 976
..... 2287
Yang, Guangshu 2208
Yang, Guifang 2282
Yang, Hai 747
Yang, Hong 2208
Yang, Hsiao-Ming 668
Yang, Hua 2265
Yang, Jd 2128
Yang, Jie 1325
..... 1998
Yang, Jing-Sui 1736
..... 2209
Yang, Jin-Hui 1268
Yang, J.y 2233
..... 2246
Yang, Kui-Feng 827
..... 1055
Yang, Kyounghee 2209
Yang, Li 2210
..... 2280
Yang, Li 1680
..... 1931
..... 2073
..... 2210
Yang, Linsheng 2211
Yang, Ming 1321
Yang, Mingjun 565
Yang, N. 991
Yang, P. 2211
Yang, Q. 2212
Yang, Shouye 957
..... 1307
..... 2212
Yang, Shui-Yuan 2213
Yang, Shun-Chung 873
..... 1030
..... 1284
Yang, Suyin 1256
Yang, T.F. 2213
Yang, W.Q. 1342
..... 2113
Yang, Xiao-Feng 2145
Yang, Xiaojing 2214
Yang, Xingye 2117
Yang, Yongqiang 2214
Yang, Yuanyuan 1322
..... 2115
Yang, Yue-Heng 1316
Yang, Yun 2181
Yang, Z.S. 1347
..... 2010
Yao, J-M. 2215
Yao, Q-Z. 2271
Yao, S. 1115
..... 1337
..... 2215
Yao, Z. 2290
Yapaskurt, V. 1620
Yarar, O.S 2216
Yardley, B. 1754
..... 2216
Yariv, S. 555
Yarmolyuk, V. 2121
Yaşar, R. 416
Yashoda, S. 1378
Yaxley, G. 522
..... 2217
Yaylali-Abanuz, G. 2217
Yazdi, M. 402
Ye, F. 901
Ye, J. 1733
Ye, K. 658
..... 1341
..... 2218
Ye, L. 1350
Ye, Y. 2252
Yeager, C. 1797
Yechieli, Y. 1193
..... 1769
Yee, N. 690
..... 1596
Yeh, E-C. 1337
Yeh, G. 2285
Yeung, L.Y. 2218
Yi, K. 2079
Yi, P. 654
Yi, X. 720
Yigini, Y. 2219
Yildirim, B 1133
Yildiz, M. 2219
Yilmaz, A. 2220
Yilmaz, İ.Ö. 2264
Yin, J. 657
Yin, Q-Z. 420
..... 665
..... 1283
..... 1857
..... 2166
..... 2220
Yin, Z-Y. 1318
Yokochi, R. 728
..... 2221
Yokouchi, Y. 1987
Yokoyama, E. 2221
Yokoyama, L. 2222
Yokoyama, Tadashi 1544
..... 2222
Yokoyama, Takaomi D. . 1027
..... 1159
..... 1564
..... 2223
Yokoyama, Takushi 818
..... 1481
..... 1772
..... 2224
Yokoyama, Tetsuya 873
..... 1564
..... 2223
Yokoyama, Y. 2223
Yondon, M. 1132
Yonezu, K. 1481
..... 1772
..... 2224
Yong, Y. 1311
Yongli, W. 1067
Yoo, C-H. 1286
Yoo, K. 1229
..... 1279
..... 2224
Yoon, Jin-Ho 1695
Yoon, Junyeon 577
Yoon, S-C. 1144
..... 1187
Yoon, Y.Y. 668
..... 1288
..... 2225
Yoshida, K. 1963
..... 2225
Yoshida, N. 1045
..... 1314
..... 1544
..... 2046
Yoshida, S. 1084
Yoshikawa, H. 1800
Yoshimura, S. 2226
Yoshimura, T. 2226
Yoshinaga, M. 1832
Yoshino, T. 2227
Yoshiya, K. 2227
You, H. 950
..... 1342
..... 1857
..... 2228
..... 2249
You, X. 2228
You, Z. 2229
Youbi, N. 1423
Young, E.D. 1382
..... 1844
..... 2218
..... 2229
..... 2284
..... 2284
Young, L. 1165
Young, Sansfica 2230
Young, Scott 1897
Young, T. 778
Yousefi, M. 2230
Yu, C. 2231
Yu, H. 666
..... 2231
Yu, Jinhai 2232
Yu, Ji-Yuan 1318
..... 2232
Yu, Q. 1799
..... 2233
Yu, X.D. 836
..... 2233
..... 2246
Yu, Yan 2114
Yu, Yao 2234
Yuan, F. 1319
..... 2251
..... 2254
Yuan, Hongji 2234
Yuan, Honglin 2235
Yuan, W. 2235
Yuan, X. 2236
Yuan, Y. 2236
Yuasa, M. 1087
Yücel, C. 2237
Yudintsev, S. 1241
Yue, F. 1317
Yue, M. 2122
Yui, M. 1999
Yui, T-F. 1268
..... 1391
Yun, J. 1680
Yun, S-T. 923
..... 1286
..... 1600
Yurimoto, H. 834
Yurkevich, N. 2237
Yurteri, C. 1566
Yuryeva, O. 2244
Yuzvinsky, T. 1538

Z

Zaarur, S. 410
Žabka, V. 2238
Zaccarini, F. 415
..... 896
..... 1214
..... 2030
..... 2055
..... 2105
..... 2238
Zachara, J. 604
..... 680
..... 865
..... 945
..... 1338
..... 1757
..... 2239
Zacharias, M. 635
Zacher, G. 2239
Zachos, J. 914
..... 1619
Zack, T. 708
..... 1219
..... 1753
..... 2240
Zadorin, A. 1632
Zaenker, H. 478
Zagnitko, V. 1526
Zagrtdenov, N. 421
Zagt, K. 1330
Zaharescu, D. 2240
Zahid, A. 1648
Zahiri, R. 1636
Zahn, R. 2063
..... 2241
Zahnle, K. 927
..... 2241
Zajacz, Z. 2242
Žák, J. 1103
Zak, K. 2242
Zambardi, T. 2243
Zammit, C. 1707
Zamudio-Resendiz, M.E. 2090
Zanda, B. 936
Zanetti, A. 555
..... 1354
..... 2283
Zanon, V. 2243
Zapata, V. 1875
Zapata-Rios, X. 1621
Zarmpas, P. 1532

https://doi.org/10.1180/S0026461X00006502 Published online by Cambridge University Press

Zarrinkoub, M.H. 668
Zarzycki, P. 915
..... 1757
..... 1757
Zavarin, M. 1064
Zavarzin, G. 2244
Zavarzina, D. 2244
Zavšek, S. 1141
Zazzo, A. 476
Zdimal, V. 2286
Zechmeister-Boltenstern, S. 1495
Zedgenizov, D. 2244
Zeebe, R. 1619
Zeglin, L. 1634
Zeh, A. 1156
Zemanova, L. 815
..... 2245
Zenáhlíková, J. 573
Zeng, L. 2245
Zeng, X. 1617
..... 2246
Zeng, Y. 836
..... 1618
..... 2123
..... 2233
..... 2246
..... 2289
Zerkle, A. 831
..... 1140
..... 1663
..... 2247
Zernack, A. 1943
Zetterberg, T. 1212
Zetzsch, C. 605
Zezin, D. 1466
..... 2247
..... 2248
Zgonnick, V. 2027
Zhamyanov, D. 2050
..... 2248
Zhan, Y. 950
..... 1342
..... 1857
..... 2249
Zhang, W.J. 2258
Zhang, Chao 2249
Zhang, Chaofeng 956
Zhang, Chengjiang 1858
..... 2129
..... 2198
..... 2250
Zhang, Chengli 2250
Zhang, Chi 835
Zhang, Chi 785
Zhang, Dayu 2251
Zhang, Dexian 2251
Zhang, Dong Mei 1057
..... 1317
Zhang, Fenfen 1016
Zhang, Fred 2252
Zhang, Guiping 931
..... 1374
Zhang, Guoping 1055
..... 1313
Zhang, Hai 1216
Zhang, Haichun 642
Zhang, Haikun 2273
Zhang, Haitao 720
Zhang, Hao 1363
Zhang, Hong 1965
..... 1966
Zhang, Hongfei 2252
..... 2254
Zhang, Hong-Fu 2191
..... 2265
Zhang, Hong Ying 643
Zhang, Jiangsu 747
..... 1618
Zhang, Jianzhong 2197
Zhang, Jin 1792
Zhang, Jing 1016
Zhang, Jing 1349
..... 1909
..... 2253
Zhang, J. ..... Q 2233
Zhang, Jun-Bo 2253
Zhang, K. 1115
Zhang, Lejun 2254
Zhang, Li 828
..... 2254
Zhang, Li-Fei 940
..... 1320
..... 2208
Zhang, Lin 956
Zhang, Lingmin 1341
Zhang, Liuyi 1618
Zhang, LiuYi 1315
Zhang, Ming 1372
Zhang, Ming-Ming 1319
Zhang, P. 1054
Zhang, Qi 2236
Zhang, Qi 1924
Zhang, Qinqin 891
Zhang, Ronghua 1058
..... 2255
..... 2259
Zhang, Rongqing 1359
Zhang, Saijin 1797
Zhang, S.h. 2123
Zhang, Shao-Bing 2255
Zhang, Shengyu 2261
Zhang, Shipeng 2256
Zhang, Shuichang 996
..... 1461
..... 1867
..... 1959
..... 2256
..... 2276
Zhang, Shunxin 1521
Zhang, Shuo 2257
Zhang, Shuwen 480
Zhang, Tong 1054
..... 2257
Zhang, Tonglin 567
Zhang, Weiming 2258
Zhang, Weiqing 709
Zhang, Wen 659
Zhang, Wen-Jing 1858
..... 1959
Zhang, Wenlan 2194
Zhang, Xiaoran 2259
Zhang, Xiaoyi 915
Zhang, Xiaoyu 2114
Zhang, Xuetong 1058
..... 2255
..... 2259
Zhang, Yan 432
Zhang, Yan 2208
Zhang, Yan 2181
Zhang, Yanlin 1055
Zhang, Yanlin 2260
Zhang, Yaping 2162
Zhang, Yi 537
Zhang, Youxue 1535
..... 2260
Zhang, Yuan 1865
Zhang, Yuling 2261
Zhang, Yx 1909
Zhang, Zhan 1378
Zhang, Zhanshi 2261
Zhang, Zhaohui 2262
Zhang, Zhaowei 892
..... 2262
Zhang, Zhigang 785
Zhang, Zhihai 833
Zhang., Zhijun 2263
Zhang, Zhiying 2263
Zhang, Zuoheng 1041
Zhang, Z.w 1113
Zhao, C. 2130
Zhao, H.L. 2264
Zhao, K-D. 2213
..... 2264
Zhao, Laishi 1060
..... 1063
..... 2252
..... 2272
Zhao, Lan 567
Zhao, Lei 709
..... 2265
Zhao, Liang 1111
..... 2276
Zhao, Lian Rong 1545
Zhao, S. 2273
Zhao, T-P. 2215
Zhao, Xiao Feng 643
Zhao, Xiaoyi 2265
Zhao, XinMiao 2265
Zhao, Yanyan 2266
Zhao, Ye 2266
Zhao, Yongwei 827
Zhao, Yuanyi 2214
Zhao, Yujia 1289
Zhao, Yusheng 2197
Zhao, Zehui 2267
Zhao, Zhi-Dan 1338
Zhao, Zhijun 2267
Zhao, Zhiqi 1317
Zhao, Zi-Fu 2268
Zhaoxian, Z. 2193
Zharkova, E. 1394
Zheng, B. 2268
Zheng, C. 945
Zheng, G. 1524
..... 2118
Zheng, M. 2269
Zheng, P-X. 2269
Zheng, X. 2270
Zheng, Yan-Ping 2116
Zheng, Yong-Fei 655
..... 658
..... 891
..... 1854
..... 2184
..... 2188
..... 2255
..... 2266
..... 2268
..... 2270
Zherebetskaya, O. 556
Zhidikova, A. 1257
Zhilina, T. 2244
Zhimulev, E. 1542
Zhmodik, S. 1278
..... 1813
Zhng, M. 2127
Zhong, H. 470
Zhong, Z. 2254
Zhou, D. 2120
Zhou, G-T. 2271
Zhou, Jian 2117
Zhou, Jie 2271
Zhou, Jin Sheng 1545
Zhou, Lian 1060
..... 1063
..... 2272
Zhou, Liya 2272
Zhou, N. 2273
Zhou, Qiang 1374
Zhou, Qunjun 2197
Zhou, S. 2273
Zhou, T-F. 1319
..... 2251
..... 2254
Zhou, W-B. 1054
..... 2274
Zhou, X. 1375
Zhou, Yan 1984
..... 2269
Zhou, Yipeng 1967
Zhou, Yongzhang 432
Zhou, Z. 1140
..... 1502
..... 2274
Zhu, Bei 2189
Zhu, Bi 2275
Zhu, Bing Quan 643
Zhu, Chen 1112
..... 2275
Zhu, Chen 2276
Zhu, Guangyou 1959
..... 2276
Zhu, Guizhi 936
Zhu, Jiang 1482
..... 2277
Zhu, Jianming 1679
..... 2236
Zhu, Jinchu 2194
Zhu, Jing 1876
..... 2277
Zhu, M-H. 2278
Zhu, R. 1601
Zhu, T. 2118
Zhu, Wei-Guang 470

https://doi.org/10.1180/S0026461X00006502 Published online by Cambridge University Press

Zhu, Wenbin 2268
..... 2278
Zhu, Xianfang 1110
..... 2279
Zhu, Xiangkun 2279
Zhu, XiangKun 2265
Zhu, Xiaobin 2181
..... 2280
Zhu, Xi Yan 1316
..... 2210
..... 2280
Zhu, Z. 2281
Zhukova, I. 2281
Zhuo, S. 2282
Zhuravlev, K. 1792
Zi, J. 2282
Ziaei, M. 2283
Ziaii, M. 2283
Ziberna, L. 1354
..... 2283
Ziegler, K. 633
..... 649
..... 2284
..... 2284
Ziegler, S. 2285
Ziemann, M.A. 1228
Ziemann, P. 1633
..... 2285
Zieringer, M. 2286
Žigon, S. 1141
Zikova, N. 2286
Zilm-Gramckow, S. 801
Zimmer, Martin 2032
Zimmer, Mindy 1190
..... 1648
Zimmerman, A. 2287
Zimmerman, G. 449
Zimmermann, C. 1706
Zimmermann, G. 577
Zimmermann, L. 473
Zimmermann, M. 746
Zimmermann, P. 494
Zimmermann, U. 1523
Zimmermannová, D. 2287
Zinchenko, O. 440
Zincone, S. 2148
..... 2288
Zinger, T. 2288
Zini, L. 1465
Zipfel, J. 928
Zivor, R. 2242
Zobrist, B 1402
Zolotov, M. 2289
Zolotova, N. 1660
Zondervan, A. 755
Zong, C-L. 1454
Zopfi, J. 535
..... 2147
Zori, M. 2026
Zorina, L. 1670
Zoroglu, O. 1133
Zotov, A. 502
Zou, F. 1066
..... 2114
..... 2289
Zou, H. 2290
Zou, X. 1321
Zouari, K. 1628
Zoulkova, V. 1520
Zral, V. 452
Zubavichus, Y. 1745
Zuddas, P. 1726
Zuend, A. 1402
Zuidema, P. 2290
Zuo, Renguang 2291
Zuo, Rui 2291
Zwingmann, H. 2204
Zyryanova, L. 2292

Zvyagina, E. A325
Zwiener, C. A1239

https://doi.org/10.1180/S0026461X00006502 Published online by Cambridge University Press